
REVIEW OF PARTICLE PHYSICS*

Particle Data Group

Abstract

This biennial *Review* summarizes much of particle physics. Using data from previous editions, plus 2158 new measurements from 551 papers, we list, evaluate, and average measured properties of gauge bosons, leptons, quarks, mesons, and baryons. We also summarize searches for hypothetical particles such as Higgs bosons, heavy neutrinos, and supersymmetric particles. All the particle properties and search limits are listed in Summary Tables. We also give numerous tables, figures, formulae, and reviews of topics such as the Standard Model, particle detectors, probability, and statistics. Among the 108 reviews are many that are new or heavily revised including those on neutrino mass, mixing, and oscillations, QCD, top quark, CKM quark-mixing matrix, V_{ud} & V_{us} , V_{cb} & V_{ub} , fragmentation functions, particle detectors for accelerator and non-accelerator physics, magnetic monopoles, cosmological parameters, and big bang cosmology.

A booklet is available containing the Summary Tables and abbreviated versions of some of the other sections of this full *Review*. All tables, listings, and reviews (and errata) are also available on the Particle Data Group website: <http://pdg.lbl.gov>.

Particle Data Group

K. Nakamura,^{1,2} K. Hagiwara,² K. Hikasa,³ H. Murayama,^{1,4,5} M. Tanabashi,⁶ T. Watari,¹ C. Amsler,⁷ M. Antonelli,⁸ D.M. Asner,⁹ H. Baer,¹⁰ H.R. Band,¹¹ R.M. Barnett,⁵ T. Basaglia,¹² E. Bergren,¹³ J. Beringer,⁵ G. Bernardi,¹³ W. Bertl,¹⁴ H. Bichsel,¹⁵ O. Biebel,¹⁶ E. Blucher,¹⁷ S. Blusk,¹⁸ R.N. Cahn,⁵ M. Carena,^{19,17} A. Ceccucci,¹² D. Chakraborty,²⁰ M.-C. Chen,²¹ R.S. Chivukula,²² G. Cowan,²³ O. Dahl,⁵ G. D'Ambrosio,²⁴ T. Damour,²⁵ D. de Florian,²⁶ A. de Gouvêa,²⁷ T. DeGrand,²⁸ G. Dissertori,²⁹ B. Dobrescu,¹⁹ M. Doser,¹² M. Drees,³⁰ D.A. Edwards,³¹ S. Eidelman,³² J. Erler,³³ V.V. Ezhela,³⁴ W. Fetscher,²⁹ B.D. Fields,³⁵ B. Foster,³⁶ T.K. Gaisser,³⁷ L. Garren,¹⁹ H.-J. Gerber,²⁹ G. Gerbier,³⁸ T. Gherghetta,³⁹ G.F. Giudice,¹² S. Golwala,⁴⁰ M. Goodman,⁴¹ C. Grab,²⁹ A.V. Gritsan,⁴² J.-F. Grivaz,⁴³ D.E. Groom,⁵ M. Grünewald,⁴⁴ A. Gurtu,^{45,12} T. Gutsche,⁴⁶ H.E. Haber,⁴⁷ C. Hagmann,⁴⁸ K.G. Hayes,⁴⁹ M. Heffner,⁴⁸ B. Heltsley,⁵⁰ J.J. Hernández-Rey,^{51†} A. Höcker,¹² J. Holder,³⁷ J. Huston,²² J.D. Jackson,⁵ K.F. Johnson,¹⁰ T. Junk,¹⁹ A. Karle,¹¹ D. Karlen,⁵² B. Kayser,¹⁹ D. Kirkby,²¹ S.R. Klein,⁵³ C. Kolda,⁵⁴ R.V. Kowalewski,⁵² B. Krusche,⁵⁵ Yu.V. Kuyanov,³⁴ Y. Kwon,⁵⁶ O. Lahav,⁵⁷ P. Langacker,⁵⁸ A. Liddle,⁵⁹ Z. Ligeti,⁵ C.-J. Lin,⁵ T.M. Liss,⁶⁰ L. Littenberg,⁶¹ K.S. Lugovsky,³⁴ S.B. Lugovsky,³⁴ J. Lys,⁵ H. Mahlke,⁵⁰ T. Mannel,⁶² A.V. Manohar,⁶³ W.J. Marciano,⁶¹ A.D. Martin,⁶⁴ A. Masoni,⁶⁵ D. Milstead,⁶⁶ R. Miquel,⁶⁷ K. Mönig,⁶⁸ M. Narain,⁶⁹ P. Nason,⁷⁰ S. Navas,^{71†} P. Nevski,⁶¹ Y. Nir,⁷² K.A. Olive,⁷³ L. Pape,²⁹ C. Patrignani,⁷⁴ J.A. Peacock,⁷⁵ S.T. Petcov,^{76,1,77} A. Piepke,⁷⁸ G. Punzi,⁷⁹ A. Quadt,⁸⁰ S. Raby,⁸¹ G. Raffelt,⁸² B.N. Ratcliff,⁸³ P. Richardson,⁶⁴ S. Roesler,¹² S. Rolli,⁸⁴ A. Romaniouk,⁸⁵ L.J. Rosenberg,¹⁵ J.L. Rosner,¹⁷ C.T. Sachrajda,⁸⁶ Y. Sakai,² G.P. Salam,⁸⁷ S. Sarkar,⁸⁸ F. Sauli,¹² O. Schneider,⁸⁹ K. Scholberg,⁹⁰ D. Scott,⁹¹ W.G. Seligman,⁹² M.H. Shaevitz,⁹³ M. Silari,¹² T. Sjöstrand,⁹⁴ J.G. Smith,²⁸ G.F. Smoot,⁵ S. Spanier,⁹⁵ H. Spieler,⁵ A. Stahl,⁹⁶ T. Stanev,³⁷ S.L. Stone,¹⁸ T. Sumiyoshi,⁹⁷ M.J. Syphers,¹⁹ J. Terning,⁹⁸ M. Titov,⁹⁹ N.P. Tkachenko,³⁴ N.A. Törnqvist,¹⁰⁰ D. Tovey,¹⁰¹ T.G. Trippe,⁵ G. Valencia,¹⁰² K. van Bibber,⁴⁸ G. Venanzoni,⁸ M.G. Vincter,¹⁰³ P. Vogel,¹⁰⁴ A. Vogt,¹⁰⁵ W. Walkowiak,⁶² C.W. Walter,⁹⁰ D.R. Ward,¹⁰⁶ B.R. Webber,¹⁰⁶ G. Weiglein,³¹ E.J. Weinberg,⁹³ J.D. Wells,¹⁰⁷ A. Wheeler,⁸³ L.R. Wiencke,¹⁰⁸ C.G. Wohl,⁵ L. Wolfenstein,¹⁰⁹ J. Womersley,¹¹⁰ C.L. Woody,⁶¹ R.L. Workman,¹¹¹ A. Yamamoto,² W.-M. Yao,⁵ O.V. Zenin,³⁴ J. Zhang,¹¹² R.-Y. Zhu,¹¹³ P.A. Zyla⁵

Technical Associates: G. Harper,⁵ V.S. Lugovsky,³⁴ P. Schaffner⁵

1. *Institute for the Physics and Mathematics of the Universe (IPMU), University of Tokyo, Kashiwa-shi, Chiba-ken 277-8583, Japan*
2. *KEK, High Energy Accelerator Research Organization, Oho, Tsukuba-shi, Ibaraki-ken 305-0801, Japan*
3. *Department of Physics, Tohoku University, Aoba-ku, Sendai 980-8578, Japan*
4. *Department of Physics, University of California, Berkeley, CA 94720, USA*
5. *Physics Division, Lawrence Berkeley National Laboratory, 1 Cyclotron Road, Berkeley, CA 94720, USA*
6. *Department of Physics, Nagoya University, Chikusa-ku, Nagoya, 464-8602, Japan*
7. *Physik-Institut, Universität Zürich, CH-8057 Zürich, Switzerland*
8. *Lab. Nazionali di Frascati dell'INFN, CP 13, via E. Fermi, 40, I-00044 Frascati (Roma), Italy*
9. *Pacific Northwest National Laboratory, 902 Battelle Boulevard, Richland, WA 99352, USA*
10. *Department of Physics, Florida State University, Tallahassee, FL 32306, USA*
11. *Department of Physics, University of Wisconsin, Madison, WI 53706, USA*
12. *CERN, European Organization for Nuclear Research, CH-1211 Genève 23, Switzerland*
13. *LPNHE, IN2P3-CNRS et Universités de Paris 6 et 7, F-75252 Paris, France*
14. *Paul Scherrer Institut, CH-5232 Villigen PSI, Switzerland*
15. *Department of Physics, University of Washington, Seattle, WA 98195, USA*
16. *Ludwig-Maximilians-Universität, Fakultät für Physik, Schellingstr. 4, D-80799 München, Germany*
17. *Enrico Fermi Institute and Department of Physics, University of Chicago, Chicago, IL 60637-1433, USA*
18. *Department of Physics, Syracuse University, Syracuse, NY, 13244-1130, USA*
19. *Fermi National Accelerator Laboratory, P.O. Box 500, Batavia, IL 60510, USA*
20. *Department of Physics, Northern Illinois University, DeKalb, IL 60115, USA*
21. *Department of Physics and Astronomy, University of California, Irvine, CA 92697-4576, USA*
22. *Michigan State University, Dept. of Physics and Astronomy, East Lansing, MI 48824-2320, USA*
23. *Department of Physics, Royal Holloway, University of London, Egham, Surrey TW20 0EX, UK*
24. *INFN - Sezione di Napoli Complesso Universitario Monte Sant'Angelo, Via Cintia, 80126 Napoli, Italy*
25. *Institut des Hautes Etudes Scientifiques, F-91440 Bures-sur-Yvette, France*
26. *Departamento de Física, FCEyN, Universidad de Buenos Aires, Pab.1, Ciudad Universitaria, (1428) Capital Federal, Argentina*
27. *Department of Physics and Astronomy, Northwestern University, Evanston, IL 60208, USA*
28. *Department of Physics, University of Colorado at Boulder, Boulder, CO 80309, USA*
29. *Institute for Particle Physics, ETH Zurich, 8093 Zurich, Switzerland*
30. *Universität Bonn, Physikalisches Institut, Nussallee 12, D-53115 Bonn, Germany*
31. *Deutsches Elektronen-Synchrotron DESY, Notkestraße 85, D-22603 Hamburg, Germany*

† J.J. Hernández-Rey and S. Navas acknowledge support from MICINN, Spain (FPA2009-07264-E)

32. *Budker Institute of Nuclear Physics, RU-630090, Novosibirsk, Russia*
33. *Departamento de Física Teórica, Instituto de Física, Universidad Nacional Autónoma de México, México D.F. 04510, México*
34. *COMPAS Group, Institute for High Energy Physics, RU-142284, Protvino, Russia*
35. *Department of Astronomy, University of Illinois, 1002 W. Green St., Urbana, IL 61801, USA*
36. *Denys Wilkinson Building, Department of Physics, University of Oxford, Oxford, OX1 3RH, UK*
37. *Bartol Research Institute, University of Delaware, Newark, DE 19716, USA*
38. *CEA/Saclay, DSM/IRFU, BP 2, F-91191 Gif s Yvette, France*
39. *School of Physics, University of Melbourne, Victoria, 3010 Australia*
40. *California Institute of Technology, Division of Physics, Mathematics, and Astronomy, Mail Code 367-17, Pasadena, CA 91125, USA*
41. *Argonne National Laboratory, 9700 S. Cass Ave., Argonne, IL 60439-4815, USA*
42. *Johns Hopkins University, Baltimore, Maryland 21218, USA*
43. *LAL, IN2P3-CNRS et Univ. de Paris 11, F-91898 Orsay CEDEX, France*
44. *Dept. of Physics and Astronomy, University of Ghent, Proeftuinstraat 86, B-9000 Ghent, Belgium*
45. *Tata Institute of Fundamental Research, Mumbai (Bombay) 400 005, India*
46. *Institut für Theoretische Physik, Universität Tübingen, Auf der Morgenstelle 14, D-72076 Tübingen, Germany*
47. *Santa Cruz Institute for Particle Physics, University of California, Santa Cruz, CA 95064, USA*
48. *Lawrence Livermore National Laboratory, 7000 East Ave., Livermore, CA 94550, USA*
49. *Department of Physics, Hillsdale College, Hillsdale, MI 49242, USA*
50. *Laboratory of Elementary-Particle Physics, Cornell University, Ithaca, NY 14853, USA*
51. *IFIC — Instituto de Física Corpuscular, Universitat de València — C.S.I.C., E-46071 Valencia, Spain*
52. *University of Victoria, Victoria, BC V8W 3P6, Canada*
53. *Nuclear Science Division, Lawrence Berkeley National Laboratory, 1 Cyclotron Road, Berkeley, CA 94720, USA*
54. *Department of Physics, University of Notre Dame, 225 Niewland Hall, Notre Dame, IN 46556, USA*
55. *Institute of Physics, University of Basel, CH-4056 Basel, Switzerland*
56. *Yonsei University, Department of Physics, 134 Sinchon-dong, Sudaemoon-gu, Seoul 120-749, South Korea*
57. *Department of Physics and Astronomy, University College London, Gower Street, London WC1E 6BT, UK*
58. *School of Natural Science, Institute for Advanced Study, Princeton, NJ 08540, USA*
59. *Astronomy Centre, University of Sussex, Falmer, Brighton BN1 9QH, UK*
60. *Department of Physics, University of Illinois, 1110 W. Green Street, Urbana, IL 61801, USA*
61. *Physics Department, Brookhaven National Laboratory, Upton, NY 11973, USA*
62. *Fachbereich Physik, Universität Siegen Walter-Flex-Str. 3, 57068 Siegen, Germany*
63. *Department of Physics, University of California at San Diego, La Jolla, CA 92093, USA*
64. *Institute for Particle Physics Phenomenology, Department of Physics, University of Durham, Durham DH1 3LE, UK*
65. *INFN Sezione di Cagliari, Cittadella Universitaria de Monserrato, Casella postale 170, I-09042 Monserrato (CA), Italy*
66. *Fysikum, Stockholms Universitet, AlbaNova University Centre, SE-106 91 Stockholm, Sweden*
67. *Institució Catalana de Recerca i Estudis Avançats, Institut de Física d'Altes Energies, E-08193 Bellaterra (Barcelona), Spain*
68. *DESY-Zeuthen, D-15735 Zeuthen, Germany*
69. *Brown University, Department of Physics, 182 Hope Street, Providence, RI 02912, USA*
70. *INFN, Sez. di Milano-Bicocca, Piazza della Scienza, 3, I-20126 Milano, Italy*
71. *Dpto. de Física Teórica y del Cosmos & C.A.F.P.E., Universidad de Granada, 18071 Granada, Spain*
72. *Weizmann Institute of Science, Department of Particle Physics and Astrophysics, P.O. Box 26 Rehovot 76100, Israel*
73. *University of Minnesota, School of Physics and Astronomy, 116 Church St. D.E., Minneapolis, MN 55455, USA*
74. *Dipartimento di Fisica e INFN, Università di Genova, I-16146 Genova, Italy*
75. *Institute for Astronomy, University of Edinburgh, Royal Observatory, Blackford Hill, Edinburgh, EH9 3JZ, Scotland, UK*
76. *SISSA/INFN, via Bonomea, 265, 34136 Trieste TS, Italy*
77. *INRNE, Bulgarian Academy of Sciences, 1784 Sofia, Bulgaria*
78. *Department of Physics and Astronomy University of Alabama, 206 Gallalee Hall, Box 870324, Tuscaloosa, AL 35487-0324, USA*
79. *INFN and Dipartimento di Fisica, Università di Pisa, I-56127 Pisa, Italy*
80. *Georg-August-Universität Göttingen, II. Physikalisches Institut, Friedrich-Hund-Platz 1, D-37077 Göttingen, Germany*
81. *Department of Physics, The Ohio State University, 191 W. Woodruff Ave., Columbus, OH 43210, USA*
82. *Max-Planck-Institut für Physik (Werner-Heisenberg-Institut), Föhringer Ring 6, D-80805 München, Germany*
83. *SLAC National Accelerator Laboratory, 2575 Sand Hill Road, Menlo Park, CA 94025, USA*
84. *Tufts University, Robinson Hall, Medford, MA 02155, USA*
85. *Moscow Engineering and Physics Institute, 31, Kashirskoye shosse, 115409 Moscow, Russia*
86. *School of Physics and Astronomy, University of Southampton, Highfield, Southampton S017 1BJ, UK*

87. *LPTHE, UPMC Université Paris 6, CNRS UMR 7589, 4 place Jussieu, Paris, France*
88. *Rudolf Peierls Centre for Theoretical Physics, University of Oxford, 1 Keble Road, Oxford OX1 3NP, UK*
89. *Ecole Polytechnique Fédérale de Lausanne (EPFL), CH-1015 Lausanne, Switzerland*
90. *Physics Department, Duke University, Durham, NC 27708, USA*
91. *Department of Physics and Astronomy, University of British Columbia, Vancouver, BC V6T 1Z1, Canada*
92. *Columbia University, Nevis Labs, PO Box 137, Irvington, NY 10533, USA*
93. *Department of Physics, Columbia University, 538 West 120th St., New York, NY 10027, USA*
94. *Department of Theoretical Physics, Lund University, S-223 62 Lund, Sweden*
95. *Department of Physics and Astronomy, University of Tennessee, Knoxville, TN 37996, USA*
96. *III. Physikalisches Institut, Physikzentrum, RWTH Aachen University, 52056 Aachen, Germany*
97. *High Energy Physics Laboratory, Tokyo Metropolitan University, Tokyo, 192-0397, Japan*
98. *Department of Physics, University of California, Davis, CA 95616, USA*
99. *CEA/Saclay, B.P.2, Orme des Merisiers, F-91191 Gif-sur-Yvette Cedex, France*
100. *Department of Physics, POB 64 FIN-00014 University of Helsinki, Finland*
101. *Department of Physics and Astronomy, University of Sheffield, Sheffield S3 7RH, UK*
102. *Department of Physics, Iowa State University, Ames, IA 50011, USA*
103. *Department of Physics, Carleton University, 1125 Colonel By Drive, Ottawa, ON K1S 5B6, Canada*
104. *California Institute of Technology, Kellogg Radiation Laboratory 106-38, Pasadena, CA 91125, USA*
105. *Division of Theoretical Physics, Department of Mathematical Sciences, The University of Liverpool, Liverpool, L69 3BX, United Kingdom*
106. *Cavendish Laboratory, J.J. Thomson Avenue, Cambridge CB3 0HE, UK*
107. *Michigan Center for Theoretical Physics, Physics Dept., 2477 Randall Laboratory, University of Michigan, Ann Arbor, MI 48109, USA*
108. *Dept. of Physics, Colorado School of Mines, Golden Colorado, 80401 USA*
109. *Department of Physics, Carnegie Mellon University, Pittsburgh, PA 15213, USA*
110. *STFC Rutherford Appleton Laboratory, Didcot, OX11 0QX, UK*
111. *Department of Physics, George Washington University Virginia Campus, Ashburn, VA 20147-2604, USA*
112. *IHEP, Chinese Academy of Sciences, Beijing 100049, P.R. China*
113. *California Institute of Technology, High Energy Physics, MC 256-48, Pasadena, CA 91125, USA*

HIGHLIGHTS OF THE 2010 EDITION OF THE REVIEW OF PARTICLE PHYSICS

551 new papers with 2158 new measurements.

- Latest from ***B*-meson** physics: 132 papers with 714 measurements:
 - *CP* violation
 - B_s mixing
 - Determination of V_{cb} , and V_{ub} CKM elements
 - New *b*-hadron states
- Many new results in the sections on strongly-decaying **mesons**: 130 papers with 698 measurements.
- New measurements of D_s^+ **branching fractions** and a new review of them.
- Nine new **top quark mass** results.
- **Astrophysics** sections updated with the 5-year WMAP analysis.
- The **Table of Astrophysical Constants** extended to include more cosmological parameters from the 5-year WMAP analysis.
- New “**Magnetic Monopoles**” review on searches.

108 reviews (most are revised or new).

- Major update of the reviews on:
 - **QCD**
 - **Top quark**
 - **Fragmentation functions**
- “**High-Energy Collider Parameters**” review includes SuperB and SuperKEKB.
- New “**Neutrino Mass, Mixing, and Oscillations**” review.
- “**Particle Detectors for Accelerator Physics**” review has substantial updates and a new section.
- New review on “**Particle Detectors for Non-Accelerator Physics**” covers
 - Atmospheric fluorescence and Cherenkov detectors
 - Large TPCs for rare event detection
 - Sub-Kelvin detectors
 - Low-radioactivity background techniques

See pdgLive.lbl.gov for online access to PDG database.

See pdg.lbl.gov/AtomicNuclearProperties for Atomic Properties of Materials.

COLOR VERSIONS OF MANY FIGURES AVAILABLE AT END OF BOOK.

TABLE OF CONTENTS

HIGHLIGHTS	5		
INTRODUCTION		Astrophysics and Cosmology	
1. Overview	11	18. Experimental tests of gravitational theory (rev.)	225
2. Particle Listings responsibilities	11	19. Big-Bang cosmology (rev.)	230
3. Consultants	12	20. Big-Bang nucleosynthesis (rev.)	241
4. Naming scheme for hadrons	13	21. The cosmological parameters (rev.)	246
5. Procedures	13	22. Dark matter (rev.)	255
5.1 Selection and treatment of data	13	23. Cosmic microwave background (rev.)	261
5.2 Averages and fits	14	24. Cosmic rays (rev.)	269
5.2.1 Treatment of errors	14	Experimental Methods and Colliders	
5.2.2 Unconstrained averaging	14	25. Accelerator physics of colliders (rev.)	277
5.2.3 Constrained fits	15	26. High-energy collider parameters (rev.)	281
5.3 Rounding	16	27. Passage of particles through matter (rev.)	285
5.4 Discussion	16	28. Particle detectors at accelerators (rev.)	300
History plots (rev.)	17	29. Particle detectors for non-accelerator phys. (new)	328
Online particle physics information (rev.)	18	30. Radioactivity and radiation protection (rev.)	341
		31. Commonly used radioactive sources	345
PARTICLE PHYSICS SUMMARY TABLES		Mathematical Tools or Statistics, Monte Carlo, Group Theory	
Gauge and Higgs bosons	25	32. Probability (rev.)	346
Leptons	27	33. Statistics (rev.)	350
Quarks	30	34. Monte Carlo techniques (rev.)	361
Mesons	31	35. Monte Carlo particle numbering scheme (rev.)	364
Baryons	72	36. Clebsch-Gordan coefficients, spherical harmonics, and d functions	368
Searches (Supersymmetry, Compositeness, <i>etc.</i>)	87	37. SU(3) isoscalar factors and representation matrices	369
Tests of conservation laws	89	38. SU(n) multiplets and Young diagrams	370
REVIEWS, TABLES, AND PLOTS		Kinematics, Cross-Section Formulae, and Plots	
Constants, Units, Atomic and Nuclear Properties		39. Kinematics (rev.)	371
1. Physical constants (rev.)	101	40. Cross-section formulae for specific processes (rev.)	376
2. Astrophysical constants (rev.)	102	41. Plots of cross sections and related quantities (rev.)	385
3. International System of Units (SI)	104		
4. Periodic table of the elements (rev.)	105		
5. Electronic structure of the elements	106		
6. Atomic and nuclear properties of materials	108		
7. Electromagnetic relations	110		
8. Naming scheme for hadrons	112		
Standard Model and Related Topics			
9. Quantum chromodynamics (new)	114		
10. Electroweak model and constraints on new physics (rev.)	126		
11. The Cabibbo-Kobayashi-Maskawa quark-mixing matrix (rev.)	146		
12. CP violation (rev.)	154		
13. Neutrino Mass, Mixing, and Oscillations (new)	164		
14. Quark model (rev.)	184		
15. Grand Unified Theories	193		
16. Structure functions (rev.)	201		
17. Fragmentation functions in e^+e^- , ep and pp collisions (rev.)	215		

(Continued on next page.)

PARTICLE LISTINGS*

Illustrative key and abbreviations	405
Gauge and Higgs bosons	
(γ , gluon, graviton, W , Z , Higgs, Axions)	417
Leptons	
(e , μ , τ , Heavy-charged lepton searches, Neutrino properties, Number of neutrino types, Double- β decay, Neutrino mixing, Heavy-neutral lepton searches)	515
Quarks	
(u , d , s , c , b , t , b' , t' (4^{th} generation), Free quarks)	583
Mesons	
Light unflavored (π , ρ , a , b) (η , ω , f , ϕ , h)	619
Other light unflavored	735
Strange (K , K^*)	740
Charmed (D , D^*)	803
Charmed, strange (D_s , D_s^* , D_{sJ})	856
Bottom (B , V_{cb}/V_{ub} , B^* , B_J^*)	877
Bottom, strange (B_s , B_s^* , B_{sJ}^*)	1031
Bottom, charmed (B_c)	1039
$c\bar{c}$ (η_c , $J/\psi(1S)$, χ_c , ψ)	1040
$b\bar{b}$ (Υ , χ_b)	1109
Non- $q\bar{q}$ candidates	1131
Baryons	
N	1135
Δ	1178
Exotic	1199
Λ	1201
Σ	1217
Ξ	1241
Ω	1254
Charmed (Λ_c , Σ_c , Ξ_c , Ω_c)	1257
Doubly charmed (Ξ_{cc})	1277
Bottom (Λ_b , Σ_b , Σ_b^* , Ξ_b , b -baryon admixture)	1278
Miscellaneous searches	
Monopoles	1285
Supersymmetry	1292
Technicolor	1340
Compositeness	1347
Extra Dimensions	1354
Searches for WIMPs and Other Particles	1365
INDEX	1373
COLOR FIGURES	1391

MAJOR REVIEWS IN THE PARTICLE LISTINGS

Gauge and Higgs bosons	
The Mass of the W Boson (rev.)	418
Triple Gauge Couplings (rev.)	422
Anomalous W/Z Quartic Couplings	424
The Z Boson (rev.)	426
Anomalous $ZZ\gamma$, $Z\gamma\gamma$, and ZZV Couplings	445
Searches for Higgs Bosons (rev.)	448
The W' Searches (rev.)	480
The Z' Searches (rev.)	483
Leptoquarks	490
Axions and Other Very Light Bosons (rev.)	496
Leptons	
Muon Anomalous Magnetic Moment (rev.)	521
Muon Decay Parameters (rev.)	521
τ Branching Fractions (rev.)	529
τ -Lepton Decay Parameters	548
Number of Light Neutrino Types	561
Neutrinoless Double- β Decay (rev.)	562
Quarks	
Quark Masses (rev.)	583
The Top Quark (rev.)	596
Free Quark Searches	613
Mesons	
Form Factors for Rad. Pion & Kaon Decays (rev.)	620
Note on Scalar Mesons (rev.)	630
The $\eta(1405)$, $\eta(1475)$, $f_1(1420)$, and $f_1(1510)$ (rev.)	680
Rare Kaon Decays (rev.)	742
$K_{\ell 3}^{\pm}$ and $K_{\ell 3}^0$ Form Factors (rev.)	753
CPT Invariance Tests in Neutral Kaon Decay (rev.)	759
CP Violation in $K_S \rightarrow 3\pi$	764
V_{ud} , V_{us} , Cabibbo Angle, and CKM Unitarity (rev.)	771
CP -Violation in K_L Decays (rev.)	779
Dalitz-Plot Analysis Formalism	807
Review of Charm Dalitz-Plot Analyses (rev.)	811
$D^0-\bar{D}^0$ Mixing (rev.)	820
D_s^+ Branching Fractions (new)	858
Decay Cons. of Charged Pseudoscalar Mesons (rev.)	861
Production and Decay of b -flavored Hadrons (rev.)	877
Polarization in B Decays (rev.)	967
$B^0-\bar{B}^0$ Mixing (rev.)	973
Determination of V_{cb} and V_{ub} (rev.)	1014
Branching Ratios of $\psi(2S)$ and $\chi_{c0,1,2}$ (rev.)	1060
Baryons	
Baryon Decay Parameters	1146
N and Δ Resonances	1149
Pentaquarks	1199
Radiative Hyperon Decays	1242
Charmed Baryons (rev.)	1257
Λ_c^+ Branching Fractions	1260
Miscellaneous searches	
Magnetic Monopoles (new)	1285
Supersymmetry (rev.)	1292
Dynamical Electroweak Symmetry Breaking (rev.)	1340
Searches for Quark & Lepton Compositeness	1347
Extra Dimensions	1354

*The divider sheets give more detailed indices for each main section of the Particle Listings.

INTRODUCTION

1. Overview	11
2. Particle Listings responsibilities	11
3. Consultants	12
4. Naming scheme for hadrons	13
5. Procedures	13
5.1 Selection and treatment of data	13
5.2 Averages and fits	14
5.2.1 Treatment of errors	14
5.2.2 Unconstrained averaging	14
5.2.3 Constrained fits	15
5.3 Rounding	16
5.4 Discussion	16
History plots	17

ONLINE PARTICLE PHYSICS INFORMATION

1. Introduction	18
2. Particles and Properties Databases	18
3. Open Access Databases (arXiv, SPIRES,...)	18
4. Conference Databases	19
5. Particle Physics Journals and Reviews	19
6. Research Institutions	19
7. People	19
8. Collaborations & Experiments	19
9. Jobs	20
10. Software Repositories	20
11. Particle Physics Education Sites	20
12. Physics Topic Pages	21
13. Further Reading	21



INTRODUCTION

1. Overview

The *Review of Particle Physics* and the abbreviated version, the *Particle Physics Booklet*, are reviews of the field of Particle Physics. This complete *Review* includes a compilation/evaluation of data on particle properties, called the “Particle Listings.” These Listings include 2,158 new measurements from 551 papers, in addition to the 27,337 measurements from 7,749 papers that first appeared in previous editions [1].

Both books include Summary Tables with our best values and limits for particle properties such as masses, widths or lifetimes, and branching fractions, as well as an extensive summary of searches for hypothetical particles. In addition, we give a long section of “Reviews, Tables, and Plots” on a wide variety of theoretical and experimental topics, a quick reference for the practicing particle physicist.

The *Review* and the *Booklet* are published in even-numbered years. This edition is an updating through January 2010 (and, in some areas, well into 2010). As described in the section “Using Particle Physics Databases” following this introduction, the content of this *Review* is available on the World-Wide Web, and is updated between printed editions (<http://pdg.lbl.gov/>).

The Summary Tables give our best values of the properties of the particles we consider to be well established, a summary of search limits for hypothetical particles, and a summary of experimental tests of conservation laws.

The Particle Listings contain all the data used to get the values given in the Summary Tables. Other measurements considered recent enough or important enough to mention, but which for one reason or another are not used to get the best values, appear separately just beneath the data we do use for the Summary Tables. The Particle Listings also give information on unconfirmed particles and on particle searches, as well as short “reviews” on subjects of particular interest or controversy.

The Particle Listings were once an archive of all published data on particle properties. This is no longer possible because of the large quantity of data. We refer interested readers to earlier editions for data now considered to be obsolete.

We organize the particles into six categories:

- Gauge and Higgs bosons
- Leptons
- Quarks
- Mesons
- Baryons
- Searches for monopoles, supersymmetry, compositeness, extra dimensions, *etc.*

The last category only includes searches for particles that do not belong to the previous groups; searches for heavy charged leptons and massive neutrinos, by contrast, are with the leptons.

In Sec. 2 of this Introduction, we list the main areas of responsibility of the authors, and also list our large number of consultants, without whom we would not have been able to produce this *Review*. In Sec. 4, we mention briefly the naming scheme for hadrons. In Sec. 5, we discuss our procedures for choosing among measurements of particle properties and for obtaining best values of the properties

from the measurements.

The accuracy and usefulness of this *Review* depend in large part on interaction between its users and the authors. We appreciate comments, criticisms, and suggestions for improvements of any kind. Please send them to the appropriate author, according to the list of responsibilities in Sec. 2 below, or to the LBNL addresses below.

To order a copy of the *Review* or the *Particle Physics Booklet* from North and South America, Australia, and the Far East, send email to PDG@LBL.GOV

or via the web at:

<http://pdg.lbl.gov/pdgmail>

or write to:

Particle Data Group, MS 50R6008
Lawrence Berkeley National Laboratory
Berkeley, CA 94720-8166, USA

From all other areas, see

<http://library.web.cern.ch/library/Library/request.html>

or write to

CERN Scientific Information Service
CH-1211 Geneva 23, Switzerland

2. Particle Listings responsibilities

* Asterisk indicates the people to contact with questions or comments about Particle Listings sections.

Gauge and Higgs bosons

γ	C. Grab, D.E. Groom*
Gluons	R.M. Barnett,* A.V. Manohar
Graviton	D.E. Groom*
W, Z	A. Gurtu,* M. Grünewald*
Higgs bosons	K. Hikasa, G. Weiglein*
Heavy bosons	M. Tanabashi, T. Watari*
Axions	G. Raffelt*

Leptons

Neutrinos	M. Goodman, R. Miquel,* K. Nakamura, K.A. Olive, A. Piepke, P. Vogel
e, μ	J. Beringer,* C. Grab
τ	K.G. Hayes, K. Mönig*

Quarks

Quarks	R.M. Barnett,* A.V. Manohar
Top quark	J. Beringer,* K. Hagiwara
b', t'	K. Hagiwara, W.-M. Yao*
Free quark	J. Beringer*

Mesons

π, η	J. Beringer,* C. Grab
Unstable mesons	C. Amsler, M. Doser,* S. Eidelman,* T. Gutsche, B. Heltsley, J.J. Hernández-Rey, H. Mahlke, A. Masoni, S. Navas, C. Patrignani, S. Spanier, N.A. Törnqvist, G. Venanzoni
K (stable)	G. D'Ambrosio, C.-J. Lin*
D (stable)	D.M. Asner, S. Blusk, C.G. Wohl*
B (stable)	Y. Kwon, G. Punzi, J.G. Smith, W.-M. Yao*

Baryons

Stable baryons	C. Grab, C.G. Wohl*
Unstable baryons	C.G. Wohl,* R.L. Workman
Charmed baryons	S. Blusk, C.G. Wohl*
Bottom baryons	Y. Kwon, J.G. Smith, G. Punzi, W.-M. Yao*

Miscellaneous searches

Monopole	D. Milstead*
Supersymmetry	A. de Gouvêa, G. Weiglein,* K.A. Olive, L. Pape
Technicolor	M. Tanabashi, J. Terning*
Compositeness	M. Tanabashi, J. Terning*
Extra Dimensions	T. Gherghetta*, C. Kolda
WIMPs and Other	K. Hikasa,*

3. Consultants

The Particle Data Group benefits greatly from the assistance of some 700 physicists who are asked to verify every piece of data entered into this *Review*. Of special value is the advice of the PDG Advisory Committee which meets biennially and thoroughly reviews all aspects of our operation. The members of the 2010 committee are:

H. Aihara (Tokyo), Chair
G. Brooijmans (Columbia)
D. Harris (FNAL)
P. Janot (CERN)
G. Perez (Stony Brook)

We have especially relied on the expertise of the following people for advice on particular topics:

- S.I. Alekhin (COMPAS Group, IHEP, Protvino)
- M. Artuso (Syracuse University)
- E. Barberio (University of Melbourne, Australia)
- M. Bardeen (FNAL)
- R. Barlow (Manchester U.)
- A. Belyaev (University of Southampton)
- G. Bernardi (LPNHE-Paris)
- S. Bethke (MPI, Munich)
- I.I. Bigi (Notre Dame University)
- M. Billing (Cornell University)
- T. Brooks (SLAC)
- T. Browder (University of Hawaii)
- O. Bruening (CERN)
- D. Bugg (Queen Mary, London)
- F. Canelli (Enrico Fermi Institute, University of Chicago)
- D. Cassel (Cornell U.)
- G.L. Cassiday (U. Utah)
- G. Cavoto (University of Rome, Italy)
- M. Chanowitz (LBNL)
- H.-C. Cheng (UC Davis)
- J. Coleman (SLAC)
- B. Dawson (U. Adelaide, Australia)
- P. de Jong (NIKHEF)
- F. Deliot (CEA, Saclay)
- L. Demortier (Rockefeller University)
- D. Denisov (FNAL)
- F. Di Lodovico (University of Lodon)
- A. Donnachie (University of Manchester)
- R. Escribano (IFAE, Barcelona)
- M. Fidecaro (CERN)
- W. Fischer (BNL)
- P. Franzini (Rome U. & INFN, Frascati)
- B.K. Fujikawa (LBNL)
- P. Gambino (Univ. degli Studi di Torino)
- A. Georges (Univ. Montreal, Canada)
- T. Gerasis (INP, NCSR, Athens)
- T. Gershon (U. of Warwick, UK)
- A. Glazov (DESY)
- D. Glenzinski (FNAL)
- R. Godang (University of South Alabama)
- B. Golob (U. Ljubljana)
- G. Gomez-Ceballos (MIT)
- F. Harris (University of Hawaii)
- S. Heinemeyer (IFCA (CSIC-UC), Santander, Spain)
- J. Heinrich (University of Pennsylvania)
- A. Hoang (Max-Planck-Institut, Germany)
- T. Iijima (KEK)
- K. Inoue (Tohoku)
- G. Isidori (INFN, Frascati)
- R. Itoh (KEK)
- J. Jowett (CERN)
- R.W. Kadel (LBNL)
- J. Kadyk (LBNL)
- A. Kagan (University of Cincinnati)
- S.G. Karshenboim (VNIIM, St-Petersburg)
- A.G. Kharlamov (BINP, Novosibirsk)
- K. Kleinknecht (U. Mainz)
- J.R. Klein (U. Pennsylvania)
- B.A. Kniehl (University of Hamburg)
- T. Komatsubara (KEK)
- J. Konigsberg (University of Florida)
- F. Krauss (University of Durham)
- A. Kronfeld (FNAL)
- S.-I. Kurokawa (KEK)
- H. Lacker (LAL-Orsay)
- E.B. Levichev (BINP, Novosibirsk)
- J. Libby (Indian Inst. of Technology, Madras)
- E. Linder (LBNL)
- O. Long (UC Riverside)
- D. Lopes Pegna (Princeton)
- V. Luth (SLAC)
- G.R. Lynch (LBNL)
- L. Lyons (Oxford U.)
- M.L. Mangano (CERN)
- P. Massarotti (Naples U.&INFN)
- B. Meadows (U. of Cincinnati)
- J.P. Miller (Boston University)
- S. Moch (DESY)
- P.J. Mohr (NIST)
- S. Monteil (Univ. Blaise Pascal, France)
- R. Moore (FNAL)
- M. Neubert (Cornell University)
- D. Newell (INST, Gaithersburg)
- J. Nico (NIST)
- H.P. Nilles (Bonn University)
- H. O'Connell (FNAL)
- Y. Ohnishi (KEK, Japan)
- K. Oide (KEK, Japan)
- S. Olsen (University of Hawaii)
- M. Palutan (INFN, Frascati)
- M. Paulini (Carnegie Mellon University)
- M.R. Pennington (University of Durham)
- A. Pich (IFIC, Valencia)
- T. Plehn (University of Edinburgh)
- P. Raimondi (INFN, Frascati)
- M. Ramsey-Musolf (Univ. Wisconsin)
- B.L. Roberts (Boston University)
- M. Roney (University of Victoria)

- M. Ross (FNAL)
- M. Ruspa (INFN-Torin)
- K. Sachs (Carleton Univ.)
- V.D. Samoylenko (IHEP, Serpukhov)
- M. Schmitt (Northwestern University)
- C. Schwanda (HEPHY, Vienna)
- C. Schwanenberger (University of Manchester)
- A.J. Schwartz (University of Cincinnati)
- J.T. Seeman (SLAC)
- E. Shabalina (University of Illinois at Chicago)
- S. Sharpe (University of Washington)
- Yu.M. Shatunov (BINP, Novosibirsk)
- T. Sloan (Lancaster Univ.)
- A.R. Smith (LBNL)
- S. Soldner-Rembold (University of Manchester)
- V. Sorin (Universitat Autònoma de Barcelona)
- M.S. Sozzi (Pisa, Scuola Normale Superiore)
- A. Stocchi (Orsay, LAL)
- S.I. Striganov (COMPAS Group, IHEP, Protvino)
- Z. Sullivan (ANL & Southern Methodist U.)
- W.M. Sun (Cornell U.)
- T. Tait (ANL)
- B.N. Taylor (NIST)
- R. Tesarek (FNAL)
- J. Thaler (MIT)
- E. Thorndike (U. Rochester)
- K. Trabelsi (KEK)
- R. Van Kooten (Indiana University)
- G. Velev (Fermilab)
- L.-T. Wang (Princeton University)
- T.C. Weekes (Center for Astrophysics-Whipple Observ.)
- C. Weiser (University of Freiburg, Germany)
- G. Wilkinson (Oxford)
- M. Wobisch (Louisiana Tech. University)
- D. Wood (Northeastern University)
- C.-P. Yuan (Michigan State University)
- G. Zanderighi (University of Oxford)
- C. Zhang (IHEP, Beijing)

4. Naming scheme for hadrons

We introduced in the 1986 edition [2] a new naming scheme for the hadrons. Changes from older terminology affected mainly the heavier mesons made of u , d , and s quarks. Otherwise, the only important change to known hadrons was that the F^\pm became the D_s^\pm . None of the lightest pseudoscalar or vector mesons changed names, nor did the $c\bar{c}$ or $b\bar{b}$ mesons (we do, however, now use χ_c for the $c\bar{c}$ χ states), nor did any of the established baryons. The Summary Tables give both the new and old names whenever a change has occurred.

The scheme is described in “Naming Scheme for Hadrons” (p. 112) of this *Review*.

We give here our conventions on type-setting style. Particle symbols are italic (or slanted) characters: e^- , p , Λ , π^0 , K_L , D_s^+ , b . Charge is indicated by a superscript: B^- , Δ^{++} . Charge is not normally indicated for p , n , or the quarks, and is optional for neutral isosinglets: η or η^0 . Antiparticles and particles are distinguished by charge for charged leptons and mesons: τ^+ , K^- . Otherwise, distinct antiparticles are indicated by a bar (overline): $\bar{\nu}_\mu$, \bar{t} , \bar{p} , \bar{K}^0 , and $\bar{\Sigma}^+$ (the antiparticle of the Σ^-).

5. Procedures

5.1. Selection and treatment of data : The Particle Listings contain all relevant data known to us that are published in journals. With very few exceptions, we do not include results from preprints or conference reports. Nor do we include data that are of historical importance only (the Listings are not an archival record). We search every volume of 20 journals through our cutoff date for relevant data. We also include later published papers that are sent to us by the authors (or others).

In the Particle Listings, we clearly separate measurements that are used to calculate or estimate values given in the Summary Tables from measurements that are not used. We give explanatory comments in many such cases. Among the reasons a measurement might be excluded are the following:

- It is superseded by or included in later results.
- No error is given.
- It involves assumptions we question.
- It has a poor signal-to-noise ratio, low statistical significance, or is otherwise of poorer quality than other data available.
- It is clearly inconsistent with other results that appear to be more reliable. Usually we then state the criterion, which sometimes is quite subjective, for selecting “more reliable” data for averaging. See Sec. 5.4.
- It is not independent of other results.
- It is not the best limit (see below).
- It is quoted from a preprint or a conference report.

In some cases, *none* of the measurements is entirely reliable and no average is calculated. For example, the masses of many of the baryon resonances, obtained from partial-wave analyses, are quoted as estimated ranges thought to probably include the true values, rather than as averages with errors. This is discussed in the Baryon Particle Listings.

For upper limits, we normally quote in the Summary Tables the strongest limit. We do not average or combine upper limits except in a very few cases where they may be re-expressed as measured numbers with Gaussian errors.

As is customary, we assume that particle and antiparticle share the same spin, mass, and mean life. The Tests of Conservation Laws table, following the Summary Tables, lists tests of CPT as well as other conservation laws.

We use the following indicators in the Particle Listings to tell how we get values from the tabulated measurements:

- OUR AVERAGE—From a weighted average of selected data.
- OUR FIT—From a constrained or overdetermined multi-parameter fit of selected data.
- OUR EVALUATION—Not from a direct measurement, but evaluated from measurements of related quantities.
- OUR ESTIMATE—Based on the observed range of the data. Not from a formal statistical procedure.
- OUR LIMIT—For special cases where the limit is evaluated by us from measured ratios or other data. Not from a direct measurement.

An experimentalist who sees indications of a particle will of course want to know what has been seen in that region in the past. Hence we include in the Particle Listings all

reported states that, in our opinion, have sufficient statistical merit and that have not been disproved by more reliable data. However, we promote to the Summary Tables only those states that we feel are well established. This judgment is, of course, somewhat subjective and no precise criteria can be given. For more detailed discussions, see the minireviews in the Particle Listings.

5.2. Averages and fits: We divide this discussion on obtaining averages and errors into three sections: (1) treatment of errors; (2) unconstrained averaging; (3) constrained fits.

5.2.1. Treatment of errors: In what follows, the “error” δx means that the range $x \pm \delta x$ is intended to be a 68.3% confidence interval about the central value x . We treat this error as if it were Gaussian. Thus when the error is Gaussian, δx is the usual one standard deviation (1σ). Many experimenters now give statistical and systematic errors separately, in which case we usually quote both errors, with the statistical error first. For averages and fits, we then add the two errors in quadrature and use this combined error for δx .

When experimenters quote asymmetric errors $(\delta x)^+$ and $(\delta x)^-$ for a measurement x , the error that we use for that measurement in making an average or a fit with other measurements is a continuous function of these three quantities. When the resultant average or fit \bar{x} is less than $x - (\delta x)^-$, we use $(\delta x)^-$; when it is greater than $x + (\delta x)^+$, we use $(\delta x)^+$. In between, the error we use is a linear function of x . Since the errors we use are functions of the result, we iterate to get the final result. Asymmetric output errors are determined from the input errors assuming a linear relation between the input and output quantities.

In fitting or averaging, we usually do not include correlations between different measurements, but we try to select data in such a way as to reduce correlations. Correlated errors are, however, treated explicitly when there are a number of results of the form $A_i \pm \sigma_i \pm \Delta$ that have identical systematic errors Δ . In this case, one can first average the $A_i \pm \sigma_i$ and then combine the resulting statistical error with Δ . One obtains, however, the same result by averaging $A_i \pm (\sigma_i^2 + \Delta_i^2)^{1/2}$, where $\Delta_i = \sigma_i \Delta [\sum (1/\sigma_j^2)]^{1/2}$. This procedure has the advantage that, with the modified systematic errors Δ_i , each measurement may be treated as independent and averaged in the usual way with other data. Therefore, when appropriate, we adopt this procedure. We tabulate Δ and invoke an automated procedure that computes Δ_i before averaging and we include a note saying that there are common systematic errors.

Another common case of correlated errors occurs when experimenters measure two quantities and then quote the two and their difference, *e.g.*, m_1 , m_2 , and $\Delta = m_2 - m_1$. We cannot enter all of m_1 , m_2 and Δ into a constrained fit because they are not independent. In some cases, it is a good approximation to ignore the quantity with the largest error and put the other two into the fit. However, in some cases correlations are such that the errors on m_1 , m_2 and Δ are comparable and none of the three values can be ignored. In this case, we put all three values into the fit and invoke an automated procedure to increase the errors prior to fitting such that the three quantities can be treated as independent measurements in the constrained fit. We include a note saying that this has been done.

5.2.2. Unconstrained averaging: To average data, we use a standard weighted least-squares procedure and in some cases, discussed below, increase the errors with a “scale factor.” We begin by assuming that measurements of a given quantity are uncorrelated, and calculate a weighted average and error as

$$\bar{x} \pm \delta\bar{x} = \frac{\sum_i w_i x_i}{\sum_i w_i} \pm (\sum_i w_i)^{-1/2}, \quad (1)$$

where

$$w_i = 1/(\delta x_i)^2.$$

Here x_i and δx_i are the value and error reported by the i th experiment, and the sums run over the N experiments. We then calculate $\chi^2 = \sum w_i (\bar{x} - x_i)^2$ and compare it with $N - 1$, which is the expectation value of χ^2 if the measurements are from a Gaussian distribution.

If $\chi^2/(N - 1)$ is less than or equal to 1, and there are no known problems with the data, we accept the results.

If $\chi^2/(N - 1)$ is very large, we may choose not to use the average at all. Alternatively, we may quote the calculated average, but then make an educated guess of the error, a conservative estimate designed to take into account known problems with the data.

Finally, if $\chi^2/(N - 1)$ is greater than 1, but not greatly so, we still average the data, but then also do the following:

(a) We increase our quoted error, $\delta\bar{x}$ in Eq. (1), by a scale factor S defined as

$$S = [\chi^2/(N - 1)]^{1/2}. \quad (2)$$

Our reasoning is as follows. The large value of the χ^2 is likely to be due to underestimation of errors in at least one of the experiments. Not knowing which of the errors are underestimated, we assume they are all underestimated by the same factor S . If we scale up all the input errors by this factor, the χ^2 becomes $N - 1$, and of course the output error $\delta\bar{x}$ scales up by the same factor. See Ref. 3.

When combining data with widely varying errors, we modify this procedure slightly. We evaluate S using only the experiments with smaller errors. Our cutoff or ceiling on δx_i is arbitrarily chosen to be

$$\delta_0 = 3N^{1/2} \delta\bar{x},$$

where $\delta\bar{x}$ is the unscaled error of the mean of all the experiments. Our reasoning is that although the low-precision experiments have little influence on the values \bar{x} and $\delta\bar{x}$, they can make significant contributions to the χ^2 , and the contribution of the high-precision experiments thus tends to be obscured. Note that if each experiment has the same error δx_i , then $\delta\bar{x}$ is $\delta x_i/N^{1/2}$, so each δx_i is well below the cutoff. (More often, however, we simply exclude measurements with relatively large errors from averages and fits: new, precise data chase out old, imprecise data.)

Our scaling procedure has the property that if there are two values with comparable errors separated by much more than their stated errors (with or without a number of other values of lower accuracy), the scaled-up error $\delta\bar{x}$ is approximately half the interval between the two discrepant values.

We emphasize that our scaling procedure for *errors* in no way affects central values. And if you wish to recover the unscaled error $\delta\bar{x}$, simply divide the quoted error by S .

(b) If the number M of experiments with an error smaller than δ_0 is at least three, and if $\chi^2/(M-1)$ is greater than 1.25, we show in the Particle Listings an ideogram of the data. Figure 1 is an example. Sometimes one or two data points lie apart from the main body; other times the data split into two or more groups. We extract no numbers from these ideograms; they are simply visual aids, which the reader may use as he or she sees fit.

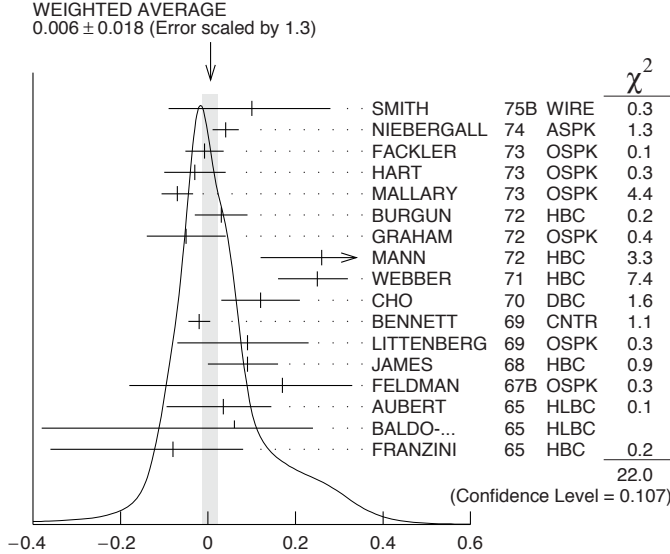


Figure 1: A typical ideogram. The arrow at the top shows the position of the weighted average, while the width of the shaded pattern shows the error in the average after scaling by the factor S . The column on the right gives the χ^2 contribution of each of the experiments. Note that the next-to-last experiment, denoted by the incomplete error flag (\perp), is not used in the calculation of S (see the text).

Each measurement in an ideogram is represented by a Gaussian with a central value x_i , error δx_i , and area proportional to $1/\delta x_i$. The choice of $1/\delta x_i$ for the area is somewhat arbitrary. With this choice, the center of gravity of the ideogram corresponds to an average that uses weights $1/\delta x_i$ rather than the $(1/\delta x_i)^2$ actually used in the averages. This may be appropriate when some of the experiments have seriously underestimated systematic errors. However, since for this choice of area the height of the Gaussian for each measurement is proportional to $(1/\delta x_i)^2$, the peak position of the ideogram will often favor the high-precision measurements at least as much as does the least-squares average. See our 1986 edition [2] for a detailed discussion of the use of ideograms.

5.2.3. Constrained fits: In some cases, such as branching ratios or masses and mass differences, a constrained fit may be needed to obtain the best values of a set of parameters. For example, most branching ratios and rate measurements are analyzed by making a simultaneous least-squares fit to all the data and extracting the partial decay fractions P_i , the partial widths Γ_i , the full width Γ (or mean life), and the associated error matrix.

Assume, for example, that a state has m partial decay fractions P_i , where $\sum P_i = 1$. These have been measured in N_r different ratios R_r , where, e.g., $R_1 = P_1/P_2$, R_2

$= P_1/P_3$, etc. [We can handle any ratio R of the form $\sum \alpha_i P_i / \sum \beta_j P_j$, where α_i and β_j are constants, usually 1 or 0. The forms $R = P_i P_j$ and $R = (P_i P_j)^{1/2}$ are also allowed.] Further assume that each ratio R has been measured by N_k experiments (we designate each experiment with a subscript k , e.g., R_{1k}). We then find the best values of the fractions P_i by minimizing the χ^2 as a function of the $m-1$ independent parameters:

$$\chi^2 = \sum_{r=1}^{N_r} \sum_{k=1}^{N_k} \left(\frac{R_{rk} - R_r}{\delta R_{rk}} \right)^2, \quad (3)$$

where the R_{rk} are the measured values and R_r are the fitted values of the branching ratios.

In addition to the fitted values \bar{P}_i , we calculate an error matrix $\langle \delta \bar{P}_i \delta \bar{P}_j \rangle$. We tabulate the diagonal elements of $\delta \bar{P}_i = \langle \delta \bar{P}_i \delta \bar{P}_i \rangle^{1/2}$ (except that some errors are scaled as discussed below). In the Particle Listings, we give the complete correlation matrix; we also calculate the fitted value of each ratio, for comparison with the input data, and list it above the relevant input, along with a simple unconstrained average of the same input.

Three comments on the example above:

(1) There was no connection assumed between measurements of the full width and the branching ratios. But often we also have information on partial widths Γ_i as well as the total width Γ . In this case we must introduce Γ as a parameter in the fit, along with the P_i , and we give correlation matrices for the widths in the Particle Listings.

(2) We try to pick those ratios and widths that are as independent and as close to the original data as possible. When one experiment measures all the branching fractions and constrains their sum to be one, we leave one of them (usually the least well-determined one) out of the fit to make the set of input data more nearly independent. We now do allow for correlations between input data.

(3) We calculate scale factors for both the R_r and P_i when the measurements for any R give a larger-than-expected contribution to the χ^2 . According to Eq. (3), the double sum for χ^2 is first summed over experiments $k = 1$ to N_k , leaving a single sum over ratios $\chi^2 = \sum \chi_r^2$. One is tempted to define a scale factor for the ratio r as $S_r = \chi_r^2 / \langle \chi_r^2 \rangle$. However, since $\langle \chi_r^2 \rangle$ is not a fixed quantity (it is somewhere between N_k and N_{k-1}), we do not know how to evaluate this expression. Instead we define

$$S_r^2 = \frac{1}{N_k} \sum_{k=1}^{N_k} \frac{(R_{rk} - \bar{R}_r)^2}{\langle (R_{rk} - \bar{R}_r)^2 \rangle}. \quad (4)$$

With this definition the expected value of S_r^2 is one. We can show that

$$\langle (R_{rk} - \bar{R}_r)^2 \rangle = \langle (\delta R_{rk})^2 \rangle - (\delta \bar{R}_r)^2, \quad (5)$$

where $\delta \bar{R}_r$ is the fitted error for ratio r .

The fit is redone using errors for the branching ratios that are scaled by the larger of S_r and unity, from which new and often larger errors $\delta \bar{P}_i'$ are obtained. The scale factors we finally list in such cases are defined by $S_i = \delta \bar{P}_i' / \delta \bar{P}_i$. However, in line with our policy of not letting S affect the central values, we give the values of \bar{P}_i obtained from the original (unscaled) fit.

There is one special case in which the errors that are obtained by the preceding procedure may be changed. When a fitted branching ratio (or rate) \overline{P}_i turns out to be less than three standard deviations ($\delta\overline{P}_i'$) from zero, a new smaller error ($\delta\overline{P}_i''$)⁻ is calculated on the low side by requiring the area under the Gaussian between $\overline{P}_i - (\delta\overline{P}_i'')^-$ and \overline{P}_i to be 68.3% of the area between zero and \overline{P}_i . A similar correction is made for branching fractions that are within three standard deviations of one. This keeps the quoted errors from overlapping the boundary of the physical region.

5.3. Rounding: While the results shown in the Particle Listings are usually exactly those published by the experiments, the numbers that appear in the Summary Tables (means, averages and limits) are subject to a set of rounding rules.

The basic rule states that if the three highest order digits of the error lie between 100 and 354, we round to two significant digits. If they lie between 355 and 949, we round to one significant digit. Finally, if they lie between 950 and 999, we round up to 1000 and keep two significant digits. In all cases, the central value is given with a precision that matches that of the error. So, for example, the result (coming from an average) 0.827 ± 0.119 would appear as 0.83 ± 0.12 , while 0.827 ± 0.367 would turn into 0.8 ± 0.4 .

Rounding is not performed if a result in a Summary Table comes from a single measurement, without any averaging. In that case, the number of digits published in the original paper is kept, unless we feel it inappropriate. Note that, even for a single measurement, when we combine statistical and systematic errors in quadrature, rounding rules apply to the result of the combination. It should be noted also that most of the limits in the Summary Tables come from a single source (the best limit) and, therefore, are not subject to rounding.

Finally, we should point out that in several instances, when a group of results come from a single fit to a set of data, we have chosen to keep two significant digits for all the results. This happens, for instance, for several properties of the W and Z bosons and the τ lepton.

5.4. Discussion: The problem of averaging data containing discrepant values is nicely discussed by Taylor in Ref. 4. He considers a number of algorithms that attempt to incorporate inconsistent data into a meaningful average. However, it is difficult to develop a procedure that handles simultaneously in a reasonable way two basic types of situations: (a) data that lie apart from the main body of the data are incorrect (contain unreported errors); and (b) the opposite—it is the main body of data that is incorrect. Unfortunately, as Taylor shows, case (b) is not infrequent. He concludes that the choice of procedure is less significant than the initial choice of data to include or exclude.

We place much emphasis on this choice of data. Often we solicit the help of outside experts (consultants). Sometimes, however, it is simply impossible to determine which of a set of discrepant measurements are correct. Our scale-factor technique is an attempt to address this ignorance by increasing the error. In effect, we are saying that present experiments do not allow a precise determination of this quantity because of unresolvable discrepancies, and one must await further measurements. The reader is warned of this situation by the size of the scale factor, and if he or she desires can go back to the literature (via the Particle

Listings) and redo the average with a different choice of data.

Our situation is less severe than most of the cases Taylor considers, such as estimates of the fundamental constants like \hbar , *etc.* Most of the errors in his case are dominated by systematic effects. For our data, statistical errors are often at least as large as systematic errors, and statistical errors are usually easier to estimate. A notable exception occurs in partial-wave analyses, where different techniques applied to the same data yield different results. In this case, as stated earlier, we often do not make an average but just quote a range of values.

A brief history of early Particle Data Group averages is given in Ref. 3. Figure 2 shows some histories of our values of a few particle properties. Sometimes large changes occur. These usually reflect the introduction of significant new data or the discarding of older data. Older data are discarded in favor of newer data when it is felt that the newer data have smaller systematic errors, or have more checks on systematic errors, or have made corrections unknown at the time of the older experiments, or simply have much smaller errors. Sometimes, the scale factor becomes large near the time at which a large jump takes place, reflecting the uncertainty introduced by the new and inconsistent data. By and large, however, a full scan of our history plots shows a dull progression toward greater precision at central values quite consistent with the first data points shown.

We conclude that the reliability of the combination of experimental data and our averaging procedures is usually good, but it is important to be aware that fluctuations outside of the quoted errors can and do occur.

ACKNOWLEDGMENTS

The publication of the *Review of Particle Physics* is supported by the Director, Office of Science, Office of High Energy and Nuclear Physics, the Division of High Energy Physics of the U.S. Department of Energy under Contract No. DE-AC02-05CH11231; by the U.S. National Science Foundation under Agreement No. PHY-0652989; by the European Laboratory for Particle Physics (CERN); by an implementing arrangement between the governments of Japan (Monbusho) and the United States (DOE) on cooperative research and development; and by the Italian National Institute of Nuclear Physics (INFN).

We thank all those who have assisted in the many phases of preparing this *Review*. We particularly thank the many who have responded to our requests for verification of data entered in the Listings, and those who have made suggestions or pointed out errors.

REFERENCES

1. The previous edition was Particle Data Group: C. Amsler *et al.*, Phys. Lett. **B667**, 1 (2008).
2. Particle Data Group: M. Aguilar-Benitez *et al.*, Phys. Lett. **170B** (1986).
3. A.H. Rosenfeld, Ann. Rev. Nucl. Sci. **25**, 555 (1975).
4. B.N. Taylor, "Numerical Comparisons of Several Algorithms for Treating Inconsistent Data in a Least-Squares Adjustment of the Fundamental Constants," U.S. National Bureau of Standards NBSIR 81-2426 (1982).

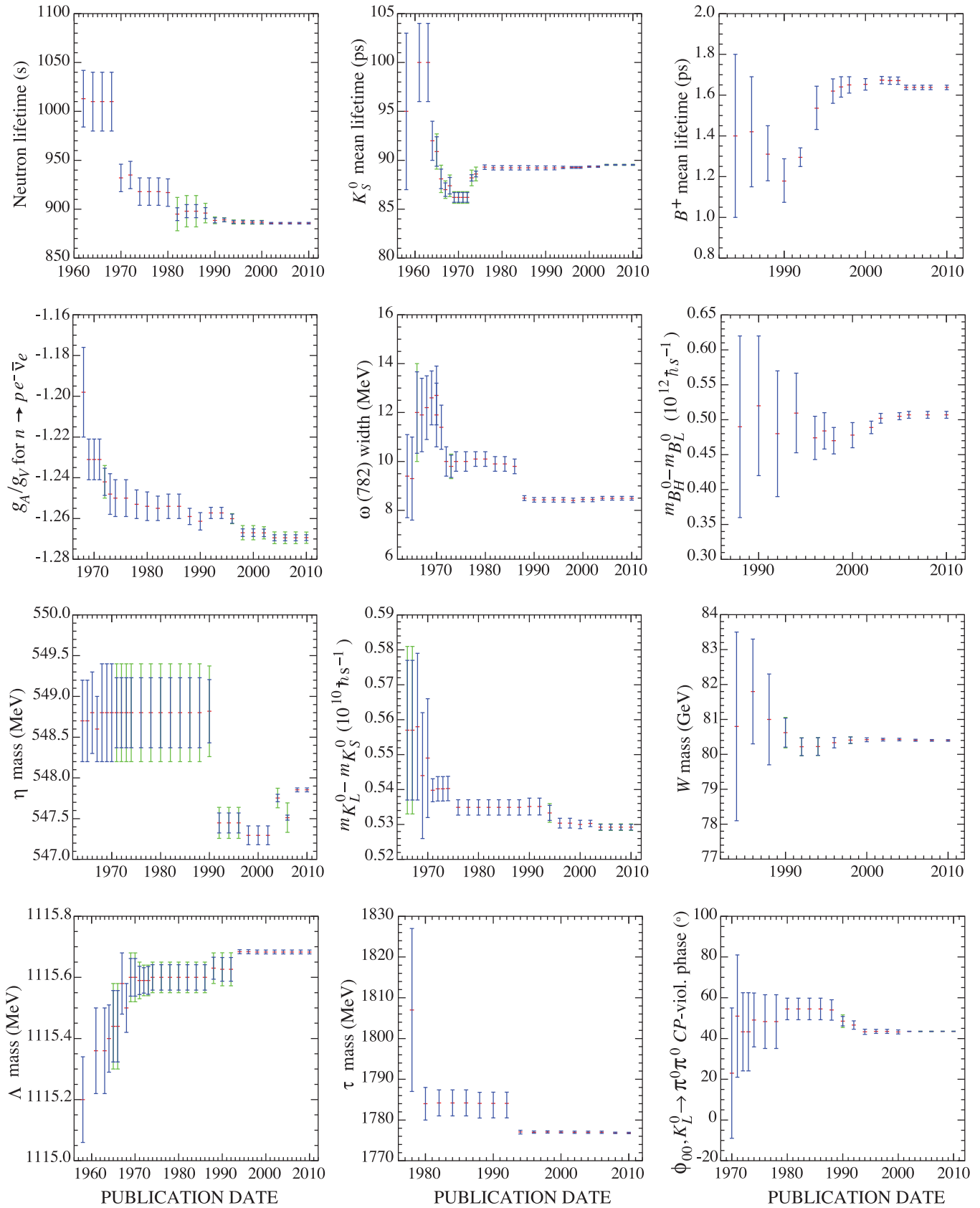


Figure 2: A historical perspective of values of a few particle properties tabulated in this *Review* as a function of date of publication of the *Review*. A full error bar indicates the quoted error; a thick-lined portion indicates the same but without the “scale factor.”

ONLINE PARTICLE PHYSICS INFORMATION

Written August 2009 by T. Basaglia (CERN).[†]

1. Introduction	18
2. Particles and Properties Databases	18
3. Open Access Databases (arXiv, SPIRES, INSPIRE, . . .)	18
4. Conference Databases	19
5. Particle Physics Journals & Reviews	19
6. Research Institutions	19
7. People	19
8. Collaborations & Experiments	19
9. Jobs	20
10. Software Repositories	20
11. Particle Physics Education Sites	20
12. Physics Topics Pages	21
13. Further Reading	21

1. Introduction

The last two years witnessed an interesting evolution of the publishing landscape in High-Energy Physics, the emergence of Open Access publishing being one of the main events. See the "Further Reading" section for a short bibliography on Open Access projects, projects on preservation of digital information, user behavior studies, and studies on the evolution of the publishing landscape in High-Energy Physics.

2. Particles and Properties Databases

Particle Data Group resources

- REVIEW OF PARTICLE PHYSICS (RPP): A biennial comprehensive review summarizing much of the known data about the field of particle physics produced by the international Particle Data Group (PDG). Includes compilations and evaluation of data on particle properties, summary tables with best values and limits for particle properties, extensive summaries of searches for hypothetical particles, and a long section of reviews, tables, and plots on a wide variety of theoretical and experimental topics of interest to particle physicists and astrophysicists. The Review of Particle Physics online:

<http://pdg.lbl.gov>

- PARTICLE PHYSICS BOOKLET: Although this booklet is produced in print only and has no online access, it is included in this guide because it is one of the most useful summary sets of physics data available. Its small size and ease of ordering from the Particle Data Group make it one of the most useful and frequently used tools for particle physicists. This pocket-sized 300-page booklet contains data abstracted from the most recent edition of the full Review of Particle Physics. Includes summary tables and abbreviated versions of some review articles. Contains useful plots and figures. Order a copy from:

[†] Starting with this edition of the Review of Particle Physics, the CERN Scientific Information Service will take over the responsibility to update and maintain this list of selected resources of interest to the particle physics community. We would like to thank our colleagues of the SLAC Research Library, who put together along the years a list of high quality resources, that we integrated and partly reorganized. An extended and updated version of this list is going to be available at:

<http://library.cern.ch/library/pdg/>

Please send comments and corrections to tullio.basaglia@cern.ch.

http://pdg.lbl.gov/2009/html/receive_our_products.html

- PDGLive:
 - <http://pdglive.lbl.gov>
- COMPUTER-READABLE FILES: Currently available from the PDG: Tables of masses, widths, and PDG Monte Carlo particle numbers and cross-section data, including hadronic total and elastic cross sections vs laboratory momenta, and total center-of-mass energy. The PDG Monte Carlo particle numbering scheme has been updated for the recent edition of the RPP and is also available as a MobileDB database. These files are updated in even-numbered years coinciding with the production of the *Review of Particle Properties*:
 - http://pdg.lbl.gov/2009/mcdata/mc_particle_id_contents.html

Other Particles and Properties Databases

- HEPDATA databases at University of Durham/RAL, this database is compiled by the Durham Database Group (UK) with help from the COMPAS Group (Russia). Contains numerical values of HEP reaction data such as total and differential cross sections, fragmentation functions, structure functions, and polarization measurements from a wide range of experiments. Updated at regular intervals. Provides data reviews which contain precompiled reviewed data such as 'Structure Functions in DIS,' 'Single Photon Production in Hadronic Interactions,' and 'Drell-Yan Cross Sections:'

<http://durpdg.dur.ac.uk/HEPDATA/REAC>

- NIST PHYSICS LABORATORY: This unit of the National Institute of Standards and Technology provides measurement services and research for electronic, optical, and radiation technologies. Three sub-pages, on Physical Reference Data, on Constants, Units & Uncertainty, and on Measurements & Calibrations, are extremely useful. Additional links to other physical properties and data of tangential interest to particle physics are also available from this page:

<http://physics.nist.gov/>

3. Open Access Databases (arXiv, SPIRES, INSPIRE, . . .)

- arXiv.org E-PRINT ARCHIVE: The arXiv.org is a repository of full text papers in physics, mathematics, computer, statistics, nonlinear sciences, quantitative finance and quantitative biology. Papers are usually sent by their authors to arXiv in advance of submission to a journal for publication. Primarily covers 1991 to the present but authors are encouraged to post older papers retroactively. Permits searching by author, title, and keyword in abstract. Allows limiting by subfield archive or by date:

<http://arXiv.org>

- SPIRES-HEP: Contains over 850,000 bibliographic records for particle physics articles, including journal papers, preprints, technical reports, conference papers and theses. Comprehensively indexed with multiple links to full text as well as links to author and institutional information. Covers 1974 to the present with substantial older materials added. Updated daily with links to electronic texts, Durham Reaction Data, PDGLive etc. Searchable by citation, by all authors and authors' affiliations, title, topic, report number, e-print archive number, date, journal, etc. A joint project of the SLAC, DESY and Fermilab with the collaboration of Durham:

<http://www.slac.stanford.edu/spires/hep/>

- INSPIRE Beta: INSPIRE combines the most successful aspects of SPIRES with the modern technology of Invenio (the CERN open-source digital-library software). However, INSPIRE takes its own inspiration from more than just SPIRES and Invenio. In searching for a paper, INSPIRE will not only fully understand the search syntax of SPIRES, but will also support free-text searches like those in Google:

<http://inspirebeta.net>

More information about the project:

<http://www.projecthepinpire.net/>

- The CERN Document Server: contains records of more than 1,000,000 CERN and non-CERN articles, preprints, theses. Includes records for internal and technical notes, official CERN committee documents, and multimedia objects:
<http://cdsweb.cern.ch/>
- NASA ASTROPHYSICS DATA SYSTEM: The ADS Abstract Service provides a search interface for four bibliographic databases covering: Astronomy and Astrophysics, Instrumentation, Physics and Geophysics, Science Education, and arXiv Preprints. Contains abstracts from articles and monographs as well as conference proceedings:
http://adsabs.harvard.edu/ads_abstracts.html
- JACoW: This Joint Accelerator Conference Website. It contains the full text of all the papers of these accelerator conferences. Search by conference name, author, title, keyword or full text of the paper:
<http://www.JACoW.org/>
- KISS (KEK INFORMATION SERVICE SYSTEM) FOR PREPRINTS: KEK Library preprint and technical report database. Contains bibliographic records of preprints and technical reports held in the KEK library with links to the full text images of more than 100,000 papers scanned from their worldwide collection of preprints. Particularly useful for older scanned preprints:
http://www-lib.kek.jp/KISS/kiss_prepri.html

4. Conference Databases

- SPIRES CONFERENCES: Database of more than 17,000 past, present and future conferences, schools, and meetings of interest to high-energy physics and related fields. Covers 1973 to the future and over 200 earlier conferences. Recent years have listed between 700 and 900 events. Search or browse by title, acronym, date, location. Includes information about published proceedings, links to submitted papers from the SPIRES-HEP database, and links to the conference Web site when available. Links to a form with which one can submit a new conference or edit an existing one:
<http://www.slac.stanford.edu/spires/conferences/additions.shtml>
to submit a new conference. Can also search for any conferences occurring by day, month, quarter, or year:
<http://www.slac.stanford.edu/spires/conferences/>
- CERN & HEP EVENTS: A list of current and upcoming conferences, schools, workshops, *etc.*, of interest to high-energy physicists. Organized by year and then by date. Covers from 1993 onwards:
<http://cdsweb.cern.ch/events/>

5. Particle Physics Journals & Reviews

A full list of URLs for journals can be found at:

<http://library.cern.ch/library/pdg/journals.html>

Please note that some of these journals may limit access to subscribers. If you encounter access problems, check with your institution's library.

6. Research Institutions

- SPIRES HEP and Astrophysics INSTITUTIONS: database of over 9,000 high-energy physics and astroparticle physics institutes, laboratories, and university departments in which research on particle physics is performed. Covers six continents and over a hundred countries. Provides an alphabetical list by country or an interface that is searchable by name, acronym, location, *etc.* Includes address, phone and fax numbers, e-mail address, and Web links where available. Has links to the recent HEP papers from each institution. Maintained by SLAC, DESY and Fermilab libraries. To search the Institutions database:
<http://www.slac.stanford.edu/spires/institutions/>

To search the top 500 HEP and astrophysics institutions by country:

<http://www.slac.stanford.edu/spires/inst/major.shtml>

- HEP INSTITUTES: Contains almost a thousand institutional addresses used in the CERN Library catalog. Includes, where available, the following: phone and fax numbers, e-mail addresses, and Web links. Provides free text searching and result sorting by organization, country, or town:
<http://cdsweb.cern.ch/collection/HEP%20Institutes>

7. People

- HEPNAMES: Searchable worldwide database of over 40,000 people associated with particle physics, astroparticle physics, synchrotron radiation, and related fields. Provides e-mail addresses, country in which the person is currently working, and a SPIRES HEP database search for their papers. If the person has supplied the following information, it lists the countries in which they did their undergraduate and graduate work, their URL, and their graduate students. It also provides information on the institutional affiliation of each researcher (as well as their affiliation history back to undergrad in many cases). It provides listings of Nobel Laureates, country statistics, Lab Directors, *etc.*:
<http://www.slac.stanford.edu/spires/hepnames/>

8. Collaborations & Experiments

- SPIRES EXPERIMENTS Database: Contains more than 2,400 past, present, and future experiments in elementary particle physics. Lists both accelerator and non-accelerator experiments. Includes official experiment name and number, location, spokespersons, and collaboration lists. Simple searches by participant, title, experiment number, institution, date approved, accelerator, or detector, return a result that fully describes the experiment, including a complete list of authors, title, description of the experiment's goals and methods, and a link to the experiment's Web page if available. Publication lists distinguish articles in refereed journals, theses, technical or instrumentation papers, and those which make the Topcite at 50+ subsequent citations or more:
<http://www.slac.stanford.edu/spires/experiments/>
- COSMIC RAY/GAMMA RAY/NEUTRINO AND SIMILAR EXPERIMENTS: This is an extensive collection of experimental Web sites organized by focus of study and also by location. Additional sections link to educational materials, organizations and related Web sites, *etc.* Maintained at the Max Planck Institute for Nuclear Physics, Heidelberg:
<http://www.mpi-hd.mpg.de/hfm/CosmicRay/CosmicRaySites.html>

9. Jobs

- AIP Employment and Industry: American Institute of Physics career network for physics, engineering and related physical sciences:
<http://www.aip.org/careersvc/>
- APS Careers in Physics: The American Physical Society Jobs/careers page:
<http://www.aps.org/jobs/>
- Careers with Physics: Advice and resources from the UK Institute of Physics:
http://www.iop.org/activity/careers/Careers/Resources/Career_resources/page_3964.html
- HEPJOBS DATABASE: Maintained by Fermilab and SLAC libraries, this database lists jobs in the fields of core interest to the particle physics and astroparticle physics communities. Use this page to post a job or to receive email notices of new job listings:
<http://www.slac.stanford.edu/spires/jobs/>
- Physicsweb.org: Listing of physics openings for all degree levels:
<http://physicsweb.org/jobs/>

10. Software Repositories

- CERNLIB: CERN PROGRAM LIBRARY: A large collection of general purpose libraries and modules offered in both source code and object code forms from the CERN central computing division. Provides programs applicable to a wide range of physics research problems such as general mathematics, data analysis, detectors simulation, data-handling, *etc.* Also includes links to commercial, free, and other software:
<http://wwwasd.web.cern.ch/wwwasd/index.html>
- FREEHEP: A collection of software and information about software useful in high-energy physics. Searching can be done by title, subject, date acquired, date updated, or by browsing an alphabetical list of all packages:
<http://www.freehep.org/>
- FERMITOOLS: Fermilab's software tools program provides a repository of Fermilab-developed software packages of value to the HEP community. Permits searching for packages by title or subject category:
<http://www.fnal.gov/fermitools/>
- HEPFORGE: HepForge is a development environment for any sort of academic software projects related to High-Energy Physics:
<http://www.hepforge.org/>
- HEPIC: SOFTWARE & TOOLS USED IN HEP RESEARCH: A meta-level site with links to other sites of HEP-related software and computing tools:
<http://www.hep.net/resources/software.html>
- GRID PHYSICS NETWORK: The GriPhyN Project is developing grid technologies for scientific and engineering projects that collect and analyze distributed, petabyte-scale datasets. Provides links to project information such as documents, education, workspace, virtual data toolkits, Chimera and Sphinx, as well as people, activities, news, and related projects:
<http://www.griphyn.org/>
- PARTICLE PHYSICS DATA GRID: The Web site for the U.S. collaboration of federal laboratories and universities to build a worldwide distributed computing model for current and future particle and nuclear physics experiments:
<http://www.ppdg.net/>

11. Particle Physics Education Sites

Particle Physics Education: General Sites:

- CONTEMPORARY PHYSICS EDUCATION PROJECT (CPEP): Provides charts, brochures, Web links, and classroom activities. Online interactive courses include: Fundamental Particles and Interactions; Plasma Physics and Fusion; and Nuclear Science:
<http://www.cpepweb.org/>

Particle Physics Education: Background Knowledge:

- ANTIMATTER: MIRROR OF THE UNIVERSE: Find out what antimatter is, where it is made, the history behind its discovery, and how it is a part of our lives. Features colorful photos and illustrations, a Kids Corner, and CERN physicists answering your questions on antimatter:
<http://livefromcern.web.cern.ch/livefromcern/antimatter/>
- BIG BANG SCIENCE—EXPLORING THE ORIGINS OF MATTER: This Web site, produced by the Particle Physics and Astronomy Research Council of the UK (PPARC), explains what physicists are looking for with their giant instruments called accelerators and particle detectors. Big Bang Science focuses on CERN particle detectors and on United Kingdom scientists' contribution to the search for the fundamental building blocks of matter.
<http://hepwww.rl.ac.uk/pub/bigbang/part1.html>

- Stanford Linear Accelerator Center: This Stanford Linear Accelerator Center Web site explains basic particle physics, linear and synchrotron accelerators, electron gamma showers, cosmic rays, and the experiments conducted at SLAC, including real-world applications. Intended for the general public as well as teachers and students:

<http://www2.slac.stanford.edu/vvc/>

- THE WORLD OF BEAMS: A site to visit if you wish to know a little or a lot about laser beams, particle beams, and other kinds of beams. Includes interactive tutorials, such as: What are Beams?, Working with Beams, and Beam Research and Technology. A good resource for physical science units involving energy, structure and properties of matter, and motion and forces for Grades 8-12. The information here is also helpful if you plan to tour any of the national laboratories listed in the "Libraries" section of this guide:
http://bc1.lbl.gov/CBP_pages/educational/WoB/home.htm

Particle Physics Education: Particle Physics Lessons & Activities:

- FERMLAB EDUCATION OFFICE: Outstanding collection of resources from the "grandmother" of all physics lab educational programs. Thoughtful unit and lesson plans in both physics and the environment (Fermilab is located on a rare, protected prairie in Illinois). Sections are organized by grade level:
<http://www-ed.fnal.gov/>
- THE PARTICLE ADVENTURE: One of the most popular Web sites for learning the fundamentals of matter and force. Created by the Particle Data Group of Lawrence Berkeley National Laboratory. An award-winning, interactive tour of the atom, with visits to quarks, neutrinos, antimatter, extra dimensions, dark matter, accelerators and particle detectors. Simple elegant graphics and translations into eleven languages:
<http://ParticleAdventure.org>
- QUARKNET: QuarkNet brings the excitement of particle physics research to high school teachers and their students. Teachers join research groups at sixty universities and labs across the country. These research groups are part of particle physics experiments at CERN, Fermilab, or SLAC. Students learn fundamental physics as they participate in inquiry-oriented investigations and analyze live, online data. QuarkNet is supported in part by the National Science Foundation and the U.S. Department of Energy:
<http://QuarkNet.fnal.gov>

Particle Physics Education: Art in Physics:

Note: This modest collection of physics art links is provided for high school art, photography, and literature teachers who may be interested in the intersections between science and technology and art and literature, or who wish to take an interdisciplinary approach to the curriculum in collaborating with their science department colleagues.

- **HIDDEN CATHEDRALS—SCIENCE OR ART?:** This page provides roughly seventeen dramatic color images of the inner workings of particle detectors at the European Organisation for Nuclear Research (CERN) which is the world's largest particle physics center:
<http://public.web.cern.ch/public/about/how/art/art.html>
- **PHYSICS ICONS:** A video by Chip Dalby, SLAC InfoMedia Solutions, showing particle physics as delicate, experiential art. This meditation on the shifting nature of physics iconography was featured in the New York Museum of Modern Art's P.S.1 exhibit, *Signatures of the Invisible*:
<http://www-project.slac.stanford.edu/streaming-media/Sub-Movies.html>

12. Physics Topics Pages**Topics Pages**

- **CAMBRIDGE RELATIVITY: PUBLIC HOME PAGE:** These pages focus on the non-technical learner and explain aspects of relativity such as: cosmology, black holes, cosmic strings, inflation, and quantum gravity. Provides links to movies, research-level home pages and to Stephen Hawking's Web site:
<http://www.damtp.cam.ac.uk/user/gr/public/>
- **THE OFFICIAL STRING THEORY WEB SITE:** Outstanding compilation of information about string theory includes: basics, mathematics, experiments, cosmology, black holes, people (including interviews with string theorists), history, theater, links to other Web sites and a discussion forum:
<http://superstringtheory.com/>
- **SUPERSTRINGS:** An online introduction to superstring theory for the advanced student. Includes further links:
<http://www.sukidog.com/jpierre/strings/>
- **THE ULTIMATE NEUTRINO PAGE:** This page provides a gateway to an extremely useful compilation of experimental data and results:
<http://cupp.oulu.fi/neutrino/>

13. Further Reading**Open Access Related Projects**

- **SCOAP3:** The Sponsoring Consortium for Open Access Publishing in Particle Physics is a consortium of High-Energy Physics funding agencies, High-Energy Physics laboratories and leading national and international libraries and library consortia. Its aim is to facilitate Open Access publishing in High Energy Physics. The Open Access (OA) tenets of granting unrestricted access to the results of publicly-funded research are in contrast with current models of scientific publishing, where access is restricted to journal customers. In this model, HEP funding agencies and libraries, which today purchase journal subscriptions to implicitly support the peer-review service, federate to explicitly cover its cost, while publishers make the electronic versions of their journals free to read. Authors are not directly charged to publish their articles OA. The SCOAP3 web site:
<http://www.scoap3.org>

- **PARSE.Insight:** Permanent Access to the Records of Science in Europe is a two-year project co-funded by the European Union under the Seventh Framework Programme. It is concerned with the preservation of digital information in science, from primary data through analysis to the final publications resulting from the research:

www.parse-insight.eu

A recent article about PARSE.Insight:

First results from the PARSE.Insight project: HEP survey on data preservation, re-use and (open) access Authors: Andre Holzner, Peter Igo-Kemenes, Salvatore Mele arXiv:0906.0485v1. 2 Jun 2009. The online article:

<http://arxiv.org/abs/0906.0485>

Data Preservation

- **ICFA Study Group on Data Preservation and Long Term Analysis in High Energy Physics.** High Energy Physics experiments initiated with this Study Group a common reflection on data persistency and long term analysis in order to get a common vision on these issues and create a multi-experiment dynamics for further reference:

<https://www.dphép.org/>

Demographic Studies

- Two studies have been recently published, which provide an insight in some aspects of scientific publication production in HEP. These articles are useful background readings for anyone interested in how the SCOAP3 project started and evolved:

Quantitative Analysis of the Publishing Landscape in High-Energy Physics Salvatore Mele, David Dallman, Jens Vigen, Joanne Yeomans arXiv:cs/0611130v1 [cs.DL]. 26 Nov 2006. These results provide quantitative input to the ongoing debate on the possible transition of HEP publishing to an Open Access model.

<http://arxiv.org/abs/cs/0611130>

Quantitative Study of the Geographical Distribution of the Authorship of High-Energy Physics Journals Jan Krause; Carl Marten Lindqvist; Salvatore Mele CERN-OPEN-2007-014. 16 July 2007.

<http://www.scoap3.org/files/cer-002691702.pdf>

User Behaviour Studies

- *Information resources in High-Energy Physics: Surveying the present landscape and charting the future course* Anne Gentil-Beccot, Salvatore Mele, Annette Holtkamp, Heath B. O'Connell, Travis C. Brooks arXiv:0804.2701v2. 16 Apr 2008. These results inform the future evolution of information management in HEP and, as these researchers are traditionally "early adopters" of innovation in scholarly communication, can inspire developments of disciplinary repositories serving other communities.

<http://arxiv.org/abs/0804.2701v2>

Published version:

<http://www.slac.stanford.edu/spires/find/hep/www?eprint?=arXiv:0804.2701>

- *Citing and Reading Behaviours in High-Energy Physics. How a Community Stopped Worrying about Journals and Learned to Love Repositories* Anne Gentil-Beccot, Salvatore Mele, Travis C. Brooks arXiv:0906.5418v1. 30 Jun 2009. CERN-OPEN-2009-007, SLAC-PUB-13693.

<http://arxiv.org/abs/0906.5418>

SUMMARY TABLES OF PARTICLE PHYSICS

Gauge and Higgs Bosons	25
Leptons	27
Quarks	30
Mesons	31
Baryons	73
Miscellaneous searches*	87
Tests of conservation laws	89
Meson Quick Reference Table	71
Baryon Quick Reference Table	72

* There are also search limits in the Summary Tables for the Gauge and Higgs Bosons, the Leptons, the Quarks, and the Mesons.



Gauge & Higgs Boson Summary Table

SUMMARY TABLES OF PARTICLE PROPERTIES

Extracted from the Particle Listings of the
Review of Particle Physics
 K. Nakamura *et al.*, JPG **37**, 075021 (2010)
 Available at <http://pdg.lbl.gov>

Particle Data Group

K. Nakamura, K. Hagiwara, K. Hikasa, H. Murayama, M. Tanabashi,
 T. Watari, C. Amsler, M. Antonelli, D.M. Asner, H. Baer, H.R. Band,
 R.M. Barnett, T. Basaglia, E. Bergren, J. Beringer, G. Bernardi, W. Bertl,
 H. Bichsel, O. Biebel, E. Blucher, S. Blusk, R.N. Cahn, M. Carena,
 A. Ceccucci, D. Chakraborty, M.-C. Chen, R.S. Chivukula, G. Cowan,
 O. Dahl, G. D'Ambrosio, T. Damour, D. de Florian, A. de Gouvêa,
 T. DeGrand, G. Dissertori, B. Dobrescu, M. Doser, M. Drees,
 D.A. Edwards, S. Eidelman, J. Erler, V.V. Ezhela, W. Fetscher,
 B.D. Fields, B. Foster, T.K. Gaiser, L. Garren, H.-J. Gerber, G. Gerbier,
 T. Gherghetta, G.F. Giudice, S. Golwala, M. Goodman, C. Grab,
 A.V. Gritsan, J.-F. Grivaz, D.E. Groom, M. Grünwald, A. Gurtu,
 T. Gutsche, H.E. Haber, C. Hagmann, K.G. Hayes, M. Heffner, B. Heltsley,
 J.J. Hernández-Rey, A. Höcker, J. Holder, J. Huston, J.D. Jackson,
 K.F. Johnson, T. Junk, A. Karle, D. Karlen, B. Kayser, D. Kirkby,
 S.R. Klein, C. Kolda, R.V. Kowalewski, B. Krusche, Yu.V. Kuyanov,
 Y. Kwon, O. Lahav, P. Langacker, A. Liddle, Z. Ligeti, C.-J. Lin,
 T.M. Liss, L. Littenberg, K.S. Lugovsky, S.B. Lugovsky, J. Lys, H. Mahlke,
 T. Mannel, A.V. Manohar, W.J. Marciano, A.D. Martin, A. Masoni,
 D. Milstead, R. Miquel, K. Mönig, M. Narain, P. Nason, S. Navas,
 P. Nevski, Y. Nir, K.A. Olive, L. Pape, C. Patrignani, J.A. Peacock,
 S.T. Petcov, A. Piepke, G. Punzi, A. Quadt, S. Raby, G. Raffelt,
 B.N. Ratcliff, P. Richardson, S. Roesler, S. Rolli, A. Romanouk,
 L.J. Rosenberg, J.L. Rosner, C.T. Sachrajda, Y. Sakai, G.P. Salam,
 S. Sarkar, F. Sauli, O. Schneider, K. Scholberg, D. Scott, W.G. Seligman,
 M.H. Shaevitz, M. Silari, T. Sjöstrand, J.G. Smith, G.F. Smoot, S. Spanier,
 H. Spieler, A. Stahl, T. Stanev, S.L. Stone, T. Sumiyoshi, M.J. Syphers,
 J. Terning, M. Titov, N.P. Tkachenko, N.A. Törnqvist, D. Tovey,
 T.G. Trippe, G. Valencia, K. van Bibber, G. Venanzoni, M.G. Vinter,
 P. Vogel, A. Vogt, W. Walkowiak, C.W. Walter, D.R. Ward, B.R. Webber,
 G. Weiglein, E.J. Weinberg, J.D. Wells, A. Wheeler, L.R. Wiencke,
 C.G. Wohl, L. Wolfenstein, J. Womersley, C.L. Woody, R.L. Workman,
 A. Yamamoto, W.-M. Yao, O.V. Zenin, J. Zhang, R.-Y. Zhu, P.A. Zyla

Technical Associates:

G. Harper, V.S. Lugovsky, P. Schaffner

©Regents of the University of California
 (Approximate closing date for data: January 15, 2010)

GAUGE AND HIGGS BOSONS

γ $I(J^{PC}) = 0,1(1^{--})$

Mass $m < 1 \times 10^{-18}$ eV
 Charge $q < 1 \times 10^{-35}$ e
 Mean life $\tau = \text{Stable}$

g or gluon $I(J^P) = 0(1^-)$

Mass $m = 0$ [a]
 SU(3) color octet

W $J = 1$

Charge = ± 1 e
 Mass $m = 80.399 \pm 0.023$ GeV
 $m_Z - m_W = 10.4 \pm 1.6$ GeV
 $m_{W^+} - m_{W^-} = -0.2 \pm 0.6$ GeV
 Full width $\Gamma = 2.085 \pm 0.042$ GeV
 $\langle N_{\pi^\pm} \rangle = 15.70 \pm 0.35$
 $\langle N_{K^\pm} \rangle = 2.20 \pm 0.19$
 $\langle N_p \rangle = 0.92 \pm 0.14$
 $\langle N_{\text{charged}} \rangle = 19.39 \pm 0.08$

W^- modes are charge conjugates of the modes below.

W^+ DECAY MODES	Fraction (Γ_i/Γ)	Confidence level	p (MeV/c)
$\ell^+ \nu$	[b] (10.80 ± 0.09) %		—
$e^+ \nu$	(10.75 ± 0.13) %		40199
$\mu^+ \nu$	(10.57 ± 0.15) %		40199
$\tau^+ \nu$	(11.25 ± 0.20) %		40180
hadrons	(67.60 ± 0.27) %		—
$\pi^+ \gamma$	< 8	$\times 10^{-5}$	95% 40199
$D_s^+ \gamma$	< 1.3	$\times 10^{-3}$	95% 40175
cX	(33.4 ± 2.6) %		—
$c\bar{s}$	(31 ± ⁺¹³ / ₋₁₁) %		—
invisible	[c] (1.4 ± 2.9) %		—

Z $J = 1$

Charge = 0

Mass $m = 91.1876 \pm 0.0021$ GeV [d]
 Full width $\Gamma = 2.4952 \pm 0.0023$ GeV
 $\Gamma(\ell^+ \ell^-) = 83.984 \pm 0.086$ MeV [d]
 $\Gamma(\text{invisible}) = 499.0 \pm 1.5$ MeV [e]
 $\Gamma(\text{hadrons}) = 1744.4 \pm 2.0$ MeV
 $\Gamma(\mu^+ \mu^-)/\Gamma(e^+ e^-) = 1.0009 \pm 0.0028$
 $\Gamma(\tau^+ \tau^-)/\Gamma(e^+ e^-) = 1.0019 \pm 0.0032$ [f]

Average charged multiplicity

$\langle N_{\text{charged}} \rangle = 20.76 \pm 0.16$ ($S = 2.1$)

Couplings to leptons

$g_V^\ell = -0.03783 \pm 0.00041$
 $g_V^u = 0.29^{+0.10}_{-0.08}$
 $g_V^d = -0.33^{+0.05}_{-0.07}$
 $g_A^\ell = -0.50123 \pm 0.00026$
 $g_A^u = 0.50^{+0.04}_{-0.07}$
 $g_A^d = -0.524^{+0.050}_{-0.030}$
 $g^{V\ell} = 0.5008 \pm 0.0008$
 $g^{Ve} = 0.53 \pm 0.09$
 $g^{V\mu} = 0.502 \pm 0.017$

Asymmetry parameters [g]

$A_e = 0.1515 \pm 0.0019$
 $A_\mu = 0.142 \pm 0.015$
 $A_\tau = 0.143 \pm 0.004$
 $A_S = 0.90 \pm 0.09$
 $A_C = 0.670 \pm 0.027$
 $A_b = 0.923 \pm 0.020$

Charge asymmetry (%) at Z pole

$A_{FB}^{(0\ell)} = 1.71 \pm 0.10$
 $A_{FB}^{(0u)} = 4 \pm 7$
 $A_{FB}^{(0s)} = 9.8 \pm 1.1$
 $A_{FB}^{(0c)} = 7.07 \pm 0.35$
 $A_{FB}^{(0b)} = 9.92 \pm 0.16$

Z DECAY MODES	Fraction (Γ_i/Γ)	Scale factor/ Confidence level	p (MeV/c)
$e^+ e^-$	(3.363 ± 0.004) %		45594
$\mu^+ \mu^-$	(3.366 ± 0.007) %		45594
$\tau^+ \tau^-$	(3.367 ± 0.008) %		45559
$\ell^+ \ell^-$	[b] (3.3658 ± 0.0023) %		—
invisible	(20.00 ± 0.06) %		—
hadrons	(69.91 ± 0.06) %		—
$(u\bar{u} + c\bar{c})/2$	(11.6 ± 0.6) %		—
$(d\bar{d} + s\bar{s} + b\bar{b})/3$	(15.6 ± 0.4) %		—
$c\bar{c}$	(12.03 ± 0.21) %		—
$b\bar{b}$	(15.12 ± 0.05) %		—
$b\bar{b}b\bar{b}$	(3.6 ± 1.3) $\times 10^{-4}$		—
$g\bar{g}g$	< 1.1	% CL=95%	—
$\pi^0 \gamma$	< 5.2	$\times 10^{-5}$ CL=95%	45594
$\eta \gamma$	< 5.1	$\times 10^{-5}$ CL=95%	45592
$\omega \gamma$	< 6.5	$\times 10^{-4}$ CL=95%	45590
$\eta'(958) \gamma$	< 4.2	$\times 10^{-5}$ CL=95%	45589
$\gamma \gamma$	< 5.2	$\times 10^{-5}$ CL=95%	45594
$\gamma \gamma \gamma$	< 1.0	$\times 10^{-5}$ CL=95%	45594
$\pi^\pm W^\mp$	[h] < 7	$\times 10^{-5}$ CL=95%	10150

Gauge & Higgs Boson Summary Table

$\rho^\pm W^\mp$	$[h] < 8.3$	$\times 10^{-5}$	CL=95%	10124
$J/\psi(1S)X$	$(3.51 \pm_{-0.25}^{+0.23}) \times 10^{-3}$		S=1.1	–
$\psi(2S)X$	$(1.60 \pm 0.29) \times 10^{-3}$			–
$\chi_{c1}(1P)X$	$(2.9 \pm 0.7) \times 10^{-3}$			–
$\chi_{c2}(1P)X$	< 3.2	$\times 10^{-3}$	CL=90%	–
$\Upsilon(1S)X + \Upsilon(2S)X$	$(1.0 \pm 0.5) \times 10^{-4}$			–
$+ \Upsilon(3S)X$				
$\Upsilon(1S)X$	< 4.4	$\times 10^{-5}$	CL=95%	–
$\Upsilon(2S)X$	< 1.39	$\times 10^{-4}$	CL=95%	–
$\Upsilon(3S)X$	< 9.4	$\times 10^{-5}$	CL=95%	–
$(D^0/\bar{D}^0)X$	$(20.7 \pm 2.0) \%$			–
$D^\pm X$	$(12.2 \pm 1.7) \%$			–
$D^*(2010)^\pm X$	$[h] (11.4 \pm 1.3) \%$			–
$D_{s1}(2536)^\pm X$	$(3.6 \pm 0.8) \times 10^{-3}$			–
$D_{sJ}(2573)^\pm X$	$(5.8 \pm 2.2) \times 10^{-3}$			–
$D^*(2629)^\pm X$	searched for			–
$B^+ X$	$[i] (6.08 \pm 0.13) \%$			–
$B_s^0 X$	$[i] (1.59 \pm 0.13) \%$			–
$B_c^\pm X$	searched for			–
$A_c^\pm X$	$(1.54 \pm 0.33) \%$			–
$\Xi_c^0 X$	seen			–
$\Xi_b X$	seen			–
b -baryon X	$[i] (1.38 \pm 0.22) \%$			–
anomalous $\gamma +$ hadrons	$[j] < 3.2$	$\times 10^{-3}$	CL=95%	–
$e^+ e^- \gamma$	$[j] < 5.2$	$\times 10^{-4}$	CL=95%	45594
$\mu^+ \mu^- \gamma$	$[j] < 5.6$	$\times 10^{-4}$	CL=95%	45594
$\tau^+ \tau^- \gamma$	$[j] < 7.3$	$\times 10^{-4}$	CL=95%	45559
$\ell^+ \ell^- \gamma \gamma$	$[k] < 6.8$	$\times 10^{-6}$	CL=95%	–
$q\bar{q}\gamma\gamma$	$[k] < 5.5$	$\times 10^{-6}$	CL=95%	–
$\nu\bar{\nu}\gamma\gamma$	$[k] < 3.1$	$\times 10^{-6}$	CL=95%	45594
$e^\pm \mu^\mp$	LF $[h] < 1.7$	$\times 10^{-6}$	CL=95%	45594
$e^\pm \tau^\mp$	LF $[h] < 9.8$	$\times 10^{-6}$	CL=95%	45576
$\mu^\pm \tau^\mp$	LF $[h] < 1.2$	$\times 10^{-5}$	CL=95%	45576
pe	L,B < 1.8	$\times 10^{-6}$	CL=95%	45589
$p\mu$	L,B < 1.8	$\times 10^{-6}$	CL=95%	45589

Higgs Bosons — H^0 and H^\pm , Searches for

The limits for H_1^0 and A_0 refer to the m_h^{max} benchmark scenario for the supersymmetric parameters.

H^0 Mass $m > 114.4$ GeV, CL = 95%

H_1^0 in Supersymmetric Models ($m_{H_1^0} < m_{H_2^0}$)

Mass $m > 92.8$ GeV, CL = 95%

A^0 Pseudoscalar Higgs Boson in Supersymmetric Models [1]

Mass $m > 93.4$ GeV, CL = 95% $\tan\beta > 0.4$

H^\pm Mass $m > 79.3$ GeV, CL = 95%

See the Particle Listings for a Note giving details of Higgs Bosons.

Heavy Bosons Other Than Higgs Bosons, Searches for

Additional W Bosons

W' with standard couplings decaying to $e\nu$
Mass $m > 1.000 \times 10^3$ GeV, CL = 95%

Additional Z Bosons

Z'_{SM} with standard couplings
Mass $m > 1.030 \times 10^3$ GeV, CL = 95% ($p\bar{p}$ direct search)
Mass $m > 1500$ GeV, CL = 95% (electroweak fit)
 Z_{LR} of $SU(2)_L \times SU(2)_R \times U(1)$ (with $g_L = g_R$)
Mass $m > 630$ GeV, CL = 95% ($p\bar{p}$ direct search)
Mass $m > 998$ GeV, CL = 95% (electroweak fit)
 Z_χ of $SO(10) \rightarrow SU(5) \times U(1)_\chi$ (with $g_\chi = e/\cos\theta_W$)
Mass $m > 892$ GeV, CL = 95% ($p\bar{p}$ direct search)
Mass $m > 781$ GeV, CL = 95% (electroweak fit)

Z_ψ of $E_6 \rightarrow SO(10) \times U(1)_\psi$ (with $g_\psi = e/\cos\theta_W$)
Mass $m > 878$ GeV, CL = 95% ($p\bar{p}$ direct search)
Mass $m > 475$ GeV, CL = 95% (electroweak fit)
 Z_η of $E_6 \rightarrow SU(3) \times SU(2) \times U(1) \times U(1)_\eta$ (with $g_\eta = e/\cos\theta_W$)
Mass $m > 904$ GeV, CL = 95% ($p\bar{p}$ direct search)
Mass $m > 619$ GeV, CL = 95% (electroweak fit)

Scalar Leptoquarks

Mass $m > 299$ GeV, CL = 95% (1st generation, pair prod.)
Mass $m > 298$ GeV, CL = 95% (1st gener., single prod.)
Mass $m > 316$ GeV, CL = 95% (2nd gener., pair prod.)
Mass $m > 73$ GeV, CL = 95% (2nd gener., single prod.)
Mass $m > 229$ GeV, CL = 95% (3rd gener., pair prod.)
(See the Particle Listings for assumptions on leptoquark quantum numbers and branching fractions.)

Axions (A^0) and Other Very Light Bosons, Searches for

The standard Peccei-Quinn axion is ruled out. Variants with reduced couplings or much smaller masses are constrained by various data. The Particle Listings in the full Review contain a Note discussing axion searches.

The best limit for the half-life of neutrinoless double beta decay with Majoron emission is $> 7.2 \times 10^{24}$ years (CL = 90%).

NOTES

In this Summary Table:

When a quantity has “(S = ...)” to its right, the error on the quantity has been enlarged by the “scale factor” S, defined as $S = \sqrt{\chi^2/(N-1)}$, where N is the number of measurements used in calculating the quantity. We do this when $S > 1$, which often indicates that the measurements are inconsistent. When $S > 1.25$, we also show in the Particle Listings an ideogram of the measurements. For more about S, see the Introduction.

A decay momentum p is given for each decay mode. For a 2-body decay, p is the momentum of each decay product in the rest frame of the decaying particle. For a 3-or-more-body decay, p is the largest momentum any of the products can have in this frame.

- [a] Theoretical value. A mass as large as a few MeV may not be precluded.
- [b] ℓ indicates each type of lepton (e , μ , and τ), not sum over them.
- [c] This represents the width for the decay of the W boson into a charged particle with momentum below detectability, $p < 200$ MeV.
- [d] The Z -boson mass listed here corresponds to a Breit-Wigner resonance parameter. It lies approximately 34 MeV above the real part of the position of the pole (in the energy-squared plane) in the Z -boson propagator.
- [e] This partial width takes into account Z decays into $\nu\bar{\nu}$ and any other possible undetected modes.
- [f] This ratio has not been corrected for the τ mass.
- [g] Here $A \equiv 2g_V g_A / (g_V^2 + g_A^2)$.
- [h] The value is for the sum of the charge states or particle/antiparticle states indicated.
- [i] This value is updated using the product of (i) the $Z \rightarrow b\bar{b}$ fraction from this listing and (ii) the b -hadron fraction in an unbiased sample of weakly decaying b -hadrons produced in Z -decays provided by the Heavy Flavor Averaging Group (HFAG, <http://www.slac.stanford.edu/xorg/hfag/osc/PDG2009/#FRACZ>).
- [j] See the Z Particle Listings for the γ energy range used in this measurement.
- [k] For $m_{\gamma\gamma} = (60 \pm 5)$ GeV.
- [l] The limits assume no invisible decays.

LEPTONS

e

$$J = \frac{1}{2}$$

Mass $m = (548.57990943 \pm 0.00000023) \times 10^{-6}$ u
 Mass $m = 0.510998910 \pm 0.00000013$ MeV
 $|m_{e^+} - m_{e^-}|/m < 8 \times 10^{-9}$, CL = 90%
 $|q_{e^+} + q_{e^-}|/e < 4 \times 10^{-8}$
 Magnetic moment anomaly
 $(g-2)/2 = (1159.65218073 \pm 0.00000028) \times 10^{-6}$
 $(g_{e^+} - g_{e^-}) / g_{\text{average}} = (-0.5 \pm 2.1) \times 10^{-12}$
 Electric dipole moment $d = (0.07 \pm 0.07) \times 10^{-26}$ ecm
 Mean life $\tau > 4.6 \times 10^{26}$ yr, CL = 90% [a]

 μ

$$J = \frac{1}{2}$$

Mass $m = 0.1134289256 \pm 0.0000000029$ u
 Mass $m = 105.658367 \pm 0.000004$ MeV
 Mean life $\tau = (2.197034 \pm 0.000021) \times 10^{-6}$ s (S = 1.2)
 $\tau_{\mu^+}/\tau_{\mu^-} = 1.00002 \pm 0.00008$
 $c\tau = 658.654$ m
 Magnetic moment anomaly $(g-2)/2 = (11659209 \pm 6) \times 10^{-10}$
 $(g_{\mu^+} - g_{\mu^-}) / g_{\text{average}} = (-0.11 \pm 0.12) \times 10^{-8}$
 Electric dipole moment $d = (-0.1 \pm 0.9) \times 10^{-19}$ ecm

Decay parameters [b]

$\rho = 0.7503 \pm 0.0004$
 $\eta = 0.057 \pm 0.034$
 $\delta = 0.7504 \pm 0.0006$
 $\xi P_{\mu} = 1.0007 \pm 0.0035$ [c]
 $\xi P_{\mu} \delta / \rho > 0.99682$, CL = 90% [c]
 $\xi' = 1.00 \pm 0.04$
 $\xi'' = 0.7 \pm 0.4$
 $\alpha/A = (0 \pm 4) \times 10^{-3}$
 $\alpha'/A = (-10 \pm 20) \times 10^{-3}$
 $\beta/A = (4 \pm 6) \times 10^{-3}$
 $\beta'/A = (2 \pm 7) \times 10^{-3}$
 $\overline{\eta} = 0.02 \pm 0.08$

μ^+ modes are charge conjugates of the modes below.

μ^- DECAY MODES	Fraction (Γ_i/Γ)	Confidence level	p (MeV/c)
$e^- \overline{\nu}_e \nu_{\mu}$	$\approx 100\%$		53
$e^- \overline{\nu}_e \nu_{\mu} \gamma$	[d] (1.4±0.4) %		53
$e^- \overline{\nu}_e \nu_{\mu} e^+ e^-$	[e] (3.4±0.4) × 10 ⁻⁵		53
Lepton Family number (LF) violating modes			
$e^- \nu_e \overline{\nu}_{\mu}$	LF [f] < 1.2	%	90%
$e^- \gamma$	LF < 1.2	× 10 ⁻¹¹	90%
$e^- e^+ e^-$	LF < 1.0	× 10 ⁻¹²	90%
$e^- 2\gamma$	LF < 7.2	× 10 ⁻¹¹	90%

 τ

$$J = \frac{1}{2}$$

Mass $m = 1776.82 \pm 0.16$ MeV
 $(m_{\tau^+} - m_{\tau^-})/m_{\text{average}} < 2.8 \times 10^{-4}$, CL = 90%
 Mean life $\tau = (290.6 \pm 1.0) \times 10^{-15}$ s
 $c\tau = 87.11$ μ m
 Magnetic moment anomaly > -0.052 and < 0.013 , CL = 95%
 $\text{Re}(d_{\tau}) = -0.22$ to 0.45×10^{-16} ecm, CL = 95%
 $\text{Im}(d_{\tau}) = -0.25$ to 0.008×10^{-16} ecm, CL = 95%

Weak dipole moment

$\text{Re}(d_{\tau}^W) < 0.50 \times 10^{-17}$ ecm, CL = 95%
 $\text{Im}(d_{\tau}^W) < 1.1 \times 10^{-17}$ ecm, CL = 95%

Weak anomalous magnetic dipole moment

$\text{Re}(\alpha_{\tau}^W) < 1.1 \times 10^{-3}$, CL = 95%
 $\text{Im}(\alpha_{\tau}^W) < 2.7 \times 10^{-3}$, CL = 95%

Decay parameters

See the τ Particle Listings for a note concerning τ -decay parameters.

$\rho(e \text{ or } \mu) = 0.745 \pm 0.008$
 $\rho(e) = 0.747 \pm 0.010$
 $\rho(\mu) = 0.763 \pm 0.020$
 $\xi(e \text{ or } \mu) = 0.985 \pm 0.030$
 $\xi(e) = 0.994 \pm 0.040$
 $\xi(\mu) = 1.030 \pm 0.059$
 $\eta(e \text{ or } \mu) = 0.013 \pm 0.020$
 $\eta(\mu) = 0.094 \pm 0.073$
 $(\delta\xi)(e \text{ or } \mu) = 0.746 \pm 0.021$
 $(\delta\xi)(e) = 0.734 \pm 0.028$
 $(\delta\xi)(\mu) = 0.778 \pm 0.037$
 $\xi(\pi) = 0.993 \pm 0.022$
 $\xi(\rho) = 0.994 \pm 0.008$
 $\xi(a_1) = 1.001 \pm 0.027$
 $\xi(\text{all hadronic modes}) = 0.995 \pm 0.007$

τ^+ modes are charge conjugates of the modes below. " h^{\pm} " stands for π^{\pm} or K^{\pm} . " e " stands for e or μ . "Neutrals" stands for γ 's and/or π^0 's.

τ^- DECAY MODES	Fraction (Γ_i/Γ)	Scale factor/ Confidence level	p (MeV/c)
Modes with one charged particle			
particle ⁻ ≥ 0 neutrals $\geq 0K^0 \nu_{\tau}$	(85.36±0.08) %	S=1.3	-
("1-prong")			
particle ⁻ ≥ 0 neutrals $\geq 0K_L^0 \nu_{\tau}$	(84.72±0.08) %	S=1.4	-
$\mu^- \overline{\nu}_{\mu} \nu_{\tau}$	[g] (17.36±0.05) %		885
$\mu^- \overline{\nu}_{\mu} \nu_{\tau} \gamma$	[e] (3.6±0.4) × 10 ⁻³		885
$e^- \overline{\nu}_e \nu_{\tau}$	[g] (17.85±0.05) %		888
$e^- \overline{\nu}_e \nu_{\tau} \gamma$	[e] (1.75±0.18) %		888
$h^- \geq 0K_L^0 \nu_{\tau}$	(12.13±0.07) %	S=1.1	883
$h^- \nu_{\tau}$	(11.61±0.06) %	S=1.1	883
$\pi^- \nu_{\tau}$	[g] (10.91±0.07) %	S=1.1	883
$K^- \nu_{\tau}$	[g] (6.96±0.23) × 10 ⁻³	S=1.1	820
$h^- \geq 1$ neutrals ν_{τ}	(37.06±0.10) %	S=1.2	-
$h^- \geq 1\pi^0 \nu_{\tau}$ (ex. K^0)	(36.54±0.11) %	S=1.2	-
$h^- \pi^0 \nu_{\tau}$	(25.94±0.09) %	S=1.1	878
$\pi^- \pi^0 \nu_{\tau}$	[g] (25.51±0.09) %	S=1.1	878
$\pi^- \pi^0$ non- $\rho(770) \nu_{\tau}$	(3.0±3.2) × 10 ⁻³		878
$K^- \pi^0 \nu_{\tau}$	[g] (4.29±0.15) × 10 ⁻³		814
$h^- \geq 2\pi^0 \nu_{\tau}$	(10.85±0.12) %	S=1.3	-
$h^- 2\pi^0 \nu_{\tau}$	(9.51±0.11) %	S=1.2	862
$h^- 2\pi^0 \nu_{\tau}$ (ex. K^0)	(9.35±0.11) %	S=1.2	862
$\pi^- 2\pi^0 \nu_{\tau}$ (ex. K^0)	[g] (9.29±0.11) %	S=1.2	862
$\pi^- 2\pi^0 \nu_{\tau}$ (ex. K^0), scajar	< 9 × 10 ⁻³	CL=95%	862
$\pi^- 2\pi^0 \nu_{\tau}$ (ex. K^0), vector	< 7 × 10 ⁻³	CL=95%	862
$K^- 2\pi^0 \nu_{\tau}$ (ex. K^0)	[g] (6.5±2.3) × 10 ⁻⁴		796
$h^- \geq 3\pi^0 \nu_{\tau}$	(1.34±0.07) %	S=1.1	-
$h^- \geq 3\pi^0 \nu_{\tau}$ (ex. K^0)	(1.25±0.07) %	S=1.1	-
$h^- 3\pi^0 \nu_{\tau}$	(1.18±0.08) %		836
$\pi^- 3\pi^0 \nu_{\tau}$ (ex. K^0)	[g] (1.04±0.07) %		836
$K^- 3\pi^0 \nu_{\tau}$ (ex. K^0), η	[g] (4.9±2.3) × 10 ⁻⁴	S=1.1	765
$h^- 4\pi^0 \nu_{\tau}$ (ex. K^0)	(1.5±0.4) × 10 ⁻³		800
$h^- 4\pi^0 \nu_{\tau}$ (ex. K^0, η)	[g] (1.1±0.4) × 10 ⁻³		800
$K^- \geq 0\pi^0 \geq 0K^0 \geq 0\gamma \nu_{\tau}$	(1.57±0.04) %	S=1.1	820
$K^- \geq 1(\pi^0 \text{ or } K^0 \text{ or } \gamma) \nu_{\tau}$	(8.72±0.32) × 10 ⁻³	S=1.1	-
Modes with K^0 's			
K_S^0 (partides) ⁻ ν_{τ}	(9.2±0.4) × 10 ⁻³	S=1.5	-
$h^- \overline{K}^0 \nu_{\tau}$	(1.00±0.05) %	S=1.8	812
$\pi^- \overline{K}^0 \nu_{\tau}$	[g] (8.4±0.4) × 10 ⁻³	S=2.1	812
$\pi^- \overline{K}^0$	(5.4±2.1) × 10 ⁻⁴		812
(non- $K^*(892)^-$) ν_{τ}			
$K^- K^0 \nu_{\tau}$	[g] (1.59±0.16) × 10 ⁻³		737
$K^- K^0 \geq 0\pi^0 \nu_{\tau}$	(3.18±0.24) × 10 ⁻³		737
$h^- \overline{K}^0 \pi^0 \nu_{\tau}$	(5.5±0.4) × 10 ⁻³		794
$\pi^- \overline{K}^0 \pi^0 \nu_{\tau}$	[g] (4.0±0.4) × 10 ⁻³		794
$\overline{K}^0 \rho^- \nu_{\tau}$	(2.2±0.5) × 10 ⁻³		612
$K^- K^0 \pi^0 \nu_{\tau}$	[g] (1.59±0.20) × 10 ⁻³		685

Lepton Summary Table

$e^- \phi$	LF	< 3.1	$\times 10^{-8}$	CL=90%	596
$\mu^- \phi$	LF	< 1.3	$\times 10^{-7}$	CL=90%	590
$e^- e^+ e^-$	LF	< 3.6	$\times 10^{-8}$	CL=90%	888
$e^- \mu^+ \mu^-$	LF	< 3.7	$\times 10^{-8}$	CL=90%	882
$e^+ \mu^- \mu^-$	LF	< 2.3	$\times 10^{-8}$	CL=90%	882
$\mu^- e^+ e^-$	LF	< 2.7	$\times 10^{-8}$	CL=90%	885
$\mu^+ e^- e^-$	LF	< 2.0	$\times 10^{-8}$	CL=90%	885
$\mu^- \mu^+ \mu^-$	LF	< 3.2	$\times 10^{-8}$	CL=90%	873
$e^- \pi^+ \pi^-$	LF	< 4.4	$\times 10^{-8}$	CL=90%	877
$e^+ \pi^- \pi^-$	L	< 8.8	$\times 10^{-8}$	CL=90%	877
$\mu^- \pi^+ \pi^-$	LF	< 3.3	$\times 10^{-8}$	CL=90%	866
$\mu^+ \pi^- \pi^-$	L	< 3.7	$\times 10^{-8}$	CL=90%	866
$e^- \pi^+ K^-$	LF	< 5.8	$\times 10^{-8}$	CL=90%	813
$e^+ \pi^- K^+$	LF	< 5.2	$\times 10^{-8}$	CL=90%	813
$e^+ \pi^- K^-$	L	< 6.7	$\times 10^{-8}$	CL=90%	813
$e^- K_S^0 K_S^0$	LF	< 2.2	$\times 10^{-6}$	CL=90%	736
$e^- K^+ K^-$	LF	< 5.4	$\times 10^{-8}$	CL=90%	738
$e^+ K^- K^-$	L	< 6.0	$\times 10^{-8}$	CL=90%	738
$\mu^- \pi^+ K^-$	LF	< 1.6	$\times 10^{-7}$	CL=90%	800
$\mu^- \pi^- K^+$	LF	< 1.0	$\times 10^{-7}$	CL=90%	800
$\mu^+ \pi^- K^-$	L	< 9.4	$\times 10^{-8}$	CL=90%	800
$\mu^- K_S^0 K_S^0$	LF	< 3.4	$\times 10^{-6}$	CL=90%	696
$\mu^- K^+ K^-$	LF	< 6.8	$\times 10^{-8}$	CL=90%	699
$\mu^+ K^- K^-$	L	< 9.6	$\times 10^{-8}$	CL=90%	699
$e^- \pi^0 \pi^0$	LF	< 6.5	$\times 10^{-6}$	CL=90%	878
$\mu^- \pi^0 \pi^0$	LF	< 1.4	$\times 10^{-5}$	CL=90%	867
$e^- \eta \eta$	LF	< 3.5	$\times 10^{-5}$	CL=90%	699
$\mu^- \eta \eta$	LF	< 6.0	$\times 10^{-5}$	CL=90%	653
$e^- \pi^0 \eta$	LF	< 2.4	$\times 10^{-5}$	CL=90%	798
$\mu^- \pi^0 \eta$	LF	< 2.2	$\times 10^{-5}$	CL=90%	784
$\bar{p} \gamma$	L,B	< 3.5	$\times 10^{-6}$	CL=90%	641
$\bar{p} \pi^0$	L,B	< 1.5	$\times 10^{-5}$	CL=90%	632
$\bar{p} 2\pi^0$	L,B	< 3.3	$\times 10^{-5}$	CL=90%	604
$\bar{p} \eta$	L,B	< 8.9	$\times 10^{-6}$	CL=90%	475
$\bar{p} \pi^0 \eta$	L,B	< 2.7	$\times 10^{-5}$	CL=90%	360
$\bar{\Lambda} \pi^-$	L,B	< 7.2	$\times 10^{-8}$	CL=90%	525
$\bar{\Lambda} \pi^-$	L,B	< 1.4	$\times 10^{-7}$	CL=90%	525
$e^- \text{light boson}$	LF	< 2.7	$\times 10^{-3}$	CL=95%	-
$\mu^- \text{light boson}$	LF	< 5	$\times 10^{-3}$	CL=95%	-

Heavy Charged Lepton Searches

 L^\pm – charged leptonMass $m > 100.8$ GeV, CL = 95% ^[h] Decay to νW . L^\pm – stable charged heavy leptonMass $m > 102.6$ GeV, CL = 95%

Neutrino Properties

See the note on “Neutrino properties listings” in the Particle Listings.

Mass $m < 2$ eV (tritium decay)Mean life/mass, $\tau/m > 300$ s/eV, CL = 90% (reactor)Mean life/mass, $\tau/m > 7 \times 10^9$ s/eV (solar)Mean life/mass, $\tau/m > 15.4$ s/eV, CL = 90% (accelerator)Magnetic moment $\mu < 0.54 \times 10^{-10} \mu_B$, CL = 90% (solar)

Number of Neutrino Types

Number $N = 2.984 \pm 0.008$ (Standard Model fits to LEP data)Number $N = 2.92 \pm 0.05$ ($S = 1.2$) (Direct measurement of invisible Z width)

Neutrino Mixing

The following values are obtained through data analyses based on the 3-neutrino mixing scheme described in the review “Neutrino Mass, Mixing, and Oscillations” by K. Nakamura and S.T. Petcov in this Review.

$$\sin^2(2\theta_{12}) = 0.87 \pm 0.03$$

$$\Delta m_{21}^2 = (7.59 \pm 0.20) \times 10^{-5} \text{ eV}^2$$

$$\sin^2(2\theta_{23}) > 0.92 \text{ [i]}$$

$$\Delta m_{32}^2 = (2.43 \pm 0.13) \times 10^{-3} \text{ eV}^2 \text{ [j]}$$

$$\sin^2(2\theta_{13}) < 0.15, \text{ CL} = 90\%$$

Heavy Neutral Leptons, Searches for

For excited leptons, see Compositeness Limits below.

Stable Neutral Heavy Lepton Mass Limits

Mass $m > 45.0$ GeV, CL = 95% (Dirac)Mass $m > 39.5$ GeV, CL = 95% (Majorana)

Neutral Heavy Lepton Mass Limits

Mass $m > 90.3$ GeV, CL = 95%(Dirac ν_L coupling to e, μ, τ ; conservative case(τ))Mass $m > 80.5$ GeV, CL = 95%(Majorana ν_L coupling to e, μ, τ ; conservative case(τ))

NOTES

In this Summary Table:

When a quantity has “(S = ...)” to its right, the error on the quantity has been enlarged by the “scale factor” S, defined as $S = \sqrt{\chi^2/(N-1)}$, where N is the number of measurements used in calculating the quantity. We do this when $S > 1$, which often indicates that the measurements are inconsistent. When $S > 1.25$, we also show in the Particle Listings an ideogram of the measurements. For more about S, see the Introduction.

A decay momentum p is given for each decay mode. For a 2-body decay, p is the momentum of each decay product in the rest frame of the decaying particle. For a 3-or-more-body decay, p is the largest momentum any of the products can have in this frame.

[a] This is the best limit for the mode $e^- \rightarrow \nu \gamma$. The best limit for “electron disappearance” is 6.4×10^{24} yr.

[b] See the “Note on Muon Decay Parameters” in the μ Particle Listings for definitions and details.

[c] P_μ is the longitudinal polarization of the muon from pion decay. In standard $V-A$ theory, $P_\mu = 1$ and $\rho = \delta = 3/4$.

[d] This only includes events with the γ energy > 10 MeV. Since the $e^- \bar{\nu}_e \nu_\mu$ and $e^- \bar{\nu}_e \nu_\mu \gamma$ modes cannot be clearly separated, we regard the latter mode as a subset of the former.

[e] See the relevant Particle Listings for the energy limits used in this measurement.

[f] A test of additive vs. multiplicative lepton family number conservation.

[g] Basis mode for the τ .

[h] L^\pm mass limit depends on decay assumptions; see the Full Listings.

[i] The limit quoted corresponds to the projection onto the $\sin^2(2\theta_{23})$ axis of the 90% CL contour in the $\sin^2(2\theta_{23}) - \Delta m_{32}^2$ plane.

[j] The sign of Δm_{32}^2 is not known at this time. The range quoted is for the absolute value.

Quark Summary Table

QUARKS

The u -, d -, and s -quark masses are estimates of so-called "current-quark masses," in a mass-independent subtraction scheme such as \overline{MS} at a scale $\mu \approx 2$ GeV. The c - and b -quark masses are the "running" masses in the \overline{MS} scheme. For the b -quark we also quote the 1S mass. These can be different from the heavy quark masses obtained in potential models.

u	$I(J^P) = \frac{1}{2}(\frac{1}{2}^+)$
$m_u = 1.7\text{--}3.3$ MeV	Charge = $\frac{2}{3} e$ $I_z = +\frac{1}{2}$
$m_u/m_d = 0.35\text{--}0.60$	
d	$I(J^P) = \frac{1}{2}(\frac{1}{2}^+)$
$m_d = 4.1\text{--}5.8$ MeV	Charge = $-\frac{1}{3} e$ $I_z = -\frac{1}{2}$
$m_s/m_d = 17$ to 22	
$\overline{m} = (m_u + m_d)/2 = 3.0\text{--}4.8$ MeV	
s	$I(J^P) = 0(\frac{1}{2}^+)$
$m_s = 101^{+29}_{-21}$ MeV	Charge = $-\frac{1}{3} e$ Strangeness = -1
$m_s / ((m_u + m_d)/2) = 22$ to 30	
c	$I(J^P) = 0(\frac{1}{2}^+)$
$m_c = 1.27^{+0.07}_{-0.09}$ GeV	Charge = $\frac{2}{3} e$ Charm = $+1$
b	$I(J^P) = 0(\frac{1}{2}^+)$
	Charge = $-\frac{1}{3} e$ Bottom = -1
$m_b(\overline{MS}) = 4.19^{+0.18}_{-0.06}$ GeV	
$m_b(1S) = 4.67^{+0.18}_{-0.06}$ GeV	
t	$I(J^P) = 0(\frac{1}{2}^+)$
	Charge = $\frac{2}{3} e$ Top = $+1$
Mass $m = 172.0 \pm 0.9 \pm 1.3$ GeV [a] (direct observation of top events)	
Full width $\Gamma < 13.1$ GeV, CL = 95%	
$\Gamma(Wb)/\Gamma(Wq(q = b, s, d)) = 0.99^{+0.09}_{-0.08}$	
t DECAY MODES	Fraction (Γ_i/Γ) Confidence level (MeV/c)
$Wq(q = b, s, d)$	—
Wb	—
$\ell\nu_\ell$ anything	[b,c] (9.4±2.4) %
$\gamma q(q=u,c)$	[d] < 5.9 × 10 ⁻³ 95% —
$\Delta T = 1$ weak neutral current (TI) modes	
$Zq(q=u,c)$	TI [e] < 3.7 % 95% —

b' (4th Generation) Quark, Searches for

Mass $m > 190$ GeV, CL = 95% ($p\overline{p}$, quasi-stable b')
 Mass $m > 199$ GeV, CL = 95% ($p\overline{p}$, neutral-current decays)
 Mass $m > 128$ GeV, CL = 95% ($p\overline{p}$, charged-current decays)
 Mass $m > 46.0$ GeV, CL = 95% (e^+e^- , all decays)

t' (4th Generation) Quark, Searches for

Mass $m > 256$ GeV, CL = 95% ($p\overline{p}$, $t'\overline{t}'$ prod., $t' \rightarrow Wq$)

Free Quark Searches

All searches since 1977 have had negative results.

NOTES

[a] Based on published top mass measurements using data from Tevatron Run-I and Run-II. Including also the most recent unpublished results from Run-II, the Tevatron Electroweak Working Group reports a top mass of $173.1 \pm 0.6 \pm 1.1$ GeV. See the note "The Top Quark" in the Quark Particle Listings of this Review.

[b] ℓ means e or μ decay mode, not the sum over them.

[c] Assumes lepton universality and W -decay acceptance.

[d] This limit is for $\Gamma(t \rightarrow \gamma q)/\Gamma(t \rightarrow Wb)$.

[e] This limit is for $\Gamma(t \rightarrow Zq)/\Gamma(t \rightarrow Wb)$.

Meson Summary Table

LIGHT UNFLAVORED MESONS ($S = C = B = 0$)

For $I = 1$ (π, b, ρ, a): $u\bar{d}, (u\bar{u}-d\bar{d})/\sqrt{2}, d\bar{u}$;
for $I = 0$ ($\eta, \eta', h, h', \omega, \phi, f, f'$): $c_1(u\bar{u} + d\bar{d}) + c_2(s\bar{s})$

 π^\pm

$$I^G(J^{PC}) = 1^-(0^-)$$

Mass $m = 139.57018 \pm 0.00035$ MeV ($S = 1.2$)
Mean life $\tau = (2.6033 \pm 0.0005) \times 10^{-8}$ s ($S = 1.2$)
 $c\tau = 7.8045$ m

$\pi^\pm \rightarrow \ell^\pm \nu \gamma$ form factors [a]

$F_V = 0.0254 \pm 0.0017$
 $F_A = 0.0119 \pm 0.0001$
 F_V slope parameter $a = 0.10 \pm 0.06$
 $R = 0.059^{+0.009}_{-0.008}$

π^- modes are charge conjugates of the modes below.

For decay limits to particles which are not established, see the section on Searches for Axions and Other Very Light Bosons.

π^\pm DECAY MODES	Fraction (Γ_i/Γ)	Confidence level	p (MeV/c)
$\mu^+ \nu_\mu$	[b] (99.98770 \pm 0.00004) %		30
$\mu^+ \nu_\mu \gamma$	[c] (2.00 \pm 0.25) $\times 10^{-4}$		30
$e^+ \nu_e$	[b] (1.230 \pm 0.004) $\times 10^{-4}$		70
$e^+ \nu_e \gamma$	[c] (7.39 \pm 0.05) $\times 10^{-7}$		70
$e^+ \nu_e \pi^0$	(1.036 \pm 0.006) $\times 10^{-8}$		4
$e^+ \nu_e e^+ e^-$	(3.2 \pm 0.5) $\times 10^{-9}$		70
$e^+ \nu_e \nu \bar{\nu}$	< 5 $\times 10^{-6}$	90%	70
Lepton Family number (LF) or Lepton number (L) violating modes			
$\mu^+ \bar{\nu}_e$	L [d] < 1.5	$\times 10^{-3}$ 90%	30
$\mu^+ \nu_e$	LF [d] < 8.0	$\times 10^{-3}$ 90%	30
$\mu^- e^+ e^+ \nu$	LF < 1.6	$\times 10^{-6}$ 90%	30

 π^0

$$I^G(J^{PC}) = 1^-(0^{++})$$

Mass $m = 134.9766 \pm 0.0006$ MeV ($S = 1.1$)
 $m_{\pi^\pm} - m_{\pi^0} = 4.5936 \pm 0.0005$ MeV
Mean life $\tau = (8.4 \pm 0.5) \times 10^{-17}$ s ($S = 2.6$)
 $c\tau = 25.1$ nm

For decay limits to particles which are not established, see the appropriate Search sections (A^0 (axion) and Other Light Boson (X^0) Searches, etc.).

π^0 DECAY MODES	Fraction (Γ_i/Γ)	Scale factor/ Confidence level	p (MeV/c)
2γ	(98.823 \pm 0.034) %	S=1.5	67
$e^+ e^- \gamma$	(1.174 \pm 0.035) %	S=1.5	67
γ positronium	(1.82 \pm 0.29) $\times 10^{-9}$		67
$e^+ e^+ e^- e^-$	(3.34 \pm 0.16) $\times 10^{-5}$		67
$e^+ e^-$	(6.46 \pm 0.33) $\times 10^{-8}$		67
4γ	< 2 $\times 10^{-8}$	CL=90%	67
$\nu \bar{\nu}$	[e] < 2.7 $\times 10^{-7}$	CL=90%	67
$\nu_e \bar{\nu}_e$	< 1.7 $\times 10^{-6}$	CL=90%	67
$\nu_\mu \bar{\nu}_\mu$	< 1.6 $\times 10^{-6}$	CL=90%	67
$\nu_\tau \bar{\nu}_\tau$	< 2.1 $\times 10^{-6}$	CL=90%	67
$\gamma \nu \bar{\nu}$	< 6 $\times 10^{-4}$	CL=90%	67
Charge conjugation (C) or Lepton Family number (LF) violating modes			
3γ	C < 3.1 $\times 10^{-8}$	CL=90%	67
$\mu^+ e^-$	LF < 3.8 $\times 10^{-10}$	CL=90%	26
$\mu^- e^+$	LF < 3.4 $\times 10^{-9}$	CL=90%	26
$\mu^+ e^- + \mu^- e^+$	LF < 3.6 $\times 10^{-10}$	CL=90%	26

 η

$$I^G(J^{PC}) = 0^+(0^{-+})$$

Mass $m = 547.853 \pm 0.024$ MeV
Full width $\Gamma = 1.30 \pm 0.07$ keV

C-nonconserving decay parameters

$\pi^+ \pi^- \pi^0$ left-right asymmetry = $(0.09 \pm 0.11) \times 10^{-2}$
 $\pi^+ \pi^- \pi^0$ sextant asymmetry = $(0.12 \pm 0.11) \times 10^{-2}$
 $\pi^+ \pi^- \pi^0$ quadrant asymmetry = $(-0.09 \pm 0.09) \times 10^{-2}$
 $\pi^+ \pi^- \gamma$ left-right asymmetry = $(0.9 \pm 0.4) \times 10^{-2}$
 $\pi^+ \pi^- \gamma$ β (D-wave) = -0.02 ± 0.07 ($S = 1.3$)

CP-nonconserving decay parameters

$\pi^+ \pi^- e^+ e^-$ decay-plane asymmetry $A_\phi = (-0.6 \pm 3.1) \times 10^{-2}$

Dalitz plot parameter

$\pi^0 \pi^0 \pi^0$ $\alpha = -0.0317 \pm 0.0016$

η DECAY MODES	Fraction (Γ_i/Γ)	Scale factor/ Confidence level	p (MeV/c)
Neutral modes			
neutral modes	(71.90 \pm 0.34) %	S=1.2	-
2γ	(39.31 \pm 0.20) %	S=1.1	274
$3\pi^0$	(32.57 \pm 0.23) %	S=1.1	179
$\pi^0 2\gamma$	(2.7 \pm 0.5) $\times 10^{-4}$	S=1.1	257
$2\pi^0 2\gamma$	< 1.2 $\times 10^{-3}$	CL=90%	238
4γ	< 2.8 $\times 10^{-4}$	CL=90%	274
invisible	< 6 $\times 10^{-4}$	CL=90%	-
Charged modes			
charged modes	(28.10 \pm 0.34) %	S=1.2	-
$\pi^+ \pi^- \pi^0$	(22.74 \pm 0.28) %	S=1.2	174
$\pi^+ \pi^- \gamma$	(4.60 \pm 0.16) %	S=2.1	236
$e^+ e^- \gamma$	(7.0 \pm 0.7) $\times 10^{-3}$	S=1.5	274
$\mu^+ \mu^- \gamma$	(3.1 \pm 0.4) $\times 10^{-4}$		253
$e^+ e^-$	< 2.7 $\times 10^{-5}$	CL=90%	274
$\mu^+ \mu^-$	(5.8 \pm 0.8) $\times 10^{-6}$		253
$2e^+ 2e^-$	< 6.9 $\times 10^{-5}$	CL=90%	274
$\pi^+ \pi^- e^+ e^- (\gamma)$	(2.68 \pm 0.11) $\times 10^{-4}$		235
$e^+ e^- \mu^+ \mu^-$	< 1.6 $\times 10^{-4}$	CL=90%	253
$2\mu^+ 2\mu^-$	< 3.6 $\times 10^{-4}$	CL=90%	161
$\mu^+ \mu^- \pi^+ \pi^-$	< 3.6 $\times 10^{-4}$	CL=90%	113
$\pi^+ \pi^- 2\gamma$	< 2.0 $\times 10^{-3}$		236
$\pi^+ \pi^- \pi^0 \gamma$	< 5 $\times 10^{-4}$	CL=90%	174
$\pi^0 \mu^+ \mu^- \gamma$	< 3 $\times 10^{-6}$	CL=90%	210

Charge conjugation (C), Parity (P), Charge conjugation \times Parity (CP), or Lepton Family number (LF) violating modes

$\pi^0 \gamma$	C	< 9 $\times 10^{-5}$	CL=90%	257
$\pi^+ \pi^-$	P, CP	< 1.3 $\times 10^{-5}$	CL=90%	236
$2\pi^0$	P, CP	< 3.5 $\times 10^{-4}$	CL=90%	238
$2\pi^0 \gamma$	C	< 5 $\times 10^{-4}$	CL=90%	238
$3\pi^0 \gamma$	C	< 6 $\times 10^{-5}$	CL=90%	179
3γ	C	< 1.6 $\times 10^{-5}$	CL=90%	274
$4\pi^0$	P, CP	< 6.9 $\times 10^{-7}$	CL=90%	40
$\pi^0 e^+ e^-$	C	[f] < 4 $\times 10^{-5}$	CL=90%	257
$\pi^0 \mu^+ \mu^-$	C	[f] < 5 $\times 10^{-6}$	CL=90%	210
$\mu^+ e^- + \mu^- e^+$	LF	< 6 $\times 10^{-6}$	CL=90%	264

$f_0(600)$ [g]
or σ

$$I^G(J^{PC}) = 0^+(0^{++})$$

Mass $m = (400-1200)$ MeV
Full width $\Gamma = (600-1000)$ MeV

$f_0(600)$ DECAY MODES	Fraction (Γ_i/Γ)	p (MeV/c)
$\pi \pi$	dominant	-
$\gamma \gamma$	seen	-

$\rho(770)$ [h]

$$I^G(J^{PC}) = 1^+(1^{--})$$

Mass $m = 775.49 \pm 0.34$ MeV
Full width $\Gamma = 149.1 \pm 0.8$ MeV
 $\Gamma_{ee} = 7.04 \pm 0.06$ keV

Meson Summary Table

$\rho(770)$ DECAY MODES	Fraction (Γ_i/Γ)	Scale factor/ Confidence level	ρ (MeV/c)
$\pi\pi$	~ 100	%	363
$\rho(770)^\pm$ decays			
$\pi^\pm\gamma$	(4.5 \pm 0.5) $\times 10^{-4}$	S=2.2	375
$\pi^\pm\eta$	< 6 $\times 10^{-3}$	CL=84%	153
$\pi^\pm\pi^+\pi^-\pi^0$	< 2.0 $\times 10^{-3}$	CL=84%	254
$\rho(770)^0$ decays			
$\pi^+\pi^-\gamma$	(9.9 \pm 1.6) $\times 10^{-3}$		362
$\pi^0\gamma$	(6.0 \pm 0.8) $\times 10^{-4}$		376
$\eta\gamma$	(3.00 \pm 0.20) $\times 10^{-4}$		194
$\pi^0\pi^0\gamma$	(4.5 \pm 0.8) $\times 10^{-5}$		363
$\mu^+\mu^-$	[i] (4.55 \pm 0.28) $\times 10^{-5}$		373
e^+e^-	[i] (4.72 \pm 0.05) $\times 10^{-5}$		388
$\pi^+\pi^-\pi^0$	(1.01 \pm 0.54 \pm 0.34) $\times 10^{-4}$		323
$\pi^+\pi^-\pi^+\pi^-$	(1.8 \pm 0.9) $\times 10^{-5}$		251
$\pi^+\pi^-\pi^0\pi^0$	(1.6 \pm 0.8) $\times 10^{-5}$		257
$\pi^0e^+e^-$	< 1.2 $\times 10^{-5}$	CL=90%	376

 $\omega(782)$

$$J^G(J^{PC}) = 0^-(1^{--})$$

Mass $m = 782.65 \pm 0.12$ MeV (S = 1.9)
 Full width $\Gamma = 8.49 \pm 0.08$ MeV
 $\Gamma_{ee} = 0.60 \pm 0.02$ keV

$\omega(782)$ DECAY MODES	Fraction (Γ_i/Γ)	Scale factor/ Confidence level	ρ (MeV/c)
$\pi^+\pi^-\pi^0$	(89.2 \pm 0.7) %		327
$\pi^0\gamma$	(8.28 \pm 0.28) %	S=2.1	380
$\pi^+\pi^-$	(1.53 \pm 0.11) %	S=1.2	366
neutrals (excluding $\pi^0\gamma$)	(8 \pm 5) $\times 10^{-3}$	S=1.1	-
$\eta\gamma$	(4.6 \pm 0.4) $\times 10^{-4}$	S=1.1	200
$\pi^0e^+e^-$	(7.7 \pm 0.6) $\times 10^{-4}$		380
$\pi^0\mu^+\mu^-$	(1.3 \pm 0.4) $\times 10^{-4}$	S=2.1	349
e^+e^-	(7.28 \pm 0.14) $\times 10^{-5}$	S=1.3	391
$\pi^+\pi^-\pi^0\pi^0$	< 2 $\times 10^{-4}$	CL=90%	262
$\pi^+\pi^-\gamma$	< 3.6 $\times 10^{-3}$	CL=95%	366
$\pi^+\pi^-\pi^+\pi^-$	< 1 $\times 10^{-3}$	CL=90%	256
$\pi^0\pi^0\gamma$	(6.6 \pm 1.1) $\times 10^{-5}$		367
$\eta\pi^0\gamma$	< 3.3 $\times 10^{-5}$	CL=90%	162
$\mu^+\mu^-$	(9.0 \pm 3.1) $\times 10^{-5}$		377
3γ	< 1.9 $\times 10^{-4}$	CL=95%	391

Charge conjugation (C) violating modes

$\eta\pi^0$	C	< 2.1 $\times 10^{-4}$	CL=90%	162
$2\pi^0$	C	< 2.1 $\times 10^{-4}$	CL=90%	367
$3\pi^0$	C	< 2.3 $\times 10^{-4}$	CL=90%	330

 $\eta'(958)$

$$J^G(J^{PC}) = 0^+(0^{-+})$$

Mass $m = 957.78 \pm 0.06$ MeV
 Full width $\Gamma = 0.194 \pm 0.009$ MeV

$\eta'(958)$ DECAY MODES	Fraction (Γ_i/Γ)	Confidence level	ρ (MeV/c)
$\pi^+\pi^-\eta$	(43.2 \pm 0.7) %		232
$\rho^0\gamma$ (including non-resonant $\pi^+\pi^-\gamma$)	(29.3 \pm 0.5) %		165
$\pi^0\pi^0\eta$	(21.7 \pm 0.8) %		239
$\omega\gamma$	(2.75 \pm 0.22) %		159
$\gamma\gamma$	(2.22 \pm 0.08) %		479
$3\pi^0$	(1.68 \pm 0.22) $\times 10^{-3}$		430
$\mu^+\mu^-\gamma$	(1.09 \pm 0.27) $\times 10^{-4}$		467
$\pi^+\pi^-\mu^+\mu^-$	< 2.2 $\times 10^{-4}$	90%	401
$\pi^+\pi^-\pi^0$	(3.6 \pm 1.1) $\times 10^{-3}$		428
$\pi^0\rho^0$	< 4 %	90%	111
$2(\pi^+\pi^-)$	< 2.4 $\times 10^{-4}$	90%	372
$\pi^+\pi^-2\pi^0$	< 2.5 $\times 10^{-3}$	90%	376
$2(\pi^+\pi^-)$ neutrals	< 1 %	95%	-
$2(\pi^+\pi^-)\pi^0$	< 1.9 $\times 10^{-3}$	90%	298
$2(\pi^+\pi^-)2\pi^0$	< 1 %	95%	197

$3(\pi^+\pi^-)$	< 5 $\times 10^{-4}$	90%	189
$\pi^+\pi^-\pi^+e^-$	(2.4 \pm 1.3 \pm 1.0) $\times 10^{-3}$		458
γe^+e^-	< 9 $\times 10^{-4}$	90%	479
$\pi^0\gamma\gamma$	< 8 $\times 10^{-4}$	90%	469
$4\pi^0$	< 5 $\times 10^{-4}$	90%	380
e^+e^-	< 2.1 $\times 10^{-7}$	90%	479
invisible	< 9 $\times 10^{-4}$	90%	-

**Charge conjugation (C), Parity (P),
Lepton family number (LF) violating modes**

$\pi^+\pi^-$	P, CP	< 2.9 $\times 10^{-3}$	90%	458
$\pi^0\pi^0$	P, CP	< 1.0 $\times 10^{-3}$	90%	459
$\pi^0e^+e^-$	C	[f] < 1.4 $\times 10^{-3}$	90%	469
ηe^+e^-	C	[f] < 2.4 $\times 10^{-3}$	90%	322
3γ	C	< 1.0 $\times 10^{-4}$	90%	479
$\mu^+\mu^-\pi^0$	C	[f] < 6.0 $\times 10^{-5}$	90%	445
$\mu^+\mu^-\eta$	C	[f] < 1.5 $\times 10^{-5}$	90%	273
$e\mu$	LF	< 4.7 $\times 10^{-4}$	90%	473

 $f_0(980)$ [i]

$$J^G(J^{PC}) = 0^+(0^{++})$$

Mass $m = 980 \pm 10$ MeV
 Full width $\Gamma = 40$ to 100 MeV

$f_0(980)$ DECAY MODES	Fraction (Γ_i/Γ)	ρ (MeV/c)
$\pi\pi$	dominant	471
$K\bar{K}$	seen	†
$\gamma\gamma$	seen	490

 $a_0(980)$ [i]

$$J^G(J^{PC}) = 1^-(0^{++})$$

Mass $m = 980 \pm 20$ MeV
 Full width $\Gamma = 50$ to 100 MeV

$a_0(980)$ DECAY MODES	Fraction (Γ_i/Γ)	ρ (MeV/c)
$\eta\pi$	dominant	319
$K\bar{K}$	seen	†
$\gamma\gamma$	seen	490

 $\phi(1020)$

$$J^G(J^{PC}) = 0^-(1^{--})$$

Mass $m = 1019.455 \pm 0.020$ MeV (S = 1.1)
 Full width $\Gamma = 4.26 \pm 0.04$ MeV (S = 1.4)

$\phi(1020)$ DECAY MODES	Fraction (Γ_i/Γ)	Scale factor/ Confidence level	ρ (MeV/c)
K^+K^-	(48.9 \pm 0.5) %	S=1.1	127
$K_L^0K_S^0$	(34.2 \pm 0.4) %	S=1.1	110
$\rho\pi + \pi^+\pi^-\pi^0$	(15.32 \pm 0.32) %	S=1.1	-
$\eta\gamma$	(1.309 \pm 0.024) %	S=1.2	363
$\pi^0\gamma$	(1.27 \pm 0.06) $\times 10^{-3}$		501
$\ell^+\ell^-$	-		510
e^+e^-	(2.954 \pm 0.030) $\times 10^{-4}$	S=1.1	510
$\mu^+\mu^-$	(2.87 \pm 0.19) $\times 10^{-4}$		499
ηe^+e^-	(1.15 \pm 0.10) $\times 10^{-4}$		363
$\pi^+\pi^-$	(7.4 \pm 1.3) $\times 10^{-5}$		490
$\omega\pi^0$	(4.7 \pm 0.5) $\times 10^{-5}$		171
$\omega\gamma$	< 5 %	CL=84%	209
$\rho\gamma$	< 1.2 $\times 10^{-5}$	CL=90%	215
$\pi^+\pi^-\gamma$	(4.1 \pm 1.3) $\times 10^{-5}$		490
$f_0(980)\gamma$	(3.22 \pm 0.19) $\times 10^{-4}$	S=1.1	39
$\pi^0\pi^0\gamma$	(1.13 \pm 0.06) $\times 10^{-4}$		492
$\pi^+\pi^-\pi^+\pi^-$	(4.0 \pm 2.8 \pm 2.2) $\times 10^{-6}$		410
$\pi^+\pi^+\pi^-\pi^-\pi^0$	< 4.6 $\times 10^{-6}$	CL=90%	342
$\pi^0e^+e^-$	(1.12 \pm 0.28) $\times 10^{-5}$		501
$\pi^0\eta\gamma$	(7.27 \pm 0.30) $\times 10^{-5}$	S=1.5	346
$a_0(980)\gamma$	(7.6 \pm 0.6) $\times 10^{-5}$		39
$K^0\bar{K}^0\gamma$	< 1.9 $\times 10^{-8}$	CL=90%	110
$\eta'(958)\gamma$	(6.25 \pm 0.21) $\times 10^{-5}$		60
$\eta\pi^0\pi^0\gamma$	< 2 $\times 10^{-5}$	CL=90%	293
$\mu^+\mu^-\gamma$	(1.4 \pm 0.5) $\times 10^{-5}$		499
$\rho\gamma\gamma$	< 1.2 $\times 10^{-4}$	CL=90%	215
$\eta\pi^+\pi^-$	< 1.8 $\times 10^{-5}$	CL=90%	288
$\eta\mu^+\mu^-$	< 9.4 $\times 10^{-6}$	CL=90%	321

Meson Summary Table

 $h_1(1170)$

$$I^G(J^{PC}) = 0^-(1^+ -)$$

Mass $m = 1170 \pm 20$ MeV
 Full width $\Gamma = 360 \pm 40$ MeV

$h_1(1170)$ DECAY MODES	Fraction (Γ_i/Γ)	ρ (MeV/c)
$\rho\pi$	seen	307

 $b_1(1235)$

$$I^G(J^{PC}) = 1^+(1^+ -)$$

Mass $m = 1229.5 \pm 3.2$ MeV ($S = 1.6$)
 Full width $\Gamma = 142 \pm 9$ MeV ($S = 1.2$)

$b_1(1235)$ DECAY MODES	Fraction (Γ_i/Γ)	Confidence level	ρ (MeV/c)
$\omega\pi$	dominant		348
$\pi^\pm\gamma$	$[D/S \text{ amplitude ratio} = 0.277 \pm 0.027]$ (1.6 ± 0.4) $\times 10^{-3}$		607
$\eta\rho$	seen		†
$\pi^+\pi^-\pi^+\pi^0$	< 50 %	84%	535
$(K\bar{K})^\pm\pi^0$	< 8 %	90%	248
$K_S^0 K_S^0 \pi^\pm$	< 6 %	90%	235
$K_S^0 K_S^0 \pi^\pm$	< 2 %	90%	235
$\phi\pi$	< 1.5 %	84%	147

 $a_1(1260)$ [k]

$$I^G(J^{PC}) = 1^-(1^+ +)$$

Mass $m = 1230 \pm 40$ MeV [l]
 Full width $\Gamma = 250$ to 600 MeV

$a_1(1260)$ DECAY MODES	Fraction (Γ_i/Γ)	ρ (MeV/c)
$(\rho\pi)_{S\text{-wave}}$	seen	353
$(\rho\pi)_{D\text{-wave}}$	seen	353
$(\rho(1450)\pi)_{S\text{-wave}}$	seen	†
$(\rho(1450)\pi)_{D\text{-wave}}$	seen	†
$\sigma\pi$	seen	-
$f_0(980)\pi$	not seen	189
$f_0(1370)\pi$	seen	†
$f_2(1270)\pi$	seen	†
$K\bar{K}^*(892) + \text{c.c.}$	seen	†
$\pi\gamma$	seen	608

 $f_2(1270)$

$$I^G(J^{PC}) = 0^+(2^+ +)$$

Mass $m = 1275.1 \pm 1.2$ MeV ($S = 1.1$)
 Full width $\Gamma = 185.1^{+2.9}_{-2.4}$ MeV ($S = 1.5$)

$f_2(1270)$ DECAY MODES	Fraction (Γ_i/Γ)	Scale factor/ Confidence level	ρ (MeV/c)
$\pi\pi$	(84.8 ± 2.4) % (-1.2) %	$S=1.2$	623
$\pi^+\pi^-2\pi^0$	(7.1 ± 1.4) % (-2.7) %	$S=1.3$	562
$K\bar{K}$	(4.6 ± 0.4) %	$S=2.8$	403
$2\pi^+2\pi^-$	(2.8 ± 0.4) %	$S=1.2$	559
$\eta\eta$	(4.0 ± 0.8) $\times 10^{-3}$	$S=2.1$	326
$4\pi^0$	(3.0 ± 1.0) $\times 10^{-3}$		564
$\gamma\gamma$	(1.64 ± 0.19) $\times 10^{-5}$	$S=1.9$	638
$\eta\pi\pi$	< 8 $\times 10^{-3}$	CL=95%	477
$K^0 K^- \pi^+ + \text{c.c.}$	< 3.4 $\times 10^{-3}$	CL=95%	293
e^+e^-	< 6 $\times 10^{-10}$	CL=90%	638

 $f_1(1285)$

$$I^G(J^{PC}) = 0^+(1^+ +)$$

Mass $m = 1281.8 \pm 0.6$ MeV ($S = 1.6$)
 Full width $\Gamma = 24.3 \pm 1.1$ MeV ($S = 1.4$)

 $f_1(1285)$ DECAY MODES

	Fraction (Γ_i/Γ)	Scale factor/ Confidence level	ρ (MeV/c)
4π	(33.1 ± 2.1) % (-1.8) %	$S=1.3$	568
$\pi^0\pi^0\pi^+\pi^-$	(22.0 ± 1.4) % (-1.2) %	$S=1.3$	566
$2\pi^+2\pi^-$	(11.0 ± 0.7) % (-0.6) %	$S=1.3$	563
$\rho^0\pi^+\pi^-$	(11.0 ± 0.7) % (-0.6) %	$S=1.3$	336
$4\pi^0$	seen		†
$\eta\pi\pi$	< 7 $\times 10^{-4}$	CL=90%	568
$a_0(980)\pi$ [ignoring $a_0(980) \rightarrow K\bar{K}$]	(52 ± 5) %		482
$\eta\pi\pi$ [excluding $a_0(980)\pi$]	(36 ± 7) %		238
$K\bar{K}\pi$	(16 ± 7) %		482
$K\bar{K}^*(892)$	(9.0 ± 0.4) %	$S=1.1$	308
$\gamma\rho^0$	not seen		†
$\phi\gamma$	(5.5 ± 1.3) %	$S=2.8$	406
	(7.4 ± 2.6) $\times 10^{-4}$		236

 $\eta(1295)$

$$I^G(J^{PC}) = 0^+(0^- +)$$

Mass $m = 1294 \pm 4$ MeV ($S = 1.6$)
 Full width $\Gamma = 55 \pm 5$ MeV

 $\eta(1295)$ DECAY MODES

	Fraction (Γ_i/Γ)	ρ (MeV/c)
$\eta\pi^+\pi^-$	seen	487
$a_0(980)\pi$	seen	248
$\eta\pi^0\pi^0$	seen	490
$\eta(\pi\pi)_{S\text{-wave}}$	seen	-

 $\pi(1300)$

$$I^G(J^{PC}) = 1^-(0^- +)$$

Mass $m = 1300 \pm 100$ MeV [l]
 Full width $\Gamma = 200$ to 600 MeV

 $\pi(1300)$ DECAY MODES

	Fraction (Γ_i/Γ)	ρ (MeV/c)
$\rho\pi$	seen	404
$\pi(\pi\pi)_{S\text{-wave}}$	seen	-

 $a_2(1320)$

$$I^G(J^{PC}) = 1^-(2^+ +)$$

Mass $m = 1318.3 \pm 0.6$ MeV ($S = 1.2$)
 Full width $\Gamma = 107 \pm 5$ MeV [l]

 $a_2(1320)$ DECAY MODES

	Fraction (Γ_i/Γ)	Scale factor/ Confidence level	ρ (MeV/c)
3π	(70.1 ± 2.7) %	$S=1.2$	624
$\eta\pi$	(14.5 ± 1.2) %		535
$\omega\pi\pi$	(10.6 ± 3.2) %	$S=1.3$	366
$K\bar{K}$	(4.9 ± 0.8) %		437
$\eta'(958)\pi$	(5.3 ± 0.9) $\times 10^{-3}$		288
$\pi^\pm\gamma$	(2.68 ± 0.31) $\times 10^{-3}$		652
$\gamma\gamma$	(9.4 ± 0.7) $\times 10^{-6}$		659
e^+e^-	< 5 $\times 10^{-9}$	CL=90%	659

 $f_0(1370)$ [j]

$$I^G(J^{PC}) = 0^+(0^+ +)$$

Mass $m = 1200$ to 1500 MeV
 Full width $\Gamma = 200$ to 500 MeV

 $f_0(1370)$ DECAY MODES

	Fraction (Γ_i/Γ)	ρ (MeV/c)
$\pi\pi$	seen	672
4π	seen	617
$4\pi^0$	seen	617
$2\pi^+2\pi^-$	seen	612
$\pi^+\pi^-2\pi^0$	seen	615
$\rho\rho$	dominant	†
$2(\pi\pi)_{S\text{-wave}}$	seen	-
$\pi(1300)\pi$	seen	†
$a_1(1260)\pi$	seen	35

Meson Summary Table

$\eta\eta$	seen	411
$K\bar{K}$	seen	475
$K\bar{K}n\pi$	not seen	†
6π	not seen	508
$\omega\omega$	not seen	†
$\gamma\gamma$	seen	685
e^+e^-	not seen	685

$$\boxed{\pi_1(1400)^{[m]}} \quad I^G(J^{PC}) = 1^-(1^-+)$$

Mass $m = 1354 \pm 25$ MeV ($S = 1.8$)
Full width $\Gamma = 330 \pm 35$ MeV

$\pi_1(1400)$ DECAY MODES	Fraction (Γ_i/Γ)	ρ (MeV/c)
$\eta\pi^0$	seen	557
$\eta\pi^-$	seen	556

$$\boxed{\eta(1405)^{[n]}} \quad I^G(J^{PC}) = 0^+(0^-+)$$

Mass $m = 1409.8 \pm 2.5$ MeV $^{[l]}$ ($S = 2.2$)
Full width $\Gamma = 51.1 \pm 3.4$ MeV $^{[l]}$ ($S = 2.0$)

$\eta(1405)$ DECAY MODES	Fraction (Γ_i/Γ)	Confidence level	ρ (MeV/c)
$K\bar{K}\pi$	seen		425
$\eta\pi\pi$	seen		563
$a_0(980)\pi$	seen		345
$\eta(\pi\pi)$ s-wave	seen		–
$f_0(980)\eta$	seen	†	
4π	seen		639
$\rho\rho$	<58 %	99.85%	†
$\rho^0\gamma$	seen		492
$K^*(892)K$	seen		125

$$\boxed{f_1(1420)^{[o]}} \quad I^G(J^{PC}) = 0^+(1^++)$$

Mass $m = 1426.4 \pm 0.9$ MeV ($S = 1.1$)
Full width $\Gamma = 54.9 \pm 2.6$ MeV

$f_1(1420)$ DECAY MODES	Fraction (Γ_i/Γ)	ρ (MeV/c)
$K\bar{K}\pi$	dominant	438
$K\bar{K}^*(892) + \text{c.c.}$	dominant	163
$\eta\pi\pi$	possibly seen	573
$\phi\gamma$	seen	349

$$\boxed{\omega(1420)^{[p]}} \quad I^G(J^{PC}) = 0^-(1^-+)$$

Mass m (1400–1450) MeV
Full width Γ (180–250) MeV

$\omega(1420)$ DECAY MODES	Fraction (Γ_i/Γ)	ρ (MeV/c)
$\rho\pi$	dominant	486
$\omega\pi\pi$	seen	444
$b_1(1235)\pi$	seen	125
e^+e^-	seen	710

$$\boxed{a_0(1450)^{[l]}} \quad I^G(J^{PC}) = 1^-(0^++)$$

Mass $m = 1474 \pm 19$ MeV
Full width $\Gamma = 265 \pm 13$ MeV

$a_0(1450)$ DECAY MODES	Fraction (Γ_i/Γ)	ρ (MeV/c)
$\pi\eta$	seen	627
$\pi\eta'(958)$	seen	410
$K\bar{K}$	seen	547
$\omega\pi\pi$	seen	484
$a_0(980)\pi\pi$	seen	342
$\gamma\gamma$	seen	737

$$\boxed{\rho(1450)^{[q]}} \quad I^G(J^{PC}) = 1^+(1^-+)$$

Mass $m = 1465 \pm 25$ MeV $^{[l]}$
Full width $\Gamma = 400 \pm 60$ MeV $^{[l]}$

$\rho(1450)$ DECAY MODES	Fraction (Γ_i/Γ)	ρ (MeV/c)
$\pi\pi$	seen	720
4π	seen	669
e^+e^-	seen	732
$\eta\rho$	possibly seen	310
$a_2(1320)\pi$	not seen	55
$K\bar{K}$	not seen	541
$K\bar{K}^*(892) + \text{c.c.}$	possibly seen	229
$\eta\gamma$	possibly seen	630

$$\boxed{\eta(1475)^{[n]}} \quad I^G(J^{PC}) = 0^+(0^-+)$$

Mass $m = 1476 \pm 4$ MeV ($S = 1.3$)
Full width $\Gamma = 85 \pm 9$ MeV ($S = 1.5$)

$\eta(1475)$ DECAY MODES	Fraction (Γ_i/Γ)	ρ (MeV/c)
$K\bar{K}\pi$	dominant	477
$K\bar{K}^*(892) + \text{c.c.}$	seen	245
$a_0(980)\pi$	seen	396
$\gamma\gamma$	seen	738

$$\boxed{f_0(1500)^{[m]}} \quad I^G(J^{PC}) = 0^+(0^++)$$

Mass $m = 1505 \pm 6$ MeV ($S = 1.3$)
Full width $\Gamma = 109 \pm 7$ MeV

$f_0(1500)$ DECAY MODES	Fraction (Γ_i/Γ)	Scale factor	ρ (MeV/c)
$\pi\pi$	(34.9±2.3) %	1.2	741
$\pi^+\pi^-$	seen		740
$2\pi^0$	seen		741
4π	(49.5±3.3) %	1.2	691
$4\pi^0$	seen		691
$2\pi^+2\pi^-$	seen		687
$2(\pi\pi)$ s-wave	seen		–
$\rho\rho$	seen		†
$\pi(1300)\pi$	seen		144
$a_1(1260)\pi$	seen		218
$\eta\eta$	(5.1±0.9) %	1.4	516
$\eta\eta'(958)$	(1.9±0.8) %	1.7	†
$K\bar{K}$	(8.6±1.0) %	1.1	568
$\gamma\gamma$	not seen		753

$$\boxed{f_2'(1525)} \quad I^G(J^{PC}) = 0^+(2^++)$$

Mass $m = 1525 \pm 5$ MeV $^{[l]}$
Full width $\Gamma = 73^{+6}_{-5}$ MeV $^{[l]}$

$f_2'(1525)$ DECAY MODES	Fraction (Γ_i/Γ)	ρ (MeV/c)
$K\bar{K}$	(88.7 ± 2.2) %	581
$\eta\eta$	(10.4 ± 2.2) %	530
$\pi\pi$	(8.2 ± 1.5) × 10 ⁻³	750
$\gamma\gamma$	(1.11 ± 0.14) × 10 ⁻⁶	763

$$\boxed{\pi_1(1600)^{[m]}} \quad I^G(J^{PC}) = 1^-(1^-+)$$

Mass $m = 1662^{+15}_{-11}$ MeV ($S = 1.2$)
Full width $\Gamma = 234 \pm 50$ MeV ($S = 1.7$)

$\pi_1(1600)$ DECAY MODES	Fraction (Γ_i/Γ)	ρ (MeV/c)
$\pi\pi\pi$	not seen	803
$\rho^0\pi^-$	not seen	641
$f_2(1270)\pi^-$	not seen	319
$b_1(1235)\pi$	seen	357
$\eta'(958)\pi^-$	seen	543
$f_1(1285)\pi$	seen	315

Meson Summary Table

 $\eta_2(1645)$

$$I^G(J^{PC}) = 0^+(2^-)$$

Mass $m = 1617 \pm 5$ MeV
Full width $\Gamma = 181 \pm 11$ MeV

$\eta_2(1645)$ DECAY MODES	Fraction (Γ_i/Γ)	ρ (MeV/c)
$a_2(1320)\pi$	seen	242
$K\bar{K}\pi$	seen	580
$K^*\bar{K}$	seen	404
$\eta\pi^+\pi^-$	seen	685
$a_0(980)\pi$	seen	499
$f_2(1270)\eta$	not seen	†

 $\omega(1650)$ [1]

$$I^G(J^{PC}) = 0^-(1^-)$$

Mass $m = 1670 \pm 30$ MeV
Full width $\Gamma = 315 \pm 35$ MeV

$\omega(1650)$ DECAY MODES	Fraction (Γ_i/Γ)	ρ (MeV/c)
$\rho\pi$	seen	646
$\omega\pi\pi$	seen	617
$\omega\eta$	seen	500
e^+e^-	seen	835

 $\omega_3(1670)$

$$I^G(J^{PC}) = 0^-(3^-)$$

Mass $m = 1667 \pm 4$ MeV
Full width $\Gamma = 168 \pm 10$ MeV [1]

$\omega_3(1670)$ DECAY MODES	Fraction (Γ_i/Γ)	ρ (MeV/c)
$\rho\pi$	seen	645
$\omega\pi\pi$	seen	615
$b_1(1235)\pi$	possibly seen	361

 $\pi_2(1670)$

$$I^G(J^{PC}) = 1^-(2^-)$$

Mass $m = 1672.4 \pm 3.2$ MeV [1] ($S = 1.4$)
Full width $\Gamma = 259 \pm 9$ MeV [1] ($S = 1.3$)

$\pi_2(1670)$ DECAY MODES	Fraction (Γ_i/Γ)	Confidence level	ρ (MeV/c)
3π	(95.8±1.4) %		809
$f_2(1270)\pi$	(56.3±3.2) %		329
$\rho\pi$	(31 ± 4) %		648
$\sigma\pi$	(10.9±3.4) %		–
$(\pi\pi)$ s-wave	(8.7±3.4) %		–
$K\bar{K}^*(892) + \text{c.c.}$	(4.2±1.4) %		455
$\omega\rho$	(2.7±1.1) %		304
$\gamma\gamma$	< 2.8	$\times 10^{-7}$ 90%	836
$\rho(1450)\pi$	< 3.6	$\times 10^{-3}$ 97.7%	148
$b_1(1235)\pi$	< 1.9	$\times 10^{-3}$ 97.7%	366
$f_1(1285)\pi$	possibly seen		323
$a_2(1320)\pi$	not seen		292

 $\phi(1680)$

$$I^G(J^{PC}) = 0^-(1^-)$$

Mass $m = 1680 \pm 20$ MeV [1]
Full width $\Gamma = 150 \pm 50$ MeV [1]

$\phi(1680)$ DECAY MODES	Fraction (Γ_i/Γ)	ρ (MeV/c)
$K\bar{K}^*(892) + \text{c.c.}$	dominant	462
$K_S^0 K\pi$	seen	621
$K\bar{K}$	seen	680
e^+e^-	seen	840
$\omega\pi\pi$	not seen	623
$K^+K^-\pi^+\pi^-$	seen	544

 $\rho_3(1690)$

$$I^G(J^{PC}) = 1^+(3^-)$$

Mass $m = 1688.8 \pm 2.1$ MeV [1]
Full width $\Gamma = 161 \pm 10$ MeV [1] ($S = 1.5$)

 $\rho_3(1690)$ DECAY MODES

	Fraction (Γ_i/Γ)	Scale factor	ρ (MeV/c)
4π	(71.1 ± 1.9) %		790
$\pi^\pm\pi^+\pi^-\pi^0$	(67 ± 22) %		787
$\omega\pi$	(16 ± 6) %		655
$\pi\pi$	(23.6 ± 1.3) %		834
$K\bar{K}\pi$	(3.8 ± 1.2) %		629
$K\bar{K}$	(1.58 ± 0.26) %	1.2	685
$\eta\pi^+\pi^-$	seen		727
$\rho(770)\eta$	seen		520
$\pi\pi\rho$	seen		633
Excluding 2ρ and $a_2(1320)\pi$.			
$a_2(1320)\pi$	seen		307
$\rho\rho$	seen		334

 $\rho(1700)$ [q]

$$I^G(J^{PC}) = 1^+(1^-)$$

Mass $m = 1720 \pm 20$ MeV [1] ($\eta\rho^0$ and $\pi^+\pi^-$ modes)
Full width $\Gamma = 250 \pm 100$ MeV [1] ($\eta\rho^0$ and $\pi^+\pi^-$ modes)

 $\rho(1700)$ DECAY MODES

	Fraction (Γ_i/Γ)	ρ (MeV/c)
$2(\pi^+\pi^-)$	large	803
$\rho\pi\pi$	dominant	653
$\rho^0\pi^+\pi^-$	large	650
$\rho^\pm\pi^\mp\pi^0$	large	652
$a_1(1260)\pi$	seen	404
$h_1(1170)\pi$	seen	447
$\pi(1300)\pi$	seen	349
$\rho\rho$	seen	372
$\pi^+\pi^-$	seen	849
$\pi\pi$	seen	849
$K\bar{K}^*(892) + \text{c.c.}$	seen	496
$\eta\rho$	seen	545
$a_2(1320)\pi$	not seen	334
$K\bar{K}$	seen	704
e^+e^-	seen	860
$\pi^0\omega$	seen	674

 $f_0(1710)$ [s]

$$I^G(J^{PC}) = 0^+(0^+)$$

Mass $m = 1720 \pm 6$ MeV ($S = 1.6$)
Full width $\Gamma = 135 \pm 8$ MeV ($S = 1.1$)

 $f_0(1710)$ DECAY MODES

	Fraction (Γ_i/Γ)	ρ (MeV/c)
$K\bar{K}$	seen	704
$\eta\eta$	seen	663
$\pi\pi$	seen	849
$\omega\omega$	seen	357

 $\pi(1800)$

$$I^G(J^{PC}) = 1^-(0^-)$$

Mass $m = 1816 \pm 14$ MeV ($S = 2.3$)
Full width $\Gamma = 208 \pm 12$ MeV

 $\pi(1800)$ DECAY MODES

	Fraction (Γ_i/Γ)	ρ (MeV/c)
$\pi^+\pi^-\pi^-$	seen	881
$f_0(600)\pi^-$	seen	–
$f_0(980)\pi^-$	seen	634
$f_0(1370)\pi^-$	seen	371
$f_0(1500)\pi^-$	not seen	254
$\rho\pi^-$	not seen	735
$\eta\eta\pi^-$	seen	664
$a_0(980)\eta$	seen	477
$a_2(1320)\eta$	not seen	†
$f_2(1270)\pi$	not seen	445
$f_0(1370)\pi^-$	not seen	371
$f_0(1500)\pi^-$	seen	254
$\eta\eta'(958)\pi^-$	seen	380
$K_0^*(1430)K^-$	seen	†
$K^*(892)K^-$	not seen	573

Meson Summary Table

$\phi_3(1850)$	$I^G(J^{PC}) = 0^-(3^{--})$	
Mass $m = 1854 \pm 7$ MeV		
Full width $\Gamma = 87_{-23}^{+28}$ MeV ($S = 1.2$)		
$\phi_3(1850)$ DECAY MODES	Fraction (Γ_i/Γ)	ρ (MeV/c)
$K\bar{K}$	seen	785
$K\bar{K}^*(892) + c.c.$	seen	602

$\pi_2(1880)$	$I^G(J^{PC}) = 1^-(2^{-+})$
Mass $m = 1895 \pm 16$ MeV	
Full width $\Gamma = 235 \pm 34$ MeV	

$f_2(1950)$	$I^G(J^{PC}) = 0^+(2^{++})$
Mass $m = 1944 \pm 12$ MeV ($S = 1.5$)	
Full width $\Gamma = 472 \pm 18$ MeV	

$f_2(1950)$ DECAY MODES	Fraction (Γ_i/Γ)	ρ (MeV/c)
$K^*(892)\bar{K}^*(892)$	seen	387
$\pi^+\pi^-\pi^0$	seen	962
$\pi^0\pi^0$	seen	963
4π	seen	925
$\eta\eta$	seen	803
$K\bar{K}$	seen	837
$\gamma\gamma$	seen	972

$f_2(2010)$	$I^G(J^{PC}) = 0^+(2^{++})$
Mass $m = 2011_{-80}^{+60}$ MeV	
Full width $\Gamma = 202 \pm 60$ MeV	

$f_2(2010)$ DECAY MODES	Fraction (Γ_i/Γ)	ρ (MeV/c)
$\phi\phi$	seen	†
$K\bar{K}$	seen	876

$a_4(2040)$	$I^G(J^{PC}) = 1^-(4^{++})$
Mass $m = 2001 \pm 10$ MeV	
Full width $\Gamma = 235 \pm 29$ MeV ($S = 1.3$)	

$a_4(2040)$ DECAY MODES	Fraction (Γ_i/Γ)	ρ (MeV/c)
$K\bar{K}$	seen	870
$\pi^+\pi^-\pi^0$	seen	976
$\rho\pi$	seen	844
$f_2(1270)\pi$	seen	583
$\omega\pi^-\pi^0$	seen	821
$\omega\rho$	seen	627
$\eta\pi^0$	seen	920
$\eta'(958)\pi$	seen	764

$f_4(2050)$	$I^G(J^{PC}) = 0^+(4^{++})$
Mass $m = 2018 \pm 11$ MeV ($S = 2.1$)	
Full width $\Gamma = 237 \pm 18$ MeV ($S = 1.9$)	

$f_4(2050)$ DECAY MODES	Fraction (Γ_i/Γ)	ρ (MeV/c)
$\omega\omega$	seen	637
$\pi\pi$	(17.0±1.5) %	1000
$K\bar{K}$	(6.8 $^{+3.4}_{-1.8}$) × 10 ⁻³	880
$\eta\eta$	(2.1±0.8) × 10 ⁻³	848
$4\pi^0$	< 1.2 %	964
$a_2(1320)\pi$	seen	567

$\phi(2170)$	$I^G(J^{PC}) = 0^-(1^{--})$
Mass $m = 2175 \pm 15$ MeV ($S = 1.6$)	
Full width $\Gamma = 61 \pm 18$ MeV	

$\phi(2170)$ DECAY MODES	Fraction (Γ_i/Γ)	ρ (MeV/c)
e^+e^-	seen	1087
$\phi f_0(980)$	seen	427
$K^+K^-f_0(980) \rightarrow$	seen	—
$K^+K^-\pi^+\pi^-$	—	—
$K^+K^-f_0(980) \rightarrow K^+K^-\pi^0\pi^0$	seen	—
$K^{*0}K^\pm\pi^\mp$	not seen	770

$f_2(2300)$	$I^G(J^{PC}) = 0^+(2^{++})$
Mass $m = 2297 \pm 28$ MeV	
Full width $\Gamma = 149 \pm 40$ MeV	

$f_2(2300)$ DECAY MODES	Fraction (Γ_i/Γ)	ρ (MeV/c)
$\phi\phi$	seen	529
$K\bar{K}$	seen	1037
$\gamma\gamma$	seen	1149

$f_2(2340)$	$I^G(J^{PC}) = 0^+(2^{++})$
Mass $m = 2339 \pm 60$ MeV	
Full width $\Gamma = 319_{-70}^{+80}$ MeV	

$f_2(2340)$ DECAY MODES	Fraction (Γ_i/Γ)	ρ (MeV/c)
$\phi\phi$	seen	573
$\eta\eta$	seen	1033

STRANGE MESONS ($S = \pm 1, C = B = 0$)

$K^+ = u\bar{s}, K^0 = d\bar{s}, \bar{K}^0 = \bar{d}s, K^- = \bar{u}s$, similarly for K^{*} 's

K^\pm	$I(J^P) = \frac{1}{2}(0^-)$
Mass $m = 493.677 \pm 0.016$ MeV [1] ($S = 2.8$)	
Mean life $\tau = (1.2380 \pm 0.0021) \times 10^{-8}$ s ($S = 1.9$)	
$c\tau = 3.712$ m	

Slope parameter g [4]

(See Particle Listings for quadratic coefficients and alternative parametrization related to $\pi\pi$ scattering)

$$K^\pm \rightarrow \pi^\pm\pi^+\pi^- \quad g = -0.21134 \pm 0.00017$$

$$(g_+ - g_-) / (g_+ + g_-) = (-1.5 \pm 2.2) \times 10^{-4}$$

$$K^\pm \rightarrow \pi^\pm\pi^0\pi^0 \quad g = 0.626 \pm 0.007$$

$$(g_+ - g_-) / (g_+ + g_-) = (1.8 \pm 1.8) \times 10^{-4}$$

K^\pm decay form factors [a,v]

Assuming μ -e universality

$$\lambda_+(K_{\mu 3}^+) = \lambda_+(K_{e 3}^+) = (2.97 \pm 0.05) \times 10^{-2}$$

$$\lambda_0(K_{\mu 3}^+) = (1.95 \pm 0.12) \times 10^{-2}$$

Not assuming μ -e universality

$$\lambda_+(K_{e 3}^+) = (2.98 \pm 0.05) \times 10^{-2}$$

$$\lambda_+(K_{\mu 3}^+) = (2.96 \pm 0.17) \times 10^{-2}$$

$$\lambda_0(K_{\mu 3}^+) = (1.96 \pm 0.13) \times 10^{-2}$$

$K_{e 3}$ form factor quadratic fit

$$\lambda'_+(K_{e 3}^\pm) \text{ linear coeff.} = (2.48 \pm 0.17) \times 10^{-2}$$

$$\lambda''_+(K_{e 3}^\pm) \text{ quadratic coeff.} = (0.19 \pm 0.09) \times 10^{-2}$$

$$K_{e 3}^+ \quad |f_S/f_+| = (-0.3_{-0.7}^{+0.8}) \times 10^{-2}$$

$$K_{e 3}^+ \quad |f_T/f_+| = (-1.2 \pm 2.3) \times 10^{-2}$$

$$K_{\mu 3}^+ \quad |f_S/f_+| = (0.2 \pm 0.6) \times 10^{-2}$$

$$K_{\mu 3}^+ \quad |f_T/f_+| = (-0.1 \pm 0.7) \times 10^{-2}$$

$$K^+ \rightarrow e^+\nu_e\gamma \quad |F_A + F_V| = 0.133 \pm 0.008 \quad (S = 1.3)$$

$$K^+ \rightarrow \mu^+\nu_\mu\gamma \quad |F_A + F_V| = 0.165 \pm 0.013$$

$$K^+ \rightarrow e^+\nu_e\gamma \quad |F_A - F_V| < 0.49$$

$$K^+ \rightarrow \mu^+\nu_\mu\gamma \quad |F_A - F_V| = -0.24 \text{ to } 0.04, \text{ CL} = 90\%$$

Meson Summary Table

Charge Radius

$$\langle r \rangle = 0.560 \pm 0.031 \text{ fm}$$

CP violation parameters

$$\Delta(K_{\pi e e}^{\pm}) = (-2.2 \pm 1.6) \times 10^{-2}$$

$$\Delta(K_{\pi \mu \mu}^{\pm}) = -0.02 \pm 0.12$$

T violation parameters

$$K^+ \rightarrow \pi^0 \mu^+ \nu_{\mu} \quad P_T = (-1.7 \pm 2.5) \times 10^{-3}$$

$$K^+ \rightarrow \mu^+ \nu_{\mu} \gamma \quad P_T = (-0.6 \pm 1.9) \times 10^{-2}$$

$$K^+ \rightarrow \pi^0 \mu^+ \nu_{\mu} \quad \text{Im}(\xi) = -0.006 \pm 0.008$$

K^- modes are charge conjugates of the modes below.

K^+ DECAY MODES	Fraction (Γ_i/Γ)	Scale factor/ Confidence level	ρ (MeV/c)
Leptonic and semileptonic modes			
$K^+ \rightarrow e^+ \nu_e$	$(1.584 \pm 0.020) \times 10^{-5}$		247
$K^+ \rightarrow \mu^+ \nu_{\mu}$	$(63.55 \pm 0.11) \%$	S=1.2	236
$K^+ \rightarrow \pi^0 e^+ \nu_e$	$(5.07 \pm 0.04) \%$	S=2.1	228
Called K_{e3}^+ .			
$K^+ \rightarrow \pi^0 \mu^+ \nu_{\mu}$	$(3.353 \pm 0.034) \%$	S=1.8	215
Called $K_{\mu 3}^+$.			
$K^+ \rightarrow \pi^0 \pi^0 e^+ \nu_e$	$(2.2 \pm 0.4) \times 10^{-5}$		206
$K^+ \rightarrow \pi^+ \pi^- e^+ \nu_e$	$(4.09 \pm 0.10) \times 10^{-5}$		203
$K^+ \rightarrow \pi^+ \pi^- \mu^+ \nu_{\mu}$	$(1.4 \pm 0.9) \times 10^{-5}$		151
$K^+ \rightarrow \pi^0 \pi^0 \pi^0 e^+ \nu_e$	$< 3.5 \times 10^{-6}$	CL=90%	135
Hadronic modes			
$K^+ \rightarrow \pi^+ \pi^0$	$(20.66 \pm 0.08) \%$	S=1.2	205
$K^+ \rightarrow \pi^+ \pi^0 \pi^0$	$(1.761 \pm 0.022) \%$	S=1.1	133
$K^+ \rightarrow \pi^+ \pi^+ \pi^-$	$(5.59 \pm 0.04) \%$	S=1.3	125
Leptonic and semileptonic modes with photons			
$K^+ \rightarrow \mu^+ \nu_{\mu} \gamma$	$[w,x] (6.2 \pm 0.8) \times 10^{-3}$		236
$K^+ \rightarrow \mu^+ \nu_{\mu} \gamma (\text{SD}^+)$	$[a,y] (1.33 \pm 0.22) \times 10^{-5}$		-
$K^+ \rightarrow \mu^+ \nu_{\mu} \gamma (\text{SD}^+ \text{INT})$	$[a,y] < 2.7 \times 10^{-5}$	CL=90%	-
$K^+ \rightarrow \mu^+ \nu_{\mu} \gamma (\text{SD}^- + \text{SD}^- \text{INT})$	$[a,y] < 2.6 \times 10^{-4}$	CL=90%	-
$K^+ \rightarrow e^+ \nu_e \gamma$	$(9.4 \pm 0.4) \times 10^{-6}$		247
$K^+ \rightarrow \pi^0 e^+ \nu_e \gamma$	$[w,x] (2.56 \pm 0.16) \times 10^{-4}$		228
$K^+ \rightarrow \pi^0 e^+ \nu_e \gamma (\text{SD})$	$[a,y] < 5.3 \times 10^{-5}$	CL=90%	228
$K^+ \rightarrow \pi^0 \mu^+ \nu_{\mu} \gamma$	$[w,x] (1.5 \pm 0.4) \times 10^{-5}$		215
$K^+ \rightarrow \pi^0 \pi^0 e^+ \nu_e \gamma$	$< 5 \times 10^{-6}$	CL=90%	206
Hadronic modes with photons or $\ell\bar{\ell}$ pairs			
$K^+ \rightarrow \pi^+ \pi^0 \gamma$	$[w,x] (2.75 \pm 0.15) \times 10^{-4}$		205
$K^+ \rightarrow \pi^+ \pi^0 \gamma (\text{DE})$	$[x,z] (4.3 \pm 0.7) \times 10^{-6}$		205
$K^+ \rightarrow \pi^+ \pi^0 \pi^0 \gamma$	$[w,x] (7.6 \pm 6.0_{-3.0}) \times 10^{-6}$		133
$K^+ \rightarrow \pi^+ \pi^+ \pi^- \gamma$	$[w,x] (1.04 \pm 0.31) \times 10^{-4}$		125
$K^+ \rightarrow \pi^+ \gamma \gamma$	$[x] (1.10 \pm 0.32) \times 10^{-6}$		227
$K^+ \rightarrow \pi^+ 3\gamma$	$[x] < 1.0 \times 10^{-4}$	CL=90%	227
$K^{\pm} \rightarrow \pi^{\pm} e^{\pm} e^{\mp} \gamma$	$(1.19 \pm 0.13) \times 10^{-8}$		227
Leptonic modes with $\ell\bar{\ell}$ pairs			
$K^+ \rightarrow e^+ \nu_e \nu_{\bar{e}}$	$< 6 \times 10^{-5}$	CL=90%	247
$K^+ \rightarrow \mu^+ \nu_{\mu} \nu_{\bar{\mu}}$	$< 6.0 \times 10^{-6}$	CL=90%	236
$K^+ \rightarrow e^+ \nu_e e^+ e^-$	$(2.48 \pm 0.20) \times 10^{-8}$		247
$K^+ \rightarrow \mu^+ \nu_{\mu} e^+ e^-$	$(7.06 \pm 0.31) \times 10^{-8}$		236
$K^+ \rightarrow e^+ \nu_e \mu^+ \mu^-$	$(1.7 \pm 0.5) \times 10^{-8}$		223
$K^+ \rightarrow \mu^+ \nu_{\mu} \mu^+ \mu^-$	$< 4.1 \times 10^{-7}$	CL=90%	185
Lepton Family number (LF), Lepton number (L), $\Delta S = \Delta Q$ (SQ) violating modes, or $\Delta S = 1$ weak neutral current (S1) modes			
$K^+ \rightarrow \pi^+ \pi^+ e^- \bar{\nu}_e$	SQ $< 1.2 \times 10^{-8}$	CL=90%	203
$K^+ \rightarrow \pi^+ \pi^+ \mu^- \bar{\nu}_{\mu}$	SQ $< 3.0 \times 10^{-6}$	CL=95%	151
$K^+ \rightarrow \pi^+ e^+ e^-$	S1 $(3.00 \pm 0.09) \times 10^{-7}$		227
$K^+ \rightarrow \pi^+ \mu^+ \mu^-$	S1 $(8.1 \pm 1.4) \times 10^{-8}$	S=2.7	172
$K^+ \rightarrow \pi^+ \nu_{\bar{e}}$	S1 $(1.7 \pm 1.1) \times 10^{-10}$		227
$K^+ \rightarrow \pi^+ \pi^0 \nu_{\bar{e}}$	S1 $< 4.3 \times 10^{-5}$	CL=90%	205
$K^+ \rightarrow \mu^- \nu e^+ e^+$	LF $< 2.0 \times 10^{-8}$	CL=90%	236
$K^+ \rightarrow \mu^+ \nu_e$	LF $[d] < 4 \times 10^{-3}$	CL=90%	236
$K^+ \rightarrow \pi^+ \mu^+ e^-$	LF $< 1.3 \times 10^{-11}$	CL=90%	214

$K^+ \rightarrow \pi^+ \mu^- e^+$	LF	$< 5.2 \times 10^{-10}$	CL=90%	214
$K^+ \rightarrow \pi^- \mu^+ e^+$	L	$< 5.0 \times 10^{-10}$	CL=90%	214
$K^+ \rightarrow \pi^- e^+ e^+$	L	$< 6.4 \times 10^{-10}$	CL=90%	227
$K^+ \rightarrow \pi^- \mu^+ \mu^+$	L	$[d] < 3.0 \times 10^{-9}$	CL=90%	172
$K^+ \rightarrow \mu^+ \bar{\nu}_e$	L	$[d] < 3.3 \times 10^{-3}$	CL=90%	236
$K^+ \rightarrow \pi^0 e^+ \bar{\nu}_e$	L	$< 3 \times 10^{-3}$	CL=90%	228
$K^+ \rightarrow \pi^+ \gamma$	[aa]	$< 2.3 \times 10^{-9}$	CL=90%	227

 K^0

$$I(J^P) = \frac{1}{2}(0^-)$$

50% K_S , 50% K_L

$$\text{Mass } m = 497.614 \pm 0.024 \text{ MeV} \quad (S = 1.6)$$

$$m_{K^0} - m_{K^{\pm}} = 3.937 \pm 0.028 \text{ MeV} \quad (S = 1.8)$$

Mean Square Charge Radius

$$\langle r^2 \rangle = -0.077 \pm 0.010 \text{ fm}^2$$

T-violation parameters in K^0 - \bar{K}^0 mixing [v]

$$\text{Asymmetry } A_T \text{ in } K^0$$
- \bar{K}^0 mixing = $(6.6 \pm 1.6) \times 10^{-3}$

CPT-violation parameters [v]

$$\text{Re } \delta = (2.3 \pm 2.7) \times 10^{-4}$$

$$\text{Im } \delta = (0.4 \pm 2.1) \times 10^{-5}$$

$$\text{Re}(y), K_{e3} \text{ parameter} = (0.4 \pm 2.5) \times 10^{-3}$$

$$\text{Re}(x_-), K_{e3} \text{ parameter} = (-2.9 \pm 2.0) \times 10^{-3}$$

$$|m_{K^0} - m_{\bar{K}^0}| / m_{\text{average}} < 8 \times 10^{-19}, \text{ CL} = 90\% \text{ [bb]}$$

$$(\Gamma_{K^0} - \Gamma_{\bar{K}^0}) / m_{\text{average}} = (8 \pm 8) \times 10^{-18}$$

Tests of $\Delta S = \Delta Q$

$$\text{Re}(x_+), K_{e3} \text{ parameter} = (-0.9 \pm 3.0) \times 10^{-3}$$

 K_S^0

$$I(J^P) = \frac{1}{2}(0^-)$$

$$\text{Mean life } \tau = (0.8953 \pm 0.0005) \times 10^{-10} \text{ s} \quad (S = 1.1) \quad \text{Assuming } CPT$$

$$\text{Mean life } \tau = (0.8958 \pm 0.0005) \times 10^{-10} \text{ s} \quad \text{Not assuming } CPT$$

$$c\tau = 2.6842 \text{ cm} \quad \text{Assuming } CPT$$

CP-violation parameters [cc]

$$\text{Im}(\eta_{+-0}) = -0.002 \pm 0.009$$

$$\text{Im}(\eta_{000}) = (-0.1 \pm 1.6) \times 10^{-2}$$

$$|\eta_{000}| = |A(K_S^0 \rightarrow 3\pi^0)/A(K_L^0 \rightarrow 3\pi^0)| < 0.018, \text{ CL} = 90\%$$

$$CP \text{ asymmetry } A \text{ in } \pi^+ \pi^- e^+ e^- = (-1 \pm 4) \%$$

 K_S^0 DECAY MODES

K_S^0 DECAY MODES	Fraction (Γ_i/Γ)	Scale factor/ Confidence level	ρ (MeV/c)
Hadronic modes			
$\pi^0 \pi^0$	$(30.69 \pm 0.05) \%$		209
$\pi^+ \pi^-$	$(69.20 \pm 0.05) \%$		206
$\pi^+ \pi^- \pi^0$	$(3.5 \pm 1.1_{-0.9}) \times 10^{-7}$		133
Modes with photons or $\ell\bar{\ell}$ pairs			
$\pi^+ \pi^- \gamma$	$[w,dd] (1.79 \pm 0.05) \times 10^{-3}$		206
$\pi^+ \pi^- e^+ e^-$	$(4.69 \pm 0.30) \times 10^{-5}$		206
$\pi^0 \gamma \gamma$	$[dd] (4.9 \pm 1.8) \times 10^{-8}$		231
$\gamma \gamma$	$(2.63 \pm 0.17) \times 10^{-6}$	S=3.0	249
Semileptonic modes			
$\pi^{\pm} e^{\mp} \nu_e$	$[ee] (7.04 \pm 0.08) \times 10^{-4}$		229
CP violating (CP) and $\Delta S = 1$ weak neutral current (S1) modes			
$3\pi^0$	CP $< 1.2 \times 10^{-7}$	CL=90%	139
$\mu^+ \mu^-$	S1 $< 3.2 \times 10^{-7}$	CL=90%	225
$e^+ e^-$	S1 $< 9 \times 10^{-9}$	CL=90%	249
$\pi^0 e^+ e^-$	S1 $[dd] (3.0 \pm 1.5_{-1.2}) \times 10^{-9}$		230
$\pi^0 \mu^+ \mu^-$	S1 $(2.9 \pm 1.5_{-1.2}) \times 10^{-9}$		177

 K_L^0

$$I(J^P) = \frac{1}{2}(0^-)$$

 $m_{K_L} - m_{K_S}$

$$= (0.5292 \pm 0.0009) \times 10^{10} \hbar \text{ s}^{-1} \quad (S = 1.2) \quad \text{Assuming } CPT$$

$$= (3.483 \pm 0.006) \times 10^{-12} \text{ MeV} \quad \text{Assuming } CPT$$

$$= (0.5290 \pm 0.0015) \times 10^{10} \hbar \text{ s}^{-1} \quad (S = 1.1) \quad \text{Not assuming } CPT$$

Mean life $\tau = (5.116 \pm 0.020) \times 10^{-8} \text{ s}$

$$c\tau = 15.34 \text{ m}$$

Meson Summary Table

Slope parameter g [u]

(See Particle Listings for quadratic coefficients)

$$K_L^0 \rightarrow \pi^+ \pi^- \pi^0: g = 0.678 \pm 0.008 \quad (S = 1.5)$$

 K_L decay form factors [v]Linear parametrization assuming μ - e universality

$$\lambda_+(K_{\mu 3}^0) = \lambda_+(K_{e 3}^0) = (2.82 \pm 0.04) \times 10^{-2} \quad (S = 1.1)$$

$$\lambda_0(K_{\mu 3}^0) = (1.38 \pm 0.18) \times 10^{-2} \quad (S = 2.2)$$

Quadratic parametrization assuming μ - e universality

$$\lambda'_+(K_{\mu 3}^0) = \lambda'_+(K_{e 3}^0) = (2.40 \pm 0.12) \times 10^{-2} \quad (S = 1.2)$$

$$\lambda''_+(K_{\mu 3}^0) = \lambda''_+(K_{e 3}^0) = (0.20 \pm 0.05) \times 10^{-2} \quad (S = 1.2)$$

$$\lambda_0(K_{\mu 3}^0) = (1.16 \pm 0.09) \times 10^{-2} \quad (S = 1.2)$$

Pole parametrization assuming μ - e universality

$$M_V^{\mu}(K_{\mu 3}^0) = M_V^e(K_{e 3}^0) = 878 \pm 6 \text{ MeV} \quad (S = 1.1)$$

$$M_S^{\mu}(K_{\mu 3}^0) = 1252 \pm 90 \text{ MeV} \quad (S = 2.6)$$

$$K_{e 3}^0 \quad |f_S/f_+| = (1.5^{+1.4}_{-1.6}) \times 10^{-2}$$

$$K_{e 3}^0 \quad |f_T/f_+| = (5^{+4}_{-5}) \times 10^{-2}$$

$$K_{\mu 3}^0 \quad |f_T/f_+| = (12 \pm 12) \times 10^{-2}$$

$$K_L \rightarrow \ell^+ \ell^- \gamma, K_L \rightarrow \ell^+ \ell^- \ell'^+ \ell'^-: \alpha_{K^*} = -0.205 \pm 0.022 \quad (S = 1.8)$$

$$K_L^0 \rightarrow \ell^+ \ell^- \gamma, K_L^0 \rightarrow \ell^+ \ell^- \ell'^+ \ell'^-: \alpha_{DIP} = -1.69 \pm 0.08 \quad (S = 1.7)$$

$$K_L \rightarrow \pi^+ \pi^- e^+ e^-: a_1/a_2 = -0.737 \pm 0.014 \text{ GeV}^2$$

$$K_L \rightarrow \pi^0 2\gamma: a_V = -0.43 \pm 0.06 \quad (S = 1.5)$$

CP-violation parameters [cc]

$$A_L = (0.332 \pm 0.006)\%$$

$$|\eta_{00}| = (2.221 \pm 0.011) \times 10^{-3} \quad (S = 1.8)$$

$$|\eta_{+-}| = (2.232 \pm 0.011) \times 10^{-3} \quad (S = 1.8)$$

$$|\epsilon| = (2.228 \pm 0.011) \times 10^{-3} \quad (S = 1.8)$$

$$|\eta_{00}/\eta_{+-}| = 0.9951 \pm 0.0008 [f] \quad (S = 1.6)$$

$$\text{Re}(\epsilon'/\epsilon) = (1.65 \pm 0.26) \times 10^{-3} [f] \quad (S = 1.6)$$

Assuming CPT

$$\phi_{+-} = (43.51 \pm 0.05)^\circ \quad (S = 1.1)$$

$$\phi_{00} = (43.52 \pm 0.05)^\circ \quad (S = 1.1)$$

$$\phi_\epsilon = \phi_{SW} = (43.51 \pm 0.05)^\circ \quad (S = 1.1)$$

Not assuming CPT

$$\phi_{+-} = (43.4 \pm 0.7)^\circ \quad (S = 1.3)$$

$$\phi_{00} = (43.7 \pm 0.8)^\circ \quad (S = 1.2)$$

$$\phi_\epsilon = (43.5 \pm 0.7)^\circ \quad (S = 1.3)$$

$$\text{CP asymmetry } A \text{ in } K_L^0 \rightarrow \pi^+ \pi^- e^+ e^- = (13.7 \pm 1.5)\%$$

$$\beta_{CP} \text{ from } K_L^0 \rightarrow e^+ e^- e^+ e^- = -0.19 \pm 0.07$$

$$\gamma_{CP} \text{ from } K_L^0 \rightarrow e^+ e^- e^+ e^- = 0.01 \pm 0.11 \quad (S = 1.6)$$

$$j \text{ for } K_L^0 \rightarrow \pi^+ \pi^- \pi^0 = 0.0012 \pm 0.0008$$

$$f \text{ for } K_L^0 \rightarrow \pi^+ \pi^- \pi^0 = 0.004 \pm 0.006$$

$$|\eta_{+-\gamma}| = (2.35 \pm 0.07) \times 10^{-3}$$

$$\phi_{+-\gamma} = (44 \pm 4)^\circ$$

$$|\epsilon'_{+-\gamma}|/\epsilon < 0.3, \text{ CL} = 90\%$$

$$|g_{E1}| \text{ for } K_L^0 \rightarrow \pi^+ \pi^- \gamma < 0.21, \text{ CL} = 90\%$$

T-violation parameters

$$\text{Im}(\xi) \text{ in } K_{\mu 3}^0 = -0.007 \pm 0.026$$

CPT invariance tests

$$\phi_{00} - \phi_{+-} = (0.2 \pm 0.4)^\circ$$

$$\text{Re}(\frac{2}{3}\eta_{+-} + \frac{1}{3}\eta_{00}) - \frac{A_L}{2} = (-3 \pm 35) \times 10^{-6}$$

 $\Delta S = -\Delta Q$ in K_{23}^0 decay

$$\text{Re } x = -0.002 \pm 0.006$$

$$\text{Im } x = 0.0012 \pm 0.0021$$

 K_L^0 DECAY MODES

	Fraction (Γ_i/Γ)	Scale factor/ Confidence level	p (MeV/c)
Semileptonic modes			
$\pi^\pm e^\mp \nu_e$ Called $K_{e 3}^0$.	[ee] (40.55 \pm 0.12) %	S=1.9	229
$\pi^\pm \mu^\mp \nu_\mu$ Called $K_{\mu 3}^0$.	[ee] (27.04 \pm 0.07) %	S=1.1	216
$(\pi \mu \text{ atom}) \nu$	(1.05 \pm 0.11) $\times 10^{-7}$		188
$\pi^0 \pi^\pm e^\mp \nu$	[ee] (5.20 \pm 0.11) $\times 10^{-5}$		207
$\pi^\pm e^\mp \nu e^+ e^-$	[ee] (1.26 \pm 0.04) $\times 10^{-5}$		229
Hadronic modes, including Charge conjugation \times Parity Violating (CPV) modes			
$3\pi^0$	(19.52 \pm 0.12) %	S=1.7	139
$\pi^+ \pi^- \pi^0$	(12.54 \pm 0.05) %		133
$\pi^+ \pi^-$	CPV [gg] (1.966 \pm 0.010) $\times 10^{-3}$	S=1.6	206
$\pi^0 \pi^0$	CPV (8.65 \pm 0.06) $\times 10^{-4}$	S=1.8	209
Semileptonic modes with photons			
$\pi^\pm e^\mp \nu_e \gamma$	[w,ee,hh] (3.79 \pm 0.06) $\times 10^{-3}$		229
$\pi^\pm \mu^\mp \nu_\mu \gamma$	(5.65 \pm 0.23) $\times 10^{-4}$		216
Hadronic modes with photons or $\ell\bar{\ell}$ pairs			
$\pi^0 \pi^0 \gamma$	< 2.43 $\times 10^{-7}$	CL=90%	209
$\pi^+ \pi^- \gamma$	[w,hh] (4.15 \pm 0.15) $\times 10^{-5}$	S=2.8	206
$\pi^+ \pi^- \gamma$ (DE)	(2.84 \pm 0.11) $\times 10^{-5}$	S=2.0	206
$\pi^0 2\gamma$	[hh] (1.273 \pm 0.034) $\times 10^{-6}$		231
$\pi^0 \gamma e^+ e^-$	(1.62 \pm 0.17) $\times 10^{-8}$		230
Other modes with photons or $\ell\bar{\ell}$ pairs			
2γ	(5.47 \pm 0.04) $\times 10^{-4}$	S=1.2	249
3γ	< 2.4 $\times 10^{-7}$	CL=90%	249
$e^+ e^- \gamma$	(9.4 \pm 0.4) $\times 10^{-6}$	S=2.0	249
$\mu^+ \mu^- \gamma$	(3.59 \pm 0.11) $\times 10^{-7}$	S=1.3	225
$e^+ e^- \gamma \gamma$	[hh] (5.95 \pm 0.33) $\times 10^{-7}$		249
$\mu^+ \mu^- \gamma \gamma$	[hh] (1.0 \pm 0.8 \pm 0.6) $\times 10^{-8}$		225
Charge conjugation \times Parity (CP) or Lepton Family number (LF) violating modes, or $\Delta S = 1$ weak neutral current (S1) modes			
$\mu^+ \mu^-$	S1 (6.84 \pm 0.11) $\times 10^{-9}$		225
$e^+ e^-$	S1 (9 \pm 6 \pm 4) $\times 10^{-12}$		249
$\pi^+ \pi^- e^+ e^-$	S1 [hh] (3.11 \pm 0.19) $\times 10^{-7}$		206
$\pi^0 \pi^0 e^+ e^-$	S1 < 6.6 $\times 10^{-9}$	CL=90%	209
$\mu^+ \mu^- e^+ e^-$	S1 (2.69 \pm 0.27) $\times 10^{-9}$		225
$e^+ e^- e^+ e^-$	S1 (3.56 \pm 0.21) $\times 10^{-8}$		249
$\pi^0 \mu^+ \mu^-$	CP,S1 [ij] < 3.8 $\times 10^{-10}$	CL=90%	177
$\pi^0 e^+ e^-$	CP,S1 [ij] < 2.8 $\times 10^{-10}$	CL=90%	230
$\pi^0 \nu \bar{\nu}$	CP,S1 [jj] < 6.7 $\times 10^{-8}$	CL=90%	231
$\pi^0 \pi^0 \nu \bar{\nu}$	S1 < 4.7 $\times 10^{-5}$	CL=90%	209
$e^\pm \mu^\mp$	LF [ee] < 4.7 $\times 10^{-12}$	CL=90%	238
$e^\pm e^\pm \mu^\mp \mu^\mp$	LF [ee] < 4.12 $\times 10^{-11}$	CL=90%	225
$\pi^0 \mu^\pm e^\mp$	LF [ee] < 7.6 $\times 10^{-11}$	CL=90%	217
$\pi^0 \pi^0 \mu^\pm e^\mp$	LF < 1.7 $\times 10^{-10}$	CL=90%	159

 $K^*(892)$

$$I(J^P) = \frac{1}{2}(1^-)$$

$$K^*(892)^\pm \text{ mass } m = 891.66 \pm 0.26 \text{ MeV}$$

$$\text{Mass } m = 895.5 \pm 0.8 \text{ MeV}$$

$$K^*(892)^0 \text{ mass } m = 895.94 \pm 0.22 \text{ MeV} \quad (S = 1.4)$$

$$K^*(892)^\pm \text{ full width } \Gamma = 50.8 \pm 0.9 \text{ MeV}$$

$$\text{Full width } \Gamma = 46.2 \pm 1.3 \text{ MeV}$$

$$K^*(892)^0 \text{ full width } \Gamma = 48.7 \pm 0.8 \text{ MeV} \quad (S = 1.7)$$

 $K^*(892)$ DECAY MODES

	Fraction (Γ_i/Γ)	Confidence level	p (MeV/c)
$K\pi$	~ 100 %		289
$K^0 \gamma$	(2.39 \pm 0.21) $\times 10^{-3}$		307
$K^\pm \gamma$	(9.9 \pm 0.9) $\times 10^{-4}$		309
$K\pi\pi$	< 7 $\times 10^{-4}$	95%	223

 $K_1(1270)$

$$I(J^P) = \frac{1}{2}(1^+)$$

$$\text{Mass } m = 1272 \pm 7 \text{ MeV} [1]$$

$$\text{Full width } \Gamma = 90 \pm 20 \text{ MeV} [1]$$

Meson Summary Table

$K_1(1270)$ DECAY MODES	Fraction (Γ_i/Γ)	ρ (MeV/c)
$K\rho$	(42 \pm 6) %	45
$K_0^*(1430)\pi$	(28 \pm 4) %	†
$K^*(892)\pi$	(16 \pm 5) %	302
$K\omega$	(11.0 \pm 2.0) %	†
$Kf_0(1370)$	(3.0 \pm 2.0) %	†
γK^0	seen	539

$$K_1(1400) \quad I(J^P) = \frac{1}{2}(1^+)$$

Mass $m = 1403 \pm 7$ MeV

Full width $\Gamma = 174 \pm 13$ MeV (S = 1.6)

$K_1(1400)$ DECAY MODES	Fraction (Γ_i/Γ)	ρ (MeV/c)
$K^*(892)\pi$	(94 \pm 6) %	402
$K\rho$	(1.2 \pm 0.6) %	292
$Kf_0(1370)$	(2.0 \pm 2.0) %	†
$K\omega$	(1.0 \pm 1.0) %	284
$K_0^*(1430)\pi$	not seen	†
γK^0	seen	613

$$K^*(1410) \quad I(J^P) = \frac{1}{2}(1^-)$$

Mass $m = 1414 \pm 15$ MeV (S = 1.3)

Full width $\Gamma = 232 \pm 21$ MeV (S = 1.1)

$K^*(1410)$ DECAY MODES	Fraction (Γ_i/Γ)	Confidence level	ρ (MeV/c)
$K^*(892)\pi$	> 40 %	95%	410
$K\pi$	(6.6 \pm 1.3) %		612
$K\rho$	< 7 %	95%	305
γK^0	seen		619

$$K_0^*(1430) [kk] \quad I(J^P) = \frac{1}{2}(0^+)$$

Mass $m = 1425 \pm 50$ MeV

Full width $\Gamma = 270 \pm 80$ MeV

$K_0^*(1430)$ DECAY MODES	Fraction (Γ_i/Γ)	ρ (MeV/c)
$K\pi$	(93 \pm 10) %	619

$$K_2^*(1430) \quad I(J^P) = \frac{1}{2}(2^+)$$

$K_2^*(1430)^\pm$ mass $m = 1425.6 \pm 1.5$ MeV (S = 1.1)

$K_2^*(1430)^0$ mass $m = 1432.4 \pm 1.3$ MeV

$K_2^*(1430)^\pm$ full width $\Gamma = 98.5 \pm 2.7$ MeV (S = 1.1)

$K_2^*(1430)^0$ full width $\Gamma = 109 \pm 5$ MeV (S = 1.9)

$K_2^*(1430)$ DECAY MODES	Fraction (Γ_i/Γ)	Scale factor/ Confidence level	ρ (MeV/c)
$K\pi$	(49.9 \pm 1.2) %		619
$K^*(892)\pi$	(24.7 \pm 1.5) %		419
$K^*(892)\pi\pi$	(13.4 \pm 2.2) %		372
$K\rho$	(8.7 \pm 0.8) %	S=1.2	318
$K\omega$	(2.9 \pm 0.8) %		311
$K^+\gamma$	(2.4 \pm 0.5) $\times 10^{-3}$	S=1.1	627
$K\eta$	(1.5 \pm 3.4 -1.0) $\times 10^{-3}$	S=1.3	486
$K\omega\pi$	< 7.2 $\times 10^{-4}$	CL=95%	100
$K^0\gamma$	< 9 $\times 10^{-4}$	CL=90%	626

$$K^*(1680) \quad I(J^P) = \frac{1}{2}(1^-)$$

Mass $m = 1717 \pm 27$ MeV (S = 1.4)

Full width $\Gamma = 322 \pm 110$ MeV (S = 4.2)

$K^*(1680)$ DECAY MODES	Fraction (Γ_i/Γ)	ρ (MeV/c)
$K\pi$	(38.7 \pm 2.5) %	781
$K\rho$	(31.4 \pm 5.0 -2.1) %	570
$K^*(892)\pi$	(29.9 \pm 2.2 -5.0) %	618

$$K_2(1770) [ll] \quad I(J^P) = \frac{1}{2}(2^-)$$

Mass $m = 1773 \pm 8$ MeV

Full width $\Gamma = 186 \pm 14$ MeV

$K_2(1770)$ DECAY MODES	Fraction (Γ_i/Γ)	ρ (MeV/c)
$K\pi\pi$		794
$K_2^*(1430)\pi$	dominant	288
$K^*(892)\pi$	seen	654
$Kf_2(1270)$	seen	55
$K\phi$	seen	441
$K\omega$	seen	607

$$K_3^*(1780) \quad I(J^P) = \frac{1}{2}(3^-)$$

Mass $m = 1776 \pm 7$ MeV (S = 1.1)

Full width $\Gamma = 159 \pm 21$ MeV (S = 1.3)

$K_3^*(1780)$ DECAY MODES	Fraction (Γ_i/Γ)	Confidence level	ρ (MeV/c)
$K\rho$	(31 \pm 9) %		613
$K^*(892)\pi$	(20 \pm 5) %		656
$K\pi$	(18.8 \pm 1.0) %		813
$K\eta$	(30 \pm 13) %		719
$K_2^*(1430)\pi$	< 16 %	95%	291

$$K_2(1820) [mm] \quad I(J^P) = \frac{1}{2}(2^-)$$

Mass $m = 1816 \pm 13$ MeV

Full width $\Gamma = 276 \pm 35$ MeV

$K_2(1820)$ DECAY MODES	Fraction (Γ_i/Γ)	ρ (MeV/c)
$K_2^*(1430)\pi$	seen	327
$K^*(892)\pi$	seen	681
$Kf_2(1270)$	seen	186
$K\omega$	seen	638

$$K_4^*(2045) \quad I(J^P) = \frac{1}{2}(4^+)$$

Mass $m = 2045 \pm 9$ MeV (S = 1.1)

Full width $\Gamma = 198 \pm 30$ MeV

$K_4^*(2045)$ DECAY MODES	Fraction (Γ_i/Γ)	ρ (MeV/c)
$K\pi$	(9.9 \pm 1.2) %	958
$K^*(892)\pi\pi$	(9 \pm 5) %	802
$K^*(892)\pi\pi\pi$	(7 \pm 5) %	768
$\rho K\pi$	(5.7 \pm 3.2) %	741
$\omega K\pi$	(5.0 \pm 3.0) %	738
$\phi K\pi$	(2.8 \pm 1.4) %	594
$\phi K^*(892)$	(1.4 \pm 0.7) %	363

Meson Summary Table

T-violation decay-rate asymmetry

$$A_T(K^+ K^- \pi^+ \pi^-) = 0.01 \pm 0.07$$

CPT-violation decay-rate asymmetry

$$A_{CPT}(K^\mp \pi^\pm) = 0.008 \pm 0.008$$

Form factors

$$\begin{aligned} r_V &\equiv V(0)/A_1(0) \text{ in } D^0 \rightarrow K^*(892)^- \ell^+ \nu_\ell = 1.7 \pm 0.8 \\ r_2 &\equiv A_2(0)/A_1(0) \text{ in } D^0 \rightarrow K^*(892)^- \ell^+ \nu_\ell = 0.9 \pm 0.4 \\ f_+(0)|V_{cs}| &\text{ in } D^0 \rightarrow K^- \ell^+ \nu_\ell = 0.726 \pm 0.009 \\ r_1 &\equiv a_1/a_0 \text{ in } D^0 \rightarrow K^- \ell^+ \nu_\ell = -2.65 \pm 0.35 \\ r_2 &\equiv a_1/a_0 \text{ in } D^0 \rightarrow K^- \ell^+ \nu_\ell = 13 \pm 9 \\ f_+(0)|V_{cd}| &\text{ in } D^0 \rightarrow \pi^- \ell^+ \nu_\ell = 0.152 \pm 0.005 \\ r_1 &\equiv a_1/a_0 \text{ in } D^0 \rightarrow \pi^- \ell^+ \nu_\ell = -2.8 \pm 0.5 \\ r_2 &\equiv a_1/a_0 \text{ in } D^0 \rightarrow \pi^- \ell^+ \nu_\ell = 6 \pm 3.0 \end{aligned}$$

Most decay modes (other than the semileptonic modes) that involve a neutral K meson are now given as K_S^0 modes, not as \bar{K}^0 modes. Nearly always it is a K_S^0 that is measured, and interference between Cabibbo-allowed and doubly Cabibbo-suppressed modes can invalidate the assumption that $2\Gamma(K_S^0) = \Gamma(\bar{K}^0)$.

D^0 DECAY MODES	Fraction (Γ_i/Γ)	Scale factor/ Confidence level	p (MeV/c)
Topological modes			
0-prongs	[uu] (17 ± 6) %	—	—
2-prongs	(69 ± 6) %	—	—
4-prongs	[vv] (14.3 ± 0.5) %	—	—
6-prongs	[ww] (6.4 ± 1.3) × 10 ⁻⁴	—	—
Inclusive modes			
e ⁺ anything	[xx] (6.49 ± 0.11) %	—	—
μ ⁺ anything	(6.7 ± 0.6) %	—	—
K ⁻ anything	(54.7 ± 2.8) %	S=1.3	—
\bar{K}^0 anything + K ⁰ anything	(47 ± 4) %	—	—
K ⁺ anything	(3.4 ± 0.4) %	—	—
K*(892) ⁻ anything	(15 ± 9) %	—	—
$\bar{K}^*(892)^0$ anything	(9 ± 4) %	—	—
K*(892) ⁺ anything	< 3.6 %	CL=90%	—
K*(892) ⁰ anything	(2.8 ± 1.3) %	—	—
η anything	(9.5 ± 0.9) %	—	—
η' anything	(2.48 ± 0.27) %	—	—
φ anything	(1.05 ± 0.11) %	—	—
Semileptonic modes			
K ⁻ e ⁺ ν _e	(3.55 ± 0.05) %	S=1.2	867
K ⁻ μ ⁺ ν _μ	(3.31 ± 0.13) %	—	864
K*(892) ⁻ e ⁺ ν _e	(2.17 ± 0.16) %	—	719
K*(892) ⁻ μ ⁺ ν _μ	(1.98 ± 0.24) %	—	714
K ⁻ π ⁰ e ⁺ ν _e	(1.6 ± 1.3 / 0.5) %	—	861
\bar{K}^0 π ⁻ e ⁺ ν _e	(2.7 ± 0.9 / 0.7) %	—	860
K ⁻ π ⁺ π ⁻ e ⁺ ν _e	(2.8 ± 1.4 / 1.1) × 10 ⁻⁴	—	843
K ₁ (1270) ⁻ e ⁺ ν _e	(7.6 ± 4.0 / 3.1) × 10 ⁻⁴	—	498
K ⁻ π ⁺ π ⁻ μ ⁺ ν _μ	< 1.2 × 10 ⁻³	CL=90%	821
($\bar{K}^*(892)^-$) π ⁻ μ ⁺ ν _μ	< 1.4 × 10 ⁻³	CL=90%	692
π ⁻ e ⁺ ν _e	(2.89 ± 0.08) × 10 ⁻³	S=1.1	927
π ⁻ μ ⁺ ν _μ	(2.37 ± 0.24) × 10 ⁻³	—	924
ρ ⁻ e ⁺ ν _e	(1.9 ± 0.4) × 10 ⁻³	—	771
Hadronic modes with one \bar{K}			
K ⁻ π ⁺	(3.89 ± 0.05) %	S=1.2	861
K _S ⁰ π ⁰	(1.22 ± 0.05) %	—	860
K _L ⁰ π ⁰	(10.0 ± 0.7) × 10 ⁻³	—	860
K _S ⁰ π ⁺ π ⁻	[oo] (2.94 ± 0.16) %	S=1.1	842
K _S ⁰ ρ ⁰	(6.6 ± 0.6 / 0.8) × 10 ⁻³	—	674
K _S ⁰ ω, ω → π ⁺ π ⁻	(2.1 ± 0.6) × 10 ⁻⁴	—	670
K _S ⁰ (π ⁺ π ⁻) _{S-wave}	(3.5 ± 0.8) × 10 ⁻³	—	842
K _S ⁰ f ₀ (980), f ₀ (980) → π ⁺ π ⁻	(1.27 ± 0.40 / 0.24) × 10 ⁻³	—	549
K _S ⁰ f ₀ (1370), f ₀ (1370) → π ⁺ π ⁻	(2.9 ± 0.9 / 1.3) × 10 ⁻³	†	—
K _S ⁰ f ₂ (1270), f ₂ (1270) → π ⁺ π ⁻	(9 ± 10 / 6) × 10 ⁻⁵	—	262

K*(892) ⁻ π ⁺ ,	(1.73 ± 0.14 / 0.17) %	—	711
K*(892) ⁻ → K _S ⁰ π ⁻	—	—	—
K ₀ ⁰ (1430) ⁻ π ⁺ ,	(2.81 ± 0.40 / 0.33) × 10 ⁻³	—	378
K ₀ ⁰ (1430) ⁻ → K _S ⁰ π ⁻	—	—	—
K ₂ ⁰ (1430) ⁻ π ⁺ ,	(3.5 ± 2.0 / 1.1) × 10 ⁻⁴	—	367
K ₂ ⁰ (1430) ⁻ → K _S ⁰ π ⁻	—	—	—
K*(1680) ⁻ π ⁺ ,	(5 ± 4) × 10 ⁻⁴	—	46
K*(1680) ⁻ → K _S ⁰ π ⁻	—	—	—
K*(892) ⁺ π ⁻ ,	[yy] (1.18 ± 0.60 / 0.35) × 10 ⁻⁴	—	711
K*(892) ⁺ → K _S ⁰ π ⁺	—	—	—
K ₀ ⁰ (1430) ⁺ π ⁻ ,	[yy] < 1.5 × 10 ⁻⁵	CL=95%	—
K ₀ ⁰ (1430) ⁺ → K _S ⁰ π ⁺	—	—	—
K ₂ ⁰ (1430) ⁺ π ⁻ ,	[yy] < 3.5 × 10 ⁻⁵	CL=95%	—
K ₂ ⁰ (1430) ⁺ → K _S ⁰ π ⁺	—	—	—
K _S ⁰ π ⁺ π ⁻ nonresonant	(2.7 ± 6.0 / 1.7) × 10 ⁻⁴	—	842
K ⁻ π ⁺ π ⁰	[oo] (13.9 ± 0.5) %	S=1.7	844
K ⁻ ρ ⁺	(10.8 ± 0.7) %	—	675
K ⁻ ρ(1700) ⁺ ,	(7.9 ± 1.7) × 10 ⁻³	—	†
ρ(1700) ⁺ → π ⁺ π ⁰	—	—	—
K*(892) ⁻ π ⁺ ,	(2.22 ± 0.40 / 0.19) %	—	711
K*(892) ⁻ → K ⁻ π ⁰	—	—	—
$\bar{K}^*(892)^0$ π ⁰ ,	(1.88 ± 0.23) %	—	711
$\bar{K}^*(892)^0$ → K ⁻ π ⁺	—	—	—
K ₀ ⁰ (1430) ⁻ π ⁺ ,	(4.6 ± 2.1) × 10 ⁻³	—	378
K ₀ ⁰ (1430) ⁻ → K ⁻ π ⁰	—	—	—
$\bar{K}_0^*(1430)^0$ π ⁰ ,	(5.7 ± 5.0 / 1.5) × 10 ⁻³	—	379
$\bar{K}_0^*(1430)^0$ → K ⁻ π ⁺	—	—	—
K*(1680) ⁻ π ⁺ ,	(1.8 ± 0.7) × 10 ⁻³	—	46
K*(1680) ⁻ → K ⁻ π ⁰	—	—	—
K ⁻ π ⁺ π ⁰ nonresonant	(1.11 ± 0.50 / 0.19) %	—	844
K _S ⁰ 2π ⁰	(8.3 ± 0.6) × 10 ⁻³	—	843
$\bar{K}^*(892)^0$ π ⁰ ,	(6.7 ± 1.8 / 1.5) × 10 ⁻³	—	711
$\bar{K}^*(892)^0$ → K _S ⁰ π ⁰	—	—	—
K _S ⁰ 2π ⁰ nonresonant	(4.5 ± 1.1) × 10 ⁻³	—	843
K ⁻ 2π ⁺ π ⁻	[oo] (8.09 ± 0.21 / 0.18) %	S=1.3	813
K ⁻ π ⁺ ρ ⁰ total	(6.76 ± 0.33) %	—	609
K ⁻ π ⁺ ρ ⁰ 3-body	(5.1 ± 2.3) × 10 ⁻³	—	609
$\bar{K}^*(892)^0$ ρ ⁰ ,	(1.06 ± 0.23) %	—	416
$\bar{K}^*(892)^0$ → K ⁻ π ⁺	—	—	—
K ⁻ a ₁ (1260) ⁺ ,	(3.6 ± 0.6) %	—	327
a ₁ (1260) ⁺ → 2π ⁺ π ⁻	—	—	—
$\bar{K}^*(892)^0$ π ⁺ π ⁻ total,	(1.6 ± 0.4) %	—	685
$\bar{K}^*(892)^0$ → K ⁻ π ⁺	—	—	—
$\bar{K}^*(892)^0$ π ⁺ π ⁻ 3-body,	(9.9 ± 2.3) × 10 ⁻³	—	685
$\bar{K}^*(892)^0$ → K ⁻ π ⁺	—	—	—
K ₁ (1270) ⁻ π ⁺ ,	[zz] (2.9 ± 0.3) × 10 ⁻³	—	484
K ₁ (1270) ⁻ → K ⁻ π ⁺ π ⁻	—	—	—
K ⁻ 2π ⁺ π ⁻ nonresonant	(1.88 ± 0.26) %	—	813
K _S ⁰ π ⁺ π ⁻ π ⁰	[aaa] (5.4 ± 0.6) %	—	813
K _S ⁰ η, η → π ⁺ π ⁻ π ⁰	(9.8 ± 0.6) × 10 ⁻⁴	—	772
K _S ⁰ ω, ω → π ⁺ π ⁻ π ⁰	(9.9 ± 0.5) × 10 ⁻³	—	670
K ⁻ 2π ⁺ π ⁻ π ⁰	(4.2 ± 0.4) %	—	771
$\bar{K}^*(892)^0$ π ⁺ π ⁻ π ⁰ ,	(1.3 ± 0.6) %	—	643
$\bar{K}^*(892)^0$ → K ⁻ π ⁺	—	—	—
K ⁻ π ⁺ ω, ω → π ⁺ π ⁻ π ⁰	(2.7 ± 0.5) %	—	605
$\bar{K}^*(892)^0$ ω,	(6.5 ± 3.0) × 10 ⁻³	—	410
$\bar{K}^*(892)^0$ → K ⁻ π ⁺ ,	—	—	—
ω → π ⁺ π ⁻ π ⁰	—	—	—
K _S ⁰ η π ⁰	(5.6 ± 1.2) × 10 ⁻³	—	721
K _S ⁰ a ₀ (980), a ₀ (980) → η π ⁰	(6.7 ± 2.1) × 10 ⁻³	—	—
$\bar{K}^*(892)^0$ η,	(1.6 ± 0.5) × 10 ⁻³	—	—
$\bar{K}^*(892)^0$ → K _S ⁰ π ⁰	—	—	—
K _S ⁰ 2π ⁺ 2π ⁻	(2.80 ± 0.30) × 10 ⁻³	—	768
K _S ⁰ ρ ⁰ π ⁺ π ⁻ , no K*(892) ⁻	(1.1 ± 0.7) × 10 ⁻³	—	—
K*(892) ⁻ 2π ⁺ π ⁻ ,	(5 ± 8) × 10 ⁻⁴	—	642
K*(892) ⁻ → K _S ⁰ π ⁻ ,	—	—	—
no ρ ⁰	—	—	—
K*(892) ⁻ ρ ⁰ π ⁺ ,	(1.7 ± 0.7) × 10 ⁻³	—	230
K*(892) ⁻ → K _S ⁰ π ⁻	—	—	—
K _S ⁰ 2π ⁺ 2π ⁻ nonresonant	< 1.3 × 10 ⁻³	CL=90%	768
K ⁻ 3π ⁺ 2π ⁻	(2.2 ± 0.6) × 10 ⁻⁴	—	713

Meson Summary Table

Doubly Cabibbo suppressed (DC) modes or $\Delta C = 2$ forbidden via mixing (C2M) modes			
$K^+ \ell^- \bar{\nu}_\ell$ via \bar{D}^0		< 2.2	$\times 10^{-5}$ CL=90%
K^+ or $K^*(892)^+ e^- \bar{\nu}_e$ via \bar{D}^0		< 6	$\times 10^{-5}$ CL=90%
$K^+ \pi^-$	DC	(1.48 ± 0.07)	$\times 10^{-4}$
$K^+ \pi^-$ via DCS		(1.31 ± 0.08)	$\times 10^{-4}$
$K^+ \pi^-$ via \bar{D}^0		< 1.6	$\times 10^{-5}$ CL=95%
$K_S^0 \pi^+ \pi^-$ in $D^0 \rightarrow \bar{D}^0$		< 1.9	$\times 10^{-4}$ CL=95%
$K^*(892)^+ \pi^-$, $K^*(892)^+ \rightarrow K_S^0 \pi^+$	DC	$(1.18 \pm_{-0.35}^{0.60})$	$\times 10^{-4}$
$K_0^*(1430)^+ \pi^-$, $K_0^*(1430)^+ \rightarrow K_S^0 \pi^+$	DC	< 1.5	$\times 10^{-5}$
$K_2^*(1430)^+ \pi^-$, $K_2^*(1430)^+ \rightarrow K_S^0 \pi^+$	DC	< 3.5	$\times 10^{-5}$
$K^+ \pi^- \pi^0$	DC	(3.05 ± 0.17)	$\times 10^{-4}$
$K^+ \pi^- \pi^0$ via \bar{D}^0		(7.3 ± 0.5)	$\times 10^{-4}$
$K^+ \pi^+ 2\pi^-$	DC	$(2.62 \pm_{-0.19}^{0.21})$	$\times 10^{-4}$
$K^+ \pi^+ 2\pi^-$ via \bar{D}^0		< 4	$\times 10^{-4}$ CL=90%
μ^- anything via \bar{D}^0		< 4	$\times 10^{-4}$ CL=90%
$\Delta C = 1$ weak neutral current (C1) modes, Lepton Family number (LF) violating modes, Lepton (L) or Baryon (B) number violating modes			
$\gamma\gamma$	C1	< 2.7	$\times 10^{-5}$ CL=90%
$e^+ e^-$	C1	< 1.2	$\times 10^{-6}$ CL=90%
$\mu^+ \mu^-$	C1	< 1.3	$\times 10^{-6}$ CL=90%
$\pi^0 e^+ e^-$	C1	< 4.5	$\times 10^{-5}$ CL=90%
$\pi^0 \mu^+ \mu^-$	C1	< 1.8	$\times 10^{-4}$ CL=90%
$\eta e^+ e^-$	C1	< 1.1	$\times 10^{-4}$ CL=90%
$\eta \mu^+ \mu^-$	C1	< 5.3	$\times 10^{-4}$ CL=90%
$\pi^+ \pi^- e^+ e^-$	C1	< 3.73	$\times 10^{-4}$ CL=90%
$\rho^0 e^+ e^-$	C1	< 1.0	$\times 10^{-4}$ CL=90%
$\pi^+ \pi^- \mu^+ \mu^-$	C1	< 3.0	$\times 10^{-5}$ CL=90%
$\rho^0 \mu^+ \mu^-$	C1	< 2.2	$\times 10^{-5}$ CL=90%
$\omega e^+ e^-$	C1	< 1.8	$\times 10^{-4}$ CL=90%
$\omega \mu^+ \mu^-$	C1	< 8.3	$\times 10^{-4}$ CL=90%
$K^- K^+ e^+ e^-$	C1	< 3.15	$\times 10^{-4}$ CL=90%
$\phi e^+ e^-$	C1	< 5.2	$\times 10^{-5}$ CL=90%
$K^- K^+ \mu^+ \mu^-$	C1	< 3.3	$\times 10^{-5}$ CL=90%
$\phi \mu^+ \mu^-$	C1	< 3.1	$\times 10^{-5}$ CL=90%
$\bar{K}^0 e^+ e^-$	[tt]	< 1.1	$\times 10^{-4}$ CL=90%
$\bar{K}^0 \mu^+ \mu^-$	[tt]	< 2.6	$\times 10^{-4}$ CL=90%
$K^- \pi^+ e^+ e^-$	C1	< 3.85	$\times 10^{-4}$ CL=90%
$\bar{K}^*(892)^0 e^+ e^-$	[tt]	< 4.7	$\times 10^{-5}$ CL=90%
$K^- \pi^+ \mu^+ \mu^-$	C1	< 3.59	$\times 10^{-4}$ CL=90%
$\bar{K}^*(892)^0 \mu^+ \mu^-$	[tt]	< 2.4	$\times 10^{-5}$ CL=90%
$\pi^+ \pi^- \pi^0 \mu^+ \mu^-$	C1	< 8.1	$\times 10^{-4}$ CL=90%
$\mu^\pm e^\mp$	LF [ee]	< 8.1	$\times 10^{-7}$ CL=90%
$\pi^0 e^\pm \mu^\mp$	LF [ee]	< 8.6	$\times 10^{-5}$ CL=90%
$\eta e^\pm \mu^\mp$	LF [ee]	< 1.0	$\times 10^{-4}$ CL=90%
$\pi^+ \pi^- e^\pm \mu^\mp$	LF [ee]	< 1.5	$\times 10^{-5}$ CL=90%
$\rho^0 e^\pm \mu^\mp$	LF [ee]	< 4.9	$\times 10^{-5}$ CL=90%
$\omega e^\pm \mu^\mp$	LF [ee]	< 1.2	$\times 10^{-4}$ CL=90%
$K^- K^+ e^\pm \mu^\mp$	LF [ee]	< 1.8	$\times 10^{-4}$ CL=90%
$\phi e^\pm \mu^\mp$	LF [ee]	< 3.4	$\times 10^{-5}$ CL=90%
$\bar{K}^0 e^\pm \mu^\mp$	LF [ee]	< 1.0	$\times 10^{-4}$ CL=90%
$K^- \pi^+ e^\pm \mu^\mp$	LF [ee]	< 5.53	$\times 10^{-4}$ CL=90%
$\bar{K}^*(892)^0 e^\pm \mu^\mp$	LF [ee]	< 8.3	$\times 10^{-5}$ CL=90%
$2\pi^- 2e^+ + c.c.$	L	< 1.12	$\times 10^{-4}$ CL=90%
$2\pi^- 2\mu^+ + c.c.$	L	< 2.9	$\times 10^{-5}$ CL=90%
$K^- \pi^- 2e^+ + c.c.$	L	< 2.06	$\times 10^{-4}$ CL=90%
$K^- \pi^- 2\mu^+ + c.c.$	L	< 3.9	$\times 10^{-4}$ CL=90%
$2K^- 2e^+ + c.c.$	L	< 1.52	$\times 10^{-4}$ CL=90%
$2K^- 2\mu^+ + c.c.$	L	< 9.4	$\times 10^{-5}$ CL=90%
$\pi^- \pi^- e^+ \mu^+ + c.c.$	L	< 7.9	$\times 10^{-5}$ CL=90%
$K^- \pi^- e^+ \mu^+ + c.c.$	L	< 2.18	$\times 10^{-4}$ CL=90%
$2K^- e^+ \mu^+ + c.c.$	L	< 5.7	$\times 10^{-5}$ CL=90%
$p e^-$	L,B [eee]	< 1.0	$\times 10^{-5}$ CL=90%
$\bar{p} e^+$	L,B [fff]	< 1.1	$\times 10^{-5}$ CL=90%

 $D^*(2007)^0$

$$I(J^P) = \frac{1}{2}(1^-)$$

I, J, P need confirmation.

Mass $m = 2006.96 \pm 0.16$ MeV
 $m_{D^{*0}} - m_{D^0} = 142.12 \pm 0.07$ MeV
 Full width $\Gamma < 2.1$ MeV, CL = 90%

$\bar{D}^*(2007)^0$ modes are charge conjugates of modes below.

$D^*(2007)^0$ DECAY MODES	Fraction (Γ_i/Γ)	ρ (MeV/c)
$D^0 \pi^0$	$(61.9 \pm 2.9)\%$	43
$D^0 \gamma$	$(38.1 \pm 2.9)\%$	137

 $D^*(2010)^\pm$

$$I(J^P) = \frac{1}{2}(1^-)$$

I, J, P need confirmation.

Mass $m = 2010.25 \pm 0.14$ MeV
 $m_{D^*(2010)^+} - m_{D^+} = 140.65 \pm 0.10$ MeV ($S = 1.1$)
 $m_{D^*(2010)^+} - m_{D^0} = 145.421 \pm 0.010$ MeV ($S = 1.1$)
 Full width $\Gamma = 96 \pm 22$ keV

$D^*(2010)^-$ modes are charge conjugates of the modes below.

$D^*(2010)^\pm$ DECAY MODES	Fraction (Γ_i/Γ)	ρ (MeV/c)
$D^0 \pi^+$	$(67.7 \pm 0.5)\%$	39
$D^+ \pi^0$	$(30.7 \pm 0.5)\%$	38
$D^+ \gamma$	$(1.6 \pm 0.4)\%$	136

 $D_0^*(2400)^0$

$$I(J^P) = \frac{1}{2}(0^+)$$

Mass $m = 2318 \pm 29$ MeV ($S = 1.7$)
 Full width $\Gamma = 267 \pm 40$ MeV

$D_0^*(2400)^0$ DECAY MODES	Fraction (Γ_i/Γ)	ρ (MeV/c)
$D^+ \pi^-$	seen	385

 $D_1(2420)^0$

$$I(J^P) = \frac{1}{2}(1^+)$$

I, J, P need confirmation.

Mass $m = 2422.0 \pm 0.6$ MeV
 $m_{D_1^0} - m_{D^{*+}} = 411.7 \pm 0.6$
 Full width $\Gamma = 20.4 \pm 1.7$ MeV

$\bar{D}_1(2420)^0$ modes are charge conjugates of modes below.

$D_1(2420)^0$ DECAY MODES	Fraction (Γ_i/Γ)	ρ (MeV/c)
$D^*(2010)^+ \pi^-$	seen	354
$D^0 \pi^+ \pi^-$	seen	426
$D^+ \pi^-$	not seen	473
$D^{*0} \pi^+ \pi^-$	not seen	280

 $D_2^*(2460)^0$

$$I(J^P) = \frac{1}{2}(2^+)$$

$J^P = 2^+$ assignment strongly favored.

Mass $m = 2462.8 \pm 1.0$ MeV ($S = 1.5$)
 $m_{D_2^0} - m_{D^+} = 593.2 \pm 1.0$ MeV ($S = 1.5$)
 $m_{D_2^0} - m_{D^{*+}} = 452.6 \pm 1.0$ MeV ($S = 1.5$)
 Full width $\Gamma = 42.9 \pm 3.1$ MeV ($S = 1.7$)

$\bar{D}_2^*(2460)^0$ modes are charge conjugates of modes below.

$D_2^*(2460)^0$ DECAY MODES	Fraction (Γ_i/Γ)	ρ (MeV/c)
$D^+ \pi^-$	seen	507
$D^*(2010)^+ \pi^-$	seen	391
$D^0 \pi^+ \pi^-$	not seen	464
$D^{*0} \pi^+ \pi^-$	not seen	326

 $D_2^*(2460)^\pm$

$$I(J^P) = \frac{1}{2}(2^+)$$

$J^P = 2^+$ assignment strongly favored.

Mass $m = 2460.1^{+2.6}_{-3.5}$ MeV ($S = 1.5$)
 $m_{D_2^*(2460)^\pm} - m_{D_2^*(2460)^0} = 2.4 \pm 1.7$ MeV
 Full width $\Gamma = 37 \pm 6$ MeV ($S = 1.4$)

Meson Summary Table

$D_2^*(2460)^-$ modes are charge conjugates of modes below.

$D_2^*(2460)^\pm$ DECAY MODES	Fraction (Γ_i/Γ)	p (MeV/c)
$D^0 \pi^+$	seen	508
$D^{*0} \pi^+$	seen	391
$D^+ \pi^+ \pi^-$	not seen	457
$D^{*+} \pi^+ \pi^-$	not seen	320

CHARMED, STRANGE MESONS ($C = S = \pm 1$)

$D_S^\pm = c\bar{s}, D_S^\mp = \bar{c}s$, similarly for $D_S^{*\pm}$'s

D_S^\pm

$$I(J^P) = 0(0^-)$$

Mass $m = 1968.47 \pm 0.33$ MeV ($S = 1.3$)

$m_{D_S^\pm} - m_{D^\pm} = 98.88 \pm 0.30$ MeV ($S = 1.4$)

Mean life $\tau = (500 \pm 7) \times 10^{-15}$ s ($S = 1.3$)

$c\tau = 149.9$ μ m

CP-violating decay-rate asymmetries

$$A_{CP}(\mu^\pm \nu) = 0.05 \pm 0.06$$

$$A_{CP}(K^\pm K_S^0) = 0.049 \pm 0.023$$

$$A_{CP}(K^+ K^- \pi^\pm) = 0.003 \pm 0.014$$

$$A_{CP}(K^+ K^- \pi^\pm \pi^0) = -0.06 \pm 0.04$$

$$A_{CP}(K_S^0 K^\mp 2\pi^\pm) = -0.01 \pm 0.04$$

$$A_{CP}(\pi^+ \pi^- \pi^\pm) = 0.02 \pm 0.05$$

$$A_{CP}(\pi^\pm \eta) = -0.08 \pm 0.05$$

$$A_{CP}(\pi^\pm \eta') = -0.06 \pm 0.04$$

$$A_{CP}(K^\pm \pi^0) = 0.02 \pm 0.29$$

$$A_{CP}(K_S^0 \pi^\pm) = 0.27 \pm 0.11$$

$$A_{CP}(K^\pm \pi^+ \pi^-) = 0.11 \pm 0.07$$

$$A_{CP}(K^\pm \eta) = -0.20 \pm 0.18$$

$$A_{CP}(K^\pm \eta'(958)) = -0.2 \pm 0.4$$

T-violating decay-rate asymmetry

$$A_T(K_S^0 K^\pm \pi^+ \pi^-) = -0.04 \pm 0.07$$
 [ggg]

$D_S^\pm \rightarrow \phi \ell^+ \nu_\ell$ form factors

$$r_2 = 0.84 \pm 0.11$$
 ($S = 2.4$)

$$r_\nu = 1.80 \pm 0.08$$

$$\Gamma_L/\Gamma_T = 0.72 \pm 0.18$$

Unless otherwise noted, the branching fractions for modes with a resonance in the final state include all the decay modes of the resonance. D_S^\pm modes are charge conjugates of the modes below.

D_S^\pm DECAY MODES	Fraction (Γ_i/Γ)	Scale factor/ Confidence level	p (MeV/c)
Inclusive modes			
e^+ semileptonic	[hhh] (6.5 \pm 0.4) %	—	—
π^+ anything	(119.3 \pm 1.4) %	—	—
π^- anything	(43.2 \pm 0.9) %	—	—
π^0 anything	(123 \pm 7) %	—	—
K^- anything	(18.7 \pm 0.5) %	—	—
K^+ anything	(28.9 \pm 0.7) %	—	—
K_S^0 anything	(19.0 \pm 1.1) %	—	—
η anything	[iii] (29.9 \pm 2.8) %	—	—
ω anything	(6.1 \pm 1.4) %	—	—
η' anything	[jjj] (11.7 \pm 1.8) %	—	—
$f_0(980)$ anything, $f_0 \rightarrow \pi^+ \pi^-$	< 1.3	CL=90%	—
ϕ anything	(15.7 \pm 1.0) %	—	—
$K^+ K^-$ anything	(15.8 \pm 0.7) %	—	—
$K_S^0 K^+$ anything	(5.8 \pm 0.5) %	—	—
$K_S^0 K^-$ anything	(1.9 \pm 0.4) %	—	—
$2K_S^0$ anything	(1.70 \pm 0.32) %	—	—
$2K^+$ anything	< 2.6 $\times 10^{-3}$	CL=90%	—
$2K^-$ anything	< 6 $\times 10^{-4}$	CL=90%	—

Leptonic and semileptonic modes

$e^+ \nu_e$	< 1.2 $\times 10^{-4}$	CL=90%	984
$\mu^+ \nu_\mu$	(5.8 \pm 0.4) $\times 10^{-3}$	[kkk]	981
$\tau^+ \nu_\tau$	(5.6 \pm 0.4) %		182
$K^+ K^- e^+ \nu_e$	—		851
$\phi e^+ \nu_e$	[kkk] (2.49 \pm 0.14) %		720
$\eta e^+ \nu_e + \eta'(958) e^+ \nu_e$	[kkk] (3.66 \pm 0.37) %		—
$\eta e^+ \nu_e$	[kkk] (2.67 \pm 0.29) %	S=1.1	908
$\eta'(958) e^+ \nu_e$	[kkk] (9.9 \pm 2.3) $\times 10^{-3}$		751
$K^0 e^+ \nu_e$	(3.7 \pm 1.0) $\times 10^{-3}$		921
$K^*(892)^0 e^+ \nu_e$	[kkk] (1.8 \pm 0.7) $\times 10^{-3}$		782
$f_0(980) e^+ \nu_e, f_0 \rightarrow \pi^+ \pi^-$	(2.00 \pm 0.32) $\times 10^{-3}$		—

Hadronic modes with a $K\bar{K}$ pair

$K^+ K_S^0$	(1.49 \pm 0.08) %		850
$K^+ K^- \pi^+$	[oo] (5.50 \pm 0.27) %		805
$\phi \pi^+$	[kkk,III] (4.5 \pm 0.4) %		712
$\phi \pi^+, \phi \rightarrow K^+ K^-$	[III] (2.32 \pm 0.14) %		712
$K^+ \bar{K}^*(892)^0, \bar{K}^{*0} \rightarrow$	(2.60 \pm 0.15) %		416
$K^- \pi^+$			
$f_0(980) \pi^+, f_0 \rightarrow K^+ K^-$	(1.55 \pm 0.16) %		732
$f_0(1370) \pi^+, f_0 \rightarrow K^+ K^-$	(2.4 \pm 0.4) $\times 10^{-3}$		—
$f_0(1710) \pi^+, f_0 \rightarrow K^+ K^-$	(1.87 \pm 0.33) $\times 10^{-3}$		198
$K^+ \bar{K}_0^*(1430)^0, \bar{K}_0^{*0} \rightarrow$	(2.1 \pm 0.4) $\times 10^{-3}$		218
$K^0 \bar{K}^0 \pi^+$	—		802
$K^*(892)^+ \bar{K}^0$	[kkk] (5.4 \pm 1.2) %		683
$K^+ K^- \pi^+ \pi^0$	(5.6 \pm 0.5) %		748
$\phi \rho^+$	[kkk] (8.4 $^{+1.9}_{-2.3}$) %		401
$K_S^0 K^- 2\pi^+$	(1.64 \pm 0.12) %		744
$K^*(892)^+ \bar{K}^*(892)^0$	[kkk] (7.2 \pm 2.6) %		417
$K^+ K_S^0 \pi^+ \pi^-$	(9.6 \pm 1.3) $\times 10^{-3}$		744
$K^+ K^- 2\pi^+ \pi^-$	(8.8 \pm 1.6) $\times 10^{-3}$		673
$\phi 2\pi^+ \pi^-$	[kkk] (1.21 \pm 0.16) %		640
$K^+ K^- \rho^0 \pi^+$ non- ϕ	< 2.6 $\times 10^{-4}$	CL=90%	249
$\phi \rho^0 \pi^+, \phi \rightarrow K^+ K^-$	(6.6 \pm 1.3) $\times 10^{-3}$		181
$\phi a_1(1260)^+, \phi \rightarrow$	(7.5 \pm 1.3) $\times 10^{-3}$		†
$K^+ K^-, a_1^+ \rightarrow \rho^0 \pi^+$			
$K^+ K^- 2\pi^+ \pi^-$ nonresonant	(9 \pm 7) $\times 10^{-4}$		673
$2K_S^0 2\pi^+ \pi^-$	(8.4 \pm 3.5) $\times 10^{-4}$		669

Hadronic modes without K 's

$\pi^+ \pi^0$	< 6 $\times 10^{-4}$	CL=90%	975
$2\pi^+ \pi^-$	(1.10 \pm 0.06) %		959
$\rho^0 \pi^+$	(2.0 \pm 1.2) $\times 10^{-4}$		825
$\pi^+ (\pi^+ \pi^-)_{S\text{-wave}}$	[mmm] (9.2 \pm 0.6) $\times 10^{-3}$		959
$f_2(1270) \pi^+, f_2 \rightarrow \pi^+ \pi^-$	(1.11 \pm 0.20) $\times 10^{-3}$		559
$\rho(1450)^0 \pi^+, \rho^0 \rightarrow \pi^+ \pi^-$	(3.0 \pm 2.0) $\times 10^{-4}$		421
$\pi^+ 2\pi^0$	(6.5 \pm 1.3) $\times 10^{-3}$		961
$2\pi^+ \pi^- \pi^0$	—		935
$\eta \pi^+$	[kkk] (1.56 \pm 0.20) %		902
$\omega \pi^+$	[kkk] (2.3 \pm 0.6) $\times 10^{-3}$		822
$3\pi^+ 2\pi^-$	(8.0 \pm 0.9) $\times 10^{-3}$		899
$2\pi^+ \pi^- 2\pi^0$	—		902
$\eta \rho^+$	[kkk] (8.9 \pm 0.8) %		724
$\eta \pi^+ \pi^0$ 3-body	[kkk] < 5 %	CL=90%	886
$\omega \pi^+ \pi^0$	[kkk] (2.8 \pm 0.7) %		802
$3\pi^+ 2\pi^- \pi^0$	(4.9 \pm 3.2) %		856
$\omega 2\pi^+ \pi^-$	[kkk] (1.6 \pm 0.5) %		766
$\eta'(958) \pi^+$	[jjj,kkk] (3.8 \pm 0.4) %		743
$3\pi^+ 2\pi^- 2\pi^0$	—		803
$\omega \eta \pi^+$	[kkk] < 2.13 %	CL=90%	654
$\eta'(958) \rho^+$	[jjj,kkk] (12.5 \pm 2.2) %		465
$\eta'(958) \pi^+ \pi^0$ 3-body	[kkk] < 1.8 %	CL=90%	720

Modes with one or three K 's

$K^+ \pi^0$	(8.2 \pm 2.2) $\times 10^{-4}$		917
$K_S^0 \pi^+$	(1.20 \pm 0.08) $\times 10^{-3}$		916
$K^+ \eta$	[kkk] (1.39 \pm 0.30) $\times 10^{-3}$		835
$K^+ \omega$	[kkk] < 2.4 $\times 10^{-3}$	CL=90%	741
$K^+ \eta'(958)$	[kkk] (1.6 \pm 0.5) $\times 10^{-3}$		646
$K^+ \pi^+ \pi^-$	(6.9 \pm 0.5) $\times 10^{-3}$		900
$K^+ \rho^0$	(2.7 \pm 0.5) $\times 10^{-3}$		745
$K^+ \rho(1450)^0, \rho^0 \rightarrow \pi^+ \pi^-$	(7.3 \pm 2.6) $\times 10^{-4}$		—
$K^*(892)^0 \pi^+, K^{*0} \rightarrow$	(1.50 \pm 0.26) $\times 10^{-3}$		775
$K^+ \pi^-$			
$K^*(1410)^0 \pi^+, K^{*0} \rightarrow$	(1.30 \pm 0.31) $\times 10^{-3}$		—
$K^+ \pi^-$			

Meson Summary Table

$K^*(1430)^0 \pi^+, K^{*0} \rightarrow$	$(5 \pm 4) \times 10^{-4}$	-
$K^+ \pi^-$ nonresonant	$(1.1 \pm 0.4) \times 10^{-3}$	900
$K_S^0 \pi^+ \pi^0$	$(1.00 \pm 0.18) \%$	900
$K_S^0 2\pi^+ \pi^-$	$(2.9 \pm 1.1) \times 10^{-3}$	870
$K^+ \omega \pi^0$	$[kkk] < 8.2 \times 10^{-3}$	CL=90% 684
$K^+ \omega \pi^+ \pi^-$	$[kkk] < 5.4 \times 10^{-3}$	CL=90% 603
$K^+ \omega \eta$	$[kkk] < 7.9 \times 10^{-3}$	CL=90% 367
$2K^+ K^-$	$(4.9 \pm 1.7) \times 10^{-4}$	628
ϕK^+	$[kkk] < 6 \times 10^{-4}$	CL=90% 607

Doubly Cabibbo-suppressed modes

$2K^+ \pi^-$	$(1.29 \pm 0.18) \times 10^{-4}$	805
--------------	----------------------------------	-----

Baryon-antibaryon mode

$p\bar{n}$	$(1.3 \pm 0.4) \times 10^{-3}$	295
------------	--------------------------------	-----

 $\Delta C = 1$ weak neutral current (CI) modes, Lepton family number (LF), or Lepton number (L) violating modes

$\pi^+ e^+ e^-$	$[tt] < 2.7 \times 10^{-4}$	CL=90% 979
$\pi^+ \mu^+ \mu^-$	$[tt] < 2.6 \times 10^{-5}$	CL=90% 968
$K^+ e^+ e^-$	CI $< 1.6 \times 10^{-3}$	CL=90% 922
$K^+ \mu^+ \mu^-$	CI $< 3.6 \times 10^{-5}$	CL=90% 909
$K^*(892)^+ \mu^+ \mu^-$	CI $< 1.4 \times 10^{-3}$	CL=90% 765
$\pi^+ e^\pm \mu^\mp$	LF $[ee] < 6.1 \times 10^{-4}$	CL=90% 976
$K^+ e^\pm \mu^\mp$	LF $[ee] < 6.3 \times 10^{-4}$	CL=90% 919
$\pi^- 2e^+$	L $< 6.9 \times 10^{-4}$	CL=90% 979
$\pi^- 2\mu^+$	L $< 2.9 \times 10^{-5}$	CL=90% 968
$\pi^- e^+ \mu^+$	L $< 7.3 \times 10^{-4}$	CL=90% 976
$K^- 2e^+$	L $< 6.3 \times 10^{-4}$	CL=90% 922
$K^- 2\mu^+$	L $< 1.3 \times 10^{-5}$	CL=90% 909
$K^- e^+ \mu^+$	L $< 6.8 \times 10^{-4}$	CL=90% 919
$K^*(892)^- 2\mu^+$	L $< 1.4 \times 10^{-3}$	CL=90% 765

 $D_S^{*\pm}$

$$I(J^P) = 0(2^?)$$

J^P is natural, width and decay modes consistent with 1^- .

Mass $m = 2112.3 \pm 0.5$ MeV ($S = 1.1$)

$m_{D_S^{*\pm}} - m_{D_S^\pm} = 143.8 \pm 0.4$ MeV

Full width $\Gamma < 1.9$ MeV, CL = 90%

D_S^{*-} modes are charge conjugates of the modes below.

$D_S^{*\pm}$ DECAY MODES	Fraction (Γ_i/Γ)	ρ (MeV/c)
$D_S^+ \gamma$	$(94.2 \pm 0.7) \%$	139
$D_S^+ \pi^0$	$(5.8 \pm 0.7) \%$	48

 $D_{S0}^*(2317)^\pm$

$$I(J^P) = 0(0^+)$$

J, P need confirmation.

J^P is natural, low mass consistent with 0^+ .

Mass $m = 2317.8 \pm 0.6$ MeV ($S = 1.1$)

$m_{D_{S0}^*(2317)^\pm} - m_{D_S^\pm} = 349.3 \pm 0.6$ MeV ($S = 1.1$)

Full width $\Gamma < 3.8$ MeV, CL = 95%

$D_{S0}^*(2317)^-$ modes are charge conjugates of modes below.

$D_{S0}^*(2317)^\pm$ DECAY MODES	Fraction (Γ_i/Γ)	ρ (MeV/c)
$D_S^+ \pi^0$	seen	298
$D_S^+ \pi^0 \pi^0$	not seen	205

 $D_{S1}(2460)^\pm$

$$I(J^P) = 0(1^+)$$

Mass $m = 2459.5 \pm 0.6$ MeV ($S = 1.1$)

$m_{D_{S1}(2460)^\pm} - m_{D_S^{*\pm}} = 347.2 \pm 0.8$ MeV ($S = 1.2$)

$m_{D_{S1}(2460)^\pm} - m_{D_S^\pm} = 491.1 \pm 0.7$ MeV ($S = 1.1$)

Full width $\Gamma < 3.5$ MeV, CL = 95%

$D_{S1}(2460)^-$ modes are charge conjugates of the modes below.

$D_{S1}(2460)^+$ DECAY MODES	Fraction (Γ_i/Γ)	Scale factor/ Confidence level	ρ (MeV/c)
$D_S^{*+} \pi^0$	$(48 \pm 11) \%$		297
$D_S^+ \gamma$	$(18 \pm 4) \%$		442
$D_S^+ \pi^+ \pi^-$	$(4.3 \pm 1.3) \%$	$S=1.1$	363
$D_S^{*+} \gamma$	$< 8 \%$	CL=90%	323
$D_{S0}^*(2317)^+ \gamma$	$(3.7 \pm 5.0) \%$		138

 $D_{S1}(2536)^\pm$

$$I(J^P) = 0(1^+)$$

J, P need confirmation.

Mass $m = 2535.29 \pm 0.20$ MeV

Full width $\Gamma < 2.3$ MeV, CL = 90%

$D_{S1}(2536)^-$ modes are charge conjugates of the modes below.

$D_{S1}(2536)^+$ DECAY MODES	Fraction (Γ_i/Γ)	ρ (MeV/c)
$D^*(2010)^+ K^0$	seen	149
$D^*(2007)^0 K^+$	seen	168
$D^+ K^0$	not seen	382
$D^0 K^+$	not seen	391
$D_S^{*+} \gamma$	possibly seen	388
$D_S^+ \pi^+ \pi^-$	seen	437

 $D_{S2}^*(2573)$

$$I(J^P) = 0(2^?)$$

J^P is natural, width and decay modes consistent with 2^+ .

Mass $m = 2572.6 \pm 0.9$ MeV

Full width $\Gamma = 20 \pm 5$ MeV ($S = 1.3$)

$D_{S2}^*(2573)^-$ modes are charge conjugates of the modes below.

$D_{S2}^*(2573)^+$ DECAY MODES	Fraction (Γ_i/Γ)	ρ (MeV/c)
$D^0 K^+$	seen	435
$D^*(2007)^0 K^+$	not seen	244

BOTTOM MESONS
($B = \pm 1$)

$$B^+ = u\bar{b}, B^0 = d\bar{b}, \bar{B}^0 = \bar{d}b, B^- = \bar{u}b, \text{ similarly for } B^*s$$

 B -particle organization

Many measurements of B decays involve admixtures of B hadrons. Previously we arbitrarily included such admixtures in the B^\pm section, but because of their importance we have created two new sections: " B^\pm/B^0 Admixture" for $\Upsilon(4S)$ results and " $B^\pm/B^0/B_S^0/b$ -baryon Admixture" for results at higher energies. Most inclusive decay branching fractions and χ_b at high energy are found in the Admixture sections. B^0 - \bar{B}^0 mixing data are found in the B^0 section, while B_S^0 - \bar{B}_S^0 mixing data and B - \bar{B} mixing data for a B^0/B_S^0 admixture are found in the B_S^0 section. CP -violation data are found in the B^\pm, B^0 , and $B^\pm B^0$ Admixture sections. b -baryons are found near the end of the Baryon section.

The organization of the B sections is now as follows, where bullets indicate particle sections and brackets indicate reviews.

- B^\pm
mass, mean life, CP violation, branching fractions
- B^0
mass, mean life, B^0 - \bar{B}^0 mixing, CP violation, branching fractions
- $B^\pm B^0$ Admixtures
 CP violation, branching fractions

Meson Summary Table

- $B^\pm/B^0/B_s^0/b$ -baryon Admixtures
mean life, production fractions, branching fractions
 - B^*
mass
 - $B_1(5721)^0$
mass
 - $B_2^*(5747)^0$
mass
 - B_s^0
mass, mean life, $B_s^0\bar{B}_s^0$ mixing, CP violation,
branching fractions
 - B_s^*
mass
 - $B_{s1}(5830)^0$
mass
 - $B_{s2}^0(5840)^0$
mass
 - B_c^\pm
mass, mean life, branching fractions
- At the end of Baryon Listings:
- Λ_b
mass, mean life, branching fractions
 - Σ_b
mass
 - Σ_b^*
mass
 - Ξ_b^0, Ξ_b^-
mass, mean life, branching fractions
 - Ω_b^-
mass, branching fractions
 - b -baryon Admixture
mean life, branching fractions

 B^\pm

$$I(J^P) = \frac{1}{2}(0^-)$$

I, J, P need confirmation. Quantum numbers shown are quark-model predictions.

$$\begin{aligned} \text{Mass } m_{B^\pm} &= 5279.17 \pm 0.29 \text{ MeV} \\ \text{Mean life } \tau_{B^\pm} &= (1.638 \pm 0.011) \times 10^{-12} \text{ s} \\ c\tau &= 491.1 \text{ } \mu\text{m} \end{aligned}$$

CP violation

$$\begin{aligned} A_{CP}(B^+ \rightarrow J/\psi(1S)K^+) &= 0.009 \pm 0.008 \quad (S = 1.3) \\ A_{CP}(B^+ \rightarrow J/\psi(1S)\pi^+) &= 0.01 \pm 0.07 \quad (S = 1.3) \\ A_{CP}(B^+ \rightarrow J/\psi\rho^+) &= -0.11 \pm 0.14 \\ A_{CP}(B^+ \rightarrow J/\psi K^*(892)^+) &= -0.048 \pm 0.033 \\ A_{CP}(B^+ \rightarrow \eta_c K^+) &= -0.16 \pm 0.08 \\ A_{CP}(B^+ \rightarrow \psi(2S)\pi^+) &= 0.02 \pm 0.09 \\ A_{CP}(B^+ \rightarrow \psi(2S)K^+) &= -0.025 \pm 0.024 \\ A_{CP}(B^+ \rightarrow \psi(2S)K^*(892)^+) &= 0.08 \pm 0.21 \\ A_{CP}(B^+ \rightarrow \chi_{c1}(1P)\pi^+) &= 0.07 \pm 0.18 \\ A_{CP}(B^+ \rightarrow \chi_{c0}K^+) &= -0.11 \pm 0.12 \\ A_{CP}(B^+ \rightarrow \chi_{c1}K^+) &= -0.009 \pm 0.033 \\ A_{CP}(B^+ \rightarrow \chi_{c1}K^*(892)^+) &= 0.5 \pm 0.5 \\ A_{CP}(B^+ \rightarrow \bar{D}^0\pi^+) &= -0.008 \pm 0.008 \\ A_{CP}(B^+ \rightarrow D_{CP(+1)}\pi^+) &= 0.035 \pm 0.024 \\ A_{CP}(B^+ \rightarrow D_{CP(-1)}\pi^+) &= 0.017 \pm 0.026 \\ A_{CP}(B^+ \rightarrow \bar{D}^0 K^+) &= 0.07 \pm 0.04 \\ r_B(B^+ \rightarrow D^0 K^+) &= 0.101 \pm 0.032 \\ \delta_B(B^+ \rightarrow D^0 K^+) &= 126 \pm 21 \text{ degrees} \\ r_B(B^+ \rightarrow DK^{*+}) &= 0.34 \pm 0.09 \quad (S = 1.3) \\ \delta_B(B^+ \rightarrow DK^{*+}) &= 157 \pm 70 \text{ degrees} \quad (S = 2.0) \\ A_{CP}(B^+ \rightarrow [K^-\pi^+]_D K^+) &= -0.1^{+0.9}_{-1.1} \\ A_{CP}(B^+ \rightarrow [K^-\pi^+]_{\bar{D}} K^*(892)^+) &= -0.3 \pm 0.5 \\ A_{CP}(B^+ \rightarrow [K^-\pi^+]_D \pi^+) &= -0.02 \pm 0.16 \end{aligned}$$

$$\begin{aligned} A_{CP}(B^+ \rightarrow [\pi^+\pi^-\pi^0]_D K^+) &= -0.02 \pm 0.15 \\ A_{CP}(B^+ \rightarrow D_{CP(+1)}K^+) &= 0.24 \pm 0.08 \quad (S = 1.1) \\ A_{CP}(B^+ \rightarrow D_{CP(-1)}K^+) &= -0.10 \pm 0.08 \\ A_{CP}(B^+ \rightarrow \bar{D}^{*0}\pi^+) &= -0.014 \pm 0.015 \\ A_{CP}(B^+ \rightarrow (D_{CP(+1)}^*)^0\pi^+) &= -0.02 \pm 0.05 \\ A_{CP}(B^+ \rightarrow (D_{CP(-1)}^*)^0\pi^+) &= -0.09 \pm 0.05 \\ A_{CP}(B^+ \rightarrow D^{*0}K^+) &= -0.07 \pm 0.04 \\ r_B^*(B^+ \rightarrow D^{*0}K^+) &= 0.14 \pm 0.05 \\ \delta_B^*(B^+ \rightarrow D^{*0}K^+) &= 299 \pm 24 \text{ degrees} \\ A_{CP}(B^+ \rightarrow D_{CP(+1)}^{*0}K^+) &= -0.12 \pm 0.08 \\ A_{CP}(B^+ \rightarrow D_{CP(-1)}^*K^+) &= 0.07 \pm 0.10 \\ A_{CP}(B^+ \rightarrow D_{CP(+1)}K^*(892)^+) &= 0.09 \pm 0.14 \\ A_{CP}(B^+ \rightarrow D_{CP(-1)}K^*(892)^+) &= -0.23 \pm 0.22 \\ A_{CP}(B^+ \rightarrow D^{*+}\bar{D}^{*0}) &= -0.15 \pm 0.11 \\ A_{CP}(B^+ \rightarrow D^{*+}\bar{D}^0) &= -0.06 \pm 0.13 \\ A_{CP}(B^+ \rightarrow D^+\bar{D}^{*0}) &= 0.13 \pm 0.18 \\ A_{CP}(B^+ \rightarrow D^+\bar{D}^0) &= -0.03 \pm 0.07 \\ A_{CP}(B^+ \rightarrow K_S^0\pi^+) &= 0.009 \pm 0.029 \quad (S = 1.2) \\ A_{CP}(B^+ \rightarrow K^+\pi^0) &= 0.051 \pm 0.025 \\ A_{CP}(B^+ \rightarrow \eta'K^+) &= 0.013 \pm 0.017 \\ A_{CP}(B^+ \rightarrow \eta'K^*(892)^+) &= -0.30^{+0.33}_{-0.40} \\ A_{CP}(B^+ \rightarrow \eta K^+) &= -0.37 \pm 0.09 \\ A_{CP}(B^+ \rightarrow \eta K^*(892)^+) &= 0.02 \pm 0.06 \\ A_{CP}(B^+ \rightarrow \eta K_0^*(1430)^+) &= 0.05 \pm 0.13 \\ A_{CP}(B^+ \rightarrow \eta K_S^*(1430)^+) &= -0.45 \pm 0.30 \\ A_{CP}(B^+ \rightarrow \omega K^+) &= 0.02 \pm 0.05 \\ A_{CP}(B^+ \rightarrow \omega K^{*+}) &= 0.29 \pm 0.35 \\ A_{CP}(B^+ \rightarrow \omega(K\pi_0^{*+})^+) &= -0.10 \pm 0.09 \\ A_{CP}(B^+ \rightarrow \omega K_2^*(1430)^+) &= 0.14 \pm 0.15 \\ A_{CP}(B^+ \rightarrow K^*(892)^+\pi^0) &= 0.04 \pm 0.29 \\ A_{CP}(B^+ \rightarrow K^{*0}\pi^+) &= -0.04 \pm 0.09 \quad (S = 2.1) \\ A_{CP}(B^+ \rightarrow K^+\pi^-\pi^+) &= 0.038 \pm 0.022 \\ A_{CP}(B^+ \rightarrow f_0(980)K^+) &= -0.10^{+0.05}_{-0.04} \\ A_{CP}(B^+ \rightarrow f_2(1270)K^+) &= -0.68^{+0.19}_{-0.17} \\ A_{CP}(B^+ \rightarrow f'_X(1300)K^+) &= 0.28 \pm 0.30 \\ A_{CP}(B^+ \rightarrow \rho^0 K^+) &= 0.37 \pm 0.10 \\ A_{CP}(B^+ \rightarrow K_S^*(1430)^0\pi^+) &= 0.055 \pm 0.033 \\ A_{CP}(B^+ \rightarrow K_S^*(1430)^0\pi^+) &= 0.05^{+0.29}_{-0.24} \\ A_{CP}(B^+ \rightarrow K^0\rho^+) &= (-0.12 \pm 0.17) \times 10^{-6} \\ A_{CP}(B^+ \rightarrow K^{*+}\pi^+\pi^-) &= 0.07 \pm 0.08 \\ A_{CP}(B^+ \rightarrow \rho\bar{\Lambda}\gamma) &= 0.17 \pm 0.17 \\ A_{CP}(B^+ \rightarrow \rho\bar{\Lambda}\pi^0) &= 0.01 \pm 0.17 \\ A_{CP}(B^+ \rightarrow \rho^0 K^*(892)^+) & \\ A_{CP}(B^+ \rightarrow K^*(892)^+ f_0(980)) &= -0.34 \pm 0.21 \\ A_{CP}(B^+ \rightarrow a_1^+ K^0) &= 0.12 \pm 0.11 \\ A_{CP}(B^+ \rightarrow b_1^+ K^0) &= -0.03 \pm 0.15 \\ A_{CP}(B^+ \rightarrow K^*(892)^0\rho^+) &= -0.01 \pm 0.16 \\ A_{CP}(B^+ \rightarrow b_1^0 K^+) &= -0.46 \pm 0.20 \\ A_{CP}(B^+ \rightarrow K^0 K^+) &= 0.12 \pm 0.18 \\ A_{CP}(B^+ \rightarrow K^+ K_S^0 K_S^0) &= -0.04 \pm 0.11 \\ A_{CP}(B^+ \rightarrow K^+ K^-\pi^+) &= 0.00 \pm 0.10 \\ A_{CP}(B^+ \rightarrow K^+ K^- K^+) &= -0.017 \pm 0.030 \\ A_{CP}(B^+ \rightarrow \phi K^+) &= -0.01 \pm 0.06 \\ A_{CP}(B^+ \rightarrow X_0(1550)K^+) &= -0.04 \pm 0.07 \\ A_{CP}(B^+ \rightarrow K^{*+}K^+K^-) &= 0.11 \pm 0.09 \\ A_{CP}(B^+ \rightarrow \phi K^*(892)^+) &= -0.01 \pm 0.08 \\ A_{CP}(B^+ \rightarrow \phi(K\pi_0^{*+})^+) &= 0.04 \pm 0.16 \\ A_{CP}(B^+ \rightarrow \phi K_1(1270)^+) &= 0.15 \pm 0.20 \\ A_{CP}(B^+ \rightarrow \phi K_S^*(1430)^+) &= -0.23 \pm 0.20 \\ A_{CP}(B^+ \rightarrow K^*(892)^+\gamma) &= 0.018 \pm 0.029 \\ A_{CP}(B^+ \rightarrow \eta K^+\gamma) &= -0.12 \pm 0.07 \\ A_{CP}(B^+ \rightarrow \phi K^+\gamma) &= -0.26 \pm 0.15 \\ A_{CP}(B^+ \rightarrow \rho^+\gamma) &= -0.11 \pm 0.33 \\ A_{CP}(B^+ \rightarrow \pi^+\pi^0) &= 0.06 \pm 0.05 \\ A_{CP}(B^+ \rightarrow \pi^+\pi^-\pi^+) &= 0.03 \pm 0.06 \\ A_{CP}(B^+ \rightarrow \rho^0\pi^+) &= 0.18^{+0.09}_{-0.17} \\ A_{CP}(B^+ \rightarrow f_2(1270)\pi^+) &= 0.41 \pm 0.30 \\ A_{CP}(B^+ \rightarrow \rho^0(1450)\pi^+) &= -0.1^{+0.4}_{-0.5} \\ A_{CP}(B^+ \rightarrow f_0(1370)\pi^+) &= 0.72 \pm 0.22 \\ A_{CP}(B^+ \rightarrow \pi^+\pi^-\pi^+ \text{ nonresonant}) &= -0.14^{+0.23}_{-0.16} \\ A_{CP}(B^+ \rightarrow \rho^+\pi^0) &= 0.02 \pm 0.11 \end{aligned}$$

Meson Summary Table

$$\begin{aligned}
A_{CP}(B^+ \rightarrow \rho^+ \rho^0) &= -0.05 \pm 0.05 \\
A_{CP}(B^+ \rightarrow b_1^0 \pi^+) &= 0.05 \pm 0.16 \\
A_{CP}(B^+ \rightarrow \omega \pi^+) &= -0.04 \pm 0.06 \\
A_{CP}(B^+ \rightarrow \omega \rho^+) &= -0.20 \pm 0.09 \\
A_{CP}(B^+ \rightarrow \eta \pi^+) &= -0.13 \pm 0.10 \quad (S = 1.5) \\
A_{CP}(B^+ \rightarrow \eta' \pi^+) &= 0.06 \pm 0.16 \\
A_{CP}(B^+ \rightarrow \eta \rho^+) &= 0.11 \pm 0.11 \\
A_{CP}(B^+ \rightarrow \eta' \rho^+) &= 0.04 \pm 0.28 \\
A_{CP}(B^+ \rightarrow \rho \bar{\rho} \pi^+) &= 0.00 \pm 0.04 \\
A_{CP}(B^+ \rightarrow \rho \bar{\rho} K^+) &= -0.16 \pm 0.07 \\
A_{CP}(B^+ \rightarrow \rho \bar{\rho} K^*(892)^+) &= 0.21 \pm 0.16 \quad (S = 1.4) \\
A_{CP}(B^+ \rightarrow K^+ \ell^+ \ell^-) &= -0.01 \pm 0.09 \quad (S = 1.1) \\
A_{CP}(B^+ \rightarrow K^+ e^+ e^-) &= 0.14 \pm 0.14 \\
A_{CP}(B^+ \rightarrow K^+ \mu^+ \mu^-) &= -0.05 \pm 0.13 \\
A_{CP}(B^+ \rightarrow K^* \ell^+ \ell^-) &= -0.09 \pm 0.14 \\
A_{CP}(B^+ \rightarrow K^* e^+ e^-) &= -0.14 \pm 0.23 \\
A_{CP}(B^+ \rightarrow K^* \mu^+ \mu^-) &= -0.12 \pm 0.24 \\
\gamma(B^+ \rightarrow D^*(*) K^*(*)^+) &= (62 \pm 15)^\circ
\end{aligned}$$

B^- modes are charge conjugates of the modes below. Modes which do not identify the charge state of the B are listed in the B^\pm/B^0 ADMIXTURE section.

The branching fractions listed below assume 50% $B^0 \bar{B}^0$ and 50% $B^+ B^-$ production at the $\Upsilon(4S)$. We have attempted to bring older measurements up to date by rescaling their assumed $\Upsilon(4S)$ production ratio to 50:50 and their assumed D, D_s, D^* , and ψ branching ratios to current values whenever this would affect our averages and best limits significantly.

Indentation is used to indicate a subchannel of a previous reaction. All resonant subchannels have been corrected for resonance branching fractions to the final state so the sum of the subchannel branching fractions can exceed that of the final state.

For inclusive branching fractions, e.g., $B \rightarrow D^\pm$ anything, the values usually are multiplicities, not branching fractions. They can be greater than one.

B^+ DECAY MODES	Fraction (Γ_i/Γ)	Scale factor / Confidence level (MeV/c)	ρ
Semileptonic and leptonic modes			
$\ell^+ \nu_\ell$ anything	[<i>nnn</i>] (10.99 ± 0.28) %		–
$e^+ \nu_e X_c$	(10.8 ± 0.4) %		–
$D \ell^+ \nu_\ell$ anything	(9.8 ± 0.7) %		–
$\bar{D}^0 \ell^+ \nu_\ell$	[<i>nnn</i>] (2.23 ± 0.11) %		2310
$\bar{D}^0 \tau^+ \nu_\tau$	(7 ± 4) × 10 ⁻³		1911
$\bar{D}^*(2007)^0 \ell^+ \nu_\ell$	[<i>nnn</i>] (5.68 ± 0.19) %		2258
$\bar{D}^*(2007)^0 \tau^+ \nu_\tau$	(2.0 ± 0.5) %		1839
$D^- \pi^+ \ell^+ \nu_\ell$	(4.2 ± 0.5) × 10 ⁻³		2306
$\bar{D}_0^*(2420)^0 \ell^+ \nu_\ell \times$ B($\bar{D}_0^* \rightarrow D^+ \pi^-$)	(2.5 ± 0.5) × 10 ⁻³		–
$\bar{D}_2^*(2460)^0 \ell^+ \nu_\ell \times$ B($\bar{D}_2^* \rightarrow D^+ \pi^-$)	(1.67 ± 0.30) × 10 ⁻³	S=1.2	2065
$D^{(*)} n \pi^+ \ell^+ \nu_\ell$ ($n \geq 1$)	(1.86 ± 0.26) %		–
$D^{*-} \pi^+ \ell^+ \nu_\ell$	(6.1 ± 0.6) × 10 ⁻³		2254
$\bar{D}_1(2420)^0 \ell^+ \nu_\ell \times$ B($\bar{D}_1^0 \rightarrow D^{*+} \pi^-$)	(3.03 ± 0.20) × 10 ⁻³		2084
$\bar{D}_1'(2430)^0 \ell^+ \nu_\ell \times$ B($\bar{D}_1'^0 \rightarrow D^{*+} \pi^-$)	(2.7 ± 0.6) × 10 ⁻³		–
$\bar{D}_2^*(2460)^0 \ell^+ \nu_\ell \times$ B($\bar{D}_2^{*0} \rightarrow D^{*+} \pi^-$)	(1.85 ± 0.27) × 10 ⁻³	S=1.3	2065
$\pi^0 \ell^+ \nu_\ell$	(7.7 ± 1.2) × 10 ⁻⁵		2638
$\eta \ell^+ \nu_\ell$	(3.7 ± 1.3) × 10 ⁻⁵	S=1.5	2611
$\eta' \ell^+ \nu_\ell$	(1.7 ± 2.2) × 10 ⁻⁵		2553
$\omega \ell^+ \nu_\ell$	[<i>nnn</i>] (1.15 ± 0.17) × 10 ⁻⁴		2582
$\rho^0 \ell^+ \nu_\ell$	[<i>nnn</i>] (1.28 ± 0.18) × 10 ⁻⁴		2583
$\rho \bar{\rho} e^+ \nu_e$	< 5.2 × 10 ⁻³	CL=90%	2467
$e^+ \nu_e$	< 1.9 × 10 ⁻⁶	CL=90%	2640
$\mu^+ \nu_\mu$	< 1.0 × 10 ⁻⁶	CL=90%	2639
$\tau^+ \nu_\tau$	(1.8 ± 0.5) × 10 ⁻⁴		2341
$\ell^+ \nu_\ell \gamma$	< 1.56 × 10 ⁻⁵	CL=90%	2640
$e^+ \nu_e \gamma$	< 1.7 × 10 ⁻⁵	CL=90%	2640
$\mu^+ \nu_\mu \gamma$	< 2.4 × 10 ⁻⁵	CL=90%	2639

	Inclusive modes	
$D^0 X$	(8.6 ± 0.7) %	–
$\bar{D}^0 X$	(7.9 ± 0.4) %	–
$D^+ X$	(2.5 ± 0.5) %	–
$D^- X$	(9.9 ± 1.2) %	–
$D_s^+ X$	(7.9 ± 1.4 / -1.3) %	–
$D_s^- X$	(1.10 ± 0.40 / -0.32) %	–
$\Lambda_c^+ X$	(2.1 ± 0.9 / -0.6) %	–
$\bar{\Lambda}_c^- X$	(2.8 ± 1.1 / -0.9) %	–
$\bar{c} X$	(97 ± 4) %	–
$c X$	(23.4 ± 2.2 / -1.8) %	–
$\bar{c} X$	(120 ± 6) %	–

D, D*, or D_s modes

$\bar{D}^0 \pi^+$	(4.84 ± 0.15) × 10 ⁻³	2308
$D_{CP(+1)} \pi^+$	[<i>ooo</i>] (2.3 ± 0.4) × 10 ⁻³	–
$D_{CP(-1)} \pi^+$	[<i>ooo</i>] (2.0 ± 0.4) × 10 ⁻³	–
$\bar{D}^0 \rho^+$	(1.34 ± 0.18) %	2237
$\bar{D}^0 K^+$	(3.68 ± 0.33) × 10 ⁻⁴	2280
$D_{CP(+1)} K^+$	[<i>ooo</i>] (2.01 ± 0.26) × 10 ⁻⁴	–
$D_{CP(-1)} K^+$	[<i>ooo</i>] (1.89 ± 0.27) × 10 ⁻⁴	–
$[K^- \pi^+]_D K^+$	[<i>ppp</i>] < 2.8 × 10 ⁻⁷	CL=90%
$[K^+ \pi^-]_D K^+$	[<i>ppp</i>] < 4 × 10 ⁻⁵	CL=90%
$[K^- \pi^+]_D \pi^+$	[<i>ppp</i>] (6.3 ± 1.1) × 10 ⁻⁷	–
$[K^+ \pi^-]_D \pi^+$	(1.9 ± 0.4) × 10 ⁻⁴	–
$[\pi^+ \pi^- \pi^0]_D K^-$	(4.6 ± 0.9) × 10 ⁻⁶	–
$\bar{D}^0 K^*(892)^+$	(5.3 ± 0.4) × 10 ⁻⁴	2213
$D_{CP(-1)} K^*(892)^+$	[<i>ooo</i>] (2.7 ± 0.8) × 10 ⁻⁴	–
$D_{CP(+1)} K^*(892)^+$	[<i>ooo</i>] (5.8 ± 1.1) × 10 ⁻⁴	–
$\bar{D}^0 K^+ \bar{K}^0$	(5.5 ± 1.6) × 10 ⁻⁴	2189
$\bar{D}^0 K^+ \bar{K}^*(892)^0$	(7.5 ± 1.7) × 10 ⁻⁴	2071
$\bar{D}^0 \pi^+ \pi^+ \pi^-$	(1.1 ± 0.4) %	2289
$\bar{D}^0 \pi^+ \pi^+ \pi^-$ nonresonant	(5 ± 4) × 10 ⁻³	2289
$\bar{D}^0 \pi^+ \rho^0$	(4.2 ± 3.0) × 10 ⁻³	2207
$\bar{D}^0 a_1(1260)^+$	(4 ± 4) × 10 ⁻³	2123
$\bar{D}^0 \omega \pi^+$	(4.1 ± 0.9) × 10 ⁻³	2206
$D^*(2010)^- \pi^+ \pi^+$	(1.35 ± 0.22) × 10 ⁻³	2247
$D^- \pi^+ \pi^+$	(1.07 ± 0.05) × 10 ⁻³	2299
$D^+ K^0$	< 5.0 × 10 ⁻⁶	CL=90%
$\bar{D}^*(2007)^0 \pi^+$	(5.19 ± 0.26) × 10 ⁻³	2256
$\bar{D}_{CP(+1)}^* \pi^+$	[<i>qqq</i>] (2.9 ± 0.7) × 10 ⁻³	–
$\bar{D}_{CP(-1)}^* \pi^+$	[<i>qqq</i>] (2.6 ± 1.0) × 10 ⁻³	–
$\bar{D}^*(2007)^0 \omega \pi^+$	(4.5 ± 1.2) × 10 ⁻³	2149
$\bar{D}^*(2007)^0 \rho^+$	(9.8 ± 1.7) × 10 ⁻³	2181
$\bar{D}^*(2007)^0 K^+$	(4.21 ± 0.35) × 10 ⁻⁴	2227
$\bar{D}_{CP(+1)}^* K^+$	[<i>qqq</i>] (2.8 ± 0.4) × 10 ⁻⁴	–
$\bar{D}_{CP(-1)}^* K^+$	[<i>qqq</i>] (2.32 ± 0.33) × 10 ⁻⁴	–
$\bar{D}^*(2007)^0 K^*(892)^+$	(8.1 ± 1.4) × 10 ⁻⁴	2156
$\bar{D}^*(2007)^0 K^+ \bar{K}^0$	< 1.06 × 10 ⁻³	CL=90%
$\bar{D}^*(2007)^0 K^+ K^*(892)^0$	(1.5 ± 0.4) × 10 ⁻³	2008
$\bar{D}^*(2007)^0 \pi^+ \pi^+ \pi^-$	(1.03 ± 0.12) %	2236
$\bar{D}^*(2007)^0 a_1(1260)^+$	(1.9 ± 0.5) %	2062
$\bar{D}^*(2007)^0 \pi^- \pi^+ \pi^+ \pi^0$	(1.8 ± 0.4) %	2219
$\bar{D}^{*0} 3\pi^+ 2\pi^-$	(5.7 ± 1.2) × 10 ⁻³	2196
$D^*(2010)^+ \pi^0$	< 3.6 × 10 ⁻⁶	2255
$D^*(2010)^+ K^0$	< 9.0 × 10 ⁻⁶	CL=90%
$D^*(2010)^- \pi^+ \pi^+ \pi^0$	(1.5 ± 0.7) %	2235
$D^*(2010)^- \pi^+ \pi^+ \pi^+ \pi^-$	(2.6 ± 0.4) × 10 ⁻³	2217
$\bar{D}^{*0} \pi^+$	[<i>rrr</i>] (5.9 ± 1.3) × 10 ⁻³	–
$\bar{D}_1^*(2420)^0 \pi^+$	(1.5 ± 0.6) × 10 ⁻³	S=1.3
$\bar{D}_1(2420)^0 \pi^+ \times$ B($\bar{D}_1^0 \rightarrow \bar{D}^0 \pi^+ \pi^-$)	(1.9 ± 0.5 / -0.6) × 10 ⁻⁴	2081
$\bar{D}_2^*(2462)^0 \pi^+$	(3.5 ± 0.4) × 10 ⁻⁴	–
\times B($\bar{D}_2^*(2462)^0 \rightarrow D^- \pi^+$)		
$\bar{D}_0^*(2400)^0 \pi^+$	(6.4 ± 1.4) × 10 ⁻⁴	2128
\times B($\bar{D}_0^*(2400)^0 \rightarrow D^- \pi^+$)		
$\bar{D}_1(2421)^0 \pi^+$	(6.8 ± 1.5) × 10 ⁻⁴	–
\times B($\bar{D}_1(2421)^0 \rightarrow D^{*-} \pi^+$)		
$\bar{D}_2^*(2462)^0 \pi^+$	(1.8 ± 0.5) × 10 ⁻⁴	–
\times B($\bar{D}_2^*(2462)^0 \rightarrow D^{*-} \pi^+$)		

Meson Summary Table

 $B^0-\bar{B}^0$ mixing parameters

$$\begin{aligned} \chi_d &= 0.1872 \pm 0.0024 \\ \Delta m_{B^0} &= m_{B_H^0} - m_{B_L^0} = (0.507 \pm 0.005) \times 10^{12} \text{ h s}^{-1} \\ &= (3.337 \pm 0.033) \times 10^{-10} \text{ MeV} \\ x_d &= \Delta m_{B^0} / \Gamma_{B^0} = 0.774 \pm 0.008 \\ \text{Re}(\lambda_{CP} / |\lambda_{CP}|) \text{ Re}(z) &= 0.01 \pm 0.05 \\ \Delta\Gamma \text{ Re}(z) &= -0.007 \pm 0.004 \\ \text{Re}(z) &= 0.00 \pm 0.12 \\ \text{Im}(z) &= -0.015 \pm 0.008 \end{aligned}$$

CP violation parameters

$$\begin{aligned} \text{Re}(\epsilon_{B^0}) / (1 + |\epsilon_{B^0}|^2) &= (-0.1 \pm 1.4) \times 10^{-3} \\ A_{T/CP} &= 0.005 \pm 0.018 \\ A_{CP}(B^0 \rightarrow D^*(2010)^+ D^-) &= 0.02 \pm 0.04 \\ A_{CP}(B^0 \rightarrow K^+ \pi^-) &= -0.098 \pm 0.013 \\ A_{CP}(B^0 \rightarrow \eta' K^*(892)^0) &= 0.08 \pm 0.25 \\ A_{CP}(B^0 \rightarrow \eta K^*(892)^0) &= 0.19 \pm 0.05 \\ A_{CP}(B^0 \rightarrow \omega K^*0) &= 0.45 \pm 0.25 \\ A_{CP}(B^0 \rightarrow \omega(K\pi)_0^*0) &= -0.07 \pm 0.09 \\ A_{CP}(B^0 \rightarrow \omega K_2^*(1430)^0) &= -0.37 \pm 0.17 \\ A_{CP}(B^0 \rightarrow K^0 K^0) &= (-0.6 \pm 0.7) \times 10^{-6} \\ A_{CP}(B^0 \rightarrow \eta K_0^*(1430)^0) &= 0.06 \pm 0.13 \\ A_{CP}(B^0 \rightarrow \eta K_2^*(1430)^0) &= -0.07 \pm 0.19 \\ A_{CP}(B^0 \rightarrow K^+ \pi^- \pi^0) &= (0 \pm 6) \times 10^{-2} \\ A_{CP}(B^0 \rightarrow \rho^- K^+) &= 0.15 \pm 0.13 \\ A_{CP}(B^0 \rightarrow K^+ \pi^- \pi^0 \text{ nonresonant}) &= 0.23_{-0.22}^{+0.22} \\ A_{CP}(B^0 \rightarrow (K\pi)_0^* \pi^-) &= 0.10 \pm 0.07 \\ A_{CP}(B^0 \rightarrow (K\pi)_0^*0 \pi^0) &= -0.22 \pm 0.32 \\ A_{CP}(B^0 \rightarrow K^*(892)^+ \pi^-) &= -0.19 \pm 0.07 \\ A_{CP}(B^0 \rightarrow K^*0 \pi^0) &= -0.09_{-0.26}^{+0.23} \\ A_{CP}(B^0 \rightarrow K^0 \pi^+ \pi^-) &= -0.01 \pm 0.05 \\ A_{CP}(B^0 \rightarrow K^*(892)^0 \pi^+ \pi^-) &= 0.07 \pm 0.05 \\ A_{CP}(B^0 \rightarrow K^*(892)^0 \rho^0) &= 0.09 \pm 0.19 \\ A_{CP}(B^0 \rightarrow a_1^- K^+) &= -0.16 \pm 0.12 \\ A_{CP}(B^0 \rightarrow b_1^- K^+) &= -0.07 \pm 0.12 \\ A_{CP}(B^0 \rightarrow K^*(892)^0 K^+ K^-) &= 0.01 \pm 0.05 \\ A_{CP}(B^0 \rightarrow K^*(892)^0 \phi) &= 0.01 \pm 0.05 \\ A_{CP}(B^0 \rightarrow K^*(892)^0 K^- \pi^+) &= 0.2 \pm 0.4 \\ A_{CP}(B^0 \rightarrow \phi(K\pi)_0^*0) &= 0.20 \pm 0.15 \\ A_{CP}(B^0 \rightarrow \phi K_2^*(1430)^0) &= -0.08 \pm 0.13 \\ A_{CP}(B^0 \rightarrow \rho^+ \pi^-) &= 0.08 \pm 0.12 \quad (S = 2.0) \\ A_{CP}(B^0 \rightarrow \rho^- \pi^+) &= -0.16 \pm 0.23 \quad (S = 1.7) \\ A_{CP}(B^0 \rightarrow a_1(1260)^\pm \pi^\mp) &= -0.07 \pm 0.07 \\ A_{CP}(B^0 \rightarrow b_1 \pi^+) &= -0.05 \pm 0.10 \\ A_{CP}(B^0 \rightarrow K^*(892)^0 \gamma) &= -0.016 \pm 0.023 \\ A_{CP}(B^0 \rightarrow K^*(1430) \gamma) &= -0.08 \pm 0.15 \\ A_{CP}(B^0 \rightarrow \rho \bar{\rho} K^*(892)^0) &= 0.05 \pm 0.12 \\ A_{CP}(B^0 \rightarrow \rho \bar{\rho} \pi^-) &= 0.04 \pm 0.07 \\ A_{CP}(B^0 \rightarrow K^*0 \ell^+ \ell^-) &= -0.05 \pm 0.10 \\ A_{CP}(B^0 \rightarrow K^*0 e^+ e^-) &= -0.21 \pm 0.19 \\ A_{CP}(B^0 \rightarrow K^*0 \mu^+ \mu^-) &= 0.00 \pm 0.15 \\ C_{D^+ D^+} (B^0 \rightarrow D^*(2010)^+ D^+) &= 0.07 \pm 0.14 \\ S_{D^+ D^+} (B^0 \rightarrow D^*(2010)^+ D^+) &= -0.78 \pm 0.21 \\ C_{D^+ D^-} (B^0 \rightarrow D^*(2010)^+ D^-) &= -0.09 \pm 0.22 \quad (S = 1.6) \\ S_{D^+ D^-} (B^0 \rightarrow D^*(2010)^+ D^-) &= -0.61 \pm 0.19 \\ C_{D^+ D^*} (B^0 \rightarrow D^+ D^{*-}) &= -0.01 \pm 0.09 \quad (S = 1.2) \\ S_{D^+ D^*} (B^0 \rightarrow D^+ D^{*-}) &= -0.76 \pm 0.14 \\ C_{\pm} (B^0 \rightarrow D^{*+} D^{*-}) &= 0.00 \pm 0.12 \\ S_{\pm} (B^0 \rightarrow D^{*+} D^{*-}) &= -0.76 \pm 0.16 \\ C_{-} (B^0 \rightarrow D^{*+} D^{*-}) &= 0.4 \pm 0.5 \\ S_{-} (B^0 \rightarrow D^{*+} D^{*-}) &= -1.8 \pm 0.7 \\ C(B^0 \rightarrow D^*(2010)^+ D^*(2010)^- K_S^0) &= 0.01 \pm 0.29 \\ S(B^0 \rightarrow D^*(2010)^+ D^*(2010)^- K_S^0) &= 0.1 \pm 0.4 \\ C_{D^+ D^-} (B^0 \rightarrow D^+ D^-) &= -0.5 \pm 0.4 \quad (S = 2.5) \\ S_{D^+ D^-} (B^0 \rightarrow D^+ D^-) &= -0.87 \pm 0.26 \\ C_{J/\psi(1S) \pi^0} (B^0 \rightarrow J/\psi(1S) \pi^0) &= -0.13 \pm 0.13 \\ S_{J/\psi(1S) \pi^0} (B^0 \rightarrow J/\psi(1S) \pi^0) &= -0.94 \pm 0.29 \quad (S = 1.9) \\ C_{D_{CP}^* h^0} (B^0 \rightarrow D_{CP}^* h^0) &= -0.23 \pm 0.16 \\ S_{D_{CP}^* h^0} (B^0 \rightarrow D_{CP}^* h^0) &= -0.56 \pm 0.24 \end{aligned}$$

$$\begin{aligned} C_{K_S^0 \pi^0} (B^0 \rightarrow K^0 \pi^0) &= 0.00 \pm 0.13 \quad (S = 1.4) \\ S_{K_S^0 \pi^0} (B^0 \rightarrow K^0 \pi^0) &= 0.58 \pm 0.17 \\ C_{\eta'(958) K} (B^0 \rightarrow \eta'(958) K_S^0) &= -0.04 \pm 0.20 \quad (S = 2.5) \\ S_{\eta'(958) K} (B^0 \rightarrow \eta'(958) K_S^0) &= 0.43 \pm 0.17 \quad (S = 1.5) \\ C_{\eta' K^0} (B^0 \rightarrow \eta' K^0) &= -0.05 \pm 0.05 \\ S_{\eta' K^0} (B^0 \rightarrow \eta' K^0) &= 0.60 \pm 0.07 \\ C_{\omega K_S^0} (B^0 \rightarrow \omega K_S^0) &= -0.30 \pm 0.28 \quad (S = 1.6) \\ S_{\omega K_S^0} (B^0 \rightarrow \omega K_S^0) &= 0.43 \pm 0.24 \\ C(B^0 \rightarrow K_S^0 \pi^0 \pi^0) &= 0.2 \pm 0.5 \\ S(B^0 \rightarrow K_S^0 \pi^0 \pi^0) &= 0.7 \pm 0.7 \\ C_{\rho^0 K_S^0} (B^0 \rightarrow \rho^0 K_S^0) &= -0.04 \pm 0.20 \\ S_{\rho^0 K_S^0} (B^0 \rightarrow \rho^0 K_S^0) &= 0.50_{-0.21}^{+0.17} \\ C_{f_0 K_S^0} (B^0 \rightarrow f_0(980) K_S^0) &= 0.07 \pm 0.14 \\ S_{f_0 K_S^0} (B^0 \rightarrow f_0(980) K_S^0) &= -0.73_{-0.09}^{+0.27} \quad (S = 1.6) \\ S_{f_2 K_S^0} (B^0 \rightarrow f_2(1270) K_S^0) &= -0.5 \pm 0.5 \\ C_{f_2 K_S^0} (B^0 \rightarrow f_2(1270) K_S^0) &= 0.3 \pm 0.4 \\ S_{f_x K_S^0} (B^0 \rightarrow f_x(1300) K_S^0) &= -0.2 \pm 0.5 \\ C_{f_x K_S^0} (B^0 \rightarrow f_x(1300) K_S^0) &= 0.13 \pm 0.35 \\ S_{K^0 \pi^+ \pi^-} (B^0 \rightarrow K^0 \pi^+ \pi^- \text{ nonresonant}) &= -0.01 \pm 0.33 \\ C_{K^0 \pi^+ \pi^-} (B^0 \rightarrow K^0 \pi^+ \pi^- \text{ nonresonant}) &= 0.01 \pm 0.26 \\ C_{K_S^0 K_S^0} (B^0 \rightarrow K_S^0 K_S^0) &= 0.0 \pm 0.4 \quad (S = 1.4) \\ S_{K_S^0 K_S^0} (B^0 \rightarrow K_S^0 K_S^0) &= -0.8 \pm 0.5 \\ C_{K^+ K^- K_S^0} (B^0 \rightarrow K^+ K^- K_S^0) &= 0.07 \pm 0.08 \\ S_{K^+ K^- K_S^0} (B^0 \rightarrow K^+ K^- K_S^0) &= -0.74_{-0.10}^{+0.12} \\ C_{K^+ K^- K_S^0} (B^0 \rightarrow K^+ K^- K_S^0 \text{ inclusive}) &= 0.01 \pm 0.09 \\ S_{K^+ K^- K_S^0} (B^0 \rightarrow K^+ K^- K_S^0 \text{ inclusive}) &= -0.65 \pm 0.12 \\ C_{\phi K_S^0} (B^0 \rightarrow \phi K_S^0) &= -0.01 \pm 0.12 \\ S_{\phi K_S^0} (B^0 \rightarrow \phi K_S^0) &= 0.39 \pm 0.17 \\ C_{K_S K_S K_S} (B^0 \rightarrow K_S K_S K_S) &= -0.15 \pm 0.16 \quad (S = 1.1) \\ S_{K_S K_S K_S} (B^0 \rightarrow K_S K_S K_S) &= -0.4 \pm 0.5 \quad (S = 2.5) \\ C_{K_S^0 \pi^0 \gamma} (B^0 \rightarrow K_S^0 \pi^0 \gamma) &= 0.36 \pm 0.33 \\ S_{K_S^0 \pi^0 \gamma} (B^0 \rightarrow K_S^0 \pi^0 \gamma) &= -0.8 \pm 0.6 \\ C_{K^*0 \gamma} (B^0 \rightarrow K^*(892)^0 \gamma) &= -0.04 \pm 0.16 \quad (S = 1.2) \\ S_{K^*0 \gamma} (B^0 \rightarrow K^*(892)^0 \gamma) &= -0.15 \pm 0.22 \\ C_{\eta K^0 \gamma} (B^0 \rightarrow \eta K^0 \gamma) &= -0.3 \pm 0.4 \\ S_{\eta K^0 \gamma} (B^0 \rightarrow \eta K^0 \gamma) &= -0.2 \pm 0.5 \\ C(B^0 \rightarrow K_S^0 \rho^0 \gamma) &= -0.05 \pm 0.19 \\ S(B^0 \rightarrow K_S^0 \rho^0 \gamma) &= 0.11 \pm 0.34 \\ C(B^0 \rightarrow \rho^0 \gamma) &= 0.4 \pm 0.5 \\ S(B^0 \rightarrow \rho^0 \gamma) &= -0.8 \pm 0.7 \\ C_{\pi \pi} (B^0 \rightarrow \pi^+ \pi^-) &= -0.38 \pm 0.17 \quad (S = 2.6) \\ S_{\pi \pi} (B^0 \rightarrow \pi^+ \pi^-) &= -0.61 \pm 0.08 \\ C_{\pi^0 \pi^0} (B^0 \rightarrow \pi^0 \pi^0) &= -0.48 \pm 0.30 \\ C_{\rho \pi} (B^0 \rightarrow \rho^+ \pi^-) &= 0.01 \pm 0.14 \quad (S = 1.9) \\ S_{\rho \pi} (B^0 \rightarrow \rho^+ \pi^-) &= 0.01 \pm 0.09 \\ \Delta C_{\rho \pi} (B^0 \rightarrow \rho^+ \pi^-) &= 0.37 \pm 0.08 \\ \Delta S_{\rho \pi} (B^0 \rightarrow \rho^+ \pi^-) &= -0.05 \pm 0.10 \\ C_{\rho^0 \pi^0} (B^0 \rightarrow \rho^0 \pi^0) &= 0.3 \pm 0.4 \\ S_{\rho^0 \pi^0} (B^0 \rightarrow \rho^0 \pi^0) &= 0.1 \pm 0.4 \\ C_{a_1 \pi} (B^0 \rightarrow a_1(1260)^+ \pi^-) &= -0.10 \pm 0.17 \\ S_{a_1 \pi} (B^0 \rightarrow a_1(1260)^+ \pi^-) &= 0.37 \pm 0.22 \\ \Delta C_{a_1 \pi} (B^0 \rightarrow a_1(1260)^+ \pi^-) &= 0.26 \pm 0.17 \\ \Delta S_{a_1 \pi} (B^0 \rightarrow a_1(1260)^+ \pi^-) &= -0.14 \pm 0.22 \\ C(B^0 \rightarrow b_1^- K^+) &= -0.22 \pm 0.24 \\ \Delta C(B^0 \rightarrow b_1^- \pi^+) &= -1.04 \pm 0.24 \\ C_{\rho^0 \rho^0} (B^0 \rightarrow \rho^0 \rho^0) &= 0.2 \pm 0.9 \\ S_{\rho^0 \rho^0} (B^0 \rightarrow \rho^0 \rho^0) &= 0.3 \pm 0.7 \\ C_{\rho \rho} (B^0 \rightarrow \rho^+ \rho^-) &= -0.05 \pm 0.13 \\ S_{\rho \rho} (B^0 \rightarrow \rho^+ \rho^-) &= -0.06 \pm 0.17 \\ |\lambda| (B^0 \rightarrow J/\psi K^*(892)^0) &< 0.25, \text{ CL} = 95\% \\ \cos 2\beta (B^0 \rightarrow J/\psi K^*(892)^0) &= 1.7_{-0.9}^{+0.7} \quad (S = 1.6) \end{aligned}$$

Meson Summary Table

$\cos 2\beta (B^0 \rightarrow [K_S^0 \pi^+ \pi^-]_{D^{(*)}} h^0) = 1.0_{-0.7}^{+0.6}$ ($S = 1.8$)
$(S_+ + S_-)/2 (B^0 \rightarrow D^{*-} \pi^+) = -0.037 \pm 0.012$
$(S_- - S_+)/2 (B^0 \rightarrow D^{*-} \pi^+) = -0.006 \pm 0.016$
$(S_+ + S_-)/2 (B^0 \rightarrow D^- \pi^+) = -0.046 \pm 0.023$
$(S_- - S_+)/2 (B^0 \rightarrow D^- \pi^+) = -0.022 \pm 0.021$
$(S_+ + S_-)/2 (B^0 \rightarrow D^- \rho^+) = -0.024 \pm 0.032$
$(S_- - S_+)/2 (B^0 \rightarrow D^- \rho^+) = -0.10 \pm 0.06$
$C_{\eta_c K_S^0} (B^0 \rightarrow \eta_c K_S^0) = 0.08 \pm 0.13$
$S_{\eta_c K_S^0} (B^0 \rightarrow \eta_c K_S^0) = 0.93 \pm 0.17$
$C_{c\bar{c}K^{(*)0}} (B^0 \rightarrow c\bar{c}K^{(*)0}) = 0.004 \pm 0.019$
$\sin(2\beta) = 0.671 \pm 0.023$
$C_{J/\psi(nS)K^0} (B^0 \rightarrow J/\psi(nS)K^0) = (-0.2 \pm 2.0) \times 10^{-2}$
$S_{J/\psi(nS)K^0} (B^0 \rightarrow J/\psi(nS)K^0) = 0.658 \pm 0.024$
$C_{J/\psi K^{*0}} (B^0 \rightarrow J/\psi K^{*0}) = 0.03 \pm 0.10$
$S_{J/\psi K^{*0}} (B^0 \rightarrow J/\psi K^{*0}) = 0.60 \pm 0.25$
$C_{\chi_{c0} K_S^0} (B^0 \rightarrow \chi_{c0} K_S^0) = -0.3_{-0.4}^{+0.5}$
$S_{\chi_{c0} K_S^0} (B^0 \rightarrow \chi_{c0} K_S^0) = -0.7 \pm 0.5$
$C_{\chi_{c1} K_S^0} (B^0 \rightarrow \chi_{c1} K_S^0) = 0.13 \pm 0.11$
$S_{\chi_{c1} K_S^0} (B^0 \rightarrow \chi_{c1} K_S^0) = 0.61 \pm 0.16$
$\sin(2\beta_{\text{eff}}) (B^0 \rightarrow \phi K^0) = 0.22 \pm 0.30$
$\sin(2\beta_{\text{eff}}) (B^0 \rightarrow \phi K_0^0 (1430)^0) = 0.97_{-0.52}^{+0.03}$
$\sin(2\beta_{\text{eff}}) (B^0 \rightarrow K^+ K^- K_S^0) = 0.77_{-0.12}^{+0.13}$
$\sin(2\beta_{\text{eff}}) (B^0 \rightarrow [K_S^0 \pi^+ \pi^-]_{D^{(*)}} h^0) = 0.45 \pm 0.28$
$ \lambda (B^0 \rightarrow [K_S^0 \pi^+ \pi^-]_{D^{(*)}} h^0) = 1.01 \pm 0.08$
$ \sin(2\beta + \gamma) > 0.40, \text{CL} = 90\%$
$2\beta + \gamma = (83 \pm 60)^\circ$
$\gamma (B^0 \rightarrow D^0 K^{*0}) = (162 \pm 60)^\circ$
$\alpha = (90 \pm 5)^\circ$

\bar{B}^0 modes are charge conjugates of the modes below. Reactions indicate the weak decay vertex and do not include mixing. Modes which do not identify the charge state of the B are listed in the B^\pm/B^0 ADMIXTURE section.

The branching fractions listed below assume 50% $B^0 \bar{B}^0$ and 50% $B^+ B^-$ production at the $\Upsilon(4S)$. We have attempted to bring older measurements up to date by rescaling their assumed $\Upsilon(4S)$ production ratio to 50:50 and their assumed D, D_s, D^* , and ψ branching ratios to current values whenever this would affect our averages and best limits significantly.

Indentation is used to indicate a subchannel of a previous reaction. All resonant subchannels have been corrected for resonance branching fractions to the final state so the sum of the subchannel branching fractions can exceed that of the final state.

For inclusive branching fractions, e.g., $B \rightarrow D^\pm \text{anything}$, the values usually are multiplicities, not branching fractions. They can be greater than one.

B^0 DECAY MODES	Fraction (Γ_i/Γ)	Scale factor/ Confidence level	p (MeV/c)
$\ell^+ \nu_\ell$ anything	[nnn] (10.33 ± 0.28) %		-
$e^+ \nu_e X_c$	(10.1 ± 0.4) %		-
$D \ell^+ \nu_\ell$ anything	(9.3 ± 0.9) %		-
$D^- \ell^+ \nu_\ell$	[nnn] (2.17 ± 0.12) %		2309
$D^- \tau^+ \nu_\tau$	(1.1 ± 0.4) %		1909
$D^*(2010)^- \ell^+ \nu_\ell$	[nnn] (5.01 ± 0.12) %		2257
$D^*(2010)^- \tau^+ \nu_\tau$	(1.5 ± 0.5) %	S=1.3	1837
$\bar{D}^0 \pi^- \ell^+ \nu_\ell$	(4.3 ± 0.6) × 10 ⁻³		2308
$D_0^*(2400)^- \ell^+ \nu_\ell \times$ $B(D_0^{*-} \rightarrow \bar{D}^0 \pi^-)$	(3.0 ± 1.2) × 10 ⁻³	S=1.8	-
$D_2^*(2460)^- \ell^+ \nu_\ell \times$ $B(D_2^{*-} \rightarrow \bar{D}^0 \pi^-)$	(2.2 ± 0.6) × 10 ⁻³		2067
$\bar{D}^{(*)0} n \pi \ell^+ \nu_\ell (n \geq 1)$	(2.3 ± 0.5) %		-
$\bar{D}^{*0} \pi^- \ell^+ \nu_\ell$	(4.9 ± 0.8) × 10 ⁻³		2256
$D_1(2420)^- \ell^+ \nu_\ell \times$ $B(D_1^- \rightarrow \bar{D}^{*0} \pi^-)$	(2.80 ± 0.28) × 10 ⁻³		-
$D_1'(2430)^- \ell^+ \nu_\ell \times$ $B(D_1'^- \rightarrow \bar{D}^{*0} \pi^-)$	(3.1 ± 0.9) × 10 ⁻³		-
$D_2^*(2460)^- \ell^+ \nu_\ell \times$ $B(D_2^{*-} \rightarrow \bar{D}^{*0} \pi^-)$	(1.2 ± 0.5) × 10 ⁻³	S=2.7	2067
$\rho^- \ell^+ \nu_\ell$	[nnn] (2.47 ± 0.33) × 10 ⁻⁴		2583
$\pi^- \ell^+ \nu_\ell$	[nnn] (1.34 ± 0.08) × 10 ⁻⁴		2638

	Inclusive modes		
K^\pm anything	(78 ± 8) %		-
$D^0 X$	(8.1 ± 1.5) %		-
$\bar{D}^0 X$	(47.4 ± 2.8) %		-
$D^+ X$	< 3.9 %	CL=90%	-
$D^- X$	(36.9 ± 3.3) %		-
$D_S^+ X$	(10.3 ± 2.1) %		-
$D_S^- X$	< 2.6 %	CL=90%	-
$\Lambda_c^+ X$	< 3.1 %	CL=90%	-
$\bar{\Lambda}_c^+ X$	(5.0 ± 2.1) %		-
$\bar{c} X$	(95 ± 5) %		-
$c X$	(24.6 ± 3.1) %		-
$\bar{c} X$	(119 ± 6) %		-

 D, D^* , or D_s modes

$D^- \pi^+$	(2.68 ± 0.13) × 10 ⁻³		2306
$D^- \rho^+$	(7.6 ± 1.3) × 10 ⁻³		2235
$D^- K^0 \pi^+$	(4.9 ± 0.9) × 10 ⁻⁴		2259
$D^- K^*(892)^+$	(4.5 ± 0.7) × 10 ⁻⁴		2211
$D^- \omega \pi^+$	(2.8 ± 0.6) × 10 ⁻³		2204
$D^- K^+$	(2.0 ± 0.6) × 10 ⁻⁴		2279
$D^- K^+ \bar{K}^0$	< 3.1 × 10 ⁻⁴	CL=90%	2188
$D^- K^+ \bar{K}^*(892)^0$	(8.8 ± 1.9) × 10 ⁻⁴		2070
$\bar{D}^0 \pi^+ \pi^-$	(8.4 ± 0.9) × 10 ⁻⁴		2301
$D^*(2010)^- \pi^+$	(2.76 ± 0.13) × 10 ⁻³		2255
$D^- \pi^+ \pi^+ \pi^-$	(8.0 ± 2.5) × 10 ⁻³		2287
($D^- \pi^+ \pi^+ \pi^- $) nonresonant	(3.9 ± 1.9) × 10 ⁻³		2287
$D^- \pi^+ \rho^0$	(1.1 ± 1.0) × 10 ⁻³		2206
$D^- a_1(1260)^+$	(6.0 ± 3.3) × 10 ⁻³		2121
$D^*(2010)^- \pi^+ \pi^0$	(1.5 ± 0.5) %		2247
$D^*(2010)^- \rho^+$	(6.8 ± 0.9) × 10 ⁻³		2180
$D^*(2010)^- K^+$	(2.14 ± 0.16) × 10 ⁻⁴		2226
$D^*(2010)^- K^0 \pi^+$	(3.0 ± 0.8) × 10 ⁻⁴		2205
$D^*(2010)^- K^*(892)^+$	(3.3 ± 0.6) × 10 ⁻⁴		2155
$D^*(2010)^- K^+ \bar{K}^0$	< 4.7 × 10 ⁻⁴	CL=90%	2131
$D^*(2010)^- K^+ \bar{K}^*(892)^0$	(1.29 ± 0.33) × 10 ⁻³		2007
$D^*(2010)^- \pi^+ \pi^+ \pi^-$	(7.0 ± 0.8) × 10 ⁻³	S=1.3	2235
($D^*(2010)^- \pi^+ \pi^+ \pi^- $) non-resonant	(0.0 ± 2.5) × 10 ⁻³		2235
$D^*(2010)^- \pi^+ \rho^0$	(5.7 ± 3.2) × 10 ⁻³		2150
$D^*(2010)^- a_1(1260)^+$	(1.30 ± 0.27) %		2061
$D^*(2010)^- \pi^+ \pi^+ \pi^- \pi^0$	(1.76 ± 0.27) %		2218
$D^{*-} 3\pi^+ 2\pi^-$	(4.7 ± 0.9) × 10 ⁻³		2195
$\bar{D}^*(2010)^- \omega \pi^+$	(2.89 ± 0.30) × 10 ⁻³		2148
$D_1(2430)^0 \omega \times$ $B(D_1(2430)^0 \rightarrow$ $D^{*-} \pi^+)$	(4.1 ± 1.6) × 10 ⁻⁴		1992
$\bar{D}^{*-} \pi^+$	[rrr] (2.1 ± 1.0) × 10 ⁻³		-
$D_1(2420)^- \pi^+ \times B(D_1^- \rightarrow$ $D^- \pi^+ \pi^-)$	(8.9 ± 2.3) × 10 ⁻⁵		-
$D_1(2420)^- \pi^+ \times B(D_1^- \rightarrow$ $D^{*-} \pi^+ \pi^-)$	< 3.3 × 10 ⁻⁵	CL=90%	-
$\bar{D}_2^*(2460)^- \pi^+ \times$ $B(D_2^{*-}(2460)^- \rightarrow D^0 \pi^-)$	(2.15 ± 0.35) × 10 ⁻⁴		2064
$\bar{D}_0^*(2400)^- \pi^+ \times$ $B(D_0^{*-}(2400)^- \rightarrow D^0 \pi^-)$	(6.0 ± 3.0) × 10 ⁻⁵		2090
$D_2^*(2460)^- \pi^+ \times B((D_2^*)^- \rightarrow$ $D^{*-} \pi^+ \pi^-)$	< 2.4 × 10 ⁻⁵	CL=90%	-
$\bar{D}_2^*(2460)^- \rho^+$	< 4.9 × 10 ⁻³	CL=90%	1977
$D^0 \bar{D}^0$	< 4.3 × 10 ⁻⁵	CL=90%	1868
$D^{*0} \bar{D}^0$	< 2.9 × 10 ⁻⁴	CL=90%	1794
$D^- D^+$	(2.11 ± 0.31) × 10 ⁻⁴	S=1.2	1864
$D^- D_S^+$	(7.2 ± 0.8) × 10 ⁻³		1812
$D^*(2010)^- D_S^+$	(8.0 ± 1.1) × 10 ⁻³		1735
$D^- D_S^{*+}$	(7.4 ± 1.6) × 10 ⁻³		1731
$D^*(2010)^- D_S^{*+}$	(1.77 ± 0.14) %		1649
$D_{S0}(2317)^- K^+ \times$ $B(D_{S0}(2317)^- \rightarrow D_S^- \pi^0)$	(4.2 ± 1.4) × 10 ⁻⁵		2097
$D_{S0}(2317)^- \pi^+ \times$ $B(D_{S0}(2317)^- \rightarrow D_S^- \pi^0)$	< 2.5 × 10 ⁻⁵	CL=90%	2128
$D_{S,J}(2457)^- K^+ \times$ $B(D_{S,J}(2457)^- \rightarrow D_S^- \pi^0)$	< 9.4 × 10 ⁻⁶	CL=90%	-
$D_{S,J}(2457)^- \pi^+ \times$ $B(D_{S,J}(2457)^- \rightarrow D_S^- \pi^0)$	< 4.0 × 10 ⁻⁶	CL=90%	-

Meson Summary Table

The branching fraction measurements are for an admixture of B mesons at the $\Upsilon(4S)$. The values quoted assume that $B(\Upsilon(4S) \rightarrow B\bar{B}) = 100\%$.

For inclusive branching fractions, e.g., $B \rightarrow D^\pm$ anything, the treatment of multiple D 's in the final state must be defined. One possibility would be to count the number of events with one-or-more D 's and divide by the total number of B 's. Another possibility would be to count the total number of D 's and divide by the total number of B 's, which is the definition of average multiplicity. The two definitions are identical if only one D is allowed in the final state. Even though the "one-or-more" definition seems sensible, for practical reasons inclusive branching fractions are almost always measured using the multiplicity definition. For heavy final state particles, authors call their results inclusive branching fractions while for light particles some authors call their results multiplicities. In the B sections, we list all results as inclusive branching fractions, adopting a multiplicity definition. This means that inclusive branching fractions can exceed 100% and that inclusive partial widths can exceed total widths, just as inclusive cross sections can exceed total cross section.

\bar{B} modes are charge conjugates of the modes below. Reactions indicate the weak decay vertex and do not include mixing.

B DECAY MODES	Fraction (Γ_i/Γ)	Scale factor/ Confidence level (MeV/c)	p
Semileptonic and leptonic modes			
$B \rightarrow e^+ \nu_e$ anything	[zzz] (10.74 \pm 0.16) %		—
$B \rightarrow \bar{p} e^+ \nu_e$ anything	< 5.9 $\times 10^{-4}$	CL=90%	—
$B \rightarrow \mu^+ \nu_\mu$ anything	[zzz] (10.74 \pm 0.16) %		—
$B \rightarrow \ell^+ \nu_\ell$ anything	[nnn,zzz] (10.74 \pm 0.16) %		—
$B \rightarrow D^- \ell^+ \nu_\ell$ anything	[nnn] (2.8 \pm 0.9) %		—
$B \rightarrow \bar{D}^0 \ell^+ \nu_\ell$ anything	[nnn] (7.2 \pm 1.4) %		—
$B \rightarrow \bar{D} \ell \nu_\ell$	(2.40 \pm 0.12) %		2310
$B \rightarrow D \tau^+ \nu_\tau$	(8.6 \pm 2.7) $\times 10^{-3}$		1911
$B \rightarrow D^{*-} \ell^+ \nu_\ell$ anything	[aaaa] (6.7 \pm 1.3) $\times 10^{-3}$		—
$B \rightarrow D^{*+} \nu_\tau$	(1.62 \pm 0.33) %		1837
$B \rightarrow \bar{D}^{*+} \ell^+ \nu_\ell$	[nnn,bbbb] (2.7 \pm 0.7) %		—
$B \rightarrow \bar{D}_1(2420) \ell^+ \nu_\ell$ anything	(3.8 \pm 1.3) $\times 10^{-3}$	S=2.4	—
$B \rightarrow D \pi \ell^+ \nu_\ell$ anything + $D^* \pi \ell^+ \nu_\ell$ anything	(2.6 \pm 0.5) %	S=1.5	—
$B \rightarrow D \pi \ell^+ \nu_\ell$ anything	(1.5 \pm 0.6) %		—
$B \rightarrow D^* \pi \ell^+ \nu_\ell$ anything	(1.9 \pm 0.4) %		—
$B \rightarrow \bar{D}_2^*(2460) \ell^+ \nu_\ell$ anything	(4.4 \pm 1.6) $\times 10^{-3}$		—
$B \rightarrow D^{*-} \pi^+ \ell^+ \nu_\ell$ anything	(1.00 \pm 0.34) %		—
$B \rightarrow D_s^- \ell^+ \nu_\ell$ anything	[nnn] < 7 $\times 10^{-3}$	CL=90%	—
$B \rightarrow D_s^- \ell^+ \nu_\ell K^+$ anything	[nnn] < 5 $\times 10^{-3}$	CL=90%	—
$B \rightarrow D_s^- \ell^+ \nu_\ell K^0$ anything	[nnn] < 7 $\times 10^{-3}$	CL=90%	—
$B \rightarrow \ell^+ \nu_\ell$ charm	(10.58 \pm 0.15) %		—
$B \rightarrow X_u \ell^+ \nu_\ell$	(2.33 \pm 0.22) $\times 10^{-3}$		—
$B \rightarrow \pi \ell \nu_\ell$	(1.35 \pm 0.10) $\times 10^{-4}$		2638
$B \rightarrow K^+ \ell^+ \nu_\ell$ anything	[nnn] (6.2 \pm 0.5) %		—
$B \rightarrow K^- \ell^+ \nu_\ell$ anything	[nnn] (10 \pm 4) $\times 10^{-3}$		—
$B \rightarrow K^0 / \bar{K}^0 \ell^+ \nu_\ell$ anything	[nnn] (4.5 \pm 0.5) %		—
D, D*, or D_s modes			
$B \rightarrow D^\pm$ anything	(23.1 \pm 1.5) %		—
$B \rightarrow D^0 / \bar{D}^0$ anything	(62.5 \pm 2.9) %	S=1.3	—
$B \rightarrow D^*(2010)^\pm$ anything	(22.5 \pm 1.5) %		—
$B \rightarrow D^*(2007)^0$ anything	(26.0 \pm 2.7) %		—
$B \rightarrow D_s^\pm$ anything	[ee] (8.3 \pm 0.8) %		—
$B \rightarrow D_s^{*\pm}$ anything	(6.3 \pm 1.0) %		—
$B \rightarrow D_s^{*\pm} \bar{D}^0(*)$	(3.4 \pm 0.6) %		—
$B \rightarrow D^0(*) \bar{D}^0(*) K^0 + D^0(*) \bar{D}^0(*) K^\pm$	[ee,cccc] (7.1 \pm 2.7 / 1.7) %		—
$b \rightarrow c \bar{c} s$	(22 \pm 4) %		—
$B \rightarrow D_s^0(*) \bar{D}^0(*)$	[ee,cccc] (3.9 \pm 0.4) %		—
$B \rightarrow D^* D^*(2010)^\pm$	[ee] < 5.9 $\times 10^{-3}$	CL=90%	1711
$B \rightarrow D D^*(2010)^\pm + D^* D^\pm$	[ee] < 5.5 $\times 10^{-3}$	CL=90%	—
$B \rightarrow D D^\pm$	[ee] < 3.1 $\times 10^{-3}$	CL=90%	1866
$B \rightarrow D_s^0(*) \bar{D}^0(*) X (n \pi^\pm)$	[ee,cccc] (9 \pm 5 / 4) %		—

$B \rightarrow D^*(2010) \gamma$	< 1.1 $\times 10^{-3}$	CL=90%	2257
$B \rightarrow D_s^+ \pi^-, D_s^{*+} \pi^-, D_s^+ \rho^-, D_s^{*+} \rho^-, D_s^+ \pi^0, D_s^{*+} \pi^0, D_s^+ \eta, D_s^{*+} \eta, D_s^+ \rho^0, D_s^{*+} \rho^0, D_s^+ \omega, D_s^{*+} \omega$	[ee] < 4 $\times 10^{-4}$	CL=90%	—
$B \rightarrow D_{s1}(2536)^+$ anything	< 9.5 $\times 10^{-3}$	CL=90%	—
Charmonium modes			
$B \rightarrow J/\psi(1S)$ anything	(1.094 \pm 0.032) %	S=1.1	—
$B \rightarrow J/\psi(1S)$ (direct) anything	(7.8 \pm 0.4) $\times 10^{-3}$	S=1.1	—
$B \rightarrow \psi(2S)$ anything	(3.07 \pm 0.21) $\times 10^{-3}$		—
$B \rightarrow \chi_{c1}(1P)$ anything	(3.86 \pm 0.27) $\times 10^{-3}$		—
$B \rightarrow \chi_{c1}(1P)$ (direct) anything	(3.22 \pm 0.25) $\times 10^{-3}$		—
$B \rightarrow \chi_{c2}(1P)$ anything	(1.3 \pm 0.4) $\times 10^{-3}$	S=1.9	—
$B \rightarrow \chi_{c2}(1P)$ (direct) anything	(1.65 \pm 0.31) $\times 10^{-3}$		—
$B \rightarrow \eta_c(1S)$ anything	< 9 $\times 10^{-3}$	CL=90%	—
$B \rightarrow KX(3872) \times B(X \rightarrow D^0 \bar{D}^0 \pi^0)$	(1.2 \pm 0.4) $\times 10^{-4}$		1141
$B \rightarrow KX(3872) \times B(X \rightarrow D^{*0} D^0)$	(8.0 \pm 2.2) $\times 10^{-5}$		1141
$B \rightarrow KX(3940) \times B(X \rightarrow D^{*0} D^0)$	< 6.7 $\times 10^{-5}$	CL=90%	1084
$B \rightarrow KX(3945) \times B(X \rightarrow \omega J/\psi)$	[dddd] (7.1 \pm 3.4) $\times 10^{-5}$		1106
K or K* modes			
$B \rightarrow K^\pm$ anything	[ee] (78.9 \pm 2.5) %		—
$B \rightarrow K^+$ anything	(66 \pm 5) %		—
$B \rightarrow K^-$ anything	(13 \pm 4) %		—
$B \rightarrow K^0 / \bar{K}^0$ anything	[ee] (64 \pm 4) %		—
$B \rightarrow K^*(892)^\pm$ anything	(18 \pm 6) %		—
$B \rightarrow K^*(892)^0 / \bar{K}^*(892)^0$ anything	[ee] (14.6 \pm 2.6) %		—
$B \rightarrow K^*(892) \gamma$	(4.2 \pm 0.6) $\times 10^{-5}$		2564
$B \rightarrow \eta K \gamma$	(8.5 \pm 1.8 / 1.6) $\times 10^{-6}$		2588
$B \rightarrow K_1(1400) \gamma$	< 1.27 $\times 10^{-4}$	CL=90%	2453
$B \rightarrow K_2^*(1430) \gamma$	(1.7 \pm 0.6 / 0.5) $\times 10^{-5}$		2447
$B \rightarrow K_2(1770) \gamma$	< 1.2 $\times 10^{-3}$	CL=90%	2342
$B \rightarrow K_3^*(1780) \gamma$	< 3.7 $\times 10^{-5}$	CL=90%	2341
$B \rightarrow K_4^*(2045) \gamma$	< 1.0 $\times 10^{-3}$	CL=90%	2244
$B \rightarrow K \eta'(958)$	(8.3 \pm 1.1) $\times 10^{-5}$		2528
$B \rightarrow K^*(892) \eta'(958)$	(4.1 \pm 1.1) $\times 10^{-6}$		2472
$B \rightarrow K \eta$	< 5.2 $\times 10^{-6}$	CL=90%	2588
$B \rightarrow K^*(892) \eta$	(1.8 \pm 0.5) $\times 10^{-5}$		2534
$B \rightarrow K \phi$	(2.3 \pm 0.9) $\times 10^{-6}$		2306
$B \rightarrow \bar{b} \rightarrow \bar{s} \gamma$	(3.60 \pm 0.23) $\times 10^{-4}$		—
$B \rightarrow \bar{b} \rightarrow \bar{d} \gamma$	(1.2 \pm 0.6) $\times 10^{-5}$		—
$B \rightarrow \bar{b} \rightarrow \bar{s} \text{gluon}$	< 6.8 %	CL=90%	—
$B \rightarrow \eta$ anything	< 4.4 $\times 10^{-4}$	CL=90%	—
$B \rightarrow \eta'$ anything	(4.2 \pm 0.9) $\times 10^{-4}$		—
Light unflavored meson modes			
$B \rightarrow \rho \gamma$	(1.39 \pm 0.25) $\times 10^{-6}$	S=1.2	2583
$B \rightarrow \rho / \omega \gamma$	(1.30 \pm 0.23) $\times 10^{-6}$	S=1.2	—
$B \rightarrow \pi^\pm$ anything	[ee,eeee] (358 \pm 7) %		—
$B \rightarrow \pi^0$ anything	(235 \pm 11) %		—
$B \rightarrow \eta$ anything	(17.6 \pm 1.6) %		—
$B \rightarrow \rho^0$ anything	(21 \pm 5) %		—
$B \rightarrow \omega$ anything	< 81 %	CL=90%	—
$B \rightarrow \phi$ anything	(3.43 \pm 0.12) %		—
$B \rightarrow \phi K^*(892)$	< 2.2 $\times 10^{-5}$	CL=90%	2460
Baryon modes			
$B \rightarrow \Lambda_c^+ / \bar{\Lambda}_c^-$ anything	(4.5 \pm 1.2) %		—
$B \rightarrow \bar{\Lambda}_c^- e^+$ anything	< 2.3 $\times 10^{-3}$	CL=90%	—
$B \rightarrow \bar{\Lambda}_c^- p$ anything	(2.6 \pm 0.8) %		—
$B \rightarrow \bar{\Lambda}_c^- p e^+ \nu_e$	< 1.0 $\times 10^{-3}$	CL=90%	2021
$B \rightarrow \bar{\Sigma}_c^{--}$ anything	(4.2 \pm 2.4) $\times 10^{-3}$		—
$B \rightarrow \bar{\Sigma}_c^-$ anything	< 9.6 $\times 10^{-3}$	CL=90%	—
$B \rightarrow \bar{\Sigma}_c^0$ anything	(4.6 \pm 2.4) $\times 10^{-3}$		—
$B \rightarrow \bar{\Sigma}_c^0 N (N = p \text{ or } n)$	< 1.5 $\times 10^{-3}$	CL=90%	1938

Meson Summary Table

$B \rightarrow \Xi_c^0$ anything	$(1.93 \pm 0.30) \times 10^{-4}$	S=1.1	-
$\times B(\Xi_c^0 \rightarrow \Xi^- \pi^+)$			
$B \rightarrow \Xi_c^+ \text{ anything}$	$(4.5 \pm 1.3) \times 10^{-4}$		-
$\times B(\Xi_c^+ \rightarrow \Xi^- \pi^+ \pi^+)$			
$B \rightarrow p/\bar{p}$ anything	[ee] $(8.0 \pm 0.4) \%$		-
$B \rightarrow p/\bar{p}$ (direct) anything	[ee] $(5.5 \pm 0.5) \%$		-
$B \rightarrow \Lambda/\bar{\Lambda}$ anything	[ee] $(4.0 \pm 0.5) \%$		-
$B \rightarrow \Xi^-/\bar{\Xi}^+$ anything	[ee] $(2.7 \pm 0.6) \times 10^{-3}$		-
$B \rightarrow$ baryons anything	$(6.8 \pm 0.6) \%$		-
$B \rightarrow p\bar{p}$ anything	$(2.47 \pm 0.23) \%$		-
$B \rightarrow \Lambda\bar{\Lambda}/\bar{\Lambda}p$ anything	[ee] $(2.5 \pm 0.4) \%$		-
$B \rightarrow \Lambda\bar{\Lambda}$ anything	$< 5 \times 10^{-3}$	CL=90%	-

Lepton Family number (LF) violating modes or $\Delta B = 1$ weak neutral current (BI) modes

$B \rightarrow s e^+ e^-$	BI	$(4.7 \pm 1.3) \times 10^{-6}$	-
$B \rightarrow s \mu^+ \mu^-$	BI	$(4.3 \pm 1.2) \times 10^{-6}$	-
$B \rightarrow s \ell^+ \ell^-$	BI [nnn]	$(4.5 \pm 1.0) \times 10^{-6}$	-
$B \rightarrow \pi \ell^+ \ell^-$		$< 6.2 \times 10^{-8}$	CL=90% 2638
$B \rightarrow K e^+ e^-$	BI	$(4.4 \pm 0.6) \times 10^{-7}$	2617
$B \rightarrow K^*(892) e^+ e^-$	BI	$(1.19 \pm 0.20) \times 10^{-6}$	S=1.2 2564
$B \rightarrow K \mu^+ \mu^-$	BI	$(4.8 \pm 0.6) \times 10^{-7}$	2612
$B \rightarrow K^*(892) \mu^+ \mu^-$	BI	$(1.15 \pm 0.15) \times 10^{-6}$	2560
$B \rightarrow K \ell^+ \ell^-$	BI	$(4.5 \pm 0.4) \times 10^{-7}$	2617
$B \rightarrow K^*(892) \ell^+ \ell^-$	BI	$(1.08 \pm 0.11) \times 10^{-6}$	2564
$B \rightarrow K^* \nu \bar{\nu}$		$< 8 \times 10^{-5}$	CL=90% -
$B \rightarrow s e^\pm \mu^\mp$	LF [ee]	$< 2.2 \times 10^{-5}$	CL=90% -
$B \rightarrow \pi e^\pm \mu^\mp$	LF	$< 9.2 \times 10^{-8}$	CL=90% 2637
$B \rightarrow \rho e^\pm \mu^\mp$	LF	$< 3.2 \times 10^{-6}$	CL=90% 2582
$B \rightarrow K e^\pm \mu^\mp$	LF	$< 3.8 \times 10^{-8}$	CL=90% 2616
$B \rightarrow K^*(892) e^\pm \mu^\mp$	LF	$< 5.1 \times 10^{-7}$	CL=90% 2563

$B^\pm/B^0/B_s^0/b$ -baryon ADMIXTURE

These measurements are for an admixture of bottom particles at high energy (LEP, Tevatron, $Spp\bar{S}$).

$$\text{Mean life } \tau = (1.568 \pm 0.009) \times 10^{-12} \text{ s}$$

$$\text{Mean life } \tau = (1.72 \pm 0.10) \times 10^{-12} \text{ s} \quad \text{Charged } b\text{-hadron admixture}$$

$$\text{Mean life } \tau = (1.58 \pm 0.14) \times 10^{-12} \text{ s} \quad \text{Neutral } b\text{-hadron admixture}$$

$$\tau_{\text{charged } b\text{-hadron}}/\tau_{\text{neutral } b\text{-hadron}} = 1.09 \pm 0.13$$

$$|\Delta\tau_b|/\tau_{b,\bar{b}} = -0.001 \pm 0.014$$

The branching fraction measurements are for an admixture of B mesons and baryons at energies above the $T(4S)$. Only the highest energy results (LEP, Tevatron, $Spp\bar{S}$) are used in the branching fraction averages. In the following, we assume that the production fractions are the same at the LEP and at the Tevatron.

For inclusive branching fractions, e.g., $B \rightarrow D^\pm$ anything, the values usually are multiplicities, not branching fractions. They can be greater than one.

The modes below are listed for a \bar{b} initial state. b modes are their charge conjugates. Reactions indicate the weak decay vertex and do not include mixing.

\bar{b} DECAY MODES	Fraction (Γ_i/Γ)	Scale factor/ Confidence level	p (MeV/c)
-----------------------	--------------------------------	-----------------------------------	----------------

PRODUCTION FRACTIONS

The production fractions for weakly decaying b -hadrons at high energy have been calculated from the best values of mean lives, mixing parameters, and branching fractions in this edition by the Heavy Flavor Averaging Group (HFAG) as described in the note " B^0 - \bar{B}^0 Mixing" in the B^0 Particle Listings. The production fractions in b -hadronic Z decay or $p\bar{p}$ collisions at the Tevatron are also listed at the end of the section. Values assume

$$B(\bar{b} \rightarrow B^+) = B(\bar{b} \rightarrow B^0)$$

$$B(\bar{b} \rightarrow B^+) + B(\bar{b} \rightarrow B^0) + B(\bar{b} \rightarrow B_s^0) + B(b \rightarrow b\text{-baryon}) = 100 \%$$

The correlation coefficients between production fractions are also reported:

$$\text{cor}(B_s^0, b\text{-baryon}) = -0.041$$

$$\text{cor}(B_s^0, B^\pm = B^0) = -0.483$$

$$\text{cor}(b\text{-baryon}, B^\pm = B^0) = -0.855.$$

The notation for production fractions varies in the literature ($f_d, d_{B^0}, f(b \rightarrow \bar{B}^0), \text{Br}(b \rightarrow \bar{B}^0)$). We use our own branching fraction notation here, $B(\bar{b} \rightarrow B^0)$.

B^+	$(40.1 \pm 1.3) \%$	-
B^0	$(40.1 \pm 1.3) \%$	-
B_s^0	$(11.3 \pm 1.3) \%$	-
b -baryon	$(8.5 \pm 2.2) \%$	-
B_c	-	-

DECAY MODES

Semileptonic and leptonic modes

ν anything	$(23.1 \pm 1.5) \%$	-
$\ell^+ \nu_\ell$ anything	[nnn] $(10.69 \pm 0.22) \%$	-
$e^+ \nu_e$ anything	$(10.86 \pm 0.35) \%$	-
$\mu^+ \nu_\mu$ anything	$(10.95 \pm 0.29) \%$	-
$D^- \ell^+ \nu_\ell$ anything	[nnn] $(2.2 \pm 0.4) \%$	S=1.8 -
$D^- \pi^+ \ell^+ \nu_\ell$ anything	$(4.9 \pm 1.9) \times 10^{-3}$	-
$D^- \pi^- \ell^+ \nu_\ell$ anything	$(2.6 \pm 1.6) \times 10^{-3}$	-
$\bar{D}^0 \ell^+ \nu_\ell$ anything	[nnn] $(6.84 \pm 0.35) \%$	-
$\bar{D}^0 \pi^- \ell^+ \nu_\ell$ anything	$(1.07 \pm 0.27) \%$	-
$\bar{D}^0 \pi^+ \ell^+ \nu_\ell$ anything	$(2.3 \pm 1.6) \times 10^{-3}$	-
$D^{*-} \ell^+ \nu_\ell$ anything	[nnn] $(2.75 \pm 0.19) \%$	-
$D^{*-} \pi^- \ell^+ \nu_\ell$ anything	$(6 \pm 7) \times 10^{-4}$	-
$D^{*-} \pi^+ \ell^+ \nu_\ell$ anything	$(4.8 \pm 1.0) \times 10^{-3}$	-
$\bar{D}_j^0 \ell^+ \nu_\ell$ anything \times	[nnn,ffff] $(2.6 \pm 0.9) \times 10^{-3}$	-
$B(\bar{D}_j^0 \rightarrow D^{*+} \pi^-)$		
$D_j^- \ell^+ \nu_\ell$ anything \times	[nnn,ffff] $(7.0 \pm 2.3) \times 10^{-3}$	-
$B(D_j^- \rightarrow D^0 \pi^-)$		
$\bar{D}_2^*(2460)^0 \ell^+ \nu_\ell$ anything	$< 1.4 \times 10^{-3}$	CL=90% -
$\times B(\bar{D}_2^*(2460)^0 \rightarrow D^{*-} \pi^+)$		
$D_2^*(2460)^- \ell^+ \nu_\ell$ anything	$(4.2 \pm 1.5) \times 10^{-3}$	-
$\times B(D_2^*(2460)^- \rightarrow D^0 \pi^-)$		
$\bar{D}_2^*(2460)^0 \ell^+ \nu_\ell$ anything	$(1.6 \pm 0.8) \times 10^{-3}$	-
$\times B(\bar{D}_2^*(2460)^0 \rightarrow D^- \pi^+)$		
charmless $\ell \bar{\nu}_\ell$	[nnn] $(1.7 \pm 0.5) \times 10^{-3}$	-
$\tau^+ \nu_\tau$ anything	$(2.41 \pm 0.23) \%$	-
$D^{*-} \tau \nu_\tau$ anything	$(9 \pm 4) \times 10^{-3}$	-
$\bar{c} \rightarrow \ell^- \bar{\nu}_\ell$ anything	[nnn] $(8.02 \pm 0.19) \%$	-
$c \rightarrow \ell^+ \nu$ anything	$(1.6 \pm 0.4) \%$	-

Charmed meson and baryon modes

\bar{D}^0 anything	$(59.6 \pm 2.9) \%$	-
$D^0 D_s^\pm$ anything	[ee] $(9.1 \pm 4.0) \%$	-
$D^\mp D_s^\pm$ anything	[ee] $(4.0 \pm 2.3) \%$	-
$\bar{D}^0 D^0$ anything	[ee] $(5.1 \pm 2.0) \%$	-
$D^0 D^\pm$ anything	[ee] $(2.7 \pm 1.8) \%$	-
$D^\pm D^\mp$ anything	[ee] $< 9 \times 10^{-3}$	CL=90% -
D^- anything	$(22.7 \pm 1.8) \%$	-
$D^*(2010)^+$ anything	$(17.3 \pm 2.0) \%$	-
$D_1(2420)^0$ anything	$(5.0 \pm 1.5) \%$	-
$D^*(2010)^\mp D_s^\pm$ anything	[ee] $(3.3 \pm 1.6) \%$	-
$D^0 D^*(2010)^\pm$ anything	[ee] $(3.0 \pm 1.1) \%$	-
$D^*(2010)^\pm D^\mp$ anything	[ee] $(2.5 \pm 1.2) \%$	-
$D^*(2010)^\pm D^*(2010)^\mp$ anything	[ee] $(1.2 \pm 0.4) \%$	-
$\bar{D} D$ anything	$(10 \pm 11) \%$	-
$D_2^*(2460)^0$ anything	$(4.7 \pm 2.7) \%$	-
D_s^- anything	$(14.7 \pm 2.1) \%$	-
D_s^+ anything	$(10.1 \pm 3.1) \%$	-
Λ_c^+ anything	$(9.7 \pm 2.9) \%$	-
\bar{c}/c anything	[eeee] $(116.2 \pm 3.2) \%$	-

Charmonium modes

$J/\psi(1S)$ anything	$(1.16 \pm 0.10) \%$	-
$\psi(2S)$ anything	$(4.8 \pm 2.4) \times 10^{-3}$	-
$\chi_{c1}(1P)$ anything	$(1.4 \pm 0.4) \%$	-

Meson Summary Table

K or K* modes		
$\bar{3}\gamma$	$(3.1 \pm 1.1) \times 10^{-4}$	-
$\bar{3}\bar{p}\nu$	$< 6.4 \times 10^{-4}$ CL=90%	-
K^\pm anything	$(74 \pm 6) \%$	-
K_S^0 anything	$(29.0 \pm 2.9) \%$	-
Pion modes		
π^\pm anything	$(397 \pm 21) \%$	-
π^0 anything	[eeee] $(278 \pm 60) \%$	-
ϕ anything	$(2.82 \pm 0.23) \%$	-
Baryon modes		
p/\bar{p} anything	$(13.1 \pm 1.1) \%$	-
Other modes		
charged anything	[eeee] $(497 \pm 7) \%$	-
hadron ⁺ hadron ⁻	$(1.7 \pm \frac{1.0}{0.7}) \times 10^{-5}$	-
charmless	$(7 \pm 21) \times 10^{-3}$	-
Baryon modes		
$\Lambda/\bar{\Lambda}$ anything	$(5.9 \pm 0.6) \%$	-
b-baryon anything	$(10.2 \pm 2.8) \%$	-
$\Delta B = 1$ weak neutral current (B1) modes		
$\mu^+ \mu^-$ anything	B1 $< 3.2 \times 10^{-4}$ CL=90%	-

B*		$I(J^P) = \frac{1}{2}(1^-)$
<i>I, J, P</i> need confirmation. Quantum numbers shown are quark-model predictions.		
Mass $m_{B^*} = 5325.1 \pm 0.5$ MeV		
$m_{B^*} - m_B = 45.78 \pm 0.35$ MeV		
B* DECAY MODES	Fraction (Γ_i/Γ)	ρ (MeV/c)
$B\gamma$	dominant	45

B₁(5721)⁰		$I(J^P) = \frac{1}{2}(1^+)$
<i>I, J, P</i> need confirmation.		
$B_1(5721)^0$ MASS = 5723.4 ± 2.0 MeV (<i>S</i> = 1.1)		
$m_{B_1^0} - m_{B^+} = 444.3 \pm 2.0$ MeV (<i>S</i> = 1.1)		
B ₁ (5721) ⁰ DECAY MODES	Fraction (Γ_i/Γ)	ρ (MeV/c)
$B^{*+} \pi^-$	dominant	-

B₂[*](5747)⁰		$I(J^P) = \frac{1}{2}(2^+)$
<i>I, J, P</i> need confirmation.		
$B_2^*(5747)^0$ MASS = 5743 ± 5 MeV (<i>S</i> = 2.8)		
Full width $\Gamma = 23_{-11}^{+5}$ MeV		
$m_{B_2^0} - m_{B_1^0} = 19 \pm 6$ MeV (<i>S</i> = 3.0)		
B ₂ [*] (5747) ⁰ DECAY MODES	Fraction (Γ_i/Γ)	ρ (MeV/c)
$B^+ \pi^-$	dominant	424
$B^{*+} \pi^-$	dominant	-

BOTTOM, STRANGE MESONS (*B* = ±1, *S* = ∓1)

$$B_S^0 = s\bar{b}, \bar{B}_S^0 = \bar{s}b, \text{ similarly for } B_S^{*0}$$

B_S⁰		$I(J^P) = 0(0^-)$
<i>I, J, P</i> need confirmation. Quantum numbers shown are quark-model predictions.		
Mass $m_{B_S^0} = 5366.3 \pm 0.6$ MeV (<i>S</i> = 1.1)		
Mean life $\tau = (1.472_{-0.026}^{+0.024}) \times 10^{-12}$ s		
$c\tau = 441 \mu\text{m}$		
$\Delta\Gamma_{B_S^0} = \Gamma_{B_S^0} - \Gamma_{B_S^0} = (0.062_{-0.037}^{+0.034}) \times 10^{12} \text{ s}^{-1}$		
$= 18.6_{-11.1}^{+10.2} \mu\text{m}$		

B_S⁰- \bar{B}_S^0 mixing parameters

$$\Delta m_{B_S^0} = m_{B_S^0} - m_{\bar{B}_S^0} = (17.77 \pm 0.12) \times 10^{12} \hbar \text{ s}^{-1}$$

$$= (117.0 \pm 0.8) \times 10^{-10} \text{ MeV}$$

$$x_s = \Delta m_{B_S^0} / \Gamma_{B_S^0} = 26.2 \pm 0.5$$

$$\chi_s = 0.49927 \pm 0.00003$$

CP violation parameters in B_S⁰

$$\text{Re}(\epsilon_{B_S^0}) / (1 + |\epsilon_{B_S^0}|^2) = (-0.9 \pm 2.6) \times 10^{-3}$$

$$\text{CP Violation phase } \beta_s = 0.47_{-0.21}^{+0.13} \text{ or } 1.09_{-0.13}^{+0.21}$$

These branching fractions all scale with $B(\bar{B} \rightarrow B_S^0)$, the LEP B_S^0 production fraction. The first four were evaluated using $B(\bar{B} \rightarrow B_S^0) = (10.7 \pm 1.2)\%$ and the rest assume $B(\bar{B} \rightarrow B_S^0) = 12\%$.

The branching fraction $B(B_S^0 \rightarrow D_S^- \ell^+ \nu_\ell \text{ anything})$ is not a pure measurement since the measured product branching fraction $B(\bar{B} \rightarrow B_S^0) \times B(B_S^0 \rightarrow D_S^- \ell^+ \nu_\ell \text{ anything})$ was used to determine $B(\bar{B} \rightarrow B_S^0)$, as described in the note on " B^0 - \bar{B}^0 Mixing"

For inclusive branching fractions, e.g., $B \rightarrow D^\pm \text{ anything}$, the values usually are multiplicities, not branching fractions. They can be greater than one.

B _S ⁰ DECAY MODES	Fraction (Γ_i/Γ)	Confidence level	ρ (MeV/c)
D_S^- anything	(93 ± 25) %	-	-
$D_S^- \ell^+ \nu_\ell \text{ anything}$	[gggg] (7.9 ± 2.4) %	-	-
$D_{S1}(2536)^- \mu^+ \nu_\mu X \times B(D_{S1}^- \rightarrow D^{*-} K_S^0)$	(2.4 ± 0.7) × 10 ⁻³	-	-
$D_S^- \pi^+$	(3.2 ± 0.5) × 10 ⁻³		2320
$D_S^- \pi^+ \pi^+ \pi^-$	(8.4 ± 3.3) × 10 ⁻³		2301
$D_S^\mp K^\pm$	(3.0 ± 0.7) × 10 ⁻⁴		2292
$D_S^+ D_S^-$	(1.04 ± 0.35) %		1823
$D_S^{*+} D_S^-$	< 12.1 %	90%	1742
$D_S^{*+} D_S^{*-}$	< 25.7 %	90%	1655
$D_S^{(*)+} D_S^{(*)-}$	(4.0 ± 1.5) %		-
$J/\psi(1S) \phi$	(1.3 ± 0.4) × 10 ⁻³		1587
$J/\psi(1S) \pi^0$	< 1.2 × 10 ⁻³	90%	1786
$J/\psi(1S) \eta$	< 3.8 × 10 ⁻³	90%	1733
$\psi(2S) \phi$	(6.8 ± 2.7) × 10 ⁻⁴		1119
$\pi^+ \pi^-$	< 1.2 × 10 ⁻⁶	90%	2680
$\pi^0 \pi^0$	< 2.1 × 10 ⁻⁴	90%	2680
$\eta \pi^0$	< 1.0 × 10 ⁻³	90%	2653
$\eta \eta$	< 1.5 × 10 ⁻³	90%	2627
$\rho^0 \rho^0$	< 3.20 × 10 ⁻⁴	90%	2569
$\phi \rho^0$	< 6.17 × 10 ⁻⁴	90%	2526
$\phi \phi$	(1.4 ± 0.8) × 10 ⁻⁵		2482
$\pi^+ K^-$	(4.9 ± 1.0) × 10 ⁻⁶		2659
$K^+ K^-$	(3.3 ± 0.9) × 10 ⁻⁵		2637
$\bar{K}^*(892)^0 \rho^0$	< 7.67 × 10 ⁻⁴	90%	2550
$\bar{K}^*(892)^0 K^*(892)^0$	< 1.681 × 10 ⁻³	90%	2531
$\phi K^*(892)^0$	< 1.013 × 10 ⁻³	90%	2507
$p\bar{p}$	< 5.9 × 10 ⁻⁵	90%	2514
$\gamma\gamma$	B1 < 8.7 × 10 ⁻⁶	90%	2683
$\phi\gamma$	(5.7 ± 2.2) × 10 ⁻⁵		2586

Lepton Family number (LF) violating modes or $\Delta B = 1$ weak neutral current (B1) modes

$\mu^+ \mu^-$	B1	< 4.7	× 10 ⁻⁸	90%	2681
$e^+ e^-$	B1	< 2.8	× 10 ⁻⁷	90%	2683
$e^\pm \mu^\mp$	LF [ee]	< 2.0	× 10 ⁻⁷	90%	2682
$\phi(1020) \mu^+ \mu^-$	B1	< 3.2	× 10 ⁻⁶	90%	2582
$\phi\nu\bar{\nu}$	B1	< 5.4	× 10 ⁻³	90%	2586

B_S[*]		$I(J^P) = 0(1^-)$
<i>I, J, P</i> need confirmation. Quantum numbers shown are quark-model predictions.		
Mass $m = 5415.4 \pm 1.4$ MeV (<i>S</i> = 2.5)		
$m_{B_S^*} - m_{B_S} = 49.0 \pm 1.5$ MeV (<i>S</i> = 2.0)		

Meson Summary Table

B_s^* DECAY MODES	Fraction (Γ_i/Γ)	ρ (MeV/c)
$B_s \gamma$	dominant	–

$B_{s1}(5830)^0$ $I(J^P) = \frac{1}{2}(1^+)$
I, J, P need confirmation.

Mass $m = 5829.4 \pm 0.7$ MeV

$m_{B_{s1}^0} - m_{B^{*+}} = 504.41 \pm 0.25$ MeV

$B_{s1}(5830)^0$ DECAY MODES	Fraction (Γ_i/Γ)	ρ (MeV/c)
$B^{*+} K^-$	dominant	–

$B_{s2}^*(5840)^0$ $I(J^P) = \frac{1}{2}(2^+)$
I, J, P need confirmation.

Mass $m = 5839.7 \pm 0.6$ MeV

$m_{B_{s2}^0} - m_{B_{s1}^0} = 10.5 \pm 0.6$ MeV

$B_{s2}^*(5840)^0$ DECAY MODES	Fraction (Γ_i/Γ)	ρ (MeV/c)
$B^+ K^-$	dominant	252

BOTTOM, CHARMED MESONS ($B = C = \pm 1$)

$B_c^+ = c\bar{b}, B_c^- = \bar{c}b$, similarly for $B_c^{* \pm}$'s

B_c^\pm $I(J^P) = 0(0^-)$
I, J, P need confirmation.

Quantum numbers shown are quark-model predictions.

Mass $m = 6.277 \pm 0.006$ GeV ($S = 1.6$)

Mean life $\tau = (0.453 \pm 0.041) \times 10^{-12}$ s

B_c^- modes are charge conjugates of the modes below.

B_c^\pm DECAY MODES $\times B(\bar{b} \rightarrow B_c)$	Fraction (Γ_i/Γ)	Confidence level	ρ (MeV/c)
---	--------------------------------	------------------	----------------

The following quantities are not pure branching ratios; rather the fraction $\Gamma_i/\Gamma \times B(\bar{b} \rightarrow B_c)$.

$J/\psi(1S) \ell^+ \nu_\ell \text{ anything}$	$(5.2^{+2.4}_{-2.1}) \times 10^{-5}$	–	
$J/\psi(1S) \pi^+$	$< 8.2 \times 10^{-5}$	90%	2372
$J/\psi(1S) \pi^+ \pi^+ \pi^-$	$< 5.7 \times 10^{-4}$	90%	2352
$J/\psi(1S) a_1(1260)$	$< 1.2 \times 10^{-3}$	90%	2171
$D^*(2010)^+ \bar{D}^0$	$< 6.2 \times 10^{-3}$	90%	2468

$c\bar{c}$ MESONS

$\eta_c(1S)$ $I^G(J^{PC}) = 0^+(0^{-+})$

Mass $m = 2980.3 \pm 1.2$ MeV ($S = 1.6$)

Full width $\Gamma = 28.6 \pm 2.2$ MeV ($S = 2.0$)

$\eta_c(1S)$ DECAY MODES	Fraction (Γ_i/Γ)	Confidence level	ρ (MeV/c)
--------------------------	--------------------------------	------------------	----------------

Decays involving hadronic resonances

$\eta'(958) \pi \pi$	$(4.1 \pm 1.7) \%$		1321
$\rho \rho$	$(2.0 \pm 0.7) \%$		1272
$K^*(892)^0 K^- \pi^+ + \text{c.c.}$	$(2.0 \pm 0.7) \%$		1276
$K^*(892) \bar{K}^*(892)$	$(9.2 \pm 3.4) \times 10^{-3}$		1194
$K^{*0} \bar{K}^{*0} \pi^+ \pi^-$	$(1.1 \pm 0.5) \%$		1071
$\phi K^+ K^-$	$(2.9 \pm 1.4) \times 10^{-3}$		1102
$\phi \phi$	$(2.7 \pm 0.9) \times 10^{-3}$		1087
$\phi 2(\pi^+ \pi^-)$	$< 3.5 \times 10^{-3}$	90%	1249
$a_0(980) \pi$	$< 2 \%$	90%	1325

$a_2(1320) \pi$	$< 2 \%$		90%	1194
$K^*(892) \bar{K} + \text{c.c.}$	$< 1.28 \%$		90%	1308
$f_2(1270) \eta$	$< 1.1 \%$		90%	1143
$\omega \omega$	$< 3.1 \times 10^{-3}$		90%	1268
$\omega \phi$	$< 1.7 \times 10^{-3}$		90%	1183
$f_2(1270) f_2(1270)$	$(7.6 \pm 3.0_{3.4}) \times 10^{-3}$			771
$f_2(1270) f_2'(1525)$	$(2.7 \pm 1.5) \%$			509

Decays into stable hadrons

$K \bar{K} \pi$	$(7.0 \pm 1.2) \%$			1379
$\eta \pi \pi$	$(4.9 \pm 1.8) \%$			1427
$\pi^+ \pi^- K^+ K^-$	$(1.5 \pm 0.6) \%$			1343
$K^+ K^- 2(\pi^+ \pi^-)$	$(7.1 \pm 2.9) \times 10^{-3}$			1252
$2(K^+ K^-)$	$(1.6 \pm 0.7) \times 10^{-3}$			1053
$2(\pi^+ \pi^-)$	$(1.20 \pm 0.30) \%$			1457
$3(\pi^+ \pi^-)$	$(1.5 \pm 0.5) \%$			1405
$\rho \bar{\rho}$	$(1.3 \pm 0.4) \times 10^{-3}$			1158
$\Lambda \bar{\Lambda}$	$(1.04 \pm 0.31) \times 10^{-3}$			988
$K \bar{K} \eta$	$< 3.1 \%$		90%	1263
$\pi^+ \pi^- \rho \bar{\rho}$	$< 1.2 \%$		90%	1024

Radiative decays

$\gamma \gamma$	$(6.3 \pm 2.9) \times 10^{-5}$			1490
-----------------	--------------------------------	--	--	------

Charge conjugation (C), Parity (P), Lepton family number (LF) violating modes

$\pi^+ \pi^-$	$P, CP < 6 \times 10^{-4}$	90%	1484
$\pi^0 \pi^0$	$P, CP < 4 \times 10^{-4}$	90%	1484
$K^+ K^-$	$P, CP < 6 \times 10^{-4}$	90%	1406
$K_S^0 K_S^0$	$P, CP < 3.1 \times 10^{-4}$	90%	1405

$J/\psi(1S)$

$I^G(J^{PC}) = 0^-(1^{--})$

Mass $m = 3096.916 \pm 0.011$ MeV

Full width $\Gamma = 92.9 \pm 2.8$ keV ($S = 1.1$)

$\Gamma_{ee} = 5.55 \pm 0.14 \pm 0.02$ keV

$J/\psi(1S)$ DECAY MODES	Fraction (Γ_i/Γ)	Scale factor/ Confidence level	ρ (MeV/c)
hadrons	$(87.7 \pm 0.5) \%$		–
virtual $\gamma \rightarrow$ hadrons	$(13.50 \pm 0.30) \%$		–
$g g g$	$(64.1 \pm 1.0) \%$		–
$\gamma g g$	$(8.8 \pm 0.5) \%$		–
$e^+ e^-$	$(5.94 \pm 0.06) \%$		1548
$\mu^+ \mu^-$	$(5.93 \pm 0.06) \%$		1545

Decays involving hadronic resonances

$\rho \pi$	$(1.69 \pm 0.15) \%$	$S=2.4$	1448
$\rho^0 \pi^0$	$(5.6 \pm 0.7) \times 10^{-3}$		1448
$a_2(1320) \rho$	$(1.09 \pm 0.22) \%$		1123
$\omega \pi^+ \pi^+ \pi^- \pi^-$	$(8.5 \pm 3.4) \times 10^{-3}$		1392
$\omega \pi^+ \pi^- \pi^0$	$(4.0 \pm 0.7) \times 10^{-3}$		1418
$\omega \pi^+ \pi^-$	$(8.6 \pm 0.7) \times 10^{-3}$	$S=1.1$	1435
$\omega f_2(1270)$	$(4.3 \pm 0.6) \times 10^{-3}$		1142
$K^*(892)^0 \bar{K}_2^*(1430)^0 + \text{c.c.}$	$(6.0 \pm 0.6) \times 10^{-3}$		1012
$K^*(892)^0 \bar{K}_2^*(1770)^0 + \text{c.c.} \rightarrow$ $K^*(892)^0 K^- \pi^+ + \text{c.c.}$	$(6.9 \pm 0.9) \times 10^{-4}$		–
$\omega K^*(892) \bar{K} + \text{c.c.}$	$(6.1 \pm 0.9) \times 10^{-3}$		1097
$K^+ \bar{K}^*(892)^- + \text{c.c.}$	$(5.12 \pm 0.30) \times 10^{-3}$		1373
$K^+ \bar{K}^*(892)^- + \text{c.c.} \rightarrow$ $K^+ K^- \pi^0$	$(1.97 \pm 0.20) \times 10^{-3}$		–
$K^+ \bar{K}^*(892)^- + \text{c.c.} \rightarrow$ $K^+ K^- \pi^+ \pi^-$	$(3.0 \pm 0.4) \times 10^{-3}$		–
$K^0 \bar{K}^*(892)^0 + \text{c.c.}$	$(4.39 \pm 0.31) \times 10^{-3}$		1373
$K^0 \bar{K}^*(892)^0 + \text{c.c.} \rightarrow$ $K^0 K^+ \pi^-$	$(3.2 \pm 0.4) \times 10^{-3}$		–
$K_1(1400)^\pm K^\mp$	$(3.8 \pm 1.4) \times 10^{-3}$		1170
$\bar{K}^*(892)^0 K^+ \pi^- + \text{c.c.}$	seen		1343
$\omega \pi^0 \pi^0$	$(3.4 \pm 0.8) \times 10^{-3}$		1436
$b_1(1235)^\pm \pi^\mp$	[ee] $(3.0 \pm 0.5) \times 10^{-3}$		1300
$\omega K^\pm K_S^0 \pi^\mp$	[ee] $(3.4 \pm 0.5) \times 10^{-3}$		1210
$b_1(1235)^0 \pi^0$	$(2.3 \pm 0.6) \times 10^{-3}$		1300
$\eta K^\pm K_S^0 \pi^\mp$	[ee] $(2.2 \pm 0.4) \times 10^{-3}$		1278
$\phi K^*(892) \bar{K} + \text{c.c.}$	$(2.18 \pm 0.23) \times 10^{-3}$		969
$\omega K \bar{K}$	$(1.6 \pm 0.5) \times 10^{-4}$		1268
$\omega f_0(1710) \rightarrow \omega K \bar{K}$	$(4.8 \pm 1.1) \times 10^{-4}$		878
$\phi 2(\pi^+ \pi^-)$	$(1.66 \pm 0.23) \times 10^{-3}$		1318
$\Delta(1232)^{++} \bar{p} \pi^-$	$(1.6 \pm 0.5) \times 10^{-3}$		1030
$\omega \eta$	$(1.74 \pm 0.20) \times 10^{-3}$	$S=1.6$	1394

Meson Summary Table

Weak decays				
$D^- e^+ \nu_e + c.c.$	< 1.2	$\times 10^{-5}$	CL=90%	984
$\overline{D}^0 e^+ e^- + c.c.$	< 1.1	$\times 10^{-5}$	CL=90%	987
$D_s^- e^+ \nu_e + c.c.$	< 3.6	$\times 10^{-5}$	CL=90%	923
$D^- \pi^+ + c.c.$	< 7.5	$\times 10^{-5}$	CL=90%	977
$\overline{D}^0 \overline{K}^0 + c.c.$	< 1.7	$\times 10^{-4}$	CL=90%	898
$D_s^- \pi^+ + c.c.$	< 1.3	$\times 10^{-4}$	CL=90%	915
Charge conjugation (C), Parity (P), Lepton Family number (LF) violating modes				
$\gamma\gamma$	C	< 5	$\times 10^{-6}$	CL=90% 1548
$e^\pm \mu^\mp$	LF	< 1.1	$\times 10^{-6}$	CL=90% 1547
$e^\pm \tau^\mp$	LF	< 8.3	$\times 10^{-6}$	CL=90% 1039
$\mu^\pm \tau^\mp$	LF	< 2.0	$\times 10^{-6}$	CL=90% 1035
Other decays				
invisible	< 7	$\times 10^{-4}$	CL=90%	-

 $\chi_{c0}(1P)$

$$J^{PC} = 0^+(0^{++})$$

Mass $m = 3414.75 \pm 0.31$ MeVFull width $\Gamma = 10.3 \pm 0.6$ MeV

$\chi_{c0}(1P)$ DECAY MODES	Fraction (Γ_i/Γ)	Scale factor/ Confidence level	ρ (MeV/c)
-----------------------------	--------------------------------	-----------------------------------	-------------------

Hadronic decays

$2(\pi^+ \pi^-)$	(2.27±0.19) %		1679
$\rho^0 \pi^+ \pi^-$	(8.9 ± 2.8) $\times 10^{-3}$		1607
$f_0(980) f_0(980)$	(6.8 ± 2.2) $\times 10^{-4}$		1398
$\pi^+ \pi^- \pi^0 \pi^0$	(3.4 ± 0.4) %		1680
$\rho^+ \pi^- \pi^0 + c.c.$	(2.9 ± 0.4) %		1607
$\pi^+ \pi^- K^+ K^-$	(1.80±0.15) %		1580
$K_0^*(1430)^0 \overline{K}_0^*(1430)^0 \rightarrow \pi^+ \pi^- K^+ K^-$	(1.00 $^{+0.40}_{-0.29}$) $\times 10^{-3}$		-
$K_0^*(1430)^0 \overline{K}_2^*(1430)^0 + c.c. \rightarrow \pi^+ \pi^- K^+ K^-$	(8.1 $^{+2.0}_{-2.5}$) $\times 10^{-4}$		-
$K_1(1270)^+ K^- + c.c. \rightarrow \pi^+ \pi^- K^+ K^-$	(6.4 ± 1.9) $\times 10^{-3}$		-
$K_1(1400)^+ K^- + c.c. \rightarrow \pi^+ \pi^- K^+ K^-$	< 2.7 $\times 10^{-3}$	CL=90%	-
$f_0(980) f_0(980)$	(1.7 $^{+1.1}_{-0.9}$) $\times 10^{-4}$		1398
$f_0(980) f_0(2200)$	(8.1 $^{+2.1}_{-2.6}$) $\times 10^{-4}$		595
$f_0(1370) f_0(1370)$	< 2.8 $\times 10^{-4}$	CL=90%	1019
$f_0(1370) f_0(1500)$	< 1.7 $\times 10^{-4}$	CL=90%	920
$f_0(1370) f_0(1710)$	(6.8 $^{+4.0}_{-2.4}$) $\times 10^{-4}$		723
$f_0(1500) f_0(1370)$	< 1.3 $\times 10^{-4}$	CL=90%	920
$f_0(1500) f_0(1500)$	< 5 $\times 10^{-5}$	CL=90%	805
$f_0(1500) f_0(1710)$	< 7 $\times 10^{-5}$	CL=90%	559
$K^+ K^- \pi^0 \pi^0$	(5.7 ± 0.9) $\times 10^{-3}$		1582
$K^+ \pi^- K^0 \pi^0 + c.c.$	(2.53±0.34) %		1581
$\rho^+ K^- K^0 + c.c.$	(1.23±0.22) %		1458
$K^*(892)^- K^+ \pi^0 \rightarrow K^+ \pi^- K^0 \pi^0 + c.c.$	(4.7 ± 1.2) $\times 10^{-3}$		-
$K_S^0 K_S^0 \pi^+ \pi^-$	(5.8 ± 1.1) $\times 10^{-3}$		1579
$K^+ K^- \eta \pi^0$	(3.1 ± 0.7) $\times 10^{-3}$		1468
$3(\pi^+ \pi^-)$	(1.20±0.18) %		1633
$K^+ \overline{K}^*(892)^0 \pi^- + c.c.$	(7.3 ± 1.6) $\times 10^{-3}$		1523
$K^*(892)^0 \overline{K}^*(892)^0$	(1.7 ± 0.6) $\times 10^{-3}$		1456
$\pi \pi$	(8.4 ± 0.4) $\times 10^{-3}$		1702
$\pi^0 \eta$	< 1.8 $\times 10^{-4}$		1661
$\pi^0 \eta'$	< 1.1 $\times 10^{-3}$		1570
$\eta \eta$	(2.68±0.28) $\times 10^{-3}$		1617
$\eta \eta'$	< 2.4 $\times 10^{-4}$	CL=90%	1521
$\eta' \eta'$	(2.03±0.22) $\times 10^{-3}$		1413
$\omega \omega$	(2.2 ± 0.7) $\times 10^{-3}$		1517
$K^+ K^-$	(6.10±0.35) $\times 10^{-3}$		1634
$K_S^0 K_S^0$	(3.16±0.18) $\times 10^{-3}$		1633
$\pi^+ \pi^- \eta$	< 2.0 $\times 10^{-4}$	CL=90%	1651
$\pi^+ \pi^- \eta'$	< 4 $\times 10^{-4}$	CL=90%	1560
$\overline{K}^0 K^+ \pi^- + c.c.$	< 1.0 $\times 10^{-4}$	CL=90%	1610
$K^+ K^- \pi^0$	< 6 $\times 10^{-5}$	CL=90%	1611
$K^+ K^- \eta$	< 2.3 $\times 10^{-4}$	CL=90%	1512
$K^+ K^- K_S^0 K_S^0$	(1.4 ± 0.5) $\times 10^{-3}$		1331
$K^+ K^- K^+ K^-$	(2.81±0.30) $\times 10^{-3}$		1333
$K^+ K^- \phi$	(9.9 ± 2.5) $\times 10^{-4}$		1381

$\phi \phi$	(9.2 ± 1.9) $\times 10^{-4}$		1370
$p \overline{p}$	(2.28±0.13) $\times 10^{-4}$		1426
$p \overline{p} \pi^0$	(5.7 ± 1.2) $\times 10^{-4}$		1379
$p \overline{p} \eta$	(3.7 ± 1.1) $\times 10^{-4}$		1187
$\pi^+ \pi^- p \overline{p}$	(2.1 ± 0.7) $\times 10^{-3}$	S=1.4	1320
$\pi^0 \pi^0 p \overline{p}$	(1.05±0.28) $\times 10^{-3}$		1324
$K_S^0 K_S^0 p \overline{p}$	< 8.8 $\times 10^{-4}$	CL=90%	884
$p \overline{p} \pi^-$	(1.14±0.31) $\times 10^{-3}$		1376
$\Lambda \overline{\Lambda}$	(3.3 ± 0.4) $\times 10^{-4}$		1292
$\Lambda \overline{\Lambda} \pi^+ \pi^-$	< 4.0 $\times 10^{-3}$	CL=90%	1153
$K^+ \overline{p} \Lambda + c.c.$	(1.03±0.20) $\times 10^{-3}$		1132
$\Sigma^0 \overline{\Sigma}^0$	(4.2 ± 0.7) $\times 10^{-4}$		1222
$\Sigma^+ \overline{\Sigma}^-$	(3.1 ± 0.7) $\times 10^{-4}$		1225
$\Xi^0 \overline{\Xi}^0$	(3.2 ± 0.8) $\times 10^{-4}$		1089
$\Xi^- \overline{\Xi}^+$	(4.9 ± 0.7) $\times 10^{-4}$		1081

Radiative decays

$\gamma J/\psi(1S)$	(1.16±0.08) %		303
$\gamma \rho^0$	< 9 $\times 10^{-6}$	CL=90%	1619
$\gamma \omega$	< 8 $\times 10^{-6}$	CL=90%	1618
$\gamma \phi$	< 6 $\times 10^{-6}$	CL=90%	1555
$\gamma \gamma$	(2.22±0.17) $\times 10^{-4}$		1707

 $\chi_{c1}(1P)$

$$J^{PC} = 0^+(1^{++})$$

Mass $m = 3510.66 \pm 0.07$ MeV (S = 1.5)Full width $\Gamma = 0.86 \pm 0.05$ MeV

$\chi_{c1}(1P)$ DECAY MODES	Fraction (Γ_i/Γ)	Scale factor/ Confidence level	ρ (MeV/c)
-----------------------------	--------------------------------	-----------------------------------	-------------------

Hadronic decays

$3(\pi^+ \pi^-)$	(5.8 ± 1.4) $\times 10^{-3}$	S=1.2	1683
$2(\pi^+ \pi^-)$	(7.6 ± 2.6) $\times 10^{-3}$		1728
$\pi^+ \pi^- \pi^0 \pi^0$	(1.26±0.17) %		1729
$\rho^+ \pi^- \pi^0 + c.c.$	(1.53±0.26) %		1658
$\rho^0 \pi^+ \pi^-$	(3.9 ± 3.5) $\times 10^{-3}$		1657
$\pi^+ \pi^- K^+ K^-$	(4.5 ± 1.0) $\times 10^{-3}$		1632
$K^+ K^- \pi^0 \pi^0$	(1.18±0.29) $\times 10^{-3}$		1634
$K^+ \pi^- K^0 \pi^0 + c.c.$	(9.0 ± 1.5) $\times 10^{-3}$		1632
$\rho^+ K^- K^0 + c.c.$	(5.3 ± 1.3) $\times 10^{-3}$		1514
$K^*(892)^0 K^0 \pi^0 \rightarrow K^+ \pi^- K^0 \pi^0 + c.c.$	(2.5 ± 0.7) $\times 10^{-3}$		-
$K^+ K^- \eta \pi^0$	(1.2 ± 0.4) $\times 10^{-3}$		1523
$\pi^+ \pi^- K_S^0 K_S^0$	(7.2 ± 3.1) $\times 10^{-4}$		1630
$K^+ K^- \eta$	(3.3 ± 1.0) $\times 10^{-4}$		1566
$K^0 K^+ \pi^- + c.c.$	(7.3 ± 0.6) $\times 10^{-3}$		1661
$K^*(892)^0 \overline{K}^0 + c.c.$	(1.0 ± 0.4) $\times 10^{-3}$		1602
$K^*(892)^+ K^- + c.c.$	(1.5 ± 0.7) $\times 10^{-3}$		1602
$K_S^*(1430)^0 \overline{K}^0 + c.c. \rightarrow K_S^0 K^+ \pi^- + c.c.$	< 8 $\times 10^{-4}$	CL=90%	-
$K_S^*(1430)^+ K^- + c.c. \rightarrow K_S^0 K^+ \pi^- + c.c.$	< 2.3 $\times 10^{-3}$	CL=90%	-
$K^+ K^- \pi^0$	(1.91±0.26) $\times 10^{-3}$		1662
$\eta \pi^+ \pi^-$	(5.0 ± 0.5) $\times 10^{-3}$		1701
$a_0(980)^+ \pi^- + c.c. \rightarrow \eta \pi^+ \pi^-$	(1.9 ± 0.7) $\times 10^{-3}$		-
$f_2(1270) \eta$	(2.8 ± 0.8) $\times 10^{-3}$		1468
$\pi^+ \pi^- \eta'$	(2.4 ± 0.5) $\times 10^{-3}$		1612
$K^+ \overline{K}^*(892)^0 \pi^- + c.c.$	(3.2 ± 2.1) $\times 10^{-3}$		1577
$K^*(892)^0 \overline{K}^*(892)^0$	(1.5 ± 0.4) $\times 10^{-3}$		1512
$K^+ K^- K_S^0 K_S^0$	< 5 $\times 10^{-4}$	CL=90%	1390
$K^+ K^- K^+ K^-$	(5.6 ± 1.2) $\times 10^{-4}$		1393
$K^+ K^- \phi$	(4.3 ± 1.6) $\times 10^{-4}$		1440
$p \overline{p}$	(7.3 ± 0.4) $\times 10^{-5}$		1484
$p \overline{p} \pi^0$	(1.2 ± 0.5) $\times 10^{-4}$		1438
$p \overline{p} \eta$	< 1.6 $\times 10^{-4}$	CL=90%	1254
$\pi^+ \pi^- p \overline{p}$	(5.0 ± 1.9) $\times 10^{-4}$		1381
$K_S^0 K_S^0 p \overline{p}$	< 4.5 $\times 10^{-4}$	CL=90%	968
$\Lambda \overline{\Lambda}$	(1.18±0.19) $\times 10^{-4}$		1355
$\Lambda \overline{\Lambda} \pi^+ \pi^-$	< 1.5 $\times 10^{-3}$	CL=90%	1223
$K^+ \overline{p} \Lambda$	(3.2 ± 1.0) $\times 10^{-4}$		1203
$\Sigma^0 \overline{\Sigma}^0$	< 4 $\times 10^{-5}$	CL=90%	1288
$\Sigma^+ \overline{\Sigma}^-$	< 6 $\times 10^{-5}$	CL=90%	1291
$\Xi^0 \overline{\Xi}^0$	< 6 $\times 10^{-5}$	CL=90%	1163
$\Xi^- \overline{\Xi}^+$	(8.4 ± 2.3) $\times 10^{-5}$		1155
$\pi^+ \pi^- + K^+ K^-$	< 2.1 $\times 10^{-3}$		-
$K_S^0 K_S^0$	< 6 $\times 10^{-5}$	CL=90%	1683

Meson Summary Table

Radiative decays			
$\gamma J/\psi(1S)$	$(34.4 \pm 1.5) \%$		389
$\gamma \rho^0$	$(2.29 \pm 0.27) \times 10^{-4}$		1670
$\gamma \omega$	$(7.8 \pm 1.8) \times 10^{-5}$		1668
$\gamma \phi$	$< 2.4 \times 10^{-5}$	CL=90%	1607

 $h_c(1P)$

$$I^G(J^{PC}) = ?^?(1^{+-})$$

Mass $m = 3525.42 \pm 0.29$ MeV ($S = 1.7$)
 Full width $\Gamma < 1$ MeV

$h_c(1P)$ DECAY MODES	Fraction (Γ_i/Γ)	ρ (MeV/c)
$J/\psi(1S)\pi\pi$	not seen	312
$\eta_c\gamma$	seen	503
$\pi^+\pi^-\pi^0$	not seen	1749
$2\pi^+2\pi^-\pi^0$	seen	1716
$3\pi^+3\pi^-\pi^0$	not seen	1661

 $\chi_{c2}(1P)$

$$I^G(J^{PC}) = 0^+(2^{++})$$

Mass $m = 3556.20 \pm 0.09$ MeV
 Full width $\Gamma = 1.97 \pm 0.11$ MeV

$\chi_{c2}(1P)$ DECAY MODES	Fraction (Γ_i/Γ)	Confidence level	ρ (MeV/c)
Hadronic decays			
$2(\pi^+\pi^-)$	$(1.11 \pm 0.11) \%$		1751
$\pi^+\pi^-\pi^0\pi^0$	$(2.00 \pm 0.26) \%$		1752
$\rho^+\pi^-\pi^0 + c.c.$	$(2.4 \pm 0.4) \%$		1682
$K^+K^-\pi^0\pi^0$	$(2.2 \pm 0.4) \times 10^{-3}$		1658
$K^+\pi^-K^0\pi^0 + c.c.$	$(1.50 \pm 0.22) \%$		1657
$\rho^+K^-K^0 + c.c.$	$(4.5 \pm 1.4) \times 10^{-3}$		1540
$K^*(892)^0 K^+\pi^- \rightarrow$ $K^+\pi^-K^0\pi^0 + c.c.$	$(3.2 \pm 0.9) \times 10^{-3}$		-
$K^*(892)^0 K^0\pi^0 \rightarrow$ $K^+\pi^-K^0\pi^0 + c.c.$	$(4.2 \pm 0.9) \times 10^{-3}$		-
$K^*(892)^- K^+\pi^0 \rightarrow$ $K^+\pi^-K^0\pi^0 + c.c.$	$(4.1 \pm 0.9) \times 10^{-3}$		-
$K^*(892)^+ K^0\pi^- \rightarrow$ $K^+\pi^-K^0\pi^0 + c.c.$	$(3.2 \pm 0.9) \times 10^{-3}$		-
$K^+K^-\eta\pi^0$	$(1.4 \pm 0.5) \times 10^{-3}$		1549
$\pi^+\pi^-K^+K^-$	$(9.2 \pm 1.1) \times 10^{-3}$		1656
$K^+\bar{K}^*(892)^0\pi^-\pi^0 + c.c.$	$(2.3 \pm 1.2) \times 10^{-3}$		1602
$K^*(892)^0\bar{K}^*(892)^0$	$(2.5 \pm 0.5) \times 10^{-3}$		1538
$3(\pi^+\pi^-)$	$(8.6 \pm 1.8) \times 10^{-3}$		1707
$\phi\phi$	$(1.48 \pm 0.28) \times 10^{-3}$		1457
$\omega\omega$	$(1.9 \pm 0.6) \times 10^{-3}$		1597
$\pi\pi$	$(2.39 \pm 0.14) \times 10^{-3}$		1773
$\rho^0\pi^+\pi^-$	$(4.0 \pm 1.7) \times 10^{-3}$		1681
$\pi^+\pi^-\eta$	$(5.2 \pm 1.4) \times 10^{-4}$		1724
$\pi^+\pi^-\eta'$	$(5.4 \pm 2.0) \times 10^{-4}$		1636
$\eta\eta$	$(5.4 \pm 0.8) \times 10^{-4}$		1692
K^+K^-	$(1.09 \pm 0.08) \times 10^{-3}$		1708
$K_S^0 K_S^0$	$(5.8 \pm 0.5) \times 10^{-4}$		1707
$\bar{K}^0 K^+\pi^- + c.c.$	$(1.32 \pm 0.20) \times 10^{-3}$		1685
$K^+K^-\pi^0$	$(3.3 \pm 0.8) \times 10^{-4}$		1686
$K^+K^-\eta$	$< 3.5 \times 10^{-4}$	90%	1592
$\eta\eta'$	$< 6 \times 10^{-5}$	90%	1600
$\eta'\eta'$	$< 1.1 \times 10^{-4}$	90%	1498
$\pi^+\pi^-K_S^0 K_S^0$	$(2.4 \pm 0.6) \times 10^{-3}$		1655
$K^+K^-K_S^0 K_S^0$	$< 4 \times 10^{-4}$	90%	1418
$K^+K^-K^+K^-$	$(1.78 \pm 0.22) \times 10^{-3}$		1421
$K^+K^-\phi$	$(1.55 \pm 0.32) \times 10^{-3}$		1468
$K_S^0 K_S^0 \rho\bar{\rho}$	$< 7.9 \times 10^{-4}$	90%	1007
$\rho\bar{\rho}$	$(7.2 \pm 0.4) \times 10^{-5}$		1510
$\rho\bar{\rho}\pi^0$	$(4.7 \pm 1.0) \times 10^{-4}$		1465
$\rho\bar{\rho}\eta$	$(2.0 \pm 0.8) \times 10^{-4}$		1285
$\pi^+\pi^-\rho\bar{\rho}$	$(1.32 \pm 0.34) \times 10^{-3}$		1410
$\pi^0\pi^0\rho\bar{\rho}$	$(8.5 \pm 2.6) \times 10^{-4}$		1414
$\rho\bar{\rho}\pi^-\pi^+$	$(1.1 \pm 0.4) \times 10^{-3}$		1463
$\Lambda\bar{\Lambda}$	$(1.86 \pm 0.27) \times 10^{-4}$		1385
$\Lambda\bar{\Lambda}\pi^+\pi^-$	$< 3.5 \times 10^{-3}$	90%	1255
$K^+\bar{K}\Lambda + c.c.$	$(9.1 \pm 1.8) \times 10^{-4}$		1236
$\Sigma^0\bar{\Sigma}^0$	$< 8 \times 10^{-5}$	90%	1319
$\Sigma^+\bar{\Sigma}^-$	$< 7 \times 10^{-5}$	90%	1322

$\Xi^0\Xi^0$	$< 1.1 \times 10^{-4}$	90%	1197
$\Xi^-\Xi^+$	$(1.55 \pm 0.35) \times 10^{-4}$		1189
$J/\psi(1S)\pi^+\pi^-\pi^0$	$< 1.5 \%$	90%	185

Radiative decays

$\gamma J/\psi(1S)$	$(19.5 \pm 0.8) \%$		430
$\gamma \rho^0$	$< 5 \times 10^{-5}$	90%	1694
$\gamma \omega$	$< 6 \times 10^{-6}$	90%	1692
$\gamma \phi$	$< 1.2 \times 10^{-5}$	90%	1632
$\gamma\gamma$	$(2.56 \pm 0.16) \times 10^{-4}$		1778

 $\eta_c(2S)$

$$I^G(J^{PC}) = 0^+(0^{-+})$$

Quantum numbers are quark model predictions.

Mass $m = 3637 \pm 4$ MeV ($S = 1.7$)
 Full width $\Gamma = 14 \pm 7$ MeV

$\eta_c(2S)$ DECAY MODES	Fraction (Γ_i/Γ)	Confidence level	ρ (MeV/c)
hadrons	not seen		-
$K\bar{K}\pi$	$(1.9 \pm 1.2) \%$		1729
$2\pi^+2\pi^-$	not seen		1792
$3\pi^+3\pi^-$	not seen		1749
$K^+K^-\pi^+\pi^-$	not seen		1700
$K^+K^-\pi^+\pi^-\pi^0$	not seen		1667
$K^+K^-\pi^+2\pi^-$	not seen		1627
$K_S^0 K^-2\pi^+\pi^- + c.c.$	not seen		1666
$2K^+2K^-$	not seen		1470
$\rho\bar{\rho}$	not seen		1558
$\gamma\gamma$	$< 5 \times 10^{-4}$	90%	1819
$\pi^+\pi^-\eta$	not seen		1766
$\pi^+\pi^-\eta'$	not seen		1680
$K^+K^-\eta$	not seen		1637
$\pi^+\pi^-\eta_c(1S)$	not seen		541

 $\psi(2S)$

$$I^G(J^{PC}) = 0^-(1^{--})$$

Mass $m = 3686.09 \pm 0.04$ MeV ($S = 1.6$)
 Full width $\Gamma = 304 \pm 9$ keV
 $\Gamma_{ee} = 2.35 \pm 0.04$ keV

$\psi(2S)$ DECAY MODES	Fraction (Γ_i/Γ)	Scale factor/ Confidence level	ρ (MeV/c)
hadrons	$(97.85 \pm 0.13) \%$		-
virtual $\gamma \rightarrow$ hadrons	$(1.73 \pm 0.14) \%$	S=1.5	-
ggg	$(10.6 \pm 1.6) \%$		-
γgg	$(1.02 \pm 0.29) \%$		-
light hadrons	$(15.4 \pm 1.5) \%$		-
e^+e^-	$(7.72 \pm 0.17) \times 10^{-3}$		1843
$\mu^+\mu^-$	$(7.7 \pm 0.8) \times 10^{-3}$		1840
$\tau^+\tau^-$	$(3.0 \pm 0.4) \times 10^{-3}$		490

Decays into $J/\psi(1S)$ and anything

$J/\psi(1S)$ anything	$(59.5 \pm 0.8) \%$		-
$J/\psi(1S)$ neutrals	$(24.5 \pm 0.4) \%$		-
$J/\psi(1S)\pi^+\pi^-$	$(33.6 \pm 0.4) \%$		477
$J/\psi(1S)\pi^0\pi^0$	$(17.73 \pm 0.34) \%$		481
$J/\psi(1S)\eta$	$(3.28 \pm 0.07) \%$		199
$J/\psi(1S)\pi^0$	$(1.30 \pm 0.10) \times 10^{-3}$	S=1.4	528

Hadronic decays

$\pi^0 h_c(1P)$	seen		85
$3(\pi^+\pi^-)\pi^0$	$(3.5 \pm 1.6) \times 10^{-3}$		1746
$2(\pi^+\pi^-)\pi^0$	$(2.9 \pm 1.0) \times 10^{-3}$	S=4.6	1799
$\rho\omega_2(1320)$	$(2.6 \pm 0.9) \times 10^{-4}$		1500
$\rho\bar{\rho}$	$(2.76 \pm 0.12) \times 10^{-4}$		1586
$\Delta^{++}\bar{\Delta}^{--}$	$(1.28 \pm 0.35) \times 10^{-4}$		1371
$\Lambda\bar{\Lambda}\pi^0$	$< 1.2 \times 10^{-4}$	CL=90%	1412
$\Lambda\bar{\Lambda}\eta$	$< 4.9 \times 10^{-5}$	CL=90%	1197
$\Lambda\bar{\Lambda}K^+$	$(1.00 \pm 0.14) \times 10^{-4}$		1327
$\Lambda\bar{\Lambda}K^+\pi^+\pi^-$	$(1.8 \pm 0.4) \times 10^{-4}$		1167
$\Lambda\bar{\Lambda}\pi^+\pi^-$	$(2.8 \pm 0.6) \times 10^{-4}$		1346
$\Lambda\bar{\Lambda}$	$(2.8 \pm 0.5) \times 10^{-4}$	S=2.6	1467
$\Sigma^+\bar{\Sigma}^-$	$(2.6 \pm 0.8) \times 10^{-4}$		1408
$\Sigma^0\bar{\Sigma}^0$	$(2.2 \pm 0.4) \times 10^{-4}$	S=1.5	1405
$\Sigma(1385)^+\bar{\Sigma}(1385)^-$	$(1.1 \pm 0.4) \times 10^{-4}$		1218
$\Xi^-\Xi^+$	$(1.8 \pm 0.6) \times 10^{-4}$	S=2.8	1284
$\Xi^0\Xi^0$	$(2.8 \pm 0.9) \times 10^{-4}$		1291

Meson Summary Table

$K^+ K^- \rho^0 \pi^0$	< 8	$\times 10^{-4}$	CL=90%	1624
$K^+ K^- \rho^+ \pi^-$	< 1.46	%	CL=90%	1622
$\omega K^+ K^-$	< 3.4	$\times 10^{-4}$	CL=90%	1664
$\phi \pi^+ \pi^- \pi^0$	< 3.8	$\times 10^{-3}$	CL=90%	1722
$K^{*0} K^- \pi^+ \pi^0 + \text{c.c.}$	< 1.62	%	CL=90%	1693
$K^{*+} K^- \pi^+ \pi^- + \text{c.c.}$	< 3.23	%	CL=90%	1692
$K^+ K^- \pi^+ \pi^- 2\pi^0$	< 2.67	%	CL=90%	1705
$K^+ K^- 2(\pi^+ \pi^-)$	< 1.03	%	CL=90%	1702
$K^+ K^- 2(\pi^+ \pi^-) \pi^0$	< 3.60	%	CL=90%	1660
$\eta K^+ K^-$	< 4.1	$\times 10^{-4}$	CL=90%	1711
$\rho^0 K^+ K^-$	< 5.0	$\times 10^{-3}$	CL=90%	1665
$2(K^+ K^-)$	< 6.0	$\times 10^{-4}$	CL=90%	1551
$\phi K^+ K^-$	< 7.5	$\times 10^{-4}$	CL=90%	1597
$2(K^+ K^-) \pi^0$	< 2.9	$\times 10^{-4}$	CL=90%	1493
$2(K^+ K^-) \pi^+ \pi^-$	< 3.2	$\times 10^{-3}$	CL=90%	1425
$K_S^0 K^- \pi^+$	< 3.2	$\times 10^{-3}$	CL=90%	1799
$K_S^0 K^- \pi^+ \pi^0$	< 1.33	%	CL=90%	1773
$K_S^0 K^- \rho^+$	< 6.6	$\times 10^{-3}$	CL=90%	1664
$K_S^0 K^- 2\pi^+ \pi^-$	< 8.7	$\times 10^{-3}$	CL=90%	1739
$K_S^0 K^- \pi^+ \rho^0$	< 1.6	%	CL=90%	1621
$K_S^0 K^- \pi^+ \eta$	< 1.3	%	CL=90%	1669
$K_S^0 K^- 2\pi^+ \pi^- \pi^0$	< 4.18	%	CL=90%	1703
$K_S^0 K^- 2\pi^+ \pi^- \eta$	< 4.8	%	CL=90%	1570
$K_S^0 K^- \pi^+ 2(\pi^+ \pi^-)$	< 1.22	%	CL=90%	1658
$K_S^0 K^- \pi^+ 2\pi^0$	< 2.65	%	CL=90%	1741
$K_S^0 K^- K^+ K^- \pi^+$	< 4.9	$\times 10^{-3}$	CL=90%	1490
$K_S^0 K^- K^+ K^- \pi^+ \pi^0$	< 3.0	%	CL=90%	1427
$K_S^0 K^- K^+ K^- \pi^+ \eta$	< 2.2	%	CL=90%	1214
$K^{*0} K^- \pi^+ + \text{c.c.}$	< 9.7	$\times 10^{-3}$	CL=90%	1721
$\rho \bar{p} \pi^0$	< 1.2	$\times 10^{-3}$		1595
$\rho \bar{p} \pi^+ \pi^-$	< 5.8	$\times 10^{-4}$	CL=90%	1544
$\Lambda \bar{\Lambda}$	< 1.2	$\times 10^{-4}$	CL=90%	1521
$\rho \bar{p} \pi^+ \pi^- \pi^0$	< 1.85	$\times 10^{-3}$	CL=90%	1490
$\omega \rho \bar{p}$	< 2.9	$\times 10^{-4}$	CL=90%	1309
$\Lambda \bar{\Lambda} \pi^0$	< 1.2	$\times 10^{-3}$	CL=90%	1468
$\rho \bar{p} 2(\pi^+ \pi^-)$	< 2.6	$\times 10^{-3}$	CL=90%	1425
$\eta \rho \bar{p}$	< 5.4	$\times 10^{-4}$	CL=90%	1430
$\rho^0 \rho \bar{p}$	< 1.7	$\times 10^{-3}$	CL=90%	1313
$\rho \bar{p} K^+ K^-$	< 3.2	$\times 10^{-4}$	CL=90%	1185
$\phi \rho \bar{p}$	< 1.3	$\times 10^{-4}$	CL=90%	1178
$\Lambda \bar{\Lambda} \pi^+ \pi^-$	< 2.5	$\times 10^{-4}$	CL=90%	1404
$\Lambda \bar{p} K^+$	< 2.8	$\times 10^{-4}$	CL=90%	1387
$\Lambda \bar{p} K^+ \pi^+ \pi^-$	< 6.3	$\times 10^{-4}$	CL=90%	1234
$\pi^+ \pi^- \pi^0$	not seen			1874
$\rho \pi$	not seen			1804
$\omega \pi^0$	not seen			1803
$\rho \eta$	not seen			1763
$\omega \eta$	not seen			1762
$\rho \eta'$	not seen			1674
$\omega \eta'$	not seen			1672
$\phi \eta'$	not seen			1606
$K^{*0} \bar{K}^0$	not seen			1744
$K^{*+} K^-$	not seen			1745
$b_1 \pi$	not seen			1683
Radiative decays				
$\gamma \pi^0$	< 2	$\times 10^{-4}$	CL=90%	1884
$\gamma \eta$	< 1.5	$\times 10^{-4}$	CL=90%	1847
$\gamma \eta'$	< 1.8	$\times 10^{-4}$	CL=90%	1765

X(3872)

$$I^G(J^{PC}) = 0^?(?^{?+})$$

Quantum numbers not established.

Mass $m = 3871.56 \pm 0.22$ MeV $m_{X(3872)} - m_{J/\psi} = 775 \pm 4$ MeV $m_{X(3872)} - m_{\psi(2S)}$ Full width $\Gamma < 2.3$ MeV, CL = 90%

X(3872) DECAY MODES	Fraction (Γ_i/Γ)	ρ (MeV/c)
$\pi^+ \pi^- J/\psi(1S)$	>2.6 %	650
$D^0 \bar{D}^0 \pi^0$	>3.2 $\times 10^{-3}$	116
$\bar{D}^{*0} D^0$	>5 $\times 10^{-3}$	†
$\gamma J/\psi$	>9 $\times 10^{-3}$	697
$\gamma \psi(2S)$	>3.0 %	181

 $\psi(4040)$ [iiv]

$$I^G(J^{PC}) = 0^-(1^{--})$$

Mass $m = 4039 \pm 1$ MeVFull width $\Gamma = 80 \pm 10$ MeV $\Gamma_{ee} = 0.86 \pm 0.07$ keV

$\psi(4040)$ DECAY MODES	Fraction (Γ_i/Γ)	Confidence level	ρ (MeV/c)
$e^+ e^-$	(1.07 \pm 0.16) $\times 10^{-5}$		2019
$D \bar{D}$	seen		775
$D^0 \bar{D}^0$	seen		775
$D^+ D^-$	seen		764
$D^* \bar{D} + \text{c.c.}$	seen		569
$D^*(2007)^0 \bar{D}^0 + \text{c.c.}$	seen		575
$D^*(2010)^+ D^- + \text{c.c.}$	seen		561
$D^* \bar{D}^*$	not seen		193
$D^*(2007)^0 \bar{D}^*(2007)^0$	not seen		225
$D^*(2010)^+ D^*(2010)^-$	not seen		193
$J/\psi \pi^+ \pi^-$	< 4	$\times 10^{-3}$	90% 794
$J/\psi \pi^0 \pi^0$	< 2	$\times 10^{-3}$	90% 797
$J/\psi \eta$	< 7	$\times 10^{-3}$	90% 675
$J/\psi \pi^0$	< 2	$\times 10^{-3}$	90% 823
$J/\psi \pi^+ \pi^- \pi^0$	< 2	$\times 10^{-3}$	90% 746
$\chi_{c1} \gamma$	< 1.1	%	90% 494
$\chi_{c2} \gamma$	< 1.7	%	90% 454
$\chi_{c1} \pi^+ \pi^- \pi^0$	< 1.1	%	90% 306
$\chi_{c2} \pi^+ \pi^- \pi^0$	< 3.2	%	90% 233
$\phi \pi^+ \pi^-$	< 3	$\times 10^{-3}$	90% 1880

 $\psi(4160)$ [iiv]

$$I^G(J^{PC}) = 0^-(1^{--})$$

Mass $m = 4153 \pm 3$ MeVFull width $\Gamma = 103 \pm 8$ MeV $\Gamma_{ee} = 0.83 \pm 0.07$ keV

$\psi(4160)$ DECAY MODES	Fraction (Γ_i/Γ)	Confidence level	ρ (MeV/c)
$e^+ e^-$	(8.1 \pm 0.9) $\times 10^{-6}$		2076
$D \bar{D}$	not seen		913
$D^0 \bar{D}^0$	not seen		913
$D^+ D^-$	not seen		904
$D^* \bar{D} + \text{c.c.}$	not seen		746
$D^*(2007)^0 \bar{D}^0 + \text{c.c.}$	not seen		751
$D^*(2010)^+ D^- + \text{c.c.}$	not seen		740
$D^* \bar{D}^*$	seen		520
$D^*(2007)^0 \bar{D}^*(2007)^0$	seen		533
$D^*(2010)^+ D^*(2010)^-$	seen		520
$J/\psi \pi^+ \pi^-$	< 3	$\times 10^{-3}$	90% 888
$J/\psi \pi^0 \pi^0$	< 3	$\times 10^{-3}$	90% 891
$J/\psi K^+ K^-$	< 2	$\times 10^{-3}$	90% 324
$J/\psi \eta$	< 8	$\times 10^{-3}$	90% 786
$J/\psi \pi^0$	< 1	$\times 10^{-3}$	90% 914
$J/\psi \eta'$	< 5	$\times 10^{-3}$	90% 385
$J/\psi \pi^+ \pi^- \pi^0$	< 1	$\times 10^{-3}$	90% 847
$\psi(2S) \pi^+ \pi^-$	< 4	$\times 10^{-3}$	90% 353
$\chi_{c1} \gamma$	< 7	$\times 10^{-3}$	90% 593
$\chi_{c2} \gamma$	< 1.3	%	90% 554
$\chi_{c1} \pi^+ \pi^- \pi^0$	< 2	$\times 10^{-3}$	90% 452
$\chi_{c2} \pi^+ \pi^- \pi^0$	< 8	$\times 10^{-3}$	90% 398
$\phi \pi^+ \pi^-$	< 2	$\times 10^{-3}$	90% 1941

X(4260)

$$I^G(J^{PC}) = ?^?(1^{--})$$

Mass $m = 4263^{+8}_{-9}$ MeV ($S = 1$)Full width $\Gamma = 95 \pm 14$ MeV

X(4260) DECAY MODES	Fraction (Γ_i/Γ)	ρ (MeV/c)
$J/\psi \pi^+ \pi^-$	seen	976
$J/\psi \pi^0 \pi^0$	[iiv] seen	978
$J/\psi K^+ K^-$	[iiv] seen	530
$J/\psi \eta$	[iiv] not seen	886
$J/\psi \pi^0$	[iiv] not seen	999
$J/\psi \eta'$	[iiv] not seen	569
$J/\psi \pi^+ \pi^- \pi^0$	[iiv] not seen	939
$J/\psi \eta \eta$	[iiv] not seen	339
$\psi(2S) \pi^+ \pi^-$	[iiv] not seen	470

Meson Summary Table

$\psi(2S)\eta$	[<i>iiii</i>] not seen	167
$\chi_{c0}\omega$	[<i>iiii</i>] not seen	292
$\chi_{c1}\gamma$	[<i>iiii</i>] not seen	686
$\chi_{c2}\gamma$	[<i>iiii</i>] not seen	648
$\chi_{c1}\pi^+\pi^-\pi^0$	[<i>iiii</i>] not seen	571
$\chi_{c2}\pi^+\pi^-\pi^0$	[<i>iiii</i>] not seen	524
$\phi\pi^+\pi^-$	[<i>iiii</i>] not seen	1999
$\phi f_0(980) \rightarrow \phi\pi^+\pi^-$	not seen	—
$D\bar{D}$	not seen	1032
$D^0 D^{*-}\pi^+$	not seen	716
$D^*\bar{D}$	not seen	887
$D^*\bar{D}^*$	not seen	708
$D^*\bar{D}\pi$	not seen	723
$D^*\bar{D}^*\pi$	not seen	474
$D_s^+ D_s^-$	not seen	817
$D_s^{*+} D_s^-$	not seen	615
$D_s^{*+} D_s^{*-}$	not seen	284
$\rho\bar{\rho}$	not seen	1914
$K_S^0 K^\pm\pi^\mp$	not seen	2054
$K^+ K^- \pi^0$	not seen	2055

 $\psi(4415)$ [*iiii*]

$$J^G(JPC) = 0^-(1^{--})$$

Mass $m = 4421 \pm 4$ MeV
 Full width $\Gamma = 62 \pm 20$ MeV
 $\Gamma_{ee} = 0.58 \pm 0.07$ keV

$\psi(4415)$ DECAY MODES	Fraction (Γ_i/Γ)	Confidence level	$\frac{p}{(\text{MeV}/c)}$
hadrons	dominant	—	—
$D\bar{D}$	not seen	1187	—
$D^0\bar{D}^0$	not seen	1187	—
$D^+ D^-$	not seen	1179	—
$D^*\bar{D} + \text{c.c.}$	not seen	1063	—
$D^*(2007)^0\bar{D}^0 + \text{c.c.}$	not seen	1067	—
$D^*(2010)^+ D^- + \text{c.c.}$	not seen	1059	—
$D^*\bar{D}^*$	not seen	919	—
$D^*(2007)^0\bar{D}^*(2007)^0 + \text{c.c.}$	not seen	927	—
$D^*(2010)^+ D^*(2010)^- + \text{c.c.}$	not seen	919	—
$(D^0 D^- \pi^+)_{\text{non-res}}$	< 2.3 %	90%	—
$D\bar{D}_2^*(2460) \rightarrow D^0 D^- \pi^+$	(10 ± 4) %	—	—
$D^0 D^* \pi^+$	< 11 %	90%	926
$e^+ e^-$	$(9.4 \pm 3.2) \times 10^{-6}$	—	2210

 $b\bar{b}$ MESONS **$T(1S)$**

$$J^G(JPC) = 0^-(1^{--})$$

Mass $m = 9460.30 \pm 0.26$ MeV ($S = 3.3$)
 Full width $\Gamma = 54.02 \pm 1.25$ keV
 $\Gamma_{ee} = 1.340 \pm 0.018$ keV

$T(1S)$ DECAY MODES	Fraction (Γ_i/Γ)	Confidence level	$\frac{p}{(\text{MeV}/c)}$
$\tau^+ \tau^-$	(2.60 ± 0.10) %	—	4384
$e^+ e^-$	(2.48 ± 0.07) %	—	4730
$\mu^+ \mu^-$	(2.48 ± 0.05) %	—	4729
Hadronic decays			
$g g g$	(81.7 ± 0.7) %	—	—
$\gamma g g$	(2.21 ± 0.22) %	—	—
$\eta'(958)$ anything	(2.94 ± 0.24) %	—	—
$J/\psi(1S)$ anything	$(6.5 \pm 0.7) \times 10^{-4}$	4223	—
χ_{c0} anything	$< 5 \times 10^{-3}$	90%	—
χ_{c1} anything	$(2.3 \pm 0.7) \times 10^{-4}$	—	—
χ_{c2} anything	$(3.4 \pm 1.0) \times 10^{-4}$	—	—
$\psi(2S)$ anything	$(2.7 \pm 0.9) \times 10^{-4}$	—	—
$\rho\pi$	$< 2 \times 10^{-4}$	90%	4697
$\pi^+ \pi^-$	$< 5 \times 10^{-4}$	90%	4728
$K^+ K^-$	$< 5 \times 10^{-4}$	90%	4704
$\rho\bar{\rho}$	$< 5 \times 10^{-4}$	90%	4636
$\pi^0 \pi^+ \pi^-$	$< 1.84 \times 10^{-5}$	90%	4725
$D^*(2010)^\pm$ anything	(2.52 ± 0.20) %	—	—
\bar{d} anything	$(2.86 \pm 0.28) \times 10^{-5}$	—	—

Radiative decays

$\gamma\pi^+\pi^-$	$(6.3 \pm 1.8) \times 10^{-5}$	4728
$\gamma\pi^0\pi^0$	$(1.7 \pm 0.7) \times 10^{-5}$	4728
$\gamma\pi^0\eta$	$< 2.4 \times 10^{-6}$	90% 4713
$\gamma K^+ K^-$	[<i>kkkk</i>] $(1.14 \pm 0.13) \times 10^{-5}$	4704
$\gamma\rho\bar{\rho}$	[<i>iiii</i>] $< 6 \times 10^{-6}$	90% 4636
$\gamma 2h^+ 2h^-$	$(7.0 \pm 1.5) \times 10^{-4}$	4720
$\gamma 3h^+ 3h^-$	$(5.4 \pm 2.0) \times 10^{-4}$	4703
$\gamma 4h^+ 4h^-$	$(7.4 \pm 3.5) \times 10^{-4}$	4679
$\gamma\pi^+\pi^- K^+ K^-$	$(2.9 \pm 0.9) \times 10^{-4}$	4686
$\gamma 2\pi^+ 2\pi^-$	$(2.5 \pm 0.9) \times 10^{-4}$	4720
$\gamma 3\pi^+ 3\pi^-$	$(2.5 \pm 1.2) \times 10^{-4}$	4703
$\gamma 2\pi^+ 2\pi^- K^+ K^-$	$(2.4 \pm 1.2) \times 10^{-4}$	4658
$\gamma\pi^+\pi^- \rho\bar{\rho}$	$(1.5 \pm 0.6) \times 10^{-4}$	4604
$\gamma 2\pi^+ 2\pi^- \rho\bar{\rho}$	$(4 \pm 6) \times 10^{-5}$	4563
$\gamma 2K^+ 2K^-$	$(2.0 \pm 2.0) \times 10^{-5}$	4601
$\gamma\eta'(958)$	$< 1.9 \times 10^{-6}$	90% 4682
$\gamma\eta$	$< 1.0 \times 10^{-6}$	90% 4714
$\gamma f_0(980)$	$< 3 \times 10^{-5}$	90% 4679
$\gamma f_2'(1525)$	$(3.7 \pm 1.2 \pm 1.1) \times 10^{-5}$	4607
$\gamma f_2(1270)$	$(1.01 \pm 0.09) \times 10^{-4}$	4644
$\gamma\eta(1405)$	$< 8.2 \times 10^{-5}$	90% 4625
$\gamma f_0(1500)$	$< 1.5 \times 10^{-5}$	90% 4610
$\gamma f_0(1710)$	$< 2.6 \times 10^{-4}$	90% 4574
$\gamma f_0(1710) \rightarrow \gamma K^+ K^-$	$< 7 \times 10^{-6}$	90% —
$\gamma f_0(1710) \rightarrow \gamma\pi^0\pi^0$	$< 1.4 \times 10^{-6}$	90% —
$\gamma f_0(1710) \rightarrow \gamma\eta\eta$	$< 1.8 \times 10^{-6}$	90% —
$\gamma f_4(2050)$	$< 5.3 \times 10^{-5}$	90% 4515
$\gamma f_0(2200) \rightarrow \gamma K^+ K^-$	$< 2 \times 10^{-4}$	90% 4475
$\gamma f_J(2220) \rightarrow \gamma K^+ K^-$	$< 8 \times 10^{-7}$	90% 4469
$\gamma f_J(2220) \rightarrow \gamma\pi^+\pi^-$	$< 6 \times 10^{-7}$	90% —
$\gamma f_J(2220) \rightarrow \gamma\rho\bar{\rho}$	$< 1.1 \times 10^{-6}$	90% —
$\gamma\eta(2225) \rightarrow \gamma\phi\phi$	$< 3 \times 10^{-3}$	90% 4469
γX	[<i>m m m m</i>] $< 3 \times 10^{-5}$	90% —
$\gamma X\bar{X}$	[<i>n n n n</i>] $< 1 \times 10^{-3}$	90% —
$\gamma X \rightarrow \gamma + \geq 4$ prongs	[<i>o o o o</i>] $< 1.78 \times 10^{-4}$	95% —
$\gamma a_1^0 \rightarrow \gamma\mu^+ \mu^-$	[<i>p p p p</i>] $< 9 \times 10^{-6}$	90% —
$\gamma a_1^0 \rightarrow \gamma\tau^+ \tau^-$	[<i>k k k k</i>] $< 5.0 \times 10^{-5}$	90% —

Lepton Flavor (LF) violating or invisible decays

$\mu^\pm\tau^\mp$	LF $< 6.0 \times 10^{-6}$	95% 4563
invisible	$< 3.0 \times 10^{-4}$	90% —

 $\chi_{b0}(1P)$ [*qqqq*]

$$J^G(JPC) = 0^+(0^{++})$$

J needs confirmation.

Mass $m = 9859.44 \pm 0.42 \pm 0.31$ MeV

$\chi_{b0}(1P)$ DECAY MODES	Fraction (Γ_i/Γ)	Confidence level	$\frac{p}{(\text{MeV}/c)}$
$\gamma T(1S)$	< 6 %	90%	391
$D^0 X$	< 10.4 %	90%	—
$\pi^+ \pi^- K^+ K^- \pi^0$	$< 1.6 \times 10^{-4}$	90%	4875
$2\pi^+ \pi^- K^- K_S^0$	$< 5 \times 10^{-5}$	90%	4875
$2\pi^+ \pi^- K^- K_S^0 2\pi^0$	$< 5 \times 10^{-4}$	90%	4846
$2\pi^+ 2\pi^- 2\pi^0$	$< 2.1 \times 10^{-4}$	90%	4905
$2\pi^+ 2\pi^- K^+ K^-$	$(1.1 \pm 0.6) \times 10^{-4}$	—	4861
$2\pi^+ 2\pi^- K^+ K^- \pi^0$	$< 2.7 \times 10^{-4}$	90%	4846
$2\pi^+ 2\pi^- K^+ K^- 2\pi^0$	$< 5 \times 10^{-4}$	90%	4828
$3\pi^+ 2\pi^- K^- K_S^0 \pi^0$	$< 1.6 \times 10^{-4}$	90%	4827
$3\pi^+ 3\pi^-$	$< 8 \times 10^{-5}$	90%	4904
$3\pi^+ 3\pi^- 2\pi^0$	$< 6 \times 10^{-4}$	90%	4881
$3\pi^+ 3\pi^- K^+ K^-$	$(2.4 \pm 1.2) \times 10^{-4}$	—	4827
$3\pi^+ 3\pi^- K^+ K^- \pi^0$	$< 1.0 \times 10^{-3}$	90%	4808
$4\pi^+ 4\pi^-$	$< 8 \times 10^{-5}$	90%	4880
$4\pi^+ 4\pi^- 2\pi^0$	$< 2.1 \times 10^{-3}$	90%	4850

 $\chi_{b1}(1P)$ [*qqqq*]

$$J^G(JPC) = 0^+(1^{++})$$

J needs confirmation.

Mass $m = 9892.78 \pm 0.26 \pm 0.31$ MeV

Meson Summary Table

$2\pi^+ 2\pi^- K^+ K^- \pi^0$	$(2.4 \pm 1.1) \times 10^{-4}$	5054
$2\pi^+ 2\pi^- K^+ K^- 2\pi^0$	$(4.7 \pm 2.3) \times 10^{-4}$	5037
$3\pi^+ 2\pi^- K^- K_S^0 \pi^0$	$< 4 \times 10^{-4}$	90%
$3\pi^+ 3\pi^-$	$(9 \pm 4) \times 10^{-5}$	5110
$3\pi^+ 3\pi^- 2\pi^0$	$(1.2 \pm 0.4) \times 10^{-3}$	5088
$3\pi^+ 3\pi^- K^+ K^-$	$(1.4 \pm 0.7) \times 10^{-4}$	5036
$3\pi^+ 3\pi^- K^+ K^- \pi^0$	$(4.2 \pm 1.7) \times 10^{-4}$	5017
$4\pi^+ 4\pi^-$	$(9 \pm 5) \times 10^{-5}$	5087
$4\pi^+ 4\pi^- 2\pi^0$	$(1.3 \pm 0.5) \times 10^{-3}$	5058

 $\Upsilon(3S)$

$$I^G(J^{PC}) = 0^-(1^{--})$$

Mass $m = 10.3552 \pm 0.0005$ GeV
 Full width $\Gamma = 20.32 \pm 1.85$ keV
 $\Gamma_{ee} = 0.443 \pm 0.008$ keV

$\Upsilon(3S)$ DECAY MODES	Fraction (Γ_i/Γ)	Scale factor/ Confidence level	p (MeV/c)
$\Upsilon(2S)$ anything	$(10.6 \pm 0.8) \%$		296
$\Upsilon(2S) \pi^+ \pi^-$	$(2.45 \pm 0.23) \%$	S=1.1	177
$\Upsilon(2S) \pi^0 \pi^0$	$(1.85 \pm 0.14) \%$		190
$\Upsilon(2S) \gamma \gamma$	$(5.0 \pm 0.7) \%$		327
$\Upsilon(2S) \pi^0$	$< 5.1 \times 10^{-4}$	CL=90%	298
$\Upsilon(1S) \pi^+ \pi^-$	$(4.40 \pm 0.10) \%$		813
$\Upsilon(1S) \pi^0 \pi^0$	$(2.20 \pm 0.13) \%$		816
$\Upsilon(1S) \eta$	$< 1.8 \times 10^{-4}$	CL=90%	677
$\Upsilon(1S) \pi^0$	$< 7 \times 10^{-5}$	CL=90%	846
$\tau^+ \tau^-$	$(2.29 \pm 0.30) \%$		4863
$\mu^+ \mu^-$	$(2.18 \pm 0.21) \%$	S=2.1	5177
$e^+ e^-$	seen		5178
$g g g$	$(35.7 \pm 2.6) \%$		-
$\gamma g g$	$(9.7 \pm 1.8) \times 10^{-3}$		-

Radiative decays

$\gamma \chi_{b2}(2P)$	$(13.1 \pm 1.6) \%$	S=3.4	86
$\gamma \chi_{b1}(2P)$	$(12.6 \pm 1.2) \%$	S=2.4	99
$\gamma \chi_{b0}(2P)$	$(5.9 \pm 0.6) \%$	S=1.4	122
$\gamma \chi_{b2}(1P)$	$< 1.9 \%$	CL=90%	434
$\gamma \chi_{b1}(1P)$	$< 1.7 \times 10^{-3}$	CL=90%	452
$\gamma \chi_{b0}(1P)$	$(3.0 \pm 1.1) \times 10^{-3}$		484
$\gamma \eta_b(2S)$	$< 6.2 \times 10^{-4}$	CL=90%	-
$\gamma \eta_b(1S)$	$(5.1 \pm 0.7) \times 10^{-4}$		919
$\gamma X \rightarrow \gamma + \geq 4$ prongs	[ssss] $< 2.2 \times 10^{-4}$	CL=95%	-
$\gamma a_1^0 \rightarrow \gamma \tau^+ \tau^-$	[tttt] $< 1.6 \times 10^{-4}$	CL=90%	-

Lepton Flavor (LF) violating decays

$\mu^\pm \tau^\mp$	LF $< 2.03 \times 10^{-5}$	CL=95%	5025
--------------------	----------------------------	--------	------

 **$\Upsilon(4S)$
or $\Upsilon(10580)$**

$$I^G(J^{PC}) = 0^-(1^{--})$$

Mass $m = 10.5794 \pm 0.0012$ GeV
 Full width $\Gamma = 20.5 \pm 2.5$ MeV
 $\Gamma_{ee} = 0.272 \pm 0.029$ keV (S = 1.5)

$\Upsilon(4S)$ DECAY MODES	Fraction (Γ_i/Γ)	Confidence level	p (MeV/c)
$B\bar{B}$	$> 96 \%$	95%	328
$B^+ B^-$	$(51.6 \pm 0.6) \%$		334
D_s^+ anything + c.c.	$(17.8 \pm 2.6) \%$		-
$B^0 \bar{B}^0$	$(48.4 \pm 0.6) \%$		328
$J/\psi K_S^0 (J/\psi, \eta_c) K_S^0$	$< 4 \times 10^{-7}$	90%	-
non- $B\bar{B}$	$< 4 \%$	95%	-
$e^+ e^-$	$(1.57 \pm 0.08) \times 10^{-5}$		5290
$\rho^+ \rho^-$	$< 5.7 \times 10^{-6}$	90%	5233
$J/\psi(1S)$ anything	$< 1.9 \times 10^{-4}$	95%	-
D^{*+} anything + c.c.	$< 7.4 \%$	90%	5099
ϕ anything	$(7.1 \pm 0.6) \%$		5240
$\phi \eta$	$< 1.8 \times 10^{-6}$	90%	5226
$\phi \eta'$	$< 4.3 \times 10^{-6}$	90%	5196
$\rho \eta$	$< 1.3 \times 10^{-6}$	90%	5247
$\rho \eta'$	$< 2.5 \times 10^{-6}$	90%	5217
$\Upsilon(1S)$ anything	$< 4 \times 10^{-3}$	90%	1053
$\Upsilon(1S) \pi^+ \pi^-$	$(8.1 \pm 0.6) \times 10^{-5}$		1026
$\Upsilon(1S) \eta$	$(1.96 \pm 0.11) \times 10^{-4}$		924
$\Upsilon(2S) \pi^+ \pi^-$	$(8.6 \pm 1.3) \times 10^{-5}$		468
\bar{d} anything	$< 1.3 \times 10^{-5}$	90%	-

 $\Upsilon(10860)$

$$I^G(J^{PC}) = 0^-(1^{--})$$

Mass $m = 10.865 \pm 0.008$ GeV (S = 1.1)
 Full width $\Gamma = 110 \pm 13$ MeV
 $\Gamma_{ee} = 0.31 \pm 0.07$ keV (S = 1.3)

$\Upsilon(10860)$ DECAY MODES	Fraction (Γ_i/Γ)	Confidence level	p (MeV/c)
$e^+ e^-$	$(2.8 \pm 0.7) \times 10^{-6}$		5432
$B\bar{B}X$	$(59 \pm 14) \%$		-
$B\bar{B}$	$< 13.8 \%$	90%	1280
$B\bar{B}^* +$ c.c.	$(14 \pm 6) \%$		-
$B^* \bar{B}^*$	$(44 \pm 11) \%$		-
$B\bar{B}^*(*) \pi$	$< 19.7 \%$	90%	-
$B\bar{B} \pi \pi$	$< 8.9 \%$	90%	442
$B_s^{(*)} \bar{B}_s^{(*)}$	$(19.3 \pm 2.9) \%$		-
$B_s \bar{B}_s$	$(5 \pm 5) \times 10^{-3}$		-
$B_s \bar{B}_s^* +$ c.c.	$(1.4 \pm 0.6) \%$		-
$B_s^* \bar{B}_s^*$	$(17.4 \pm 2.7) \%$		-
$\Upsilon(1S) \pi^+ \pi^-$	$(5.3 \pm 0.6) \times 10^{-3}$		1288
$\Upsilon(2S) \pi^+ \pi^-$	$(7.8 \pm 1.3) \times 10^{-3}$		763
$\Upsilon(3S) \pi^+ \pi^-$	$(4.8 \pm 1.9) \times 10^{-3}$		416
$\Upsilon(1S) K^+ K^-$	$(6.1 \pm 1.8) \times 10^{-4}$		933

Inclusive Decays.

These decay modes are submodes of one or more of the decay modes above.

ϕ anything	$(13.8 \pm 2.4) \%$	-
D^0 anything + c.c.	$(108 \pm 8) \%$	-
D_s anything + c.c.	$(46 \pm 6) \%$	-
J/ψ anything	$(2.06 \pm 0.21) \%$	-

 $\Upsilon(11020)$

$$I^G(J^{PC}) = 0^-(1^{--})$$

Mass $m = 11.019 \pm 0.008$ GeV
 Full width $\Gamma = 79 \pm 16$ MeV
 $\Gamma_{ee} = 0.130 \pm 0.030$ keV

$\Upsilon(11020)$ DECAY MODES	Fraction (Γ_i/Γ)	p (MeV/c)
$e^+ e^-$	$(1.6 \pm 0.5) \times 10^{-6}$	5510

NOTES

In this Summary Table:

When a quantity has "(S = ...)" to its right, the error on the quantity has been enlarged by the "scale factor" S, defined as $S = \sqrt{\chi^2/(N-1)}$, where N is the number of measurements used in calculating the quantity. We do this when $S > 1$, which often indicates that the measurements are inconsistent. When $S > 1.25$, we also show in the Particle Listings an ideogram of the measurements. For more about S, see the Introduction.

A decay momentum p is given for each decay mode. For a 2-body decay, p is the momentum of each decay product in the rest frame of the decaying particle. For a 3-or-more-body decay, p is the largest momentum any of the products can have in this frame.

[a] See the "Note on $\pi^\pm \rightarrow \ell^\pm \nu \gamma$ and $K^\pm \rightarrow \ell^\pm \nu \gamma$ Form Factors" in the π^\pm Particle Listings for definitions and details.

[b] Measurements of $\Gamma(e^+ \nu_e)/\Gamma(\mu^+ \nu_\mu)$ always include decays with γ 's, and measurements of $\Gamma(e^+ \nu_e \gamma)$ and $\Gamma(\mu^+ \nu_\mu \gamma)$ never include low-energy γ 's. Therefore, since no clean separation is possible, we consider the modes with γ 's to be subreactions of the modes without them, and let $[\Gamma(e^+ \nu_e) + \Gamma(\mu^+ \nu_\mu)]/\Gamma_{\text{total}} = 100\%$.

[c] See the π^\pm Particle Listings for the energy limits used in this measurement; low-energy γ 's are not included.

[d] Derived from an analysis of neutrino-oscillation experiments.

[e] Astrophysical and cosmological arguments give limits of order 10^{-13} ; see the π^0 Particle Listings.

[f] C parity forbids this to occur as a single-photon process.

[g] See the "Note on scalar mesons" in the $f_0(1370)$ Particle Listings. The interpretation of this entry as a particle is controversial.

[h] See the "Note on $\rho(770)$ " in the $\rho(770)$ Particle Listings.

Meson Summary Table

[i] The $\omega\rho$ interference is then due to $\omega\rho$ mixing only, and is expected to be small. If $e\mu$ universality holds, $\Gamma(\rho^0 \rightarrow \mu^+\mu^-) = \Gamma(\rho^0 \rightarrow e^+e^-) \times 0.99785$.

- [j] See the “Note on scalar mesons” in the $f_0(1370)$ Particle Listings .
 [k] See the “Note on $a_1(1260)$ ” in the $a_1(1260)$ Particle Listings in PDG 06, Journal of Physics, G **33** 1 (2006).
 [l] This is only an educated guess; the error given is larger than the error on the average of the published values. See the Particle Listings for details.
 [m] See the “Note on non- $q\bar{q}$ mesons” in the Particle Listings in PDG 06, Journal of Physics, G **33** 1 (2006).
 [n] See the “Note on the $\eta(1405)$ ” in the $\eta(1405)$ Particle Listings.
 [o] See the “Note on the $f_1(1420)$ ” in the $\eta(1405)$ Particle Listings.
 [p] See also the $\omega(1650)$ Particle Listings.
 [q] See the “Note on the $\rho(1450)$ and the $\rho(1700)$ ” in the $\rho(1700)$ Particle Listings.
 [r] See also the $\omega(1420)$ Particle Listings.
 [s] See the “Note on $f_0(1710)$ ” in the $f_0(1710)$ Particle Listings in 2004 edition of *Review of Particle Physics*.
 [t] See the note in the K^\pm Particle Listings.
 [u] The definition of the slope parameter g of the $K \rightarrow 3\pi$ Dalitz plot is as follows (see also “Note on Dalitz Plot Parameters for $K \rightarrow 3\pi$ Decays” in the K^\pm Particle Listings):

$$|M|^2 = 1 + g(s_3 - s_0)/m_{\pi^+}^2 + \dots$$

- [v] For more details and definitions of parameters see the Particle Listings.
 [w] Most of this radiative mode, the low-momentum γ part, is also included in the parent mode listed without γ 's.
 [x] See the K^\pm Particle Listings for the energy limits used in this measurement.
 [y] Structure-dependent part.
 [z] Direct-emission branching fraction.
 [aa] Violates angular-momentum conservation.
 [bb] Derived from measured values of ϕ_{+-} , ϕ_{00} , $|\eta|$, $|m_{K_L^0} - m_{K_S^0}|$, and $\tau_{K_S^0}$, as described in the introduction to “Tests of Conservation Laws.”
 [cc] The CP -violation parameters are defined as follows (see also “Note on CP Violation in $K_S \rightarrow 3\pi$ ” and “Note on CP Violation in K_L^0 Decay” in the Particle Listings):

$$\eta_{+-} = |\eta_{+-}|e^{i\phi_{+-}} = \frac{A(K_L^0 \rightarrow \pi^+\pi^-)}{A(K_S^0 \rightarrow \pi^+\pi^-)} = \epsilon + \epsilon'$$

$$\eta_{00} = |\eta_{00}|e^{i\phi_{00}} = \frac{A(K_L^0 \rightarrow \pi^0\pi^0)}{A(K_S^0 \rightarrow \pi^0\pi^0)} = \epsilon - 2\epsilon'$$

$$\delta = \frac{\Gamma(K_L^0 \rightarrow \pi^-\ell^+\nu) - \Gamma(K_L^0 \rightarrow \pi^+\ell^-\nu)}{\Gamma(K_L^0 \rightarrow \pi^-\ell^+\nu) + \Gamma(K_L^0 \rightarrow \pi^+\ell^-\nu)},$$

$$\text{Im}(\eta_{+-0})^2 = \frac{\Gamma(K_S^0 \rightarrow \pi^+\pi^-\pi^0)_{CP \text{ viol.}}}{\Gamma(K_L^0 \rightarrow \pi^+\pi^-\pi^0)},$$

$$\text{Im}(\eta_{000})^2 = \frac{\Gamma(K_S^0 \rightarrow \pi^0\pi^0\pi^0)}{\Gamma(K_L^0 \rightarrow \pi^0\pi^0\pi^0)}.$$

where for the last two relations CPT is assumed valid, *i.e.*, $\text{Re}(\eta_{+-0}) \simeq 0$ and $\text{Re}(\eta_{000}) \simeq 0$.

- [dd] See the K_S^0 Particle Listings for the energy limits used in this measurement.
 [ee] The value is for the sum of the charge states or particle/antiparticle states indicated.
 [ff] $\text{Re}(\epsilon'/\epsilon) = \epsilon'/\epsilon$ to a very good approximation provided the phases satisfy CPT invariance.
 [gg] This mode includes gammas from inner bremsstrahlung but not the direct emission mode $K_L^0 \rightarrow \pi^+\pi^-\gamma(\text{DE})$.
 [hh] See the K_L^0 Particle Listings for the energy limits used in this measurement.
 [ii] Allowed by higher-order electroweak interactions.
 [jj] Violates CP in leading order. Test of direct CP violation since the indirect CP -violating and CP -conserving contributions are expected to be suppressed.
 [kk] See the “Note on $f_0(1370)$ ” in the $f_0(1370)$ Particle Listings and in the 1994 edition.

[ll] See the note in the $L(1770)$ Particle Listings in Reviews of Modern Physics **56** S1 (1984), p. S200. See also the “Note on $K_2(1770)$ and the $K_2(1820)$ ” in the $K_2(1770)$ Particle Listings .

- [mm] See the “Note on $K_2(1770)$ and the $K_2(1820)$ ” in the $K_2(1770)$ Particle Listings .
 [nn] This result applies to $Z^0 \rightarrow c\bar{c}$ decays only. Here ℓ^+ is an average (not a sum) of e^+ and μ^+ decays.
 [oo] The branching fraction for this mode may differ from the sum of the submodes that contribute to it, due to interference effects. See the relevant papers in the Particle Listings.
 [pp] These subfractions of the $K^-2\pi^+$ mode are uncertain: see the Particle Listings.
 [qq] Submodes of the $D^+ \rightarrow K^-2\pi^+\pi^0$ and $K_S^0 2\pi^+\pi^-$ modes were studied by ANJOS 92C and COFFMAN 92B, but with at most 142 events for the first mode and 229 for the second – not enough for precise results. With nothing new for 18 years, we refer to our 2008 edition, Physics Letters **B667** 1 (2008), for those results.
 [rr] The unseen decay modes of the resonances are included.
 [ss] This is *not* a test for the $\Delta C=1$ weak neutral current, but leads to the $\pi^+\ell^+\ell^-$ final state.
 [tt] This mode is not a useful test for a $\Delta C=1$ weak neutral current because both quarks must change flavor in this decay.
 [uu] This value is obtained by subtracting the branching fractions for 2-, 4- and 6-prongs from unity.
 [vv] This is the sum of our $K^-2\pi^+\pi^-$, $K^-2\pi^+\pi^-\pi^0$, $\bar{K}^0 2\pi^+2\pi^-$, $K^+2K^-\pi^+$, $2\pi^+2\pi^-$, $2\pi^+2\pi^-\pi^0$, $K^+K^-\pi^+\pi^-$, and $K^+K^-\pi^+\pi^-\pi^0$, branching fractions.
 [ww] This is the sum of our $K^-3\pi^+2\pi^-$ and $3\pi^+3\pi^-$ branching fractions.
 [xx] The branching fractions for the $K^-e^+\nu_e$, $K^*(892)^-e^+\nu_e$, $\pi^-e^+\nu_e$, and $\rho^-e^+\nu_e$ modes add up to $6.20 \pm 0.17\%$.
 [yy] This is a doubly Cabibbo-suppressed mode.
 [zz] The two experiments measuring this fraction are in serious disagreement. See the Particle Listings.
 [aaa] Submodes of the $D^0 \rightarrow K_S^0\pi^+\pi^-\pi^0$ mode with a K^* and/or ρ were studied by COFFMAN 92B, but with only 140 events. With nothing new for 18 years, we refer to our 2008 edition, Physics Letters **B667** 1 (2008), for those results.
 [bbb] This branching fraction includes all the decay modes of the resonance in the final state.
 [ccc] The experiments on the division of this charge mode amongst its submodes disagree, and the submode branching fractions here add up to considerably more than the charged-mode fraction.
 [ddd] However, these upper limits are in serious disagreement with values obtained in another experiment.
 [eee] This limit is for either D^0 or \bar{D}^0 to $p e^-$.
 [fff] This limit is for either D^0 or \bar{D}^0 to $\bar{p} e^+$.
 [ggg] See the Particle Listings for the (complicated) definition of this quantity.
 [hhh] This is the purely e^+ semileptonic branching fraction: the e^+ fraction from τ^+ decays has been subtracted off. The sum of our (non- τ) e^+ exclusive fractions — an $e^+\nu_e$ with an η , η' , ϕ , K^0 , K^{*0} , or $f_0(980)$ — is $6.90 \pm 0.4\%$.
 [iii] This fraction includes η from η' decays.
 [jjj] Two times (to include μ decays) the $\eta' e^+\nu_e$ branching fraction, plus the $\eta' \pi^+$, $\eta' \rho^+$, and $\eta' K^+$ fractions, is $(18.4 \pm 2.3)\%$, which considerably exceeds the inclusive η' fraction of $(11.7 \pm 1.8)\%$. Our best guess is that the $\eta' \rho^+$ fraction, $(12.5 \pm 2.2)\%$, is too large.
 [kkk] This branching fraction includes all the decay modes of the final-state resonance.
 [lll] We decouple the $D_S^+ \rightarrow \phi\pi^+$ branching fraction obtained from mass projections (and used to get some of the other branching fractions) from the $D_S^+ \rightarrow \phi\pi^+$, $\phi \rightarrow K^+K^-$ branching fraction obtained from the Dalitz-plot analysis of $D_S^+ \rightarrow K^+K^-\pi^+$. That is, the ratio of these two branching fractions is not exactly the $\phi \rightarrow K^+K^-$ branching fraction 0.491.
 [mmm] This comes from a model-independent and a K -matrix parametrization of the $\pi^+\pi^- S$ -wave and is a sum over several f_0 mesons.
 [nnn] An ℓ indicates an e or a μ mode, not a sum over these modes.
 [ooo] An $CP(\pm 1)$ indicates the $CP=+1$ and $CP=-1$ eigenstates of the D^0 - \bar{D}^0 system.
 [ppp] D denotes D^0 or \bar{D}^0 .

Meson Summary Table

[*qqq*] D_{CP+}^0 decays into $D^0\pi^0$ with the D^0 reconstructed in CP -even eigenstates K^+K^- and $\pi^+\pi^-$.

[*rrr*] \bar{D}^{**} represents an excited state with mass $2.2 < M < 2.8 \text{ GeV}/c^2$.

[*sss*] $X(3872)^+$ is a hypothetical charged partner of the $X(3872)$.

[*ttt*] $\Theta(1710)^{++}$ is a possible narrow pentaquark state and $G(2220)$ is a possible glueball resonance.

[*uuu*] $(\bar{\Lambda}_c^- p)_s$ denotes a low-mass enhancement near $3.35 \text{ GeV}/c^2$.

[*vvv*] Stands for the possible candidates of $K^*(1410)$, $K_0^*(1430)$ and $K_2^*(1430)$.

[*www*] B^0 and B_s^0 contributions not separated. Limit is on weighted average of the two decay rates.

[*xxx*] This decay refers to the coherent sum of resonant and nonresonant $J^P = 0^+ K\pi$ components with $1.60 < m_{K\pi} < 2.15 \text{ GeV}/c^2$.

[*yyy*] $\Theta(1540)^+$ denotes a possible narrow pentaquark state.

[*zzz*] These values are model dependent.

[*aaaa*] Here “anything” means at least one particle observed.

[*bbbb*] D^{**} stands for the sum of the $D(1^1P_1)$, $D(1^3P_0)$, $D(1^3P_1)$, $D(1^3P_2)$, $D(2^1S_0)$, and $D(2^1S_1)$ resonances.

[*cccc*] $D^{(*)}\bar{D}^{(*)}$ stands for the sum of $D^*\bar{D}^*$, $D^*\bar{D}$, $D\bar{D}^*$, and $D\bar{D}$.

[*ddd*] $X(3945)$ denotes a near-threshold enhancement in the $\omega J/\psi$ mass spectrum.

[*eeee*] Inclusive branching fractions have a multiplicity definition and can be greater than 100%.

[*ffff*] D_j represents an unresolved mixture of pseudoscalar and tensor D^{**} (P -wave) states.

[*gggg*] Not a pure measurement. See note at head of B_s^0 Decay Modes.

[*hhhh*] Includes $\rho\bar{\rho}\pi^+\pi^-\gamma$ and excludes $\rho\bar{\rho}\eta$, $\rho\bar{\rho}\omega$, $\rho\bar{\rho}\eta'$.

[*iiii*] J^{PC} known by production in e^+e^- via single photon annihilation. I^G is not known; interpretation of this state as a single resonance is unclear because of the expectation of substantial threshold effects in this energy region.

[*jjjj*] See COAN 06 for details.

[*kkkk*] $2m_\tau < M(\tau^+\tau^-) < 7500 \text{ MeV}$.

[*llll*] $2 < m_{K^+K^-} < 3 \text{ GeV}$.

[*mmmm*] $X =$ pseudoscalar with $m < 7.2 \text{ GeV}$

[*nnnn*] $X\bar{X} =$ vectors with $m < 3.1 \text{ GeV}$

[*oooo*] $1.5 \text{ GeV} < m_X < 5.0 \text{ GeV}$

[*pppp*] $201 < M(\mu^+\mu^-) < 3565 \text{ MeV}$.

[*qqqq*] Spectroscopic labeling for these states is theoretical, pending experimental information.

[*rrrr*] $1.5 \text{ GeV} < m_X < 5.0 \text{ GeV}$

[*ssss*] $1.5 \text{ GeV} < m_X < 5.0 \text{ GeV}$

[*tttt*] For $m_{\tau^+\tau^-}$ in the ranges 4.03–9.52 and 9.61–10.10 GeV.

Baryon Summary Table

This short table gives the name, the quantum numbers (where known), and the status of baryons in the Review. Only the baryons with 3- or 4-star status are included in the main Baryon Summary Table. Due to insufficient data or uncertain interpretation, the other entries in the short table are not established baryons. The names with masses are of baryons that decay strongly. For Λ , Δ , and Ξ resonances, the πN partial wave is indicated by the symbol $L_{2l,2J}$, where L is the orbital angular momentum (S, P, D, \dots), l is the isospin, and J is the total angular momentum. For Λ and Σ resonances, the $\bar{K}N$ partial wave is labeled $L_{l,2J}$. The nucleon is a pole in the P_{11} wave, and similar comments apply to the Λ and Σ .

p	P_{11}	****	$\Delta(1232)$	P_{33}	****	Σ^+	P_{11}	****	Ξ^0	P_{11}	****	Λ_c^+	****
n	P_{11}	****	$\Delta(1600)$	P_{33}	***	Σ^0	P_{11}	****	Ξ^-	P_{11}	****	$\Lambda_c(2595)^+$	***
$N(1440)$	P_{11}	****	$\Delta(1620)$	S_{31}	****	Σ^-	P_{11}	****	$\Xi(1530)$	P_{13}	****	$\Lambda_c(2625)^+$	***
$N(1520)$	D_{13}	****	$\Delta(1700)$	D_{33}	****	$\Sigma(1385)$	P_{13}	****	$\Xi(1620)$	*		$\Lambda_c(2765)^+$	*
$N(1535)$	S_{11}	****	$\Delta(1750)$	P_{31}	*	$\Sigma(1480)$	*		$\Xi(1690)$	***		$\Lambda_c(2880)^+$	***
$N(1650)$	S_{11}	****	$\Delta(1900)$	S_{31}	**	$\Sigma(1560)$	**		$\Xi(1820)$	D_{13}	***	$\Lambda_c(2940)^+$	***
$N(1675)$	D_{15}	****	$\Delta(1905)$	F_{35}	****	$\Sigma(1580)$	D_{13}	*	$\Xi(1950)$	***		$\Sigma_c(2455)$	****
$N(1680)$	F_{15}	****	$\Delta(1910)$	P_{31}	****	$\Sigma(1620)$	S_{11}	**	$\Xi(2030)$	***		$\Sigma_c(2520)$	***
$N(1700)$	D_{13}	***	$\Delta(1920)$	P_{33}	***	$\Sigma(1660)$	P_{11}	***	$\Xi(2120)$	*		$\Sigma_c(2800)$	***
$N(1710)$	P_{11}	***	$\Delta(1930)$	D_{35}	***	$\Sigma(1670)$	D_{13}	****	$\Xi(2250)$	**		Ξ_c^+	***
$N(1720)$	P_{13}	****	$\Delta(1940)$	D_{33}	*	$\Sigma(1690)$	*		$\Xi(2370)$	**		Ξ_c^0	***
$N(1900)$	P_{13}	**	$\Delta(1950)$	F_{37}	****	$\Sigma(1750)$	S_{11}	***	$\Xi(2500)$	*		$\Xi_c^{'+}$	***
$N(1990)$	F_{17}	**	$\Delta(2000)$	F_{35}	**	$\Sigma(1770)$	P_{11}	*				Ξ_c^0	***
$N(2000)$	F_{15}	**	$\Delta(2150)$	S_{31}	*	$\Sigma(1775)$	D_{15}	****	Ω^-	****		$\Xi_c(2645)$	***
$N(2080)$	D_{13}	**	$\Delta(2200)$	G_{37}	*	$\Sigma(1840)$	P_{13}	*	$\Omega(2250)^-$	***		$\Xi_c(2790)$	***
$N(2090)$	S_{11}	*	$\Delta(2300)$	H_{39}	**	$\Sigma(1880)$	P_{11}	**	$\Omega(2380)^-$	**		$\Xi_c(2815)$	***
$N(2100)$	P_{11}	*	$\Delta(2350)$	D_{35}	*	$\Sigma(1915)$	F_{15}	****	$\Omega(2470)^-$	**		$\Xi_c(2930)$	*
$N(2190)$	G_{17}	****	$\Delta(2390)$	F_{37}	*	$\Sigma(1940)$	D_{13}	***				$\Xi_c(2980)$	***
$N(2200)$	D_{15}	**	$\Delta(2400)$	G_{39}	**	$\Sigma(2000)$	S_{11}	*				$\Xi_c(3055)$	**
$N(2220)$	H_{19}	****	$\Delta(2420)$	$H_{3,11}$	****	$\Sigma(2030)$	F_{17}	****				$\Xi_c(3080)$	***
$N(2250)$	G_{19}	****	$\Delta(2750)$	$l_{3,13}$	**	$\Sigma(2070)$	F_{15}	*				$\Xi_c(3123)$	*
$N(2600)$	$l_{1,11}$	***	$\Delta(2950)$	$K_{3,15}$	**	$\Sigma(2080)$	P_{13}	**				Ω_c^0	***
$N(2700)$	$K_{1,13}$	**				$\Sigma(2100)$	G_{17}	*				$\Omega_c(2770)^0$	***
			Λ	P_{01}	****	$\Sigma(2250)$		***					
			$\Lambda(1405)$	S_{01}	****	$\Sigma(2455)$		**				Ξ_{cc}^+	*
			$\Lambda(1520)$	D_{03}	****	$\Sigma(2620)$		**					
			$\Lambda(1600)$	P_{01}	***	$\Sigma(3000)$		*				Λ_b^0	***
			$\Lambda(1670)$	S_{01}	****	$\Sigma(3170)$		*				Σ_b	***
			$\Lambda(1690)$	D_{03}	****							Σ_b^*	***
			$\Lambda(1800)$	S_{01}	***							Ξ_b^0, Ξ_b^-	***
			$\Lambda(1810)$	P_{01}	***							Ω_b^-	***
			$\Lambda(1820)$	F_{05}	****								
			$\Lambda(1830)$	D_{05}	****								
			$\Lambda(1890)$	P_{03}	****								
			$\Lambda(2000)$	*									
			$\Lambda(2020)$	F_{07}	*								
			$\Lambda(2100)$	G_{07}	****								
			$\Lambda(2110)$	F_{05}	***								
			$\Lambda(2325)$	D_{03}	*								
			$\Lambda(2350)$	H_{09}	***								
			$\Lambda(2585)$	**									

**** Existence is certain, and properties are at least fairly well explored.

*** Existence ranges from very likely to certain, but further confirmation is desirable and/or quantum numbers, branching fractions, etc. are not well determined.

** Evidence of existence is only fair.

* Evidence of existence is poor.

Baryon Summary Table

Mean-square charge radius $\langle r_n^2 \rangle = -0.1161 \pm 0.0022$
 fm^2 ($S = 1.3$)
 Electric polarizability $\alpha = (11.6 \pm 1.5) \times 10^{-4} \text{fm}^3$
 Magnetic polarizability $\beta = (3.7 \pm 2.0) \times 10^{-4} \text{fm}^3$
 Charge $q = (-0.4 \pm 1.1) \times 10^{-21} e$
 Mean $n\bar{n}$ -oscillation time $> 8.6 \times 10^7 \text{s}$, CL = 90% (free n)
 Mean $n\bar{n}$ -oscillation time $> 1.3 \times 10^8 \text{s}$, CL = 90% [e] (bound n)
 Mean $n\bar{n}'$ -oscillation time $> 414 \text{s}$, CL = 90% [f]

 $p e^- \nu_e$ decay parameters [g]

$\lambda \equiv g_A / g_V = -1.2694 \pm 0.0028$ ($S = 2.0$)
 $A = -0.1173 \pm 0.0013$ ($S = 2.3$)
 $B = 0.9807 \pm 0.0030$
 $C = -0.2377 \pm 0.0026$
 $a = -0.103 \pm 0.004$
 $\phi_{AV} = (180.06 \pm 0.07)^\circ$ [h]
 $D = (-4 \pm 6) \times 10^{-4}$ [i]
 $R = 0.008 \pm 0.016$ [j]

n DECAY MODES	Fraction (Γ_i/Γ)	Confidence level	ρ (MeV/c)
$p e^- \bar{\nu}_e$	100	%	1
$p e^- \bar{\nu}_e \gamma$	[j] (3.13 ± 0.35) $\times 10^{-3}$		1

Charge conservation (Q) violating mode

$p \nu_e \bar{\nu}_e$	Q	< 8	$\times 10^{-27}$	68%	1
-----------------------	---	-------	-------------------	-----	---

 $N(1440) P_{11}$

$$I(J^P) = \frac{1}{2}(\frac{1}{2}^+)$$

Breit-Wigner mass = 1420 to 1470 (≈ 1440) MeV
 Breit-Wigner full width = 200 to 450 (≈ 300) MeV
 $p_{\text{beam}} = 0.61 \text{ GeV}/c$ $4\pi\lambda^2 = 31.0 \text{ mb}$
 Re(pole position) = 1350 to 1380 (≈ 1365) MeV
 $-2\text{Im}(\text{pole position}) = 160$ to 220 (≈ 190) MeV

$N(1440)$ DECAY MODES	Fraction (Γ_i/Γ)	ρ (MeV/c)
$N\pi$	0.55 to 0.75	398
$N\pi\pi$	30–40 %	347
$\Delta\pi$	20–30 %	147
$N\rho$	< 8 %	†
$N(\pi\pi)_{S\text{-wave}}^{J=0}$	5–10 %	–
$p\gamma$	0.035–0.048 %	414
$p\gamma$, helicity=1/2	0.035–0.048 %	414
$n\gamma$	0.009–0.032 %	413
$n\gamma$, helicity=1/2	0.009–0.032 %	413

 $N(1520) D_{13}$

$$I(J^P) = \frac{1}{2}(\frac{3}{2}^-)$$

Breit-Wigner mass = 1515 to 1525 (≈ 1520) MeV
 Breit-Wigner full width = 100 to 125 (≈ 115) MeV
 $p_{\text{beam}} = 0.74 \text{ GeV}/c$ $4\pi\lambda^2 = 23.5 \text{ mb}$
 Re(pole position) = 1505 to 1515 (≈ 1510) MeV
 $-2\text{Im}(\text{pole position}) = 105$ to 120 (≈ 110) MeV

$N(1520)$ DECAY MODES	Fraction (Γ_i/Γ)	ρ (MeV/c)
$N\pi$	0.55 to 0.65	457
$N\eta$	(2.3 ± 0.4) $\times 10^{-3}$	154
$N\pi\pi$	40–50 %	414
$\Delta\pi$	15–25 %	230
$N\rho$	15–25 %	†
$N(\pi\pi)_{S\text{-wave}}^{J=0}$	< 8 %	–
$p\gamma$	0.46–0.56 %	470
$p\gamma$, helicity=1/2	0.001–0.034 %	470
$p\gamma$, helicity=3/2	0.44–0.53 %	470
$n\gamma$	0.30–0.53 %	470
$n\gamma$, helicity=1/2	0.04–0.10 %	470
$n\gamma$, helicity=3/2	0.25–0.45 %	470

 $N(1535) S_{11}$

$$I(J^P) = \frac{1}{2}(\frac{1}{2}^-)$$

Breit-Wigner mass = 1525 to 1545 (≈ 1535) MeV
 Breit-Wigner full width = 125 to 175 (≈ 150) MeV
 $p_{\text{beam}} = 0.76 \text{ GeV}/c$ $4\pi\lambda^2 = 22.5 \text{ mb}$
 Re(pole position) = 1490 to 1530 (≈ 1510) MeV
 $-2\text{Im}(\text{pole position}) = 90$ to 250 (≈ 170) MeV

$N(1535)$ DECAY MODES	Fraction (Γ_i/Γ)	ρ (MeV/c)
$N\pi$	35–55 %	468
$N\eta$	45–60 %	186
$N\pi\pi$	1–10 %	426
$\Delta\pi$	< 1 %	244
$N\rho$	< 4 %	†
$N(\pi\pi)_{S\text{-wave}}^{J=0}$	< 3 %	–
$N(1440)\pi$	< 7 %	†
$p\gamma$	0.15–0.35 %	481
$p\gamma$, helicity=1/2	0.15–0.35 %	481
$n\gamma$	0.004–0.29 %	480
$n\gamma$, helicity=1/2	0.004–0.29 %	480

 $N(1650) S_{11}$

$$I(J^P) = \frac{1}{2}(\frac{1}{2}^-)$$

Breit-Wigner mass = 1645 to 1670 (≈ 1655) MeV
 Breit-Wigner full width = 145 to 185 (≈ 165) MeV
 $p_{\text{beam}} = 0.97 \text{ GeV}/c$ $4\pi\lambda^2 = 16.2 \text{ mb}$
 Re(pole position) = 1640 to 1670 (≈ 1655) MeV
 $-2\text{Im}(\text{pole position}) = 150$ to 180 (≈ 165) MeV

$N(1650)$ DECAY MODES	Fraction (Γ_i/Γ)	ρ (MeV/c)
$N\pi$	0.60 to 0.95	551
$N\eta$	3–10 %	354
ΛK	3–11 %	179
$N\pi\pi$	10–20 %	517
$\Delta\pi$	1–7 %	349
$N\rho$	4–12 %	†
$N(\pi\pi)_{S\text{-wave}}^{J=0}$	< 4 %	–
$N(1440)\pi$	< 5 %	156
$p\gamma$	0.04–0.18 %	562
$p\gamma$, helicity=1/2	0.04–0.18 %	562
$n\gamma$	0.003–0.17 %	561
$n\gamma$, helicity=1/2	0.003–0.17 %	561

 $N(1675) D_{15}$

$$I(J^P) = \frac{1}{2}(\frac{5}{2}^-)$$

Breit-Wigner mass = 1670 to 1680 (≈ 1675) MeV
 Breit-Wigner full width = 130 to 165 (≈ 150) MeV
 $p_{\text{beam}} = 1.01 \text{ GeV}/c$ $4\pi\lambda^2 = 15.4 \text{ mb}$
 Re(pole position) = 1655 to 1665 (≈ 1660) MeV
 $-2\text{Im}(\text{pole position}) = 125$ to 150 (≈ 135) MeV

$N(1675)$ DECAY MODES	Fraction (Γ_i/Γ)	ρ (MeV/c)
$N\pi$	0.35 to 0.45	564
$N\eta$	(0.0 ± 1.0) %	376
ΛK	< 1 %	216
$N\pi\pi$	50–60 %	532
$\Delta\pi$	50–60 %	366
$N\rho$	< 1 –3 %	†
$p\gamma$	0.004–0.023 %	575
$p\gamma$, helicity=1/2	0.0–0.015 %	575
$p\gamma$, helicity=3/2	0.0–0.011 %	575
$n\gamma$	0.02–0.12 %	574
$n\gamma$, helicity=1/2	0.006–0.046 %	574
$n\gamma$, helicity=3/2	0.01–0.08 %	574

Baryon Summary Table

 $N(1680) F_{15}$

$$I(J^P) = \frac{1}{2}(\frac{5}{2}^+)$$

Breit-Wigner mass = 1680 to 1690 (≈ 1685) MeV
 Breit-Wigner full width = 120 to 140 (≈ 130) MeV
 $p_{\text{beam}} = 1.02 \text{ GeV}/c$ $4\pi\lambda^2 = 15.0 \text{ mb}$
 Re(pole position) = 1665 to 1680 (≈ 1675) MeV
 $-2\text{Im}(\text{pole position}) = 110 \text{ to } 135$ (≈ 120) MeV

$N(1680)$ DECAY MODES	Fraction (Γ_i/Γ)	ρ (MeV/c)
$N\pi$	0.65 to 0.70	571
$N\eta$	(0.0 \pm 1.0) %	386
$N\pi\pi$	30–40 %	539
$\Delta\pi$	5–15 %	374
$N\rho$	3–15 %	†
$N(\pi\pi)_{S\text{-wave}}^{I=0}$	5–20 %	–
$p\gamma$	0.21–0.32 %	581
$p\gamma$, helicity=1/2	0.001–0.011 %	581
$p\gamma$, helicity=3/2	0.20–0.32 %	581
$n\gamma$	0.021–0.046 %	581
$n\gamma$, helicity=1/2	0.004–0.029 %	581
$n\gamma$, helicity=3/2	0.01–0.024 %	581

 $N(1700) D_{13}$

$$I(J^P) = \frac{1}{2}(\frac{3}{2}^-)$$

Breit-Wigner mass = 1650 to 1750 (≈ 1700) MeV
 Breit-Wigner full width = 50 to 150 (≈ 100) MeV
 $p_{\text{beam}} = 1.05 \text{ GeV}/c$ $4\pi\lambda^2 = 14.5 \text{ mb}$
 Re(pole position) = 1630 to 1730 (≈ 1680) MeV
 $-2\text{Im}(\text{pole position}) = 50 \text{ to } 150$ (≈ 100) MeV

$N(1700)$ DECAY MODES	Fraction (Γ_i/Γ)	ρ (MeV/c)
$N\pi$	5–15 %	581
$N\eta$	(0.0 \pm 1.0) %	402
ΛK	< 3 %	255
$N\pi\pi$	85–95 %	550
$N\rho$	< 35 %	†
$p\gamma$	0.01–0.05 %	591
$p\gamma$, helicity=1/2	0.0–0.024 %	591
$p\gamma$, helicity=3/2	0.002–0.026 %	591
$n\gamma$	0.01–0.13 %	590
$n\gamma$, helicity=1/2	0.0–0.09 %	590
$n\gamma$, helicity=3/2	0.01–0.05 %	590

 $N(1710) P_{11}$

$$I(J^P) = \frac{1}{2}(\frac{1}{2}^+)$$

Breit-Wigner mass = 1680 to 1740 (≈ 1710) MeV
 Breit-Wigner full width = 50 to 250 (≈ 100) MeV
 $p_{\text{beam}} = 1.07 \text{ GeV}/c$ $4\pi\lambda^2 = 14.2 \text{ mb}$
 Re(pole position) = 1670 to 1770 (≈ 1720) MeV
 $-2\text{Im}(\text{pole position}) = 80 \text{ to } 380$ (≈ 230) MeV

$N(1710)$ DECAY MODES	Fraction (Γ_i/Γ)	ρ (MeV/c)
$N\pi$	10–20 %	588
$N\eta$	(6.2 \pm 1.0) %	412
$N\omega$	(13.0 \pm 2.0) %	†
ΛK	5–25 %	269
$N\pi\pi$	40–90 %	557
$\Delta\pi$	15–40 %	394
$N\rho$	5–25 %	†
$N(\pi\pi)_{S\text{-wave}}^{I=0}$	10–40 %	–
$p\gamma$	0.002–0.05 %	598
$p\gamma$, helicity=1/2	0.002–0.05 %	598
$n\gamma$	0.0–0.02 %	597
$n\gamma$, helicity=1/2	0.0–0.02 %	597

 $N(1720) P_{13}$

$$I(J^P) = \frac{1}{2}(\frac{3}{2}^+)$$

Breit-Wigner mass = 1700 to 1750 (≈ 1720) MeV
 Breit-Wigner full width = 150 to 300 (≈ 200) MeV
 $p_{\text{beam}} = 1.09 \text{ GeV}/c$ $4\pi\lambda^2 = 13.9 \text{ mb}$
 Re(pole position) = 1660 to 1690 (≈ 1675) MeV
 $-2\text{Im}(\text{pole position}) = 115 \text{ to } 275$ MeV

$N(1720)$ DECAY MODES	Fraction (Γ_i/Γ)	ρ (MeV/c)
$N\pi$	10–20 %	594
$N\eta$	(4.0 \pm 1.0) %	422
ΛK	1–15 %	283
$N\pi\pi$	> 70 %	564
$N\rho$	70–85 %	73
$p\gamma$	0.003–0.10 %	604
$p\gamma$, helicity=1/2	0.003–0.08 %	604
$p\gamma$, helicity=3/2	0.001–0.03 %	604
$n\gamma$	0.002–0.39 %	603
$n\gamma$, helicity=1/2	0.0–0.002 %	603
$n\gamma$, helicity=3/2	0.001–0.39 %	603

 $N(2190) G_{17}$

$$I(J^P) = \frac{1}{2}(\frac{7}{2}^-)$$

Breit-Wigner mass = 2100 to 2200 (≈ 2190) MeV
 Breit-Wigner full width = 300 to 700 (≈ 500) MeV
 $p_{\text{beam}} = 2.07 \text{ GeV}/c$ $4\pi\lambda^2 = 6.21 \text{ mb}$
 Re(pole position) = 2050 to 2100 (≈ 2075) MeV
 $-2\text{Im}(\text{pole position}) = 400 \text{ to } 520$ (≈ 450) MeV

$N(2190)$ DECAY MODES	Fraction (Γ_i/Γ)	ρ (MeV/c)
$N\pi$	10–20 %	888
$N\eta$	(0.0 \pm 1.0) %	791
$N\omega$	seen	676
ΛK	seen	712
$N\pi\pi$	seen	870
$N\rho$	seen	680

 $N(2220) H_{19}$

$$I(J^P) = \frac{1}{2}(\frac{9}{2}^+)$$

Breit-Wigner mass = 2200 to 2300 (≈ 2250) MeV
 Breit-Wigner full width = 350 to 500 (≈ 400) MeV
 $p_{\text{beam}} = 2.21 \text{ GeV}/c$ $4\pi\lambda^2 = 5.74 \text{ mb}$
 Re(pole position) = 2130 to 2200 (≈ 2170) MeV
 $-2\text{Im}(\text{pole position}) = 400 \text{ to } 560$ (≈ 480) MeV

$N(2220)$ DECAY MODES	Fraction (Γ_i/Γ)	ρ (MeV/c)
$N\pi$	10–20 %	924

 $N(2250) G_{19}$

$$I(J^P) = \frac{1}{2}(\frac{9}{2}^-)$$

Breit-Wigner mass = 2200 to 2350 (≈ 2275) MeV
 Breit-Wigner full width = 230 to 800 (≈ 500) MeV
 $p_{\text{beam}} = 2.27 \text{ GeV}/c$ $4\pi\lambda^2 = 5.56 \text{ mb}$
 Re(pole position) = 2150 to 2250 (≈ 2200) MeV
 $-2\text{Im}(\text{pole position}) = 350 \text{ to } 550$ (≈ 450) MeV

$N(2250)$ DECAY MODES	Fraction (Γ_i/Γ)	ρ (MeV/c)
$N\pi$	5–15 %	938

 $N(2600) h_{1,11}$

$$I(J^P) = \frac{1}{2}(\frac{11}{2}^-)$$

Breit-Wigner mass = 2550 to 2750 (≈ 2600) MeV
 Breit-Wigner full width = 500 to 800 (≈ 650) MeV
 $p_{\text{beam}} = 3.12 \text{ GeV}/c$ $4\pi\lambda^2 = 3.86 \text{ mb}$

$N(2600)$ DECAY MODES	Fraction (Γ_i/Γ)	ρ (MeV/c)
$N\pi$	5–10 %	1126

Baryon Summary Table

 Δ BARYONS
($S = 0, I = 3/2$)

$$\Delta^{++} = uuu, \Delta^+ = uud, \Delta^0 = udd, \Delta^- = ddd$$

 $\Delta(1232) P_{33}$

$$I(J^P) = \frac{3}{2}(\frac{3}{2}^+)$$

Breit-Wigner mass (mixed charges) = 1231 to 1233 (\approx 1232) MeV

Breit-Wigner full width (mixed charges) = 116 to 120 (\approx 118) MeV

$$p_{\text{beam}} = 0.30 \text{ GeV}/c \quad 4\pi\lambda^2 = 94.8 \text{ mb}$$

Re(pole position) = 1209 to 1211 (\approx 1210) MeV

$-2\text{Im}(\text{pole position}) = 98 \text{ to } 102$ (\approx 100) MeV

$\Delta(1232)$ DECAY MODES	Fraction (Γ_i/Γ)	ρ (MeV/c)
$N\pi$	100 %	229
$N\gamma$	0.52-0.60 %	259
$N\gamma$, helicity=1/2	0.11-0.13 %	259
$N\gamma$, helicity=3/2	0.41-0.47 %	259

 $\Delta(1600) P_{33}$

$$I(J^P) = \frac{3}{2}(\frac{3}{2}^+)$$

Breit-Wigner mass = 1550 to 1700 (\approx 1600) MeV

Breit-Wigner full width = 250 to 450 (\approx 350) MeV

$$p_{\text{beam}} = 0.87 \text{ GeV}/c \quad 4\pi\lambda^2 = 18.6 \text{ mb}$$

Re(pole position) = 1500 to 1700 (\approx 1600) MeV

$-2\text{Im}(\text{pole position}) = 200 \text{ to } 400$ (\approx 300) MeV

$\Delta(1600)$ DECAY MODES	Fraction (Γ_i/Γ)	ρ (MeV/c)
$N\pi$	10-25 %	513
$N\pi\pi$	75-90 %	477
$\Delta\pi$	40-70 %	303
$N\rho$	<25 %	†
$N(1440)\pi$	10-35 %	82
$N\gamma$	0.001-0.02 %	525
$N\gamma$, helicity=1/2	0.0-0.02 %	525
$N\gamma$, helicity=3/2	0.001-0.005 %	525

 $\Delta(1620) S_{31}$

$$I(J^P) = \frac{3}{2}(\frac{1}{2}^-)$$

Breit-Wigner mass = 1600 to 1660 (\approx 1630) MeV

Breit-Wigner full width = 135 to 150 (\approx 145) MeV

$$p_{\text{beam}} = 0.93 \text{ GeV}/c \quad 4\pi\lambda^2 = 17.2 \text{ mb}$$

Re(pole position) = 1590 to 1610 (\approx 1600) MeV

$-2\text{Im}(\text{pole position}) = 115 \text{ to } 120$ (\approx 118) MeV

$\Delta(1620)$ DECAY MODES	Fraction (Γ_i/Γ)	ρ (MeV/c)
$N\pi$	20-30 %	534
$N\pi\pi$	70-80 %	499
$\Delta\pi$	30-60 %	328
$N\rho$	7-25 %	†
$N\gamma$	0.004-0.044 %	545
$N\gamma$, helicity=1/2	0.004-0.044 %	545

 $\Delta(1700) D_{33}$

$$I(J^P) = \frac{3}{2}(\frac{3}{2}^-)$$

Breit-Wigner mass = 1670 to 1750 (\approx 1700) MeV

Breit-Wigner full width = 200 to 400 (\approx 300) MeV

$$p_{\text{beam}} = 1.05 \text{ GeV}/c \quad 4\pi\lambda^2 = 14.5 \text{ mb}$$

Re(pole position) = 1620 to 1680 (\approx 1650) MeV

$-2\text{Im}(\text{pole position}) = 160 \text{ to } 240$ (\approx 200) MeV

$\Delta(1700)$ DECAY MODES	Fraction (Γ_i/Γ)	ρ (MeV/c)
$N\pi$	10-20 %	581
$N\pi\pi$	80-90 %	550
$\Delta\pi$	30-60 %	386
$N\rho$	30-55 %	†
$N\gamma$	0.12-0.26 %	591
$N\gamma$, helicity=1/2	0.08-0.16 %	591
$N\gamma$, helicity=3/2	0.025-0.12 %	591

 $\Delta(1905) F_{35}$

$$I(J^P) = \frac{3}{2}(\frac{5}{2}^+)$$

Breit-Wigner mass = 1865 to 1915 (\approx 1890) MeV

Breit-Wigner full width = 270 to 400 (\approx 330) MeV

$$p_{\text{beam}} = 1.42 \text{ GeV}/c \quad 4\pi\lambda^2 = 9.89 \text{ mb}$$

Re(pole position) = 1825 to 1835 (\approx 1830) MeV

$-2\text{Im}(\text{pole position}) = 265 \text{ to } 300$ (\approx 280) MeV

$\Delta(1905)$ DECAY MODES	Fraction (Γ_i/Γ)	ρ (MeV/c)
$N\pi$	0.09 to 0.15	704
$N\pi\pi$	85-95 %	680
$\Delta\pi$	<25 %	531
$N\rho$	>60 %	397
$N\gamma$	0.01-0.03 %	712
$N\gamma$, helicity=1/2	0.0-0.1 %	712
$N\gamma$, helicity=3/2	0.004-0.03 %	712

 $\Delta(1910) P_{31}$

$$I(J^P) = \frac{3}{2}(\frac{1}{2}^+)$$

Breit-Wigner mass = 1870 to 1920 (\approx 1910) MeV

Breit-Wigner full width = 190 to 270 (\approx 250) MeV

$$p_{\text{beam}} = 1.46 \text{ GeV}/c \quad 4\pi\lambda^2 = 9.54 \text{ mb}$$

Re(pole position) = 1830 to 1880 (\approx 1855) MeV

$-2\text{Im}(\text{pole position}) = 200 \text{ to } 500$ (\approx 350) MeV

$\Delta(1910)$ DECAY MODES	Fraction (Γ_i/Γ)	ρ (MeV/c)
$N\pi$	15-30 %	717
$N\gamma$	0.0-0.2 %	725
$N\gamma$, helicity=1/2	0.0-0.2 %	725

 $\Delta(1920) P_{33}$

$$I(J^P) = \frac{3}{2}(\frac{3}{2}^+)$$

Breit-Wigner mass = 1900 to 1970 (\approx 1920) MeV

Breit-Wigner full width = 150 to 300 (\approx 200) MeV

$$p_{\text{beam}} = 1.48 \text{ GeV}/c \quad 4\pi\lambda^2 = 9.37 \text{ mb}$$

Re(pole position) = 1850 to 1950 (\approx 1900) MeV

$-2\text{Im}(\text{pole position}) = 200 \text{ to } 400$ (\approx 300) MeV

$\Delta(1920)$ DECAY MODES	Fraction (Γ_i/Γ)	ρ (MeV/c)
$N\pi$	5-20 %	723
ΣK	(2.10 ± 0.30) %	431

 $\Delta(1930) D_{35}$

$$I(J^P) = \frac{3}{2}(\frac{5}{2}^-)$$

Breit-Wigner mass = 1900 to 2020 (\approx 1960) MeV

Breit-Wigner full width = 220 to 500 (\approx 360) MeV

$$p_{\text{beam}} = 1.56 \text{ GeV}/c \quad 4\pi\lambda^2 = 8.76 \text{ mb}$$

Re(pole position) = 1840 to 1960 (\approx 1900) MeV

$-2\text{Im}(\text{pole position}) = 175 \text{ to } 360$ (\approx 270) MeV

$\Delta(1930)$ DECAY MODES	Fraction (Γ_i/Γ)	ρ (MeV/c)
$N\pi$	0.05 to 0.15	748
$N\gamma$	0.0-0.02 %	755
$N\gamma$, helicity=1/2	0.0-0.01 %	755
$N\gamma$, helicity=3/2	0.0-0.01 %	755

Baryon Summary Table

 $\Delta(1950) F_{37}$

$$I(J^P) = \frac{3}{2}(\frac{7}{2}^+)$$

Breit-Wigner mass = 1915 to 1950 (\approx 1930) MeV
 Breit-Wigner full width = 235 to 335 (\approx 285) MeV
 $p_{\text{beam}} = 1.50 \text{ GeV}/c$ $4\pi\lambda^2 = 9.21 \text{ mb}$
 Re(pole position) = 1870 to 1890 (\approx 1880) MeV
 $-2\text{Im}(\text{pole position}) = 220 \text{ to } 260$ (\approx 240) MeV

$\Delta(1950)$ DECAY MODES	Fraction (Γ_i/Γ)	ρ (MeV/c)
$N\pi$	0.35 to 0.45	729
$N\pi\pi$		706
$\Delta\pi$	20–30 %	560
$N\rho$	<10 %	442
$N\gamma$	0.08–0.13 %	737
$N\gamma$, helicity=1/2	0.03–0.055 %	737
$N\gamma$, helicity=3/2	0.05–0.075 %	737

 $\Delta(2420) H_{3,11}$

$$I(J^P) = \frac{3}{2}(\frac{11}{2}^+)$$

Breit-Wigner mass = 2300 to 2500 (\approx 2420) MeV
 Breit-Wigner full width = 300 to 500 (\approx 400) MeV
 $p_{\text{beam}} = 2.64 \text{ GeV}/c$ $4\pi\lambda^2 = 4.68 \text{ mb}$
 Re(pole position) = 2260 to 2400 (\approx 2330) MeV
 $-2\text{Im}(\text{pole position}) = 350 \text{ to } 750$ (\approx 550) MeV

$\Delta(2420)$ DECAY MODES	Fraction (Γ_i/Γ)	ρ (MeV/c)
$N\pi$	5–15 %	1023

Λ BARYONS

$(S = -1, I = 0)$

$\Lambda^0 = uds$

 Λ

$$I(J^P) = 0(\frac{1}{2}^+)$$

Mass $m = 1115.683 \pm 0.006 \text{ MeV}$
 $(m_\Lambda - m_\pi) / m_\Lambda = (-0.1 \pm 1.1) \times 10^{-5}$ ($S = 1.6$)
 Mean life $\tau = (2.631 \pm 0.020) \times 10^{-10} \text{ s}$ ($S = 1.6$)
 $(\tau_\Lambda - \tau_{\bar{\Lambda}}) / \tau_\Lambda = -0.001 \pm 0.009$
 $c\tau = 7.89 \text{ cm}$
 Magnetic moment $\mu = -0.613 \pm 0.004 \mu_N$
 Electric dipole moment $d < 1.5 \times 10^{-16} \text{ ecm}$, CL = 95%

Decay parameters

$p\pi^-$	$\alpha_- = 0.642 \pm 0.013$
$\bar{p}\pi^+$	$\alpha_+ = -0.71 \pm 0.08$
$p\pi^-$	$\phi_- = (-6.5 \pm 3.5)^\circ$
"	$\gamma_- = 0.76 [k]$
"	$\Delta_- = (8 \pm 4)^\circ [k]$
$n\pi^0$	$\alpha_0 = 0.65 \pm 0.04$
$p e^- \bar{\nu}_e$	$g_A/g_V = -0.718 \pm 0.015 [g]$

Λ DECAY MODES	Fraction (Γ_i/Γ)	ρ (MeV/c)
$p\pi^-$	(63.9 \pm 0.5) %	101
$n\pi^0$	(35.8 \pm 0.5) %	104
$n\gamma$	(1.75 \pm 0.15) $\times 10^{-3}$	162
$p\pi^- \gamma$	[1] (8.4 \pm 1.4) $\times 10^{-4}$	101
$p e^- \bar{\nu}_e$	(8.32 \pm 0.14) $\times 10^{-4}$	163
$p\mu^- \bar{\nu}_\mu$	(1.57 \pm 0.35) $\times 10^{-4}$	131

 $\Lambda(1405) S_{01}$

$$I(J^P) = 0(\frac{1}{2}^-)$$

Mass $m = 1406 \pm 4 \text{ MeV}$
 Full width $\Gamma = 50 \pm 2 \text{ MeV}$
 Below $\bar{K}N$ threshold

$\Lambda(1405)$ DECAY MODES	Fraction (Γ_i/Γ)	ρ (MeV/c)
$\Sigma\pi$	100 %	157

 $\Lambda(1520) D_{03}$

$$I(J^P) = 0(\frac{3}{2}^-)$$

Mass $m = 1519.5 \pm 1.0 \text{ MeV} [m]$
 Full width $\Gamma = 15.6 \pm 1.0 \text{ MeV} [m]$
 $p_{\text{beam}} = 0.39 \text{ GeV}/c$ $4\pi\lambda^2 = 82.8 \text{ mb}$

$\Lambda(1520)$ DECAY MODES	Fraction (Γ_i/Γ)	ρ (MeV/c)
$N\bar{K}$	45 \pm 1%	243
$\Sigma\pi$	42 \pm 1%	268
$\Lambda\pi\pi$	10 \pm 1%	259
$\Sigma\pi\pi$	0.9 \pm 0.1%	169
$\Lambda\gamma$	0.85 \pm 0.15%	350

 $\Lambda(1600) P_{01}$

$$I(J^P) = 0(\frac{1}{2}^-)$$

Mass $m = 1560 \text{ to } 1700$ (\approx 1600) MeV
 Full width $\Gamma = 50 \text{ to } 250$ (\approx 150) MeV
 $p_{\text{beam}} = 0.58 \text{ GeV}/c$ $4\pi\lambda^2 = 41.6 \text{ mb}$

$\Lambda(1600)$ DECAY MODES	Fraction (Γ_i/Γ)	ρ (MeV/c)
$N\bar{K}$	15–30 %	343
$\Sigma\pi$	10–60 %	338

 $\Lambda(1670) S_{01}$

$$I(J^P) = 0(\frac{1}{2}^-)$$

Mass $m = 1660 \text{ to } 1680$ (\approx 1670) MeV
 Full width $\Gamma = 25 \text{ to } 50$ (\approx 35) MeV
 $p_{\text{beam}} = 0.74 \text{ GeV}/c$ $4\pi\lambda^2 = 28.5 \text{ mb}$

$\Lambda(1670)$ DECAY MODES	Fraction (Γ_i/Γ)	ρ (MeV/c)
$N\bar{K}$	20–30 %	414
$\Sigma\pi$	25–55 %	394
$\Lambda\eta$	10–25 %	69

 $\Lambda(1690) D_{03}$

$$I(J^P) = 0(\frac{3}{2}^-)$$

Mass $m = 1685 \text{ to } 1695$ (\approx 1690) MeV
 Full width $\Gamma = 50 \text{ to } 70$ (\approx 60) MeV
 $p_{\text{beam}} = 0.78 \text{ GeV}/c$ $4\pi\lambda^2 = 26.1 \text{ mb}$

$\Lambda(1690)$ DECAY MODES	Fraction (Γ_i/Γ)	ρ (MeV/c)
$N\bar{K}$	20–30 %	433
$\Sigma\pi$	20–40 %	410
$\Lambda\pi\pi$	\sim 25 %	419
$\Sigma\pi\pi$	\sim 20 %	358

 $\Lambda(1800) S_{01}$

$$I(J^P) = 0(\frac{1}{2}^-)$$

Mass $m = 1720 \text{ to } 1850$ (\approx 1800) MeV
 Full width $\Gamma = 200 \text{ to } 400$ (\approx 300) MeV
 $p_{\text{beam}} = 1.01 \text{ GeV}/c$ $4\pi\lambda^2 = 17.5 \text{ mb}$

$\Lambda(1800)$ DECAY MODES	Fraction (Γ_i/Γ)	ρ (MeV/c)
$N\bar{K}$	25–40 %	528
$\Sigma\pi$	seen	494
$\Sigma(1385)\pi$	seen	349
$N\bar{K}^*(892)$	seen	†

Baryon Summary Table

$\Lambda(1810) P_{01}$		$I(J^P) = 0(\frac{1}{2}^+)$
Mass $m = 1750$ to 1850 (≈ 1810) MeV		
Full width $\Gamma = 50$ to 250 (≈ 150) MeV		
$\rho_{\text{beam}} = 1.04$ GeV/c $4\pi\lambda^2 = 17.0$ mb		
$\Lambda(1810)$ DECAY MODES	Fraction (Γ_i/Γ)	ρ (MeV/c)
$N\bar{K}$	20–50 %	537
$\Sigma\pi$	10–40 %	501
$\Sigma(1385)\pi$	seen	357
$N\bar{K}^*(892)$	30–60 %	†

$\Lambda(1820) F_{05}$		$I(J^P) = 0(\frac{5}{2}^+)$
Mass $m = 1815$ to 1825 (≈ 1820) MeV		
Full width $\Gamma = 70$ to 90 (≈ 80) MeV		
$\rho_{\text{beam}} = 1.06$ GeV/c $4\pi\lambda^2 = 16.5$ mb		
$\Lambda(1820)$ DECAY MODES	Fraction (Γ_i/Γ)	ρ (MeV/c)
$N\bar{K}$	55–65 %	545
$\Sigma\pi$	8–14 %	509
$\Sigma(1385)\pi$	5–10 %	366

$\Lambda(1830) D_{05}$		$I(J^P) = 0(\frac{5}{2}^-)$
Mass $m = 1810$ to 1830 (≈ 1830) MeV		
Full width $\Gamma = 60$ to 110 (≈ 95) MeV		
$\rho_{\text{beam}} = 1.08$ GeV/c $4\pi\lambda^2 = 16.0$ mb		
$\Lambda(1830)$ DECAY MODES	Fraction (Γ_i/Γ)	ρ (MeV/c)
$N\bar{K}$	3–10 %	553
$\Sigma\pi$	35–75 %	516
$\Sigma(1385)\pi$	>15 %	374

$\Lambda(1890) P_{03}$		$I(J^P) = 0(\frac{3}{2}^+)$
Mass $m = 1850$ to 1910 (≈ 1890) MeV		
Full width $\Gamma = 60$ to 200 (≈ 100) MeV		
$\rho_{\text{beam}} = 1.21$ GeV/c $4\pi\lambda^2 = 13.6$ mb		
$\Lambda(1890)$ DECAY MODES	Fraction (Γ_i/Γ)	ρ (MeV/c)
$N\bar{K}$	20–35 %	599
$\Sigma\pi$	3–10 %	560
$\Sigma(1385)\pi$	seen	423
$N\bar{K}^*(892)$	seen	236

$\Lambda(2100) G_{07}$		$I(J^P) = 0(\frac{7}{2}^-)$
Mass $m = 2090$ to 2110 (≈ 2100) MeV		
Full width $\Gamma = 100$ to 250 (≈ 200) MeV		
$\rho_{\text{beam}} = 1.68$ GeV/c $4\pi\lambda^2 = 8.68$ mb		
$\Lambda(2100)$ DECAY MODES	Fraction (Γ_i/Γ)	ρ (MeV/c)
$N\bar{K}$	25–35 %	751
$\Sigma\pi$	~ 5 %	705
$\Lambda\eta$	<3 %	617
ΞK	<3 %	491
$\Lambda\omega$	<8 %	443
$N\bar{K}^*(892)$	10–20 %	515

$\Lambda(2110) F_{05}$		$I(J^P) = 0(\frac{5}{2}^+)$
Mass $m = 2090$ to 2140 (≈ 2110) MeV		
Full width $\Gamma = 150$ to 250 (≈ 200) MeV		
$\rho_{\text{beam}} = 1.70$ GeV/c $4\pi\lambda^2 = 8.53$ mb		

$\Lambda(2110)$ DECAY MODES	Fraction (Γ_i/Γ)	ρ (MeV/c)
$N\bar{K}$	5–25 %	757
$\Sigma\pi$	10–40 %	711
$\Lambda\omega$	seen	455
$\Sigma(1385)\pi$	seen	591
$N\bar{K}^*(892)$	10–60 %	525

$\Lambda(2350) H_{09}$		$I(J^P) = 0(\frac{9}{2}^+)$
Mass $m = 2340$ to 2370 (≈ 2350) MeV		
Full width $\Gamma = 100$ to 250 (≈ 150) MeV		
$\rho_{\text{beam}} = 2.29$ GeV/c $4\pi\lambda^2 = 5.85$ mb		
$\Lambda(2350)$ DECAY MODES	Fraction (Γ_i/Γ)	ρ (MeV/c)
$N\bar{K}$	~ 12 %	915
$\Sigma\pi$	~ 10 %	867

Σ BARYONS ($S = -1, I = 1$)

$\Sigma^+ = uus, \Sigma^0 = uds, \Sigma^- = dds$

Σ^+		$I(J^P) = 1(\frac{1}{2}^+)$
Mass $m = 1189.37 \pm 0.07$ MeV ($S = 2.2$)		
Mean life $\tau = (0.8018 \pm 0.0026) \times 10^{-10}$ s		
$c\tau = 2.404$ cm		
$(\tau_{\Sigma^+} - \tau_{\Sigma^-}) / \tau_{\Sigma^+} = (-0.6 \pm 1.2) \times 10^{-3}$		
Magnetic moment $\mu = 2.458 \pm 0.010 \mu_N$ ($S = 2.1$)		
$(\mu_{\Sigma^+} + \mu_{\Sigma^-}) / \mu_{\Sigma^+} = 0.014 \pm 0.015$		
$\Gamma(\Sigma^+ \rightarrow n\ell^+\nu) / \Gamma(\Sigma^- \rightarrow n\ell^-\bar{\nu}) < 0.043$		
Decay parameters		
$\rho\pi^0$	$\alpha_0 = -0.980^{+0.017}_{-0.015}$	
"	$\phi_0 = (36 \pm 34)^\circ$	
"	$\gamma_0 = 0.16$ [k]	
"	$\Delta_0 = (187 \pm 6)^\circ$ [k]	
$n\pi^+$	$\alpha_+ = 0.068 \pm 0.013$	
"	$\phi_+ = (167 \pm 20)^\circ$ ($S = 1.1$)	
"	$\gamma_+ = -0.97$ [k]	
"	$\Delta_+ = (-73^{+133}_{-10})^\circ$ [k]	
$\rho\gamma$	$\alpha_\gamma = -0.76 \pm 0.08$	

Σ^+ DECAY MODES	Fraction (Γ_i/Γ)	Confidence level	ρ (MeV/c)
$\rho\pi^0$	(51.57 ± 0.30) %		189
$n\pi^+$	(48.31 ± 0.30) %		185
$\rho\gamma$	(1.23 ± 0.05) × 10 ⁻³		225
$n\pi^+\gamma$	[] (4.5 ± 0.5) × 10 ⁻⁴		185
$\Lambda e^+\nu_e$	(2.0 ± 0.5) × 10 ⁻⁵		71

$\Delta S = \Delta Q$ (SQ) violating modes or $\Delta S = 1$ weak neutral current (S1) modes			
$n e^+\nu_e$	SQ	< 5	× 10 ⁻⁶ 90% 224
$n \mu^+\nu_\mu$	SQ	< 3.0	× 10 ⁻⁵ 90% 202
$\rho e^+ e^-$	S1	< 7	× 10 ⁻⁶ 225
$\rho \mu^+ \mu^-$	S1	(9 $\frac{+9}{-8}$) × 10 ⁻⁸	121

Σ^0		$I(J^P) = 1(\frac{1}{2}^+)$
Mass $m = 1192.642 \pm 0.024$ MeV		
$m_{\Sigma^-} - m_{\Sigma^0} = 4.807 \pm 0.035$ MeV ($S = 1.1$)		
$m_{\Sigma^0} - m_\Lambda = 76.959 \pm 0.023$ MeV		
Mean life $\tau = (7.4 \pm 0.7) \times 10^{-20}$ s		
$c\tau = 2.22 \times 10^{-11}$ m		
Transition magnetic moment $ \mu_{\Sigma\Lambda} = 1.61 \pm 0.08 \mu_N$		

Baryon Summary Table

Σ^0 DECAY MODES	Fraction (Γ_i/Γ)	Confidence level	ρ (MeV/c)
$\Lambda\gamma$	100 %		74
$\Lambda\gamma\gamma$	< 3 %	90%	74
$\Lambda e^+ e^-$	[n] 5×10^{-3}		74

 Σ^-

$$I(J^P) = 1(\frac{1}{2}^+)$$

Mass $m = 1197.449 \pm 0.030$ MeV (S = 1.2)
 $m_{\Sigma^-} - m_{\Sigma^+} = 8.08 \pm 0.08$ MeV (S = 1.9)
 $m_{\Sigma^-} - m_{\Lambda} = 81.766 \pm 0.030$ MeV (S = 1.2)
Mean life $\tau = (1.479 \pm 0.011) \times 10^{-10}$ s (S = 1.3)
 $c\tau = 4.434$ cm
Magnetic moment $\mu = -1.160 \pm 0.025 \mu_N$ (S = 1.7)
 Σ^- charge radius = 0.78 ± 0.10 fm

Decay parameters

$n\pi^-$ $\alpha_- = -0.068 \pm 0.008$
" $\phi_- = (10 \pm 15)^\circ$
" $\gamma_- = 0.98$ [k]
" $\Delta_- = (249^+_{-120})^\circ$ [k]
 $n e^- \bar{\nu}_e$ $g_A/g_V = 0.340 \pm 0.017$ [g]
" $f_2(0)/f_1(0) = 0.97 \pm 0.14$
" $D = 0.11 \pm 0.10$
 $\Lambda e^- \bar{\nu}_e$ $g_V/g_A = 0.01 \pm 0.10$ [g] (S = 1.5)
" $g_{WM}/g_A = 2.4 \pm 1.7$ [g]

Σ^- DECAY MODES	Fraction (Γ_i/Γ)	ρ (MeV/c)
$n\pi^-$	(99.848 ± 0.005) %	193
$n\pi^- \gamma$	[l] (4.6 ± 0.6) × 10 ⁻⁴	193
$n e^- \bar{\nu}_e$	(1.017 ± 0.034) × 10 ⁻³	230
$n \mu^- \bar{\nu}_\mu$	(4.5 ± 0.4) × 10 ⁻⁴	210
$\Lambda e^- \bar{\nu}_e$	(5.73 ± 0.27) × 10 ⁻⁵	79

 $\Sigma(1385) P_{13}$

$$I(J^P) = 1(\frac{3}{2}^+)$$

$\Sigma(1385)^+$ mass $m = 1382.8 \pm 0.4$ MeV (S = 2.0)
 $\Sigma(1385)^0$ mass $m = 1383.7 \pm 1.0$ MeV (S = 1.4)
 $\Sigma(1385)^-$ mass $m = 1387.2 \pm 0.5$ MeV (S = 2.2)
 $\Sigma(1385)^+$ full width $\Gamma = 35.8 \pm 0.8$ MeV
 $\Sigma(1385)^0$ full width $\Gamma = 36 \pm 5$ MeV
 $\Sigma(1385)^-$ full width $\Gamma = 39.4 \pm 2.1$ MeV (S = 1.7)
Below $\bar{K}N$ threshold

$\Sigma(1385)$ DECAY MODES	Fraction (Γ_i/Γ)	Confidence level	ρ (MeV/c)
$\Lambda\pi$	(87.0 ± 1.5) %		208
$\Sigma\pi$	(11.7 ± 1.5) %		129
$\Lambda\gamma$	(1.3 ± 0.4) %		241
$\Sigma^- \gamma$	< 2.4 × 10 ⁻⁴	90%	173

 $\Sigma(1660) P_{11}$

$$I(J^P) = 1(\frac{1}{2}^+)$$

Mass $m = 1630$ to 1690 (≈ 1660) MeV
Full width $\Gamma = 40$ to 200 (≈ 100) MeV
 $\rho_{\text{beam}} = 0.72$ GeV/c $4\pi\lambda^2 = 29.9$ mb

$\Sigma(1660)$ DECAY MODES	Fraction (Γ_i/Γ)	ρ (MeV/c)
$N\bar{K}$	10–30 %	405
$\Lambda\pi$	seen	440
$\Sigma\pi$	seen	387

 $\Sigma(1670) D_{13}$

$$I(J^P) = 1(\frac{3}{2}^-)$$

Mass $m = 1665$ to 1685 (≈ 1670) MeV
Full width $\Gamma = 40$ to 80 (≈ 60) MeV
 $\rho_{\text{beam}} = 0.74$ GeV/c $4\pi\lambda^2 = 28.5$ mb

$\Sigma(1670)$ DECAY MODES	Fraction (Γ_i/Γ)	ρ (MeV/c)
$N\bar{K}$	7–13 %	414
$\Lambda\pi$	5–15 %	448
$\Sigma\pi$	30–60 %	394

 $\Sigma(1750) S_{11}$

$$I(J^P) = 1(\frac{1}{2}^-)$$

Mass $m = 1730$ to 1800 (≈ 1750) MeV
Full width $\Gamma = 60$ to 160 (≈ 90) MeV
 $\rho_{\text{beam}} = 0.91$ GeV/c $4\pi\lambda^2 = 20.7$ mb

$\Sigma(1750)$ DECAY MODES	Fraction (Γ_i/Γ)	ρ (MeV/c)
$N\bar{K}$	10–40 %	486
$\Lambda\pi$	seen	507
$\Sigma\pi$	< 8 %	456
$\Sigma\eta$	15–55 %	98

 $\Sigma(1775) D_{15}$

$$I(J^P) = 1(\frac{5}{2}^-)$$

Mass $m = 1770$ to 1780 (≈ 1775) MeV
Full width $\Gamma = 105$ to 135 (≈ 120) MeV
 $\rho_{\text{beam}} = 0.96$ GeV/c $4\pi\lambda^2 = 19.0$ mb

$\Sigma(1775)$ DECAY MODES	Fraction (Γ_i/Γ)	ρ (MeV/c)
$N\bar{K}$	37–43%	508
$\Lambda\pi$	14–20%	525
$\Sigma\pi$	2–5%	475
$\Sigma(1385)\pi$	8–12%	327
$\Lambda(1520)\pi$	17–23%	201

 $\Sigma(1915) F_{15}$

$$I(J^P) = 1(\frac{5}{2}^+)$$

Mass $m = 1900$ to 1935 (≈ 1915) MeV
Full width $\Gamma = 80$ to 160 (≈ 120) MeV
 $\rho_{\text{beam}} = 1.26$ GeV/c $4\pi\lambda^2 = 12.8$ mb

$\Sigma(1915)$ DECAY MODES	Fraction (Γ_i/Γ)	ρ (MeV/c)
$N\bar{K}$	5–15 %	618
$\Lambda\pi$	seen	623
$\Sigma\pi$	seen	577
$\Sigma(1385)\pi$	< 5 %	443

 $\Sigma(1940) D_{13}$

$$I(J^P) = 1(\frac{3}{2}^-)$$

Mass $m = 1900$ to 1950 (≈ 1940) MeV
Full width $\Gamma = 150$ to 300 (≈ 220) MeV
 $\rho_{\text{beam}} = 1.32$ GeV/c $4\pi\lambda^2 = 12.1$ mb

$\Sigma(1940)$ DECAY MODES	Fraction (Γ_i/Γ)	ρ (MeV/c)
$N\bar{K}$	< 20 %	637
$\Lambda\pi$	seen	640
$\Sigma\pi$	seen	595
$\Sigma(1385)\pi$	seen	463
$\Lambda(1520)\pi$	seen	355
$\Delta(1232)\bar{K}$	seen	410
$N\bar{K}^*(892)$	seen	322

 $\Sigma(2030) F_{17}$

$$I(J^P) = 1(\frac{7}{2}^+)$$

Mass $m = 2025$ to 2040 (≈ 2030) MeV
Full width $\Gamma = 150$ to 200 (≈ 180) MeV
 $\rho_{\text{beam}} = 1.52$ GeV/c $4\pi\lambda^2 = 9.93$ mb

Baryon Summary Table

$\Sigma(2030)$ DECAY MODES	Fraction (Γ_i/Γ)	ρ (MeV/c)
$N\bar{K}$	17-23 %	702
$\Lambda\pi$	17-23 %	700
$\Sigma\pi$	5-10 %	657
ΞK	<2 %	422
$\Sigma(1385)\pi$	5-15 %	532
$\Lambda(1520)\pi$	10-20 %	430
$\Delta(1232)\bar{K}$	10-20 %	498
$N\bar{K}^*(892)$	<5 %	439

$\Sigma(2250)$ $I(J^P) = 1(??)$

Mass $m = 2210$ to 2280 (≈ 2250) MeV
 Full width $\Gamma = 60$ to 150 (≈ 100) MeV
 $\rho_{\text{beam}} = 2.04$ GeV/c $4\pi\lambda^2 = 6.76$ mb

$\Sigma(2250)$ DECAY MODES	Fraction (Γ_i/Γ)	ρ (MeV/c)
$N\bar{K}$	<10 %	851
$\Lambda\pi$	seen	842
$\Sigma\pi$	seen	803

Ξ BARYONS ($S = -2, I = 1/2$)

$$\Xi^0 = uss, \quad \Xi^- = dss$$

Ξ^0 $I(J^P) = \frac{1}{2}(\frac{1}{2}^+)$

P is not yet measured; + is the quark model prediction.

Mass $m = 1314.86 \pm 0.20$ MeV
 $m_{\Xi^-} - m_{\Xi^0} = 6.85 \pm 0.21$ MeV
 Mean life $\tau = (2.90 \pm 0.09) \times 10^{-10}$ s
 $c\tau = 8.71$ cm

Magnetic moment $\mu = -1.250 \pm 0.014 \mu_N$

Decay parameters

$\Lambda\pi^0$	$\alpha = -0.411 \pm 0.022$ ($S = 2.1$)
"	$\phi = (21 \pm 12)^\circ$
"	$\gamma = 0.85$ [k]
"	$\Delta = (218^{+12}_{-19})^\circ$ [k]
$\Lambda\gamma$	$\alpha = -0.73 \pm 0.17$
$\Lambda e^+ e^-$	$\alpha = -0.8 \pm 0.2$
$\Sigma^0\gamma$	$\alpha = -0.63 \pm 0.09$
$\Sigma^+ e^- \bar{\nu}_e$	$g_1(0)/f_1(0) = 1.21 \pm 0.05$
$\Sigma^+ e^- \bar{\nu}_e$	$f_2(0)/f_1(0) = 2.0 \pm 1.3$

Ξ^0 DECAY MODES	Fraction (Γ_i/Γ)	Confidence level	ρ (MeV/c)
$\Lambda\pi^0$	$(99.525 \pm 0.012) \%$		135
$\Lambda\gamma$	$(1.17 \pm 0.07) \times 10^{-3}$		184
$\Lambda e^+ e^-$	$(7.6 \pm 0.6) \times 10^{-6}$		184
$\Sigma^0\gamma$	$(3.33 \pm 0.10) \times 10^{-3}$		117
$\Sigma^+ e^- \bar{\nu}_e$	$(2.53 \pm 0.08) \times 10^{-4}$		120
$\Sigma^+ \mu^- \bar{\nu}_\mu$	$(4.6^{+1.8}_{-1.4}) \times 10^{-6}$		64

$\Delta S = \Delta Q$ (SQ) violating modes or $\Delta S = 2$ forbidden ($S2$) modes

$\Sigma^- e^+ \nu_e$	$SQ < 9$	$\times 10^{-4}$	90%	112
$\Sigma^- \mu^+ \nu_\mu$	$SQ < 9$	$\times 10^{-4}$	90%	49
$\rho\pi^-$	$S2 < 8$	$\times 10^{-6}$	90%	299
$\rho e^- \bar{\nu}_e$	$S2 < 1.3$	$\times 10^{-3}$		323
$\rho \mu^- \bar{\nu}_\mu$	$S2 < 1.3$	$\times 10^{-3}$		309

Ξ^-

$$I(J^P) = \frac{1}{2}(\frac{1}{2}^+)$$

P is not yet measured; + is the quark model prediction.

Mass $m = 1321.71 \pm 0.07$ MeV

$$(m_{\Xi^-} - m_{\Xi^+}) / m_{\Xi^-} = (-3 \pm 9) \times 10^{-5}$$

$$\text{Mean life } \tau = (1.639 \pm 0.015) \times 10^{-10} \text{ s}$$

$$c\tau = 4.91 \text{ cm}$$

$$(\tau_{\Xi^-} - \tau_{\Xi^+}) / \tau_{\Xi^-} = -0.01 \pm 0.07$$

$$\text{Magnetic moment } \mu = -0.6507 \pm 0.0025 \mu_N$$

$$(\mu_{\Xi^-} + \mu_{\Xi^+}) / |\mu_{\Xi^-}| = +0.01 \pm 0.05$$

Decay parameters

$\Lambda\pi^-$	$\alpha = -0.458 \pm 0.012$ ($S = 1.8$)
$[\alpha(\Xi^-)\alpha_{\Lambda} - \alpha(\Xi^+)\alpha_{\Lambda}]/[\text{sum}] = (0 \pm 7) \times 10^{-4}$	
"	$\phi = (-2.1 \pm 0.8)^\circ$
"	$\gamma = 0.89$ [k]
"	$\Delta = (175.9 \pm 1.5)^\circ$ [k]
$\Lambda e^- \bar{\nu}_e$	$g_A/g_V = -0.25 \pm 0.05$ [g]

Ξ^- DECAY MODES	Fraction (Γ_i/Γ)	Confidence level	ρ (MeV/c)
$\Lambda\pi^-$	$(99.887 \pm 0.035) \%$		140
$\Sigma^- \gamma$	$(1.27 \pm 0.23) \times 10^{-4}$		118
$\Lambda e^- \bar{\nu}_e$	$(5.63 \pm 0.31) \times 10^{-4}$		190
$\Lambda \mu^- \bar{\nu}_\mu$	$(3.5^{+3.5}_{-2.2}) \times 10^{-4}$		163
$\Sigma^0 e^- \bar{\nu}_e$	$(8.7 \pm 1.7) \times 10^{-5}$		123
$\Sigma^0 \mu^- \bar{\nu}_\mu$	< 8	$\times 10^{-4}$	90% 70
$\Xi^0 e^- \bar{\nu}_e$	< 2.3	$\times 10^{-3}$	90% 7

$\Delta S = 2$ forbidden ($S2$) modes

$n\pi^-$	$S2 < 1.9$	$\times 10^{-5}$	90%	304
$n e^- \bar{\nu}_e$	$S2 < 3.2$	$\times 10^{-3}$	90%	327
$n \mu^- \bar{\nu}_\mu$	$S2 < 1.5$		90%	314
$\rho\pi^- \pi^-$	$S2 < 4$	$\times 10^{-4}$	90%	223
$\rho\pi^- e^- \bar{\nu}_e$	$S2 < 4$	$\times 10^{-4}$	90%	305
$\rho\pi^- \mu^- \bar{\nu}_\mu$	$S2 < 4$	$\times 10^{-4}$	90%	251
$\rho \mu^- \bar{\nu}_\mu$	$L < 4$	$\times 10^{-8}$	90%	272

$\Xi(1530) P_{13}$

$$I(J^P) = \frac{1}{2}(\frac{3}{2}^+)$$

$$\Xi(1530)^0 \text{ mass } m = 1531.80 \pm 0.32 \text{ MeV} \quad (S = 1.3)$$

$$\Xi(1530)^- \text{ mass } m = 1535.0 \pm 0.6 \text{ MeV}$$

$$\Xi(1530)^0 \text{ full width } \Gamma = 9.1 \pm 0.5 \text{ MeV}$$

$$\Xi(1530)^- \text{ full width } \Gamma = 9.9^{+1.7}_{-1.9} \text{ MeV}$$

$\Xi(1530)$ DECAY MODES	Fraction (Γ_i/Γ)	Confidence level	ρ (MeV/c)
$\Xi\pi$	100 %		158
$\Xi\gamma$	<4 %	90%	202

$\Xi(1690)$

$$I(J^P) = \frac{1}{2}(??)$$

Mass $m = 1690 \pm 10$ MeV [m]

Full width $\Gamma < 30$ MeV

$\Xi(1690)$ DECAY MODES	Fraction (Γ_i/Γ)	ρ (MeV/c)
$\Lambda\bar{K}$	seen	240
$\Sigma\bar{K}$	seen	70
$\Xi\pi$	seen	311
$\Xi^- \pi^+ \pi^-$	possibly seen	213

Baryon Summary Table

 $\Xi(1820) D_{13}$

$$I(J^P) = \frac{1}{2}(\frac{3}{2}^-)$$

Mass $m = 1823 \pm 5$ MeV [m]
 Full width $\Gamma = 24_{-10}^{+15}$ MeV [m]

$\Xi(1820)$ DECAY MODES	Fraction (Γ_i/Γ)	ρ (MeV/c)
$\Lambda \bar{K}$	large	402
$\Sigma \bar{K}$	small	324
$\Xi \pi$	small	421
$\Xi(1530)\pi$	small	237

 $\Xi(1950)$

$$I(J^P) = \frac{1}{2}(?^?)$$

Mass $m = 1950 \pm 15$ MeV [m]
 Full width $\Gamma = 60 \pm 20$ MeV [m]

$\Xi(1950)$ DECAY MODES	Fraction (Γ_i/Γ)	ρ (MeV/c)
$\Lambda \bar{K}$	seen	522
$\Sigma \bar{K}$	possibly seen	460
$\Xi \pi$	seen	519

 $\Xi(2030)$

$$I(J^P) = \frac{1}{2}(\geq \frac{5}{2}^?)$$

Mass $m = 2025 \pm 5$ MeV [m]
 Full width $\Gamma = 20_{-5}^{+15}$ MeV [m]

$\Xi(2030)$ DECAY MODES	Fraction (Γ_i/Γ)	ρ (MeV/c)
$\Lambda \bar{K}$	$\sim 20\%$	585
$\Sigma \bar{K}$	$\sim 80\%$	529
$\Xi \pi$	small	574
$\Xi(1530)\pi$	small	416
$\Lambda \bar{K} \pi$	small	499
$\Sigma \bar{K} \pi$	small	428

Ω BARYONS ($S = -3, I = 0$)

$$\Omega^- = sss$$

 Ω^-

$$I(J^P) = 0(\frac{3}{2}^+)$$

$J^P = \frac{3}{2}^+$ is the quark-model prediction; and $J = 3/2$ is fairly well established.

Mass $m = 1672.45 \pm 0.29$ MeV
 $(m_{\Omega^-} - m_{\bar{\Omega}^+}) / m_{\Omega^-} = (-1 \pm 8) \times 10^{-5}$
 Mean life $\tau = (0.821 \pm 0.011) \times 10^{-10}$ s
 $c\tau = 2.461$ cm
 $(\tau_{\Omega^-} - \tau_{\bar{\Omega}^+}) / \tau_{\Omega^-} = 0.00 \pm 0.05$
 Magnetic moment $\mu = -2.02 \pm 0.05 \mu_N$

Decay parameters

ΛK^- $\alpha = 0.0180 \pm 0.0024$
 $\Lambda K^-, \bar{\Lambda} K^+ (\alpha + \bar{\alpha}) / (\alpha - \bar{\alpha}) = -0.02 \pm 0.13$
 $\Xi^0 \pi^-$ $\alpha = 0.09 \pm 0.14$
 $\Xi^- \pi^0$ $\alpha = 0.05 \pm 0.21$

Ω^- DECAY MODES	Fraction (Γ_i/Γ)	Confidence level	ρ (MeV/c)
ΛK^-	(67.8±0.7) %		211
$\Xi^0 \pi^-$	(23.6±0.7) %		294
$\Xi^- \pi^0$	(8.6±0.4) %		289
$\Xi^- \pi^+ \pi^-$	(4.3±3.4, -1.3) $\times 10^{-4}$		189
$\Xi(1530)^0 \pi^-$	(6.4±5.0, -2.0) $\times 10^{-4}$		17
$\Xi^0 e^- \bar{\nu}_e$	(5.6±2.8) $\times 10^{-3}$		319
$\Xi^- \gamma$	< 4.6 $\times 10^{-4}$	90%	314
$\Delta S = 2$ forbidden (S_2) modes			
$\Lambda \pi^-$	S_2 < 2.9 $\times 10^{-6}$	90%	449

 $\Omega(2250)^-$

$$I(J^P) = 0(?^?)$$

Mass $m = 2252 \pm 9$ MeV
 Full width $\Gamma = 55 \pm 18$ MeV

$\Omega(2250)^-$ DECAY MODES	Fraction (Γ_i/Γ)	ρ (MeV/c)
$\Xi^- \pi^+ K^-$	seen	532
$\Xi(1530)^0 K^-$	seen	437

CHARMED BARYONS ($C = +1$)

$$\Lambda_c^+ = udc, \quad \Sigma_c^{++} = uuc, \quad \Sigma_c^+ = udc, \quad \Sigma_c^0 = ddc,$$

$$\Xi_c^+ = usc, \quad \Xi_c^0 = dsc, \quad \Omega_c^0 = ssc$$

 Λ_c^+

$$I(J^P) = 0(\frac{1}{2}^+)$$

J is not well measured; $\frac{1}{2}$ is the quark-model prediction.

Mass $m = 2286.46 \pm 0.14$ MeV
 Mean life $\tau = (200 \pm 6) \times 10^{-15}$ s ($S = 1.6$)
 $c\tau = 59.9 \mu\text{m}$

Decay asymmetry parameters

$\Lambda \pi^+$ $\alpha = -0.91 \pm 0.15$
 $\Sigma^+ \pi^0$ $\alpha = -0.45 \pm 0.32$
 $\Lambda \ell^+ \nu_\ell$ $\alpha = -0.86 \pm 0.04$
 $(\alpha + \bar{\alpha}) / (\alpha - \bar{\alpha})$ in $\Lambda_c^+ \rightarrow \Lambda \pi^+, \bar{\Lambda}_c^- \rightarrow \bar{\Lambda} \pi^- = -0.07 \pm 0.31$
 $(\alpha + \bar{\alpha}) / (\alpha - \bar{\alpha})$ in $\Lambda_c^+ \rightarrow \Lambda e^+ \nu_e, \bar{\Lambda}_c^- \rightarrow \bar{\Lambda} e^- \bar{\nu}_e = 0.00 \pm 0.04$

Nearly all branching fractions of the Λ_c^+ are measured relative to the $p K^- \pi^+$ mode, but there are no model-independent measurements of this branching fraction. We explain how we arrive at our value of $B(\Lambda_c^+ \rightarrow p K^- \pi^+)$ in a Note at the beginning of the branching-ratio measurements in the Listings. When this branching fraction is eventually well determined, all the other branching fractions will slide up or down proportionally as the true value differs from the value we use here.

 Λ_c^+ DECAY MODES

Scale factor /
Confidence level (ρ) (MeV/c)

Hadronic modes with a p: $S = -1$ final states		
$p \bar{K}^0$	(2.3 ± 0.6) %	873
$p K^- \pi^+$	[o] (5.0 ± 1.3) %	823
$p \bar{K}^*(892)^0$	[p] (1.6 ± 0.5) %	685
$\Delta(1232)^{++} K^-$	(8.6 ± 3.0) $\times 10^{-3}$	710
$\Lambda(1520) \pi^+$	[p] (1.8 ± 0.6) %	627
$p K^- \pi^+$ nonresonant	(2.8 ± 0.8) %	823
$p \bar{K}^0 \pi^0$	(3.3 ± 1.0) %	823
$p \bar{K}^0 \eta$	(1.2 ± 0.4) %	568
$p \bar{K}^0 \pi^+ \pi^-$	(2.6 ± 0.7) %	754
$p K^- \pi^+ \pi^0$	(3.4 ± 1.0) %	759
$p K^*(892)^- \pi^+$	[p] (1.1 ± 0.5) %	580
$p (K^- \pi^+)$ nonresonant π^0	(3.6 ± 1.2) %	759
$\Delta(1232) \bar{K}^*(892)$	seen	419
$p K^- \pi^+ \pi^+ \pi^-$	(1.1 ± 0.8) $\times 10^{-3}$	671
$p K^- \pi^+ \pi^0 \pi^0$	(8 ± 4) $\times 10^{-3}$	678

Hadronic modes with a p: $S = 0$ final states		
$p \pi^+ \pi^-$	(3.5 ± 2.0) $\times 10^{-3}$	927
$p f_0(980)$	[p] (2.8 ± 1.9) $\times 10^{-3}$	622
$p \pi^+ \pi^+ \pi^- \pi^-$	(1.8 ± 1.2) $\times 10^{-3}$	852
$p K^+ K^-$	(7.7 ± 3.5) $\times 10^{-4}$	616
$p \phi$	[p] (8.2 ± 2.7) $\times 10^{-4}$	590
$p K^+ K^-$ non- ϕ	(3.5 ± 1.7) $\times 10^{-4}$	616

Hadronic modes with a hyperon: $S = -1$ final states		
$\Lambda \pi^+$	(1.07 ± 0.28) %	864
$\Lambda \pi^+ \pi^0$	(3.6 ± 1.3) %	844
$\Lambda \rho^+$	< 5 %	CL=95% 635
$\Lambda \pi^+ \pi^+ \pi^-$	(2.6 ± 0.7) %	807
$\Sigma(1385)^+ \pi^+ \pi^-, \Sigma^{*+} \rightarrow$	(7 ± 4) $\times 10^{-3}$	688
$\Lambda \pi^+$		
$\Sigma(1385)^- \pi^+ \pi^+, \Sigma^{*-} \rightarrow$	(5.5 ± 1.7) $\times 10^{-3}$	688
$\Lambda \pi^-$		
$\Lambda \pi^+ \rho^0$	(1.1 ± 0.5) %	523
$\Sigma(1385)^+ \rho^0, \Sigma^{*+} \rightarrow \Lambda \pi^+$	(3.7 ± 3.1) $\times 10^{-3}$	363

Baryon Summary Table

$\Lambda\pi^+\pi^+\pi^-\pi^0$ nonresonant	< 8	$\times 10^{-3}$	CL=90%	807
$\Lambda\pi^+\pi^+\pi^-\pi^0$ total	(1.8 ± 0.8) %			757
$\Lambda\pi^+\eta$	[ρ] (1.8 ± 0.6) %			691
$\Sigma(1385)^+\eta$	[ρ] (8.5 ± 3.3) $\times 10^{-3}$			570
$\Lambda\pi^+\omega$	[ρ] (1.2 ± 0.5) %			517
$\Lambda\pi^+\pi^+\pi^-\pi^0$, no η or ω	< 7	$\times 10^{-3}$	CL=90%	757
$\Lambda K^+\bar{K}^0$	(4.7 ± 1.5) $\times 10^{-3}$		S=1.2	443
$\Xi(1690)^0 K^+, \Xi^{*0} \rightarrow \Lambda\bar{K}^0$	(1.3 ± 0.5) $\times 10^{-3}$			286
$\Sigma^0\pi^+$	(1.05 ± 0.28) %			825
$\Sigma^+\pi^0$	(1.00 ± 0.34) %			827
$\Sigma^+\eta$	(5.5 ± 2.3) $\times 10^{-3}$			713
$\Sigma^+\pi^+\pi^-$	(3.6 ± 1.0) %			804
$\Sigma^+\rho^0$	< 1.4	%	CL=95%	575
$\Sigma^-\pi^+\pi^+$	(1.7 ± 0.5) %			799
$\Sigma^0\pi^+\pi^0$	(1.8 ± 0.8) %			803
$\Sigma^0\pi^+\pi^+\pi^-$	(8.3 ± 3.1) $\times 10^{-3}$			763
$\Sigma^+\pi^+\pi^-\pi^0$	—			767
$\Sigma^+\omega$	[ρ] (2.7 ± 1.0) %			569
$\Sigma^+ K^+ K^-$	(2.8 ± 0.8) $\times 10^{-3}$			349
$\Sigma^+\phi$	[ρ] (3.1 ± 0.9) $\times 10^{-3}$			295
$\Xi(1690)^0 K^+, \Xi^{*0} \rightarrow \Sigma^+ K^+ K^-$	(8.1 ± 3.0) $\times 10^{-4}$			286
$\Sigma^+ K^+ K^-$ nonresonant	< 6	$\times 10^{-4}$	CL=90%	349
$\Xi^0 K^+$	(3.9 ± 1.4) $\times 10^{-3}$			653
$\Xi^- K^+ \pi^+$	(5.1 ± 1.4) $\times 10^{-3}$			565
$\Xi(1530)^0 K^+$	[ρ] (2.6 ± 1.0) $\times 10^{-3}$			473

Hadronic modes with a hyperon: S = 0 final states

ΛK^+	(5.0 ± 1.6) $\times 10^{-4}$			781
$\Lambda K^+ \pi^+ \pi^-$	< 4	$\times 10^{-4}$	CL=90%	637
$\Sigma^0 K^+$	(4.2 ± 1.3) $\times 10^{-4}$			735
$\Sigma^0 K^+ \pi^+ \pi^-$	< 2.1	$\times 10^{-4}$	CL=90%	574
$\Sigma^+ K^+ \pi^-$	(1.7 ± 0.7) $\times 10^{-3}$			670
$\Sigma^+ K^*(892)^0$	[ρ] (2.8 ± 1.1) $\times 10^{-3}$			470
$\Sigma^- K^+ \pi^+$	< 1.0	$\times 10^{-3}$	CL=90%	664

Doubly Cabibbo-suppressed modes

$\rho K^+ \pi^-$	< 2.3	$\times 10^{-4}$	CL=90%	823
------------------	-------	------------------	--------	-----

Semileptonic modes

$\Lambda\ell^+ \nu_\ell$	[q] (2.0 ± 0.6) %			871
$\Lambda e^+ \nu_e$	(2.1 ± 0.6) %			871
$\Lambda\mu^+ \nu_\mu$	(2.0 ± 0.7) %			867

Inclusive modes

e^+ anything	(4.5 ± 1.7) %			—
$p e^+$ anything	(1.8 ± 0.9) %			—
ρ anything	(50 ± 16) %			—
ρ anything (no Λ)	(12 ± 19) %			—
n anything	(50 ± 16) %			—
n anything (no Λ)	(29 ± 17) %			—
Λ anything	(35 ± 11) %		S=1.4	—
Σ^\pm anything	[r] (10 ± 5) %			—
3prongs	(24 ± 8) %			—

 $\Delta C = 1$ weak neutral current (C1) modes, or Lepton number (L) violating modes

$\rho\mu^+\mu^-$	C1 < 3.4	$\times 10^{-4}$	CL=90%	937
$\Sigma^-\mu^+\mu^+$	L < 7.0	$\times 10^{-4}$	CL=90%	812

 $\Lambda_c(2595)^+$

$$I(J^P) = 0(\frac{1}{2}^-)$$

The spin-parity follows from the fact that $\Sigma_c(2455)\pi$ decays, with little available phase space, are dominant. This assumes that $J^P = 1/2^+$ for the $\Sigma_c(2455)$.

$$\text{Mass } m = 2595.4 \pm 0.6 \text{ MeV} \quad (S = 1.1)$$

$$m - m_{\Lambda_c^+} = 308.9 \pm 0.6 \text{ MeV} \quad (S = 1.1)$$

$$\text{Full width } \Gamma = 3.6_{-1.3}^{+2.0} \text{ MeV}$$

$\Lambda_c^+ \pi \pi$ and its submode $\Sigma_c(2455)\pi$ — the latter just barely — are the only strong decays allowed to an excited Λ_c^+ having this mass; and the submode seems to dominate.

 $\Lambda_c(2595)^+$ DECAY MODES

Decay Mode	Fraction (Γ_i/Γ)	ρ (MeV/c)
$\Lambda_c^+ \pi^+ \pi^-$	[s] $\approx 67\%$	124
$\Sigma_c(2455)^{++} \pi^-$	24 ± 7 %	28
$\Sigma_c(2455)^0 \pi^+$	24 ± 7 %	28
$\Lambda_c^+ \pi^+ \pi^-$ 3-body	18 ± 10 %	124
$\Lambda_c^+ \pi^0$	[t] not seen	261
$\Lambda_c^+ \gamma$	not seen	291

 $\Lambda_c(2625)^+$

$$I(J^P) = 0(\frac{3}{2}^-)$$

J^P has not been measured; $\frac{3}{2}^-$ is the quark-model prediction.

$$\text{Mass } m = 2628.1 \pm 0.6 \text{ MeV} \quad (S = 1.5)$$

$$m - m_{\Lambda_c^+} = 341.7 \pm 0.6 \text{ MeV} \quad (S = 1.6)$$

$$\text{Full width } \Gamma < 1.9 \text{ MeV, CL} = 90\%$$

$\Lambda_c^+ \pi \pi$ and its submode $\Sigma(2455)\pi$ are the only strong decays allowed to an excited Λ_c^+ having this mass.

 $\Lambda_c(2625)^+$ DECAY MODES

Decay Mode	Fraction (Γ_i/Γ)	Confidence level	ρ (MeV/c)
$\Lambda_c^+ \pi^+ \pi^-$	[s] $\approx 67\%$		184
$\Sigma_c(2455)^{++} \pi^-$	<5	90%	102
$\Sigma_c(2455)^0 \pi^+$	<5	90%	102
$\Lambda_c^+ \pi^+ \pi^-$ 3-body	large		184
$\Lambda_c^+ \pi^0$	[t] not seen		293
$\Lambda_c^+ \gamma$	not seen		319

 $\Lambda_c(2880)^+$

$$I(J^P) = 0(\frac{5}{2}^+)$$

There is some good evidence that indeed $J^P = 5/2^+$

$$\text{Mass } m = 2881.53 \pm 0.35 \text{ MeV}$$

$$m - m_{\Lambda_c^+} = 595.1 \pm 0.4 \text{ MeV}$$

$$\text{Full width } \Gamma = 5.8 \pm 1.1 \text{ MeV}$$

 $\Lambda_c(2880)^+$ DECAY MODES

Decay Mode	Fraction (Γ_i/Γ)	ρ (MeV/c)
$\Lambda_c^+ \pi^+ \pi^-$	seen	471
$\Sigma_c(2455)^0, ++ \pi^\pm$	seen	376
$\Sigma_c(2520)^0, ++ \pi^\pm$	seen	317
ρD^0	seen	316

 $\Lambda_c(2940)^+$

$$I(J^P) = 0(?^?)$$

$$\text{Mass } m = 2939.3_{-1.5}^{+1.4} \text{ MeV}$$

$$\text{Full width } \Gamma = 17_{-6}^{+8} \text{ MeV}$$

 $\Lambda_c(2940)^+$ DECAY MODES

Decay Mode	Fraction (Γ_i/Γ)	ρ (MeV/c)
ρD^0	seen	420
$\Sigma_c(2455)^0, ++ \pi^\pm$	seen	—

 $\Sigma_c(2455)$

$$I(J^P) = 1(\frac{1}{2}^+)$$

J^P has not been measured; $\frac{1}{2}^+$ is the quark-model prediction.

$$\Sigma_c(2455)^{++} \text{ mass } m = 2454.02 \pm 0.18 \text{ MeV}$$

$$\Sigma_c(2455)^+ \text{ mass } m = 2452.9 \pm 0.4 \text{ MeV}$$

$$\Sigma_c(2455)^0 \text{ mass } m = 2453.76 \pm 0.18 \text{ MeV}$$

$$m_{\Sigma_c^{++}} - m_{\Lambda_c^+} = 167.56 \pm 0.11 \text{ MeV}$$

$$m_{\Sigma_c^+} - m_{\Lambda_c^+} = 166.4 \pm 0.4 \text{ MeV}$$

$$m_{\Sigma_c^0} - m_{\Lambda_c^+} = 167.30 \pm 0.11 \text{ MeV}$$

$$m_{\Sigma_c^{++}} - m_{\Sigma_c^0} = 0.27 \pm 0.11 \text{ MeV} \quad (S = 1.1)$$

$$m_{\Sigma_c^+} - m_{\Sigma_c^0} = -0.9 \pm 0.4 \text{ MeV}$$

Baryon Summary Table

$\Sigma_c(2455)^{++}$ full width $\Gamma = 2.23 \pm 0.30$ MeV
 $\Sigma_c(2455)^+$ full width $\Gamma < 4.6$ MeV, CL = 90%
 $\Sigma_c(2455)^0$ full width $\Gamma = 2.2 \pm 0.4$ MeV ($S = 1.4$)

$\Lambda_c^+ \pi$ is the only strong decay allowed to a Σ_c having this mass.

$\Sigma_c(2455)$ DECAY MODES	Fraction (Γ_i/Γ)	ρ (MeV/c)
$\Lambda_c^+ \pi$	≈ 100 %	94

 $\Sigma_c(2520)$

$$I(J^P) = 1(\frac{3}{2}^+)$$

J^P has not been measured; $\frac{3}{2}^+$ is the quark-model prediction.

$\Sigma_c(2520)^{++}$ mass $m = 2518.4 \pm 0.6$ MeV ($S = 1.4$)
 $\Sigma_c(2520)^+$ mass $m = 2517.5 \pm 2.3$ MeV
 $\Sigma_c(2520)^0$ mass $m = 2518.0 \pm 0.5$ MeV
 $m_{\Sigma_c(2520)^{++}} - m_{\Lambda_c^+} = 231.9 \pm 0.6$ MeV ($S = 1.5$)
 $m_{\Sigma_c(2520)^+} - m_{\Lambda_c^+} = 231.0 \pm 2.3$ MeV
 $m_{\Sigma_c(2520)^0} - m_{\Lambda_c^+} = 231.6 \pm 0.5$ MeV ($S = 1.1$)
 $m_{\Sigma_c(2520)^{++}} - m_{\Sigma_c(2520)^0} = 0.3 \pm 0.6$ MeV ($S = 1.2$)
 $\Sigma_c(2520)^{++}$ full width $\Gamma = 14.9 \pm 1.9$ MeV
 $\Sigma_c(2520)^+$ full width $\Gamma < 17$ MeV, CL = 90%
 $\Sigma_c(2520)^0$ full width $\Gamma = 16.1 \pm 2.1$ MeV

$\Lambda_c^+ \pi$ is the only strong decay allowed to a Σ_c having this mass.

$\Sigma_c(2520)$ DECAY MODES	Fraction (Γ_i/Γ)	ρ (MeV/c)
$\Lambda_c^+ \pi$	≈ 100 %	180

 $\Sigma_c(2800)$

$$I(J^P) = 1(2^?)$$

$\Sigma_c(2800)^{++}$ mass $m = 2801^{+4}_{-6}$ MeV
 $\Sigma_c(2800)^+$ mass $m = 2792^{+14}_{-5}$ MeV
 $\Sigma_c(2800)^0$ mass $m = 2802^{+4}_{-7}$ MeV
 $m_{\Sigma_c(2800)^{++}} - m_{\Lambda_c^+} = 514^{+4}_{-6}$ MeV
 $m_{\Sigma_c(2800)^+} - m_{\Lambda_c^+} = 505^{+14}_{-5}$ MeV
 $m_{\Sigma_c(2800)^0} - m_{\Lambda_c^+} = 515^{+4}_{-7}$ MeV
 $\Sigma_c(2800)^{++}$ full width $\Gamma = 75^{+22}_{-17}$ MeV
 $\Sigma_c(2800)^+$ full width $\Gamma = 62^{+60}_{-40}$ MeV
 $\Sigma_c(2800)^0$ full width $\Gamma = 61^{+28}_{-18}$ MeV

$\Sigma_c(2800)$ DECAY MODES	Fraction (Γ_i/Γ)	ρ (MeV/c)
$\Lambda_c^+ \pi$	seen	443

 Ξ_c^+

$$I(J^P) = \frac{1}{2}(\frac{1}{2}^+)$$

J^P has not been measured; $\frac{1}{2}^+$ is the quark-model prediction.

Mass $m = 2467.8^{+0.4}_{-0.6}$ MeV
Mean life $\tau = (442 \pm 26) \times 10^{-15}$ s ($S = 1.3$)
 $c\tau = 132$ μ m

Ξ_c^+ DECAY MODES	Fraction (Γ_i/Γ)	Confidence level	ρ (MeV/c)
-----------------------	--------------------------------	------------------	----------------

No absolute branching fractions have been measured.
The following are branching ratios relative to $\Xi^- 2\pi^+$.

Cabibbo-favored ($S = -2$) decays

$p 2K_S^0$	[u]	0.087 ± 0.022	767
$\Lambda \bar{K}^0 \pi^+$		—	852
$\Sigma(1385)^+ \bar{K}^0$	[ρ, u]	1.0 ± 0.5	746
$\Lambda K^- 2\pi^+$	[u]	0.323 ± 0.033	787
$\Lambda \bar{K}^*(892)^0 \pi^+$	[ρ, u]	< 0.2	90% 608
$\Sigma(1385)^+ K^- \pi^+$	[ρ, u]	< 0.3	90% 678
$\Sigma^+ K^- \pi^+$	[u]	0.94 ± 0.11	810
$\Sigma^+ \bar{K}^*(892)^0$	[ρ, u]	0.81 ± 0.15	658

$\Sigma^0 K^- 2\pi^+$	[u]	0.29 ± 0.16	735
$\Xi^0 \pi^+$	[u]	0.55 ± 0.16	877
$\Xi^- 2\pi^+$	[u]	DEFINED AS 1	851
$\Xi(1530)^0 \pi^+$	[ρ, u]	< 0.1	90% 750
$\Xi^0 \pi^+ \pi^0$	[u]	2.34 ± 0.68	856
$\Xi^0 \pi^- 2\pi^+$	[u]	1.74 ± 0.50	818
$\Xi^0 e^+ \nu_e$	[u]	$2.3^{+0.7}_{-0.9}$	884
$\Omega^- K^+ \pi^+$	[u]	0.07 ± 0.04	399

Cabibbo-suppressed decays

$\rho K^- \pi^+$	[u]	0.21 ± 0.03	944
$\rho \bar{K}^*(892)^0$	[ρ, u]	0.12 ± 0.02	828
$\Sigma^+ \pi^+ \pi^-$	[u]	0.48 ± 0.20	922
$\Sigma^- 2\pi^+$	[u]	0.18 ± 0.09	918
$\Sigma^+ K^+ K^-$	[u]	0.15 ± 0.07	579
$\Sigma^+ \phi$	[ρ, u]	< 0.11	90% 549
$\Xi(1690)^0 K^+, \Xi(1690)^0 \rightarrow \Sigma^+ K^-$	[u]	< 0.05	90% 501

 Ξ_c^0

$$I(J^P) = \frac{1}{2}(\frac{1}{2}^+)$$

J^P has not been measured; $\frac{1}{2}^+$ is the quark-model prediction.

Mass $m = 2470.88^{+0.34}_{-0.80}$ MeV ($S = 1.1$)
 $m_{\Xi_c^0} - m_{\Xi_c^+} = 3.1^{+0.4}_{-0.5}$ MeV
Mean life $\tau = (112^{+13}_{-10}) \times 10^{-15}$ s
 $c\tau = 33.6$ μ m

Decay asymmetry parameters

$$\Xi^- \pi^+ \quad \alpha = -0.6 \pm 0.4$$

No absolute branching fractions have been measured. Several measurements of ratios of fractions may be found in the Listings that follow.

Ξ_c^0 DECAY MODES	Fraction (Γ_i/Γ)	ρ (MeV/c)
$p K^- K^- \pi^+$	seen	676
$\rho K^- \bar{K}^*(892)^0$	seen	413
$\rho K^- K^- \pi^+$ no $\bar{K}^*(892)^0$	seen	676
ΛK_S^0	seen	906
$\Lambda \bar{K}^0 \pi^+ \pi^-$	seen	787
$\Lambda K^- \pi^+ \pi^+ \pi^-$	seen	703
$\Xi^- \pi^+$	seen	875
$\Xi^- \pi^+ \pi^+ \pi^-$	seen	816
$\Omega^- K^+$	seen	522
$\Xi^- e^+ \nu_e$	seen	882
$\Xi^- \ell^+$ anything	seen	—

 $\Xi_c^{'+}$

$$I(J^P) = \frac{1}{2}(\frac{1}{2}^+)$$

J^P has not been measured; $\frac{1}{2}^+$ is the quark-model prediction.

Mass $m = 2575.6 \pm 3.1$ MeV
 $m_{\Xi_c^{'+}} - m_{\Xi_c^+} = 107.8 \pm 3.0$ MeV

The $\Xi_c^{'+} - \Xi_c^+$ mass difference is too small for any strong decay to occur.

$\Xi_c^{'+}$ DECAY MODES	Fraction (Γ_i/Γ)	ρ (MeV/c)
$\Xi_c^{'+} \gamma$	seen	106

 $\Xi_c^{'0}$

$$I(J^P) = \frac{1}{2}(\frac{1}{2}^+)$$

J^P has not been measured; $\frac{1}{2}^+$ is the quark-model prediction.

Mass $m = 2577.9 \pm 2.9$ MeV
 $m_{\Xi_c^{'0}} - m_{\Xi_c^0} = 107.0 \pm 2.9$ MeV

The $\Xi_c^{'0} - \Xi_c^0$ mass difference is too small for any strong decay to occur.

$\Xi_c^{'0}$ DECAY MODES	Fraction (Γ_i/Γ)	ρ (MeV/c)
$\Xi_c^{'0} \gamma$	seen	105

Baryon Summary Table

 $\Xi_c(2645)$

$$I(J^P) = \frac{1}{2}(\frac{3}{2}^+)$$

J^P has not been measured; $\frac{3}{2}^+$ is the quark-model prediction.

$$\Xi_c(2645)^+ \text{ mass } m = 2645.9^{+0.5}_{-0.6} \text{ MeV} \quad (S = 1.1)$$

$$\Xi_c(2645)^0 \text{ mass } m = 2645.9 \pm 0.5 \text{ MeV}$$

$$m_{\Xi_c(2645)^+} - m_{\Xi_c^0} = 175.0^{+0.8}_{-0.6} \text{ MeV} \quad (S = 1.2)$$

$$m_{\Xi_c(2645)^0} - m_{\Xi_c^+} = 178.1 \pm 0.6 \text{ MeV}$$

$$m_{\Xi_c(2645)^+} - m_{\Xi_c(2645)^0} = 0.0 \pm 0.5 \text{ MeV}$$

$$\Xi_c(2645)^+ \text{ full width } \Gamma < 3.1 \text{ MeV, CL} = 90\%$$

$$\Xi_c(2645)^0 \text{ full width } \Gamma < 5.5 \text{ MeV, CL} = 90\%$$

$\Xi_c \pi$ is the only strong decay allowed to a Ξ_c resonance having this mass.

$\Xi_c(2645)$ DECAY MODES	Fraction (Γ_i/Γ)	ρ (MeV/c)
$\Xi_c^0 \pi^+$	seen	102
$\Xi_c^+ \pi^-$	seen	107

 $\Xi_c(2790)$

$$I(J^P) = \frac{1}{2}(\frac{1}{2}^-)$$

J^P has not been measured; $\frac{1}{2}^-$ is the quark-model prediction.

$$\Xi_c(2790)^+ \text{ mass } = 2789.1 \pm 3.2 \text{ MeV}$$

$$\Xi_c(2790)^0 \text{ mass } = 2791.8 \pm 3.3 \text{ MeV}$$

$$m_{\Xi_c(2790)^+} - m_{\Xi_c^0} = 318.2 \pm 3.2 \text{ MeV}$$

$$m_{\Xi_c(2790)^0} - m_{\Xi_c^+} = 324.0 \pm 3.3 \text{ MeV}$$

$$\Xi_c(2790)^+ \text{ width } < 15 \text{ MeV, CL} = 90\%$$

$$\Xi_c(2790)^0 \text{ width } < 12 \text{ MeV, CL} = 90\%$$

$\Xi_c(2790)$ DECAY MODES	Fraction (Γ_i/Γ)	ρ (MeV/c)
$\Xi_c^+ \pi^-$	seen	159

 $\Xi_c(2815)$

$$I(J^P) = \frac{1}{2}(\frac{3}{2}^-)$$

J^P has not been measured; $\frac{3}{2}^-$ is the quark-model prediction.

$$\Xi_c(2815)^+ \text{ mass } m = 2816.6 \pm 0.9 \text{ MeV}$$

$$\Xi_c(2815)^0 \text{ mass } m = 2819.6 \pm 1.2 \text{ MeV}$$

$$m_{\Xi_c(2815)^+} - m_{\Xi_c^+} = 348.8 \pm 0.9 \text{ MeV}$$

$$m_{\Xi_c(2815)^0} - m_{\Xi_c^0} = 348.7 \pm 1.2 \text{ MeV}$$

$$m_{\Xi_c(2815)^+} - m_{\Xi_c(2815)^0} = -3.1 \pm 1.3 \text{ MeV}$$

$$\Xi_c(2815)^+ \text{ full width } \Gamma < 3.5 \text{ MeV, CL} = 90\%$$

$$\Xi_c(2815)^0 \text{ full width } \Gamma < 6.5 \text{ MeV, CL} = 90\%$$

The $\Xi_c \pi \pi$ modes are consistent with being entirely via $\Xi_c(2645) \pi$.

$\Xi_c(2815)$ DECAY MODES	Fraction (Γ_i/Γ)	ρ (MeV/c)
$\Xi_c^+ \pi^+ \pi^-$	seen	196
$\Xi_c^0 \pi^+ \pi^-$	seen	191

 $\Xi_c(2980)$

$$I(J^P) = \frac{1}{2}(\frac{3}{2}^?)$$

$$\Xi_c(2980)^+ m = 2971.4 \pm 3.3 \text{ MeV} \quad (S = 2.1)$$

$$\Xi_c(2980)^0 m = 2968.0 \pm 2.6 \text{ MeV} \quad (S = 1.2)$$

$$\Xi_c(2980)^+ \text{ width } \Gamma = 26 \pm 7 \text{ MeV} \quad (S = 1.5)$$

$$\Xi_c(2980)^0 \text{ width } \Gamma = 20 \pm 7 \text{ MeV} \quad (S = 1.3)$$

$\Xi_c(2980)$ DECAY MODES	Fraction (Γ_i/Γ)	ρ (MeV/c)
$\Lambda_c^+ \bar{K} \pi$	seen	231
$\Sigma_c(2455) \bar{K}$	seen	134
$\Lambda_c^+ \bar{K}$	not seen	414
$\Xi_c 2\pi$	seen	-
$\Xi_c(2645) \pi$	seen	277

 $\Xi_c(3080)$

$$I(J^P) = \frac{1}{2}(\frac{3}{2}^?)$$

$$\Xi_c(3080)^+ m = 3077.0 \pm 0.4 \text{ MeV}$$

$$\Xi_c(3080)^0 m = 3079.9 \pm 1.4 \text{ MeV} \quad (S = 1.3)$$

$$\Xi_c(3080)^+ \text{ width } \Gamma = 5.8 \pm 1.0 \text{ MeV}$$

$$\Xi_c(3080)^0 \text{ width } \Gamma = 5.6 \pm 2.2 \text{ MeV}$$

$\Xi_c(3080)$ DECAY MODES	Fraction (Γ_i/Γ)	ρ (MeV/c)
$\Lambda_c^+ \bar{K} \pi$	seen	415
$\Sigma_c(2455) \bar{K}$	seen	342
$\Sigma_c(2455) \bar{K} + \Sigma_c(2520) \bar{K}$	seen	-
$\Lambda_c^+ \bar{K}$	not seen	536
$\Lambda_c^+ \bar{K} \pi^+ \pi^-$	not seen	143

 Ω_c^0

$$I(J^P) = 0(\frac{1}{2}^+)$$

J^P has not been measured; $\frac{1}{2}^+$ is the quark-model prediction.

$$\text{Mass } m = 2695.2 \pm 1.7 \text{ MeV} \quad (S = 1.3)$$

$$\text{Mean life } \tau = (69 \pm 12) \times 10^{-15} \text{ s}$$

$$c\tau = 21 \mu\text{m}$$

No absolute branching fractions have been measured.

Ω_c^0 DECAY MODES	Fraction (Γ_i/Γ)	ρ (MeV/c)
$\Sigma^+ K^- K^- \pi^+$	seen	689
$\Xi^0 K^- \pi^+$	seen	901
$\Xi^- K^- \pi^+ \pi^+$	seen	830
$\Omega^- e^+ \nu_e$	seen	829
$\Omega^- \pi^+$	seen	821
$\Omega^- \pi^+ \pi^0$	seen	797
$\Omega^- \pi^- \pi^+ \pi^+$	seen	753

 $\Omega_c(2770)^0$

$$I(J^P) = 0(\frac{3}{2}^+)$$

J^P has not been measured; $\frac{3}{2}^+$ is the quark-model prediction.

$$\text{Mass } m = 2765.9 \pm 2.0 \text{ MeV} \quad (S = 1.2)$$

$$m_{\Omega_c(2770)^0} - m_{\Omega_c^0} = 70.7^{+0.8}_{-0.9} \text{ MeV}$$

The $\Omega_c(2770)^0 - \Omega_c^0$ mass difference is too small for any strong decay to occur.

$\Omega_c(2770)^0$ DECAY MODES	Fraction (Γ_i/Γ)	ρ (MeV/c)
$\Omega_c^0 \gamma$	presumably 100%	70

BOTTOM BARYONS
($B = -1$)

$$\Lambda_b^0 = udb, \Xi_b^0 = usb, \Xi_b^- = dsb, \Omega_b^- = ssb$$

 Λ_b^0

$$I(J^P) = 0(\frac{1}{2}^+)$$

$I(J^P)$ not yet measured; $0(\frac{1}{2}^+)$ is the quark model prediction.

$$\text{Mass } m = 5620.2 \pm 1.6 \text{ MeV}$$

$$m_{\Lambda_b} - m_{B^0} = 339.2 \pm 1.4 \text{ MeV}$$

$$\text{Mean life } \tau = (1.391^{+0.038}_{-0.037}) \times 10^{-12} \text{ s}$$

$$c\tau = 417 \mu\text{m}$$

The branching fractions $B(b\text{-baryon}) \rightarrow \Lambda \ell^- \bar{\nu}_\ell \text{ anything}$ and $B(\Lambda_b^0 \rightarrow \Lambda_c^+ \ell^- \bar{\nu}_\ell \text{ anything})$ are not pure measurements because the underlying measured products of these with $B(b \rightarrow b\text{-baryon})$ were used to determine $B(b \rightarrow b\text{-baryon})$, as described in the note "Production and Decay of b -Flavored Hadrons."

For inclusive branching fractions, e.g., $\Lambda_b \rightarrow \bar{\Lambda}_c \text{ anything}$, the values usually are multiplicities, not branching fractions. They can be greater than one.

Baryon Summary Table

For inclusive branching fractions, e.g., $B \rightarrow D^\pm$ anything, the values usually are multiplicities, not branching fractions. They can be greater than one.

Λ_b^0 DECAY MODES	Fraction (Γ_i/Γ)	Confidence level	p (MeV/c)
$J/\psi(1S)\Lambda \times B(b \rightarrow \Lambda_b^0)$	$(4.7 \pm 2.3) \times 10^{-5}$		1741
$\Lambda_c^+ \pi^-$	$(8.8 \pm 3.2) \times 10^{-3}$		2343
$\Lambda_c^+ a_1(1260)^-$	seen		2153
$\Lambda_c^+ \ell^- \bar{\nu}_\ell$ anything	[v] $(10.7 \pm 3.2) \%$		—
$\Lambda_c^+ \ell^- \bar{\nu}_\ell$	$(5.0^{+1.9}_{-1.4}) \%$		2345
$\Lambda_c^+ \pi^+ \pi^- \ell^- \bar{\nu}_\ell$	$(5.6 \pm 3.1) \%$		2335
$\Lambda_c(2595)^+ \ell^- \bar{\nu}_\ell$	$(6.3^{+4.0}_{-3.1}) \times 10^{-3}$		2211
$\Lambda_c(2625)^+ \ell^- \bar{\nu}_\ell$	$(1.1^{+0.6}_{-0.4}) \%$		2196
$p h^-$	[w] $< 2.3 \times 10^{-5}$	90%	2730
$p \pi^-$	$(3.8 \pm 1.3) \times 10^{-6}$		2730
$p K^-$	$(6.0 \pm 1.9) \times 10^{-6}$		2709
$\Lambda \gamma$	$< 1.3 \times 10^{-3}$	90%	2699

$$\Sigma_b \quad I(J^P) = 1(\frac{1}{2}^+)$$

I, J, P need confirmation.

$$\text{Mass } m(\Sigma_b^+) = 5807.8 \pm 2.7 \text{ MeV}$$

$$\text{Mass } m(\Sigma_b^-) = 5815.2 \pm 2.0 \text{ MeV}$$

Σ_b DECAY MODES	Fraction (Γ_i/Γ)	p (MeV/c)
$\Lambda_b^0 \pi$	dominant	128

$$\Sigma_b^* \quad I(J^P) = 1(\frac{3}{2}^+)$$

I, J, P need confirmation.

$$\text{Mass } m(\Sigma_b^{*+}) = 5829.0 \pm 3.4 \text{ MeV}$$

$$\text{Mass } m(\Sigma_b^{*-}) = 5836.4 \pm 2.8 \text{ MeV}$$

$$m_{\Sigma_b^*} - m_{\Sigma_b} = 21.2 \pm 2.0 \text{ MeV}$$

Σ_b^* DECAY MODES	Fraction (Γ_i/Γ)	p (MeV/c)
$\Lambda_b^0 \pi$	dominant	156

$$\Xi_b^0, \Xi_b^- \quad I(J^P) = \frac{1}{2}(\frac{1}{2}^+)$$

I, J, P need confirmation.

$$\text{Mass } m = 5790.5 \pm 2.7 \text{ MeV}$$

$$\text{Mean life } \tau_{\Xi_b^-} = (1.56 \pm 0.26) \times 10^{-12} \text{ s}$$

$$\text{Mean life } \tau_{\Xi_b^0} = (1.49^{+0.19}_{-0.18}) \times 10^{-12} \text{ s}$$

Ξ_b DECAY MODES	Fraction (Γ_i/Γ)	Scale factor	p (MeV/c)
$\Xi_b^- \rightarrow \Xi^- \ell^- \bar{\nu}_\ell X \times B(\bar{b} \rightarrow \Xi_b^-)$	$(3.9 \pm 1.2) \times 10^{-4}$	1.4	—
$\Xi_b^- \rightarrow J/\psi \Xi^- \times B(b \rightarrow \Xi_b^-)$	$(8 \pm 4) \times 10^{-6}$		—

$$\Omega_b^- \quad I(J^P) = 0(\frac{1}{2}^+)$$

I, J, P need confirmation.

$$\text{Mass } m = 6071 \pm 40 \text{ MeV} \quad (S = 6.2)$$

$$\text{Mean life } \tau = (1.1^{+0.5}_{-0.4}) \times 10^{-12} \text{ s}$$

Ω_b^- DECAY MODES	Fraction (Γ_i/Γ)	p (MeV/c)
$J/\psi \Omega^- \times B(b \rightarrow \Omega_b^-)$	$(2.4 \pm 1.2) \times 10^{-6}$	1826

b-baryon ADMIXTURE ($\Lambda_b, \Xi_b, \Sigma_b, \Omega_b$)

$$\text{Mean life } \tau = (1.345 \pm 0.032) \times 10^{-12} \text{ s}$$

These branching fractions are actually an average over weakly decaying b -baryons weighted by their production rates in Z decay (or high-energy $p\bar{p}$), branching ratios, and detection efficiencies. They scale with the LEP b -baryon production fraction $B(b \rightarrow b\text{-baryon})$ and are evaluated for our value $B(b \rightarrow b\text{-baryon}) = (9.2 \pm 1.8) \%$.

The branching fractions $B(b\text{-baryon} \rightarrow \Lambda \ell^- \bar{\nu}_\ell \text{ anything})$ and $B(\Lambda_b^0 \rightarrow \Lambda_c^+ \ell^- \bar{\nu}_\ell \text{ anything})$ are not pure measurements because the underlying measured products of these with $B(b \rightarrow b\text{-baryon})$ were used to determine $B(b \rightarrow b\text{-baryon})$, as described in the note "Production and Decay of b -Flavored Hadrons."

b-baryon ADMIXTURE DECAY MODES ($\Lambda_b, \Xi_b, \Sigma_b, \Omega_b$)

Decay Mode	Fraction (Γ_i/Γ)	p (MeV/c)
$p \mu^- \bar{\nu}$ anything	$(5.8 \pm \frac{2.6}{2.4}) \%$	—
$p \ell \bar{\nu}_\ell$ anything	$(5.6 \pm 1.7) \%$	—
p anything	$(69 \pm 27) \%$	—
$\Lambda \ell^- \bar{\nu}_\ell$ anything	$(3.7 \pm 1.0) \%$	—
$\Lambda/\bar{\Lambda}$ anything	$(39 \pm 11) \%$	—
$\Xi^- \ell^- \bar{\nu}_\ell$ anything	$(6.5 \pm 2.2) \times 10^{-3}$	—

NOTES

This Summary Table only includes established baryons. The Particle Listings include evidence for other baryons. The masses, widths, and branching fractions for the resonances in this Table are Breit-Wigner parameters, but pole positions are also given for most of the N and Δ resonances.

For most of the resonances, the parameters come from various partial-wave analyses of more or less the same sets of data, and it is not appropriate to treat the results of the analyses as independent or to average them together. Furthermore, the systematic errors on the results are not well understood. Thus, we usually only give ranges for the parameters. We then also give a best guess for the mass (as part of the name of the resonance) and for the width. The *Note on N and Δ Resonances* and the *Note on Λ and Σ Resonances* in the Particle Listings review the partial-wave analyses.

When a quantity has "($S = \dots$)" to its right, the error on the quantity has been enlarged by the "scale factor" S , defined as $S = \sqrt{\chi^2/(N-1)}$, where N is the number of measurements used in calculating the quantity. We do this when $S > 1$, which often indicates that the measurements are inconsistent. When $S > 1.25$, we also show in the Particle Listings an ideogram of the measurements. For more about S , see the Introduction.

A decay momentum p is given for each decay mode. For a 2-body decay, p is the momentum of each decay product in the rest frame of the decaying particle. For a 3-or-more-body decay, p is the largest momentum any of the products can have in this frame. For any resonance, the *nominal* mass is used in calculating p . A dagger ("†") in this column indicates that the mode is forbidden when the nominal masses of resonances are used, but is in fact allowed due to the nonzero widths of the resonances.

[a] The masses of the p and n are most precisely known in u (unified atomic mass units). The conversion factor to MeV, $1 u = 931.494028(23) \text{ MeV}$, is less well known than are the masses in u .

[b] The $|m_p - m_{\bar{p}}|/m_p$ and $|q_p + q_{\bar{p}}|/e$ are not independent, and both use the more precise measurement of $|q_{\bar{p}}/m_{\bar{p}}|/(q_p/m_p)$.

[c] The limit is from neutrality-of-matter experiments; it assumes $q_n = q_p + q_e$. See also the charge of the neutron.

[d] The first limit is for $p \rightarrow$ anything or "disappearance" modes of a bound proton. The second entry, a rough range of limits, assumes the dominant decay modes are among those investigated. For antiprotons the best limit, inferred from the observation of cosmic ray \bar{p} 's is $\tau_{\bar{p}} > 10^7$ yr, the cosmic-ray storage time, but this limit depends on a number of assumptions. The best direct observation of stored antiprotons gives $\tau_{\bar{p}}/B(\bar{p} \rightarrow e^- \gamma) > 7 \times 10^5$ yr.

[e] There is some controversy about whether nuclear physics and model dependence complicate the analysis for bound neutrons (from which the best limit comes). The first limit here is from reactor experiments with free neutrons.

[f] Lee and Yang in 1956 proposed the existence of a mirror world in an attempt to restore global parity symmetry—thus a search for oscillations between the two worlds. Oscillations between the worlds would be maximal when the magnetic fields B and B' were equal. The limit for any B' in the range 0 to 12.5 μT is $>12 \text{ s}$ (95% CL).

[g] The parameters $g_A, g_V,$ and g_{WM} for semileptonic modes are defined by $\bar{B}_f[\gamma_\lambda(g_V + g_A\gamma_5) + i(g_{WM}/m_B)\sigma_{\lambda\nu}q^\nu]B_i$, and ϕ_{AV} is defined by $g_A/g_V = |g_A/g_V|e^{i\phi_{AV}}$. See the "Note on Baryon Decay Parameters" in the neutron Particle Listings.

[h] Time-reversal invariance requires this to be 0° or 180° .

[i] This coefficient is zero if time invariance is not violated.

[j] This limit is for γ energies between 15 and 340 keV.

[k] The decay parameters γ and Δ are calculated from α and ϕ using

Baryon Summary Table

$$\gamma = \sqrt{1-\alpha^2} \cos\phi, \quad \tan\Delta = -\frac{1}{\alpha} \sqrt{1-\alpha^2} \sin\phi.$$

See the "Note on Baryon Decay Parameters" in the neutron Particle Listings.

- [l] See the Listings for the pion momentum range used in this measurement.
- [m] The error given here is only an educated guess. It is larger than the error on the weighted average of the published values.
- [n] A theoretical value using QED.
- [o] See the note on " Λ_c^+ Branching Fractions" in the Λ_c^+ Particle Listings.
- [p] This branching fraction includes all the decay modes of the final-state resonance.

[q] An ℓ indicates an e or a μ mode, not a sum over these modes.

[r] The value is for the sum of the charge states or particle/antiparticle states indicated.

[s] Assuming isospin conservation, so that the other third is $\Lambda_c^+ \pi^0 \pi^0$.

[t] A test that the isospin is indeed 0, so that the particle is indeed a Λ_c^+ .

[u] No absolute branching fractions have been measured. The value here is the branching *ratio* relative to $\Xi^- 2\pi^+$.

[v] Not a pure measurement. See note at head of Λ_b^0 Decay Modes.

[w] Here h^- means π^- or K^- .

SEARCHES FOR MONOPOLES, SUPERSYMMETRY, TECHNICOLOR, COMPOSITENESS, EXTRA DIMENSIONS, etc.

Magnetic Monopole Searches

Isolated supermassive monopole candidate events have not been confirmed. The most sensitive experiments obtain negative results.

Best cosmic-ray supermassive monopole flux limit:

$$< 1.0 \times 10^{-15} \text{ cm}^{-2}\text{s}^{-1}\text{s}^{-1} \quad \text{for } 1.1 \times 10^{-4} < \beta < 0.1$$

Supersymmetric Particle Searches

Limits are based on the Minimal Supersymmetric Standard Model.

Assumptions include: 1) $\tilde{\chi}_1^0$ (or $\tilde{\gamma}$) is lightest supersymmetric particle; 2) R -parity is conserved; 3) With the exception of \tilde{t} and \tilde{b} , all scalar quarks are assumed to be degenerate in mass and $m_{\tilde{q}_R} = m_{\tilde{q}_L}$. 4) Limits for sleptons refer to the \tilde{L}_R states. 5) Gaugino mass unification at the GUT scale.

See the Particle Listings for a Note giving details of supersymmetry.

$\tilde{\chi}_i^0$ — neutralinos (mixtures of $\tilde{\gamma}$, \tilde{Z}^0 , and \tilde{H}_i^0)

Mass $m_{\tilde{\chi}_1^0} > 46$ GeV, CL = 95%

[all $\tan\beta$, all m_0 , all $m_{\tilde{\chi}_2^0} - m_{\tilde{\chi}_1^0}$]

Mass $m_{\tilde{\chi}_2^0} > 62.4$ GeV, CL = 95%

[$1 < \tan\beta < 40$, all m_0 , all $m_{\tilde{\chi}_2^0} - m_{\tilde{\chi}_1^0}$]

Mass $m_{\tilde{\chi}_3^0} > 99.9$ GeV, CL = 95%

[$1 < \tan\beta < 40$, all m_0 , all $m_{\tilde{\chi}_3^0} - m_{\tilde{\chi}_1^0}$]

Mass $m_{\tilde{\chi}_4^0} > 116$ GeV, CL = 95%

[$1 < \tan\beta < 40$, all m_0 , all $m_{\tilde{\chi}_4^0} - m_{\tilde{\chi}_1^0}$]

$\tilde{\chi}_i^\pm$ — charginos (mixtures of \tilde{W}^\pm and \tilde{H}_i^\pm)

Mass $m_{\tilde{\chi}_1^\pm} > 94$ GeV, CL = 95%

[$\tan\beta < 40$, $m_{\tilde{\chi}_1^\pm} - m_{\tilde{\chi}_1^0} > 3$ GeV, all m_0]

\tilde{e} — scalar electron (selectron)

Mass $m > 107$ GeV, CL = 95% [all $m_{\tilde{e}_R} - m_{\tilde{\chi}_1^0}$]

$\tilde{\mu}$ — scalar muon (smuon)

Mass $m > 94$ GeV, CL = 95%

[$1 \leq \tan\beta \leq 40$, $m_{\tilde{\mu}_R} - m_{\tilde{\chi}_1^0} > 10$ GeV]

$\tilde{\tau}$ — scalar tau (stau)

Mass $m > 81.9$ GeV, CL = 95%

[$m_{\tilde{\tau}_R} - m_{\tilde{\chi}_1^0} > 15$ GeV, all θ_τ]

\tilde{q} — scalar quark (squark)

These limits include the effects of cascade decays, evaluated assuming a fixed value of the parameters μ and $\tan\beta$. The limits are weakly sensitive to these parameters over much of parameter space. Limits assume GUT relations between gaugino masses and the gauge coupling.

Mass $m > 379$ GeV, CL = 95% [$\tan\beta=3$, $\mu < 0$, $A=0$, any $m_{\tilde{g}}$]

\tilde{b} — scalar bottom (sbottom)

Mass $m > 89$ GeV, CL = 95% [$m_{\tilde{b}_1} - m_{\tilde{\chi}_1^0} > 8$ GeV, all θ_b]

\tilde{t} — scalar top (stop)

Mass $m > 95.7$ GeV, CL = 95%

[$\tilde{t} \rightarrow c\tilde{\chi}_1^0$, all θ_t , $m_{\tilde{t}} - m_{\tilde{\chi}_1^0} > 10$ GeV]

\tilde{g} — gluino

The limits summarised here refer to the high-mass region ($m_{\tilde{g}} \gtrsim 5$ GeV), and include the effects of cascade decays, evaluated assuming a fixed value of the parameters μ and $\tan\beta$.

The limits are weakly sensitive to these parameters over much of parameter space. Limits assume GUT relations between gaugino masses and the gauge coupling,

Mass $m > 308$ GeV, CL = 95% [any $m_{\tilde{q}}$]

Mass $m > 392$ GeV, CL = 95% [$m_{\tilde{q}} = m_{\tilde{g}}$]

Technicolor

Searches for a color-octet techni- ρ constrain its mass to be greater than 260 to 480 GeV, depending on allowed decay channels. Similar bounds exist on the color-octet techni- ω .

Quark and Lepton Compositeness, Searches for

Scale Limits Λ for Contact Interactions (the lowest dimensional interactions with four fermions)

If the Lagrangian has the form

$$\pm \frac{g^2}{2\lambda^2} \bar{\psi}_L \gamma_\mu \psi_L \bar{\psi}_L \gamma^\mu \psi_L$$

(with $g^2/4\pi$ set equal to 1), then we define $\Lambda \equiv \Lambda_{LL}^\pm$. For the full definitions and for other forms, see the Note in the Listings on Searches for Quark and Lepton Compositeness in the full Review and the original literature.

$$\Lambda_{LL}^+ (eeee) > 8.3 \text{ TeV, CL} = 95\%$$

$$\Lambda_{LL}^- (eeee) > 10.3 \text{ TeV, CL} = 95\%$$

$$\Lambda_{LL}^+ (ee\mu\mu) > 8.5 \text{ TeV, CL} = 95\%$$

$$\Lambda_{LL}^- (ee\mu\mu) > 9.5 \text{ TeV, CL} = 95\%$$

$$\Lambda_{LL}^+ (ee\tau\tau) > 7.9 \text{ TeV, CL} = 95\%$$

$$\Lambda_{LL}^- (ee\tau\tau) > 7.2 \text{ TeV, CL} = 95\%$$

$$\Lambda_{LL}^+ (\ell\ell\ell\ell) > 9.1 \text{ TeV, CL} = 95\%$$

$$\Lambda_{LL}^- (\ell\ell\ell\ell) > 10.3 \text{ TeV, CL} = 95\%$$

$$\Lambda_{LL}^+ (eeuu) > 23.3 \text{ TeV, CL} = 95\%$$

$$\Lambda_{LL}^- (eeuu) > 12.5 \text{ TeV, CL} = 95\%$$

$$\Lambda_{LL}^+ (eedd) > 11.1 \text{ TeV, CL} = 95\%$$

$$\Lambda_{LL}^- (eedd) > 26.4 \text{ TeV, CL} = 95\%$$

$$\Lambda_{LL}^+ (eccc) > 9.4 \text{ TeV, CL} = 95\%$$

$$\Lambda_{LL}^- (eccc) > 5.6 \text{ TeV, CL} = 95\%$$

$$\Lambda_{LL}^+ (eebb) > 9.4 \text{ TeV, CL} = 95\%$$

$$\Lambda_{LL}^- (eebb) > 4.9 \text{ TeV, CL} = 95\%$$

$$\Lambda_{LL}^+ (\mu\mu qq) > 2.9 \text{ TeV, CL} = 95\%$$

$$\Lambda_{LL}^- (\mu\mu qq) > 4.2 \text{ TeV, CL} = 95\%$$

$$\Lambda(\ell\nu\ell\nu) > 3.10 \text{ TeV, CL} = 90\%$$

$$\Lambda(e\nu qq) > 2.81 \text{ TeV, CL} = 95\%$$

$$\Lambda_{LL}^+ (qqqq) > 2.7 \text{ TeV, CL} = 95\%$$

$$\Lambda_{LL}^- (qqqq) > 2.4 \text{ TeV, CL} = 95\%$$

$$\Lambda_{LL}^+ (\nu\nu qq) > 5.0 \text{ TeV, CL} = 95\%$$

$$\Lambda_{LL}^- (\nu\nu qq) > 5.4 \text{ TeV, CL} = 95\%$$

Excited Leptons

The limits from $\ell^{*+}\ell^{*-}$ do not depend on λ (where λ is the $\ell\ell^*$ transition coupling). The λ -dependent limits assume chiral coupling.

$e^{*\pm}$ — excited electron

Mass $m > 103.2$ GeV, CL = 95% (from e^*e^*)

Mass $m > 272$ GeV, CL = 95% (from e^*e^*)

Mass $m > 310$ GeV, CL = 95% (if $\lambda_\gamma = 1$)

Searches Summary Table

$\mu^{*\pm}$ — excited muon

Mass $m > 103.2$ GeV, CL = 95% (from $\mu^* \mu^*$)

Mass $m > 221$ GeV, CL = 95% (from $\mu \mu^*$)

$\tau^{*\pm}$ — excited tau

Mass $m > 103.2$ GeV, CL = 95% (from $\tau^* \tau^*$)

Mass $m > 185$ GeV, CL = 95% (from $\tau \tau^*$)

ν^* — excited neutrino

Mass $m > 102.6$ GeV, CL = 95% (from $\nu^* \nu^*$)

Mass $m > 213$ GeV, CL = 95% (from $\nu \nu^*$)

q^* — excited quark

Mass $m > 45.6$ GeV, CL = 95% (from $q^* q^*$)

Mass m (from $q^* X$)

Color Sextet and Octet Particles

Color Sextet Quarks (q_6)

Mass $m > 84$ GeV, CL = 95% (Stable q_6)

Color Octet Charged Leptons (ℓ_8)

Mass $m > 86$ GeV, CL = 95% (Stable ℓ_8)

Color Octet Neutrinos (ν_8)

Mass $m > 110$ GeV, CL = 90% ($\nu_8 \rightarrow \nu g$)

Extra Dimensions

Please refer to the Extra Dimensions section of the full *Review* for a discussion of the model-dependence of these bounds, and further constraints.

Constraints on the fundamental gravity scale

$M_H > 1.1$ TeV, CL = 95% (dim-8 operators; $p\bar{p} \rightarrow e^+ e^-, \gamma\gamma$)

$M_D > 1.1$ TeV, CL = 95% ($e^+ e^- \rightarrow G\gamma$; 2-flat dimensions)

$M_D > 3\text{--}1000$ TeV (astrophys. and cosmology; 2-flat dimensions; limits depend on technique and assumptions)

Constraints on the radius of the extra dimensions, for the case of two-flat dimensions of equal radii

$r < 90\text{--}660$ nm (astrophysics; limits depend on technique and assumptions)

$r < 0.22$ mm, CL = 95% (direct tests of Newton's law; cited in Extra Dimensions review)

TESTS OF CONSERVATION LAWS

Updated May 2010 by L. Wolfenstein (Carnegie-Mellon University), T.G. Trippe (LBNL), and C.-J. Lin (LBNL).

In keeping with the current interest in tests of conservation laws, we collect together a Table of experimental limits on all weak and electromagnetic decays, mass differences, and moments, and on a few reactions, whose observation would violate conservation laws. The Table is given only in the full *Review of Particle Physics*, not in the Particle Physics Booklet. For the benefit of Booklet readers, we include the best limits from the Table in the following text. Limits in this text are for CL=90% unless otherwise specified. The Table is in two parts: “Discrete Space-Time Symmetries,” *i.e.*, C , P , T , CP , and CPT ; and “Number Conservation Laws,” *i.e.*, lepton, baryon, hadronic flavor, and charge conservation. The references for these data can be found in the the Particle Listings in the *Review*. A discussion of these tests follows.

CPT INVARIANCE

General principles of relativistic field theory require invariance under the combined transformation CPT . The simplest tests of CPT invariance are the equality of the masses and lifetimes of a particle and its antiparticle. The best test comes from the limit on the mass difference between K^0 and \bar{K}^0 . Any such difference contributes to the CP -violating parameter ϵ . Assuming CPT invariance, ϕ_ϵ , the phase of ϵ should be very close to 44° . (See the review “ CP Violation in K_L decay” in this edition.) In contrast, if the entire source of CP violation in K^0 decays were a $K^0 - \bar{K}^0$ mass difference, ϕ_ϵ would be $44^\circ + 90^\circ$.

Assuming that there is no other source of CPT violation than this mass difference, it is possible to deduce that[1]

$$m_{\bar{K}^0} - m_{K^0} \approx \frac{2(m_{K_L^0} - m_{K_S^0}) |\eta| (\frac{2}{3}\phi_{+-} + \frac{1}{3}\phi_{00} - \phi_{SW})}{\sin \phi_{SW}},$$

where $\phi_{SW} = (43.51 \pm 0.05)^\circ$, the superweak angle. Using our best values of the CP -violation parameters, we get $|(m_{\bar{K}^0} - m_{K^0})/m_{K^0}| \leq 0.8 \times 10^{-18}$ at CL=90%. Limits can also be placed on specific CPT -violating decay amplitudes. Given the small value of $(1 - |\eta_{00}/\eta_{+-}|)$, the value of $\phi_{00} - \phi_{+-}$ provides a measure of CPT violation in $K_L^0 \rightarrow 2\pi$ decay. Results from CERN [1] and Fermilab [2] indicate no CPT -violating effect.

CP AND T INVARIANCE

Given CPT invariance, CP violation and T violation are equivalent. The original evidence for CP violation came from the measurement of $|\eta_{+-}| = |A(K_L^0 \rightarrow \pi^+\pi^-)/A(K_S^0 \rightarrow \pi^+\pi^-)| = (2.232 \pm 0.011) \times 10^{-3}$. This could be explained in terms of $K^0 - \bar{K}^0$ mixing, which also leads to the asymmetry $[\Gamma(K_L^0 \rightarrow \pi^- e^+ \nu) - \Gamma(K_L^0 \rightarrow \pi^+ e^- \bar{\nu})]/[\text{sum}] = (0.334 \pm 0.007)\%$. Evidence for CP violation in the kaon decay amplitude comes from the measurement of $(1 - |\eta_{00}/\eta_{+-}|)/3 = \text{Re}(\epsilon'/\epsilon) = (1.65 \pm 0.26) \times 10^{-3}$. In the Standard Model much larger CP -violating effects are expected. The first of these, which is associated with $B - \bar{B}$ mixing, is the parameter $\sin(2\beta)$ now measured

quite accurately to be 0.671 ± 0.023 . A number of other CP -violating observables are being measured in B decays; direct evidence for CP violation in the B decay amplitude comes from the asymmetry $[\Gamma(\bar{B}^0 \rightarrow K^-\pi^+) - \Gamma(B^0 \rightarrow K^+\pi^-)]/[\text{sum}] = -0.098 \pm 0.013$. Direct tests of T violation are much more difficult; a measurement by CPLEAR of the difference between the oscillation probabilities of K^0 to \bar{K}^0 and \bar{K}^0 to K^0 is related to T violation [3]. Other searches for CP or T violation involve effects that are expected to be unobservable in the Standard Model. The most sensitive are probably the searches for an electric dipole moment of the neutron, measured to be $< 2.9 \times 10^{-26}$ e cm, and the electron $(0.07 \pm 0.07) \times 10^{-26}$ e cm. A nonzero value requires both P and T violation.

CONSERVATION OF LEPTON NUMBERS

Present experimental evidence and the standard electroweak theory are consistent with the absolute conservation of three separate lepton numbers: electron number L_e , muon number L_μ , and tau number L_τ , except for the effect of neutrino mixing associated with neutrino masses. Searches for violations are of the following types:

a) $\Delta L = 2$ for one type of charged lepton. The best limit comes from the search for neutrinoless double beta decay $(Z, A) \rightarrow (Z + 2, A) + e^- + e^-$. The best laboratory limit is $t_{1/2} > 1.9 \times 10^{25}$ yr (CL=90%) for ^{76}Ge .

b) Conversion of one charged-lepton type to another. For purely leptonic processes, the best limits are on $\mu \rightarrow e\gamma$ and $\mu \rightarrow 3e$, measured as $\Gamma(\mu \rightarrow e\gamma)/\Gamma(\mu \rightarrow \text{all}) < 1.2 \times 10^{-11}$ and $\Gamma(\mu \rightarrow 3e)/\Gamma(\mu \rightarrow \text{all}) < 1.0 \times 10^{-12}$. For semileptonic processes, the best limit comes from the coherent conversion process in a muonic atom, $\mu^- + (Z, A) \rightarrow e^- + (Z, A)$, measured as $\Gamma(\mu^- \text{Ti} \rightarrow e^- \text{Ti})/\Gamma(\mu^- \text{Ti} \rightarrow \text{all}) < 4.3 \times 10^{-12}$. Of special interest is the case in which the hadronic flavor also changes, as in $K_L \rightarrow e\mu$ and $K^+ \rightarrow \pi^+ e^- \mu^+$, measured as $\Gamma(K_L \rightarrow e\mu)/\Gamma(K_L \rightarrow \text{all}) < 4.7 \times 10^{-12}$ and $\Gamma(K^+ \rightarrow \pi^+ e^- \mu^+)/\Gamma(K^+ \rightarrow \text{all}) < 1.3 \times 10^{-11}$. Limits on the conversion of τ into e or μ are found in τ decay and are much less stringent than those for $\mu \rightarrow e$ conversion, *e.g.*, $\Gamma(\tau \rightarrow \mu\gamma)/\Gamma(\tau \rightarrow \text{all}) < 4.4 \times 10^{-8}$ and $\Gamma(\tau \rightarrow e\gamma)/\Gamma(\tau \rightarrow \text{all}) < 3.3 \times 10^{-8}$.

c) Conversion of one type of charged lepton into another type of charged antilepton. The case most studied is $\mu^- + (Z, A) \rightarrow e^+ + (Z - 2, A)$, the strongest limit being $\Gamma(\mu^- \text{Ti} \rightarrow e^+ \text{Ca})/\Gamma(\mu^- \text{Ti} \rightarrow \text{all}) < 3.6 \times 10^{-11}$.

d) Neutrino oscillations. It is expected even in the standard electroweak theory that the lepton numbers are not separately conserved, as a consequence of lepton mixing analogous to Cabibbo-Kobayashi-Maskawa quark mixing. However, if the only source of lepton-number violation is the mixing of low-mass neutrinos then processes such as $\mu \rightarrow e\gamma$ are expected to have extremely small unobservable probabilities. For small neutrino masses, the lepton-number violation would be observed first in neutrino oscillations, which have been the subject of extensive experimental searches. Strong evidence for neutrino mixing has come from atmospheric and solar neutrinos. The

Tests of Conservation Laws

SNO experiment has detected the total flux of neutrinos from the sun measured via neutral current interactions and found it greater than the flux of ν_e . This confirms previous indications of a deficit of ν_e . Furthermore, evidence for such oscillations for reactor $\bar{\nu}$ has been found by the KAMLAND detector. A global analysis combining all solar neutrino data (SNO, Borexino, Super-Kamiokande, Chlorine, Gallium) and the KamLAND data yields $\Delta(m^2) = (7.59 \pm 0.20) \times 10^{-5} \text{ eV}^2$ [4].

Underground detectors observing neutrinos produced by cosmic rays in the atmosphere have found a factor of 2 deficiency of upward going ν_μ compared to downward. This provides compelling evidence for ν_μ disappearance, for which the most probable explanation is $\nu_\mu \rightarrow \nu_\tau$ oscillations with nearly maximal mixing. This mixing space can also be explored by accelerator-based long-baseline experiments. The most recent result from MINOS gives $\Delta(m^2) = (2.43 \pm 0.13) \times 10^{-3} \text{ eV}^2$ [5].

CONSERVATION OF HADRONIC FLAVORS

In strong and electromagnetic interactions, hadronic flavor is conserved, *i.e.* the conversion of a quark of one flavor (d, u, s, c, b, t) into a quark of another flavor is forbidden. In the Standard Model, the weak interactions violate these conservation laws in a manner described by the Cabibbo-Kobayashi-Maskawa mixing (see the section “Cabibbo-Kobayashi-Maskawa Mixing Matrix”). The way in which these conservation laws are violated is tested as follows:

(a) $\Delta S = \Delta Q$ rule. In the strangeness-changing semileptonic decay of strange particles, the strangeness change equals the change in charge of the hadrons. Tests come from limits on decay rates such as $\Gamma(\Sigma^+ \rightarrow ne^+\nu)/\Gamma(\Sigma^+ \rightarrow \text{all}) < 5 \times 10^{-6}$, and from a detailed analysis of $K_L \rightarrow \pi e \nu$, which yields the parameter x , measured to be $(\text{Re } x, \text{Im } x) = (-0.002 \pm 0.006, 0.0012 \pm 0.0021)$. Corresponding rules are $\Delta C = \Delta Q$ and $\Delta B = \Delta Q$.

(b) **Change of flavor by two units.** In the Standard Model this occurs only in second-order weak interactions. The classic example is $\Delta S = 2$ via $K^0 - \bar{K}^0$ mixing, which is directly measured by $m(K_L) - m(K_S) = (0.5292 \pm 0.0009) \times 10^{10} \hbar s^{-1}$. The $\Delta B = 2$ transitions in the B^0 and B_s^0 systems via mixing are also well established. The measured mass differences between the eigenstates are $(m_{B_H^0} - m_{B_L^0}) = (0.507 \pm 0.005) \times 10^{12} \hbar s^{-1}$ and $(m_{B_{sH}^0} - m_{B_{sL}^0}) = (17.77 \pm 0.12) \times 10^{12} \hbar s^{-1}$. There is now strong evidence of $\Delta C = 2$ transition in the charm sector with the mass difference $m_{D_H^0} - m_{D_L^0} = (2.39^{+0.59}_{-0.63}) \times 10^{10} \hbar s^{-1}$. All results are consistent with the second-order calculations in the Standard Model.

(c) **Flavor-changing neutral currents.** In the Standard Model the neutral-current interactions do not change flavor. The low rate $\Gamma(K_L \rightarrow \mu^+ \mu^-)/\Gamma(K_L \rightarrow \text{all}) = (6.84 \pm 0.11) \times 10^{-9}$ puts limits on such interactions; the nonzero value for this rate is attributed to a combination of the weak and electromagnetic interactions. The

best test should come from $K^+ \rightarrow \pi^+ \nu \bar{\nu}$, which occurs in the Standard Model only as a second-order weak process with a branching fraction of $(0.4 \text{ to } 1.2) \times 10^{-10}$. Combining results from BNL-E787 and BNL-E949 experiments yield $\Gamma(K^+ \rightarrow \pi^+ \nu \bar{\nu})/\Gamma(K^+ \rightarrow \text{all}) = (1.7 \pm 1.1) \times 10^{-10}$ [6]. Limits for charm-changing or bottom-changing neutral currents are much less stringent: $\Gamma(D^0 \rightarrow \mu^+ \mu^-)/\Gamma(D^0 \rightarrow \text{all}) < 1.3 \times 10^{-6}$ and $\Gamma(B^0 \rightarrow \mu^+ \mu^-)/\Gamma(B^0 \rightarrow \text{all}) < 1.5 \times 10^{-8}$. One cannot isolate flavor-changing neutral current (FCNC) effects in non leptonic decays. For example, the FCNC transition $s \rightarrow d + (\bar{u} + u)$ is equivalent to the charged-current transition $s \rightarrow u + (\bar{u} + d)$. Tests for FCNC are therefore limited to hadron decays into lepton pairs. Such decays are expected only in second-order in the electroweak coupling in the Standard Model.

References

1. R. Carosi *et al.*, Phys. Lett. **B237**, 303 (1990).
2. A. Alavi-Harati *et al.*, Phys. Rev. **D67**, 012005 (2003); B. Schwingerheuer *et al.*, Phys. Rev. Lett. **74**, 4376 (1995).
3. A. Angelopoulos *et al.*, Phys. Lett. **B444**, 43 (1998); L. Wolfenstein, Phys. Rev. Lett. **83**, 911 (1999).
4. B. Aharmim *et al.*, Phys. Rev. Lett. **101**, 111301 (2008).
5. P. Adamson *et al.*, Phys. Rev. Lett. **101**, 131802 (2008).
6. A.V. Artamonov *et al.*, Phys. Rev. Lett. **101**, 191802 (2008).

TESTS OF DISCRETE SPACE-TIME SYMMETRIES

CHARGE CONJUGATION (C) INVARIANCE

$\Gamma(\pi^0 \rightarrow 3\gamma)/\Gamma_{\text{total}}$	$< 3.1 \times 10^{-8}$, CL = 90%
η C-nonconserving decay parameters	
$\pi^+ \pi^- \pi^0$ left-right asymmetry	$(0.09^{+0.11}_{-0.12}) \times 10^{-2}$
$\pi^+ \pi^- \pi^0$ sextant asymmetry	$(0.12^{+0.10}_{-0.11}) \times 10^{-2}$
$\pi^+ \pi^- \pi^0$ quadrant asymmetry	$(-0.09 \pm 0.09) \times 10^{-2}$
$\pi^+ \pi^- \gamma$ left-right asymmetry	$(0.9 \pm 0.4) \times 10^{-2}$
$\pi^+ \pi^- \gamma$ parameter β (<i>D</i> -wave)	-0.02 ± 0.07 ($S = 1.3$)
$\Gamma(\eta \rightarrow \pi^0 \gamma)/\Gamma_{\text{total}}$	$< 9 \times 10^{-5}$, CL = 90%
$\Gamma(\eta \rightarrow 2\pi^0 \gamma)/\Gamma_{\text{total}}$	$< 5 \times 10^{-4}$, CL = 90%
$\Gamma(\eta \rightarrow 3\pi^0 \gamma)/\Gamma_{\text{total}}$	$< 6 \times 10^{-5}$, CL = 90%
$\Gamma(\eta \rightarrow 3\gamma)/\Gamma_{\text{total}}$	$< 1.6 \times 10^{-5}$, CL = 90%
$\Gamma(\eta \rightarrow \pi^0 e^+ e^-)/\Gamma_{\text{total}}$	[a] $< 4 \times 10^{-5}$, CL = 90%
$\Gamma(\eta \rightarrow \pi^0 \mu^+ \mu^-)/\Gamma_{\text{total}}$	[a] $< 5 \times 10^{-6}$, CL = 90%
$\Gamma(\omega(782) \rightarrow \eta \pi^0)/\Gamma_{\text{total}}$	$< 2.1 \times 10^{-4}$, CL = 90%
$\Gamma(\omega(782) \rightarrow 2\pi^0)/\Gamma_{\text{total}}$	$< 2.1 \times 10^{-4}$, CL = 90%
$\Gamma(\omega(782) \rightarrow 3\pi^0)/\Gamma_{\text{total}}$	$< 2.3 \times 10^{-4}$, CL = 90%
asymmetry parameter for $\eta'(958) \rightarrow \pi^+ \pi^- \gamma$ decay	-0.03 ± 0.04
$\Gamma(\eta'(958) \rightarrow \pi^0 e^+ e^-)/\Gamma_{\text{total}}$	[a] $< 1.4 \times 10^{-3}$, CL = 90%
$\Gamma(\eta'(958) \rightarrow \eta e^+ e^-)/\Gamma_{\text{total}}$	[a] $< 2.4 \times 10^{-3}$, CL = 90%
$\Gamma(\eta'(958) \rightarrow 3\gamma)/\Gamma_{\text{total}}$	$< 1.0 \times 10^{-4}$, CL = 90%
$\Gamma(\eta'(958) \rightarrow \mu^+ \mu^- \pi^0)/\Gamma_{\text{total}}$	[a] $< 6.0 \times 10^{-5}$, CL = 90%
$\Gamma(\eta'(958) \rightarrow \mu^+ \mu^- \eta)/\Gamma_{\text{total}}$	[a] $< 1.5 \times 10^{-5}$, CL = 90%
$\Gamma(J/\psi(1S) \rightarrow \gamma \gamma)/\Gamma_{\text{total}}$	$< 5 \times 10^{-6}$, CL = 90%

Tests of Conservation Laws

PARITY (P) INVARIANCE

e electric dipole moment	$(0.07 \pm 0.07) \times 10^{-26}$ e cm
μ electric dipole moment	$(-0.1 \pm 0.9) \times 10^{-19}$ e cm
$\text{Re}(d_r = \tau$ electric dipole moment)	-0.22 to 0.45×10^{-16} e cm, CL = 95%
$\Gamma(\eta \rightarrow \pi^+ \pi^-) / \Gamma_{\text{total}}$	$< 1.3 \times 10^{-5}$, CL = 90%
$\Gamma(\eta \rightarrow 2\pi^0) / \Gamma_{\text{total}}$	$< 3.5 \times 10^{-4}$, CL = 90%
$\Gamma(\eta \rightarrow 4\pi^0) / \Gamma_{\text{total}}$	$< 6.9 \times 10^{-7}$, CL = 90%
$\Gamma(\eta'(958) \rightarrow \pi^+ \pi^-) / \Gamma_{\text{total}}$	$< 2.9 \times 10^{-3}$, CL = 90%
$\Gamma(\eta'(958) \rightarrow \pi^0 \pi^0) / \Gamma_{\text{total}}$	$< 1.0 \times 10^{-3}$, CL = 90%
$\Gamma(\eta_c(1S) \rightarrow \pi^+ \pi^-) / \Gamma_{\text{total}}$	$< 6 \times 10^{-4}$, CL = 90%
$\Gamma(\eta_c(1S) \rightarrow \pi^0 \pi^0) / \Gamma_{\text{total}}$	$< 4 \times 10^{-4}$, CL = 90%
$\Gamma(\eta_c(1S) \rightarrow K^+ K^-) / \Gamma_{\text{total}}$	$< 6 \times 10^{-4}$, CL = 90%
$\Gamma(\eta_c(1S) \rightarrow K_S^0 K_S^0) / \Gamma_{\text{total}}$	$< 3.1 \times 10^{-4}$, CL = 90%
p electric dipole moment	$< 0.54 \times 10^{-23}$ e cm
n electric dipole moment	$< 0.29 \times 10^{-25}$ e cm, CL = 90%
Λ electric dipole moment	$< 1.5 \times 10^{-16}$ e cm, CL = 95%

TIME REVERSAL (T) INVARIANCE

e electric dipole moment	$(0.07 \pm 0.07) \times 10^{-26}$ e cm
μ electric dipole moment	$(-0.1 \pm 0.9) \times 10^{-19}$ e cm
μ decay parameters	
transverse e^+ polarization normal to plane of μ spin, e^+ momentum	$(-2 \pm 8) \times 10^{-3}$
α'/A	$(-10 \pm 20) \times 10^{-3}$
β'/A	$(2 \pm 7) \times 10^{-3}$
$\text{Re}(d_r = \tau$ electric dipole moment)	-0.22 to 0.45×10^{-16} e cm, CL = 95%
P_T in $K^+ \rightarrow \pi^0 \mu^+ \nu_\mu$	$(-1.7 \pm 2.5) \times 10^{-3}$
P_T in $K^+ \rightarrow \mu^+ \nu_\mu \gamma$	$(-0.6 \pm 1.9) \times 10^{-2}$
$\text{Im}(\xi)$ in $K^+ \rightarrow \pi^0 \mu^+ \nu_\mu$ decay (from transverse μ pol.)	-0.006 ± 0.008
asymmetry A_T in $K^0 \bar{K}^0$ mixing	$(6.6 \pm 1.6) \times 10^{-3}$
$\text{Im}(\xi)$ in $K_{\mu 3}^0$ decay (from transverse μ pol.)	-0.007 ± 0.026
$A_T(D^\pm \rightarrow K_S^0 K^\pm \pi^\pm \pi^\mp)$	0.02 ± 0.07
$A_T(D^0 \rightarrow K^+ K^- \pi^+ \pi^-)$	0.01 ± 0.07
$A_T(D_S^\pm \rightarrow K_S^0 K^\pm \pi^\pm \pi^\mp)$	[b] -0.04 ± 0.07
p electric dipole moment	$< 0.54 \times 10^{-23}$ e cm
n electric dipole moment	$< 0.29 \times 10^{-25}$ e cm, CL = 90%
$n \rightarrow pe^- \bar{\nu}_e$ decay parameters	
ϕ_{AV} , phase of g_A relative to g_V	[c] $(180.06 \pm 0.07)^\circ$
triple correlation coefficient D	[d] $(-4 \pm 6) \times 10^{-4}$
triple correlation coefficient R	[d] 0.008 ± 0.016
Λ electric dipole moment	$< 1.5 \times 10^{-16}$ e cm, CL = 95%
triple correlation coefficient D for $\Sigma^- \rightarrow ne^- \bar{\nu}_e$	0.11 ± 0.10

CP INVARIANCE

$\text{Re}(d_r^W)$	$< 0.50 \times 10^{-17}$ e cm, CL = 95%
$\text{Im}(d_r^W)$	$< 1.1 \times 10^{-17}$ e cm, CL = 95%
$\eta \rightarrow \pi^+ \pi^- e^+ e^-$ decay-plane asymmetry	$(-0.6 \pm 3.1) \times 10^{-2}$
$\Gamma(\eta \rightarrow \pi^+ \pi^-) / \Gamma_{\text{total}}$	$< 1.3 \times 10^{-5}$, CL = 90%
$\Gamma(\eta \rightarrow 2\pi^0) / \Gamma_{\text{total}}$	$< 3.5 \times 10^{-4}$, CL = 90%
$\Gamma(\eta \rightarrow 4\pi^0) / \Gamma_{\text{total}}$	$< 6.9 \times 10^{-7}$, CL = 90%
$\Gamma(\eta'(958) \rightarrow \pi^+ \pi^-) / \Gamma_{\text{total}}$	$< 2.9 \times 10^{-3}$, CL = 90%
$\Gamma(\eta'(958) \rightarrow \pi^0 \pi^0) / \Gamma_{\text{total}}$	$< 1.0 \times 10^{-3}$, CL = 90%
$K^\pm \rightarrow \pi^\pm \pi^+ \pi^-$ rate difference/average	$(0.08 \pm 0.12)\%$
$K^\pm \rightarrow \pi^\pm \pi^0 \pi^0$ rate difference/average	$(0.0 \pm 0.6)\%$
$K^\pm \rightarrow \pi^\pm \pi^0 \gamma$ rate difference/average	$(0.9 \pm 3.3)\%$
$K^\pm \rightarrow \pi^\pm \pi^+ \pi^- (g_+ - g_-) / (g_+ + g_-)$	$(-1.5 \pm 2.2) \times 10^{-4}$
$K^\pm \rightarrow \pi^\pm \pi^0 \pi^0 (g_+ - g_-) / (g_+ + g_-)$	$(1.8 \pm 1.8) \times 10^{-4}$
$\Delta(K_{\pi e e}^\pm) = \frac{\Gamma(K_{\pi e e}^+) - \Gamma(K_{\pi e e}^-)}{\Gamma(K_{\pi e e}^+) + \Gamma(K_{\pi e e}^-)}$	$(-2.2 \pm 1.6) \times 10^{-2}$
$\Delta(K_{\pi \mu \mu}^\pm) = \frac{\Gamma(K_{\pi \mu \mu}^+) - \Gamma(K_{\pi \mu \mu}^-)}{\Gamma(K_{\pi \mu \mu}^+) + \Gamma(K_{\pi \mu \mu}^-)}$	-0.02 ± 0.12
$A_S = [\Gamma(K_S^0 \rightarrow \pi^- e^+ \nu_e) - \Gamma(K_S^0 \rightarrow \pi^+ e^- \bar{\nu}_e)] / \text{SUM}$	$(2 \pm 10) \times 10^{-3}$

$\text{Im}(\eta_{+-0}) = \text{Im}(A(K_S^0 \rightarrow \pi^+ \pi^- \pi^0, CP\text{-violating}) / A(K_L^0 \rightarrow \pi^+ \pi^- \pi^0))$	-0.002 ± 0.009
$\text{Im}(\eta_{000}) = \text{Im}(A(K_S^0 \rightarrow \pi^0 \pi^0 \pi^0) / A(K_L^0 \rightarrow \pi^0 \pi^0 \pi^0))$	$(-0.1 \pm 1.6) \times 10^{-2}$
$ \eta_{000} = A(K_S^0 \rightarrow 3\pi^0) / A(K_L^0 \rightarrow 3\pi^0) $	< 0.018 , CL = 90%
CP asymmetry A in $K_S^0 \rightarrow \pi^+ \pi^- e^+ e^-$	$(-1 \pm 4)\%$
$\Gamma(K_S^0 \rightarrow 3\pi^0) / \Gamma_{\text{total}}$	$< 1.2 \times 10^{-7}$, CL = 90%
linear coefficient j for $K_L^0 \rightarrow \pi^+ \pi^- \pi^0$	0.0012 ± 0.0008
quadratic coefficient f for $K_L^0 \rightarrow \pi^+ \pi^- \pi^0$	0.004 ± 0.006
$ \epsilon_{+-\gamma}' / \epsilon$ for $K_L^0 \rightarrow \pi^+ \pi^- \gamma$	< 0.3 , CL = 90%
$ g_{E1} $ for $K_L^0 \rightarrow \pi^+ \pi^- \gamma$	< 0.21 , CL = 90%
$\Gamma(K_L^0 \rightarrow \pi^0 \mu^+ \mu^-) / \Gamma_{\text{total}}$	[e] $< 3.8 \times 10^{-10}$, CL = 90%
$\Gamma(K_L^0 \rightarrow \pi^0 e^+ e^-) / \Gamma_{\text{total}}$	[e] $< 2.8 \times 10^{-10}$, CL = 90%
$\Gamma(K_L^0 \rightarrow \pi^0 \nu \bar{\nu}) / \Gamma_{\text{total}}$	[f] $< 6.7 \times 10^{-8}$, CL = 90%
$ACP(D^\pm \rightarrow \mu^\pm \nu)$	0.08 ± 0.08
$ACP(D^\pm \rightarrow K_S^0 \pi^\pm)$	-0.009 ± 0.009
$ACP(D^\pm \rightarrow K^\mp 2\pi^\pm)$	-0.005 ± 0.010
$ACP(D^\pm \rightarrow K^\mp \pi^\pm \pi^\pm \pi^0)$	0.010 ± 0.013
$ACP(D^\pm \rightarrow K_S^0 \pi^\pm \pi^0)$	0.003 ± 0.009
$ACP(D^\pm \rightarrow K_S^0 \pi^\pm \pi^+ \pi^-)$	0.001 ± 0.013
$ACP(D^\pm \rightarrow K_S^0 K^\pm)$	0.07 ± 0.06
$ACP(D^\pm \rightarrow K^+ K^- \pi^\pm)$	$(0.3 \pm 0.6)\%$
$ACP(D^\pm \rightarrow K^\pm K^0)$	$(0.1 \pm 1.3)\%$
$ACP(D^\pm \rightarrow \phi \pi^\pm)$	$(-0.9 \pm 1.1)\%$
$ACP(D^\pm \rightarrow K^\pm K_S^0(1430)^0)$	$(8_{-6}^{+7})\%$
$ACP(D^\pm \rightarrow K^\pm K_S^0(1430)^0)$	$(43_{-26}^{+20})\%$
$ACP(D^\pm \rightarrow K^\pm K_S^0(800))$	$(-12_{-13}^{+18})\%$
$ACP(D^\pm \rightarrow a_0(1450)^0 \pi^\pm)$	$(-19_{-16}^{+14})\%$
$ACP(D^\pm \rightarrow \phi(1680) \pi^\pm)$	$(-9 \pm 26)\%$
$ACP(D^\pm \rightarrow \pi^+ \pi^- \pi^\pm)$	-0.02 ± 0.04
$ACP(D^\pm \rightarrow K_S^0 K^\pm \pi^+ \pi^-)$	-0.04 ± 0.07
$ a / b $ of $D^0 \bar{D}^0$ mixing	$0.86_{-0.15}^{+0.18}$
A_T of $D^0 \bar{D}^0$ mixing	$(1.4 \pm 2.7) \times 10^{-3}$

Where there is ambiguity, the CP test is labelled by the D^0 decay mode.

$ACP(D^0 \rightarrow K^+ K^-)$	$(-0.17 \pm 0.31) \times 10^{-2}$ ($S = 1.3$)
$ACP(D^0 \rightarrow K_S^0 K_S^0)$	-0.23 ± 0.19
$ACP(D^0 \rightarrow \pi^+ \pi^-)$	$(0.2 \pm 0.4) \times 10^{-2}$
$ACP(D^0 \rightarrow \pi^0 \pi^0)$	0.00 ± 0.05
$ACP(D^0 \rightarrow \pi^+ \pi^- \pi^0)$	$(0.3 \pm 0.4)\%$
$ACP(D^0 \rightarrow \rho(770)^+ \pi^- \rightarrow \pi^+ \pi^- \pi^0)$	$(1.6 \pm 1.2)\%$
$ACP(D^0 \rightarrow \rho(770)^0 \pi^0 \rightarrow \pi^+ \pi^- \pi^0)$	$(-1.6 \pm 1.5)\%$
$ACP(D^0 \rightarrow \rho(770)^- \pi^+ \rightarrow \pi^+ \pi^- \pi^0)$	$(-0.7 \pm 1.2)\%$
$ACP(D^0 \rightarrow \rho(1450)^+ \pi^- \rightarrow \pi^+ \pi^- \pi^0)$	$(0.0 \pm 0.14)\%$
$ACP(D^0 \rightarrow \rho(1450)^0 \pi^0 \rightarrow \pi^+ \pi^- \pi^0)$	$(-0.1 \pm 0.22)\%$
$ACP(D^0 \rightarrow \rho(1450)^- \pi^+ \rightarrow \pi^+ \pi^- \pi^0)$	$(0.2 \pm 0.32)\%$
$ACP(D^0 \rightarrow \rho(1700)^+ \pi^- \rightarrow \pi^+ \pi^- \pi^0)$	$(-0.4 \pm 1.1)\%$
$ACP(D^0 \rightarrow \rho(1700)^0 \pi^0 \rightarrow \pi^+ \pi^- \pi^0)$	$(1.3 \pm 0.9)\%$
$ACP(D^0 \rightarrow \rho(1700)^- \pi^+ \rightarrow \pi^+ \pi^- \pi^0)$	$(0.5 \pm 0.7)\%$
$ACP(D^0 \rightarrow f_0(980) \pi^0 \rightarrow \pi^+ \pi^- \pi^0)$	$(0.0 \pm 0.14)\%$
$ACP(D^0 \rightarrow f_0(1370) \pi^0 \rightarrow \pi^+ \pi^- \pi^0)$	$(0.2 \pm 0.14)\%$
$ACP(D^0 \rightarrow f_0(1500) \pi^0 \rightarrow \pi^+ \pi^- \pi^0)$	$(0.0 \pm 0.14)\%$
$ACP(D^0 \rightarrow f_0(1710) \pi^0 \rightarrow \pi^+ \pi^- \pi^0)$	$(0.0 \pm 0.14)\%$
$ACP(D^0 \rightarrow f_2(1270) \pi^0 \rightarrow \pi^+ \pi^- \pi^0)$	$(-0.1 \pm 0.14)\%$
$ACP(D^0 \rightarrow \sigma(400) \pi^0 \rightarrow \pi^+ \pi^- \pi^0)$	$(0.1 \pm 0.14)\%$
$ACP(\text{nonresonant } D^0 \rightarrow \pi^+ \pi^- \pi^0)$	$(-0.2 \pm 0.4)\%$
$ACP(D^0 \rightarrow K^+ K^- \pi^0)$	$(-1.0 \pm 1.7)\%$
$ACP(D^0 \rightarrow K^*(892)^+ K^- \rightarrow K^+ K^- \pi^0)$	$(-0.8 \pm 1.2)\%$
$ACP(D^0 \rightarrow K^*(1410)^+ K^- \rightarrow K^+ K^- \pi^0)$	$(-1.7 \pm 1.9)\%$
$ACP(D^0 \rightarrow (K^+ \pi^0)_S\text{-wave } K^- \rightarrow K^+ K^- \pi^0)$	$(2 \pm 5)\%$
$ACP(D^0 \rightarrow \phi(1020) \pi^0 \rightarrow K^+ K^- \pi^0)$	$(0.4 \pm 0.8)\%$
$ACP(D^0 \rightarrow f_0(980) \pi^0 \rightarrow K^+ K^- \pi^0)$	$(-0.4 \pm 2.6)\%$
$ACP(D^0 \rightarrow a_0(980)^0 \pi^0 \rightarrow K^+ K^- \pi^0)$	$(-0.6 \pm 1.9)\%$
$ACP(D^0 \rightarrow f_2'(1525) \pi^0 \rightarrow K^+ K^- \pi^0)$	$(0.0 \pm 0.32)\%$
$ACP(D^0 \rightarrow K^*(892)^- K^+ \rightarrow K^+ K^- \pi^0)$	$(-1.7 \pm 1.4)\%$
$ACP(D^0 \rightarrow K^*(1410)^- K^+ \rightarrow K^+ K^- \pi^0)$	$(-1.7 \pm 2.9)\%$

Tests of Conservation Laws

$A_{CP}(D^0 \rightarrow (K^- \pi^0)_{S\text{-wave}} K^+ \rightarrow K^+ K^- \pi^0)$	$(-0.4 \pm 2.5)\%$	$A_{CP}(B^+ \rightarrow D^{*0} K^+)$	-0.07 ± 0.04
$A_{CP}(D^0 \rightarrow K_S^0 \phi)$	-0.03 ± 0.09	$r_B^*(B^+ \rightarrow D^{*0} K^+)$	0.14 ± 0.05
$A_{CP}(D^0 \rightarrow K_S^0 \pi^0)$	0.001 ± 0.013	$\delta_B^*(B^+ \rightarrow D^{*0} K^+)$	$299 \pm 24 \text{ degrees}$
$A_{CP}(D^0 \rightarrow K^- \pi^+)$	-0.004 ± 0.010	$A_{CP}(B^+ \rightarrow D_{CP(+1)}^{*0} K^+)$	-0.12 ± 0.08
$A_{CP}(D^0 \rightarrow K^+ \pi^-)$	0.022 ± 0.032	$A_{CP}(B^+ \rightarrow D_{CP(-1)}^{*0} K^+)$	0.07 ± 0.10
$A_{CP}(D^0 \rightarrow K^- \pi^+ \pi^0)$	0.002 ± 0.009	$A_{CP}(B^+ \rightarrow D_{CP(+1)} K^*(892)^+)$	0.09 ± 0.14
$A_{CP}(D^0 \rightarrow K^+ \pi^- \pi^0)$	0.00 ± 0.05	$A_{CP}(B^+ \rightarrow D_{CP(-1)} K^*(892)^+)$	-0.23 ± 0.22
$A_{CP}(D^0 \rightarrow K_S^0 \pi^+ \pi^-)$	$-0.009^{+0.026}_{-0.060}$	$A_{CP}(B^+ \rightarrow D^{*+} \bar{D}^{*0})$	-0.15 ± 0.11
$A_{CP}(D^0 \rightarrow K^*(892)^- \pi^+ \rightarrow K_S^0 \pi^+ \pi^-)$	$<3.5 \times 10^{-4}, \text{CL} = 95\%$	$A_{CP}(B^+ \rightarrow D^{*+} \bar{D}^0)$	-0.06 ± 0.13
$A_{CP}(D^0 \rightarrow K^*(892)^+ \pi^- \rightarrow K_S^0 \pi^+ \pi^-)$	$<7.8 \times 10^{-4}, \text{CL} = 95\%$	$A_{CP}(B^+ \rightarrow D^+ \bar{D}^{*0})$	0.13 ± 0.18
$A_{CP}(D^0 \rightarrow K_S^0 \rho^0 \rightarrow K_S^0 \pi^+ \pi^-)$	$<4.8 \times 10^{-4}, \text{CL} = 95\%$	$A_{CP}(B^+ \rightarrow D^+ \bar{D}^0)$	-0.03 ± 0.07
$A_{CP}(D^0 \rightarrow K_S^0 \omega \rightarrow K_S^0 \pi^+ \pi^-)$	$<9.2 \times 10^{-4}, \text{CL} = 95\%$	$A_{CP}(B^+ \rightarrow K_S^0 \pi^+)$	$0.009 \pm 0.029 \text{ (S} = 1.2)$
$A_{CP}(D^0 \rightarrow K_S^0 f_0(980) \rightarrow K_S^0 \pi^+ \pi^-)$	$<6.8 \times 10^{-4}, \text{CL} = 95\%$	$A_{CP}(B^+ \rightarrow K^+ \pi^0)$	0.051 ± 0.025
$A_{CP}(D^0 \rightarrow K_S^0 f_2(1270) \rightarrow K_S^0 \pi^+ \pi^-)$	$<13.5 \times 10^{-4}, \text{CL} = 95\%$	$A_{CP}(B^+ \rightarrow \eta' K^+)$	0.013 ± 0.017
$A_{CP}(D^0 \rightarrow K_S^0 f_0(1370) \rightarrow K_S^0 \pi^+ \pi^-)$	$<25.5 \times 10^{-4}, \text{CL} = 95\%$	$A_{CP}(B^+ \rightarrow \eta' K^*(892)^+)$	$-0.30^{+0.33}_{-0.40}$
$A_{CP}(D^0 \rightarrow K_S^0(1430)^- \pi^+ \rightarrow K_S^0 \pi^+ \pi^-)$	$<9.0 \times 10^{-4}, \text{CL} = 95\%$	$A_{CP}(B^+ \rightarrow \eta K^+)$	-0.37 ± 0.09
$A_{CP}(D^0 \rightarrow K_S^0(1430)^- \pi^+ \rightarrow K_S^0 \pi^+ \pi^-)$	$<6.5 \times 10^{-4}, \text{CL} = 95\%$	$A_{CP}(B^+ \rightarrow \eta K^*(892)^+)$	0.02 ± 0.06
$A_{CP}(D^0 \rightarrow K^*(1680)^- \pi^+ \rightarrow K_S^0 \pi^+ \pi^-)$	$<28.4 \times 10^{-4}, \text{CL} = 95\%$	$A_{CP}(B^+ \rightarrow \eta K_0^*(1430)^+)$	0.05 ± 0.13
$A_{CP}(D^0 \rightarrow K^- \pi^+ \pi^+ \pi^-)$	0.007 ± 0.010	$A_{CP}(B^+ \rightarrow \eta K_2^*(1430)^+)$	-0.45 ± 0.30
$A_{CP}(D^0 \rightarrow K^+ \pi^- \pi^+ \pi^-)$	-0.02 ± 0.04	$A_{CP}(B^+ \rightarrow \omega K^+)$	0.02 ± 0.05
$A_{CP}(D^0 \rightarrow K^+ K^- \pi^+ \pi^-)$	-0.08 ± 0.07	$A_{CP}(B^+ \rightarrow \omega K^{*+})$	0.29 ± 0.35
$A_{CP}(D_S^\pm \rightarrow \mu^\pm \nu)$	0.05 ± 0.06	$A_{CP}(B^+ \rightarrow \omega(K\pi)_0^{*+})$	-0.10 ± 0.09
$A_{CP}(D_S^\pm \rightarrow K^\pm K_S^0)$	0.049 ± 0.023	$A_{CP}(B^+ \rightarrow \omega K_2^*(1430)^+)$	0.14 ± 0.15
$A_{CP}(D_S^\pm \rightarrow K^+ K^- \pi^\pm)$	0.003 ± 0.014	$A_{CP}(B^+ \rightarrow K^*(892)^+ \pi^0)$	0.04 ± 0.29
$A_{CP}(D_S^\pm \rightarrow K^+ K^- \pi^\pm \pi^0)$	-0.06 ± 0.04	$A_{CP}(B^+ \rightarrow K^{*0} \pi^+)$	$-0.04 \pm 0.09 \text{ (S} = 2.1)$
$A_{CP}(D_S^\pm \rightarrow K_S^0 K^\mp 2\pi^\pm)$	-0.01 ± 0.04	$A_{CP}(B^+ \rightarrow K^+ \pi^- \pi^+)$	0.038 ± 0.022
$A_{CP}(D_S^\pm \rightarrow \pi^+ \pi^- \pi^\pm)$	0.02 ± 0.05	$A_{CP}(B^+ \rightarrow f_0(980) K^+)$	$-0.10^{+0.05}_{-0.04}$
$A_{CP}(D_S^\pm \rightarrow \pi^\pm \eta)$	-0.08 ± 0.05	$A_{CP}(B^+ \rightarrow f_2(1270) K^+)$	$-0.68^{+0.19}_{-0.17}$
$A_{CP}(D_S^\pm \rightarrow \pi^\pm \eta')$	-0.06 ± 0.04	$A_{CP}(B^+ \rightarrow f_X(1300) K^+)$	0.28 ± 0.30
$A_{CP}(D_S^\pm \rightarrow K^\pm \pi^0)$	0.02 ± 0.29	$A_{CP}(B^+ \rightarrow \rho^0 K^+)$	0.37 ± 0.10
$A_{CP}(D_S^\pm \rightarrow K_S^0 \pi^\pm)$	0.27 ± 0.11	$A_{CP}(B^+ \rightarrow K_S^0(1430)^0 \pi^+)$	0.055 ± 0.033
$A_{CP}(D_S^\pm \rightarrow K^\pm \pi^+ \pi^-)$	0.11 ± 0.07	$A_{CP}(B^+ \rightarrow K_S^0(1430)^0 \pi^+)$	$0.05^{+0.29}_{-0.24}$
$A_{CP}(D_S^\pm \rightarrow K^\pm \eta)$	-0.20 ± 0.18	$A_{CP}(B^+ \rightarrow K^0 \rho^+)$	$(-0.12 \pm 0.17) \times 10^{-6}$
$A_{CP}(D_S^\pm \rightarrow K^\pm \eta'(958))$	-0.2 ± 0.4	$A_{CP}(B^+ \rightarrow K^{*+} \pi^+ \pi^-)$	0.07 ± 0.08
$A_{CP}(B^+ \rightarrow J/\psi(1S) K^+)$	$0.009 \pm 0.008 \text{ (S} = 1.3)$	$A_{CP}(B^+ \rightarrow \rho \bar{A} \gamma)$	0.17 ± 0.17
$A_{CP}(B^+ \rightarrow J/\psi(1S) \pi^+)$	$0.01 \pm 0.07 \text{ (S} = 1.3)$	$A_{CP}(B^+ \rightarrow \rho \bar{A} \pi^0)$	0.01 ± 0.17
$A_{CP}(B^+ \rightarrow J/\psi \rho^+)$	-0.11 ± 0.14	$A_{CP}(B^+ \rightarrow \rho^0 K^*(892)^+)$	—
$A_{CP}(B^+ \rightarrow J/\psi K^*(892)^+)$	-0.048 ± 0.033	$A_{CP}(B^+ \rightarrow K^*(892)^+ f_0(980))$	-0.34 ± 0.21
$A_{CP}(B^+ \rightarrow \eta_c K^+)$	-0.16 ± 0.08	$A_{CP}(B^+ \rightarrow a_1^+ K^0)$	0.12 ± 0.11
$A_{CP}(B^+ \rightarrow \psi(2S) \pi^+)$	0.02 ± 0.09	$A_{CP}(B^+ \rightarrow b_1^+ K^0)$	-0.03 ± 0.15
$A_{CP}(B^+ \rightarrow \psi(2S) K^+)$	-0.025 ± 0.024	$A_{CP}(B^+ \rightarrow K^*(892)^0 \rho^+)$	-0.01 ± 0.16
$A_{CP}(B^+ \rightarrow \psi(2S) K^*(892)^+)$	0.08 ± 0.21	$A_{CP}(B^+ \rightarrow b_1^0 K^+)$	-0.46 ± 0.20
$A_{CP}(B^+ \rightarrow \chi_{c1}(1P) \pi^+)$	0.07 ± 0.18	$A_{CP}(B^+ \rightarrow K^0 K^+)$	0.12 ± 0.18
$A_{CP}(B^+ \rightarrow \chi_{c0} K^+)$	-0.11 ± 0.12	$A_{CP}(B^+ \rightarrow K^+ K_S^0 K_S^0)$	-0.04 ± 0.11
$A_{CP}(B^+ \rightarrow \chi_{c1} K^+)$	-0.009 ± 0.033	$A_{CP}(B^+ \rightarrow K^+ K^- K^+)$	-0.017 ± 0.030
$A_{CP}(B^+ \rightarrow \chi_{c1} K^*(892)^+)$	0.5 ± 0.5	$A_{CP}(B^+ \rightarrow \phi K^+)$	-0.01 ± 0.06
$A_{CP}(B^+ \rightarrow \bar{D}^0 \pi^+)$	-0.008 ± 0.008	$A_{CP}(B^+ \rightarrow X_0(1550) K^+)$	-0.04 ± 0.07
$A_{CP}(B^+ \rightarrow D_{CP(+1)} \pi^+)$	0.035 ± 0.024	$A_{CP}(B^+ \rightarrow K^{*+} K^+ K^-)$	0.11 ± 0.09
$A_{CP}(B^+ \rightarrow D_{CP(-1)} \pi^+)$	0.017 ± 0.026	$A_{CP}(B^+ \rightarrow \phi K^*(892)^+)$	-0.01 ± 0.08
$A_{CP}(B^+ \rightarrow \bar{D}^0 K^+)$	0.07 ± 0.04	$A_{CP}(B^+ \rightarrow \phi(K\pi)_0^{*+})$	0.04 ± 0.16
$r_B(B^+ \rightarrow D^0 K^+)$	0.101 ± 0.032	$A_{CP}(B^+ \rightarrow \phi K_1(1270)^+)$	0.15 ± 0.20
$\delta_B(B^+ \rightarrow D^0 K^+)$	$126 \pm 21 \text{ degrees}$	$A_{CP}(B^+ \rightarrow \phi K_2^*(1430)^+)$	-0.23 ± 0.20
$r_B(B^+ \rightarrow D K^{*+})$	$0.34 \pm 0.09 \text{ (S} = 1.3)$	$A_{CP}(B^+ \rightarrow K^*(892)^+ \gamma)$	0.018 ± 0.029
$\delta_B(B^+ \rightarrow D K^{*+})$	$157 \pm 70 \text{ degrees (S} = 2.0)$	$A_{CP}(B^+ \rightarrow \eta K^+ \gamma)$	-0.12 ± 0.07
$A_{CP}(B^+ \rightarrow [K^- \pi^+]_D K^+)$	$-0.1^{+0.9}_{-1.1}$	$A_{CP}(B^+ \rightarrow \phi K^+ \gamma)$	-0.26 ± 0.15
$A_{CP}(B^+ \rightarrow [K^- \pi^+]_{\bar{D}} K^*(892)^+)$	-0.3 ± 0.5	$A_{CP}(B^+ \rightarrow \rho^+ \gamma)$	-0.11 ± 0.33
$A_{CP}(B^+ \rightarrow [K^- \pi^+]_D \pi^+)$	-0.02 ± 0.16	$A_{CP}(B^+ \rightarrow \pi^+ \pi^0)$	0.06 ± 0.05
$A_{CP}(B^+ \rightarrow [\pi^+ \pi^- \pi^0]_D K^+)$	-0.02 ± 0.15	$A_{CP}(B^+ \rightarrow \pi^+ \pi^- \pi^+)$	0.03 ± 0.06
$A_{CP}(B^+ \rightarrow D_{CP(+1)} K^+)$	$0.24 \pm 0.08 \text{ (S} = 1.1)$	$A_{CP}(B^+ \rightarrow \rho^0 \pi^+)$	$0.18^{+0.09}_{-0.17}$
$A_{CP}(B^+ \rightarrow D_{CP(-1)} K^+)$	-0.10 ± 0.08	$A_{CP}(B^+ \rightarrow f_2(1270) \pi^+)$	0.41 ± 0.30
$A_{CP}(B^+ \rightarrow \bar{D}^{*0} \pi^+)$	-0.014 ± 0.015	$A_{CP}(B^+ \rightarrow \rho^0(1450) \pi^+)$	$-0.1^{+0.4}_{-0.5}$
$A_{CP}(B^+ \rightarrow (D_{CP(+1)}^*)^0 \pi^+)$	-0.02 ± 0.05	$A_{CP}(B^+ \rightarrow f_0(1370) \pi^+)$	0.72 ± 0.22
$A_{CP}(B^+ \rightarrow (D_{CP(-1)}^*)^0 \pi^+)$	-0.09 ± 0.05	$A_{CP}(B^+ \rightarrow \pi^+ \pi^- \pi^+ \text{ nonresonant})$	$-0.14^{+0.23}_{-0.16}$
		$A_{CP}(B^+ \rightarrow \rho^+ \pi^0)$	0.02 ± 0.11
		$A_{CP}(B^+ \rightarrow \rho^+ \rho^0)$	-0.05 ± 0.05
		$A_{CP}(B^+ \rightarrow b_1^0 \pi^+)$	0.05 ± 0.16
		$A_{CP}(B^+ \rightarrow \omega \pi^+)$	-0.04 ± 0.06
		$A_{CP}(B^+ \rightarrow \omega \rho^+)$	-0.20 ± 0.09

Tests of Conservation Laws

$A_{CP}(B^+ \rightarrow \eta\pi^+)$	-0.13 ± 0.10 (S = 1.5)	$C_{\omega K_S^0}(B^0 \rightarrow \omega K_S^0)$	-0.30 ± 0.28 (S = 1.6)
$A_{CP}(B^+ \rightarrow \eta'\pi^+)$	0.06 ± 0.16	$S_{\omega K_S^0}(B^0 \rightarrow \omega K_S^0)$	0.43 ± 0.24
$A_{CP}(B^+ \rightarrow \eta\rho^+)$	0.11 ± 0.11	$C(B^0 \rightarrow K_S^0\pi^0\pi^0)$	0.2 ± 0.5
$A_{CP}(B^+ \rightarrow \eta'\rho^+)$	0.04 ± 0.28	$S(B^0 \rightarrow K_S^0\pi^0\pi^0)$	0.7 ± 0.7
$A_{CP}(B^+ \rightarrow p\bar{p}\pi^+)$	0.00 ± 0.04	$C_{\rho^0 K_S^0}(B^0 \rightarrow \rho^0 K_S^0)$	-0.04 ± 0.20
$A_{CP}(B^+ \rightarrow p\bar{p}K^+)$	-0.16 ± 0.07	$S_{\rho^0 K_S^0}(B^0 \rightarrow \rho^0 K_S^0)$	$0.50^{+0.17}_{-0.21}$
$A_{CP}(B^+ \rightarrow p\bar{p}K^*(892)^+)$	0.21 ± 0.16 (S = 1.4)	$C_{f_0(980) K_S^0}(B^0 \rightarrow f_0(980) K_S^0)$	0.07 ± 0.14
$A_{CP}(B^+ \rightarrow K^+\ell^+\ell^-)$	-0.01 ± 0.09 (S = 1.1)	$S_{f_0(980) K_S^0}(B^0 \rightarrow f_0(980) K_S^0)$	$-0.73^{+0.27}_{-0.09}$ (S = 1.6)
$A_{CP}(B^+ \rightarrow K^+e^+e^-)$	0.14 ± 0.14	$S_{f_2(1270) K_S^0}(B^0 \rightarrow f_2(1270) K_S^0)$	-0.5 ± 0.5
$A_{CP}(B^+ \rightarrow K^+\mu^+\mu^-)$	-0.05 ± 0.13	$C_{f_2(1270) K_S^0}(B^0 \rightarrow f_2(1270) K_S^0)$	0.3 ± 0.4
$A_{CP}(B^+ \rightarrow K^{*+}\ell^+\ell^-)$	-0.09 ± 0.14	$S_{f_x(1300) K_S^0}(B^0 \rightarrow f_x(1300) K_S^0)$	-0.2 ± 0.5
$A_{CP}(B^+ \rightarrow K^{*+}e^+e^-)$	-0.14 ± 0.23	$C_{f_x(1300) K_S^0}(B^0 \rightarrow f_x(1300) K_S^0)$	0.13 ± 0.35
$A_{CP}(B^+ \rightarrow K^{*+}\mu^+\mu^-)$	-0.12 ± 0.24	$S_{K^0\pi^+\pi^-}(B^0 \rightarrow K^0\pi^+\pi^- \text{ nonresonant})$	-0.01 ± 0.33
$\gamma(B^+ \rightarrow D^{(*)}K^{(*)+})$	$(62 \pm 15)^\circ$	$C_{K^0\pi^+\pi^-}(B^0 \rightarrow K^0\pi^+\pi^- \text{ nonresonant})$	0.01 ± 0.26
$\text{Re}(\epsilon_{B^0})/(1+ \epsilon_{B^0} ^2)$	$(-0.1 \pm 1.4) \times 10^{-3}$	$C_{K_S^0 K_S^0}(B^0 \rightarrow K_S^0 K_S^0)$	0.0 ± 0.4 (S = 1.4)
$A_{T/CP}$	0.005 ± 0.018	$S_{K_S^0 K_S^0}(B^0 \rightarrow K_S^0 K_S^0)$	-0.8 ± 0.5
$A_{CP}(B^0 \rightarrow D^*(2010)^+ D^-)$	0.02 ± 0.04	$C_{K^+K^- K_S^0}(B^0 \rightarrow K^+K^- K_S^0)$	0.07 ± 0.08
$A_{CP}(B^0 \rightarrow \eta' K^*(892)^0)$	0.08 ± 0.25	$C_{K^+K^- K_S^0}(B^0 \rightarrow K^+K^- K_S^0 \text{ inclusive})$	0.01 ± 0.09
$A_{CP}(B^0 \rightarrow \omega K^{*0})$	0.45 ± 0.25	$C_{\phi K_S^0}(B^0 \rightarrow \phi K_S^0)$	-0.01 ± 0.12
$A_{CP}(B^0 \rightarrow \omega(K\pi)_0^{*0})$	-0.07 ± 0.09	$S_{\phi K_S^0}(B^0 \rightarrow \phi K_S^0)$	0.39 ± 0.17
$A_{CP}(B^0 \rightarrow \omega K_2^*(1430)^0)$	-0.37 ± 0.17	$C_{K_S K_S K_S}(B^0 \rightarrow K_S K_S K_S)$	-0.15 ± 0.16 (S = 1.1)
$A_{CP}(B^0 \rightarrow K^0 K^0)$	$(-0.6 \pm 0.7) \times 10^{-6}$	$S_{K_S K_S K_S}(B^0 \rightarrow K_S K_S K_S)$	-0.4 ± 0.5 (S = 2.5)
$A_{CP}(B^0 \rightarrow \eta K_0^*(1430)^0)$	0.06 ± 0.13	$C_{K_S^0\pi^0\gamma}(B^0 \rightarrow K_S^0\pi^0\gamma)$	0.36 ± 0.33
$A_{CP}(B^0 \rightarrow \eta K_2^*(1430)^0)$	-0.07 ± 0.19	$S_{K_S^0\pi^0\gamma}(B^0 \rightarrow K_S^0\pi^0\gamma)$	-0.8 ± 0.6
$A_{CP}(B^0 \rightarrow K^+\pi^-\pi^0)$	$(0 \pm 6) \times 10^{-2}$	$C_{K^*(892)^0\gamma}(B^0 \rightarrow K^*(892)^0\gamma)$	-0.04 ± 0.16 (S = 1.2)
$A_{CP}(B^0 \rightarrow \rho^- K^+)$	0.15 ± 0.13	$S_{K^*(892)^0\gamma}(B^0 \rightarrow K^*(892)^0\gamma)$	-0.15 ± 0.22
$A_{CP}(B^0 \rightarrow K^+\pi^-\pi^0 \text{ nonresonant})$	$0.23^{+0.22}_{-0.29}$	$C_{\eta K^0\gamma}(B^0 \rightarrow \eta K^0\gamma)$	-0.3 ± 0.4
$A_{CP}(B^0 \rightarrow (K\pi)_0^{*+}\pi^-)$	0.10 ± 0.07	$S_{\eta K^0\gamma}(B^0 \rightarrow \eta K^0\gamma)$	-0.2 ± 0.5
$A_{CP}(B^0 \rightarrow (K\pi)_0^{*0}\pi^0)$	-0.22 ± 0.32	$C(B^0 \rightarrow K_S^0\rho^0\gamma)$	-0.05 ± 0.19
$A_{CP}(B^0 \rightarrow K^*(892)^+\pi^-)$	-0.19 ± 0.07	$S(B^0 \rightarrow K_S^0\rho^0\gamma)$	0.11 ± 0.34
$A_{CP}(B^0 \rightarrow K^{*0}\pi^0)$	$-0.09^{+0.23}_{-0.26}$	$C(B^0 \rightarrow \rho^0\gamma)$	0.4 ± 0.5
$A_{CP}(B^0 \rightarrow K^0\pi^+\pi^-)$	-0.01 ± 0.05	$S(B^0 \rightarrow \rho^0\gamma)$	-0.8 ± 0.7
$A_{CP}(B^0 \rightarrow K^*(892)^0\pi^+\pi^-)$	0.07 ± 0.05	$C_{\pi\pi}(B^0 \rightarrow \pi^+\pi^-)$	-0.38 ± 0.17 (S = 2.6)
$A_{CP}(B^0 \rightarrow K^*(892)^0\rho^0)$	0.09 ± 0.19	$C_{\pi^0\pi^0}(B^0 \rightarrow \pi^0\pi^0)$	-0.48 ± 0.30
$A_{CP}(B^0 \rightarrow a_1^- K^+)$	-0.16 ± 0.12	$C_{\rho\pi}(B^0 \rightarrow \rho^+\pi^-)$	0.01 ± 0.14 (S = 1.9)
$A_{CP}(B^0 \rightarrow b_1 K^+)$	-0.07 ± 0.12	$S_{\rho\pi}(B^0 \rightarrow \rho^+\pi^-)$	0.01 ± 0.09
$A_{CP}(B^0 \rightarrow K^*(892)^0 K^+ K^-)$	0.01 ± 0.05	$\Delta S_{\rho\pi}(B^0 \rightarrow \rho^+\pi^-)$	-0.05 ± 0.10
$A_{CP}(B^0 \rightarrow K^*(892)^0\phi)$	0.01 ± 0.05	$C_{\rho^0\pi^0}(B^0 \rightarrow \rho^0\pi^0)$	0.3 ± 0.4
$A_{CP}(B^0 \rightarrow K^*(892)^0 K^-\pi^+)$	0.2 ± 0.4	$S_{\rho^0\pi^0}(B^0 \rightarrow \rho^0\pi^0)$	0.1 ± 0.4
$A_{CP}(B^0 \rightarrow \phi(K\pi)_0^{*0})$	0.20 ± 0.15	$C_{a_1\pi}(B^0 \rightarrow a_1(1260)^+\pi^-)$	-0.10 ± 0.17
$A_{CP}(B^0 \rightarrow \phi K_2^*(1430)^0)$	-0.08 ± 0.13	$S_{a_1\pi}(B^0 \rightarrow a_1(1260)^+\pi^-)$	0.37 ± 0.22
$A_{CP}(B^0 \rightarrow \rho^+\pi^-)$	0.08 ± 0.12 (S = 2.0)	$\Delta C_{a_1\pi}(B^0 \rightarrow a_1(1260)^+\pi^-)$	0.26 ± 0.17
$A_{CP}(B^0 \rightarrow \rho^-\pi^+)$	-0.16 ± 0.23 (S = 1.7)	$\Delta S_{a_1\pi}(B^0 \rightarrow a_1(1260)^+\pi^-)$	-0.14 ± 0.22
$A_{CP}(B^0 \rightarrow a_1(1260)^\pm\pi^\mp)$	-0.07 ± 0.07	$C(B^0 \rightarrow b_1^- K^+)$	-0.22 ± 0.24
$A_{CP}(B^0 \rightarrow b_1\pi^+)$	-0.05 ± 0.10	$\Delta C(B^0 \rightarrow b_1^- \pi^+)$	-1.04 ± 0.24
$A_{CP}(B^0 \rightarrow K^*(1430)\gamma)$	-0.08 ± 0.15	$C_{\rho^0\rho^0}(B^0 \rightarrow \rho^0\rho^0)$	0.2 ± 0.9
$A_{CP}(B^0 \rightarrow p\bar{p}K^*(892)^0)$	0.05 ± 0.12	$S_{\rho^0\rho^0}(B^0 \rightarrow \rho^0\rho^0)$	0.3 ± 0.7
$A_{CP}(B^0 \rightarrow p\bar{p}\pi^-)$	0.04 ± 0.07	$C_{\rho\rho}(B^0 \rightarrow \rho^+\rho^-)$	-0.05 ± 0.13
$A_{CP}(B^0 \rightarrow K^{*0}\ell^+\ell^-)$	-0.05 ± 0.10	$S_{\rho\rho}(B^0 \rightarrow \rho^+\rho^-)$	-0.06 ± 0.17
$A_{CP}(B^0 \rightarrow K^{*0}e^+e^-)$	-0.21 ± 0.19	$ \lambda (B^0 \rightarrow J/\psi K^*(892)^0)$	<0.25 , CL = 95%
$A_{CP}(B^0 \rightarrow K^{*0}\mu^+\mu^-)$	0.00 ± 0.15	$\cos 2\beta(B^0 \rightarrow J/\psi K^*(892)^0)$	$1.7^{+0.7}_{-0.9}$ (S = 1.6)
$C_{D^*(2010)^- D^+}(B^0 \rightarrow D^*(2010)^- D^+)$	0.07 ± 0.14	$\cos 2\beta(B^0 \rightarrow [K_S^0\pi^+\pi^-]_{D^{(*)}} h^0)$	$1.0^{+0.6}_{-0.7}$ (S = 1.8)
$C_{D^*(2010)^+ D^-}(B^0 \rightarrow D^*(2010)^+ D^-)$	-0.09 ± 0.22 (S = 1.6)	$(S_+ + S_-)/2(B^0 \rightarrow D^{*-}\pi^+)$	-0.037 ± 0.012
$C_+(B^0 \rightarrow D^{*+} D^{*-})$	0.00 ± 0.12	$(S_- - S_+)/2(B^0 \rightarrow D^{*-}\pi^+)$	-0.006 ± 0.016
$C_-(B^0 \rightarrow D^{*+} D^{*-})$	0.4 ± 0.5	$(S_+ + S_-)/2(B^0 \rightarrow D^-\pi^+)$	-0.046 ± 0.023
$S_-(B^0 \rightarrow D^{*+} D^{*-})$	-1.8 ± 0.7	$(S_- - S_+)/2(B^0 \rightarrow D^-\pi^+)$	-0.022 ± 0.021
$C(B^0 \rightarrow D^*(2010)^+ D^*(2010)^- K_S^0)$	0.01 ± 0.29	$C_{\eta_c K_S^0}(B^0 \rightarrow \eta_c K_S^0)$	0.08 ± 0.13
$S(B^0 \rightarrow D^*(2010)^+ D^*(2010)^- K_S^0)$	0.1 ± 0.4	$C_{c\bar{c}K^{(*)0}}(B^0 \rightarrow c\bar{c}K^{(*)0})$	0.004 ± 0.019
$C_{D^+ D^-}(B^0 \rightarrow D^+ D^-)$	-0.5 ± 0.4 (S = 2.5)		
$C_{J/\psi(1S)\pi^0}(B^0 \rightarrow J/\psi(1S)\pi^0)$	-0.13 ± 0.13		
$C_{D_{CP}^{(*)} h^0}(B^0 \rightarrow D_{CP}^{(*)} h^0)$	-0.23 ± 0.16		
$S_{D_{CP}^{(*)} h^0}(B^0 \rightarrow D_{CP}^{(*)} h^0)$	-0.56 ± 0.24		
$C_{K_S^0\pi^0}(B^0 \rightarrow K^0\pi^0)$	0.00 ± 0.13 (S = 1.4)		
$C_{\eta'(958) K}(B^0 \rightarrow \eta'(958) K_S^0)$	-0.04 ± 0.20 (S = 2.5)		
$S_{\eta'(958) K}(B^0 \rightarrow \eta'(958) K_S^0)$	0.43 ± 0.17 (S = 1.5)		
$C_{\eta' K^0}(B^0 \rightarrow \eta' K^0)$	-0.05 ± 0.05		

Unless otherwise stated, limits are given at the 90% confidence level, while errors are given as ± 1 standard deviation.

Tests of Conservation Laws

$C_{J/\psi(nS)K^0} (B^0 \rightarrow J/\psi(nS)K^0)$	$(-0.2 \pm 2.0) \times 10^{-2}$
$C_{J/\psi K^{*0}} (B^0 \rightarrow J/\psi K^{*0})$	0.03 ± 0.10
$S_{J/\psi K^{*0}} (B^0 \rightarrow J/\psi K^{*0})$	0.60 ± 0.25
$C_{\chi_{c0} K_S^0} (B^0 \rightarrow \chi_{c0} K_S^0)$	$-0.3^{+0.5}_{-0.4}$
$S_{\chi_{c0} K_S^0} (B^0 \rightarrow \chi_{c0} K_S^0)$	-0.7 ± 0.5
$C_{\chi_{c1} K_S^0} (B^0 \rightarrow \chi_{c1} K_S^0)$	0.13 ± 0.11
$\sin(2\beta_{\text{eff}})(B^0 \rightarrow \phi K^0)$	0.22 ± 0.30
$\sin(2\beta_{\text{eff}})(B^0 \rightarrow \phi K_{00}^{*0}(1430)^0)$	$0.97^{+0.03}_{-0.52}$
$\sin(2\beta_{\text{eff}})(B^0 \rightarrow [K_S^0 \pi^+ \pi^-]_{D(\pi^+) h^0})$	0.45 ± 0.28

$A_{CP}(B \rightarrow K^*(892)\gamma)$	-0.003 ± 0.017
$A_{CP}(B \rightarrow s\gamma)$	-0.014 ± 0.028
$A_{CP}(b \rightarrow (s+d)\gamma)$	-0.11 ± 0.12
$A_{CP}(b \rightarrow X_S \ell^+ \ell^-)$	-0.22 ± 0.26
$A_{CP}(B \rightarrow K^* \ell^+ \ell^-)$	-0.07 ± 0.08
$A_{CP}(B \rightarrow K^* e^+ e^-)$	-0.18 ± 0.15
$A_{CP}(B \rightarrow K^* \mu^+ \mu^-)$	-0.03 ± 0.13
$\Gamma(\eta_c(1S) \rightarrow \pi^+ \pi^-) / \Gamma_{\text{total}}$	$< 6 \times 10^{-4}$, CL = 90%
$\Gamma(\eta_c(1S) \rightarrow \pi^0 \pi^0) / \Gamma_{\text{total}}$	$< 4 \times 10^{-4}$, CL = 90%
$\Gamma(\eta_c(1S) \rightarrow K^+ K^-) / \Gamma_{\text{total}}$	$< 6 \times 10^{-4}$, CL = 90%
$\Gamma(\eta_c(1S) \rightarrow K_S^0 K_S^0) / \Gamma_{\text{total}}$	$< 3.1 \times 10^{-4}$, CL = 90%
$(\alpha + \bar{\alpha}) / (\alpha - \bar{\alpha})$ in $\Lambda \rightarrow p \pi^-, \bar{\Lambda} \rightarrow \bar{p} \pi^+$	0.006 ± 0.021
$\frac{[\alpha(\Xi^-) - \alpha(\Lambda) - \alpha(\Xi^+) + \alpha(\Lambda)]}{[\alpha(\Xi^-) - \alpha(\Lambda) + \alpha(\Xi^+) + \alpha(\Lambda)]}$	$(0 \pm 7) \times 10^{-4}$
$(\alpha + \bar{\alpha}) / (\alpha - \bar{\alpha})$ in $\Omega^- \rightarrow \Lambda K^-, \bar{\Omega}^+ \rightarrow \bar{\Lambda} K^+$	-0.02 ± 0.13
$(\alpha + \bar{\alpha}) / (\alpha - \bar{\alpha})$ in $\Lambda_c^+ \rightarrow \Lambda \pi^+, \bar{\Lambda}_c^- \rightarrow \bar{\Lambda} \pi^-$	-0.07 ± 0.31
$(\alpha + \bar{\alpha}) / (\alpha - \bar{\alpha})$ in $\Lambda_c^+ \rightarrow \Lambda e^+ \nu_e, \bar{\Lambda}_c^- \rightarrow \bar{\Lambda} e^- \bar{\nu}_e$	0.00 ± 0.04

CP VIOLATION OBSERVED

$\text{Re}(\epsilon)$	$(1.596 \pm 0.013) \times 10^{-3}$
charge asymmetry in K_{S3}^0 decays	
$A_L =$ weighted average of $A_L(\mu)$ and $A_L(e)$	$(0.332 \pm 0.006)\%$
$A_L(\mu) = [\Gamma(\pi^- \mu^+ \nu_\mu) - \Gamma(\pi^+ \mu^- \bar{\nu}_\mu)] / \text{sum}$	$(0.304 \pm 0.025)\%$
$A_L(e) = [\Gamma(\pi^- e^+ \nu_e) - \Gamma(\pi^+ e^- \bar{\nu}_e)] / \text{sum}$	$(0.334 \pm 0.007)\%$
parameters for $K_L^0 \rightarrow 2\pi$ decay	
$ \eta_{00} = A(K_L^0 \rightarrow 2\pi^0) / A(K_S^0 \rightarrow 2\pi^0) $	$(2.221 \pm 0.011) \times 10^{-3}$ (S = 1.8)
$ \eta_{+-} = A(K_L^0 \rightarrow \pi^+ \pi^-) / A(K_S^0 \rightarrow \pi^+ \pi^-) $	$(2.232 \pm 0.011) \times 10^{-3}$ (S = 1.8)
$ \epsilon = (2 \eta_{+-} + \eta_{00}) / 3$	$(2.228 \pm 0.011) \times 10^{-3}$ (S = 1.8)
$ \eta_{00} / \eta_{+-} $	[g] 0.9951 ± 0.0008 (S = 1.6)
$\text{Re}(\epsilon' / \epsilon) = (1 - \eta_{00} / \eta_{+-}) / 3$	[g] $(1.65 \pm 0.26) \times 10^{-3}$ (S = 1.6)
Assuming CPT	
ϕ_{+-} , phase of η_{+-}	$(43.51 \pm 0.05)^\circ$ (S = 1.1)
ϕ_{00} , phase of η_{00}	$(43.52 \pm 0.05)^\circ$ (S = 1.1)
$\phi_e = (2\phi_{+-} + \phi_{00}) / 3$	$(43.51 \pm 0.05)^\circ$ (S = 1.1)
Not assuming CPT	
ϕ_{+-} , phase of η_{+-}	$(43.4 \pm 0.7)^\circ$ (S = 1.3)
ϕ_{00} , phase of η_{00}	$(43.7 \pm 0.8)^\circ$ (S = 1.2)
$\phi_e = (2\phi_{+-} + \phi_{00}) / 3$	$(43.5 \pm 0.7)^\circ$ (S = 1.3)
CP asymmetry A in $K_L^0 \rightarrow \pi^+ \pi^- e^+ e^-$	$(13.7 \pm 1.5)\%$
β_{CP} from $K_L^0 \rightarrow e^+ e^- e^+ e^-$	-0.19 ± 0.07
γ_{CP} from $K_L^0 \rightarrow e^+ e^- e^+ e^-$	0.01 ± 0.11 (S = 1.6)
parameters for $K_L^0 \rightarrow \pi^+ \pi^- \gamma$ decay	
$ \eta_{+-\gamma} = A(K_L^0 \rightarrow \pi^+ \pi^- \gamma, CP \text{ violating}) / A(K_S^0 \rightarrow \pi^+ \pi^- \gamma) $	$(2.35 \pm 0.07) \times 10^{-3}$
$\phi_{+-\gamma} =$ phase of $\eta_{+-\gamma}$	$(44 \pm 4)^\circ$
$\Gamma(K_L^0 \rightarrow \pi^+ \pi^-) / \Gamma_{\text{total}}$	[h] $(1.966 \pm 0.010) \times 10^{-3}$ (S = 1.6)
$\Gamma(K_L^0 \rightarrow \pi^0 \pi^0) / \Gamma_{\text{total}}$	$(8.65 \pm 0.06) \times 10^{-4}$ (S = 1.8)
$A_{CP}(B^0 \rightarrow K^+ \pi^-)$	-0.098 ± 0.013
$A_{CP}(B^0 \rightarrow \eta K^*(892)^0)$	0.19 ± 0.05
$S_{D^*(2010)-D^+}(B^0 \rightarrow D^*(2010)^- D^+)$	-0.78 ± 0.21

$S_{D^*(2010)+D^-}(B^0 \rightarrow D^*(2010)^+ D^-)$	-0.61 ± 0.19
$C_{D^{*+}D^{*-}}(B^0 \rightarrow D^{*+}D^{*-})$	-0.01 ± 0.09 (S = 1.2)
$S_{D^{*+}D^{*-}}(B^0 \rightarrow D^{*+}D^{*-})$	-0.76 ± 0.14
$S_+(B^0 \rightarrow D^{*+}D^{*-})$	-0.76 ± 0.16
$S_{D^+D^-}(B^0 \rightarrow D^+D^-)$	-0.87 ± 0.26
$S_{J/\psi(1S)\pi^0}(B^0 \rightarrow J/\psi(1S)\pi^0)$	-0.94 ± 0.29 (S = 1.9)
$S_{K_S^0\pi^0}(B^0 \rightarrow K_S^0\pi^0)$	0.58 ± 0.17
$S_{\eta'K^0}(B^0 \rightarrow \eta'K^0)$	0.60 ± 0.07
$S_{K^+K^-K_S^0}(B^0 \rightarrow K^+K^-K_S^0)$	$-0.74^{+0.12}_{-0.10}$
$S_{K^+K^-K_S^0}(B^0 \rightarrow K^+K^-K_S^0 \text{ inclusive})$	-0.65 ± 0.12
$S_{\pi\pi}(B^0 \rightarrow \pi^+\pi^-)$	-0.61 ± 0.08
$\Delta C_{\rho\pi}(B^0 \rightarrow \rho^+\pi^-)$	0.37 ± 0.08
$S_{\eta_c K_S^0}(B^0 \rightarrow \eta_c K_S^0)$	0.93 ± 0.17
$\sin(2\beta)(B^0 \rightarrow J/\psi K_S^0)$	0.671 ± 0.023
$S_{J/\psi(nS)K^0}(B^0 \rightarrow J/\psi(nS)K^0)$	0.658 ± 0.024
$S_{\chi_{c1}K_S^0}(B^0 \rightarrow \chi_{c1}K_S^0)$	0.61 ± 0.16
$\sin(2\beta_{\text{eff}})(B^0 \rightarrow K^+K^-K_S^0)$	$0.77^{+0.13}_{-0.12}$

CPT INVARIANCE

$(m_{W^+} - m_{W^-}) / m_{\text{average}}$	-0.002 ± 0.007
$(m_{e^+} - m_{e^-}) / m_{\text{average}}$	$< 8 \times 10^{-9}$, CL = 90%
$ q_{e^+} + q_{e^-} / e$	$< 4 \times 10^{-8}$
$(g_{e^+} - g_{e^-}) / g_{\text{average}}$	$(-0.5 \pm 2.1) \times 10^{-12}$
$(\tau_{\mu^+} - \tau_{\mu^-}) / \tau_{\text{average}}$	$(2 \pm 8) \times 10^{-5}$
$(g_{\mu^+} - g_{\mu^-}) / g_{\text{average}}$	$(-0.11 \pm 0.12) \times 10^{-8}$
$(m_{\tau^+} - m_{\tau^-}) / m_{\text{average}}$	$< 2.8 \times 10^{-4}$, CL = 90%
$2(m_t - m_{\bar{t}}) / (m_t + m_{\bar{t}})$	0.022 ± 0.022
$(m_{\pi^+} - m_{\pi^-}) / m_{\text{average}}$	$(2 \pm 5) \times 10^{-4}$
$(\tau_{\pi^+} - \tau_{\pi^-}) / \tau_{\text{average}}$	$(6 \pm 7) \times 10^{-4}$
$(m_{K^+} - m_{K^-}) / m_{\text{average}}$	$(-0.6 \pm 1.8) \times 10^{-4}$
$(\tau_{K^+} - \tau_{K^-}) / \tau_{\text{average}}$	$(0.10 \pm 0.09)\%$ (S = 1.2)
$K^\pm \rightarrow \mu^\pm \nu_\mu$ rate difference/average	$(-0.5 \pm 0.4)\%$
$K^\pm \rightarrow \pi^\pm \pi^0$ rate difference/average	[j] $(0.8 \pm 1.2)\%$
δ in $K^0 - \bar{K}^0$ mixing	
real part of δ	$(2.3 \pm 2.7) \times 10^{-4}$
imaginary part of δ	$(0.4 \pm 2.1) \times 10^{-5}$
$\text{Re}(y)$, K_{e3} parameter	$(0.4 \pm 2.5) \times 10^{-3}$
$\text{Re}(x_-)$, K_{e3} parameter	$(-2.9 \pm 2.0) \times 10^{-3}$
$ m_{K^0} - m_{\bar{K}^0} / m_{\text{average}}$	[j] $< 8 \times 10^{-19}$, CL = 90%
$(\Gamma_{K^0} - \Gamma_{\bar{K}^0}) / m_{\text{average}}$	$(8 \pm 8) \times 10^{-18}$
phase difference $\phi_{00} - \phi_{+-}$	$(0.2 \pm 0.4)^\circ$
$\text{Re}(\frac{2}{3}\eta_{+-} + \frac{1}{3}\eta_{00}) - \frac{A_L}{\epsilon}$	$(-3 \pm 35) \times 10^{-6}$
$A_{CPT}(D^0 \rightarrow K^- \pi^+)$	0.008 ± 0.008
$ m_{\rho^-} - m_{\bar{\rho}^-} / m_\rho$	[k] $< 2 \times 10^{-9}$, CL = 90%
$(\frac{q_{\bar{\rho}^-}}{m_{\bar{\rho}^-}} - \frac{q_\rho}{m_\rho}) / \frac{q_\rho}{m_\rho}$	$(-9 \pm 9) \times 10^{-11}$
$ q_\rho + q_{\bar{\rho}} / e$	[k] $< 2 \times 10^{-9}$, CL = 90%
$(\mu_\rho + \mu_{\bar{\rho}}) / \mu_\rho$	$(-0.1 \pm 2.1) \times 10^{-3}$
$(m_n - m_{\bar{n}}) / m_n$	$(9 \pm 6) \times 10^{-5}$
$(m_\Lambda - m_{\bar{\Lambda}}) / m_\Lambda$	$(-0.1 \pm 1.1) \times 10^{-5}$ (S = 1.6)
$(\tau_\Lambda - \tau_{\bar{\Lambda}}) / \tau_\Lambda$	-0.001 ± 0.009
$(\tau_{\Sigma^+} - \tau_{\bar{\Sigma}^-}) / \tau_{\Sigma^+}$	$(-0.6 \pm 1.2) \times 10^{-3}$
$(\mu_{\Sigma^+} + \mu_{\bar{\Sigma}^-}) / \mu_{\Sigma^+}$	0.014 ± 0.015
$(m_{\Xi^-} - m_{\bar{\Xi}^+}) / m_{\Xi^-}$	$(-3 \pm 9) \times 10^{-5}$
$(\tau_{\Xi^-} - \tau_{\bar{\Xi}^+}) / \tau_{\Xi^-}$	-0.01 ± 0.07
$(\mu_{\Xi^-} + \mu_{\bar{\Xi}^+}) / \mu_{\Xi^-} $	$+0.01 \pm 0.05$
$(m_{\Omega^-} - m_{\bar{\Omega}^+}) / m_{\Omega^-}$	$(-1 \pm 8) \times 10^{-5}$
$(\tau_{\Omega^-} - \tau_{\bar{\Omega}^+}) / \tau_{\Omega^-}$	0.00 ± 0.05

Tests of Conservation Laws

TOTAL LEPTON NUMBER

Violation of total lepton number conservation also implies violation of lepton family number conservation.

$\Gamma(Z \rightarrow pe)/\Gamma_{\text{total}}$	$<1.8 \times 10^{-6}$, CL = 95%
$\Gamma(Z \rightarrow p\mu)/\Gamma_{\text{total}}$	$<1.8 \times 10^{-6}$, CL = 95%
limit on $\mu^- \rightarrow e^+$ conversion	
$\sigma(\mu^- 32\text{S} \rightarrow e^+ 32\text{Si}^*) / \sigma(\mu^- 32\text{S} \rightarrow \nu_{\mu} 32\text{P}^*)$	$<9 \times 10^{-10}$, CL = 90%
$\sigma(\mu^- 127\text{I} \rightarrow e^+ 127\text{Sb}^*) / \sigma(\mu^- 127\text{I} \rightarrow \text{anything})$	$<3 \times 10^{-10}$, CL = 90%
$\sigma(\mu^- \text{Ti} \rightarrow e^+ \text{Ca}) / \sigma(\mu^- \text{Ti} \rightarrow \text{capture})$	$<3.6 \times 10^{-11}$, CL = 90%
$\Gamma(\tau^- \rightarrow e^+ \pi^- \pi^-)/\Gamma_{\text{total}}$	$<8.8 \times 10^{-8}$, CL = 90%
$\Gamma(\tau^- \rightarrow \mu^+ \pi^- \pi^-)/\Gamma_{\text{total}}$	$<3.7 \times 10^{-8}$, CL = 90%
$\Gamma(\tau^- \rightarrow e^+ \pi^- K^-)/\Gamma_{\text{total}}$	$<6.7 \times 10^{-8}$, CL = 90%
$\Gamma(\tau^- \rightarrow e^+ K^- K^-)/\Gamma_{\text{total}}$	$<6.0 \times 10^{-8}$, CL = 90%
$\Gamma(\tau^- \rightarrow \mu^+ \pi^- K^-)/\Gamma_{\text{total}}$	$<9.4 \times 10^{-8}$, CL = 90%
$\Gamma(\tau^- \rightarrow \mu^+ K^- K^-)/\Gamma_{\text{total}}$	$<9.6 \times 10^{-8}$, CL = 90%
$\Gamma(\tau^- \rightarrow \bar{p}\gamma)/\Gamma_{\text{total}}$	$<3.5 \times 10^{-6}$, CL = 90%
$\Gamma(\tau^- \rightarrow \bar{p}\pi^0)/\Gamma_{\text{total}}$	$<1.5 \times 10^{-5}$, CL = 90%
$\Gamma(\tau^- \rightarrow \bar{p}2\pi^0)/\Gamma_{\text{total}}$	$<3.3 \times 10^{-5}$, CL = 90%
$\Gamma(\tau^- \rightarrow \bar{p}\eta)/\Gamma_{\text{total}}$	$<8.9 \times 10^{-6}$, CL = 90%
$\Gamma(\tau^- \rightarrow \bar{p}\pi^0\eta)/\Gamma_{\text{total}}$	$<2.7 \times 10^{-5}$, CL = 90%
$\Gamma(\tau^- \rightarrow \Lambda\pi^-)/\Gamma_{\text{total}}$	$<7.2 \times 10^{-8}$, CL = 90%
$\Gamma(\tau^- \rightarrow \bar{\Lambda}\pi^-)/\Gamma_{\text{total}}$	$<1.4 \times 10^{-7}$, CL = 90%
$t_{1/2}(^{76}\text{Ge} \rightarrow ^{76}\text{Se} + 2e^-)$	$>1.9 \times 10^{25}$ yr, CL = 90%
$\Gamma(\pi^+ \rightarrow \mu^+ \bar{\nu}_e)/\Gamma_{\text{total}}$	[p] $<1.5 \times 10^{-3}$, CL = 90%
$\Gamma(K^+ \rightarrow \pi^- \mu^+ e^+)/\Gamma_{\text{total}}$	$<5.0 \times 10^{-10}$, CL = 90%
$\Gamma(K^+ \rightarrow \pi^- e^+ e^+)/\Gamma_{\text{total}}$	$<6.4 \times 10^{-10}$, CL = 90%
$\Gamma(K^+ \rightarrow \pi^- \mu^+ \mu^+)/\Gamma_{\text{total}}$	[p] $<3.0 \times 10^{-9}$, CL = 90%
$\Gamma(K^+ \rightarrow \mu^+ \bar{\nu}_e)/\Gamma_{\text{total}}$	[p] $<3.3 \times 10^{-3}$, CL = 90%
$\Gamma(K^+ \rightarrow \pi^0 e^+ \bar{\nu}_e)/\Gamma_{\text{total}}$	$<3 \times 10^{-3}$, CL = 90%
$\Gamma(D^+ \rightarrow \pi^- 2e^+)/\Gamma_{\text{total}}$	$<3.6 \times 10^{-6}$, CL = 90%
$\Gamma(D^+ \rightarrow \pi^- 2\mu^+)/\Gamma_{\text{total}}$	$<4.8 \times 10^{-6}$, CL = 90%
$\Gamma(D^+ \rightarrow \pi^- e^+ \mu^+)/\Gamma_{\text{total}}$	$<5.0 \times 10^{-5}$, CL = 90%
$\Gamma(D^+ \rightarrow \rho^- 2\mu^+)/\Gamma_{\text{total}}$	$<5.6 \times 10^{-4}$, CL = 90%
$\Gamma(D^+ \rightarrow K^- 2e^+)/\Gamma_{\text{total}}$	$<4.5 \times 10^{-6}$, CL = 90%
$\Gamma(D^+ \rightarrow K^- 2\mu^+)/\Gamma_{\text{total}}$	$<1.3 \times 10^{-5}$, CL = 90%
$\Gamma(D^+ \rightarrow K^- e^+ \mu^+)/\Gamma_{\text{total}}$	$<1.3 \times 10^{-4}$, CL = 90%
$\Gamma(D^+ \rightarrow K^*(892)^- 2\mu^+)/\Gamma_{\text{total}}$	$<8.5 \times 10^{-4}$, CL = 90%
$\Gamma(D^0 \rightarrow 2\pi^- 2e^+ + \text{c.c.})/\Gamma_{\text{total}}$	$<1.12 \times 10^{-4}$, CL = 90%
$\Gamma(D^0 \rightarrow 2\pi^- 2\mu^+ + \text{c.c.})/\Gamma_{\text{total}}$	$<2.9 \times 10^{-5}$, CL = 90%
$\Gamma(D^0 \rightarrow K^- \pi^- 2e^+ + \text{c.c.})/\Gamma_{\text{total}}$	$<2.06 \times 10^{-4}$, CL = 90%
$\Gamma(D^0 \rightarrow K^- \pi^- 2\mu^+ + \text{c.c.})/\Gamma_{\text{total}}$	$<3.9 \times 10^{-4}$, CL = 90%
$\Gamma(D^0 \rightarrow 2K^- 2e^+ + \text{c.c.})/\Gamma_{\text{total}}$	$<1.52 \times 10^{-4}$, CL = 90%
$\Gamma(D^0 \rightarrow 2K^- 2\mu^+ + \text{c.c.})/\Gamma_{\text{total}}$	$<9.4 \times 10^{-5}$, CL = 90%
$\Gamma(D^0 \rightarrow \pi^- \pi^- e^+ \mu^+ + \text{c.c.})/\Gamma_{\text{total}}$	$<7.9 \times 10^{-5}$, CL = 90%
$\Gamma(D^0 \rightarrow K^- \pi^- e^+ \mu^+ + \text{c.c.})/\Gamma_{\text{total}}$	$<2.18 \times 10^{-4}$, CL = 90%
$\Gamma(D^0 \rightarrow 2K^- e^+ \mu^+ + \text{c.c.})/\Gamma_{\text{total}}$	$<5.7 \times 10^{-5}$, CL = 90%
$\Gamma(D^0 \rightarrow \rho^- e^-)/\Gamma_{\text{total}}$	[q] $<1.0 \times 10^{-5}$, CL = 90%
$\Gamma(D^0 \rightarrow \bar{p}e^+)/\Gamma_{\text{total}}$	[r] $<1.1 \times 10^{-5}$, CL = 90%
$\Gamma(D_s^+ \rightarrow \pi^- 2e^+)/\Gamma_{\text{total}}$	$<6.9 \times 10^{-4}$, CL = 90%
$\Gamma(D_s^+ \rightarrow \pi^- 2\mu^+)/\Gamma_{\text{total}}$	$<2.9 \times 10^{-5}$, CL = 90%
$\Gamma(D_s^+ \rightarrow \pi^- e^+ \mu^+)/\Gamma_{\text{total}}$	$<7.3 \times 10^{-4}$, CL = 90%
$\Gamma(D_s^+ \rightarrow K^- 2e^+)/\Gamma_{\text{total}}$	$<6.3 \times 10^{-4}$, CL = 90%
$\Gamma(D_s^+ \rightarrow K^- 2\mu^+)/\Gamma_{\text{total}}$	$<1.3 \times 10^{-5}$, CL = 90%
$\Gamma(D_s^+ \rightarrow K^- e^+ \mu^+)/\Gamma_{\text{total}}$	$<6.8 \times 10^{-4}$, CL = 90%
$\Gamma(D_s^+ \rightarrow K^*(892)^- 2\mu^+)/\Gamma_{\text{total}}$	$<1.4 \times 10^{-3}$, CL = 90%
$\Gamma(B^+ \rightarrow \pi^- e^+ e^+)/\Gamma_{\text{total}}$	$<1.6 \times 10^{-6}$, CL = 90%
$\Gamma(B^+ \rightarrow \pi^- \mu^+ \mu^+)/\Gamma_{\text{total}}$	$<1.4 \times 10^{-6}$, CL = 90%
$\Gamma(B^+ \rightarrow \pi^- e^+ \mu^+)/\Gamma_{\text{total}}$	$<1.3 \times 10^{-6}$, CL = 90%
$\Gamma(B^+ \rightarrow \rho^- e^+ e^+)/\Gamma_{\text{total}}$	$<2.6 \times 10^{-6}$, CL = 90%
$\Gamma(B^+ \rightarrow \rho^- \mu^+ \mu^+)/\Gamma_{\text{total}}$	$<5.0 \times 10^{-6}$, CL = 90%
$\Gamma(B^+ \rightarrow \rho^- e^+ \mu^+)/\Gamma_{\text{total}}$	$<3.3 \times 10^{-6}$, CL = 90%
$\Gamma(B^+ \rightarrow K^- e^+ e^+)/\Gamma_{\text{total}}$	$<1.0 \times 10^{-6}$, CL = 90%
$\Gamma(B^+ \rightarrow K^- \mu^+ \mu^+)/\Gamma_{\text{total}}$	$<1.8 \times 10^{-6}$, CL = 90%
$\Gamma(B^+ \rightarrow K^- e^+ \mu^+)/\Gamma_{\text{total}}$	$<2.0 \times 10^{-6}$, CL = 90%
$\Gamma(B^+ \rightarrow K^*(892)^- e^+ e^+)/\Gamma_{\text{total}}$	$<2.8 \times 10^{-6}$, CL = 90%
$\Gamma(B^+ \rightarrow K^*(892)^- \mu^+ \mu^+)/\Gamma_{\text{total}}$	$<8.3 \times 10^{-6}$, CL = 90%

$\Gamma(B^+ \rightarrow K^*(892)^- e^+ \mu^+)/\Gamma_{\text{total}}$	$<4.4 \times 10^{-6}$, CL = 90%
$\Gamma(\Xi^- \rightarrow p\mu^- \mu^-)/\Gamma_{\text{total}}$	$<4 \times 10^{-8}$, CL = 90%
$\Gamma(\Lambda_c^+ \rightarrow \Sigma^- \mu^+ \mu^+)/\Gamma_{\text{total}}$	$<7.0 \times 10^{-4}$, CL = 90%

BARYON NUMBER

$\Gamma(Z \rightarrow pe)/\Gamma_{\text{total}}$	$<1.8 \times 10^{-6}$, CL = 95%
$\Gamma(Z \rightarrow p\mu)/\Gamma_{\text{total}}$	$<1.8 \times 10^{-6}$, CL = 95%
$\Gamma(\tau^- \rightarrow \bar{p}\gamma)/\Gamma_{\text{total}}$	$<3.5 \times 10^{-6}$, CL = 90%
$\Gamma(\tau^- \rightarrow \bar{p}\pi^0)/\Gamma_{\text{total}}$	$<1.5 \times 10^{-5}$, CL = 90%
$\Gamma(\tau^- \rightarrow \bar{p}2\pi^0)/\Gamma_{\text{total}}$	$<3.3 \times 10^{-5}$, CL = 90%
$\Gamma(\tau^- \rightarrow \bar{p}\eta)/\Gamma_{\text{total}}$	$<8.9 \times 10^{-6}$, CL = 90%
$\Gamma(\tau^- \rightarrow \bar{p}\pi^0\eta)/\Gamma_{\text{total}}$	$<2.7 \times 10^{-5}$, CL = 90%
$\Gamma(\tau^- \rightarrow \Lambda\pi^-)/\Gamma_{\text{total}}$	$<7.2 \times 10^{-8}$, CL = 90%
$\Gamma(\tau^- \rightarrow \bar{\Lambda}\pi^-)/\Gamma_{\text{total}}$	$<1.4 \times 10^{-7}$, CL = 90%
$\Gamma(D^0 \rightarrow pe^-)/\Gamma_{\text{total}}$	[q] $<1.0 \times 10^{-5}$, CL = 90%
$\Gamma(D^0 \rightarrow \bar{p}e^+)/\Gamma_{\text{total}}$	[r] $<1.1 \times 10^{-5}$, CL = 90%
p mean life	[s] $>2.1 \times 10^{29}$ years, CL = 90%

A few examples of proton or bound neutron decay follow. For limits on many other nucleon decay channels, see the Baryon Summary Table.

$\tau(N \rightarrow e^+ \pi)$	>158 (n), >1600 (p) $\times 10^{30}$ years, CL = 90%
$\tau(N \rightarrow \mu^+ \pi)$	>100 (n), >473 (p) $\times 10^{30}$ years, CL = 90%
$\tau(N \rightarrow e^+ K)$	>17 (n), >150 (p) $\times 10^{30}$ years, CL = 90%
$\tau(N \rightarrow \mu^+ K)$	>26 (n), >120 (p) $\times 10^{30}$ years, CL = 90%
limit on $n\bar{n}$ oscillations (free n)	$>0.86 \times 10^8$ s, CL = 90%
limit on $n\bar{n}$ oscillations (bound n)	[t] $>1.3 \times 10^9$ s, CL = 90%

ELECTRIC CHARGE (Q)

$e \rightarrow \nu_e \gamma$ and astrophysical limits	[u] $>4.6 \times 10^{26}$ yr, CL = 90%
$\Gamma(n \rightarrow p\nu_e \bar{\nu}_e)/\Gamma_{\text{total}}$	$<8 \times 10^{-27}$, CL = 68%

$\Delta S = \Delta Q$ RULE

Violations allowed in second-order weak interactions.

$\Gamma(K^+ \rightarrow \pi^+ \pi^+ e^- \bar{\nu}_e)/\Gamma_{\text{total}}$	$<1.2 \times 10^{-8}$, CL = 90%
$\Gamma(K^+ \rightarrow \pi^+ \pi^+ \mu^- \bar{\nu}_\mu)/\Gamma_{\text{total}}$	$<3.0 \times 10^{-6}$, CL = 95%
Re(x_+), K_{e3} parameter	$(-0.9 \pm 3.0) \times 10^{-3}$
$x = A(\bar{K}^0 \rightarrow \pi^- \ell^+ \nu)/A(K^0 \rightarrow \pi^- \ell^+ \nu) = A(\Delta S = -\Delta Q)/A(\Delta S = \Delta Q)$	
real part of x	-0.002 ± 0.006
imaginary part of x	0.0012 ± 0.0021
$\Gamma(\Sigma^+ \rightarrow n\ell^+ \nu)/\Gamma(\Sigma^- \rightarrow n\ell^- \bar{\nu})$	<0.043
$\Gamma(\Sigma^+ \rightarrow ne^+ \nu_e)/\Gamma_{\text{total}}$	$<5 \times 10^{-6}$, CL = 90%
$\Gamma(\Sigma^+ \rightarrow n\mu^+ \nu_\mu)/\Gamma_{\text{total}}$	$<3.0 \times 10^{-5}$, CL = 90%
$\Gamma(\Xi^0 \rightarrow \Sigma^- e^+ \nu_e)/\Gamma_{\text{total}}$	$<9 \times 10^{-4}$, CL = 90%
$\Gamma(\Xi^0 \rightarrow \Sigma^- \mu^+ \nu_\mu)/\Gamma_{\text{total}}$	$<9 \times 10^{-4}$, CL = 90%

$\Delta S = 2$ FORBIDDEN

Allowed in second-order weak interactions.

$\Gamma(\Xi^0 \rightarrow p\pi^-)/\Gamma_{\text{total}}$	$<8 \times 10^{-6}$, CL = 90%
$\Gamma(\Xi^0 \rightarrow pe^- \bar{\nu}_e)/\Gamma_{\text{total}}$	$<1.3 \times 10^{-3}$
$\Gamma(\Xi^0 \rightarrow p\mu^- \bar{\nu}_\mu)/\Gamma_{\text{total}}$	$<1.3 \times 10^{-3}$
$\Gamma(\Xi^- \rightarrow n\pi^-)/\Gamma_{\text{total}}$	$<1.9 \times 10^{-5}$, CL = 90%
$\Gamma(\Xi^- \rightarrow ne^- \bar{\nu}_e)/\Gamma_{\text{total}}$	$<3.2 \times 10^{-3}$, CL = 90%
$\Gamma(\Xi^- \rightarrow n\mu^- \bar{\nu}_\mu)/\Gamma_{\text{total}}$	$<1.5 \times 10^{-2}$, CL = 90%
$\Gamma(\Xi^- \rightarrow p\pi^- \pi^-)/\Gamma_{\text{total}}$	$<4 \times 10^{-4}$, CL = 90%
$\Gamma(\Xi^- \rightarrow p\pi^- e^- \bar{\nu}_e)/\Gamma_{\text{total}}$	$<4 \times 10^{-4}$, CL = 90%
$\Gamma(\Xi^- \rightarrow p\pi^- \mu^- \bar{\nu}_\mu)/\Gamma_{\text{total}}$	$<4 \times 10^{-4}$, CL = 90%
$\Gamma(\Omega^- \rightarrow \Lambda\pi^-)/\Gamma_{\text{total}}$	$<2.9 \times 10^{-6}$, CL = 90%

Tests of Conservation Laws

 $\Delta S = 2$ VIA MIXING

Allowed in second-order weak interactions, e.g. mixing.

$$m_{K_L^0} - m_{K_S^0} \quad (0.5292 \pm 0.0009) \times 10^{10} \text{ h s}^{-1} \quad (S = 1.2)$$

$$m_{K_L^0} - m_{K_S^0} \quad (3.483 \pm 0.006) \times 10^{-12} \text{ MeV}$$

 $\Delta C = 2$ VIA MIXING

Allowed in second-order weak interactions, e.g. mixing.

$$|m_{D_1^0} - m_{D_2^0}| = x\Gamma \quad (2.39 \pm_{-0.63}^{+0.59}) \times 10^{10} \text{ h s}^{-1}$$

$$(\Gamma_{D_1^0} - \Gamma_{D_2^0})/\Gamma = 2y \quad (1.66 \pm 0.32) \times 10^{-2}$$

 $\Delta B = 2$ VIA MIXING

Allowed in second-order weak interactions, e.g. mixing.

$$x_d \quad 0.1872 \pm 0.0024$$

$$\Delta m_{B^0} = m_{B_H^0} - m_{B_L^0} \quad (0.507 \pm 0.005) \times 10^{12} \text{ h s}^{-1}$$

$$x_d = \Delta m_{B^0}/\Gamma_{B^0} \quad 0.774 \pm 0.008$$

$$\Delta m_{B_s^0} = m_{B_{sH}^0} - m_{B_{sL}^0} \quad (17.77 \pm 0.12) \times 10^{12} \text{ h s}^{-1}$$

$$x_s = \Delta m_{B_s^0}/\Gamma_{B_s^0} \quad 26.2 \pm 0.5$$

$$x_s \quad 0.49927 \pm 0.00003$$

 $\Delta S = 1$ WEAK NEUTRAL CURRENT FORBIDDEN

Allowed by higher-order electroweak interactions.

$$\Gamma(K^+ \rightarrow \pi^+ e^+ e^-)/\Gamma_{\text{total}} \quad (3.00 \pm 0.09) \times 10^{-7}$$

$$\Gamma(K^+ \rightarrow \pi^+ \mu^+ \mu^-)/\Gamma_{\text{total}} \quad (8.1 \pm 1.4) \times 10^{-8} \quad (S = 2.7)$$

$$\Gamma(K^+ \rightarrow \pi^+ \nu \bar{\nu})/\Gamma_{\text{total}} \quad (1.7 \pm 1.1) \times 10^{-10}$$

$$\Gamma(K^+ \rightarrow \pi^+ \pi^0 \nu \bar{\nu})/\Gamma_{\text{total}} \quad < 4.3 \times 10^{-5}, \text{ CL} = 90\%$$

$$\Gamma(K_S^0 \rightarrow \mu^+ \mu^-)/\Gamma_{\text{total}} \quad < 3.2 \times 10^{-7}, \text{ CL} = 90\%$$

$$\Gamma(K_S^0 \rightarrow e^+ e^-)/\Gamma_{\text{total}} \quad < 9 \times 10^{-9}, \text{ CL} = 90\%$$

$$\Gamma(K_S^0 \rightarrow \pi^0 e^+ e^-)/\Gamma_{\text{total}} \quad [v] \quad (3.0 \pm_{-1.2}^{+1.5}) \times 10^{-9}$$

$$\Gamma(K_S^0 \rightarrow \pi^0 \mu^+ \mu^-)/\Gamma_{\text{total}} \quad (2.9 \pm_{-1.2}^{+1.5}) \times 10^{-9}$$

$$\Gamma(K_L^0 \rightarrow \mu^+ \mu^-)/\Gamma_{\text{total}} \quad (6.84 \pm 0.11) \times 10^{-9}$$

$$\Gamma(K_L^0 \rightarrow e^+ e^-)/\Gamma_{\text{total}} \quad (9 \pm_4^6) \times 10^{-12}$$

$$\Gamma(K_L^0 \rightarrow \pi^+ \pi^- e^+ e^-)/\Gamma_{\text{total}} \quad [w] \quad (3.11 \pm 0.19) \times 10^{-7}$$

$$\Gamma(K_L^0 \rightarrow \pi^0 \pi^0 e^+ e^-)/\Gamma_{\text{total}} \quad < 6.6 \times 10^{-9}, \text{ CL} = 90\%$$

$$\Gamma(K_L^0 \rightarrow \mu^+ \mu^- e^+ e^-)/\Gamma_{\text{total}} \quad (2.69 \pm 0.27) \times 10^{-9}$$

$$\Gamma(K_L^0 \rightarrow e^+ e^- e^+ e^-)/\Gamma_{\text{total}} \quad (3.56 \pm 0.21) \times 10^{-8}$$

$$\Gamma(K_L^0 \rightarrow \pi^0 \mu^+ \mu^-)/\Gamma_{\text{total}} \quad < 3.8 \times 10^{-10}, \text{ CL} = 90\%$$

$$\Gamma(K_L^0 \rightarrow \pi^0 e^+ e^-)/\Gamma_{\text{total}} \quad < 2.8 \times 10^{-10}, \text{ CL} = 90\%$$

$$\Gamma(K_L^0 \rightarrow \pi^0 \nu \bar{\nu})/\Gamma_{\text{total}} \quad < 6.7 \times 10^{-8}, \text{ CL} = 90\%$$

$$\Gamma(K_L^0 \rightarrow \pi^0 \pi^0 \nu \bar{\nu})/\Gamma_{\text{total}} \quad < 4.7 \times 10^{-5}, \text{ CL} = 90\%$$

$$\Gamma(\Sigma^+ \rightarrow p e^+ e^-)/\Gamma_{\text{total}} \quad < 7 \times 10^{-6}$$

$$\Gamma(\Sigma^+ \rightarrow p \mu^+ \mu^-)/\Gamma_{\text{total}} \quad (9 \pm_8^9) \times 10^{-8}$$

 $\Delta C = 1$ WEAK NEUTRAL CURRENT FORBIDDEN

Allowed by higher-order electroweak interactions.

$$\Gamma(D^+ \rightarrow \pi^+ e^+ e^-)/\Gamma_{\text{total}} \quad < 7.4 \times 10^{-6}, \text{ CL} = 90\%$$

$$\Gamma(D^+ \rightarrow \pi^+ \mu^+ \mu^-)/\Gamma_{\text{total}} \quad < 3.9 \times 10^{-6}, \text{ CL} = 90\%$$

$$\Gamma(D^+ \rightarrow \rho^+ \mu^+ \mu^-)/\Gamma_{\text{total}} \quad < 5.6 \times 10^{-4}, \text{ CL} = 90\%$$

$$\Gamma(D^0 \rightarrow \gamma \gamma)/\Gamma_{\text{total}} \quad < 2.7 \times 10^{-5}, \text{ CL} = 90\%$$

$$\Gamma(D^0 \rightarrow e^+ e^-)/\Gamma_{\text{total}} \quad < 1.2 \times 10^{-6}, \text{ CL} = 90\%$$

$$\Gamma(D^0 \rightarrow \mu^+ \mu^-)/\Gamma_{\text{total}} \quad < 1.3 \times 10^{-6}, \text{ CL} = 90\%$$

$$\Gamma(D^0 \rightarrow \pi^0 e^+ e^-)/\Gamma_{\text{total}} \quad < 4.5 \times 10^{-5}, \text{ CL} = 90\%$$

$$\Gamma(D^0 \rightarrow \pi^0 \mu^+ \mu^-)/\Gamma_{\text{total}} \quad < 1.8 \times 10^{-4}, \text{ CL} = 90\%$$

$$\Gamma(D^0 \rightarrow \eta e^+ e^-)/\Gamma_{\text{total}} \quad < 1.1 \times 10^{-4}, \text{ CL} = 90\%$$

$$\Gamma(D^0 \rightarrow \eta \mu^+ \mu^-)/\Gamma_{\text{total}} \quad < 5.3 \times 10^{-4}, \text{ CL} = 90\%$$

$$\Gamma(D^0 \rightarrow \pi^+ \pi^- e^+ e^-)/\Gamma_{\text{total}} \quad < 3.73 \times 10^{-4}, \text{ CL} = 90\%$$

$$\Gamma(D^0 \rightarrow \rho^0 e^+ e^-)/\Gamma_{\text{total}} \quad < 1.0 \times 10^{-4}, \text{ CL} = 90\%$$

$$\Gamma(D^0 \rightarrow \pi^+ \pi^- \mu^+ \mu^-)/\Gamma_{\text{total}} \quad < 3.0 \times 10^{-5}, \text{ CL} = 90\%$$

$$\Gamma(D^0 \rightarrow \rho^0 \mu^+ \mu^-)/\Gamma_{\text{total}} \quad < 2.2 \times 10^{-5}, \text{ CL} = 90\%$$

$$\Gamma(D^0 \rightarrow \omega e^+ e^-)/\Gamma_{\text{total}} \quad < 1.8 \times 10^{-4}, \text{ CL} = 90\%$$

$$\Gamma(D^0 \rightarrow \omega \mu^+ \mu^-)/\Gamma_{\text{total}} \quad < 8.3 \times 10^{-4}, \text{ CL} = 90\%$$

$$\Gamma(D^0 \rightarrow K^- K^+ e^+ e^-)/\Gamma_{\text{total}} \quad < 3.15 \times 10^{-4}, \text{ CL} = 90\%$$

$$\Gamma(D^0 \rightarrow \phi e^+ e^-)/\Gamma_{\text{total}} \quad < 5.2 \times 10^{-5}, \text{ CL} = 90\%$$

$$\Gamma(D^0 \rightarrow K^- K^+ \mu^+ \mu^-)/\Gamma_{\text{total}} \quad < 3.3 \times 10^{-5}, \text{ CL} = 90\%$$

$$\Gamma(D^0 \rightarrow \phi \mu^+ \mu^-)/\Gamma_{\text{total}} \quad < 3.1 \times 10^{-5}, \text{ CL} = 90\%$$

$$\Gamma(D^0 \rightarrow K^- \pi^+ e^+ e^-)/\Gamma_{\text{total}} \quad < 3.85 \times 10^{-4}, \text{ CL} = 90\%$$

$$\Gamma(D^0 \rightarrow K^- \pi^+ \mu^+ \mu^-)/\Gamma_{\text{total}} \quad < 3.59 \times 10^{-4}, \text{ CL} = 90\%$$

$$\Gamma(D^0 \rightarrow \pi^+ \pi^- \pi^0 \mu^+ \mu^-)/\Gamma_{\text{total}} \quad < 8.1 \times 10^{-4}, \text{ CL} = 90\%$$

$$\Gamma(D_S^+ \rightarrow K^+ e^+ e^-)/\Gamma_{\text{total}} \quad < 1.6 \times 10^{-3}, \text{ CL} = 90\%$$

$$\Gamma(D_S^+ \rightarrow K^+ \mu^+ \mu^-)/\Gamma_{\text{total}} \quad < 3.6 \times 10^{-5}, \text{ CL} = 90\%$$

$$\Gamma(D_S^+ \rightarrow K^*(892)^+ \mu^+ \mu^-)/\Gamma_{\text{total}} \quad < 1.4 \times 10^{-3}, \text{ CL} = 90\%$$

$$\Gamma(\Lambda_c^+ \rightarrow p \mu^+ \mu^-)/\Gamma_{\text{total}} \quad < 3.4 \times 10^{-4}, \text{ CL} = 90\%$$

 $\Delta B = 1$ WEAK NEUTRAL CURRENT FORBIDDEN

Allowed by higher-order electroweak interactions.

$$\Gamma(B^+ \rightarrow \pi^+ \ell^+ \ell^-)/\Gamma_{\text{total}} \quad < 4.9 \times 10^{-8}, \text{ CL} = 90\%$$

$$\Gamma(B^+ \rightarrow \pi^+ e^+ e^-)/\Gamma_{\text{total}} \quad < 8.0 \times 10^{-8}, \text{ CL} = 90\%$$

$$\Gamma(B^+ \rightarrow \pi^+ \mu^+ \mu^-)/\Gamma_{\text{total}} \quad < 6.9 \times 10^{-8}, \text{ CL} = 90\%$$

$$\Gamma(B^+ \rightarrow \pi^+ \nu \bar{\nu})/\Gamma_{\text{total}} \quad < 1.0 \times 10^{-4}, \text{ CL} = 90\%$$

$$\Gamma(B^+ \rightarrow K^+ \ell^+ \ell^-)/\Gamma_{\text{total}} \quad [x] \quad (5.1 \pm 0.5) \times 10^{-7}$$

$$\Gamma(B^+ \rightarrow K^+ e^+ e^-)/\Gamma_{\text{total}} \quad (5.5 \pm 0.7) \times 10^{-7}$$

$$\Gamma(B^+ \rightarrow K^+ \mu^+ \mu^-)/\Gamma_{\text{total}} \quad (5.2 \pm 0.7) \times 10^{-7}$$

$$\Gamma(B^+ \rightarrow K^+ \nu \bar{\nu})/\Gamma_{\text{total}} \quad < 1.4 \times 10^{-5}, \text{ CL} = 90\%$$

$$\Gamma(B^+ \rightarrow \rho^+ \nu \bar{\nu})/\Gamma_{\text{total}} \quad < 1.5 \times 10^{-4}, \text{ CL} = 90\%$$

$$\Gamma(B^+ \rightarrow K^*(892)^+ \ell^+ \ell^-)/\Gamma_{\text{total}} \quad [x] \quad (1.29 \pm 0.21) \times 10^{-6}$$

$$\Gamma(B^+ \rightarrow K^*(892)^+ e^+ e^-)/\Gamma_{\text{total}} \quad (1.55 \pm_{-0.31}^{+0.40}) \times 10^{-6}$$

$$\Gamma(B^+ \rightarrow K^*(892)^+ \mu^+ \mu^-)/\Gamma_{\text{total}} \quad (1.16 \pm_{-0.27}^{+0.31}) \times 10^{-6}$$

$$\Gamma(B^+ \rightarrow K^*(892)^+ \nu \bar{\nu})/\Gamma_{\text{total}} \quad < 8 \times 10^{-5}, \text{ CL} = 90\%$$

$$\Gamma(B^0 \rightarrow \gamma \gamma)/\Gamma_{\text{total}} \quad < 6.2 \times 10^{-7}, \text{ CL} = 90\%$$

$$\Gamma(B^0 \rightarrow e^+ e^-)/\Gamma_{\text{total}} \quad < 8.3 \times 10^{-8}, \text{ CL} = 90\%$$

$$\Gamma(B^0 \rightarrow e^+ e^- \gamma)/\Gamma_{\text{total}} \quad < 1.2 \times 10^{-7}, \text{ CL} = 90\%$$

$$\Gamma(B^0 \rightarrow \mu^+ \mu^-)/\Gamma_{\text{total}} \quad < 1.5 \times 10^{-8}, \text{ CL} = 90\%$$

$$\Gamma(B^0 \rightarrow \mu^+ \mu^- \gamma)/\Gamma_{\text{total}} \quad < 1.6 \times 10^{-7}, \text{ CL} = 90\%$$

$$\Gamma(B^0 \rightarrow \tau^+ \tau^-)/\Gamma_{\text{total}} \quad < 4.1 \times 10^{-3}, \text{ CL} = 90\%$$

$$\Gamma(B^0 \rightarrow \pi^0 \ell^+ \ell^-)/\Gamma_{\text{total}} \quad < 1.2 \times 10^{-7}, \text{ CL} = 90\%$$

$$\Gamma(B^0 \rightarrow \pi^0 e^+ e^-)/\Gamma_{\text{total}} \quad < 1.4 \times 10^{-7}, \text{ CL} = 90\%$$

$$\Gamma(B^0 \rightarrow \pi^0 \mu^+ \mu^-)/\Gamma_{\text{total}} \quad < 1.8 \times 10^{-7}, \text{ CL} = 90\%$$

$$\Gamma(B^0 \rightarrow \pi^0 \nu \bar{\nu})/\Gamma_{\text{total}} \quad < 2.2 \times 10^{-4}, \text{ CL} = 90\%$$

$$\Gamma(B^0 \rightarrow K^0 \ell^+ \ell^-)/\Gamma_{\text{total}} \quad [x] \quad (3.1 \pm_{-0.7}^{+0.8}) \times 10^{-7}$$

$$\Gamma(B^0 \rightarrow K^0 e^+ e^-)/\Gamma_{\text{total}} \quad (1.6 \pm_{-0.8}^{+1.0}) \times 10^{-7}$$

$$\Gamma(B^0 \rightarrow K^0 \mu^+ \mu^-)/\Gamma_{\text{total}} \quad (4.5 \pm_{-1.0}^{+1.2}) \times 10^{-7}$$

$$\Gamma(B^0 \rightarrow K^0 \nu \bar{\nu})/\Gamma_{\text{total}} \quad < 1.6 \times 10^{-4}, \text{ CL} = 90\%$$

$$\Gamma(B^0 \rightarrow \rho^0 \nu \bar{\nu})/\Gamma_{\text{total}} \quad < 4.4 \times 10^{-4}, \text{ CL} = 90\%$$

$$\Gamma(B^0 \rightarrow K^*(892)^0 \ell^+ \ell^-)/\Gamma_{\text{total}} \quad [x] \quad (9.9 \pm_{-1.1}^{+1.2}) \times 10^{-7}$$

$$\Gamma(B^0 \rightarrow K^*(892)^0 e^+ e^-)/\Gamma_{\text{total}} \quad (1.03 \pm_{-0.17}^{+0.19}) \times 10^{-6}$$

$$\Gamma(B^0 \rightarrow K^*(892)^0 \mu^+ \mu^-)/\Gamma_{\text{total}} \quad (1.05 \pm_{-0.13}^{+0.16}) \times 10^{-6}$$

$$\Gamma(B^0 \rightarrow K^*(892)^0 \nu \bar{\nu})/\Gamma_{\text{total}} \quad < 1.2 \times 10^{-4}, \text{ CL} = 90\%$$

$$\Gamma(B^0 \rightarrow \phi \nu \bar{\nu})/\Gamma_{\text{total}} \quad < 5.8 \times 10^{-5}, \text{ CL} = 90\%$$

$$\Gamma(B^0 \rightarrow \text{invisible})/\Gamma_{\text{total}} \quad < 2.2 \times 10^{-4}, \text{ CL} = 90\%$$

$$\Gamma(B^0 \rightarrow \nu \bar{\nu} \gamma)/\Gamma_{\text{total}} \quad < 4.7 \times 10^{-5}, \text{ CL} = 90\%$$

$$\Gamma(B \rightarrow s e^+ e^-)/\Gamma_{\text{total}} \quad (4.7 \pm 1.3) \times 10^{-6}$$

$$\Gamma(B \rightarrow s \mu^+ \mu^-)/\Gamma_{\text{total}} \quad (4.3 \pm 1.2) \times 10^{-6}$$

$$\Gamma(B \rightarrow s \ell^+ \ell^-)/\Gamma_{\text{total}} \quad [x] \quad (4.5 \pm 1.0) \times 10^{-6}$$

$$\Gamma(B \rightarrow K e^+ e^-)/\Gamma_{\text{total}} \quad (4.4 \pm 0.6) \times 10^{-7}$$

$$\Gamma(B \rightarrow K^*(892) e^+ e^-)/\Gamma_{\text{total}} \quad (1.19 \pm 0.20) \times 10^{-6} \quad (S = 1.2)$$

$$\Gamma(B \rightarrow K \mu^+ \mu^-)/\Gamma_{\text{total}} \quad (4.8 \pm 0.6) \times 10^{-7}$$

$$\Gamma(B \rightarrow K^*(892) \mu^+ \mu^-)/\Gamma_{\text{total}} \quad (1.15 \pm 0.15) \times 10^{-6}$$

$$\Gamma(B \rightarrow K \ell^+ \ell^-)/\Gamma_{\text{total}} \quad (4.5 \pm 0.4) \times 10^{-7}$$

$$\Gamma(B \rightarrow K^*(892) \ell^+ \ell^-)/\Gamma_{\text{total}} \quad (1.08 \pm 0.11) \times 10^{-6}$$

$$\Gamma(\bar{D} \rightarrow \mu^+ \mu^- \text{ anything})/\Gamma_{\text{total}} \quad < 3.2 \times 10^{-4}, \text{ CL} = 90\%$$

$$\Gamma(B_S^0 \rightarrow \gamma \gamma)/\Gamma_{\text{total}} \quad < 8.7 \times 10^{-6}, \text{ CL} = 90\%$$

$$\Gamma(B_S^0 \rightarrow \mu^+ \mu^-)/\Gamma_{\text{total}} \quad < 4.7 \times 10^{-8}, \text{ CL} = 90\%$$

$$\Gamma(B_S^0 \rightarrow e^+ e^-)/\Gamma_{\text{total}} \quad < 2.8 \times 10^{-7}, \text{ CL} = 90\%$$

Tests of Conservation Laws

$$\Gamma(B_S^0 \rightarrow \phi(1020)\mu^+\mu^-)/\Gamma_{\text{total}} < 3.2 \times 10^{-6}, \text{ CL} = 90\%$$

$$\Gamma(B_S^0 \rightarrow \phi\nu\bar{\nu})/\Gamma_{\text{total}} < 5.4 \times 10^{-3}, \text{ CL} = 90\%$$

$\Delta T = 1$ WEAK NEUTRAL CURRENT FORBIDDEN

Allowed by higher-order electroweak interactions.

$$\Gamma(t \rightarrow Zq(q=u,c))/\Gamma_{\text{total}} [y] < 3.7 \times 10^{-2}, \text{ CL} = 95\%$$

NOTES

In this Summary Table:

When a quantity has “(S = ...)” to its right, the error on the quantity has been enlarged by the “scale factor” S, defined as $S = \sqrt{\chi^2/(N-1)}$, where N is the number of measurements used in calculating the quantity. We do this when $S > 1$, which often indicates that the measurements are inconsistent. When $S > 1.25$, we also show in the Particle Listings an ideogram of the measurements. For more about S, see the Introduction.

- [a] C parity forbids this to occur as a single-photon process.
- [b] See the Particle Listings for the (complicated) definition of this quantity.
- [c] Time-reversal invariance requires this to be 0° or 180° .
- [d] This coefficient is zero if time invariance is not violated.
- [e] Allowed by higher-order electroweak interactions.
- [f] Violates CP in leading order. Test of direct CP violation since the indirect CP-violating and CP-conserving contributions are expected to be suppressed.
- [g] $\text{Re}(\epsilon'/\epsilon) = \epsilon'/\epsilon$ to a very good approximation provided the phases satisfy CPT invariance.
- [h] This mode includes gammas from inner bremsstrahlung but not the direct emission mode $K_L^0 \rightarrow \pi^+\pi^-\gamma(\text{DE})$.
- [i] Neglecting photon channels. See, e.g., A. Pais and S.B. Treiman, Phys. Rev. **D12**, 2744 (1975).

[j] Derived from measured values of ϕ_{+-} , ϕ_{00} , $|\eta|$, $|m_{K_L^0} - m_{K_S^0}|$, and $\tau_{K_S^0}$, as described in the introduction to “Tests of Conservation Laws.”

[k] The $|m_p - m_{\bar{p}}|/m_p$ and $|q_p + q_{\bar{p}}|/e$ are not independent, and both use the more precise measurement of $|q_{\bar{p}}/m_{\bar{p}}|/(q_p/m_p)$.

[l] The value is for the sum of the charge states or particle/antiparticle states indicated.

[m] A test of additive vs. multiplicative lepton family number conservation.

[n] The limit quoted corresponds to the projection onto the $\sin^2(2\theta_{23})$ axis of the 90% CL contour in the $\sin^2(2\theta_{23}) - \Delta m_{32}^2$ plane.

[o] The sign of Δm_{32}^2 is not known at this time. The range quoted is for the absolute value.

[p] Derived from an analysis of neutrino-oscillation experiments.

[q] This limit is for either D^0 or \bar{D}^0 to $p e^-$.

[r] This limit is for either D^0 or \bar{D}^0 to $\bar{p} e^+$.

[s] The first limit is for $p \rightarrow$ anything or “disappearance” modes of a bound proton. The second entry, a rough range of limits, assumes the dominant decay modes are among those investigated. For antiprotons the best limit, inferred from the observation of cosmic ray \bar{p} 's is $\tau_{\bar{p}} > 10^7$ yr, the cosmic-ray storage time, but this limit depends on a number of assumptions. The best direct observation of stored antiprotons gives $\tau_{\bar{p}}/B(\bar{p} \rightarrow e^- \gamma) > 7 \times 10^5$ yr.

[t] There is some controversy about whether nuclear physics and model dependence complicate the analysis for bound neutrons (from which the best limit comes). The first limit here is from reactor experiments with free neutrons.

[u] This is the best limit for the mode $e^- \rightarrow \nu \gamma$. The best limit for “electron disappearance” is 6.4×10^{24} yr.

[v] See the K_S^0 Particle Listings for the energy limits used in this measurement.

[w] See the K_L^0 Particle Listings for the energy limits used in this measurement.

[x] An ℓ indicates an e or a μ mode, not a sum over these modes.

[y] This limit is for $\Gamma(t \rightarrow Zq)/\Gamma(t \rightarrow Wb)$.

REVIEWS, TABLES, AND PLOTS

Constants, Units, Atomic and Nuclear Properties

1. Physical constants (rev.)	101
2. Astrophysical constants (rev.)	102
3. International System of Units (SI)	104
4. Periodic table of the elements (rev.)	105
5. Electronic structure of the elements	106
6. Atomic and nuclear properties of materials	108
7. Electromagnetic relations	110
8. Naming scheme for hadrons	112

Standard Model and Related Topics

9. Quantum chromodynamics (new)	114
10. Electroweak model and constraints on new physics (rev.)	126
11. The Cabibbo-Kobayashi-Maskawa quark-mixing matrix (rev.)	146
12. CP violation (rev.)	154
13. Neutrino Mass, Mixing, & Oscillations (new)	164
14. Quark model (rev.)	184
15. Grand Unified Theories	193
16. Structure functions (rev.)	201
17. Fragmentation functions in e^+e^- , ep and pp collisions (rev.)	215

Astrophysics and cosmology

18. Experimental tests of gravitational theory (rev.)	225
19. Big-Bang cosmology (rev.)	230
20. Big-Bang nucleosynthesis (rev.)	241
21. The cosmological parameters (rev.)	246
22. Dark matter (rev.)	255
23. Cosmic microwave background (rev.)	261
24. Cosmic rays (rev.)	269

Experimental Methods and Colliders

25. Accelerator physics of colliders (rev.)	277
26. High-energy collider parameters (rev.)	281
27. Passage of particles through matter (rev.)	285
28. Particle detectors at accelerators (rev.)	300
28. Particle detectors for non-accelerators (new)	328
30. Radioactivity and radiation protection (rev.)	341
31. Commonly used radioactive sources	345

Mathematical Tools or Statistics, Monte Carlo,

Group Theory	
32. Probability (rev.)	346
33. Statistics (rev.)	350
34. Monte Carlo techniques (rev.)	361
35. Monte Carlo particle numbering scheme (rev.)	364
36. Clebsch-Gordan coefficients, spherical harmonics, and d functions	368
37. $SU(3)$ isoscalar factors and representation matrices	369
38. $SU(n)$ multiplets and Young diagrams	370

Kinematics, Cross-Section Formulae, and Plots

39. Kinematics (rev.)	371
40. Cross-section formulae for specific proc. (rev.)	376
41. Plots of cross secs. and related quant. (rev.)	385

MAJOR REVIEWS IN THE PARTICLE LISTINGS

Gauge and Higgs bosons

The Mass of the W Boson (rev.)	418
Triple Gauge Couplings (rev.)	422
Anomalous W/Z Quartic Couplings	424
The Z Boson (rev.)	426
Anomalous $ZZ\gamma$, $Z\gamma\gamma$, and ZZV Couplings	445
Searches for Higgs Bosons (rev.)	448
The W' Searches (rev.)	480
The Z' Searches (rev.)	483
Leptoquarks	490
Axions and Other Very Light Bosons (rev.)	496

Leptons

Muon Anomalous Magnetic Moment (rev.)	521
Muon Decay Parameters (rev.)	521
τ Branching Fractions (rev.)	529
τ -Lepton Decay Parameters	548
Number of Light Neutrino Types	561
Neutrinoless Double- β Decay (rev.)	562

Quarks

Quark Masses (rev.)	583
The Top Quark (rev.)	596
Free Quark Searches	613

Mesons

Form Factors for Rad. Pion & Kaon Decays (rev.)	620
Note on Scalar Mesons (rev.)	630
The $\eta(1405)$, $\eta(1475)$, $f_1(1420)$, and $f_1(1510)$ (rev.)	680
Rare Kaon Decays (rev.)	742
$K_{\ell 3}^{\pm}$ and $K_{\ell 3}^0$ Form Factors (rev.)	753
CPT Invariance Tests in Neutral Kaon Decay (rev.)	759
CP Violation in $K_S \rightarrow 3\pi$	764
V_{ud} , V_{us} , Cabibbo Angle, and CKM Unitarity (new)	771
CP -Violation in K_L Decays (rev.)	779
Dalitz-Plot Analysis Formalism	807
Review of Charm Dalitz-Plot Analyses (rev.)	811
$D^0-\bar{D}^0$ Mixing (rev.)	820
D_s^+ Branching Fractions (new)	858
Decay Cons. of Charged Pseudoscalar Mesons (rev.)	861
Production and Decay of b -flavored Hadrons (rev.)	877
Polarization in B Decays (rev.)	967
$B^0-\bar{B}^0$ Mixing (rev.)	973
Determination of V_{cb} and V_{ub} (rev.)	1014
Branching Ratios of $\psi(2S)$ and $\chi_{c0,1,2}$ (rev.)	1060

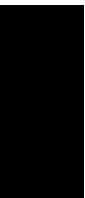
Baryons

Baryon Decay Parameters	1146
N and Δ Resonances	1149
Pentaquarks	1199
Radiative Hyperon Decays	1242
Charmed Baryons (rev.)	1257
Λ_c^+ Branching Fractions	1260

Miscellaneous searches

Magnetic Monopoles (new)	1285
Supersymmetry (rev.)	1292
Dynamical Electroweak Symmetry Breaking (rev.)	1340
Searches for Quark & Lepton Compositeness	1347
Extra Dimensions	1354

Additional Reviews and Notes related to specific particles are located in the Particle Listings.



1. PHYSICAL CONSTANTS

Table 1.1. Reviewed 2010 by P.J. Mohr (NIST). Mainly from the “CODATA Recommended Values of the Fundamental Physical Constants: 2006” by P.J. Mohr, B.N. Taylor, and D.B. Newell in Rev. Mod. Phys. **80** (2008) 633. The last group of constants (beginning with the Fermi coupling constant) comes from the Particle Data Group. The figures in parentheses after the values give the 1-standard-deviation uncertainties in the last digits; the corresponding fractional uncertainties in parts per 10⁹ (ppb) are given in the last column. This set of constants (aside from the last group) is recommended for international use by CODATA (the Committee on Data for Science and Technology). The full 2006 CODATA set of constants may be found at <http://physics.nist.gov/constants>. See also P.J. Mohr and D.B. Newell, “Resource Letter FC-1: The Physics of Fundamental Constants,” Am. J. Phys, **78** (2010) 338.

Quantity	Symbol, equation	Value	Uncertainty (ppb)
speed of light in vacuum	c	299 792 458 m s ⁻¹	exact*
Planck constant	h	6.626 068 96(33) × 10 ⁻³⁴ J s	50
Planck constant, reduced	$\hbar \equiv h/2\pi$	1.054 571 628(53) × 10 ⁻³⁴ J s = 6.582 118 99(16) × 10 ⁻²² MeV s	50 25
electron charge magnitude	e	1.602 176 487(40) × 10 ⁻¹⁹ C = 4.803 204 27(12) × 10 ⁻¹⁰ esu	25, 25
conversion constant	$\hbar c$	197.326 9631(49) MeV fm	25
conversion constant	$(\hbar c)^2$	0.389 379 304(19) GeV ² mbarn	50
electron mass	m_e	0.510 998 910(13) MeV/c ² = 9.109 382 15(45) × 10 ⁻³¹ kg	25, 50
proton mass	m_p	938.272 013(23) MeV/c ² = 1.672 621 637(83) × 10 ⁻²⁷ kg = 1.007 276 466 77(10) u = 1836.152 672 47(80) m_e	25, 50 0.10, 0.43
deuteron mass	m_d	1875.612 793(47) MeV/c ²	25
unified atomic mass unit (u)	(mass ¹² C atom)/12 = (1 g)/(N _A mol)	931.494 028(23) MeV/c ² = 1.660 538 782(83) × 10 ⁻²⁷ kg	25, 50
permittivity of free space	$\epsilon_0 = 1/\mu_0 c^2$	8.854 187 817 ... × 10 ⁻¹² F m ⁻¹	exact
permeability of free space	μ_0	4π × 10 ⁻⁷ N A ⁻² = 12.566 370 614 ... × 10 ⁻⁷ N A ⁻²	exact
fine-structure constant	$\alpha = e^2/4\pi\epsilon_0\hbar c$	7.297 352 5376(50) × 10 ⁻³ = 1/137.035 999 679(94) [†]	0.68, 0.68
classical electron radius	$r_e = e^2/4\pi\epsilon_0 m_e c^2$	2.817 940 2894(58) × 10 ⁻¹⁵ m	2.1
(e ⁻ Compton wavelength)/2π	$\lambda_e = \hbar/m_e c = r_e \alpha^{-1}$	3.861 592 6459(53) × 10 ⁻¹³ m	1.4
Bohr radius ($m_{\text{nucleus}} = \infty$)	$a_\infty = 4\pi\epsilon_0 \hbar^2 / m_e e^2 = r_e \alpha^{-2}$	0.529 177 208 59(36) × 10 ⁻¹⁰ m	0.68
wavelength of 1 eV/c particle	$\hbar c / (1 \text{ eV})$	1.239 841 875(31) × 10 ⁻⁶ m	25
Rydberg energy	$\hbar c R_\infty = m_e c^4 / 2(4\pi\epsilon_0)^2 \hbar^2 = m_e c^2 \alpha^2 / 2$	13.605 691 93(34) eV	25
Thomson cross section	$\sigma_T = 8\pi r_e^2 / 3$	0.665 245 8558(27) barn	4.1
Bohr magneton	$\mu_B = e\hbar/2m_e$	5.788 381 7555(79) × 10 ⁻¹¹ MeV T ⁻¹	1.4
nuclear magneton	$\mu_N = e\hbar/2m_p$	3.152 451 2326(45) × 10 ⁻¹⁴ MeV T ⁻¹	1.4
electron cyclotron freq./field	$\omega_{\text{cycl}}^e / B = e/m_e$	1.758 820 150(44) × 10 ¹¹ rad s ⁻¹ T ⁻¹	25
proton cyclotron freq./field	$\omega_{\text{cycl}}^p / B = e/m_p$	9.578 833 92(24) × 10 ⁷ rad s ⁻¹ T ⁻¹	25
gravitational constant [‡]	G_N	6.674 28(67) × 10 ⁻¹¹ m ³ kg ⁻¹ s ⁻² = 6.708 81(67) × 10 ⁻³⁹ $\hbar c$ (GeV/c ²) ⁻²	1.0 × 10 ⁵ 1.0 × 10 ⁵
standard gravitational accel.	g_N	9.806 65 m s ⁻²	exact
Avogadro constant	N_A	6.022 141 79(30) × 10 ²³ mol ⁻¹	50
Boltzmann constant	k	1.380 6504(24) × 10 ⁻²³ J K ⁻¹ = 8.617 343(15) × 10 ⁻⁵ eV K ⁻¹	1700 1700
molar volume, ideal gas at STP	$N_A k (273.15 \text{ K}) / (101 325 \text{ Pa})$	22.413 996(39) × 10 ⁻³ m ³ mol ⁻¹	1700
Wien displacement law constant	$b = \lambda_{\text{max}} T$	2.897 7685(51) × 10 ⁻³ m K	1700
Stefan-Boltzmann constant	$\sigma = \pi^2 k^4 / 60 \hbar^3 c^2$	5.670 400(40) × 10 ⁻⁸ W m ⁻² K ⁻⁴	7000
Fermi coupling constant**	$G_F / (\hbar c)^3$	1.166 37(1) × 10 ⁻⁵ GeV ⁻²	9000
weak-mixing angle	$\sin^2 \hat{\theta}(M_Z) (\overline{\text{MS}})$	0.231 16(13) ^{††}	5.6 × 10 ⁵
W [±] boson mass	m_W	80.399(23) GeV/c ²	2.9 × 10 ⁵
Z ⁰ boson mass	m_Z	91.1876(21) GeV/c ²	2.3 × 10 ⁴
strong coupling constant	$\alpha_s(m_Z)$	0.1184(7)	5.9 × 10 ⁶
$\pi = 3.141 592 653 589 793 238$		$e = 2.718 281 828 459 045 235$	$\gamma = 0.577 215 664 901 532 861$
1 in ≡ 0.0254 m	1 G ≡ 10 ⁻⁴ T	1 eV = 1.602 176 487(40) × 10 ⁻¹⁹ J	kT at 300 K = [38.681 685(68)] ⁻¹ eV
1 Å ≡ 0.1 nm	1 dyne ≡ 10 ⁻⁵ N	1 eV/c ² = 1.782 661 758(44) × 10 ⁻³⁶ kg	0 °C ≡ 273.15 K
1 barn ≡ 10 ⁻²⁸ m ²	1 erg ≡ 10 ⁻⁷ J	2.997 924 58 × 10 ⁹ esu = 1 C	1 atmosphere ≡ 760 Torr ≡ 101 325 Pa

* The meter is the length of the path traveled by light in vacuum during a time interval of 1/299 792 458 of a second.

† At $Q^2 = 0$. At $Q^2 \approx m_W^2$ the value is $\sim 1/128$.

‡ Absolute lab measurements of G_N have been made only on scales of about 1 cm to 1 m.

** See the discussion in Sec. 10, “Electroweak model and constraints on new physics.”

†† The corresponding $\sin^2 \theta$ for the effective angle is 0.23146(12).

2. ASTROPHYSICAL CONSTANTS AND PARAMETERS

Table 2.1. Revised May 2010 by E. Bergren and D.E. Groom (LBNL). The figures in parentheses after some values give the one standard deviation uncertainties in the last digit(s). Physical constants are from Ref. 1. While every effort has been made to obtain the most accurate current values of the listed quantities, the table does not represent a critical review or adjustment of the constants, and is not intended as a primary reference.

The values and uncertainties for the cosmological parameters depend on the exact data sets, priors, and basis parameters used in the fit. Many of the parameters reported in this table are derived parameters or have non-Gaussian likelihoods. The quoted errors may be highly correlated with those of other parameters, so care must be taken in propagating them. Unless otherwise specified, cosmological parameters are best fits of a spatially-flat Λ CDM cosmology with a power-law initial spectrum to 5-year WMAP data alone [2]. For more information see Ref. 3 and the original papers.

Quantity	Symbol, equation	Value	Reference, footnote
speed of light	c	299 792 458 m s ⁻¹	exact[4]
Newtonian gravitational constant	G_N	6.674 3(7) $\times 10^{-11}$ m ³ kg ⁻¹ s ⁻²	[1]
Planck mass	$\sqrt{\hbar c/G_N}$	1.220 89(6) $\times 10^{19}$ GeV/c ² = 2.176 44(11) $\times 10^{-8}$ kg	[1]
Planck length	$\sqrt{\hbar G_N/c^3}$	1.616 25(8) $\times 10^{-35}$ m	[1]
standard gravitational acceleration	g_N	9.806 65 m s ⁻² $\approx \pi^2$	exact[1]
jansky (flux density)	Jy	10 ⁻²⁶ W m ⁻² Hz ⁻¹	definition
tropical year (equinox to equinox) (2011)	yr	31 556 925.2 s $\approx \pi \times 10^7$ s	[5]
sidereal year (fixed star to fixed star) (2011)		31 558 149.8 s $\approx \pi \times 10^7$ s	[5]
mean sidereal day (2011) (time between vernal equinox transits)		23 ^h 56 ^m 04 ^s .090 53	[5]
astronomical unit	au, A	149 597 870 700(3) m	[6]
parsec (1 au/1 arc sec)	pc	3.085 677 6 $\times 10^{16}$ m = 3.262 ... ly	[7]
light year (deprecated unit)	ly	0.306 6 ... pc = 0.946 053 ... $\times 10^{16}$ m	
Schwarzschild radius of the Sun	$2G_N M_\odot/c^2$	2.953 250 077 0(2) km	[8]
Solar mass	M_\odot	1.988 4(2) $\times 10^{30}$ kg	[9]
Solar equatorial radius	R_\odot	6.9551(4) $\times 10^8$ m	[10]
Solar luminosity	L_\odot	3.842 7(1 4) $\times 10^{26}$ W	[11]
Schwarzschild radius of the Earth	$2G_N M_\oplus/c^2$	8.870 055 94(2) mm	[12]
Earth mass	M_\oplus	5.972 2(6) $\times 10^{24}$ kg	[13]
Earth mean equatorial radius	R_\oplus	6.378 137 $\times 10^6$ m	[5]
luminosity conversion (deprecated)	L	3.02 $\times 10^{28} \times 10^{-0.4 M_{\text{bol}}}$ W	[14]
flux conversion (deprecated)	\mathcal{F}	(M_{bol} = absolute bolometric magnitude = bolometric magnitude at 10 pc) 2.52 $\times 10^{-8} \times 10^{-0.4 m_{\text{bol}}}$ W m ⁻²	from above
ABsolute monochromatic magnitude	AB	(m_{bol} = apparent bolometric magnitude) -2.5 log ₁₀ f_ν - 56.10 (for f_ν in W m ⁻² Hz ⁻¹) = -2.5 log ₁₀ f_ν + 8.90 (for f_ν in Jy)	[15]
Solar distance from Galactic center	R_0	8.4(4) kpc	[16]
[Solar circular velocity at R_0]/ R_0	v_\odot/R_0	30.2 \pm 0.2 km s ⁻¹ kpc ⁻¹	[17]
circular velocity at R_0	Θ_0	240(10) km s ⁻¹	[18]
local disk density	ρ_{disk}	3-12 $\times 10^{-24}$ g cm ⁻³ \approx 2-7 GeV/c ² cm ⁻³	[19]
local dark matter density	ρ_χ	canonical value 0.3 GeV/c ² cm ⁻³ within factor 2-3	[20]
escape velocity from Galaxy	v_{esc}	498 km/s < v_{esc} < 608 km/s	[21]
present day CMB temperature	T_0	2.725(1) K	[22]
present day CMB dipole amplitude		3.355(8) mK	[2]
Solar velocity with respect to CMB		369(1) km/s towards (ℓ, b) = (263.99(14) $^\circ$, 48.26(3) $^\circ$)	[2]
Local Group velocity with respect to CMB	v_{LG}	627(22) km/s towards (ℓ, b) = (276(3) $^\circ$, 30(3) $^\circ$)	[23]
entropy density/Boltzmann constant	s/k	2 889.2 (T/2.725) ³ cm ⁻³	[14]
number density of CMB photons	n_γ	410.5 (T/2.725) ³ cm ⁻³	[24]
baryon-to-photon ratio [†]	$\eta = n_b/n_\gamma$	6.23(17) $\times 10^{-10}$ 5.1 $\times 10^{-10} \leq \eta \leq 6.5 \times 10^{-10}$ (95% CL)	[2] [25]
number density of baryons [†]	n_b	(2.56 \pm 0.07) $\times 10^{-7}$ cm ⁻³ (2.1 $\times 10^{-7} < n_b < 2.7 \times 10^{-7}$) cm ⁻³ (95% CL)	from η in [2] from η in [25]
present day Hubble expansion rate	H_0	100 h km s ⁻¹ Mpc ⁻¹ = $h \times (9.777 752 \text{ Gyr})^{-1}$	[26]
present day normalized Hubble expansion rate [†]	h	0.72(3)	[2,3]
Hubble length	c/H_0	0.925 063 $\times 10^{26}$ h ⁻¹ m = 1.28(5) $\times 10^{26}$ m	
scale factor for cosmological constant	$c^2/3H_0^2$	2.852 $\times 10^{51}$ h ⁻² m ² = 5.5(5) $\times 10^{51}$ m ²	
critical density of the Universe	$\rho_c = 3H_0^2/8\pi G_N$	2.775 366 27 $\times 10^{11}$ h ² M _⊙ Mpc ⁻³ = 1.878 35(19) $\times 10^{-29}$ h ² g cm ⁻³ = 1.053 68(11) $\times 10^{-5}$ h ² (GeV/c ²) cm ⁻³	
pressureless matter density of the Universe [†]	$\Omega_m = \rho_m/\rho_c$	0.133(6) h ⁻² = 0.26(2)	[2,3]
baryon density of the Universe [†]	$\Omega_b = \rho_b/\rho_c$	0.0227(6) h ⁻² = 0.044(4)	[2,3]
dark matter density of the universe [†]	$\Omega_{\text{cdm}} = \Omega_m - \Omega_b - \Omega_\nu$	0.110(6) h ⁻² = 0.21(2)	[2,3]
dark energy density of the Λ CDM Universe [†]	Ω_Λ	0.74(3)	[2,3]
dark energy equation of state parameter	w	-1.04 ^{+0.09} _{-0.10}	[27]
CMB radiation density of the Universe	$\Omega_\gamma = \rho_\gamma/\rho_c$	2.471 $\times 10^{-5}$ (T/2.725) ⁴ h ⁻² = 4.8(4) $\times 10^{-5}$	[24]
neutrino density of the Universe [†]	Ω_ν	0.0005 < $\Omega_\nu h^2$ < 0.025 \Rightarrow 0.0009 < Ω_ν < 0.048	[28]
total energy density of the Universe [†]	$\Omega_{\text{tot}} = \Omega_m + \dots + \Omega_\Lambda$	1.006(6)	[2,3]

Quantity	Symbol, equation	Value	Reference, footnote
fluctuation amplitude at $8 h^{-1}$ Mpc scale [‡]	σ_8	0.80(4)	[2,3]
curvature fluctuation amplitude, $k_0 = 0.002$ Mpc ⁻¹ [‡]	$\Delta_{\mathcal{R}}^2$	$2.41(11) \times 10^{-9}$	[2,3]
scalar spectral index [‡]	n_s	0.96(1)	[2,3]
running spectral index slope, $k_0 = 0.002$ Mpc ⁻¹ [‡]	$dn_s/d \ln k$	-0.04(3)	[2]
tensor-to-scalar field perturbations ratio, $k_0 = 0.002$ Mpc ⁻¹ [‡]	$r = T/S$	< 0.43 at 95% C.L.	[2,3]
redshift at decoupling [‡]	z_*	1090(1)	[2]
age at decoupling [‡]	t_*	$3.80(6) \times 10^5$ yr	[2]
sound horizon at decoupling [‡]	$r_s(z_*)$	147(2) Mpc	[2]
redshift of matter-radiation equality [‡]	z_{eq}	3180 ± 150	[2]
redshift of reionization [‡]	z_{reion}	11.0 ± 1.4	[2]
age at reionization [‡]	t_{reion}	430^{+90}_{-70} Myr	[2,29]
reionization optical depth [‡]	τ	0.09(2)	[2,3]
age of the Universe [‡]	t_0	13.69 ± 0.13 Gyr	[2]

[‡] Best fit of a spatially-flat Λ CDM cosmology with a power-law initial spectrum to 5-year WMAP data alone [2].

References:

- P.J. Mohr, B.N. Taylor, & D.B. Newell, *CODATA Recommended Values of the Fundamental Constants: 2006*, Rev. Mod. Phys. **80**, 663 (2008); physics.nist.gov/constants.
- G. Hinshaw *et al.*, Astrophys. J. Supp. **180**, 225 (2009); J. Dunkley *et al.*, Astrophys. J. Supp. **180**, 306 (2009); E. Komatsu *et al.*, Astrophys. J. Supp. **180**, 330 (2009). Post-deadline 7-year WMAP values* have not been used. In any case, they vary by less than 1σ from the 5-year WMAP values.
- O. Lahav & A.R. Liddle, “The Cosmological Parameters,” in this *Review*.
- B.W. Petley, Nature **303**, 373 (1983).
- The Astronomical Almanac for the year 2011*, U.S. Government Printing Office, Washington, and The U.K. Hydrographic Office (2010).
- While A is approximately equal to the semi-major axis of the Earth’s orbit, it is not exactly so. Nor is it exactly the mean Earth-Sun distance. There are a number of reasons: a) the Earth’s orbit is not exactly Keplerian due to relativity and to perturbations from other planets; b) the adopted value for the Gaussian gravitational constant k is not exactly equal to the Earth’s mean motion; and c) the mean distance in a Keplerian orbit is not equal to the semi-major axis a : $\langle r \rangle = a(1 + e^2/2)$, where e is the eccentricity. (Discussion courtesy of Myles Standish, JPL).
- The distance at which 1 A subtends 1 arc sec: 1 A divided by $\pi/648000$.
- Product of $2/c^2$ and the heliocentric gravitational constant $G_N M_\odot = A^3 k^2 / 86400^2$, where k is the Gaussian gravitational constant, 0.01720209895 (exact) [5]. The value and error for A given in this table are used.
- Obtained from the heliocentric gravitational constant [5] and G_N [1]. The error is the 100 ppm standard deviation of G_N .
- T. M. Brown & J. Christensen-Dalsgaard, Astrophys. J. **500**, L195 (1998) Many values for the Solar radius have been published, most of which are consistent with this result.
- $4\pi A^2 \times (1366.4 \pm 0.5)$ W m⁻² [30]. Assumes isotropic irradiance.
- Schwarzschild radius of the Sun (above) scaled by the Earth/Sun mass ratio given in Ref. 5.
- Obtained from the geocentric gravitational constant [5] and G_N [1]. The error is the 100 ppm standard deviation of G_N .
- E.W. Kolb & M.S. Turner, *The Early Universe*, Addison-Wesley (1990); The IAU (Commission 36) has recommended 3.055×10^{28} W for the zero point. Based on newer Solar measurements, the value and significance given in the table seems more appropriate.
- J. B. Oke & J. E. Gunn, Astrophys. J. **266**, 713 (1983). Note that in the definition of AB the sign of the constant is wrong.
- A. M. Ghez *et al.*, Astrophys. J. **689**, 1044 (2008); S. Gillessen *et al.*, Astrophys. J. **692**, 1075 (2009); M. Shen & Z. Zhu, Chin. Astron. Astrophys. **7**, 120 (2007). In their Fig.2 Zhu & Chin present a summary of a dozen values published 1984–2007. Most are closer to $R_0 = 8.0(5)$ kpc than those cited above.
- M.J. Reid & A. Brunthaler, Astrophys. J. **616**, 872 (2004) as corrected using new value for Solar proper motion in Ref. 18. Note that v_\odot/R_0 is better determined than either Θ_0 or R_0 .
- C. McCabe, [arXiv:1005.0579](https://arxiv.org/abs/1005.0579) Other papers report values closer to 220(20) km s⁻¹; S.E. Kuposov, H.-W. Rix, & D.W. Hogg (2009), [arXiv:0907.1085](https://arxiv.org/abs/0907.1085); P.J. McMillan & J.J. Binney, [arXiv:0907.4685](https://arxiv.org/abs/0907.4685).
- G. Gilmore, R.F.G. Wyse, & K. Kuijken, Ann. Rev. Astron. Astrophys. **27**, 555 (1989).
- Sampling of many references: M. Mori *et al.*, Phys. Lett. **B289**, 463 (1992); E.I. Gates *et al.*, Astrophys. J. **449**, L133 (1995); M. Kamionkowski & A. Kinkhabwala, Phys. Rev. **D57**, 325 (1998); M. Weber and W. de Boer (2009), [arXiv:0910.4272](https://arxiv.org/abs/0910.4272); P. Salucci *et al.*, (2010), [arXiv:1003.3101](https://arxiv.org/abs/1003.3101).
- M. C. Smith *et al.*, Mon. Not. R. Astr. Soc. **379**, 755 (2007) ([astro-ph/0611671](https://arxiv.org/abs/astro-ph/0611671)).
- J. Mather *et al.*, Astrophys. J. **512**, 511 (1999). This paper gives $T_0 = (2.725 \pm 0.002)$ K at 95% CL. We take 0.001 as the one standard deviation uncertainty.
- D. Scott & G.F. Smoot, “Cosmic Microwave Background,” in this *Review*.
- $n_\gamma = \frac{2\zeta(3)}{\pi^2} \left(\frac{kT}{hc}\right)^3$ and $\rho_\gamma = \frac{\pi^2 (kT)^4}{15 (hc)^3 c^2}$; $\frac{kT_0}{hc} = 11.900(4)/\text{cm}$.
- B.D. Fields & S. Sarkar, “Big-Bang Nucleosynthesis,” in this *Review*.
- Conversion using length of sidereal year.
- R. Amanullah *et al.*, Astrophys. J. **716**, 712 (2010). Fit with curvature unconstrained. For a flat Universe, $w = -1.00 \pm 0.08$.
- $\Omega_\nu h^2 = \sum m_{\nu_j} / 93 \text{ eV}$, where the sum is over all neutrino mass eigenstates. The lower limit follows from neutrino mixing results reported in this *Review* combined with the assumptions that there are three light neutrinos ($m_\nu < 45 \text{ GeV}/c^2$) and that the lightest neutrino is substantially less massive than the others: $\Delta m_{32}^2 = (2.43 \pm 0.13) \times 10^{-3} \text{ eV}^2$, so $\sum m_{\nu_j} \geq m_{\nu_3} \approx \sqrt{\Delta m_{32}^2} = 0.05 \text{ eV}$. (This becomes 0.10 eV if the mass hierarchy is inverted, with $m_{\nu_1} \approx m_{\nu_2} \gg m_{\nu_3}$.) Astrophysical determinations of $\sum m_{\nu_j}$, reported in the Full Listings of this *Review* under “Sum of the neutrino masses,” range from $< 0.17 \text{ eV}$ to $< 2.3 \text{ eV}$ in papers published since 2002. Alternatively, if the limit obtained from tritium decay experiments ($m_\nu < 2 \text{ eV}$) is used for the upper limit, then $\Omega_\nu < 0.04$.
- If the Universe were reionized instantaneously at z_{reion} .
- R.C. Willson & A.V. Mordvinov, Geophys. Res. Lett. **30**, 1119 (2003); C. Frölich, Space Sci. Rev. **125**, 53–65 (2006).

* lambda.gsfc.nasa.gov/product/map/current/map_bibliography.cfm

3. INTERNATIONAL SYSTEM OF UNITS (SI)

See “The International System of Units (SI),” NIST Special Publication **330**, B.N. Taylor, ed. (USGPO, Washington, DC, 1991); and “Guide for the Use of the International System of Units (SI),” NIST Special Publication **811**, 1995 edition, B.N. Taylor (USGPO, Washington, DC, 1995).

Physical quantity	Name of unit	Symbol
<i>Base units</i>		
length	meter	m
mass	kilogram	kg
time	second	s
electric current	ampere	A
thermodynamic temperature	kelvin	K
amount of substance	mole	mol
luminous intensity	candela	cd
<i>Derived units with special names</i>		
plane angle	radian	rad
solid angle	steradian	sr
frequency	hertz	Hz
energy	joule	J
force	newton	N
pressure	pascal	Pa
power	watt	W
electric charge	coulomb	C
electric potential	volt	V
electric resistance	ohm	Ω
electric conductance	siemens	S
electric capacitance	farad	F
magnetic flux	weber	Wb
inductance	henry	H
magnetic flux density	tesla	T
luminous flux	lumen	lm
illuminance	lux	lx
celsius temperature	degree celsius	$^{\circ}\text{C}$
activity (of a radioactive source)*	becquerel	Bq
absorbed dose (of ionizing radiation)*	gray	Gy
dose equivalent*	sievert	Sv

SI prefixes

10^{24}	yotta	(Y)
10^{21}	zetta	(Z)
10^{18}	exa	(E)
10^{15}	peta	(P)
10^{12}	tera	(T)
10^9	giga	(G)
10^6	mega	(M)
10^3	kilo	(k)
10^2	hecto	(h)
10	deca	(da)
10^{-1}	deci	(d)
10^{-2}	centi	(c)
10^{-3}	milli	(m)
10^{-6}	micro	(μ)
10^{-9}	nano	(n)
10^{-12}	pico	(p)
10^{-15}	femto	(f)
10^{-18}	atto	(a)
10^{-21}	zepto	(z)
10^{-24}	yocto	(y)

*See our section 30, on “Radioactivity and radiation protection,” p. 341.

Table 4.1. Revised 2010 by D.E. Groom (LBNL), and E. Bergren. Atomic weights of stable elements are adapted from the Commission on Isotopic Abundances and Atomic Weights, "Atomic Weights of the Elements 2007," <http://www.chem.qmul.ac.uk/iupac/AtWt/>. The atomic number (top left) is the number of protons in the nucleus. The atomic mass (bottom) of a stable elements is weighted by isotopic abundances in the Earth's surface. If the element has no stable isotope, the atomic mass (in parentheses) of the most stable isotope currently known is given. In this case the mass is from <http://www.nndc.bnl.gov/amc/masstabes/Ame2003/mass.mas03> and the longest-lived isotope is from www.nndc.bnl.gov/ensdf/za_form.jsp. The exceptions are Th, Pa, and U, which do have characteristic terrestrial compositions. Atomic masses are relative to the mass of ^{12}C , defined to be exactly 12 unified atomic mass units (u) (approx. g/mole). Relative isotopic abundances often vary considerably, both in natural and commercial samples; this is reflected in the number of significant figures given. Previously confirmed element 112 was named Copernicium (Cp). The discovery of element 114 was confirmed in 2009. There are no other confirmed elements with $Z > 112$.

PERIODIC TABLE OF THE ELEMENTS																					
1 1A H Hydrogen 1.00794																	18 VIII He Helium 4.002602				
3 Li Lithium 6.941	4 IIA Be Beryllium 9.012182															5 III B Boron 10.811	6 IV C Carbon 12.0107	7 V N Nitrogen 14.0067	8 VI O Oxygen 15.9994	9 VII F Fluorine 18.9984032	10 Ne Neon 20.1797
11 Na Sodium 22.98976928	12 Mg Magnesium 24.3050	3 IIIB	4 IVB	5 VB	6 VIB	7 VIIB	8 VIII	9 VIII	10 VIII	11 IB	12 IIB	13 Al Aluminum 26.9815386	14 Si Silicon 28.0855	15 P Phosph. 30.973762	16 S Sulfur 32.065	17 Cl Chlorine 35.453	18 Ar Argon 39.948				
19 K Potassium 39.0983	20 Ca Calcium 40.078	21 Sc Scandium 44.955912	22 Ti Titanium 47.867	23 V Vanadium 50.9415	24 Cr Chromium 51.9961	25 Mn Manganese 54.938045	26 Fe Iron 55.845	27 Co Cobalt 58.933195	28 Ni Nickel 58.6934	29 Cu Copper 63.546	30 Zn Zinc 65.38	31 Ga Gallium 69.723	32 Ge German. 72.64	33 As Arsenic 74.92160	34 Se Selenium 78.96	35 Br Bromine 79.904	36 Kr Krypton 83.798				
37 Rb Rubidium 85.4678	38 Sr Strontium 87.62	39 Y Yttrium 88.90585	40 Zr Zirconium 91.224	41 Nb Niobium 92.90638	42 Mo Molybd. 95.96	43 Tc Technet. (97.90722)	44 Ru Ruthen. 101.07	45 Rh Rhodium 102.90550	46 Pd Palladium 106.42	47 Ag Silver 107.8682	48 Cd Cadmium 112.411	49 In Indium 114.818	50 Sn Tin 118.710	51 Sb Antimony 121.760	52 Te Tellurium 127.60	53 I Iodine 126.90447	54 Xe Xenon 131.293				
55 Cs Cesium 132.9054519	56 Ba Barium 137.327	57-71 Lanthe- nides	72 Hf Hafnium 178.49	73 Ta Tantalum 180.94788	74 W Tungsten 183.84	75 Re Rhenium 186.207	76 Os Osmium 190.23	77 Ir Iridium 192.217	78 Pt Platinum 195.084	79 Au Gold 196.966569	80 Hg Mercury 200.59	81 Tl Thallium 204.3833	82 Pb Lead 207.2	83 Bi Bismuth 208.98040	84 Po Polonium (208.98243)	85 At Astatine (209.98715)	86 Rn Radon (222.01758)				
87 Fr Francium (223.01974)	88 Ra Radium (226.02541)	89-103 Actinides	104 Rf Rutherford. (267.122)	105 Db Dubnium (268.125)	106 Sg Seaborg. (271.133)	107 Bh Bohrium (270.134)	108 Hs Hassium (269.134)	109 Mt Meitner. (276.151)	110 Ds Darmstadt. (281.162)	111 Rg Roentgen. (280.164)	112 Cp Copernicium (277)		114 (288)								

Lanthanide series	57 La Lanthan. 138.90547	58 Ce Cerium 140.116	59 Pr Praseodym. 140.90765	60 Nd Neodym. 144.242	61 Pm Prometh. (144.91275)	62 Sm Samarium 150.36	63 Eu Europium 151.964	64 Gd Gadolin. 157.25	65 Tb Terbium 158.92535	66 Dy Dyspros. 162.500	67 Ho Holmium 164.93032	68 Er Erbium 167.259	69 Tm Thulium 168.93421	70 Yb Ytterbium 173.054	71 Lu Lutetium 174.9668
Actinide series	89 Ac Actinium (227.02775)	90 Th Thorium 232.03806	91 Pa Protactin. 231.03588	92 U Uranium 238.02891	93 Np Neptunium (237.04817)	94 Pu Plutonium (244.06420)	95 Am Americ. (243.06138)	96 Cm Curium (247.07035)	97 Bk Berkelium (247.07031)	98 Cf Californ. (251.07959)	99 Es Einstein. (252.0830)	100 Fm Fermium (257.09510)	101 Md Mendelev. (258.09843)	102 No Nobelium (259.1010)	103 Lr Lawrenc. (262.110)

5. ELECTRONIC STRUCTURE OF THE ELEMENTS

Table 5.1. Reviewed 2005 by C.G. Wohl (LBNL). The electronic configurations and the ionization energies are from the NIST database, “Ground Levels and Ionization Energies for the Neutral Atoms,” W.C. Martin, A. Musgrove, S. Kotochigova, and J.E. Sansonetti (2003), <http://physics.nist.gov> (select “Physical Reference Data”). The electron configuration for, say, iron indicates an argon electronic core (see argon) plus six $3d$ electrons and two $4s$ electrons. The ionization energy is the least energy necessary to remove to infinity one electron from an atom of the element.

	Element	Electron configuration ($3d^5 =$ five $3d$ electrons, <i>etc.</i>)	Ground state $2S+1L_J$	Ionization energy (eV)
1	H Hydrogen	$1s$	$^2S_{1/2}$	13.5984
2	He Helium	$1s^2$	1S_0	24.5874
3	Li Lithium	(He) $2s$	$^2S_{1/2}$	5.3917
4	Be Beryllium	(He) $2s^2$	1S_0	9.3227
5	B Boron	(He) $2s^2 2p$	$^2P_{1/2}$	8.2980
6	C Carbon	(He) $2s^2 2p^2$	3P_0	11.2603
7	N Nitrogen	(He) $2s^2 2p^3$	$^4S_{3/2}$	14.5341
8	O Oxygen	(He) $2s^2 2p^4$	3P_2	13.6181
9	F Fluorine	(He) $2s^2 2p^5$	$^2P_{3/2}$	17.4228
10	Ne Neon	(He) $2s^2 2p^6$	1S_0	21.5645
11	Na Sodium	(Ne) $3s$	$^2S_{1/2}$	5.1391
12	Mg Magnesium	(Ne) $3s^2$	1S_0	7.6462
13	Al Aluminum	(Ne) $3s^2 3p$	$^2P_{1/2}$	5.9858
14	Si Silicon	(Ne) $3s^2 3p^2$	3P_0	8.1517
15	P Phosphorus	(Ne) $3s^2 3p^3$	$^4S_{3/2}$	10.4867
16	S Sulfur	(Ne) $3s^2 3p^4$	3P_2	10.3600
17	Cl Chlorine	(Ne) $3s^2 3p^5$	$^2P_{3/2}$	12.9676
18	Ar Argon	(Ne) $3s^2 3p^6$	1S_0	15.7596
19	K Potassium	(Ar) $4s$	$^2S_{1/2}$	4.3407
20	Ca Calcium	(Ar) $4s^2$	1S_0	6.1132
21	Sc Scandium	(Ar) $3d 4s^2$	$^2D_{3/2}$	6.5615
22	Ti Titanium	(Ar) $3d^2 4s^2$	3F_2	6.8281
23	V Vanadium	(Ar) $3d^3 4s^2$	$^4F_{3/2}$	6.7462
24	Cr Chromium	(Ar) $3d^5 4s$	7S_3	6.7665
25	Mn Manganese	(Ar) $3d^5 4s^2$	$^6S_{5/2}$	7.4340
26	Fe Iron	(Ar) $3d^6 4s^2$	5D_4	7.9024
27	Co Cobalt	(Ar) $3d^7 4s^2$	$^4F_{9/2}$	7.8810
28	Ni Nickel	(Ar) $3d^8 4s^2$	3F_4	7.6398
29	Cu Copper	(Ar) $3d^{10} 4s$	$^2S_{1/2}$	7.7264
30	Zn Zinc	(Ar) $3d^{10} 4s^2$	1S_0	9.3942
31	Ga Gallium	(Ar) $3d^{10} 4s^2 4p$	$^2P_{1/2}$	5.9993
32	Ge Germanium	(Ar) $3d^{10} 4s^2 4p^2$	3P_0	7.8994
33	As Arsenic	(Ar) $3d^{10} 4s^2 4p^3$	$^4S_{3/2}$	9.7886
34	Se Selenium	(Ar) $3d^{10} 4s^2 4p^4$	3P_2	9.7524
35	Br Bromine	(Ar) $3d^{10} 4s^2 4p^5$	$^2P_{3/2}$	11.8138
36	Kr Krypton	(Ar) $3d^{10} 4s^2 4p^6$	1S_0	13.9996
37	Rb Rubidium	(Kr) $5s$	$^2S_{1/2}$	4.1771
38	Sr Strontium	(Kr) $5s^2$	1S_0	5.6949
39	Y Yttrium	(Kr) $4d 5s^2$	$^2D_{3/2}$	6.2173
40	Zr Zirconium	(Kr) $4d^2 5s^2$	3F_2	6.6339
41	Nb Niobium	(Kr) $4d^4 5s$	$^6D_{1/2}$	6.7589
42	Mo Molybdenum	(Kr) $4d^5 5s$	7S_3	7.0924
43	Tc Technetium	(Kr) $4d^5 5s^2$	$^6S_{5/2}$	7.28
44	Ru Ruthenium	(Kr) $4d^7 5s$	5F_5	7.3605
45	Rh Rhodium	(Kr) $4d^8 5s$	$^4F_{9/2}$	7.4589
46	Pd Palladium	(Kr) $4d^{10}$	1S_0	8.3369
47	Ag Silver	(Kr) $4d^{10} 5s$	$^2S_{1/2}$	7.5762
48	Cd Cadmium	(Kr) $4d^{10} 5s^2$	1S_0	8.9938

49	In	Indium	(Kr) $4d^{10}5s^2$	$5p$		$^2P_{1/2}$	5.7864
50	Sn	Tin	(Kr) $4d^{10}5s^2$	$5p^2$		3P_0	7.3439
51	Sb	Antimony	(Kr) $4d^{10}5s^2$	$5p^3$		$^4S_{3/2}$	8.6084
52	Te	Tellurium	(Kr) $4d^{10}5s^2$	$5p^4$		3P_2	9.0096
53	I	Iodine	(Kr) $4d^{10}5s^2$	$5p^5$		$^2P_{3/2}$	10.4513
54	Xe	Xenon	(Kr) $4d^{10}5s^2$	$5p^6$		1S_0	12.1298
55	Cs	Cesium	(Xe)	$6s$		$^2S_{1/2}$	3.8939
56	Ba	Barium	(Xe)	$6s^2$		1S_0	5.2117
57	La	Lanthanum	(Xe)	$5d$	$6s^2$	$^2D_{3/2}$	5.5769
58	Ce	Cerium	(Xe) $4f$	$5d$	$6s^2$	1G_4	5.5387
59	Pr	Praseodymium	(Xe) $4f^3$		$6s^2$	$^4I_{9/2}$	5.473
60	Nd	Neodymium	(Xe) $4f^4$		$6s^2$	5I_4	5.5250
61	Pm	Promethium	(Xe) $4f^5$		$6s^2$	$^6H_{5/2}$	5.582
62	Sm	Samarium	(Xe) $4f^6$		$6s^2$	7F_0	5.6437
63	Eu	Europium	(Xe) $4f^7$		$6s^2$	$^8S_{7/2}$	5.6704
64	Gd	Gadolinium	(Xe) $4f^7$	$5d$	$6s^2$	9D_2	6.1498
65	Tb	Terbium	(Xe) $4f^9$		$6s^2$	$^6H_{15/2}$	5.8638
66	Dy	Dysprosium	(Xe) $4f^{10}$		$6s^2$	5I_8	5.9389
67	Ho	Holmium	(Xe) $4f^{11}$		$6s^2$	$^4I_{15/2}$	6.0215
68	Er	Erbium	(Xe) $4f^{12}$		$6s^2$	3H_6	6.1077
69	Tm	Thulium	(Xe) $4f^{13}$		$6s^2$	$^2F_{7/2}$	6.1843
70	Yb	Ytterbium	(Xe) $4f^{14}$		$6s^2$	1S_0	6.2542
71	Lu	Lutetium	(Xe) $4f^{14}5d$		$6s^2$	$^2D_{3/2}$	5.4259
72	Hf	Hafnium	(Xe) $4f^{14}5d^2$		$6s^2$	3F_2	6.8251
73	Ta	Tantalum	(Xe) $4f^{14}5d^3$		$6s^2$	$^4F_{3/2}$	7.5496
74	W	Tungsten	(Xe) $4f^{14}5d^4$		$6s^2$	5D_0	7.8640
75	Re	Rhenium	(Xe) $4f^{14}5d^5$		$6s^2$	$^6S_{5/2}$	7.8335
76	Os	Osmium	(Xe) $4f^{14}5d^6$		$6s^2$	5D_4	8.4382
77	Ir	Iridium	(Xe) $4f^{14}5d^7$		$6s^2$	$^4F_{9/2}$	8.9670
78	Pt	Platinum	(Xe) $4f^{14}5d^9$		$6s$	3D_3	8.9588
79	Au	Gold	(Xe) $4f^{14}5d^{10}6s$			$^2S_{1/2}$	9.2255
80	Hg	Mercury	(Xe) $4f^{14}5d^{10}6s^2$			1S_0	10.4375
81	Tl	Thallium	(Xe) $4f^{14}5d^{10}6s^2$		$6p$	$^2P_{1/2}$	6.1082
82	Pb	Lead	(Xe) $4f^{14}5d^{10}6s^2$		$6p^2$	3P_0	7.4167
83	Bi	Bismuth	(Xe) $4f^{14}5d^{10}6s^2$		$6p^3$	$^4S_{3/2}$	7.2855
84	Po	Polonium	(Xe) $4f^{14}5d^{10}6s^2$		$6p^4$	3P_2	8.414
85	At	Astatine	(Xe) $4f^{14}5d^{10}6s^2$		$6p^5$	$^2P_{3/2}$	
86	Rn	Radon	(Xe) $4f^{14}5d^{10}6s^2$		$6p^6$	1S_0	10.7485
87	Fr	Francium	(Rn)		$7s$	$^2S_{1/2}$	4.0727
88	Ra	Radium	(Rn)		$7s^2$	1S_0	5.2784
89	Ac	Actinium	(Rn)	$6d$	$7s^2$	$^2D_{3/2}$	5.17
90	Th	Thorium	(Rn)	$6d^2$	$7s^2$	3F_2	6.3067
91	Pa	Protactinium	(Rn) $5f^2$	$6d$	$7s^2$	$^4K_{11/2}^*$	5.89
92	U	Uranium	(Rn) $5f^3$	$6d$	$7s^2$	$^5L_6^*$	6.1941
93	Np	Neptunium	(Rn) $5f^4$	$6d$	$7s^2$	$^6L_{11/2}^*$	6.2657
94	Pu	Plutonium	(Rn) $5f^6$		$7s^2$	7F_0	6.0260
95	Am	Americium	(Rn) $5f^7$		$7s^2$	$^8S_{7/2}$	5.9738
96	Cm	Curium	(Rn) $5f^7$	$6d$	$7s^2$	9D_2	5.9914
97	Bk	Berkelium	(Rn) $5f^9$		$7s^2$	$^6H_{15/2}$	6.1979
98	Cf	Californium	(Rn) $5f^{10}$		$7s^2$	5I_8	6.2817
99	Es	Einsteinium	(Rn) $5f^{11}$		$7s^2$	$^4I_{15/2}$	6.42
100	Fm	Fermium	(Rn) $5f^{12}$		$7s^2$	3H_6	6.50
101	Md	Mendelevium	(Rn) $5f^{13}$		$7s^2$	$^2F_{7/2}$	6.58
102	No	Nobelium	(Rn) $5f^{14}$		$7s^2$	1S_0	6.65
103	Lr	Lawrencium	(Rn) $5f^{14}$		$7s^2$	$^2P_{1/2}^?$	4.9?
104	Rf	Rutherfordium	(Rn) $5f^{14}6d^2$		$7s^2?$	$^3F_2?$	6.0?

* The usual LS coupling scheme does not apply for these three elements. See the introductory note to the NIST table from which this table is taken.

6. ATOMIC AND NUCLEAR PROPERTIES OF MATERIALS

Table 6.1 Abridged from pdg.lbl.gov/AtomicNuclearProperties by D. E. Groom (2007). See web pages for more detail about entries in this table including chemical formulae, and for several hundred other entries. Quantities in parentheses are for NTP (20°C and 1 atm), and square brackets indicate quantities evaluated at STP. Boiling points are at 1 atm. Refractive indices n are evaluated at the sodium D line blend (589.2 nm); values $\gg 1$ in brackets are for $(n - 1) \times 10^6$ (gases).

Material	Z	A	$\langle Z/A \rangle$	Nucl.coll. length λ_T {g cm ⁻² }	Nucl.inter. length λ_I {g cm ⁻² }	Rad.len. X_0 {g cm ⁻² }	$dE/dx _{\min}$ { MeV g ⁻¹ cm ² }	Density {g cm ⁻³ } {gℓ ⁻¹ }	Melting point (K)	Boiling point (K)	Refract. index (@ Na D)
H ₂	1	1.00794(7)	0.99212	42.8	52.0	63.04	(4.103)	0.071(0.084)	13.81	20.28	1.11[132.]
D ₂	1	2.01410177803(8)	0.49650	51.3	71.8	125.97	(2.053)	0.169(0.168)	18.7	23.65	1.11[138.]
He	2	4.002602(2)	0.49967	51.8	71.0	94.32	(1.937)	0.125(0.166)		4.220	1.02[35.0]
Li	3	6.941(2)	0.43221	52.2	71.3	82.78	1.639	0.534	453.6	1615.	
Be	4	9.012182(3)	0.44384	55.3	77.8	65.19	1.595	1.848	1560.	2744.	
C diamond	6	12.0107(8)	0.49955	59.2	85.8	42.70	1.725	3.520			2.42
C graphite	6	12.0107(8)	0.49955	59.2	85.8	42.70	1.742	2.210			
N ₂	7	14.0067(2)	0.49976	61.1	89.7	37.99	(1.825)	0.807(1.165)	63.15	77.29	1.20[298.]
O ₂	8	15.9994(3)	0.50002	61.3	90.2	34.24	(1.801)	1.141(1.332)	54.36	90.20	1.22[271.]
F ₂	9	18.9984032(5)	0.47372	65.0	97.4	32.93	(1.676)	1.507(1.580)	53.53	85.03	[195.]
Ne	10	20.1797(6)	0.49555	65.7	99.0	28.93	(1.724)	1.204(0.839)	24.56	27.07	1.09[67.1]
Al	13	26.9815386(8)	0.48181	69.7	107.2	24.01	1.615	2.699	933.5	2792.	
Si	14	28.0855(3)	0.49848	70.2	108.4	21.82	1.664	2.329	1687.	3538.	3.95
Cl ₂	17	35.453(2)	0.47951	73.8	115.7	19.28	(1.630)	1.574(2.980)	171.6	239.1	[773.]
Ar	18	39.948(1)	0.45059	75.7	119.7	19.55	(1.519)	1.396(1.662)	83.81	87.26	1.23[281.]
Ti	22	47.867(1)	0.45961	78.8	126.2	16.16	1.477	4.540	1941.	3560.	
Fe	26	55.845(2)	0.46557	81.7	132.1	13.84	1.451	7.874	1811.	3134.	
Cu	29	63.546(3)	0.45636	84.2	137.3	12.86	1.403	8.960	1358.	2835.	
Ge	32	72.64(1)	0.44053	86.9	143.0	12.25	1.370	5.323	1211.	3106.	
Sn	50	118.710(7)	0.42119	98.2	166.7	8.82	1.263	7.310	505.1	2875.	
Xe	54	131.293(6)	0.41129	100.8	172.1	8.48	(1.255)	2.953(5.483)	161.4	165.1	1.39[701.]
W	74	183.84(1)	0.40252	110.4	191.9	6.76	1.145	19.300	3695.	5828.	
Pt	78	195.084(9)	0.39983	112.2	195.7	6.54	1.128	21.450	2042.	4098.	
Au	79	196.966569(4)	0.40108	112.5	196.3	6.46	1.134	19.320	1337.	3129.	
Pb	82	207.2(1)	0.39575	114.1	199.6	6.37	1.122	11.350	600.6	2022.	
U	92	[238.02891(3)]	0.38651	118.6	209.0	6.00	1.081	18.950	1408.	4404.	
Air (dry, 1 atm)			0.49919	61.3	90.1	36.62	(1.815)	(1.205)		78.80	
Shielding concrete			0.50274	65.1	97.5	26.57	1.711	2.300			
Borosilicate glass (Pyrex)			0.49707	64.6	96.5	28.17	1.696	2.230			
Lead glass			0.42101	95.9	158.0	7.87	1.255	6.220			
Standard rock			0.50000	66.8	101.3	26.54	1.688	2.650			
Methane (CH ₄)			0.62334	54.0	73.8	46.47	(2.417)	(0.667)	90.68	111.7	[444.]
Ethane (C ₂ H ₆)			0.59861	55.0	75.9	45.66	(2.304)	(1.263)	90.36	184.5	
Propane (C ₃ H ₈)			0.58962	55.3	76.7	45.37	(2.262)	0.493(1.868)	85.52	231.0	
Butane (C ₄ H ₁₀)			0.59497	55.5	77.1	45.23	(2.278)	(2.489)	134.9	272.6	
Octane (C ₈ H ₁₈)			0.57778	55.8	77.8	45.00	2.123	0.703	214.4	398.8	
Paraffin (CH ₃ (CH ₂) _n ≈23CH ₃)			0.57275	56.0	78.3	44.85	2.088	0.930			
Nylon (type 6, 6/6)			0.54790	57.5	81.6	41.92	1.973	1.18			
Polycarbonate (Lexan)			0.52697	58.3	83.6	41.50	1.886	1.20			
Polyethylene ([CH ₂ CH ₂] _n)			0.57034	56.1	78.5	44.77	2.079	0.89			
Polyethylene terephthalate (Mylar)			0.52037	58.9	84.9	39.95	1.848	1.40			
Polyimide film (Kapton)			0.51264	59.2	85.5	40.58	1.820	1.42			
Polymethylmethacrylate (acrylic)			0.53937	58.1	82.8	40.55	1.929	1.19			1.49
Polypropylene			0.55998	56.1	78.5	44.77	2.041	0.90			
Polystyrene ([C ₆ H ₅ CHCH ₂] _n)			0.53768	57.5	81.7	43.79	1.936	1.06			1.59
Polytetrafluoroethylene (Teflon)			0.47992	63.5	94.4	34.84	1.671	2.20			
Polyvinyltoluene			0.54141	57.3	81.3	43.90	1.956	1.03			1.58
Aluminum oxide (sapphire)			0.49038	65.5	98.4	27.94	1.647	3.970	2327.	3273.	1.77
Barium fluoride (BaF ₂)			0.42207	90.8	149.0	9.91	1.303	4.893	1641.	2533.	1.47
Bismuth germanate (BGO)			0.42065	96.2	159.1	7.97	1.251	7.130	1317.		2.15
Carbon dioxide gas (CO ₂)			0.49989	60.7	88.9	36.20	1.819	(1.842)			[449.]
Solid carbon dioxide (dry ice)			0.49989	60.7	88.9	36.20	1.787	1.563	Sublimes at 194.7 K		
Cesium iodide (CsI)			0.41569	100.6	171.5	8.39	1.243	4.510	894.2	1553.	1.79
Lithium fluoride (LiF)			0.46262	61.0	88.7	39.26	1.614	2.635	1121.	1946.	1.39
Lithium hydride (LiH)			0.50321	50.8	68.1	79.62	1.897	0.820	965.		
Lead tungstate (PbWO ₄)			0.41315	100.6	168.3	7.39	1.229	8.300	1403.		2.20
Silicon dioxide (SiO ₂ , fused quartz)			0.49930	65.2	97.8	27.05	1.699	2.200	1986.	3223.	1.46
Sodium chloride (NaCl)			0.55509	71.2	110.1	21.91	1.847	2.170	1075.	1738.	1.54
Sodium iodide (NaI)			0.42697	93.1	154.6	9.49	1.305	3.667	933.2	1577.	1.77
Water (H ₂ O)			0.55509	58.5	83.3	36.08	1.992	1.000(0.756)	273.1	373.1	1.33
Silica aerogel			0.50093	65.0	97.3	27.25	1.740	0.200	(0.03 H ₂ O, 0.97 SiO ₂)		

Material	Dielectric constant ($\kappa = \epsilon/\epsilon_0$) () is $(\kappa-1)\times 10^6$ for gas	Young's modulus [10^6 psi]	Coeff. of thermal expansion [10^{-6} cm/cm- $^{\circ}$ C]	Specific heat [cal/g- $^{\circ}$ C]	Electrical resistivity [$\mu\Omega$ cm(@ $^{\circ}$ C)]	Thermal conductivity [cal/cm- $^{\circ}$ C-sec]
H ₂	(253.9)	—	—	—	—	—
He	(64)	—	—	—	—	—
Li	—	—	56	0.86	8.55(0 $^{\circ}$)	0.17
Be	—	37	12.4	0.436	5.885(0 $^{\circ}$)	0.38
C	—	0.7	0.6–4.3	0.165	1375(0 $^{\circ}$)	0.057
N ₂	(548.5)	—	—	—	—	—
O ₂	(495)	—	—	—	—	—
Ne	(127)	—	—	—	—	—
Al	—	10	23.9	0.215	2.65(20 $^{\circ}$)	0.53
Si	11.9	16	2.8–7.3	0.162	—	0.20
Ar	(517)	—	—	—	—	—
Ti	—	16.8	8.5	0.126	50(0 $^{\circ}$)	—
Fe	—	28.5	11.7	0.11	9.71(20 $^{\circ}$)	0.18
Cu	—	16	16.5	0.092	1.67(20 $^{\circ}$)	0.94
Ge	16.0	—	5.75	0.073	—	0.14
Sn	—	6	20	0.052	11.5(20 $^{\circ}$)	0.16
Xe	—	—	—	—	—	—
W	—	50	4.4	0.032	5.5(20 $^{\circ}$)	0.48
Pt	—	21	8.9	0.032	9.83(0 $^{\circ}$)	0.17
Pb	—	2.6	29.3	0.038	20.65(20 $^{\circ}$)	0.083
U	—	—	36.1	0.028	29(20 $^{\circ}$)	0.064

7. ELECTROMAGNETIC RELATIONS

Revised September 2005 by H.G. Spieler (LBNL).

Quantity	Gaussian CGS	SI
Conversion factors:		
Charge:	$2.997\,924\,58 \times 10^9$ esu	$= 1\text{ C} = 1\text{ A s}$
Potential:	$(1/299.792\,458)$ statvolt (ergs/esu)	$= 1\text{ V} = 1\text{ J C}^{-1}$
Magnetic field:	10^4 gauss = 10^4 dyne/esu	$= 1\text{ T} = 1\text{ N A}^{-1}\text{m}^{-1}$
	$\mathbf{F} = q(\mathbf{E} + \frac{\mathbf{v}}{c} \times \mathbf{B})$	$\mathbf{F} = q(\mathbf{E} + \mathbf{v} \times \mathbf{B})$
	$\nabla \cdot \mathbf{D} = 4\pi\rho$ $\nabla \times \mathbf{H} - \frac{1}{c} \frac{\partial \mathbf{D}}{\partial t} = \frac{4\pi}{c} \mathbf{J}$ $\nabla \cdot \mathbf{B} = 0$ $\nabla \times \mathbf{E} + \frac{1}{c} \frac{\partial \mathbf{B}}{\partial t} = 0$	$\nabla \cdot \mathbf{D} = \rho$ $\nabla \times \mathbf{H} - \frac{\partial \mathbf{D}}{\partial t} = \mathbf{J}$ $\nabla \cdot \mathbf{B} = 0$ $\nabla \times \mathbf{E} + \frac{\partial \mathbf{B}}{\partial t} = 0$
Constitutive relations:	$\mathbf{D} = \mathbf{E} + 4\pi\mathbf{P}$, $\mathbf{H} = \mathbf{B} - 4\pi\mathbf{M}$	$\mathbf{D} = \epsilon_0\mathbf{E} + \mathbf{P}$, $\mathbf{H} = \mathbf{B}/\mu_0 - \mathbf{M}$
Linear media:	$\mathbf{D} = \epsilon\mathbf{E}$, $\mathbf{H} = \mathbf{B}/\mu$ 1 1	$\mathbf{D} = \epsilon\mathbf{E}$, $\mathbf{H} = \mathbf{B}/\mu$ $\epsilon_0 = 8.854\,187 \dots \times 10^{-12}$ F m ⁻¹ $\mu_0 = 4\pi \times 10^{-7}$ N A ⁻²
	$\mathbf{E} = -\nabla V - \frac{1}{c} \frac{\partial \mathbf{A}}{\partial t}$ $\mathbf{B} = \nabla \times \mathbf{A}$	$\mathbf{E} = -\nabla V - \frac{\partial \mathbf{A}}{\partial t}$ $\mathbf{B} = \nabla \times \mathbf{A}$
	$V = \sum_{\text{charges}} \frac{q_i}{r_i} = \int \frac{\rho(\mathbf{r}')}{ \mathbf{r} - \mathbf{r}' } d^3x'$ $\mathbf{A} = \frac{1}{c} \oint \frac{I d\boldsymbol{\ell}}{ \mathbf{r} - \mathbf{r}' } = \frac{1}{c} \int \frac{\mathbf{J}(\mathbf{r}')}{ \mathbf{r} - \mathbf{r}' } d^3x'$	$V = \frac{1}{4\pi\epsilon_0} \sum_{\text{charges}} \frac{q_i}{r_i} = \frac{1}{4\pi\epsilon_0} \int \frac{\rho(\mathbf{r}')}{ \mathbf{r} - \mathbf{r}' } d^3x'$ $\mathbf{A} = \frac{\mu_0}{4\pi} \oint \frac{I d\boldsymbol{\ell}}{ \mathbf{r} - \mathbf{r}' } = \frac{\mu_0}{4\pi} \int \frac{\mathbf{J}(\mathbf{r}')}{ \mathbf{r} - \mathbf{r}' } d^3x'$
	$\mathbf{E}'_{\parallel} = \mathbf{E}_{\parallel}$ $\mathbf{E}'_{\perp} = \gamma(\mathbf{E}_{\perp} + \frac{1}{c}\mathbf{v} \times \mathbf{B})$ $\mathbf{B}'_{\parallel} = \mathbf{B}_{\parallel}$ $\mathbf{B}'_{\perp} = \gamma(\mathbf{B}_{\perp} - \frac{1}{c}\mathbf{v} \times \mathbf{E})$	$\mathbf{E}'_{\parallel} = \mathbf{E}_{\parallel}$ $\mathbf{E}'_{\perp} = \gamma(\mathbf{E}_{\perp} + \mathbf{v} \times \mathbf{B})$ $\mathbf{B}'_{\parallel} = \mathbf{B}_{\parallel}$ $\mathbf{B}'_{\perp} = \gamma(\mathbf{B}_{\perp} - \frac{1}{c^2}\mathbf{v} \times \mathbf{E})$
	$\frac{1}{4\pi\epsilon_0} = c^2 \times 10^{-7} \text{ N A}^{-2} = 8.987\,55 \dots \times 10^9 \text{ m F}^{-1}$; $\frac{\mu_0}{4\pi} = 10^{-7} \text{ N A}^{-2}$; $c = \frac{1}{\sqrt{\mu_0\epsilon_0}} = 2.997\,924\,58 \times 10^8 \text{ m s}^{-1}$	

7.1. Impedances (SI units)

ρ = resistivity at room temperature in $10^{-8} \Omega \text{ m}$:
 ~ 1.7 for Cu ~ 5.5 for W
 ~ 2.4 for Au ~ 73 for SS 304
 ~ 2.8 for Al ~ 100 for Nichrome
(Al alloys may have double the Al value.)

For alternating currents, instantaneous current I , voltage V , angular frequency ω :

$$V = V_0 e^{j\omega t} = ZI. \quad (7.1)$$

Impedance of self-inductance L : $Z = j\omega L$.

Impedance of capacitance C : $Z = 1/j\omega C$.

Impedance of free space: $Z = \sqrt{\mu_0/\epsilon_0} = 376.7 \Omega$.

High-frequency surface impedance of a good conductor:

$$Z = \frac{(1+j)\rho}{\delta}, \quad \text{where } \delta = \text{skin depth}; \quad (7.2)$$

$$\delta = \sqrt{\frac{\rho}{\pi\nu\mu}} \approx \frac{6.6 \text{ cm}}{\sqrt{\nu \text{ (Hz)}}} \quad \text{for Cu}. \quad (7.3)$$

7.2. Capacitors, inductors, and transmission Lines

The capacitance between two parallel plates of area A spaced by the distance d and enclosing a medium with the dielectric constant ϵ is

$$C = K\epsilon A/d, \quad (7.4)$$

where the correction factor K depends on the extent of the fringing field. If the dielectric fills the capacitor volume without extending beyond the electrodes, the correction factor $K \approx 0.8$ for capacitors of typical geometry.

The inductance at high frequencies of a straight wire whose length ℓ is much greater than the wire diameter d is

$$L \approx 2.0 \left[\frac{\text{nH}}{\text{cm}} \right] \cdot \ell \left(\ln \left(\frac{4\ell}{d} \right) - 1 \right). \quad (7.5)$$

For very short wires, representative of vias in a printed circuit board, the inductance is

$$L(\text{in nH}) \approx \ell/d. \quad (7.6)$$

A transmission line is a pair of conductors with inductance L and capacitance C . The characteristic impedance $Z = \sqrt{L/C}$ and the phase velocity $v_p = 1/\sqrt{LC} = 1/\sqrt{\mu\epsilon}$, which decreases with the inverse square root of the dielectric constant of the medium. Typical coaxial and ribbon cables have a propagation delay of about 5 ns/cm. The impedance of a coaxial cable with outer diameter D and inner diameter d is

$$Z = 60 \Omega \cdot \frac{1}{\sqrt{\epsilon_r}} \ln \frac{D}{d}, \quad (7.7)$$

where the relative dielectric constant $\epsilon_r = \epsilon/\epsilon_0$. A pair of parallel wires of diameter d and spacing $a > 2.5d$ has the impedance

$$Z = 120 \Omega \cdot \frac{1}{\sqrt{\epsilon_r}} \ln \frac{2a}{d}. \quad (7.8)$$

This yields the impedance of a wire at a spacing h above a ground plane,

$$Z = 60 \Omega \cdot \frac{1}{\sqrt{\epsilon_r}} \ln \frac{4h}{d}. \quad (7.9)$$

A common configuration utilizes a thin rectangular conductor above a ground plane with an intermediate dielectric (microstrip). Detailed calculations for this and other transmission line configurations are given by Gunston.*

7.3. Synchrotron radiation (CGS units)

For a particle of charge e , velocity $v = \beta c$, and energy $E = \gamma mc^2$, traveling in a circular orbit of radius R , the classical energy loss per revolution δE is

$$\delta E = \frac{4\pi}{3} \frac{e^2}{R} \beta^3 \gamma^4. \quad (7.10)$$

For high-energy electrons or positrons ($\beta \approx 1$), this becomes

$$\delta E \text{ (in MeV)} \approx 0.0885 [E(\text{in GeV})]^4 / R(\text{in m}). \quad (7.11)$$

For $\gamma \gg 1$, the energy radiated per revolution into the photon energy interval $d(\hbar\omega)$ is

$$dI = \frac{8\pi}{9} \alpha \gamma F(\omega/\omega_c) d(\hbar\omega), \quad (7.12)$$

where $\alpha = e^2/\hbar c$ is the fine-structure constant and

$$\omega_c = \frac{3\gamma^3 c}{2R} \quad (7.13)$$

is the critical frequency. The normalized function $F(y)$ is

$$F(y) = \frac{9}{8\pi} \sqrt{3} y \int_y^\infty K_{5/3}(x) dx, \quad (7.14)$$

where $K_{5/3}(x)$ is a modified Bessel function of the third kind. For electrons or positrons,

$$\hbar\omega_c \text{ (in keV)} \approx 2.22 [E(\text{in GeV})]^3 / R(\text{in m}). \quad (7.15)$$

Fig. 7.1 shows $F(y)$ over the important range of y .

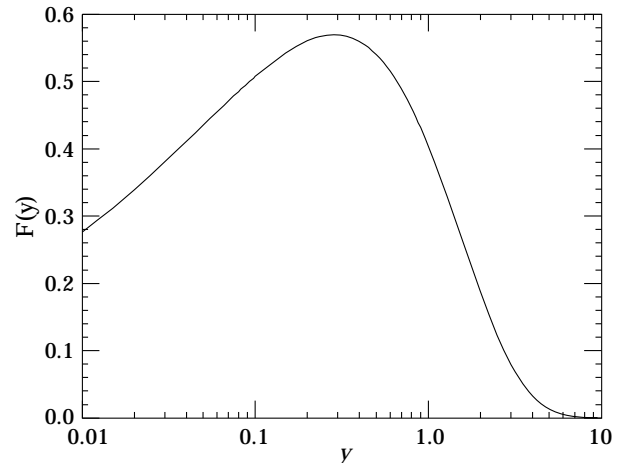


Figure 7.1: The normalized synchrotron radiation spectrum $F(y)$.

For $\gamma \gg 1$ and $\omega \ll \omega_c$,

$$\frac{dI}{d(\hbar\omega)} \approx 3.3\alpha (\omega R/c)^{1/3}, \quad (7.16)$$

whereas for

$$\gamma \gg 1 \text{ and } \omega \gtrsim 3\omega_c,$$

$$\frac{dI}{d(\hbar\omega)} \approx \sqrt{\frac{3\pi}{2}} \alpha \gamma \left(\frac{\omega}{\omega_c} \right)^{1/2} e^{-\omega/\omega_c} \left[1 + \frac{55}{72} \frac{\omega_c}{\omega} + \dots \right]. \quad (7.17)$$

The radiation is confined to angles $\lesssim 1/\gamma$ relative to the instantaneous direction of motion. For $\gamma \gg 1$, where Eq. (7.12) applies, the mean number of photons emitted per revolution is

$$N_\gamma = \frac{5\pi}{\sqrt{3}} \alpha \gamma, \quad (7.18)$$

and the mean energy per photon is

$$\langle \hbar\omega \rangle = \frac{8}{15\sqrt{3}} \hbar\omega_c. \quad (7.19)$$

When $\langle \hbar\omega \rangle \gtrsim O(E)$, quantum corrections are important.

* M.A.R. Gunston. Microwave Transmission Line Data, Noble Publishing Corp., Atlanta (1997) ISBN 1-884932-57-6, TK6565.T73G85.

See J.D. Jackson, *Classical Electrodynamics*, 3rd edition (John Wiley & Sons, New York, 1998) for more formulae and details. (Note that earlier editions had ω_c twice as large as Eq. (7.13).)

8. NAMING SCHEME FOR HADRONS

Revised 2004 by M. Roos (University of Finland) and C.G. Wohl (LBNL).

8.1. Introduction

We introduced in the 1986 edition [1] a new naming scheme for the hadrons. Changes from older terminology affected mainly the heavier mesons made of the light (u , d , and s) quarks. Old and new names were listed alongside until 1994. Names also change from edition to edition because some characteristic like mass or spin changes. The Summary Tables give both the new and old names whenever a change occurred.

8.2. “Neutral-flavor” mesons ($S=C=B=T=0$)

Table 8.1 shows the names for mesons having the strangeness and all heavy-flavor quantum numbers equal to zero. The scheme is designed for all ordinary non-exotic mesons, but it will work for many exotic types too, if needed.

Table 8.1: Symbols for mesons with the strangeness and all heavy-flavor quantum numbers equal to zero.

J^{PC}	$\begin{cases} 0^{-+} \\ 2^{-+} \\ \vdots \end{cases}$	$\begin{cases} 1^{+-} \\ 3^{+-} \\ \vdots \end{cases}$	$\begin{cases} 1^{--} \\ 2^{--} \\ \vdots \end{cases}$	$\begin{cases} 0^{++} \\ 1^{++} \\ \vdots \end{cases}$	
$q\bar{q}$ content	$2^{S+1}L_J$	${}^1(L\text{ even})_J$	${}^1(L\text{ odd})_J$	${}^3(L\text{ even})_J$	${}^3(L\text{ odd})_J$
$u\bar{d}, u\bar{u} - d\bar{d}, d\bar{u}$ ($I=1$)	π	b	ρ	a	
$d\bar{d} + u\bar{u}$ and/or $s\bar{s}$ } ($I=0$)	η, η'	h, h'	ω, ϕ	f, f'	
$c\bar{c}$	η_c	h_c	ψ^\dagger	χ_c	
$b\bar{b}$	η_b	h_b	Υ	χ_b	
$t\bar{t}$	η_t	h_t	θ	χ_t	

[†]The J/ψ remains the J/ψ .

First, we assign names to those states with quantum numbers compatible with being $q\bar{q}$ states. The rows of the Table give the possible $q\bar{q}$ content. The columns give the possible parity/charge-conjugation states,

$$PC = --, +-, --, \text{ and } ++;$$

these combinations correspond one-to-one with the angular-momentum state ${}^{2S+1}L_J$ of the $q\bar{q}$ system being

$${}^1(L\text{ even})_J, {}^1(L\text{ odd})_J, {}^3(L\text{ even})_J, \text{ or } {}^3(L\text{ odd})_J.$$

Here S , L , and J are the spin, orbital, and total angular momenta of the $q\bar{q}$ system. The quantum numbers are related by $P = (-1)^{L+1}$, $C = (-1)^{L+S}$, and G parity $= (-1)^{L+S+I}$, where of course the C quantum number is only relevant to neutral mesons.

The entries in the Table give the meson names. The spin J is added as a subscript except for pseudoscalar and vector mesons, and the mass is added in parentheses for mesons that decay strongly. However, for the lightest meson resonances, we omit the mass.

Measurements of the mass, quark content (where relevant), and quantum numbers I , J , P , and C (or G) of a meson thus fix its symbol. Conversely, these properties may be inferred unambiguously from the symbol.

If the main symbol cannot be assigned because the quantum numbers are unknown, X is used. Sometimes it is not known whether a meson is mainly the isospin-0 mix of $u\bar{u}$ and $d\bar{d}$ or is mainly $s\bar{s}$. A prime (or pair ω , ϕ) may be used to distinguish two such mixing states.

We follow custom and use spectroscopic names such as $\Upsilon(1S)$ as the primary name for most of those ψ , Υ , and χ states whose spectroscopic identity is known. We use the form $\Upsilon(9460)$ as an alternative, and as the primary name when the spectroscopic identity is not known.

Names are assigned for $t\bar{t}$ mesons, although the top quark is evidently so heavy that it is expected to decay too rapidly for bound states to form.

Gluonium states or other mesons that are not $q\bar{q}$ states are, if the quantum numbers are *not* exotic, to be named just as are the $q\bar{q}$ mesons. Such states will probably be difficult to distinguish from $q\bar{q}$ states and will likely mix with them, and we make no attempt to distinguish those “mostly gluonium” from those “mostly $q\bar{q}$.”

An “exotic” meson with J^{PC} quantum numbers that a $q\bar{q}$ system cannot have, namely $J^{PC} = 0^{--}, 0^{+-}, 1^{-+}, 2^{+-}, 3^{-+}, \dots$, would use the same symbol as does an ordinary meson with all the same quantum numbers as the exotic meson except for the C parity. But then the J subscript may still distinguish it; for example, an isospin-0 1^{-+} meson could be denoted ω_1 .

8.3. Mesons with nonzero S , C , B , and/or T

Since the strangeness or a heavy flavor of these mesons is nonzero, none of them are eigenstates of charge conjugation, and in each of them one of the quarks is heavier than the other. The rules are:

1. The main symbol is an upper-case italic letter indicating the heavier quark as follows:

$$s \rightarrow \bar{K} \quad c \rightarrow D \quad b \rightarrow \bar{B} \quad t \rightarrow T.$$

We use the convention that *the flavor and the charge of a quark have the same sign*. Thus the strangeness of the s quark is negative, the charm of the c quark is positive, and the bottom of the b quark is negative. In addition, I_3 of the u and d quarks are positive and negative, respectively. The effect of this convention is as follows: *Any flavor carried by a charged meson has the same sign as its charge*. Thus the K^+ , D^+ , and B^+ have positive strangeness, charm, and bottom, respectively, and all have positive I_3 . The D_s^+ has positive charm *and* strangeness. Furthermore, the $\Delta(\text{flavor}) = \Delta Q$ rule, best known for the kaons, applies to every flavor.

2. If the lighter quark is not a u or a d quark, its identity is given by a subscript. The D_s^+ is an example.
3. If the spin-parity is in the “normal” series, $J^P = 0^+, 1^-, 2^+, \dots$, a superscript “*” is added.
4. The spin is added as a subscript except for pseudoscalar or vector mesons.

8.4. Ordinary (3-quark) baryons

The symbols N , Δ , Λ , Σ , Ξ , and Ω used for more than 30 years for the baryons made of light quarks (u , d , and s quarks) tell the isospin and quark content, and the same information is conveyed by the symbols used for the baryons containing one or more heavy quarks (c and b quarks). The rules are:

1. Baryons with *three* u and/or d quarks are N 's (isospin 1/2) or Δ 's (isospin 3/2).
2. Baryons with *two* u and/or d quarks are Λ 's (isospin 0) or Σ 's (isospin 1). If the third quark is a c , b , or t quark, its identity is given by a subscript.
3. Baryons with *one* u or d quark are Ξ 's (isospin 1/2). One or two subscripts are used if one or both of the remaining quarks are heavy: thus Ξ_c , Ξ_{cc} , Ξ_b , *etc.**
4. Baryons with *no* u or d quarks are Ω 's (isospin 0), and subscripts indicate any heavy-quark content.
5. A baryon that decays strongly has its mass as part of its name. Thus p , $\Sigma^-, \Omega^-, \Lambda_c^+$, *etc.*, but $\Delta(1232)^0, \Sigma(1385)^-, \Xi_c(2645)^+$, *etc.*

In short, the number of u plus d quarks together with the isospin determine the main symbol, and subscripts indicate any content of heavy quarks. A Σ always has isospin 1, an Ω always has isospin 0, *etc.*

8.5. Exotic baryons

In 2003, several experiments reported finding a strangeness $S = +1$, charge $Q = +1$ baryon, and one experiment reported finding an $S = -2$, $Q = -2$ baryon. Baryons with such quantum numbers cannot be made from three quarks, and thus they are exotic. The $S = +1$ baryon, which once would have been called a Z , was quickly dubbed the $\Theta(1540)^+$, and we proposed to name the $S = -2$ baryon the $\Phi(1860)$. However, these “discoveries” were then completely ruled out by many experiments with far larger statistics: See our 2008 *Review* [2].

Footnote and Reference:

- * Sometimes a prime is necessary to distinguish two Ξ_c 's in the same $SU(n)$ multiplet. See the “Note on Charmed Baryons” in the Charmed Baryon Listings.
1. Particle Data Group: M. Aguilar-Benitez *et al.*, Phys. Lett. **170B** (1986).
 2. Particle Data Group: C. Amsler *et al.*, Phys. Lett. **B667**, 1 (2008).

9. QUANTUM CHROMODYNAMICS

Written October 2009 by G. Dissertori (ETH, Zurich) and G.P. Salam (LPTHE, Paris).

9.1. Basics

Quantum Chromodynamics (QCD), the gauge field theory that describes the strong interactions of colored quarks and gluons, is the SU(3) component of the SU(3)×SU(2)×U(1) Standard Model of Particle Physics.

The Lagrangian of QCD is given by

$$\mathcal{L} = \sum_q \bar{\psi}_{q,a} (i\gamma^\mu \partial_\mu \delta_{ab} - g_s \gamma^\mu t_{ab}^C A_\mu^C - m_q \delta_{ab}) \psi_{q,b} - \frac{1}{4} F_{\mu\nu}^A F^{A\mu\nu}, \quad (9.1)$$

where repeated indices are summed over. The γ^μ are the Dirac γ -matrices. The $\psi_{q,a}$ are quark-field spinors for a quark of flavor q and mass m_q , with a color-index a that runs from $a = 1$ to $N_c = 3$, *i.e.* quarks come in three “colors.” Quarks are said to be in the fundamental representation of the SU(3) color group.

The A_μ^C correspond to the gluon fields, with C running from 1 to $N_c^2 - 1 = 8$, *i.e.* there are eight kinds of gluon. Gluons are said to be in the adjoint representation of the SU(3) color group. The t_{ab}^C correspond to eight 3×3 matrices and are the generators of the SU(3) group (cf. the section on “SU(3) isoscalar factors and representation matrices” in this *Review* with $t_{ab}^C \equiv \lambda_{ab}^C/2$). They encode the fact that a gluon’s interaction with a quark rotates the quark’s color in SU(3) space. The quantity g_s is the QCD coupling constant. Finally, the field tensor $F_{\mu\nu}^A$ is given by

$$F_{\mu\nu}^A = \partial_\mu A_\nu^A - \partial_\nu A_\mu^A - g_s f_{ABC} A_\mu^B A_\nu^C \quad [t^A, t^B] = i f_{ABC} t^C, \quad (9.2)$$

where the f_{ABC} are the structure constants of the SU(3) group.

Neither quarks nor gluons are observed as free particles. Hadrons are color-singlet (*i.e.* color-neutral) combinations of quarks, anti-quarks, and gluons.

Ab-initio predictive methods for QCD include lattice gauge theory and perturbative expansions in the coupling. The Feynman rules of QCD involve a quark-antiquark-gluon ($q\bar{q}g$) vertex, a 3-gluon vertex (both proportional to g_s), and a 4-gluon vertex (proportional to g_s^2). A full set of Feynman rules is to be found for example in Ref. 1.

Useful color-algebra relations include: $t_{ab}^A t_{bc}^A = C_F \delta_{ac}$, where $C_F \equiv (N_c^2 - 1)/(2N_c) = 4/3$ is the color-factor (“Casimir”) associated with gluon emission from a quark; $f^{ACD} f^{BCD} = C_A \delta_{AB}$ where $C_A \equiv N_c = 3$ is the color-factor associated with gluon emission from a gluon; $t_{ab}^A t_{ab}^B = T_R \delta_{AB}$, where $T_R = 1/2$ is the color-factor for a gluon to split to a $q\bar{q}$ pair.

The fundamental parameters of QCD are the coupling g_s (or $\alpha_s = \frac{g_s^2}{4\pi}$) and the quark masses m_q .

This review will concentrate mainly on perturbative aspects of QCD as they relate to collider physics. Related textbooks include Refs. 1–3. Some discussion of non-perturbative aspects, including lattice QCD, is to be found in the reviews on “Quark Masses” and “The CKM quark-mixing matrix” in this *Review*. Lattice-QCD textbooks and lecture notes include Refs. 4–6, while recent developments are summarized for example in Ref. 7. For a review of some of the QCD issues in heavy-ion physics, see for example Ref. 8.

9.1.1. Running coupling :

In the framework of perturbative QCD (pQCD), predictions for observables are expressed in terms of the renormalized coupling $\alpha_s(\mu_R^2)$, a function of an (unphysical) renormalization scale μ_R . When one takes μ_R close to the scale of the momentum transfer Q in a given process, then $\alpha_s(\mu_R^2 \simeq Q^2)$ is indicative of the effective strength of the strong interaction in that process.

The coupling satisfies the following renormalization group equation (RGE):

$$\mu_R^2 \frac{d\alpha_s}{d\mu_R^2} = \beta(\alpha_s) = -(b_0 \alpha_s^2 + b_1 \alpha_s^3 + b_2 \alpha_s^4 + \dots) \quad (9.3)$$

where $b_0 = (11C_A - 4n_f T_R)/(12\pi) = (33 - 2n_f)/(12\pi)$ is referred to as the 1-loop beta-function coefficient, the 2-loop coefficient is $b_1 = (17C_A^2 - n_f T_R(10C_A + 6C_F))/(24\pi^2) = (153 - 19n_f)/(24\pi^2)$, and the 3-loop coefficient is $b_2 = (2857 - \frac{5033}{9}n_f + \frac{325}{27}n_f^2)/(128\pi^3)$. The 4-loop coefficient, b_3 , is to be found in Refs. 9, 10[†]. The minus sign in Eq. (9.3) is the origin of asymptotic freedom, *i.e.* the fact that the strong coupling becomes weak for processes involving large momentum transfers (“hard processes”), $\alpha_s \sim 0.1$ for momentum transfers in the 100 GeV –TeV range.

The β -function coefficients, the b_i , are given for the coupling of an *effective theory* in which n_f of the quark flavors are considered light ($m_q \ll \mu_R$), and in which the remaining heavier quark flavors decouple from the theory. One may relate the coupling for the theory with $n_f + 1$ light flavors to that with n_f flavors through an equation of the form

$$\alpha_s^{(n_f+1)}(\mu_R^2) = \alpha_s^{(n_f)}(\mu_R^2) \left(1 + \sum_{n=1}^{\infty} \sum_{\ell=0}^n c_{n\ell} [\alpha_s^{(n_f)}(\mu_R^2)]^n \ln^\ell \frac{\mu_R^2}{m_h^2} \right), \quad (9.4)$$

where m_h is the mass of the $(n_f + 1)$ th flavor, and the first few $c_{n\ell}$ coefficients are $c_{11} = \frac{1}{6\pi}$, $c_{10} = 0$, $c_{22} = c_{11}^2$, $c_{21} = \frac{19}{24\pi^2}$, and $c_{20} = -\frac{11}{72\pi^2}$ when m_h is the $\overline{\text{MS}}$ mass at scale m_h ($c_{20} = \frac{7}{24\pi^2}$ when m_h is the pole mass — mass definitions are discussed below and in the review on “Quark Masses”). Terms up to $c_{4\ell}$ are to be found in Refs. 11, 12. Numerically, when one chooses $\mu_R = m_h$, the matching is a small effect, owing to the zero value for the c_{10} coefficient.

Working in an energy range where the number of flavors is constant, a simple exact analytic solution exists for Eq. (9.3) only if one neglects all but the b_0 term, giving $\alpha_s(\mu_R^2) = (b_0 \ln(\mu_R^2/\Lambda^2))^{-1}$. Here Λ is a constant of integration, which corresponds to the scale where the perturbatively-defined coupling would diverge, *i.e.* it is the non-perturbative scale of QCD. A convenient approximate analytic solution to the RGE that includes also the b_1 , b_2 , and b_3 terms is given by (see for example Ref. 13),

$$\alpha_s(\mu_R^2) \simeq \frac{1}{b_0 t} \left(1 - \frac{b_1 \ln t}{b_0^2 t} + \frac{b_1^2 (\ln^2 t - \ln t - 1) + b_0 b_2}{b_0^4 t^2} - \frac{b_1^3 (\ln^3 t - \frac{5}{2} \ln^2 t - 2 \ln t + \frac{1}{2}) + 3b_0 b_1 b_2 \ln t - \frac{1}{2} b_0^2 b_3}{b_0^6 t^3} \right), \quad t \equiv \ln \frac{\mu_R^2}{\Lambda^2}, \quad (9.5)$$

again parametrized in terms of a constant Λ . Note that Eq. (9.5) is one of several possible approximate 4-loop solutions for $\alpha_s(\mu_R^2)$, and that a value for Λ only defines $\alpha_s(\mu_R^2)$ once one knows which particular approximation is being used. An alternative to the use of formulas such as Eq. (9.5) is to solve the RGE exactly, numerically (including the discontinuities, Eq. (9.4), at flavor thresholds). In such cases the quantity Λ is not defined at all. For these reasons, in determinations of the coupling, it has become standard practice to quote the value of α_s at a given scale (typically M_Z) rather than to quote a value for Λ .

The value of the coupling, as well as the exact forms of the b_2 , c_{10} (and higher order) coefficients, depend on the renormalization scheme in which the coupling is defined, *i.e.* the convention used to subtract infinities in the context of renormalization. The coefficients given above hold for a coupling defined in the modified minimal subtraction ($\overline{\text{MS}}$) scheme [14], by far the most widely used scheme.

A discussion of determinations of the coupling and a graph illustrating its scale dependence (“running”) are to be found in Section 9.3.4.

[†] One should be aware that the b_2 and b_3 coefficients are renormalization-scheme-dependent, and given here in the $\overline{\text{MS}}$ scheme, as discussed below.

9.1.2. Quark masses :

Free quarks are never observed, *i.e.* a quark never exists on its own for a time longer than $\sim 1/\Lambda$: up, down, strange, charm, and bottom quarks all *hadronize*, *i.e.* become part of a meson or baryon, on a timescale $\sim 1/\Lambda$; the top quark instead decays before it has time to hadronize. This means that the question of what one means by the quark mass is a complex one, which requires that one adopts a specific prescription. A perturbatively defined prescription is the pole mass, m_q , which corresponds to the position of the divergence of the propagator. This is close to one's physical picture of mass. However, when relating it to observable quantities, it suffers from substantial non-perturbative ambiguities (see *e.g.* Ref. 15). An alternative is the $\overline{\text{MS}}$ mass, $\overline{m}_q(\mu_R^2)$, which depends on the renormalization scale μ_R .

Results for the masses of heavier quarks are often quoted either as the pole mass or as the $\overline{\text{MS}}$ mass evaluated at a scale equal to the mass, $\overline{m}_q(\overline{m}_q^2)$; light quark masses are generally quoted in the $\overline{\text{MS}}$ scheme at a scale $\mu_R \sim 2 \text{ GeV}$. The pole and $\overline{\text{MS}}$ masses are related by a slowly converging series that starts $m_q = \overline{m}_q(\overline{m}_q^2)(1 + \frac{4\alpha_s(\overline{m}_q^2)}{3\pi} + \mathcal{O}(\alpha_s^2))$, while the scale-dependence of $\overline{\text{MS}}$ masses is given by

$$\mu_R^2 \frac{d\overline{m}_q(\mu_R^2)}{d\mu_R^2} = \left[-\frac{\alpha_s(\mu_R^2)}{\pi} + \mathcal{O}(\alpha_s^2) \right] \overline{m}_q(\mu_R^2). \quad (9.6)$$

Quark masses are discussed in detail in a dedicated section of the *Review*, “Quark Masses.”

9.2. Structure of QCD predictions

9.2.1. Inclusive cross sections :

The simplest observables in QCD are those that do not involve initial-state hadrons and that are fully inclusive with respect to details of the final state. One example is the total cross section for $e^+e^- \rightarrow \text{hadrons}$ at center-of-mass energy Q , for which one can write

$$\frac{\sigma(e^+e^- \rightarrow \text{hadrons}, Q)}{\sigma(e^+e^- \rightarrow \mu^+\mu^-, Q)} \equiv R(Q) = R_{\text{EW}}(Q)(1 + \delta_{\text{QCD}}(Q)), \quad (9.7)$$

where $R_{\text{EW}}(Q)$ is the purely electroweak prediction for the ratio and $\delta_{\text{QCD}}(Q)$ is the correction due to QCD effects. To keep the discussion simple, we can restrict our attention to energies $Q \ll M_Z$, where the process is dominated by photon exchange ($R_{\text{EW}} = 3 \sum_q e_q^2$, neglecting finite-quark-mass corrections),

$$\delta_{\text{QCD}}(Q) = \sum_{n=1}^{\infty} c_n \cdot \left(\frac{\alpha_s(Q^2)}{\pi} \right)^n + \mathcal{O}\left(\frac{\Lambda^4}{Q^4}\right). \quad (9.8)$$

The first four terms in the α_s series expansion are then to be found in Refs. 16, 17

$$c_1 = 1, \quad c_2 = 1.9857 - 0.1152n_f, \quad (9.9a)$$

$$c_3 = -6.63694 - 1.20013n_f - 0.00518n_f^2 - 1.240\eta \quad (9.9b)$$

$$c_4 = -156.61 + 18.77n_f - 0.7974n_f^2 + 0.0215n_f^3 + C\eta, \quad (9.9c)$$

with $\eta = (\sum e_q)^2 / (3 \sum e_q^2)$ and where the coefficient C of the η -dependent piece in the α_s^4 term has yet to be determined. For corresponding expressions including also Z exchange and finite-quark-mass effects, see Ref. 18.

A related series holds also for the QCD corrections to the hadronic decay width of the τ lepton, which essentially involves an integral of $R(Q)$ over the allowed range of invariant masses of the hadronic part of the τ decay (see *e.g.* Ref. 16). The series expansions for QCD corrections to Higgs-boson (partial) decay widths are summarized in Refs. 19, 20.

One characteristic feature of the Eq. (9.8) is that the coefficients of α_s^n increase rapidly order by order: calculations in perturbative QCD tend to converge more slowly than would be expected based

just on the size of $\alpha_s^{\dagger\dagger}$. Another feature is the existence of an extra “power-correction” term $\mathcal{O}(\Lambda^4/Q^4)$ in Eq. (9.8), which accounts for contributions that are fundamentally non-perturbative. All high-energy QCD predictions involve such corrections, though the exact power of Λ/Q depends on the observable.

Scale dependence. In Eq. (9.8) the renormalization scale for α_s has been chosen equal to Q . The result can also be expressed in terms of the coupling at an arbitrary renormalization scale μ_R ,

$$\delta_{\text{QCD}}(Q) = \sum_{n=1}^{\infty} \overline{c}_n \left(\frac{\mu_R^2}{Q^2} \right) \cdot \left(\frac{\alpha_s(\mu_R^2)}{\pi} \right)^n + \mathcal{O}\left(\frac{\Lambda^4}{Q^4}\right), \quad (9.10)$$

where $\overline{c}_1(\mu_R^2/Q^2) \equiv c_1$, $\overline{c}_2(\mu_R^2/Q^2) = c_2 + \pi b_0 c_1 \ln(\mu_R^2/Q^2)$, $\overline{c}_3(\mu_R^2/Q^2) = c_3 + (2b_0 c_2 \pi + b_1 c_1 \pi^2) \ln(\mu_R^2/Q^2) + b_0^2 c_1 \pi^2 \ln^2(\mu_R^2/Q^2)$, *etc.*. Given an infinite number of terms in the α_s expansion, the μ_R dependence of the $\overline{c}_n(\mu_R^2/Q^2)$ coefficients will exactly cancel that of $\alpha_s(\mu_R^2)$, and the final result will be independent of the choice of μ_R : physical observables do not depend on unphysical scales.

With just terms up to $n = N$, a residual μ_R dependence will remain, which implies an uncertainty on the prediction of $R(Q)$ due to the arbitrariness of the scale choice. This uncertainty will be $\mathcal{O}(\alpha_s^{N+1})$, *i.e.* of the same order as the neglected terms. For this reason it is standard to use QCD predictions' scale dependence as an estimate of the uncertainties due to neglected terms. One usually takes a central value for $\mu_R \sim Q$, in order to avoid the poor convergence of the perturbative series that results from the large $\ln^{n-1}(\mu_R^2/Q^2)$ terms in the \overline{c}_n coefficients when $\mu_R \ll Q$ or $\mu_R \gg Q$.

9.2.1.1. Processes with initial-state hadrons:

Deep Inelastic Scattering. To illustrate the key features of QCD cross sections in processes with initial-state hadrons, let us consider deep-inelastic scattering (DIS), $ep \rightarrow e + X$, where an electron e with four-momentum k emits a highly off-shell photon (momentum q) that interacts with the proton (momentum p). For photon virtualities $Q^2 \equiv -q^2$ far above the squared proton mass (but far below the Z mass), the differential cross section in terms of the kinematic variables Q^2 , $x = Q^2/(2p \cdot q)$ and $y = (q \cdot p)/(k \cdot p)$ is

$$\frac{d^2\sigma}{dx dQ^2} = \frac{4\pi\alpha}{2xQ^4} \left[(1 + (1-y)^2)F_2(x, Q^2) - y^2 F_L(x, Q^2) \right], \quad (9.11)$$

where α is the electromagnetic coupling and $F_2(x, Q^2)$ and $F_L(x, Q^2)$ are proton structure functions, which encode the interaction between the photon (in given polarization states) and the proton (for an extended review, see Sec. 16).

Structure functions are not calculable in perturbative QCD, nor is any other cross section that involves initial-state hadrons. To zeroth order in α_s , the structure functions are given directly in terms of non-perturbative parton (quark or gluon) distribution functions (PDFs),

$$F_2(x, Q^2) = x \sum_q e_q^2 f_{q/p}(x), \quad F_L(x, Q^2) = 0, \quad (9.12)$$

where $f_{q/p}(x)$ is the PDF for quarks of type q inside the proton, *i.e.* the number density of quarks of type q inside a fast-moving proton that carry a fraction x of its longitudinal momentum (the quark flavor index q , here, is not to be confused with the photon momentum q in the lines preceding Eq. (9.11)). Since PDFs are non-perturbative, and difficult to calculate in lattice QCD [22], they must be extracted from data.

The above result, with PDFs $f_{q/p}(x)$ that are independent of the scale Q , corresponds to the “quark-parton model” picture in which the photon interacts with point-like free quarks, or equivalently, one has incoherent elastic scattering between the electron and individual

^{††} The situation is significantly worse near thresholds, *e.g.* the $t\bar{t}$ production threshold. An overview of some of the “effective field theory” techniques used in such cases is to be found for example in Ref. 21.

constituents of the proton. As a consequence, in this picture also F_2 and F_L are independent of Q . When including higher orders in pQCD, Eq. (9.12) becomes

$$F_2(x, Q^2) = x \sum_{n=0}^{\infty} \frac{\alpha_s^n(\mu_R^2)}{(2\pi)^n} \sum_{i=q,g} \int_x^1 \frac{dz}{z} C_{2,i}^{(n)}(z, Q^2, \mu_R^2, \mu_F^2) f_{i/p}\left(\frac{x}{z}, \mu_F^2\right) + \mathcal{O}\left(\frac{\Lambda^2}{Q^2}\right). \quad (9.13)$$

Just as in Eq. (9.10), we have a series in powers $\alpha_s(\mu_R^2)$, each term involving a coefficient $C_{2,i}^{(n)}$ that can be calculated using Feynman graphs. An important difference relative to Eq. (9.10) stems from the fact that the quark's momentum, when it interacts with the photon, can differ from its momentum when it was extracted from the proton, because it may have radiated gluons in between. As a result, the $C_{2,i}^{(n)}$ coefficients are functions that depend on the ratio, z , of these two momenta, and one must integrate over z . At zeroth order, $C_{2,q}^{(0)} = e_q^2 \delta(1-z)$ and $C_{2,g}^{(0)} = 0$.

The majority of the emissions that modify a parton's momentum are actually collinear (parallel) to that parton, and don't depend on the fact that the parton is destined to interact with a photon. It is natural to view these emissions as modifying the proton's structure rather than being part of the coefficient function for the parton's interaction with the photon. The separation between the two categories is somewhat arbitrary and parametrized by a *factorization scale*, μ_F . Technically, one uses a procedure known as *factorization* to give rigorous meaning to this distinction, most commonly through the $\overline{\text{MS}}$ factorization scheme, defined in the context of dimensional regularization. The $\overline{\text{MS}}$ factorization scheme involves an arbitrary choice of *factorization scale*, μ_F , whose meaning can be understood roughly as follows: emissions with transverse momenta above μ_F are included in the $C_{2,i}^{(n)}(z, Q^2, \mu_R^2, \mu_F^2)$; emissions with transverse momenta below μ_F are accounted for within the PDFs, $f_{i/p}(x, \mu_F^2)$.

The PDFs' resulting dependence on μ_F is described by the Dokshitzer-Gribov-Lipatov-Altarelli-Parisi (DGLAP) equations [23], which to leading order (LO) read*

$$\frac{\partial f_{i/p}(x, \mu_F^2)}{\partial \mu_F^2} = \sum_j \frac{\alpha_s(\mu_F^2)}{2\pi} \int_x^1 \frac{dz}{z} P_{i \leftarrow j}^{(1)}(z) f_{j/p}\left(\frac{x}{z}, \mu_F^2\right), \quad (9.14)$$

with, for example, $P_{q \leftarrow g}^{(1)}(z) = T_R(z^2 + (1-z)^2)$. The other LO splitting functions are listed in Sec. 16 of this *Review*, while results up to next-to-next-to-leading order (NNLO), α_s^3 , are given in Refs. 24, 25. The coefficient functions are also μ_F dependent, for example $C_{2,i}^{(1)}(x, Q^2, \mu_R^2, \mu_F^2) = C_{2,i}^{(1)}(x, Q^2, \mu_R^2, Q^2) - \ln\left(\frac{\mu_F^2}{Q^2}\right) \sum_j \int_x^1 \frac{dz}{z} P_{i \leftarrow j}^{(1)}(z) C_{2,j}^{(0)}\left(\frac{x}{z}\right)$. For the electromagnetic component of DIS with light quarks and gluons they are known to $\mathcal{O}(\alpha_s^3)$ (N³LO) [26]. For weak currents they are known fully to α_s^2 (NNLO) [27] with substantial results known also at N³LO [28]. For heavy quark production they are known to $\mathcal{O}(\alpha_s^2)$ [29] (next-to-leading order (NLO) insofar as the series starts at $\mathcal{O}(\alpha_s)$), with work ongoing towards NNLO [30].

As with the renormalization scale, the choice of factorization scale is arbitrary, but if one has an infinite number of terms in the

* LO is generally taken to mean the lowest order at which a quantity is non-zero. This definition is nearly always unambiguous, the one major exception being for the case of the hadronic branching ratio of virtual photons, Z , τ , etc., for which two conventions exist: LO can either mean the lowest order that contributes to the hadronic branching fraction, *i.e.* the term “1” in Eq. (9.7); or it can mean the lowest order at which the hadronic branching ratio becomes sensitive to the coupling, $n = 1$ in Eq. (9.8), as is relevant when extracting the value of the coupling from a measurement of the branching ratio. Because of this ambiguity, we avoided use of the term “LO” in that context.

perturbative series, the μ_F -dependences of the coefficient functions and PDFs will compensate each other fully. Given only N terms of the series, a residual uncertainty $\mathcal{O}(\alpha_s^{N+1})$ is associated with the ambiguity in the choice of μ_F . As with μ_R , varying μ_F provides an input in estimating uncertainties on predictions. In inclusive DIS predictions, the default choice for the scales is usually $\mu_R = \mu_F = Q$.

Hadron-hadron collisions. The extension to processes with two initial-state hadrons is straightforward, and for example the total (inclusive) cross section for W boson production in $p\bar{p}$ collisions can be written as

$$\sigma(p\bar{p} \rightarrow W + X) = \sum_{n=0}^{\infty} \alpha_s^n(\mu_R^2) \sum_{i,j} \int dx_1 dx_2 f_{i/p}(x_1, \mu_F^2) f_{j/\bar{p}}(x_2, \mu_F^2) \times \hat{\sigma}_{ij \rightarrow W+X}^{(n)}(x_1 x_2 s, \mu_R^2, \mu_F^2), \quad (9.15)$$

where s is the squared center-of-mass energy of the collision. At LO, $n = 0$, the hard (partonic) cross section $\hat{\sigma}_{ij \rightarrow W+X}^{(0)}(x_1 x_2 s, \mu_R^2, \mu_F^2)$ is simply proportional to $\delta(x_1 x_2 s - M_W^2)$, in the narrow W -boson width approximation (see Sec. 40 of this *Review* for detailed expressions for this and other hard scattering cross sections). It is non-zero only for choices of i, j that can directly give a W , such as $i = u$, $j = \bar{d}$. At higher orders, $n \geq 1$, new partonic channels contribute, such as gg , and there is no restriction $x_1 x_2 s = M_W^2$.

Equation 9.15 involves a factorization between hard cross section and PDFs, just like Eq. (9.13). As long as the same factorization scheme is used in DIS and pp or $p\bar{p}$ (usually the $\overline{\text{MS}}$ scheme), then PDFs extracted in DIS can be directly used in pp and $p\bar{p}$ predictions [31].

The fully inclusive hard cross sections are known to NNLO, α_s^2 , for Drell-Yan (DY) lepton-pair and vector-boson production [32,33], and for Higgs-boson production [33–36].

Photoproduction. γp (and $\gamma\gamma$) collisions are similar to pp collisions, with the subtlety that the photon can behave in two ways: there is “direct” photoproduction, in which the photon behaves as a point-like particle and takes part directly in the hard collision, with hard subprocesses such as $\gamma g \rightarrow q\bar{q}$; there is also resolved photoproduction, in which the photon behaves like a hadron, with non-perturbative partonic substructure and a corresponding PDF for its quark and gluon content, $f_{i/\gamma}(x, Q^2)$.

While useful to understand the general structure of γp collisions, the distinction between direct and resolved photoproduction is not well defined beyond leading order, as discussed for example in Ref. 37.

The high-energy limit. In situations in which the total center-of-mass energy \sqrt{s} is much larger than other scales in the problem (*e.g.* Q in DIS, m_b for $b\bar{b}$ production in pp collisions, *etc.*), each power of α_s beyond LO can be accompanied by a power of $\ln(s/Q^2)$ (or $\ln(s/m_b^2)$, *etc.*). This is known as the high-energy or Balitsky-Fadin-Kuraev-Lipatov (BFKL) limit [38–40]. Currently it is possible to account for the dominant and first subdominant [41,42] power of $\ln s$ at each order of α_s , and also to estimate further subdominant contributions that are numerically large (see Refs. 43–45 and references therein).

Physically, the summation of all orders in α_s can be understood as leading to a growth with s of the gluon density in the proton. At sufficiently high energies this implies non-linear effects, whose treatment has been the subject of intense study (see for example Refs. 46, 47 and references thereto).

9.2.2. Non-inclusive cross-sections :

QCD final states always consist of hadrons, while perturbative QCD calculations deal with partons. Physically, an energetic parton fragments (“showers”) into many further partons, which then, on later timescales, undergo a transition to hadrons (“hadronization”). Fixed-order perturbation theory captures only a small part of these dynamics.

This does not matter for the fully inclusive cross sections discussed above: the showering and hadronization stages are “unitary”, *i.e.* they do not change the overall probability of hard scattering, because they occur long after it has taken place.

Non-inclusive measurements, in contrast, may be affected by the extra dynamics. For those sensitive just to the main directions of energy flow (jet rates, event shapes, cf. Sec. 9.3.1) fixed order perturbation theory is often still adequate, because showering and hadronization don't substantially change the overall energy flow. This means that one can make a prediction using just a small number of partons, which should correspond well to a measurement of the same observable carried out on hadrons. For observables that instead depend on distributions of individual hadrons (which, e.g., are the inputs to detector simulations), it is mandatory to account for showering and hadronization. The range of predictive techniques available for QCD final states reflects this diversity of needs of different measurements.

While illustrating the different methods, we shall for simplicity mainly use expressions that hold for e^+e^- scattering. The extension to cases with initial-state partons will be mostly straightforward (space constraints unfortunately prevent us from addressing diffraction and exclusive hadron-production processes; extensive discussion is to be found in Refs. 48, 49).

9.2.2.1. Preliminaries: Soft and collinear limits:

Before examining specific predictive methods, it is useful to be aware of a general property of QCD matrix elements in the soft and collinear limits. Consider a squared tree-level matrix element $|M_n^2(p_1, \dots, p_n)|$ for the production of n partons with momenta p_1, \dots, p_n , and a corresponding phase-space integration measure $d\Phi_n$. If particle n is a gluon, and additionally it becomes collinear (parallel) to another particle i and its momentum tends to zero (it becomes "soft"), the matrix element simplifies as follows,

$$\lim_{\theta_{in} \rightarrow 0, E_n \rightarrow 0} d\Phi_n |M_n^2(p_1, \dots, p_n)| = d\Phi_{n-1} |M_{n-1}^2(p_1, \dots, p_{n-1})| \frac{\alpha_s C_i}{\pi} \frac{d\theta_{in}^2}{\theta_{in}^2} \frac{dE_n}{E_n}, \quad (9.16)$$

where $C_i = C_F$ (C_A) if i is a quark (gluon). This formula has non-integrable divergences both for the inter-parton angle $\theta_{in} \rightarrow 0$ and for the gluon energy $E_n \rightarrow 0$, which are mirrored also in the structure of divergences in loop diagrams. These divergences are important for at least two reasons: firstly, they govern the typical structure of events (inducing many emissions either with low energy or at small angle with respect to hard partons); secondly, they will determine which observables can be calculated within perturbative QCD.

9.2.2.2. Fixed-order predictions:

Let us consider an observable \mathcal{O} that is a function $\mathcal{O}_m(p_1, \dots, p_m)$ of the four-momenta of the m particles in an event (whether partons or hadrons). In what follows, we shall consider the cross section for events weighted with the value of the observable, $\sigma_{\mathcal{O}}$. As examples, if $\mathcal{O}_m \equiv 1$ for all m , then $\sigma_{\mathcal{O}}$ is just the total cross section; if $\mathcal{O}_m \equiv \hat{\tau}(p_1, \dots, p_m)$ where $\hat{\tau}$ is the value of the thrust for that event (see Sec. 9.3.1.2), then the average value of the thrust is $\langle \tau \rangle = \sigma_{\mathcal{O}} / \sigma_{\text{tot}}$; if $\mathcal{O}_m \equiv \delta(\tau - \hat{\tau}(p_1, \dots, p_m))$ then one gets the differential cross section as a function of the thrust, $\sigma_{\mathcal{O}} \equiv d\sigma/d\tau$.

In the expressions below, we shall omit to write the non-perturbative power correction term, which for most common observables is proportional to a single power of Λ/Q .

LO. If the observable \mathcal{O} is non-zero only for events with at least n particles, then the LO QCD prediction for the weighted cross section in e^+e^- annihilation is

$$\sigma_{\mathcal{O}, LO} = \alpha_s^{n-2} (\mu_R^2)^2 \int d\Phi_n |M_n^2(p_1, \dots, p_n)| \mathcal{O}_n(p_1, \dots, p_n), \quad (9.17)$$

where the squared tree-level matrix element, $|M_n^2(p_1, \dots, p_n)|$, includes relevant symmetry factors, has been summed over all subprocesses (e.g. $e^+e^- \rightarrow q\bar{q}q\bar{q}$, $e^+e^- \rightarrow q\bar{q}gg$) and has had all factors of α_s extracted in front. In processes other than e^+e^- collisions, the powers of the coupling are often brought inside the integrals, with the scale μ_R chosen event by event, as a function of the event kinematics.

Other than in the simplest cases (see the review on Cross Sections in this *Review*), the matrix elements in Eq. (9.17) are usually calculated

automatically with programs such as CompHEP [50], MadGraph [51], Alpgen [52], Comix/Sherpa [53], and Helac/Phegas [54]. Some of these (CompHEP, MadGraph) use formulae obtained from direct evaluations of Feynman diagrams. Others (Alpgen, Helac/Phegas and Comix/Sherpa) use methods designed to be particularly efficient at high multiplicities, such as Berends-Giele recursion [55] (see also the review Ref. 56), which builds up amplitudes for complex processes from simpler ones.

The phase-space integration is usually carried out by Monte Carlo sampling, in order to deal with the sometimes complicated cuts that are used in corresponding experimental measurements. Because of the divergences in the matrix element, Eq. (9.16), the integral converges only if the observable vanishes for kinematic configurations in which one of the n particles is arbitrarily soft or it is collinear to another particle. As an example, the cross section for producing any configuration of n partons will lead to an infinite integral, whereas a finite result will be obtained for the cross section for producing n deposits of energy (or jets, see Sec. 9.3.1.1), each above some energy threshold and well separated from each other in angle.

LO calculations can be carried out for $2 \rightarrow n$ processes with $n \lesssim 6-10$. The exact upper limit depends on the process, the method used to evaluate the matrix elements (recursive methods are more efficient), and the extent to which the phase-space integration can be optimized to work around the large variations in the values of the matrix elements.

NLO. Given an observable that is non-zero starting from n particles, its prediction at NLO involves supplementing the LO result with the $(n+1)$ -particle tree-level matrix element ($|M_{n+1}^2|$), and the interference of a n -particle tree-level and n -particle 1-loop amplitude ($2\text{Re}(M_n M_{n,1\text{-loop}}^*)$),

$$\begin{aligned} \sigma_{\mathcal{O}}^{NLO} &= \sigma_{\mathcal{O}}^{LO} + \alpha_s^{n-1} (\mu_R^2) \int d\Phi_{n+1} \\ &|M_{n+1}^2(p_1, \dots, p_{n+1})| \mathcal{O}_{n+1}(p_1, \dots, p_{n+1}) \\ &+ \alpha_s^{n-1} (\mu_R^2) \int d\Phi_n 2\text{Re}(M_n(p_1, \dots, p_n) \\ &M_{n,1\text{-loop}}^*(p_1, \dots, p_n)) \mathcal{O}_n(p_1, \dots, p_n). \end{aligned} \quad (9.18)$$

Relative to LO calculations, two important issues appear in the NLO calculations. Firstly, the extra complexity of loop-calculations relative to tree-level calculations means that they have yet to be fully automated, though considerable progress is being made in this direction (see Refs. 57–60 and references therein). Secondly, loop amplitudes are infinite in 4 dimensions, while tree-level amplitudes are finite, but their *integrals* are infinite, due to the divergences of Eq. (9.16). These two sources of infinities have the same soft and collinear origins and cancel after the integration only if the observable \mathcal{O} satisfies the property of infrared and collinear safety,

$$\begin{aligned} \mathcal{O}_{n+1}(p_1, \dots, p_s, \dots, p_n) &\rightarrow \mathcal{O}_n(p_1, \dots, p_n) && \text{if } p_s \rightarrow 0 \\ \mathcal{O}_{n+1}(p_1, \dots, p_a, p_b, \dots, p_n) &\rightarrow \mathcal{O}_n(p_1, \dots, p_a + p_b, \dots, p_n) \\ &&& \text{if } p_a \parallel p_b. \end{aligned} \quad (9.19)$$

Examples of infrared safe quantities include event-shape distributions and jet cross sections (with appropriate jet algorithms, see below). Unsafe quantities include the distribution of the momentum of the hardest QCD particle (which is not conserved under collinear splitting), observables that require the complete absence of radiation in some region of phase-space (e.g. rapidity gaps or 100% isolation cuts, which are affected by soft emissions), or the particle multiplicity (affected by both soft and collinear emissions). The non-cancellation of divergences at NLO due to infrared or collinear unsafety compromises the usefulness not only of the NLO calculation, but also that of a LO calculation, since LO is only an acceptable approximation if one can prove that higher order terms are smaller. Infrared and collinear unsafety usually also imply large non-perturbative effects.

As with LO calculations, the phase-space integrals in Eq. (9.18) are usually carried out by Monte Carlo integration, so as to facilitate the study of arbitrary observables. Various methods exist to obtain numerically efficient cancellation among the different infinities. The

most widely used in current NLO computer codes is known as dipole subtraction [61]; other methods that have seen numerous applications include FKS [62] and antenna [63] subtraction.

NLO calculations exist for nearly all $2 \rightarrow n$ processes with $n \leq 3$ (and for $1 \rightarrow 4$ in $e^+e^- \rightarrow \gamma/Z \rightarrow \text{hadrons}$), as reviewed in Ref. 64. Some of the corresponding codes are public, and those that provide access to multiple processes include NLOJet++ [65] for e^+e^- , DIS, and hadron-hadron processes involving just light partons in the final state, MCFM [66] for hadron-hadron processes with vector bosons and/or heavy quarks in the final state, VBFNLO for vector-boson fusion processes [67], and the Phox family [68] for processes with photons in the final state. The current forefront of NLO calculations is $2 \rightarrow 4$ processes in pp scattering, for which results exist on $t\bar{t}b\bar{b}$ [59,60] and $pp \rightarrow W+3\text{jets}$ [57,58].

NNLO. Conceptually, NNLO and NLO calculations are similar, except that one must add a further order in α_s , consisting of: the squared $(n+2)$ -parton tree-level amplitude, the interference of the $(n+1)$ -parton tree-level and 1-loop amplitudes, the interference of the n -parton tree-level and 2-loop amplitudes, and the squared n -parton 1-loop amplitude.

Each of these elements involves large numbers of soft and collinear divergences. Arranging for their cancellation after numerical Monte Carlo integration is one of the significant challenges of NNLO calculations, as is the determination of the relevant 2-loop amplitudes. The processes for which fully exclusive NNLO calculations exist include the 3-jet cross section in e^+e^- collisions [69,70] (for which NNLO means α_s^3), as well as vector- [71,72] and Higgs-boson [73,74] production in pp and $p\bar{p}$ collisions (for which NNLO means α_s^2).

9.2.2.3. Resummation:

Many experimental measurements place tight constraints on emissions in the final state, for example, in e^+e^- events, that the thrust should be less than some value $\tau \ll 1$, or in $pp \rightarrow Z$ events that the Z -boson transverse momentum should be much smaller than its mass, $p_{t,Z} \ll M_Z$. A further example is the production of heavy particles or jets near threshold (so that little energy is left over for real emissions) in DIS and pp collisions.

In such cases the constraint vetoes a significant part of the integral over the soft and collinear divergence of Eq. (9.16). As a result, there is only a partial cancellation between real emission terms (subject to the constraint) and loop (virtual) contributions (not subject to the constraint), causing each order of α_s to be accompanied by a large coefficient $\sim L^2$, where *e.g.* $L = \ln \tau$ or $L = \ln(M_Z/p_{t,Z})$. One ends up with a perturbative series whose terms go as $\sim (\alpha_s L^2)^n$. It is not uncommon that $\alpha_s L^2 \gg 1$, so that the perturbative series converges very poorly if at all.** In such cases one may carry out a “resummation,” which accounts for the dominant logarithmically enhanced terms to all orders in α_s , by making use of known properties of matrix elements for multiple soft and collinear emissions, and of the all-orders properties of the divergent parts of virtual corrections, following original works such as Refs. 75–84 (or more recently through soft-collinear effective theory, cf. the review in Ref. 85).

For cases with double logarithmic enhancements (two powers of logarithm per power of α_s), there are two classification schemes for resummation accuracy. Writing the cross section including the constraint as $\sigma(L)$ and the unconstrained (total) cross section as σ_{tot} , the series expansion takes the form

$$\sigma(L) \simeq \sigma_{\text{tot}} \sum_{n=0}^{\infty} \sum_{k=0}^{2n} R_{nk} \alpha_s^n (\mu_R^2) L^k, \quad L \gg 1 \quad (9.20)$$

and leading log (LL) resummation means that one accounts for all terms with $k = 2n$, next-to-leading-log (NLL) includes additionally

** To be precise one should distinguish two causes of the divergence of perturbative series. That which interests us here is associated with the presence of a new large parameter (*e.g.* ratio of scales). Nearly all perturbative series also suffer from “renormalon” divergences $\alpha_s^n n!$ (reviewed in Ref. 15), which however have an impact only at very high perturbative orders and have a deep connection with non-perturbative uncertainties.

all terms with $k = 2n - 1$, *etc.*. Often $\sigma(L)$ (or its Fourier or Mellin transform) *exponentiates*[‡],

$$\sigma(L) \simeq \sigma_{\text{tot}} \exp \left[\sum_{n=1}^{\infty} \sum_{k=0}^{n+1} G_{nk} \alpha_s^n (\mu_R^2) L^k \right], \quad L \gg 1, \quad (9.21)$$

where one notes the different upper limit on k compared to Eq. (9.20). This is a more powerful form of resummation: the G_{12} term alone reproduces the full LL series in Eq. (9.20). With the form Eq. (9.21) one still uses the nomenclature LL, but this now means that all terms with $k = n + 1$ are included, and NLL implies all terms with $k = n$, *etc.*

For a large number of observables, the state-of-the-art for resummation is NLL in the sense of Eq. (9.21) (see Refs. 89–91 and references therein). NNLL has been achieved for the DY and Higgs-boson p_t distributions [92,93] (in addition the NLL ResBos program [94] is still widely used), the back-to-back energy-energy correlation in e^+e^- [95], and the production of top anti-top pairs near threshold [96–100]. Finally, the parts believed to be dominant in the N³LL resummation are available for the thrust variable in e^+e^- annihilations [101], and for Higgs- and vector-boson production near threshold [102,103] in hadron collisions. The inputs and methods involved in these various calculations are somewhat too diverse to discuss in detail here, so we recommend that the interested reader consults the original references for further details.

9.2.2.4. Fragmentation functions:

Since the parton-hadron transition is non-perturbative, it is not possible to perturbatively calculate quantities such as the energy-spectra of specific hadrons in high-energy collisions. However, one can factorize perturbative and non-perturbative contributions via the concept of fragmentation functions. These are the final-state analogue of the parton distribution functions that are used for initial-state hadrons.

It should be added that if one ignores the non-perturbative difficulties and just calculates the energy and angular spectrum of partons in perturbative QCD with some low cutoff scale $\sim \Lambda$ (using resummation to sum large logarithms of \sqrt{s}/Λ), then this reproduces many features of the corresponding hadron spectra. This is often taken to suggest that hadronization is “local” in momentum space.

Sec. 17 of this *Review* provides further information (and references) on these topics, including also the question of heavy-quark fragmentation.

9.2.2.5. Parton-shower Monte Carlo generators:

Parton-shower Monte Carlo (MC) event generators like PYTHIA [104–106], HERWIG [107–109], SHERPA [110], and ARIADNE [111] provide fully exclusive simulations of QCD events. Because they provide access to “hadron-level” events they are a crucial tool for all applications that involve simulating the response of detectors to QCD events. Here we give only a brief outline of how they work and refer the reader to [112] and references therein for a more complete overview.

The MC generation of an event involves several stages. It starts with the random generation of the kinematics and partonic channels of whatever *hard scattering process* the user has requested.

This is then followed by a *parton shower*, usually based on a resummed calculation of the probability $\Delta(Q_0, Q_1)$ for each parton, that it does not split into other partons (*e.g.* radiate a gluon) between the hard scale Q_0 and some smaller scale Q_1 . $\Delta(Q_0, Q_1)$, known as a Sudakov form factor, takes the form $\Delta(Q_0, Q_1) \sim \exp(-G_{12} \alpha_s \ln^2(Q_0/Q_1) + \dots)$. By choosing a random number r uniformly in the range $0 < r < 1$ and finding the Q_1 value that solves $r = \Delta(Q_0, Q_1)$, the MC determines the scale of the first

‡ Whether or not this happens depends on the quantity being resummed. A classic example involves jet rates in e^+e^- collisions as a function of a jet-resolution parameter y_{cut} . The logarithms of $1/y_{\text{cut}}$ exponentiate for the k_t (Durham) jet algorithm [86], but not [87] for the JADE algorithm [88] (both are discussed below in Sec. 9.3.1.1).

emission of the shower. The procedure is repeated to obtain Q_2 , the scale of the next emission, and so forth down to a scale ~ 1 GeV that separates the perturbative and non-perturbative part of the simulation.

Once it has generated a partonic configuration, the MC “hadronizes” it according to some *hadronization* model. One widely-used model involves stretching a color “string” across quarks and gluons, and breaking it up into hadrons [113,114]. For a discussion of the implementation of this “Lund” model in the MC program PYTHIA, with further improvements and extensions, see Ref. 104 and references therein. Another model breaks each gluon into a $q\bar{q}$ pair and then groups quarks and anti-quarks into colorless “clusters”, which then give the hadrons. This cluster hadronization is implemented in the HERWIG event generator [107–109].

For processes with initial-state hadrons, the showering off the incoming partons must additionally take into account the scale-dependence of the PDFs and the non-perturbative part must account also for the proton remnants. In pp and γp scattering, the collision between the hadron remnants generates an *underlying event* (UE), usually by implementing additional $2 \rightarrow 2$ scatterings (“multiple parton interactions”) at a scale of a few GeV. The separation between the UE and other parts of the shower and hadronization is somewhat ambiguous, because they are all interconnected in terms of their color flow.

Parton showers usually generate a correct distribution of soft and collinear emission, but they often fail to reproduce the pattern of hard wide-angle emissions that would be given by the exact multi-parton matrix elements. In cases where this matters, it is usual to “merge” the parton showers with the generation of exact LO multi-parton matrix elements (Sec. 9.2.2.2), including a prescription to avoid double or under-counting of real and virtual corrections (*e.g.* CKKW [115] or MLM prescriptions [116]).

MCs as described above generate cross sections for the requested hard process that are correct at LO. For hadron-collider applications it is common to multiply these cross sections by an inclusive K -factor, *i.e.* the ratio of (N)NLO to LO results for a related inclusive cross section. For measurements with cuts, this may not always be adequate: higher-order corrections in a restricted phase-space region can be substantially different from those in the inclusive case. For a number of processes there also exist MC implementations that are correct to NLO, using the MC@NLO [117] or POWHEG [118] prescriptions to avoid double counting the approximate NLO pieces already implicitly included in the MCs through their showering.

9.2.3. Accuracy of predictions :

LO calculations are often said to be accurate to within a factor of two. This is based on the observed impact of scale variation across a range of observables and of the experience with NLO corrections in the cases where these are available. In processes involving new partonic scattering channels at NLO and/or large ratios of scales (such as the production of high- p_t jets containing B -hadrons), the NLO to LO K -factors can be substantially larger than 2.

The accuracy of a given particular perturbative QCD prediction is usually estimated by varying the renormalization and factorization scales around a central value Q that is taken close to the physical scale of the process.^{‡‡} A conventional range of variation is $Q/2 < \mu_R, \mu_F < 2Q$.

There does not seem to be a broad consensus on whether μ_R and μ_F should be kept identical or varied independently. One option is to vary them independently with the restriction $\frac{1}{2}\mu_R < \mu_F < 2\mu_R$ [119]. This limits the risk of misleadingly small uncertainties due to fortuitous cancellations between the μ_F and μ_R dependence when both are varied together, while avoiding the appearance of large logarithms of μ_R^2/μ_F^2 when both are varied completely independently.

Calculations that involve resummations usually have an additional source of uncertainty associated with the choice of argument of the logarithms being resummed, *e.g.* $\ln(2\frac{p_{t,Z}}{M_Z})$ as opposed to $\ln(\frac{1}{2}\frac{p_{t,Z}}{M_Z})$.

^{‡‡} A more conservative scheme is to take the uncertainty to be the size of the last known perturbative order.

In addition to varying renormalization and factorization scales, it is therefore also advisable to vary the argument of the logarithm by a factor of two in either direction with respect to the “natural” argument.

The accuracy of QCD predictions is limited also by non-perturbative corrections, which typically scale as a power of Λ/Q . For measurements that are directly sensitive to the structure of the hadronic final state the corrections are usually linear in Λ/Q . The non-perturbative corrections are further enhanced in processes with a significant underlying event (*i.e.* in pp and $p\bar{p}$ collisions) and in cases where the perturbative cross sections fall steeply as a function of p_t or some other kinematic variable.

Non-perturbative corrections are commonly estimated from the difference between Monte Carlo events at the parton-level and after hadronization, though methods exist also to analytically deduce non-perturbative effects in one observable based on measurements of other observables (see the reviews [15,120]).

9.3. Experimental QCD

Since we are not able to directly measure partons (quarks or gluons), but only hadrons and their decay products, a central issue for every experimental test of QCD is establishing a correspondence between observables obtained at the partonic and the hadronic level. The only theoretically sound correspondence is achieved by means of *infrared and collinear safe* quantities, which allow one to obtain finite predictions at any order of perturbative QCD.

As stated above, the simplest case of infrared and collinear safe observables are total cross sections. More generally, when measuring inclusive observables, the final state is not analyzed at all regarding its (topological, kinematical) structure or its composition. Basically the relevant information consists in the rate of a process ending up in a partonic or hadronic final state. In e^+e^- annihilation, widely used examples are the ratios of partial widths or branching ratios for the electroweak decay of particles into hadrons or leptons, such as Z or τ decays, (cf. Sec. 9.2.1). Such ratios are often favored over absolute cross sections or partial widths because of large cancellations of experimental and theoretical systematic uncertainties. The strong suppression of non-perturbative effects, $\mathcal{O}(\Lambda^4/Q^4)$, is one of the attractive features of such observables, however, at the same time the sensitivity to radiative QCD corrections is small, which for example affects the statistical uncertainty when using them for the determination of the strong coupling constant. In the case of τ decays not only the hadronic branching ratio is of interest, but also moments of the spectral functions of hadronic tau decays, which sample different parts of the decay spectrum and thus provide additional information. Other examples of inclusive observables are structure functions (and related sum rules) in DIS. These are extensively discussed in Sec. 16 of this *Review*.

As soon as (parts) of the structure or composition of the final state are analyzed and cross section differential in one or more variables characterizing this structure are of interest, we talk about exclusive observables, such as jet rates, jet substructure and event-shape distributions. Furthermore, any cross section differential in some characteristic kinematic quantity of the final state falls into this category, such as transverse momentum distributions of jets or vector bosons in hadron collisions. The case of fragmentation functions, *i.e.* the measurement of hadron production as a function of the hadron momentum relative to some hard scattering scale, is discussed in Sec. 17 of this *Review*.

It is worth mentioning that, besides the correspondence between the parton and hadron level, also a correspondence between the hadron level and the actually measured quantities in the detector has to be established. The simplest examples are corrections for finite experimental acceptance and efficiencies. However, measurements of exclusive observables such as jet rates require more involved corrections in order to relate, *e.g.* the energy deposits in a calorimeter to the jets at the hadron level. Typically detector simulations are used in order to obtain these corrections. Care should be taken here in order to have a clear separation between the parton-to-hadron level and hadron-to-detector level corrections, as well as to ensure

the independence of the latter from the MC model used in the simulations. Finally, it is strongly suggested to provide, whenever possible, measurements corrected for detector effects which then can be easily compared to the results of other experiments and/or theoretical calculations.

9.3.1. Hadronic final-state observables :

9.3.1.1. Jets:

In hard interactions, final-state partons and hadrons appear predominantly in collimated bunches. These bunches are generically called *jets*. To a first approximation, a jet can be thought of as a hard parton that has undergone soft and collinear showering and then hadronization. Jets are used both for testing our understanding and predictions of high-energy QCD processes, and also for identifying the hard partonic structure of decays of massive particles like top quarks.

In order to map observed hadrons onto a set of jets, one uses a *jet definition*. The mapping involves explicit choices: for example when a gluon is radiated from a quark, for what range of kinematics should the gluon be part of the quark jet, or instead form a separate jet? Good jet definitions are infrared and collinear safe, simple to use in theoretical and experimental contexts, applicable to any type of inputs (parton or hadron momenta, charged particle tracks, and/or energy deposits in the detectors) and lead to jets that are not too sensitive to non-perturbative effects. An extensive treatment of the topic of jet definitions is given in Ref. 121 (for e^+e^- collisions) and Refs. 122, 123 (for pp or $p\bar{p}$ collisions). Here we briefly review the two main classes: cone algorithms, extensively used at hadron colliders, and sequential recombination algorithms, more widespread in e^+e^- and ep colliders.

Very generically, most (iterative) cone algorithms start with some seed particle i , sum the momenta of all particles j within a cone of opening-angle R , typically defined in terms of (pseudo-)rapidity and azimuthal angle. They then take the direction of this sum as a new seed and repeat until the cone is stable, and call the contents of the resulting stable cone a jet if its transverse momentum is above some threshold $p_{t,\min}$. The parameters R and $p_{t,\min}$ should be chosen according to the needs of a given analysis.

There are many variants of cone algorithm, and they differ in the set of seeds they use and the manner in which they ensure a one-to-one mapping of particles to jets, given that two stable cones may share particles (“overlap”). The use of seed particles is a problem w.r.t. infrared and collinear safety, and seeded algorithms are generally not compatible with higher-order (or sometimes even leading-order) QCD calculations, especially in multi-jet contexts, as well as potentially subject to large non-perturbative corrections and instabilities. Seeded algorithms (JetCLU, MidPoint, and various other experiment-specific iterative cone algorithms) are therefore to be deprecated. A modern alternative is to use a seedless variant, SIScone [124].

Sequential recombination algorithms at hadron colliders (and in DIS) are characterized by a distance $d_{ij} = \min(k_{t,i}^{2p}, k_{t,j}^{2p})\Delta_{ij}^2/R^2$ between all pairs of particles i, j , where Δ_{ij} is their distance in the rapidity-azimuthal plane, $k_{t,i}$ is the transverse momentum w.r.t. the incoming beams, and R is a free parameter. They also involve a “beam” distance $d_{iB} = k_{t,i}^{2p}$. One identifies the smallest of all the d_{ij} and d_{iB} , and if it is a d_{ij} , then i and j are merged into a new pseudo-particle (with some prescription, a recombination scheme, for the definition of the merged four-momentum). If the smallest distance is a d_{iB} , then i is removed from the list of particles and called a jet. As with cone algorithms, one usually considers only jets above some transverse-momentum threshold $p_{t,\min}$. The parameter p determines the kind of algorithm: $p = 1$ corresponds to the (inclusive)- k_t algorithm [86,125,126], $p = 0$ defines the *Cambridge-Aachen* algorithm [127,128], while for $p = -1$ we have the *anti- k_t* algorithm [129]. All these variants are infrared and collinear safe to all orders of perturbation theory. Whereas the former two lead to irregularly shaped jet boundaries, the latter results in cone-like boundaries.

The k_t algorithm in e^+e^- annihilations [86] uses $y_{ij} = 2 \min(E_i^2, E_j^2)(1 - \cos\theta_{ij})/Q^2$ as distance measure and repeatedly merges the pair with smallest y_{ij} , until all y_{ij} distances are above some threshold y_{cut} , the jet resolution parameter. The (pseudo)-particles

that remain at this point are called the jets. Here it is y_{cut} (rather than R and $p_{t,\min}$) that should be chosen according to the needs of the analysis. As mentioned above, the k_t algorithm has the property that logarithms $\ln(1/y_{\text{cut}})$ exponentiate in resummation calculations. This is one reason why it is preferred over the earlier JADE algorithm [88], which uses the distance measure $y_{ij} = 2 E_i E_j (1 - \cos\theta_{ij})/Q^2$.

Efficient implementations of the above algorithms are available through the *FastJet* package [130], which is also packaged within *SpartyJet* [131].

9.3.1.2. Event Shapes:

Event-shape variables are functions of the four momenta in the hadronic final state that characterize the topology of an event’s energy flow. They are sensitive to QCD radiation (and correspondingly to the strong coupling) insofar as gluon emission changes the shape of the energy flow.

The classic example of an event shape is the *thrust* [132,133] in e^+e^- annihilations, defined as

$$\hat{\tau} = \max_{\vec{n}_\tau} \frac{\sum_i |\vec{p}_i \cdot \vec{n}_\tau|}{\sum_i |\vec{p}_i|}, \quad (9.22)$$

where \vec{p}_i are the momenta of the final-state particles and the maximum is obtained for the thrust axis \vec{n}_τ . In the Born limit of the production of a perfect back-to-back $q\bar{q}$ pair the limit $\hat{\tau} \rightarrow 1$ is obtained, whereas a perfectly symmetric many-particle configuration leads to $\hat{\tau} \rightarrow 1/2$. Further event shapes of similar nature have been defined and extensively measured at LEP and at HERA, and for their definitions and reviews we refer to Refs. 1,2,120,134,135. Some discussion of hadron-collider event shapes is given in Ref. 136.

Event shapes are used for many purposes. These include measuring the strong coupling, tuning the parameters of Monte Carlo showering programs, investigating analytical models of hadronization and distinguishing QCD events from events that might involve decays of new particles (giving event-shape values closer to the spherical limit).

9.3.1.3. Jet substructure, quark vs. gluon jets:

Jet substructure, which can be resolved by finding subjets or by measuring jet shapes, is sensitive to the details of QCD radiation in the shower development inside a jet and has been extensively used to study differences in the properties of quark and gluon induced jets, strongly related to their different color charges. In general there is clear experimental evidence that gluon jets are “broader” and have a softer particle spectrum than (light-) quark jets, whereas b-quark jets are similar to gluon jets. As an example for an observable, the jet shape $\Psi(r/R)$ is the fractional transverse momentum contained within a sub-cone of cone-size r for jets of cone-size R . It is sensitive to the relative fractions of quark and gluon jets in an inclusive jet sample and receives contributions from soft-gluon initial-state radiation and beam remnant-remnant interactions. Therefore, it has been widely employed for validation and tuning of Monte Carlo models. CDF has measured the jet shape $\Psi(r/R)$ for an inclusive jet sample [137] as well as for b-jets [138]. Similar measurements in DIS have been reported in Refs. 139, 140. Further discussions, references and, recent summaries can be found in Refs. 135, 141, 142.

The use of jet substructure has also been suggested in order to distinguish QCD jets from jets that originate from hadronic decays of boosted massive particles (high- p_t electroweak bosons, top quarks and hypothesized new particles). For a review and detailed references, see sec. 5.3 of Ref. 122.

9.3.2. State of the art QCD measurements at colliders :

There exists an enormous wealth of data on QCD-related measurements in e^+e^- , ep , pp , and $p\bar{p}$ collisions, to which a short overview like this would not be able to do any justice. Extensive reviews of the subject have been published in Refs. 134, 135 for e^+e^- colliders, whereas for hadron colliders comprehensive overviews are given in Refs. 123, 143, and recent summaries can be found in, e.g. Refs. 144–146, 142. Below we concentrate our discussion on measurements that are most sensitive to hard QCD processes.

9.3.2.1. e^+e^- colliders: The analyses of jet production in e^+e^- collisions, mostly from JADE data at center-of-mass energies between 14 and 44 GeV, as well as from LEP data at the Z resonance and up to 209 GeV, covered the measurements of (differential or exclusive) jet rates (with multiplicities typically up to 4, 5 or 6 jets), the study of 3-jet events and particle production between the jets as a tool for testing hadronization models, as well as 4-jet production and angular correlations in 4-jet events, useful for measurements of the strong coupling constant and putting constraints on the QCD color factors, thus probing the non-abelian nature of QCD. There have also been extensive measurements of event shapes. The tuning of parton shower MC models, typically matched to matrix elements for 3-jet production, has led to good descriptions of the available, highly precise data. Especially for the large LEP data sample at the Z peak, the statistical errors are mostly negligible, whereas the experimental systematic uncertainties are at the per-cent level or even below. These are usually dominated by the uncertainties related to the MC model dependence of the efficiency and acceptance corrections (often referred to as “detector corrections”).

9.3.2.2. DIS and photoproduction: Multi-jet production in ep collisions at HERA, both in the DIS and photoproduction regime, allows for tests of QCD factorization (one initial-state proton and its associated PDF versus the hard scattering which leads to high- p_T jets) and NLO calculations which exist for 2- and 3-jet final states. Sensitivity is also obtained to the product of the coupling constant and the gluon PDF. By now experimental uncertainties of the order of 5 – 10% have been achieved, mostly dominated by jet energy scale uncertainties, whereas statistical errors are negligible to a large extent. For comparison to theoretical predictions, at large jet p_T the PDF uncertainty dominates the theoretical error (typically of order 5 - 10%, in some regions of phase-space up to 20%), therefore jet observables become useful inputs for PDF fits. In general, for Q^2 above $\sim 100 \text{ GeV}^2$ the data are well described by NLO matrix element calculations, combined with DGLAP evolution equations. Results at lower values ($Q^2 < 100 \text{ GeV}^2$) point to the necessity of including NNLO effects. Also, at low values of Q^2 and x , in particular for large jet pseudo-rapidities, there are indications for the need of BFKL-type evolution, though the predictions for such schemes are still limited. In the case of photoproduction, the data-theory comparisons are hampered by the uncertainties related to the photon PDF.

A few examples of recent measurements can be found in Refs. 147–150 for DIS and in Refs. 151–153 for photoproduction.

9.3.2.3. Hadron colliders: Jet measurements at the TEVATRON are now published for data samples up to $\sim 2 \text{ fb}^{-1}$. Among the most important cross sections measured is the inclusive jet production as a function of the jet transverse energy (E_T) or the jet transverse momentum (p_T), now available for several rapidity regions and for p_T up to 700 GeV. Most notably, the TEVATRON experiments now have measurements based on the infrared- and collinear-safe k_T algorithm in addition to the more widely used Midpoint and JetCLU algorithms of the past. Recent results by the CDF and D0 collaborations can be found in Refs. 154, 155, where we observe a good description of the data by the NLO QCD predictions. The experimental systematic uncertainties are dominated by the jet energy scale error, by now quoted to less than 3% and thus leading to uncertainties of 10 to 60% on the cross section, increasing with p_T . The PDF uncertainties dominate the theoretical error. In fact, inclusive jet data are important inputs to global PDF fits, in particular for constraining the high- x gluon PDF.

A rather comprehensive summary, comparing NLO QCD predictions to data for inclusive jet production in DIS, pp , and $p\bar{p}$ collisions, is given in Ref. 156 and reproduced here in Fig. 9.1.

Dijet events are analyzed in terms of their invariant mass and angular distributions, which allow one to put stringent limits on deviations from the Standard Model, such as quark compositeness (two recent examples can be found in Refs. 158, 159). Furthermore, dijet azimuthal correlations between the two leading jets, normalized to the total dijet cross section, are an extremely valuable tool for studying the spectrum of gluon radiation in the event. As shown in Ref. 160, the LO (non-trivial) prediction for this observable, with at

most three partons in the final state, is not able to describe the data for an azimuthal separation below $2\pi/3$, where NLO contributions (with 4 partons) restore the agreement with data. In addition, this observable can be employed to tune Monte Carlo predictions of soft gluon radiation in the final state.

Similarly important tests of QCD arise from measurements of vector boson (photon, W , Z) production together with jets. A recent analysis of photon+jet production by D0 [161] indicates that NLO calculations, combined with modern PDF sets, are unable to describe the shape of the photon p_T across the entire measured range, showing the need for an improved and consistent theoretical description of this process.

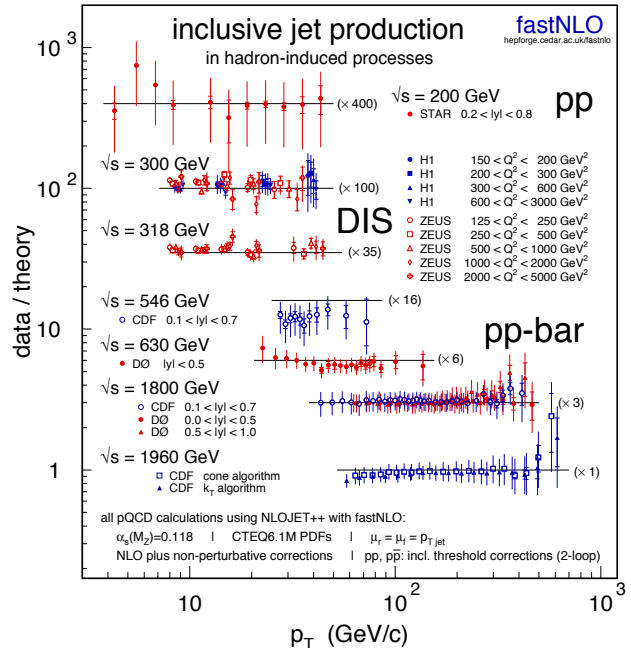


Figure 9.1: A compilation of data-over-theory ratios for inclusive jet cross sections as a function of jet transverse momentum (p_T), measured in different hadron-induced processes at different center-of-mass energies; from Ref. 156, including some updates [157]. The various ratios are scaled by arbitrary numbers (indicated between parentheses) for better readability of the plot. The theoretical predictions have been obtained at NLO accuracy, for parameter choices (coupling constant, PDFs, renormalization, and factorization scales) as indicated at the bottom of the figure. Color version at end of book.

In the case of Z +jets, the Z momentum can be precisely reconstructed using the leptons, allowing for a precise determination of the Z p_T distribution, which is sensitive to QCD radiation both at high and low scales and thus probes perturbative as well as non-perturbative effects. For example, a recent D0 result [162] quotes experimental statistical and systematic uncertainties of the order of 10%, increasing up to 20% in the lowest momentum range. The data are compared to predictions from NLO QCD and from different Monte Carlo models, where, for example, LO matrix elements for up to three partons are matched to a parton shower. Whereas the total cross section is underestimated, the shape is well reproduced over a large phase-space region. Further examples of recent results for Z (or W) plus jets production are found in Refs. 161, 163, 164. Among the most important recent developments is the completion of a NLO calculation for W +3jet production [57,58], which will be relevant also for future LHC background estimations. This type of process is an example, where jets need to be found with an infrared and collinear safe jet algorithm, such as SISCone, in order to obtain finite NLO predictions. This would not be possible with algorithms such as Midpoint or JetCLU. The latter is used for a CDF measurement [164], which is

compared to the NLO QCD prediction with SISCone as jet algorithm. Besides this inconsistency, the agreement appears to be good.

Finally, TEVATRON measurements of heavy quark (b , c) jet production, inclusive or in association with vector bosons, have led to stringent tests of NLO predictions (see Refs. 165–170 for examples of recent analyses).

9.3.3. Tests of the non-abelian nature of QCD :

QCD is a gauge theory with SU(3) as underlying gauge group. For a general gauge theory with a simple Lie group, the couplings of the fermion fields to the gauge fields and the self-interactions in the non-abelian case are determined by the coupling constant and Casimir operators of the gauge group, as introduced in Sec. 9.1. Measuring the eigenvalues of these operators, called color factors, probes the underlying structure of the theory in a gauge invariant way and provides evidence of the gluon self-interactions. Typically, cross sections can be expressed as functions of the color factors, for example $\sigma = f(\alpha_s C_F, C_A/C_F, n_f T_R/C_F)$. Sensitivity at leading order in perturbation theory can be achieved by measuring angular correlations in 4-jet events in e^+e^- annihilation or 3-jet events in DIS. Some sensitivity, although only at NLO, is also obtained from event-shape distributions. Scaling violations of fragmentation functions and the different subjet structure in quark and gluon induced jets also give access to these color factors. In order to extract absolute values, *e.g.* for C_F and C_A , certain assumptions have to be made for other parameters, such as T_R, n_f or α_s , since typically only combinations (ratios, products) of all the relevant parameters appear in the perturbative prediction. A recent compilation of results [135] quotes world average values of $C_A = 2.89 \pm 0.03(\text{stat}) \pm 0.21(\text{syst})$ and $C_F = 1.30 \pm 0.01(\text{stat}) \pm 0.09(\text{syst})$, with a correlation coefficient of 82%. These results are in perfect agreement with the expectations from SU(3) of $C_A = 3$ and $C_F = 4/3$. An overview of the history and the current status of tests of asymptotic freedom, closely related to the non-abelian nature of QCD, can be found in Ref. 171.

9.3.4. Measurements of the strong coupling constant :

If the quark masses are fixed, there is only one free parameter in the QCD Lagrangian, the strong coupling constant α_s . The coupling constant in itself is not a physical observable, but rather a quantity defined in the context of perturbation theory, which enters predictions for experimentally measurable observables, such as R in Eq. (9.7).

Many experimental observables are used to determine α_s . Considerations in such determinations include:

- The observable's sensitivity to α_s as compared to the experimental precision. For example, for the e^+e^- cross section to hadrons (cf. R in Sec. 9.2.1), QCD effects are only a small correction, since the perturbative series starts at order α_s^0 ; 3-jet production or event shapes in e^+e^- annihilations are directly sensitive to α_s since they start at order α_s ; the hadronic decay width of heavy quarkonia, $\Gamma(\Upsilon \rightarrow \text{hadrons})$, is very sensitive to α_s since its leading order term is $\propto \alpha_s^3$.
- The accuracy of the perturbative prediction, or equivalently of the relation between α_s and the value of the observable. The minimal requirement is generally considered to be an NLO prediction. Some observables are predicted to NNLO (many inclusive observables, 3-jet rates and event shapes in e^+e^- collisions) or even N³LO (e^+e^- hadronic cross section and τ branching fraction to hadrons). In certain cases, fixed-order predictions are supplemented with resummation. The precise magnitude of theory uncertainties is usually estimated as discussed in Sec. 9.2.3.
- The size of uncontrolled non-perturbative effects (except for lattice-based determinations of α_s). Sufficiently inclusive quantities, like the e^+e^- cross section to hadrons, have small non-perturbative uncertainties $\sim \Lambda^4/Q^4$. Others, such as event-shape distributions, have uncertainties $\sim \Lambda/Q$.
- The scale at which the measurement is performed. An uncertainty δ on a measurement of $\alpha_s(Q^2)$, at a scale Q , translates to an uncertainty $\delta' = (\alpha_s^2(M_Z^2)/\alpha_s^2(Q^2)) \cdot \delta$ on $\alpha_s(M_Z^2)$. For example, this enhances the already important impact of precise low- Q measurements, such as from τ decays, in combinations performed at the M_Z scale.

In this review, we make no attempt to compile a full list of measurements of α_s or to produce a new world average value from them. We rather prefer to quote a recent analysis by Bethke [172], which incorporates results with recently improved theoretical predictions and/or experimental precision[‡]. For detailed comments on the selected set of recent results we refer to Ref. 172. Here we quote the main inputs:

- Several re-analyses of the hadronic τ decay width [16,174–179], based on the new N³LO predictions, have been performed, with different approaches towards the detailed treatment of the perturbative (fixed order or contour improved perturbative expansions) and non-perturbative contributions. In Ref. 172 a value of $\alpha_s(M_Z^2) = 0.1197 \pm 0.0016$ is quoted as average, where the uncertainty spans the difference of those recent analyses.
- The N³LO calculation of the hadronic Z decay width was used in a recent revision of the global fit to electroweak precision data [180], resulting in $\alpha_s(M_Z^2) = 0.1193^{+0.0028}_{-0.0027} \pm 0.0005$, where the first error is of experimental and the second of theoretical origin.
- A combined analysis of non-singlet structure functions from DIS [181], based on QCD predictions up to N³LO, gives $\alpha_s(M_Z^2) = 0.1142 \pm 0.0023$. This uncertainty includes a theoretical error of ± 0.0008 .
- A recent re-analysis of event shapes, measured by ALEPH at the Z peak and LEP2 energies up to 209 GeV, using NNLO predictions matched to NLL resummation, has resulted in $\alpha_s(M_Z^2) = 0.1224 \pm 0.0039$ [182], with a dominant theoretical uncertainty of 0.0035. Similarly, an analysis of JADE data [183] at center-of-mass energies between 14 and 46 GeV gives $\alpha_s(M_Z^2) = 0.1172 \pm 0.0051$, with contributions from hadronization model (perturbative QCD) uncertainties of 0.0035 (0.0030).
- A new combination [184] of precision measurements at HERA, based on NLO fits to inclusive jet cross sections in neutral current DIS at high Q^2 , quotes a combined result of $\alpha_s(M_Z^2) = 0.1198 \pm 0.0032$, which includes a theoretical uncertainty of ± 0.0026 .
- An improved extraction of the strong coupling constant from a NLO analysis of radiative Υ decays [185] resulted in $\alpha_s(M_Z) = 0.119^{+0.006}_{-0.005}$.
- The HPQCD collaboration [186] computes Wilson loops and similar short-distance quantities with lattice QCD and analyzes them with NNLO perturbative QCD. This yields a value for α_s , but the lattice scale must be related to a physical energy/momentum scale. This is achieved with the Υ - Υ mass difference, however, many other quantities could be used as well [187]. HPQCD obtains $\alpha_s(M_Z^2) = 0.1183 \pm 0.0008$, where the uncertainty includes effects from truncating perturbation theory, finite lattice spacing and extrapolation of lattice data. An independent perturbative analysis of the same lattice-QCD data yields $\alpha_s(M_Z^2) = 0.1192 \pm 0.0011$ [188]. The HPQCD value [186] is taken for the average. It is the most precise of all inputs used in Ref. 172. It is worth noting that there is a more recent result in Ref. 189, which avoids the staggered fermion treatment of Ref. 186. There a value of $\alpha_s(M_Z^2) = 0.1205 \pm 0.0008 \pm 0.0005^{+0.0000}_{-0.0017}$ [189] is found, where the first uncertainty is statistical and the others are from systematics. Since this approach uses a different discretization of lattice fermions and a different general methodology, it provides an important cross check of other lattice extractions of α_s .

A non-trivial exercise consists in the evaluation of a world-average value for $\alpha_s(M_Z^2)$. A certain arbitrariness and subjective component is inevitable because of the choice of measurements to be included in the average, the treatment of (non-Gaussian) systematic uncertainties of mostly theoretical nature, as well as the treatment of correlations among the various inputs, again mostly of theoretical origin. In Ref. 172 an attempt has been made to take account of

[‡] The time evolution of α_s combinations can be followed by consulting Refs. 171, 173 as well as earlier editions of this *Review*.

such correlations, using methods as proposed, *e.g.*, in Ref. 190. The central value is determined as the weighted average of the individual measurements. For the error an overall, a-priori unknown, correlation coefficient is introduced and determined by requiring that the total χ^2 of the combination equals the number of degrees of freedom. The world average quoted in Ref. 172 is

$$\alpha_s(M_Z^2) = 0.1184 \pm 0.0007,$$

with an astonishing precision of 0.6%. It is worth noting that a cross check performed in Ref. 172, consisting in excluding each of the single measurements from the combination, resulted in variations of the central value well below the quoted uncertainty, and in a maximal increase of the combined error up to 0.0012. Most notably, excluding the most precise determination from lattice QCD gives only a marginally different average value. Nevertheless, there remains an apparent and long-standing systematic difference between the results from structure functions and other determinations of similar accuracy. This is evidenced in Fig. 9.2 (left), where the various inputs to this combination, evolved to the Z mass scale, are shown. Fig. 9.2 (right) provides strongest evidence for the correct prediction by QCD of the scale dependence of the strong coupling.

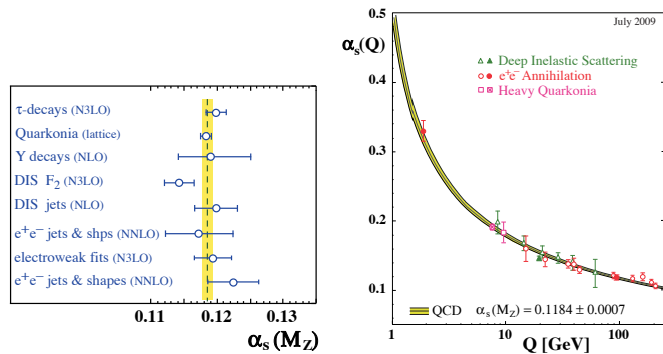


Figure 9.2: Left: Summary of measurements of $\alpha_s(M_Z^2)$, used as input for the world average value; Right: Summary of measurements of α_s as a function of the respective energy scale Q . Both plots are taken from Ref. 172.

9.4. Acknowledgments

We are grateful to S. Bethke, J. Butterworth, M. Cacciari, L. del Debbio, P. Gambino, A. Kronfeld, M. d’Onofrio, S. Sharpe, D. Treille, N. Varelas, M. Wobisch, W.M. Yao, C.P. Yuan, and G. Zanderighi for their suggestions and comments.

References:

- R.K. Ellis, W.J. Stirling, and B.R. Webber, “*QCD and collider physics*,” *Camb. Monogr. Part. Phys. Nucl. Phys. Cosmol.* **81** (1996).
- G. Dissertori, I.G. Knowles, and M. Schmelling, “*High energy experiments and theory*,” Oxford, UK: Clarendon (2003).
- R. Brock *et al.*, [CTEQ Collaboration], *Rev. Mod. Phys.* **67**, 157 (1995), see also <http://www.phys.psu.edu/~cteq/handbook/v1.1/handbook.pdf>.
- J. Smit, “*Introduction to quantum fields on a lattice: A robust mate*,” *Cambridge Lect. Notes Phys.* **15** (2002), p. 1.
- T. DeGrand and C.E. Detar, *Lattice methods for quantum chromodynamics*, *World Scientific* (2006).
- “*Perspectives in Lattice QCD*,” *Proceedings of the Workshop, Nara International Seminar House (2005)*, Ed. Y. Kuramashi, World Scientific 2008.
- T. Onogi, [arXiv:0906.2344](https://arxiv.org/abs/0906.2344) [hep-ph].
- D. d’Enterria, [arXiv:0902.2488](https://arxiv.org/abs/0902.2488) [nucl-ex].
- T. van Ritbergen, J.A.M. Vermaseren, and S.A. Larin, *Phys. Lett.* **B400**, 379 (1997) [[arXiv:hep-ph/9701390](https://arxiv.org/abs/hep-ph/9701390)].
- M. Czakon, *Nucl. Phys.* **B710**, 485 (2005) [[arXiv:hep-ph/0411261](https://arxiv.org/abs/hep-ph/0411261)].
- Y. Schroder and M. Steinhauser, *JHEP* **0601**, 051 (2006) [[arXiv:hep-ph/0512058](https://arxiv.org/abs/hep-ph/0512058)].
- K.G. Chetyrkin, J.H. Kuhn, and C. Sturm, *Nucl. Phys.* **B744**, 121 (2006) [[arXiv:hep-ph/0512060](https://arxiv.org/abs/hep-ph/0512060)].
- K.G. Chetyrkin, B.A. Kniehl, and M. Steinhauser, *Nucl. Phys.* **B510**, 61 (1998) [[arXiv:hep-ph/9708255](https://arxiv.org/abs/hep-ph/9708255)].
- See for example section 11.4 of M.E. Peskin and D.V. Schroeder, “*An Introduction To Quantum Field Theory*,” Reading, USA: Addison-Wesley (1995), 842 p.
- M. Beneke, *Phys. Reports* **317**, 1 (1999) [[arXiv:hep-ph/9807443](https://arxiv.org/abs/hep-ph/9807443)].
- P.A. Baikov, K.G. Chetyrkin, and J.H. Kuhn, *Phys. Rev. Lett.* **101**, 012002 (2008) [[arXiv:0801.1821](https://arxiv.org/abs/0801.1821) [hep-ph]].
- P.A. Baikov, K.G. Chetyrkin, and J.H. Kuhn, [arXiv:0906.2987](https://arxiv.org/abs/0906.2987) [hep-ph].
- K.G. Chetyrkin, J.H. Kuhn, and A. Kwiatkowski, *Phys. Reports* **277**, 189 (1996).
- M. Spira, *Fortsch. Phys.* **46**, 203 (1998) [[arXiv:hep-ph/9705337](https://arxiv.org/abs/hep-ph/9705337)].
- A. Djouadi, *Phys. Reports* **457**, 1 (2008) [[arXiv:hep-ph/0503172](https://arxiv.org/abs/hep-ph/0503172)].
- A.H. Hoang, *PoS TOP2006* 032, (2006) [[arXiv:hep-ph/0604185](https://arxiv.org/abs/hep-ph/0604185)].
- J.M. Zanotti, *PoS LC2008* 051 (2008).
- V.N. Gribov and L.N. Lipatov, *Sov. J. Nucl. Phys.* **15**, 438 (1972); G. Altarelli and G. Parisi, *Nucl. Phys.* **B126**, 298 (1977); Yu.L. Dokshitzer, *Sov. Phys. JETP* **46**, 641 (1977).
- A. Vogt, S. Moch, and J.A.M. Vermaseren, *Nucl. Phys.* **B691**, 129 (2004) [[arXiv:hep-ph/0404111](https://arxiv.org/abs/hep-ph/0404111)].
- S. Moch, J.A.M. Vermaseren, and A. Vogt, *Nucl. Phys.* **B688**, 101 (2004) [[arXiv:hep-ph/0403192](https://arxiv.org/abs/hep-ph/0403192)].
- J.A.M. Vermaseren, A. Vogt, and S. Moch, *Nucl. Phys.* **B724**, 3 (2005) [[arXiv:hep-ph/0504242](https://arxiv.org/abs/hep-ph/0504242)].
- E.B. Zijlstra and W.L. van Neerven, *Phys. Lett.* **B297**, 377 (1992).
- S. Moch, J.A.M. Vermaseren, and A. Vogt, [arXiv:0812.4168](https://arxiv.org/abs/0812.4168) [hep-ph].
- E. Laenen *et al.*, *Nucl. Phys.* **B392**, 162 (1993); S. Riemersma, J. Smith, and W.L. van Neerven, *Phys. Lett.* **B347**, 143 (1995) [[arXiv:hep-ph/9411431](https://arxiv.org/abs/hep-ph/9411431)].
- I. Bierenbaum, J. Blumlein, and S. Klein, *Nucl. Phys.* **B820**, 417 (2009) [[arXiv:0904.3563](https://arxiv.org/abs/0904.3563) [hep-ph]].
- J.C. Collins, D.E. Soper, and G. Sterman, *Nucl. Phys.* **B261**, 104 (1985).
- R. Hamberg, W.L. van Neerven, and T. Matsuura, *Nucl. Phys.* **B359**, 343 (1991); Erratum *ibid.*, **B 644** 403, (2002).
- R.V. Harlander and W.B. Kilgore, *Phys. Rev. Lett.* **88**, 201801 (2002) [[arXiv:hep-ph/0201206](https://arxiv.org/abs/hep-ph/0201206)].
- C. Anastasiou and K. Melnikov, *Nucl. Phys.* **B646**, 220 (2002) [[arXiv:hep-ph/0207004](https://arxiv.org/abs/hep-ph/0207004)].
- V. Ravindran, J. Smith, and W.L. van Neerven, *Nucl. Phys.* **B665**, 325 (2003) [[arXiv:hep-ph/0302135](https://arxiv.org/abs/hep-ph/0302135)].
- R.V. Harlander and K. J. Ozeren, [arXiv:0909.3420](https://arxiv.org/abs/0909.3420) [hep-ph].
- M. Greco and A. Vicini, *Nucl. Phys.* **B415**, 386 (1994).
- L.N. Lipatov, *Sov. J. Nucl. Phys.* **23**, 338 (1976) [*Yad. Fiz.* **23**, 642 (1976)].
- E.A. Kuraev, L.N. Lipatov, and V.S. Fadin, *Sov. Phys. JETP* **45**, 199 (1977) [*Zh. Eksp. Teor. Fiz.* **72**, 377 (1977)].
- I.I. Balitsky and L.N. Lipatov, *Sov. J. Nucl. Phys.* **28**, 822 (1978) [*Yad. Fiz.* **28**, 1597 (1978)].
- V.S. Fadin and L.N. Lipatov, *Phys. Lett.* **B429**, 127 (1998) [[arXiv:hep-ph/9802290](https://arxiv.org/abs/hep-ph/9802290)].
- M. Ciafaloni and G. Camici, *Phys. Lett.* **B430**, 329 (1998) [[arXiv:hep-ph/9803389](https://arxiv.org/abs/hep-ph/9803389)].
- S. Marzani *et al.*, *Nucl. Phys.* **B783**, 143 (2007) [[arXiv:0704.2404](https://arxiv.org/abs/0704.2404) [hep-ph]].
- M. Ciafaloni *et al.*, *JHEP* **0708**, 046 (2007) [[arXiv:0707.1453](https://arxiv.org/abs/0707.1453) [hep-ph]].

45. C.D. White and R.S. Thorne, Phys. Rev. **D75**, 034005 (2007) [arXiv:hep-ph/0611204].
46. I. Balitsky, Nucl. Phys. **B463**, 99 (1996) [arXiv:hep-ph/9509348].
47. Y.V. Kovchegov, Phys. Rev. **D60**, 034008 (1999) [arXiv:hep-ph/9901281].
48. A. Hebecker, Phys. Reports **331**, 1 (2000) [arXiv:hep-ph/9905226].
49. A.V. Belitsky and A.V. Radyushkin, Phys. Reports **418**, 1 (2005) [arXiv:hep-ph/0504030].
50. E. Boos *et al.*, [CompHEP Collaboration], Nucl. Instrum. Methods **A534**, 250 (2004) [arXiv:hep-ph/0403113]; <http://comphep.sinp.msu.ru/>.
51. J. Alwall *et al.*, JHEP **0709**, 028 (2007) [arXiv:0706.2334 [hep-ph]]; <http://madgraph.hep.uiuc.edu/>.
52. M.L. Mangano *et al.*, JHEP **0307**, 001 (2003) [arXiv:hep-ph/0206293]; <http://cern.ch/mlm/alpgen/>.
53. T. Gleisberg and S. Hoche, JHEP **0812**, 039 (2008) [arXiv:0808.3674 [hep-ph]].
54. A. Cafarella, C.G. Papadopoulos, and M. Worek, arXiv:0710.2427 [hep-ph]; <http://cern.ch/helac-phegas/>.
55. F.A. Berends and W.T. Giele, Nucl. Phys. **B306**, 759 (1988).
56. L.J. Dixon, arXiv:hep-ph/9601359.
57. C.F. Berger *et al.*, arXiv:0907.1984 [hep-ph].
58. R. Keith Ellis, K. Melnikov, and G. Zanderighi, arXiv:0906.1445 [hep-ph].
59. G. Bevilacqua *et al.*, arXiv:0907.4723 [hep-ph].
60. A. Bredenstein *et al.*, arXiv:0905.0110 [hep-ph].
61. S. Catani and M.H. Seymour, Nucl. Phys. **B485**, 291 (1997) [Erratum-ibid. B **510** (1998) 503] [arXiv:hep-ph/9605323].
62. S. Frixione, Z. Kunszt, and A. Signer, Nucl. Phys. **B467**, 399 (1996) [arXiv:hep-ph/9512328].
63. D.A. Kosower, Phys. Rev. **D57**, 5410 (1998) [arXiv:hep-ph/9710213]; J.M. Campbell, M.A. Cullen, and E.W.N. Glover, Eur. Phys. J. **C9**, 245 (1999) [arXiv:hep-ph/9809429]; D.A. Kosower, Phys. Rev. **D71**, 045016 (2005) [arXiv:hep-ph/0311272].
64. Z. Bern *et al.*, [NLO Multileg Working Group], arXiv:0803.0494 [hep-ph].
65. Z. Nagy, Phys. Rev. **D68**, 094002 (2003) [arXiv:hep-ph/0307268]; <http://cern.ch/nagy/z/Site/NLOJet++.html>.
66. J.M. Campbell and R.K. Ellis, Phys. Rev. **D62**, 114012 (2000) [arXiv:hep-ph/0006304]; <http://mcfm.fnal.gov/>.
67. K. Arnold *et al.*, Comput. Phys. Commun. **180** 1661, (2009) [arXiv:0811.4559 [hep-ph]]; <http://www-itsp.particle.uni-karlsruhe.de/~vbfnlweb/>.
68. T. Binoth *et al.*, Eur. Phys. J. **C16**, 311 (2000) [arXiv:hep-ph/9911340]; http://lappweb.in2p3.fr/lapth/PHOX_FAMILY/.
69. A. Gehrmann-De Ridder *et al.*, JHEP **0712**, 094 (2007) [arXiv:0711.4711 [hep-ph]].
70. S. Weinzierl, Phys. Rev. Lett. **101**, 162001 (2008) [arXiv:0807.3241 [hep-ph]]; JHEP **0906**, 041 (2009) [arXiv:0904.1077 [hep-ph]].
71. K. Melnikov and F. Petriello, Phys. Rev. **D74**, 114017 (2006) [arXiv:hep-ph/0609070].
72. S. Catani *et al.*, arXiv:0903.2120 [hep-ph].
73. C. Anastasiou, K. Melnikov, and F. Petriello, Nucl. Phys. **B724**, 197 (2005) [arXiv:hep-ph/0501130].
74. S. Catani and M. Grazzini, Phys. Rev. Lett. **98**, 222002 (2007) [arXiv:hep-ph/0703012].
75. Y.L. Dokshitzer, D. Diakonov, and S.I. Troian, Phys. Reports **58**, 269 (1980).
76. G. Parisi and R. Petronzio, Nucl. Phys. **B154**, 427 (1979).
77. G. Curci, M. Greco, and Y. Srivastava, Nucl. Phys. **B159**, 451 (1979).
78. A. Bassetto, M. Ciafaloni, and G. Marchesini, Nucl. Phys. **B163**, 477 (1980).
79. J.C. Collins and D.E. Soper, Nucl. Phys. **B193**, 381 (1981) [Erratum-*ibid.* **B213**, 545 (1983)].
80. J.C. Collins and D.E. Soper, Nucl. Phys. **B197**, 446 (1982).
81. J. Kodaira and L. Trentadue, Phys. Lett. **B112**, 66 (1982).
82. J. Kodaira and L. Trentadue, Phys. Lett. **B123**, 335 (1983).
83. J.C. Collins, D.E. Soper, and G. Sterman, Nucl. Phys. **B250**, 199 (1985).
84. S. Catani, *et al.*, Nucl. Phys. **B407**, 3 (1993).
85. S. Fleming, arXiv:0907.3897 [hep-ph].
86. S. Catani, *et al.*, Phys. Lett. **B269**, 432 (1991).
87. N. Brown and W.J. Stirling, Phys. Lett. **B252**, 657 (1990).
88. W. Bartel, *et al.*, [JADE Collaboration], Z. Phys. **C33**, 23 (1986).
89. N. Kidonakis, G. Oderda, and G. Sterman, Nucl. Phys. **B531**, 365 (1998) [arXiv:hep-ph/9803241].
90. R. Bonciani *et al.*, Phys. Lett. **B575**, 268 (2003) [arXiv:hep-ph/0307035].
91. A. Banfi, G.P. Salam, and G. Zanderighi, JHEP **0503**, 073 (2005) [arXiv:hep-ph/0407286].
92. D. de Florian and M. Grazzini, Phys. Rev. Lett. **85**, 4678 (2000) [arXiv:hep-ph/0008152].
93. G. Bozzi *et al.*, Phys. Lett. **B564**, 65 (2003) [arXiv:hep-ph/0302104].
94. C. Balazs and C.P. Yuan, Phys. Rev. **D56**, 5558 (1997) [arXiv:hep-ph/9704258].
95. D. de Florian and M. Grazzini, Nucl. Phys. **B704**, 387 (2005) [arXiv:hep-ph/0407241].
96. S. Moch and P. Uwer, Phys. Rev. **D78**, 034003 (2008) [arXiv:0804.1476 [hep-ph]].
97. N. Kidonakis and R. Vogt, Phys. Rev. **D78**, 074005 (2008) [arXiv:0805.3844 [hep-ph]].
98. M. Beneke, P. Falgari, and C. Schwinn, arXiv:0907.1443 [hep-ph].
99. M. Czakon, A. Mitov, and G. Sterman, arXiv:0907.1790 [hep-ph].
100. A. Ferroglia *et al.*, arXiv:0907.4791 [hep-ph].
101. T. Becher and M.D. Schwartz, JHEP **0807**, 034 (2008) [arXiv:0803.0342 [hep-ph]].
102. S. Moch and A. Vogt, Phys. Lett. **B631**, 48 (2005) [arXiv:hep-ph/0508265].
103. E. Laenen and L. Magnea, Phys. Lett. **B632**, 270 (2006) [arXiv:hep-ph/0508284].
104. T. Sjostrand *et al.*, Comput. Phys. Commun. **135** 238, (2001) [arXiv:hep-ph/0010017].
105. T. Sjostrand, S. Mrenna, and P. Skands, JHEP **0605**, 026 (2006) [arXiv:hep-ph/0603175]; <http://projects.hepforge.org/pythia6/>.
106. T. Sjostrand, S. Mrenna, and P. Skands, Comput. Phys. Commun. **178** 852, (2008) [arXiv:0710.3820 [hep-ph]]; <http://home.thep.lu.se/~torbjorn/Pythia.html>.
107. B.R. Webber, Nucl. Phys. **B238**, 492 (1984).
108. G. Corcella *et al.*, JHEP **0101**, 010 (2001) [arXiv:hep-ph/0011363]; <http://hepwww.rl.ac.uk/theory/seymour/herwig/>.
109. M. Bahr *et al.*, Eur. Phys. J. **C58**, 639 (2008) [arXiv:0803.0883 [hep-ph]]; <http://projects.hepforge.org/herwig/>.
110. T. Gleisberg *et al.*, JHEP **0902**, 007 (2009) [arXiv:0811.4622 [hep-ph]]; <http://projects.hepforge.org/sherpa/>.
111. L. Lonnblad, Comput. Phys. Commun. **71** 15, (1992).
112. T. Sjostrand, arXiv:hep-ph/0611247.
113. B. Andersson *et al.*, Phys. Reports **97**, 31 (1983).
114. T. Sjostrand, Nucl. Phys. **B248**, 469 (1984).
115. S. Catani *et al.*, JHEP **0111**, 063 (2001) [arXiv:hep-ph/0109231].
116. J. Alwall *et al.*, Eur. Phys. J. **C53**, 473 (2008) [arXiv:0706.2569 [hep-ph]].
117. S. Frixione and B.R. Webber, JHEP **0206**, 029 (2002) [arXiv:hep-ph/0204244].
118. P. Nason, JHEP **0411**, 040 (2004) [arXiv:hep-ph/0409146].
119. M. Cacciari *et al.*, JHEP **0404**, 068 (2004) [arXiv:hep-ph/0303085].

120. M. Dasgupta and G.P. Salam, *J. Phys.* **G30**, R143 (2004) [arXiv:hep-ph/0312283].
121. S. Moretti, L. Lonnblad, and T. Sjostrand, *JHEP* **9808**, 001 (1998) [arXiv:hep-ph/9804296].
122. G.P. Salam, arXiv:0906.1833 [hep-ph].
123. S.D. Ellis *et al.*, *Prog. in Part. Nucl. Phys.* **60**, 484 (2008) [arXiv:0712.2447 [hep-ph]].
124. G.P. Salam and G. Soyez, *JHEP* **0705**, 086 (2007) [arXiv:0704.0292 [hep-ph]].
125. S. Catani *et al.*, *Nucl. Phys.* **B406**, 187 (1993).
126. S.D. Ellis and D.E. Soper, *Phys. Rev.* **D48**, 3160 (1993) [arXiv:hep-ph/9305266].
127. Y.L. Dokshitzer *et al.*, *JHEP* **9708**, 001 (1997) [arXiv:hep-ph/9707323].
128. M. Wobisch and T. Wengler, arXiv:hep-ph/9907280.
129. M. Cacciari, G.P. Salam, and G. Soyez, *JHEP* **0804**, 063 (2008) [arXiv:0802.1189 [hep-ph]].
130. M. Cacciari and G.P. Salam, *Phys. Lett.* **B641**, 57 (2006) [arXiv:hep-ph/0512210]; M. Cacciari, G.P. Salam, and G. Soyez, <http://fastjet.fr/>.
131. P.A. Delsart, K. Geerlins, and J. Huston, <http://www.pa.msu.edu/~huston/SpartyJet/SpartyJet.html>.
132. S. Brandt *et al.*, *Phys. Lett.* **12**, 57 (1964).
133. E. Farhi, *Phys. Rev. Lett.* **39**, 1587 (1977).
134. O. Biebel, *Phys. Reports* **340**, 165 (2001).
135. S. Kluth, *Rept. on Prog. in Phys.* **69**, 1771 (2006) [arXiv:hep-ex/0603011].
136. A. Banfi, G.P. Salam, and G. Zanderighi, *JHEP* **0408**, 062 (2004) [arXiv:hep-ph/0407287].
137. D.E. Acosta *et al.*, [CDF Collaboration], *Phys. Rev.* **D71**, 112002 (2005) [arXiv:hep-ex/0505013].
138. T. Aaltonen *et al.*, [CDF Collaboration], *Phys. Rev.* **D78**, 072005 (2008) [arXiv:0806.1699 [hep-ex]].
139. C. Adloff *et al.*, [H1 Collaboration], *Nucl. Phys.* **B545**, 3 (1999) [arXiv:hep-ex/9901010].
140. S. Chekanov *et al.*, [ZEUS Collaboration], *Nucl. Phys.* **B700**, 3 (2004) [arXiv:hep-ex/0405065].
141. C. Glasman [H1 Collaboration and ZEUS Collaboration], *Nucl. Phys. (Proc. Supp.)* **191**, 121 (2009) [arXiv:0812.0757 [hep-ex]].
142. M. Martinez, arXiv:0905.2727 [hep-ex].
143. J.M. Campbell, J.W. Huston, and W.J. Stirling, *Rept. on Prog. in Phys.* **70**, 89 (2007) [arXiv:hep-ph/0611148].
144. C. Royon, arXiv:0811.1544 [hep-ex].
145. V.D. Elvira [D0 Collaboration and CDF Collaboration], arXiv:0808.0901 [hep-ex].
146. C. Glasman, arXiv:0810.3570 [hep-ex].
147. F.D. Aaron *et al.*, [H1 Collaboration], arXiv:0904.3870 [hep-ex].
148. F.D. Aaron *et al.*, [H1 Collaboration], *Eur. Phys. J.* **C54**, 389 (2008) [arXiv:0711.2606 [hep-ex]].
149. S. Chekanov *et al.*, [ZEUS Collaboration], *Eur. Phys. J.* **C52**, 515 (2007) [arXiv:0707.3093 [hep-ex]].
150. S. Chekanov *et al.*, [ZEUS Collaboration], *Phys. Rev.* **D78**, 032004 (2008) [arXiv:0802.3955 [hep-ex]].
151. S. Chekanov *et al.*, [ZEUS Collaboration], *Nucl. Phys.* **B792**, 1 (2008) [arXiv:0707.3749 [hep-ex]].
152. S. Chekanov *et al.*, [ZEUS Collaboration], *Phys. Rev.* **D76**, 072011 (2007) [arXiv:0706.3809 [hep-ex]].
153. A. Aktas *et al.*, [H1 Collaboration], *Phys. Lett.* **B639**, 21 (2006) [arXiv:hep-ex/0603014].
154. A. Abulencia *et al.*, [CDF - Run II Collaboration], *Phys. Rev.* **D75**, 092006 (2007) [Erratum-ibid. 119901] [arXiv:hep-ex/0701051].
155. V.M. Abazov *et al.*, [D0 Collaboration], *Phys. Rev. Lett.* **101**, 062001 (2008) [arXiv:0802.2400 [hep-ex]].
156. T. Kluge, K. Rabbertz, and M. Wobisch, arXiv:hep-ph/0609285.
157. K. Rabbertz, private communication, Aug 2009.
158. T. Aaltonen *et al.*, [CDF Collaboration], *Phys. Rev.* **D79**, 112002 (2009) [arXiv:0812.4036 [hep-ex]].
159. V.M. Abazov *et al.*, [D0 Collaboration], arXiv:0906.4819 [hep-ex], submitted to *Phys. Rev. Lett.*
160. V.M. Abazov *et al.*, [D0 Collaboration], *Phys. Rev. Lett.* **94**, 221801 (2005) [arXiv:hep-ex/0409040].
161. V.M. Abazov *et al.*, [D0 Collaboration], *Phys. Rev. Lett.* **678**, 45 (2009) [arXiv:0903.1748 [hep-ex]].
162. V.M. Abazov *et al.*, [D0 Collaboration], *Phys. Lett.* **B669**, 278 (2008) [arXiv:0808.1296 [hep-ex]].
163. T. Aaltonen *et al.*, [CDF - Run II Collaboration], *Phys. Rev. Lett.* **100**, 102001 (2008) [arXiv:0711.3717 [hep-ex]].
164. T. Aaltonen *et al.*, [CDF Collaboration], *Phys. Rev.* **D77**, 011108 (2008) [arXiv:0711.4044 [hep-ex]].
165. CDF Collaboration, public note 8418, July 2006; see also http://www-cdf.fnal.gov/physics/new/qcd/abstracts/bjet_05.html.
166. V.M. Abazov *et al.*, [D0 Collaboration], *Phys. Rev. Lett.* **102**, 192002 (2009) [arXiv:0901.0739 [hep-ex]].
167. V.M. Abazov *et al.*, [D0 Collaboration], *Phys. Lett.* **B666**, 23 (2008) [arXiv:0803.2259 [hep-ex]].
168. T. Aaltonen *et al.*, [CDF Collaboration], *Phys. Rev. Lett.* **100**, 091803 (2008) [arXiv:0711.2901 [hep-ex]].
169. A. Abulencia *et al.*, [CDF Collaboration], *Phys. Rev.* **D74**, 032008 (2006) [arXiv:hep-ex/0605099].
170. T. Aaltonen *et al.*, [CDF collaboration], arXiv:0812.4458 [hep-ex], submitted to *Phys. Rev. D.*
171. S. Bethke, *Prog. in Part. Nucl. Phys.* **58**, 351 (2007) [arXiv:hep-ex/0606035].
172. S. Bethke, arXiv:0908.1135 [hep-ph].
173. S. Bethke, *J. Phys.* **G26**, R27 (2000) [arXiv:hep-ex/0004021].
174. M. Beneke and M. Jamin, *JHEP* **0809**, 044 (2008) [arXiv:0806.3156 [hep-ph]].
175. M. Davier *et al.*, *Eur. Phys. J.* **C56**, 305 (2008) [arXiv:0803.0979 [hep-ph]].
176. K. Maltman and T. Yavin, *Phys. Rev.* **D78**, 094020 (2008) [arXiv:0807.0650 [hep-ph]].
177. S. Menke, arXiv:0904.1796 [hep-ph].
178. S. Narison, *Phys. Lett.* **B673**, 30 (2009) [arXiv:0901.3823 [hep-ph]].
179. I. Caprini and J. Fischer, arXiv:0906.5211 [hep-ph], acc. by *Eur. Phys. J. C.*
180. H. Flacher *et al.*, *Eur. Phys. J.* **C60**, 543 (2009) [arXiv:0811.0009 [hep-ph]].
181. J. Blumlein, H. Bottcher, and A. Guffanti, *Nucl. Phys.* **B774**, 182 (2007) [arXiv:hep-ph/0607200].
182. G. Dissertori *et al.*, *JHEP* **0908**, 036 (2009) [arXiv:0906.3436 [hep-ph]].
183. S. Bethke *et al.*, [JADE Collaboration], arXiv:0810.1389 [hep-ex].
184. C. Glasman [H1 Collaboration and ZEUS Collaboration], *J. Phys. Conf. Ser.* **110** 022013 (2008) [arXiv:0709.4426 [hep-ex]].
185. N. Brambilla *et al.*, *Phys. Rev.* **D75**, 074014 (2007) [arXiv:hep-ph/0702079].
186. C.T.H. Davies *et al.*, [HPQCD Collaboration], *Phys. Rev.* **D78**, 114507 (2008) [arXiv:0807.1687 [hep-lat]].
187. C.T.H. Davies *et al.*, [HPQCD Collaboration, UKQCD Collaboration, and MILC Collaboration], *Phys. Rev. Lett.* **92**, 022001 (2004) [arXiv:hep-lat/0304004].
188. K. Maltman, *et al.*, *Phys. Rev.* **D78**, 114504 (2008) [arXiv:0807.2020 [hep-lat]].
189. S. Aoki, *et al.*, [PACS-CS Collaboration], arXiv:0906.3906 [hep-lat].
190. M. Schmelling, *Phys. Scripta* **51**, 676 (1995).

10. ELECTROWEAK MODEL AND CONSTRAINTS ON NEW PHYSICS

Revised November 2009 by J. Erler (U. Mexico) and P. Langacker (Institute for Advanced Study).

- 10.1 Introduction
- 10.2 Renormalization and radiative corrections
- 10.3 Low energy electroweak observables
- 10.4 W and Z boson physics
- 10.5 Precision flavor physics
- 10.6 Experimental results
- 10.7 Constraints on new physics

10.1. Introduction

The standard electroweak model (SM) is based on the gauge group [1] $SU(2) \times U(1)$, with gauge bosons W_μ^i , $i = 1, 2, 3$, and B_μ for the $SU(2)$ and $U(1)$ factors, respectively, and the corresponding gauge coupling constants g and g' . The left-handed fermion fields of the i^{th} fermion family transform as doublets $\Psi_i = \begin{pmatrix} \nu_i \\ \ell_i^- \end{pmatrix}$ and $\begin{pmatrix} u_i \\ d_i^- \end{pmatrix}$ under $SU(2)$, where $d_i^- \equiv \sum_j V_{ij} d_j$, and V is the Cabibbo-Kobayashi-Maskawa mixing matrix. (Constraints on V and tests of universality are discussed in Ref. 2 and in the Section on “The CKM Quark-Mixing Matrix”. The extension of the formalism to allow an analogous leptonic mixing matrix is discussed in the Section on “Neutrino Mass, Mixing, and Flavor Change”.) The right-handed fields are $SU(2)$ singlets. In the minimal model there are three fermion families and a single complex Higgs doublet $\phi \equiv \begin{pmatrix} \phi^+ \\ \phi^0 \end{pmatrix}$ which is introduced for mass generation.

After spontaneous symmetry breaking the Lagrangian for the fermion fields, ψ_i , is

$$\begin{aligned} \mathcal{L}_F = & \sum_i \bar{\psi}_i \left(i \not{\partial} - m_i - \frac{gm_i H}{2M_W} \right) \psi_i \\ & - \frac{g}{2\sqrt{2}} \sum_i \bar{\Psi}_i \gamma^\mu (1 - \gamma^5) (T^+ W_\mu^+ + T^- W_\mu^-) \Psi_i \\ & - e \sum_i q_i \bar{\psi}_i \gamma^\mu \psi_i A_\mu \\ & - \frac{g}{2 \cos \theta_W} \sum_i \bar{\psi}_i \gamma^\mu (g_V^i - g_A^i \gamma^5) \psi_i Z_\mu. \end{aligned} \quad (10.1)$$

$\theta_W \equiv \tan^{-1}(g'/g)$ is the weak angle; $e = g \sin \theta_W$ is the positron electric charge; and $A \equiv B \cos \theta_W + W^3 \sin \theta_W$ is the (massless) photon field. $W^\pm \equiv (W^1 \mp iW^2)/\sqrt{2}$ and $Z \equiv -B \sin \theta_W + W^3 \cos \theta_W$ are the massive charged and neutral weak boson fields, respectively. T^+ and T^- are the weak isospin raising and lowering operators. The vector and axial-vector couplings are

$$g_V^i \equiv t_{3L}(i) - 2q_i \sin^2 \theta_W, \quad (10.2a)$$

$$g_A^i \equiv t_{3L}(i), \quad (10.2b)$$

where $t_{3L}(i)$ is the weak isospin of fermion i (+1/2 for u_i and ν_i ; -1/2 for d_i and e_i) and q_i is the charge of ψ_i in units of e .

The second term in \mathcal{L}_F represents the charged-current weak interaction [3,4]. For example, the coupling of a W to an electron and a neutrino is

$$-\frac{e}{2\sqrt{2} \sin \theta_W} \left[W_\mu^- \bar{\nu} \gamma^\mu (1 - \gamma^5) \nu + W_\mu^+ \bar{e} \gamma^\mu (1 - \gamma^5) e \right]. \quad (10.3)$$

For momenta small compared to M_W , this term gives rise to the effective four-fermion interaction with the Fermi constant given (at tree level, *i.e.*, lowest order in perturbation theory) by $G_F/\sqrt{2} = g^2/8M_W^2$. CP violation is incorporated in the SM by a single observable phase in V_{ij} . The third term in \mathcal{L}_F describes electromagnetic interactions (QED), and the last is the weak neutral-current interaction.

In Eq. (10.1), m_i is the mass of the i^{th} fermion ψ_i . For the quarks these are the current masses. For the light quarks, as described in the note on “Quark Masses” in the Quark Listings, $\hat{m}_u = 2.5_{-1.0}^{+0.8}$ MeV, $\hat{m}_d = 5.0_{-1.5}^{+1.0}$ MeV, and $\hat{m}_s = 105_{-35}^{+25}$ MeV. These are running $\overline{\text{MS}}$ masses evaluated at the scale $\mu = 2$ GeV. (In this Section we denote

quantities defined in the modified minimal subtraction ($\overline{\text{MS}}$) scheme by a caret; the exception is the strong coupling constant, α_s , which will always correspond to the $\overline{\text{MS}}$ definition and where the caret will be dropped.) For the heavier quarks we use QCD sum rule constraints [5] and recalculate their masses in each call of our fits to account for their direct α_s dependence. We find, $\hat{m}_c(\mu = \hat{m}_c) = 1.266_{-0.036}^{+0.031}$ GeV and $\hat{m}_b(\mu = \hat{m}_b) = 4.198 \pm 0.023$ GeV, with a correlation of 25%. The top quark “pole” mass, $m_t = 173.1 \pm 1.3$ GeV, is an average [6] of published and preliminary CDF and $D\bar{O}$ results from run I and II. We are working, however, with $\overline{\text{MS}}$ masses in all expressions to minimize theoretical uncertainties, and therefore convert this result to the top quark $\overline{\text{MS}}$ mass,

$$\hat{m}_t(\mu = \hat{m}_t) = m_t \left[1 - \frac{4\alpha_s}{3\pi} + \mathcal{O}(\alpha_s^2) \right],$$

using the three-loop formula [7]. This introduces an additional uncertainty which we estimate to 0.5 GeV (the size of the three-loop term). We are assuming that the kinematic mass extracted from the collider events corresponds within this uncertainty to the pole mass. Using the BLM optimized [8] version of the two-loop perturbative QCD formula [9] (as we did in previous editions of this *Review*) gives virtually identical results. Thus, we will use $m_t = 173.1 \pm 0.6$ (stat.) ± 1.1 (syst.) ± 0.5 (QCD) GeV $\approx 173.1 \pm 1.35$ GeV (together with $M_H = 117$ GeV) for the numerical values quoted in Sec. 10.2–Sec. 10.5. In the presence of right-handed neutrinos, Eq. (10.1) gives rise also to Dirac neutrino masses. The possibility of Majorana masses is discussed in the Section on “Neutrino Mass, Mixing, and Flavor Change”.

H is the physical neutral Higgs scalar which is the only remaining part of ϕ after spontaneous symmetry breaking. The Yukawa coupling of H to ψ_i , which is flavor diagonal in the minimal model, is $gm_i/2M_W$. In non-minimal models there are additional charged and neutral scalar Higgs particles [10].

10.2. Renormalization and radiative corrections

The SM has three parameters (not counting the Higgs boson mass, M_H , and the fermion masses and mixings). A particularly useful set contains the Z mass, the fine structure constant, and the Fermi constant, which will be discussed in turn:

The Z boson mass, $M_Z = 91.1876 \pm 0.0021$ GeV, has been determined from the Z lineshape scan at LEP 1 [11].

The fine structure constant, $\alpha = 1/137.035999084(51)$, is currently best determined from the e^\pm anomalous magnetic moment [12] using the revised 4-loop QED result from Ref. 13. (For other determinations, see Ref. 14.) In most electroweak renormalization schemes, it is convenient to define a running α dependent on the energy scale of the process, with $\alpha^{-1} \sim 137$ appropriate at very low energy, *i.e.* close to the Thomson limit. (The running has also been observed [15] directly.) For scales above a few hundred MeV this introduces an uncertainty due to the low energy hadronic contribution to vacuum polarization. In the modified minimal subtraction ($\overline{\text{MS}}$) scheme [16] (used for this *Review*), and with $\alpha_s(M_Z) = 0.120$ for the QCD coupling at M_Z , we have $\hat{\alpha}(m_\tau)^{-1} = 133.444 \pm 0.015$ and $\hat{\alpha}(M_Z)^{-1} = 127.916 \pm 0.015$. The latter corresponds to a quark sector contribution (without the top) to the conventional (on-shell) QED coupling, $\alpha(M_Z) = \frac{\alpha}{1 - \Delta\alpha(M_Z)}$,

of $\Delta\alpha_{\text{had}}^{(5)}(M_Z) \approx 0.02793 \pm 0.00011$. These values are updated from Ref. 17 with $\Delta\alpha_{\text{had}}^{(5)}(M_Z)$ moved upwards and its uncertainty almost halved (mostly due to a more precise $\hat{m}_c(\hat{m}_c)$). Its correlation with the μ^\pm anomalous magnetic moment (see Sec. 10.5), as well as the non-linear α_s dependence of $\hat{\alpha}(M_Z)$ and the resulting correlation with the input variable α_s , are fully taken into account in the fits. This is done by using as actual input (fit constraint) instead of $\Delta\alpha_{\text{had}}^{(5)}(M_Z)$ the analogous low energy contribution by the three light quarks, $\Delta\alpha_{\text{had}}^{(3)}(1.8 \text{ GeV}) = (57.29 \pm 0.90) \times 10^{-4}$, and by calculating the perturbative and heavy quark contributions to $\hat{\alpha}(M_Z)$ in each call of the fits according to Ref. 17. The uncertainty is from e^+e^- annihilation data below 1.8 GeV and τ decay data; from isospin breaking effects (affecting the interpretation of the τ data); from

uncalculated higher order perturbative and non-perturbative QCD corrections; and from the $\overline{\text{MS}}$ quark masses. Such a short distance mass definition (unlike the pole mass) is free from non-perturbative and renormalon [18] uncertainties. Various recent evaluations of $\Delta\alpha_{\text{had}}^{(5)}$ are summarized in Table 10.1. where the leading order relation between the $\overline{\text{MS}}$ and on-shell definitions is given by,

$$\Delta\hat{\alpha}(M_Z) - \Delta\alpha(M_Z) = \frac{\alpha}{\pi} \left(\frac{100}{27} - \frac{1}{6} - \frac{7}{4} \ln \frac{M_Z^2}{M_W^2} \right) \approx 0.0072,$$

and where the first term is from fermions and the other two are from W^\pm loops which are usually excluded from the on-shell definition. Most of the older results relied on $e^+e^- \rightarrow \text{hadrons}$ cross-section measurements up to energies of 40 GeV, which were somewhat higher than the QCD prediction, suggested stronger running, and were less precise. The most recent results typically assume the validity of perturbative QCD (PQCD) at scales of 1.8 GeV and above, and are in reasonable agreement with each other. (Evaluations in the on-shell scheme utilize threshold data from BES [38] as further input.) There is, however, some discrepancy between analyzes based on $e^+e^- \rightarrow \text{hadrons}$ cross-section data and those based on τ decay spectral functions [39,40]. The latter utilize data from OPAL [41], CLEO [42], ALEPH [43], and Belle [44] and imply lower central values for the extracted M_H of about 6%. This discrepancy is smaller than in the past and at least some of it appears to be experimental. The dominant $e^+e^- \rightarrow \pi^+\pi^-$ cross-section was measured with the CMD-2 [45] and SND [46] detectors at the VEPP-2M e^+e^- collider at Novosibirsk and the results are (after an initial discrepancy due to a flaw in the Monte Carlo event generator used by SND) in good agreement with each other. As an alternative to cross-section scans, one can use the high statistics radiative return events at e^+e^- accelerators operating at resonances such as the Φ or the $\Upsilon(4S)$. The method [47] is systematic dominated. The BaBar collaboration [48] studied multi-hadron events radiatively returned from the $\Upsilon(4S)$, reconstructing the radiated photon and normalizing to $\mu^\pm\gamma$ final states. Their result is higher compared to VEPP-2M and in fact agrees quite well with the τ analysis including the energy dependence (shape). In contrast, the shape and smaller overall cross-section from the $\pi^+\pi^-$ radiative return results from the Φ obtained by the KLOE collaboration [49] differs significantly from what is observed by BaBar. The discrepancy originates from the kinematic region $\sqrt{s} \gtrsim 0.6$ GeV, and is most pronounced for $\sqrt{s} \gtrsim 0.85$ GeV. For a recent review on these e^+e^- data, see Ref. 50. All measurements including older data [51] are accounted for in the fits on the basis of results in Refs. [28,40,50]. Further improvement of this dominant theoretical uncertainty in the interpretation of precision data will require better measurements of the cross-section for $e^+e^- \rightarrow \text{hadrons}$ below the charmonium resonances including multi-pion and other final states. To improve the precisions in $\hat{m}_c(\hat{m}_c)$ and $\hat{m}_b(\hat{m}_b)$ it would help to remeasure the threshold regions of the heavy quarks as well as the electronic decay widths of the narrow $c\bar{c}$ and $b\bar{b}$ resonances.

The Fermi constant, $G_F = 1.166364(5) \times 10^{-5}$ GeV $^{-2}$, is derived from the muon lifetime formula*,

$$\tau_\mu^{-1} = \frac{G_F^2 m_\mu^5}{192\pi^3} F(\rho) \left(1 + \frac{3}{5} \frac{m_\mu^2}{M_W^2} \right) \left[1 + H_1(\rho) \frac{\hat{\alpha}(m_\mu)}{\pi} + H_2(\rho) \frac{\hat{\alpha}^2(m_\mu)}{\pi^2} \right], \quad (10.4)$$

where $\rho = m_c^2/m_\mu^2$, and where

$$\begin{aligned} F(\rho) &= 1 - 8\rho + 8\rho^3 - \rho^4 - 12\rho^2 \ln \rho = 0.999813, \\ H_1(\rho) &= \frac{25}{8} - \frac{\pi^2}{2} - (9 + 4\pi^2 + 12 \ln \rho) \rho \\ &\quad + 16\rho^2 \rho^{3/2} + \mathcal{O}(\rho^2) = -1.8079, \end{aligned}$$

* In the spirit of the Fermi theory, the propagator correction proportional to m_μ^2 could instead be incorporated into Δr (see below), but we choose to leave it in the definition of G_F for historical consistency.

$$\begin{aligned} H_2(\rho) &= \frac{156815}{5184} - \frac{518}{81} \pi^2 - \frac{895}{36} \zeta(3) + \frac{67}{720} \pi^4 \\ &\quad + \frac{53}{6} \pi^2 \ln 2 - \frac{5}{4} \pi^2 \sqrt{\rho} + \mathcal{O}(\rho) = 6.7, \\ \hat{\alpha}(m_\mu)^{-1} &= \alpha^{-1} + \frac{1}{3\pi} \ln \rho = 135.9. \end{aligned}$$

The massless corrections to H_1 and H_2 have been obtained in Refs. 52 and 53, respectively. The mass corrections to H_1 have been known for some time [54], while those to H_2 are very recent [55]. Notice the term linear in m_e whose appearance was unforeseen and can be traced to the use of the muon pole mass in the prefactor [55]. The remaining uncertainty in G_F is experimental and has recently been halved by the MuLan [56] and FAST [57] collaborations.

With these inputs, $\sin^2 \theta_W$ and the W boson mass, M_W , can be calculated when values for m_t and M_H are given; conversely (as is done at present), M_H can be constrained by $\sin^2 \theta_W$ and M_W . The value of $\sin^2 \theta_W$ is extracted from Z pole observables and neutral-current processes [11,60], and depends on the renormalization prescription. There are a number of popular schemes [61–68] leading to values which differ by small factors depending on m_t and M_H . The notation for these schemes is shown in Table 10.1.

Table 10.1: Notations used to indicate the various schemes discussed in the text. Each definition of $\sin^2 \theta_W$ leads to values that differ by small factors depending on m_t and M_H . Approximate values are also given for illustration.

Scheme	Notation	Value
On-shell	s_W^2	0.2233
NOV	$s_{M_Z}^2$	0.2311
$\overline{\text{MS}}$	\hat{s}_Z^2	0.2313
$\overline{\text{MS}}$ ND	\hat{s}_{ND}^2	0.2315
Effective angle	\hat{s}_f^2	0.2316

- (i) The on-shell scheme [61] promotes the tree-level formula $\sin^2 \theta_W = 1 - M_W^2/M_Z^2$ to a definition of the renormalized $\sin^2 \theta_W$ to all orders in perturbation theory, *i.e.*, $\sin^2 \theta_W \rightarrow s_W^2 \equiv 1 - M_W^2/M_Z^2$:

$$M_W = \frac{A_0}{s_W(1 - \Delta r)^{1/2}}, \quad M_Z = \frac{M_W}{c_W}, \quad (10.5)$$

where $c_W \equiv \cos \theta_W$, $A_0 = (\pi\alpha/\sqrt{2}G_F)^{1/2} = 37.28061(8)$ GeV, and Δr includes the radiative corrections relating α , $\alpha(M_Z)$, G_F , M_W , and M_Z . One finds $\Delta r \sim \Delta r_0 - \rho_t/\tan^2 \theta_W$, where $\Delta r_0 = 1 - \alpha/\hat{\alpha}(M_Z) = 0.06655(11)$ is due to the running of α , and $\rho_t = 3G_F m_t^2/8\sqrt{2}\pi^2 = 0.00939(m_t/173.1 \text{ GeV})^2$ represents the dominant (quadratic) m_t dependence. There are additional contributions to Δr from bosonic loops, including those which depend logarithmically on M_H . One has $\Delta r = 0.0362 \mp 0.0005 \pm 0.00011$, where the second uncertainty is from $\alpha(M_Z)$. Thus the value of s_W^2 extracted from M_Z includes an uncertainty (∓ 0.00019) from the currently allowed range of m_t . This scheme is simple conceptually. However, the relatively large ($\sim 3\%$) correction from ρ_t causes large spurious contributions in higher orders.

- (ii) A more precisely determined quantity $s_{M_Z}^2$ [62] can be obtained from M_Z by removing the (m_t, M_H) dependent term from Δr [63], *i.e.*,

$$s_{M_Z}^2(1 - s_{M_Z}^2) \equiv \frac{\pi\alpha(M_Z)}{\sqrt{2}G_F M_Z^2}. \quad (10.6)$$

Using $\alpha(M_Z)^{-1} = 128.91 \pm 0.02$ yields $s_{M_Z}^2 = 0.23108 \mp 0.00005$. The small uncertainty in $s_{M_Z}^2$ compared to other schemes is because the m_t dependence has been removed by definition. However, the m_t uncertainty reemerges when other quantities

(e.g., M_W or other Z pole observables) are predicted in terms of M_Z .

Both s_W^2 and $s_{M_Z}^2$ depend not only on the gauge couplings but also on the spontaneous-symmetry breaking, and both definitions are awkward in the presence of any extension of the SM which perturbs the value of M_Z (or M_W). Other definitions are motivated by the tree-level coupling constant definition $\theta_W = \tan^{-1}(g'/g)$:

(iii) In particular, the modified minimal subtraction ($\overline{\text{MS}}$) scheme introduces the quantity $\sin^2 \hat{\theta}_W(\mu) \equiv \hat{g}'^2(\mu)/[\hat{g}^2(\mu) + \hat{g}'^2(\mu)]$, where the couplings \hat{g} and \hat{g}' are defined by modified minimal subtraction and the scale μ is conveniently chosen to be M_Z for many electroweak processes. The value of $\hat{s}_Z^2 = \sin^2 \hat{\theta}_W(M_Z)$ extracted from M_Z is less sensitive than s_W^2 to m_t (by a factor of $\tan^2 \theta_W$), and is less sensitive to most types of new physics than s_W^2 or $s_{M_Z}^2$. It is also very useful for comparing with the predictions of grand unification. There are actually several variant definitions of $\sin^2 \hat{\theta}_W(M_Z)$, differing according to whether or how finite $\alpha \ln(m_t/M_Z)$ terms are decoupled (subtracted from the couplings). One cannot entirely decouple the $\alpha \ln(m_t/M_Z)$ terms from all electroweak quantities because $m_t \gg m_b$ breaks SU(2) symmetry. The scheme that will be adopted here decouples the $\alpha \ln(m_t/M_Z)$ terms from the γ - Z mixing [16,64], essentially eliminating any $\ln(m_t/M_Z)$ dependence in the formulae for asymmetries at the Z pole when written in terms of \hat{s}_Z^2 . (A similar definition is used for $\hat{\alpha}$.) The various definitions are related by

$$\hat{s}_Z^2 = c(m_t, M_H) s_W^2 = \bar{c}(m_t, M_H) s_{M_Z}^2, \quad (10.7)$$

where $c = 1.0361 \pm 0.0005$ and $\bar{c} = 1.0010 \mp 0.0002$. The quadratic m_t dependence is given by $c \sim 1 + \rho_t/\tan^2 \theta_W$ and $\bar{c} \sim 1 - \rho_t/(1 - \tan^2 \theta_W)$, respectively. The expressions for M_W and M_Z in the $\overline{\text{MS}}$ scheme are

$$M_W = \frac{A_0}{\hat{s}_Z(1 - \Delta\hat{r}_W)^{1/2}}, \quad M_Z = \frac{M_W}{\hat{\rho}^{1/2} \hat{c}_Z}, \quad (10.8)$$

and one predicts $\Delta\hat{r}_W = 0.06971 \pm 0.00002 \pm 0.00011$. $\Delta\hat{r}_W$ has no quadratic m_t dependence, because shifts in M_W are absorbed into the observed G_F , so that the error in $\Delta\hat{r}_W$ is dominated by $\Delta r_0 = 1 - \alpha/\hat{\alpha}(M_Z)$ which induces the second quoted uncertainty. The quadratic m_t dependence has been shifted into $\hat{\rho} \sim 1 + \rho_t$, where including bosonic loops, $\hat{\rho} = 1.01047 \pm 0.00015$. Quadratic M_H effects are deferred to two-loop order, while the leading logarithmic M_H effect is a good approximation only for large M_H values which are currently disfavored by the precision data. As an illustration, the shift in M_W due to a large M_H (for fixed M_Z) is given by

$$\begin{aligned} \Delta_H M_W &= -\frac{11}{96} \frac{\alpha}{\pi} \frac{M_W}{c_W^2 - s_W^2} \ln \frac{M_H^2}{M_W^2} + \mathcal{O}(\alpha^2) \\ &\sim -200 \text{ MeV (for } M_H = 10 M_W). \end{aligned}$$

(iv) A variant $\overline{\text{MS}}$ quantity \hat{s}_{ND}^2 (used in the 1992 edition of this *Review*) does not decouple the $\alpha \ln(m_t/M_Z)$ terms [65]. It is related to \hat{s}_Z^2 by

$$\hat{s}_Z^2 = \hat{s}_{\text{ND}}^2 \left(1 + \frac{\hat{\alpha}}{\pi} d\right), \quad (10.9a)$$

$$d = \frac{1}{3} \left(\frac{1}{\hat{s}^2} - \frac{8}{3} \right) \left[\left(1 + \frac{\alpha_s}{\pi}\right) \ln \frac{m_t}{M_Z} - \frac{15\alpha_s}{8\pi} \right], \quad (10.9b)$$

Thus, $\hat{s}_Z^2 - \hat{s}_{\text{ND}}^2 \sim -0.0002$ for $m_t = 173.1$ GeV.

(v) Yet another definition, the effective angle [66–68] \hat{s}_f^2 for the Z vector coupling to fermion f , is described in Sec. 10.3.

Experiments are at such level of precision that complete $\mathcal{O}(\alpha)$ radiative corrections must be applied. For neutral-current and Z pole processes, these corrections are conveniently divided into two classes:

1. QED diagrams involving the emission of real photons or the exchange of virtual photons in loops, but not including vacuum polarization diagrams. These graphs often yield finite and gauge-invariant contributions to observable processes. However, they are dependent on energies, experimental cuts, *etc.*, and must be calculated individually for each experiment.
2. Electroweak corrections, including $\gamma\gamma$, γZ , ZZ , and WW vacuum polarization diagrams, as well as vertex corrections, box graphs, *etc.*, involving virtual W and Z bosons. Many of these corrections are absorbed into the renormalized Fermi constant defined in Eq. (10.4). Others modify the tree-level expressions for Z pole observables and neutral-current amplitudes in several ways [58]. One-loop corrections are included for all processes. In addition, certain two-loop corrections are also important. In particular, two-loop corrections involving the top quark modify ρ_t in $\hat{\rho}$, Δr , and elsewhere by

$$\rho_t \rightarrow \rho_t [1 + R(M_H, m_t) \rho_t / 3]. \quad (10.10)$$

$R(M_H, m_t)$ is best described as an expansion in M_Z^2/m_t^2 . The unsuppressed terms were first obtained in Ref. 69, and are known analytically [70]. Contributions suppressed by M_Z^2/m_t^2 were first studied in Ref. 71 with the help of small and large Higgs mass expansions, which can be interpolated. These contributions are about as large as the leading ones in Refs. 69 and 70. The complete two-loop calculation of Δr (without further approximation) has been performed in Refs. 72 and 73 for fermionic and purely bosonic diagrams, respectively. Similarly, the electroweak two-loop calculation for the relation between \hat{s}_e^2 and s_W^2 is complete [74] including the recently obtained purely bosonic contribution [75]. For M_H above its lower direct limit, $-17 < R \leq -13$.

Mixed QCD-electroweak contributions to gauge boson self-energies of order $\alpha\alpha_s m_t^2$ [76] and $\alpha\alpha_s^2 m_t^2$ [77] increase the predicted value of m_t by 6%. This is, however, almost entirely an artifact of using the pole mass definition for m_t . The equivalent corrections when using the $\overline{\text{MS}}$ definition $\hat{m}_t(\hat{m}_t)$ increase m_t by less than 0.5%. The subleading $\alpha\alpha_s$ corrections [78] are also included. Further three-loop corrections of order $\alpha\alpha_s^2$ [79], $\alpha^3 m_t^6$ [80,81], and $\alpha^2 \alpha_s m_t^4$ (for $M_H = 0$) [80], are rather small. The same is true for $\alpha^3 M_H^4$ [82] corrections unless M_H approaches 1 TeV. Also known are the singlet contributions (pure gluonic intermediate states) of order $\alpha\alpha_s^2$ [83] and $\alpha\alpha_s^3$ [84]. Recently, the corresponding non-singlet contributions have been computed as well [85].

The leading electroweak two-loop terms for the $Z \rightarrow b\bar{b}$ -vertex of $\mathcal{O}(\alpha^2 m_t^4)$ have been obtained in Refs. 69 and 70, and the mixed QCD-electroweak contributions in Refs. 86 and 87. Very recently, the authors of Ref. 88 completed the two-loop electroweak fermionic corrections to \hat{s}_b^2 . The $\mathcal{O}(\alpha\alpha_s)$ -vertex corrections involving massless quarks [89] add coherently, resulting in a sizable effect and shift $\alpha_s(M_Z)$ when extracted from Z lineshape observables (see Sec. 10.3) by $\approx +0.0007$.

Throughout this *Review* we utilize electroweak radiative corrections from the program GAPP [90], which works entirely in the $\overline{\text{MS}}$ scheme, and which is independent of the package ZFITTER [68].

10.3. Low energy electroweak observables

It is convenient to write the four-fermion interactions relevant to ν -hadron, ν - e , as well as parity violating e -hadron and e - e neutral-current processes in a form that is valid in an arbitrary gauge theory (assuming massless left-handed neutrinos). One has,

$$\begin{aligned} -\mathcal{L}^{\nu h} &= \frac{G_F}{\sqrt{2}} \bar{\nu} \gamma^\mu (1 - \gamma^5) \nu \sum_i \left[\epsilon_L(i) \bar{q}_i \gamma_\mu (1 - \gamma^5) q_i \right. \\ &\quad \left. + \epsilon_R(i) \bar{q}_i \gamma_\mu (1 + \gamma^5) q_i \right], \quad (10.11) \end{aligned}$$

$$-\mathcal{L}^{\nu e} = \frac{G_F}{\sqrt{2}} \bar{\nu} \gamma^\mu (1 - \gamma^5) \nu_\mu \bar{e} \gamma_\mu (g_V^{\nu e} - g_A^{\nu e} \gamma^5) e, \quad (10.12)$$

$$-\mathcal{L}^{eh} = -\frac{G_F}{\sqrt{2}} \sum_i \left[C_{1i} \bar{e} \gamma_\mu \gamma^5 e \bar{q}_i \gamma^\mu q_i + C_{2i} \bar{e} \gamma_\mu e \bar{q}_i \gamma^\mu \gamma^5 q_i \right], \quad (10.13)$$

$$-\mathcal{L}^{ee} = -\frac{G_F}{\sqrt{2}} C_{2e} \bar{e} \gamma_\mu \gamma^5 e \bar{e} \gamma^\mu e, \quad (10.14)$$

where one must include the charged-current contribution for ν_e - e and $\bar{\nu}_e$ - e and the parity-conserving QED contribution for electron scattering.

The SM expressions for $\epsilon_{L,R}(i)$, $g_{V,A}^{\nu e}$, and C_{ij} are given in Table 10.2. Note, that $g_{V,A}^{\nu e}$ and the other quantities are coefficients of effective four-Fermi operators, which differ from the quantities defined in Eq. (10.2) in the radiative corrections and in the presence of possible physics beyond the SM.

Table 10.2: Standard Model expressions for the neutral-current parameters for ν -hadron, ν - e , and e^- -scattering processes.

At tree level, $\rho = \kappa = 1$, $\lambda = 0$. If radiative corrections are included, $\rho_{\nu N} = 1.0081$, $\hat{\kappa}_{\nu N}(\langle Q^2 \rangle) = -20 \text{ GeV}^2 = 0.9972$, $\hat{\kappa}_{\nu N}(\langle Q^2 \rangle) = -35 \text{ GeV}^2 = 0.9964$, $\lambda_{uL} = -0.0031$, $\lambda_{dL} = -0.0025$ and $\lambda_R = 3.7 \times 10^{-5}$. For ν - e scattering, $\rho_{\nu e} = 1.0127$ and $\hat{\kappa}_{\nu e} = 0.9965$ (at $\langle Q^2 \rangle = 0$). For atomic parity violation and the polarized DIS experiment at SLAC, $\rho'_e = 0.9877$, $\rho_e = 1.0006$, $\hat{\kappa}'_e = 1.0026$, $\hat{\kappa}_e = 1.0299$, $\lambda' = -1.8 \times 10^{-5}$, $\lambda_u = -0.0118$ and $\lambda_d = 0.0029$. And for polarized Möller scattering with SLAC (JLab) kinematics, $\lambda_e = -0.0002$ ($\lambda_e = -0.0004$). The dominant m_t dependence is given by $\rho \sim 1 + \rho_t$, while $\hat{\kappa} \sim 1$ ($\overline{\text{MS}}$) or $\kappa \sim 1 + \rho_t / \tan^2 \theta_W$ (on-shell).

Quantity	Standard Model Expression
$\epsilon_L(u)$	$\rho_{\nu N} \left(\frac{1}{2} - \frac{2}{3} \hat{\kappa}_{\nu N} \hat{s}_Z^2 \right) + \lambda_{uL}$
$\epsilon_L(d)$	$\rho_{\nu N} \left(-\frac{1}{2} + \frac{1}{3} \hat{\kappa}_{\nu N} \hat{s}_Z^2 \right) + \lambda_{dL}$
$\epsilon_R(u)$	$\rho_{\nu N} \left(-\frac{2}{3} \hat{\kappa}_{\nu N} \hat{s}_Z^2 \right) + \lambda_R$
$\epsilon_R(d)$	$\rho_{\nu N} \left(\frac{1}{3} \hat{\kappa}_{\nu N} \hat{s}_Z^2 \right) + 2 \lambda_R$
$g_V^{\nu e}$	$\rho_{\nu e} \left(-\frac{1}{2} + 2 \hat{\kappa}_{\nu e} \hat{s}_Z^2 \right)$
$g_A^{\nu e}$	$\rho_{\nu e} \left(-\frac{1}{2} \right)$
C_{1u}	$\rho'_e \left(-\frac{1}{2} + \frac{4}{3} \hat{\kappa}'_e \hat{s}_Z^2 \right) + \lambda'$
C_{1d}	$\rho'_e \left(\frac{1}{2} - \frac{2}{3} \hat{\kappa}'_e \hat{s}_Z^2 \right) - 2 \lambda'$
C_{2u}	$\rho_e \left(-\frac{1}{2} + 2 \hat{\kappa}_e \hat{s}_Z^2 \right) + \lambda_u$
C_{2d}	$\rho_e \left(\frac{1}{2} - 2 \hat{\kappa}_e \hat{s}_Z^2 \right) + \lambda_d$
C_{2e}	$\rho_e \left(\frac{1}{2} - 2 \hat{\kappa}_e \hat{s}_Z^2 \right) + \lambda_e$

10.3.1. Neutrino scattering :

A precise determination of the on-shell s_W^2 , which depends only very weakly on m_t and M_H , is obtained from deep inelastic scattering (DIS) of neutrinos from (approximately) isoscalar targets [91]. The ratio $R_\nu \equiv \sigma_{\nu N}^{NC} / \sigma_{\nu N}^{CC}$ of neutral-to-charged-current cross-sections has been measured to 1% accuracy by the CDHS [92] and CHARM [93] collaborations at CERN. The CCFR [94] collaboration at Fermilab has obtained an even more precise result, so it is important to obtain theoretical expressions for R_ν and $R_{\bar{\nu}} \equiv \sigma_{\bar{\nu} N}^{NC} / \sigma_{\bar{\nu} N}^{CC}$ to comparable accuracy. Fortunately, many of the uncertainties from the strong interactions and neutrino spectra cancel in the ratio. A large theoretical uncertainty is associated with the c -threshold, which mainly affects σ^{CC} . Using the slow rescaling prescription [95] the central value of $\sin^2 \theta_W$ from CCFR varies as $0.0111(m_c [\text{GeV}] - 1.31)$, where m_c is the effective mass which is numerically close to the $\overline{\text{MS}}$ mass $\hat{m}_c(\hat{m}_c)$, but their exact relation is unknown at higher orders.

For $m_c = 1.31 \pm 0.24 \text{ GeV}$ (determined from ν -induced dimuon production [96]) this contributes ± 0.003 to the total uncertainty $\Delta \sin^2 \theta_W \sim \pm 0.004$. (The experimental uncertainty is also ± 0.003 .) This uncertainty largely cancels, however, in the Paschos-Wolfenstein ratio [97],

$$R^- = \frac{\sigma_{\nu N}^{NC} - \sigma_{\bar{\nu} N}^{NC}}{\sigma_{\nu N}^{CC} - \sigma_{\bar{\nu} N}^{CC}}. \quad (10.15)$$

It was measured by Fermilab's NuTeV collaboration [98] for the first time, and required a high-intensity and high-energy anti-neutrino beam.

A simple zeroth-order approximation is

$$R_\nu = g_L^2 + g_R^2, \quad R_{\bar{\nu}} = g_L^2 + \frac{g_R^2}{r}, \quad R^- = g_L^2 - g_R^2, \quad (10.16)$$

where

$$g_L^2 \equiv \epsilon_L(u)^2 + \epsilon_L(d)^2 \approx \frac{1}{2} - \sin^2 \theta_W + \frac{5}{9} \sin^4 \theta_W, \quad (10.17a)$$

$$g_R^2 \equiv \epsilon_R(u)^2 + \epsilon_R(d)^2 \approx \frac{5}{9} \sin^4 \theta_W, \quad (10.17b)$$

and $r \equiv \sigma_{\bar{\nu} N}^{CC} / \sigma_{\nu N}^{CC}$ is the ratio of $\bar{\nu}$ to ν charged-current cross-sections, which can be measured directly. (In the simple parton model, ignoring hadron energy cuts, $r \approx (\frac{1}{3} + \epsilon) / (1 + \frac{1}{3}\epsilon)$, where $\epsilon \sim 0.125$ is the ratio of the fraction of the nucleon's momentum carried by anti-quarks to that carried by quarks.) In practice, Eq. (10.16) must be corrected for quark mixing, quark sea effects, c -quark threshold effects, non-isoscalarity, W - Z propagator differences, the finite muon mass, QED and electroweak radiative corrections. Details of the neutrino spectra, experimental cuts, x and Q^2 dependence of structure functions, and longitudinal structure functions enter only at the level of these corrections and therefore lead to very small uncertainties. The CCFR group quotes $s_W^2 = 0.2236 \pm 0.0041$ for $(m_t, M_H) = (175, 150) \text{ GeV}$ with very little sensitivity to (m_t, M_H) .

The NuTeV collaboration found $s_W^2 = 0.2277 \pm 0.0016$ (for the same reference values), which was 3.0σ higher than the SM prediction [98]. Since then a number of experimental and theoretical developments implied shifts in the extracted s_W^2 , most of them reducing the discrepancy: (i) NuTeV also measured [99] the difference between the strange and anti-strange quark momentum distributions, $S^- \equiv \int_0^1 dx [s(x) - \bar{s}(x)] = 0.00196 \pm 0.00143$, from dimuon events utilizing the first complete next-to-leading order QCD description [100] and parton distribution functions (PDFs) according to Ref. 101. The magnitude of the central value agrees with the earlier result [102] but differs in sign. The effect of $S^- \neq 0$ on the NuTeV value for s_W^2 has been studied in Ref. 102, and the S^- above translates into a shift $\delta s_W^2 = -0.0014 \pm 0.0010$. On the other hand, there are theoretical arguments (see Ref. 103 and references therein) favoring a zero crossing of $x[s(x) - \bar{s}(x)]$ at values much larger than seen by NuTeV and suggesting an effect of much smaller and perhaps negligible size. We will therefore take half of the above shift as an estimate of both the S^- effect and the associated uncertainty, $\delta s_W^2 = -0.0007 \pm 0.0007$, replacing the original uncertainty [98] of ± 0.00047 . (ii) The measured branching ratio for K_{e3} decays enters crucially in the determination of the $\nu_e(\bar{\nu}_e)$ contamination of the $\nu_\mu(\bar{\nu}_\mu)$ beam. This branching ratio has moved from $4.82 \pm 0.06\%$ at the time of the original publication [98] to the current value of $5.07 \pm 0.04\%$, *i.e.*, a change by more than 4σ . To reflect this, we move s_W^2 by $+0.0016$ and reduce the $\nu_e(\bar{\nu}_e)$ uncertainty by a factor of $2/3$. (iii) PDFs seem to violate isospin symmetry at levels much stronger than generally expected [104]. A minimum χ^2 set of PDFs generalized in this sense [105,106] shows a reduction in the NuTeV discrepancy in s_W^2 by 0.0015 . But isospin symmetry violating PDFs are currently not well constrained phenomenologically and within uncertainties the NuTeV anomaly could be accounted for in full or conversely made larger [105]. Still, the leading contribution from quark mass differences turns out to be largely model-independent [107] and a shift, $\delta s_W^2 = -0.0015 \pm 0.0003$ [103], is applied. (iv) QED splitting effects also violate isospin symmetry with an effect on s_W^2 whose sign (reducing the discrepancy) is model-independent. The corresponding shift of $\delta s_W^2 = -0.0011$ has been calculated in Ref. 108

and a 100% uncertainty is assigned to it. (v) Nuclear shadowing effects [109] are likely to affect the interpretation of the NuTeV result at some level, but the NuTeV collaboration argues that their data are dominated by values of Q^2 at which nuclear shadowing is expected to be relatively small so that we do not apply a correction. However, another nuclear effect, the isovector EMC effect [110], is much larger (because it affects all neutrons in the nucleus, not just the excess ones) and model-independently works to reduce the discrepancy. It is estimated to lead to a shift of $\delta s_W^2 = -0.0019 \pm 0.0006$ [103]. (vi) The extracted s_W^2 may also shift at the level of the quoted uncertainty when analyzed using the most recent QED and electroweak radiative corrections [111,112], as well as QCD corrections to the structure functions [113]. However, their precise impact can be estimated only after the NuTeV data have been analyzed with a new set of PDFs including these new radiative corrections while simultaneously allowing isospin breaking and asymmetric strange seas. Remaining one- and two-loop radiative corrections have been estimated [112] to induce uncertainties in the extracted s_W^2 of ± 0.0004 and ± 0.0003 , respectively, compared to the initial error of ± 0.00011 [102]. Most of the s_W^2 dependence and the NuTeV discrepancy reside in g_L^2 (initially 2.7σ low). Thus, the total shift of $\delta s_W^2 = -0.0036 \pm 0.0015$ corresponds to $\delta g_L^2 = +0.0027 \mp 0.0011$ and we arrive at $g_L^2 = 0.3027 \pm 0.0018$ which we use as a constraint in the fits. The right-handed coupling, $g_R^2 = 0.0308 \pm 0.0011$ (which is 0.7σ high) and the other ν -DIS data are expected to exhibit shifts as well, but these ought to be less significant since their relative experimental uncertainties are larger. In view of these developments and caveats, we use the NuTeV result in this *Review* but consider it along with the other ν -DIS data as preliminary until a re-analysis using PDFs including all experimental and theoretical information and correlations has been completed.

The cross-section in the laboratory system for $\nu_\mu e \rightarrow \nu_\mu e$ or $\bar{\nu}_\mu e \rightarrow \bar{\nu}_\mu e$ elastic scattering is

$$\frac{d\sigma_{\nu,\bar{\nu}}}{dy} = \frac{G_F^2 m_e E_\nu}{2\pi} \left[(g_V^{\nu e} \pm g_A^{\nu e})^2 + (g_V^{\nu e} \mp g_A^{\nu e})^2 (1-y)^2 - (g_V^{\nu e 2} - g_A^{\nu e 2}) \frac{y m_e}{E_\nu} \right], \quad (10.18)$$

where the upper (lower) sign refers to ν_μ ($\bar{\nu}_\mu$), and $y \equiv T_e/E_\nu$ (which runs from 0 to $(1 + m_e/2E_\nu)^{-1}$) is the ratio of the kinetic energy of the recoil electron to the incident ν or $\bar{\nu}$ energy. For $E_\nu \gg m_e$ this yields a total cross-section

$$\sigma = \frac{G_F^2 m_e E_\nu}{2\pi} \left[(g_V^{\nu e} \pm g_A^{\nu e})^2 + \frac{1}{3} (g_V^{\nu e} \mp g_A^{\nu e})^2 \right]. \quad (10.19)$$

The most accurate measurements [114–117] of $\sin^2 \theta_W$ from ν -lepton scattering are from the ratio $R \equiv \sigma_{\nu\mu e}/\sigma_{\bar{\nu}\mu e}$ in which many of the systematic uncertainties cancel. Radiative corrections (other than m_t effects) are small compared to the precision of present experiments and have negligible effect on the extracted $\sin^2 \theta_W$. The most precise experiment (CHARM II) [116] determined not only $\sin^2 \theta_W$ but $g_{V,A}^{\nu e}$ as well. The cross-sections for $\nu_e e$ and $\bar{\nu}_e e$ may be obtained from Eq. (10.18) by replacing $g_{V,A}^{\nu e}$ by $g_{V,A}^{\nu e} + 1$, where the 1 is due to the charged-current contribution [117,118].

10.3.2. Parity violation :

The SLAC polarized electron-deuteron DIS experiment [119] measured the right-left asymmetry,

$$A = \frac{\sigma_R - \sigma_L}{\sigma_R + \sigma_L}, \quad (10.20)$$

where $\sigma_{R,L}$ is the cross-section for the deep-inelastic scattering of a right- or left-handed electron: $e_{R,L} N \rightarrow eX$. In the quark parton model,

$$\frac{A}{Q^2} = a_1 + a_2 \frac{1 - (1-y)^2}{1 + (1-y)^2}, \quad (10.21)$$

where $Q^2 > 0$ is the momentum transfer and y is the fractional energy transfer from the electron to the hadrons. For the deuteron or other isoscalar targets, one has, neglecting the s -quark and anti-quarks,

$$a_1 = \frac{3G_F}{5\sqrt{2}\pi\alpha} \left(C_{1u} - \frac{1}{2} C_{1d} \right) \approx \frac{3G_F}{5\sqrt{2}\pi\alpha} \left(-\frac{3}{4} + \frac{5}{3} \sin^2 \theta_W \right), \quad (10.22a)$$

$$a_2 = \frac{3G_F}{5\sqrt{2}\pi\alpha} \left(C_{2u} - \frac{1}{2} C_{2d} \right) \approx \frac{9G_F}{5\sqrt{2}\pi\alpha} \left(\sin^2 \theta_W - \frac{1}{4} \right). \quad (10.22b)$$

In another polarized-electron scattering experiment on deuterons, but in the quasi-elastic kinematic regime, the SAMPLE experiment [120] at MIT-Bates extracted the combination $C_{2u} - C_{2d}$ at Q^2 values of 0.1 GeV^2 and 0.038 GeV^2 . What was actually determined were nucleon form factors from which the quoted results were obtained by the removal of a multi-quark radiative correction [121]. Other linear combinations of the C_{iq} have been determined in polarized-lepton scattering at CERN in μ -C DIS, at Mainz in e -Be (quasi-elastic), and at Bates in e -C (elastic). See the review articles in Refs. 59 and 122 for more details. Recent polarized electron asymmetry experiments, *i.e.*, SAMPLE, the PVA4 experiment at Mainz, and the HAPPEX and G0 experiments at Jefferson Lab, have focussed on the strange quark content of the nucleon. These are reviewed in Ref. 123, where it is shown that they can also provide significant constraints on C_{1u} and C_{1d} which complement those from atomic parity violation.

The parity violating asymmetry, A_{PV} , in fixed target polarized Moller scattering, $e^- e^- \rightarrow e^- e^-$, is defined as in Eq. (10.20) and reads [124],

$$\frac{A_{PV}}{Q^2} = -2C_{2e} \frac{G_F}{\sqrt{2}\pi\alpha} \frac{1-y}{1+y^4+(1-y)^4}, \quad (10.23)$$

where y is again the energy transfer. It has been measured at low $Q^2 = 0.026 \text{ GeV}^2$ in the SLAC E158 experiment [125], with the result $A_{PV} = (-1.31 \pm 0.14 \text{ (stat.)} \pm 0.10 \text{ (syst.)}) \times 10^{-7}$. Expressed in terms of the weak mixing angle in the $\overline{\text{MS}}$ scheme, this yields $\hat{s}^2(Q^2) = 0.2403 \pm 0.0013$, and established the scale dependence of the weak mixing (see Fig. 10.1) at the level of 6.4 standard deviations. One can also define the so-called weak charge of the electron (*cf.* Eq. (10.24) below) as $Q_W(e) \equiv -2C_{2e} = -0.0403 \pm 0.0053$ (the implications are discussed in Ref. 126). In a similar experiment and at about the same Q^2 , Qweak at Jefferson Lab [127] will be able to measure the weak charge of the proton, $Q_W(p) = -2[2C_{1u} + C_{1d}]$, and $\sin^2 \theta_W$ in polarized ep scattering with relative precisions of 4% and 0.3%, respectively. These experiments will provide the most precise determinations of the weak mixing angle off the Z peak and will be sensitive to various types of physics beyond the SM.

There are precise experiments measuring atomic parity violation (APV) [131] in cesium [132,133] (at the 0.4% level [132]), thallium [134], lead [135], and bismuth [136]. The electroweak physics is contained in the weak charges which are defined by,

$$Q_W(Z, N) \equiv -2[C_{1u}(2Z + N) + C_{1d}(Z + 2N)] \approx Z(1 - 4 \sin^2 \theta_W) - N. \quad (10.24)$$

E.g., $Q_W(^{133}\text{Cs})$ is extracted by measuring experimentally the ratio of the parity violating amplitude, E_{PNC} , to the Stark vector transition polarizability, β , and by calculating theoretically E_{PNC} in terms of Q_W . One can then write,

$$Q_W = N \left(\frac{\text{Im } E_{\text{PNC}}}{\beta} \right)_{\text{exp.}} \left(\frac{|e| a_B Q_W}{\text{Im } E_{\text{PNC}} N} \right)_{\text{th.}} \left(\frac{\beta}{a_B^3} \right)_{\text{exp.+th.}} \left(\frac{a_B^2}{|e|} \right).$$

The uncertainties associated with atomic wave functions are quite small for cesium [137]. In the past, the semi-empirical value of β added another source of theoretical uncertainty [138]. The ratio of the off-diagonal hyperfine amplitude to the polarizability has now been measured directly by the Boulder group [139]. Combined with the precisely known hyperfine amplitude [140] one finds, $\beta = 26.991 \pm 0.046$, in excellent agreement with the earlier results, reducing the overall theory uncertainty (while slightly increasing the experimental error). The very recent state-of-the-art many body calculation [141] yields, $\text{Im } E_{\text{PNC}} = (0.8906 \pm 0.0026) \times 10^{-11} |e| a_B Q_W/N$, while the two measurements [132,133] combine to give $\text{Im } E_{\text{PNC}}/\beta = -1.5924 \pm 0.0055 \text{ mV/cm}$, and we obtain $Q_W(^{133}\text{Cs}) = -73.20 \pm 0.35$. Thus, the various theoretical efforts in Refs. 141 and 142 together with an update of the SM calculation [128] removed an earlier 2.3σ deviation from the SM (see the year 2000 edition of this *Review*). The theoretical uncertainties are 3% for thallium [143] but larger for the other atoms. The Boulder experiment in cesium also observed the parity-violating weak corrections to the nuclear electromagnetic vertex (the anapole moment [144]).

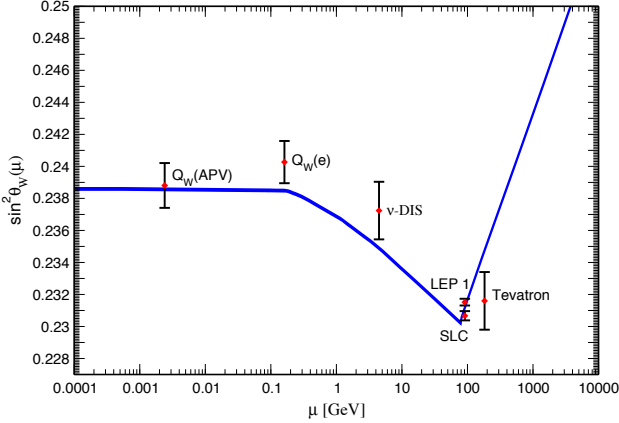


Figure 10.1: Scale dependence of the weak mixing angle defined in the $\overline{\text{MS}}$ scheme [129] (for the scale dependence of the weak mixing angle defined in a mass-dependent renormalization scheme, see Ref. 126). The minimum of the curve corresponds to $Q = M_W$, below which we switch to an effective theory with the W^\pm bosons integrated out, and where the β -function for the weak mixing angle changes sign. At the location of the W boson mass and each fermion mass, there are also discontinuities arising from scheme dependent matching terms which are necessary to ensure that the various effective field theories within a given loop order describe the same physics. However, in the $\overline{\text{MS}}$ scheme these are very small numerically and barely visible in the figure provided one decouples quarks at $Q = \widehat{m}_q(\widehat{m}_q)$. The width of the curve reflects the theory uncertainty from strong interaction effects which at low energies is at the level of $\pm 7 \times 10^{-5}$ [129]. Following the estimate [130] of the typical momentum transfer for parity violation experiments in Cs, the location of the APV data point is given by $\mu = 2.4$ MeV. For ν -DIS we chose $\mu = 20$ GeV which is about half-way between the averages of $\sqrt{Q^2}$ for ν and $\bar{\nu}$ interactions at NuTeV. The Tevatron measurements are strongly dominated by invariant masses of the final state dilepton pair of $\mathcal{O}(M_Z)$ and can thus be considered as additional Z pole data points, yielding $\overline{s}_Z^2 = 0.2316 \pm 0.0018$. However, for clarity we displayed the point horizontally to the right.

In the future it could be possible to further reduce the theoretical wave function uncertainties by taking the ratios of parity violation in different isotopes [131,145]. There would still be some residual uncertainties from differences in the neutron charge radii, however [146]. Experiments in hydrogen and deuterium are another possibility for reducing the uncertainties [147].

10.4. W and Z boson physics

10.4.1. e^+e^- scattering below the Z pole :

The forward-backward asymmetry for $e^+e^- \rightarrow \ell^+\ell^-$, $\ell = \mu$ or τ , is defined as

$$A_{FB} \equiv \frac{\sigma_F - \sigma_B}{\sigma_F + \sigma_B}, \quad (10.25)$$

where $\sigma_F(\sigma_B)$ is the cross-section for ℓ^- to travel forward (backward) with respect to the e^- direction. A_{FB} and R , the total cross-section relative to pure QED, are given by

$$R = F_1, \quad A_{FB} = \frac{3F_2}{4F_1}, \quad (10.26)$$

where

$$F_1 = 1 - 2\chi_0 g_V^e g_V^\ell \cos \delta_R + \chi_0^2 (g_V^{e2} + g_A^{e2}) (g_V^{\ell 2} + g_A^{\ell 2}), \quad (10.27a)$$

$$F_2 = -2\chi_0 g_A^e g_A^\ell \cos \delta_R + 4\chi_0^2 g_A^e g_A^\ell g_V^e g_V^\ell, \quad (10.27b)$$

$$\tan \delta_R = \frac{M_Z \Gamma_Z}{M_Z^2 - s}, \quad \chi_0 = \frac{G_F}{2\sqrt{2}\pi\alpha} \frac{sM_Z^2}{[(M_Z^2 - s)^2 + M_Z^2 \Gamma_Z^2]^{1/2}}, \quad (10.28)$$

and where \sqrt{s} is the CM energy. Eq. (10.27) is valid at tree level. If the data are radiatively corrected for QED effects (as described above), then the remaining electroweak corrections can be incorporated [148,149] (in an approximation adequate for existing PEP, PETRA, and TRISTAN data, which are well below the Z pole) by replacing χ_0 by $\chi(s) \equiv (1 + \rho_t)\chi_0(s)\alpha/\alpha(s)$, where $\alpha(s)$ is the running QED coupling, and evaluating g_V in the $\overline{\text{MS}}$ scheme. Reviews and formulae for $e^+e^- \rightarrow \text{hadrons}$ may be found in Ref. 150.

10.4.2. Z pole physics :

At LEP 1 and SLC, there were high-precision measurements of various Z pole observables [11,151–156], as summarized in Table 10.6. These include the Z mass and total width, Γ_Z , and partial widths $\Gamma(f\bar{f})$ for $Z \rightarrow f\bar{f}$ where fermion $f = e, \mu, \tau, \text{hadrons}, b, \text{or } c$. It is convenient to use the variables $M_Z, \Gamma_Z, R_\ell \equiv \Gamma(\text{had})/\Gamma(\ell^+\ell^-)$ ($\ell = e, \mu, \tau$), $\sigma_{\text{had}} \equiv 12\pi\Gamma(e^+e^-)\Gamma(\text{had})/M_Z^2\Gamma_Z^2$, $R_b \equiv \Gamma(b\bar{b})/\Gamma(\text{had})$, and $R_c \equiv \Gamma(c\bar{c})/\Gamma(\text{had})$, most of which are weakly correlated experimentally. ($\Gamma(\text{had})$ is the partial width into hadrons.) The three values for R_ℓ are not inconsistent with lepton universality (although R_τ is somewhat low), but we use the general analysis in which the three observables are treated as independent. Similar remarks apply to $A_{FB}^{0,\ell}$ below ($A_{FB}^{0,\tau}$ is somewhat high). $\mathcal{O}(\alpha^3)$ QED corrections introduce a large anti-correlation (-30%) between Γ_Z and σ_{had} . The anti-correlation between R_b and R_c is -18% [11]. The R_ℓ are insensitive to m_t except for the $Z \rightarrow b\bar{b}$ vertex and final state corrections and the implicit dependence through $\sin^2\theta_W$. Thus, they are especially useful for constraining α_s . The width for invisible decays [11], $\Gamma(\text{inv}) = \Gamma_Z - 3\Gamma(\ell^+\ell^-) - \Gamma(\text{had}) = 499.0 \pm 1.5$ MeV, can be used to determine the number of neutrino flavors much lighter than $M_Z/2$, $N_\nu = \Gamma(\text{inv})/\Gamma^{\text{theory}}(\nu\bar{\nu}) = 2.984 \pm 0.009$ for $(m_t, M_H) = (173.1, 117)$ GeV.

There were also measurements of various Z pole asymmetries. These include the polarization or left-right asymmetry

$$A_{LR} \equiv \frac{\sigma_L - \sigma_R}{\sigma_L + \sigma_R}, \quad (10.29)$$

where $\sigma_L(\sigma_R)$ is the cross-section for a left-(right)-handed incident electron. A_{LR} was measured precisely by the SLD collaboration at the SLC [152], and has the advantages of being extremely sensitive to $\sin^2\theta_W$ and that systematic uncertainties largely cancel. In addition, SLD extracted the final-state couplings (defined below), A_b, A_c [11], A_s [153], A_τ , and A_μ [154], from left-right forward-backward asymmetries, using

$$A_{LR}^{FB}(f) = \frac{\sigma_{LF}^f - \sigma_{LB}^f - \sigma_{RF}^f + \sigma_{RB}^f}{\sigma_{LF}^f + \sigma_{LB}^f + \sigma_{RF}^f + \sigma_{RB}^f} = \frac{3}{4}A_f, \quad (10.30)$$

where, for example, σ_{LF}^f is the cross-section for a left-handed incident electron to produce a fermion f traveling in the forward hemisphere. Similarly, A_τ was measured at LEP 1 [11] through the negative total τ polarization, \mathcal{P}_τ , and A_e was extracted from the angular distribution of \mathcal{P}_τ . An equation such as (10.30) assumes that initial state QED corrections, photon exchange, γ - Z interference, the tiny electroweak boxes, and corrections for $\sqrt{s} \neq M_Z$ are removed from the data, leaving the pure electroweak asymmetries. This allows the use of effective tree-level expressions,

$$A_{LR} = A_e P_e, \quad A_{FB} = \frac{3}{4}A_f \frac{A_e + P_e}{1 + P_e A_e}, \quad (10.31)$$

where

$$A_f \equiv \frac{2\overline{g}_V^f \overline{g}_A^f}{\overline{g}_V^{f2} + \overline{g}_A^{f2}}, \quad (10.32)$$

and

$$\overline{g}_V^f = \sqrt{\rho_f} (t_{3L}^{(f)} - 2q_f \kappa_f \sin^2\theta_W), \quad \overline{g}_A^f = \sqrt{\rho_f} t_{3L}^{(f)}. \quad (10.33)$$

P_e is the initial e^- polarization, so that the second equality in Eq. (10.30) is reproduced for $P_e = 1$, and the Z pole forward-backward asymmetries at LEP 1 ($P_e = 0$) are given by $A_{FB}^{(0,f)} = \frac{3}{4}A_e A_f$ where

$f = e, \mu, \tau, b, c, s$ [155], and q , and where $A_{FB}^{(0,q)}$ refers to the hadronic charge asymmetry. Corrections for t -channel exchange and s/t -channel interference cause $A_{FB}^{(0,e)}$ to be strongly anti-correlated with R_e (-37%). The correlation between $A_{FB}^{(0,b)}$ and $A_{FB}^{(0,c)}$ amounts to 15%. The initial state coupling, A_e , was also determined through the left-right charge asymmetry [156] and in polarized Bhabha scattering [154] at the SLC. The forward-backward asymmetry, A_{FB} , for e^+e^- final states (with invariant masses restricted to or dominated by values around M_Z) in $p\bar{p}$ collisions has been measured by the CDF [157] and DØ [158] collaborations and values for \bar{s}_ℓ^2 were extracted, which combine to $\bar{s}_\ell^2 = 0.2316 \pm 0.0018$. By varying the invariant mass and the scattering angle (and assuming the electron couplings), the effective Z couplings to light quarks, $\bar{g}_{V,A}^{u,d}$, resulted, as well, but with large uncertainties and mutual correlations and not independently of \bar{s}_ℓ^2 above. Similar analyses have also been reported by the H1 and ZEUS collaborations at HERA [159] and by the LEP collaborations [11].

The electroweak radiative corrections have been absorbed into corrections $\rho_f - 1$ and $\kappa_f - 1$, which depend on the fermion f and on the renormalization scheme. In the on-shell scheme, the quadratic m_t dependence is given by $\rho_f \sim 1 + \rho_t$, $\kappa_f \sim 1 + \rho_t / \tan^2 \theta_W$, while in $\overline{\text{MS}}$, $\hat{\rho}_f \sim \hat{\kappa}_f \sim 1$, for $f \neq b$ ($\hat{\rho}_b \sim 1 - \frac{4}{3}\rho_t$, $\hat{\kappa}_b \sim 1 + \frac{2}{3}\rho_t$). In the $\overline{\text{MS}}$ scheme the normalization is changed according to $G_F M_Z^2 / 2\sqrt{2}\pi \rightarrow \hat{\alpha} / 4\hat{s}_Z^2 \hat{c}_Z^2$. (If one continues to normalize amplitudes by $G_F M_Z^2 / 2\sqrt{2}\pi$, as in the 1996 edition of this *Review*, then $\hat{\rho}_f$ contains an additional factor of $\hat{\rho}$.) In practice, additional bosonic and fermionic loops, vertex corrections, leading higher order contributions, *etc.*, must be included. For example, in the $\overline{\text{MS}}$ scheme one has $\hat{\rho}_\ell = 0.9981$, $\hat{\kappa}_\ell = 1.0013$, $\hat{\rho}_b = 0.9870$, and $\hat{\kappa}_b = 1.0067$. It is convenient to define an effective angle $\bar{s}_f^2 \equiv \sin^2 \bar{\theta}_{Wf} \equiv \hat{\kappa}_f \hat{s}_Z^2 = \kappa_f s_W^2$, in terms of which \bar{g}_V^f and \bar{g}_A^f are given by $\sqrt{\rho_f}$ times their tree-level formulae. Because \bar{g}_V^f is very small, not only $A_{LR}^0 = A_e, A_{FB}^{(0,\ell)}$, and \mathcal{P}_τ , but also $A_{FB}^{(0,b)}, A_{FB}^{(0,c)}, A_{FB}^{(0,s)}$, and the hadronic asymmetries are mainly sensitive to \bar{s}_ℓ^2 . One finds that $\hat{\kappa}_f$ ($f \neq b$) is almost independent of (m_t, M_H) , so that one can write

$$\bar{s}_\ell^2 \sim \hat{s}_Z^2 + 0.00029. \quad (10.34)$$

Thus, the asymmetries determine values of \bar{s}_ℓ^2 and \hat{s}_Z^2 almost independent of m_t , while the κ 's for the other schemes are m_t dependent.

10.4.3. LEP 2 :

LEP 2 [160] ran at several energies above the Z pole up to ~ 209 GeV. Measurements were made of a number of observables, including the cross-sections for $e^+e^- \rightarrow f\bar{f}$ for $f = q, \mu, \tau, \nu$; the differential cross-sections for $f = e^-, \mu^-, \tau^-$; R_q for $q = b, c$; $A_{FB}(f)$ for $f = \mu, \tau, b, c$; W branching ratios; and $WW, WW\gamma, ZZ$, single W , and single Z cross-sections. They are in good agreement with the SM predictions, with the exceptions of the total hadronic cross-section (1.7 σ high), R_b (2.1 σ low), and $A_{FB}(b)$ (1.6 σ low). Also, the negative result of the direct search for the SM Higgs boson excluded M_H values below 114.4 GeV at the 95% CL [161]. This result is complementary to and can be combined with [162] the limits inferred from the electroweak precision data.

The Z boson properties are extracted assuming the SM expressions for the γ - Z interference terms. These have also been tested experimentally by performing more general fits [160,163] to the LEP 1 and LEP 2 data. Assuming family universality this approach introduces three additional parameters relative to the standard fit [11], describing the γ - Z interference contribution to the total hadronic and leptonic cross-sections, $j_{\text{had}}^{\text{tot}}$ and j_ℓ^{tot} , and to the leptonic forward-backward asymmetry, j_ℓ^{fb} . *E.g.*,

$$j_{\text{had}}^{\text{tot}} \sim g_V^\ell g_V^{\text{had}} = 0.277 \pm 0.065, \quad (10.35)$$

which is in agreement with the SM expectation [11] of 0.21 ± 0.01 . These are valuable tests of the SM; but it should be cautioned that new physics is not expected to be described by this set of parameters, since (i) they do not account for extra interactions beyond the standard

weak neutral-current, and (ii) the photonic amplitude remains fixed to its SM value.

Strong constraints on anomalous triple and quartic gauge couplings have been obtained at LEP 2 and the Tevatron as described in the Gauge & Higgs Bosons Particle Listings.

10.4.4. W and Z decays :

The partial decay width for gauge bosons to decay into massless fermions $f_1\bar{f}_2$ (the numerical values include the small electroweak radiative corrections and final state mass effects) is

$$\Gamma(W^+ \rightarrow e^+\nu_e) = \frac{G_F M_W^3}{6\sqrt{2}\pi} \approx 226.31 \pm 0.07 \text{ MeV}, \quad (10.36a)$$

$$\Gamma(W^+ \rightarrow u_i\bar{d}_j) = \frac{CG_F M_W^3}{6\sqrt{2}\pi} |V_{ij}|^2 \approx 706.18 \pm 0.22 \text{ MeV} |V_{ij}|^2, \quad (10.36b)$$

$$\Gamma(Z \rightarrow \psi_i\bar{\psi}_i) = \frac{CG_F M_Z^3}{6\sqrt{2}\pi} [g_V^i{}^2 + g_A^i{}^2] \approx \begin{cases} 167.21 \pm 0.02 \text{ MeV} (\nu\bar{\nu}), \\ 83.99 \pm 0.01 \text{ MeV} (e^+e^-), \\ 300.20 \pm 0.06 \text{ MeV} (u\bar{u}), \\ 382.98 \pm 0.06 \text{ MeV} (d\bar{d}), \\ 375.94 \mp 0.04 \text{ MeV} (b\bar{b}). \end{cases} \quad (10.36c)$$

For leptons $C = 1$, while for quarks

$$C = 3 \left[1 + \frac{\alpha_s(M_Z)}{\pi} + 1.409 \frac{\alpha_s^2}{\pi^2} - 12.77 \frac{\alpha_s^3}{\pi^3} - 80.0 \frac{\alpha_s^4}{\pi^4} \right], \quad (10.37)$$

where the 3 is due to color and the factor in brackets represents the universal part of the QCD corrections [164] for massless quarks [165]. The $\mathcal{O}(\alpha_s^4)$ contribution in Eq. (10.37) is new [166]. The $Z \rightarrow f\bar{f}$ widths contain a number of additional corrections: universal (non-singlet) top quark mass contributions [167]; fermion mass effects and further QCD corrections proportional to $\hat{m}_q^2(M_Z^2)$ [168] which are different for vector and axial-vector partial widths; and singlet contributions starting from two-loop order which are large, strongly top quark mass dependent, family universal, and flavor non-universal [169]. The QED factor $1 + 3\alpha q_f^2/4\pi$, as well as two-loop order $\alpha\alpha_s$ and α^2 self-energy corrections [170] are also included. Working in the on-shell scheme, *i.e.*, expressing the widths in terms of $G_F M_{W,Z}^3$, incorporates the largest radiative corrections from the running QED coupling [61,171]. Electroweak corrections to the Z widths are then incorporated by replacing $g_{V,A}^i{}^2$ by $\bar{g}_{V,A}^i{}^2$. Hence, in the on-shell scheme the Z widths are proportional to $\rho_i \sim 1 + \rho_t$. The $\overline{\text{MS}}$ normalization accounts also for the leading electroweak corrections [66]. There is additional (negative) quadratic m_t dependence in the $Z \rightarrow b\bar{b}$ vertex corrections [172] which causes $\Gamma(b\bar{b})$ to decrease with m_t . The dominant effect is to multiply $\Gamma(b\bar{b})$ by the vertex correction $1 + \delta\rho_{b\bar{b}}$, where $\delta\rho_{b\bar{b}} \sim 10^{-2}(-\frac{1}{2}\frac{m_t^2}{M_Z^2} + \frac{1}{5})$. In practice, the corrections are included in ρ_b and κ_b , as discussed before.

For 3 fermion families the total widths are predicted to be

$$\Gamma_Z \approx 2.4957 \pm 0.0003 \text{ GeV}, \quad \Gamma_W \approx 2.0910 \pm 0.0007 \text{ GeV}. \quad (10.38)$$

We have assumed $\alpha_s(M_Z) = 0.1200$. An uncertainty in α_s of ± 0.0016 introduces an additional uncertainty of 0.05% in the hadronic widths, corresponding to ± 0.8 MeV in Γ_Z . These predictions are to be compared with the experimental results $\Gamma_Z = 2.4952 \pm 0.0023$ GeV [11] and $\Gamma_W = 2.085 \pm 0.042$ GeV [173] (see the Gauge & Higgs Boson Particle Listings for more details).

Table 10.3: Correlation matrix for measurements of $b \rightarrow s\gamma$.

CLEO	1.000	0.175	0.048	0.038
BaBar (inclusive)	0.175	1.000	0.029	0.033
BaBar (exclusive)	0.048	0.029	1.000	0.019
Belle	0.038	0.033	0.019	1.000

10.5. Precision flavor physics

In addition to cross-sections, asymmetries, parity violation, W and Z decays, there is a large number of experiments and observables testing the flavor structure of the SM. These are addressed elsewhere in this *Review*, and generally not included in this Section. However, we identify three precision observables with sensitivity to similar types of new physics as the other processes discussed here. The branching fraction of the flavor changing transition $b \rightarrow s\gamma$ is of comparatively low precision, but since it is a loop-level process (in the SM) its sensitivity to new physics (and SM parameters, such as heavy quark masses) is enhanced. The τ -lepton lifetime and leptonic branching ratios are primarily sensitive to α_s and not affected significantly by many types of new physics. However, having an independent and reliable low energy measurement of α_s in a global analysis allows the comparison with the Z lineshape determination of α_s which shifts easily in the presence of new physics contributions. By far the most precise observable discussed here is the anomalous magnetic moment of the muon (the electron magnetic moment is measured to even greater precision, but its new physics sensitivity is suppressed by an additional factor of m_e^2/m_μ^2). Its combined experimental and theoretical uncertainty is comparable to typical new physics contributions.

The CLEO [174], BaBar [175] and Belle [176] collaborations reported precise measurements of the process $b \rightarrow s\gamma$. We extrapolated these results to the full photon spectrum which is defined according to the recommendation in Ref. 177. The results for the branching fractions are then given by,

$$\text{CLEO} : 3.32 \times 10^{-4} [1 \pm 0.134 \pm 0.076 \pm 0.038 \pm 0.048 \pm 0.003],$$

$$\text{BaBar (incl.)} : 3.99 \times 10^{-4} [1 \pm 0.080 \pm 0.091 \pm 0.079 \pm 0.026 \pm 0.003],$$

$$\text{BaBar (excl.)} : 3.57 \times 10^{-4} [1 \pm 0.055_{-0.122}^{+0.168} \pm 0 \pm 0.026 \pm 0],$$

$$\text{Belle} : 3.61 \times 10^{-4} [1 \pm 0.043 \pm 0.116 \pm 0.003 \pm 0.014 \pm 0.003],$$

where the first two errors are the statistical and systematic uncertainties (taken uncorrelated). In the cases of CLEO and Belle, the error component from the signal models are moved from the systematic error to the model (third) error. The fourth error accounts for the extrapolation from the finite photon energy cutoff [177–179] (2.0 GeV, 1.9 GeV, and 1.7 GeV, respectively, for CLEO, BaBar and Belle) to the full theoretical branching ratio. For this we use the results of Ref. 177 for $m_b = 4.70$ GeV which is in good agreement with the more recent Ref. 179. The uncertainty reflects the difference due to choosing $m_b = 4.60$ GeV, instead. The last error is from the correction (0.957 ± 0.003) for the $b \rightarrow d\gamma$ component which is common to all inclusive measurements, but absent for the exclusive BaBar measurement in the third line. The last three errors are taken as 100% correlated, resulting in the correlation matrix in Table 10.3. It is advantageous [180] to normalize the result with respect to the semi-leptonic branching fraction, $\mathcal{B}(b \rightarrow X\ell\nu) = 0.1074 \pm 0.0016$, yielding,

$$R = \frac{\mathcal{B}(b \rightarrow s\gamma)}{\mathcal{B}(b \rightarrow X\ell\nu)} = (3.38 \pm 0.27 \pm 0.37) \times 10^{-3}. \quad (10.39)$$

In the fits we use the variable $\ln R = -5.69 \pm 0.14$ to assure an approximately Gaussian error [181]. The second uncertainty in Eq. (10.39) is an 11% theory uncertainty (excluding parametric errors such as from α_s) in the SM prediction which is based on the next-to-leading order calculations of Refs. 180 and 182. There is a coordinated effort underway to obtain the SM prediction at next-to-next-to-leading order [183].

The extraction of α_s from the τ lifetime is standing out from other determinations because of a variety of independent reasons: (i) the τ -scale is low, so that upon extrapolation to the Z scale (where it can be compared to the theoretically clean Z lineshape determinations) the α_s error shrinks by about an order of magnitude; (ii) yet, this scale is high enough that perturbation theory and the operator product expansion (OPE) can be applied; (iii) these observables are fully inclusive and thus free of fragmentation and hadronization effects that would have to be modeled or measured; (iv) OPE breaking effects are most problematic near the branch cut but there they are suppressed by a double zero at $s = m_\tau^2$; (v) there are enough data [41,43] to constrain non-perturbative effects both within and breaking the OPE; (vi) a complete four-loop order QCD calculation is available [166]; (vii) large effects associated with the QCD β -function can be re-summed [184] in what has become known as contour improved perturbation theory (CIPT). However, while there is no doubt that CIPT shows faster convergence in the lower (calculable) orders, doubts have been cast on the method by the observation that at least in a specific model [185], which includes the exactly known coefficients and theoretical constraints on the large-order behavior, ordinary fixed order perturbation theory (FOPT) may nevertheless give a better approximation to the full result. We therefore use the expressions [5,165,166,186],

$$\tau_\tau = \hbar \frac{1 - \mathcal{B}_\tau^s}{\Gamma_\tau^e + \Gamma_\tau^\mu + \Gamma_\tau^{ud}} = 291.09 \pm 0.48 \text{ fs}, \quad (10.40)$$

$$\Gamma_\tau^{ud} = \frac{G_F^2 m_\tau^5 |V_{ud}|^2}{64\pi^3} S(m_\tau, M_Z) \left(1 + \frac{3}{5} \frac{m_\tau^2}{M_W^2} \right) \times \left[1 + \frac{\alpha_s(m_\tau)}{\pi} + 5.202 \frac{\alpha_s^2}{\pi^2} + 26.37 \frac{\alpha_s^3}{\pi^3} + 127.1 \frac{\alpha_s^4}{\pi^4} + \frac{\hat{\alpha}}{\pi} \left(\frac{85}{24} - \frac{\pi^2}{2} \right) \right], \quad (10.41)$$

and Γ_τ^e and Γ_τ^μ can be taken from Eq. (10.4) with obvious replacements. The relative fraction of decays with $\Delta S = -1$, $\mathcal{B}_\tau^s = 0.0286 \pm 0.0007$, is based on experimental data since the value for the strange quark mass, $\hat{m}_s(m_\tau)$, is not well known and the QCD expansion proportional to \hat{m}_s^2 converges poorly and cannot be trusted. $S(m_\tau, M_Z) = 1.01907 \pm 0.0003$ is a logarithmically enhanced electroweak correction factor with higher orders re-summed [187]. Also included (but not shown) are quark mass effects and condensate contributions [188]. The largest uncertainty arises from the truncation of the FOPT series and is conservatively taken as the α_s^4 term (this is re-calculated in each call of the fits, leading to an α_s -dependent and thus asymmetric error) until a better understanding of the numerical differences between FOPT and CIPT has been gained. Incidentally, the τ spectral functions are better described in CIPT than in FOPT [188]. Our error almost covers the entire range from using CIPT to assuming that the nearly geometric series in Eq. (10.41) continues to higher orders. The next largest uncertainties (± 0.6 fs) are from the condensates [188] and the evolution to the Z scale, followed by the experimental uncertainty in Eq. (10.40), which is from combining the two leptonic branching ratios with the direct τ_τ . Included are also various smaller uncertainties from other sources. In total we obtain a $\sim 1.5\%$ determination of $\alpha_s(M_Z) = 0.1174_{-0.0016}^{+0.0018}$ which updates the result of Ref. 5. For more details, see Refs. 50 and 188 where the τ spectral functions are used as additional input.

The world average of the muon anomalous magnetic moment**,

$$a_\mu^{\text{exp}} = \frac{g_\mu - 2}{2} = (1165920.80 \pm 0.63) \times 10^{-9}, \quad (10.42)$$

** In what follows, we summarize the most important aspects of $g_\mu - 2$, and give some details about the evaluation in our fits. For more details see the dedicated contribution by A. Höcker and W. Marciano in this *Review*. There are some small numerical differences (at the level of 0.1 standard deviation), which are well understood and mostly arise because internal consistency of the fits requires the calculation of all observables from analytical expressions and common inputs and fit parameters, so that an independent evaluation is necessary for this Section. Note, that in the spirit of a global analysis based on all avail-

is dominated by the final result of the E821 collaboration at BNL [189]. The QED contribution has been calculated to four loops [190] (fully analytically to three loops [191,192]), and the leading logarithms are included to five loops [193,194]. The estimated SM electroweak contribution [195–197], $a_\mu^{\text{EW}} = (1.52 \pm 0.03) \times 10^{-9}$, which includes leading two-loop [196] and three-loop [197] corrections, is at the level of twice the current uncertainty.

The limiting factor in the interpretation of the result is the uncertainty from the two-loop hadronic contribution. *E.g.*, Ref. 50 obtained the value $a_\mu^{\text{had}} = (69.55 \pm 0.41) \times 10^{-9}$ which combines CMD-2 [45] and SND [46] $e^+e^- \rightarrow$ hadrons cross-section data with radiative return results from BaBar [48] and KLOE [49]. This value suggests a 3.1σ discrepancy between Eq. (10.42) and the SM prediction. Updating an alternative analysis [39] the authors of Ref. 40 quote $a_\mu^{\text{had}} = (70.53 \pm 0.45) \times 10^{-9}$ using τ decay data and isospin symmetry (CVC). This result implies a smaller conflict (1.8σ) with Eq. (10.42). Thus, there is also a discrepancy between the 2π and 4π spectral functions obtained from the two methods, contributing 70% and 30% of the discrepancy, respectively. For example, if one uses the e^+e^- data and CVC to predict the branching ratio for $\tau^- \rightarrow \nu_\tau \pi^- \pi^0$ decays one obtains $24.78 \pm 0.25\%$ [40], while the average of the directly measured branching ratio yields $25.51 \pm 0.09\%$ which is 2.7σ higher. It is important to understand the origin of this difference, but two observations point to the conclusion that at least some of it is experimental: (i) The $\tau^- \rightarrow \nu_\tau 2\pi^- \pi^+ \pi^0$ spectral function also disagrees with the corresponding e^+e^- data by 1.7σ , which translates to a 20% effect [40,50] and seems too large to arise from isospin violation. (ii) Isospin violating corrections have been studied in detail in Refs. 40 and 198 and found to be largely under control. The largest effect is due to higher-order electroweak corrections [52] but introduces a negligible uncertainty [187]. Nevertheless, a_μ^{had} is often evaluated excluding the τ decay data arguing [199] that CVC breaking effects (*e.g.*, through a relatively large mass difference between the ρ^\pm and ρ^0 vector mesons) may be larger than expected. (This may also be relevant [199] in the context of the NuTeV result discussed above.) Experimentally [43], this mass difference is indeed larger than expected, but then one would also expect a significant width difference which is contrary to observation [43]. Fortunately, due to the suppression at large s (from where the conflicts originate) these problems are less pronounced as far as a_μ^{had} is concerned. In the following we view all differences in spectral functions as (systematic) fluctuations and average the results.

Table 10.4: Principal SM fit result including mutual correlations (all masses in GeV).

M_Z	91.1874 ± 0.0021	1.00	-0.01	0.00	0.00	-0.01	0.00	0.12
$\hat{m}_t(\hat{m}_t)$	163.5 ± 1.3	-0.01	1.00	0.00	0.00	-0.10	0.00	0.39
$\hat{m}_b(\hat{m}_b)$	4.198 ± 0.023	0.00	0.00	1.00	0.25	-0.04	0.01	0.04
$\hat{m}_c(\hat{m}_c)$	$1.266^{+0.031}_{-0.036}$	0.00	0.00	0.25	1.00	0.08	0.02	0.12
$\alpha_s(M_Z)$	0.1183 ± 0.0015	-0.01	-0.10	-0.04	0.08	1.00	0.00	-0.04
$\Delta\alpha_{\text{had}}^{(3)}(1.8 \text{ GeV})$	0.00574 ± 0.00010	0.00	-0.01	0.01	0.02	0.00	1.00	-0.18
M_H	90^{+27}_{-22}	0.12	0.39	0.04	0.12	-0.04	-0.18	1.00

An additional uncertainty is induced by the hadronic three-loop light-by-light scattering contribution. Two recent and inherently different model calculations yield $a_\mu^{\text{LBS}} = (+1.36 \pm 0.25) \times 10^{-9}$ [200] and $a_\mu^{\text{LBS}} = +1.37^{+0.15}_{-0.27} \times 10^{-9}$ [201] which are higher than previous evaluations [202,203]. The sign of this effect is opposite [202] to the one quoted in the 2002 edition of this *Review*, and has subsequently been confirmed by two other groups [203]. There is also the upper bound $a_\mu^{\text{LBS}} < 1.59 \times 10^{-9}$ [201] but this requires

able information we have chosen here to average in the τ decay and radiative return (KLOE and BaBar) data, as well.

an ad hoc assumption, too. The very recent Ref. 204 quotes the value $a_\mu^{\text{LBS}} = (+1.05 \pm 0.26) \times 10^{-9}$, which we shift by 2×10^{-11} to account for the more accurate charm quark treatment of Ref. 201. We also increase the error to cover all evaluations, and we will use $a_\mu^{\text{LBS}} = (+1.07 \pm 0.32) \times 10^{-9}$ in the fits.

Other hadronic effects at three-loop order contribute [205] $a_\mu^{\text{had}}(\alpha^3) = (-1.00 \pm 0.06) \times 10^{-9}$. Correlations with the two-loop hadronic contribution and with $\Delta\alpha(M_Z)$ (see Sec. 10.2) were considered in Ref. 192 which also contains analytic results for the perturbative QCD contribution.

Altogether, the SM prediction is

$$a_\mu^{\text{theory}} = (1165918.90 \pm 0.44) \times 10^{-9}, \quad (10.43)$$

where the error is from the hadronic uncertainties excluding parametric ones such as from α_s and the heavy quark masses. We estimate its correlation with $\Delta\alpha(M_Z)$ to 14%. The overall 2.5σ discrepancy between the experimental and theoretical values could be due to fluctuations (the E821 result is statistics dominated) or underestimates of the theoretical uncertainties. On the other hand, $g_\mu - 2$ is also affected by many types of new physics, such as supersymmetric models with large $\tan\beta$ and moderately light superparticle masses [206]. Thus, the deviation could also arise from physics beyond the SM.

10.6. Experimental results

The values for m_t [6], M_W [160,207], neutrino scattering [98,114–116], the weak charges of the electron [125], cesium [132,133] and thallium [134], the $b \rightarrow s\gamma$ observable [174–175], the muon anomalous magnetic moment [189], and the τ lifetime are listed in Table 10.5. Likewise, the principal Z pole observables can be found in Table 10.6 where the LEP 1 averages of the ALEPH, DELPHI, L3, and OPAL results include common systematic errors and correlations [11]. The heavy flavor results of LEP 1 and SLD are based on common inputs and correlated, as well [11]. Note that the values of $\Gamma(\ell^+\ell^-)$, $\Gamma(\text{had})$, and $\Gamma(\text{inv})$ are not independent of Γ_Z , the R_ℓ , and σ_{had} and that the SM errors in those latter are largely dominated by the uncertainty in α_s . Also shown in both Tables are the SM predictions for the values of M_Z , M_H , $\alpha_s(M_Z)$, $\Delta\alpha_{\text{had}}^{(3)}$ and the heavy quark masses shown in Table 10.4. The predictions result from a global least-square (χ^2) fit to all data using the minimization

package MINUIT [208] and the electroweak library GAPP [90]. In most cases, we treat all input errors (the uncertainties of the values) as Gaussian. The reason is not that we assume that theoretical and systematic errors are intrinsically bell-shaped (which they are not) but because in most cases the input errors are combinations of many different (including statistical) error sources, which should yield approximately Gaussian *combined* errors by the large number theorem. Thus, it suffices if either the statistical components dominate or there are many components of similar size. An exception is the theory dominated error on the τ lifetime, which we recalculate in each χ^2 -function call since it depends itself on α_s . Sizes and shapes

are included. The theoretical correlations between $\Delta\alpha_{\text{had}}^{(5)}$ and $g_\mu - 2$, and between the charm and bottom quark masses, are also accounted for.

The data allow a simultaneous determination of M_Z , M_H , m_t , and the strong coupling $\alpha_s(M_Z)$. (\hat{m}_c , \hat{m}_b , and $\Delta\alpha_{\text{had}}^{(3)}$ are also allowed to float in the fits, subject to the theoretical constraints [5,17] described in Sec. 10.1–Sec. 10.2. These are correlated with α_s .) α_s is determined mainly from R_ℓ , Γ_Z , σ_{had} , and τ_τ and is only weakly correlated with the other variables. The global fit to all data, including the CDF/DØ average $m_t = 173.1 \pm 1.3$ GeV, yields the result in Table 10.4 (the $\overline{\text{MS}}$ top quark mass given there corresponds to $m_t = 173.2 \pm 1.3$ GeV). The weak mixing angle is determined to

$$\hat{s}_Z^2 = 0.23116 \pm 0.00013, \quad s_W^2 = 0.22292 \pm 0.00028,$$

where the larger error in the on-shell scheme is due to the stronger sensitivity to m_t , while the corresponding effective angle is related by Eq. (10.34), *i.e.*, $\hat{s}_\ell^2 = 0.23146 \pm 0.00012$.

As described at the beginning of Sec. 10.2 and the paragraph following Eq. (10.42) in Sec. 10.5, there is considerable stress in the experimental e^+e^- spectral functions and also conflict when these are compared with τ decay spectral functions. These are below or above the 2σ level (depending on what is actually compared) but not larger than the deviations of some other quantities entering our analyzes. The number and size of these deviations are not inconsistent with what one would expect to happen as a result of random fluctuations. It is nevertheless instructive to study the effect of doubling the uncertainty in $\Delta\alpha_{\text{had}}^{(3)}$ (1.8 GeV) = $(57.29 \pm 0.90) \times 10^{-4}$, (see the beginning of Sec. 10.2) on the extracted Higgs mass. The result, $M_H = 87_{-22}^{+28}$ GeV, demonstrates that the uncertainty in $\Delta\alpha_{\text{had}}$ is currently of only secondary importance. Note also, that the uncertainty of about ± 0.0001 in $\Delta\alpha_{\text{had}}^{(3)}$ (1.8 GeV) corresponds to a shift of ∓ 5 GeV in M_H or about one fifth of its total uncertainty. The hadronic contribution to $\alpha(M_Z)$ is correlated with $g_\mu - 2$ (see Sec. 10.5). The measurement of the latter is higher than the SM prediction, and its inclusion in the fit favors a larger $\alpha(M_Z)$ and a lower M_H (currently by about 2 GeV).

The weak mixing angle can be determined from Z pole observables, M_W , and from a variety of neutral-current processes spanning a very wide Q^2 range. The results (for the older low energy neutral-current data see Refs. 58 and 59) shown in Table 10.7 are in reasonable agreement with each other, indicating the quantitative success of the SM. The largest discrepancy is the value $\hat{s}_Z^2 = 0.23193 \pm 0.00028$ from the forward-backward asymmetries into bottom and charm quarks, which is 2.7σ above the value 0.23116 ± 0.00013 from the global fit to all data. Similarly, $\hat{s}_Z^2 = 0.23067 \pm 0.00029$ from the SLD asymmetries (in both cases when combined with M_Z) is 1.7σ low. The SLD result has the additional difficulty (within the SM) of implying very low and excluded [161] Higgs masses. This is also true for $\hat{s}_Z^2 = 0.23100 \pm 0.00023$ from M_W and M_Z and — as a consequence — for the global fit. We have therefore included in Table 10.5 and Table 10.6 an additional column (denoted Deviation) indicating the deviations if $M_H = 117$ GeV is fixed.

The extracted Z pole value of $\alpha_s(M_Z)$ is based on a formula with negligible theoretical uncertainty if one assumes the exact validity of the SM. One should keep in mind, however, that this value, $\alpha_s(M_Z) = 0.1198 \pm 0.0028$, is very sensitive to such types of new physics as non-universal vertex corrections. In contrast, the value derived from τ decays, $\alpha_s(M_Z) = 0.1174_{-0.0016}^{+0.0018}$, is theory dominated but less sensitive to new physics. The two values are in remarkable agreement with each other. They are also in agreement with other recent values, such as from jet-event shapes at LEP [215] (0.1202 ± 0.0050) the average from HERA [216] (0.1198 ± 0.0032), and the most recent quenched lattice calculation [217] (0.1183 ± 0.0008). For more details and other determinations, see our Section 9 on “Quantum Chromodynamics” in this *Review*.

Using $\alpha(M_Z)$ and \hat{s}_Z^2 as inputs, one can predict $\alpha_s(M_Z)$ assuming grand unification. One predicts [218] $\alpha_s(M_Z) = 0.130 \pm 0.001 \pm 0.01$ for the simplest theories based on the minimal supersymmetric extension of the SM, where the first (second) uncertainty is from the inputs (thresholds). This is slightly larger, but consistent with the

Table 10.7: Values of \hat{s}_Z^2 , s_W^2 , α_s , and M_H [in GeV] for various (combinations of) observables. Unless indicated otherwise, the top quark mass, $m_t = 170.9 \pm 1.9$ GeV, is used as an additional constraint in the fits. The (†) symbol indicates a fixed parameter.

Data	\hat{s}_Z^2	s_W^2	$\alpha_s(M_Z)$	M_H
All data	0.23116(13)	0.22292(28)	0.1183(15)	90_{-22}^{+27}
All indirect (no m_t)	0.23118(14)	0.22283(34)	0.1183(16)	112_{-52}^{+110}
Z pole (no m_t)	0.23121(17)	0.22311(59)	0.1198(28)	90_{-44}^{+114}
LEP 1 (no m_t)	0.23152(21)	0.22376(67)	0.1213(30)	170_{-93}^{+234}
SLD + M_Z	0.23067(29)	0.22201(54)	0.1183 (†)	33_{-17}^{+27}
$A_{FB}^{(b,c)} + M_Z$	0.23193(28)	0.22484(76)	0.1183 (†)	389_{-158}^{+264}
$M_W + M_Z$	0.23100(23)	0.22262(48)	0.1183 (†)	67_{-28}^{+38}
M_Z	0.23128(6)	0.22321(17)	0.1183 (†)	117 (†)
Q_W (APV)	0.2314(14)	0.2233(14)	0.1183 (†)	117 (†)
$Q_W(e)$	0.2332(15)	0.2251(15)	0.1183 (†)	117 (†)
ν_μ -N DIS (isoscalar)	0.2335(18)	0.2254(18)	0.1183 (†)	117 (†)
Elastic $\nu_\mu(\bar{\nu}_\mu)$ -e	0.2311(77)	0.2230(77)	0.1183 (†)	117 (†)
e-D DIS (SLAC)	0.222(18)	0.213(19)	0.1183 (†)	117 (†)
Elastic $\nu_\mu(\bar{\nu}_\mu)$ -p	0.211(33)	0.203(33)	0.1183 (†)	117 (†)

experimental $\alpha_s(M_Z) = 0.1183 \pm 0.0015$ from the Z lineshape and the τ lifetime, as well as with other determinations. Non-supersymmetric unified theories predict the low value $\alpha_s(M_Z) = 0.073 \pm 0.001 \pm 0.001$. See also the note on “Supersymmetry” in the Searches Particle Listings.

The data indicate a preference for a small Higgs mass. There is a strong correlation between the quadratic m_t and logarithmic M_H terms in $\hat{\rho}$ in all of the indirect data except for the $Z \rightarrow b\bar{b}$ vertex. Therefore, observables (other than R_b) which favor m_t values higher than the Tevatron range favor lower values of M_H . M_W has additional M_H dependence through $\Delta\hat{r}_W$ which is not coupled to m_t^2 effects. The strongest individual pulls toward smaller M_H are from M_W and A_{LR}^0 , while $A_{FB}^{(b,c)}$ favors higher values. The difference in χ^2 for the global fit is $\Delta\chi^2 = \chi^2(M_H = 300 \text{ GeV}) - \chi_{\text{min}}^2 \approx 25$. Hence, the data favor a small value of M_H , as in supersymmetric extensions of the SM. The central value of the global fit result, $M_H = 90_{-22}^{+27}$ GeV, is below the direct lower bound, $M_H \geq 114.4$ GeV (95% CL) [161].

The 90% central confidence range from all precision data is

$$55 \text{ GeV} \leq M_H \leq 135 \text{ GeV}. \quad (10.44)$$

Including the results of the direct searches at LEP 2 [161] and the Tevatron [219] as extra contributions to the likelihood function drives the 95% upper limit to $M_H \leq 147$ GeV. As two further refinements, we account for (i) theoretical uncertainties from uncalculated higher order contributions by allowing the T parameter (see next subsection) subject to the constraint $T = 0 \pm 0.02$, (ii) the M_H dependence of the correlation matrix which gives slightly more weight to lower Higgs masses [220]. The resulting limits at 95 (90, 99)% CL are, respectively,

$$M_H \leq 149 \text{ (145, 194) GeV}. \quad (10.45)$$

One can also carry out a fit to the indirect data alone, *i.e.*, without including the constraint, $m_t = 173.1 \pm 1.3$ GeV, obtained by CDF and DØ. (The indirect prediction is for the $\overline{\text{MS}}$ mass, $\hat{m}_t(\hat{m}_t) = 166.2_{-6.6}^{+8.1}$ GeV, which is in the end converted to the pole mass). One obtains $m_t = 176.0_{-7.0}^{+8.5}$ GeV, in perfect agreement with the direct CDF/DØ average. Using this indirect top mass value, the tendency for a light Higgs persists and Eq. (10.44) becomes 46 GeV

$\leq M_H \leq 306$ GeV. The relations between M_H and m_t for various observables are shown in Fig. 10.2.

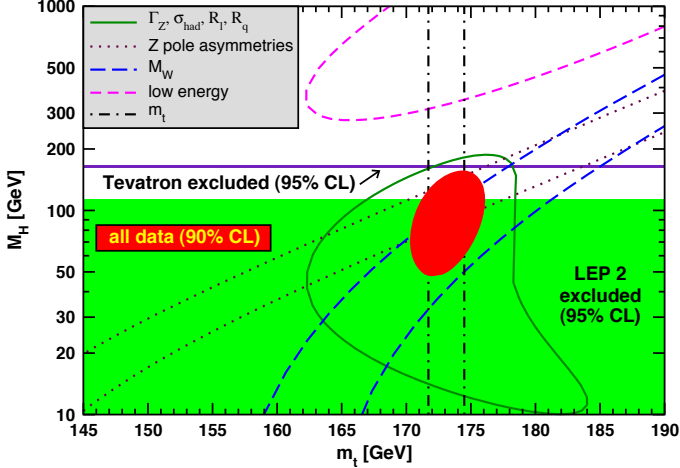


Figure 10.2: One-standard-deviation (39.35%) uncertainties in M_H as a function of m_t for various inputs, and the 90% CL region ($\Delta\chi^2 = 4.605$) allowed by all data. $\alpha_s(M_Z) = 0.1183$ is assumed except for the fits including the Z lineshape or low energy data. The direct lower limit from LEP 2 and the excluded window from the Tevatron [221] (both at the 95% CL) are also shown. Color version at end of book.

One can also determine the radiative correction parameters Δr : from the global fit one obtains $\Delta r = 0.0351 \pm 0.0009$ and $\Delta\hat{r}_W = 0.06950 \pm 0.00021$. M_W measurements [160,207] (when combined with M_Z) are equivalent to measurements of $\Delta r = 0.0342 \pm 0.0014$, which is 0.9 σ below the result from all other data, $\Delta r = 0.0357 \pm 0.0011$. Fig. 10.3 shows the 1σ contours in the M_W - m_t plane from the direct and indirect determinations, as well as the combined 90% CL region. The indirect determination uses M_Z from LEP 1 as input, which is defined assuming an s -dependent decay width. M_W then corresponds to the s -dependent width definition, as well, and can be directly compared with the results from the Tevatron and LEP 2 which have been obtained using the same definition. The difference to a constant width definition is formally only of $\mathcal{O}(\alpha^2)$, but is strongly enhanced since the decay channels add up coherently. It is about 34 MeV for M_Z and 27 MeV for M_W . The residual difference between working consistently with one or the other definition is about 3 MeV, *i.e.*, of typical size for non-enhanced $\mathcal{O}(\alpha^2)$ corrections [72–75].

Most of the parameters relevant to ν -hadron, ν - e , e -hadron, and e^-e^+ processes are determined uniquely and precisely from the data in “model-independent” fits (*i.e.*, fits which allow for an arbitrary electroweak gauge theory). The values for the parameters defined in Eqs. (10.11)–(10.14) are given in Table 10.8 along with the predictions of the SM. The agreement is very good. (The ν -hadron results without the NuTeV data can be found in the 1998 edition of this *Review*, and the fits using the original NuTeV data in the 2006 edition.) The off Z pole e^+e^- results are difficult to present in a model-independent way because Z propagator effects are non-negligible at TRISTAN, PETRA, PEP, and LEP 2 energies. However, assuming e - μ - τ universality, the low energy lepton asymmetries imply [150] $4(g_A^e)^2 = 0.99 \pm 0.05$, in good agreement with the SM prediction $\simeq 1$.

10.7. Constraints on new physics

The Z pole, W mass, and low energy data can be used to search for and set limits on deviations from the SM. In particular, the combination of these indirect data with the direct CDF and $D\bar{O}$ average for m_t allows one to set stringent limits on new physics. We will mainly discuss the effects of exotic particles (with heavy masses $M_{\text{new}} \gg M_Z$ in an expansion in M_Z/M_{new}) on the gauge boson self-energies. (Brief remarks are made on new physics which is not of this type.) Most of the effects on precision measurements can be

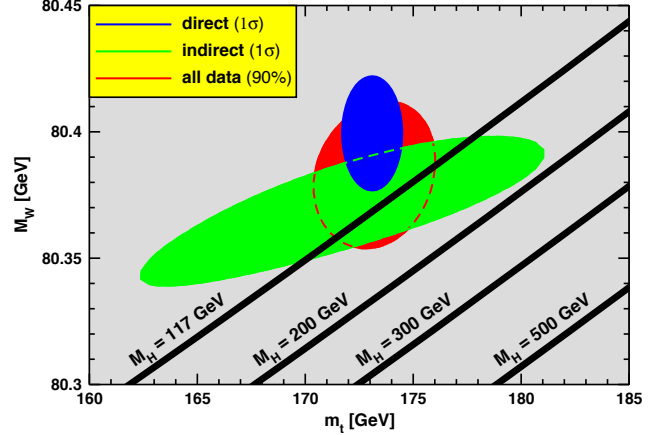


Figure 10.3: One-standard-deviation (39.35%) region in M_W as a function of m_t for the direct and indirect data, and the 90% CL region ($\Delta\chi^2 = 4.605$) allowed by all data. The SM prediction as a function of M_H is also indicated. The widths of the M_H bands reflect the theoretical uncertainty from $\alpha(M_Z)$. Color version at end of book.

Table 10.8: Values of the model-independent neutral-current parameters, compared with the SM predictions. There is a second $g_{V,A}^{\nu e}$ solution, given approximately by $g_{V,A}^{\nu e} \leftrightarrow g_{V,A}^{\nu e}$, which is eliminated by e^+e^- data under the assumption that the neutral current is dominated by the exchange of a single Z boson. The ϵ_L , as well as the ϵ_R , are strongly correlated and non-Gaussian, so that for implementations we recommend the parametrization using g_i^2 and $\theta_i = \tan^{-1}[\epsilon_i(u)/\epsilon_i(d)]$, $i = L$ or R . The analysis of more recent low energy experiments in polarized electron scattering performed in Ref. 123 is included by means of the two orthogonal constraints, $\cos\gamma C_{1d} - \sin\gamma C_{1u} = 0.342 \pm 0.063$ and $\sin\gamma C_{1d} + \cos\gamma C_{1u} = -0.0285 \pm 0.0043$, where $\tan\gamma \approx 0.445$. In the SM predictions, the uncertainty is from M_Z , M_H , m_t , m_b , m_c , $\hat{\alpha}(M_Z)$, and α_s .

Quantity	Experimental Value	SM	Correlation		
$\epsilon_L(u)$	0.338 ± 0.016	0.3461(1)			
$\epsilon_L(d)$	-0.434 ± 0.012	-0.4292(1)			non-
$\epsilon_R(u)$	$-0.174^{+0.013}_{-0.004}$	-0.1549(1)			Gaussian
$\epsilon_R(d)$	$-0.023^{+0.071}_{-0.047}$	0.0775			
g_L^2	0.3025 ± 0.0014	0.3040(2)	-0.18	-0.21	-0.02
g_R^2	0.0309 ± 0.0010	0.0300		-0.03	-0.07
θ_L	2.48 ± 0.036	2.4630(1)			0.24
θ_R	$4.58^{+0.41}_{-0.28}$	5.1765			
$g_{V,A}^{\nu e}$	-0.040 ± 0.015	-0.0398(3)			-0.05
$g_A^{\nu e}$	-0.507 ± 0.014	-0.5064(1)			
$C_{1u} + C_{1d}$	0.1537 ± 0.0011	0.1528(1)	0.64	-0.18	-0.01
$C_{1u} - C_{1d}$	-0.516 ± 0.014	-0.5300(3)		-0.27	-0.02
$C_{2u} + C_{2d}$	-0.21 ± 0.57	-0.0089			-0.30
$C_{2u} - C_{2d}$	-0.077 ± 0.044	-0.0625(5)			
$Q_W(e) = -2C_{2e}$	-0.0403 ± 0.0053	-0.0473(5)			

described by three gauge self-energy parameters S , T , and U . We define these, as well as related parameters, such as ρ_0 , ϵ_i , and $\hat{\epsilon}_i$, to arise from new physics only. *I.e.*, they are equal to zero ($\rho_0 = 1$) exactly in the SM, and do not include any contributions from m_t or M_H , which are treated separately. Our treatment differs from most of

where $t_{3L,R}(i)$ is the third component of weak isospin of the left-(right-)handed component of fermion i and C is the number of colors. For example, a heavy degenerate ordinary or mirror family would contribute $2/3\pi$ to S . In Technicolor models with QCD-like dynamics, one expects [226] $S \sim 0.45$ for an iso-doublet of techni-fermions, assuming $N_{TC} = 4$ techni-colors, while $S \sim 1.62$ for a full techni-generation with $N_{TC} = 4$; T is harder to estimate because it is model-dependent. In these examples one has $S \geq 0$. However, the QCD-like models are excluded on other grounds (flavor changing neutral-currents, and too-light quarks and pseudo-Goldstone bosons [234]). In particular, these estimates do not apply to models of walking Technicolor [234], for which S can be smaller or even negative [235]. Other situations in which $S < 0$, such as loops involving scalars or Majorana particles, are also possible [236]. The simplest origin of $S < 0$ would probably be an additional heavy Z' boson [223], which could mimic $S < 0$. Supersymmetric extensions of the SM generally give very small effects. See Refs. 181 and 237 and the note on ‘‘Supersymmetry’’ in the Searches Particle Listings for a complete set of references.

Most simple types of new physics yield $U = 0$, although there are counter-examples, such as the effects of anomalous triple gauge vertices [228].

The SM expressions for observables are replaced by

$$M_Z^2 = M_{Z0}^2 \frac{1 - \hat{\alpha}(M_Z)T}{1 - G_F M_{Z0}^2 S / 2\sqrt{2}\pi},$$

$$M_W^2 = M_{W0}^2 \frac{1}{1 - G_F M_{W0}^2 (S + U) / 2\sqrt{2}\pi}, \quad (10.59)$$

where M_{Z0} and M_{W0} are the SM expressions (as functions of m_t and M_H) in the $\overline{\text{MS}}$ scheme. Furthermore,

$$\Gamma_Z = \frac{M_Z^3 \beta_Z}{1 - \hat{\alpha}(M_Z)T}, \quad \Gamma_W = M_W^3 \beta_W, \quad A_i = \frac{A_{i0}}{1 - \hat{\alpha}(M_Z)T}, \quad (10.60)$$

where β_Z and β_W are the SM expressions for the reduced widths Γ_{Z0}/M_{Z0}^3 and Γ_{W0}/M_{W0}^3 , M_Z and M_W are the physical masses, and $A_i(A_{i0})$ is a neutral-current amplitude (in the SM).

The data allow a simultaneous determination of \hat{s}_Z^2 (from the Z pole asymmetries), S (from M_Z), U (from M_W), T (mainly from Γ_Z), α_s (from R_ℓ , σ_{had} , and τ_τ), and m_t (from CDF and $D\mathcal{O}$), with little correlation among the SM parameters:

$$S = 0.01 \pm 0.10 (-0.08),$$

$$T = 0.03 \pm 0.11 (+0.09),$$

$$U = 0.06 \pm 0.10 (+0.01), \quad (10.61)$$

and $\hat{s}_Z^2 = 0.23124 \pm 0.00016$, $\alpha_s(M_Z) = 0.1183 \pm 0.0016$, $m_t = 173.0 \pm 1.3$ GeV, where the uncertainties are from the inputs. The central values assume $M_H = 117$ GeV and in parentheses we show the difference to assuming $M_H = 300$ GeV instead. As can be seen, the SM parameters (U) can be determined with no (little) M_H dependence. On the other hand, S , T , and M_H cannot be obtained simultaneously, because the Higgs boson loops themselves are resembled approximately by oblique effects. Eqs. (10.61) show that negative (positive) contributions to the S (T) parameter can weaken or entirely remove the strong constraints on M_H from the SM fits. Specific models in which a large M_H is compensated by new physics are reviewed in Ref. 238. The parameters in Eqs. (10.61), which by definition are due to new physics only, are in reasonable agreement with the SM values of zero. Fixing $U = 0$ (as is also done in Fig. 10.4) moves S and T slightly upwards,

$$S = 0.03 \pm 0.09 (-0.07),$$

$$T = 0.07 \pm 0.08 (+0.09). \quad (10.62)$$

The correlation between S and T in this fit amounts to 87%.

Using Eq. (10.57), the value of ρ_0 corresponding to T in Eq. (10.61) is $1.0002 \pm 0.0009 (+0.0007)$, while the one corresponding to Eq. (10.62)

is $1.0006 \pm 0.0006 (+0.0007)$. The values of the $\hat{\epsilon}$ parameters defined in Eq. (10.56) are

$$\hat{\epsilon}_3 = 0.0000 \pm 0.0009 (-0.0006),$$

$$\hat{\epsilon}_1 = 0.0002 \pm 0.0008 (+0.0007),$$

$$\hat{\epsilon}_2 = -0.0005 \pm 0.0009 (-0.0001). \quad (10.63)$$

Unlike the original definition, we defined the quantities in Eqs. (10.63) to vanish identically in the absence of new physics and to correspond directly to the parameters S , T , and U in Eqs. (10.61). There is a strong correlation (88%) between the S and T parameters. The allowed regions in S - T are shown in Fig. 10.4. From Eqs. (10.61) one obtains $S \leq 0.16$ (0.08) and $T \leq 0.21$ (0.29) at 95% CL for $M_H = 117$ GeV (300 GeV). If one fixes $M_H = 600$ GeV and requires the constraint $S \geq 0$ (as is appropriate in QCD-like Technicolor models) then $S \leq 0.13$ (Bayesian) or $S \leq 0.10$ (frequentist). This rules out simple Technicolor models with many techni-doublets and

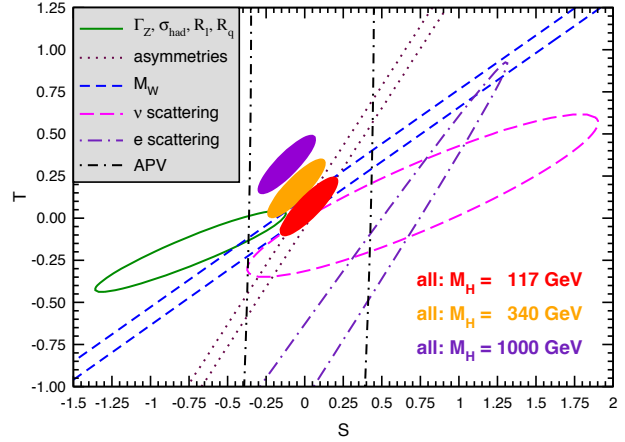


Figure 10.4: 1σ constraints (39.35%) on S and T from various inputs combined with M_Z . S and T represent the contributions of new physics only. (Uncertainties from m_t are included in the errors.) The contours assume $M_H = 117$ GeV except for the central and upper 90% CL contours allowed by all data, which are for $M_H = 340$ GeV and 1000 GeV, respectively. Data sets not involving M_W are insensitive to U . Due to higher order effects, however, $U = 0$ has to be assumed in all fits. α_s is constrained using the τ lifetime as additional input in all fits. Because this has changed significantly since the 2008 edition of this Review (see the discussion in Sec. 10.5), the strongly α_s -dependent solid (green) contour from Z lineshape and cross-section measurements has moved significantly towards negative S and T . The long-dashed (magenta) contour from ν scattering has moved closer towards the global averages (see Sec. 10.3). The long-dash-dotted (indigo) contour from polarized e scattering [123,125] is the upper tip of an elongated ellipse centered at around $S = -15$ and $T = -21$. At first sight it looks as if it is deviating strongly but it is off by only 1.8σ . This illusion arises because $\Delta\chi^2 > 0.8$ everywhere on the visible part of the contour. Color version at end of book.

An extra generation of SM fermions is excluded at the 6σ level on the basis of the S parameter alone, corresponding to $N_F = 2.85 \pm 0.20$ for the number of families. This result assumes that there are no new contributions to T or U and therefore that any new families are degenerate, and is in agreement with a fit to the number of light neutrinos, $N_\nu = 2.991 \pm 0.007$. However, the S parameter fits are valid even for a very heavy fourth family neutrino. This restriction can be relaxed by allowing T to vary as well, since $T > 0$ is expected from a non-degenerate extra family. Fixing $S = 2/3\pi$, the global fit favors a fourth family contribution to T of 0.22 ± 0.04 . However, the quality of the fit deteriorates ($\Delta\chi^2 = 3.2$ relative to the SM fit with

M_H forced not to drop below its LEP 2 bound of 114.4 GeV) so that this tuned T scenario is also disfavored but only at about the 90% CL which is weaker compared to the 2008 edition of this *Review*, *i.e.* before the latest developments in APV and the ν -DIS interpretation. In fact, tuned mass splittings of the extra leptons and quarks [239] can now yield fits with only moderately higher χ^2 values (by about 1 unit) than for the SM. A more detailed analysis is also required if the extra neutrino (or the extra down-type quark) is close to its direct mass limit [240]. Thus, a fourth family is disfavored but not excluded by current data. Similar remarks apply to a heavy mirror family [241] involving right-handed SU(2) doublets and left-handed singlets. A more detailed discussion based on the same data set as used for this *Review* can be found in Ref. 242. Additional heavy ordinary or mirror generations may also require large Yukawa and Higgs couplings that may lead to Landau poles at low scales [243]. In contrast, heavy degenerate non-chiral (also known as vector-like or exotic) multiplets, which are predicted in many grand unified theories [244] and other extensions of the SM, do not contribute to S , T , and U (or to ρ_0), and do not require large coupling constants. Such exotic multiplets may occur in partial families, as in E_6 models, or as complete vector-like families [245].

There is no simple parametrization to describe the effects of every type of new physics on every possible observable. The S , T , and U formalism describes many types of heavy physics which affect only the gauge self-energies, and it can be applied to all precision observables. However, new physics which couples directly to ordinary fermions, such as heavy Z' bosons [223], mixing with exotic fermions [246], or leptoquark exchange [160,247] cannot be fully parametrized in the S , T , and U framework. It is convenient to treat these types of new physics by parameterizations that are specialized to that particular class of theories (*e.g.*, extra Z' bosons), or to consider specific models (which might contain, *e.g.*, Z' bosons and exotic fermions with correlated parameters). Fits to Supersymmetric models are described in Refs. 181 and 248. Models involving strong dynamics (such as (extended) Technicolor) for electroweak breaking are considered in Ref. 249. The effects of compactified extra spatial dimensions at the TeV scale are reviewed in Ref. 250, and constraints on Little Higgs models in Ref. 251. The implications of non-standard Higgs sectors, *e.g.*, involving Higgs singlets or triplets, are discussed in Ref. 252. Limits on new four-Fermi operators and on leptoquarks using LEP 2 and lower energy data are given in Refs. [160,253]. Constraints on various types of new physics are reviewed in Refs. [59,128,254,255], and implications for the LHC in Ref. 256.

An alternate formalism [257] defines parameters, ϵ_1 , ϵ_2 , ϵ_3 , and ϵ_b in terms of the specific observables M_W/M_Z , $\Gamma_{\ell\ell}$, $A_{FB}^{(0,\ell)}$, and R_b . The definitions coincide with those for $\hat{\epsilon}_i$ in Eqs. (10.55) and (10.56) for physics which affects gauge self-energies only, but the ϵ_i 's now parametrize arbitrary types of new physics. However, the ϵ_i 's are not related to other observables unless additional model-dependent assumptions are made. Another approach [258] parametrizes new physics in terms of gauge-invariant sets of operators. It is especially powerful in studying the effects of new physics on non-Abelian gauge vertices. The most general approach introduces deviation vectors [254]. Each type of new physics defines a deviation vector, the components of which are the deviations of each observable from its SM prediction, normalized to the experimental uncertainty. The length (direction) of the vector represents the strength (type) of new physics.

One of the best motivated kinds of physics beyond the SM besides Supersymmetry are extra Z' bosons [259]. They do not spoil the observed approximate gauge coupling unification, and appear copiously in many Grand Unified Theories (GUTs), most Superstring models [260], as well as in dynamical symmetry breaking [249] and Little Higgs models [251]. For example, the SO(10) GUT contains an extra U(1) as can be seen from its maximal subgroup, $SU(5) \times U(1)_\chi$. Similarly, the E_6 GUT contains the subgroup $SO(10) \times U(1)_\psi$. The Z_ψ possesses only axial-vector couplings to the ordinary fermions, and its mass is generally less constrained. The Z_η boson is the linear combination $\sqrt{3/8}Z_\chi - \sqrt{5/8}Z_\psi$. The Z_{LR} boson occurs in left-right models with gauge group $SU(3)_C \times SU(2)_L \times SU(2)_R \times U(1)_{B-L} \subset SO(10)$, and the secluded

Table 10.9: 95% CL lower mass limits (in GeV) from low energy and Z pole data on various extra Z' gauge bosons, appearing in models of unification and string theory. More general parametrizations are described in Refs. 259,264. The electroweak results [265] are for Higgs sectors consisting of doublets and singlets only ($\rho_0 = 1$) with unspecified $U(1)'$ charges. The CDF [266] and DØ [267] bounds from searches for $\bar{p}p \rightarrow \mu^+\mu^-$ and e^+e^- , respectively, are listed in the next two columns, followed by the LEP 2 $e^+e^- \rightarrow f\bar{f}$ bounds [160] (assuming $\theta = 0$). (The Tevatron bounds would be moderately weakened if there are open supersymmetric or exotic decay channels [268]). The last column shows the 1σ ranges for M_H when it is left unconstrained in the electroweak fits.

Z'	electroweak	CDF	DØ	LEP 2	M_H
Z_χ	1, 141	892	800	673	171^{+493}_{-89}
Z_ψ	147	878	763	481	97^{+31}_{-25}
Z_η	427	982	810	434	423^{+577}_{-350}
Z_{LR}	998	630	—	804	804^{+174}_{-35}
Z_S	1, 257	821	719	—	149^{+353}_{-68}
Z_{SM}	1, 403	1, 030	950	1, 787	331^{+669}_{-246}
Z_{string}	1, 362	—	—	—	134^{+209}_{-58}

Z_S emerges in a supersymmetric bottom-up scenario [261]. The sequential Z_{SM} boson is defined to have the same couplings to fermions as the SM Z boson. Such a boson is not expected in the context of gauge theories unless it has different couplings to exotic fermions than the ordinary Z boson. However, it serves as a useful reference case when comparing constraints from various sources. It could also play the role of an excited state of the ordinary Z boson in models with extra dimensions at the weak scale [250]. Finally, we consider a Superstring motivated Z_{string} boson appearing in a specific model [262]. The potential Z' boson is in general a superposition of the SM Z and the new boson associated with the extra U(1). The mixing angle θ satisfies,

$$\tan^2 \theta = \frac{M_{Z_1}^2 - M_Z^2}{M_{Z'}^2 - M_{Z_1}^2},$$

where M_{Z_1} is the SM value for M_Z in the absence of mixing. Note, that $M_Z < M_{Z_1}$, and that the SM Z couplings are changed by the mixing. The couplings of the heavier Z' may also be modified by kinetic mixing [259,263]. If the Higgs U(1)' quantum numbers are known, there will be an extra constraint,

$$\theta = C \frac{g_2 M_Z^2}{g_1 M_{Z'}^2},$$

where $g_{1,2}$ are the U(1) and U(1)' gauge couplings with $g_2 = \sqrt{\frac{5}{3}} \sin \theta_W \sqrt{\lambda} g_1$ and $g_1 = \sqrt{g^2 + g'^2}$. $\lambda \sim 1$ (which we assume) if the GUT group breaks directly to $SU(3) \times SU(2) \times U(1) \times U(1)'$. C is a function of vacuum expectation values. For minimal Higgs sectors it can be found in Ref. 223. Table 10.9 shows the 95% CL lower mass limits [265] for $\rho_0 = 1$ and $114.4 \text{ GeV} \leq M_H \leq 1 \text{ TeV}$. The last column shows the 1σ ranges for M_H when it is left unconstrained. In cases of specific minimal Higgs sectors where C is known, the Z' mass limits are generally pushed into the TeV region. The limits on $|\theta|$ are typically smaller than a few $\times 10^{-3}$. For more details see [259,265,269] and the note on “The Z' Searches” in the Gauge & Higgs Boson Particle Listings. Also listed in Table 10.9 are the direct lower limits on Z' production from the Tevatron [266,267] and LEP 2 bounds [160].

Acknowledgments:

This work was supported in part by CONACyT (México) contract 82291-F by an IBM Einstein Fellowship, and by NSF grant PHY-0503584.

The calculation of the ratio of the kaon and pion decay constants enables one to extract $|V_{us}/V_{ud}|$ from $K \rightarrow \mu\nu(\gamma)$ and $\pi \rightarrow \mu\nu(\gamma)$, where (γ) indicates that radiative decays are included [15]. The KLOE measurement of the $K^+ \rightarrow \mu^+\nu(\gamma)$ branching ratio [16], combined with the lattice QCD calculation, $f_K/f_\pi = 1.189 \pm 0.007$ [17], leads to $|V_{us}| = 0.2259 \pm 0.0014$, where the accuracy is limited by the knowledge of the ratio of the decay constants. The average of these two determinations is quoted by Ref. [9] as

$$|V_{us}| = 0.2252 \pm 0.0009. \quad (11.8)$$

The latest determination from hyperon decays can be found in Ref. [19]. The authors focus on the analysis of the vector form factor, protected from first order $SU(3)$ breaking effects by the Ademollo-Gatto theorem [20], and treat the ratio between the axial and vector form factors g_1/f_1 as experimental input, thus avoiding first order $SU(3)$ breaking effects in the axial-vector contribution. They find $|V_{us}| = 0.2250 \pm 0.0027$, although this does not include an estimate of the theoretical uncertainty due to second-order $SU(3)$ breaking, contrary to Eq. (11.8). Concerning hadronic τ decays to strange particles, the latest determinations based on LEP, and recent *BABAR* and *Belle* data yield $|V_{us}| = 0.2208 \pm 0.0039$ [21]. A recent measurement of the ratio of branching fractions $\mathcal{B}(\tau \rightarrow K\nu)/\mathcal{B}(\tau \rightarrow \pi\nu)$ by *BABAR* [22] combined with the above f_K/f_π value gives $|V_{us}| = 0.2255 \pm 0.0024$.

11.2.3. $|V_{cd}|$:

The magnitude of V_{cd} can be extracted from semileptonic charm decays if theoretical knowledge of the form factors is available. Three-flavor unquenched lattice QCD calculations for $D \rightarrow K\ell\nu$ and $D \rightarrow \pi\ell\nu$ have been published [23]. Using these estimates and the average of recent CLEO-c [24] and *Belle* [25] measurements of $D \rightarrow \pi\ell\nu$ decays, one obtains $|V_{cd}| = 0.229 \pm 0.006 \pm 0.024$, where the first uncertainty is experimental, and the second is from the theoretical uncertainty of the form factor.

This determination is not yet as precise as the one based on neutrino and antineutrino interactions. The difference of the ratio of double-muon to single-muon production by neutrino and antineutrino beams is proportional to the charm cross section off valence d -quarks, and therefore to $|V_{cd}|^2$ times the average semileptonic branching ratio of charm mesons, \mathcal{B}_μ . The method was used first by CDHS [26] and then by CCFR [27,28] and CHARM II [29]. Averaging these results is complicated, not only because it requires assumptions about the scale of the QCD corrections, but also because \mathcal{B}_μ is an effective quantity, which depends on the specific neutrino beam characteristics. Given that no new experimental input is available, we quote the average provided in a previous review, $\mathcal{B}_\mu|V_{cd}|^2 = (0.463 \pm 0.034) \times 10^{-2}$ [30]. Analysis cuts make these experiments insensitive to neutrino energies smaller than 30 GeV. Thus, \mathcal{B}_μ should be computed using only neutrino interactions with visible energy larger than 30 GeV. An appraisal [31] based on charm-production fractions measured in neutrino interactions [32,33] gives $\mathcal{B}_\mu = 0.088 \pm 0.006$. Data from the CHORUS experiment [34] are sufficiently precise to extract \mathcal{B}_μ directly, by comparing the number of charm decays with a muon to the total number of charmed hadrons found in the nuclear emulsions. Requiring the visible energy to be larger than 30 GeV, CHORUS finds $\mathcal{B}_\mu = 0.085 \pm 0.009 \pm 0.006$. To extract $|V_{cd}|$, we use the average of these two determinations, $\mathcal{B}_\mu = 0.087 \pm 0.005$, and obtain

$$|V_{cd}| = 0.230 \pm 0.011. \quad (11.9)$$

11.2.4. $|V_{cs}|$:

The determination of $|V_{cs}|$ from neutrino and antineutrino scattering suffers from the uncertainty of the s -quark sea content. Measurements sensitive to $|V_{cs}|$ from on-shell W^\pm decays were performed at LEP-2. The branching ratios of the W depend on the six CKM matrix elements involving quarks with masses smaller than M_W . The W branching ratio to each lepton flavor is given by $1/\mathcal{B}(W \rightarrow \ell\bar{\nu}_\ell) = 3[1 + \sum_{u,c,d,s,b} |V_{ij}|^2 (1 + \alpha_s(m_W)/\pi)]$. The measurement assuming lepton universality, $\mathcal{B}(W \rightarrow \ell\bar{\nu}_\ell) = (10.83 \pm 0.07 \pm 0.07) \%$ [35],

implies $\sum_{u,c,d,s,b} |V_{ij}|^2 = 2.002 \pm 0.027$. This is a precise test of unitarity, but only flavor-tagged W -decay measurements determine $|V_{cs}|$ directly. DELPHI measured tagged $W^+ \rightarrow c\bar{s}$ decays, obtaining $|V_{cs}| = 0.94^{+0.32}_{-0.26} \pm 0.13$ [36]. Hereafter, the first error is statistical and the second is systematic, unless mentioned otherwise.

The direct determination of $|V_{cs}|$ is possible from semileptonic D or leptonic D_s decays, using unquenched lattice QCD calculations of the semileptonic D form factor or the D_s decay constant. For muonic decays, the average of *Belle* [37] and CLEO-c [38] gives $\mathcal{B}(D_s^+ \rightarrow \mu^+\nu) = (5.81 \pm 0.43) \times 10^{-3}$ [39]. The adjusted *BABAR* [40] measurement gives $\mathcal{B}(D_s^+ \rightarrow \mu^+\nu) = (4.81 \pm 0.68) \times 10^{-3}$ [39]. For decays with τ leptons, the average of recent CLEO-c measurements [38,41] gives $\mathcal{B}(D_s^+ \rightarrow \tau^+\nu) = (5.61 \pm 0.44) \times 10^{-2}$ [39]. From each of these values, determinations of $|V_{cs}|$ can be obtained by using the PDG values for the mass and lifetime of the D_s , the masses of the leptons, and $f_{D_s} = (242.8 \pm 3.2 \pm 5.3) \text{ MeV}$ [42]. The average of these three determinations gives $|V_{cs}| = 1.030 \pm 0.038$, where the error is dominated by the lattice QCD determination of f_{D_s} . In semileptonic D decays, unquenched lattice QCD calculations have predicted the normalization and the shape (dependence on the invariant mass of the lepton pair, q^2) of the form factors in $D \rightarrow K\ell\nu$ and $D \rightarrow \pi\ell\nu$ [23]. Using these theoretical results and the average of recent CLEO-c [24], *Belle* [25] and *BABAR* [43] measurements of $B \rightarrow K\ell\nu$ decays, one obtains $|V_{cs}| = 0.98 \pm 0.01 \pm 0.10$, where the first error is experimental and the second, which is dominant, is from the theoretical uncertainty of the form factor. Averaging the determinations from leptonic and semileptonic decays, we find

$$|V_{cs}| = 1.023 \pm 0.036. \quad (11.10)$$

11.2.5. $|V_{cb}|$:

This matrix element can be determined from exclusive and inclusive semileptonic decays of B mesons to charm. The inclusive determinations use the semileptonic decay rate measurement, together with the leptonic energy and the hadronic invariant-mass spectra. The theoretical foundation of the calculation is the operator product expansion [44,45]. It expresses the total rate and moments of differential energy and invariant-mass spectra as expansions in α_s , and inverse powers of the heavy quark mass. The dependence on m_b , m_c , and the parameters that occur at subleading order is different for different moments, and a large number of measured moments overconstrains all the parameters, and tests the consistency of the determination. The precise extraction of $|V_{cb}|$ requires using a “threshold” quark mass definition [46,47]. Inclusive measurements have been performed using B mesons from Z^0 decays at LEP, and at e^+e^- machines operated at the $\Upsilon(4S)$. At LEP, the large boost of B mesons from the Z^0 allows the determination of the moments throughout phase space, which is not possible otherwise, but the large statistics available at the B factories lead to more precise determinations. An average of the measurements and a compilation of the references are provided by Ref. [48]: $|V_{cb}| = (41.5 \pm 0.7) \times 10^{-3}$.

Exclusive determinations are based on semileptonic B decays to D and D^* . In the $m_{b,c} \gg \Lambda_{\text{QCD}}$ limit, all form factors are given by a single Isgur-Wise function [49], which depends on the product of the four-velocities of the B and $D^{(*)}$ mesons, $w = v \cdot v'$. Heavy quark symmetry determines the normalization of the rate at $w = 1$, the maximum momentum transfer to the leptons, and $|V_{cb}|$ is obtained from an extrapolation to $w = 1$. The exclusive determination, $|V_{cb}| = (38.7 \pm 1.1) \times 10^{-3}$ [48], is less precise than the inclusive one because of the theoretical uncertainty in the form factor and the experimental uncertainty in the rate near $w = 1$. Ref. [48] quotes a combination with a scaled error as

$$|V_{cb}| = (40.6 \pm 1.3) \times 10^{-3}. \quad (11.11)$$

11.2.6. $|V_{ub}|$:

The determination of $|V_{ub}|$ from inclusive $B \rightarrow X_u \ell \bar{\nu}$ decay suffers from large $B \rightarrow X_c \ell \bar{\nu}$ backgrounds. In most regions of phase space where the charm background is kinematically forbidden, the hadronic physics enters via unknown nonperturbative functions, so-called shape functions. (In contrast, the nonperturbative physics for $|V_{cb}|$ is encoded in a few parameters.) At leading order in Λ_{QCD}/m_b , there is only one shape function, which can be extracted from the photon energy spectrum in $B \rightarrow X_s \gamma$ [50,51], and applied to several spectra in $B \rightarrow X_u \ell \bar{\nu}$. The subleading shape functions are modeled in the current determinations. Phase space cuts for which the rate has only subleading dependence on the shape function are also possible [52]. The measurements of both the hadronic and the leptonic systems are important for an optimal choice of phase space. A different approach is to make the measurements more inclusive by extending them deeper into the $B \rightarrow X_c \ell \bar{\nu}$ region, and thus reduce the theoretical uncertainties. Analyses of the electron-energy endpoint from CLEO [53], BABAR [54], and Belle [55] quote $B \rightarrow X_u e \bar{\nu}$ partial rates for $|\vec{p}_e| \geq 2.0 \text{ GeV}$ and 1.9 GeV , which are well below the charm endpoint. The large and pure $B\bar{B}$ samples at the B factories permit the selection of $B \rightarrow X_u \ell \bar{\nu}$ decays in events where the other B is fully reconstructed [56]. With this full-reconstruction tag method, the four-momenta of both the leptonic and the hadronic systems can be measured. It also gives access to a wider kinematic region because of improved signal purity. Ref. [48] quotes an inclusive average as $|V_{ub}| = (4.27 \pm 0.38) \times 10^{-3}$.

To extract $|V_{ub}|$ from an exclusive channel, the form factors have to be known. Experimentally, better signal-to-background ratios are offset by smaller yields. The $B \rightarrow \pi \ell \bar{\nu}$ branching ratio is now known to 5%. Unquenched lattice QCD calculations of the $B \rightarrow \pi \ell \bar{\nu}$ form factor are available [57,58] for the high q^2 region ($q^2 > 16$ or 18 GeV^2). A simultaneous fit to the experimental partial rates and lattice points versus q^2 yields $|V_{ub}| = (3.38 \pm 0.36) \times 10^{-3}$ [58]. Light-cone QCD sum rules are applicable for $q^2 < 14 \text{ GeV}^2$ [59] and yield similar results.

The theoretical uncertainties in extracting $|V_{ub}|$ from inclusive and exclusive decays are different. A combination of the determinations is quoted by Ref. [48] as

$$|V_{ub}| = (3.89 \pm 0.44) \times 10^{-3}. \quad (11.12)$$

11.2.7. $|V_{td}|$ and $|V_{ts}|$:

The CKM elements $|V_{td}|$ and $|V_{ts}|$ cannot be measured from tree-level decays of the top quark, so one has to rely on determinations from B - \bar{B} oscillations mediated by box diagrams with top quarks, or loop-mediated rare K and B decays. Theoretical uncertainties in hadronic effects limit the accuracy of the current determinations. These can be reduced by taking ratios of processes that are equal in the flavor $SU(3)$ limit to determine $|V_{td}/V_{ts}|$.

The mass difference of the two neutral B meson mass eigenstates is very well measured, $\Delta m_d = (0.507 \pm 0.005) \text{ ps}^{-1}$ [60]. For the B_s^0 system, CDF measured $\Delta m_s = (17.77 \pm 0.10 \pm 0.07) \text{ ps}^{-1}$ [61] with more than 5σ significance (the $D\bar{D}$ result [62] is compatible and has about 2σ significance). Using the unquenched lattice QCD calculations [63] $f_{B_d} \sqrt{\hat{B}_{B_d}} = (216 \pm 9 \pm 13) \text{ MeV}$, $f_{B_s} \sqrt{\hat{B}_{B_s}} = (275 \pm 7 \pm 13) \text{ MeV}$, and assuming $|V_{tb}| = 1$, one finds

$$|V_{td}| = (8.4 \pm 0.6) \times 10^{-3}, \quad |V_{ts}| = (38.7 \pm 2.1) \times 10^{-3}. \quad (11.13)$$

The uncertainties are dominated by lattice QCD. Several uncertainties are reduced in the calculation of the ratio $\xi = (f_{B_s} \sqrt{\hat{B}_{B_s}})/(f_{B_d} \sqrt{\hat{B}_{B_d}}) = 1.243 \pm 0.021 \pm 0.021$, and therefore the constraint on $|V_{td}/V_{ts}|$ from $\Delta m_d/\Delta m_s$ is more reliable theoretically. These provide a new, theoretically clean, and significantly improved constraint

$$|V_{td}/V_{ts}| = 0.211 \pm 0.001 \pm 0.005. \quad (11.14)$$

The inclusive branching ratio $\mathcal{B}(B \rightarrow X_s \gamma) = (3.52 \pm 0.25) \times 10^{-4}$ extrapolated to $E_\gamma > E_0 = 1.6 \text{ GeV}$ [64] is also sensitive to $V_{tb}V_{ts}^*$.

In addition to t -quark penguins, a large part of the sensitivity comes from charm contributions proportional to $V_{cb}V_{cs}^*$ via the application of 3×3 CKM unitarity (which is used here; any CKM determination from loop processes necessarily assumes the SM). With the NNLO calculation of $\mathcal{B}(B \rightarrow X_s \gamma)_{E_\gamma > E_0}/\mathcal{B}(B \rightarrow X_c e \bar{\nu})$ [65], we obtain $|V_{ts}/V_{cb}| = (1.04 \pm 0.05)$.

A complementary determination of $|V_{td}/V_{ts}|$ is possible from the ratio of $B \rightarrow \rho \gamma$ and $K^* \gamma$ rates. The ratio of the neutral modes is theoretically cleaner than that of the charged ones, because the poorly known spectator-interaction contribution is expected to be smaller (W -exchange vs. weak annihilation). For now, because of low statistics we average the charged and neutral rates assuming the isospin symmetry and heavy quark limit motivated relation, $|V_{td}/V_{ts}|^2/\xi_\gamma^2 = [\Gamma(B^+ \rightarrow \rho^+ \gamma) + 2\Gamma(B^0 \rightarrow \rho^0 \gamma)]/[\Gamma(B^+ \rightarrow K^{*+} \gamma) + \Gamma(B^0 \rightarrow K^{*0} \gamma)] = (3.19 \pm 0.46)\%$ [64]. Here ξ_γ contains the poorly known hadronic physics. Using $\xi_\gamma = 1.2 \pm 0.2$ [66], and combining the experimental and theoretical errors in quadrature, gives $|V_{td}/V_{ts}| = 0.21 \pm 0.04$.

A theoretically clean determination of $|V_{td}V_{ts}^*|$ is possible from $K^+ \rightarrow \pi^+ \nu \bar{\nu}$ decay [67]. Experimentally, only seven events have been observed [68] and the rate is consistent with the SM with large uncertainties. Much more data are needed for a precision measurement.

11.2.8. $|V_{tb}|$:

The determination of $|V_{tb}|$ from top decays uses the ratio of branching fractions $R = \mathcal{B}(t \rightarrow Wb)/\mathcal{B}(t \rightarrow Wq) = |V_{tb}|^2/(\sum_q |V_{tq}|^2) = |V_{tb}|^2$, where $q = b, s, d$. The CDF and $D\bar{D}$ measurements performed on data collected during Run II of the Tevatron give $|V_{tb}| > 0.78$ [69] and $|V_{tb}| > 0.89$ [70], respectively, at 95% CL. The direct determination of $|V_{tb}|$ without assuming unitarity is possible from the single top-quark-production cross section. The $(2.76_{-0.47}^{+0.58}) \text{ pb}$ [71] average cross section measured by $D\bar{D}$ [72] and CDF [73] implies

$$|V_{tb}| = 0.88 \pm 0.07. \quad (11.15)$$

An attempt at constraining $|V_{tb}|$ from the precision electroweak data was made in [74]. The result, mostly driven by the top-loop contributions to $\Gamma(Z \rightarrow b\bar{b})$, gives $|V_{tb}| = 0.77_{-0.24}^{+0.18}$.

11.3. Phases of CKM elements

As can be seen from Fig. 11.1, the angles of the unitarity triangle are

$$\begin{aligned} \beta = \phi_1 &= \arg \left(-\frac{V_{cd}V_{cb}^*}{V_{td}V_{tb}^*} \right), \\ \alpha = \phi_2 &= \arg \left(-\frac{V_{td}V_{tb}^*}{V_{ud}V_{ub}^*} \right), \\ \gamma = \phi_3 &= \arg \left(-\frac{V_{ud}V_{ub}^*}{V_{cd}V_{cb}^*} \right). \end{aligned} \quad (11.16)$$

Since CP violation involves phases of CKM elements, many measurements of CP -violating observables can be used to constrain these angles and the $\bar{\rho}, \bar{\eta}$ parameters.

11.3.1. ϵ and ϵ' :

The measurement of CP violation in K^0 - \bar{K}^0 mixing, $|\epsilon| = (2.233 \pm 0.015) \times 10^{-3}$ [75], provides important information about the CKM matrix. In the SM, in the basis where $V_{ud}V_{us}^*$ is real [76]

$$\begin{aligned} |\epsilon| = \frac{G_F^2 f_K^2 m_K m_W^2}{12\sqrt{2}\pi^2 \Delta m_K} \hat{B}_K \left\{ \eta_1 S(x_c) \text{Im}[(V_{cs}V_{cd}^*)^2] \right. \\ \left. + \eta_2 S(x_t) \text{Im}[(V_{ts}V_{td}^*)^2] + 2\eta_3 S(x_c, x_t) \text{Im}(V_{cs}V_{cd}^* V_{ts}V_{td}^*) \right\}, \end{aligned} \quad (11.17)$$

where S is an Inami-Lim function [77], $x_q = m_q^2/m_W^2$, and η_i are perturbative QCD corrections. The constraint from ϵ in the $\bar{\rho}, \bar{\eta}$ plane is bounded by approximate hyperbolae. The dominant uncertainties are due to the bag parameter, for which we use $\hat{B}_K = 0.725 \pm 0.026$

than $\mathcal{B}(B^0 \rightarrow \rho^+\rho^-) = (24.2^{+3.1}_{-3.2}) \times 10^{-6}$ and $\mathcal{B}(B^+ \rightarrow \rho^+\rho^0) = (24.0^{+1.9}_{-2.0}) \times 10^{-6}$ [64], which implies that the effect of the penguin diagrams is small. The isospin analysis using the world averages, $S_{\rho^+\rho^-} = -0.05 \pm 0.17$ and $C_{\rho^+\rho^-} = -0.06 \pm 0.13$ [64], together with the time-dependent CP asymmetry, $S_{\rho^0\rho^0} = -0.3 \pm 0.7$ and $C_{\rho^0\rho^0} = -0.2 \pm 0.9$ [97], and the above-mentioned branching fractions, gives $\alpha = (89.9 \pm 5.4)^\circ$ [95], with a mirror solution at $3\pi/2 - \alpha$. A possible small violation of Eq. (11.22) due to the finite width of the ρ [98] is neglected.

11.3.3.3. $B \rightarrow \rho\pi$:

The final state in $B^0 \rightarrow \rho^+\pi^-$ decay is not a CP eigenstate, but this decay proceeds via the same quark-level diagrams as $B^0 \rightarrow \pi^+\pi^-$, and both B^0 and \bar{B}^0 can decay to $\rho^+\pi^-$. Consequently, mixing-induced CP violations can occur in four decay amplitudes, $B^0 \rightarrow \rho^\pm\pi^\mp$ and $\bar{B}^0 \rightarrow \rho^\pm\pi^\mp$. The time-dependent Dalitz plot analysis of $B^0 \rightarrow \pi^+\pi^-\pi^0$ decays permits the extraction of α with a single discrete ambiguity, $\alpha \rightarrow \alpha + \pi$, since one knows the variation of the strong phases in the interference regions of the $\rho^+\pi^-$, $\rho^-\pi^+$, and $\rho^0\pi^0$ amplitudes in the Dalitz plot [99]. The combination of Belle [100] and BABAR [101] measurements gives $\alpha = (120^{+11}_{-7})^\circ$ [95]. This constraint is still moderate, and there are also solutions around 30° and 90° within 2σ significance level.

Combining the above-mentioned three decay modes [95], α is constrained as

$$\alpha = (89.0^{+4.4}_{-4.2})^\circ. \quad (11.23)$$

A different statistical approach [102] gives similar constraint from the combination of these measurements.

11.3.4. γ / ϕ_3 :

By virtue of Eq. (11.16), γ does not depend on CKM elements involving the top quark, so it can be measured in tree-level B decays. This is an important distinction from the measurements of α and β , and implies that the measurements of γ are unlikely to be affected by physics beyond the SM.

11.3.4.1. $B^\pm \rightarrow DK^\pm$:

The interference of $B^- \rightarrow D^0K^-$ ($b \rightarrow c\bar{u}s$) and $B^- \rightarrow \bar{D}^0K^-$ ($b \rightarrow u\bar{c}s$) transitions can be studied in final states accessible in both D^0 and \bar{D}^0 decays [85]. In principle, it is possible to extract the B and D decay amplitudes, the relative strong phases, and the weak phase γ from the data.

A practical complication is that the precision depends sensitively on the ratio of the interfering amplitudes

$$r_B = \left| \frac{A(B^- \rightarrow \bar{D}^0K^-)}{A(B^- \rightarrow D^0K^-)} \right|, \quad (11.24)$$

which is around 0.1–0.2. The original GLW method [103,104] considers D decays to CP eigenstates, such as $B^\pm \rightarrow D_{CP}^{(*)}(\rightarrow \pi^+\pi^-)K^\pm$. To alleviate the smallness of r_B and make the interfering amplitudes (which are products of the B and D decay amplitudes) comparable in magnitude, the ADS method [105] considers final states where Cabibbo-allowed \bar{D}^0 and doubly-Cabibbo-suppressed D^0 decays interfere. Extensive measurements have been made by the B factories using both methods [106].

It was realized that both D^0 and \bar{D}^0 have large branching fractions to certain three-body final states, such as $K_S\pi^+\pi^-$, and the analysis can be optimized by studying the Dalitz plot dependence of the interferences [107,108]. The best present determination of γ comes from this method. Belle [109] and BABAR [110] obtained $\gamma = (76^{+12}_{-13} \pm 4 \pm 9)^\circ$ and $\gamma = (76 \pm 22 \pm 5 \pm 5)^\circ$, respectively, where the last uncertainty is due to the D -decay modeling. The error is sensitive to the central value of the amplitude ratio r_B (and r_B^* for the D^*K mode), for which Belle found somewhat larger central values than BABAR. The same values of $r_B^{(*)}$ enter the ADS analyses, and the data can be combined to fit for $r_B^{(*)}$ and γ . The D^0 - \bar{D}^0 -mixing has been neglected in all measurements, but its effect on γ is far below the present experimental accuracy [111], unless D^0 - \bar{D}^0 -mixing is due

to CP -violating new physics, in which case it can be included in the analysis [112].

Combining the GLW, ADS, and Dalitz analyses [95], γ is constrained as

$$\gamma = (73^{+22}_{-25})^\circ. \quad (11.25)$$

Similar results are found in [102].

11.3.4.2. $B^0 \rightarrow D^{(*)\pm}\pi^\mp$:

The interference of $b \rightarrow u$ and $b \rightarrow c$ transitions can be studied in $\bar{B}^0 \rightarrow D^{(*)+}\pi^-$ ($b \rightarrow c\bar{u}d$) and $\bar{B}^0 \rightarrow B^0 \rightarrow D^{(*)+}\pi^-$ ($\bar{b} \rightarrow \bar{u}c\bar{d}$) decays and their CP conjugates, since both B^0 and \bar{B}^0 decay to $D^{(*)\pm}\pi^\mp$ (or $D^\pm\rho^\mp$, etc.). Since there are only tree and no penguin contributions to these decays, in principle, it is possible to extract from the four time-dependent rates the magnitudes of the two hadronic amplitudes, their relative strong phase, and the weak phase between the two-decay paths, which is $2\beta + \gamma$.

A complication is that the ratio of the interfering amplitudes is very small, $r_{D\pi} = A(B^0 \rightarrow D^+\pi^-)/A(\bar{B}^0 \rightarrow D^+\pi^-) = \mathcal{O}(0.01)$ (and similarly for $r_{D^*\pi}$ and $r_{D\rho}$), and therefore it has not been possible to measure it. To obtain $2\beta + \gamma$, $SU(3)$ flavor symmetry and dynamical assumptions have been used to relate $A(\bar{B}^0 \rightarrow D^-\pi^+)$ to $A(\bar{B}^0 \rightarrow D_s^-\pi^+)$, so this measurement is not model-independent at present. Combining the $D^\pm\pi^\mp$, $D^{*\pm}\pi^\mp$ and $D^\pm\rho^\mp$ measurements [113] gives $\sin(2\beta + \gamma) > 0.68$ at 68% CL [95], consistent with the previously discussed results for β and γ . The amplitude ratio is much larger in the analogous $B_s^0 \rightarrow D_s^\pm K^\mp$ decays, so it will be possible at LHCb to measure it and model-independently extract $\gamma - 2\beta_s$ [114] (where $\beta_s = \arg(-V_{ts}V_{tb}^*/V_{cs}V_{cb}^*)$ is related to the phase of B_s mixing).

11.4. Global fit in the Standard Model

Using the independently measured CKM elements mentioned in the previous sections, the unitarity of the CKM matrix can be checked. We obtain $|V_{ud}|^2 + |V_{us}|^2 + |V_{ub}|^2 = 0.9999 \pm 0.0006$ (1st row), $|V_{cd}|^2 + |V_{cs}|^2 + |V_{cb}|^2 = 1.101 \pm 0.074$ (2nd row), $|V_{ud}|^2 + |V_{cd}|^2 + |V_{td}|^2 = 1.002 \pm 0.005$ (1st column), and $|V_{us}|^2 + |V_{cs}|^2 + |V_{ts}|^2 = 1.098 \pm 0.074$ (2nd column), respectively. The uncertainties in the second row and column are dominated by that of $|V_{cs}|$. For the second row, a more stringent check is obtained from the measurement of $\sum_{u,c,d,s,b} |V_{ij}|^2$ in Sec. 11.2.4 minus the sum in the first row above: $|V_{cd}|^2 + |V_{cs}|^2 + |V_{cb}|^2 = 1.002 \pm 0.027$. These provide strong tests of the unitarity of the CKM matrix. The sum of the three angles of the unitarity triangle, $\alpha + \beta + \gamma = (183^{+22}_{-25})^\circ$, is also consistent with the SM expectation.

The CKM matrix elements can be most precisely determined by a global fit that uses all available measurements and imposes the SM constraints (*i.e.*, three generation unitarity). The fit must also use theory predictions for hadronic matrix elements, which sometimes have significant uncertainties. There are several approaches to combining the experimental data. CKMfitter [6,95] and Ref. [115] (which develops [116,117] further) use frequentist statistics, while UTfit [102,118] uses a Bayesian approach. These approaches provide similar results.

The constraints implied by the unitarity of the three generation CKM matrix significantly reduce the allowed range of some of the CKM elements. The fit for the Wolfenstein parameters defined in Eq. (11.4) gives

$$\begin{aligned} \lambda &= 0.2253 \pm 0.0007, & A &= 0.808^{+0.022}_{-0.015}, \\ \bar{\rho} &= 0.132^{+0.022}_{-0.014}, & \bar{\eta} &= 0.341 \pm 0.013. \end{aligned} \quad (11.26)$$

These values are obtained using the method of Refs. [6,95]. Using the prescription of Refs. [102,118] gives $\lambda = 0.2246 \pm 0.0011$, $A = 0.832 \pm 0.017$, $\bar{\rho} = 0.130 \pm 0.018$, $\bar{\eta} = 0.350 \pm 0.013$ [119]. The fit results for the magnitudes of all nine CKM elements are.

$$V_{\text{CKM}} = \begin{pmatrix} 0.97428 \pm 0.00015 & 0.2253 \pm 0.0007 & 0.00347^{+0.00016}_{-0.00012} \\ 0.2252 \pm 0.0007 & 0.97345^{+0.00015}_{-0.00016} & 0.0410^{+0.0011}_{-0.0007} \\ 0.00862^{+0.00026}_{-0.00020} & 0.0403^{+0.0011}_{-0.0007} & 0.999152^{+0.000030}_{-0.000045} \end{pmatrix}, \quad (11.27)$$

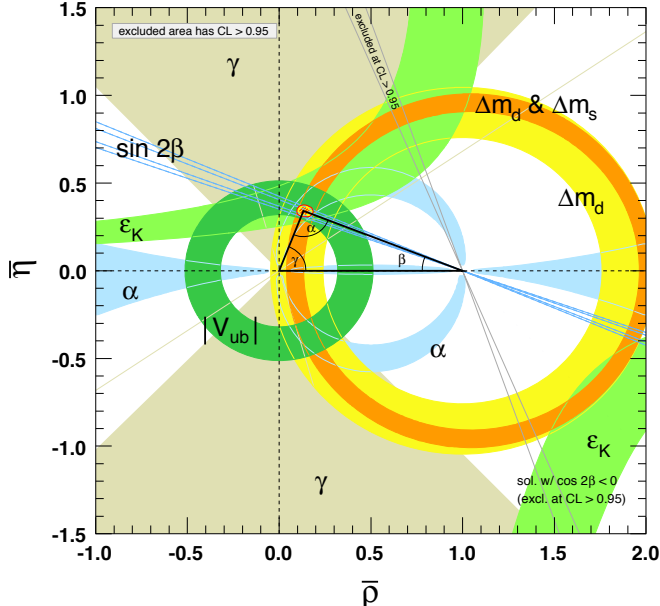


Figure 11.2: Constraints on the $\bar{\rho}, \bar{\eta}$ plane. The shaded areas have 95% CL. Color version at end of book.

and the Jarlskog invariant is $J = (2.91_{-0.11}^{+0.19}) \times 10^{-5}$.

Fig. 11.2 illustrates the constraints on the $\bar{\rho}, \bar{\eta}$ plane from various measurements and the global fit result. The shaded 95% CL regions all overlap consistently around the global fit region, though the consistency of $|V_{ub}/V_{cb}|$ and $\sin 2\beta$ is not very good.

11.5. Implications beyond the SM

The effects in B , K , and D decays and mixings due to high-scale physics (W , Z , t , h in the SM, and new physics particles) can be parameterized by operators made of SM fields, obeying the $SU(3) \times SU(2) \times U(1)$ gauge symmetry. The non-SM contributions to the coefficients of these operators are suppressed by powers of the scale of new physics. At lowest order, there are of order a hundred flavor-changing operators of dimension-6, and the observable effects of non-SM interactions are encoded in their coefficients. In the SM, these coefficients are determined by just the four CKM parameters, and the W , Z , and quark masses. For example, Δm_d , $\Gamma(B \rightarrow \rho\gamma)$, and $\Gamma(B \rightarrow X_d \ell^+ \ell^-)$ are all proportional to $|V_{td}^* V_{tb}^*|^2$ in the SM, however, they may receive unrelated contributions from new physics. The new physics contributions may or may not obey the SM relations. (For example, the flavor sector of the MSSM contains 69 CP -conserving parameters and 41 CP -violating phases, *i.e.*, 40 new ones [120]). Thus, similar to the measurements of $\sin 2\beta$ in tree- and loop-dominated decay modes, overconstraining measurements of the magnitudes and phases of flavor-changing neutral current amplitudes give good sensitivity to new physics.

To illustrate the level of suppression required for non-SM contributions, consider a class of models in which the unitarity of the CKM matrix is maintained, and the dominant effect of new physics is to modify the neutral meson mixing amplitudes [121] by $(z_{ij}/\Lambda^2)(\bar{q}_i \gamma^\mu P_L q_j)^2$ (for recent reviews, see [122,123]). It is only known since the measurements of γ and α that the SM gives the leading contribution to $B^0 - \bar{B}^0$ mixing [6,124]. Nevertheless, new physics with a generic weak phase may still contribute to neutral meson mixings at a significant fraction of the SM [125,118]. The existing data imply that $\Lambda/|z_{ij}|^{1/2}$ has to exceed about 10^4 TeV for $K^0 - \bar{K}^0$ mixing, 10^3 TeV for $D^0 - \bar{D}^0$ mixing, 500 TeV for $B^0 - \bar{B}^0$ mixing, and 100 TeV for $B_s^0 - \bar{B}_s^0$ mixing [118,123]. (Some other operators are even better constrained [118].) The constraints are the strongest in the kaon sector, because the CKM suppression is the most severe. Thus, if there is new physics at the TeV scale, $|z_{ij}| \ll 1$ is required. Even if $|z_{ij}|$ are suppressed by a loop factor and $|V_{ti}^* V_{tj}|^2$ (in the down quark sector), similar to the SM, one expects percent-level effects, which may be observable in forthcoming

flavor physics experiments. To constrain such extensions of the SM, many measurements irrelevant for the SM-CKM fit, such as the CP asymmetry in semileptonic B decays [126], are important.

Many key measurements, which are sensitive to non-SM flavor physics, are not useful to think about in terms of constraining CKM parameters. For example, besides the angles in Eq. (11.16), a key quantity in the B_s sector is $\beta_s = \arg(-V_{ts}V_{tb}^*/V_{cs}V_{cb}^*)$, which is the small, λ^2 -suppressed, angle of a “squashed” unitarity triangle, obtained by taking the scalar product of the second and third columns. The angle β_s can be measured via time-dependent CP violation in $B_s^0 \rightarrow J/\psi\phi$, similar to β in $B^0 \rightarrow J/\psi K^0$. Checking if β_s agrees with its SM prediction, $\beta_s = 0.018 \pm 0.001$ [95], is an equally important test of the theory. The first flavor-tagged time-dependent CP -asymmetry measurements of $B_s^0 \rightarrow J/\psi\phi$ decay appeared recently [127], giving a mild hint of a possible deviation.

In the kaon sector, the two measured CP -violating observables ϵ and ϵ' are tiny, so models in which all sources of CP violation are small were viable before the B -factory measurements. Since the measurement of $\sin 2\beta$, we know that CP violation can be an $\mathcal{O}(1)$ effect, and only flavor mixing is suppressed between the three quark generations. Thus, many models with spontaneous CP violation are excluded. In the kaon sector, a very clean test of the SM will come from measurements of $K^+ \rightarrow \pi^+ \nu \bar{\nu}$ and $K_L^0 \rightarrow \pi^0 \nu \bar{\nu}$. These loop-induced rare decays are sensitive to new physics, and will allow a determination of β independent of its value measured in B decays [128].

The CKM elements are fundamental parameters, so they should be measured as precisely as possible. The overconstraining measurements of CP asymmetries, mixing, semileptonic, and rare decays have started to severely constrain the magnitudes and phases of possible new physics contributions to flavor-changing interactions. When new particles are observed at the LHC, it will be important to know the flavor parameters as precisely as possible to understand the underlying physics.

References:

1. N. Cabibbo, Phys. Rev. Lett. **10**, 531 (1963).
2. M. Kobayashi and T. Maskawa, Prog. Theor. Phys. **49**, 652 (1973).
3. L. L. Chau and W. Y. Keung, Phys. Rev. Lett. **53**, 1802 (1984).
4. L. Wolfenstein, Phys. Rev. Lett. **51**, 1945 (1983).
5. A. J. Buras *et al.*, Phys. Rev. **D50**, 3433 (1994) [hep-ph/9403384].
6. J. Charles *et al.* [CKMfitter Group], Eur. Phys. J. **C41**, 1 (2005) [hep-ph/0406184].
7. C. Jarlskog, Phys. Rev. Lett. **55**, 1039 (1985).
8. J. C. Hardy and I. S. Towner, Phys. Rev. **C70**, 055502 (2009) [arXiv:0812.1202 [nucl-ex]].
9. E. Blucher and W.J. Marciano, “ V_{ud} , V_{us} , the Cabibbo Angle and CKM Unitarity,” in this Review.
10. D. Pocanic *et al.*, Phys. Rev. Lett. **93**, 181803 (2004) [hep-ex/0312030].
11. M. Antonelli *et al.* [The FlaviaNet Kaon Working Group], arXiv:0801.1817; see also <http://www.lnf.infn.it/wg/vus>.
12. P. A. Boyle *et al.*, Phys. Rev. Lett. **100**, 141601 (2008) [arXiv:0710.5136].
13. H. Leutwyler and M. Roos, Z. Phys. **C25**, 91 (1984).
14. J. Bijnens and P. Talavera, Nucl. Phys. **B669**, 341 (2003) [hep-ph/0303103]; M. Jamin *et al.*, JHEP **402**, 047 (2004) [hep-ph/0401080]; V. Cirigliano *et al.*, JHEP **504**, 6 (2005) [hep-ph/0503108]; C. Dawson *et al.*, PoS **LAT2005**, 337 (2005) [hep-lat/0510018]; N. Tsutsui *et al.* [JLQCD Collab.], PoS **LAT2005**, 357 (2005) [hep-lat/0510068]; M. Okamoto [Fermilab Lattice Collab.], hep-lat/0412044.
15. W. J. Marciano, Phys. Rev. Lett. **93**, 231803 (2004) [hep-ph/0402299].
16. F. Ambrosino *et al.* [KLOE Collab.], Phys. Lett. **B632**, 76 (2006) [hep-ex/0509045].

12. *CP VIOLATION IN MESON DECAYS*

Revised August 2009 by D. Kirkby (UC Irvine) and Y. Nir (Weizmann Institute).

The *CP* transformation combines charge conjugation *C* with parity *P*. Under *C*, particles and antiparticles are interchanged, by conjugating all internal quantum numbers, e.g., $Q \rightarrow -Q$ for electromagnetic charge. Under *P*, the handedness of space is reversed, $\vec{x} \rightarrow -\vec{x}$. Thus, for example, a left-handed electron e_L^- is transformed under *CP* into a right-handed positron, e_R^+ .

If *CP* were an exact symmetry, the laws of Nature would be the same for matter and for antimatter. We observe that most phenomena are *C*- and *P*-symmetric, and therefore, also *CP*-symmetric. In particular, these symmetries are respected by the gravitational, electromagnetic, and strong interactions. The weak interactions, on the other hand, violate *C* and *P* in the strongest possible way. For example, the charged *W* bosons couple to left-handed electrons, e_L^- , and to their *CP*-conjugate right-handed positrons, e_R^+ , but to neither their *C*-conjugate left-handed positrons, e_L^+ , nor their *P*-conjugate right-handed electrons, e_R^- . While weak interactions violate *C* and *P* separately, *CP* is still preserved in most weak interaction processes. The *CP* symmetry is, however, violated in certain rare processes, as discovered in neutral *K* decays in 1964 [1], and observed in recent years in *B* decays. A K_L meson decays more often to $\pi^- e^+ \bar{\nu}_e$ than to $\pi^+ e^- \nu_e$, thus allowing electrons and positrons to be unambiguously distinguished, but the decay-rate asymmetry is only at the 0.003 level. The *CP*-violating effects observed in *B* decays are larger: the *CP* asymmetry in B^0/\bar{B}^0 meson decays to *CP* eigenstates like $J/\psi K_S$ is about 0.70 [2,3]. These effects are related to $K^0 - \bar{K}^0$ and $B^0 - \bar{B}^0$ mixing, but *CP* violation arising solely from decay amplitudes has also been observed, first in $K \rightarrow \pi\pi$ decays [4–6] and more recently in various neutral [7,8] and charged [9,10] *B* decays. *CP* violation has not yet been observed in *D* or B_s meson decays, or in the lepton sector.

In addition to parity and to continuous Lorentz transformations, there is one other spacetime operation that could be a symmetry of the interactions: time reversal *T*, $t \rightarrow -t$. Violations of *T* symmetry have been observed in neutral *K* decays [11], and are expected as a corollary of *CP* violation if the combined *CPT* transformation is a fundamental symmetry of Nature [12]. All observations indicate that *CPT* is indeed a symmetry of Nature. Furthermore, one cannot build a Lorentz-invariant quantum field theory with a Hermitian Hamiltonian that violates *CPT*. (At several points in our discussion, we avoid assumptions about *CPT*, in order to identify cases where evidence for *CP* violation relies on assumptions about *CPT*.)

Within the Standard Model, *CP* symmetry is broken by complex phases in the Yukawa couplings (that is, the couplings of the Higgs scalar to quarks). When all manipulations to remove unphysical phases in this model are exhausted, one finds that there is a single *CP*-violating parameter [13]. In the basis of mass eigenstates, this single phase appears in the 3×3 unitary matrix that gives the *W*-boson couplings to an up-type antiquark and a down-type quark. (If the Standard Model is supplemented with Majorana mass terms for the neutrinos, the analogous mixing matrix for leptons has three *CP*-violating phases.) The beautifully consistent and economical Standard-Model description of *CP* violation in terms of Yukawa couplings, known as the Kobayashi-Maskawa (KM) mechanism [13], agrees with all measurements to date. Furthermore, one can fit the data allowing new physics contributions to loop processes to compete with, or even dominate over, the Standard Model ones [14,15]. Such an analysis provides a model-independent proof that the KM phase is different from zero, and that the matrix of three-generation quark mixing is the dominant source of *CP* violation in meson decays.

The current level of experimental accuracy and the theoretical uncertainties involved in the interpretation of the various observations leave room, however, for additional subdominant sources of *CP* violation from new physics. Indeed, almost all extensions of the Standard Model imply that there are such additional sources. Moreover, *CP* violation is a necessary condition for baryogenesis, the process of dynamically generating the matter-antimatter asymmetry of the Universe [16]. Despite the phenomenological success of the KM

mechanism, it fails (by several orders of magnitude) to accommodate the observed asymmetry [17]. This discrepancy strongly suggests that Nature provides additional sources of *CP* violation beyond the KM mechanism. (Recent evidence for neutrino masses implies that *CP* can be violated also in the lepton sector. This situation makes leptogenesis [18], a scenario where *CP*-violating phases in the Yukawa couplings of the neutrinos play a crucial role in the generation of the baryon asymmetry, a very attractive possibility.) The expectation of new sources motivates the large ongoing experimental effort to find deviations from the predictions of the KM mechanism.

CP violation can be experimentally searched for in a variety of processes, such as meson decays, electric dipole moments of neutrons, electrons and nuclei, and neutrino oscillations. Meson decays probe flavor-changing *CP* violation. The search for electric dipole moments may find (or constrain) sources of *CP* violation that, unlike the KM phase, are not related to flavor-changing couplings. Future searches for *CP* violation in neutrino oscillations might provide further input on leptogenesis.

The present measurements of *CP* asymmetries provide some of the strongest constraints on the weak couplings of quarks. Future measurements of *CP* violation in *K*, *D*, *B*, and B_s meson decays will provide additional constraints on the flavor parameters of the Standard Model, and can probe new physics. In this review, we give the formalism and basic physics that are relevant to present and near future measurements of *CP* violation in meson decays.

Before going into details, we list here the independent *CP*-violating observables where a signal has been established [19,20,21]:

1. Indirect *CP* violation in $K \rightarrow \pi\pi$ decays and in $K \rightarrow \pi\ell\nu$ decays is given by

$$|\epsilon| = (2.228 \pm 0.011) \times 10^{-3}. \quad (12.1)$$

2. Direct *CP* violation in $K \rightarrow \pi\pi$ decays is given by

$$\mathcal{R}e(\epsilon'/\epsilon) = (1.65 \pm 0.26) \times 10^{-3}. \quad (12.2)$$

3. *CP* violation in the interference of mixing and decay in the $B \rightarrow \psi K^0$ and other related modes is given by (we use K^0 throughout to denote results that combine K_S and K_L modes, but use the sign appropriate to K_S):

$$S_{\psi K^0} = +0.673 \pm 0.023. \quad (12.3)$$

4. *CP* violation in the interference of mixing and decay in the $B \rightarrow \eta' K^0$ modes is given by

$$S_{\eta' K^0} = +0.60 \pm 0.07. \quad (12.4)$$

5. *CP* violation in the interference of mixing and decay in the $B \rightarrow K^+ K^- K_S$ mode is given by

$$S_{(K^+ K^- K_0)_+} = -0.74_{-0.10}^{+0.12}. \quad (12.5)$$

6. *CP* violation in the interference of mixing and decay in the $B \rightarrow \pi^+ \pi^-$ mode is given by

$$S_{\pi^+ \pi^-} = -0.61 \pm 0.08. \quad (12.6)$$

7. *CP* violation in the interference of mixing and decay in the $B \rightarrow \psi \pi^0$ mode is given by

$$S_{\psi \pi^0} = -0.94 \pm 0.29. \quad (12.7)$$

8. *CP* violation in the interference of mixing and decay in the $B \rightarrow D^+ D^-$ mode is given by

$$S_{D^+ D^-} = -0.87 \pm 0.26. \quad (12.8)$$

9. *CP* violation in the interference of mixing and decay in the $B \rightarrow D^{*+} D^{*-}$ mode is given by

$$S_{D^{*+} D^{*-}} = -0.70 \pm 0.16. \quad (12.9)$$

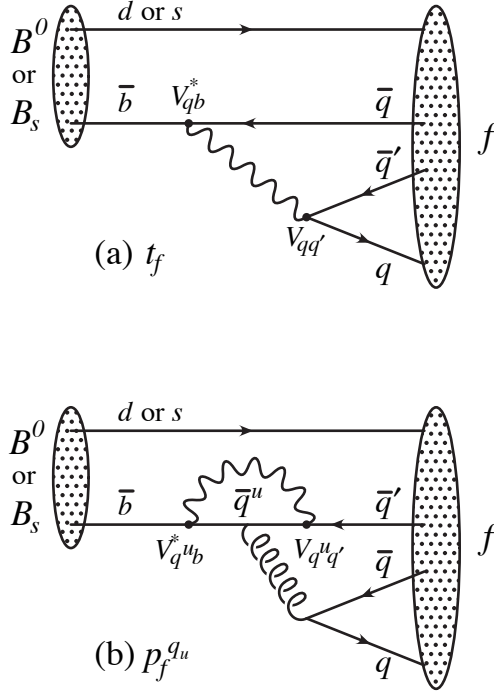


Figure 12.2: Feynman diagrams for (a) tree and (b) penguin amplitudes contributing to $B^0 \rightarrow f$ or $B_s \rightarrow f$ via a $\bar{b} \rightarrow \bar{q}q'$ quark-level process.

Table 12.1: Summary of $\bar{b} \rightarrow \bar{q}q'$ modes with $q' = s$ or d . The second and third columns give examples of final hadronic states. The fourth column gives the CKM dependence of the amplitude A_f , using the notation of Eqs. (12.76, 12.78, 12.80), with the dominant term first and the subdominant second. The suppression factor of the second term compared to the first is given in the last column. ‘‘Loop’’ refers to a penguin versus tree-suppression factor (it is mode-dependent and roughly $\mathcal{O}(0.2 - 0.3)$) and $\lambda = 0.23$ is the expansion parameter of Eq. (12.48).

$\bar{b} \rightarrow \bar{q}q'$	$B^0 \rightarrow f$	$B_s \rightarrow f$	CKM dependence of A_f	Suppression
$\bar{b} \rightarrow \bar{c}c\bar{s}$	ψK_S	$\psi\phi$	$(V_{cb}^*V_{cs})T + (V_{ub}^*V_{us})P^u$	loop $\times \lambda^2$
$\bar{b} \rightarrow \bar{s}s\bar{s}$	ϕK_S	$\phi\phi$	$(V_{cb}^*V_{cs})P^c + (V_{ub}^*V_{us})P^u$	λ^2
$\bar{b} \rightarrow \bar{u}u\bar{s}$	$\pi^0 K_S$	K^+K^-	$(V_{cb}^*V_{cs})P^c + (V_{ub}^*V_{us})T$	λ^2/loop
$\bar{b} \rightarrow \bar{c}c\bar{d}$	D^+D^-	ψK_S	$(V_{cb}^*V_{cd})T + (V_{ub}^*V_{td})P^t$	loop
$\bar{b} \rightarrow \bar{s}s\bar{d}$	$\phi\pi$	ϕK_S	$(V_{tb}^*V_{td})P^t + (V_{cb}^*V_{cd})P^c$	$\lesssim 1$
$\bar{b} \rightarrow \bar{u}u\bar{d}$	$\pi^+\pi^-$	$\pi^0 K_S$	$(V_{ub}^*V_{ud})T + (V_{tb}^*V_{td})P^t$	loop

The cleanliness of the theoretical interpretation of S_f can be assessed from the information in the last column of Table 12.1. In case of small uncertainties, the expression for S_f in terms of CKM phases can be deduced from the fourth column of Table 12.1 in combination with Eq. (12.73) (and, for $b \rightarrow \bar{q}q's$ decays, the example in Eq. (12.79)). Here we consider several interesting examples.

For $B \rightarrow J/\psi K_S$ and other $\bar{b} \rightarrow \bar{c}c\bar{s}$ processes, we can neglect the P^u contribution to A_f , in the Standard Model, to an approximation that is better than one percent:

$$\lambda_{\psi K_S} = -e^{-2i\beta} \Rightarrow S_{\psi K_S} = \sin 2\beta, \quad C_{\psi K_S} = 0. \quad (12.81)$$

In the presence of new physics, A_f is still likely to be dominated by the

T term, but the mixing amplitude might be modified. We learn that, model-independently, $C_f \approx 0$ while S_f cleanly determines the mixing phase ($\phi_M - 2 \arg(V_{cb}V_{cd}^*)$). The experimental measurement [21], $S_{\psi K} = 0.673 \pm 0.023$, gave the first precision test of the Kobayashi-Maskawa mechanism, and its consistency with the predictions for $\sin 2\beta$ makes it very likely that this mechanism is indeed the dominant source of CP violation in meson decays.

For $B \rightarrow \phi K_S$ and other $\bar{b} \rightarrow \bar{s}s\bar{s}$ processes (as well as some $\bar{b} \rightarrow \bar{u}u\bar{s}$ processes), we can neglect the subdominant contributions, in the Standard Model, to an approximation that is good on the order of a few percent:

$$\lambda_{\phi K_S} = -e^{-2i\beta} \Rightarrow S_{\phi K_S} = \sin 2\beta, \quad C_{\phi K_S} = 0. \quad (12.82)$$

In the presence of new physics, both A_f and \mathbf{M}_{12} can get contributions that are comparable in size to those of the Standard Model and carry new weak phases. Such a situation gives several interesting consequences for penguin-dominated $b \rightarrow \bar{q}q's$ decays ($q = u, d, s$) to a final state f :

1. The value of $-\eta_f S_f$ may be different from $S_{\psi K_S}$ by more than a few percent, where η_f is the CP eigenvalue of the final state.
2. The values of $\eta_f S_f$ for different final states f may be different from each other by more than a few percent (for example, $S_{\phi K_S} \neq S_{\eta' K_S}$).
3. The value of C_f may be different from zero by more than a few percent.

While a clear interpretation of such signals in terms of Lagrangian parameters will be difficult because, under these circumstances, hadronic parameters do play a role, any of the above three options will clearly signal new physics. Fig. 12.3 summarizes the present experimental results: none of the possible signatures listed above is unambiguously established, but there is definitely still room for new physics.

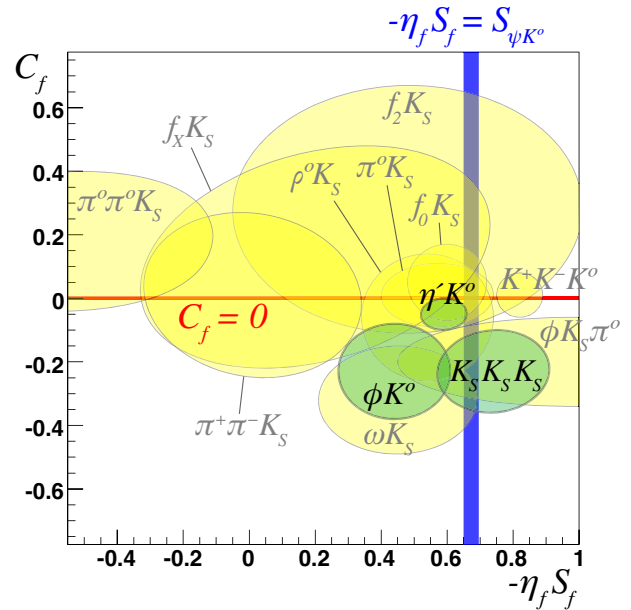


Figure 12.3: Summary of the results [21] of time-dependent analyses of $b \rightarrow \bar{q}q's$ decays, which are potentially sensitive to new physics. Subdominant corrections are expected to be smallest for the modes shown in green (darker). Results for final states including K^0 mesons combine CP -conjugate K_S and K_L measurements. The final state $K^+K^-K^0$ is not a CP eigenstate; the mixture of CP -even and CP -odd components is taken into account in obtaining an effective value for $\eta_f S_f$. Correlations between C_f and S_f are included when available. Color version at end of book.

For $B \rightarrow \pi\pi$ and other $\bar{b} \rightarrow \bar{u}d$ processes, the penguin-to-tree ratio can be estimated using SU(3) relations and experimental data on related $B \rightarrow K\pi$ decays. The result is that the suppression is on the order of 0.2–0.3 and so cannot be neglected. The expressions for $S_{\pi\pi}$ and $C_{\pi\pi}$ to leading order in $R_{PT} \equiv (|V_{tb}V_{td}|P_{\pi\pi}^t)/(|V_{ub}V_{ud}|T_{\pi\pi})$ are:

$$\lambda_{\pi\pi} = e^{2i\alpha} \left[(1 - R_{PT}e^{-i\alpha}) / (1 - R_{PT}e^{+i\alpha}) \right] \Rightarrow$$

$$S_{\pi\pi} \approx \sin 2\alpha + 2 \operatorname{Re}(R_{PT}) \cos 2\alpha \sin \alpha, \quad C_{\pi\pi} \approx 2 \operatorname{Im}(R_{PT}) \sin \alpha. \quad (12.83)$$

Note that R_{PT} is mode-dependent and, in particular, could be different for $\pi^+\pi^-$ and $\pi^0\pi^0$. If strong phases can be neglected, then R_{PT} is real, resulting in $C_{\pi\pi} = 0$. The size of $C_{\pi\pi}$ is an indicator of how large the strong phase is. The present experimental range is $C_{\pi\pi} = -0.38 \pm 0.06$ [21]. As concerns $S_{\pi\pi}$, it is clear from Eq. (12.83) that the relative size or strong phase of the penguin contribution must be known to extract α . This is the problem of penguin pollution.

The cleanest solution involves isospin relations among the $B \rightarrow \pi\pi$ amplitudes [46]:

$$\frac{1}{\sqrt{2}}A_{\pi^+\pi^-} + A_{\pi^0\pi^0} = A_{\pi^+\pi^0}. \quad (12.84)$$

The method exploits the fact that the penguin contribution to $P_{\pi\pi}^t$ is pure $\Delta I = \frac{1}{2}$ (this is not true for the electroweak penguins which, however, are expected to be small), while the tree contribution to $T_{\pi\pi}$ contains pieces which are both $\Delta I = \frac{1}{2}$ and $\Delta I = \frac{3}{2}$. A simple geometric construction then allows one to find R_{PT} and extract α cleanly from $S_{\pi^+\pi^-}$. The key experimental difficulty is that one must measure accurately the separate rates for $B^0, \bar{B}^0 \rightarrow \pi^0\pi^0$.

CP asymmetries in $B \rightarrow \rho\pi$ and $B \rightarrow \rho\rho$ can also be used to determine α . In particular, the $B \rightarrow \rho\rho$ measurements are presently very significant in constraining α . The extraction proceeds via isospin analysis similar to that of $B \rightarrow \pi\pi$. There are, however, several important differences. First, due to the finite width of the ρ mesons, a final $(\rho\rho)_{I=1}$ state is possible [47]. The effect is, however, small, on the order of $(\Gamma_\rho/m_\rho)^2 \sim 0.04$. Second, due to the presence of three helicity states for the two-vector mesons, angular analysis is needed to separate the CP -even and CP -odd components. The theoretical expectation is, however, that the CP -odd component is small. This expectation is supported by experiments which find that the $\rho^+\rho^-$ and $\rho^\pm\rho^0$ modes are dominantly longitudinally polarized. Third, an important advantage of the $\rho\rho$ modes is that the penguin contribution is expected to be small due to different hadronic dynamics. This expectation is confirmed by the smallness of the upper bound on $\mathcal{B}(B^0 \rightarrow \rho^0\rho^0)$. Thus, $S_{\rho^+\rho^-}$ is not far from $\sin 2\alpha$. Finally, both $S_{\rho^0\rho^0}$ and $C_{\rho^0\rho^0}$ are experimentally accessible, which may allow a precision determination of α . The consistency between the range of α determined by the $B \rightarrow \pi\pi, \rho\pi, \rho\rho$ measurements and the range allowed by CKM fits (excluding these direct determinations) provides further support to the Kobayashi-Maskawa mechanism.

An interesting class of decay modes is that of the tree level decays $B^\pm \rightarrow D^{(*)0}K^\pm$. These decays provide golden methods for a clean determination of the angle γ [48–51]. The method uses the decays $B^+ \rightarrow D^0K^+$, which proceeds via the quark transition $\bar{b} \rightarrow \bar{u}c\bar{s}$, and $B^+ \rightarrow \bar{D}^0K^+$, which proceeds via the quark transition $\bar{b} \rightarrow \bar{c}u\bar{s}$, with the D^0 and \bar{D}^0 decaying into a common final state. The decays into common final states, such $(\pi^0 K_S)_D K^+$, involve interference effects between the two amplitudes, with sensitivity to the relative phase, $\delta + \gamma$ (δ is the relevant strong phase). The CP -conjugate processes are sensitive to $\delta - \gamma$. Measurements of branching ratios and CP asymmetries allow an extraction of γ and δ from amplitude triangle relations. The extraction suffers from discrete ambiguities but involves no hadronic uncertainties. However, the smallness of the CKM-suppressed $b \rightarrow u$ transitions makes it difficult at present to use the simplest methods [48–50] to determine γ . These difficulties are overcome by performing a Dalitz plot analysis for multi-body D decays [51]. The consistency between the range of γ determined by the $B \rightarrow DK$ measurements and the range allowed by CKM fits

(excluding these direct determinations) provides further support to the Kobayashi-Maskawa mechanism.

For B_s decays, one has to replace Eq. (12.73) with $e^{-i\phi_{M(B_s)}} = (V_{tb}^*V_{ts})/(V_{cb}V_{cs}^*)$. Note that one expects $\Delta\Gamma/\Gamma = \mathcal{O}(0.1)$, and therefore, y should not be put to zero in Eqs. (12.30, 12.31), but $|q/p| = 1$ is expected to hold to an even better approximation than for B mesons. The CP asymmetry in $B_s \rightarrow J/\psi\phi$ will determine (with angular analysis to disentangle the CP -even and CP -odd components of the final state) $\sin 2\beta_s$, where

$$\beta_s \equiv \arg \left(-\frac{V_{ts}V_{tb}^*}{V_{cs}V_{cb}^*} \right). \quad (12.85)$$

Other observables, such as the width difference between the neutral B_s -mesons and the semileptonic asymmetry in their decay, are also sensitive to $\phi_{M(B_s)}$. The CDF and D0 experiments are now providing first constraints on these observables.

12.7. Summary and Outlook

CP violation has been experimentally established in neutral K and B meson decays:

1. All three types of CP violation have been observed in $K \rightarrow \pi\pi$ decays:

$$\operatorname{Re}(\epsilon') = \frac{1}{6} \left(\left| \frac{\bar{A}_{\pi^0\pi^0}}{A_{\pi^0\pi^0}} \right| - \left| \frac{\bar{A}_{\pi^+\pi^-}}{A_{\pi^+\pi^-}} \right| \right) = (2.5 \pm 0.4) \times 10^{-6} \text{(I)}$$

$$\operatorname{Re}(\epsilon) = \frac{1}{2} \left(1 - \left| \frac{q}{p} \right| \right) = (1.66 \pm 0.02) \times 10^{-3} \quad \text{(II)}$$

$$\operatorname{Im}(\epsilon) = -\frac{1}{2} \operatorname{Im}(\lambda_{(\pi\pi)_{I=0}}) = (1.57 \pm 0.02) \times 10^{-3}. \quad \text{(III)} \quad (12.86)$$

2. Direct CP violation has been observed, first in $B^0 \rightarrow K^+\pi^-$ decays (and more recently also in $B \rightarrow \pi^+\pi^-, B^0 \rightarrow \eta K^{*0}$, and $B^+ \rightarrow \rho^0 K^+$ decays), and CP violation in interference of decays with and without mixing has been observed, first in $B \rightarrow J/\psi K_S$ decays and related modes (as well as other final CP eigenstates: $\eta' K_S, K^+K^- K_S, J/\psi\pi^0$ and $\pi^+\pi^-$):

$$\mathcal{A}_{K^+\pi^-} = \frac{|\bar{A}_{K^-\pi^+}/A_{K^+\pi^-}|^2 - 1}{|\bar{A}_{K^-\pi^+}/A_{K^+\pi^-}|^2 + 1} = -0.098 \pm 0.013 \quad \text{(I)}$$

$$S_{\psi K} = \operatorname{Im}(\lambda_{\psi K}) = 0.673 \pm 0.023. \quad \text{(III)} \quad (12.87)$$

Searches for additional CP asymmetries are ongoing in B, D , and K decays, and current limits are consistent with Standard Model expectations.

Based on Standard Model predictions, further observation of CP violation in B decays seems promising for the near future, both at LHCb [52] and a possible higher-luminosity asymmetric-energy B factory [53,54]. Observables that are subject to clean theoretical interpretation, such as $S_{\psi K_S}$ and $\mathcal{B}(K_L \rightarrow \pi^0 \nu \bar{\nu})$, are of particular value for constraining the values of the CKM parameters and probing the flavor sector of extensions to the Standard Model. Other probes of CP violation now being pursued experimentally include the electric dipole moments of the neutron and electron, and the decays of tau leptons. Additional processes that are likely to play an important role in future CP studies include top-quark production and decay, and neutrino oscillations.

All measurements of CP violation to date are consistent with the predictions of the Kobayashi-Maskawa mechanism of the Standard Model. Actually, it is now established that the KM mechanism plays a major role in the CP violation measured in meson decays. However, a dynamically-generated matter-antimatter asymmetry of the universe requires additional sources of CP violation, and such sources are naturally generated by extensions to the Standard Model. New sources might eventually reveal themselves as small deviations from the predictions of the KM mechanism in meson decay rates, or

else might not be observable in meson decays at all, but observable with future probes such as neutrino oscillations or electric dipole moments. We cannot guarantee that new sources of CP violation will ever be found experimentally, but the fundamental nature of CP violation demands a vigorous effort.

A number of excellent reviews of CP violation are available [55–62], where the interested reader may find a detailed discussion of the various topics that are briefly reviewed here.

References:

1. J.H. Christenson *et al.*, Phys. Rev. Lett. **13**, 138 (1964).
2. B. Aubert *et al.*, [BABAR Collab.], Phys. Rev. Lett. **87**, 091801 (2001).
3. K. Abe *et al.*, [Belle Collab.], Phys. Rev. Lett. **87**, 091802 (2001).
4. H. Burkhardt *et al.*, [NA31 Collab.], Phys. Lett. **B206**, 169 (1988).
5. V. Fanti *et al.*, [NA48 Collab.], Phys. Lett. **B465**, 335 (1999).
6. A. Alavi-Harati *et al.*, [KTeV Collab.], Phys. Rev. Lett. **83**, 22 (1999).
7. B. Aubert *et al.*, [BABAR Collab.], Phys. Rev. Lett. **93**, 131801 (2004).
8. K. Abe *et al.*, [Belle Collab.], arXiv:hep-ex/0507045.
9. B. Aubert *et al.*, [BABAR Collab.], Phys. Rev. **D72**, 072003 (2005).
10. A. Garmash *et al.*, [Belle Collab.], Phys. Rev. Lett. **96**, 251803 (2006).
11. See results on the “Time reversal invariance,” within the review on “Tests of Conservation Laws,” in this *Review*.
12. See, for example, R. F. Streater and A. S. Wightman, *CPT, Spin and Statistics, and All That*, reprinted by Addison-Wesley, New York (1989).
13. M. Kobayashi and T. Maskawa, Prog. Theor. Phys. **49**, 652 (1973).
14. J. Charles *et al.*, [CKMfitter Group], Eur. Phys. J. **C41**, 1 (2005), updated results and plots available at: <http://ckmfitter.in2p3.fr>.
15. M. Bona *et al.*, [UTfit Collab.], JHEP **0603**, 080 (2006), updated results and plots available at: <http://babar.roma1.infn.it/ckm/>.
16. A.D. Sakharov, Pisma Zh. Eksp. Teor. Fiz. **5**, 32 (1967) [Sov. Phys. JETP Lett. **5**, 24 (1967)].
17. For a review, see *e.g.* A. Riotto, “Theories of baryogenesis,” arXiv:hep-ph/9807454.
18. M. Fukugita and T. Yanagida, Phys. Lett. **B174**, 45 (1986).
19. See the K -Meson Listings in this *Review*.
20. See the B -Meson Listings in this *Review*.
21. E. Barberio *et al.*, [HFAG Collab.], arXiv:0808.1297 [hep-ex], and online update at <http://www.slac.stanford.edu/xorg/hfag>.
22. V. Weisskopf and E. P. Wigner, Z. Phys. **63**, 54 (1930); Z. Phys. **65**, 18 (1930). [See also Appendix A of P.K. Kabir, *The CP Puzzle: Strange Decays of the Neutral Kaon*, Academic Press (1968)].
23. O. Long *et al.*, Phys. Rev. **D68**, 034010 (2003).
24. L. Wolfenstein, Phys. Rev. Lett. **13**, 562 (1964).
25. See the review on “Cabibbo-Kobayashi-Maskawa Mixing Matrix,” in this *Review*.
26. L. Wolfenstein, Phys. Rev. Lett. **51**, 1945 (1983).
27. A.J. Buras, M.E. Lautenbacher, and G. Ostermaier, Phys. Rev. **D50**, 3433 (1994).
28. C. Jarlskog, Phys. Rev. Lett. **55**, 1039 (1985).
29. See the review on “ CP violation in $K_S \rightarrow 3\pi$,” in this *Review*.
30. Y. Grossman and Y. Nir, Phys. Lett. **B398**, 163 (1997).
31. L.S. Littenberg, Phys. Rev. **D39**, 3322 (1989).
32. A.J. Buras, Phys. Lett. **B333**, 476 (1994).
33. G. Buchalla and A.J. Buras, Nucl. Phys. **B400**, 225 (1993).
34. B. Aubert *et al.*, [BABAR Collab.], Phys. Rev. Lett. **98**, 211802 (2007).
35. M. Staric *et al.*, [Belle Collab.], Phys. Rev. Lett. **98**, 211803 (2007).
36. T. Aaltonen *et al.*, [CDF Collab.], Phys. Rev. Lett. **100**, 121802 (2008).
37. See the D -Meson Listings in this *Review*.
38. S. Bergmann *et al.*, Phys. Lett. **B486**, 418 (2000).
39. See the review on “ $D^0 - \bar{D}^0$ Mixing” in this *Review*.
40. A.B. Carter and A.I. Sanda, Phys. Rev. Lett. **45**, 952 (1980); Phys. Rev. **D23**, 1567 (1981).
41. I.I. Bigi and A.I. Sanda, Nucl. Phys. **B193**, 85 (1981).
42. I. Dunietz and J.L. Rosner, Phys. Rev. **D34**, 1404 (1986).
43. Ya.I. Azimov, N.G. Uraltsev, and V.A. Khoze, Sov. J. Nucl. Phys. **45**, 878 (1987) [Yad. Fiz. **45**, 1412 (1987)].
44. I.I. Bigi and A.I. Sanda, Nucl. Phys. **B281**, 41 (1987).
45. G. Buchalla, A.J. Buras, and M.E. Lautenbacher, Rev. Mod. Phys. **68**, 1125 (1996).
46. M. Gronau and D. London, Phys. Rev. Lett. **65**, 3381 (1990).
47. A. F. Falk *et al.*, Phys. Rev. **D69**, 011502 (2004).
48. M. Gronau and D. London, Phys. Lett. **B253**, 483 (1991).
49. M. Gronau and D. Wyler, Phys. Lett. **B265**, 172 (1991).
50. D. Atwood, I. Dunietz, and A. Soni, Phys. Rev. Lett. **78**, 3257 (1997).
51. A. Giri *et al.*, Phys. Rev. **D68**, 054018 (2003).
52. A.A. Alves *et al.*, [LHCb Collab.], “The LHCb Detector at the LHC,” JINST **3:S08005** (2008).
53. A.G. Akeroyd *et al.*, “Physics at Super B Factory,” KEK **04-4** (2004) arXiv:hep-ex/0406071.
54. M. Bona *et al.*, “SuperB: A High-Luminosity Asymmetric e^+e^- Super Flavor Factory. Conceptual Design Report,” INFN/AE-07/2, SLAC-R-856, LAL-07-15 (2007) arXiv:0709.0451.
55. G.C. Branco, L. Lavoura, and J.P. Silva, *CP Violation*, Oxford University Press, Oxford (1999).
56. I.I. Y. Bigi and A.I. Sanda, *CP Violation*, Cambridge Monogr., Part. Phys. Nucl. Phys. Cosmol. **9**, 1 (2000).
57. P.F. Harrison and H.R. Quinn, editors [BABAR Collab.], *The BABAR physics book: Physics at an asymmetric B factory*, SLAC-R-0504.
58. K. Anikeev *et al.*, arXiv:hep-ph/0201071.
59. K. Kleinknecht, “Uncovering CP Violation,” Springer tracts in modern physics **195** (2003).
60. H.R. Quinn and Y. Nir, “The Mystery of the Missing Antimatter,” Princeton University Press, Princeton (2008).
61. J. Hewett *et al.*, arXiv:hep-ph/0503261.
62. A. G. Akeroyd *et al.*, [SuperKEKB Physics Working Group], arXiv:hep-ex/0406071.

13. NEUTRINO MASS, MIXING, AND OSCILLATIONS

Written May 2010 by K. Nakamura (IPMU, U. Tokyo, KEK) and S.T. Petcov (SISSA/INFN Trieste, IPMU, U. Tokyo, Bulgarian Academy of Sciences).

The experiments with solar, atmospheric, reactor and accelerator neutrinos have provided compelling evidences for oscillations of neutrinos caused by nonzero neutrino masses and neutrino mixing. The data imply the existence of 3-neutrino mixing in vacuum. We review the theory of neutrino oscillations, the phenomenology of neutrino mixing, the problem of the nature - Dirac or Majorana, of massive neutrinos, the issue of CP violation in the lepton sector, and the current data on the neutrino masses and mixing parameters. The open questions and the main goals of future research in the field of neutrino mixing and oscillations are outlined.

13.1. Introduction: Massive neutrinos and neutrino mixing

It is a well-established experimental fact that the neutrinos and antineutrinos which take part in the standard charged current (CC) and neutral current (NC) weak interaction are of three varieties (types) or flavours: electron, ν_e and $\bar{\nu}_e$, muon, ν_μ and $\bar{\nu}_\mu$, and tauon, ν_τ and $\bar{\nu}_\tau$. The notion of neutrino type or flavour is dynamical: ν_e is the neutrino which is produced with e^+ , or produces an e^- in CC weak interaction processes; ν_μ is the neutrino which is produced with μ^+ , or produces μ^- , etc. The flavour of a given neutrino is Lorentz invariant. Among the three different flavour neutrinos and antineutrinos, no two are identical. Correspondingly, the states which describe different flavour neutrinos must be orthogonal (within the precision of the corresponding data): $\langle \nu_l | \nu_l \rangle = \delta_{ll}$, $\langle \bar{\nu}_l | \bar{\nu}_l \rangle = \delta_{ll}$, $\langle \bar{\nu}_l | \nu_l \rangle = 0$.

It is also well-known from the existing data (all neutrino experiments were done so far with relativistic neutrinos or antineutrinos), that the flavour neutrinos ν_l (antineutrinos $\bar{\nu}_l$), are always produced in weak interaction processes in a state that is predominantly left-handed (LH) (right-handed (RH)). To account for this fact, ν_l and $\bar{\nu}_l$ are described in the Standard Model (SM) by a chiral LH flavour neutrino field $\nu_{lL}(x)$, $l = e, \mu, \tau$. For massless ν_l , the state of ν_l ($\bar{\nu}_l$) which the field $\nu_{lL}(x)$ annihilates (creates) is with helicity $(-1/2)$ (helicity $+1/2$). If ν_l has a non-zero mass $m(\nu_l)$, the state of ν_l ($\bar{\nu}_l$) is a linear superposition of the helicity $(-1/2)$ and $(+1/2)$ states, but the helicity $+1/2$ state (helicity $-1/2$ state) enters into the superposition with a coefficient $\propto m(\nu_l)/E$, E being the neutrino energy, and thus is strongly suppressed. Together with the LH charged lepton field $l_L(x)$, $\nu_{lL}(x)$ forms an $SU(2)_L$ doublet. In the absence of neutrino mixing and zero neutrino masses, $\nu_{lL}(x)$ and $l_L(x)$ can be assigned one unit of the additive lepton charge L_l and the three charges L_l , $l = e, \mu, \tau$, are conserved by the weak interaction.

At present there is no evidence for the existence of states of relativistic neutrinos (antineutrinos), which are predominantly right-handed, ν_R (left-handed, $\bar{\nu}_L$). If RH neutrinos and LH antineutrinos exist, their interaction with matter should be much weaker than the weak interaction of the flavour LH neutrinos ν_l and RH antineutrinos $\bar{\nu}_l$, *i.e.*, ν_R ($\bar{\nu}_L$) should be “sterile” or “inert” neutrinos (antineutrinos) [1]. In the formalism of the Standard Model, the sterile ν_R and $\bar{\nu}_L$ can be described by $SU(2)_L$ singlet RH neutrino fields $\nu_R(x)$. In this case, ν_R and $\bar{\nu}_L$ will have no gauge interactions, *i.e.*, will not couple to the weak W^\pm and Z^0 bosons. If present in an extension of the Standard Model, the RH neutrinos can play a crucial role i) in the generation of neutrino masses and mixing, ii) in understanding the remarkable disparity between the magnitudes of neutrino masses and the masses of the charged leptons and quarks, and iii) in the generation of the observed matter-antimatter asymmetry of the Universe (via the leptogenesis mechanism [2]). In this scenario which is based on the see-saw theory [3], there is a link between the generation of neutrino masses and the generation of the baryon asymmetry of the Universe. The simplest hypothesis is that to each LH flavour neutrino field $\nu_{lL}(x)$ there corresponds a RH neutrino field $\nu_{lR}(x)$, $l = e, \mu, \tau$.

The experiments with solar, atmospheric and reactor neutrinos [4–16] have provided compelling evidences for the existence of neutrino

oscillations [17,18], transitions in flight between the different flavour neutrinos ν_e, ν_μ, ν_τ (antineutrinos $\bar{\nu}_e, \bar{\nu}_\mu, \bar{\nu}_\tau$), caused by nonzero neutrino masses and neutrino mixing. Strong evidences for oscillations of muon neutrinos were obtained also in the long-baseline accelerator neutrino experiments K2K [20] and MINOS [21,22]. In addition, a short-baseline accelerator experiment LSND [23] observed a possible indication of $\bar{\nu}_\mu \rightarrow \bar{\nu}_e$ oscillations. If confirmed, this result required the existence of at least one additional neutrino type. More recently, MiniBooNE searched for $\nu_\mu \rightarrow \nu_e$ transitions, and if the neutrinos oscillate in the same way as antineutrinos, the MiniBooNE result [24] does not support the interpretation of the LSND data in terms of $\bar{\nu}_\mu \rightarrow \bar{\nu}_e$ oscillations.

The existence of flavour neutrino oscillations implies that if a neutrino of a given flavour, say ν_μ , with energy E is produced in some weak interaction process, at a sufficiently large distance L from the ν_μ source the probability to find a neutrino of a different flavour, say ν_τ , $P(\nu_\mu \rightarrow \nu_\tau; E, L)$, is different from zero. $P(\nu_\mu \rightarrow \nu_\tau; E, L)$ is called the $\nu_\mu \rightarrow \nu_\tau$ oscillation or transition probability. If $P(\nu_\mu \rightarrow \nu_\tau; E, L) \neq 0$, the probability that ν_μ will not change into a neutrino of a different flavour, *i.e.*, the “ ν_μ survival probability” $P(\nu_\mu \rightarrow \nu_\mu; E, L)$, will be smaller than one. If only muon neutrinos ν_μ are detected in a given experiment and they take part in oscillations, one would observe a “disappearance” of muon neutrinos on the way from the ν_μ source to the detector. As a consequence of the results of the experiments quoted above the existence of oscillations or transitions of the solar ν_e , atmospheric ν_μ and $\bar{\nu}_\mu$, accelerator ν_μ (at $L \sim 250$ km and $L \sim 730$ km) and reactor $\bar{\nu}_e$ (at $L \sim 180$ km), driven by nonzero neutrino masses and neutrino mixing, was firmly established. There are strong indications that the solar ν_e transitions are affected by the solar matter [25,26].

Oscillations of neutrinos are a consequence of the presence of flavour neutrino mixing, or lepton mixing, in vacuum. In the formalism of local quantum field theory, used to construct the Standard Model, this means that the LH flavour neutrino fields $\nu_{lL}(x)$, which enter into the expression for the lepton current in the CC weak interaction Lagrangian, are linear combinations of the fields of three (or more) neutrinos ν_j , having masses $m_j \neq 0$:

$$\nu_{lL}(x) = \sum_j U_{lj} \nu_j(x), \quad l = e, \mu, \tau, \quad (13.1)$$

where $\nu_{jL}(x)$ is the LH component of the field of ν_j possessing a mass m_j and U is a unitary matrix - the neutrino mixing matrix [1,17,18]. The matrix U is often called the Pontecorvo-Maki-Nakagawa-Sakata (PMNS) or Maki-Nakagawa-Sakata (MNS) mixing matrix. Obviously, Eq. (13.1) implies that the individual lepton charges L_l , $l = e, \mu, \tau$, are not conserved.

All existing neutrino oscillation data, except for the LSND result [23], can be described assuming 3-flavour neutrino mixing in vacuum. The data on the invisible decay width of the Z^0 -boson is compatible with only 3 light flavour neutrinos coupled to Z^0 [19]. The number of massive neutrinos ν_j , n , can, in general, be bigger than 3, $n > 3$, if, for instance, there exist sterile neutrinos and they mix with the flavour neutrinos. It follows from the existing data that at least 3 of the neutrinos ν_j , say ν_1, ν_2, ν_3 , must be light, $m_{1,2,3} \lesssim 1$ eV, and must have different masses, $m_1 \neq m_2 \neq m_3$. At present there are no compelling experimental evidences for the existence of more than 3 light neutrinos.

Being electrically neutral, the neutrinos with definite mass ν_j can be Dirac fermions or Majorana particles [27,28]. The first possibility is realised when there exists a lepton charge carried by the neutrinos ν_j , which is conserved by the particle interactions. This could be, *e.g.*, the total lepton charge $L = L_e + L_\mu + L_\tau$: $L(\nu_j) = 1$, $j = 1, 2, 3$. In this case the neutrino ν_j has a distinctive antiparticle $\bar{\nu}_j$: $\bar{\nu}_j$ differs from ν_j by the value of the lepton charge L it carries, $L(\bar{\nu}_j) = -1$. The massive neutrinos ν_j can be Majorana particles if no lepton charge is conserved (see, *e.g.*, Ref. 29). A massive Majorana particle χ_j is identical with its antiparticle $\bar{\chi}_j$: $\chi_j \equiv \bar{\chi}_j$. On the basis of the existing neutrino data it is impossible to determine whether the massive neutrinos are Dirac or Majorana fermions.

In the case of n neutrino flavours and n massive neutrinos, the $n \times n$ unitary neutrino mixing matrix U can be parametrised by $n(n-1)/2$ Euler angles and $n(n+1)/2$ phases. If the massive neutrinos ν_j are Dirac particles, only $(n-1)(n-2)/2$ phases are physical and can be responsible for CP violation in the lepton sector. In this respect the neutrino (lepton) mixing with Dirac massive neutrinos is similar to the quark mixing. For $n=3$ there is just one CP violating phase in U , which is usually called “the Dirac CP violating phase.” CP invariance holds if (in a certain standard convention) U is real, $U^* = U$.

If, however, the massive neutrinos are Majorana fermions, $\nu_j \equiv \chi_j$, the neutrino mixing matrix U contains $n(n-1)/2$ CP violation phases [30,31], i.e., by $(n-1)$ phases more than in the Dirac neutrino case: in contrast to Dirac fields, the massive Majorana neutrino fields cannot “absorb” phases. In this case U can be cast in the form [30]

$$U = V P \quad (13.2)$$

where the matrix V contains the $(n-1)(n-2)/2$ Dirac CP violation phases, while P is a diagonal matrix with the additional $(n-1)$ Majorana CP violation phases $\alpha_{21}, \alpha_{31}, \dots, \alpha_{n1}$,

$$P = \text{diag} \left(1, e^{i\frac{\alpha_{21}}{2}}, e^{i\frac{\alpha_{31}}{2}}, \dots, e^{i\frac{\alpha_{n1}}{2}} \right). \quad (13.3)$$

The Majorana phases will conserve CP if [32] $\alpha_{j1} = \pi q_j$, $q_j = 0, 1, 2$, $j = 2, 3, \dots, n$. In this case $\exp[i(\alpha_{j1} - \alpha_{k1})] = \pm 1$ has a simple physical interpretation: this is the relative CP-parity of Majorana neutrinos χ_j and χ_k . The condition of CP invariance of the leptonic CC weak interaction in the case of mixing and massive Majorana neutrinos reads [29]:

$$U_{lj}^* = U_{lj} \rho_j, \quad \rho_j = \frac{1}{i} \eta_{CP}(\chi_j) = \pm 1, \quad (13.4)$$

where $\eta_{CP}(\chi_j) = i\rho_j = \pm i$ is the CP parity of the Majorana neutrino χ_j [32]. Thus, if CP invariance holds, the elements of U are either real or purely imaginary.

In the case of $n=3$ there are altogether 3 CP violation phases - one Dirac and two Majorana. Even in the mixing involving only 2 massive Majorana neutrinos there is one physical CP violation Majorana phase. In contrast, the CC weak interaction is automatically CP-invariant in the case of mixing of two massive Dirac neutrinos or of two quarks.

13.2. Neutrino oscillations in vacuum

Neutrino oscillations are a quantum mechanical consequence of the existence of nonzero neutrino masses and neutrino (lepton) mixing, Eq. (13.1), and of the relatively small splitting between the neutrino masses. The neutrino mixing and oscillation phenomena are analogous to the $K^0 - \bar{K}^0$ and $B^0 - \bar{B}^0$ mixing and oscillations.

In what follows we will present a simplified version of the derivation of the expressions for the neutrino and antineutrino oscillation probabilities. The complete derivation would require the use of the wave packet formalism for the evolution of the massive neutrino states, or, alternatively, of the field-theoretical approach, in which one takes into account the processes of production, propagation and detection of neutrinos [33].

Suppose the flavour neutrino ν_l is produced in a CC weak interaction process and after a time T it is observed by a neutrino detector, located at a distance L from the neutrino source and capable of detecting also neutrinos $\nu_{l'}$, $l' \neq l$. We will consider the evolution of the neutrino state $|\nu_l\rangle$ in the frame in which the detector is at rest (laboratory frame). The oscillation probability, as we will see, is a Lorentz invariant quantity. If lepton mixing, Eq. (13.1), takes place and the masses m_j of all neutrinos ν_j are sufficiently small, the state of the neutrino ν_l , $|\nu_l\rangle$, will be a coherent superposition of the states $|\nu_j\rangle$ of neutrinos ν_j :

$$|\nu_l\rangle = \sum_j U_{lj}^* |\nu_j; \tilde{p}_j\rangle, \quad l = e, \mu, \tau, \quad (13.5)$$

where U is the neutrino mixing matrix and \tilde{p}_j is the 4-momentum of ν_j [34].

We will consider the case of relativistic neutrinos ν_j , which corresponds to the conditions in both past and currently planned future neutrino oscillation experiments [36]. In this case the state $|\nu_j; \tilde{p}_j\rangle$ practically coincides with the helicity (-1) state $|\nu_j, L; \tilde{p}_j\rangle$ of the neutrino ν_j , the admixture of the helicity (+1) state $|\nu_j, R; \tilde{p}_j\rangle$ in $|\nu_j; \tilde{p}_j\rangle$ being suppressed due to the factor $\sim m_j/E_j$, where E_j is the energy of ν_j . If ν_j are Majorana particles, $\nu_j \equiv \chi_j$, due to the presence of the helicity (+1) state $|\chi_j, R; \tilde{p}_j\rangle$ in $|\chi_j; \tilde{p}_j\rangle$, the neutrino ν_l can produce an l^+ (instead of l^-) when it interacts with nucleons. The cross section of such a $|\Delta L| = 2$ process is suppressed by the factor $(m_j/E_j)^2$, which renders the process unobservable at present.

If the number n of massive neutrinos ν_j is bigger than 3 due to a mixing between the active flavour and sterile neutrinos, one will have additional relations similar to that in Eq. (13.5) for the state vectors of the (predominantly LH) sterile antineutrinos. In the case of just one RH sterile neutrino field $\nu_{sR}(x)$, for instance, we will have in addition to Eq. (13.5):

$$|\bar{\nu}_{sL}\rangle = \sum_{j=1}^4 U_{sj}^* |\nu_j; \tilde{p}_j\rangle \cong \sum_{j=1}^4 U_{sj}^* |\nu_j, L; \tilde{p}_j\rangle, \quad (13.6)$$

where the neutrino mixing matrix U is now a 4×4 unitary matrix.

For the state vector of RH flavour antineutrino $\bar{\nu}_l$, produced in a CC weak interaction process we similarly get:

$$|\bar{\nu}_l\rangle = \sum_j U_{lj} |\bar{\nu}_j; \tilde{p}_j\rangle \cong \sum_{j=1} U_{lj} |\bar{\nu}_j, R; \tilde{p}_j\rangle, \quad l = e, \mu, \tau, \quad (13.7)$$

where $|\bar{\nu}_j, R; \tilde{p}_j\rangle$ is the helicity (+1) state of the antineutrino $\bar{\nu}_j$ if ν_j are Dirac fermions, or the helicity (+1) state of the neutrino $\nu_j \equiv \bar{\nu}_j \equiv \chi_j$ if the massive neutrinos are Majorana particles. Thus, in the latter case we have in Eq. (13.7): $|\bar{\nu}_j; \tilde{p}_j\rangle \cong |\nu_j, R; \tilde{p}_j\rangle \equiv |\chi_j, R; \tilde{p}_j\rangle$. The presence of the matrix U in Eq. (13.7) (and not of U^*) follows directly from Eq. (13.1).

We will assume in what follows that the spectrum of masses of neutrinos is not degenerate: $m_j \neq m_k$, $j \neq k$. Then the states $|\nu_j; \tilde{p}_j\rangle$ in the linear superposition in the r.h.s. of Eq. (13.5) will have, in general, different energies and different momenta, independently of whether they are produced in a decay or interaction process: $\tilde{p}_j \neq \tilde{p}_k$, or $E_j \neq E_k$, $\mathbf{p}_j \neq \mathbf{p}_k$, $j \neq k$, where $E_j = \sqrt{p_j^2 + m_j^2}$, $p_j \equiv |\mathbf{p}_j|$. The deviations of E_j and p_j from the values for a massless neutrino E and $p = E$ are proportional to m_j^2/E_0 , E_0 being a characteristic energy of the process, and are extremely small. In the case of $\pi^+ \rightarrow \mu^+ + \nu_\mu$ decay at rest, for instance, we have: $E_j = E + m_j^2/(2m_\pi)$, $p_j = E - \xi m_j^2/(2E)$, where $E = (m_\pi/2)(1 - m_\mu^2/m_\pi^2) \cong 30$ MeV, $\xi = (1 + m_\mu^2/m_\pi^2)/2 \cong 0.8$, and m_μ and m_π are the μ^+ and π^+ masses. Taking $m_j = 1$ eV we find: $E_j \cong E(1 + 1.2 \times 10^{-16})$ and $p_j \cong E(1 - 4.4 \times 10^{-16})$.

Suppose that the neutrinos are observed via a CC weak interaction process and that in the detector's rest frame they are detected after time T after emission, after traveling a distance L . Then the amplitude of the probability that neutrino $\nu_{l'}$ will be observed if neutrino ν_l was produced by the neutrino source can be written as [33,35,37]:

$$A(\nu_l \rightarrow \nu_{l'}) = \sum_j \bar{U}_{l'j} D_j U_{lj}^\dagger, \quad l, l' = e, \mu, \tau, \quad (13.8)$$

where $D_j = D_j(p_j; L, T)$ describes the propagation of ν_j between the source and the detector, U_{lj}^\dagger and $\bar{U}_{l'j}$ are the amplitudes to find ν_j in the initial and in the final flavour neutrino state, respectively. It follows from relativistic Quantum Mechanics considerations that [33,35]

$$D_j \equiv D_j(\tilde{p}_j; L, T) = e^{-i\tilde{p}_j(x_f - x_0)} = e^{-i(E_j T - p_j L)}, \quad p_j \equiv |\mathbf{p}_j|, \quad (13.9)$$

where [38] x_0 and x_f are the space-time coordinates of the points of neutrino production and detection, $T = (t_f - t_0)$ and $L = \mathbf{k}(\mathbf{x}_f - \mathbf{x}_0)$, \mathbf{k} being the unit vector in the direction of neutrino momentum,

$\mathbf{p}_j = k\mathbf{p}_j$. What is relevant for the calculation of the probability $P(\nu_l \rightarrow \nu_{l'}) = |A(\nu_l \rightarrow \nu_{l'})|^2$ is the interference factor $D_j D_k^*$ which depends on the phase

$$\begin{aligned} \delta\varphi_{jk} &= (E_j - E_k)T - (p_j - p_k)L = (E_j - E_k) \left[T - \frac{E_j + E_k}{p_j + p_k} L \right] \\ &+ \frac{m_j^2 - m_k^2}{p_j + p_k} L. \end{aligned} \quad (13.10)$$

Some authors [39] have suggested that the distance traveled by the neutrinos L and the time interval T are related by $T = (E_j + E_k)L/(p_j + p_k) = L/\bar{v}$, $\bar{v} = (E_j/(E_j + E_k))v_j + (E_k/(E_j + E_k))v_k$ being the “average” velocity of ν_j and ν_k , where $v_{j,k} = p_{j,k}/E_{j,k}$. In this case the first term in the r.h.s. of Eq. (13.10) vanishes. The indicated relation has not emerged so far from any dynamical wave packet calculations. We arrive at the same conclusion concerning the term under discussion in Eq. (13.10) if one assumes [40] that $E_j = E_k = E_0$. Finally, it was proposed in Ref. 37 and Ref. 41 that the states of ν_j and $\bar{\nu}_j$ in Eq. (13.5) and Eq. (13.7) have the same 3-momentum, $p_j = p_k = p$. Under this condition the first term in the r.h.s. of Eq. (13.10) is negligible, being suppressed by the additional factor $(m_j^2 + m_k^2)/p^2$ since for relativistic neutrinos $L = T$ up to terms $\sim m_{j,k}^2/p^2$. We arrive at the same conclusion if $E_j \neq E_k$, $p_j \neq p_k$, $j \neq k$, and we take into account that neutrinos are relativistic and therefore, up to corrections $\sim m_{j,k}^2/E_{j,k}^2$, we have $L \cong T$ (see, e.g., C. Giunti quoted in Ref. 33).

Although the cases considered above are physically quite different, they lead to the same result for the phase difference $\delta\varphi_{jk}$. Thus, we have:

$$\delta\varphi_{jk} \cong \frac{m_j^2 - m_k^2}{2p} L = 2\pi \frac{L}{L_{jk}^v} \text{sgn}(m_j^2 - m_k^2), \quad (13.11)$$

where $p = (p_j + p_k)/2$ and

$$L_{jk}^v = 4\pi \frac{p}{|\Delta m_{jk}^2|} \cong 2.48 \text{ m} \frac{p[\text{MeV}]}{|\Delta m_{jk}^2|[\text{eV}^2]} \quad (13.12)$$

is the neutrino oscillation length associated with Δm_{jk}^2 . We can safely neglect the dependence of p_j and p_k on the masses m_j and m_k and consider p to be the zero neutrino mass momentum, $p = E$. The phase difference $\delta\varphi_{jk}$, Eq. (13.11), is Lorentz-invariant.

Eq. (13.9) corresponds to a plane-wave description of the propagation of neutrinos ν_j . It accounts only for the movement of the center of the wave packet describing ν_j . In the wave packet treatment of the problem, the interference between the states of ν_j and ν_k is subject to a number of conditions [33], the localisation condition and the condition of overlapping of the wave packets of ν_j and ν_k at the detection point being the most important. For relativistic neutrinos, the localisation condition reads: $\sigma_{xP}, \sigma_{xD} < L_{jk}^v/(2\pi)$, $\sigma_{xP(D)}$ being the spatial width of the production (detection) wave packet. Thus, the interference will not be suppressed if the spatial width of the neutrino wave packets determined by the neutrino production and detection processes is smaller than the corresponding oscillation length in vacuum. In order for the interference to be nonzero, the wave packets describing ν_j and ν_k should also overlap in the point of neutrino detection. This requires that the spatial separation between the two wave packets at the point of neutrinos detection, caused by the two wave packets having different group velocities $v_j \neq v_k$, satisfies $|(v_j - v_k)T| \ll \max(\sigma_{xP}, \sigma_{xD})$. If the interval of time T is not measured, T in the preceding condition must be replaced by the distance L between the neutrino source and the detector (for further discussion see, e.g., [33,35,37]).

For the $\nu_l \rightarrow \nu_{l'}$ and $\bar{\nu}_l \rightarrow \bar{\nu}_{l'}$ oscillation probabilities we get from Eq. (13.8), Eq. (13.9), and Eq. (13.11):

$$\begin{aligned} P(\nu_l \rightarrow \nu_{l'}) &= \sum_j |U_{l'j}|^2 |U_{lj}|^2 + 2 \sum_{j>k} |U_{l'j} U_{lj}^* U_{lk} U_{l'k}^*| \\ &\cos \left(\frac{\Delta m_{jk}^2}{2p} L - \phi_{l'l';jk} \right), \end{aligned} \quad (13.13)$$

$$\begin{aligned} P(\bar{\nu}_l \rightarrow \bar{\nu}_{l'}) &= \sum_j |U_{l'j}|^2 |U_{lj}|^2 + 2 \sum_{j>k} |U_{l'j} U_{lj}^* U_{lk} U_{l'k}^*| \\ &\cos \left(\frac{\Delta m_{jk}^2}{2p} L + \phi_{l'l';jk} \right), \end{aligned} \quad (13.14)$$

where $l, l' = e, \mu, \tau$ and $\phi_{l'l';jk} = \arg(U_{l'j} U_{lj}^* U_{lk} U_{l'k}^*)$. It follows from Eq. (13.8) - Eq. (13.10) that in order for neutrino oscillations to occur, at least two neutrinos ν_j should not be degenerate in mass and lepton mixing should take place, $U \neq \mathbf{1}$. The neutrino oscillations effects can be large if we have

$$\frac{|\Delta m_{jk}^2|}{2p} L = 2\pi \frac{L}{L_{jk}^v} \gtrsim 1, \quad j \neq k. \quad (13.15)$$

at least for one Δm_{jk}^2 . This condition has a simple physical interpretation: the neutrino oscillation length L_{jk}^v should be of the order of, or smaller, than source-detector distance L , otherwise the oscillations will not have time to develop before neutrinos reach the detector.

We see from Eq. (13.13) and Eq. (13.14) that $P(\nu_l \rightarrow \nu_{l'}) = P(\bar{\nu}_l \rightarrow \bar{\nu}_{l'})$, $l, l' = e, \mu, \tau$. This is a consequence of CPT invariance. The conditions of CP and T invariance read [30,42,43]: $P(\nu_l \rightarrow \nu_{l'}) = P(\bar{\nu}_l \rightarrow \bar{\nu}_{l'})$, $l, l' = e, \mu, \tau$ (CP), $P(\nu_l \rightarrow \nu_{l'}) = P(\nu_{l'} \rightarrow \nu_l)$, $P(\bar{\nu}_l \rightarrow \bar{\nu}_{l'}) = P(\bar{\nu}_{l'} \rightarrow \bar{\nu}_l)$, $l, l' = e, \mu, \tau$ (T). In the case of CPT invariance, which we will assume to hold throughout this article, we get for the survival probabilities: $P(\nu_l \rightarrow \nu_l) = P(\bar{\nu}_l \rightarrow \bar{\nu}_l)$, $l, l' = e, \mu, \tau$. Thus, the study of the “disappearance” of ν_l and $\bar{\nu}_l$, caused by oscillations in vacuum, cannot be used to test whether CP invariance holds in the lepton sector. It follows from Eq. (13.13) and Eq. (13.14) that we can have CP violation effects in neutrino oscillations only if $\phi_{l'l';jk} \neq \pi q$, $q = 0, 1, 2$, i.e., if $U_{l'j} U_{lj}^* U_{lk} U_{l'k}^*$, and therefore U itself, is not real. As a measure of CP and T violation in neutrino oscillations we can consider the asymmetries:

$$A_{\text{CP}}^{(l'l')} \equiv P(\nu_l \rightarrow \nu_{l'}) - P(\bar{\nu}_l \rightarrow \bar{\nu}_{l'}), \quad A_{\text{T}}^{(l'l')} \equiv P(\nu_l \rightarrow \nu_{l'}) - P(\nu_{l'} \rightarrow \nu_l). \quad (13.16)$$

CPT invariance implies: $A_{\text{CP}}^{(l'l')} = -A_{\text{CP}}^{(l'l')}$, $A_{\text{T}}^{(l'l')} = P(\bar{\nu}_{l'} \rightarrow \bar{\nu}_l) - P(\bar{\nu}_l \rightarrow \bar{\nu}_{l'}) = A_{\text{CP}}^{(l'l')}$. It follows further directly from Eq. (13.13) and Eq. (13.14) that

$$A_{\text{CP}}^{(l'l')} = 4 \sum_{j>k} \text{Im} \left(U_{l'j} U_{lj}^* U_{lk} U_{l'k}^* \right) \sin \frac{\Delta m_{jk}^2}{2p} L, \quad l, l' = e, \mu, \tau. \quad (13.17)$$

Eq. (13.2) and Eq. (13.13) - Eq. (13.14) imply that $P(\nu_l \rightarrow \nu_{l'})$ and $P(\bar{\nu}_l \rightarrow \bar{\nu}_{l'})$ do not depend on the Majorana CP violation phases in the neutrino mixing matrix U [30]. Thus, the experiments investigating the $\nu_l \rightarrow \nu_{l'}$ and $\bar{\nu}_l \rightarrow \bar{\nu}_{l'}$ oscillations, $l, l' = e, \mu, \tau$, cannot provide information on the nature - Dirac or Majorana, of massive neutrinos. The same conclusions hold also when the $\nu_l \rightarrow \nu_{l'}$ and $\bar{\nu}_l \rightarrow \bar{\nu}_{l'}$ oscillations take place in matter [44]. In the case of $\nu_l \leftrightarrow \nu_{l'}$ and $\bar{\nu}_l \leftrightarrow \bar{\nu}_{l'}$ oscillations in vacuum, only the Dirac phase(s) in U can cause CP violating effects leading to $P(\nu_l \rightarrow \nu_{l'}) \neq P(\bar{\nu}_l \rightarrow \bar{\nu}_{l'})$, $l \neq l'$.

In the case of 3-neutrino mixing all different $\text{Im}(U_{l'j} U_{lj}^* U_{lk} U_{l'k}^*)$ coincide up to a sign as a consequence of the unitarity of U . Therefore one has [45]:

$$\begin{aligned} A_{\text{CP}}^{(\mu e)} &= -A_{\text{CP}}^{(\tau e)} = A_{\text{CP}}^{(\tau \mu)} = \\ &4 J_{\text{CP}} \left(\sin \frac{\Delta m_{32}^2}{2p} L + \sin \frac{\Delta m_{21}^2}{2p} L + \sin \frac{\Delta m_{13}^2}{2p} L \right) \end{aligned} \quad (13.18)$$

where

$$J_{\text{CP}} = \text{Im} \left(U_{\mu 3} U_{e 3}^* U_{e 2} U_{\mu 2}^* \right), \quad (13.19)$$

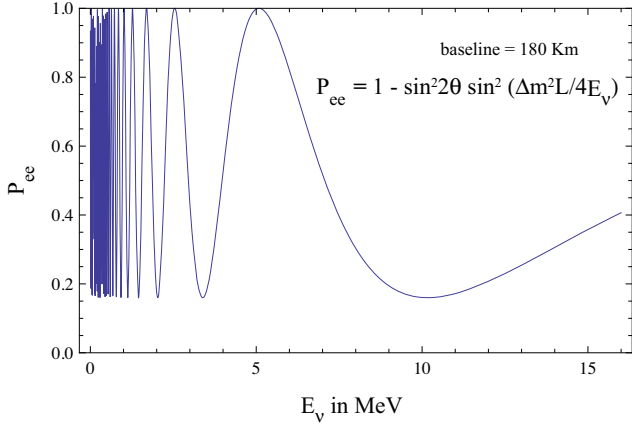


Figure 13.1: The ν_e ($\bar{\nu}_e$) survival probability $P(\nu_e \rightarrow \nu_e) = P(\bar{\nu}_e \rightarrow \bar{\nu}_e)$, Eq. (13.30), as a function of the neutrino energy for $L = 180$ km, $\Delta m^2 = 7.0 \times 10^{-5}$ eV² and $\sin^2 2\theta = 0.84$ (from [48]).

is the “rephasing invariant” associated with the Dirac CP violation phase in U . It is analogous to the rephasing invariant associated with the Dirac CP violating phase in the CKM quark mixing matrix [46]. It is clear from Eq. (13.18) that J_{CP} controls the magnitude of CP violation effects in neutrino oscillations in the case of 3-neutrino mixing. If $\sin(\Delta m_{ij}^2/(2p))L \cong 0$ for $(ij) = (32)$, or (21) , or (13) ,

we get $A_{CP}^{(l'l')} \cong 0$. Thus, if as a consequence of the production, propagation and/or detection of neutrinos, effectively oscillations due only to one non-zero neutrino mass squared difference take place, the CP violating effects will be strongly suppressed. In particular, we get $A_{CP}^{(l'l')} = 0$, unless all three $\Delta m_{ij}^2 \neq 0$, $(ij) = (32)$, (21) , (13) .

If the number of massive neutrinos n is equal to the number of neutrino flavours, $n = 3$, one has as a consequence of the unitarity of the neutrino mixing matrix: $\sum_{l'=e,\mu,\tau} P(\nu_l \rightarrow \nu_{l'}) = 1$, $l = e, \mu, \tau$, $\sum_{l=e,\mu,\tau} P(\nu_l \rightarrow \nu_{l'}) = 1$, $l' = e, \mu, \tau$. Similar “probability conservation” equations hold for $P(\bar{\nu}_l \rightarrow \bar{\nu}_{l'})$. If, however, the number of light massive neutrinos is bigger than the number of flavour neutrinos as a consequence, *e.g.*, of a flavour neutrino - sterile neutrino mixing, we would have $\sum_{l'=e,\mu,\tau} P(\nu_l \rightarrow \nu_{l'}) = 1 - P(\nu_l \rightarrow \bar{\nu}_s L)$, $l = e, \mu, \tau$, where we have assumed the existence of just one sterile neutrino. Obviously, in this case $\sum_{l'=e,\mu,\tau} P(\nu_l \rightarrow \nu_{l'}) < 1$ if $P(\nu_l \rightarrow \bar{\nu}_s L) \neq 0$. The former inequality is used in the searches for oscillations between active and sterile neutrinos.

Consider next neutrino oscillations in the case of one neutrino mass squared difference “dominance”: suppose that $|\Delta m_{j1}^2| \ll |\Delta m_{n1}^2|$, $j = 2, \dots, (n-1)$, $|\Delta m_{n1}^2| L/(2p) \gtrsim 1$ and $|\Delta m_{j1}^2| L/(2p) \ll 1$, so that $\exp[i(\Delta m_{j1}^2 L/(2p))] \cong 1$, $j = 2, \dots, (n-1)$. Under these conditions we obtain from Eq. (13.13) and Eq. (13.14), keeping only the oscillating terms involving Δm_{n1}^2 :

$$P(\nu_{l(l')} \rightarrow \nu_{l(l')}) \cong P(\bar{\nu}_{l(l')} \rightarrow \bar{\nu}_{l(l')}) \cong \delta_{ll'} - 2|U_{ln}|^2 \left[\delta_{ll'} - |U_{l'n}|^2 \right] \left(1 - \cos \frac{\Delta m_{n1}^2 L}{2p} \right). \quad (13.20)$$

It follows from the neutrino oscillation data (Sections 13.4 and 13.5) that in the case of 3-neutrino mixing, one of the two independent neutrino mass squared differences, say Δm_{21}^2 , is much smaller in absolute value than the second one, Δm_{31}^2 : $|\Delta m_{21}^2| \ll |\Delta m_{31}^2|$. The data imply:

$$\begin{aligned} |\Delta m_{21}^2| &\cong 7.6 \times 10^{-5} \text{ eV}^2, \\ |\Delta m_{31}^2| &\cong 2.4 \times 10^{-3} \text{ eV}^2, \\ |\Delta m_{21}^2|/|\Delta m_{31}^2| &\cong 0.032. \end{aligned} \quad (13.21)$$

Neglecting the effects due to Δm_{21}^2 we get from Eq. (13.20) by setting $n = 3$ and choosing, *e.g.*, i) $l = l' = e$ and ii) $l = e(\mu)$, $l' = \mu(e)$ [47]:

$$P(\nu_e \rightarrow \nu_e) = P(\bar{\nu}_e \rightarrow \bar{\nu}_e) \cong 1 - 2|U_{e3}|^2 \left(1 - |U_{e3}|^2 \right) \left(1 - \cos \frac{\Delta m_{31}^2 L}{2p} \right), \quad (13.22)$$

$$\begin{aligned} P(\nu_{\mu(e)} \rightarrow \nu_{e(\mu)}) &\cong 2|U_{\mu3}|^2 |U_{e3}|^2 \left(1 - \cos \frac{\Delta m_{31}^2 L}{2p} \right) \\ &= \frac{|U_{\mu3}|^2}{1 - |U_{e3}|^2} P^{2\nu} \left(|U_{e3}|^2, m_{31}^2 \right), \end{aligned} \quad (13.23)$$

Table 13.1: Sensitivity of different oscillation experiments.

Source	Type of ν	\bar{E} [MeV]	L [km]	$\min(\Delta m^2)$ [eV ²]
Reactor	$\bar{\nu}_e$	~ 1	1	$\sim 10^{-3}$
Reactor	$\bar{\nu}_e$	~ 1	100	$\sim 10^{-5}$
Accelerator	$\nu_\mu, \bar{\nu}_\mu$	$\sim 10^3$	1	~ 1
Accelerator	$\nu_\mu, \bar{\nu}_\mu$	$\sim 10^3$	1000	$\sim 10^{-3}$
Atmospheric ν 's	$\nu_{\mu,e}, \bar{\nu}_{\mu,e}$	$\sim 10^3$	10^4	$\sim 10^{-4}$
Sun	ν_e	~ 1	1.5×10^8	$\sim 10^{11}$

and $P(\bar{\nu}_{\mu(e)} \rightarrow \bar{\nu}_{e(\mu)}) = P(\nu_{\mu(e)} \rightarrow \nu_{e(\mu)})$. Here $P^{2\nu}(|U_{e3}|^2, m_{31}^2)$ is the probability of the 2-neutrino transition $\nu_e \rightarrow (s_{23}\nu_\mu + c_{23}\nu_\tau)$ due to Δm_{31}^2 and a mixing with angle θ_{13} , where

$$\begin{aligned} \sin^2 \theta_{13} &= |U_{e3}|^2, \quad s_{23}^2 \equiv \sin^2 \theta_{23} = \frac{|U_{\mu3}|^2}{1 - |U_{e3}|^2}, \\ c_{23}^2 &\equiv \cos^2 \theta_{23} = \frac{|U_{\tau3}|^2}{1 - |U_{e3}|^2}. \end{aligned} \quad (13.24)$$

Eq. (13.22) describes with a relatively high precision the oscillations of reactor $\bar{\nu}_e$ on a distance $L \sim 1$ km in the case of 3-neutrino mixing. It was used in the analysis of the results of the CHOOZ experiment and can be used in the analyses of the data of the Double Chooz, Daya Bay and RENO experiments, which are under preparation. Eq. (13.20) with $n = 3$ and $l = l' = \mu$ describes with a relatively good precision the effects of oscillations of the accelerator ν_μ , seen in the K2K and MINOS experiments. The $\nu_\mu \rightarrow \nu_\tau$ oscillations, which the OPERA experiment is aiming to detect, can be described by Eq. (13.20) with $n = 3$ and $l = \mu$, $l' = \tau$. Finally, the probability Eq. (13.23) describes with a good precision the $\nu_\mu \rightarrow \nu_e$ and $\bar{\nu}_\mu \rightarrow \bar{\nu}_e$ oscillations under the conditions of the MINOS experiment.

In certain cases the dimensions of the neutrino source, ΔL , are not negligible in comparison with the oscillation length. Similarly, when analyzing neutrino oscillation data one has to include the energy resolution of the detector, ΔE , *etc.* in the analysis. As can be shown [29], if $2\pi\Delta L/L_{jk}^v \gg 1$, and/or $2\pi(L/L_{jk}^v)(\Delta E/E) \gg 1$, the oscillating terms in the neutrino oscillation probabilities will be strongly suppressed. In this case (as well as in the case of sufficiently large separation of the ν_j and ν_k wave packets at the detection point) the interference terms in $P(\nu_l \rightarrow \nu_{l'})$ and $P(\bar{\nu}_{l'} \rightarrow \bar{\nu}_l)$ will be negligibly small and the neutrino flavour conversion will be determined by the average probabilities:

$$\bar{P}(\nu_l \rightarrow \nu_{l'}) = \bar{P}(\bar{\nu}_l \rightarrow \bar{\nu}_{l'}) \cong \sum_j |U_{lj}|^2 |U_{l'j}|^2. \quad (13.25)$$

Suppose next that in the case of 3-neutrino mixing, $|\Delta m_{21}^2| L/(2p) \sim 1$, while at the same time $|\Delta m_{31(32)}^2| L/(2p) \gg 1$, and the oscillations due to Δm_{31}^2 and Δm_{32}^2 are strongly suppressed (averaged out) due to integration over the region of neutrino production, the energy resolution function, *etc.* In this case we get for the ν_e and $\bar{\nu}_e$ survival probabilities:

$$P(\nu_e \rightarrow \nu_e) = P(\bar{\nu}_e \rightarrow \bar{\nu}_e) \cong |U_{e3}|^4 + \left(1 - |U_{e3}|^2 \right)^2 P^{2\nu}(\nu_e \rightarrow \nu_e), \quad (13.26)$$

$$P^{2\nu}(\nu_e \rightarrow \nu_e) = P^{2\nu}(\bar{\nu}_e \rightarrow \bar{\nu}_e) \equiv P_{ee}^{2\nu}(\theta_{12}, \Delta m_{21}^2) \\ = 1 - \frac{1}{2} \sin^2 2\theta_{12} \left(1 - \cos \frac{\Delta m_{21}^2}{2p} L \right) \quad (13.27)$$

being the ν_e and $\bar{\nu}_e$ survival probability in the case of 2-neutrino oscillations “driven” by the angle θ_{12} and Δm_{21}^2 , with θ_{12} determined by

$$\cos^2 \theta_{12} = \frac{|U_{e1}|^2}{1 - |U_{e3}|^2}, \quad \sin^2 \theta_{12} = \frac{|U_{e2}|^2}{1 - |U_{e3}|^2}. \quad (13.28)$$

Eq. (13.26) with $P^{2\nu}(\bar{\nu}_e \rightarrow \bar{\nu}_e)$ given by Eq. (13.27) describes the effects of neutrino oscillations of reactor $\bar{\nu}_e$ observed by the KamLAND experiment.

In the case of 3-neutrino mixing with $0 < \Delta m_{21}^2 < |\Delta m_{31(32)}^2|$ and $|U_{e3}|^2 = |\sin \theta_{13}|^2 \ll 1$ (see Section 13.6), one can identify Δm_{21}^2 and θ_{12} as the neutrino mass squared difference and mixing angle responsible for the solar ν_e oscillations, and Δm_{31}^2 and θ_{23} as those associated with the dominant atmospheric ν_μ and $\bar{\nu}_\mu$ oscillations. Thus, θ_{12} and θ_{23} are often called “solar” and “atmospheric” neutrino mixing angles and denoted as $\theta_{12} = \theta_\odot$ and $\theta_{23} = \theta_\Lambda$ (or θ_{atm}), while Δm_{21}^2 and Δm_{31}^2 are often referred to as the “solar” and “atmospheric” neutrino mass squared differences and denoted as $\Delta m_{21}^2 \equiv \Delta m_\odot^2$ and $\Delta m_{31}^2 \equiv \Delta m_\Lambda^2$ (or Δm_{atm}^2).

The data of ν -oscillations experiments is often analyzed assuming 2-neutrino mixing:

$$|\nu_l\rangle = |\nu_l\rangle \cos \theta + |\nu_x\rangle \sin \theta, \quad |\nu_x\rangle = -|\nu_l\rangle \sin \theta + |\nu_x\rangle \cos \theta, \quad (13.29)$$

where θ is the neutrino mixing angle in vacuum and ν_x is another flavour neutrino or sterile (anti-) neutrino, $x = l' \neq l$ or $\nu_x \equiv \bar{\nu}_{sL}$. In this case we have [41]:

$$P^{2\nu}(\nu_l \rightarrow \nu_l) = 1 - \frac{1}{2} \sin^2 2\theta \left(1 - \cos 2\pi \frac{L}{L^v} \right), \\ P^{2\nu}(\nu_l \rightarrow \nu_x) = 1 - P^{2\nu}(\nu_l \rightarrow \nu_l), \quad (13.30)$$

where $L^v = 4\pi p/\Delta m^2$, $\Delta m^2 = m_2^2 - m_1^2 > 0$. Combining the CPT invariance constraints with the probability conservation one obtains: $P(\nu_l \rightarrow \nu_x) = P(\bar{\nu}_l \rightarrow \bar{\nu}_x) = P(\nu_x \rightarrow \nu_l) = P(\bar{\nu}_x \rightarrow \bar{\nu}_l)$. These equalities and Eq. (13.30) with $l = \mu$ and $x = \tau$ were used, for instance, in the analysis of the Super-K atmospheric neutrino data [13], in which the first compelling evidence for oscillations of neutrinos was obtained. The probability $P^{2\nu}(\nu_l \rightarrow \nu_x)$, Eq. (13.30), depends on two factors: on $(1 - \cos 2\pi L/L^v)$, which exhibits oscillatory dependence on the distance L and on the neutrino energy $p = E$ (hence the name “neutrino oscillations”), and on $\sin^2 2\theta$, which determines the amplitude of the oscillations. In order to have $P^{2\nu}(\nu_l \rightarrow \nu_x) \cong 1$, two conditions have to be fulfilled: one should have $\sin^2 2\theta \cong 1$ and $L^v \lesssim 2\pi L$ with $\cos 2\pi L/L^v \cong -1$. If $L^v \gg 2\pi L$, the oscillations do not have enough time to develop on the way to the neutrino detector and $P(\nu_l \rightarrow \nu_x) \cong 0$. This is illustrated in Fig. 1 showing the dependence of the probability $P^{2\nu}(\nu_e \rightarrow \nu_e) = P^{2\nu}(\bar{\nu}_e \rightarrow \bar{\nu}_e)$ on the neutrino energy.

A given experiment searching for neutrino oscillations is specified, in particular, by the average energy of the neutrinos being studied, \bar{E} , and by the source-detector distance L . The requirement $L_{jk}^v \lesssim 2\pi L$ determines the minimal value of a generic neutrino mass squared difference $\Delta m^2 > 0$, to which the experiment is sensitive (figure of merit of the experiment): $\min(\Delta m^2) \sim 2\bar{E}/L$. Because of the interference nature of neutrino oscillations, experiments can probe, in general, rather small values of Δm^2 (see, e.g., Ref. 37). Values of $\min(\Delta m^2)$, characterizing qualitatively the sensitivity of different experiments are given in Table 1. They correspond to the reactor experiments CHOOZ ($L \sim 1$ km) and KamLAND ($L \sim 100$ km), to accelerator experiments - past ($L \sim 1$ km), recent, current and future (K2K, MINOS, OPERA, T2K, NO ν A), $L \sim (300 \div 1000)$ km), to the Super-Kamiokande experiment studying atmospheric neutrino oscillations, and to the solar neutrino experiments.

13.3. Matter effects in neutrino oscillations

The presence of matter can change drastically the pattern of neutrino oscillations: neutrinos can interact with the particles forming the matter. Accordingly, the Hamiltonian of the neutrino system in matter H_m , differs from the Hamiltonian in vacuum H_0 , $H_m = H_0 + H_{int}$, where H_{int} describes the interaction of neutrinos with the particles of matter. When, for instance, ν_e and ν_μ propagate in matter, they can scatter (due to H_{int}) on the electrons (e^-), protons (p) and neutrons (n) present in matter. The incoherent elastic and the quasi-elastic scattering, in which the states of the initial particles change in the process (destroying the coherence between the neutrino states), are not of interest - they have a negligible effect on the solar neutrino propagation in the Sun and on the solar, atmospheric and reactor neutrino propagation in the Earth [49]: even in the center of the Sun, where the matter density is relatively high (~ 150 g/cm³), a ν_e with energy of 1 MeV has a mean free path with respect to the indicated scattering processes $\sim 10^{10}$ km. We recall that the solar radius is much smaller: $R_\odot = 6.96 \times 10^5$ km. The oscillating ν_e and ν_μ can scatter also elastically in the forward direction on the e^- , p and n , with the momenta and the spin states of the particles remaining unchanged. In such a process the coherence of the neutrino states is preserved.

The ν_e and ν_μ coherent elastic scattering on the particles of matter generates nontrivial indices of refraction of the ν_e and ν_μ in matter [25]: $\kappa(\nu_e) \neq 1$, $\kappa(\nu_\mu) \neq 1$. Most importantly, we have $\kappa(\nu_e) \neq \kappa(\nu_\mu)$. The difference $\kappa(\nu_e) - \kappa(\nu_\mu)$ is determined essentially by the difference of the real parts of the forward $\nu_e - e^-$ and $\nu_\mu - e^-$ elastic scattering amplitudes [25] $\text{Re} [F_{\nu_e e^-}(0)] - \text{Re} [F_{\nu_\mu e^-}(0)]$: due to the flavour symmetry of the neutrino - quark (neutrino - nucleon) neutral current interaction, the forward $\nu_e - p, n$ and $\nu_\mu - p, n$ elastic scattering amplitudes are equal and therefore do not contribute to the difference of interest [50]. The imaginary parts of the forward scattering amplitudes (responsible, in particular, for decoherence effects) are proportional to the corresponding total scattering cross-sections and in the case of interest are negligible in comparison with the real parts. The real parts of the amplitudes $F_{\nu_e e^-}(0)$ and $F_{\nu_\mu e^-}(0)$ can be calculated in the Standard Model. To leading order in the Fermi constant G_F , only the term in $F_{\nu_e e^-}(0)$ due to the diagram with exchange of a virtual W^\pm -boson contributes to $F_{\nu_e e^-}(0) - F_{\nu_\mu e^-}(0)$. One finds the following result for $\kappa(\nu_e) - \kappa(\nu_\mu)$ in the rest frame of the scatters [25,52,53]:

$$\kappa(\nu_e) - \kappa(\nu_\mu) = \frac{2\pi}{p^2} \left(\text{Re} [F_{\nu_e e^-}(0)] - \text{Re} [F_{\nu_\mu e^-}(0)] \right) \\ = - \frac{1}{p} \sqrt{2} G_F N_e, \quad (13.31)$$

where N_e is the electron number density in matter. Given $\kappa(\nu_e) - \kappa(\nu_\mu)$, the system of evolution equations describing the $\nu_e \leftrightarrow \nu_\mu$ oscillations in matter reads [25]:

$$i \frac{d}{dt} \begin{pmatrix} A_e(t, t_0) \\ A_\mu(t, t_0) \end{pmatrix} = \begin{pmatrix} -\epsilon(t) & \epsilon' \\ \epsilon' & \epsilon(t) \end{pmatrix} \begin{pmatrix} A_e(t, t_0) \\ A_\mu(t, t_0) \end{pmatrix} \quad (13.32)$$

where $A_e(t, t_0)$ ($A_\mu(t, t_0)$) is the amplitude of the probability to find ν_e (ν_μ) at time t of the evolution of the system if at time $t_0 \leq t$ the neutrino ν_e or ν_μ has been produced and

$$\epsilon(t) = \frac{1}{2} \left[\frac{\Delta m^2}{2E} \cos 2\theta - \sqrt{2} G_F N_e(t) \right], \quad \epsilon' = \frac{\Delta m^2}{4E} \sin 2\theta. \quad (13.33)$$

The term $\sqrt{2} G_F N_e(t)$ in $\epsilon(t)$ accounts for the effects of matter on neutrino oscillations. The system of evolution equations describing the oscillations of antineutrinos $\bar{\nu}_e \leftrightarrow \bar{\nu}_\mu$ in matter has exactly the same form except for the matter term in $\epsilon(t)$ which changes sign. The effect of matter in neutrino oscillations is usually called the Mikheyev, Smirnov, Wolfenstein (or MSW) effect.

Consider first the case of $\nu_e \leftrightarrow \nu_\mu$ oscillations in matter with constant density: $N_e(t) = N_e = \text{const}$. Due to the interaction term H_{int} in H_m , the eigenstates of the Hamiltonian of the neutrino system

in vacuum, $|\nu_{1,2}\rangle$ are not eigenstates of H_m . For the eigenstates $|\nu_{1,2}^m\rangle$ of H_m , which diagonalize the evolution matrix in the r.h.s. of the system Eq. (13.32) we have:

$$|\nu_e\rangle = |\nu_1^m\rangle \cos\theta_m + |\nu_2^m\rangle \sin\theta_m, \quad |\nu_\mu\rangle = -|\nu_1^m\rangle \sin\theta_m + |\nu_2^m\rangle \cos\theta_m. \quad (13.34)$$

Here θ_m is the neutrino mixing angle in matter [25],

$$\sin 2\theta_m = \frac{\tan 2\theta}{\sqrt{\left(1 - \frac{N_e}{N_e^{res}}\right)^2 + \tan^2 2\theta}}, \quad \cos 2\theta_m = \frac{1 - N_e/N_e^{res}}{\sqrt{\left(1 - \frac{N_e}{N_e^{res}}\right)^2 + \tan^2 2\theta}}, \quad (13.35)$$

where the quantity

$$N_e^{res} = \frac{\Delta m^2 \cos 2\theta}{2E\sqrt{2}G_F} \cong 6.56 \times 10^6 \frac{\Delta m^2[\text{eV}^2]}{E[\text{MeV}]} \cos 2\theta \text{ cm}^{-3} N_A, \quad (13.36)$$

is called (for $\Delta m^2 \cos 2\theta > 0$) ‘‘resonance density’’ [26,52], N_A being Avogadro’s number. The ‘‘adiabatic’’ states $|\nu_{1,2}^m\rangle$ have energies $E_{1,2}^m$ whose difference is given by

$$E_2^m - E_1^m = \frac{\Delta m^2}{2E} \left(\left(1 - \frac{N_e}{N_e^{res}}\right)^2 \cos^2 2\theta + \sin^2 2\theta \right)^{\frac{1}{2}} \cong \frac{\Delta M^2}{2E}. \quad (13.37)$$

The probability of $\nu_e \rightarrow \nu_\mu$ transition in matter with $N_e = \text{const.}$ has the form [25,52]

$$P_m^{2\nu}(\nu_e \rightarrow \nu_\mu) = |A_\mu(t)|^2 = \frac{1}{2} \sin^2 2\theta_m \left[1 - \cos 2\pi \frac{L}{L_m} \right] \\ L_m = 2\pi/(E_2^m - E_1^m), \quad (13.38)$$

where L_m is the oscillation length in matter. As Eq. (13.35) indicates, the dependence of $\sin^2 2\theta_m$ on N_e has a resonance character [26]. Indeed, if $\Delta m^2 \cos 2\theta > 0$, for any $\sin^2 2\theta \neq 0$ there exists a value of N_e given by N_e^{res} , such that when $N_e = N_e^{res}$ we have $\sin^2 2\theta_m = 1$ independently of the value of $\sin^2 2\theta < 1$. This implies that the presence of matter can lead to a strong enhancement of the oscillation probability $P_m^{2\nu}(\nu_e \rightarrow \nu_\mu)$ even when the $\nu_e \leftrightarrow \nu_\mu$ oscillations in vacuum are suppressed due to a small value of $\sin^2 2\theta$. For obvious reasons

$$N_e = N_e^{res} \cong \frac{\Delta m^2 \cos 2\theta}{2E\sqrt{2}G_F}, \quad (13.39)$$

is called the ‘‘resonance condition’’ [26,52], while the energy at which Eq. (13.39) holds for given N_e and $\Delta m^2 \cos 2\theta$, is referred to as the ‘‘resonance energy’’, E^{res} . The oscillation length at resonance is given by [26] $L_m^{res} = L^v/\sin 2\theta$, while the width in N_e of the resonance at half height reads $\Delta N_e^{res} = 2N_e^{res} \tan 2\theta$. Thus, if the mixing angle in vacuum is small, the resonance is narrow, $\Delta N_e^{res} \ll N_e^{res}$, and $L_m^{res} \gg L^v$. The energy difference $E_2^m - E_1^m$ has a minimum at the resonance: $(E_2^m - E_1^m)^{res} = \min (E_2^m - E_1^m) = (\Delta m^2/(2E)) \sin 2\theta$.

It is instructive to consider two limiting cases. If $N_e \ll N_e^{res}$, we have from Eq. (13.35) and Eq. (13.37), $\theta_m \cong \theta$, $L_m \cong L^v$ and neutrinos oscillate practically as in vacuum. In the limit $N_e \gg N_e^{res}$, $N_e^{res} \tan^2 2\theta$, one finds $\theta_m \cong \pi/2$ ($\cos 2\theta_m \cong -1$) and the presence of matter suppresses the $\nu_e \leftrightarrow \nu_\mu$ oscillations. In this case $|\nu_e\rangle \cong |\nu_2^m\rangle$, $|\nu_\mu\rangle = -|\nu_1^m\rangle$, i.e., ν_e practically coincides with the heavier matter-eigenstate, while ν_μ coincides with the lighter one.

Since the neutral current weak interaction of neutrinos in the Standard Model is flavour symmetric, the formulae and results we have obtained are valid for the case of $\nu_e - \nu_\tau$ mixing and $\nu_e \leftrightarrow \nu_\tau$ oscillations in matter as well. The case of $\nu_\mu - \nu_\tau$ mixing, however, is different: to a relatively good precision we have [54] $\kappa(\nu_\mu) \cong \kappa(\nu_\tau)$ and the $\nu_\mu \leftrightarrow \nu_\tau$ oscillations in the matter of the Earth and the Sun proceed practically as in vacuum [55].

The analogs of Eq. (13.35) to Eq. (13.38) for oscillations of antineutrinos, $\bar{\nu}_e \leftrightarrow \bar{\nu}_\mu$, in matter can formally be obtained by replacing N_e with $(-N_e)$ in the indicated equations. It should be clear that depending on the sign of $\Delta m^2 \cos 2\theta$, the presence of matter can lead to resonance enhancement either of the $\nu_e \leftrightarrow \nu_\mu$ or of the $\bar{\nu}_e \leftrightarrow \bar{\nu}_\mu$ oscillations, but not of both types of oscillations [52]. For $\Delta m^2 \cos 2\theta < 0$, for instance, the matter can only suppress the

$\nu_e \rightarrow \nu_\mu$ oscillations, while it can enhance the $\bar{\nu}_e \rightarrow \bar{\nu}_\mu$ transitions. This disparity between the behavior of neutrinos and that of antineutrinos is a consequence of the fact that the matter in the Sun or in the Earth we are interested in is not charge-symmetric (it contains e^- , p and n , but does not contain their antiparticles) and therefore the oscillations in matter are neither CP- nor CPT- invariant [44]. Thus, even in the case of 2-neutrino mixing and oscillations we have, e.g., $P_m^{2\nu}(\nu_e \rightarrow \nu_\mu(\tau)) \neq P_m^{2\nu}(\bar{\nu}_e \rightarrow \bar{\nu}_\mu(\tau))$.

The matter effects in the $\nu_e \leftrightarrow \nu_\mu(\tau)$ ($\bar{\nu}_e \leftrightarrow \bar{\nu}_\mu(\tau)$) oscillations will be invariant with respect to the operation of time reversal if the N_e distribution along the neutrino path is symmetric with respect to this operation [45,56]. The latter condition is fulfilled (to a good approximation) for the N_e distribution along a path of a neutrino crossing the Earth [57].

13.3.1. Effects of Earth matter on oscillations of neutrinos :

The formalism we have developed can be applied, e.g., to the study of matter effects in the $\nu_e \leftrightarrow \nu_\mu(\tau)$ ($\nu_\mu(\tau) \leftrightarrow \nu_e$) and $\bar{\nu}_e \leftrightarrow \bar{\nu}_\mu(\tau)$ ($\bar{\nu}_\mu(\tau) \leftrightarrow \bar{\nu}_e$) oscillations of neutrinos which traverse the Earth [58]. Indeed, the Earth density distribution in the existing Earth models [57] is assumed to be spherically symmetric and there are two major density structures - the core and the mantle, and a certain number of substructures (shells or layers). The Earth radius is $R_\oplus = 6371$ km; the Earth core has a radius of $R_c = 3486$ km, so the Earth mantle depth is 2885 km. For a spherically symmetric Earth density distribution, the neutrino trajectory in the Earth is specified by the value of the Nadir angle θ_n of the trajectory. For $\theta_n \leq 33.17^\circ$, or path lengths $L \geq 10660$ km, neutrinos cross the Earth core. The path length for neutrinos which cross only the Earth mantle is given by $L = 2R_\oplus \cos\theta_n$. If neutrinos cross the Earth core, the lengths of the paths in the mantle, $2L^{\text{man}}$, and in the core, L^{core} , are determined by: $L^{\text{man}} = R_\oplus \cos\theta_n - (R_c^2 - R_\oplus^2 \sin^2\theta_n)^{\frac{1}{2}}$, $L^{\text{core}} = 2(R_c^2 - R_\oplus^2 \sin^2\theta_n)^{\frac{1}{2}}$. The mean electron number densities in the mantle and in the core according to the PREM model read [57]: $\bar{N}_e^{\text{man}} \cong 2.2 \text{ cm}^{-3} N_A$, $\bar{N}_e^c \cong 5.4 \text{ cm}^{-3} N_A$. Thus, we have $\bar{N}_e^c \cong 2.5 \bar{N}_e^{\text{man}}$. The change of N_e from the mantle to the core can well be approximated by a step function [57]. The electron number density N_e changes relatively little around the indicated mean values along the trajectories of neutrinos which cross a substantial part of the Earth mantle, or the mantle and the core, and the two-layer constant density approximation, $N_e^{\text{man}} = \text{const.} = \bar{N}_e^{\text{man}}$, $N_e^c = \text{const.} = \bar{N}_e^c$, \bar{N}_e^{man} and \bar{N}_e^c being the mean densities along the given neutrino path in the Earth, was shown to be sufficiently accurate in what concerns the calculation of neutrino oscillation probabilities [45,60,63] (and references quoted in [60,63]) in a large number of specific cases. This is related to the fact that the relatively small changes of density along the path of the neutrinos in the mantle (or in the core) take place over path lengths which are typically considerably smaller than the corresponding oscillation length in matter.

In the case of 3-neutrino mixing and for neutrino energies of $E \gtrsim 2$ GeV, the effects due to Δm_{21}^2 ($|\Delta m_{21}^2| \ll |\Delta m_{31}^2|$, see Eq. (13.21)) in the neutrino oscillation probabilities are sub-dominant and to leading order can be neglected: the corresponding resonance density $|N_{e21}^{res}| \lesssim 0.25 \text{ cm}^{-3} N_A \ll \bar{N}_e^{\text{man,c}}$ and the Earth matter strongly suppresses the oscillations due to Δm_{21}^2 . For oscillations in vacuum this approximation is valid as long as the leading order contribution due to Δm_{31}^2 in the relevant probabilities is bigger than approximately 10^{-3} . In this case the 3-neutrino $\nu_e \rightarrow \nu_\mu(\tau)$ ($\bar{\nu}_e \rightarrow \bar{\nu}_\mu(\tau)$) and $\nu_\mu(\tau) \rightarrow \nu_e$ ($\bar{\nu}_\mu(\tau) \rightarrow \bar{\nu}_e$) transition probabilities for neutrinos traversing the Earth, reduce effectively to a 2-neutrino transition probability (see, e.g., [61–63]), with Δm_{31}^2 and θ_{13} playing the role of the relevant 2-neutrino vacuum oscillation parameters. The 3-neutrino oscillation probabilities of the atmospheric and accelerator $\nu_{e,\mu}$ having energy E and crossing the Earth along a trajectory characterized by a Nadir angle θ_n , for instance, have the following form:

$$P_m^{3\nu}(\nu_e \rightarrow \nu_e) \cong 1 - P_m^{2\nu}, \quad (13.40)$$

$$P_m^{3\nu}(\nu_e \rightarrow \nu_\mu) \cong P_m^{3\nu}(\nu_\mu \rightarrow \nu_e) \cong s_{23}^2 P_m^{2\nu}, \quad P_m^{3\nu}(\nu_e \rightarrow \nu_\tau) \cong c_{23}^2 P_m^{2\nu}, \quad (13.41)$$

$$P_m^{3\nu}(\nu_\mu \rightarrow \nu_\mu) \cong 1 - s_{23}^4 P_m^{2\nu} - 2c_{23}s_{23}^2 \left[1 - \text{Re}(e^{-i\kappa} A_m^{2\nu}(\nu' \rightarrow \nu')) \right], \quad (13.42)$$

13.3.2. Oscillations of solar neutrinos :

Consider next the oscillations of solar ν_e while they propagate from the central part of the Sun, where they are produced, to the surface of the Sun [26,59] (see also, e.g., [70]). Details concerning the production, spectrum, magnitude and particularities of the solar neutrino flux, the methods of detection of solar neutrinos, description of solar neutrino experiments and of the data they provided will be discussed in the next section (see also Ref. 71). The electron number density N_e changes considerably along the neutrino path in the Sun: it decreases monotonically from the value of $\sim 100 \text{ cm}^{-3} N_A$ in the center of the Sun to 0 at the surface of the Sun. According to the contemporary solar models (see, e.g., [71,72]), N_e decreases approximately exponentially in the radial direction towards the surface of the Sun:

$$N_e(t) = N_e(t_0) \exp \left\{ -\frac{t-t_0}{r_0} \right\}, \quad (13.50)$$

where $(t-t_0) \cong d$ is the distance traveled by the neutrino in the Sun, $N_e(t_0)$ is the electron number density at the point of ν_e production in the Sun, r_0 is the scale-height of the change of $N_e(t)$ and one has [71,72] $r_0 \sim 0.1 R_\odot$.

Consider the case of 2-neutrino mixing, Eq. (13.34). Obviously, if N_e changes with t (or equivalently with the distance) along the neutrino trajectory, the matter-eigenstates, their energies, the mixing angle and the oscillation length in matter, become, through their dependence on N_e , also functions of t : $|\nu_{1,2}^m(t)\rangle = |\nu_{1,2}^m(t)\rangle$, $E_{1,2}^m = E_{1,2}^m(t)$, $\theta_m = \theta_m(t)$ and $L_m = L_m(t)$. It is not difficult to understand qualitatively the possible behavior of the neutrino system when solar neutrinos propagate from the center to the surface of the Sun if one realizes that one is dealing effectively with a two-level system whose Hamiltonian depends on time and admits “jumps” from one level to the other (see Eq. (13.32)). Consider the case of $\Delta m^2 \cos 2\theta > 0$. Let us assume first for simplicity that the electron number density at the point of a solar ν_e production in the Sun is much bigger than the resonance density, $N_e(t_0) \gg N_e^{res}$. Actually, this is one of the cases relevant to the solar neutrinos. In this case we have $\theta_m(t_0) \cong \pi/2$ and the state of the electron neutrino in the initial moment of the evolution of the system practically coincides with the heavier of the two matter-eigenstates:

$$|\nu_e\rangle \cong |\nu_2^m(t_0)\rangle. \quad (13.51)$$

Thus, at t_0 the neutrino system is in a state corresponding to the “level” with energy $E_2^m(t_0)$. When neutrinos propagate to the surface of the Sun they cross a layer of matter in which $N_e = N_e^{res}$: in this layer the difference between the energies of the two “levels” ($E_2^m(t) - E_1^m(t)$) has a minimal value on the neutrino trajectory (Eq. (13.37) and Eq. (13.39)). Correspondingly, the evolution of the neutrino system can proceed basically in two ways. First, the system can stay on the “level” with energy $E_2^m(t)$, i.e., can continue to be in the state $|\nu_2^m(t)\rangle$ up to the final moment t_s , when the neutrino reaches the surface of the Sun. At the surface of the Sun $N_e(t_s) = 0$ and therefore $\theta_m(t_s) = \theta$, $|\nu_{1,2}^m(t_s)\rangle \equiv |\nu_{1,2}\rangle$ and $E_{1,2}^m(t_s) = E_{1,2}$. Thus, in this case the state describing the neutrino system at t_0 will evolve continuously into the state $|\nu_2\rangle$ at the surface of the Sun. Using Eq. (13.29) with $l=e$ and $x=\mu$, it is easy to obtain the probabilities to find ν_e and ν_μ at the surface of the Sun:

$$\begin{aligned} P(\nu_e \rightarrow \nu_e; t_s, t_0) &\cong |\langle \nu_e | \nu_2 \rangle|^2 = \sin^2 \theta \\ P(\nu_e \rightarrow \nu_\mu; t_s, t_0) &\cong |\langle \nu_\mu | \nu_2 \rangle|^2 = \cos^2 \theta. \end{aligned} \quad (13.52)$$

It is clear that under the assumption made and if $\sin^2 \theta \ll 1$, practically a total $\nu_e \rightarrow \nu_\mu$ conversion is possible. This type of evolution of the neutrino system and the $\nu_e \rightarrow \nu_\mu$ transitions taking place during the evolution, are called [26] “adiabatic.” They are characterized by the fact that the probability of the “jump” from the upper “level” (having energy $E_2^m(t)$) to the lower “level” (with energy $E_1^m(t)$), P' , or equivalently the probability of the $\nu_2^m(t_0) \rightarrow \nu_1^m(t_s)$ transition, $P' \equiv P'(\nu_2^m(t_0) \rightarrow \nu_1^m(t_s))$, on the whole neutrino trajectory is negligible:

$$P' \equiv P'(\nu_2^m(t_0) \rightarrow \nu_1^m(t_s)) \cong 0 : \text{adiabatic transitions.} \quad (13.53)$$

The second possibility is realized if in the resonance region, where the two “levels” approach each other closest the system “jumps” from the upper “level” to the lower “level” and after that continues to be in the state $|\nu_1^m(t)\rangle$ until the neutrino reaches the surface of the Sun. Evidently, now we have $P' \equiv P'(\nu_2^m(t_0) \rightarrow \nu_1^m(t_s)) \sim 1$. In this case the neutrino system ends up in the state $|\nu_1^m(t_s)\rangle \equiv |\nu_1\rangle$ at the surface of the Sun and

$$\begin{aligned} P(\nu_e \rightarrow \nu_e; t_s, t_0) &\cong |\langle \nu_e | \nu_1 \rangle|^2 = \cos^2 \theta \\ P(\nu_e \rightarrow \nu_\mu; t_s, t_0) &\cong |\langle \nu_\mu | \nu_1 \rangle|^2 = \sin^2 \theta. \end{aligned} \quad (13.54)$$

Obviously, if $\sin^2 \theta \ll 1$, practically no transitions of the solar ν_e into ν_μ will occur. The considered regime of evolution of the neutrino system and the corresponding $\nu_e \rightarrow \nu_\mu$ transitions are usually referred to as “extremely nonadiabatic.”

Clearly, the value of the “jump” probability P' plays a crucial role in the the $\nu_e \rightarrow \nu_\mu$ transitions: it fixes the type of the transition and determines to a large extent the $\nu_e \rightarrow \nu_\mu$ transition probability [59,73,74]. We have considered above two limiting cases. Obviously, there exists a whole spectrum of possibilities since P' can have any value from 0 to $\cos^2 \theta$ [75,76]. In general, the transitions are called “nonadiabatic” if P' is non-negligible.

Numerical studies have shown [26] that solar neutrinos can undergo both adiabatic and nonadiabatic $\nu_e \rightarrow \nu_\mu$ transitions in the Sun and the matter effects can be substantial in the solar neutrino oscillations for $10^{-8} \text{ eV}^2 \lesssim \Delta m^2 \lesssim 10^{-4} \text{ eV}^2$, $10^{-4} \lesssim \sin^2 2\theta < 1.0$.

The condition of adiabaticity of the solar ν_e transitions in Sun can be written as [59,73]

$$\begin{aligned} \gamma(t) \equiv \sqrt{2} G_F \frac{(N_e^{res})^2}{|N_e(t)|} \tan^2 2\theta \left(1 + \tan^{-2} 2\theta_m(t) \right)^{\frac{3}{2}} &\gg 1 \\ \text{adiabatic transitions,} & \end{aligned} \quad (13.55)$$

while if $\gamma(t) \lesssim 1$ the transitions are nonadiabatic (see also Ref. 76), where $N_e(t) \equiv \frac{d}{dt} N_e(t)$. Condition in Eq. (13.55) implies that the $\nu_e \rightarrow \nu_\mu(\tau)$ transitions in the Sun will be adiabatic if $N_e(t)$ changes sufficiently slowly along the neutrino path. In order for the transitions to be adiabatic, condition in Eq. (13.55) has to be fulfilled at any point of the neutrino’s path in the Sun.

Actually, the system of evolution equations Eq. (13.32) can be solved exactly for N_e changing exponentially, Eq. (13.50), along the neutrino path in the Sun [75,77]. More specifically, the system in Eq. (13.32) is equivalent to one second order differential equation (with appropriate initial conditions). The latter can be shown [78] to coincide in form, in the case of N_e given by Eq. (13.50), with the Schroedinger equation for the radial part of the nonrelativistic wave function of the Hydrogen atom [79]. On the basis of the exact solution, which is expressed in terms of confluent hypergeometric functions, it was possible to derive a complete, simple and very accurate analytic description of the matter-enhanced transitions of solar neutrinos in the Sun for any values of Δm^2 and θ [25,75,76,80,81] (see also [26,59,74,82,83]).

The probability that a ν_e , produced at time t_0 in the central part of the Sun, will not transform into $\nu_\mu(\tau)$ on its way to the surface of the Sun (reached at time t_s) is given by

$$P_\odot^{2\nu}(\nu_e \rightarrow \nu_e; t_s, t_0) = \bar{P}_\odot^{2\nu}(\nu_e \rightarrow \nu_e; t_s, t_0) + \text{Oscillating terms.} \quad (13.56)$$

Here

$$\bar{P}_\odot^{2\nu}(\nu_e \rightarrow \nu_e; t_s, t_0) \equiv \bar{P}_\odot = \frac{1}{2} + \left(\frac{1}{2} - P' \right) \cos 2\theta_m(t_0) \cos 2\theta, \quad (13.57)$$

is the average survival probability for ν_e having energy $E \cong p$ [74], where

$$P' = \frac{\exp \left[-2\pi r_0 \frac{\Delta m^2}{2E} \sin^2 \theta \right] - \exp \left[-2\pi r_0 \frac{\Delta m^2}{2E} \right]}{1 - \exp \left[-2\pi r_0 \frac{\Delta m^2}{2E} \right]}, \quad (13.58)$$

is [75] the “jump” probability for exponentially varying N_e , and $\theta_m(t_0)$ is the mixing angle in matter at the point of ν_e production [82]. The expression for $\bar{P}_{\odot}^{2\nu}(\nu_e \rightarrow \nu_e; t_s, t_0)$ with P' given by Eq. (13.58) is valid for $\Delta m^2 > 0$, but for both signs of $\cos 2\theta \neq 0$ [75,83]; it is valid for any given value of the distance along the neutrino trajectory and does not take into account the finite dimensions of the region of ν_e production in the Sun. This can be done by integrating over the different neutrino paths, *i.e.*, over the region of ν_e production.

The oscillating terms in the probability $P_{\odot}^{2\nu}(\nu_e \rightarrow \nu_e; t_s, t_0)$ [80,78] were shown [81] to be strongly suppressed for $\Delta m^2 \gtrsim 10^{-7}$ eV² by the various averagings one has to perform when analyzing the solar neutrino data. The current solar neutrino and KamLAND data suggest that $\Delta m^2 \cong 7.6 \times 10^{-5}$ eV². For $\Delta m^2 \gtrsim 10^{-7}$ eV², the averaging over the region of neutrino production in the Sun *etc.* renders negligible all interference terms which appear in the probability of ν_e survival due to the $\nu_e \leftrightarrow \nu_{\mu(\tau)}$ oscillations in vacuum taking place on the way of the neutrinos from the surface of the Sun to the surface of the Earth. Thus, the probability that ν_e will remain ν_e while it travels from the central part of the Sun to the surface of the Earth is effectively equal to the probability of survival of the ν_e while it propagates from the central part to the surface of the Sun and is given by the average probability $\bar{P}_{\odot}(\nu_e \rightarrow \nu_e; t_s, t_0)$ (determined by Eq. (13.57) and Eq. (13.58)).

If the solar ν_e transitions are adiabatic ($P' \cong 0$) and $\cos 2\theta_m(t_0) \cong -1$ (*i.e.*, $N_e(t_0)/|N_e^{res}| \gg 1, |\tan 2\theta|$, the ν_e are born “above” (in N_e) the resonance region), one has [26]

$$\bar{P}^{2\nu}(\nu_e \rightarrow \nu_e; t_s, t_0) \cong \frac{1}{2} - \frac{1}{2} \cos 2\theta. \quad (13.59)$$

The regime under discussion is realised for $\sin^2 2\theta \cong 0.8$ (suggested by the data, Section 13.4), if $E/\Delta m^2$ lies approximately in the range ($2 \times 10^4 - 3 \times 10^7$) MeV/eV² (see Ref. 76). This result is relevant for the interpretation of the Super-Kamiokande and SNO solar neutrino data. We see that depending on the sign of $\cos 2\theta \neq 0$, $\bar{P}^{2\nu}(\nu_e \rightarrow \nu_e)$ is either bigger or smaller than 1/2. It follows from the solar neutrino data that in the range of validity (in $E/\Delta m^2$) of Eq. (13.59) we have $\bar{P}^{2\nu}(\nu_e \rightarrow \nu_e) \cong 0.3$. Thus, the possibility of $\cos 2\theta \leq 0$ is ruled out by the data. Given the choice $\Delta m^2 > 0$ we made, the data imply that $\Delta m^2 \cos 2\theta > 0$.

If $E/\Delta m^2$ is sufficiently small so that $N_e(t_0)/|N_e^{res}| \ll 1$, we have $P' \cong 0$, $\theta_m(t_0) \cong \theta$ and the oscillations take place in the Sun as in vacuum [26]:

$$\bar{P}^{2\nu}(\nu_e \rightarrow \nu_e; t_s, t_0) \cong 1 - \frac{1}{2} \sin^2 2\theta, \quad (13.60)$$

which is the average two-neutrino vacuum oscillation probability. This expression describes with good precision the transitions of the solar pp neutrinos (Section 13.4). The extremely nonadiabatic ν_e transitions in the Sun, characterised by $\gamma(t) \ll 1$, are also described by the average vacuum oscillation probability (Eq. (13.60)) (for $\Delta m^2 \cos 2\theta > 0$ in this case we have (see *e.g.*, [75,76]) $\cos 2\theta_m(t_0) \cong -1$ and $P' \cong \cos^2 \theta$).

The probability of ν_e survival in the case 3-neutrino mixing takes a simple form for $|\Delta m_{31}^2| \cong 2.4 \times 10^{-3}$ eV² $\gg |\Delta m_{21}^2|$. Indeed, for the energies of solar neutrinos $E \lesssim 10$ MeV, N_e^{res} corresponding to $|\Delta m_{31}^2|$ satisfies $N_e^{res} \gtrsim 10^3$ cm⁻³ N_A and is by a factor of 10 bigger than N_e in the center of the Sun. As a consequence, the oscillations due to Δm_{31}^2 proceed as in vacuum. The oscillation length associated with $|\Delta m_{31}^2|$ satisfies $L_{31}^v \lesssim 10$ km $\ll \Delta R$, ΔR being the dimension of the region of ν_e production in the Sun. We have for the different components of the solar ν_e flux [71] $\Delta R \cong (0.04 - 0.20) R_{\odot}$. Therefore the averaging over ΔR strongly suppresses the oscillations due to Δm_{31}^2 and we get [61,84]:

$$P_{\odot}^{3\nu} \cong \sin^4 \theta_{13} + \cos^4 \theta_{13} P_{\odot}^{2\nu}(\Delta m_{21}^2, \theta_{12}; N_e \cos^2 \theta_{13}), \quad (13.61)$$

where $P_{\odot}^{2\nu}(\Delta m_{21}^2, \theta_{12}; N_e \cos^2 \theta_{13})$ is given by Eq. (13.56) to Eq. (13.58) in which $\Delta m^2 = \Delta m_{21}^2$, $\theta = \theta_{12}$ and the solar e^- number density N_e is replaced by $N_e \cos^2 \theta_{13}$. Thus, the solar ν_e

transitions observed by the Super-Kamiokande and SNO experiments are described approximately by:

$$P_{\odot}^{3\nu} \cong \sin^4 \theta_{13} + \cos^4 \theta_{13} \sin^2 \theta_{12}. \quad (13.62)$$

The data show that $P_{\odot}^{3\nu} \cong 0.3$, which is a strong evidence for matter effects in the solar ν_e transitions [85] since in the case of oscillations in vacuum $P_{\odot}^{3\nu} \cong \sin^4 \theta_{13} + (1 - 0.5 \sin^2 2\theta_{12}) \cos^4 \theta_{13} \gtrsim 0.48$, where we used $\sin^2 \theta_{13} < 0.056$ and $\sin^2 2\theta_{12} \lesssim 0.93$.

13.4. Measurements of Δm_{\odot}^2 and θ_{\odot}

13.4.1. Solar neutrino observations :

Observation of solar neutrinos directly addresses the theory of stellar structure and evolution, which is the basis of the standard solar model (SSM). The Sun as a well-defined neutrino source also provides extremely important opportunities to investigate nontrivial neutrino properties such as nonzero mass and mixing, because of the wide range of matter density and the great distance from the Sun to the Earth.

The solar neutrinos are produced by some of the fusion reactions in the pp chain or CNO cycle. The combined effect of these reactions is written as

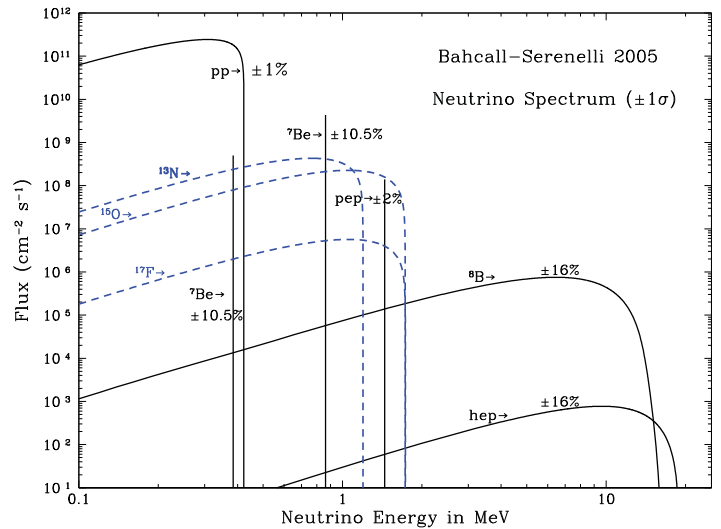
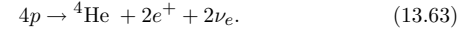
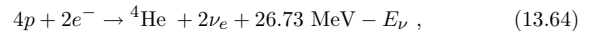


Figure 13.2: The solar neutrino spectrum predicted by the BS05(OP) standard solar model [86]. The neutrino fluxes are given in units of cm⁻²s⁻¹MeV⁻¹ for continuous spectra and cm⁻²s⁻¹ for line spectra. The numbers associated with the neutrino sources show theoretical errors of the fluxes. This figure is taken from the late John Bahcall’s web site, <http://www.sns.ias.edu/~jnb/>.

Positrons annihilate with electrons. Therefore, when considering the solar thermal energy generation, a relevant expression is



where E_{ν} represents the energy taken away by neutrinos, with an average value being $\langle E_{\nu} \rangle \sim 0.6$ MeV. There have been efforts to calculate solar neutrino fluxes from these reactions on the basis of SSM. A variety of input information is needed in the evolutionary calculations. The most elaborate SSM calculations have been developed by Bahcall and his collaborators, who define their SSM as the solar model which is constructed with the best available physics and input data. Therefore, their SSM calculations have been rather frequently updated. SSM’s labelled as BS05(OP) [86], BSB06(GS) and BSB06(AGS) [72], and BPS08(GS) and BPS08(AGS) [87] represent recent model calculations. (Bahcall passed away in 2005, but his program to improve SSM is still pursued by his collaborators.)

Here, “OP” means that newly calculated radiative opacities from the “Opacity Project” are used. The later models are also calculated with OP opacities. “GS” and “AGS” refer to old and new determinations of solar abundances of heavy elements. There are significant differences between the old, higher heavy element abundances (GS) and the new, lower heavy element abundances (AGS). The BS05(OP) model was calculated with GS, but it adopted conservative theoretical uncertainties in the solar neutrino fluxes to account for the differences between GS and AGS. The models with GS are consistent with helioseismological data, but the models with AGS are not. The BPS08(GS) model may be considered to be the currently preferred SSM. Its prediction for the fluxes from neutrino-producing reactions is given in Table 13.2. Fig. 13.2 shows the solar-neutrino spectra calculated with the BS05(OP) model which is similar to the BPS08(GS) model.

Table 13.2: Neutrino-producing reactions in the Sun (first column) and their abbreviations (second column). The neutrino fluxes predicted by the BPS08(GS) model [87] are listed in the third column.

Reaction	Abbr.	Flux ($\text{cm}^{-2} \text{s}^{-1}$)
$pp \rightarrow de^+ \nu$	pp	$5.97(1 \pm 0.006) \times 10^{10}$
$pe^- p \rightarrow d \nu$	pep	$1.41(1 \pm 0.011) \times 10^8$
${}^3\text{He } p \rightarrow {}^4\text{He } e^+ \nu$	hep	$7.90(1 \pm 0.15) \times 10^3$
${}^7\text{Be } e^- \rightarrow {}^7\text{Li } \nu + (\gamma)$	${}^7\text{Be}$	$5.07(1 \pm 0.06) \times 10^9$
${}^8\text{B} \rightarrow {}^8\text{Be}^* e^+ \nu$	${}^8\text{B}$	$5.94(1 \pm 0.11) \times 10^6$
${}^{13}\text{N} \rightarrow {}^{13}\text{C } e^+ \nu$	${}^{13}\text{N}$	$2.88(1 \pm 0.15) \times 10^8$
${}^{15}\text{O} \rightarrow {}^{15}\text{N } e^+ \nu$	${}^{15}\text{O}$	$2.15(1_{-0.16}^{+0.17}) \times 10^8$
${}^{17}\text{F} \rightarrow {}^{17}\text{O } e^+ \nu$	${}^{17}\text{F}$	$5.82(1_{-0.17}^{+0.19}) \times 10^6$

So far, solar neutrinos have been observed by chlorine (Homestake) and gallium (SAGE, GALLEX, and GNO) radiochemical detectors and water Cherenkov detectors using light water (Kamiokande and Super-Kamiokande) and heavy water (SNO). Recently, a liquid scintillation detector (Borexino) successfully observed low energy solar neutrinos.

A pioneering solar neutrino experiment by Davis and collaborators at Homestake using the ${}^{37}\text{Cl} - {}^{37}\text{Ar}$ method proposed by Pontecorvo [88] started in the late 1960’s. This experiment exploited ν_e absorption on ${}^{37}\text{Cl}$ nuclei followed by the produced ${}^{37}\text{Ar}$ decay through orbital e^- capture,



The ${}^{37}\text{Ar}$ atoms produced are radioactive, with a half life ($\tau_{1/2}$) of 34.8 days. After an exposure of the detector for two to three times $\tau_{1/2}$, the reaction products were chemically extracted and introduced into a low-background proportional counter, where they were counted for a sufficiently long period to determine the exponentially decaying signal and a constant background. Solar-model calculations predict that the dominant contribution in the chlorine experiment came from ${}^8\text{B}$ neutrinos, but ${}^7\text{Be}$, pep , ${}^{13}\text{N}$, and ${}^{15}\text{O}$ neutrinos also contributed (for notations, refer to Table 13.2).

From the very beginning of the solar-neutrino observation [89], it was recognized that the observed flux was significantly smaller than the SSM prediction, provided nothing happens to the electron neutrinos after they are created in the solar interior. This deficit has been called “the solar-neutrino problem.”

Gallium experiments (GALLEX and GNO at Gran Sasso in Italy and SAGE at Baksan in Russia) utilize the reaction



They are sensitive to the most abundant pp solar neutrinos. However, the solar-model calculations predict almost half of the capture rate

in gallium is due to other solar neutrinos. GALLEX presented the first evidence of pp solar-neutrino observation in 1992 [7]. The GALLEX Collaboration finished observations in early 1997 [8]. Since April, 1998, a newly defined collaboration, GNO (Gallium Neutrino Observatory) continued the observations until April 2003. The GNO results are published in Ref. 9. The GNO + GALLEX joint analysis results are also presented in Ref. 9. SAGE initially reported very low flux [90], but later observed similar flux to that of GALLEX. The latest SAGE results are published in Ref. 6. The SAGE experiment continues to collect data.

In 1987, the Kamiokande experiment in Japan succeeded in real-time solar neutrino observation, utilizing νe scattering,

$$\nu_x + e^- \rightarrow \nu_x + e^-, \quad (13.67)$$

in a large water-Cherenkov detector. This experiment takes advantage of the directional correlation between the incoming neutrino and the recoil electron. This feature greatly helps the clear separation of the solar-neutrino signal from the background. The Kamiokande result gave the first direct evidence that neutrinos come from the direction of the Sun [91]. Later, the high-statistics Super-Kamiokande experiment [92,93] with a 50-kton water Cherenkov detector replaced the Kamiokande experiment. Due to the high thresholds (7 MeV in Kamiokande and 5 MeV at present in Super-Kamiokande) the experiments observe pure ${}^8\text{B}$ solar neutrinos. It should be noted that the reaction (Eq. (13.67)) is sensitive to all active neutrinos, $x = e, \mu$, and τ . However, the sensitivity to ν_μ and ν_τ is much smaller than the sensitivity to ν_e , $\sigma(\nu_{\mu,\tau}e) \approx 0.16 \sigma(\nu_e e)$.

In 1999, a new real time solar-neutrino experiment, SNO (Sudbury Neutrino Observatory), in Canada started observation. This experiment used 1000 tons of ultra-pure heavy water (D_2O) contained in a spherical acrylic vessel, surrounded by an ultra-pure H_2O shield. SNO measured ${}^8\text{B}$ solar neutrinos via the charged-current (CC) and neutral-current (NC) reactions

$$\nu_e + d \rightarrow e^- + p + p \quad (\text{CC}), \quad (13.68)$$

and

$$\nu_x + d \rightarrow \nu_x + p + n \quad (\text{NC}), \quad (13.69)$$

as well as νe scattering, (Eq. (13.67)). The CC reaction, (Eq. (13.68)), is sensitive only to ν_e , while the NC reaction, (Eq. (13.69)), is sensitive to all active neutrinos. This is a key feature to solve the solar neutrino problem. If it is caused by flavour transitions such as neutrino oscillations, the solar neutrino fluxes measured by CC and NC reactions would show a significant difference.

The Q -value of the CC reaction is -1.4 MeV and the e^- energy is strongly correlated with the ν_e energy. Thus, the CC reaction provides an accurate measure of the shape of the ${}^8\text{B}$ neutrino spectrum. The contributions from the CC reaction and νe scattering can be distinguished by using different $\cos \theta$ distributions, where θ is the angle of the e^- momentum with respect to the Sun-Earth axis. While the νe scattering events have a strong forward peak, CC events have an approximate angular distribution of $1 - 1/3 \cos \theta$.

The neutrino energy threshold of the NC reaction is 2.2 MeV. In the pure D_2O [11,12], the signal of the NC reaction was neutron capture in deuterium, producing a 6.25-MeV γ -ray. In this case, the capture efficiency was low and the deposited energy was close to the detection threshold of 5 MeV. In order to enhance both the capture efficiency and the total γ -ray energy (8.6 MeV), 2 tons of NaCl were added to the heavy water in the second phase of the experiment [94]. Subsequently NaCl was removed and an array of ${}^3\text{He}$ neutron counters were installed for the third phase measurement [95]. These neutron counters provided independent NC measurement with different systematics from that of the second phase, and thus strengthened the reliability of the NC measurement.

Another real time solar neutrino experiment, Borexino at Gran Sasso in Italy, started solar neutrino observation in 2007. This experiment measures solar neutrinos via νe scattering in 300 tons of ultra-pure liquid scintillator. With a detection threshold as low as 250 keV, the flux of monochromatic 0.862 MeV ${}^7\text{Be}$ solar

neutrinos has been directly observed for the first time. The observed energy spectrum shows the characteristic Compton-edge over the background [96]. Measurements of low energy solar neutrinos are important not only to test the SSM further, but also to study the MSW effect over the energy region spanning from sub-MeV to 10 MeV.

Table 13.3: Results from radiochemical solar-neutrino experiments. The predictions of a recent standard solar model BPS08(GS) are also shown. The first and the second errors in the experimental results are the statistical and systematic errors, respectively. SNU (Solar Neutrino Unit) is defined as 10^{-36} neutrino captures per atom per second.

	$^{37}\text{Cl} \rightarrow ^{37}\text{Ar}$ (SNU)	$^{71}\text{Ga} \rightarrow ^{71}\text{Ge}$ (SNU)
Homestake [4]	$2.56 \pm 0.16 \pm 0.16$	–
GALLEX [8]	–	$77.5 \pm 6.2^{+4.3}_{-4.7}$
GNO [9]	–	$62.9^{+5.5}_{-5.3} \pm 2.5$
GNO+GALLEX [9]	–	$69.3 \pm 4.1 \pm 3.6$
SAGE [6]	–	$65.4^{+3.1+2.6}_{-3.0-2.8}$
SSM [BPS08(GS)] [87]	$8.46^{+0.87}_{-0.88}$	$127.9^{+8.1}_{-8.2}$

Table 13.3 and Table 13.4 show the results from solar-neutrino experiments compared with the SSM calculations. Table 13.4 includes the results from the SNO group's recent joint analysis of the SNO Phase I and Phase II data with the analysis threshold as low as 3.5 MeV (effective electron kinetic energy) and significantly improved

Table 13.4: Results from real time solar-neutrino experiments. The predictions of a recent standard solar model BPS08(GS) are also shown. The first and the second errors in the experimental results are the statistical and systematic errors, respectively.

	Reaction	^8B ν flux ($10^6 \text{cm}^{-2}\text{s}^{-1}$)	^7Be ν flux ($10^9 \text{cm}^{-2}\text{s}^{-1}$)
Kamiokande [5]	ν_e	$2.80 \pm 0.19 \pm 0.33$	–
Super-Kamiokande [93]	ν_e	$2.35 \pm 0.02 \pm 0.08$	–
SNO Phase I [12]	CC	$1.76^{+0.06}_{-0.05} \pm 0.09$	–
(pure D_2O)	ν_e	$2.39^{+0.24}_{-0.23} \pm 0.12$	–
	NC	$5.09^{+0.44+0.46}_{-0.43-0.43}$	–
SNO Phase II [94]	CC	$1.68 \pm 0.06^{+0.08}_{-0.09}$	–
(NaCl in D_2O)	ν_e	$2.35 \pm 0.22 \pm 0.15$	–
	NC	$4.94 \pm 0.21^{+0.38}_{-0.34}$	–
SNO Phase III [95]	CC	$1.67^{+0.05+0.07}_{-0.04-0.08}$	–
(^3He counters)	ν_e	$1.77^{+0.24+0.09}_{-0.21-0.10}$	–
	NC	$5.54^{+0.33+0.36}_{-0.31-0.34}$	–
SNO Phase I+II [97]	NC	$5.140^{+0.160+0.132}_{-0.158-0.117}$	–
(Joint Analysis)	ϕ_{SB} from fit to all data	$5.046^{+0.159+0.107}_{-0.152-0.123}$	–
Borexino [96]	ν_e	–	3.36 ± 0.34
SSM [BPS08(GS)] [87]	–	$5.94(1 \pm 0.11)$	$5.07(1 \pm 0.06)$

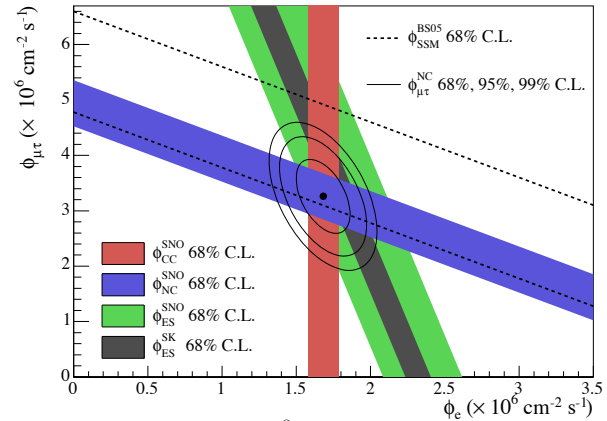


Figure 13.3: Fluxes of ^8B solar neutrinos, $\phi(\nu_e)$, and $\phi(\nu_\mu \text{ or } \tau)$, deduced from the SNO's CC, ES, and NC results of the salt phase measurement [94]. The Super-Kamiokande ES flux is from Ref. 99. The BS05(OP) standard solar model prediction [86] is also shown. The bands represent the 1σ error. The contours show the 68%, 95%, and 99% joint probability for $\phi(\nu_e)$ and $\phi(\nu_\mu \text{ or } \tau)$. The figure is from Ref. 94. Color version at end of book.

systematic uncertainties [97]. It is seen from these tables that the results from all the solar-neutrino experiments, except SNO's NC result, indicate significantly less flux than expected from the solar-model predictions.

13.4.2. Evidence for solar neutrino flavour conversion :

Solar neutrino experiments achieved remarkable progress in the past ten years, and the solar-neutrino problem, which had remained unsolved for more than 30 years, has been understood as due to neutrino flavour conversion. In 2001, the initial SNO CC result combined with the Super-Kamiokande's high-statistics ν_e elastic scattering result [98] provided direct evidence for flavour conversion of solar neutrinos [11]. Later, SNO's NC measurements further strengthened this conclusion [12,94,95]. From the salt-phase measurement [94], the fluxes measured with CC, ES, and NC events were obtained as

$$\phi_{\text{SNO}}^{\text{CC}} = (1.68 \pm 0.06^{+0.08}_{-0.09}) \times 10^6 \text{cm}^{-2} \text{s}^{-1}, \quad (13.70)$$

$$\phi_{\text{SNO}}^{\text{ES}} = (2.35 \pm 0.22 \pm 0.15) \times 10^6 \text{cm}^{-2} \text{s}^{-1}, \quad (13.71)$$

$$\phi_{\text{SNO}}^{\text{NC}} = (4.94 \pm 0.21^{+0.38}_{-0.34}) \times 10^6 \text{cm}^{-2} \text{s}^{-1}, \quad (13.72)$$

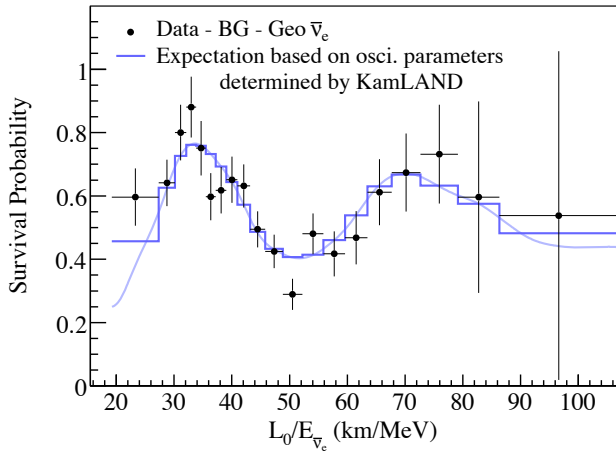


Figure 13.4: The ratio of the background and geoneutrino-subtracted $\bar{\nu}_e$ spectrum to the predicted one without oscillations (survival probability) as a function of L_0/E , where $L_0=180$ km. The curves show the best-fit expectations for $\bar{\nu}_e$ oscillations. The figure is from Ref. [101].

where the first errors are statistical and the second errors are systematic. In the case of $\nu_e \rightarrow \nu_{\mu,\tau}$ transitions, Eq. (13.72) is a mixing-independent result and therefore tests solar models. It shows good agreement with the ^8B solar-neutrino flux predicted by the solar model [86]. Fig. 13.3 shows the salt phase result of $\phi(\nu_\mu$ or $\tau)$ versus the flux of electron neutrinos $\phi(\nu_e)$ with the 68%, 95%, and 99% joint probability contours. The flux of non- ν_e active neutrinos, $\phi(\nu_\mu$ or $\tau)$, can be deduced from these results. It is

$$\phi(\nu_\mu \text{ or } \tau) = (3.26 \pm 0.25^{+0.40}_{-0.35}) \times 10^6 \text{cm}^{-2} \text{s}^{-1}. \quad (13.73)$$

The non-zero $\phi(\nu_\mu$ or $\tau)$ is strong evidence for neutrino flavor conversion. These results are consistent with those expected from the LMA (large mixing angle) solution of solar neutrino oscillation in matter [25,26] with $\Delta m_\odot^2 \sim 5 \times 10^{-5} \text{eV}^2$ and $\tan^2 \theta_\odot \sim 0.45$. However, with the SNO data alone, the possibility of other solutions cannot be excluded with sufficient statistical significance.

13.4.3. KamLAND experiment : KamLAND is a 1-kton ultra-pure liquid scintillator detector located at the old Kamiokande's site in Japan. The primary goal of the KamLAND experiment was a long-baseline (flux-weighted average distance of ~ 180 km) neutrino oscillation studies using $\bar{\nu}_e$'s emitted from nuclear power reactors. The reaction $\bar{\nu}_e + p \rightarrow e^+ + n$ is used to detect reactor $\bar{\nu}_e$'s and a delayed coincidence of the positron with a 2.2 MeV γ -ray from neutron capture on a proton is used to reduce the backgrounds. With the reactor $\bar{\nu}_e$'s energy spectrum (< 8 MeV) and a prompt-energy analysis threshold of 2.6 MeV, this experiment has a sensitive Δm^2

range down to $\sim 10^{-5} \text{eV}^2$. Therefore, if the LMA solution is the real solution of the solar neutrino problem, KamLAND should observe reactor $\bar{\nu}_e$ disappearance, assuming CPT invariance.

The first KamLAND results [15] with 162 ton-yr exposure were reported in December 2002. The ratio of observed to expected (assuming no $\bar{\nu}_e$ oscillations) number of events was

$$\frac{N_{\text{obs}} - N_{\text{BG}}}{N_{\text{NoOsc}}} = 0.611 \pm 0.085 \pm 0.041 \quad (13.74)$$

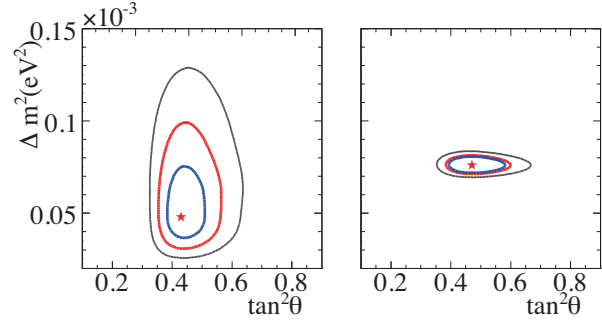


Figure 13.5: 68%, 95%, and 99.73% confidence level allowed parameter regions as well as the best-fit points are shown for (left) global solar neutrino data analysis and (right) global solar neutrino + KamLAND data analysis. This figure is taken from Ref. 95.

with obvious notation. This result showed clear evidence of an event deficit expected from neutrino oscillations. The 95% CL allowed regions are obtained from the oscillation analysis with the observed event rates and positron spectrum shape. A combined global solar + KamLAND analysis showed that the LMA is a unique solution to the solar neutrino problem with $> 5\sigma$ CL [100]. With increased statistics [16,101], KamLAND observed not only the distortion of the $\bar{\nu}_e$ spectrum, but also the periodic feature of the $\bar{\nu}_e$ survival probability expected from neutrino oscillations for the first time (see Fig. 13.4). A two-neutrino oscillation analysis gave $\Delta m_\odot^2 = 7.58^{+0.14+0.15}_{-0.13-0.15} \times 10^{-5} \text{eV}^2$ and $\tan^2 \theta_\odot = 0.56^{+0.10+0.10}_{-0.07-0.06}$.

13.4.4. Global neutrino oscillation analysis :

The SNO Collaboration updated [95] a two-neutrino oscillation analysis including all the solar neutrino data (SNO, Super-Kamiokande, chlorine, gallium, and Borexino) and the KamLAND data [101]. The best fit parameters obtained from this global solar + KamLAND analysis are $\Delta m_\odot^2 = 7.59^{+0.19}_{-0.21} \times 10^{-5} \text{eV}^2$ and $\theta_\odot = 34.4^{+1.3}_{-1.2}$ degrees ($\tan^2 \theta_\odot = 0.468^{+0.048}_{-0.040}$). The global solar analysis, however, gives the best fit parameters of $\Delta m_\odot^2 = 4.90 \times 10^{-5} \text{eV}^2$ and $\tan^2 \theta_\odot = 0.437$. The allowed parameter regions obtained from these two analyses are shown in Fig. 13.5. The best-fit values of Δm_\odot^2 from the two analyses show a rather large difference. However, according to the recent SNO's two-neutrino oscillation analyses using its Phase I and Phase II joint analysis [97] results, this difference has become smaller. Namely, the best fit parameters obtained from the new global solar + KamLAND analysis are $\Delta m_\odot^2 = 7.59^{+0.20}_{-0.21} \times 10^{-5} \text{eV}^2$ and $\theta_\odot = 34.06^{+1.16}_{-0.84}$ degrees ($\tan^2 \theta_\odot = 0.457^{+0.040}_{-0.029}$), and those from the global solar analysis are $\Delta m_\odot^2 = 5.89^{+2.13}_{-2.16} \times 10^{-5} \text{eV}^2$ and $\tan^2 \theta_\odot = 0.457^{+0.038}_{-0.041}$ [97].

13.5. Measurements of $|\Delta m_A^2|$ and θ_A

13.5.1. Atmospheric neutrino results :

The first compelling evidence for the neutrino oscillation was presented by the Super-Kamiokande Collaboration in 1998 [13] from the observation of atmospheric neutrinos produced by cosmic-ray interactions in the atmosphere. The zenith-angle distributions of the μ -like events which are mostly muon-neutrino and muon antineutrino initiated charged-current interactions, showed a clear deficit compared to the no-oscillation expectation. Note that a water

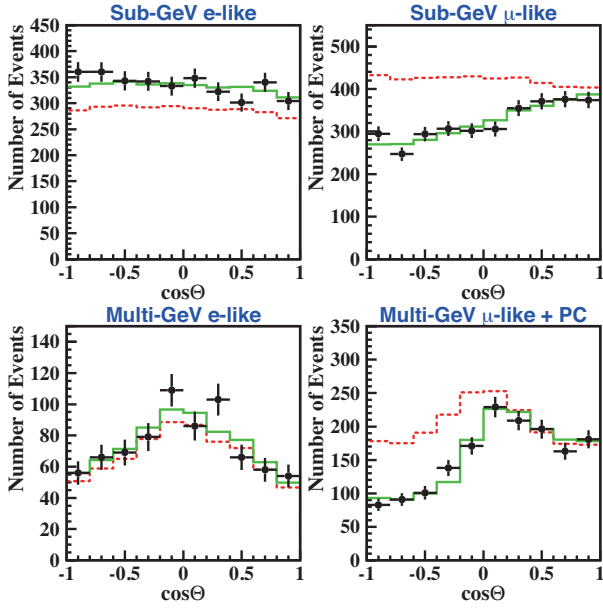


Figure 13.6: The zenith angle distributions for fully contained 1-ring e -like and μ -like events with visible energy < 1.33 GeV (sub-GeV) and > 1.33 GeV (multi-GeV). For multi-GeV μ -like events, a combined distribution with partially contained (PC) events is shown. The dotted histograms show the non-oscillated Monte Carlo events, and the solid histograms show the best-fit expectations for $\nu_\mu \leftrightarrow \nu_\tau$ oscillations. (This figure is provided by the Super-Kamiokande Collab.) Color version at end of book.

Cherenkov detector cannot measure the charge of the final-state leptons, and therefore neutrino and antineutrino induced events cannot be discriminated. Neutrino events having their vertex in the 22.5 kton fiducial volume in Super-Kamiokande are classified into fully contained (FC) events and partially contained (PC) events. The FC events are required to have no activity in the anti-counter. The total visible energy (proportional to the total number of photoelectrons measured by the photomultiplier tubes in the inner detector) can be measured for the FC events.

FC events are subjected to particle identification of the final-state particles. Single-ring events have only one charged lepton which radiates Cherenkov light in the final state, and particle identification is particularly clean for single-ring FC events. The method adopted for the FC events identifies the particle types as e -like or μ -like based on the pattern of each Cherenkov ring. A ring produced by an e -like (e^\pm, γ) particle exhibits a more diffuse pattern than that produced by a μ -like (μ^\pm, π^\pm) particle, since an e -like particle produces an electromagnetic shower and low-energy electrons suffer considerable multiple Coulomb scattering in water. All the PC events were assumed to be μ -like since the PC events comprise a 98% pure charged-current ν_μ sample.

Fig. 13.6 shows the zenith-angle distributions of e -like and μ -like events from the SK-I measurement [102]. $\cos\theta = 1$ corresponds to the downward direction, while $\cos\theta = -1$ corresponds to the upward direction. Events included in these plots are single-ring FC events subdivided into sub-GeV (visible energy < 1.33 GeV) events and multi-GeV (visible energy > 1.33 GeV) events. Note that the zenith-angle distribution of the multi-GeV μ -like events is shown combined with that of the PC events. The final-state leptons in these events have good directional correlation with the parent neutrinos. The dotted histograms show the Monte Carlo expectation for neutrino events. If the produced flux of atmospheric neutrinos of a given flavour remains unchanged at the detector, the data should have similar distributions to the expectation. However, the zenith-angle distribution of the μ -like events shows a strong deviation from the expectation. On the other hand, the zenith-angle distribution of the e -like events is consistent with the expectation. This characteristic feature may be interpreted that muon neutrinos coming from the

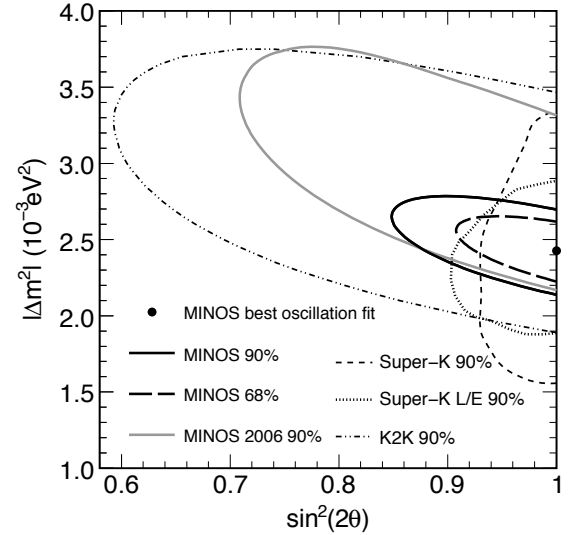


Figure 13.7: Allowed region for the $\nu_\mu \leftrightarrow \nu_\tau$ oscillation parameters from the MINOS results published in 2008. The 68 % and 90 % CL allowed regions are shown together with the SK-I and K2K 90 % CL allowed regions. This figure is taken from Ref. 22.

opposite side of the Earth's atmosphere, having travelled $\sim 10,000$ km, oscillate into other neutrinos and disappeared, while oscillations still do not take place for muon neutrinos coming from above the detector, having travelled a few km. Disappeared muon neutrinos may have oscillated into tau neutrinos because there is no indication of electron neutrino appearance. The atmospheric neutrinos corresponding to the events shown in Fig. 13.6 have $E = 1 \sim 10$ GeV. With $L = 10000$ km, the hypothesis of neutrino oscillations suggests $\Delta m^2 \sim 10^{-3} - 10^{-4}$ eV^2 . The solid histograms show the best-fit results of a two-neutrino oscillation analysis with the hypothesis of $\nu_\mu \leftrightarrow \nu_\tau$. (To constrain the flux of atmospheric neutrinos through the accurately predicted ν_μ/ν_e ratio, e -like events are included in the fit.) They reproduce the observed data well. The oscillation parameters determined by the SK-I atmospheric neutrino data are $\sin^2 2\theta_A > 0.92$ and $1.5 \times 10^{-3} < |\Delta m_A^2| < 3.4 \times 10^{-3}$ eV^2 at 90% confidence level. For the allowed parameter region, see Fig. 13.7.

Though the SK-I atmospheric neutrino observations gave compelling evidence for muon neutrino disappearance which is consistent with two-neutrino oscillation $\nu_\mu \leftrightarrow \nu_\tau$ [103], the question may be asked whether the observed muon neutrino disappearance is really due to neutrino oscillations. First, other exotic explanations such as neutrino decay [104] and quantum decoherence [105] cannot be completely ruled out from the zenith-angle distributions alone. To provide firm evidence for neutrino oscillation, we need to confirm the characteristic sinusoidal behavior of the conversion probability as a function of neutrino energy E for a fixed distance L in the case of long-baseline neutrino oscillation experiments, or as a function of L/E in the case of atmospheric neutrino experiments. By selecting events with high L/E resolution, evidence for the dip in the L/E distribution was observed at the right place expected from the interpretation of the SK-I data in terms of $\nu_\mu \leftrightarrow \nu_\tau$ oscillations [14], Fig. 13.8. This dip cannot be explained by alternative hypotheses of neutrino decay and neutrino decoherence, and they are excluded at more than 3σ in comparison with the neutrino oscillation interpretation. At 90% CL, the constraints obtained from the L/E analysis are $1.9 \times 10^{-3} < |\Delta m_A^2| < 3.0 \times 10^{-3}$ eV^2 and $\sin^2 2\theta_A > 0.90$. (see Fig. 13.7).

Second, a natural question is whether appearance of tau neutrinos has been observed in the Super-Kamiokande detector. Detection of ν_τ CC reactions in a water Cherenkov detector is not easy. In addition to the low flux of atmospheric neutrinos above the threshold of these reactions, 3.5 GeV, the interactions are mostly deep inelastic scattering, leading to complicated multiring event pattern. Nevertheless, search for a ν_τ appearance signal by using criteria to enhance ν_τ CC events

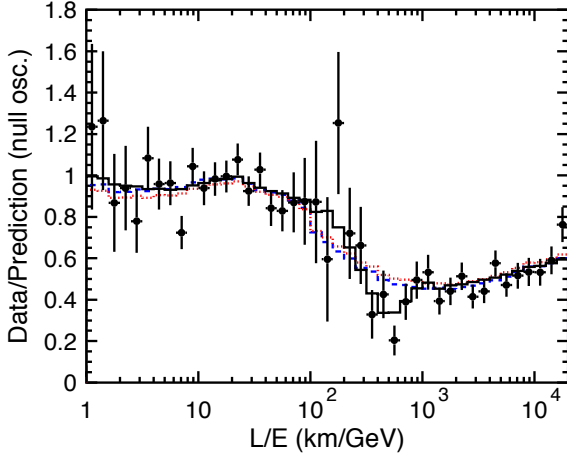


Figure 13.8: Results of the L/E analysis of SK-I atmospheric neutrino data. The points show the ratio of the data to the Monte Carlo prediction without oscillations, as a function of the reconstructed L/E. The error bars are statistical only. The solid line shows the best fit with 2-flavour $\nu_\mu \leftrightarrow \nu_\tau$ oscillations. The dashed and dotted lines show the best fit expectations for neutrino decay and neutrino decoherence hypotheses, respectively. (From Ref. 14.)

(high visible energy, high average multiplicity, etc.) found candidate events in the upward-going direction as expected [103]. However, the significance of the signal is yet marginal; no ν_τ appearance hypothesis is disfavored at only 2.4σ .

13.5.2. Results from accelerator experiments :

The $\Delta m^2 \geq 2 \times 10^{-3} \text{ eV}^2$ region can be explored by accelerator-based long-baseline experiments with typically $E \sim 1 \text{ GeV}$ and $L \sim$ several hundred km. With a fixed baseline distance and a narrower, well understood neutrino spectrum, the value of $|\Delta m_A^2|$ and, with higher statistics, also the mixing angle, are potentially better constrained in accelerator experiments than from atmospheric neutrino observations.

The K2K (KEK-to-Kamioka) long-baseline neutrino oscillation experiment [20] is the first accelerator-based experiment with a neutrino path length extending hundreds of kilometers. K2K aimed at confirmation of the neutrino oscillation in ν_μ disappearance in the $|\Delta m_A^2| \geq 2 \times 10^{-3} \text{ eV}^2$ region. A horn-focused wide-band muon neutrino beam having an average $L/E_\nu \sim 200$ ($L = 250 \text{ km}$, $\langle E_\nu \rangle \sim 1.3 \text{ GeV}$), was produced by 12-GeV protons from the KEK-PS and directed to the Super-Kamiokande detector. The spectrum and profile of the neutrino beam were measured by a near neutrino detector system located 300 m downstream from the production target.

The construction of the K2K neutrino beam line and the near detector began before Super-Kamiokande's discovery of atmospheric neutrino oscillations, and the stable data-taking started in June 1999. Super-Kamiokande events caused by accelerator-produced neutrinos were selected using the timing information from the global positioning system. Data were intermittently taken until November 2004. The total number of protons on target (POT) for physics analysis amounted to 0.92×10^{20} . The observed number of beam-originated FC events in the 22.5 kton fiducial volume of Super-Kamiokande was 112, compared with an expectation of $158.1_{-8.6}^{+9.2}$ events without oscillation. For 58 1-ring μ -like subset of the data, the neutrino energy was reconstructed from measured muon momentum and angle, assuming CC quasidestic kinematics. The measured energy spectrum showed the distortion expected from neutrino oscillations. From a 2-flavour neutrino oscillation analysis, the allowed parameter region shown in Fig. 13.7 is obtained. At $\sin^2 2\theta_A = 1.0$, $1.9 \times 10^{-3} < |\Delta m_A^2| < 3.5 \times 10^{-3} \text{ eV}^2$ at the 90% CL with the best-fit value of $2.8 \times 10^{-3} \text{ eV}^2$. The probability that the observations are due to a statistical fluctuation instead of neutrino oscillation is 0.0015% or 4.3σ [20].

MINOS is the second long-baseline neutrino oscillation experiment with near and far detectors. Neutrinos are produced by the NuMI

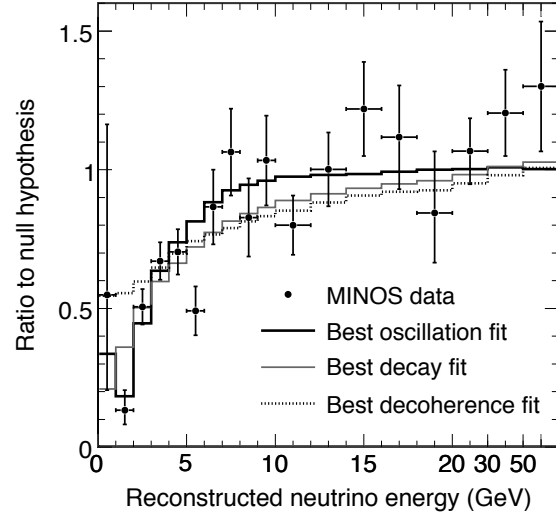


Figure 13.9: Ratio of the MINOS far detector data and the expected spectrum for no oscillations. The best-fit with the hypothesis of $\nu_\mu \rightarrow \nu_\tau$ oscillations as well as the best fit to alternative models (neutrino decay and decoherence) is also shown. This figure is taken from Ref. 22.

(Neutrinos at the Main Injector) facility using 120 GeV protons from the Fermilab Main Injector. The far detector is a 5.4 kton (total mass) iron-scintillator tracking calorimeter with toroidal magnetic field, located underground in the Soudan mine. The baseline distance is 735 km. The near detector is also an iron-scintillator tracking calorimeter with toroidal magnetic field, with a total mass of 0.98 kton. The neutrino beam is a horn-focused wide-band beam. Its energy spectrum can be varied by moving the target position relative to the first horn and changing the horn current.

MINOS started the neutrino-beam run in 2005. Initial results were reported [21] using the data taken between May 2005 and February 2006 with 1.27×10^{20} POT, and the updated results corresponding to a total POT of 3.36×10^{20} (May 2005 to July 2007) were published [22] recently. During this period, a “low-energy” option was mostly chosen for the spectrum of the neutrino beam so that the flux was enhanced in the 1-5 GeV energy range. In the far detector, a total of 848 CC events were produced by the NuMI beam, compared to the unoscillated expectation of 1065 ± 60 (syst) events. Fig. 13.9 shows the ratio of observed energy spectrum and the expected one with no oscillation. Fig. 13.7 shows the 68% and 90% CL allowed regions obtained from the $\nu_\mu \rightarrow \nu_\tau$ oscillation analysis. The results are compared with the 90% CL allowed regions obtained from the initial MINOS [21], SK-I zenith-angle dependence [102], the SK-I L/E analysis [14], and the K2K results [20]. The MINOS results are consistent with the SK-I and K2K results, and constrain the oscillation parameters as $|\Delta m_A^2| = (2.43 \pm 0.13) \times 10^{-3} \text{ eV}^2$ (68% CL) and $\sin^2 2\theta_A > 0.90$ at 90% CL. The alternative models to explain the ν_μ disappearance, neutrino decay and quantum decoherence of neutrinos, are disfavored at the 3.7 and 5.7σ , respectively, by the MINOS data (see Fig. 13.9).

The regions of neutrino parameter space favoured or excluded by various neutrino oscillation experiments are shown in Fig. 13.10.

A promising method to confirm the appearance of ν_τ from $\nu_\mu \rightarrow \nu_\tau$ oscillations is an accelerator long-baseline experiment using emulsion technique to identify short-lived τ leptons event-by-event. The only experiment of this kind is OPERA [106] with a neutrino source at CERN and a detector at Gran Sasso with the baseline distance of 732 km. The detector is a combination of the “Emulsion Cloud Chamber” and magnetized spectrometer. The CNGS (CERN Neutrinos to Gran Sasso) neutrino beam with $\langle E_\nu \rangle = 17 \text{ GeV}$ is produced by high-energy protons from the CERN SPS. With so-called shared SPS operation, 4.5×10^{19} POT/yr is expected. With this beam and 1.35 kt target mass, a ν_τ appearance signal of about 10 events is expected in 5 years run with full intensity.

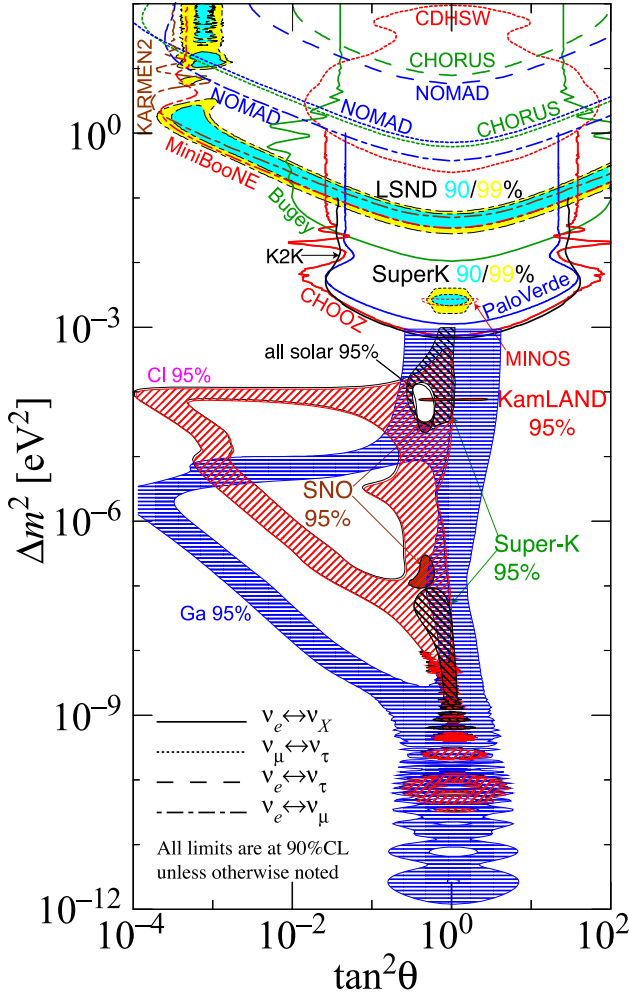


Figure 13.10: The regions of squared-mass splitting and mixing angle favored or excluded by various experiments. The figure was contributed by H. Murayama (University of California, Berkeley, and IPMU, University of Tokyo). References to the data used in the figure can be found at <http://hitoshi.berkeley.edu/neutrino>. Color version at end of book.

13.6. Measurements of θ_{13}

Reactor $\bar{\nu}_e$ disappearance experiments with $L \sim 1$ km, $\langle E \rangle \sim 3$ MeV are sensitive to $\sim E/L \sim 3 \times 10^{-3} \text{ eV}^2 \sim |\Delta m_{\Delta}^2|$. At this baseline distance, the reactor $\bar{\nu}_e$ oscillations driven by Δm_{\odot}^2 are negligible. Therefore, as can be seen from Eq. (13.22) and Eq. (13.24), θ_{13} can be directly measured. A reactor neutrino oscillation experiment at the Chooz nuclear power station in France [107] was the first experiment of this kind. The detector was located in an underground laboratory with 300 mwe (meter water equivalent) rock overburden, at about 1 km from the neutrino source. It consisted of a central 5-ton target filled with 0.09% gadolinium loaded liquid scintillator, surrounded by an intermediate 17-ton and outer 90-ton regions filled with undoped liquid scintillator. Reactor $\bar{\nu}_e$'s were detected via the reaction $\bar{\nu}_e + p \rightarrow e^+ + n$. Gd-doping was chosen to maximize the neutron capture efficiency. The CHOOZ experiment [107] found no evidence for $\bar{\nu}_e$ disappearance. The 90% CL upper limit for $\Delta m^2 = 2.0 \times 10^{-3} \text{ eV}^2$ is $\sin^2 2\theta_{13} < 0.19$ and for the MINOS measurement [22] of $|\Delta m_{\Delta}^2| = 2.43 \times 10^{-3} \text{ eV}^2$, $\sin^2 2\theta_{13} < 0.15$, both at 90% CL.

A similar reactor neutrino oscillation experiment was also conducted at the Palo Verde Nuclear Generating Station in Arizona [108]. This experiment used a segmented Gd-loaded liquid scintillator detector with a total mass of 11.34 tons. The detector was located at a

shallow underground site with only 32 mwe. This experiment found no evidence for $\bar{\nu}_e$ disappearance either [108]. The excluded oscillation parameter region is consistent with, but less restrictive than, the CHOOZ results.

In the accelerator neutrino oscillation experiments with conventional neutrino beams, θ_{13} can be measured using $\nu_{\mu} \rightarrow \nu_e$ appearance. The K2K experiment searched for the $\nu_{\mu} \rightarrow \nu_e$ appearance signal [109], but no evidence was found. Using the dominant term in the probability of $\nu_{\mu} \rightarrow \nu_e$ appearance (see Eq. (13.23) and Eq. (13.24)),

$$P(\nu_{\mu} \rightarrow \nu_e) = \sin^2 2\theta_{13} \cdot \sin^2 2\theta_{23} \cdot \sin^2(1.27\Delta m^2 L/E) \\ \sim \frac{1}{2} \sin^2 2\theta_{13} \sin^2(1.27\Delta m^2 L/E), \quad (13.75)$$

the 90% CL upper limit $\sin^2 2\theta_{13} < 0.26$ was obtained at the K2K measurement of $\Delta m^2 = 2.8 \times 10^{-3} \text{ eV}^2$. Though this limit is less significant than the CHOOZ limit, it is the first result obtained from an accelerator ν_e appearance experiment.

By examining the exact expression for the oscillation probability, however, it is understood that some of the neglected terms could have rather large effects and the unknown CP-violating phase δ causes uncertainties in determining the value of θ_{13} . Actually, from the measurement of $\nu_{\mu} \rightarrow \nu_e$ appearance, θ_{13} is given as a function of δ for a given sign of Δm_{32}^2 . Also, deviations from maximal θ_{23} mixing would cause a further uncertainty. Therefore, a single experiment with a neutrino beam cannot determine the value of θ_{13} though it is possible to establish non-zero θ_{13} .

Turning to atmospheric and solar neutrino observations, Eq. (13.40) to Eq. (13.43) and Eq. (13.62) indicate that they are sensitive to θ_{13} through sub-leading effects. So far the SK group analyzed its atmospheric neutrino data [64] and the SNO group analyzed [97] the data from all solar neutrino experiments, with or without the KamLAND data, in terms of 3-neutrino oscillations.

The SK-I atmospheric neutrino data were analyzed in the three-neutrino oscillation framework with the approximation of one mass scale dominance ($\Delta m_{\odot}^2 = 0$) [64]. Since the matter effects in $\nu_e \leftrightarrow \nu_{\mu,\tau}$ oscillations cause differences for the normal and inverted mass hierarchy cases, both cases were analyzed. For the $\Delta m_{\Delta}^2 > 0$ case, $\sin^2 \theta_{13} < 0.14$ and $0.37 < \sin^2 \theta_{23} < 0.65$ was obtained at 90% CL, while for the $\Delta m_{\Delta}^2 < 0$ case, weaker constraints, $\sin^2 \theta_{13} < 0.27$ and $0.37 < \sin^2 \theta_{23} < 0.69$ were obtained at 90% CL.

The recent SNO's three-neutrino oscillation analysis using its Phase I and Phase II joint analysis [97] results and the results from all other solar neutrino experiments and the KamLAND experiment has yielded the best fit value of $\sin^2 \theta_{13} = 2.00_{-1.63}^{+2.09} \times 10^{-2}$ [97]. At the 95% CL, this result implies $\sin^2 \theta_{13} < 0.057$ [97].

Finally, it should be noted that a global analysis [110] of all available neutrino oscillation data gave a hint of non-zero $\sin^2 \theta_{13}$; $\sin^2 \theta_{13} = 0.016 \pm 0.010$ at 1σ CL.

13.7. The three neutrino mixing

All existing compelling data on neutrino oscillations can be described assuming 3-flavour neutrino mixing in vacuum. This is the minimal neutrino mixing scheme which can account for the currently available data on the oscillations of the solar (ν_e), atmospheric (ν_{μ} and $\bar{\nu}_{\mu}$), reactor ($\bar{\nu}_e$) and accelerator (ν_{μ}) neutrinos. The (left-handed) fields of the flavour neutrinos ν_e , ν_{μ} and ν_{τ} in the expression for the weak charged lepton current in the CC weak interaction Lagrangian, are linear combinations of the LH components of the fields of three massive neutrinos ν_j :

$$\mathcal{L}_{CC} = -\frac{g}{\sqrt{2}} \sum_{l=e,\mu,\tau} \bar{l}_L(x) \gamma_{\alpha} \nu_{lL}(x) W^{\alpha\dagger}(x) + h.c., \\ \nu_{lL}(x) = \sum_{j=1}^3 U_{lj} \nu_{jL}(x), \quad (13.76)$$

where U is the 3×3 unitary neutrino mixing matrix [17,18]. The mixing matrix U can be parameterized by 3 angles, and, depending on

whether the massive neutrinos ν_j are Dirac or Majorana particles, by 1 or 3 CP violation phases [30,31]:

$$U = \begin{bmatrix} c_{12}c_{13} & & s_{12}c_{13} & s_{13}e^{-i\delta} \\ -s_{12}c_{23} - c_{12}s_{23}s_{13}e^{i\delta} & c_{12}c_{23} & -s_{12}s_{23}s_{13}e^{i\delta} & s_{23}c_{13} \\ s_{12}s_{23} - c_{12}c_{23}s_{13}e^{i\delta} & -c_{12}s_{23} & -s_{12}c_{23}s_{13}e^{i\delta} & c_{23}c_{13} \end{bmatrix} \\ \times \text{diag}(1, e^{i\frac{\alpha_{21}}{2}}, e^{i\frac{\alpha_{31}}{2}}). \quad (13.77)$$

where $c_{ij} = \cos \theta_{ij}$, $s_{ij} = \sin \theta_{ij}$, the angles $\theta_{ij} \in [0, \pi/2]$, $\delta \in [0, 2\pi]$ is the Dirac CP violation phase and α_{21}, α_{31} are two Majorana CP violation phases. Thus, in the case of massive Dirac neutrinos, the neutrino mixing matrix U is similar, in what concerns the number of mixing angles and CP violation phases, to the CKM quark mixing matrix. The presence of two additional physical CP violation phases in U if ν_j are Majorana particles is a consequence of the special properties of the latter (see, *e.g.*, [29,30]).

As we see, the fundamental parameters characterizing the 3-neutrino mixing are: i) the 3 angles $\theta_{12}, \theta_{23}, \theta_{13}$, ii) depending on the nature of massive neutrinos ν_j - 1 Dirac (δ), or 1 Dirac + 2 Majorana ($\delta, \alpha_{21}, \alpha_{31}$), CP violation phases, and iii) the 3 neutrino masses, m_1, m_2, m_3 . Thus, depending on whether the massive neutrinos are Dirac or Majorana particles, this makes 7 or 9 additional parameters in the ‘‘Standard’’ Model of particle interactions.

The neutrino oscillation probabilities depend (Section 13.2), in general, on the neutrino energy, E , the source-detector distance L , on the elements of U and, for relativistic neutrinos used in all neutrino experiments performed so far, on $\Delta m_{ij}^2 \equiv (m_i^2 - m_j^2)$, $i \neq j$. In the case of 3-neutrino mixing there are only two independent neutrino mass squared differences, say $\Delta m_{21}^2 \neq 0$ and $\Delta m_{31}^2 \neq 0$. The numbering of massive neutrinos ν_j is arbitrary. It proves convenient from the point of view of relating the mixing angles θ_{12}, θ_{23} and θ_{13} to observables, to identify $|\Delta m_{21}^2|$ with the smaller of the two neutrino mass squared differences, which, as it follows from the data, is responsible for the solar ν_e and, the observed by KamLAND, reactor $\bar{\nu}_e$ oscillations. We will number (just for convenience) the massive neutrinos in such a way that $m_1 < m_2$, so that $\Delta m_{21}^2 > 0$. With these choices made, there are two possibilities: either $m_1 < m_2 < m_3$, or $m_3 < m_1 < m_2$. Then the larger neutrino mass square difference $|\Delta m_{31}^2|$ or $|\Delta m_{32}^2|$, can be associated with the experimentally observed oscillations of the atmospheric ν_μ and $\bar{\nu}_\mu$ and accelerator ν_μ . The effects of Δm_{31}^2 or Δm_{32}^2 in the oscillations of solar ν_e , and of Δm_{21}^2 in the oscillations of atmospheric ν_μ and $\bar{\nu}_\mu$ and of accelerator ν_μ , are relatively small and subdominant as a consequence of the facts that i) L, E and L/E in the experiments with solar ν_e and with atmospheric ν_μ and $\bar{\nu}_\mu$ or accelerator ν_μ , are very different, ii) the conditions of production and propagation (on the way to the detector) of the solar ν_e and of the atmospheric ν_μ and $\bar{\nu}_\mu$ or accelerator ν_μ , are very different, and iii) $|\Delta m_{21}^2|$ and $|\Delta m_{31}^2|$ ($|\Delta m_{32}^2|$) in the case of $m_1 < m_2 < m_3$ ($m_3 < m_1 < m_2$), as it follows from the data, differ by approximately a factor of 30, $|\Delta m_{21}^2| \ll |\Delta m_{31(32)}^2|$, $|\Delta m_{21}^2|/|\Delta m_{31(32)}^2| \cong 0.03$. This implies that in both cases of $m_1 < m_2 < m_3$ and $m_3 < m_1 < m_2$ we have $\Delta m_{32}^2 \cong \Delta m_{31}^2$ with $|\Delta m_{31}^2 - \Delta m_{32}^2| = |\Delta m_{21}^2| \ll |\Delta m_{31,32}^2|$.

It follows from the results of CHOOZ and Palo Verde experiments with reactor $\bar{\nu}_e$ [107,108] that, in the convention we use, in which $0 < \Delta m_{21}^2 < |\Delta m_{31(32)}^2|$, the element $|U_{e3}| = \sin \theta_{13}$ of the neutrino mixing matrix U is small (we will quantify this statement below). This makes it possible to identify the angles θ_{12} and θ_{23} as the neutrino mixing angles associated with the solar ν_e and the dominant atmospheric ν_μ (and $\bar{\nu}_\mu$) oscillations, respectively. The angles θ_{12} and θ_{23} are often called ‘‘solar’’ and ‘‘atmospheric’’ neutrino mixing angles, and are often denoted as $\theta_{12} = \theta_\odot$ and $\theta_{23} = \theta_A$ (or θ_{atm}) while Δm_{21}^2 and Δm_{31}^2 are often referred to as the ‘‘solar’’ and ‘‘atmospheric’’ neutrino mass squared differences and are often denoted as $\Delta m_{21}^2 \equiv \Delta m_\odot^2$, $\Delta m_{31}^2 \equiv \Delta m_A^2$ (or Δm_{atm}^2).

The solar neutrino data tell us that $\Delta m_{21}^2 \cos 2\theta_{12} > 0$. In the convention employed by us we have $\Delta m_{21}^2 > 0$. Correspondingly, in this convention one must have $\cos 2\theta_{12} > 0$.

The existing neutrino oscillation data allow us to determine the parameters which drive the solar neutrino and the dominant

atmospheric neutrino oscillations, $\Delta m_\odot^2 = \Delta m_{21}^2$, θ_{12} , and $|\Delta m_A^2| = |\Delta m_{31}^2| \cong |\Delta m_{32}^2|$, θ_{23} , with a relatively good precision, and to obtain rather stringent limits on the angle θ_{13} [107,108]. The best fit values and the 99.73% C.L. allowed ranges of Δm_{21}^2 , $\sin^2 \theta_{12}$, $|\Delta m_{31(32)}^2|$ and $\sin^2 \theta_{23}$, read [111,112]:

$$(\Delta m_{21}^2)_{\text{BF}} = 7.65 \times 10^{-5} \text{ eV}^2, \\ 7.05 \times 10^{-5} \text{ eV}^2 \leq \Delta m_{21}^2 \leq 8.34 \times 10^{-5} \text{ eV}^2, \quad (13.78)$$

$$(\sin^2 \theta_{12})_{\text{BF}} = 0.304, \quad 0.25 \leq \sin^2 \theta_{12} \leq 0.37, \quad (13.79)$$

$$(|\Delta m_{31}^2|)_{\text{BF}} = 2.40 \times 10^{-3} \text{ eV}^2, \\ 2.07 \times 10^{-3} \text{ eV}^2 \leq |\Delta m_{31}^2| \leq 2.75 \times 10^{-3} \text{ eV}^2, \quad (13.80)$$

$$(\sin^2 \theta_{23})_{\text{BF}} = 0.5, \quad 0.36 \leq \sin^2 \theta_{23} \leq 0.67. \quad (13.81)$$

The existing SK atmospheric neutrino, K2K and MINOS data do not allow to determine the sign of $\Delta m_{31(32)}^2$. Maximal solar neutrino mixing, *i.e.*, $\theta_{12} = \pi/4$, is ruled out at more than 6 σ by the data. Correspondingly, one has $\cos 2\theta_{12} \geq 0.26$ (at 99.73% C.L.). A stringent upper limit on the angle θ_{13} was provided by the CHOOZ experiment with reactor $\bar{\nu}_e$ [107]: at $|\Delta m_{31}^2| \cong 2.4 \times 10^{-3} \text{ eV}^2$ the limit reads

$$\sin^2 2\theta_{13} < 0.15 \quad \text{at 90\% C.L.} \quad (13.82)$$

A combined 3-neutrino oscillation analysis of the global data gives [112]:

$$\sin^2 \theta_{13} < 0.035 \text{ (0.056)} \quad \text{at 90\% (99.73\%) C.L.} \quad (13.83)$$

These results imply that $\theta_{23} \cong \pi/4$, $\theta_{12} \cong \pi/5.4$ and that $\theta_{13} < \pi/13$. Correspondingly, the pattern of neutrino mixing is drastically different from the pattern of quark mixing.

At present no experimental information on the Dirac and Majorana CP violation phases in the neutrino mixing matrix is available. Thus, the status of CP symmetry in the lepton sector is unknown. If $\theta_{13} \neq 0$, the Dirac phase δ can generate CP violation effects in neutrino oscillations [30,42,43]. The magnitude of CP violation in $\nu_l \rightarrow \nu_{l'}$ and $\bar{\nu}_l \rightarrow \bar{\nu}_{l'}$ oscillations, $l \neq l' = e, \mu, \tau$, is determined, as we have seen, by the rephasing invariant J_{CP} (see Eq. (13.19)), which in the ‘‘standard’’ parametrisation of the neutrino mixing matrix (Eq. (13.77)) has the form:

$$J_{CP} \equiv \text{Im}(U_{\mu 3} U_{e 3}^* U_{e 2} U_{\mu 2}^*) = \frac{1}{8} \cos \theta_{13} \sin 2\theta_{12} \sin 2\theta_{23} \sin 2\theta_{13} \sin \delta. \quad (13.84)$$

Thus, the size of CP violation effects in neutrino oscillations depends on the magnitude of the currently unknown values of the ‘‘small’’ angle θ_{13} and the Dirac phase δ .

As we have indicated, the existing data do not allow one to determine the sign of $\Delta m_A^2 = \Delta m_{31(2)}^2$. In the case of 3-neutrino mixing, the two possible signs of $\Delta m_{31(2)}^2$ correspond to two types of neutrino mass spectrum. In the widely used conventions of numbering the neutrinos with definite mass in the two cases, the two spectra read: *i) spectrum with normal ordering*: $m_1 < m_2 < m_3$, $\Delta m_A^2 = \Delta m_{31}^2 > 0$, $\Delta m_\odot^2 \equiv \Delta m_{21}^2 > 0$, $m_{2(3)} = (m_1^2 + \Delta m_{21(31)}^2)^{\frac{1}{2}}$; *ii) spectrum with inverted ordering (IO)*: $m_3 < m_1 < m_2$, $\Delta m_A^2 = \Delta m_{32}^2 < 0$, $\Delta m_\odot^2 \equiv \Delta m_{21}^2 > 0$, $m_2 = (m_3^2 + \Delta m_{23}^2)^{\frac{1}{2}}$, $m_1 = (m_3^2 + \Delta m_{23}^2 - \Delta m_{21}^2)^{\frac{1}{2}}$. Depending on the values of the lightest neutrino mass [113], $\min(m_j)$, the neutrino mass spectrum can also be:

- Normal Hierarchical (NH): $m_1 \ll m_2 < m_3$, $m_2 \cong (\Delta m_\odot^2)^{\frac{1}{2}}$, $m_3 \cong |\Delta m_A^2|^{\frac{1}{2}}$; or
- Inverted Hierarchical (IH): $m_3 \ll m_1 < m_2$, with $m_{1,2} \cong |\Delta m_A^2|^{\frac{1}{2}} \sim 0.05 \text{ eV}$; or
- Quasi-Degenerate (QD): $m_1 \cong m_2 \cong m_3 \cong m_0$, $m_j^2 \gg |\Delta m_A^2|$, $m_0 \gtrsim 0.10 \text{ eV}$.

All three types of spectrum are compatible with the existing constraints on the absolute scale of neutrino masses m_j . Information about the latter can be obtained, *e.g.*, by measuring the spectrum of electrons near the end point in ${}^3\text{H}$ β -decay experiments [115–117] and from cosmological and astrophysical data. The most stringent upper bounds on the $\bar{\nu}_e$ mass were obtained in the Troitzk [116] and Mainz [117] experiments:

$$m_{\bar{\nu}_e} < 2.3 \text{ eV} \quad \text{at 95\% C.L.} \quad (13.85)$$

We have $m_{\bar{\nu}_e} \cong m_{1,2,3}$ in the case of QD spectrum. The KATRIN experiment [117] is planned to reach sensitivity of $m_{\bar{\nu}_e} \sim 0.20 \text{ eV}$, *i.e.*, it will probe the region of the QD spectrum.

The Cosmic Microwave Background (CMB) data of the WMAP experiment, combined with supernovae data and data on galaxy clustering can be used to obtain an upper limit on the sum of neutrinos masses [118] (see review on Cosmological Parameters): $\sum_j m_j \lesssim 0.68 \text{ eV}$, 95% C.L. A more conservative estimate of the uncertainties in the astrophysical data leads to a somewhat weaker constraint (see *e.g.*, Ref. 119): $\sum_j m_j \lesssim 1.7 \text{ eV}$, 95% C.L.

It follows from these data that neutrino masses are much smaller than the masses of charged leptons and quarks. If we take as an indicative upper limit $m_j \lesssim 0.5 \text{ eV}$, we have $m_j/m_{l,q} \lesssim 10^{-6}$, $l = e, \mu, \tau$, $q = d, s, b, u, c, t$. It is natural to suppose that the remarkable smallness of neutrino masses is related to the existence of a new fundamental mass scale in particle physics, and thus to new physics beyond that predicted by the Standard Model.

13.7.1. The see-saw mechanism and the baryon asymmetry of the Universe :

A natural explanation of the smallness of neutrino masses is provided by the see-saw mechanism of neutrino mass generation [3]. An integral part of the simplest version of this mechanism - the so-called “type I see-saw”, are the RH neutrinos ν_{lR} (RH neutrino fields $\nu_{lR}(x)$). The latter are assumed to possess a Majorana mass term as well as Yukawa type coupling $\mathcal{L}_Y(x)$ with the Standard Model lepton and Higgs doublets, $\psi_{lL}(x)$ and $\Phi(x)$, respectively, $(\psi_{lL}(x))^T = (\nu_{lL}^T(x) \quad l_L^T(x))$, $l = e, \mu, \tau$, $(\Phi(x))^T = (\Phi^{(0)} \quad \Phi^{(-)})$. In the basis in which the Majorana mass matrix of RH neutrinos is diagonal, we have:

$$\mathcal{L}_{Y,M}(x) = \left(\lambda_{il} \overline{N_{iR}}(x) \Phi^\dagger(x) \psi_{lL}(x) + \text{h.c.} \right) - \frac{1}{2} M_i \overline{N_i}(x) N_i(x), \quad (13.86)$$

where λ_{il} is the matrix of neutrino Yukawa couplings and N_i ($N_i(x)$) is the heavy RH Majorana neutrino (field) possessing a mass $M_i > 0$. When the electroweak symmetry is broken spontaneously, the neutrino Yukawa coupling generates a Dirac mass term: $m_{il}^D \overline{N_{iR}}(x) \nu_{lL}(x) + \text{h.c.}$, with $m^D = v\lambda$, $v = 174 \text{ GeV}$ being the Higgs doublet v.e.v. In the case when the elements of m^D are much smaller than M_k , $|m_{il}^D| \ll M_k$, $i, k = 1, 2, 3$, $l = e, \mu, \tau$, the interplay between the Dirac mass term and the mass term of the heavy (RH) Majorana neutrinos N_i generates an effective Majorana mass (term) for the LH flavour neutrinos [3]: $m_{il}^{LL} \cong -(m^D)_{ij}^T M_j^{-1} m_{jl}^D$. In grand unified theories, m^D is typically of the order of the charged fermion masses. In $SO(10)$ theories, for instance, m^D coincides with the up-quark mass matrix. Taking indicatively $m^{LL} \sim 0.1 \text{ eV}$, $m^D \sim 100 \text{ GeV}$, one finds $M \sim 10^{14} \text{ GeV}$, which is close to the scale of unification of the electroweak and strong interactions, $M_{GUT} \cong 2 \times 10^{16} \text{ GeV}$. In GUT theories with RH neutrinos one finds that indeed the heavy Majorana neutrinos N_j naturally obtain masses which are by few to several orders of magnitude smaller than M_{GUT} . Thus, the enormous disparity between the neutrino and charged fermion masses is explained in this approach by the huge difference between effectively the electroweak symmetry breaking scale and M_{GUT} .

An additional attractive feature of the see-saw scenario is that the generation and smallness of neutrino masses is related via the leptogenesis mechanism [2] to the generation of the baryon asymmetry of the Universe. The Yukawa coupling in Eq. (13.86), in general, is not CP conserving. Due to this CP-nonconserving coupling the heavy Majorana neutrinos undergo, *e.g.*, the decays

$N_j \rightarrow l^+ + \Phi^{(-)}$, $N_j \rightarrow l^- + \Phi^{(+)}$, which have different rates: $\Gamma(N_j \rightarrow l^+ + \Phi^{(-)}) \neq \Gamma(N_j \rightarrow l^- + \Phi^{(+)})$. When these decays occur in the Early Universe at temperatures somewhat below the mass of, say, N_1 , so that the latter are out of equilibrium with the rest of the particles present at that epoch, CP violating asymmetries in the individual lepton charges L_l , and in the total lepton charge L , of the Universe are generated. These lepton asymmetries are converted into a baryon asymmetry by $(B - L)$ conserving, but $(B + L)$ violating, sphaleron processes, which exist in the Standard Model and are effective at temperatures $T \sim (100 - 10^{12}) \text{ GeV}$. If the heavy neutrinos N_j have hierarchical spectrum, $M_1 \ll M_2 \ll M_3$, the observed baryon asymmetry can be reproduced provided the mass of the lightest one satisfies $M_1 \gtrsim 10^9 \text{ GeV}$ [120]. Thus, in this scenario, the neutrino masses and mixing and the baryon asymmetry have the same origin - the neutrino Yukawa couplings and the existence of (at least two) heavy Majorana neutrinos. Moreover, quantitative studies based on recent advances in leptogenesis theory [121] have shown that the Dirac and/or Majorana phases in the neutrino mixing matrix U can provide the CP violation, necessary in leptogenesis for the generation of the observed baryon asymmetry of the Universe [122]. This implies, in particular, that if the CP symmetry is established not to hold in the lepton sector due to U , at least some fraction (if not all) of the observed baryon asymmetry might be due to the Dirac and/or Majorana CP violation present in the neutrino mixing.

13.7.2. The nature of massive neutrinos :

The experiments studying flavour neutrino oscillations cannot provide information on the nature - Dirac or Majorana, of massive neutrinos [30,44]. Establishing whether the neutrinos with definite mass ν_j are Dirac fermions possessing distinct antiparticles, or Majorana fermions, *i.e.* spin 1/2 particles that are identical with their antiparticles, is of fundamental importance for understanding the origin of ν -masses and mixing and the underlying symmetries of particle interactions (see *e.g.*, Ref. 51). The neutrinos with definite mass ν_j will be Dirac fermions if the particle interactions conserve some additive lepton number, *e.g.*, the total lepton charge $L = L_e + L_\mu + L_\tau$. If no lepton charge is conserved, ν_j will be Majorana fermions (see *e.g.*, Ref. 29). The massive neutrinos are predicted to be of Majorana nature by the see-saw mechanism of neutrino mass generation [3]. The observed patterns of neutrino mixing and of neutrino mass squared differences can be related to Majorana massive neutrinos and the existence of an approximate symmetry in the lepton sector corresponding, *e.g.*, to the conservation of the lepton charge $L' = L_e - L_\mu - L_\tau$ [123]. Determining the nature of massive neutrinos ν_j is one of the fundamental and most challenging problems in the future studies of neutrino mixing.

The Majorana nature of massive neutrinos ν_j manifests itself in the existence of processes in which the total lepton charge L changes by two units: $K^+ \rightarrow \pi^- + \mu^+ + \mu^+$, $\mu^- + (A, Z) \rightarrow \mu^+ + (A, Z - 2)$, *etc.* Extensive studies have shown that the only feasible experiments having the potential of establishing that the massive neutrinos are Majorana particles are at present the experiments searching for $(\beta\beta)_{0\nu}$ -decay: $(A, Z) \rightarrow (A, Z + 2) + e^- + e^-$ (see *e.g.*, Ref. 124). The observation of $(\beta\beta)_{0\nu}$ -decay and the measurement of the corresponding half-life with sufficient accuracy, would not only be a proof that the total lepton charge is not conserved, but might also provide unique information on the i) type of neutrino mass spectrum (see, *e.g.*, Ref. 125), ii) Majorana phases in U [114,126] and iii) the absolute scale of neutrino masses (for details see Ref. 124 to Ref. 127 and references quoted therein).

Under the assumptions of 3- ν mixing, of massive neutrinos ν_j being Majorana particles, and of $(\beta\beta)_{0\nu}$ -decay generated only by the (V-A) charged current weak interaction via the exchange of the three Majorana neutrinos ν_j having masses $m_j \lesssim$ few MeV, the $(\beta\beta)_{0\nu}$ -decay amplitude has the form (see, *e.g.*, Ref. 29 and Ref. 124): $A(\beta\beta)_{0\nu} \cong \langle m \rangle / M$, where M is the corresponding nuclear matrix element which does not depend on the neutrino mixing parameters, and

$$\begin{aligned} |\langle m \rangle| &= \left| m_1 U_{e1}^2 + m_2 U_{e2}^2 + m_3 U_{e3}^2 \right| \\ &= \left| \left(m_1 c_{12}^2 + m_2 s_{12}^2 e^{i\alpha_{21}} \right) c_{13}^2 + m_3 s_{13}^2 e^{i(\alpha_{31} - 2\delta)} \right|, \quad (13.87) \end{aligned}$$

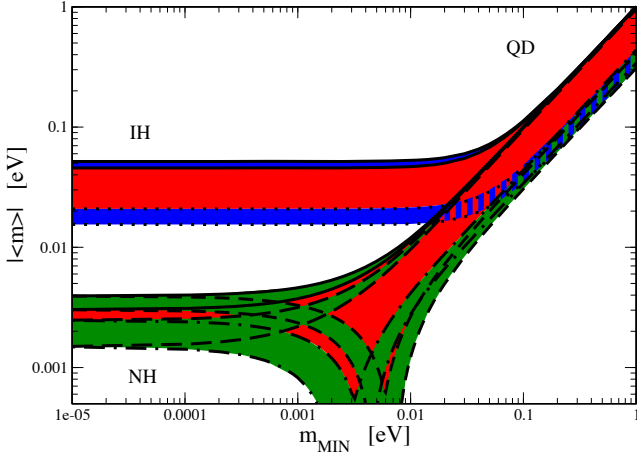


Figure 13.11: The effective Majorana mass $\langle m \rangle$ (including a 2σ uncertainty) as a function of $\min(m_j)$. The figure is obtained using the best fit values and 1σ errors of Δm_{21}^2 , $\sin^2 \theta_{12}$, and $|\Delta m_{31}^2| \cong |\Delta m_{32}^2|$ from Ref. 112, fixed $\sin^2 \theta_{13} = 0.01$ and $\delta = 0$. The phases $\alpha_{21,31}$ are varied in the interval $[0, \pi]$. The predictions for the NH, IH and QD spectra are indicated. The black lines determine the ranges of values of $\langle m \rangle$ for the different pairs of CP conserving values of $\alpha_{21,31}$: $(\alpha_{21}, \alpha_{31}) = (0, 0)$ solid, $(0, \pi)$ long dashed, $(\pi, 0)$ dash-dotted, (π, π) short dashed, lines. The red regions correspond to at least one of the phases $\alpha_{21,31}$ and $(\alpha_{31} - \alpha_{21})$ having a CP violating value. (Update by S. Pascoli of a figure from the last article quoted in Ref. 127.) See full-color version on color pages at end of book.

is the effective Majorana mass in $(\beta\beta)_{0\nu}$ -decay. In the case of CP-invariance one has [32], $\eta_{21} \equiv e^{i\alpha_{21}} = \pm 1$, $\eta_{31} \equiv e^{i\alpha_{31}} = \pm 1$, $e^{-i2\delta} = 1$. The three neutrino masses $m_{1,2,3}$ can be expressed in terms of the two measured Δm_{jk}^2 and, e.g., $\min(m_j)$. Thus, given the neutrino oscillation parameters Δm_{21}^2 , $\sin^2 \theta_{12}$, Δm_{31}^2 and $\sin^2 \theta_{13}$, $\langle m \rangle$ is a function of the lightest neutrino mass $\min(m_j)$, the Majorana (and Dirac) CP violation phases in U and of the type of neutrino mass spectrum. In the case of NH, IH and QD spectrum we have (see, e.g., Ref. 114 and Ref. 127):

$$\langle m \rangle \cong \left| \sqrt{\Delta m_{21}^2 s_{12}^2 c_{13}^2} + \sqrt{\Delta m_{31}^2 s_{13}^2} e^{i(\alpha_{31} - \alpha_{21} - 2\delta)} \right|, \quad \text{NH}, \quad (13.88)$$

$$\langle m \rangle \cong \tilde{m} \left(1 - \sin^2 2\theta_{12} \sin^2 \frac{\alpha_{21}}{2} \right)^{\frac{1}{2}}, \quad \text{IH (IO) and QD}, \quad (13.89)$$

where $\tilde{m} \equiv \sqrt{\Delta m_{23}^2 + m_3^2}$ and $\tilde{m} \equiv m_0$ for IH (IO) and QD spectrum, respectively. In Eq. (13.89) we have exploited the fact that $\sin^2 \theta_{13} \ll \cos 2\theta_{12}$. The CP conserving values of the Majorana phases $(\alpha_{31} - \alpha_{21})$ and α_{21} determine the ranges of possible values of $\langle m \rangle$, corresponding to the different types of neutrino mass spectrum. Using the best fit values of neutrino oscillation parameters, Eq. (13.78) to Eq. (13.80), and the upper limit on θ_{13} , Eq. (13.83), one finds that: i) $\langle m \rangle \lesssim 0.005$ eV in the case of NH spectrum; ii) $\sqrt{\Delta m_{23}^2} \cos 2\theta_{12} \lesssim \langle m \rangle \lesssim \sqrt{\Delta m_{23}^2}$, or 10^{-2} eV $\lesssim \langle m \rangle \lesssim 0.05$ eV in the case of IH spectrum; iii) $m_0 \cos 2\theta_{12} \lesssim \langle m \rangle \lesssim m_0$, or 0.03 eV $\lesssim \langle m \rangle \lesssim m_0$ eV, $m_0 \gtrsim 0.10$ eV, in the case of QD spectrum. The difference in the ranges of $\langle m \rangle$ in the cases of NH, IH and QD spectrum opens up the possibility to get information about the type of neutrino mass spectrum from a measurement of $\langle m \rangle$ [125]. The predicted $(\beta\beta)_{0\nu}$ -decay effective Majorana mass $\langle m \rangle$ as a function of the lightest neutrino mass $\min(m_j)$ is shown in Fig. 13.11.

13.8. Outlook

After the spectacular experimental progress made in the studies of neutrino oscillations, further understanding of the pattern of neutrino masses and neutrino mixing, of their origins and of the status of CP symmetry in the lepton sector requires an extensive and challenging program of research. The main goals of such a research program include:

- Determining the nature - Dirac or Majorana, of massive neutrinos ν_j . This is of fundamental importance for making progress in our understanding of the origin of neutrino masses and mixing and of the symmetries governing the lepton sector of particle interactions.
- Determination of the sign of Δm_A^2 (Δm_{31}^2) and of the type of neutrino mass spectrum.
- Determining or obtaining significant constraints on the absolute scale of neutrino masses.
- Measurement of, or improving by at least a factor of (5 - 10) the existing upper limit on, the small neutrino mixing angle θ_{13} . Together with the Dirac CP-violating phase, the angle θ_{13} determines the magnitude of CP-violation effects in neutrino oscillations.
- Determining the status of CP symmetry in the lepton sector.
- High precision measurement of Δm_{21}^2 , θ_{12} , and $|\Delta m_{31}^2|$, θ_{23} .
- Understanding at a fundamental level the mechanism giving rise to neutrino masses and mixing and to L_I -non-conservation. This includes understanding the origin of the patterns of ν -mixing and ν -masses suggested by the data. Are the observed patterns of ν -mixing and of $\Delta m_{21,31}^2$ related to the existence of a new fundamental symmetry of particle interactions? Is there any relation between quark mixing and neutrino mixing, e.g., does the relation $\theta_{12} + \theta_c = \pi/4$, where θ_c is the Cabibbo angle, hold? What is the physical origin of CP violation phases in the neutrino mixing matrix U ? Is there any relation (correlation) between the (values of) CP violation phases and mixing angles in U ? Progress in the theory of neutrino mixing might also lead to a better understanding of the mechanism of generation of baryon asymmetry of the Universe.

The successful realization of this research program would be a formidable task and would require many years. We are at the beginning of the "road" leading to a comprehensive understanding of the patterns of neutrino masses and mixing and of their origin.

References:

1. B. Pontecorvo, Zh. Eksp. Teor. Fiz. **53**, 1717 (1967) [Sov. Phys. JETP **26**, 984 (1968)].
2. M. Fukugita and T. Yanagida, Phys. Lett. **B174**, 45 (1986); V.A. Kuzmin, V.A. Rubakov, and M.E. Shaposhnikov, Phys. Lett. **B155**, 36 (1985).
3. P. Minkowski, Phys. Lett. **B67**, 421 (1977); see also: M. Gell-Mann, P. Ramond, and R. Slansky in *Supergravity*, p. 315, edited by F. Nieuwenhuizen and D. Friedman, North Holland, Amsterdam, 1979; T. Yanagida, *Proc. of the Workshop on Unified Theories and the Baryon Number of the Universe*, edited by O. Sawada and A. Sugamoto, KEK, Japan 1979; R.N. Mohapatra and G. Senjanović, Phys. Rev. Lett. **44**, 912 (1980).
4. B.T. Cleveland *et al.*, Astrophys. J. **496**, 505 (1988).
5. Y. Fukuda *et al.*, [Kamiokande Collab.], Phys. Rev. Lett. **77**, 1683 (1996).
6. J.N. Abdurashitov *et al.*, Phys. Rev. **C80**, 015807 (2009).
7. P. Anselmann *et al.*, Phys. Lett. **B285**, 376 (1992).
8. W. Hampel *et al.*, Phys. Lett. **B447**, 127 (1999).
9. M. Altmann *et al.*, Phys. Lett. **B616**, 174 (2005).
10. S. Fukuda *et al.*, [Super-Kamiokande Collab.], Phys. Lett. **B539**, 179 (2002).
11. Q.R. Ahmad *et al.*, [SNO Collab.], Phys. Rev. Lett. **87**, 071301 (2001).
12. Q.R. Ahmad *et al.*, [SNO Collab.], Phys. Rev. Lett. **89**, 011301 (2002).

13. Y. Fukuda *et al.*, [Super-Kamiokande Collab.], Phys. Rev. Lett. **81**, 1562 (1998).
14. Y. Ashie *et al.*, [Super-Kamiokande Collab.], Phys. Rev. Lett. **93**, 101801 (2004).
15. K. Eguchi *et al.*, [KamLAND Collab.], Phys. Rev. Lett. **90**, 021802 (2003).
16. T. Araki *et al.*, [KamLAND Collab.], Phys. Rev. Lett. **94**, 081801 (2005).
17. B. Pontecorvo, Zh. Eksp. Teor. Fiz. **33**, 549 (1957) and **34**, 247 (1958).
18. Z. Maki, M. Nakagawa, and S. Sakata, Prog. Theor. Phys. **28**, 870 (1962).
19. D. Karlen in RPP2010.
20. M.H. Ahn *et al.*, [K2K Collab.], Phys. Rev. **D74**, 072003 (2006).
21. D.G. Michael *et al.*, [MINOS Collab.], Phys. Rev. Lett. **97**, 191801 (2006).
22. P. Adamson *et al.*, [MINOS Collab.], Phys. Rev. Lett. **101**, 131802 (2008).
23. A. Aguilar *et al.*, Phys. Rev. **D64**, 112007 (2001).
24. A.A. Aguilar-Arevalo *et al.*, Phys. Rev. Lett. **98**, 231801 (2007).
25. L. Wolfenstein, Phys. Rev. **D17**, 2369 (1978); *Proc. of the 8th International Conference on Neutrino Physics and Astrophysics - "Neutrino'78"* (ed. E.C. Fowler, Purdue University Press, West Lafayette, 1978), p. C3.
26. S.P. Mikheev and A.Y. Smirnov, Sov. J. Nucl. Phys. **42**, 913 (1985); Nuovo Cimento **9C**, 17 (1986).
27. E. Majorana, Nuovo Cimento **5**, 171 (1937).
28. Majorana particles, in contrast to Dirac fermions, are their own antiparticles. An electrically charged particle (like the electron) cannot coincide with its antiparticle (the positron) which carries the opposite non-zero electric charge.
29. S.M. Bilenky and S.T. Petcov, Rev. Mod. Phys. **59**, 671 (1987).
30. S.M. Bilenky, J. Hosek, and S.T. Petcov, Phys. Lett. **B94**, 495 (1980).
31. J. Schechter and J.W.F. Valle, Phys. Rev. **D23**, 2227 (1980); M. Doi *et al.*, Phys. Lett. **B102**, 323 (1981).
32. L. Wolfenstein, Phys. Lett. **B107**, 77 (1981); S.M. Bilenky, N.P. Nedelcheva, and S.T. Petcov, Nucl. Phys. **B247**, 61 (1984); B. Kayser, Phys. Rev. **D30**, 1023 (1984).
33. S. Nussinov, Phys. Lett. **B63**, 201 (1976); B. Kayser, Phys. Rev. **D24**, 110 (1981); J. Rich, Phys. Rev. **D48**, 4318 (1993); H. Lipkin, Phys. Lett. **B348**, 604 (1995); W. Grimus and P. Stockinger, Phys. Rev. **D54**, 3414 (1996); L. Stodolski, Phys. Rev. **D58**, 036006 (1998); W. Grimus, P. Stockinger, and S. Mohanty, Phys. Rev. **D59**, 013011 (1999); L.B. Okun, Surv. High Energy Physics **15**, 75 (2000); J.-M. Levy, hep-ph/0004221 and arXiv:0901.0408; A.D. Dolgov, Phys. Reports **370**, 333 (2002); C. Giunti, Phys. Scripta **67**, 29 (2003) and Phys. Lett. **B17**, 103 (2004); M. Beuthe, Phys. Reports **375**, 105 (2003); H. Lipkin, Phys. Lett. **B642**, 366 (2006); S.M. Bilenky, F. von Feilitzsch, and W. Potzel, J. Phys. **G34**, 987 (2007); C. Giunti and C.W. Kim, *Fundamentals of Neutrino Physics and Astrophysics* (Oxford University Press, Oxford, 2007); E.Kh. Akhmedov, J. Kopp, and M. Lindner, JHEP **0805**, 005 (2008); E.Kh. Akhmedov and A.Yu. Smirnov, Phys. Atom. Nucl. **72**, 1363 (2009).
34. For the subtleties involved in the step leading from Eq. (13.1) to Eq. (13.5) see, *e.g.*, Ref. 35.
35. A.G. Cohen, S.L. Glashow, and Z. Ligeti, arXiv:0810.4602.
36. The neutrino masses do not exceed approximately 1 eV, $m_j \lesssim 1$, while in neutrino oscillation experiments neutrinos with energy $E \gtrsim 100$ keV are detected.
37. S.M. Bilenky and B. Pontecorvo, Phys. Reports **41**, 225 (1978).
38. In Eq. (13.9) we have neglected the possible instability of neutrinos ν_j . In most theoretical models with nonzero neutrino masses and neutrino mixing, the predicted half life-time of neutrinos with mass of 1 eV exceeds the age of the Universe, see, *e.g.*, S.T. Petcov, Yad. Fiz. **25**, 641 (1977), (E) *ibid.*, **25** (1977) 1336 [Sov. J. Nucl. Phys. **25**, 340 (1977)], (E) *ibid.*, **25**, (1977), 698], and Phys. Lett. **B115**, 401 (1982); W. Marciano and A.I. Sanda, Phys. Lett. **B67**, 303 (1977); P. Pal and L. Wolfenstein, Phys. Rev. **D25**, 766 (1982).
39. L.B. Okun (2000), J.-M. Levy (2000) and H. Lipkin (2006) quoted in Ref. 33 and Ref. 35.
40. The articles by L. Stodolsky (1998) and H. Lipkin (1995) quoted in Ref. 33.
41. V. Gribov and B. Pontecorvo, Phys. Lett. **B28**, 493 (1969).
42. N. Cabibbo, Phys. Lett. **B72**, 333 (1978).
43. V. Barger *et al.*, Phys. Rev. Lett. **45**, 2084 (1980).
44. P. Langacker *et al.*, Nucl. Phys. **B282**, 589 (1987).
45. P.I. Krastev and S.T. Petcov, Phys. Lett. **B205**, 84 (1988).
46. C. Jarlskog, Z. Phys. **C29**, 491 (1985).
47. A. De Rujula *et al.*, Nucl. Phys. **B168**, 54 (1980).
48. S. Goswami *et al.*, Nucl. Phys. (Proc. Supp.) **B143**, 121 (2005).
49. These processes are important, however, for the supernova neutrinos see, *e.g.*, G. Raffelt, *Proc. International School of Physics "Enrico Fermi", CLII Course "Neutrino Physics"*, 23 July-2 August 2002, Varenna, Italy [hep-ph/0208024], and articles quoted therein.
50. We standardly assume that the weak interaction of the flavour neutrinos ν_l and antineutrinos $\bar{\nu}_l$ is described by the Standard Model (for alternatives see, *e.g.*, [25]; M.M. Guzzo *et al.*, Phys. Lett. **B260**, 154 (1991); E. Roulet, Phys. Rev. **D44**, R935 (1991) and Ref. 51).
51. R. Mohapatra *et al.*, Rept. on Prog. in Phys. **70**, 1757 (2007); A. Bandyopadhyay *et al.*, Rept. on Prog. in Phys. **72**, 106201 (2009).
52. V. Barger *et al.*, Phys. Rev. **D22**, 2718 (1980).
53. P. Langacker, J.P. Leveille, and J. Sheiman, Phys. Rev. **D27**, 1228 (1983).
54. The difference between the ν_μ and ν_τ indices of refraction arises at one-loop level and can be relevant for the $\nu_\mu - \nu_\tau$ oscillations in very dense media, like the core of supernovae, *etc.*; see F.J. Botella, C.S. Lim, and W.J. Marciano, Phys. Rev. **D35**, 896 (1987).
55. The relevant formulae for the oscillations between the ν_e and a sterile neutrino ν_s , $\nu_e \leftrightarrow \nu_s$, can be obtained from those derived for the case of $\nu_e \leftrightarrow \nu_{\mu(\tau)}$ oscillations by [44,53] replacing N_e with $(N_e - 1/2N_n)$, N_n being the neutron number density in matter.
56. T.K. Kuo and J. Pantaleone, Phys. Lett. **B198**, 406 (1987).
57. A.D. Dziewonski and D.L. Anderson, Physics of the Earth and Planetary Interiors **25**, 297 (1981).
58. The first studies of the effects of Earth matter on the oscillations of neutrinos were performed numerically in [52,59] and in E.D. Carlson, Phys. Rev. **D34**, 1454 (1986); A. Dar *et al.*, *ibid.*, **D35**, 3607 (1988); in [45] and in G. Auremma *et al.*, *ibid.*, **D37**, 665 (1988).
59. A.Yu. Smirnov and S.P. Mikheev, *Proc. of the VIth Moriond Workshop* (eds. O. Fackler, J. Tran Thanh Van, Frontières, Gif-sur-Yvette, 1986), p. 355.
60. S.T. Petcov, Phys. Lett. **B434**, 321 (1998), (E) *ibid.* **B444**, 584 (1998).
61. S.T. Petcov, Phys. Lett. **B214**, 259 (1988).
62. E.Kh. Akhmedov *et al.*, Nucl. Phys. **B542**, 3 (1999).
63. M.V. Chizhov, M. Maris, and S.T. Petcov, hep-ph/9810501; see also: S.T. Petcov, Nucl. Phys. (Proc. Supp.) **B77**, 93 (1999) (hep-ph/9809587).
64. J. Hosaka *et al.*, [Super-Kamiokande collab.], Phys. Rev. **D74**, 032002 (2006).
65. E.Kh. Akhmedov, Nucl. Phys. **B538**, 25 (1999).
66. M.V. Chizhov and S.T. Petcov, Phys. Rev. Lett. **83**, 1096 (1999) and Phys. Rev. Lett. **85**, 3979 (2000); Phys. Rev. **D63**, 073003 (2001).
67. J. Bernabéu, S. Palomares-Ruiz, and S.T. Petcov, Nucl. Phys. **B669**, 255 (2003); S.T. Petcov and T. Schwetz, Nucl. Phys. **B740**, 1 (2006); R. Gandhi *et al.*, Phys. Rev. **D76**, 073012 (2007); E.Kh. Akhmedov, M. Maltoni, and A.Yu. Smirnov, JHEP **0705**, 077 (2007).

68. The mantle-core enhancement maxima, *e.g.*, in $P_{m}^{2\nu}(\nu_{\mu} \rightarrow \nu_{\mu})$, appeared in some of the early numerical calculations, but with incorrect interpretation (see, *e.g.*, the articles quoted in Ref. 58).
69. M. Freund, Phys. Rev. **D64**, 053003 (2001).
70. M.C. Gonzalez-Garcia and Y. Nir, Rev. Mod. Phys. **75**, 345 (2003); S.M. Bilenky, W. Grimus, and C. Giunti, Prog. in Part. Nucl. Phys. **43**, 1 (1999); S.T. Petcov, Lecture Notes in Physics **512**, (eds. H. Gausterer, C.B. Lang, Springer, 1998), p. 281.
71. J.N. Bahcall, *Neutrino Astrophysics*, Cambridge University Press, Cambridge, 1989; J.N. Bahcall and M. Pinsonneault, Phys. Rev. Lett. **92**, 121301 (2004).
72. J.N. Bahcall, A.M. Serenelli, and S. Basu, Astrophys. J. Supp. **165**, 400 (2006).
73. A. Messiah, *Proc. of the VIth Moriond Workshop* (eds. O. Fackler, J. Tran Thanh Van, Frontières, Gif-sur-Yvette, 1986), p. 373.
74. S.J. Parke, Phys. Rev. Lett. **57**, 1275 (1986).
75. S.T. Petcov, Phys. Lett. **B200**, 373 (1988).
76. P.I. Krastev and S.T. Petcov, Phys. Lett. **B207**, 64 (1988); M. Bruggen, W.C. Haxton, and Y.-Z. Quian, Phys. Rev. **D51**, 4028 (1995).
77. T. Kaneko, Prog. Theor. Phys. **78**, 532 (1987); S. Toshev, Phys. Lett. **B196**, 170 (1987); M. Ito, T. Kaneko, and M. Nakagawa, Prog. Theor. Phys. **79**, 13 (1988), (E) *ibid.*, **79**, 555 (1988).
78. S.T. Petcov, Phys. Lett. **B406**, 355 (1997).
79. C. Cohen-Tannoudji, B. Diu, and F. Laloe, *Quantum Mechanics*, vol. 1 (Hermann, Paris, and John Wiley & Sons, New York, 1977).
80. S.T. Petcov, Phys. Lett. **B214**, 139 (1988); E. Lisi *et al.*, Phys. Rev. **D63**, 093002 (2000); A. Friedland, Phys. Rev. **D64**, 013008 (2001).
81. S.T. Petcov and J. Rich, Phys. Lett. **B224**, 401 (1989).
82. An expression for the “jump” probability P' for N_e varying linearly along the neutrino path was derived in W.C. Haxton, Phys. Rev. Lett. **57**, 1271 (1986) and in Ref. 74 on the basis of the old Landau-Zener result: L.D. Landau, Phys. Z. USSR **1**, 426 (1932), C. Zener, Proc. R. Soc. A **137**, 696 (1932). An analytic description of the solar ν_e transitions based on the Landau-Zener jump probability was proposed in Ref. 74 and in W.C. Haxton, Phys. Rev. **D35**, 2352 (1987). The precision limitations of this description, which is less accurate than that based on the exponential density approximation, were discussed in S.T. Petcov, Phys. Lett. **B191**, 299 (1987) and in Ref. 76.
83. A. de Gouvea, A. Friedland, and H. Murayama, JHEP **0103**, 009 (2001).
84. C.-S. Lim, Report BNL 52079, 1987; S.P. Mikheev and A.Y. Smirnov, Phys. Lett. **B200**, 560 (1988).
85. G.L. Fogli *et al.*, Phys. Lett. **B583**, 149 (2004).
86. J.N. Bahcall, A.M. Serenelli, and S. Basu, Astrophys. J. **621**, L85 (2005).
87. C. Peña-Garay and A.M. Serenelli, arXiv:0811.2424.
88. B. Pontecorvo, Chalk River Lab. report PD-205, 1946.
89. D. Davis, Jr., D.S. Harmer, and K.C. Hoffman, Phys. Rev. Lett. **20**, 1205 (1968).
90. A.I. Abazov *et al.*, Phys. Rev. Lett. **67**, 3332 (1991).
91. K.S. Hirata *et al.*, Phys. Rev. Lett. **63**, 16 (1989).
92. Y. Fukuda *et al.*, Phys. Rev. Lett. **81**, 1158 (1998).
93. J. Hosaka *et al.*, Phys. Rev. **D73**, 112001 (2006).
94. B. Aharmim *et al.*, Phys. Rev. **C72**, 055502 (2005).
95. B. Aharmim *et al.*, Phys. Rev. Lett. **101**, 111301 (2008).
96. C. Arpesella *et al.*, Phys. Lett. **B658**, 101 (2008); Phys. Rev. Lett. **101**, 091302 (2008).
97. B. Aharmim *et al.*, arXiv:0910.2984.
98. Y. Fukuda *et al.*, Phys. Rev. Lett. **86**, 5651 (2001).
99. Y. Fukuda *et al.*, Phys. Lett. **B539**, 179 (2002).
100. G. L. Fogli *et al.*, Phys. Rev. **D67**, 073002 (2003); M. Maltoni, T. Schwetz, and J.W. Valle, Phys. Rev. **D67**, 093003 (2003); A. Bandyopadhyay *et al.*, Phys. Lett. **B559**, 121 (2003); J.N. Bahcall, M.C. Gonzalez-Garcia, and C. Peña-Garay, JHEP **0302**, 009 (2003); P.C. de Holanda and A.Y. Smirnov, JCAP **0302**, 001 (2003).
101. S. Abe *et al.*, Phys. Rev. Lett. **100**, 221803 (2008).
102. Y. Ashie *et al.*, Phys. Rev. **D71**, 112005 (2005).
103. K. Abe *et al.*, Phys. Rev. Lett. **97**, 171801 (2006).
104. V. Barger *et al.*, Phys. Rev. Lett. **82**, 2640 (1999).
105. E. Lisi *et al.*, Phys. Rev. Lett. **85**, 1166 (2000).
106. M. Guler *et al.*, [OPERA Collab.], CERN/SPSC 2000-028 (2000).
107. M. Apollonio *et al.*, Phys. Lett. **B466**, 415 (1999); Eur. Phys. J. **C27**, 331 (2003).
108. F. Boehm *et al.*, Phys. Rev. Lett. **84**, 3764 (2000); Phys. Rev. **D64**, 112001 (2001).
109. S. Yamamoto *et al.*, Phys. Rev. Lett. **96**, 181801 (2006).
110. G.L. Fogli *et al.*, Phys. Rev. Lett. **101**, 141801 (2008).
111. G.L. Fogli *et al.*, Phys. Rev. **D78**, 033010 (2008).
112. T. Schwetz, M. Tortola, and J.W. F. Valle, arXiv:0808.2016.
113. In the convention we use, the neutrino masses are not ordered in magnitude according to their index number: $\Delta m_{31}^2 < 0$ corresponds to $m_3 < m_1 < m_2$. We can also number the massive neutrinos in such a way that one always has $m_1 < m_2 < m_3$, see, *e.g.*, Ref. 114.
114. S.M. Bilenky, S. Pascoli, and S.T. Petcov, Phys. Rev. **D64**, 053010 (2001) and *ibid.*, 113003; S.T. Petcov, Physica Scripta **T121**, 94 (2005).
115. F. Perrin, Comptes Rendus **197**, 868 (1933); E. Fermi, Nuovo Cim. **11**, 1 (1934).
116. V. Lobashev *et al.*, Nucl. Phys. **A719**, 153c, (2003).
117. K. Eitel *et al.*, Nucl. Phys. (Proc. Supp.) **B143**, 197 (2005).
118. D.N. Spergel *et al.*, Astrophys. J. Supp. **170**, 377 (2007).
119. M. Fukugita *et al.*, Phys. Rev. **D74**, 027302 (2006).
120. S. Davidson and A. Ibarra, Phys. Lett. **B535**, 25 (2002).
121. A. Abada *et al.*, JCAP **0604**, 004 (2006); E. Nardi *et al.*, JHEP **0601**, 164 (2006).
122. S. Pascoli, S.T. Petcov, and A. Riotto, Phys. Rev. **D75**, 083511 (2007) and Nucl. Phys. **B774**, 1 (2007); E. Molinaro and S.T. Petcov, Phys. Lett. **B671**, 60 (2009).
123. S.T. Petcov, Phys. Lett. **B110**, 245 (1982); R. Barbieri *et al.*, JHEP **9812**, 017 (1998); P.H. Frampton, S.T. Petcov, and W. Rodejohann, Nucl. Phys. **B687**, 31 (2004).
124. A. Morales and J. Morales, Nucl. Phys. (Proc. Supp.) **B114**, 141 (2003); C. Aalseth *et al.*, hep-ph/0412300; S.R. Elliott and P. Vogel, Ann. Rev. Nucl. Part. Sci. **52**, 115 (2002).
125. S. Pascoli and S.T. Petcov, Phys. Lett. **B544**, 239 (2002); *ibid.*, **B580**, 280 (2004); see also: S. Pascoli, S.T. Petcov, and L. Wolfenstein, Phys. Lett. **B524**, 319 (2002).
126. S.M. Bilenky *et al.*, Phys. Rev. **D54**, 4432 (1996).
127. S.M. Bilenky *et al.*, Phys. Lett. **B465**, 193 (1999); F. Vissani, JHEP **06**, 022 (1999); K. Matsuda *et al.*, Phys. Rev. **D62**, 093001 (2000); K. Czakov *et al.*, hep-ph/0003161; H.V. Klapdor-Kleingrothaus, H. Päs and A.Yu. Smirnov, Phys. Rev. **D63**, 073005 (2001) S. Pascoli, S.T. Petcov and W. Rodejohann, Phys. Lett. **B549**, 177 (2002), and *ibid.* **B558**, 141 (2003); H. Murayama and Peña-Garay, Phys. Rev. **D69**, 031301 (2004); S. Pascoli, S.T. Petcov, and T. Schwetz, Nucl. Phys. **B734**, 24 (2006); M. Lindner, A. Merle, and W. Rodejohann, Phys. Rev. **D73**, 053005 (2006); A. Faessler *et al.*, Phys. Rev. **D79**, 053001 (2009); S. Pascoli and S.T. Petcov, Phys. Rev. **D77**, 113003 (2008).

14. QUARK MODEL

Revised September 2009 by C. Amsler (University of Zürich), T. DeGrand (University of Colorado, Boulder), and B. Krusche (University of Basel).

14.1. Quantum numbers of the quarks

Quarks are strongly interacting fermions with spin 1/2 and, by convention, positive parity. Antiquarks have negative parity. Quarks have the additive baryon number 1/3, antiquarks -1/3. Table 14.1 gives the other additive quantum numbers (flavors) for the three generations of quarks. They are related to the charge Q (in units of the elementary charge e) through the generalized Gell-Mann-Nishijima formula

$$Q = I_z + \frac{B + S + C + B + T}{2}, \quad (14.1)$$

where B is the baryon number. The convention is that the *flavor* of a quark (I_z , S , C , B , or T) has the same sign as its *charge* Q . With this convention, any flavor carried by a charged meson has the same sign as its charge, *e.g.*, the strangeness of the K^+ is +1, the bottomness of the B^+ is +1, and the charm and strangeness of the D_s^- are each -1. Antiquarks have the opposite flavor signs.

Table 14.1: Additive quantum numbers of the quarks.

Property \ Quark	d	u	s	c	b	t
Q – electric charge	$-\frac{1}{3}$	$+\frac{2}{3}$	$-\frac{1}{3}$	$+\frac{2}{3}$	$-\frac{1}{3}$	$+\frac{2}{3}$
I – isospin	$\frac{1}{2}$	$\frac{1}{2}$	0	0	0	0
I_z – isospin z -component	$-\frac{1}{2}$	$+\frac{1}{2}$	0	0	0	0
S – strangeness	0	0	-1	0	0	0
C – charm	0	0	0	+1	0	0
B – bottomness	0	0	0	0	-1	0
T – topness	0	0	0	0	0	+1

14.2. Mesons

Mesons have baryon number $B = 0$. In the quark model, they are $q\bar{q}'$ bound states of quarks q and antiquarks \bar{q}' (the flavors of q and q' may be different). If the orbital angular momentum of the $q\bar{q}'$ state is ℓ , then the parity P is $(-1)^{\ell+1}$. The meson spin J is given by the usual relation $|\ell - s| \leq J \leq |\ell + s|$, where s is 0 (antiparallel quark spins) or 1 (parallel quark spins). The charge conjugation, or C -parity $C = (-1)^{\ell+s}$, is defined only for the $q\bar{q}$ states made of quarks and their own antiquarks. The C -parity can be generalized to the G -parity $G = (-1)^{I+\ell+s}$ for mesons made of quarks and their own antiquarks (isospin $I_z = 0$), and for the charged $u\bar{d}$ and $d\bar{u}$ states (isospin $I = 1$).

The mesons are classified in J^{PC} multiplets. The $\ell = 0$ states are the pseudoscalars (0^{-+}) and the vectors ($1^{- -}$). The orbital excitations $\ell = 1$ are the scalars (0^{++}), the axial vectors (1^{++}) and (1^{+-}), and the tensors (2^{++}). Assignments for many of the known mesons are given in Tables 14.2 and 14.3. Radial excitations are denoted by the principal quantum number n . The very short lifetime of the t quark makes it likely that bound-state hadrons containing t quarks and/or antiquarks do not exist.

States in the natural spin-parity series $P = (-1)^J$ must, according to the above, have $s = 1$ and hence, $CP = +1$. Thus, mesons with natural spin-parity and $CP = -1$ (0^{+-} , 1^{+-} , 2^{+-} , 3^{+-} , *etc.*) are forbidden in the $q\bar{q}'$ model. The $J^{PC} = 0^{- -}$ state is forbidden as well. Mesons with such *exotic* quantum numbers may exist, but would lie outside the $q\bar{q}'$ model (see section below on exotic mesons).

Following SU(3), the nine possible $q\bar{q}'$ combinations containing the light u , d , and s quarks are grouped into an octet and a singlet of light quark mesons:

$$3 \otimes \bar{3} = 8 \oplus 1. \quad (14.2)$$

A fourth quark such as charm c can be included by extending SU(3) to SU(4). However, SU(4) is badly broken owing to the much heavier c quark. Nevertheless, in an SU(4) classification, the sixteen mesons are grouped into a 15-plet and a singlet:

$$4 \otimes \bar{4} = 15 \oplus 1. \quad (14.3)$$

The *weight diagrams* for the ground-state pseudoscalar (0^{-+}) and vector ($1^{- -}$) mesons are depicted in Fig. 14.1. The light quark mesons are members of nonets building the middle plane in Fig. 14.1(a) and (b).

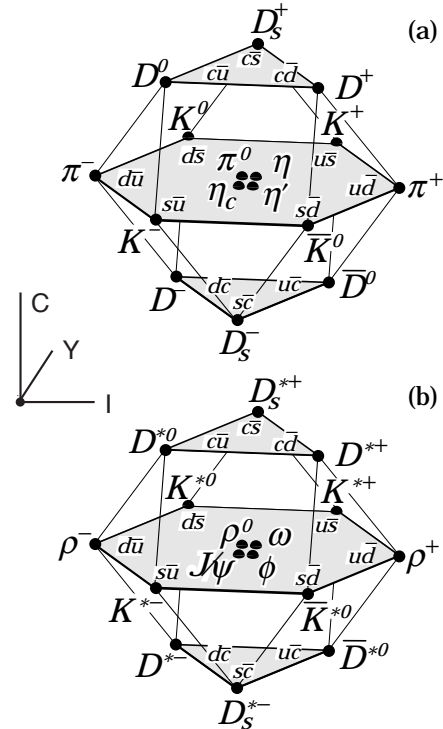


Figure 14.1: SU(4) weight diagram showing the 16-plets for the pseudoscalar (a) and vector mesons (b) made of the u , d , s , and c quarks as a function of isospin I , charm C , and hypercharge $Y = S+B - \frac{C}{3}$. The nonets of light mesons occupy the central planes to which the $c\bar{c}$ states have been added.

Isoscalar states with the same J^{PC} will mix, but mixing between the two light quark isoscalar mesons, and the much heavier charmonium or bottomonium states, are generally assumed to be negligible. In the following, we shall use the generic names a for the $I = 1$, K for the $I = 1/2$, and f and f' for the $I = 0$ members of the light quark nonets. Thus, the physical isoscalars are mixtures of the SU(3) wave function ψ_8 and ψ_1 :

$$f' = \psi_8 \cos \theta - \psi_1 \sin \theta, \quad (14.4)$$

$$f = \psi_8 \sin \theta + \psi_1 \cos \theta, \quad (14.5)$$

where θ is the nonet mixing angle and

$$\psi_8 = \frac{1}{\sqrt{6}}(u\bar{u} + d\bar{d} - 2s\bar{s}), \quad (14.6)$$

$$\psi_1 = \frac{1}{\sqrt{3}}(u\bar{u} + d\bar{d} + s\bar{s}). \quad (14.7)$$

The mixing angle has to be determined experimentally.

Table 14.2: Suggested $q\bar{q}$ quark-model assignments for some of the observed light mesons. Mesons in bold face are included in the Meson Summary Table. The wave functions f and f' are given in the text. The singlet-octet mixing angles from the quadratic and linear mass formulae are also given for the well established nonets. The classification of the 0^{++} mesons is tentative and the mixing angle uncertain due to large uncertainties in some of the masses. Also, the $f_0(1710)$ and $f_0(1370)$ are expected to mix with the $f_0(1500)$. The latter is not in this table as it is hard to accommodate in the scalar nonet. The light scalars $a_0(980)$, $f_0(980)$, and $f_0(600)$ are often considered as meson-meson resonances or four-quark states, and are therefore not included in the table. See the “Note on Scalar Mesons” in the Meson Listings for details and alternative schemes.

$n^{2s+1}\ell_J$	J^{PC}	$l = 1$ $u\bar{d}, \bar{u}d, \frac{1}{\sqrt{2}}(d\bar{d} - u\bar{u})$	$l = \frac{1}{2}$ $u\bar{s}, \bar{d}s; \bar{d}s, -\bar{u}s$	$l = 0$ f'	$l = 0$ f	θ_{quad} [°]	θ_{lin} [°]
1^1S_0	0^{-+}	π	K	η	$\eta'(958)$	-11.5	-24.6
1^3S_1	1^{--}	$\rho(770)$	$K^*(892)$	$\phi(1020)$	$\omega(782)$	38.7	36.0
1^1P_1	1^{+-}	$b_1(1235)$	K_{1B}^\dagger	$h_1(1380)$	$h_1(1170)$		
1^3P_0	0^{++}	$a_0(1450)$	$K_0^*(1430)$	$f_0(1710)$	$f_0(1370)$		
1^3P_1	1^{++}	$a_1(1260)$	K_{1A}^\dagger	$f_1(1420)$	$f_1(1285)$		
1^3P_2	2^{++}	$a_2(1320)$	$K_2^*(1430)$	$f_2'(1525)$	$f_2(1270)$	29.6	28.0
1^1D_2	2^{-+}	$\pi_2(1670)$	$K_2(1770)^\dagger$	$\eta_2(1870)$	$\eta_2(1645)$		
1^3D_1	1^{--}	$\rho(1700)$	$K^*(1680)$		$\omega(1650)$		
1^3D_2	2^{--}		$K_2(1820)$				
1^3D_3	3^{--}	$\rho_3(1690)$	$K_3^*(1780)$	$\phi_3(1850)$	$\omega_3(1670)$	32.0	31.0
1^3F_4	4^{++}	$a_4(2040)$	$K_4^*(2045)$		$f_4(2050)$		
1^3G_5	5^{--}	$\rho_5(2350)$					
1^3H_6	6^{++}	$a_6(2450)$			$f_6(2510)$		
2^1S_0	0^{-+}	$\pi(1300)$	$K(1460)$	$\eta(1475)$	$\eta(1295)$		
2^3S_1	1^{--}	$\rho(1450)$	$K^*(1410)$	$\phi(1680)$	$\omega(1420)$		

† The $1^{+\pm}$ and $2^{-\pm}$ isospin $\frac{1}{2}$ states mix. In particular, the K_{1A} and K_{1B} are nearly equal (45°) mixtures of the $K_1(1270)$ and $K_1(1400)$. The physical vector mesons listed under 1^3D_1 and 2^3S_1 may be mixtures of 1^3D_1 and 2^3S_1 , or even have hybrid components.

Table 14.3: $q\bar{q}$ quark-model assignments for the observed heavy mesons. Mesons in bold face are included in the Meson Summary Table.

$n^{2s+1}\ell_J$	J^{PC}	$l = 0$ $c\bar{c}$	$l = 0$ $b\bar{b}$	$l = \frac{1}{2}$ $c\bar{u}, \bar{c}d; \bar{c}u, \bar{c}d$	$l = 0$ $c\bar{s}; \bar{c}s$	$l = \frac{1}{2}$ $b\bar{u}, \bar{b}d; \bar{b}u, \bar{b}d$	$l = 0$ $b\bar{s}; \bar{b}s$	$l = 0$ $b\bar{c}; \bar{b}c$
1^1S_0	0^{-+}	$\eta_c(1S)$	$\eta_b(1S)$	D	D_s^\pm	B	B_s^0	B_c^\pm
1^3S_1	1^{--}	$J/\psi(1S)$	$\Upsilon(1S)$	D^*	$D_s^{*\pm}$	B^*	B_s^*	
1^1P_1	1^{+-}	$h_c(1P)$		$D_1(2420)$	$D_{s1}(2536)^\pm$	$B_1(5721)$	$B_{s1}(5830)^0$	
1^3P_0	0^{++}	$\chi_{c0}(1P)$	$\chi_{b0}(1P)$	$D_0^*(2400)$	$D_{s0}^*(2317)^\pm$			
1^3P_1	1^{++}	$\chi_{c1}(1P)$	$\chi_{b1}(1P)$	$D_1(2430)$	$D_{s1}(2460)^\pm$			
1^3P_2	2^{++}	$\chi_{c2}(1P)$	$\chi_{b2}(1P)$	$D_2^*(2460)$	$D_{s2}^*(2573)^\pm$	$B_2^*(5747)$	$B_{s2}^*(5840)^0$	
1^3D_1	1^{--}	$\psi(3770)$			$D_{s1}^*(2700)^\pm$			
2^1S_0	0^{-+}	$\eta_c(2S)$						
2^3S_1	1^{--}	$\psi(2S)$	$\Upsilon(2S)$					
$2^3P_{0,1,2}$	$0^{++}, 1^{++}, 2^{++}$		$\chi_{b0,1,2}(2P)$					

† The masses of these states are considerably smaller than most theoretical predictions. They have also been considered as four-quark states (See the “Note on Non- $q\bar{q}$ Mesons” at the end of the Meson Listings). The open flavor states in the 1^{+-} and 1^{++} rows are mixtures of the $1^{+\pm}$ states.

These mixing relations are often rewritten to exhibit the $u\bar{u} + d\bar{d}$ and $s\bar{s}$ components which decouple for the “ideal” mixing angle θ_i , such that $\tan \theta_i = 1/\sqrt{2}$ (or $\theta_i=35.3^\circ$). Defining $\alpha = \theta + 54.7^\circ$, one obtains the physical isoscalar in the flavor basis

$$f' = \frac{1}{\sqrt{2}}(u\bar{u} + d\bar{d}) \cos \alpha - s\bar{s} \sin \alpha, \quad (14.8)$$

and its orthogonal partner f (replace α by $\alpha - 90^\circ$). Thus for ideal mixing ($\alpha_i = 90^\circ$), the f' becomes pure $s\bar{s}$ and the f pure $u\bar{u} + d\bar{d}$. The mixing angle θ can be derived from the mass relation

$$\tan \theta = \frac{4m_K - m_a - 3m_{f'}}{2\sqrt{2}(m_a - m_K)}, \quad (14.9)$$

which also determines its sign or, alternatively, from

$$\tan^2 \theta = \frac{4m_K - m_a - 3m_{f'}}{-4m_K + m_a + 3m_{f'}}. \quad (14.10)$$

Eliminating θ from these equations leads to the sum rule [1]

$$(m_f + m_{f'})(4m_K - m_a) - 3m_{f'}m_a = 8m_K^2 - 8m_K m_a + 3m_a^2. \quad (14.11)$$

This relation is verified for the ground-state vector mesons. We identify the $\phi(1020)$ with the f' and the $\omega(783)$ with the f . Thus

$$\phi(1020) = \psi_8 \cos \theta_V - \psi_1 \sin \theta_V, \quad (14.12)$$

$$\omega(782) = \psi_8 \sin \theta_V + \psi_1 \cos \theta_V, \quad (14.13)$$

with the vector mixing angle $\theta_V = 35^\circ$ from Eq. (14.9), very close to ideal mixing. Thus $\phi(1020)$ is nearly pure $s\bar{s}$. For ideal mixing, Eq. (14.9) and Eq. (14.10) lead to the relations

$$m_K = \frac{m_f + m_{f'}}{2}, \quad m_a = m_f, \quad (14.14)$$

which are satisfied for the vector mesons. However, for the pseudoscalar (and scalar mesons), Eq. (14.11) is satisfied only approximately. Then Eq. (14.9) and Eq. (14.10) lead to somewhat different values for the mixing angle. Identifying the η with the f' one gets

$$\eta = \psi_8 \cos \theta_P - \psi_1 \sin \theta_P, \quad (14.15)$$

$$\eta' = \psi_8 \sin \theta_P + \psi_1 \cos \theta_P. \quad (14.16)$$

Following chiral perturbation theory, the meson masses in the mass formulae (Eq. (14.9) and Eq. (14.10)) should be replaced by their squares. Table 14.2 lists the mixing angle θ_{lin} from Eq. (14.10) and the corresponding θ_{quad} obtained by replacing the meson masses by their squares throughout.

The pseudoscalar mixing angle θ_P can also be measured by comparing the partial widths for radiative J/ψ decay into a vector and a pseudoscalar [2], radiative $\phi(1020)$ decay into η and η' [3], or $\bar{p}p$ annihilation at rest into a pair of vector and pseudoscalar or into two pseudoscalars [4,5]. One obtains a mixing angle between -10° and -20° .

The nonet mixing angles can be measured in $\gamma\gamma$ collisions, *e.g.*, for the 0^{-+} , 0^{++} , and 2^{++} nonets. In the quark model, the amplitude for the coupling of neutral mesons to two photons is proportional to $\sum_i Q_i^2$, where Q_i is the charge of the i -th quark. The 2γ partial width of an isoscalar meson with mass m is then given in terms of the mixing angle α by

$$\Gamma_{2\gamma} = C(5 \cos \alpha - \sqrt{2} \sin \alpha)^2 m^3, \quad (14.17)$$

for f' and f ($\alpha \rightarrow \alpha - 90^\circ$). The coupling C may depend on the meson mass. It is often assumed to be a constant in the nonet. For the isovector a , one then finds $\Gamma_{2\gamma} = 9 C m^3$. Thus the members of an ideally mixed nonet couple to 2γ with partial widths in the ratios $f' : a = 25 : 2 : 9$. For tensor mesons, one finds from the ratios of the measured 2γ partial widths for the $f_2(1270)$ and $f_2'(1525)$ mesons a mixing angle α_T of $(81 \pm 1)^\circ$, or $\theta_T = (27 \pm 1)^\circ$, in accord with the linear mass formula. For the pseudoscalars, one finds from the ratios of partial widths $\Gamma(\eta' \rightarrow 2\gamma)/\Gamma(\eta \rightarrow 2\gamma)$ a mixing angle $\theta_P = (-18 \pm 2)^\circ$, while the ratio $\Gamma(\eta' \rightarrow 2\gamma)/\Gamma(\pi^0 \rightarrow 2\gamma)$ leads to $\sim -24^\circ$. SU(3) breaking effects for pseudoscalars are discussed in Ref. 6.

Table 14.4: SU(3) couplings γ^2 for quarkonium decays as a function of nonet mixing angle α , up to a common multiplicative factor C ($\phi \equiv 54.7^\circ + \theta_P$).

Isospin	Decay channel	γ^2
0	$\pi\pi$	$3 \cos^2 \alpha$
	$K\bar{K}$	$(\cos \alpha - \sqrt{2} \sin \alpha)^2$
	$\eta\eta$	$(\cos \alpha \cos^2 \phi - \sqrt{2} \sin \alpha \sin^2 \phi)^2$
	$\eta\eta'$	$\frac{1}{2} \sin^2 2\phi (\cos \alpha + \sqrt{2} \sin \alpha)^2$
1	$\eta\pi$	$2 \cos^2 \phi$
	$\eta'\pi$	$2 \sin^2 \phi$
	$K\bar{K}$	1
$\frac{1}{2}$	$K\pi$	$\frac{3}{2}$
	$K\eta$	$(\sin \phi - \frac{\cos \phi}{\sqrt{2}})^2$
	$K\eta'$	$(\cos \phi + \frac{\sin \phi}{\sqrt{2}})^2$

The partial width for the decay of a scalar or a tensor meson into a pair of pseudoscalar mesons is model-dependent. Following Ref. 7,

$$\Gamma = C \times \gamma^2 \times |F(q)|^2 \times q. \quad (14.18)$$

C is a nonet constant, q the momentum of the decay products, $F(q)$ a form factor, and γ^2 the SU(3) coupling. The model-dependent form factor may be written as

$$|F(q)|^2 = q^{2\ell} \times \exp\left(-\frac{q^2}{8\beta^2}\right), \quad (14.19)$$

where ℓ is the relative angular momentum between the decay products. The decay of a $q\bar{q}$ meson into a pair of mesons involves the creation of a $q\bar{q}$ pair from the vacuum, and SU(3) symmetry assumes that the matrix elements for the creation of $s\bar{s}$, $u\bar{u}$, and $d\bar{d}$ pairs are equal. The couplings γ^2 are given in Table 14.4, and their dependence upon the mixing angle α is shown in Fig. 14.2 for isoscalar decays. The generalization to unequal $s\bar{s}$, $u\bar{u}$, and $d\bar{d}$ couplings is given in Ref. 7. An excellent fit to the tensor meson decay widths is obtained assuming SU(3) symmetry, with $\beta \simeq 0.5 \text{ GeV}/c$, $\theta_V \simeq 26^\circ$ and $\theta_P \simeq -17^\circ$ [7].

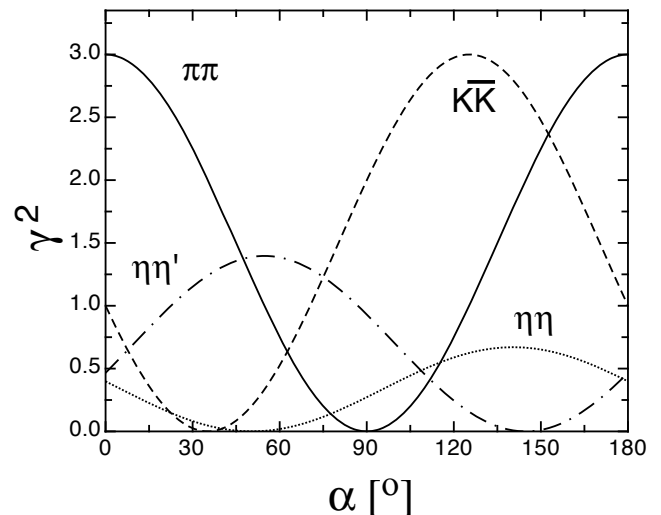


Figure 14.2: SU(3) couplings as a function of mixing angle α for isoscalar decays, up to a common multiplicative factor C and for $\theta_P = -17.3^\circ$.

14.3. Exotic mesons

The existence of a light nonet composed of four quarks with masses below 1 GeV was suggested a long time ago [8]. Coupling two triplets of light quarks u , d , and s , one obtains nine states, of which the six symmetric (uu , dd , ss , $ud + du$, $us + su$, $ds + sd$) form the six dimensional representation $\mathbf{6}$, while the three antisymmetric ($ud - du$, $us - su$, $ds - sd$) form the three dimensional representation $\bar{\mathbf{3}}$ of SU(3):

$$\mathbf{3} \otimes \mathbf{3} = \mathbf{6} \oplus \bar{\mathbf{3}}. \quad (14.20)$$

Combining with spin and color and requiring antisymmetry, one finds that the most deeply bound diquark (and hence the lightest) is the one in the $\bar{\mathbf{3}}$ and spin singlet state. The combination of the diquark with an antiquark in the $\mathbf{3}$ representation then gives a light nonet of four-quark scalar states. Letting the number of strange quarks determine the mass splitting, one obtains a mass inverted spectrum with a light isosinglet ($ud\bar{u}\bar{d}$), a medium heavy isodoublet (*e.g.*, $ud\bar{s}\bar{d}$) and a heavy isotriplet (*e.g.*, $ds\bar{u}\bar{s}$) + isosinglet (*e.g.*, $us\bar{u}\bar{s}$). It is then tempting to identify the lightest state with the $f_0(600)$, and the heaviest states with the $a_0(980)$, and $f_0(980)$. Then the meson with strangeness $\kappa(800)$ would lie in between.

QCD predicts the existence of extra isoscalar mesons. In the pure gauge theory, they contain only gluons, and are called the glueballs. The ground state glueball is predicted by lattice gauge theories to be 0^{++} , the first excited state 2^{++} . Errors on the mass predictions are large. From Ref. 10 one obtains 1750 (50) (80) MeV for the mass of the lightest 0^{++} glueball from quenched QCD. As an example for the glueball mass spectrum, we show in Fig. 14.3 a recent calculation from the quenched lattice [9]. A mass of 1710 MeV is predicted for the ground state, also with an error of about 100 MeV. Earlier work by other groups produced masses at 1650 MeV [11] and 1550 MeV [12] (see also Ref. 13) The first excited state has a mass of about 2.4 GeV, and the lightest glueball with exotic quantum numbers (2^{+-}) has a mass of about 4 GeV.

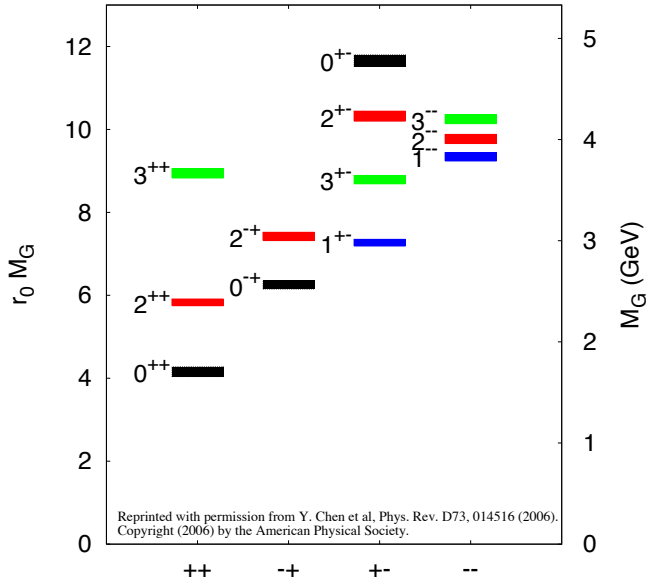


Figure 14.3: Predicted glueball mass spectrum from the lattice, in quenched approximation, (from Ref. 9).

These calculations assume that the quark masses are infinite (quenched approximation) and neglect $q\bar{q}$ loops. However, both glue and $q\bar{q}$ states will couple to singlet scalar mesons. Therefore glueballs will mix with nearby $q\bar{q}$ states of the same quantum numbers. For example, the two isoscalar 0^{++} mesons around 1500 MeV will mix with the pure ground state glueball to generate the observed physical states $f_0(1370)$, $f_0(1500)$, and $f_0(1710)$ [7,14]. Lattice calculations are only beginning to include these effects. Unquenched QCD with a coarse lattice suggests that the mass of the singlet scalar meson is very low [15]. However, in quenched QCD, the mass of the 0^{++} glueball strongly depends on lattice spacing, and therefore

continuum extrapolation cannot be attempted yet in unquenched lattice simulations for flavor-singlet scalar mesons [16].

The existence of three singlet scalar mesons around 1.5 GeV suggests additional degrees of freedom such as glue, since only two mesons are predicted in this mass range. The $f_0(1500)$ [7,14] or, alternatively, the $f_0(1710)$ [11], have been proposed as candidates for the scalar glueball, both states having considerable mixing also with the $f_0(1370)$. Other mixing schemes, in particular with the $f_0(600)$ and the $f_0(980)$, have also been proposed (more details can be found in the “Note on Scalar Mesons” in the Meson Listings and in Ref. 17).

Mesons made of $q\bar{q}$ pairs bound by excited gluons g , the hybrid states $q\bar{q}g$, are also predicted. They should lie in the 1.9 GeV mass region, according to gluon flux tube models [18]. Lattice QCD also predicts the lightest hybrid, an exotic 1^{-+} , at a mass of 1.8 to 1.9 GeV [19]. However, the bag model predicts four nonets, among them an exotic 1^{-+} around or above 1.4 GeV [20,21]. There are so far two candidates for exotic states with quantum numbers 1^{-+} , the $\pi_1(1400)$ and $\pi_1(1600)$, which could be hybrids or four-quark states (see the “Note on Non- $q\bar{q}$ Mesons” in the 2006 issue of this Review [22] and in Ref. 17).

14.4. Baryons: qqq states

Baryons are fermions with baryon number $\mathcal{B} = 1$, *i.e.*, in the most general case, they are composed of three quarks plus any number of quark - antiquark pairs. Although recently some experimental evidence for ($qqq\bar{q}$) pentaquark states has been claimed (see review on Possible Exotic Baryon Resonance), so far all established baryons are 3-quark (qqq) configurations. The color part of their state functions is an SU(3) singlet, a completely antisymmetric state of the three colors. Since the quarks are fermions, the state function must be antisymmetric under interchange of any two equal-mass quarks (up and down quarks in the limit of isospin symmetry). Thus it can be written as

$$|qqq\rangle_A = |\text{color}\rangle_A \times |\text{space, spin, flavor}\rangle_S, \quad (14.21)$$

where the subscripts S and A indicate symmetry or antisymmetry under interchange of any two equal-mass quarks. Note the contrast with the state function for the three nucleons in ${}^3\text{H}$ or ${}^3\text{He}$:

$$|NNN\rangle_A = |\text{space, spin, isospin}\rangle_A. \quad (14.22)$$

This difference has major implications for internal structure, magnetic moments, *etc.* (For a nice discussion, see Ref. 23.)

The “ordinary” baryons are made up of u , d , and s quarks. The three flavors imply an approximate flavor SU(3), which requires that baryons made of these quarks belong to the multiplets on the right side of

$$\mathbf{3} \otimes \mathbf{3} \otimes \mathbf{3} = \mathbf{10}_S \oplus \mathbf{8}_M \oplus \mathbf{8}_M \oplus \mathbf{1}_A \quad (14.23)$$

(see Sec. 38, on “SU(n) Multiplets and Young Diagrams”). Here the subscripts indicate symmetric, mixed-symmetry, or antisymmetric states under interchange of any two quarks. The $\mathbf{1}$ is a uds state (Λ_1), and the octet contains a similar state (Λ_8). If these have the same spin and parity, they can mix. The mechanism is the same as for the mesons (see above). In the ground state multiplet, the SU(3) flavor singlet Λ_1 is forbidden by Fermi statistics. Section 37, on “SU(3) Isoscalar Factors and Representation Matrices,” shows how relative decay rates in, say, $\mathbf{10} \rightarrow \mathbf{8} \otimes \mathbf{8}$ decays may be calculated.

The addition of the c quark to the light quarks extends the flavor symmetry to SU(4). However, due to the large mass of the c quark, this symmetry is much more strongly broken than the SU(3) of the three light quarks. Figures 14.4(a) and 14.4(b) show the SU(4) baryon multiplets that have as their bottom levels an SU(3) octet, such as the octet that includes the nucleon, or an SU(3) decuplet, such as the decuplet that includes the $\Delta(1232)$. All particles in a given SU(4) multiplet have the same spin and parity. The charmed baryons are discussed in more detail in the “Note on Charmed Baryons” in the Particle Listings. The addition of a b quark extends the flavor symmetry to SU(5); the existence of baryons with t -quarks is very unlikely due to the short lifetime of the top.

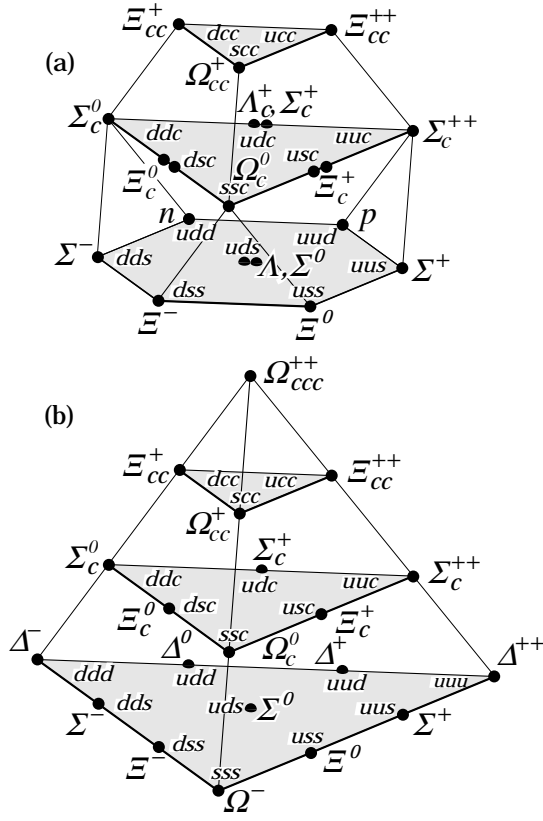


Figure 14.4: SU(4) multiplets of baryons made of u , d , s , and c quarks. (a) The 20-plet with an SU(3) octet. (b) The 20-plet with an SU(3) decuplet.

For the “ordinary” baryons (no c or b quark), flavor and spin may be combined in an approximate flavor-spin SU(6), in which the six basic states are $d \uparrow$, $d \downarrow$, \dots , $s \downarrow$ (\uparrow, \downarrow = spin up, down). Then the baryons belong to the multiplets on the right side of

$$\mathbf{6} \otimes \mathbf{6} \otimes \mathbf{6} = \mathbf{56}_S \oplus \mathbf{70}_M \oplus \mathbf{70}_M \oplus \mathbf{20}_A. \quad (14.24)$$

These SU(6) multiplets decompose into flavor SU(3) multiplets as follows:

$$\mathbf{56} = \mathbf{4}\mathbf{10} \oplus \mathbf{2}\mathbf{8} \quad (14.25a)$$

$$\mathbf{70} = \mathbf{2}\mathbf{10} \oplus \mathbf{4}\mathbf{8} \oplus \mathbf{2}\mathbf{8} \oplus \mathbf{2}\mathbf{1} \quad (14.25b)$$

$$\mathbf{20} = \mathbf{2}\mathbf{8} \oplus \mathbf{4}\mathbf{1}, \quad (14.25c)$$

where the superscript ($2S + 1$) gives the net spin S of the quarks for each particle in the SU(3) multiplet. The $J^P = 1/2^+$ octet containing the nucleon and the $J^P = 3/2^+$ decuplet containing the $\Delta(1232)$ together make up the “ground-state” 56-plet, in which the orbital angular momenta between the quark pairs are zero (so that the spatial part of the state function is trivially symmetric). The $\mathbf{70}$ and $\mathbf{20}$ require some excitation of the spatial part of the state function in order to make the overall state function symmetric. States with nonzero orbital angular momenta are classified in SU(6) \otimes O(3) supermultiplets.

It is useful to classify the baryons into bands that have the same number N of quanta of excitation. Each band consists of a number of supermultiplets, specified by (D, L_N^P) , where D is the dimensionality of the SU(6) representation, L is the total quark orbital angular momentum, and P is the total parity. Supermultiplets contained in bands up to $N = 12$ are given in Ref. 25. The $N = 0$ band, which contains the nucleon and $\Delta(1232)$, consists only of the $(56, 0_0^+)$ supermultiplet. The $N = 1$ band consists only of the $(70, 1_1^-)$ multiplet and contains the negative-parity baryons with masses below about 1.9 GeV. The $N = 2$ band contains five supermultiplets: $(56, 0_2^+)$, $(70, 0_2^+)$, $(56, 2_2^+)$, $(70, 2_2^+)$, and $(20, 1_2^+)$.

Table 14.5: N and Δ states in the $N=0,1,2$ harmonic oscillator bands. L^P denotes angular momentum and parity, S the three-quark spin and ‘sym’=A,S,M the symmetry of the spatial wave function.

N	sym	L^P	S	$N(I = 1/2)$	$\Delta(I = 3/2)$
2	A	1^+	$1/2$	$1/2^+$	$3/2^+$
2	M	2^+	$3/2$	$1/2^+$	$3/2^+$
2	M	2^+	$1/2$	$3/2^+$	$5/2^+$
2	M	0^+	$3/2$	$3/2^+$	$3/2^+$
2	M	0^+	$1/2$	$1/2^+$	$1/2^+$
2	S	2^+	$3/2$		$1/2^+$
2	S	2^+	$1/2$	$3/2^+$	$5/2^+$
2	S	0^+	$3/2$		$3/2^+$
2	S	0^+	$1/2$	$1/2^+$	
1	M	1^-	$3/2$	$1/2^-$	$3/2^-$
1	M	1^-	$1/2$	$1/2^-$	$3/2^-$
0	S	0^+	$3/2$		$3/2^+$
0	S	0^+	$1/2$	$1/2^+$	

Table 14.6: Quark-model assignments for some of the known baryons in terms of a flavor-spin SU(6) basis. Only the dominant representation is listed. Assignments for several states, especially for the $\Lambda(1810)$, $\Lambda(2350)$, $\Xi(1820)$, and $\Xi(2030)$, are merely educated guesses. \dagger Recent suggestions for assignments and re-assignments from Ref. 28. For assignments of the charmed baryons, see the “Note on Charmed Baryons” in the Particle Listings.

J^P	$(D, L_N^P)S$	Octet members	Singlets
$1/2^+$	$(56, 0_0^+)$	$1/2 N(939)$	$\Lambda(1116)$
$1/2^+$	$(56, 0_2^+)$	$1/2 N(1440)$	$\Lambda(1600)$
$1/2^-$	$(70, 1_1^-)$	$1/2 N(1535)$	$\Lambda(1670)$
$3/2^-$	$(70, 1_1^-)$	$1/2 N(1520)$	$\Lambda(1690)$
$1/2^-$	$(70, 1_1^-)$	$3/2 N(1650)$	$\Lambda(1800)$
$3/2^-$	$(70, 1_1^-)$	$3/2 N(1700)$	$\Lambda(?)$
$5/2^-$	$(70, 1_1^-)$	$3/2 N(1675)$	$\Lambda(1830)$
$1/2^+$	$(70, 0_2^+)$	$1/2 N(1710)$	$\Lambda(1810)$
$3/2^+$	$(56, 2_2^+)$	$1/2 N(1720)$	$\Lambda(1890)$
$5/2^+$	$(56, 2_2^+)$	$1/2 N(1680)$	$\Lambda(1820)$
$7/2^-$	$(70, 3_3^-)$	$1/2 N(2190)$	$\Lambda(?)$
$9/2^-$	$(70, 3_3^-)$	$3/2 N(2250)$	$\Lambda(?)$
$9/2^+$	$(56, 4_4^+)$	$1/2 N(2220)$	$\Lambda(2350)$

Decuplet members			
$3/2^+$	$(56, 0_0^+)$	$3/2 \Delta(1232)$	$\Sigma(1385)$
$3/2^+$	$(56, 0_2^+)$	$3/2 \Delta(1600)$	$\Sigma(1690)$
$1/2^-$	$(70, 1_1^-)$	$1/2 \Delta(1620)$	$\Sigma(1750)$
$3/2^-$	$(70, 1_1^-)$	$1/2 \Delta(1700)$	$\Sigma(?)$
$5/2^+$	$(56, 2_2^+)$	$3/2 \Delta(1905)$	$\Sigma(?)$
$7/2^+$	$(56, 2_2^+)$	$3/2 \Delta(1950)$	$\Sigma(2030)$
$11/2^+$	$(56, 4_4^+)$	$3/2 \Delta(2420)$	$\Sigma(?)$

The wave functions of the non-strange baryons in the harmonic oscillator basis are often labeled by $|X^{2S+1}L_N J^P\rangle$, where S, L, J, P

are as above, $X = N$ or Δ , and $\pi = S, M$ or A denotes the symmetry of the spatial wave function. The possible states for the bands with $N=0,1,2$ are given in Table 14.5.

In Table 14.6, quark-model assignments are given for many of the established baryons whose $SU(6)\otimes O(3)$ compositions are relatively unmixed. One must, however, keep in mind that apart from the mixing of the Λ singlet and octet states, states with same J^P but different L, S combinations can also mix. In the quark model with one-gluon exchange motivated interactions, the size of the mixing is determined by the relative strength of the tensor term with respect to the contact term (see below). The mixing is more important for the decay patterns of the states than for their positions. An example are the lowest lying $(70, 1^-)$ states with $J^P=1/2^-$ and $3/2^-$. The physical states are:

$$|S_{11}(1535)\rangle = \cos(\Theta_S)|N^2P_M1/2^-\rangle - \sin(\Theta_S)|N^4P_M1/2^-\rangle \quad (14.26)$$

$$|D_{13}(1520)\rangle = \cos(\Theta_D)|N^2P_M3/2^-\rangle - \sin(\Theta_D)|N^4P_M3/2^-\rangle \quad (14.27)$$

and the orthogonal combinations for $S_{11}(1650)$ and $D_{13}(1700)$. The mixing is large for the $J^P=1/2^-$ states ($\Theta_S \approx -32^\circ$), but small for the $J^P=3/2^-$ states ($\Theta_D \approx +6^\circ$) [26,30].

All baryons of the ground state multiplets are known. Many of their properties, in particular their masses, are in good agreement even with the most basic versions of the quark model, including harmonic (or linear) confinement and a spin-spin interaction, which is responsible for the octet - decuplet mass shifts. A consistent description of the ground-state electroweak properties, however, requires refined relativistic constituent quark models.

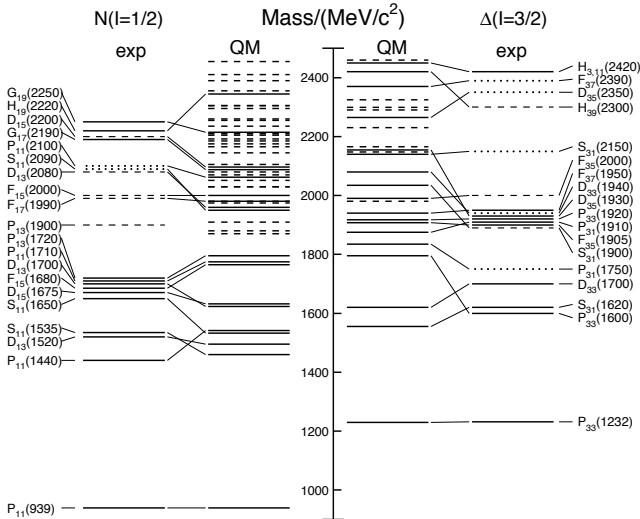


Figure 14.5: Excitation spectrum of the nucleon. Compared are the positions of the excited states identified in experiment, to those predicted by a relativized quark model calculation. Left hand side: isospin $I = 1/2$ N -states, right hand side: isospin $I = 3/2$ Δ -states. Experimental: (columns labeled 'exp'), three- and four-star states are indicated by full lines (two-star dashed lines, one-star dotted lines). At the very left and right of the figure, the spectroscopic notation of these states is given. Quark model [27]: (columns labeled 'QM'), all states for the $N=1,2$ bands, low-lying states for the $N=3,4,5$ bands. Full lines: at least tentative assignment to observed states, dashed lines: so far no observed counterparts. Many of the assignments between predicted and observed states are highly tentative.

The situation for the excited states is much less clear. The assignment of some experimentally observed states with strange quarks to model configurations is only tentative and in many cases candidates are completely missing. Recently, Melde, Plessas, and Sengl [28] have calculated baryon properties in relativistic constituent quark models, using one-gluon exchange and Goldstone-boson exchange for the modelling of the hyperfine interactions (see Sec. 14.5 on

Dynamics). Both types of models give qualitatively comparable results, and underestimate in general experimentally observed decay widths. Nevertheless, in particular on the basis of the observed decay patterns, the authors have assigned some additional states with strangeness to the $SU(3)$ multiplets and suggest re-assignments for a few others. Among the new assignments are states with weak experimental evidence (two or three star ratings) and partly without firm spin/parity assignments, so that further experimental efforts are necessary before final conclusions can be drawn. We have added their suggestions in Table 14.6.

In the non-strange sector there are two main problems which are illustrated in Fig. 14.5, where the experimentally observed excitation spectrum of the nucleon (N and Δ resonances) is compared to the results of a typical quark model calculation [27]. Many more states are predicted than observed, but on the other hand, states with certain quantum numbers appear in the spectrum at excitation energies much lower than predicted. Up to an excitation energy of 2.4 GeV, about 45 N states are predicted, but only 12 are established (four- or three-star; see Note on N and Δ Resonances for the rating of the status of resonances) and 7 are tentative (two- or one-star). Even for the $N=1,2$ bands, up to now only half of the predicted states have been observed. This has been known for a long time as the 'missing resonance' problem [26]. On the other hand, the lowest states from the $N=2$ band, the $P_{11}(1440)$, and the $P_{33}(1600)$, appear lower than the negative parity states from the $N=1$ band, and much lower than predicted by most models. Also negative parity Δ states from the $N=3$ band ($S_{31}(1900)$, $D_{33}(1940)$, and $D_{35}(1930)$) are too low in energy. Part of the problem could be experimental. Among the negative parity Δ states, only the D_{35} has three stars and the uncertainty in the position of the $P_{33}(1600)$ is large (1550 - 1700 MeV). For the missing resonance problem, selection rules could play a role [26]. The states are broad and overlapping, and most studies of baryon resonances have been done with pion-induced reactions, so that there is bias in the database against resonances, which couple only weakly to the $N\pi$ channel. Quark model predictions for the couplings to other hadronic channels and to photons are given in Ref. 27. A large experimental effort is ongoing at several electron accelerators to study the baryon resonance spectrum with real and virtual photon-induced meson production reactions. This includes the search for as-yet-unobserved states, as well as detailed studies of the properties of the low lying states (decay patterns, electromagnetic couplings, magnetic moments, *etc.*) (see Ref. 29 for recent reviews).

In quark models, the number of excited states is determined by the effective degrees of freedom, while their ordering and decay properties are related to the residual quark - quark interaction. A recent overview of quark models for baryons is given in Ref. 30. The effective degrees of freedom in the standard nonrelativistic quark model are three equivalent valence quarks with one-gluon exchange-motivated, flavor-independent color-magnetic interactions. A different class of models uses interactions which give rise to a quark - diquark clustering of the baryons (for a review see Ref. 31). If there is a tightly bound diquark, only two degrees of freedom are available at low energies, and thus *fewer* states are predicted. Furthermore, selection rules in the decay pattern may arise from the quantum numbers of the diquark. *More* states are predicted by collective models of the baryon like the algebraic approach in Ref. 32. In this approach, the quantum numbers of the valence quarks are distributed over a Y-shaped string-like configuration, and additional states arise *e.g.*, from vibrations of the strings. *More* states are also predicted in the framework of flux-tube models (see Ref. 33), which are motivated by lattice QCD. In addition to the quark degrees of freedom, flux-tubes responsible for the confinement of the quarks are considered as degrees of freedom. These models include hybrid baryons containing explicit excitations of the gluon fields. However, since all half integral J^P quantum numbers are possible for ordinary baryons, such 'exotics' will be very hard to identify, and probably always mix with ordinary states. So far, the experimentally observed number of states is still far lower even than predicted by the quark-diquark models.

Recently, the influence of chiral symmetry on the excitation spectrum of the nucleon has been hotly debated from a somewhat new perspective. Chiral symmetry, the fundamental symmetry of QCD, is strongly broken for the low lying states, resulting in large mass

differences of parity partners like the $J^P=1/2^+$ $P_{11}(938)$ ground state and the $J^P=1/2^-$ $S_{11}(1535)$ excitation. However, at higher excitation energies there is some evidence for parity doublets and even some very tentative suggestions for full chiral multiplets of N^* and Δ resonances. An effective restoration of chiral symmetry at high excitation energies due to a decoupling from the quark condensate of the vacuum has been controversially discussed (see Ref. 34 for recent reviews) as a possible cause. In this case, the mass generating mechanisms for low and high lying states would be essentially different. As a further consequence, the parity doublets would decouple from pions, so that experimental bias would be worse. However, parity doublets might also arise from the spin-orbital dynamics of the 3-quark system. Presently, the status of data does not allow final conclusions.

14.5. Dynamics

Many specific quark models exist, but most contain a similar basic set of dynamical ingredients. These include:

- i) A confining interaction, which is generally spin-independent (*e.g.*, harmonic oscillator or linear confinement);
- ii) Different types of spin-dependent interactions:
 - a) commonly used is a color-magnetic flavor-independent interaction modeled after the effects of gluon exchange in QCD (see *e.g.*, Ref. 36). For example, in the S -wave states, there is a spin-spin hyperfine interaction of the form

$$H_{HF} = -\alpha_S M \sum_{i>j} (\vec{\sigma} \lambda_a)_i (\vec{\sigma} \lambda_a)_j, \quad (14.28)$$

where M is a constant with units of energy, λ_a ($a = 1, \dots, 8$) is the set of SU(3) unitary spin matrices, defined in Sec. 37, on “SU(3) Isoscalar Factors and Representation Matrices,” and the sum runs over constituent quarks or antiquarks. Spin-orbit interactions, although allowed, seem to be small in general, but a tensor term is responsible for the mixing of states with the same J^P but different L, S combinations.

b) other approaches include flavor-dependent short-range quark forces from instanton effects (see *e.g.*, Ref. 37). This interaction acts only on scalar, isoscalar pairs of quarks in a relative S -wave state:

$$\langle q^2; S, L, T | W | q^2; S, L, T \rangle = -4g\delta_{S,0}\delta_{L,0}\delta_{T,0}\mathcal{W} \quad (14.29)$$

where \mathcal{W} is the radial matrix element of the contact interaction.

c) a rather different and controversially discussed approach is based on flavor-dependent spin-spin forces arising from one-boson exchange. The interaction term is of the form:

$$H_{HF} \propto \sum_{i<j} V(\vec{r}_{ij}) \lambda_i^F \cdot \lambda_j^F \vec{\sigma}_i \cdot \vec{\sigma}_j \quad (14.30)$$

where the λ_i^F are in flavor space (see *e.g.*, Ref. 38).

- iii) A strange quark mass somewhat larger than the up and down quark masses, in order to split the SU(3) multiplets;
- iv) In the case of spin-spin interactions (iia,c), a flavor-symmetric interaction for mixing $q\bar{q}$ configurations of different flavors (*e.g.*, $u\bar{u} \leftrightarrow d\bar{d} \leftrightarrow s\bar{s}$), in isoscalar channels, so as to reproduce *e.g.*, the $\eta - \eta'$ and $\omega - \Phi$ mesons.

These ingredients provide the basic mechanisms that determine the hadron spectrum in the standard quark model.*

* However, recently, in a radically different approach [35], it has been suggested that most baryon and meson resonances can be generated by chiral coupled-channel dynamics.

14.6. Lattice Calculations of Hadronic Spectroscopy

Lattice calculations predict the spectrum of bound states in QCD from first principles, beginning with the Lagrangian of full QCD or of various approximations to it. This is typically done using the Euclidean path integral formulation of quantum field theory, where the analog of a partition function for a field theory containing some generic fields $\phi(x)$, with action $S(\phi)$, is

$$Z = \int [d\phi] \exp(-S(\phi)). \quad (14.31)$$

The expectation value of any observable O is

$$\langle O \rangle = \frac{1}{Z} \int [d\phi] O(\phi) \exp(-S(\phi)). \quad (14.32)$$

The theory is regulated by introducing a space-time lattice, with lattice spacing a . This converts the functional integral Eq. (14.31) into an ordinary integral (of very large dimensionality). The integral is replaced by a Monte Carlo sampling over an ensemble of configurations of field variables, using an algorithm which insures that a field configuration is present in the ensemble with a probability proportional to $\exp(-S(\phi_j))$. Then ensemble averages become sample averages,

$$\langle O \rangle = \frac{1}{N} \sum_{j=1}^N O(\phi_j). \quad (14.33)$$

This is all quite similar to the kind of Monte Carlo simulation done by experiments, except that the ensembles of field configurations are created sequentially, as a so-called “Markov chain.”

In QCD, the field variables correspond to gauge fields and quark fields. In a lattice calculation, the lattice spacing (which serves as an ultraviolet cutoff) and the (current) quark masses are inputs; hadron masses and other observables are predicted as a function of those masses. The lattice spacing is unphysical, and it is necessary to extrapolate to the limit of zero lattice spacing. Lattice predictions are for dimensionless ratios of dimensionful parameters (like mass ratios), and predictions of dimensionful quantities require using one experimental input to set the scale. Interpolation or extrapolation of lattice results in the light quark masses involves formulas of chiral perturbation theory.

For conventional hadronic states, lattice calculations use the quark model to construct operators, which are taken as interpolating fields. This does not mean that the hadronic states have minimal quark content: the operators create multi-quark states with particular quantum numbers, but they are connected by quark propagators which include all effects of relativity, and could include the effects of virtual quark-antiquark pairs in the vacuum.

Constituent gluons do not appear naturally in lattice calculations; instead, gauge fields appear as link variables, which allow color to be parallel transported across the lattice in a gauge covariant way. Calculations of glueballs on the lattice use interpolating fields of the form $O_j \sim \exp i \oint \vec{A} \cdot \vec{d}l$ integrated about some path. The fields look like closed tubes of chromoelectric and chromomagnetic flux. Calculations of exotics are done with interpolating fields involving quark and antiquark creation operators joined by flux tubes.

Calculations with heavy quarks typically use Non-Relativistic QCD (NRQCD) or Heavy Quark Effective Theory (HQET), systematic expansions of the QCD Lagrangian in powers of the heavy quark velocity, or the inverse heavy quark mass. Terms in the Lagrangian have obvious quark model analogs, but are derived directly from QCD. The heavy quark potential is a derived quantity, measured in simulations.

Lattice calculations are as specialized as the experiments which produce the data in this book, and it is not easy to give a blanket answer to the question: “How well can lattice calculations predict any specific quantity?” However, let us try:

The cleanest lattice predictions come from measurements of processes in which there is only one particle in the simulation volume. These quantities include masses of hadrons, simple decay constants, like pseudoscalar meson decay constants, and semileptonic form factors

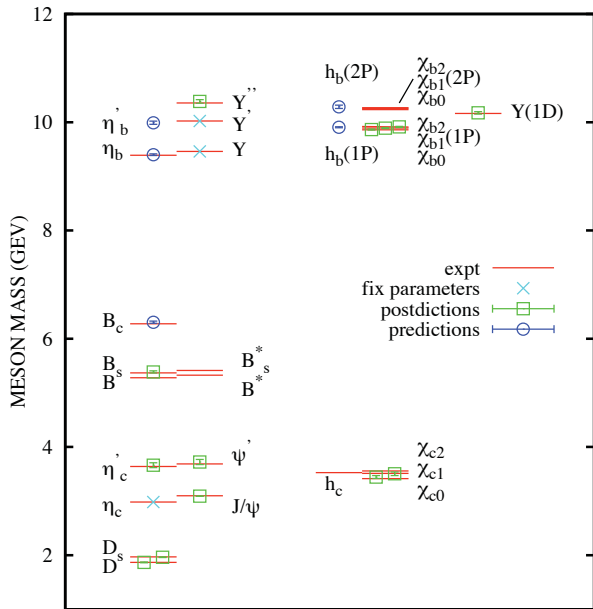


Figure 14.7: Spectroscopy for mesonic systems containing one or more heavy quarks (adapted from Ref. 43). Particles whose masses are used to fix lattice parameters are shown with crosses; the authors distinguish between “predictions” and “postdictions” of their calculation. Lines represent experiment.

(such as the ones appropriate to $B \rightarrow D\nu, K\nu, \pi\nu$). The cleanest predictions for masses are for states which have narrow decay widths and are far below any thresholds to open channels, since the effects of final state interactions are not yet under complete control on the lattice. “Difficult” states for the quark model (such as exotics) are also difficult for the lattice because of the lack of simple operators which couple well to them. Technical issues presently prevent lattice practitioners from directly computing matrix elements for weak decays with more than one strongly interacting particle in the final state.

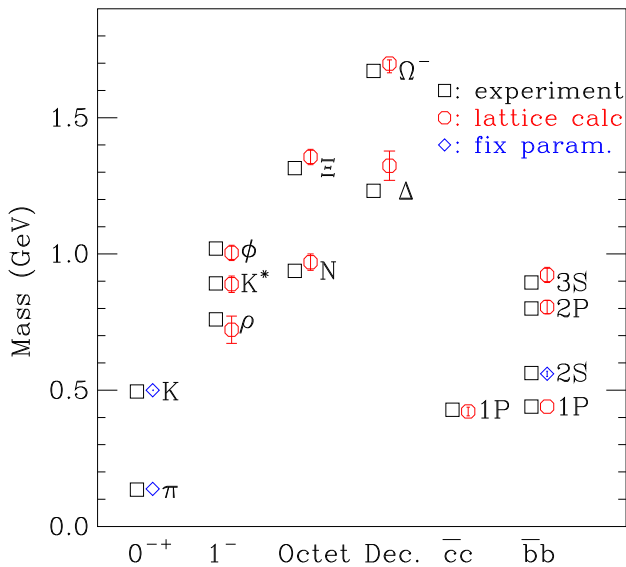


Figure 14.6: A recent calculation of spectroscopy with dynamical $u, d,$ and s quarks. The pion and kaon fix the light quark masses. Only the mass splittings relative to the $1S$ states in the heavy quark sectors are shown. The $\Upsilon 1P - 1S$ splitting sets the overall energy scale.

Good-quality modern lattice calculations will present multi-part error budgets with their predictions. Users are advised to read them carefully! A small part of the uncertainty is statistical, from sample size. Typically, the quoted statistical uncertainty includes uncertainty from a fit: it is rare that a simulation measures one global quantity which is the desired observable. Simulations which include virtual quark-antiquark pairs (also known as “dynamical quarks” or “sea quarks”) are typically done at mass values heavier than the experimental ones, and it is necessary to extrapolate in the quark mass. A major goal of lattice groups is to be able to work directly at the physical values of the light quark masses. (For an example of work in that direction, see Ref. 39.) They are always done at nonzero lattice spacing, and so it is necessary to extrapolate to zero lattice spacing. Some theoretical input is needed to do this. Much of the uncertainty in these extrapolations is systematic, from the choice of fitting function. Other systematics include the effect of finite simulation volume, the number of flavors of dynamical quarks actually simulated, and technical issues with how these dynamical quarks are included. The particular choice of a fiducial mass (to normalize other predictions) is not standardized; there are many possible choices, each with its own set of strengths and weaknesses, and determining it usually requires a second lattice simulation from that used to calculate the quantity under consideration.

A systematic of major historical interest is the “quenched approximation,” in which dynamical quarks are simply left out of the simulation. This was done because the addition of these virtual pairs presented an expensive computational problem. No generally-accepted methodology has ever allowed one to correct for quenching effects, short of redoing all calculations with dynamical quarks. Recent advances in algorithms and computer hardware have rendered it obsolete.

Of course, there is much more to lattice calculations besides spectroscopy; please refer to the mini-review on Quark Masses in the Quarks section of the Listings for more lattice-based phenomenology.

We conclude with a few representative pictures of spectroscopy from recent state-of-the-art simulations. They illustrate (better than any discussion) the size of lattice uncertainties.

A recent calculation of spectroscopy with dynamical $u, d,$ and s quarks is shown in Fig. 14.6. The pion and kaon masses are used to set the light quark masses. The $\Upsilon 1P - 1S$ splitting is used to set the lattice spacing or equivalently, the overall energy scale in the lattice calculation. This is an updated figure from Ref. 40, using results from Ref. 41 and Ref. 42 (D. Toussaint, private communication).

Fig. 14.7 shows the mass spectrum for mesons containing at least one heavy (b or c) quark from Ref. 43. The calculation uses a discretization of nonrelativistic QCD for its heavy quarks, and includes three flavors of light dynamical fermions.

References:

1. J. Schwinger, Phys. Rev. Lett. **12**, 237 (1964).
2. A. Bramon *et al.*, Phys. Lett. **B403**, 339 (1997).
3. A. Aloisio *et al.*, Phys. Lett. **B541**, 45 (2002).
4. C. Amsler *et al.*, Phys. Lett. **B294**, 451 (1992).
5. C. Amsler, Rev. Mod. Phys. **70**, 1293 (1998).
6. T. Feldmann, Int. J. Mod. Phys. **A915**, 159 (2000).
7. C. Amsler and F.E. Close, Phys. Rev. **D53**, 295 (1996).
8. R.L. Jaffe, Phys. Rev. **D 15** 267, 281 (1977).
9. Y. Chen *et al.*, Phys. Rev. **D73**, 014516 (2006).
10. C. Morningstar and M. Peardon, Phys. Rev. **D60**, 034509 (1999).
11. W. J. Lee and D. Weingarten, Phys. Rev. **D61**, 014015 (2000).
12. G. S. Bali, *et. al.* Phys. Lett. **B309**, 378 (1993).
13. C. Michael, AIP Conf. Proc. **432**, 657 (1998).
14. F.E. Close and A. Kirk, Eur. Phys. J. **C21**, 531 (2001).
15. A. Hart *et al.*, Phys. Rev. **D74**, 114504 (2006).
16. C. McNeile, *XXV Int. Symp. on Lattice Field Theory*, Regensburg, 2007, [arXiv:0710.0985v1[hep-lat]].
17. C. Amsler and N.A. Törnqvist, Phys. Reports **389**, 61 (2004).
18. N. Isgur and J. Paton, Phys. Rev. **D31**, 2910 (1985).

19. P. Lacock *et al.*, Phys. Lett. **B401**, 308 (1997);
C. Bernard *et al.*, Phys. Rev. **D56**, 7039 (1997);
C. Bernard *et al.*, Phys. Rev. **D68**, 074505 (2003).
20. M. Chanowitz and S. Sharpe, Nucl. Phys. **B222**, 211 (1983).
21. T. Barnes *et al.*, Nucl. Phys. **B224**, 241 (1983).
22. W.-M Yao *et al.*, J. Phys. **G33**, 1 (2006).
23. F.E. Close, in *Quarks and Nuclear Forces* (Springer-Verlag, 1982), p. 56.
24. Particle Data Group, Phys. Lett. **111B** (1982).
25. R.H. Dalitz and L.J. Reinders, in “Hadron Structure as Known from Electromagnetic and Strong Interactions,” *Proceedings of the Hadron '77 Conference* (Veda, 1979), p. 11.
26. N. Isgur and G. Karl, Phys. Rev. **D18**, 4187 (1978); *ibid.*, **D19**, 2653 (1979); *ibid.*, **D20**, 1191 (1979);
K.-T. Chao *et al.*, Phys. Rev. **D23**, 155 (1981).
27. S. Capstick and W. Roberts, Phys. Rev. **D49**, 4570 (1994); *ibid.*, **D57**, 4301 (1998); *ibid.*, **D58**, 074011 (1998).
28. T. Melde, W. Plessas, and B. Sengl, Phys. Rev. **D77**, 114002 (2008);
S. Capstick, Phys. Rev. **D46**, 2864 (1992).
29. B. Krusche and S. Schadmand, Prog. Part. Nucl. Phys. **51**, 399 (2003);
V.D. Burkert and T.-S.H. Lee, Int. J. Mod. Phys. **E13**, 1035 (2004).
30. S. Capstick and W. Roberts, Prog. Part. Nucl. Phys. **45**, 241 (2000);
see also A.J.G. Hey and R.L. Kelly, Phys. Reports **96**, 71 (1983).
31. M. Anselmino *et al.*, Rev. Mod. Phys. **65**, 1199 (1993).
32. R. Bijker *et al.*, Ann. of Phys. **236** 69 (1994).
33. N. Isgur and J. Paton, Phys. Rev. **D31**, 2910 (1985);
S. Capstick and P.R. Page, Phys. Rev. **C66**, 065204 (2002).
34. R.L. Jaffe, D. Pirjol, A. Scardicchio, Phys. Rept. **435** 157 (2006);
L. Ya. Glozman, Phys. Rept. **444** 1 (2007).
35. M.F.M Lutz and E.E. Kolomeitsev, Nucl. Phys. **A700**, 193 (2002);
M.F.M Lutz and E.E. Kolomeitsev, Nucl. Phys. **A730**, 392 (2004);
E.E. Kolomeitsev and M.F.M Lutz, Phys. Lett. **B585**, 243 (2004).
36. A. De Rujula *et al.*, Phys. Rev. **D12**, 147 (1975).
37. W.H. Blask *et al.*, Z. Phys. **A337** 327 (1990);
U. Löring *et al.*, Eur. Phys. J. **A10** 309 (2001);
U. Löring *et al.*, Eur. Phys. J. **A10** 395 (2001); *ibid.*, **A10** 447 (2001).
38. L.Y. Glozman and D.O. Riska, Phys. Rept. **268** 263 (1996);
L.Y. Glozman *et al.*, Phys. Rev. **D58**, 094030 (1998).
39. S. Aoki *et al.* [PACS-CS Collab.]. Phys. Rev. **D79**, 034503 (2009) [arXiv:0807.1661[hep-lat]].
40. C. Aubin *et al.* [MILC Collab.], Phys. Rev. **D70**, 094505 (2004) [arXiv:hep-lat/0407028].
41. C. T. H. Davies *et al.* [HPQCD Collaboration], Phys. Rev. Lett. **92**, 022001 (2004) [arXiv:hep-lat/0304004].
42. M. Wingate *et al.*, Phys. Rev. Lett. **92**, 162001 (2004) [arXiv:hep-ph/0311130].
43. E. Follana, C. T. H. Davies, G. P. Lepage and J. Shigemitsu [HPQCD Collaboration and UKQCD Collaboration], Phys. Rev. Lett. **100**, 062002 (2008) [arXiv:0706.1726[hep-lat]], E. Follana *et al.*, [HPQCD Collaboration and UKQCD Collaboration], Phys. Rev. D **75**, 054502 (2007) [arXiv:hep-lat/0610092], C. T. H. Davies *et al.*, [HPQCD Collaboration], [arXiv:0810.3548[hep-lat]], A. Gray *et al.*, [HPQCD Collaboration], Phys. Rev. D **72**, 094507 (2005) [arXiv:hep-lat/0507013], I. F. Allison, C. T. H. Davies, A. Gray, A. S. Kronfeld, P. B. Mackenzie and J. N. Simone [HPQCD Collaboration and Fermilab Lattice Collaboration and UKQCD Colla], Phys. Rev. Lett. **94**, 172001 (2005).

15. GRAND UNIFIED THEORIES

Revised October 2005 by S. Raby (Ohio State University).

15.1. Grand Unification

15.1.1. Standard Model: An Introduction :

In spite of all the successes of the Standard Model [SM], it is unlikely to be the final theory. It leaves many unanswered questions. Why the local gauge interactions $SU(3)_C \times SU(2)_L \times U(1)_Y$, and why 3 families of quarks and leptons? Moreover, why does one family consist of the states $[Q, u^c, d^c; L, e^c]$ transforming as $[(3, 2, 1/3), (\bar{3}, 1, -4/3), (\bar{3}, 1, 2/3); (1, 2, -1), (1, 1, 2)]$, where $Q = (u, d)$, and $L = (\nu, e)$ are $SU(2)_L$ doublets, and u^c, d^c, e^c are charge conjugate $SU(2)_L$ singlet fields with the $U(1)_Y$ quantum numbers given? [We use the convention that electric charge $Q_{EM} = T_{3L} + Y/2$ and all fields are left-handed.] Note the SM gauge interactions of quarks and leptons are completely fixed by their gauge charges. Thus, if we understood the origin of this charge quantization, we would also understand why there are no fractionally charged hadrons. Finally, what is the origin of quark and lepton masses, or the apparent hierarchy of family masses and quark mixing angles? Perhaps if we understood this, we would also know the origin of CP violation, the solution to the strong CP problem, the origin of the cosmological matter-antimatter asymmetry, or the nature of dark matter.

The SM has 19 arbitrary parameters; their values are chosen to fit the data. Three arbitrary gauge couplings: g_3, g, g' (where g, g' are the $SU(2)_L, U(1)_Y$ couplings, respectively) or equivalently, $\alpha_s = (g_3^2/4\pi), \alpha_{EM} = (e^2/4\pi)$ ($e = g \sin \theta_W$), and $\sin^2 \theta_W = (g')^2/(g^2 + (g')^2)$. In addition, there are 13 parameters associated with the 9 charged fermion masses and the four mixing angles in the CKM matrix. The remaining 3 parameters are v, λ [the Higgs VEV (vacuum expectation value) and quartic coupling] (or equivalently, M_Z, m_h^0), and the QCD θ parameter. In addition, data from neutrino oscillation experiments provide convincing evidence for neutrino masses. With 3 light Majorana neutrinos, there are at least 9 additional parameters in the neutrino sector; 3 masses, 3 mixing angles and 3 phases. In summary, the SM has too many arbitrary parameters, and leaves open too many unresolved questions to be considered complete. These are the problems which grand unified theories hope to address.

15.1.2. Charge Quantization :

In the Standard Model, quarks and leptons are on an equal footing; both fundamental particles without substructure. It is now clear that they may be two faces of the same coin; unified, for example, by extending QCD (or $SU(3)_C$) to include leptons as the fourth color, $SU(4)_C$ [1]. The complete Pati-Salam gauge group is $SU(4)_C \times SU(2)_L \times SU(2)_R$, with the states of one family $[(Q, L), (Q^c, L^c)]$ transforming as $[(4, 2, 1), (\bar{4}, 1, \bar{2})]$, where $Q^c = (d^c, u^c), L^c = (e^c, \nu^c)$ are doublets under $SU(2)_R$. Electric charge is now given by the relation $Q_{EM} = T_{3L} + T_{3R} + 1/2(B-L)$, and $SU(4)_C$ contains the subgroup $SU(3)_C \times (B-L)$ where B (L) is baryon (lepton) number. Note ν^c has no SM quantum numbers and is thus completely "sterile." It is introduced to complete the $SU(2)_R$ lepton doublet. This additional state is desirable when considering neutrino masses.

Although quarks and leptons are unified with the states of one family forming two irreducible representations of the gauge group, there are still 3 independent gauge couplings (two if one also imposes parity, *i.e.*, $L \leftrightarrow R$ symmetry). As a result, the three low-energy gauge couplings are still independent arbitrary parameters. This difficulty is resolved by embedding the SM gauge group into the simple unified gauge group, Georgi-Glashow $SU(5)$, with one universal gauge coupling α_G defined at the grand unification scale M_G [2]. Quarks and leptons still sit in two irreducible representations, as before, with a $\mathbf{10} = [Q, u^c, e^c]$ and $\mathbf{\bar{5}} = [d^c, L]$. Nevertheless, the three low energy gauge couplings are now determined in terms of two independent parameters: α_G and M_G . Hence, there is one prediction.

In order to break the electroweak symmetry at the weak scale and give mass to quarks and leptons, Higgs doublets are needed which can sit in either a $\mathbf{5}_H$ or $\mathbf{\bar{5}}_H$. The additional 3 states are color triplet Higgs scalars. The couplings of these color triplets violate baryon and lepton number, and nucleons decay via the exchange of a single

color triplet Higgs scalar. Hence, in order not to violently disagree with the non-observation of nucleon decay, their mass must be greater than $\sim 10^{10-11}$ GeV. Moreover, in supersymmetric GUTs, in order to cancel anomalies, as well as give mass to both up and down quarks, both Higgs multiplets $\mathbf{5}_H, \mathbf{\bar{5}}_H$ are required. As we shall discuss later, nucleon decay now constrains the color triplet Higgs states in a SUSY GUT to have mass significantly greater than M_G .

Complete unification is possible with the symmetry group $SO(10)$, with one universal gauge coupling α_G , and one family of quarks and leptons sitting in the 16-dimensional spinor representation $\mathbf{16} = [\mathbf{10} + \mathbf{\bar{5}} + \mathbf{1}]$ [3]. The $SU(5)$ singlet $\mathbf{1}$ is identified with ν^c . In Table 15.1 we present the states of one family of quarks and leptons, as they appear in the $\mathbf{16}$. It is an amazing and perhaps even profound fact that all the states of a single family of quarks and leptons can be represented digitally as a set of 5 zeros and/or ones or equivalently as the tensor product of 5 "spin" $1/2$ states with $\pm = |\pm \frac{1}{2}\rangle$ and with the condition that we have an even number of $|- \rangle$ spins. The first three "spins" correspond to $SU(3)_C$ color quantum numbers, while the last two are $SU(2)_L$ weak quantum numbers. In fact, an $SU(3)_C$ rotation just raises one color index and lowers another, thereby changing colors $\{r, b, g\}$. Similarly an $SU(2)_L$ rotation raises one weak index and lowers another, thereby flipping the weak isospin from up to down or vice versa. In this representation, weak hypercharge Y is given by the simple relation $Y = 2/3(\sum \text{color spins}) - (\sum \text{weak spins})$. $SU(5)$ rotations [not in the Standard Model] then raise (or lower) a color index, while at the same time lowering (or raising) a weak index. It is easy to see that such rotations can mix the states $\{Q, u^c, e^c\}$ and $\{d^c, L\}$ among themselves, and ν^c is a singlet. The new $SO(10)$ rotations [not in $SU(5)$] are then given by either raising or lowering any two spins. For example, by lowering the two weak indices, ν^c rotates into e^c , etc.

Table 15.1: The quantum numbers of the $\mathbf{16}$ dimensional representation of $SO(10)$.

State	Y	Color	Weak
ν^c	0	+++	++
e^c	2	+++	--
u_r	1/3	-++	+-
d_r	1/3	-++	-+
u_b	1/3	+ - +	+-
d_b	1/3	+ - +	-+
u_y	1/3	+ + -	+-
d_y	1/3	+ + -	-+
u_r^c	-4/3	+ - -	++
u_b^c	-4/3	- + -	++
u_y^c	-4/3	- - +	++
d_r^c	2/3	+ - -	--
d_b^c	2/3	- + -	--
d_y^c	2/3	- - +	--
ν	-1	- - -	+-
e	-1	- - -	-+

$SO(10)$ has two inequivalent maximal breaking patterns: $SO(10) \rightarrow SU(5) \times U(1)_X$ and $SO(10) \rightarrow SU(4)_C \times SU(2)_L \times SU(2)_R$. In the first case, we obtain Georgi-Glashow $SU(5)$ if Q_{EM} is given in terms of $SU(5)$ generators alone, or so-called flipped $SU(5)$ [4] if Q_{EM} is partly in $U(1)_X$. In the latter case, we have the Pati-Salam symmetry. If $SO(10)$ breaks directly to the SM at M_G , then we retain the prediction for gauge coupling unification. However, more possibilities for breaking (hence more breaking scales and more parameters) are available in $SO(10)$. Nevertheless with one breaking pattern $SO(10) \rightarrow SU(5) \rightarrow SM$, where the last breaking scale is M_G , the predictions from gauge coupling unification are preserved. The Higgs multiplets in minimal $SO(10)$ are contained in the fundamental

$10_{\mathbf{H}} = [5_{\mathbf{H}}, \bar{5}_{\mathbf{H}}]$ representation. Note, only in SO(10) does the gauge symmetry distinguish quark and lepton multiplets from Higgs multiplets.

Finally, larger symmetry groups have been considered. For example, $E(6)$ has a fundamental representation 27 , which under SO(10) transforms as a $[16 + 10 + 1]$. The breaking pattern $E(6) \rightarrow SU(3)_C \times SU(3)_L \times SU(3)_R$ is also possible. With the additional permutation symmetry $Z(3)$ interchanging the three SU(3)s, we obtain so-called “trification [5],” with a universal gauge coupling. The latter breaking pattern has been used in phenomenological analyses of the heterotic string [6]. However, in larger symmetry groups, such as $E(6)$, $SU(6)$, *etc.*, there are now many more states which have not been observed and must be removed from the effective low-energy theory. In particular, three families of 27 s in $E(6)$ contain three Higgs type multiplets transforming as 10 s of SO(10). This makes these larger symmetry groups unattractive starting points for model building.

15.1.3. String Theory and Orbifold GUTs :

Orbifold compactification of the heterotic string [7–9], and recent field theoretic constructions known as orbifold GUTs [10], contain grand unified symmetries realized in 5 and 6 dimensions. However, upon compactifying all but four of these extra dimensions, only the MSSM is recovered as a symmetry of the effective four dimensional field theory.¹ These theories can retain many of the nice features of four dimensional SUSY GUTs, such as charge quantization, gauge coupling unification and sometimes even Yukawa unification; while at the same time resolving some of the difficulties of 4d GUTs, in particular problems with unwieldy Higgs sectors necessary for spontaneously breaking the GUT symmetry, problems with doublet-triplet Higgs splitting or rapid proton decay. We will comment further on the corrections to the four dimensional GUT picture due to orbifold GUTs in the following sections.

15.1.4. Gauge coupling unification :

The biggest paradox of grand unification is to understand how it is possible to have a universal gauge coupling g_G in a grand unified theory [GUT], and yet have three unequal gauge couplings at the weak scale with $g_3 > g > g'$. The solution is given in terms of the concept of an effective field theory [EFT] [16]. The GUT symmetry is spontaneously broken at the scale M_G , and all particles not in the SM obtain mass of order M_G . When calculating Green’s functions with external energies $E \gg M_G$, we can neglect the mass of all particles in the loop and hence all particles contribute to the renormalization group running of the universal gauge coupling. However, for $E \ll M_G$, one can consider an effective field theory including only the states with mass $< E \ll M_G$. The gauge symmetry of the EFT is $SU(3)_C \times SU(2)_L \times U(1)_Y$, and the three gauge couplings renormalize independently. The states of the EFT include only those of the SM; 12 gauge bosons, 3 families of quarks and leptons, and one or more Higgs doublets. At M_G , the two effective theories [the GUT

¹ Also, in recent years there has been a great deal of progress in constructing three and four family models in Type IIA string theory with intersecting D6 branes [11]. Although these models can incorporate SU(5) or a Pati-Salam symmetry group in four dimensions, they typically have problems with gauge coupling unification. In the former case this is due to charged exotics which affect the RG running, while in the latter case the $SU(4) \times SU(2)_L \times SU(2)_R$ symmetry never unifies. Note, heterotic string theory models also exist whose low energy effective 4d field theory is a SUSY GUT [12]. These models have all the virtues and problems of 4d GUTs. Finally, many heterotic string models have been constructed with the standard model gauge symmetry in 4d and no intermediate GUT symmetry in less than 10d. Recently some minimal 3 family supersymmetric models have been constructed [13,14]. These theories may retain some of the symmetry relations of GUTs, however the unification scale would typically be the string scale, of order 5×10^{17} GeV, which is inconsistent with low energy data. A way out of this problem was discovered in the context of the strongly coupled heterotic string, defined in an effective 11 dimensions [15]. In this case the 4d Planck scale (which controls the value of the string scale) now unifies with the GUT scale.

itself is most likely the EFT of a more fundamental theory defined at a higher scale] must give identical results; hence we have the boundary conditions $g_3 = g_2 = g_1 \equiv g_G$, where at any scale $\mu < M_G$, we have $g_2 \equiv g$ and $g_1 = \sqrt{5/3} g'$. Then using two low-energy couplings, such as $\alpha_s(M_Z)$, $\alpha_{EM}(M_Z)$, the two independent parameters α_G , M_G can be fixed. The third gauge coupling, $\sin^2 \theta_W$ in this case, is then predicted. This was the procedure up until about 1991 [17,18]. Subsequently, the uncertainties in $\sin^2 \theta_W$ were reduced tenfold. Since then, $\alpha_{EM}(M_Z)$, $\sin^2 \theta_W$ have been used as input to predict α_G , M_G , and $\alpha_s(M_Z)$ [19].

We emphasize that the above boundary condition is only valid when using one-loop-renormalization group [RG] running. With precision electroweak data, however, it is necessary to use two-loop-RG running. Hence, one must include one-loop-threshold corrections to gauge coupling boundary conditions at both the weak and GUT scales. In this case, it is always possible to define the GUT scale as the point where $\alpha_1(M_G) = \alpha_2(M_G) \equiv \bar{\alpha}_G$ and $\alpha_3(M_G) = \bar{\alpha}_G (1 + \epsilon_3)$. The threshold correction ϵ_3 is a logarithmic function of all states with mass of order M_G and $\bar{\alpha}_G = \alpha_G + \Delta$, where α_G is the GUT coupling constant above M_G , and Δ is a one-loop-threshold correction. To the extent that gauge coupling unification is perturbative, the GUT threshold corrections are small and calculable. This presumes that the GUT scale is sufficiently below the Planck scale or any other strong coupling extension of the GUT, such as a strongly coupled string theory.

Supersymmetric grand unified theories [SUSY GUTs] are an extension of non-SUSY GUTs [20]. The key difference between SUSY GUTs and non-SUSY GUTs is the low-energy effective theory. The low-energy effective field theory in a SUSY GUT is assumed to satisfy $N = 1$ supersymmetry down to scales of order the weak scale, in addition to the SM gauge symmetry. Hence, the spectrum includes all the SM states, plus their supersymmetric partners. It also includes one pair (or more) of Higgs doublets; one to give mass to up-type quarks, and the other to down-type quarks and charged leptons. Two doublets with opposite hypercharge Y are also needed to cancel fermionic triangle anomalies. Finally, it is important to recognize that a low-energy SUSY-breaking scale (the scale at which the SUSY partners of SM particles obtain mass) is necessary to solve the gauge hierarchy problem.

Simple non-SUSY SU(5) is ruled out, initially by the increased accuracy in the measurement of $\sin^2 \theta_W$, and by early bounds on the proton lifetime (see below) [18]. However, by now LEP data [19] has conclusively shown that SUSY GUTs is the new Standard Model; by which we mean the theory used to guide the search for new physics beyond the present SM (see Fig. 15.1). SUSY extensions of the SM have the property that their effects decouple as the effective SUSY-breaking scale is increased. Any theory beyond the SM must have this property simply because the SM works so well. However, the SUSY-breaking scale cannot be increased with impunity, since this would reintroduce a gauge hierarchy problem. Unfortunately there is no clear-cut answer to the question, “When is the SUSY-breaking scale too high?” A conservative bound would suggest that the third generation squarks and sleptons must be lighter than about 1 TeV, in order that the one-loop corrections to the Higgs mass from Yukawa interactions remain of order the Higgs mass bound itself.

At present, gauge coupling unification within SUSY GUTs works extremely well. Exact unification at M_G , with two-loop-RG running from M_G to M_Z , and one-loop-threshold corrections at the weak scale, fits to within 3σ of the present precise low-energy data. A small threshold correction at M_G ($\epsilon_3 \sim -3$ to -4%) is sufficient to fit the low-energy data precisely [22–24].² This may be compared to non-SUSY GUTs, where the fit misses by $\sim 12 \sigma$, and a precise

² This result implicitly assumes universal GUT boundary conditions for soft SUSY-breaking parameters at M_G . In the simplest case, we have a universal gaugino mass $M_{1/2}$, a universal mass for squarks and sleptons m_{16} , and a universal Higgs mass m_{10} , as motivated by SO(10). In some cases, threshold corrections to gauge coupling unification can be exchanged for threshold corrections to soft SUSY parameters. See for example, Ref. 25 and references therein.

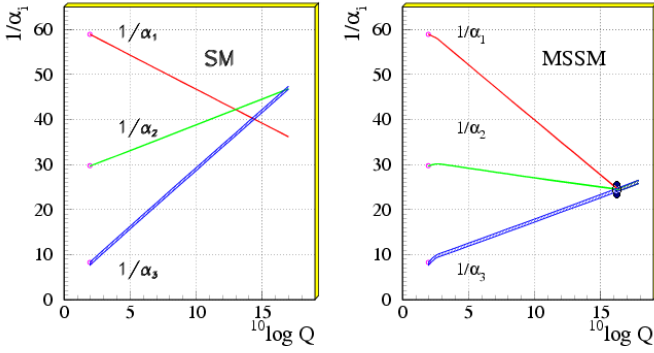


Figure 15.1: Gauge coupling unification in non-SUSY GUTs on the left vs. SUSY GUTs on the right using the LEP data as of 1991. Note, the difference in the running for SUSY is the inclusion of supersymmetric partners of standard model particles at scales of order a TeV (Fig. taken from Ref. 21). Given the present accurate measurements of the three low energy couplings, in particular $\alpha_s(M_Z)$, GUT scale threshold corrections are now needed to precisely fit the low energy data. The dark blob in the plot on the right represents these model dependent corrections.

fit requires new weak-scale states in incomplete GUT multiplets, or multiple GUT-breaking scales.³

Following the analysis of Ref. 24 let us try to understand the need for the GUT threshold correction and its order of magnitude. The renormalization group equations relate the low energy gauge coupling constants $\alpha_i(M_Z)$, $i = 1, 2, 3$ to the value of the unification scale Λ_U and the GUT coupling α_U by the expression

$$\frac{1}{\alpha_i(M_Z)} = \frac{1}{\alpha_U} + \frac{b_i}{2\pi} \log \left(\frac{\Lambda_U}{M_Z} \right) + \delta_i \quad (15.1)$$

where Λ_U is the GUT scale evaluated at one loop and the threshold corrections, δ_i , are given by $\delta_i = \delta_i^{(2)} + \delta_i^{(l)} + \delta_i^{(g)}$ with $\delta_i^{(2)}$ representing two loop running effects, $\delta_i^{(l)}$ the light threshold corrections at the SUSY breaking scale and $\delta_i^{(g)} = \delta_i^{(h)} + \delta_i^{(b)}$ representing GUT scale threshold corrections. Note, in this analysis, the two loop RG running is treated on the same footing as weak and GUT scale threshold corrections. One then obtains the prediction

$$(\alpha_3(M_Z) - \alpha_3^{LO}(M_Z))/\alpha_3^{LO}(M_Z) = -\alpha_3^{LO}(M_Z) \delta_s \quad (15.2)$$

where $\alpha_3^{LO}(M_Z)$ is the leading order one loop RG result and $\delta_s = \frac{1}{7}(5\delta_1 - 12\delta_2 + 7\delta_3)$ is the net threshold correction. [A similar formula applies at the GUT scale with the GUT threshold correction, ϵ_3 , given by $\epsilon_3 = -\bar{\alpha}_G \delta_s^{(g)}$.] Given the experimental inputs [28]:

$$\begin{aligned} \alpha_{em}^{-1}(M_Z) &= 127.906 \pm 0.019 \\ \sin^2 \theta_W(M_Z) &= 0.2312 \pm 0.0002 \\ \alpha_3(M_Z) &= 0.1187 \pm 0.0020 \end{aligned} \quad (15.3)$$

and taking into account the light threshold corrections, assuming an ensemble of 10 SUSY spectra [24] (corresponding to the Snowmass benchmark points), we have

$$\alpha_3^{LO}(M_Z) \approx 0.118 \quad (15.4)$$

³ Non-SUSY GUTs with a more complicated breaking pattern can still fit the data. For example, non-SUSY $SO(10) \rightarrow SU(4)_C \times SU(2)_L \times SU(2)_R \rightarrow SM$, with the second breaking scale of order an intermediate scale, determined by light neutrino masses using the see-saw mechanism, can fit the low-energy data for gauge couplings [26], and at the same time survive nucleon decay bounds [27], discussed in the following section.

and

$$\begin{aligned} \delta_s^{(2)} &\approx -0.82 \\ \delta_s^{(l)} &\approx -0.50 + \frac{19}{28\pi} \log \frac{M_{SUSY}}{M_Z}. \end{aligned}$$

For $M_{SUSY} = 1$ TeV, we have $\delta_s^{(2)} + \delta_s^{(l)} \approx -0.80$. Since the one loop result $\alpha_3^{LO}(M_Z)$ is very close to the experimental value, we need $\delta_s \approx 0$ or equivalently, $\delta_s^{(g)} \approx 0.80$. This corresponds, at the GUT scale, to $\epsilon_3 \approx -3\%$.⁴

In four dimensional SUSY GUTs, the threshold correction ϵ_3 receives a positive contribution from Higgs doublets and triplets.⁵ Thus a larger, negative contribution must come from the GUT breaking sector of the theory. This is certainly possible in specific $SO(10)$ [29] or $SU(5)$ [30] models, but it is clearly a significant constraint on the 4d GUT sector of the theory. In five or six dimensional orbifold GUTs, on the other hand, the ‘‘GUT scale’’ threshold correction comes from the Kaluza-Klein modes between the compactification scale, M_c , and the effective cutoff scale M_* .⁶ Thus, in orbifold GUTs, gauge coupling unification at two loops is only consistent with the low energy data with a fixed value for M_c and M_* .⁷ Typically, one finds $M_c < M_G = 3 \times 10^{16}$ GeV, where M_G is the 4d GUT scale. Since the grand unified gauge bosons, responsible for nucleon decay, get mass at the compactification scale, the result $M_c < M_G$ for orbifold GUTs has significant consequences for nucleon decay.

A few final comments are in order. We do not consider the scenario of split supersymmetry [33] in this review. In this scenario squarks and sleptons have mass at a scale $\tilde{m} \gg M_Z$, while gauginos and Higgsinos have mass of order the weak scale. Gauge coupling unification occurs at a scale of order 10^{16} GeV, provided that the scale \tilde{m} lies in the range $10^3 - 10^{11}$ GeV [34]. A serious complaint concerning the split SUSY scenario is that it does not provide a solution to the gauge hierarchy problem. Moreover, it is only consistent with grand unification if it also postulates an ‘‘intermediate’’ scale, \tilde{m} , for scalar masses. In addition, it is in conflict with $b - \tau$ Yukawa unification, unless $\tan \beta$ is fine-tuned to be close to 1 [34].⁸

We have also neglected to discuss non-supersymmetric GUTs in four dimensions which still survive once one allows for several scales

⁴ In order to fit the low energy data for gauge coupling constants we require a relative shift in $\alpha_3(M_G)$ of order 3% due to GUT scale threshold corrections. If these GUT scale corrections were not present, however, weak scale threshold corrections of order 9% (due to the larger value of α_3 at M_Z) would be needed to resolve the discrepancy with the data for exact gauge coupling unification at M_G . Leaving out the fact that any consistent GUT necessarily contributes threshold corrections at the GUT scale, it is much more difficult to find the necessary larger corrections at the weak scale. For example, we need $M_{SUSY} \approx 40$ TeV for the necessary GUT scale threshold correction to vanish.

⁵ Note, the Higgs contribution is given by $\epsilon_3 = \frac{3\bar{\alpha}_G}{5\pi} \log \left| \frac{\tilde{M}_t \gamma}{M_G} \right|$ where \tilde{M}_t is the effective color triplet Higgs mass (setting the scale for dimension 5 baryon and lepton number violating operators) and $\gamma = \lambda_b/\lambda_t$ at M_G . Since \tilde{M}_t is necessarily greater than M_G , the Higgs contribution to ϵ_3 is positive.

⁶ In string theory, the cutoff scale is the string scale.

⁷ It is interesting to note that a ratio $M_*/M_c \sim 100$, needed for gauge coupling unification to work in orbifold GUTs is typically the maximum value for this ratio consistent with perturbativity [31]. In addition, in orbifold GUTs brane-localized gauge kinetic terms may destroy the successes of gauge coupling unification. However, for values of $M_*/M_c = M_*\pi R \gg 1$ the unified bulk gauge kinetic terms can dominate over the brane-localized terms [32].

⁸ $b - \tau$ Yukawa unification only works for $\tilde{m} < 10^4$ for $\tan \beta \geq 1.5$. This is because the effective theory between the gaugino mass scale and \tilde{m} includes only one Higgs doublet, as in the standard model. In this case, the large top quark Yukawa coupling tends to increase the ratio λ_b/λ_τ as one runs down in energy below \tilde{m} . This is opposite to what happens in MSSM where the large top quark Yukawa coupling decreases the ratio λ_b/λ_τ [35].

of GUT symmetry breaking [26]. Finally, it has been shown that non-supersymmetric GUTs in warped 5 dimensional orbifolds can be consistent with gauge coupling unification, assuming that the right-handed top quark and the Higgs doublets are composite-like objects with a compositeness scale of order a TeV [36].

15.1.5. Nucleon Decay :

Baryon number is necessarily violated in any GUT [37]. In SU(5), nucleons decay via the exchange of gauge bosons with GUT scale masses, resulting in dimension-6 baryon-number-violating operators suppressed by $(1/M_G^2)$. The nucleon lifetime is calculable and given by $\tau_N \propto M_G^4/(\alpha_G^2 m_p^5)$. The dominant decay mode of the proton (and the baryon-violating decay mode of the neutron), via gauge exchange, is $p \rightarrow e^+ \pi^0$ ($n \rightarrow e^+ \pi^-$). In any simple gauge symmetry, with one universal GUT coupling and scale (α_G , M_G), the nucleon lifetime from gauge exchange is calculable. Hence, the GUT scale may be directly observed via the extremely rare decay of the nucleon. Experimental searches for nucleon decay began with the Kolar Gold Mine, Homestake, Soudan, NUSEX, Frejus, HPW, and IMB detectors [17]. The present experimental bounds come from Super-Kamiokande and Soudan II. We discuss these results shortly. Non-SUSY GUTs are also ruled out by the non-observation of nucleon decay [18]. In SUSY GUTs, the GUT scale is of order 3×10^{16} GeV, as compared to the GUT scale in non-SUSY GUTs, which is of order 10^{15} GeV. Hence, the dimension-6 baryon-violating operators are significantly suppressed in SUSY GUTs [20] with $\tau_p \sim 10^{34-38}$ yrs.

However, in SUSY GUTs, there are additional sources for baryon-number violation—dimension-4 and -5 operators [38]. Although the notation does not change, when discussing SUSY GUTs, all fields are implicitly bosonic superfields, and the operators considered are the so-called F terms, which contain two fermionic components, and the rest scalars or products of scalars. Within the context of SU(5), the dimension-4 and -5 operators have the form $(\mathbf{10} \mathbf{5} \mathbf{5}) \supset (u^c d^c d^c) + (Q L d^c) + (e^c L L)$, and $(\mathbf{10} \mathbf{10} \mathbf{10} \mathbf{5}) \supset (Q Q Q L) + (u^c u^c d^c e^c) + B$ and L conserving terms, respectively. The dimension-4 operators are renormalizable with dimensionless couplings; similar to Yukawa couplings. On the other hand, the dimension-5 operators have a dimensionful coupling of order $(1/M_G)$.

The dimension-4 operators violate baryon number or lepton number, respectively, but not both. The nucleon lifetime is extremely short if both types of dimension-4 operators are present in the low-energy theory. However, both types can be eliminated by requiring R parity. In SU(5), the Higgs doublets reside in a $\mathbf{5}_H$, $\mathbf{5}_H$, and R parity distinguishes the $\mathbf{5}$ (quarks and leptons) from $\mathbf{5}_H$ (Higgs). R parity [39] (or more precisely, its cousin, family reflection symmetry) (see Dimopoulos and Georgi [20] and DRW [40]) takes $F \rightarrow -F$, $H \rightarrow H$ with $F = \{\mathbf{10}, \mathbf{5}\}$, $H = \{\mathbf{5}_H, \mathbf{5}_H\}$. This forbids the dimension-4 operator $(\mathbf{10} \mathbf{5} \mathbf{5})$, but allows the Yukawa couplings of the form $(\mathbf{10} \mathbf{5} \mathbf{5}_H)$ and $(\mathbf{10} \mathbf{10} \mathbf{5}_H)$. It also forbids the dimension-3, lepton-number-violating operator $(\mathbf{5} \mathbf{5}_H) \supset (L H_u)$, with a coefficient with dimensions of mass which, like the μ parameter, could be of order the weak scale and the dimension-5, baryon-number-violating operator $(\mathbf{10} \mathbf{10} \mathbf{10} \mathbf{5}_H) \supset (Q Q Q H_d) + \dots$.

Note, in the MSSM, it is possible to retain R -parity-violating operators at low energy, as long as they violate either baryon number or lepton number only, but not both. Such schemes are natural if one assumes a low-energy symmetry, such as lepton number, baryon number, or a baryon parity [41]. However, these symmetries cannot be embedded in a GUT. Thus, in a SUSY GUT, only R parity can prevent unwanted dimension four operators. Hence, by naturalness arguments, R parity must be a symmetry in the effective low-energy theory of any SUSY GUT. This does not mean to say that R parity is guaranteed to be satisfied in any GUT.

Note also, R parity distinguishes Higgs multiplets from ordinary families. In SU(5), Higgs and quark/lepton multiplets have identical quantum numbers; while in $E(6)$, Higgs and families are unified within the fundamental $\mathbf{27}$ representation. Only in SO(10) are Higgs and ordinary families distinguished by their gauge quantum numbers. Moreover, the $Z(4)$ center of SO(10) distinguishes $\mathbf{10}_s$ from $\mathbf{16}_s$, and can be associated with R parity [42].

In SU(5), dimension-5 baryon-number-violating operators may be forbidden at tree level by additional symmetries. These symmetries are typically broken, however, by the VEVs responsible for the color triplet Higgs masses. Consequently, these dimension-5 operators are generically generated via color triplet Higgsino exchange. Hence, the color triplet partners of Higgs doublets must necessarily obtain mass of order the GUT scale. The dominant decay modes from dimension-5 operators are $p \rightarrow K^+ \bar{\nu}$ ($n \rightarrow K^0 \bar{\nu}$). This is due to a simple symmetry argument; the operators $(Q_i Q_j Q_k L_l)$, $(u_i^c u_j^c d_k^c e_l^c)$ (where $i, j, k, l = 1, 2, 3$ are family indices, and color and weak indices are implicit) must be invariant under SU(3) $_C$ and SU(2) $_L$. As a result, their color and weak doublet indices must be anti-symmetrized. However, since these operators are given by bosonic superfields, they must be totally symmetric under interchange of all indices. Thus, the first operator vanishes for $i = j = k$, and the second vanishes for $i = j$. Hence, a second or third generation member must exist in the final state [40].

Recent Super-Kamiokande bounds on the proton lifetime severely constrain these dimension-6 and dimension-5 operators with $\tau_{(p \rightarrow e^+ \pi^0)} > 5.0 \times 10^{33}$ yrs (79.3 ktyr exposure), $\tau_{(n \rightarrow e^+ \pi^-)} > 5 \times 10^{33}$ yrs (61 ktyr), and $\tau_{(p \rightarrow K^+ \bar{\nu})} > 1.6 \times 10^{33}$ yrs (79.3 ktyr), $\tau_{(n \rightarrow K^0 \bar{\nu})} > 1.7 \times 10^{32}$ yrs (61 ktyr) at (90% CL) based on the listed exposures [43]. These constraints are now sufficient to rule out minimal SUSY SU(5) [44].⁹ Non-minimal Higgs sectors in SU(5) or SO(10) theories still survive [23,30]. The upper bound on the proton lifetime from these theories is approximately a factor of 5 above the experimental bounds. They are, however, being pushed to their theoretical limits. Hence, if SUSY GUTs are correct, nucleon decay should be seen soon.

Is there a way out of this conclusion? Orbifold GUTs and string theories, see Sect. 15.1.3, contain grand unified symmetries realized in higher dimensions. In the process of compactification and GUT symmetry breaking, color triplet Higgs states are removed (projected out of the massless sector of the theory). In addition, the same projections typically rearrange the quark and lepton states so that the massless states which survive emanate from different GUT multiplets. In these models, proton decay due to dimension 5 operators can be severely suppressed or eliminated completely. However, proton decay due to dimension 6 operators may be enhanced, since the gauge bosons mediating proton decay obtain mass at the compactification scale, M_c , which is less than the 4d GUT scale (see the discussion at the end of Section 15.1.4), or suppressed, if the states of one family come from different irreducible representations. Which effect dominates is a model dependent issue. In some complete 5d orbifold GUT models [47,24] the lifetime for the decay $\tau(p \rightarrow e^+ \pi^0)$ can be near the excluded bound of 5×10^{33} years with, however, large model dependent and/or theoretical uncertainties. In other cases, the modes $p \rightarrow K^+ \bar{\nu}$ and $p \rightarrow K^0 \mu^+$ may be dominant [24]. To summarize, in either 4d or orbifold string/field theories, nucleon decay remains a premier signature for SUSY GUTs. Moreover, the observation of nucleon decay may distinguish extra-dimensional orbifold GUTs from four dimensional ones.

Before concluding the topic of baryon-number violation, consider the status of $\Delta B = 2$ neutron- anti-neutron oscillations. Generically, the leading operator for this process is the dimension-9 six-quark operator $G_{(\Delta B=2)} (u^c d^c d^c u^c d^c d^c)$, with dimensionful coefficient $G_{(\Delta B=2)} \sim 1/M^5$. The present experimental bound $\tau_{n-\bar{n}} \geq 0.86 \times 10^8$ sec. at 90% CL [48] probes only up to the scale $M \leq 10^6$ GeV. For $M \sim M_G$, $n-\bar{n}$ oscillations appear to be unobservable for any GUT (for a recent discussion see Ref. 49).

⁹ This conclusion relies on the mild assumption that the three-by-three matrices diagonalizing squark and slepton mass matrices are not so different from their fermionic partners. It has been shown that if this caveat is violated, then dimension five proton decay in minimal SUSY SU(5) may not be ruled out [45].

15.1.6. Yukawa coupling unification :

15.1.6.1. 3rd generation, b - τ or t - b - τ unification:

If quarks and leptons are two sides of the same coin, related by a new grand unified gauge symmetry, then that same symmetry relates the Yukawa couplings (and hence the masses) of quarks and leptons. In SU(5), there are two independent renormalizable Yukawa interactions given by $\lambda_t (\mathbf{10} \mathbf{10} \mathbf{5}_H) + \lambda (\mathbf{10} \mathbf{5} \mathbf{5}_H)$. These contain the SM interactions $\lambda_t (\mathbf{Q} \mathbf{u}^c \mathbf{H}_u) + \lambda (\mathbf{Q} \mathbf{d}^c \mathbf{H}_d + \mathbf{e}^c \mathbf{L} \mathbf{H}_d)$. Hence, at the GUT scale, we have the tree-level relation, $\lambda_b = \lambda_\tau \equiv \lambda$ [35]. In SO(10), there is only one independent renormalizable Yukawa interaction given by $\lambda (\mathbf{16} \mathbf{16} \mathbf{10}_H)$, which gives the tree-level relation, $\lambda_t = \lambda_b = \lambda_\tau \equiv \lambda$ [50,51]. Note, in the discussion above, we assume the minimal Higgs content, with Higgs in $\mathbf{5}$, $\mathbf{5}$ for SU(5) and $\mathbf{10}$ for SO(10). With Higgs in higher-dimensional representations, there are more possible Yukawa couplings. [58–60]

In order to make contact with the data, one now renormalizes the top, bottom, and τ Yukawa couplings, using two-loop-RG equations, from M_G to M_Z . One then obtains the running quark masses $m_t(M_Z) = \lambda_t(M_Z) v_u$, $m_b(M_Z) = \lambda_b(M_Z) v_d$, and $m_\tau(M_Z) = \lambda_\tau(M_Z) v_d$, where $\langle H_u^0 \rangle \equiv v_u = \sin \beta v / \sqrt{2}$, $\langle H_d^0 \rangle \equiv v_d = \cos \beta v / \sqrt{2}$, $v_u/v_d \equiv \tan \beta$, and $v \sim 246$ GeV is fixed by the Fermi constant, G_μ .

Including one-loop-threshold corrections at M_Z , and additional RG running, one finds the top, bottom, and τ -pole masses. In SUSY, b - τ unification has two possible solutions, with $\tan \beta \sim 1$ or 40–50. The small $\tan \beta$ solution is now disfavored by the LEP limit, $\tan \beta > 2.4$ [52].¹⁰ The large $\tan \beta$ limit overlaps the SO(10) symmetry relation.

When $\tan \beta$ is large, there are significant weak-scale threshold corrections to down quark and charged lepton masses, from either gluino and/or chargino loops [54]. Yukawa unification (consistent with low energy data) is only possible in a restricted region of SUSY parameter space with important consequences for SUSY searches [55].

15.1.6.2. Three families:

Simple Yukawa unification is not possible for the first two generations, of quarks and leptons. Consider the SU(5) GUT scale relation $\lambda_b = \lambda_\tau$. If extended to the first two generations, one would have $\lambda_s = \lambda_\mu$, $\lambda_d = \lambda_e$, which gives $\lambda_s/\lambda_d = \lambda_\mu/\lambda_e$. The last relation is a renormalization group invariant, and is thus satisfied at any scale. In particular, at the weak scale, one obtains $m_s/m_d = m_\mu/m_e$, which is in serious disagreement with the data, namely $m_s/m_d \sim 20$ and $m_\mu/m_e \sim 200$. An elegant solution to this problem was given by Georgi and Jarlskog [56]. Of course, a three-family model must also give the observed CKM mixing in the quark sector. Note, although there are typically many more parameters in the GUT theory above M_G , it is possible to obtain effective low-energy theories with many fewer parameters making strong predictions for quark and lepton masses.

It is important to note that grand unification alone is not sufficient to obtain predictive theories of fermion masses and mixing angles. Other ingredients are needed. In one approach additional global family symmetries are introduced (non-abelian family symmetries can significantly reduce the number of arbitrary parameters in the Yukawa matrices). These family symmetries constrain the set of effective higher dimensional fermion mass operators. In addition, sequential breaking of the family symmetry is correlated with the hierarchy of fermion masses. Three-family models exist which fit all the data, including neutrino masses and mixing [57]. In a completely separate approach for SO(10) models, the Standard Model Higgs bosons are contained in the higher dimensional Higgs representations including the $\mathbf{10}$, $\mathbf{126}$ and/or $\mathbf{120}$. Such theories have been shown to make predictions for neutrino masses and mixing angles [58–60].

15.1.7. Neutrino Masses :

Atmospheric and solar neutrino oscillations require neutrino masses. Adding three “sterile” neutrinos ν^c with the Yukawa coupling $\lambda_\nu (\nu^c \mathbf{L} \mathbf{H}_u)$, one easily obtains three massive Dirac neutrinos with mass $m_\nu = \lambda_\nu v_u$.¹¹ However, in order to obtain a tau neutrino with mass of order 0.1 eV, one needs $\lambda_{\nu\tau}/\lambda_\tau \leq 10^{-10}$. The see-saw mechanism, on the other hand, can naturally explain such small neutrino masses [61,62]. Since ν^c has no SM quantum numbers, there is no symmetry (other than global lepton number) which prevents the mass term $\frac{1}{2} \nu^c M \nu^c$. Moreover, one might expect $M \sim M_G$. Heavy “sterile” neutrinos can be integrated out of the theory, defining an effective low-energy theory with only light active Majorana neutrinos, with the effective dimension-5 operator $\frac{1}{2} (\mathbf{L} \mathbf{H}_u) \lambda_\nu^T M^{-1} \lambda_\nu (\mathbf{L} \mathbf{H}_u)$. This then leads to a 3×3 Majorana neutrino mass matrix $\mathbf{m} = m_\nu^T M^{-1} m_\nu$.

Atmospheric neutrino oscillations require neutrino masses with $\Delta m_\nu^2 \sim 3 \times 10^{-3}$ eV² with maximal mixing, in the simplest two-neutrino scenario. With hierarchical neutrino masses, $m_{\nu\tau} = \sqrt{\Delta m_\nu^2} \sim 0.055$ eV. Moreover, via the “see-saw” mechanism, $m_{\nu\tau} = m_t(m_t)^2/(3M)$. Hence, one finds $M \sim 2 \times 10^{14}$ GeV; remarkably close to the GUT scale. Note we have related the neutrino-Yukawa coupling to the top-quark-Yukawa coupling $\lambda_{\nu\tau} = \lambda_t$ at M_G , as given in SO(10) or SU(4) \times SU(2)_L \times SU(2)_R. However, at low energies they are no longer equal, and we have estimated this RG effect by $\lambda_{\nu\tau}(M_Z) \approx \lambda_t(M_Z)/\sqrt{3}$.

15.1.8. Selected Topics :

15.1.8.1. Magnetic Monopoles:

In the broken phase of a GUT, there are typically localized classical solutions carrying magnetic charge under an unbroken U(1) symmetry [63]. These magnetic monopoles with mass of order M_G/α_G are produced during the GUT phase transition in the early universe. The flux of magnetic monopoles is experimentally found to be less than $\sim 10^{-16}$ cm⁻² s⁻¹ sr⁻¹ [64]. Many more are predicted however, hence the GUT monopole problem. In fact, one of the original motivations for an inflationary universe is to solve the monopole problem by invoking an epoch of rapid inflation after the GUT phase transition [65]. This would have the effect of diluting the monopole density as long as the reheat temperature is sufficiently below M_G . Other possible solutions to the monopole problem include: sweeping them away by domain walls [66], U(1) electromagnetic symmetry breaking at high temperature [67] or GUT symmetry non-restoration [68]. Parenthetically, it was also shown that GUT monopoles can catalyze nucleon decay [69]. A significantly lower bound on the monopole flux can then be obtained by considering X-ray emission from radio pulsars due to monopole capture and the subsequent nucleon decay catalysis [70].

15.1.8.2. Baryogenesis via Leptogenesis:

Baryon-number-violating operators in SU(5) or SO(10) preserve the global symmetry $B-L$. Hence, the value of the cosmological $B-L$ density is an initial condition of the theory, and is typically assumed to be zero. On the other hand, anomalies of the electroweak symmetry violate $B+L$ while also preserving $B-L$. Hence, thermal fluctuations in the early universe, via so-called sphaleron processes, can drive $B+L$ to zero, washing out any net baryon number generated in the early universe at GUT temperatures [71].

One way out of this dilemma is to generate a net $B-L$ dynamically in the early universe. We have just seen that neutrino oscillations suggest a new scale of physics of order 10^{14} GeV. This scale is associated with heavy Majorana neutrinos with mass M . If in the early universe, the decay of the heavy neutrinos is out of equilibrium and violates both lepton number and CP , then a net lepton number may be generated. This lepton number will then be partially converted into baryon number via electroweak processes [72].

¹⁰ However, this bound disappears if one takes $M_{SUSY} = 2$ TeV and $m_t = 180$ GeV [53].

¹¹ Note, these “sterile” neutrinos are quite naturally identified with the right-handed neutrinos necessarily contained in complete families of SO(10) or Pati-Salam.

15.1.8.3. GUT symmetry breaking:

The grand unification symmetry is necessarily broken spontaneously. Scalar potentials (or superpotentials) exist whose vacua spontaneously break SU(5) and SO(10). These potentials are ad hoc (just like the Higgs potential in the SM), and, therefore it is hoped that they may be replaced with better motivated sectors. Gauge coupling unification now tests GUT-breaking sectors, since it is one of the two dominant corrections to the GUT threshold correction e_3 . The other dominant correction comes from the Higgs sector and doublet-triplet splitting. This latter contribution is always positive $e_3 \propto \ln(M_T/M_G)$ (where M_T is an effective color triplet Higgs mass), while the low-energy data requires $e_3 < 0$. Hence, the GUT-breaking sector must provide a significant (of order -8%) contribution to e_3 to be consistent with the Super-K bound on the proton lifetime [23,29,30,57].

In string theory (and GUTs in extra-dimensions), GUT breaking may occur due to boundary conditions in the compactified dimensions [7,10]. This is still ad hoc. The major benefits are that it does not require complicated GUT-breaking sectors.

15.1.8.4. Doublet-triplet splitting:

The Minimal Supersymmetric Standard Model has a μ problem: why is the coefficient of the bilinear Higgs term in the superpotential μ ($\mathbf{H}_u \mathbf{H}_d$) of order the weak scale when, since it violates no low-energy symmetry, it could be as large as M_G ? In a SUSY GUT, the μ problem is replaced by the problem of *doublet-triplet* splitting—giving mass of order M_G to the color triplet Higgs, and mass μ to the Higgs doublets. Several mechanisms for natural doublet-triplet splitting have been suggested, such as the sliding singlet, missing partner or missing VEV [73], and pseudo-Nambu-Goldstone boson mechanisms. Particular examples of the missing partner mechanism for SU(5) [30], the missing VEV mechanism for SO(10) [23,57], and the pseudo-Nambu-Goldstone boson mechanism for SU(6) [74], have been shown to be consistent with gauge coupling unification and proton decay. There are also several mechanisms for explaining why μ is of order the SUSY-breaking scale [75]. Finally, for a recent review of the μ problem and some suggested solutions in SUSY GUTs and string theory, see Refs. [76,9] and references therein.

Once again, in string theory (and orbifold GUTs), the act of breaking the GUT symmetry via orbifolding projects certain states out of the theory. It has been shown that it is possible to remove the color triplet Higgs while retaining the Higgs doublets in this process. Hence the doublet-triplet splitting problem is finessed. As discussed earlier (see Section 15.1.5), this has the effect of eliminating the contribution of dimension 5 operators to nucleon decay.

15.2. Conclusion

Grand unification of the strong and electroweak interactions requires that the three low energy gauge couplings unify (up to small threshold corrections) at a unique scale, M_G . Supersymmetric grand unified theories provide, by far, the most predictive and economical framework allowing for perturbative unification.

The three pillars of SUSY GUTs are:

- gauge coupling unification at $M_G \sim 3 \times 10^{16}$ GeV;
- low-energy supersymmetry [with a large SUSY desert], and
- nucleon decay.

The first prediction has already been verified (see Fig. 15.1). Perhaps the next two will soon be seen. Whether or not Yukawa couplings unify is more model dependent. Nevertheless, the “digital” 16-dimensional representation of quarks and leptons in SO(10) is very compelling, and may yet lead to an understanding of fermion masses and mixing angles.

In any event, the experimental verification of the first three pillars of SUSY GUTs would forever change our view of Nature. Moreover, the concomitant evidence for a vast SUSY desert would expose a huge lever arm for discovery. For then it would become clear that experiments probing the TeV scale could reveal physics at the GUT scale and perhaps beyond. Of course, some questions will still remain: Why do we have three families of quarks and leptons? How is the

grand unified symmetry and possible family symmetries chosen by Nature? At what scale might stringy physics become relevant? *Etc.*

References:

1. J. Pati and A. Salam, Phys. Rev. **D8**, 1240 (1973);
For more discussion on the standard charge assignments in this formalism, see A. Davidson, Phys. Rev. **D20**, 776 (1979); and R.N. Mohapatra and R.E. Marshak, Phys. Lett. **B91**, 222 (1980).
2. H. Georgi and S.L. Glashow, Phys. Rev. Lett. **32**, 438 (1974).
3. H. Georgi, Particles and Fields, *Proceedings of the APS Div. of Particles and Fields*, ed. C. Carlson, p. 575 (1975);
H. Fritzsch and P. Minkowski, Ann. Phys. **93**, 193 (1975).
4. S.M. Barr, Phys. Lett. **B112**, 219 (1982).
5. A. de Rujula *et al.*, p. 88, *5th Workshop on Grand Unification*, ed. K. Kang *et al.*, World Scientific, Singapore (1984);
See also earlier paper by Y. Achiman and B. Stech, p. 303, “New Phenomena in Lepton-Hadron Physics,” ed. D.E.C. Fries and J. Wess, Plenum, NY (1979).
6. B.R. Greene *et al.*, Nucl. Phys. **B278**, 667 (1986);
ibid., Nucl. Phys. **B292**, 606 (1987);
B.R. Greene *et al.*, Nucl. Phys. **B325**, 101 (1989).
7. P. Candelas *et al.*, Nucl. Phys. **B258**, 46 (1985);
L.J. Dixon *et al.*, Nucl. Phys. **B261**, 678 (1985);
ibid., Nucl. Phys. **B274**, 285 (1986);
L. E. Ibanez *et al.*, Phys. Lett. **B187**, 25 (1987);
ibid., Phys. Lett. **B191**, 282 (1987);
J.E. Kim *et al.*, Nucl. Phys. **B712**, 139 (2005).
8. T. Kobayashi *et al.*, Phys. Lett. **B593**, 262 (2004);
S. Forste *et al.*, Phys. Rev. **D70**, 106008 (2004);
T. Kobayashi *et al.*, Nucl. Phys. **B704**, 3 (2005);
W. Buchmuller *et al.*, Nucl. Phys. **B712**, 139 (2005).
9. E. Witten, [hep-ph/0201018];
M. Dine *et al.*, Phys. Rev. **D66**, 115001 (2002), [hep-ph/0206268].
10. Y. Kawamura, Prog. Theor. Phys. **103**, 613 (2000);
ibid., **105**, 999 (2001);
G. Altarelli *et al.*, Phys. Lett. **B5111**, 257 (2001);
L.J. Hall *et al.*, Phys. Rev. **D64**, 055003 (2001);
A. Hebecker and J. March-Russell, Nucl. Phys. **B613**, 3 (2001);
T. Asaka *et al.*, Phys. Lett. **B523**, 199 (2001);
L.J. Hall *et al.*, Phys. Rev. **D65**, 035008 (2002);
R. Dermisek and A. Mafi, Phys. Rev. **D65**, 055002 (2002);
H.D. Kim and S. Raby, JHEP **0301**, 056 (2003).
11. For a recent review see, R. Blumenhagen *et al.*, “Toward realistic intersecting D-brane models,” hep-th/0502005.
12. G. Aldazabal *et al.*, Nucl. Phys. **B452**, 3 (1995);
Z. Kakushadze and S.H.H. Tye, Phys. Rev. **D54**, 7520 (1996);
Z. Kakushadze *et al.*, Int. J. Mod. Phys. **A13**, 2551 (1998).
13. G. B. Cleaver *et al.*, Int. J. Mod. Phys. **A16**, 425 (2001),
hep-ph/9904301;
ibid., Nucl. Phys. **B593**, 471 (2001) hep-ph/9910230.
14. V. Braun *et al.*, Phys. Lett. **B618**, 252 (2005), hep-th/0501070;
ibid., JHEP **506**, 039 (2005), [hep-th/0502155].
15. E. Witten, Nucl. Phys. **B471**, 135 (1996), [hep-th/9602070].
16. H. Georgi *et al.*, Phys. Rev. Lett. **33**, 451 (1974);
See also the definition of effective field theories by S. Weinberg, Phys. Lett. **91B**, 51 (1980).
17. See talks on proposed and running nucleon decay experiments, and theoretical talks by P. Langacker, p. 131, and W.J. Marciano and A. Sirlin, p. 151, in *The Second Workshop on Grand Unification*, eds. J.P. Leveille *et al.*, Birkhäuser, Boston (1981).
18. W.J. Marciano, p. 190, *Eighth Workshop on Grand Unification*, ed. K. Wali, World Scientific Publishing Co., Singapore (1987).
19. U. Amaldi *et al.*, Phys. Lett. **B260**, 447 (1991);
J. Ellis *et al.*, Phys. Lett. **B260**, 131 (1991);
P. Langacker and M. Luo, Phys. Rev. **D44**, 817 (1991);
P. Langacker and N. Polonsky, Phys. Rev. **D47**, 4028 (1993);
M. Carena *et al.*, Nucl. Phys. **B406**, 59 (1993);
see also the review by S. Dimopoulos *et al.*, Physics Today, 25–33, October (1991).
20. S. Dimopoulos *et al.*, Phys. Rev. **D24**, 1681 (1981);
S. Dimopoulos and H. Georgi, Nucl. Phys. **B193**, 150 (1981);

- L. Ibanez and G.G. Ross, Phys. Lett. **105B**, 439 (1981);
N. Sakai, Z. Phys. **C11**, 153 (1981);
M.B. Einhorn and D.R.T. Jones, Nucl. Phys. **B196**, 475 (1982);
W.J. Marciano and G. Senjanovic, Phys. Rev. **D25**, 3092 (1982).
21. D.I. Kazakov, Lectures given at the European School on High Energy Physics, Aug.-Sept. 2000, Caramulo, Portugal [hep-ph/0012288v2].
 22. V. Lucas and S. Raby, Phys. Rev. **D54**, 2261 (1996) [hep-ph/9601303];
T. Blazek *et al.*, Phys. Rev. **D56**, 6919 (1997) [hep-ph/9611217];
G. Altarelli *et al.*, JHEP **0011**, 040 (2000) [hep-ph/0007254].
 23. R. Dermisek *et al.*, Phys. Rev. **D63**, 035001 (2001);
K.S. Babu *et al.*, Nucl. Phys. **B566**, 33 (2000).
 24. M. L. Alciati *et al.*, JHEP **0503**, 054 (2005) [hep-ph/0501086].
 25. G. Anderson *et al.*, eConf **C960625**, SUP107 (1996) [hep-ph/9609457].
 26. R.N. Mohapatra and M.K. Parida, Phys. Rev. **D47**, 264 (1993).
 27. D.G. Lee *et al.*, Phys. Rev. **D51**, 229 (1995).
 28. S. Eidelman *et al.* [Particle Data Group], Phys. Lett. **B592**, 1 (2004).
 29. K.S. Babu and S.M. Barr, Phys. Rev. **D48**, 5354 (1993);
V. Lucas and S. Raby, Phys. Rev. **D54**, 2261 (1996);
S.M. Barr and S. Raby, Phys. Rev. Lett. **79**, 4748 (1997) and references therein.
 30. G. Altarelli *et al.*, JHEP **0011**, 040 (2000) See also earlier papers by A. Masiero *et al.*, Phys. Lett. **B115**, 380 (1982);
B. Grinstein, Nucl. Phys. **B206**, 387 (1982).
 31. K.R. Dienes *et al.*, Phys. Rev. Lett. **91**, 061601 (2003).
 32. L. J. Hall *et al.*, Phys. Rev. **D64**, 055003 (2001).
 33. N. Arkani-Hamed and S. Dimopoulos, JHEP **0506**, 073 (2005) [hep-th/0405159].
 34. G. F. Giudice and A. Romanino, Nucl. Phys. **B6999**, 65 (2004) [Erratum: *ibid.*, Nucl. Phys. **B706**, 65 (2005)] [hep-ph/0406088].
 35. M. Chanowitz *et al.*, Nucl. Phys. **B135**, 66 (1978);
For the corresponding SUSY analysis, see M. Einhorn and D.R.T. Jones, Nucl. Phys. **B196**, 475 (1982);
K. Inoue *et al.*, Prog. Theor. Phys. **67**, 1889 (1982);
L. E. Ibanez and C. Lopez, Phys. Lett. **B126**, 54 (1983);
ibid., Nucl. Phys. **B233**, 511 (1984).
 36. K. Agashe *et al.*, [hep-ph/0502222].
 37. M. Gell-Mann *et al.*, in *Supergravity*, eds. P. van Nieuwenhuizen and D.Z. Freedman, North-Holland, Amsterdam, 1979, p. 315.
 38. S. Weinberg, Phys. Rev. **D26**, 287 (1982);
N. Sakai and T. Yanagida, Nucl. Phys. **B197**, 533 (1982).
 39. G. Farrar and P. Fayet, Phys. Lett. **B76**, 575 (1978).
 40. S. Dimopoulos *et al.*, Phys. Lett. **112B**, 133 (1982);
J. Ellis *et al.*, Nucl. Phys. **B202**, 43 (1982).
 41. L.E. Ibanez and G.G. Ross, Nucl. Phys. **B368**, 3 (1992).
 42. For a recent discussion, see C.S. Aulakh *et al.*, Nucl. Phys. **B597**, 89 (2001).
 43. See talks by Matthew Earl, *NNN workshop*, Irvine, February (2000);
Y. Totsuka, *SUSY2K*, CERN, June (2000);
Y. Suzuki, *International Workshop on Neutrino Oscillations and their Origins*, Tokyo, Japan, December (2000), and *Baksan School, Baksan Valley*, Russia, April (2001), hep-ex/0110005;
K. Kobayashi [Super-Kamiokande Collaboration], "Search for nucleon decay from Super-Kamiokande," *Prepared for 27th International Cosmic Ray Conference (ICRC 2001), Hamburg, Germany, 7-15 Aug 2001*. For published results see : Y. Hayato *et al.* (Super-Kamiokande Collab.), Phys. Rev. Lett. **83**, 1529 (1999);
K. Kobayashi *et al.* [Super-Kamiokande Collaboration], [hep-ex/0502026].
 44. T. Goto and T. Nihei, Phys. Rev. **D59**, 115009 (1999) [hep-ph/9808255];
H. Murayama and A. Pierce, Phys. Rev. **D65**, 055009 (2002) hep-ph/0108104.
 45. B. Bajc *et al.*, Phys. Rev. **D66**, 075005 (2002) [hep-ph/0204311].
 46. J. L. Chkareuli and I. G. Gogoladze, Phys. Rev. **D58**, 055011 (1998) [hep-ph/9803335].
 47. L. J. Hall and Y. Nomura, Phys. Rev. **D66**, 075004 (2002);
H. D. Kim *et al.*, JHEP **0505**, 036 (2005).
 48. M. Baldoceolin *et al.*, Z. Phys. **C63**, 409 (1994).
 49. K. S. Babu and R. N. Mohapatra, Phys. Lett. **B518**, 269 (2001) [hep-ph/0108089].
 50. H. Georgi and D.V. Nanopoulos, Nucl. Phys. **B159**, 16 (1979);
J. Harvey *et al.*, Phys. Lett. **B92**, 309 (1980);
ibid., Nucl. Phys. **B199**, 223 (1982).
 51. T. Banks, Nucl. Phys. **B303**, 172 (1988);
M. Olechowski and S. Pokorski, Phys. Lett. **B214**, 393 (1988);
S. Pokorski, Nucl. Phys. (Proc. Supp.) **B13**, 606 (1990);
B. Ananthanarayan *et al.*, Phys. Rev. **D44**, 1613 (1991);
Q. Shafi and B. Ananthanarayan, ICTP Summer School lectures (1991);
S. Dimopoulos *et al.*, Phys. Rev. Lett. **68**, 1984 (1992);
ibid., Phys. Rev. **D45**, 4192 (1992);
G. Anderson *et al.*, Phys. Rev. **D47**, 3702 (1993);
B. Ananthanarayan *et al.*, Phys. Lett. **B300**, 245 (1993);
G. Anderson *et al.*, Phys. Rev. **D49**, 3660 (1994);
B. Ananthanarayan *et al.*, Phys. Rev. **D50**, 5980 (1994).
 52. LEP Higgs Working Group and ALEPH collaboration and DELPHI collaboration and L3 collaboration and OPAL Collaboration, Preliminary results, [hep-ex/0107030] (2001).
 53. M. Carena and H. E. Haber, Prog. in Part. Nucl. Phys. **50**, 63 (2003) [hep-ph/0208209].
 54. L.J. Hall *et al.*, Phys. Rev. **D50**, 7048 (1994);
M. Carena *et al.*, Nucl. Phys. **B419**, 213 (1994);
R. Rattazzi and U. Sarid, Nucl. Phys. **B501**, 297 (1997).
 55. Blazek *et al.*, Phys. Rev. Lett. **88**, 111804 (2002) [hep-ph/0107097];
ibid., Phys. Rev. **D65**, 115004 (2002) [hep-ph/0201081];
K. Tobe and J. D. Wells, Nucl. Phys. **B663**, 123 (2003) [hep-ph/0301015];
D. Auto *et al.*, JHEP **0306**, 023 (2003) [hep-ph/0302155].
 56. H. Georgi and C. Jarlskog, Phys. Lett. **B86**, 297 (1979).
 57. K.S. Babu and R.N. Mohapatra, Phys. Rev. Lett. **74**, 2418 (1995);
V. Lucas and S. Raby, Phys. Rev. **D54**, 2261 (1996);
T. Blazek *et al.*, Phys. Rev. **D56**, 6919 (1997);
R. Barbieri *et al.*, Nucl. Phys. **B493**, 3 (1997);
T. Blazek *et al.*, Phys. Rev. **D60**, 113001 (1999);
ibid., Phys. Rev. **D62**, 055001 (2000);
Q. Shafi and Z. Tavartkiladze, Phys. Lett. **B487**, 145 (2000);
C.H. Albright and S.M. Barr, Phys. Rev. Lett. **85**, 244 (2000);
K.S. Babu *et al.*, Nucl. Phys. **B566**, 33 (2000);
G. Altarelli *et al.*, Ref. 30;
Z. Berezhiani and A. Rossi, Nucl. Phys. **B594**, 113 (2001);
C. H. Albright and S. M. Barr, Phys. Rev. **D64**, 073010 (2001) [hep-ph/0104294];
R. Dermisek and S. Raby, Phys. Lett. **B622**, 327 (2005) [hep-ph/0507045].
 58. G. Lazarides *et al.*, Nucl. Phys. **B181**, 287 (1981);
T. E. Clark *et al.*, Phys. Lett. **B115**, 26 (1982);
K. S. Babu and R. N. Mohapatra, Phys. Rev. Lett. **70**, 2845 (1993) [hep-ph/9209215].
 59. B. Bajc *et al.*, Phys. Rev. Lett. **90**, 051802 (2003) [hep-ph/0210207].
 60. H. S. Goh *et al.*, Phys. Lett. **B570**, 215 (2003) [hep-ph/0303055];
ibid., Phys. Rev. **D68**, 115008 (2003) [hep-ph/0308197];
B. Dutta *et al.*, Phys. Rev. **D69**, 115014 (2004) [hep-ph/0402113];
S. Bertolini and M. Malinsky, [hep-ph/0504241];
K. S. Babu and C. Macesanu, [hep-ph/0505200].
 61. P. Minkowski, Phys. Lett. **B67**, 421 (1977).
 62. T. Yanagida, in *Proceedings of the Workshop on the Unified Theory and the Baryon Number of the Universe*, eds. O. Sawada and A. Sugamoto, KEK report No. 79-18, Tsukuba, Japan, 1979;
S. Glashow, Quarks and leptons, published in Proceedings of the Cargèse Lectures, M. Levy (ed.), Plenum Press, New York, (1980);

- M. Gell-Mann *et al.*, in *Supergravity*, ed. P. van Nieuwenhuizen *et al.*, North-Holland, Amsterdam, (1979), p. 315;
R.N. Mohapatra and G. Senjanovic, *Phys. Rev. Lett.* **44**, 912 (1980).
63. G. 't Hooft, *Nucl. Phys.* **B79**, 276 (1974);
A.M. Polyakov, *Pis'ma Zh. Eksp. Teor. Fiz.* **20**, 430 (1974) [*JETP Lett.* **20**, 194 (1974)];
For a pedagogical introduction, see S. Coleman, in *Aspects of Symmetry*, Selected Erice Lectures, Cambridge University Press, Cambridge, (1985), and P. Goddard and D. Olive, *Rep. Prog. Phys.* **41**, 1357 (1978).
64. I. De Mitri, (MACRO Collab.), *Nucl. Phys. (Proc. Suppl.)* **B95**, 82 (2001).
65. For a review, see A.D. Linde, *Particle Physics and Inflationary Cosmology*, Harwood Academic, Switzerland (1990).
66. G. R. Dvali *et al.*, *Phys. Rev. Lett.* **80**, 2281 (1998) [[hep-ph/9710301](#)].
67. P. Langacker and S. Y. Pi, *Phys. Rev. Lett.* **45**, 1 (1980).
68. G. R. Dvali *et al.*, *Phys. Rev. Lett.* **75**, 4559 (1995) [[hep-ph/9507230](#)].
69. V. Rubakov, *Nucl. Phys.* **B203**, 311 (1982), Institute of Nuclear Research Report No. P-0211, Moscow (1981), unpublished;
C. Callan, *Phys. Rev.* **D26**, 2058 (1982);
F. Wilczek, *Phys. Rev. Lett.* **48**, 1146 (1982);
See also, S. Dawson and A.N. Schellekens, *Phys. Rev.* **D27**, 2119 (1983).
70. K. Freese *et al.*, *Phys. Rev. Lett.* **51**, 1625 (1983).
71. V. A. Kuzmin *et al.*, *Phys. Lett.* **B155**, 36 (1985).
72. M. Fukugita and T. Yanagida, *Phys. Lett.* **B174**, 45 (1986);
See also the recent review by W. Buchmuller *et al.*, [hep-ph/0502169](#) and references therein.
73. S. Dimopoulos and F. Wilczek, *Proceedings Erice Summer School*, ed. A. Zichichi (1981);
K.S. Babu and S.M. Barr, *Phys. Rev.* **D50**, 3529 (1994).
74. R. Barbieri *et al.*, *Nucl. Phys.* **B391**, 487 (1993);
Z. Berezhiani *et al.*, *Nucl. Phys.* **B444**, 61 (1995);
Q. Shafi and Z. Tavartkiladze, *Phys. Lett.* **B522**, 102 (2001).
75. G.F. Giudice and A. Masiero, *Phys. Lett.* **B206**, 480 (1988);
J.E. Kim and H.P. Nilles, *Mod. Phys. Lett.* **A9**, 3575 (1994).
76. L. Randall and C. Csaki, [hep-ph/9508208](#).

16. STRUCTURE FUNCTIONS

Updated July 2009 by B. Foster (University of Oxford), A.D. Martin (University of Durham), and M.G. Vinster (Carleton University).

16.1. Deep inelastic scattering

High-energy lepton-nucleon scattering (deep inelastic scattering) plays a key role in determining the partonic structure of the proton. The process $\ell N \rightarrow \ell' X$ is illustrated in Fig. 16.1. The filled circle in this figure represents the internal structure of the proton which can be expressed in terms of structure functions.

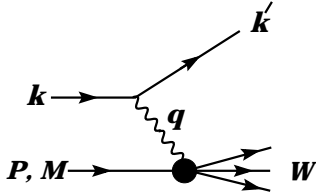


Figure 16.1: Kinematic quantities for the description of deep inelastic scattering. The quantities k and k' are the four-momenta of the incoming and outgoing leptons, P is the four-momentum of a nucleon with mass M , and W is the mass of the recoiling system X . The exchanged particle is a γ , W^\pm , or Z ; it transfers four-momentum $q = k - k'$ to the nucleon.

Invariant quantities:

$\nu = \frac{q \cdot P}{M} = E - E'$ is the lepton's energy loss in the nucleon rest frame (in earlier literature sometimes $\nu = q \cdot P$). Here, E and E' are the initial and final lepton energies in the nucleon rest frame.

$Q^2 = -q^2 = 2(E E' - \vec{k} \cdot \vec{k}') - m_\ell^2 - m_{\ell'}^2$ where $m_\ell(m_{\ell'})$ is the initial (final) lepton mass. If $E E' \sin^2(\theta/2) \gg m_\ell^2, m_{\ell'}^2$, then

$\approx 4E E' \sin^2(\theta/2)$, where θ is the lepton's scattering angle with respect to the lepton beam direction.

$x = \frac{Q^2}{2M\nu}$ where, in the parton model, x is the fraction of the nucleon's momentum carried by the struck quark.

$y = \frac{q \cdot P}{k \cdot P} = \frac{\nu}{E}$ is the fraction of the lepton's energy lost in the nucleon rest frame.

$W^2 = (P + q)^2 = M^2 + 2M\nu - Q^2$ is the mass squared of the system X recoiling against the scattered lepton.

$s = (k + P)^2 = \frac{Q^2}{xy} + M^2 + m_\ell^2$ is the center-of-mass energy squared of the lepton-nucleon system.

The process in Fig. 16.1 is called deep ($Q^2 \gg M^2$) inelastic ($W^2 \gg M^2$) scattering (DIS). In what follows, the masses of the initial and scattered leptons, m_ℓ and $m_{\ell'}$, are neglected.

16.1.1. DIS cross sections :

$$\frac{d^2\sigma}{dx dy} = x(s - M^2) \frac{d^2\sigma}{dx dQ^2} = \frac{2\pi M\nu}{E'} \frac{d^2\sigma}{d\Omega_{N\text{rest}} dE'} . \quad (16.1)$$

In lowest-order perturbation theory, the cross section for the scattering of polarized leptons on polarized nucleons can be expressed in terms of the products of leptonic and hadronic tensors associated with the coupling of the exchanged bosons at the upper and lower vertices in Fig. 16.1 (see Refs. 1–4)

$$\frac{d^2\sigma}{dx dy} = \frac{2\pi y \alpha^2}{Q^4} \sum_j \eta_j L_j^{\mu\nu} W_{\mu\nu}^j . \quad (16.2)$$

For neutral-current processes, the summation is over $j = \gamma, Z$ and γZ representing photon and Z exchange and the interference between

them, whereas for charged-current interactions there is only W exchange, $j = W$. (For transverse nucleon polarization, there is a dependence on the azimuthal angle of the scattered lepton.) $L_{\mu\nu}$ is the lepton tensor associated with the coupling of the exchange boson to the leptons. For incoming leptons of charge $e = \pm 1$ and helicity $\lambda = \pm 1$,

$$\begin{aligned} L_{\mu\nu}^\gamma &= 2 \left(k_\mu k'_\nu + k'_\mu k_\nu - k \cdot k' g_{\mu\nu} - i \lambda \varepsilon_{\mu\nu\alpha\beta} k^\alpha k'^\beta \right), \\ L_{\mu\nu}^{\gamma Z} &= (g_V^e + e \lambda g_A^e) L_{\mu\nu}^\gamma, \quad L_{\mu\nu}^Z = (g_V^e + e \lambda g_A^e)^2 L_{\mu\nu}^\gamma, \\ L_{\mu\nu}^W &= (1 + e \lambda)^2 L_{\mu\nu}^\gamma, \end{aligned} \quad (16.3)$$

where $g_V^e = -\frac{1}{2} + 2 \sin^2 \theta_W$, $g_A^e = -\frac{1}{2}$.

Although here the helicity formalism is adopted, an alternative approach is to express the tensors in Eq. (16.3) in terms of the polarization of the lepton.

The factors η_j in Eq. (16.2) denote the ratios of the corresponding propagators and couplings to the photon propagator and coupling squared

$$\begin{aligned} \eta_\gamma &= 1 \quad ; \quad \eta_{\gamma Z} = \left(\frac{G_F M_Z^2}{2\sqrt{2}\pi\alpha} \right) \left(\frac{Q^2}{Q^2 + M_Z^2} \right); \\ \eta_Z &= \eta_{\gamma Z}^2 \quad ; \quad \eta_W = \frac{1}{2} \left(\frac{G_F M_W^2}{4\pi\alpha} \frac{Q^2}{Q^2 + M_W^2} \right)^2. \end{aligned} \quad (16.4)$$

The hadronic tensor, which describes the interaction of the appropriate electroweak currents with the target nucleon, is given by

$$W_{\mu\nu} = \frac{1}{4\pi} \int d^4z e^{iq \cdot z} \langle P, S | [J_\mu^\dagger(z), J_\nu(0)] | P, S \rangle, \quad (16.5)$$

where S denotes the nucleon-spin 4-vector, with $S^2 = -M^2$ and $S \cdot P = 0$.

16.2. Structure functions of the proton

The structure functions are defined in terms of the hadronic tensor (see Refs. 1–3)

$$\begin{aligned} W_{\mu\nu} &= \left(-g_{\mu\nu} + \frac{q_\mu q_\nu}{q^2} \right) F_1(x, Q^2) + \frac{\hat{P}_\mu \hat{P}_\nu}{P \cdot q} F_2(x, Q^2) \\ &\quad - i \varepsilon_{\mu\nu\alpha\beta} \frac{q^\alpha P^\beta}{2P \cdot q} F_3(x, Q^2) \\ &\quad + i \varepsilon_{\mu\nu\alpha\beta} \frac{q^\alpha}{P \cdot q} \left[S^\beta g_1(x, Q^2) + \left(S^\beta - \frac{S \cdot q}{P \cdot q} P^\beta \right) g_2(x, Q^2) \right] \\ &\quad + \frac{1}{P \cdot q} \left[\frac{1}{2} \left(\hat{P}_\mu \hat{S}_\nu + \hat{S}_\mu \hat{P}_\nu \right) - \frac{S \cdot q}{P \cdot q} \hat{P}_\mu \hat{P}_\nu \right] g_3(x, Q^2) \\ &\quad + \frac{S \cdot q}{P \cdot q} \left[\frac{\hat{P}_\mu \hat{P}_\nu}{P \cdot q} g_4(x, Q^2) + \left(-g_{\mu\nu} + \frac{q_\mu q_\nu}{q^2} \right) g_5(x, Q^2) \right] \end{aligned} \quad (16.6)$$

where

$$\hat{P}_\mu = P_\mu - \frac{P \cdot q}{q^2} q_\mu, \quad \hat{S}_\mu = S_\mu - \frac{S \cdot q}{q^2} q_\mu . \quad (16.7)$$

In Ref. [2], the definition of $W_{\mu\nu}$ with $\mu \leftrightarrow \nu$ is adopted, which changes the sign of the $\varepsilon_{\mu\nu\alpha\beta}$ terms in Eq. (16.6), although the formulae given here below are unchanged. Ref. [1] tabulates the relation between the structure functions defined in Eq. (16.6) and other choices available in the literature.

The cross sections for neutral- and charged-current deep inelastic scattering on unpolarized nucleons can be written in terms of the structure functions in the generic form

$$\begin{aligned} \frac{d^2\sigma^i}{dx dy} &= \frac{4\pi\alpha^2}{xyQ^2} \eta^i \left\{ \left(1 - y - \frac{x^2 y^2 M^2}{Q^2} \right) F_2^i \right. \\ &\quad \left. + y^2 x F_1^i \mp \left(y - \frac{y^2}{2} \right) x F_3^i \right\}, \end{aligned} \quad (16.8)$$

where $i = \text{NC, CC}$ corresponds to neutral-current ($eN \rightarrow eX$) or charged-current ($eN \rightarrow \nu X$ or $\nu N \rightarrow eX$) processes, respectively. For incoming neutrinos, $L_{\mu\nu}^W$ of Eq. (16.3) is still true, but with e, λ corresponding to the outgoing charged lepton. In the last term of Eq. (16.8), the $-$ sign is taken for an incoming e^+ or $\bar{\nu}$ and the $+$ sign for an incoming e^- or ν . The factor $\eta^{\text{NC}} = 1$ for unpolarized e^\pm beams, whereas*

$$\eta^{\text{CC}} = (1 \pm \lambda)^2 \eta_W \quad (16.9)$$

with \pm for ℓ^\pm ; and where λ is the helicity of the incoming lepton and η_W is defined in Eq. (16.4); for incoming neutrinos $\eta^{\text{CC}} = 4\eta_W$. The CC structure functions, which derive exclusively from W exchange, are

$$F_1^{\text{CC}} = F_1^W, \quad F_2^{\text{CC}} = F_2^W, \quad xF_3^{\text{CC}} = xF_3^W. \quad (16.10)$$

The NC structure functions $F_2^\gamma, F_2^{\gamma Z}, F_2^Z$ are, for $e^\pm N \rightarrow e^\pm X$, given by Ref. [5],

$$F_2^{\text{NC}} = F_2^\gamma - (g_V^e \pm \lambda g_A^e) \eta_{\gamma Z} F_2^{\gamma Z} + (g_V^e \pm \lambda g_A^e \pm 2\lambda g_V^e g_A^e) \eta_Z F_2^Z \quad (16.11)$$

and similarly for F_1^{NC} , whereas

$$xF_3^{\text{NC}} = -(g_A^e \pm \lambda g_V^e) \eta_{\gamma Z} xF_3^{\gamma Z} + [2g_V^e g_A^e \pm \lambda(g_V^e \pm g_A^e)] \eta_Z xF_3^Z. \quad (16.12)$$

The polarized cross-section difference

$$\Delta\sigma = \sigma(\lambda_n = -1, \lambda_\ell) - \sigma(\lambda_n = 1, \lambda_\ell), \quad (16.13)$$

where λ_ℓ, λ_n are the helicities (± 1) of the incoming lepton and nucleon, respectively, may be expressed in terms of the five structure functions $g_{1,\dots,5}(x, Q^2)$ of Eq. (16.6). Thus,

$$\begin{aligned} \frac{d^2 \Delta\sigma^i}{dx dy} &= \frac{8\pi\alpha^2}{xyQ^2} \eta^i \left\{ -\lambda_\ell y \left(2 - y - 2x^2 y^2 \frac{M^2}{Q^2} \right) x g_1^i + \lambda_\ell 4x^3 y^2 \frac{M^2}{Q^2} g_2^i \right. \\ &+ 2x^2 y \frac{M^2}{Q^2} \left(1 - y - x^2 y^2 \frac{M^2}{Q^2} \right) g_3^i \\ &\left. - \left(1 + 2x^2 y \frac{M^2}{Q^2} \right) \left[\left(1 - y - x^2 y^2 \frac{M^2}{Q^2} \right) g_4^i + xy^2 g_5^i \right] \right\} \quad (16.14) \end{aligned}$$

with $i = \text{NC or CC}$ as before. The Eq. (16.13) corresponds to the difference of antiparallel minus parallel spins of the incoming particles for e^- or ν initiated reactions, but the difference of parallel minus antiparallel for e^+ or $\bar{\nu}$ initiated processes. For longitudinal nucleon polarization, the contributions of g_2 and g_3 are suppressed by powers of M^2/Q^2 . These structure functions give an unsuppressed contribution to the cross section for transverse polarization [1], but in this case the cross-section difference vanishes as $M/Q \rightarrow 0$.

Because the same tensor structure occurs in the spin-dependent and spin-independent parts of the hadronic tensor of Eq. (16.6) in the $M^2/Q^2 \rightarrow 0$ limit, the differential cross-section difference of Eq. (16.14) may be obtained from the differential cross section Eq. (16.8) by replacing

$$F_1 \rightarrow -g_5, \quad F_2 \rightarrow -g_4, \quad F_3 \rightarrow 2g_1, \quad (16.15)$$

and multiplying by two, since the total cross section is the average over the initial-state polarizations. In this limit, Eq. (16.8) and Eq. (16.14) may be written in the form

$$\begin{aligned} \frac{d^2 \sigma^i}{dx dy} &= \frac{2\pi\alpha^2}{xyQ^2} \eta^i \left[Y_+ F_2^i \mp Y_- x F_3^i - y^2 F_L^i \right], \\ \frac{d^2 \Delta\sigma^i}{dx dy} &= \frac{4\pi\alpha^2}{xyQ^2} \eta^i \left[-Y_+ g_4^i \mp Y_- 2x g_1^i + y^2 g_L^i \right], \quad (16.16) \end{aligned}$$

with $i = \text{NC or CC}$, where $Y_\pm = 1 \pm (1 - y)^2$ and

$$F_L^i = F_2^i - 2x F_1^i, \quad g_L^i = g_4^i - 2x g_5^i. \quad (16.17)$$

In the naive quark-parton model, the analogy with the Callan-Gross relations [6] $F_L^i = 0$, are the Dicus relations [7] $g_L^i = 0$. Therefore, there are only two independent polarized structure functions: g_1 (parity conserving) and g_5 (parity violating), in analogy with the unpolarized structure functions F_1 and F_3 .

16.2.1. Structure functions in the quark-parton model :

In the quark-parton model [8,9], contributions to the structure functions F^i and g^i can be expressed in terms of the quark distribution functions $q(x, Q^2)$ of the proton, where $q = u, \bar{u}, d, \bar{d}$ etc. The quantity $q(x, Q^2) dx$ is the number of quarks (or antiquarks) of designated flavor that carry a momentum fraction between x and $x + dx$ of the proton's momentum in a frame in which the proton momentum is large.

For the neutral-current processes $ep \rightarrow eX$,

$$\begin{aligned} \left[F_2^\gamma, F_2^{\gamma Z}, F_2^Z \right] &= x \sum_q \left[e_q^2, 2e_q g_V^q, g_V^{q^2} + g_A^{q^2} \right] (q + \bar{q}), \\ \left[F_3^\gamma, F_3^{\gamma Z}, F_3^Z \right] &= \sum_q \left[0, 2e_q g_A^q, 2g_V^q g_A^q \right] (q - \bar{q}), \\ \left[g_1^\gamma, g_1^{\gamma Z}, g_1^Z \right] &= \frac{1}{2} \sum_q \left[e_q^2, 2e_q g_V^q, g_V^{q^2} + g_A^{q^2} \right] (\Delta q + \Delta \bar{q}), \\ \left[g_5^\gamma, g_5^{\gamma Z}, g_5^Z \right] &= \sum_q \left[0, e_q g_A^q, g_V^q g_A^q \right] (\Delta q - \Delta \bar{q}), \quad (16.18) \end{aligned}$$

where $g_V^q = \pm \frac{1}{2} - 2e_q \sin^2 \theta_W$ and $g_A^q = \pm \frac{1}{2}$, with \pm according to whether q is a u - or d -type quark respectively. The quantity Δq is the difference $q \uparrow - q \downarrow$ of the distributions with the quark spin parallel and antiparallel to the proton spin.

For the charged-current processes $e^- p \rightarrow \nu X$ and $\bar{\nu} p \rightarrow e^+ X$, the structure functions are:

$$\begin{aligned} F_2^{W^-} &= 2x(u + \bar{d} + \bar{s} + c \dots), \\ F_3^{W^-} &= 2(u - \bar{d} - \bar{s} + c \dots), \\ g_1^{W^-} &= (\Delta u + \Delta \bar{d} + \Delta \bar{s} + \Delta c \dots), \\ g_5^{W^-} &= (-\Delta u + \Delta \bar{d} + \Delta \bar{s} - \Delta c \dots), \quad (16.19) \end{aligned}$$

where only the active flavors are to be kept and where CKM mixing has been neglected. For $e^+ p \rightarrow \bar{\nu} X$ and $\nu p \rightarrow e^- X$, the structure functions F^{W^+}, g^{W^+} are obtained by the flavor interchanges $d \leftrightarrow u, s \leftrightarrow c$ in the expressions for F^{W^-}, g^{W^-} . The structure functions for scattering on a neutron are obtained from those of the proton by the interchange $u \leftrightarrow d$. For both the neutral- and charged-current processes, the quark-parton model predicts $2xF_1^i = F_2^i$ and $g_4^i = 2xg_5^i$.

Neglecting masses, the structure functions g_2 and g_3 contribute only to scattering from transversely polarized nucleons (for which $S \cdot q = 0$), and have no simple interpretation in terms of the quark-parton model. They arise from off-diagonal matrix elements $\langle P, \lambda' | [J_\mu^\dagger(z), J_\nu(0)] | P, \lambda \rangle$, where the proton helicities satisfy $\lambda' \neq \lambda$. In fact, the leading-twist contributions to both g_2 and g_3 are both twist-2 and twist-3, which contribute at the same order of Q^2 . The Wandzura-Wilczek relation [10] expresses the twist-2 part of g_2 in terms of g_1 as

$$g_2^i(x) = -g_1^i(x) + \int_x^1 \frac{dy}{y} g_1^i(y). \quad (16.20)$$

However, the twist-3 component of g_2 is unknown. Similarly, there is a relation expressing the twist-2 part of g_3 in terms of g_4 . A complete set of relations, including M^2/Q^2 effects, can be found in Ref. [11].

16.2.2. Structure functions and QCD :

One of the most striking predictions of the quark-parton model is that the structure functions F_i, g_i scale, i.e., $F_i(x, Q^2) \rightarrow F_i(x)$ in the Bjorken limit that Q^2 and $\nu \rightarrow \infty$ with x fixed [12]. This property is related to the assumption that the transverse momentum of the partons in the infinite-momentum frame of the proton is small. In QCD, however, the radiation of hard gluons from the quarks violates this assumption, leading to logarithmic scaling violations, which are particularly large at small x , see Fig. 16.2. The radiation of gluons produces the evolution of the structure functions. As Q^2 increases, more and more gluons are radiated, which in turn split into $q\bar{q}$ pairs. This process leads both to the softening of the initial quark momentum distributions and to the growth of the gluon density and the $q\bar{q}$ sea as x decreases.

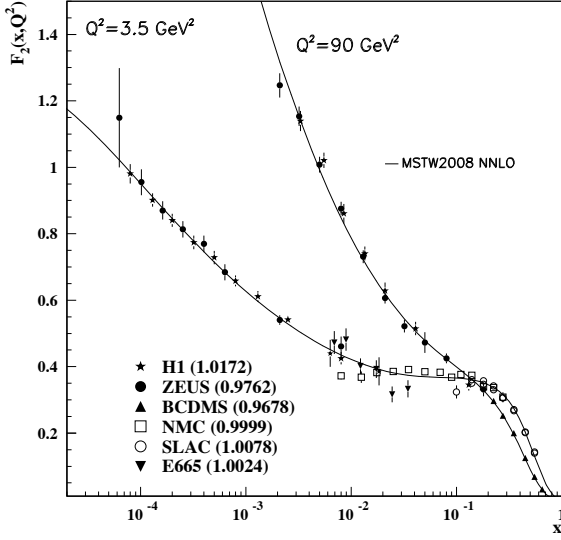


Figure 16.2: The proton structure function F_2^p given at two Q^2 values (3.5 GeV^2 and 90 GeV^2), which exhibit scaling at the ‘pivot’ point $x \sim 0.14$. See the captions in Fig. 16.7 and Fig. 16.10 for the references of the data. The various data sets have been renormalised by the factors shown in brackets in the key to the plot, which were determined in the NNLO MSTW2008 global analysis, see Table 3 of [13].

In QCD, the above process is described in terms of scale-dependent parton distributions $f_a(x, \mu^2)$, where $a = g$ or q and, typically, μ is the scale of the probe Q . For $Q^2 \gg M^2$, the structure functions are of the form

$$F_i = \sum_a C_i^a \otimes f_a, \quad (16.21)$$

where \otimes denotes the convolution integral

$$C \otimes f = \int_x^1 \frac{dy}{y} C(y) f\left(\frac{x}{y}\right), \quad (16.22)$$

and where the coefficient functions C_i^a are given as a power series in α_s . The parton distribution f_a corresponds, at a given x , to the density of parton a in the proton integrated over transverse momentum k_t up to μ . Its evolution in μ is described in QCD by a DGLAP equation (see Refs. 14–17) which has the schematic form

$$\frac{\partial f_a}{\partial \ln \mu^2} \sim \frac{\alpha_s(\mu^2)}{2\pi} \sum_b (P_{ab} \otimes f_b), \quad (16.23)$$

where the P_{ab} , which describe the parton splitting $b \rightarrow a$, are also given as a power series in α_s . Although perturbative QCD can predict, via Eq. (16.23), the evolution of the parton distribution functions from a particular scale, μ_0 , these DGLAP equations cannot predict them *a priori* at any particular μ_0 . Thus they must be measured at a starting point μ_0 before the predictions of QCD can be compared to the data at other scales, μ . In general, all observables involving a hard hadronic interaction (such as structure functions) can be expressed as a convolution of calculable, process-dependent coefficient functions and these universal parton distributions, e.g. Eq. (16.21).

It is often convenient to write the evolution equations in terms of the gluon, non-singlet (q^{NS}) and singlet (q^S) quark distributions, such that

$$q^{NS} = q_i - \bar{q}_i \quad (\text{or } q_i - q_j), \quad q^S = \sum_i (q_i + \bar{q}_i). \quad (16.24)$$

The non-singlet distributions have non-zero values of flavor quantum numbers, such as isospin and baryon number. The DGLAP evolution equations then take the form

$$\begin{aligned} \frac{\partial q^{NS}}{\partial \ln \mu^2} &= \frac{\alpha_s(\mu^2)}{2\pi} P_{qq} \otimes q^{NS}, \\ \frac{\partial}{\partial \ln \mu^2} \begin{pmatrix} q^S \\ g \end{pmatrix} &= \frac{\alpha_s(\mu^2)}{2\pi} \begin{pmatrix} P_{qq} & 2n_f P_{qg} \\ P_{gq} & P_{gg} \end{pmatrix} \otimes \begin{pmatrix} q^S \\ g \end{pmatrix}, \end{aligned} \quad (16.25)$$

where P are splitting functions that describe the probability of a given parton splitting into two others, and n_f is the number of (active) quark flavors. The leading-order Altarelli-Parisi [16] splitting functions are

$$P_{qq} = \frac{4}{3} \left[\frac{1+x^2}{(1-x)} \right]_+ = \frac{4}{3} \left[\frac{1+x^2}{(1-x)_+} \right] + 2\delta(1-x), \quad (16.26)$$

$$P_{qg} = \frac{1}{2} \left[x^2 + (1-x)^2 \right], \quad (16.27)$$

$$P_{gq} = \frac{4}{3} \left[\frac{1+(1-x)^2}{x} \right], \quad (16.28)$$

$$\begin{aligned} P_{gg} &= 6 \left[\frac{1-x}{x} + x(1-x) + \frac{x}{(1-x)_+} \right] \\ &+ \left[\frac{11}{2} - \frac{n_f}{3} \right] \delta(1-x), \end{aligned} \quad (16.29)$$

where the notation $[F(x)]_+$ defines a distribution such that for any sufficiently regular test function, $f(x)$,

$$\int_0^1 dx f(x) [F(x)]_+ = \int_0^1 dx (f(x) - f(1)) F(x). \quad (16.30)$$

In general, the splitting functions can be expressed as a power series in α_s . The series contains both terms proportional to $\ln \mu^2$ and to $\ln 1/x$. The leading-order DGLAP evolution sums up the $(\alpha_s \ln \mu^2)^n$ contributions, while at next-to-leading order (NLO) the sum over the $\alpha_s (\alpha_s \ln \mu^2)^{n-1}$ terms is included [18,19]. In fact, the NNLO contributions to the splitting functions and the DIS coefficient functions are now also all known [20–22].

In the kinematic region of very small x , it is essential to sum leading terms in $\ln 1/x$, independent of the value of $\ln \mu^2$. At leading order, LLx, this is done by the BFKL equation for the unintegrated distributions (see Refs. [23,24]). The leading-order $(\alpha_s \ln(1/x))^n$ terms result in a power-like growth, $x^{-\omega}$ with $\omega = (12\alpha_s \ln 2)/\pi$, at asymptotic values of $\ln 1/x$. More recently, the next-to-leading $\ln 1/x$ (NLLx) contributions have become available [25,26]. They are so large (and negative) that the result appears to be perturbatively unstable. Methods, based on a combination of collinear and small x resummations, have been developed which reorganize the perturbative series into a more stable hierarchy [27–30]. There are indications that small x resummations become necessary for real precision for $x \lesssim 10^{-3}$ at low scales. On the other hand, there is no convincing indication that, for $Q^2 \gtrsim 2 \text{ GeV}^2$, we have entered the ‘non-linear’ regime where the gluon density is so high that gluon-gluon recombination effects become significant.

The precision of the contemporary experimental data demands that at least NLO, and preferably NNLO, DGLAP evolution be used in comparisons between QCD theory and experiment. Beyond the leading order, it is necessary to specify, and to use consistently, both a renormalization and a factorization scheme. The renormalization scheme used is almost universally the modified minimal subtraction ($\overline{\text{MS}}$) scheme [31,32]. There are two popular choices for factorization scheme, in which the form of the correction for each structure function is different. The most-used factorization scheme is again $\overline{\text{MS}}$ [33]. However, sometimes the DIS [34] scheme is adopted, in which there are no higher-order corrections to the F_2 structure function. The two schemes differ in how the non-divergent pieces are assimilated in the parton distribution functions.

The u , d , and s quarks are taken to be massless, and the effects of the c and b -quark masses have been studied up to NNLO, for example, in [35–41]. An approach using a variable flavor number is now generally adopted, in which evolution with $n_f = 3$ is matched to that with $n_f = 4$ at the charm threshold, with an analogous matching at the bottom threshold.

The discussion above relates to the Q^2 behavior of leading-twist (twist-2) contributions to the structure functions. Higher-twist terms, which involve their own non-perturbative input, exist. These die off as powers of Q ; specifically twist- n terms are damped by $1/Q^{n-2}$. The higher-twist terms appear to be numerically unimportant for Q^2 above a few GeV^2 , except for x close to 1.

Table 16.1: The main processes included in the current global PDF analyses, ordered in three groups: fixed-target experiments, HERA and the Tevatron. For each process we give an indication of their dominant partonic subprocesses, the primary partons which are probed and the approximate range of x constrained by the data. The Table is taken from [13].

Process	Subprocess	Partons	x range
$\ell^\pm \{p, n\} \rightarrow \ell^\pm X$	$\gamma^* q \rightarrow q$	q, \bar{q}, g	$x \gtrsim 0.01$
$\ell^\pm n/p \rightarrow \ell^\pm X$	$\gamma^* d/u \rightarrow d/u$	d/u	$x \gtrsim 0.01$
$pp \rightarrow \mu^+ \mu^- X$	$u\bar{u}, d\bar{d} \rightarrow \gamma^*$	\bar{q}	$0.015 \lesssim x \lesssim 0.35$
$pn/pp \rightarrow \mu^+ \mu^- X$	$(u\bar{d})/(u\bar{u}) \rightarrow \gamma^*$	\bar{d}/\bar{u}	$0.015 \lesssim x \lesssim 0.35$
$\nu(\bar{\nu}) N \rightarrow \mu^-(\mu^+) X$	$W^* q \rightarrow q'$	q, \bar{q}	$0.01 \lesssim x \lesssim 0.5$
$\nu N \rightarrow \mu^- \mu^+ X$	$W^* s \rightarrow c$	s	$0.01 \lesssim x \lesssim 0.2$
$\bar{\nu} N \rightarrow \mu^+ \mu^- X$	$W^* \bar{s} \rightarrow \bar{c}$	\bar{s}	$0.01 \lesssim x \lesssim 0.2$
$e^\pm p \rightarrow e^\pm X$	$\gamma^* q \rightarrow q$	g, q, \bar{q}	$0.0001 \lesssim x \lesssim 0.1$
$e^+ p \rightarrow \bar{\nu} X$	$W^+ \{d, s\} \rightarrow \{u, c\}$	d, s	$x \gtrsim 0.01$
$e^\pm p \rightarrow e^\pm c\bar{c} X$	$\gamma^* c \rightarrow c, \gamma^* g \rightarrow c\bar{c}$	c, g	$0.0001 \lesssim x \lesssim 0.01$
$e^\pm p \rightarrow \text{jet}+X$	$\gamma^* g \rightarrow q\bar{q}$	g	$0.01 \lesssim x \lesssim 0.1$
$p\bar{p} \rightarrow \text{jet}+X$	$gg, qq, q\bar{q} \rightarrow 2j$	g, q	$0.01 \lesssim x \lesssim 0.5$
$p\bar{p} \rightarrow (W^\pm \rightarrow \ell^\pm \nu) X$	$ud \rightarrow W, \bar{u}\bar{d} \rightarrow W$	u, d, \bar{u}, \bar{d}	$x \gtrsim 0.05$
$p\bar{p} \rightarrow (Z \rightarrow \ell^+ \ell^-) X$	$uu, dd \rightarrow Z$	d	$x \gtrsim 0.05$

16.3. Determination of parton distributions

The parton distribution functions (PDFs) can be determined from data for deep inelastic lepton-nucleon scattering and for related hard-scattering processes initiated by nucleons. Table 16.1 highlights some processes and their primary sensitivity to PDFs.

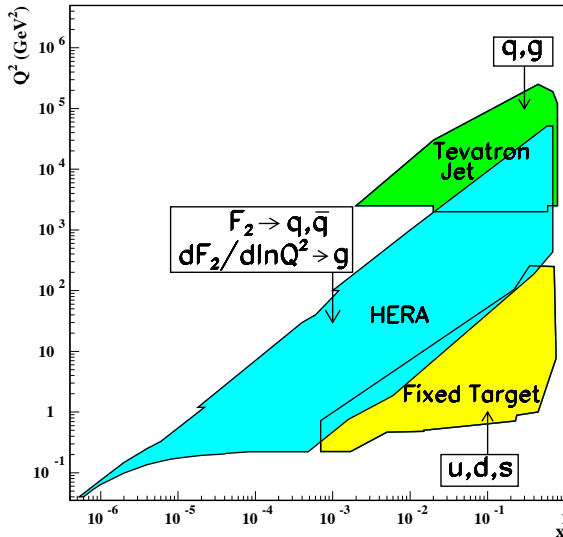


Figure 16.3: Kinematic domains in x and Q^2 probed by fixed-target and collider experiments, shown together with the parton distributions that are most strongly constrained by the indicated regions.

The kinematic ranges of fixed-target and collider experiments are complementary (as is shown in Fig. 16.3), which enables the determination of PDFs over a wide range in x and Q^2 . Recent determinations of the unpolarized PDFs from NLO global analyses are given in Ref. [13,42], see also Ref. [43] for progress towards a neural network global analysis. NNLO global analyses are given in Ref. [13,44]. The results of one analysis are shown in Fig. 16.4 at scales $\mu^2 = 10$ and 10^4 GeV².

Spin-dependent (or polarized) PDFs have been obtained through NLO global analyses which include measurements of the g_1 structure function in inclusive polarized DIS, ‘flavour-tagged’ semi-inclusive DIS data, and results from polarized pp scattering at RHIC. Recent NLO analyses are given in Refs. [45–47]. Improved parton-to-hadron fragmentation functions, needed to describe the semi-inclusive DIS data, can be found in [48–50]. Fig. 16.5 shows several global analyses at a scale of 2.5 GeV² along with the data from semi-inclusive DIS.

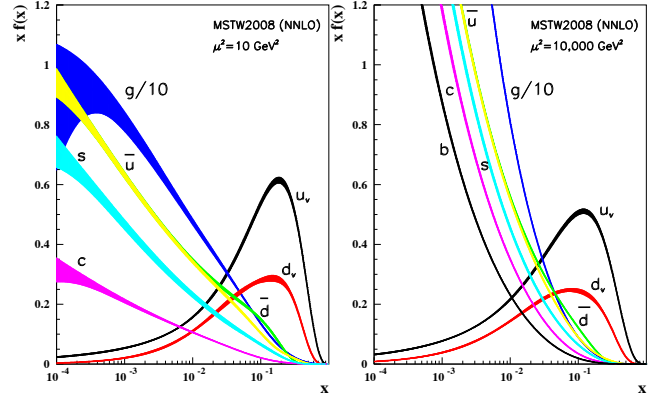


Figure 16.4: Distributions of x times the unpolarized parton distributions $f(x)$ (where $f = u_v, d_v, \bar{u}, \bar{d}, s, c, b, g$) and their associated uncertainties using the NNLO MSTW2008 parameterization [13] at a scale $\mu^2 = 10$ GeV² and $\mu^2 = 10,000$ GeV². Color version at end of book.

Comprehensive sets of PDFs are available as program-callable functions from the HepData website [55], which includes comparison graphics of PDFs, and from the LHAPDF library [56], which can be linked directly into a users programme to provide access to recent PDFs in a standard format.

16.4. DIS determinations of α_s

Table 16.2 shows the values of $\alpha_s(M_Z^2)$ found in recent fits to DIS and related data in which the coupling is left as a free parameter. There have been several other studies of α_s using subsets of inclusive DIS data, and also from measurements of spin-dependent structure functions, see the Quantum Chromodynamics section of this *Review*.

Table 16.2: The values of $\alpha_s(M_Z^2)$ found in NLO and NNLO fits to DIS and related data. CTEQ [57] and MSTW [58] are global fits. H1 [59] fit only a subset of the F_2^{ep} data, while Alekhin [61] also includes F_2^{ed} and ZEUS [60] in addition include their charged current and jet data. At NNLO, Alekhin *et al.* [44] include Drell-Yan data in their fit. The experimental errors quoted correspond to 68% C.L. See [58] for an extended comparative discussion.

	$\alpha_s(M_Z^2) \pm \text{expt} \pm \text{theory} \pm \text{model}$		
NLO			
CTEQ	0.1170	± 0.0047	
MSTW08	0.1202	$^{+0.0012}_{-0.0015}$	± 0.003
ZEUS	0.1183	± 0.0028	± 0.0008
H1	0.115	± 0.0017	$^{+0.0009}_{-0.0005}$
Alekhin	0.1171	± 0.0015	± 0.0033
NNLO			
MSTW08	0.1171	± 0.0014	± 0.003
Alekhin	0.1128	± 0.0015	

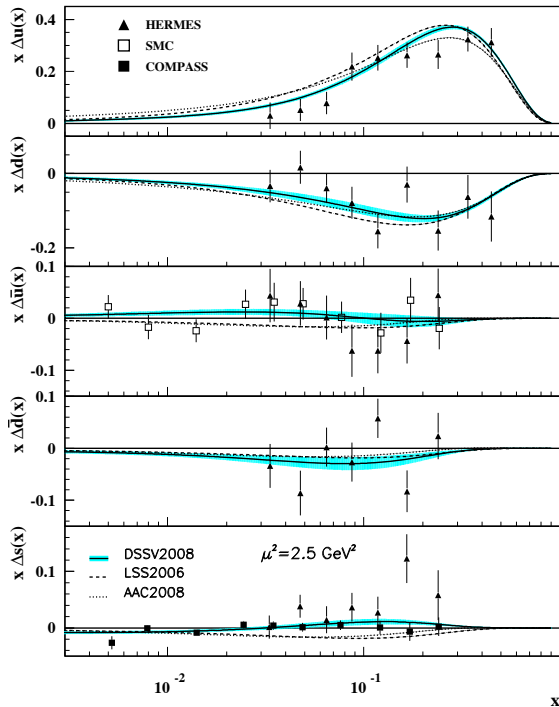


Figure 16.5: Distributions of x times the polarized parton distributions $\Delta q(x)$ (where $q = u, d, \bar{u}, \bar{d}, s$) using the LSS2006 [45], AAC2008 [46], and DSSV2008 [47] parameterizations at a scale $\mu^2 = 2.5 \text{ GeV}^2$, showing the error corridor of the latter set (corresponding to a one-unit increase in χ^2). Points represent data from semi-inclusive positron (HERMES [51,52]) and muon (SMC [53] and COMPASS [54]) deep inelastic scattering given at $Q^2 = 2.5 \text{ GeV}^2$. SMC results are extracted under the assumption that $\Delta \bar{u}(x) = \Delta \bar{d}(x)$.

16.5. The hadronic structure of the photon

Besides the *direct* interactions of the photon, it is possible for it to fluctuate into a hadronic state via the process $\gamma \rightarrow q\bar{q}$. While in this state, the partonic content of the photon may be *resolved*, for example, through the process $e^+e^- \rightarrow e^+e^-\gamma^* \rightarrow e^+e^-X$, where the virtual photon emitted by the DIS lepton probes the hadronic structure of the quasi-real photon emitted by the other lepton. The perturbative LO contributions, $\gamma \rightarrow q\bar{q}$ followed by $\gamma^*q \rightarrow q$, are subject to QCD corrections due to the coupling of quarks to gluons.

Often the equivalent-photon approximation is used to express the differential cross section for deep inelastic electron–photon scattering in terms of the structure functions of the transverse quasi-real photon times a flux factor N_γ^T (for these incoming quasi-real photons of transverse polarization)

$$\frac{d^2\sigma}{dx dQ^2} = N_\gamma^T \frac{2\pi\alpha^2}{xQ^4} \left[\left(1 + (1-y)^2\right) F_2^\gamma(x, Q^2) - y^2 F_L^\gamma(x, Q^2) \right],$$

where we have used $F_2^\gamma = 2xF_T^\gamma + F_L^\gamma$, not to be confused with F_2^γ of Sec. 16.2. Complete formulae are given, for example, in the comprehensive review of Ref. [62].

The hadronic photon structure function, F_2^γ , evolves with increasing Q^2 from the ‘hadron-like’ behavior, calculable via the vector-meson-dominance model, to the dominating ‘point-like’ behaviour, calculable in perturbative QCD. Due to the point-like coupling, the logarithmic evolution of F_2^γ with Q^2 has a *positive* slope for all values of x , see Fig. 16.14. The ‘loss’ of quarks at large x due to gluon radiation is over-compensated by the ‘creation’ of quarks via the point-like $\gamma \rightarrow q\bar{q}$ coupling. The logarithmic evolution was first predicted in the quark–parton model ($\gamma^*\gamma \rightarrow q\bar{q}$) [63,64], and then in QCD in the limit of large Q^2 [65]. The evolution is now known to NLO [66–68]. NLO data analyses to determine the parton densities of the photon can be found in [69–71].

16.6. Diffractive DIS (DDIS)

Some 10% of DIS events are diffractive, $\gamma^*p \rightarrow X + p$, in which the slightly deflected proton and the cluster X of outgoing hadrons are well-separated in rapidity. Besides x and Q^2 , two extra variables are needed to describe a DDIS event: the fraction x_{IP} of the proton’s momentum transferred across the rapidity gap and t , the square of the 4-momentum transfer of the proton. The DDIS data [72–76] are usually analyzed using two levels of factorization. First, the diffractive structure function F_2^D satisfies *collinear factorization*, and can be expressed as the convolution [77]

$$F_2^D = \sum_{a=q,g} C_2^a \otimes f_{a/p}^D, \quad (16.31)$$

with the same coefficient functions as in DIS (see Eq. (16.21)), and where the diffractive parton distributions $f_{a/p}^D$ ($a = q, g$) satisfy DGLAP evolution. Second, *Regge factorization* is assumed [78],

$$f_{a/p}^D(x_{IP}, t, z, \mu^2) = f_{IP/p}(x_{IP}, t) f_{a/IP}(z, \mu^2), \quad (16.32)$$

where $f_{a/IP}$ are the parton densities of the Pomeron, which itself is treated like a hadron, and $z \in [x/x_{IP}, 1]$ is the fraction of the Pomeron’s momentum carried by the parton entering the hard subprocess. The Pomeron flux factor $f_{IP/p}(x_{IP}, t)$ is taken from Regge phenomenology. There are also secondary Reggeon contributions to Eq. (16.32). A sample of the t -integrated diffractive parton densities, obtained in this way, is shown in Fig. 16.6 as Fit A.

Although collinear factorization holds as $\mu^2 \rightarrow \infty$, there are non-negligible corrections for finite μ^2 and small x_{IP} . Besides the *resolved* interactions of the Pomeron, the perturbative QCD Pomeron may also interact *directly* with the hard subprocess, giving rise to an inhomogeneous evolution equation for the diffractive parton densities analogous to the photon case. The results of the MRW analysis [79], which includes these contributions, are also shown in Fig. 16.6. Unlike the inclusive case, the diffractive parton densities cannot be directly used to calculate diffractive hadron–hadron cross sections, since account must first be taken of ‘soft’ rescattering effects.

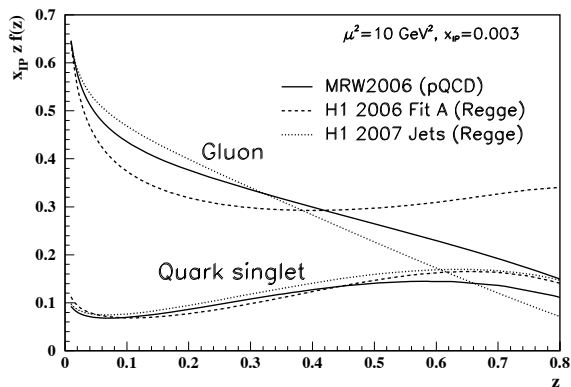


Figure 16.6: Diffractive parton distributions, $x_{IP} z f_{a/p}^D$, obtained from fitting to the H1 data with $Q^2 > 8.5 \text{ GeV}^2$ assuming Regge factorization [75], and using a more perturbative QCD approach [79]. Only the Pomeron contributions are shown and not the secondary Reggeon contributions which are negligible at the value of $x_{IP} = 0.003$ chosen here. Diffractive DIS dijet data [80,81,82] favour a smaller gluon at high z than that in H1 Fit A, more like MRW, as shown by the H1 Jets curve [81].

* The value of η^{CC} deduced from Ref. [1] is found to be a factor of two too small; η^{CC} of Eq. (16.9) agrees with Refs. [2,3].

References:

1. J. Blümlein and N. Kochelev, Nucl. Phys. **B498**, 285 (1997).
2. S. Forte *et al.*, Nucl. Phys. **B602**, 585 (2001).
3. M. Anselmino *et al.*, Z. Phys. **C64**, 267 (1994).
4. M. Anselmino *et al.*, Phys. Rep. **261**, 1 (1995).
5. M. Klein and T. Riemann, Z. Phys. **C24**, 151 (1984).
6. C.G. Callan and D.J. Gross, Phys. Rev. Lett. **22**, 156 (1969).
7. D.A. Dicus, Phys. Rev. **D5**, 1367 (1972).
8. J.D. Bjorken and E.A. Paschos, Phys. Rev. **185**, 1975 (1969).
9. R.P. Feynman, Photon Hadron Interactions (Benjamin, New York, 1972).
10. S. Wandzura and F. Wilczek, Phys. Rev. **B72**, 195 (1977).
11. J. Blümlein and A. Tkabladze, Nucl. Phys. **B553**, 427 (1999).
12. J.D. Bjorken, Phys. Rev. **179**, 1547 (1969).
13. MSTW, A.D. Martin *et al.*, Eur. Phys. J. **C63**, 189 (2009).
14. V.N. Gribov and L.N. Lipatov, Sov. J. Nucl. Phys. **15**, 438 (1972).
15. L.N. Lipatov, Sov. J. Nucl. Phys. **20**, 95 (1975).
16. G. Altarelli and G. Parisi, Nucl. Phys. **B126**, 298 (1977).
17. Yu.L. Dokshitzer, Sov. Phys. JETP **46**, 641 (1977).
18. G. Curci *et al.*, Nucl. Phys. **B175**, 27 (1980); W. Furmanski, and R. Petronzio, Phys. Lett. **B97**, 437 (1980).
19. R.K. Ellis *et al.*, QCD and Collider Physics (Cambridge UP, 1996).
20. E.B. Zijlstra and W.L. van Neerven, Phys. Lett. **B272**, 127 (1991); Phys. Lett. **B273**, 476 (1991); Phys. Lett. **B297**, 377 (1992); Nucl. Phys. **B383**, 525 (1992).
21. S. Moch and J.A.M. Vermaseren, Nucl. Phys. **B573**, 853 (2000).
22. S. Moch *et al.*, Nucl. Phys. **B688**, 101 (2004); Nucl. Phys. **B691**, 129 (2004); Phys. Lett. **B606**, 123 (2005); Nucl. Phys. **B724**, 3 (2005).
23. E.A. Kuraev *et al.*, Phys. Lett. **B60**, 50 (1975); Sov. Phys. JETP **44**, 443 (1976); Sov. Phys. JETP **45**, 199 (1977).
24. Ya.Ya. Balitsky and L.N. Lipatov, Sov. J. Nucl. Phys. **28**, 822 (1978).
25. V.S. Fadin, and L.N. Lipatov, Phys. Lett. **B429**, 127 (1998).
26. G. Camici and M. Ciafaloni, Phys. Lett. **B412**, 396 (1997), erratum-Phys. Lett. **B147**, 390 (1997); Phys. Lett. **B430**, 349 (1998).
27. M. Ciafaloni *et al.*, Phys. Rev. **D60**, 114036 (1999); JHEP **0007** 054 (2000).
28. M. Ciafaloni *et al.*, Phys. Lett. **B576**, 143 (2003); Phys. Rev. **D68**, 114003 (2003).
29. G. Altarelli *et al.*, Nucl. Phys. **B742**, 1 (2006); Nucl. Phys. **B799**, 199 (2008).
30. C.D. White and R.S. Thorne, Phys. Rev. **D75**, 034005 (2007).
31. G. 't Hooft and M. Veltman, Nucl. Phys. **B44**, 189 (1972).
32. G. 't Hooft, Nucl. Phys. **B61**, 455 (1973).
33. W.A. Bardeen *et al.*, Phys. Rev. **D18**, 3998 (1978).
34. G. Altarelli *et al.*, Nucl. Phys. **B143**, 521 (1978) and erratum: Nucl. Phys. **B146**, 544 (1978).
35. M.A.G. Aivazis *et al.*, Phys. Rev. **D50**, 3102 (1994).
36. J.C. Collins, Phys. Rev. **D58**, 094002 (1998).
37. A. Chuvakin *et al.*, Phys. Rev. **D61**, 096004 (2000).
38. R.S. Thorne and R.G. Roberts, Eur. Phys. J. **C19**, 339 (2001).
39. S. Kretzer *et al.*, Phys. Rev. **D69**, 114005 (2004).
40. R.S. Thorne, Phys. Rev. **D73**, 054019 (2006).
41. R.S. Thorne and W.-K. Tung, Proc. 4th HERA-LHC Workshop, arXiv:0809.0714.
42. CTEQ: P.M. Nadolsky *et al.*, Phys. Rev. **D78**, 013004 (2008).
43. NNPDF: R.D. Ball *et al.*, Nucl. Phys. **B809**, 1 (2009), erratum Nucl. Phys. **B816**, 293 (2009); Nucl. Phys. **B823**, 195 (2009).
44. S. Alekhin *et al.*, Phys. Rev. **D74**, 054033 (2006).
45. E. Leader *et al.*, Phys. Rev. **D75**, 0704027 (2007).
46. M. Hirai *et al.*, Nucl. Phys. **B813**, 106 (2009).
47. D. de Florian *et al.*, Phys. Rev. Lett. **101**, 072001 (2008); Phys. Rev. **D80**, 034030 (2009).
48. M. Hirai *et al.*, Phys. Rev. **D75**, 094009 (2007).
49. D. de Florian *et al.*, Phys. Rev. **D75**, 114010 (2007); Phys. Rev. **D76**, 074033 (2007).
50. S. Albino *et al.*, Nucl. Phys. **B803**, 42 (2008).
51. HERMES, A. Airpetian *et al.*, Phys. Rev. Lett. **92**, 012005 (2004); A. Airpetian *et al.*, Phys. Rev. **D71**, 012003 (2005).
52. HERMES, A. Airpetian *et al.*, Phys. Lett. **B666**, 446 (2008).
53. SMC, B. Adeva *et al.*, Phys. Lett. **B420**, 180 (1998).
54. COMPASS, M. Alekseev *et al.*, Phys. Lett. **B680**, 217 (2009).
55. <http://durpdg.dur.ac.uk/hepdata/pdf>.
56. <http://projects.hepforge.org/lhapdf>, see hep-ph/0508110.
57. J. Pumplin *et al.*, JHEP **0602**, 032 (2006).
58. MSTW, A.D. Martin *et al.*, Eur. Phys. J. **C64**, 653 (2009).
59. H1, C. Adloff *et al.*, Eur. Phys. J. **C21**, 33 (2001).
60. ZEUS, S. Chekanov *et al.*, Eur. Phys. J. **C42**, 1 (2005).
61. S. Alekhin, JHEP **0302**, 015 (2003).
62. R. Nisius, Phys. Reports **332**, 165 (2000).
63. T.F. Walsh and P.M. Zerwas, Phys. Lett. **B44**, 195 (1973).
64. R.L. Kingsley, Nucl. Phys. **B60**, 45 (1973).
65. E. Witten, Nucl. Phys. **B120**, 189 (1977).
66. W.A. Bardeen and A.J. Buras, Phys. Rev. **D20**, 166 (1979), erratum Phys. Rev. **D21**, 2041 (1980).
67. M. Fontannaz and E. Pilon, Phys. Rev. **D45**, 382 (1992), erratum Phys. Rev. **D46**, 484 (1992).
68. M. Glück *et al.*, Phys. Rev. **D45**, 3986 (1992).
69. F. Cornet *et al.*, Phys. Rev. **D70**, 093004 (2004).
70. P. Aurenche, *et al.*, Eur. Phys. J. **C44**, 395 (2005).
71. W. Slominski *et al.*, Eur. Phys. J. **C45**, 633 (2006).
72. ZEUS, S. Chekanov *et al.*, Eur. Phys. J. **C38**, 43 (2004).
73. ZEUS, S. Chekanov *et al.*, Nucl. Phys. **B713**, 3 (2005).
74. H1, A. Aktas *et al.*, Eur. Phys. J. **C48**, 749 (2006).
75. H1, A. Aktas *et al.*, Eur. Phys. J. **C48**, 715 (2006).
76. ZEUS, S. Chekanov *et al.*, Nucl. Phys. **B816**, 1 (2009).
77. J. C. Collins, Phys. Rev. **D57**, 3051 (1998); Erratum Phys. Rev. **D61**, 019902 (2000).
78. G. Ingelman and P. E. Schlein, Phys. Lett. **B152**, 256 (1985).
79. A. D. Martin, M. G. Ryskin and G. Watt, Phys. Lett. **B644**, 131 (2007).
80. H1, A. Aktas *et al.*, Eur. Phys. J. **C51**, 549 (2007).
81. H1, A. Aktas *et al.*, JHEP **0710**, 042 (2007).
82. ZEUS, S. Chekanov *et al.*, Eur. Phys. J. **C52**, 813 (2007).

NOTE: THE FIGURES IN THIS SECTION ARE INTENDED TO SHOW THE REPRESENTATIVE DATA. THEY ARE NOT MEANT TO BE COMPLETE COMPILATIONS OF ALL THE WORLD'S RELIABLE DATA.

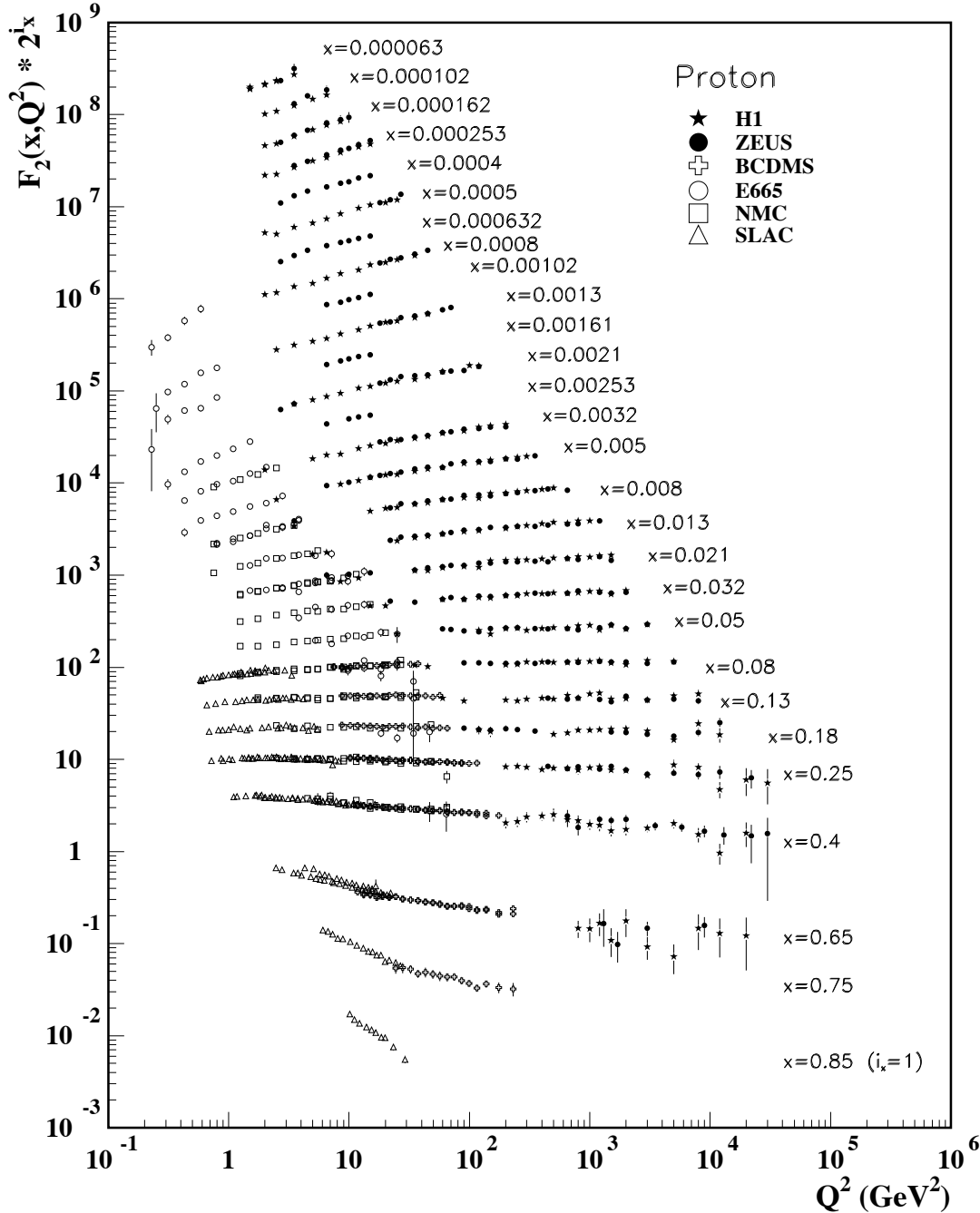


Figure 16.7: The proton structure function F_2^p measured in electromagnetic scattering of positrons on protons (collider experiments ZEUS and H1), in the kinematic domain of the HERA data, for $x > 0.00006$ (*cf.* Fig. 16.10 for data at smaller x and Q^2), and for electrons (SLAC) and muons (BCDMS, E665, NMC) on a fixed target. Statistical and systematic errors added in quadrature are shown. The data are plotted as a function of Q^2 in bins of fixed x . Some points have been slightly offset in Q^2 for clarity. The ZEUS binning in x is used in this plot; all other data are rebinned to the x values of the ZEUS data. For the purpose of plotting, F_2^p has been multiplied by 2^{i_x} , where i_x is the number of the x bin, ranging from $i_x = 1$ ($x = 0.85$) to $i_x = 28$ ($x = 0.000063$). References: **H1**—C. Adloff *et al.*, *Eur. Phys. J.* **C21**, 33 (2001); C. Adloff *et al.*, *Eur. Phys. J.* **C30**, 1 (2003); **ZEUS**—S. Chekanov *et al.*, *Eur. Phys. J.* **C21**, 443 (2001); S. Chekanov *et al.*, *Phys. Rev.* **D70**, 052001 (2004); **BCDMS**—A.C. Benvenuti *et al.*, *Phys. Lett.* **B223**, 485 (1989) (as given in [55]); **E665**—M.R. Adams *et al.*, *Phys. Rev.* **D54**, 3006 (1996); **NMC**—M. Arneodo *et al.*, *Nucl. Phys.* **B483**, 3 (1997); **SLAC**—L.W. Whitlow *et al.*, *Phys. Lett.* **B282**, 475 (1992).

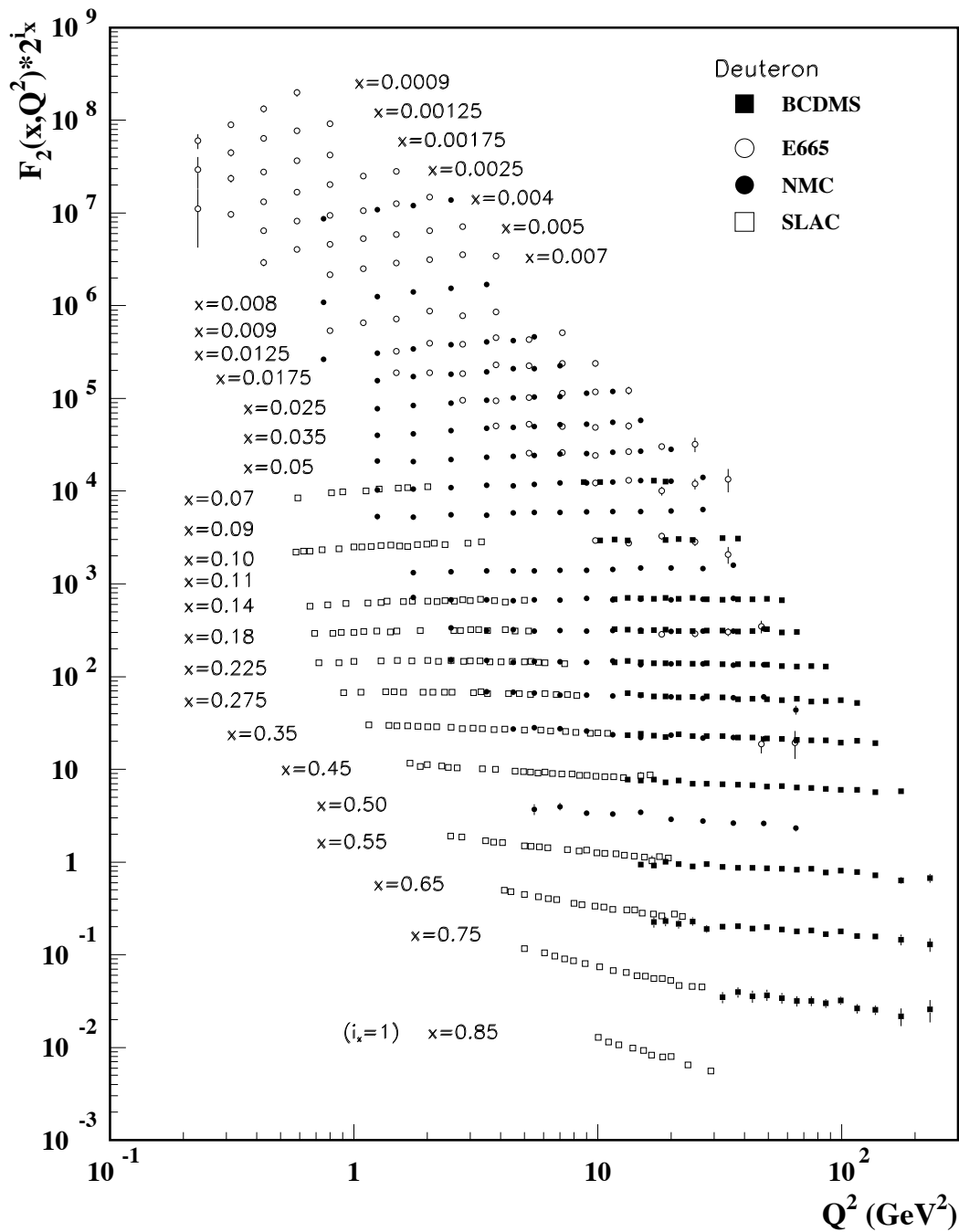


Figure 16.8: The deuteron structure function F_2^d measured in electromagnetic scattering of electrons (SLAC) and muons (BCDMS, E665, NMC) on a fixed target, shown as a function of Q^2 for bins of fixed x . Statistical and systematic errors added in quadrature are shown. For the purpose of plotting, F_2^d has been multiplied by 2^{i_x} , where i_x is the number of the x bin, ranging from 1 ($x = 0.85$) to 29 ($x = 0.0009$). References: **BCDMS**—A.C. Benvenuti *et al.*, Phys. Lett. **B237**, 592 (1990). **E665**, **NMC**, **SLAC**—same references as Fig. 16.7.

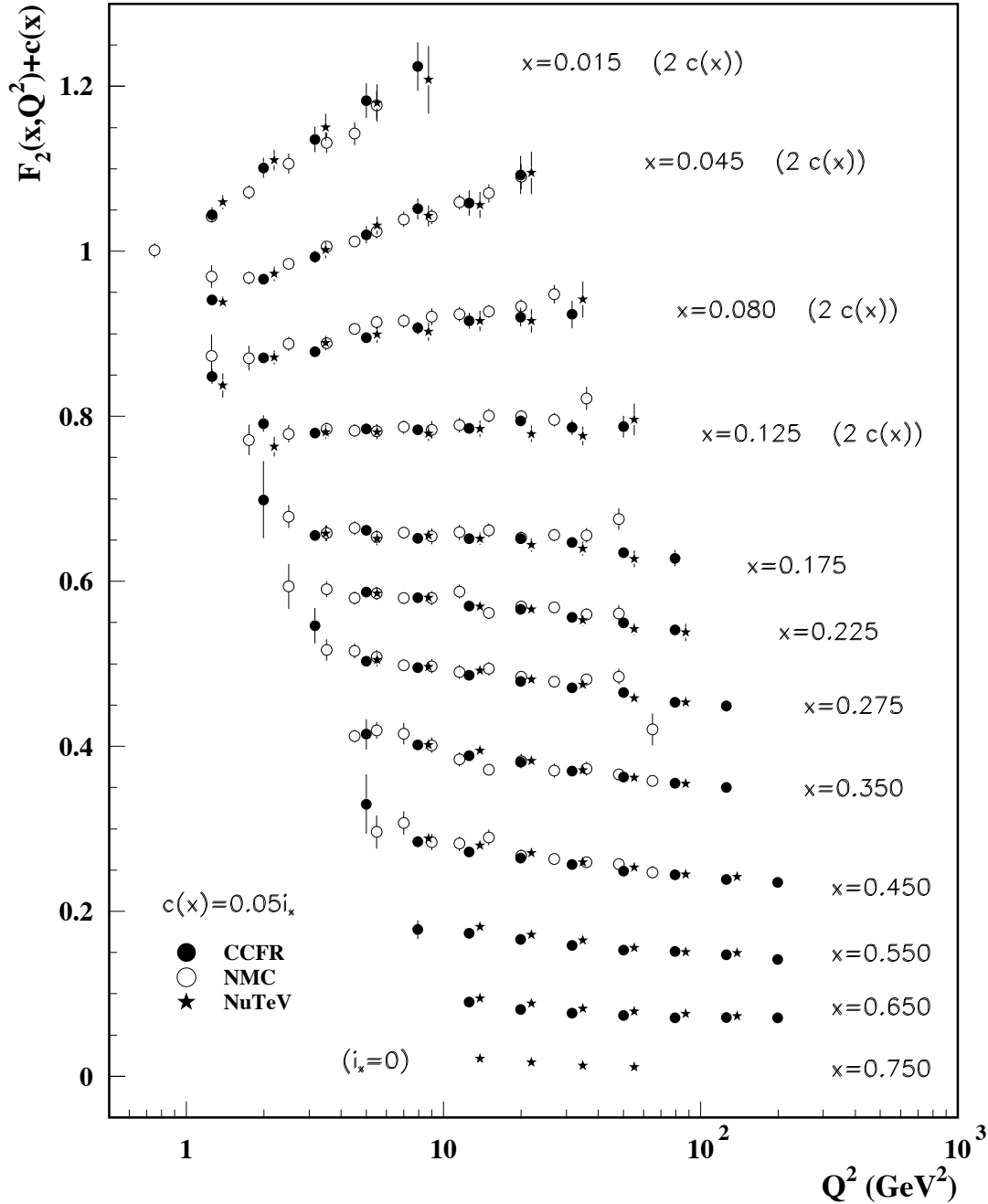


Figure 16.9: The deuteron structure function F_2 measured in deep inelastic scattering of muons on a fixed target (NMC) is compared to the structure function F_2 from neutrino-iron scattering (CCFR and NuTeV) using $F_2^{\mu} = (5/18)F_2^{\nu} - x(s + \bar{s})/6$, where heavy-target effects have been taken into account. The data are shown versus Q^2 , for bins of fixed x . The NMC data have been rebinned to CCFR and NuTeV x values. Statistical and systematic errors added in quadrature are shown. For the purpose of plotting, a constant $c(x) = 0.05i_x$ is added to F_2 , where i_x is the number of the x bin, ranging from 0 ($x = 0.75$) to 7 ($x = 0.175$). For $i_x = 8$ ($x = 0.125$) to 11 ($x = 0.015$), $2c(x)$ has been added. References: NMC—M. Arneodo *et al.*, Nucl. Phys. **B483**, 3 (1997); CCFR/NuTeV—U.K. Yang *et al.*, Phys. Rev. Lett. **86**, 2741 (2001); NuTeV—M. Tzanov *et al.*, Phys. Rev. **D74**, 012008 (2006).

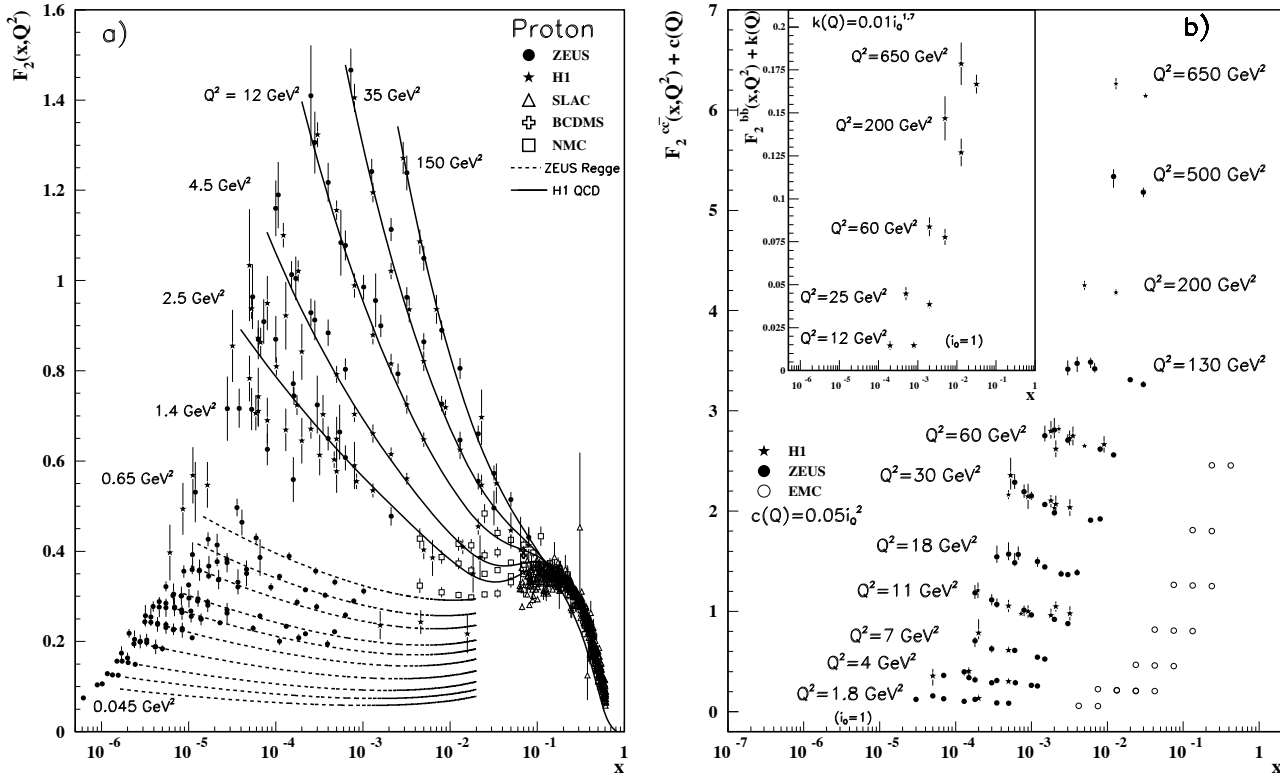


Figure 16.10: a) The proton structure function F_2^p mostly at small x and Q^2 , measured in electromagnetic scattering of positrons (H1, ZEUS), electrons (SLAC), and muons (BCDMS, NMC) on protons. Lines are ZEUS and H1 parameterizations for lower (Regge) and higher (QCD) Q^2 . The width of the bins can be up to 10% of the stated Q^2 . Some points have been slightly offset in x for clarity. References: **ZEUS**—J. Breitweg *et al.*, Phys. Lett. **B407**, 432 (1997); J. Breitweg *et al.*, Eur. Phys. J. **C7**, 609 (1999); J. Breitweg *et al.*, Phys. Lett. **B487**, 53 (2000) (both data and ZEUS Regge parameterization); S. Chekanov *et al.*, Eur. Phys. J. **C21**, 443 (2001); S. Chekanov *et al.*, Phys. Rev. **D70**, 052001 (2004); **H1**—C. Adloff *et al.*, Nucl. Phys. **B497**, 3 (1997); C. Adloff *et al.*, Eur. Phys. J. **C21**, 33 (2001) (both data and H1 QCD parameterization); C. Adloff *et al.*, Eur. Phys. J. **C30**, 1 (2003); A. Aktas *et al.*, Phys. Lett. **B598**, 159 (2004); **BCDMS, NMC, SLAC**—same references as Fig. 16.7.

b) The charm structure function $F_2^{c\bar{c}}(x)$, i.e. that part of the inclusive structure function F_2^p arising from the production of charm quarks, measured in electromagnetic scattering of positrons on protons (H1, ZEUS) and muons on iron (EMC). The H1 points have been slightly offset in x for clarity. For the purpose of plotting, a constant $c(Q) = 0.05i_Q^2$ is added to $F_2^{c\bar{c}}$ where i_Q is the number of the Q^2 bin, ranging from 1 ($Q^2 = 1.8 \text{ GeV}^2$) to 11 ($Q^2 = 650 \text{ GeV}^2$). References: **ZEUS**—J. Breitweg *et al.*, Eur. Phys. J. **C12**, 35 (2000); S. Chekanov *et al.*, Phys. Rev. **D69**, 012004 (2004); S. Chekanov *et al.*, JHEP **07**, 074 (2007); **H1**—C. Adloff *et al.*, Z. Phys. **C72**, 593 (1996); C. Adloff *et al.*, Phys. Lett. **B528**, 199 (2002); A. Aktas *et al.*, Eur. Phys. J. **C40**, 349 (2005); A. Aktas *et al.*, Eur. Phys. J. **C45**, 23 (2006); **EMC**—J.J. Aubert *et al.*, Nucl. Phys. **B213**, 31 (1983).

Inset: The bottom quark structure function $F_2^{b\bar{b}}(x)$. For the purpose of plotting, a constant $k(Q) = 0.01i_Q^{1.7}$ is added to $F_2^{b\bar{b}}$ where i_Q is the number of the Q^2 bin, ranging from 1 ($Q^2 = 12 \text{ GeV}^2$) to 5 ($Q^2 = 650 \text{ GeV}^2$). References: **H1**—A. Aktas *et al.*, Eur. Phys. J. **C40**, 349 (2005); A. Aktas *et al.*, Eur. Phys. J. **C45**, 23 (2006).

Statistical and systematic errors added in quadrature are shown for both plots. The data are given as a function of x in bins of Q^2 .

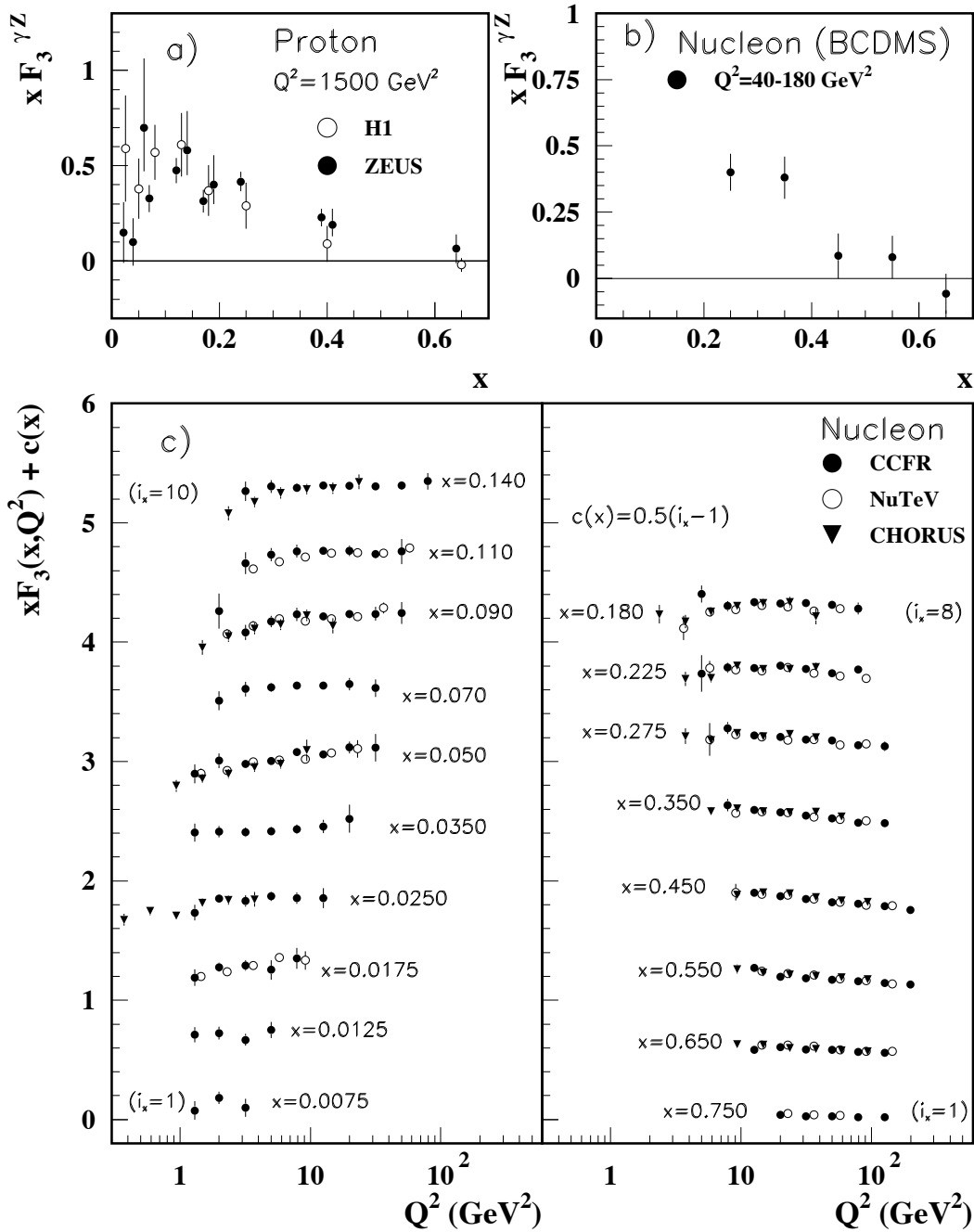


Figure 16.11: The structure function $x F_3^{\gamma Z}$ measured in electroweak scattering of **a)** electrons on protons (H1 and ZEUS) and **b)** muons on carbon (BCDMS). The ZEUS points have been slightly offset in x for clarity. References: **H1**—C. Adloff *et al.*, *Eur. Phys. J. C* **30**, 1 (2003); **ZEUS**—S. Chekanov *et al.*, *Eur. Phys. J. C* **28**, 175 (2003); S. Chekanov *et al.*, *Eur. Phys. J. C* **62**, 625 (2009); **BCDMS**—A. Argento *et al.*, *Phys. Lett. B* **140**, 142 (1984).

c) The structure function $x F_3$ of the nucleon measured in ν -Fe scattering. The data are plotted as a function of Q^2 in bins of fixed x . For the purpose of plotting, a constant $c(x) = 0.5(i_x - 1)$ is added to $x F_3$, where i_x is the number of the x bin as shown in the plot. The NuTeV and CHORUS points have been shifted to the nearest corresponding x bin as given in the plot and slightly offset in Q^2 for clarity. References: **CCFR**—W.G. Seligman *et al.*, *Phys. Rev. Lett.* **79**, 1213 (1997); **NuTeV**—M. Tzanov *et al.*, *Phys. Rev. D* **74**, 012008 (2006); **CHORUS**—G. Önençüt *et al.*, *Phys. Lett. B* **632**, 65 (2006).

Statistical and systematic errors added in quadrature are shown for all plots.

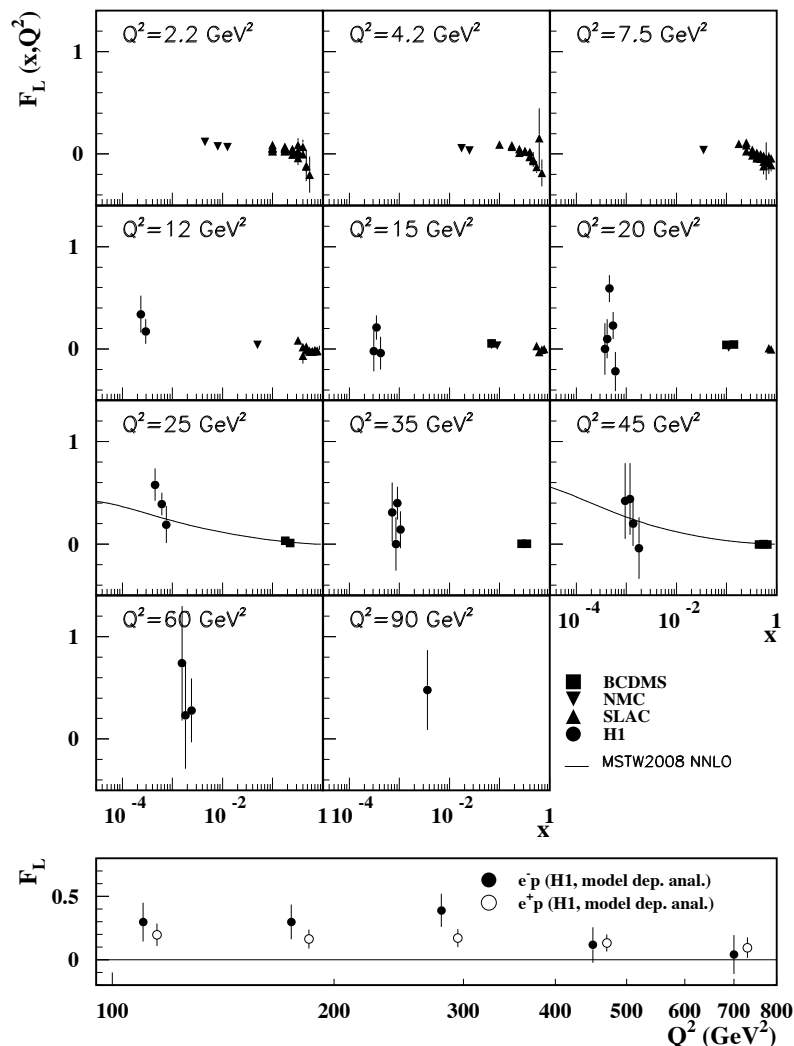


Figure 16.12: Top panel: The longitudinal structure function F_L as a function of x in bins of fixed Q^2 measured on the proton (except for the SLAC data which also contain deuterium data). BCDMS, NMC, and SLAC results are from measurements of R (the ratio of longitudinal to transverse photon absorption cross sections) which are converted to F_L by using the BDCMS parameterization of F_2 (A.C. Benvenuti *et al.*, Phys. Lett. **B223**, 485 (1989)). It is assumed that the Q^2 dependence of the fixed-target data is small within a given Q^2 bin. Also shown is the MSTW2008 parameterization given at two Q^2 values (A.D. Martin *et al.*, Eur. Phys. J. **C63**, 189 (2009)). References: **H1**—F.D. Aaron *et al.*, Phys. Lett. **B665**, 139 (2008); **BCDMS**—A. Benvenuti *et al.*, Phys. Lett. **B223**, 485 (1989); **NMC**—M. Arneodo *et al.*, Nucl. Phys. **B483**, 3 (1997); **SLAC**—L.W. Whitlow *et al.*, Phys. Lett. **B250**, 193 (1990) and numerical values from the thesis of L.W. Whitlow (SLAC-357).

Bottom panel: Higher Q^2 values of the longitudinal structure function F_L as a function of Q^2 given at the measured x for e^+/e^- -proton scattering. Points have been slightly offset in Q^2 for clarity. References: **H1**—C. Adloff *et al.*, Eur. Phys. J. **C30**, 1 (2003).

The H1 results shown in the bottom plot require the assumption of the validity of the QCD form for the F_2 structure function in order to extract F_L . Statistical and systematic errors added in quadrature are shown for both plots.

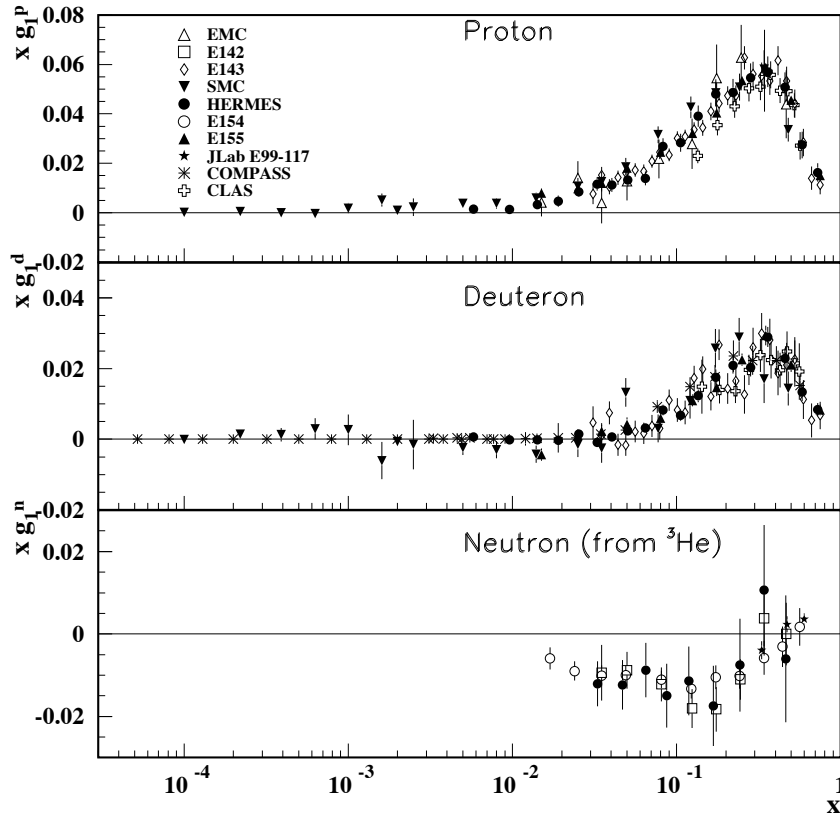


Figure 16.13: The spin-dependent structure function $xg_1(x)$ of the proton, deuteron, and neutron (from ${}^3\text{He}$ target) measured in deep inelastic scattering of polarized electrons/positrons: E142 ($Q^2 \sim 0.3 - 10 \text{ GeV}^2$), E143 ($Q^2 \sim 0.3 - 10 \text{ GeV}^2$), E154 ($Q^2 \sim 1 - 17 \text{ GeV}^2$), E155 ($Q^2 \sim 1 - 40 \text{ GeV}^2$), JLab E99-117 ($Q^2 \sim 2.71 - 4.83 \text{ GeV}^2$), HERMES ($Q^2 \sim 0.18 - 20 \text{ GeV}^2$), CLAS ($Q^2 \sim 1 - 5 \text{ GeV}^2$) and muons: EMC ($Q^2 \sim 1.5 - 100 \text{ GeV}^2$), SMC ($Q^2 \sim 0.01 - 100 \text{ GeV}^2$), COMPASS ($Q^2 \sim 0.001 - 100 \text{ GeV}^2$), shown at the measured Q^2 (except for EMC data given at $Q^2 = 10.7 \text{ GeV}^2$ and E155 data given at $Q^2 = 5 \text{ GeV}^2$). Note that $g_1^n(x)$ may also be extracted by taking the difference between $g_1^d(x)$ and $g_1^p(x)$, but these values have been omitted in the bottom plot for clarity. Statistical and systematic errors added in quadrature are shown. References: **EMC**—J. Ashman *et al.*, Nucl. Phys. **B328**, 1 (1989); **E142**—P.L. Anthony *et al.*, Phys. Rev. **D54**, 6620 (1996); **E143**—K. Abe *et al.*, Phys. Rev. **D58**, 112003 (1998); **SMC**—B. Adeva *et al.*, Phys. Rev. **D58**, 112001 (1998), B. Adeva *et al.*, Phys. Rev. **D60**, 072004 (1999) and Erratum-Phys. Rev. **D62**, 079902 (2000); **HERMES**—A. Airapetian *et al.*, Phys. Rev. **D75**, 012007 (2007) and K. Ackerstaff *et al.*, Phys. Lett. **B404**, 383 (1997); **E154**—K. Abe *et al.*, Phys. Rev. Lett. **79**, 26 (1997); **E155**—P.L. Anthony *et al.*, Phys. Lett. **B463**, 339 (1999) and P.L. Anthony *et al.*, Phys. Lett. **B493**, 19 (2000); **Jlab-E99-117**—X. Zheng *et al.*, Phys. Rev. **C70**, 065207 (2004); **COMPASS**—V.Yu. Alexakhin *et al.*, Phys. Lett. **B647**, 8 (2007) and E.S. Ageev *et al.*, Phys. Lett. **B647**, 330 (2007); **CLAS**—K.V. Dharmawardane *et al.*, Phys. Lett. **B641**, 11 (2006) (which also includes resonance region data not shown on this plot).

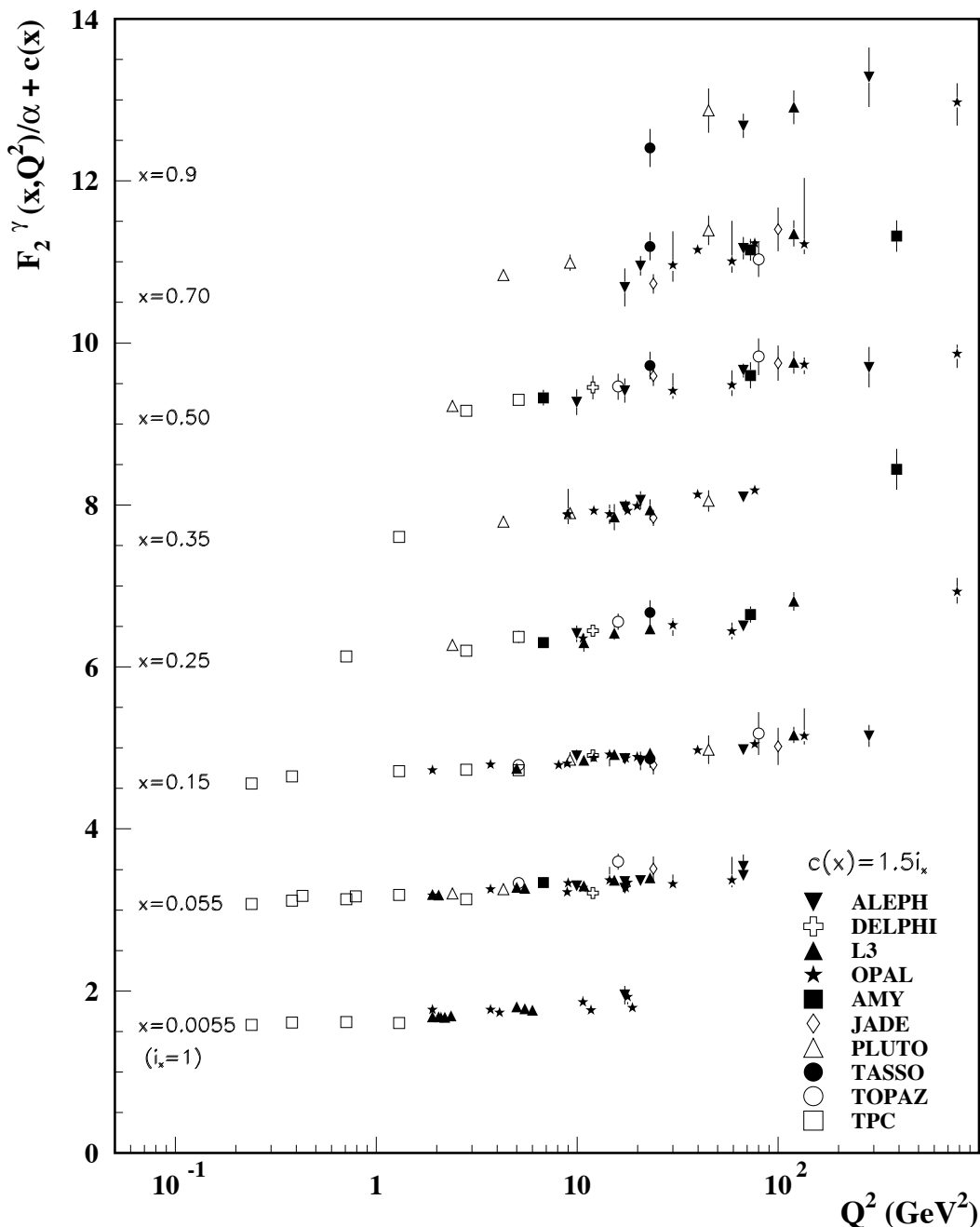


Figure 16.14: The hadronic structure function of the photon F_2^γ divided by the fine structure constant α measured in e^+e^- scattering, shown as a function of Q^2 for bins of x . Data points have been shifted to the nearest corresponding x bin as given in the plot. Some points have been offset in Q^2 for clarity. Statistical and systematic errors added in quadrature are shown. For the purpose of plotting, a constant $c(x) = 1.5i_x$ is added to F_2^γ/α where i_x is the number of the x bin, ranging from 1 ($x = 0.0055$) to 8 ($x = 0.9$). References: **ALEPH**—R. Barate *et al.*, Phys. Lett. **B458**, 152 (1999); A. Heister *et al.*, Eur. Phys. J. **C30**, 145 (2003); **DELPHI**—P. Abreu *et al.*, Z. Phys. **C69**, 223 (1995); **L3**—M. Acciarri *et al.*, Phys. Lett. **B436**, 403 (1998); M. Acciarri *et al.*, Phys. Lett. **B447**, 147 (1999); M. Acciarri *et al.*, Phys. Lett. **B483**, 373 (2000); **OPAL**—A. Ackerstaff *et al.*, Phys. Lett. **B411**, 387 (1997); A. Ackerstaff *et al.*, Z. Phys. **C74**, 33 (1997); G. Abbiendi *et al.*, Eur. Phys. J. **C18**, 15 (2000); G. Abbiendi *et al.*, Phys. Lett. **B533**, 207 (2002) (note that there is overlap of the data samples in these last two papers); **AMY**—S.K. Sahu *et al.*, Phys. Lett. **B346**, 208 (1995); T. Kojima *et al.*, Phys. Lett. **B400**, 395 (1997); **JADE**—W. Bartel *et al.*, Z. Phys. **C24**, 231 (1984); **PLUTO**—C. Berger *et al.*, Phys. Lett. **142B**, 111 (1984); C. Berger *et al.*, Nucl. Phys. **B281**, 365 (1987); **TASSO**—M. Althoff *et al.*, Z. Phys. **C31**, 527 (1986); **TOPAZ**—K. Muramatsu *et al.*, Phys. Lett. **B332**, 477 (1994); **TPC/Two Gamma**—H. Aihara *et al.*, Z. Phys. **C34**, 1 (1987).

17. FRAGMENTATION FUNCTIONS IN e^+e^- , ep AND pp COLLISIONS

Revised October 2009 by O. Biebel (Ludwig-Maximilians-Universität, Munich, Germany), D. de Florian (Dep. de Física, FCEyN-UBA, Buenos Aires, Argentina), D. Milstead (Fysikum, Stockholms Universitet, Sweden), and A. Vogt (Dep. of Mathematical Sciences, University of Liverpool, UK).

17.1. Introduction to fragmentation

The term ‘fragmentation functions’ is widely used for two related if conceptually different sets of functions describing final-state single particle energy distributions in hard scattering processes (see Refs. [1,2] for introductory reviews, and Refs. [3,4] for summaries of recent experimental and theoretical research in this field).

The first are cross-section observables such as the functions $F_{T,L,A}(x,s)$ in semi-inclusive e^+e^- annihilation at center-of-mass (CM) energy \sqrt{s} via an intermediate photon or Z -boson, $e^+e^- \rightarrow \gamma/Z \rightarrow h+X$, given by

$$\frac{1}{\sigma_0} \frac{d^2\sigma^h}{dx d\cos\theta} = \frac{3}{8}(1 + \cos^2\theta)F_T^h + \frac{3}{4}\sin^2\theta F_L^h + \frac{3}{4}\cos\theta F_A^h. \quad (17.1)$$

Here $x = 2E_h/\sqrt{s} \leq 1$ is the scaled energy of the hadron h (in practice the approximation $x \simeq x_p = 2p_h/\sqrt{s}$ is often used), and θ is its angle relative to the electron beam in the CM frame. Eq. (17.1) is the most general form for unpolarized inclusive single-particle production via vector bosons [5]. The transverse and longitudinal fragmentation functions F_T and F_L represent the contributions from γ/Z polarizations transverse or longitudinal with respect to the direction of motion of the hadron. The parity-violating term with the asymmetric fragmentation function F_A arises from the interference between vector and axial-vector contributions. Normalization factors σ_0 used in the literature range from the total cross section σ_{tot} for $e^+e^- \rightarrow$ hadrons, including all weak and QCD contributions, to $\sigma_0 = 4\pi\alpha^2 N_c/3s$ with $N_c = 3$, the lowest-order QED cross section for $e^+e^- \rightarrow \mu^+\mu^-$ times the number of colors N_c . LEP1 measurements of all three fragmentation functions are shown in Fig. 17.1.

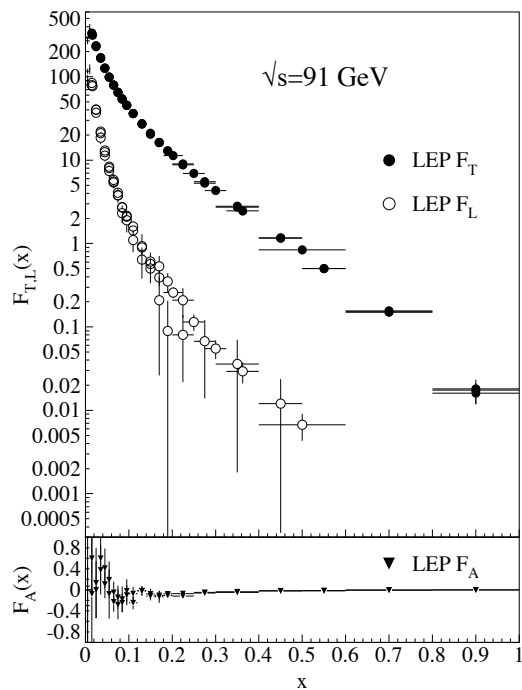


Figure 17.1: LEP1 measurements of total transverse (F_T), longitudinal (F_L), and asymmetric (F_A) fragmentation functions [6,7,8]. Data points with relative errors greater than 100% are omitted.

Integration of Eq. (17.1) over θ yields the total fragmentation function $F^h = F_T^h + F_L^h$,

$$\frac{1}{\sigma_0} \frac{d\sigma^h}{dx} = F^h(x,s) = \sum_i \int_x^1 \frac{dz}{z} C_i(z, \alpha_s(\mu), \frac{s}{\mu^2}) D_i^h(\frac{x}{z}, \mu^2) + \mathcal{O}(\frac{1}{\sqrt{s}}) \quad (17.2)$$

with $i = u, \bar{u}, d, \bar{d}, \dots, g$. Here we have introduced the second set of functions mentioned in the first paragraph, the parton fragmentation functions (or fragmentation densities) D_i^h . These functions are the final-state analogue of the initial-state parton distributions addressed in Section 16 of this Review. Due to the different sign of the squared four-momentum q^2 of the intermediate gauge boson these two sets of distributions are also referred to as the timelike (e^+e^- annihilation, $q^2 > 0$) and spacelike (deep-inelastic scattering (DIS), $q^2 < 0$) parton distributions. The function $D_i^h(z, \mu^2)$ encodes the

probability that the parton i fragments into a hadron h carrying a fraction z of the parton’s momentum. Beyond the leading order (LO) of perturbative QCD these universal functions are factorization-scheme dependent, with ‘reasonable’ scheme choices retaining certain quark-parton-model (QPM) constraints such as the momentum sum rule

$$\sum_h \int_0^1 dz z D_i^h(z, \mu^2) = 1. \quad (17.3)$$

The dependence of the functions D_i^h on the factorization (or fragmentation) scale μ^2 (in Eq. (17.2) and below identified with the renormalization scale) is discussed in Section 17.2.

The second ingredient in Eq. (17.2), and analogous expressions for the functions $F_{T,L,A}$, are the observable-dependent coefficient functions C_i . At the zeroth order in the strong coupling α_s the coefficient functions C_g for gluons are zero, while for (anti-)quarks $C_i = g_i(s)\delta(1-z)$ except for F_L , where $g_i(s)$ is the appropriate electroweak coupling. In particular, $g_i(s)$ is proportional to the squared charge of the quark i at $s \ll M_Z^2$, when weak effects can be neglected. The full electroweak prefactors $g_i(s)$ can be found in Ref. [5]. The power corrections in Eq. (17.2) arise from quark and hadron mass terms and from non-perturbative effects.

Measurements of fragmentation in lepton-hadron and hadron-hadron scattering are complementary to those in e^+e^- annihilation. The latter provides a clean environment (no initial-state hadron remnant) and stringent constraints on the combinations $D_{q_i}^h + D_{\bar{q}_i}^h$. However e^+e^- annihilation is far less sensitive to D_g^h and insensitive to the charge asymmetries $D_{q_i}^h - D_{\bar{q}_i}^h$. These quantities are best constrained in proton-(anti-)proton and electron-proton scattering, respectively. Especially the latter provides a more complicated environment with which it is possible to study the influence on the fragmentation process from initial state QCD radiation, the partonic and spin structure of the hadron target, and the target remnant system (see Ref. [9] for a comprehensive review of the measurements and models of fragmentation in lepton-hadron scattering).

Moreover, unlike e^+e^- annihilation where $q^2 = s$ is fixed by the collider energy, lepton-hadron scattering has two independent scales, $Q^2 = -q^2$ and the invariant mass W^2 of the hadronic final state, which both can vary by several orders of magnitudes for a given CM energy, thus allowing the study of fragmentation in different environments by a single experiment. E.g., in photoproduction the exchanged photon is quasi-real ($Q^2 \approx 0$) leading to processes akin to hadron-hadron scattering. In DIS ($Q^2 \gg 1 \text{ GeV}^2$), using the QPM, the hadronic fragments of the struck quark can be directly compared with quark fragmentation in e^+e^- in a suitable frame. Results from lepton-hadron experiments quoted in this report primarily concern fragmentation in the DIS regime. Studies performed by lepton-hadron experiments of fragmentation with photoproduction data containing high transverse momentum jets or particles are also reported, when these are directly comparable to DIS and e^+e^- results.

Fragmentation studies at HERA are usually performed in one of two frames in which the target hadron and the exchanged boson are collinear. The hadronic center-of-mass frame (HCMS) is defined as the rest system of the exchanged boson and incoming hadron, with the z^* -axis defined along the direction of the exchanged

boson. The positive z^* direction defines the so-called current region. Fragmentation measurements performed in the HCMS often use the Feynman- x variable $x_F = 2p_z^*/W$, where p_z^* is the longitudinal momentum of the particle in this frame. As W is the invariant mass of the hadronic final state, x_F ranges between -1 and 1 .

The Breit system [10] is connected to the HCMS by a longitudinal boost such that the time component of q vanishes, i.e. $q = (0, 0, 0, -Q)$. In the QPM, the struck parton then has the longitudinal momentum $Q/2$ which becomes $-Q/2$ after the collision. As compared with the HCMS, the current region of the Breit frame is more closely matched to the partonic scattering process, and is thus appropriate for direct comparisons of fragmentation functions in DIS with those from e^+e^- annihilation. The variable $x_p = 2p^*/Q$ is used at HERA for measurements in the Breit frame, ensuring rather directly comparable DIS and e^+e^- results, where p^* is the particle's momentum in the current region of the Breit frame.

17.2. Scaling violation

The simplest parton-model approach would predict scale-independent x -distributions ('scaling') for both the fragmentation function F^h and the parton fragmentation functions D_i^h . Perturbative QCD corrections lead, after factorization of the final-state collinear singularities for light partons, to logarithmic scaling violations via the evolution equations

$$\frac{\partial}{\partial \ln \mu^2} D_i(x, \mu^2) = \sum_j \int_x^1 \frac{dz}{z} P_{ji}(z, \alpha_s(\mu^2)) D_j\left(\frac{x}{z}, \mu^2\right). \quad (17.4)$$

Usually this system of equations is decomposed into a 2×2 flavour-singlet sector comprising gluon and the sum of all quark and antiquark fragmentation functions, and scalar ('non-singlet') equations for quark-antiquark and flavour differences. Notice that the singlet splitting-function matrix is now P_{ji} , rather than P_{ij} as for the initial-state parton distributions, since D_j represents the fragmentation of the final parton.

The splitting functions in Eq. (17.4) have perturbative expansion of the form

$$P_{ji}(z, \alpha_s) = \frac{\alpha_s}{2\pi} P_{ji}^{(0)}(z) + \left(\frac{\alpha_s}{2\pi}\right)^2 P_{ji}^{(1)}(z) + \left(\frac{\alpha_s}{2\pi}\right)^3 P_{ji}^{(2)}(z) + \dots \quad (17.5)$$

where the leading-order (LO) functions $P^{(0)}(z)$ [11,12] are the same as those for the initial-state parton distributions. The next-to-leading order (NLO) corrections $P^{(1)}(z)$ have been calculated in Refs. [13–17] (there are well-known misprints in the journal version of Ref. [14]). Ref. [17] also includes the spin-dependent case. These functions are different from, but related to their space-like counterparts, see also Ref. [18]. These relations have facilitated recent calculations of the next-to-next-to-leading order (NNLO) quantities $P_{qq}^{(2)}(z)$ and $P_{gg}^{(2)}(z)$ in Eq. (17.5) [19,20]. The corresponding off-diagonal quantities $P_{qg}^{(2)}$ and $P_{gq}^{(2)}$ are not yet known except for their second moments fixed by the momentum sum rule, Eq. (17.3) [20]. All these results refer to the standard $\overline{\text{MS}}$ scheme, with the exception of Refs. [16], with a fixed number n_f of light flavours. The NLO treatment of flavour thresholds in the evolution has been addressed in Ref. [21].

The QCD parts of the coefficient functions for $F_{T,L,A}(x, s)$ in Eq. (17.1) and the total fragmentation function $F_2^h \equiv F^h$ in Eq. (17.2) are given by

$$C_{a,i}(z, \alpha_s) = (1 - \delta_{aL}) \delta_{iq} + \frac{\alpha_s}{2\pi} c_{a,i}^{(1)}(z) + \left(\frac{\alpha_s}{2\pi}\right)^2 c_{a,i}^{(2)}(z) + \dots \quad (17.6)$$

The first-order corrections have been calculated a long time ago in Refs. [22], and the second-order terms in [23]. The latter results have recently been verified (and some typos corrected) in Refs. [19,24]. Thus the coefficient functions are known to NNLO except for F_L where the leading contribution is of order α_s .

The effect of the evolution is similar in the timelike and spacelike cases: as the scale increases, one observes a scaling violation in which the x -distribution is shifted towards lower values. This can be seen from Fig. 17.2 where a large amount of measurements of the total fragmentation function in e^+e^- annihilation are summarized. QCD analyses of these data are discussed in Section 17.5 below.

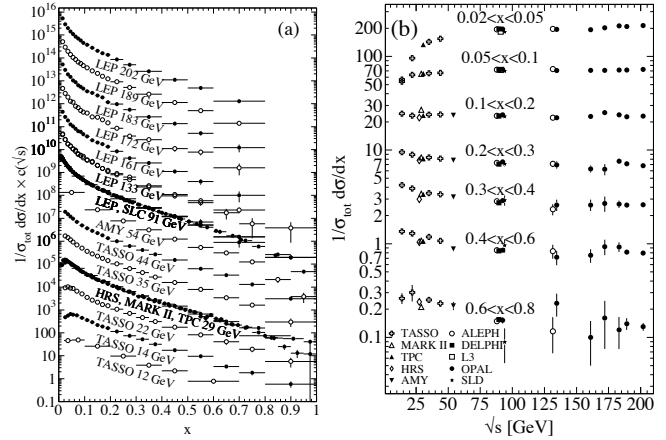


Figure 17.2: The e^+e^- fragmentation function for all charged particles is shown [8,25–41] (a) for different CM energies \sqrt{s} versus x and (b) for various ranges of x versus \sqrt{s} . For the purpose of plotting (a), the distributions were scaled by $c(\sqrt{s}) = 10^i$ with i ranging from $i = 0$ ($\sqrt{s} = 12$ GeV) to $i = 13$ ($\sqrt{s} = 202$ GeV).

Unlike the splitting functions in Eq. (17.5), see Refs. [18–20], the coefficient functions for $F_{2,T,A}$ in Eq. (17.6) show a threshold enhancement with terms up to $\alpha_s^n (1-z)^{-1} \ln^{2n-1}(1-z)$. Such logarithms can be resummed to all orders in α_s using standard soft-gluon techniques [42–44]. Recently this resummation has been extended to the subleading (and for F_L leading) class $\alpha_s^n \ln^k(1-z)$ of large- x logarithms [45].

In Refs. [22] the NLO coefficient functions have been calculated also for single hadron production in lepton-proton scattering, $ep \rightarrow e + h + X$. More recently corresponding results have been obtained for the case that a non-vanishing transverse momentum is required in the HCMS frame [46].

Scaling violations in DIS are shown in Fig. 17.3 for both HCMS and Breit frame. In Fig. 1.3(a) the distribution in terms of $x_F = 2p_z^*/W$ shows a steeper slope in ep data than for the lower-energy μp data for $x_F > 0.15$, indicating the scaling violations. At smaller values of x_F in the current jet region, the multiplicity of particles substantially increases with W owing to the increased phase space available for the fragmentation process. The EMC data access both the current region and the region of the fragmenting target remnant system. At higher values of $|x_F|$, due to the extended nature of the remnant, the multiplicity in the target region far exceeds that in the current region. For acceptance reasons the remnant hemisphere of the HCMS is only accessible by the lower-energy fixed-target experiments.

Using hadrons from the current hemisphere in the Breit frame, measurements of fragmentation functions and the production properties of particles in ep scattering have been made by Refs. [51–56]. Fig. 17.3(b) compares results from ep scattering and e^+e^- experiments, the latter results are halved as they cover both event hemispheres. The agreement between the DIS and e^+e^- results is fairly good. However, processes in DIS which are not present in e^+e^- annihilation, such as boson-gluon fusion and initial state QCD radiation, can depopulate the current region. These effects become most prominent at low values of Q and x_p . Hence, when compared with e^+e^- annihilation data at $\sqrt{s} = 5.2, 6.5$ GeV [58] not shown here, the DIS particle rates tend to lie below those from e^+e^- annihilation. A recent ZEUS study [59] finds that the direct comparability of the ep data to e^+e^- results at low scales is improved if twice the energy in the current hemisphere of the Breit frame, $2E_B^{\text{CT}}$, is used instead of Q as the fragmentation scale.

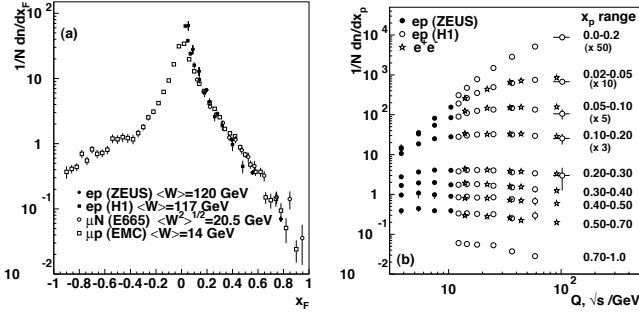


Figure 17.3: (a) The distribution $1/N \cdot dN/dx_F$ for all charged particles in DIS lepton-hadron experiments at different values of W , and measured in the HCMS [47–50]. (b) Scaling violations of the fragmentation function for all charged particles in the current region of the Breit frame of DIS [51,56] and in e^+e^- interactions [40,57]. The data are shown as a function of \sqrt{s} for e^+e^- results, and as a function of Q^2 for the DIS results, each within the same indicated intervals of the scaled momentum x_p . The data for the four lowest intervals of x_p are multiplied by factors 50, 10, 5, and 3, respectively for clarity.

17.3. Fragmentation functions for small particle momenta

The higher-order timelike splitting functions in Eq. (17.5) are very singular at small x . They show a double-logarithmic (LL) enhancement with leading terms of the form $\alpha_s^n \ln^{2n-2}x$ corresponding to poles $\alpha_s^n (N-1)^{1-2n}$ for the Mellin moments

$$P^{(n)}(N) = \int_0^1 dx x^{N-1} P^{(n)}(x). \quad (17.7)$$

Despite large cancellations between leading and non-leading logarithms at non-asymptotic value of x , the resulting small- x rise in the timelike splitting functions dwarfs that of their spacelike counterparts for the evolution of the parton distributions in Section 16 of this *Review*, see Fig. 1 of Ref. [20]. Consequently the fixed-order approximation to the evolution breaks down orders of magnitude in x earlier in fragmentation than in DIS.

The pattern of the known coefficients and other considerations suggest that the LL terms sum to all-order expressions without any pole at $N=1$ such as [60,61]

$$P_{gg}^{LL}(N) = -\frac{1}{4}(N-1 - \sqrt{(N-1)^2 \cdot 24 \alpha_s/\pi}). \quad (17.8)$$

Keeping the first three terms in the resulting expansion of Eq. (17.4) around $N=1$ yields a Gaussian in the variable $\xi = \ln(1/x)$ for the small- x fragmentation functions,

$$xD(x, s) \propto \exp\left[-\frac{1}{2\sigma^2}(\xi - \xi_p)^2\right], \quad (17.9)$$

with the peak position and width varying with the energy as [62] (see also Ref. [2])

$$\xi_p \simeq \frac{1}{4} \ln\left(\frac{s}{\Lambda^2}\right), \quad \sigma \propto \left[\ln\left(\frac{s}{\Lambda^2}\right)\right]^{3/4}. \quad (17.10)$$

Next-to-leading corrections to the above predictions have been calculated [63]. In the method of Ref. [64], see also Refs. [65,66], the corrections are included in an analytical form known as the ‘modified leading logarithmic approximation’ (MLLA). Alternatively they can be used to compute higher-moment corrections to the shape in Eq. (17.9) [67].

Fig. 17.4 shows the ξ distribution for charged particles produced in the current region of the Breit frame in DIS and in e^+e^- annihilation. Consistent with Eq. (17.9) (the ‘hump backed plateau’) and Eq. (17.10) the distributions have a Gaussian shape with the peak position and area increasing with the CM energy (e^+e^-) and Q^2 (DIS).

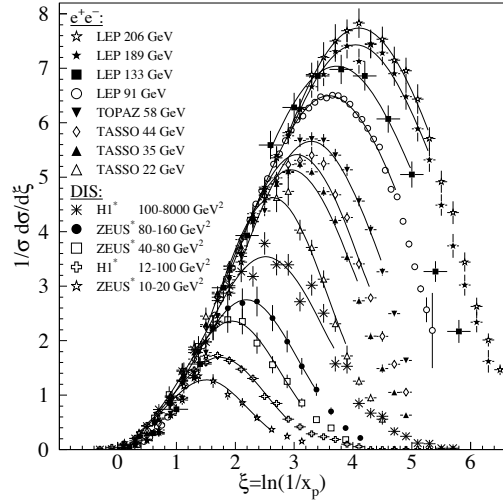


Figure 17.4: Distribution of $\xi = \ln(1/x_p)$ at several CM energies (e^+e^-) [25–27,32–35,40,68–71] and intervals of Q^2 (DIS) [54,55]. At each energy only one representative measurement is displayed. For clarity some measurements at intermediate CM energies (e^+e^-) or Q^2 ranges (DIS) are not shown. The DIS measurements (*) have been scaled by a factor of 2 for direct comparability with the e^+e^- results. Fits of simple Gaussian functions are overlaid for illustration.

The predicted energy dependence Eq. (17.10) of the peak in the ξ distribution is explained by soft gluon coherence (angular ordering) which correctly predicts the suppression of hadron production at small x . Of course, a decrease at very small x is expected on purely kinematical grounds, but this would occur at particle energies proportional to their masses, *i.e.*, at $x \propto m/\sqrt{s}$ and hence $\xi \sim \frac{1}{2} \ln s$. Thus, if the suppression were purely kinematic, the peak position ξ_p would vary twice as rapidly with the energy, which is ruled out by the data in Fig. 17.5. The e^+e^- and DIS data agree well with each other, demonstrating the universality of hadronization, and the MLLA prediction. Measurements of the higher moments of the ξ distribution in e^+e^- [40,71–73] and DIS [55] have also been performed and show consistency with each other.

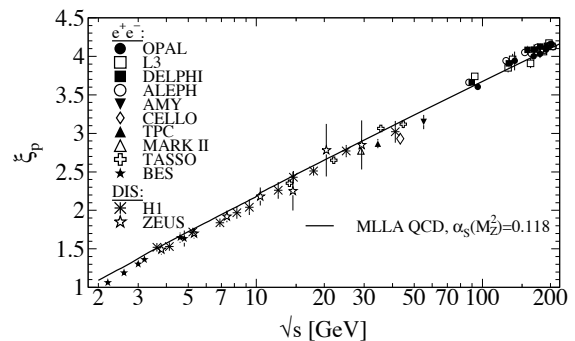


Figure 17.5: Evolution of the peak position, ξ_p , of the ξ distribution with the CM energy \sqrt{s} . The MLLA QCD prediction using $\alpha_s(s = M_Z^2) = 0.118$ is superimposed to the data of Refs. [25,27,28,31–33,35,40,53,54,69,70,73–81].

17.4. Fragmentation models

Although the scaling violation can be calculated perturbatively, the actual form of the parton fragmentation functions is non-perturbative. Perturbative evolution gives rise to a shower of quarks and gluons (partons). Multi-parton final states from leading and higher order matrix element calculations are linked to these parton showers using factorization prescriptions, also called matching schemes, see Ref. [82]

for an overview. Phenomenological schemes are then used to model the carry-over of parton momenta and flavor to the hadrons. Two of the very popular models are the *string fragmentation* [83,84], implemented in the JETSET [85], PYTHIA [86] and UCLA [87] Monte Carlo event generation programs, and the *cluster fragmentation* of the HERWIG [88] and SHERPA [89] Monte Carlo event generators.

17.4.1. String fragmentation: The string-fragmentation scheme considers the color field between the partons, *i.e.*, quarks and gluons, to be the fragmenting entity rather than the partons themselves. The string can be viewed as a color flux tube formed by gluon self-interaction as two colored partons move apart. Energetic gluon emission is regarded as energy-momentum carrying “kinks” on the string. When the energy stored in the string is sufficient, a $q\bar{q}$ pair may be created from the vacuum. Thus, the string breaks up repeatedly into color singlet systems, as long as the invariant mass of the string pieces exceeds the on-shell mass of a hadron. The $q\bar{q}$ pairs are created according to the probability of a tunneling process $\exp(-\pi m_{q,\perp}^2/\kappa)$, which depends on the transverse mass squared $m_{q,\perp}^2 \equiv m_q^2 + p_{q,\perp}^2$ and the string tension $\kappa \approx 1$ GeV/fm. The transverse momentum $p_{q,\perp}$ is locally compensated between quark and antiquark. Due to the dependence on the parton mass, m_q , and/or hadron mass, m_h , the production of strange and, in particular, heavy-quark hadrons is suppressed. The light-cone momentum fraction $z = (E+p_{||})_h/(E+p)_{q\bar{q}}$, where $p_{||}$ is the momentum of the formed hadron h along the direction of the quark q , is given by the string-fragmentation function

$$f(z) \sim \frac{1}{z}(1-z)^a \exp\left(-\frac{bm_{h,\perp}^2}{z}\right), \quad (17.11)$$

where a and b are free parameters. These parameters need to be adjusted to bring the fragmentation into accordance with measured data, *e.g.*, $a = 0.11$ and $b = 0.52$ GeV $^{-2}$ as determined in [90] (for an overview on tuned parameters see [91]).

17.4.2. Cluster fragmentation: Assuming a local compensation of color based on the *pre-confinement* property of perturbative QCD [92], the remaining gluons at the end of the parton shower evolution are split non-perturbatively into quark-antiquark pairs. Color singlet clusters of typical mass of a couple of GeV are then formed from quark and antiquark of color-connected splittings. These clusters decay directly into two hadrons unless they are either too heavy, when they decay into two clusters, or too light, in which case a cluster decays into a single hadron, requiring a small rearrangement of energy and momentum with neighboring clusters. The decay of a cluster into two hadrons is assumed to be isotropic in the rest frame of the cluster except if a perturbative-formed quark is involved. A decay channel is chosen based on the phase-space probability, the density of states, and the spin degeneracy of the hadrons. Cluster fragmentation has a compact description with few parameters, due to the phase-space dominance in the hadron formation.

17.5. Quark and gluon fragmentation functions

The fragmentation functions are solutions to the evolution equations Eq. (17.4), but need to be parametrized at some initial scale μ_0^2 (usually around 1 GeV 2 for light quarks and gluons and m_Q^2 for heavy quarks). A usual parametrization for light hadrons is [93–98]

$$D_i^h(x, \mu_0^2) = N x^\alpha (1-x)^\beta \left(1 + \gamma(1-x)^\delta\right), \quad (17.12)$$

where the normalization N , and the parameters α , β , γ and δ in general depend on the energy scale μ_0^2 , and also on the type of the parton, i , and the hadron, h . Frequently the term involving γ and δ is left out [95–98]. Heavy flavor fragmentation into heavy mesons is discussed in Sect. 17.9. The parameters of Eq. (17.12) (see [93–98]) are obtained by performing global fits to data on various hadron types for different combinations of partons and hadrons in e^+e^- , lepton-hadron and hadron-hadron collisions.

Data from e^+e^- annihilation present the cleanest experimental source for the measurement of fragmentation functions, but can

not contribute to disentangle quark from antiquark distributions. Since the bulk of the e^+e^- annihilation data is obtained at the mass of the Z -boson, where the electroweak couplings are roughly the same for the different partons, it provides the most precise determination of the flavor-singlet quark fragmentation. Flavor tagged results [99], distinguishing between the light quark, charm and bottom contributions are of particular value for flavor decomposition, even though those measurements can not be unambiguously interpreted in perturbative QCD.

The most relevant source for quark-antiquark (and also flavor) separation is provided by data from semi-inclusive DIS (SIDIS). Semi-inclusive measurements are usually performed at much lower scales than for e^+e^- annihilation. The inclusion of SIDIS data in global fits allows for a wider coverage in the evolution of the fragmentation functions, resulting at the same time in a stringent test of the universality of these distributions. Charged-hadron production data in hadronic collisions also presents a sensitivity on (anti-)quark fragmentation functions.

The gluon fragmentation function $D_g(x)$ can be extracted, in principle, from the longitudinal fragmentation function F_L in Eq. (17.2), as the coefficient functions $C_{L,i}$ for quarks and gluons are comparable at order α_s . However at NLO, *i.e.*, including the $\mathcal{O}(\alpha_s^2)$ coefficient functions $C_{L,i}^{(2)}$ [23], quark fragmentation is dominant in F_L over a large part of the kinematic range, reducing the sensitivity on D_g . This distribution could be determined also analyzing the evolution of the fragmentation functions. This possibility is limited by the lack of sufficiently precise data at energy scales away from the Z -resonance and the dominance of the quark contributions and at medium and large values of x .

D_g can also be deduced from the fragmentation of three-jet events in which the gluon jet is identified, for example, by tagging the other two jets with heavy quark decays. To leading order, the measured distributions of $x = E_{\text{had}}/E_{\text{jet}}$ for particles in gluon jets can be identified directly with the gluon fragmentation functions $D_g(x)$. At higher orders the theoretical interpretation of this observable is ambiguous.

A direct constraint on D_g is provided by $pp, p\bar{p} \rightarrow hX$ data. At variance with e^+e^- annihilation and SIDIS, for this process gluon fragmentation starts to contribute at the lowest order in the coupling constant, introducing a strong sensitivity on D_g . At large $x \gtrsim 0.5$, where information from e^+e^- is sparse, data from hadronic colliders facilitate significantly improved extractions of D_g [93,94].

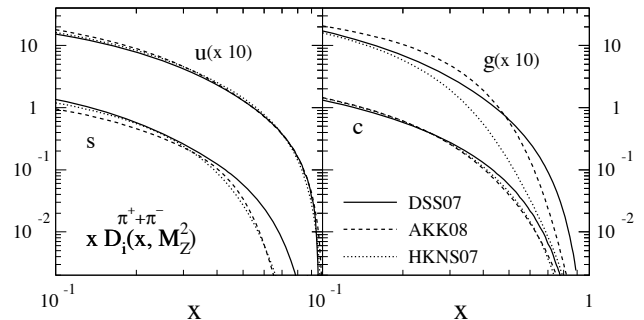


Figure 17.6: Comparison of up, strange, charm and gluon NLO fragmentation functions for $\pi^+ + \pi^-$ at the mass of the Z . The different lines correspond to the result of the most recent analyses performed in Refs. [93,94,98].

A comparison of recent fits of NLO fragmentation functions for $\pi^+ + \pi^-$ obtained by DSS07 [93], AKK08 [94] and HKNS07 [98] is shown in Fig. 17.6. Differences between the sets are large especially for the gluon fragmentation function over the full range of x and for the quark distribution at large momentum fractions. Those discrepancies can be considered as a first estimate of the present uncertainties involved in the extraction of the fragmentation functions. The differences are even larger for other species of hadrons like kaons and protons [93,94,98].

17.6. Identified particles in e^+e^- and semi-inclusive DIS

A great wealth of measurements of e^+e^- fragmentation into identified particles exists. A collection of references for data on fragmentation into identified particles is given on Table 41.1. Representative of this body of data is Fig. 17.7 which shows fragmentation functions as the scaled momentum spectra of charged particles at several CM energies.

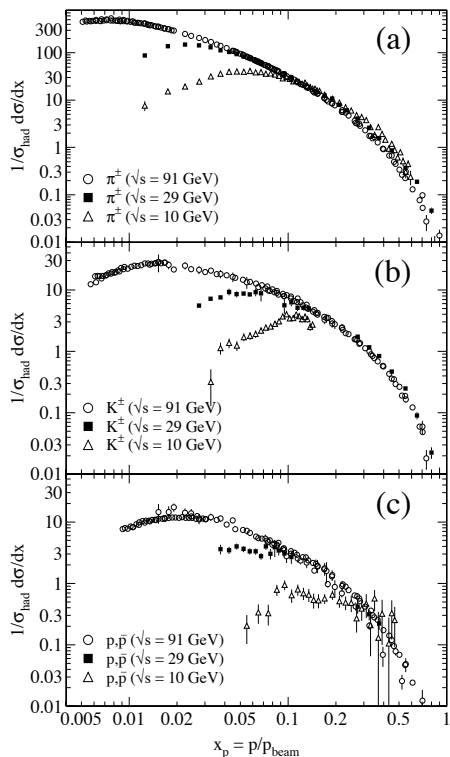


Figure 17.7: Scaled momentum spectra of (a) π^\pm , (b) K^\pm , and (c) p/\bar{p} at $\sqrt{s} = 10, 29$, and 91 GeV [37,41,78,100].

Quantitative results of studies of scaling violation in e^+e^- fragmentation have been reported in [6,38,101,102]. The values of α_s obtained are consistent with the world average (see review on QCD in Section 9 of this *Review*).

Many studies have been made of identified particles produced in lepton-hadron scattering, although fewer particle species have been measured than in e^+e^- collisions. References [103–108] and [109–115] are representative of the data from fixed target and ep collider experiments, respectively.

QCD calculations performed at NLO provide an overall good description of the HERA data [50,51,55,110,116,117] for both SIDIS [118] and the hadron transverse momentum distribution [46] in the kinematic regions in which the calculations are predictive.

Fig. 17.8(a) compares lower-energy fixed-target and HERA data on strangeness production, showing that the HERA spectra have substantially increased multiplicities, albeit with insufficient statistical precision to study scaling violations. The fixed-target data show that the Λ rate substantially exceeds the $\bar{\Lambda}$ rate in the remnant region, owing to the conserved baryon number from the baryon target. Fig. 17.8(b) shows neutral and charged pion fragmentation functions $1/N \cdot dn/dz$, where z is defined as the ratio of the pion energy to that of the exchanged boson, both measured in the laboratory frame. Results are shown from HERMES and the EMC experiments, where HERMES data have been evolved with NLO QCD to $\langle Q^2 \rangle = 25$ GeV² in order to be consistent with the EMC. Each of the experiments uses various kinematic cuts to ensure that the measured particles lie in the region which is expected to be associated with the struck quark.

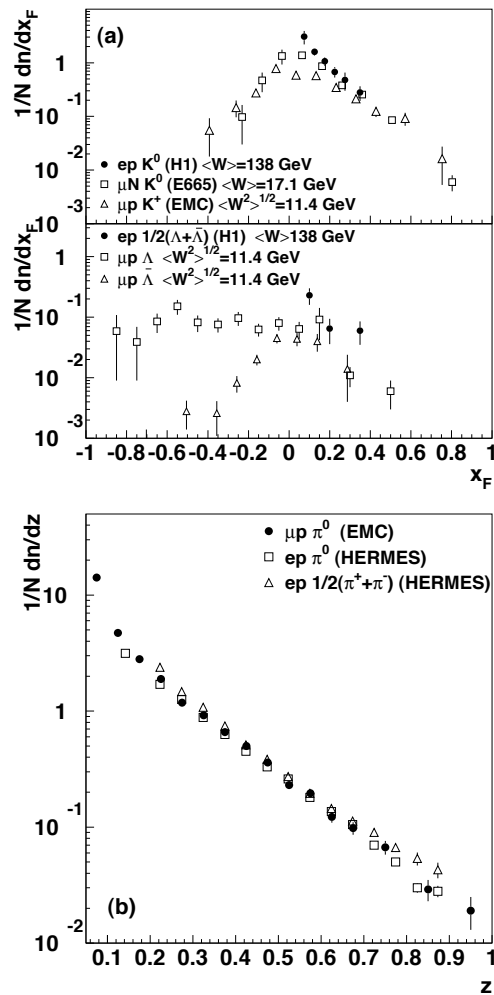


Figure 17.8: (a) $1/N \cdot dn/dx_F$ for identified strange particles in DIS at various values of W [103,106,109]. (b) $1/N \cdot dn/dz$ for measurements of pions from fixed-target DIS experiment [104,107,108].

In the DIS kinematic regime accessed at these experiments, and over the range in z shown in Fig. 17.8, the z and x_F variables have similar values [47]. The precision data on identified particles can be used in the study of the quark flavor content of the proton [119].

Data on identified particle production can aid the investigation of the universality of jet fragmentation in e^+e^- and DIS. The strangeness suppression factor γ_s , as derived principally from tuning the Lund string model [84] within JETSET [85], is typically found to be around 0.3 in e^+e^- experiments [68], although values closer to 0.2 [120] have also been obtained. A number of measurements of so-called V^0 -particles (K^0 , Λ^0) and the relative rates of V^0 's and inclusively produced charged particles have been performed at HERA [109,111,115] and fixed target experiments [103]. These typically favour a stronger suppression ($\gamma_s \approx 0.2$) than usually obtained from e^+e^- data although values close to 0.3 have also been obtained [121,122].

However, when comparing the description of QCD-based models for lepton-hadron interactions and e^+e^- collisions, it is important to note that the overall description by event generators of inclusively produced hadronic final states is more accurate in e^+e^- collisions than lepton-hadron interactions [123]. Predictions of particle rates in lepton-hadron scattering are affected by uncertainties in the modelling of the parton composition of the proton and photon, the extended target remnant, and initial and final state QCD radiation. Furthermore, the tuning of event generators for e^+e^-

collisions is typically based on a larger set of parameters and uses more observables [68] than are used when optimizing models for lepton-hadron data [124].

17.7. Fragmentation in hadron-hadron collisions

An extensive set on high-transverse momentum (p_T) single-inclusive hadron data has been collected in $h_1 h_2 \rightarrow hX$ scattering processes, both at high energy colliders and fixed-target experiments [125–143]. Only the transverse momentum p_T is considered in hadron-hadron collisions because of lack of knowledge of the longitudinal momentum of the hard subprocess. Fig. 17.9 shows a compilation of neutral pion and charged hadron production data for energies in the range $\sqrt{s} \approx 23$ – 800 GeV.

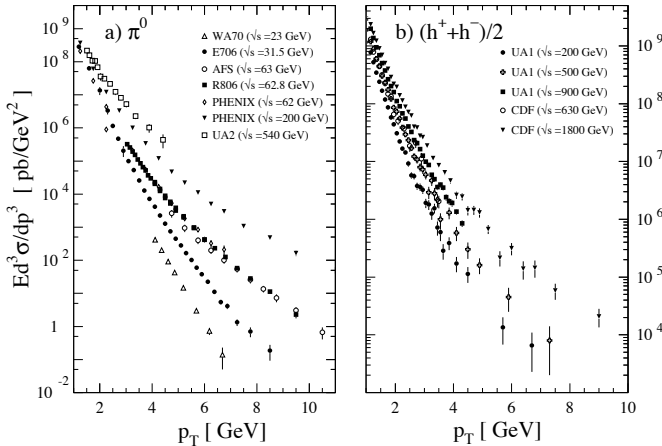


Figure 17.9: Selection of inclusive (a) π^0 and (b) charged-hadron production data from pp [133,140–143] and $p\bar{p}$ [125,128,131] collisions.

The differential cross-section for high-transverse momentum distributions has been computed to next-to-leading order accuracy in perturbative QCD [144]. NLO calculations yield a good description of the collider data, but significantly under-predict the cross-section for several fixed-target energy data sets [145,146]. Data collected at high energy colliders are either included in global fit analyses or used as a test for the universality of fragmentation functions.

Different strategies have been developed to ameliorate the theoretical description at fixed-target energies. A possible phenomenological approach involves the introduction of a non-perturbative intrinsic partonic transverse momentum [143,147,148]. From the perturbative side, the resummation of the dominant higher order corrections at threshold produces an enhancement of the theoretical calculation that significantly improves the description of the data [149].

Measurements of hadron production in longitudinally polarized pp collisions are used mainly in the determination of the polarized gluon distribution in the proton [150,151].

Hadron production provides a critical observable for probing the high energy-density matter produced in heavy-ion collisions. Measurements at colliders show a suppression of inclusive hadron yields at high transverse momentum for AA collisions compared to pp scattering, indicating the formation of a dense medium opaque to quark and gluons, see e.g. [152].

17.8. Spin-dependent fragmentation

Measurements of charged-hadron production in unpolarized lepton-hadron scattering provide a unique tool to perform a flavor-separation determination of polarized parton densities from DIS interactions with longitudinally polarized targets [153–157].

Polarized scattering presents the possibility to measure the spin transfer from the struck quark to the final hadron, and thus develop spin-dependent fragmentation functions [158,159]. Early measurements of the longitudinal spin transfer to Lambda hyperons

have been presented in [160,161]. This process is also useful in the study of the quark transversity distribution [162], which describes the probability of finding a transversely polarized quark with its spin aligned or anti-aligned with the spin of a transversely polarized nucleon. The transversity function is chiral-odd, and therefore not accessible through measurements of inclusive lepton-hadron scattering. Semi-inclusive DIS, in which another chiral-odd observable may be involved, provides a valuable tool to probe transversity. The Collins fragmentation function [163] relates the transverse polarization of the quark to that of the final hadron. It is chiral-odd and naive T-odd, leading to a characteristic single spin asymmetry in the azimuthal angular distribution of the produced hadron in the hadron scattering plane. Azimuthal angular distributions in semi-inclusive DIS can also be produced by other processes requiring non-polarized fragmentation functions, like the Sivers mechanism [164].

A number of experiments have measured these asymmetries [165–173]. Collins and Sivers asymmetries have been shown experimentally to be non zero by the HERMES measurements on transversely polarized proton targets [166–168]. Independent information on the Collins function has been provided by the BELLE Collaboration [169–170]. Measurements performed by the COMPASS collaboration on deuteron targets show results compatible with zero for both asymmetries [171–173].

17.9. Heavy quark fragmentation

It was recognized very early [174] that a heavy flavored meson should retain a large fraction of the momentum of the primordial heavy quark, and therefore its fragmentation function should be much harder than that of a light hadron. In the limit of a very heavy quark, one expects the fragmentation function for a heavy quark to go into any heavy hadron to be peaked near $x = 1$.

When the heavy quark is produced at a momentum much larger than its mass, one expects important perturbative effects, enhanced by powers of the logarithm of the transverse momentum over the heavy quark mass, to intervene and modify the shape of the fragmentation function. In leading logarithmic order (*i.e.*, including all powers of $\alpha_s \log m_Q/p_T$), the total (*i.e.*, summed over all hadron types) perturbative fragmentation function is simply obtained by solving the leading evolution equation for fragmentation functions, Eq. (17.4), with the initial condition at a scale $\mu^2 = m_Q^2$ given by $D_Q(z, m_Q^2) = \delta(1 - z)$ and $D_i(z, m_Q^2) = 0$ for $i \neq Q$ (here $D_i(z)$, stands for the probability to produce a heavy quark Q from parton i with a fraction z of the parton momentum).

Several extensions of the leading logarithmic result have appeared in the literature. Next-to-leading-log (NLL) order results for the perturbative heavy quark fragmentation function have been obtained in [175]. The resummation of the dominant logarithmic contributions at large z was performed in [42] to next-to-leading-log accuracy. Fixed-order calculations of the fragmentation function at order α_s^2 in e^+e^- annihilation have appeared in [176] while the initial condition for the perturbative heavy quark fragmentation function has been extended to NNLO in [177].

Inclusion of non-perturbative effects in the calculation of the heavy-quark fragmentation function is done by convoluting the perturbative result with a phenomenological non-perturbative form [178–183], see also section 17.8 of [184]. The parameters entering the non-perturbative forms are fitted together with some model of hard radiation, which can be either a shower Monte Carlo, a leading-log or NLL calculation (which may or may not include Sudakov resummation), or a fixed order calculation [176,185].

A more conventional approach [186] involves the introduction of a unique set of heavy quark fragmentation functions of non-perturbative nature that obey the usual massless evolution equations in Eq. (17.4). Finite mass terms of the form $(m_Q/p_T)^n$ are kept in the corresponding short distance coefficient function for each scattering process. Within this approach, the initial condition for the perturbative fragmentation function provides the term needed to define the correct subtraction scheme to match the massless limit for the coefficient function (see e.g. [187]). Such implementation is in line with the variable flavor

number scheme introduced for parton distributions functions, as described in Section 16 of this *Review*.

High statistics data for charmed mesons production near the Υ resonance (excluding decay products of B mesons) have been published [188,189]. They include results for D and D^* , D_s (see also [190,191]) and Λ_c . Shown in Fig. 17.10(a) are the CLEO and BELLE inclusive cross-sections times branching ratio \mathcal{B} , $s \cdot \mathcal{B} d\sigma/dx_p$, for the production of D^0 and D^{*+} . The variable x_p approximates the light-cone momentum fraction z , but is not identical to it. The two measurements are consistent with each other.

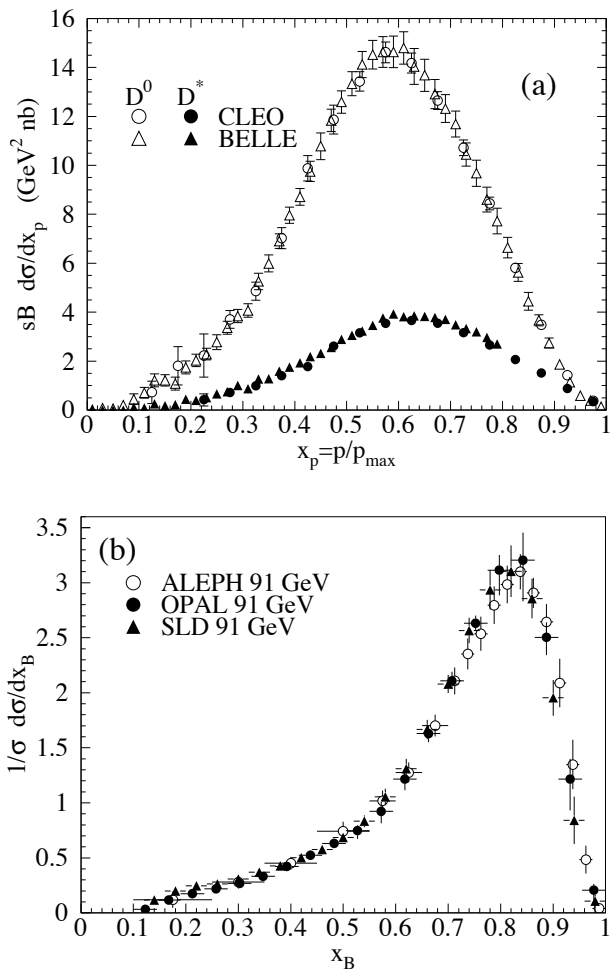


Figure 17.10: (a) Efficiency-corrected inclusive cross-section measurements for the production of D^0 and D^{*+} in e^+e^- measurements at $\sqrt{s} \approx 10.6$ GeV, excluding B decay products [188,189]. (b) Measured e^+e^- fragmentation function of b quarks into B hadrons at $\sqrt{s} \approx 91$ GeV [200].

The branching ratio \mathcal{B} represents $D^0 \rightarrow K^-\pi^+$ for the D^0 results and for the D^{*+} the product branching fraction: $D^{*+} \rightarrow D^0\pi^+$, $D^0 \rightarrow K^-\pi^+$. Given the high precision of CLEO's and BELLE's data, a superposition of different parametric forms for the non-perturbative contribution is needed to obtain a good fit [21]. Older studies are reported in Refs. [192–194]. Charmed meson spectra on the Z peak have been published by OPAL and ALEPH [90,195].

Charm quark production has also been extensively studied at HERA by the H1 and ZEUS collaborations. Measurements have been made of $D^{*\pm}$, D^\pm , and D_s^\pm mesons; see, for example, Refs. [196,197]. The production of the Λ_c baryon has also been studied [198].

Experimental studies of the fragmentation function for b quarks, shown in Fig. 17.10(b), have been performed at LEP and SLD [199–201]. Commonly used methods identify the B meson through its semileptonic decay or based upon tracks emerging from

the B secondary vertex. The studies in [200] fit the B spectrum using a Monte Carlo shower model supplemented with non-perturbative fragmentation functions yielding consistent results.

The experiments measure primarily the spectrum of B mesons. This defines a fragmentation function which includes the effect of the decay of higher mass excitations, like the B^* and B^{**} . In the literature, there is sometimes ambiguity in what is defined to be the bottom fragmentation function. Instead of using what is directly measured (*i.e.*, the B meson spectrum) corrections are applied to account for B^* or B^{**} production in some cases. For a more detailed discussion see section 17.8 of [184].

Heavy-flavor production in e^+e^- collisions is the primary source of information for the role of fragmentation effects in heavy-flavor production in hadron-hadron and lepton-hadron collisions. The QCD calculations tend to underestimate the data in certain regions of phase space. The discrepancy observed between theoretical calculations and the measured B meson spectrum at the hadron colliders [202] is substantially reduced when a more refined use of information on heavy flavor production from e^+e^- data is made [203] and when up-to-date parton distributions and strong coupling constant values are considered [204].

Both bottomed- and charmed-mesons spectra have been measured at the Tevatron with unprecedented accuracy [205]. The measured spectra are in good agreement with QCD calculations (including non-perturbative fragmentation effects inferred from e^+e^- data [206]), no longer supporting the previously reported discrepancies [202].

The HERA collaborations have produced a number of measurements of beauty production; see, for example, Refs. [196,207–209]. As for the Tevatron data, the HERA results are described well by QCD-based calculations using fragmentation models optimised with e^+e^- data.

Besides degrading the fragmentation function by gluon radiation, QCD evolution can also generate soft heavy quarks, increasing in the small x region as \sqrt{s} increases. Several theoretical studies are available on the issue of how often $b\bar{b}$ or $c\bar{c}$ pairs are produced indirectly, via a gluon splitting mechanism [210–212]. Experimental results from studies on charm and bottom production via gluon splitting, given in [195,213–217], yield weighted averages of $\bar{\pi}_{g \rightarrow c\bar{c}} = 3.05 \pm 0.45\%$ and $\bar{\pi}_{g \rightarrow b\bar{b}} = 0.277 \pm 0.072\%$, respectively.

References:

1. G. Altarelli, *Phys. Reports* **81**, 1 (1982).
2. R.K. Ellis *et al.*, *QCD and Collider Physics*, Cambridge University Press (1996).
3. S. Albino *et al.*, arXiv:0804.2021 [hep-ph].
4. F. Arleo, *Eur. Phys. J.* **C61**, 603 (2009).
5. P. Nason and B.R. Webber, *Nucl. Phys.* **B421**, 473 (1994); Erratum *ibid.* **B480**, 755 (1996).
6. ALEPH Collab.: D. Barate *et al.*, *Phys. Lett.* **B357**, 487 (1995); Erratum *ibid.*, **B364**, 247 (1995).
7. OPAL Collab.: R. Akers *et al.*, *Z. Phys.* **C86**, 203 (1995).
8. DELPHI Collab.: P. Abreu *et al.*, *Eur. Phys. J.* **C6**, 19 (1999).
9. W. Kittel and E.A. De Wolf, *Soft Multihadron Dynamics*, World Scientific (2005).
10. H.F. Jones, *Nuovo Cimento* **40A**, 1018 (1965); K.H. Streng *et al.*, *Z. Phys.* **C2**, 237 (1979).
11. V.N. Gribov and L.N. Lipatov, *Sov. J. Nucl. Phys.* **15**, 438 (1972); V.N. Gribov and L.N. Lipatov, *Sov. J. Nucl. Phys.* **15**, 675 (1972); G. Altarelli and G. Parisi, *Nucl. Phys.* **B126**, 298 (1977); Yu.L. Dokshitzer, *Sov. Phys. JETP Lett.* **46**, 641 (1977).
12. H. Georgi and H.D. Politzer, *Nucl. Phys.* **B136**, 445 (1978); J.F. Owens, *Phys. Lett.* **B76**, 85 (1978); T. Uematsu, *Phys. Lett.* **B79**, 97 (1978).
13. G. Curci *et al.*, *Nucl. Phys.* **B175**, 27 (1980).
14. W. Furmanski and R. Petronzio, *Phys. Lett.* **97B**, 437 (1980).
15. E.G. Floratos *et al.*, *Nucl. Phys.* **B192**, 417 (1981); T. Muehisa *et al.*, *Prog. Theor. Phys.* **67**, 609 (1982).
16. J. Kalinowski *et al.*, *Nucl. Phys.* **B181**, 221 (1981); J. Kalinowski *et al.*, *Nucl. Phys.* **B181**, 253 (1981).

17. M. Stratmann and W. Vogelsang, Nucl. Phys. **B496**, 41 (1997).
18. Yu.L. Dokshitzer *et al.*, Phys. Lett. **B634**, 504 (2006).
19. A. Mitov *et al.*, Phys. Lett. **B638**, 61 (2006).
20. S. Moch and A. Vogt, Phys. Lett. **B659**, 290 (2008).
21. M. Cacciari *et al.*, JHEP **0604**, 006 (2006).
22. G. Altarelli *et al.*, Nucl. Phys. **B160**, 301 (1979);
R. Baier and K. Fey, Z. Phys. **C2**, 339 (1979).
23. P.J. Rijken and W.L. van Neerven, Phys. Lett. **B386**, 422 (1996);
P.J. Rijken and W.L. van Neerven, Phys. Lett. **B392**, 207 (1997);
P.J. Rijken and W.L. van Neerven, Nucl. Phys. **B487**, 233 (1997).
24. A. Mitov and S. Moch, Nucl. Phys. **B751**, 18 (2006).
25. ALEPH Collab.: D. Buskulic *et al.*, Z. Phys. **C73**, 409 (1997).
26. ALEPH Collab.: E. Barate *et al.*, Phys. Reports **294**, 1 (1998).
27. L3 Collab.: B. Adeva *et al.*, Phys. Lett. **B259**, 199 (1991).
28. AMY Collab.: Y.K. Li *et al.*, Phys. Rev. **D41**, 2675 (1990).
29. HRS Collab.: D. Bender *et al.*, Phys. Rev. **D31**, 1 (1984).
30. MARK II Collab.: G.S. Abrams *et al.*, Phys. Rev. Lett. **64**, 1334 (1990).
31. MARK II Collab.: A. Petersen *et al.*, Phys. Rev. **D37**, 1 (1988).
32. OPAL Collab.: R. Akers *et al.*, Z. Phys. **C72**, 191 (1996).
33. OPAL Collab.: K. Ackerstaff *et al.*, Z. Phys. **C75**, 193 (1997).
34. OPAL Collab.: K. Ackerstaff *et al.*, Eur. Phys. J. **C7**, 369 (1998).
35. OPAL Collab.: G. Abbiendi *et al.*, Eur. Phys. J. **C16**, 185 (2000);
OPAL Collab.: G. Abbiendi *et al.*, Eur. Phys. J. **C27**, 467 (2003).
36. OPAL Collab.: G. Abbiendi *et al.*, Eur. Phys. J. **C37**, 25 (2004).
37. SLD Collab.: K. Abe *et al.*, Phys. Rev. **D69**, 072003 (2004).
38. DELPHI Collab.: P. Abreu *et al.*, Phys. Lett. **B398**, 194 (1997).
39. TASSO Collab.: R. Brandelik *et al.*, Phys. Lett. **B114**, 65 (1982).
40. TASSO Collab.: W. Braunschweig *et al.*, Z. Phys. **C47**, 187 (1990).
41. TPC Collab.: H. Aihara *et al.*, Phys. Rev. Lett. **61**, 1263 (1988).
42. M. Cacciari and S. Catani, Nucl. Phys. **B617**, 253 (2001).
43. J. Blümlein and V. Ravindran, Phys. Lett. **B640**, 40 (2006).
44. S. Moch and A. Vogt, Phys. Lett. **B680**, 239 (2009).
45. S. Moch and A. Vogt, JHEP **0911**, 099 (2009).
46. P. Aurenche *et al.*, Eur. Phys. J. **C34**, 277 (2004);
A. Daleo *et al.*, Phys. Rev. **D71**, 034013 (2005);
B.A. Kniehl *et al.*, Nucl. Phys. **B711**, 345 (2005);
Erratum *ibid.* **B720**, 231 (2005).
47. E665 Collab.: M.R. Adams *et al.*, Phys. Lett. **B272**, 163 (1991).
48. EMC Collab.: M. Arneodo *et al.*, Z. Phys. **C35**, 417 (1987).
49. H1 Collab.: I. Abt *et al.*, Z. Phys. **C63**, 377 (1994).
50. ZEUS Collab.: M. Derrick *et al.*, Z. Phys. **C70**, 1 (1996).
51. ZEUS Collab.: J. Breitweg *et al.*, Phys. Lett. **B414**, 428 (1997).
52. H1 Collab.: S. Aid *et al.*, Nucl. Phys. **B445**, 3 (1995).
53. ZEUS Collab.: M. Derrick *et al.*, Z. Phys. **C67**, 93 (1995).
54. H1 Collab.: C. Adloff *et al.*, Nucl. Phys. **B504**, 3 (1997).
55. ZEUS Collab.: J. Breitweg *et al.*, Eur. Phys. J. **C11**, 251 (1999).
56. H1 Collab.: F.D. Aaron *et al.*, Phys. Lett. **B654**, 148 (2007).
57. DELPHI Collab.: P. Abreu *et al.*, Phys. Lett. **B311**, 408 (1993).
58. MARK II Collab.: J.F. Patrick *et al.*, Phys. Rev. Lett. **49**, 1232, (1982).
59. ZEUS Collab.: S. Chekanov *et al.*, JHEP **0608**, 061 (2008).
60. A.H. Mueller, Phys. Lett. **B104**, 161 (1981).
61. A. Bassetto *et al.*, Nucl. Phys. **B207**, 189 (1982).
62. Yu.L. Dokshitzer *et al.*, Z. Phys. **C15**, 324 (1982).
63. A.H. Mueller, Nucl. Phys. **B213**, 85 (1983);
Erratum in *ibid.* **B241**, 141 (196).
64. Yu.L. Dokshitzer *et al.*, Int. J. Mod. Phys. **A7**, 1875 (1992).
65. Yu.L. Dokshitzer *et al.*, *Basics of Perturbative QCD*, Editions Frontières (1991).
66. V.A. Khoze and W. Ochs, Int. J. Mod. Phys. **A12**, 2949 (1997).
67. C.P. Fong and B.R. Webber, Nucl. Phys. **B355**, 54 (1992).
68. DELPHI Collab.: P. Abreu *et al.*, Z. Phys. **C73**, 11 (1996).
69. DELPHI Collab.: P. Abreu *et al.*, Z. Phys. **C73**, 229 (1997).
70. L3 Collab.: P. Achard *et al.*, Phys. Reports **399**, 71 (2004).
71. TOPAZ Collab.: R. Itoh *et al.*, Phys. Lett. **B345**, 335 (1995).
72. TASSO Collab.: W. Braunschweig *et al.*, Z. Phys. **C22**, 307 (1990).
73. OPAL Collab.: M.Z. Akrawy *et al.*, Phys. Lett. **B247**, 617 (1990).
74. BES Collab.: J.Z. Bai *et al.*, Phys. Rev. **D69**, 072002 (2004).
75. ALEPH Collab.: D. Buskulic *et al.*, Z. Phys. **C55**, 209 (1992).
76. ALEPH Collab.: A. Heister *et al.*, Eur. Phys. J. **C35**, 457 (2004).
77. DELPHI Collab.: P. Abreu *et al.*, Phys. Lett. **B275**, 231 (1992).
78. DELPHI Collab.: P. Abreu *et al.*, Eur. Phys. J. **C5**, 585 (1998).
79. DELPHI Collab.: P. Abreu *et al.*, Phys. Lett. **B459**, 397 (1999).
80. L3 Collab.: M. Acciarri *et al.*, Phys. Lett. **B444**, 569 (1998).
81. TPC/TWO-GAMMA Collab.: H. Aihara *et al.*, LBL 23737.
82. S. Höche *et al.*, arXiv:hep-ph/0602031;
J. Alwall *et al.*, Eur. Phys. J. **C53**, 473 (2008);
S. Mrenna and P. Richardson, JHEP **0405**, 040 (2004).
83. X. Artru and G. Mennessier, Nucl. Phys. **B70**, 93 (1974).
84. B. Andersson *et al.*, Phys. Reports **97**, 31 (1983).
85. T. Sjöstrand and M. Bengtsson, Comp. Phys. Comm. **43**, 367 (1987);
T. Sjöstrand, Comp. Phys. Comm. **82**, 74 (1994).
86. T. Sjöstrand, S. Mrenna, P. Skands, JHEP **0605**, 026 (2006);
T. Sjöstrand, S. Mrenna, P. Skands, Comp. Phys. Comm. **178**, 852 (2008).
87. S. Chun and C. Buchanan, Phys. Reports **292**, 239 (1998).
88. G. Marchesini *et al.*, Comp. Phys. Comm. **67**, 465 (1992);
G. Corcella *et al.*, JHEP **0101**, 010 (2001);
M. Bähr *et al.*, Eur. Phys. J. **C58**, 639 (2008).
89. T. Gleisberg *et al.*, JHEP **0902**, 007 (2009).
90. OPAL Collab.: G. Alexander *et al.*, Z. Phys. **C69**, 543 (1996).
91. M. Schmelling, Phys. Scripta **51**, 683 (1995).
92. D. Amati and G. Veneziano, Phys. Lett. **B83**, 87 (1979).
93. D. de Florian *et al.*, Phys. Rev. **D76**, 074033 (2007);
D. de Florian *et al.*, Phys. Rev. **D75**, 114010 (2007).
94. S. Albino *et al.*, Nucl. Phys. **B803**, 42 (2008).
95. S. Kretzer *et al.*, Eur. Phys. J. **C22**, 269 (2001).
96. S. Kretzer, Phys. Rev. **D62**, 054001 (2000).
97. L. Bourhis *et al.*, Eur. Phys. J. **C19**, 89 (2001).
98. M. Hirai *et al.*, Phys. Rev. **D75**, 094009 (2007).
99. ALEPH Collab.: R. Barate *et al.*, Eur. Phys. J. **C17**, 1 (2000);
OPAL Collab.: R. Akers *et al.*, Z. Phys. **C68**, 179 (1995);
OPAL Collab.: G. Abbiendi *et al.*, Eur. Phys. J. **C11**, 217 (1999).
100. ALEPH Collab.: D. Buskulic *et al.*, Z. Phys. **C66**, 355 (1995);
ARGUS Collab.: H. Albrecht *et al.*, Z. Phys. **C44**, 547 (1989);
OPAL Collab.: R. Akers *et al.*, Z. Phys. **C63**, 181 (1994);
SLD Collab.: K. Abe *et al.*, Phys. Rev. **D59**, 052001 (1999).
101. DELPHI Collab.: P. Abreu *et al.*, Eur. Phys. J. **C13**, 573 (2000).
102. B.A. Kniehl *et al.*, Phys. Rev. Lett. **85**, 5288 (2000).
103. E665 Collab.: M.R. Adams *et al.*, Z. Phys. **C61**, 539 (1994).
104. EMC Collab.: J.J. Aubert *et al.*, Z. Phys. **C18**, 189 (1983);
EMC Collab.: M. Arneodo *et al.*, Phys. Lett. **B150**, 458 (1985).
105. EMC Collab.: M. Arneodo *et al.*, Z. Phys. **C33**, 167 (1986).
106. EMC Collab.: M. Arneodo *et al.*, Z. Phys. **C34**, 283 (1987).
107. HERMES Collab.: A. Airapetian *et al.*, Eur. Phys. J. **C21**, 599 (2001).
108. T.P. McPharlin *et al.*, Phys. Lett. **B90**, 479 (1980).
109. H1 Collab.: S. Aid *et al.*, Nucl. Phys. **B480**, 3 (1996).
110. H1 Collab.: C. Adloff *et al.*, Eur. Phys. J. **C18**, 293 (2000);
H1 Collab.: A. Aktas *et al.*, Eur. Phys. J. **C36**, 413 (2004).
111. ZEUS Collab.: M. Derrick *et al.*, Z. Phys. **C68**, 29 (1995);
ZEUS Collab.: J. Breitweg *et al.*, Eur. Phys. J. **C2**, 77 (1998).
112. ZEUS Collab.: S. Chekanov *et al.*, Phys. Lett. **B553**, 141 (2003).

113. ZEUS Collab.: S. Chekanov *et al.*, Nucl. Phys. **B786**, 181 (2007).
114. H1 Collab.: F. D. Aaron *et al.*, Eur. Phys. J. **C61**, 185 (2009).
115. H1 Collab.: F. D. Aaron *et al.*, Phys. Lett. **B673**, 119 (2009).
116. P. Dixon *et al.*, J. Phys. **G25**, 1453 (1999).
117. H1 Collab.: C. Adloff *et al.*, Phys. Lett. **B462**, 440 (1999).
118. D. Graudenz, Fortsch. Phys. **45**, 629 (1997).
119. S. Albino *et al.*, Phys. Rev. **D75**, 034018 (2007).
120. OPAL Collab.: P.D. Acton *et al.*, Phys. Lett. **B305**, 407 (1993).
121. E632 Collab.: D. DeProspero *et al.*, Phys. Rev. **D50**, 6691 (1994).
122. ZEUS Collab.: S. Chekanov *et al.*, Eur. Phys. J. **C51**, 1 (2007).
123. G. Grindhammer *et al.*, in: *Proceedings of the Workshop on Monte Carlo Generators for HERA Physics*, Hamburg, Germany, 1998/1999.
124. N. Brook *et al.*, in: *Proceedings of the Workshop for Future HERA Physics at HERA*, Hamburg, Germany, 1996.
125. CDF Collab.: F. Abe *et al.*, Phys. Rev. Lett. **61**, 1819 (1988).
126. CDF Collab.: D. E. Acosta *et al.*, Phys. Rev. **D72**, 052001 (2005).
127. UA1 Collab.: G. Arnison *et al.*, Phys. Lett. **B118**, 167 (1982).
128. UA1 Collab.: C. Albajar *et al.*, Nucl. Phys. **B335**, 261 (1990).
129. UA1 Collab.: G. Bocquet *et al.*, Phys. Lett. **B366**, 434 (1996).
130. UA2 Collab.: M. Banner *et al.*, Phys. Lett. **B122**, 322 (1983).
131. UA2 Collab.: M. Banner *et al.*, Phys. Lett. **B115**, 59 (1982).
132. UA2 Collab.: M. Banner *et al.*, Z. Phys. **C27**, 329 (1985).
133. PHENIX Collab.: S. S. Adler *et al.*, Phys. Rev. Lett. **91**, 241803 (2003).
134. BRAHMS Collab.: I. Arsene *et al.*, Phys. Rev. Lett. **98**, 252001 (2007).
135. STAR Collab.: J. Adams *et al.*, Phys. Lett. **B637**, 161 (2006).
136. STAR Collab.: J. Adams *et al.*, Phys. Rev. Lett. **97**, 152302 (2006).
137. STAR Collab.: B. I. Abelev *et al.*, Phys. Rev. **C75**, 064901 (2007).
138. E706 Collab.: L. Apanasevich *et al.*, Phys. Rev. Lett. **81**, 2642 (1998).
139. UA6 Collab.: G. Balocchi *et al.*, Phys. Lett. **B436**, 222 (1998).
140. WA70 Collab.: M. Bonesini *et al.*, Z. Phys. **C38**, 371 (1988).
141. AFS Collab.: E. Anassontzis *et al.*, Sov. J. Nucl. Phys. **51**, 836 (1990).
142. R806 Collab.: C. Kourkoumelis *et al.*, Z. Phys. **C5**, 95 (1980).
143. E706 Collab.: L. Apanasevich *et al.*, Phys. Rev. **D68**, 052001 (2003).
144. F. Aversa *et al.*, Nucl. Phys. **B327**, 105 (1989);
D. de Florian, Phys. Rev. **D67**, 054004 (2003);
B. Jager *et al.*, Phys. Rev. **D67**, 054005 (2003).
145. U. Baur *et al.*, arXiv:hep-ph/0005226.
146. P. Aurenche *et al.*, Eur. Phys. J. **C13**, 347 (2000).
147. L. Apanasevich *et al.*, Phys. Rev. **D59**, 074007 (1999).
148. U. D'Alesio and F. Murgia, Phys. Rev. **D70**, 074009 (2004).
149. D. de Florian and W. Vogelsang, Phys. Rev. **D71**, 114004 (2005).
150. PHENIX Collab.: A. Adare *et al.*, Phys. Rev. **D76**, 051106 (2007).
151. PHENIX Collab.: A. Adare *et al.*, Phys. Rev. **D79**, 012003 (2009).
152. PHENIX Collab.: K. Adcox *et al.*, Phys. Rev. Lett. **88**, 022301 (2002);
STAR Collab.: C. Adler *et al.*, Phys. Rev. Lett. **90**, 082302 (2003).
153. COMPASS Collab.: M. Alekseev *et al.*, Phys. Lett. **B660**, 458, (2008).
154. HERMES Collab.: A. Airapetian *et al.*, Phys. Rev. **D71**, 012003 (2005).
155. SMC Collab.: B. Adeva *et al.*, Phys. Lett. **B420**, 180 (1998).
156. HERMES Collab.: A. Airapetian *et al.*, Phys. Lett. **B666**, 446 (2008).
157. D. de Florian *et al.*, Phys. Rev. Lett. **101**, 072001 (2008).
158. P.J. Mulders and R.D. Tangerman, Nucl. Phys. **B461**, 197 (1996);
Erratum *ibid.*, **B484**, 538 (1997).
159. R. Jacob, Nucl. Phys. **A711**, 35 (2002).
160. COMPASS Collab.: M. Alekseev *et al.*, Eur. Phys. J. **C64**, 171 (2009).
161. HERMES Collab.: A. Airapetian *et al.*, Phys. Rev. **D74**, 072004 (2006).
162. J.P. Ralston and D.E. Soper, Nucl. Phys. **B152**, 109 (1979).
163. J. Collins, Nucl. Phys. **B396**, 161 (1993).
164. D. Sivers, Phys. Rev. **D43**, 261 (1991).
165. CLAS Collab.: H. Avakian *et al.*, Phys. Rev. **D69**, 112004 (2004).
166. HERMES Collab.: A. Airapetian *et al.*, Phys. Rev. Lett. **84**, 4047 (2000).
167. HERMES Collab.: A. Airapetian *et al.*, Phys. Rev. **D64**, 097101 (2001).
168. HERMES Collab.: A. Airapetian *et al.*, Phys. Rev. Lett. **94**, 012002 (2005).
169. BELLE Collab.: K. Abe *et al.*, Phys. Rev. Lett. **96**, 232002 (2006).
170. BELLE Collab.: K. Abe *et al.*, Phys. Rev. **D78**, 032011 (2008).
171. COMPASS Collab.: V.Y. Alexakhin *et al.*, Phys. Rev. Lett. **94**, 202002 (2005).
172. COMPASS Collab.: V.Y. Alexakhin *et al.*, Nucl. Phys. **B765**, 31 (2007).
173. COMPASS Collab.: M. Alekseev *et al.*, Phys. Lett. **B673**, 127 (2009).
174. V.A. Khoze *et al.*, *Proceedings, Conference on High-Energy Physics, Tbilisi 1976*;
J.D. Bjorken, Phys. Rev. **D17**, 171 (1978).
175. B. Mele and P. Nason, Phys. Lett. **B245**, 635 (1990);
B. Mele and P. Nason, Nucl. Phys. **B361**, 626 (1991).
176. P. Nason and C. Oleari, Phys. Lett. **B418**, 199 (1998);
P. Nason and C. Oleari, Phys. Lett. **B447**, 327 (1999);
P. Nason and C. Oleari, Nucl. Phys. **B565**, 245 (2000).
177. K. Melnikov and A. Mitov, Phys. Rev. **D70**, 034027 (2004).
178. C. Peterson *et al.*, Phys. Rev. **D27**, 105 (1983).
179. V.G. Kartvelishvili *et al.*, Phys. Lett. **B78**, 615 (1978).
180. P. Collins and T. Spiller, J. Phys. **G11**, 1289 (1985).
181. G. Colangelo and P. Nason, Phys. Lett. **B285**, 167 (1992).
182. M.G. Bowler, Z. Phys. **C11**, 169 (1981).
183. E. Braaten *et al.*, Phys. Rev. **D51**, 4819 (1995).
184. Particle Data Group: C. Amsler *et al.*, Phys. Lett. **B667**, 1 (2008).
185. J. Chrin, Z. Phys. **C36**, 163 (1987).
186. J. Collins, Phys. Rev. **D58**, 094002 (1998).
187. B.A. Kniehl *et al.*, Eur. Phys. J. **C41**, 199 (2005).
188. CLEO Collab.: M. Artuso *et al.*, Phys. Rev. **D70**, 112001 (2004).
189. BELLE Collab.: R. Seuster *et al.*, Phys. Rev. **D73**, 032002 (2006).
190. CLEO Collab.: R.A. Briere *et al.*, Phys. Rev. **D62**, 112003 (2000).
191. BABAR Collab.: B. Aubert *et al.*, Phys. Rev. **D65**, 091104 (2002).
192. CLEO Collab.: D. Bortoletto *et al.*, Phys. Rev. **D37**, 1719 (1988).
193. ARGUS Collab.: H. Albrecht *et al.*, Z. Phys. **C52**, 353 (1991).
194. ARGUS Collab.: H. Albrecht *et al.*, Z. Phys. **C54**, 1 (1992).
195. ALEPH Collab.: R. Barate *et al.*, Phys. Lett. **B561**, 213 (2003).
196. H1 Collab.: F.D. Aaron *et al.*, Eur. Phys. J. **C65**, 89 (2010).
197. ZEUS Collab.: S. Chekanov *et al.*, JHEP **0707**, 074 (2007);
ZEUS Collab.: S. Chekanov *et al.*, JHEP **0904**, 82 (2009);
ZEUS Collab.: S. Chekanov *et al.*, Eur. Phys. J. **C63**, 171 (2009);
H1 Collab.: A. Aktas *et al.*, Eur. Phys. J. **C51**, 271 (2007);
H1 Collab.: F. D. Aaron *et al.*, Eur. Phys. J. **C59**, 589 (2009).
198. ZEUS Collab.: S. Chekanov *et al.*, Eur. Phys. J. **C44**, 351 (2005).
199. ALEPH Collab.: D. Buskulic *et al.*, Phys. Lett. **B357**, 699 (1995).

200. ALEPH Collab.: A. Heister *et al.*, Phys. Lett. **B512**, 30 (2001);
OPAL Collab.: G. Abbiendi *et al.*, Eur. Phys. J. **C29**, 463 (2003);
SLD Collab.: K. Abe *et al.*, Phys. Rev. **D65**, 092006 (2002);
Erratum *ibid.*, **D66**, 079905 (2002).
201. L3 Collab.: B. Adeva *et al.*, Phys. Lett. **B261**, 177 (1991).
202. CDF Collab.: F. Abe *et al.*, Phys. Rev. Lett. **71**, 500 (1993);
CDF Collab.: F. Abe *et al.*, Phys. Rev. Lett. **71**, 2396 (1993);
CDF Collab.: F. Abe *et al.*, Phys. Rev. **D50**, 4252 (1994);
CDF Collab.: F. Abe *et al.*, Phys. Rev. Lett. **75**, 1451 (1995);
CDF Collab.: D. Acosta *et al.*, Phys. Rev. **D66**, 032002 (2002);
CDF Collab.: D. Acosta *et al.*, Phys. Rev. **D65**, 052005 (2002);
D0 Collab.: S. Abachi *et al.*, Phys. Rev. Lett. **74**, 3548 (1995);
UA1 Collab.: C. Albajar *et al.*, Phys. Lett. **B186**, 237 (1987);
UA1 Collab.: C. Albajar *et al.*, Phys. Lett. **B256**, 121 (1991);
Erratum *ibid.*, **B272**, 497 (1991).
203. M. Cacciari and P. Nason, Phys. Rev. Lett. **89**, 122003 (2002).
204. B.A. Kniehl *et al.*, Phys. Rev. **D77**, 014011 (2008).
205. CDF Collab.: D. Acosta *et al.*, Phys. Rev. Lett. **91**, 241804 (2003);
CDF Collab.: D. Acosta *et al.*, Phys. Rev. **D71**, 032001 (2005).
206. M. Cacciari and P. Nason, JHEP **0309**, 006 (2003);
M. Cacciari *et al.*, JHEP **0407**, 033 (2004);
B.A. Kniehl *et al.*, Phys. Rev. Lett. **96**, 012001 (2006).
207. ZEUS Collab.: S. Chekanov *et al.*, Phys. Rev. **D78**, 072001 (2008).
208. ZEUS Collab.: S. Chekanov *et al.*, JHEP **0902**, 032 (2009).
209. H1 Collab.: A. Aktas *et al.*, Eur. Phys. J. **C47**, 597 (2006).
210. A.H. Mueller and P. Nason, Nucl. Phys. **B266**, 265 (1986);
M.L. Mangano and P. Nason, Phys. Lett. **B285**, 160 (1992).
211. M.H. Seymour, Nucl. Phys. **B436**, 163 (1995).
212. D.J. Miller and M.H. Seymour, Phys. Lett. **B435**, 213 (1998).
213. ALEPH Collab.: R. Barate *et al.*, Phys. Lett. **B434**, 437 (1998).
214. DELPHI Collab.: P. Abreu *et al.*, Phys. Lett. **B405**, 202 (1997).
215. L3 Collab.: M. Acciarri *et al.*, Phys. Lett. **B476**, 243 (2000).
216. OPAL Collab.: G. Abbiendi *et al.*, Eur. Phys. J. **C13**, 1 (2000).
217. SLD Collab.: K. Abe *et al.*, SLAC-PUB-8157, hep-ex/9908028.

18. EXPERIMENTAL TESTS OF GRAVITATIONAL THEORY

Revised November 2009 by T. Damour (IHES, Bures-sur-Yvette, France).

Einstein's General Relativity, the current "standard" theory of gravitation, describes gravity as a universal deformation of the Minkowski metric:

$$g_{\mu\nu}(x^\lambda) = \eta_{\mu\nu} + h_{\mu\nu}(x^\lambda), \text{ where } \eta_{\mu\nu} = \text{diag}(-1, +1, +1, +1). \quad (18.1)$$

Alternatively, it can be defined as the unique, consistent, local theory of a massless spin-2 field $h_{\mu\nu}$, whose source must then be the total, conserved energy-momentum tensor [1]. General Relativity is classically defined by two postulates. One postulate states that the Lagrangian density describing the propagation and self-interaction of the gravitational field is

$$\mathcal{L}_{\text{Ein}}[g_{\mu\nu}] = \frac{c^4}{16\pi G_N} \sqrt{g} g^{\mu\nu} R_{\mu\nu}(g), \quad (18.2)$$

$$R_{\mu\nu}(g) = \partial_\alpha \Gamma_{\mu\nu}^\alpha - \partial_\nu \Gamma_{\mu\alpha}^\alpha + \Gamma_{\alpha\beta}^\beta \Gamma_{\mu\nu}^\alpha - \Gamma_{\alpha\nu}^\beta \Gamma_{\mu\beta}^\alpha, \quad (18.3)$$

$$\Gamma_{\mu\nu}^\lambda = \frac{1}{2} g^{\lambda\sigma} (\partial_\mu g_{\nu\sigma} + \partial_\nu g_{\mu\sigma} - \partial_\sigma g_{\mu\nu}), \quad (18.4)$$

where G_N is Newton's constant, $g = -\det(g_{\mu\nu})$, and $g^{\mu\nu}$ is the matrix inverse of $g_{\mu\nu}$. A second postulate states that $g_{\mu\nu}$ couples universally, and minimally, to all the fields of the Standard Model by replacing everywhere the Minkowski metric $\eta_{\mu\nu}$. Schematically (suppressing matrix indices and labels for the various gauge fields and fermions and for the Higgs doublet),

$$\begin{aligned} \mathcal{L}_{\text{SM}}[\psi, A_\mu, H, g_{\mu\nu}] = & -\frac{1}{4} \sum \sqrt{g} g^{\mu\alpha} g^{\nu\beta} F_{\mu\nu}^\alpha F_{\alpha\beta}^\alpha \\ & - \sum \sqrt{g} \bar{\psi} \gamma^\mu D_\mu \psi \\ & - \frac{1}{2} \sqrt{g} g^{\mu\nu} \overline{D_\mu H} D_\nu H - \sqrt{g} V(H) \\ & - \sum \lambda \sqrt{g} \bar{\psi} H \psi, \end{aligned} \quad (18.5)$$

where $\gamma^\mu \gamma^\nu + \gamma^\nu \gamma^\mu = 2g^{\mu\nu}$, and where the covariant derivative D_μ contains, besides the usual gauge field terms, a (spin-dependent) gravitational contribution $\Gamma_\mu(x)$ [2]. From the total action follow Einstein's field equations,

$$R_{\mu\nu} - \frac{1}{2} R g_{\mu\nu} = \frac{8\pi G_N}{c^4} T_{\mu\nu}. \quad (18.6)$$

Here $R = g^{\mu\nu} R_{\mu\nu}$, $T_{\mu\nu} = g_{\mu\alpha} g_{\nu\beta} T^{\alpha\beta}$, and $T^{\mu\nu} = (2/\sqrt{g}) \delta \mathcal{L}_{\text{SM}} / \delta g_{\mu\nu}$ is the (symmetric) energy-momentum tensor of the Standard Model matter. The theory is invariant under arbitrary coordinate transformations: $x'^\mu = f^\mu(x^\nu)$. To solve the field equations Eq. (18.6), one needs to fix this coordinate gauge freedom. *E.g.*, the "harmonic gauge" (which is the analogue of the Lorenz gauge, $\partial_\mu A^\mu = 0$, in electromagnetism) corresponds to imposing the condition $\partial_\nu (\sqrt{g} g^{\mu\nu}) = 0$.

In this *Review*, we only consider the classical limit of gravitation (*i.e.* classical matter and classical gravity). Considering quantum matter in a classical gravitational background already poses interesting challenges, notably the possibility that the zero-point fluctuations of the matter fields generate a nonvanishing vacuum energy density ρ_{vac} , corresponding to a term $-\sqrt{g} \rho_{\text{vac}}$ in \mathcal{L}_{SM} [3]. This is equivalent to adding a "cosmological constant" term $+\Lambda g_{\mu\nu}$ on the left-hand side of Einstein's equations Eq. (18.6), with $\Lambda = 8\pi G_N \rho_{\text{vac}}/c^4$. Recent cosmological observations (see the following *Reviews*) suggest a positive value of Λ corresponding to $\rho_{\text{vac}} \approx (2.3 \times 10^{-3} \text{eV})^4$. Such a small value has a negligible effect on the tests discussed below. Quantizing the gravitational field itself poses a very difficult challenge because of the perturbative non-renormalizability of Einstein's Lagrangian. Superstring theory offers a promising avenue toward solving this challenge.

18.1. Experimental tests of the coupling between matter and gravity

The universality of the coupling between $g_{\mu\nu}$ and the Standard Model matter postulated in Eq. (18.5) ("Equivalence Principle") has many observable consequences. First, it predicts that the outcome of a local non-gravitational experiment, referred to local standards, does not depend on where, when, and in which locally inertial frame, the experiment is performed. This means, for instance, that local experiments should neither feel the cosmological evolution of the universe (constancy of the "constants"), nor exhibit preferred directions in spacetime (isotropy of space, local Lorentz invariance). These predictions are consistent with many experiments and observations. Stringent limits on a possible time variation of the basic coupling constants have been obtained by analyzing a natural fission reactor phenomenon which took place at Oklo, Gabon, two billion years ago [4,5]. These limits are at the 1×10^{-7} level for the fractional variation of the fine-structure constant α_{em} [5], and at the 4×10^{-9} level for the fractional variation of the ratio between the light quark masses and Λ_{QCD} [6]. The determination of the lifetime of Rhenium 187 from isotopic measurements of some meteorites dating back to the formation of the solar system (about 4.6 Gyr ago) yields comparably strong limits [7]. Measurements of absorption lines in astronomical spectra also give stringent limits on the variability of both α_{em} (at the 10^{-5} level [8]), and $\mu = m_p/m_e$, namely [9]

$$|\Delta\mu/\mu| < 1.8 \times 10^{-6}, \quad (18.7)$$

at a redshift $z = 0.68466$. Direct laboratory limits on the (present) time variation of α_{em} (based on monitoring the frequency ratio of several different atomic clocks) have recently reached the impressive level [10]:

$$\dot{\alpha}_{\text{em}}/\alpha_{\text{em}} = (-1.6 \pm 2.3) \times 10^{-17} \text{yr}^{-1}.$$

There are also experimental limits on a possible dependence of coupling constants on the gravitational potential [11]. See Refs. [12,13] for reviews of the issue of "variable constants."

The highest precision tests of the isotropy of space have been performed by looking for possible quadrupolar shifts of nuclear energy levels [14]. The (null) results can be interpreted as testing the fact that the various pieces in the matter Lagrangian Eq. (18.5) are indeed coupled to one and the same external metric $g_{\mu\nu}$ to the 10^{-27} level. For astrophysical constraints on possible Planck-scale violations of Lorentz invariance, see Ref. 15.

The universal coupling to $g_{\mu\nu}$ postulated in Eq. (18.5) implies that two (electrically neutral) test bodies dropped at the same location and with the same velocity in an external gravitational field fall in the same way, independently of their masses and compositions. The universality of the acceleration of free fall has been verified at the 10^{-13} level for laboratory bodies, notably Beryllium and Titanium test bodies [16],

$$(\Delta a/a)_{\text{BeTi}} = (0.3 \pm 1.8) \times 10^{-13}, \quad (18.8)$$

as well as for the gravitational accelerations of the Earth and the Moon toward the Sun [17],

$$(\Delta a/a)_{\text{EarthMoon}} = (-1.0 \pm 1.4) \times 10^{-13}. \quad (18.9)$$

The latter result constrains not only how $g_{\mu\nu}$ couples to matter, but also how it couples to itself [18] ("strong equivalence principle"; see Eq. (18.15) below, and the end of the section on binary pulsar tests). See also Ref. 19 for a review of torsion balance experiments.

Finally, Eq. (18.5) also implies that two identically constructed clocks located at two different positions in a static external Newtonian potential $U(\mathbf{x}) = \sum G_N m/r$ exhibit, when intercompared by means of electromagnetic signals, the (apparent) difference in clock rate, $\tau_1/\tau_2 = \nu_2/\nu_1 = 1 + [U(\mathbf{x}_1) - U(\mathbf{x}_2)]/c^2 + O(1/c^4)$, independently of their nature and constitution. This universal gravitational redshift of clock rates has been verified at the 10^{-4} level by comparing a hydrogen-maser clock flying on a rocket up to an altitude $\sim 10,000$ km to a similar clock on the ground [20]. For more details and references on experimental gravity see, *e.g.*, Refs. 21 and 22.

18.2. Tests of the dynamics of the gravitational field in the weak field regime

The effect on matter of one-graviton exchange, *i.e.*, the interaction Lagrangian obtained when solving Einstein’s field equations Eq. (18.6) written in, say, the harmonic gauge at first order in $h_{\mu\nu}$,

$$\square h_{\mu\nu} = -\frac{16\pi G_N}{c^4} \left(T_{\mu\nu} - \frac{1}{2} T \eta_{\mu\nu} \right) + O(h^2) + O(hT), \quad (18.10)$$

reads $-(8\pi G_N/c^4) T^{\mu\nu} \square^{-1} (T_{\mu\nu} - \frac{1}{2} T \eta_{\mu\nu})$. For a system of N moving

point masses, with free Lagrangian $L^{(1)} = \sum_{A=1}^N -m_A c^2 \sqrt{1 - v_A^2/c^2}$,

this interaction, expanded to order v^2/c^2 , reads (with $r_{AB} \equiv |\mathbf{x}_A - \mathbf{x}_B|$, $\mathbf{n}_{AB} \equiv (\mathbf{x}_A - \mathbf{x}_B)/r_{AB}$)

$$L^{(2)} = \frac{1}{2} \sum_{A \neq B} \frac{G_N m_A m_B}{r_{AB}} \left[1 + \frac{3}{2c^2} (v_A^2 + v_B^2) - \frac{7}{2c^2} (\mathbf{v}_A \cdot \mathbf{v}_B) - \frac{1}{2c^2} (\mathbf{n}_{AB} \cdot \mathbf{v}_A) (\mathbf{n}_{AB} \cdot \mathbf{v}_B) + O\left(\frac{1}{c^4}\right) \right]. \quad (18.11)$$

The two-body interactions (Eq. (18.11)) exhibit v^2/c^2 corrections to Newton’s $1/r$ potential induced by spin-2 exchange (“gravitomagnetism”). Consistency at the “post-Newtonian” level $v^2/c^2 \sim G_N m/r c^2$ requires that one also considers the three-body interactions induced by some of the three-graviton vertices and other nonlinearities (terms $O(h^2)$ and $O(hT)$ in Eq. (18.10)),

$$L^{(3)} = -\frac{1}{2} \sum_{B \neq A \neq C} \frac{G_N^2 m_A m_B m_C}{r_{AB} r_{AC} c^2} + O\left(\frac{1}{c^4}\right). \quad (18.12)$$

All currently performed gravitational experiments in the solar system, including perihelion advances of planetary orbits, the bending and delay of electromagnetic signals passing near the Sun, and very accurate ranging data to the Moon obtained by laser echoes, are compatible with the post-Newtonian results Eqs. (18.10)–(18.12). The “gravito-magnetic” interactions contained in Eq. (18.11) are involved in many of these experimental tests. They have been particularly tested in some lunar [23] and satellite experiments [24,25].

Similar to what is done in discussions of precision electroweak experiments, it is useful to quantify the significance of precision gravitational experiments by parameterizing plausible deviations from General Relativity. The addition of a mass-term in Einstein’s field equations leads to a score of theoretical difficulties [26] which have not yet received any consensual solution. We shall, therefore, not consider here the ill-defined “mass of the graviton” as a possible deviation parameter from General Relativity (see, however, the phenomenological limits quoted in the Section “Gauge and Higgs Bosons” of this *Review*). Deviations from Einstein’s pure spin-2 theory are then defined by adding new, bosonic light or massless, macroscopically coupled fields. The possibility of new gravitational-strength couplings leading (on small, and possibly large, scales) to deviations from Einsteinian (and Newtonian) gravity is suggested by String Theory [27], and by Brane World ideas [28]. For compilations of experimental constraints on Yukawa-type additional interactions, see Refs. [19,29] and the Section “Extra Dimensions” in this *Review*. Recent experiments have set limits on non-Newtonian forces below 0.056 mm [30].

Here, we shall focus on the parametrization of long-range deviations from relativistic gravity obtained by adding a strictly massless (*i.e.* without self-interaction $V(\varphi) = 0$) scalar field φ coupled to the trace of the energy-momentum tensor $T = g_{\mu\nu} T^{\mu\nu}$ [31]. The most general such theory contains an arbitrary function $a(\varphi)$ of the scalar field, and can be defined by the Lagrangian

$$\mathcal{L}_{\text{tot}}[g_{\mu\nu}, \varphi, \psi, A_\mu, H] = \frac{c^4}{16\pi G} \sqrt{g}(R(g_{\mu\nu}) - 2g^{\mu\nu} \partial_\mu \varphi \partial_\nu \varphi) + \mathcal{L}_{\text{SM}}[\psi, A_\mu, H, \tilde{g}_{\mu\nu}], \quad (18.13)$$

where G is a “bare” Newton constant, and where the Standard Model matter is coupled not to the “Einstein” (pure spin-2) metric $g_{\mu\nu}$, but to the conformally related (“Jordan-Fierz”) metric $\tilde{g}_{\mu\nu} = \exp(2a(\varphi))g_{\mu\nu}$. The scalar field equation $\square_g \varphi = -(4\pi G/c^4) a(\varphi) T$ displays $a(\varphi) \equiv \partial a(\varphi)/\partial \varphi$ as the basic (field-dependent) coupling between φ and matter [32]. The one-parameter (ω) Jordan-Fierz-Brans-Dicke theory [31] is the special case $a(\varphi) = \alpha_0 \varphi$ leading to a field-independent coupling $a(\varphi) = \alpha_0$ (with $\alpha_0^2 = 1/(2\omega + 3)$). The addition of a self-interaction term $V(\varphi)$ in Eq. (18.13) introduces new phenomenological possibilities; notably the “chameleon mechanism” [33].

In the weak-field slow-motion limit appropriate to describing gravitational experiments in the solar system, the addition of φ modifies Einstein’s predictions only through the appearance of two “post-Einstein” dimensionless parameters: $\bar{\gamma} = -2\alpha_0^2/(1 + \alpha_0^2)$ and $\bar{\beta} = +\frac{1}{2}\beta_0\alpha_0^2/(1 + \alpha_0^2)^2$, where $\alpha_0 \equiv \alpha(\varphi_0)$, $\beta_0 \equiv \partial \alpha(\varphi_0)/\partial \varphi_0$, φ_0 denoting the vacuum expectation value of φ . These parameters show up also naturally (in the form $\gamma_{\text{PPN}} = 1 + \bar{\gamma}$, $\beta_{\text{PPN}} = 1 + \bar{\beta}$) in phenomenological discussions of possible deviations from General Relativity [21,34]. The parameter $\bar{\gamma}$ measures the admixture of spin 0 to Einstein’s graviton, and contributes an extra term $+\bar{\gamma}(\mathbf{v}_A - \mathbf{v}_B)^2/c^2$ in the square brackets of the two-body Lagrangian Eq. (18.11). The parameter $\bar{\beta}$ modifies the three-body interaction Eq. (18.12) by an overall multiplicative factor $1 + 2\bar{\beta}$. Moreover, the combination $\eta \equiv 4\bar{\beta} - \bar{\gamma}$ parameterizes the lowest order effect of the self-gravity of orbiting masses by modifying the Newtonian interaction energy terms in Eq. (18.11) into $G_{AB} m_A m_B / r_{AB}$, with a body-dependent gravitational “constant” $G_{AB} = G_N [1 + \eta (E_A^{\text{grav}}/m_A c^2 + E_B^{\text{grav}}/m_B c^2) + O(1/c^4)]$, where $G_N = G \exp[2a(\varphi_0)](1 + \alpha_0^2)$ and where E_A^{grav} denotes the gravitational binding energy of body A .

The best current limits on the post-Einstein parameters $\bar{\gamma}$ and $\bar{\beta}$ are (at the 68% confidence level):

$$\bar{\gamma} = (2.1 \pm 2.3) \times 10^{-5}, \quad (18.14)$$

deduced from the additional Doppler shift experienced by radio-wave beams connecting the Earth to the Cassini spacecraft when they passed near the Sun [35], and

$$4\bar{\beta} - \bar{\gamma} = (4.4 \pm 4.5) \times 10^{-4}, \quad (18.15)$$

from Lunar Laser Ranging measurements [17] of a possible polarization of the Moon toward the Sun [18]. More stringent limits on $\bar{\gamma}$ are obtained in models (*e.g.*, string-inspired ones [27]) where scalar couplings violate the Equivalence Principle.

18.3. Tests of the dynamics of the gravitational field in the radiative and/or strong field regimes

The discovery of pulsars (*i.e.*, rotating neutron stars emitting a beam of radio noise) in gravitationally bound orbits [36,37] has opened up an entirely new testing ground for relativistic gravity, giving us an experimental handle on the regime of radiative and/or strong gravitational fields. In these systems, the finite velocity of propagation of the gravitational interaction between the pulsar and its companion generates damping-like terms at order $(v/c)^5$ in the equations of motion [38]. These damping forces are the local counterparts of the gravitational radiation emitted at infinity by the system (“gravitational radiation reaction”). They cause the binary orbit to shrink and its orbital period P_b to decrease. The remarkable stability of pulsar clocks has allowed one to measure the corresponding very small orbital period decay $\dot{P}_b \equiv dP_b/dt \sim -(v/c)^5 \sim -10^{-12}$ in several binary systems, thereby giving us a direct experimental confirmation of the propagation properties of the gravitational field, and, in particular, an experimental confirmation that the speed of propagation of gravity is equal to the velocity of light to better than a part in a thousand. In addition, the surface gravitational potential of a neutron star $h_{00}(R) \simeq 2Gm/c^2 R \simeq 0.4$ being a factor $\sim 10^8$ higher than the surface potential of the Earth, and a mere factor 2.5 below the black hole limit ($h_{00} = 1$), pulsar data have allowed one to obtain several accurate tests of the strong-gravitational-field regime, as we discuss next.

Binary pulsar timing data record the times of arrival of successive electromagnetic pulses emitted by a pulsar orbiting around the center of mass of a binary system. After correcting for the Earth motion around the Sun and for the dispersion due to propagation in the interstellar plasma, the time of arrival of the N th pulse t_N can be described by a generic, parameterized “timing formula” [39] whose functional form is common to the whole class of tensor-scalar gravitation theories:

$$t_N - t_0 = F[T_N(\nu_p, \dot{\nu}_p, \ddot{\nu}_p); \{p^K\}; \{p^{PK}\}]. \quad (18.16)$$

Here, T_N is the pulsar proper time corresponding to the N th turn given by $N/2\pi = \nu_p T_N + \frac{1}{2}\dot{\nu}_p T_N^2 + \frac{1}{6}\ddot{\nu}_p T_N^3$ (with $\nu_p \equiv 1/P_p$ the spin frequency of the pulsar, *etc.*), $\{p^K\} = \{P_b, T_0, e, \omega_0, x\}$ is the set of “Keplerian” parameters (notably, orbital period P_b , eccentricity e , periastron longitude ω_0 and projected semi-major axis $x = a \sin i/c$), and $\{p^{PK}\} = \{k, \gamma_{\text{timing}}, \dot{P}_b, r, s, \delta_\theta, \dot{e}, \dot{x}\}$ denotes the set of (separately measurable) “post-Keplerian” parameters. Most important among these are: the fractional periastron advance per orbit $k \equiv \dot{\omega} P_b / 2\pi$, a dimensionful time-dilation parameter γ_{timing} , the orbital period derivative \dot{P}_b , and the “range” and “shape” parameters of the gravitational time delay caused by the companion, r and s .

Without assuming any specific theory of gravity, one can phenomenologically analyze the data from any binary pulsar by least-squares fitting the observed sequence of pulse arrival times to the timing formula Eq. (18.16). This fit yields the “measured” values of the parameters $\{\nu_p, \dot{\nu}_p, \ddot{\nu}_p\}$, $\{p^K\}$, $\{p^{PK}\}$. Now, each specific relativistic theory of gravity predicts that, for instance, k , γ_{timing} , \dot{P}_b , r and s (to quote parameters that have been successfully measured from some binary pulsar data) are some theory-dependent functions of the Keplerian parameters and of the (unknown) masses m_1 , m_2 of the pulsar and its companion. For instance, in General Relativity, one finds (with $M \equiv m_1 + m_2$, $n \equiv 2\pi/P_b$)

$$\begin{aligned} k^{\text{GR}}(m_1, m_2) &= 3(1 - e^2)^{-1} (G_N M n / c^3)^{2/3}, \\ \gamma_{\text{timing}}^{\text{GR}}(m_1, m_2) &= e n^{-1} (G_N M n / c^3)^{2/3} m_2 (m_1 + 2m_2) / M^2, \\ \dot{P}_b^{\text{GR}}(m_1, m_2) &= - (192\pi/5) (1 - e^2)^{-7/2} \left(1 + \frac{73}{24} e^2 + \frac{37}{96} e^4 \right) \\ &\quad \times (G_N M n / c^3)^{5/3} m_1 m_2 / M^2, \\ r(m_1, m_2) &= G_N m_2 / c^3, \\ s(m_1, m_2) &= n x (G_N M n / c^3)^{-1/3} M / m_2. \end{aligned} \quad (18.17)$$

In tensor-scalar theories, each of the functions $k^{\text{theory}}(m_1, m_2)$, $\gamma_{\text{timing}}^{\text{theory}}(m_1, m_2)$, $\dot{P}_b^{\text{theory}}(m_1, m_2)$, *etc.*, is modified by quasi-static strong field effects (associated with the self-gravities of the pulsar and its companion), while the particular function $\dot{P}_b^{\text{theory}}(m_1, m_2)$ is further modified by radiative effects (associated with the spin 0 propagator) [32,40,41].

Let us give some highlights of the current experimental situation (see Ref. 42 for a more extensive review). In the first discovered binary pulsar PSR1913 + 16 [36,37], it has been possible to measure with accuracy *three* post-Keplerian parameters: k , γ_{timing} and \dot{P}_b . The three equations $k^{\text{measured}} = k^{\text{theory}}(m_1, m_2)$, $\gamma_{\text{timing}}^{\text{measured}} = \gamma_{\text{timing}}^{\text{theory}}(m_1, m_2)$, $\dot{P}_b^{\text{measured}} = \dot{P}_b^{\text{theory}}(m_1, m_2)$ determine, for each given theory, three curves in the two-dimensional mass plane. This yields *one* (combined radiative/strong-field) test of the specified theory, according to whether the three curves meet at one point, as they should. After subtracting a small ($\sim 10^{-14}$ level in $\dot{P}_b^{\text{obs}} = (-2.4184 \pm 0.0009) \times 10^{-12}$), but significant, Newtonian perturbing effect caused by the Galaxy [43], one finds that General Relativity passes this $(k - \gamma_{\text{timing}} - \dot{P}_b)_{1913+16}$ test with complete success at the 10^{-3} level [37,44,45]

$$\begin{aligned} \left[\frac{\dot{P}_b^{\text{obs}} - \dot{P}_b^{\text{galactic}}}{\dot{P}_b^{\text{GR}}[k^{\text{obs}}, \gamma_{\text{timing}}^{\text{obs}}]} \right]_{1913+16} &= 1.00132 \pm 0.00037(\text{obs}) \pm 0.00208(\text{galactic}) \\ &= 1.0013 \pm 0.0021. \end{aligned} \quad (18.18)$$

Here $\dot{P}_b^{\text{GR}}[k^{\text{obs}}, \gamma_{\text{timing}}^{\text{obs}}]$ is the result of inserting in $\dot{P}_b^{\text{GR}}(m_1, m_2)$ the values of the masses predicted by the two equations $k^{\text{obs}} = k^{\text{GR}}(m_1, m_2)$, $\gamma_{\text{timing}}^{\text{obs}} = \gamma_{\text{timing}}^{\text{GR}}(m_1, m_2)$. This yields experimental evidence for the reality of gravitational radiation damping forces at the $(0.13 \pm 0.21)\%$ level.

The discovery of the binary pulsar PSR1534 + 12 [46] has allowed one to measure *five* post-Keplerian parameters: k , γ_{timing} , r , s , and (with less accuracy) \dot{P}_b [47,48]. This allows one to obtain *three* (five observables minus two masses) tests of relativistic gravity. Two among these tests probe strong field gravity, without mixing of radiative effects [47]. General Relativity passes all these tests within the measurement accuracy. The most precise of the new, pure strong-field tests is the one obtained by combining the measurements of k , γ , and s . Using the most recent data [48], one finds agreement at the 1% level:

$$\left[\frac{s^{\text{obs}}}{s^{\text{GR}}[k^{\text{obs}}, \gamma_{\text{timing}}^{\text{obs}}]} \right]_{1534+12} = 1.000 \pm 0.007. \quad (18.19)$$

The discovery of the binary pulsar PSR J1141 – 6545 [49] (whose companion is probably a white dwarf) has allowed one to measure *four* observable parameters: k , γ_{timing} , \dot{P}_b [50,51], and the parameter s [52,51]. The latter parameter (which is equal to the sine of the inclination angle, $s = \sin i$) was consistently measured in two ways: from a scintillation analysis [52], and from timing measurements [51]. General Relativity passes all the corresponding tests within measurement accuracy. See Fig. 18.1 which uses the (more precise) scintillation measurement of $s = \sin i$.

The discovery of the remarkable *double* binary pulsar PSR J0737 – 3039 A and B [53,54] has led to the measurement of *seven* independent parameters [55,56]: five of them are the post-Keplerian parameters k , γ_{timing} , r , s and \dot{P}_b entering the relativistic timing formula of the fast-spinning pulsar PSR J0737 – 3039 A, a sixth is the ratio $R = x_B/x_A$ between the projected semi-major axis of the more slowly spinning companion pulsar PSR J0737 – 3039 B, and that of PSR J0737 – 3039 A. [The theoretical prediction for the ratio $R = x_B/x_A$, considered as a function of the (inertial) masses $m_1 = m_A$ and $m_2 = m_B$, is $R^{\text{theory}} = m_1/m_2 + O((v/c)^4)$ [39], independently of the gravitational theory considered.] Finally, the seventh parameter $\Omega_{\text{SO,B}}$ is the angular rate of (spin-orbit) precession of PSR J0737 – 3039 B around the total angular momentum [56]. These seven measurements give us *five* tests of relativistic gravity [55,57]. General Relativity passes all those tests with flying colors (see Fig. 18.1). Let us highlight here two of them.

One test is a new, precise confirmation of the reality of gravitational radiation

$$\left[\frac{\dot{P}_b^{\text{obs}}}{\dot{P}_b^{\text{GR}}[k^{\text{obs}}, R^{\text{obs}}]} \right]_{0737-3039} = 1.003 \pm 0.014. \quad (18.20)$$

Another one is an accurate (5×10^{-4} level) new strong-field confirmation of General Relativity:

$$\left[\frac{s^{\text{obs}}}{s^{\text{GR}}[k^{\text{obs}}, R^{\text{obs}}]} \right]_{0737-3039} = 0.99987 \pm 0.00050. \quad (18.21)$$

Fig. 18.1 illustrates all the tests of strong-field and radiative gravity derived from the above-mentioned binary pulsars: (3 – 2 =) one test from PSR1913 + 16, (5 – 2 =) 3 tests from PSR1534 + 12, (4 – 2 =) 2 tests from PSR J1141 – 6545, and (7 – 2 =) 5 tests from PSR J0737 – 3039. In addition, data from several nearly circular binary systems (made of a neutron star and a white dwarf) have led to strong-field confirmations (at the 5.6×10^{-3} level) of the ‘strong equivalence principle,’ *i.e.*, the fact that neutron stars and white dwarfs fall with the same acceleration in the gravitational field of the Galaxy [58,59].

The constraints on tensor-scalar theories provided by the various binary-pulsar “experiments” have been analyzed in [41,60] and

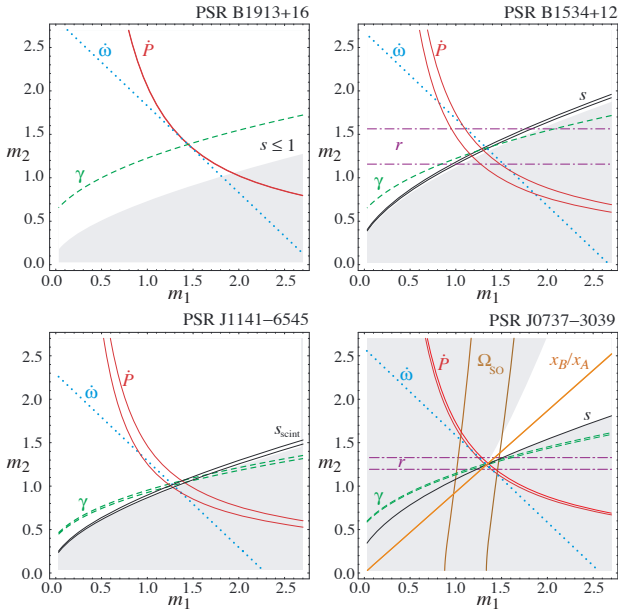


Figure 18.1: Illustration of the *eleven* tests of relativistic gravity obtained in the four different binary pulsar systems: PSR1913 + 16 (one test), PSR1534 + 12 (3 tests), PSR J1141 – 6545 (2 tests), and PSR J0737 – 3039 A,B (5 tests). Each curve (or strip) in the mass plane corresponds to the interpretation, within General Relativity, of some observable parameter among: \dot{P}_b , $k \equiv \dot{\omega}P_b/2\pi$, γ_{timing} , r , $s = \sin i$, $\Omega_{\text{SO},B}$ and R . (Figure updated from [60]; courtesy of G. Esposito-Farèse.)

shown to exclude a large portion of the parameter space allowed by solar-system tests.

Finally, measurements over several years of the pulse profiles of various pulsars have detected secular profile changes compatible with the prediction [61] that the general relativistic spin-orbit coupling should cause a secular change in the orientation of the pulsar beam with respect to the line of sight (“geodetic precession”). Such confirmations of general-relativistic spin-orbit effects were obtained in PSR 1913+16 [62], PSR B1534+12 [63], PSR J1141–6545 [64], and PSR J0737 – 3039 [56].

The tests considered above have examined the gravitational interaction on scales between a fraction of a millimeter and a few astronomical units. On the other hand, the general relativistic action on light and matter of an external gravitational field have been verified on much larger scales in many gravitational lensing systems. For quantitative tests on kiloparsec scales see Ref. 65. Some tests on cosmological scales are also available. In particular, Big Bang Nucleosynthesis (see Section 20 of this *Review*) has been used to set significant constraints on the variability of the “constants” [12,13].

18.4. Conclusions

All present experimental tests are compatible with the predictions of the current “standard” theory of gravitation: Einstein’s General Relativity. The universality of the coupling between matter and gravity (Equivalence Principle) has been verified around the 10^{-13} level. Solar system experiments have tested the weak-field predictions of Einstein’s theory at the 10^{-4} level (and down to the 2×10^{-5} level for the post-Einstein parameter $\bar{\gamma}$). The propagation properties of relativistic gravity, as well as several of its strong-field aspects, have been verified at the 10^{-3} level in binary pulsar experiments. Recent laboratory experiments have set strong constraints on sub-millimeter modifications of Newtonian gravity.

Several important new developments in experimental gravitation are expected in the near future. The improved lunar laser ranging experiment APOLLO [66] is currently accumulating data with a range accuracy of about one millimeter. The approved European Space Agency’s Atomic Clock Ensemble in Space (ACES) Mission [67] should

provide improved tests of gravitational redshift and of the ‘variability of constants’ by comparing several types of ultrastable clocks in space. The universality of free-fall acceleration should soon be tested to much better than the 10^{-13} level by some satellite experiments: the approved CNES MICROSCOPE [68] mission (10^{-15} level), and the planned (cryogenic) NASA-ESA STEP [69] mission (10^{-18} level). The recently constructed kilometer-size laser interferometers (notably LIGO [70] in the USA and VIRGO [71] and GEO600 [72] in Europe) should soon directly detect gravitational waves arriving on Earth. See [73] for some of the first scientific results. Note also that arrays of millisecond pulsars are sensitive detectors of (very low frequency) gravitational waves [74]. They constrain the contribution $\Omega_{gw}(f)$ to the critical cosmological density of a stochastic background of gravitational waves to the level $\Omega_{gw}(1/(8\text{yr})) < 2 \times 10^{-8}h^{-2}$ [75] (here, h denotes the normalized Hubble expansion rate). See finally Ref. [76] for a review of recently proposed space-based gravitational experiments.

References:

- R.P. Feynman, F.B. Morinigo, and W.G. Wagner, *Feynman Lectures on Gravitation*, ed. by B. Hatfield, (Addison-Wesley, Reading, 1995);
S. Weinberg, Phys. Rev. **138**, B988 (1965);
V.I. Ogievetsky and I.V. Polubarinov, Ann. Phys. (NY) **35**, 167 (1965);
W. Wyss, Helv. Phys. Acta **38**, 469 (1965);
S. Deser, Gen. Rel. Grav. **1**, 9 (1970);
D.G. Boulware and S. Deser, Ann. Phys. (NY) **89**, 193 (1975);
J. Fang and C. Fronsdal, J. Math. Phys. **20**, 2264 (1979);
R.M. Wald, Phys. Rev. **D33**, 3613 (1986);
C. Cutler and R.M. Wald, Class. Quantum Grav. **4**, 1267 (1987);
R.M. Wald, Class. Quantum Grav. **4**, 1279 (1987);
N. Boulanger *et al.*, Nucl. Phys. **B597**, 127 (2001).
- S. Weinberg, *Gravitation and Cosmology* (John Wiley, New York, 1972).
- S. Weinberg, Rev. Mod. Phys. **61**, 1 (1989).
- A.I. Shlyakhter, Nature **264**, 340 (1976).
- T. Damour and F. Dyson, Nucl. Phys. **B480**, 37 (1996);
C.R. Gould, E.I. Sharapov, and S.K. Lamoreaux, Phys. Rev. **C74**, 024607 (2006);
Yu.V. Petrov *et al.*, Phys. Rev. **C74**, 064610 (2006).
- V.V. Flambaum and R.B. Wiringa, Phys. Rev. **C79**, 034302 (2009).
- K.A. Olive *et al.*, Phys. Rev. **D66**, 045022 (2002);
K.A. Olive *et al.*, Phys. Rev. **D69**, 027701 (2004).
- J.K. Webb *et al.*, Phys. Rev. Lett. **87**, 091301 (2001);
M.T. Murphy, J.K. Webb, and V.V. Flambaum, Mon. Not. Roy. Astron. Soc. **384**, 1053 (2008).
- M.T. Murphy *et al.*, Science **320**, 1611 (2008).
- T. Rosenband *et al.*, Science, **319**, 1808 (2008).
- T.M. Fortier *et al.*, Phys. Rev. Lett. **98**, 070801 (2007);
S. Blatt *et al.*, Phys. Rev. Lett. **100**, 140801 (2008);
T. Dent, Phys. Rev. Lett. **101**, 041102 (2008).
- J.P. Uzan, Rev. Mod. Phys. **75**, 403 (2003).
- V. V. Flambaum, Eur. Phys. J. ST **163**, 159 (2008).
- J.D. Prestage *et al.*, Phys. Rev. Lett. **54**, 2387 (1985);
S.K. Lamoreaux *et al.*, Phys. Rev. Lett. **57**, 3125 (1986);
T.E. Chupp *et al.*, Phys. Rev. Lett. **63**, 1541 (1989).
- T. Jacobson, S. Liberati, and D. Mattingly, Ann. Phys. **321**, 150 (2006).
- S. Schlamminger *et al.*, Phys. Rev. Lett. **100**, 041101 (2008).
- J.G. Williams, S.G. Turyshev, and D.H. Boggs, Phys. Rev. Lett. **93**, 261101 (2004); Int. J. Mod. Phys. **D18**, 1129 (2009).
- K. Nordtvedt, Phys. Rev. **170**, 1186 (1968).
- E.G. Adelberger *et al.*, Prog. in Part. Nucl. Phys. **62**, 102 (2009).
- R.F.C. Vessot and M.W. Levine, Gen. Rel. Grav. **10**, 181 (1978);
R.F.C. Vessot *et al.*, Phys. Rev. Lett. **45**, 2081 (1980).
- C.M. Will, *Theory and Experiment in Gravitational Physics* (Cambridge University Press, Cambridge, 1993); and Living Rev. Rel. **9**, 3 (2006).

22. T. Damour, in *Gravitation and Quantizations*, ed. B. Julia and J. Zinn-Justin, Les Houches, Session LVII (Elsevier, Amsterdam, 1995), pp. 1–61.
23. I.I. Shapiro *et al.*, Phys. Rev. Lett. **61**, 2643 (1988).
24. I. Ciufolini and E.C. Pavlis, Nature **431**, 958 (2004).
25. <http://einstein.stanford.edu>.
26. H. van Dam and M.J. Veltman, Nucl. Phys. **B22**, 397 (1970); V.I. Zakharov, Sov. Phys. JETP Lett. **12**, 312 (1970); D.G. Boulware and S. Deser, Phys. Rev. **D6**, 3368 (1972); C. Aragone and J. Chela-Flores, Nuovo Cimento **10A**, 818 (1972); A.I. Vainshtein, Phys. Lett. **B39**, 393 (1972); C. Deffayet *et al.*, Phys. Rev. **D65**, 044026 (2002); M. Porrati, Phys. Lett. **B534**, 209 (2002); N. Arkani-Hamed, H. Georgi, and M.D. Schwartz, Nucl. Phys. **305**, 96 (2003); T. Damour, I.I. Kogan, and A. Papazoglou, Phys. Rev. **D67**, 064009 (2003); G. Dvali, A. Gruzinov, and M. Zaldarriaga, Phys. Rev. **D68**, 024012 (2003); E. Babichev, C. Deffayet, and R. Ziour, JHEP **0905**, 098 (2009).
27. T.R. Taylor and G. Veneziano, Phys. Lett. **B213**, 450 (1988); T. Damour and A.M. Polyakov, Nucl. Phys. **B423**, 532 (1994); S. Dimopoulos and G. Giudice, Phys. Lett. **B379**, 105 (1996); I. Antoniadis, S. Dimopoulos, and G. Dvali, Nucl. Phys. **B516**, 70 (1998).
28. V.A. Rubakov, Phys. Usp **44**, 871 (2001); R. Maartens, Living Rev. Rel. **7**, 7 (2004).
29. E. Fischbach and C.L. Talmadge, *The search for Non-Newtonian gravity*, (Springer-Verlag, New York, 1999).
30. D.J. Kapner *et al.*, Phys. Rev. Lett. **98**, 021101 (2007).
31. P. Jordan, *Schwerkraft und Weltall* (Vieweg, Braunschweig, 1955); M. Fierz, Helv. Phys. Acta **29**, 128 (1956); C. Brans and R.H. Dicke, Phys. Rev. **124**, 925 (1961).
32. T. Damour and G. Esposito-Farèse, Class. Quantum Grav. **9**, 2093 (1992).
33. J. Khoury and A. Weltman, Phys. Rev. Lett. **93**, 171104 (2004).
34. A.S. Eddington, *The Mathematical Theory of Relativity*, (Cambridge University Press, Cambridge, 1923); K. Nordtvedt, Phys. Rev. **169**, 1017 (1968); C.M. Will, Astrophys. J. **163**, 611 (1971).
35. B. Bertotti, L. Iess, and P. Tortora, Nature, 425,374 (2003).
36. R.A. Hulse, Rev. Mod. Phys. **66**, 699 (1994).
37. J.H. Taylor, Rev. Mod. Phys. **66**, 711 (1994).
38. T. Damour and N. Deruelle, Phys. Lett. **A87**, 81 (1981); T. Damour, C.R. Acad. Sci. Paris **294**, 1335 (1982).
39. T. Damour and N. Deruelle, Ann. Inst. H. Poincaré A, **44**, 263 (1986); T. Damour and J.H. Taylor, Phys. Rev. **D45**, 1840 (1992).
40. C.M. Will and H.W. Zaglauer, Astrophys. J. **346**, 366 (1989).
41. T. Damour and G. Esposito-Farèse, Phys. Rev. **D54**, 1474 (1996); and Phys. Rev. **D58**, 042001 (1998).
42. I.H. Stairs, Living Rev. Rel. **6** 5 (2003).
43. T. Damour and J.H. Taylor, Astrophys. J. **366**, 501 (1991).
44. J.H. Taylor, Class. Quantum Grav. **10**, S167 (Supplement 1993).
45. J. Weisberg and J.H. Taylor, in *Radio Pulsars, ASP Conference Series 328*, 25 (2005); astro-ph/0407149.
46. A. Wolszczan, Nature **350**, 688 (1991).
47. J.H. Taylor *et al.*, Nature **355**, 132 (1992).
48. I.H. Stairs *et al.*, Astrophys. J. **505**, 352 (1998); I.H. Stairs *et al.*, Astrophys. J. **581**, 501 (2002).
49. V.M. Kaspi *et al.*, Astrophys. J. **528**, 445 (2000).
50. M. Bailes *et al.*, Astrophys. J. **595**, L49 (2003).
51. N.D.R. Bhat, M. Bailes, and J.P.W. Verbiest, Phys. Rev. **D77**, 124017 (2008).
52. S.M. Ord *et al.*, Astrophys. J. **574**, L75 (2002).
53. M. Burgay *et al.*, Nature **426**, 531 (2003).
54. A.G. Lyne *et al.*, Science **303**, 1153 (2004).
55. M. Kramer *et al.*, Science **314**, 97 (2006).
56. R.P. Breton *et al.*, Science **321**, 104 (2008).
57. M. Kramer and N. Wex, Class. Quantum Grav. **26**, 073001 (2009).
58. T. Damour and G. Schäfer, Phys. Rev. Lett. **66**, 2549 (1991).
59. I.H. Stairs *et al.*, Astrophys. J. **632**, 1060 (2005).
60. G. Esposito-Farèse, in *Proceedings of the 10th Marcel Grossmann Meeting on Recent Developments in Theoretical and Experimental General Relativity*, edited by M. Novello *et al.*, (World Scientific, 2006), part A, pp 647-666.
61. T. Damour and R. Ruffini, C. R. Acad. Sc. Paris **279**, série A, 971 (1974); B.M. Barker and R.F. O'Connell, Phys. Rev. **D12**, 329 (1975).
62. M. Kramer, Astrophys. J. **509**, 856 (1998); J.M. Weisberg and J.H. Taylor, Astrophys. J. **576**, 942 (2002).
63. I.H. Stairs, S.E. Thorsett, and Z. Arzumianian, Phys. Rev. Lett. **93**, 141101 (2004).
64. A.W. Hotan, M. Bailes, and S.M. Ord, Astrophys. J. **624**, 906 (2005).
65. A.S. Bolton, S. Rappaport, and S. Burles, Phys. Rev. **D74**, 061501 (2006); T.L. Smith, [arXiv:0907.4829](http://arxiv.org/abs/0907.4829) [astro-ph.CO]; J. Schwab, A.S. Bolton and S.A. Rappaport, [arXiv:0907.4992](http://arxiv.org/abs/0907.4992) [astro-ph.CO].
66. <http://physics.ucsd.edu/~tmurphy/apollo/apollo.html>.
67. <http://www.phys.ens.fr/~salomon/horlogesfin.pdf>.
68. <http://microscope.onera.fr/>.
69. <http://einstein.stanford.edu/STEP/>.
70. <http://www.ligo.caltech.edu>.
71. <http://www.virgo.infn.it>.
72. <http://www.geo600.uni-hannover.de>.
73. <https://www.lsc-group.phys.uwm.edu/ppcomm/Papers.html>.
74. A.N. Lommen and D.C. Backer, Bulletin of the American Astronomical Society **33**, 1347 (2001); and Astrophys. J. **562**, 297 (2001).
75. F.A. Jenet *et al.*, Astrophys. J. **653**, 1571 (2006).
76. S.G. Turyshev, Usp. Fiz. Nauk **179**, 3034 (2009) [Phys. Usp. **52**, 1 (2009)].

19. BIG-BANG COSMOLOGY

Revised September 2009 by K.A. Olive (University of Minnesota) and J.A. Peacock (University of Edinburgh).

19.1. Introduction to Standard Big-Bang Model

The observed expansion of the Universe [1,2,3] is a natural (almost inevitable) result of any homogeneous and isotropic cosmological model based on general relativity. However, by itself, the Hubble expansion does not provide sufficient evidence for what we generally refer to as the Big-Bang model of cosmology. While general relativity is in principle capable of describing the cosmology of any given distribution of matter, it is extremely fortunate that our Universe appears to be homogeneous and isotropic on large scales. Together, homogeneity and isotropy allow us to extend the Copernican Principle to the Cosmological Principle, stating that all spatial positions in the Universe are essentially equivalent.

The formulation of the Big-Bang model began in the 1940s with the work of George Gamow and his collaborators, Alpher and Herman. In order to account for the possibility that the abundances of the elements had a cosmological origin, they proposed that the early Universe which was once very hot and dense (enough so as to allow for the nucleosynthetic processing of hydrogen), and has expanded and cooled to its present state [4,5]. In 1948, Alpher and Herman predicted that a direct consequence of this model is the presence of a relic background radiation with a temperature of order a few K [6,7]. Of course this radiation was observed 16 years later as the microwave background radiation [8]. Indeed, it was the observation of the 3 K background radiation that singled out the Big-Bang model as the prime candidate to describe our Universe. Subsequent work on Big-Bang nucleosynthesis further confirmed the necessity of our hot and dense past. (See the review on BBN—Sec. 20 of this *Review* for a detailed discussion of BBN.) These relativistic cosmological models face severe problems with their initial conditions, to which the best modern solution is inflationary cosmology, discussed in Sec. 19.3.5. If correct, these ideas would strictly render the term ‘Big Bang’ redundant, since it was first coined by Hoyle to represent a criticism of the lack of understanding of the initial conditions.

19.1.1. The Robertson-Walker Universe :

The observed homogeneity and isotropy enable us to describe the overall geometry and evolution of the Universe in terms of two cosmological parameters accounting for the spatial curvature and the overall expansion (or contraction) of the Universe. These two quantities appear in the most general expression for a space-time metric which has a (3D) maximally symmetric subspace of a 4D space-time, known as the Robertson-Walker metric:

$$ds^2 = dt^2 - R^2(t) \left[\frac{dr^2}{1 - kr^2} + r^2 (d\theta^2 + \sin^2 \theta d\phi^2) \right]. \quad (19.1)$$

Note that we adopt $c = 1$ throughout. By rescaling the radial coordinate, we can choose the curvature constant k to take only the discrete values $+1$, -1 , or 0 corresponding to closed, open, or spatially flat geometries. In this case, it is often more convenient to re-express the metric as

$$ds^2 = dt^2 - R^2(t) \left[d\chi^2 + S_k^2(\chi) (d\theta^2 + \sin^2 \theta d\phi^2) \right], \quad (19.2)$$

where the function $S_k(\chi)$ is $(\sin \chi, \chi, \sinh \chi)$ for $k = (+1, 0, -1)$. The coordinate r (in Eq. (19.1)) and the ‘angle’ χ (in Eq. (19.2)) are both dimensionless; the dimensions are carried by $R(t)$, which is the cosmological scale factor which determines proper distances in terms of the comoving coordinates. A common alternative is to define a dimensionless scale factor, $a(t) = R(t)/R_0$, where $R_0 \equiv R(t_0)$ is R at the present epoch. It is also sometimes convenient to define a dimensionless or conformal time coordinate, η , by $d\eta = dt/R(t)$. Along constant spatial sections, the proper time is defined by the time coordinate, t . Similarly, for $dt = d\theta = d\phi = 0$, the proper distance is given by $R(t)\chi$. For standard texts on cosmological models see *e.g.*, Refs. [9–16].

19.1.2. The redshift :

The cosmological redshift is a direct consequence of the Hubble expansion, determined by $R(t)$. A local observer detecting light from a distant emitter sees a redshift in frequency. We can define the redshift as

$$z \equiv \frac{\nu_1 - \nu_2}{\nu_2} \simeq \frac{v_{12}}{c}, \quad (19.3)$$

where ν_1 is the frequency of the emitted light, ν_2 is the observed frequency and v_{12} is the relative velocity between the emitter and the observer. While the definition, $z = (\nu_1 - \nu_2)/\nu_2$ is valid on all distance scales, relating the redshift to the relative velocity in this simple way is only true on small scales (*i.e.*, less than cosmological scales) such that the expansion velocity is non-relativistic. For light signals, we can use the metric given by Eq. (19.1) and $ds^2 = 0$ to write

$$\frac{v_{12}}{c} = \dot{R} \delta r = \frac{\dot{R}}{R} \delta t = \frac{\delta R}{R} = \frac{R_2 - R_1}{R_1}, \quad (19.4)$$

where $\delta r(\delta t)$ is the radial coordinate (temporal) separation between the emitter and observer. Thus, we obtain the simple relation between the redshift and the scale factor

$$1 + z = \frac{\nu_1}{\nu_2} = \frac{R_2}{R_1}. \quad (19.5)$$

This result does not depend on the non-relativistic approximation.

19.1.3. The Friedmann-Lemaître equations of motion :

The cosmological equations of motion are derived from Einstein’s equations

$$\mathcal{R}_{\mu\nu} - \frac{1}{2}g_{\mu\nu}\mathcal{R} = 8\pi G_N T_{\mu\nu} + \Lambda g_{\mu\nu}. \quad (19.6)$$

Gliner [17] and Zeldovich [18] have pioneered the modern view, in which the Λ term is taken to the rhs and interpreted as an effective energy–momentum tensor $T_{\mu\nu}$ for the vacuum of $\Lambda g_{\mu\nu}/8\pi G_N$. It is common to assume that the matter content of the Universe is a perfect fluid, for which

$$T_{\mu\nu} = -p g_{\mu\nu} + (p + \rho) u_\mu u_\nu, \quad (19.7)$$

where $g_{\mu\nu}$ is the space-time metric described by Eq. (19.1), p is the isotropic pressure, ρ is the energy density and $u = (1, 0, 0, 0)$ is the velocity vector for the isotropic fluid in co-moving coordinates. With the perfect fluid source, Einstein’s equations lead to the Friedmann-Lemaître equations

$$H^2 \equiv \left(\frac{\dot{R}}{R} \right)^2 = \frac{8\pi G_N \rho}{3} - \frac{k}{R^2} + \frac{\Lambda}{3}, \quad (19.8)$$

and

$$\frac{\ddot{R}}{R} = \frac{\Lambda}{3} - \frac{4\pi G_N}{3} (\rho + 3p), \quad (19.9)$$

where $H(t)$ is the Hubble parameter and Λ is the cosmological constant. The first of these is sometimes called the Friedmann equation. Energy conservation via $T^{\mu\nu}_{;\mu} = 0$, leads to a third useful equation [which can also be derived from Eq. (19.8) and Eq. (19.9)]

$$\dot{\rho} = -3H(\rho + p). \quad (19.10)$$

Eq. (19.10) can also be simply derived as a consequence of the first law of thermodynamics.

Eq. (19.8) has a simple classical mechanical analog if we neglect (for the moment) the cosmological term Λ . By interpreting $-k/R^2$ Newtonianly as a ‘total energy’, then we see that the evolution of the Universe is governed by a competition between the potential energy, $8\pi G_N \rho/3$, and the kinetic term $(\dot{R}/R)^2$. For $\Lambda = 0$, it is clear that the Universe must be expanding or contracting (except at the turning point prior to collapse in a closed Universe). The ultimate fate of the Universe is determined by the curvature constant k . For $k = +1$, the Universe will recollapse in a finite time, whereas for $k = 0, -1$, the Universe will expand indefinitely. These simple conclusions can be altered when $\Lambda \neq 0$ or more generally with some component with $(\rho + 3p) < 0$.

19.1.4. Definition of cosmological parameters :

In addition to the Hubble parameter, it is useful to define several other measurable cosmological parameters. The Friedmann equation can be used to define a critical density such that $k = 0$ when $\Lambda = 0$,

$$\begin{aligned} \rho_c &\equiv \frac{3H^2}{8\pi G_N} = 1.88 \times 10^{-26} h^2 \text{ kg m}^{-3} \\ &= 1.05 \times 10^{-5} h^2 \text{ GeV cm}^{-3}, \end{aligned} \quad (19.11)$$

where the scaled Hubble parameter, h , is defined by

$$\begin{aligned} H &\equiv 100 h \text{ km s}^{-1} \text{ Mpc}^{-1} \\ \Rightarrow H^{-1} &= 9.78 h^{-1} \text{ Gyr} \\ &= 2998 h^{-1} \text{ Mpc}. \end{aligned} \quad (19.12)$$

The cosmological density parameter Ω_{tot} is defined as the energy density relative to the critical density,

$$\Omega_{\text{tot}} = \rho/\rho_c. \quad (19.13)$$

Note that one can now rewrite the Friedmann equation as

$$k/R^2 = H^2(\Omega_{\text{tot}} - 1). \quad (19.14)$$

From Eq. (19.14), one can see that when $\Omega_{\text{tot}} > 1$, $k = +1$ and the Universe is closed, when $\Omega_{\text{tot}} < 1$, $k = -1$ and the Universe is open, and when $\Omega_{\text{tot}} = 1$, $k = 0$, and the Universe is spatially flat.

It is often necessary to distinguish different contributions to the density. It is therefore convenient to define present-day density parameters for pressureless matter (Ω_m) and relativistic particles (Ω_r), plus the quantity $\Omega_\Lambda = \Lambda/3H^2$. In more general models, we may wish to drop the assumption that the vacuum energy density is constant, and we therefore denote the present-day density parameter of the vacuum by Ω_v . The Friedmann equation then becomes

$$k/R_0^2 = H_0^2(\Omega_m + \Omega_r + \Omega_v - 1), \quad (19.15)$$

where the subscript 0 indicates present-day values. Thus, it is the sum of the densities in matter, relativistic particles, and vacuum that determines the overall sign of the curvature. Note that the quantity $-k/R_0^2 H_0^2$ is sometimes referred to as Ω_k . This usage is unfortunate: it encourages one to think of curvature as a contribution to the energy density of the Universe, which is not correct.

19.1.5. Standard Model solutions :

Much of the history of the Universe in the standard Big-Bang model can be easily described by assuming that either matter or radiation dominates the total energy density. During inflation and again today the expansion rate for the Universe is accelerating, and domination by a cosmological constant or some other form of dark energy should be considered. In the following, we shall delineate the solutions to the Friedmann equation when a single component dominates the energy density. Each component is distinguished by an equation of state parameter $w = p/\rho$.

19.1.5.1. Solutions for a general equation of state:

Let us first assume a general equation of state parameter for a single component, w which is constant. In this case, Eq. (19.10) can be written as $\dot{\rho} = -3(1+w)\rho\dot{R}/R$ and is easily integrated to yield

$$\rho \propto R^{-3(1+w)}. \quad (19.16)$$

Note that at early times when R is small, the less singular curvature term k/R^2 in the Friedmann equation can be neglected so long as $w > -1/3$. Curvature domination occurs at rather late times (if a cosmological constant term does not dominate sooner). For $w \neq -1$, one can insert this result into the Friedmann equation Eq. (19.8), and if one neglects the curvature and cosmological constant terms, it is easy to integrate the equation to obtain,

$$R(t) \propto t^{2/[3(1+w)]}. \quad (19.17)$$

19.1.5.2. A Radiation-dominated Universe:

In the early hot and dense Universe, it is appropriate to assume an equation of state corresponding to a gas of radiation (or relativistic particles) for which $w = 1/3$. In this case, Eq. (19.16) becomes $\rho \propto R^{-4}$. The ‘extra’ factor of $1/R$ is due to the cosmological redshift; not only is the number density of particles in the radiation background decreasing as R^{-3} since volume scales as R^3 , but in addition, each particle’s energy is decreasing as $E \propto \nu \propto R^{-1}$. Similarly, one can substitute $w = 1/3$ into Eq. (19.17) to obtain

$$R(t) \propto t^{1/2}; \quad H = 1/2t. \quad (19.18)$$

19.1.5.3. A Matter-dominated Universe:

At relatively late times, non-relativistic matter eventually dominates the energy density over radiation (see Sec. 19.3.8). A pressureless gas ($w = 0$) leads to the expected dependence $\rho \propto R^{-3}$ from Eq. (19.16) and, if $k = 0$, we get

$$R(t) \propto t^{2/3}; \quad H = 2/3t. \quad (19.19)$$

19.1.5.4. A Universe dominated by vacuum energy:

If there is a dominant source of vacuum energy, V_0 , it would act as a cosmological constant with $\Lambda = 8\pi G_N V_0$ and equation of state $w = -1$. In this case, the solution to the Friedmann equation is particularly simple and leads to an exponential expansion of the Universe

$$R(t) \propto e^{\sqrt{\Lambda/3}t}. \quad (19.20)$$

A key parameter is the equation of state of the vacuum, $w \equiv p/\rho$: this need not be the $w = -1$ of Λ , and may not even be constant [19,20,21]. There is now much interest in the more general possibility of a dynamically evolving vacuum energy, for which the name ‘dark energy’ has become commonly used. A variety of techniques exist whereby the vacuum density as a function of time may be measured, usually expressed as the value of w as a function of epoch [22,23]. The best current measurement for the equation of state (assumed constant) is $w = -1.006^{+0.067}_{-0.068}$ [24]. Unless stated otherwise, we will assume that the vacuum energy is a cosmological constant with $w = -1$ exactly.

The presence of vacuum energy can dramatically alter the fate of the Universe. For example, if $\Lambda < 0$, the Universe will eventually recollapse independent of the sign of k . For large values of $\Lambda > 0$ (larger than the Einstein static value needed to halt any cosmological expansion or contraction), even a closed Universe will expand forever. One way to quantify this is the deceleration parameter, q_0 , defined as

$$q_0 = - \left. \frac{R\ddot{R}}{\dot{R}^2} \right|_0 = \frac{1}{2}\Omega_m + \Omega_r + \frac{(1+3w)}{2}\Omega_v. \quad (19.21)$$

This equation shows us that $w < -1/3$ for the vacuum may lead to an accelerating expansion. To the continuing astonishment of cosmologists, such an effect has been observed; one piece of direct evidence is the Supernova Hubble diagram [26–30] (see Fig. 19.1 below); current data indicate that vacuum energy is indeed the largest contributor to the cosmological density budget, with $\Omega_v = 0.74 \pm 0.03$ and $\Omega_m = 0.26 \pm 0.03$ if $k = 0$ is assumed (5-year mean WMAP) [24].

The existence of this constituent is without doubt the greatest puzzle raised by the current cosmological model; the final section of this review discusses some of the ways in which the vacuum-energy problem is being addressed.

19.2. Introduction to Observational Cosmology

19.2.1. Fluxes, luminosities, and distances :

The key quantities for observational cosmology can be deduced quite directly from the metric.

(1) The *proper* transverse size of an object seen by us to subtend an angle $d\psi$ is its comoving size $d\psi S_k(\chi)$ times the scale factor at the time of emission:

$$d\ell = d\psi R_0 S_k(\chi)/(1+z) . \quad (19.22)$$

(2) The apparent flux density of an object is deduced by allowing its photons to flow through a sphere of current radius $R_0 S_k(\chi)$; but photon energies and arrival rates are redshifted, and the bandwidth $d\nu$ is reduced. The observed photons at frequency ν_0 were emitted at frequency $\nu_0(1+z)$, so the flux density is the luminosity at this frequency, divided by the total area, divided by $1+z$:

$$S_\nu(\nu_0) = \frac{L_\nu([1+z]\nu_0)}{4\pi R_0^2 S_k^2(\chi)(1+z)} . \quad (19.23)$$

These relations lead to the following common definitions:

$$\begin{aligned} \text{angular-diameter distance: } D_A &= (1+z)^{-1} R_0 S_k(\chi) \\ \text{luminosity distance: } D_L &= (1+z) R_0 S_k(\chi) . \end{aligned} \quad (19.24)$$

These distance-redshift relations are expressed in terms of observables by using the equation of a null radial geodesic ($R(t)d\chi = dt$) plus the Friedmann equation:

$$\begin{aligned} R_0 d\chi &= \frac{1}{H(z)} dz = \frac{1}{H_0} \left[(1 - \Omega_m - \Omega_v - \Omega_r)(1+z)^2 \right. \\ &\quad \left. + \Omega_v(1+z)^{3+3w} + \Omega_m(1+z)^3 + \Omega_r(1+z)^4 \right]^{-1/2} dz . \end{aligned} \quad (19.25)$$

The main scale for the distance here is the Hubble length, $1/H_0$.

The flux density is the product of the specific intensity I_ν and the solid angle $d\Omega$ subtended by the source: $S_\nu = I_\nu d\Omega$. Combining the angular size and flux-density relations thus gives the relativistic version of surface-brightness conservation:

$$I_\nu(\nu_0) = \frac{B_\nu([1+z]\nu_0)}{(1+z)^3} , \quad (19.26)$$

where B_ν is surface brightness (luminosity emitted into unit solid angle per unit area of source). We can integrate over ν_0 to obtain the corresponding total or bolometric formula:

$$I_{\text{tot}} = \frac{B_{\text{tot}}}{(1+z)^4} . \quad (19.27)$$

This cosmology-independent form expresses Liouville's Theorem: photon phase-space density is conserved along rays.

19.2.2. Distance data and geometrical tests of cosmology :

In order to confront these theoretical predictions with data, we have to bridge the divide between two extremes. Nearby objects may have their distances measured quite easily, but their radial velocities are dominated by deviations from the ideal Hubble flow, which typically have a magnitude of several hundred kms^{-1} . On the other hand, objects at redshifts $z \gtrsim 0.01$ will have observed recessional velocities that differ from their ideal values by $\lesssim 10\%$, but absolute distances are much harder to supply in this case. The traditional solution to this problem is the construction of the distance ladder: an interlocking set of methods for obtaining relative distances between various classes of object, which begins with absolute distances at the 10 to 100 pc level, and terminates with galaxies at significant redshifts. This is reviewed in the review on Cosmological Parameters—Sec. 21 of this *Review*.

By far the most exciting development in this area has been the use of type Ia Supernovae (SNe), which now allow measurement of relative distances with 5% precision. In combination with Cepheid data from the HST and a direct geometrical distance to the maser

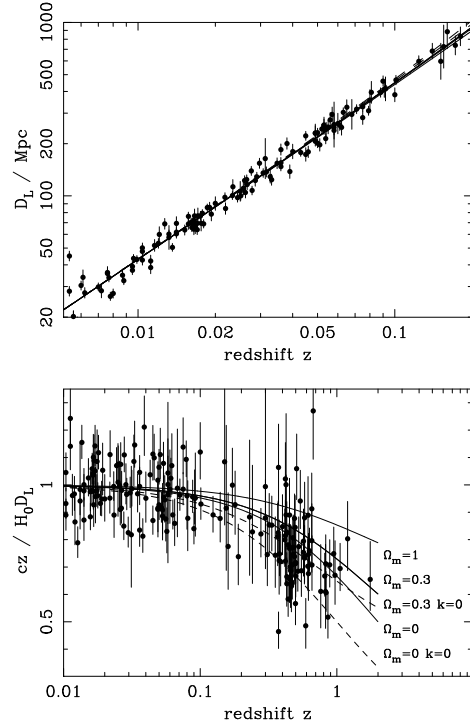


Figure 19.1: The type Ia supernova Hubble diagram [26–28]. The first panel shows that for $z \ll 1$ the large-scale Hubble flow is indeed linear and uniform; the second panel shows an expanded scale, with the linear trend divided out, and with the redshift range extended to show how the Hubble law becomes nonlinear. ($\Omega_r = 0$ is assumed.) Comparison with the prediction of Friedmann-Lemaître models appears to favor a vacuum-dominated Universe.

galaxy NGC4258, SNe results extend the distance ladder to the point where deviations from uniform expansion are negligible, leading to the best existing direct value for H_0 : $74.2 \pm 3.6 \text{ km s}^{-1} \text{ Mpc}^{-1}$ [25]. Better still, the analysis of high- z SNe has allowed the first meaningful test of cosmological geometry to be carried out: as shown in Fig. 19.1 and Fig. 19.2, a combination of supernova data and measurements of microwave-background anisotropies strongly favors a $k = 0$ model dominated by vacuum energy. (See the review on Cosmological Parameters—Sec. 21 of this *Review* for a more comprehensive review of Hubble parameter determinations.)

19.2.3. Age of the Universe :

The most striking conclusion of relativistic cosmology is that the Universe has not existed forever. The dynamical result for the age of the Universe may be written as

$$\begin{aligned} H_0 t_0 &= \int_0^\infty \frac{dz}{(1+z)H(z)} \\ &= \int_0^\infty \frac{dz}{(1+z) [(1+z)^2(1+\Omega_m z) - z(2+z)\Omega_v]^{1/2}} , \end{aligned} \quad (19.28)$$

where we have neglected Ω_r and chosen $w = -1$. Over the range of interest ($0.1 \lesssim \Omega_m \lesssim 1$, $|\Omega_v| \lesssim 1$), this exact answer may be approximated to a few % accuracy by

$$H_0 t_0 \simeq \frac{2}{3} (0.7\Omega_m + 0.3 - 0.3\Omega_v)^{-0.3} . \quad (19.29)$$

For the special case that $\Omega_m + \Omega_v = 1$, the integral in Eq. (19.28) can be expressed analytically as

$$H_0 t_0 = \frac{2}{3\sqrt{\Omega_v}} \ln \frac{1 + \sqrt{\Omega_v}}{\sqrt{1 - \Omega_v}} \quad (\Omega_m < 1) . \quad (19.30)$$

The most accurate means of obtaining ages for astronomical objects is based on the natural clocks provided by radioactive decay. The use of these clocks is complicated by a lack of knowledge of the initial conditions of the decay. In the Solar System, chemical fractionation of different elements helps pin down a precise age for the pre-Solar nebula of 4.6 Gyr, but for stars it is necessary to attempt an a priori calculation of the relative abundances of nuclei that result from supernova explosions. In this way, a lower limit for the age of stars in the local part of the Milky Way of about 11 Gyr is obtained [34,35].

The other major means of obtaining cosmological age estimates is based on the theory of stellar evolution. In principle, the main-sequence turnoff point in the color-magnitude diagram of a globular cluster should yield a reliable age. However, these have been controversial owing to theoretical uncertainties in the evolution model, as well as observational uncertainties in the distance, dust extinction, and metallicity of clusters. The present consensus favors ages for the oldest clusters of about 12 Gyr [36,37].

These methods are all consistent with the age deduced from studies of structure formation, using the microwave background and large-scale structure: $t_0 = 13.69 \pm 0.13$ Gyr [24], where the extra accuracy comes at the price of assuming the Cold Dark Matter model to be true.

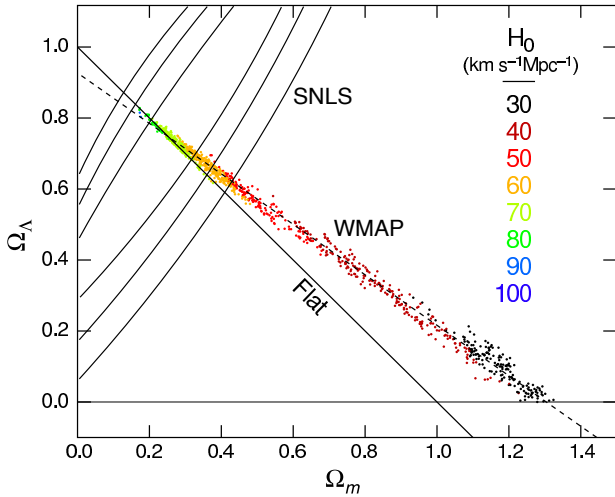


Figure 19.2: Likelihood-based probability densities on the plane Ω_Λ (i.e., Ω_v assuming $w = -1$) vs Ω_m . The colored Monte-Carlo points derive from WMAP [32] and show that the CMB alone requires a flat universe $\Omega_v + \Omega_m \simeq 1$ if the Hubble constant is not too high. The SNe Ia results [33] very nearly constrain the orthogonal combination $\Omega_v - \Omega_m$. The intersection of these constraints is the most direct (but far from the only) piece of evidence favoring a flat model with $\Omega_m \simeq 0.25$. See full-color version on color pages at end of book.

19.2.4. Horizon, isotropy, flatness problems :

For photons, the radial equation of motion is just $c dt = R d\chi$. How far can a photon get in a given time? The answer is clearly

$$\Delta\chi = \int_{t_1}^{t_2} \frac{dt}{R(t)} \equiv \Delta\eta, \quad (19.31)$$

i.e., just the interval of conformal time. We can replace dt by dR/\dot{R} , which the Friedmann equation says is $\propto dR/\sqrt{\rho R^2}$ at early times. Thus, this integral converges if $\rho R^2 \rightarrow \infty$ as $t_1 \rightarrow 0$, otherwise it diverges. Provided the equation of state is such that ρ changes faster than R^{-2} , light signals can only propagate a finite distance between the Big Bang and the present; there is then said to be a particle horizon. Such a horizon therefore exists in conventional Big-Bang models, which are dominated by radiation ($\rho \propto R^{-4}$) at early times.

At late times, the integral for the horizon is largely determined by the matter-dominated phase, for which

$$D_H = R_0 \chi_H \equiv R_0 \int_0^{t(z)} \frac{dt}{R(t)} \simeq \frac{6000}{\sqrt{\Omega_z}} h^{-1} \text{Mpc} \quad (z \gg 1). \quad (19.32)$$

The horizon at the time of formation of the microwave background ('last scattering,' $z \simeq 1100$) was thus of order 100 Mpc in size, subtending an angle of about 1° . Why then are the large number of causally disconnected regions we see on the microwave sky all at the same temperature? The Universe is very nearly isotropic and homogeneous, even though the initial conditions appear not to permit such a state to be constructed.

A related problem is that the $\Omega = 1$ Universe is unstable:

$$\Omega(a) - 1 = \frac{\Omega - 1}{1 - \Omega + \Omega_v a^2 + \Omega_m a^{-1} + \Omega_r a^{-2}}, \quad (19.33)$$

where Ω with no subscript is the total density parameter, and $a(t) = R(t)/R_0$. This requires $\Omega(t)$ to be unity to arbitrary precision as the initial time tends to zero; a universe of non-zero curvature today requires very finely tuned initial conditions.

19.3. The Hot Thermal Universe

19.3.1. Thermodynamics of the early Universe :

As alluded to above, we expect that much of the early Universe can be described by a radiation-dominated equation of state. In addition, through much of the radiation-dominated period, thermal equilibrium is established by the rapid rate of particle interactions relative to the expansion rate of the Universe (see Sec. 19.3.3 below). In equilibrium, it is straightforward to compute the thermodynamic quantities, ρ , p , and the entropy density, s . In general, the energy density for a given particle type i can be written as

$$\rho_i = \int E_i dn_{q_i}, \quad (19.34)$$

with the density of states given by

$$dn_{q_i} = \frac{g_i}{2\pi^2} (\exp[(E_{q_i} - \mu_i)/T_i] \pm 1)^{-1} q_i^2 dq_i, \quad (19.35)$$

where g_i counts the number of degrees of freedom for particle type i , $E_{q_i}^2 = m_i^2 + q_i^2$, μ_i is the chemical potential, and the \pm corresponds to either Fermi or Bose statistics. Similarly, we can define the pressure of a perfect gas as

$$p_i = \frac{1}{3} \int \frac{q_i^2}{E_i} dn_{q_i}. \quad (19.36)$$

The number density of species i is simply

$$n_i = \int dn_{q_i}, \quad (19.37)$$

and the entropy density is

$$s_i = \frac{\rho_i + p_i - \mu_i n_i}{T_i}. \quad (19.38)$$

In the Standard Model, a chemical potential is often associated with baryon number, and since the net baryon density relative to the photon density is known to be very small (of order 10^{-10}), we can neglect any such chemical potential when computing total thermodynamic quantities.

For photons, we can compute all of the thermodynamic quantities rather easily. Taking $g_i = 2$ for the 2 photon polarization states, we have (in units where $\hbar = k_B = 1$)

$$\rho_\gamma = \frac{\pi^2}{15} T^4; \quad p_\gamma = \frac{1}{3} \rho_\gamma; \quad s_\gamma = \frac{4\rho_\gamma}{3T}; \quad n_\gamma = \frac{2\zeta(3)}{\pi^2} T^3, \quad (19.39)$$

with $2\zeta(3)/\pi^2 \simeq 0.2436$. Note that Eq. (19.10) can be converted into an equation for entropy conservation. Recognizing that $\dot{p} = s\dot{T}$, Eq. (19.10) becomes

$$d(sR^3)/dt = 0. \quad (19.40)$$

For radiation, this corresponds to the relationship between expansion and cooling, $T \propto R^{-1}$ in an adiabatically expanding universe. Note also that both s and n_γ scale as T^3 .

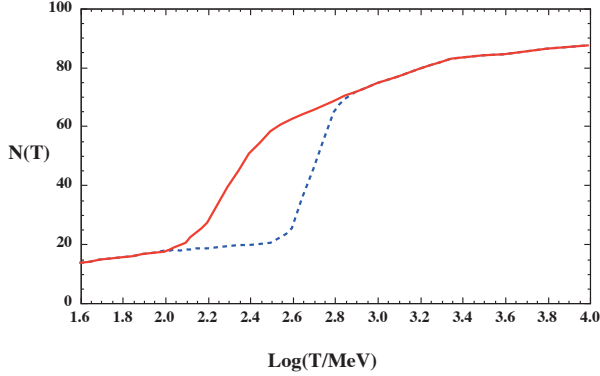


Figure 19.3: The effective numbers of relativistic degrees of freedom as a function of temperature. The sharp drop corresponds to the quark-hadron transition. The solid curve assume a QCD scale of 150 MeV, while the dashed curve assumes 450 MeV.

19.3.2. Radiation content of the Early Universe :

At the very high temperatures associated with the early Universe, massive particles are pair produced, and are part of the thermal bath. If for a given particle species i we have $T \gg m_i$, then we can neglect the mass in Eq. (19.34) to Eq. (19.38), and the thermodynamic quantities are easily computed as in Eq. (19.39). In general, we can approximate the energy density (at high temperatures) by including only those particles with $m_i \ll T$. In this case, we have

$$\rho = \left(\sum_B g_B + \frac{7}{8} \sum_F g_F \right) \frac{\pi^2}{30} T^4 \equiv \frac{\pi^2}{30} N(T) T^4, \quad (19.41)$$

where $g_{B(F)}$ is the number of degrees of freedom of each boson (fermion) and the sum runs over all boson and fermion states with $m \ll T$. The factor of 7/8 is due to the difference between the Fermi and Bose integrals. Eq. (19.41) defines the effective number of degrees of freedom, $N(T)$, by taking into account new particle degrees of freedom as the temperature is raised. This quantity is plotted in Fig. 19.3 [38].

The value of $N(T)$ at any given temperature depends on the particle physics model. In the standard $SU(3) \times SU(2) \times U(1)$ model, we can specify $N(T)$ up to temperatures of $O(100)$ GeV. The change in N (ignoring mass effects) can be seen in the table below.

Temperature	New Particles	$4N(T)$
$T < m_e$	γ 's + ν 's	29
$m_e < T < m_\mu$	e^\pm	43
$m_\mu < T < m_\pi$	μ^\pm	57
$m_\pi < T < T_c^\dagger$	π 's	69
$T_c < T < m_{\text{strange}}$	π 's + u, \bar{u}, d, \bar{d} + gluons	205
$m_s < T < m_{\text{charm}}$	s, \bar{s}	247
$m_c < T < m_\tau$	c, \bar{c}	289
$m_\tau < T < m_{\text{bottom}}$	τ^\pm	303
$m_b < T < m_{W,Z}$	b, \bar{b}	345
$m_{W,Z} < T < m_{\text{Higgs}}$	W^\pm, Z	381
$m_H < T < m_{\text{top}}$	H^0	385
$m_t < T$	t, \bar{t}	427

$^\dagger T_c$ corresponds to the confinement-deconfinement transition between quarks and hadrons.

At higher temperatures, $N(T)$ will be model-dependent. For example, in the minimal $SU(5)$ model, one needs to add 24 states to $N(T)$ for the X and Y gauge bosons, another 24 from the adjoint Higgs, and another 6 (in addition to the 4 already counted in W^\pm, Z , and H) from the $\bar{5}$ of Higgs. Hence for $T > m_X$ in minimal $SU(5)$, $N(T) = 160.75$. In a supersymmetric model this would at least double, with some changes possibly necessary in the table if the lightest supersymmetric particle has a mass below m_t .

In the radiation-dominated epoch, Eq. (19.10) can be integrated (neglecting the T -dependence of N) giving us a relationship between the age of the Universe and its temperature

$$t = \left(\frac{90}{32\pi^3 G_N N(T)} \right)^{1/2} T^{-2}. \quad (19.42)$$

Put into a more convenient form

$$t T_{\text{MeV}}^2 = 2.4 [N(T)]^{-1/2}, \quad (19.43)$$

where t is measured in seconds and T_{MeV} in units of MeV.

19.3.3. Neutrinos and equilibrium : Due to the expansion of the Universe, certain rates may be too slow to either establish or maintain equilibrium. Quantitatively, for each particle i , as a minimal condition for equilibrium, we will require that some rate Γ_i involving that type be larger than the expansion rate of the Universe or

$$\Gamma_i > H. \quad (19.44)$$

Recalling that the age of the Universe is determined by H^{-1} , this condition is equivalent to requiring that on average, at least one interaction has occurred over the lifetime of the Universe.

A good example for a process which goes in and out of equilibrium is the weak interactions of neutrinos. On dimensional grounds, one can estimate the thermally averaged scattering cross section

$$\langle \sigma v \rangle \sim O(10^{-2}) T^2 / m_W^4 \quad (19.45)$$

for $T \lesssim m_W$. Recalling that the number density of leptons is $n \propto T^3$, we can compare the weak interaction rate, $\Gamma_{\text{wk}} \sim n \langle \sigma v \rangle$, with the expansion rate,

$$H = \left(\frac{8\pi G_N \rho}{3} \right)^{1/2} = \left(\frac{8\pi^3}{90} N(T) \right)^{1/2} T^2 / M_{\text{P}} \sim 1.66 N(T)^{1/2} T^2 / M_{\text{P}}, \quad (19.46)$$

where the Planck mass $M_{\text{P}} = G_N^{-1/2} = 1.22 \times 10^{19}$ GeV.

Neutrinos will be in equilibrium when $\Gamma_{\text{wk}} > H$ or

$$T > (500 m_W^4 / M_{\text{P}})^{1/3} \sim 1 \text{ MeV}. \quad (19.47)$$

However, this condition assumes $T \ll m_W$; for higher temperatures, we should write $\langle \sigma v \rangle \sim O(10^{-2}) / T^2$, so that $\Gamma \sim 10^{-2} T$. Thus, in the very early stages of expansion, at temperatures $T \gtrsim 10^{-2} M_{\text{P}} / \sqrt{N}$, equilibrium will not have been established.

Having attained a quasi-equilibrium stage, the Universe then cools further to the point where the interaction and expansion timescales match once again. The temperature at which these rates are equal is commonly referred to as the neutrino decoupling or freeze-out temperature and is defined by $\Gamma_{\text{wk}}(T_d) = H(T_d)$. For $T < T_d$, neutrinos drop out of equilibrium. The Universe becomes transparent to neutrinos and their momenta simply redshift with the cosmic expansion. The effective neutrino temperature will simply fall with $T \sim 1/R$.

Soon after decoupling, e^\pm pairs in the thermal background begin to annihilate (when $T \lesssim m_e$). Because the neutrinos are decoupled, the energy released due to annihilation heats up the photon background relative to the neutrinos. The change in the photon temperature can be easily computed from entropy conservation. The neutrino entropy must be conserved separately from the entropy of interacting particles. A straightforward computation yields

$$T_\nu = (4/11)^{1/3} T_\gamma \simeq 1.9 \text{ K}. \quad (19.48)$$

Today, the total entropy density is therefore given by

$$s = \frac{4}{3} \frac{\pi^2}{30} \left(2 + \frac{21}{4} (T_\nu / T_\gamma)^3 \right) T_\gamma^3 = \frac{4}{3} \frac{\pi^2}{30} \left(2 + \frac{21}{11} \right) T_\gamma^3 = 7.04 n_\gamma. \quad (19.49)$$

Similarly, the total relativistic energy density today is given by

$$\rho_r = \frac{\pi^2}{30} \left[2 + \frac{21}{4} (T_\nu/T_\gamma)^4 \right] T_\gamma^4 \simeq 1.68 \rho_\gamma. \quad (19.50)$$

In practice, a small correction is needed to this, since neutrinos are not totally decoupled at e^\pm annihilation: the effective number of massless neutrino species is 3.04, rather than 3 [39].

This expression ignores neutrino rest masses, but current oscillation data require at least one neutrino eigenstate to have a mass exceeding 0.05 eV. In this minimal case, $\Omega_\nu h^2 = 5 \times 10^{-4}$, so the neutrino contribution to the matter budget would be negligibly small (which is our normal assumption). However, a nearly degenerate pattern of mass eigenstates could allow larger densities, since oscillation experiments only measure differences in m^2 values. Note that a 0.05-eV neutrino has $kT_\nu = m_\nu$ at $z \simeq 297$, so the above expression for the total present relativistic density is really only an extrapolation. However, neutrinos are almost certainly relativistic at all epochs where the radiation content of the Universe is dynamically significant.

19.3.4. Field Theory and Phase transitions :

It is very likely that the Universe has undergone one or more phase transitions during the course of its evolution [40–43]. Our current vacuum state is described by $SU(3)_c \times U(1)_{em}$, which in the Standard Model is a remnant of an unbroken $SU(3)_c \times SU(2)_L \times U(1)_Y$ gauge symmetry. Symmetry breaking occurs when a non-singlet gauge field (the Higgs field in the Standard Model) picks up a non-vanishing vacuum expectation value, determined by a scalar potential. For example, a simple (non-gauged) potential describing symmetry breaking is $V(\phi) = \frac{1}{4} \lambda \phi^4 - \frac{1}{2} \mu^2 \phi^2 + V(0)$. The resulting expectation value is simply $\langle \phi \rangle = \mu/\sqrt{\lambda}$.

In the early Universe, finite temperature radiative corrections typically add terms to the potential of the form $\phi^2 T^2$. Thus, at very high temperatures, the symmetry is restored and $\langle \phi \rangle = 0$. As the Universe cools, depending on the details of the potential, symmetry breaking will occur via a first order phase transition in which the field tunnels through a potential barrier, or via a second order transition in which the field evolves smoothly from one state to another (as would be the case for the above example potential).

The evolution of scalar fields can have a profound impact on the early Universe. The equation of motion for a scalar field ϕ can be derived from the energy-momentum tensor

$$T_{\mu\nu} = \partial_\mu \phi \partial_\nu \phi - \frac{1}{2} g_{\mu\nu} \partial_\rho \phi \partial^\rho \phi - g_{\mu\nu} V(\phi). \quad (19.51)$$

By associating $\rho = T_{00}$ and $p = R^{-2}(t)T_{ii}$ we have

$$\begin{aligned} \rho &= \frac{1}{2} \dot{\phi}^2 + \frac{1}{2} R^{-2}(t) (\nabla \phi)^2 + V(\phi) \\ p &= \frac{1}{2} \dot{\phi}^2 - \frac{1}{6} R^{-2}(t) (\nabla \phi)^2 - V(\phi), \end{aligned} \quad (19.52)$$

and from Eq. (19.10) we can write the equation of motion (by considering a homogeneous region, we can ignore the gradient terms)

$$\ddot{\phi} + 3H\dot{\phi} = -\partial V/\partial \phi. \quad (19.53)$$

19.3.5. Inflation :

In Sec. 19.2.4, we discussed some of the problems associated with the standard Big-Bang model. However, during a phase transition, our assumptions of an adiabatically expanding universe are generally not valid. If, for example, a phase transition occurred in the early Universe such that the field evolved slowly from the symmetric state to the global minimum, the Universe may have been dominated by the vacuum energy density associated with the potential near $\phi \simeq 0$. During this period of slow evolution, the energy density due to radiation will fall below the vacuum energy density, $\rho \ll V(0)$. When this happens, the expansion rate will be dominated by the constant $V(0)$, and we obtain the exponentially expanding solution given in Eq. (19.20). When the field evolves towards the global minimum it will

begin to oscillate about the minimum, energy will be released during its decay, and a hot thermal universe will be restored. If released fast enough, it will produce radiation at a temperature $NT_R^4 \lesssim V(0)$. In this reheating process, entropy has been created and the final value of RT is greater than the initial value of RT . Thus, we see that, during a phase transition, the relation $RT \sim \text{constant}$ need not hold true. This is the basis of the inflationary Universe scenario [44–46].

If, during the phase transition, the value of RT changed by a factor of $O(10^{29})$, the cosmological problems discussed above would be solved. The observed isotropy would be generated by the immense expansion; one small causal region could get blown up, and hence, our entire visible Universe would have been in thermal contact some time in the past. In addition, the density parameter Ω would have been driven to 1 (with exponential precision). Density perturbations will be stretched by the expansion, $\lambda \sim R(t)$. Thus it will appear that $\lambda \gg H^{-1}$ or that the perturbations have left the horizon, where in fact the size of the causally connected region is now no longer simply H^{-1} . However, not only does inflation offer an explanation for large scale perturbations, it also offers a source for the perturbations themselves through quantum fluctuations.

Early models of inflation were based on a first order phase transition of a Grand Unified Theory [47]. Although these models led to sufficient exponential expansion, completion of the transition through bubble percolation did not occur. Later models of inflation [48,49], also based on Grand Unified symmetry breaking, through second order transitions were also doomed. While they successfully inflated and reheated, and in fact produced density perturbations due to quantum fluctuations during the evolution of the scalar field, they predicted density perturbations many orders of magnitude too large. Most models today are based on an unknown symmetry breaking involving a new scalar field, the inflaton, ϕ .

19.3.6. Baryogenesis :

The Universe appears to be populated exclusively with matter rather than antimatter. Indeed antimatter is only detected in accelerators or in cosmic rays. However, the presence of antimatter in the latter is understood to be the result of collisions of primary particles in the interstellar medium. There is in fact strong evidence against primary forms of antimatter in the Universe. Furthermore, the density of baryons compared to the density of photons is extremely small, $\eta \sim 10^{-10}$.

The production of a net baryon asymmetry requires baryon number violating interactions, C and CP violation and a departure from thermal equilibrium [50]. The first two of these ingredients are expected to be contained in grand unified theories as well as in the non-perturbative sector of the Standard Model, the third can be realized in an expanding universe where as we have seen interactions come in and out of equilibrium.

There are several interesting and viable mechanisms for the production of the baryon asymmetry. While, we can not review any of them here in any detail, we mention some of the important scenarios. In all cases, all three ingredients listed above are incorporated. One of the first mechanisms was based on the out of equilibrium decay of a massive particle such as a superheavy GUT gauge of Higgs boson [51,52]. A novel mechanism involving the decay of flat directions in supersymmetric models is known as the Affleck-Dine scenario [53]. Recently, much attention has been focused on the possibility of generating the baryon asymmetry at the electro-weak scale using the non-perturbative interactions of sphalerons [54]. Because these interactions conserve the sum of baryon and lepton number, $B + L$, it is possible to first generate a lepton asymmetry (*e.g.*, by the out-of-equilibrium decay of a superheavy right-handed neutrino), which is converted to a baryon asymmetry at the electro-weak scale [55]. This mechanism is known as leptobaryogenesis.

19.3.7. Nucleosynthesis :

An essential element of the standard cosmological model is Big-Bang nucleosynthesis (BBN), the theory which predicts the abundances of the light element isotopes D, ^3He , ^4He , and ^7Li . Nucleosynthesis takes place at a temperature scale of order 1 MeV. The nuclear processes lead primarily to ^4He , with a primordial mass fraction of about 25%. Lesser amounts of the other light elements are produced: about 10^{-5} of D and ^3He and about 10^{-10} of ^7Li by number relative to H. The abundances of the light elements depend almost solely on one key parameter, the baryon-to-photon ratio, η . The nucleosynthesis predictions can be compared with observational determinations of the abundances of the light elements. Consistency between theory and observations leads to a conservative range of

$$5.1 \times 10^{-10} < \eta < 6.5 \times 10^{-10}. \quad (19.54)$$

η is related to the fraction of Ω contained in baryons, Ω_b

$$\Omega_b = 3.66 \times 10^7 \eta h^{-2}, \quad (19.55)$$

or $10^{10} \eta = 274 \Omega_b h^2$. The WMAP result [24] for $\Omega_b h^2$ of 0.0227 ± 0.0006 translates into a value of $\eta = 6.23 \pm 0.17$. This result can be used to ‘predict’ the light element abundance which can in turn be compared with observation [56]. The resulting D/H abundance is in excellent agreement with that found in quasar absorption systems. It is in reasonable agreement with the helium abundance observed in extra-galactic HII regions (once systematic uncertainties are accounted for), but is in poor agreement with the Li abundance observed in the atmospheres of halo dwarf stars [57]. (See the review on BBN—Sec. 20 of this *Review* for a detailed discussion of BBN or references [58,59].)

19.3.8. The transition to a matter-dominated Universe :

In the Standard Model, the temperature (or redshift) at which the Universe undergoes a transition from a radiation dominated to a matter dominated Universe is determined by the amount of dark matter. Assuming three nearly massless neutrinos, the energy density in radiation at temperatures $T \ll 1$ MeV, is given by

$$\rho_r = \frac{\pi^2}{30} \left[2 + \frac{21}{4} \left(\frac{4}{11} \right)^{4/3} \right] T^4. \quad (19.56)$$

In the absence of non-baryonic dark matter, the matter density can be written as

$$\rho_m = m_N \eta n_\gamma, \quad (19.57)$$

where m_N is the nucleon mass. Recalling that $n_\gamma \propto T^3$ [cf. Eq. (19.39)], we can solve for the temperature or redshift at the matter-radiation equality when $\rho_r = \rho_m$,

$$T_{\text{eq}} = 0.22 m_N \eta \quad \text{or} \quad (1 + z_{\text{eq}}) = 0.22 \eta \frac{m_N}{T_0}, \quad (19.58)$$

where T_0 is the present temperature of the microwave background. For $\eta = 6.2 \times 10^{-10}$, this corresponds to a temperature $T_{\text{eq}} \simeq 0.13$ eV or $(1 + z_{\text{eq}}) \simeq 550$. A transition this late is very problematic for structure formation (see Sec. 19.4.5).

The redshift of matter domination can be pushed back significantly if non-baryonic dark matter is present. If instead of Eq. (19.57), we write

$$\rho_m = \Omega_m \rho_c \left(\frac{T}{T_0} \right)^3, \quad (19.59)$$

we find that

$$T_{\text{eq}} = 0.9 \frac{\Omega_m \rho_c}{T_0^3} \quad \text{or} \quad (1 + z_{\text{eq}}) = 2.4 \times 10^4 \Omega_m h^2. \quad (19.60)$$

19.4. The Universe at late times

19.4.1. The CMB :

One form of the infamous Olbers’ paradox says that, in Euclidean space, surface brightness is independent of distance. Every line of sight will terminate on matter that is hot enough to be ionized and so scatter photons: $T \gtrsim 10^3$ K; the sky should therefore shine as brightly as the surface of the Sun. The reason the night sky is dark is entirely due to the expansion, which cools the radiation temperature to 2.73 K. This gives a Planck function peaking at around 1 mm to produce the microwave background (CMB).

The CMB spectrum is a very accurate match to a Planck function [60]. (See the review on CBR—Sec. 23 of this *Review*.) The COBE estimate of the temperature is [61]

$$T = 2.725 \pm 0.001 \text{ K}. \quad (19.61)$$

The lack of any distortion of the Planck spectrum is a strong physical constraint. It is very difficult to account for in any expanding universe other than one that passes through a hot stage. Alternative schemes for generating the radiation, such as thermalization of starlight by dust grains, inevitably generate a superposition of temperatures. What is required in addition to thermal equilibrium is that $T \propto 1/R$, so that radiation from different parts of space appears identical.

Although it is common to speak of the CMB as originating at ‘recombination,’ a more accurate terminology is the era of ‘last scattering.’ In practice, this takes place at $z \simeq 1100$, almost independently of the main cosmological parameters, at which time the fractional ionization is very small. This occurred when the age of the Universe was a few hundred thousand years. (See the review on CBR—Sec. 23 of this *Review* for a full discussion of the CMB.)

19.4.2. Matter in the Universe :

One of the main tasks of cosmology is to measure the density of the Universe, and how this is divided between dark matter and baryons. The baryons consist partly of stars, with $0.002 \lesssim \Omega_* \lesssim 0.003$ [62] but mainly inhabit the intergalactic medium (IGM). One powerful way in which this can be studied is via the absorption of light from distant luminous objects such as quasars. Even very small amounts of neutral hydrogen can absorb rest-frame UV photons (the Gunn-Peterson effect), and should suppress the continuum by a factor $\exp(-\tau)$, where

$$\tau \simeq 10^{4.62} h^{-1} \left[\frac{n_{\text{HI}}(z)/m^{-3}}{(1+z)\sqrt{1+\Omega_m z}} \right], \quad (19.62)$$

and this expression applies while the Universe is matter dominated ($z \gtrsim 1$ in the $\Omega_m = 0.3$ $\Omega_v = 0.7$ model). It is possible that this general absorption has now been seen at $z = 6.2 - 6.4$ [63]. In any case, the dominant effect on the spectrum is a ‘forest’ of narrow absorption lines, which produce a mean $\tau = 1$ in the Ly α forest at about $z = 3$, and so we have $\Omega_{\text{HI}} \simeq 10^{-6.7} h^{-1}$. This is such a small number that clearly the IGM is very highly ionized at these redshifts.

The Ly α forest is of great importance in pinning down the abundance of deuterium. Because electrons in deuterium differ in reduced mass by about 1 part in 4000 compared to hydrogen, each absorption system in the Ly α forest is accompanied by an offset deuterium line. By careful selection of systems with an optimal HI column density, a measurement of the D/H ratio can be made. This has now been done in 7 quasars, with relatively consistent results [64]. Combining these determinations with the theory of primordial nucleosynthesis yields a baryon density of $\Omega_b h^2 = 0.019 - 0.024$ (95% confidence). (See also the review on BBN—Sec. 20 of this *Review*.)

Ionized IGM can also be detected in emission when it is densely clumped, via bremsstrahlung radiation. This generates the spectacular X-ray emission from rich clusters of galaxies. Studies of this phenomenon allow us to achieve an accounting of the total baryonic material in clusters. Within the central $\simeq 1$ Mpc, the masses in stars, X-ray emitting gas and total dark matter can be determined with reasonable accuracy (perhaps 20% rms), and this allows a minimum baryon fraction to be determined [65,66]:

$$\frac{M_{\text{baryons}}}{M_{\text{total}}} \gtrsim 0.009 + (0.066 \pm 0.003) h^{-3/2}. \quad (19.63)$$

Because clusters are the largest collapsed structures, it is reasonable to take this as applying to the Universe as a whole. This equation implies a minimum baryon fraction of perhaps 12% (for reasonable h), which is too high for $\Omega_m = 1$ if we take $\Omega_b h^2 \simeq 0.02$ from nucleosynthesis. This is therefore one of the more robust arguments in favor of $\Omega_m \simeq 0.3$. (See the review on Cosmological Parameters—Sec. 21 of this *Review*.) This argument is also consistent with the inference on Ω_m that can be made from Fig. 19.2.

This method is much more robust than the older classical technique for weighing the Universe: ‘ $L \times M/L$.’ The overall light density of the Universe is reasonably well determined from redshift surveys of galaxies, so that a good determination of mass M and luminosity L for a single object suffices to determine Ω_m if the mass-to-light ratio is universal.

19.4.3. Gravitational lensing :

A robust method for determining masses in cosmology is to use gravitational light deflection. Most systems can be treated as a geometrically thin gravitational lens, where the light bending is assumed to take place only at a single distance. Simple geometry then determines a mapping between the coordinates in the intrinsic source plane and the observed image plane:

$$\alpha(D_L \theta_I) = \frac{D_S}{D_{LS}}(\theta_I - \theta_S), \quad (19.64)$$

where the angles θ_I, θ_S and α are in general two-dimensional vectors on the sky. The distances D_{LS} etc. are given by an extension of the usual distance-redshift formula:

$$D_{LS} = \frac{R_0 S_k(\chi_S - \chi_L)}{1 + z_S}. \quad (19.65)$$

This is the angular-diameter distance for objects on the source plane as perceived by an observer on the lens.

Solutions of this equation divide into weak lensing, where the mapping between source plane and image plane is one-to-one, and strong lensing, in which multiple imaging is possible. For circularly-symmetric lenses, an on-axis source is multiply imaged into a ‘caustic’ ring, whose radius is the Einstein radius:

$$\begin{aligned} \theta_E &= \left(4GM \frac{D_{LS}}{D_L D_S} \right)^{1/2} \\ &= \left(\frac{M}{10^{11.09} M_\odot} \right)^{1/2} \left(\frac{D_L D_S / D_{LS}}{\text{Gpc}} \right)^{-1/2} \text{ arcsec}. \end{aligned} \quad (19.66)$$

The observation of ‘arcs’ (segments of near-perfect Einstein rings) in rich clusters of galaxies has thus given very accurate masses for the central parts of clusters—generally in good agreement with other indicators, such as analysis of X-ray emission from the cluster IGM [67].

Gravitational lensing has also developed into a particularly promising probe of cosmological structure on 10 to 100 Mpc scales. Weak image distortions manifest themselves as an additional ellipticity of galaxy images (‘shear’), which can be observed by averaging many images together (the corresponding flux amplification is less readily detected). The result is a ‘cosmic shear’ field of order 1% ellipticity, coherent over scales of around 30 arcmin, which is directly related to the cosmic mass field, without any astrophysical uncertainties. For this reason, weak lensing is seen as potentially the cleanest probe of matter fluctuations, next to the CMB. Already, impressive results have been obtained in measuring cosmological parameters, based on survey data from only $\sim 10 \text{ deg}^2$ [68]. The particular current strength of this technique is the ability to measure the amplitude of mass fluctuations; this can be deduced from the CMB only subject to uncertainty over the optical depth due to Thomson scattering after reionization.

19.4.4. Density Fluctuations :

The overall properties of the Universe are very close to being homogeneous; and yet telescopes reveal a wealth of detail on scales varying from single galaxies to large-scale structures of size exceeding 100 Mpc. The existence of these structures must be telling us something important about the initial conditions of the Big Bang, and about the physical processes that have operated subsequently. This motivates the study of the density perturbation field, defined as

$$\delta(\mathbf{x}) \equiv \frac{\rho(\mathbf{x}) - \langle \rho \rangle}{\langle \rho \rangle}. \quad (19.67)$$

A critical feature of the δ field is that it inhabits a universe that is isotropic and homogeneous in its large-scale properties. This suggests that the statistical properties of δ should also be statistically homogeneous—*i.e.*, it is a stationary random process.

It is often convenient to describe δ as a Fourier superposition:

$$\delta(\mathbf{x}) = \sum \delta_{\mathbf{k}} e^{-i\mathbf{k} \cdot \mathbf{x}}. \quad (19.68)$$

We avoid difficulties with an infinite universe by applying periodic boundary conditions in a cube of some large volume V . The cross-terms vanish when we compute the variance in the field, which is just a sum over modes of the power spectrum

$$\langle \delta^2 \rangle = \sum |\delta_{\mathbf{k}}|^2 \equiv \sum P(k). \quad (19.69)$$

Note that the statistical nature of the fluctuations must be isotropic, so we write $P(k)$ rather than $P(\mathbf{k})$. The $\langle \dots \rangle$ average here is a volume average. Cosmological density fields are an example of an ergodic process, in which the average over a large volume tends to the same answer as the average over a statistical ensemble.

The statistical properties of discrete objects sampled from the density field are often described in terms of N -point correlation functions, which represent the excess probability over random for finding one particle in each of N boxes in a given configuration. For the 2-point case, the correlation function is readily shown to be identical to the autocorrelation function of the δ field: $\xi(r) = \langle \delta(x)\delta(x+r) \rangle$.

The power spectrum and correlation function are Fourier conjugates, and thus are equivalent descriptions of the density field (similarly, k -space equivalents exist for the higher-order correlations). It is convenient to take the limit $V \rightarrow \infty$ and use k -space integrals, defining a dimensionless power spectrum, which measures the contribution to the fractional variance in density per unit logarithmic range of scale, as $\Delta^2(k) = d\langle \delta^2 \rangle / d \ln k = V k^3 P(k) / 2\pi^2$:

$$\xi(r) = \int \Delta^2(k) \frac{\sin kr}{kr} d \ln k; \quad \Delta^2(k) = \frac{2}{\pi} k^3 \int_0^\infty \xi(r) \frac{\sin kr}{kr} r^2 dr. \quad (19.70)$$

For many years, an adequate approximation to observational data on galaxies was $\xi = (r/r_0)^{-\gamma}$, with $\gamma \simeq 1.8$ and $r_0 \simeq 5 h^{-1} \text{ Mpc}$. Modern surveys are now able to probe into the large-scale linear regime where unaltered traces of the curved post-recombination spectrum can be detected [69,70,71].

19.4.5. Formation of cosmological structure :

The simplest model for the generation of cosmological structure is gravitational instability acting on some small initial fluctuations (for the origin of which a theory such as inflation is required). If the perturbations are adiabatic (*i.e.*, fractionally perturb number densities of photons and matter equally), the linear growth law for matter perturbations is simple:

$$\delta \propto \begin{cases} a^2(t) & (\text{radiation domination; } \Omega_r = 1) \\ a(t) & (\text{matter domination; } \Omega_m = 1). \end{cases} \quad (19.71)$$

For low density universes, the present-day amplitude is suppressed by a factor $g(\Omega)$, where

$$g(\Omega) \simeq \frac{5}{2} \Omega_m \left[\Omega_m^{4/7} - \Omega_v + (1 + \Omega_m/2)(1 + \frac{1}{70} \Omega_v) \right]^{-1} \quad (19.72)$$

is an accurate fit for models with matter plus cosmological constant. The alternative perturbation mode is isocurvature: only the equation of state changes, and the total density is initially unperturbed. These modes perturb the total entropy density, and thus induce additional large-scale CMB anisotropies [72]. Although the character of perturbations in the simplest inflationary theories are purely adiabatic, correlated adiabatic and isocurvature modes are predicted in many models; the simplest example is the curvaton, which is a scalar field that decays to yield a perturbed radiation density. If the matter content already exists at this time, the overall perturbation field will have a significant isocurvature component. Such a prediction is inconsistent with current CMB data [73], and most analyses of CMB and LSS data assume the adiabatic case to hold exactly.

Linear evolution preserves the shape of the power spectrum. However, a variety of processes mean that growth actually depends on the matter content:

- (1) Pressure opposes gravity effectively for wavelengths below the horizon length while the Universe is radiation dominated. The *comoving* horizon size at z_{eq} is therefore an important scale:

$$D_{\text{H}}(z_{\text{eq}}) = \frac{2(\sqrt{2}-1)}{(\Omega_{\text{m}} z_{\text{eq}})^{1/2} H_0} = \frac{16.0}{\Omega_{\text{m}} h^2} \text{Mpc} . \quad (19.73)$$

- (2) At early times, dark matter particles will undergo free streaming at the speed of light, and so erase all scales up to the horizon—a process that only ceases when the particles go nonrelativistic. For light massive neutrinos, this happens at z_{eq} ; all structure up to the horizon-scale power-spectrum break is in fact erased. Hot(cold) dark matter models are thus sometimes dubbed large(small)-scale damping models.
- (3) A further important scale arises where photon diffusion can erase perturbations in the matter–radiation fluid; this process is named Silk damping.

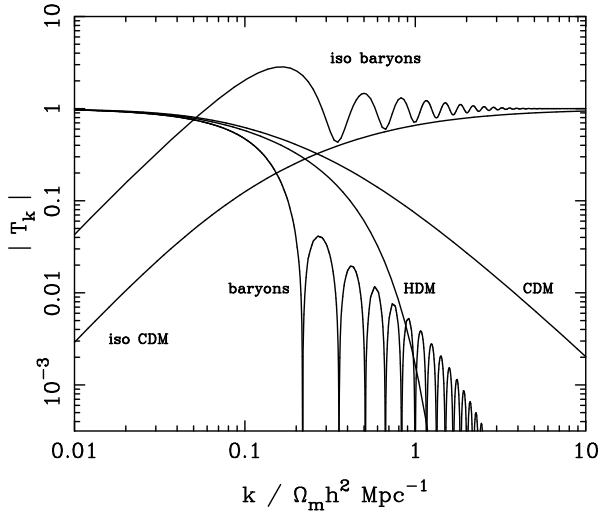


Figure 19.4: A plot of transfer functions for various models. For adiabatic models, $T_k \rightarrow 1$ at small k , whereas the opposite is true for isocurvature models. For dark-matter models, the characteristic wavenumber scales proportional to $\Omega_{\text{m}} h^2$. The scaling for baryonic models does not obey this exactly; the plotted cases correspond to $\Omega_{\text{m}} = 1$, $h = 0.5$.

The overall effect is encapsulated in the transfer function, which gives the ratio of the late-time amplitude of a mode to its initial value (see Fig. 19.4). The overall power spectrum is thus the primordial power-law, times the square of the transfer function:

$$P(k) \propto k^n T_k^2 . \quad (19.74)$$

The most generic power-law index is $n = 1$: the ‘Zeldovich’ or ‘scale-invariant’ spectrum. Inflationary models tend to predict a small ‘tilt’: $|n - 1| \lesssim 0.03$ [12,13]. On the assumption that the dark matter

is cold, the power spectrum then depends on 5 parameters: n , h , Ω_{b} , Ω_{cdm} ($\equiv \Omega_{\text{m}} - \Omega_{\text{b}}$) and an overall amplitude. The latter is often specified as σ_8 , the linear-theory fractional rms in density when a spherical filter of radius $8 h^{-1} \text{Mpc}$ is applied in linear theory. This scale can be probed directly via weak gravitational lensing, and also via its effect on the abundance of rich galaxy clusters. The favored value is approximately [32,74]

$$\sigma_8 \simeq (0.803 \pm 0.011) (\Omega_{\text{m}}/0.25)^{-0.47} . \quad (19.75)$$

A direct measure of mass inhomogeneity is valuable, since the galaxies inevitably are biased with respect to the mass. This means that the fractional fluctuations in galaxy number, $\delta n/n$, may differ from the mass fluctuations, $\delta \rho/\rho$. It is commonly assumed that the two fields obey some proportionality on large scales where the fluctuations are small, $\delta n/n = b \delta \rho/\rho$, but even this is not guaranteed [75].

The main shape of the transfer function is a break around the horizon scale at z_{eq} , which depends just on $\Omega_{\text{m}} h$ when wavenumbers are measured in observable units ($h \text{Mpc}^{-1}$). For reasonable baryon content, weak oscillations in the transfer function are also expected, and these BAOs (Baryon Acoustic Oscillations) have been clearly detected [76,77]. As well as directly measuring the baryon fraction, the scale of the oscillations directly measures the acoustic horizon at decoupling; this can be used as an additional standard ruler for cosmological tests, and the BAO method is likely to be important in future large galaxy surveys. Overall, current power-spectrum data [69,70,71] favor $\Omega_{\text{m}} h \simeq 0.20$ and a baryon fraction of about 0.15 for $n = 1$ (see Fig. 19.5).

In principle, accurate data over a wide range of k could determine both Ωh and n , but in practice there is a strong degeneracy between these. In order to constrain n itself, it is necessary to examine data on anisotropies in the CMB.

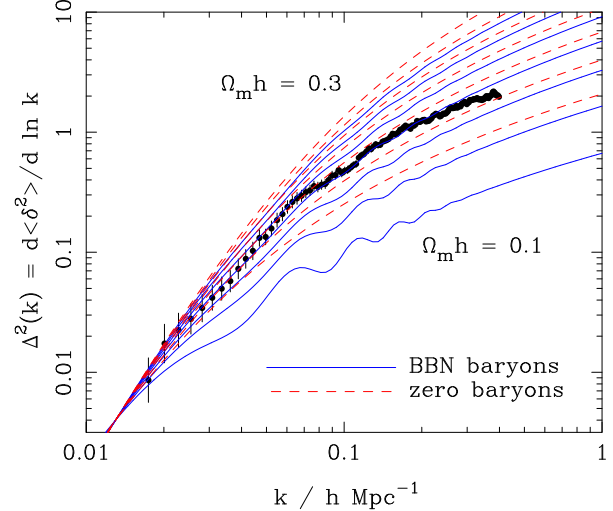


Figure 19.5: The galaxy power spectrum from the 2dFGRS [70], shown in dimensionless form, $\Delta^2(k) \propto k^3 P(k)$. The solid points with error bars show the power estimate. The window function correlates the results at different k values, and also distorts the large-scale shape of the power spectrum. An approximate correction for the latter effect has been applied. The solid and dashed lines show various CDM models, all assuming $n = 1$. For the case with non-negligible baryon content, a big-bang nucleosynthesis value of $\Omega_{\text{b}} h^2 = 0.02$ is assumed, together with $h = 0.7$. A good fit is clearly obtained for $\Omega_{\text{m}} h \simeq 0.2$.

19.4.6. CMB anisotropies :

The CMB has a clear dipole anisotropy, of magnitude 1.23×10^{-3} . This is interpreted as being due to the Earth’s motion, which is equivalent to a peculiar velocity for the Milky Way of

$$v_{\text{MW}} \simeq 600 \text{ km s}^{-1} \text{ towards } (\ell, b) \simeq (270^\circ, 30^\circ) . \quad (19.76)$$

All higher-order multipole moments of the CMB are however much smaller (of order 10^{-5}), and interpreted as signatures of density fluctuations at last scattering ($\simeq 1100$). To analyze these, the sky is expanded in spherical harmonics as explained in the review on CBR—Sec. 23 of this *Review*. The dimensionless power per $\ln k$ or ‘bandpower’ for the CMB is defined as

$$\mathcal{T}^2(\ell) = \frac{\ell(\ell+1)}{2\pi} C_\ell. \quad (19.77)$$

This function encodes information from the three distinct mechanisms that cause CMB anisotropies:

- (1) Gravitational (Sachs–Wolfe) perturbations. Photons from high-density regions at last scattering have to climb out of potential wells, and are thus redshifted.
- (2) Intrinsic (adiabatic) perturbations. In high-density regions, the coupling of matter and radiation can compress the radiation also, giving a higher temperature.
- (3) Velocity (Doppler) perturbations. The plasma has a non-zero velocity at recombination, which leads to Doppler shifts in frequency and hence shifts in brightness temperature.

Because the potential fluctuations obey Poisson’s equation, $\nabla^2\Phi = 4\pi G\rho\delta$, and the velocity field satisfies the continuity equation $\nabla \cdot \mathbf{u} = -\dot{\delta}$, the resulting different powers of k ensure that the Sachs–Wolfe effect dominates on large scales and adiabatic effects on small scales.

The relation between angle and comoving distance on the last-scattering sphere requires the comoving angular-diameter distance to the last-scattering sphere; because of its high redshift, this is effectively identical to the horizon size at the present epoch, D_H :

$$\begin{aligned} D_H &= \frac{2}{\Omega_m H_0} \quad (\Omega_v = 0) \\ D_H &\simeq \frac{2}{\Omega_m^{0.4} H_0} \quad (\text{flat} : \Omega_m + \Omega_v = 1). \end{aligned} \quad (19.78)$$

These relations show how the CMB is strongly sensitive to curvature: the horizon length at last scattering is $\propto 1/\sqrt{\Omega_m}$, so that this subtends an angle that is virtually independent of Ω_m for a flat model. Observations of a peak in the CMB power spectrum at relatively large scales ($\ell \simeq 225$) are thus strongly inconsistent with zero- Λ models with low density: current CMB + BAO +SN data require $\Omega_m + \Omega_v = 1.005 \pm 0.006$ [24]. (See *e.g.*, Fig. 19.2).

In addition to curvature, the CMB encodes information about several other key cosmological parameters. Within the compass of simple adiabatic CDM models, there are 9 of these:

$$\omega_c, \omega_b, \Omega_t, h, \tau, n_s, n_t, r, Q. \quad (19.79)$$

The symbol ω denotes the physical density, Ωh^2 : the transfer function depends only on the densities of CDM (ω_c) and baryons (ω_b). Transcribing the power spectrum at last scattering into an angular power spectrum brings in the total density parameter ($\Omega_t \equiv \Omega_m + \Omega_v = \Omega_c + \Omega_b + \Omega_v$) and h : there is an exact geometrical degeneracy [78] between these that keeps the angular-diameter distance to last scattering invariant, so that models with substantial spatial curvature and large vacuum energy cannot be ruled out without prior knowledge of the Hubble parameter. Alternatively, the CMB alone cannot measure the Hubble parameter.

The other main parameter degeneracy involves the tensor contribution to the CMB anisotropies. These are important at large scales (up to the horizon scales); for smaller scales, only scalar fluctuations (density perturbations) are important. Each of these components is characterized by a spectral index, n , and a ratio between the power spectra of tensors and scalars (r). See the review on Cosmological Parameters—Sec. 21 of this *Review* for a technical definition of the r parameter. Finally, the overall amplitude of the spectrum must be specified (Q), together with the optical depth to Compton scattering owing to recent reionization (τ). The tensor degeneracy operates as follows: the main effect of adding a large tensor contribution is to reduce the contrast between low ℓ and the peak at

$\ell \simeq 225$ (because the tensor spectrum has no acoustic component). The required height of the peak can be recovered by increasing n_s to increase the small-scale power in the scalar component; this in turn over-predicts the power at $\ell \sim 1000$, but this effect can be counteracted by raising the baryon density [79]. In order to break this degeneracy, additional data are required. For example, an excellent fit to the CMB data is obtained with a scalar-only model with zero curvature and $\omega_b = 0.0227$, $\omega_c = 0.1099$, $h = 0.719$, $n_s = 0.963$ [24]. However, this is indistinguishable from a model where tensors dominate at $\ell \lesssim 100$, if we raise ω_b to 0.03 and n_s to 1.2. This baryon density is too high for nucleosynthesis, which disfavors the high-tensor solution [80].

The reason the tensor component is introduced, and why it is so important, is that it is the only non-generic prediction of inflation. Slow-roll models of inflation involve two dimensionless parameters:

$$\epsilon \equiv \frac{M_{\text{P}}^2}{16\pi} \left(\frac{V'}{V}\right)^2 \quad \eta \equiv \frac{M_{\text{P}}^2}{8\pi} \left(\frac{V''}{V}\right), \quad (19.80)$$

where V is the inflaton potential, and dashes denote derivatives with respect to the inflation field. In terms of these, the tensor-to-scalar ratio is $r \simeq 16\epsilon$, and the spectral indices are $n_s = 1 - 6\epsilon + 2\eta$ and $n_t = -2\epsilon$. The natural expectation of inflation is that the quasi-exponential phase ends once the slow-roll parameters become significantly non-zero, so that both $n_s \neq 1$ and a significant tensor component are expected. These prediction can be avoided in some models, but it is undeniable that observation of such features would be a great triumph for inflation. Cosmology therefore stands at a fascinating point given that the most recent CMB data appear to reject the zero-tensor $n_s = 1$ model at around 2.5σ : $n_s = 0.963^{+0.014}_{-0.015}$ [24]. If we insist on $n_s = 1$, then a very substantial tensor fraction would be required ($r \simeq 0.3$), although the fit is better with $r = 0$. Assuming that no systematic error in this result can be identified, cosmology has passed a critical hurdle; the years ahead will be devoted to the task of breaking the tensor degeneracy — for which the main tool will be the polarization of the CMB [14].

19.4.7. Probing dark energy and the nature of gravity :

The most radical element of our current cosmological model is the dark energy that accelerates the expansion. The energy density of this component is approximately $(2.4 \text{ meV})^4$ (for $w = -1$, $\Omega_v = 0.75$, $h = 0.73$), or roughly $10^{-123} M_{\text{P}}^4$, and such a small number is hard to understand. Various quantum effects (most simply zero-point energy) should make contributions to the vacuum energy density: these may be truncated by new physics at high energy, but this presumably occurs at $> 1 \text{ TeV}$ scales, not meV. If the truncation is placed at the Planck scale (something of an extreme position), the natural value for the vacuum density is then over 120 orders of magnitude larger than observed. This situation is well analysed in [81], which lists extreme escape routes — especially the multiverse viewpoint, according to which low values of Λ are rare, but high values suppress the formation of structure and observers. It is certainly impressive that Weinberg used such reasoning to predict the value of Λ before any data strongly indicated a non-zero value.

But it may be that the phenomenon of dark energy is entirely illusory. The necessity for this constituent arises from using the Friedmann equation to describe the evolution of the cosmic expansion; if this equation is incorrect, it would require the replacement of Einstein’s relativistic theory of gravity with some new alternative. A frontier of current cosmological research is to distinguish these possibilities [82,83]. We also note that it has been suggested that dark energy might be an illusion even within general relativity, owing to an incorrect treatment of averaging in an inhomogeneous Universe [84,85]. Many would argue that a standard Newtonian treatment of such issues should be adequate inside the cosmological horizon, but debate on this issue continues.

Dark Energy can differ from a classical cosmological constant in being a dynamical phenomenon [31,86], *e.g.*, a rolling scalar field (sometimes dubbed ‘quintessence’). Empirically, this means that it is endowed with two thermodynamic properties that astronomers can try to measure: the bulk equation of state and the sound speed. If the sound speed is close to the speed of light, the effect of this property

is confined to very large scales, and mainly manifests itself in the large-angle multipoles of the CMB anisotropies [87]. The equation of state parameter governs the rate of change of the vacuum density: $d \ln \rho_v / d \ln a = -3(1+w)$, so it can be accessed via the evolving expansion rate, $H(a)$. This can be measured most cleanly by using the inbuilt natural ruler of large-scale structure: the Baryon Acoustic Oscillation horizon scale [88]:

$$D_{\text{BAO}} \simeq 147 (\Omega_m h^2 / 0.13)^{-0.25} (\Omega_b h^2 / 0.023)^{-0.08} \text{ Mpc}. \quad (19.81)$$

$H(a)$ is measured by radial clustering, since $dr/dz = c/H$; clustering in the plane of the sky measures the integral of this. The expansion rate is also measured by the growth of density fluctuations, where the pressure-free growth equation for the density perturbation is $\ddot{\delta} + 2H(a)\dot{\delta} = 4\pi G\rho_0 \delta$. Thus, both the scale and amplitude of density fluctuations are sensitive to $w(a)$ – but only weakly. These observables change by only typically 0.2% for a 1% change in w . Current constraints [24] are $-1.14 < w < -0.88$ (95% confidence), so a substantial improvement will require us to limit systematics in data to a few parts in 1000.

Testing whether theories of gravity require revision can also be done using the growth of perturbations. Informally, we can regard many theories of modified gravity as involving a change of the strength of gravity with scale, so that the properties inferred from the global expansion can differ from those obtained from clustering at 10 Mpc. An increasingly common parameterization is to assume that the growth rate can be tied to the density parameter: $d \ln \delta / d \ln a = \Omega_m^\gamma(a)$ [89]. The parameter γ is close to 0.55 for standard relativistic gravity, but can differ by around 0.1 from this value in many non-standard models. Clearly this parameterization is incomplete, since it explicitly rejects the possibility of early dark energy ($\Omega_m(a) \rightarrow 1$ as $a \rightarrow 0$), but it is a convenient way of capturing the power of various experiments.

Current planning envisages a set of satellite probes that, a decade hence, will pursue these tests via gravitational lensing measurements over thousands of square degrees, $> 10^8$ redshifts, and photometry of > 1000 supernovae (JDEM in the USA, Euclid in Europe) [22,23]. These experiments will measure both w and the perturbation growth rate to an accuracy of around 1%. The outcome will be either a validation of the standard relativistic vacuum-dominated big bang cosmology at a level of precision far beyond anything attempted to date, or the opening of entirely new directions in cosmological models.

References:

1. V.M. Slipher, *Pop. Astr.* **23**, 21 (1915).
2. K. Lundmark, *MNRAS* **84**, 747 (1924).
3. E. Hubble and M.L. Humason, *Ap. J.* **74**, 43 (1931).
4. G. Gamow, *Phys. Rev.* **70**, 572 (1946).
5. R.A. Alpher *et al.*, *Phys. Rev.* **73**, 803 (1948).
6. R.A. Alpher and R.C. Herman, *Phys. Rev.* **74**, 1737 (1948).
7. R.A. Alpher and R.C. Herman, *Phys. Rev.* **75**, 1089 (1949).
8. A.A. Penzias and R.W. Wilson, *Ap. J.* **142**, 419 (1965).
9. P.J.E. Peebles, *Principles of Physical Cosmology* Princeton University Press (1993).
10. G. Börner, *The Early Universe: Facts and Fiction*, Springer-Verlag (1988).
11. E.W. Kolb and M.S. Turner, *The Early Universe*, Addison-Wesley (1990).
12. J.A. Peacock, *Cosmological Physics*, Cambridge Univ. Press (1999).
13. A.R. Liddle and D. Lyth, *Cosmological Inflation and Large-Scale Structure*, Cambridge University Press (2000).
14. S. Dodelson, *Modern Cosmology*, Academic Press (2003).
15. V. Mukhanov, *Physical Foundations of Cosmology*, Cambridge University Press (2005).
16. S. Weinberg, *Cosmology*, Oxford Press (2008).
17. E.B. Gliner, *Sov. Phys. JETP* **22**, 378 (1966).
18. Y.B. Zeldovich, (1967), *Sov. Phys. Uspekhi*, **11**, 381 (1968).
19. P.M. Garnavich *et al.*, *Ap. J.* **507**, 74 (1998).
20. S. Perlmutter *et al.*, *Phys. Rev. Lett.* **83**, 670 (1999).
21. I. Maor *et al.*, *Phys. Rev.* **D65**, 123003 (2002).
22. A. Albrecht *et al.*, *astro-ph/0609591*.
23. J. Peacock *et al.*, *astro-ph/0610906*.
24. E. Komatsu *et al.*, *Astrophys. J. Supp.* **180**, 330 (2009).
25. A.G. Riess *et al.*, *Astrophys. J.* **699**, 539 (2009).
26. A.G. Riess *et al.*, *A. J.* **116**, 1009 (1998).
27. S. Perlmutter *et al.*, *Ap. J.* **517**, 565 (1999).
28. A.G. Riess, *PASP*, **112**, 1284 (2000).
29. J.L. Tonry *et al.*, *Ap. J.* **594**, 1 (2003).
30. M. Kowalski *et al.*, *Ap. J.* **686**, 749 (2008).
31. I. Zlatev *et al.*, *Phys. Rev. Lett.* **82**, 896 (1999).
32. D.N. Spergel *et al.*, *Astrophys. J. Supp.* **170**, 377 (2007).
33. P. Astier *et al.*, *A&A*, **447** 31 (2006).
34. J.A. Johnson and M. Bolte, *Astrophys. J.* **554**, 888 (2001).
35. R. Cayrel *et al.*, *Nature* **409**, 691 (2001).
36. R. Jimenez and P. Padoan, *Astrophys. J.* **498**, 704 (1998).
37. E. Carretta *et al.*, *Astrophys. J.* **533**, 215 (2000).
38. M. Srednicki *et al.*, *Nucl. Phys. B* **310**, 693 (1988).
39. G. Mangano *et al.*, *Phys. Lett.* **B534**, 8 (2002).
40. A. Linde, *Phys. Rev.* **D14**, 3345 (1976).
41. A. Linde, *Rep. Prog. Phys.* **42**, 389 (1979).
42. C.E. Vayonakis, *Surveys High Energ. Phys.* **5**, 87 (1986).
43. S.A. Bonometto and A. Masiéro, *Riv. Nuovo Cim.* **9N5**, 1 (1986).
44. A. Linde, *Particle Physics And Inflationary Cosmology*, Harwood (1990).
45. K.A. Olive, *Phys. Rep.* **190**, 3345 (1990).
46. D. Lyth and A. Riotto, *Phys. Rep.* **314**, 1 (1999).
47. A.H. Guth, *Phys. Rev.* **D23**, 347 (1981).
48. A.D. Linde, *Phys. Lett.* **108B**, 389 (1982).
49. A. Albrecht and P.J. Steinhardt, *Phys. Rev. Lett.* **48**, 1220 (1982).
50. A.D. Sakharov, *Sov. Phys. JETP Lett.* **5**, 24 (1967).
51. S. Weinberg, *Phys. Rev. Lett.* **42**, 850 (1979).
52. D. Toussaint *et al.*, *Phys. Rev.* **D19**, 1036 (1979).
53. I. Affleck and M. Dine, *Nucl. Phys.* **B249**, 361 (1985).
54. V. Kuzmin *et al.*, *Phys. Lett.* **B155**, 36 (1985).
55. M. Fukugita and T. Yanagida, *Phys. Lett.* **B174**, 45 (1986).
56. R.H. Cyburt *et al.*, *Phys. Lett.* **B567**, 227 (2003).
57. R.H. Cyburt *et al.*, *JCAP* **0811**, 012 (2008).
58. K.A. Olive *et al.*, *Phys. Rept.* **333**, 389 (2000).
59. J. M. O’meara *et al.*, *Ap. J.* **649**, L61 (2006).
60. D.J. Fixsen *et al.*, *Astrophys. J.* **473**, 576 (1996).
61. J.C. Mather *et al.*, *Astrophys. J.* **512**, 511 (1999).
62. S.M. Cole *et al.*, *MNRAS* **326**, 255 (2001).
63. A. Mesinger and Z. Haiman, *Ap. J.* **660**, 923 (2007).
64. M. Pettini *et al.*, *MNRAS* **391**, 1499 (2008).
65. S.D.M. White *et al.*, *Nature* **366**, 429 (1993).
66. S.W. Allen *et al.*, *MNRAS*, **334**, L11 (2002).
67. S.W. Allen, *MNRAS* **296**, 392 (1998).
68. H. Hoekstra *et al.*, *Astrophys. J.* **647**, 116 (2006).
69. W.J. Percival *et al.*, *MNRAS* **327**, 1297 (2001).
70. S.M. Cole *et al.*, *MNRAS* **362**, 505 (2005).
71. W.J. Percival *et al.*, *Astrophys. J.* **657**, 645 (2007).
72. G. Efstathiou and J.R. Bond, *MNRAS* **218**, 103 (1986).
73. C. Gordon and A. Lewis, *Phys. Rev.* **D67**, 123513 (2003).
74. A. Vikhlinin *et al.*, *arXiv:0812.2720* (2008).
75. A. Dekel and O. Lahav, *Astrophys. J.* **520**, 24 (1999).
76. W.J. Percival *et al.*, *MNRAS*, **381**, 1053 (2007).
77. W.J. Percival *et al.*, *arXiv:0907.1660* [*astro-ph.CO*].
78. G. Efstathiou and J.R. Bond, *MNRAS*, **304**, 75 (1999).
79. G.P. Efstathiou *et al.*, *MNRAS* **330**, L29 (2002).
80. G.P. Efstathiou, *MNRAS* **332**, 193 (2002).
81. S. Weinberg, *Rev. Mod. Phys.* **60**, 1 (1989).
82. W. Hu and I. Sawicki, *Phys. Rev.* **D76**, 4043 (2007).
83. B. Jain and P. Zhang, *Phys. Rev.* **D78**, 3503 (2008).
84. D.L. Wiltshire, *Phys. Rev. Lett.* **99**, 251101 (2007).
85. T. Buchert, *GRG* **40**, 467 (2008).
86. C. Armendariz-Picon, V. Mukhanov and P.J. Steinhardt, *Phys. Rev.* **D63**, 3510 (2001).
87. S. DeDeo, R.R. Caldwell and P.J. Steinhardt, *Phys. Rev.* **D67**, 3509 (2003).
88. W. Hu, *arXiv:astro-ph/0407158* (2004).
89. E. Linder, *Phys. Rev.* **D72**, 43529 (2005).

20. BIG-BANG NUCLEOSYNTHESIS

Revised August 2009 by B.D. Fields (Univ. of Illinois) and S. Sarkar (Univ. of Oxford).

Big-Bang nucleosynthesis (BBN) offers the deepest reliable probe of the early Universe, being based on well-understood Standard Model physics [1–5]. Predictions of the abundances of the light elements, D, ^3He , ^4He , and ^7Li , synthesized at the end of the ‘first three minutes’, are in good overall agreement with the primordial abundances inferred from observational data, thus validating the standard hot Big-Bang cosmology (see [6] for a review). This is particularly impressive given that these abundances span nine orders of magnitude – from $^4\text{He}/\text{H} \sim 0.08$ down to $^7\text{Li}/\text{H} \sim 10^{-10}$ (ratios by number). Thus BBN provides powerful constraints on possible deviations from the standard cosmology [2], and on new physics beyond the Standard Model [3,4].

20.1. Theory

The synthesis of the light elements is sensitive to physical conditions in the early radiation-dominated era at a temperature $T \sim 1$ MeV, corresponding to an age $t \sim 1$ s. At higher temperatures, weak interactions were in thermal equilibrium, thus fixing the ratio of the neutron and proton number densities to be $n/p = e^{-Q/T}$, where $Q = 1.293$ MeV is the neutron-proton mass difference. As the temperature dropped, the neutron-proton inter-conversion rate, $\Gamma_{n-p} \sim G_F^2 T^5$, fell faster than the Hubble expansion rate, $H \sim \sqrt{g_* G_N} T^2$, where g_* counts the number of relativistic particle species determining the energy density in radiation (see ‘Big Bang Cosmology’ review). This resulted in departure from chemical equilibrium (‘freeze-out’) at $T_{\text{fr}} \sim (g_* G_N / G_F^4)^{1/6} \simeq 1$ MeV. The neutron fraction at this time, $n/p = e^{-Q/T_{\text{fr}}} \simeq 1/6$, is thus sensitive to every known physical interaction, since Q is determined by both strong and electromagnetic interactions while T_{fr} depends on the weak as well as gravitational interactions. Moreover, the sensitivity to the Hubble expansion rate affords a probe of *e.g.*, the number of relativistic neutrino species [7]. After freeze-out, the neutrons were free to β -decay, so the neutron fraction dropped to $n/p \simeq 1/7$ by the time nuclear reactions began. A simplified analytic model of freeze-out yields the n/p ratio to an accuracy of $\sim 1\%$ [8,9].

The rates of these reactions depend on the density of baryons (strictly speaking, nucleons), which is usually expressed normalized to the relic blackbody photon density as $\eta \equiv n_b/n_\gamma$. As we shall see, all the light-element abundances can be explained with $\eta_{10} \equiv \eta \times 10^{10}$ in the range 5.1–6.5 (95% CL). With n_γ fixed by the present CMB temperature 2.725 K (see ‘Cosmic Microwave Background’ review), this can be stated as the allowed range for the baryon mass density today, $\rho_b = (3.5\text{--}4.5) \times 10^{-31} \text{ g cm}^{-3}$, or as the baryonic fraction of the critical density, $\Omega_b = \rho_b/\rho_{\text{crit}} \simeq \eta_{10} h^{-2}/274 = (0.019\text{--}0.024)h^{-2}$, where $h \equiv H_0/100 \text{ km s}^{-1} \text{ Mpc}^{-1} = 0.72 \pm 0.08$ is the present Hubble parameter (see Cosmological Parameters review).

The nucleosynthesis chain begins with the formation of deuterium in the process $p(n, \gamma)\text{D}$. However, photo-dissociation by the high number density of photons delays production of deuterium (and other complex nuclei) well after T drops below the binding energy of deuterium, $\Delta_{\text{D}} = 2.23$ MeV. The quantity $\eta^{-1} e^{-\Delta_{\text{D}}/T}$, *i.e.*, the number of photons per baryon above the deuterium photo-dissociation threshold, falls below unity at $T \simeq 0.1$ MeV; nuclei can then begin to form without being immediately photo-dissociated again. Only 2-body reactions, such as $\text{D}(p, \gamma)^3\text{He}$, $^3\text{He}(\text{D}, p)^4\text{He}$, are important because the density by this time has become rather low – comparable to that of air!

Nearly all the surviving neutrons when nucleosynthesis begins end up bound in the most stable light element ^4He . Heavier nuclei do not form in any significant quantity both because of the absence of stable nuclei with mass number 5 or 8 (which impedes nucleosynthesis via $n^4\text{He}$, $p^4\text{He}$ or $^4\text{He}^4\text{He}$ reactions), and the large Coulomb barriers for reactions such as $\text{T}(^4\text{He}, \gamma)^7\text{Li}$ and $^3\text{He}(^4\text{He}, \gamma)^7\text{Be}$. Hence the primordial mass fraction of ^4He , conventionally referred to as Y_{p} , can be estimated by the simple counting argument

$$Y_{\text{p}} = \frac{2(n/p)}{1 + n/p} \simeq 0.25. \quad (20.1)$$

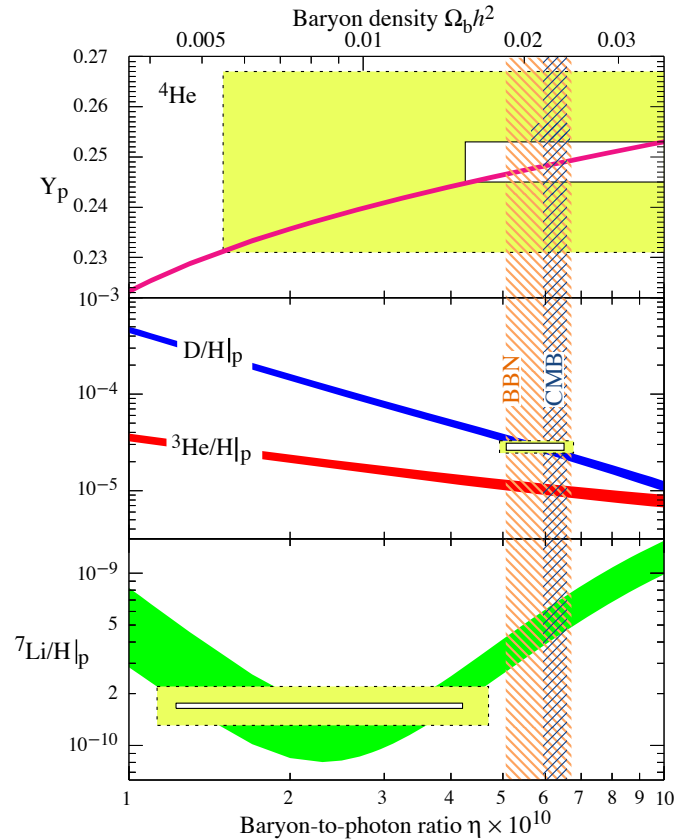


Figure 20.1: The abundances of ^4He , D, ^3He , and ^7Li as predicted by the standard model of Big-Bang nucleosynthesis [11] – the bands show the 95% CL range. Boxes indicate the observed light element abundances (smaller boxes: $\pm 2\sigma$ statistical errors; larger boxes: $\pm 2\sigma$ statistical and systematic errors). The narrow vertical band indicates the CMB measure of the cosmic baryon density, while the wider band indicates the BBN concordance range (both at 95% CL). Color version at end of book.

There is little sensitivity here to the actual nuclear reaction rates, which are, however, important in determining the other ‘left-over’ abundances: D and ^3He at the level of a few times 10^{-5} by number relative to H, and $^7\text{Li}/\text{H}$ at the level of about 10^{-10} (when η_{10} is in the range 1–10). These values can be understood in terms of approximate analytic arguments [9,10]. The experimental parameter most important in determining Y_{p} is the neutron lifetime, τ_n , which normalizes (the inverse of) Γ_{n-p} . The experimental uncertainty in τ_n used to be a source of concern, but has been reduced substantially: $\tau_n = 885.7 \pm 0.8$ s (see *N* Baryons Listing).

The elemental abundances shown in Fig. 20.1 as a function of η_{10} were calculated [11] using an updated version [12] of the Wagoner code [1]; other modern versions [13,14] are publicly available. The ^4He curve includes small corrections due to radiative processes at zero and finite temperatures [15], non-equilibrium neutrino heating during e^\pm annihilation [16], and finite nucleon mass effects [17]; the range reflects primarily the 2σ uncertainty in the neutron lifetime. The spread in the curves for D, ^3He , and ^7Li corresponds to the 2σ uncertainties in nuclear cross sections, as estimated by Monte Carlo methods [18–19]. The input nuclear data have been carefully reassessed [11, 20–23], leading to improved precision in the abundance predictions. In particular, the uncertainty in $^7\text{Li}/\text{H}$ at interesting values of η has been reduced recently by a factor ~ 2 , a consequence of a similar reduction in the error budget [24] for the dominant mass-7 production channel $\text{T}(^4\text{He}, \gamma)^7\text{Be}$. Polynomial fits to the predicted abundances and the error correlation matrix have been given [19,25]. The boxes in Fig. 20.1 show the observationally inferred primordial abundances with their associated statistical and systematic uncertainties, as discussed below.

20.2. Light Element Abundances

BBN theory predicts the universal abundances of D, ${}^3\text{He}$, ${}^4\text{He}$, and ${}^7\text{Li}$, which are essentially fixed by $t \sim 180$ s. Abundances are, however, observed at much later epochs, after stellar nucleosynthesis has commenced. The ejected remains of this stellar processing can alter the light element abundances from their primordial values, and also produce heavy elements such as C, N, O, and Fe (‘metals’). Thus, one seeks astrophysical sites with low metal abundances, in order to measure light element abundances which are closer to primordial. For all of the light elements, systematic errors are an important (and often dominant) limitation to the precision with which primordial abundances can be inferred.

High-resolution spectra reveal the presence of D in high-redshift, low-metallicity quasar absorption systems via its isotope-shifted Lyman- α absorption [26–29]. It is believed that there are no astrophysical sources of deuterium [30], so any detection provides a lower limit to primordial D/H, and thus an upper limit on η ; for example, the local interstellar value of $\text{D}/\text{H}|_{\text{p}} = (1.56 \pm 0.04) \times 10^{-5}$ [31] requires $\eta_{10} \leq 9$. Recent observations find an unexpected scatter of a factor of ~ 2 [32], as well as correlations with heavy element abundances which suggest that interstellar D may suffer stellar processing (astration), but also partly reside in dust particles which evade gas-phase observations. This is supported by a measurement in the lower halo [33], which indicates that the Galactic D abundance has been reduced by a factor of only 1.12 ± 0.13 since its formation. For the high-redshift systems, conventional models of galactic nucleosynthesis (chemical evolution) do not predict either of these effects for D/H [34].

The observed extragalactic D values are bracketed by the non-detection of D in a high-redshift system, $\text{D}/\text{H}|_{\text{p}} < 6.7 \times 10^{-5}$ at 1σ [35], and low values in some (damped Lyman- α) systems [26,27]. Averaging the seven most precise observations of deuterium in quasar absorption systems gives $\text{D}/\text{H} = (2.82 \pm 0.12) \times 10^{-5}$, where the error is statistical only [28,29]. However, there remains concern over systematic errors, the dispersion between the values being much larger than is expected from the individual measurement errors ($\chi^2 = 17.7$ for $\nu = 6$ d.o.f.). Increasing the error by a factor $\sqrt{\chi^2/\nu}$ gives, as shown in Fig. 20.1:

$$\text{D}/\text{H}|_{\text{p}} = (2.82 \pm 0.21) \times 10^{-5}. \quad (20.2)$$

${}^4\text{He}$ can be observed in clouds of ionized hydrogen (H II regions), the most metal-poor of which are in dwarf galaxies. There is now a large body of data on ${}^4\text{He}$ and CNO in such systems [36]. These data confirm that the small stellar contribution to helium is positively correlated with metal production. Extrapolating to zero metallicity gives the primordial ${}^4\text{He}$ abundance [37]

$$Y_{\text{p}} = 0.249 \pm 0.009. \quad (20.3)$$

Here the latter error is a careful (and significantly enlarged) estimate of the systematic uncertainties which dominate, and is based on the scatter in different analyses of the physical properties of the H II regions [36,37]. Other recent extrapolations to zero metallicity give $Y_{\text{p}} = 0.247 \pm 0.001$ or 0.252 ± 0.001 depending on which set of He I emissivities are used [38], and $Y_{\text{p}} = 0.248 \pm 0.003$ [39]. These are consistent (given the systematic errors) with the above estimate [37], which appears in Fig. 20.1.

As we will see in more detail below, the primordial abundance of lithium now plays a central role in BBN, and possibly points to new physics. The systems best suited for Li observations are metal-poor stars in the spheroid (Pop II) of our Galaxy, which have metallicities going down to at least 10^{-4} , and perhaps 10^{-5} of the Solar value [40]. Observations have long shown [41–45] that Li does not vary significantly in Pop II stars with metallicities $\lesssim 1/30$ of Solar — the ‘Spite plateau’ [41]. Precision data suggest a small but significant correlation between Li and Fe [42], which can be understood as the result of Li production from Galactic cosmic rays [43]. Extrapolating to zero metallicity, one arrives at a primordial value $\text{Li}/\text{H}|_{\text{p}} = (1.23 \pm 0.06^{+0.68}_{-0.32}) \times 10^{-10}$ [44], where the first error given is statistical and is very small due to the

relatively large sample of 22 stars used. One source of systematic error stems from the differences in techniques used to determine the physical parameters (*e.g.*, the temperature) of the stellar atmosphere in which the Li absorption line is formed. Alternative analyses, using methods that give systematically higher temperatures, and in some cases different stars and stellar systems (globular clusters), yield $\text{Li}/\text{H}|_{\text{p}} = (2.19 \pm 0.28) \times 10^{-10}$ [45], $\text{Li}/\text{H}|_{\text{p}} = (2.34 \pm 0.32) \times 10^{-10}$ [46], and $\text{Li}/\text{H}|_{\text{p}} = (1.26 \pm 0.26) \times 10^{-10}$ [47]; the differences with [44] indicate a systematic uncertainty of a factor of ~ 2 . Moreover, it is possible that the Li in Pop II stars has been partially destroyed, due to mixing of the outer layers with the hotter interior [48]. Such processes can be constrained by the absence of significant scatter in Li versus Fe [42], and by observations of the fragile isotope ${}^6\text{Li}$ [43]. Nevertheless, some depletion is likely to exist, though this is difficult to quantify with confidence — a factor as large as ~ 1.8 has been suggested [49]. Including these systematics, we estimate a primordial Li range which spans the ranges above, as shown in Fig. 20.1:

$$\text{Li}/\text{H}|_{\text{p}} = (1.7 \pm 0.06 \pm 0.44) \times 10^{-10}. \quad (20.4)$$

Stellar determination of Li abundances typically sum over both stable isotopes ${}^6\text{Li}$ and ${}^7\text{Li}$. Recent high-precision measurements are sensitive to the tiny isotopic shift in Li absorption (which manifests itself in the shape of the blended, thermally broadened line) and indicate ${}^6\text{Li}/{}^7\text{Li} \leq 0.15$ [50]. This confirms that ${}^7\text{Li}$ is dominant, but surprisingly there is indication of a ${}^6\text{Li}$ plateau (analogous to the ${}^7\text{Li}$ plateau) which suggests a significant primordial ${}^6\text{Li}$ abundance. However, caution must be exercised since convective motions in the star can generate similar asymmetries in the line shape, hence the deduced ${}^6\text{Li}$ abundance is presently best interpreted as an upper limit [51].

Turning to ${}^3\text{He}$, the only data available are from the Solar system and (high-metallicity) H II regions in our Galaxy [52]. This makes inferring the primordial abundance difficult, a problem compounded by the fact that stellar nucleosynthesis models for ${}^3\text{He}$ are in conflict with observations [53]. Consequently, it is no longer appropriate to use ${}^3\text{He}$ as a cosmological probe; instead, one might hope to turn the problem around and constrain stellar astrophysics using the predicted primordial ${}^3\text{He}$ abundance [54].

20.3. Concordance, Dark Matter, and the CMB

We now use the observed light element abundances to test the theory. We first consider standard BBN, which is based on Standard Model physics alone, so $N_{\nu} = 3$ and the only free parameter is the baryon-to-photon ratio η . (The implications of BBN for physics beyond the Standard Model will be considered below, §4). Thus, any abundance measurement determines η , while additional measurements overconstrain the theory and thereby provide a consistency check.

First we note that the overlap in the η ranges spanned by the larger boxes in Fig. 20.1 indicates overall concordance. More quantitatively, when we account for theoretical uncertainties, as well as the statistical and systematic errors in observations, there is acceptable agreement among the abundances when

$$5.1 \leq \eta_{10} \leq 6.5 \text{ (95\% CL)}. \quad (20.5)$$

However, the agreement is much less satisfactory if we use only the quoted statistical errors in the observations. In particular, as seen in Fig. 20.1, D and ${}^4\text{He}$ are consistent with each other, but favor a value of η which is higher by a factor of at least 2.4, and by at least $\sim 4.2\sigma$ from that indicated by the ${}^7\text{Li}$ abundance determined in stars. Furthermore, if the ${}^6\text{Li}$ plateau [50] reflects a primordial component, it is ~ 1000 times that expected in standard BBN; both these ‘lithium problems’ may indicate new physics (see below).

Even so, the overall concordance is remarkable: using well-established microphysics we have extrapolated back to an age of ~ 1 s to correctly predict light element abundances spanning 9 orders of magnitude. This is a major success for the standard cosmology, and inspires confidence in extrapolation back to still earlier times.

This concordance provides a measure of the baryon content

$$0.019 \leq \Omega_{\text{b}} h^2 \leq 0.024 \text{ (95\% CL)}, \quad (20.6)$$

a result that plays a key role in our understanding of the matter budget of the Universe. First we note that $\Omega_b \ll 1$, *i.e.*, baryons cannot close the Universe [55]. Furthermore, the cosmic density of (optically) luminous matter is $\Omega_{\text{lum}} \simeq 0.0024h^{-1}$ [56], so that $\Omega_b \gg \Omega_{\text{lum}}$: most baryons are optically dark, probably in the form of a diffuse intergalactic medium [57]. Finally, given that $\Omega_m \sim 0.3$ (see Dark Matter and Cosmological Parameters reviews), we infer that most matter in the Universe is not only dark, but also takes some non-baryonic (more precisely, non-nucleonic) form.

The BBN prediction for the cosmic baryon density can be tested through precision observations of CMB temperature fluctuations (see Cosmic Microwave Background review). One can determine η from the amplitudes of the acoustic peaks in the CMB angular power spectrum [58], making it possible to compare two measures of η using very different physics, at two widely separated epochs. In the standard cosmology, there is no change in η between BBN and CMB decoupling, thus, a comparison of η_{BBN} and η_{CMB} is a key test. Agreement would endorse the standard picture while disagreement could point to new physics during/between the BBN and CMB epochs.

The release of the WMAP results was a landmark event in this test of BBN. As with other cosmological parameter determinations from CMB data, the derived η_{CMB} depends on the adopted priors [59], in particular the form assumed for the power spectrum of primordial density fluctuations. If this is taken to be a scale-free power-law, the five-year WMAP data imply $\Omega_b h^2 = 0.02273 \pm 0.00062$ or $\eta_{10} = 6.23 \pm 0.17$ [60] as shown in Fig. 20.1. Other assumptions for the shape of the power spectrum can lead to baryon densities as low as $\Omega_b h^2 = 0.0175 \pm 0.0007$ [61]. Thus, outstanding uncertainties regarding priors are a source of systematic error which presently exceeds the statistical error in the prediction for η .

It is remarkable that the CMB estimate of the baryon density is consistent with the BBN range quoted in Eq. (20.6), and in very good agreement with the value inferred from recent high-redshift D/H measurements [29] and ${}^4\text{He}$ determinations; together these observations span diverse environments from redshifts $z = 1000$ to the present.

Bearing in mind the importance of priors, the promise of precision determinations of the baryon density using the CMB motivates the use of this value as an input to BBN calculations. Within the context of the Standard Model, BBN then becomes a zero-parameter theory, and the light element abundances are completely determined to within the uncertainties in η_{CMB} and the BBN theoretical errors. Comparison with the observed abundances then can be used to test the astrophysics of post-BBN light element evolution [64]. Alternatively, one can consider possible physics beyond the Standard Model (*e.g.*, which might change the expansion rate during BBN) and then use all of the abundances to test such models; this is the subject of our final section.

20.4. The Lithium Problem

As Fig. 20.1 shows, stellar Li/H measurements are inconsistent with the CMB (and D/H), given the error budgets we have quoted. Recent updates in nuclear cross sections, stellar abundance systematics, and the WMAP results all *increase* the discrepancy to as much as 5.3σ , depending on the stellar abundance analysis adopted. [11].

The question then becomes more pressing as to whether this mismatch comes from systematic errors in the observed abundances, and/or uncertainties in stellar astrophysics, or whether there might be new physics at work. Nucleosynthesis models in which the baryon-to-photon ratio is inhomogeneous can alter abundances for a given η_{BBN} , but will overproduce ${}^7\text{Li}$ [62]. Entropy generation by some non-standard process could have decreased η between the BBN era and CMB decoupling, however the lack of spectral distortions in the CMB rules out any significant energy injection upto a redshift $z \sim 10^7$ [63]. The most intriguing resolution of the lithium problem thus involves new physics during BBN [4].

For now this is a central unresolved issue in BBN. Nevertheless, the remarkable concordance between the CMB and D/H, as well as ${}^4\text{He}$, remain as non-trivial successes, and open windows onto the early Universe and particle physics, as we now discuss.

20.5. Beyond the Standard Model

Given the simple physics underlying BBN, it is remarkable that it still provides the most effective test for the cosmological viability of ideas concerning physics beyond the Standard Model. Although baryogenesis and inflation must have occurred at higher temperatures in the early Universe, we do not as yet have ‘standard models’ for these, so BBN still marks the boundary between the established and the speculative in Big Bang cosmology. It might appear possible to push the boundary back to the quark-hadron transition at $T \sim \Lambda_{\text{QCD}}$, or electroweak symmetry breaking at $T \sim 1/\sqrt{G_{\text{F}}}$; however, so far no observable relics of these epochs have been identified, either theoretically or observationally. Thus, although the Standard Model provides a precise description of physics up to the Fermi scale, cosmology cannot be traced in detail before the BBN era.

Limits on particle physics beyond the Standard Model come mainly from the observational bounds on the ${}^4\text{He}$ abundance. This is proportional to the n/p ratio which is determined when the weak-interaction rates fall behind the Hubble expansion rate at $T_{\text{fr}} \sim 1$ MeV. The presence of additional neutrino flavors (or of any other relativistic species) at this time increases g_* , hence the expansion rate, leading to a larger value of T_{fr} , n/p , and therefore Y_{p} [7,65]. In the Standard Model, the number of relativistic particle species at 1 MeV is $g_* = 5.5 + \frac{7}{4}N_\nu$, where the factor 5.5 accounts for photons and e^\pm , and N_ν is the *effective* number of (nearly massless) neutrino flavors (see Big Bang Cosmology review). The helium curves in Fig. 20.1 were computed taking $N_\nu = 3$; small corrections for non-equilibrium neutrino heating [16] are included in the thermal evolution and lead to an effective $N_\nu = 3.04$ compared to assuming instantaneous neutrino freezeout (see, *e.g.*, Big Bang Cosmology review). The computed ${}^4\text{He}$ abundance scales as $\Delta Y_{\text{p}} \simeq 0.013\Delta N_\nu$ [8]. Clearly the central value for N_ν from BBN will depend on η , which is independently determined (with weaker sensitivity to N_ν) by the adopted D or ${}^7\text{Li}$ abundance. For example, if the best value for the observed primordial ${}^4\text{He}$ abundance is 0.249, then, for $\eta_{10} \sim 6$, the central value for N_ν is very close to 3. This limit depends sensitively on the adopted light element abundances, particularly Y_{p} . A maximum likelihood analysis on η and N_ν based on the above ${}^4\text{He}$ and D abundances finds the (correlated) 95% CL ranges to be $4.9 < \eta_{10} < 7.1$ and $1.8 < N_\nu < 4.5$ [66]. Similar results were obtained in another study [67] which presented a simpler method to extract such bounds based on χ^2 statistics, given a set of input abundances. Using the CMB determination of η improves the constraints: with a ‘low’ ${}^4\text{He}$, $N_\nu = 3$ is barely allowed at 2σ [68], but using the ${}^4\text{He}$ (and D) abundance quoted above gives $5.66 < \eta_{10} < 6.58$ ($\Omega_b h^2 = 0.0226 \pm 0.0017$) and $N_\nu = 3.2 \pm 1.2$ (95% CL) [66].

Just as one can use the measured helium abundance to place limits on g_* [65], any changes in the strong, weak, electromagnetic, or gravitational coupling constants, arising *e.g.*, from the dynamics of new dimensions, can be similarly constrained [69], as can be any speed-up of the expansion rate in *e.g.* scalar-tensor theories of gravity [70].

The limits on N_ν can be translated into limits on other types of particles or particle masses that would affect the expansion rate of the Universe during nucleosynthesis. For example, consider ‘sterile’ neutrinos with only right-handed interactions of strength $G_{\text{R}} < G_{\text{F}}$. Such particles would decouple at higher temperature than (left-handed) neutrinos, so their number density ($\propto T^3$) relative to neutrinos would be reduced by any subsequent entropy release, *e.g.*, due to annihilations of massive particles that become non-relativistic between the two decoupling temperatures. Thus (relativistic) particles with less than full strength weak interactions contribute less to the energy density than particles that remain in equilibrium up to the time of nucleosynthesis [71]. If we impose $N_\nu < 4$ as an illustrative constraint, then the three right-handed neutrinos must have a temperature $3(T_{\nu_{\text{R}}}/T_{\nu_{\text{L}}})^4 < 1$. Since the temperature of the decoupled ν_{R} ’s is determined by entropy conservation (see Big Bang Cosmology review), $T_{\nu_{\text{R}}}/T_{\nu_{\text{L}}} = [(43/4)/g_*(T_{\text{d}})]^{1/3} < 0.76$, where T_{d} is the decoupling temperature of the ν_{R} ’s. This requires $g_*(T_{\text{d}}) > 24$, so decoupling must have occurred at $T_{\text{d}} > 140$ MeV. The decoupling temperature is related to G_{R} through $(G_{\text{R}}/G_{\text{F}})^2 \sim (T_{\text{d}}/3 \text{ MeV})^{-3}$,

where 3 MeV is the decoupling temperature for ν_L s. This yields a limit $G_R \lesssim 10^{-2} G_F$. The above argument sets lower limits on the masses of new Z' gauge bosons to which right-handed neutrinos would be coupled in models of superstrings [72], or extended technicolor [73]. Similarly a Dirac magnetic moment for neutrinos, which would allow the right-handed states to be produced through scattering and thus increase g_* , can be significantly constrained [74], as can any new interactions for neutrinos which have a similar effect [75]. Right-handed states can be populated directly by helicity-flip scattering if the neutrino mass is large enough, and this property has been used to infer a bound of $m_{\nu\tau} \lesssim 1$ MeV taking $N_\nu < 4$ [76]. If there is mixing between active and sterile neutrinos then the effect on BBN is more complicated [77].

The limit on the expansion rate during BBN can also be translated into bounds on the mass/lifetime of non-relativistic particles which decay during BBN. This results in an even faster speed-up rate, and typically also change the entropy [78]. If the decays include Standard Model particles, the resulting electromagnetic [79–80] and/or hadronic [81] cascades can strongly perturb the light elements, which leads to even stronger constraints. Such arguments have been applied to rule out a MeV mass ν_τ , which decays during nucleosynthesis [82].

Such arguments have proved very effective in constraining supersymmetry. For example, if the gravitino is very light and contributes to g_* , the illustrative BBN limit $N_\nu < 4$ requires its mass to exceed ~ 1 eV [83]. Alternatively, much recent interest has focussed on the case in which the next-to-lightest supersymmetric particle is metastable and decays during or after BBN. The constraints on unstable particles discussed above imply stringent bounds on the allowed abundance of such particles [81]; if the metastable particle is charged (*e.g.*, the stau), then it is possible for it to form atom-like electromagnetic bound states with nuclei, and the resulting impact on light elements can be quite complex [84]. Such decays can destroy ${}^7\text{Li}$ and/or produce ${}^6\text{Li}$, leading to a possible supersymmetric solution to the lithium problems noted above [85] (see [4] for a review). In addition, these arguments impose powerful constraints on supersymmetric inflationary cosmology [80–81], in particular thermal leptogenesis [86]. These can be evaded only if the gravitino is massive enough to decay before BBN, *i.e.*, $m_{3/2} \gtrsim 50$ TeV [87] (which would be unnatural), or if it is in fact the lightest supersymmetric particle and thus stable [80,88]. Similar constraints apply to moduli – very weakly coupled fields in string theory which obtain an electroweak-scale mass from supersymmetry breaking [89].

Finally, we mention that BBN places powerful constraints on the possibility that there are new large dimensions in nature, perhaps enabling the scale of quantum gravity to be as low as the electroweak scale [90]. Thus, Standard Model fields may be localized on a ‘brane,’ while gravity alone propagates in the ‘bulk.’ It has been further noted that the new dimensions may be non-compact, even infinite [91], and the cosmology of such models has attracted considerable attention. The expansion rate in the early Universe can be significantly modified, so BBN is able to set interesting constraints on such possibilities [92].

References:

- R.V. Wagoner *et al.*, *Astrophys. J.* **148**, 3 (1967).
- R.A. Malaney & G.J. Mathews, *Phys. Reports* **229**, 145 (1993).
- S. Sarkar, *Rept. on Prog. in Phys.* **59**, 1493 (1996).
- K. Jedamzik & M. Pospelov, *New J. Phys.* **11**, 105028 (2009).
- D.N. Schramm & M.S. Turner, *Rev. Mod. Phys.* **70**, 303 (1998).
- K.A. Olive *et al.*, *Phys. Reports* **333**, 389 (2000).
- P.J.E. Peebles, *Phys. Rev. Lett.* **16**, 411 (1966).
- J. Bernstein *et al.*, *Rev. Mod. Phys.* **61**, 25 (1989).
- S. Mukhanov, *Int. J. Theor. Phys.* **143**, 669 (2004).
- R. Esmailzadeh *et al.*, *Astrophys. J.* **378**, 504 (1991).
- R.H. Cyburt *et al.*, *JCAP* **0811**, 012 (2008).
- R.H. Cyburt *et al.*, *New Astron.* **6**, 215 (2001).
- L. Kawano, FERMILAB-PUB-92/04-A.
- O. Pisanti *et al.*, *Comput. Phys. Commun.* **178**, 956 (2008).
- S. Esposito *et al.*, *Nucl. Phys.* **B568**, 421 (2000).
- S. Dodelson & M.S. Turner, *Phys. Rev.* **D46**, 3372 (1992).
- D. Seckel, *hep-ph/9305311*;
R. Lopez & M.S. Turner, *Phys. Rev.* **D59**, 103502 (1999).
- M.S. Smith *et al.*, *Astrophys. J. Supp.* **85**, 219 (1993).
- G. Fiorentini *et al.*, *Phys. Rev.* **D58**, 063506 (1998).
- K.M. Nollett & S. Burles, *Phys. Rev.* **D61**, 123505 (2000).
- A. Coc *et al.*, *Astrophys. J.* **600**, 544 (2004).
- R.H. Cyburt, *Phys. Rev.* **D70**, 023505 (2004).
- P.D. Serpico *et al.*, *JCAP* **12**, 010 (2004).
- R.H. Cyburt & B. Davids, *Phys. Rev.* **C78**, 012 (2008).
- K.M. Nollett *et al.*, *Astrophys. J. Lett.* **552**, L1 (2001).
- S. D’Odorico *et al.*, *Astron. & Astrophys.* **368**, L21 (2001).
- M. Pettini & D. Bowen, *Astrophys. J.* **560**, 41 (2001).
- J.M. O’Meara *et al.*, *Astrophys. J. Lett.* **649**, L61 (2006).
- M. Pettini *et al.*, *MNRAS* **391**, 1499 (2008).
- R.I. Epstein *et al.*, *Nature* **263**, 198 (1976).
- B.E. Wood *et al.*, *Astrophys. J.* **609**, 838 (2004).
- J.L. Linsky *et al.*, *Astrophys. J.* **647**, 1106 (2006).
- B.D. Savage *et al.*, *Astrophys. J.* **659**, 1222 (2007).
- B.D. Fields, *Astrophys. J.* **456**, 678 (1996).
- D. Kirkman *et al.*, *Astrophys. J.* **529**, 655 (2000).
- Y.I. Izotov *et al.*, *Astrophys. J.* **527**, 757 (1999).
- K.A. Olive & E. Skillman, *Astrophys. J.* **617**, 29 (2004).
- Y.I. Izotov *et al.*, *Astrophys. J.* **662**, 15 (2007).
- M. Peimbert *et al.*, *Astrophys. J.* **667**, 636 (2007).
- N. Christlieb *et al.*, *Nature* **419**, 904 (2002).
- M. Spite & F. Spite, *Nature* **297**, 483 (1982).
- S.G. Ryan *et al.*, *Astrophys. J.* **523**, 654 (1999).
- E. Vangioni-Flam *et al.*, *New Astron.* **4**, 245 (1999).
- S.G. Ryan *et al.*, *Astrophys. J. Lett.* **530**, L57 (2000).
- P. Bonifacio *et al.*, *Astron. & Astrophys.* **390**, 91 (2002).
- J. Meléndez & I. Ramirez, *Astrophys. J. Lett.* **615**, 33 (2004).
- P. Bonifacio *et al.*, *Astron. & Astrophys.* **462**, 851 (2007).
- M.H. Pinsonneault *et al.*, *Astrophys. J.* **574**, 389 (2002).
- A.J. Korn *et al.*, *Nature* **442**, 657 (2006).
- M. Asplund *et al.*, *Astrophys. J.* **644**, 229 (2006).
- R. Cayrel *et al.*, *Astron. & Astrophys.* **473**, L37 (2007).
- T.M. Bania *et al.*, *Nature* **415**, 54 (2002).
- K.A. Olive *et al.*, *Astrophys. J.* **479**, 752 (1997).
- E. Vangioni-Flam *et al.*, *Astrophys. J.* **585**, 611 (2003).
- H. Reeves *et al.*, *Astrophys. J.* **179**, 909 (1973).
- M. Fukugita & P.J.E. Peebles, *Astrophys. J.* **616**, 643 (2004).
- R. Cen & J.P. Ostriker, *Astrophys. J.* **514**, 1 (1999).
- G. Jungman *et al.*, *Phys. Rev.* **D54**, 1332 (1996).
- M. Tegmark *et al.*, *Phys. Rev.* **D63**, 043007 (2001).
- J. Dunkley *et al.*, *Astrophys. J. Supp.* **180**, 306 (2009).
- P. Hunt & S. Sarkar, *Phys. Rev.* **D76**, 123504 (2007).
- K. Jedamzik & J.B. Rehm, *Phys. Rev.* **D64**, 023510 (2001).
- D.J. Fixsen *et al.*, *Astrophys. J.* **473**, 576 (1996).
- R.H. Cyburt *et al.*, *Phys. Lett.* **B567**, 227 (2003).
- G. Steigman *et al.*, *Phys. Lett.* **B66**, 202 (1977).
- R.H. Cyburt *et al.*, *Astropart. Phys.* **23**, 313 (2005).
- E. Lisi *et al.*, *Phys. Rev.* **D59**, 123520 (1999).
- V. Barger *et al.*, *Phys. Lett.* **B566**, 8 (2003).
- E.W. Kolb *et al.*, *Phys. Rev.* **D33**, 869 (1986);
F.S. Accetta *et al.*, *Phys. Lett.* **B248**, 146 (1990);
B.A. Campbell & K.A. Olive, *Phys. Lett.* **B345**, 429 (1995);
K.M. Nollett & R. Lopez, *Phys. Rev.* **D66**, 063507 (2002);
C. Bambi *et al.*, *Phys. Rev.* **D71**, 123524 (2005).
- A. Coc *et al.*, *Phys. Rev.* **D73**, 083525 (2006).
- K.A. Olive *et al.*, *Nucl. Phys.* **B180**, 497 (1981).
- J. Ellis *et al.*, *Phys. Lett.* **B167**, 457 (1986).
- L.M. Krauss *et al.*, *Phys. Rev. Lett.* **71**, 823 (1993).
- J.A. Morgan, *Phys. Lett.* **B102**, 247 (1981).
- E.W. Kolb *et al.*, *Phys. Rev.* **D34**, 2197 (1986);
J.A. Grifols & E. Massó, *Mod. Phys. Lett.* **A2**, 205 (1987);
K.S. Babu *et al.*, *Phys. Rev. Lett.* **67**, 545 (1991).
- A.D. Dolgov *et al.*, *Nucl. Phys.* **B524**, 621 (1998).
- K. Enqvist *et al.*, *Nucl. Phys.* **B373**, 498 (1992);
A.D. Dolgov, *Phys. Reports* **370**, 333 (2002).
- K. Sato & M. Kobayashi, *Prog. Theor. Phys.* **58**, 1775 (1977);
D.A. Dicus *et al.*, *Phys. Rev.* **D17**, 1529 (1978);
R.J. Scherrer & M.S. Turner, *Astrophys. J.* **331**, 19 (1988).
- D. Lindley, *MNRAS* **188**, 15 (1979), *Astrophys. J.* **294**, 1 (1985).

-
80. J. Ellis *et al.*, Nucl. Phys. **B259**, 175 (1985);
J. Ellis *et al.*, Nucl. Phys. **B373**, 399 (1992);
R.H. Cyburt *et al.*, Phys. Rev. **D67**, 103521 (2003).
81. M.H. Reno & D. Seckel, Phys. Rev. **D37**, 3441 (1988);
S. Dimopoulos *et al.*, Nucl. Phys. **B311**, 699 (1989);
K. Kohri *et al.*, Phys. Rev. **D71**, 083502 (2005).
82. S. Sarkar & A.M. Cooper, Phys. Lett. **B148**, 347 (1984).
83. J.A. Grifols *et al.*, Phys. Lett. **B400**, 124 (1997).
84. M. Pospelov *et al.*, Phys. Rev. Lett. **98**, 231301 (2007);
R.H. Cyburt *et al.*, JCAP **11**, 014 (2006);
M. Kawasaki *et al.*, Phys. Lett. **B649**, 436 (2007).
85. K. Jedamzik *et al.*, JCAP **07**, 007 (2006).
86. S. Davidson *et al.*, Phys. Rev. **466**, 105 (2008).
87. S. Weinberg, Phys. Rev. Lett. **48**, 1303 (1979).
88. M. Bolz *et al.*, Nucl. Phys. **B606**, 518 (2001).
89. G. Coughlan *et al.*, Phys. Lett. **B131**, 59 (1983).
90. N. Arkani-Hamed *et al.*, Phys. Rev. **D59**, 086004 (1999).
91. L. Randall & R. Sundrum, Phys. Rev. Lett. **83**, 3370 (1999).
92. J.M. Cline *et al.*, Phys. Rev. Lett. **83**, 4245 (1999);
P. Binetruy *et al.*, Phys. Lett. **B477**, 285 (2000).

21. THE COSMOLOGICAL PARAMETERS

Updated September 2009, by O. Lahav (University College London) and A.R. Liddle (University of Sussex).

21.1. Parametrizing the Universe

Rapid advances in observational cosmology have led to the establishment of a precision cosmological model, with many of the key cosmological parameters determined to one or two significant figure accuracy. Particularly prominent are measurements of cosmic microwave background (CMB) anisotropies, led by the five-year results from the Wilkinson Microwave Anisotropy Probe (WMAP) [1–3]. However the most accurate model of the Universe requires consideration of a wide range of different types of observation, with complementary probes providing consistency checks, lifting parameter degeneracies, and enabling the strongest constraints to be placed.

The term ‘cosmological parameters’ is forever increasing in its scope, and nowadays includes the parametrization of some functions, as well as simple numbers describing properties of the Universe. The original usage referred to the parameters describing the global dynamics of the Universe, such as its expansion rate and curvature. Also now of great interest is how the matter budget of the Universe is built up from its constituents: baryons, photons, neutrinos, dark matter, and dark energy. We need to describe the nature of perturbations in the Universe, through global statistical descriptors such as the matter and radiation power spectra. There may also be parameters describing the physical state of the Universe, such as the ionization fraction as a function of time during the era since recombination. Typical comparisons of cosmological models with observational data now feature between five and ten parameters.

21.1.1. The global description of the Universe :

Ordinarily, the Universe is taken to be a perturbed Robertson–Walker space-time with dynamics governed by Einstein’s equations. This is described in detail by Olive and Peacock in this volume. Using the density parameters Ω_i for the various matter species and Ω_Λ for the cosmological constant, the Friedmann equation can be written

$$\sum_i \Omega_i + \Omega_\Lambda - 1 = \frac{k}{R^2 H^2}, \quad (21.1)$$

where the sum is over all the different species of material in the Universe. This equation applies at any epoch, but later in this article we will use the symbols Ω_i and Ω_Λ to refer to the present values. A typical collection would be baryons, photons, neutrinos, and dark matter (given charge neutrality, the electron density is guaranteed to be too small to be worth considering separately and is included with the baryons).

The complete present state of the homogeneous Universe can be described by giving the current values of all the density parameters and of the Hubble parameter h . These also allow us to track the history of the Universe back in time, at least until an epoch where interactions allow interchanges between the densities of the different species, which is believed to have last happened at neutrino decoupling, shortly before Big Bang Nucleosynthesis (BBN). To probe further back into the Universe’s history requires assumptions about particle interactions, and perhaps about the nature of physical laws themselves.

21.1.2. Neutrinos :

The standard neutrino sector has three flavors. For neutrinos of mass in the range 5×10^{-4} eV to 1 MeV, the density parameter in neutrinos is predicted to be

$$\Omega_\nu h^2 = \frac{\sum m_\nu}{93 \text{ eV}}, \quad (21.2)$$

where the sum is over all families with mass in that range (higher masses need a more sophisticated calculation). We use units with $c = 1$ throughout. Results on atmospheric and Solar neutrino oscillations [4] imply non-zero mass-squared differences between the three neutrino flavors. These oscillation experiments cannot tell us the absolute neutrino masses, but within the simple assumption of a mass hierarchy suggest a lower limit of $\Omega_\nu \approx 0.001$ on the neutrino mass density parameter.

For a total mass as small as 0.1 eV, this could have a potentially observable effect on the formation of structure, as neutrino free-streaming damps the growth of perturbations. Present cosmological observations have shown no convincing evidence of any effects from either neutrino masses or an otherwise non-standard neutrino sector, and impose quite stringent limits, which we summarize in Section 21.3.4. Accordingly, the usual assumption is that the masses are too small to have a significant cosmological impact at present data accuracy. However, we note that the inclusion of neutrino mass as a free parameter can affect the derived values of other cosmological parameters.

The cosmological effect of neutrinos can also be modified if the neutrinos have decay channels, or if there is a large asymmetry in the lepton sector manifested as a different number density of neutrinos versus anti-neutrinos. This latter effect would need to be of order unity to be significant (rather than the 10^{-9} seen in the baryon sector), which may be in conflict with nucleosynthesis [5].

21.1.3. Inflation and perturbations :

A complete model of the Universe should include a description of deviations from homogeneity, at least in a statistical way. Indeed, some of the most powerful probes of the parameters described above come from the evolution of perturbations, so their study is naturally intertwined in the determination of cosmological parameters.

There are many different notations used to describe the perturbations, both in terms of the quantity used to describe the perturbations and the definition of the statistical measure. We use the dimensionless power spectrum Δ^2 as defined in Olive and Peacock (also denoted \mathcal{P} in some of the literature). If the perturbations obey Gaussian statistics, the power spectrum provides a complete description of their properties.

From a theoretical perspective, a useful quantity to describe the perturbations is the curvature perturbation \mathcal{R} , which measures the spatial curvature of a comoving slicing of the space-time. A case of particular interest is the Harrison–Zel’dovich spectrum, which corresponds to a constant $\Delta_{\mathcal{R}}^2$. More generally, one can approximate the spectrum by a power-law, writing

$$\Delta_{\mathcal{R}}^2(k) = \Delta_{\mathcal{R}}^2(k_*) \left[\frac{k}{k_*} \right]^{n-1}, \quad (21.3)$$

where n is known as the spectral index, always defined so that $n = 1$ for the Harrison–Zel’dovich spectrum, and k_* is an arbitrarily chosen scale. The initial spectrum, defined at some early epoch of the Universe’s history, is usually taken to have a simple form such as this power-law, and we will see that observations require n close to one, which corresponds to the perturbations in the curvature being independent of scale. Subsequent evolution will modify the spectrum from its initial form.

The simplest viable mechanism for generating the observed perturbations is the inflationary cosmology, which posits a period of accelerated expansion in the Universe’s early stages [6]. It is a useful working hypothesis that this is the sole mechanism for generating perturbations, and it may further be assumed to be the simplest class of inflationary model, where the dynamics are equivalent to that of a single scalar field ϕ slowly rolling on a potential $V(\phi)$. One may seek to verify that this simple picture can match observations and to determine the properties of $V(\phi)$ from the observational data. Alternatively, more complicated models, perhaps motivated by contemporary fundamental physics ideas, may be tested on a model-by-model basis.

Inflation generates perturbations through the amplification of quantum fluctuations, which are stretched to astrophysical scales by the rapid expansion. The simplest models generate two types, density perturbations which come from fluctuations in the scalar field and its corresponding scalar metric perturbation, and gravitational waves which are tensor metric fluctuations. The former experience gravitational instability and lead to structure formation, while the latter can influence the CMB anisotropies. Defining slow-roll parameters, with primes indicating derivatives with respect to the scalar field, as

$$\epsilon = \frac{m_{\text{Pl}}^2}{16\pi} \left(\frac{V'}{V} \right)^2 ; \quad \eta = \frac{m_{\text{Pl}}^2}{8\pi} \frac{V''}{V}, \quad (21.4)$$

which should satisfy $\epsilon, |\eta| \ll 1$, the spectra can be computed using the slow-roll approximation as

$$\begin{aligned} \Delta_{\mathcal{R}}^2(k) &\simeq \frac{8}{3m_{\text{Pl}}^4} \left. \frac{V}{\epsilon} \right|_{k=aH}; \\ \Delta_{\text{grav}}^2(k) &\simeq \frac{128}{3m_{\text{Pl}}^4} \left. V \right|_{k=aH}. \end{aligned} \quad (21.5)$$

In each case, the expressions on the right-hand side are to be evaluated when the scale k is equal to the Hubble radius during inflation. The symbol ‘ \simeq ’ here indicates use of the slow-roll approximation, which is expected to be accurate to a few percent or better.

From these expressions, we can compute the spectral indices

$$n \simeq 1 - 6\epsilon + 2\eta \quad ; \quad n_{\text{grav}} \simeq -2\epsilon. \quad (21.6)$$

Another useful quantity is the ratio of the two spectra, defined by

$$r \equiv \frac{\Delta_{\text{grav}}^2(k_*)}{\Delta_{\mathcal{R}}^2(k_*)}. \quad (21.7)$$

This convention matches that of recent versions of the CMBFAST code [7] and that used by WMAP [8] (there are some alternative historical definitions which lead to a slightly different prefactor in the following equation). We have

$$r \simeq 16\epsilon \simeq -8n_{\text{grav}}, \quad (21.8)$$

which is known as the consistency equation.

In general, one could consider corrections to the power-law approximation, which we discuss later. However, for now we make the working assumption that the spectra can be approximated by power laws. The consistency equation shows that r and n_{grav} are not independent parameters, and so the simplest inflation models give initial conditions described by three parameters, usually taken as $\Delta_{\mathcal{R}}^2$, n , and r , all to be evaluated at some scale k_* , usually the ‘statistical center’ of the range explored by the data. Alternatively, one could use the parametrization V , ϵ , and η , all evaluated at a point on the putative inflationary potential.

After the perturbations are created in the early Universe, they undergo a complex evolution up until the time they are observed in the present Universe. While the perturbations are small, this can be accurately followed using a linear theory numerical code such as CMBFAST [7]. This works right up to the present for the CMB, but for density perturbations on small scales non-linear evolution is important and can be addressed by a variety of semi-analytical and numerical techniques. However the analysis is made, the outcome of the evolution is in principle determined by the cosmological model, and by the parameters describing the initial perturbations, and hence can be used to determine them.

Of particular interest are CMB anisotropies. Both the total intensity and two independent polarization modes are predicted to have anisotropies. These can be described by the radiation angular power spectra C_ℓ as defined in the article of Scott and Smoot in this volume, and again provide a complete description if the density perturbations are Gaussian.

21.1.4. The standard cosmological model :

We now have most of the ingredients in place to describe the cosmological model. Beyond those of the previous subsections, there are two parameters which are essential — a measure of the ionization state of the Universe and the galaxy bias parameter. The Universe is known to be highly ionized at low redshifts (otherwise radiation from distant quasars would be heavily absorbed in the ultra-violet), and the ionized electrons can scatter microwave photons altering the pattern of observed anisotropies. The most convenient parameter to describe this is the optical depth to scattering τ (*i.e.*, the probability that a given photon scatters once); in the approximation of instantaneous and complete reionization, this could equivalently be described by the redshift of reionization z_{ion} . The bias parameter, described fully later, is needed to relate the observed galaxy power spectrum to the predicted dark matter power spectrum. The basic set of cosmological parameters is therefore as shown in Table 21.1. The spatial curvature does not appear in the list, because it can be determined from the other parameters using Eq. (21.1). The total present matter density $\Omega_{\text{m}} = \Omega_{\text{cdm}} + \Omega_{\text{b}}$ is usually used in place of the dark matter density.

Table 21.1: The basic set of cosmological parameters. We give values (with some additional rounding) as obtained using a fit of a Λ CDM cosmology with a power-law initial spectrum to WMAP5 data alone [2]. Tensors are assumed zero except in quoting a limit on them. The exact values and uncertainties depend on both the precise data-sets used and the choice of parameters allowed to vary (see Table 21.2 for the former). Limits on Ω_{Λ} and h weaken if the Universe is not assumed flat. The density perturbation amplitude is specified by the derived parameter σ_8 . Uncertainties are one-sigma/68% confidence unless otherwise stated.

Parameter	Symbol	Value
Hubble parameter	h	0.72 ± 0.03
Total matter density	Ω_{m}	$\Omega_{\text{m}}h^2 = 0.133 \pm 0.006$
Baryon density	Ω_{b}	$\Omega_{\text{b}}h^2 = 0.0227 \pm 0.0006$
Cosmological constant	Ω_{Λ}	$\Omega_{\Lambda} = 0.74 \pm 0.03$
Radiation density	Ω_{r}	$\Omega_{\text{r}}h^2 = 2.47 \times 10^{-5}$
Neutrino density	Ω_{ν}	See Sec. 21.1.2
Density perturb. amplitude at $k=2\text{Kpc}$	$\Delta_{\mathcal{R}}^2$	$(2.41 \pm 0.11) \times 10^{-9}$
Density perturb. spectral index	n	$n = 0.963^{+0.014}_{-0.015}$
Tensor to scalar ratio	r	$r < 0.43$ (95% conf.)
Ionization optical depth	τ	$\tau = 0.087 \pm 0.017$
Bias parameter	b	See Sec. 21.3.4

Most attention to date has been on parameter estimation, where a set of parameters is chosen by hand and the aim is to constrain them. Interest has been growing towards the higher-level inference problem of model selection, which compares different choices of parameter sets. Bayesian inference offers an attractive framework for cosmological model selection, setting a tension between model predictiveness and ability to fit the data.

As described in Sec. 21.4, models based on these eleven parameters are able to give a good fit to the complete set of high-quality data available at present, and indeed some simplification is possible. Observations are consistent with spatial flatness, and indeed the inflation models so far described automatically generate negligible spatial curvature, so we can set $k = 0$; the density parameters then must sum to unity, and so one can be eliminated. The neutrino energy density is often not taken as an independent parameter. Provided the neutrino sector has the standard interactions, the neutrino energy density, while relativistic, can be related to the photon density using thermal physics arguments, and it is currently difficult to see the effect of the neutrino mass, although observations of large-scale structure have already placed interesting upper limits. This reduces the standard parameter set to nine. In addition, there is no observational evidence for the existence of tensor perturbations (though the upper limits are quite weak), and so r could be set to zero. Presently n is in a somewhat controversial position regarding whether it needs to be varied in a fit, or can be set to the Harrison–Zel’dovich value $n = 1$. Parameter estimation [2] suggests $n = 1$ is ruled out at some significance, but Bayesian model selection techniques [9] suggest the data is not conclusive. With n set to one, this leaves seven parameters, which is the smallest set that can usefully be compared to the present cosmological data set. This model (usually with n kept as a parameter) is referred to by various names, including Λ CDM, the concordance cosmology, and the standard cosmological model.

Of these parameters, only Ω_{r} is accurately measured directly. The radiation density is dominated by the energy in the CMB, and the COBE satellite FIRAS experiment determined its temperature to be $T = 2.725 \pm 0.001$ K [10], corresponding to $\Omega_{\text{r}} = 2.47 \times 10^{-5}h^{-2}$. It typically need not be varied in fitting other data. If galaxy clustering data are not included in a fit, then the bias parameter is also unnecessary.

In addition to this minimal set, there is a range of other parameters which might prove important in future as the data-sets further improve, but for which there is so far no direct evidence, allowing

them to be set to a specific value for now. We discuss various speculative options in the next section. For completeness at this point, we mention one other interesting parameter, the helium fraction, which is a non-zero parameter that can affect the CMB anisotropies at a subtle level. Presently, BBN provides the best measurement of this parameter (see the Fields and Sarkar article in this volume), and it is usually fixed in microwave anisotropy studies, but the data are just reaching a level where allowing its variation may become mandatory.

21.1.5. Derived parameters :

The parameter list of the previous subsection is sufficient to give a complete description of cosmological models which agree with observational data. However, it is not a unique parametrization, and one could instead use parameters derived from that basic set. Parameters which can be obtained from the set given above include the age of the Universe, the present horizon distance, the present neutrino background temperature, the epoch of matter–radiation equality, the epochs of recombination and decoupling, the epoch of transition to an accelerating Universe, the baryon-to-photon ratio, and the baryon to dark matter density ratio. In addition, the physical densities of the matter components, $\Omega_i h^2$, are often more useful than the density parameters. The density perturbation amplitude can be specified in many different ways other than the large-scale primordial amplitude, for instance, in terms of its effect on the CMB, or by specifying a short-scale quantity, a common choice being the present linear-theory mass dispersion on a scale of $8 h^{-1} \text{Mpc}$, known as σ_8 , whose WMAP5 value is 0.80 ± 0.04 .

Different types of observation are sensitive to different subsets of the full cosmological parameter set, and some are more naturally interpreted in terms of some of the derived parameters of this subsection than on the original base parameter set. In particular, most types of observation feature degeneracies whereby they are unable to separate the effects of simultaneously varying several of the base parameters.

21.2. Extensions to the standard model

This section discusses some ways in which the standard model could be extended. At present, there is no positive evidence in favor of any of these possibilities, which are becoming increasingly constrained by the data, though there always remains the possibility of trace effects at a level below present observational capability.

21.2.1. More general perturbations :

The standard cosmology assumes adiabatic, Gaussian perturbations. Adiabaticity means that all types of material in the Universe share a common perturbation, so that if the space-time is foliated by constant-density hypersurfaces, then all fluids and fields are homogeneous on those slices, with the perturbations completely described by the variation of the spatial curvature of the slices. Gaussianity means that the initial perturbations obey Gaussian statistics, with the amplitudes of waves of different wavenumbers being randomly drawn from a Gaussian distribution of width given by the power spectrum. Note that gravitational instability generates non-Gaussianity; in this context, Gaussianity refers to a property of the initial perturbations, before they evolve significantly.

The simplest inflation models, based on one dynamical field, predict adiabatic fluctuations and a level of non-Gaussianity which is too small to be detected by any experiment so far conceived. For present data, the primordial spectra are usually assumed to be power laws.

21.2.1.1. Non-power-law spectra:

For typical inflation models, it is an approximation to take the spectra as power laws, albeit usually a good one. As data quality improves, one might expect this approximation to come under pressure, requiring a more accurate description of the initial spectra, particularly for the density perturbations. In general, one can write a Taylor expansion of $\ln \Delta_{\mathcal{R}}^2$ as

$$\ln \Delta_{\mathcal{R}}^2(k) = \ln \Delta_{\mathcal{R}}^2(k_*) + (n_* - 1) \ln \frac{k}{k_*} + \frac{1}{2} \frac{dn}{d \ln k} \Big|_* \ln^2 \frac{k}{k_*} + \dots, \quad (21.9)$$

where the coefficients are all evaluated at some scale k_* . The term $dn/d \ln k|_*$ is often called the running of the spectral index [11]. Once

non-power-law spectra are allowed, it is necessary to specify the scale k_* at which the spectral index is defined.

21.2.1.2. Isocurvature perturbations:

An isocurvature perturbation is one which leaves the total density unperturbed, while perturbing the relative amounts of different materials. If the Universe contains N fluids, there is one growing adiabatic mode and $N - 1$ growing isocurvature modes (for reviews see Ref. 12 and Ref. 13). These can be excited, for example, in inflationary models where there are two or more fields which acquire dynamically-important perturbations. If one field decays to form normal matter, while the second survives to become the dark matter, this will generate a cold dark matter isocurvature perturbation.

In general, there are also correlations between the different modes, and so the full set of perturbations is described by a matrix giving the spectra and their correlations. Constraining such a general construct is challenging, though constraints on individual modes are beginning to become meaningful, with no evidence that any other than the adiabatic mode must be non-zero.

21.2.1.3. Non-Gaussianity:

Multi-field inflation models can also generate primordial non-Gaussianity (reviewed, *e.g.*, in Ref. 13). The extra fields can either be in the same sector of the underlying theory as the inflaton, or completely separate, an interesting example of the latter being the curvaton model [14]. Current upper limits on non-Gaussianity are becoming stringent, but there remains much scope to push down those limits and perhaps reveal trace non-Gaussianity in the data. If non-Gaussianity is observed, its nature may favor an inflationary origin, or a different one such as topological defects. A plausible possibility is non-Gaussianity caused by defects forming in a phase transition which ended inflation.

21.2.2. Dark matter properties :

Dark matter properties are discussed in the article by Drees and Gerber in this volume. The simplest assumption concerning the dark matter is that it has no significant interactions with other matter, and that its particles have a negligible velocity as far as structure formation is concerned. Such dark matter is described as ‘cold,’ and candidates include the lightest supersymmetric particle, the axion, and primordial black holes. As far as astrophysicists are concerned, a complete specification of the relevant cold dark matter properties is given by the density parameter Ω_{cdm} , though those seeking to directly detect it are as interested in its interaction properties.

Cold dark matter is the standard assumption and gives an excellent fit to observations, except possibly on the shortest scales where there remains some controversy concerning the structure of dwarf galaxies and possible substructure in galaxy halos. It has long been excluded for all the dark matter to have a large velocity dispersion, so-called ‘hot’ dark matter, as it does not permit galaxies to form; for thermal relics the mass must be below about 1 keV to satisfy this constraint, though relics produced non-thermally, such as the axion, need not obey this limit. However, in future further parameters might need to be introduced to describe dark matter properties relevant to astrophysical observations. Suggestions which have been made include a modest velocity dispersion (warm dark matter) and dark matter self-interactions. There remains the possibility that the dark matter comprises two separate components, *e.g.*, a cold one and a hot one, an example being if massive neutrinos have a non-negligible effect.

21.2.3. Dark energy :

While the standard cosmological model given above features a cosmological constant, in order to explain observations indicating that the Universe is presently accelerating, further possibilities exist under the general heading ‘dark energy’.[†] A particularly attractive possibility (usually called quintessence, though that word is used

[†] Unfortunately this is rather a misnomer, as it is the negative pressure of this material, rather than its energy, that is responsible for giving the acceleration. Furthermore, while generally in physics matter and energy are interchangeable terms, dark matter and dark energy are quite distinct concepts.

with various different meanings in the literature) is that a scalar field is responsible, with the mechanism mimicking that of early Universe inflation [15]. As described by Olive and Peacock, a fairly model-independent description of dark energy can be given just using the equation of state parameter w , with $w = -1$ corresponding to a cosmological constant. In general, the function w could itself vary with redshift, though practical experiments devised so far would be sensitive primarily to some average value weighted over recent epochs. For high-precision predictions of CMB anisotropies, it is better to use a scalar-field description in order to have a self-consistent evolution of the ‘sound speed’ associated with the dark energy perturbations.

A competing possibility is that the observed acceleration is due to a modification of gravity, *i.e.*, the left-hand side of Einstein’s equation rather than the right. Observations of expansion kinematics alone cannot distinguish these two possibilities, but probes of the growth rate of structure formation may be able to.

Present observations are consistent with a cosmological constant, but often w is kept as a free parameter to be added to the set described in the previous section. Most, but not all, researchers assume the weak energy condition $w \geq -1$. In the future, it may be necessary to use a more sophisticated parametrization of the dark energy.

21.2.4. Complex ionization history :

The full ionization history of the Universe is given by the ionization fraction as a function of redshift z . The simplest scenario takes the ionization to have the small residual value left after recombination up to some redshift z_{ion} , at which point the Universe instantaneously reionizes completely. Then there is a one-to-one correspondence between τ and z_{ion} (that relation, however, also depending on other cosmological parameters). An accurate treatment of this process will track separate histories for hydrogen and helium. While currently rapid ionization appears to be a good approximation, as data improve a more complex ionization history may need to be considered.

21.2.5. Varying ‘constants’ :

Variation of the fundamental constants of Nature over cosmological times is another possible enhancement of the standard cosmology. There is a long history of study of variation of the gravitational constant G , and more recently attention has been drawn to the possibility of small fractional variations in the fine-structure constant. There is presently no observational evidence for the former, which is tightly constrained by a variety of measurements. Evidence for the latter has been claimed from studies of spectral line shifts in quasar spectra at redshifts of order two [16], but this is presently controversial and in need of further observational study.

More broadly, one can ask whether general relativity is valid at all epochs under consideration.

21.2.6. Cosmic topology :

The usual hypothesis is that the Universe has the simplest topology consistent with its geometry, for example that a flat Universe extends forever. Observations cannot tell us whether that is true, but they can test the possibility of a non-trivial topology on scales up to roughly the present Hubble scale. Extra parameters would be needed to specify both the type and scale of the topology, for example, a cuboidal topology would need specification of the three principal axis lengths. At present, there is no direct evidence for cosmic topology, though the low values of the observed cosmic microwave quadrupole and octupole have been cited as a possible signature [17].

21.3. Probes

The goal of the observational cosmologist is to utilize astronomical information to derive cosmological parameters. The transformation from the observables to the key parameters usually involves many assumptions about the nature of the objects, as well as about the nature of the dark matter. Below we outline the physical processes involved in each probe, and the main recent results. The first two subsections concern probes of the homogeneous Universe, while the remainder consider constraints from perturbations.

In addition to statistical uncertainties we note three sources of systematic uncertainties that will apply to the cosmological

parameters of interest: (i) due to the assumptions on the cosmological model and its priors (*i.e.*, the number of assumed cosmological parameters and their allowed range); (ii) due to the uncertainty in the astrophysics of the objects (*e.g.*, light curve fitting for supernovae or the mass–temperature relation of galaxy clusters); and (iii) due to instrumental and observational limitations (*e.g.*, the effect of ‘seeing’ on weak gravitational lensing measurements, or beam shape on CMB anisotropy measurements).

21.3.1. Direct measures of the Hubble constant :

In 1929, Edwin Hubble discovered the law of expansion of the Universe by measuring distances to nearby galaxies. The slope of the relation between the distance and recession velocity is defined to be the Hubble constant H_0 . Astronomers argued for decades on the systematic uncertainties in various methods and derived values over the wide range, $40 \text{ km s}^{-1} \text{ Mpc}^{-1} \lesssim H_0 \lesssim 100 \text{ km s}^{-1} \text{ Mpc}^{-1}$.

One of the most reliable results on the Hubble constant comes from the Hubble Space Telescope Key Project [18]. This study used the empirical period–luminosity relations for Cepheid variable stars to obtain distances to 31 galaxies, and calibrated a number of secondary distance indicators (Type Ia Supernovae, Tully–Fisher relation, surface brightness fluctuations, and Type II Supernovae) measured over distances of 400 to 600 Mpc. They estimated $H_0 = 72 \pm 3$ (statistical) ± 7 (systematic) $\text{km s}^{-1} \text{ Mpc}^{-1}$.[‡] A recent study [19] of 240 Cepheids observed with an improved camera onboard the Hubble Space Telescope has yielded an even more accurate figure, $H_0 = 74 \pm 4 \text{ km s}^{-1} \text{ Mpc}^{-1}$ (including both statistical and systematic errors). The major sources of uncertainty in these results are due to the heavy element abundance of the Cepheids and the distance to the fiducial nearby galaxy (called the Large Magellanic Cloud) relative to which all Cepheid distances are measured. Nevertheless, it is remarkable that this result is in such good agreement with the result derived from the WMAP CMB measurements combined with other probes (see Table 21.2).

21.3.2. Supernovae as cosmological probes :

The relation between observed flux and the intrinsic luminosity of an object depends on the luminosity distance D_L , which in turn depends on cosmological parameters. More specifically

$$D_L = (1+z)r_e(z), \quad (21.10)$$

where $r_e(z)$ is the coordinate distance. For example, in a flat Universe

$$r_e(z) = \int_0^z \frac{dz'}{H(z')}. \quad (21.11)$$

For a general dark energy equation of state $w(z) = p_{\text{de}}(z)/\rho_{\text{de}}(z)$, the Hubble parameter is, still considering only the flat case,

$$\frac{H^2(z)}{H_0^2} = (1+z)^3 \Omega_m + \Omega_{\text{de}} \exp[3X(z)], \quad (21.12)$$

where

$$X(z) = \int_0^z [1+w(z')](1+z')^{-1} dz', \quad (21.13)$$

and Ω_m and Ω_{de} are the present density parameters of matter and dark energy components. If a general equation of state is allowed, then one has to solve for $w(z)$ (parametrized, for example, as $w(z) = w = \text{const.}$, or $w(z) = w_0 + w_1 z$) as well as for Ω_{de} .

Empirically, the peak luminosity of supernovae of Type Ia (SNe Ia) can be used as an efficient distance indicator (*e.g.*, Ref. 20). The favorite theoretical explanation for SNe Ia is the thermonuclear disruption of carbon-oxygen white dwarfs. Although not perfect ‘standard candles,’ it has been demonstrated that by correcting for a relation between the light curve shape, color, and the luminosity at maximum brightness, the dispersion of the measured luminosities can be greatly reduced. There are several possible systematic effects which may affect the accuracy of the use of SNe Ia as distance indicators, for example, evolution with redshift and interstellar extinction in the host galaxy and in the Milky Way.

[‡] Unless stated otherwise, all quoted uncertainties in this article are one-sigma/68% confidence. Cosmological parameters often have significantly non-Gaussian uncertainties. Throughout we have rounded central values, and especially uncertainties, from original sources in cases where they appear to be given to excessive precision.

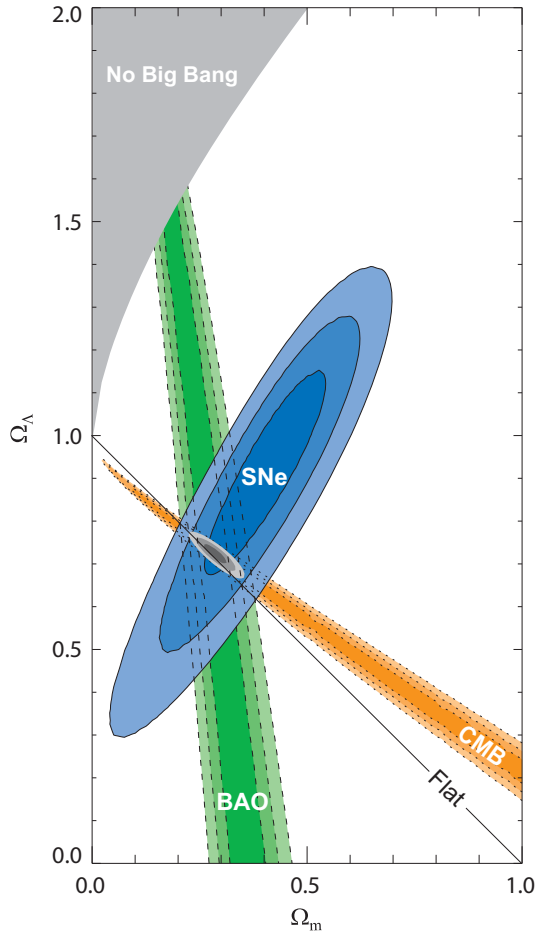


Figure 21.1: Confidence level contours of 68.3%, 95.4% and 99.7% in the Ω_Λ - Ω_m plane from the Cosmic Microwave Background, Baryonic Acoustic Oscillations and the Union SNe Ia set, as well as their combination (assuming $w = -1$). [Courtesy of Kowalski *et al.* [22]]

Two major studies, the ‘Supernova Cosmology Project’ and the ‘High- z Supernova Search Team’, found evidence for an accelerating Universe [21], interpreted as due to a cosmological constant, or to a more general dark energy component. Current results from the ‘Union sample’ [22] of over 300 SNe Ia are shown in Fig. 21.1 (see also earlier results in Ref. 23). When combined with the CMB data (which indicates flatness, *i.e.*, $\Omega_m + \Omega_\Lambda \approx 1$), the best-fit values are $\Omega_m \approx 0.3$ and $\Omega_\Lambda \approx 0.7$. Most results in the literature are consistent with Einstein’s $w = -1$ cosmological constant case.

For example, Kowalski *et al.* [22] deduced from SNe Ia combined with CMB and Baryonic Acoustic Oscillations (BAO) data (see next section), assuming a flat universe, that $w = -0.97 \pm 0.06 \pm 0.06$ (stat, sys) and $\Omega_m = 0.274 \pm 0.016 \pm 0.012$. Similarly Kessler *et al.* [24] estimated $w = -0.96 \pm 0.06 \pm 0.12$ and $\Omega_m = 0.265 \pm 0.016 \pm 0.025$, but they note a sensitivity to the light-curve fitter used.

Future experiments will aim to set constraints on the cosmic equation of state $w(z)$. However, given the integral relation between the luminosity distance and $w(z)$, it is not straightforward to recover $w(z)$ (*e.g.*, Ref. 25).

21.3.3. Cosmic microwave background :

The physics of the CMB is described in detail by Scott and Smoot in this volume. Before recombination, the baryons and photons are tightly coupled, and the perturbations oscillate in the potential wells generated primarily by the dark matter perturbations. After decoupling, the baryons are free to collapse into those potential wells. The CMB carries a record of conditions at the time of last scattering, often called primary anisotropies. In addition, it is affected by various processes as it propagates towards us, including the effect

of a time-varying gravitational potential (the integrated Sachs-Wolfe effect), gravitational lensing, and scattering from ionized gas at low redshift.

The primary anisotropies, the integrated Sachs-Wolfe effect, and scattering from a homogeneous distribution of ionized gas, can all be calculated using linear perturbation theory, a widely-used implementation being the CMBFAST code of Seljak and Zaldarriaga [7] (CAMB is a popular alternative, often used embedded in the analysis package CosmoMC [26]). Gravitational lensing is also calculated in this code. Secondary effects such as inhomogeneities in the reionization process, and scattering from gravitationally-collapsed gas (the Sunyaev-Zel’dovich effect), require more complicated, and more uncertain, calculations.

The upshot is that the detailed pattern of anisotropies depends on all of the cosmological parameters. In a typical cosmology, the anisotropy power spectrum [usually plotted as $\ell(\ell+1)C_\ell$] features a flat plateau at large angular scales (small ℓ), followed by a series of oscillatory features at higher angular scales, the first and most prominent being at around one degree ($\ell \simeq 200$). These features, known as acoustic peaks, represent the oscillations of the photon-baryon fluid around the time of decoupling. Some features can be closely related to specific parameters—for instance, the location of the first peak probes the spatial geometry, while the relative heights of the peaks probes the baryon density—but many other parameters combine to determine the overall shape.

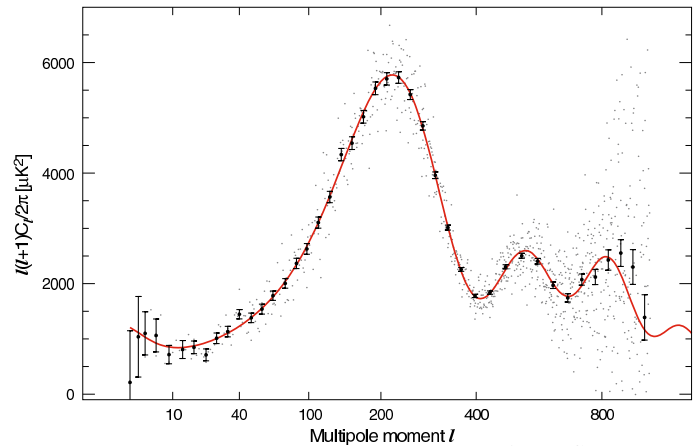


Figure 21.2: The angular power spectrum of the CMB temperature anisotropies from WMAP5 from Ref. 2. The grey points are the unbinned data, and the solid are binned data with error estimates including cosmic variance. The solid line shows the prediction from the best-fitting Λ CDM model. [Figure courtesy NASA/WMAP Science Team.]

The five-year data release from the WMAP satellite [1], henceforth WMAP5, has provided the most powerful results to date on the spectrum of CMB fluctuations, with a precision determination of the temperature power spectrum up to $\ell \simeq 900$, shown in Fig. 21.2, as well as measurements of the spectrum of E -polarization anisotropies and the correlation spectrum between temperature and polarization (those spectra having first been detected by DASI [27]). These are consistent with models based on the parameters we have described, and provide accurate determinations of many of those parameters [2].

WMAP5 provides an exquisite measurement of the location of the first acoustic peak, determining the angular-diameter distance of the last-scattering surface. In combination with other data this strongly constrains the spatial geometry, in a manner consistent with spatial flatness and excluding significantly-curved Universes. WMAP5 also gives a precision measurement of the age of the Universe. It gives a baryon density consistent with, and at higher precision than, that coming from BBN. It affirms the need for both dark matter and dark energy. It shows no evidence for dynamics of the dark energy, being consistent with a pure cosmological constant ($w = -1$). The density perturbations are consistent with a power-law primordial spectrum, with indications that the spectral slope may be less than

the Harrison–Zel’dovich value $n = 1$ [2]. There is no indication of tensor perturbations, but the upper limit is quite weak. WMAP5’s current best-fit for the reionization optical depth, $\tau = 0.087$, is in reasonable agreement with models of how early structure formation induces reionization.

WMAP5 is consistent with other experiments and its dynamic range can be enhanced by including information from small-angle CMB experiments including ACBAR, CBI, and QUaD, which gives extra constraining power on some parameters.

21.3.4. Galaxy clustering :

The power spectrum of density perturbations depends on the nature of the dark matter. Within the Cold Dark Matter model, the shape of the power spectrum depends primarily on the primordial power spectrum and on the combination $\Omega_m h$, which determines the horizon scale at matter–radiation equality, with a subdominant dependence on the baryon density. The matter distribution is most easily probed by observing the galaxy distribution, but this must be done with care as the galaxies do not perfectly trace the dark matter distribution. Rather, they are a ‘biased’ tracer of the dark matter. The need to allow for such bias is emphasized by the observation that different types of galaxies show bias with respect to each other. Further, the observed 3D galaxy distribution is in redshift space, *i.e.*, the observed redshift is the sum of the Hubble expansion and the line-of-sight peculiar velocity, leading to linear and non-linear dynamical effects which also depend on the cosmological parameters. On the largest length scales, the galaxies are expected to trace the location of the dark matter, except for a constant multiplier b to the power spectrum, known as the linear bias parameter. On scales smaller than $20 h^{-1}$ Mpc or so, the clustering pattern is ‘squashed’ in the radial direction due to coherent infall, which depends approximately on the parameter $\beta \equiv \Omega_m^{0.6}/b$ (on these shorter scales, more complicated forms of biasing are not excluded by the data). On scales of a few h^{-1} Mpc, there is an effect of elongation along the line of sight (colloquially known as the ‘finger of God’ effect) which depends on the galaxy velocity dispersion.

21.3.4.1. Baryonic Acoustic Oscillations:

The Fourier power spectra of the 2-degree Field (2dF) Galaxy Redshift Survey** and the Sloan Digital Sky Survey (SDSS)†† are well fitted by a Λ CDM model and both surveys show evidence for BAOs. Cole *et al.* [28] estimate from 2dF a baryon fraction $\Omega_b/\Omega_m = 0.18 \pm 0.05$ ($1\text{-}\sigma$ uncertainties). The shape of the power spectrum has been characterized by $\Omega_m h = 0.168 \pm 0.016$, and in combination with WMAP data gives $\Omega_m = 0.23 \pm 0.02$ (see also Ref. 29). Eisenstein *et al.* [30] reported a detection of the BAO peak in the large-scale correlation function of the SDSS sample of nearly 47,000 Luminous Red Galaxies (LRG). By using the baryon acoustic peak as a ‘standard ruler’ they found, independent of WMAP, that $\Omega_m = 0.27 \pm 0.03$ for a flat Λ CDM model. Signatures of BAOs have also been measured [31,32] from samples of nearly 600,000 LRGs with photometric redshifts (which are less accurate than spectroscopic redshifts, but easier to obtain for large samples).

The most recent work uses the SDSS LRG 7th Data Release [33,34]. Combining the so-called ‘halo’ power spectrum measurement with the WMAP5 results, for the flat Λ CDM model they find $\Omega_m = 0.289 \pm 0.019$ and $H_0 = 69.4 \pm 1.6$ km s $^{-1}$ Mpc $^{-1}$. Allowing for massive neutrinos in Λ CDM, they find $\sum m_\nu < 0.62$ eV at the 95% confidence level [33].

Combination of the 2dF data with the CMB indicates a ‘biasing’ parameter $b \sim 1$, in agreement with a 2dF-alone analysis of higher-order clustering statistics. However, results for biasing also depend on the length scale over which a fit is done, and the selection of the objects by luminosity, spectral type, or color. In particular, on scales smaller than $10 h^{-1}$ Mpc, different galaxy types are clustered differently. This ‘biasing’ introduces a systematic effect on the determination of cosmological parameters from redshift surveys. Prior knowledge from simulations of galaxy formation or from gravitational lensing data could help.

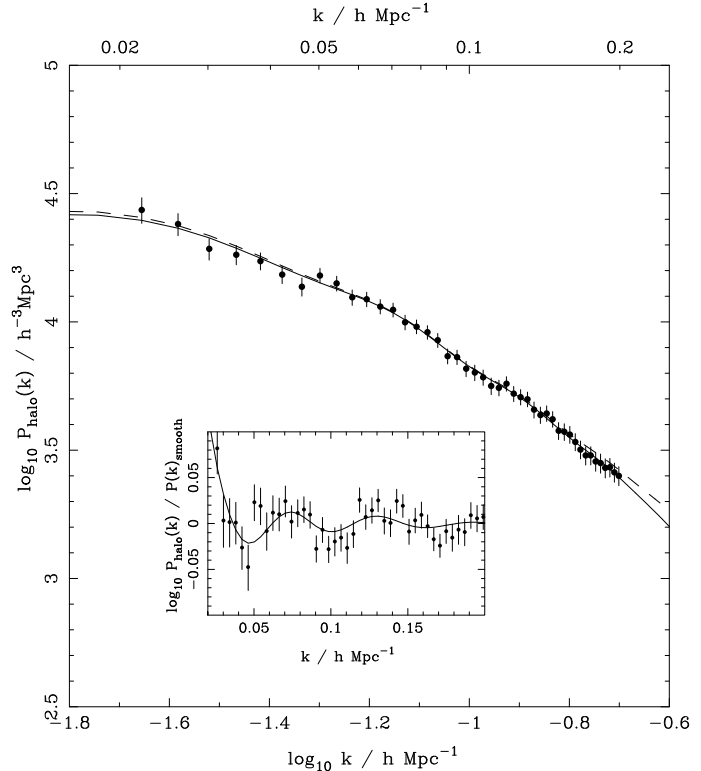


Figure 21.3: The galaxy power spectrum from the SDSS Luminous Red Galaxies (LRG). The best-fit LRG+WMAP Λ CDM model is shown for two sets of nuisance parameters (solid and dashed lines). The BAO inset shows the same data and model divided by a spline fit to the smooth component. [Figure provided by B. Reid and W. Percival; see Ref. 33 and Ref. 34.]

21.3.4.2. Integrated Sachs–Wolfe effect:

The integrated Sachs–Wolfe effect, described in the article by Scott and Smoot, is the change in CMB photon energy when propagating through the changing gravitational potential wells of developing cosmic structures. Correlating the large-angle CMB anisotropies with very large scale structures, first proposed in Ref. 35, has provided detections of this effect typically of significance 2 to 4σ [36]. As gravitational potentials do not evolve in critical density models, this provides direct evidence of a sub-critical matter density, and hence in combination with other probes supports the existence of dark energy.

21.3.4.3. Limits on neutrino mass from galaxy surveys and other probes:

Large-scale structure data can put an upper limit on the ratio Ω_ν/Ω_m due to the neutrino ‘free streaming’ effect [37,38]. For example, by comparing the 2dF galaxy power spectrum with a four-component model (baryons, cold dark matter, a cosmological constant, and massive neutrinos), it is estimated that $\Omega_\nu/\Omega_m < 0.13$ (95% confidence limit), giving $\Omega_\nu < 0.04$ if a concordance prior of $\Omega_m = 0.3$ is imposed. The latter corresponds to an upper limit of about 2 eV on the total neutrino mass, assuming a prior of $h \approx 0.7$ [39]. Potential systematic effects include biasing of the galaxy distribution and non-linearities of the power spectrum. A similar upper limit of 2 eV has been derived from CMB anisotropies alone [40–42]. The above analyses assume that the primordial power spectrum is adiabatic, scale-invariant and Gaussian. Additional cosmological data sets have improved the results [43,44]. An upper limit on the total neutrino mass of 0.17 eV was reported by combining a large number of cosmological probes [45].

Laboratory limits on absolute neutrino masses from tritium beta decay and especially from neutrinoless double-beta decay should, within the next decade, push down towards (or perhaps even beyond) the 0.1 eV level that has cosmological significance.

** See <http://www.mso.anu.edu.au/2dFGRS>

†† See <http://www.sdss.org>

21.3.5. Clusters of galaxies :

A cluster of galaxies is a large collection of galaxies held together by their mutual gravitational attraction. The largest ones are around 10^{15} Solar masses, and are the largest gravitationally-collapsed structures in the Universe. Even at the present epoch they are relatively rare, with only a few percent of galaxies being in clusters. They provide various ways to study the cosmological parameters; here we discuss constraints from the measurements of the cluster number density and the baryon fraction in clusters.

21.3.5.1. Cluster number density:

The first objects of a given kind form at the rare high peaks of the density distribution, and if the primordial density perturbations are Gaussian distributed, their number density is exponentially sensitive to the size of the perturbations, and hence can strongly constrain it. Clusters are an ideal application in the present Universe. They are usually used to constrain the amplitude σ_8 , as a box of side $8h^{-1}$ Mpc contains about the right amount of material to form a cluster. The most useful observations at present are of X-ray emission from hot gas lying within the cluster, whose temperature is typically a few keV, and which can be used to estimate the mass of the cluster. A theoretical prediction for the mass function of clusters can come either from semi-analytic arguments or from numerical simulations. At present, the main uncertainty is the relation between the observed gas temperature and the cluster mass, despite extensive study using simulations. Ref. 46 uses Chandra satellite X-ray data to obtain

$$\sigma_8 = 0.803 \pm 0.011 \text{ (stat.)} \pm 0.020 \text{ (sys.)} \quad (68\% \text{ conf.}) \quad (21.14)$$

for $\Omega_m = 0.25$. This result agrees well with the values predicted in cosmologies compatible with WMAP5.

The same approach can be adopted at high redshift (which for clusters means redshifts approaching one) to attempt to measure σ_8 at an earlier epoch. The evolution of σ_8 is primarily driven by the value of the matter density Ω_m , with a sub-dominant dependence on the dark energy density. Such analyses favor a low matter density, again compatible with measurements from the CMB.

21.3.5.2. Cluster baryon fraction:

If clusters are representative of the mass distribution in the Universe, the fraction of the mass in baryons to the overall mass distribution would be $f_b = \Omega_b/\Omega_m$. If Ω_b , the baryon density parameter, can be inferred from the primordial nucleosynthesis abundance of the light elements, the cluster baryon fraction f_b can then be used to constrain Ω_m and h (*e.g.*, Ref. 47). The baryons in clusters are primarily in the form of X-ray-emitting gas that falls into the cluster, and secondarily in the form of stellar baryonic mass. Hence, the baryon fraction in clusters is estimated to be

$$f_b = \frac{\Omega_b}{\Omega_m} \simeq f_{\text{gas}} + f_{\text{gal}}, \quad (21.15)$$

where $f_b = M_b/M_{\text{grav}}$, $f_{\text{gas}} = M_{\text{gas}}/M_{\text{grav}}$, $f_{\text{gal}} = M_{\text{gal}}/M_{\text{grav}}$, and M_{grav} is the total gravitating mass. This leads to an approximate relation between Ω_m and h :

$$\Omega_m = \frac{\Omega_b}{f_{\text{gas}} + f_{\text{gal}}} \simeq \frac{\Omega_b}{0.08h^{-1.5} + 0.01h^{-1}}. \quad (21.16)$$

The ratio Ω_b/Ω_m is consistent with other measures, and Allen *et al.* [48] give examples of constraints that can be obtained this way on both dark matter and dark energy using Chandra data across a range of redshifts.

21.3.6. Clustering in the inter-galactic medium :

It is commonly assumed, based on hydrodynamic simulations, that the neutral hydrogen in the inter-galactic medium (IGM) can be related to the underlying mass distribution. It is then possible to estimate the matter power spectrum on scales of a few megaparsecs from the absorption observed in quasar spectra, the so-called Lyman- α forest. The usual procedure is to measure the power spectrum of the transmitted flux, and then to infer the mass power spectrum. Photo-ionization heating by the ultraviolet background radiation and

adiabatic cooling by the expansion of the Universe combine to give a simple power-law relation between the gas temperature and the baryon density. It also follows that there is a power-law relation between the optical depth τ and ρ_b . Therefore, the observed flux $F = \exp(-\tau)$ is strongly correlated with ρ_b , which itself traces the mass density. The matter and flux power spectra can be related by

$$P_m(k) = b^2(k) P_F(k), \quad (21.17)$$

where $b(k)$ is a bias function which is calibrated from simulations. Croft *et al.* [49] derived cosmological parameters from Keck Telescope observations of the Lyman- α forest at redshifts $z = 2 - 4$. Their derived power spectrum corresponds to that of a CDM model, which is in good agreement with the 2dF galaxy power spectrum. A recent study using VLT spectra [50] agrees with the flux power spectrum of Ref. 49. This method depends on various assumptions. Seljak *et al.* [51] pointed out that errors are sensitive to the range of cosmological parameters explored in the simulations, and the treatment of the mean transmitted flux. Nevertheless, this method has the potential of measuring accurately the power spectrum of mass fluctuations in a way different from the other methods.

21.3.7. Gravitational lensing :

Images of background galaxies get distorted due to the gravitational effect of mass fluctuations along the line of sight. Deep gravitational potential wells such as galaxy clusters generate ‘strong lensing,’ *i.e.*, arcs, arclets and multiple images, while more moderate fluctuations give rise to ‘weak lensing’. Weak lensing is now widely used to measure the mass power spectrum in random regions of the sky (see Ref. 52 for recent reviews). As the signal is weak, the image of deformed galaxy shapes (‘shear map’) is analyzed statistically to measure the power spectrum, higher moments, and cosmological parameters.

The shear measurements are mainly sensitive to the combination of Ω_m and the amplitude σ_8 . For example, the weak lensing signal detected by the CFHT Legacy Survey has been analyzed to yield $\sigma_8(\Omega_m/0.25)^{0.64} = 0.78 \pm 0.04$ [53] and $\sigma_8(\Omega_m/0.24)^{0.59} = 0.84 \pm 0.05$ [54] assuming a Λ CDM model. Earlier results are summarized in Ref. 52. There are various systematic effects in the interpretation of weak lensing, *e.g.*, due to atmospheric distortions during observations, the redshift distribution of the background galaxies, intrinsic correlation of galaxy shapes, and non-linear modeling uncertainties.

21.3.8. Peculiar velocities :

Deviations from the Hubble flow directly probe the mass fluctuations in the Universe, and hence provide a powerful probe of the dark matter. Peculiar velocities are deduced from the difference between the redshift and the distance of a galaxy. The observational difficulty is in accurately measuring distances to galaxies. Even the best distance indicators (*e.g.*, the Tully–Fisher relation) give an error of 15% per galaxy, hence limiting the application of the method at large distances. Peculiar velocities are mainly sensitive to Ω_m , not to Ω_Λ or quintessence. Extensive analyses in the early 1990s (*e.g.*, Ref. 55) suggested a value of Ω_m close to unity. Further analysis [56], which takes into account non-linear corrections, gives $\sigma_8\Omega_m^{0.6} = 0.49 \pm 0.06$ and $\sigma_8\Omega_m^{0.6} = 0.63 \pm 0.08$ (90% errors) for two independent data sets. Analysis from pairwise velocities [57] gives $\sigma_8 = 1.1 \pm 0.2$, while bulk flows [58] give a lower limit $\sigma_8 > 1.11$ (95% CL), in disagreement with WMAP5. While at present cosmological parameters derived from peculiar velocities are strongly affected by random and systematic errors, a new generation of surveys may improve their accuracy. Three promising approaches are the 6dF near-infrared survey of 15,000 peculiar velocities^{‡‡}, supernovae Type Ia, and the kinematic Sunyaev–Zel’dovich effect.

There is also a renewed interest in ‘redshift distortion’. As the measured redshift of a galaxy is the sum of its redshift due to the Hubble expansion and its peculiar velocity, this distortion depends on cosmological parameters (Ref. 59) via the growth rate $f(z) = d\ln\delta/d\ln a \approx \Omega^\gamma(z)$, where $\gamma = 0.55$ for a concordance Λ CDM model, and is different for a modified gravity model. Recent observational results [60] show that by measuring $f(z)$ with redshift it is feasible to constrain γ .

^{‡‡} See <http://www.mso.anu.edu.au/6dFGS/>

Table 21.2: Parameter constraints reproduced from Dunkley *et al.* [2] and Komatsu *et al.* [3], with some additional rounding. All columns assume the Λ CDM cosmology with a power-law initial spectrum, no tensors, spatial flatness, and a cosmological constant as dark energy. Above the line are the six parameter combinations actually fit to the data; those below the line are derived from these. Two different data combinations are shown to highlight the extent to which this choice matters. The first column is WMAP5 alone, while the second column shows a combination of WMAP5 with BAO and SNe data as described in Ref. 3. The perturbation amplitude $\Delta_{\mathcal{R}}^2$ is specified at the scale 0.002 Mpc^{-1} . Uncertainties are shown at 68% confidence, and caution is needed in extrapolating them to higher significance levels due to non-Gaussian likelihoods and assumed priors.

	WMAP5 alone	WMAP5 + BAO + SN
$\Omega_b h^2$	0.0227 ± 0.0006	0.0227 ± 0.0006
$\Omega_{\text{cdm}} h^2$	0.110 ± 0.006	0.113 ± 0.003
Ω_Λ	0.74 ± 0.03	0.726 ± 0.015
n	$0.963_{-0.015}^{+0.014}$	0.960 ± 0.013
τ	0.087 ± 0.017	0.084 ± 0.016
$\Delta_{\mathcal{R}}^2 \times 10^9$	2.41 ± 0.11	2.44 ± 0.10
h	0.72 ± 0.03	0.705 ± 0.013
σ_8	0.80 ± 0.04	0.81 ± 0.03
$\Omega_m h^2$	0.133 ± 0.006	0.136 ± 0.004

21.4. Bringing observations together

Although it contains two ingredients—dark matter and dark energy—which have not yet been verified by laboratory experiments, the Λ CDM model is almost universally accepted by cosmologists as the best description of the present data. The basic ingredients are given by the parameters listed in Sec. 21.1.4, with approximate values of some of the key parameters being $\Omega_b \approx 0.04$, $\Omega_{\text{cdm}} \approx 0.21$, $\Omega_\Lambda \approx 0.74$, and a Hubble constant $h \approx 0.72$. The spatial geometry is very close to flat (and usually assumed to be precisely flat), and the initial perturbations Gaussian, adiabatic, and nearly scale-invariant.

The most powerful single experiment is WMAP5, which on its own supports all these main tenets. Values for some parameters, as given in Dunkley *et al.* [2] and Komatsu *et al.* [3], are reproduced in Table 21.2. These particular results presume a flat Universe. The constraints are somewhat strengthened by adding additional data-sets, as shown in the Table, though most of the constraining power resides in the WMAP5 data.

If the assumption of spatial flatness is lifted, it turns out that WMAP5 on its own only weakly constrains the spatial curvature, due to a parameter degeneracy in the angular-diameter distance. However inclusion of other data readily removes this, *e.g.*, inclusion of BAO and SNe data, plus the assumption that the dark energy is a cosmological constant, yields a constraint on $\Omega_{\text{tot}} \equiv \sum \Omega_i + \Omega_\Lambda$ of [3]

$$\Omega_{\text{tot}} = 1.006 \pm 0.006. \quad (21.18)$$

Results of this type are normally taken as justifying the restriction to flat cosmologies.

The baryon density Ω_b is now measured with quite high accuracy from the CMB and large-scale structure, and is consistent with the determination from BBN; Fields and Sarkar in this volume quote the range $0.019 \leq \Omega_b h^2 \leq 0.024$ (95% confidence).

While Ω_Λ is measured to be non-zero with very high confidence, there is no evidence of evolution of the dark energy density. The WMAP team find the limit $w < -0.86$ at 95% confidence from a

compilation of data including SNe Ia, with the cosmological constant case $w = -1$ giving an excellent fit to the data.

The data provide strong support for the main predictions of the simplest inflation models: spatial flatness and adiabatic, Gaussian, nearly scale-invariant density perturbations. But it is disappointing that there is no sign of primordial gravitational waves, with WMAP5 alone providing only a weak upper limit $r < 0.43$ at 95% confidence [2] (this assumes no running, and weakens to 0.58 if running is allowed). The spectral index n is placed in an interesting position by WMAP5, with indications that $n < 1$ is required by the data. However, the confidence with which $n = 1$ is ruled out is still rather weak, and in our view it is premature to conclude that $n = 1$ is no longer viable.

Tests have been made for various types of non-Gaussianity, a particular example being a parameter f_{NL} which measures a quadratic contribution to the perturbations. Tests distinguish between non-Gaussianity of ‘local’ and ‘equilateral’ type (see Ref. 3 for details), and current constraints give $-9 < f_{\text{NL}}^{\text{local}} < 110$ and $-150 < f_{\text{NL}}^{\text{equil}} < 250$ at 95% confidence (these look weak, but prominent non-Gaussianity requires the product $f_{\text{NL}} \Delta_{\mathcal{R}}$ to be large, and $\Delta_{\mathcal{R}}$ is of order 10^{-5}). It will be interesting to watch if the tendency of the former to have a positive value reaches significance in future data.

One parameter which is very robust is the age of the Universe, as there is a useful coincidence that for a flat Universe the position of the first peak is strongly correlated with the age. The WMAP5 result is 13.69 ± 0.13 Gyr (assuming flatness). This is in good agreement with the ages of the oldest globular clusters [61] and radioactive dating [62].

21.5. Outlook for the future

The concordance model is now well established, and there seems little room left for any dramatic revision of this paradigm. A measure of the strength of that statement is how difficult it has proven to formulate convincing alternatives.

Should there indeed be no major revision of the current paradigm, we can expect future developments to take one of two directions. Either the existing parameter set will continue to prove sufficient to explain the data, with the parameters subject to ever-tightening constraints, or it will become necessary to deploy new parameters. The latter outcome would be very much the more interesting, offering a route towards understanding new physical processes relevant to the cosmological evolution. There are many possibilities on offer for striking discoveries, for example:

- The cosmological effects of a neutrino mass may be unambiguously detected, shedding light on fundamental neutrino properties;
- Compelling detection of deviations from scale-invariance in the initial perturbations would indicate dynamical processes during perturbation generation by, for instance, inflation;
- Detection of primordial non-Gaussianities would indicate that non-linear processes influence the perturbation generation mechanism;
- Detection of variation in the dark-energy density (*i.e.*, $w \neq -1$) would provide much-needed experimental input into the question of the properties of the dark energy.

These provide more than enough motivation for continued efforts to test the cosmological model and improve its precision.

Over the coming years, there are a wide range of new observations which will bring further precision to cosmological studies. Indeed, there are far too many for us to be able to mention them all here, and so we will just highlight a few areas.

The CMB observations will improve in several directions. The current frontier is the study of polarization, first detected in 2002 by DASI and for which power spectrum measurements have now been made by several experiments. Future measurements may be able to separately detect the two modes of polarization. Another area of development is pushing accurate power spectrum measurements to smaller angular scales, with the Atacama Cosmology Telescope (ACT) and South Pole Telescope (SPT) both now in operation. Finally, we mention the Planck satellite, launched in May 2009, which will make high-precision all-sky maps of temperature and polarization, utilizing

a very wide frequency range for observations to improve understanding of foreground contaminants, and to compile a large sample of clusters via the Sunyaev–Zeldovich effect.

On the supernova side, the most ambitious initiatives at present are satellite missions JDEM (Joint Dark Energy Mission), proposed to NASA and DOE, and Euclid proposed to ESA. An impressive array of ground-based dark energy surveys are already operational, under construction, or proposed, including the ESSENCE project, the Dark Energy Survey, Pan-Starrs, and LSST. With large samples, it may be possible to detect evolution of the dark energy density, thus measuring its equation of state and perhaps even its variation.

An exciting new area for the future will be radio surveys of the redshifted 21-cm line of hydrogen. Because of the intrinsic narrowness of this line, by tuning of the bandpass the emission from narrow redshift slices of the Universe will be measured to extremely high redshift, probing the details of the reionization process at redshifts up to perhaps 20. LOFAR is the first instrument able to do this and is at an advanced construction stage. In the longer term, the Square Kilometer Array (SKA) will take these studies to a precision level.

The above future surveys will address fundamental questions of physics well beyond just testing the ‘concordance’ Λ CDM model and minor variations. By learning about both the geometry of the universe and the growth of perturbations, it would be possible to test theories of modified gravity and inhomogeneous universes.

The development of the first precision cosmological model is a major achievement. However, it is important not to lose sight of the motivation for developing such a model, which is to understand the underlying physical processes at work governing the Universe’s evolution. On that side, progress has been much less dramatic. For instance, there are many proposals for the nature of the dark matter, but no consensus as to which is correct. The nature of the dark energy remains a mystery. Even the baryon density, now measured to an accuracy of a few percent, lacks an underlying theory able to predict it even within orders of magnitude. Precision cosmology may have arrived, but at present many key questions remain unanswered.

References:

1. G. Hinshaw *et al.*, *Astrophys. J. Supp.* **180**, 225 (2009).
2. J. Dunkley *et al.*, *Astrophys. J. Supp.* **180**, 306 (2009).
3. E. Komatsu *et al.*, *Astrophys. J. Supp.* **180**, 330 (2009).
4. S. Fukuda *et al.*, *Phys. Rev. Lett.* **85**, 3999 (2000);
Q.R. Ahmad *et al.*, *Phys. Rev. Lett.* **87**, 071301 (2001).
5. A.D. Dolgov *et al.*, *Nucl. Phys.* **B632**, 363 (2002).
6. For detailed accounts of inflation see E.W. Kolb and M.S. Turner, *The Early Universe*, Addison–Wesley (Redwood City, 1990);
A.R. Liddle and D.H. Lyth, *Cosmological Inflation and Large-Scale Structure*, Cambridge University Press (2000).
7. U. Seljak and M. Zaldarriaga, *Astrophys. J.* **469**, 1 (1996).
8. H.V. Peiris *et al.*, *Astrophys. J. Supp.* **148**, 213 (2003).
9. D. Parkinson *et al.*, *Phys. Rev.* **D73**, 123523 (2006).
10. J.C. Mather *et al.*, *Astrophys. J.* **512**, 511 (1999).
11. A. Kosowsky and M.S. Turner, *Phys. Rev.* **D52**, 1739 (1995).
12. K.A. Malik and D. Wands, *Physics Reports* **475**, 1 (2009).
13. D.H. Lyth and A.R. Liddle, *The Primordial Density Perturbation*, Cambridge University Press (2009).
14. D.H. Lyth and D. Wands, *Phys. Lett.* **B524**, 5 (2002);
K. Enqvist and M.S. Sloth, *Nucl. Phys.* **B626**, 395 (2002);
T. Moroi and T. Takahashi, *Phys. Lett.* **B522**, 215 (2001).
15. B. Ratra and P.J.E. Peebles, *Phys. Rev.* **D37**, 3406 (1988);
C. Wetterich, *Nucl. Phys.* **B302**, 668 (1988);
T. Padmanabhan, *Phys. Rept.* **380**, 235 (2003);
V. Sahni and A. Starobinsky, *Int. J. Mod. Phys.* **D9**, 373 (2000).
16. J.K. Webb *et al.*, *Phys. Rev. Lett.* **82**, 884 (1999);
J.K. Webb *et al.*, *Phys. Rev. Lett.* **87**, 091301 (2001);
J.K. Webb *et al.*, *Astrophys. Sp. Sci.* **283**, 565 (2003);
H. Chand *et al.*, *Astron. Astrophys.* **417**, 853 (2004);
R. Srianand *et al.*, *Phys. Rev. Lett.* **92**, 121302 (2004).
17. J. Levin, *Physics Reports* **365**, 251 (2002).
18. W.L. Freedman *et al.*, *Astrophys. J.* **553**, 47 (2001).
19. A.G. Riess *et al.*, *Astrophys. J.* **699**, 539 (2009).
20. B. Leibundgut, *Ann. Rev. Astron. Astrophys.* **39**, 67 (2001).
21. A.G. Riess *et al.*, *Astron. J.* **116**, 1009 (1998);
P. Garnavich *et al.*, *Astrophys. J.* **509**, 74 (1998);
S. Perlmutter *et al.*, *Astrophys. J.* **517**, 565 (1999).
22. M. Kowalski *et al.*, *Astrophys. J.* **686**, 749 (2008).
23. J.L. Tonry *et al.*, *Astrophys. J.* **594**, 1 (2003);
A.G. Riess *et al.*, *Astrophys. J.* **659**, 98 (2007);
S. Jha, A.G. Riess, and R.P. Kirshner *et al.*, *Astrophys. J.* **659**, 122 (2007);
R.A. Knop *et al.*, *Astrophys. J.* **598**, 102 (2003);
W.M. Wood-Vasey *et al.*, *Astrophys. J.* **666**, 694 (2007).
24. R. Kessler *et al.*, *Astrophys. J. Supp.* in press, [arXiv:0908.4274](https://arxiv.org/abs/0908.4274) (2009).
25. I. Maor *et al.*, *Phys. Rev.* **D65**, 123003 (2002).
26. A. Lewis and S. Bridle, *Phys. Rev.* **D66**, 103511 (2002).
27. J. Kovac *et al.*, *Nature* **420**, 772 (2002).
28. S. Cole *et al.*, *Mon. Not. Roy. Astr. Soc.* **362**, 505 (2005).
29. A. Sanchez *et al.*, *Mon. Not. Roy. Astr. Soc.* **366**, 189 (2006).
30. D. Eisenstein *et al.*, *Astrophys. J.* **633**, 560 (2005).
31. C. Blake *et al.*, *Mon. Not. Roy. Astr. Soc.* **374**, 1527 (2007).
32. N. Padmanabhan *et al.*, *Mon. Not. Roy. Astr. Soc.* **378**, 852 (2007).
33. B. Reid *et al.*, [arXiv:0907.1659](https://arxiv.org/abs/0907.1659) [astro-ph] (2009).
34. W.J. Percival *et al.*, [arXiv:0907.1660](https://arxiv.org/abs/0907.1660) [astro-ph] (2009).
35. R.G. Crittenden and N. Turok, *Phys. Rev. Lett.* **75**, 2642 (1995).
36. S.P. Boughn and R.G. Crittenden, *Nature* **427**, 45 (20034);
T. Giannantonio *et al.*, *Phys. Rev.* **D77**, 123520 (2008).
37. W. Hu *et al.*, *Phys. Rev. Lett.* **80**, 5255 (1998).
38. J. Lesgourgues and S. Pastor, *Physics Reports*, **429**, 307 (2006).
39. O. Elgaroy and O. Lahav, *JCAP* **0304**, 004 (2003).
40. D. N. Spergel *et al.*, *Astrophys. J. Supp.* **170**, 377 (2007).
41. K. Ichikawa *et al.*, *Phys. Rev.* **D71**, 043001 (2005).
42. M. Fukugita *et al.*, *Phys. Rev.* **D74**, 027302 (2006).
43. S. Hannestad, *JCAP* **0305**, 004 (2003).
44. O. Elgaroy and O. Lahav, *New J. Physics*, **7**, 61 (2005).
45. U. Seljak *et al.*, *JCAP* **0610**, 014 (2006).
46. A. Vikhlinin *et al.*, *Astrophys. J.* **692**, 1060 (2009).
47. S.D.M. White *et al.*, *Nature* **366**, 429 (1993).
48. S.W. Allen *et al.*, *Mon. Not. Roy. Astr. Soc.* **383**, 879 (2008).
49. R.A.C. Croft *et al.*, *Astrophys. J.* **581**, 20 (2002).
50. S. Kim *et al.*, *Mon. Not. Roy. Astr. Soc.* **347**, 355 (2004).
51. U. Seljak *et al.*, *Mon. Not. Roy. Astr. Soc.* **342**, L79 (2003);
U. Seljak *et al.*, *Phys. Rev.* **D71**, 103515 (2005).
52. P. Schneider, [astro-ph/0306465](https://arxiv.org/abs/astro-ph/0306465);
A. Refregier, *Ann. Rev. Astron. Astrophys.* **41**, 645 (2003);
H. Hoekstra, B. Jain, *Ann. Rev. Nuc. Particle Physics*, **58** (2008);
R. Massey *et al.*, *Nature*, **445**, 286, (2007).
53. L. Fu *et al.*, *Astron. Astrophys.* **479**, 9 (2008).
54. J. Benjamin *et al.*, *Mon. Not. Roy. Astr. Soc.* **381**, 702 (2007).
55. A. Dekel, *Ann. Rev. Astron. Astrophys.* **32**, 371 (1994).
56. L. Silberman *et al.*, *Astrophys. J.* **557**, 102 (2001).
57. H.A. Feldman *et al.*, *Astrophys. J.* **596**, L131 (2003).
58. R. Watkins, H.A. Feldman, M.J. Hudson, *Mon. Not. Roy. Astr. Soc.* **392**, 743 (2009).
59. N. Kaiser, *Mon. Not. Roy. Astr. Soc.* **227**, 1 (1987).
60. L. Guzzo, *et al.*, *Nature* **451**, 541 (2008).
61. B. Chaboyer and L.M. Krauss, *Science* **299**, 65 (2003).
62. R. Cayrel *et al.*, *Nature* **409**, 691 (2001).
63. C.J. MacTavish *et al.*, *Astrophys. J.* **647**, 833 (2006).

22. DARK MATTER

Revised September 2009 by M. Drees (Bonn University) and G. Gerbier (Saclay, CEA).

22.1. Theory

22.1.1. Evidence for Dark Matter :

The existence of Dark (*i.e.*, non-luminous and non-absorbing) Matter (DM) is by now well established. The earliest [1], and perhaps still most convincing, evidence for DM came from the observation that various luminous objects (stars, gas clouds, globular clusters, or entire galaxies) move faster than one would expect if they only felt the gravitational attraction of other visible objects. An important example is the measurement of galactic rotation curves. The rotational velocity v of an object on a stable Keplerian orbit with radius r around a galaxy scales like $v(r) \propto \sqrt{M(r)/r}$, where $M(r)$ is the mass inside the orbit. If r lies outside the visible part of the galaxy and mass tracks light, one would expect $v(r) \propto 1/\sqrt{r}$. Instead, in most galaxies one finds that v becomes approximately constant out to the largest values of r where the rotation curve can be measured; in our own galaxy, $v \simeq 220$ km/s at the location of our solar system, with little change out to the largest observable radius. This implies the existence of a *dark halo*, with mass density $\rho(r) \propto 1/r^2$, *i.e.*, $M(r) \propto r$; at some point ρ will have to fall off faster (in order to keep the total mass of the galaxy finite), but we do not know at what radius this will happen. This leads to a lower bound on the DM mass density, $\Omega_{\text{DM}} \gtrsim 0.1$, where $\Omega_X \equiv \rho_X/\rho_{\text{crit}}$, ρ_{crit} being the critical mass density (*i.e.*, $\Omega_{\text{tot}} = 1$ corresponds to a flat Universe).

The observation of clusters of galaxies tends to give somewhat larger values, $\Omega_{\text{DM}} \simeq 0.2$. These observations include measurements of the peculiar velocities of galaxies in the cluster, which are a measure of their potential energy if the cluster is virialized; measurements of the *X-ray* temperature of hot gas in the cluster, which again correlates with the gravitational potential felt by the gas; and—most directly—studies of (weak) gravitational lensing of background galaxies on the cluster.

A particularly compelling example involves the bullet cluster (1E0657-558) which recently (on cosmological time scales) passed through another cluster. As a result, the hot gas forming most of the clusters' baryonic mass was shocked and decelerated, whereas the galaxies in the clusters proceeded on ballistic trajectories. Gravitational lensing shows that most of the total mass also moved ballistically, indicating that DM self-interaction are indeed weak [2].

The currently most accurate, if somewhat indirect, determination of Ω_{DM} comes from global fits of cosmological parameters to a variety of observations; see the Section on Cosmological Parameters for details. For example, using measurements of the anisotropy of the cosmic microwave background (CMB) and of the spatial distribution of galaxies, Ref. 3 finds a density of cold, non-baryonic matter

$$\Omega_{\text{nbm}} h^2 = 0.110 \pm 0.006, \quad (22.1)$$

where h is the Hubble constant in units of 100 km/(s·Mpc). Some part of the baryonic matter density [3],

$$\Omega_{\text{b}} h^2 = 0.0227 \pm 0.0006, \quad (22.2)$$

may well contribute to (baryonic) DM, *e.g.*, MACHOs [4] or cold molecular gas clouds [5].

The DM density in the “neighborhood” of our solar system is also of considerable interest. This was first estimated as early as 1922 by J.H. Jeans, who analyzed the motion of nearby stars transverse to the galactic plane [1]. He concluded that in our galactic neighborhood, the average density of DM must be roughly equal to that of luminous matter (stars, gas, dust). Remarkably enough, the most recent estimates, based on a detailed model of our galaxy, find quite similar results [6]:

$$\rho_{\text{DM}}^{\text{local}} \simeq 0.3 \frac{\text{GeV}}{\text{cm}^3}; \quad (22.3)$$

this value is known to within a factor of two or so.

22.1.2. Candidates for Dark Matter :

Analyses of structure formation in the Universe [7] indicate that most DM should be “cold,” *i.e.*, should have been non-relativistic at the onset of galaxy formation (when there was a galactic mass inside the causal horizon). This agrees well with the upper bound [3] on the contribution of light neutrinos to Eq. (22.1),

$$\Omega_{\nu} h^2 \leq 0.0067 \quad 95\% \text{ CL}. \quad (22.4)$$

Candidates for non-baryonic DM in Eq. (22.1) must satisfy several conditions: they must be stable on cosmological time scales (otherwise they would have decayed by now), they must interact very weakly with electromagnetic radiation (otherwise they wouldn't qualify as *dark matter*), and they must have the right relic density. Candidates include primordial black holes, axions, and weakly interacting massive particles (WIMPs).

Primordial black holes must have formed before the era of Big-Bang nucleosynthesis, since otherwise they would have been counted in Eq. (22.2) rather than Eq. (22.1). Such an early creation of a large number of black holes is possible only in certain somewhat contrived cosmological models [8].

The existence of axions [9] was first postulated to solve the strong CP problem of QCD; they also occur naturally in superstring theories. They are pseudo Nambu-Goldstone bosons associated with the (mostly) spontaneous breaking of a new global “Peccei-Quinn” (PQ) U(1) symmetry at scale f_a ; see the Section on Axions in this *Review* for further details. Although very light, axions would constitute cold DM, since they were produced non-thermally. At temperatures well above the QCD phase transition, the axion is massless, and the axion field can take any value, parameterized by the “misalignment angle” θ_i . At $T \lesssim 1$ GeV, the axion develops a mass m_a due to instanton effects. Unless the axion field happens to find itself at the minimum of its potential ($\theta_i = 0$), it will begin to oscillate once m_a becomes comparable to the Hubble parameter H . These coherent oscillations transform the energy originally stored in the axion field into physical axion quanta. The contribution of this mechanism to the present axion relic density is [9]

$$\Omega_a h^2 = \kappa_a \left(f_a / 10^{12} \text{ GeV} \right)^{1.175} \theta_i^2, \quad (22.5)$$

where the numerical factor κ_a lies roughly between 0.5 and a few. If $\theta_i \sim \mathcal{O}(1)$, Eq. (22.5) will saturate Eq. (22.1) for $f_a \sim 10^{11}$ GeV, comfortably above laboratory and astrophysical constraints [9]; this would correspond to an axion mass around 0.1 meV. However, if the post-inflationary reheating temperature $T_R > f_a$, cosmic strings will form during the PQ phase transition at $T \simeq f_a$. Their decay will give an additional contribution to Ω_a , which is often bigger than that in Eq. (22.5) [10], leading to a smaller preferred value of f_a , *i.e.*, larger m_a . On the other hand, values of f_a near the Planck scale become possible if θ_i is for some reason very small.

Weakly interacting massive particles (WIMPs) χ are particles with mass roughly between 10 GeV and a few TeV, and with cross sections of approximately weak strength. Within standard cosmology, their present relic density can be calculated reliably if the WIMPs were in thermal and chemical equilibrium with the hot “soup” of Standard Model (SM) particles after inflation. In this case, their density would become exponentially (Boltzmann) suppressed at $T < m_\chi$. The WIMPs therefore drop out of thermal equilibrium (“freeze out”) once the rate of reactions that change SM particles into WIMPs or vice versa, which is proportional to the product of the WIMP number density and the WIMP pair annihilation cross section into SM particles σ_A times velocity, becomes smaller than the Hubble expansion rate of the Universe. After freeze out, the co-moving WIMP density remains essentially constant; if the Universe evolved adiabatically after WIMP decoupling, this implies a constant WIMP number to entropy density ratio. Their present relic density is then approximately given by (ignoring logarithmic corrections) [11]

$$\Omega_\chi h^2 \simeq \text{const.} \cdot \frac{T_0^3}{M_{\text{Pl}}^3 \langle \sigma_A v \rangle} \simeq \frac{0.1 \text{ pb} \cdot c}{\langle \sigma_A v \rangle}. \quad (22.6)$$

Here T_0 is the current CMB temperature, M_{Pl} is the Planck mass, c is the speed of light, σ_A is the total annihilation cross section of a pair of WIMPs into SM particles, v is the relative velocity between the two WIMPs in their cms system, and $\langle \dots \rangle$ denotes thermal averaging. Freeze out happens at temperature $T_F \simeq m_\chi/20$ almost independently of the properties of the WIMP. This means that WIMPs are already non-relativistic when they decouple from the thermal plasma; it also implies that Eq. (22.6) is applicable if $T_R > T_F$. Notice that the 0.1 pb in Eq. (22.6) contains factors of T_0 and M_{Pl} ; it is, therefore, quite intriguing that it “happens” to come out near the typical size of weak interaction cross sections.

The seemingly most obvious WIMP candidate is a heavy neutrino. However, an SU(2) doublet neutrino will have too small a relic density if its mass exceeds $M_Z/2$, as required by LEP data. One can suppress the annihilation cross section, and hence increase the relic density, by postulating mixing between a heavy SU(2) doublet and some “sterile” SU(2) \times U(1) $_Y$ singlet neutrino. However, one also has to require the neutrino to be stable; it is not obvious why a massive neutrino should not be allowed to decay.

The currently best motivated WIMP candidate is, therefore, the lightest superparticle (LSP) in supersymmetric models [12] with exact R-parity (which guarantees the stability of the LSP). Searches for exotic isotopes [13] imply that a stable LSP has to be neutral. This leaves basically two candidates among the superpartners of ordinary particles, a sneutrino, and a neutralino. Sneutrinos again have quite large annihilation cross sections; their masses would have to exceed several hundred GeV for them to make good DM candidates. This is uncomfortably heavy for the lightest sparticle, in view of naturalness arguments. Moreover, the negative outcome of various WIMP searches (see below) rules out “ordinary” sneutrinos as primary component of the DM halo of our galaxy. (In models with gauge-mediated SUSY breaking, the lightest “messenger sneutrino” could make a good WIMP [14].) The most widely studied WIMP is therefore the lightest neutralino. Detailed calculations [15] show that the lightest neutralino will have the desired thermal relic density Eq. (22.1) in at least four distinct regions of parameter space. χ could be (mostly) a bino or photino (the superpartner of the U(1) $_Y$ gauge boson and photon, respectively), if both χ and some sleptons have mass below ~ 150 GeV, or if m_χ is close to the mass of some sfermion (so that its relic density is reduced through co-annihilation with this sfermion), or if $2m_\chi$ is close to the mass of the CP-odd Higgs boson present in supersymmetric models. Finally, Eq. (22.1) can also be satisfied if χ has a large higgsino or wino component.

Many non-supersymmetric extensions of the Standard Model also contain viable WIMP candidates. Examples are the lightest T -odd particle in “Little Higgs” models with conserved T -parity [16], or “techni-baryons” in scenarios with an additional, strongly interacting (“technicolor” or similar) gauge group [17].

Recently there has been a flurry of developments of models where the DM particles, while interacting only weakly with ordinary matter, have quite strong interactions within an extended “dark sector” of the theory. These were spurred by measurements by the PAMELA, ATIC and Fermi satellites indicating excesses in the cosmic e^+ and/or e^- fluxes at high energies. However, these excesses are relative to background estimates that are clearly too simplistic (*e.g.*, neglecting primary sources of electrons and positrons, and modeling the galaxy as a homogeneous cylinder). Moreover, the excesses, if real, are far too large to be due to usual WIMPs, but can be explained by astrophysical sources. It therefore seems unlikely that they are due to Dark Matter [18].

Although thermally produced WIMPs are attractive DM candidates because their relic density naturally has at least the right order of magnitude, non-thermal production mechanisms have also been suggested, *e.g.*, LSP production from the decay of some moduli fields [19], from the decay of the inflaton [20], or from the decay of “Q-balls” (non-topological solitons) formed in the wake of Affleck-Dine baryogenesis [21]. Although LSPs from these sources are typically highly relativistic when produced, they quickly achieve kinetic (but not chemical) equilibrium if T_R exceeds a few MeV [22] (but stays below $m_\chi/20$). They therefore also contribute to cold DM.

Primary black holes (as MACHOs), axions, and WIMPs are all (in principle) detectable with present or near-future technology (see below). There are also particle physics DM candidates which currently seem almost impossible to detect, unless they decay; the present lower limit on their lifetime is of order 10^{25} to 10^{26} s for 100 GeV particles. These include the gravitino (the spin-3/2 superpartner of the graviton) [23], states from the “hidden sector” thought responsible for supersymmetry breaking [14], and the axino (the spin-1/2 superpartner of the axion) [24].

22.2. Experimental detection of Dark Matter

22.2.1. The case of baryonic matter in our galaxy :

The search for hidden galactic baryonic matter in the form of Massive Compact Halo Objects (MACHOs) has been initiated following the suggestion that they may represent a large part of the galactic DM and could be detected through the microlensing effect [4]. The MACHO, EROS, and OGLE collaborations have performed a program of observation of such objects by monitoring the luminosity of millions of stars in the Large and Small Magellanic Clouds for several years. EROS concluded that MACHOs cannot contribute more than 8% to the mass of the galactic halo [25], while MACHO observed a signal at 0.4 solar mass and put an upper limit of 40%. Overall, this strengthens the need for non-baryonic DM, also supported by the arguments developed above.

22.2.2. Axion searches :

Axions can be detected by looking for $a \rightarrow \gamma$ conversion in a strong magnetic field [26]. Such a conversion proceeds through the loop-induced $a\gamma\gamma$ coupling, whose strength $g_{a\gamma\gamma}$ is an important parameter of axion models. There currently are two experiments searching for axionic DM. They both employ high quality cavities. The cavity “Q factor” enhances the conversion rate on resonance, *i.e.*, for $m_a c^2 = \hbar\omega_{\text{res}}$. One then needs to scan the resonance frequency in order to cover a significant range in m_a or, equivalently, f_a . The bigger of the two experiments, the ADMX experiment [27], originally situated at the LLNL in California but recently moved to the University of Washington, started taking data in the first half of 1996. It now uses SQUIDs as first-stage amplifiers; their extremely low noise temperature (1.2 K) enhances the conversion signal. Their first published results [28], obtained with conventional amplifiers, exclude axions with mass between 1.9 and 3.3 μeV , corresponding to $f_a \simeq 4 \cdot 10^{13}$ GeV, as a major component of the dark halo of our galaxy, if $g_{a\gamma\gamma}$ is near the upper end of the theoretically expected range. Later, the experiment achieved [29] an about five times better limit on $g_{a\gamma\gamma}$ for $1.98 \mu\text{eV} \leq m_a \leq 2.18 \mu\text{eV}$, if a large fraction of the local DM density is due to a single flow of axions with very low velocity dispersion. The ADMX experiment is being upgraded by reducing the cavity temperature from the current 1.2 K to about 0.1 K. This should increase the frequency scanning speed for given sensitivity by more than two orders of magnitude, or increase the sensitivity for fixed observation time.

The smaller “CARRACK” experiment now being developed in Kyoto, Japan [30] uses Rydberg atoms (atoms excited to a very high state, $n = 111$) to detect the microwave photons that would result from axion conversion. This allows almost noise-free detection of single photons. Their ultimate goal is to probe the range between 2 and 50 μeV with sensitivity to all plausible axion models, if axions form most of DM.

22.2.3. Basics of direct WIMP search :

As stated above, WIMPs should be gravitationally trapped inside galaxies and should have the adequate density profile to account for the observed rotational curves. These two constraints determine the main features of experimental detection of WIMPs, which have been detailed in the reviews [31].

Their rms velocity inside our galaxy relative to its center is expected to be similar to that of stars, *i.e.*, a few hundred kilometers per second at the location of our solar system. For these velocities, WIMPs interact with ordinary matter through elastic scattering on nuclei. With expected WIMP masses in the range 10 GeV to 10 TeV, typical nuclear recoil energies are of order of 1 to 100 keV.

The shape of the nuclear recoil spectrum results from a convolution of the WIMP velocity distribution, usually taken as a Maxwellian distribution in the galactic rest frame, shifted into the Earth rest frame, with the angular scattering distribution, which is isotropic to first approximation but forward-peaked for high nuclear mass (typically higher than Ge mass) due to the nuclear form factor. Overall, this results in a roughly exponential spectrum. The higher the WIMP mass, the higher the mean value of the exponential. This points to the need for low nuclear energy threshold detectors.

On the other hand, expected interaction rates depend on the product of the local WIMP flux and the interaction cross section. The first term is fixed by the local density of dark matter, taken as 0.3 GeV/cm^3 (see above), the mean WIMP velocity, typically 220 km/s , and the mass of the WIMP. The expected interaction rate then mainly depends on two unknowns, the mass and cross section of the WIMP (with some uncertainty [6] due to the halo model). This is why the experimental observable, which is basically the scattering rate as a function of energy, is usually expressed as a contour in the WIMP mass–cross section plane.

The cross section depends on the nature of the couplings. For non-relativistic WIMPs, one in general has to distinguish spin-independent and spin-dependent couplings. The former can involve scalar and vector WIMP and nucleon currents (vector currents are absent for Majorana WIMPs, *e.g.*, the neutralino), while the latter involve axial vector currents (and obviously only exist if χ carries spin). Due to coherence effects, the spin-independent cross section scales approximately as the square of the mass of the nucleus, so higher mass nuclei, from Ge to Xe, are preferred for this search. For spin-dependent coupling, the cross section depends on the nuclear spin factor; used target nuclei include ^{19}F , ^{23}Na , ^{73}Ge , ^{127}I , ^{129}Xe , ^{131}Xe , and ^{133}Cs .

Cross sections calculated in MSSM models induce rates of at most $1 \text{ evt day}^{-1} \text{ kg}^{-1}$ of detector, much lower than the usual radioactive backgrounds. This indicates the need for underground laboratories to protect against cosmic ray induced backgrounds, and for the selection of extremely radio-pure materials.

The typical shape of exclusion contours can be anticipated from this discussion: at low WIMP mass, the sensitivity drops because of the detector energy threshold, whereas at high masses, the sensitivity also decreases because, for a fixed mass density, the WIMP flux decreases $\propto 1/m_\chi$. The sensitivity is best for WIMP masses near the mass of the recoiling nucleus.

22.2.4. Status and prospects of direct WIMP searches :

The first searches have been performed with ultra-pure semiconductors installed in pure lead and copper shields in underground environments [32]. Combining a priori excellent energy resolutions and very pure detector material, they produced the first limits on WIMP searches (Heidelberg-Moscow, IGEX, COSME-II, HDMS) [32]. Without positive identification of nuclear recoil events, however, these experiments could only set limits, *e.g.*, excluding sneutrinos as major component of the galactic halo. Still, planned experiments using several tens of kg to a ton of Germanium (many of which were designed for double-beta decay search)—GERDA, MAJORANA—are based on only passive reduction of the external and internal electromagnetic and neutron background by using segmented detectors, minimal detector housing, close electronics, and large liquid nitrogen shields. Their sensitivity to WIMP interactions will depend on their ability to lower the energy threshold sufficiently, while keeping the background rate small.

New results have recently been obtained with non-cryogenic detectors with sub-keV thresholds. The TEXONO collaboration has operated four ultra low energy Germanium 5 g detectors, in a reactor environment, with threshold of order of 200 eV [33]. The CoGENT collaboration has operated a 475 g Germanium detector with point contact electrode, with a very small capacitance which allowed to reach an effective threshold of 500 eV in a physics run performed in rather shallow site [34]. Both results allowed to set best limits for spin independent coupling WIMPs in the 5 to 8 GeV WIMP mass range, at a cross section around 10^{-4} pb , a bit below the allowed

range for the low WIMP mass DAMA solution without channeling (see below).

To make further progress, in particular at higher masses, active background rejection and signal identification questions have to be addressed. This has been the focus of many recent investigations and improvements. Active background rejection in detectors relies on the relatively small ionization in nuclear recoils due to their low velocity. This induces a reduction—quenching—of the ionization/scintillation signal for nuclear recoil signal events relative to e or γ induced backgrounds. Energies calibrated with gamma sources are then called “electron equivalent energies” (eee). This effect has been both calculated and measured [32]. It is exploited in cryogenic detectors described later. In scintillation detectors, it induces in addition a difference in decay times of pulses induced by e/γ events vs nuclear recoils. Due to the limited resolution and discrimination power of this technique at low energies, this effect allows only a statistical background rejection. It has been used in NaI(Tl) (DAMA, LIBRA, NAIAD, Saclay NaI), in CsI(Tl)(KIMS), and Xe (ZEPLIN I) [32]. No observation of nuclear recoils has been reported by these experiments.

Two experimental signatures are predicted for true WIMP signals. One is a strong daily forward/backward asymmetry of the nuclear recoil direction, due to the alternate sweeping of the WIMP cloud by the rotating Earth. Detection of this effect requires gaseous detectors or anisotropic response scintillators (stilbene). The second is a few percent annual modulation of the recoil rate due to the Earth speed adding to or subtracting from the speed of the Sun. This tiny effect can only be detected with large masses; nuclear recoil identification should also be performed, as the much larger background may also be subject to seasonal modulation.

After the report of an observed annual modulation with a statistical significance of 6.3σ , through operation of 100 kg of NaI(Tl) in Gran Sasso for 7 years, the DAMA collaboration has reported a new result with the LIBRA phase, involving 250 kg of detectors and an exposure of 0.53 t-y [35]. The modulation signal phases are compatible in both sets of data with the phase expected for a homogenous halo. The significance of the combined sets of data, corresponding to an exposure of 0.82 t-y, is between 8.3 and 8.9σ depending on the width of the analyzed energy window. If interpreted within the standard halo model described above, it would require a WIMP with $m_\chi \simeq 50 \text{ GeV}$ and $\sigma_{\chi p} \simeq 7 \cdot 10^{-6} \text{ pb}$ (central values) or at low mass, in the 6 to 10 GeV range with $\sigma_{\chi p} \sim 10^{-3} \text{ pb}$, and lower if there is a significant channeling effect. Such solutions would induce a sizeable fraction of nuclear recoils in the total measured rate in the 2 to 6 keV bin. No pulse shape analysis has been reported by the authors to check whether the signal was detectable this way. The shape of the residual e/γ -induced, background is also an unresolved issue [36]. Concerning compatibility with other experiments, there is now severe tension for the high mass solution (see below) and a small phase space available for the low mass solution (according to [36] this loophole is closed if the energy spectrum measured by DAMA/LIBRA is taken into account). The reported large significance of the signal has triggered new activity with non minimal WIMP models to reconcile DAMA result with limits from other experiments [35].

No other annual modulation analysis with comparable sensitivity has been reported by any experiment. KIMS, an experiment operating 12 crystals of CsI(Tl) with a total mass of 104.4 kg in the Yang Yang laboratory in Korea, has now accumulated 1 year of continuous operation. They should be able to set an upper limit on annual modulation amplitude lower than DAMA value if no annual modulation is present, and would need 2 years of running to confirm the DAMA value at 3σ . They currently provide the best limit on pure proton spin-dependent couplings [37] above 30 GeV.

The simultaneous measurement of the phonon signal and the ionization signal in semiconductor detectors permits event by event discrimination between nuclear and electronic recoils down to 5 to 10 keV recoil energy. Currently the largest such experiment is the Cryogenic Dark Matter Search (CDMS). They reject surface detector interactions, which can mimic nuclear recoils, using timing information. New limits on the spin-independent coupling of WIMPs were obtained by this collaboration, which has operated 19 Ge cryogenic detectors at the Soudan mine, during new runs involving

total exposure of around 400 kg·d (121 kg·d fiducial) [38], without any event in the pre-defined signal region. Combined with earlier data sets, these data provide an upper limit on the spin-independent cross section for the scattering of a 60 GeV/c² WIMP on a nucleon of 4.6×10^{-8} pb, at 90% CL. This experiment has achieved the best sensitivity for WIMP masses above 44 GeV/c².

Assuming conventional WIMP halo parameters described above, and spin-independent coupling WIMP interactions, the CDMS limit and DAMA signal are clearly incompatible. Varying the halo parameters, and/or including spin-dependent interactions compatible with the neutrino flux limit from the Sun, does not allow reconciliation of both results without fine tuning [36,39].

EDELWEISS, who is using similar technique as CDMS, but with different sensors has shown substantial instrumental progress with an interleaved electrodes scheme prototype able to reject surface interactions at the level of one in 100 000. They are building and going to operate these new detectors [41] in the Modane underground lab. Other cryogenic experiments like CRESST and ROSEBUD [40] use the scintillation of CaWO₄ or other inorganic scintillators as second variable for background discrimination. They set weaker limits than the best current experiments. The cryogenic experimental programs of CDMS II, EDELWEISS II, and CRESST II [40] intend to increase their sensitivity by a factor of 10, by operating from a few to 40 kg of detectors.

Noble gas dual (liquid and gas) phase detectors allow one to measure both the primary scintillation and the ionization electrons drifted through the liquid and amplified in the gas, which can be used for background rejection. The limit obtained by XENON-10, an experiment involving 5.4 kg of fiducial mass of Xenon, run at the Gran Sasso laboratory, on spin-independent couplings of WIMPs is still the best for masses lower than 44 GeV/c² [42]. This was obtained thanks to a very low threshold of 4 keV recoil energy and the high A of Xenon nuclei. Xenon10, by exploiting the presence of ¹²⁹Xe and ¹³¹Xe isotopes in natural Xenon has set the best limit for spin-dependent WIMPs with pure neutron couplings at all masses [43]. Xenon100, the next stage of the experiment with a fiducial mass of 30 to 50 kg and lower radioactivity components, has been operated and calibrated, and is expected to take data in 2010.

ZEPLIN III, using a similar principle and with an active mass of 12 kg of Xenon, operated in the Boulby laboratory for 83 days, reports a lower sensitivity. XMASS in Japan has operated a single-phase 100 kg detector (few kg fiducial mass) at the SuperKamiokande site, and demonstrated the self-shielding effect to lower the background [44]. They are currently building the 800 kg (100 kg fiducial mass) detector, installed in a large pure water shield.

The WARP collaboration is now installing a 100 l Argon detector at the Gran Sasso laboratory. They have demonstrated that, thanks to a double-background rejection method based on the asymmetry between scintillating and ionizing pulses and pulse shape discrimination of scintillating pulses, they could achieve very high background rejection, even in the presence of the radioactive isotope ³⁹Ar, although with a final sensitivity still lower than that of CDMS or XENON. The ArDM project will use a similar technique with a much larger (1,100 kg) volume. Many other projects (CLEAN, DEAP, HPGS, and SIGN) are developing with the aim of using Argon, Xenon, or Neon in liquid, double-phase, or high-pressure gas form [44].

There is also continuous development of the low pressure Time Projection Chamber technique, the only convincing way to measure the direction of nuclear recoils [45]. DRIFT, a 1 m³ volume detector, has been operated underground, but suffered high background due to internal radon contamination. A background rejection technique has been developed, the recoil track head tail effect has been demonstrated, but no new operation underground was reported. A sub-keV energy threshold gaseous detector using Helium 3, the Mimac project, is being investigated for WIMP searches [45]. Very sensitive measurements of quenching factor of Helium nuclei have been performed recently down to 1 keV and are shown to depend on the pressure of the gas [46]. Other groups developing similar techniques are DMTPC in the US and NewAge in Japan.

A bubble chamber like detector, COUPP, run at Fermilab [47],

has provided the best limits for spin-dependent proton-coupling WIMPs for masses lower than 30 GeV. The performance was limited by alpha background from radon internal contamination. Other exotic techniques include the superheated droplet detectors SIMPLE and PICASSO, which has obtained interesting but not competitive limits on spin-dependent couplings. An ultra cold pure ³He detector (ULTIMA) has been operated with a very small sensitive mass.

Sensitivities down to $\sigma_{\chi p}$ of 10^{-10} pb, as needed to probe large regions of MSSM parameter space [48], can be reached with detectors of typical masses of 1 ton [40], assuming nearly perfect background discrimination capabilities. More and more projects are envisaged such EURECA (European multi-array, multi-target 1 ton cryogenic set up), Xenon1T (Extension of Xenon100), LUX/LZ (US 300 kg liquid Xenon, then multiton project), DARWIN European consortium (liquid Xe and Ar multiton project) [40,44]. Note that the expected WIMP rate is then 5 evts/ton/year for Ge. The ultimate neutron background will only be identified by its multiple interactions in a finely segmented or multiple-interaction-sensitive detector, and/or by operating detectors containing different target materials within the same set-up. Information on various neutron background calculations and measurements can be found in [49]. With an intermediate mass of 10 to 30 kg, and therefore less efficient multiple interaction detection, a muon veto seems mandatory in most existing underground laboratories.

22.2.5. Status and prospects of indirect WIMP searches :

WIMPs can annihilate and their annihilation products can be detected; these include neutrinos, gamma rays, positrons, antiprotons, and antinuclei [50]. These methods are complementary to direct detection and can explore higher masses and different coupling scenarios. “Smoking gun” signals for indirect detection are neutrinos coming from the center of the Sun or Earth, and monoenergetic photons from WIMP annihilation in space.

WIMPs can be slowed down, captured, and trapped in celestial objects like the Earth or the Sun, thus enhancing their density and their probability of annihilation. This is a source of muon neutrinos which can interact in the Earth. Upward going muons can then be detected in large neutrino telescopes such as MACRO, BAKSAN, SuperKamiokande, Baikal, AMANDA, ANTARES, NESTOR, and the large sensitive area IceCube [50]. The best upper limits, of $\simeq 1000$ muons/km²/year, have initially been set by SuperKamiokande [51]. A new limit has been set by AMANDA and IceCube22 (using 22 strings) at around few hundreds of muons/km²/year for muons from the sun [52]. In the framework of the MSSM and with standard halo velocity profiles, only the limits from the Sun, which mostly probe spin-dependent couplings, are competitive with direct WIMP search limits. IceCube80 will increase this sensitivity by a factor $\simeq 5$ at masses higher than 200 GeV while IceCube Deep Core will allow one to reach masses down to 50 GeV.

WIMP annihilation in the halo can give a continuous spectrum of gamma rays and (at one-loop level) also monoenergetic photon contributions from the $\gamma\gamma$ and γZ channels. These channels also allow to search for WIMPs for which direct detection experiments have little sensitivity, *e.g.*, almost pure higgsinos. However, the size of this signal depends very strongly on the halo model, but is expected to be most prominent towards the galactic center. Existing limits come from the EGRET satellite below 10 GeV, and from the WHIPPLE ground based telescope above 100 GeV [53]. The FERMI/LAT apparatus, now taking data, will soon bring new quality data in the galactic center region. Atmospheric Cherenkov Telescopes like MAGIC, VERITAS, and H.E.S.S. did not claim so far any significant excess which could be attributed to Dark Matter annihilation.

Diffuse continuum gammas could also give a signature due to their anisotropic distribution tracking the halo density as seen from Earth. According to [54], a re-analysis of EGRET data shows an excess in the energy spectrum at the GeV range, if one normalizes the experimental spectrum to that expected from model calculations at lower energies, assuming that the cosmic ray spectrum has the same shape (but different normalization) everywhere in our galaxy. The excess has been explained in terms of WIMP annihilation, with WIMP mass near 80 GeV, only if one assumes a rather clumpy halo. However, with newly

accumulated high accuracy data [55] the FERMI/LAT instrument has found agreement with a pure secondary production model (from CR interactions), and does not confirm the EGRET excess.

Antiprotons arise as another WIMP annihilation product in the halo. The signal is expected to be detectable above background only at very low energies. The BESS balloon-borne experiment indeed observed antiprotons below 1 GeV [56]. However, the uncertainties in the calculation of the expected signal and background energy spectra are too large to reach a firm conclusion. PAMELA measurement of the antiproton spectrum between 2 and 20 GeV [57], of higher accuracy, shows a good agreement with secondary production and propagation models.

Positrons arise as well as another WIMP annihilation product in the halo. A cosmic-ray positron flux excess at around 8 GeV measured by HEAT [58] has given rise to numerous calculations and conjectures concerning a possible WIMP interpretation. New positron/(electron+positron) ratio measurement performed by PAMELA [59] between 1 and 100 GeV showed a rather marked rise between 10 and 100 GeV. The observed spectrum falls within the one order of magnitude span (largely due to differences in the propagation model used) of positron fraction values predicted by secondary production models [60]. Measurements of the total electron+positrons energy spectrum by ATIC [61], FERMI/LAT [62] and HESS [63] between 100 and 1000 GeV also exceed the predicted purely secondary spectrum, but with very large dispersion of the magnitude of these excesses. While it has been recognized that astrophysical sources may account for all these features, many ad-hoc Dark Matter models have been built to account for these excesses. As mentioned in section 1, given the amount of jerking and twisting needed to build such models not to contradict any observation, it seems very unlikely that Dark Matter is at the origin of these excesses.

Last but not least, an antideuteron signal [64], as potentially observable by AMS2 or PAMELA, could constitute a signal for WIMP annihilation in the halo.

An interesting comparison of respective sensitivities to MSSM parameter space of future direct and various indirect searches has been performed with the DARKSUSY tool [65]. A web-based up-to-date collection of results from direct WIMP searches, theoretical predictions, and sensitivities of future experiments can be found in Ref. 66. Also, a new web page, initiated by ILIAS [67], a European underground science and infrastructure network, allows to make predictions for WIMP signals in various experiments, within a variety of SUSY models. Its long-term goal is to propose an interactive integrated analysis of all relevant data. These should ultimately include not only data from direct and indirect WIMP detection experiments, but also from high-energy colliders such as the LHC. If a positive WIMP signal is found anywhere, such a comprehensive approach will be required to fully unravel the mysteries of dark matter.

References:

1. For a brief but delightful history of DM, see V. Trimble, in *Proceedings of the First International Symposium on Sources of Dark Matter in the Universe*, Bel Air, California, 1994, published by World Scientific, Singapore (ed. D.B. Cline). See also the recent review G. Bertone, D. Hooper, and J. Silk, *Phys. Rep.* **405**, 279 (2005).
2. D. Clowe et al., *Astrophys. J.* **648**, L109 (2006).
3. See *Cosmological Parameters* in this Review.
4. B. Paczynski, *Astrophys. J.* **304**, 1 (1986); K. Griest, *Astrophys. J.* **366**, 412 (1991).
5. F. De Paolis et al., *Phys. Rev. Lett.* **74**, 14 (1995).
6. M. Kamionkowski and A. Kinkhabwala, *Phys. Rev.* **D57**, 3256 (1998).
7. See e.g., J.R. Primack, in the *Proceedings of Midrasha Mathematicae in Jerusalem: Winter School in Dynamical Systems*, Jerusalem, Israel, January 1997, astro-ph/9707285. There is currently some debate whether cold DM models correctly reproduce the DM density profile near the center of galactic haloes. See e.g., R.A. Swaters et al., *Astrophys. J.* **583**, 732 (2003).
8. K. Kohri, D.H. Lyth and A. Melchiorri, *JCAP* **0804**, 038 (2008).
9. See *Axions and Other Very Light Bosons* in this Review.
10. R.A. Battye and E.P.S. Shellard, *Phys. Rev. Lett.* **73**, 2954 (1994); Erratum-ibid. **76**, 2203 (1996).
11. E.W. Kolb and M.E. Turner, *The Early Universe*, Addison-Wesley (1990).
12. For a review, see G. Jungman, M. Kamionkowski, and K. Griest, *Phys. Reports* **267**, 195 (1996).
13. See *Searches for WIMPs and Other Particles* in this Review.
14. S. Dimopoulos, G.F. Giudice, and A. Pomarol, *Phys. Lett.* **B389**, 37 (1996).
15. See e.g., J.R. Ellis et al., *Nucl. Phys.* **B652**, 259 (2003); J.R. Ellis et al., *Phys. Lett.* **B565**, 176 (2003); H. Baer et al., *JHEP* **0306**, 054 (2003); A. Bottino et al., *Phys. Rev.* **D68**, 043506 (2003).
16. See e.g., A. Birkedal et al., *Phys. Rev.* **D74**, 035002 (2006).
17. See e.g., S. B. Gudnason, C. Kouvaris, and F. Sannino, *Phys. Rev.* **D74**, 095008 (2006).
18. For a recent discussion and further references, see the talk by M. Cirelli at PASCOS2009, DESY, Hamburg, <http://pascos2009.desy.de>.
19. T. Moroi and L. Randall, *Nucl. Phys.* **B570**, 455 (2000).
20. R. Allahverdi and M. Drees, *Phys. Rev. Lett.* **89**, 091302 (2002).
21. M. Fujii and T. Yanagida, *Phys. Lett.* **B542**, 80 (2002).
22. J. Hisano, K. Kohri, and M.M. Nojiri, *Phys. Lett.* **B505**, 169 (2001); X. Chen, M. Kamionkowski, and X. Zhang, *Phys. Rev.* **D64**, 021302 (2001).
23. M. Bolz, W. Buchmüller, and M. Plümacher, *Phys. Lett.* **B443**, 209 (1998).
24. L. Covi et al., *JHEP* **0105**, 033 (2001).
25. MACHO Collab., C. Alcock et al., *Astrophys. J.* **542**, 257 (2000); EROS Collab., AA **469**, 387 (2007); OGLE Collab., AA **343**, 10 (1999).
26. P. Sikivie, *Phys. Rev. Lett.* **51**, 1415 (1983), Erratum-ibid. **52**, 695 (1984).
27. H. Peng et al., *Nucl. Instrum. Methods* **A444**, 569 (2000).
28. S. Asztalos et al., *Phys. Rev.* **D69**, 011101 (2004).
29. L.D. Duffy et al., *Phys. Rev.* **D74**, 012006 (2006).
30. M. Shibata et al., *J. Low Temp. Phys.* **151**, 1043 (2008); M. Tada et al., *Phys. Lett.* **A349**, 488 (2006).
31. P.F. Smith and J.D. Lewin, *Phys. Reports* **187**, 203 (1990); J.R. Primack, D. Seckel, and B. Sadoulet, *Ann. Rev. Nucl. Part. Sci.* **38** 751 (1988); R.J. Gaitskill, *Ann. Rev. Nucl. and Part. Sci.* **54**, 315 (2004).
32. Early non cryogenic detectors are described in e.g., A. Morales, *Nucl. Phys. (Proc. Suppl.)* **B138** 135 (2005); *Proceedings of Topics in Astroparticles and Underground Physics TAUP 2005*, J. Phys. Conf. Ser. **39**, (2006); *Proceedings of Identification of Dark Matter*. IDM 2004, World Scientific, ed. N. Spooner and V. Kudryavtsev (York, UK, 2004).
33. TEXONO Collab., S.T. Lin et al., *Phys. Rev.* **D79**, 061101 (2009).
34. C.E. Aalseth et al., *Phys. Rev. Lett.* **101**, 251301 (2008).
35. DAMA Collab., R. Bernabei et al., *Eur. Phys. J. C Phys. Lett.* **56**, (2008) 333-355.
36. M Fairbairn and T Schwetz, *JCAP* 0901:037,2009.
37. KIMS Collab., H.S. Lee et al., *Phys. Rev. Lett.* **99**, 091301 (2007).
38. CDMS Collab., Z. Ahmed et al., *Phys. Rev. Lett.* **102**, 011301 (2009).
39. C.J. Copi and L.M. Krauss, *Phys. Rev.* **67**, 103507 (2003); G. Gelmini and P. Gondolo, *Phys. Rev.* **D71**, 123520 (2005); A. Kurylov and M. Kamionkowski, *Phys. Rev.* **D69**, 063503 (2004); C.J. Copi and L.M. Krauss, *New Astron. Rev.* **49**, 185 (2005).

40. For a recent review on cryogenic detectors, see *e.g.*, W. Seidel, Nucl. Phys. (Proc. Suppl.) **B138** 130 (2005). Up-to-date information can be found in the proceedings of IDM2008 (<http://pos.sissa.it/cgi-bin/reader/conf.cgi?confid=64>) and of TAUP2007 [K. Inoue *et al.*, J. Phys.: Conf. Ser. **120**, 001001 (2008)]. See also the *Proceedings of Int. Workshop on Low Temperature Detectors*, LTD10, NIM A (2003).
41. EDELWEISS Collab., A. Broniatowski *et al.*, arXiv:0905.0753, submitted to PLB.
42. XENON10 Collab., J. Angle *et al.*, Phys. Rev. Lett. **100**, 021303 (2008).
43. XENON10 Collab., J. Angle *et al.*, Phys. Rev. Lett. **101**, 091301 (2008).
44. For recent reviews on noble gas detectors, in addition to IDM and TAUP proceedings, see also the *Proceedings of 7th UCLA Symposium on Sources and Detection of Dark Matter and Dark Energy in the Universe*, Nucl. Phys. B – Proc. Suppl. **173** (2007).
45. Fourth symposium on large TPCs for low energy rare event detection, Paris, December 2008, <http://www-tpc-paris.cea.fr/>.
46. D. Santos *et al.*, arxiv:0810.1137v1, submitted for publi..
47. E. Behnke *et al.*, Science 319:933-936 (2008).
48. For a general introduction to SUSY, see the section devoted in this *Review of Particle Physics*. For a review on cross sections for direct detection, see J. Ellis *et al.*, Phys. Rev. **D67**, 123502 (2003) and for a recent update Phys. Rev. **D77**, 065026 (2008).
49. These sites gather informations on neutrons from various underground labs:
<http://www.physics.ucla.edu/wimps/nBG/nBG.html>;
http://ilias-darkmatter.uni-tuebingen.de/BSNS_WG.html.
50. L. Bergstrom, Rept. on Prog. in Phys. **63**, 793 (2000); L. Bergstrom *et al.*, Phys. Rev. **D59**, 043506 (1999); C. Tao, Phys. Scripta **T93**, 82 (2001); Y. Mambrini and C. Muñoz, Journ. of Cosm. And Astrop. Phys., **10**, 3(2004).
51. SuperKamiokande Collab., S. Desai *et al.*, Phys. Rev. **D70**, 109901 (2004).
52. AMANDA/IceCube Collab., A. Rizzo *et al.*, AIP Conf. Proc. 1115:42-48 (2009).
53. EGRET Collab., D. Dixon *et al.*, New Astron. **3**, 539 (1998).
54. W. de Boer *et al.*, Astron. Astrophys. **444** (2005) 51, and Phys. Lett. **B636**, 13 (2006).
55. FERMI/LAT collab, T A Porter *et al.*, PROCEEDINGS OF THE 31 th ICRC, LODZ, 2009.
56. BESS Collab., S. Orito *et al.*, Phys. Rev. Lett. **84**, 1078 (2000).
57. PAMELA collab, O. Adriani *et al.*, Phys. Rev. Lett. **102**, 051101 (2009).
58. HEAT Collab., S. W. Barwick *et al.*, Astrophys. J. **482**, L191 (2000).
59. PAMELA collab, O. Adriani *et al.*, Nature 458, 607 (2009).
60. T. Delahaye *et al.*, Astronomy and Astrophysics, 501- 3, 821 (2009).
61. ATIC collab, J. Chang *et al.*, Nature (London) 456, 362 (2008).
62. FERMI/LAT collab, A. A. Abdo *et al.*, Phys. Rev. Lett. **102**, 181101 (2009).
63. HESS collab, F. Aharonian *et al.*, Phys. Rev. Lett. **101**, 261104, (2008).
64. F. Donato, N. Fornengo, and P. Salati, Phys. Rev. **D62**, 043003 (2000).
65. DARKSUSY site: <http://www.physto.se/edsjo/darksusy/>.
66. <http://dmtools.brown.edu>.
67. ILIAS web page: <http://pisrv0.pit.physik.uni-tuebingen.de/darkmatter/>.

23. COSMIC MICROWAVE BACKGROUND

Revised August 2009 by D. Scott (University of British Columbia) and G.F. Smoot (UCB/LBNL).

23.1. Introduction

The energy content in radiation from beyond our Galaxy is dominated by the Cosmic Microwave Background (CMB), discovered in 1965 [1]. The spectrum of the CMB is well described by a blackbody function with $T = 2.725$ K. This spectral form is one of the main pillars of the hot Big Bang model for the early Universe. The lack of any observed deviations from a blackbody spectrum constrains physical processes over cosmic history at redshifts $z \lesssim 10^7$ (see earlier versions of this review). All viable cosmological models predict a very nearly Planckian spectrum inside the current observational limits.

Another observable quantity inherent in the CMB is the variation in temperature (or intensity) from one part of the microwave sky to another [2]. Since the first detection of these anisotropies by the *COBE* satellite [3], there has been intense activity to map the sky at increasing levels of sensitivity and angular resolution by ground-based and balloon-borne measurements. These were joined in 2003 by the first results from NASA's Wilkinson Microwave Anisotropy Probe (*WMAP*) [4], which were improved upon by analysis of the 3 year and 5 year *WMAP* data [5,6]. Together these observations have led to a stunning confirmation of the 'Standard Model of Cosmology.' In combination with other astrophysical data, the CMB anisotropy measurements place quite precise constraints on a number of cosmological parameters, and have launched us into an era of precision cosmology. This is expected to continue with the improved capabilities of the *Planck* satellite.

23.2. Description of CMB Anisotropies

Observations show that the CMB contains anisotropies at the 10^{-5} level, over a wide range of angular scales. These anisotropies are usually expressed by using a spherical harmonic expansion of the CMB sky:

$$T(\theta, \phi) = \sum_{\ell m} a_{\ell m} Y_{\ell m}(\theta, \phi).$$

The vast majority of the cosmological information is contained in the temperature 2-point function, *i.e.*, the variance as a function only of angular separation, since we notice no preferred direction. Equivalently, the power per unit $\ln \ell$ is $\ell \sum_m |a_{\ell m}|^2 / 4\pi$.

23.2.1. The Monopole :

The CMB has a mean temperature of $T_\gamma = 2.725 \pm 0.001$ K (1σ) [7], which can be considered as the monopole component of CMB maps, a_{00} . Since all mapping experiments involve difference measurements, they are insensitive to this average level. Monopole measurements can only be made with absolute temperature devices, such as the FIRAS instrument on the *COBE* satellite [7]. Such measurements of the spectrum are consistent with a blackbody distribution over more than three decades in frequency (with some recent evidence for deviation at low frequencies [8]). A blackbody of the measured temperature corresponds to $n_\gamma = (2\zeta(3)/\pi^2) T_\gamma^3 \simeq 411 \text{ cm}^{-3}$ and $\rho_\gamma = (\pi^2/15) T_\gamma^4 \simeq 4.64 \times 10^{-34} \text{ g cm}^{-3} \simeq 0.260 \text{ eV cm}^{-3}$.

23.2.2. The Dipole :

The largest anisotropy is in the $\ell = 1$ (dipole) first spherical harmonic, with amplitude 3.355 ± 0.008 mK [6]. The dipole is interpreted to be the result of the Doppler shift caused by the solar system motion relative to the nearly isotropic blackbody field, as confirmed by measurements of the radial velocities of local galaxies [9]. The motion of an observer with velocity $\beta \equiv v/c$ relative to an isotropic Planckian radiation field of temperature T_0 produces a Doppler-shifted temperature pattern

$$\begin{aligned} T(\theta) &= T_0(1 - \beta^2)^{1/2} / (1 - \beta \cos \theta) \\ &\simeq T_0 \left(1 + \beta \cos \theta + (\beta^2/2) \cos 2\theta + O(\beta^3) \right). \end{aligned}$$

At every point in the sky, one observes a blackbody spectrum, with temperature $T(\theta)$. The spectrum of the dipole is the differential of a blackbody spectrum, as confirmed by Ref. 10.

The implied velocity for the solar system barycenter is $v = 369.0 \pm 0.9 \text{ km s}^{-1}$, assuming a value $T_0 = T_\gamma$, towards $(\ell, b) = (263.99^\circ \pm 0.14^\circ, 48.26^\circ \pm 0.03^\circ)$ [6,11]. Such a solar system motion implies a velocity for the Galaxy and the Local Group of galaxies relative to the CMB. The derived value is $v_{\text{LG}} = 627 \pm 22 \text{ km s}^{-1}$ towards $(\ell, b) = (276^\circ \pm 3^\circ, 30^\circ \pm 3^\circ)$, where most of the error comes from uncertainty in the velocity of the solar system relative to the Local Group.

The dipole is a frame-dependent quantity, and one can thus determine the 'absolute rest frame' as that in which the CMB dipole would be zero. Our velocity relative to the Local Group, as well as the velocity of the Earth around the Sun, and any velocity of the receiver relative to the Earth, is normally removed for the purposes of CMB anisotropy study.

23.2.3. Higher-Order Multipoles :

The variations in the CMB temperature maps at higher multipoles ($\ell \geq 2$) are interpreted as being mostly the result of perturbations in the density of the early Universe, manifesting themselves at the epoch of the last scattering of the CMB photons. In the hot Big Bang picture, the expansion of the Universe cools the plasma so that by a redshift $z \simeq 1100$ (with little dependence on the details of the model), the hydrogen and helium nuclei can bind electrons into neutral atoms, a process usually referred to as recombination [12]. Before this epoch, the CMB photons are tightly coupled to the baryons, while afterwards they can freely stream towards us.

Theoretical models generally predict that the $a_{\ell m}$ modes are Gaussian random fields to high precision, *e.g.*, standard slow-roll inflation's non-Gaussian contribution is expected to be one or two orders of magnitude below current observational limits [13]. Although non-Gaussianity of various forms is possible in early Universe models, tests show that Gaussianity is an extremely good simplifying approximation [14], with only some relatively weak indications of non-Gaussianity or statistical anisotropy at large scales. Such signatures found in existing *WMAP* data are generally considered to be subtle foreground or instrumental artefacts [15,16].

A statistically isotropic sky means that all m s are equivalent, *i.e.*, there is no preferred axis. Together with the assumption of Gaussian statistics, the variance of the temperature field (or equivalently the power spectrum in ℓ) then fully characterizes the anisotropies. The power summed over all m s at each ℓ is $(2\ell + 1)C_\ell / (4\pi)$, where $C_\ell \equiv \langle |a_{\ell m}|^2 \rangle$. Thus averages of $a_{\ell m}$ s over m can be used as estimators of the C_ℓ s to constrain their expectation values, which are the quantities predicted by a theoretical model. For an idealized full-sky observation, the variance of each measured C_ℓ (*i.e.*, the variance of the variance) is $[2/(2\ell + 1)]C_\ell^2$. This sampling uncertainty (known as 'cosmic variance') comes about because each C_ℓ is χ^2 distributed with $(2\ell + 1)$ degrees of freedom for our observable volume of the Universe. For fractional sky coverage, f_{sky} , this variance is increased by $1/f_{\text{sky}}$ and the modes become partially correlated.

It is important to understand that theories predict the expectation value of the power spectrum, whereas our sky is a single realization. Hence the cosmic variance is an unavoidable source of uncertainty when constraining models; it dominates the scatter at lower ℓ s, while the effects of instrumental noise and resolution dominate at higher ℓ s [17].

23.2.4. Angular Resolution and Binning :

There is no one-to-one conversion between multipole ℓ and the angle subtended by a particular spatial scale projected onto the sky. However, a single spherical harmonic $Y_{\ell m}$ corresponds to angular variations of $\theta \sim \pi/\ell$. CMB maps contain anisotropy information from the size of the map (or in practice some fraction of that size) down to the beam-size of the instrument, σ . One can think of the effect of a Gaussian beam as rolling off the power spectrum with the function $e^{-\ell(\ell+1)\sigma^2}$.

For less than full sky coverage, the ℓ modes become correlated. Hence, experimental results are usually quoted as a series of 'band powers', defined as estimators of $\ell(\ell + 1)C_\ell / 2\pi$ over different ranges of ℓ . Because of the strong foreground signals in the Galactic Plane, even 'all-sky' surveys, such as *COBE* and *WMAP* involve a cut sky. The amount of binning required to obtain uncorrelated estimates of power also depends on the map size.

23.3. Cosmological Parameters

The current ‘Standard Model’ of cosmology contains around 10 free parameters (see The Cosmological Parameters—Sec. 21 of this *Review*). The basic framework is the Friedmann-Robertson-Walker (FRW) metric (*i.e.*, a universe that is approximately homogeneous and isotropic on large scales), with density perturbations laid down at early times and evolving into today’s structures (see Big-Bang cosmology—Sec. 19 of this *Review*). The most general possible set of density perturbations is a linear combination of an adiabatic density perturbation and some isocurvature perturbations. Adiabatic means that there is no change to the entropy per particle for each species, *i.e.*, $\delta\rho/\rho$ for matter is $(3/4)\delta\rho/\rho$ for radiation. Isocurvature means that the set of individual density perturbations adds to zero, for example, matter perturbations compensate radiation perturbations so that the total energy density remains unperturbed, *i.e.*, $\delta\rho$ for matter is $-\delta\rho$ for radiation. These different modes give rise to distinct (temporal) phases during growth, with those of the adiabatic scenario being strongly preferred by the data. Models that generate mainly isocurvature type perturbations (such as most topological defect scenarios) are no longer considered to be viable. However, an admixture of the adiabatic mode with up to about 10% isocurvature contribution is still allowed [18].

Within the adiabatic family of models, there is, in principle, a free function describing how the comoving curvature perturbations, $\mathcal{R}(\mathbf{x}, t)$, vary with length scale. The great virtue of \mathcal{R} is that it is constant for a purely adiabatic perturbation. There are physical reasons to anticipate that the variance of these perturbations will be described well by a power-law in scale, *i.e.*, in Fourier space $\langle |\mathcal{R}_k|^2 \rangle \propto k^{n-4}$, where k is wavenumber and n is the usual definition of spectral index. So-called ‘scale-invariant’ initial conditions (meaning gravitational potential fluctuations which are independent of k) correspond to $n = 1$. In inflationary models [19], perturbations are generated by quantum fluctuations, which are set by the energy scale of inflation, together with the slope and higher derivatives of the inflationary potential. One generally expects that the Taylor series expansion of $\ln \mathcal{R}_k(\ln k)$ has terms of steadily decreasing size. For the simplest models, there are thus 2 parameters describing the initial conditions for density perturbations: the amplitude and slope of the power spectrum. These can be explicitly defined, for example, through:

$$\Delta_{\mathcal{R}}^2 \equiv (k^3/2\pi^2) \langle |\mathcal{R}_k|^2 \rangle = A (k/k_0)^{n-1},$$

with $A \equiv \Delta_{\mathcal{R}}^2(k_0)$ and $k_0 = 0.002 \text{ Mpc}^{-1}$, say. There are many other equally valid definitions of the amplitude parameter (see also Sec. 19 and Sec. 21 of this *Review*), and we caution that the relationships between some of them can be cosmology-dependent. In ‘slow roll’ inflationary models, this normalization is proportional to the combination $V^3/(V')^2$, for the inflationary potential $V(\phi)$. The slope n also involves V'' , and so the combination of A and n can, in principle, constrain potentials.

Inflation generates tensor (gravitational wave) modes, as well as scalar (density perturbation) modes. This fact introduces another parameter, measuring the amplitude of a possible tensor component, or equivalently the ratio of the tensor to scalar contributions. The tensor amplitude is $A_T \propto V$, and thus one expects a larger gravitational wave contribution in models where inflation happens at higher energies. The tensor power spectrum also has a slope, often denoted n_T , but since this seems unlikely to be measured in the near future, it is sufficient for now to focus only on the amplitude of the gravitational wave component. It is most common to define the tensor contribution through r , the ratio of tensor to scalar perturbation spectra at some small value of k (although sometimes it is defined in terms of the ratio of contributions at $\ell = 2$). Different inflationary potentials will lead to different predictions, *e.g.*, for $\lambda\phi^4$ inflation with 50 e-folds, $r = 0.32$, and for $m^2\phi^2$ inflation $r \simeq 0.15$, while other models can have arbitrarily small values of r . In any case, whatever the specific definition, and whether they come from inflation or something else, the ‘initial conditions’ give rise to a minimum of 3 parameters: A , n , and r .

The background cosmology requires an expansion parameter (the Hubble Constant, H_0 , often represented through $H_0 = 100 h \text{ km s}^{-1} \text{ Mpc}^{-1}$) and several parameters to describe the matter and energy content of the Universe. These are usually given in terms

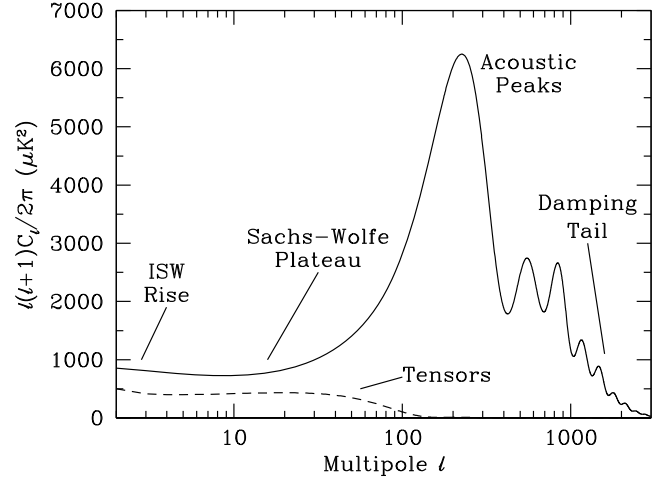


Figure 23.1: The theoretical CMB anisotropy power spectrum, using a standard Λ CDM model from CMBFAST. The x -axis is logarithmic here. The regions, each covering roughly a decade in ℓ , are labeled as in the text: the ISW rise; Sachs-Wolfe plateau; acoustic peaks; and damping tail. Also shown is the shape of the tensor (gravitational wave) contribution, with an arbitrary normalization.

of the critical density, *i.e.*, for species ‘x’, $\Omega_x \equiv \rho_x/\rho_{\text{crit}}$, where $\rho_{\text{crit}} \equiv 3H_0^2/8\pi G$. Since physical densities $\rho_x \propto \Omega_x h^2 \equiv \omega_x$ are what govern the physics of the CMB anisotropies, it is these ω s that are best constrained by CMB data. In particular CMB observations constrain $\Omega_b h^2$ for baryons and $\Omega_m h^2$ for baryons plus Cold Dark Matter.

The contribution of a cosmological constant Λ (or other form of Dark Energy) is usually included via a parameter which quantifies the curvature, $\Omega_K \equiv 1 - \Omega_{\text{tot}}$, where $\Omega_{\text{tot}} = \Omega_m + \Omega_\Lambda$. The radiation content, while in principle a free parameter, is precisely enough determined by the measurement of T_γ , and makes a $< 10^{-4}$ contribution to Ω_{tot} today.

The main effect of astrophysical processes on the C_ℓ s comes through reionization. The Universe became reionized at some redshift z_i , long after recombination, affecting the CMB through the integrated Thomson scattering optical depth:

$$\tau = \int_0^{z_i} \sigma_T n_e(z) \frac{dt}{dz} dz,$$

where σ_T is the Thomson cross-section, $n_e(z)$ is the number density of free electrons (which depends on astrophysics), and dt/dz is fixed by the background cosmology. In principle, τ can be determined from the small-scale matter power spectrum, together with the physics of structure formation and feedback processes. However, this is a sufficiently intricate calculation that τ needs to be considered as a free parameter.

Thus, we have 8 basic cosmological parameters: A , n , r , h , $\Omega_b h^2$, $\Omega_m h^2$, Ω_{tot} , and τ . One can add additional parameters to this list, particularly when using the CMB in combination with other data sets. The next most relevant ones might be: $\Omega_\nu h^2$, the massive neutrino contribution; w ($\equiv p/\rho$), the equation of state parameter for the Dark Energy; and $dn/d\ln k$, measuring deviations from a constant spectral index. To these 11 one could of course add further parameters describing additional physics, such as details of the reionization process, features in the initial power spectrum, a sub-dominant contribution of isocurvature modes, *etc.*

As well as these underlying parameters, there are other quantities that can be obtained from them. Such derived parameters include the actual Ω s of the various components (*e.g.*, Ω_m), the variance of density perturbations at particular scales (*e.g.*, σ_8), the age of the Universe today (t_0), the age of the Universe at recombination, reionization, *etc.*

23.4. Physics of Anisotropies

The cosmological parameters affect the anisotropies through the well understood physics of the evolution of linear perturbations within a background FRW cosmology. There are very effective, fast, and publicly-available software codes for computing the CMB anisotropy, polarization, and matter power spectra, *e.g.*, CMBFAST [20] and CAMB [21]. These have been tested over a wide range of cosmological parameters and are considered to be accurate to better than the 1% level [22].

A description of the physics underlying the C_ℓ s can be separated into 3 main regions, as shown in Fig. 23.1.

23.4.1. The ISW rise, $\ell \lesssim 10$, and Sachs-Wolfe plateau, $10 \lesssim \ell \lesssim 100$:

The horizon scale (or more precisely, the angle subtended by the Hubble radius) at last scattering corresponds to $\ell \simeq 100$. Anisotropies at larger scales have not evolved significantly, and hence directly reflect the ‘initial conditions’. $\delta T/T = -(1/5)\mathcal{R}(\mathbf{x}_{\text{LSS}}) \simeq (1/3)\delta\phi/c^2$, here $\delta\phi$ is the perturbation to the gravitational potential, evaluated on the last scattering surface (LSS). This is a result of the combination of gravitational redshift and intrinsic temperature fluctuations and is usually referred to as the ‘Sachs-Wolfe’ effect [23].

Assuming that a nearly scale-invariant spectrum of curvature and corresponding density perturbations was laid down at early times (*i.e.*, $n \simeq 1$, meaning equal power per decade in k), then $\ell(\ell+1)C_\ell \simeq \text{constant}$ at low ℓ s. This effect is hard to see unless the multipole axis is plotted logarithmically (as in Fig. 23.1, but not Fig. 23.2).

Time variation of the potentials (*i.e.*, time-dependent metric perturbations) leads to an upturn in the C_ℓ s in the lowest several multipoles; any deviation from a total equation of state $w = 0$ has such an effect. So the dominance of the Dark Energy at low redshift makes the lowest ℓ s rise above the plateau. This is sometimes called the ‘integrated Sachs-Wolfe effect’ (or ISW rise), since it comes from the line integral of $\dot{\phi}$; it has been confirmed through correlations between the large-angle anisotropies and large-scale structure [24]. Specific models can also give additional contributions at low ℓ (*e.g.*, perturbations in the Dark Energy component itself [25]), but typically these are buried in the cosmic variance.

In principle, the mechanism that produces primordial perturbations could generate scalar, vector, and tensor modes. However, the vector (vorticity) modes decay with the expansion of the Universe. The tensors (transverse trace-free perturbations to the metric) generate temperature anisotropies through the integrated effect of the locally anisotropic expansion of space. Since the tensor modes also redshift away after they enter the horizon, they contribute only to angular scales above about 1° (see Fig. 23.1). Hence some fraction of the low ℓ signal could be due to a gravitational wave contribution, although small amounts of tensors are essentially impossible to discriminate from other effects that might raise the level of the plateau. However, the tensors *can* be distinguished using polarization information (see Sec. 23.6).

23.4.2. The acoustic peaks, $100 \lesssim \ell \lesssim 1000$:

On sub-degree scales, the rich structure in the anisotropy spectrum is the consequence of gravity-driven acoustic oscillations occurring before the atoms in the Universe became neutral. Perturbations inside the horizon at last scattering have been able to evolve causally and produce anisotropy at the last scattering epoch, which reflects this evolution. The frozen-in phases of these sound waves imprint a dependence on the cosmological parameters, which gives CMB anisotropies their great constraining power.

The underlying physics can be understood as follows. Before the Universe became neutral, the proton-electron plasma was tightly coupled to the photons, and these components behaved as a single ‘photon-baryon fluid.’ Perturbations in the gravitational potential, dominated by the Dark Matter component, were steadily evolving. They drove oscillations in the photon-baryon fluid, with photon pressure providing most of the restoring force and baryons giving some additional inertia. The perturbations were quite small in amplitude, $O(10^{-5})$, and so evolved linearly. That means each Fourier mode developed independently, and hence can be described by a driven harmonic oscillator, with frequency determined by the sound speed in

the fluid. Thus the fluid density underwent oscillations, giving time variations in temperature. These combine with a velocity effect which is $\pi/2$ out of phase and has its amplitude reduced by the sound speed.

After the Universe recombined, the radiation decoupled from the baryons and could travel freely towards us. At that point, the phases of the oscillations were frozen-in, and became projected on the sky as a harmonic series of peaks. The main peak is the mode that went through $1/4$ of a period, reaching maximal compression. The even peaks are maximal *under*-densities, which are generally of smaller amplitude because the rebound has to fight against the baryon inertia. The troughs, which do not extend to zero power, are partially filled by the Doppler effect because they are at the velocity maxima.

The physical length scale associated with the peaks is the sound horizon at last scattering, which can be straightforwardly calculated. This length is projected onto the sky, leading to an angular scale that depends on the geometry of space, as well as the distance to last scattering. Hence the angular position of the peaks is a sensitive probe of the spatial curvature of the Universe (*i.e.*, Ω_{tot}), with the peaks lying at higher ℓ in open universes and lower ℓ in closed geometry.

One additional effect arises from reionization at redshift z_i . A fraction of photons (τ) will be isotropically scattered at $z < z_i$, partially erasing the anisotropies at angular scales smaller than those subtended by the Hubble radius at z_i . This corresponds typically to ℓ s above about a few 10s, depending on the specific reionization model. The acoustic peaks are therefore reduced by a factor $e^{-2\tau}$ relative to the plateau.

These peaks were a clear theoretical prediction going back to about 1970 [26]. One can think of them as a snapshot of stochastic standing waves. Since the physics governing them is simple and their structure rich, then one can see how they encode extractable information about the cosmological parameters. Their empirical existence started to become clear around 1994 [27], and the emergence, over the following decade, of a coherent series of acoustic peaks and troughs is a triumph of modern cosmology. This picture has received further confirmation with the detection in the power spectrum of galaxies (at redshifts close to zero) of the imprint of these same acoustic oscillations in the baryon component [28,29,34].

23.4.3. The damping tail, $\ell \gtrsim 1000$:

The recombination process is not instantaneous, giving a thickness to the last scattering surface. This leads to a damping of the anisotropies at the highest ℓ s, corresponding to scales smaller than that subtended by this thickness. One can also think of the photon-baryon fluid as having imperfect coupling, so that there is diffusion between the two components, and hence the amplitudes of the oscillations decrease with time. These effects lead to a damping of the C_ℓ s, sometimes called Silk damping [31], which cuts off the anisotropies at multipoles above about 2000.

An extra effect at high ℓ s comes from gravitational lensing, caused mainly by non-linear structures at low redshift. The C_ℓ s are convolved with a smoothing function in a calculable way, partially flattening the peaks, generating a power-law tail at the highest multipoles, and complicating the polarization signal [32]. The effects of lensing on the CMB have recently been detected by correlating temperature gradients and small-scale filtered anisotropies from WMAP with lensing potentials traced using galaxies [33]. This is an example of a ‘secondary effect,’ *i.e.*, the processing of anisotropies due to relatively nearby structures (see Sec. 23.7.2). Galaxies and clusters of galaxies give several such effects; all are expected to be of low amplitude and typically affect only the highest ℓ s, but they carry additional cosmological information and will be increasingly important as experiments push to higher sensitivity and angular resolution.

23.5. Current Anisotropy Data

There has been a steady improvement in the quality of CMB data that has led to the development of the present-day cosmological model. Probably the most robust constraints currently available come from the combination of the WMAP five year data [34] with smaller scale results from the ACBAR [35] and QUAD [36] experiments (together with constraints from other cosmological data-sets). We plot power spectrum estimates from these experiments, as well as BOOMERANG [38] and CBI [39] in Fig. 23.2. Other recent

experiments also give powerful constraints, which are quite consistent with what we describe below. There have been some comparisons among data-sets [37,41], which indicate very good agreement, both in maps and in derived power spectra (up to systematic uncertainties in the overall calibration for some experiments). This makes it clear that systematic effects are largely under control. However, a fully self-consistent joint analysis of all the current data sets has not been attempted, one of the reasons being that it requires a careful treatment of the overlapping sky coverage.

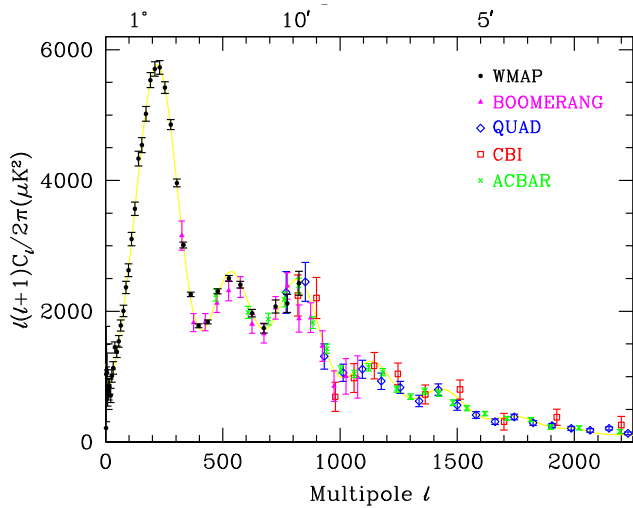


Figure 23.2: Band-power estimates from the WMAP, BOOMERANG, QUAD, CBI, and ACBAR experiments. Some of the low- ℓ and high- ℓ band-powers which have large error bars have been omitted. Note also that the widths of the ℓ -bands varies between experiments and have not been plotted. This figure represent only a selection of available experimental results, with some other data-sets being of similar quality. The multipole axis here is linear, so the Sachs-Wolfe plateau is hard to see. However, the acoustic peaks and damping region are very clearly observed, with no need for a theoretical curve to guide the eye; the curve plotted is a best-fit model from WMAP 5-year plus other CMB data. Color version at end of book.

The band-powers shown in Fig. 23.2 are in very good agreement with a ‘ Λ CDM’ type model, as described earlier, with several of the peaks and troughs quite apparent. For details of how these estimates were arrived at, the strength of any correlations between band-powers and other information required to properly interpret them, the original papers should be consulted.

23.6. CMB Polarization

Since Thomson scattering of an anisotropic radiation field also generates linear polarization, the CMB is predicted to be polarized at the roughly 5% level of the temperature anisotropies [42]. Polarization is a spin-2 field on the sky, and the algebra of the modes in ℓ -space is strongly analogous to spin-orbit coupling in quantum mechanics [43]. The linear polarization pattern can be decomposed in a number of ways, with two quantities required for each pixel in a map, often given as the Q and U Stokes parameters. However, the most intuitive and physical decomposition is a geometrical one, splitting the polarization pattern into a part that comes from a divergence (often referred to as the ‘E-mode’) and a part with a curl (called the ‘B-mode’) [44]. More explicitly, the modes are defined in terms of second derivatives of the polarization amplitude, with the Hessian for the E-modes having principle axes in the same sense as the polarization, while the B-mode pattern can be thought of simply as a 45° rotation of the E-mode pattern. Globally one sees that the E-modes have $(-1)^\ell$ parity (like the spherical harmonics), while the B-modes have $(-1)^{\ell+1}$ parity.

The existence of this linear polarization allows for 6 different cross power spectra to be determined from data that measure the

full temperature and polarization anisotropy information. Parity considerations make 2 of these zero, and we are left with 4 potential observables: C_ℓ^{TT} , C_ℓ^{TE} , C_ℓ^{EE} , and C_ℓ^{BB} . Because scalar perturbations have no handedness, the B-mode power spectrum can only be sourced by vectors or tensors. Moreover, since inflationary scalar perturbations give only E-modes, while tensors generate roughly equal amounts of E- and B-modes, then the determination of a non-zero B-mode signal is a way to measure the gravitational wave contribution (and thus potentially derive the energy scale of inflation), even if it is rather weak. However, one must first eliminate the foreground contributions and other systematic effects down to very low levels.

The oscillating photon-baryon fluid also results in a series of acoustic peaks in the polarization C_ℓ s. The main ‘EE’ power spectrum has peaks that are out of phase with those in the ‘TT’ spectrum, because the polarization anisotropies are sourced by the fluid velocity. The ‘TE’ part of the polarization and temperature patterns comes from correlations between density and velocity perturbations on the last scattering surface, which can be both positive and negative, and is of larger amplitude than the EE signal. There is no polarization ‘Sachs-Wolfe’ effect, and hence no large-angle plateau. However, scattering during a recent period of reionization can create a polarization ‘bump’ at large angular scales.

Because the polarization anisotropies have only a fraction of the amplitude of the temperature anisotropies, they took longer to detect. The first measurement of a polarization signal came in 2002 from the DASI experiment [45], which provided a convincing detection, confirming the general paradigm, but of low enough significance that it lent little constraint to models. As well as the E-mode signal, DASI also made a statistical detection of the TE correlation.

In 2003, the WMAP experiment demonstrated that it was able to measure the TE cross-correlation power spectrum with high precision [46], and this was improved upon in the 3- and 5-year results, which also included EE measurements [34,47]. The TE signal has been mapped out quite accurately now through a combination of data from WMAP, together with the BOOMERANG [54], QUAD [37], CBI [51], DASI [52] and BICEP [49,50] experiments, which are shown in Fig. 23.3. The anti-correlation at $\ell \simeq 150$ and the peak at $\ell \simeq 300$ are now quite distinct. The measured shape of the cross-correlation power spectrum provides supporting evidence for the adiabatic nature of the perturbations, as well as directly constraining the thickness of the last scattering surface. Since the polarization anisotropies are generated in this scattering surface, the existence of correlations at angles above about a degree demonstrates that there were super-Hubble fluctuations at the recombination epoch. The sign of this correlation also confirms the adiabatic paradigm.

Experimental band-powers for C_ℓ^{EE} from WMAP plus CAPMAP [48], CBI [51], DASI [52], BOOMERANG [53], QUAD [37] and BICEP [50] are shown in Fig. 23.4. Without the benefit of correlating with the temperature anisotropies (*i.e.*, measuring C_ℓ^{TE}), the polarization anisotropies are very weak and challenging to measure. Nevertheless, there is a highly significant overall detection which is consistent with expectation. The QUAD data convincingly show the peak at $\ell \simeq 400$ (corresponding to the first trough in C_ℓ^{TT}) and the generally oscillatory structure, while the new BICEP data show the lower peak at $\ell \simeq 140$.

Several experiments have reported upper limits on C_ℓ^{BB} , but they are currently not very constraining. This situation should change as increasingly ambitious experiments report results.

The most distinctive result from the polarization measurements is at the largest angular scales ($\ell < 10$) in C_ℓ^{TE} , where there is an excess signal compared to that expected from the temperature power spectrum alone. This is precisely the signal anticipated from an early period of reionization, arising from Doppler shifts during the partial scattering at $z < z_i$. The effect is also confirmed in the WMAP C_ℓ^{EE} results at $\ell = 2-6$. The amplitude of the signal indicates that the first stars, presumably the source of the ionizing radiation, formed around $z \simeq 10$ (somewhat lower than the value suggested by the first year WMAP results, although the uncertainty is still quite large). Since this corresponds to scattering optical depth $\tau \simeq 0.1$, then roughly 10% of CMB photons were rescattered at the reionization epoch, with the other 90% last scattering at $z \simeq 1100$.

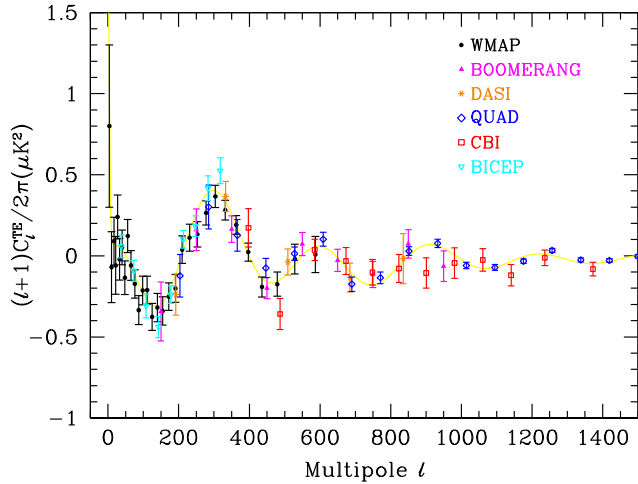


Figure 23.3: Cross power spectrum of the temperature anisotropies and E-mode polarization signal from WMAP [47], together with estimates from BOOMERANG, DASI, QUAD, CBI and BICEP, several of which extend to higher ℓ . Note that the widths of the bands have been suppressed for clarity, but that in some cases they are almost as wide as the features in the power spectrum. Also note that the y -axis here is not multiplied by the additional ℓ , which helps to show both the large and small angular scale features. Color version at end of book.

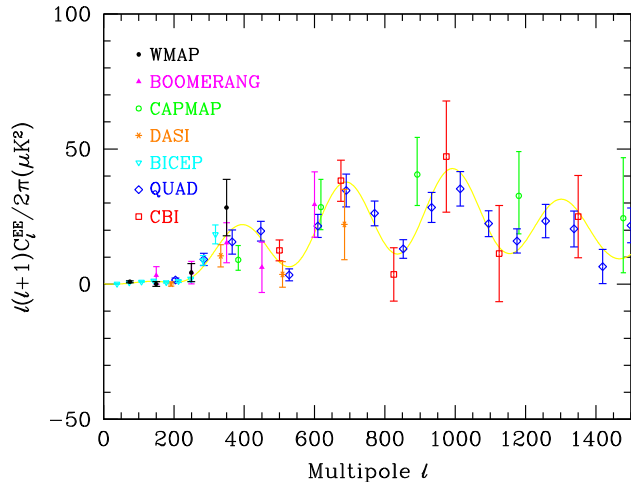


Figure 23.4: Power spectrum of E-mode polarization from several different experiments, plotted along with a theoretical model which fits WMAP plus other CMB data. Color version at end of book.

23.7. Complications

There are a number of issues which complicate the interpretation of CMB anisotropy data (and are considered to be *signal* by many astrophysicists), some of which we sketch out below.

23.7.1. Foregrounds :

The microwave sky contains significant emission from our Galaxy and from extra-galactic sources [55]. Fortunately, the frequency dependence of these various sources is in general substantially different from that of the CMB anisotropy signals. The combination of Galactic synchrotron, bremsstrahlung, and dust emission reaches a minimum at a wavelength of roughly 3 mm (or about 100 GHz). As one moves to greater angular resolution, the minimum moves to slightly higher frequencies, but becomes more sensitive to unresolved (point-like) sources.

At frequencies around 100 GHz, and for portions of the sky away from the Galactic Plane, the foregrounds are typically 1 to 10% of the CMB anisotropies. By making observations at multiple frequencies,

it is relatively straightforward to separate the various components and determine the CMB signal to the few per cent level. For greater sensitivity, it is necessary to use the spatial information and statistical properties of the foregrounds to separate them from the CMB.

The foregrounds for CMB polarization are expected to follow a similar pattern, but are less well studied, and are intrinsically more complicated. The three year WMAP data have shown that the polarized foregrounds dominate at large angular scales, and that they must be well characterized in order to be discriminated [56]. Whether it is possible to achieve sufficient separation to detect B-mode CMB polarization is still an open question. However, for the time being, foreground contamination is not a fundamental limit for CMB experiments.

23.7.2. Secondary Anisotropies :

With increasingly precise measurements of the primary anisotropies, there is growing theoretical and experimental interest in ‘secondary anisotropies,’ pushing experiments to higher angular resolution and sensitivity. These secondary effects arise from the processing of the CMB due to ionization history and the evolution of structure, including gravitational lensing and patchy reionization effects [57]. Additional information can thus be extracted about the Universe at $z \ll 1000$. This tends to be most effectively done through correlating CMB maps with other cosmological probes of structure. Secondary signals are also typically non-Gaussian, unlike the primary CMB anisotropies.

23.7.3. Sunyaev-Zel’dovich Effect :

A secondary signal of great current interest is the Sunyaev-Zel’dovich (SZ) effect [58], which is Compton scattering ($\gamma e \rightarrow \gamma' e'$) of the CMB photons by hot electron gas, which creates spectral distortions by transferring energy from the electrons to the photons. It is particularly important for clusters of galaxies, through which one observes a partially Comptonized spectrum, resulting in a decrement at radio wavelengths and an increment in the submillimeter.

The imprint on the CMB sky is of the form $\Delta T/T = y f(x)$, with the y -parameter being the integral of Thomson optical depth times $kT_e/m_e c^2$ through the cluster, and $f(x)$ describing the frequency dependence. This is simply $x \coth(x/2) - 4$ for a non-relativistic gas (the electron temperature in a cluster is typically a few keV), where the dimensionless frequency $x \equiv h\nu/kT_\gamma$. As well as this ‘thermal’ SZ effect, there is also a smaller ‘kinetic’ effect due to the bulk motion of the cluster gas, this being $\Delta T/T \sim \tau(v/c)$, with either sign, but having the same spectrum as the primary CMB anisotropies.

A significant advantage in finding galaxy clusters this way is that the SZ effect is largely independent of redshift, so in principle clusters can be found to arbitrarily large distances. The SZ effect can be used to find and study individual clusters, and to obtain estimates of the Hubble constant. There is also the potential to constrain the equation of state of the Dark Energy through counts of detected clusters as a function of redshift [59]. Many experiments (including the *Planck* satellite) are currently in operation which will probe clusters in this way. The promise of the method has been realised through the first detections of clusters purely through the SZ effect, by the SPT [60] and ACT [61] experiments.

23.7.4. Higher-order Statistics :

Although most of the CMB anisotropy information is contained in the power spectra, there will also be weak signals present in higher-order statistics. These statistics can measure any primordial non-Gaussianity in the perturbations, as well as non-linear growth of the fluctuations on small scales and other secondary effects (plus residual foreground contamination of course). Although there are an infinite variety of ways in which the CMB could be non-Gaussian, there is a generic form to consider for the initial conditions, where a quadratic contribution to the curvature perturbations is parameterized through a dimensionless number f_{NL} . This weakly non-linear component can be constrained through measurements of the bispectrum or Minkowski functionals, for example. The constraints depend on the shape of the triangles in harmonic space, and it has become common to distinguish the ‘local’ or ‘squeezed’ configuration (in which one side is much smaller than the other two) from the ‘equilateral’ configuration. The results from the WMAP team are

$-9 < f_{\text{NL}} < 111$ (95% confidence region), for the local mode and $-151 < f_{\text{NL}} < 253$ for the equilateral mode [14]. Different estimators used by other authors give results of similar magnitude [62].

The level of f_{NL} expected is small, so that a detection of $f_{\text{NL}} \gtrsim 10$ would rule out all single field, slow-roll inflationary models. However, with the capabilities of *Planck* and other future experiments, it seems that a measurement of primordial non-Gaussianity may be feasible for a wide class of models, and therefore much effort is expected to be devoted to predictions and measurements in the coming years.

23.8. Constraints on Cosmologies

The most striking outcome of the newer experimental results is that the standard cosmological paradigm is in very good shape. A large amount of high precision data on the power spectrum is adequately fit with fewer than 10 free parameters. The framework is that of FRW models, which have nearly flat geometry, containing Dark Matter and Dark Energy, and with adiabatic perturbations having close to scale invariant initial conditions.

Within this framework, bounds can be placed on the values of the cosmological parameters. Of course, much more stringent constraints can be placed on models which cover a restricted parameter space, *e.g.*, assuming that $\Omega_{\text{tot}} = 1$, $n = 1$ or $r = 0$. More generally, the constraints depend upon the adopted prior probability distributions, even if they are implicit, for example by restricting the parameter freedom or their ranges (particularly where likelihoods peak near the boundaries), or by using different choices of other data in combination with the CMB. When the data become even more precise, these considerations will be less important, but for now we caution that restrictions on model space and choice of priors need to be kept in mind when adopting specific parameter values and uncertainties.

There are some combinations of parameters that fit the CMB anisotropies almost equivalently. For example, there is a nearly exact geometric degeneracy, where any combination of Ω_{m} and Ω_{Λ} that gives the same angular diameter distance to last scattering will give nearly identical C_{ℓ} s. There are also other less exact degeneracies among the parameters. Such degeneracies can be broken when using the CMB results in combination with other cosmological data sets. Particularly useful are complementary constraints from galaxy clustering, the abundance of galaxy clusters, baryon acoustic oscillations, weak gravitational lensing measurements, Type Ia supernova distances, and the distribution of Lyman α forest clouds. For an overview of some of these other cosmological constraints, see The Cosmological Parameters—Sec. 21 of this *Review*.

The 5-year *WMAP* data alone, together with constraints from Hubble constant determination [18], supernovae [64] and baryon acoustic oscillations [29], within the context of a 6 parameter family of models (which fixes $\Omega_{\text{tot}} = 1$ and $r = 0$), yield the following results [14]: $A = (2.44 \pm 0.10) \times 10^{-9}$, $n = 0.960 \pm 0.013$, $h = 0.705 \pm 0.013$, $\Omega_{\text{b}}h^2 = 0.0227 \pm 0.0006$, $\Omega_{\text{m}}h^2 = 0.136 \pm 0.004$ and $\tau = 0.084 \pm 0.016$. There has been little substantive change compared with the 3-year data, although the error bars are reduced with more integration time and the inclusion of lower frequency polarization data. The better measurement of the third acoustic peak, together with improved understanding of calibration issues has led to tighter error bars on dark matter density and overall normalization. The evidence for non-zero reionization optical depth is now very compelling, while the evidence for $n < 1$ is still only at the roughly 3σ level.

Other combinations of data, *e.g.*, including additional CMB measurements, or using cosmological constraints, lead to consistent results to those given above, sometimes with smaller error bars, and with the precise values depending on data selection [34,37,65]. Note that for h , the CMB data alone provide only a very weak constraint, unless spatial flatness or some other cosmological data are used. For $\Omega_{\text{b}}h^2$, the precise value depends sensitively on how much freedom is allowed in the shape of the primordial power spectrum (see Big-Bang nucleosynthesis—Sec. 20 of this *Review*). The addition of other data-sets also allows for constraints to be placed on further parameters.

For Ω_{tot} , perhaps the best *WMAP* constraint is 1.006 ± 0.006 , from the combination with supernova and baryon acoustic oscillation constraints (and setting $w = -1$). The 95% confidence upper limit on r is 0.43 using *WMAP* alone, tightening to $r < 0.22$ with the

addition of other data [14]. This limit depends on how the slope n is restricted and whether $dn/d\ln k \neq 0$ is allowed. Nevertheless, it is clear that $\lambda\phi^4$ (sometimes called self-coupled) inflation is disfavored by the data, while the $m^2\phi^2$ (sometimes called mass term) inflationary model is still allowed [14]. Gravity wave constraints coming directly from B-mode limits are at the level of $r < 0.73$ [50].

There are also constraints on parameters over and above the basic 8 that we have described, usually requiring extra cosmological data to break degeneracies. For example, the addition of the Dark Energy equation of state w adds the partial degeneracy of being able to fit a ridge in (w, h) space, extending to low values of both parameters. This degeneracy is broken when the CMB is used in combination with independent H_0 limits, or other data. *WMAP* plus supernova and large-scale structure data yield $-0.14 < 1 + w < 0.12$ (95% confidence), with stronger constraints for flat models.

For the optical depth τ , the best-fit corresponds to a reionization redshift centered on 11 in the best-fit cosmology, and assuming instantaneous reionization. This redshift appears to be higher than that suggested from studies of absorption in high- z quasar spectra [66]. The excitement here is that we have direct information from CMB polarization which can be combined with other astrophysical measurements to understand when the first stars formed and brought about the end of the cosmic dark ages.

23.9. Particle Physics Constraints

CMB data are beginning to put limits on parameters which are directly relevant for particle physics models. For example, there is a limit on the neutrino contribution $\Omega_{\nu}h^2 < 0.0071$ (95% confidence) from a combination of *WMAP* and other data [14]. This directly implies a limit on neutrino mass, $\sum m_{\nu} < 0.67$ eV, assuming the usual number density of fermions which decoupled when they were relativistic. Some tighter constraints can be derived using the CMB in combination with other data-sets [67].

The current suite of data suggest that $n < 1$, with a best-fitting value about 5% below unity. If borne out, this would be quite constraining for inflationary models. Moreover, this gives a real target for B-mode searches, since the value of r in simple models may be in the range of detectability, *e.g.*, $r \sim 0.2$ for $m^2\phi^2$ inflation if $n \simeq 0.95$. In addition, a combination of the *WMAP* data with other data-sets constrains the running of the spectral index, although at the moment there is no evidence for $dn/d\ln k \neq 0$ [14].

One other hint of new physics lies in the fact that the quadrupole and possibly some of the other low ℓ modes seem anomalously low compared with the best-fit Λ CDM model [6]. Additionally there is some weak evidence for a large scale modulation of the smaller-scale power [16]. These effects might be expected in a universe which has a large-scale cut-off or anisotropy in the initial power spectrum, or is topologically non-trivial. However, cosmic variance, possible foregrounds, apparent correlations between modes (as mentioned in Sec. 23.2), *etc.*, limit the significance of these anomalies.

In addition, it is also possible to put limits on other pieces of physics [68], for example the neutrino chemical potentials, contribution of Warm Dark Matter, decaying particles, time variation of the fine-structure constant, or physics beyond general relativity. Further particle physics constraints will follow as the anisotropy measurements increase in precision.

Careful measurement of the CMB power spectra and non-Gaussianity can in principle put constraints on physics at the highest energies, including ideas of string theory, extra dimensions, colliding branes, *etc.* At the moment any calculation of predictions appears to be far from definitive. However, there is a great deal of activity on implications of string theory for the early Universe, and hence a very real chance that there might be observational implications for specific scenarios.

23.10. Fundamental Lessons

More important than the precise values of parameters is what we have learned about the general features which describe our observable Universe. Beyond the basic hot Big Bang picture, the CMB has taught us that:

- The Universe recombined at $z \simeq 1100$ and started to become ionized again at $z \simeq 10$.
- The geometry of the Universe is close to flat.
- Both Dark Matter and Dark Energy are required.
- Gravitational instability is sufficient to grow all of the observed large structures in the Universe.
- Topological defects were not important for structure formation.
- There are ‘synchronized’ super-Hubble modes generated in the early Universe.
- The initial perturbations were adiabatic in nature.
- The perturbations had close to Gaussian (*i.e.*, maximally random) initial conditions.

It is very tempting to make an analogy between the status of the cosmological ‘Standard Model’ and that of particle physics (see earlier Sections of this *Review*). In cosmology there are about 10 free parameters, each of which is becoming well determined, and with a great deal of consistency between different measurements. However, none of these parameters can be calculated from a fundamental theory, and so hints of the bigger picture, ‘physics beyond the Standard Model,’ are being searched for with ever more ambitious experiments.

Despite this analogy, there are some basic differences. For one thing, many of the cosmological parameters change with cosmic epoch, and so the measured values are simply the ones determined today, and hence they are not ‘constants,’ like particle masses for example (although they *are* deterministic, so that if one knows their values at one epoch, they can be calculated at another). Moreover, the number of parameters is not as fixed as it is in the particle physics Standard Model; different researchers will not necessarily agree on what the free parameters are, and new ones can be added as the quality of the data improves. In addition, parameters like τ , which come from astrophysics, are in principle calculable from known physical processes. On top of all this, other parameters might be ‘stochastic’ in that they may be fixed only in our observable patch of the Universe or among certain vacuum states in the ‘Landscape’ [70].

In a more general sense, the cosmological ‘Standard Model’ is much further from the underlying ‘fundamental theory,’ which will ultimately provide the values of the parameters from first principles. Nevertheless, any genuinely complete ‘theory of everything’ must include an explanation for the values of these cosmological parameters as well as the parameters of the Standard Model of particle physics.

23.11. Future Directions

Given the significant progress in measuring the CMB sky, which has been instrumental in tying down cosmological parameters, what can we anticipate for the future? There will be a steady improvement in the precision and confidence with which we can determine the appropriate cosmological model and its parameters. Ground-based experiments operating at smaller angular scales will over the next few years provide significantly tighter constraints on the damping tail. New polarization experiments will continue to push down the constraints on primordial B-modes. The third generation CMB satellite mission, *Planck* was launched successfully in May 2009, and the first results are keenly anticipated.

Despite the increasing improvement in the results, the addition of the latest experiments has not significantly changed the established cosmological model. It is, therefore, appropriate to ask: what should we expect to come from *Planck* and from other future experiments, including those being discussed in the U.S. and in Europe? *Planck* certainly has the advantage of high sensitivity and a full-sky survey. A precise measurement of the third acoustic peak provides a good determination of the matter density; this can only be done by measurements which are accurate relative to the first two peaks (which themselves constrain the curvature and the baryon density). A detailed measurement of the damping tail region will also significantly improve the determination of n and any running of the slope. *Planck*

should be capable of measuring C_{ℓ}^{EE} quite well, providing both a strong check on the cosmological Standard Model and extra constraints that will improve parameter estimation.

A set of cosmological parameters is now known to roughly 10% accuracy, and that may seem sufficient for many people. However, we should certainly demand more of measurements which describe *the entire observable Universe!* Hence a lot of activity in the coming years will continue to focus on determining those parameters with increasing precision. This necessarily includes testing for consistency among different predictions of the cosmological Standard Model, and searching for signals which might require additional physics.

A second area of focus will be the smaller scale anisotropies and ‘secondary effects.’ There is a great deal of information about structure formation at $z \ll 1000$ encoded in the CMB sky. This may involve higher-order statistics as well as spectral signatures, with many new experiments targeting the galaxy cluster SZ effect. Such investigations can also provide constraints on the Dark Energy equation of state, for example. *Planck*, as well as new telescopes aimed at the highest ℓ s, should be able to make a lot of progress in this arena.

A third direction is increasingly sensitive searches for specific signatures of physics at the highest energies. The most promising of these may be the primordial gravitational wave signals in C_{ℓ}^{BB} , which could be a probe of the $\sim 10^{16}$ GeV energy range. As well as *Planck*, there are several ground- and balloon-based experiments underway which are designed to probe the polarization B-modes. Whether the amplitude of the effect coming from inflation will be detectable is unclear, but the prize makes the effort worthwhile, and the indications that $n \simeq 0.95$ give some genuine optimism that $r(= T/S)$ may be of order 0.1, and hence within reach soon.

Anisotropies in the CMB have proven to be the premier probe of cosmology and the early Universe. Theoretically the CMB involves well-understood physics in the linear regime, and is under very good calculational control. A substantial and improving set of observational data now exists. Systematics appear to be well understood and not a limiting factor. And so for the next few years we can expect an increasing amount of cosmological information to be gleaned from CMB anisotropies, with the prospect also of some genuine surprises.

References:

1. A.A. Penzias and R. Wilson, *Astrophys. J.* **142**, 419 (1965); R.H. Dicke *et al.*, *Astrophys. J.* **142**, 414 (1965).
2. M. White, D. Scott, and J. Silk, *Ann. Rev. Astron. & Astrophys.* **32**, 329 (1994); W. Hu and S. Dodelson, *Ann. Rev. Astron. & Astrophys.* **40**, 171 (2002).
3. G.F. Smoot *et al.*, *Astrophys. J.* **396**, L1 (1992).
4. C.L. Bennett *et al.*, *Astrophys. J. Supp.* **148**, 1 (2003).
5. N. Jarosik *et al.*, *Astrophys. J. Supp.* **170**, 263 (2007).
6. G. Hinshaw *et al.*, *Astrophys. J. Supp.* **180**, 225 (2009).
7. J.C. Mather *et al.*, *Astrophys. J.* **512**, 511 (1999).
8. D.J. Fixsen *et al.*, [arXiv:0901.0555](https://arxiv.org/abs/0901.0555).
9. S. Courteau *et al.*, *Astrophys. J.* **544**, 636 (2000).
10. D.J. Fixsen *et al.*, *Astrophys. J.* **420**, 445 (1994).
11. D.J. Fixsen *et al.*, *Astrophys. J.* **473**, 576 (1996); A. Kogut *et al.*, *Astrophys. J.* **419**, 1 (1993).
12. S. Seager, D.D. Sasselov, and D. Scott, *Astrophys. J. Supp.* **128**, 407 (2000).
13. N. Bartolo *et al.*, *Phys. Rep.* **402**, 103 (2004).
14. E. Komatsu *et al.*, *Astrophys. J. Supp.* **180**, 330 (2009).
15. A. de Oliveira-Costa *et al.*, *Phys. Rev.* **D69**, 063516 (2004); J.D. McEwen *et al.*, *Monthly Not. Royal Astron. Soc.* **388**, 659 (2008).
16. J. Hoftuft *et al.*, *Astrophys. J.* **699**, 985 (2009).
17. L. Knox, *Phys. Rev.* **D52**, 4307 (1995).
18. I. Sollom, A. Challinor, and M.P. Hobson, *Phys. Rev.* **D79**, 123521 (2009).
19. A.R. Liddle and D.H. Lyth, *Cosmological Inflation and Large-Scale Structure*, Cambridge University Press (2000).
20. U. Seljak and M. Zaldarriaga, *Astrophys. J.* **469**, 437 (1996).
21. A. Lewis, A. Challinor, and A. Lasenby, *Astrophys. J.* **538**, 473 (2000).

22. U. Seljak *et al.*, Phys. Rev. **D68**, 083507 (2003).
23. R.K. Sachs and A.M. Wolfe, Astrophys. J. **147**, 73 (1967).
24. R. Crittenden and N. Turok, Phys. Rev. Lett. **76**, 575 (1996); T. Giannantonio *et al.*, Phys. Rev. **D77**, 123520 (2008); S. Ho *et al.*, Phys. Rev. **D78**, 043519 (2008).
25. W. Hu and D.J. Eisenstein, Phys. Rev. **D59**, 083509 (1999); W. Hu *et al.*, Phys. Rev. **D59**, 023512 (1999).
26. P.J.E. Peebles and J.T. Yu, Astrophys. J. **162**, 815 (1970); R.A. Sunyaev and Ya.B. Zel'dovich, Astrophys. & Space Sci. **7**, 3 (1970).
27. D. Scott, J. Silk, and M. White, Science **268**, 829 (1995).
28. D.J. Eisenstein *et al.*, Astrophys. J. **633**, 560 (2005).
29. W.J. Percival *et al.*, Monthly Not. Royal Astron. Soc. **381**, 1053 (2007).
30. W.J. Percival *et al.*, arXiv:0907.1660.
31. J. Silk, Astrophys. J. **151**, 459 (1968).
32. M. Zaldarriaga and U. Seljak, Phys. Rev. **D58**, 023003 (1998); A. Lewis and A. Challinor, Phys. Rep. **429**, 1 (2006).
33. K.M. Smith, O. Zahn, and O. Doré, Phys. Rev. **D76**, 3510 (2007); C.M. Hirata *et al.*, Phys. Rev. **D78**, 043520 (2008).
34. M.R. Nolta *et al.*, Astrophys. J. Supp. **180**, 296 (2009).
35. M.C. Runyan *et al.*, Astrophys. J. Supp. **149**, 265 (2003); C.L. Reichardt *et al.*, Astrophys. J. **694**, 1200 (2009).
36. J.R. Hinderks *et al.*, Astrophys. J. **692**, 1221 (2009); R.B. Friedman *et al.*, Astrophys. J. **700**, L187 (2009).
37. M.L. Brown *et al.*, arXiv:0906.1003.
38. S. Masi *et al.*, Astron. & Astrophys. **458**, 687 (2006); W.C. Jones *et al.*, Astrophys. J. **647**, 823 (2006).
39. S. Padin *et al.*, Publ. Astron. Soc. Pacific **114**, 83 (2002); J.L. Sievers *et al.*, arXiv:0901.4540.
40. N.W. Halverson *et al.*, Astrophys. J. **568**, 38 (2002).
41. M.E. Abroe *et al.*, Astrophys. J. **605**, 607 (2004); N. Rajguru *et al.*, Monthly Not. Royal Astron. Soc. **363**, 1125 (2005).
42. W. Hu and M. White, New Astron. **2**, 323 (1997).
43. W. Hu and M. White, Phys. Rev. **D56**, 596 (1997).
44. M. Zaldarriaga and U. Seljak, Phys. Rev. **D55**, 1830 (1997); M. Kamionkowski, A. Kosowsky, and A. Stebbins, Phys. Rev. **D55**, 7368 (1997).
45. J. Kovac *et al.*, Nature, **420**, 772 (2002).
46. A. Kogut *et al.*, Astrophys. J. Supp. **148**, 161 (2003).
47. L. Page *et al.*, Astrophys. J. Supp. **170**, 335 (2007).
48. D. Barkats *et al.*, Astrophys. J. **619**, L127 (2005); C. Bischoff *et al.*, Astrophys. J. **684**, 771 (2008).
49. Y.D. Takahashi *et al.*, arXiv:0906.4069.
50. H.C. Chiang *et al.*, arXiv:0906.1181.
51. A.C.S. Readhead *et al.*, Science, **306**, 836 (2004); J.L. Sievers *et al.*, Astrophys. J. **660**, 976 (2007).
52. E.M. Leitch *et al.*, Astrophys. J. **624**, 10 (2005).
53. T.E. Montroy *et al.*, Astrophys. J. **647**, 813 (2006).
54. F. Piacentini *et al.*, Astrophys. J. **647**, 833 (2006).
55. A. de Oliveira-Costa, M. Tegmark (eds.), Microwave Foregrounds, Astron. Soc. of the Pacific, San Francisco (1999).
56. B. Gold *et al.*, Astrophys. J. Supp. **180**, 265 (2009).
57. N. Aghanim, S. Majumdar, and J. Silk, Rept. Prog. Phys., **71**, 066902 (2008).
58. R.A. Sunyaev and Ya.B. Zel'dovich, Ann. Rev. Astron. Astrophys. **18**, 537 (1980); M. Birkinshaw, Phys. Rep. **310**, 98 (1999).
59. J.E. Carlstrom, G.P. Holder, and E.D. Reese, Ann. Rev. Astron. & Astrophys. **40**, 643 (2002).
60. Z. Staniszewski *et al.*, Astrophys. J. **701**, 32 (2009).
61. A.D. Hincks *et al.*, arXiv:0907.0461.
62. A.P.S. Yadav and D. Wandelt, Phys. Rev. Lett. **100**, 1301 (2008); K.M. Smith, L. Senatore, and M. Zaldarriaga, arXiv:0901.2572.
63. W.L. Freedman *et al.*, Astrophys. J. **553**, 47 (2001).
64. M. Kowalski *et al.*, Astrophys. J. **686**, 749 (2008).
65. J. Dunkley *et al.*, Astrophys. J. Supp. **180**, 306 (2009).
66. X. Fan *et al.*, Astrophys. J. **123**, 1247 (2002).
67. U. Seljak, A. Slosar, and P. McDonald, JCAP, **10**, 014 (2006); A. Goobar *et al.*, J. Cosm. & Astropart. Phys. **6**, 019 (2006); G.L. Fogli *et al.*, Phys. Rev. **D75**, 053001 (2007).
68. M. Kamionkowski and A. Kosowsky, Ann. Rev. Nucl. Part. Sci. **49**, 77 (1999).
69. R. Maartens, Living Rev. Rel. **7**, 7 (2004).
70. R. Bousso and J. Polchinski, JHEP 0006, 006 (2000); L. Susskind, The Davis Meeting On Cosmic Inflation (2003), hep-th/0302219.

24. COSMIC RAYS

Revised August 2009 by T.K. Gaisser and T. Stanev (Bartol Research Inst., Univ. of Delaware)

24.1. Primary spectra

The cosmic radiation incident at the top of the terrestrial atmosphere includes all stable charged particles and nuclei with lifetimes of order 10^6 years or longer. Technically, “primary” cosmic rays are those particles accelerated at astrophysical sources and “secondaries” are those particles produced in interaction of the primaries with interstellar gas. Thus electrons, protons and helium, as well as carbon, oxygen, iron, and other nuclei synthesized in stars, are primaries. Nuclei such as lithium, beryllium, and boron (which are not abundant end-products of stellar nucleosynthesis) are secondaries. Antiprotons and positrons are also in large part secondary. Whether a small fraction of these particles may be primary is a question of current interest.

Apart from particles associated with solar flares, the cosmic radiation comes from outside the solar system. The incoming charged particles are “modulated” by the solar wind, the expanding magnetized plasma generated by the Sun, which decelerates and partially excludes the lower energy galactic cosmic rays from the inner solar system. There is a significant anticorrelation between solar activity (which has an alternating eleven-year cycle) and the intensity of the cosmic rays with energies below about 10 GeV. In addition, the lower-energy cosmic rays are affected by the geomagnetic field, which they must penetrate to reach the top of the atmosphere. Thus the intensity of any component of the cosmic radiation in the GeV range depends both on the location and time.

There are four different ways to describe the spectra of the components of the cosmic radiation: (1) By particles per unit rigidity. Propagation (and probably also acceleration) through cosmic magnetic fields depends on gyroradius or *magnetic rigidity*, R , which is gyroradius multiplied by the magnetic field strength:

$$R = \frac{pc}{Ze} = r_L B. \quad (24.1)$$

(2) By particles per energy-per-nucleon. Fragmentation of nuclei propagating through the interstellar gas depends on energy per nucleon, since that quantity is approximately conserved when a nucleus breaks up on interaction with the gas. (3) By nucleons per energy-per-nucleon. Production of secondary cosmic rays in the atmosphere depends on the intensity of nucleons per energy-per-nucleon, approximately independently of whether the incident nucleons are free protons or bound in nuclei. (4) By particles per energy-per-nucleus. Air shower experiments that use the atmosphere as a calorimeter generally measure a quantity that is related to total energy per particle.

The units of differential intensity I are $[\text{m}^{-2} \text{s}^{-1} \text{sr}^{-1} \mathcal{E}^{-1}]$, where \mathcal{E} represents the units of one of the four variables listed above.

The intensity of primary nucleons in the energy range from several GeV to somewhat beyond 100 TeV is given approximately by

$$I_N(E) \approx 1.8 \times 10^4 (E/1 \text{ GeV})^{-\alpha} \frac{\text{nucleons}}{\text{m}^2 \text{ s sr GeV}}, \quad (24.2)$$

where E is the energy-per-nucleon (including rest mass energy) and α ($\equiv \gamma + 1$) = 2.7 is the differential spectral index of the cosmic ray flux and γ is the integral spectral index. About 79% of the primary nucleons are free protons and about 70% of the rest are nucleons bound in helium nuclei. The fractions of the primary nuclei are nearly constant over this energy range (possibly with small but interesting variations). Fractions of both primary and secondary incident nuclei are listed in Table 24.1. Figure 24.1 shows the major components for energies greater than 2 GeV/nucleon.

The composition and energy spectra of nuclei are typically interpreted in the context of propagation models, in which the sources of the primary cosmic radiation are located within the galaxy [13]. The ratio of secondary to primary nuclei is observed to decrease with increasing energy, a fact interpreted to mean that the lifetime of cosmic rays in the galaxy decreases with energy. Measurements of radioactive “clock” isotopes in the low energy cosmic radiation are consistent with a lifetime in the galaxy of about 15 Myr.

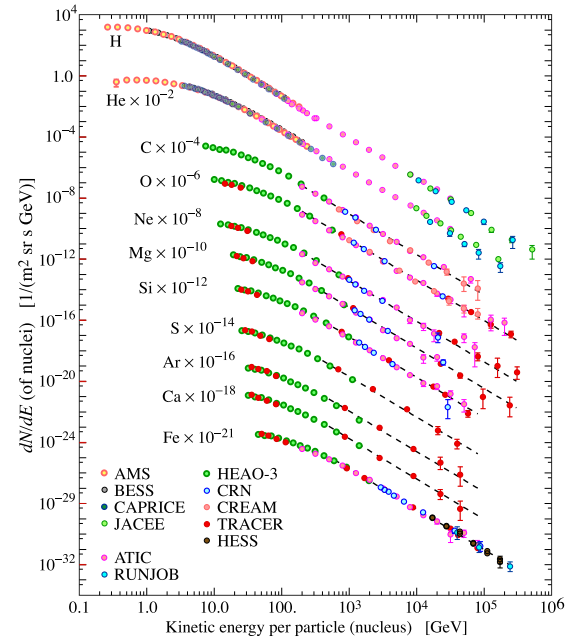


Figure 24.1: Major components of the primary cosmic radiation from Refs. [1–12]. The figure was created by P. Boyle and D. Muller. Color version at end of book.

Table 24.1: Relative abundances F of cosmic-ray nuclei at 10.6 GeV/nucleon normalized to oxygen ($\equiv 1$) [6]. The oxygen flux at kinetic energy of 10.6 GeV/nucleon is $3.26 \times 10^{-2} (\text{m}^2 \text{ s sr GeV/nucleon})^{-1}$. Abundances of hydrogen and helium are from Ref. [2,3]. Note that one can not use these values to extend the cosmic ray flux to high energy because the power law spectrum is not fully established yet.

Z	Element	F	Z	Element	F
1	H	540	13–14	Al-Si	0.19
2	He	26	15–16	P-S	0.03
3–5	Li-B	0.40	17–18	Cl-Ar	0.01
6–8	C-O	2.20	19–20	K-Ca	0.02
9–10	F-Ne	0.30	21–25	Sc-Mn	0.05
11–12	Na-Mg	0.22	26–28	Fe-Ni	0.12

The spectrum of electrons and positrons incident at the top of the is expected to steepen by one power of E at energy ~ 5 GeV because of the strong synchrotron energy loss in the galactic magnetic fields. The ATIC experiment [19] measured an excess of electrons above 100 GeV followed by a steepening above 1,000 GeV. The Fermi/LAT γ -ray observatory confirmed the relatively flat electron spectrum [21] without confirming the peak of the ATIC excess at ~ 800 GeV.

The PAMELA satellite experiment measured the positron to electron ratio to increase above 10 GeV instead of the expected decrease [23] at higher energy. The structure in the electron spectrum as well as the increase in the positron fraction could be related to contributions from individual nearby sources emerging above a background suppressed at high energy by synchrotron losses [24]. The low positron to electron ratio below 10 GeV is due to the new solar magnetic field polarity after the year 2001.

The ratio of antiprotons to protons is $\sim 2 \times 10^{-4}$ [25] at around 10–20 GeV, and there is clear evidence [26] for the kinematic suppression at lower energy that is the signature of secondary antiprotons. The \bar{p}/p ratio also shows a strong dependence on the phase and polarity of the solar cycle [27] in the opposite sense to that of the positron fraction. There is at this time no evidence for a significant primary

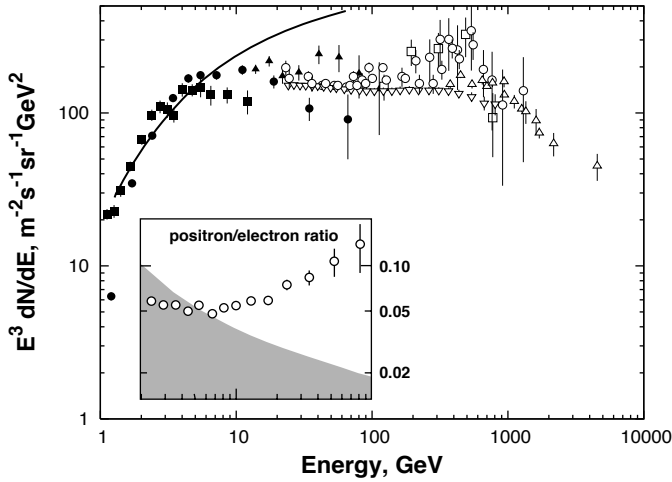


Figure 24.2: Differential spectrum of electrons plus positrons multiplied by E^3 (data from [15–21]). The line shows the proton spectrum multiplied by 0.01. The inset shows the positron to electron ratio measured by PAMELA compared to the expected [23] decrease.

component of antiprotons. No antihelium or antideuteron has been found in the cosmic radiation. The best measured upper limit on the ratio antihelium/helium is currently approximately 7×10^{-7} [28]. The upper limit on the flux of antideuterons around 1 GeV/nucleon is approximately $2 \times 10^{-4} (\text{m}^2 \text{ sr GeV/nucleon})^{-1}$ [29].

24.2. Cosmic rays in the atmosphere

Figure 24.3 shows the vertical fluxes of the major cosmic ray components in the atmosphere in the energy region where the particles are most numerous (except for electrons, which are most numerous near their critical energy, which is about 81 MeV in air). Except for protons and electrons near the top of the atmosphere, all particles are produced in interactions of the primary cosmic rays in the air. Muons and neutrinos are products of the decay of charged mesons, while electrons and photons originate in decays of neutral mesons.

Most measurements are made at ground level or near the top of the atmosphere, but there are also measurements of muons and electrons from airplanes and balloons. Fig. 24.3 includes recent measurements of negative muons [31,30–33]. Since $\mu^+(\mu^-)$ are produced in association with $\nu_\mu(\bar{\nu}_\mu)$, the measurement of muons near the maximum of the intensity curve for the parent pions serves to calibrate the atmospheric ν_μ beam [34]. Because muons typically lose almost two GeV in passing through the atmosphere, the comparison near the production altitude is important for the sub-GeV range of $\nu_\mu(\bar{\nu}_\mu)$ energies.

The flux of cosmic rays through the atmosphere is described by a set of coupled cascade equations with boundary conditions at the top of the atmosphere to match the primary spectrum. Numerical or Monte Carlo calculations are needed to account accurately for decay and energy-loss processes, and for the energy-dependences of the cross sections and of the primary spectral index γ . Approximate analytic solutions are, however, useful in limited regions of energy [35,36]. For example, the vertical intensity of charged pions with energy $E_\pi \ll \epsilon_\pi = 115$ GeV is

$$I_\pi(E_\pi, X) \approx \frac{Z_{N\pi}}{\lambda_N} I_N(E_\pi, 0) e^{-X/\Lambda} \frac{X E_\pi}{\epsilon_\pi}, \quad (24.3)$$

where Λ is the characteristic length for exponential attenuation of the parent nucleon flux in the atmosphere. This expression has a maximum at $X = \Lambda \approx 121 \pm 4 \text{ g cm}^{-2}$ [37], which corresponds to an altitude of 15 kilometers. The quantity $Z_{N\pi}$ is the spectrum-weighted moment of the inclusive distribution of charged pions in interactions of nucleons with nuclei of the atmosphere. The intensity of low-energy pions is much less than that of nucleons because $Z_{N\pi} \approx 0.079$ is small

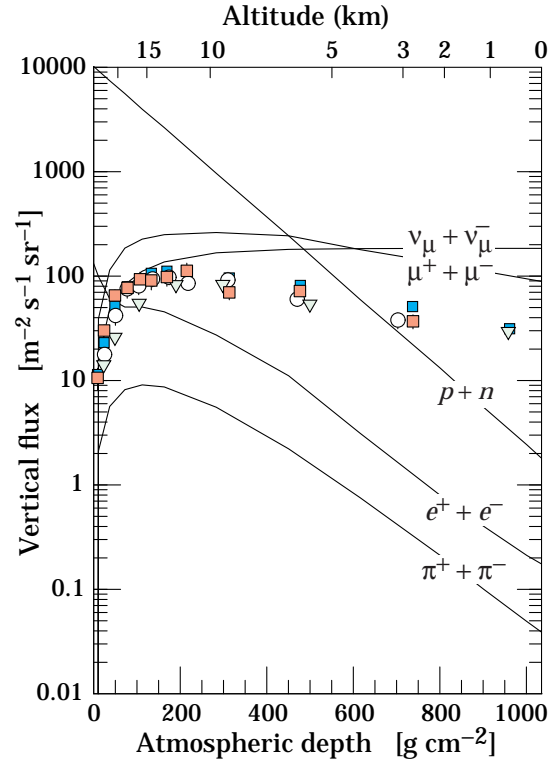


Figure 24.3: Vertical fluxes of cosmic rays in the atmosphere with $E > 1$ GeV estimated from the nucleon flux of Eq. (24.2). The points show measurements of negative muons with $E_\mu > 1$ GeV [31,30–33].

and because most pions with energy much less than the critical energy ϵ_π decay rather than interact.

24.3. Cosmic rays at the surface

24.3.1. Muons: Muons are the most numerous charged particles at sea level (see Fig. 24.3). Most muons are produced high in the atmosphere (typically 15 km) and lose about 2 GeV to ionization before reaching the ground. Their energy and angular distribution reflect a convolution of production spectrum, energy loss in the atmosphere, and decay. For example, 2.4 GeV muons have a decay length of 15 km, which is reduced to 8.7 km by energy loss. The mean energy of muons at the ground is ≈ 4 GeV. The energy spectrum is almost flat below 1 GeV, steepens gradually to reflect the primary spectrum in the 10–100 GeV range, and steepens further at higher energies because pions with $E_\pi > \epsilon_\pi$ tend to interact in the atmosphere before they decay. Asymptotically ($E_\mu \gg 1$ TeV), the energy spectrum of atmospheric muons is one power steeper than the primary spectrum. The integral intensity of vertical muons above 1 GeV/c at sea level is $\approx 70 \text{ m}^{-2} \text{ s}^{-1} \text{ sr}^{-1}$ [38,39], with recent measurements [40–42] tending to give lower normalization by 10–15%. Experimentalists are familiar with this number in the form $I \approx 1 \text{ cm}^{-2} \text{ min}^{-1}$ for horizontal detectors. The overall angular distribution of muons at the ground is $\propto \cos^2 \theta$, which is characteristic of muons with $E_\mu \sim 3$ GeV. At lower energy the angular distribution becomes increasingly steep, while at higher energy it flattens, approaching a $\sec \theta$ distribution for $E_\mu \gg \epsilon_\pi$ and $\theta < 70^\circ$.

Figure 24.4 shows the muon energy spectrum at sea level for two angles. At large angles low energy muons decay before reaching the surface and high energy pions decay before they interact, thus the average muon energy increases. An approximate extrapolation formula valid when muon decay is negligible ($E_\mu > 100/\cos \theta$ GeV) and the curvature of the Earth can be neglected ($\theta < 70^\circ$) is

$$\frac{dN_\mu}{dE_\mu d\Omega} \approx \frac{0.14 E_\mu^{-2.7}}{\text{cm}^2 \text{ s sr GeV}} \times \left\{ \frac{1}{1 + \frac{1.1 E_\mu \cos \theta}{115 \text{ GeV}}} + \frac{0.054}{1 + \frac{1.1 E_\mu \cos \theta}{850 \text{ GeV}}} \right\}, \quad (24.4)$$

where the two terms give the contribution of pions and charged kaons. Eq. (24.4) neglects a small contribution from charm and heavier flavors which is negligible except at very high energy [47].

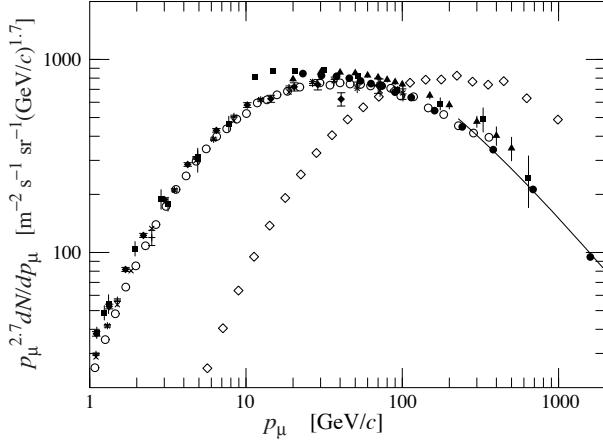


Figure 24.4: Spectrum of muons at $\theta = 0^\circ$ (\blacklozenge [38], \blacksquare [43], \blacktriangledown [44], \blacktriangle [45], \times , $+$ [40], \circ [41], and \bullet [42] and $\theta = 75^\circ$ \diamond [46]). The line plots the result from Eq. (24.4) for vertical showers.

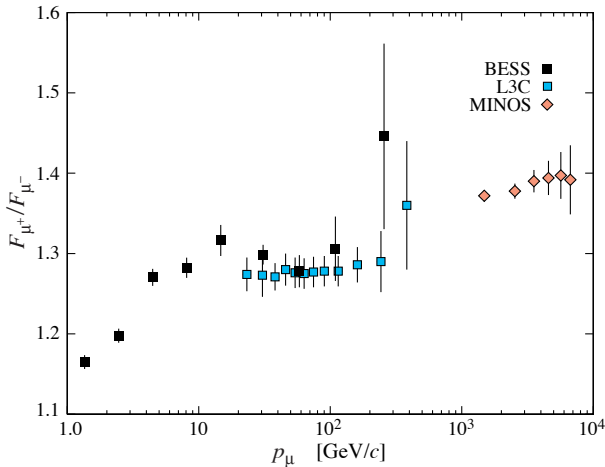


Figure 24.5: Muon charge ratio as a function of the muon momentum from Refs. [41,42,48].

The muon charge ratio reflects the excess of π^+ over π^- and K^+ over K^- in the forward fragmentation region of proton initiated interactions together with the fact that there are more protons than neutrons in the primary spectrum. The increase with energy of μ^+/μ^- shown in Fig. 24.5 reflects the increasing importance of kaons in the TeV range [48] and indicates a significant contribution of associated production by cosmic-ray protons ($p \rightarrow \Lambda + K^+$). The same process is even more important for atmospheric neutrinos at high energy.

24.3.2. Electromagnetic component: At the ground, this component consists of electrons, positrons, and photons primarily from electromagnetic cascades initiated by decay of neutral and charged mesons. Muon decay is the dominant source of low-energy electrons at sea level. Decay of neutral pions is more important at high altitude or when the energy threshold is high. Knock-on electrons also make a small contribution at low energy [49]. The integral vertical intensity of electrons plus positrons is very approximately 30, 6, and

0.2 $\text{m}^{-2}\text{s}^{-1}\text{sr}^{-1}$ above 10, 100, and 1000 MeV respectively [39,50], but the exact numbers depend sensitively on altitude, and the angular dependence is complex because of the different altitude dependence of the different sources of electrons [49–51]. The ratio of photons to electrons plus positrons is approximately 1.3 above a GeV and 1.7 below the critical energy [51].

24.3.3. Protons: Nucleons above 1 GeV/c at ground level are degraded remnants of the primary cosmic radiation. The intensity is approximately $I_N(E,0) \times \exp(-X/\cos\theta\Lambda)$ for $\theta < 70^\circ$. At sea level, about 1/3 of the nucleons in the vertical direction are neutrons (up from $\approx 10\%$ at the top of the atmosphere as the n/p ratio approaches equilibrium). The integral intensity of vertical protons above 1 GeV/c at sea level is $\approx 0.9 \text{ m}^{-2}\text{s}^{-1}\text{sr}^{-1}$ [39,52].

24.4. Cosmic rays underground

Only muons and neutrinos penetrate to significant depths underground. The muons produce tertiary fluxes of photons, electrons, and hadrons.

24.4.1. Muons: As discussed in Section 27.6 of this *Review*, muons lose energy by ionization and by radiative processes: bremsstrahlung, direct production of e^+e^- pairs, and photonuclear interactions. The total muon energy loss may be expressed as a function of the amount of matter traversed as

$$-\frac{dE_\mu}{dX} = a + b E_\mu, \quad (24.5)$$

where a is the ionization loss and b is the fractional energy loss by the three radiation processes. Both are slowly varying functions of energy. The quantity $\epsilon \equiv a/b$ (≈ 500 GeV in standard rock) defines a critical energy below which continuous ionization loss is more important than radiative losses. Table 24.2 shows a and b values for standard rock as a function of muon energy. The second column of Table 24.2 shows the muon range in standard rock ($A = 22$, $Z = 11$, $\rho = 2.65 \text{ g cm}^{-3}$). These parameters are quite sensitive to the chemical composition of the rock, which must be evaluated for each location.

Table 24.2: Average muon range R and energy loss parameters calculated for standard rock [53]. Range is given in km-water-equivalent, or 10^5 g cm^{-2} .

E_μ GeV	R km.w.e.	a MeV $\text{g}^{-1} \text{cm}^2$	b_{brems}	b_{pair} $10^{-6} \text{ g}^{-1} \text{cm}^2$	b_{nucl}	$\sum b_i$	$\sum b(\text{ice})$
10	0.05	2.17	0.70	0.70	0.50	1.90	1.66
100	0.41	2.44	1.10	1.53	0.41	3.04	2.51
1000	2.45	2.68	1.44	2.07	0.41	3.92	3.17
10000	6.09	2.93	1.62	2.27	0.46	4.35	3.78

The intensity of muons underground can be estimated from the muon intensity in the atmosphere and their rate of energy loss. To the extent that the mild energy dependence of a and b can be neglected, Eq. (24.5) can be integrated to provide the following relation between the energy $E_{\mu,0}$ of a muon at production in the atmosphere and its average energy E_μ after traversing a thickness X of rock (or ice or water):

$$E_\mu = (E_{\mu,0} + \epsilon) e^{-bX} - \epsilon. \quad (24.6)$$

Especially at high energy, however, fluctuations are important and an accurate calculation requires a simulation that accounts for stochastic energy-loss processes [54].

There are two depth regimes for Eq. (24.6). For $X \ll b^{-1} \approx 2.5$ km water equivalent, $E_{\mu,0} \approx E_\mu(X) + aX$, while for $X \gg b^{-1}$ $E_{\mu,0} \approx (\epsilon + E_\mu(X)) \exp(bX)$. Thus at shallow depths the differential muon energy spectrum is approximately constant for $E_\mu < aX$ and steepens to reflect the surface muon spectrum for $E_\mu > aX$, whereas for $X > 2.5$ km.w.e. the differential spectrum underground is again

constant for small muon energies but steepens to reflect the surface muon spectrum for $E_\mu > \epsilon \approx 0.5$ TeV. In the deep regime the shape is independent of depth although the intensity decreases exponentially with depth. In general the muon spectrum at slant depth X is

$$\frac{dN_\mu(X)}{dE_\mu} = \frac{dN_\mu}{dE_{\mu,0}} \frac{dE_{\mu,0}}{dE_\mu} = \frac{dN_\mu}{dE_{\mu,0}} e^{bX}, \quad (24.7)$$

where $E_{\mu,0}$ is the solution of Eq. (24.6) in the approximation neglecting fluctuations.

Fig. 24.6 shows the vertical muon intensity versus depth. In constructing this “depth-intensity curve,” each group has taken account of the angular distribution of the muons in the atmosphere, the map of the overburden at each detector, and the properties of the local medium in connecting measurements at various slant depths and zenith angles to the vertical intensity. Use of data from a range of angles allows a fixed detector to cover a wide range of depths. The flat portion of the curve is due to muons produced locally by charged-current interactions of ν_μ . The inset shows the vertical intensity curve for water and ice published in Refs. [56–59]. It is not as steep as the one for rock because of the lower muon energy loss in water.

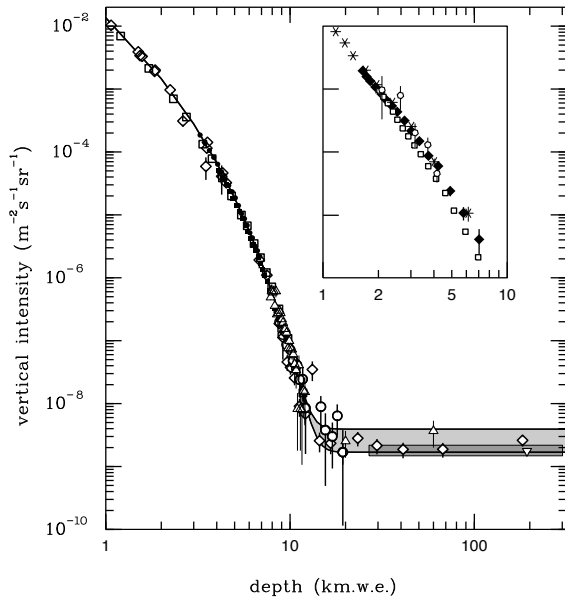


Figure 24.6: Vertical muon intensity vs depth (1 km.w.e. = 10^5 g cm^{-2} of standard rock). The experimental data are from: \diamond : the compilations of Crouch [55], \square : Baksan [60], \circ : LVD [61], \bullet : MACRO [62], \blacksquare : Frejus [63], and \triangle : SNO [64]. The shaded area at large depths represents neutrino-induced muons of energy above 2 GeV. The upper line is for horizontal neutrino-induced muons, the lower one for vertically upward muons. Darker shading shows the muon flux measured by the SuperKamiokande experiment.

24.4.2. Neutrinos :

Because neutrinos have small interaction cross sections, measurements of atmospheric neutrinos require a deep detector to avoid backgrounds. There are two types of measurements: contained (or semi-contained) events, in which the vertex is determined to originate inside the detector, and neutrino-induced muons. The latter are muons that enter the detector from zenith angles so large (*e.g.*, nearly horizontal or upward) that they cannot be muons produced in the atmosphere. In neither case is the neutrino flux measured directly. What is measured is a convolution of the neutrino flux and cross section with the properties of the detector (which includes the surrounding medium in the case of entering muons).

Contained and semi-contained events reflect neutrinos in the sub-GeV to multi-GeV region where the product of increasing cross

section and decreasing flux is maximum. In the GeV region the neutrino flux and its angular distribution depend on the geomagnetic location of the detector and, to a lesser extent, on the phase of the solar cycle. Naively, we expect $\nu_\mu/\nu_e = 2$ from counting neutrinos of the two flavors coming from the chain of pion and muon decay. Contrary to expectation, however, the numbers of the two classes of events are similar rather than different by a factor of two. This is now understood to be a consequence of neutrino flavor oscillations [69]. (See the article on neutrino properties in this *Review*.)

Various details need to be understood to reach this conclusion. For example, the fraction of electron neutrinos gradually decreases above a GeV as parent muons begin to reach the ground before decaying. At low energy, three-dimensional effects of cascade development and muon bending in the atmosphere need to be accounted for [70] in the calculations used for interpreting the data [66,67]. Experimental measurements have to account for the ratio of $\bar{\nu}/\nu$, which have cross sections different by a factor of 3 in this energy range. In addition, detectors generally have different efficiencies for detecting muon neutrinos and electron neutrinos which need to be accounted for in comparing measurements with expectation.

Two well-understood properties of atmospheric cosmic rays provide a standard for comparison of the measurements of atmospheric neutrinos to expectation. These are the “sec θ effect” and the “east-west effect” [68]. The former refers originally to the enhancement of the flux of > 10 GeV muons (and neutrinos) at large zenith angles because the parent pions propagate more in the low density upper atmosphere where decay is enhanced relative to interaction. For neutrinos from muon decay, the enhancement near the horizontal becomes important for $E_\nu > 1$ GeV and arises mainly from the increased pathlength through the atmosphere for muon decay in flight. Fig. 24.7 from Ref. 65 shows a comparison between measurement and expectation for the zenith angle dependence of multi-GeV electron-like (mostly ν_e) and muon-like (mostly ν_μ) events separately. The ν_e show an enhancement near the horizontal and approximate equality for nearly upward ($\cos\theta \approx -1$) and nearly downward ($\cos\theta \approx 1$) events. There is, however, a very significant deficit of upward ($\cos\theta < 0$) ν_μ events, which have long pathlengths comparable to the radius of the Earth. This feature is the principal signature for oscillations [69].

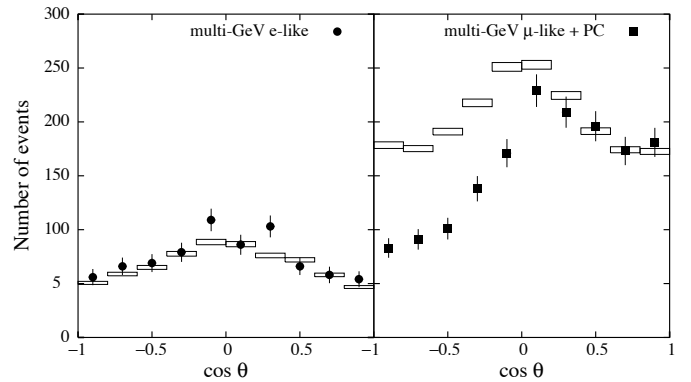


Figure 24.7: Zenith-angle dependence of multi-GeV neutrino interactions from SuperKamiokande [65]. The shaded boxes show the expectation in the absence of any oscillations.

Muons that enter the detector from outside after production in charged-current interactions of neutrinos naturally reflect a higher energy portion of the neutrino spectrum than contained events because the muon range increases with energy as well as the cross section. The relevant energy range is $\sim 10 < E_\nu < 1000$ GeV, depending somewhat on angle. Neutrinos in this energy range show a sec θ effect similar to muons (see Eq. (24.4)). This causes the flux of horizontal neutrino-induced muons to be approximately a factor two higher than the vertically upward flux. The upper and lower edges of the horizontal shaded region in Fig. 24.6 correspond to horizontal and vertical intensities of neutrino-induced muons. Table 24.3 gives the measured fluxes of upward-moving neutrino-induced muons averaged

Table 24.3: Measured fluxes ($10^{-9} \text{ m}^{-2} \text{ s}^{-1} \text{ sr}^{-1}$) of neutrino-induced muons as a function of the effective minimum muon energy E_μ .

$E_\mu >$	1 GeV	1 GeV	1 GeV	2 GeV	3 GeV	3 GeV
Ref.	CWI [71]	Baksan [72]	MACRO [73]	IMB [74]	Kam [75]	SuperK [76]
F_μ	2.17 ± 0.21	2.77 ± 0.17	2.29 ± 0.15	2.26 ± 0.11	1.94 ± 0.12	1.74 ± 0.07

over the lower hemisphere. Generally the definition of minimum muon energy depends on where it passes through the detector. The tabulated effective minimum energy estimates the average over various accepted trajectories.

24.5. Air showers

So far we have discussed inclusive or uncorrelated fluxes of various components of the cosmic radiation. An air shower is caused by a single cosmic ray with energy high enough for its cascade to be detectable at the ground. The shower has a hadronic core, which acts as a collimated source of electromagnetic subshowers, generated mostly from $\pi^0 \rightarrow \gamma\gamma$ decays. The resulting electrons and positrons are the most numerous particles in the shower. The number of muons, produced by decays of charged mesons, is an order of magnitude lower. Air showers spread over a large area on the ground, and arrays of detectors operated for long times are useful for studying cosmic rays with primary energy $E_0 > 100$ TeV, where the low flux makes measurements with small detectors in balloons and satellites difficult.

Greisen [77] gives the following approximate expressions for the numbers and lateral distributions of particles in showers at ground level. The total number of muons N_μ with energies above 1 GeV is

$$N_{\mu}(> 1 \text{ GeV}) \approx 0.95 \times 10^5 \left(N_e / 10^6 \right)^{3/4}, \quad (24.8)$$

where N_e is the total number of charged particles in the shower (not just e^\pm). The number of muons per square meter, ρ_μ , as a function of the lateral distance r (in meters) from the center of the shower is

$$\rho_\mu = \frac{1.25 N_\mu}{2\pi \Gamma(1.25)} \left(\frac{1}{320} \right)^{1.25} r^{-0.75} \left(1 + \frac{r}{320} \right)^{-2.5}, \quad (24.9)$$

where Γ is the gamma function. The number density of charged particles is

$$\rho_e = C_1(s, d, C_2) x^{(s-2)} (1+x)^{(s-4.5)} (1+C_2 x^d). \quad (24.10)$$

Here s , d , and C_2 are parameters in terms of which the overall normalization constant $C_1(s, d, C_2)$ is given by

$$C_1(s, d, C_2) = \frac{N_e}{2\pi r_1^2} [B(s, 4.5 - 2s) + C_2 B(s + d, 4.5 - d - 2s)]^{-1}, \quad (24.11)$$

where $B(m, n)$ is the beta function. The values of the parameters depend on shower size (N_e), depth in the atmosphere, identity of the primary nucleus, etc. For showers with $N_e \approx 10^6$ at sea level, Greisen uses $s = 1.25$, $d = 1$, and $C_2 = 0.088$. Finally, x is r/r_1 , where r_1 is the Molière radius, which depends on the density of the atmosphere and hence on the altitude at which showers are detected. At sea level $r_1 \approx 78$ m. It increases with altitude as the air density decreases.

The lateral spread of a shower is determined largely by Coulomb scattering of the many low-energy electrons and is characterized by the Molière radius. The lateral spread of the muons (ρ_μ) is larger and depends on the transverse momenta of the muons at production as well as multiple scattering.

There are large fluctuations in development from shower to shower, even for showers of the same energy and primary mass—especially for small showers, which are usually well past maximum development when observed at the ground. Thus the shower size N_e and primary

energy E_0 are only related in an average sense, and even this relation depends on depth in the atmosphere. One estimate of the relation is [78]

$$E_0 \sim 3.9 \times 10^6 \text{ GeV} (N_e / 10^6)^{0.9} \quad (24.12)$$

for vertical showers with $10^{14} < E < 10^{17}$ eV at 920 g cm^{-2} (965 m above sea level). As E_0 increases the shower maximum (on average) moves down into the atmosphere and the relation between N_e and E_0 changes. Moreover, because of fluctuations, N_e as a function of E_0 is not correctly obtained by inverting Eq. (24.12). At the maximum of shower development, there are approximately 2/3 particles per GeV of primary energy.

There are three types of air shower detectors: shower arrays that study the shower size N_e and the lateral distribution on the ground, Cherenkov detectors that detect the Cherenkov radiation emitted by the charged particles of the shower, and fluorescence detectors that study the nitrogen fluorescence excited by the charged particles in the shower. The fluorescence light is emitted isotropically so the showers can be observed from the side. Detailed simulations and cross-calibrations between different types of detectors are necessary to establish the primary energy spectrum from air-shower experiments.

Figure 24.8 shows the “all-particle” spectrum. The differential energy spectrum has been multiplied by $E^{2.7}$ in order to display the features of the steep spectrum that are otherwise difficult to discern. The steepening that occurs between 10^{15} and 10^{16} eV is known as the *knee* of the spectrum. The feature around 10^{19} eV is called the *ankle* of the spectrum.

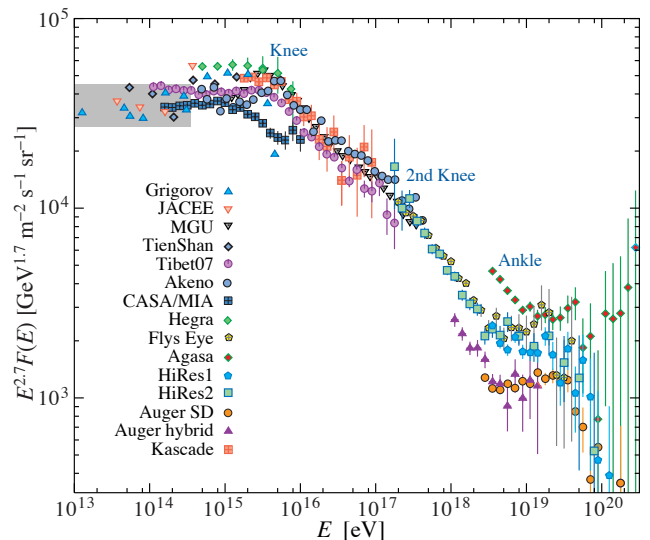


Figure 24.8: The all-particle spectrum from air shower measurements. The shaded area shows the range of the direct cosmic ray spectrum measurements. See full-color version on color pages at end of book.

Measurements with small air shower experiments in the knee region differ by as much as a factor of two, indicative of systematic uncertainties in interpretation of the data. (For a review see Ref. 79.) In establishing the spectrum shown in Fig. 24.8, efforts have been made to minimize the dependence of the spectrum on the primary composition. Ref. 80 uses an unfolding procedure to obtain the

spectra of the individual components, giving a result for the all-particle spectrum between 10^{15} and 10^{17} eV that lies toward the upper range of the data shown in Fig. 24.8. In the energy range above 10^{17} eV, the fluorescence technique [82] is particularly useful because it can establish the primary energy in a model-independent way by observing most of the longitudinal development of each shower, from which E_0 is obtained by integrating the energy deposition in the atmosphere. The result, however, depends strongly on the light absorption in the atmosphere and the calculation of the detector's aperture.

Assuming the cosmic ray spectrum below 10^{18} eV is of galactic origin, the *knee* could reflect the fact that most cosmic accelerators in the galaxy have reached their maximum energy. Some types of expanding supernova remnants, for example, are estimated not to be able to accelerate protons above energies in the range of 10^{15} eV. Effects of propagation and confinement in the galaxy [83] also need to be considered.

Concerning the ankle, one possibility is that it is the result of a higher energy population of particles overtaking a lower energy population, for example an extragalactic flux beginning to dominate over the galactic flux (e.g. Ref. [82]). Another possibility is that the dip structure in the region of the ankle is due to $\gamma p \rightarrow e^+ + e^-$ energy losses of extragalactic protons on the 2.7 K cosmic microwave radiation (CMB) [85]. This dip structure has been cited as a robust signature of both the protonic and extragalactic nature of the highest energy cosmic rays [84]. If this interpretation is correct, then the end of the galactic cosmic ray spectrum would be at an energy lower than 10^{18} eV, consistent with the maximum expected range of acceleration by supernova remnants.

Energy-dependence of the composition from the knee through the ankle holds the key to discriminating between these two viewpoints. The HiRes and Auger experiments, however, present very different data on the UHECR composition from the observation of the depth of shower maximum X_{max} . The HiRes data [86] is fully consistent with a cosmic ray composition getting lighter and containing only protons and helium above 10^{19} eV. Auger [87–88] sees a composition getting lighter up to 2×10^{18} eV and becoming heavier after that to become intermediate between protons and iron at 3×10^{19} eV. This may mean that the extragalactic cosmic rays have a mixed composition at acceleration similar to the GeV galactic cosmic rays.

If the cosmic ray flux at the highest energies is cosmological in origin, there should be a rapid steepening of the spectrum (called the GZK feature) around 5×10^{19} eV, resulting from the onset of inelastic interactions of UHE cosmic rays with the cosmic microwave background [89,90]. Photo-dissociation of heavy nuclei in the mixed composition model [91] would have a similar effect. Although all UHECR experiments have detected events of energy above 10^{20} eV [82], [92–94], the spectral shape above the ankle is still not well determined. The AGASA experiment [92] claimed 11 events above 10^{20} eV (although a recent re-analysis has decreased that number) while HiRes [93] detected only two. The Auger observatory [94–95] presented spectra based on its surface detector (with an exposure of $12,790 \text{ km}^2 \text{ sr yr}$) and on events detected in hybrid mode, i.e. with both the surface and the fluorescence detectors. The energy scale of the surface detector is calibrated by the longitudinal shower profile in hybrid events of high quality. Both the HiRes and Auger spectra show a significant steepening of the cosmic ray spectrum above $3\text{--}5 \times 10^{19}$ eV which is consistent with the onset of inelastic interactions with astrophysical photon fields, mostly the CMB [89–90].

Figure 24.9 gives an expanded view of the high energy end of the spectrum, showing only the more recent data, including the spectrum derived by HiRes in stereo mode [102]. This figure shows the differential flux multiplied by $E^{2.6}$ which the Auger observatory finds around 10^{19} eV. The two experiments are actually consistent in normalization if one takes quoted systematic errors in the energy scales into account. The continued power law type of flux beyond the GZK cutoff claimed by the AGASA experiment is not supported by the HiRes and Auger data.

One half of the energy that UHECR protons lose in photoproduction interactions that cause the GZK effects ends up in neutrinos [96].

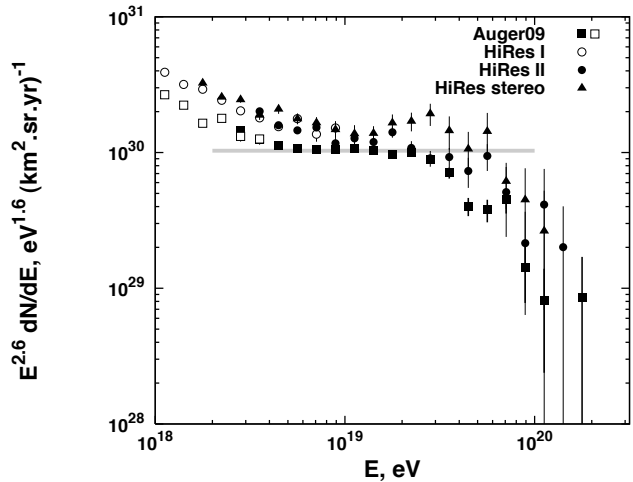


Figure 24.9: Expanded view of the highest energy portion of the cosmic-ray spectrum from data of the Auger Observatory (hybrid events shown with empty squares and HiRes in monocular and stereo modes). The differential cosmic ray flux is multiplied by $E^{2.6}$.

Measuring this *cosmogenic* neutrino flux above 10^{18} eV would help resolve the UHECR uncertainties mentioned above. The magnitude of this flux depends strongly on the cosmic ray spectrum at acceleration, the cosmic ray composition, and the cosmological evolution of the cosmic ray sources. In the case that UHECR have mixed composition only the proton fraction would produce cosmogenic neutrinos. Heavy nuclei propagation produces mostly $\bar{\nu}_e$ at lower energy from neutron decay.

The expected rate of cosmogenic neutrinos is lower than current limits obtained by RICE [97], the Auger observatory [98] and ANITA [99], which are shown in Figure 24.10 together with a model for cosmogenic neutrino production [100] and an upper limit of the neutrinos that can be accelerated at the cosmic ray sources [101]. One has to note that the limits are calculated in different ways. Those of ANITA and RICE are for all neutrino flavors, where the contribution of different flavors is energy dependent. The limit of Auger is only for ν_τ and $\bar{\nu}_\tau$ which should be about 1/3 of the total neutrino flux after oscillations on propagation.

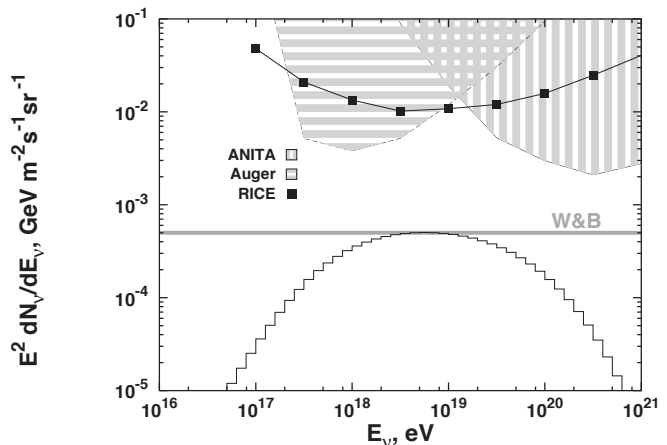


Figure 24.10: Limits on the flux of cosmogenic neutrinos set by three neutrino experiments. The histogram shows the sum of all neutrino flavors.

References:

1. M. Boezio *et al.*, *Astropart. Phys.* **19**, 583 (2003).
2. AMS Collaboration, *Phys. Lett.* **B490**, 27 (2000); *Phys. Lett.* **B494**, 193 (2000).
3. T. Sanuki *et al.*, *Astrophys. J.* **545**, 1135 (2000).
4. S. Haino *et al.*, *Phys. Lett.* **B594**, 35 (2004).
5. CREAM Collaboration, *Proc. 30th Int. Cosmic Ray Conf.*, (Merida, Yucatan, 2007), paper 0301.
6. J.J. Engelmann *et al.*, *Astron. & Astrophys.* **233**, 96 (1990).
7. D. Müller *et al.*, *Ap J*, **374**, 356 (1991).
8. P.J. Boyle *et al.*, *Ap J* submitted. See also P.J. Boyle *et al.*, *Proc. 30th Int. Cosmic Ray Conf.*, (Merida, Yucatan, 2007), paper 1192.
9. A.D. Panov *et al.*, *Bull Russian Acad of Science, Physics*, **71**, 494 (2007).
10. V.A. Derbina *et al.*, *Astrophys. J.* **628**, L41 (2005).
11. K. Asakimori *et al.* (JACEE Collaboration), *Astrophys. J.* **502**, 278 (1998).
12. F. Aharonian *et al.* (HESS Collaboration), *Phys. Rev.* **D75**, 042004 (2007).
13. A.W. Strong *et al.*, *Ann. Rev. Nucl. and Part. Sci.* **57**, 285 (2007).
14. N.E. Yanasak *et al.*, *Astrophys. J.* **563**, 768 (2001).
15. M.A. DuVernois *et al.*, *Astrophys. J.* **559**, 296 (2000).
16. S. Torii *et al.*, *Astrophys. J.* **559**, 973 (2001).
17. M. Boezio *et al.*, *Astrophys. J.* **532**, 635 (2000).
18. K. Yoshida *et al.*, *Adv. Spa. Research*, **42**, 1670 (2008).
19. J. Chang *et al.* (ATIC Collaboration), *Nature* **456**, 362 (2008).
20. F. Aharonian *et al.* (HESS Collaboration), *Phys. Rev. Lett.* **101**, 261104 (2008) and [arXiv:0905.0105](https://arxiv.org/abs/0905.0105).
21. A.A. Abdo *et al.* (Fermi/LAT Collaboration), *Phys. Rev. Lett.* **102**, 181101 (2009).
22. O. Adriani *et al.* (Pamela Collaboration), *Nature* **458**, 607 (2009), *Phys. Rev. Lett.* **102**, 051101 (2009).
23. I.V. Moskalenko and A.W. Strong, *Astrophys. J.* **493**, 694 (1998).
24. J. Nishimura *et al.*, *Adv. Space Research* **19**, 767 (1997).
25. A.S. Beach *et al.*, *Phys. Rev. Lett.* **87**, 271101 (2001).
26. A. Yamamoto *et al.*, *Adv. Space Research* (2007) in press.
27. Y. Asaoka *et al.*, *Phys. Rev. Lett.* **88**, 51101 (2002).
28. M. Sasaki *et al.*, *Nucl. Phys.* **B113**, (Proc. Suppl.) 202(2002).
29. H. Fuke *et al.*, *Phys. Rev. Lett.* **95**, 081101 (2005).
30. R. Bellotti *et al.*, *Phys. Rev.* **D53**, 35 (1996).
31. R. Bellotti *et al.*, *Phys. Rev.* **D60**, 052002 (1999).
32. M. Boezio *et al.*, *Phys. Rev.* **D62**, 032007 (2000).
33. S. Coutu *et al.*, *Phys. Rev.* **D62**, 032001 (2000).
34. T. Sanuki *et al.*, *Phys. Rev.* **D75**, 043005 (2007).
35. T.K. Gaisser, *Cosmic Rays and Particle Physics*, Cambridge University Press (1990).
36. P. Lipari, *Astropart. Phys.* **1**, 195 (1993).
37. E. Mocchiutto *et al.*, in *Proc. 28th Int. Cosmic Ray Conf.*, Tsukuba, 1627 (2003).
38. M.P. De Pascale *et al.*, *J. Geophys. Res.* **98**, 3501 (1993).
39. P.K.F. Grieder, *Cosmic Rays at Earth*, Elsevier Science (2001).
40. J. Kremer *et al.*, *Phys. Rev. Lett.* **83**, 4241 (1999).
41. S. Haino *et al.* (BESS Collaboration), *Phys. Lett.* **B594**, 35 (2004).
42. P. Archard *et al.* (L3+C Collaboration), *Phys. Lett.* **B598**, 15 (2004).
43. O.C. Allkofer, K. Carstensen, and W.D. Dau, *Phys. Lett.* **B36**, 425 (1971).
44. B.C. Rastin, *J. Phys.* **G10**, 1609 (1984).
45. C.A. Ayre *et al.*, *J. Phys.* **G1**, 584 (1975).
46. H. Jokisch *et al.*, *Phys. Rev.* **D19**, 1368 (1979).
47. C.G.S. Costa, *Astropart. Phys.* **16**, 193 (2001).
48. P. Adamson *et al.* (MINOS Collaboration), *Phys. Rev.* **D76**, 052003 (2007).
49. S. Hayakawa, *Cosmic Ray Physics*, Wiley, Interscience, New York (1969).
50. R.R. Daniel and S.A. Stephens, *Revs. Geophysics & Space Sci.* **12**, 233 (1974).
51. K.P. Beuermann and G. Wibberenz, *Can. J. Phys.* **46**, S1034 (1968).
52. I.S. Diggory *et al.*, *J. Phys.* **A7**, 741 (1974).
53. D.E. Groom, N.V. Mokhov, and S.I. Striganov, "Muon stopping-power and range tables," *Atomic Data and Nuclear Data Tables*, **78**, 183 (2001).
54. P. Lipari and T. Stanev, *Phys. Rev.* **D44**, 3543 (1991).
55. M. Crouch, in *Proc. 20th Int. Cosmic Ray Conf.*, Moscow, **6**, 165 (1987).
56. I.A. Belolaptikov *et al.*, *Astropart. Phys.* **7**, 263 (1997).
57. J. Babson *et al.*, *Phys. Rev.* **D42**, 3613 (1990).
58. P. Desiati *et al.*, in *Proc. 28th Int. Cosmic Ray Conf.*, Tsukuba, 1373 (2003).
59. T. Pradier *et al.* (ANTARES Collaboration), [arXiv:0805.2545](https://arxiv.org/abs/0805.2545) and 31st ICRC, 7-15 July 2009, Łódź, Poland (paper #0340).
60. Yu.M. Andreev, V.I. Gurentzov, and I.M. Kogai, in *Proc. 20th Int. Cosmic Ray Conf.*, Moscow, **6**, 200 (1987).
61. M. Aglietta *et al.* (LVD Collaboration), *Astropart. Phys.* **3**, 311 (1995).
62. M. Ambrosio *et al.* (MACRO Collaboration), *Phys. Rev.* **D52**, 3793 (1995).
63. Ch. Berger *et al.* (Frejus Collaboration), *Phys. Rev.* **D40**, 2163 (1989).
64. C. Waltham *et al.*, in *Proc. 27th Int. Cosmic Ray Conf.*, Hamburg, 991 (2001).
65. Y. Ashie *et al.* (SuperKamiokande Collaboration), *Phys. Rev.* **D71**, 112005 (2005).
66. G. Barr *et al.*, *Phys. Rev.* **D70**, 023006 (2004).
67. M. Honda *et al.*, *Phys. Rev.* **D75**, 096005 (2007).
68. T. Futagami *et al.*, *Phys. Rev. Lett.* **82**, 5194 (1999).
69. Y. Fukuda *et al.*, *Phys. Rev. Lett.* **81**, 1562 (1998).
70. G. Battistoni *et al.*, *Astropart. Phys.* **12**, 315 (2000).
71. F. Reines *et al.*, *Phys. Rev. Lett.* **15**, 429 (1965).
72. M.M. Boliev *et al.*, in *Proc. 3rd Int. Workshop on Neutrino Telescopes* (ed. Milla Baldo Ceolin), 235 (1991).
73. M. Ambrosio *et al.*, (MACRO) *Phys. Lett.* **B434**, 451 (1998). The number quoted for MACRO is the average over 90% of the lower hemisphere, $\cos\theta < -0.1$; see F. Ronga *et al.*, [hep-ex/9905025](https://arxiv.org/abs/hep-ex/9905025).
74. R. Becker-Szendy *et al.*, *Phys. Rev. Lett.* **69**, 1010 (1992); *Proc. 25th Int. Conf. High-Energy Physics*, Singapore (eds. K.K. Phua and Y. Yamaguchi, World Scientific), 662 (1991).
75. S. Hatakeyama *et al.*, *Phys. Rev. Lett.* **81**, 2016 (1998).
76. Y. Fukuda *et al.*, *Phys. Rev. Lett.* **82**, 2644 (1999).
77. K. Greisen, *Ann. Rev. Nucl. Sci.* **10**, 63 (1960).
78. M. Nagano *et al.*, *J. Phys.* **G10**, 1295 (1984).
79. S.P. Swordy *et al.*, *Astropart. Phys.* **18**, 129 (2002).
80. T. Antoni *et al.* (Kascade Collaboration), *Astropart. Phys.* **24**, 1 (2005).
81. M. Amenomori *et al.*, *Proc. 30th Int. Cosmic Ray Conf.*, (Merida, Yucatan, 2007), paper 0277.
82. D.J. Bird *et al.*, *Astrophys. J.* **424**, 491 (1994).
83. V.S. Ptuskin *et al.*, *Astron. & Astrophys.* **268**, 726 (1993).
84. V.S. Berezinsky and S.I. Grigor'eva, *Astron. & Astrophys.* **199**, 1 (1988).
85. V. Berezinsky, A. Gazizov, and S. Grigor'eva, *Phys. Rev.* **D74**, 043005 (2006).
86. R.U. Abbasi *et al.* (The HiRes Collaboration), *Astrophys. J.* **622**, 910 (2005).
87. M. Unger *et al.* (Auger Collaboration), *Proc. 30th Int. Cosmic Ray Conf.*, Merida, Mexico, 2007 ([arXiv:0706.1495](https://arxiv.org/abs/0706.1495)).
88. J. Abraham *et al.* (Auger Collaboration), *Proc. 31st Int. Cosmic Ray Conf.*, Lodz, Poland, 2009; ([arXiv:0906.2319](https://arxiv.org/abs/0906.2319)).
89. K. Greisen, *Phys. Rev. Lett.* **16**, 748 (1966).
90. G.T. Zatsepin and V.A. Kuz'min, *Sov. Phys. JETP Lett.* **4**, 78 (1966).
91. D. Allard *et al.*, *Astron. & Astrophys.* **443**, L29 (2005).
92. M. Takeda *et al.* (The AGASA Collaboration), *Astropart. Phys.* **19**, 447 (2003).
93. R. Abbasi *et al.* (HiRes Collaboration), *Phys. Rev. Lett.* **100**, 101101 (2008).

-
94. J. Abraham *et al.* (Auger Collaboration), *Phys. Rev. Lett.* **101**, 061101 (2008).
 95. F. Schüssler *et al.* (Auger Collaboration), in *Proc. 31st Int. Cosmic Ray Conf.*, Lodz, Poland; ([arXiv:0906.2319](#)).
 96. V.S. Berezinsky and G.T. Zatsepin, *Phys. Lett.* **B28**, 423 (1969).
 97. I. Kravchenko *et al.* (RICE Collaboration), *Phys. Rev.* **D73**, 082002 (2006).
 98. J. Abraham *et al.* (Auger Collaboration), *Phys. Rev. Lett.* **100**, 211101 (2008).
 99. P. Gorham *et al.* (Anita Collaboration), *Phys. Rev. Lett.* **103**, 051103 (2009).
 100. R. Engel, D. Seckel, and T. Stanev, *Phys. Rev.* **D64**, 09310 (2001).
 101. E. Waxman and J. Bahcall, *Phys. Rev.* **D59**, 023002 (1999).
 102. R.U. Abbasi *et al.* (HiRes Collaboration), *Astropart. Phys.* **32**, 53 (2009).

25. ACCELERATOR PHYSICS OF COLLIDERS

Revised July 2009 by D.A. Edwards (DESY) and M.J. Syphers (FNAL).

25.1. Luminosity

This article provides background for the High-Energy Collider Parameter Tables that follow. Of prime importance in a collider run is the *integrated luminosity*; the ratio of yield to cross section. Integrated luminosity is the integral over time of the instantaneous *luminosity* denoted here by \mathcal{L} .

Today's colliders all employ bunched beams. If two bunches containing n_1 and n_2 particles collide head-on with frequency f , the luminosity is

$$\mathcal{L} = f \frac{n_1 n_2}{4\pi\sigma_x\sigma_y} \quad (25.1)$$

where σ_x and σ_y characterize the transverse beam profiles in the horizontal (bend) and vertical directions. In this form it is assumed that the bunches are identical in transverse profile, that the profiles are independent of position along the bunch, and the particle distributions are not altered during bunch passage.

Whatever the distribution at the source, by the time the beam reaches high energy, the normal form is a useful approximation as suggested by the σ -notation. In the case of an electron storage ring, synchrotron radiation leads to a Gaussian distribution in equilibrium, but even in the absence of radiation the central limit theorem of probability and the diminished importance of space charge effects produces a similar result.

The n 's and σ 's in Eq. (25.1) may change with time during a "store", and control of that time variation is a major factor in integrated luminosity. The integral achieved over a period such as a week is a measure of overall systems performance, as it will include such influences as turn-around time for refill. The formula needs a variety of modifications depending on the type of collider; for example, the angular distribution of particle velocities in a bunch may cause a significant variation in transverse beam size through the collision overlap region. This effect and others specific to collider type will be discussed in later sections.

In the Tables, luminosity is stated in units of $\text{cm}^{-2}\text{s}^{-1}$. Integrated luminosity, on the other hand, is usually quoted as the inverse of the standard measures of cross section such as femtobarns and, recently, attobarns.

Subsequent sections in this report enlarge briefly on the dynamics behind collider design, comment on the realization of collider performance in a selection of today's facilities, and end with some remarks on future possibilities.

25.2. Single Particle Dynamics

Today's operating HEP colliders are all alternating-gradient synchrotrons [1,2], and the material of this section reflects that circumstance. The single particle transverse motion in this focusing structure is not a simple sinusoid; rather it may be expressed in the form

$$x(s) = A\sqrt{\beta(s)} \cos[\psi(s) + \delta], \quad (25.2)$$

where s is path length in the beam direction, A and δ are constants of integration and the envelope of the motion is modulated by the *amplitude function*, β . The phase advances according to $d\psi/ds = 1/\beta$; that is, β also plays the role of a local $\lambda/2\pi$, and the *tune*, ν , is the number of such oscillations per turn about the closed path. In the neighborhood of an interaction point, the beam optics of the ring is configured so as to produce a near focus; the value of the amplitude function at this point is designated β^* .

The motion as it develops with s describes an ellipse in $\{x, x' (\equiv dx/ds)\}$ phase space the area of which is πA^2 , where A is the constant above. If the interior of that ellipse is populated by an ensemble of particles, that area, given the name *emittance* and denoted by ε , would change only with beam energy in the absence of other processes. For a beam with a Gaussian distribution in x, x' , the area containing one standard deviation σ_x is the definition of emittance in the Tables:

$$\varepsilon_x \equiv \pi \frac{\sigma_x^2}{\beta_x}, \quad (25.3)$$

with a corresponding expression in the other transverse direction, y . This definition includes 39% of the beam.

To complete the coordinates used to describe the motion, we add to the transverse phase space $\{x, x', y, y'\}$ the longitudinal variables $\{z, \delta p/p\}$, where z is the distance by which the particle leads the "ideal" particle along the design trajectory. Radiofrequency electric fields in the s direction provide the means for longitudinal oscillations, and the frequency determines the bunch length. The frequency of this system appears in the Tables as does $\delta p/p$ characterized as "energy spread".

For HEP bunch length is a significant quantity for a variety of reasons, but in the present context if the bunch length becomes larger than β^* the luminosity is adversely affected. This is because β grows parabolically as one proceeds away from the IP and so the beam size increases thus lowering the contribution to the luminosity from such locations. This is often called the "hour glass" effect as is the factor by which the luminosity is reduced.

The other major external electromagnetic field interaction in the single particle context is the production of synchrotron radiation due to centripetal acceleration, given by the Larmor formula multiplied by a relativistic magnification factor of γ^4 [3,4]. In the case of electron rings this process determines the equilibrium emittance through a balance between radiation damping and excitation of oscillations, and further serves as the barrier to future higher energy versions in this variety of collider.

25.3. Impediments to High Luminosity

Eq. (25.1) can be recast in terms of emittances and amplitude functions as

$$\mathcal{L} = f \frac{n_1 n_2}{4\sqrt{\varepsilon_x \beta_x^* \varepsilon_y \beta_y^*}}. \quad (25.4)$$

So to achieve high luminosity, all one has to do is make high population bunches of low emittance to collide at high frequency at locations where the beam optics provides as low values of the amplitude functions as possible.

While there are no fundamental limits to this process, there are certainly challenges. Here we have space to mention only a few of these. The beam-beam tune shift appears in the Tables. A bunch in one beam presents a (nonlinear) lens to a particle in the other beam resulting in changes to the particle's transverse oscillation tune with a range characterized by the parameter [5]

$$\xi_{y,2} = \frac{r_2 n_1 \beta_{y,2}^*}{2\pi\gamma_2 \sigma_{y,1} (\sigma_{x,1} + \sigma_{y,1})} \quad (25.5)$$

where $r_2 = e^2/(4\pi\epsilon_0 m_2 c^2)$ is the classical radius of the affected particle. The transverse oscillations are susceptible to resonant perturbations from a variety of sources such as imperfections in the magnetic guide field, so certain values of the tune must be avoided. Accordingly, the tune spread arising from ξ is limited, but limited to a value difficult to predict. But a glance at the Tables shows that electrons are more forgiving than protons thanks to the damping effects of synchrotron radiation; the ξ -values for the former are about an order of magnitude larger than those for protons.

A subject of present intense interest is the *electron-cloud effect* [6,7]; actually a variety of related processes come under this heading. They typically involve a buildup of electron density in the vacuum chamber due to emission from the chamber walls stimulated by electrons or photons originating from the beam itself. For instance, there is a process closely resembling the multipacting effects familiar from radiofrequency system commissioning. Low energy electrons are ejected from the walls by photons from positron or proton beam-produced synchrotron radiation. These electrons are accelerated toward a beam bunch, but by the time they reach the center of the vacuum chamber the bunch has gone and so the now-energetic electrons strike the opposite wall to produce more secondaries. These secondaries are now accelerated by a subsequent bunch, and so on. Among the disturbances that this electron accumulation can produce is enhancement of the tune spread within the bunch; the near-cancellation of bunch induced electric and magnetic fields is no longer in effect.

The benefits of low emittance are clear in Eq. (25.4), so a few words are in order on that subject. For electron synchrotrons, radiation damping provides an automatic route. For hadrons, particularly antiprotons, two inventions have played a prominent role. Stochastic cooling [8] was employed first in the Sp̄pS and subsequently in the Tevatron. Electron cooling [9] is currently also in use in the Tevatron complex. Further innovations are underway due to the needs of potential future projects; these are noted in the final section.

25.4. Comments on Present Facilities

Collider accelerator physics of course goes far beyond the elements of the preceding sections. In this section elaboration is made on various issues associated with some of the recently operating colliders, particularly issues which impact integrated luminosity. The various colliders utilizing hadrons have important unique differences and hence are broken out separately. As space is limited, general references are provided where much further information can be obtained.

25.4.1. LHC : [10] Once commissioning is complete, the superconducting Large Hadron Collider will emerge as the world's highest energy collider. To meet its luminosity goals the LHC will have to contend with a high beam current of 0.5 A, leading to stored energies of several hundred MJ per beam. Component protection, beam collimation, and controlled energy deposition will be given very high priorities. Additionally, at energies of 5-7 TeV per particle, synchrotron radiation will move from being a curiosity to a challenge in a hadron accelerator for the first time. At design beam current the system must remove roughly 7 kW at 1.8 K due to synchrotron radiation. As the photons are emitted their interactions with the vacuum chamber wall can generate free electrons, with consequent "electron cloud" development. Much care was taken to design a special liner for the chamber to mitigate this issue.

The two proton beams are contained in separate pipes throughout most of the circumference, but naturally must be brought together into a single pipe at the interaction points (IP's). The large number of bunches, and subsequent short bunch spacing, would lead to approximately 30 head-on collisions through 120 m of common beam pipe at each IP. Thus, a small crossing angle is employed, which reduces the luminosity by about 15%. Still, the bunches moving in one direction will have long-range encounters with the counter-rotating bunches and the resulting perturbations of the particle motion constitute a continued course of study.

As with all hadron colliders, emittance preservation and optimization throughout the injector chain and through to collision conditions is paramount to obtaining the highest luminosity possible.

25.4.2. Tevatron : [11] The route to high integrated luminosity in the Tevatron has been governed by the antiproton production rate, the turn-around time to produce another store, and the resulting optimization of store time. The overall reliability of the accelerator complex plays a crucial role, as it can take many hours to produce an adequate number of antiprotons for collisions. The first superconducting synchrotron in history, the Tevatron has operated as the highest energy collider for approximately 25 years.

Though the bunches in the Tevatron are collided without a crossing angle they are of long enough extent that the luminous region takes on an "hour glass" shape along the direction of motion as the beam is focused toward the interaction point. This leads to its own reduction in luminosity, roughly 40% in this case. Unlike the LHC, the beams in the Tevatron circulate in a single vacuum pipe and thus are placed on separated orbits which wrap around each other in a helical pattern outside of the interaction regions. Hence, long-range encounters play an important role here as well, though the effects can be different than in the LHC where the encounters are more or less "in phase" with each other through a single interaction region. In the Tevatron, the 70 long-range encounters are distributed about the synchrotron and their mitigation is limited by the available aperture.

In recent years the antiproton bunch intensities have approached those of the proton bunches, and their emittances have been greatly reduced using improved beam cooling, so much so that detrimental effects on the proton beam have become apparent. The antiproton beam emittance is now adjusted prior to collision conditions to

optimize the proton bunch lifetime during the store. Eq. (25.1) can be re-written as

$$\mathcal{L} = \frac{2f_0\gamma}{\beta^*r_0} \xi \frac{\mathcal{H}}{1 + \bar{\varepsilon}/\varepsilon} \bar{N}_{tot} \approx 10^{30} \text{cm}^{-2}\text{s}^{-1} \left(\bar{N}_{tot}/10^{10} \right)$$

where f_0 is the revolution frequency, $\gamma = E/mc^2$, β^* is the amplitude function at the IP, r_0 is the classical radius of the proton, ξ is the beam-beam tune shift parameter, \mathcal{H} is the hour glass factor, and $\bar{\varepsilon}/\varepsilon$ is the ratio of the emittances of the antiproton to proton beams. After many years the first three factors have become saturated operationally, so that the luminosity depends almost entirely upon the production of antiprotons. In these units, the Tevatron has achieved luminosities of over 350, where its original design luminosity was 1 [12].

25.4.3. e^+e^- Rings : As should be expected, synchrotron radiation plays a major role in the design and optimization of the e^+e^- colliders. While vacuum stability and electron clouds can be of concern in the positron rings, synchrotron radiation along with the restoration of longitudinal momentum by the RF system have the positive effect of generating very small transverse beam sizes and small momentum spread. Further reduction of beam size at the interaction points using standard beam optics techniques and successfully contending with high beam currents has led to record luminosities in these rings, far exceeding those of hadron colliders. To maximize integrated luminosity the beam can be "topped off" by injecting new particles without removing existing ones – a feature difficult to imitate in hadron colliders.

Asymmetric energies of the two beams have allowed for the enhancement of B-physics research and for interesting interaction region designs. As the bunch spacing can be quite short, the lepton beams sometimes pass through each other at an angle and hence have reduced luminosity. Recently, however, the invention of high frequency "crab crossing" schemes have been successfully tested wherein bunches are rotated at the IP to produce full restoration of the luminous region. KEK-B has attained over 1fb^{-1} of integrated luminosity in a single day, and its upgrade plans is aiming for initial luminosities of $8 \times 10^{35} \text{cm}^{-2}\text{s}^{-1}$ [13].

25.4.4. HERA : [14] Now decommissioned, HERA was the first facility to employ both applications of superconductivity: magnets and accelerating structures. Its next-generation cold-iron superconducting magnets for the proton beam were the culmination of lessons learned from the Tevatron experience and extensive development of the technology since then. The HERA team felt comfortable with a larger dynamic range of the magnet system, enabling the use of the existing DESY complex for injection. Though the HERA magnets could reach fields consistent with energies above 1 TeV, other accelerator systems precluded operation above 920 GeV.

The lepton beam (positrons or electrons) were provided by the existing complex, and were accelerated to 27.5 GeV using conventional magnets. The interaction region where the beams had common vacuum chambers had the interesting feature that the lepton beam could be manipulated without detrimental effects on the proton beam due to the large difference in magnetic rigidity. A 4-times higher frequency RF system was used at collision to generate shorter bunches, thus helping alleviate the hour glass effect at the collision points. As in any high energy lepton storage ring, the lepton beam naturally would become transversely polarized (within about 40 minutes, for HERA). "Spin rotators" were implemented on either side of an IP to produce longitudinal polarization at the experiment.

25.4.5. RHIC : [15] The Relativistic Heavy Ion Collider employs superconducting magnets, and collides combinations of fully-stripped ions such as H-H (p-p), Au-Au, Cu-Cu, and d-Au.

The high charge per particle (+79 for gold, for instance) makes intra-beam scattering of particles within the bunch of special concern, even for seemingly modest bunch intensities. Another special feature of accelerating heavy ions in RHIC is that the beams experience a "transition energy" during acceleration – a point where the derivative with respect to momentum of the revolution period is zero. This is more typical of low-energy accelerators, where the necessary phase jump required of the RF system is implemented rapidly and little time

is spent near this condition. In the case of RHIC with heavy ions, the superconducting magnets do not ramp very quickly and the period of time spent crossing transition is long and must be dealt with carefully. For p-p operation the beams are always above their transition energy and so this condition is completely avoided.

RHIC is also distinctive in its ability to accelerate and collide polarized proton beams. As proton beam polarization must be maintained from its low-energy source, successful acceleration through the myriad of depolarizing resonance conditions in high energy circular accelerators has taken years to accomplish. A record energy of 250 GeV per proton with ~35% final polarization per beam has recently been realized.

25.5. Future Prospects

Present design activity emphasizes a lepton collider as the next major HEP project following initial results from the LHC. Synchrotron radiation precludes a higher energy successor to LEP. Four alternatives are noted in this section: two approaches to an electron-positron linear collider, a muon ring collider, and potential use of a plasma as the acceleration medium.

25.5.1. Electron-Positron Linear Colliders :

The only linear collider ever operated is the ground-breaking Stanford Linear Collider (SLC), which ran from 1989 until 1998. A major problem confronting a future high energy, high luminosity single pass collider design is the power requirement, so measures must be taken to keep the demand within bounds as illustrated in a transformed Eq. (25.1) as developed in the *TESLA Design Report* [16]:

$$\mathcal{L} = \frac{1}{4\pi r_e^3} \frac{P_b}{E_{cm}} \left(\frac{\pi \delta_E}{\gamma \varepsilon_y} \right)^{1/2} H_D. \quad (25.6)$$

Here, r_e is the classical electron radius, P_b is the total power of both beams and E_{cm} their cms energy. Management of P_b leads to an upward push on the product of collision frequency and bunch population with an attendant rise in the energy radiated due to the electromagnetic field on one bunch acting on the particles of the other. The fractional spread in the collision energy that results from this radiation is represented by δ_E and keeping a significant fraction of the luminosity within a percent or so of the nominal energy represents a design goal. A consequence is the use of flat beams, where δ_E is managed by the beam width, and luminosity adjusted by the beam height, thus the explicit appearance of the vertical emittance ε_y . The final factor in Eq. (25.6), H_D , represents the enhancement of luminosity due to the pinch effect during bunch passage.

The approach designated the International Linear Collider (ILC) is presented in the Tables, and the contrast with the collision-point parameters of the circular colliders is striking, though reminiscent in direction of those of the SLAC Linear Collider that are no longer shown. The *ILC Reference Design Report* [17] has a baseline of a cms energy of 500 GeV with upgrade provision for 1 TeV, and luminosity comparable to the LHC. The ILC is based on superconducting accelerating structures of the 1.3 GHz TESLA variety.

At CERN, a design effort is underway on the Compact Linear Collider (CLIC), each linac of which is itself a two-beam accelerator, in that a high energy, low current beam is fed by a low energy, high current driver [18]. The CLIC design employs normal conducting 12 GHz accelerating structures at a gradient of 100 MeV/m, some three times the current capability of the superconducting ILC cavities. The design cms energy is 3 TeV.

25.5.2. Muon Collider :

The muon to electron mass ratio of 210 implies less concern about synchrotron radiation by a factor of about 2×10^9 and its 1.6 μ s lifetime means that it will last for some 150B turns in a ring about half of which is occupied by bend magnets with average field B (tesla). Design effort became serious in the mid 1990s and a collider outline emerged quickly [19].

Removal of the synchrotron radiation barrier reduces collider facility scale to a level compatible with on-site placement at some locations. If a Higgs particle is detected the $(m_\mu/m_e)^2$ cross section advantage

in s-channel production would be valuable. And a neutrino factory could potentially be realized in the course of construction [20].

The challenges to luminosity achievement were clear and very attractive for R&D: targetting, collection, and emittance reduction are three that come immediately to mind. The proton source will deliver a beam power of several MW; muon collection would be aided by ultra-high magnetic fields, with solenoids to produce them currently under development. The emittance requirements have inspired fascinating investigations into phase space manipulation that are finding application in other facilities. A summary of the status may be found in a recent presentation to the HEPAP P5 Subpanel [21].

25.5.3. Plasma Acceleration :

At the 1956 CERN Symposium, a paper by Veksler in which he suggested acceleration of protons to the TeV scale using a bunch of electrons anticipated current interest in plasma acceleration [22]. A half-century later this is more than a suggestion, with the demonstration, as a striking example, of energy enhancement of 28.5 GeV at SLAC [23].

How plasma acceleration will find application in an HEP facility is not yet clear, given the likely necessity of sequential impulses. Active R&D is underway; for recent discussion of parameters for a laser-plasma based electron positron collider, see, for example, relevant papers in the recent Advanced Accelerator Concepts Workshop [24]. In the relatively near-term, there is the likelihood of application outside of HEP in compact multi-GeV accelerators [25].

References:

1. E.D. Courant and H.S. Snyder, *Ann. Phys.* **3**, 1 (1958). This is the classic article on the alternating gradient synchrotron.
2. A.W. Chao and M. Tigner (eds.), *Handbook of Accelerator Physics and Engineering*, World Science Publishing Co. (Singapore, 2nd printing, 2002.), Sec. 2.1, 2.2.
3. H. Wiedemann, *Handbook of Accelerator Physics and Engineering*, *op cit*, Sec. 3.1.
4. Basic synchrotron radiation material is given in Sec. 7.3, p 113 in RPP-2008 (C. Amsler *et al.*, *Phys. Lett.* **B667**, 1 (2008)).
5. M.A. Furman and M.S. Zisman, *Handbook of Accelerator Physics and Engineering*, *op cit*, Sec. 4.1.
6. M.A. Furman, *Handbook of Accelerator Physics and Engineering*, *op cit*, Sec. 2.5.11.
7. <http://ab-abp-rlc.web.cern.ch/ab-abp-rlc-ecloud/>. This site contains many references as well as videos of electron cloud simulations.
8. D. Möhl *et al.*, *Phys. Reports* **58**, 73 (1980).
9. G.I. Budker, *Proc. Int. Symp. Electron & Positron Storage Rings* (1966).
10. Detailed information from the multi-volume design report to present status may be found at <http://lhc.web.cern.ch/lhc/>.
11. H.T. Edwards, "The Tevatron Energy Doubler: A Superconducting Accelerator," *Ann. Rev. Nucl. and Part. Sci.* **35**, 605 (1985).
12. C. Gattuso, M. Convery, M. Syphers, "Optimization of integrated luminosity in the Tevatron," FERMILAB-CONF-09-132-AD (Apr 2009).
13. An overview of electron-positron colliders past and present may be found in ICFA Beam Dynamics Newsletter No. 46, April 2009, www-bd.fnal.gov/icfabd/. A day-by-day account of the luminosity progress at KEK-B may be found at <http://www-acc.kek.jp/kekb/>.
14. A brief history of HERA may be found at <http://zms.desy.de/research/accelerators/>.
15. M. Harrison, T. Ludlam, and S. Ozaki, *eds*, "Special Issue: The Relativistic Heavy Ion Collider Project: RHIC and its Detectors," *Nucl. Instrum. Methods* **A499**, 235 (2003).
16. http://tesla.desy.de/new_pages/TDR_CD/start.html.
17. Information on ILC R&D status as well as the 2007 Reference Design Report may be obtained from <http://www.linearcollider.org/cms/>.
18. <http://clic-study.web.cern.ch/clic2Dstudy/>.

19. R.B. Palmer, A. Tollestrup, and A. Sessler “*Status Report of a High Luminosity Muon Collider and Future Research and Development Plans*,” MC-047, www.fnal.gov/projects/muon Collider/notes/fnal_notes.html.
20. http://en.wikipedia.org/wiki/Neutrino_Factory.
21. www.cap.bnl.gov/mumu/polit/palmer-p5.pdf.
22. V.I. Veksler, CERN Symposium on High Energy Accelerators and Pion Physics, 11–23 June 1956, page 80. This paper may be downloaded from http://documents.cern.ch/cgi-bin/setlink?base=cernrep&categ=Yellow_Report&id=1956-025.
23. <http://slac.stanford.edu/grp/arb/siemann.pdf>.
24. “*Advanced Accelerator Concepts*,” ed. by C. Schroeder, W. Leemans, and E. Esarey, AIP Conference Proceedings 1086, Santa Cruz CA 27 July – 2 August 2008.
25. <http://accelconf.web.cern.ch/Accelconf/106/PAPERS/THP094.PDF>.

HIGH-ENERGY COLLIDER PARAMETERS: e^+e^- Colliders (I)

Updated in early 2010 with numbers received from representatives of the colliders (contact J. Beringer, LBNL). For existing (future) colliders the latest achieved (design) values are given. Quantities are, where appropriate, r.m.s.; H and V indicate horizontal and vertical directions; s.c. stands for superconducting. Parameters for the defunct SPEAR, DORIS, PETRA, PEP, SLC, TRISTAN, and VEPP-2M colliders may be found in our 1996 edition (Phys. Rev. **D54**, 1 July 1996, Part I).

	VEPP-2000 (Novosibirsk)	VEPP-4M (Novosibirsk)	BEPC (China)	BEPC-II (China)	DAΦNE (Frascati)
Physics start date	2008	1994	1989	2008	1999
Physics end date	—	—	2005	—	2013
Maximum beam energy (GeV)	1.0	6	2.2	1.89 (2.3 max)	0.700
Luminosity (10^{30} cm $^{-2}$ s $^{-1}$)	100	20	12.6 at 1.843 GeV/beam 5 at 1.55 GeV/beam	330	450 (1000 achievable)
Time between collisions (μ s)	0.04	0.6	0.8	0.008	0.0027
Full crossing angle (μ rad)	0	0	0	2.2×10^4	5×10^4
Energy spread (units 10^{-3})	0.64	1	0.58 at 2.2 GeV	0.52	0.40
Bunch length (cm)	4	5	≈ 5	1.3	low current: 1 high current: 2
Beam radius (10^{-6} m)	125 (round)	H : 1000 V : 30	H : 890 V : 37	H : 380 V : 5.7	H : 800 V : 4.8
Free space at interaction point (m)	± 1	± 2	± 2.15	± 0.63	± 0.40
Luminosity lifetime (hr)	continuous	2	7–12	1.5	0.3
Turn-around time (min)	continuous	18	32	26	3
Injection energy (GeV)	0.2–1.0	1.8	1.55	1.89	on energy
Transverse emittance ($10^{-9}\pi$ rad-m)	H : 250 V : 250	H : 200 V : 20	H : 660 V : 28	H : 144 V : 2.2	H : 260 V : 0.52
β^* , amplitude function at interaction point (m)	H : 0.06 – 0.11 V : 0.06 – 0.10	H : 0.75 V : 0.05	H : 1.2 V : 0.05	H : 1.0 V : 0.015	H : 0.25 V : 0.009
Beam-beam tune shift per crossing (units 10^{-4})	H : 750 V : 750	500	350	200	250
RF frequency (MHz)	172	180	199.53	499.8	368
Particles per bunch (units 10^{10})	16	15	20 at 2 GeV 11 at 1.55 GeV	3.6	e^- : 3.3 e^+ : 2.4
Bunches per ring per species	1	2	1	93	120 (incl. 10 bunch gap)
Average beam current per species (mA)	150	80	40 at 2 GeV 22 at 1.55 GeV	580	e^- : 1800 e^+ : 1300
Circumference or length (km)	0.024	0.366	0.2404	0.23753	0.098
Interaction regions	2	1	2	1	1
Magnetic length of dipole (m)	1.2	2	1.6	Outer ring: 1.6 Inner ring: 1.41	1
Length of standard cell (m)	12	7.2	6.6	Outer ring: 6.6 Inner ring: 6.2	12
Phase advance per cell (deg)	H : 738 V : 378	65	≈ 60	60–90 non-standard cells	360
Dipoles in ring	8	78	40 + 4 weak	84 + 8 weak	8
Quadrupoles in ring	20	150	68	134+2 s.c.	48
Peak magnetic field (T)	2.4	0.6	0.903 at 2.8 GeV	Outer ring: 0.677 Inner ring: 0.766	1.7

HIGH-ENERGY COLLIDER PARAMETERS: e^+e^- Colliders (II)

Updated in early 2010 with numbers received from representatives of the colliders (contact J. Beringer, LBNL). For existing (future) colliders the latest achieved (design) values are given. Quantities are, where appropriate, r.m.s.; H and V indicate horizontal and vertical directions; s.c. stands for superconducting.

	CESR (Cornell)	CESR-C (Cornell)	LEP (CERN)	ILC (TBD)
Physics start date	1979	2002	1989	TBD
Physics end date	2002	2008	2000	—
Maximum beam energy (GeV)	6	6	100 - 104.6	250 (upgradeable to 500)
Luminosity ($10^{30} \text{ cm}^{-2}\text{s}^{-1}$)	1280 at 5.3 GeV/beam	76 at 2.08 GeV/beam	24 at Z^0 100 at > 90 GeV	2×10^4
Time between collisions (μs)	0.014 to 0.22	0.014 to 0.22	22	0.3^{\ddagger}
Full crossing angle (μ rad)	± 2000	± 3300	0	14000
Energy spread (units 10^{-3})	0.6 at 5.3 GeV/beam	0.82 at 2.08 GeV/beam	0.7→1.5	1
Bunch length (cm)	1.8	1.2	1.0	0.03
Beam radius (μm)	H : 460 V : 4	H : 340 V : 6.5	H : 200 → 300 V : 2.5 → 8	H : 0.639 V : 0.0057
Free space at interaction point (m)	± 2.2 (± 0.6 to REC quads)	± 2.2 (± 0.3 to PM quads)	± 3.5	± 3.5
Luminosity lifetime (hr)	2-3	2-3	20 at Z^0 10 at > 90 GeV	n/a
Turn-around time (min)	5 (topping up)	1.5 (topping up)	50	n/a
Injection energy (GeV)	1.8-6	1.5-6	22	n/a
Transverse emittance ($10^{-9}\pi$ rad-m)	H : 210 V : 1	H : 120 V : 3.5	H : 20-45 V : 0.25 → 1	H : 0.02 V : 8×10^{-5} (at 250 GeV)
β^* , amplitude function at interaction point (m)	H : 1.0 V : 0.018	H : 0.94 V : 0.012	H : 1.5 V : 0.05	H : 0.02 V : 0.0004
Beam-beam tune shift per crossing (units 10^{-4})	H : 250 V : 620	e^- : 420 (H), 280 (V) e^+ : 410 (H), 270 (V)	830	n/a
RF frequency (MHz)	500	500	352.2	1300
Particles per bunch (units 10^{10})	1.15	4.7	45 in collision 60 in single beam	2
Bunches per ring per species	9 trains of 5 bunches	8 trains of 3 bunches	4 trains of 1 or 2	2625
Average beam current per species (mA)	340	72	4 at Z^0 4→6 at > 90 GeV	9 (in pulse)
Beam polarization (%)	—	—	55 at 45 GeV 5 at 61 GeV	e^- : $> 80\%$ e^+ : $> 60\%$
Circumference or length (km)	0.768	0.768	26.66	31
Interaction regions	1	1	4	1
Magnetic length of dipole (m)	1.6-6.6	1.6-6.6	11.66/pair	n/a
Length of standard cell (m)	16	16	79	n/a
Phase advance per cell (deg)	45-90 (no standard cell)	45-90 (no standard cell)	102/90	n/a
Dipoles in ring	86	84	3280+24 inj. + 64 weak	n/a
Quadrupoles in ring	101 + 4 s.c.	101 + 4 s.c.	520+288 + 8 s.c.	n/a
Peak magnetic field (T)	0.3 / 0.8 at 8 GeV	0.3 / 0.8 at 8 GeV, 2.1 wigglers at 1.9 GeV	0.135	n/a

‡ Time between bunch trains: 200ms.

HIGH-ENERGY COLLIDER PARAMETERS: e^+e^- Colliders (III)

Updated in early 2010 with numbers received from representatives of the colliders (contact J. Beringer, LBNL). For existing (future) colliders the latest achieved (design) values are given. Quantities are, where appropriate, r.m.s.; H and V indicate horizontal and vertical directions; s.c. stands for superconducting.

	KEKB (KEK)	PEP-II (SLAC)	SuperB (Italy)	SuperKEKB (KEK)
Physics start date	1999	1999	TBD	2014 ?
Physics end date	—	2008	—	—
Maximum beam energy (GeV)	e^- : 8.33 (8.0 nominal) e^+ : 3.64 (3.5 nominal)	e^- : 7–12 (9.0 nominal) e^+ : 2.5–4 (3.1 nominal) (nominal $E_{cm} = 10.5$ GeV)	e^- : 4.2 e^+ : 6.7	e^- : 7 e^+ : 4
Luminosity (10^{30} cm $^{-2}$ s $^{-1}$)	21083	12069 (design: 3000)	1.0×10^6	8×10^5
Time between collisions (μ s)	0.00590 or 0.00786	0.0042	0.0042	0.004
Full crossing angle (μ rad)	$\pm 11000^\dagger$	0	± 33000	± 41500
Energy spread (units 10^{-3})	0.7	e^-/e^+ : 0.61/0.77	e^-/e^+ : 0.73/0.64	e^-/e^+ : 0.58/0.84
Bunch length (cm)	0.65	e^-/e^+ : 1.1/1.0	0.5	e^-/e^+ : 0.5/0.6
Beam radius (μ m)	H: 124 (e^-), 117 (e^+) V: 0.94	H: 157 V: 4.7	H: 8 V: 0.04	e^- : 11 (H), 0.062 (V) e^+ : 10 (H), 0.048 (V)
Free space at interaction point (m)	+0.75/−0.58 (+300/−500) mrad cone	± 0.2 , ± 300 mrad cone	± 0.35	e^- : +1.20/−1.28, e^+ : +0.78/−0.73 (+300/−500) mrad cone
Luminosity lifetime (hr)	continuous	continuous	continuous	continuous
Turn-around time (min)	continuous	continuous	continuous	continuous
Injection energy (GeV)	e^-/e^+ : 8/3.5	2.5–12	e^-/e^+ : 4.2/6.7	e^-/e^+ : 7/4
Transverse emittance ($10^{-9}\pi$ rad-m)	e^- : 24 (57*) (H), 0.61 (V) e^+ : 18 (55*) (H), 0.56 (V)	e^- : 48 (H), 1.5 (V) e^+ : 24 (H), 1.5 (V)	e^- : 2.5 (H), 0.006 (V) e^+ : 2.0 (H), 0.005 (V)	5 (H), 3 (V)
β^* , amplitude function at interaction point (m)	e^- : 1.2 (0.27*) (H), 0.0059 (V) e^+ : 1.2 (0.23*) (H), 0.0059 (V)	e^- : 0.50 (H), 0.012 (V) e^+ : 0.50 (H), 0.012 (V)	e^- : 0.032 (H), 0.00021 (V) e^+ : 0.026 (H), 0.00025 (V)	e^- : 0.025 (H), 3×10^{-4} (V) e^+ : 0.032 (H), 2.7×10^{-4} (V)
Beam-beam tune shift per crossing (units 10^{-4})	e^- : 1020 (H), 900 (V) e^+ : 1270 (H), 1290 (V)	e^- : 703 (H), 498 (V) e^+ : 510 (H), 727 (V)	20 (H), 950 (V)	e^- : 12 (H), 807 (V) e^+ : 28 (H), 893 (V)
RF frequency (MHz)	508.887	476	476	508.887
Particles per bunch (units 10^{10})	e^-/e^+ : 4.7/6.4	e^-/e^+ : 5.2/8.0	e^-/e^+ : 5.1/6.5	e^-/e^+ : 6.53/9.04
Bunches per ring per species	1585	1732	978	2500
Average beam current per species (mA)	e^-/e^+ : 1188/1637	e^-/e^+ : 1960/3026	e^-/e^+ : 1900/2400	e^-/e^+ : 2600/3600
Beam polarization (%)	—	—	> 80	—
Circumference or length (km)	3.016	2.2	1.258	3.016
Interaction regions	1	1	1	1
Magnetic length of dipole (m)	e^-/e^+ : 5.86/0.915	e^-/e^+ : 5.4/0.45	e^-/e^+ : 0.9/5.4	e^-/e^+ : 5.9/4.0
Length of standard cell (m)	e^-/e^+ : 75.7/76.1	15.2	40	e^-/e^+ : 75.7/76.1
Phase advance per cell (deg)	450	e^-/e^+ : 60/90	360 (V), 1080 (H)	450
Dipoles in ring	e^-/e^+ : 116/112	e^-/e^+ : 192/192	e^-/e^+ : 186/102	e^-/e^+ : 116/112
Quadrupoles in ring	e^-/e^+ : 452/452	e^-/e^+ : 290/326	e^-/e^+ : 290/300	e^-/e^+ : 466/460
Peak magnetic field (T)	e^-/e^+ : 0.25/0.72	e^-/e^+ : 0.18/0.75	e^-/e^+ : 0.52/0.25	e^-/e^+ : 0.22/0.19

† KEKB is operating with crab crossing since February 2007.

*With dynamic beam-beam effect.

HIGH-ENERGY COLLIDER PARAMETERS: ep , $p\bar{p}$, pp , and Heavy Ion Colliders

Updated in early 2010 with numbers received from representatives of the colliders (contact J. Beringer, LBNL). For existing (future) colliders the latest achieved (design) values are given. Quantities are, where appropriate, r.m.s.; H and V indicate horizontal and vertical directions; s.c. stands for superconducting; pk and ave denote peak and average values.

	HERA (DESY)	TEVATRON* (Fermilab)	RHIC (Brookhaven)				LHC† (CERN)	
			2001	2000	2004	2002	2009	2010
Physics start date	1992	1987	2001	2000	2004	2002	2009	2010
Physics end date	2007	—	—	—	—	—	—	—
Particles collided	ep	$p\bar{p}$	pp (pol.)	Au Au	Cu Cu	d Au	pp	Pb Pb
Maximum beam energy (TeV)	e : 0.030 p : 0.92	0.980	0.25 34% pol	0.1 TeV/n	0.1 TeV/n	0.1 TeV/n	7.0 (3.5)	2.76 TeV/n (1.38 TeV/n)
Luminosity (10^{30} cm $^{-2}$ s $^{-1}$)	75	402	85 (pk) 55 (ave)	0.0040 (pk) 0.0020 (ave)	0.020 (pk) 0.0008 (ave)	0.27 (pk) 0.14 (ave)	1.0×10^4 (170)	1.0×10^{-3} (1.3×10^{-5})
Time between collisions (ns)	96	396	107	107	321	107	24.95 (49.90)	99.8 (1347)
Full crossing angle (μ rad)	0	0	0				≈ 300	≤ 100 (0)
Energy spread (units 10^{-3})	e : 0.91 p : 0.2	0.14	0.15	0.75	0.75	0.75	0.113 (0.116)	0.11
Bunch length (cm)	e : 0.83 p : 8.5	p : 50 \bar{p} : 45	55	30	30	30	7.55 (5.87)	7.94 (5.83)
Beam radius (10^{-6} m)	e : 280(H), 50(V) p : 265(H), 50(V)	p : 28 \bar{p} : 16	90	135	145	145	16.6 (45)	15.9 (45)
Free space at interaction point (m)	± 2	± 6.5	16				38	38
Initial luminosity decay time, $-L/(dL/dt)$ (hr)	10	6 (average)	2.0	1.1	1.8	1.5	14.9 (8)	10.9 - 3.6‡ (150 - 50)‡
Turn-around time (min)	e : 75, p : 135	90	200	100	145	145	≈ 180	
Injection energy (TeV)	e : 0.012 p : 0.040	0.15	0.023	0.011 TeV/n	0.011 TeV/n	0.012 TeV/n	0.450	0.177 TeV/n
Transverse emittance ($10^{-9}\pi$ rad-m)	e : 20(H), 3.5(V) p : 5(H), 5(V)	p : 3 \bar{p} : 1	11	25	23	25	0.5 (1.0)	0.5 (1.0)
β^* , ampl. function at interaction point (m)	e : 0.6(H), 0.26(V) p : 2.45(H), 0.18(V)	0.28	0.7	0.75	0.9	0.85	0.55 (2.0)	0.5 (2.0)
Beam-beam tune shift per crossing (units 10^{-4})	e : 190(H), 450(V) p : 12(H), 9(V)	p : 120 \bar{p} : 120	47	16	30	d: 21 Au: 17	34 (23)	—
RF frequency (MHz)	e : 499.7 p : 208.2/52.05	53	accel: 28 store: 28	accel: 28 store: 197	accel: 28 store: 197	accel: 28 store: 197	400.8	400.8
Particles per bunch (units 10^{10})	e : 3 p : 7	p : 26 \bar{p} : 9	11	0.12	0.45	d: 10 Au: 0.1	11.5 (7)	0.007
Bunches per ring per species	e : 189 p : 180	36	111	111	37	95	2808 (796)	592 (62)
Average beam current per species (mA)	e : 40 p : 90	p : 70 \bar{p} : 24	152	127	60	d: 119 Au: 94	584 (100)	6.12 (0.641)
Circumference (km)	6.336	6.28	3.834				26.659	
Interaction regions	2 colliding beams 1 fixed target (e beam)	2 high \mathcal{L}	6 total, 2 high \mathcal{L}				2 high \mathcal{L} +2	1 dedicated +2
Magnetic length of dipole (m)	e : 9.185 p : 8.82	6.12	9.45				14.3	
Length of standard cell (m)	e : 23.5 p : 47	59.5	29.7				106.90	
Phase advance per cell (deg)	e : 60 p : 90	67.8	84	93	84	d: 84 Au: 93	90	
Dipoles in ring	e : 396 p : 416	774	192 per ring + 12 common				1232 main dipoles	
Quadrupoles in ring	e : 580 p : 280	216	246 per ring				482 2-in-1 24 1-in-1	
Magnet type	e : C-shaped p : s.c., collared, cold iron	s.c. $\cos\theta$ warm iron	s.c. $\cos\theta$ cold iron				s.c. 2 in 1 cold iron	
Peak magnetic field (T)	e : 0.274, p : 5	4.4	3.5				8.3	

* Additional TEVATRON parameters: \bar{p} source accum. rate: 25×10^{10} hr $^{-1}$; max. no. of \bar{p} stored: 3.1×10^{12} (Accumulator), 5.4×10^{12} (Recycler).

† Numbers in parentheses refer to goals for operation in 2010.

‡ For 1 - 3 experiments.

27. PASSAGE OF PARTICLES THROUGH MATTER

Revised January 2010 by H. Bichsel (University of Washington),
D.E. Groom (LBNL), and S.R. Klein (LBNL).

27. PASSAGE OF PARTICLES THROUGH MATTER	285
27.1. Notation	285
27.2. Electronic energy loss by heavy particles	285
27.2.1. Moments and cross sections	285
27.2.2. Stopping power at intermediate energies	286
27.2.3. Energy loss at low energies	288
27.2.4. Density effect	288
27.2.5. Energetic knock-on electrons (δ rays)	288
27.2.6. Restricted energy loss rates for relativistic ionizing particles	289
27.2.7. Fluctuations in energy loss	289
27.2.8. Energy loss in mixtures and compounds	290
27.2.9. Ionization yields	290
27.3. Multiple scattering through small angles	290
27.4. Photon and electron interactions in matter	291
27.4.1. Radiation length	291
27.4.2. Energy loss by electrons	291
27.4.3. Critical energy	292
27.4.4. Energy loss by photons	292
27.4.5. Bremsstrahlung and pair production at very high energies	293
27.4.6. Photomuclear and electronuclear interactions at still higher energies	294
27.5. Electromagnetic cascades	294
27.6. Muon energy loss at high energy	296
27.7. Cherenkov and transition radiation	297

27.1. Notation

Table 27.1: Summary of variables used in this section. The kinematic variables β and γ have their usual meanings.

Symbol	Definition	Units or Value
α	Fine structure constant ($e^2/4\pi\epsilon_0\hbar c$)	1/137.035 999 11(46)
M	Incident particle mass	MeV/ c^2
E	Incident part. energy γMc^2	MeV
T	Kinetic energy	MeV
$m_e c^2$	Electron mass $\times c^2$	0.510 998 918(44) MeV
r_e	Classical electron radius $e^2/4\pi\epsilon_0 m_e c^2$	2.817 940 325(28) fm
N_A	Avogadro's number	6.022 1415(10) $\times 10^{23}$ mol $^{-1}$
ze	Charge of incident particle	
Z	Atomic number of absorber	
A	Atomic mass of absorber	g mol $^{-1}$
K/A	$4\pi N_A r_e^2 m_e c^2 / A$	0.307 075 MeV g $^{-1}$ cm 2 for A = 1 g mol $^{-1}$
I	Mean excitation energy	eV (<i>Nota bene!</i>)
$\delta(\beta\gamma)$	Density effect correction to ionization energy loss	
$\hbar\omega_p$	Plasma energy ($\sqrt{4\pi N_e r_e^3 m_e c^2 / \alpha}$)	$\sqrt{\rho \langle Z/A \rangle} \times 28.816$ eV (ρ in g cm $^{-3}$)
N_e	Electron density	(units of r_e) $^{-3}$
w_j	Weight fraction of the j th element in a compound or mixture	
n_j	α number of j th kind of atoms in a compound or mixture	
—	$4\alpha r_e^2 N_A / A$	(716.408 g cm $^{-2}$) $^{-1}$ for A = 1 g mol $^{-1}$
X_0	Radiation length	g cm $^{-2}$
E_c	Critical energy for electrons	MeV
$E_{\mu c}$	Critical energy for muons	GeV
E_s	Scale energy $\sqrt{4\pi/\alpha} m_e c^2$	21.2052 MeV
R_M	Molière radius	g cm $^{-2}$

27.2. Electronic energy loss by heavy particles [1–32]

27.2.1. Moments and cross sections :

The electronic interactions of fast charged particles with speed $v = \beta c$ occur in *single collisions with energy losses* E [1], leading to ionization, atomic, or collective excitation. Most frequently the energy losses are small (for 90% of all collisions the energy losses are less than 100 eV). In thin absorbers few collisions will take place and the total energy loss will show a large variance [1]; also see Sec. 27.2.7 below. For particles with charge ze more massive than electrons (“heavy” particles), scattering from free electrons is adequately described by the Rutherford differential cross section [2], *

$$\frac{d\sigma_R(E; \beta)}{dE} = \frac{2\pi r_e^2 m_e c^2 z^2 (1 - \beta^2 E/T_{\max})}{\beta^2 E^2}, \quad (27.1)$$

where T_{\max} is the maximum energy transfer possible in a single collision. But in matter electrons are not free. E must be finite and depends on atomic and bulk structure. For electrons bound in atoms Bethe [3] used “Born Theorie” to obtain the differential cross section

$$\frac{d\sigma_B(E; \beta)}{dE} = \frac{d\sigma_R(E, \beta)}{dE} B(E). \quad (27.2)$$

Examples of $B(E)$ and $d\sigma_B/dE$ can be seen in Figs. 5 and 6 of Ref. 1.

* For spin 0 particles. The β dependence in the parentheses is different for spin 1/2 and spin 1 particles, but it is not important except at energies far above atomic binding energies.

Bethe's theory extends only to some energy above which atomic effects were not important. The free-electron cross section (Eq. (27.1)) can be used to extend the cross section to T_{\max} . At high energies σ_B is further modified by polarization of the medium, and this "density effect," discussed in Sec. 27.2.4, must also be included. Less important corrections are discussed below.

The mean number of collisions with energy loss between E and $E + dE$ occurring in a distance δx is $N_e \delta x (d\sigma/dE) dE$, where $d\sigma(E; \beta)/dE$ contains all contributions. It is convenient to define the moments

$$M_j(\beta) = N_e \delta x \int E^j \frac{d\sigma(E; \beta)}{dE} dE,$$

so that M_0 is the mean number of collisions in δx , M_1 is the mean energy loss in δx , $M_2 - M_1^2$ is the variance, etc. The number of collisions is Poisson-distributed with mean M_0 . N_e is either measured in electrons/g ($N_e = N_A Z/A$) or electrons/cm³ ($N_e = N_A \rho Z/A$). The former is used throughout this chapter, since quantities of interest (dE/dx , X_0 , etc.) vary smoothly with composition when there is no density dependence.

collision, and the other variables are defined in Table 27.1. A minor dependence on M at the highest energies is introduced through T_{\max} , but for all practical purposes $\langle dE/dx \rangle$ in a given material is a function of β alone. With the symbol definitions and values given in Table 27.1, the units are MeV g⁻¹cm².

Few concepts in high-energy physics are as misused as $\langle dE/dx \rangle$. The main problem is that the mean is weighted by very rare events with large single-collision energy deposits. Even with samples of hundreds of events a dependable value for the mean energy loss cannot be obtained. Far better and more easily measured is the most probable energy loss, discussed in Sec. 27.2.7. The most probable energy loss in a detector is considerably below the mean given by the Bethe equation.

In a TPC (Sec. 28.6.5), the mean of 50%–70% of the samples with the smallest signals is often used as an estimator.

Although it must be used with cautions and caveats, $\langle dE/dx \rangle$ as described in Eq. (27.3) still forms the basis of much of our understanding of energy loss by charged particles. Extensive tables are available[5,4, pdg.lbl.gov/AtomicNuclearProperties/].

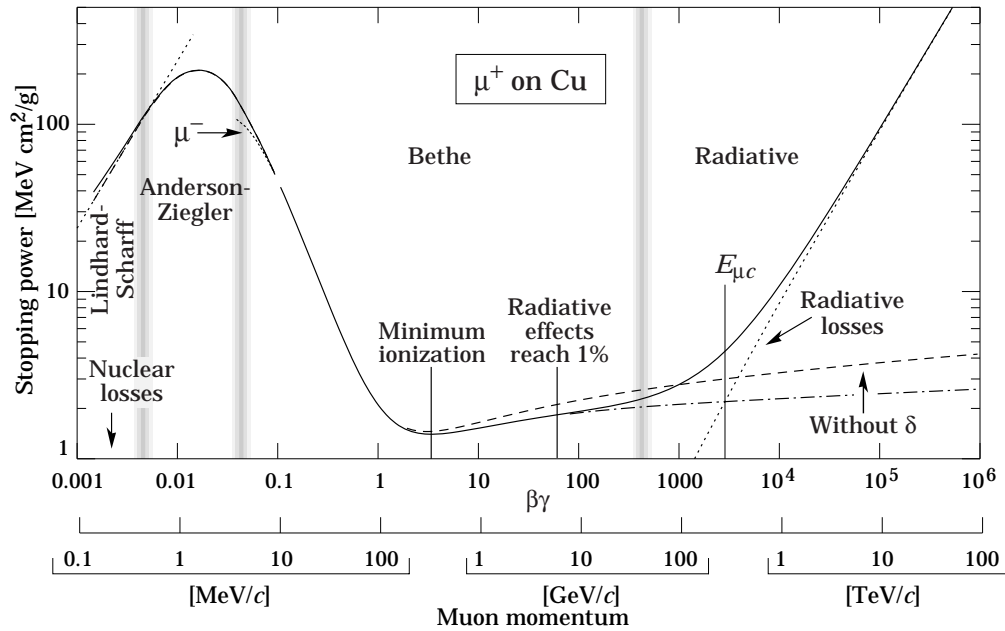


Fig. 27.1: Stopping power ($= \langle -dE/dx \rangle$) for positive muons in copper as a function of $\beta\gamma = p/Mc$ over nine orders of magnitude in momentum (12 orders of magnitude in kinetic energy). Solid curves indicate the total stopping power. Data below the break at $\beta\gamma \approx 0.1$ are taken from ICRU 49 [4], and data at higher energies are from Ref. 5. Vertical bands indicate boundary boundaries between different approximations discussed in the text. The short dotted lines labeled " μ^- " illustrate the "Barkas effect," the dependence of stopping power on projectile charge at very low energies [6].

27.2.2. Stopping power at intermediate energies :

The mean rate of energy loss by moderately relativistic charged heavy particles, $M_1/\delta x$, is well-described by the "Bethe" equation,

$$-\left\langle \frac{dE}{dx} \right\rangle = K z^2 \frac{Z}{A} \frac{1}{\beta^2} \left[\frac{1}{2} \ln \frac{2m_e c^2 \beta^2 \gamma^2 T_{\max}}{I^2} - \beta^2 - \frac{\delta(\beta\gamma)}{2} \right]. \quad (27.3)$$

It describes the mean rate of energy loss in the region $0.1 \lesssim \beta\gamma \lesssim 1000$ for intermediate- Z materials with an accuracy of a few %. At the lower limit the projectile velocity becomes comparable to atomic electron "velocities" (Sec. 27.2.3), and at the upper limit radiative effects begin to be important (Sec. 27.6). Both limits are Z dependent. Here T_{\max} is the maximum kinetic energy which can be imparted to a free electron in a single

The function as computed for muons on copper is shown as the "Bethe" region of Fig. 27.1. Mean energy loss behavior below this region is discussed in Sec. 27.2.3, and the radiative effects at high energy are discussed in Sec. 27.6. Only in the Bethe region is it a function of β alone; the mass dependence is more complicated elsewhere. The stopping power in several other materials is shown in Fig. 27.2. Except in hydrogen, particles with the same velocity have similar rates of energy loss in different materials, although there is a slow decrease in the rate of energy loss with increasing Z . The qualitative behavior difference at high energies between a gas (He in the figure) and the other materials shown in the figure is due to the density-effect correction, $\delta(\beta\gamma)$, discussed in Sec. 27.2.4. The stopping power functions are characterized by broad minima whose position

drops from $\beta\gamma = 3.5$ to 3.0 as Z goes from 7 to 100. The values of minimum ionization as a function of atomic number are shown in Fig. 27.3. In practical cases, most relativistic particles (*e.g.*, cosmic-ray muons) have mean energy loss rates close to the minimum; they are “minimum-ionizing particles,” or mip’s.

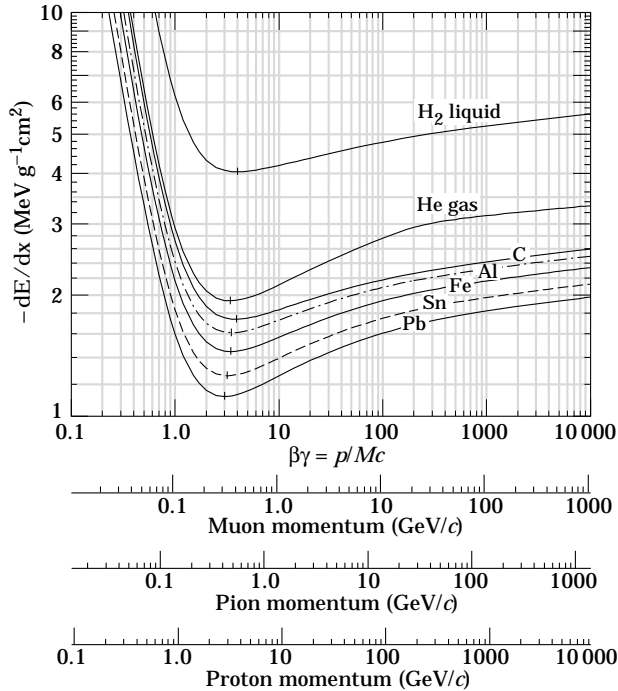


Figure 27.2: Mean energy loss rate in liquid (bubble chamber) hydrogen, gaseous helium, carbon, aluminum, iron, tin, and lead. Radiative effects, relevant for muons and pions in iron for $\beta\gamma \gtrsim 1000$, and at lower momenta for muons in higher- Z absorbers. See Fig. 27.21.

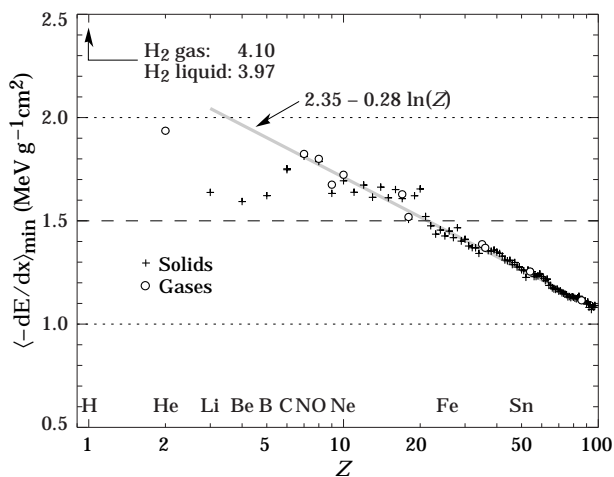


Figure 27.3: Stopping power at minimum ionization for the chemical elements. The straight line is fitted for $Z > 6$. A simple functional dependence on Z is not to be expected, since $\langle -dE/dx \rangle$ also depends on other variables.

Eq. (27.3) may be integrated to find the total (or partial) “continuous slowing-down approximation” (CSDA) range R for a particle which loses energy only through ionization and atomic excitation. Since dE/dx depends only on β , R/M is a function

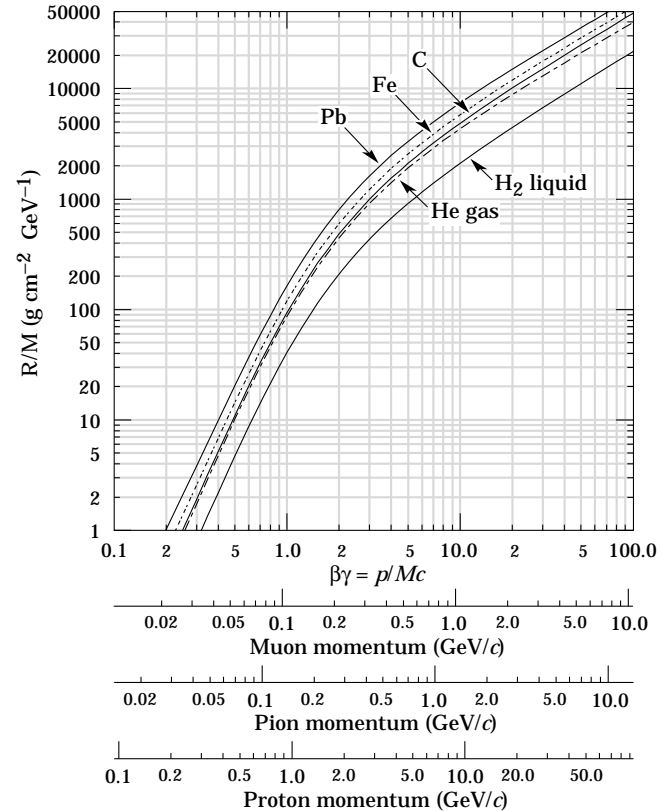


Figure 27.4: Range of heavy charged particles in liquid (bubble chamber) hydrogen, helium gas, carbon, iron, and lead. For example: For a K^+ whose momentum is 700 MeV/c, $\beta\gamma = 1.42$. For lead we read $R/M \approx 396$, and so the range is 195 cm^{-2} .

of E/M or pc/M . In practice, range is a useful concept only for low-energy hadrons ($R \lesssim \lambda_I$, where λ_I is the nuclear interaction length), and for muons below a few hundred GeV (above which radiative effects dominate). R/M as a function of $\beta\gamma = p/Mc$ is shown for a variety of materials in Fig. 27.4.

The mass scaling of dE/dx and range is valid for the electronic losses described by the Bethe equation, but not for radiative losses, relevant only for muons and pions.

For a particle with mass M and momentum $M\beta\gamma c$, T_{\max} is given by

$$T_{\max} = \frac{2m_e c^2 \beta^2 \gamma^2}{1 + 2\gamma m_e/M + (m_e/M)^2}. \quad (27.4)$$

In older references [2,7] the “low-energy” approximation $T_{\max} = 2m_e c^2 \beta^2 \gamma^2$, valid for $2\gamma m_e/M \ll 1$, is often implicit. For a pion in copper, the error thus introduced into dE/dx is greater than 6% at 100 GeV.

At energies of order 100 GeV, the maximum 4-momentum transfer to the electron can exceed 1 GeV/c, where hadronic structure effects significantly modify the cross sections. This problem has been investigated by J.D. Jackson [8], who concluded that for hadrons (but not for large nuclei) corrections to dE/dx are negligible below energies where radiative effects dominate. While the cross section for rare hard collisions is modified, the average stopping power, dominated by many softer collisions, is almost unchanged.

“The determination of the mean excitation energy is the principal non-trivial task in the evaluation of the Bethe stopping-power formula” [9]. Recommended values have varied substantially with time. Estimates based on experimental

stopping-power measurements for protons, deuterons, and alpha particles and on oscillator-strength distributions and dielectric-response functions were given in ICRU 49 [4]. See also ICRU 37 [10]. These values, shown in Fig. 27.5, have since been widely used. Machine-readable versions can also be found [11]. These values are widely used.

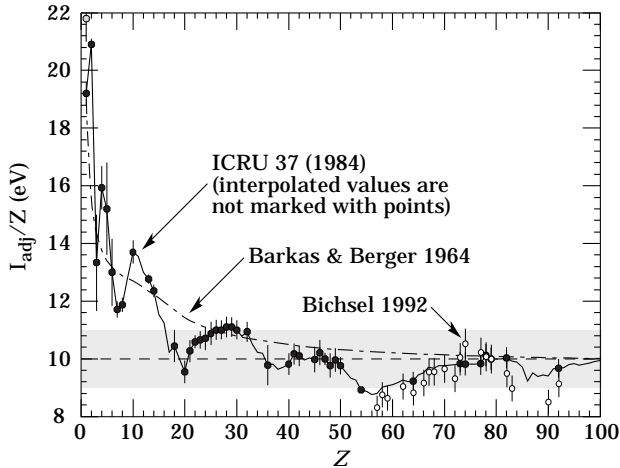


Figure 27.5: Mean excitation energies (divided by Z) as adopted by the ICRU [10]. Those based on experimental measurements are shown by symbols with error flags; the interpolated values are simply joined. The grey point is for liquid H_2 ; the black point at 19.2 eV is for H_2 gas. The open circles show more recent determinations by Bichsel [12]. The dotted curve is from the approximate formula of Barkas [13] used in early editions of this *Review*.

27.2.3. Energy loss at low energies : Shell corrections C/Z must be included in the square brackets of Eq. (27.3) [4,10,12,13] to correct for atomic binding having been neglected in calculating some of the contributions to Eq. (27.3). The Barkas form [13] was used in generating Fig. 27.1. For copper it contributes about 1% at $\beta\gamma = 0.3$ (kinetic energy 6 MeV for a pion), and the correction decreases very rapidly with increasing energy.

Equation 27.2, and therefore Eq. (27.3), are based on a first-order Born approximation. Higher-order corrections, again important only at lower energy, are normally included by adding the “Bloch correction” $z^2 L_2(\beta)$ inside the square brackets (Eq.(2.5) in [4]).

An additional “Barkas correction” $zL_1(\beta)$ makes the stopping power for a negative particle somewhat smaller than for a positive particle with the same mass and velocity. In a 1956 paper, Barkas *et al.* noted that negative pions had a longer range than positive pions [6]. The effect has been measured for a number of negative/positive particle pairs, most recently for antiprotons at the CERN LEAR facility [14].

A detailed discussion of low-energy corrections to the Bethe formula is given in ICRU Report 49 [4]. When the corrections are properly included, the Bethe treatment is accurate to about 1% down to $\beta \approx 0.05$, or about 1 MeV for protons.

For $0.01 < \beta < 0.05$, there is no satisfactory theory. For protons, one usually relies on the phenomenological fitting formulae developed by Andersen and Ziegler [4,15]. For particles moving more slowly than $\approx 0.01c$ (more or less the velocity of the outer atomic electrons), Lindhard has been quite successful in describing electronic stopping power, which is proportional to β [16]. Finally, we note that at even lower energies, *e.g.*, for protons of less than several hundred eV, non-ionizing nuclear recoil energy loss dominates the total energy loss [4,16,17].

As shown in ICRU 49 [4] (using data taken from Ref. 15), the nuclear plus electronic proton stopping power in copper is $113 \text{ MeV cm}^2 \text{ g}^{-1}$ at $T = 10 \text{ keV}$, rises to a maximum of $210 \text{ MeV cm}^2 \text{ g}^{-1}$ at 100–150 keV, then falls to $120 \text{ MeV cm}^2 \text{ g}^{-1}$ at 1 MeV. Above 0.5–1.0 MeV the corrected Bethe theory is adequate.

27.2.4. Density effect : As the particle energy increases, its electric field flattens and extends, so that the distant-collision contribution to Eq. (27.3) increases as $\ln \beta\gamma$. However, real media become polarized, limiting the field extension and effectively truncating this part of the logarithmic rise [2–7,18–20]. At very high energies,

$$\delta/2 \rightarrow \ln(\hbar\omega_p/I) + \ln \beta\gamma - 1/2, \quad (27.5)$$

where $\delta(\beta\gamma)/2$ is the density effect correction introduced in Eq. (27.3) and $\hbar\omega_p$ is the plasma energy defined in Table 27.1. A comparison with Eq. (27.3) shows that $|dE/dx|$ then grows as $\ln \beta\gamma$ rather than $\ln \beta^2\gamma^2$, and that the mean excitation energy I is replaced by the plasma energy $\hbar\omega_p$. The ionization stopping power as calculated with and without the density effect correction is shown in Fig. 27.1. Since the plasma frequency scales as the square root of the electron density, the correction is much larger for a liquid or solid than for a gas, as is illustrated by the examples in Fig. 27.2.

The density effect correction is usually computed using Sternheimer’s parameterization [18]:

$$\delta(\beta\gamma) = \begin{cases} 2(\ln 10)x - \bar{C} & \text{if } x \geq x_1; \\ 2(\ln 10)x - \bar{C} + a(x_1 - x)^k & \text{if } x_0 \leq x < x_1; \\ 0 & \text{if } x < x_0 \text{ (nonconductors);} \\ \delta_0 10^{2(x-x_0)} & \text{if } x < x_0 \text{ (conductors)} \end{cases} \quad (27.6)$$

Here $x = \log_{10} \eta = \log_{10}(p/Mc)$. \bar{C} (the negative of the C used in Ref. 18) is obtained by equating the high-energy case of Eq. (27.6) with the limit given in Eq. (27.5). The other parameters are adjusted to give a best fit to the results of detailed calculations for momenta below $Mc \exp(x_1)$. Parameters for elements and nearly 200 compounds and mixtures of interest are published in a variety of places, notably in Ref. 20. A recipe for finding the coefficients for nontabulated materials is given by Sternheimer and Peierls [21], and is summarized in Ref. 5.

The remaining relativistic rise comes from the $\beta^2\gamma^2$ growth of T_{\max} , which in turn is due to (rare) large energy transfers to a few electrons. When these events are excluded, the energy deposit in an absorbing layer approaches a constant value, the Fermi plateau (see Sec. 27.2.6 below). At extreme energies (*e.g.*, $> 332 \text{ GeV}$ for muons in iron, and at a considerably higher energy for protons in iron), radiative effects are more important than ionization losses. These are especially relevant for high-energy muons, as discussed in Sec. 27.6.

27.2.5. Energetic knock-on electrons (δ rays) : The distribution of secondary electrons with kinetic energies $T \gg I$ is [2]

$$\frac{d^2 N}{dT dx} = \frac{1}{2} K z^2 \frac{Z}{A} \frac{1}{\beta^2} \frac{F(T)}{T^2} \quad (27.7)$$

for $I \ll T \leq T_{\max}$, where T_{\max} is given by Eq. (27.4). Here β is the velocity of the primary particle. The factor F is spin-dependent, but is about unity for $T \ll T_{\max}$. For spin-0 particles $F(T) = (1 - \beta^2 T/T_{\max})$; forms for spins 1/2 and 1 are also given by Rossi [2]. For incident electrons, the indistinguishability of projectile and target means that the range of T extends only to half the kinetic energy of the incident particle. Additional formulae are given in Ref. 22. Equation (27.7) is inaccurate for T close to I .

δ rays of even modest energy are rare. For $\beta \approx 1$ particle, for example, on average only one collision with $T_e > 1 \text{ keV}$ will occur along a path length of 90 cm of Ar gas [1].

A δ ray with kinetic energy T_e and corresponding momentum p_e is produced at an angle θ given by

$$\cos \theta = (T_e/p_e)(p_{\max}/T_{\max}), \quad (27.8)$$

where p_{\max} is the momentum of an electron with the maximum possible energy transfer T_{\max} .

27.2.6. Restricted energy loss rates for relativistic ionizing particles: Further insight can be obtained by examining the mean energy deposit by an ionizing particle when energy transfers are restricted to $T \leq T_{\text{cut}} \leq T_{\max}$. The restricted energy loss rate is

$$-\frac{dE}{dx}\Big|_{T < T_{\text{cut}}} = Kz^2 \frac{Z}{A} \frac{1}{\beta^2} \left[\frac{1}{2} \ln \frac{2m_e c^2 \beta^2 \gamma^2 T_{\text{cut}}}{I^2} - \frac{\beta^2}{2} \left(1 + \frac{T_{\text{cut}}}{T_{\max}} \right) - \frac{\delta}{2} \right]. \quad (27.9)$$

This form approaches the normal Bethe function (Eq. (27.3)) as $T_{\text{cut}} \rightarrow T_{\max}$. It can be verified that the difference between Eq. (27.3) and Eq. (27.9) is equal to $\int_{T_{\text{cut}}}^{T_{\max}} T(d^2N/dTdx)dT$, where $d^2N/dTdx$ is given by Eq. (27.7).

Since T_{cut} replaces T_{\max} in the argument of the logarithmic term of Eq. (27.3), the $\beta\gamma$ term producing the relativistic rise in the close-collision part of dE/dx is replaced by a constant, and $|dE/dx|_{T < T_{\text{cut}}}$ approaches the constant ‘‘Fermi plateau.’’ (The density effect correction δ eliminates the explicit $\beta\gamma$ dependence produced by the distant-collision contribution.) This behavior is illustrated in Fig. 27.6, where restricted loss rates for two examples of T_{cut} are shown in comparison with the full Bethe dE/dx and the Landau-Vavilov most probable energy loss (to be discussed in Sec. 27.2.7 below).

27.2.7. Fluctuations in energy loss: For detectors of moderate thickness x (e.g. scintillators or LAr cells),* the energy loss probability distribution $f(\Delta; \beta\gamma, x)$ is adequately described by the highly-skewed Landau (or Landau-Vavilov) distribution [24,25]. The most probable energy loss is [26]

$$\Delta_p = \xi \left[\ln \frac{2mc^2 \beta^2 \gamma^2}{I} + \ln \frac{\xi}{I} + j - \beta^2 - \delta(\beta\gamma) \right], \quad (27.10)$$

where $\xi = (K/2) \langle Z/A \rangle (x/\beta^2)$ MeV for a detector with a thickness x in g cm^{-2} , and $j = 0.200$ [26].[†] While dE/dx is independent of thickness, Δ_p/x scales as $a \ln x + b$. The density correction $\delta(\beta\gamma)$ was not included in Landau’s or Vavilov’s work, but it was later included by Bichsel [26]. The high-energy behavior of $\delta(\beta\gamma)$ (Eq. (27.5)), is such that

$$\Delta_p \xrightarrow{\beta\gamma \gtrsim 100} \xi \left[\ln \frac{2mc^2 \xi}{(h\omega_p)^2} + j \right]. \quad (27.11)$$

Thus the Landau-Vavilov most probable energy loss, like the restricted energy loss, reaches a Fermi plateau. The Bethe dE/dx and Landau-Vavilov-Bichsel Δ_p/x in silicon are shown as a function of muon energy in Fig. 27.6. The case $x/\rho = 1600 \mu\text{m}$ was chosen since it has about the same stopping power as does 3 mm of plastic scintillator. Folding in experimental resolution displaces the peak of the distribution, usually toward a higher value.

The mean of the energy-loss given by the Bethe equation, Eq. (27.3), is ill-defined experimentally and is not useful for describing energy loss by single particles. (It finds its application in dosimetry, where only bulk deposit is of relevance.) It rises as $\ln \beta\gamma$ because T_{\max} increases as $\beta^2 \gamma^2$. The large single-collision

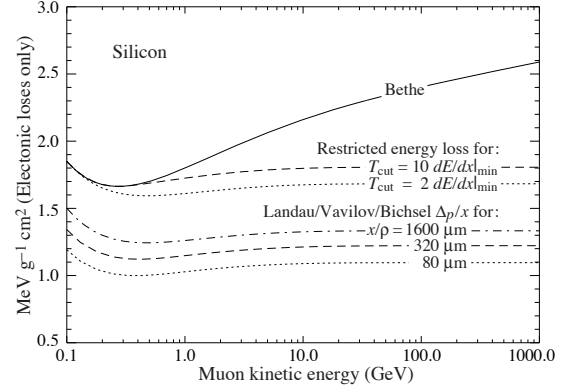


Figure 27.6: Bethe dE/dx , two examples of restricted energy loss, and the Landau most probable energy per unit thickness in silicon. The change of Δ_p/x with thickness x illustrates its $a \ln x + b$ dependence. Minimum ionization ($dE/dx|_{\min}$) is $1.664 \text{ MeV g}^{-1} \text{ cm}^2$. Radiative losses are excluded. The incident particles are muons.

energy transfers that increasingly extend the long tail are rare, making the mean of an experimental distribution consisting of a few hundred events subject to large fluctuations and sensitive to cuts as well as to background. The most probable energy loss should be used.

For very thick absorbers the distribution is less skewed but never approaches a Gaussian. In the case of Si illustrated in Fig. 27.6, the most probable energy loss per unit thickness for $x \approx 35 \text{ g cm}^{-2}$ is very close to the restricted energy loss with $T_{\text{cut}} = 2 dE/dx|_{\min}$.

The Landau distribution fails to describe energy loss in thin absorbers such as gas TPC cells [1] and Si detectors [26], as shown clearly in Fig. 1 of Ref. 1 for an argon-filled TPC cell. Also see Talman [27]. While Δ_p/x may be calculated adequately with Eq. (27.10), the distributions are significantly wider than the Landau width $w = 4\xi$ [Ref. 26, Fig. 15]. Examples for thin silicon detectors are shown in Fig. 27.7.

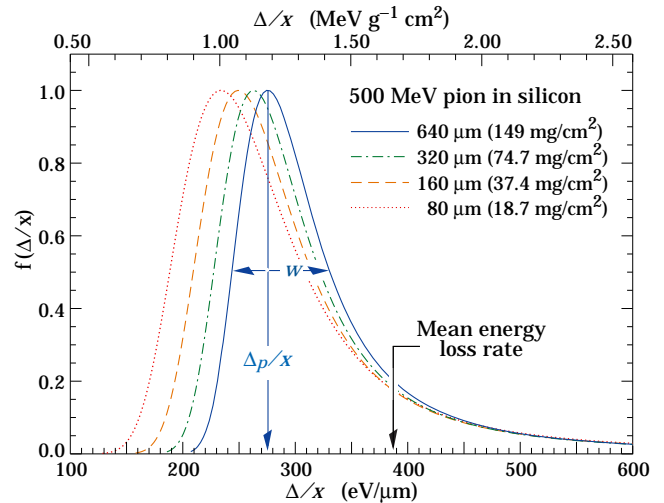


Figure 27.7: Straggling functions in silicon for 500 MeV pions, normalized to unity at the most probable value δ_p/x . The width w is the full width at half maximum.

* $G \lesssim 0.05\text{--}0.1$, where G is given by Rossi [Ref. 2, Eq. 2.7.10]. It is Vavilov’s κ [25].

[†] Rossi [2], Talman [27], and others give somewhat different values for j . The most probable loss is not sensitive to its value.

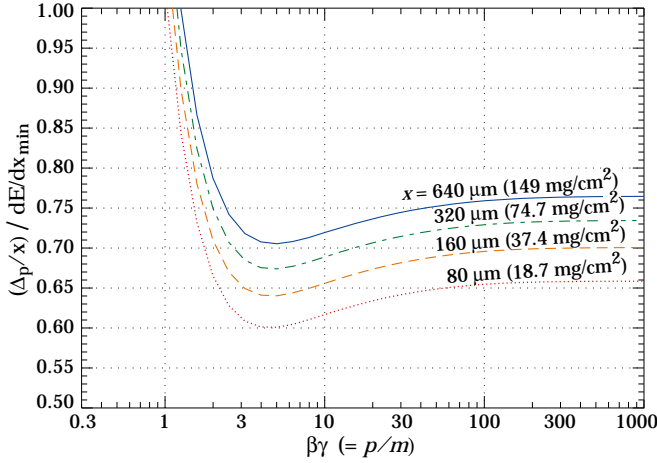


Figure 27.8: Most probable energy loss in silicon, scaled to the mean loss of a minimum ionizing particle, $388 \text{ eV}/\mu\text{m}$ ($1.66 \text{ MeV g}^{-1}\text{cm}^2$).

27.2.8. Energy loss in mixtures and compounds : A mixture or compound can be thought of as made up of thin layers of pure elements in the right proportion (Bragg additivity). In this case,

$$\frac{dE}{dx} = \sum w_j \left. \frac{dE}{dx} \right|_j, \quad (27.12)$$

where $dE/dx|_j$ is the mean rate of energy loss (in MeV g cm^{-2}) in the j th element. Eq. (27.3) can be inserted into Eq. (27.12) to find expressions for $\langle Z/A \rangle$, $\langle I \rangle$, and $\langle \delta \rangle$; for example, $\langle Z/A \rangle = \sum w_j Z_j/A_j = \sum n_j Z_j / \sum n_j A_j$. However, $\langle I \rangle$ as defined this way is an underestimate, because in a compound electrons are more tightly bound than in the free elements, and $\langle \delta \rangle$ as calculated this way has little relevance, because it is the electron density that matters. If possible, one uses the tables given in Refs. 20 and 28, which include effective excitation energies and interpolation coefficients for calculating the density effect correction for the chemical elements and nearly 200 mixtures and compounds. If a compound or mixture is not found, then one uses the recipe for δ given in Ref. 21 (repeated in Ref. 5), and calculates $\langle I \rangle$ according to the discussion in Ref. 9. (Note the “13%” rule!)

27.2.9. Ionization yields : Physicists frequently relate total energy loss to the number of ion pairs produced near the particle’s track. This relation becomes complicated for relativistic particles due to the wandering of energetic knock-on electrons whose ranges exceed the dimensions of the fiducial volume. For a qualitative appraisal of the nonlocality of energy deposition in various media by such modestly energetic knock-on electrons, see Ref. 29. The mean local energy dissipation per local ion pair produced, W , while essentially constant for relativistic particles, increases at slow particle speeds [30]. For gases, W can be surprisingly sensitive to trace amounts of various contaminants [30]. Furthermore, ionization yields in practical cases may be greatly influenced by such factors as subsequent recombination [31].

27.3. Multiple scattering through small angles

A charged particle traversing a medium is deflected by many small-angle scatters. Most of this deflection is due to Coulomb scattering from nuclei, and hence the effect is called multiple Coulomb scattering. (However, for hadronic projectiles, the strong interactions also contribute to multiple scattering.) The Coulomb scattering distribution is well represented by the theory of Molière [33]. It is roughly Gaussian for small deflection angles, but at larger angles (greater than a few θ_0 , defined below)

it behaves like Rutherford scattering, with larger tails than does a Gaussian distribution.

If we define

$$\theta_0 = \theta_{\text{plane}}^{\text{rms}} = \frac{1}{\sqrt{2}} \theta_{\text{space}}^{\text{rms}}. \quad (27.13)$$

then it is sufficient for many applications to use a Gaussian approximation for the central 98% of the projected angular distribution, with a width given by [34,35]

$$\theta_0 = \frac{13.6 \text{ MeV}}{\beta c p} z \sqrt{x/X_0} \left[1 + 0.038 \ln(x/X_0) \right]. \quad (27.14)$$

Here p , βc , and z are the momentum, velocity, and charge number of the incident particle, and x/X_0 is the thickness in radiation lengths (defined below). This value of θ_0 is from a fit to Molière distribution [33] for singly charged particles with $\beta = 1$ for all Z , and is accurate to 11% or better for $10^{-3} < x/X_0 < 100$.

Eq. (27.14) describes scattering from a single material, while the usual problem involves the multiple scattering of a particle traversing many different layers and mixtures. Since it is from a fit to a Molière distribution, it is incorrect to add the individual θ_0 contributions in quadrature; the result is systematically too small. It is much more accurate to apply Eq. (27.14) once, after finding x and X_0 for the combined scatterer.

Lynch and Dahl have extended this phenomenological approach, fitting Gaussian distributions to a variable fraction of the Molière distribution for arbitrary scatterers [35], and achieve accuracies of 2% or better.

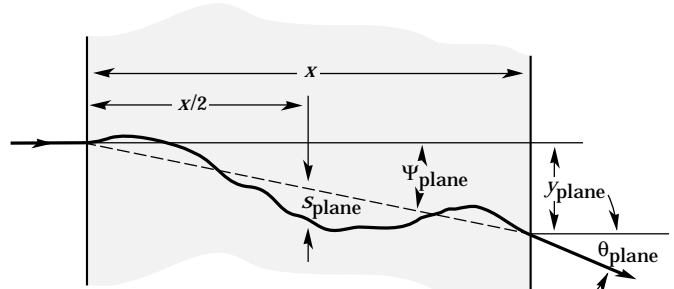


Figure 27.9: Quantities used to describe multiple Coulomb scattering. The particle is incident in the plane of the figure.

The nonprojected (space) and projected (plane) angular distributions are given approximately by [33]

$$\frac{1}{2\pi \theta_0^2} \exp \left(-\frac{\theta_{\text{space}}^2}{2\theta_0^2} \right) d\Omega, \quad (27.15)$$

$$\frac{1}{\sqrt{2\pi} \theta_0} \exp \left(-\frac{\theta_{\text{plane}}^2}{2\theta_0^2} \right) d\theta_{\text{plane}}, \quad (27.16)$$

where θ is the deflection angle. In this approximation, $\theta_{\text{space}}^2 \approx (\theta_{\text{plane},x}^2 + \theta_{\text{plane},y}^2)$, where the x and y axes are orthogonal to the direction of motion, and $d\Omega \approx d\theta_{\text{plane},x} d\theta_{\text{plane},y}$. Deflections into $\theta_{\text{plane},x}$ and $\theta_{\text{plane},y}$ are independent and identically distributed.

Figure 27.9 shows these and other quantities sometimes used to describe multiple Coulomb scattering. They are

$$\psi_{\text{plane}}^{\text{rms}} = \frac{1}{\sqrt{3}} \theta_{\text{plane}}^{\text{rms}} = \frac{1}{\sqrt{3}} \theta_0, \quad (27.17)$$

$$y_{\text{plane}}^{\text{rms}} = \frac{1}{\sqrt{3}} x \theta_{\text{plane}}^{\text{rms}} = \frac{1}{\sqrt{3}} x \theta_0, \quad (27.18)$$

$$s_{\text{plane}}^{\text{rms}} = \frac{1}{4\sqrt{3}} x \theta_{\text{plane}}^{\text{rms}} = \frac{1}{4\sqrt{3}} x \theta_0. \quad (27.19)$$

All the quantitative estimates in this section apply only in the limit of small $\theta_{\text{plane}}^{\text{rms}}$ and in the absence of large-angle scatters.

The random variables s , ψ , y , and θ in a given plane are distributed in a correlated fashion (see Sec. 32.1 of this *Review* for the definition of the correlation coefficient). Obviously, $y \approx x\psi$. In addition, y and θ have the correlation coefficient $\rho_{y\theta} = \sqrt{3}/2 \approx 0.87$. For Monte Carlo generation of a joint $(y_{\text{plane}}, \theta_{\text{plane}})$ distribution, or for other calculations, it may be most convenient to work with independent Gaussian random variables (z_1, z_2) with mean zero and variance one, and then set

$$\begin{aligned} y_{\text{plane}} &= z_1 x \theta_0 (1 - \rho_{y\theta}^2)^{1/2} / \sqrt{3} + z_2 \rho_{y\theta} x \theta_0 / \sqrt{3} \\ &= z_1 x \theta_0 / \sqrt{12} + z_2 x \theta_0 / 2 ; \end{aligned} \quad (27.20)$$

$$\theta_{\text{plane}} = z_2 \theta_0 . \quad (27.21)$$

Note that the second term for y_{plane} equals $x \theta_{\text{plane}}/2$ and represents the displacement that would have occurred had the deflection θ_{plane} all occurred at the single point $x/2$.

For heavy ions the multiple Coulomb scattering has been measured and compared with various theoretical distributions [36].

27.4. Photon and electron interactions in matter

27.4.1. Radiation length: High-energy electrons predominantly lose energy in matter by bremsstrahlung, and high-energy photons by e^+e^- pair production. The characteristic amount of matter traversed for these related interactions is called the radiation length X_0 , usually measured in g cm^{-2} . It is both (a) the mean distance over which a high-energy electron loses all but $1/e$ of its energy by bremsstrahlung, and (b) $\frac{7}{9}$ of the mean free path for pair production by a high-energy photon [37]. It is also the appropriate scale length for describing high-energy electromagnetic cascades. X_0 has been calculated and tabulated by Y.S. Tsai [38]:

$$\frac{1}{X_0} = 4\alpha r_e^2 \frac{N_A}{A} \left\{ Z^2 [L_{\text{rad}} - f(Z)] + Z L'_{\text{rad}} \right\} . \quad (27.22)$$

For $A = 1 \text{ g mol}^{-1}$, $4\alpha r_e^2 N_A/A = (716.408 \text{ g cm}^{-2})^{-1}$. L_{rad} and L'_{rad} are given in Table 27.2. The function $f(Z)$ is an infinite sum, but for elements up to uranium can be represented to 4-place accuracy by

$$\begin{aligned} f(Z) &= a^2[(1 + a^2)^{-1} + 0.20206 \\ &\quad - 0.0369 a^2 + 0.0083 a^4 - 0.002 a^6] , \end{aligned} \quad (27.23)$$

where $a = \alpha Z$ [39].

Table 27.2: Tsai's L_{rad} and L'_{rad} , for use in calculating the radiation length in an element using Eq. (27.22).

Element	Z	L_{rad}	L'_{rad}
H	1	5.31	6.144
He	2	4.79	5.621
Li	3	4.74	5.805
Be	4	4.71	5.924
Others	> 4	$\ln(184.15 Z^{-1/3})$	$\ln(1194 Z^{-2/3})$

Although it is easy to use Eq. (27.22) to calculate X_0 , the functional dependence on Z is somewhat hidden. Dahl provides a compact fit to the data [40]:

$$X_0 = \frac{716.4 \text{ g cm}^{-2} A}{Z(Z+1) \ln(287/\sqrt{Z})} . \quad (27.24)$$

Results using this formula agree with Tsai's values to better than 2.5% for all elements except helium, where the result is about 5% low.

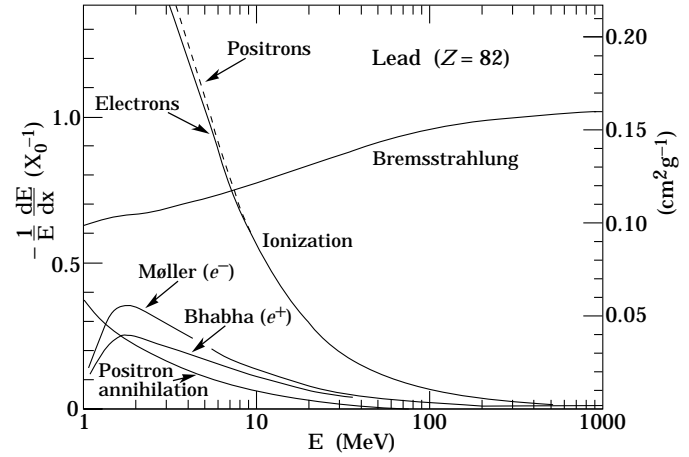


Figure 27.10: Fractional energy loss per radiation length in lead as a function of electron or positron energy. Electron (positron) scattering is considered as ionization when the energy loss per collision is below 0.255 MeV, and as Møller (Bhabha) scattering when it is above. Adapted from Fig. 3.2 from Messel and Crawford, *Electron-Photon Shower Distribution Function Tables for Lead, Copper, and Air Absorbers*, Pergamon Press, 1970. Messel and Crawford use $X_0(\text{Pb}) = 5.82 \text{ g cm}^{-2}$, but we have modified the figures to reflect the value given in the Table of Atomic and Nuclear Properties of Materials ($X_0(\text{Pb}) = 6.37 \text{ g cm}^{-2}$).

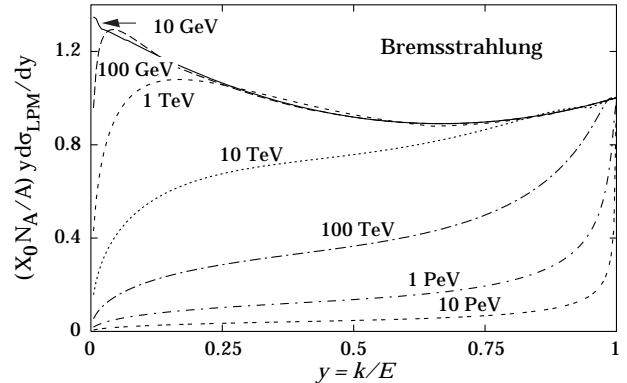


Figure 27.11: The normalized bremsstrahlung cross section $k d\sigma_{\text{LPM}}/dk$ in lead versus the fractional photon energy $y = k/E$. The vertical axis has units of photons per radiation length.

The radiation length in a mixture or compound may be approximated by

$$1/X_0 = \sum w_j/X_j , \quad (27.25)$$

where w_j and X_j are the fraction by weight and the radiation length for the j th element.

27.4.2. Energy loss by electrons: At low energies electrons and positrons primarily lose energy by ionization, although other processes (Møller scattering, Bhabha scattering, e^+ annihilation) contribute, as shown in Fig. 27.10. While ionization loss rates rise logarithmically with energy, bremsstrahlung losses rise nearly linearly (fractional loss is nearly independent of energy), and dominates above a few tens of MeV in most materials

Ionization loss by electrons and positrons differs from loss by heavy particles because of the kinematics, spin, and the identity of the incident electron with the electrons which it ionizes. Complete discussions and tables can be found in Refs. 9, 10, and 28.

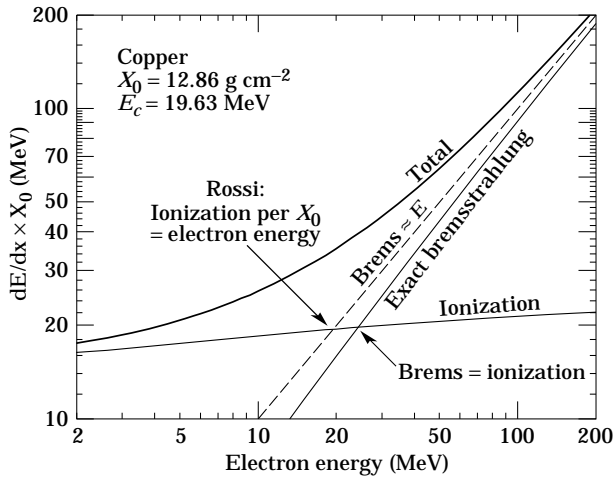


Figure 27.12: Two definitions of the critical energy E_c .

At very high energies and except at the high-energy tip of the bremsstrahlung spectrum, the cross section can be approximated in the “complete screening case” as [38]

$$d\sigma/dk = (1/k)4\alpha r_e^2 \left\{ \left(\frac{4}{3} - \frac{4}{3}y + y^2 \right) [Z^2(L_{\text{rad}} - f(Z)) + ZL'_{\text{rad}}] + \frac{1}{9}(1-y)(Z^2 + Z) \right\}, \quad (27.26)$$

where $y = k/E$ is the fraction of the electron’s energy transferred to the radiated photon. At small y (the “infrared limit”) the term on the second line ranges from 1.7% (low Z) to 2.5% (high Z) of the total. If it is ignored and the first line simplified with the definition of X_0 given in Eq. (27.22), we have

$$\frac{d\sigma}{dk} = \frac{A}{X_0 N_A k} \left(\frac{4}{3} - \frac{4}{3}y + y^2 \right). \quad (27.27)$$

This cross section (times k) is shown by the top curve in Fig. 27.11.

This formula is accurate except in near $y = 1$, where screening may become incomplete, and near $y = 0$, where the infrared divergence is removed by the interference of bremsstrahlung amplitudes from nearby scattering centers (the LPM effect) [41,42] and dielectric suppression [43,44]. These and other suppression effects in bulk media are discussed in Sec. 27.4.5.

With decreasing energy ($E \lesssim 10$ GeV) the high- y cross section drops and the curves become rounded as $y \rightarrow 1$. Curves of this familiar shape can be seen in Rossi [2] (Figs. 2.11.2,3); see also the review by Koch & Motz [45].

Except at these extremes, and still in the complete-screening approximation, the number of photons with energies between k_{min} and k_{max} emitted by an electron travelling a distance $d \ll X_0$ is

$$N_\gamma = \frac{d}{X_0} \left[\frac{4}{3} \ln \left(\frac{k_{\text{max}}}{k_{\text{min}}} \right) - \frac{4(k_{\text{max}} - k_{\text{min}})}{3E} + \frac{k_{\text{max}}^2 - k_{\text{min}}^2}{2E^2} \right]. \quad (27.28)$$

We obtain

$$E_c = \frac{610 \text{ MeV}}{Z + 1.24} \quad (\text{solids and liquids}), \quad = \frac{710 \text{ MeV}}{Z + 0.92} \quad (\text{gases}).$$

Data from [49]; parameters for $\sigma_{\text{g.d.r.}}$ from [50]. Curves for these and other elements, compounds, and mixtures may be obtained from <http://physics.nist.gov/PhysRefData>. The photon total cross section is approximately flat for at least two decades beyond the energy range shown. Original figures courtesy J.H. Hubbell (NIST).

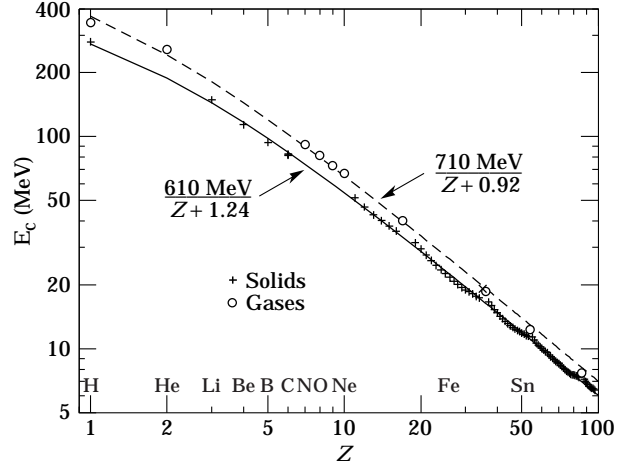


Figure 27.13: Electron critical energy for the chemical elements, using Rossi’s definition [2]. The fits shown are for solids and liquids (solid line) and gases (dashed line). The rms deviation is 2.2% for the solids and 4.0% for the gases. (Computed with code supplied by A. Fassó.)

27.4.3. Critical energy : An electron loses energy by bremsstrahlung at a rate nearly proportional to its energy, while the ionization loss rate varies only logarithmically with the electron energy. The *critical energy* E_c is sometimes defined as the energy at which the two loss rates are equal [46]. Berger and Seltzer [46] also give the approximation $E_c = (800 \text{ MeV})/(Z + 1.2)$. This formula has been widely quoted, and has been given in older editions of this *Review* [47]. Among alternate definitions is that of Rossi [2], who defines the critical energy as the energy at which the ionization loss per radiation length is equal to the electron energy. Equivalently, it is the same as the first definition with the approximation $|dE/dx|_{\text{brems}} \approx E/X_0$. This form has been found to describe transverse electromagnetic shower development more accurately (see below). These definitions are illustrated in the case of copper in Fig. 27.12.

The accuracy of approximate forms for E_c has been limited by the failure to distinguish between gases and solid or liquids, where there is a substantial difference in ionization at the relevant energy because of the density effect. We distinguish these two cases in Fig. 27.13. Fits were also made with functions of the form $a/(Z + b)^\alpha$, but α was found to be essentially unity. Since E_c also depends on A , I , and other factors, such forms are at best approximate.

27.4.4. Energy loss by photons : Contributions to the photon cross section in a light element (carbon) and a heavy element (lead) are shown in Fig. 27.14. At low energies it is seen that the photoelectric effect dominates, although Compton scattering, Rayleigh scattering, and photonuclear absorption also contribute. The photoelectric cross section is characterized by discontinuities (absorption edges) as thresholds for photoionization of various atomic levels are reached. Photon attenuation lengths for a variety of elements are shown in Fig. 27.16, and data for $30 \text{ eV} < k < 100 \text{ GeV}$ for all elements is available from the web pages given in the caption. Here k is the photon energy.

The increasing domination of pair production as the energy increases is shown in Fig. 27.17. Using approximations similar to those used to obtain Eq. (27.27), Tsai’s formula for the differential cross section [38] reduces to

$$\frac{d\sigma}{dx} = \frac{A}{X_0 N_A} \left[1 - \frac{4}{3}x(1-x) \right] \quad (27.29)$$

in the complete-screening limit valid at high energies. Here $x = E/k$ is the fractional energy transfer to the pair-produced

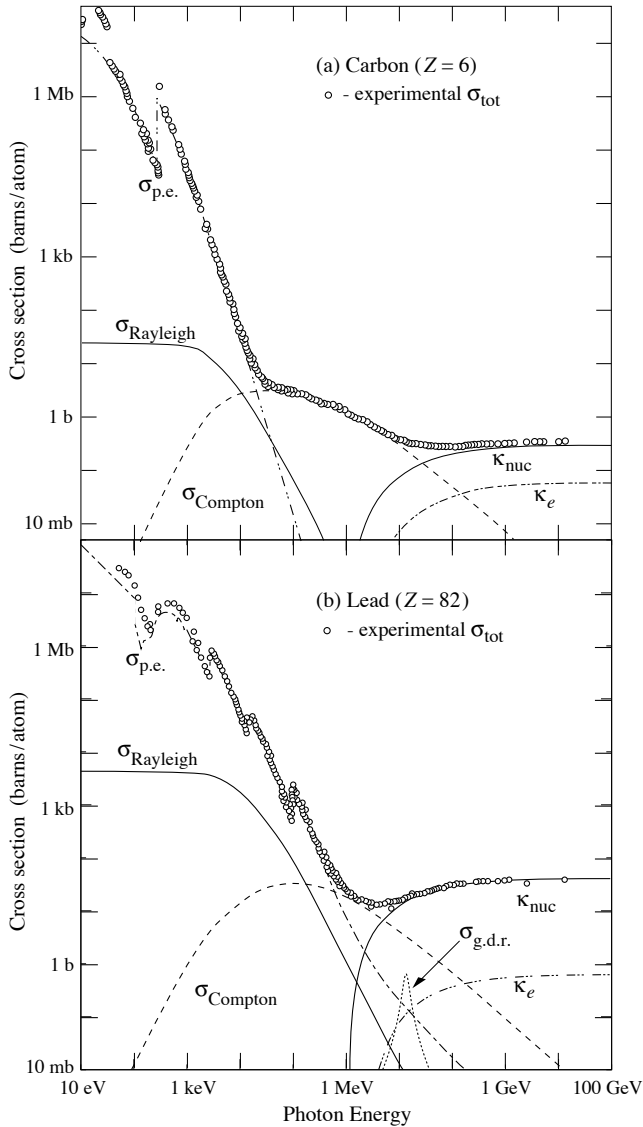


Figure 27.14: Photon total cross sections as a function of energy in carbon and lead, showing the contributions of different processes:

- $\sigma_{p.e.}$ = Atomic photoelectric effect (electron ejection, photon absorption)
- σ_{Rayleigh} = Rayleigh (coherent) scattering—atom neither ionized nor excited
- σ_{Compton} = Incoherent scattering (Compton scattering off an electron)
- κ_{nuc} = Pair production, nuclear field
- κ_e = Pair production, electron field
- $\sigma_{g.d.r.}$ = Photonuclear interactions, most notably the Giant Dipole Resonance [48]. In these interactions, the target nucleus is broken up.

electron (or positron), and k is the incident photon energy. The cross section is very closely related to that for bremsstrahlung, since the Feynman diagrams are variants of one another. The cross section is of necessity symmetric between x and $1 - x$, as can be seen by the solid curve in Fig. 27.15. See the review by Motz, Olsen, & Koch for a more detailed treatment [51].

Eq. (27.29) may be integrated to find the high-energy limit for the total e^+e^- pair-production cross section:

$$\sigma = \frac{7}{9}(A/X_0 N_A) . \quad (27.30)$$

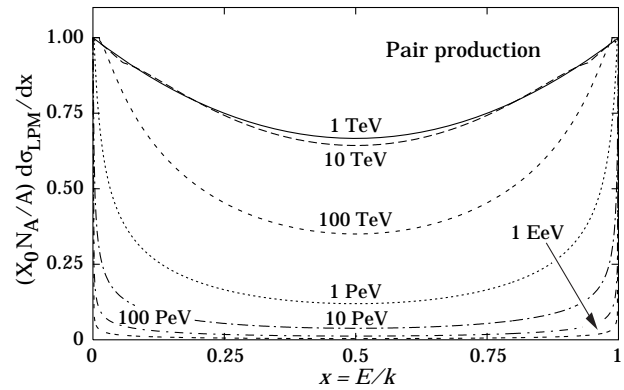


Figure 27.15: The normalized pair production cross section $d\sigma_{LPM}/dy$, versus fractional electron energy $x = E/k$.

Equation Eq. (27.30) is accurate to within a few percent down to energies as low as 1 GeV, particularly for high- Z materials.

27.4.5. Bremsstrahlung and pair production at very high energies : At ultrahigh energies, Eqns. 27.26–27.30 will fail because of quantum mechanical interference between amplitudes from different scattering centers. Since the longitudinal momentum transfer to a given center is small ($\propto k/E(E - k)$, in the case of bremsstrahlung), the interaction is spread over a comparatively long distance called the formation length ($\propto E(E - k)/k$) via the uncertainty principle. In alternate language, the formation length is the distance over which the highly relativistic electron and the photon “split apart.” The interference is usually destructive. Calculations of the “Landau-Pomeranchuk-Migdal” (LPM) effect may be made semi-classically based on the average multiple scattering, or more rigorously using a quantum transport approach [41,42].

In amorphous media, bremsstrahlung is suppressed if the photon energy k is less than $E^2/(E + E_{LPM})$ [42], where*

$$E_{LPM} = \frac{(m_e c^2)^2 \alpha X_0}{4\pi \hbar c \rho} = (7.7 \text{ TeV/cm}) \times \frac{X_0}{\rho} . \quad (27.31)$$

Since physical distances are involved, X_0/ρ , in cm, appears. The energy-weighted bremsstrahlung spectrum for lead, $k d\sigma_{LPM}/dk$, is shown in Fig. 27.11. With appropriate scaling by X_0/ρ , other materials behave similarly.

For photons, pair production is reduced for $E(k - E) > k E_{LPM}$. The pair-production cross sections for different photon energies are shown in Fig. 27.15.

If $k \ll E$, several additional mechanisms can also produce suppression. When the formation length is long, even weak factors can perturb the interaction. For example, the emitted photon can coherently forward scatter off of the electrons in the media. Because of this, for $k < \omega_p E/m_e \sim 10^{-4}$, bremsstrahlung is suppressed by a factor $(k m_e / \omega_p E)^2$ [44]. Magnetic fields can also suppress bremsstrahlung.

In crystalline media, the situation is more complicated, with coherent enhancement or suppression possible. The cross section depends on the electron and photon energies and the angles between the particle direction and the crystalline axes [53].

* This definition differs from that of Ref. 52 by a factor of two. E_{LPM} scales as the 4th power of the mass of the incident particle, so that $E_{LPM} = (1.4 \times 10^{10} \text{ TeV/cm}) \times X_0/\rho$ for a muon.

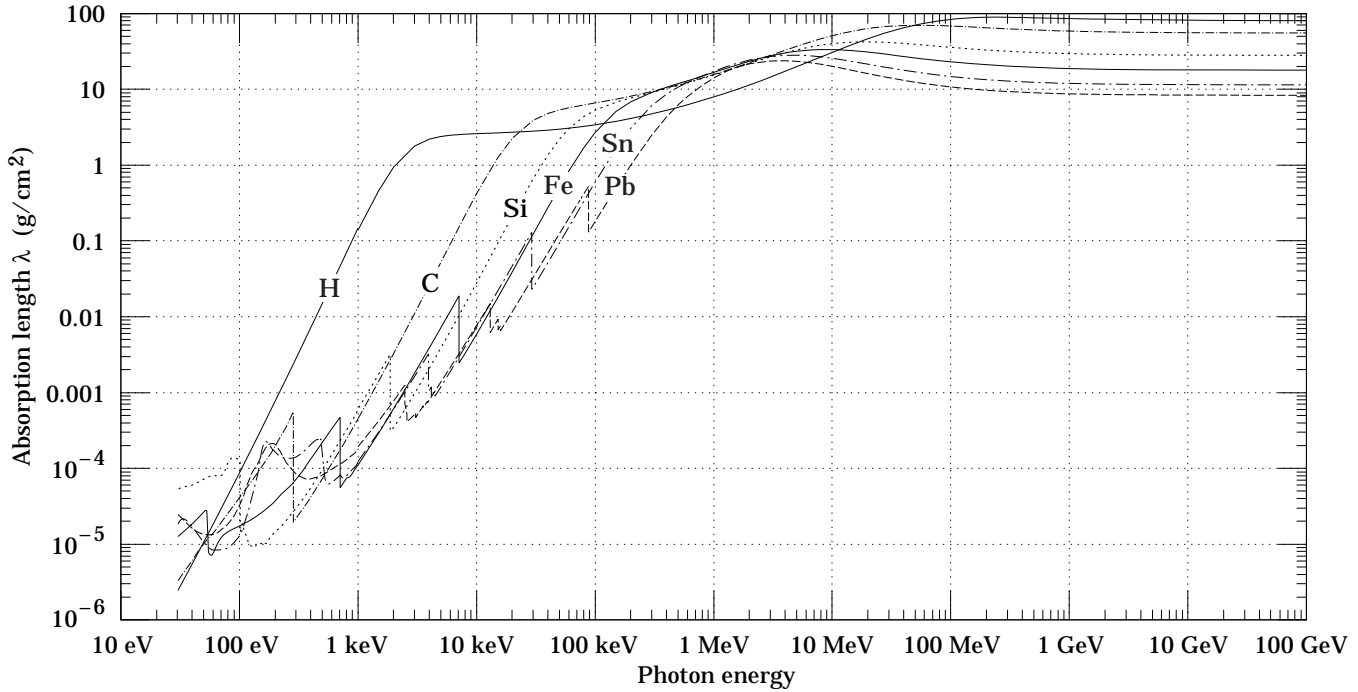


Fig. 27.16: The photon mass attenuation length (or mean free path) $\lambda = 1/(\mu/\rho)$ for various elemental absorbers as a function of photon energy. The mass attenuation coefficient is μ/ρ , where ρ is the density. The intensity I remaining after traversal of thickness t (in mass/unit area) is given by $I = I_0 \exp(-t/\lambda)$. The accuracy is a few percent. For a chemical compound or mixture, $1/\lambda_{\text{eff}} \approx \sum_{\text{elements}} w_Z/\lambda_Z$, where w_Z is the proportion by weight of the element with atomic number Z . The processes responsible for attenuation are given in Fig. 27.10. Since coherent processes are included, not all these processes result in energy deposition. The data for $30 \text{ eV} < E < 1 \text{ keV}$ are obtained from http://www-cxro.lbl.gov/optical_constants (courtesy of Eric M. Gullikson, LBNL). The data for $1 \text{ keV} < E < 100 \text{ GeV}$ are from <http://physics.nist.gov/PhysRefData>, through the courtesy of John H. Hubbell (NIST).

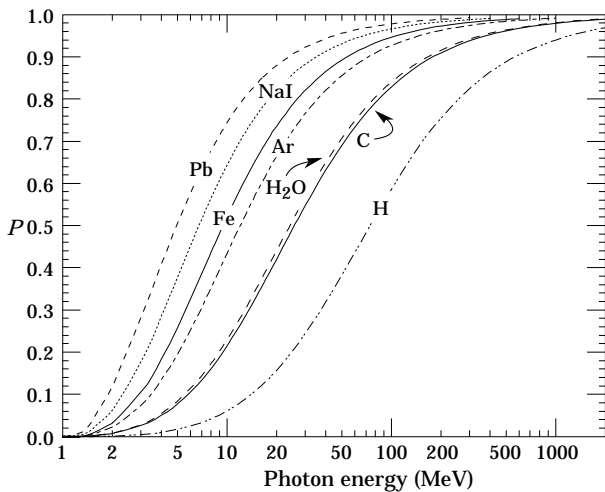


Figure 27.17: Probability P that a photon interaction will result in conversion to an e^+e^- pair. Except for a few-percent contribution from photonuclear absorption around 10 or 20 MeV, essentially all other interactions in this energy range result in Compton scattering off an atomic electron. For a photon attenuation length λ (Fig. 27.16), the probability that a given photon will produce an electron pair (without first Compton scattering) in thickness t of absorber is $P[1 - \exp(-t/\lambda)]$.

27.4.6. Photonuclear and electronuclear interactions at still higher energies :

At very high photon and electron energies, where the bremsstrahlung and pair production cross-sections are heavily suppressed by the LPM effect, photonuclear and electronuclear interactions predominate over electromagnetic interactions. At photon energies above about 10^{20} eV , for example, photons usually interact hadronically. The exact cross-over energy depends on the model used for the photonuclear interactions. At still higher energies ($\gtrsim 10^{23} \text{ eV}$), photonuclear interactions can become coherent, with the photon interaction spread over multiple nuclei. Essentially, the photon coherently converts to a ρ^0 , in a process that is somewhat similar to kaon regeneration [54].

27.5. Electromagnetic cascades

When a high-energy electron or photon is incident on a thick absorber, it initiates an electromagnetic cascade as pair production and bremsstrahlung generate more electrons and photons with lower energy. The longitudinal development is governed by the high-energy part of the cascade, and therefore scales as the radiation length in the material. Electron energies eventually fall below the critical energy, and then dissipate their energy by ionization and excitation rather than by the generation of more shower particles. In describing shower behavior, it is therefore convenient to introduce the scale variables

$$t = x/X_0, \quad y = E/E_c, \quad (27.32)$$

so that distance is measured in units of radiation length and energy in units of critical energy.

Longitudinal profiles from an EGS4 [55] simulation of a 30 GeV electron-induced cascade in iron are shown in Fig. 27.18. The number of particles crossing a plane (very close to Rossi's

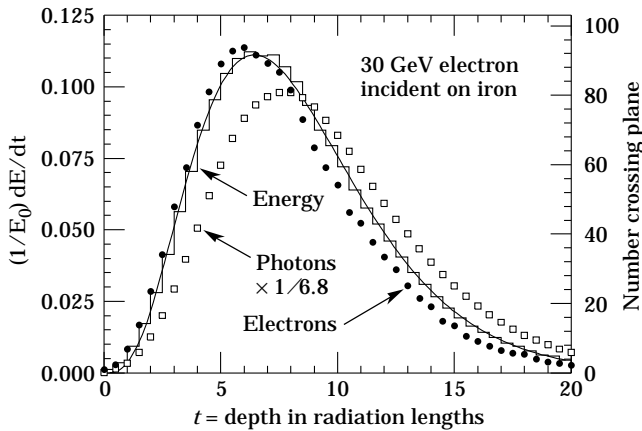


Figure 27.18: An EGS4 simulation of a 30 GeV electron-induced cascade in iron. The histogram shows fractional energy deposition per radiation length, and the curve is a gamma-function fit to the distribution. Circles indicate the number of electrons with total energy greater than 1.5 MeV crossing planes at $X_0/2$ intervals (scale on right) and the squares the number of photons with $E \geq 1.5$ MeV crossing the planes (scaled down to have same area as the electron distribution).

Π function [2]) is sensitive to the cutoff energy, here chosen as a total energy of 1.5 MeV for both electrons and photons. The electron number falls off more quickly than energy deposition. This is because, with increasing depth, a larger fraction of the cascade energy is carried by photons. Exactly what a calorimeter measures depends on the device, but it is not likely to be exactly any of the profiles shown. In gas counters it may be very close to the electron number, but in glass Cherenkov detectors and other devices with “thick” sensitive regions it is closer to the energy deposition (total track length). In such detectors the signal is proportional to the “detectable” track length T_d , which is in general less than the total track length T . Practical devices are sensitive to electrons with energy above some detection threshold E_d , and $T_d = T F(E_d/E_c)$. An analytic form for $F(E_d/E_c)$ obtained by Rossi [2] is given by Fabjan [56]; see also Amaldi [57].

The mean longitudinal profile of the energy deposition in an electromagnetic cascade is reasonably well described by a gamma distribution [58]:

$$\frac{dE}{dt} = E_0 b \frac{(bt)^{a-1} e^{-bt}}{\Gamma(a)} \quad (27.33)$$

The maximum t_{\max} occurs at $(a-1)/b$. We have made fits to shower profiles in elements ranging from carbon to uranium, at energies from 1 GeV to 100 GeV. The energy deposition profiles are well described by Eq. (27.33) with

$$t_{\max} = (a-1)/b = 1.0 \times (\ln y + C_j), \quad j = e, \gamma, \quad (27.34)$$

where $C_e = -0.5$ for electron-induced cascades and $C_\gamma = +0.5$ for photon-induced cascades. To use Eq. (27.33), one finds $(a-1)/b$ from Eq. (27.34) and Eq. (27.32), then finds a either by assuming $b \approx 0.5$ or by finding a more accurate value from Fig. 27.19. The results are very similar for the electron number profiles, but there is some dependence on the atomic number of the medium. A similar form for the electron number maximum was obtained by Rossi in the context of his “Approximation B,” [2] (see Fabjan’s review in Ref. 56), but with $C_e = -1.0$ and $C_\gamma = -0.5$; we regard this as superseded by the EGS4 result.

The “shower length” $X_s = X_0/b$ is less conveniently parameterized, since b depends upon both Z and incident energy, as

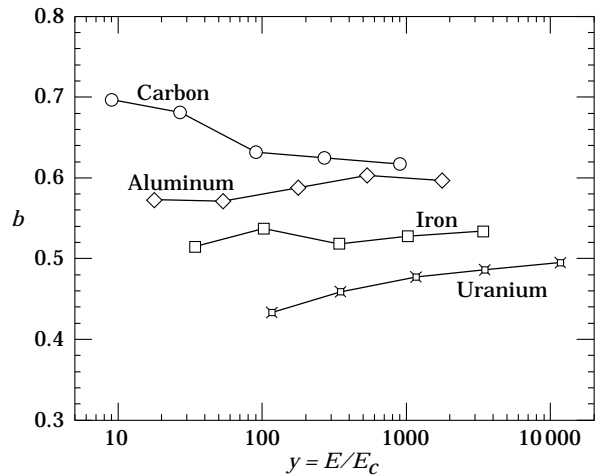


Figure 27.19: Fitted values of the scale factor b for energy deposition profiles obtained with EGS4 for a variety of elements for incident electrons with $1 \leq E_0 \leq 100$ GeV. Values obtained for incident photons are essentially the same.

shown in Fig. 27.19. As a corollary of this Z dependence, the number of electrons crossing a plane near shower maximum is underestimated using Rossi’s approximation and seriously overestimated for carbon and seriously underestimated for uranium. Essentially the same b values are obtained for incident electrons and photons. For many purposes it is sufficient to take $b \approx 0.5$.

The gamma function distribution is very flat near the origin, while the EGS4 cascade (or a real cascade) increases more rapidly. As a result Eq. (27.33) fails badly for about the first two radiation lengths; it was necessary to exclude this region in making fits.

Because fluctuations are important, Eq. (27.33) should be used only in applications where average behavior is adequate. Grindhammer *et al.* have developed fast simulation algorithms in which the variance and correlation of a and b are obtained by fitting Eq. (27.33) to individually simulated cascades, then generating profiles for cascades using a and b chosen from the correlated distributions [59].

The transverse development of electromagnetic showers in different materials scales fairly accurately with the *Molière radius* R_M , given by [60,61]

$$R_M = X_0 E_s / E_c, \quad (27.35)$$

where $E_s \approx 21$ MeV (Table 27.1), and the Rossi definition of E_c is used.

In a material containing a weight fraction w_j of the element with critical energy E_{cj} and radiation length X_j , the Molière radius is given by

$$\frac{1}{R_M} = \frac{1}{E_s} \sum \frac{w_j E_{cj}}{X_j}. \quad (27.36)$$

Measurements of the lateral distribution in electromagnetic cascades are shown in Refs. 60 and 61. On the average, only 10% of the energy lies outside the cylinder with radius R_M . About 99% is contained inside of $3.5R_M$, but at this radius and beyond composition effects become important and the scaling with R_M fails. The distributions are characterized by a narrow core, and broaden as the shower develops. They are often represented as the sum of two Gaussians, and Grindhammer [59] describes them with the function

$$f(r) = \frac{2r R^2}{(r^2 + R^2)^2}, \quad (27.37)$$

where R is a phenomenological function of x/X_0 and $\ln E$.

At high enough energies, the LPM effect (Sec. 27.4.5) reduces the cross sections for bremsstrahlung and pair production, and hence can cause significant elongation of electromagnetic cascades [42].

27.6. Muon energy loss at high energy

At sufficiently high energies, radiative processes become more important than ionization for all charged particles. For muons and pions in materials such as iron, this “critical energy” occurs at several hundred GeV. (There is no simple scaling with particle mass, but for protons the “critical energy” is much, much higher.) Radiative effects dominate the energy loss of energetic muons found in cosmic rays or produced at the newest accelerators. These processes are characterized by small cross sections, hard spectra, large energy fluctuations, and the associated generation of electromagnetic and (in the case of photonuclear interactions) hadronic showers [62–70]. As a consequence, at these energies the treatment of energy loss as a uniform and continuous process is for many purposes inadequate.

It is convenient to write the average rate of muon energy loss as [71]

$$-dE/dx = a(E) + b(E)E. \quad (27.38)$$

Here $a(E)$ is the ionization energy loss given by Eq. (27.3), and $b(E)$ is the sum of e^+e^- pair production, bremsstrahlung, and photonuclear contributions. To the approximation that these slowly-varying functions are constant, the mean range x_0 of a muon with initial energy E_0 is given by

$$x_0 \approx (1/b) \ln(1 + E_0/E_{\mu c}), \quad (27.39)$$

where $E_{\mu c} = a/b$. Figure 27.20 shows contributions to $b(E)$ for iron. Since $a(E) \approx 0.002 \text{ GeV g}^{-1} \text{ cm}^2$, $b(E)E$ dominates the energy loss above several hundred GeV, where $b(E)$ is nearly constant. The rates of energy loss for muons in hydrogen, uranium, and iron are shown in Fig. 27.21 [5].

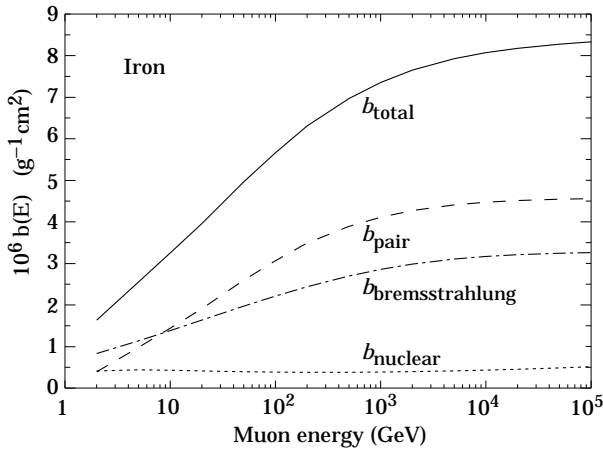


Figure 27.20: Contributions to the fractional energy loss by muons in iron due to e^+e^- pair production, bremsstrahlung, and photonuclear interactions, as obtained from Groom *et al.* [5] except for post-Born corrections to the cross section for direct pair production from atomic electrons.

The “muon critical energy” $E_{\mu c}$ can be defined more exactly as the energy at which radiative and ionization losses are equal, and can be found by solving $E_{\mu c} = a(E_{\mu c})/b(E_{\mu c})$. This definition corresponds to the solid-line intersection in Fig. 27.12, and is different from the Rossi definition we used for electrons. It serves the same function: below $E_{\mu c}$ ionization losses dominate, and above $E_{\mu c}$ radiative effects dominate. The dependence of $E_{\mu c}$ on atomic number Z is shown in Fig. 27.22.

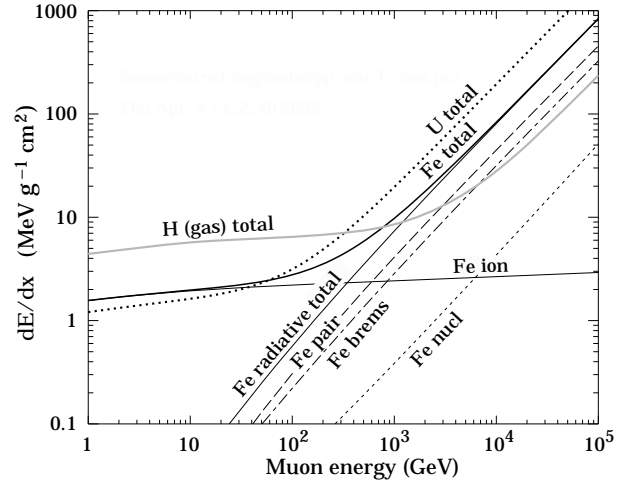


Figure 27.21: The average energy loss of a muon in hydrogen, iron, and uranium as a function of muon energy. Contributions to dE/dx in iron from ionization and the processes shown in Fig. 27.20 are also shown.

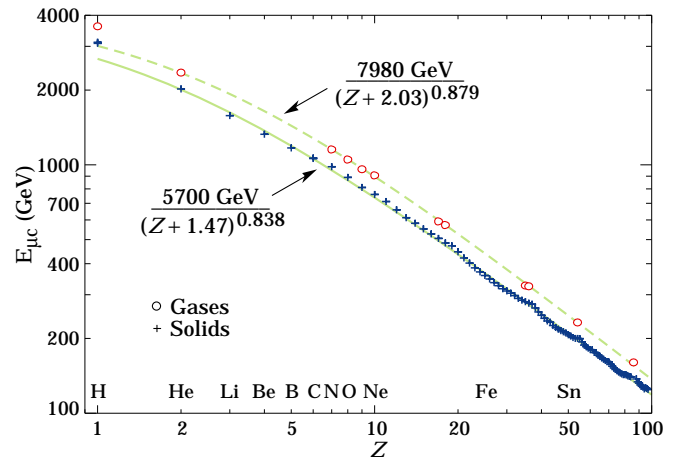


Figure 27.22: Muon critical energy for the chemical elements, defined as the energy at which radiative and ionization energy loss rates are equal [5]. The equality comes at a higher energy for gases than for solids or liquids with the same atomic number because of a smaller density effect reduction of the ionization losses. The fits shown in the figure exclude hydrogen. Alkali metals fall 3–4% above the fitted function, while most other solids are within 2% of the function. Among the gases the worst fit is for radon (2.7% high).

The radiative cross sections are expressed as functions of the fractional energy loss ν . The bremsstrahlung cross section goes roughly as $1/\nu$ over most of the range, while for the pair production case the distribution goes as ν^{-3} to ν^{-2} [72]. “Hard” losses are therefore more probable in bremsstrahlung, and in fact energy losses due to pair production may very nearly be treated as continuous. The simulated [70] momentum distribution of an incident 1 TeV/c muon beam after it crosses 3 m of iron is shown in Fig. 27.23. The most probable loss is 8 GeV, or $3.4 \text{ MeV g}^{-1} \text{ cm}^2$. The full width at half maximum is 9 GeV/c, or 0.9%. The radiative tail is almost entirely due to bremsstrahlung, although most of the events in which more than 10% of the incident energy lost experienced relatively hard photonuclear interactions. The latter can exceed detector resolution [73], necessitating the reconstruction of lost energy.

Tables [5] list the stopping power as $9.82 \text{ MeV g}^{-1}\text{cm}^2$ for a 1 TeV muon, so that the mean loss should be 23 GeV ($\approx 23 \text{ GeV}/c$), for a final momentum of $977 \text{ GeV}/c$, far below the peak. This agrees with the indicated mean calculated from the simulation. Electromagnetic and hadronic cascades in detector materials can obscure muon tracks in detector planes and reduce tracking efficiency [74].

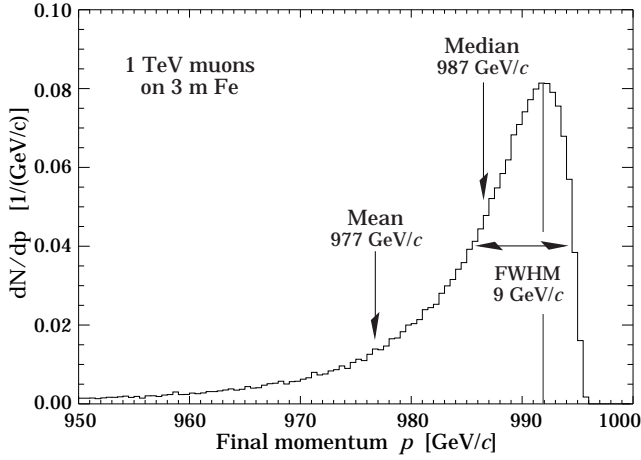


Figure 27.23: The momentum distribution of 1 TeV/ c muons after traversing 3 m of iron as calculated with the MARS15 Monte Carlo code [70] by S.I. Striganov [5].

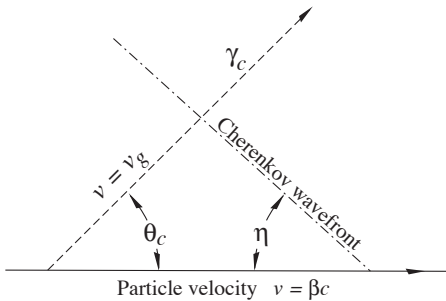


Figure 27.24: Cherenkov light emission and wavefront angles. In a dispersive medium, $\theta_c + \eta \neq 90^\circ$.

27.7. Cherenkov and transition radiation [75,76,32]

A charged particle radiates if its velocity is greater than the local phase velocity of light (Cherenkov radiation) or if it crosses suddenly from one medium to another with different optical properties (transition radiation). Neither process is important for energy loss, but both are used in high-energy physics detectors.

Cherenkov Radiation. The angle θ_c of Cherenkov radiation, relative to the particle's direction, for a particle with velocity βc in a medium with index of refraction n is

$$\begin{aligned} \cos \theta_c &= (1/n\beta) \\ \text{or } \tan \theta_c &= \sqrt{\beta^2 n^2 - 1} \\ &\approx \sqrt{2(1 - 1/n\beta)} \quad \text{for small } \theta_c, \text{ e.g. in gas} \end{aligned} \quad (27.40)$$

The threshold velocity β_t is $1/n$, and $\gamma_t = 1/(1 - \beta_t^2)^{1/2}$. Therefore, $\beta_t \gamma_t = 1/(2\delta + \delta^2)^{1/2}$, where $\delta = n - 1$. Values of δ for various commonly used gases are given as a function of pressure and wavelength in Ref. 77. For values at atmospheric pressure, see Table 6.1. Data for other commonly used materials are given in Ref. 78.

Practical Cherenkov radiator materials are dispersive. Let ω be the photon's frequency, and let $k = 2\pi/\lambda$ be its wavenumber. The photons propagate at the group velocity $v_g = d\omega/dk = c/[n(\omega) + \omega(dn/d\omega)]$. In a non-dispersive medium, this simplifies to $v_g = c/n$.

In his classical paper, Tamm [79] showed that for dispersive media the radiation is concentrated in a thin conical shell whose vertex is at the moving charge, and whose opening half-angle η is given by

$$\begin{aligned} \cot \eta &= \left[\frac{d}{d\omega} (\omega \tan \theta_c) \right]_{\omega_0} \\ &= \left[\tan \theta_c + \beta^2 \omega n(\omega) \frac{dn}{d\omega} \cot \theta_c \right]_{\omega_0}, \end{aligned} \quad (27.41)$$

where ω_0 is the central value of the small frequency range under consideration. (See Fig. 27.24.) This cone has an opening half-angle η , and, unless the medium is non-dispersive ($dn/d\omega = 0$), $\theta_c + \eta \neq 90^\circ$. The Cherenkov wavefront 'sideslips' along with the particle [80]. This effect may have timing implications for ring imaging Cherenkov counters [81], but it is probably unimportant for most applications.

The number of photons produced per unit path length of a particle with charge ze and per unit energy interval of the photons is

$$\begin{aligned} \frac{d^2 N}{dE dx} &= \frac{\alpha z^2}{hc} \sin^2 \theta_c = \frac{\alpha^2 z^2}{r_e m_e c^2} \left(1 - \frac{1}{\beta^2 n^2(E)} \right) \\ &\approx 370 \sin^2 \theta_c(E) \text{ eV}^{-1} \text{ cm}^{-1} \quad (z = 1), \end{aligned} \quad (27.42)$$

or, equivalently,

$$\frac{d^2 N}{dx d\lambda} = \frac{2\pi \alpha z^2}{\lambda^2} \left(1 - \frac{1}{\beta^2 n^2(\lambda)} \right). \quad (27.43)$$

The index of refraction n is a function of photon energy $E = \hbar\omega$, as is the sensitivity of the transducer used to detect the light. For practical use, Eq. (27.42) must be multiplied by the the transducer response function and integrated over the region for which $\beta n(\omega) > 1$. Further details are given in the discussion of Cherenkov detectors in the Particle Detectors section (Sec. 28 of this Review).

When two particles are close together (within $\lesssim 1$ wavelength), the electromagnetic fields from the particles may add coherently, affecting the Cherenkov radiation. The radiation from an e^+e^- pair at close separation is suppressed compared to two independent leptons [82].

Coherent radio Cherenkov radiation from electromagnetic showers (containing a net excess of e^- over e^+) is significant [83], and has been used to study cosmic ray air showers [84] and to search for ν_e induced showers.

Transition radiation. The energy radiated when a particle with charge ze crosses the boundary between vacuum and a medium with plasma frequency ω_p is

$$I = \alpha z^2 \gamma \hbar \omega_p / 3, \quad (27.44)$$

where

$$\hbar \omega_p = \sqrt{4\pi N_e r_e^3} m_e c^2 / \alpha = \sqrt{\rho \text{ (in g/cm}^3\text{)} \langle Z/A \rangle} \times 28.81 \text{ eV}. \quad (27.45)$$

For styrene and similar materials, $\hbar \omega_p \approx 20 \text{ eV}$; for air it is 0.7 eV .

The number spectrum $dN_\gamma/d(\hbar\omega)$ diverges logarithmically at low energies and decreases rapidly for $\hbar\omega/\gamma\hbar\omega_p > 1$. About half the energy is emitted in the range $0.1 \leq \hbar\omega/\gamma\hbar\omega_p \leq 1$. Inevitable absorption in a practical detector removes the divergence. For a particle with $\gamma = 10^3$, the radiated photons are in the soft x-ray range 2 to 40 keV. The γ dependence of the emitted energy thus comes from the hardening of the spectrum rather than from an increased quantum yield.

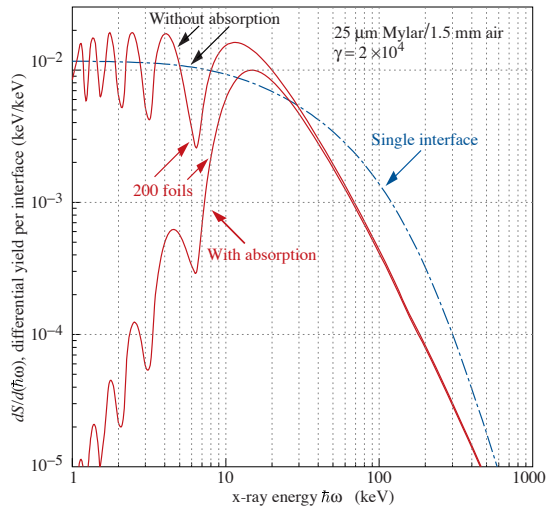


Figure 27.25: X-ray photon energy spectra for a radiator consisting of 200 25 μm thick foils of Mylar with 1.5 mm spacing in air (solid lines) and for a single surface (dashed line). Curves are shown with and without absorption. Adapted from Ref. 85.

The number of photons with energy $h\omega > h\omega_0$ is given by the answer to problem 13.15 in Ref. 32,

$$N_\gamma(h\omega > h\omega_0) = \frac{\alpha z^2}{\pi} \left[\left(\ln \frac{\gamma h\omega_p}{h\omega_0} - 1 \right)^2 + \frac{\pi^2}{12} \right], \quad (27.46)$$

within corrections of order $(h\omega_0/\gamma h\omega_p)^2$. The number of photons above a fixed energy $h\omega_0 \ll \gamma h\omega_p$ thus grows as $(\ln \gamma)^2$, but the number above a fixed fraction of $\gamma h\omega_p$ (as in the example above) is constant. For example, for $h\omega > \gamma h\omega_p/10$, $N_\gamma = 2.519 \alpha z^2/\pi = 0.59\% \times z^2$.

The particle stays “in phase” with the x ray over a distance called the formation length, $d(\omega)$. Most of the radiation is produced in a distance $d(\omega) = (2c/\omega)(1/\gamma^2 + \theta^2 + \omega_p^2/\omega^2)^{-1}$. Here θ is the x-ray emission angle, characteristically $1/\gamma$. For $\theta = 1/\gamma$ the formation length has a maximum at $d(\gamma\omega_p/\sqrt{2}) = \gamma c/\sqrt{2}\omega_p$. In practical situations it is tens of μm .

Since the useful x-ray yield from a single interface is low, in practical detectors it is enhanced by using a stack of N foil radiators—foils L thick, where L is typically several formation lengths—separated by gas-filled gaps. The amplitudes at successive interfaces interfere to cause oscillations about the single-interface spectrum. At increasing frequencies above the position of the last interference maximum ($L/d(\omega) = \pi/2$), the formation zones, which have opposite phase, overlap more and more and the spectrum saturates, $dI/d\omega$ approaching zero as $L/d(\omega) \rightarrow 0$. This is illustrated in Fig. 27.25 for a realistic detector configuration.

For regular spacing of the layers fairly complicated analytic solutions for the intensity have been obtained [85]. (See also Ref. 86 and references therein.) Although one might expect the intensity of coherent radiation from the stack of foils to be proportional to N^2 , the angular dependence of the formation length conspires to make the intensity $\propto N$.

References:

1. H. Bichsel, Nucl. Instrum. Methods **A562**, 154–197 (2006).
2. B. Rossi, *High Energy Particles*, Prentice-Hall, Inc., Englewood Cliffs, NJ, 1952.
3. H.A. Bethe, *Zur Theorie des Durchgangs schneller Korpuskularstrahlen durch Materie*, H. Bethe, Ann. Phys. **5**, 325 (1930).
4. “Stopping Powers and Ranges for Protons and Alpha

Particles,” ICRU Report No. 49 (1993); Tables and graphs of these data are available at <http://physics.nist.gov/PhysRefData/>.

5. D.E. Groom, N.V. Mokhov, and S.I. Striganov, “Muon stopping-power and range tables: 10 MeV–100 TeV,” Atomic Data and Nuclear Data Tables **78**, 183–356 (2001). Since submission of this paper it has become likely that post-Born corrections to the direct pair production cross section should be made. Code used to make Figs. 27.20–27.22 included these corrections [D.Yu. Ivanov *et al.*, Phys. Lett. **B442**, 453 (1998)]. The effect is negligible for except at high Z . (It is less than 1% for iron.); More extensive printable and machine-readable tables are given at <http://pdg.lbl.gov/AtomicNuclearProperties/>.
6. W.H. Barkas, W. Birnbaum, and F.M. Smith, Phys. Rev. **101**, 778 (1956).
7. U. Fano, Ann. Rev. Nucl. Sci. **13**, 1 (1963).
8. J. D. Jackson, Phys. Rev. **D59**, 017301 (1999).
9. S.M. Seltzer and M.J. Berger, Int. J. of Applied Rad. **33**, 1189 (1982).
10. “Stopping Powers for Electrons and Positrons,” ICRU Report No. 37 (1984).
11. <http://physics.nist.gov/PhysRefData/XrayMassCoef/tab1.html>.
12. H. Bichsel, Phys. Rev. **A46**, 5761 (1992).
13. W.H. Barkas and M.J. Berger, *Tables of Energy Losses and Ranges of Heavy Charged Particles*, NASA-SP-3013 (1964).
14. M. Agnello *et al.*, Phys. Rev. Lett. **74**, 371 (1995).
15. H.H. Andersen and J.F. Ziegler, *Hydrogen: Stopping Powers and Ranges in All Elements*. Vol. 3 of *The Stopping and Ranges of Ions in Matter* (Pergamon Press 1977).
16. J. Lindhard, Kgl. Danske Videnskab. Selskab, Mat.-Fys. Medd. **28**, No. 8 (1954); J. Lindhard, M. Scharff, and H.E. Schiøtt, Kgl. Danske Videnskab. Selskab, Mat.-Fys. Medd. **33**, No. 14 (1963).
17. J.F. Ziegler, J.F. Biersac, and U. Littmark, *The Stopping and Range of Ions in Solids*, Pergamon Press 1985.
18. R.M. Sternheimer, Phys. Rev. **88**, 851 (1952).
19. A. Crispin and G.N. Fowler, Rev. Mod. Phys. **42**, 290 (1970).
20. R.M. Sternheimer, S.M. Seltzer, and M.J. Berger, “The Density Effect for the Ionization Loss of Charged Particles in Various Substances,” Atomic Data and Nuclear Data Tables **30**, 261 (1984). Minor errors are corrected in Ref. 5. Chemical composition for the tabulated materials is given in Ref. 9.
21. R.M. Sternheimer and R.F. Peierls, Phys. Rev. **B3**, 3681 (1971).
22. For unit-charge projectiles, see E.A. Uehling, Ann. Rev. Nucl. Sci. **4**, 315 (1954). For highly charged projectiles, see J.A. Doggett and L.V. Spencer, Phys. Rev. **103**, 1597 (1956). A Lorentz transformation is needed to convert these center-of-mass data to knock-on energy spectra.
23. N.F. Mott and H.S.W. Massey, *The Theory of Atomic Collisions*, Oxford Press, London, 1965.
24. L.D. Landau, J. Exp. Phys. (USSR) **8**, 201 (1944).
25. P.V. Vavilov, Sov. Phys. JETP **5**, 749 (1957).
26. H. Bichsel, Rev. Mod. Phys. **60**, 663 (1988).
27. R. Talman, Nucl. Instrum. Methods **159**, 189 (1979).
28. S.M. Seltzer and M.J. Berger, Int. J. of Applied Rad. **35**, 665 (1984). This paper corrects and extends the results of Ref. 9.
29. L.V. Spencer “Energy Dissipation by Fast Electrons,” Nat’l Bureau of Standards Monograph No. 1 (1959).
30. “Average Energy Required to Produce an Ion Pair,” ICRU Report No. 31 (1979).

31. N. Hadley *et al.*, "List of Poisoning Times for Materials," Lawrence Berkeley Lab Report TPC-LBL-79-8 (1981).
32. J.D. Jackson, *Classical Electrodynamics*, 3rd edition, (John Wiley & Sons, New York, 1998).
33. H.A. Bethe, *Phys. Rev.* **89**, 1256 (1953). A thorough review of multiple scattering is given by W.T. Scott, *Rev. Mod. Phys.* **35**, 231 (1963). However, the data of Shen *et al.*, (*Phys. Rev.* **D20**, 1584 (1979)) show that Bethe's simpler method of including atomic electron effects agrees better with experiment than does Scott's treatment. For a thorough discussion of simple formulae for single scatters and methods of compounding these into multiple-scattering formulae, see W.T. Scott, *Rev. Mod. Phys.* **35**, 231 (1963). Detailed summaries of formulae for computing single scatters are given in J.W. Motz, H. Olsen, and H.W. Koch, *Rev. Mod. Phys.* **36**, 881 (1964).
34. V.L. Highland, *Nucl. Instrum. Methods* **129**, 497 (1975), and *Nucl. Instrum. Methods* **161**, 171 (1979).
35. G.R. Lynch and O.I. Dahl, *Nucl. Instrum. Methods* **B58**, 6 (1991).
36. M. Wong *et al.*, *Med. Phys.* **17**, 163 (1990).
37. E. Segré, *Nuclei and Particles*, New York, Benjamin (1964) p. 65 ff.
38. Y.S. Tsai, *Rev. Mod. Phys.* **46**, 815 (1974).
39. H. Davies, H.A. Bethe, and L.C. Maximon, *Phys. Rev.* **93**, 788 (1954).
40. O.I. Dahl, private communication.
41. L.D. Landau and I.J. Pomeranchuk, *Dokl. Akad. Nauk. SSSR* **92**, 535 (1953); **92**, 735 (1953). These papers are available in English in L. Landau, *The Collected Papers of L.D. Landau*, Pergamon Press, 1965; A.B. Migdal, *Phys. Rev.* **103**, 1811 (1956).
42. S. Klein, *Rev. Mod. Phys.* **71**, 1501 (1999).
43. M. L. Ter-Mikaelian, *SSSR* **94**, 1033 (1954); M. L. Ter-Mikaelian, *High Energy Electromagnetic Processes in Condensed Media* (John Wiley & Sons, New York, 1972).
44. P. Anthony *et al.*, *Phys. Rev. Lett.* **76**, 3550 (1996).
45. H. W. Koch and J. W. Motz, *Rev. Mod. Phys.* **31**, 920 (1959).
46. M.J. Berger and S.M. Seltzer, "Tables of Energy Losses and Ranges of Electrons and Positrons," National Aeronautics and Space Administration Report NASA-SP-3012 (Washington DC 1964).
47. K. Hikasa *et al.*, *Review of Particle Properties*, *Phys. Rev.* **D46** (1992) S1.
48. B. L. Berman and S. C. Fultz, *Rev. Mod. Phys.* **47**, 713 (1975).
49. J.S. Hubbell, H. Gimm, and I. Øverbø, *J. Phys. Chem. Ref. Data* **9**, 1023 (1980).
50. A. Veyssiere *et al.*, *Nucl. Phys.* **A159**, 561 (1970).
51. J. W. Motz, H. A. Olsen, and H. W. Koch, *Rev. Mod. Phys.* **41**, 581 (1969).
52. P. Anthony *et al.*, *Phys. Rev. Lett.* **75**, 1949 (1995).
53. U.I. Uggerhoj, *Rev. Mod. Phys.* **77**, 1131 (2005).
54. FIND IT..
55. W.R. Nelson, H. Hirayama, and D.W.O. Rogers, "The EGS4 Code System," SLAC-265, Stanford Linear Accelerator Center (Dec. 1985).
56. *Experimental Techniques in High Energy Physics*, ed. by T. Ferbel (Addison-Wesley, Menlo Park CA 1987).
57. U. Amaldi, *Phys. Scripta* **23**, 409 (1981).
58. E. Longo and I. Sestili, *Nucl. Instrum. Methods* **128**, 283 (1975).
59. G. Grindhammer *et al.*, in *Proceedings of the Workshop on Calorimetry for the Supercollider*, Tuscaloosa, AL, March 13–17, 1989, edited by R. Donaldson and M.G.D. Gilchriese (World Scientific, Teaneck, NJ, 1989), p. 151.
60. W.R. Nelson *et al.*, *Phys. Rev.* **149**, 201 (1966).
61. G. Bathow *et al.*, *Nucl. Phys.* **B20**, 592 (1970).
62. H.A. Bethe and W. Heitler, *Proc. Roy. Soc.* **A146**, 83 (1934); H.A. Bethe, *Proc. Cambridge Phil. Soc.* **30**, 542 (1934).
63. A.A. Petrukhin and V.V. Shestakov, *Can. J. Phys.* **46**, S377 (1968).
64. V.M. Galitskii and S.R. Kel'ner, *Sov. Phys. JETP* **25**, 948 (1967).
65. S.R. Kel'ner and Yu.D. Kotov, *Sov. J. Nucl. Phys.* **7**, 237 (1968).
66. R.P. Kokoulin and A.A. Petrukhin, in *Proceedings of the International Conference on Cosmic Rays*, Hobart, Australia, August 16–25, 1971, Vol. 4, p. 2436.
67. A.I. Nikishov, *Sov. J. Nucl. Phys.* **27**, 677 (1978).
68. Y.M. Andreev *et al.*, *Phys. Atom. Nucl.* **57**, 2066 (1994).
69. L.B. Bezrukov and E.V. Bugaev, *Sov. J. Nucl. Phys.* **33**, 635 (1981).
70. N.V. Mokhov, "The MARS Code System User's Guide," Fermilab-FN-628 (1995); N. V. Mokhov *et al.*, *Radiation Protection and Dosimetry*, vol. 116, part 2, pp. 99 (2005); Fermilab-Conf-04/053 (2004); N. V. Mokhov *et al.*, in *Proc. of Intl. Conf. on Nuclear Data for Science and Tech.* (Santa Fe, NM, 2004), AIP Conf. Proc. 769, part 2, p. 1618; Fermilab-Conf-04/269-AD (2004); <http://www-ap.fnal.gov/MARS/>.
71. P.H. Barrett *et al.*, *Rev. Mod. Phys.* **24**, 133 (1952).
72. A. Van Ginneken, *Nucl. Instrum. Methods* **A251**, 21 (1986).
73. U. Becker *et al.*, *Nucl. Instrum. Methods* **A253**, 15 (1986).
74. J.J. Eastman and S.C. Loken, in *Proceedings of the Workshop on Experiments, Detectors, and Experimental Areas for the Supercollider*, Berkeley, CA, July 7–17, 1987, edited by R. Donaldson and M.G.D. Gilchriese (World Scientific, Singapore, 1988), p. 542.
75. *Methods of Experimental Physics*, L.C.L. Yuan and C.-S. Wu, editors, Academic Press, 1961, Vol. 5A, p. 163.
76. W.W.M. Allison and P.R.S. Wright, "The Physics of Charged Particle Identification: dE/dx , Cherenkov Radiation, and Transition Radiation," p. 371 in *Experimental Techniques in High Energy Physics*, T. Ferbel, editor, (Addison-Wesley 1987).
77. E.R. Hayes, R.A. Schluter, and A. Tamosaitis, "Index and Dispersion of Some Cherenkov Counter Gases," ANL-6916 (1964).
78. T. Ypsilantis, "Particle Identification at Hadron Colliders", CERN-EP/89-150 (1989), or ECFA 89-124, **2** 661 (1989).
79. I. Tamm, *J. Phys. U.S.S.R.*, **1**, 439 (1939).
80. H. Motz and L. I. Schiff, *Am. J. Phys.* **21**, 258 (1953).
81. B. N. Ratcliff, *Nucl. Instrum. & Meth.* **A502**, 211 (2003).
82. S. K. Mandal, S. R. Klein, and J. D. Jackson, *Phys. Rev.* **D72**, 093003 (2005).
83. E. Zas, F. Halzen and T. Stanev, *Phys. Rev.* **D45**, 362 (1991).
84. H. Falcke *et al.*, *Nature* **435**, 313 (2005).
85. M. L. Cherry, *Phys. Rev.* **D10**, 3594–3607 (1974); M. L. Cherry, *Phys. Rev.* **D17**, 2245–2260 (1978).
86. B. Dolgoshein, *Nucl. Instrum. Methods* **A326**, 434–469 (1993).

28. PARTICLE DETECTORS AT ACCELERATORS

Revised 2010. See the various sections for authors.

28. PARTICLE DETECTORS AT ACCELERATORS	300
28.1. Summary of detector spatial resolution, temporal resolution, and deadtime	300
28.2. Photon detectors	300
28.2.1. Vacuum photodetectors	301
28.2.1.1. Photomultiplier tubes	301
28.2.1.2. Microchannel plates	302
28.2.1.3. Hybrid photon detectors	302
28.2.2. Gaseous photon detectors	302
28.2.3. Solid-state photon detectors	302
28.3. Organic scintillators	303
28.3.1. Scintillation mechanism	303
28.3.2. Caveats and cautions	304
28.3.3. Scintillating and wavelength-shifting fibers	304
28.4. Inorganic scintillators:	305
28.5. Cherenkov detectors	307
28.6. Gaseous detectors	308
28.6.1. Energy loss and charge transport in gases	308
28.6.2. Multi-Wire Proportional and Drift Chambers	310
28.6.3. High Rate Effects	311
28.6.4. Micro-Pattern Gas Detectors	312
28.6.5. Time-projection chambers	313
28.6.6. Transition radiation detectors (TRD's)	315
28.6.7. Resistive-plate chambers	316
28.7. Semiconductor detectors	316
28.7.1. Materials Requirements	317
28.7.2. Detector Configurations	317
28.7.3. Signal Formation	317
28.7.4. Radiation Damage	318
28.8. Low-noise electronics	318
28.9. Calorimeters	320
28.9.1. Electromagnetic calorimeters	320
28.9.2. Hadronic calorimeters	321
28.9.3. Free electron drift velocities in liquid ionization chambers	323
28.10. Superconducting magnets for collider detectors	323
28.10.1. Solenoid Magnets	323
28.10.2. Properties of collider detector magnets	324
28.10.3. Toroidal magnets	325
28.11. Measurement of particle momenta in a uniform magnetic field	325
References	325

28.1. Summary of detector spatial resolution, temporal resolution, and deadtime

In this section we give various parameters for common detector components. The quoted numbers are usually based on typical devices, and should be regarded only as rough approximations for new designs. More detailed discussions of detectors and their underlying physics can be found in books by Ferbel [1], Kleinknecht [2], Knoll [3], Green [4], Leroy & Rancoita [5], and Grupen [6]. In Table 28.1 are given typical resolutions and deadtimes of common detectors.

Table 28.1: Typical resolutions and deadtimes of common detectors. Revised September 2009.

Detector Type	Accuracy (rms)	Resolution Time	Dead Time
Bubble chamber	10–150 μm	1 ms	50 ms ^a
Streamer chamber	300 μm	2 μs	100 ms
Proportional chamber	50–100 μm ^{b,c}	2 ns	200 ns
Drift chamber	50–100 μm	2 ns ^d	100 ns
Scintillator	—	100 ps/ <i>n</i> ^e	10 ns
Emulsion	1 μm	—	—
Liquid argon drift [7]	~175–450 μm	~ 200 ns	~ 2 μs
Micro-pattern gas detectors [8]	30–40 μm	< 10 ns	20 ns
Resistive plate chamber [9]	~ 10 μm	1–2 ns	—
Silicon strip	pitch/(3 to 7) ^f	<i>g</i>	<i>g</i>
Silicon pixel	2 μm ^h	<i>g</i>	<i>g</i>

^a Multiple pulsing time.

^b 300 μm is for 1 mm pitch (wirespacing/ $\sqrt{12}$).

^c Delay line cathode readout can give ± 150 μm parallel to anode wire.

^d For two chambers.

^e *n* = index of refraction.

^f The highest resolution (“7”) is obtained for small-pitch detectors ($\lesssim 25$ μm) with pulse-height-weighted center finding.

^g Limited by the readout electronics [10]. (Time resolution of ≤ 25 ns is planned for the ATLAS SCT.)

^h Analog readout of 34 μm pitch, monolithic pixel detectors.

28.2. Photon detectors

Updated September 2009 by D. Chakraborty (Northern Illinois U) and T. Sumiyoshi (Tokyo Metro U).

Most detectors in high-energy, nuclear, and astrophysics rely on the detection of photons in or near the visible range, $100 \text{ nm} \lesssim \lambda \lesssim 1000 \text{ nm}$, or $E \approx$ a few eV. This range covers scintillation and Cherenkov radiation as well as the light detected in many astronomical observations.

Generally, photodetection involves generating a detectable electrical signal proportional to the (usually very small) number of incident photons. The process involves three distinct steps:

1. Generation of a primary photoelectron or electron-hole (*e-h*) pair by an incident photon by the photoelectric or photoconductive effect,
2. Amplification of the p.e. signal to detectable levels by one or more multiplicative bombardment steps and/or an avalanche process (usually), and,
3. Collection of the secondary electrons to form the electrical signal. The important characteristics of a photodetector include the following in statistical averages:
 1. Quantum efficiency (QE or ϵ_Q): the number of primary photoelectrons generated per incident photon ($0 \leq \epsilon_Q \leq 1$; in silicon more than one *e-h* pair per incident photon can be generated for $\lambda \lesssim 165 \text{ nm}$),
 2. Collection efficiency (CE or ϵ_C): the overall acceptance factor other than the generation of photoelectrons ($0 \leq \epsilon_C \leq 1$),
 3. Gain (*G*): the number of electrons collected for each photoelectron generated,
 4. Dark current or dark noise: the electrical signal when there is no photon,
 5. Energy resolution: electronic noise (ENC or N_e) and statistical fluctuations in the amplification process compound the Poisson distribution of n_γ photons from a given source:

$$\frac{\sigma(E)}{\langle E \rangle} = \sqrt{\frac{f_N}{n_\gamma \epsilon_Q \epsilon_C} + \left(\frac{N_e}{G n_\gamma \epsilon_Q \epsilon_C} \right)^2}, \quad (28.1)$$

where f_N , or the excess noise factor (ENF), is the contribution to the energy distribution variance due to amplification statistics [11],

6. Dynamic range: the maximum signal available from the detector (this is usually expressed in units of the response to noise-equivalent power, or NEP, which is the optical input power that produces a signal-to-noise ratio of 1),
7. Time dependence of the response: this includes the transit time, which is the time between the arrival of the photon and the electrical pulse, and the transit time spread, which contributes to the pulse rise time and width, and
8. Rate capability: inversely proportional to the time needed, after the arrival of one photon, to get ready to receive the next.

typically 10 times in series to generate a sufficient number of electrons, which are collected at the anode for delivery to the external circuit. The total gain of a PMT depends on the applied high voltage V as $G = AV^{kn}$, where $k \approx 0.7$ – 0.8 (depending on the dynode material), n is the number of dynodes in the chain, and A a constant (which also depends on n). Typically, G is in the range of 10^5 – 10^6 . Pulse risetimes are usually in the few nanosecond range. With *e.g.* two-level discrimination the effective time resolution can be much better.

Table 28.2: Representative characteristics of some photodetectors commonly used in particle physics. The time resolution of the devices listed here vary in the 10–2000 ps range.

Type	λ (nm)	$\epsilon_Q \epsilon_C$	Gain	Risetime (ns)	Area (mm ²)	1-p.e noise (Hz)	HV (V)	Price (USD)
PMT*	115–1700	0.15–0.25	10^3 – 10^7	0.7–10	10^2 – 10^5	10 – 10^4	500–3000	100–5000
MCP*	100–650	0.01–0.10	10^3 – 10^7	0.15–0.3	10^2 – 10^4	0.1–200	500–3500	10–6000
HPD*	115–850	0.1–0.3	10^3 – 10^4	7	10^2 – 10^5	10 – 10^3	$\sim 2 \times 10^4$	~ 600
GPM*	115–500	0.15–0.3	10^3 – 10^6	$O(0.1)$	$O(10)$	10 – 10^3	300–2000	$O(10)$
APD	300–1700	~ 0.7	10 – 10^8	$O(1)$	10 – 10^3	1 – 10^3	400–1400	$O(100)$
PPD	320–900	0.15–0.3	10^5 – 10^6	~ 1	1–10	$O(10^6)$	30–60	$O(100)$
VLPC	500–600	~ 0.9	$\sim 5 \times 10^4$	~ 10	1	$O(10^4)$	~ 7	~ 1

*These devices often come in multi-anode configurations. In such cases, area, noise, and price are to be considered on a “per readout-channel” basis.

The QE is a strong function of the photon wavelength (λ), and is usually quoted at maximum, together with a range of λ where the QE is comparable to its maximum. Spatial uniformity and linearity with respect to the number of photons are highly desirable in a photodetector’s response.

Optimization of these factors involves many trade-offs and vary widely between applications. For example, while a large gain is desirable, attempts to increase the gain for a given device also increases the ENF and after-pulsing (“echos” of the main pulse). In solid-state devices, a higher QE often requires a compromise in the timing properties. In other types, coverage of large areas by focusing increases the transit time spread.

Other important considerations also are highly application-specific. These include the photon flux and wavelength range, the total area to be covered and the efficiency required, the volume available to accommodate the detectors, characteristics of the environment such as chemical composition, temperature, magnetic field, ambient background, as well as ambient radiation of different types and, mode of operation (continuous or triggered), bias (high-voltage) requirements, power consumption, calibration needs, aging, cost, and so on. Several technologies employing different phenomena for the three steps described above, and many variants within each, offer a wide range of solutions to choose from. The salient features of the main technologies and the common variants are described below. Some key characteristics are summarized in Table 28.2.

28.2.1. Vacuum photodetectors: Vacuum photodetectors can be broadly subdivided into three types: photomultiplier tubes, microchannel plates, and hybrid photodetectors.

28.2.1.1. Photomultiplier tubes: A versatile class of photon detectors, vacuum photomultiplier tubes (PMT) has been employed by a vast majority of all particle physics experiments to date [11]. Both “transmission-” and “reflection-type” PMT’s are widely used. In the former, the photocathode material is deposited on the inside of a transparent window through which the photons enter, while in the latter, the photocathode material rests on a separate surface that the incident photons strike. The cathode material has a low work function, chosen for the wavelength band of interest. When a photon hits the cathode and liberates an electron (the photoelectric effect), the latter is accelerated and guided by electric fields to impinge on a secondary-emission electrode, or dynode, which then emits a few (~ 5) secondary electrons. The multiplication process is repeated

A large variety of PMT’s, including many just recently developed, covers a wide span of wavelength ranges from infrared (IR) to extreme ultraviolet (XUV) [12]. They are categorized by the window materials, photocathode materials, dynode structures, anode configurations, *etc.* Common window materials are borosilicate glass for IR to near-UV, fused quartz and sapphire (Al_2O_3) for UV, and MgF_2 or LiF for XUV. The choice of photocathode materials include a variety of mostly Cs- and/or Sb-based compounds such as CsI, CsTe, bi-alkali (SbRbCs, SbKCs), multi-alkali (SbNa₂KCs), GaAs(Cs), GaAsP, *etc.* Sensitive wavelengths and peak quantum efficiencies for these materials are summarized in Table 28.3. Typical dynode structures used in PMT’s are circular cage, line focusing, box and grid, venetian blind, and fine mesh. In some cases, limited spatial resolution can be obtained by using a mosaic of multiple anodes. Fast PMT’s with very large windows—measuring up to 508 mm across—have been developed in recent years for detection of Cherenkov radiation in neutrino experiments such as Super-Kamiokande and KamLAND among many others. Specially prepared low-radioactivity glass is used to make these PMT’s, and they are also able to withstand the high pressure of the surrounding liquid.

PMT’s are vulnerable to magnetic fields—sometimes even the geomagnetic field causes large orientation-dependent gain changes. A high-permeability metal shield is often necessary. However, proximity-focused PMT’s, *e.g.* the fine-mesh types, can be used even in a high magnetic field (≥ 1 T) if the electron drift direction is parallel to the field. CMS uses custom-made vacuum phototriodes (VPT) mounted on the back face of projective lead tungstate crystals to detect scintillation light in the endcap sections of its electromagnetic calorimeters, which are inside a 3.8 T superconducting solenoid. A VPT employs a single dynode (thus, $G \approx 10$) placed close to the photocathode, and a mesh anode plane between the two, to help it cope with the strong magnetic field, which is not too unfavorably oriented with respect to the photodetector axis in the endcaps (within 25°), but where the radiation level is too high for APD’s like those used in the barrel section.

28.2.1.2. Microchannel plates: A typical Microchannel plate (MCP) photodetector consists of one or more ~ 2 mm thick glass plates with densely packed $O(10 \mu\text{m})$ -diameter cylindrical holes, or “channels”, sitting between the transmission-type photocathode and anode planes, separated by $O(1 \text{ mm})$ gaps. Instead of discrete dynodes, the inner surface of each cylindrical tube serves as a continuous dynode for the entire cascade of multiplicative bombardments initiated by a photoelectron. Gain fluctuations can be minimized by operating in a saturation mode, whence each channel is only capable of a binary output, but the sum of all channel outputs remains proportional to the number of photons received so long as the photon flux is low enough to ensure that the probability of a single channel receiving more than one photon during a single time gate is negligible. MCP’s are thin, offer good spatial resolution, have excellent time resolution (~ 20 ps), and can tolerate random magnetic fields up to 0.1 T and axial fields up to ~ 1 T. However, they suffer from relatively long recovery time per channel and short lifetime. MCP’s are widely employed as image-intensifiers, although not so much in HEP or astrophysics.

28.2.1.3. Hybrid photon detectors: Hybrid photon detectors (HPD) combine the sensitivity of a vacuum PMT with the excellent spatial and energy resolutions of a Si sensor [13]. A single photoelectron ejected from the photocathode is accelerated through a potential difference of ~ 20 kV before it impinges on the silicon sensor/anode. The gain nearly equals the maximum number of e - h pairs that could be created from the entire kinetic energy of the accelerated electron: $G \approx eV/w$, where e is the electronic charge, V is the applied potential difference, and $w \approx 3.7$ eV is the mean energy required to create an e - h pair in Si at room temperature. Since the gain is achieved in a single step, one might expect to have the excellent resolution of a simple Poisson statistic with large mean, but in fact it is even better, thanks to the Fano effect discussed in Sec. 28.7.

Low-noise electronics must be used to read out HPD’s if one intends to take advantage of the low fluctuations in gain, *e.g.* when counting small numbers of photons. HPD’s can have the same $\epsilon_Q \epsilon_C$ and window geometries as PMT’s and can be segmented down to $\sim 50 \mu\text{m}$. However, they require rather high biases and will not function in a magnetic field. The exception is proximity-focused devices (\Rightarrow no (de)magnification) in an axial field. With time resolutions of ~ 10 ps and superior rate capability, proximity-focused HPD’s can be an alternative to MCP’s. Current applications of HPD’s include the CMS hadronic calorimeter and the RICH detector in LHCb. Large-size HPD’s with sophisticated focusing may be suitable for future water Cherenkov experiments.

Hybrid APD’s (HAPD’s) add an avalanche multiplication step following the electron bombardment to boost the gain by a factor of ~ 50 . This affords a higher gain and/or lower electrical bias, but also degrades the signal definition.

Table 28.3: Properties of photocathode and window materials commonly used in vacuum photodetectors [12].

Photocathode material	λ (nm)	Window material	Peak ϵ_Q (λ/nm)
CsI	115–200	MgF ₂	0.15 (135)
CsTe	115–240	MgF ₂	0.18 (210)
Bi-alkali	300–650	Borosilicate	0.27 (390)
	160–650	Quartz	0.27 (390)
Multi-alkali	300–850	Borosilicate	0.20 (360)
	160–850	Quartz	0.23 (280)
GaAs(Cs)*	160–930	Quartz	0.23 (280)
GaAsP(Cs)	300–750	Borosilicate	0.42 (560)
InP/InGaAsP [†]	350–1700	Borosilicate	0.01 (1500)

*Reflection type photocathode is used. [†]Requires cooling to $\sim -80^\circ\text{C}$.

28.2.2. Gaseous photon detectors: In gaseous photomultipliers (GPM) a photoelectron in a suitable gas mixture initiates an avalanche in a high-field region, producing a large number of secondary impact-ionization electrons. In principle the charge multiplication and collection processes are identical to those employed in gaseous tracking detectors such as multiwire proportional chambers, micromesh gaseous detectors (Micromegas), or gas electron multipliers (GEM). These are discussed in Sec. 28.6.4.

The devices can be divided into two types depending on the photocathode material. One type uses solid photocathode materials much in the same way as PMT’s. Since it is resistant to gas mixtures typically used in tracking chambers, CsI is a common choice. In the other type, photoionization occurs on suitable molecules vaporized and mixed in the drift volume. Most gases have photoionization work functions in excess of 10 eV, which would limit their sensitivity to wavelengths far too short. However, vapors of TMAE (tetrakis dimethyl-amine ethylene) or TEA (tri-ethyl-amine), which have smaller work functions (5.3 eV for TMAE and 7.5 eV for TEA), are suited for XUV photon detection [14]. Since devices like GEM’s offer sub-mm spatial resolution, GPM’s are often used as position-sensitive photon detectors. They can be made into flat panels to cover large areas ($O(1 \text{ m}^2)$), can operate in high magnetic fields, and are relatively inexpensive. Many of the ring imaging Cherenkov (RICH) detectors to date have used GPM’s for the detection of Cherenkov light [15]. Special care must be taken to suppress the photon-feedback process in GPM’s. It is also important to maintain high purity of the gas as minute traces of O₂ can significantly degrade the detection efficiency.

28.2.3. Solid-state photon detectors: In a phase of rapid development, solid-state photodetectors are competing with vacuum- or gas-based devices for many existing applications and making way for a multitude of new ones. Compared to traditional vacuum- and gaseous photodetectors, solid-state devices are more compact, lightweight, rugged, tolerant to magnetic fields, and often cheaper. They also allow fine pixelization, are easy to integrate into large systems, and can operate at low electric potentials, while matching or exceeding most performance criteria. They are particularly well suited for detection of γ - and X-rays. Except for applications where coverage of very large areas or dynamic range is required, solid-state detectors are proving to be the better choice. Some hybrid devices attempt to combine the best features of different technologies while applications of nanotechnology are opening up exciting new possibilities.

Silicon photodiodes (PD) are widely used in high-energy physics as particle detectors and in a great number of applications (including solar cells!) as light detectors. The structure is discussed in some detail in Sec. 28.7. In its simplest form, the PD is a reverse-biased p - n junction. Photons with energies above the indirect bandgap energy (wavelengths shorter than about 1050 nm, depending on the temperature) can create e - h pairs (the photoconductive effect), which are collected on the p and n sides, respectively. Often, as in the PD’s used for crystal scintillator readout in CLEO, L3, Belle, BaBar, and GLAST, intrinsic silicon is doped to create a p - i - n structure. The reverse bias increases the thickness of the depleted region; in the case of these particular detectors, to full depletion at a depth of about 100 μm . Increasing the depletion depth decreases the capacitance (and hence electronic noise) and extends the red response. Quantum efficiency can exceed 90%, but falls toward the red because of the increasing absorption length of light in silicon. The absorption length reaches 100 μm at 985 nm. However, since $G = 1$, amplification is necessary. Optimal low-noise amplifiers are slow, but, even so, noise limits the minimum detectable signal in room-temperature devices to several hundred photons.

Very large arrays containing $O(10^7)$ of $O(10 \mu\text{m}^2)$ -sized photodiodes pixelizing a plane are widely used to photograph all sorts of things from everyday subjects at visible wavelengths to crystal structures with X-rays and astronomical objects from infrared to UV. To limit the number of readout channels, these are made into charge-coupled devices (CCD), where pixel-to-pixel signal transfer takes place over thousands of synchronous cycles with sequential output through shift registers [16]. Thus, high spatial resolution is achieved at the expense of speed and timing precision. Custom-made CCD’s have virtually replaced photographic plates and other imagers

for astronomy and in spacecraft. Typical QE's exceed 90% over much of the visible spectrum, and "thick" CCD's have useful QE up to $\lambda = 1 \mu\text{m}$. Active Pixel Sensor (APS) arrays with a preamplifier on each pixel and CMOS processing afford higher speeds, but are challenged at longer wavelengths. Much R&D is underway to overcome the limitations of both CCD and CMOS imagers.

In avalanche photodiodes (APD), an exponential cascade of impact ionizations initiated by the initial photogenerated e - h pair under a large reverse-bias voltage leads to an avalanche breakdown [17]. As a result, detectable electrical response can be obtained from low-intensity optical signals down to single photons. Excellent junction uniformity is critical, and a guard ring is generally used as a protection against edge breakdown. Well-designed APD's, such as those used in CMS' crystal-based electromagnetic calorimeter, have achieved $\epsilon_Q \epsilon_C \approx 0.7$ with sub-ns response time. The sensitive wavelength window and gain depend on the semiconductor used. The gain is typically 10–200 in linear and up to 10^8 in Geiger mode of operation. Stability and close monitoring of the operating temperature are important for linear-mode operation, and substantial cooling is often necessary. Position-sensitive APD's use time information at multiple anodes to calculate the hit position.

One of the most promising recent developments in the field is that of devices consisting of large arrays ($O(10^3)$) of tiny APD's packed over a small area ($O(1 \text{ mm}^2)$) and operated in a limited Geiger mode [18]. Among different names used for this class of photodetectors, "PPD" (for "Pixelized Photon Detector") is most widely accepted (formerly "SiPM"). Although each cell only offers a binary output, linearity with respect to the number of photons is achieved by summing the cell outputs in the same way as with a MCP in saturation mode (see above). PPD's are being adopted as the preferred solution for various purposes including medical imaging, *e.g.* positron emission tomography (PET). These compact, rugged, and economical devices allow auto-calibration through decent separation of photoelectron peaks and offer gains of $O(10^6)$ at a moderate bias voltage ($\sim 50 \text{ V}$). However, the single-photoelectron noise of a PPD, being the logical "or" of $O(10^3)$ Geiger APD's, is rather large: $O(1 \text{ MHz/mm}^2)$ at room temperature. PPD's are particularly well-suited for applications where triggered pulses of several photons are expected over a small area, *e.g.* fiber-guided scintillation light. Intense R&D is expected to lower the noise level and improve radiation hardness, resulting in coverage of larger areas and wider applications. Attempts are being made to combine the fabrication of the sensors and the front-end electronics (ASIC) in the same process with the goal of making PPD's and other finely pixelized solid-state photodetectors extremely easy to use.

Of late, much R&D has been directed to p - i - n diode arrays based on thin polycrystalline diamond films formed by chemical vapor deposition (CVD) on a hot substrate ($\sim 1000 \text{ K}$) from a hydrocarbon-containing gas mixture under low pressure ($\sim 100 \text{ mbar}$). These devices have maximum sensitivity in the extreme- to moderate-UV region [19]. Many desirable characteristics, including high tolerance to radiation and temperature fluctuations, low dark noise, blindness to most of the solar radiation spectrum, and relatively low cost make them ideal for space-based UV/XUV astronomy, measurement of synchrotron radiation, and luminosity monitoring at (future) lepton collider(s).

Visible-light photon counters (VLPC) utilize the formation of an impurity band only 50 meV below the conduction band in As-doped Si to generate strong ($G \approx 5 \times 10^4$) yet sharp response to single photons with $\epsilon_Q \approx 0.9$ [20]. The smallness of the band gap considerably reduces the gain dispersion. Only a very small bias ($\sim 7 \text{ V}$) is needed, but high sensitivity to infrared photons requires cooling below 10 K. The dark noise increases sharply and exponentially with both temperature and bias. The Run 2 DØ detector uses 86000 VLPC's to read the optical signal from its scintillating-fiber tracker and scintillator-strip preshower detectors.

28.3. Organic scintillators

Revised September 2007 by K.F. Johnson (FSU).

Organic scintillators are broadly classed into three types, crystalline, liquid, and plastic, all of which utilize the ionization produced by charged particles (see Sec. 27.2) of this *Review*) to generate optical photons, usually in the blue to green wavelength regions [21]. Plastic scintillators are by far the most widely used. Crystal organic scintillators are practically unused in high-energy physics.

Densities range from 1.03 to 1.20 g cm⁻³. Typical photon yields are about 1 photon per 100 eV of energy deposit [22]. A one-cm-thick scintillator traversed by a minimum-ionizing particle will therefore yield $\approx 2 \times 10^4$ photons. The resulting photoelectron signal will depend on the collection and transport efficiency of the optical package and the quantum efficiency of the photodetector.

Plastic scintillators do not respond linearly to the ionization density. Very dense ionization columns emit less light than expected on the basis of dE/dx for minimum-ionizing particles. A widely used semi-empirical model by Birks posits that recombination and quenching effects between the excited molecules reduce the light yield [23]. These effects are more pronounced the greater the density of the excited molecules. Birks' formula is

$$\frac{d\mathcal{L}}{dx} = \mathcal{L}_0 \frac{dE/dx}{1 + k_B dE/dx}, \quad (28.2)$$

where \mathcal{L} is the luminescence, \mathcal{L}_0 is the luminescence at low specific ionization density, and k_B is Birks' constant, which must be determined for each scintillator by measurement.

Decay times are in the ns range; rise times are much faster. The combination of high light yield and fast response time allows the possibility of sub-ns timing resolution [24]. The fraction of light emitted during the decay "tail" can depend on the exciting particle. This allows pulse shape discrimination as a technique to carry out particle identification. Because of the hydrogen content (carbon to hydrogen ratio ≈ 1) plastic scintillator is sensitive to proton recoils from neutrons. Ease of fabrication into desired shapes and low cost has made plastic scintillators a common detector component. Recently, plastic scintillators in the form of scintillating fibers have found widespread use in tracking and calorimetry [25].

28.3.1. Scintillation mechanism :

Scintillation: A charged particle traversing matter leaves behind it a wake of excited molecules. Certain types of molecules, however, will release a small fraction ($\approx 3\%$) of this energy as optical photons. This process, scintillation, is especially marked in those organic substances which contain aromatic rings, such as polystyrene (PS) and polyvinyltoluene (PVT). Liquids which scintillate include toluene and xylene.

Fluorescence: In fluorescence, the initial excitation takes place via the absorption of a photon, and de-excitation by emission of a longer wavelength photon. Fluors are used as "wavelength shifters" to shift scintillation light to a more convenient wavelength. Occurring in complex molecules, the absorption and emission are spread out over a wide band of photon energies, and have some overlap, that is, there is some fraction of the emitted light which can be re-absorbed [26]. This "self-absorption" is undesirable for detector applications because it causes a shortened attenuation length. The wavelength difference between the major absorption and emission peaks is called the Stokes' shift. It is usually the case that the greater the Stokes' shift, the smaller the self absorption—thus, a large Stokes' shift is a desirable property for a fluor.

Scintillators: The plastic scintillators used in high-energy physics are binary or ternary solutions of selected fluors in a plastic base containing aromatic rings. (See the appendix in Ref. 27 for a comprehensive list of components.) Virtually all plastic scintillators contain as a base either PVT or PS. PVT-based scintillator can be up to 50% brighter.

Ionization in the plastic base produces UV photons with short attenuation length (several mm). Longer attenuation lengths are obtained by dissolving a "primary" fluor in high concentration (1% by weight) into the base, which is selected to efficiently re-radiate absorbed energy at wavelengths where the base is more transparent.

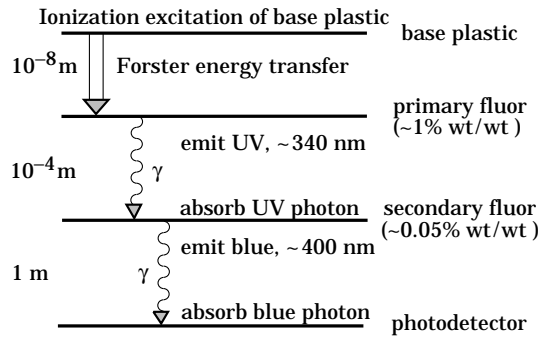


Figure 28.1: Cartoon of scintillation “ladder” depicting the operating mechanism of plastic scintillator. Approximate fluor concentrations and energy transfer distances for the separate sub-processes are shown.

The primary fluor has a second important function. The decay time of the scintillator base material can be quite long—in pure polystyrene it is 16 ns, for example. The addition of the primary fluor in high concentration can shorten the decay time by an order of magnitude and increase the total light yield. At the concentrations used (1% and greater), the average distance between a fluor molecule and an excited base unit is around 100 Å, much less than a wavelength of light. At these distances the predominant mode of energy transfer from base to fluor is not the radiation of a photon, but a resonant dipole-dipole interaction, first described by Foerster, which strongly couples the base and fluor [28]. The strong coupling sharply increases the speed and the light yield of the plastic scintillators.

Unfortunately, a fluor which fulfills other requirements is usually not completely adequate with respect to emission wavelength or attenuation length, so it is necessary to add yet another wavelifter (the “secondary” fluor), at fractional percent levels, and occasionally a third (not shown in Fig. 28.1).

External wavelength shifters: Light emitted from a plastic scintillator may be absorbed in a (nonscintillating) base doped with a wavelength shifter. Such wavelength shifters are widely used to aid light collection in complex geometries. The wavelength shifter must be insensitive to ionizing radiation and Cherenkov light. A typical wavelength shifter uses an acrylic base because of its good optical qualities, a single fluor to shift the light emerging from the plastic scintillator to the blue-green, and contains ultra-violet absorbing additives to deaden response to Cherenkov light.

28.3.2. Caveats and cautions: Plastic scintillators are reliable, robust, and convenient. However, they possess quirks to which the experimenter must be alert.

Aging and Handling: Plastic scintillators are subject to aging which diminishes the light yield. Exposure to solvent vapors, high temperatures, mechanical flexing, irradiation, or rough handling will aggravate the process. A particularly fragile region is the surface which can “craze”—develop microcracks—which rapidly destroy the capability of plastic scintillators to transmit light by total internal reflection. Crazeing is particularly likely where oils, solvents, or *fingerprints* have contacted the surface.

Attenuation length: The Stokes’ shift is not the only factor determining attenuation length. Others are the concentration of fluors (the higher the concentration of a fluor, the greater will be its self-absorption); the optical clarity and uniformity of the bulk material; the quality of the surface; and absorption by additives, such as stabilizers, which may be present.

Afterglow: Plastic scintillators have a long-lived luminescence which does not follow a simple exponential decay. Intensities at the 10^{-4} level of the initial fluorescence can persist for hundreds of ns [21,29].

Atmospheric quenching: Plastic scintillators will decrease their light yield with increasing partial pressure of oxygen. This can be a 10% effect in an artificial atmosphere [30]. It is not excluded that other gases may have similar quenching effects.

Magnetic field: The light yield of plastic scintillators may be changed by a magnetic field. The effect is very nonlinear and apparently not all types of plastic scintillators are so affected. Increases of $\approx 3\%$ at 0.45 T have been reported [31]. Data are sketchy and mechanisms are not understood.

Radiation damage: Irradiation of plastic scintillators creates color centers which absorb light more strongly in the UV and blue than at longer wavelengths. This poorly understood effect appears as a reduction both of light yield and attenuation length. Radiation damage depends not only on the integrated dose, but on the dose rate, atmosphere, and temperature, before, during and after irradiation, as well as the materials properties of the base such as glass transition temperature, polymer chain length, *etc.* Annealing also occurs, accelerated by the diffusion of atmospheric oxygen and elevated temperatures. The phenomena are complex, unpredictable, and not well understood [32]. Since color centers are less intrusive at longer wavelengths, the most reliable method of mitigating radiation damage is to shift emissions at every step to the longest practical wavelengths, *e.g.*, utilize fluors with large Stokes’ shifts (aka the “Better red than dead” strategy).

28.3.3. Scintillating and wavelength-shifting fibers :

The clad optical fiber is an incarnation of scintillator and wavelength shifter (WLS) which is particularly useful [33]. Since the initial demonstration of the scintillating fiber (SCIFI) calorimeter [34], SCIFI techniques have become mainstream [35].

SCIFI calorimeters are fast, dense, radiation hard, and can have leadglass-like resolution. SCIFI trackers can handle high rates and are radiation tolerant, but the low photon yield at the end of a long fiber (see below) forces the use of sensitive photodetectors. WLS scintillator readout of a calorimeter allows a very high level of hermeticity since the solid angle blocked by the fiber on its way to the photodetector is very small. The sensitive region of scintillating fibers can be controlled by splicing them onto clear (non-scintillating/non-WLS) fibers.

A typical configuration would be fibers with a core of polystyrene-based scintillator or WLS (index of refraction $n = 1.59$), surrounded by a cladding of PMMA ($n = 1.49$) a few microns thick, or, for added light capture, with another cladding of fluorinated PMMA with $n = 1.42$, for an overall diameter of 0.5 to 1 mm. The fiber is drawn from a boule and great care is taken during production to ensure that the intersurface between the core and the cladding has the highest possible uniformity and quality, so that the signal transmission via total internal reflection has a low loss. The fraction of generated light which is transported down the optical pipe is denoted the capture fraction and is about 6% for the single-clad fiber and 10% for the double-clad fiber.

The number of photons from the fiber available at the photodetector is always smaller than desired, and increasing the light yield has proven difficult. A minimum-ionizing particle traversing a high-quality 1 mm diameter fiber perpendicular to its axis will produce fewer than 2000 photons, of which about 200 are captured. Attenuation may eliminate 95% of these photons in a large collider tracker.

A scintillating or WLS fiber is often characterized by its “attenuation length,” over which the signal is attenuated to $1/e$ of its original value. Many factors determine the attenuation length, including the importance of re-absorption of emitted photons by the polymer base or dissolved fluors, the level of crystallinity of the base polymer, and the quality of the total internal reflection boundary. Attenuation lengths of several meters are obtained by high quality fibers. However, it should be understood that the attenuation length is not necessarily a measure of fiber quality. Among other things, it is not constant with distance from the excitation source and it is wavelength dependent. So-called “cladding light” causes some of the distance dependence [36], but not all. The wavelength dependence is usually related to the higher re-absorption of shorter wavelength photons—once absorbed, re-emitted isotropically and lost with 90% probability—and to the lower absorption of longer wavelengths by polystyrene. Experimenters should be aware that measurements of attenuation length by a phototube with a bialkali photocathode, whose quantum efficiency drops below 10% at 480 nm, should not be naively compared to measurements utilizing a silicon photodiode, whose quantum efficiency is still rising at 600 nm.

28.4. Inorganic scintillators:

Revised September 2009 by R.-Y. Zhu (California Institute of Technology) and C.L. Woody (BNL).

Inorganic crystals form a class of scintillating materials with much higher densities than organic plastic scintillators (typically $\sim 4\text{--}8\text{ g/cm}^3$) with a variety of different properties for use as scintillation detectors. Due to their high density and high effective atomic number, they can be used in applications where high stopping power or a high conversion efficiency for electrons or photons is required. These include total absorption electromagnetic calorimeters (see Sec. 28.9.1), which consist of a totally active absorber (as opposed to a sampling calorimeter), as well as serving as gamma ray detectors over a wide range of energies. Many of these crystals also have very high light output, and can therefore provide excellent energy resolution down to very low energies (\sim few hundred keV).

Some crystals are intrinsic scintillators in which the luminescence is produced by a part of the crystal lattice itself. However, other crystals require the addition of a dopant, typically fluorescent ions such as thallium (Tl) or cerium (Ce) which is responsible for producing the scintillation light. However, in both cases, the scintillation mechanism is the same. Energy is deposited in the crystal by ionization, either directly by charged particles, or by the conversion of photons into electrons or positrons which subsequently produce ionization. This energy is transferred to the luminescent centers which then radiate scintillation photons. The efficiency η for the conversion of energy deposit in the crystal to scintillation light can be expressed by the relation [37]

$$\eta = \beta \cdot S \cdot Q . \quad (28.3)$$

where β is the efficiency of the energy conversion process, S is the efficiency of energy transfer to the luminescent center, and Q is the quantum efficiency of the luminescent center. The value of η ranges between 0.1 and ~ 1 depending on the crystal, and is the main factor in determining the intrinsic light output of the scintillator. In addition, the scintillation decay time is primarily determined by the energy transfer and emission process. The decay time of the scintillator is mainly dominated by the decay time of the luminescent center. For example, in the case of thallium doped sodium iodide (NaI(Tl)), the value of η is ~ 0.5 , which results in a light output $\sim 40,000$ photons per MeV of energy deposit. This high light output is largely due to the high quantum efficiency of the thallium ion ($Q \sim 1$), but the decay time is rather slow ($\tau \sim 250$ ns).

Table 28.4 lists the basic properties of some commonly used inorganic crystal scintillators. NaI(Tl) is one of the most common and widely used scintillators, with an emission that is well matched to a bi-alkali photomultiplier tube, but it is highly hygroscopic and difficult to work with, and has a rather low density. CsI(Tl) has high light yield, an emission that is well matched to solid state photodiodes, and is mechanically robust (high plasticity and resistance to cracking). However, it needs careful surface treatment and is slightly hygroscopic. Compared with CsI(Tl), pure CsI has identical mechanical properties, but faster emission at shorter wavelengths and light output approximately an order of magnitude lower. BaF₂ has a fast component with a sub-nanosecond decay time, and is the fastest known scintillator. However, it also has a slow component with a much longer decay time (~ 630 ns). Bismuth germanate (Bi₄Ge₃O₁₂ or BGO) has a high density, and consequently a short radiation length X_0 and Molière radius R_M . BGO's emission is well-matched to the spectral sensitivity of photodiodes, and it is easy to handle and not hygroscopic. Lead tungstate (PbWO₄ or PWO) has a very high density, with a very short X_0 and R_M , but its intrinsic light yield is rather low.

Cerium doped lutetium oxyorthosilicate (Lu₂SiO₅:Ce, or LSO:Ce) [38] and cerium doped lutetium-yttrium oxyorthosilicate (Lu_{2(1-x)}Y_{2x}SiO₅, LYSO:Ce) [39] are dense crystal scintillators which have a high light yield and a fast decay time. Only properties of LSO:Ce is listed in Table 28.4 since the properties of LYSO:Ce are similar to that of LSO:Ce except a little lower density than LSO:Ce depending on the yttrium fraction in LYSO:Ce. This material is also featured with excellent radiation hardness [40], so is expected to be used where extraordinary radiation hardness is required.

Table 28.4 also includes cerium doped lanthanum tri-halides, such as LaBr₃ [41], which is brighter and faster than LSO:Ce, but it is highly hygroscopic and has a lower density. The FWHM energy resolution measured for this material coupled to a PMT with bi-alkali photocathode for 0.662 MeV γ -rays from a ¹³⁷Cs source is about 3%, which is the best among all inorganic crystal scintillators. For this reason, LaBr₃ is expected to be widely used in applications where a good energy resolution for low energy photons are required, such as homeland security.

Beside the crystals listed in Table 28.4, a number of new crystals are being developed that may have potential applications in high energy or nuclear physics. Of particular interest is the family of yttrium and lutetium perovskites, which include YAP (YAlO₃:Ce) and LuAP (LuAlO₃:Ce) and their mixed compositions. These have been shown to be linear over a large energy range [42], and have the potential for providing extremely good intrinsic energy resolution. In addition, other fluoride crystals such as CeF₃ have been shown to provide excellent energy resolution in calorimeter applications.

Table 28.4 gives the light output of other crystals relative to NaI(Tl) and their dependence to the temperature variations measured for crystal samples of 1.5 X_0 cube with a Tyvek paper wrapping and a full end face coupled to a photodetector [43]. The quantum efficiencies of the photodetector is taken out to facilitate a direct comparison of crystal's light output. However, the useful signal produced by a scintillator is usually quoted in terms of the number of photoelectrons per MeV produced by a given photodetector. The relationship between the number of photons/MeV produced and photoelectrons/MeV detected involves the factors for the light collection efficiency L and the quantum efficiency QE of the photodetector:

$$N_{p.e./MeV} = L \cdot QE \cdot N_{\gamma}/MeV \quad (28.4)$$

L includes the transmission of scintillation light within the crystal (*i.e.*, the bulk attenuation length of the material), reflections and scattering from the surfaces, and the size and shape of the crystal. These factors can vary considerably depending on the sample, but can be in the range of $\sim 10\text{--}60\%$. The internal light transmission depends on the intrinsic properties of the material, *e.g.* the density and type of the scattering centers and defects that can produce internal absorption within the crystal, and can be highly affected by factors such as radiation damage, as discussed below.

The quantum efficiency depends on the type of photodetector used to detect the scintillation light, which is typically $\sim 15\text{--}20\%$ for photomultiplier tubes and $\sim 70\%$ for silicon photodiodes for visible wavelengths. The quantum efficiency of the detector is usually highly wavelength dependent and should be matched to the particular crystal of interest to give the highest quantum yield at the wavelength corresponding to the peak of the scintillation emission. Fig. 28.2 shows the quantum efficiencies of two photodetectors, a Hamamatsu R2059 PMT with bi-alkali cathode and quartz window and a Hamamatsu S8664 avalanche photodiode (APD) as a function of wavelength. Also shown in the figure are emission spectra of three crystal scintillators, BGO, LSO:Ce/LYSO:Ce and CsI(Tl), and the numerical values of the emission weighted quantum efficiency. The area under each emission spectrum is proportional to crystal's light yield, as shown in Table 28.4, where the quantum efficiencies of the photodetector has been taken out. Results with different photodetectors can be significantly different. For example, the response of CsI(Tl) relative to NaI(Tl) with a standard photomultiplier tube with a bi-alkali photo-cathode, *e.g.* Hamamatsu R2059, would be 45 rather than 165 because of the photomultiplier's low quantum efficiency at longer wavelengths. For scintillators which emit in the UV, a detector with a quartz window should be used.

For very low energy applications (typically below 1 MeV), non-proportionality of the scintillation light yield may be important. It has been known for a long time that the conversion factor between the energy deposited in a crystal scintillator and the number of photons produced is not constant. It is also known that the energy resolution measured by all crystal scintillators for low energy γ -rays is significantly worse than the contribution from photo-electron statistics alone, indicating an intrinsic contribution from the scintillator itself. Precision measurement using low energy electron beam shows that

this non-proportionality is crystal dependent [44]. Recent study on this issue also shows that this effect is also sample dependent even for the same crystal [45]. Further work is therefore needed to fully understand this subject.

One important issue related to the application of a crystal scintillator is its radiation hardness. Stability of its light output, or the ability to track and monitor the variation of its light output in a radiation environment, is required for high resolution and precision calibration [46]. All known crystal scintillators suffer from radiation damage. A common damage phenomenon is the appearance of radiation induced absorption caused by the formation of color centers originated from the impurities or point defects in the crystal. This radiation induced absorption reduces the light attenuation length in the crystal, and hence its light output. For crystals with high defect density, a severe reduction of light attenuation length may cause a distortion of the light response uniformity, leading to a degradation of the energy resolution. Additional radiation damage effects may include a reduced intrinsic scintillation light yield (damage to the luminescent centers) and an increased phosphorescence (afterglow). For crystals to be used in the construction a high precision calorimeter in a radiation environment, its scintillation mechanism must not be damaged and its light attenuation length in the expected radiation environment must be long enough so that its light response uniformity, and thus its energy resolution, does not change [47].

Most of the crystals listed in Table 28.4 have been used in high energy or nuclear physics experiments when the ultimate energy resolution for electrons and photons is desired. Examples are the Crystal Ball NaI(Tl) calorimeter at SPEAR, the L3 BGO calorimeter at LEP, the CLEO CsI(Tl) calorimeter at CESR, the KTeV CsI calorimeter at the Tevatron, the BaBar, BELLE and BES II CsI(Tl) calorimeters at PEP-II, KEK and BEPC III. Because of its high density and low cost, PWO calorimeters are widely used by CMS and ALICE at LHC, by CLAS and PrimEx at CEBAF, and by PANDA at GSI. Recently, investigations have been made aiming at using LSO:Ce or LYSO:Ce crystals for future high energy or nuclear physics experiments [40].

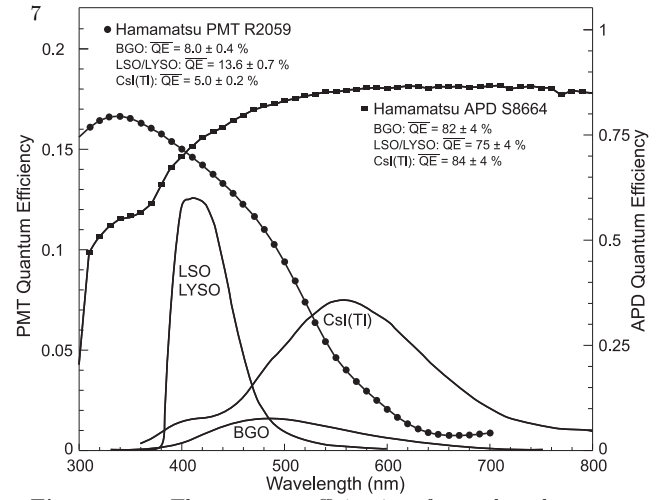


Figure 28.2: The quantum efficiencies of two photodetectors, a Hamamatsu R2059 PMT with bi-alkali cathode and a Hamamatsu S8664 avalanche photodiode (APD), are shown as a function of wavelength. Also shown in the figure are emission spectra of three crystal scintillators, BGO, LSO and CsI(Tl), and the numerical values of the emission weighted quantum efficiency. The area under each emission spectrum is proportional to crystal's light yield.

Table 28.4: Properties of several inorganic crystal scintillators. Most of the notation is defined in Sec. 6 of this *Review*.

Parameter:	ρ	MP	X_0^*	R_M^*	dE^*/dx	λ_I^*	τ_{decay}	λ_{max}	n^\ddagger	Relative output [†]	Hygroscopic?	$d(\text{LY})/dT$
Units:	g/cm^3	$^\circ\text{C}$	cm	cm	MeV/cm	cm	ns	nm				$\%/^\circ\text{C}^\ddagger$
NaI(Tl)	3.67	651	2.59	4.13	4.8	42.9	230	410	1.85	100	yes	-0.2
BGO	7.13	1050	1.12	2.23	9.0	22.8	300	480	2.15	21	no	-0.9
BaF ₂	4.89	1280	2.03	3.10	6.5	30.7	630 ^s 0.9 ^f	300 ^s 220 ^f	1.50	36 ^s 3.4 ^f	no	-1.3 ^s $\sim 0^f$
CsI(Tl)	4.51	621	1.86	3.57	5.6	39.3	1300	560	1.79	165	slight	0.3
CsI(pure)	4.51	621	1.86	3.57	5.6	39.3	35 ^s 6 ^f	420 ^s 310 ^f	1.95	3.6 ^s 1.1 ^f	slight	-1.3
PbWO ₄	8.3	1123	0.89	2.00	10.1	20.7	30 ^s 10 ^f	425 ^s 420 ^f	2.20	0.083 ^s 0.29 ^f	no	-2.7
LSO(Ce)	7.40	2050	1.14	2.07	9.6	20.9	40	402	1.82	83	no	-0.2
LaBr ₃ (Ce)	5.29	788	1.88	2.85	6.9	30.4	20	356	1.9	130	yes	0.2

* Numerical values calculated using formulae in this review.

[‡] Refractive index at the wavelength of the emission maximum.

[†] Relative light output measured for samples of 1.5 X_0 cube with a Tyvek paper wrapping and a full end face coupled to a photodetector. The quantum efficiencies of the photodetector is taken out.

[‡] Variation of light yield with temperature evaluated at the room temperature.

f = fast component, s = slow component

28.5. Cherenkov detectors

Revised September 2009 by B.N. Ratcliff (SLAC).

Although devices using Cherenkov radiation are often thought of as only particle identification (PID) detectors, in practice they are used over a broader range of applications including; (1) fast particle counters; (2) hadronic PID; and (3) tracking detectors performing complete event reconstruction. Examples of applications from each category include; (1) the BaBar luminosity detector [48]; (2) the hadronic PID detectors at the B factory detectors—DIRC in BaBar [9] and the aerogel threshold Cherenkov in Belle [49]; and (3) large water Cherenkov counters such as Super-Kamiokande [51]. Cherenkov counters contain two main elements; (1) a radiator through which the charged particle passes, and (2) a photodetector. As Cherenkov radiation is a weak source of photons, light collection and detection must be as efficient as possible. The refractive index n and the particle's path length through the radiator L appear in the Cherenkov relations allowing the tuning of these quantities for particular applications.

Cherenkov detectors utilize one or more of the properties of Cherenkov radiation discussed in the Passages of Particles through Matter section (Sec. 27 of this *Review*): the prompt emission of a light pulse; the existence of a velocity threshold for radiation; and the dependence of the Cherenkov cone half-angle θ_c and the number of emitted photons on the velocity of the particle and the refractive index of the medium.

The number of photoelectrons ($N_{p.e.}$) detected in a given device is

$$N_{p.e.} = L \frac{\alpha^2 z^2}{r_e m_e c^2} \int \epsilon(E) \sin^2 \theta_c(E) dE, \quad (28.5)$$

where $\epsilon(E)$ is the efficiency for collecting the Cherenkov light and transducing it into photoelectrons, and $\alpha^2/(r_e m_e c^2) = 370 \text{ cm}^{-1} \text{ eV}^{-1}$.

The quantities ϵ and θ_c are functions of the photon energy E . As the typical energy dependent variation of the index of refraction is modest, a quantity called the *Cherenkov detector quality factor* N_0 can be defined as

$$N_0 = \frac{\alpha^2 z^2}{r_e m_e c^2} \int \epsilon dE, \quad (28.6)$$

so that, taking $z = 1$ (the usual case in high-energy physics),

$$N_{p.e.} \approx LN_0 \langle \sin^2 \theta_c \rangle. \quad (28.7)$$

This definition of the quality factor N_0 is not universal, nor, indeed, very useful for those common situations where ϵ factorizes as $\epsilon = \epsilon_{\text{coll}} \epsilon_{\text{det}}$ with the geometrical photon collection efficiency (ϵ_{coll}) varying substantially for different tracks while the photon detector efficiency (ϵ_{det}) remains nearly track independent. In this case, it can be useful to explicitly remove (ϵ_{coll}) from the definition of N_0 . A typical value of N_0 for a photomultiplier (PMT) detection system working in the visible and near UV, and collecting most of the Cherenkov light, is about 100 cm^{-1} . Practical counters, utilizing a variety of different photodetectors, have values ranging between about 30 and 180 cm^{-1} . Radiators can be chosen from a variety of transparent materials (Sec. 27 of this *Review* and Table 6.1). In addition to refractive index, the choice requires consideration of factors such as material density, radiation length and radiation hardness, transmission bandwidth, absorption length, chromatic dispersion, optical workability (for solids), availability, and cost. When the momenta of particles to be identified is high, the refractive index must be set close to one, so that the photon yield per unit length is low and a long particle path in the radiator is required. Recently, the gap in refractive index that has traditionally existed between gases and liquid or solid materials has been partially closed with transparent *silica aerogels* with indices that range between about 1.007 and 1.13.

Cherenkov counters may be classified as either *imaging* or *threshold* types, depending on whether they do or do not make use of Cherenkov angle (θ_c) information. Imaging counters may be used to track particles as well as identify them. The recent development of very fast photodetectors such as micro-channel plate PMTs (MCP PMT) (see Sec. 28.2 of this *Review*) also potentially allows very fast Cherenkov based time of flight (TOF) detectors of either class [55].

Threshold Cherenkov detectors [52], in their simplest form, make a yes/no decision based on whether the particle is above or below the Cherenkov threshold velocity $\beta_t = 1/n$. A straightforward enhancement of such detectors uses the number of observed photoelectrons (or a calibrated pulse height) to discriminate between species or to set probabilities for each particle species [53]. This strategy can increase the momentum range of particle separation by a modest amount (to a momentum some 20% above the threshold momentum of the heavier particle in a typical case).

Careful designs give $\langle \epsilon_{\text{coll}} \rangle \gtrsim 90\%$. For a photomultiplier with a typical alkali cathode, $\int \epsilon_{\text{det}} dE \approx 0.27 \text{ eV}$, so that

$$N_{p.e.}/L \approx 90 \text{ cm}^{-1} \langle \sin^2 \theta_c \rangle \quad (\text{i.e., } N_0 = 90 \text{ cm}^{-1}). \quad (28.8)$$

Suppose, for example, that n is chosen so that the threshold for species a is p_t ; that is, at this momentum species a has velocity $\beta_a = 1/n$. A second, lighter, species b with the same momentum has velocity β_b , so $\cos \theta_c = \beta_a/\beta_b$, and

$$N_{p.e.}/L \approx 90 \text{ cm}^{-1} \frac{m_a^2 - m_b^2}{p_t^2 + m_a^2}. \quad (28.9)$$

For K/π separation at $p = p_t = 1(5) \text{ GeV}/c$, $N_{p.e.}/L \approx 16(0.8) \text{ cm}^{-1}$ for π 's and (by design) 0 for K 's.

For limited path lengths $N_{p.e.}$ will usually be small. The overall efficiency of the device is controlled by Poisson fluctuations, which can be especially critical for separation of species where one particle type is dominant. Moreover, the effective number of photoelectrons is often less than the average number calculated above due to additional equivalent noise from the photodetector (see the discussion of the excess noise factor in Sec. 28.2 of this *Review*). It is common to design for at least 10 photoelectrons for the high velocity particle in order to obtain a robust counter. As rejection of the particle that is below threshold depends on *not* seeing a signal, electronic and other background noise can be important. Physics sources of light production for the below threshold particle, such as decay to an above threshold particle or the production of delta rays in the radiator, often limit the separation attainable, and need to be carefully considered. Well designed, modern multi-channel counters, such as the ACC at Belle [49], can attain adequate particle separation performance over a substantial momentum range for essentially the full solid angle of the spectrometer.

Imaging counters make the most powerful use of the information available by measuring the ring-correlated angles of emission of the individual Cherenkov photons. Since low-energy photon detectors can measure only the position (and, perhaps, a precise detection time) of the individual Cherenkov photons (not the angles directly), the photons must be “imaged” onto a detector so that their angles can be derived [54]. Typically the optics map the Cherenkov cone onto (a portion of) a distorted “circle” at the photodetector. Though the imaging process is directly analogous to familiar imaging techniques used in telescopes and other optical instruments, there is a somewhat bewildering variety of methods used in a wide variety of counter types with different names. Some of the imaging methods used include (1) focusing by a lens; (2) proximity focusing (i.e., focusing by limiting the emission region of the radiation); and (3) focusing through an aperture (a pinhole). In addition, the prompt Cherenkov emission coupled with the speed of modern photon detectors allows the use of (4) time imaging, a method which is little used in conventional imaging technology. Finally, (5) correlated tracking (and event reconstruction) can be performed in large water counters by combining the individual space position and time of each photon together with the constraint that Cherenkov photons are emitted from each track at the same polar angle (Sec. 29.3.1 of this *Review*).

In a simple model of an imaging PID counter, the fractional error on the particle velocity (δ_β) is given by

$$\delta_\beta = \frac{\sigma_\beta}{\beta} = \tan \theta_c \sigma(\theta_c), \quad (28.10)$$

where

$$\sigma(\theta_c) = \frac{\langle \sigma(\theta_i) \rangle}{\sqrt{N_{p.e.}}} \oplus C, \quad (28.11)$$

and $\langle\sigma(\theta_i)\rangle$ is the average single photoelectron resolution, as defined by the optics, detector resolution and the intrinsic chromaticity spread of the radiator index of refraction averaged over the photon detection bandwidth. C combines a number of other contributions to resolution including, (1) correlated terms such as tracking, alignment, and multiple scattering, (2) hit ambiguities, (3) background hits from random sources, and (4) hits coming from other tracks. The actual separation performance is also limited by physics effects such as decays in flight and particle interactions in the material of the detector. In many practical cases, the performance is limited by these effects.

For a $\beta \approx 1$ particle of momentum (p) well above threshold entering a radiator with index of refraction (n), the number of σ separation (N_σ) between particles of mass m_1 and m_2 is approximately

$$N_\sigma \approx \frac{|m_1^2 - m_2^2|}{2p^2\sigma(\theta_c)\sqrt{n^2 - 1}}. \quad (28.12)$$

In practical counters, the angular resolution term $\sigma(\theta_c)$ varies between about 0.1 and 5 mrad depending on the size, radiator, and photodetector type of the particular counter. The range of momenta over which a particular counter can separate particle species extends from the point at which the number of photons emitted becomes sufficient for the counter to operate efficiently as a threshold device ($\sim 20\%$ above the threshold for the lighter species) to the value in the imaging region given by the equation above. For example, for $\sigma(\theta_c) = 2\text{mrad}$, a fused silica radiator ($n = 1.474$), or a fluorocarbon gas radiator (C_5F_{12} , $n = 1.0017$), would separate π/K 's from the threshold region starting around 0.15(3) GeV/ c through the imaging region up to about 4.2(18) GeV/ c at better than 3σ .

Many different imaging counters have been built during the last several decades [55]. Among the earliest examples of this class of counters are the very limited acceptance Differential Cherenkov detectors, designed for particle selection in high momentum beam lines. These devices use optical focusing and/or geometrical masking to select particles having velocities in a specified region. With careful design, a velocity resolution of $\sigma_\beta/\beta \approx 10^{-4}$ – 10^{-5} can be obtained [52].

Practical multi-track Ring-Imaging Cherenkov detectors (generically called RICH counters) are a more recent development. RICH counters are sometimes further classified by ‘generations’ that differ based on historical timing, performance, design, and photodetection techniques.

Prototypical examples of first generation RICH counters are those used in the DELPHI and SLD detectors at the LEP and SLC Z factory e^+e^- colliders [55]. They have both liquid (C_6F_{14} , $n = 1.276$) and gas (C_5F_{12} , $n = 1.0017$) radiators, the former being proximity imaged with the latter using mirrors. The phototransducers are a TPC/wire-chamber combination. They are made sensitive to photons by doping the TPC gas (usually, ethane/methane) with $\sim 0.05\%$ TMAE (tetrakis(dimethylamino)ethylene). Great attention to detail is required, (1) to avoid absorbing the UV photons to which TMAE is sensitive, (2) to avoid absorbing the single photoelectrons as they drift in the long TPC, and (3) to keep the chemically active TMAE vapor from interacting with materials in the system. In spite of their unforgiving operational characteristics, these counters attained good $e/\pi/K/p$ separation over wide momentum ranges (from about 0.25 to 20 GeV/ c) during several years of operation at LEP and SLC. Related but smaller acceptance devices include the OMEGA RICH at the CERN SPS, and the RICH in the balloon-borne CAPRICE detector [55].

Later generation counters [55] generally operate at much higher rates, with more detection channels, than the first generation detectors just described. They also utilize faster, more forgiving photon detectors, covering different photon detection bandwidths. Radiator choices have broadened to include materials such as lithium fluoride, fused silica, and aerogel. Vacuum based photodetection systems (*e.g.*, single or multi anode PMTs, MCP PMTs, or hybrid photodiodes (HPD)) have become increasingly common (see Sec. 28.2 of this *Review*). They handle high rates, and can be used with a wide choice of radiators. Examples include (1) the SELEX RICH at Fermilab, which mirror focuses the Cherenkov photons from a neon radiator onto a camera array made of ~ 2000 PMTs to separate hadrons over a wide momentum range (to well above 200 GeV/ c for heavy hadrons);

(2) the HERMES RICH at HERA, which mirror focuses photons from C_4F_{10} ($n = 1.00137$) and aerogel ($n = 1.0304$) radiators within the same volume onto a PMT camera array to separate hadrons in the momentum range from 2 to 15 GeV/ c ; and (3) the LHCb detector now being brought into operation at the LHC. It uses two separate counters. One volume, like HERMES, contains two radiators (aerogel and C_4F_{10}) while the second volume contains CF_4 . Photons are mirror focused onto detector arrays of HPDs to cover a π/K separation momentum range between 1 and 150 GeV/ c .

Other fast detection systems that use solid cesium iodide (CsI) photocathodes or triethylamine (TEA) doping in proportional chambers are useful with certain radiator types and geometries. Examples include (1) the CLEO-III RICH at CESR that uses a LiF radiator with TEA doped proportional chambers; (2) the ALICE detector at the LHC that uses proximity focused liquid (C_6F_{14} radiators and solid CSI photocathodes (similar photodetectors have been used for several years by the HADES and COMPASS detectors), and the hadron blind detector (HBD) in the PHENIX detector at RHIC that couples a low index CF_4 radiator to a photodetector based on electron multiplier (GEM) chambers with reflective CSI photocathodes [55].

A DIRC (Detection [of] Internally Reflected Cherenkov [light]) is a distinctive, compact RICH subtype first used in the BaBar detector [50]. A DIRC ‘inverts’ the usual RICH principle for use of light from the radiator by collecting and imaging the total internally reflected light rather than the transmitted light. It utilizes the optical material of the radiator in two ways, simultaneously; first as a Cherenkov radiator, and second, as a light pipe. The magnitudes of the photon angles are preserved during transport by the flat, rectangular cross section radiators, allowing the photons to be efficiently transported to a detector outside the path of the particle where they may be imaged in up to three independent dimensions (the usual two in space and, due to the long photon paths lengths, one in time). Because the index of refraction in the radiator is large (~ 1.48 for fused silica), the momentum range with good π/K separation is rather low. The BaBar DIRC range extends up to ~ 4 GeV/ c . It is plausible, but difficult, to extend it up to about 10 GeV/ c with an improved design. New DIRC detectors are being developed that take advantage of the new, very fast, pixelated photodetectors becoming available, such as flat panel PMTs and MCP PMTs. They typically utilize either time imaging or mirror focused optics, or both, leading not only to a precision measurement of the Cherenkov angle, but in some cases, to a precise measurement of the particle time of flight, and/or to correction of the chromatic dispersion in the radiator. Examples include (1) the time of propagation (TOP) counter being developed for the BELLE-II upgrade at KEKB which emphasizes precision timing for both Cherenkov imaging and TOF; (2) the full 3-dimensional imaging FDIRC for the SuperB detector at the Italian SuperB collider which uses precision timing not only for improving the angle reconstruction and TOF, but also to correct the chromatic dispersion; and (3) the DIRCs being developed for the PANDA detector at FAIR that use elegant focusing optics and fast timing [55].

28.6. Gaseous detectors

28.6.1. Energy loss and charge transport in gases : Revised March 2010 by F. Sauli (CERN) and M. Titov (CEA Saclay).

Gas-filled detectors localize the ionization produced by charged particles, generally after charge multiplication. The statistics of ionization processes having asymmetries in the ionization trails, affect the coordinate determination deduced from the measurement of drift time, or of the center of gravity of the collected charge. For thin gas layers, the width of the energy loss distribution can be larger than its average, requiring multiple sample or truncated mean analysis to achieve good particle identification. In the truncated mean method for calculating $\langle dE/dx \rangle$, the ionization measurements along the track length are broken into many samples and then a fixed fraction of high-side (and sometimes also low-side) values are rejected [56].

The energy loss of charged particles and photons in matter is discussed in Sec. 27. Table 28.5 provides values of relevant parameters in some commonly used gases at NTP (normal temperature, 20°C ,

and pressure, 1 atm) for unit-charge minimum-ionizing particles (MIPs) [57–63]. Values often differ, depending on the source, so those in the table should be taken only as approximate. For different conditions and for mixtures, and neglecting internal energy transfer processes (*e.g.*, Penning effect), one can scale the density, N_P , and N_T with temperature and pressure assuming a perfect gas law.

Table 28.5: Properties of noble and molecular gases at normal temperature and pressure (NTP: 20° C, one atm). E_X , E_I : first excitation, ionization energy; W_I : average energy per ion pair; $dE/dx|_{\min}$, N_P , N_T : differential energy loss, primary and total number of electron-ion pairs per cm, for unit charge minimum ionizing particles.

Gas	Density, mg cm ⁻³	E_x eV	E_I eV	W_I eV	$dE/dx _{\min}$ keV cm ⁻¹	N_P cm ⁻¹	N_T cm ⁻¹
He	0.179	19.8	24.6	41.3	0.32	3.5	8
Ne	0.839	16.7	21.6	37	1.45	13	40
Ar	1.66	11.6	15.7	26	2.53	25	97
Xe	5.495	8.4	12.1	22	6.87	41	312
CH ₄	0.667	8.8	12.6	30	1.61	28	54
C ₂ H ₆	1.26	8.2	11.5	26	2.91	48	112
iC ₄ H ₁₀	2.49	6.5	10.6	26	5.67	90	220
CO ₂	1.84	7.0	13.8	34	3.35	35	100
CF ₄	3.78	10.0	16.0	54	6.38	63	120

When an ionizing particle passes through the gas it creates electron-ion pairs, but often the ejected electrons have sufficient energy to further ionize the medium. As shown in Table 28.5, the total number of electron-ion pairs (N_T) is usually a few times larger than the number of primaries (N_P).

The probability for a released electron to have an energy E or larger follows an approximate $1/E^2$ dependence (Rutherford law), shown in Fig. 28.3 for Ar/CH₄ at NTP (dotted line, left scale). More detailed estimates taking into account the electronic structure of the medium are shown in the figure, for three values of the particle velocity factor $\beta\gamma$ [58]. The dot-dashed line provides, on the right scale, the practical range of electrons (including scattering) of energy E . As an example, about 0.6% of released electrons have 1 keV or more energy, substantially increasing the ionization loss rate. The practical range of 1 keV electrons in argon (dot-dashed line, right scale) is 70 μm and this can contribute to the error in the coordinate determination.

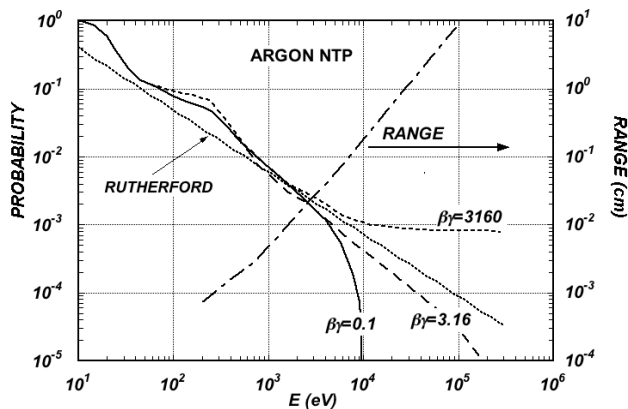


Figure 28.3: Probability of single collisions in which released electrons have an energy E or larger (left scale) and practical range of electrons in Ar/CH₄ (P10) at NTP (dot-dashed curve, right scale) [58].

The number of electron-ion pairs per primary ionization, or cluster size, has an exponentially decreasing probability; for argon, there is about 1% probability for primary clusters to contain ten or more electron-ion pairs [59].

Once released in the gas, and under the influence of an applied electric field, electrons and ions drift in opposite directions and diffuse towards the electrodes. The scattering cross section is determined by the details of atomic and molecular structure. Therefore, the drift velocity and diffusion of electrons depend very strongly on the nature of the gas, specifically on the inelastic cross-section involving the rotational and vibrational levels of molecules. In noble gases, the inelastic cross section is zero below excitation and ionization thresholds. Large drift velocities are achieved by adding polyatomic gases (usually CH₄, CO₂, or CF₄) having large inelastic cross sections at moderate energies, which results in “cooling” electrons into the energy range of the Ramsauer-Townsend minimum (at ~ 0.5 eV) of the elastic cross-section of argon. The reduction in both the total electron scattering cross-section and the electron energy results in a large increase of electron drift velocity (for a compilation of electron-molecule cross sections see Ref. 60). Another principal role of the polyatomic gas is to absorb the ultraviolet photons emitted by the excited noble gas atoms. Extensive collections of experimental data [61] and theoretical calculations based on transport theory [62] permit estimates of drift and diffusion properties in pure gases and their mixtures. In a simple approximation, gas kinetic theory provides the drift velocity v as a function of the mean collision time τ and the electric field E : $v = eE\tau/m_e$ (Townsend’s expression). Values of drift velocity and diffusion for some commonly used gases at NTP are given in Fig. 28.4 and Fig. 28.5. These have been computed with the MAGBOLTZ program [63]. For different conditions, the horizontal axis must be scaled inversely with the gas density. Standard deviations for longitudinal (σ_L) and transverse diffusion (σ_T) are given for one cm of drift, and scale with the the square root of the drift distance. Since the collection time is inversely proportional to the drift velocity, diffusion is less in gases such as CF₄ that have high drift velocities. In the presence of an external magnetic field, the Lorentz force acting on electrons between collisions deflects the drifting electrons and modifies the drift properties. The electron trajectories, velocities and diffusion parameters can be computed with MAGBOLTZ. A simple theory, the friction force model, provides an expression for the vector drift velocity \mathbf{v} as a function of electric and magnetic field vectors \mathbf{E} and \mathbf{B} , of the Larmor frequency $\omega = eB/m_e$, and of the mean collision time τ :

$$\mathbf{v} = \frac{e}{m_e} \frac{\tau}{1 + \omega^2\tau^2} \left(\mathbf{E} + \frac{\omega\tau}{B} (\mathbf{E} \times \mathbf{B}) + \frac{\omega^2\tau^2}{B^2} (\mathbf{E} \cdot \mathbf{B}) \mathbf{B} \right) \quad (28.13)$$

To a good approximation, and for moderate fields, one can assume that the energy of the electrons is not affected by B , and use for τ the values deduced from the drift velocity at $B = 0$ (the Townsend expression). For \mathbf{E} perpendicular to \mathbf{B} , the drift angle to the relative to the electric field vector is $\tan \theta_B = \omega\tau$ and $v = (E/B)(\omega\tau/\sqrt{1 + \omega^2\tau^2})$. For parallel electric and magnetic fields, drift velocity and longitudinal diffusion are not affected, while the transverse diffusion can be strongly reduced: $\sigma_T(B) = \sigma_T(B = 0)/\sqrt{1 + \omega^2\tau^2}$. The dotted line in Fig. 28.5 represents σ_T for the classic Ar/CH₄ (90:10) mixture at 4 T. Large values of $\omega\tau \sim 20$ at 5 T are consistent with the measurement of diffusion coefficient in Ar/CF₄/iC₄H₁₀ (95:3:2). This reduction is exploited in time projection chambers (Sec. 28.6.5) to improve spatial resolution.

In mixtures containing electronegative molecules, such as O₂ or H₂O, electrons can be captured to form negative ions. Capture cross-sections are strongly energy-dependent, and therefore the capture probability is a function of applied field. For example, the electron is attached to the oxygen molecule at energies below 1 eV. The three-body electron attachment coefficients may differ greatly for the same additive in different mixtures. As an example, at moderate fields (up to 1 kV/cm) the addition of 0.1% of oxygen to an Ar/CO₂ mixture results in an electron capture probability about twenty times larger than the same addition to Ar/CH₄.

Carbon tetrafluoride is not electronegative at low and moderate fields, making its use attractive as drift gas due to its very low diffusion. However, CF₄ has a large electron capture cross section at fields above ~ 8 kV/cm, before reaching avalanche field strengths. Depending on detector geometry, some signal reduction and resolution loss can be expected using this gas.

If the electric field is increased sufficiently, electrons gain enough energy between collisions to ionize molecules. Above a gas-dependent

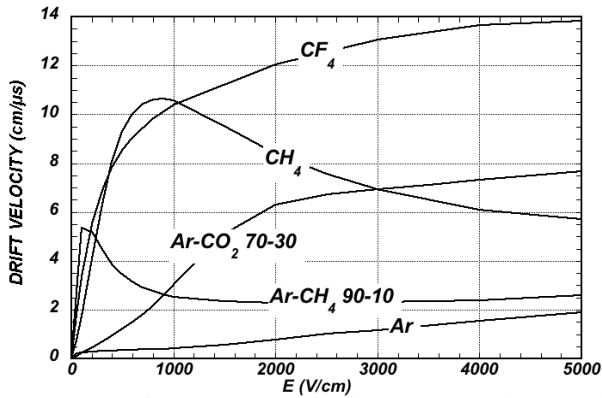


Figure 28.4: Computed electron drift velocity as a function of electric field in several gases at NTP and $B = 0$ [63].

threshold, the mean free path for ionization, λ_i , decreases exponentially with the field; its inverse, $\alpha = 1/\lambda_i$, is the first Townsend coefficient. In wire chambers, most of the increase of avalanche particle density occurs very close to the anode wires, and a simple electrostatic consideration shows that the largest fraction of the detected signal is due to the motion of positive ions receding from the wires. The electron component, although very fast, contributes very little to the signal. This determines the characteristic shape of the detected signals in the proportional mode: a fast rise followed by a gradual increase. The slow component, the so-called “ion tail” that limits the time resolution of the detector, is usually removed by differentiation of the signal. In uniform fields, N_0 initial electrons multiply over a length x forming an electron avalanche of size $N = N_0 e^{\alpha x}$; N/N_0 is the gain of the detector. Fig. 28.6 shows examples of Townsend coefficients for several gas mixtures, computed with MAGBOLTZ [63].

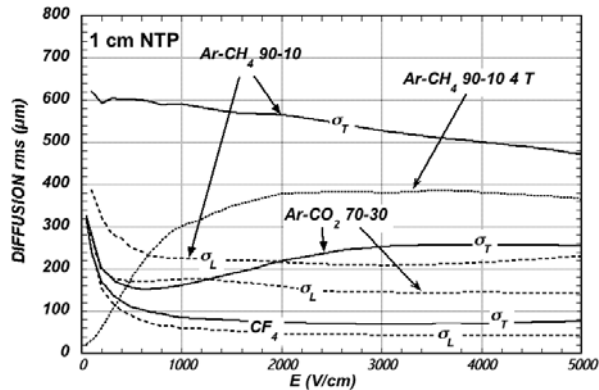


Figure 28.5: Electron longitudinal diffusion (σ_L) (dashed lines) and transverse diffusion (σ_T) (full lines) for 1 cm of drift at NTP and $B = 0$. The dotted line shows σ_T for the P10 mixture at 4T [63].

Positive ions released by the primary ionization or produced in the avalanches drift and diffuse under the influence of the electric field. Negative ions may also be produced by electron attachment to gas molecules. The drift velocity of ions in the fields encountered in gaseous detectors (up to few kV/cm) is typically about three orders of magnitude less than for electrons. The ion mobility μ , the ratio of drift velocity to electric field, is constant for a given ion type up to very high fields. Values of mobility at NTP for ions in their own and other gases are given in Table 28.6 [64]. For different temperatures and pressures, the mobility can be scaled inversely with the density assuming an ideal gas law. For mixtures, due to a very effective charge transfer mechanism, only ions with the lowest ionization potential survive after a short path in the gas. Both the lateral and transverse diffusion of ions are proportional to the square root of the drift time, with a coefficient that depends on temperature but not on the ion

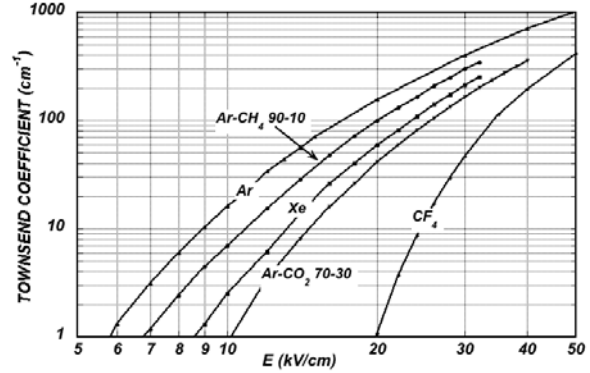


Figure 28.6: Computed first Townsend coefficient α as a function of electric field in several gases at NTP [63].

mass. Accumulation of ions in the gas drift volume may induce field distortions (see Sec. 28.6.5).

Table 28.6: Mobility of ions in gases at NTP [64].

Gas	Ion	Mobility μ ($\text{cm}^2 \text{V}^{-1} \text{s}^{-1}$)
He	He^+	10.4
Ne	Ne^+	4.7
Ar	Ar^+	1.54
Ar/ CH_4	CH_4^+	1.87
Ar/ CO_2	CO_2^+	1.72
CH_4	CH_4^+	2.26
CO_2	CO_2^+	1.09

28.6.2. Multi-Wire Proportional and Drift Chambers : Revised March 2010 by Fabio Sauli (CERN) and Maxim Titov (CEA Saclay).

Single-wire counters that detect the ionization produced in a gas by a charged particle, followed by charge multiplication and collection around a thin wire have been used for decades. Good energy resolution is obtained in the proportional amplification mode, while very large saturated pulses can be detected in the streamer and Geiger modes [3].

Multiwire proportional chambers (MWPCs) [65,66], introduced in the late '60's, detect, localize and measure energy deposit by charged particles over large areas. A mesh of parallel anode wires at a suitable potential, inserted between two cathodes, acts almost as a set of independent proportional counters (see Fig. 28.7a). Electrons released in the gas volume drift towards the anodes and produce avalanches in the increasing field. Analytic expressions for the electric field can be found in many textbooks. The fields close to the wires $E(r)$, in the drift region E_D , and the capacitance C per unit length of anode wire are approximately given by

$$E(r) = \frac{CV_0}{2\pi\epsilon_0 r} \quad E_D = \frac{CV_0}{2\epsilon_0 s} \quad C = \frac{2\pi\epsilon_0}{\pi(\ell/s) - \ln(2\pi a/s)}, \quad (28.14)$$

where r is the distance from the center of the anode, s the wire spacing, ℓ and V_0 the distance and potential difference between anode and cathode, and a the anode wire radius.

Because of electrostatic forces, anode wires are in equilibrium only for a perfect geometry. Small deviations result in forces displacing the wires alternatively below and above the symmetry plane, sometimes with catastrophic results. These displacement forces are countered by the mechanical tension of the wire, up to a maximum unsupported stable length, L_M [56], above which the wire deforms:

$$L_M = \frac{s}{CV_0} \sqrt{4\pi\epsilon_0 T_M} \quad (28.15)$$

The maximum tension T_M depends on the wire diameter and modulus of elasticity. Table 28.7 gives approximate values for tungsten and the corresponding maximum stable wire length under reasonable assumptions for the operating voltage ($V_0 = 5$ kV) [67]. Internal supports and spacers can be used in the construction of longer detectors to overcome limits on the wire length imposed by Eq. (28.15).

Table 28.7: Maximum tension T_M and stable unsupported length L_M for tungsten wires with spacing s , operated at $V_0 = 5$ kV. No safety factor is included.

Wire diameter (μm)	T_M (newton)	s (mm)	L_M (cm)
10	0.16	1	25
20	0.65	2	85

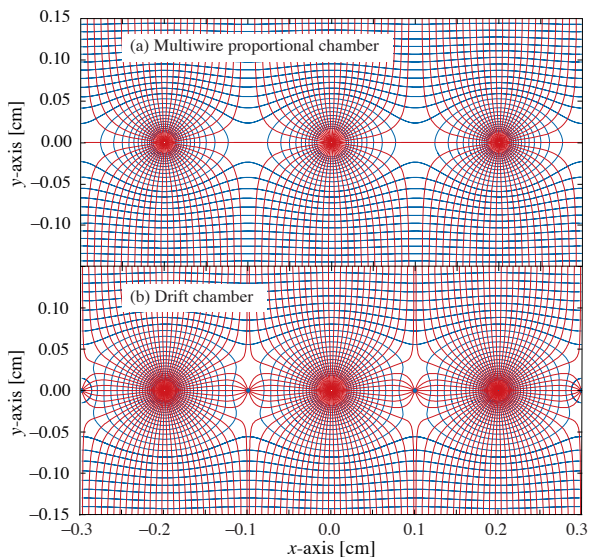


Figure 28.7: Electric field lines and equipotentials in (a) a multiwire proportional chamber and (b) a drift chamber.

Detection of charge on the wires over a predefined threshold provides the transverse coordinate to the wire with an accuracy comparable to that of the wire spacing. The coordinate along each wire can be obtained by measuring the ratio of collected charge at the two ends of resistive wires. Making use of the charge profile induced on segmented cathodes, the so-called center-of gravity (COG) method, permits localization of tracks to sub-mm accuracy. Due to the statistics of energy loss and asymmetric ionization clusters, the position accuracy is $\sim 50 \mu\text{m}$ rms for tracks perpendicular to the wire plane, but degrades to $\sim 250 \mu\text{m}$ at 30° to the normal [68]. The intrinsic bi-dimensional characteristic of the COG readout has found numerous applications in medical imaging.

Drift chambers, developed in the early '70's, can be used to estimate the longitudinal position of a track by exploiting the arrival time of electrons at the anodes if the time of interaction is known [69]. The distance between anode wires is usually several cm, allowing coverage of large areas at reduced cost. In the original design, a thicker wire (the field wire) at the proper voltage, placed between the anode wires, reduces the field at the mid-point between anodes and improves charge collection (Fig. 28.7b). In some drift chamber designs, and with the help of suitable voltages applied to field-shaping electrodes, the electric field structure is adjusted to improve the linearity of space-to-drift-time relation, resulting in better spatial resolution [70].

Drift chambers can reach a longitudinal spatial resolution from timing measurement of order $100 \mu\text{m}$ (rms) or better for minimum ionizing particles, depending on the geometry and operating conditions. However, a degradation of resolution is observed [71] due to primary ionization statistics for tracks close to the anode wires, caused by the

spread in arrival time of the nearest ionization clusters. The effect can be reduced by operating the detector at higher pressures. Sampling the drift time on rows of anodes led to the concept of multiple arrays such as the multi-drift module [72] and the JET chamber [73]. A measurement of drift time, together with the recording of charge sharing from the two ends of the anode wires provides the coordinates of segments of tracks. The total charge gives information on the differential energy loss and is exploited for particle identification. The time projection chamber (TPC) [74] combines a measurement of drift time and charge induction on cathodes, to obtain excellent tracking for high multiplicity topologies occurring at moderate rates (see Sec. 28.6.5). In all cases, a good knowledge of electron drift velocity and diffusion properties is required. This has to be combined with the knowledge of the electric fields in the structures, computed with commercial or custom-developed software [63,75]. For an overview of detectors exploiting the drift time for coordinate measurement see Refs. 6 and 56.

Multiwire and drift chambers have been operated with a variety of gas fillings and operating modes, depending on experimental requirements. The so-called "Magic Gas," a mixture of argon, isobutane and Freon [66], permits very high and saturated gains ($\sim 10^6$). This gas mixture was used in early wire chambers, but was found to be susceptible to severe aging processes. With present-day electronics, proportional gains around 10^4 are sufficient for detection of minimum ionizing particles, and noble gases with moderate amounts of polyatomic gases, such as methane or carbon dioxide, are used.

Although very powerful in terms of performance, multi-wire structures have reliability problems when used in harsh or hard-to-access environments, since a single broken wire can disable the entire detector. Introduced in the '80's, straw and drift tube systems make use of large arrays of wire counters encased in individual enclosures, each acting as an independent wire counter [76]. Techniques for low-cost mass production of these detectors have been developed for large experiments, such as the Transition Radiation Tracker and the Drift Tubes arrays for CERN's LHC experiments [77].

28.6.3. High Rate Effects : Revised March 2010 by Fabio Sauli (CERN) and Maxim Titov (CEA Saclay).

The production of positive ions in the avalanches and their slow drift before neutralization result in a rate-dependent accumulation of positive charge in the detector. This may result in significant field distortion, gain reduction and degradation of spatial resolution. As shown in Fig. 28.8 [78], the proportional gain drops above a charge production rate around 10^9 electrons per second and mm of wire, independently of the avalanche size. For a proportional gain of 10^4 and 100 electrons per track, this corresponds to a particle flux of $10^3 \text{ s}^{-1} \text{ mm}^{-1}$ (1 kHz/mm² for 1 mm wire spacing).

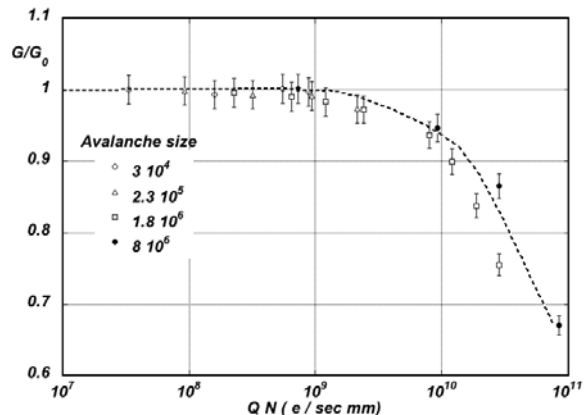


Figure 28.8: Charge rate dependence of normalized gas gain G/G_0 (relative to zero counting rate) in proportional thin-wire detectors [78]. Q is the total charge in single avalanche; N is the particle rate per wire length.

At high radiation fluxes, a fast degradation of detectors due to the formation of polymers deposits (aging) is often observed. The process

has been extensively investigated, often with conflicting results. Several causes have been identified, including organic pollutants and silicone oils. Addition of small amounts of water in many (but not all) cases has been shown to extend the lifetime of the detectors. Addition of fluorinated gases (*e.g.*, CF_4) or oxygen may result in an etching action that can overcome polymer formation, or even eliminate already existing deposits. However, the issue of long-term survival of gas detectors with these gases is controversial [79]. Under optimum operating conditions, a total collected charge of a few coulombs per cm of wire can usually be reached before noticeable degradation occurs. This corresponds, for one mm spacing and at a gain of 10^4 , to a total particle flux of $\sim 10^{14}$ MIPs/cm².

28.6.4. Micro-Pattern Gas Detectors : Revised March 2010 by Fabio Sauli (CERN) and Maxim Titov (CEA Saclay)

Despite various improvements, position-sensitive detectors based on wire structures are limited by basic diffusion processes and space charge effects to localization accuracies of 50–100 μm [80]. Modern photolithographic technology led to the development of novel Micro-Pattern Gas Detector (MPGD) concepts [81], revolutionizing cell size limitations for many gas detector applications. By using pitch size of a few hundred μm , an order of magnitude improvement in granularity over wire chambers, these detectors offer intrinsic high rate capability ($> 10^6$ Hz/mm²), excellent spatial resolution (~ 30 μm), multi-particle resolution (~ 500 μm), and single photo-electron time resolution in the ns range.

The Micro-Strip Gas Chamber (MSGC), invented in 1988, was the first of the micro-structure gas chambers [82]. It consists of a set of tiny parallel metal strips laid on a thin resistive support, alternatively connected as anodes and cathodes. Owing to the small anode-to-cathode distance (~ 100 μm), the fast collection of positive ions reduces space charge build-up, and provides a greatly increased rate capability. Unfortunately, the fragile electrode structure of the MSGC turned out to be easily destroyed by discharges induced by heavily ionizing particles [83]. Nevertheless, detailed studies of their properties, and in particular, on the radiation-induced processes leading to discharge breakdown, led to the development of the more powerful devices: GEM and Micromegas. These have improved reliability and radiation hardness. The absence of space-charge effects in GEM detectors at the highest rates reached so far and the fine granularity of MPGDs improve the maximum rate capability by more than two orders of magnitude (Fig. 28.9) [70,84]. Even larger rate capability has been reported for Micromegas [85].

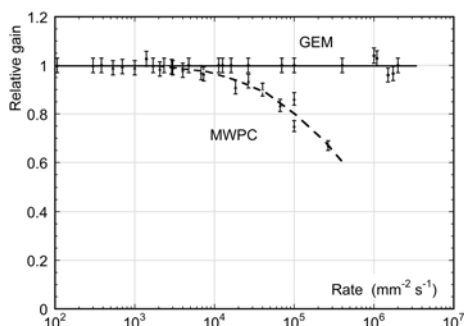


Figure 28.9: Normalized gas gain as a function of particle rate for MWPC [70] and GEM [84].

The Gas Electron Multiplier (GEM) detector consists of a thin-foil copper-insulator-copper sandwich chemically perforated to obtain a high density of holes in which avalanches occur [86]. The hole diameter is typically between 25 μm and 150 μm , while the corresponding distance between holes varies between 50 μm and 200 μm . The central insulator is usually (in the original design) the polymer Kapton, with a thickness of 50 μm . Application of a potential difference between the two sides of the GEM generates the electric fields indicated in Fig. 28.10. Each hole acts as an independent proportional counter. Electrons released by the primary ionization particle in the upper conversion region (above the GEM foil) drift into the holes, where charge multiplication occurs in the high electric

field (50–70 kV/cm). Most of avalanche electrons are transferred into the gap below the GEM. Several GEM foils can be cascaded, allowing the multi-layer GEM detectors to operate at overall gas gain above 10^4 in the presence of highly ionizing particles, while strongly reducing the risk of discharges. This is a major advantage of the GEM technology [87]. Localization can then be performed by collecting the charge on a patterned one- or two-dimensional readout board of arbitrary pattern, placed below the last GEM.

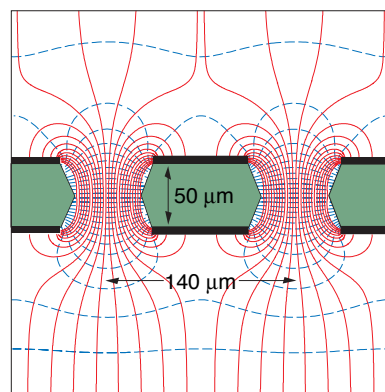


Figure 28.10: Schematic view and typical dimensions of the hole structure in the GEM amplification cell. Electric field lines (solid) and equipotentials (dashed) are shown.

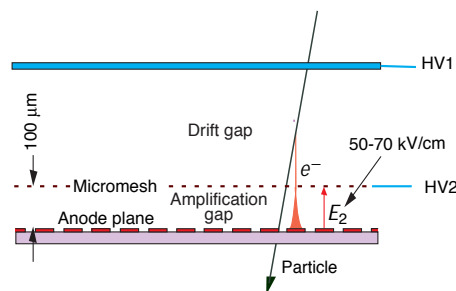


Figure 28.11: Schematic drawing of the Micromegas detector.

The micro-mesh gaseous structure (Micromegas) is a thin parallel-plate avalanche counter, as shown in Fig. 28.11 [88]. It consists of a drift region and a narrow multiplication gap (25–150 μm) between a thin metal grid (micromesh) and the readout electrode (strips or pads of conductor printed on an insulator board). Electrons from the primary ionization drift through the holes of the mesh into the narrow multiplication gap, where they are amplified. The electric field is homogeneous both in the drift (electric field ~ 1 kV/cm) and amplification (50–70 kV/cm) gaps. In the narrow multiplication region, gain variations due to small variations of the amplification gap are approximately compensated by an inverse variation of the amplification coefficient, resulting in a more uniform gain. The small amplification gap produces a narrow avalanche, giving rise to excellent spatial resolution: 12 μm accuracy, limited by the micro-mesh pitch, has been achieved for MIPs, as well as very good time resolution and energy resolution ($\sim 12\%$ FWHM with 6 keV x rays) [89].

The performance and robustness of GEM and Micromegas have encouraged their use in high-energy and nuclear physics, UV and visible photon detection, astroparticle and neutrino physics, neutron detection and medical physics. Most structures were originally optimized for high-rate particle tracking in nuclear and high-energy physics experiments. COMPASS, a high-luminosity experiment at CERN, pioneered the use of large-area ($\sim 40 \times 40$ cm²) GEM and Micromegas detectors close to the beam line with particle rates of 25 kHz/mm². Both technologies achieved a tracking efficiency of close to 100% at gas gains of about 10^4 , a spatial resolution of 70–100 μm and a time resolution of ~ 10 ns. GEM detectors are also used for triggering in the LHCb Muon System and for tracking in the TOTEM

Telescopes. Both GEM and Micromegas devices are foreseen for the upgrade of the LHC experiments and for one of the readout options for the Time Projection Chamber (TPC) at the International Linear Collider (ILC). The development of new fabrication techniques—“bulk” Micromegas technology [90] and single-mask GEMs [91]—is a big step toward industrial production of large-size MPGDs. In some applications requiring very large-area coverage with moderate spatial resolution, coarse macro-patterned detectors, such as Thick GEMs (THGEM) [92] or patterned resistive-plate devices [93] might offer economically interesting solutions.

Sensitive and low-noise electronics enlarge the range of the MPGD applications. Recently, the GEM and Micromegas detectors were read out by high-granularity ($\sim 50 \mu\text{m}$ pitch) CMOS chips assembled directly below the GEM or Micromegas amplification structures [94]. These detectors use the bump-bonding pads of a pixel chip as an integrated charge collecting anode. With this arrangement signals are induced at the input gate of a charge-sensitive preamplifier (top metal layer of the CMOS chip). Every pixel is then directly connected to the amplification and digitization circuits, integrated in the underlying active layers of the CMOS technology, yielding timing and charge measurements as well as precise spatial information in 3D.

The operation of a MPGD with a Timepix CMOS chip has demonstrated the possibility of reconstructing 3D-space points of individual primary electron clusters with $\sim 30 \mu\text{m}$ spatial resolution and event-time resolution with nanosecond precision. This has become indispensable for tracking and triggering and also for discriminating between ionizing tracks and photon conversions. The GEM, in conjunction with a CMOS ASIC,* can directly view the absorption process of a few keV x-ray quanta and simultaneously reconstruct the direction of emission, which is sensitive to the x-ray polarization. Thanks to these developments, a micro-pattern device with finely segmented CMOS readout can serve as a high-precision “electronic bubble chamber.” This may open new opportunities for x-ray polarimeters, detection of weakly interacting massive particles (WIMPs) and axions, Compton telescopes, and 3D imaging of nuclear recoils.

An elegant solution for the construction of the Micromegas with pixel readout is the integration of the amplification grid and CMOS chip by means of an advanced “wafer post-processing” technology [95]. This novel concept is called “Ingrid” (see Fig. 28.12). With this technique, the structure of a thin ($1 \mu\text{m}$) aluminum grid is fabricated on top of an array of insulating pillars, which stands $\sim 50 \mu\text{m}$ above the CMOS chip. The sub- μm precision of the grid dimensions and avalanche gap size results in a uniform gas gain. The grid hole size, pitch and pattern can be easily adapted to match the geometry of any pixel readout chip.

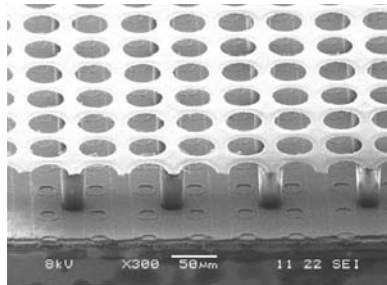


Figure 28.12: Photo of the Micromegas “Ingrid” detector. The grid holes can be accurately aligned with readout pixels of CMOS chip. The insulating pillars are centered between the grid holes, thus avoiding dead regions.

Recent developments in radiation hardness research with state-of-the-art MPGDs are reviewed in Ref. 96. Earlier aging studies of GEM and Micromegas concepts revealed that they might be even less vulnerable to radiation-induced performance degradation than standard silicon microstrip detectors.

* Application Specific Integrated Circuit

The RD51 collaboration was established in 2008 to further advance technological developments of micro-pattern detectors and associated electronic-readout systems for applications in basic and applied research [97].

28.6.5. Time-projection chambers : Written September 2007 by D. Karlen (U. of Victoria and TRIUMF, Canada)

The Time Projection Chamber (TPC) concept, invented by David Nygren in the late 1970’s [74], is the basis for charged particle tracking in a large number of particle and nuclear physics experiments. A uniform electric field drifts tracks of electrons produced by charged particles traversing a medium, either gas or liquid, towards a surface segmented into 2D readout pads. The signal amplitudes and arrival times are recorded to provide full 3D measurements of the particle trajectories. The intrinsic 3D segmentation gives the TPC a distinct advantage over other large volume tracking detector designs which record information only in a 2D projection with less overall segmentation, particularly for pattern recognition in events with large numbers of particles.

Gaseous TPC’s are often designed to operate within a strong magnetic field (typically parallel to the drift field) so that particle momenta can be estimated from the track curvature. For this application, precise spatial measurements in the plane transverse to the magnetic field are most important. Since the amount of ionization along the length of the track depends on the velocity of the particle, ionization and momentum measurements can be combined to identify the types of particles observed in the TPC. The estimator for the energy deposit by a particle is usually formed as the truncated mean of the energy deposits, using the 50%–70% of the samples with the smallest signals. Variance due to energetic δ -ray production is thus reduced.

Gas amplification of 10^3 – 10^4 at the readout endplate is usually required in order to provide signals with sufficient amplitude for conventional electronics to sense the drifted ionization. Until recently, the gas amplification system used in TPC’s have exclusively been planes of anode wires operated in proportional mode placed close to the readout pads. Performance has been recently improved by replacing these wire planes with micro-pattern gas detectors, namely GEM [86] and Micromegas [88] devices. Advances in electronics miniaturization have been important in this development, allowing pad areas to be reduced to the 10 mm^2 scale or less, well matched to the narrow extent of signals produced with micro-pattern gas detectors. Presently, the ultimate in fine segmentation TPC readout are silicon sensors, with $0.05 \text{ mm} \times 0.05 \text{ mm}$ pixels, in combination with GEM or Micromegas [98]. With such fine granularity it is possible to count the number of ionization clusters along the length of a track which, in principle, can improve the particle identification capability.

Examples of two modern large volume gaseous TPC’s are shown in Fig. 28.13 and Fig. 28.14. The particle identification performance is illustrated in Fig. 28.15, for the original TPC in the PEP-4/9 experiment [99].

The greatest challenges for a large TPC arise from the long drift distance, typically 100 times further than in a comparable wire chamber design. In particular, the long drift distance can make the device sensitive to small distortions in the electric field. Distortions can arise from a number of sources, such as imperfections in the TPC construction, deformations of the readout surface, or the presence of ions in the active medium.

For a gaseous TPC operated in a magnetic field, the electron drift velocity v is defined by Eq. (28.13). With a strong magnetic field parallel to the electric field and a gas with a large value of $\omega\tau$ (also favored to reduce transverse diffusion as discussed below), the transverse displacements of the drifting electrons due to electric field distortions are reduced. In this mode of operation, it is essential to precisely map the magnetic field as the electron drift lines closely follow the magnetic field lines. Corrections for electric and/or magnetic field non-uniformities can be determined from control samples of electrons produced by ionizing the gas with UV laser beams, from photoelectrons produced on the cathode, or from tracks emanating from calibration reactions.

The long drift distance means that there is a delay, typically

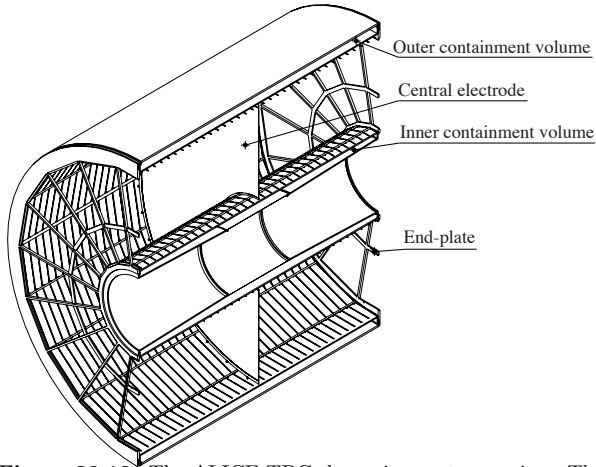


Figure 28.13: The ALICE TPC shown in a cutaway view. The drift volume is 5 m long with a 5 m diameter. Gas amplification is provided by planes of anode wires.

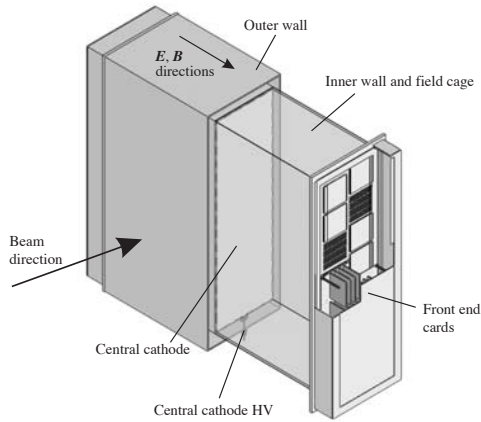


Figure 28.14: One of the 3 TPC modules for the near detector of the T2K experiment. The drift volume is 2 m×2 m×0.8 m. Micromegas devices are used for gas amplification and readout.

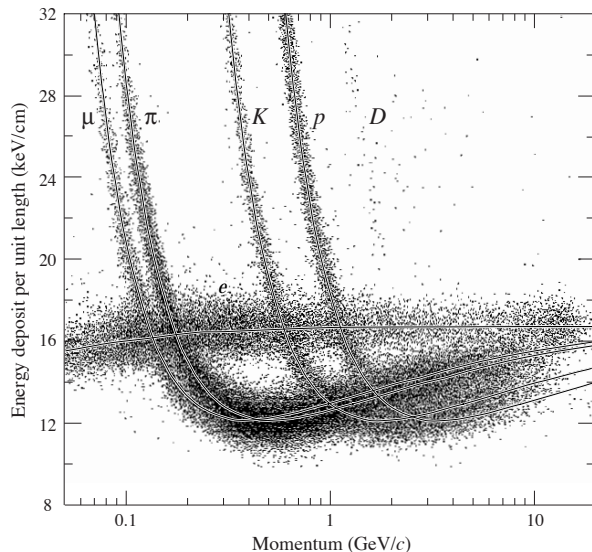


Figure 28.15: The PEP4/9-TPC energy deposit measurements (185 samples, 8.5 atm Ar-CH₄ 80:20). The ionization rate at the Fermi plateau (at high β) is 1.4 times that for the minimum at lower β . This ratio increases to 1.6 at atmospheric pressure.

10–100 μ s in a large gaseous TPC, for signals to arrive at the endplate. For experiments with shorter intervals between events, this can produce ambiguities in the starting time for the drift of ionization. This can be resolved by matching the TPC data with that from an auxiliary detector providing additional spatial or timing information.

In a gaseous TPC, the motion of positive ions is much slower than the electrons, and so the positive ions produced by many events may exist in the active volume. Of greatest concern is the ions produced in the gas amplification stage. Large gaseous TPC's built until now with wire planes have included a gating grid that prevent the positive ions from escaping into the drift volume in the interval between event triggers. Micro-pattern gas detectors release much less positive ions than wire planes operating at the same gain, which may allow operation of a TPC without a gating grid.

Given the long drift distance in a large TPC, the active medium must remain very pure, as small amounts of contamination can absorb the ionization signal. For example, in a typical large gaseous TPC, O₂ must be kept below a few parts in 10⁵, otherwise a large fraction of the drifting electrons will become attached. Special attention must be made in the choice of construction materials in order to avoid the release of other electronegative contaminants.

Diffusion degrades the position information of ionization that drifts a long distance. For a gaseous TPC, the effect can be alleviated by the choice of a gas with low intrinsic diffusion or by operating in a strong magnetic field parallel to the drift field with a gas which exhibits a significant reduction in transverse diffusion with magnetic field. For typical operation without magnetic field, the transverse extent of the electrons, σ_{Dx} , is a few mm after drifting 1 m due to diffusion. With a strong magnetic field, σ_{Dx} can be reduced by as much as a factor of 10,

$$\sigma_{Dx}(B)/\sigma_{Dx}(0) = \frac{1}{\sqrt{1 + \omega^2\tau^2}} \quad (28.16)$$

where $\omega\tau$ is defined above. The diffusion limited position resolution from the information collected by a single row of pads is

$$\sigma_x = \frac{\sigma_{Dx}}{\sqrt{n}} \quad (28.17)$$

where n is the effective number of electrons collected by the pad row, giving an ultimate single row resolution of order 100 μ m.

Diffusion is significantly reduced in a negative-ion TPC [100], which uses a special gas mixture that attaches electrons immediately as they are produced. The drifting negative ions exhibit much less diffusion than electrons. The slow drift velocity and small $\omega\tau$ of negative ions must be compatible with the experimental environment.

The spatial resolution achieved by a TPC is determined by a number of factors in addition to diffusion. Non-uniform ionization along the length of the track is a particularly important factor, and is responsible for the so-called “track angle” and “ $\mathbf{E} \times \mathbf{B}$ ” effects. If the boundaries between pads in a row are not parallel to the track, the ionization fluctuations will increase the variance in the position estimate from that row. For this reason, experiments with a preferred track direction should have pad boundaries aligned with that direction. Traditional TPC's with wire plane amplification suffer from the effects of non-parallel electric and magnetic fields near the wires that rotate ionization segments, thereby degrading the resolution because of the non-uniform ionization. Micro-pattern gas detectors exhibit a much smaller $\mathbf{E} \times \mathbf{B}$ effect, since their feature size is much smaller than that of a wire grid.

28.6.6. Transition radiation detectors (TRD's) : Written August 2007 by P. Nevski (BNL) and A. Romaniouk (Moscow Eng. & Phys. Inst.)

Transition radiation (TR) x rays are produced when a highly relativistic particle ($\gamma \gtrsim 10^3$) crosses a refractive index interface, as discussed in Sec. 27.7. The x rays, ranging from a few keV to a few dozen keV, are emitted at a characteristic angle $1/\gamma$ from the particle trajectory. Since the TR yield is about 1% per boundary crossing, radiation from multiple surface crossings is used in practical detectors. In the simplest concept, a detector module might consist of low- Z foils followed by a high- Z active layer made of proportional counters filled with a Xe-rich gas mixture. The atomic number considerations follow from the dominant photoelectric absorption cross section per atom going roughly as Z^n/E_x^3 , where n varies between 4 and 5 over the region of interest, and the x-ray energy is E_x .^{*} To minimize self-absorption, materials such as polypropylene, Mylar, carbon, and (rarely) lithium are used as radiators. The TR signal in the active regions is in most cases superimposed upon the particle's ionization losses. These drop a little faster than Z/A with increasing Z , providing another reason for active layers with high Z .

The TR intensity for a single boundary crossing always increases with γ , but for multiple boundary crossings interference leads to saturation near a Lorentz factor $\gamma_{\text{sat}} = 0.6 \omega_1 \sqrt{\ell_1 \ell_2} / c$ [101], where ω_1 is the radiator plasma frequency, ℓ_1 is its thickness, and ℓ_2 the spacing. In most of the detectors used in particle physics the radiator parameters are chosen to provide $\gamma_{\text{sat}} \approx 2000$. Those detectors normally work as threshold devices, ensuring the best electron/pion separation in the momentum range $1 \text{ GeV}/c \lesssim p \lesssim 150 \text{ GeV}/c$.

One can distinguish two design concepts—"thick" and "thin" detectors:

1. The radiator, optimized for a minimum total radiation length at maximum TR yield and total TR absorption, consists of few hundred foils (for instance 300 20 μm thick polypropylene foils). A dominant fraction of the soft TR photons is absorbed in the radiator itself. To increase the average TR photon energy further, part of the radiator far from the active layers is often made of thicker foils. The detector thickness, about 2 cm for Xe-filled gas chambers, is optimized to absorb the shaped x-ray spectrum. A classical detector is composed of several similar modules which respond nearly independently. Such detectors were used in the NA34 [102], and are being used in the ALICE experiment [103].
2. In another TRD concept a fine granular radiator/detector structure exploits the soft part of the TR spectrum more efficiently. This can be achieved, for instance, by distributing small-diameter straw-tube detectors uniformly or in thin layers throughout the radiator material (foils or fibers). Even with a relatively thin radiator stack, radiation below 5 keV is mostly lost in the radiators themselves. However for photon energies above this value the absorption becomes smaller and the radiation can be registered by several consecutive detector layers, thus creating a strong TR build-up effect. Descriptions of detectors using this approach can be found in both accelerator and space experiments [103]. For example, in the ATLAS TR tracker charged particles cross about 35 effective straw tube layers embedded in the radiator material [103]. The effective thickness of the Xe gas per straw is about 2.3 mm and the average number of foils per straw is about 40 with an effective foil thickness of about 20 μm .

Both TR photon absorption and the TR build-up significantly affect the detector performance. Although the values mentioned above are typical for most of the plastic radiators used with Xe-based detectors, they vary significantly depending on detector parameters: radiator material, thickness and spacing, the construction of the sensitive chambers, their position, *etc.* Thus careful simulations are usually needed to build a detector optimized for a particular application.

The discrimination between electrons and pions can be based on the charge deposition measured in each detection module, on the number of clusters—energy depositions observed above an optimal

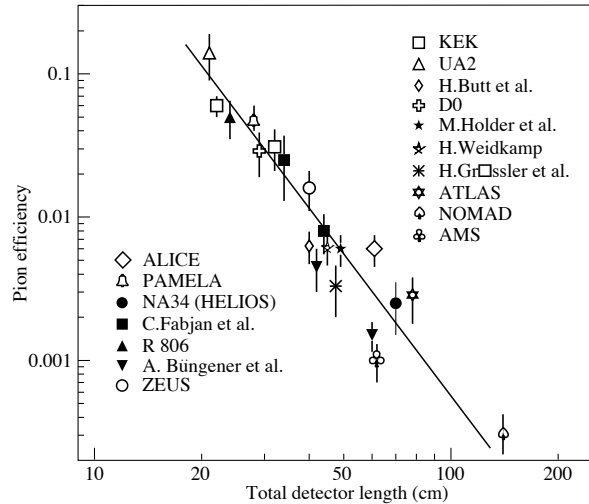


Figure 28.16: Pion efficiency measured (or predicted) for different TRDs as a function of the detector length for a fixed electron efficiency of 90%. The plot is taken from [102] with efficiencies of more recent detectors added [103].

threshold (usually in the 5 to 7 keV region), or on more sophisticated methods analyzing the pulse shape as a function of time. The total energy measurement technique is more suitable for thick gas volumes, which absorb most of the TR radiation and where the ionization loss fluctuations are small. The cluster-counting method works better for detectors with thin gas layers, where the fluctuations of the ionization losses are big. Cluster-counting replaces the Landau-Vavilov distribution of background ionization energy losses with the Poisson statistics of δ -electrons, responsible for the distribution tails. The latter distribution is narrower than the Landau-Vavilov distribution.

The major factor in the performance of any TRD is its overall length. This is illustrated in Fig. 28.16, which shows, for a variety of detectors, the pion efficiency at a fixed electron efficiency of 90% as a function of the overall detector length. The experimental data, covering a range of particle energies from a few GeV to 40 GeV, are rescaled to an energy of 10 GeV when possible. Phenomenologically, the rejection power against pions increases as $5 \cdot 10^{L/38}$, where the range of validity is $L \approx 20$ –100 cm.

Many recent TRDs combine particle identification with charged-track measurement in the same detector [103]. This provides a powerful tool for electron identification even at very high particle densities. Another example of this combination is described by Brigida *et al.* in Ref. 103. In this work Si-microstrip detectors operating in a magnetic field are used both for particle and TR detection. The excellent coordinate resolution of the Si detectors allows spatial separation of the TR photons from particle ionization tracks with relatively modest distances between radiator and detector.

Recent TRDs for particle astrophysics are designed to directly measure the Lorentz factor of high-energy nuclei by using the quadratic dependence of the TR yield on nuclear charge; see Cherry and Müller papers in Ref. 103. The radiator configuration (ℓ_1, ℓ_2) is tuned to extend the TR yield rise up to $\gamma \lesssim 10^5$ using more energetic part of the TR spectrum (up to 100 keV). Exotic radiator materials such as aluminum and unusual TR detection methods (Compton scattering) are used such cases.

^{*} Photon absorption coefficients for the elements (via a NIST link), and dE/dx_{min} and plasma energies for many materials are given in pdg.lbl.gov/AtomicNuclearProperties.

28.6.7. Resistive-plate chambers : Revised September 2007 by H.R. Band (U. Wisconsin).

The resistive-plate chamber (RPC) was developed by Santonico and Cardarelli in the early 1980's [104] as a low-cost alternative to large scintillator planes.* Most commonly, an RPC is constructed from two parallel high-resistivity (10^9 – 10^{13} Ω -cm) glass or phenolic (Bakelite)/melamine laminate plates with a few-mm gap between them which is filled with atmospheric-pressure gas. The gas is chosen to absorb UV photons in order to limit transverse growth of discharges. The backs of the plates are coated with a lower-resistivity paint or ink ($\sim 10^5$ Ω/\square), and a high potential (7–12 kV) is maintained between them. The passage of a charged particle initiates an electric discharge, whose size and duration are limited since the current reduces the local potential to below that needed to maintain the discharge. The sensitivity of the detector outside of this region is unaffected. The signal readout is via capacitive coupling to metallic strips on both sides of the detector which are separated from the high voltage coatings by thin insulating sheets. The x and y position of the discharge can be measured if the strips on opposite sides of the gap are orthogonal. When operated in streamer mode, the induced signals on the strips can be quite large (~ 300 mV), making sensitive electronics unnecessary. An example of an RPC structure is shown in Fig. 28.17.

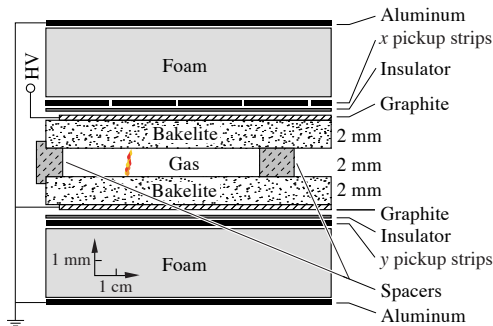


Figure 28.17: Schematic cross section of a typical RPC, in this case the single-gap streamer-mode BaBar RPC.

RPC's have inherent rate limitations since the time needed to re-establish the field after a discharge is proportional to the chamber capacitance and plate resistance. The average charge per streamer is 100–1000 pC. Typically, the efficiency of streamer-mode glass RPC's begins to fall above ~ 0.4 Hz/cm². Because of Bakelite's lower bulk resistivity, Bakelite RPC's can be efficient at 10–100 Hz/cm². The need for higher rate capability led to the development of avalanche-mode RPC's, in which the gas and high voltage have been tuned to limit the growth of the electric discharge, preventing streamer formation. Typical avalanche-mode RPC's have a signal charge of about 10 pC and can be efficient at 1 kHz/cm². The avalanche discharge produces a much smaller induced signal on the pickup strips (~ 1 mV) than streamers, and thus requires a more sophisticated and careful electronic design.

Many variations of the initial RPC design have been built for operation in either mode. Efficiencies of $\gtrsim 92\%$ for single gaps can be improved by the use of two or more gas gaps with shared pickup strips. Non-flammable and more environmentally friendly gas mixtures have been developed. In streamer mode, various mixtures of argon with isobutane and tetrafluoroethane have been used. For avalanche mode operation, a gas mixture of tetrafluoroethane (C₂H₂F₄) with 2–5% isobutane and 0.4–10% sulfur hexafluoride (SF₆) is typical. An example of large-scale RPC use is provided by the muon system being built for the ATLAS detector, where three layers of pairs of RPC's are used to trigger the drift tube arrays between the pairs. The total area is about 10,000 m². These RPC's provide a spatial resolution of 1 cm and a time resolution of 1 ns at an efficiency $\geq 99\%$.

Developments of multiple-gap RPC's [106] lead to RPC designs with much better timing resolution (~ 50 ps) for use in time-of-flight

* It was based on earlier work on a spark counter with one high-resistivity plate [105].

particle identification systems. A pioneering design used by the HARP experiment [107] has two sets of 2 thin gas gaps (0.3 mm) separated by thin (0.7 mm) glass plates. The outer plates are connected to high voltage and ground while the inner plate is electrically isolated and floats to a stable equilibrium potential. The observed RPC intrinsic time resolution of 127 ps may have been limited by amplifier noise. Fonte provides useful review [108] of other RPC designs.

Operational experience with RPC's has been mixed. Several experiments (*e.g.*, L3 and HARP) have reported reliable performance. However, the severe problems experienced with the BaBar RPC's have raised concerns about the long-term reliability of Bakelite RPC's.

Glass RPC's have had fewer problems, as seen by the history of the BELLE chambers. A rapid growth in the noise rate and leakage current in some of the BELLE glass RPC's was observed during commissioning. It was found that water vapor in the input gas was reacting with fluorine (produced by the disassociation of the tetrafluoroethane in the streamers) to produce hydrofluoric acid. The acid etched the glass surfaces, leading to increased noise rates and lower efficiencies. The use of copper gas piping to insure the dryness of the input gas stopped the problem. The BELLE RPC's have now operated reliably for more than 5 years.

Several different failure modes diagnosed in the first-generation BaBar Bakelite RPC's caused the average efficiency of the barrel RPC's to fall from $\gtrsim 90\%$ to 35% in five years. The linseed oil which is used in Bakelite RPC's to coat the inner surface [109] had not been completely cured. Under warm conditions (32°C) and high voltage, oil collected on the spacers between the gaps or formed oil-drop bridges between the gaps. This led to large leakage currents (50–100 μ A in some chambers) which persisted even when the temperature was regulated at 20°C. In addition, the graphite layer used to distribute the high voltage over the Bakelite became highly resistive (100 k Ω/\square \rightarrow 10 M Ω/\square), resulting in lowered efficiency in some regions and the complete death of whole chambers.

The BaBar problems and the proposed use of Bakelite RPC's in the LHC detectors prompted detailed studies of RPC aging and have led to improved construction techniques and a better understanding of RPC operational limits. The graphite layer has been improved and should be stable with integrated currents of $\lesssim 600$ mC/cm². Molded gas inlets and improved cleanliness during construction have reduced the noise rate of new chambers. Unlike glass RPC's, Bakelite RPC's have been found to require humid input gases to prevent drying of the Bakelite (increasing the bulk resistivity) which would decrease the rate capability. Second-generation BaBar RPC's incorporating many of the above improvements have performed reliably for over two years [110].

With many of these problems solved, new-generation RPC's are now being or soon will be used in about a dozen cosmic-ray and HEP detectors. Their comparatively low cost, ease of construction, good time resolution, high efficiency, and moderate spatial resolution make them attractive in many situations, particularly those requiring fast timing and/or large-area coverage.

28.7. Semiconductor detectors

Updated September 2009 by H. Spieler (LBNL).

Semiconductor detectors provide a unique combination of energy and position resolution. In collider detectors they are most widely used as position sensing devices and photodetectors (Sec. 28.2). Integrated circuit technology allows the formation of high-density micron-scale electrodes on large (15–20 cm diameter) wafers, providing excellent position resolution. Furthermore, the density of silicon and its small ionization energy yield adequate signals with active layers only 100–300 μ m thick, so the signals are also fast (typically tens of ns). The high energy resolution is a key parameter in x-ray, gamma, and charged particle spectroscopy, *e.g.*, in neutrinoless double beta decay searches. Silicon and germanium are the most commonly used materials, but gallium-arsenide, CdTe, CdZnTe, and other materials are also useful. CdZnTe provides a higher stopping power and the ratio of Cd to Zn concentrations changes the bandgap. Ge detectors are commonly operated at liquid nitrogen temperature to reduce the bias current, which depends exponentially on temperature. Semiconductor detectors depend crucially on low-noise electronics (see Sec. 28.8), so the detection sensitivity is determined by signal charge

and capacitance. For a comprehensive discussion of semiconductor detectors and electronics see Ref. 111.

28.7.1. Materials Requirements :

Semiconductor detectors are essentially solid state ionization chambers. Absorbed energy forms electron-hole pairs, *i.e.*, negative and positive charge carriers, which under an applied electric field move towards their respective collection electrodes, where they induce a signal current. The energy required to form an electron-hole pair is proportional to the bandgap. In tracking detectors the energy loss in the detector should be minimal, whereas for energy spectroscopy the stopping power should be maximized, so for gamma rays high- Z materials are desirable.

Measurements on silicon photodiodes [112] show that for photon energies below 4 eV one electron-hole ($e-h$) pair is formed per incident photon. The mean energy E_i required to produce an $e-h$ pair peaks at 4.4 eV for a photon energy around 6 eV. Above ~ 1.5 keV it assumes a constant value, 3.67 eV at room temperature. It is larger than the bandgap energy because momentum conservation requires excitation of lattice vibrations (phonons). For minimum-ionizing particles, the most probable charge deposition in a 300 μm thick silicon detector is about 3.5 fC (22000 electrons). Other typical ionization energies are 2.96 eV in Ge, 4.2 eV in GaAs, and 4.43 eV in CdTe.

Since both electronic and lattice excitations are involved, the variance in the number of charge carriers $N = E/E_i$ produced by an absorbed energy E is reduced by the Fano factor F (about 0.1 in Si and Ge). Thus, $\sigma_N = \sqrt{FN}$ and the energy resolution $\sigma_E/E = \sqrt{FE_i}/E$. However, the measured signal fluctuations are usually dominated by electronic noise or energy loss fluctuations in the detector. The electronic noise contributions depend on the pulse shaping in the signal processing electronics, so the choice of the shaping time is critical (see Sec. 28.8).

A smaller bandgap would produce a larger signal and improve energy resolution, but the intrinsic resistance of the material is critical. Thermal excitation, given by the Fermi-Dirac distribution, promotes electrons into the conduction band, so the thermally excited carrier concentration increases exponentially with decreasing bandgaps. In pure Si the carrier concentration is $\sim 10^{10} \text{cm}^{-3}$ at 300 K, corresponding to a resistivity $\rho \approx 400 \text{k}\Omega \text{cm}$. In reality, crystal imperfections and minute impurity concentrations limit Si carrier concentrations to $\sim 10^{11} \text{cm}^{-3}$ at 300 K, corresponding to a resistivity $\rho \approx 40 \text{k}\Omega \text{cm}$. In practice, resistivities up to 20 $\text{k}\Omega \text{cm}$ are available, with mass production ranging from 5 to 10 $\text{k}\Omega \text{cm}$. Signal currents at keV scale energies are of order μA . However, for a resistivity of $10^4 \Omega \text{cm}$ a 300 μm thick sensor with 1 cm^2 area would have a resistance of 300 Ω , so 30 V would lead to a current flow of 100 mA and a power dissipation of 3 W. On the other hand, high-quality single crystals of Si and Ge can be grown economically with suitably large volumes, so to mitigate the effect of resistivity one resorts to reverse-biased diode structures. Although this reduces the bias current relative to a resistive material, the thermally excited leakage current can still be excessive at room temperature, so Ge diodes are typically operated at liquid nitrogen temperature (77 K).

A major effort is to find high- Z materials with a bandgap that is sufficiently high to allow room-temperature operation while still providing good energy resolution. Compound semiconductors, *e.g.*, CdZnTe, can allow this, but typically suffer from charge collection problems, characterized by the product $\mu\tau$ of mobility and carrier lifetime. In Si and Ge $\mu\tau > 1 \text{cm}^2 \text{V}^{-1}$ for both electrons and holes, whereas in compound semiconductors it is in the range 10^{-3} – 10^{-8} . Since for holes $\mu\tau$ is typically an order of magnitude smaller than for electrons, detector configurations where the electron contribution to the charge signal dominates—*e.g.*, strip or pixel structures—can provide better performance.

28.7.2. Detector Configurations :

A $p-n$ junction operated at reverse bias forms a sensitive region depleted of mobile charge and sets up an electric field that sweeps charge liberated by radiation to the electrodes. Detectors typically use an asymmetric structure, *e.g.*, a highly doped p electrode and a lightly doped n region, so that the depletion region extends predominantly into the lightly doped volume.

In a planar device the thickness of the depleted region is

$$W = \sqrt{2\epsilon(V + V_{bi})/Ne} = \sqrt{2\rho\mu\epsilon(V + V_{bi})}, \quad (28.18)$$

where V = external bias voltage

V_{bi} = “built-in” voltage (≈ 0.5 V for resistivities typically used in Si detectors)

N = doping concentration

e = electronic charge

ϵ = dielectric constant = $11.9 \epsilon_0 \approx 1 \text{pF/cm}$ in Si

ρ = resistivity (typically 1–10 $\text{k}\Omega \text{cm}$ in Si)

μ = charge carrier mobility

= $1350 \text{cm}^2 \text{V}^{-1} \text{s}^{-1}$ for electrons in Si

= $450 \text{cm}^2 \text{V}^{-1} \text{s}^{-1}$ for holes in Si

In Si

$$W = 0.5 [\mu\text{m}/\sqrt{\Omega\text{-cm} \cdot \text{V}}] \times \sqrt{\rho(V + V_{bi})} \text{ for } n\text{-type Si, and}$$

$$W = 0.3 [\mu\text{m}/\sqrt{\Omega\text{-cm} \cdot \text{V}}] \times \sqrt{\rho(V + V_{bi})} \text{ for } p\text{-type Si.}$$

The conductive p and n regions together with the depleted volume form a capacitor with the capacitance per unit area

$$C = \epsilon/W \approx 1 [\text{pF/cm}]/W. \quad (28.19)$$

In strip and pixel detectors the capacitance is dominated by the fringing capacitance. For example, the strip-to-strip fringing capacitance is ~ 1 – 1.5pF cm^{-1} of strip length at a strip pitch of 25–50 μm .

Large volume ($\sim 10^2$ – 10^3cm^3) Ge detectors are commonly configured as coaxial detectors, *e.g.*, a cylindrical n -type crystal with 5–10 cm diameter and 10 cm length with an inner 5–10 mm diameter n^+ electrode and an outer p^+ layer forming the diode junction. Ge can be grown with very low impurity levels, 10^9 – 10^{10}cm^{-3} (HPGe), so these large volumes can be depleted with several kV.

28.7.3. Signal Formation :

The signal pulse shape depends on the instantaneous carrier velocity $v(x) = \mu E(x)$ and the electrode geometry, which determines the distribution of induced charge (*e.g.*, see Ref. 111, pp. 71–83). Charge collection time decreases with increasing bias voltage, and can be reduced further by operating the detector with “overbias,” *i.e.*, a bias voltage exceeding the value required to fully deplete the device. The collection time is limited by velocity saturation at high fields (in Si approaching 10^7cm/s at $E > 10^4 \text{V/cm}$); at an average field of 10^4V/cm the collection time is about 15 ps/ μm for electrons and 30 ps/ μm for holes. In typical fully-depleted detectors 300 μm thick, electrons are collected within about 10 ns, and holes within about 25 ns.

Position resolution is limited by transverse diffusion during charge collection (typically 5 μm for 300 μm thickness) and by knock-on electrons. Resolutions of 2–4 μm (rms) have been obtained in beam tests. In magnetic fields, the Lorentz drift deflects the electron and hole trajectories and the detector must be tilted to reduce spatial spreading (see “Hall effect” in semiconductor textbooks).

Electrodes can be in the form of cm-scale pads, strips, or μm -scale pixels. Various readout structures have been developed for pixels, *e.g.*, CCDs, DEPFETs, monolithic pixel devices that integrate sensor and electronics (MAPS), and hybrid pixel devices that utilize separate sensors and readout ICs connected by two-dimensional arrays of solder bumps. For an overview and further discussion see Ref. 111.

In gamma ray spectroscopy ($E_\gamma > 10^2 \text{keV}$) Compton scattering dominates, so for a significant fraction of events the incident gamma energy is not completely absorbed, *i.e.*, the Compton scattered photon escapes from the detector and the energy deposited by the Compton electron is only a fraction of the total. Distinguishing

multi-interaction events, *e.g.*, multiple Compton scatters with a final photoelectric absorption, from single Compton scatters allows background suppression. Since the individual interactions take place in different parts of the detector volume, these events can be distinguished by segmenting the outer electrode of a coaxial detector and analyzing the current pulse shapes. The different collection times can be made more distinguishable by using “point” electrodes, where most of the signal is induced when charges are close to the electrode, similarly to strip or pixel detectors. Charge clusters arriving from different positions in the detector will arrive at different times and produce current pulses whose major components are separated in time. Point electrodes also reduce the electrode capacitance, which reduces electronic noise, but careful design is necessary to avoid low-field regions in the detector volume.

28.7.4. Radiation Damage: Radiation damage occurs through two basic mechanisms:

1. Bulk damage due to displacement of atoms from their lattice sites. This leads to increased leakage current, carrier trapping, and build-up of space charge that changes the required operating voltage. Displacement damage depends on the nonionizing energy loss and the energy imparted to the recoil atoms, which can initiate a chain of subsequent displacements, *i.e.*, damage clusters. Hence, it is critical to consider both particle type and energy.
2. Surface damage due to charge build-up in surface layers, which leads to increased surface leakage currents. In strip detectors the inter-strip isolation is affected. The effects of charge build-up are strongly dependent on the device structure and on fabrication details. Since the damage is proportional to the absorbed energy (when ionization dominates), the dose can be specified in rad (or Gray) independent of particle type.

The increase in reverse bias current due to bulk damage is $\Delta I_r = \alpha \Phi$ per unit volume, where Φ is the particle fluence and α the damage coefficient ($\alpha \approx 3 \times 10^{-17}$ A/cm for minimum ionizing protons and pions after long-term annealing; $\alpha \approx 2 \times 10^{-17}$ A/cm for 1 MeV neutrons). The reverse bias current depends strongly on temperature

$$\frac{I_R(T_2)}{I_R(T_1)} = \left(\frac{T_2}{T_1}\right)^2 \exp\left[-\frac{E}{2k} \left(\frac{T_1 - T_2}{T_1 T_2}\right)\right] \quad (28.20)$$

where $E = 1.2$ eV, so rather modest cooling can reduce the current substantially (~ 6 -fold current reduction in cooling from room temperature to 0°C).

Displacement damage forms acceptor-like states. These trap electrons, building up a negative space charge, which in turn requires an increase in the applied voltage to sweep signal charge through the detector thickness. This has the same effect as a change in resistivity, *i.e.*, the required voltage drops initially with fluence, until the positive and negative space charge balance and very little voltage is required to collect all signal charge. At larger fluences the negative space charge dominates, and the required operating voltage increases ($V \propto N$). The safe limit on operating voltage ultimately limits the detector lifetime. Strip detectors specifically designed for high voltages have been extensively operated at bias voltages >500 V. Since the effect of radiation damage depends on the electronic activity of defects, various techniques have been applied to neutralize the damage sites. For example, additional doping with oxygen can increase the allowable charged hadron fluence roughly three-fold [113]. Detectors with columnar electrodes normal to the surface can also extend operational lifetime [114]. The increase in leakage current with fluence, on the other hand, appears to be unaffected by resistivity and whether the material is *n* or *p*-type. At fluences beyond 10^{15} cm^{-2} decreased carrier lifetime becomes critical [115,116].

Strip and pixel detectors have remained functional at fluences beyond 10^{15} cm^{-2} for minimum ionizing protons. At this damage level, charge loss due to recombination and trapping becomes significant and the high signal-to-noise ratio obtainable with low-capacitance pixel structures extends detector lifetime. The higher mobility of electrons makes them less sensitive to carrier lifetime than holes, so detector configurations that emphasize the electron contribution to the charge signal are advantageous, *e.g.*, n^+ strips or

pixels on a *p*-substrate. The occupancy of the defect charge states is strongly temperature dependent; competing processes can increase or decrease the required operating voltage. It is critical to choose the operating temperature judiciously (-10 to 0°C in typical collider detectors) and limit warm-up periods during maintenance. For a more detailed summary see Ref. 117 and the web-sites of the ROSE and RD50 collaborations at <http://RD48.web.cern.ch/rd48> and <http://RD50.web.cern.ch/rd50>. Materials engineering, *e.g.*, introducing oxygen interstitials, can improve certain aspects and is under investigation. At high fluences diamond is an alternative, but operates as an insulator rather than a reverse-biased diode.

Currently, the lifetime of detector systems is still limited by the detectors; in the electronics use of standard “deep submicron” CMOS fabrication processes with appropriately designed circuitry has increased the radiation resistance to fluences $> 10^{15}$ cm^{-2} of minimum ionizing protons or pions. For a comprehensive discussion of radiation effects see Ref. 118.

28.8. Low-noise electronics

Revised September 2009 by H. Spieler (LBNL).

Many detectors rely critically on low-noise electronics, either to improve energy resolution or to allow a low detection threshold. A typical detector front-end is shown in Fig. 28.18.

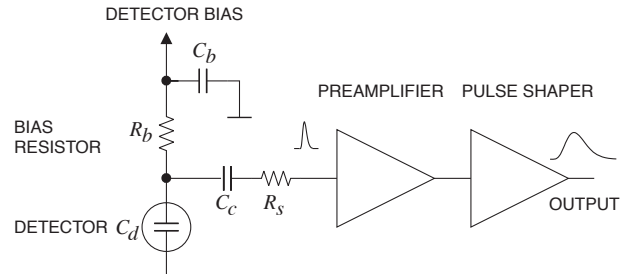


Figure 28.18: Typical detector front-end circuit.

The detector is represented by a capacitance C_d , a relevant model for most detectors. Bias voltage is applied through resistor R_b and the signal is coupled to the preamplifier through a blocking capacitor C_c . The series resistance R_s represents the sum of all resistances present in the input signal path, *e.g.* the electrode resistance, any input protection networks, and parasitic resistances in the input transistor. The preamplifier provides gain and feeds a pulse shaper, which tailors the overall frequency response to optimize signal-to-noise ratio while limiting the duration of the signal pulse to accommodate the signal pulse rate. Even if not explicitly stated, all amplifiers provide some form of pulse shaping due to their limited frequency response.

The equivalent circuit for the noise analysis (Fig. 28.19) includes both current and voltage noise sources. The leakage current of a semiconductor detector, for example, fluctuates due to electron emission statistics. This “shot noise” i_{nd} is represented by a current noise generator in parallel with the detector. Resistors exhibit noise due to thermal velocity fluctuations of the charge carriers. This noise source can be modeled either as a voltage or current generator. Generally, resistors shunting the input act as noise current sources and resistors in series with the input act as noise voltage sources (which is why some in the detector community refer to current and voltage noise as “parallel” and “series” noise). Since the bias resistor effectively shunts the input, as the capacitor C_b passes current fluctuations to ground, it acts as a current generator i_{nb} and its noise current has the same effect as the shot noise current from the detector. Any other shunt resistances can be incorporated in the same way. Conversely, the series resistor R_s acts as a voltage generator. The electronic noise of the amplifier is described fully by a combination of voltage and current sources at its input, shown as e_{na} and i_{na} .

Shot noise and thermal noise have a “white” frequency distribution, *i.e.* the spectral power densities $dP_n/df \propto di_n^2/df \propto de_n^2/df$ are constant with the magnitudes

$$i_{nd}^2 = 2eI_d,$$

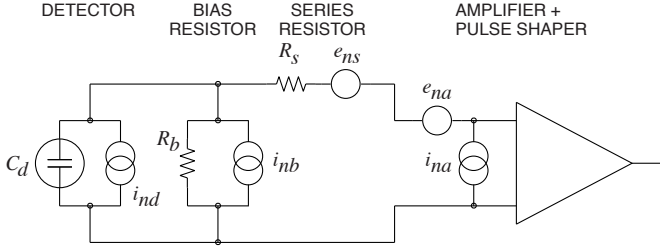


Figure 28.19: Equivalent circuit for noise analysis.

$$\begin{aligned} i_{nb}^2 &= \frac{4kT}{R_b}, \\ e_{ns}^2 &= 4kTR_s, \end{aligned} \quad (28.21)$$

where e is the electronic charge, I_d the detector bias current, k the Boltzmann constant and T the temperature. Typical amplifier noise parameters e_{na} and i_{na} are of order $\text{nV}/\sqrt{\text{Hz}}$ and $\text{pA}/\sqrt{\text{Hz}}$. Trapping and detrapping processes in resistors, dielectrics and semiconductors can introduce additional fluctuations whose noise power frequently exhibits a $1/f$ spectrum. The spectral density of the $1/f$ noise voltage is

$$e_{nf}^2 = \frac{A_f}{f}, \quad (28.22)$$

where the noise coefficient A_f is device specific and of order 10^{-10} – 10^{-12} V^2 .

A fraction of the noise current flows through the detector capacitance, resulting in a frequency-dependent noise voltage $i_n/(\omega C_d)$, which is added to the noise voltage in the input circuit. Since the individual noise contributions are random and uncorrelated, they add in quadrature. The total noise at the output of the pulse shaper is obtained by integrating over the full bandwidth of the system. Superimposed on repetitive detector signal pulses of constant magnitude, purely random noise produces a Gaussian signal distribution.

Since radiation detectors typically convert the deposited energy into charge, the system's noise level is conveniently expressed as an equivalent noise charge Q_n , which is equal to the detector signal that yields a signal-to-noise ratio of one. The equivalent noise charge is commonly expressed in Coulombs, the corresponding number of electrons, or the equivalent deposited energy (eV). For a capacitive sensor

$$Q_n^2 = i_n^2 F_i T_S + e_n^2 F_v \frac{C^2}{T_S} + F_{vf} A_f C^2, \quad (28.23)$$

where C is the sum of all capacitances shunting the input, F_i , F_v , and F_{vf} depend on the shape of the pulse determined by the shaper and T_S is a characteristic time, for example, the peaking time of a semi-gaussian pulse or the sampling interval in a correlated double sampler. The form factors F_i , F_v are easily calculated

$$F_i = \frac{1}{2T_S} \int_{-\infty}^{\infty} [W(t)]^2 dt, \quad F_v = \frac{T_S}{2} \int_{-\infty}^{\infty} \left[\frac{dW(t)}{dt} \right]^2 dt, \quad (28.24)$$

where for time-invariant pulse-shaping $W(t)$ is simply the system's impulse response (the output signal seen on an oscilloscope) for a short input pulse with the peak output signal normalized to unity. For more details see Refs. 119 and 120.

A pulse shaper formed by a single differentiator and integrator with equal time constants has $F_i = F_v = 0.9$ and $F_{vf} = 4$, independent of the shaping time constant. The overall noise bandwidth, however, depends on the time constant, *i.e.* the characteristic time T_S . The contribution from noise currents increases with shaping time, *i.e.*, pulse duration, whereas the voltage noise decreases with increasing shaping time. Noise with a $1/f$ spectrum depends only on the ratio of upper to lower cutoff frequencies (integrator to differentiator time constants), so for a given shaper topology the $1/f$ contribution to Q_n is independent of T_S . Furthermore, the contribution of noise voltage sources to Q_n increases with detector capacitance. Pulse shapers can be designed to reduce the effect of current noise, *e.g.*, mitigate radiation damage. Increasing pulse symmetry tends to decrease F_i

and increase F_v (*e.g.*, to 0.45 and 1.0 for a shaper with one CR differentiator and four cascaded integrators). For the circuit shown in Fig. 28.19,

$$\begin{aligned} Q_n^2 &= \left(2eI_d + 4kT/R_b + i_{na}^2 \right) F_i T_S \\ &\quad + (4kTR_s + e_{na}^2) F_v C_d^2 / T_S + F_{vf} A_f C_d^2. \end{aligned} \quad (28.25)$$

As the characteristic time T_S is changed, the total noise goes through a minimum, where the current and voltage contributions are equal. Fig. 28.20 shows a typical example. At short shaping times the voltage noise dominates, whereas at long shaping times the current noise takes over. The noise minimum is flattened by the presence of $1/f$ noise. Increasing the detector capacitance will increase the voltage noise and shift the noise minimum to longer shaping times.

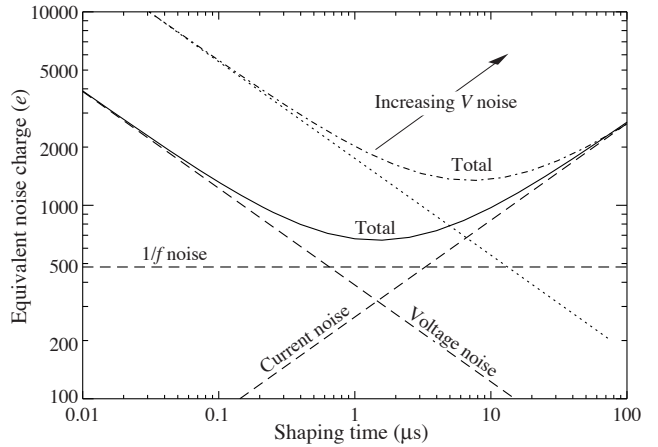


Figure 28.20: Equivalent noise charge vs shaping time. Changing the voltage or current noise contribution shifts the noise minimum. Increased voltage noise is shown as an example.

For quick estimates, one can use the following equation, which assumes an FET amplifier (negligible i_{na}) and a simple CR - RC shaper with time constants τ (equal to the peaking time):

$$\begin{aligned} (Q_n/e)^2 &= 12 \left[\frac{1}{\text{nA} \cdot \text{ns}} \right] I_d \tau + 6 \times 10^5 \left[\frac{\text{k}\Omega}{\text{ns}} \right] \frac{\tau}{R_b} \\ &\quad + 3.6 \times 10^4 \left[\frac{\text{ns}}{(\text{pF})^2 (\text{nV})^2 / \text{Hz}} \right] e_n^2 \frac{C^2}{\tau}. \end{aligned} \quad (28.26)$$

Noise is improved by reducing the detector capacitance and leakage current, judiciously selecting all resistances in the input circuit, and choosing the optimum shaping time constant.

The noise parameters of the amplifier depend primarily on the input device. In field effect transistors, the noise current contribution is very small, so reducing the detector leakage current and increasing the bias resistance will allow long shaping times with correspondingly lower noise. In bipolar transistors, the base current sets a lower bound on the noise current, so these devices are best at short shaping times. In special cases where the noise of a transistor scales with geometry, *i.e.*, decreasing noise voltage with increasing input capacitance, the lowest noise is obtained when the input capacitance of the transistor is equal to the detector capacitance, albeit at the expense of power dissipation. Capacitive matching is useful with field-effect transistors, but not bipolar transistors. In bipolar transistors, the minimum obtainable noise is independent of shaping time, but only at the optimum collector current I_C , which does depend on shaping time.

$$Q_{n,\min}^2 = 4kT \frac{C}{\sqrt{\beta_{DC}}} \sqrt{F_i F_v} \quad \text{at} \quad I_C = \frac{kT}{e} C \sqrt{\beta_{DC}} \sqrt{\frac{F_v}{F_i} \frac{1}{T_S}}, \quad (28.27)$$

where β_{DC} is the DC current gain. For a CR - RC shaper and $\beta_{DC} = 100$,

$$Q_{n,\min}/e \approx 250 \sqrt{C/\text{pF}}. \quad (28.28)$$

Practical noise levels range from $\sim 1e$ for CCD's at long shaping times to $\sim 10^4 e$ in high-capacitance liquid argon calorimeters. Silicon strip detectors typically operate at $\sim 10^3 e$ electrons, whereas pixel detectors with fast readout provide noise of several hundred electrons.

In timing measurements, the slope-to-noise ratio must be optimized, rather than the signal-to-noise ratio alone, so the rise time t_r of the pulse is important. The "jitter" σ_t of the timing distribution is

$$\sigma_t = \frac{\sigma_n}{(dS/dt)_{S_T}} \approx \frac{t_r}{S/N}, \quad (28.29)$$

where σ_n is the rms noise and the derivative of the signal dS/dt is evaluated at the trigger level S_T . To increase dS/dt without incurring excessive noise, the amplifier bandwidth should match the rise-time of the detector signal. The 10 to 90% rise time of an amplifier with bandwidth f_U is $0.35/f_U$. For example, an oscilloscope with 350 MHz bandwidth has a 1 ns rise time. When amplifiers are cascaded, which is invariably necessary, the individual rise times add in quadrature.

$$t_r \approx \sqrt{t_{r1}^2 + t_{r2}^2 + \dots + t_{rn}^2}$$

Increasing signal-to-noise ratio also improves time resolution, so minimizing the total capacitance at the input is also important. At high signal-to-noise ratios, the time jitter can be much smaller than the rise time. The timing distribution may shift with signal level ("walk"), but this can be corrected by various means, either in hardware or software [10].

For a more detailed introduction to detector signal processing and electronics see Ref. 111.

28.9. Calorimeters

A calorimeter is designed to measure the energy deposition and its direction for a contained electromagnetic (EM) or hadronic shower. The characteristic interaction distance for an electromagnetic interaction is the radiation length X_0 , which ranges from 13.8 g cm^{-2} in iron to 6.0 g cm^{-2} in uranium.* Similarly, the characteristic nuclear interaction length λ_I varies from 132.1 g cm^{-2} (Fe) to 209 g cm^{-2} (U).† In either case, a calorimeter must be many interaction lengths deep, where "many" is determined by physical size, cost, and other factors. EM calorimeters tend to be $15\text{--}30 X_0$ deep, while hadronic calorimeters are usually compromised at $5\text{--}8 \lambda_I$. In real experiments there is likely to be an EM calorimeter in front of the hadronic section, which in turn has less sampling density in the back, so the hadronic cascade occurs in a succession of different structures.

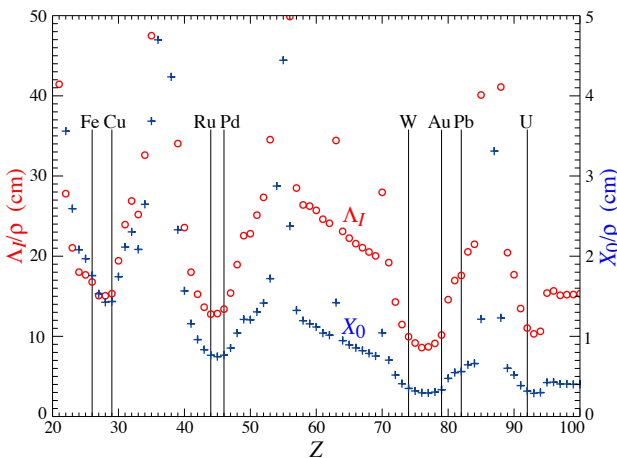


Figure 28.21: Nuclear interaction length λ_I/ρ (circles) and radiation length X_0/ρ (+’s) in cm for the chemical elements with $Z > 20$ and $\lambda_I < 50 \text{ cm}$.

* $X_0 = 120 \text{ g cm}^{-2} Z^{-2/3}$ to better than 5% for $Z > 23$.

† $\lambda_I = 37.8 \text{ g cm}^{-2} A^{0.312}$ to within 0.8% for $Z > 15$.

See pdg.lbl.gov/AtomicNuclearProperties for actual values.

In all cases there is a premium on small λ_I/ρ and X_0/ρ (both with units of length). These quantities are shown for $Z > 20$ for the chemical elements in Fig. 28.21. For the hadronic case, metallic absorbers in the W–Au region are best, followed by U. The Ru–Pd region elements are rare and expensive. Lead is a bad choice. Given cost considerations, Fe and Cu might be appropriate choices. For EM calorimeters high Z is preferred, and lead is not a bad choice.

These considerations are for *sampling calorimeters* consisting of metallic absorber sandwiched or (threaded) with an active material which generates signal. The active medium may be a scintillator, an ionizing noble liquid, a gas chamber, a semiconductor, or a Cherenkov radiator. The average interaction length is thus greater than that of the absorber alone, sometimes substantially so.

There are also *homogeneous calorimeters*, in which the entire volume is sensitive, *i.e.*, contributes signal. Homogeneous calorimeters (so far usually electromagnetic) may be built with inorganic heavy (high density, high $\langle Z \rangle$) scintillating crystals, or non-scintillating Cherenkov radiators such as lead glass and lead fluoride. Scintillation light and/or ionization in noble liquids can be detected. Nuclear interaction lengths in inorganic crystals range from 17.8 cm (LuAlO_3) to 42.2 cm (NaI). Popular choices have been BGO with $\lambda_I = 22.3 \text{ cm}$ and $X_0 = 1.12 \text{ cm}$, and PbWO_4 (20.3 cm and 0.89 cm). Properties of these and other commonly used inorganic crystal scintillators can be found in Table 28.4.

28.9.1. Electromagnetic calorimeters :

Revised October 2009 by R.-Y. Zhu (California Inst. of Technology).

The development of electromagnetic showers is discussed in the section on "Passage of Particles Through Matter" (Sec. 27 of this Review).

Formulae are given which approximately describe average showers, but since the physics of electromagnetic showers is well understood, detailed and reliable Monte Carlo simulation is possible. EGS4 [121] and GEANT [122] have emerged as the standards.

There are homogeneous and sampling electromagnetic calorimeters. In a homogeneous calorimeter the entire volume is sensitive, *i.e.*, contributes signal. Homogeneous electromagnetic calorimeters may be built with inorganic heavy (high- Z) scintillating crystals such as BGO, CsI, NaI, and PWO, non-scintillating Cherenkov radiators such as lead glass and lead fluoride, or ionizing noble liquids. Properties of commonly used inorganic crystal scintillators can be found in Table 28.4. A sampling calorimeter consists of an active medium which generates signal and a passive medium which functions as an absorber. The active medium may be a scintillator, an ionizing noble liquid, a gas chamber, or a semiconductor. The passive medium is usually a material of high density, such as lead, iron, copper, or depleted uranium.

The energy resolution σ_E/E of a calorimeter can be parametrized as $a/\sqrt{E} \oplus b \oplus c/E$, where \oplus represents addition in quadrature and E is in GeV. The stochastic term a represents statistics-related fluctuations such as intrinsic shower fluctuations, photoelectron statistics, dead material at the front of the calorimeter, and sampling fluctuations. For a fixed number of radiation lengths, the stochastic term a for a sampling calorimeter is expected to be proportional to $\sqrt{t/f}$, where t is plate thickness and f is sampling fraction [123,124]. While a is at a few percent level for a homogeneous calorimeter, it is typically 10% for sampling calorimeters. The main contributions to the systematic, or constant, term b are detector non-uniformity and calibration uncertainty. In the case of the hadronic cascades discussed below, non-compensation also contributes to the constant term. One additional contribution to the constant term for calorimeters built for modern high-energy physics experiments, operated in a high-beam intensity environment, is radiation damage of the active medium. This can be minimized by developing radiation-hard active media [47] and by frequent *in situ* calibration and monitoring [46,124]. With effort, the constant term b can be reduced to below one percent. The term c is due to electronic noise summed over readout channels within a few Molière radii. The best energy resolution for electromagnetic shower measurement is obtained in total absorption homogeneous calorimeters, *e.g.* calorimeters built with heavy crystal scintillators. These are used when ultimate performance is pursued.

The position resolution depends on the effective Molière radius

and the transverse granularity of the calorimeter. Like the energy resolution, it can be factored as $a/\sqrt{E} \oplus b$, where a is a few to 20 mm and b can be as small as a fraction of mm for a dense calorimeter with fine granularity. Electromagnetic calorimeters may also provide direction measurement for electrons and photons. This is important for photon-related physics when there are uncertainties in event origin, since photons do not leave information in the particle tracking system. Typical photon angular resolution is about $45 \text{ mrad}/\sqrt{E}$, which can be provided by implementing longitudinal segmentation [125] for a sampling calorimeter or by adding a preshower detector [126] for a homogeneous calorimeter without longitudinal segmentation.

Table 28.8: Resolution of typical electromagnetic calorimeters. E is in GeV.

Technology (Experiment)	Depth	Energy resolution	Date
NaI(Tl) (Crystal Ball)	$20X_0$	$2.7\%/E^{1/4}$	1983
$\text{Bi}_4\text{Ge}_3\text{O}_{12}$ (BGO) (L3)	$22X_0$	$2\%/\sqrt{E} \oplus 0.7\%$	1993
CsI (KTeV)	$27X_0$	$2\%/\sqrt{E} \oplus 0.45\%$	1996
CsI(Tl) (BaBar)	$16\text{--}18X_0$	$2.3\%/E^{1/4} \oplus 1.4\%$	1999
CsI(Tl) (BELLE)	$16X_0$	1.7% for $E_\gamma > 3.5 \text{ GeV}$	1998
PbWO_4 (PWO) (CMS)	$25X_0$	$3\%/\sqrt{E} \oplus 0.5\% \oplus 0.2/E$	1997
Lead glass (OPAL)	$20.5X_0$	$5\%/\sqrt{E}$	1990
Liquid Kr (NA48)	$27X_0$	$3.2\%/\sqrt{E} \oplus 0.42\% \oplus 0.09/E$	1998
Scintillator/depleted U (ZEUS)	$20\text{--}30X_0$	$18\%/\sqrt{E}$	1988
Scintillator/Pb (CDF)	$18X_0$	$13.5\%/\sqrt{E}$	1988
Scintillator fiber/Pb spaghetti (KLOE)	$15X_0$	$5.7\%/\sqrt{E} \oplus 0.6\%$	1995
Liquid Ar/Pb (NA31)	$27X_0$	$7.5\%/\sqrt{E} \oplus 0.5\% \oplus 0.1/E$	1988
Liquid Ar/Pb (SLD)	$21X_0$	$8\%/\sqrt{E}$	1993
Liquid Ar/Pb (H1)	$20\text{--}30X_0$	$12\%/\sqrt{E} \oplus 1\%$	1998
Liquid Ar/depl. U (DØ)	$20.5X_0$	$16\%/\sqrt{E} \oplus 0.3\% \oplus 0.3/E$	1993
Liquid Ar/Pb accordion (ATLAS)	$25X_0$	$10\%/\sqrt{E} \oplus 0.4\% \oplus 0.3/E$	1996

Novel technologies have been developed for electromagnetic calorimetry. New heavy crystal scintillators, such as PWO and LSO:Ce (see Sec. 28.4), have attracted much attention for homogeneous calorimetry. In some cases, such as PWO, it has received broad applications in high-energy and nuclear physics experiments. The “spaghetti” structure has been developed for sampling calorimetry with scintillating fibers as the sensitive medium. The “accordion” structure has been developed for sampling calorimetry with ionizing noble liquid as the sensitive medium. Table 28.8 provides a brief description of typical electromagnetic calorimeters built recently for high-energy physics experiments. Also listed in this table are calorimeter depths in radiation lengths (X_0) and the achieved energy resolution. Whenever possible, the performance of calorimeters *in situ* is quoted, which is usually in good agreement with prototype test beam results as well as EGS or GEANT simulations, provided that all systematic effects are properly included. Detailed references on detector design and performance can be found in Appendix C of reference [124] and Proceedings of the International Conference series on Calorimetry in Particle Physics.

28.9.2. Hadronic calorimeters : [1–5,124]

Written April 2008 by D. E. Groom (LBNL).

Most large hadron calorimeters are sampling calorimeters which are parts of complicated 4π detectors at colliding beam facilities. Typically, the basic structure is plates of absorber (Fe, Pb, Cu, or occasionally U or W) alternating with plastic scintillators (plates, tiles, bars), liquid argon (LAr), or gaseous detectors. The ionization is measured directly, as in LAr calorimeters, or via scintillation light observed by photodetectors (usually PMT’s). Wavelength-shifting fibers are often used to solve difficult problems of geometry and light collection uniformity. Silicon sensors are being studied for ILC detectors; in this case $e\text{-}h$ pairs are collected. There are as many variants of these schemes as there are calorimeters, including variations in geometry of the absorber and sensors, *e.g.*, scintillating fibers threading an absorber [127], and the “accordion” LAr detector, with zig-zag absorber plates to minimize channeling effects. Another departure from the traditional sandwich structure is the LAr-tube design shown in Fig. 28.22(a).

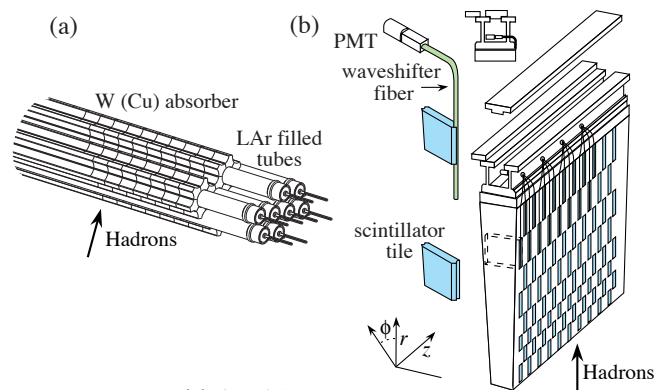


Figure 28.22: (a) ATLAS forward hadronic calorimeter structure (FCal2, 3). Tubes containing LAr are embedded in a mainly tungsten matrix. (b) ATLAS central calorimeter wedge; iron with plastic scintillator tile with wavelength-shifting fiber readout.

A relatively new variant is the use of Cerenkov light in hadron calorimetry. Such a calorimeter is sensitive to e^\pm ’s in the EM showers plus a few relativistic pions. An example is the radiation-hard forward calorimeter in CMS, with iron absorber and quartz fiber readout by PMTs.

Ideally, the calorimeter is segmented in ϕ and θ (or $\eta = -\ln \tan(\theta/2)$). Fine segmentation, while desirable, is limited by cost, readout complexity, practical geometry, and the transverse size of the cascades. An example, a wedge of the ATLAS central barrel calorimeter, is shown in Fig. 28.22(b).

In an inelastic hadronic collision a significant fraction f_{em} of the energy is removed from further hadronic interaction by the production of secondary π^0 ’s and η ’s, whose decay photons generate high-energy electromagnetic (EM) cascades. Charged secondaries (π^\pm , p , ...) deposit energy via ionization and excitation, but also interact with nuclei, producing spallation protons and neutrons, evaporation neutrons, and recoiling nuclei in highly excited states. The charged collision products produce detectable ionization, as do the showering γ -rays from the prompt de-excitation of highly excited nuclei. The recoiling nuclei generate little or no detectable signal. The neutrons lose kinetic energy in elastic collisions over hundreds of ns, gradually thermalize and are captured, with the production of more γ -rays—usually outside the acceptance gate of the electronics. Between endothermic spallation losses, nuclear recoils, and late neutron capture, a significant fraction of the hadronic energy (20%–35%, depending on the absorber and energy of the incident particle) is invisible.

In contrast to EM showers, hadronic cascade processes are characterized by relatively few high-energy particles being produced. The lost energy and the $\pi^0 \rightarrow \gamma\gamma$ fraction f_{em} are highly variable from event to event. Until there is event-by-event knowledge of both the invisible energy loss and EM deposit (to be discussed below), the energy resolution of a hadron calorimeter will remain significantly

worse than that of an EM calorimeter.

It has been shown by a simple induction argument and verified by experiment, that the decrease in the average value of the hadronic energy fraction ($\langle f_h \rangle = 1 - \langle f_{em} \rangle$) as the projectile energy E increases is fairly well described by the power law [128,129]

$$\langle f_h \rangle \approx (E/E_0)^{m-1} \quad (\text{for } E > E_0), \quad (28.30)$$

up to at least a few hundred GeV. The exponent m depends logarithmically on the mean multiplicity and the mean fractional loss to π^0 production in a single interaction. It is in the range 0.80–0.87, but must be obtained experimentally for each calorimeter configuration. E_0 is roughly the energy for the onset of inelastic collisions. It is 1 GeV or a little less for incident pions.

In a hadron-nucleus collision a large fraction of the incident energy is carried by a “leading particle” with the same quark content as the incident hadron. If the projectile is a charged pion, the leading particle is usually a pion, which can be neutral and hence contributes to the EM sector. This is not true for incident protons. The result is an increased mean hadronic fraction for incident protons: in Eq. (28.31b) $E_0 \approx 2.6$ GeV [127–131].

The EM energy deposit is usually detected more efficiently than the hadronic energy deposit. If the detection efficiency for the EM sector is e and that for the hadronic sector is h , then the ratio of the mean response to a pion to that for an electron is

$$\pi/e = \langle f_{em} \rangle + \langle f_h \rangle h/e = 1 - (1 - h/e)\langle f_h \rangle \quad (28.31a)$$

$$\approx 1 - (1 - h/e)(E/E_0)^{m-1}. \quad (28.31b)$$

If $h \neq e$ the hadronic response is not a linear function of energy. Only the product $(1 - h/e)E_0^{1-m}$ can be obtained by measuring π/e as a function of energy. Since $1 - m$ is small and $E_0 \approx 1$ GeV for the usual pion-induced cascades, this fact is usually ignored and h/e is reported.

The discussion above assumes an idealized calorimeter, with the same structure throughout and without leakage. “Real” calorimeters usually have an EM detector in front and a coarse “catcher” in the back. Complete containment is generally impractical.

By definition, $0 \leq f_{em} \leq 1$. Its variance changes only slowly with energy, but perforce $\langle f_{em} \rangle \rightarrow 1$ as the projectile energy increases. An empirical power law $\sigma_{f_{em}} = (E/E_1)^{1-\ell}$ (where $\ell < 1$) describes the energy dependence adequately and has the right asymptotic properties. For $h/e \neq 1$, fluctuations in f_{em} significantly contribute to the resolution, in particular contributing a larger fraction of the variance at high energies. Since the f_{em} distribution has a tail on the high side, the calorimeter response is non-Gaussian with a high-energy tail if $h/e < 1$. *Noncompensation* ($h/e \neq 1$) thus seriously degrades resolution as well as producing a nonlinear response.

It is clearly desirable to *compensate* the response, *i.e.*, to design the calorimeter such that $h/e = 1$. This is possible only in a sampling calorimeter, where several variables can be chosen or tuned:

1. Decrease the EM sensitivity. Because the EM cross sections increase with Z ,* and the absorber usually has higher $\langle Z \rangle$ than does the sensor, the EM energy deposit rate, relative to minimum ionization, is greater than this ratio in the sensor. Lower- Z inactive cladding, such as the steel cladding on ZEUS U plates, preferentially absorbs low-energy γ 's in EM showers and thus also lowers the electronic response. G10 signal boards in the DØ calorimeters have the same effect.
2. Increase the hadronic sensitivity. The abundant neutrons have a large n - p scattering cross section, with the production of low-energy scattered protons in hydrogenous sampling materials such as butane-filled proportional counters or plastic scintillator. (When scattering off a nucleus with mass number A , a neutron can at most lose $4/(1+A)^2$ of its kinetic energy.) The down side in the scintillator case is that the signal from a highly-ionizing proton stub can be reduced by as much as 90% by recombination and quenching (Birk's Law, Eq. (28.2)).
3. Fabjan and Willis proposed that the additional signal generated in the aftermath of fission in ^{238}U absorber plates should compensate

nuclear fluctuations [132]. The production of fission fragments due to fast n capture was later observed [133]. However, while a very large amount of energy is released, it is mostly carried by low-velocity fission fragments which produce very little observable signal. The approach seemed promising for awhile.

The compensation observed with the ZEUS ^{238}U /scintillator calorimeter was mainly the result of methods 2 and 3 above.

Motivated very much by the work of Brau, Gabriel, Brückmann, and Wigmans [134], several groups built calorimeters which were very nearly compensating. The degree of compensation was sensitive to the acceptance gate width, and so could be somewhat tuned. These included (a) HELIOS with 2.5 mm thick scintillator plates sandwiched between 2 mm thick ^{238}U plates (one of several structures); $\sigma/E = 0.34/\sqrt{E}$ was obtained, (b) ZEUS, 2.6 cm thick scintillator plates between 3.3 mm ^{238}U plates; $\sigma/E = 0.35/\sqrt{E}$, (c) a ZEUS prototype with 10 mm Pb plates and 2.5 mm scintillator sheets; $\sigma/E = 0.44/\sqrt{E}$, and (d) DØ, where the sandwich cell consists of a 4–6 mm thick ^{238}U plate, 2.3 mm LAr, a G-10 signal board, and another 2.3 mm LAr gap.

A more versatile approach to compensation is provided by a *dual-readout calorimeter*, in which the signal is sensed by two readout systems with highly contrasting h/e . Although the concept is more than two decades old [135], it has only recently been implemented by the DREAM collaboration [136]. The test beam calorimeter consisted of copper tubes, each filled with scintillator and quartz fibers. If the two signals Q and S (quartz and scintillator) are both normalized to electrons, then for each event Eq. (28.31) takes the form:

$$\begin{aligned} Q &= E[f_{em} + h/e|_Q(1 - f_{em})] \\ S &= E[f_{em} + h/e|_S(1 - f_{em})] \end{aligned} \quad (28.32)$$

These equations are linear in $1/E$ and f_{em} , and are easily solved for estimators of the *corrected* energy and f_{em} for each event. Both are subject to resolution effects, but effects due to fluctuations in f_{em} are eliminated. The solution for the corrected energy is given by [129]:

$$E = \frac{RS - Q}{R - 1}, \quad \text{where } R = \frac{1 - h/e|_Q}{1 - h/e|_S} \quad (28.33)$$

R is the energy-independent slope of the event locus on a plot of Q vs S . It can be found either from the fitted slope or by measuring π/e as a function of E .

The fractional resolution can be represented by

$$\frac{\sigma}{E} = \frac{a_1(E)}{\sqrt{E}} \oplus \left| 1 - \frac{h}{e} \right| \left(\frac{E}{E_1} \right)^{1-\ell} \quad (28.34)$$

The coefficient a_1 is expected to have mild energy dependence for a number of reasons. For example, the sampling variance is $(\pi/e)E$ rather than E . $(E/E_1)^{1-\ell}$ is the parameterization of $\sigma_{f_{em}}$ discussed above. At a time when data were of lower quality, a plot of $(\sigma/E)^2$ vs $1/E$ was apparently well-described by a straight line (constant a_1) with a finite intercept—the square of the right term in Eq. (28.34), then called “the constant term.” Modern data show the slight downturn [127].

The average longitudinal distribution rises to a smooth peak, increasing slowly with energy but about one nuclear interaction length (λ_I) into the calorimeter. After several interaction lengths its fall is reasonably exponential. Examples from the CDHS magnetized iron-scintillator sandwich calorimeter test beam calibration runs [137] are shown in Fig. 28.23. Proton-induced cascades are somewhat shorter and broader than pion-induced cascades [131]. It has been found that a gamma distribution fairly well describes the longitudinal development of an EM shower, as discussed in Sec. 27.5. Following this logic, Bock *et al.* suggested that the profile of a hadronic cascade could be fit by the sum of two gamma distributions, one with a characteristic length X_0 and the other with length λ_I [138]. Fits to this 4-parameter function are commonly used, *e.g.*, by the ATLAS Tilecal collaboration [131]. If the interaction point is not known (the usual case), the distribution must be convoluted with an exponential in the interaction length of the incident particle. Adragna *et al.* give an analytic form for the convoluted function [131]

* The asymptotic pair-production cross section scales roughly as $Z^{0.75}$, and $|dE/dx|$ slowly decreases with increasing Z .

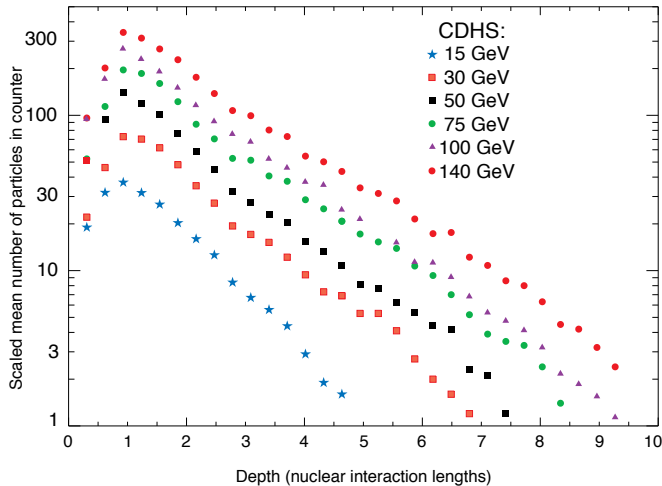


Figure 28.23: Mean profiles of π^+ (mostly) induced cascades in the CDHS neutrino detector [137]. See full-color version on color pages at end of book.

The transverse energy deposit is characterized by a central core dominated by EM cascades, together with a wide “skirt” produced by wide-angle hadronic interactions [139].

28.9.3. Free electron drift velocities in liquid ionization chambers :

Written August 2009 by W. Walkowiak (U. Siegen)

Drift velocities of free electrons in LAr [140] are given as a function of electric field strength for different temperatures of the medium in Fig. 28.24. The drift velocities in LAr have been measured using a double-gridded drift chamber with electrons produced by a laser pulse on a gold-plated cathode. The average temperature gradient of the drift velocity of the free electrons in LAr is described [140] by

$$\frac{\Delta v_d}{\Delta T v_d} = (-1.72 \pm 0.08) \% / \text{K}.$$

Earlier measurements [141–144] used different techniques and show systematic deviations of the drift velocities for free electrons which cannot be explained by the temperature dependence mentioned above.

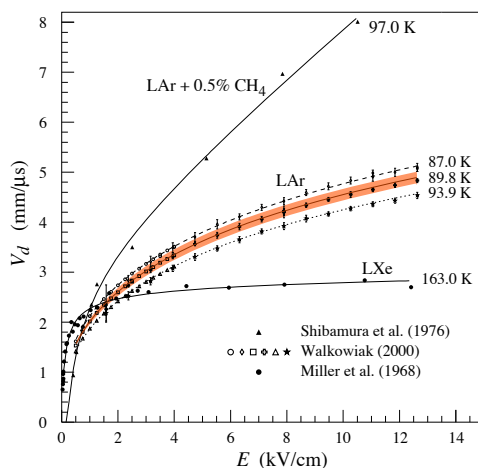


Figure 28.24: Drift velocity of free electrons as a function of electric field strength for LAr [140], LAr + 0.5% CH_4 [142] and LXe [141]. The average temperatures of the liquids are indicated. Results of a fit to an empirical function [146] are superimposed. In case of LAr at 91 K the error band for the global fit [140] including statistical and systematic errors as well as correlations of the data points is given. Only statistical errors are shown for the individual LAr data points.

Drift velocities of free electrons in LXe [142] as a function of electric field strength are also displayed in Fig. 28.24. The drift

velocity saturates for $|\mathbf{E}| > 3$ kV/cm, and decreases with increasing temperature for LXe as well as measured e.g. by [145].

The addition of small concentrations of other molecules like N_2 , H_2 and CH_4 in solution to the liquid typically increases the drift velocities of free electrons above the saturation value [142,143], see example for CH_4 admixture to LAr in Fig. 28.24. Therefore, actual drift velocities are critically dependent on even small additions or contaminations.

28.10. Superconducting magnets for collider detectors

Revised January 2010 by A. Yamamoto (KEK); revised October 2001 by R.D. Kephart (FNAL)

28.10.1. Solenoid Magnets : In all cases SI unit are assumed, so that the magnetic field, B , is in Tesla, the stored energy, E , is in joules, the dimensions are in meters, and $\mu_0 = 4\pi \times 10^{-7}$.

The magnetic field (B) in an ideal solenoid with a flux return iron yoke, in which the magnetic field is < 2 T, is given by

$$B = \mu_0 n I \quad (28.35)$$

where n is the number of turns/meter and I is the current. In an air-core solenoid, the central field is given by

$$B(0,0) = \mu_0 n I \frac{L}{\sqrt{L^2 + 4R^2}}, \quad (28.36)$$

where L is the coil length and R is the coil radius.

In most cases, momentum analysis is made by measuring the circular trajectory of the passing particles according to $p = mv\gamma = qrB$, where p is the momentum, m the mass, q the charge, r the bending radius. The sagitta, s , of the trajectory is given by

$$s = qB\ell^2/8p, \quad (28.37)$$

where ℓ is the path length in the magnetic field. In a practical momentum measurement in colliding beam detectors, it is more effective to increase the magnetic volume than the field strength, since

$$dp/p \propto p/B\ell^2, \quad (28.38)$$

where ℓ corresponds to the solenoid coil radius R . The energy stored in the magnetic field of any magnet is calculated by integrating B^2 over all space:

$$E = \frac{1}{2\mu_0} \int B^2 dV \quad (28.39)$$

If the coil thin, (which is the case if it is to superconducting coil), then

$$E \approx (B^2/2\mu_0)\pi R^2 L. \quad (28.40)$$

For a detector in which the calorimetry is outside the aperture of the solenoid, the coil must be thin in terms of radiation and absorption lengths. This usually means that the coil is superconducting and that the vacuum vessel encasing it is of minimum real thickness and fabricated of a material with long radiation length. There are two major contributors to the thickness of a thin solenoid:

- 1) The conductor consisting of the current-carrying superconducting material (usually NbTi/Cu) and the quench protecting stabilizer (usually aluminum) are wound on the inside of a structural support cylinder (usually aluminum also). The coil thickness scales as $B^2 R$, so the thickness in radiation lengths (X_0) is

$$t_{\text{coil}}/X_0 = (R/\sigma_h X_0)(B^2/2\mu_0), \quad (28.41)$$

where t_{coil} is the physical thickness of the coil, X_0 the average radiation length of the coil/stabilizer material, and σ_h is the hoop stress in the coil [149]. $B^2/2\mu_0$ is the magnetic pressure. In large detector solenoids, the aluminum stabilizer and support cylinders dominate the thickness; the superconductor (NbTi/Cu) contributes a smaller fraction. The main coil and support cylinder components typically contribute about 2/3 of the total thickness in radiation lengths.

Table 28.9: Progress of superconducting magnets for particle physics detectors.

Experiment	Laboratory	B [T]	Radius [m]	Length [m]	Energy [MJ]	X/X_0	E/M [kJ/kg]
TOPAZ*	KEK	1.2	1.45	5.4	20	0.70	4.3
CDF	Tsukuba/Fermi	1.5	1.5	5.07	30	0.84	5.4
VENUS*	KEK	0.75	1.75	5.64	12	0.52	2.8
AMY*	KEK	3	1.29	3	40	†	
CLEO-II	Cornell	1.5	1.55	3.8	25	2.5	3.7
ALEPH*	Saclay/CERN	1.5	2.75	7.0	130	2.0	5.5
DELPHI*	RAL/CERN	1.2	2.8	7.4	109	1.7	4.2
ZEUS*	INFN/DESY	1.8	1.5	2.85	11	0.9	5.5
H1*	RAL/DESY	1.2	2.8	5.75	120	1.8	4.8
BaBar*	INFN/SLAC	1.5	1.5	3.46	27	†	3.6
D0	Fermi	2.0	0.6	2.73	5.6	0.9	3.7
BELLE	KEK	1.5	1.8	4	42	†	5.3
BES-III	IHEP	1.0	1.475	3.5	9.5	†	2.6
ATLAS-CS	ATLAS/CERN	2.0	1.25	5.3	38	0.66	7.0
ATLAS-BT	ATLAS/CERN	1	4.7–9.75	26	1080	(Toroid)†	
ATLAS-ET	ATLAS/CERN	1	0.825–5.35	5	2 × 250	(Toroid)†	
CMS	CMS/CERN	4	6	12.5	2600	†	12

* No longer in service

† EM calorimeter is inside solenoid, so small X/X_0 is not a goal

2) Another contribution to the material comes from the outer cylindrical shell of the vacuum vessel. Since this shell is susceptible to buckling collapse, its thickness is determined by the diameter, length and the modulus of the material of which it is fabricated. The outer vacuum shell represents about 1/3 of the total thickness in radiation length.

28.10.2. Properties of collider detector magnets :

The physical dimensions, central field stored energy and thickness in radiation lengths normal to the beam line of the superconducting solenoids associated with the major collider are given in Table 28.9 [148]. Fig. 28.25 shows thickness in radiation lengths as a function of B^2R in various collider detector solenoids.

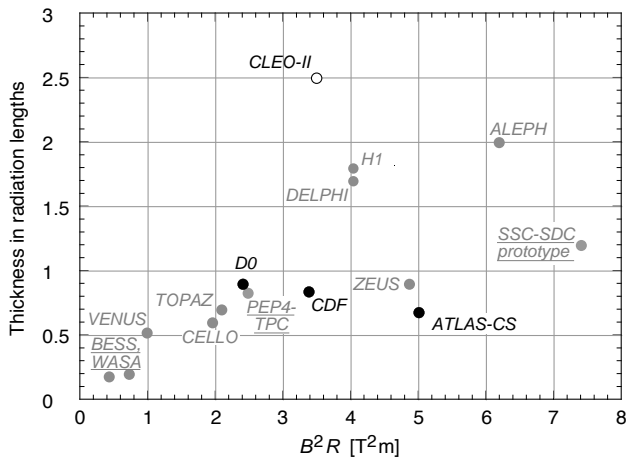


Figure 28.25: Magnet wall thickness in radiation length as a function of B^2R for various detector solenoids. Gray entries are for magnets no longer in use, and entries underlined are not listed in Table 28.9. Open circles are for magnets not designed to be “thin.” The SSC-SDC prototype provided important R&D for LHC magnets.

The ratio of stored energy to cold mass (E/M) is a useful performance measure. It can also be expressed as the ratio of the stress, σ_h , to twice the equivalent density, ρ , in the coil [149]:

$$\frac{E}{M} = \frac{\int (B^2/2\mu_0)dV}{\rho V_{\text{coil}}} \approx \frac{\sigma_h}{2\rho} \quad (28.42)$$

The E/M ratio in the coil is approximately equivalent to H ,* the enthalpy of the coil, and it determines the average coil temperature rise after energy absorption in a quench:

$$E/M = H(T_2) - H(T_1) \approx H(T_2) \quad (28.43)$$

where T_2 is the average coil temperature after the full energy absorption in a quench, and T_1 is the initial temperature. E/M ratios of 5, 10, and 20 kJ/kg correspond to ~ 65 , ~ 80 , and ~ 100 K, respectively. The E/M ratios of various detector magnets are shown in Fig. 28.26 as a function of total stored energy. One would like the cold mass to be as small as possible to minimize the thickness, but temperature rise during a quench must also be minimized. An E/M ratio as large as 12 kJ/kg is designed into the CMS solenoid, with the possibility that about half of the stored energy can go to an external dump resistor. Thus the coil temperature can be kept below 80 K if the energy extraction system work well. The limit is set by the maximum temperature that the coil design can tolerate during a quench. This maximum local temperature should be < 130 K (50 K + 80 K), so that thermal expansion effects in the coil are manageable.

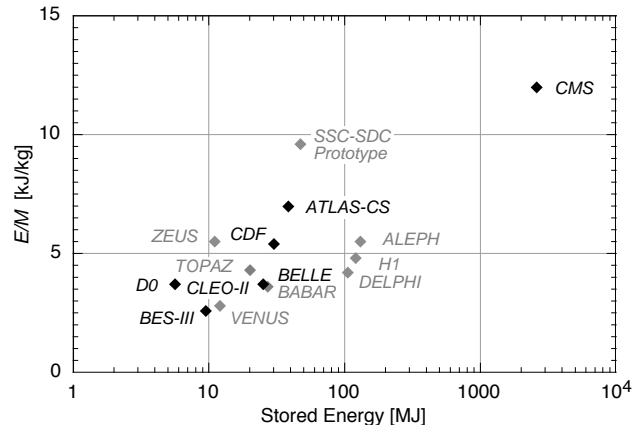


Figure 28.26: Ratio of stored energy to cold mass for thin detector solenoids. Gray indicates magnets no longer in operation.

* The enthalpy, or heat content, is called H in the thermodynamics literature. It is not to be confused with the magnetic field intensity B/μ .

28.10.3. Toroidal magnets :

Toroidal coils uniquely provide a closed magnetic field without the necessity of an iron flux-return yoke. Because no field exists at the collision point and along the beam line, there is, in principle, no effect on the beam. On the other hand, the field profile generally has $1/r$ dependence. The particle momentum may be determined by measurements of the deflection angle combined with the sagitta. The deflection (bending) power BL is

$$BL \approx \int_{R_i}^{R_0} \frac{B_i R_i dR}{R \sin \theta} = \frac{B_i R_i}{\sin \theta} \ln(R_0/R_i), \quad (28.44)$$

where R_i is the inner coil radius, R_0 is the outer coil radius, and θ is the angle between the particle trajectory and the beam line axis. The momentum resolution given by the deflection may be expressed as

$$\frac{\Delta p}{p} \propto \frac{p}{BL} \approx \frac{p \sin \theta}{B_i R_i \ln(R_0/R_i)}. \quad (28.45)$$

The momentum resolution is better in the forward/backward (smaller θ) direction. The geometry has been found to be optimal when $R_0/R_i \approx 3-4$. In practical designs, the coil is divided into 6-12 lumped coils in order to have reasonable acceptance and accessibility. This causes the coil design to be much more complex. The mechanical structure needs to sustain the decentering force between adjacent coils, and the peak field in the coil is 3-5 times higher than the useful magnetic field for the momentum analysis [147].

28.11. Measurement of particle momenta in a uniform magnetic field [150,151]

The trajectory of a particle with momentum p (in GeV/c) and charge ze in a constant magnetic field \vec{B} is a helix, with radius of curvature R and pitch angle λ . The radius of curvature and momentum component perpendicular to \vec{B} are related by

$$p \cos \lambda = 0.3 z B R, \quad (28.46)$$

where B is in tesla and R is in meters.

The distribution of measurements of the curvature $k \equiv 1/R$ is approximately Gaussian. The curvature error for a large number of uniformly spaced measurements on the trajectory of a charged particle in a uniform magnetic field can be approximated by

$$(\delta k)^2 = (\delta k_{\text{res}})^2 + (\delta k_{\text{ms}})^2, \quad (28.47)$$

where δk = curvature error

δk_{res} = curvature error due to finite measurement resolution

δk_{ms} = curvature error due to multiple scattering.

If many (≥ 10) uniformly spaced position measurements are made along a trajectory in a uniform medium,

$$\delta k_{\text{res}} = \frac{\epsilon}{L'^2} \sqrt{\frac{720}{N+4}}, \quad (28.48)$$

where N = number of points measured along track

L' = the projected length of the track onto the bending plane

ϵ = measurement error for each point, perpendicular to the trajectory.

If a vertex constraint is applied at the origin of the track, the coefficient under the radical becomes 320.

For arbitrary spacing of coordinates s_i measured along the projected trajectory and with variable measurement errors ϵ_i the curvature error δk_{res} is calculated from:

$$(\delta k_{\text{res}})^2 = \frac{4}{w} \frac{V_{ss}}{V_{ss} V_{s^2 s^2} - (V_{ss^2})^2}, \quad (28.49)$$

where V are covariances defined as $V_{s^m s^n} = \langle s^m s^n \rangle - \langle s^m \rangle \langle s^n \rangle$ with $\langle s^m \rangle = w^{-1} \sum (s_i^m / \epsilon_i^2)$ and $w = \sum \epsilon_i^{-2}$.

The contribution due to multiple Coulomb scattering is approximately

$$\delta k_{\text{ms}} \approx \frac{(0.016)(\text{GeV}/c)z}{Lp\beta \cos^2 \lambda} \sqrt{\frac{L}{X_0}}, \quad (28.50)$$

where p = momentum (GeV/c)

z = charge of incident particle in units of e

L = the total track length

X_0 = radiation length of the scattering medium (in units of length; the X_0 defined elsewhere must be multiplied by density)

β = the kinematic variable v/c .

More accurate approximations for multiple scattering may be found in the section on Passage of Particles Through Matter (Sec. 27 of this Review). The contribution to the curvature error is given approximately by $\delta k_{\text{ms}} \approx 8 s_{\text{plane}}^{\text{rms}} / L^2$, where $s_{\text{plane}}^{\text{rms}}$ is defined there.

References:

1. *Experimental Techniques in High Energy Physics*, T. Ferbel (ed.) (Addison-Wesley, Menlo Park, CA, 1987).
2. K. Kleinknecht, *Detectors for Particle Radiation*, Cambridge University Press (1998).
3. G.F. Knoll, *Radiation Detection and Measurement*, 3rd edition, John Wiley & Sons, New York (1999).
4. D.R. Green, *The Physics of Particle Detectors*, Cambridge Monographs on Particle Physics, Nuclear Physics and Cosmology, # 12, Cambridge University Press (2000).
5. C. Leroy & P.-G. Rancoita, *Principles of Radiation Interaction in Matter and Detection*, (World Scientific, Singapore, 2004).
6. C. Grupen, *Particle Detectors*, Cambridge Monographs on Particle Physics, Nuclear Physics and Cosmology, Cambridge University Press (2008).
7. [Icarus Collaboration], ICARUS-TM/2001-09; LGNS-EXP 13/89 add 2-01.
8. M. Titov, Nucl. Instrum. Methods **A581**, 25 (2007).
9. B. Aubert, *et al.*, [BaBar Collaboration], Nucl. Instrum. Methods **A479**, 1 (2002).
10. H. Spieler, IEEE Trans. **NS29**, 1142 (1982).
11. K. Arisaka, Nucl. Instrum. Methods **A442**, 80 (2000).
12. Hamamatsu K.K. Electron Tube Division, *Photomultiplier Tubes: Basics and Applications*, 2nd edition (2002); Can be found under "Photomultiplier Tube Handbook" at sales.hamamatsu.com/en/products/electron-tube-division/detectors/photomultiplier-tubes-pmts.php.
13. A. Braem *et al.*, Nucl. Instrum. Methods **A518**, 574 (2004).
14. R. Arnold *et al.*, Nucl. Instrum. Methods **A314**, 465 (1992).
15. P. Mangeot *et al.*, Nucl. Instrum. Methods **A216**, 79 (1983); R. Apsimon *et al.*, IEEE. Trans. Nucl. Sci. **33**, 122 (1986); R. Arnold *et al.*, Nucl. Instrum. Methods **A270**, 255, 289 (1988); D. Aston *et al.*, Nucl. Instrum. Methods **A283**, 582 (1989).
16. J. Janesick *Scientific charge-coupled devices*, SPIE Press, Bellingham, WA (2001).
17. R. Haitz *et al.*, J. Appl. Phys. **36**, 3123 (1965); R. McIntyre, IEEE Trans. Electron Devices **13**, 164 (1966); H. Dautet *et al.*, Applied Optics, **32**, (21), 3894 (1993); Perkin-Elmer Optoelectronics, *Avalanche Photodiodes: A User's Guide*.
18. P. Buzhan *et al.*, Nucl. Instrum. Methods **A504**, 48 (2003); Z. Sadygov *et al.*, Nucl. Instrum. Methods **A504**, 301 (2003); V. Golovin and V. Saveliev, Nucl. Instrum. Methods **A518**, 560 (2004).
19. M. Landstrass *et al.*, Diam. & Rel. Matter, **2**, 1033 (1993); R. McKeag and R. Jackman, Diam. & Rel. Matter, **7**, 513 (1998); R. Brascia *et al.*, Phys. Stat. Sol., **199**, 113 (2003).
20. M. Petrov, M. Stapelbroek, and W. Kleinhans, Appl. Phys. Lett. **51**, 406 (1987); M. Atac, M. Petrov, IEEE Trans. Nucl. Sci. **36** 163 (1989); M. Atac *et al.*, Nucl. Instrum. Methods **A314**, 56 (1994).
21. J.B. Birks, *The Theory and Practice of Scintillation Counting*, (Pergamon, London, 1964).
22. D. Clark, Nucl. Instrum. Methods **117**, 295 (1974).
23. J.B. Birks, Proc. Phys. Soc. **A64**, 874 (1951).
24. B. Bengston and M. Moszynski, Nucl. Instrum. Methods **117**, 227 (1974); J. Bialkowski, *et al.*, Nucl. Instrum. Methods **117**, 221 (1974).

25. C. P. Achenbach, "Active optical fibres in modern particle physics experiments," [arXiv:nuc1-ex/0404008v1](https://arxiv.org/abs/nuc1-ex/0404008v1).
26. I.B. Berلمان, *Handbook of Fluorescence Spectra of Aromatic Molecules*, 2nd edition (Academic Press, New York, 1971).
27. C. Zorn, in *Instrumentation in High Energy Physics*, ed. F. Sauli, (1992, World Scientific, Singapore) pp. 218–279.
28. T. Foerster, *Ann. Phys.* **2**, 55 (1948).
29. J.M. Fluornoy, Conference on Radiation-Tolerant Plastic Scintillators and Detectors, K.F. Johnson and R.L. Clough editors, *Rad. Phys. and Chem.*, **41** 389 (1993).
30. D. Horstman and U. Holm, *ibid*, 395.
31. D. Blomker, *et al.*, *Nucl. Instrum. Methods* **A311**, 505 (1992); J. Mainusch, *et al.*, *Nucl. Instrum. Methods* **A312**, 451 (1992).
32. Conference on Radiation-Tolerant Plastic Scintillators and Detectors, K.F. Johnson and R.L. Clough editors, *Rad. Phys. and Chem.*, **41** (1993).
33. S.R. Borenstein and R.C. Strand, *IEEE Trans. Nuc. Sci.* **NS-31(1)**, 396 (1984).
34. P. Sonderegger, *Nucl. Instrum. Methods* **A257**, 523 (1987).
35. Achenbach, *ibid*.
36. C.M. Hawkes, *et al.*, *Nucl. Instrum. Methods* **A292**, 329 (1990).
37. A. Lempicki *et al.*, *Nucl. Instrum. Methods* **A333**, 304 (1993); G. Blasse, *Proceedings of the Crystal 2000 International Workshop on Heavy Scintillators for Scientific and Industrial Applications*, Chamonix, France, Sept. (1992), Edition Frontieres.
38. C. Melcher and J. Schweitzer, *Nucl. Instrum. Methods* **A314**, 212 (1992).
39. D.W. Cooke *et al.*, *J. Appl. Phys.* **88** (2000) 7360 (2000); T. Kimble, M Chou and B.H.T. Chai, in *Proc. IEEE Nuclear Science Symposium Conference* (2002).
40. J.M. Chen, R.H. Mao, L.Y. Zhang and R.Y. Zhu, *IEEE Trans. Nuc. Sci.* **NS-54(3)**, 718 (2007) and **NS-54(4)**, 1319 (2007).
41. E.V.D. van Loef, P. Dorenbos, C.W.E. van Eijk, K.W. Kraemer, and H.U. Gudel, *Nucl. Instrum. Methods* **A486**, 254 (2002).
42. C. Kuntner *et al.*, *Nucl. Instrum. Methods* **A493**, 131 (2002).
43. R.H. Mao, L.Y. Zhang and R.Y. Zhu, *IEEE Trans. Nuc. Sci.* **NS-55(4)**, 2425 (2008)..
44. B.D. Rooney and J.D. Valentine, *IEEE Trans. Nuc. Sci.* **NS-44(3)**, 509 (1997).
45. W.W. Moses, S.A. Payne, W.-S. Choong, G. Hull and B.W. Reutter, *IEEE Trans. Nuc. Sci.* **NS-55(3)**, 1049 (2008).
46. G. Gratta, H. Newman, and R.Y. Zhu, *Ann. Rev. Nucl. and Part. Sci.* **44**, 453 (1994).
47. R.Y. Zhu, *Nucl. Instrum. Methods* **A413**, 297 (1998).
48. S. Ecklund, *et al.*, *Nucl. Instrum. Methods* **A463**, 68 (2001).
49. A. Abashian, *et al.*, *Nucl. Instrum. Methods* **A479**, 117 (2002).
50. I. Adam, *et al.*, *Nucl. Instrum. Methods* **A538**, 281 (2005).
51. M. Shiozawa, [Super-Kamiokande Collaboration], *Nucl. Instrum. Methods* **A433**, 240 (1999).
52. J. Litt and R. Meunier, *Ann. Rev. Nucl. Sci.* **23**, 1 (1973).
53. D. Bartlett, *et al.*, *Nucl. Instrum. Methods* **A260**, 55 (1987).
54. B. Ratcliff, *Nucl. Instrum. Methods* **A502**, 211 (2003).
55. See the RICH Workshop series: *Nucl. Instrum. Methods* **A343**, 1 (1993); *Nucl. Instrum. Methods* **A371**, 1 (1996); *Nucl. Instrum. Methods* **A433**, 1 (1999); *Nucl. Instrum. Methods* **A502**, 1 (2003); *Nucl. Instrum. Methods* **A553**, 1 (2005); *Nucl. Instrum. Methods* **A595**, 1 (2008).
56. W. Blum, W. Riegler, L. Rolandi, *Particle Detection with Drift Chambers* (Springer-Verlag, 2008).
57. L. G. Christophorou, *Atomic and Molecular Radiation Physics* (Wiley, 1971); I.B. Smirnov, *Nucl. Instrum. Methods* **A554**, 474 (2005); J. Berkowitz, *Atomic and Molecular Photo Absorption* (Academic Press, 2002); <http://pdg.lbl.gov/2007/AtomicNuclearProperties>.
58. H. Bichsel, *Nucl. Instrum. Methods* **A562**, 154 (2006).
59. H. Fischle *et al.*, *Nucl. Instrum. Methods* **A301**, 202 (1991).
60. <http://rjd.web.cern.ch/rjd/cgi-bin/cross>.
61. A. Peisert & F. Sauli, "Drift and Diffusion of Electrons in Gases," CERN 84-08 (1984).
62. S. Biagi, *Nucl. Instrum. Methods* **A421**, 234 (1999).
63. <http://consult.cern.ch/writeup/magboltz/>.
64. E. McDaniel & E. Mason, *The Mobility and Diffusion of Ions in Gases* (Wiley, 1973); G. Shultz *et al.*, *Rev. Phys. Appl.* **12**, 67(1977).
65. G. Charpak *et al.*, *Nucl. Instrum. Methods* **A62**, 262 (1968).
66. G. Charpak & F. Sauli, *Ann. Rev. Nucl. Sci.* **34**, 285 (1984).
67. F. Sauli, "Principles of Operation of Multiwire Proportional and Drift Chambers," in *Experimental Techniques in High Energy Physics*, T. Ferbel (ed.) (Addison-Wesley, Menlo Park, CA, 1987).
68. G. Charpak *et al.*, *Nucl. Instrum. Methods* **A167**, 455 (1979).
69. A.H. Walenta *et al.*, *Nucl. Instrum. Methods* **A92**, 373 (1971).
70. A. Breskin *et al.*, *Nucl. Instrum. Methods* **A124**, 189 (1975).
71. A. Breskin *et al.*, *Nucl. Instrum. Methods* **A156**, 147 (1978).
72. R. Bouclier *et al.*, *Nucl. Instrum. Methods* **A265**, 78 (1988).
73. H. Drumm *et al.*, *Nucl. Instrum. Methods* **A176**, 333 (1980).
74. D.R. Nygren & J.N. Marx, *Phys. Today* **31N10**, 46 (1978).
75. <http://www.ansoft.com>.
76. P. Beringer *et al.*, *Nucl. Instrum. Methods* **A254**, 542 (1987).
77. J. Virdee, *Phys. Rep.* 403-404,401(2004).
78. H. Walenta, *Phys. Scripta* **23**, 354 (1981).
79. J. Va'vra, *Nucl. Instrum. Methods* **A515**, 1 (2003); M. Titov, "Radiation damage and long-term aging in gas detectors," [arXiv: physics/0403055](https://arxiv.org/abs/physics/0403055).
80. M. Aleksa *et al.*, *Nucl. Instrum. Methods* **A446**, 435 (2000).
81. F. Sauli and A. Sharma, *Ann. Rev. Nucl. Part. Sci.* **49**, 341 (1999).
82. A. Oed, *Nucl. Instrum. Methods* **A263**, 351 (1988); A. Barr *et al.*, *Nucl. Phys. B (Proc. Suppl.)*, **61B**, 264 (1988).
83. Y. Bagaturia *et al.*, *Nucl. Instrum. Methods* **A490**, 223 (2002).
84. J. Benloch *et al.*, *IEEE Trans. Nucl. Sci.*, **NS-45** (1998) 234.
85. Y. Giomataris, *Nucl. Instrum. Methods* **A419**, 239 (1998).
86. F. Sauli, *Nucl. Instrum. Methods* **A386**, 531 (1997); A. Bressan *et al.*, *Nucl. Instrum. Methods* **A425**, 262 (1999).
87. S. Bachmann *et al.*, *Nucl. Instrum. Methods* **A479**, 294 (2002); A. Bressan *et al.*, *Nucl. Instrum. Methods* **A424**, 321 (1999).
88. Y. Giomataris *et al.*, *Nucl. Instrum. Methods* **A376**, 29 (1996).
89. J. Dere *et al.*, *Nucl. Instrum. Methods* **A459**, 523 (2001); G. Charpak *et al.*, *Nucl. Instrum. Methods* **A478**, 26 (2002).
90. I. Giomataris *et al.*, *Nucl. Instrum. Methods* **A560**, 405 (2006).
91. S. Duarte Pinto *et al.*, *IEEE NSS/MIC Conference Record* (2008).
92. L. Periale *et al.*, *Nucl. Instrum. Methods* **A478**, 377 (2002); R. Chechik *et al.*, *Nucl. Instrum. Methods* **A535**, 303 (2004); A. Breskin *et al.*, *Nucl. Instrum. Methods* **A598**, 107 (2009).
93. A. Di Mauro *et al.*, *Nucl. Instrum. Methods* **A581**, 225 (2007).
94. R. Bellazzini *et al.*, *Nucl. Instrum. Methods* **A535**, 477 (2004); M. Campbell *et al.*, *Nucl. Instrum. Methods* **A540**, 295 (2005); A. Bamberger *et al.*, *Nucl. Instrum. Methods* **A573**, 361 (2007); T.Kim *et al.*, *Nucl. Instrum. Methods* **A599**, 173–184 (2008).
95. M. Chefdeville *et al.*, *Nucl. Instrum. Methods* **A556**, 490 (2006).
96. M. Titov, [arXiv: physics/0403055](https://arxiv.org/abs/physics/0403055); *Proc. of the Workshop of the INFN ELOISATRON Project*, "Innovative Detectors For Super-Colliders," Erice, Italy, Sept. 28–Oct. 4 (2003).
97. <http://rd51-public.web.cern.ch/RD51-Public>.
98. P. Colas *et al.*, *Nucl. Instrum. Methods* **A535**, 506 (2004); M. Campbell *et al.*, *Nucl. Instrum. Methods* **A540**, 295 (2005).
99. H. Aihara *et al.*, *IEEE Trans. NS30*, 63 (1983).
100. C.J. Martoff *et al.*, *Nucl. Instrum. Methods* **A440**, 355 (2000).
101. X. Artru *et al.*, *Phys. Rev.* **D12**, 1289 (1975); G.M. Garibian *et al.*, *Nucl. Instrum. Methods* **125**, 133 (1975).
102. B. Dolgoshein, *Nucl. Instrum. Methods* **A326**, 434 (1993).
103. *TRDs for the Third Millenium: Proc. 2nd Workshop on Advanced Transition Radiation Detectors for Accelerator and Space Applications*, *Nucl. Instrum. Methods* **A522**, 1–170 (2004).

104. R. Santonico and R. Cardarelli, Nucl. Instrum. Methods **A187**, 377 (1981).
105. V. V. Parkhomchuk, Yu. N. Pestov, & N. V. Petrovykh, Nucl. Instrum. Methods **93**, 269 (1971).
106. E. Cerron Zeballos *et al.*, Nucl. Instrum. Methods **A374**, 132 (1996).
107. V. Ammosov *et al.*, Nucl. Instrum. Methods **A578**, 119 (2007).
108. P. Fonte, IEEE Trans. Nucl. Sci. **49**, 881 (2002).
109. M. Abbrescia *et al.*, Nucl. Instrum. Methods **A394**, 13 (1997).
110. F. Anulli *et al.*, Nucl. Instrum. Methods **A552**, 276 (2005).
111. H. Spieler, *Semiconductor Detector Systems*, Oxford Univ. Press, Oxford (2005) ISBN 0-19-852784-5.
112. F. Scholze *et al.*, Nucl. Instrum. Methods **A439**, 208 (2000).
113. G. Lindström *et al.*, Nucl. Instrum. Methods **A465**, 60 (2001).
114. C. Da Via *et al.*, Nucl. Instrum. Methods **A509**, 86 (2003).
115. G. Kramberger *et al.*, Nucl. Instrum. Methods **A481**, 297 (2002).
116. O. Krasel *et al.*, IEEE Trans. Nucl. Sci. NS-51/6,3055 (2004).
117. G. Lindström *et al.*, Nucl. Instrum. Methods **A426**, 1 (1999).
118. A. Holmes-Siedle and L. Adams, *Handbook of Radiation Effects*, 2nd ed., Oxford 2002, ISBN 0-19-850733-X, QC474.H59 2001.
119. V. Radeka, IEEE Trans. Nucl. Sci. **NS-15/3**, 455 (1968); V. Radeka, IEEE Trans. Nucl. Sci. **NS-21**, 51 (1974).
120. F.S. Goulding, Nucl. Instrum. Methods **100**, 493 (1972); F.S. Goulding and D.A. Landis, IEEE Trans. Nucl. Sci. **NS-29**, 1125 (1982).
121. W.R. Nelson, H. Hirayama, and D.W.O. Rogers, "The EGS4 Code System," SLAC-265, Stanford Linear Accelerator Center (Dec. 1985).
122. R. Brun *et al.*, *GEANT3*, CERN DD/EE/84-1 (1987).
123. D. Hitlin *et al.*, Nucl. Instrum. Methods **137**, 225 (1976). See also W. J. Willis and V. Radeka, Nucl. Instrum. Methods **120**, 221 (1974), for a more detailed discussion.
124. R. Wigmans, *Calorimetry: Energy Measurement in Particle Physics*, Inter. Series of Monographs on Phys. **107**, Clarendon, Oxford (2000).
125. ATLAS Collaboration, *The ATLAS Liquid Argon Calorimeter Technical Design Report*, CERN/LHCC 96-41 (1996).
126. CMS Collaboration, *The CMS Electromagnetic Calorimeter Technical Design Report*, CERN/LHCC 97-33 (1997).
127. N. Akchurin, *et al.*, Nucl. Instrum. Methods **A399**, 202 (1997).
128. T.A. Gabriel *et al.*, Nucl. Instrum. Methods **A338**, 336-347 (1994).
129. D.E. Groom, Nucl. Instrum. Methods **A572**, 633-653 (2007); Erratum: D.E. Groom, Nucl. Instrum. Methods **A593**, 638 (2008).
130. N. Akchurin, *et al.*, Nucl. Instrum. Methods **A408**, 380 (1998).
131. P. Adragna *et al.*, Nucl. Instrum. Methods **A615**, 158-181 (2010).
132. C.W. Fabjan *et al.*, Phys. Lett. **B60**, 105-108 (1975).
133. C. Leroy, J. Sirois, and R. Wigmans, Nucl. Instrum. Methods **A252**, 4 (1986).
134. J.E. Brau and T.A. Gabriel, Nucl. Instrum. Methods **A238**, 489 (1985); H. Brückmann and H. Kowalski, ZEUS Int. Note 86/026 DESY, Hamburg (1986); R. Wigmans, Nucl. Instrum. Methods **A259**, 389 (1987); R. Wigmans, Nucl. Instrum. Methods **A265**, 273 (1988).
135. P. Mockett, "A review of the physics and technology of high-energy calorimeter devices," *Proc. 11th SLAC Summer Inst. Part. Phy.*, July 1983, SLAC Report No. 267 (July 1983), p. 42, www.slac.stanford.edu/pubs/confproc/ssi83/ssi83-008.html.
136. R. Wigmans, "Quartz Fibers and the Prospects for Hadron Calorimetry at the 1% Resolution Level," *Proc. 7th Inter. Conf. on Calorimetry in High Energy Physics*, Tucson, AZ, Nov. 9-14, 1997, eds. E. Cheu, T. Embry, J. Rutherford, R. Wigmans (World Scientific, River Edge, NJ, 1998), p. 182; N. Akchurin *et al.*, Nucl. Instrum. Methods **A537**, 537 (2005).
137. M. Holder *et al.*, Nucl. Instrum. Methods **151**, 69-80 (1978).
138. R.K. Bock, T. Hansl-Kozanecka, and T.P. Shah, Nucl. Instrum. Methods **186**, 533 (1981); Y.A. Kulchitsky and V.B. Vinogradov, Nucl. Instrum. Methods **A455**, 499 (2000).
139. D. Acosta *et al.*, Nucl. Instrum. Methods **A316**, 184 (1997).
140. W. Walkowiak, Nucl. Instrum. Methods **A449**, 288 (2000).
141. L.S. Miller *et al.*, Phys. Rev. **166**, 871 (1968).
142. E. Shibamura *et al.*, Nucl. Instrum. Methods **A316**, 184 (1975).
143. K. Yoshino *et al.*, Phys. Rev. **A14**, 438 (1976).
144. A.O. Allen *et al.*, "Drift mobilities and conduction band energies of excess electrons in dielectric liquids," NSRDS-NBS-58 (1976).
145. P. Benetti *et al.*, Nucl. Instrum. Methods **A32**, 361 (1993).
146. A.M. Kalinin *et al.*, "Temperature and electric field strength dependence of electron drift velocity in liquid argon," ATLAS Internal Note, ATLAS-LARG-NO-058, CERN (1996).
147. T. Taylor, Phys. Scr. **23**, 459 (1980).
148. A. Yamamoto, Nucl. Instr. Meth. **A494**, 255 (2003).
149. A. Yamamoto, Nucl. Instr. Meth. **A453**, 445 (2000).
150. R.L. Gluckstern, Nucl. Instrum. Methods **24**, 381 (1963).
151. V. Karimäki, Nucl. Instrum. Methods **A410**, 284 (1998).

29. PARTICLE DETECTORS FOR NON-ACCELERATOR PHYSICS

Written 2009 (see the various sections for authors).

29. PARTICLE DETECTORS FOR NON-ACCELERATOR PHYSICS	328
29.1. Introduction	328
29.2. High-energy cosmic-ray hadron and gamma-ray detectors	328
29.2.1. Atmospheric fluorescence detectors	328
29.2.2. Atmospheric Cherenkov telescopes for high-energy γ -ray astronomy	329
29.3. Large neutrino detectors	330
29.3.1. Deep liquid detectors for rare processes	330
29.3.1.1. Liquid scintillator detectors	330
29.3.1.2. Water Cherenkov detectors	331
29.3.2. Neutrino telescopes	332
29.4. Large time-projection chambers for rare event detection	334
29.5. Sub-Kelvin detectors	335
29.5.1. Thermal Phonons	335
29.5.2. Athermal Phonons and Superconducting Quasiparticles	337
29.5.3. Ionization and Scintillation	337
29.6. Low-radioactivity background techniques	338
29.6.1. Defining the problem	338
29.6.2. Environmental radioactivity	338
29.6.3. Radioimpurities in detector or shielding components	338
29.6.4. Radon and its progeny	339
29.6.5. Cosmic rays	339
29.6.6. Neutrons	339

29.1. Introduction

Non-accelerator experiments have become increasingly important in particle physics. These include classical cosmic ray experiments, neutrino oscillation measurements, and searches for double-beta decay, dark matter candidates, and magnetic monopoles. The experimental methods are sometimes those familiar at accelerators (plastic scintillators, drift chambers, TRD's, *etc.*) but there is also instrumentation either not found at accelerators or applied in a radically different way. Examples are atmospheric scintillation detectors (Fly's Eye), massive Cherenkov detectors (Super-Kamiokande, IceCube), ultracold solid state detectors (CDMS). And, except for the cosmic ray detectors, there is a demand for radiologically ultra-pure materials.

In this section, some more important detectors special to terrestrial non-accelerator experiments are discussed. Techniques used in both accelerator and non-accelerator experiments are described in Sec. 28, Particle Detectors at Accelerators, some of which have been modified to accommodate the non-accelerator nuances. Space-based detectors also use some unique methods, but these are beyond the present scope of *RPP*.

29.2. High-energy cosmic-ray hadron and gamma-ray detectors

29.2.1. Atmospheric fluorescence detectors :

Written September 2009 by L.R. Wiencke (Colorado School of Mines).

Cosmic-ray fluorescence detectors (FD) use the atmosphere as a giant calorimeter to measure isotropic scintillation light that traces the development profiles of extensive air showers (EAS). The EASs observed are produced by the interactions of high-energy ($E > 10^{17}$ eV) subatomic particles in the stratosphere and upper troposphere. The amount of scintillation light generated is proportional to energy deposited in the atmosphere and nearly independent of the primary species. Experiments with FDs include the pioneering Fly's Eye [1],

HiRes [2], the Telescope Array [3], and the Pierre Auger Observatory [4].

The scintillation light is emitted between 290 and 430 nm (Fig. 29.1), when relativistic charged particles, primarily electrons and positrons, excite nitrogen molecules in air, resulting in transitions of the 1P and 2P systems. Reviews and references for the pioneering and ongoing laboratory measurements of fluorescence yield, $Y(\lambda, P, T, u)$, including dependence on wavelength (λ), temperature (T), pressure (p), and humidity (u) may be found in Refs. 5 and 6.

An FD element (telescope) consists of a non-tracking spherical mirror (3.5–13 m² and less than astronomical quality), a close-packed “camera” of PMTs (for example, Hamamatsu R9508 or Photonis XP3062) near the focal plane, and flash ADC readout system with a pulse and track-finding trigger scheme [7]. Simple reflector optics (12° × 16° degree field of view (FOV) on 256 PMTs) and Schmidt optics (30° × 30° FOV on 440 PMTs), including a correcting element, have been used. Segmented mirrors have been fabricated from slumped or slumped/polished glass with anodized aluminized coating and from chemically anodized AlMgSiO₅ affixed to shaped aluminum. A broadband UV pass filter (custom fabricated or Schott MUG-6) covers the camera face or much larger entrance aperture to reduce background light such as starlight, airglow, man-made light pollution, and airplane strobelights.

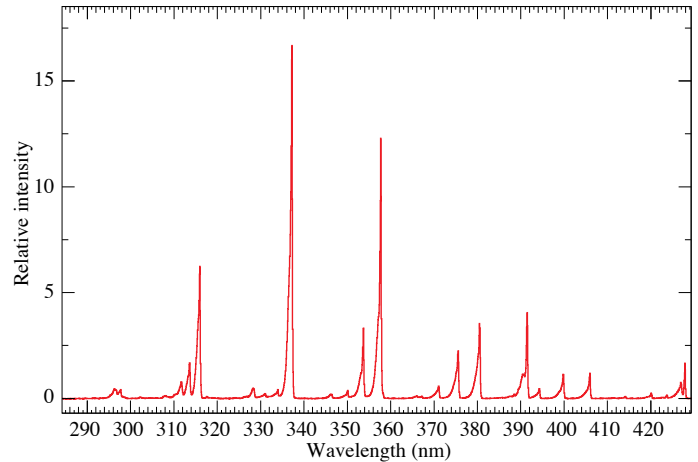


Figure 29.1: Measured fluorescence spectrum excited by 3 MeV electrons in dry air at 800 hPa and 293 K [8].

At 10^{20} eV, where the flux drops to roughly 1 EAS/km²century, the aperture for an eye of adjacent FD telescopes that span the horizon can reach 10^4 km² sr. FD operation requires (nearly) moonless nights and clear atmospheric conditions, which imposes a duty cycle of about 10%. Arrangements of LEDs, calibrated diffuse sources [9], pulsed UV lasers [10], LIDARs* [11] and cloud monitors are used for photometric calibration, periodic measurement of atmospheric clarity [12], and identification of clear periods.

The EAS generates a track consistent with a light source moving at $v = c$ across the FOV. The number of photons (N_γ) as a function of atmospheric depth (X) can be expressed as [6]

$$\frac{dN_\gamma}{dX} = \frac{dE_{\text{dep}}^{\text{tot}}}{dX} \int Y(\lambda, P, T, u) \cdot \tau_{\text{atm}}(\lambda, X) \cdot \varepsilon_{\text{FD}}(\lambda) d\lambda, \quad (29.1)$$

where $\tau_{\text{atm}}(\lambda, X)$ is atmospheric transmission, including wavelength (λ) dependence, and $\varepsilon_{\text{FD}}(\lambda)$ is FD efficiency. $\varepsilon_{\text{FD}}(\lambda)$ includes geometric factors and collection efficiency of the optics, quantum efficiency of the PMTs, and other throughput factors. The typical systematic uncertainties, Y (10–15%), τ_{atm} (10%) and ε_{FD} (photometric calibration 10%), currently dominate the total reconstructed EAS energy uncertainty. $\Delta E/E$ of 20–25% is possible, provided the geometric fit

* This acronym for “Light Detection and Ranging,” refers here to systems that measure atmospheric properties from the light scattered backwards from laser pulses directed into the sky.

of the EAS axis is constrained by multi-eye stereo projection, or by timing from a colocated sparse array of surface detectors.

Analysis methods to reconstruct the EAS profile and deconvolute the contributions of re-scattered scintillation light, and direct and scattered Cherenkov light are described in [1] and more recently in [13]. The EAS energy is typically obtained by integrating over the Gaisser-Hillas function [14]

$$E_{\text{cal}} = \int_0^{\infty} w_{\text{max}} \left(\frac{X - X_0}{X_{\text{max}} - X_0} \right)^{(X_{\text{max}} - X_0)/\lambda} e^{(X_{\text{max}} - X)/\lambda} dX, \quad (29.2)$$

where X_{max} is the depth at which the shower reaches its maximum energy deposit w_{max} and X_0 and λ are two shape parameters.

29.2.2. Atmospheric Cherenkov telescopes for high-energy γ -ray astronomy :

Written August 2009 by J. Holder (Bartol Research Inst., Univ. of Delaware).

A wide variety of astrophysical objects are now known to produce high-energy γ -ray photons. Leptonic or hadronic particle populations, accelerated to relativistic energies in the source, produce γ rays typically through inverse Compton boosting of ambient photons, or through the decay of neutral pions produced in hadronic interactions. At energies below ~ 30 GeV, γ -ray emission can be detected directly using satellite or balloon-borne instrumentation, with an effective area approximately equal to the size of the detector ($< 1 \text{ m}^2$). At higher energies, a technique with much larger effective collection area is required to measure astrophysical γ -ray fluxes, which decrease rapidly with increasing energy. Atmospheric Cherenkov detectors achieve effective collection areas of $\sim 10^5 \text{ m}^2$ by employing the Earth's atmosphere as an intrinsic part of the detection technique.

As described in Chapter 24, a hadronic cosmic ray or high energy γ -ray incident on the Earth's atmosphere triggers a particle cascade, or air shower. Relativistic charged particles in the cascade produce Cherenkov radiation, which is emitted along the shower direction, resulting in a light pool on the ground with a radius of $\sim 130 \text{ m}$. Cherenkov light is produced throughout the cascade development, with the maximum emission occurring when the number of particles in the cascade is largest, at an altitude of $\sim 10 \text{ km}$ for primary energies of 100 GeV–1 TeV. Following absorption and scattering in the atmosphere, the Cherenkov light at ground level peaks at a wavelength, $\lambda \approx 300\text{--}350 \text{ nm}$. The photon density is typically ~ 100 photons/ m^2 at 1 TeV, arriving in a brief flash of a few nanoseconds duration. This Cherenkov pulse can be detected from any point within the light pool radius by using large reflecting surfaces to focus the Cherenkov light on to fast photon detectors (Fig. 29.2).

Modern atmospheric Cherenkov telescopes, such as those built and operated by the H.E.S.S. [16], MAGIC [17] and VERITAS [15] collaborations, consist of large ($> 100 \text{ m}^2$) segmented mirrors on steerable altitude-azimuth mounts. A camera, made from an array of up to 1000 photomultiplier tubes (PMTs) covering a field-of-view of up to 5.0° in diameter, is placed at the mirror focus and used to record a Cherenkov image of each air shower. Images are recorded at a rate of a few hundred Hz, the vast majority of which are due to showers with hadronic cosmic-ray primaries. The shape and orientation of the Cherenkov images are used to discriminate γ -ray photon events from this cosmic-ray background, and to reconstruct the photon energy and arrival direction. γ -ray images result from purely electromagnetic cascades and appear as narrow, elongated ellipses in the camera plane. The long axis of the ellipse corresponds to the vertical extension of the air shower, and points back towards the source position in the field-of-view. If multiple telescopes are used to view the same shower ("stereoscopy"), the source position is simply the intersection point of the various image axes. Cosmic-ray primaries produce secondaries with large transverse momenta, which initiate sub-showers. Their images are consequently wider and less regular than those with γ -ray primaries and, since the original charged particle has been deflected by galactic magnetic fields before reaching the Earth, the images have no preferred orientation.

The measurable differences in Cherenkov image orientation and morphology provide the background discrimination which makes

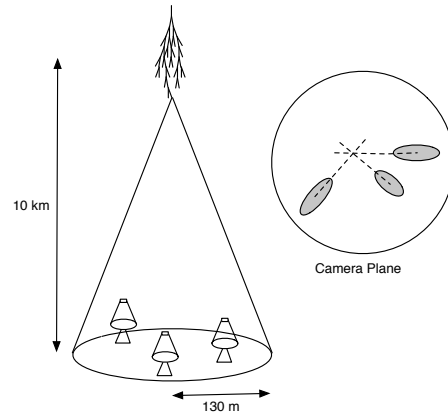


Figure 29.2: A schematic illustration of an atmospheric Cherenkov telescope array. The primary particle initiates an air shower, resulting in a cone of Cherenkov radiation. Telescopes within the Cherenkov light pool record elliptical images; the intersection of the long axes of these images indicates the arrival direction of the primary, and hence the location of a γ -ray source in the sky.

ground-based γ -ray astronomy possible. For point-like sources, such as distant Active Galactic Nuclei (AGNs), modern instruments can reject up to 99.999% of the triggered cosmic-ray events, while retaining up to 50% of the γ -ray population. In the case of spatially extended sources, such as Galactic supernova remnants (SNR), the background rejection is less efficient, but the technique can be used to produce γ -ray maps of the emission from the source. The angular resolution depends upon the energy of the primary γ -ray, but is typically 0.1° per event (68% containment radius) at energies above a few hundred GeV.

The total Cherenkov yield from the air shower is proportional to the energy of the primary particle. The image intensity, combined with the reconstructed distance of the shower core from each telescope, can therefore be used to estimate the primary energy. The energy resolution of this technique, also energy-dependent, is typically 15–20 at energies above a few hundred GeV. Energy spectra of γ -ray sources can be measured over a wide range; potentially from ~ 50 GeV to ~ 100 TeV, depending upon the instrument characteristics, source strength, and exposure time. To a first approximation, the lower energy threshold at the trigger level, E_T , depends upon the mirror area, A , the photon collection efficiency, $\eta(\lambda)$, the Cherenkov light yield, $C(\lambda)$, the night sky background light, $B(\lambda)$, the solid angle, Ω , and the trigger resolving time, τ , as follows [18]:

$$E_T \propto \frac{1}{C(\lambda)} \sqrt{\frac{B(\lambda)\Omega\tau}{\eta(\lambda)A}} \quad (29.3)$$

In practice, this function may be modified by the properties of the detector; for example, by complex, multi-level, combinatorial trigger systems and highly pixellated fields of view. In addition, the useful scientific threshold, after the application of analysis cuts to select γ -ray events, is always somewhat higher than this.

The first astrophysical source to be convincingly detected using the imaging atmospheric Cherenkov technique was the Crab Nebula [19], with a flux of 2.1×10^{-11} photons $\text{cm}^{-2} \text{ s}^{-1}$ above 1 TeV [20]. Modern arrays have sensitivity sufficient to detect sources with 1% of the Crab Nebula flux in a few tens of hours, and the TeV source catalog now consists of more than 80 sources. The majority of these have been detected by scanning the Galactic plane from the southern hemisphere with the H.E.S.S. telescope array [21].

29.3. Large neutrino detectors

Table 29.1: Properties of large detectors for rare processes. If total target mass is divided into large submodules, the number of subdetectors is indicated in parentheses.

Detector	Fid. mass, kton (modules)	PMTs (diameter, cm)	ξ	pe/MeV	Dates
Baksan	0.33, scint (3150)	1/module (15)	segmented	40	1980–
MACRO	0.6, scint (476)	2-4/module (20)	segmented	18	1989–2000
LVD	1, scint. (840)	3/module (15)	segmented	15	1992–
KamLAND	1, scint	1325 (43)+554 (51)*	34%	460	2002–
Borexino	0.1, scint	2212 (20)	30%	500	2005–
SNO+	0.78, scint	9438 (20)	54%	400–900	Future
Chooz	0.005, scint (Gd)	192 (20)	15%	130	1997–1998
Double Chooz	0.020 scint (Gd) (2)	534/module (20)	13%	180	Future
Daya Bay	0.160, scint (Gd) (8)	192/module (20)	5.6% [†]	100	Future
RENO	0.030, scint (Gd) (2)	342/module (25)	12.6%	100	Future
IMB-1	3.3, H ₂ O	2048 (12.5)	1%	0.25	1982–1985
IMB-2	3.3, H ₂ O	2048 (20)	4.5%	1.1	1987–1990
Kam I	0.88/0.78, H ₂ O	1000/948 (50)	20%	3.4	1986–1990
Kam II	1.04, H ₂ O	948 (50)	20%	3.4	1993–1998
SK I	22.5, H ₂ O	11146 (50)	39%	6	1996–2001
SK II	22.5, H ₂ O	5182 (50)	19%	3	2002–2005
SK III+	22.5, H ₂ O	11129 (50)	39%	6	2006–
SNO	1, D ₂ O/1.7 H ₂ O	9438 (20)	54%	9	1999–2006

* The 51 cm PMTs were added in 2003.

[†] The effective Daya Bay coverage is 12% with top and bottom reflectors.**29.3.1. Deep liquid detectors for rare processes :**

Written September 2009 by K. Scholberg & C.W. Walter (Duke University)

Deep, large detectors for rare processes tend to be multi-purpose with physics reach that includes not only solar, reactor, supernova and atmospheric neutrinos, but also searches for baryon number violation, searches for exotic particles such as magnetic monopoles, and neutrino and cosmic ray astrophysics in different energy regimes. The detectors may also serve as targets for long-baseline neutrino beams for neutrino oscillation physics studies. In general, detector design considerations can be divided into high- and low-energy regimes, for which background and event reconstruction issues differ. The high-energy regime, from about 100 MeV to a few hundred GeV, is relevant for proton decay searches, atmospheric neutrinos and high-energy astrophysical neutrinos. The low-energy regime (a few tens of MeV or less) is relevant for supernova, solar, reactor and geological neutrinos.

Large water Cherenkov and scintillator detectors (see Table 29.1) usually consist of a volume of transparent liquid viewed by photomultiplier tubes (PMTs) (see Sec. 28.2); the liquid serves as active target. PMT hit charges and times are recorded and digitized, and triggering is usually based on coincidence of PMTs hits within a time window comparable to the detector's light-crossing time. Because photosensors lining an inner surface represent a driving cost that scales as surface area, very large volumes can be used for comparatively reasonable cost. Some detectors are segmented into subvolumes individually viewed by PMTs, and may include other detector elements (*e.g.*, tracking detectors). Devices to increase light collection, *e.g.*, reflectors or waveshifter plates, may be employed. A common configuration is to have at least one concentric outer layer of liquid material separated from the inner part of the detector to serve as shielding against ambient background. If optically separated and instrumented with PMTs, an outer layer may also serve as an active veto against entering cosmic rays and other background

events. The PMTs for large detectors typically range in size from 20 cm to 50 cm diameter, and typical quantum efficiencies are in the 20–25% range. The active liquid volume requires purification and there may be continuous recirculation of liquid. For large homogeneous detectors, the event interaction vertex is determined using relative timing of PMT hits, and energy deposition is determined from the number of recorded photoelectrons. A “fiducial volume” is usually defined within the full detector volume, some distance away from the PMT array. Inside the fiducial volume, enough PMTs are illuminated per event that reconstruction is considered reliable, and furthermore, entering background from the enclosing walls is suppressed by a buffer of self-shielding. PMT and detector optical parameters are calibrated using laser, LED, or other light sources. Quality of event reconstruction typically depends on photoelectron yield, pixelization and timing.

Because in most cases one is searching for rare events, large detectors are usually sited underground to reduce cosmic-ray related background (see Chapter 24). The minimum depth required varies according to the physics goals [22].

29.3.1.1. Liquid scintillator detectors:

Past and current large underground detectors based on hydrocarbon scintillators include LVD, MACRO, Baksan, Borexino, KamLAND and SNO+. Experiments at nuclear reactors include Chooz, Double Chooz, Daya Bay, and RENO. Organic liquid scintillators (see Sec. 28.3.0) for large detectors are chosen for high light yield and attenuation length, good stability, compatibility with other detector materials, high flash point, low toxicity, appropriate density for mechanical stability, and low cost. They may be doped with waveshifters and stabilizing agents. Popular choices are pseudocumene (1,2,4-trimethylbenzene) with a few g/L of the PPO (2,5-diphenyloxazole) fluor, and linear alkylbenzene (LAB). In a typical detector configuration there will be active or passive regions of undoped scintillator, non-scintillating mineral oil or water surrounding the inner neutrino target volume. A thin vessel or balloon made of nylon, acrylic or other material transparent to

scintillation light may contain the inner target; if the scintillator is buoyant with respect to its buffer, ropes may hold the balloon in place. For phototube surface coverages in the 20–40% range, yields in the few hundreds of photoelectrons per MeV of energy deposition can be obtained. Typical energy resolution is about $7\%/\sqrt{E(\text{MeV})}$, and typical position reconstruction resolution is a few tens of cm at ~ 1 MeV, scaling as $\sim N^{-1/2}$, where N is the number of photoelectrons detected.

Shallow detectors for reactor neutrino oscillation experiments require excellent muon veto capabilities. For $\bar{\nu}_e$ detection via inverse beta decay on free protons, $\bar{\nu}_e + p \rightarrow n + e^+$, the neutron is captured by a proton on a ~ 180 μs timescale, resulting in a 2.2 MeV γ ray, observable by Compton scattering and which can be used as a tag in coincidence with the positron signal. The positron annihilation γ rays may also contribute. Inverse beta decay tagging may be improved by addition of Gd at $\sim 0.1\%$ by mass, which for natural isotope abundance has a $\sim 49,000$ barn cross-section for neutron capture (in contrast to the 0.3 barn cross-section for capture on free protons). Gd capture takes ~ 30 μs , and is followed by a cascade of γ rays adding up to about 8 MeV. Gadolinium doping of scintillator requires specialized formulation to ensure adequate attenuation length and stability.

Scintillation detectors have an advantage over water Cherenkov detectors in the lack of Cherenkov threshold and the high light yield. However, scintillation light emission is nearly isotropic, and therefore directional capabilities are relatively weak. Liquid scintillator is especially suitable for detection of low-energy events. Radioactive backgrounds are a serious issue, and include long-lived cosmogenics. To go below a few MeV, very careful selection of materials and purification of the scintillator is required (see Sec. 29.6). Fiducialization and tagging can reduce background. A recent idea, not yet realized, is to dissolve neutrinoless double beta decay ($0\nu\beta\beta$) isotopes in scintillator (for instance ^{150}Nd in SNO+). Although energy resolution is poor compared to typical $0\nu\beta\beta$ search experiments, the quantity of isotope could be so large that the kinematic signature would be visible as a clear feature in the spectrum.

29.3.1.2. Water Cherenkov detectors:

Very large-imaging water detectors reconstruct ten-meter-scale Cherenkov rings produced by charged particles (see Sec. 28.5.0). The first such large detectors were IMB and Kamiokande. The only currently existing instance of this class, with fiducial volume of 22.5 kton and total mass of 50 kton, is Super-Kamiokande (Super-K). For volumes of this scale, absorption and scattering of Cherenkov light are non-negligible, and a wavelength-dependent factor $\exp(-d/L(\lambda))$ (where d is the distance from emission to the sensor and $L(\lambda)$ is the attenuation length of the medium) must be included in the integral of Eq. (28.5) for the photoelectron yield. Attenuation lengths on the order of 100 meters have been achieved.

Cherenkov detectors are excellent electromagnetic calorimeters, and the number of Cherenkov photons produced by an e/γ is nearly proportional to its kinetic energy. For massive particles, the number of photons produced is also related to the energy, but not linearly. For any type of particle, the *visible energy* E_{vis} is defined as the energy of an electron which would produce the same number of Cherenkov photons. The number of collected photoelectrons depends on the scattering and attenuation in the water along with the photocathode coverage, quantum efficiency and the optical parameters of any external light collection systems or protective material surrounding them. Event-by-event corrections are made for geometry and attenuation. For a typical case, in water $N_{\text{p.e.}} \sim 15 \xi E_{\text{vis}}(\text{MeV})$, where ξ is the effective fractional photosensor coverage. Cherenkov photoelectron yield per MeV of energy is relatively small compared to that for scintillator, e.g., ~ 6 pe/MeV for Super-K with a PMT surface coverage of $\sim 40\%$. In spite of light yield and Cherenkov threshold issues, the intrinsic directionality of Cherenkov light allows individual particle tracks to be reconstructed. Vertex and direction fits are performed using PMT hit charges and times, requiring that the hit pattern be consistent with a Cherenkov ring.

High-energy (~ 100 MeV or more) neutrinos from the atmosphere or beams interact with nucleons; for the nucleons bound inside the ^{16}O nucleus, the nuclear effects both at the interaction, and as the particles leave the nucleus must be considered when reconstructing

the interaction. Various event topologies can be distinguished by their timing and fit patterns, and by presence or absence of light in a veto. “Fully-contained” events are those for which the neutrino interaction final state particles do not leave the inner part of the detector; these have their energies relatively well measured. Neutrino interactions for which the lepton is not contained in the inner detector sample higher-energy parent neutrino energy distributions. For example, in “partially-contained” events, the neutrino interacts inside the inner part of the detector but the lepton (almost always a muon, since only muons are penetrating) exits. “Upward-going muons” can arise from neutrinos which interact in the rock below the detector and create muons which enter the detector and either stop, or go all the way through (entering downward-going muons cannot be distinguished from cosmic rays). At high energies, multi-photoelectron hits are likely and the charge collected by each PMT (rather than the number of PMTs firing) must be used; this degrades the energy resolution to approximately $2\%/\sqrt{\xi E_{\text{vis}}(\text{GeV})}$. The absolute energy scale in this regime can be known to ≈ 2 –3% using cosmic-ray muon energy deposition, Michel electrons and π^0 from atmospheric neutrino interactions. Typical vertex resolutions for GeV energies are a few tens of cm [23]. Angular resolution for determination of the direction of a charged particle track is a few degrees. For a neutrino interaction, because some final-state particles are usually below Cherenkov threshold, knowledge of direction of the incoming neutrino direction itself is generally worse than that of the lepton direction, and dependent on neutrino energy.

Multiple particles in an interaction (so long as they are above Cherenkov threshold) may be reconstructed, allowing for the exclusive reconstruction of final states. In searches for proton decay, multiple particles can be kinematically reconstructed to form a decaying nucleon. High-quality particle identification is also possible: γ rays and electrons shower, and electrons scatter, which results in fuzzy rings, whereas muons, pions and protons make sharp rings. These patterns can be quantitatively separated with high reliability using maximum likelihood methods [24]. A e/μ misidentification probability of $\sim 0.4\%/\xi$ in the sub-GeV range is consistent with the performance of several experiments for $4\% < \xi < 40\%$. Sources of background for high energy interactions include misidentified cosmic muons and anomalous light patterns when the PMTs sometimes “flash” and emit photons themselves. The latter class of events can be removed using its distinctive PMT signal patterns, which may be repeated. More information about high energy event selection and reconstruction may be found in reference [25].

In spite of the fairly low light yield, large water Cherenkov detectors may be employed for reconstructing low-energy events, down to e.g. ~ 4 –5 MeV for Super-K [26]. Low-energy neutrino interactions of solar neutrinos in water are predominantly elastic scattering off atomic electrons; single electron events are then reconstructed. At solar neutrino energies, the visible energy resolution ($\sim 30\%/\sqrt{\xi E_{\text{vis}}(\text{MeV})}$) is about 20% worse than photoelectron counting statistics would imply. Using an electron LINAC and/or nuclear sources, 0.5–1.5% determination of the absolute energy scale has been achieved at solar neutrino energies. Angular resolution is limited by multiple scattering in this energy regime (25–30°). At these energies, radioactive backgrounds become a dominant issue. These backgrounds include radon in the water itself or emanated by detector materials, and γ rays from the rock and detector materials. In the few to few tens of MeV range, radioactive products of cosmic ray muon-induced spallation are troublesome, and are removed by proximity in time and space to preceding muons, at some cost in dead time.

The Sudbury Neutrino Observatory (SNO) detector [27] is the only instance of a large heavy water detector and deserves mention here. In addition to an outer 1.7 kton of light water, SNO contained 1 kton of D_2O , giving it unique sensitivity to neutrino neutral current ($\nu_x + d \rightarrow \nu_x + p + n$), and charged current ($\nu_e + d \rightarrow p + p + e^-$) deuteron breakup reactions. The neutrons were detected in three ways: In the first phase, via the reaction $n + d \rightarrow t + \gamma + 6.25$ MeV; Cherenkov radiation from electrons Compton-scattered by the γ rays was observed. In the second phase, NaCl was dissolved in the water. ^{35}Cl captures neutrons, $n + ^{35}\text{Cl} \rightarrow ^{36}\text{Cl} + \gamma + 8.6$ MeV.

The γ rays were observed via Compton scattering. In a final phase, specialized low-background ^3He counters (“neutral current detectors” or NCDs) were deployed in the detector. These detected neutrons via $n + ^3\text{He} \rightarrow p + t + 0.76 \text{ MeV}$, and ionization charge from energy loss of the products was recorded in proportional counters.

29.3.2. Neutrino telescopes :

Written November 2009 by A. Karle (University of Wisconsin).

Neutrino telescopes are large water or ice Cherenkov detectors designed to do neutrino astronomy in the energy range 10^{11} – 10^{18} eV. The primary physics goal is the detection of high-energy extra-terrestrial neutrinos. Neutrinos offer a unique view of the high-energy Universe because they are not deflected by magnetic fields like charged cosmic rays, and can travel vast distances without being absorbed like high-energy photons. Establishing correlations with the known high-energy objects in the sky and a measurement of the cosmic high-energy neutrino flux will provide an important insight into the most violent processes of the Universe.

Atmospheric neutrinos, *i.e.*, neutrinos produced in air showers initiated by the cosmic rays entering the Earth’s atmosphere, form a background that can be rejected by

- a) measuring the energy of neutrinos (astrophysical fluxes will have a harder spectrum),
- b) identifying point sources, hot spots on the sky, or
- c) finding a burst-like neutrino emission.

The latter, *e.g.*, neutrino detection of γ -ray bursts, might be correlated with observations by other terrestrial or extraterrestrial observatories.

Neutrino telescopes detect neutrinos via the process $\nu_l(\bar{\nu}_l) + N \rightarrow l^\pm + X$ of primarily upward-going or horizontal neutrinos interacting with a nucleon N of the matter comprising or surrounding the detector volume. A significant fraction of the neutrino energy E_ν will be carried away by the produced lepton. For the important case of a lepton being a muon, the angle $\Delta\psi$ between the parent neutrino and the muon is $\approx 0.7^\circ (E_\nu/\text{TeV})^{-0.7}$ [28]. At energies above a few TeV, the angular resolution is dominated by the reconstructed muon direction, which is well below 1° for the newest instruments [29]. The quality of event reconstruction is determined primarily by the optical properties of the medium, and by the instrumented density of sensors.

The small cross sections combined with small expected fluxes of high-energy cosmic neutrinos necessitate very large, km-scale detection volumes. Neutrino telescopes make use of large natural transparent target media such as deep sea water or the deep glacial ice in Antarctica. The target volume is instrumented with large photomultipliers (PMTs). The goal is to maximize the number of detected Cherenkov photons produced by energetic charged particles, and thus to maximize the number of well reconstructed events while keeping the density of PMTs (and thus the cost of the experiment) low. The sensors are deployed at depths of one to several km to reduce backgrounds from the cosmic-ray-generated muon flux. Underground detectors such as MACRO and Super-Kamiokande can also act as neutrino telescopes. These detectors, however, are not scalable to reach the sensitivities required for the detection of the predicted astrophysical neutrino fluxes.

When designing a neutrino telescope, one is faced with significant technical challenges in dealing with the conditions of the natural medium and the installation of large number of optical sensors and of electronics in the deep water and ice. Over the past decade, high-energy neutrino astronomy has evolved from exploratory experiments to the first second-generation neutrino telescope, the IceCube Neutrino Observatory. The first attempts were made by the DUMAND project [30] in the deep Pacific Ocean near Hawaii and by the Baikal collaboration. In the 1990’s, the first-generation neutrino experiments were designed and built, including the the Lake Baikal neutrino detector [31] and the Antarctic Muon And Neutrino Detection Array (AMANDA) [32]. The NT-200 configuration of the Lake Baikal experiment was completed in 1998. It consists of 192 optical modules (OMs), mounted on 8 vertical strings, each with 24 OMs arranged in pairs. The entire structure forms a cylinder 40m in diameter and 72m in height. Each OM contains a 37cm diameter photomultiplier. The optical properties of the water are characterized by a long scattering length and a relatively short absorption length. For the installation and maintenance, the Baikal collaboration takes

advantage of the cold winters in Siberia, which cause the surface of the lake to stay frozen over several months. Several additional strings have since been added to increase the effective volume for cascades.

AMANDA-II was completed in 2000 with 677 optical sensors on 19 strings (cables instrumented with 20–40 sensors each). The optical sensor strings form an instrumented cylinder 200m in diameter and 450m in height from 1450m to 1900m in the glacial ice at the South Pole. AMANDA-II played a role of a precursor to IceCube, establishing the feasibility of using the ice as medium for neutrino telescopes. The South Pole ice is characterized by a very large absorption length (100m to 200m) for blue and UV light and a relatively short scattering length of 20 to 40m. AMANDA relied on minimum amount of electronics in the ice. Each optical sensor with a 20cm diameter PMT (Hamamatsu R5912-2), operating at a gain of 3×10^8 , was connected to electronics on the surface with an electrical cable, which supplied high voltage, and an optical fiber cable which transmitted the PMT signal and was used for calibration purposes. The photomultiplier signals were converted to infrared pulses by LEDs and then transmitted with almost no loss in bandwidth and amplitude to the surface counting house. One of the guiding principles was to keep the complexity in the ice at a minimum since the modules can never be accessed after they are frozen into the ice. This approach facilitated fast construction with small technological risk. Only one string was instrumented with additional digital data acquisition circuitry, serving as a prototype string for IceCube.

In the Mediterranean Sea NESTOR [33] deployed prototype detector modules off the coast of Greece at depths of up to 4km. The design of the NESTOR array proposed the deployment of optical sensors with large hemispherical PMTs that are arranged in 12 hexagonal floors.

The ANTARES neutrino telescope [34] has been operating with five strings (lines) at an average depth of 2200m off the shore of La Seyne sur mer, near Toulon, France, since 2008. Various studies of the optical properties of the sea water indicated a relatively large effective scattering length (>200 m) in the blue and shorter absorption length of about 60m [35] and a factor of 2 smaller values in the UV region. The full ANTARES array will have 12 strings of optical sensors. Like in all water-based neutrino telescopes, the strings are anchored to the sea floor and form approximately vertical lines with the aid of buoys.

The European km3Net consortium has completed a design study and is planning a km-scale neutrino telescope in the Mediterranean Sea [36].

The IceCube Neutrino Observatory [37] is a km-scale detector which will be completed in 2011. In 2009 IceCube has been operating with 59 strings and its construction is more than 65% complete. In its final configuration, IceCube will consist of 5160 optical sensors deployed on 86 strings covering a volume of 1 km^3 . A surface detector component, IceTop, forms an air shower array with 320 standard photomultipliers deployed in 160 IceTop tanks on the ice surface directly above the strings. Fig. 29.3 summarizes the status of IceCube, the largest neutrino telescope in operation in 2009.

The optical sensors are located at depths between 1450m and 2450m. Each sensor contains a 25cm diameter hemispherical photomultiplier (Hamamatsu R7081-02) with electronics to operate the PMT, digitize and time-stamp the signals and provide calibration signals [38]. Each sensor, referred to as a Digital Optical Module (DOM), collects data autonomously, sending data packets to the surface. Each DOM consists of a 33.0cm diameter pressurized glass sphere holding the PMT and associated electronics. The digitized signals are sent to a central data acquisition system, which forms triggered events. The 40-string configuration of IceCube (2008) detects about 10000 atmospheric neutrinos per year with energies above 500 GeV with some events above 100 TeV. The pulses from PMTs are processed with waveform recording electronics. The system has a large linear dynamic range and can resolve more than 300 photoelectrons/10ns. Events are reconstructed when more than ~ 10 PMTs detect at least one photoelectron each. Highest-energy events may consist of hits in more than 1000 PMTs.

The detector is constructed by drilling holes in the ice with a hot-water drill. The strings are deployed into the water filled hole in less than 24 hours. The holes freeze back within 1 – 2 weeks. This

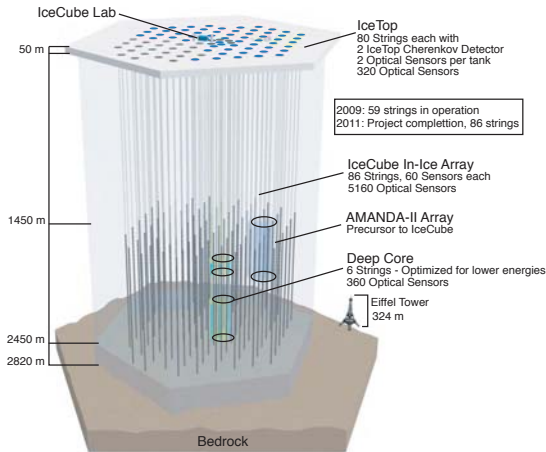


Figure 29.3: Schematic view of the IceCube Neutrino Observatory located at the South Pole.

method was pioneered and developed by AMANDA. Up to 19 strings have been installed in an Antarctic summer season, which lasts from November to mid-February when the South Pole Station is accessible.

The optical properties of water and ice have been investigated by collaborations mentioned in this section in great detail. Optical absorption and scattering length in the spectral range of 300 nm–500 nm are relevant for typical alkali photomultipliers. Deep sea water sites show a relatively large effective scattering length (>100 m) and a shorter absorption length (~ 50 m) in the region around 400 nm. South Pole ice has a larger absorption length (100–200 m) and a shorter scattering length (20–40 m). A large scattering length should result in good angular resolution. Radio- and biological activity in the medium contribute to the optical noise background. PMT noise rates in sea water are typically 100 kHz and may spike significantly higher to beyond 1 MHz due to biological activity. Noise rates in the deep South Pole ice are about 0.5 kHz and are almost entirely due to the background created by the sensor itself.

Neutrino telescopes are sensitive to a very wide range of neutrino energies from about 100 GeV to 10^{18} eV. The rise in the neutrino cross section with energy combined with the increasing range of muons results in a strong increase of the neutrino effective area of the detectors with energy as shown in Fig. 29.4. The trigger-level neutrino effective area of IceCube increases from 0.5 m^2 at 1 TeV to 300 m^2 at 1 PeV. The neutrino effective area is a useful quantity as it can be folded directly with the astrophysical or terrestrial neutrino flux to obtain event rates. A km scale detector like the 86-string IceCube configuration will detect $\sim 5 \cdot 10^4$ atmospheric neutrinos in the energy range of 0.5 to 200 TeV.

The muon effective area approaches the geometric area if the energy of the muons is large enough so that they pass the entire detector. In case of IceCube, it increases from 0.8 km^2 to just about 1.2 km^2 over the same energy range from 1 TeV to 1 PeV [41]. The energy resolution of the muons is estimated from their energy loss within the detector and is typically ~ 0.3 in $\log_{10}(E)$ for energies above 10 TeV.

Figure 29.5 contains three different predictions for the flux of neutrinos associated with the still-enigmatic sources of the highest energy cosmic rays. Kilometer-scale neutrino detectors have the sensitivity to reveal generic cosmic-ray sources with an energy density in neutrinos comparable to their energy density in cosmic rays and in TeV γ rays. If one assumes that γ ray bursts are the sources of the cosmic rays, then protons (nuclei) and synchrotron photons coexist in the expanding fireball prior to it reaching transparency and producing the observed γ ray fluxes. The protons interact to produce pions that are the source of the neutrino flux shown in the figure. Also shown is a flux with an E^{-2} energy spectrum (Waxman-Bahcall [42]) that is obtained from the assumption that highest energy cosmic rays lose all their energy by interaction regardless of their origin. Finally, cosmic

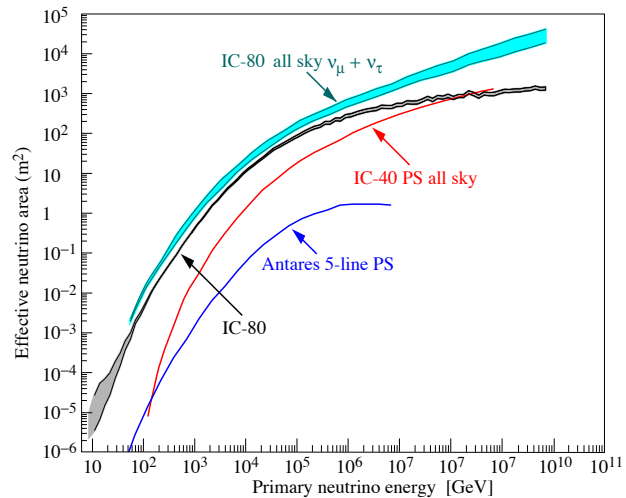


Figure 29.4: Neutrino effective area of large neutrino telescopes: The neutrino effective area is shown for several IceCube configurations and detection channels (ν_μ , ν_τ , 40, 80 strings) [39], and for the ANTARES 5-string configuration [40]. The effective area increases strongly with energy. The growth in effective area in the energy range above 1 PeV is dominated by events in the downgoing direction (all sky).

rays inevitably interact with relic photons leading to the absorption feature seen in the primary flux, the so-called GZK cutoff. In the interactions, pions are produced that decay into the cosmogenic neutrino flux [43] shown in the figure.

The atmospheric neutrino flux has been measured by AMANDA [44]. These measurements are in reasonable agreement with predicted atmospheric neutrino spectra [45], [46], [47]. While the figure focuses on diffuse fluxes, it is clear that some of these diffuse fluxes may be detected as point sources.

No detection of astrophysical neutrinos has been made yet. Two limits from AMANDA to such E^{-2} neutrino fluxes are shown: one is a diffuse muon neutrino flux limit [48], the other is a limit based on all flavor analysis of non-contained events in the PeV to EeV energy region [49]

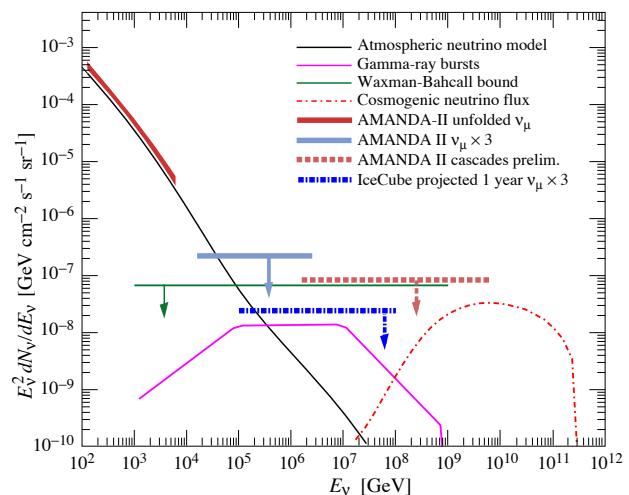


Figure 29.5: Measured atmospheric neutrino fluxes above 100 GeV are shown together with a few generic models for astrophysical neutrinos and some limits. See full-color version on color pages at end of book.

Neutrino telescopes can detect neutrinos of all flavors. If the primary interaction is caused by a ν_e , ν_τ or a neutral current interaction within the volume of the detector, the resulting event signature is a short cascade of particles, as opposed to the track-like signature left by a muon produced in a ν_μ charged-current interaction within or outside the volume of the detector. The extension of the

cascade shower in ice or water is small compared to the size of the detector, which effectively becomes a fully active calorimeter for these events. The energy resolution $\Delta E/E$ can be well below 10%. Thus, in studying the astrophysical diffuse fluxes, the small atmospheric ν_e background can be effectively suppressed by energy discrimination. The resulting sensitivity to diffuse astrophysical fluxes of all flavors can therefore be comparable to that of the muon channel.

The atmospheric neutrino background can be much more effectively suppressed in the search for point sources, where even in a km-scale detector only of order 10 atmospheric neutrino events are counted in a search bin. Unbinned search methods improve the sensitivity by using the point spread function and the energy information in the significance analysis, see *e.g.*, Ref. 50. The search for neutrinos from transient sources such as γ -ray bursts, where the typical duration of a burst is only 10 s, permits background reduction to $< 10^{-2}$, so that even 2 or 3 events are enough for discovery.

The sensitivity in the search for neutrinos from astrophysical point sources continues to increase rapidly as bigger detectors with better resolution improve. It should be added that neutrino telescopes can explore a variety of particle physics and astrophysics topics, such as cosmic-ray muons, cosmic-ray physics including cosmic-ray mass composition, atmospheric neutrinos of very high energies, indirect searches for dark matter and other searches for new physics. A detailed discussion is beyond the scope of this report. A very recent review can be found in Ref. 51.

29.4. Large time-projection chambers for rare event detection

Written August 2009 by M. Hefner (LLNL).

The Time Projection Chamber (TPC) concept (Sec. 28.6.5) has been applied to many projects outside of particle physics and the accelerator-based experiments for which it was initially developed. TPCs in non-accelerator particle physics experiments are principally focused on rare event detection (*e.g.*, neutrino and dark matter experiments) and the physics of these experiments can place dramatically different constraints on the TPC design (only extensions of the traditional TPCs are discussed here). The drift gas or liquid is usually the target or matter under observation and due to very low signal rates a TPC with the largest possible active mass is desired. The large mass complicates particle tracking of short and sometimes very low-energy particles. Other special design issues include efficient light collection, background rejection, internal triggering, and optimal energy resolution.

Backgrounds from γ rays and neutrons are significant design issues in the construction of these TPCs. These are generally placed deep underground to shield them from cosmogenic particles and are surrounded with shielding to reduce radiation from the local surroundings. The construction materials are carefully screened for radiopurity, as they are in close contact with the active mass and can be a significant source of background. The TPC excels in reducing this internal background because the mass inside the field cage forms one monolithic volume from which fiducial cuts can be made *ex post facto* to isolate quiet drift mass. The liquid (gas) can be circulated and purified to a very high level. Self-shielding in these large mass systems can be significant and the effect improves with density and size. (See Sec. 29.6.)

The liquid-phase TPC can have a high density at low pressure that results in very good self-shielding and compact installation with lightweight containment. The down sides are the need for cryogenics, slower charge drift, tracks shorter than typical electron diffusion distances, lower-energy resolution (*e.g.*, xenon) and limited charge readout options. Slower charge drift requires long electron lifetimes, placing strict limits on the oxygen and other impurities with high electron affinity. A significant variation of the liquid-phase TPC that improves the charge readout is the dual-phase TPC, where a gas phase layer is formed above the liquid into which the drifting electrons are extracted and amplified, typically with electroluminescence (*i.e.*, secondary scintillation or proportional scintillation (Fig. 29.6)). The successful transfer of electrons across the phase boundary requires careful control of its position and setting up an appropriate electric field.

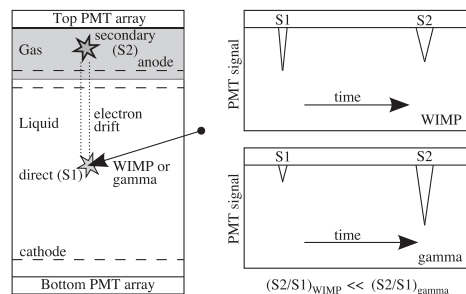


Figure 29.6: The configuration of a dual phase detector is shown on the left with the locations of where the primary and secondary light are generated. On the right is a schematic view of the signals of both an electron and nuclear interaction illustrating the discrimination power of this method. This figure is a slightly modified version of the figure in Ref. 61.

A high-pressure gas phase TPC has no cryogenics and density is easily optimized for the signal, but a large heavy-pressure vessel is required. Although self shielding is reduced, it can in some cases approach that of the liquid phase; in xenon at 50 atm the density is about half that of water or about 1/6 of liquid xenon. A significant feature of high pressure xenon gas is the energy resolution. Below a density of about 0.5 g cm^{-3} the intrinsic resolution is only a few times that of high purity germanium [62]. A neutrinoless double beta decay ($0\nu 2\beta$) search with a TPC operated below this density limit could enjoy excellent energy resolution and maintain particle tracking for background rejection.

An observable interaction with the TPC results in a charged particle that travels in the drift matter, exciting and ionizing the atoms until the initial energy is converted into ionization, scintillation, or heat with relatively large fluctuations around the mean. Rare-event TPCs can be designed to detect scintillation light as well as charge to exploit the anti-correlation to improve energy resolution and/or signal to noise [63]. An electric drift field separates the electrons and positive ions from the ionization although the separation is not complete and some electrons are captured, exciting atoms and releasing more light than the primary excitation alone. The average partition between the scintillation and ionization can be manipulated to increase the ionization (at the expense of scintillation) by a number of methods, such as increasing the strength of the electric field up to saturation of the ionization yield, increasing the temperature to enhance the diffusion of the ionized electrons, and adding dopants such as triethylamine that can be photoionized by the scintillation photons releasing more ionization.

Scintillation light is typically collected with photomultiplier tubes (PMTs) and avalanche photo diodes (APDs) although any fast (compared to the ionization drift speed) light collector capable of detecting the typically UV photons, maintaining high radiopurity, and perhaps withstanding pressure would work. (CCDs are slow and therefore only record two dimensions, integrating over the time direction. Some of the 3D information can be recovered by a few PMTs.) In most cases, coating the optics or adding a wavelength shifter is required [63], although some work has been done to directly readout the 175 nm light from xenon with a silicon detector. In a typical cylindrical geometry, the light detectors are placed at the ends on an equipotential of the field cage simplifying the design, but limiting the collection efficiency. The field cage can be made of UV-reflective materials such as Teflon, to increase the light-collection efficiency.

Charge collection can be accomplished with proportional avalanche in the manner used in a traditional TPC (even in the liquid state), although the final signal suffers from rather large fluctuations caused by small fluctuations early in the avalanche that are amplified by the process. Inductive readout of passing charges and direct collection of the unamplified charge do not rely on an avalanche, and are effective where energy resolution is of paramount importance, but depend on low-noise amplifiers and relatively large signals (*e.g.*, in $0\nu 2\beta$ decay).

Electroluminescence can be used to proportionally amplify the

the drifted ionization, and it does not suffer the fluctuations of an avalanche or the small signals of direct collection. It works by setting up at the positive end of the drift volume parallel meshes or wire arrays with an electric field larger than the drift field, but less than the field needed for avalanche. In xenon, this is $3\text{--}6\text{ kV cm}^{-1}\text{ bar}^{-1}$ for good energy resolution. Eq. (29.4) shows the dependence of the yield (Y) in xenon in units of photons/(electron cm bar) as a function of pressure (p) in units of bar and electric field (E) in units of kV/cm [58]:

$$Y/p = 140 E/p - 116 . \quad (29.4)$$

The amplification can be adjusted with the length of the electroluminescence region, pressure and electric field.

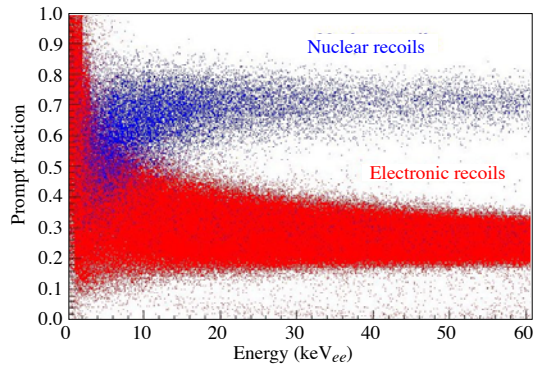


Figure 29.7: An example of pulse-shape discrimination of nuclear recoils and electrons in argon. The prompt fraction is a measure of the pulse shape that clearly separates the two interactions down to very low energy. Figure from Ref. 59.

Differentiation of nuclear and electron recoils at low-energy deposition is important as a means of background rejection. The nuclear recoil deposits a higher density of ionization than an electron recoil and this results in a higher geminate recombination resulting in a higher output of primary scintillation and lower charge. The ratio of scintillation to charge can be used to distinguish the two. In the case of an electroluminescence readout, this is done simply with the ratio of primary light to secondary light. Optically transparent grids with PMT or APD readout combine to make a elegant setup wherein the same array can measure the primary scintillation (S1), and the electroluminescence (S2) eliminating the necessity of two sets of readout detectors. Fig. 29.6 illustrates this method that works in the gas phase and in dual phase detectors. The time evolution of the primary light is also affected by the type of recoil that results from different populations of excimers in the singlet and triplet states [59]. This alone has resulted in excellent discrimination, particularly in gases where the decay times are significantly different (see Table 29.2). An example of the discrimination is displayed in Fig. 29.7, where nuclear recoils and electrons can be identified down to 10's of keVee, in argon. Nuclear recoils deposit less ionization than electrons at a given energy. For this reason, nuclear recoil energy is typically reported in equivalent electron energy loss, keVee, when compared with electrons.

The composition of the drift matter is an important choice in TPC design, and the noble gases are frequently selected as the bulk element in the mix (Table 29.2). The noble gases have no electron affinity in the ground state, resulting in good free-electron lifetime and a good amount of scintillation that is useful for particle identification and t_0 determination. In the case of argon and xenon, the low average energy to produce an ion pair results in good energy resolution. The noble gases are easily purified to a high level that, combined with moderate cost, enables the construction of large monolithic detectors. Of the noble gasses one isotope of xenon (^{136}Xe) is a candidate for ($0\nu 2\beta$).

The negative-ion TPC [60] uses an electronegative gas (*e.g.*, CS_2) either as the drift gas or as a dopant to the drift gas that captures the primary electrons, forming negative ions that drift in the electric field. Upon reaching the gas-gain region of the TPC, the electron is stripped from the ion in the high electric field, and the electron avalanches in

Table 29.2: Properties of the noble gasses typically used in non-accelerator TPCs [56,57]. W is the average energy spent to produce one electron ion pair.

Element	W (eV)	photon yield (γ/keV)	wave- length (nm)	decay time (fast/slow)	cost (\$/kg)
Helium	46.0	50	80	10 ns/1.6 μs	\$5
Neon	36.6	30	77	10 ns/3.9 μs	\$60
Argon	26.4	40	128	4 ns/1.6 μs	\$2
Xenon	21.7	42	175	4 ns/22 ns	\$1000

the normal manner. The larger mass of the the negative ion keeps the kinetic energy of the ion thermal at high electric fields, and therefore such a TPC exhibits far less diffusion. The reduction of diffusion over large distance (time) enables detailed tracking of small tracks in a large volume without the benefit of a magnetic field to limit diffusion (which would be prohibitively expensive for a large volume). The trade-off is orders-of-magnitude slower drift, placing a limit on the trigger rate.

29.5. Sub-Kelvin detectors

Written September 2009 by S. Golwala (Caltech).

Detectors operating below 1 K, also known as “low-temperature” or “cryogenic” detectors, use $\lesssim\text{meV}$ quanta (phonons, superconducting quasiparticles) to provide better energy resolution than is typically available from conventional technologies. Such resolution can provide unique advantages to applications reliant on energy resolution, such as beta-decay experiments seeking to measure the ν_e mass or searches for neutrinoless double-beta decay. In addition, the sub-Kelvin mode is combined with conventional (eV quanta) ionization or scintillation measurements to provide discrimination of nuclear recoils from electron recoils, critical for searches for WIMP dark matter and for coherent neutrino-nucleus scattering. We describe the techniques in generic fashion in the text and provide a list of experiments using these techniques in An excellent review [52] is available that covers this material and other applications of low-temperature detectors. The proceedings of the Low Temperature Detectors Workshops are also useful [53].

Table 29.3.

29.5.1. Thermal Phonons :

The most basic kind of low-temperature detector employs a dielectric absorber coupled to a thermal bath via a weak link. A thermistor monitors the temperature of the absorber. The energy E deposited by a particle interaction causes a calorimetric temperature change by increasing the population of thermal phonons. The fundamental sensitivity is

$$\sigma_E^2 = \xi^2 kT [TC(T) + \beta E] , \quad (29.5)$$

where C is the heat capacity of the detector, T is the temperature of operation, k is Boltzmann's constant, and ξ is a dimensionless factor of order unity that is precisely calculable from the nature of the thermal link and the non-thermodynamic noises (*e.g.*, Johnson and/or readout noise). The first term is imposed by statistical fluctuations in the number of thermally excited phonons and on the energy in the absorber due to exchange with the thermal bath (see, *e.g.*, Ref. 54 and references therein). The second term is due to statistical fluctuations in the number of phonons excited by the absorbed radiation. The factor β is also dimensionless and $\mathcal{O}(1)$ and is also precisely calculable from the nature of the thermal link. The ratio of the second term to the first term is equal to the fractional absorber temperature change due to an energy deposition. Thus, the second term becomes appreciable when this fractional temperature change is appreciable, at which point nonlinear effects also come into play. The energy resolution typically acquires an additional energy dependence due to deviations from an ideal calorimetric model that cause position and/or energy dependence in the signal shape.

Table 29.3: Selected experiments using sub-Kelvin detectors. The table is not exhaustive. Operation mode, detector and excitation sensor construction, baseline energy resolution, and energy resolution at a particular energy of interest E_0 are given. We quote the energy and energy resolution for “total” phonon signal, where the total phonon signal includes both recoil energy and, where relevant, drift heating. Ionization and scintillation energies are normalized so that, for electron recoils, the energy in these channels is equal to the recoil energy (“electron-equivalent” energies). For scintillation energy, this is the electron-equivalent energy deposited in the target detector, not the energy received by the photon absorber. Approximate dates of operation are also given. Key to comments: “a-Si” and “a-Ge” = amorphous silicon or germanium layers in ionization electrodes; “H-a-Si” = hydrogenated amorphous silicon. “P-implanted” = phosphorous implantation. “Interdig.” = interdigitated ionization electrode design that provides some z information from ionization signal asymmetry. “Surface-event discrimination” = ability to reject events near surfaces that suffer reduced ionization yield and can be misidentified as WIMPs. “w/phonons” = using athermal phonon pulse rising edge (faster for surface events). “w/ioniz. asym.” = using the asymmetry of the ionization signal on electrodes on opposite faces of interdigitated-electrode detectors. “w/phonon asym.” = using the asymmetry of the phonon signal detected on opposite detector faces. SuperCDMS energy resolutions have not been fully reported yet but are likely no worse than CDMS II.

Experiment	technique	substrate + mass	sensor	ΔE_{FWHM} at $E = 0$	[keV] at E_0	E_0 [keV]	comments
WIMP dark matter							
CDMS I (1996-2000)	thermal	Ge	NTD Ge	0.3	0.7	12	nuclear recoil discrimination
	phonon, ionization	0.16 kg	thermistor, H-a-Si/Al electrode	0.9	1.1	10.4	w/ ionization yield
CDMS II (2001-2008)	athermal	Ge	tungsten	0.4	2.4	20.7	CDMS I+ surface-event discrimination
	phonon, ionization	0.25 kg	TES, a-Si/Al electrode	0.7	0.8	10.4	w/phonons
SuperCDMS- SNOLAB, in develop- ment	athermal	Ge	tungsten	0.4	N/A	N/A	CDMS II+ surface-event
	phonon, ionization	0.64 kg	TES, a-Si/Al interdig.	0.7	N/A	N/A	discr. w/ioniz.+ phonon z asym.
EDELWEISS I (1996-2005)	thermal	Ge	NTD Ge	2.3	2.3	24.2	nuclear recoil discrimination
	phonon, ionization	0.32 kg	thermistor, a-Si/Al a-Ge/Al	1.1	1.1	10.4	w/ionization yield
EDELWEISS II (2006-)	thermal	Ge	NTD Ge	3.6	3.6	38.0	EDELWEISS I +surface-event discrimination
	phonon, ionization	0.4 kg	thermistor, a-Si/Al interdig.	1.0	1.0	10.4	w/ioniz. asym.
CRESST I (1996-2002)	athermal phonon	Al ₂ O ₃ 0.26 kg	tungsten SPT	0.20	0.24	1.5	no NR discr.
CRESST II (2003-)	athermal	CaWO ₄	tungsten	0.3	0.3	8.1	NR discr.
	phonon, scint.	0.3 kg (ZnWO ₄)	SPT (target and photon abs.)	1.0	3.5	10	w/scint. yield
α decay							
ROSEBUD (1996-)	athermal phonon, scintillation	BGO 46 g	NTD Ge thermistor (target & photon abs.)	6 N/A	5500 N/A	18 N/A	α discr. w/scint. yield, first detection of ²⁰⁹ Bi α decay
β decay							
Oxford ⁶³ Ni (1994-1995)	athermal phonon	InSb 3.3 g	Al STJ	1.24	1.24	67	
MARE (2009-)	thermal phonon	AgReO ₄ 0.5 mg	P-implanted Si thermistor	N/A	0.033	2.6	
$0\nu\beta\beta$ decay							
CUORE (2003-)	thermal phonon	TeO ₂ * 0.75 kg	NTD Ge thermistor	N/A	7	2527	

* The CUORE energy resolution is worse than can be obtained with Ge diode detectors.

The rise time of response is limited by the internal thermal conductivity of the absorber. The decay time constant, describing the time required for the absorbed energy to flow out to the bath, is $\tau = C/G$, where G is the thermal conductance of the weak link. The above formula immediately suggests the use of crystalline dielectric absorbers and low temperatures because of the linear factor of T and because C for crystalline dielectrics drops as T^3 for T well below the material's Debye temperature (Θ_D , typically hundreds of K). Specifically, the Debye model indicates that a crystal consisting of N atoms has

$$C = \frac{12\pi^4}{5} N k \left(\frac{T}{\Theta_D} \right)^3 \quad (29.6)$$

which gives $\sigma_E = 5.2\xi$ eV for 1 kg of germanium operated at $T = 10$ mK. (For a detector of this size the 2nd term in Eq. (29.5) is negligible.) In practice, a number of factors degrade the above result by about an order of magnitude (thermistor heat capacity and power dissipation, readout noise, etc.), but the predicted energy resolution for such a large mass remains attractive.

Neutron-transmutation-doped (NTD) germanium and implanted silicon semiconductors are used for thermistors. Conduction is via phonon-assisted hopping between impurity sites, yielding an exponentially decreasing resistance as a function of temperature, $R(T)$, with negative slope, dR/dT . Attachment to the absorber is usually by eutectic bonding or epoxy or by direct implantation into the absorber. Another type of temperature sensor is the superconducting phase-transition thermometers (SPT) or transition-edge sensor (TES). A SPT or TES is a superconducting film operated in the transition from superconductive to normal resistance at the transition temperature, T_c , where its resistance is a strong function of temperature with positive dR/dT . This can provide strong electrothermal negative feedback, which improves linearity, speeds up response, and mitigates variations in T_c among multiple TESs on the same absorber. $\text{Nb}_x\text{Si}_{1-x}$ is another thermistor material that ranges between the semiconducting and superconducting regimes as a function of the stoichiometry (defined by x). SPTs/TESs and $\text{Nb}_x\text{Si}_{1-x}$ thermistors are frequently deposited directly onto the absorber by sputtering or evaporation.

The readout method depends on the type of thermometer used. Doped semiconductors typically have high impedances and are well matched to low-noise JFET-based readout while SPTs/TESs are low-impedance devices requiring SQUID amplifiers.

29.5.2. Athermal Phonons and Superconducting Quasiparticles :

The advantage of thermal phonons is also a disadvantage: energy resolution degrades as \sqrt{M} where M is the detector mass. This motivates the use of athermal phonons. There are three steps in the development of the phonon signal. The recoiling particle deposits energy along its track, with the majority going directly into phonons. (A minority of the energy goes directly into scintillation and ionization. Energy deposited in ionization is recovered when the carriers recombine.) The recoil and bandgap energy scales (keV and higher, and eV, respectively) are much larger than phonon energies (meV), so the full energy spectrum of phonons is populated, with phase space favoring the most energetic phonons. However, these initial energetic phonons do not propagate because of isotopic scattering (scattering due to variations in lattice ion atomic mass, rate $\propto \nu^4$ where ν is the phonon frequency) and anharmonic decay (scattering wherein a single phonon splits into two phonons, rate $\propto \nu^5$). Anharmonic decay downshifts the phonon spectrum, which increases the phonon mean free path, so that eventually phonons can propagate the characteristic dimension of the detector. These phonons travel quasiballistically, preserve information about the position of the parent interaction, and are not affected by an increase in detector mass (modulo the concomitant larger distance to the surface where they can be sensed). Anharmonic decay continues until a thermal distribution is reached (μeV at mK temperatures), which is exhibited as a thermal increase in the temperature of the detector. If one can detect the athermal phonons at the crystal surface, keep the density of such sensors fixed as the detector surface area increases with mass, and the crystals are pure enough that the athermal phonons can propagate to the surface prior to thermalization, then an increase in detector mass need not degrade energy resolution, and can in fact

improve position reconstruction. Sensors for athermal phonons are similar to those for superconducting quasiparticles described below.

Another mode is detection of superconducting quasiparticles in superconducting crystals. Energy absorption breaks superconducting Cooper pairs and yields quasiparticles, electron-like excitations that can diffuse through the material and that recombine after the quasiparticle lifetime. In crystals with very large mean free path against scattering, the diffusion length (distance traveled in a quasiparticle lifetime) is large enough (mm to cm) that the quasiparticles reach the surface and can be detected, usually in a superconducting tunnel junction (STJ) or TES/SPT.

A similar technique is applied to detect athermal phonons. Athermal phonons reaching a superconducting film on the detector surface generate quasiparticles as above. Such thin films have diffusion lengths much shorter than for superconducting crystalline substrates, only of order $100 \mu\text{m}$ to 1 mm. Thus, the superconducting film must be segmented on this length scale and have a quasiparticle sensor for each segment. The sensors may, however, be connected in series or parallel in large groups to reduce readout channel count.

The readout for athermal phonon and quasiparticle sensing depends on the type of quasiparticle detector. Tunnel junctions match well to JFET-based readouts, while TESs/SPTs use SQUID amplifiers.

29.5.3. Ionization and Scintillation :

While ionization and scintillation detectors usually operate at much higher temperatures, ionization and scintillation can be measured at low temperature and can be combined with a "sub-Kelvin" technique to discriminate nuclear recoils from background interactions producing electron recoils, which is critical for WIMP searches and coherent neutrino-nucleus scattering. With ionization, such techniques are based on Lindhard theory [55], which predicts substantially reduced ionization yield for nuclear recoils relative to electron recoils. For scintillation, application of Birks' law (Sec. 28.3.0) yields a similar prediction. (The reduced ionization or scintillation yield for nuclear recoils is frequently referred to as "quenching".)

Specifically, consider the example of measuring thermal phonons and ionization. All the deposited energy eventually appears in the thermal phonon channel, regardless of recoil type (modulo some loss to permanent crystal defect creation). Thus, the ionization yield—the number of charge pairs detected per unit detected energy in phonons—provides a means to discriminate nuclear recoils from electron recoils. Similar discrimination is observed with athermal phonons and ionization and with phonons and scintillation.

In semiconducting materials of sufficient purity—germanium and silicon—electron-hole pairs created by recoiling particles can be drifted to surface electrodes by applying an electric field, similar to how this is done at 77 K in high-purity germanium photon spectrometers (Sec. 28.7). There are three important differences, however, that result in the use of low fields—of order 1 V/cm—instead of the hundreds to thousands of V/cm used in 77 K detectors. First, high fields are required at 77 K to deplete the active volume of thermally excited mobile carriers. At low temperature and in crystals of purity high enough to drift ionization with negligible trapping, the population of thermally excited carriers is exponentially suppressed due to the low ambient thermal energy. Second, high fields in 77 K operation prevent trapping of drifting carriers on ionized impurities and crystalline defects and/or overcome space charge effects. At low temperatures, ionized impurities and space charge can be neutralized (using free charge created by photons from LEDs or radioactive sources) and remain in this state for minutes to hours. This reduces trapping exponentially and allows low-field drift. Third, a high field in a sub-Kelvin detector would result in a massive phonon signal from the drifting carriers, fully correlated with the ionization signal and thereby eliminating nuclear recoil discrimination. Readout of the charge signal is typically done with a conventional JFET-based transimpedance amplifier.

A number of materials that scintillate on their own (*i.e.*, without doping) continue to do so at low temperatures, including BaF_2 , BGO, CaWO_4 , ZnWO_4 , PbWO_4 , and other tungstates and molybdates. In and of itself, there is little advantage to a low-temperature scintillation measurement because detecting the scintillation is nontrivial, the quanta are large, and the detection efficiency is usually poor.

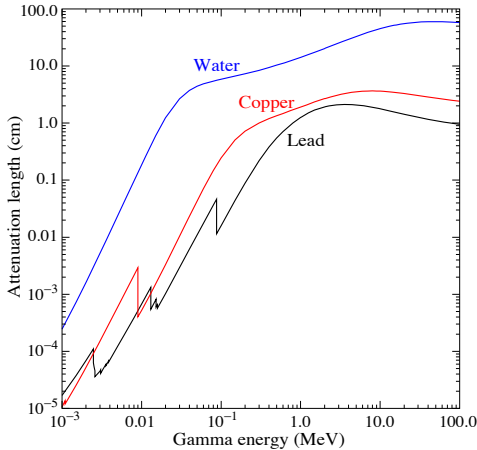


Figure 29.8: γ -ray attenuation lengths in some common shielding materials. The mass attenuation data has been taken from the NIST data base XCOM; see “Atomic Nuclear Properties” at pdg.lbl.gov.

Such techniques are pursued only in order to obtain nuclear-recoil discrimination. Conventional photodetectors do not operate at such low temperatures, so one typically detects the scintillation photons in an adjacent low-temperature detector that is thermally disconnected from but resides in an optically reflective cavity with the target detector.

29.6. Low-radioactivity background techniques

Written August 2009 by A. Piepke (University of Alabama).

The physics reach of low-energy rare event searches *e.g.* for dark matter, neutrino oscillations, or double beta decay is often limited by background caused by radioactivity. Depending on the chosen detector design, the separation of the physics signal from this unwanted interference can be achieved on an event-by-event basis by active event tagging, utilizing some unique event feature, or by reducing the radiation background by appropriate shielding and material selection. In both cases, the background rate is proportional to the flux of background-creating radiation. Its reduction is thus essential for realizing the full physics potential of the experiment. In this context, “low energy” may be defined as the regime of natural, anthropogenic, or cosmogenic radioactivity, all at energies up to about 10 MeV. Following the classification of [64], sources of background may be categorized into the following classes:

1. environmental radioactivity,
2. radioimpurities in detector or shielding components,
3. radon and its progeny,
4. cosmic rays,
5. neutrons from natural fission, (α , n) reactions and from cosmic-ray muon spallation and capture.

29.6.1. Defining the problem: The application defines the requirements. Background goals can be as demanding as a few low-energy events per year in a ton-size detector. The strength of the physics signal to be measured can often be estimated theoretically or from limits derived by earlier experiments. The experiments are then designed for the desired signal-to-background ratio. This requires finding the right balance between clarity of measurement, ease of construction, and budget. In a practical sense, it is important to formulate background goals that are sufficient for the task at hand but doable, in a finite time. It is now standard practice to use a detector simulation to translate the background requirements into limits for the radioactivity content of various detector components, requirements for the radiation shielding, and allowable cosmic-ray flux. This strategy allows identifying the most critical components early and the allocation of analysis and development resources accordingly. The CERN code GEANT4 is a widely used tool for this task. It contains sufficient nuclear physics to allow accurate background estimations. Custom-written event generators, modeling particle correlations in complex decay schemes, are used as well.

29.6.2. Environmental radioactivity: The long-lived natural radioisotopes ^{40}K , ^{232}Th , and ^{238}U have average abundances of 2.4, 9.6 and 2.7 ppm in the earth’s crust, with large local variations. In most applications, γ radiation emitted by natural radioactivity constitutes the dominant contribution to the local radiation field. Typical low-background applications require levels of natural radioactivity on the order of ppb or ppt in the detector components. Passive or active shielding is used to suppress external γ radiation down to that level. Fig. 29.8 shows the energy-dependent attenuation length $\lambda(E_\gamma)$ as a function of γ ray energy E_γ for three common shielding materials (water, copper, lead). The thickness ℓ required to reduce the external flux by a factor $f > 1$ is estimated assuming exponential damping:

$$\ell = \lambda(E_\gamma) \cdot \ln f. \quad (29.7)$$

At 100 keV, a typical energy scale for dark matter searches (or 2.615 MeV, for a typical double-beta decay experiment), attenuation by a factor $f = 10^5$ requires 67(269) cm of H_2O , 2.8(34) cm of Cu, or 0.18(23) cm of Pb. Such estimates allows for an order-of-magnitude estimate of the experiment dimensions. A precise estimation of the leakage of external γ radiation, including scattering and the effect of energy cuts, requires Monte Carlo simulations and determination of the radioactivity present in the laboratory. Detailed modeling of the γ flux in a large laboratory, or inside hermetic shielding, needs to cope with very small detector-hit efficiencies. It is often advantageous to calculate solid angle and mass attenuation separately. This approach reduces the computation time required for a statistically meaningful number of detector hits to manageable levels.

Because of its low density, water has relatively long attenuation lengths, resulting in rather voluminous shields. However, because water can be obtained relatively cheaply in large amounts, it has become the medium of choice for most large detectors. Water purification technology is effective and commercially available, an important consideration in view of the intrinsic radioactivity of the shield, to be discussed below. High-purity water, instrumented with photo multiplier tubes, can further serve as a Cherenkov cosmic-ray veto detector. Liquefied gases are being used for shielding as well.

29.6.3. Radioimpurities in detector or shielding components

: After suppressing the effect of external radioactivity, radioactive impurities contained in the detector components or attached to its surfaces become important. Any material is radioactive at some level. The activity can be natural, cosmogenic, or man-made. The determination of the activity content of a specific material or component requires case-by-case analysis, and is almost never obtainable from the manufacturer. However, there are some general rules than can be used to guide the pre-selection. For detectors designed to look for electrons (for example in double-beta decay searches or neutrino detection via inverse beta decay or elastic scattering), this is the principal source of background. For devices detecting nuclear recoils (for example in dark matter searches), this is often of secondary importance as ionization signals can be actively suppressed on an event-by-event basis.

For natural radioactivity, a rule of thumb is that synthetic substances are cleaner than natural materials. Typically, more highly processed materials have lower activity content. Substances with smaller chemical reactivity tend to be cleaner. The refining process tends to remove K, Th, and U. For example, Al is often found to contain considerable amounts of Th and U, while electrolytic Cu is very low in primordial activities. Plastics or liquid hydrocarbons, having been refined by distillation, are often quite radiopure. Tabulated radioactivity screening results for a wide range of materials can be found in Refs. 65 and 66.

The long-lived ^{238}U daughter ^{210}Pb ($T_{1/2}=22.3$ y) is found in all shielding lead, and is a background concern at low energies. This is due to the relatively high endpoint energy ($Q_\beta=1.162$ MeV) of its beta-unstable daughter ^{210}Bi . Lead parts made from selected low-U ores have specific activities of about 5–30 mBq/kg. For lower activity, ancient lead (for example from Roman ships) has been used. Because the ore processing and lead refining removed most of the ^{238}U , the ^{210}Pb decayed during the long waiting time to the level supported by the U-content of the refined lead. Lining the lead with copper

to range out the low-energy radiation is another remedy. However, intermediate Z materials are an activation risk when handled above ground, as will be discussed below. ^{210}Pb is also found in solders.

The fission product ^{137}Cs can be found attached to the surface of materials. The radioactive noble gas ^{85}Kr , released into the atmosphere by nuclear reactors and nuclear fuel re-processing, is also important, especially due to its high solubility in organic materials. Post-World War II steel typically contains a few tens of mBq/kg of ^{60}Co .

Surface activity is not a material property but is added during manufacturing and handling. It can often be effectively removed by etching. Installation of low-background detectors is often done in clean rooms to avoid this contamination. Surface contamination can be quantified by means of wipe-testing with acid or alcohol wetted Whatman 41 filters. The paper filters are ashed after wiping and the residue is digested in acid. Subsequent analysis by means of mass spectroscopy or neutron activation analysis is capable of detecting less than 1 pg/cm^2 of Th and U. The most demanding low-rate experiments require screening of *all* components, which can be a time consuming task. The requirements for activity characterization depend on the experiment and the location and amount of a particular component. Monte Carlo simulations are used to quantify these requirements. Activities of the order $\mu\text{Bq/kg}$ or even below may need to be detected in the process. At such level of sensitivity, the characterization becomes a challenging problem in itself. Low-background α , β , and γ ray counting, mass spectroscopy, and neutron activation analysis are used.

29.6.4. Radon and its progeny: The noble gas ^{222}Rn , a pure α -emitter, is a ^{238}U decay product. Due to its half-life of 3.8 d it is released by surface soil and is found in the atmosphere everywhere. ^{220}Rn (^{232}Th decay product) is unimportant because of its short half-life. ^{222}Rn activity in air ranges from 10 to 100 mBq/L outdoors and 100 to thousands of mBq/L indoors. The natural radon concentration depends on the weather and shows daily and seasonal variations. Radon levels are lowest above the oceans. For electron detectors, it is not the Rn itself that creates background, but its progeny ^{214}Pb , ^{214}Bi , ^{210}Bi , which emit energetic beta and γ radiation. Thus, not only the detector itself has to be separated from contact with air, but also internal voids in the shield which contain air can be a background concern. Radon is quite soluble in water and even more so in organic solvents. For large liquid scintillation detectors, radon mobility due to convection and diffusion is a concern. To define a scale: typical double-beta-decay searches are disturbed by a μBq (or $1/11.6\text{ d}$) activity of ^{222}Rn contained in the detector medium. This corresponds to a steady-state population of 0.5 atoms in $50\ \mu\text{L}$ of air (assuming 20 mBq/L of radon in the air). The criteria for leak tightness are thus quite demanding. The decay of Rn itself is a concern for some recoil type detectors, as nuclear recoil energies in α decays are substantial (76 keV in case of ^{222}Rn).

Low-activity detectors are often kept sealed from the air and continuously flushed with boil-off nitrogen, which contains only small amounts of Rn. For the most demanding applications, the nitrogen is purified by multiple distillations. Then only the Rn outgassing of the piping (due to its U internal content) determines the radon concentration. Radon diffuses readily through thin plastic barriers. If the detector is to be isolated from its environment by means of a membrane, the right choice of material is important [67].

If energies below 1 MeV are to be measured, additional care has to be taken to avoid plate-out of the long-lived radon daughter ^{210}Pb on the surfaces. This can be reduced by keeping the parts under a protective low-radon cover gas.

Radon can be detected even at the level of few atoms with solid state, scintillation, or gas detectors by exploiting the fast decay sequences of ^{214}Bi and ^{214}Po . The efficiency of these devices is sometimes boosted by electrostatic collection of charged radon into a small detector.

29.6.5. Cosmic rays: Cosmic radiation, discussed in detail in Chapter 24, is a source of background for just about any non-accelerator experiment. Primary cosmic rays are about 90% protons, 9% alpha particles, and the rest heavier nuclei (Fig. 24.1). They are totally attenuated within the first few hg/cm² of atmospheric thickness. At sea level secondary particles ($\pi^\pm : p : e^\pm : n : \mu^\pm$) are observed with relative intensities 1 : 13 : 340 : 480 : 1420 (Ref. 68; also see Fig. 24.3).

All but the muon and the neutron components are readily absorbed by overburden such as building ceilings and passive shielding. Only if there is very little overburden ($\lesssim 1\text{ g/cm}^2$ or so) do pions and protons need to be considered when estimating the production rate of cosmogenic radioactivity.

Sensitive experiments are thus operated deep underground where essentially only muons penetrate. As shown in Fig. 24.6, the muon intensity falls off rapidly with depth. Active detection systems capable of tagging events correlated in time with cosmic-ray activity are needed, depending on the overburden. Such experiments are described in Sec. 29.3.1.

The muonic background is only related to low-radioactivity techniques insofar as photonuclear interactions of muons can produce long-lived radioactivity. This happens at any depth, and it constitutes an essentially irreducible background.

Cosmogenic activation of components brought from the surface is also an issue. Proper management of parts and materials above ground during machining and detector assembly minimizes the accumulation of long-lived activity. Cosmogenic activation is most important for intermediate Z materials such as Cu and Fe. For the most demanding applications, metals are stored and transported under sufficient shielding to stop the hadronic component of the cosmic rays. Parts, *e.g.*, the nickel tubes for the ^3He counters in SNO, can be stored underground for long periods before being used. Underground machine shops are also sometimes used to limit the duration of exposure at the surface.

29.6.6. Neutrons: Neutrons contribute to the background of low-energy experiments in different ways: directly through nuclear recoil in the detector medium, and indirectly, through the production of radio nuclides inside the detector and its components. The latter mechanism allows even remote materials to contribute to the background by means of penetrating γ radiation, since inelastic scattering of fast neutrons or radiative capture of slow neutrons can result in the emission of γ radiation. Neutrons are thus an important source of low-energy background. They are produced in different ways:

1. At the earth's surface neutrons are the most intense cosmic-ray secondary other than muons;
2. Energetic tertiary neutrons are produced by cosmic-ray muons in nuclear spallation reactions with the detector and laboratory walls;
3. In high Z materials, often used in radiation shields, nuclear capture of negative muons results in emission of neutrons;
4. Natural radioactivity has a neutron component through spontaneous fission and (α, n) -reactions.

A calculation with the hadronic simulation code FLUKA, using the known energy distribution of secondary neutrons at the earth's surface [69], yields a mass attenuation of 1.5 hg/cm^2 in concrete for secondary neutrons. If energy-dependent neutron-capture cross sections are known, then such calculations can be used to obtain the production rate of radio nuclides.

At an overburden of only few meters, water equivalent neutron production by muons becomes the dominant mechanism. Neutron production rates are high in high- Z shielding materials. A high- Z radiation shield, discussed earlier as being effective in reducing background due to external radioactivity, thus acts as a source for cosmogenic tertiary high-energy neutrons. Depending on the overburden and the radioactivity content of the laboratory, there is an optimal shielding thickness. Water shields, although bulky, are an attractive alternative due to their low neutron production yield and self-shielding.

Neutron shields made from plastic or water are commonly used to reduce the neutron flux. The shield is sometimes doped with a substance having a high thermal neutron capture cross section (such

as boron) to absorb thermal neutrons more quickly. The hydrogen serves as a target for elastic scattering, and is effective in reducing the neutron energy. Neutrons from natural radioactivity have relatively low energies and can be effectively suppressed by a neutron shield. Such a neutron shield should be inside the lead to be effective for tertiary neutrons. However, this is rarely done as it increases the neutron production target (in form of the passive shield), and costs increase as the cube of the dimensions. An active cosmic-ray veto is an effective solution, correlating a neutron with its parent muon. This solution works best if the veto system is as far removed from the detector as feasible (outside the radiation shield) to correlate as many background-producing muons with neutrons as possible. The vetoed time after a muon hit needs to be sufficiently long to assure neutron thermalization. The average thermalization and capture time in lead is about 900 μ s [64]. The veto-induced deadtime, and hence muon hit rate on the veto detector, is the limiting factor for the physical size of the veto system (besides the cost). The background caused by neutron-induced radioactivity with live times exceeding the veto time cannot be addressed in this way. Moving the detector deep underground, and thus reducing the muon flux, is the only technique addressing all sources of neutron background.

References:

- R.M. Baltrusaitis *et al.*, Nucl. Instrum. Methods **A20**, 410 (1985).
- T. Abu-Zayyad *et al.*, Nucl. Instrum. Methods **A450**, 253 (2000).
- H. Kawai *et al.*, Nucl. Phys. Proc. Suppl. **175–176**, 253, (2008).
- J. Abraham *et al.*, [Pierre Auger Collab.], Nucl. Instrum. Methods **A523**, 50 (2004).
- F. Arqueros, J. Hrandel, & B. Keilhauer, Nucl. Instrum. Methods **A597**, 23 (2008).
- F. Arqueros, J. Hrandel, & B. Keilhauer, Nucl. Instrum. Methods **A597**, 1 (2008).
- J. Boyer *et al.*, Nucl. Instrum. Methods **A482**, 457 (2002); M. Kleifges for the Pierre Auger Collab., Nucl. Instrum. Methods **A518**, 180 (2004).
- M. Ave *et al.*, [AIRFLY Collab.], Astropart. Phys. **28**, 41 (2007).
- J.T. Brack *et al.*, Astropart. Phys. **20**, 653, (2004).
- B. Rick *et al.*, JINST **1**, 11003, (2006).
- S.Y. Benzvi *et al.*, Nucl. Instrum. Methods **A574**, 171 (2007).
- R. Abassi *et al.*, Astropart. Phys. **25**, 74 (2006).
- M. Unger *et al.*, Nucl. Instrum. Methods **A588**, 433 (2008).
- T.K. Gaisser & A.M. Hillas, *Proc. 15th Int. Cosmic Ray Conf.* (Plovdiv, Bulgaria, 13–26 Aug. 1977).
- J. Holder *et al.*, *Proc. 4th International Meeting on High Energy Gamma-Ray Astron.*, eds. F.A. Aharonian, W. Hofmann & F. Rieger, AIP Conf. Proc. **1085**, 657 (2008).
- J.A. Hinton, *New Astron. Rev.* **48**, 331 (2004).
- J. Albert *et al.*, *Astrophys. J.* **674**, 1037 (2008).
- astro-ph/0508253** Lectures given at the International Heraeus Summer School, “Physics with Cosmic Accelerators,” Bad Honnef, Germany, July 5–16 (2004).
- T.C. Weekes *et al.*, *Astrophys. J.* **342**, 379 (1989).
- A.M. Hillas *et al.*, *Astrophys. J.* **503**, 744 (1998).
- F.A. Aharonian, *et al.*, *Astrophys. J.* **636**, 777 (2006).
- L.A. Bernstein *et al.*, “Report on the Depth Requirements for a Massive Detector at Homestake” (2009); **arXiv:0907.4183**.
- Y. Ashie *et al.*, *Phys. Rev.* **D71**, 112005 (2005).
- S. Kasuga *et al.*, *Phys. Lett.* **B374**, 238 (1996).
- M. Shiozawa, Nucl. Instrum. Methods **A433**, 240 (1999).
- J. Hosaka *et al.*, *Phys. Rev.* **D73**, 112001 (2006).
- J. Boger *et al.*, Nucl. Instrum. Methods **A449**, 172 (2000).
- J. Ahrens, *et al.*, Nucl. Instrum. Methods **A524**, 169–194 (2004); J.G. Learned, K. Mannheim, *Ann. Rev. Nucl. and Part. Sci.* **50**, 679 (2000).
- R. Abbasi, *et al.*, (IceCube collaboration), *Astrophys. J. Lett.* **701**, (2009).
- A. Roberts, *Rev. Mod. Phys.* **64**, 259 (1992).
- I. Belolapcticov, *et al.*, (Baikal collaboration), *Astropart. Phys.* **7**, 263 (1997); G.V. Domogatsky, for the Baikal coll., *Proc. XXth Int. Conf. Neutrino Phys. & Astrophys.* (Munich, 25–30 May, 2002); **astro-ph/0211571**.
- E. Andres, *et al.*, (The AMANDA collaboration), *Nature* **410**, 441–443 (2001).
- G. Aggouras *et al.*, *Nucl. Instrum. Methods* **A552**, 420–439 (2005).
- G. Giacomelli, for the ANTARES Coll., “The ANTARES Neutrino Telescope,” **arXiv:0812.1945v1**.
- J.A. Aguilar, *et al.*, (ANTARES Collaboration), *Astropart. Phys.* **26**, 131 (2005).
- KM3NeT: **http://www.kmenet.org**.
- A. Achterberg, *et al.*, *Astropart. Phys.* **26**, 155–230 (2006); **astro-ph/0604450**.
- R. Abbasi, *et al.* (IceCube collaboration), *Nucl. Instrum. Methods* **A601**, 294–316 (2009).
- A. Karle (IceCube collaboration), *Proc. 31th Int. Cosmic Ray Conf.* (Łódź, Poland, 7–15 July 2009), and references therein.
- S. Toscano, for the ANTARES Coll., *Proc. 31th Int. Cosmic Ray Conf.* (Łódź, Poland, 7–15 July 2009), **arXiv:0908.0864v1**.
- J. Ahrens *et al.*, *Astropart. Phys.* **20**, 507–532 (2004).
- S. Razzaque, P. Meszaros, & E. Waxman, *Phys. Rev.* **D68**, 083001 (2003).
- R. Engel, D. Seckel, & T. Stanev, *Phys. Rev.* **D64**, 093010 (2001).
- A. Achterberg, *et al.*, (IceCube collaboration), *Phys. Rev.* **D79**, 102005 (2009).
- E.V. Bugaev, *Nuovo Cimento* **C12**, 41 (1989).
- G. Barr, *et al.*, *Physical Review D*, **V70**, 023006 (2004).
- M. Honda, *et al.*, *Physical Review D*, **V70**, 043008 (2004).
- A. Achterberg, *et al.*, (IceCube collaboration), *Phys. Rev.* **D76**, 042008 (2007).
- M. Ackermann, *et al.*, (IceCube collaboration), *Astrophys. J.* **675**, 1014–1024 (2008).
- J. Braum *et al.*, *Astropart. Phys.* **29**, 299–305 (2008).
- L.A. Anchordoqui & T. Montaruli, *Ann. Rev. Nucl. Sci.* **60**, in press (2010),.
- Cryogenic Particle Detection*, ed. by C. Enss, (Springer-Verlag: Berlin, 2005).
- Proc. 13th Inter. Workshop on Low Temperature Detectors*, AIP Conference Proc. (2009); see also Proceedings of previous occurrences of this workshop.
- S.H. Moseley, J.C. Mather, & D. McCammon, *J. Appl. Phys.* **56**, 1257 (1984).
- J. Lindhard *et al.*, *Mat. Fys. Medd. K. Dan. Vidensk. Selsk.* **33**, 10 (1963).
- W. Blum, L. Rolandi, *Particle Detection with Drift Chambers*, Springer-Verlag (1994).
- R.S. Chandrasekharan, “Noble Gas Scintillation-Based Radiation Portal Monitor and Active Interrogation Systems,” *IEEE Nucl. Sci. Symposium Conference Record* (2006).
- C.M.B. Monteiro *et al.*, “Secondary scintillation yield in pure xenon,” *JINST* **2** P05001 (2007), doi 10.1088/1748-0221/2/05/P05001.
- W.H. Lippincott *et al.*, *Phys. Rev.* **C78**, 035801 (2008).
- C.J. Martoff *et al.*, Nucl. Instrum. Methods **A440**, 355 (2000).
- M. Schaumann, “The XENON 100 Dark Matter Experiment,” *10th Conf. on the Intersections of Part. & Nucl. Phys.*, (2009), to be published in AIP Conf. Proc.
- A. Bolotnikov and B. Ramsey, Nucl. Instrum. Methods **A496**, 360 (1997).
- E. Aprile *et al.*, *Phys. Rev.* **B76**, 014115 (2007).
- G. Heusser, *Ann. Rev. Nucl. and Part. Sci.* **45**, 543 (1995).
- P. Jagam and J.J. Simpson, Nucl. Instrum. Methods **A324**, 389 (1993).
- D.S. Leonard *et al.*, Nucl. Instrum. Methods **A591**, 490 (2008).
- M. Wojcik *et al.*, Nucl. Instrum. Methods **A449**, 158 (2000).
- National Council on Radiation Protection and Measurement, Report 94, Bethesda, MD (1987).
- M.S. Gordon *et al.*, *IEEE Trans.* **NS51**, 3427 (2004).

30. RADIOACTIVITY AND RADIATION PROTECTION

Revised September 2009 by S. Roesler and M. Silari (CERN).

30.1. Definitions [1,2]

30.1.1. Physical quantities :

• **Fluence, Φ** (unit: $1/\text{m}^2$): The fluence is the quotient of dN by da , where dN is the number of particles incident upon a small sphere of cross-sectional area da

$$\Phi = dN/da . \quad (30.1)$$

In dosimetric calculations, fluence is frequently expressed in terms of the lengths of the particle trajectories. It can be shown that the fluence, Φ , is given by

$$\Phi = dl/dV,$$

where dl is the sum of the particle trajectory lengths in the volume dV .

• **Absorbed dose, D** (unit: gray, $1 \text{ Gy}=1 \text{ J/kg}=100 \text{ rad}$): The absorbed dose is the energy imparted by ionizing radiation in a volume element of a specified material divided by the mass of this volume element.

• **Kerma, K** (unit: gray): Kerma is the sum of the initial kinetic energies of all charged particles liberated by indirectly ionizing radiation in a volume element of the specified material divided by the mass of this volume element.

• **Linear energy transfer, L or LET** (unit: J/m , often given in $\text{keV}/\mu\text{m}$): The linear energy transfer is the mean energy, dE , lost by a charged particle owing to collisions with electrons in traversing a distance dl in matter. *Low-LET radiation*: X-rays and gamma rays (accompanied by charged particles due to interactions with the surrounding medium) or light charged particles such as electrons that produce sparse ionizing events far apart at a molecular scale ($L < 10 \text{ keV}/\mu\text{m}$). *High-LET radiation*: neutrons and heavy charged particles that produce ionizing events densely spaced at a molecular scale ($L > 10 \text{ keV}/\mu\text{m}$).

• **Activity, A** (unit: becquerel, $1 \text{ Bq}=1/\text{s}=27 \text{ picocurie}$): Activity is the expectation value of the number of nuclear decays occurring in a given quantity of material per unit time.

30.1.2. Protection quantities :

Protection quantities are dose quantities developed for radiological protection that allow quantification of the extent of exposure of the human body to ionizing radiation from both whole and partial body external irradiation and from intakes of radionuclides.

• **Organ absorbed dose, D_T** (unit: gray): The mean absorbed dose in an organ or tissue T of mass m_T is defined as

$$D_T = \frac{1}{m_T} \int_{m_T} D dm .$$

• **Equivalent dose, H_T** (unit: sievert, $1 \text{ Sv}=100 \text{ rem}$): The equivalent dose H_T in an organ or tissue T is equal to the sum of the absorbed doses $D_{T,R}$ in the organ or tissue caused by different radiation types R weighted with so-called radiation weighting factors w_R :

$$H_T = \sum_R w_R \times D_{T,R} . \quad (30.2)$$

It expresses long-term risks (primarily cancer and leukemia) from low-level chronic exposure. The values for w_R recommended by ICRP [2] are given in Table 30.1.

• **Effective dose, E** (unit: sievert): The sum of the equivalent doses, weighted by the tissue weighting factors w_T ($\sum_T w_T = 1$) of several organs and tissues T of the body that are considered to be most sensitive [2], is called “effective dose”:

$$E = \sum_T w_T \times H_T . \quad (30.3)$$

Table 30.1: Radiation weighting factors, w_R .

Radiation type	w_R
Photons, electrons and muons	1
Neutrons, $E_n < 1 \text{ MeV}$	$2.5 + 18.2 \times \exp[-(\ln E_n)^2/6]$
$1 \text{ MeV} \leq E_n \leq 50 \text{ MeV}$	$5.0 + 17.0 \times \exp[-(\ln(2E_n))^2/6]$
$E_n > 50 \text{ MeV}$	$2.5 + 3.25 \times \exp[-(\ln(0.04E_n))^2/6]$
Protons and charged pions	2
Alpha particles, fission fragments, heavy ions	20

30.1.3. Operational quantities :

The body-related protection quantities, equivalent dose and effective dose, are not measurable in practice. Therefore, operational quantities are used for the assessment of effective dose or mean equivalent doses in tissues or organs. These quantities aim to provide a conservative estimate for the value of the protection quantity.

• **Ambient dose equivalent, $H^*(10)$** (unit: sievert): The dose equivalent at a point in a radiation field that would be produced by the corresponding expanded and aligned field in a 30 cm diameter sphere of unit density tissue (ICRU sphere) at a depth of 10 mm on the radius vector opposing the direction of the aligned field. Ambient dose equivalent is the operational quantity for *area monitoring*.

• **Personal dose equivalent, $H_p(d)$** (unit: sievert): The dose equivalent in ICRU tissue at an appropriate depth, d , below a specified point on the human body. The specified point is normally taken to be where the individual dosimeter is worn. For the assessment of effective dose, $H_p(10)$ with a depth $d = 10 \text{ mm}$ is chosen, and for the assessment of the dose to the skin and to the hands and feet the personal dose equivalent, $H_p(0.07)$, with a depth $d = 0.07 \text{ mm}$, is used. Personal dose equivalent is the operational quantity for *individual monitoring*.

30.2. Radiation levels [3]

• **Natural background radiation**: On a worldwide average, the annual whole-body dose equivalent due to all sources of natural background radiation ranges from 1.0 to 13 mSv (0.1-1.3 rem) with an annual average of 2.4 mSv [4]. In certain areas values up to 50 mSv (5 rem) have been measured. A large fraction (typically more than 50%) originate from inhaled natural radioactivity, mostly radon and radon daughters. The latter can vary by more than one order of magnitude: it is 0.1–0.2 mSv in open areas, 2 mSv on average in a house and more than 20 mSv in poorly ventilated mines.

• **Cosmic ray background radiation**: At sea level, the whole-body dose equivalent due to cosmic ray background radiation is dominated by muons; at higher altitudes also nucleons contribute. Dose equivalent rates range from less than 0.1 $\mu\text{Sv/h}$ at sea level to a few $\mu\text{Sv/h}$ at aircraft altitudes. Details on cosmic ray fluence levels are given in the Cosmic Rays section (Sec. 24 of this Review).

• **Fluence to deposit one Gy: Charged particles**: The fluence necessary to deposit a dose of one Gy (in units of cm^{-2}) is about $6.24 \times 10^9 / (dE/dx)$, where dE/dx (in units of $\text{MeV g}^{-1} \text{ cm}^2$) is the mean energy loss rate that may be obtained from Figs. 27.2 and 27.4 in Sec. 27 of this Review, and from <http://pdg.lbl.gov/AtomicNuclearProperties>. For example, it is approximately $3.5 \times 10^9 \text{ cm}^{-2}$ for minimum-ionizing singly-charged particles in carbon. *Photons*: This fluence is about $6.24 \times 10^9 / (Ef/\ell)$ for photons of energy E (in MeV), an attenuation length ℓ (in g cm^{-2}), and a fraction $f \lesssim 1$, expressing the fraction of the photon energy deposited in a small volume of thickness $\ll \ell$ but large enough to contain the secondary electrons. For example, it is approximately $2 \times 10^{11} \text{ cm}^{-2}$ for 1 MeV photons on carbon ($f \approx 1/2$).

30.3. Health effects of ionizing radiation

There are two types of health effects caused by radiation, deterministic and stochastic:

- **Tissue reactions** (also called non-stochastic effects or deterministic effects): injury to a population of cells which only occurs if a given threshold of absorbed dose is exceeded. The severity of the reaction increases with dose. The quantity in use for tissue reactions is the absorbed dose, D . When particles other than photons and electrons (low-LET radiation) are involved, a Relative Biological Effectiveness (RBE)-weighted dose may be used. The RBE of a given radiation is the reciprocal of the ratio of the absorbed dose of that radiation to the absorbed dose of a reference radiation (usually X-rays) required to produce the same degree of biological effect.

- **Stochastic effects:** malignant disease and heritable effects for which the probability of an effect occurring, but not its severity, is a function of dose without threshold.

- **Lethal dose:** The whole-body dose from penetrating ionizing radiation resulting in 50% mortality in 30 days (assuming no medical treatment) is 2.5–4.5 Gy (250–450 rad)[†], as measured internally on the body longitudinal center line. The surface dose varies due to variable body attenuation and may be a strong function of energy.

- **Cancer induction:** The cancer induction probability is about 5% per Sv on average for the entire population [2].

- **Recommended limits of effective dose to radiation workers** (whole-body dose): The ICRP recommendation is 20 mSv per year averaged over 5 years, with the provision that the dose should not exceed 50 mSv in any single year [2]. The limit in the EU-countries and Switzerland is 20 mSv per year, in the U.S. it is 50 mSv per year (5 rem per year). Many physics laboratories in the U.S. and elsewhere set lower limits.

30.4. Prompt neutrons at accelerators

Neutrons dominate the particle environment outside thick shielding (*e.g.*, > 1 m of concrete) for high energy (> a few hundred MeV) electron and hadron accelerators.

30.4.1. Electron accelerators :

At electron accelerators, neutrons are generated via photonuclear reactions from bremsstrahlung photons. In the photon energy range from threshold (few MeV) to about 30 MeV, neutron production is via the Giant Dipole Resonance (GDR) mechanism. The reaction consists in a collective excitation of the nucleus, in which neutrons and protons oscillate in the direction of the photon electric field. The oscillation is damped by friction in a few cycles, with the photon energy being transferred to the nucleus in a process similar to evaporation. Nucleons emitted in the dipolar interaction have an anisotropic angular distribution, with a maximum at 90°, while those leaving the nucleus as a result of evaporation are emitted isotropically with a Maxwellian energy distribution described as [5]:

$$\frac{dN}{dE_n} = \frac{E_n}{T^2} e^{-E_n/T}, \quad (30.4)$$

where T is a nuclear 'temperature' (in units of MeV) characteristic of the particular target nucleus and its excitation energy. For heavy nuclei the 'temperature' generally lies in the range of $T = 0.5$ – 1.0 MeV. For higher energy photons, the quasi-deuteron (between about 30 MeV and 250 MeV), delta resonance (250 MeV–1.2 GeV) and vector meson dominance ($\gtrsim 1.2$ GeV) mechanisms become important.

Neutron yields from semi-infinite targets per kW of electron beam power are plotted in Fig. 30.1 as a function of the electron beam energy [5].

Typical neutron energy spectra outside of concrete (80 cm thick, 2.35 g/cm³) and iron (40 cm thick) shields are shown in Fig. 30.2. In order to compare these spectra to those caused by proton beams (see below) the spectra are scaled by a factor of 100, which roughly corresponds to the difference in the high energy hadronic cross sections

[†] RBE-weighted when necessary

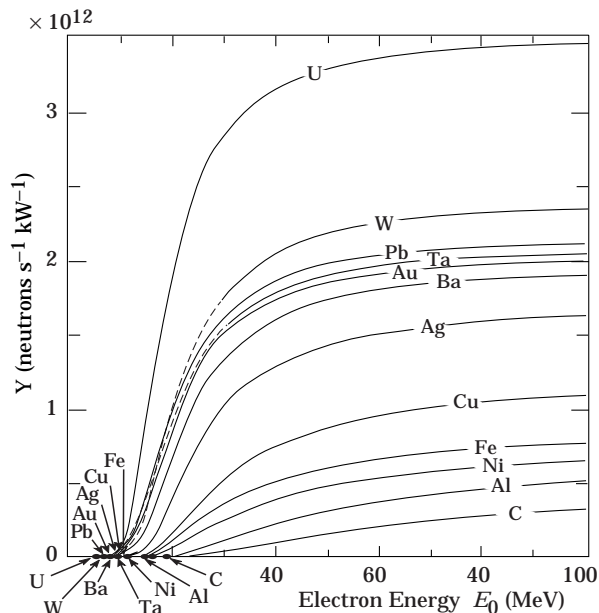


Figure 30.1: Neutron yields from semi-infinite targets per kW of electron beam power, as a function of the electron beam energy, disregarding target self-shielding [5].

for photons and hadrons (*e.g.*, the fine structure constant). The shape of these spectra are generally characterized by a low-energy peak at around 1 MeV (evaporation neutrons) and a high-energy shoulder at around 70–80 MeV. In case of concrete shielding, the spectrum also shows a pronounced peak at thermal neutron energies.

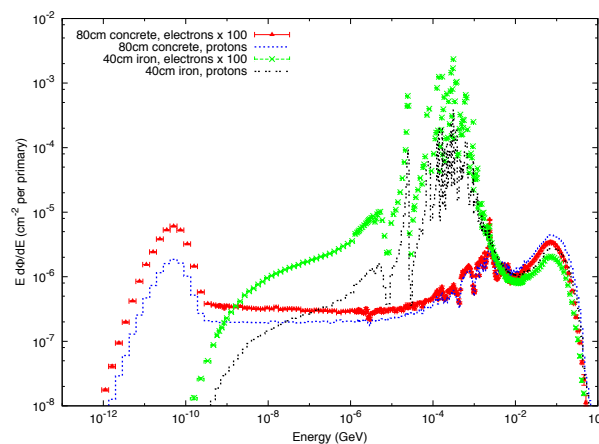


Figure 30.2: Neutron energy spectra calculated with the FLUKA code [6,7] from 25 GeV proton and electron beams on a thick copper target. Spectra are evaluated at 90° to the beam direction behind 80 cm of concrete or 40 cm of iron. All spectra are normalized per beam particle. In addition, spectra for electron beam are multiplied by a factor of 100. See full-color version on color pages at end of book.

30.4.2. Proton accelerators :

At proton accelerators, neutron yields emitted per incident proton by different target materials are roughly independent of proton energy between 20 MeV and 1 GeV, and are given by the ratio C:Al:Cu:Fe:Sn:Ta:Pb = 0.3 : 0.6 : 1.0 : 1.5 : 1.7 [8]. Above about 1 GeV, the neutron yield is proportional to E^m , where $0.80 \leq m \leq 0.85$ [9].

Typical neutron energy spectra outside of concrete and iron shielding are shown in Fig. 30.2. Here, the radiation fields are caused by a 25 GeV proton beam interacting with a thick copper target.

The comparison of these spectra with those for an electron beam of the same energy reflects the difference in the hadronic cross sections between photons and hadrons above a few 100 MeV. Differences are increasing towards lower energies because of different interaction mechanisms. Furthermore, the slight shift in energy above about 100 MeV follows from the fact that the energies of the interacting photons are lower than 25 GeV. Apart from this the shapes of the two spectra are similar.

The neutron-attenuation length is shown in Fig. 30.3 for concrete and mono-energetic broad-beam conditions. As can be seen in the figure it reaches a value of about 117 g/cm^2 above 200 MeV. As the cascade through thick shielding is carried by high-energy particles this value is equal to the equilibrium attenuation length at 90 degrees in concrete.

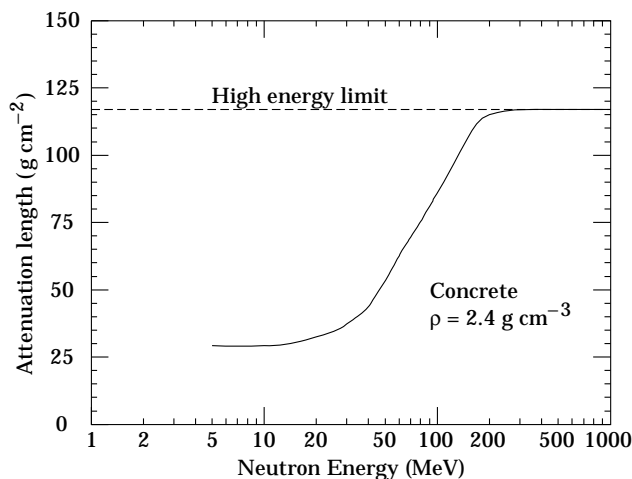


Figure 30.3: The variation of the attenuation length for mono-energetic neutrons in concrete as a function of neutron energy [8].

30.5. Photon sources

The dose equivalent rate in tissue (in mSv/h) from a gamma point source emitting one photon of energy E (in MeV) per second at a distance of 1 m is $4.6 \times 10^{-9} \mu_{en}/\rho E$, where μ_{en}/ρ is the mass energy absorption coefficient. The latter has a value of $0.029 \pm 0.004 \text{ cm}^2/\text{g}$ for photons in tissue over an energy range between 60 keV and 2 MeV (see Ref. 10 for tabulated values).

Similarly, the dose equivalent rate in tissue (in mSv/h) at the surface of a semi-infinite slab of uniformly activated material containing 1 Bq/g of a gamma emitter of energy E (in MeV) is $2.9 \times 10^{-4} R_{\mu} E$, where R_{μ} is the ratio of the mass energy absorption coefficients of the photons in tissue and in the material.

30.6. Dose conversion coefficients

Conversion coefficients from fluence to effective dose are given for anterior-posterior irradiation and various particles in Fig. 30.4 [11]. These coefficients can be used for converting particle fluence to dose for personnel protection purposes. For example, the effective dose from an anterior-posterior irradiation in a field of 1-MeV neutrons with a fluence of 1 neutron per cm^2 is about 290 pSv.

30.7. Accelerator-induced radioactivity

Typical medium- and long-lived activation products in metallic components of accelerators are ^{22}Na , ^{46}Sc , ^{48}V , ^{51}Cr , ^{54}Mn , ^{55}Fe , ^{59}Fe , ^{56}Co , ^{57}Co , ^{58}Co , ^{60}Co , ^{63}Ni and ^{65}Zn . Gamma-emitting nuclides dominate doses by external irradiation at longer decay times (more than one day) while at short decay times β^+ emitters are also important (through photons produced by β^+ annihilation). Due to their short range, β^- emitters are relevant, for example, only for dose to the skin and eyes or for doses due to inhalation or ingestion.

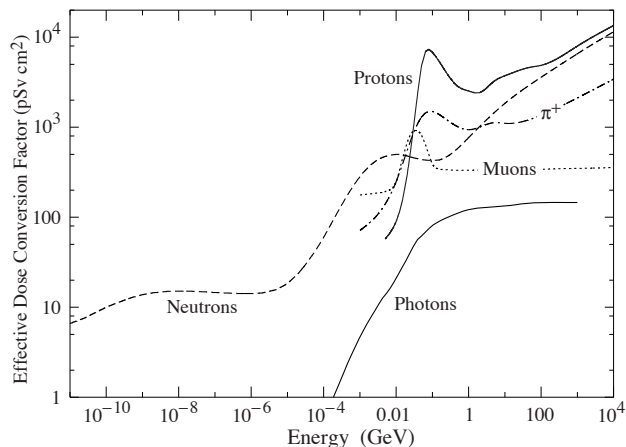


Figure 30.4: Fluence to effective dose conversion coefficients for anterior-posterior irradiation and various particles [11].

Fig. 30.5 and Fig. 30.6 show the contributions of gamma and β^+ emitters to the total dose rate at 12.4 cm distance to an activated copper sample [12]. Typically, dose rates at a certain decay time are mainly determined by radionuclides having a half-life of the order of the decay time. Extended irradiation periods might be an exception to this general rule as in this case the activity of long-lived nuclides can build up sufficiently so that it dominates that one of short-lived even at short cooling times.

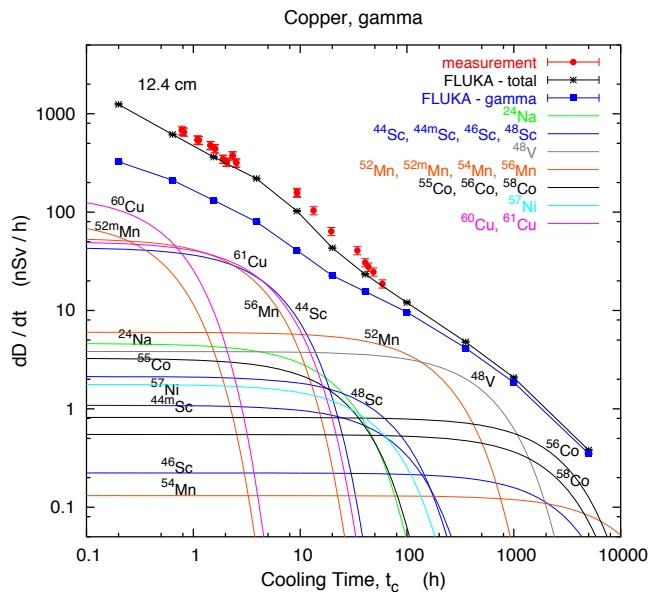


Figure 30.5: Contribution of individual gamma-emitting nuclides to the total dose rate at 12.4 cm distance to an activated copper sample [12]. See full-color version on color pages at end of book.

Activation in concrete is dominated by ^{24}Na (short decay times) and ^{22}Na (long decay times). Both nuclides can be produced either by low-energy neutron reactions on the sodium-component in the concrete or by spallation reactions on silicon and calcium. At long decay times nuclides of radiological interest in activated concrete can also be ^{60}Co , ^{152}Eu , ^{154}Eu and ^{134}Cs , all of which produced by (n,γ) -reactions with traces of natural cobalt, europium and cesium. Thus, such trace elements might be important even if their content in concrete is only a few parts per million or less by weight.

The explicit simulation of radionuclide production with general-purpose Monte Carlo codes has become the most commonly applied method to calculate induced radioactivity and its radiological

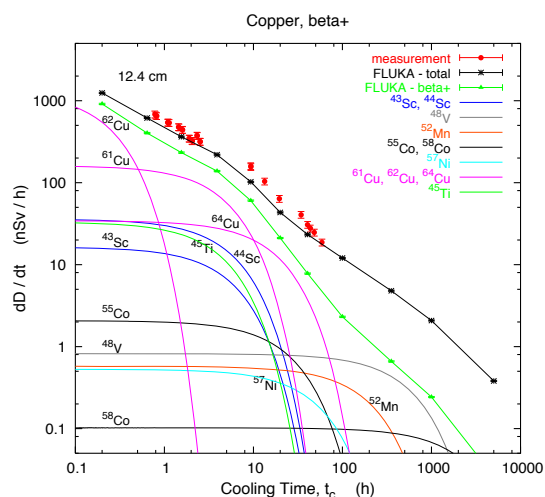


Figure 30.6: Contribution of individual positron-emitting nuclides to the total dose rate at 12.4 cm distance to an activated copper sample [12]. See full-color version on color pages at end of book.

consequences. Nevertheless, other more approximative approaches, such as “ ω -factors” [8], can still be useful for fast order-of-magnitude estimates. These ω -factors give the dose rate per unit star density (inelastic reactions above a certain energy threshold, e.g. 50 MeV) on contact to an extended, uniformly activated object after a 30-day irradiation and 1-day decay. The ω factor for steel or iron is $\approx 3 \times 10^{-12}$ (Sv cm³/star). This does not include possible contributions from thermal-neutron activation.

References:

1. International Commission on Radiation Units and Measurements, *Fundamental Quantities and Units for Ionizing Radiation*, ICRU Report 60 (1998).
2. ICRP Publication 103, *The 2007 Recommendations of the International Commission on Radiological Protection*, Annals of the ICRP, Elsevier (2007).
3. E. Pochin, *Nuclear Radiation: Risks and Benefits*, Clarendon Press, Oxford, 1983.
4. United Nations, *Report of the United Nations Scientific Committee on the Effect of Atomic Radiation*, General Assembly, Official Records A/63/46 (2008).
5. W.P. Swanson, *Radiological Safety Aspects of the Operation of Electron Linear Accelerators*, IAEA Technical Reports Series No. 188 (1979).
6. A. Ferrari *et al.*, FLUKA, A Multi-particle Transport Code (Program Version 2005), CERN-2005-010 (2005).
7. G. Battistoni *et al.*, The FLUKA code: Description and benchmarking, *Proceedings of the Hadronic Shower Simulation Workshop 2006*, Fermilab 6-8 September 2006, M. Albrow, R. Raja eds., *AIP Conference Proceeding 896*, p. 31-49, (2007).
8. R.H. Thomas and G.R. Stevenson, *Radiological Safety Aspects of the Operation of Proton Accelerators*, IAEA Technical Report Series No. 283 (1988).
9. T.A. Gabriel *et al.*, Nucl. Instrum. Methods **A338**, 336 (1994).
10. <http://physics.nist.gov/PhysRefData/XrayMassCoef/cover.html>.
11. M. Pelliccioni, Radiation Protection Dosimetry **88**, 279 (2000).
12. S. Roesler *et al.*, “Simulation of Remanent Dose Rates and Benchmark Measurements at the CERN-EU High Energy Reference Field Facility,” in *Proceedings of the Sixth International Meeting on Nuclear Applications of Accelerator Technology*, San Diego, CA, 1-5 June 2003, pp. 655-662 (2003).

31. COMMONLY USED RADIOACTIVE SOURCES

Table 31.1. Revised November 1993 by E. Browne (LBNL).

Nuclide	Half-life	Type of decay	Particle		Photon							
			Energy (MeV)	Emission prob.	Energy (MeV)	Emission prob.						
$^{22}_{11}\text{Na}$	2.603 y	β^+ , EC	0.545	90%	0.511 Annih. 1.275 100%							
$^{54}_{25}\text{Mn}$	0.855 y	EC			0.835 100% Cr K x rays 26%							
$^{55}_{26}\text{Fe}$	2.73 y	EC			Mn K x rays: 0.00590 24.4% 0.00649 2.86%							
$^{57}_{27}\text{Co}$	0.744 y	EC			0.014 9% 0.122 86% 0.136 11% Fe K x rays 58%							
$^{60}_{27}\text{Co}$	5.271 y	β^-	0.316	100%	1.173 100% 1.333 100%							
$^{68}_{32}\text{Ge}$	0.742 y	EC			Ga K x rays 44%							

	\rightarrow	$^{68}_{31}\text{Ga}$	β^+ , EC	1.899	90%	0.511 Annih. 1.077 3%						
$^{90}_{38}\text{Sr}$	28.5 y	β^-	0.546	100%								

	\rightarrow	$^{90}_{39}\text{Y}$	β^-	2.283	100%							
$^{106}_{44}\text{Ru}$	1.020 y	β^-	0.039	100%								

	\rightarrow	$^{106}_{45}\text{Rh}$	β^-	3.541	79%	0.512 21% 0.622 10%						
$^{109}_{48}\text{Cd}$	1.267 y	EC	0.063 e^- 0.084 e^- 0.087 e^-	41% 45% 9%	0.088 3.6% Ag K x rays 100%							
$^{113}_{50}\text{Sn}$	0.315 y	EC	0.364 e^- 0.388 e^-	29% 6%	0.392 65% In K x rays 97%							
$^{137}_{55}\text{Cs}$	30.2 y	β^-	0.514 1.176	94% 6%	0.662 85%							
$^{133}_{56}\text{Ba}$	10.54 y	EC	0.045 e^- 0.075 e^-	50% 6%	0.081 34% 0.356 62% Cs K x rays 121%							
$^{207}_{83}\text{Bi}$	31.8 y	EC	0.481 e^- 0.975 e^- 1.047 e^-	2% 7% 2%	0.569 98% 1.063 75% 1.770 7% Pb K x rays 78%							
$^{228}_{90}\text{Th}$	1.912 y	6α : $3\beta^-$:	5.341 to 8.785 0.334 to 2.246		0.239 44% 0.583 31% 2.614 36%							

	$(\rightarrow$	$^{224}_{88}\text{Ra}$	\rightarrow	$^{220}_{86}\text{Rn}$	\rightarrow	$^{216}_{84}\text{Po}$	\rightarrow	$^{212}_{82}\text{Pb}$	\rightarrow	$^{212}_{83}\text{Bi}$	\rightarrow	$^{212}_{84}\text{Po}$)
$^{241}_{95}\text{Am}$	432.7 y	α	5.443 5.486	13% 85%	0.060 36% Np L x rays 38%							
$^{241}\text{Am/Be}$	432.2 y	6×10^{-5} neutrons (4–8 MeV) and 4×10^{-5} γ 's (4.43 MeV) per Am decay										
$^{244}_{96}\text{Cm}$	18.11 y	α	5.763 5.805	24% 76%	Pu L x rays \sim 9%							
$^{252}_{98}\text{Cf}$	2.645 y	α (97%) Fission (3.1%)	6.076 6.118	15% 82%								

≈ 20 γ 's/fission; 80% < 1 MeV ≈ 4 neutrons/fission; $\langle E_n \rangle = 2.14$ MeV												

“Emission probability” is the probability per decay of a given emission; because of cascades these may total more than 100%. Only principal emissions are listed. EC means electron capture, and e^- means monoenergetic internal conversion (Auger) electron. The intensity of 0.511 MeV e^+e^- annihilation photons depends upon the number of stopped positrons. Endpoint β^\pm energies are listed. In some cases when energies are closely spaced, the γ -ray values are approximate weighted averages. Radiation from short-lived daughter isotopes is included where relevant.

Half-lives, energies, and intensities are from E. Browne and R.B. Firestone, *Table of Radioactive Isotopes* (John Wiley & Sons, New York, 1986), recent *Nuclear Data Sheets*, and *X-ray and Gamma-ray Standards for Detector Calibration*, IAEA-TECDOC-619 (1991).

Neutron data are from *Neutron Sources for Basic Physics and Applications* (Pergamon Press, 1983).

32. PROBABILITY

Revised September 2009 by G. Cowan (RHUL).

32.1. General [1–8]

An abstract definition of probability can be given by considering a set S , called the sample space, and possible subsets A, B, \dots , the interpretation of which is left open. The probability P is a real-valued function defined by the following axioms due to Kolmogorov [9]:

1. For every subset A in S , $P(A) \geq 0$;
2. For disjoint subsets (*i.e.*, $A \cap B = \emptyset$), $P(A \cup B) = P(A) + P(B)$;
3. $P(S) = 1$.

In addition, one defines the conditional probability $P(A|B)$ (read P of A given B) as

$$P(A|B) = \frac{P(A \cap B)}{P(B)}. \quad (32.1)$$

From this definition and using the fact that $A \cap B$ and $B \cap A$ are the same, one obtains *Bayes' theorem*,

$$P(A|B) = \frac{P(B|A)P(A)}{P(B)}. \quad (32.2)$$

From the three axioms of probability and the definition of conditional probability, one obtains the *law of total probability*,

$$P(B) = \sum_i P(B|A_i)P(A_i), \quad (32.3)$$

for any subset B and for disjoint A_i with $\cup_i A_i = S$. This can be combined with Bayes' theorem (Eq. (32.2)) to give

$$P(A|B) = \frac{P(B|A)P(A)}{\sum_i P(B|A_i)P(A_i)}, \quad (32.4)$$

where the subset A could, for example, be one of the A_i .

The most commonly used interpretation of the subsets of the sample space are outcomes of a repeatable experiment. The probability $P(A)$ is assigned a value equal to the limiting frequency of occurrence of A . This interpretation forms the basis of *frequentist statistics*.

The subsets of the sample space can also be interpreted as *hypotheses*, *i.e.*, statements that are either true or false, such as ‘The mass of the W boson lies between 80.3 and 80.5 GeV.’ In the frequency interpretation, such statements are either always or never true, *i.e.*, the corresponding probabilities would be 0 or 1. Using *subjective probability*, however, $P(A)$ is interpreted as the degree of belief that the hypothesis A is true. Subjective probability is used in *Bayesian* (as opposed to frequentist) statistics. Bayes' theorem can be written

$$P(\text{theory}|\text{data}) \propto P(\text{data}|\text{theory})P(\text{theory}), \quad (32.5)$$

where ‘theory’ represents some hypothesis and ‘data’ is the outcome of the experiment. Here $P(\text{theory})$ is the *prior* probability for the theory, which reflects the experimenter's degree of belief before carrying out the measurement, and $P(\text{data}|\text{theory})$ is the probability to have gotten the data actually obtained, given the theory, which is also called the *likelihood*.

Bayesian statistics provides no fundamental rule for obtaining the prior probability; this is necessarily subjective and may depend on previous measurements, theoretical prejudices, *etc.* Once this has been specified, however, Eq. (32.5) tells how the probability for the theory must be modified in the light of the new data to give the *posterior* probability, $P(\text{theory}|\text{data})$. As Eq. (32.5) is stated as a proportionality, the probability must be normalized by summing (or integrating) over all possible hypotheses.

32.2. Random variables

A *random variable* is a numerical characteristic assigned to an element of the sample space. In the frequency interpretation of probability, it corresponds to an outcome of a repeatable experiment. Let x be a possible outcome of an observation. If x can take on any value from a continuous range, we write $f(x;\theta)dx$ as the probability that the measurement's outcome lies between x and $x + dx$. The function $f(x;\theta)$ is called the *probability density function* (p.d.f.), which may depend on one or more parameters θ . If x can take on only discrete values (*e.g.*, the non-negative integers), then $f(x;\theta)$ is itself a probability.

The p.d.f. is always normalized to unit area (unit sum, if discrete). Both x and θ may have multiple components and are then often written as vectors. If θ is unknown, we may wish to estimate its value from a given set of measurements of x ; this is a central topic of *statistics* (see Sec. 33).

The *cumulative distribution function* $F(a)$ is the probability that $x \leq a$:

$$F(a) = \int_{-\infty}^a f(x) dx. \quad (32.6)$$

Here and below, if x is discrete-valued, the integral is replaced by a sum. The endpoint a is expressly included in the integral or sum. Then $0 \leq F(x) \leq 1$, $F(x)$ is nondecreasing, and $P(a < x \leq b) = F(b) - F(a)$. If x is discrete, $F(x)$ is flat except at allowed values of x , where it has discontinuous jumps equal to $f(x)$.

Any function of random variables is itself a random variable, with (in general) a different p.d.f. The *expectation value* of any function $u(x)$ is

$$E[u(x)] = \int_{-\infty}^{\infty} u(x) f(x) dx, \quad (32.7)$$

assuming the integral is finite. For $u(x)$ and $v(x)$, any two functions of x , $E[u+v] = E[u] + E[v]$. For c and k constants, $E[cu+k] = cE[u] + k$.

The n^{th} moment of a random variable is

$$\alpha_n \equiv E[x^n] = \int_{-\infty}^{\infty} x^n f(x) dx, \quad (32.8a)$$

and the n^{th} central moment of x (or moment about the mean, α_1) is

$$m_n \equiv E[(x - \alpha_1)^n] = \int_{-\infty}^{\infty} (x - \alpha_1)^n f(x) dx. \quad (32.8b)$$

The most commonly used moments are the mean μ and variance σ^2 :

$$\mu \equiv \alpha_1, \quad (32.9a)$$

$$\sigma^2 \equiv V[x] \equiv m_2 = \alpha_2 - \mu^2. \quad (32.9b)$$

The mean is the location of the ‘center of mass’ of the p.d.f., and the variance is a measure of the square of its width. Note that $V[cx+k] = c^2V[x]$. It is often convenient to use the *standard deviation* of x , σ , defined as the square root of the variance.

Any odd moment about the mean is a measure of the skewness of the p.d.f. The simplest of these is the dimensionless coefficient of skewness $\gamma_1 = m_3/\sigma^3$.

The fourth central moment m_4 provides a convenient measure of the tails of a distribution. For the Gaussian distribution (see Sec. 32.4), one has $m_4 = 3\sigma^4$. The *kurtosis* is defined as $\gamma_2 = m_4/\sigma^4 - 3$, *i.e.*, it is zero for a Gaussian, positive for a *leptokurtic* distribution with longer tails, and negative for a *platykurtic* distribution with tails that die off more quickly than those of a Gaussian.

Besides the mean, another useful indicator of the ‘middle’ of the probability distribution is the *median*, x_{med} , defined by $F(x_{\text{med}}) = 1/2$, *i.e.*, half the probability lies above and half lies below x_{med} . (More rigorously, x_{med} is a median if $P(x \geq x_{\text{med}}) \geq 1/2$ and $P(x \leq x_{\text{med}}) \geq 1/2$. If only one value exists, it is called ‘the median.’)

Let x and y be two random variables with a *joint* p.d.f. $f(x,y)$. The *marginal* p.d.f. of x (the distribution of x with y unobserved) is

$$f_1(x) = \int_{-\infty}^{\infty} f(x,y) dy, \quad (32.10)$$

and similarly for the marginal p.d.f. $f_2(y)$. The *conditional* p.d.f. of y given fixed x (with $f_1(x) \neq 0$) is defined by $f_3(y|x) = f(x, y)/f_1(x)$, and similarly $f_4(x|y) = f(x, y)/f_2(y)$. From these, we immediately obtain Bayes' theorem (see Eqs. (32.2) and (32.4)),

$$f_4(x|y) = \frac{f_3(y|x)f_1(x)}{f_2(y)} = \frac{f_3(y|x)f_1(x)}{\int f_3(y|x')f_1(x') dx'} . \quad (32.11)$$

The mean of x is

$$\mu_x = \int_{-\infty}^{\infty} \int_{-\infty}^{\infty} x f(x, y) dx dy = \int_{-\infty}^{\infty} x f_1(x) dx , \quad (32.12)$$

and similarly for y . The *covariance* of x and y is

$$\text{cov}[x, y] = E[(x - \mu_x)(y - \mu_y)] = E[xy] - \mu_x \mu_y . \quad (32.13)$$

A dimensionless measure of the covariance of x and y is given by the *correlation coefficient*,

$$\rho_{xy} = \text{cov}[x, y] / \sigma_x \sigma_y , \quad (32.14)$$

where σ_x and σ_y are the standard deviations of x and y . It can be shown that $-1 \leq \rho_{xy} \leq 1$.

Two random variables x and y are *independent* if and only if

$$f(x, y) = f_1(x)f_2(y) . \quad (32.15)$$

If x and y are independent, then $\rho_{xy} = 0$; the converse is not necessarily true. If x and y are independent, $E[u(x)v(y)] = E[u(x)]E[v(y)]$, and $V[x + y] = V[x] + V[y]$; otherwise, $V[x + y] = V[x] + V[y] + 2\text{cov}[x, y]$, and $E[uv]$ does not necessarily factorize.

Consider a set of n continuous random variables $\mathbf{x} = (x_1, \dots, x_n)$ with joint p.d.f. $f(\mathbf{x})$, and a set of n new variables $\mathbf{y} = (y_1, \dots, y_n)$, related to \mathbf{x} by means of a function $\mathbf{y}(\mathbf{x})$ that is one-to-one, *i.e.*, the inverse $\mathbf{x}(\mathbf{y})$ exists. The joint p.d.f. for \mathbf{y} is given by

$$g(\mathbf{y}) = f(\mathbf{x}(\mathbf{y}))|J| , \quad (32.16)$$

where $|J|$ is the absolute value of the determinant of the square matrix $J_{ij} = \partial x_i / \partial y_j$ (the Jacobian determinant). If the transformation from \mathbf{x} to \mathbf{y} is not one-to-one, the \mathbf{x} -space must be broken in to regions where the function $\mathbf{y}(\mathbf{x})$ can be inverted, and the contributions to $g(\mathbf{y})$ from each region summed.

Given a set of functions $\mathbf{y} = (y_1, \dots, y_m)$ with $m < n$, one can construct $n - m$ additional independent functions, apply the procedure above, then integrate the resulting $g(\mathbf{y})$ over the unwanted y_i to find the marginal distribution of those of interest.

For a one-to-one transformation of discrete random variables, simply substitute; no Jacobian is necessary because now f is a probability rather than a probability density. If the transformation is not one-to-one, then sum the probabilities for all values of the original variable that contribute to a given value of the transformed variable. If f depends on a set of parameters $\boldsymbol{\theta}$, a change to a different parameter set $\boldsymbol{\eta}(\boldsymbol{\theta})$ is made by simple substitution; no Jacobian is used.

32.3. Characteristic functions

The characteristic function $\phi(u)$ associated with the p.d.f. $f(x)$ is essentially its Fourier transform, or the expectation value of e^{iux} :

$$\phi(u) = E[e^{iux}] = \int_{-\infty}^{\infty} e^{iux} f(x) dx . \quad (32.17)$$

Once $\phi(u)$ is specified, the p.d.f. $f(x)$ is uniquely determined and vice versa; knowing one is equivalent to the other. Characteristic functions are useful in deriving a number of important results about moments and sums of random variables.

It follows from Eqs. (32.8a) and (32.17) that the n^{th} moment of a random variable x that follows $f(x)$ is given by

$$i^{-n} \left. \frac{d^n \phi}{du^n} \right|_{u=0} = \int_{-\infty}^{\infty} x^n f(x) dx = \alpha_n . \quad (32.18)$$

Thus it is often easy to calculate all the moments of a distribution defined by $\phi(u)$, even when $f(x)$ cannot be written down explicitly.

If the p.d.f.s $f_1(x)$ and $f_2(y)$ for independent random variables x and y have characteristic functions $\phi_1(u)$ and $\phi_2(u)$, then the characteristic function of the weighted sum $ax + by$ is $\phi_1(au)\phi_2(bu)$. The additional rules for several important distributions (*e.g.*, that the sum of two Gaussian distributed variables also follows a Gaussian distribution) easily follow from this observation.

Let the (partial) characteristic function corresponding to the conditional p.d.f. $f_2(x|z)$ be $\phi_2(u|z)$, and the p.d.f. of z be $f_1(z)$. The characteristic function after integration over the conditional value is

$$\phi(u) = \int \phi_2(u|z)f_1(z) dz . \quad (32.19)$$

Suppose we can write ϕ_2 in the form

$$\phi_2(u|z) = A(u)e^{ig(u)z} . \quad (32.20)$$

Then

$$\phi(u) = A(u)\phi_1(g(u)) . \quad (32.21)$$

The cumulants (semi-invariants) κ_n are defined by

$$\phi(u) = \exp \left[\sum_{n=1}^{\infty} \frac{\kappa_n}{n!} (iu)^n \right] = \exp \left(i\kappa_1 u - \frac{1}{2}\kappa_2 u^2 + \dots \right) . \quad (32.22)$$

The values κ_n are related to the moments α_n and m_n . The first few relations are

$$\begin{aligned} \kappa_1 &= \alpha_1 (= \mu, \text{ the mean}) \\ \kappa_2 &= m_2 = \alpha_2 - \alpha_1^2 (= \sigma^2, \text{ the variance}) \\ \kappa_3 &= m_3 = \alpha_3 - 3\alpha_1\alpha_2 + 2\alpha_1^3 . \end{aligned} \quad (32.23)$$

32.4. Some probability distributions

Table 32.1 gives a number of common probability density functions and corresponding characteristic functions, means, and variances. Further information may be found in Refs. [1–8], [10], and [11], which has particularly detailed tables. Monte Carlo techniques for generating each of them may be found in our Sec. 34.4 and in Ref. 10. We comment below on all except the trivial uniform distribution.

32.4.1. Binomial distribution :

A random process with exactly two possible outcomes which occur with fixed probabilities is called a *Bernoulli* process. If the probability of obtaining a certain outcome (a “success”) in an individual trial is p , then the probability of obtaining exactly r successes ($r = 0, 1, 2, \dots, N$) in N independent trials, without regard to the order of the successes and failures, is given by the binomial distribution $f(r; N, p)$ in Table 32.1. If r and s are binomially distributed with parameters (N_r, p) and (N_s, p) , then $t = r + s$ follows a binomial distribution with parameters $(N_r + N_s, p)$.

32.4.2. Poisson distribution :

The Poisson distribution $f(n; \nu)$ gives the probability of finding exactly n events in a given interval of x (*e.g.*, space or time) when the events occur independently of one another and of x at an average rate of ν per the given interval. The variance σ^2 equals ν . It is the limiting case $p \rightarrow 0, N \rightarrow \infty, Np = \nu$ of the binomial distribution. The Poisson distribution approaches the Gaussian distribution for large ν .

For example, a large number of radioactive nuclei of a given type will result in a certain number of decays in a fixed time interval. If this interval is small compared to the mean lifetime, then the probability for a given nucleus to decay is small, and thus the number of decays in the time interval is well modeled as a Poisson variable.

Table 32.1. Some common probability density functions, with corresponding characteristic functions and means and variances. In the Table, $\Gamma(k)$ is the gamma function, equal to $(k - 1)!$ when k is an integer; ${}_1F_1$ is the confluent hypergeometric function of the 1st kind [11].

Distribution	Probability density function f (variable; parameters)	Characteristic function $\phi(u)$	Mean	Variance σ^2
Uniform	$f(x; a, b) = \begin{cases} 1/(b - a) & a \leq x \leq b \\ 0 & \text{otherwise} \end{cases}$	$\frac{e^{ibu} - e^{iau}}{(b - a)iu}$	$\frac{a + b}{2}$	$\frac{(b - a)^2}{12}$
Binomial	$f(r; N, p) = \frac{N!}{r!(N - r)!} p^r q^{N-r}$ $r = 0, 1, 2, \dots, N; \quad 0 \leq p \leq 1; \quad q = 1 - p$	$(q + pe^{iu})^N$	Np	Npq
Poisson	$f(n; \nu) = \frac{\nu^n e^{-\nu}}{n!}; \quad n = 0, 1, 2, \dots; \quad \nu > 0$	$\exp[\nu(e^{iu} - 1)]$	ν	ν
Normal (Gaussian)	$f(x; \mu, \sigma^2) = \frac{1}{\sigma\sqrt{2\pi}} \exp(-(x - \mu)^2/2\sigma^2)$ $-\infty < x < \infty; \quad -\infty < \mu < \infty; \quad \sigma > 0$	$\exp(i\mu u - \frac{1}{2}\sigma^2 u^2)$	μ	σ^2
Multivariate Gaussian	$f(\mathbf{x}; \boldsymbol{\mu}, V) = \frac{1}{(2\pi)^n \sqrt{ V }}$ $\times \exp[-\frac{1}{2}(\mathbf{x} - \boldsymbol{\mu})^T V^{-1}(\mathbf{x} - \boldsymbol{\mu})]$ $-\infty < x_j < \infty; \quad -\infty < \mu_j < \infty; \quad V > 0$	$\exp[i\boldsymbol{\mu} \cdot \mathbf{u} - \frac{1}{2}\mathbf{u}^T V \mathbf{u}]$	$\boldsymbol{\mu}$	V_{jk}
χ^2	$f(z; n) = \frac{z^{n/2-1} e^{-z/2}}{2^{n/2} \Gamma(n/2)}; \quad z \geq 0$	$(1 - 2iu)^{-n/2}$	n	$2n$
Student's t	$f(t; n) = \frac{1}{\sqrt{n\pi}} \frac{\Gamma[(n+1)/2]}{\Gamma(n/2)} \left(1 + \frac{t^2}{n}\right)^{-(n+1)/2}$ $-\infty < t < \infty; \quad n$ not required to be integer	—	0 for $n > 1$	$n/(n - 2)$ for $n > 2$
Gamma	$f(x; \lambda, k) = \frac{x^{k-1} \lambda^k e^{-\lambda x}}{\Gamma(k)}; \quad 0 \leq x < \infty;$ k not required to be integer	$(1 - iu/\lambda)^{-k}$	k/λ	k/λ^2
Beta	$f(x; \alpha, \beta) = \frac{\Gamma(\alpha + \beta)}{\Gamma(\alpha)\Gamma(\beta)} x^{\alpha-1} (1 - x)^{\beta-1}$ $0 \leq x \leq 1$	${}_1F_1(\alpha; \alpha + \beta; iu)$	$\frac{\alpha}{\alpha + \beta}$	$\frac{\alpha\beta}{(\alpha + \beta)^2(\alpha + \beta + 1)}$

32.4.3. Normal or Gaussian distribution :

The normal (or Gaussian) probability density function $f(x; \mu, \sigma^2)$ given in Table 32.1 has mean $E[x] = \mu$ and variance $V[x] = \sigma^2$. Comparison of the characteristic function $\phi(u)$ given in Table 32.1 with Eq. (32.22) shows that all cumulants κ_n beyond κ_2 vanish; this is a unique property of the Gaussian distribution. Some other properties are:

$P(x \text{ in range } \mu \pm \sigma) = 0.6827,$
 $P(x \text{ in range } \mu \pm 0.6745\sigma) = 0.5,$
 $E[|x - \mu|] = \sqrt{2/\pi}\sigma = 0.7979\sigma,$
 half-width at half maximum = $\sqrt{2 \ln 2}\sigma = 1.177\sigma.$

For a Gaussian with $\mu = 0$ and $\sigma^2 = 1$ (the *standard* Gaussian), the cumulative distribution, Eq. (32.6), is related to the error function $\text{erf}(y)$ by

$$F(x; 0, 1) = \frac{1}{2} \left[1 + \text{erf}(x/\sqrt{2}) \right]. \quad (32.24)$$

The error function and standard Gaussian are tabulated in many references (e.g., Ref. [11]) and are available in software packages such as ROOT [12] and CERNLIB [13]. For a mean μ and variance σ^2 , replace x by $(x - \mu)/\sigma$. The probability of x in a given range can be calculated with Eq. (33.53).

For x and y independent and normally distributed, $z = ax + by$ follows $f(z; a\mu_x + b\mu_y, a^2\sigma_x^2 + b^2\sigma_y^2)$; that is, the weighted means and variances add.

The Gaussian derives its importance in large part from the *central limit theorem*:

If independent random variables x_1, \dots, x_n are distributed according to any p.d.f. with finite mean and variance, then the sum $y = \sum_{i=1}^n x_i$ will have a p.d.f. that approaches a Gaussian for large n . If the p.d.f.s of the x_i are not identical, the theorem still holds under somewhat more restrictive conditions. The mean and variance are given by the sums of corresponding terms from the individual x_i . Therefore, the sum of a large number of fluctuations x_i will be distributed as a Gaussian, even if the x_i themselves are not.

(Note that the *product* of a large number of random variables is not Gaussian, but its logarithm is. The p.d.f. of the product is *log-normal*. See Ref. [8] for details.)

For a set of n Gaussian random variables \mathbf{x} with means $\boldsymbol{\mu}$ and covariances $V_{ij} = \text{cov}[x_i, x_j]$, the p.d.f. for the one-dimensional Gaussian is generalized to

$$f(\mathbf{x}; \boldsymbol{\mu}, V) = \frac{1}{(2\pi)^n \sqrt{|V|}} \exp \left[-\frac{1}{2}(\mathbf{x} - \boldsymbol{\mu})^T V^{-1}(\mathbf{x} - \boldsymbol{\mu}) \right], \quad (32.25)$$

where the determinant $|V|$ must be greater than 0. For diagonal V (independent variables), $f(\mathbf{x}; \boldsymbol{\mu}, V)$ is the product of the p.d.f.s of n Gaussian distributions.

For $n = 2$, $f(\mathbf{x}; \boldsymbol{\mu}, V)$ is

$$f(x_1, x_2; \mu_1, \mu_2, \sigma_1, \sigma_2, \rho) = \frac{1}{2\pi\sigma_1\sigma_2\sqrt{1-\rho^2}} \times \exp \left\{ \frac{-1}{2(1-\rho^2)} \left[\frac{(x_1 - \mu_1)^2}{\sigma_1^2} - \frac{2\rho(x_1 - \mu_1)(x_2 - \mu_2)}{\sigma_1\sigma_2} + \frac{(x_2 - \mu_2)^2}{\sigma_2^2} \right] \right\}. \quad (32.26)$$

The characteristic function for the multivariate Gaussian is

$$\phi(\mathbf{u}; \boldsymbol{\mu}, V) = \exp \left[i\boldsymbol{\mu} \cdot \mathbf{u} - \frac{1}{2}\mathbf{u}^T V \mathbf{u} \right]. \quad (32.27)$$

If the components of \mathbf{x} are independent, then Eq. (32.27) is the product of the c.f.s of n Gaussians.

The marginal distribution of any x_i is a Gaussian with mean μ_i and variance V_{ii} . V is $n \times n$, symmetric, and positive definite. Therefore, for any vector \mathbf{X} , the quadratic form $\mathbf{X}^T V^{-1} \mathbf{X} = C$, where C is any positive number, traces an n -dimensional ellipsoid as \mathbf{X} varies. If $X_i = x_i - \mu_i$, then C is a random variable obeying the χ^2 distribution with n degrees of freedom, discussed in the following section. The probability that \mathbf{X} corresponding to a set of Gaussian random variables x_i lies outside the ellipsoid characterized by a given value of C ($= \chi^2$) is given by $1 - F_{\chi^2}(C; n)$, where F_{χ^2} is the cumulative χ^2 distribution. This may be read from Fig. 33.1. For example, the “ s -standard-deviation ellipsoid” occurs at $C = s^2$. For the two-variable case ($n = 2$), the point \mathbf{X} lies outside the one-standard-deviation ellipsoid with 61% probability. The use of these ellipsoids as indicators of probable error is described in Sec. 33.3.2.4; the validity of those indicators assumes that $\boldsymbol{\mu}$ and V are correct.

32.4.4. χ^2 distribution :

If x_1, \dots, x_n are independent Gaussian random variables, the sum $z = \sum_{i=1}^n (x_i - \mu_i)^2 / \sigma_i^2$ follows the χ^2 p.d.f. with n degrees of freedom, which we denote by $\chi^2(n)$. More generally, for n correlated Gaussian variables as components of a vector \mathbf{X} with covariance matrix V , $z = \mathbf{X}^T V^{-1} \mathbf{X}$ follows $\chi^2(n)$ as in the previous section. For a set of z_i , each of which follows $\chi^2(n_i)$, $\sum z_i$ follows $\chi^2(\sum n_i)$. For large n , the χ^2 p.d.f. approaches a Gaussian with a mean and variance give by $\mu = n$ and $\sigma^2 = 2n$, respectively (here the formulae for μ and σ^2 are valid for all n).

The χ^2 p.d.f. is often used in evaluating the level of compatibility between observed data and a hypothesis for the p.d.f. that the data might follow. This is discussed further in Sec. 33.2.2 on tests of goodness-of-fit.

32.4.5. Student's t distribution :

Suppose that x and x_1, \dots, x_n are independent and Gaussian distributed with mean 0 and variance 1. We then define

$$z = \sum_{i=1}^n x_i^2 \quad \text{and} \quad t = \frac{x}{\sqrt{z/n}}. \quad (32.28)$$

The variable z thus follows a $\chi^2(n)$ distribution. Then t is distributed according to Student's t distribution with n degrees of freedom, $f(t; n)$, given in Table 32.1.

The Student's t distribution resembles a Gaussian but has wider tails. As $n \rightarrow \infty$, the distribution approaches a Gaussian. If $n = 1$, it is a *Cauchy* or *Breit-Wigner* distribution. The mean is finite only for $n > 1$ and the variance is finite only for $n > 2$, so the central limit theorem is not applicable to sums of random variables following the t distribution for $n = 1$ or 2.

As an example, consider the *sample mean* $\bar{x} = \sum x_i / n$ and the *sample variance* $s^2 = \sum (x_i - \bar{x})^2 / (n - 1)$ for normally distributed x_i with unknown mean μ and variance σ^2 . The sample mean has a Gaussian distribution with a variance σ^2 / n , so the variable $(\bar{x} - \mu) / \sqrt{\sigma^2 / n}$ is normal with mean 0 and variance 1. The quantity $(n - 1)s^2 / \sigma^2$ is independent of this and follows $\chi^2(n - 1)$. The ratio

$$t = \frac{(\bar{x} - \mu) / \sqrt{\sigma^2 / n}}{\sqrt{(n - 1)s^2 / \sigma^2 / (n - 1)}} = \frac{\bar{x} - \mu}{\sqrt{s^2 / n}} \quad (32.29)$$

is distributed as $f(t; n - 1)$. The unknown variance σ^2 cancels, and t can be used to test the hypothesis that the true mean is some particular value μ .

In Table 32.1, n in $f(t; n)$ is not required to be an integer. A Student's t distribution with non-integral $n > 0$ is useful in certain applications.

32.4.6. Gamma distribution :

For a process that generates events as a function of x (e.g., space or time) according to a Poisson distribution, the distance in x from an arbitrary starting point (which may be some particular event) to the k^{th} event follows a *gamma* distribution, $f(x; \lambda, k)$. The Poisson parameter μ is λ per unit x . The special case $k = 1$ (i.e., $f(x; \lambda, 1) = \lambda e^{-\lambda x}$) is called the *exponential* distribution. A sum of k' exponential random variables x_i is distributed as $f(\sum x_i; \lambda, k')$.

The parameter k is not required to be an integer. For $\lambda = 1/2$ and $k = n/2$, the gamma distribution reduces to the $\chi^2(n)$ distribution.

32.4.7. Beta distribution :

The beta distribution describes a continuous random variable x in the interval $[0, 1]$; this can easily be generalized by scaling and translation to have arbitrary endpoints. In Bayesian inference about the parameter p of a binomial process, if the prior p.d.f. is a beta distribution $f(p; \alpha, \beta)$ then the observation of r successes out of N trials gives a posterior beta distribution $f(p; r + \alpha, N - r + \beta)$ (Bayesian methods are discussed further in Sec. 33). The uniform distribution is a beta distribution with $\alpha = \beta = 1$.

References:

1. H. Cramér, *Mathematical Methods of Statistics*, (Princeton Univ. Press, New Jersey, 1958).
2. A. Stuart and J.K. Ord, *Kendall's Advanced Theory of Statistics*, Vol. 1 *Distribution Theory* 6th Ed., (Halsted Press, New York, 1994), and earlier editions by Kendall and Stuart.
3. F.E. James, *Statistical Methods in Experimental Physics*, 2nd ed., (World Scientific, Singapore, 2006).
4. L. Lyons, *Statistics for Nuclear and Particle Physicists*, (Cambridge University Press, New York, 1986).
5. B.R. Roe, *Probability and Statistics in Experimental Physics*, 2nd Ed., (Springer, New York, 2001).
6. R.J. Barlow, *Statistics: A Guide to the Use of Statistical Methods in the Physical Sciences*, (John Wiley, New York, 1989).
7. S. Brandt, *Data Analysis*, 3rd Ed., (Springer, New York, 1999).
8. G. Cowan, *Statistical Data Analysis*, (Oxford University Press, Oxford, 1998).
9. A.N. Kolmogorov, *Grundbegriffe der Wahrscheinlichkeitsrechnung*, (Springer, Berlin 1933); *Foundations of the Theory of Probability*, 2nd Ed., (Chelsea, New York 1956).
10. Ch. Walck, *Hand-book on Statistical Distributions for Experimentalists*, University of Stockholm Internal Report SUF-PFY/96-01, available from www.physto.se/~walck.
11. M. Abramowitz and I. Stegun, eds., *Handbook of Mathematical Functions*, (Dover, New York, 1972).
12. Rene Brun and Fons Rademakers, Nucl. Inst. Meth. A **389**, 81 (1997); see also root.cern.ch.
13. The CERN Program Library (CERNLIB); see cernlib.web.cern.ch/cernlib.

33. STATISTICS

Revised September 2009 by G. Cowan (RHUL).

This chapter gives an overview of statistical methods used in high-energy physics. In statistics, we are interested in using a given sample of data to make inferences about a probabilistic model, *e.g.*, to assess the model's validity or to determine the values of its parameters. There are two main approaches to statistical inference, which we may call frequentist and Bayesian. In frequentist statistics, probability is interpreted as the frequency of the outcome of a repeatable experiment. The most important tools in this framework are parameter estimation, covered in Section 33.1, and statistical tests, discussed in Section 33.2. Frequentist confidence intervals, which are constructed so as to cover the true value of a parameter with a specified probability, are treated in Section 33.3.2. Note that in frequentist statistics one does not define a probability for a hypothesis or for a parameter.

Frequentist statistics provides the usual tools for reporting the outcome of an experiment objectively, without needing to incorporate prior beliefs concerning the parameter being measured or the theory being tested. As such, they are used for reporting most measurements and their statistical uncertainties in high-energy physics.

In Bayesian statistics, the interpretation of probability is more general and includes *degree of belief* (called subjective probability). One can then speak of a probability density function (p.d.f.) for a parameter, which expresses one's state of knowledge about where its true value lies. Bayesian methods allow for a natural way to input additional information, such as physical boundaries and subjective information; in fact they *require* the *prior* p.d.f. as input for the parameters, *i.e.*, the degree of belief about the parameters' values before carrying out the measurement. Using Bayes' theorem Eq. (32.4), the prior degree of belief is updated by the data from the experiment. Bayesian methods for interval estimation are discussed in Sections 33.3.1 and 33.3.2.6

Bayesian techniques are often used to treat systematic uncertainties, where the author's beliefs about, say, the accuracy of the measuring device may enter. Bayesian statistics also provides a useful framework for discussing the validity of different theoretical interpretations of the data. This aspect of a measurement, however, will usually be treated separately from the reporting of the result.

For many inference problems, the frequentist and Bayesian approaches give similar numerical answers, even though they are based on fundamentally different interpretations of probability. For small data samples, however, and for measurements of a parameter near a physical boundary, the different approaches may yield different results, so we are forced to make a choice. For a discussion of Bayesian vs. non-Bayesian methods, see References written by a statistician[1], by a physicist[2], or the more detailed comparison in Ref. [3].

Following common usage in physics, the word "error" is often used in this chapter to mean "uncertainty." More specifically it can indicate the size of an interval as in "the standard error" or "error propagation," where the term refers to the standard deviation of an estimator.

33.1. Parameter estimation

Here we review *point estimation* of parameters, first with an overview of the frequentist approach and its two most important methods, maximum likelihood and least squares, treated in Sections 33.1.2 and 33.1.3. The Bayesian approach is outlined in Sec. 33.1.4.

An *estimator* $\hat{\theta}$ (written with a hat) is a function of the data whose value, the *estimate*, is intended as a meaningful guess for the value of the parameter θ . There is no fundamental rule dictating how an estimator must be constructed. One tries, therefore, to choose that estimator which has the best properties. The most important of these are (a) *consistency*, (b) *bias*, (c) *efficiency*, and (d) *robustness*.

(a) An estimator is said to be *consistent* if the estimate $\hat{\theta}$ converges to the true value θ as the amount of data increases. This property is so important that it is possessed by all commonly used estimators.

(b) The *bias*, $b = E[\hat{\theta}] - \theta$, is the difference between the expectation value of the estimator and the true value of the parameter. The expectation value is taken over a hypothetical set of similar

experiments in which $\hat{\theta}$ is constructed in the same way. When $b = 0$, the estimator is said to be unbiased. The bias depends on the chosen metric, *i.e.*, if θ is an unbiased estimator of θ , then $\hat{\theta}^2$ is not in general an unbiased estimator for θ^2 . If we have an estimate \hat{b} for the bias, we can subtract it from $\hat{\theta}$ to obtain a new $\hat{\theta}' = \hat{\theta} - \hat{b}$. The estimate \hat{b} may, however, be subject to statistical or systematic uncertainties that are larger than the bias itself, so that the new $\hat{\theta}'$ may not be better than the original.

(c) *Efficiency* is the inverse of the ratio of the variance $V[\hat{\theta}]$ to the minimum possible variance for any estimator of θ . Under rather general conditions, the minimum variance is given by the Rao-Cramér-Frechet bound,

$$\sigma_{\min}^2 = \left(1 + \frac{\partial b}{\partial \theta}\right)^2 / I(\theta), \quad (33.1)$$

where

$$I(\theta) = E \left[\left(\frac{\partial}{\partial \theta} \sum_i \ln f(x_i; \theta) \right)^2 \right] \quad (33.2)$$

is the *Fisher information*. The sum is over all data, assumed independent, and distributed according to the p.d.f. $f(x; \theta)$, b is the bias, if any, and the allowed range of x must not depend on θ .

The *mean-squared error*,

$$\text{MSE} = E[(\hat{\theta} - \theta)^2] = V[\hat{\theta}] + b^2, \quad (33.3)$$

is a measure of an estimator's quality which combines the uncertainties due to bias and variance.

(d) *Robustness* is the property of being insensitive to departures from assumptions in the p.d.f., *e.g.*, owing to uncertainties in the distribution's tails.

Simultaneously optimizing for all the measures of estimator quality described above can lead to conflicting requirements. For example, there is in general a trade-off between bias and variance. For some common estimators, the properties above are known exactly. More generally, it is possible to evaluate them by Monte Carlo simulation. Note that they will often depend on the unknown θ .

33.1.1. Estimators for mean, variance and median :

Suppose we have a set of N independent measurements, x_i , assumed to be unbiased measurements of the same unknown quantity μ with a common, but unknown, variance σ^2 . Then

$$\hat{\mu} = \frac{1}{N} \sum_{i=1}^N x_i \quad (33.4)$$

$$\hat{\sigma}^2 = \frac{1}{N-1} \sum_{i=1}^N (x_i - \hat{\mu})^2 \quad (33.5)$$

are unbiased estimators of μ and σ^2 . The variance of $\hat{\mu}$ is σ^2/N and the variance of $\hat{\sigma}^2$ is

$$V[\hat{\sigma}^2] = \frac{1}{N} \left(m_4 - \frac{N-3}{N-1} \sigma^4 \right), \quad (33.6)$$

where m_4 is the 4th central moment of x . For Gaussian distributed x_i , this becomes $2\sigma^4/(N-1)$ for any $N \geq 2$, and for large N , the standard deviation of $\hat{\sigma}^2$ (the "error of the error") is $\sigma/\sqrt{2N}$. Again, if the x_i are Gaussian, $\hat{\mu}$ is an efficient estimator for μ , and the estimators $\hat{\mu}$ and $\hat{\sigma}^2$ are uncorrelated. Otherwise the arithmetic mean (33.4) is not necessarily the most efficient estimator; this is discussed further in Sec. 8.7 of Ref. [4].

If σ^2 is known, it does not improve the estimate $\hat{\mu}$, as can be seen from Eq. (33.4); however, if μ is known, substitute it for $\hat{\mu}$ in Eq. (33.5) and replace $N-1$ by N to obtain an estimator of σ^2 still with zero bias but smaller variance. If the x_i have different, known variances σ_i^2 , then the weighted average

$$\hat{\mu} = \frac{1}{w} \sum_{i=1}^N w_i x_i \quad (33.7)$$

is an unbiased estimator for μ with a smaller variance than an unweighted average; here $w_i = 1/\sigma_i^2$ and $w = \sum_i w_i$. The standard deviation of $\hat{\mu}$ is $1/\sqrt{w}$.

As an estimator for the median x_{med} , one can use the value \hat{x}_{med} such that half the x_i are below and half above (the sample median). If the sample median lies between two observed values, it is set by convention halfway between them. If the p.d.f. of x has the form $f(x - \mu)$ and μ is both mean and median, then for large N the variance of the sample median approaches $1/[4Nf^2(0)]$, provided $f(0) > 0$. Although estimating the median can often be more difficult computationally than the mean, the resulting estimator is generally more robust, as it is insensitive to the exact shape of the tails of a distribution.

33.1.2. The method of maximum likelihood :

Suppose we have a set of N measured quantities $\mathbf{x} = (x_1, \dots, x_N)$ described by a joint p.d.f. $f(\mathbf{x}; \boldsymbol{\theta})$, where $\boldsymbol{\theta} = (\theta_1, \dots, \theta_n)$ is set of n parameters whose values are unknown. The *likelihood function* is given by the p.d.f. evaluated with the data \mathbf{x} , but viewed as a function of the parameters, *i.e.*, $L(\boldsymbol{\theta}) = f(\mathbf{x}; \boldsymbol{\theta})$. If the measurements x_i are statistically independent and each follow the p.d.f. $f(x; \boldsymbol{\theta})$, then the joint p.d.f. for \mathbf{x} factorizes and the likelihood function is

$$L(\boldsymbol{\theta}) = \prod_{i=1}^N f(x_i; \boldsymbol{\theta}). \quad (33.8)$$

The method of maximum likelihood takes the estimators $\hat{\boldsymbol{\theta}}$ to be those values of $\boldsymbol{\theta}$ that maximize $L(\boldsymbol{\theta})$.

Note that the likelihood function is *not* a p.d.f. for the parameters $\boldsymbol{\theta}$; in frequentist statistics this is not defined. In Bayesian statistics, one can obtain from the likelihood the posterior p.d.f. for $\boldsymbol{\theta}$, but this requires multiplying by a prior p.d.f. (see Sec. 33.3.1).

It is usually easier to work with $\ln L$, and since both are maximized for the same parameter values $\boldsymbol{\theta}$, the maximum likelihood (ML) estimators can be found by solving the *likelihood equations*,

$$\frac{\partial \ln L}{\partial \theta_i} = 0, \quad i = 1, \dots, n. \quad (33.9)$$

Often the solution must be found numerically. Maximum likelihood estimators are important because they are approximately unbiased and efficient for large data samples, under quite general conditions, and the method has a wide range of applicability.

In evaluating the likelihood function, it is important that any normalization factors in the p.d.f. that involve $\boldsymbol{\theta}$ be included. However, we will only be interested in the maximum of L and in ratios of L at different values of the parameters; hence any multiplicative factors that do not involve the parameters that we want to estimate may be dropped, including factors that depend on the data but not on $\boldsymbol{\theta}$.

Under a one-to-one change of parameters from $\boldsymbol{\theta}$ to $\boldsymbol{\eta}$, the ML estimators $\hat{\boldsymbol{\theta}}$ transform to $\boldsymbol{\eta}(\hat{\boldsymbol{\theta}})$. That is, the ML solution is invariant under change of parameter. However, other properties of ML estimators, in particular the bias, are not invariant under change of parameter.

The inverse V^{-1} of the covariance matrix $V_{ij} = \text{cov}[\hat{\theta}_i, \hat{\theta}_j]$ for a set of ML estimators can be estimated by using

$$(\hat{V}^{-1})_{ij} = - \left. \frac{\partial^2 \ln L}{\partial \theta_i \partial \theta_j} \right|_{\hat{\boldsymbol{\theta}}}. \quad (33.10)$$

For finite samples, however, Eq. (33.10) can result in an underestimate of the variances. In the large sample limit (or in a linear model with Gaussian errors), L has a Gaussian form and $\ln L$ is (hyper)parabolic. In this case, it can be seen that a numerically equivalent way of determining s -standard-deviation errors is from the contour given by the $\boldsymbol{\theta}'$ such that

$$\ln L(\boldsymbol{\theta}') = \ln L_{\text{max}} - s^2/2, \quad (33.11)$$

where $\ln L_{\text{max}}$ is the value of $\ln L$ at the solution point (compare with Eq. (33.56)). The extreme limits of this contour on the θ_i axis give

an approximate s -standard-deviation confidence interval for θ_i (see Section 33.3.2.4).

In the case where the size n of the data sample x_1, \dots, x_n is small, the unbinned maximum likelihood method, *i.e.*, use of equation (33.8), is preferred since binning can only result in a loss of information, and hence larger statistical errors for the parameter estimates. The sample size n can be regarded as fixed, or the user can choose to treat it as a Poisson-distributed variable; this latter option is sometimes called “extended maximum likelihood” (see, *e.g.*, [6–8]).

If the sample is large, it can be convenient to bin the values in a histogram, so that one obtains a vector of data $\mathbf{n} = (n_1, \dots, n_N)$ with expectation values $\boldsymbol{\nu} = E[\mathbf{n}]$ and probabilities $f(\mathbf{n}; \boldsymbol{\nu})$. Then one may maximize the likelihood function based on the contents of the bins (so i labels bins). This is equivalent to maximizing the likelihood ratio $\lambda(\boldsymbol{\theta}) = f(\mathbf{n}; \boldsymbol{\nu}(\boldsymbol{\theta}))/f(\mathbf{n}; \mathbf{n})$, or to minimizing the equivalent quantity $-2 \ln \lambda(\boldsymbol{\theta})$. For independent Poisson distributed n_i this is [9]

$$-2 \ln \lambda(\boldsymbol{\theta}) = 2 \sum_{i=1}^N \left[\nu_i(\boldsymbol{\theta}) - n_i + n_i \ln \frac{n_i}{\nu_i(\boldsymbol{\theta})} \right], \quad (33.12)$$

where for bins with $n_i = 0$, the last term in (33.12) is zero. The expression (33.12) without the terms $\nu_i - n_i$ also gives $-2 \ln \lambda(\boldsymbol{\theta})$ for multinomially distributed n_i , *i.e.*, when the total number of entries is regarded as fixed. In the limit of zero bin width, maximizing (33.12) is equivalent to maximizing the unbinned likelihood function (33.8).

A benefit of binning is that it allows for a goodness-of-fit test (see Sec. 33.2.2). According to Wilks’ theorem, for sufficiently large ν_i and providing certain regularity conditions are met, the minimum of $-2 \ln \lambda$ as defined by Eq. (33.12) follows a χ^2 distribution (see, *e.g.*, Ref. [3]). If there are N bins and m fitted parameters, then the number of degrees of freedom for the χ^2 distribution is $N - m$ if the data are treated as Poisson-distributed, and $N - m - 1$ if the n_i are multinomially distributed.

Suppose the n_i are Poisson-distributed and the overall normalization $\nu_{\text{tot}} = \sum_i \nu_i$ is taken as an adjustable parameter, so that $\nu_i = \nu_{\text{tot}} p_i(\boldsymbol{\theta})$, where the probability to be in the i th bin, $p_i(\boldsymbol{\theta})$, does not depend on ν_{tot} . Then by minimizing Eq. (33.12), one obtains that the area under the fitted function is equal to the sum of the histogram contents, *i.e.*, $\sum_i \nu_i = \sum_i n_i$. This is not the case for parameter estimation methods based on a least-squares procedure with traditional weights (see, *e.g.*, Ref. [8]).

33.1.3. The method of least squares :

The *method of least squares* (LS) coincides with the method of maximum likelihood in the following special case. Consider a set of N independent measurements y_i at known points x_i . The measurement y_i is assumed to be Gaussian distributed with mean $F(x_i; \boldsymbol{\theta})$ and known variance σ_i^2 . The goal is to construct estimators for the unknown parameters $\boldsymbol{\theta}$. The likelihood function contains the sum of squares

$$\chi^2(\boldsymbol{\theta}) = -2 \ln L(\boldsymbol{\theta}) + \text{constant} = \sum_{i=1}^N \frac{(y_i - F(x_i; \boldsymbol{\theta}))^2}{\sigma_i^2}. \quad (33.13)$$

The set of parameters $\boldsymbol{\theta}$ which maximize L is the same as those which minimize χ^2 .

The minimum of Equation (33.13) defines the least-squares estimators $\hat{\boldsymbol{\theta}}$ for the more general case where the y_i are not Gaussian distributed as long as they are independent. If they are not independent but rather have a covariance matrix $V_{ij} = \text{cov}[y_i, y_j]$, then the LS estimators are determined by the minimum of

$$\chi^2(\boldsymbol{\theta}) = (\mathbf{y} - \mathbf{F}(\boldsymbol{\theta}))^T V^{-1} (\mathbf{y} - \mathbf{F}(\boldsymbol{\theta})), \quad (33.14)$$

where $\mathbf{y} = (y_1, \dots, y_N)$ is the vector of measurements, $\mathbf{F}(\boldsymbol{\theta})$ is the corresponding vector of predicted values (understood as a column vector in (33.14)), and the superscript T denotes transposed (*i.e.*, row) vector.

In many practical cases, one further restricts the problem to the situation where $F(x_i; \boldsymbol{\theta})$ is a linear function of the parameters, *i.e.*,

$$F(x_i; \boldsymbol{\theta}) = \sum_{j=1}^m \theta_j h_j(x_i). \quad (33.15)$$

Here the $h_j(x)$ are m linearly independent functions, *e.g.*, $1, x, x^2, \dots, x^{m-1}$, or Legendre polynomials. We require $m < N$ and at least m of the x_i must be distinct.

Minimizing χ^2 in this case with m parameters reduces to solving a system of m linear equations. Defining $H_{ij} = h_j(x_i)$ and minimizing χ^2 by setting its derivatives with respect to the θ_i equal to zero gives the LS estimators,

$$\hat{\boldsymbol{\theta}} = (H^T V^{-1} H)^{-1} H^T V^{-1} \mathbf{y} \equiv D \mathbf{y}. \quad (33.16)$$

The covariance matrix for the estimators $U_{ij} = \text{cov}[\hat{\theta}_i, \hat{\theta}_j]$ is given by

$$U = D V D^T = (H^T V^{-1} H)^{-1}, \quad (33.17)$$

or equivalently, its inverse U^{-1} can be found from

$$(U^{-1})_{ij} = \frac{1}{2} \frac{\partial^2 \chi^2}{\partial \theta_i \partial \theta_j} \Big|_{\boldsymbol{\theta}=\hat{\boldsymbol{\theta}}} = \sum_{k,l=1}^N h_i(x_k) (V^{-1})_{kl} h_j(x_l). \quad (33.18)$$

The LS estimators can also be found from the expression

$$\hat{\boldsymbol{\theta}} = U \mathbf{g}, \quad (33.19)$$

where the vector \mathbf{g} is defined by

$$g_i = \sum_{j,k=1}^N y_j h_i(x_k) (V^{-1})_{jk}. \quad (33.20)$$

For the case of uncorrelated y_i , for example, one can use (33.19) with

$$(U^{-1})_{ij} = \sum_{k=1}^N \frac{h_i(x_k) h_j(x_k)}{\sigma_k^2}, \quad (33.21)$$

$$g_i = \sum_{k=1}^N \frac{y_k h_i(x_k)}{\sigma_k^2}. \quad (33.22)$$

Expanding $\chi^2(\boldsymbol{\theta})$ about $\hat{\boldsymbol{\theta}}$, one finds that the contour in parameter space defined by

$$\chi^2(\boldsymbol{\theta}) = \chi^2(\hat{\boldsymbol{\theta}}) + 1 = \chi_{\min}^2 + 1 \quad (33.23)$$

has tangent planes located at approximately plus-or-minus-one standard deviation $\sigma_{\hat{\boldsymbol{\theta}}}$ from the LS estimates $\hat{\boldsymbol{\theta}}$.

In constructing the quantity $\chi^2(\boldsymbol{\theta})$, one requires the variances or, in the case of correlated measurements, the covariance matrix. Often these quantities are not known *a priori* and must be estimated from the data; an important example is where the measured value y_i represents a counted number of events in the bin of a histogram. If, for example, y_i represents a Poisson variable, for which the variance is equal to the mean, then one can either estimate the variance from the predicted value, $F(x_i; \boldsymbol{\theta})$, or from the observed number itself, y_i . In the first option, the variances become functions of the fitted parameters, which may lead to calculational difficulties. The second option can be undefined if y_i is zero, and in both cases for small y_i , the variance will be poorly estimated. In either case, one should constrain the normalization of the fitted curve to the correct value, *i.e.*, one should determine the area under the fitted curve directly from the number of entries in the histogram (see [8], Section 7.4). A further alternative is to use the method of maximum likelihood; for binned data this can be done by minimizing Eq. (33.12)

As the minimum value of the χ^2 represents the level of agreement between the measurements and the fitted function, it can be used for assessing the goodness-of-fit; this is discussed further in Section 33.2.2.

33.1.4. The Bayesian approach :

In the frequentist methods discussed above, probability is associated only with data, not with the value of a parameter. This is no longer the case in Bayesian statistics, however, which we introduce in this section. Bayesian methods are considered further in Sec. 33.3.1 for interval estimation and in Sec. 33.2.3 for model selection. For general introductions to Bayesian statistics see, *e.g.*, Refs. [19,20,21, 22].

Suppose the outcome of an experiment is characterized by a vector of data \mathbf{x} , whose probability distribution depends on an unknown parameter (or parameters) $\boldsymbol{\theta}$ that we wish to determine. In Bayesian statistics, all knowledge about $\boldsymbol{\theta}$ is summarized by the posterior p.d.f. $p(\boldsymbol{\theta}|\mathbf{x})$, which gives the degree of belief for $\boldsymbol{\theta}$ to take on values in a certain region given the data \mathbf{x} . It is obtained by using Bayes' theorem,

$$p(\boldsymbol{\theta}|\mathbf{x}) = \frac{L(\mathbf{x}|\boldsymbol{\theta})\pi(\boldsymbol{\theta})}{\int L(\mathbf{x}|\boldsymbol{\theta}')\pi(\boldsymbol{\theta}') d\boldsymbol{\theta}'}, \quad (33.24)$$

where $L(\mathbf{x}|\boldsymbol{\theta})$ is the likelihood function, *i.e.*, the joint p.d.f. for the data viewed as a function of $\boldsymbol{\theta}$, evaluated with the data actually obtained in the experiment, and $\pi(\boldsymbol{\theta})$ is the prior p.d.f. for $\boldsymbol{\theta}$. Note that the denominator in Eq. (33.24) serves to normalize the posterior p.d.f. to unity.

As it can be difficult to report the full posterior p.d.f. $p(\boldsymbol{\theta}|\mathbf{x})$, one would usually summarize it with statistics such as the mean (or median), and covariance matrix. In addition one may construct intervals with a given probability content, as is discussed in Sec. 33.3.1 on Bayesian interval estimation.

Bayesian statistics supplies no unique rule for determining the prior $\pi(\boldsymbol{\theta})$; this reflects the experimenter's subjective degree of belief (or state of knowledge) about $\boldsymbol{\theta}$ before the measurement was carried out. For the result to be of value to the broader community, whose members may not share these beliefs, it is important to carry out a sensitivity analysis, that is, to show how the result changes under a reasonable variation of the prior probabilities.

One might like to construct $\pi(\boldsymbol{\theta})$ to represent complete ignorance about the parameters by setting it equal to a constant. A problem here is that if the prior p.d.f. is flat in $\boldsymbol{\theta}$, then it is not flat for a nonlinear function of $\boldsymbol{\theta}$, and so a different parametrization of the problem would lead in general to a non-equivalent posterior p.d.f.

For the special case of a constant prior, one can see from Bayes' theorem (33.24) that the posterior is proportional to the likelihood, and therefore the mode (peak position) of the posterior is equal to the ML estimator. The posterior mode, however, will change in general upon a transformation of parameter. A summary statistic other than the mode may be used as the Bayesian estimator, such as the median, which is invariant under parameter transformation. But this will not in general coincide with the ML estimator.

The difficult and subjective nature of encoding personal knowledge into priors has led to what is called *objective Bayesian statistics*, where prior probabilities are based not on an actual degree of belief but rather derived from formal rules. These give, for example, priors which are invariant under a transformation of parameters or which result in a maximum gain in information for a given set of measurements. For an extensive review see, *e.g.*, Ref. [23].

Objective priors do not in general reflect degree of belief, but they could in some cases be taken as possible, although perhaps extreme, subjective priors. The posterior probabilities as well therefore do not necessarily reflect a degree of belief. However one may regard investigating a variety of objective priors to be an important part of the sensitivity analysis. Furthermore, use of objective priors with Bayes' theorem can be viewed as a recipe for producing estimators or intervals which have desirable frequentist properties.

An important procedure for deriving objective priors is due to Jeffreys. According to *Jeffreys' rule* one takes the prior as

$$\pi(\boldsymbol{\theta}) \propto \sqrt{\det(I(\boldsymbol{\theta}))}, \quad (33.25)$$

where

$$I_{ij}(\boldsymbol{\theta}) = -E \left[\frac{\partial^2 \ln L(\mathbf{x}|\boldsymbol{\theta})}{\partial \theta_i \partial \theta_j} \right] = - \int \frac{\partial^2 \ln L(\mathbf{x}|\boldsymbol{\theta})}{\partial \theta_i \partial \theta_j} L(\mathbf{x}|\boldsymbol{\theta}) d\mathbf{x} \quad (33.26)$$

is the *Fisher information matrix*. One can show that the Jeffreys prior leads to inference that is invariant under a transformation of parameters. One should note that the Jeffreys prior depends on the likelihood function, and thus contains information about the measurement model itself, which goes beyond one's degree of belief about the value of a parameter. As examples, the Jeffreys prior for the mean μ of a Gaussian distribution is a constant, and for the mean of a Poisson distribution one finds $\pi(\mu) \propto 1/\sqrt{\mu}$.

Neither the constant nor $1/\sqrt{\mu}$ priors can be normalized to unit area and are said to be *improper*. This can be allowed because the prior always appears multiplied by the likelihood function, and if the likelihood falls off sufficiently quickly then one may have a normalizable posterior density.

Bayesian statistics provides a framework for incorporating systematic uncertainties into a result. Suppose, for example, that a model depends not only on parameters of interest θ , but on *nuisance parameters* ν , whose values are known with some limited accuracy. For a single nuisance parameter ν , for example, one might have a p.d.f. centered about its nominal value with a certain standard deviation σ_ν . Often a Gaussian p.d.f. provides a reasonable model for one's degree of belief about a nuisance parameter; in other cases, more complicated shapes may be appropriate. If, for example, the parameter represents a non-negative quantity then a log-normal or gamma p.d.f. can be a more natural choice than a Gaussian truncated at zero. The likelihood function, prior, and posterior p.d.f.s then all depend on both θ and ν , and are related by Bayes' theorem, as usual. One can obtain the posterior p.d.f. for θ alone by integrating over the nuisance parameters, *i.e.*,

$$p(\theta|\mathbf{x}) = \int p(\theta, \nu|\mathbf{x}) d\nu. \quad (33.27)$$

Such integrals can often not be carried out in closed form, and if the number of nuisance parameters is large, then they can be difficult to compute with standard Monte Carlo methods. *Markov Chain Monte Carlo* (MCMC) is often used for computing integrals of this type (see Sec. 34.5).

If the prior joint p.d.f. for θ and ν factorizes, then integrating the posterior p.d.f. over ν is equivalent to replacing the likelihood function by (see [24]),

$$L'(\mathbf{x}|\theta) = \int L(\mathbf{x}|\theta, \nu)\pi(\nu) d\nu. \quad (33.28)$$

The function $L'(\mathbf{x}|\theta)$ can also be used together with frequentist methods that employ the likelihood function such as ML estimation of parameters. The results then have a mixed frequentist/Bayesian character, where the systematic uncertainty due to limited knowledge of the nuisance parameters is built in. Although this may make it more difficult to disentangle statistical from systematic effects, such a hybrid approach may satisfy the objective of reporting the result in a convenient way.

33.1.5. Propagation of errors :

Consider a set of n quantities $\theta = (\theta_1, \dots, \theta_n)$ and a set of m functions $\eta(\theta) = (\eta_1(\theta), \dots, \eta_m(\theta))$. Suppose we have estimated $\hat{\theta} = (\hat{\theta}_1, \dots, \hat{\theta}_n)$, using, say, maximum-likelihood or least-squares, and we also know or have estimated the covariance matrix $V_{ij} = \text{cov}[\hat{\theta}_i, \hat{\theta}_j]$. The goal of *error propagation* is to determine the covariance matrix for the functions, $U_{ij} = \text{cov}[\hat{\eta}_i, \hat{\eta}_j]$, where $\hat{\eta} = \eta(\hat{\theta})$. In particular, the diagonal elements $U_{ii} = V[\hat{\eta}_i]$ give the variances. The new covariance matrix can be found by expanding the functions $\eta(\theta)$ about the estimates $\hat{\theta}$ to first order in a Taylor series. Using this one finds

$$U_{ij} \approx \sum_{k,l} \frac{\partial \eta_i}{\partial \theta_k} \frac{\partial \eta_j}{\partial \theta_l} \Big|_{\hat{\theta}} V_{kl}. \quad (33.29)$$

This can be written in matrix notation as $U \approx AVA^T$ where the matrix of derivatives A is

$$A_{ij} = \frac{\partial \eta_i}{\partial \theta_j} \Big|_{\hat{\theta}}, \quad (33.30)$$

and A^T is its transpose. The approximation is exact if $\eta(\theta)$ is linear (it holds, for example, in equation (33.17)). If this is not the case, the approximation can break down if, for example, $\eta(\theta)$ is significantly nonlinear close to $\hat{\theta}$ in a region of a size comparable to the standard deviations of $\hat{\theta}$.

33.2. Statistical tests

In addition to estimating parameters, one often wants to assess the validity of certain statements concerning the data's underlying distribution. Frequentist *Hypothesis tests*, described in Sec. 33.2.1, provide a rule for accepting or rejecting hypotheses depending on the outcome of a measurement. In *significance tests*, covered in Sec. 33.2.2, one gives the probability to obtain a level of incompatibility with a certain hypothesis that is greater than or equal to the level observed with the actual data. In the Bayesian approach, the corresponding procedure is referred to as model selection, which is based fundamentally on the probabilities of competing hypotheses. In Sec. 33.2.3 we describe a related construct called the Bayes factor, which can be used to quantify the degree to which the data prefer one or another hypothesis.

33.2.1. Hypothesis tests :

Consider an experiment whose outcome is characterized by a vector of data \mathbf{x} . A *hypothesis* is a statement about the distribution of \mathbf{x} . It could, for example, define completely the p.d.f. for the data (a simple hypothesis), or it could specify only the functional form of the p.d.f., with the values of one or more parameters left open (a composite hypothesis).

A *statistical test* is a rule that states for which values of \mathbf{x} a given hypothesis (often called the null hypothesis, H_0) should be rejected in favor of its alternative H_1 . This is done by defining a region of \mathbf{x} -space called the critical region; if the outcome of the experiment lands in this region, H_0 is rejected, otherwise it is accepted.

Rejecting H_0 if it is true is called an error of the first kind. The probability for this to occur is called the *size* or *significance level* of the test, α , which is chosen to be equal to some pre-specified value. It can also happen that H_0 is false and the true hypothesis is the alternative, H_1 . If H_0 is accepted in such a case, this is called an error of the second kind, which will have some probability β . The quantity $1 - \beta$ is called the *power* of the test relative to H_1 .

In high-energy physics, the components of \mathbf{x} might represent the measured properties of candidate events, and the acceptance region is defined by the cuts that one imposes in order to select events of a certain desired type. Here H_0 could represent the background hypothesis and the alternative H_1 could represent the sought after signal.

Often rather than using the full set of quantities \mathbf{x} , it is convenient to define a *test statistic*, t , which can be a single number, or in any case a vector with fewer components than \mathbf{x} . Each hypothesis for the distribution of \mathbf{x} will determine a distribution for t , and the acceptance region in \mathbf{x} -space will correspond to a specific range of values of t . In constructing t , one attempts to reduce the volume of data without losing the ability to discriminate between different hypotheses.

Often one tries to construct a test to maximize power for a given significance level, *i.e.*, to maximize the signal efficiency for a given significance level. The *Neyman-Pearson lemma* states that this is done by defining the acceptance region such that, for \mathbf{x} in that region, the ratio of p.d.f.s for the hypotheses H_1 (signal) and H_0 (background),

$$\lambda(\mathbf{x}) = \frac{f(\mathbf{x}|H_1)}{f(\mathbf{x}|H_0)}, \quad (33.31)$$

is greater than a given constant, the value of which is chosen to give the desired signal efficiency. Here H_0 and H_1 must be simple hypotheses, *i.e.*, they should not contain undetermined parameters. The lemma is equivalent to the statement that (33.31) represents the test statistic with which one may obtain the highest signal efficiency for a given purity for the selected sample. It can be difficult in practice, however, to determine $\lambda(\mathbf{x})$, since this requires knowledge of the joint p.d.f.s $f(\mathbf{x}|H_0)$ and $f(\mathbf{x}|H_1)$.

In the usual case where the likelihood ratio (33.31) cannot be used explicitly, there exist a variety of other multivariate classifiers that effectively separate different types of events. Methods often used in HEP include *neural networks* or *Fisher discriminants* (see [10]). Recently, further classification methods from machine-learning have been applied in HEP analyses; these include *probability density estimation (PDE)* techniques, *kernel-based PDE (KDE or Parzen window)*, *support vector machines*, and *decision trees*. Techniques such as “boosting” and “bagging” can be applied to combine a number of classifiers into a stronger one with greater stability with respect to fluctuations in the training data. Descriptions of these methods can be found in [11–13], and Proceedings of the PHYSTAT conference series [14]. Software for HEP includes the *TMVA* [15] and *StatPatternRecognition* [16] packages.

33.2.2. Significance tests :

Often one wants to quantify the level of agreement between the data and a hypothesis without explicit reference to alternative hypotheses. This can be done by defining a statistic t , which is a function of the data whose value reflects in some way the level of agreement between the data and the hypothesis. The user must decide what values of the statistic correspond to better or worse levels of agreement with the hypothesis in question; for many goodness-of-fit statistics, there is an obvious choice.

The hypothesis in question, say, H_0 , will determine the p.d.f. $g(t|H_0)$ for the statistic. The significance of a discrepancy between the data and what one expects under the assumption of H_0 is quantified by giving the p -value, defined as the probability to find t in the region of equal or lesser compatibility with H_0 than the level of compatibility observed with the actual data. For example, if t is defined such that large values correspond to poor agreement with the hypothesis, then the p -value would be

$$p = \int_{t_{\text{obs}}}^{\infty} g(t|H_0) dt, \quad (33.32)$$

where t_{obs} is the value of the statistic obtained in the actual experiment. The p -value should not be confused with the size (significance level) of a test, or the confidence level of a confidence interval (Section 33.3), both of which are pre-specified constants.

The p -value is a function of the data, and is therefore itself a random variable. If the hypothesis used to compute the p -value is true, then for continuous data, p will be uniformly distributed between zero and one. Note that the p -value is not the probability for the hypothesis; in frequentist statistics, this is not defined. Rather, the p -value is the probability, under the assumption of a hypothesis H_0 , of obtaining data at least as incompatible with H_0 as the data actually observed.

When searching for a new phenomenon, one tries to reject the hypothesis H_0 that the data are consistent with known, *e.g.*, Standard Model processes. If the p -value of H_0 is sufficiently low, then one is willing to accept that some alternative hypothesis is true. Often one converts the p -value into an equivalent significance Z , defined so that a Z standard deviation upward fluctuation of a Gaussian random variable would have an upper tail area equal to p , *i.e.*,

$$Z = \Phi^{-1}(1 - p). \quad (33.33)$$

Here Φ is the cumulative distribution of the Standard Gaussian, and Φ^{-1} is its inverse (quantile) function. Often in HEP, the level of significance where an effect is said to qualify as a discovery is $Z = 5$, *i.e.*, a 5σ effect, corresponding to a p -value of 2.87×10^{-7} . One’s actual degree of belief that a new process is present, however, will depend in general on other factors as well, such as the plausibility of the new signal hypothesis and the degree to which it can describe the data, one’s confidence in the model that led to the observed p -value, and possible corrections for multiple observations out of which one focuses on the smallest p -value obtained (the “look-elsewhere effect”). For a review of how to incorporate systematic uncertainties into p -values see, *e.g.*, [17].

When estimating parameters using the method of least squares, one obtains the minimum value of the quantity χ^2 (33.13). This

statistic can be used to test the *goodness-of-fit*, *i.e.*, the test provides a measure of the significance of a discrepancy between the data and the hypothesized functional form used in the fit. It may also happen that no parameters are estimated from the data, but that one simply wants to compare a histogram, *e.g.*, a vector of Poisson distributed numbers $\mathbf{n} = (n_1, \dots, n_N)$, with a hypothesis for their expectation values $\nu_i = E[n_i]$. As the distribution is Poisson with variances $\sigma_i^2 = \nu_i$, the χ^2 (33.13) becomes *Pearson’s χ^2 statistic*,

$$\chi^2 = \sum_{i=1}^N \frac{(n_i - \nu_i)^2}{\nu_i}. \quad (33.34)$$

If the hypothesis $\boldsymbol{\nu} = (\nu_1, \dots, \nu_N)$ is correct, and if the expected values ν_i in (33.34) are sufficiently large (in practice, this will be a good approximation if all $\nu_i > 5$), then the χ^2 statistic will follow the χ^2 p.d.f. with the number of degrees of freedom equal to the number of measurements N minus the number of fitted parameters. The minimized χ^2 from Eq. (33.13) also has this property if the measurements y_i are Gaussian.

Alternatively, one may fit parameters and evaluate goodness-of-fit by minimizing $-2 \ln \lambda$ from Eq. (33.12). One finds that the distribution of this statistic approaches the asymptotic limit faster than does Pearson’s χ^2 , and thus computing the p -value with the χ^2 p.d.f. will in general be better justified (see [9] and references therein).

Assuming the goodness-of-fit statistic follows a χ^2 p.d.f., the p -value for the hypothesis is then

$$p = \int_{\chi^2}^{\infty} f(z; n_d) dz, \quad (33.35)$$

where $f(z; n_d)$ is the χ^2 p.d.f. and n_d is the appropriate number of degrees of freedom. Values can be obtained from Fig. 33.1 or from the CERNLIB routine `PROB` or the ROOT function `TMATH::Prob`. If the conditions for using the χ^2 p.d.f. do not hold, the statistic can still be defined as before, but its p.d.f. must be determined by other means in order to obtain the p -value, *e.g.*, using a Monte Carlo calculation.

If one finds a χ^2 value much greater than n_d , and a correspondingly small p -value, one may be tempted to expect a high degree of uncertainty for any fitted parameters. Although this may be true for systematic errors in the parameters, it is not in general the case for statistical uncertainties. If, for example, the error bars (or covariance matrix) used in constructing the χ^2 are underestimated, then this will lead to underestimated statistical errors for the fitted parameters. But in such a case, an estimate $\hat{\theta}$ can differ from the true value θ by an amount much greater than its estimated statistical error. The standard deviations of estimators that one finds from, say, Eq. (33.11) reflect how widely the estimates would be distributed if one were to repeat the measurement many times, assuming that the measurement errors used in the χ^2 are also correct. They do not include the systematic error which may result from an incorrect hypothesis or incorrectly estimated measurement errors in the χ^2 .

Since the mean of the χ^2 distribution is equal to n_d , one expects in a “reasonable” experiment to obtain $\chi^2 \approx n_d$. Hence the quantity χ^2/n_d is sometimes reported. Since the p.d.f. of χ^2/n_d depends on n_d , however, one must report n_d as well if one wishes to determine the p -value. The p -values obtained for different values of χ^2/n_d are shown in Fig. 33.2.

33.2.3. Bayesian model selection :

In Bayesian statistics, all of one’s knowledge about a model is contained in its posterior probability, which one obtains using Bayes’ theorem (33.24). Thus one could reject a hypothesis H if its posterior probability $P(H|\mathbf{x})$ is sufficiently small. The difficulty here is that $P(H|\mathbf{x})$ is proportional to the prior probability $P(H)$, and there will not be a consensus about the prior probabilities for the existence of new phenomena. Nevertheless one can construct a quantity called the Bayes factor (described below), which can be used to quantify the degree to which the data prefer one hypothesis over another, and is independent of their prior probabilities.

Consider two models (hypotheses), H_i and H_j , described by vectors of parameters $\boldsymbol{\theta}_i$ and $\boldsymbol{\theta}_j$, respectively. Some of the components will

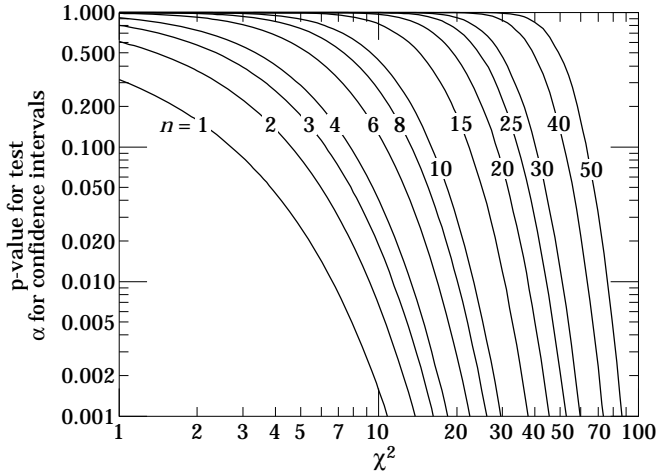


Figure 33.1: One minus the χ^2 cumulative distribution, $1 - F(\chi^2; n)$, for n degrees of freedom. This gives the p -value for the χ^2 goodness-of-fit test as well as one minus the coverage probability for confidence regions (see Sec. 33.3.2.4).

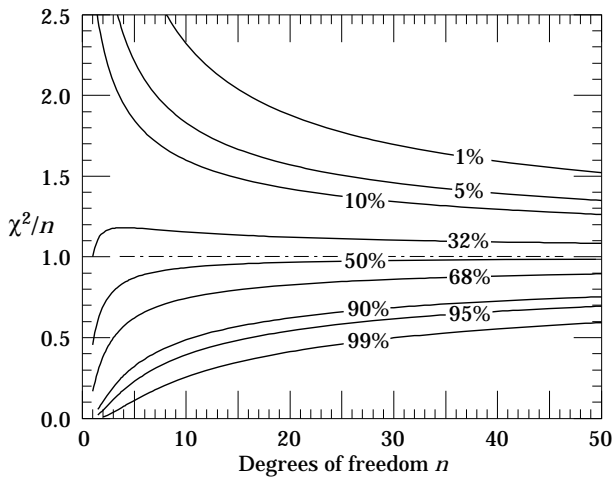


Figure 33.2: The ‘reduced’ χ^2 , equal to χ^2/n , for n degrees of freedom. The curves show as a function of n the χ^2/n that corresponds to a given p -value.

be common to both models and others may be distinct. The full prior probability for each model can be written in the form

$$\pi(H_i, \theta_i) = P(H_i)\pi(\theta_i|H_i), \tag{33.36}$$

Here $P(H_i)$ is the overall prior probability for H_i , and $\pi(\theta_i|H_i)$ is the normalized p.d.f. of its parameters. For each model, the posterior probability is found using Bayes’ theorem,

$$P(H_i|\mathbf{x}) = \frac{\int L(\mathbf{x}|\theta_i, H_i)P(H_i)\pi(\theta_i|H_i) d\theta_i}{P(\mathbf{x})}, \tag{33.37}$$

where the integration is carried out over the internal parameters θ_i of the model. The ratio of posterior probabilities for the models is therefore

$$\frac{P(H_i|\mathbf{x})}{P(H_j|\mathbf{x})} = \frac{\int L(\mathbf{x}|\theta_i, H_i)\pi(\theta_i|H_i) d\theta_i}{\int L(\mathbf{x}|\theta_j, H_j)\pi(\theta_j|H_j) d\theta_j} \frac{P(H_i)}{P(H_j)}. \tag{33.38}$$

The *Bayes factor* is defined as

$$B_{ij} = \frac{\int L(\mathbf{x}|\theta_i, H_i)\pi(\theta_i|H_i) d\theta_i}{\int L(\mathbf{x}|\theta_j, H_j)\pi(\theta_j|H_j) d\theta_j}. \tag{33.39}$$

This gives what the ratio of posterior probabilities for models i and j would be if the overall prior probabilities for the two models were

equal. If the models have no nuisance parameters *i.e.*, no internal parameters described by priors, then the Bayes factor is simply the likelihood ratio. The Bayes factor therefore shows by how much the probability ratio of model i to model j changes in the light of the data, and thus can be viewed as a numerical measure of evidence supplied by the data in favour of one hypothesis over the other.

Although the Bayes factor is by construction independent of the overall prior probabilities $P(H_i)$ and $P(H_j)$, it does require priors for all internal parameters of a model, *i.e.*, one needs the functions $\pi(\theta_i|H_i)$ and $\pi(\theta_j|H_j)$. In a Bayesian analysis where one is only interested in the posterior p.d.f. of a parameter, it may be acceptable to take an unnormalizable function for the prior (an improper prior) as long as the product of likelihood and prior can be normalized. But improper priors are only defined up to an arbitrary multiplicative constant, which does not cancel in the ratio (33.39). Furthermore, although the range of a constant normalized prior is unimportant for parameter determination (provided it is wider than the likelihood), this is not so for the Bayes factor when such a prior is used for only one of the hypotheses. So to compute a Bayes factor, all internal parameters must be described by normalized priors that represent meaningful probabilities over the entire range where they are defined.

An exception to this rule may be considered when the identical parameter appears in the models for both numerator and denominator of the Bayes factor. In this case one can argue that the arbitrary constants would cancel. One must exercise some caution, however, as parameters with the same name and physical meaning may still play different roles in the two models. Both integrals in equation (33.39) are of the form

$$m = \int L(\mathbf{x}|\theta)\pi(\theta) d\theta, \tag{33.40}$$

which is called the *marginal likelihood* (or in some fields called the *evidence*). A review of Bayes factors including a discussion of computational issues is Ref. [26].

33.3. Intervals and limits

When the goal of an experiment is to determine a parameter θ , the result is usually expressed by quoting, in addition to the point estimate, some sort of interval which reflects the statistical precision of the measurement. In the simplest case, this can be given by the parameter’s estimated value $\hat{\theta}$ plus or minus an estimate of the standard deviation of $\hat{\theta}$, $\sigma_{\hat{\theta}}$. If, however, the p.d.f. of the estimator is not Gaussian or if there are physical boundaries on the possible values of the parameter, then one usually quotes instead an interval according to one of the procedures described below.

In reporting an interval or limit, the experimenter may wish to

- communicate as objectively as possible the result of the experiment;
- provide an interval that is constructed to cover the true value of the parameter with a specified probability;
- provide the information needed by the consumer of the result to draw conclusions about the parameter or to make a particular decision;
- draw conclusions about the parameter that incorporate stated prior beliefs.

With a sufficiently large data sample, the point estimate and standard deviation (or for the multiparameter case, the parameter estimates and covariance matrix) satisfy essentially all of these goals. For finite data samples, no single method for quoting an interval will achieve all of them.

In addition to the goals listed above, the choice of method may be influenced by practical considerations such as ease of producing an interval from the results of several measurements. Of course the experimenter is not restricted to quoting a single interval or limit; one may choose, for example, first to communicate the result with a confidence interval having certain frequentist properties, and then in addition to draw conclusions about a parameter using Bayesian statistics. It is recommended, however, that there be a clear separation between these two aspects of reporting a result. In the remainder of

this section, we assess the extent to which various types of intervals achieve the goals stated here.

33.3.1. Bayesian intervals :

As described in Sec. 33.1.4, a Bayesian posterior probability may be used to determine regions that will have a given probability of containing the true value of a parameter. In the single parameter case, for example, an interval (called a Bayesian or credible interval) $[\theta_{lo}, \theta_{up}]$ can be determined which contains a given fraction $1 - \alpha$ of the posterior probability, *i.e.*,

$$1 - \alpha = \int_{\theta_{lo}}^{\theta_{up}} p(\theta|\mathbf{x}) d\theta . \tag{33.41}$$

Sometimes an upper or lower limit is desired, *i.e.*, θ_{lo} can be set to zero or θ_{up} to infinity. In other cases, one might choose θ_{lo} and θ_{up} such that $p(\theta|\mathbf{x})$ is higher everywhere inside the interval than outside; these are called *highest posterior density* (HPD) intervals. Note that HPD intervals are not invariant under a nonlinear transformation of the parameter.

If a parameter is constrained to be non-negative, then the prior p.d.f. can simply be set to zero for negative values. An important example is the case of a Poisson variable n , which counts signal events with unknown mean s , as well as background with mean b , assumed known. For the signal mean s , one often uses the prior

$$\pi(s) = \begin{cases} 0 & s < 0 \\ 1 & s \geq 0 \end{cases} . \tag{33.42}$$

This prior is regarded as providing an interval whose frequentist properties can be studied, rather than as representing a degree of belief. In the absence of a clear discovery, (*e.g.*, if $n = 0$ or if in any case n is compatible with the expected background), one usually wishes to place an upper limit on s (see, however, Sec. 33.3.2.6 on “flip-flopping” concerning frequentist coverage). Using the likelihood function for Poisson distributed n ,

$$L(n|s) = \frac{(s+b)^n}{n!} e^{-(s+b)} , \tag{33.43}$$

along with the prior (33.42) in (33.24) gives the posterior density for s . An upper limit s_{up} at confidence level (or here, rather, credibility level) $1 - \alpha$ can be obtained by requiring

$$1 - \alpha = \int_{-\infty}^{s_{up}} p(s|n) ds = \frac{\int_{-\infty}^{s_{up}} L(n|s) \pi(s) ds}{\int_{-\infty}^{\infty} L(n|s) \pi(s) ds} , \tag{33.44}$$

where the lower limit of integration is effectively zero because of the cut-off in $\pi(s)$. By relating the integrals in Eq. (33.44) to incomplete gamma functions, the equation reduces to

$$\alpha = e^{-s_{up}} \frac{\sum_{m=0}^n (s_{up} + b)^m / m!}{\sum_{m=0}^{\infty} b^m / m!} . \tag{33.45}$$

This must be solved numerically for the limit s_{up} . For the special case of $b = 0$, the sums can be related to the *quantile* $F_{\chi^2}^{-1}$ of the χ^2 distribution (inverse of the cumulative distribution) to give

$$s_{up} = \frac{1}{2} F_{\chi^2}^{-1}(1 - \alpha; n_d) , \tag{33.46}$$

where the number of degrees of freedom is $n_d = 2(n + 1)$. The quantile of the χ^2 distribution can be obtained using the CERNLIB routine CHISIN, or the ROOT function `TMath::ChisquareQuantile`. It so happens that for the case of $b = 0$, the upper limits from Eq. (33.46) coincide numerically with the values of the frequentist upper limits discussed in Section 33.3.2.5. Values for $1 - \alpha = 0.9$ and 0.95 are given by the values ν_{up} in Table 33.3. The frequentist properties of confidence intervals for the Poisson mean obtained in this way are discussed in Refs. [2] and [18].

As in any Bayesian analysis, it is important to show how the result would change if one uses different prior probabilities. For example, one could consider the Jeffreys prior as described in Sec. 33.1.4. For this problem one finds the Jeffreys prior $\pi(s) \propto 1/\sqrt{s+b}$ for $s \geq 0$ and zero otherwise. As with the constant prior, one would not regard this as representing one’s prior beliefs about s , both because it is improper and also as it depends on b . Rather it is used with Bayes’ theorem to produce an interval whose frequentist properties can be studied.

33.3.2. Frequentist confidence intervals :

The unqualified phrase “confidence intervals” refers to frequentist intervals obtained with a procedure due to Neyman [25], described below. These are intervals (or in the multiparameter case, regions) constructed so as to include the true value of the parameter with a probability greater than or equal to a specified level, called the *coverage probability*. In this section, we discuss several techniques for producing intervals that have, at least approximately, this property.

33.3.2.1. The Neyman construction for confidence intervals:

Consider a p.d.f. $f(x;\theta)$ where x represents the outcome of the experiment and θ is the unknown parameter for which we want to construct a confidence interval. The variable x could (and often does) represent an estimator for θ . Using $f(x;\theta)$, we can find for a pre-specified probability $1 - \alpha$, and for every value of θ , a set of values $x_1(\theta, \alpha)$ and $x_2(\theta, \alpha)$ such that

$$P(x_1 < x < x_2; \theta) = 1 - \alpha = \int_{x_1}^{x_2} f(x; \theta) dx . \tag{33.47}$$

This is illustrated in Fig. 33.3: a horizontal line segment $[x_1(\theta, \alpha), x_2(\theta, \alpha)]$ is drawn for representative values of θ . The union of such intervals for all values of θ , designated in the figure as $D(\alpha)$, is known as the *confidence belt*. Typically the curves $x_1(\theta, \alpha)$ and $x_2(\theta, \alpha)$ are monotonic functions of θ , which we assume for this discussion.

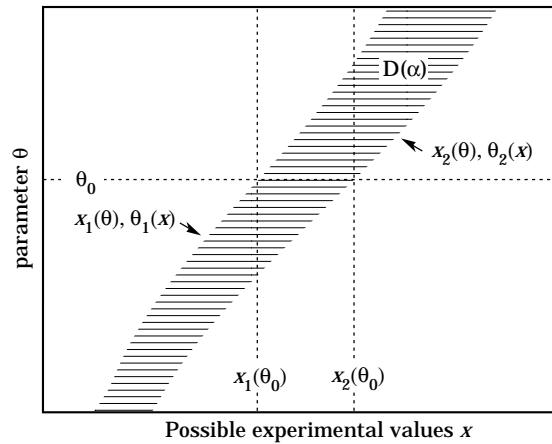


Figure 33.3: Construction of the confidence belt (see text).

Upon performing an experiment to measure x and obtaining a value x_0 , one draws a vertical line through x_0 . The confidence interval for θ is the set of all values of θ for which the corresponding line segment $[x_1(\theta, \alpha), x_2(\theta, \alpha)]$ is intercepted by this vertical line. Such confidence intervals are said to have a *confidence level* (CL) equal to $1 - \alpha$.

Now suppose that the true value of θ is θ_0 , indicated in the figure. We see from the figure that θ_0 lies between $\theta_1(x)$ and $\theta_2(x)$ if and only if x lies between $x_1(\theta_0)$ and $x_2(\theta_0)$. The two events thus have the same probability, and since this is true for any value θ_0 , we can drop the subscript 0 and obtain

$$1 - \alpha = P(x_1(\theta) < x < x_2(\theta)) = P(\theta_2(x) < \theta < \theta_1(x)) . \tag{33.48}$$

In this probability statement, $\theta_1(x)$ and $\theta_2(x)$, *i.e.*, the endpoints of the interval, are the random variables and θ is an unknown constant. If the experiment were to be repeated a large number of times, the interval $[\theta_1, \theta_2]$ would vary, covering the fixed value θ in a fraction $1 - \alpha$ of the experiments.

The condition of coverage in Eq. (33.47) does not determine x_1 and x_2 uniquely, and additional criteria are needed. The most common criterion is to choose *central intervals* such that the probabilities excluded below x_1 and above x_2 are each $\alpha/2$. In other cases, one may want to report only an upper or lower limit, in which case the probability excluded below x_1 or above x_2 can be set to zero. Another

principle based on *likelihood ratio ordering* for determining which values of x should be included in the confidence belt is discussed in Sec. 33.3.2.2

When the observed random variable x is continuous, the coverage probability obtained with the Neyman construction is $1 - \alpha$, regardless of the true value of the parameter. If x is discrete, however, it is not possible to find segments $[x_1(\theta, \alpha), x_2(\theta, \alpha)]$ that satisfy Eq. (33.47) exactly for all values of θ . By convention, one constructs the confidence belt requiring the probability $P(x_1 < x < x_2)$ to be *greater than or equal to* $1 - \alpha$. This gives confidence intervals that include the true parameter with a probability greater than or equal to $1 - \alpha$.

33.3.2.2. Relationship between intervals and tests:

An equivalent method of constructing confidence intervals is to consider a test (see Sec. 33.2) of the hypothesis that the parameter's true value is θ (assume one constructs a test for all physical values of θ). One then excludes all values of θ where the hypothesis would be rejected at a significance level less than α . The remaining values constitute the confidence interval at confidence level $1 - \alpha$.

In this procedure, one is still free to choose the test to be used; this corresponds to the freedom in the Neyman construction as to which values of the data are included in the confidence belt. One possibility is use a test statistic based on the *likelihood ratio*,

$$\lambda = \frac{f(x; \theta)}{f(x; \hat{\theta})}, \tag{33.49}$$

where $\hat{\theta}$ is the value of the parameter which, out of all allowed values, maximizes $f(x; \theta)$. This results in the intervals described in [27] by Feldman and Cousins. The same intervals can be obtained from the Neyman construction described in the previous section by including in the confidence belt those values of x which give the greatest values of λ .

Another technique that can be formulated in the language of statistical tests has been used to set limits on the Higgs mass from measurements at LEP [28,29]. For each value of the Higgs mass, a statistic called CL_s is determined from the ratio

$$CL_s = \frac{p\text{-value of signal plus background hypothesis}}{1 - p\text{-value of hypothesis of background only}}. \tag{33.50}$$

The p -values in Eq. (33.50) are themselves based on a test statistic which depends in general on the signal being tested, *i.e.*, on the hypothesized Higgs mass.

In the usual procedure for constructing confidence intervals, one would exclude the signal hypothesis if the probability to obtain a value of CL_s less than the one actually observed is less than α . The LEP Higgs group has in fact followed a more conservative approach, and excludes the signal at a confidence level $1 - \alpha$ if CL_s itself (not the probability to obtain a lower CL_s value) is less than α . This prevents exclusion of a parameter value that could result from a statistical fluctuation in situations where one has no sensitivity, *e.g.*, at very high Higgs masses. The procedure results in a coverage probability that is in general greater than $1 - \alpha$. The interpretation of such intervals is discussed in Refs.[28,29].

33.3.2.3. Profile likelihood and treatment of nuisance parameters:

As mentioned in Section 33.3.1, one may have a model containing parameters that must be determined from data, but which are not of any interest in the final result (nuisance parameters). Suppose the likelihood $L(\theta, \nu)$ depends on parameters of interest θ and nuisance parameters ν . The nuisance parameters can be effectively removed from the problem by constructing the *profile likelihood*, defined by

$$L_p(\theta) = L(\theta, \hat{\nu}(\theta)), \tag{33.51}$$

where $\hat{\nu}(\theta)$ is given by the ν that maximizes the likelihood for fixed θ . The profile likelihood may then be used to construct tests of or intervals for the parameters of interest. This is in contrast to the integrated likelihood (33.28) used in the Bayesian approach. For example, one may construct the profile likelihood ratio,

$$\lambda_p(\theta) = \frac{L_p(\theta)}{L(\hat{\theta}, \hat{\nu})}, \tag{33.52}$$

where $\hat{\theta}$ and $\hat{\nu}$ are the ML estimators. The ratio λ_p can be used in place of the likelihood ratio (33.49) for inference about θ . The resulting intervals for the parameters of interest are not guaranteed to have the exact coverage probability for all values of the nuisance parameters, but in cases of practical interest the approximation is found to be very good. Further discussion on use of the profile likelihood can be found in, *e.g.*, Refs.[33,34] and other contributions to the PHYSTAT conferences [14].

33.3.2.4. Gaussian distributed measurements:

An important example of constructing a confidence interval is when the data consists of a single random variable x that follows a Gaussian distribution; this is often the case when x represents an estimator for a parameter and one has a sufficiently large data sample. If there is more than one parameter being estimated, the multivariate Gaussian is used. For the univariate case with known σ ,

$$1 - \alpha = \frac{1}{\sqrt{2\pi}\sigma} \int_{\mu-\delta}^{\mu+\delta} e^{-(x-\mu)^2/2\sigma^2} dx = \text{erf}\left(\frac{\delta}{\sqrt{2}\sigma}\right) \tag{33.53}$$

is the probability that the measured value x will fall within $\pm\delta$ of the true value μ . From the symmetry of the Gaussian with respect to x and μ , this is also the probability for the interval $x \pm \delta$ to include μ . Fig. 33.4 shows a $\delta = 1.64\sigma$ confidence interval unshaded. The choice $\delta = \sigma$ gives an interval called the *standard error* which has $1 - \alpha = 68.27\%$ if σ is known. Values of α for other frequently used choices of δ are given in Table 33.1.

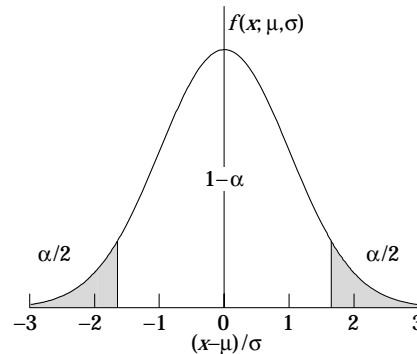


Figure 33.4: Illustration of a symmetric 90% confidence interval (unshaded) for a measurement of a single quantity with Gaussian errors. Integrated probabilities, defined by α , are as shown.

Table 33.1: Area of the tails α outside $\pm\delta$ from the mean of a Gaussian distribution.

α	δ	α	δ
0.3173	1σ	0.2	1.28σ
4.55×10^{-2}	2σ	0.1	1.64σ
2.7×10^{-3}	3σ	0.05	1.96σ
6.3×10^{-5}	4σ	0.01	2.58σ
5.7×10^{-7}	5σ	0.001	3.29σ
2.0×10^{-9}	6σ	10^{-4}	3.89σ

We can set a one-sided (upper or lower) limit by excluding above $x + \delta$ (or below $x - \delta$). The values of α for such limits are half the values in Table 33.1.

The relation (33.53) can be re-expressed using the cumulative distribution function for the χ^2 distribution as

$$\alpha = 1 - F(\chi^2; n), \tag{33.54}$$

for $\chi^2 = (\delta/\sigma)^2$ and $n = 1$ degree of freedom. This can be obtained from Fig. 33.1 on the $n = 1$ curve or by using the CERNLIB routine PROB or the ROOT function TMath::Prob.

For multivariate measurements of, say, n parameter estimates $\hat{\theta} = (\hat{\theta}_1, \dots, \hat{\theta}_n)$, one requires the full covariance matrix $V_{ij} = \text{cov}[\hat{\theta}_i, \hat{\theta}_j]$, which can be estimated as described in Sections 33.1.2 and 33.1.3. Under fairly general conditions with the methods of maximum-likelihood or least-squares in the large sample limit, the estimators will be distributed according to a multivariate Gaussian centered about the true (unknown) values θ , and furthermore, the likelihood function itself takes on a Gaussian shape.

The standard error ellipse for the pair $(\hat{\theta}_i, \hat{\theta}_j)$ is shown in Fig. 33.5, corresponding to a contour $\chi^2 = \chi^2_{\min} + 1$ or $\ln L = \ln L_{\max} - 1/2$. The ellipse is centered about the estimated values $\hat{\theta}$, and the tangents to the ellipse give the standard deviations of the estimators, σ_i and σ_j . The angle of the major axis of the ellipse is given by

$$\tan 2\phi = \frac{2\rho_{ij}\sigma_i\sigma_j}{\sigma_j^2 - \sigma_i^2}, \tag{33.55}$$

where $\rho_{ij} = \text{cov}[\hat{\theta}_i, \hat{\theta}_j]/\sigma_i\sigma_j$ is the correlation coefficient.

The correlation coefficient can be visualized as the fraction of the distance σ_i from the ellipse's horizontal centerline at which the ellipse becomes tangent to vertical, *i.e.*, at the distance $\rho_{ij}\sigma_i$ below the centerline as shown. As ρ_{ij} goes to +1 or -1, the ellipse thins to a diagonal line.

It could happen that one of the parameters, say, θ_j , is known from previous measurements to a precision much better than σ_j , so that the current measurement contributes almost nothing to the knowledge of θ_j . However, the current measurement of θ_i and its dependence on θ_j may still be important. In this case, instead of quoting both parameter estimates and their correlation, one sometimes reports the value of θ_i , which minimizes χ^2 at a fixed value of θ_j , such as the PDG best value. This θ_i value lies along the dotted line between the points where the ellipse becomes tangent to vertical, and has statistical error σ_{inner} as shown on the figure, where $\sigma_{\text{inner}} = (1 - \rho_{ij}^2)^{1/2}\sigma_i$. Instead of the correlation ρ_{ij} , one reports the dependency $d\hat{\theta}_i/d\theta_j$ which is the slope of the dotted line. This slope is related to the correlation coefficient by $d\hat{\theta}_i/d\theta_j = \rho_{ij} \times \frac{\sigma_i}{\sigma_j}$.

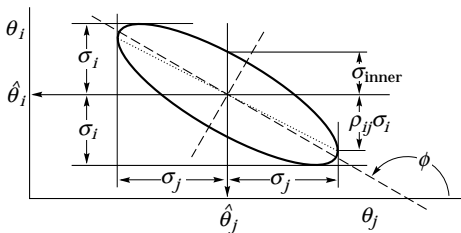


Figure 33.5: Standard error ellipse for the estimators $\hat{\theta}_i$ and $\hat{\theta}_j$. In this case the correlation is negative.

As in the single-variable case, because of the symmetry of the Gaussian function between θ and $\hat{\theta}$, one finds that contours of constant $\ln L$ or χ^2 cover the true values with a certain, fixed probability. That is, the confidence region is determined by

$$\ln L(\theta) \geq \ln L_{\max} - \Delta \ln L, \tag{33.56}$$

or where a χ^2 has been defined for use with the method of least-squares,

$$\chi^2(\theta) \leq \chi^2_{\min} + \Delta\chi^2. \tag{33.57}$$

Table 33.2: $\Delta\chi^2$ or $2\Delta \ln L$ corresponding to a coverage probability $1 - \alpha$ in the large data sample limit, for joint estimation of m parameters.

$(1 - \alpha)$ (%)	$m = 1$	$m = 2$	$m = 3$
68.27	1.00	2.30	3.53
90.	2.71	4.61	6.25
95.	3.84	5.99	7.82
95.45	4.00	6.18	8.03
99.	6.63	9.21	11.34
99.73	9.00	11.83	14.16

Values of $\Delta\chi^2$ or $2\Delta \ln L$ are given in Table 33.2 for several values of the coverage probability and number of fitted parameters.

For finite data samples, the probability for the regions determined by equations (33.56) or (33.57) to cover the true value of θ will depend on θ , so these are not exact confidence regions according to our previous definition. Nevertheless, they can still have a coverage probability only weakly dependent on the true parameter, and approximately as given in Table 33.2. In any case, the coverage probability of the intervals or regions obtained according to this procedure can in principle be determined as a function of the true parameter(s), for example, using a Monte Carlo calculation.

One of the practical advantages of intervals that can be constructed from the log-likelihood function or χ^2 is that it is relatively simple to produce the interval for the combination of several experiments. If N independent measurements result in log-likelihood functions $\ln L_i(\theta)$, then the combined log-likelihood function is simply the sum,

$$\ln L(\theta) = \sum_{i=1}^N \ln L_i(\theta). \tag{33.58}$$

This can then be used to determine an approximate confidence interval or region with Eq. (33.56), just as with a single experiment.

33.3.2.5. Poisson or binomial data:

Another important class of measurements consists of counting a certain number of events, n . In this section, we will assume these are all events of the desired type, *i.e.*, there is no background. If n represents the number of events produced in a reaction with cross section σ , say, in a fixed integrated luminosity \mathcal{L} , then it follows a Poisson distribution with mean $\nu = \sigma\mathcal{L}$. If, on the other hand, one has selected a larger sample of N events and found n of them to have a particular property, then n follows a binomial distribution where the parameter p gives the probability for the event to possess the property in question. This is appropriate, *e.g.*, for estimates of branching ratios or selection efficiencies based on a given total number of events.

For the case of Poisson distributed n , the upper and lower limits on the mean value ν can be found from the Neyman procedure to be

$$\nu_{\text{lo}} = \frac{1}{2}F_{\chi^2}^{-1}(\alpha_{\text{lo}}; 2n), \tag{33.59a}$$

$$\nu_{\text{up}} = \frac{1}{2}F_{\chi^2}^{-1}(1 - \alpha_{\text{up}}; 2(n + 1)), \tag{33.59b}$$

where the upper and lower limits are at confidence levels of $1 - \alpha_{\text{lo}}$ and $1 - \alpha_{\text{up}}$, respectively, and $F_{\chi^2}^{-1}$ is the *quantile* of the χ^2 distribution (inverse of the cumulative distribution). The quantiles $F_{\chi^2}^{-1}$ can be obtained from standard tables or from the CERNLIB routine CHISIN. For central confidence intervals at confidence level $1 - \alpha$, set $\alpha_{\text{lo}} = \alpha_{\text{up}} = \alpha/2$.

It happens that the upper limit from Eq. (33.59a) coincides numerically with the Bayesian upper limit for a Poisson parameter, using a uniform prior p.d.f. for ν . Values for confidence levels of 90% and 95% are shown in Table 33.3. For the case of binomially distributed n successes out of N trials with probability of success p , the upper and lower limits on p are found to be

$$p_{\text{lo}} = \frac{nF_F^{-1}[\alpha_{\text{lo}}; 2n, 2(N - n + 1)]}{N - n + 1 + nF_F^{-1}[\alpha_{\text{lo}}; 2n, 2(N - n + 1)]}, \tag{33.60a}$$

$$p_{\text{up}} = \frac{(n + 1)F_F^{-1}[1 - \alpha_{\text{up}}; 2(n + 1), 2(N - n)]}{(N - n) + (n + 1)F_F^{-1}[1 - \alpha_{\text{up}}; 2(n + 1), 2(N - n)]}. \tag{33.60b}$$

Table 33.3: Lower and upper (one-sided) limits for the mean ν of a Poisson variable given n observed events in the absence of background, for confidence levels of 90% and 95%.

n	$1 - \alpha = 90\%$		$1 - \alpha = 95\%$	
	ν_{lo}	ν_{up}	ν_{lo}	ν_{up}
0	–	2.30	–	3.00
1	0.105	3.89	0.051	4.74
2	0.532	5.32	0.355	6.30
3	1.10	6.68	0.818	7.75
4	1.74	7.99	1.37	9.15
5	2.43	9.27	1.97	10.51
6	3.15	10.53	2.61	11.84
7	3.89	11.77	3.29	13.15
8	4.66	12.99	3.98	14.43
9	5.43	14.21	4.70	15.71
10	6.22	15.41	5.43	16.96

Here F_F^{-1} is the quantile of the F distribution (also called the Fisher–Snedecor distribution; see [4]).

33.3.2.6. Difficulties with intervals near a boundary:

A number of issues arise in the construction and interpretation of confidence intervals when the parameter can only take on values in a restricted range. An important example is where the mean of a Gaussian variable is constrained on physical grounds to be non-negative. This arises, for example, when the square of the neutrino mass is estimated from $\hat{m}^2 = \hat{E}^2 - \hat{p}^2$, where \hat{E} and \hat{p} are independent, Gaussian-distributed estimates of the energy and momentum. Although the true m^2 is constrained to be positive, random errors in \hat{E} and \hat{p} can easily lead to negative values for the estimate \hat{m}^2 .

If one uses the prescription given above for Gaussian distributed measurements, which says to construct the interval by taking the estimate plus-or-minus one standard deviation, then this can give intervals that are partially or entirely in the unphysical region. In fact, by following strictly the Neyman construction for the central confidence interval, one finds that the interval is truncated below zero; nevertheless an extremely small or even a zero-length interval can result.

An additional important example is where the experiment consists of counting a certain number of events, n , which is assumed to be Poisson-distributed. Suppose the expectation value $E[n] = \nu$ is equal to $s + b$, where s and b are the means for signal and background processes, and assume further that b is a known constant. Then $\hat{s} = n - b$ is an unbiased estimator for s . Depending on true magnitudes of s and b , the estimate \hat{s} can easily fall in the negative region. Similar to the Gaussian case with the positive mean, the central confidence interval or even the upper limit for s may be of zero length.

The confidence interval will by construction not cover the parameter with a probability of at most α , and if a zero-length interval results, then this is evidently one of those experiments. So although the construction is behaving as it should, a null interval is an unsatisfying result to report, and several solutions to this type of problem are possible.

An additional difficulty arises when a parameter estimate is not significantly far away from the boundary, in which case it is natural to report a one-sided confidence interval (often an upper limit). It is straightforward to force the Neyman prescription to produce only an upper limit by setting $x_2 = \infty$ in Eq. 33.47. Then x_1 is uniquely determined and the upper limit can be obtained. If, however, the data come out such that the parameter estimate is not so close to the boundary, one might wish to report a central (*i.e.*, two-sided) confidence interval. As pointed out by Feldman and Cousins [27],

however, if the decision to report an upper limit or two-sided interval is made by looking at the data (“flip-flopping”), then in general there will be parameter values for which the resulting intervals have a coverage probability less than $1 - \alpha$.

With the confidence intervals suggested in [27], the prescription determines whether the interval is one- or two-sided in a way which preserves the coverage probability. Interval constructions that have this property and avoid the problem of null intervals are said to be unified. The intervals based on the Feldman-Cousins prescription are of this type. For a given choice of $1 - \alpha$, if the parameter estimate is sufficiently close to the boundary, the method gives a one-sided limit. In the case of a Poisson variable in the presence of background, for example, this would occur if the number of observed events is compatible with the expected background. For parameter estimates increasingly far away from the boundary, *i.e.*, for increasing signal significance, the interval makes a smooth transition from one- to two-sided, and far away from the boundary, one obtains a central interval.

The intervals according to this method for the mean of Poisson variable in the absence of background are given in Table 33.4. (Note that α in [27] is defined following Neyman [25] as the coverage probability; this is opposite the modern convention used here in which the coverage probability is $1 - \alpha$.) The values of $1 - \alpha$ given here refer to the coverage of the true parameter by the whole interval $[\nu_1, \nu_2]$. In Table 33.3 for the one-sided upper limit, however, $1 - \alpha$ refers to the probability to have $\nu_{\text{up}} \geq \nu$ (or $\nu_{\text{lo}} \leq \nu$ for lower limits).

Table 33.4: Unified confidence intervals $[\nu_1, \nu_2]$ for a the mean of a Poisson variable given n observed events in the absence of background, for confidence levels of 90% and 95%.

n	$1 - \alpha = 90\%$		$1 - \alpha = 95\%$	
	ν_1	ν_2	ν_1	ν_2
0	0.00	2.44	0.00	3.09
1	0.11	4.36	0.05	5.14
2	0.53	5.91	0.36	6.72
3	1.10	7.42	0.82	8.25
4	1.47	8.60	1.37	9.76
5	1.84	9.99	1.84	11.26
6	2.21	11.47	2.21	12.75
7	3.56	12.53	2.58	13.81
8	3.96	13.99	2.94	15.29
9	4.36	15.30	4.36	16.77
10	5.50	16.50	4.75	17.82

A potential difficulty with unified intervals arises if, for example, one constructs such an interval for a Poisson parameter s of some yet to be discovered signal process with, say, $1 - \alpha = 0.9$. If the true signal parameter is zero, or in any case much less than the expected background, one will usually obtain a one-sided upper limit on s . In a certain fraction of the experiments, however, a two-sided interval for s will result. Since, however, one typically chooses $1 - \alpha$ to be only 0.9 or 0.95 when setting limits, the value $s = 0$ may be found below the lower edge of the interval before the existence of the effect is well established. It must then be communicated carefully that in excluding $s = 0$ from the interval, one is not necessarily claiming to have discovered the effect.

The intervals constructed according to the unified procedure in [27] for a Poisson variable n consisting of signal and background have the property that for $n = 0$ observed events, the upper limit decreases for increasing expected background. This is counter-intuitive, since it is known that if $n = 0$ for the experiment in question, then no background was observed, and therefore one may argue that the expected background should not be relevant. The extent to which

one should regard this feature as a drawback is a subject of some controversy (see, *e.g.*, [32]).

Another possibility is to construct a Bayesian interval as described in Section 33.3.1. The presence of the boundary can be incorporated simply by setting the prior density to zero in the unphysical region. Priors based on invariance principles (rather than subjective degree of belief) for the Poisson mean are rarely used in high-energy physics. An example one may consider for the Poisson problem is a prior inversely proportional to the mean; here one obtains a posterior that diverges for the case of zero events observed, and finds upper limits which undercover when evaluated by the frequentist definition of coverage [2]. Rather, priors uniform in the Poisson mean have been used, although as previously mentioned, this is generally not done to reflect the experimenter's degree of belief, but rather as a procedure for obtaining an interval with certain frequentist properties. The resulting upper limits have a coverage probability that depends on the true value of the Poisson parameter, and is nowhere smaller than the stated probability content. Lower limits and two-sided intervals for the Poisson mean based on flat priors undercover, however, for some values of the parameter, although to an extent that in practical cases may not be too severe [2, 18]. Intervals constructed in this way have the advantage of being easy to derive; if several independent measurements are to be combined then one simply multiplies the likelihood functions (cf. Eq. (33.58)).

An additional alternative is presented by the intervals found from the likelihood function or χ^2 using the prescription of Equations (33.56) or (33.57). However, the coverage probability is not, in general, independent of the true parameter, and these intervals can for some parameter values undercover. The coverage probability can, of course, be determined with some extra effort and reported with the result. A study of the coverage of different intervals for a Poisson parameter can be found in [30].

Also as in the Bayesian case, intervals derived from the value of the likelihood function from a combination of independent experiments can be determined simply by multiplying the likelihood functions. These intervals are also invariant under transformation of the parameter; this is not true for Bayesian intervals with a conventional flat prior, because a uniform distribution in, say, θ will not be uniform if transformed to $1/\theta$. Use of the likelihood function to determine approximate confidence intervals is discussed further in [31].

In any case, it is important to always report sufficient information so that the result can be combined with other measurements. Often this means giving an unbiased estimator and its standard deviation, even if the estimated value is in the unphysical region.

It can also be useful with a frequentist interval to calculate its subjective probability content using the posterior p.d.f. based on one or several reasonable guesses for the prior p.d.f. If it turns out to be significantly less than the stated confidence level, this warns that it would be particularly misleading to draw conclusions about the parameter's value from the interval alone.

References:

1. B. Efron, *Am. Stat.* **40**, 11 (1986).
2. R.D. Cousins, *Am. J. Phys.* **63**, 398 (1995).
3. A. Stuart, J.K. Ord, and S. Arnold, *Kendall's Advanced Theory of Statistics*, Vol. 2A: *Classical Inference and the Linear Model*, 6th Ed., Oxford Univ. Press (1999), and earlier editions by Kendall and Stuart. The likelihood-ratio ordering principle is described at the beginning of Ch. 23. Chapter 26 compares different schools of statistical inference.
4. F.E. James, *Statistical Methods in Experimental Physics*, 2nd ed., (World Scientific, Singapore, 2007).
5. H. Cramér, *Mathematical Methods of Statistics*, Princeton Univ. Press, New Jersey (1958).
6. L. Lyons, *Statistics for Nuclear and Particle Physicists*, (Cambridge University Press, New York, 1986).
7. R. Barlow, *Nucl. Instrum. Methods* **A297**, 496 (1990).
8. G. Cowan, *Statistical Data Analysis*, (Oxford University Press, Oxford, 1998).
9. For a review, see S. Baker and R. Cousins, *Nucl. Instrum. Methods* **221**, 437 (1984).
10. For information on neural networks and related topics, see *e.g.*, C.M. Bishop, *Neural Networks for Pattern Recognition*, Clarendon Press, Oxford (1995); C. Peterson and T. Rönkvallsson, An Intro. to Artificial Neural Networks, in *Proc. of the 1991 CERN School of Computing*, C. Verkerk (ed.), CERN 92-02 (1992).
11. T. Hastie, R. Tibshirani, and J. Friedman, *The Elements of Statistical Learning* (2nd edition, Springer, New York, 2009).
12. A. Webb, *Statistical Pattern Recognition*, 2nd ed., (Wiley, New York, 2002).
13. L.I. Kuncheva, *Combining Pattern Classifiers*, (Wiley, New York, 2004).
14. Links to the Proceedings of the PHYSTAT conference series (Durham 2002, Stanford 2003, Oxford 2005, and Geneva 2007) can be found at phystat.org.
15. A. Höcker *et al.*, *TMVA Users Guide*, physics/0703039(2007); software available from tmva.sf.net.
16. I. Narsky, *StatPatternRecognition: A C++ Package for Statistical Analysis of High Energy Physics Data*, physics/0507143(2005); software avail. from sourceforge.net/projects/statpatrec.
17. L. Demortier, *P-Values and Nuisance Parameters*, Proceedings of PHYSTAT 2007, CERN-2008-001, p. 23..
18. B.P. Roe and M.B. Woodroffe, *Phys. Rev.* **D63**, 13009 (2001).
19. A. O'Hagan and J.J. Forster, *Bayesian Inference*, (2nd edition, volume 2B of *Kendall's Advanced Theory of Statistics*, Arnold, London, 2004).
20. Devinderjit Sivya and John Skilling, *Data Analysis: A Bayesian Tutorial*, (Oxford University Press, 2006).
21. P.C. Gregory, *Bayesian Logical Data Analysis for the Physical Sciences*, (Cambridge University Press, 2005).
22. J.M. Bernardo and A.F.M. Smith, *Bayesian Theory*, (Wiley, 2000).
23. Robert E. Kass and Larry Wasserman, *The Selection of Prior Distributions by Formal Rules*, *J. Am. Stat. Assoc.*, Vol. 91, No. 435, pp. 1343-1370 (1996).
24. P.H. Garthwaite, I.T. Jolliffe, and B. Jones, *Statistical Inference*, (Prentice Hall, 1995).
25. J. Neyman, *Phil. Trans. Royal Soc. London, Series A*, **236**, 333 (1937), reprinted in *A Selection of Early Statistical Papers on J. Neyman*, (University of California Press, Berkeley, 1967).
26. Robert E. Kass and Adrian E. Raftery, *Bayes Factors*, *J. Am. Stat. Assoc.*, Vol. 90, No. 430, pp. 773-795 (1995).
27. G.J. Feldman and R.D. Cousins, *Phys. Rev.* **D57**, 3873 (1998). This paper does not specify what to do if the ordering principle gives equal rank to some values of x . Eq. 21.6 of Ref. 3 gives the rule: all such points are included in the acceptance region (the domain $D(\alpha)$). Some authors have assumed the contrary, and shown that one can then obtain null intervals.
28. T. Junk, *Nucl. Instrum. Methods* **A434**, 435 (1999).
29. A.L. Read, *Modified frequentist analysis of search results (the CL_s method)*, in F. James, L. Lyons, and Y. Perrin (eds.), *Workshop on Confidence Limits*, CERN Yellow Report 2000-005, available through cdsweb.cern.ch.
30. Joel Heinrich, *Coverage of Error Bars for Poisson Data*, CDF Statistics Note 6438, www-cdf.fnal.gov/publications/cdf6438_coverage.pdf (2003).
31. F. Porter, *Nucl. Instrum. Methods* **A368**, 793 (1996).
32. Workshop on Confidence Limits, CERN, 17-18 Jan. 2000, www.cern.ch/CERN/Divisions/EP/Events/CLW/. The proceedings, F. James, L. Lyons, and Y. Perrin (eds.), CERN Yellow Report 2000-005, are available through cdsweb.cern.ch. See also the Fermilab workshop at conferences.fnal.gov/c12k/.
33. N. Reid, *Likelihood Inference in the Presence of Nuisance Parameters*, Proceedings of PHYSTAT2003, L. Lyons, R. Mount, and R. Reitmeyer, eds., eConf C030908, Stanford, 2003.
34. W.A. Rolke, A.M. Lopez, and J. Conrad, *Nucl. Instrum. Methods* **A551**, 493 (2005); physics/0403059.

34. MONTE CARLO TECHNIQUES

Revised September 2009 by G. Cowan (RHUL).

Monte Carlo techniques are often the only practical way to evaluate difficult integrals or to sample random variables governed by complicated probability density functions. Here we describe an assortment of methods for sampling some commonly occurring probability density functions.

34.1. Sampling the uniform distribution

Most Monte Carlo sampling or integration techniques assume a “random number generator,” which generates uniform statistically independent values on the half open interval $[0, 1)$; for reviews see, e.g., [1, 2].

Uniform random number generators are available in software libraries such as CERNLIB [3], CLHEP [4], and ROOT [5]. For example, in addition to a basic congruential generator `TRandom` (see below), ROOT provides three more sophisticated routines: `TRandom1` implements the RANLUX generator [6] based on the method by Lüscher, and allows the user to select different quality levels, trading off quality with speed; `TRandom2` is based on the maximally equidistributed combined Tausworthe generator by L’Ecuyer [7]; the `TRandom3` generator implements the Mersenne twister algorithm of Matsumoto and Nishimura [8]. All of the algorithms produce a periodic sequence of numbers, and to obtain effectively random values, one must not use more than a small subset of a single period. The Mersenne twister algorithm has an extremely long period of $2^{19937} - 1$.

The performance of the generators can be investigated with tests such as DIEHARD [9] or TestU01 [10]. Many commonly available congruential generators fail these tests and often have sequences (typically with periods less than 2^{32}), which can be easily exhausted on modern computers. A short period is a problem for the `TRandom` generator in ROOT, which, however, has the advantage that its state is stored in a single 32-bit word. The generators `TRandom1`, `TRandom2`, or `TRandom3` have much longer periods, with `TRandom3` being recommended by the ROOT authors as providing the best combination of speed and good random properties.

34.2. Inverse transform method

If the desired probability density function is $f(x)$ on the range $-\infty < x < \infty$, its cumulative distribution function (expressing the probability that $x \leq a$) is given by Eq. (32.6). If a is chosen with probability density $f(a)$, then the integrated probability up to point a , $F(a)$, is itself a random variable which will occur with uniform probability density on $[0, 1]$. If x can take on any value, and ignoring the endpoints, we can then find a unique x chosen from the p.d.f. $f(s)$ for a given u if we set

$$u = F(x) , \tag{34.1}$$

provided we can find an inverse of F , defined by

$$x = F^{-1}(u) . \tag{34.2}$$

This method is shown in Fig. 34.1a. It is most convenient when one can calculate by hand the inverse function of the indefinite integral of f . This is the case for some common functions $f(x)$ such as $\exp(x)$, $(1 - x)^n$, and $1/(1 + x^2)$ (Cauchy or Breit-Wigner), although it does not necessarily produce the fastest generator. Standard libraries contain software to implement this method numerically, working from functions or histograms in one or more dimensions, e.g., the UNU.RAN package [11], available in ROOT.

For a discrete distribution, $F(x)$ will have a discontinuous jump of size $f(x_k)$ at each allowed $x_k, k = 1, 2, \dots$. Choose u from a uniform distribution on $(0, 1)$ as before. Find x_k such that

$$F(x_{k-1}) < u \leq F(x_k) \equiv \text{Prob}(x \leq x_k) = \sum_{i=1}^k f(x_i) ; \tag{34.3}$$

then x_k is the value we seek (note: $F(x_0) \equiv 0$). This algorithm is illustrated in Fig. 34.1b.

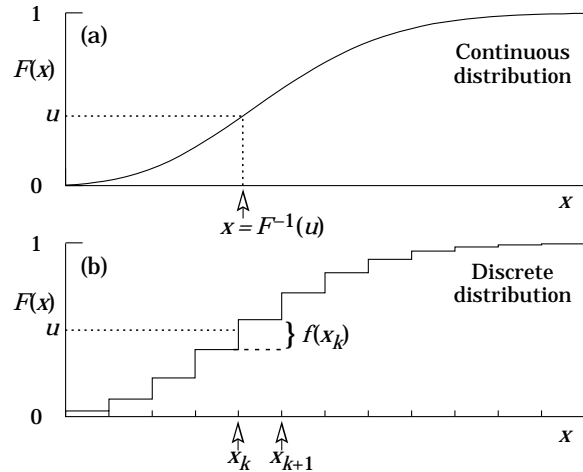


Figure 34.1: Use of a random number u chosen from a uniform distribution $(0,1)$ to find a random number x from a distribution with cumulative distribution function $F(x)$.

34.3. Acceptance-rejection method (Von Neumann)

Very commonly an analytic form for $F(x)$ is unknown or too complex to work with, so that obtaining an inverse as in Eq. (34.2) is impractical. We suppose that for any given value of x , the probability density function $f(x)$ can be computed, and further that enough is known about $f(x)$ that we can enclose it entirely inside a shape which is C times an easily generated distribution $h(x)$, as illustrated in Fig. 34.2.

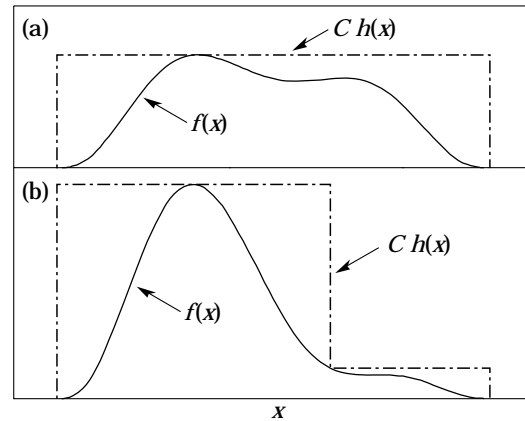


Figure 34.2: Illustration of the acceptance-rejection method. Random points are chosen inside the upper bounding figure, and rejected if the ordinate exceeds $f(x)$. The lower figure illustrates a method to increase the efficiency (see text).

Frequently $h(x)$ is uniform or is a normalized sum of uniform distributions. Note that both $f(x)$ and $h(x)$ must be normalized to unit area, and therefore, the proportionality constant $C > 1$. To generate $f(x)$, first generate a candidate x according to $h(x)$. Calculate $f(x)$ and the height of the envelope $C h(x)$; generate u and test if $u C h(x) \leq f(x)$. If so, accept x ; if not reject x and try again. If we regard x and $u C h(x)$ as the abscissa and ordinate of a point in a two-dimensional plot, these points will populate the entire area $C h(x)$ in a smooth manner; then we accept those which fall under $f(x)$. The efficiency is the ratio of areas, which must equal $1/C$; therefore we must keep C as close as possible to 1.0. Therefore, we try to choose $C h(x)$ to be as close to $f(x)$ as convenience dictates, as in the lower part of Fig. 34.2.

34.4. Algorithms

Algorithms for generating random numbers belonging to many different distributions are given for example by Press [12], Ahrens and Dieter [13], Rubinstein [14], Devroye [15], Walck [16] and Gentle [17]. For many distributions, alternative algorithms exist, varying in complexity, speed, and accuracy. For time-critical applications, these algorithms may be coded in-line to remove the significant overhead often encountered in making function calls.

In the examples given below, we use the notation for the variables and parameters given in Table 32.1. Variables named “ u ” are assumed to be independent and uniform on $[0,1]$. Denominators must be verified to be non-zero where relevant.

34.4.1. Exponential decay :

This is a common application of the inverse transform method, and uses the fact that if u is uniformly distributed in $[0,1]$, then $(1-u)$ is as well. Consider an exponential p.d.f. $f(t) = (1/\tau)\exp(-t/\tau)$ that is truncated so as to lie between two values, a and b , and renormalized to unit area. To generate decay times t according to this p.d.f., first let $\alpha = \exp(-a/\tau)$ and $\beta = \exp(-b/\tau)$; then generate u and let

$$t = -\tau \ln(\beta + u(\alpha - \beta)). \quad (34.4)$$

For $(a,b) = (0,\infty)$, we have simply $t = -\tau \ln u$. (See also Sec. 34.4.6.)

34.4.2. Isotropic direction in 3D :

Isotropy means the density is proportional to solid angle, the differential element of which is $d\Omega = d(\cos\theta)d\phi$. Hence $\cos\theta$ is uniform $(2u_1 - 1)$ and ϕ is uniform $(2\pi u_2)$. For alternative generation of $\sin\phi$ and $\cos\phi$, see the next subsection.

34.4.3. Sine and cosine of random angle in 2D :

Generate u_1 and u_2 . Then $v_1 = 2u_1 - 1$ is uniform on $(-1,1)$, and $v_2 = u_2$ is uniform on $(0,1)$. Calculate $r^2 = v_1^2 + v_2^2$. If $r^2 > 1$, start over. Otherwise, the sine (S) and cosine (C) of a random angle (*i.e.*, uniformly distributed between zero and 2π) are given by

$$S = 2v_1v_2/r^2 \quad \text{and} \quad C = (v_1^2 - v_2^2)/r^2. \quad (34.5)$$

34.4.4. Gaussian distribution :

If u_1 and u_2 are uniform on $(0,1)$, then

$$z_1 = \sin 2\pi u_1 \sqrt{-2 \ln u_2} \quad \text{and} \quad z_2 = \cos 2\pi u_1 \sqrt{-2 \ln u_2} \quad (34.6)$$

are independent and Gaussian distributed with mean 0 and $\sigma = 1$.

There are many variants of this basic algorithm, which may be faster. For example, construct $v_1 = 2u_1 - 1$ and $v_2 = 2u_2 - 1$, which are uniform on $(-1,1)$. Calculate $r^2 = v_1^2 + v_2^2$, and if $r^2 > 1$ start over. If $r^2 < 1$, it is uniform on $(0,1)$. Then

$$z_1 = v_1 \sqrt{\frac{-2 \ln r^2}{r^2}} \quad \text{and} \quad z_2 = v_2 \sqrt{\frac{-2 \ln r^2}{r^2}} \quad (34.7)$$

are independent numbers chosen from a normal distribution with mean 0 and variance 1. $z'_i = \mu + \sigma z_i$ distributes with mean μ and variance σ^2 .

For a multivariate Gaussian with an $n \times n$ covariance matrix V , one can start by generating n independent Gaussian variables, $\{\eta_j\}$, with mean 0 and variance 1 as above. Then the new set $\{x_i\}$ is obtained as $x_i = \mu_i + \sum_j L_{ij}\eta_j$, where μ_i is the mean of x_i , and L_{ij} are the components of L , the unique lower triangular matrix that fulfils $V = LL^T$. The matrix L can be easily computed by the following recursive relation (Cholesky's method):

$$L_{jj} = \left(V_{jj} - \sum_{k=1}^{j-1} L_{jk}^2 \right)^{1/2}, \quad (34.8a)$$

$$L_{ij} = \frac{V_{ij} - \sum_{k=1}^{j-1} L_{ik}L_{jk}}{L_{jj}}, \quad j = 1, \dots, n; \quad i = j + 1, \dots, n, \quad (34.8b)$$

where $V_{ij} = \rho_{ij}\sigma_i\sigma_j$ are the components of V . For $n = 2$ one has

$$L = \begin{pmatrix} \sigma_1 & 0 \\ \rho\sigma_2 & \sqrt{1 - \rho^2}\sigma_2 \end{pmatrix}, \quad (34.9)$$

and therefore the correlated Gaussian variables are generated as $x_1 = \mu_1 + \sigma_1\eta_1$, $x_2 = \mu_2 + \rho\sigma_2\eta_1 + \sqrt{1 - \rho^2}\sigma_2\eta_2$.

34.4.5. $\chi^2(n)$ distribution :

To generate variable following the χ^2 distribution for n degrees of freedom, use the Gamma distribution with $k = n/2$ and $\lambda = 1/2$ using the method of Sec. 34.4.6.

34.4.6. Gamma distribution :

All of the following algorithms are given for $\lambda = 1$. For $\lambda \neq 1$, divide the resulting random number x by λ .

- If $k = 1$ (the *exponential* distribution), accept $x = -\ln u$. (See also Sec. 34.4.1.)
- If $0 < k < 1$, initialize with $v_1 = (e + k)/e$ (with $e = 2.71828\dots$ being the natural log base). Generate u_1, u_2 . Define $v_2 = v_1u_1$.

Case 1: $v_2 \leq 1$. Define $x = v_2^{1/k}$. If $u_2 \leq e^{-x}$, accept x and stop, else restart by generating new u_1, u_2 .

Case 2: $v_2 > 1$. Define $x = -\ln([v_1 - v_2]/k)$. If $u_2 \leq x^{k-1}$, accept x and stop, else restart by generating new u_1, u_2 .

Note that, for $k < 1$, the probability density has a pole at $x = 0$, so that return values of zero due to underflow must be accepted or otherwise dealt with.

- Otherwise, if $k > 1$, initialize with $c = 3k - 0.75$. Generate u_1 and compute $v_1 = u_1(1 - u_1)$ and $v_2 = (u_1 - 0.5)\sqrt{c/v_1}$. If $x = k + v_2 - 1 \leq 0$, go back and generate new u_1 ; otherwise generate u_2 and compute $v_3 = 64v_1^3u_2^2$. If $v_3 \leq 1 - 2v_2^2/x$ or if $\ln v_3 \leq 2\{[k - 1] \ln[x/(k - 1)] - v_2\}$, accept x and stop; otherwise go back and generate new u_1 .

34.4.7. Binomial distribution :

Begin with $k = 0$ and generate u uniform in $[0,1]$. Compute $P_k = (1 - p)^n$ and store P_k into B . If $u \leq B$ accept $r_k = k$ and stop. Otherwise, increment k by one; compute the next P_k as $P_k \cdot (p/(1 - p)) \cdot (n - k)/(k + 1)$; add this to B . Again, if $u \leq B$, accept $r_k = k$ and stop, otherwise iterate until a value is accepted. If $p > 1/2$, it will be more efficient to generate r from $f(r; n, q)$, *i.e.*, with p and q interchanged, and then set $r_k = n - r$.

34.4.8. Poisson distribution :

Iterate until a successful choice is made: Begin with $k = 1$ and set $A = 1$ to start. Generate u . Replace A with uA ; if now $A < \exp(-\mu)$, where μ is the Poisson parameter, accept $n_k = k - 1$ and stop. Otherwise increment k by 1, generate a new u and repeat, always starting with the value of A left from the previous try.

Note that the Poisson generator used in ROOT's `TRandom` classes before version 5.12 (including the derived classes `TRandom1`, `TRandom2`, `TRandom3`) as well as the routine `RNPSSN` from CERNLIB, use a Gaussian approximation when μ exceeds a given threshold. This may be satisfactory (and much faster) for some applications. To do this, generate z from a Gaussian with zero mean and unit standard deviation; then use $x = \max(0, [\mu + z\sqrt{\mu} + 0.5])$ where $[\]$ signifies the greatest integer \leq the expression. The routines from Numerical Recipes [12] and CLHEP's routine `RandPoisson` do not make this approximation (see, *e.g.*, Ref. 18).

34.4.9. Student's t distribution :

Generate u_1 and u_2 uniform in $(0,1)$; then $t = \sin(2\pi u_1)[n(u_2^{-2/n} - 1)]^{1/2}$ follows the Student's t distribution for $n > 0$ degrees of freedom (n not necessarily an integer).

Alternatively, generate x from a Gaussian with mean 0 and $\sigma^2 = 1$ according to the method of 34.4.4. Next generate y , an independent gamma random variate, according to 34.4.6 with $\lambda = 1/2$ and $k = n/2$. Then $z = x/\sqrt{y/n}$ is distributed as a t with n degrees of freedom.

For the special case $n = 1$, the Breit-Wigner distribution, generate u_1 and u_2 ; set $v_1 = 2u_1 - 1$ and $v_2 = 2u_2 - 1$. If $v_1^2 + v_2^2 \leq 1$ accept $z = v_1/v_2$ as a Breit-Wigner distribution with unit area, center at 0.0, and FWHM 2.0. Otherwise start over. For center M_0 and FWHM Γ , use $W = z\Gamma/2 + M_0$.

34.4.10. Beta distribution :

The choice of an appropriate algorithm for generation of beta distributed random numbers depends on the values of the parameters α and β . For, e.g., $\alpha = 1$, one can use the transformation method to find $x = 1 - u^{1/\beta}$, and similarly if $\beta = 1$ one has $x = u^{1/\alpha}$. For more general cases see, e.g., Refs. [16,17] and references therein.

34.5. Markov Chain Monte Carlo

In applications involving generation of random numbers following a multivariate distribution with a high number of dimensions, the transformation method may not be possible and the acceptance-rejection technique may have too low of an efficiency to be practical. If it is not required to have independent random values, but only that they follow a certain distribution, then Markov Chain Monte Carlo (MCMC) methods can be used. In depth treatments of MCMC can be found, e.g., in the texts by Robert and Casella [19], Liu [20], and the review by Neal [21].

MCMC is particularly useful in connection with Bayesian statistics, where a p.d.f. $p(\boldsymbol{\theta})$ for an n -dimensional vector of parameters $\boldsymbol{\theta} = (\theta_1, \dots, \theta_n)$ is obtained, and one needs the marginal distribution of a subset of the components. Here one samples $\boldsymbol{\theta}$ from $p(\boldsymbol{\theta})$ and simply records the marginal distribution for the components of interest.

A simple and broadly applicable MCMC method is the Metropolis-Hastings algorithm, which allows one to generate multidimensional points $\boldsymbol{\theta}$ distributed according to a target p.d.f. that is proportional to a given function $p(\boldsymbol{\theta})$. It is not necessary to have $p(\boldsymbol{\theta})$ normalized to unit area, which is useful in Bayesian statistics, as posterior probability densities are often determined only up to an unknown normalization constant.

To generate points that follow $p(\boldsymbol{\theta})$, one first needs a proposal p.d.f. $q(\boldsymbol{\theta}; \boldsymbol{\theta}_0)$, which can be (almost) any p.d.f. from which independent random values $\boldsymbol{\theta}$ can be generated, and which contains as a parameter another point in the same space $\boldsymbol{\theta}_0$. For example, a multivariate Gaussian centered about $\boldsymbol{\theta}_0$ can be used. Beginning at an arbitrary starting point $\boldsymbol{\theta}_0$, the Hastings algorithm iterates the following steps:

1. Generate a value $\boldsymbol{\theta}$ using the proposal density $q(\boldsymbol{\theta}; \boldsymbol{\theta}_0)$;
2. Form the Hastings test ratio, $\alpha = \min \left[1, \frac{p(\boldsymbol{\theta})q(\boldsymbol{\theta}_0; \boldsymbol{\theta})}{p(\boldsymbol{\theta}_0)q(\boldsymbol{\theta}; \boldsymbol{\theta}_0)} \right]$;
3. Generate a value u uniformly distributed in $[0, 1]$;
4. If $u \leq \alpha$, take $\boldsymbol{\theta}_1 = \boldsymbol{\theta}$. Otherwise, repeat the old point, i.e., $\boldsymbol{\theta}_1 = \boldsymbol{\theta}_0$.

If one takes the proposal density to be symmetric in $\boldsymbol{\theta}$ and $\boldsymbol{\theta}_0$, then this is the *Metropolis-Hastings* algorithm, and the test ratio becomes $\alpha = \min[1, p(\boldsymbol{\theta})/p(\boldsymbol{\theta}_0)]$. That is, if the proposed $\boldsymbol{\theta}$ is at a value of probability higher than $\boldsymbol{\theta}_0$, the step is taken. If the proposed step is rejected, hop in place.

Methods for assessing and optimizing the performance of the algorithm are discussed in, e.g., [19–21]. One can, for example, examine the autocorrelation as a function of the lag k , i.e., the correlation of a sampled point with that k steps removed. This should decrease as quickly as possible for increasing k .

Generally one chooses the proposal density so as to optimize some quality measure such as the autocorrelation. For certain problems it has been shown that one achieves optimal performance when the acceptance fraction, that is, the fraction of points with $u \leq \alpha$, is around 40%. This can be adjusted by varying the width of the proposal density. For example, one can use for the proposal p.d.f. a multivariate Gaussian with the same covariance matrix as that of the target p.d.f., but scaled by a constant.

References:

1. F. James, *Comp. Phys. Comm.* **60**, 329-344, 1990.
2. P. L'Ecuyer, *Proc. 1997 Winter Simulation Conference*, IEEE Press, Dec. 1997, 127–134.
3. The CERN Program Library (CERNLIB); see cernlib.web.cern.ch/cernlib.
4. Leif Lönnblad, *Comp. Phys. Comm.* **84**, 307 (1994).
5. Rene Brun and Fons Rademakers, *Nucl. Inst. Meth.* **A389**, 81 (1997); see also root.cern.ch.
6. F. James, *Comp. Phys. Comm.* **79**, 111 (1994), based on M. Lüscher, *Comp. Phys. Comm.* **79**, 100 (1994).
7. P. L'Ecuyer, *Mathematics of Computation*, **65**, 213 (1996) and **65**, 225 (1999).
8. M. Matsumoto and T. Nishimura, *ACM Transactions on Modeling and Computer Simulation*, Vol. 8, No. 1, January 1998, 3–30.
9. Much of DIEHARD is described in: G. Marsaglia, *A Current View of Random Number Generators*, keynote address, *Computer Science and Statistics: 16th Symposium on the Interface*, Elsevier (1985).
10. P. L'Ecuyer and R. Simard, *ACM Transactions on Mathematical Software*, 33, 4, Article 1, December 2007.
11. UNURAN is described at statistik.wu-wien.ac.at/software/unuran; see also W. Hörmann, J. Leydold, and G. Derflinger, *Automatic Nonuniform Random Variate Generation*, (Springer, New York, 2004).
12. W.H. Press *et al.*, *Numerical Recipes*, 3rd edition, (Cambridge University Press, New York, 2007).
13. J.H. Ahrens and U. Dieter, *Computing* **12**, 223 (1974).
14. R.Y. Rubinstein, *Simulation and the Monte Carlo Method*, (John Wiley and Sons, Inc., New York, 1981).
15. L. Devroye, *Non-Uniform Random Variate Generation*, (Springer-Verlag, New York, 1986); available online at cg.scs.carleton.ca/~luc/rnbookindex.html.
16. Ch. Walck, *Handbook on Statistical Distributions for Experimentalists*, University of Stockholm Internal Report SUF-PFY/96-01, available from www.physto.se/~walck.
17. James E. Gentle, *Random Number Generation and Monte Carlo Methods*, 2nd ed., (Springer, New York, 2003).
18. J. Heinrich, CDF Note CDF/MEMO/STATISTICS/PUBLIC/8032, 2006.
19. C.P. Robert and G. Casella, *Monte Carlo Statistical Methods*, 2nd ed., (Springer, New York, 2004).
20. J.S. Liu, *Monte Carlo Strategies in Scientific Computing*, (Springer, New York, 2001).
21. R.M. Neal, *Probabilistic Inference Using Markov Chain Monte Carlo Methods*, Technical Report CRG-TR-93-1, Dept. of Computer Science, University of Toronto, available from www.cs.toronto.edu/~radford/res-mcmc.html.

35. MONTE CARLO PARTICLE NUMBERING SCHEME

Revised November 2009 by L. Garren (Fermilab), C.-J. Lin (LBNL), S. Navas (U. Granada), P. Richardson (Durham U.), T. Sjöstrand (Lund U.), and T. Trippe (LBNL).

The Monte Carlo particle numbering scheme presented here is intended to facilitate interfacing between event generators, detector simulators, and analysis packages used in particle physics. The numbering scheme was introduced in 1988 [1] and a revised version [2,3] was adopted in 1998 in order to allow systematic inclusion of quark model states which are as yet undiscovered and hypothetical particles such as SUSY particles. The numbering scheme is used in several event generators, *e.g.* HERWIG, PYTHIA, and SHERPA, and interfaces, *e.g.* /HEPEVT/ and HepMC.

The general form is a 7-digit number:

$$\pm n_r n_L n_{q_1} n_{q_2} n_{q_3} n_J .$$

This encodes information about the particle's spin, flavor content, and internal quantum numbers. The details are as follows:

1. Particles are given positive numbers, antiparticles negative numbers. The PDG convention for mesons is used, so that K^+ and B^+ are particles.
2. Quarks and leptons are numbered consecutively starting from 1 and 11 respectively; to do this they are first ordered by family and within families by weak isospin.
3. In composite quark systems (diquarks, mesons, and baryons) $n_{q_{1-3}}$ are quark numbers used to specify the quark content, while the rightmost digit $n_J = 2J + 1$ gives the system's spin (except for the K_S^0 and K_L^0). The scheme does not cover particles of spin $J > 4$.
4. Diquarks have 4-digit numbers with $n_{q_1} \geq n_{q_2}$ and $n_{q_3} = 0$.
5. The numbering of mesons is guided by the nonrelativistic (L - S decoupled) quark model, as listed in Tables 14.2 and 14.3.
 - a. The numbers specifying the meson's quark content conform to the convention $n_{q_1} = 0$ and $n_{q_2} \geq n_{q_3}$. The special case K_L^0 is the sole exception to this rule.
 - b. The quark numbers of flavorless, light (u, d, s) mesons are: 11 for the member of the isotriplet (π^0, ρ^0, \dots), 22 for the lighter isosinglet (η, ω, \dots), and 33 for the heavier isosinglet (η', ϕ, \dots). Since isosinglet mesons are often large mixtures of $u\bar{u} + d\bar{d}$ and $s\bar{s}$ states, 22 and 33 are assigned by mass and do not necessarily specify the dominant quark composition.
 - c. The special numbers 310 and 130 are given to the K_S^0 and K_L^0 respectively.
 - d. The fifth digit n_L is reserved to distinguish mesons of the same total (J) but different spin (S) and orbital (L) angular momentum quantum numbers. For $J > 0$ the numbers are: (L, S) = ($J - 1, 1$) $n_L = 0$, ($J, 0$) $n_L = 1$, ($J, 1$) $n_L = 2$ and ($J + 1, 1$) $n_L = 3$. For the exceptional case $J = 0$ the numbers are (0,0) $n_L = 0$ and (1,1) $n_L = 1$ (*i.e.* $n_L = L$). See Table 35.1.

Table 35.1: Meson numbering logic. Here qq stands for $n_{q_2} n_{q_3}$.

	$L = J - 1, S = 1$	$L = J, S = 0$	$L = J, S = 1$	$L = J + 1, S = 1$
J	code J^{PC} L	code J^{PC} L	code J^{PC} L	code J^{PC} L
0	— — —	00qq1 0 ⁺⁺ 0	— — —	10qq1 0 ⁺⁺ 1
1	00qq3 1 ⁻⁻ 0	10qq3 1 ⁺⁻ 1	20qq3 1 ⁺⁺ 1	30qq3 1 ⁻⁻ 2
2	00qq5 2 ⁺⁺ 1	10qq5 2 ⁺⁻ 2	20qq5 2 ⁻⁻ 2	30qq5 2 ⁺⁺ 3
3	00qq7 3 ⁻⁻ 2	10qq7 3 ⁺⁻ 3	20qq7 3 ⁺⁺ 3	30qq7 3 ⁻⁻ 4
4	00qq9 4 ⁺⁺ 3	10qq9 4 ⁺⁻ 4	20qq9 4 ⁻⁻ 4	30qq9 4 ⁺⁺ 5

- e. If a set of physical mesons correspond to a (non-negligible) mixture of basis states, differing in their internal quantum numbers, then the lightest physical state gets the smallest basis state number. For example the $K_1(1270)$ is numbered 10313 ($1^1P_1 K_{1B}$) and the $K_1(1400)$ is numbered 20313 ($1^3P_1 K_{1A}$).

- f. The sixth digit n_r is used to label mesons radially excited above the ground state.
- g. Numbers have been assigned for complete $n_r = 0$ S - and P -wave multiplets, even where states remain to be identified.
- h. In some instances assignments within the $q\bar{q}$ meson model are only tentative; here best guess assignments are made.
- i. Many states appearing in the Meson Listings are not yet assigned within the $q\bar{q}$ model. Here $n_{q_{2-3}}$ and n_J are assigned according to the state's likely flavors and spin; all such unassigned light isoscalar states are given the flavor code 22. Within these groups $n_L = 0, 1, 2, \dots$ is used to distinguish states of increasing mass. These states are flagged using $n = 9$. It is to be expected that these numbers will evolve as the nature of the states are elucidated. Codes are assigned to all mesons which are listed in the one-page table at the end of the Meson Summary Table as long as they have a preferred or established spin. Additional heavy meson states expected from heavy quark spectroscopy are also assigned codes.

6. The numbering of baryons is again guided by the nonrelativistic quark model, see Table 14.6.
 - a. The numbers specifying a baryon's quark content are such that in general $n_{q_1} \geq n_{q_2} \geq n_{q_3}$.
 - b. Two states exist for $J = 1/2$ baryons containing 3 different types of quarks. In the lighter baryon ($\Lambda, \Xi, \Omega, \dots$) the light quarks are in an antisymmetric ($J = 0$) state while for the heavier baryon ($\Sigma^0, \Xi', \Omega', \dots$) they are in a symmetric ($J = 1$) state. In this situation n_{q_2} and n_{q_3} are reversed for the lighter state, so that the smaller number corresponds to the lighter baryon.
 - c. At present most Monte Carlos do not include excited baryons and no systematic scheme has been developed to denote them, though one is foreseen. In the meantime, use of the PDG 96 [4] numbers for excited baryons is recommended.
 - d. For pentaquark states $n = 9$, $n_r n_L n_{q_1} n_{q_2}$ gives the four quark numbers in order $n_r \geq n_L \geq n_{q_1} \geq n_{q_2}$, n_{q_3} gives the antiquark number, and $n_J = 2J + 1$, with the assumption that $J = 1/2$ for the states currently reported.
7. The gluon, when considered as a gauge boson, has official number 21. In codes for glueballs, however, 9 is used to allow a notation in close analogy with that of hadrons.
8. The pomeron and odderon trajectories and a generic reggeon trajectory of states in QCD are assigned codes 990, 9990, and 110 respectively, where the final 0 indicates the indeterminate nature of the spin, and the other digits reflect the expected "valence" flavor content. We do not attempt a complete classification of all reggeon trajectories, since there is currently no need to distinguish a specific such trajectory from its lowest-lying member.
9. Two-digit numbers in the range 21–30 are provided for the Standard Model gauge bosons and Higgs.
10. Codes 81–100 are reserved for generator-specific pseudoparticles and concepts.
11. The search for physics beyond the Standard Model is an active area, so these codes are also standardized as far as possible.
 - a. A standard fourth generation of fermions is included by analogy with the first three.
 - b. The graviton and the boson content of a two-Higgs-doublet scenario and of additional $SU(2) \times U(1)$ groups are found in the range 31–40.
 - c. "One-of-a-kind" exotic particles are assigned numbers in the range 41–80.
 - d. Fundamental supersymmetric particles are identified by adding a nonzero n to the particle number. The superpartner of a boson or a left-handed fermion has $n = 1$ while the superpartner of a right-handed fermion has $n = 2$. When mixing occurs, such as between the winos and charged Higgsinos to give charginos, or between left and right sfermions, the lighter physical state is given the smaller basis state number.
 - e. Technicolor states have $n = 3$, with technifermions treated like ordinary fermions. States which are ordinary color singlets have $n_r = 0$. Color octets have $n_r = 1$. If a state has non-trivial quantum numbers under the topcolor groups

SU(3)₁ × SU(3)₂, the quantum numbers are specified by tech,*ij*, where *i* and *j* are 1 or 2. *n_L* is then 2*i* + *j*. The colon, V₈, is a heavy gluon color octet and thus is 3100021.

f. Excited (composite) quarks and leptons are identified by setting *n* = 4 and *n_r* = 0.

g. Within several scenarios of new physics, it is possible to have colored particles sufficiently long-lived for color-singlet hadronic states to form around them. In the context of supersymmetric scenarios, these states are called *R*-hadrons, since they carry odd *R*-parity. *R*-hadron codes, defined here, should be viewed as templates for corresponding codes also in other scenarios, for any long-lived particle that is either an unflavored color octet or a flavored color triplet. The *R*-hadron code is obtained by combining the SUSY particle code with a code for the light degrees of freedom, with as many intermediate zeros removed from the former as required to make place for the latter at the end. (To exemplify, a sparticle *n*00000*n_q* combined with quarks *q*₁ and *q*₂ obtains code *n*00*n_q**n_{q1}**n_{q2}**n_J*.) Specifically, the new-particle spin decouples in the limit of large masses, so that the final *n_J* digit is defined by the spin state of the light-quark system alone. An appropriate number of *n_q* digits is used to define the ordinary-quark content. As usual, 9 rather than 21 is used to denote a gluon/gluino in composite states. The sign of the hadron agrees with that of the constituent new particle (a color triplet) where there is a distinct new antiparticle, and else is defined as for normal hadrons. Particle names are *R* with the flavor content as lower index. A non-exhaustive list of *R*-hadron codes is given below.

h. A black hole in models with extra dimensions has code 5000040. Kaluza-Klein excitations in models with extra dimensions have *n* = 5 or *n* = 6, to distinguish excitations of left- or right-handed fermions or, in case of mixing, the lighter or heavier state (cf. 11d). The nonzero *n_r* digit gives the radial excitation number, in scenarios where the level spacing allow these to be distinguished. Should the model also contain supersymmetry, excited SUSY states would be denoted by an *n_r* > 0, with *n* = 1 or 2 as usual. Should some colored states be long-lived enough that hadrons would form around them, the coding strategy of 11g applies, with the initial two *mn_r* digits preserved in the combined code. A non-exhaustive list of codes for the Kaluza-Klein states is given below.

i. Magnetic monopoles and dyons are assumed to have one unit of Dirac monopole charge and a variable integer number *n_{q1}**n_{q2}**n_{q3}* units of electric charge. Codes 411*n_{q1}**n_{q2}**n_{q3}*0 are then used when the magnetic and electrical charge sign agree and 412*n_{q1}**n_{q2}**n_{q3}*0 when they disagree, with the overall sign of the particle set by the magnetic charge. For now no spin information is provided.

12. Occasionally program authors add their own states. To avoid confusion, these should be flagged by setting *mn_r* = 99.
13. Concerning the non-99 numbers, it may be noted that only quarks, excited quarks, squarks, and diquarks have *n_{q3}* = 0; only diquarks, baryons (including pentaquarks), and the odderon have *n_{q1}* ≠ 0; and only mesons, the reggeon, and the pomeron have *n_{q1}* = 0 and *n_{q2}* ≠ 0. Concerning mesons (not antimesons), if *n_{q1}* is odd then it labels a quark and an antiquark if even.
14. Nuclear codes are given as 10-digit numbers ±10*LZZZAAAI*. For a (hyper)nucleus consisting of *n_p* protons, *n_n* neutrons and *n_Λ* Λ's, *A* = *n_p* + *n_n* + *n_Λ* gives the total baryon number, *Z* = *n_p* the total charge and *L* = *n_Λ* the total number of strange quarks. *I* gives the isomer level, with *I* = 0 corresponding to the ground state and *I* > 0 to excitations, see [8], where states denoted *m, n, p, q* translate to *I* = 1 – 4. As examples, the deuteron is 1000010020 and ²³⁵U is 1000922350. To avoid ambiguities, nuclear codes should not be applied to a single hadron, like *p, n* or Λ⁰, where quark-contents-based codes already exist.

This text and lists of particle numbers can be found on the WWW [5]. The StdHep Monte Carlo standardization project [6] maintains the list of PDG particle numbers, as well as numbering schemes from most event generators and software to convert between the different schemes.

References:

1. G.P. Yost *et al.*, Particle Data Group, Phys. Lett. **B204**, 1 (1988).
2. I. G. Knowles *et al.*, in “Physics at LEP2”, CERN 96-01, vol. 2, p. 103.
3. C. Caso *et al.*, Particle Data Group, Eur. Phys. J. **C3**, 1 (1998).
4. R.M. Barnett *et al.*, PDG, Phys. Rev. **D54**, 1 (1996).
5. pdg.lbl.gov/2009/mcdata/mc_particle_id_contents.html.
6. L. Garren, StdHep, Monte Carlo Standardization at FNAL, Fermilab PM0091 and StdHep WWW site: <http://cepa.fnal.gov/psm/stdhep/>.
7. W.-M. Yao *et al.*, J. Phys. **G33**, 1 (2006).
8. G. Audi *et al.*, Nucl. Phys. **A729**, 3 (2003) See also http://www.nndc.bnl.gov/amdc/web/nubase_en.html.

QUARKS

<i>d</i>	1
<i>u</i>	2
<i>s</i>	3
<i>c</i>	4
<i>b</i>	5
<i>t</i>	6
<i>b'</i>	7
<i>t'</i>	8

LEPTONS

<i>e</i> [−]	11
<i>ν_e</i>	12
<i>μ</i> [−]	13
<i>ν_μ</i>	14
<i>τ</i> [−]	15
<i>ν_τ</i>	16
<i>τ</i> [−]	17
<i>ν_τ</i>	18

GAUGE AND HIGGS BOSONS

<i>g</i>	(9) 21
<i>γ</i>	22
<i>Z</i> ⁰	23
<i>W</i> ⁺	24
<i>h</i> ⁰ / <i>H</i> ₁ ⁰	25
<i>Z'</i> / <i>Z</i> ₂ ⁰	32
<i>Z''</i> / <i>Z</i> ₃ ⁰	33
<i>W'</i> / <i>W</i> ₂ ⁺	34
<i>H</i> ⁰ / <i>H</i> ₂ ⁰	35
<i>A</i> ⁰ / <i>H</i> ₃ ⁰	36
<i>H</i> ⁺	37

SPECIAL PARTICLES

<i>G</i> (graviton)	39
<i>R</i> ⁰	41
<i>LQ</i> ^c	42
<i>reggeon</i>	110
<i>pomeron</i>	990
<i>odderon</i>	9990

for MC internal use 81–100

DIQUARKS

(<i>dd</i>) ₁	1103
(<i>ud</i>) ₀	2101
(<i>ud</i>) ₁	2103
(<i>wu</i>) ₁	2203
(<i>sd</i>) ₀	3101
(<i>sd</i>) ₁	3103
(<i>su</i>) ₀	3201
(<i>su</i>) ₁	3203
(<i>ss</i>) ₁	3303
(<i>cd</i>) ₀	4101
(<i>cd</i>) ₁	4103
(<i>cu</i>) ₀	4201
(<i>cu</i>) ₁	4203
(<i>cs</i>) ₀	4301
(<i>cs</i>) ₁	4303
(<i>cc</i>) ₁	4403
(<i>bd</i>) ₀	5101
(<i>bd</i>) ₁	5103
(<i>bu</i>) ₀	5201
(<i>bu</i>) ₁	5203
(<i>bs</i>) ₀	5301
(<i>bs</i>) ₁	5303
(<i>bc</i>) ₀	5401
(<i>bc</i>) ₁	5403
(<i>bb</i>) ₁	5503

TECHNICOLOR PARTICLES

<i>π</i> _{tech} ⁰	3000111
<i>π</i> _{tech} ⁺	3000211
<i>π</i> _{tech} ⁰	3000221
<i>η</i> _{tech} ⁰	3100221
<i>ρ</i> _{tech} ⁰	3000113
<i>ρ</i> _{tech} ⁺	3000213
<i>ω</i> _{tech} ⁰	3000223
<i>V</i> ₈	3100021
<i>π</i> _{tech,22} ¹	3060111
<i>π</i> _{tech,22} ⁸	3160111
<i>ρ</i> _{tech,11}	3130113
<i>ρ</i> _{tech,12}	3140113
<i>ρ</i> _{tech,21}	3150113
<i>ρ</i> _{tech,22}	3160113

**SUSY
PARTICLES**

\tilde{d}_L	1000001
\tilde{u}_L	1000002
\tilde{s}_L	1000003
\tilde{c}_L	1000004
\tilde{b}_1	1000005 ^a
\tilde{t}_1	1000006 ^a
\tilde{e}_L	1000011
$\tilde{\nu}_{eL}$	1000012
$\tilde{\mu}_L$	1000013
$\tilde{\nu}_{\mu L}$	1000014
$\tilde{\tau}_1$	1000015 ^a
$\tilde{\nu}_{\tau L}$	1000016
\tilde{d}_R	2000001
\tilde{u}_R	2000002
\tilde{s}_R	2000003
\tilde{c}_R	2000004
\tilde{b}_2	2000005 ^a
\tilde{t}_2	2000006 ^a
\tilde{e}_R	2000011
$\tilde{\mu}_R$	2000013
$\tilde{\tau}_2$	2000015 ^a
\tilde{g}	1000021
$\tilde{\chi}_1^0$	1000022 ^b
$\tilde{\chi}_2^0$	1000023 ^b
$\tilde{\chi}_1^+$	1000024 ^b
$\tilde{\chi}_3^0$	1000025 ^b
$\tilde{\chi}_4^0$	1000035 ^b
$\tilde{\chi}_2^+$	1000037 ^b
\tilde{G}	1000039
KALUZA-KLEIN EXCITATIONS	
<i>black hole</i>	5000040*
$d_L^{(1)}$	5100001
$u_L^{(1)}$	5100002
$e_L^{(1)-}$	5100011
$\nu_{eL}^{(1)}$	5100012
$d_R^{(1)}$	6100001
$u_R^{(1)}$	6100002
$e_R^{(1)-}$	6100011
$\nu_{eR}^{(1)}$	6100012
$g^{(1)}$	5100021
$\gamma^{(1)}$	5100022
$Z^{(1)0}$	5100023
$W^{(1)+}$	5100024
$h^{(1)0}$	5100025
$G^{(1)}$	5100039

R-HADRONS

R_{gg}^0	1000993
$R_{g\bar{d}}^0$	1009113
R_{gud}^+	1009213
$R_{gu\bar{u}}^0$	1009223
$R_{g\bar{s}}^0$	1009313
$R_{gu\bar{s}}^+$	1009323
$R_{gs\bar{s}}^0$	1009333
$R_{g\bar{d}dd}^-$	1091114
R_{gudd}^0	1092114
R_{guud}^+	1092214
R_{guuu}^{++}	1092224
R_{gsdd}^-	1093114
R_{gsud}^0	1093214
R_{gsuu}^+	1093224
R_{gssd}^-	1093314
R_{gssu}^0	1093324
R_{gsss}^-	1093334
$R_{t_1\bar{d}}^+$	1000612
$R_{t_1\bar{u}}^0$	1000622
$R_{t_1\bar{s}}^+$	1000632
$R_{t_1\bar{c}}^0$	1000642
$R_{t_1\bar{b}}^+$	1000652
$R_{t_1d\bar{d}_1}^0$	1006113
$R_{t_1ud_0}^+$	1006211
$R_{t_1ud_1}^+$	1006213
$R_{t_1uu_1}^{++}$	1006223
$R_{t_1sd_0}^0$	1006311
$R_{t_1sd_1}^0$	1006313
$R_{t_1su_0}^+$	1006321
$R_{t_1su_1}^+$	1006323
$R_{t_1ss_1}^0$	1006333

**EXCITED
PARTICLES**

d^*	4000001
u^*	4000002
e^*	4000011
ν_e^*	4000012

LIGHT $I = 1$ MESONS

π^0	111
π^+	211
$a_0(980)^0$	9000111
$a_0(980)^+$	9000211
$\pi(1300)^0$	100111
$\pi(1300)^+$	100211
$a_0(1450)^0$	10111
$a_0(1450)^+$	10211
$\pi(1800)^0$	9010111
$\pi(1800)^+$	9010211
$\rho(770)^0$	113
$\rho(770)^+$	213
$b_1(1235)^0$	10113
$b_1(1235)^+$	10213
$a_1(1260)^0$	20113
$a_1(1260)^+$	20213
$\pi_1(1400)^0$	9000113
$\pi_1(1400)^+$	9000213
$\rho(1450)^0$	100113
$\rho(1450)^+$	100213
$\pi_1(1600)^0$	9010113
$\pi_1(1600)^+$	9010213
$a_1(1640)^0$	9020113
$a_1(1640)^+$	9020213
$\rho(1700)^0$	30113
$\rho(1700)^+$	30213
$\rho(1900)^0$	9030113
$\rho(1900)^+$	9030213
$\rho(2150)^0$	9040113
$\rho(2150)^+$	9040213
$a_2(1320)^0$	115
$a_2(1320)^+$	215
$\pi_2(1670)^0$	10115
$\pi_2(1670)^+$	10215
$a_2(1700)^0$	9000115
$a_2(1700)^+$	9000215
$\pi_2(2100)^0$	9010115
$\pi_2(2100)^+$	9010215
$\rho_3(1690)^0$	117
$\rho_3(1690)^+$	217
$\rho_3(1990)^0$	9000117
$\rho_3(1990)^+$	9000217
$\rho_3(2250)^0$	9010117
$\rho_3(2250)^+$	9010217
$a_4(2040)^0$	119
$a_4(2040)^+$	219

LIGHT $I = 0$ MESONS

($u\bar{u}$, $d\bar{d}$, and $s\bar{s}$ Admixtures)	
η	221
$\eta'(958)$	331
$f_0(600)$	9000221
$f_0(980)$	9010221
$\eta(1295)$	100221
$f_0(1370)$	10221
$\eta(1405)$	9020221
$\eta(1475)$	100331
$f_0(1500)$	9030221
$f_0(1710)$	10331
$\eta(1760)$	9040221
$f_0(2020)$	9050221
$f_0(2100)$	9060221
$f_0(2200)$	9070221
$\eta(2225)$	9080221
$\omega(782)$	223
$\phi(1020)$	333
$h_1(1170)$	10223
$f_1(1285)$	20223
$h_1(1380)$	10333
$f_1(1420)$	20333
$\omega(1420)$	100223
$f_1(1510)$	9000223
$h_1(1595)$	9010223
$\omega(1650)$	30223
$\phi(1680)$	100333
$f_2(1270)$	225
$f_2(1430)$	9000225
$f_2'(1525)$	335
$f_2(1565)$	9010225
$f_2(1640)$	9020225
$\eta_2(1645)$	10225
$f_2(1810)$	9030225
$\eta_2(1870)$	10335
$f_2(1910)$	9040225
$f_2(1950)$	9050225
$f_2(2010)$	9060225
$f_2(2150)$	9070225
$f_2(2300)$	9080225
$f_2(2340)$	9090225
$\omega_3(1670)$	227
$\phi_3(1850)$	337
$f_4(2050)$	229
$f_J(2220)$	9000229
$f_4(2300)$	9010229

STRANGE MESONS		CHARMED MESONS		$c\bar{c}$ MESONS		LIGHT BARYONS		BOTTOM BARYONS			
K_L^0	130	D^+	411	$\eta_c(1S)$	441	p	2212	Λ_b^0	5122		
K_S^0	310	D^0	421	$\chi_{c0}(1P)$	10441	n	2112	Σ_b^-	5112		
K^0	311	$D_0^*(2400)^+$	10411	$\eta_c(2S)$	100441	Δ^{++}	2224	Σ_b^0	5212		
K^+	321	$D_0^*(2400)^0$	10421	$J/\psi(1S)$	443	Δ^+	2214	Σ_b^+	5222		
$K_0^*(800)^0$	9000311	$D^*(2010)^+$	413	$h_c(1P)$	10443	Δ^0	2114	Σ_b^{*-}	5114		
$K_0^*(800)^+$	9000321	$D^*(2007)^0$	423	$\chi_{c1}(1P)$	20443	Δ^-	1114	Σ_b^{*0}	5214		
$K_0^*(1430)^0$	10311	$D_1(2420)^+$	10413	$\psi(2S)$	100443	STRANGE BARYONS					
$K_0^*(1430)^+$	10321	$D_1(2420)^0$	10423	$\psi(3770)$	30443	Λ	3122	Σ_b^{*+}	5224		
$K(1460)^0$	100311	$D_1(H)^+$	20413	$\psi(4040)$	9000443	Σ^+	3222	Ξ_b^-	5132		
$K(1460)^+$	100321	$D_1(2430)^0$	20423	$\psi(4160)$	9010443	Σ^0	3212	Ξ_b^0	5232		
$K(1830)^0$	9010311	$D_2^*(2460)^+$	415	$\psi(4415)$	9020443	Σ^-	3112 ^d	$\Xi_b^{\prime-}$	5312		
$K(1830)^+$	9010321	$D_2^*(2460)^0$	425	$\chi_{c2}(1P)$	445	Σ^{*+}	3224 ^d	$\Xi_b^{\prime0}$	5322		
$K_0^*(1950)^0$	9020311	D_s^+	431	$\chi_{c2}(2P)$	100445	Σ^{*0}	3214 ^d	Ξ_b^-	5314		
$K_0^*(1950)^+$	9020321	$D_{s0}^*(2317)^+$	10431	$b\bar{b}$ MESONS				Σ^{*-}	3114 ^d	Ξ_b^{*0}	5324
$K^*(892)^0$	313	D_s^{*+}	433	$\eta_b(1S)$	551	Ξ^0	3322	Ξ_b^-	5332		
$K^*(892)^+$	323	$D_{s1}(2536)^+$	10433	$\chi_{b0}(1P)$	10551	Ξ^-	3312	Ω_b^-	5332		
$K_1(1270)^0$	10313	$D_{s1}(2460)^+$	20433	$\chi_{b0}(2P)$	110551	Ξ^{*0}	3324 ^d	Ω_b^{*-}	5334		
$K_1(1270)^+$	10323	$D_{s2}^*(2573)^+$	435	$\eta_b(2S)$	100551	Ξ^{*-}	3314 ^d	Ξ_{bc}^0	5142		
$K_1(1400)^0$	20313	BOTTOM MESONS				$\chi_{b0}(3P)$	210551	Ξ_{bc}^+	5242		
$K_1(1400)^+$	20323	B^0	511	$\eta_b(3S)$	200551	$\chi_{b0}(2P)$	110551	$\Xi_{bc}^{\prime0}$	5412		
$K^*(1410)^0$	100313	B^+	521	$\chi_{b0}(3P)$	210551	$\chi_{b1}(1P)$	10553	$\Xi_{bc}^{\prime+}$	5422		
$K^*(1410)^+$	100323	B_0^*	10511	$\Upsilon(1S)$	553	$h_b(1P)$	10553	$\Xi_{bc}^{\prime*0}$	5414		
$K_1(1650)^0$	9000313	B_0^{*+}	10521	$h_b(1P)$	10553	$\chi_{b1}(1P)$	20553	$\Xi_{bc}^{\prime*+}$	5424		
$K_1(1650)^+$	9000323	B^*	513	$\Upsilon_1(1D)$	30553	$\Upsilon_1(1D)$	30553	Ω_{bc}^0	5342		
$K^*(1680)^0$	30313	B^{*+}	523	$\Upsilon(2S)$	100553	$h_b(2P)$	110553	$\Omega_{bc}^{\prime0}$	5432		
$K^*(1680)^+$	30323	$B_1(L)^0$	10513	$h_b(2P)$	110553	$\chi_{b1}(2P)$	120553	$\Omega_{bc}^{\prime*0}$	5434		
$K_2^*(1430)^0$	315	$B_1(L)^+$	10523	$\Upsilon(2S)$	100553	$\Upsilon_1(2D)$	130553	Ω_{bcc}^+	5442		
$K_2^*(1430)^+$	325	$B_1(H)^0$	20513	$h_b(3P)$	210553	$\Upsilon(3S)$	200553	$\Omega_{bcc}^{\prime*+}$	5444		
$K_2(1580)^0$	9000315	$B_1(H)^+$	20523	$\chi_{b1}(3P)$	220553	$\Upsilon(3S)$	200553	Ξ_{bb}^-	5512		
$K_2(1580)^+$	9000325	B_2^0	515	$\Upsilon(4S)$	300553	$h_b(3P)$	210553	Ξ_{bb}^0	5522		
$K_2(1770)^0$	10315	B_2^{*+}	525	$\Upsilon(10860)$	9000553	$\chi_{b1}(3P)$	220553	Ξ_{bb}^{*-}	5514		
$K_2(1770)^+$	10325	B_s^0	531	$\Upsilon(11020)$	9010553	$\Upsilon(4S)$	300553	Ξ_{bb}^{*0}	5524		
$K_2(1820)^0$	20315	B_s^*	10531	$\chi_{b2}(1P)$	555	$\Upsilon(4S)$	300553	Ω_{bb}^-	5532		
$K_2(1820)^+$	20325	B_s^0	533	$\chi_{b2}(1P)$	555	$\Upsilon(10860)$	9000553	Ω_{bb}^{*-}	5534		
$K_2^*(1980)^0$	9010315	$B_{s1}(L)^0$	10533	$\Upsilon(11020)$	9010553	$\chi_{b2}(2P)$	100555	Ω_{bbc}^0	5542		
$K_2^*(1980)^+$	9010325	$B_{s1}(H)^0$	20533	$\chi_{b2}(2P)$	100555	$\eta_{b2}(1D)$	10555	$\Omega_{bbc}^{\prime*0}$	5544		
$K_2(2250)^0$	9020315	B_{s2}^*	535	$\Upsilon_2(1D)$	20555	$\Upsilon_2(1D)$	20555	Ω_{bbb}^-	5554		
$K_2(2250)^+$	9020325	B_c^+	541	$\chi_{b2}(2P)$	100555	$\Upsilon_2(2D)$	120555				
$K_3^*(1780)^0$	317	B_c^{*+}	10541	$\eta_{b2}(2D)$	110555	$\Upsilon_2(2D)$	120555				
$K_3^*(1780)^+$	327	B_c^{*+}	543	$\Upsilon_2(2D)$	120555	$\chi_{b2}(3P)$	200555				
$K_3(2320)^0$	9010317	$B_{c1}(L)^+$	10543	$\chi_{b2}(3P)$	200555	$\Upsilon_3(1D)$	557				
$K_3(2320)^+$	9010327	$B_{c1}(H)^+$	20543	$\Upsilon_3(2D)$	100557	$\Upsilon_3(2D)$	100557				
$K_4^*(2045)^0$	319	B_{c2}^{*+}	545								
$K_4^*(2045)^+$	329										
$K_4(2500)^0$	9000319										
$K_4(2500)^+$	9000329										

CHARMED BARYONS		STRANGE BARYONS		CHARMED BARYONS		PENTAQUARKS	
Λ_c^+	4122	Λ_c^+	4122	Λ_c^+	4122	Θ^+	9221132
Σ_c^{++}	4222	Σ_c^{++}	4222	Σ_c^{++}	4222	Φ^{--}	9331122
Σ_c^+	4212	Σ_c^+	4212	Σ_c^+	4212		
Σ_c^0	4112	Σ_c^0	4112	Σ_c^0	4112		
Σ_c^{*+}	4224	Σ_c^{*+}	4224	Σ_c^{*+}	4224		
Σ_c^{*0}	4114	Σ_c^{*0}	4114	Σ_c^{*0}	4114		
Ξ_c^+	4232	Ξ_c^+	4232	Ξ_c^+	4232		
Ξ_c^0	4132	Ξ_c^0	4132	Ξ_c^0	4132		
$\Xi_c^{\prime+}$	4322	$\Xi_c^{\prime+}$	4322	$\Xi_c^{\prime+}$	4322		
$\Xi_c^{\prime0}$	4312	$\Xi_c^{\prime0}$	4312	$\Xi_c^{\prime0}$	4312		
Ξ_c^{*+}	4324	Ξ_c^{*+}	4324	Ξ_c^{*+}	4324		
Ξ_c^{*0}	4314	Ξ_c^{*0}	4314	Ξ_c^{*0}	4314		
Ω_c^0	4332	Ω_c^0	4332	Ω_c^0	4332		
Ω_c^{*0}	4334	Ω_c^{*0}	4334	Ω_c^{*0}	4334		
Ξ_{cc}^+	4412	Ξ_{cc}^+	4412	Ξ_{cc}^+	4412		
Ξ_{cc}^{*+}	4422	Ξ_{cc}^{*+}	4422	Ξ_{cc}^{*+}	4422		
Ξ_{cc}^{*0}	4414	Ξ_{cc}^{*0}	4414	Ξ_{cc}^{*0}	4414		
Ξ_{cc}^{*+}	4424	Ξ_{cc}^{*+}	4424	Ξ_{cc}^{*+}	4424		
Ω_{cc}^+	4432	Ω_{cc}^+	4432	Ω_{cc}^+	4432		
Ω_{cc}^{*+}	4434	Ω_{cc}^{*+}	4434	Ω_{cc}^{*+}	4434		
Ω_{ccc}^+	4444	Ω_{ccc}^+	4444	Ω_{ccc}^+	4444		

Footnotes to the Tables:

- *) Numbers or names in bold face are new or have changed since the 2006 *Review* [7].
- a) Particular in the third generation, the left and right sfermion states may mix, as shown. The lighter mixed state is given the smaller number.
- b) The physical $\tilde{\chi}$ states are admixtures of the pure $\tilde{\gamma}$, \tilde{Z}^0 , \tilde{W}^+ , \tilde{H}_1^0 , \tilde{H}_2^0 , and \tilde{H}^+ states.
- c) In this draft we have only provided one generic leptoquark code. More general classifications according to spin, weak isospin and flavor content would lead to a host of states, that could be added as the need arises.
- d) Σ^* and Ξ^* are alternate names for $\Sigma(1385)$ and $\Xi(1530)$.

36. CLEBSCH-GORDAN COEFFICIENTS, SPHERICAL HARMONICS, AND d FUNCTIONS

Note: A square-root sign is to be understood over every coefficient, e.g., for $-8/15$ read $-\sqrt{8/15}$.

Notation:

J	J	\dots
M	M	\dots
m_1	m_2	\dots
m_1	m_2	\dots
\vdots	\vdots	\vdots
\vdots	\vdots	\vdots
Coefficients		

$Y_0^1 = \sqrt{\frac{3}{4\pi}} \cos \theta$

$Y_1^1 = -\sqrt{\frac{3}{8\pi}} \sin \theta e^{i\phi}$

$Y_2^0 = \sqrt{\frac{5}{4\pi}} \left(\frac{3}{2} \cos^2 \theta - \frac{1}{2} \right)$

$Y_2^1 = -\sqrt{\frac{15}{8\pi}} \sin \theta \cos \theta e^{i\phi}$

$Y_2^2 = \frac{1}{4} \sqrt{\frac{15}{2\pi}} \sin^2 \theta e^{2i\phi}$

$Y_\ell^{-m} = (-1)^m Y_\ell^{m*}$

$d_{m,0}^\ell = \sqrt{\frac{4\pi}{2\ell+1}} Y_\ell^m e^{-im\phi}$

$\langle j_1 j_2 m_1 m_2 | j_1 j_2 J M \rangle$
 $= (-1)^{J-j_1-j_2} \langle j_2 j_1 m_2 m_1 | j_2 j_1 J M \rangle$

$d_{m',m}^j = (-1)^{m-m'} d_{m,m'}^j = d_{-m,-m'}^j$

$d_{0,0}^1 = \cos \theta$

$d_{1/2,1/2}^{1/2} = \cos \frac{\theta}{2}$

$d_{1/2,-1/2}^{1/2} = -\sin \frac{\theta}{2}$

$d_{1,1}^1 = \frac{1 + \cos \theta}{2}$

$d_{1,0}^1 = -\frac{\sin \theta}{\sqrt{2}}$

$d_{1,-1}^1 = \frac{1 - \cos \theta}{2}$

$d_{3/2,3/2}^{3/2} = \frac{1 + \cos \theta}{2} \cos \frac{\theta}{2}$

$d_{3/2,1/2}^{3/2} = -\sqrt{3} \frac{1 + \cos \theta}{2} \sin \frac{\theta}{2}$

$d_{3/2,-1/2}^{3/2} = \sqrt{3} \frac{1 - \cos \theta}{2} \cos \frac{\theta}{2}$

$d_{3/2,-3/2}^{3/2} = -\frac{1 - \cos \theta}{2} \sin \frac{\theta}{2}$

$d_{1/2,1/2}^{3/2} = \frac{3 \cos \theta - 1}{2} \cos \frac{\theta}{2}$

$d_{1/2,-1/2}^{3/2} = -\frac{3 \cos \theta + 1}{2} \sin \frac{\theta}{2}$

$d_{2,2}^2 = \left(\frac{1 + \cos \theta}{2} \right)^2$

$d_{2,1}^2 = -\frac{1 + \cos \theta}{2} \sin \theta$

$d_{2,0}^2 = \frac{\sqrt{6}}{4} \sin^2 \theta$

$d_{2,-1}^2 = -\frac{1 - \cos \theta}{2} \sin \theta$

$d_{2,-2}^2 = \left(\frac{1 - \cos \theta}{2} \right)^2$

$d_{1,1}^2 = \frac{1 + \cos \theta}{2} (2 \cos \theta - 1)$

$d_{1,0}^2 = -\sqrt{\frac{3}{2}} \sin \theta \cos \theta$

$d_{1,-1}^2 = \frac{1 - \cos \theta}{2} (2 \cos \theta + 1)$

$d_{0,0}^2 = \left(\frac{3}{2} \cos^2 \theta - \frac{1}{2} \right)$

Figure 36.1: The sign convention is that of Wigner (*Group Theory*, Academic Press, New York, 1959), also used by Condon and Shortley (*The Theory of Atomic Spectra*, Cambridge Univ. Press, New York, 1953), Rose (*Elementary Theory of Angular Momentum*, Wiley, New York, 1957), and Cohen (*Tables of the Clebsch-Gordan Coefficients*, North American Rockwell Science Center, Thousand Oaks, Calif., 1974).

37. SU(3) ISOSCALAR FACTORS AND REPRESENTATION MATRICES

Written by R.L. Kelly (LBNL).

The most commonly used SU(3) isoscalar factors, corresponding to the singlet, octet, and decuplet content of $8 \otimes 8$ and $10 \otimes 8$, are shown at the right. The notation uses particle names to identify the coefficients, so that the pattern of relative couplings may be seen at a glance. We illustrate the use of the coefficients below. See J.J de Swart, Rev. Mod. Phys. **35**, 916 (1963) for detailed explanations and phase conventions.

A $\sqrt{\quad}$ is to be understood over every integer in the matrices; the exponent 1/2 on each matrix is a reminder of this. For example, the $\Xi \rightarrow \Omega K$ element of the $10 \rightarrow 10 \otimes 8$ matrix is $-\sqrt{6}/\sqrt{24} = -1/2$.

Intramultiplet relative decay strengths may be read directly from the matrices. For example, in decuplet \rightarrow octet + octet decays, the ratio of $\Omega^* \rightarrow \Xi \bar{K}$ and $\Delta \rightarrow N\pi$ partial widths is, from the $10 \rightarrow 8 \times 8$ matrix,

$$\frac{\Gamma(\Omega^* \rightarrow \Xi \bar{K})}{\Gamma(\Delta \rightarrow N\pi)} = \frac{12}{6} \times (\text{phase space factors}). \quad (37.1)$$

Including isospin Clebsch-Gordan coefficients, we obtain, e.g.,

$$\frac{\Gamma(\Omega^{*-} \rightarrow \Xi^0 K^-)}{\Gamma(\Delta^+ \rightarrow p\pi^0)} = \frac{1/2}{2/3} \times \frac{12}{6} \times p.s.f. = \frac{3}{2} \times p.s.f. \quad (37.2)$$

Partial widths for $8 \rightarrow 8 \otimes 8$ involve a linear superposition of 8_1 (symmetric) and 8_2 (antisymmetric) couplings. For example,

$$\Gamma(\Xi^* \rightarrow \Xi\pi) \sim \left(-\sqrt{\frac{9}{20}} g_1 + \sqrt{\frac{3}{12}} g_2 \right)^2. \quad (37.3)$$

The relations between g_1 and g_2 (with de Swart's normalization) and the standard D and F couplings that appear in the interaction Lagrangian,

$$\mathcal{L} = -\sqrt{2} D \text{Tr}(\{\bar{B}, B\}M) + \sqrt{2} F \text{Tr}([\bar{B}, B]M), \quad (37.4)$$

where $[\bar{B}, B] \equiv \bar{B}B - B\bar{B}$ and $\{\bar{B}, B\} \equiv \bar{B}B + B\bar{B}$, are

$$D = \frac{\sqrt{30}}{40} g_1, \quad F = \frac{\sqrt{6}}{24} g_2. \quad (37.5)$$

Thus, for example,

$$\Gamma(\Xi^* \rightarrow \Xi\pi) \sim (F - D)^2 \sim (1 - 2\alpha)^2, \quad (37.6)$$

where $\alpha \equiv F/(D + F)$. (This definition of α is de Swart's. The alternative $D/(D + F)$, due to Gell-Mann, is also used.)

The generators of SU(3) transformations, λ_a ($a = 1, 8$), are 3×3 matrices that obey the following commutation and anticommutation relationships:

$$[\lambda_a, \lambda_b] \equiv \lambda_a \lambda_b - \lambda_b \lambda_a = 2i f_{abc} \lambda_c \quad (37.7)$$

$$\{\lambda_a, \lambda_b\} \equiv \lambda_a \lambda_b + \lambda_b \lambda_a = \frac{4}{3} \delta_{ab} I + 2d_{abc} \lambda_c, \quad (37.8)$$

where I is the 3×3 identity matrix, and δ_{ab} is the Kronecker delta symbol. The f_{abc} are odd under the permutation of any pair of indices, while the d_{abc} are even. The nonzero values are

$1 \rightarrow 8 \otimes 8$

$$(\Lambda) \rightarrow (N \bar{K} \ \Sigma\pi \ \Lambda\eta \ \Xi K) = \frac{1}{\sqrt{8}} (2 \ 3 \ -1 \ -2)^{1/2}$$

$8_1 \rightarrow 8 \otimes 8$

$$\begin{pmatrix} N \\ \Sigma \\ \Lambda \\ \Xi \end{pmatrix} \rightarrow \begin{pmatrix} N\pi & N\eta & \Sigma K & \Lambda K \\ N\bar{K} & \Sigma\pi & \Lambda\pi & \Sigma\eta & \Xi K \\ N\bar{K} & \Sigma\pi & \Lambda\eta & \Xi K \\ \Sigma\bar{K} & \Lambda\bar{K} & \Xi\pi & \Xi\eta \end{pmatrix} = \frac{1}{\sqrt{20}} \begin{pmatrix} 9 & -1 & -9 & -1 \\ -6 & 0 & 4 & 4 & -6 \\ 2 & -12 & -4 & -2 \\ 9 & -1 & -9 & -1 \end{pmatrix}^{1/2}$$

$8_2 \rightarrow 8 \otimes 8$

$$\begin{pmatrix} N \\ \Sigma \\ \Lambda \\ \Xi \end{pmatrix} \rightarrow \begin{pmatrix} N\pi & N\eta & \Sigma K & \Lambda K \\ N\bar{K} & \Sigma\pi & \Lambda\pi & \Sigma\eta & \Xi K \\ N\bar{K} & \Sigma\pi & \Lambda\eta & \Xi K \\ \Sigma\bar{K} & \Lambda\bar{K} & \Xi\pi & \Xi\eta \end{pmatrix} = \frac{1}{\sqrt{12}} \begin{pmatrix} 3 & 3 & 3 & -3 \\ 2 & 8 & 0 & 0 & -2 \\ 6 & 0 & 0 & 6 \\ 3 & 3 & 3 & -3 \end{pmatrix}^{1/2}$$

$10 \rightarrow 8 \otimes 8$

$$\begin{pmatrix} \Delta \\ \Sigma \\ \Xi \\ \Omega \end{pmatrix} \rightarrow \begin{pmatrix} N\pi & \Sigma K \\ N\bar{K} & \Sigma\pi & \Lambda\pi & \Sigma\eta & \Xi K \\ \Sigma\bar{K} & \Lambda\bar{K} & \Xi\pi & \Xi\eta \\ \Xi\bar{K} \end{pmatrix} = \frac{1}{\sqrt{12}} \begin{pmatrix} -6 & 6 \\ -2 & 2 & -3 & 3 & 2 \\ 3 & -3 & 3 & 3 \\ 12 \end{pmatrix}^{1/2}$$

$8 \rightarrow 10 \otimes 8$

$$\begin{pmatrix} N \\ \Sigma \\ \Lambda \\ \Xi \end{pmatrix} \rightarrow \begin{pmatrix} \Delta\pi & \Sigma K \\ \Delta\bar{K} & \Sigma\pi & \Sigma\eta & \Xi K \\ \Sigma\bar{K} & \Sigma\pi & \Xi K \\ \Xi\bar{K} & \Xi\pi & \Xi\eta & \Omega K \end{pmatrix} = \frac{1}{\sqrt{15}} \begin{pmatrix} -12 & 3 \\ 8 & -2 & -3 & 2 \\ -9 & 6 \\ 3 & -3 & -3 & 6 \end{pmatrix}^{1/2}$$

$10 \rightarrow 10 \otimes 8$

$$\begin{pmatrix} \Delta \\ \Sigma \\ \Xi \\ \Omega \end{pmatrix} \rightarrow \begin{pmatrix} \Delta\pi & \Delta\eta & \Sigma K \\ \Delta\bar{K} & \Sigma\pi & \Sigma\eta & \Xi K \\ \Sigma\bar{K} & \Xi\pi & \Xi\eta & \Omega K \\ \Xi\bar{K} & \Omega\eta \end{pmatrix} = \frac{1}{\sqrt{24}} \begin{pmatrix} 15 & 3 & -6 \\ 8 & 8 & 0 & -8 \\ 12 & 3 & -3 & -6 \\ 12 & -12 \end{pmatrix}^{1/2}$$

abc	f_{abc}	abc	d_{abc}	abc	d_{abc}
123	1	118	$1/\sqrt{3}$	355	1/2
147	1/2	146	1/2	366	-1/2
156	-1/2	157	1/2	377	-1/2
246	1/2	228	$1/\sqrt{3}$	448	$-1/(2\sqrt{3})$
257	1/2	247	-1/2	558	$-1/(2\sqrt{3})$
345	1/2	256	1/2	668	$-1/(2\sqrt{3})$
367	-1/2	338	$1/\sqrt{3}$	778	$-1/(2\sqrt{3})$
458	$\sqrt{3}/2$	344	1/2	888	$-1/\sqrt{3}$
678	$\sqrt{3}/2$				

The λ_a 's are

$$\lambda_1 = \begin{pmatrix} 0 & 1 & 0 \\ 1 & 0 & 0 \\ 0 & 0 & 0 \end{pmatrix} \quad \lambda_2 = \begin{pmatrix} 0 & -i & 0 \\ i & 0 & 0 \\ 0 & 0 & 0 \end{pmatrix} \quad \lambda_3 = \begin{pmatrix} 1 & 0 & 0 \\ 0 & -1 & 0 \\ 0 & 0 & 0 \end{pmatrix}$$

$$\lambda_4 = \begin{pmatrix} 0 & 0 & 1 \\ 0 & 0 & 0 \\ 1 & 0 & 0 \end{pmatrix} \quad \lambda_5 = \begin{pmatrix} 0 & 0 & -i \\ 0 & 0 & 0 \\ i & 0 & 0 \end{pmatrix} \quad \lambda_6 = \begin{pmatrix} 0 & 0 & 0 \\ 0 & 0 & 1 \\ 0 & 1 & 0 \end{pmatrix}$$

$$\lambda_7 = \begin{pmatrix} 0 & 0 & 0 \\ 0 & 0 & -i \\ 0 & i & 0 \end{pmatrix} \quad \lambda_8 = \frac{1}{\sqrt{3}} \begin{pmatrix} 1 & 0 & 0 \\ 0 & 1 & 0 \\ 0 & 0 & -2 \end{pmatrix}$$

Equation (37.7) defines the Lie algebra of SU(3). A general d -dimensional representation is given by a set of $d \times d$ matrices satisfying Eq. (37.7) with the f_{abc} given above. Equation (37.8) is specific to the defining 3-dimensional representation.

38. SU(n) MULTIPLETS AND YOUNG DIAGRAMMS

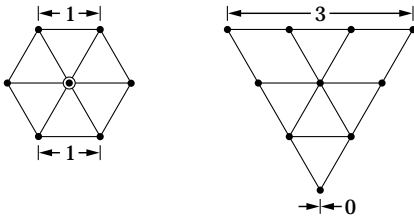
Written by C.G. Wohl (LBNL).

This note tells (1) how SU(n) particle multiplets are identified or labeled, (2) how to find the number of particles in a multiplet from its label, (3) how to draw the Young diagram for a multiplet, and (4) how to use Young diagrams to determine the overall multiplet structure of a composite system, such as a 3-quark or a meson-baryon system.

In much of the literature, the word “representation” is used where we use “multiplet,” and “tableau” is used where we use “diagram.”

38.1. Multiplet labels

An SU(n) multiplet is uniquely identified by a string of (n-1) nonnegative integers: (α, β, γ, ...). Any such set of integers specifies a multiplet. For an SU(2) multiplet such as an isospin multiplet, the single integer α is the number of steps from one end of the multiplet to the other (i.e., it is one fewer than the number of particles in the multiplet). In SU(3), the two integers α and β are the numbers of steps across the top and bottom levels of the multiplet diagram. Thus the labels for the SU(3) octet and decuplet



are (1,1) and (3,0). For larger n, the interpretation of the integers in terms of the geometry of the multiplets, which exist in an (n-1)-dimensional space, is not so readily apparent.

The label for the SU(n) singlet is (0, 0, ..., 0). In a flavor SU(n), the n quarks together form a (1, 0, ..., 0) multiplet, and the n antiquarks belong to a (0, ..., 0, 1) multiplet. These two multiplets are conjugate to one another, which means their labels are related by (α, β, ...) ↔ (... , β, α).

38.2. Number of particles

The number of particles in a multiplet, N = N(α, β, ...), is given as follows (note the pattern of the equations).

In SU(2), N = N(α) is

$$N = \frac{(\alpha + 1)}{1} \tag{38.1}$$

In SU(3), N = N(α, β) is

$$N = \frac{(\alpha + 1)}{1} \cdot \frac{(\beta + 1)}{1} \cdot \frac{(\alpha + \beta + 2)}{2} \tag{38.2}$$

In SU(4), N = N(α, β, γ) is

$$N = \frac{(\alpha+1)}{1} \cdot \frac{(\beta+1)}{1} \cdot \frac{(\gamma+1)}{1} \cdot \frac{(\alpha+\beta+2)}{2} \cdot \frac{(\beta+\gamma+2)}{2} \cdot \frac{(\alpha+\beta+\gamma+3)}{3} \tag{38.3}$$

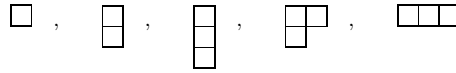
Note that in Eq. (38.3) there is no factor with (α + γ + 2): only a consecutive sequence of the label integers appears in any factor. One more example should make the pattern clear for any SU(n). In SU(5), N = N(α, β, γ, δ) is

$$N = \frac{(\alpha+1)}{1} \cdot \frac{(\beta+1)}{1} \cdot \frac{(\gamma+1)}{1} \cdot \frac{(\delta+1)}{1} \cdot \frac{(\alpha+\beta+2)}{2} \cdot \frac{(\beta+\gamma+2)}{2} \cdot \frac{(\gamma+\delta+2)}{2} \cdot \frac{(\alpha+\beta+\gamma+3)}{3} \cdot \frac{(\beta+\gamma+\delta+3)}{3} \cdot \frac{(\alpha+\beta+\gamma+\delta+4)}{4} \tag{38.4}$$

From the symmetry of these equations, it is clear that multiplets that are conjugate to one another have the same number of particles, but so can other multiplets. For example, the SU(4) multiplets (3,0,0) and (1,1,0) each have 20 particles. Try the equations and see.

38.3. Young diagrams

A Young diagram consists of an array of boxes (or some other symbol) arranged in one or more left-justified rows, with each row being at least as long as the row beneath. The correspondence between a diagram and a multiplet label is: The top row juts out α boxes to the right past the end of the second row, the second row juts out β boxes to the right past the end of the third row, etc. A diagram in SU(n) has at most n rows. There can be any number of “completed” columns of n boxes buttressing the left of a diagram; these don’t affect the label. Thus in SU(3) the diagrams



represent the multiplets (1,0), (0,1), (0,0), (1,1), and (3,0). In any SU(n), the quark multiplet is represented by a single box, the antiquark multiplet by a column of (n-1) boxes, and a singlet by a completed column of n boxes.

38.4. Coupling multiplets together

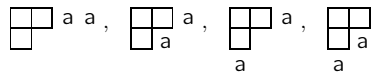
The following recipe tells how to find the multiplets that occur in coupling two multiplets together. To couple together more than two multiplets, first couple two, then couple a third with each of the multiplets obtained from the first two, etc.

First a definition: A sequence of the letters a, b, c, ... is admissible if at any point in the sequence at least as many a’s have occurred as b’s, at least as many b’s have occurred as c’s, etc. Thus abcd and aabcb are admissible sequences and abb and acb are not. Now the recipe:

(a) Draw the Young diagrams for the two multiplets, but in one of the diagrams replace the boxes in the first row with a’s, the boxes in the second row with b’s, etc. Thus, to couple two SU(3) octets (such as the π-meson octet and the baryon octet), we start with and

. The unlettered diagram forms the upper left-hand corner of all the enlarged diagrams constructed below.

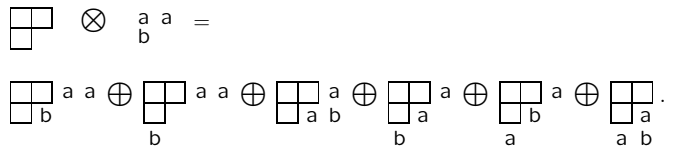
(b) Add the a’s from the lettered diagram to the right-hand ends of the rows of the unlettered diagram to form all possible legitimate Young diagrams that have no more than one a per column. In general, there will be several distinct diagrams, and all the a’s appear in each diagram. At this stage, for the coupling of the two SU(3) octets, we have:



(c) Use the b’s to further enlarge the diagrams already obtained, subject to the same rules. Then throw away any diagram in which the full sequence of letters formed by reading right to left in the first row, then the second row, etc., is not admissible.

(d) Proceed as in (c) with the c’s (if any), etc.

The final result of the coupling of the two SU(3) octets is:



Here only the diagrams with admissible sequences of a’s and b’s and with fewer than four rows (since n = 3) have been kept. In terms of multiplet labels, the above may be written

$$(1, 1) \otimes (1, 1) = (2, 2) \oplus (3, 0) \oplus (0, 3) \oplus (1, 1) \oplus (1, 1) \oplus (0, 0) .$$

In terms of numbers of particles, it may be written

$$8 \otimes 8 = 27 \oplus 10 \oplus \overline{10} \oplus 8 \oplus 8 \oplus 1 .$$

The product of the numbers on the left here is equal to the sum on the right, a useful check. (See also Sec. 14 on the Quark Model.)

39. KINEMATICS

Revised January 2000 by J.D. Jackson (LBNL) and June 2008 by D.R. Tovey (Sheffield).

Throughout this section units are used in which $\hbar = c = 1$. The following conversions are useful: $\hbar c = 197.3$ MeV fm, $(\hbar c)^2 = 0.3894$ (GeV)² mb.

39.1. Lorentz transformations

The energy E and 3-momentum \mathbf{p} of a particle of mass m form a 4-vector $p = (E, \mathbf{p})$ whose square $p^2 \equiv E^2 - |\mathbf{p}|^2 = m^2$. The velocity of the particle is $\boldsymbol{\beta} = \mathbf{p}/E$. The energy and momentum (E^*, \mathbf{p}^*) viewed from a frame moving with velocity $\boldsymbol{\beta}_f$ are given by

$$\begin{pmatrix} E^* \\ p_{\parallel}^* \end{pmatrix} = \begin{pmatrix} \gamma_f & -\gamma_f \boldsymbol{\beta}_f \\ -\gamma_f \boldsymbol{\beta}_f & \gamma_f \end{pmatrix} \begin{pmatrix} E \\ p_{\parallel} \end{pmatrix}, \quad p_T^* = p_T, \quad (39.1)$$

where $\gamma_f = (1 - \beta_f^2)^{-1/2}$ and p_T (p_{\parallel}) are the components of \mathbf{p} perpendicular (parallel) to $\boldsymbol{\beta}_f$. Other 4-vectors, such as the space-time coordinates of events, of course transform in the same way. The scalar product of two 4-momenta $p_1 \cdot p_2 = E_1 E_2 - \mathbf{p}_1 \cdot \mathbf{p}_2$ is invariant (frame independent).

39.2. Center-of-mass energy and momentum

In the collision of two particles of masses m_1 and m_2 the total center-of-mass energy can be expressed in the Lorentz-invariant form

$$\begin{aligned} E_{\text{cm}} &= \left[(E_1 + E_2)^2 - (\mathbf{p}_1 + \mathbf{p}_2)^2 \right]^{1/2}, \\ &= \left[m_1^2 + m_2^2 + 2E_1 E_2 (1 - \beta_1 \beta_2 \cos \theta) \right]^{1/2}, \end{aligned} \quad (39.2)$$

where θ is the angle between the particles. In the frame where one particle (of mass m_2) is at rest (lab frame),

$$E_{\text{cm}} = (m_1^2 + m_2^2 + 2E_{1\text{lab}} m_2)^{1/2}. \quad (39.3)$$

The velocity of the center-of-mass in the lab frame is

$$\boldsymbol{\beta}_{\text{cm}} = \mathbf{p}_{\text{lab}} / (E_{1\text{lab}} + m_2), \quad (39.4)$$

where $\mathbf{p}_{\text{lab}} \equiv \mathbf{p}_{1\text{lab}}$ and

$$\gamma_{\text{cm}} = (E_{1\text{lab}} + m_2) / E_{\text{cm}}. \quad (39.5)$$

The c.m. momenta of particles 1 and 2 are of magnitude

$$p_{\text{cm}} = p_{\text{lab}} \frac{m_2}{E_{\text{cm}}}. \quad (39.6)$$

For example, if a 0.80 GeV/c kaon beam is incident on a proton target, the center of mass energy is 1.699 GeV and the center of mass momentum of either particle is 0.442 GeV/c. It is also useful to note that

$$E_{\text{cm}} dE_{\text{cm}} = m_2 dE_{1\text{lab}} = m_2 \beta_{1\text{lab}} dp_{\text{lab}}. \quad (39.7)$$

39.3. Lorentz-invariant amplitudes

The matrix elements for a scattering or decay process are written in terms of an invariant amplitude $-i\mathcal{M}$. As an example, the S -matrix for $2 \rightarrow 2$ scattering is related to \mathcal{M} by

$$\begin{aligned} \langle p'_1 p'_2 | S | p_1 p_2 \rangle &= I - i(2\pi)^4 \delta^4(p_1 + p_2 - p'_1 - p'_2) \\ &\times \frac{\mathcal{M}(p_1, p_2; p'_1, p'_2)}{(2E_1)^{1/2} (2E_2)^{1/2} (2E'_1)^{1/2} (2E'_2)^{1/2}}. \end{aligned} \quad (39.8)$$

The state normalization is such that

$$\langle p' | p \rangle = (2\pi)^3 \delta^3(\mathbf{p} - \mathbf{p}'). \quad (39.9)$$

39.4. Particle decays

The partial decay rate of a particle of mass M into n bodies in its rest frame is given in terms of the Lorentz-invariant matrix element \mathcal{M} by

$$d\Gamma = \frac{(2\pi)^4}{2M} |\mathcal{M}|^2 d\Phi_n(P; p_1, \dots, p_n), \quad (39.10)$$

where $d\Phi_n$ is an element of n -body phase space given by

$$d\Phi_n(P; p_1, \dots, p_n) = \delta^4(P - \sum_{i=1}^n p_i) \prod_{i=1}^n \frac{d^3 p_i}{(2\pi)^3 2E_i}. \quad (39.11)$$

This phase space can be generated recursively, viz.

$$\begin{aligned} d\Phi_n(P; p_1, \dots, p_n) &= d\Phi_j(q; p_1, \dots, p_j) \\ &\times d\Phi_{n-j+1}(P; q, p_{j+1}, \dots, p_n) (2\pi)^3 dq^2, \end{aligned} \quad (39.12)$$

where $q^2 = (\sum_{i=1}^j E_i)^2 - |\sum_{i=1}^j \mathbf{p}_i|^2$. This form is particularly useful in the case where a particle decays into another particle that subsequently decays.

39.4.1. Survival probability: If a particle of mass M has mean proper lifetime τ ($= 1/\Gamma$) and has momentum (E, \mathbf{p}) , then the probability that it lives for a time t_0 or greater before decaying is given by

$$P(t_0) = e^{-t_0 \Gamma / \gamma} = e^{-M t_0 \Gamma / E}, \quad (39.13)$$

and the probability that it travels a distance x_0 or greater is

$$P(x_0) = e^{-M x_0 \Gamma / |\mathbf{p}|}. \quad (39.14)$$

39.4.2. Two-body decays:

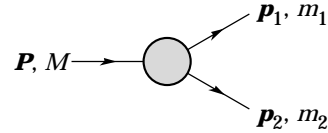


Figure 39.1: Definitions of variables for two-body decays.

In the rest frame of a particle of mass M , decaying into 2 particles labeled 1 and 2,

$$E_1 = \frac{M^2 - m_2^2 + m_1^2}{2M}, \quad (39.15)$$

$$|\mathbf{p}_1| = |\mathbf{p}_2|$$

$$= \frac{[(M^2 - (m_1 + m_2)^2)(M^2 - (m_1 - m_2)^2)]^{1/2}}{2M}, \quad (39.16)$$

and

$$d\Gamma = \frac{1}{32\pi^2} |\mathcal{M}|^2 \frac{|\mathbf{p}_1|}{M^2} d\Omega, \quad (39.17)$$

where $d\Omega = d\phi_1 d(\cos \theta_1)$ is the solid angle of particle 1. The invariant mass M can be determined from the energies and momenta using Eq. (39.2) with $M = E_{\text{cm}}$.

39.4.3. Three-body decays:

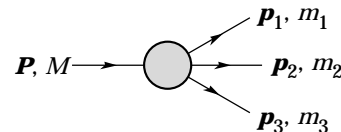


Figure 39.2: Definitions of variables for three-body decays.

Defining $p_{ij} = p_i + p_j$ and $m_{ij}^2 = p_{ij}^2$, then $m_{12}^2 + m_{23}^2 + m_{13}^2 = M^2 + m_1^2 + m_2^2 + m_3^2$ and $m_{12}^2 = (P - p_3)^2 = M^2 + m_3^2 - 2ME_3$, where E_3 is the energy of particle 3 in the rest frame of M . In that frame, the momenta of the three decay particles lie in a plane. The relative orientation of these three momenta is fixed if their energies are known. The momenta can therefore be specified in space by giving three Euler angles (α, β, γ) that specify the orientation of the final system relative to the initial particle [1]. Then

$$d\Gamma = \frac{1}{(2\pi)^5} \frac{1}{16M} |\mathcal{M}|^2 dE_1 dE_2 d\alpha d(\cos\beta) d\gamma. \quad (39.18)$$

Alternatively

$$d\Gamma = \frac{1}{(2\pi)^5} \frac{1}{16M^2} |\mathcal{M}|^2 |\mathbf{p}_1^*| |\mathbf{p}_3| dm_{12} d\Omega_1^* d\Omega_3, \quad (39.19)$$

where $(|\mathbf{p}_1^*|, \Omega_1^*)$ is the momentum of particle 1 in the rest frame of 1 and 2, and Ω_3 is the angle of particle 3 in the rest frame of the decaying particle. $|\mathbf{p}_1^*|$ and $|\mathbf{p}_3|$ are given by

$$|\mathbf{p}_1^*| = \frac{[(m_{12}^2 - (m_1 + m_2)^2)(m_{12}^2 - (m_1 - m_2)^2)]^{1/2}}{2m_{12}}, \quad (39.20a)$$

and

$$|\mathbf{p}_3| = \frac{[(M^2 - (m_{12} + m_3)^2)(M^2 - (m_{12} - m_3)^2)]^{1/2}}{2M}. \quad (39.20b)$$

[Compare with Eq. (39.16).]

If the decaying particle is a scalar or we average over its spin states, then integration over the angles in Eq. (39.18) gives

$$\begin{aligned} d\Gamma &= \frac{1}{(2\pi)^3} \frac{1}{8M} |\overline{\mathcal{M}}|^2 dE_1 dE_2 \\ &= \frac{1}{(2\pi)^3} \frac{1}{32M^3} |\overline{\mathcal{M}}|^2 dm_{12}^2 dm_{23}^2. \end{aligned} \quad (39.21)$$

This is the standard form for the Dalitz plot.

39.4.3.1. Dalitz plot: For a given value of m_{12}^2 , the range of m_{23}^2 is determined by its values when \mathbf{p}_2 is parallel or antiparallel to \mathbf{p}_3 :

$$(m_{23}^2)_{\max} = (E_2^* + E_3^*)^2 - \left(\sqrt{E_2^{*2} - m_2^2} - \sqrt{E_3^{*2} - m_3^2} \right)^2, \quad (39.22a)$$

$$(m_{23}^2)_{\min} = (E_2^* + E_3^*)^2 - \left(\sqrt{E_2^{*2} - m_2^2} + \sqrt{E_3^{*2} - m_3^2} \right)^2. \quad (39.22b)$$

Here $E_2^* = (m_{12}^2 - m_1^2 + m_2^2)/2m_{12}$ and $E_3^* = (M^2 - m_{12}^2 - m_3^2)/2m_{12}$ are the energies of particles 2 and 3 in the m_{12} rest frame. The scatter plot in m_{12}^2 and m_{23}^2 is called a Dalitz plot. If $|\overline{\mathcal{M}}|^2$ is constant, the allowed region of the plot will be uniformly populated with events [see Eq. (39.21)]. A nonuniformity in the plot gives immediate information on $|\overline{\mathcal{M}}|^2$. For example, in the case of $D \rightarrow K\pi\pi$, bands appear when $m_{(K\pi)} = m_{K^*(892)}$, reflecting the appearance of the decay chain $D \rightarrow K^*(892)\pi \rightarrow K\pi\pi$.

39.4.4. Kinematic limits :

39.4.4.1. Three-body decays: In a three-body decay (Fig. 39.2) the maximum of $|\mathbf{p}_3|$, [given by Eq. (39.20)], is achieved when $m_{12} = m_1 + m_2$, *i.e.*, particles 1 and 2 have the same vector velocity in the rest frame of the decaying particle. If, in addition, $m_3 > m_1, m_2$, then $|\mathbf{p}_3|_{\max} > |\mathbf{p}_1|_{\max}, |\mathbf{p}_2|_{\max}$. The distribution of m_{12} values possesses an end-point or maximum value at $m_{12} = M - m_3$. This can be used to constrain the mass difference of a parent particle and one invisible decay product.

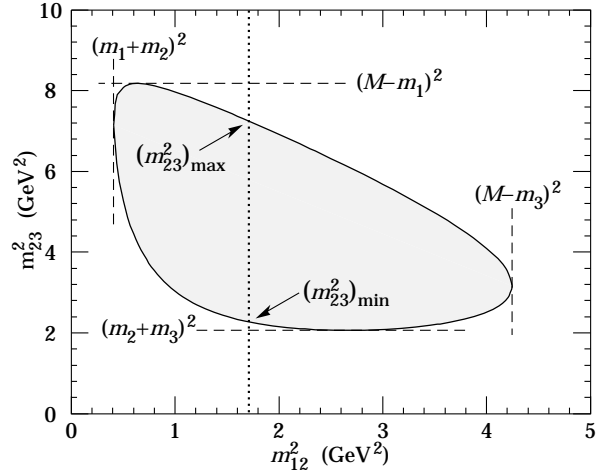


Figure 39.3: Dalitz plot for a three-body final state. In this example, the state is π^+K^0p at 3 GeV. Four-momentum conservation restricts events to the shaded region.

39.4.4.2. Sequential two-body decays:

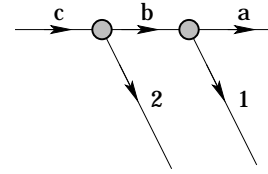


Figure 39.4: Particles participating in sequential two-body decay chain. Particles labeled 1 and 2 are visible while the particle terminating the chain (a) is invisible.

When a heavy particle initiates a sequential chain of two-body decays terminating in an invisible particle, constraints on the masses of the states participating in the chain can be obtained from end-points and thresholds in invariant mass distributions of the aggregated decay products. For the two-step decay chain depicted in Fig. 39.4 the invariant mass distribution of the two visible particles possesses an end-point given by:

$$(m_{12}^{\max})^2 = \frac{(m_c^2 - m_b^2)(m_b^2 - m_a^2)}{m_b^2}, \quad (39.23)$$

provided particles 1 and 2 are massless. If visible particle 1 has non-zero mass m_1 then Eq. (39.23) is replaced by

$$(m_{12}^{\max})^2 = m_1^2 + \frac{(m_c^2 - m_b^2)}{2m_b^2} \times \left(m_1^2 + m_b^2 - m_a^2 + \sqrt{(-m_1^2 + m_b^2 - m_a^2)^2 - 4m_1^2 m_a^2} \right). \quad (39.24)$$

See Refs. 2 and 3 for other cases.

39.4.5. Multibody decays : The above results may be generalized to final states containing any number of particles by combining some of the particles into “effective particles” and treating the final states as 2 or 3 “effective particle” states. Thus, if $p_{ijk\dots} = p_i + p_j + p_k + \dots$, then

$$m_{ijk\dots} = \sqrt{p_{ijk\dots}^2}, \quad (39.25)$$

and $m_{ijk\dots}$ may be used in place of *e.g.*, m_{12} in the relations in Sec. 39.4.3 or Sec. 39.4.4 above.

39.5. Cross sections

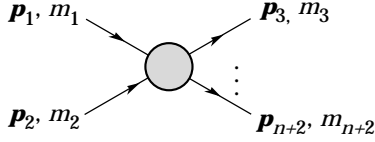


Figure 39.5: Definitions of variables for production of an n -body final state.

The differential cross section is given by

$$d\sigma = \frac{(2\pi)^4 |\mathcal{M}|^2}{4\sqrt{(p_1 \cdot p_2)^2 - m_1^2 m_2^2}} \times d\Phi_n(p_1 + p_2; p_3, \dots, p_{n+2}). \quad (39.26)$$

[See Eq. (39.11).] In the rest frame of m_2 (lab),

$$\sqrt{(p_1 \cdot p_2)^2 - m_1^2 m_2^2} = m_2 p_{1\text{lab}}; \quad (39.27a)$$

while in the center-of-mass frame

$$\sqrt{(p_1 \cdot p_2)^2 - m_1^2 m_2^2} = p_{1\text{cm}} \sqrt{s}. \quad (39.27b)$$

39.5.1. Two-body reactions :

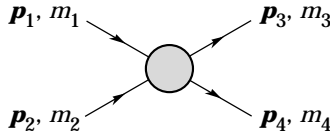


Figure 39.6: Definitions of variables for a two-body final state.

Two particles of momenta p_1 and p_2 and masses m_1 and m_2 scatter to particles of momenta p_3 and p_4 and masses m_3 and m_4 ; the Lorentz-invariant Mandelstam variables are defined by

$$s = (p_1 + p_2)^2 = (p_3 + p_4)^2 = m_1^2 + 2E_1 E_2 - 2\mathbf{p}_1 \cdot \mathbf{p}_2 + m_2^2, \quad (39.28)$$

$$t = (p_1 - p_3)^2 = (p_2 - p_4)^2 = m_1^2 - 2E_1 E_3 + 2\mathbf{p}_1 \cdot \mathbf{p}_3 + m_3^2, \quad (39.29)$$

$$u = (p_1 - p_4)^2 = (p_2 - p_3)^2 = m_1^2 - 2E_1 E_4 + 2\mathbf{p}_1 \cdot \mathbf{p}_4 + m_4^2, \quad (39.30)$$

and they satisfy

$$s + t + u = m_1^2 + m_2^2 + m_3^2 + m_4^2. \quad (39.31)$$

The two-body cross section may be written as

$$\frac{d\sigma}{dt} = \frac{1}{64\pi s} \frac{1}{|\mathbf{p}_{1\text{cm}}|^2} |\mathcal{M}|^2. \quad (39.32)$$

In the center-of-mass frame

$$t = (E_{1\text{cm}} - E_{3\text{cm}})^2 - (p_{1\text{cm}} - p_{3\text{cm}})^2 - 4p_{1\text{cm}} p_{3\text{cm}} \sin^2(\theta_{\text{cm}}/2) = t_0 - 4p_{1\text{cm}} p_{3\text{cm}} \sin^2(\theta_{\text{cm}}/2), \quad (39.33)$$

where θ_{cm} is the angle between particle 1 and 3. The limiting values t_0 ($\theta_{\text{cm}} = 0$) and t_1 ($\theta_{\text{cm}} = \pi$) for $2 \rightarrow 2$ scattering are

$$t_0(t_1) = \left[\frac{m_1^2 - m_3^2 - m_2^2 + m_4^2}{2\sqrt{s}} \right]^2 - (p_{1\text{cm}} \mp p_{3\text{cm}})^2. \quad (39.34)$$

In the literature the notation t_{min} (t_{max}) for t_0 (t_1) is sometimes used, which should be discouraged since $t_0 > t_1$. The center-of-mass energies and momenta of the incoming particles are

$$E_{1\text{cm}} = \frac{s + m_1^2 - m_2^2}{2\sqrt{s}}, \quad E_{2\text{cm}} = \frac{s + m_2^2 - m_1^2}{2\sqrt{s}}, \quad (39.35)$$

For $E_{3\text{cm}}$ and $E_{4\text{cm}}$, change m_1 to m_3 and m_2 to m_4 . Then

$$p_{i\text{cm}} = \sqrt{E_{i\text{cm}}^2 - m_i^2} \text{ and } p_{1\text{cm}} = \frac{p_{1\text{lab}} m_2}{\sqrt{s}}. \quad (39.36)$$

Here the subscript lab refers to the frame where particle 2 is at rest. [For other relations see Eqs. (39.2)–(39.4).]

39.5.2. Inclusive reactions : Choose some direction (usually the beam direction) for the z -axis; then the energy and momentum of a particle can be written as

$$E = m_T \cosh y, \quad p_x, p_y, p_z = m_T \sinh y, \quad (39.37)$$

where m_T , conventionally called the ‘transverse mass’, is given by

$$m_T^2 = m^2 + p_x^2 + p_y^2. \quad (39.38)$$

and the rapidity y is defined by

$$y = \frac{1}{2} \ln \left(\frac{E + p_z}{E - p_z} \right)$$

$$= \ln \left(\frac{E + p_z}{m_T} \right) = \tanh^{-1} \left(\frac{p_z}{E} \right). \quad (39.39)$$

Note that the definition of the transverse mass in Eq. (39.38) differs from that used by experimentalists at hadron colliders (see Sec. 39.6.1 below). Under a boost in the z -direction to a frame with velocity β , $y \rightarrow y - \tanh^{-1} \beta$. Hence the shape of the rapidity distribution dN/dy is invariant, as are differences in rapidity. The invariant cross section may also be rewritten

$$E \frac{d^3\sigma}{d^3p} = \frac{d^3\sigma}{d\phi dy p_T dp_T} \Rightarrow \frac{d^2\sigma}{\pi dy d(p_T^2)}. \quad (39.40)$$

The second form is obtained using the identity $dy/dp_z = 1/E$, and the third form represents the average over ϕ .

Feynman’s x variable is given by

$$x = \frac{p_z}{p_{z\text{max}}} \approx \frac{E + p_z}{(E + p_z)_{\text{max}}} \quad (p_T \ll |p_z|). \quad (39.41)$$

In the c.m. frame,

$$x \approx \frac{2p_{z\text{cm}}}{\sqrt{s}} = \frac{2m_T \sinh y_{\text{cm}}}{\sqrt{s}} \quad (39.42)$$

and

$$= (y_{\text{cm}})_{\text{max}} = \ln(\sqrt{s}/m). \quad (39.43)$$

The invariant mass M of the two-particle system described in Sec. 39.4.2 can be written in terms of these variables as

$$M^2 = m_1^2 + m_2^2 + 2[E_T(1)E_T(2) \cosh \Delta y - \mathbf{p}_T(1) \cdot \mathbf{p}_T(2)], \quad (39.44)$$

where

$$E_T(i) = \sqrt{|\mathbf{p}_T(i)|^2 + m_i^2}, \quad (39.45)$$

and $\mathbf{p}_T(i)$ denotes the transverse momentum vector of particle i .

For $p \gg m$, the rapidity [Eq. (39.39)] may be expanded to obtain

$$y = \frac{1}{2} \ln \frac{\cos^2(\theta/2) + m^2/4p^2 + \dots}{\sin^2(\theta/2) + m^2/4p^2 + \dots} \approx -\ln \tan(\theta/2) \equiv \eta \quad (39.46)$$

where $\cos \theta = p_z/p$. The pseudorapidity η defined by the second line is approximately equal to the rapidity y for $p \gg m$ and $\theta \gg 1/\gamma$, and in any case can be measured when the mass and momentum of the particle are unknown. From the definition one can obtain the identities

$$\sinh \eta = \cot \theta, \quad \cosh \eta = 1/\sin \theta, \quad \tanh \eta = \cos \theta. \quad (39.47)$$

39.5.3. Partial waves : The amplitude in the center of mass for elastic scattering of spinless particles may be expanded in Legendre polynomials

$$f(k, \theta) = \frac{1}{k} \sum_{\ell} (2\ell + 1) a_{\ell} P_{\ell}(\cos \theta), \quad (39.48)$$

where k is the c.m. momentum, θ is the c.m. scattering angle, $a_{\ell} = (\eta_{\ell} e^{2i\delta_{\ell}} - 1)/2i$, $0 \leq \eta_{\ell} \leq 1$, and δ_{ℓ} is the phase shift of the ℓ^{th} partial wave. For purely elastic scattering, $\eta_{\ell} = 1$. The differential cross section is

$$\frac{d\sigma}{d\Omega} = |f(k, \theta)|^2. \quad (39.49)$$

The optical theorem states that

$$\sigma_{\text{tot}} = \frac{4\pi}{k} \text{Im} f(k, 0), \quad (39.50)$$

and the cross section in the ℓ^{th} partial wave is therefore bounded:

$$\sigma_{\ell} = \frac{4\pi}{k^2} (2\ell + 1) |a_{\ell}|^2 \leq \frac{4\pi(2\ell + 1)}{k^2}. \quad (39.51)$$

The evolution with energy of a partial-wave amplitude a_{ℓ} can be displayed as a trajectory in an Argand plot, as shown in Fig. 39.7.

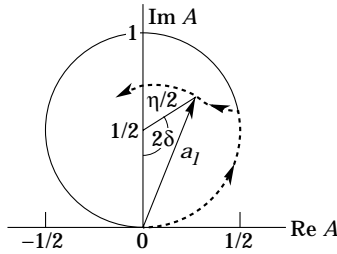


Figure 39.7: Argand plot showing a partial-wave amplitude a_{ℓ} as a function of energy. The amplitude leaves the unitary circle where inelasticity sets in ($\eta_{\ell} < 1$).

The usual Lorentz-invariant matrix element \mathcal{M} (see Sec. 39.3 above) for the elastic process is related to $f(k, \theta)$ by

$$\mathcal{M} = -8\pi\sqrt{s} f(k, \theta), \quad (39.52)$$

so

$$\sigma_{\text{tot}} = -\frac{1}{2p_{\text{lab}} m_2} \text{Im} \mathcal{M}(t = 0), \quad (39.53)$$

where s and t are the center-of-mass energy squared and momentum transfer squared, respectively (see Sec. 39.4.1).

39.5.3.1. Resonances: The Breit-Wigner (nonrelativistic) form for an elastic amplitude a_{ℓ} with a resonance at c.m. energy E_R , elastic width Γ_{el} , and total width Γ_{tot} is

$$a_{\ell} = \frac{\Gamma_{\text{el}}/2}{E_R - E - i\Gamma_{\text{tot}}/2}, \quad (39.54)$$

where E is the c.m. energy. As shown in Fig. 39.8, in the absence of background the elastic amplitude traces a counterclockwise circle with center $ix_{\text{el}}/2$ and radius $x_{\text{el}}/2$, where the elasticity $x_{\text{el}} = \Gamma_{\text{el}}/\Gamma_{\text{tot}}$. The amplitude has a pole at $E = E_R - i\Gamma_{\text{tot}}/2$.

The spin-averaged Breit-Wigner cross section for a spin- J resonance produced in the collision of particles of spin S_1 and S_2 is

$$\sigma_{BW}(E) = \frac{(2J+1)}{(2S_1+1)(2S_2+1)} \frac{\pi}{k^2} \frac{B_{\text{in}} B_{\text{out}} \Gamma_{\text{tot}}^2}{(E - E_R)^2 + \Gamma_{\text{tot}}^2/4}, \quad (39.55)$$

where k is the c.m. momentum, E is the c.m. energy, and B_{in} and B_{out} are the branching fractions of the resonance into the entrance and exit channels. The $2S+1$ factors are the multiplicities of the incident spin states, and are replaced by 2 for photons. This expression is valid only for an isolated state. If the width is not small, Γ_{tot} cannot be treated as a constant independent of E . There are many other forms for σ_{BW} , all of which are equivalent to the one given here in the narrow-width case. Some of these forms may be more appropriate if the resonance is broad.

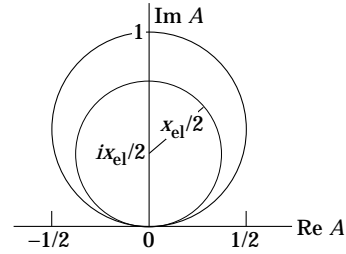


Figure 39.8: Argand plot for a resonance.

The relativistic Breit-Wigner form corresponding to Eq. (39.54) is:

$$a_{\ell} = \frac{-m\Gamma_{\text{el}}}{s - m^2 + im\Gamma_{\text{tot}}}. \quad (39.56)$$

A better form incorporates the known kinematic dependences, replacing $m\Gamma_{\text{tot}}$ by $\sqrt{s}\Gamma_{\text{tot}}(s)$, where $\Gamma_{\text{tot}}(s)$ is the width the resonance particle would have if its mass were \sqrt{s} , and correspondingly $m\Gamma_{\text{el}}$ by $\sqrt{s}\Gamma_{\text{el}}(s)$ where $\Gamma_{\text{el}}(s)$ is the partial width in the incident channel for a mass \sqrt{s} :

$$a_{\ell} = \frac{-\sqrt{s}\Gamma_{\text{el}}(s)}{s - m^2 + i\sqrt{s}\Gamma_{\text{tot}}(s)}. \quad (39.57)$$

For the Z boson, all the decays are to particles whose masses are small enough to be ignored, so on dimensional grounds $\Gamma_{\text{tot}}(s) = \sqrt{s}\Gamma_0/m_Z$, where Γ_0 defines the width of the Z , and $\Gamma_{\text{el}}(s)/\Gamma_{\text{tot}}(s)$ is constant. A full treatment of the line shape requires consideration of dynamics, not just kinematics. For the Z this is done by calculating the radiative corrections in the Standard Model.

39.6. Transverse variables

At hadron colliders, a significant and unknown proportion of the energy of the incoming hadrons in each event escapes down the beam-pipe. Consequently if invisible particles are created in the final state, their net momentum can only be constrained in the plane transverse to the beam direction. Defining the z -axis as the beam direction, this net momentum is equal to the missing transverse energy vector

$$\mathbf{E}_T^{\text{miss}} = -\sum_i \mathbf{p}_T(i), \quad (39.58)$$

where the sum runs over the transverse momenta of all visible final state particles.

39.6.1. Single production with semi-invisible final state :

Consider a single heavy particle of mass M produced in association with visible particles which decays as in Fig. 39.1 to two particles, of which one (labeled particle 1) is invisible. The mass of the parent particle can be constrained with the quantity M_T defined by

$$M_T^2 \equiv [E_T(1) + E_T(2)]^2 - [\mathbf{p}_T(1) + \mathbf{p}_T(2)]^2 = m_1^2 + m_2^2 + 2[E_T(1)E_T(2) - \mathbf{p}_T(1) \cdot \mathbf{p}_T(2)], \quad (39.59)$$

where

$$\mathbf{p}_T(1) = \mathbf{E}_T^{\text{miss}}. \quad (39.60)$$

This quantity is called the ‘transverse mass’ by hadron collider experimentalists but it should be noted that it is quite different from that used in the description of inclusive reactions [Eq. (39.38)]. The distribution of event M_T values possesses an end-point at $M_T^{\text{max}} = M$. If $m_1 = m_2 = 0$ then

$$M_T^2 = 2|\mathbf{p}_T(1)||\mathbf{p}_T(2)|(1 - \cos \phi_{12}), \quad (39.61)$$

where ϕ_{ij} is defined as the angle between particles i and j in the transverse plane.

39.6.2. Pair production with semi-invisible final states :

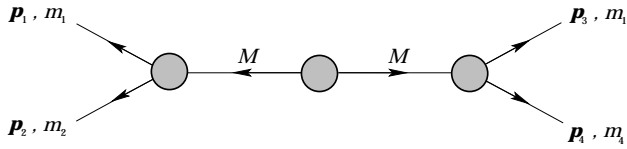


Figure 39.9: Definitions of variables for pair production of semi-invisible final states. Particles 1 and 3 are invisible while particles 2 and 4 are visible.

Consider two identical heavy particles of mass M produced such that their combined center-of-mass is at rest in the transverse plane (Fig. 39.9). Each particle decays to a final state consisting of an invisible particle of fixed mass m_1 together with an additional visible particle. M and m_1 can be constrained with the variables M_{T2} and M_{CT} which are defined in Refs. [4] and [5].

References:

1. See, for example, J.J. Sakurai, *Modern Quantum Mechanics*, Addison-Wesley (1985), p. 172, or D.M. Brink and G.R. Satchler, *Angular Momentum*, 2nd ed., Oxford University Press (1968), p. 20.
2. I. Hinchliffe *et al.*, Phys. Rev. **D55**, 5520 (1997).
3. B.C. Allanach *et al.*, JHEP **0009**, 004 (2000).
4. C.G. Lester and D.J. Summers, Phys. Lett. **B463**, 99 (1999).
5. D.R. Tovey, JHEP **0804**, 034 (2008).

40. CROSS-SECTION FORMULAE FOR SPECIFIC PROCESSES

Revised October 2009 by H. Baer (University of Oklahoma) and R.N. Cahn (LBNL).

PART I: STANDARD MODEL PROCESSES

Setting aside leptoproduction (for which, see Sec. 16 of this *Review*), the cross sections of primary interest are those with light incident particles, e^+e^- , $\gamma\gamma$, $q\bar{q}$, gq , gg , etc., where g and q represent gluons and light quarks. The produced particles include both light particles and heavy ones - t , W , Z , and the Higgs boson H . We provide the production cross sections calculated within the Standard Model for several such processes.

40.1. Resonance Formation

Resonant cross sections are generally described by the Breit-Wigner formula (Sec. 16 of this *Review*).

$$\sigma(E) = \frac{2J+1}{(2S_1+1)(2S_2+1)} \frac{4\pi}{k^2} \left[\frac{\Gamma^2/4}{(E-E_0)^2 + \Gamma^2/4} \right] B_{in} B_{out}, \quad (40.1)$$

where E is the c.m. energy, J is the spin of the resonance, and the number of polarization states of the two incident particles are $2S_1+1$ and $2S_2+1$. The c.m. momentum in the initial state is k , E_0 is the c.m. energy at the resonance, and Γ is the full width at half maximum height of the resonance. The branching fraction for the resonance into the initial-state channel is B_{in} and into the final-state channel is B_{out} . For a narrow resonance, the factor in square brackets may be replaced by $\pi\Gamma\delta(E-E_0)/2$.

40.2. Production of light particles

The production of point-like, spin-1/2 fermions in e^+e^- annihilation through a virtual photon, $e^+e^- \rightarrow \gamma^* \rightarrow ff$, at c.m. energy squared s is given by

$$\frac{d\sigma}{d\Omega} = N_c \frac{\alpha^2}{4s} \beta [1 + \cos^2\theta + (1-\beta^2)\sin^2\theta] Q_f^2, \quad (40.2)$$

where β is v/c for the produced fermions in the c.m., θ is the c.m. scattering angle, and Q_f is the charge of the fermion. The factor N_c is 1 for charged leptons and 3 for quarks. In the ultrarelativistic limit, $\beta \rightarrow 1$,

$$\sigma = N_c Q_f^2 \frac{4\pi\alpha^2}{3s} = N_c Q_f^2 \frac{86.8 \text{ nb}}{s(\text{GeV}^2)}. \quad (40.3)$$

The cross section for the annihilation of a $q\bar{q}$ pair into a distinct pair $q'\bar{q}'$ through a gluon is completely analogous up to color factors, with the replacement $\alpha \rightarrow \alpha_s$. Treating all quarks as massless, averaging over the colors of the initial quarks and defining $t = -s\sin^2(\theta/2)$, $u = -s\cos^2(\theta/2)$, one finds [1]

$$\frac{d\sigma}{d\Omega}(q\bar{q} \rightarrow q'\bar{q}') = \frac{\alpha_s^2}{9s} \frac{t^2 + u^2}{s^2}. \quad (40.4)$$

Crossing symmetry gives

$$\frac{d\sigma}{d\Omega}(qq' \rightarrow qq') = \frac{\alpha_s^2}{9s} \frac{s^2 + u^2}{t^2}. \quad (40.5)$$

If the quarks q and q' are identical, we have

$$\frac{d\sigma}{d\Omega}(q\bar{q} \rightarrow q\bar{q}) = \frac{\alpha_s^2}{9s} \left[\frac{t^2 + u^2}{s^2} + \frac{s^2 + u^2}{t^2} - \frac{2u^2}{3st} \right], \quad (40.6)$$

and by crossing

$$\frac{d\sigma}{d\Omega}(qq \rightarrow qq) = \frac{\alpha_s^2}{9s} \left[\frac{t^2 + s^2}{u^2} + \frac{s^2 + u^2}{t^2} - \frac{2s^2}{3ut} \right]. \quad (40.7)$$

Annihilation of e^+e^- into $\gamma\gamma$ has the cross section

$$\frac{d\sigma}{d\Omega}(e^+e^- \rightarrow \gamma\gamma) = \frac{\alpha^2}{2s} \frac{u^2 + t^2}{tu}. \quad (40.8)$$

The related QCD process also has a triple-gluon coupling. The cross section is

$$\frac{d\sigma}{d\Omega}(q\bar{q} \rightarrow gg) = \frac{8\alpha_s^2}{27s} (t^2 + u^2) \left(\frac{1}{tu} - \frac{9}{4s^2} \right). \quad (40.9)$$

The crossed reactions are

$$\frac{d\sigma}{d\Omega}(gq \rightarrow gq) = \frac{\alpha_s^2}{9s} (s^2 + u^2) \left(-\frac{1}{su} + \frac{9}{4t^2} \right) \quad (40.10)$$

and

$$\frac{d\sigma}{d\Omega}(gg \rightarrow q\bar{q}) = \frac{\alpha_s^2}{24s} (t^2 + u^2) \left(\frac{1}{tu} - \frac{9}{4s^2} \right). \quad (40.11)$$

Finally,

$$\frac{d\sigma}{d\Omega}(gg \rightarrow gg) = \frac{9\alpha_s^2}{8s} \left(3 - \frac{ut}{s^2} - \frac{su}{t^2} - \frac{st}{u^2} \right). \quad (40.12)$$

Lepton-quark scattering is analogous (neglecting Z exchange)

$$\frac{d\sigma}{d\Omega}(eq \rightarrow eq) = \frac{\alpha^2}{2s} e_q^2 \frac{s^2 + u^2}{t^2}. \quad (40.13)$$

where e_q is the charge of the quark. For neutrino scattering with the four-Fermi interaction

$$\frac{d\sigma}{d\Omega}(\nu d \rightarrow \ell^- u) = \frac{G_F^2 s}{4\pi^2}, \quad (40.14)$$

where the Cabibbo angle suppression is ignored. Similarly

$$\frac{d\sigma}{d\Omega}(\nu \bar{u} \rightarrow \ell^+ \bar{d}) = \frac{G_F^2 s}{4\pi^2} \frac{(1 + \cos\theta)^2}{4}. \quad (40.15)$$

To obtain the formulae for deep inelastic scattering (presented in more detail in Section 16) we consider quarks of type i carrying a fraction $x = Q^2/(2M\nu)$ of the nucleon's energy, where $\nu = E - E'$ is the energy lost by the lepton in the nucleon rest frame. With $y = \nu/E$ we have the correspondences

$$\begin{aligned} 1 + \cos\theta &\rightarrow 2(1-y), \\ d\Omega_{cm} &\rightarrow 4\pi f_i(x) dx dy, \end{aligned} \quad (40.16)$$

where the latter incorporates the quark distribution, $f_i(x)$. In this way we find

$$\begin{aligned} \frac{d\sigma}{dx dy}(eN \rightarrow eX) &= \frac{4\pi\alpha^2 x s}{Q^4} \frac{1}{2} \left[1 + (1-y)^2 \right] \\ &\times \left[\frac{4}{9}(u(x) + \bar{u}(x) + \dots) + \frac{1}{9}(d(x) + \bar{d}(x) + \dots) \right] \end{aligned} \quad (40.17)$$

where now $s = 2ME$ is the cm energy squared for the electron-nucleon collision and we have suppressed contributions from higher mass quarks.

Similarly,

$$\frac{d\sigma}{dx dy}(\nu N \rightarrow \ell^- X) = \frac{G_F^2 x s}{\pi} [(d(x) + \dots) + (1-y)^2(\bar{u}(x) + \dots)] \quad (40.18)$$

and

$$\frac{d\sigma}{dx dy}(\bar{\nu} N \rightarrow \ell^+ X) = \frac{G_F^2 x s}{\pi} [(\bar{d}(x) + \dots) + (1-y)^2(u(x) + \dots)]. \quad (40.19)$$

Quasi-elastic neutrino scattering ($\nu_\mu n \rightarrow \mu^- p$, $\bar{\nu}_\mu p \rightarrow \mu^+ n$) is directly related to the crossed reaction, neutron decay. The formula for the differential cross section is presented, for example, in N.J. Baker *et al.*, Phys. Rev. **D23**, 2499 (1981).

40.3. Hadroproduction of heavy quarks

For hadroproduction of heavy quarks $Q = c, b, t$, it is important to include mass effects in the formulae. For $q\bar{q} \rightarrow Q\bar{Q}$, one has

$$\frac{d\sigma}{d\Omega}(q\bar{q} \rightarrow Q\bar{Q}) = \frac{\alpha_s^2}{9s^3} \left[(m_Q^2 - t)^2 + (m_Q^2 - u)^2 + 2m_Q^2 s \right], \quad (40.20)$$

while for $gg \rightarrow Q\bar{Q}$ one has

$$\begin{aligned} \frac{d\sigma}{d\Omega}(gg \rightarrow Q\bar{Q}) &= \frac{\alpha_s^2}{32s} \left[\frac{6}{s^2} (m_Q^2 - t)(m_Q^2 - u) - \frac{m_Q^2 (s - 4m_Q^2)}{3(m_Q^2 - t)(m_Q^2 - u)} + \right. \\ &\quad \frac{4}{3} \frac{(m_Q^2 - t)(m_Q^2 - u) - 2m_Q^2(m_Q^2 + t)}{(m_Q^2 - t)^2} \\ &\quad + \frac{4}{3} \frac{(m_Q^2 - t)(m_Q^2 - u) - 2m_Q^2(m_Q^2 + u)}{(m_Q^2 - u)^2} \\ &\quad - \left[3 \frac{(m_Q^2 - t)(m_Q^2 - u) + m_Q^2(u - t)}{s(m_Q^2 - t)} \right. \\ &\quad \left. \left. - 3 \frac{(m_Q^2 - t)(m_Q^2 - u) + m_Q^2(t - u)}{s(m_Q^2 - u)} \right] \right]. \quad (40.21) \end{aligned}$$

40.4. Production of Weak Gauge Bosons

40.4.1. W and Z resonant production :

Resonant production of a single W or Z is governed by the partial widths

$$\Gamma(W \rightarrow \ell_i \bar{\nu}_i) = \frac{\sqrt{2} G_F m_W^3}{12\pi} \quad (40.22)$$

$$\Gamma(W \rightarrow q_i \bar{q}_j) = 3 \frac{\sqrt{2} G_F |V_{ij}|^2 m_W^3}{12\pi} \quad (40.23)$$

$$\begin{aligned} \Gamma(Z \rightarrow f\bar{f}) &= N_c \frac{\sqrt{2} G_F m_Z^3}{6\pi} \\ &\quad \times \left[(T_3 - Q_f \sin^2 \theta_W)^2 + (Q_f \sin \theta_W)^2 \right]. \quad (40.24) \end{aligned}$$

The weak mixing angle is θ_W . The CKM matrix elements are indicated by V_{ij} and N_c is 3 for $q\bar{q}$ final states and 1 for leptonic final states.

The full differential cross section for $f_i \bar{f}_j \rightarrow (W, Z) \rightarrow f'_i \bar{f}'_j$ is given by

$$\begin{aligned} \frac{d\sigma}{d\Omega} &= \frac{N_c^f}{N_c^i} \cdot \frac{1}{256\pi^2 s} \cdot \frac{s^2}{(s - M^2)^2 + s\Gamma^2} \\ &\quad \times \left[(L^2 + R^2)(L'^2 + R'^2)(1 + \cos^2 \theta) \right. \\ &\quad \left. + (L^2 - R^2)(L'^2 - R'^2) 2 \cos \theta \right] \quad (40.25) \end{aligned}$$

where M is the mass of the W or Z . The couplings for the W are $L = (8G_F m_W^2 / \sqrt{2})^{1/2} V_{ij} / \sqrt{2}$; $R = 0$ where V_{ij} is the corresponding CKM matrix element, with an analogous expression for L' and R' . For Z , the couplings are $L = (8G_F m_Z^2 / \sqrt{2})^{1/2} (T_3 - \sin^2 \theta_W Q)$; $R = -(8G_F m_Z^2 / \sqrt{2})^{1/2} \sin^2 \theta_W Q$, where T_3 is the weak isospin of the initial left-handed fermion and Q is the initial fermion's electric charge. The expressions for L' and R' are analogous. The color factors $N_c^{i,f}$ are 3 for initial or final quarks and 1 for initial or final leptons.

40.4.2. Production of pairs of weak gauge bosons :

The cross section for $f\bar{f} \rightarrow W^+ W^-$ is given in term of the couplings of the left-handed and right-handed fermion f , $\ell = 2(T_3 - Qx_W)$, $r = -2Qx_W$, where T_3 is the third component of weak isospin for the left-handed f , Q is its electric charge (in units of the proton charge), and $x_W = \sin^2 \theta_W$:

$$\begin{aligned} \frac{d\sigma}{dt} &= \frac{2\pi\alpha^2}{N_c s^2} \left\{ \left[\left(Q + \frac{\ell+r}{4x_W} \frac{s}{s-m_Z^2} \right)^2 + \left(\frac{\ell-r}{4x_W} \frac{s}{s-m_Z^2} \right)^2 \right] A(s, t, u) \right. \\ &\quad + \frac{1}{2x_W} \left(Q + \frac{\ell}{2x_W} \frac{s}{s-m_Z^2} \right) (\Theta(-Q)I(s, t, u) - \Theta(Q)I(s, u, t)) \\ &\quad \left. + \frac{1}{8x_W^2} (\Theta(-Q)E(s, t, u) + \Theta(Q)E(s, u, t)) \right\}, \quad (40.26) \end{aligned}$$

where $\Theta(x)$ is 1 for $x > 0$ and 0 for $x < 0$, and where

$$\begin{aligned} A(s, t, u) &= \left(\frac{tu}{m_W^4} - 1 \right) \left(\frac{1}{4} - \frac{m_W^2}{s} + 3 \frac{m_W^4}{s^2} \right) + \frac{s}{m_W^2} - 4, \\ I(s, t, u) &= \left(\frac{tu}{m_W^4} - 1 \right) \left(\frac{1}{4} - \frac{m_W^2}{2s} - \frac{m_W^4}{st} \right) + \frac{s}{m_W^2} - 2 + 2 \frac{m_W^2}{t}, \\ E(s, t, u) &= \left(\frac{tu}{m_W^4} - 1 \right) \left(\frac{1}{4} + \frac{m_W^4}{t^2} \right) + \frac{s}{m_W^2}, \quad (40.27) \end{aligned}$$

and s, t, u are the usual Mandelstam variables with $s = (p_f + p_{\bar{f}})^2$, $t = (p_f - p_{W^-})^2$, $u = (p_f - p_{W^+})^2$. The factor N_c is 3 for quarks and 1 for leptons.

The analogous cross-section for $q_i \bar{q}_j \rightarrow W^\pm Z^0$ is

$$\begin{aligned} \frac{d\sigma}{dt} &= \frac{\pi\alpha^2 |V_{ij}|^2}{6s^2 x_W^2} \left\{ \left(\frac{1}{s - m_W^2} \right)^2 \left[\left(\frac{9 - 8x_W}{4} \right) (ut - m_W^2 m_Z^2) \right. \right. \\ &\quad \left. \left. + (8x_W - 6) s (m_W^2 + m_Z^2) \right] \right. \\ &\quad + \left[\frac{ut - m_W^2 m_Z^2 - s(m_W^2 + m_Z^2)}{s - m_W^2} \right] \left[\frac{\ell_j}{t} - \frac{\ell_i}{u} \right] \\ &\quad \left. + \frac{ut - m_W^2 m_Z^2}{4(1 - x_W)} \left[\frac{\ell_j^2}{t^2} + \frac{\ell_i^2}{u^2} \right] + \frac{s(m_W^2 + m_Z^2)}{2(1 - x_W)} \frac{\ell_i \ell_j}{tu} \right\}, \quad (40.28) \end{aligned}$$

where ℓ_i and ℓ_j are the couplings of the left-handed q_i and q_j as defined above. The CKM matrix element between q_i and q_j is V_{ij} .

The cross section for $q_i \bar{q}_i \rightarrow Z^0 Z^0$ is

$$\frac{d\sigma}{dt} = \frac{\pi\alpha^2}{96} \frac{\ell_i^4 + r_i^4}{x_W^2 (1 - x_W^2)^2 s^2} \left[\frac{t}{u} + \frac{u}{t} + \frac{4m_Z^2 s}{tu} - m_Z^4 \left(\frac{1}{t^2} + \frac{1}{u^2} \right) \right]. \quad (40.29)$$

40.5. Production of Higgs Bosons

40.5.1. Resonant Production :

The Higgs boson of the Standard Model can be produced resonantly in the collisions of quarks, leptons, W or Z bosons, gluons, or photons. The production cross section is thus controlled by the partial width of the Higgs boson into the entrance channel and its total width. The branching fractions for the Standard Model Higgs boson are shown in Fig. 1 of the ‘‘Searches for Higgs bosons’’ review in the Particle Listings section, as a function of the Higgs boson mass. The partial widths are given by the relations

$$\Gamma(H \rightarrow f\bar{f}) = \frac{G_F m_f^2 m_H N_c}{4\pi\sqrt{2}} \left(1 - 4m_f^2/m_H^2 \right)^{3/2}, \quad (40.30)$$

$$\Gamma(H \rightarrow W^+ W^-) = \frac{G_F m_H^3 \beta_W}{32\pi\sqrt{2}} \left(4 - 4a_W + 3a_W^2 \right), \quad (40.31)$$

$$\Gamma(H \rightarrow ZZ) = \frac{G_F m_H^3 \beta_Z}{64\pi\sqrt{2}} \left(4 - 4a_Z + 3a_Z^2 \right), \quad (40.32)$$

where N_c is 3 for quarks and 1 for leptons and where $a_W = 1 - \beta_W^2 = 4m_W^2/m_H^2$ and $a_Z = 1 - \beta_Z^2 = 4m_Z^2/m_H^2$. The decay to two gluons proceeds through quark loops, with the t quark dominating [2]. Explicitly,

$$\Gamma(H \rightarrow gg) = \frac{\alpha_s^2 G_F m_H^3}{36\pi^3 \sqrt{2}} \left| \sum_q I(m_q^2/m_H^2) \right|^2, \quad (40.33)$$

where $I(z)$ is complex for $z < 1/4$. For $z < 2 \times 10^{-3}$, $|I(z)|$ is small so the light quarks contribute negligibly. For $m_H < 2m_t$, $z > 1/4$ and

$$I(z) = 3 \left[2z + 2z(1-4z) \left(\sin^{-1} \frac{1}{2\sqrt{z}} \right)^2 \right], \quad (40.34)$$

which has the limit $I(z) \rightarrow 1$ as $z \rightarrow \infty$.

40.5.2. Higgs Boson Production in W^* and Z^* decay :

The Standard Model Higgs boson can be produced in the decay of a virtual W or Z ("Higgsstrahlung") [3,4]: In particular, if k is the c.m. momentum of the Higgs boson,

$$\sigma(q_i \bar{q}_j \rightarrow WH) = \frac{\pi \alpha^2 |V_{ij}|^2}{36 \sin^4 \theta_W} \frac{2k}{\sqrt{s}} \frac{k^2 + 3m_W^2}{(s - m_W^2)^2} \quad (40.35)$$

$$\sigma(f \bar{f} \rightarrow ZH) = \frac{2\pi \alpha^2 (\ell_f^2 + r_f^2)}{48 N_c \sin^4 \theta_W \cos^4 \theta_W} \frac{2k}{\sqrt{s}} \frac{k^2 + 3m_Z^2}{(s - m_Z^2)^2}, \quad (40.36)$$

where ℓ and r are defined as above.

40.5.3. W and Z Fusion :

Just as high-energy electrons can be regarded as sources of virtual photon beams, at very high energies they are sources of virtual W and Z beams. For Higgs boson production, it is the longitudinal components of the W s and Z s that are important [5]. The distribution of longitudinal W s carrying a fraction y of the electron's energy is [6]

$$f(y) = \frac{g^2}{16\pi^2} \frac{1-y}{y}, \quad (40.37)$$

where $g = e/\sin\theta_W$. In the limit $s \gg m_H \gg m_W$, the partial decay rate is $\Gamma(H \rightarrow W_L W_L) = (g^2/64\pi)(m_H^3/m_W^2)$ and in the equivalent W approximation [7]

$$\sigma(e^+e^- \rightarrow \bar{\nu}_e \nu_e H) = \frac{1}{16m_W^2} \left(\frac{\alpha}{\sin^2 \theta_W} \right)^3 \times \left[\left(1 + \frac{m_H^2}{s} \right) \log \frac{s}{m_H^2} - 2 + 2 \frac{m_H^2}{s} \right]. \quad (40.38)$$

There are significant corrections to this relation when m_H is not large compared to m_W [8]. For $m_H = 150$ GeV, the estimate is too high by 51% for $\sqrt{s} = 1000$ GeV, 32% too high at $\sqrt{s} = 2000$ GeV, and 22% too high at $\sqrt{s} = 4000$ GeV. Fusion of ZZ to make a Higgs boson can be treated similarly. Identical formulae apply for Higgs production in the collisions of quarks whose charges permit the emission of a W^+ and a W^- , except that QCD corrections and CKM matrix elements are required. Even in the absence of QCD corrections, the fine-structure constant ought to be evaluated at the scale of the collision, say m_W . All quarks contribute to the ZZ fusion process.

40.6. Inclusive hadronic reactions

One-particle inclusive cross sections $E d^3\sigma/d^3p$ for the production of a particle of momentum p are conveniently expressed in terms of rapidity y (see above) and the momentum p_T transverse to the beam direction (in the c.m.):

$$E \frac{d^3\sigma}{d^3p} = \frac{d^3\sigma}{d\phi dy p_T dp_T^2}. \quad (40.39)$$

In appropriate circumstances, the cross section may be decomposed as a partonic cross section multiplied by the probabilities of finding partons of the prescribed momenta:

$$\sigma_{\text{hadronic}} = \sum_{ij} \int dx_1 dx_2 f_i(x_1) f_j(x_2) d\hat{\sigma}_{\text{partonic}}, \quad (40.40)$$

The probability that a parton of type i carries a fraction of the incident particle's that lies between x_1 and $x_1 + dx_1$ is $f_i(x_1)dx_1$ and similarly for partons in the other incident particle. The partonic collision is specified by its c.m. energy squared $\hat{s} = x_1 x_2 s$ and the momentum transfer squared \hat{t} . The final hadronic state is more conveniently specified by the rapidities y_1, y_2 of the two jets resulting from the collision and the transverse momentum p_T . The connection between the differentials is

$$dx_1 dx_2 d\hat{t} = dy_1 dy_2 \frac{\hat{s}}{s} dp_T^2, \quad (40.41)$$

so that

$$\frac{d^3\sigma}{dy_1 dy_2 dp_T^2} = \frac{\hat{s}}{s} \left[f_i(x_1) f_j(x_2) \frac{d\hat{\sigma}}{d\hat{t}}(\hat{s}, \hat{t}, \hat{u}) + f_i(x_2) f_j(x_1) \frac{d\hat{\sigma}}{d\hat{t}}(\hat{s}, \hat{u}, \hat{t}) \right], \quad (40.42)$$

where we have taken into account the possibility that the incident parton types might arise from either incident particle. The second term should be dropped if the types are identical: $i = j$.

40.7. Two-photon processes

In the Weizsäcker-Williams picture, a high-energy electron beam is accompanied by a spectrum of virtual photons of energies ω and invariant-mass squared $q^2 = -Q^2$, for which the photon number density is

$$dn = \frac{\alpha}{\pi} \left[1 - \frac{\omega}{E} + \frac{\omega^2}{E^2} - \frac{m_e^2 \omega^2}{Q^2 E^2} \right] \frac{d\omega dQ^2}{\omega Q^2}, \quad (40.43)$$

where E is the energy of the electron beam. The cross section for $e^+e^- \rightarrow e^+e^-X$ is then [9]

$$d\sigma_{e^+e^- \rightarrow e^+e^-X}(s) = dn_1 dn_2 d\sigma_{\gamma\gamma \rightarrow X}(W^2), \quad (40.44)$$

where $W^2 = m_X^2$. Integrating from the lower limit $Q^2 = m_e^2 \frac{\omega_i^2}{E_i(E_i - \omega_i)}$ to a maximum Q^2 gives

$$\sigma_{e^+e^- \rightarrow e^+e^-X}(s) = \frac{\alpha^2}{\pi^2} \int_{z_{th}}^1 \frac{dz}{z} \times \left[\left(\ln \frac{Q_{max}^2}{zm_e^2} - 1 \right)^2 f(z) + \frac{1}{3} (\ln z)^3 \right] \sigma_{\gamma\gamma \rightarrow X}(zs), \quad (40.45)$$

where

$$f(z) = \left(1 + \frac{1}{2}z \right)^2 \ln(1/z) - \frac{1}{2}(1-z)(3+z). \quad (40.46)$$

The appropriate value of Q_{max}^2 depends on the properties of the produced system X . For production of hadronic systems, $Q_{max}^2 \approx m_\rho^2$, while for lepton-pair production, $Q^2 \approx W^2$. For production of a resonance with spin $J \neq 1$, we have

$$\sigma_{e^+e^- \rightarrow e^+e^-R}(s) = (2J+1) \frac{8\alpha^2 \Gamma_{R \rightarrow \gamma\gamma}}{m_R^3} \times \left[f(m_V^2/s) \left(\ln \frac{m_V^2 s}{m_e^2 m_R^2} - 1 \right)^2 - \frac{1}{3} \left(\ln \frac{s}{M_R^2} \right)^3 \right], \quad (40.47)$$

where m_V is the mass that enters into the form factor for the $\gamma\gamma \rightarrow R$ transition, typically m_ρ .

PART II: PROCESSES BEYOND THE STANDARD MODEL

40.8. Production of supersymmetric particles

In supersymmetric (SUSY) theories (see Supersymmetric Particle Searches in this *Review*), every boson has a fermionic superpartner, and every fermion has a bosonic superpartner. The minimal supersymmetric Standard Model (MSSM) is a direct supersymmetrization of the Standard Model (SM), although a second Higgs doublet is needed to avoid triangle anomalies [10]. Under *soft* SUSY breaking, superpartner masses are lifted above the SM particle masses. In weak scale SUSY, the superpartners are invoked to stabilize the weak scale under radiative corrections, so the superpartners are expected to have masses of order the TeV scale.

40.8.1. Gluino and squark production :

The superpartners of gluons are the color octet, spin- $\frac{1}{2}$ gluinos (\tilde{g}), while each helicity component of quark flavor has a spin-0 *squark* partner, *e.g.* \tilde{q}_L and \tilde{q}_R . Third generation left- and right- squarks are expected to have large mixing, resulting in mass eigenstates \tilde{q}_1 and \tilde{q}_2 , with $m_{\tilde{q}_1} < m_{\tilde{q}_2}$ (here, q denotes any of the SM flavors of quarks and \tilde{q}_i the corresponding flavor and type ($i = L, R$ or $1, 2$) of squark). Gluino pair production ($\tilde{g}\tilde{g}$) takes place via either glue-gluon or quark-antiquark annihilation [11].

The subprocess cross sections are usually presented as differential distributions in the Mandelstam variables s , t and u . Note that for a $2 \rightarrow 2$ scattering subprocess $ab \rightarrow cd$, the Mandelstam variable $s = (p_a + p_b)^2 = (p_c + p_d)^2$, where p_a is the 4-momentum of particle a , and so forth. The variable $t = (p_c - p_a)^2$, where c and a are taken conventionally to be the most similar particles in the subprocess. The variable u would then be equal to $(p_d - p_a)^2$. Note that since s , t and u are squares of 4-vectors, they are invariants in any inertial reference frame.

Gluino pair production at hadron colliders is described by:

$$\begin{aligned} \frac{d\sigma}{dt}(gg \rightarrow \tilde{g}\tilde{g}) &= \frac{9\pi\alpha_s^2}{4s^2} \left\{ \frac{2(m_g^2 - t)(m_g^2 - u)}{s^2} \right. \\ &+ \frac{(m_g^2 - t)(m_g^2 - u) - 2m_g^2(m_g^2 + t)}{(m_g^2 - t)^2} \\ &+ \frac{(m_g^2 - t)(m_g^2 - u) - 2m_g^2(m_g^2 + u)}{(m_g^2 - u)^2} + \frac{m_g^2(s - 4m_g^2)}{(m_g^2 - t)(m_g^2 - u)} \\ &\left. - \frac{(m_g^2 - t)(m_g^2 - u) + m_g^2(u - t)}{s(m_g^2 - t)} - \frac{(m_g^2 - t)(m_g^2 - u) + m_g^2(t - u)}{s(m_g^2 - u)} \right\}, \quad (40.48) \end{aligned}$$

where α_s is the strong fine structure constant. Also,

$$\begin{aligned} \frac{d\sigma}{dt}(q\bar{q} \rightarrow \tilde{g}\tilde{g}) &= \frac{8\pi\alpha_s^2}{9s^2} \left\{ \frac{4}{3} \left(\frac{m_g^2 - t}{m_g^2 - t} \right)^2 + \frac{4}{3} \left(\frac{m_g^2 - u}{m_g^2 - u} \right)^2 \right. \\ &+ \frac{3}{s^2} \left[(m_g^2 - t)^2 + (m_g^2 - u)^2 + 2m_g^2 s \right] - 3 \frac{(m_g^2 - t)^2 + m_g^2 s}{s(m_g^2 - t)} \\ &\left. - 3 \frac{(m_g^2 - u)^2 + m_g^2 s}{s(m_g^2 - u)} + \frac{1}{3} \frac{m_g^2 s}{(m_g^2 - t)(m_g^2 - u)} \right\}. \quad (40.49) \end{aligned}$$

Gluinos can also be produced in association with squarks: $\tilde{g}\tilde{q}_i$ production, where \tilde{q}_i represents any of the various types (left-, right- or mixed) and flavors of squarks. The subprocess cross section is independent of whether the squark is the right-, left- or mixed type:

$$\begin{aligned} \frac{d\sigma}{dt}(gq \rightarrow \tilde{g}\tilde{q}_i) &= \frac{\pi\alpha_s^2}{24s^2} \left[\frac{16}{3}(s^2 + (m_{\tilde{q}_i}^2 - u)^2) + \frac{4}{3}s(m_{\tilde{q}_i}^2 - u) \right] \\ &\times \left((m_g^2 - u)^2 + (m_{\tilde{q}_i}^2 - m_g^2)^2 + \frac{2sm_g^2(m_{\tilde{q}_i}^2 - m_g^2)}{(m_g^2 - t)} \right). \quad (40.50) \end{aligned}$$

There are many different subprocesses for production of squark pairs. Since left- and right- squarks generally have different masses and different decay patterns, we present the differential cross section for each subprocess of \tilde{q}_i ($i = L, R$ or $1, 2$) separately. (In early literature, the following formulae were often combined into a single equation which didn't differentiate the various squark types.) The result for $gg \rightarrow \tilde{q}_i\tilde{q}_i$ is:

$$\begin{aligned} \frac{d\sigma}{dt}(gg \rightarrow \tilde{q}_i\tilde{q}_i) &= \frac{\pi\alpha_s^2}{4s^2} \left\{ \frac{1}{3} \left(\frac{m_q^2 + t}{m_q^2 - t} \right)^2 + \frac{1}{3} \left(\frac{m_q^2 + u}{m_q^2 - u} \right)^2 \right. \\ &+ \frac{3}{32s^2} \left(8s(4m_q^2 - s) + 4(u - t)^2 \right) + \frac{7}{12} \\ &- \frac{1}{48} \frac{(4m_q^2 - s)^2}{(m_q^2 - t)(m_q^2 - u)} \\ &+ \frac{3}{32} \frac{[(t - u)(4m_q^2 + 4t - s) - 2(m_q^2 - u)(6m_q^2 + 2t - s)]}{s(m_q^2 - t)} \\ &+ \frac{3}{32} \frac{[(u - t)(4m_q^2 + 4u - s) - 2(m_q^2 - t)(6m_q^2 + 2u - s)]}{s(m_q^2 - u)} \\ &\left. + \frac{7}{96} \frac{[4m_q^2 + 4t - s]}{m_q^2 - t} + \frac{7}{96} \frac{[4m_q^2 + 4u - s]}{m_q^2 - u} \right\}, \quad (40.51) \end{aligned}$$

which has an obvious $u \leftrightarrow t$ symmetry.

For $q\bar{q} \rightarrow \tilde{q}_i\tilde{q}_i$ with the same initial and final state flavors, we have

$$\begin{aligned} \frac{d\sigma}{dt}(q\bar{q} \rightarrow \tilde{q}_i\tilde{q}_i) &= \frac{2\pi\alpha_s^2}{9s^2} \left\{ \frac{1}{(t - m_{\tilde{q}_i}^2)^2} + \frac{2}{s^2} - \frac{2/3}{s(t - m_{\tilde{q}_i}^2)} \right\} \\ &\times \left[-st - (t - m_{\tilde{q}_i}^2)^2 \right], \quad (40.52) \end{aligned}$$

while if initial and final state flavors are different ($q\bar{q} \rightarrow \tilde{q}_i\tilde{q}_j$) we instead have

$$\frac{d\sigma}{dt}(q\bar{q} \rightarrow \tilde{q}_i\tilde{q}_j) = \frac{4\pi\alpha_s^2}{9s^4} \left[-st - (t - m_{\tilde{q}_i}^2)^2 \right]. \quad (40.53)$$

If the two initial state quarks are of different flavors, then we have

$$\frac{d\sigma}{dt}(q\bar{q}' \rightarrow \tilde{q}_i\tilde{q}_j) = \frac{2\pi\alpha_s^2}{9s^2} \frac{-st - (t - m_{\tilde{q}_i}^2)^2}{(t - m_{\tilde{q}_i}^2)^2}. \quad (40.54)$$

If the initial quarks are of different flavor and final state squarks are of different type ($i \neq j$) then

$$\frac{d\sigma}{dt}(q\bar{q}' \rightarrow \tilde{q}_i\tilde{q}_j) = \frac{2\pi\alpha_s^2}{9s^2} \frac{m_g^2 s}{(t - m_{\tilde{q}_i}^2)^2}. \quad (40.55)$$

For same-flavor initial state quarks, but final state unlike-type squarks, we also have

$$\frac{d\sigma}{dt}(q\bar{q} \rightarrow \tilde{q}_i\tilde{q}_j) = \frac{2\pi\alpha_s^2}{9s^2} \frac{m_g^2 s}{(t - m_{\tilde{q}_i}^2)^2}. \quad (40.56)$$

There also exist cross sections for quark-quark annihilation to squark pairs. For same flavor quark-quark annihilation to same flavor/same type final state squarks,

$$\begin{aligned} \frac{d\sigma}{dt}(qq \rightarrow \tilde{q}_i \tilde{q}_i) &= \\ &= \frac{\pi\alpha_s^2 m_g^2 s}{9s^2} \left\{ \frac{1}{(t-m_g^2)^2} + \frac{1}{(u-m_g^2)^2} - \frac{2/3}{(t-m_g^2)(u-m_g^2)} \right\}, \end{aligned} \quad (40.57)$$

while if the final type squarks are different ($i \neq j$), we have

$$\begin{aligned} \frac{d\sigma}{dt}(qq \rightarrow \tilde{q}_i \tilde{q}_j) &= \\ \frac{2\pi\alpha_s^2}{9s^2} \left\{ \frac{[-st - (t-m_{\tilde{q}_i}^2)(t-m_{\tilde{q}_j}^2)]}{(t-m_g^2)} + \frac{[-su - (u-m_{\tilde{q}_i}^2)(u-m_{\tilde{q}_j}^2)]}{(u-m_g^2)} \right\}. \end{aligned} \quad (40.58)$$

If initial/final state flavors are different, but final state squark types are the same, then

$$\frac{d\sigma}{dt}(qq' \rightarrow \tilde{q}_i \tilde{q}_i) = \frac{2\pi\alpha_s^2 m_g^2 s}{9s^2 (t-m_g^2)^2}. \quad (40.59)$$

If initial quark flavors are different and final squark types are different, then

$$\frac{d\sigma}{dt}(qq' \rightarrow \tilde{q}_i \tilde{q}_j) = \frac{2\pi\alpha_s^2 (-st - (t-m_{\tilde{q}_i}^2)(t-m_{\tilde{q}_j}^2))}{9s^2 (t-m_g^2)^2}. \quad (40.60)$$

40.8.2. Gluino and squark associated production :

In the MSSM, the charged spin- $\frac{1}{2}$ winos and higgsinos mix to make chargino states $\chi_{\pm 1}^{\pm}$ and $\chi_{\pm 2}^{\pm}$, with $m_{\chi_{\pm 1}^{\pm}} < m_{\chi_{\pm 2}^{\pm}}$. The spin- $\frac{1}{2}$ neutral bino, wino and higgsino fields mix to give four neutralino mass eigenstates $\chi_{1,2,3,4}^0$ ordered according to mass. We sometimes denote the charginos and neutralinos collectively as -inos for notational simplicity

For gluino and squark production in association with charginos and neutralinos [12], the quark-squark-neutralino couplings* are defined by the interaction Lagrangian terms $\mathcal{L}_{f\tilde{f}\tilde{\chi}_i^0} = \left[iA_{\tilde{\chi}_i^0}^f \tilde{f}_L^\dagger \tilde{\chi}_i^0 P_L f + iB_{\tilde{\chi}_i^0}^f \tilde{f}_R^\dagger \tilde{\chi}_i^0 P_R f + \text{h.c.} \right]$, where $A_{\tilde{\chi}_i^0}^f$ and $B_{\tilde{\chi}_i^0}^f$ are coupling constants involving gauge couplings, neutralino mixing elements and in the case of third generation fermions, Yukawa couplings. Their form depends on the conventions used for setting up the MSSM Lagrangian, and can be found in various reviews [13] and textbooks [14,15]. P_L and P_R are the usual left- and right-spinor projection operators and f denotes any of the SM fermions u, d, e, ν_e, \dots . The fermion-sfermion- chargino couplings have the form $\mathcal{L} = \left[iA_{\tilde{\chi}_i^{\pm}}^d \tilde{u}_L^\dagger \tilde{\chi}_i^{\pm} P_L d + iA_{\tilde{\chi}_i^{\pm}}^u \tilde{d}_L^\dagger \tilde{\chi}_i^{\pm} P_L u + \text{h.c.} \right]$ for u and d quarks, where the $A_{\tilde{\chi}_i^{\pm}}^d$ and $A_{\tilde{\chi}_i^{\pm}}^u$ couplings are again convention-dependent, and can be found in textbooks. The superscript c denotes ‘‘charge conjugate spinor’’, defined by $\psi^c \equiv C\bar{\psi}^T$.

The subprocess cross sections for chargino-squark associated production occur via squark exchange and are given by

$$\frac{d\sigma}{dt}(\bar{u}g \rightarrow \tilde{\chi}_i^+ \tilde{d}_L) = \frac{\alpha_s}{24s^2} |A_{\tilde{\chi}_i^+}^d|^2 \psi(m_{\tilde{d}_L}, m_{\tilde{\chi}_i^+}, t), \quad (40.61)$$

$$\frac{d\sigma}{dt}(dg \rightarrow \tilde{\chi}_i^- \tilde{u}_L) = \frac{\alpha_s}{24s^2} |A_{\tilde{\chi}_i^-}^d|^2 \psi(m_{\tilde{u}_L}, m_{\tilde{\chi}_i^-}, t), \quad (40.62)$$

* The couplings $A_{\tilde{\chi}_i^0}^f$ and $B_{\tilde{\chi}_i^0}^f$ are given explicitly in Ref. 15 in Eq. (8.87). Also, the couplings $A_{\tilde{\chi}_i^{\pm}}^d$ and $A_{\tilde{\chi}_i^{\pm}}^u$ are given in Eq. (8.93). The couplings X_i^j and Y_i^j are given by Eq. (8.103), while the x_i and y_i couplings are given in Eq. (8.100). Finally, the couplings W_{ij} are given in Eq. (8.101).

while neutralino-squark production is given by

$$\frac{d\sigma}{dt}(qg \rightarrow \tilde{\chi}_i^0 \tilde{q}) = \frac{\alpha_s}{24s^2} \left(|A_{\tilde{\chi}_i^0}^q|^2 + |B_{\tilde{\chi}_i^0}^q|^2 \right) \psi(m_{\tilde{q}}, m_{\tilde{\chi}_i^0}, t), \quad (40.63)$$

where

$$\begin{aligned} \psi(m_1, m_2, t) &= \frac{s+t-m_1^2}{2s} - \frac{m_1^2(m_2^2-t)}{(m_1^2-t)^2} \\ &+ \frac{t(m_2^2-m_1^2) + m_2^2(s-m_2^2+m_1^2)}{s(m_1^2-t)}. \end{aligned} \quad (40.64)$$

Here, the variable t is given by the square of ‘‘squark-minus-quark’’ four-momentum. The neutralino-gluino associated production cross section also occurs via squark exchange and is given by

$$\begin{aligned} \frac{d\sigma}{dt}(q\bar{q} \rightarrow \tilde{\chi}_i^0 \tilde{g}) &= \frac{\alpha_s}{18s^2} \left(|A_{\tilde{\chi}_i^0}^q|^2 + |B_{\tilde{\chi}_i^0}^q|^2 \right) \left[\frac{(m_{\tilde{\chi}_i^0}^2-t)(m_g^2-t)}{(m_g^2-t)^2} \right. \\ &+ \left. \frac{(m_{\tilde{\chi}_i^0}^2-u)(m_g^2-u)}{(m_g^2-u)^2} - \frac{2\eta_i \eta_{\tilde{g}} m_{\tilde{g}} m_{\tilde{\chi}_i^0} s}{(m_g^2-t)(m_g^2-u)} \right], \end{aligned} \quad (40.65)$$

where η_i is the sign of the neutralino mass eigenvalue and $\eta_{\tilde{g}}$ is the sign of the gluino mass eigenvalue. We also have chargino-gluino associated production:

$$\begin{aligned} \frac{d\sigma}{dt}(\bar{u}d \rightarrow \tilde{\chi}_i^- \tilde{g}) &= \frac{\alpha_s}{18s^2} \left[|A_{\tilde{\chi}_i^-}^u|^2 \frac{(m_{\tilde{\chi}_i^-}^2-t)(m_g^2-t)}{(m_{\tilde{d}_L}^2-t)^2} \right. \\ &+ \left. |A_{\tilde{\chi}_i^-}^d|^2 \frac{(m_{\tilde{\chi}_i^-}^2-u)(m_g^2-u)}{(m_{\tilde{u}_L}^2-u)^2} + \frac{2\eta_{\tilde{g}} \text{Re}(A_{\tilde{\chi}_i^-}^u A_{\tilde{\chi}_i^-}^d) m_{\tilde{g}} m_{\tilde{\chi}_i^-} s}{(m_{\tilde{d}_L}^2-t)(m_{\tilde{u}_L}^2-u)} \right], \end{aligned} \quad (40.66)$$

where $\hat{t} = (\tilde{g}-d)^2$ and in the third term one must take the real part of the in general complex coupling constant product.

40.8.3. Slepton and sneutrino production :

The subprocess cross section for $\tilde{\ell}_L \tilde{\nu}_{\ell L}$ production ($\ell = e$ or μ) occurs via s -channel W exchange and is given by

$$\frac{d\sigma}{dt}(d\bar{u} \rightarrow \tilde{\ell}_L \tilde{\nu}_{\ell L}) = \frac{g^4 |D_W(s)|^2}{192\pi s^2} \left(tu - m_{\tilde{\ell}_L}^2 m_{\tilde{\nu}_{\ell L}}^2 \right), \quad (40.67)$$

where $D_W(s) = 1/(s - M_W^2 + iM_W\Gamma_W)$ is the W -boson propagator denominator. The production of $\tilde{\tau}_1 \tilde{\nu}_{\tau}$ is given as above, but replacing $m_{\tilde{\ell}_L} \rightarrow m_{\tilde{\tau}_1}$, $m_{\tilde{\nu}_{\ell L}} \rightarrow m_{\tilde{\nu}_{\tau}}$ and multiplying by an overall factor of $\cos^2 \theta_{\tau}$ (where θ_{τ} is the tau-slepton mixing angle). Similar substitutions hold for $\tilde{\tau}_2 \tilde{\nu}_{\tau}$ production, except the overall factor is $\sin^2 \theta_{\tau}$.

Table 40.1: The constants α_f and β_f that appear in in the SM neutral current Lagrangian. Here $t \equiv \tan \theta_W$ and $c \equiv \cot \theta_W$.

f	q_f	α_f	β_f
ℓ	-1	$\frac{1}{4}(3t-c)$	$\frac{1}{4}(t+c)$
ν_{ℓ}	0	$\frac{1}{4}(t+c)$	$-\frac{1}{4}(t+c)$
u	$\frac{2}{3}$	$-\frac{5}{12}t + \frac{1}{4}c$	$-\frac{1}{4}(t+c)$
d	$-\frac{1}{3}$	$\frac{1}{12}t - \frac{1}{4}c$	$\frac{1}{4}(t+c)$

The subprocess cross section for $\tilde{\ell}_L \bar{\ell}_L$ production occurs via s -channel γ and Z exchange, and depends on the neutral current interaction, with fermion couplings to γ and Z^0 given by $\mathcal{L}_{\text{neutral}} = -e q_f \bar{f} \gamma^\mu f A_\mu + e \bar{f} \gamma^\mu (\alpha_f + \beta_f \gamma_5) f Z_\mu$ (with values of q_f , α_f , and β_f given in Table 40.1.

The subprocess cross section is given by

$$\begin{aligned} \frac{d\sigma}{dt}(q\bar{q} \rightarrow \tilde{\ell}_L \bar{\ell}_L) &= \frac{e^4}{24\pi s^2} (tu - m_{\tilde{\ell}_L}^4) \times \\ &\left\{ \frac{q_\ell^2 q_q^2}{s^2} + (\alpha_\ell - \beta_\ell)^2 (\alpha_q^2 + \beta_q^2) |D_Z(s)|^2 \right. \\ &\left. + \frac{2q_\ell q_q \alpha_q (\alpha_\ell - \beta_\ell) (s - M_Z^2)}{s} |D_Z(s)|^2 \right\}, \end{aligned} \quad (40.68)$$

where $D_Z(s) = 1/(s - M_Z^2 + iM_Z\Gamma_Z)$. The cross section for sneutrino production is given by the same formula, but with α_ℓ , β_ℓ , q_ℓ and $m_{\tilde{\ell}_L}$ replaced by α_ν , β_ν , 0 and $m_{\tilde{\nu}_L}$, respectively. The cross section for $\tilde{\tau}_1 \bar{\tau}_1$ production is obtained by replacing $m_{\tilde{\ell}_L} \rightarrow m_{\tilde{\tau}_1}$ and $\beta_\ell \rightarrow \beta_\ell \cos 2\theta_\tau$.

The cross section for $\tilde{\ell}_R \bar{\ell}_R$ production is given by substituting $\alpha_\ell - \beta_\ell \rightarrow \alpha_\ell + \beta_\ell$ and $m_{\tilde{\ell}_L} \rightarrow m_{\tilde{\ell}_R}$ in the equation above. The cross section for $\tilde{\tau}_2 \bar{\tau}_2$ production is obtained from the formula for $\tilde{\ell}_R \bar{\ell}_R$ production by replacing $m_{\tilde{\ell}_R} \rightarrow m_{\tilde{\tau}_2}$ and $\beta_\ell \rightarrow \beta_\ell \cos 2\theta_\tau$.

Finally, the cross section for $\tilde{\tau}_1 \bar{\tau}_2$ production occurs only via Z exchange, and is given by

$$\begin{aligned} \frac{d\sigma}{dt}(q\bar{q} \rightarrow \tilde{\tau}_1 \bar{\tau}_2) &= \frac{d\sigma}{dt}(q\bar{q} \rightarrow \tilde{\tau}_1 \bar{\tau}_2) = \\ &\frac{e^4}{24\pi s^2} (\alpha_q^2 + \beta_q^2) \beta_\ell^2 \sin^2 2\theta_\tau |D_Z(s)|^2 (ut - m_{\tilde{\tau}_1}^2 m_{\tilde{\tau}_2}^2). \end{aligned} \quad (40.69)$$

40.8.4. Chargino and neutralino pair production:

40.8.4.1. $\tilde{\chi}_i^- \tilde{\chi}_j^0$ production:

The subprocess cross section for $d\bar{u} \rightarrow \tilde{\chi}_i^- \tilde{\chi}_j^0$ depends on Lagrangian couplings $\mathcal{L}_{W\bar{u}d} = -\frac{g}{\sqrt{2}} \bar{u} \gamma_\mu P_L d W^{+\mu} + \text{h.c.}$, $\mathcal{L}_{W\tilde{\chi}_i^- \tilde{\chi}_j^0} = -g(-i)^{\theta_j} \bar{\chi}_i^- [X_i^j + Y_i^j \gamma_5] \gamma_\mu \tilde{\chi}_j^0 W^{-\mu} + \text{h.c.}$, $\mathcal{L}_{q\tilde{q}\tilde{\chi}_i^-} = iA_{\tilde{\chi}_i^-}^d \bar{u} \tilde{\chi}_i^- P_L d + iA_{\tilde{\chi}_i^-}^u \bar{d} \tilde{\chi}_i^- P_L u + \text{h.c.}$ and $\mathcal{L}_{q\tilde{q}\tilde{\chi}_j^0} = iA_{\tilde{\chi}_j^0}^q \bar{q} \tilde{\chi}_j^0 P_L q + \text{h.c.}$. Contributing diagrams include W exchange and also \tilde{d}_L and \tilde{u}_L squark exchange. The X_i^j and Y_i^j couplings are new, and again convention-dependent: the cross section formulae works if the interaction Lagrangian is written in the above form, so that the couplings can be suitably extracted. The term $\theta_j = 0$ (1) if $m_{\tilde{\chi}_j^0} > 0$ (< 0); it comes about because the neutralino field must be re-defined by a $-i\gamma_5$ transformation if its mass eigenvalue is negative [15]. The subprocess cross section is given in terms of dot products of four momenta, where particle labels are used to denote their four-momenta; note that all mass terms in the cross section formulae are positive definite, so that the signs of mass eigenstates have been absorbed into the Lagrangian couplings, as for instance in Ref. [15]. We then have

$$\begin{aligned} \frac{d\sigma}{dt}(d\bar{u} \rightarrow \tilde{\chi}_i^- \tilde{\chi}_j^0) &= \frac{1}{192\pi s^2} \\ &\left[T_W + T_{\tilde{d}_L} + T_{\tilde{u}_L} + T_{W\tilde{d}_L} + T_{W\tilde{u}_L} + T_{\tilde{d}_L \tilde{u}_L} \right] \end{aligned} \quad (40.70)$$

where

$$\begin{aligned} T_W &= 8g^4 |D_W(s)|^2 \left\{ [X_i^{j2} + Y_i^{j2}] (\tilde{\chi}_j^0 \cdot d\tilde{\chi}_i^- \cdot \bar{u} + \tilde{\chi}_j^0 \cdot \bar{u}\tilde{\chi}_i^- \cdot d) \right. \\ &\left. + 2(X_i^j Y_i^j) (\tilde{\chi}_j^0 \cdot d\tilde{\chi}_i^- \cdot \bar{u} - \tilde{\chi}_j^0 \cdot \bar{u}\tilde{\chi}_i^- \cdot d) + [X_i^{j2} - Y_i^{j2}] m_{\tilde{\chi}_i^-} m_{\tilde{\chi}_j^0} d \cdot \bar{u} \right\}, \end{aligned} \quad (40.71)$$

$$T_{\tilde{d}_L} = \frac{4|A_{\tilde{\chi}_i^-}^u|^2 |A_{\tilde{\chi}_j^0}^d|^2}{[(\tilde{\chi}_i^- - \bar{u})^2 - m_{\tilde{d}_L}^2]^2} d \cdot \tilde{\chi}_j^0 \tilde{\chi}_i^- \cdot \bar{u}, \quad (40.72)$$

$$T_{\tilde{u}_L} = \frac{4|A_{\tilde{\chi}_i^-}^d|^2 |A_{\tilde{\chi}_j^0}^u|^2}{[(\tilde{\chi}_j^0 - \bar{u})^2 - m_{\tilde{u}_L}^2]^2} \bar{u} \cdot \tilde{\chi}_j^0 \tilde{\chi}_i^- \cdot d \quad (40.73)$$

$$\begin{aligned} T_{W\tilde{d}_L} &= \frac{-\sqrt{2}g^2 \text{Re}[A_{\tilde{\chi}_j^0}^{d*} A_{\tilde{\chi}_i^-}^u (-i)^{\theta_j}] (s - M_W^2) |D_W(s)|^2}{(\tilde{\chi}_i^- - \bar{u})^2 - m_{\tilde{d}_L}^2} \\ &\times \left\{ 8(X_i^j + Y_i^j) \tilde{\chi}_j^0 \cdot d\bar{u} \cdot \tilde{\chi}_i^- + 4(X_i^j - Y_i^j) m_{\tilde{\chi}_i^-} m_{\tilde{\chi}_j^0} d \cdot \bar{u} \right\} \end{aligned} \quad (40.74)$$

$$\begin{aligned} T_{W\tilde{u}_L} &= \frac{\sqrt{2}g^2 \text{Re}[A_{\tilde{\chi}_i^-}^{d*} A_{\tilde{\chi}_j^0}^u (-i)^{\theta_j}] (s - M_W^2) |D_W(s)|^2}{(\tilde{\chi}_j^0 - \bar{u})^2 - m_{\tilde{u}_L}^2} \\ &\times \left\{ 8(X_i^j - Y_i^j) \tilde{\chi}_j^0 \cdot \bar{u}d \cdot \tilde{\chi}_i^- + 4(X_i^j + Y_i^j) m_{\tilde{\chi}_i^-} m_{\tilde{\chi}_j^0} d \cdot \bar{u} \right\} \end{aligned} \quad (40.75)$$

and

$$T_{\tilde{d}_L \tilde{u}_L} = -\frac{4\text{Re}[A_{\tilde{\chi}_j^0}^d A_{\tilde{\chi}_i^-}^{u*} A_{\tilde{\chi}_i^-}^{d*} A_{\tilde{\chi}_j^0}^u] m_{\tilde{\chi}_i^-} m_{\tilde{\chi}_j^0} d \cdot \bar{u}}{[(\tilde{\chi}_i^- - \bar{u})^2 - m_{\tilde{d}_L}^2][(\tilde{\chi}_j^0 - \bar{u})^2 - m_{\tilde{u}_L}^2]}. \quad (40.76)$$

40.8.4.2. Chargino pair production:

The subprocess cross section for $d\bar{d} \rightarrow \tilde{\chi}_i^- \tilde{\chi}_i^+$ ($i = 1, 2$) depends on Lagrangian couplings $\mathcal{L} = e\tilde{\chi}_i^- \gamma_\mu \tilde{\chi}_i^+ A^\mu - e \cot \theta_W \tilde{\chi}_i^- \gamma_\mu (x_i - y_i \gamma_5) \tilde{\chi}_i^+ Z^\mu$ and also $\mathcal{L} \ni iA_{\tilde{\chi}_i^-}^d \bar{u} \tilde{\chi}_i^- P_L d + iA_{\tilde{\chi}_i^-}^u \bar{d} \tilde{\chi}_i^- P_L u + \text{h.c.}$. Contributing diagrams include s -channel γ , Z^0 exchange and t -channel \tilde{u}_L exchange [16,17]. The couplings x_i and y_i are again new and as usual convention-dependent.

The subprocess cross section is given by

$$\frac{d\sigma}{dt}(d\bar{d} \rightarrow \tilde{\chi}_i^- \tilde{\chi}_i^+) = \frac{1}{192\pi s^2} [T_\gamma + T_Z + T_{\tilde{u}_L} + T_{\gamma\tilde{u}_L} + T_{Z\tilde{u}_L}] \quad (40.77)$$

where

$$T_\gamma = \frac{32e^4 q_d^2}{s^2} \left[d \cdot \tilde{\chi}_i^+ \bar{d} \cdot \tilde{\chi}_i^- + d \cdot \tilde{\chi}_i^- \bar{d} \cdot \tilde{\chi}_i^+ + m_{\tilde{\chi}_i^-}^2 d \cdot \bar{d} \right] \quad (40.78)$$

$$T_Z = 32e^4 \cot^2 \theta_W |D_Z(s)|^2$$

$$\begin{aligned} &\left\{ (\alpha_d^2 + \beta_d^2) (x_i^2 + y_i^2) \left[d \cdot \tilde{\chi}_i^+ \bar{d} \cdot \tilde{\chi}_i^- + d \cdot \tilde{\chi}_i^- \bar{d} \cdot \tilde{\chi}_i^+ + m_{\tilde{\chi}_i^-}^2 d \cdot \bar{d} \right] \right. \\ &\left. \mp 4\alpha_d \beta_d x_i y_i \left[d \cdot \tilde{\chi}_i^+ \bar{d} \cdot \tilde{\chi}_i^- - d \cdot \tilde{\chi}_i^- \bar{d} \cdot \tilde{\chi}_i^+ \right] - 2y_i^2 (\alpha_d^2 + \beta_d^2) m_{\tilde{\chi}_i^-}^2 d \cdot \bar{d} \right\}, \end{aligned} \quad (40.79)$$

$$T_{\tilde{u}_L} = \frac{4|A_{\tilde{\chi}_i^-}^d|^4}{[(d - \tilde{\chi}_i^-)^2 - m_{\tilde{u}_L}^2]^2} d \cdot \tilde{\chi}_i^- \bar{d} \cdot \tilde{\chi}_i^+ \quad (40.80)$$

$$\begin{aligned} T_{\gamma\tilde{u}_L} &= \frac{64e^4 \cot \theta_W q_d (s - M_Z^2) |D_Z(s)|^2}{s} \times \\ &\left\{ \alpha_d x_i \left(d \cdot \tilde{\chi}_i^+ \bar{d} \cdot \tilde{\chi}_i^- + d \cdot \tilde{\chi}_i^- \bar{d} \cdot \tilde{\chi}_i^+ + m_{\tilde{\chi}_i^-}^2 d \cdot \bar{d} \right) \right. \\ &\left. \pm \beta_d y_i (d \cdot \tilde{\chi}_i^- \bar{d} \cdot \tilde{\chi}_i^+ - d \cdot \tilde{\chi}_i^+ \bar{d} \cdot \tilde{\chi}_i^-) \right\} \end{aligned} \quad (40.81)$$

$$T_{\gamma\tilde{u}_L} = \mp \frac{8e^2 q_d}{s} \frac{|A_{\tilde{\chi}_i^-}^d|^2}{[(d - \tilde{\chi}_i^-)^2 - m_{\tilde{u}_L}^2]} \left\{ 2\bar{d} \cdot \tilde{\chi}_i^+ d \cdot \tilde{\chi}_i^- + m_{\tilde{\chi}_i^-}^2 d \cdot \bar{d} \right\} \quad (40.82)$$

and

$$T_{Z\tilde{u}_L} = \mp 8e^2 \cot \theta_W |D_Z(s)|^2 \frac{|A_{\tilde{\chi}_i^-}^d|^2 (s - M_Z^2)}{[(d - \tilde{\chi}_i^-)^2 - m_{\tilde{u}_L}^2]} (\alpha_d - \beta_d) \\ \times \left\{ 2(x_i \mp y_i) d \cdot \tilde{\chi}_i^- \bar{d} \cdot \tilde{\chi}_i^+ + m_{\tilde{\chi}_i^-}^2 (x_i \pm y_i) d \cdot \bar{d} \right\} \quad (40.83)$$

using the upper of the sign choices.

The cross section for $u\bar{u} \rightarrow \tilde{\chi}_i^+ \tilde{\chi}_i^-$ can be obtained from the above by replacing $\alpha_d \rightarrow \alpha_u$, $\beta_d \rightarrow \beta_u$, $q_d \rightarrow q_u$, $\tilde{u}_L \rightarrow \tilde{d}_L$, $A_{\tilde{\chi}_i^-}^d \rightarrow A_{\tilde{\chi}_i^-}^u$, $d \rightarrow \bar{u}$, $\bar{d} \rightarrow u$ and adopting the lower of the sign choices everywhere.

The cross section for $q\bar{q} \rightarrow \tilde{\chi}_1^- \tilde{\chi}_2^+$, $\tilde{\chi}_1^+ \tilde{\chi}_2^-$ can occur via Z and \tilde{q}_L exchange. It is usually much smaller than $\tilde{\chi}_{1,2}^- \tilde{\chi}_{1,2}^+$ production, so the cross section will not be presented here. It can be found in Appendix A of Ref. 15.

40.8.4.3. Neutralino pair production:

Neutralino pair production via $q\bar{q}$ fusion takes place via s -channel Z exchange plus t - and u -channel left- and right- squark exchange (5 diagrams) [17,18]. The Lagrangian couplings (see previous footnote*) needed include terms given above plus terms of the form $\mathcal{L} = W_{ij} \tilde{\chi}_i^0 \gamma^\mu (\gamma_5)^{\theta_i + \theta_j + 1} \tilde{\chi}_j^0 Z^\mu$. The couplings W_{ij} depend only on the *higgsino* components of the neutralinos i and j . The subprocess cross section is given by:

$$\frac{d\sigma}{dt}(q\bar{q} \rightarrow \tilde{\chi}_i^0 \tilde{\chi}_j^0) = \frac{1}{192\pi s^2} [T_Z + T_{\tilde{q}_L} + T_{\tilde{q}_R} + T_{Z\tilde{q}_L} + T_{Z\tilde{q}_R}] \quad (40.84)$$

where

$$T_Z = 128e^2 |W_{ij}|^2 (\alpha_q^2 + \beta_q^2) |D_Z(s)|^2 \\ \left[q \cdot \tilde{\chi}_i^0 \bar{q} \cdot \tilde{\chi}_j^0 + q \cdot \tilde{\chi}_j^0 \bar{q} \cdot \tilde{\chi}_i^0 - \eta_i \eta_j m_{\tilde{\chi}_i^0} m_{\tilde{\chi}_j^0} q \cdot \bar{q} \right], \quad (40.85)$$

$$T_{\tilde{q}_L} = 4 |A_{\tilde{\chi}_i^0}^q|^2 |A_{\tilde{\chi}_j^0}^q|^2 \left\{ \frac{q \cdot \tilde{\chi}_i^0 \bar{q} \cdot \tilde{\chi}_j^0}{[(\tilde{\chi}_i^0 - q)^2 - m_{\tilde{q}_L}^2]^2} + \frac{q \cdot \tilde{\chi}_j^0 \bar{q} \cdot \tilde{\chi}_i^0}{[(\tilde{\chi}_j^0 - q)^2 - m_{\tilde{q}_L}^2]^2} \right. \\ \left. - \eta_i \eta_j \frac{m_{\tilde{\chi}_i^0} m_{\tilde{\chi}_j^0} q \cdot \bar{q}}{[(\tilde{\chi}_i^0 - q)^2 - m_{\tilde{q}_L}^2][(\tilde{\chi}_j^0 - q)^2 - m_{\tilde{q}_L}^2]} \right\} \quad (40.86)$$

$$T_{\tilde{q}_R} = 4 |B_{\tilde{\chi}_i^0}^q|^2 |B_{\tilde{\chi}_j^0}^q|^2 \left\{ \frac{q \cdot \tilde{\chi}_i^0 \bar{q} \cdot \tilde{\chi}_j^0}{[(\tilde{\chi}_i^0 - q)^2 - m_{\tilde{q}_R}^2]^2} + \frac{q \cdot \tilde{\chi}_j^0 \bar{q} \cdot \tilde{\chi}_i^0}{[(\tilde{\chi}_j^0 - q)^2 - m_{\tilde{q}_R}^2]^2} \right. \\ \left. - \eta_i \eta_j \frac{m_{\tilde{\chi}_i^0} m_{\tilde{\chi}_j^0} q \cdot \bar{q}}{[(\tilde{\chi}_i^0 - q)^2 - m_{\tilde{q}_R}^2][(\tilde{\chi}_j^0 - q)^2 - m_{\tilde{q}_R}^2]} \right\} \quad (40.87)$$

$$T_{Z\tilde{q}_L} = 16e(\alpha_q - \beta_q)(s - M_Z^2) |D_Z(s)|^2 \\ \left\{ \frac{\text{Re}(W_{ij} A_{\tilde{\chi}_i^0}^{q*} A_{\tilde{\chi}_j^0}^q)}{[(\tilde{\chi}_i^0 - q)^2 - m_{\tilde{q}_L}^2]} \left[2q \cdot \tilde{\chi}_i^0 \bar{q} \cdot \tilde{\chi}_j^0 - \eta_i \eta_j m_{\tilde{\chi}_i^0} m_{\tilde{\chi}_j^0} q \cdot \bar{q} \right] \right. \\ \left. + \eta_i \eta_j \frac{\text{Re}(W_{ij} A_{\tilde{\chi}_i^0}^q A_{\tilde{\chi}_j^0}^{q*})}{[(\tilde{\chi}_j^0 - q)^2 - m_{\tilde{q}_L}^2]} \left[2q \cdot \tilde{\chi}_j^0 \bar{q} \cdot \tilde{\chi}_i^0 - \eta_i \eta_j m_{\tilde{\chi}_i^0} m_{\tilde{\chi}_j^0} q \cdot \bar{q} \right] \right\} \quad (40.88)$$

$$T_{Z\tilde{q}_R} = 16e(\alpha_q + \beta_q)(s - M_Z^2) |D_Z(s)|^2 \\ \left\{ \frac{\text{Re}(W_{ij} B_{\tilde{\chi}_i^0}^{q*} B_{\tilde{\chi}_j^0}^q)}{[(\tilde{\chi}_i^0 - q)^2 - m_{\tilde{q}_R}^2]} \left[2q \cdot \tilde{\chi}_i^0 \bar{q} \cdot \tilde{\chi}_j^0 - \eta_i \eta_j m_{\tilde{\chi}_i^0} m_{\tilde{\chi}_j^0} q \cdot \bar{q} \right] \right. \\ \left. - \frac{\text{Re}(W_{ij} B_{\tilde{\chi}_i^0}^q B_{\tilde{\chi}_j^0}^{q*})}{[(\tilde{\chi}_j^0 - q)^2 - m_{\tilde{q}_R}^2]} \left[2q \cdot \tilde{\chi}_j^0 \bar{q} \cdot \tilde{\chi}_i^0 - \eta_i \eta_j m_{\tilde{\chi}_i^0} m_{\tilde{\chi}_j^0} q \cdot \bar{q} \right] \right\}. \quad (40.89)$$

As before, $\eta_i = \pm 1$ corresponding to whether the neutralino mass eigenvalue is positive or negative. When $i = j$ in the above formula, one must remember to integrate over just 2π steradians of solid angle to avoid double counting in the total cross section.

40.9. Universal extra dimensions

In the Universal Extra Dimension (UED) model of Ref. [19] (see Ref. [20] for a review of models with extra spacetime dimensions), the Standard Model is embedded in a five dimensional theory, where the fifth dimension is compactified on an S_1/Z_2 orbifold. Each SM chirality state is then the zero mode of an infinite tower of Kaluza-Klein excitations labelled by $n = 0 - \infty$. A KK parity is usually assumed to hold, where each state is assigned KK-parity $P = (-1)^n$. If the compactification scale is around a TeV, then the $n = 1$ (or even higher) KK modes may be accessible to collider searches.

Of interest for hadron colliders are the production of massive $n \geq 1$ quark or gluon pairs. These production cross sections have been calculated in Ref. [21,22]. We list here results for the $n = 1$ case only with $M_1 = 1/R$ (R is the compactification radius) and s , t and u are the usual Mandelstam variables; more general formulae can be found in Ref. [22]. The superscript $*$ stands for any KK excited state, while \bullet stands for left chirality states and \circ stands for right chirality states.

$$\frac{d\sigma}{dt} = \frac{1}{16\pi s^2} T \quad (40.90)$$

where

$$T(q\bar{q} \rightarrow g^* g^*) = \frac{2g_s^4}{27} \left[M_1^2 \left(-\frac{4s^3}{t'^2 u'^2} + \frac{57s}{t' u'} - \frac{108}{s} \right) \right. \\ \left. + \frac{20s^2}{t' u'} - 93 + \frac{108t' u'}{s^2} \right] \quad (40.91)$$

and

$$T(gg \rightarrow g^* g^*) = \\ \frac{9g_s^4}{27} \left[3M_1^4 \frac{s^2 + t'^2 + u'^2}{t'^2 u'^2} - 3M_1^2 \frac{s^2 + t'^2 + u'^2}{s t' u'} + 1 \right. \\ \left. + \frac{(s^2 + t'^2 + u'^2)^3}{4s^2 t'^2 u'^2} - \frac{t' u'}{s^2} \right] \quad (40.92)$$

where $t' = t - M_1^2$ and $u' = u - M_1^2$.

Also,

$$T(q\bar{q} \rightarrow q_1^* \bar{q}_1^*) = \frac{4g_s^4}{9} \left[\frac{2M_1^2}{s} + \frac{t'^2 + u'^2}{s^2} \right],$$

$$T(q\bar{q} \rightarrow q_1^* \bar{q}_1^*) = \frac{g_s^4}{9} \left[2M_1^2 \left(\frac{4}{s} + \frac{s}{t'^2} - \frac{1}{t'} \right) \right. \\ \left. + \frac{23}{6} + \frac{2s^2}{t'^2} + \frac{8s}{3t'} + \frac{6t'}{s} + \frac{8t'^2}{s^2} \right],$$

$$T(qq \rightarrow q_1^* \bar{q}_1^*) = \frac{g_s^4}{27} \left[M_1^2 \left(6 \frac{t'}{u'^2} + 6 \frac{u'}{t'^2} - \frac{s}{t' u'} \right) \right. \\ \left. + 2 \left(3 \frac{t'^2}{u'^2} + 3 \frac{u'^2}{t'^2} + 4 \frac{s^2}{t' u'} - 5 \right) \right],$$

$$T(gg \rightarrow q_1^* \bar{q}_1^*) = g_s^4 \left[M_1^4 \frac{-4}{t' u'} \left(\frac{s^2}{6t' u'} - \frac{3}{8} \right) \right. \\ \left. + M_1^2 \frac{4}{s} \left(\frac{s^2}{6t' u'} - \frac{3}{8} \right) + \frac{s^2}{6t' u'} - \frac{17}{24} + \frac{3t' u'}{4s^2} \right],$$

$$T(gg \rightarrow g^* q_1^*) = \frac{-g_s^4}{3} \left[\frac{5s^2}{12t'^2} + \frac{s^3}{t'^2 u'} + \frac{11s u'}{6t'^2} + \frac{5u'^2}{12t'^2} + \frac{u'^3}{s t'^2} \right],$$

$$T(qq' \rightarrow q_1^* \bar{q}_1^*) = \frac{g_s^4}{18} \left[4M_1^4 \frac{s}{t'^2} + 5 + 4 \frac{s^2}{t'^2} + 8 \frac{s}{t'} \right],$$

$$T(qq' \rightarrow q_1^* \bar{q}_1^*) = \frac{2g_s^4}{9} \left[-M_1^2 \frac{s}{t'^2} + \frac{1}{4} + \frac{s^2}{t'^2} \right],$$

$$T(qq \rightarrow q_1^{\bullet} q_1^{\circ}) = \frac{g_s^4}{9} \left[M_1^2 \left(\frac{2s^3}{t'^2 u'^2} - \frac{4s}{t' u'} \right) + 2 \frac{s^4}{t'^2 u'^2} - 8 \frac{s^2}{t' u'} + 5 \right],$$

$$T(q\bar{q}' \rightarrow q_1^{\bullet} \bar{q}_1^{\circ}) = \frac{g_s^4}{9} \left[2M_1^2 \left(\frac{1}{t'} + \frac{u'}{t'^2} \right) + \frac{5}{2} + \frac{4u'}{t'} + \frac{2u'^2}{t'^2} \right],$$

and

$$T(qq' \rightarrow q_1^{\bullet} q_1^{\circ}) = \frac{g_s^4}{9} \left[-2M_1^2 \left(\frac{1}{t'} + \frac{u'}{t'^2} \right) + \frac{1}{2} + \frac{2u'^2}{t'^2} \right].$$

40.10. Large extra dimensions

In the ADD theory [23] with large extra dimensions (LED), the SM particles are confined to a 3-brane, while gravity propagates in the bulk. It is assumed that the n extra dimensions are compactified on an n -dimensional torus of volume $(2\pi r)^n$, so that the fundamental $4+n$ dimensional Planck scale M_* is related to the usual 4-dimensional Planck scale M_{Pl} by $M_{Pl}^2 = M_*^{n+2} (2\pi r)^n$. If $M_* \sim 1$ TeV, then the $M_W - M_{Pl}$ hierarchy problem is just due to gravity propagating in the large extra dimensions.

In these theories, the KK-excited graviton states $G_{\mu\nu}^n$ for $n = 1 - \infty$ can be produced at collider experiments. The graviton couplings to matter are suppressed by $1/M_{Pl}$, so that graviton emission cross sections $d\sigma/dt \sim 1/M_{Pl}^2$. However, the mass splittings between the excited graviton states can be tiny, so the graviton eigenstates are usually approximated by a continuum distribution. A summation (integration) over all allowed graviton emissions ends up cancelling the $1/M_{Pl}^2$ factor, so that observable cross section rates can be attained. Some of the fundamental production formulae for a KK graviton (denoted G) of mass m at hadron colliders include the subprocesses

$$\frac{d\sigma_m}{dt}(f\bar{f} \rightarrow \gamma G) = \frac{\alpha Q_f^2}{16N_f s M_{Pl}^2} F_1\left(\frac{t}{s}, \frac{m^2}{s}\right), \quad (40.93)$$

where Q_f is the charge of fermion f and N_f is the number of QCD colors of f . Also,

$$\frac{d\sigma_m}{dt}(q\bar{q} \rightarrow gG) = \frac{\alpha_s}{36 s M_{Pl}^2} F_1\left(\frac{t}{s}, \frac{m^2}{s}\right), \quad (40.94)$$

$$\frac{d\sigma_m}{dt}(qq \rightarrow qG) = \frac{\alpha_s}{96 s M_{Pl}^2} F_2\left(\frac{t}{s}, \frac{m^2}{s}\right), \quad (40.95)$$

$$\frac{d\sigma_m}{dt}(gg \rightarrow gG) = \frac{3\alpha_s}{16 s M_{Pl}^2} F_3\left(\frac{t}{s}, \frac{m^2}{s}\right), \quad (40.96)$$

where

$$F_1(x, y) = \frac{1}{x(y-1-x)} \left[-4x(1+x)(1+2x+2x^2) + y(1+6x+18x^2+16x^3) - 6y^2x(1+2x) + y^3(1+4x) \right] \quad (40.97)$$

$$F_2(x, y) = -(y-1-x)F_1\left(\frac{x}{y-1-x}, \frac{y}{y-1-x}\right) \quad (40.98)$$

and

$$F_3(x, y) = \frac{1}{x(y-1-x)} \left[1+2x+3x^2+2x^3+x^4 - 2y(1+x^3) + 3y^2(1+x^2) - 2y^3(1+x) + y^4 \right]. \quad (40.99)$$

These formulae must then be multiplied by the graviton density of states formula $dN = S_{n-1} \frac{M_{Pl}^2}{M_*^{n+2}} m^{n-1} dm$ to gain the cross section

$$\frac{d^2\sigma}{dt dm} = S_{n-1} \frac{M_{Pl}^2}{M_*^{n+2}} m^{n-1} \frac{d\sigma_m}{dt} \quad (40.100)$$

where $S_n = \frac{(2\pi)^{n/2}}{\Gamma(n/2)}$ is the surface area of an n -dimensional sphere of unit radius.

Virtual graviton processes can also be searched for at colliders. For instance, in Ref. [24] the cross section for Drell-Yan production of lepton pairs via gluon fusion was calculated, where it is found that, in the center-of-mass system

$$\frac{d\sigma}{dz}(gg \rightarrow \ell^+ \ell^-) = \frac{\lambda^2 s^3}{64\pi M_*^2} (1-z^2)(1+z^2) \quad (40.101)$$

where $z = \cos\theta$ and λ is a model-dependent coupling constant ~ 1 . Formulae for Drell-Yan production via $q\bar{q}$ fusion can also be found in Ref. [24,25].

40.11. Warped extra dimensions

In the Randall-Sundrum model [26] of warped extra dimensions, the arena for physics is a 5-d anti-deSitter (AdS_5) spacetime, for which a non-factorizable metric exists with a metric warp factor $e^{-2\sigma(\phi)}$. It is assumed that two opposite tension 3-branes exist within AdS_5 at the two ends of an S_1/Z_2 orbifold parametrized by co-ordinate ϕ which runs from $0 - \pi$. The 4-D solution of the Einstein equations yields $\sigma(\phi) = kr_c|\phi|$, where r_c is the compactification radius of the extra dimension and $k \sim M_{Pl}$. The 4-D effective action allows one to identify $\overline{M}_{Pl}^2 = \frac{M^3}{k}(1 - e^{-2kr_c\pi})$, where M is the 5-D Planck scale. Physical particles on the TeV scale (SM) brane have mass $m = e^{-kr_c\pi} m_0$, where m_0 is a fundamental mass of order the Planck scale. Thus, the weak scale-Planck scale hierarchy occurs due to the existence of the exponential warp factor if $kr_c \sim 12$.

In the simplest versions of the RS model, the TeV-scale brane contains only SM particles plus a tower of KK gravitons. The RS gravitons have mass $m_n = kx_n e^{-kr_c\pi}$, where the x_i are roots of Bessel functions $J_1(x_n) = 0$, with $x_1 \simeq 3.83$, $x_2 \simeq 7.02$ etc. While the RS zero-mode graviton couplings suppressed by $1/\overline{M}_{Pl}$ and are thus inconsequential for collider searches, the $n=1$ and higher modes have couplings suppressed instead by $\Lambda_\pi = e^{-kr_c\pi} \overline{M}_{Pl} \sim TeV$. The $n=1$ RS graviton should have width $\Gamma_1 = \rho m_1 x_1^2 (k/\overline{M}_{Pl})^2$, where ρ is a constant depending on how many decay modes are open. The formulae for dilepton production via virtual RS graviton exchange can be gained from the above formulae for the ADD scenario via the replacement [27]

$$\frac{\lambda}{M_*^4} \rightarrow \frac{i^2}{8\Lambda_\pi^2} \sum_{n=1}^{\infty} \frac{1}{s - m_n^2 + im_n\Gamma_n}. \quad (40.102)$$

References:

1. J.F. Owens *et al.*, Phys. Rev. **D18**, 1501 (1978). Note that cross section given in previous editions of RPP for $gg \rightarrow q\bar{q}$ lacked a factor of π .
2. F. Wilczek, Phys. Rev. Lett. **39**, 1304 (1977).
3. B.L. Ioffe and V.Khoze, Leningrad Report 274, 1976; Sov. J. Nucl. Phys. **9**, 50 (1978).
4. J. Ellis *et al.*, Nucl. Phys. **B106**, 292 (1976).
5. R.N. Cahn and S. Dawson, Phys. Lett. **B136**, 196 (1984), erratum, Phys. Lett. **B138**, 464 (1984).
6. S. Dawson, Nucl. Phys. **B249**, 42 (1985).
7. M.S. Chanowitz and M.K. Gaillard, Phys. Lett. **B142**, 85 (1984).
8. R.N. Cahn, Nucl. Phys. **B255**, 341 (1985).
9. For an exhaustive treatment, see V.M. Budnev *et al.*, Phys. Reports **15C**, 181 (1975).
10. See *e.g.* H. Haber, *Supersymmetry, Part I (Theory)*, this Review.
11. P.R. Harrison and C.H. Llewellyn Smith, Nucl. Phys. **B213**, 223 (1983), Erratum-*ibid.*, **B223**, 542 (1983); S. Dawson, E. Eichten, and C. Quigg, Phys. Rev. **D31**, 1581 (1985); V. Barger *et al.*, Phys. Rev. **D31**, 528 (1985); H. Baer and X. Tata, Phys. Lett. **B160**, 159 (1985).
12. H. Baer, D. Karatas, and X. Tata, Phys. Rev. **D42**, 2259 (1990).
13. H. Haber and G. Kane, Phys. Rept. **117**, 75 (1985).
14. Theory and Phenomenology of Sparticles, M. Drees, R. Godbole, and P. Roy (World Scientific) 2005.

15. Weak Scale Supersymmetry: From Superfields to Scattering Events, H. Baer and X. Tata (Cambridge University Press) 2006.
16. A. Bartl, H. Fraas, and W. Majerotto, *Z. Phys.* **C30**, 441 (1986).
17. H. Baer *et al.*, *Int. J. Mod. Phys.* **A4**, 4111 (1989).
18. A. Bartl, H. Fraas, and W. Majerotto, *Nucl. Phys.* **B278**, 1 (1986).
19. T. Appelquist, H.C. Cheng, and B. Dobrescu, *Phys. Rev.* **D64**, 035002 (2001).
20. For a review of models with extra spacetime dimensions, see G. Giudice and J. Wells, *Extra Dimensions*, this *Review*.
21. J.M. Smillie and B.R. Webber, *JHEP* **0510**, 069 (2005).
22. C. Macesanu, C.D. McMullen, and S. Nandi, *Phys. Rev.* **D66**, 015009 (2002).
23. N. Arkani-Hamed, S. Dimopoulos, and G. Dvali, *Phys. Lett.* **B429**, 263 (1998) and *Phys. Rev.* **D59**, 086004 (1999).
24. J. L. Hewett, *Phys. Rev. Lett.* **82**, 4765 (1999).
25. G. Giudice, R. Rattazzi, and J. Wells, *Nucl. Phys.* **B544**, 3 (1999); E.A. Mirabelli, M. Perelstein, and M.E. Peskin, *Phys. Rev. Lett.* **82**, 2236 (1999); T. Han, J. Lykken, and R. Zhang, *Phys. Rev.* **D59**, 105006 (1999).
26. L. Randall and R.S. Sundrum, *Phys. Rev. Lett.* **83**, 3370 (1999).
27. H. Davoudiasl, J.L. Hewett, and T.G. Rizzo, *Phys. Rev. Lett.* **84**, 2080 (2000).

41. PLOTS OF CROSS SECTIONS AND RELATED QUANTITIES

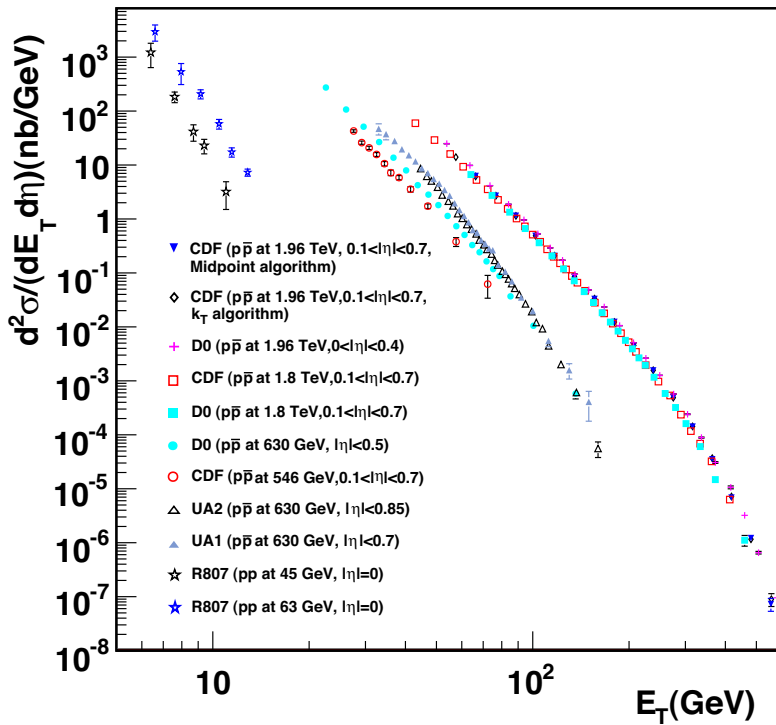
Jet Production in pp and $\bar{p}p$ Interactions

Figure 41.1: Inclusive differential jet cross sections plotted as a function of the jet transverse energy. The CDF and D0 measurements use a cone algorithm of radius 0.7 for all results shown except for the CDF measurements at 1.96 TeV which also use k_T with a D parameter of 0.7 and midpoint algorithms. The cone/ k_T results should be similar if $R_{cone} = D$. UA1 (UA2) uses a non-iterative cone algorithm with a radius of 1.0 (1.3). Recent NLO QCD predictions (such as CTEQ6M) provide a good description of the CDF and D0 jet cross sections, Rept. on Prog. in Phys. **70**, 89 (2007). Comparisons with the older cross sections are more difficult due to the nature of the jet algorithms used. **CDF**: Phys. Rev. **D75**, 092006 (2007), Phys. Rev. **D64**, 032001 (2001), Phys. Rev. Lett. **70**, 1376 (1993); **D0**: Phys. Rev. **D64**, 032003 (2001); **UA2**: Phys. Lett. **B257**, 232 (1991); **UA1**: Phys. Lett. **B172**, 461 (1986); **R807**: Phys. Lett. **B123**, 133 (1983). (Courtesy of J. Huston, Michigan State University, 2010.) See full-color version on color pages at end of book.

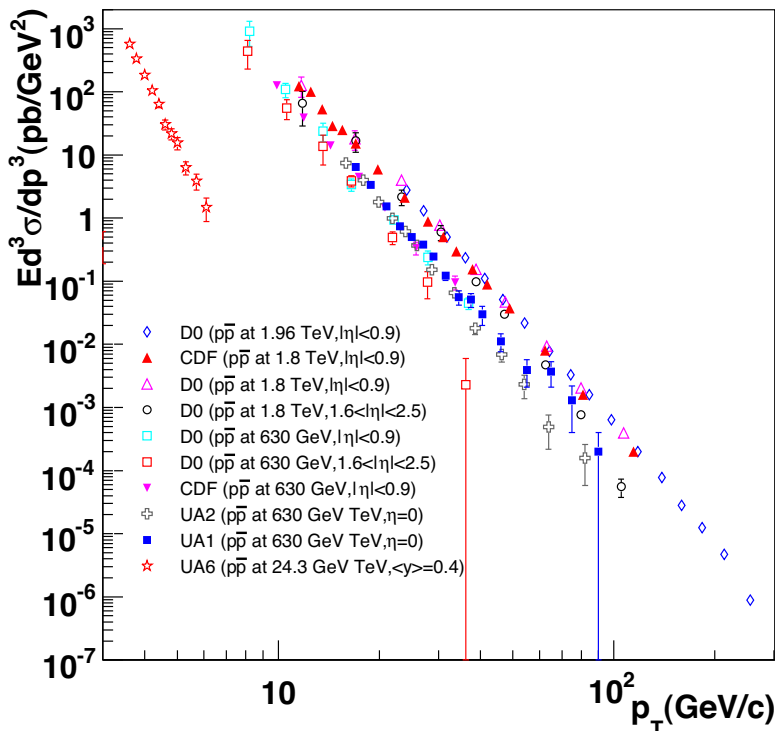
Direct γ Production in $\bar{p}p$ Interactions

Figure 41.2: Isolated photon cross sections plotted as a function of the photon transverse momentum. The errors are either statistical only (CDF, D0 (1.96 TeV), UA1, UA2, UA6) or uncorrelated (D0 1.8 TeV, 630 GeV). The data are generally in good agreement with NLO QCD predictions, albeit with a tendency for the data to be above (below) the theory for lower (large) transverse momenta, Phys. Rev. **D59**, 074007 (1999). **D0**: Phys. Lett. **B639**, 151 (2006), Phys. Rev. Lett. **87**, 251805 (2001); **CDF**: Phys. Rev. **D65**, 112003 (2002); **UA6**: Phys. Lett. **B206**, 163 (1988); **UA1**: Phys. Lett. **B209**, 385 (1988); **UA2**: Phys. Lett. **B288**, 386 (1992). (Courtesy of J. Huston, Michigan State University, 2007.) See full-color version on color pages at end of book.

Differential Cross Section for W and Z Boson Production

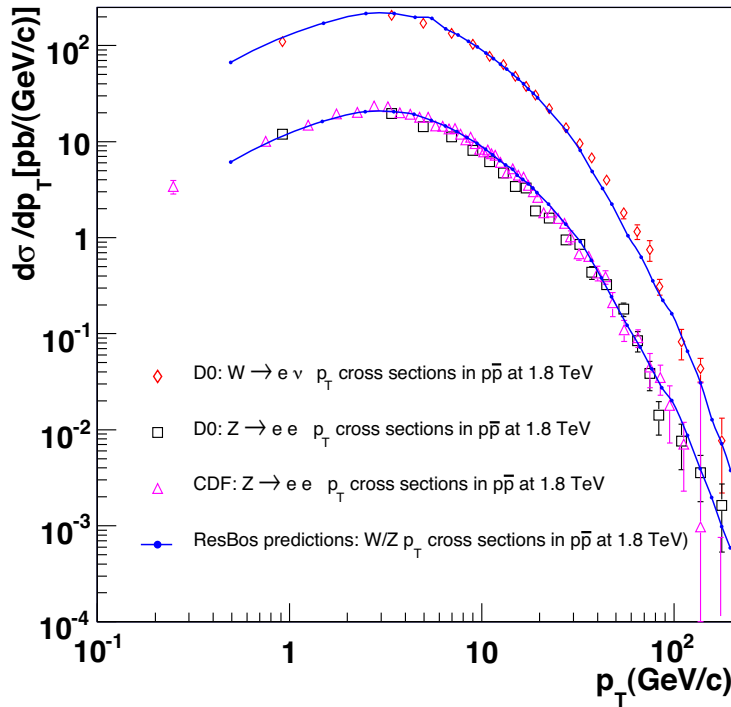


Figure 41.3: Differential cross sections for W and Z production shown as a function of the boson transverse momentum. The D0 results include only the statistical error while the CDF results include all errors except for the 3.9% integrated luminosity error. The results are in good agreement with theoretical predictions that include both the effects of NLO corrections and of q_T resummation, such as the ResBos (Phys. Rev. **D67**, 073016 (2003)) predictions indicated on the plot. **D0:** Phys. Lett. **B513**, 292 (2001), Phys. Rev. Lett. **84**, 2792 (2000). **CDF:** Phys. Rev. Lett. **84**, 845 (2000). (Courtesy of J. Huston, Michigan State University, 2007)

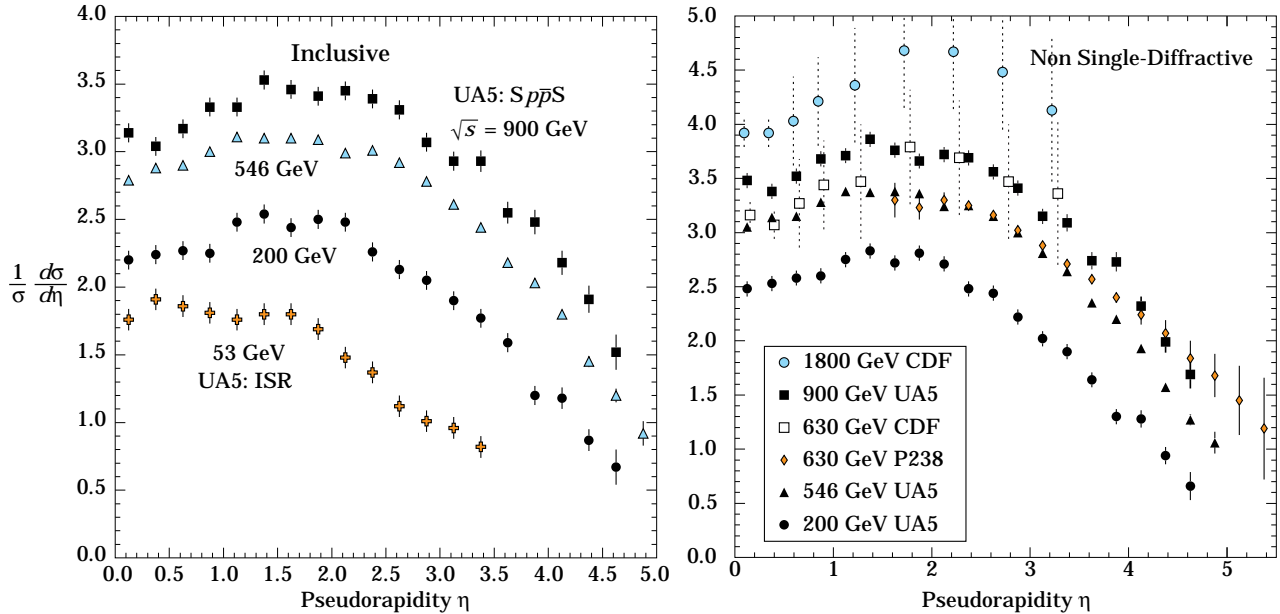
Pseudorapidity Distributions in $p\bar{p}$ Interactions

Figure 41.4: Charged particle pseudorapidity distributions in $p\bar{p}$ collisions for $53 \text{ GeV} \leq \sqrt{s} \leq 1800 \text{ GeV}$. UA5 data from the $Spp\bar{S}$ are taken from G.J. Alner *et al.*, Z. Phys. **C33**, 1 (1986), and from the ISR from K. Alpgöard *et al.*, Phys. Lett. **112B**, 193 (1982). The UA5 data are shown for both the full inelastic cross section and with singly diffractive events excluded. Additional non single-diffractive measurements are available from CDF at the Tevatron, F. Abe *et al.*, Phys. Rev. **D41**, 2330 (1990) and Experiment P238 at the $Spp\bar{S}$, R. Harr *et al.*, Phys. Lett. **B401**, 176 (1997). (Courtesy of D.R. Ward, Cambridge Univ., 1999)

Average Hadron Multiplicities in Hadronic e^+e^- Annihilation Events

Table 41.1: Average hadron multiplicities per hadronic e^+e^- annihilation event at $\sqrt{s} \approx 10, 29\text{--}35, 91,$ and $130\text{--}200$ GeV. The rates given include decay products from resonances with $c\tau < 10$ cm, and include the corresponding anti-particle state. Correlations of the systematic uncertainties were considered for the calculation of the averages. (Updated May 2010 by O. Biebel, LMU, Munich)

Particle	$\sqrt{s} \approx 10$ GeV	$\sqrt{s} = 29\text{--}35$ GeV	$\sqrt{s} = 91$ GeV	$\sqrt{s} = 130\text{--}200$ GeV
Pseudoscalar mesons:				
π^+	6.6 ± 0.2	10.3 ± 0.4	17.02 ± 0.19	21.24 ± 0.39
π^0	3.2 ± 0.3	5.83 ± 0.28	9.42 ± 0.32	
K^+	0.90 ± 0.04	1.48 ± 0.09	2.228 ± 0.059	2.82 ± 0.19
K^0	0.91 ± 0.05	1.48 ± 0.07	2.049 ± 0.026	2.10 ± 0.12
η	0.20 ± 0.04	0.61 ± 0.07	1.049 ± 0.080	
$\eta(958)$	0.03 ± 0.01	0.26 ± 0.10	0.152 ± 0.020	
D^+	$0.194 \pm 0.019^{(a)}$	0.17 ± 0.03	0.175 ± 0.016	
D^0	$0.446 \pm 0.032^{(a)}$	0.45 ± 0.07	0.454 ± 0.030	
D_s^+	$0.063 \pm 0.014^{(a)}$	$0.45 \pm 0.20^{(b)}$	0.131 ± 0.021	
$B^{(c)}$	—	—	$0.165 \pm 0.026^{(d)}$	
B^+	—	—	$0.178 \pm 0.006^{(d)}$	
B_s^0	—	—	$0.057 \pm 0.013^{(d)}$	
Scalar mesons:				
$f_0(980)$	0.024 ± 0.006	$0.05 \pm 0.02^{(e)}$	0.146 ± 0.012	
$a_0(980)^\pm$	—	—	$0.27 \pm 0.11^{(f)}$	
Vector mesons:				
$\rho(770)^0$	0.35 ± 0.04	0.81 ± 0.08	1.231 ± 0.098	
$\rho(770)^\pm$	—	—	$2.40 \pm 0.43^{(f)}$	
$\omega(782)$	0.30 ± 0.08	—	1.016 ± 0.065	
$K^*(892)^+$	0.27 ± 0.03	0.64 ± 0.05	0.715 ± 0.059	
$K^*(892)^0$	0.29 ± 0.03	0.56 ± 0.06	0.738 ± 0.024	
$\phi(1020)$	0.044 ± 0.003	0.085 ± 0.011	0.0963 ± 0.0032	
$D^*(2010)^+$	$0.177 \pm 0.022^{(a)}$	0.43 ± 0.07	$0.1937 \pm 0.0057^{(g)}$	
$D^*(2007)^0$	$0.168 \pm 0.019^{(a)}$	0.27 ± 0.11	—	
$D_s^*(2112)^+$	$0.048 \pm 0.014^{(a)}$	—	$0.101 \pm 0.048^{(h)}$	
$B^* \text{ }^{(i)}$	—	—	0.288 ± 0.026	
$J/\psi(1S)$	$0.00050 \pm 0.00005^{(a)}$	—	$0.0052 \pm 0.0004^{(j)}$	
$\psi(2S)$	—	—	$0.0023 \pm 0.0004^{(j)}$	
$\Upsilon(1S)$	—	—	$0.00014 \pm 0.00007^{(j)}$	
Pseudovector mesons:				
$f_1(1285)$	—	—	0.165 ± 0.051	
$f_1(1420)$	—	—	0.056 ± 0.012	
$\chi_{c1}(3510)$	—	—	$0.0041 \pm 0.0011^{(j)}$	
Tensor mesons:				
$f_2(1270)$	0.09 ± 0.02	0.14 ± 0.04	0.166 ± 0.020	
$f_2'(1525)$	—	—	0.012 ± 0.006	
$K_2^*(1430)^+$	—	0.09 ± 0.03	—	
$K_2^*(1430)^0$	—	0.12 ± 0.06	0.084 ± 0.022	
$B^{** \text{ }^{(k)}}$	—	—	0.118 ± 0.024	
D_{s1}^\pm	—	—	$0.0052 \pm 0.0011^{(\ell)}$	
$D_{s2}^{*\pm}$	—	—	$0.0083 \pm 0.0031^{(\ell)}$	
Baryons:				
p	0.253 ± 0.016	0.640 ± 0.050	1.050 ± 0.032	1.41 ± 0.18
Λ	0.080 ± 0.007	0.205 ± 0.010	0.3915 ± 0.0065	0.39 ± 0.03
Σ^0	0.023 ± 0.008	—	0.076 ± 0.011	
Σ^-	—	—	0.081 ± 0.010	
Σ^+	—	—	0.107 ± 0.011	
Σ^\pm	—	—	0.174 ± 0.009	
Ξ^-	0.0059 ± 0.0007	0.0176 ± 0.0027	0.0258 ± 0.0010	
$\Delta(1232)^{++}$	0.040 ± 0.010	—	0.085 ± 0.014	
$\Sigma(1385)^-$	0.006 ± 0.002	0.017 ± 0.004	0.0240 ± 0.0017	
$\Sigma(1385)^+$	0.005 ± 0.001	0.017 ± 0.004	0.0239 ± 0.0015	
$\Sigma(1385)^\pm$	0.0106 ± 0.0020	0.033 ± 0.008	0.0462 ± 0.0028	
$\Xi(1530)^0$	0.0015 ± 0.0006	—	0.0068 ± 0.0006	
Ω^-	0.0007 ± 0.0004	0.014 ± 0.007	0.0016 ± 0.0003	
Λ_c^+	$0.074 \pm 0.031^{(m)}$	0.110 ± 0.050	0.078 ± 0.017	
Λ_b^0	—	—	0.031 ± 0.016	
$\Sigma_c^{++}, \Sigma_c^0$	0.014 ± 0.007	—	—	
$\Lambda(1520)$	0.008 ± 0.002	—	0.0222 ± 0.0027	

Notes for Table 41.1:

- (a) $\sigma_{\text{had}} = 3.33 \pm 0.05 \pm 0.21$ nb (CLEO: Phys. Rev. **D29**, 1254 (1984)) has been used in converting the measured cross sections to average hadron multiplicities.
- (b) $B(D_s \rightarrow \eta\pi, \eta'\pi)$ was used (RPP 1994).
- (c) Comprises both charged and neutral B meson states.
- (d) The Standard Model $B(Z \rightarrow b\bar{b}) = 0.217$ was used.
- (e) $x_p = p/p_{\text{beam}} > 0.1$ only.
- (f) Both charge states.
- (g) $B(D^*(2010)^+ \rightarrow D^0\pi^+) \times B(D^0 \rightarrow K^-\pi^+)$ has been used (RPP 2000).
- (h) $B(D_s^* \rightarrow D_s^+\gamma)$, $B(D_s^+ \rightarrow \phi\pi^+)$, $B(\phi \rightarrow K^+K^-)$ have been used (RPP 1998).
- (i) Any charge state (i.e., B_d^* , B_u^* , or B_s^*).
- (j) $B(Z \rightarrow \text{hadrons}) = 0.699$ was used (RPP 1994).
- (k) Any charge state (i.e., B_d^{**} , B_u^{**} , or B_s^{**}).
- (l) Assumes $B(D_{s1}^+ \rightarrow D^{*+}K^0 + D^{*0}K^+) = 100\%$ and $B(D_{s2}^+ \rightarrow D^0K^+) = 45\%$.
- (m) The value was derived from the cross section of $\Lambda_c^+ \rightarrow p\pi K$ using (a) and assuming the branching fraction to be $(5.0 \pm 1.3)\%$ (RPP 2004).

References for Table 41.1:

- RPP 1992: Phys. Rev. **D45** (1992) and references therein.
- RPP 1994: Phys. Rev. **D50**, 1173 (1994) and references therein.
- RPP 1996: Phys. Rev. **D54**, 1 (1996) and references therein.
- RPP 1998: Eur. Phys. J. **C3**, 1 (1998) and references therein.
- RPP 2000: Eur. Phys. J. **C15**, 1 (2000) and references therein.
- RPP 2002: Phys. Rev. **D66**, 010001 (2002) and references therein.
- RPP 2004: Phys. Lett. **B592**, 1 (2004) and references therein.
- RPP 2006: J. Phys. **G33**, 1 (2006) and references therein.
- RPP 2008: Phys. Lett. **B667**, 1 (2008) and references therein.
- R. Marshall, Rept. on Prog. in Phys. **52**, 1329 (1989). A. De Angelis, J. Phys. **G19**, 1233 (1993) and references therein.
- ALEPH: D. Buskulic *et al.*: Phys. Lett. **B295**, 396 (1992); Z. Phys. **C64**, 361 (1994); **C69**, 15 (1996); **C69**, 379 (1996); **C73**, 409 (1997); and R. Barate *et al.*: Z. Phys. **C74**, 451 (1997); Phys. Reports **294**, 1 (1998); Eur. Phys. J. **C5**, 205 (1998); **C16**, 597 (2000); **C16**, 613 (2000); and A. Heister *et al.*: Phys. Lett. **B526**, 34 (2002); **B528**, 19 (2002).
- ARGUS: H. Albrecht *et al.*: Phys. Lett. **230B**, 169 (1989); Z. Phys. **C44**, 547 (1989); **C46**, 15 (1990); **C54**, 1 (1992); **C58**, 199 (1993); **C61**, 1 (1994); Phys. Rep. **276**, 223 (1996).
- BaBar: B. Aubert *et al.*: Phys. Rev. Lett. **87**, 162002 (2001); Phys. Rev. **D65**, 091104 (2002).
- Belle: K. Abe *et al.*, Phys. Rev. Lett. **88**, 052001 (2002); and R. Seuster *et al.*, Phys. Rev. **D73**, 032002 (2006).
- CELLO: H.J. Behrend *et al.*: Z. Phys. **C46**, 397 (1990); **C47**, 1 (1990).
- CLEO: D. Bortoletto *et al.*, Phys. Rev. **D37**, 1719 (1988); erratum *ibid.* **D39**, 1471 (1989); and M. Artuso *et al.*, Phys. Rev. **D70**, 112001 (2004).
- Crystal Ball: Ch. Bieler *et al.*, Z. Phys. **C49**, 225 (1991).
- DELPHI: P. Abreu *et al.*: Z. Phys. **C57**, 181 (1993); **C59**, 533 (1993); **C61**, 407 (1994); **C65**, 587 (1995); **C67**, 543 (1995); **C68**, 353 (1995); **C73**, 61 (1996); Nucl. Phys. **B444**, 3 (1995); Phys. Lett. **B341**, 109 (1994); **B345**, 598 (1995); **B361**, 207 (1995); **B372**, 172 (1996); **B379**, 309 (1996); **B416**, 233 (1998); **B449**, 364 (1999); **B475**, 429 (2000); Eur. Phys. J. **C6**, 19 (1999); **C5**, 585 (1998); **C18**, 203 (2000); and J. Abdallah *et al.*, Phys. Lett. **B569**, 129 (2003); Phys. Lett. **B576**, 29 (2003); Eur. Phys. J. **C44**, 299 (2005); and W. Adam *et al.*: Z. Phys. **C69**, 561 (1996); **C70**, 371 (1996).
- HRS: S. Abachi *et al.*, Phys. Rev. Lett. **57**, 1990 (1986); and M. Derrick *et al.*, Phys. Rev. **D35**, 2639 (1987).
- L3: M. Acciarri *et al.*: Phys. Lett. **B328**, 223 (1994); **B345**, 589 (1995); **B371**, 126 (1996); **B371**, 137 (1996); **B393**, 465 (1997); **B404**, 390 (1997); **B407**, 351 (1997); **B407**, 389 (1997), erratum *ibid.* **B427**, 409 (1998); **B453**, 94 (1999); **B479**, 79 (2000).
- MARK II: H. Schellman *et al.*, Phys. Rev. **D31**, 3013 (1985); and G. Wormser *et al.*, Phys. Rev. Lett. **61**, 1057 (1988).
- JADE: W. Bartel *et al.*, Z. Phys. **C20**, 187 (1983); and D.D. Pietzl *et al.*, Z. Phys. **C46**, 1 (1990).
- OPAL: R. Akers *et al.*: Z. Phys. **C63**, 181 (1994); **C66**, 555 (1995); **C67**, 389 (1995); **C68**, 1 (1995); and G. Alexander *et al.*: Phys. Lett. **B358**, 162 (1995); Z. Phys. **C70**, 197 (1996); **C72**, 1 (1996); **C72**, 191 (1996); **C73**, 569 (1997); **C73**, 587 (1997); Phys. Lett. **B370**, 185 (1996); and K. Ackerstaff *et al.*: Z. Phys. **C75**, 192 (1997); Phys. Lett. **B412**, 210 (1997); Eur. Phys. J. **C1**, 439 (1998); **C4**, 19 (1998); **C5**, 1 (1998); **C5**, 411 (1998); and G. Abbiendi *et al.*: Eur. Phys. J. **C16**, 185 (2000); **C17**, 373 (2000).
- PLUTO: Ch. Berger *et al.*, Phys. Lett. **104B**, 79 (1981).
- SLD: K. Abe, Phys. Rev. **D59**, 052001 (1999); Phys. Rev. **D69**, 072003 (2004).
- TASSO: H. Aihara *et al.*, Z. Phys. **C27**, 27 (1985).
- TPC: H. Aihara *et al.*, Phys. Rev. Lett. **53**, 2378 (1984).

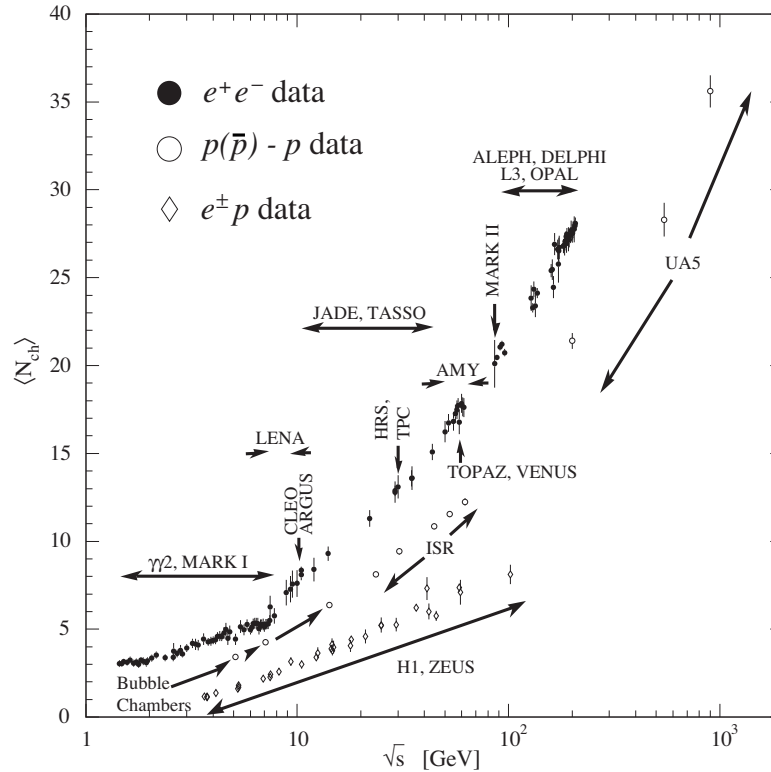
Average e^+e^- , $p\bar{p}$, and $p\bar{p}$ Multiplicity

Figure 41.5: Average multiplicity as a function of \sqrt{s} for e^+e^- and $p\bar{p}$ annihilations, and pp and ep collisions. The indicated errors are statistical and systematic errors added in quadrature, except when no systematic errors are given. Files of the data shown in this figure are given in <http://pdg.lbl.gov/current/avg-multiplicity/>.

e^+e^- : Most e^+e^- measurements include contributions from K_S^0 and Λ decays. The $\gamma\gamma 2$ and MARK I measurements contain a systematic 5% error. Points at identical energies have been spread horizontally for clarity:

ALEPH: D. Buskulic *et al.*, Z. Phys. **C69**, 15 (1995); and Z. Phys. **C73**, 409 (1997);
A. Heister *et al.*, Eur. Phys. J. **C35**, 457 (2004).

ARGUS: H. Albrecht *et al.*, Z. Phys. **C54**, 13 (1992).

DELPHI: P. Abreu *et al.*, Eur. Phys. J. **C6**, 19 (1999); Phys. Lett. **B372**, 172 (1996); Phys. Lett. **B416**, 233 (1998); and Eur. Phys. J. **C18**, 203 (2000).

L3: M. Acciarri *et al.*, Phys. Lett. **B371**, 137 (1996); Phys. Lett. **B404**, 390 (1997); and Phys. Lett. **B444**, 569 (1998);
P. Achard *et al.*, Phys. Reports **339**, 71 (2004).

OPAL: G. Abbiendi *et al.*, Eur. Phys. J. **C16**, 185 (2000); and Eur. Phys. J. **C37**, 25 (2004);
K. Ackerstaff *et al.*, Z. Phys. **C75**, 193 (1997);
P.D. Acton *et al.*, Z. Phys. **C53**, 539 (1992) and references therein;
R. Akers *et al.*, Z. Phys. **C68**, 203 (1995).

TOPAZ: K. Nakabayashi *et al.*, Phys. Lett. **B413**, 447 (1997).

VENUS: K. Okabe *et al.*, Phys. Lett. **B423**, 407 (1998).

$e^\pm p$: Multiplicities have been measured in the current fragmentation region of the Breit frame:

H1: C. Adloff *et al.*, Nucl. Phys. **B504**, 3 (1997); F.D. Aaron *et al.*, Phys. Lett. **B654**, 148 (2007).

ZEUS: J. Breitweg *et al.*, Eur. Phys. J. **C11**, 251 (1999);
S. Chekanov *et al.*, Phys. Lett. **B510**, 36 (2001).

$p(\bar{p})$: The errors of the $p(\bar{p})$ measurements are the quadratically added statistical and systematic errors, except for the bubble chamber measurements for which only statistical errors are given in the references. The values measured by UA5 exclude single diffractive dissociation:
bubble chamber: J. Benecke *et al.*, Nucl. Phys. **B76**, 29 (1976); W.M. Morse *et al.*, Phys. Rev. **D15**, 66 (1977).

ISR: A. Breakstone *et al.*, Phys. Rev. **D30**, 528 (1984).

UA5: G.J. Alner *et al.*, Phys. Lett. **167B**, 476 (1986);
R.E. Ansorge *et al.*, Z. Phys. **C43**, 357 (1989).

(Courtesy of O. Biebel, LMU, Munich, 2010)

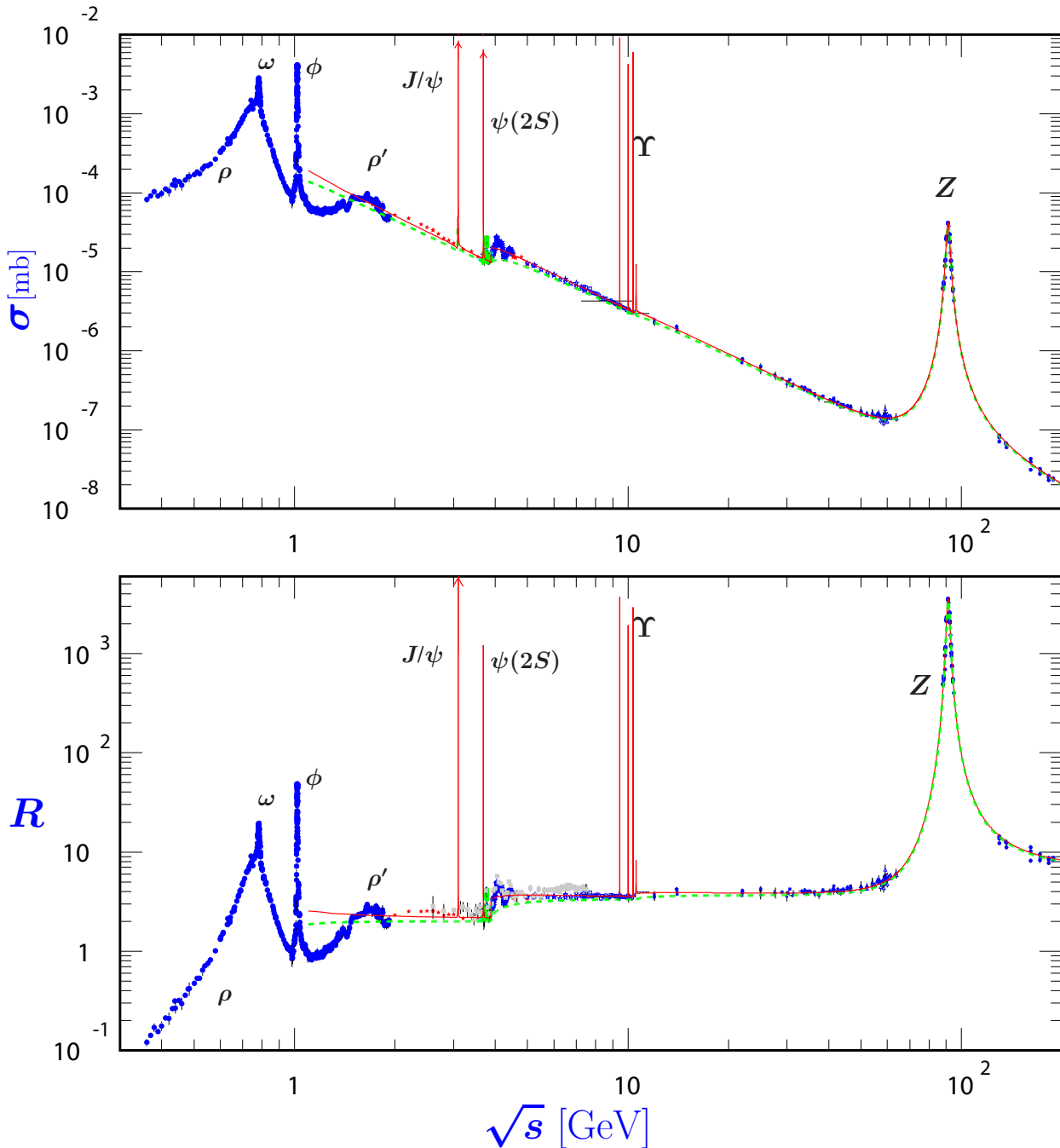
σ and R in e^+e^- Collisions

Figure 41.6: World data on the total cross section of $e^+e^- \rightarrow \text{hadrons}$ and the ratio $R(s) = \sigma(e^+e^- \rightarrow \text{hadrons}, s) / \sigma(e^+e^- \rightarrow \mu^+\mu^-, s)$. $\sigma(e^+e^- \rightarrow \text{hadrons}, s)$ is the experimental cross section corrected for initial state radiation and electron-positron vertex loops, $\sigma(e^+e^- \rightarrow \mu^+\mu^-, s) = 4\pi\alpha^2(s)/3s$. Data errors are total below 2 GeV and statistical above 2 GeV. The curves are an educative guide: the broken one (green) is a naive quark-parton model prediction, and the solid one (red) is 3-loop pQCD prediction (see “Quantum Chromodynamics” section of this Review, Eq. (9.7) or, for more details, K. G. Chetyrkin *et al.*, Nucl. Phys. **B586**, 56 (2000) (Erratum *ibid.* **B634**, 413 (2002))). Breit-Wigner parameterizations of J/ψ , $\psi(2S)$, and $\Upsilon(nS)$, $n = 1, 2, 3, 4$ are also shown. The full list of references to the original data and the details of the R ratio extraction from them can be found in [arXiv:hep-ph/0312114]. Corresponding computer-readable data files are available at <http://pdg.lbl.gov/current/xsect/>. (Courtesy of the COMPAS (Protvino) and HEPDATA (Durham) Groups, May 2010.) See full-color version on color pages at end of book.

R in Light-Flavor, Charm, and Beauty Threshold Regions

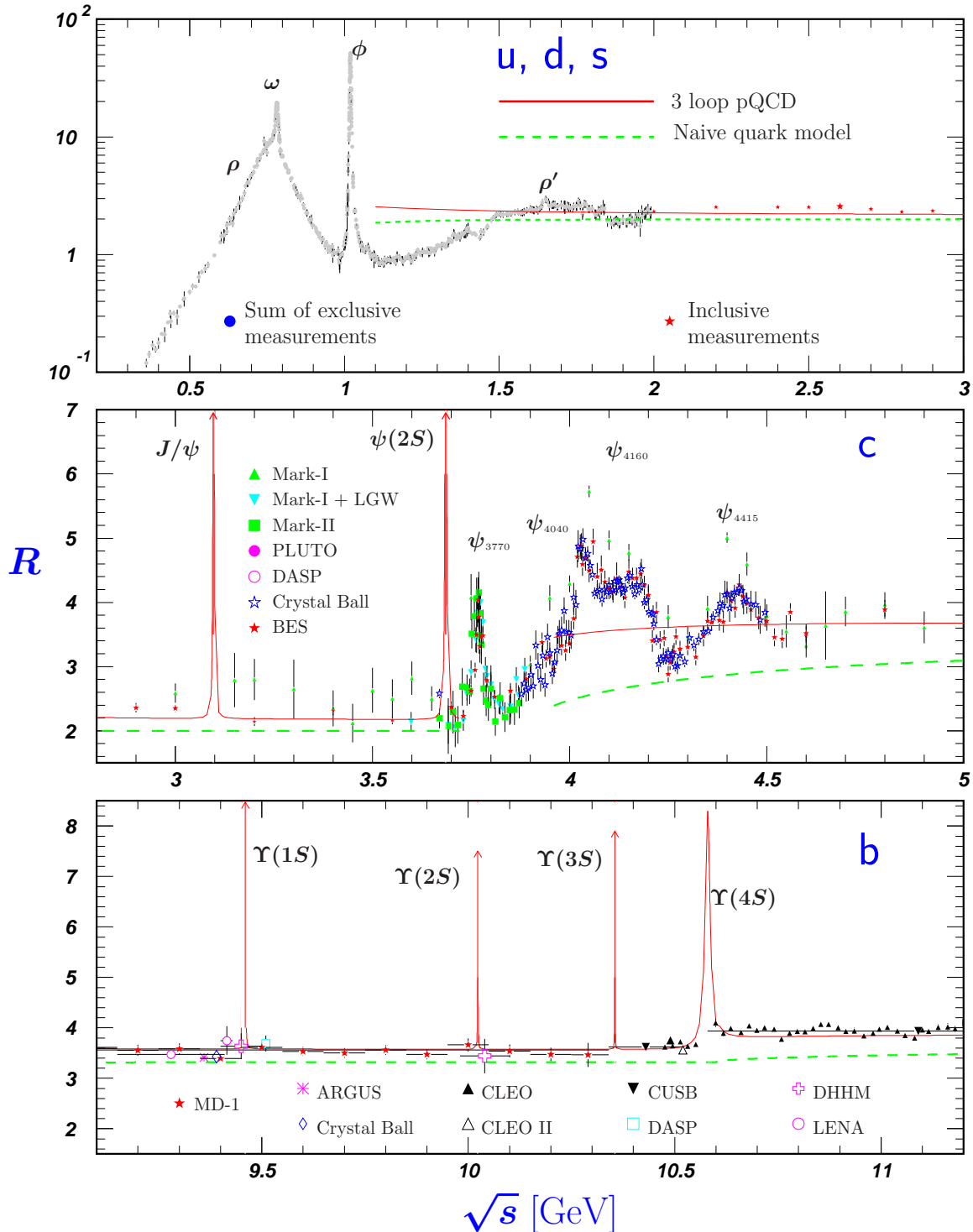


Figure 41.7: R in the light-flavor, charm, and beauty threshold regions. Data errors are total below 2 GeV and statistical above 2 GeV. The curves are the same as in Fig. 41.6. **Note:** CLEO data above $\Upsilon(4S)$ were not fully corrected for radiative effects, and we retain them on the plot only for illustrative purposes with a normalization factor of 0.8. The full list of references to the original data and the details of the R ratio extraction from them can be found in [arXiv:hep-ph/0312114]. The computer-readable data are available at <http://pdg.lbl.gov/current/xsect/>. (Courtesy of the COMPAS (Protvino) and HEPDATA (Durham) Groups, May 2010.) See full-color version on color pages at end of book.

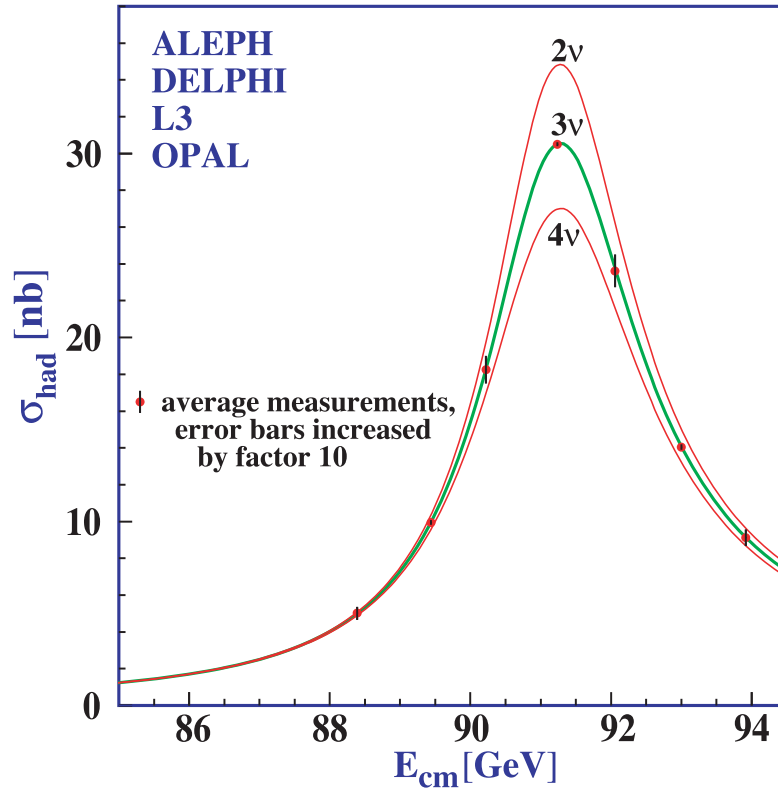
Annihilation Cross Section Near M_Z 

Figure 41.8: Combined data from the ALEPH, DELPHI, L3, and OPAL Collaborations for the cross section in e^+e^- annihilation into hadronic final states as a function of the center-of-mass energy near the Z pole. The curves show the predictions of the Standard Model with two, three, and four species of light neutrinos. The asymmetry of the curve is produced by initial-state radiation. Note that the error bars have been increased by a factor ten for display purposes. References:

ALEPH: R. Barate *et al.*, Eur. Phys. J. **C14**, 1 (2000).

DELPHI: P. Abreu *et al.*, Eur. Phys. J. **C16**, 371 (2000).

L3: M. Acciarri *et al.*, Eur. Phys. J. **C16**, 1 (2000).

OPAL: G. Abbiendi *et al.*, Eur. Phys. J. **C19**, 587 (2001).

Combination: The ALEPH, DELPHI, L3, OPAL, SLD Collaborations, the LEP Electroweak Working Group, and the SLD Electroweak and Heavy Flavor Groups, Phys. Rept. **427**, 257 (2006) [[arXiv:hep-ex/0509008](https://arxiv.org/abs/hep-ex/0509008)].

(Courtesy of M. Grünewald and the LEP Electroweak Working Group, 2007)

Muon Neutrino and Anti-Neutrino Charged-Current Total Cross Section

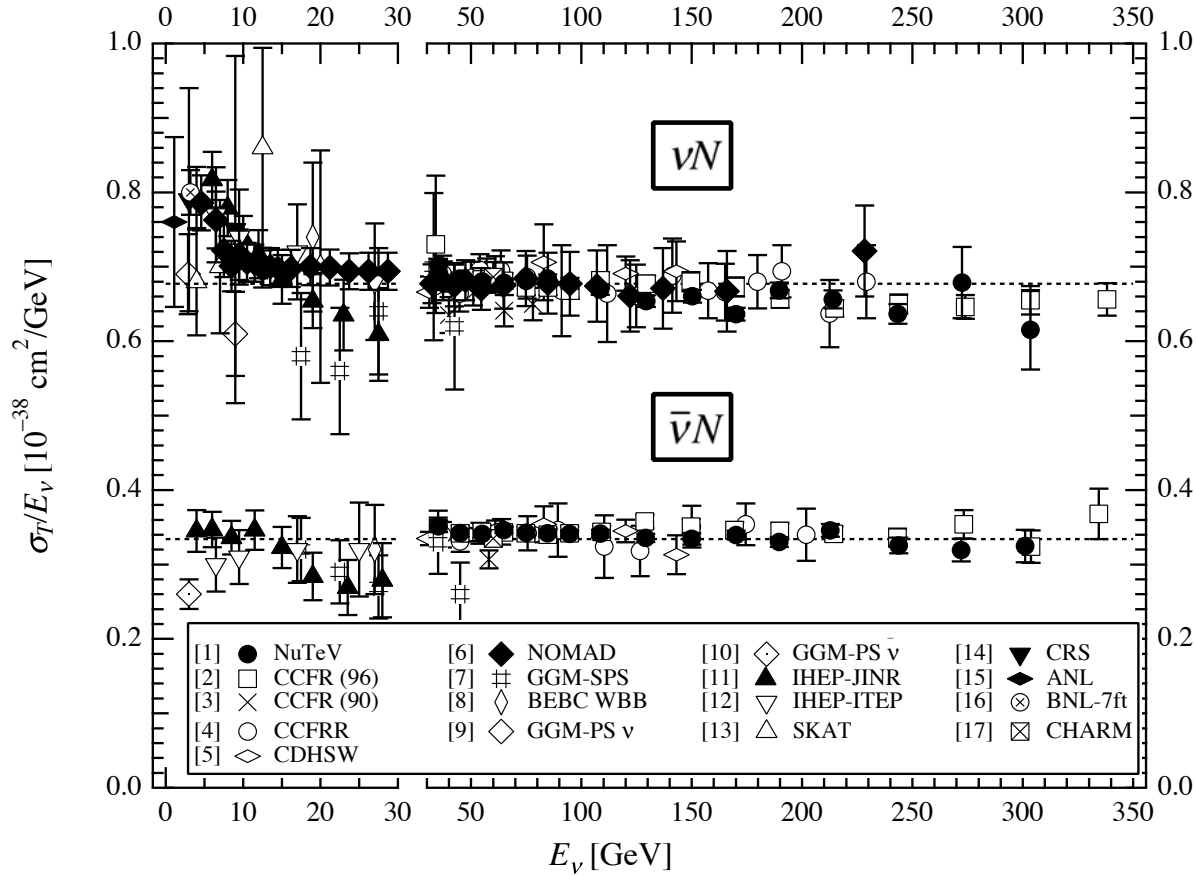


Figure 41.9: σ_T/E_ν for the muon neutrino and anti-neutrino charged-current total cross section as a function of neutrino energy. The error bars include both statistical and systematic errors. The straight lines are the isoscalar-corrected total cross-section values averaged over 30-200 GeV as measured by the experiments in Refs. [3–5]: $\sigma^{\nu Iso}/E_\nu = (0.677 \pm 0.014) \times 10^{-38} \text{cm}^2/\text{GeV}$; $\sigma^{\bar{\nu} Iso}/E_{\bar{\nu}} = (0.334 \pm 0.008) \times 10^{-38} \text{cm}^2/\text{GeV}$. The average ratio of the anti-neutrino to neutrino cross section in the energy range 30-200 GeV is $\sigma^{\bar{\nu} Iso}/\sigma^{\nu Iso} = 0.504 \pm 0.003$ as measured by Refs. [1–5]. Note the change in the energy scale at 30 GeV. (Courtesy W. Seligman and M.H. Shaevitz, Columbia University, 2010)

- | | |
|--|---|
| [1] M. Tzanov <i>et al.</i> , Phys. Rev. D74 , 012008 (2006); | [10] O. Erriquez <i>et al.</i> , Phys. Lett. B80 , 309 (1979); |
| [2] W. Seligman, Ph.D. Thesis, Nevis Report 292 (1996); | [11] V.B. Anikeev <i>et al.</i> , Z. Phys. C70 , 39 (1996); |
| [3] P.S. Auchincloss <i>et al.</i> , Z. Phys. C48 , 411 (1990); | [12] A.S. Vovenko <i>et al.</i> , Sov. J. Nucl. Phys. 30 , 527 (1979); |
| [4] D.B. MacFarlane <i>et al.</i> , Z. Phys. C26 , 1 (1984); | [13] D.S. Baranov <i>et al.</i> , Phys. Lett. B81 , 255 (1979); |
| [5] P. Berge <i>et al.</i> , Z. Phys. C35 , 443 (1987); | [14] C. Baltay <i>et al.</i> , Phys. Rev. Lett. 44 , 916 (1980); |
| [6] Q. Wu <i>et al.</i> , Phys. Lett. B660 , 19 (2008); | [15] S.J. Barish <i>et al.</i> , Phys. Lett. B66 , 291 (1977); |
| [7] J. Morfin <i>et al.</i> , Phys. Lett. B104 , 235 (1981); | [16] N.J. Baker <i>et al.</i> , Phys. Rev. D25 , 617 (1982); |
| [8] D.C. Colley <i>et al.</i> , Z. Phys. C2 , 187 (1979); | [17] J.V. Allaby <i>et al.</i> , Z. Phys. C38 , 403 (1988). |
| [9] S. Campolillo <i>et al.</i> , Phys. Lett. B84 , 281 (1979); | |

Table 41.2: Total hadronic cross section. Analytic S -matrix and Regge theory suggest a variety of parameterizations of total cross sections at high energies with different areas of applicability and fits quality.

A ranking procedure, based on measures of different aspects of the quality of the fits to the current evaluated experimental database, allows one to single out the following parameterization of highest rank[1]

$$\sigma^{ab} = Z^{ab} + B \log^2(s/s_0) + Y_1^{ab}(s_1/s)^{\eta_1} - Y_2^{ab}(s_1/s)^{\eta_2}, \quad \sigma^{\bar{a}b} = Z^{ab} + B \log^2(s/s_0) + Y_1^{ab}(s_1/s)^{\eta_1} + Y_2^{ab}(s_1/s)^{\eta_2},$$

where Z^{ab}, B, Y_i^{ab} are in mb, and $s, s_1,$ and s_0 are in GeV^2 . The scales $s_0, s_1,$ the rate of universal rise of the cross sections $B,$ and exponents η_1 and η_2 are independent of the colliding particles. The scale s_1 is fixed at 1 GeV^2 . Terms $Z^{ab} + B \log^2(s/s_0)$ represent the pomerons. The exponents η_1 and η_2 represent lower-lying C -even and C -odd exchanges, respectively. Requiring $\eta_1 = \eta_2$ results in somewhat poorer fits. In addition to total cross sections $\sigma,$ the measured ratios of the real-to-imaginary parts of the forward scattering amplitudes $\rho = \text{Re}(T)/\text{Im}(T)$ were included in the fits by using s to u crossing symmetry. Global fits were made to the 2005-updated data for $\bar{p}(p)p, \Sigma^-p, \pi^\pm p, K^\pm p, \gamma p,$ and $\gamma\gamma$ collisions.

Exact factorization hypothesis in the form $(Z^{\gamma p}, B^{\gamma p}) = \delta \cdot (Z^{pp}, B), (Z^{\gamma\gamma}, B^{\gamma\gamma}) = \delta^2 \cdot (Z^{pp}, B)$ was used to extend the universal rise of the total hadronic cross sections to the $\gamma p \rightarrow \text{hadrons}$ and $\gamma\gamma \rightarrow \text{hadrons}$ collisions. This resulted in reducing the number of adjusted parameters from 21 used for the 2002 edition to 19, and in the higher quality rank of the parameterization. The asymptotic parameters thus obtained were then fixed and used as inputs to a fit to a larger data sample that included cross sections on deuterons (d) and neutrons (n). All fits included data above $\sqrt{s_{\text{min}}} = 5 \text{ GeV}$.

Fits to $\bar{p}(p)p, \Sigma^-p, \pi^\pm p, K^\pm p, \gamma p, \gamma\gamma$			Beam/ Target	Fits to groups				χ^2/dof by groups
Z	Y_1	Y_2		Z	Y_1	Y_2	B	
35.45(48)	42.53(1.35)	33.34(1.04)	$\bar{p}(p)/p$	35.45(48)	42.53(23)	33.34(33)	0.308(10)	1.029
			$\bar{p}(p)/n$	35.80(16)	40.15(1.59)	30.00(96)	0.308(10)	
35.20(1.46)	-199(102)	-264(126)	Σ^-/p	35.20(1.41)	-199(86)	-264(112)	0.308(10)	0.565
20.86(40)	19.24(1.22)	6.03(19)	π^\pm/p	20.86(3)	19.24(18)	6.03(9)	0.308(10)	0.955
17.91(36)	7.1(1.5)	13.45(40)	K^\pm/p	17.91(3)	7.14(25)	13.45(13)	0.308(10)	0.669
			K^\pm/n	17.87(6)	5.17(50)	7.23(28)	0.308(10)	
	0.0317(6)		γ/p		0.0320(40)		0.308(10)	0.766
	-0.61(62)E-3		γ/γ		-0.58(61)E-3		0.308(10)	
$\chi^2/dof = 0.971,$	$B = 0.308(10) \text{ mb},$		$\bar{p}(p)/d$	64.35(38)	130(3)	85.5(1.3)	0.537(31)	1.432
$\eta_1 = 0.458(17),$	$\eta_2 = 0.545(7)$		π^\pm/d	38.62(21)	59.62(1.53)	1.60(41)	0.461(14)	0.735
$\delta = 0.00308(2),$	$\sqrt{s_0} = 5.38(50) \text{ GeV}$		K^\pm/d	33.41(20)	23.66(1.45)	28.70(37)	0.449(14)	0.814

The fitted functions are shown in the following figures, along with one-standard-deviation error bands. When the reduced χ^2 is greater than one, a scale factor has been included to evaluate the parameter values, and to draw the error bands. Where appropriate, statistical and systematic errors were combined quadratically in constructing weights for all fits. On the plots, only statistical error bars are shown. Vertical arrows indicate lower limits on the p_{lab} or E_{cm} range used in the fits.

One can find the details of the global fits and ranking procedure, in the paper [1]. Database is practically the same as for the 2004 edition (it was slightly changed in the low energy regions not used in the fits).

Recently, the statement in [1] that the models with $\log^2(s/s_0)$ asymptotic terms work much better than the models with $\log(s/s_0)$ or $(s/s_0)^\epsilon$ terms was confirmed in [2] and [3], based on matching traditional asymptotic parameterizations with low energy data in different ways. Both these references, however, questioned the statement in [1] on the universality of the coefficient of the $\log^2(s/s_0)$ term for all processes with nucleon and gamma targets. The two references give different predictions at superhigh energies: $\sigma_{\pi N}^{as} > \sigma_{NN}^{as}$ [2] and $\sigma_{\pi N}^{as} \sim 2/3 \sigma_{NN}^{as}$ [3]. A broader universality of σ_{tot}^{as} has been recently advocated in [4] for hadron-nucleus collisions. It should be noted that asymptotic rate universality in hadron-deuteron collisions has not been established at available energies (see Table).

Computer-readable data files are available at <http://pdg.lbl.gov/current/xsect/>. (Courtesy of the COMPAS group, IHEP, Protvino, August 2005)

On-line ‘‘Predictor’’ to calculate σ and ρ for any energy from five high rank models is also available at <http://nuclth02.phys.ulg.ac.be/compete/predictor/>.

References:

1. J.R. Cudell *et al.* (COMPETE Collab.), Phys. Rev. **D65**, 074024 (2002).
2. K. Igi and M. Ishida, Phys. Rev. **D66**, 034023 (2002), Phys. Lett. **B622**, 286 (2005).
3. M. M. Block and F. Halzen, Phys. Rev. **D70**, 091901 (2004), Phys. Rev. **D72**, 036006 (2005).
4. L. Frankfurt, M. Strikman, and M. Zhalov, Phys. Lett. **B616**, 59 (2005).

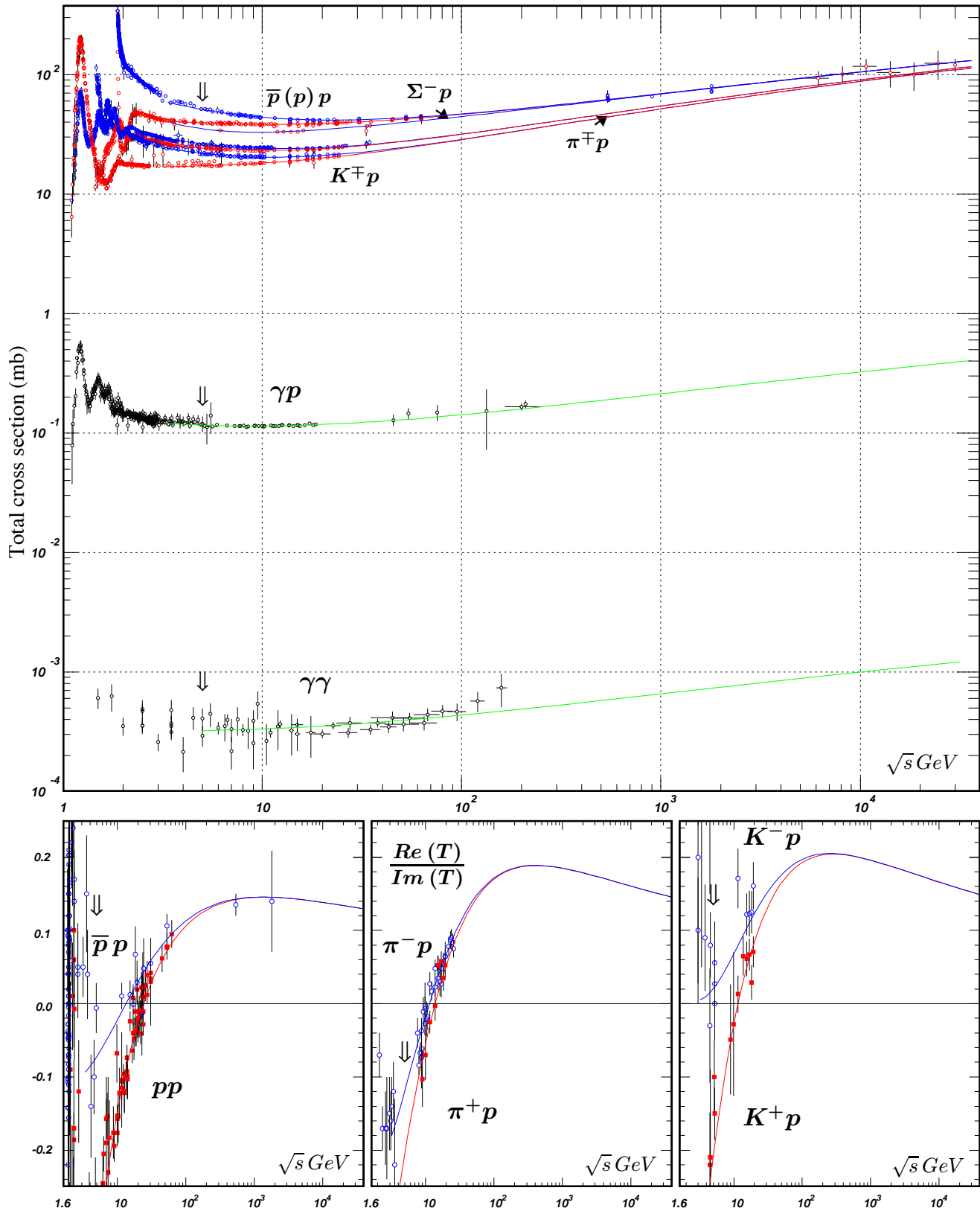


Figure 41.10: Summary of hadronic, γp , and $\gamma\gamma$ total cross sections, and ratio of the real to imaginary parts of the forward hadronic amplitudes. Corresponding computer-readable data files may be found at <http://pdg.lbl.gov/current/xsect/>. (Courtesy of the COMPAS group, IHEP, Protvino, August 2005.) See full-color version on color pages at end of book.

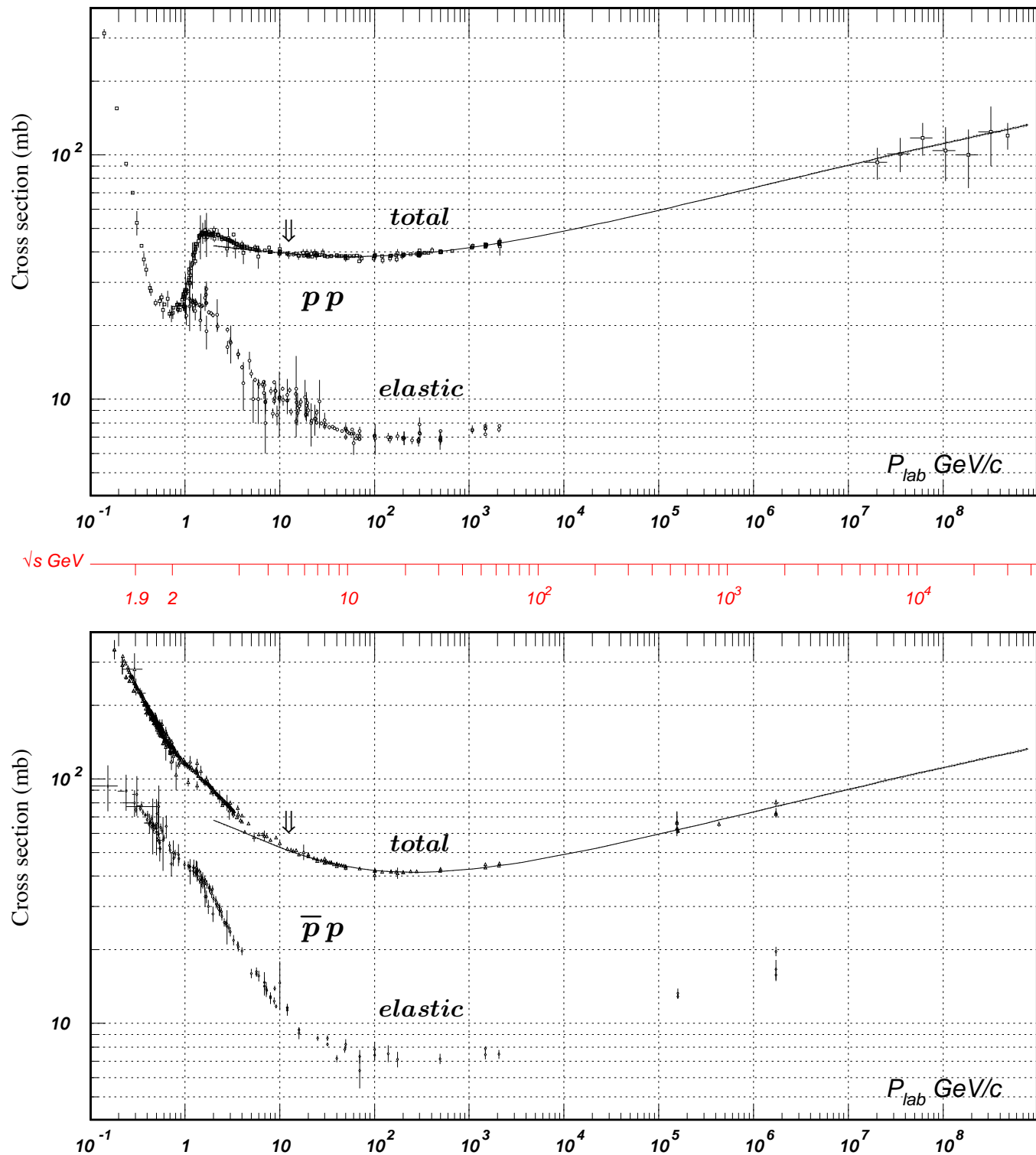


Figure 41.11: Total and elastic cross sections for pp and $\bar{p}p$ collisions as a function of laboratory beam momentum and total center-of-mass energy. Corresponding computer-readable data files may be found at <http://pdg.lbl.gov/current/xsect/>. (Courtesy of the COMPAS group, IHEP, Protvino, August 2005)

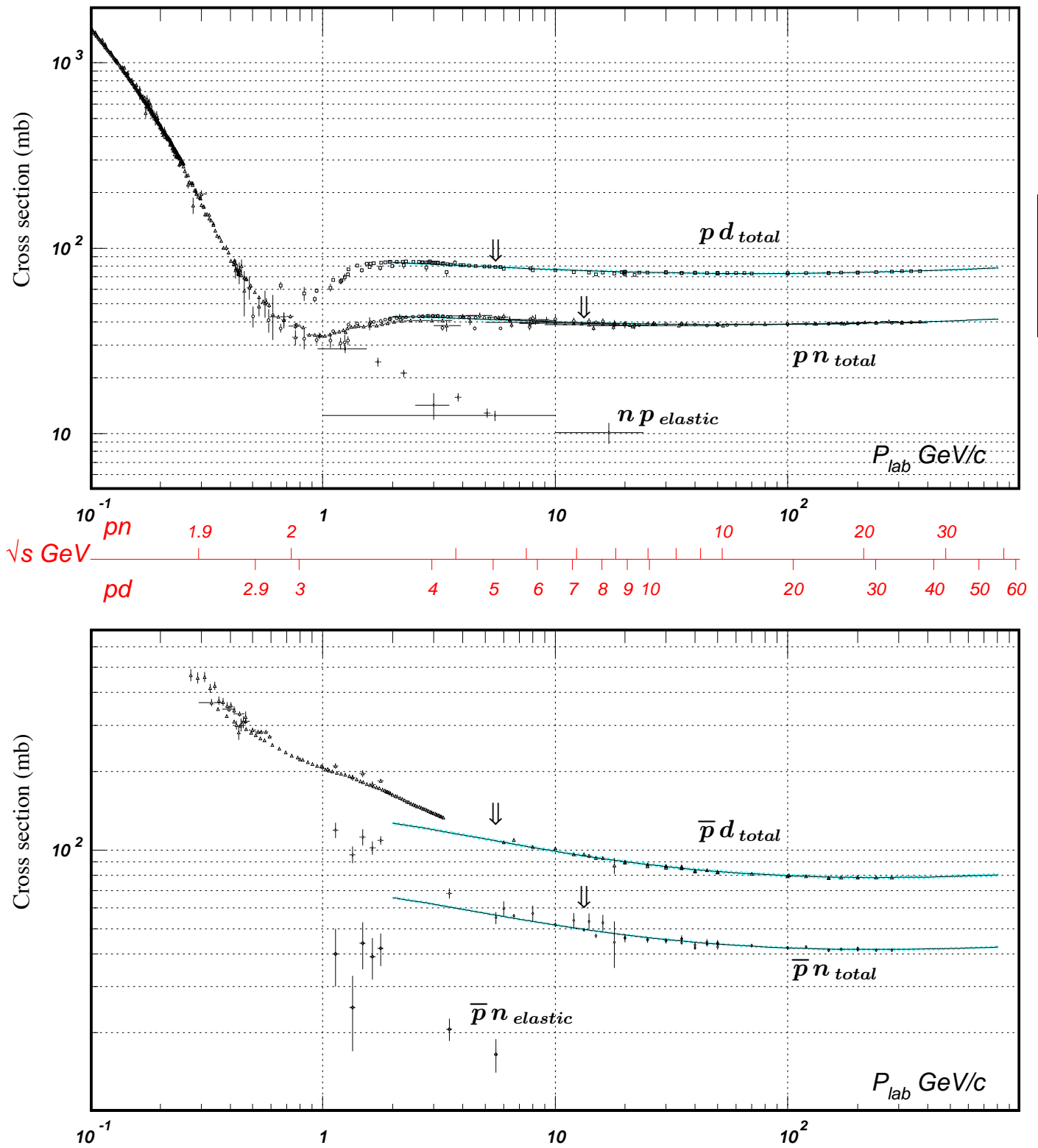


Figure 41.12: Total and elastic cross sections for pd (total only), np , $\bar{p}d$ (total only), and $\bar{p}n$ collisions as a function of laboratory beam momentum and total center-of-mass energy. Corresponding computer-readable data files may be found at <http://pdg.lbl.gov/current/xsect/>. (Courtesy of the COMPAS Group, IHEP, Protvino, August 2005)

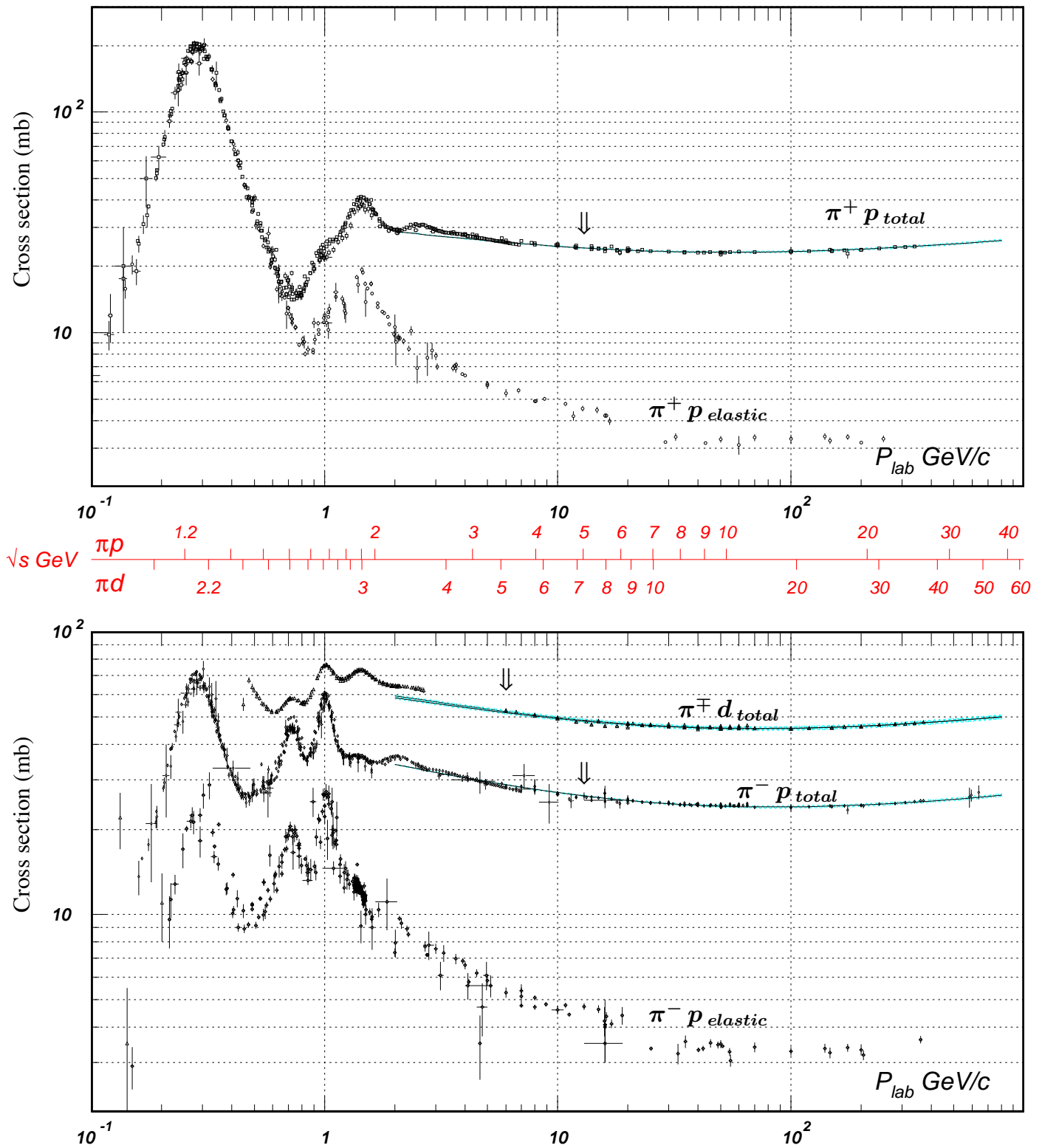


Figure 41.13: Total and elastic cross sections for $\pi^\pm p$ and $\pi^\pm d$ (total only) collisions as a function of laboratory beam momentum and total center-of-mass energy. Corresponding computer-readable data files may be found at <http://pdg.lbl.gov/current/xsect/>. (Courtesy of the COMPAS Group, IHEP, Protvino, August 2005)

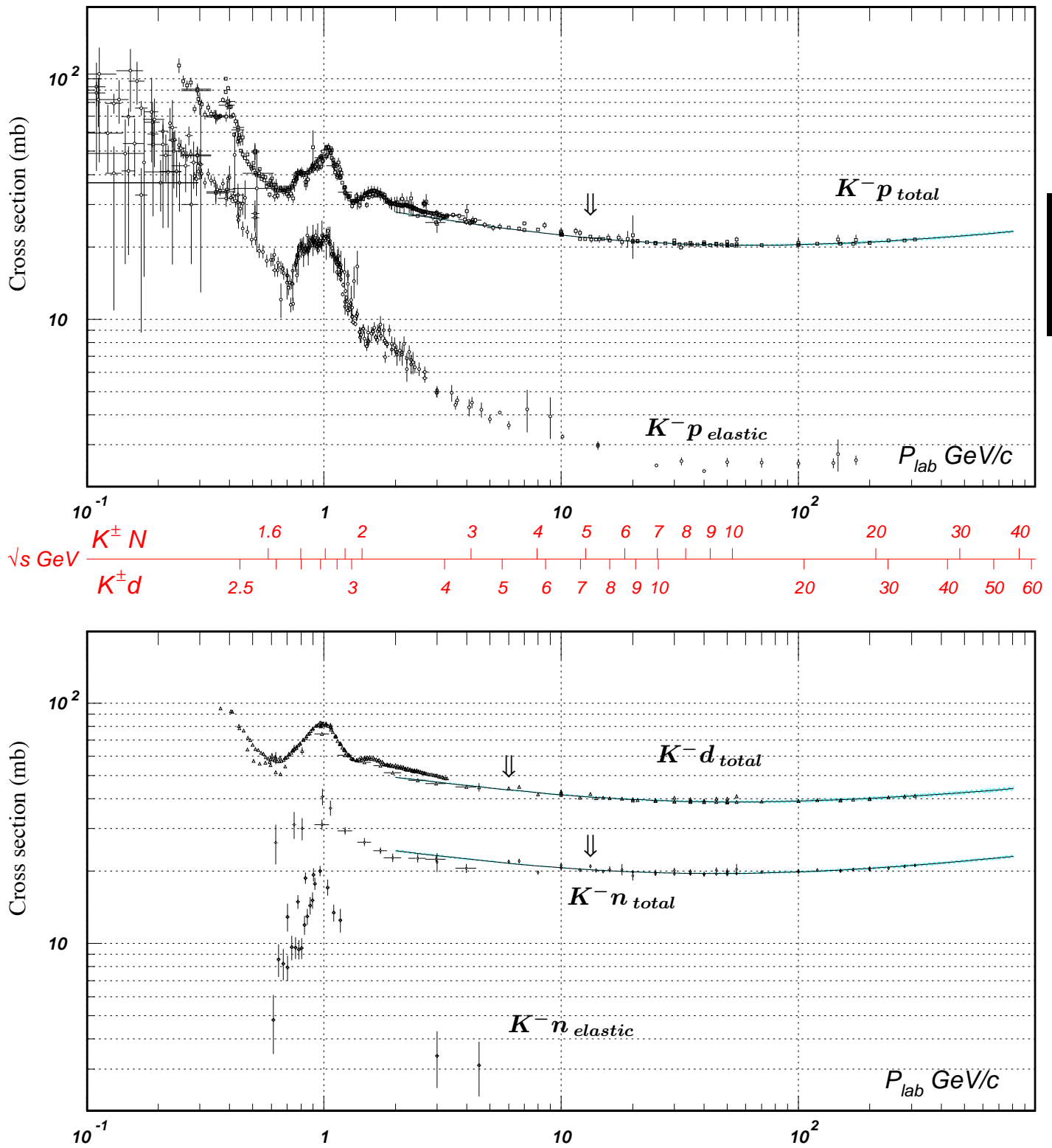


Figure 41.14: Total and elastic cross sections for K^-p and K^-d (total only), and K^-n collisions as a function of laboratory beam momentum and total center-of-mass energy. Corresponding computer-readable data files may be found at <http://pdg.lbl.gov/current/xsect/>. (Courtesy of the COMPAS Group, IHEP, Protvino, August 2005)

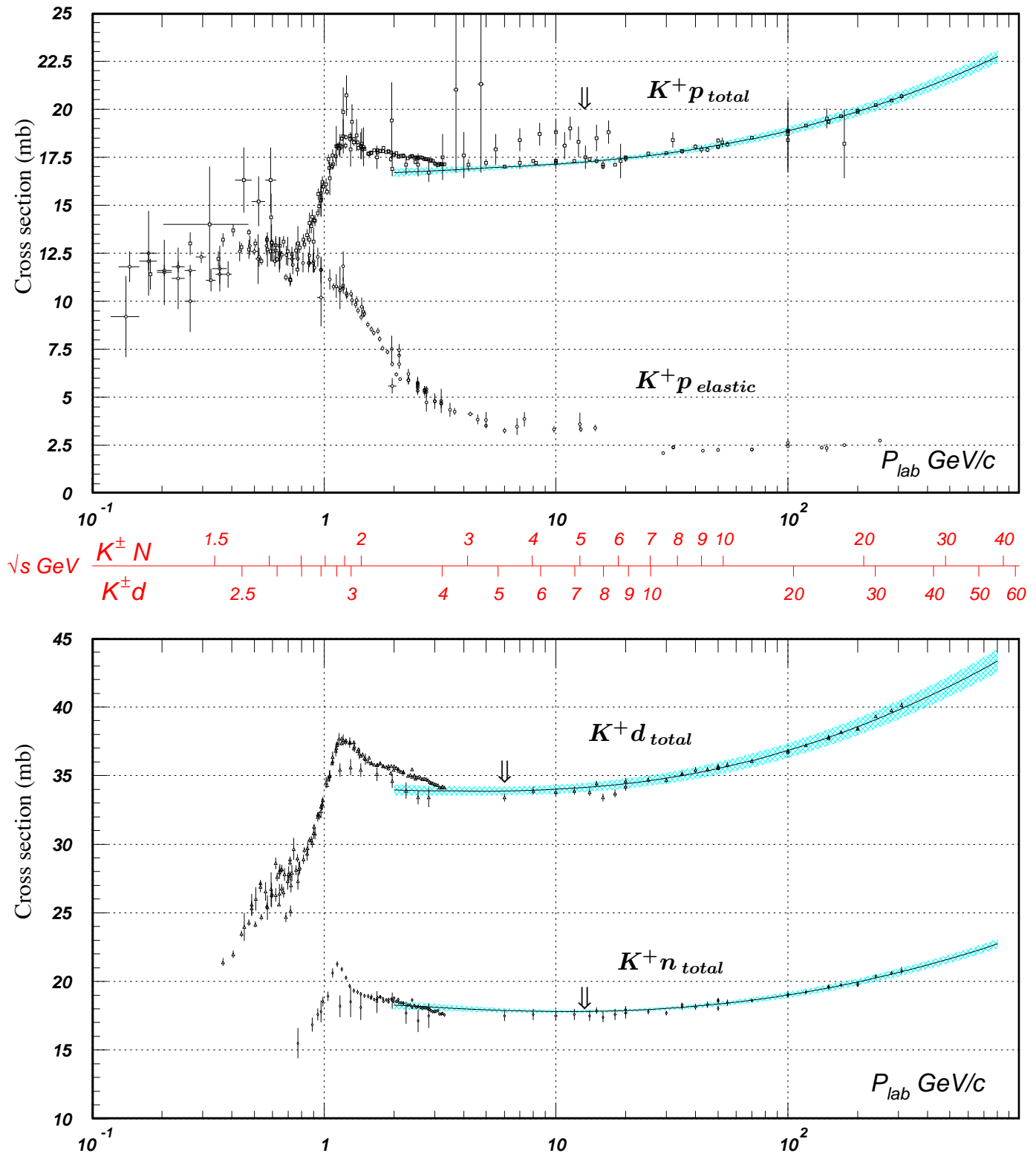


Figure 41.15: Total and elastic cross sections for K^+p and total cross sections for K^+d and K^+n collisions as a function of laboratory beam momentum and total center-of-mass energy. Corresponding computer-readable data files may be found at <http://pdg.lbl.gov/current/xsect/>. (Courtesy of the COMPAS Group, IHEP, Protvino, August 2005)

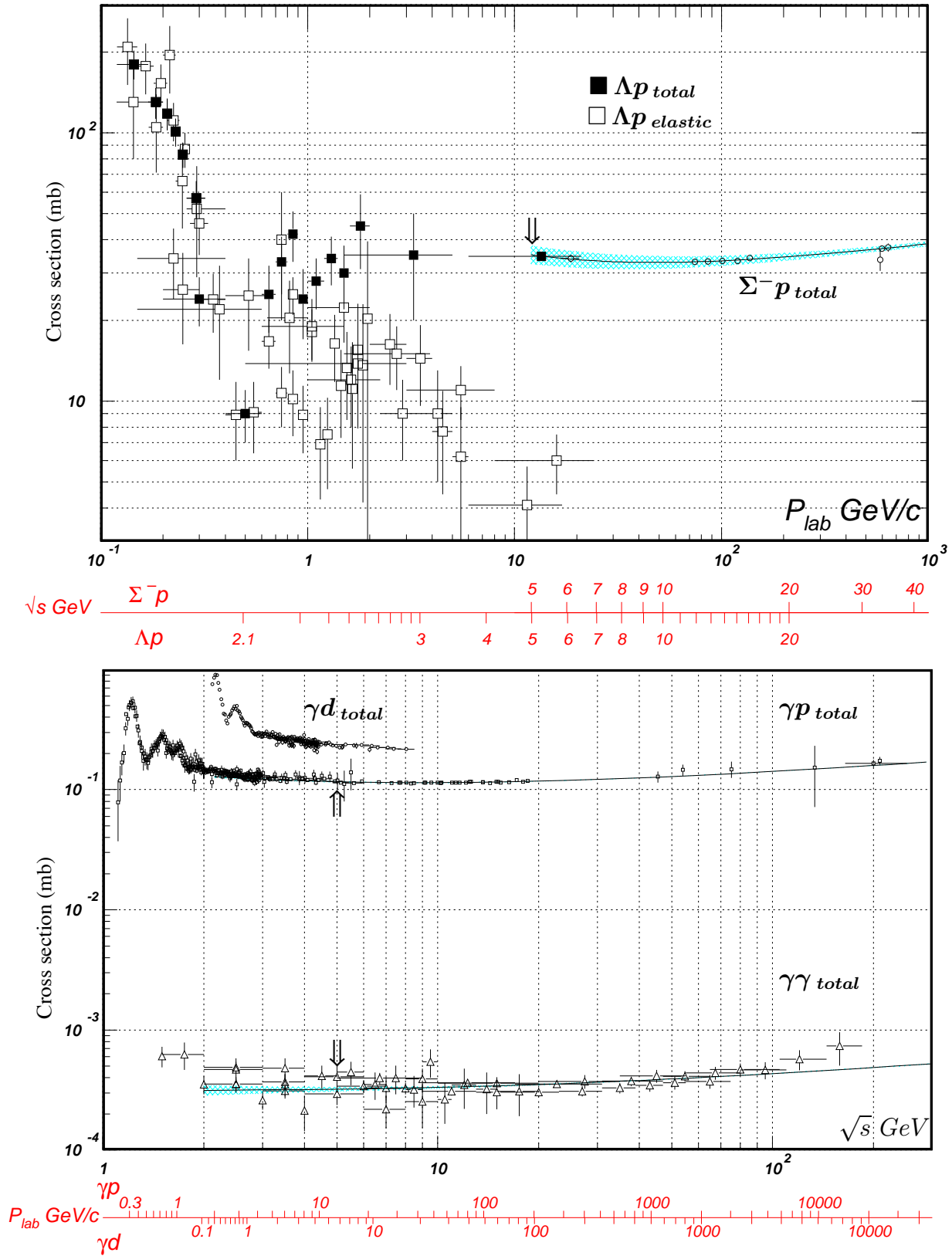


Figure 41.16: Total and elastic cross sections for Λp , total cross section for $\Sigma^- p$, and total hadronic cross sections for γd , γp , and $\gamma\gamma$ collisions as a function of laboratory beam momentum and the total center-of-mass energy. Corresponding computer-readable data files may be found at <http://pdg.lbl.gov/current/xsect/>. (Courtesy of the COMPAS group, IHEP, Protvino, August 2005)

INTRODUCTION TO THE PARTICLE LISTINGS

Illustrative key	405
Abbreviations	406





Illustrative Key to the Particle Listings

Name of particle. "Old" name used before 1986 renaming scheme also given if different. See the section "Naming Scheme for Hadrons" for details.

$a_0(1200)$

$$I^G(J^{PC}) = 1^-(0^+)$$

Particle quantum numbers (where known).

OMITTED FROM SUMMARY TABLE
Evidence not compelling, may be a kinematic effect.

Indicates particle omitted from Particle Physics Summary Table, implying particle's existence is not confirmed.

Quantity tabulated below.

$a_0(1200)$ MASS

Top line gives our best value (and error) of quantity tabulated here, based on weighted average of measurements used. Could also be from fit, best limit, estimate, or other evaluation. See next page for details.

VALUE (MeV)	EVTS	DOCUMENT ID	TECN	CHG	COMMENT
1206 ± 7 OUR AVERAGE					
1210 ± 8 ± 9	3000	FENNER 87	MMS	-	3.5 $\pi^- p$
1198 ± 10		PIERCE 83	ASPK	+	2.1 $K^- p$
1216 ± 11 ± 9	1500	MERRILL 81	HBC	0	3.2 $K^- p$
• • • We do not use the following data for averages, fits, limits, etc. • • •					
1192 ± 16		LYNCH 81	HBC	±	2.7 $\pi^- p$
¹ Systematic error was added quadratically by us in our 1986 edition.					

General comments on particle.

Footnote number linking measurement to text of footnote.

"Document id" for this result; full reference given below.

Measurement technique. (See abbreviations on next page.)

Number of events above background.

$a_0(1200)$ WIDTH

Measured value used in averages, fits, limits, etc.

VALUE (MeV)	EVTS	DOCUMENT ID	TECN	CHG	COMMENT
41 ± 11 OUR AVERAGE					Error includes scale factor of 1.8. See the ideogram below.
50 ± 8		PIERCE 83	ASPK	+	2.1 $K^- p$
70 + 30 - 20	200	LYNCH 81	HBC	±	2.7 $\pi^- p$
25 ± 5 ± 7		MERRILL 81	HBC	0	3.2 $K^- p$
• • • We do not use the following data for averages, fits, limits, etc. • • •					
<60		FENNER 87	MMS	±	3.5 $\pi^- p$

Scale factor > 1 indicates possibly inconsistent data.

Reaction producing particle, or general comments.

Error in measured value (often statistical only; followed by systematic if separately known; the two are combined in quadrature for averaging and fitting.)

"Change bar" indicates result added or changed since previous edition.

Measured value *not* used in averages, fits, limits, etc. See the Introductory Text for explanations.

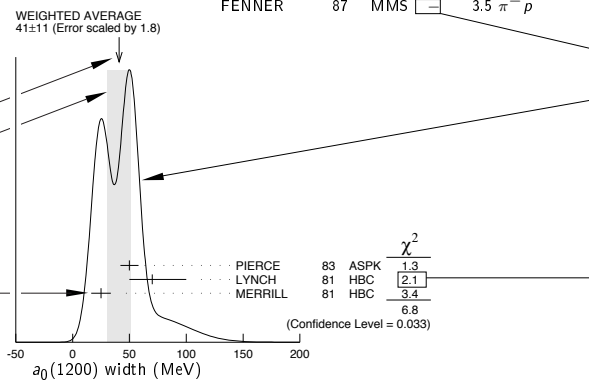
Charge(s) of particle(s) detected.

Arrow points to weighted average.

Shaded pattern extends ±1σ (scaled by "scale factor" S) from weighted average.

Ideogram to display possibly inconsistent data. Curve is sum of Gaussians, one for each experiment (area of Gaussian = 1/error; width of Gaussian = ±error). See Introductory Text for discussion.

Value and error for each experiment.



Contribution of experiment to χ^2 (if no entry present, experiment not used in calculating χ^2 or scale factor because of very large error).

$a_0(1200)$ DECAY MODES

Partial decay mode (labeled by Γ_i).

Mode	Fraction (Γ_i/Γ)	Scale factor/ Confidence level
Γ_1 3π	(65.2 ± 1.3) %	S=1.7
Γ_2 $K\bar{K}$	(34.8 ± 1.3) %	S=1.7
Γ_3 $\eta\pi^\pm$	< 4.9 × 10 ⁻⁴	CL=95%

Our best value for branching fraction as determined from data averaging, fitting, evaluating, limit selection, etc. This list is basically a compact summary of results in the Branching Ratio section below.

$a_0(1200)$ BRANCHING RATIOS

Branching ratio.

$\Gamma(3\pi)/\Gamma_{total}$	VALUE	DOCUMENT ID	TECN	CHG	COMMENT
0.652 ± 0.013 OUR FIT					Error includes scale factor of 1.7.
0.643 ± 0.010 OUR AVERAGE					
0.64 ± 0.01		PIERCE 83	ASPK	+	2.1 $K^- p$
0.74 ± 0.06		MERRILL 81	HBC	0	3.2 $K^- p$
• • • We do not use the following data for averages, fits, limits, etc. • • •					
0.48 ± 0.15		² LYNCH 81	HBC	±	2.7 $\pi^- p$
² Data has questionable background subtraction.					

Our best value (and error) of quantity tabulated, as determined from constrained fit (using *all significant* measured branching ratios for this particle).

Weighted average of measurements of this ratio only.

Footnote (referring to LYNCH 81).

Confidence level for measured upper limit.

$\Gamma(K\bar{K})/\Gamma_{total}$	VALUE	DOCUMENT ID	TECN	CHG	COMMENT	
0.348 ± 0.013 OUR FIT					Error includes scale factor of 1.7.	
0.35 ± 0.05		PIERCE 83	ASPK	+	2.1 $K^- p$	
$\Gamma(K\bar{K})/\Gamma(3\pi)$	VALUE	DOCUMENT ID	TECN	CHG	COMMENT	
0.535 ± 0.030 OUR FIT					Error includes scale factor of 1.7.	
0.50 ± 0.03		MERRILL 81	HBC	0	3.2 $K^- p$	
$\Gamma(\eta(\text{neutral decay})\pi^\pm)/\Gamma_{total}$	VALUE (units 10 ⁻⁴)	CL%	DOCUMENT ID	TECN	CHG	COMMENT
<3.5		95	PIERCE 83	ASPK	+	2.1 $K^- p$

References, ordered inversely by year, then author.

$a_0(1200)$ REFERENCES

"Document id" used on data entries above.

FENNER 87	PRL 55 14	H. Fenner et al.	(SLAC)
PIERCE 83	PL 123B 230	J.H. Pierce	(FNAL) JUP
LYNCH 81	PR D24 610	G.R. Lynch et al.	(CLEO Collab.)
MERRILL 81	PRL 47 143	D.W. Merrill et al.	(SACL, CERN)

Journal, report, preprint, etc. (See abbreviations on next page.)

Partial list of author(s) in addition to first author.

Quantum number determinations in this reference.

Institution(s) of author(s). (See abbreviations on next page.)

Abbreviations Used in the Particle Listings

Indicator of Procedure Used to Obtain Our Result

OUR AVERAGE	From a weighted average of selected data.
OUR FIT	From a constrained or overdetermined multiparameter fit of selected data.
OUR EVALUATION	Not from a direct measurement, but evaluated from measurements of other quantities.
OUR ESTIMATE	Based on the observed range of the data. Not from a formal statistical procedure.
OUR LIMIT	For special cases where the limit is evaluated by us from measured ratios or other data. Not from a direct measurement.

Measurement Techniques

(i.e., Detectors and Methods of Analysis)

ACCM	ACCMOR Collaboration
AEMS	Argonne effective mass spectrometer
ALEP	ALEPH – CERN LEP detector
AMND	AMANDA South Pole neutrino detector
AMY	AMY detector at KEK-TRISTAN
APEX	FNAL APEX Collab.
ARG	ARGUS detector at DORIS
ARGD	Fit to semicircular amplitude path on Argand diagram
ASP	Anomalous single-photon detector
ASPK	Automatic spark chambers
ASTE	ASTERIX detector at LEAR
ASTR	Astronomy
B787	BNL experiment 787 detector
B791	BNL experiment 791 detector
B845	BNL experiment 845 detector
B852	BNL E-852
B865	BNL E865 detector
B871	BNL experiment 871 detector
B949	BNL E949 detector at AGS
BABR	BaBar Collab.
BAKS	Baksan underground scintillation telescope
BC	Bubble chamber
BDMP	Beam dump
BEAT	CERN BEATRICE Collab.
BEBC	Big European bubble chamber at CERN
BELL	Belle Collab.
BES	BES Beijing Spectrometer at Beijing Electron-Positron Collider
BES2	BES Beijing Spectrometer at Beijing Electron-Positron Collider
BIS2	BIS-2 spectrometer at Serpukhov
BKEI	BENKEI spectrometer system at KEK Proton Synchrotron
BOLO	Bolometer, a cryogenic thermal detector
BONA	Bonanza nonmagnetic detector at DORIS
BORX	BOREXINO
BPWA	Barrelet-zero partial-wave analysis
CALO	Calorimeter
CAST	CAST experiment at CERN
CBAL	Crystal Ball detector at SLAC-SPEAR or DORIS
CBAR	Crystal Barrel detector at CERN-LEAR
CBOX	Crystal Box at LAMPF
CC	Cloud chamber
CCFR	Columbia-Chicago-Fermilab-Rochester detector
CDF	Collider detector at Fermilab
CDF2	CDF-II Collab.
CDHS	CDHS neutrino detector at CERN
CDMS	CDMS Collab.
CELL	CELLO detector at DESY
CGNT	CoGeNT dark matter search experiment
CHER	Cherenkov detector
CHM2	CHARM-II neutrino detector (glass) at CERN
CHOZ	Nuclear Power Station near Chooz, France
CHRM	CHARM neutrino detector (marble) at CERN
CHRS	CHORUS Collaboration – CERN SPS
CIB	Cosmic Infrared Background
CIBS	CERN-IHEP boson spectrometer
CLAS	Jefferson CLAS Collab.
CLE2	CLEO II detector at CESR
CLE3	CLEO III detector at CESR
CLEO	Cornell magnetic detector at CESR
CMB	Cosmic Microwave Background
CMD	Cryogenic magnetic detector at VEPP-2M, Novosibirsk
CMD2	Cryogenic magnetic detector 2 at VEPP-2M, Novosibirsk
CNTR	Counters
COSM	Cosmology and astrophysics
COSY	COSY-TOF Collaboration

COUP	COUPP (the Chicagoland Observatory for Underground Particle Physics) Collab.
CPLR	CPLEAR Collaboration
CRES	CRESST cryogenic detector
CRYB	Crystal Ball at BNL
CRYM	Crystal Ball detector at Mainz Microtron MAMI
CSB2	Columbia U. - Stony Brook BGO calorimeter inserted in NaI array
CSME	COSME Collaboration
CUOR	CUORICINO experiment at Gran Sasso Laboratory.
CUSB	Columbia U. - Stony Brook segmented NaI detector at CESR
D0	D0 detector at Fermilab Tevatron Collider
DAMA	DAMA, dark matter detector at Gran Sasso National Lab.
DASP	DESY double-arm spectrometer
DBC	Deuterium bubble chamber
DLCO	DELCO detector at SLAC-SPEAR or SLAC-PEP
DLPH	DELPHI detector at LEP
DM1	Magnetic detector no. 1 at Orsay DCI collider
DM2	Magnetic detector no. 2 at Orsay DCI collider
DONU	DONUT Collab.
DPWA	Energy-dependent partial-wave analysis
E621	Fermilab E621 detector
E653	Fermilab E653 detector
E665	Fermilab E665 detector
E687	Fermilab E687 detector
E691	Fermilab E691 detector
E705	Fermilab E705 Spectrometer-Calorimeter
E731	Fermilab E731 Spectrometer-Calorimeter
E756	Fermilab E756 detector
E760	Fermilab E760 detector
E761	Fermilab E761 detector
E771	Fermilab E771 detector
E773	Fermilab E773 Spectrometer-Calorimeter
E789	Fermilab E789 detector
E791	Fermilab E791 detector
E799	Fermilab E799 Spectrometer-Calorimeter
E835	Fermilab E835 detector
EDEL	EDELWEISS dark matter search Collaboration
EHS	Four-pi detector at CERN
ELEC	Electronic combination
EMC	European muon collaboration detector at CERN
EMUL	Emulsions
FAST	Fiber Active Scintillator Target detector at PSI
FBC	Freon bubble chamber
FENI	FENICE (at the ADONE collider of Frascati)
FIT	Fit to previously existing data
FMPS	Fermilab Multiparticle Spectrometer
FOCS	FNAL E831 FOCUS Collab.
FRAB	ADONE $B\bar{B}$ group detector
FRAG	ADONE $\gamma\gamma$ group detector
FRAM	ADONE MEA group detector
FREJ	FREJUS Collaboration – modular flash chamber detector (calorimeter)
GA24	Hodoscope Cherenkov γ calorimeter (IHEP GAMS-2000) (CERN GAMS-4000)
GALX	GALLEX solar neutrino detector in the Gran Sasso Underground Lab.
GAM2	IHEP hodoscope Cherenkov γ calorimeter GAMS-2000
GAM4	CERN hodoscope Cherenkov γ calorimeter GAMS-4000
GAMS	IHEP hodoscope Cherenkov γ calorimeter GAMS-4 π
GNO	Gallium Neutrino Observatory, Gran Sasso Underground Lab.
GOLI	CERN Goliath spectrometer
H1	H1 detector at DESY/HERA
HBC	Hydrogen bubble chamber
HDBC	Hydrogen and deuterium bubble chambers
HDMO	Heidelberg-Moscow Experiment
HDMS	Heidelberg Dark Matter Search Experiment
HEBC	Helium bubble chamber
HEPT	Helium proportional tubes
HERB	HERA-B detector at DESY/HERA
HERM	HERMES detector at DESY/HERA
HFS	Hyperfine structure
HLBC	Heavy-liquid bubble chamber
HOME	Homestake underground scintillation detector
HPGE	High-purity Germanium detector
HPW	Harvard-Pennsylvania-Wisconsin detector
HRS	SLAC high-resolution spectrometer
HYBR	Hybrid: bubble chamber + electronics

Abbreviations Used in the Particle Listings

HYCP	HyperCP Collab. (FNAL E-871)	PIBE	The PIBETA detector at the Paul Scherrer Institute (PSI), Switzerland.
ICAR	ICARUS experiment at Gran Sasso Laboratory.	PICA	PICASSO dark matter search experiment
ICCB	IceCube neutrino detector at South Pole	PLAS	Plastic detector
IGEX	IGEX Collab.	PLUT	DESY PLUTO detector
IMB	Irvine-Michigan-Brookhaven underground Cherenkov detector	PWA	Partial-wave analysis
IMB3	Irvine-Michigan-Brookhaven underground Cherenkov detector	REDE	Resonance depolarization
INDU	Magnetic induction	RICE	Radio Ice Cherenkov Experiment
IPWA	Energy-independent partial-wave analysis	RVUE	Review of previous data
ISTR	IHEP ISTR+ spectrometer-calorimeter	SAGE	US - Russian Gallium Experiment
JADE	JADE detector at DESY	SELX	FNAL SELEX Collab.
K246	KEK E246 detector with polarimeter	SFM	CERN split-field magnet
K2K	KEK to Super-Kamiokande	SHF	SLAC Hybrid Facility Photon Collaboration
K391	KEK E391a detector	SIGM	Serpukhov CERN-IHEP magnetic spectrometer (SIGMA)
K470	KEK-E470 Stopping K detector	SILI	Silicon detector
KAM2	KAMIOKANDE-II underground Cherenkov detector	SIMP	SIMPLE, dark matter detector at Laboratori Nazionali del Sud
KAMI	KAMIOKANDE underground Cherenkov detector	SKAM	Super-Kamiokande Collab.
KAR2	KARMEN2 calorimeter at the ISIS neutron spallation source at Rutherford	SLAX	Solar Axion Experiment in Canfranc Underground Laboratory
KARM	KARMEN calorimeter at the ISIS neutron spallation source at Rutherford	SLD	SLC Large Detector for e^+e^- colliding beams at SLAC
KEDR	detector operating at VEPP-4M collider (Novosibirsk)	SMPL	SIMPLE superheated droplet detector.
KIMS	Korea Invisible Mass Search experiment at YangYang, Korea	SND	Novosibirsk Spherical neutral detector at VEPP-2M
KLND	KamLand Collab. (Japan)	SNDR	SINDRUM spectrometer at PSI
KLOE	KLOE detector at DAFNE (the Frascati e^+e^- collider Italy)	SNO	SNO Collaboration (Sudbury Neutrino Observatory)
KOLR	Kolar Gold Field underground detector	SOU2	Soudan 2 underground detector
KTEV	KTeV Collaboration	SOUD	Soudan underground detector
L3	L3 detector at LEP	SPEC	Spectrometer
LASS	Large-angle superconducting solenoid spectrometer at SLAC	SPED	From maximum of speed plot or resonant amplitude
LATT	Lattice calculations	SPHR	Bonn SAPHIR Collab.
LEBC	Little European bubble chamber at CERN	SPNX	SPHINX spectrometer at IHEP accelerator
LEGS	BNL LEGS Collab.	SPRK	Spark chamber
LENA	Nonmagnetic lead-glass NaI detector at DORIS	SQID	SQUID device
LEP	Combination of all LEP experiments: ALEPH, DELPHI, L3, OPAL	STRC	Streamer chamber
LEPS	Low-Energy Pion Spectrometer at the Paul Scherrer Institute	SVD2	SVD-2 experiment at IHEP, Protvino
LGW	Lead Glass Wall collaboration at SPEAR/SLAC	TASS	DESY TASSO detector
LSD	Mont Blanc liquid scintillator detector	TEVA	Combined analysis of CDF and $D\bar{0}$ experiments
LSND	Liquid Scintillator Neutrino Detector	TEXN	TEXONO Collab., ultra low energy Ge detector at Kuo-Sheng Laboratory
MAC	MAC detector at PEP/SLAC	THEO	Theoretical or heavily model-dependent result
MBOO	Fermilab MiniBooNE neutrino experiment	TNF	TNF-IHEP facility at 70 GeV IHEP accelerator
MBR	Molecular beam resonance technique	TOF	Time-of-flight
MCRO	MACRO detector in Gran Sasso	TOPZ	TOPAZ detector at KEK-TRISTAN
MD1	Magnetic detector at VEPP-4, Novosibirsk	TPC	TPC detector at PEP/SLAC
MDRP	Millikan drop measurement	TPS	Tagged photon spectrometer at Fermilab
MICA	Underground mica deposits	TRAP	Penning trap
MINS	Fermilab MINOS experiment	TWST	TWIST spectrometer at TRIUMF
MIRA	MIRABELLE Liquid-hydrogen bubble chamber	UA1	UA1 detector at CERN
MLEV	Magnetic levitation	UA2	UA2 detector at CERN
MMS	Missing mass spectrometer	UA5	UA5 detector at CERN
MPS	Multiparticle spectrometer at BNL	UKDM	UK Dark Matter Collab.
MPS2	Multiparticle spectrometer upgrade at BNL	VES	Vertex Spectrometer Facility at 70 GeV IHEP accelerator
MPSF	Multiparticle spectrometer at Fermilab	VLBI	Very Long Baseline Interferometer
MPWA	Model-dependent partial-wave analysis	VNS	VENUS detector at KEK-TRISTAN
MRK1	SLAC Mark-I detector	WA75	CERN WA75 experiment
MRK2	SLAC Mark-II detector	WA82	CERN WA82 experiment
MRK3	SLAC Mark-III detector	WA89	CERN WA89 experiment
MRKJ	Mark-J detector at DESY	WARP	Liquid argon detector for CDM searches at Gran Sasso
MRS	Magnetic resonance spectrometer	WASA	WASA detector at CELSIUS, Uppsala and at COSY, Juelich
MUG2	MUON($g-2$)	WIRE	Wire chamber
MWPC	Multi-Wire Proportional Chamber	XE10	XENON10 experiment at Gran Sasso National Laboratory
NA14	CERN NA14	XEBC	Xenon bubble chamber
NA31	CERN NA31 Spectrometer-Calorimeter	ZEP2	ZEPLIN-II dark matter detector
NA32	CERN NA32 Spectrometer	ZEP3	ZEPLIN-III dark matter detector at Palmer Underground Lab.
NA48	CERN NA48 Collaboration	ZEPL	ZEPLIN-I galactic dark matter detector
NA49	CERN NA49	ZEUS	ZEUS detector at DESY/HERA
NA60	CERN NA60 Collaboration		
NAIA	NAIAD (NaI Advanced Detector) dark matter search exp.		
ND	NaI detector at VEPP-2M, Novosibirsk		
NICE	Serpukhov nonmagnetic precision spectrometer		
NMR	Nuclear magnetic resonance		
NOMD	NOMAD Collaboration, CERN SPS		
NTEV	NuTeV Collab. at Fermilab		
NUSX	Mont Blanc NUSEX underground detector		
OBLX	OBELIX detector at LEAR		
OLYA	Detector at VEPP-2M and VEPP-4, Novosibirsk		
OMEG	CERN OMEGA spectrometer		
OPAL	OPAL detector at LEP		
OSPK	Optical spark chamber		

Journals

AA	Astronomy and Astrophysics
ADVP	Advances in Physics
AFIS	Anales de Fisica
AJP	American Journal of Physics
AL	Astronomy Letters
ANP	Annals of Physics
ANPL	Annals of Physics (Leipzig)
ANYAS	Annals of the New York Academy of Sciences
AP	Atomic Physics
APAH	Acta Physica Academiae Scientiarum Hungaricae
APJ	Astrophysical Journal

Abbreviations Used in the Particle Listings

APJS	Astrophysical Journal Suppl.		
APP	Acta Physica Polonica		
APS	Acta Physica Slovaca		
ARNPS	Annual Review of Nuclear and Particle Science		
ARNS	Annual Review of Nuclear Science		
ASP	Astroparticle Physics		
BAPS	Bulletin of the American Physical Society		
BASUP	Bulletin of the Academy of Science, USSR (Physics)		
CJNP	Chinese Journal of Nuclear Physics		
CJP	Canadian Journal of Physics		
CNPP	Comments on Nuclear and Particle Physics		
CTP	Communications in Theoretical Physics		
CZJP	Czechoslovak Journal of Physics		
DANS	Doklady Akademii nauk SSSR		
EPJ	The European Physical Journal		
EPL	Europhysics Letters		
FECAJ	Fizika Elementarnykh Chastits i Atomnogo Yadra		
HADJ	Hadronic Journal		
IJMP	International Journal of Modern Physics		
JAP	Journal of Applied Physics		
JCAP	Journal of Cosmology and Astroparticle Physics		
JETP	English Translation of Soviet Physics ZETF		
JETPL	English Translation of Soviet Physics ZETF Letters		
JHEP	Journal of High Energy Physics		
JINR	Joint Inst. for Nuclear Research		
JINRRC	JINR Rapid Communications		
JPA	Journal of Physics, A		
JPB	Journal of Physics, B		
JPCRD	Journal of Physical and Chemical Reference Data		
JPG	Journal of Physics, G		
JPSJ	Journal of the Physical Society of Japan		
LNC	Lettere Nuovo Cimento		
MNRAS	Monthly Notices of the Royal Astronomical Society		
MPL	Modern Physics Letters		
NAT	Nature		
NC	Nuovo Cimento		
NIM	Nuclear Instruments and Methods		
NJP	New Journal of Physics		
NP	Nuclear Physics		
NPBPS	Nuclear Physics B Proceedings Supplement		
PAN	Physics of Atomic Nuclei (formerly SJNP)		
PD	Physics Doklady (Magazine)		
PDAT	Physik Daten		
PL	Physics Letters		
PN	Particles and Nuclei		
PPCF	Plasma Physics Control Fusion		
PPN	Physics of Particles and Nuclei (formerly SJPN)		
PPNL	Physics of Particles and Nuclei Letters		
PPNP	Progress in Particles and Nuclear Physics		
PPSL	Proc. of the Physical Society of London		
PR	Physical Review		
PRAM	Pramana		
PRL	Physical Review Letters		
PRPL	Physics Reports (Physics Letters C)		
PRSE	Proc. of the Royal Society of Edinburgh		
PRSL	Proc. of the Royal Society of London, Section A		
PS	Physica Scripta		
PTP	Progress of Theoretical Physics		
PTPS	Progress of Theoretical Physics Supplement		
PTRSL	Phil. Trans. Royal Society of London		
RA	Radiochimica Acta		
RMP	Reviews of Modern Physics		
RNC	La Rivista del Nuovo Cimento		
RPP	Reports on Progress in Physics		
RRP	Revue Roumaine de Physique		
SCI	Science		
SJNP	Soviet Journal of Nuclear Physics		
SJPN	Soviet Journal of Particles and Nuclei		
SPD	Soviet Physics Doklady (Magazine)		
SPU	Soviet Physics - Uspekhi		
UFN	Usp. Fiz. Nauk - Russian version of SPU		
YAF	Yadernaya Fizika		
ZETF	Zhurnal Eksperimental'noi i Teoreticheskoi Fiziki		
ZETFp	Zhurnal Eksperimental'noi i Teoreticheskoi Fiziki, Pis'ma v Redakts		
ZNAT	Zeitschrift fur Naturforschung		
ZPHY	Zeitschrift fur Physik		
Institutions			
AACH	Phys. Inst. der Techn. Hochschule Aachen (Historical, use for general Inst. der Techn. Hochschule)	Aachen, Germany	
AACH1	I Phys. Inst. B, RWTH Aachen	Aachen, Germany	
AACH3	III Phys. Inst. A, RWTH Aachen Univ.	Aachen, Germany	
AACHT	Inst. für Theoretische Teilchenphysik & Kosmologie, RWTH Aachen	Aachen, Germany	
AARH	Univ. of Aarhus	Aarhus C, Denmark	
ABO	Åbo Akademi Univ.	Turku, Finland	
ADEL	Adelphi Univ.	Garden City, NY, USA	
ADLD	The Univ. of Adelaide ; Dept. of Physics; Centre for Subatomic Structure of Matter (CSSM)	Adelaide, SA, Australia	
AERE	Atomic Energy Research Estab.	Didcot, United Kingdom	
AFRR	Armed Forces Radiobiology Res. Inst.	Bethesda, MD, USA	
AHMED	Physical Research Lab.	Ahmedabad , Gujarat, India	
AICH	Aichi Univ. of Education	Aichi, Japan	
AKIT	Akita Univ.	Akita, Japan	
ALAH	Univ. of Alabama (Huntsville)	Huntsville, AL, USA	
ALAT	Univ. of Alabama (Tuscaloosa)	Tuscaloosa, AL, USA	
ALBA	SUNY at Albany	Albany, NY, USA	
ALBE	Univ. of Alberta	Edmonton, AB, Canada	
AMES	Ames Lab.	Ames, IA, USA	
AMHT	Amherst College	Amherst, MA, USA	
AMST	Univ. van Amsterdam	Amsterdam, The Netherlands	
ANIK	NIKHEF	Amsterdam , The Netherlands	
ANKA	Middle East Technical Univ.; Dept. of Physics; Experimental HEP Lab	Ankara, Turkey	
ANL	Argonne National Lab.; High Energy Physics Division, Bldg. 362; Physics Division, Bldg. 203	Argonne, IL, USA	
ANSM	St. Anselm Coll.	Manchester, NH, USA	
ARCBO	Arecibo Observatory	Arecibo, PR, USA	
ARIZ	Univ. of Arizona	Tucson, AZ, USA	
ARZS	Arizona State Univ.	Tempe, AZ, USA	
ASCI	Russian Academy of Sciences	Moscow , Russian Federation	
AST	Inst. of Phys.	Nankang, Taipei, Taiwan, China	
ATEN	NCSR " Demokritos "	Aghia Paraskevi, Greece	
ATHU	Univ. of Athens	Athens, Greece	
AUCK	Univ. of Auckland	Auckland, New Zealand	
BAKU	Natl. Azerbaijan Academy of Sciences , Inst. of Physics	Baku , Azerbaijan	
BANG	Indian Inst. of Science	Bangalore , India	
BANGB	Bangabasi College	Calcutta, India	
BARC	Univ. Autónoma de Barcelona	Bellaterra (Barcelona), Spain	
BARI	Univ. di Bari	Bari, Italy	
BART	Univ. of Delaware ; Bartol Research Inst.	Newark, DE, USA	
BASL	Inst. für Physik der Univ. Basel	Basel, Switzerland	
BAYR	Univ. Bayreuth	Bayreuth, Germany	
BCEN	Centre d'Etudes Nucleaires de Bordeaux-Gradignan	Gradignan, France	
BCIP	Natl. Inst. for Physics & Nuclear Eng. "Horia Hulubei" (IFIN-HH)	Bucharest -Magurele, Romania	
BELJ	Beijing Univ.	Beijing, China	
BELJT	Inst. of Theoretical Physics	Beijing , China	
BELG	Inter-University Inst. for High Energies (ULB-VUB)	Brussel , Belgium	
BELL	AT & T Bell Labs	Murray Hill, NJ, USA	
BERG	Univ. of Bergen	Bergen, Norway	
BERL	DESY	Zeuthen , Germany	
BERN	Univ. of Berne	Berne, Switzerland	

Abbreviations Used in the Particle Listings

BGNA	Univ. di Bologna , & INFN, Sezione di Bologna; Viale C. Berti Pichat, n. 6/2; Via Irnerio, 46, I-40126 Bologna	Bologna, Italy	CENG	Centre d'Etudes Nucleaires	Grenoble , France
BHAB	Bhabha Atomic Research Center	Trombay, Bombay, India	CERN	CERN , European Organization for Nuclear Research	Genève, Switzerland
BHEP	Inst. of High Energy Physics	Beijing , China	CFPA	Univ. of California , (Berkeley)	Berkeley, CA, USA
BIEL	Univ. Bielefeld	Bielefeld, Germany	CHIC	Univ. of Chicago	Chicago, IL, USA
BING	SUNY at Binghamton	Binghamton, NY, USA	CIAE	China Institute of Atomic Energy	Beijing , China
BIRK	Birkbeck College, Univ. of London	London, United Kingdom	CINC	Univ. of Cincinnati	Cincinnati, OH, USA
BIRM	Univ. of Birmingham	Edgbaston, Birmingham, United Kingdom	CINV	CINVESTAV-IPN, Centro de Investigacion y de Estudios Avanzados del IPN	México , DF, Mexico
BLSU	Bloomsburg Univ.	Bloomsburg, PA, USA	CIT	California Inst. of Tech.	Pasadena, CA, USA
BNL	Brookhaven National Lab.	Upton, NY, USA	CLER	Univ. de Clermont-Ferrand	Aubière, France
BOCH	Ruhr Univ. Bochum	Bochum, Germany	CLEV	Cleveland State Univ.	Cleveland, OH, USA
BOHR	Niels Bohr Inst.	Copenhagen Ø, Denmark	CMNS	Comenius Univ. (FMFI UK)	Bratislava , Slovakia
BOIS	Boise State Univ.	Boise, ID, USA	CMU	Carnegie Mellon Univ.	Pittsburgh, PA, USA
BOMB	Univ. of Bombay	Bombay, India	CNEA	Comisión Nacional de Energía Atómica	Buenos Aires, Argentina
BONN	Rheinische Friedr.-Wilhelms-Univ. Bonn	Bonn, Germany	CNRC	Centre for Research in Particle Physics	Ottawa, ON, Canada
BORD	Univ. de Bordeaux I	Gradignan, France	COLO	Univ. of Colorado	Boulder, CO, USA
BOSE	S.N. Bose National Centre for Basis Sciences	Calcutta, India	COLU	Columbia Univ.	New York, NY, USA
BOSK	"Rudjer Bošković" Inst.	Zagreb, Croatia	CONC	Concordia University	Montreal, PQ, Canada
BOST	Boston Univ.	Boston, MA, USA	CORN	Cornell Univ.	Ithaca, NY, USA
BRAN	Brandeis Univ.	Waltham, MA, USA	COSU	Colorado State Univ.	Fort Collins, CO, USA
BRCO	Univ. of British Columbia	Vancouver, BC, Canada	CPPM	Centre National de la Recherche Scientifique, Luminy	Marseille , France
BRIS	Univ. of Bristol	Bristol, United Kingdom	CRAC	Henryk Niewodnicza'nski Inst. of Nuclear Physics	Kraków , Poland
BROW	Brown Univ.	Providence, RI, USA	CRNL	Chalk River Labs.	Chalk River, ON, Canada
BRUN	Brunel Univ.	Uxbridge, Middlesex, United Kingdom	CSOK	Oklahoma Central State Univ.	Edmond, OK, USA
BRUX	Univ. Libre de Bruxelles ; Service de Physique des Particules Élémentaires	Bruxelles, Belgium	CST	Univ. of Science and Technology of China	Hefei , Anhui 230026, China
BRUXT	Univ. Libre de Bruxelles ; Physique Théorique	Bruxelles, Belgium	CSULB	California State Univ.	Long Beach, CA, USA
BUCH	Univ. of Bucharest	Bucharest-Magurele, Romania	CSUS	California State Univ.	Sacramento, USA
BUDA	KFKI Research Inst. for Particle & Nuclear Physics	Budapest , Hungary	CUNY	City College of New York	New York, NY, USA
BUFF	SUNY at Buffalo	Buffalo, NY, USA	CURCP	Univ. Pierre et Marie Curie (Paris VI), LCP	Paris, France
BURE	Inst. des Hautes Etudes Scientifiques	Bures-sur-Yvette , France	CURIN	Univ. Pierre et Marie Curie (Paris VI), LPNHE	Paris, France
CAEN	Lab. de Physique Corpusculaire, ENSICAEN	Caen , France	CURIT	Univ. Pierre et Marie Curie (Paris VI), LPTHE	Paris, France
CAGL	Univ. degli Studi di Cagliari	Monserato (CA), Italy	DALH	Dalhousie Univ.	Halifax, NS, Canada
CAIR	Cairo University	Orman, Giza, Cairo, Egypt	DARE	Daresbury Lab	Cheshire, United Kingdom
CAIW	Carnegie Inst. of Washington	Washington, DC, USA	DARM	Tech. Hochschule Darmstadt	Darmstadt, Germany
CALC	Univ. of Calcutta	Calcutta, India	DELA	Univ. of Delaware ; Dept. of Physics & Astronomy; Bartol Research Inst.	Newark, DE, USA
CAMB	DAMTP	Cambridge, United Kingdom	DELH	Univ. of Delhi	Delhi, India
CAMP	Univ. Estadual de Campinas (UNICAMP)	Campinas , SP, Brasil	DESY	DESY , Deutsches Elektronen-Synchrotron	Hamburg , Germany
CANB	Australian National Univ.	Canberra, ACT, Australia	DFAB	Escuela de Ingenieros	Bilbao , Spain
CANTB	Inst. de Física de Cantabria (CSIC- Univ. Cantabria)	Santander, Spain	DOE	Department of Energy	Washington, DC, USA
CAPE	University of Cape Town	Rondebosch, Cape Town, South Africa	DORT	Technische Univ. Dortmund	Dortmund, Germany
CARA	Univ. Central de Venezuela	Caracas, Venezuela	DUKE	Duke Univ.	Durham, NC, USA
CARL	Carleton Univ.	Ottawa, ON, Canada	DURH	Univ. of Durham	Durham, United Kingdom
CARLC	Carleton College	Northfield, MN, USA	DUUC	University College Dublin	Dublin, Ireland
CASE	Case Western Reserve Univ.	Cleveland, OH, USA	EDIN	Univ. of Edinburgh	Edinburgh, United Kingdom
CAST	China Center of Advanced Science and Technology	Beijing, China	EFI	Univ. of Chicago, The Enrico Fermi Inst.	Chicago , IL, USA
CATA	Univ. di Catania	Catania, Italy	ELMT	Elmhurst College	Elmhurst, IL, USA
CATH	Catholic Univ. of America	Washington, DC, USA	ENSP	l'Ecole Normale Supérieure	Paris , France
CAVE	Cavendish Lab.	Cambridge, United Kingdom	EOTV	Eötvös University	Budapest, Hungary
CBNM	CBNM	Geel , Belgium	EPOL	École Polytechnique	Palaiseau , France
CCAC	Allegheny College	Meadville, PA, USA	ERLA	Univ. Erlangen-Nurnberg	Erlangen, Germany
CDEF	Univ. Paris VII, Denis Diderot	Paris, France	ETH	Univ. Zürich	Zürich, Switzerland
CEA	Cambridge Electron Accelerator (Historical in <i>Review</i>)	Cambridge, MA , USA	FERR	Univ. di Ferrara	Ferrara, Italy
CEADE	Center for Apl. Studies for Nuclear Physics	Havana, Cuba	FIRZ	Univ. degli Studi di Firenze	Sesto Fiorentino, Italy
CEBAF	Jefferson Lab—Thomas Jefferson National Accelerator Facility	Newport News , VA, USA	FISK	Fisk Univ.	Nashville, TN, USA
			FLOR	Univ. of Florida	Gainesville, FL, USA
			FNAL	Fermilab	Batavia, IL, USA
			FOM	FOM , Stichting voor Fundamenteel Onderzoek der Materie	JP Utrecht , The Netherlands

Abbreviations Used in the Particle Listings

FRAN	Frankfurt Inst. for Advanced Studies (FIAS)	Frankfurt am Main, Germany	IFIC	IFIC (Instituto de Física Corpuscular)	Valencia, Spain
FRAS	Lab. Nazionali di Frascati dell'INFN	Frascati (Roma), Italy	IFRJ	Univ. Federal do Rio de Janeiro	Rio de Janeiro, RJ, Brasil
FREIB	Albert-Ludwigs Univ.	Freiburg , Germany	IIT	Illinois Inst. of Tech.	Chicago, IL, USA
FREIE	Freie Univ. Berlin	Berlin, Germany	ILL	Univ. of Illinois at Urbana-Champaign	Urbana, IL, USA
FRIB	Univ. de Fribourg	Fribourg, Switzerland	ILLC	Univ. of Illinois at Chicago	Chicago, IL, USA
FSU	Florida State Univ.; High Energy Physics	Tallahassee, FL, USA	ILLG	Inst. Laue-Langevin	Grenoble, France
FSUSC	Florida State Univ.; SCS (School of Computational Science)	Tallahassee, FL, USA	IND	Indiana Univ.	Bloomington, IN, USA
FUKI	Fukui Univ.	Fukui, Japan	INEL	E G and G Idaho , Inc.	Idaho Falls, ID, USA
FUKU	Fukushima Univ.	Fukushima, Japan	INFN	Ist. Nazionale di Fisica Nucleare (Generic INFN, unknown location)	Various places, Italy
GENO	Univ. di Genova	Genova, Italy	INNS	Univ. of Innsbruck	Innsbruck , Austria
GEOR	Georgian Academy of Sciences	Tbilisi, Republic of Georgia	INPK	Inst. of Nuclear Physics	Kraków , Poland
GESC	General Electric Co.	Schenectady, NY, USA	INRM	INR , Inst. for Nucl. Research	Moscow , Russian Federation
GEVA	Univ. de Genève	Genève, Switzerland	INUS	KEK , High Energy Accelerator Research Organization	Tokyo, Japan
GIES	Univ. Giessen	Giessen, Germany	IOAN	Univ. of Ioannina	Ioannina, Greece
GIFU	Gifu Univ.	Gifu, Japan	IOFF	A.F. Ioffe Phys. Tech. Inst.	St. Petersburg , Russian Federation
GLAS	Univ. of Glasgow	Glasgow, United Kingdom	IOWA	Univ. of Iowa	Iowa City, IA, USA
GMAS	George Mason Univ.	Fairfax, VA, USA	IPN	IPN , Inst. de Phys. Nucl.	Orsay , France
GOET	Univ. Göttingen	Göttingen, Germany	IPNP	Univ. Pierre et Marie Curie (Paris VI)	Paris, France
GRAN	Univ. de Granada	Granada, Spain	IRAD	Inst. du Radium (Historical)	Paris , France
GRAZ	Univ. Graz	Graz, Austria	ISNG	Lab. de Physique Subatomique et de Cosmologie (LPSC)	Grenoble , France
GRON	Univ. of Groningen	Groningen, The Netherlands	ISU	Iowa State Univ.	Ames, IA, USA
GSCO	Geological Survey of Canada	Ottawa, ON, Canada	ITEP	ITEP , Inst. of Theor. and Exp. Physics	Moscow , Russian Federation
GSI	GSI Helmholtzzentrum für Schwerionenforschung GmbH	Darmstadt , Germany	ITHA	Ithaca College	Ithaca, NY, USA
GUAN	Univ. de Guanajuato	León, Gto., Mexico	IUPU	Indiana Univ., Purdue Univ. Indianapolis	Indianapolis, IN, USA
GUEL	Univ. of Guelph	Guelph, ON, Canada	JADA	Jadavpur Univ.	Calcutta, India
GWU	George Washington Univ.	Washington, DC, USA	JAGL	Jagiellonian Univ.	Kraków, Poland
HAHN	Hahn-Meitner Inst. Berlin GmbH	Berlin, Germany	JHU	Johns Hopkins Univ.	Baltimore, MD, USA
HAIF	Technion – Israel Inst. of Tech.	Technion, Haifa, Israel	JINR	JINR , Joint Inst. for Nucl. Research	Dubna , Russian Federation
HAMB	Univ. Hamburg	Hamburg, Germany	JULI	Forschungszentrum Jülich	Jülich, Germany
HANN	Univ. Hannover	Hannover, Germany	JYV	Univ. of Jyväskylä	Jyväskylä, Finland
HARC	Houston Advanced Research Ctr.	The Woodlands, TX, USA	KAGO	Univ. of Kagoshima	Kagoshima-shi, Japan
HARV	Harvard Univ.	Cambridge, MA, USA	KANS	Univ. of Kansas	Lawrence, KS, USA
HAWA	Univ. of Hawai'i	Honolulu, HI, USA	KARL	Univ. Karlsruhe (Historical in <i>Review</i>)	Karlsruhe, Germany
HEBR	Hebrew Univ.	Jerusalem, Israel	KARLE	Karlsruhe Inst. für Technologie KIT	Karlsruhe, Germany
HEID	Univ. Heidelberg ; (unspecified division) (Historical in <i>Review</i>)	Heidelberg, Germany	KARLK	Karlsruhe Inst. of Technology (KIT)	Eggenstein-Leopoldshafen, Germany
HEIDH	Ruprecht-Karls Univ. Heidelberg	Heidelberg, Germany	KARLT	Karlsruhe Inst. of Technology (KIT)	Karlsruhe, Germany
HEIDP	Univ. Heidelberg ; Physikalisches Inst.	Heidelberg, Germany	KAZA	Kazakh Inst. of High Energy Physics	Alma Ata, Kazakhstan
HEIDT	Univ. Heidelberg ; Inst. für Theoretische Physik	Heidelberg, Germany	KEK	KEK , High Energy Accelerator Research Organization	Ibaraki-ken, Japan
HELH	Univ. of Helsinki ; Dept. of Phys., High Energy Phys. Div. (SEFO); Dept. of Phys., Theor. Phys. Div. (TFO); Helsinki Institute of Physics (HIP)	University of Helsinki, Finland	KENT	Univ. of Kent	Canterbury, United Kingdom
HIRO	Hiroshima Univ.	Higashi-Hiroshima, Japan	KEYN	Open Univ.	Milton Keynes, UK
HOUS	Univ. of Houston	Houston, TX, USA	KFTI	Kharkov Inst. of Physics and Tech. (NSC KIPT)	Kharkov, Ukraine
HPC	Hewlett-Packard Corp.	Cupertino, CA, USA	KIAE	The Russian Research Center, Kurchatov Inst.	Moscow , Russian Federation
HSCA	Harvard-Smithsonian Center for Astrophysics	Cambridge, MA, USA	KIAM	Keldysh Inst. of Applied Math., Acad. Sci., Russia	Moscow, Russian Federation
IAS	Inst. for Advanced Study	Princeton, NJ, USA	KIDR	Vinča Inst. of Nuclear Sciences	Belgrade, Serbia and Montenegro
IASD	Dublin Inst. for Advanced Studies	Dublin, Ireland	KIEV	Institute for Nuclear Research	Kyiv , Ukraine
IBAR	Ibaraki Univ.	Ibaraki, Japan	KINK	Kinki Univ.	Osaka, Japan
IBM	IBM Corp.	Palo Alto, CA, USA	KNTY	Univ. of Kentucky	Lexington, KY, USA
IBMY	IBM	Yorktown Heights, NY, USA	KOBE	Kobe Univ.	Kobe, Japan
IBS	Inst. for Boson Studies	Pasadena, CA, USA	KOMAB	Univ. of Tokyo, Komaba	Tokyo, Japan
ICEPP	Univ. of Tokyo ; Int. Center for Elementary Particle Physics (ICEPP)	Tokyo, Japan	KONAN	Konan Univ.	Kobe, Japan
ICRR	Univ. of Tokyo	Chiba, Japan	KOSI	Inst. of Experimental Physics SAS	Košice , Slovakia
ICTP	Abdus Salam International Centre for Theoretical Physics	Trieste , Italy	KYOT	Kyoto Univ.; Dept. of Physics, Graduate School of Science	Kyoto, Japan

Abbreviations Used in the Particle Listings

KYOTU	Kyoto Univ.; Yukawa Inst. for Theor. Physics	Kyoto, Japan	MELB	Univ. of Melbourne	Victoria, Australia
KYUN	Kyungpook National Univ.	Daegu, Republic of Korea	MEUD	Observatoire de Meudon	Meudon, France
KYUSH	Kyushu Univ.	Fukuoka, Japan	MICH	Univ. of Michigan	Ann Arbor, MI, USA
LALO	LAL , Laboratoire de l'Accélérateur Linéaire	Orsay , France	MILA	Univ. di Milano	Milano, Italy
LANC	Lancaster Univ.	Lancaster, United Kingdom	MILAI	INFN, Sez. di Milano	Milano, Italy
LANL	Los Alamos National Lab. (LANL)	Los Alamos, NM, USA	MINN	Univ. of Minnesota	Minneapolis, MN, USA
LAPP	LAPP , Lab. d'Annecy-le-Vieux de Phys. des Particules	Annecy-le-Vieux , France	MISS	Univ. of Mississippi	University, MS, USA
LASL	U.C. Los Alamos Scientific Lab. (Old name for LANL)	Los Alamos, NM, USA	MISSR	Univ. of Missouri	Rolla, MO, USA
LATV	Latvian State Univ.	Riga, Latvia	MIT	MIT Massachusetts Inst. of Technology	Cambridge, MA, USA
LAUS	EPFL Lausanne	Lausanne, Switzerland	MIU	Maharishi International Univ.	Fairfield, IA, USA
LAVL	Univ. Laval	Quebec, QC, Canada	MIYA	Miyazaki Univ.	Miyazaki-shi, Japan
LBL	Lawrence Berkeley National Lab.	Berkeley, CA, USA	MONP	Univ. de Montpellier II	Montpellier, France
LCGT	Univ. di Torino	Turin, Italy	MONS	Univ. de Mons-Hainaut	Mons , Belgium
LEBD	Lebedev Physical Inst.	Moscow , Russian Federation	MONT	Univ. de Montréal ; Pavillon René-J.-A.-Lévesque	Montréal, PQ, Canada
LECE	Univ. di Lecce	Lecce, Italy	MONTC	Univ. de Montréal ; Centre de recherches mathématiques	Montréal, PQ, Canada
LEED	Univ. of Leeds	Leeds, United Kingdom	MOSU	Skobeltsyn Inst. of Nuclear Physics, Lomonosov Moscow State Univ.; Experimental, Theoretical HEP Divisions	Moscow , Russian Federation
LEHI	Lehigh Univ.	Bethlehem, PA, USA	MPCM	Max Planck Inst. für Chemie	Mainz , Germany
LEHM	Lehman College of CUNY	Bronx, NY, USA	MPEI	Moscow Physical Engineering Inst.	Moscow, Russian Federation
LEID	Univ. Leiden	Leiden, The Netherlands	MPIA	Max-Planck-Institute für Astrophysik	Garching, Germany
LEMO	Le Moyne Coll.	Syracuse, NY, USA	MPIH	Max-Planck-Inst. für Kernphysik	Heidelberg , Germany
LEUV	Katholieke Univ. Leuven	Leuven, Belgium	MPIM	Max-Planck-Inst. für Physik	München , Germany
LINZ	Univ. Linz	Linz, Austria	MSU	Michigan State Univ.	East Lansing, MI, USA
LISB	Inst. Nacional de Investigacion Cientifica	Lisboa CODEX, Portugal	MTHO	Mount Holyoke College	South Hadley, MA, USA
LISBT	Centro de Física Teórica de Partículas (CFTP)	Lisboa , Portugal	MULH	Centre Univ. du Haut-Rhin	Mulhouse, France
LIVP	Univ. of Liverpool	Liverpool, United Kingdom	MUNI	Ludwig-Maximilians-Univ. München	Garching, Germany
LLL	Lawrence Livermore Lab. (Old name for LLNL)	Livermore, CA, USA	MUNT	Tech. Univ. München	Garching, Germany
LLNL	Lawrence Livermore National Lab.	Livermore, CA, USA	MURA	Midwestern Univ. Research Assoc. (Historical in <i>Review</i>)	Stroughton, WI, USA
LOCK	Lockheed Palo Alto Res. Lab	Palo Alto, CA, USA	MURC	Univ. of Murcia	Murcia, Spain
LOIC	Imperial College of Science Tech. & Medicine	London, United Kingdom	NAAS	North America Aviation Science Center (Historical in <i>Review</i>)	Thousand Oaks, CA, USA
LOQM	Queen Mary, Univ. of London	London, United Kingdom	NAGO	Nagoya Univ.	Nagoya, Japan
LOUC	University College London	London, United Kingdom	NAPL	Univ. di Napoli "Federico II"	Napoli, Italy
LOUV	Univ. Catholique de Louvain	Louvain-la-Neuve, Belgium	NASA	NASA	Greenbelt, MD, USA
LOWC	Westfield College (Historical, see LOQM (Queen Mary and Westfield joined))	London, United Kingdom	NBS	U.S. National Bureau of Standards (Old name for NIST)	Gaithersburg, MD, USA
LRL	U.C. Lawrence Radiation Lab. (Old name for LBL)	Berkeley , CA, USA	NBSB	National Inst. Standards Tech.	Boulder, CO, USA
LSU	Louisiana State Univ.	Baton Rouge, LA, USA	NCAR	National Center for Atmospheric Research	Boulder, CO, USA
LUND	Fysiska Institutionen	Lund , Sweden	NCSU	North Carolina State Univ.	Raleigh , NC, USA
LUND	Lund Univ.	Lund, Sweden	NDAM	Univ. of Notre Dame	Notre Dame, IN, USA
LYON	Institute de Physique Nucléaire de Lyon (IPN)	Villeurbanne, France	NEAS	Northeastern Univ.	Boston, MA, USA
MADE	UAM/CSIC , Inst. de Física Teórica	Madrid , Cantoblanco, Spain	NEBR	Univ. of Nebraska	Lincoln, NE, USA
MADR	C.I.E.M.A.T	Madrid , Spain	NEUC	Univ. de Neuchâtel	Neuchâtel, Switzerland
MADU	Univ. Autónoma de Madrid	Cantoblanco, Madrid, Spain	NICEA	Univ. de Nice	Nice, France
MANI	Univ. of Manitoba	Winnipeg, MB, Canada	NICEO	Observatoire de Nice	Nice, France
MANZ	Johannes-Gutenberg-Univ. ; Inst. für Physik, Staudingerweg 7; Inst. für Kernphysik, J.-J.-Becher-Weg 45	Mainz , Germany	NIHO	Nihon Univ.	Tokyo, Japan
MARB	Univ. Marburg	Marburg, Germany	NIIG	Niigata Univ.	Niigata, Japan
MARS	Centre de Physique des Particules de Marseille	Marseille, France	NIJM	Radboud Univ. Nijmegen	ED Nijmegen , The Netherlands
MASA	Univ. of Massachusetts Amherst	Amherst , MA, USA	NIRS	Nat. Inst. Radiological Sciences	Chiba , Japan
MASB	Univ. of Massachusetts Boston	Boston , MA, USA	NIST	National Institute of Standards & Technology	Gaithersburg, MD, USA
MASD	Univ. of Massachusetts Dartmouth	North Dartmouth , MA, USA	NIU	Northern Illinois Univ.	De Kalb, IL, USA
MCGI	McGill Univ.	Montreal, QC, Canada	NMSU	New Mexico State Univ.; Dept. of Physics, MSC 3D; Part. & Nucl. Phys. Group, Box 30001/Dept.	Las Cruces, NM, USA
MCHS	Univ. of Manchester	Manchester, United Kingdom	NORD	Nordita	Stockholm, Sweden
MCMS	McMaster Univ.	Hamilton, ON, Canada	NOTT	Univ. of Nottingham	Nottingham, United Kingdom
MEHTA	Harish-Chandra Research Inst.	Allahabad, India	NOVM	Inst. of Mathematics	Novosibirsk , Russian Federation
MEIS	Meisei Univ.	Tokyo, Japan			

Abbreviations Used in the Particle Listings

NOVO	BINP, Budker Inst. of Nuclear Physics	Novosibirsk , Russian Federation	RISL	Universities Research Reactor	Risley , Warrington, United Kingdom
NPOL	Polytechnic of North London	London, United Kingdom	RISO	Riso National Laboratory	Roskilde, Denmark
NRL	Naval Research Lab	Washington, DC, USA	RL	Rutherford High Energy Lab (Old name for RAL)	Chilton, Didcot, Oxon., United Kingdom
NSF	National Science Foundation	Arlington, VA, USA	RMCS	Royal Military Coll. of Science	Swindon, Wilts., United Kingdom
NTHU	National Tsing Hua Univ.	Hsinchu, Taiwan, China	ROCH	Univ. of Rochester	Rochester, NY, USA
NTUA	National Tech. Univ. of Athens	Athens, Greece	ROCK	Rockefeller Univ.	New York, NY, USA
NWES	Northwestern Univ.	Evanston, IL, USA	ROMA	Univ. di Roma (Historical)	Roma , Italy
NYU	New York Univ.	New York, NY, USA	ROMA2	Univ. di Roma , "Tor Vergata"	Roma, Italy
OBER	Oberlin College	Oberlin, OH, USA	ROMAI	INFN, Sez. di Roma	Roma, Italy
OCH	Ochanomizu Univ.	Tokyo, Japan	ROSE	Rose-Hulman Inst. of Technology	Terre Haute IN, USA
OHIO	Ohio Univ.	Athens, OH, USA	RPI	Rensselaer Polytechnic Inst.	Troy, NY, USA
OKAY	Okayama Univ.	Okayama, Japan	RUTG	Rutgers , the State Univ. of New Jersey	Piscataway, NJ, USA
OKLA	Univ. of Oklahoma	Norman, OK, USA	SACL	CEA Saclay , IRFU	Gif-sur-Yvette, France
OKSU	Oklahoma State Univ.	Stillwater, OK, USA	SACLD	CEA Saclay (Essonne)	Gif-sur-Yvette, France
OREG	Univ. of Oregon ; Inst. of Theor. Science; U.O. Center for High Energy Physics	Eugene, OR, USA	SAGA	Saga Univ.	Saga-shi, Japan
ORNL	Oak Ridge National Lab.	Oak Ridge, TN, USA	SAHA	Saha Inst. of Nuclear Physics	Bidhan Nagar, Calcutta, India
ORSAY	Univ. de Paris Sud	Orsay CEDEX, France	SANG	Kyoto Sangyo Univ.	Kyoto-shi, Japan
ORST	Oregon State Univ.	Corvallis, OR, USA	SANI	Ist. Superiore di Sanità	Roma , Italy
OSAK	Osaka Univ.	Osaka, Japan	SASK	Univ. of Saskatchewan	Saskatoon, SK, Canada
OSKC	Osaka City Univ.	Osaka-shi, Japan	SASSO	Lab. Naz. Gran Sasso dell'INFN	Assergi (AQ), Italy
OSLO	Univ. of Oslo	Oslo, Norway	SAVO	Univ. de Savoie	Chambery, France
OSU	Ohio State Univ.	Columbus, OH, USA	SBER	California State Univ.	San Bernardino , CA, USA
OTTA	Univ. of Ottawa	Ottawa, ON, Canada	SCHAF	W.J. Schafer Assoc.	Livermore, DA, USA
OXF	University of Oxford	Oxford, United Kingdom	SCIT	Science Univ. of Tokyo	Tokyo, Japan
OXFTP	Univ. of Oxford	Oxford, United Kingdom	SCOT	Scottish Univ. Research and Reactor Ctr.	Glasgow, United Kingdom
PADO	Univ. degli Studi di Padova	Padova, Italy	SCUC	Univ. of South Carolina	Columbia, SC, USA
PARIN	Univ. Paris VI et Paris VII , IN ² P ³ /CNRS	Paris, France	SEAT	Seattle Pacific Coll.	Seattle, WA, USA
PARIS	Univ. de Paris (Historical)	Paris , France	SEIB	Austrian Research Center, Seibersdorf LTD.	Seibersdorf, Austria
PARIT	Univ. Paris VII , LP ^{THE}	Paris, France	SEOU	Korea Univ.; Dept. of Physics; HEP Group	Seoul, Republic of Korea
PARM	Gruppo Collegato INFN	Parma, Italy	SEOUL	Seoul National Univ.; Dept. of Physics & Astronomy, Coll. of Natural Sciences; Center for Theoretical Physics	Seoul, Republic of Korea
PAST	Institut Pasteur	Paris , France	SERP	IHEP , Inst. for High Energy Physics	Protvino, Russian Federation
PATR	Univ. of Patras	Patras, Greece	SETO	Seton Hall Univ.	South Orange, NJ, USA
PAVI	Univ. di Pavia	Pavia, Italy	SFLA	Univ. of South Florida	Tampa, FL, USA
PENN	Univ. of Pennsylvania	Philadelphia, PA, USA	SFRA	Simon Fraser University	Burnaby, BC, Canada
PGIA	INFN, Sezione di Perugia	Perugia, Italy	SFSU	California State Univ.	San Francisco , CA, USA
PISA	Univ. di Pisa	Pisa, Italy	SHAMS	Ain Shams University	Abbassia, Cairo, Egypt
PISAI	INFN, Sez. di Pisa	Pisa, Italy	SHEF	Univ. of Sheffield	Sheffield, United Kingdom
PITT	Univ. of Pittsburgh	Pittsburgh, PA, USA	SHMP	Univ. of Southampton	Southampton, United Kingdom
PLAT	SUNY at Plattsburgh	Plattsburgh, NY, USA	SIEG	Univ. of Siegen	Siegen, Germany
PLRM	Univ. di Palermo	Palermo, Italy	SILES	Univ. of Silesia	Katowice, Poland
PNL	Battelle Memorial Inst.	Richland, WA, USA	SIN	Swiss Inst. of Nuclear Research (Old name for VILL)	Villigen , Switzerland
PNPI	Petersburg Nuclear Physics Inst. of Russian Academy of Sciences	Gatchina, Russian Federation	SING	National Univ. of Singapore	Kent Ridge, Singapore
PPA	Princeton-Penn. Proton Accelerator (Historical in <i>Review</i>)	Princeton, NJ, USA	SISSA	Scuola Internazionale Superiore di Studi Avanzati	Trieste , Italy
PRAG	Inst. of Physics, ASCR	Prague , Czech Republic	SLAC	SLAC National Accelerator Laboratory	Menlo Park, CA, USA
PRIN	Princeton Univ.	Princeton, NJ, USA	SLOV	Inst. of Physics, Slovak Acad. of Sciences	Bratislava 45, Slovakia
PSI	Paul Scherrer Inst.	Villigen PSI, Switzerland	SMU	Southern Methodist Univ.	Dallas, TX, USA
PSLL	Physical Science Lab	Las Cruces, NM, USA	SNSP	Scuola Normale Superiore	Pisa , Italy
PSU	Penn State Univ.	University Park, PA, USA	SOFI	Inst. for Nuclear Research and Nuclear Energy	Sofia , Bulgaria
PUCB	Pontificia Univ. Católica do Rio de Janeiro	Rio de Janeiro, RJ, Brasil	SOFU	Univ. of Sofia "St. Kliment Ohridski"	Sofia, Bulgaria
PUEB	Univ. Autonoma de Puebla	Puebla , Pue, Mexico	SPAUL	Univ. de São Paulo	São Paulo, SP, Brasil
PURD	Purdue Univ.	West Lafayette, IN, USA	SPIFT	Inst. de Física Teórica (IFT)	São Paulo , SP, Brasil
QUKI	Queen's Univ.	Kingston, ON, Canada	SSL	U. of California (Berkeley)	Berkeley, CA, USA
RAL	Rutherford Appleton Lab.	Didcot, Oxfordshire, United Kingdom	STAN	Stanford Univ.	Stanford, CA, USA
REGE	Univ. Regensburg	Regensburg, Germany	STEV	Stevens Inst. of Tech.	Hoboken, NJ, USA
REHO	Weizmann Inst. of Science	Rehovot, Israel	STLO	St. Louis Univ.	St. Louis, MO, USA
RHBL	Royal Holloway, Univ. of London	Egham, Surrey, United Kingdom	STOH	Stockholm Univ.	Stockholm, Sweden
RHEL	Rutherford High Energy Lab (Old name for RAL)	Chilton, Didcot, Oxon., United Kingdom	STON	SUNY at Stony Brook	Stony Brook, NY, USA
RICE	Rice Univ.	Houston, TX, USA			
RIKEN	Riken Nishina Center for Accelerator-Based Science	Saitama, Japan			
RIKK	Rikkyo Univ.	Tokyo, Japan			
RIS	Rowland Inst. for Science	Cambridge, MA, USA			
RISC	Rockwell International	Thousand Oaks, CA, USA			

Abbreviations Used in the Particle Listings

STRB	Inst. Pluridisciplinaire Hubert Curien (CNRS)	Strasbourg, France	UCSD	Univ. of California (San Diego)	La Jolla, CA, USA
STUT	Univ. Stuttgart	Stuttgart, Germany	UGAZ	Univ. of Gaziantep	Gaziantep, Turkey
STUTM	Max-Planck-Inst.	Stuttgart , Germany	UMD	Univ. of Maryland	College Park, MD, USA
SUGI	Sugiyama Jogakuen Univ.	Aichi, Japan	UNC	Univ. of North Carolina	Greensboro, NC, USA
SURR	Univ. of Surrey	Guildford, Surrey, UK	UNCCH	Univ. of North Carolina at Chapel Hill	Chapel Hill, NC, USA
SUSS	Univ. of Sussex	Brighton, United Kingdom	UNCS	Union College	Schenectady, NY, USA
SVR	Savannah River Labs.	Aiken, SC, USA	UNESP	UNESP	Botucatu, Brasil
SYDN	Univ. of Sydney	Sydney, NSW, Australia	UNH	Univ. of New Hampshire	Durham, NH, USA
SYRA	Syracuse Univ.	Syracuse, NY, USA	UNM	Univ. of New Mexico	Albuquerque, NM, USA
TAJK	Acad. Sci., Tadjik SSR	Dushanbe , Tadjikistan	UOEH	Univ. of Occupational and Environmental Health	Kitakyushu , Japan
TAMU	Texas A&M Univ.	College Station, TX, USA	UPNJ	Uppsala College	East Orange, NJ, USA
TATA	Tata Inst. of Fundamental Research	Bombay, India	UPPS	Uppsala Univ.	Uppsala , Sweden
TBIL	Tbilisi State University	Tbilisi, Republic of Georgia	UPR	Univ. of Puerto Rico	Rio Piedras , PR, USA
TELA	Tel-Aviv Univ.	Tel Aviv, Israel	URI	Univ. of Rhode Island	Kingston, RI, USA
TELE	Teledyne Brown Engineering	Huntsville, AL, USA	USC	Univ. of Southern California	Los Angeles, CA, USA
TEMP	Temple Univ.	Philadelphia, PA, USA	USF	Univ. of San Francisco	San Francisco, CA, USA
TENN	Univ. of Tennessee	Knoxville, TN, USA	UTAH	Univ. of Utah	Salt Lake City, UT, USA
TEXA	Univ. of Texas at Austin	Austin, TX, USA	UTRE	Univ. of Utrecht	Utrecht, The Netherlands
TGAK	Tokyo Gakugei Univ.	Tokyo, Japan	UTRO	Norwegian Univ. of Science & Technology	Trondheim, Norway
TGU	Tohoku Gakuin Univ.	Miyagi, Japan	UVA	Univ. of Virginia	Charlottesville, VA, USA
THES	Aristotle Univ. of Thessaloniki (AUTh)	Thessaloniki, Greece	UZINR	Acad. Sci., Ukrainian SSR	Uzhgorod , Ukraine
TINT	Tokyo Inst. of Technology	Tokyo, Japan	VALE	Univ. de Valencia	Burjassot, Valencia , Spain
TISA	Sagamihara Inst. of Space & Astronautical Sci.	Kanagawa, Japan	VALP	Valparaiso Univ.	Valparaiso, IN, USA
TMSK	Nuclear Physics Institute	Tomsk , Russian Federation	VAND	Vanderbilt Univ.	Nashville, TN, USA
TMTC	Tokyo Metropolitan Coll. Tech.	Tokyo, Japan	VASS	Vassar College	Poughkeepsie, NY, USA
TMU	Tokyo Metropolitan Univ.	Tokyo, Japan	VICT	Univ. of Victoria	Victoria, BC, Canada
TNTO	Univ. of Toronto	Toronto, ON, Canada	VIEN	Inst. für Hochenergiephysik (HEPHY)	Vienna , Austria
TOHO	Toho Univ.	Chiba, Japan	VILL	ETH Zürich	Zürich, Switzerland
TOHOK	Tohoku Univ.	Sendai, Japan	VPI	Virginia Tech.	Blacksburg, VA, USA
TOKA	Tokai Univ.	Shimizu, Japan	VRIJ	Vrije Univ.	HV Amsterdam , The Netherlands
TOKAH	Tokai Univ.	Hiratsuka, Japan	WABRNE	Eidgenössisches Amt für Messwesen	Waber , Switzerland
TOKMS	Univ. of Tokyo ; Meson Science Laboratory	Tokyo, Japan	WARS	Univ. of Warsaw	Warsaw, Poland
TOKU	Univ. of Tokushima	Tokushima-shi, Japan	WASCR	Waseda Univ.; Cosmic Ray Division	Tokyo, Japan
TOKY	Univ. of Tokyo ; High-Energy Physics Theory Group	Tokyo, Japan	WASH	Univ. of Washington ; Elem. Particle Experiment (EPE); Particle Astrophysics (PA)	Seattle, WA, USA
TOKYC	Univ. of Tokyo ; Dept. of Chemistry	Tokyo, Japan	WASU	Waseda Univ.; Dept. of Physics, High Energy Physics Group	Tokyo, Japan
TORI	Univ. degli Studi di Torino	Torino, Italy	WAYN	Wayne State Univ.	Detroit, MI, USA
TPTI	Uzbek Academy of Sciences	Tashkent , Republic of Uzbekistan	WESL	Wesleyan Univ.	Middletown, CT, USA
TRIN	Trinity College Dublin	Dublin, Ireland	WIEN	Univ. Wien	Vienna, Austria
TRIU	TRIUMF	Vancouver, BC, Canada	WILL	Coll. of William and Mary	Williamsburg, VA, USA
TRST	Univ. di Trieste	Trieste, Italy	WINR	Andrzej Soltan Inst. for Nuclear Studies	Warsaw , Poland
TRSTI	INFN, Sez. di Trieste	Trieste, Italy	WISC	Univ. of Wisconsin	Madison, WI, USA
TRSTT	Univ. degli Studi di Trieste	Trieste , Italy	WITW	Univ. of the Witwatersrand	Wits, South Africa
TSUK	Univ. of Tsukuba	Ibaraki-ken, Japan	WMIU	Western Michigan Univ.	Kalamazoo, MI, USA
TTAM	Tamagawa Univ.	Tokyo, Japan	WONT	The Univ. of Western Ontario	London, ON, Canada
TUAT	Tokyo Univ. of Agriculture Tech.	Tokyo, Japan	WOOD	Woodstock College (No longer in existence)	Woodstock, MD, USA
TUBIN	Univ. Tübingen	Tübingen, Germany	WUPP	Bergische Univ. Wuppertal	Wuppertal , Germany
TUFTS	Tufts Univ.	Medford, MA, USA	WURZ	Univ. Würzburg	Würzburg, Germany
TUW	Technische Univ. Wien	Vienna, Austria	WUSL	Washington Univ.	St. Louis, MO, USA
TUZL	Tuzla Univ.	Tuzla, Argentina	WYOM	Univ. of Wyoming	Laramie, WY, USA
UCB	Univ. of California (Berkeley)	Berkeley, CA, USA	YALE	Yale Univ.	New Haven, CT, USA
UCD	Univ. of California (Davis)	Davis, CA, USA	YARO	Yaroslavl State Univ.	Yaroslavl, Russian Federation
UCI	Univ. of California (Irvine)	Irvine, CA, USA	YCC	Yokohama Coll. of Commerce	Yokohama, Japan
UCLA	Univ. of California (Los Angeles)	Los Angeles, CA, USA	YERE	Yerevan Physics Inst.	Yerevan, Armenia
UCND	Union Carbide Corp.	Oak Ridge, TN, USA	YOKO	Yokohama National Univ.	Yokohama-shi, Japan
UCR	U. of California (Riverside)	Riverside, CA, USA	YORKC	York Univ.	Toronto, Canada
UCSB	Univ. of California (Santa Barbara); Physics Dept., High Energy Physics Experiment	Santa Barbara, CA, USA	ZAGR	Zagreb Univ.	Zagreb, Croatia
UCSBT	Univ. of California (Santa Barbara); Kavli Inst. for Theoretical Physics	Santa Barbara, CA, USA	ZARA	Univ. de Zaragoza	Zaragoza, Spain
UCSC	Univ. of California (Santa Cruz)	Santa Cruz, CA, USA	ZEEM	Univ. van Amsterdam	TV Amsterdam, The Netherlands
			ZHZH	Zhengzhou Univ.	Zhengzhou, Henan, China
			ZURI	Univ. Zürich	Zürich, Switzerland



GAUGE AND HIGGS BOSONS

γ	417
g (gluon)	417
graviton	418
W	418
Z	426
Higgs Bosons — H^0 and H^\pm	448
Heavy Bosons Other than Higgs Bosons	480
Axions (A^0) and Other Very Light Bosons	496

Notes in the Gauge and Higgs Boson Listings

The Mass of the W Boson (rev.)	418
Triple Gauge Couplings (rev.)	422
Anomalous W/Z Quartic Couplings	424
The Z Boson (rev.)	426
Anomalous $ZZ\gamma$, $Z\gamma\gamma$, and ZZV Couplings	445
Anomalous W/Z Quartic Couplings	446
Searches for Higgs Bosons (rev.)	448
The W' Searches (rev.)	480
The Z' Searches (rev.)	483
Leptoquarks	490
Axions and Other Very Light Bosons (rev.)	496





See key on page 405

Gauge & Higgs Boson Particle Listings

 γ, g

GAUGE AND HIGGS BOSONS

 γ

$$I(J^{PC}) = 0,1(1^{-})$$

 γ MASS

Results prior to 2008 are critiqued in GOLDHABER 09.

VALUE (eV)	CL%	DOCUMENT ID	TECN	COMMENT
< 1	$\times 10^{-18}$	1 RYUTOV 07		MHD of solar wind
< 1	$\times 10^{-26}$	2 ADELBERGER 07A		Galactic field existence if Higgs mass
< 1.4	$\times 10^{-7}$	ACCIOLY 04		Dispersion of GHz radio waves by sun
< 2	$\times 10^{-16}$	FULLEKRUG 04		Speed of 5-50 Hz radiation in atmosphere
< 7	$\times 10^{-19}$	3 LUO 03		Modulation torsion balance
< 1	$\times 10^{-17}$	4 LAKES 98		Torque on toroid balance
< 6	$\times 10^{-17}$	5 RYUTOV 97		MHD of solar wind
< 9	$\times 10^{-16}$	6 FISCHBACH 94		Earth magnetic field
< (4.73 ± 0.45) × 10 ⁻¹²		7 CHERNIKOV 92	SQID	Ampere-law null test
< (9.10 ± 8.1) × 10 ⁻¹⁰		8 RYAN 85		Coulomb-law null test
< 3	$\times 10^{-27}$	9 CHIBISOV 76		Galactic magnetic field
< 6	$\times 10^{-16}$	99.7 DAVIS 75		Jupiter magnetic field
< 7.3	$\times 10^{-16}$	HOLLWEG 74		Alfvén waves
< 6	$\times 10^{-17}$	10 FRANKEN 71		Low freq. res. cir.
< 1	$\times 10^{-14}$	WILLIAMS 71	CNTR	Tests Gauss law
< 2.3	$\times 10^{-15}$	GOLDHABER 68		Satellite data
< 6	$\times 10^{-15}$	10 PATEL 65		Satellite data
< 6	$\times 10^{-15}$	GINTSBURG 64		Satellite data

- 1 RYUTOV 07 extends the method of RYUTOV 97 to the radius of Pluto's orbit.
- 2 When trying to measure m one must distinguish between measurements performed on large and small scales. If the photon acquires mass by the Higgs mechanism, the large-scale behavior of the photon might be effectively Maxwellian. If, on the other hand, one postulates the Proca regime for all scales, the very existence of the galactic field implies $m < 10^{-26}$ eV, as correctly calculated by YAMAGUCHI 59 and CHIBISOV 76.
- 3 LUO 03 determine a limit on $\mu^2 A < 1.1 \times 10^{-11}$ T m/m² (with μ^{-1} = characteristic length for photon mass; A = ambient vector potential) — similar to the LAKES 98 technique. Unlike LAKES 98 who used static, the authors used dynamic torsion balance. Assuming A to be 10^{12} T m, they obtain $\mu < 1.2 \times 10^{-51}$ g, equivalent to 6.7×10^{-19} eV. The rotating modified Cavendish balance removes dependence on the direction of A . GOLDHABER 03 argue that because plasma current effects are neglected, the LUO 03 limit does not provide the best available limit on $\mu^2 A$ nor a reliable limit at all on μ . The reason is that the A associated with cluster magnetic fields could become arbitrarily small in plasma voids, whose existence would be compatible with present knowledge. LUO 03s reply that fields of distant clusters are not accurately mapped, but assert that a zero A is unlikely given what we know about the magnetic field in our galaxy.
- 4 LAKES 98 reports limits on torque on a toroid Cavendish balance, obtaining a limit on $\mu^2 A < 2 \times 10^{-9}$ Tm/m² via the Maxwell-Proca equations, where μ^{-1} is the characteristic length associated with the photon mass and A is the ambient vector potential in the Lorentz gauge. Assuming $A \approx 1 \times 10^{12}$ Tm due to cluster fields he obtains $\mu^{-1} > 2 \times 10^{10}$ m, corresponding to $\mu < 1 \times 10^{-17}$ eV. A more conservative limit, using $A \approx (1 \mu\text{G}) \times (600 \text{ pc})$ based on the galactic field, is $\mu^{-1} > 1 \times 10^9$ m or $\mu < 2 \times 10^{-16}$ eV.
- 5 RYUTOV 97 uses a magnetohydrodynamics argument concerning survival of the Sun's field to the radius of the Earth's orbit. "To reconcile observations to theory, one has to reduce [the photon mass] by approximately an order of magnitude compared with" DAVIS 75.
- 6 FISCHBACH 94 report $< 8 \times 10^{-16}$ with unknown CL. We report Bayesian CL used elsewhere in these Listings and described in the Statistics section.
- 7 CHERNIKOV 92 measures the photon mass at 1.24 K, following a theoretical suggestion that electromagnetic gauge invariance might break down at some low critical temperature. See the erratum for a correction, included here, to the published result.
- 8 RYAN 85 measures the photon mass at 1.36 K (see the footnote to CHERNIKOV 92).
- 9 CHIBISOV 76 depends in critical way on assumptions such as applicability of virial theorem. Some of the arguments given only in unpublished references.
- 10 See criticism questioning the validity of these results in GOLDHABER 71, PARK 71 and KROLL 71. See also review GOLDHABER 71b.

 γ CHARGE

OKUN 06 has argued that schemes in which all photons are charged are inconsistent. He says that if a neutral photon is also admitted to avoid this problem, then other problems emerge, such as those connected with the emission and absorption of charged photons by charged particles. He concludes that in the absence of a self-consistent phenomenological basis, interpretation of experimental data is at best difficult.

VALUE (e)	CHARGE	DOCUMENT ID	TECN	COMMENT
< 1	$\times 10^{-46}$	11 ALTSCHUL 07B	VLBI	Aharonov-Bohm effect
< 1	$\times 10^{-35}$	12 CAPRINI 05	CMB	Isotropy constraint

• • • We do not use the following data for averages, fits, limits, etc. • • •

< 1 × 10 ⁻³²	single	11 ALTSCHUL 07B	VLBI	Aharonov-Bohm effect
< 3 × 10 ⁻³³	mixed	13 KOBYCHEV 05	VLBI	Smear as function of B·E _γ
< 4 × 10 ⁻³¹	single	13 KOBYCHEV 05	VLBI	Deflection as function of B·E _γ
< 8.5 × 10 ⁻¹⁷		14 SEMERTZIDIS 03		Laser light deflection in B-field
< 3 × 10 ⁻²⁸	single	15 SIVARAM 95	CMB	For Ω _M = 0.3, h ² = 0.5
< 5 × 10 ⁻³⁰		16 RAFFELT 94	TOF	Pulsar f ₁ - f ₂
< 2 × 10 ⁻²⁸		17 COCCONI 92		VLBA radio telescope resolution
< 2 × 10 ⁻³²		COCCONI 88	TOF	Pulsar f ₁ - f ₂ TOF

11 ALTSCHUL 07B looks for Aharonov-Bohm phase shift in addition to geometric phase shift in radio interference fringes (VSOP mission).

12 CAPRINI 05 uses isotropy of the cosmic microwave background to place stringent limits on possible charge asymmetry of the Universe. Charge limits are set on the photon, neutrino, and dark matter particles. Valid if charge asymmetries produced by different particles are not anticorrelated.

13 KOBYCHEV 05 considers a variety of observable effects of photon charge for extragalactic compact radio sources. Best limits if source observed through a foreground cluster of galaxies.

14 SEMERTZIDIS 03 reports the first laboratory limit on the photon charge in the last 30 years. Straightforward improvements in the apparatus could attain a sensitivity of 10⁻²⁰ e.

15 SIVARAM 95 requires that CMB photon charge density not overwhelm gravity. Result scales as Ω_M h².

16 RAFFELT 94 notes that COCCONI 88 neglects the fact that the time delay due to dispersion by free electrons in the interstellar medium has the same photon energy dependence as that due to bending of a charged photon in the magnetic field. His limit is based on the assumption that the entire observed dispersion is due to photon charge. It is a factor of 200 less stringent than the COCCONI 88 limit.

17 See COCCONI 92 for less stringent limits in other frequency ranges. Also see RAFFELT 94 note.

 γ REFERENCES

GOLDHABER 09	arXiv:0809.1003	A.F. Goldhaber, M.M. Nieto	(STON, LANL)
ADELBERGER 07A	PRL 98 010402	E. Adelberger, G. Dvali, A. Gruzinov	(WASH, NYU)
ALTSCHUL 07B	PRL 98 261801	B. Altschul	(IND)
	Also	ASP 29 290	(SUC)
RYUTOV 07	PPCF 49 B429	D.D. Ryutov	(LLNL)
OKUN 06	APP B37 565	L.B. Okun	(ITEP)
CAPRINI 05	JCAP 0502 006	C. Caprini, P.G. Ferreira	(GEVA, OXFPT)
KOBYCHEV 05	AL 31 147	V.V. Kobychiev, S.B. Popov	(KIEV, PADO)
ACCIOLY 04	PR D69 107501	A. Accioly, R. Paszko	
FULLEKRUG 04	PRL 93 043901	M. Fullekrug	
GOLDHABER 03	PRL 91 149101	A.S. Goldhaber, M.M. Nieto	
LUO 03	PRL 90 081801	J. Luo et al.	
LUO 03B	PRL 91 149102	J. Luo et al.	
SEMERTZIDIS 03	PR D67 017701	Y.K. Semertzidis, G.T. Danby, D.M. Lazarus	
LAKES 98	PRL 80 1826	R. Lakes	(WIS C)
RYUTOV 97	PPCF 39 A73	D.D. Ryutov	(LLNL)
SIVARAM 95	AJP 63 473	C. Sivaram	(BANG)
FISCHBACH 94	PRL 73 514	E. Fischbach et al.	(PURD, JHU+)
RAFFELT 94	PR D50 7729	G. Raffelt	(MPIM)
CHERNIKOV 92	PRL 68 3383	M.A. Chernikov et al.	(ETH)
	Also	PRL 69 2939 (erratum)	M.A. Chernikov et al.
COCCONI 88	AJP 60 750	G. Cocconi	(CERN)
COCCONI 88	PL B206 705	G. Cocconi	(CERN)
RYAN 85	PR D32 802	J.J. Ryan, F. Accetta, R.H. Austin	(PRIN)
CHIBISOV 76	SPI 19 624	G.V. Chibisov	(LEBD)
	Translated from UFN 119 551.		
DAVIS 75	PRL 35 1402	L. Davis, A.S. Goldhaber, M.M. Nieto	(CIT, STON+)
HOLLWEG 74	PRL 32 961	J.V. Hollweg	(NCAR)
FRANKEN 71	PRL 26 115	P.A. Franken, G.W. Ampulski	(MICH)
GOLDHABER 71B	PRL 26 1390	A.S. Goldhaber, M.M. Nieto	(STON, BOHR, UCSB)
GOLDHABER 71B	RMP 43 277	A.S. Goldhaber, M.M. Nieto	(STON, BOHR, UCSB)
KROLL 71	PRL 26 1395	M.M. Kroll	(SLAC)
PARK 71	PRL 26 1393	D. Park, E.R. Williams	(SLAC)
WILLIAMS 71	PRL 26 721	E.R. Williams, J.E. Faller, H.A. Hill	(WESL)
GOLDHABER 68	PRL 21 567	A.S. Goldhaber, M.M. Nieto	(STON)
PATEL 65	PL 14 105	V.L. Patel	(DUKE)
GINTSBURG 64	Sov. Astr. AJ7 536	M.A. Gintsburg	(ASCI)
YAMAGUCHI 59	PTPS 11 37	Y. Yamaguchi	

 g
or gluon

$$I(J^P) = 0(1^-)$$

SU(3) color octet

Mass $m = 0$. Theoretical value. A mass as large as a few MeV may not be precluded, see YNDURAIN 95.

VALUE	DOCUMENT ID	TECN	COMMENT
• • • We do not use the following data for averages, fits, limits, etc. • • •			
	ABREU 92E	DLPH	Spin 1, not 0
	ALEXANDER 91H	OPAL	Spin 1, not 0
	BEHREND 82D	CELL	Spin 1, not 0
	BERGER 80D	PLUT	Spin 1, not 0
	BRANDELIC 80C	TASS	Spin 1, not 0

gluon REFERENCES

YNDURAIN 95	PL B345 524	F.J. Yndurain	(MADU)
ABREU 92E	PL B274 498	P. Abreu et al.	(DELPHI Collab.)
ALEXANDER 91H	ZPHY C52 543	G. Alexander et al.	(OPAL Collab.)
BEHREND 82D	PL B110 329	H.J. Behrend et al.	(CELLO Collab.)
BERGER 80D	PL B97 459	C. Berger et al.	(PLUTO Collab.)
BRANDELIC 80C	PL B97 453	R. Brandelik et al.	(TASSO Collab.)

Gauge & Higgs Boson Particle Listings

graviton, W

graviton $J = 2$

OMITTED FROM SUMMARY TABLE

graviton MASS

All of the following limits are obtained assuming Yukawa potential in weak field limit. VANDAM 70 argue that a massive field cannot approach general relativity in the zero-mass limit; however, see GOLDHABER 09 and references therein. h_0 is the Hubble constant in units of $100 \text{ km s}^{-1} \text{ Mpc}^{-1}$.

VALUE (eV)	DOCUMENT ID	COMMENT
$< 7 \times 10^{-32}$	1 CHOUDHURY 04	Weak gravitational lensing
$< 7.6 \times 10^{-20}$	2 FINN 02	Binary Pulsars
$< 2 \times 10^{-29} h_0^{-1}$	3 DAMOUR 91	Binary pulsar PSR 1913+16
$< 7 \times 10^{-28} h_0^{-1}$	GOLDHABER 74	Rich clusters
$< 8 \times 10^4$	HARE 73	Galaxy
	HARE 73	2γ decay

- ¹ CHOUDHURY 04 sets limits based on nonobservation of a distortion in the measured values of the variance of the power spectrum.
- ² FINN 02 analyze the orbital decay rates of PSR B1913+16 and PSR B1534+12 with a possible graviton mass as a parameter. The combined frequentist mass limit is at 90%CL.
- ³ DAMOUR 91 is an analysis of the orbital period change in binary pulsar PSR 1913+16, and confirms the general relativity prediction to 0.8%. "The theoretical importance of the [rate of orbital period decay] measurement has long been recognized as a direct confirmation that the gravitational interaction propagates with velocity c (which is the immediate cause of the appearance of a damping force in the binary pulsar system) and thereby as a test of the existence of gravitational radiation and of its quadrupolar nature." TAYLOR 93 adds that orbital parameter studies now agree with general relativity to 0.5%, and set limits on the level of scalar contribution in the context of a family of tensor [spin 2]-biscalar theories.

graviton REFERENCES

GOLDHABER 09	arXiv:0809.1003	A.F. Goldhaber, M.M. Nieto	(STON, LANL)
CHOUDHURY 04	ASP 21 559	S.R. Choudhury <i>et al.</i>	(DELPH, MELB)
FINN 02	PR D65 044022	L.S. Finn, P.J. Sutton	
TAYLOR 93	NAT 365 132	J.N. Taylor <i>et al.</i>	(PRIN, ARCBO, BURE+)
DAMOUR 91	API 366 501	T. Damour, J.H. Taylor	(BURE, MEUD, PRIN)
GOLDHABER 74	PR D9 1119	A.S. Goldhaber, M.M. Nieto	(LANL, STON)
HARE 73	CJP 51 431	M.G. Hare	(SASK)
VANDAM 70	NP B22 397	H. van Dam, M. Veltman	(UTRE)

W $J = 1$

THE MASS AND WIDTH OF THE W BOSON

Revised March 2010 by M. W. Grünewald (University Ghent), and A. Gurtu (Tata Inst.).

The W mass and width definition used here corresponds to a Breit-Wigner with mass-dependent width.

Until 1995, the production and study of the W boson was the exclusive domain of the $\bar{p}p$ colliders at CERN and Fermilab. W production at hadron colliders is tagged by a high p_T lepton from W decay. Owing to unknown parton-parton effective energy and missing energy in the longitudinal direction, the experiments reconstruct only the transverse mass of the W , and derive the W mass from comparing the transverse mass distribution with Monte Carlo predictions as a function of M_{TW} . These analyses use the electron and muon decay modes of the W boson.

Beginning in 1996, the energy of the LEP accelerator increased to above 161 GeV, the threshold for W -pair production. A precise knowledge of the e^+e^- center-of-mass energy enables one to reconstruct the W mass, even if one of them decays leptonically. At LEP two methods have been used to obtain the W mass. In the first method, the measured W -pair production cross sections, $\sigma(e^+e^- \rightarrow W^+W^-)$, have been used to determine the W mass using the predicted dependence of this cross section on M_W . At 161 GeV, which is just above the

W -pair production threshold, this dependence is a much more sensitive function of the W mass than at the higher energies (172 to 209 GeV) at which LEP ran during 1996–2000. In the second method, which is used at the higher energies, the W mass has been determined by directly reconstructing the W and its invariant mass from its decay products.

Each LEP experiment has combined their own mass values, properly taking into account the common systematic errors. In order to compute the LEP average W mass, each experiment has provided its measured W mass for the $q\bar{q}q\bar{q}$ and $q\bar{q}\ell\bar{\nu}_\ell$, $\ell = e, \mu, \tau$ channels at each center-of-mass energy, along with a detailed break-up of errors (statistical and uncorrelated, partially correlated and fully correlated systematics [1]). These have been properly combined to obtain a LEP W mass of $M_W = 80.376 \pm 0.033$ GeV, which includes W mass determination from W -pair production cross section variation at threshold. Errors due to uncertainties in LEP energy (9 MeV), and possible effect of color reconnection (CR) and Bose-Einstein correlations (BEC) between quarks from different W 's (8 MeV) are included. The mass difference between $q\bar{q}q\bar{q}$ and $q\bar{q}\ell\bar{\nu}_\ell$ final states (due to possible CR and BEC effects) is -12 ± 45 MeV. In a similar manner, the width results obtained at LEP have been combined, resulting in $\Gamma_W = 2.196 \pm 0.083$ GeV [1].

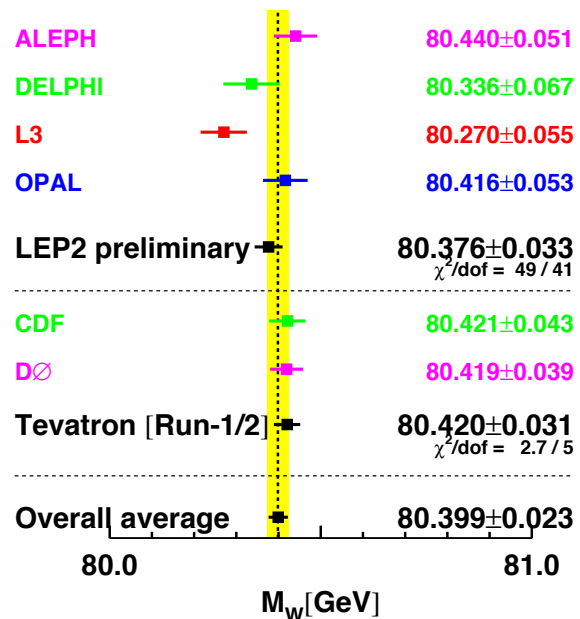


Figure 1: Measurements of the W -boson mass by the LEP and Tevatron experiments. Color version at end of book.

The two Tevatron experiments have also identified common systematic errors. Between the two experiments, uncertainties due to the production model, radiative corrections and parton distribution functions are treated as correlated. An average W mass of $M_W = 80.420 \pm 0.031$ GeV [2] and a W width of $\Gamma_W = 2.046 \pm 0.049$ GeV [3] are obtained.

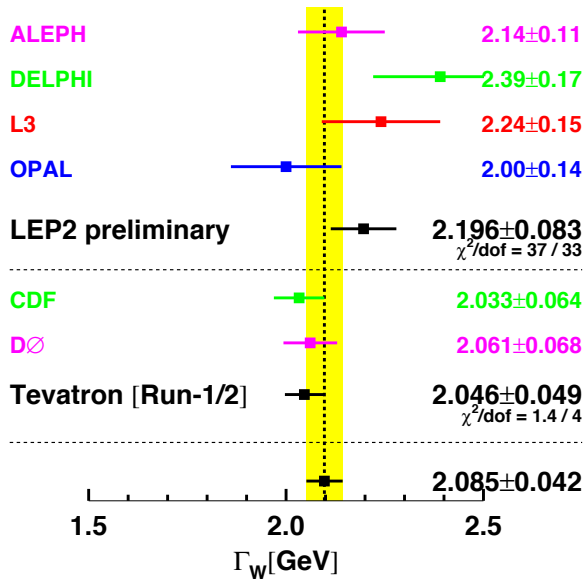


Figure 2: Measurements of the W -boson width by the LEP and Tevatron experiments. Color version at end of book.

The LEP and Tevatron results on mass and width, which are based on all results available, are compared in Fig. 1 and Fig. 2. Combining these results, assuming no common systematics between the LEP and Tevatron measurements, yields an average W mass of $M_W = 80.399 \pm 0.023$ GeV and a W width of $\Gamma_W = 2.085 \pm 0.042$ GeV.

The Standard Model prediction from the electroweak fit, using Z -pole data plus m_{top} measurement, gives a W -boson mass of $M_W = 80.364 \pm 0.020$ GeV and a W -boson width of $\Gamma_W = 2.091 \pm 0.002$ GeV [4].

References

1. The LEP Collaborations: ALEPH, DELPHI, L3, OPAL, the LEP Electroweak Working Group, CERN-PH-EP/2006-042, hep-ex/0612034 (14 December 2006).
2. The Tevatron Electroweak Working Group, for the CDF and DØ Collaborations: *Updated Combination of CDF and DØ Results for the Mass of the W Boson*, August 2009, arXiv:0908.1374 [hep-ex].
3. The Tevatron Electroweak Working Group, for the CDF and DØ Collaborations: *Combination of CDF and DØ Results on the Width of the W Boson*, March 2010, arXiv:1003.2826 [hep-ex].
4. The ALEPH, CDF, DØ, DELPHI, L3, OPAL, SLD Collaborations, the LEP Electroweak Working Group, the Tevatron Electroweak Working Group, and the SLD electroweak and heavy flavour groups, CERN-PH-EP/2009-023, arXiv:0911.2604 [hep-ex] (November 2009).

W MASS

The W -mass listed here corresponds to the mass parameter in a Breit-Wigner distribution with mass-dependent width. To obtain the world average, common systematic uncertainties between experiments are properly taken into account. The LEP-2 average W mass based on published results is 80.376 ± 0.033 GeV [CERN-PH-EP/2006-042]. The combined Tevatron data yields an average W mass of 80.420 ± 0.031 GeV [FERMILAB-TM-2439-E].

OUR FIT uses these average LEP and Tevatron mass values and combines them assuming no correlations.

VALUE (GeV)	EVTS	DOCUMENT ID	TECN	COMMENT
80.399 ± 0.023 OUR FIT				
80.401 ± 0.043	500k	1 ABAZOV	09AB D0	$E_{\text{cm}}^{\text{PD}} = 1.96$ TeV
80.336 ± 0.055 ± 0.039	10.3k	2 ABDALLAH	08A DLPH	$E_{\text{cm}}^{\text{ee}} = 161\text{--}209$ GeV
80.413 ± 0.034 ± 0.034	115k	3 AALTONEN	07F CDF	$E_{\text{cm}}^{\text{PD}} = 1.96$ TeV
80.415 ± 0.042 ± 0.031	11830	4 ABBIENDI	06 OPAL	$E_{\text{cm}}^{\text{ee}} = 170\text{--}209$ GeV
80.270 ± 0.046 ± 0.031	9909	5 ACHARD	06 L3	$E_{\text{cm}}^{\text{ee}} = 161\text{--}209$ GeV
80.440 ± 0.043 ± 0.027	8692	6 SCHAELE	06 ALEP	$E_{\text{cm}}^{\text{ee}} = 161\text{--}209$ GeV
80.483 ± 0.084	49247	7 ABAZOV	02D D0	$E_{\text{cm}}^{\text{PD}} = 1.8$ TeV
80.433 ± 0.079	53841	8 AFFOLDER	01E CDF	$E_{\text{cm}}^{\text{PD}} = 1.8$ TeV
• • • We do not use the following data for averages, fits, limits, etc. • • •				
82.87 ± 1.82 $^{+0.30}_{-0.16}$	1500	9 AKTAS	06 H1	$e^{\pm} p \rightarrow \bar{\nu}_e(\nu_e) X$, $\sqrt{s} \approx 300$ GeV
80.3 ± 2.1 ± 1.2 ± 1.0	645	10 CHEKANOV	02C ZEUS	$e^- p \rightarrow \nu_e X$, $\sqrt{s} = 318$ GeV
81.4 $^{+2.7}_{-2.6}$ ± 2.0 $^{+3.3}_{-3.0}$	1086	11 BREITWEG	00D ZEUS	$e^+ p \rightarrow \bar{\nu}_e X$, $\sqrt{s} \approx 300$ GeV
80.84 ± 0.22 ± 0.83	2065	12 ALITTI	92B UA2	See W/Z ratio below
80.79 ± 0.31 ± 0.84		13 ALITTI	90B UA2	$E_{\text{cm}}^{\text{PD}} = 546,630$ GeV
80.0 ± 3.3 ± 2.4	22	14 ABE	89I CDF	$E_{\text{cm}}^{\text{PD}} = 1.8$ TeV
82.7 ± 1.0 ± 2.7	149	15 ALBAJAR	89 UA1	$E_{\text{cm}}^{\text{PD}} = 546,630$ GeV
81.8 $^{+6.0}_{-5.3}$ ± 2.6	46	16 ALBAJAR	89 UA1	$E_{\text{cm}}^{\text{PD}} = 546,630$ GeV
89 ± 3 ± 6	32	17 ALBAJAR	89 UA1	$E_{\text{cm}}^{\text{PD}} = 546,630$ GeV
81 ± 5.	6	ARNISON	83 UA1	$E_{\text{cm}}^{\text{ee}} = 546$ GeV
80. $^{+10.}_{-6.}$	4	BANNER	83B UA2	Repl. by ALITTI 90B

¹ ABAZOV 09AB study the transverse mass, transverse electron momentum, and transverse missing energy in a sample of 0.5 million $W \rightarrow e\nu$ decays selected in Run-II data. The quoted result combines all three methods, accounting for correlations.

² ABDALLAH 08A use direct reconstruction of the kinematics of $W^+ W^- \rightarrow q\bar{q}\ell\nu$ and $W^+ W^- \rightarrow q\bar{q}q\bar{q}$ events for energies 172 GeV and above. The W mass was also extracted from the dependence of the WW cross section close to the production threshold and combined appropriately to obtain the final result. The systematic error includes ± 0.025 GeV due to final state interactions and ± 0.009 GeV due to LEP energy uncertainty.

³ AALTONEN 07F obtain high purity $W \rightarrow e\nu$ and $W \rightarrow \mu\nu$ candidate samples totaling 63,964 and 51,128 events respectively. The W mass value quoted above is derived by simultaneously fitting the transverse mass and the lepton, and neutrino p_T distributions.

⁴ ABBIENDI 06 use direct reconstruction of the kinematics of $W^+ W^- \rightarrow q\bar{q}\ell\nu$ and $W^+ W^- \rightarrow q\bar{q}q\bar{q}$ events. The result quoted here is obtained combining this mass value with the results using $W^+ W^- \rightarrow \ell\nu\ell'\nu\ell'$ events in the energy range 183–207 GeV (ABBIENDI 03c) and the dependence of the WW production cross-section on m_{WW} at threshold. The systematic error includes ± 0.009 GeV due to the uncertainty on the LEP beam energy.

⁵ ACHARD 06 use direct reconstruction of the kinematics of $W^+ W^- \rightarrow q\bar{q}\ell\nu$ and $W^+ W^- \rightarrow q\bar{q}q\bar{q}$ events in the C.M. energy range 189–209 GeV. The result quoted here is obtained combining this mass value with the results obtained from a direct W mass reconstruction at 172 and 183 GeV and with those from the dependence of the WW production cross-section on m_{WW} at 161 and 172 GeV (ACCIARRI 99).

⁶ SCHAELE 06 use direct reconstruction of the kinematics of $W^+ W^- \rightarrow q\bar{q}\ell\nu$ and $W^+ W^- \rightarrow q\bar{q}q\bar{q}$ events in the C.M. energy range 183–209 GeV. The result quoted here is obtained combining this mass value with those obtained from the dependence of the W pair production cross-section on m_{WW} at 161 and 172 GeV (BARATE 97 and BARATE 97s respectively). The systematic error includes ± 0.009 GeV due to possible effects of final state interactions in the $q\bar{q}q\bar{q}$ channel and ± 0.009 GeV due to the uncertainty on the LEP beam energy.

⁷ ABAZOV 02D improve the measurement of the W -boson mass including $W \rightarrow e\nu$ events in which the electron is close to a boundary of a central electromagnetic calorimeter module. Properly combining the results obtained by fitting $m_T(W)$, $p_T(e)$, and $p_T(\nu)$, this sample provides a mass value of 80.574 ± 0.405 GeV. The value reported here is a combination of this measurement with all previous DØ W -boson mass measurements.

⁸ AFFOLDER 01E fit the transverse mass spectrum of 30115 $W \rightarrow e\nu_e$ events ($M_W = 80.473 \pm 0.065 \pm 0.092$ GeV) and of 14740 $W \rightarrow \mu\nu_\mu$ events ($M_W = 80.465 \pm 0.100 \pm 0.103$ GeV) obtained in the run IB (1994–95). Combining the electron and muon results, accounting for correlated uncertainties, yields $M_W = 80.470 \pm 0.089$ GeV. They combine this value with their measurement of ABE 95P reported in run IA (1992–93) to obtain the quoted value.

⁹ AKTAS 06 fit the Q^2 dependence ($300 < Q^2 < 30,000$ GeV²) of the charged-current differential cross section with a propagator mass. The first error is experimental and the second corresponds to uncertainties due to input parameters and model assumptions.

¹⁰ CHEKANOV 02c fit the Q^2 dependence ($200 < Q^2 < 60,000$ GeV²) of the charged-current differential cross sections with a propagator mass fit. The last error is due to the uncertainty on the probability density functions.

¹¹ BREITWEG 00d fit the Q^2 dependence ($200 < Q^2 < 225,000$ GeV²) of the charged-current differential cross sections with a propagator mass fit. The last error is due to the uncertainty on the probability density functions.

¹² ALITTI 92B result has two contributions to the systematic error (± 0.83); one (± 0.81) cancels in m_{WW}/m_Z and one (± 0.17) is noncancelling. These were added in quadrature. We choose the ALITTI 92B value without using the LEP m_Z value, because we perform our own combined fit.

¹³ There are two contributions to the systematic error (± 0.84): one (± 0.81) which cancels in m_{WW}/m_Z and one (± 0.21) which is non-cancelling. These were added in quadrature.

¹⁴ ABE 89I systematic error dominated by the uncertainty in the absolute energy scale.

Gauge & Higgs Boson Particle Listings

W

- ¹⁵ ALBAJAR 89 result is from a total sample of 299 $W \rightarrow e\nu$ events.
¹⁶ ALBAJAR 89 result is from a total sample of 67 $W \rightarrow \mu\nu$ events.
¹⁷ ALBAJAR 89 result is from $W \rightarrow \tau\nu$ events.

W/Z MASS RATIO

VALUE	EVTS	DOCUMENT ID	TECN	COMMENT
0.8819 ± 0.0012 OUR AVERAGE				
0.8821 ± 0.0011 ± 0.0008	28323	¹⁸ ABBOTT	98N D0	$E_{cm}^{pp} = 1.8$ TeV
0.88114 ± 0.00154 ± 0.00252	5982	¹⁹ ABBOTT	98P D0	$E_{cm}^{pp} = 1.8$ TeV
0.8813 ± 0.0036 ± 0.0019	156	²⁰ ALITTI	92B UA2	$E_{cm}^{pp} = 630$ GeV

- ¹⁸ ABBOTT 98N obtain this from a study of 28323 $W \rightarrow e\nu_e$ and 3294 $Z \rightarrow e^+e^-$ decays. Of this latter sample, 2179 events are used to calibrate the electron energy scale.
¹⁹ ABBOTT 98P obtain this from a study of 5982 $W \rightarrow e\nu_e$ events. The systematic error includes an uncertainty of ± 0.00175 due to the electron energy scale.
²⁰ Scale error cancels in this ratio.

m_Z - m_W

VALUE (GeV)	DOCUMENT ID	TECN	COMMENT
10.4 ± 1.4 ± 0.8	ALBAJAR 89	UA1	$E_{cm}^{pp} = 546,630$ GeV
• • • We do not use the following data for averages, fits, limits, etc. • • •			
11.3 ± 1.3 ± 0.9	ANSARI 87	UA2	$E_{cm}^{pp} = 546,630$ GeV

m_{W+} - m_{W-}

Test of CPT invariance.

VALUE (GeV)	EVTS	DOCUMENT ID	TECN	COMMENT
-0.19 ± 0.58	1722	ABE 90G	CDF	$E_{cm}^{pp} = 1.8$ TeV

W WIDTH

The W width listed here corresponds to the width parameter in a Breit-Wigner distribution with mass-dependent width. To obtain the world average, common systematic uncertainties between experiments are properly taken into account. The LEP-2 average W width based on published results is 2.196 ± 0.083 GeV [CERN-PH-EP/2006-042]. The combined Tevatron data yields an average W width of 2.046 ± 0.049 GeV [FERMILAB-TM-2460-E].

OUR FIT uses these average LEP and Tevatron width values and combines them assuming no correlations.

VALUE (GeV)	EVTS	DOCUMENT ID	TECN	COMMENT
2.085 ± 0.042 OUR FIT				
2.028 ± 0.072	5272	²¹ ABAZOV	09AK D0	$E_{cm}^{pp} = 1.96$ GeV
2.032 ± 0.045 ± 0.057	6055	²² AALTONEN	08B CDF	$E_{cm}^{pp} = 1.96$ TeV
2.404 ± 0.140 ± 0.101	10.3k	²³ ABDALLAH	08A DLPH	$E_{cm}^{ee} = 183-209$ GeV
1.996 ± 0.096 ± 0.102	10729	²⁴ ABBIENDI	06 OPAL	$E_{cm}^{ee} = 170-209$ GeV
2.18 ± 0.11 ± 0.09	9795	²⁵ ACHARD	06 L3	$E_{cm}^{ee} = 172-209$ GeV
2.14 ± 0.09 ± 0.06	8717	²⁶ SCHAEEL	06 ALEP	$E_{cm}^{ee} = 183-209$ GeV
2.23 $^{+0.15}_{-0.14}$ ± 0.10	294	²⁷ ABAZOV	02E D0	Direct meas.
2.05 ± 0.10 ± 0.08	662	²⁸ AFFOLDER	00M CDF	Direct meas.
• • • We do not use the following data for averages, fits, limits, etc. • • •				
2.152 ± 0.066	79176	²⁹ ABBOTT	00B D0	Extracted value
2.064 ± 0.060 ± 0.059		³⁰ ABE	95W CDF	Extracted value
2.10 $^{+0.14}_{-0.13}$ ± 0.09	3559	³¹ ALITTI	92 UA2	Extracted value
2.18 $^{+0.26}_{-0.24}$ ± 0.04		³² ALBAJAR	91 UA1	Extracted value

- ²¹ ABAZOV 09AK obtain this result fitting the high-end tail (100-200 GeV) of the transverse mass spectrum in $W \rightarrow e\nu$ decays.
²² AALTONEN 08B obtain this result fitting the high-end tail (90-200 GeV) of the transverse mass spectrum in semileptonic $W \rightarrow e\nu_e$ and $W \rightarrow \mu\nu_\mu$ decays.
²³ ABDALLAH 08A use direct reconstruction of the kinematics of $W^+W^- \rightarrow q\bar{q}\ell\nu$ and $W^+W^- \rightarrow q\bar{q}q\bar{q}$ events. The systematic error includes ± 0.065 GeV due to final state interactions.
²⁴ ABBIENDI 06 use direct reconstruction of the kinematics of $W^+W^- \rightarrow q\bar{q}\ell\nu_\ell$ and $W^+W^- \rightarrow q\bar{q}q\bar{q}$ events. The systematic error includes ± 0.003 GeV due to the uncertainty on the LEP beam energy.
²⁵ ACHARD 06 use direct reconstruction of the kinematics of $W^+W^- \rightarrow q\bar{q}\ell\nu_\ell$ and $W^+W^- \rightarrow q\bar{q}q\bar{q}$ events in the C.M. energy range 189-209 GeV. The result quoted here is obtained combining this value of the width with the result obtained from a direct W mass reconstruction at 172 and 183 GeV (ACCIARRI 99).
²⁶ SCHAEEL 06 use direct reconstruction of the kinematics of $W^+W^- \rightarrow q\bar{q}\ell\nu_\ell$ and $W^+W^- \rightarrow q\bar{q}q\bar{q}$ events. The systematic error includes ± 0.05 GeV due to possible effects of final state interactions in the $q\bar{q}q\bar{q}$ channel and ± 0.01 GeV due to the uncertainty on the LEP beam energy.
²⁷ ABAZOV 02E obtain this result fitting the high-end tail (90-200 GeV) of the transverse-mass spectrum in semileptonic $W \rightarrow e\nu_e$ decays.
²⁸ AFFOLDER 00M fit the high transverse mass (100-200 GeV) $W \rightarrow e\nu_e$ and $W \rightarrow \mu\nu_\mu$ events to obtain $\Gamma(W) = 2.04 \pm 0.11(\text{stat}) \pm 0.09(\text{syst})$ GeV. This is combined with the earlier CDF measurement (ABE 95c) to obtain the quoted result.

- ²⁹ ABBOTT 00B measure $R = 10.43 \pm 0.27$ for the $W \rightarrow e\nu_e$ decay channel. They use the SM theoretical predictions for $\sigma(W)/\sigma(Z)$ and $\Gamma(W \rightarrow e\nu_e)$ and the world average for $B(Z \rightarrow ee)$. The value quoted here is obtained combining this result (2.169 ± 0.070 GeV) with that of ABBOTT 99H.
³⁰ ABE 95W measured $R = 10.90 \pm 0.32 \pm 0.29$. They use $m_W = 80.23 \pm 0.18$ GeV, $\sigma(W)/\sigma(Z) = 3.35 \pm 0.03$, $\Gamma(W \rightarrow e\nu) = 225.9 \pm 0.9$ MeV, $\Gamma(Z \rightarrow e^+e^-) = 83.98 \pm 0.18$ MeV, and $\Gamma(Z) = 2.4969 \pm 0.0038$ GeV.
³¹ ALITTI 92 measured $R = 10.4 \pm 0.7 \pm 0.6 \pm 0.3$. The values of $\sigma(Z)$ and $\sigma(W)$ come from α_s^2 calculations using $m_W = 80.14 \pm 0.27$ GeV, and $m_Z = 91.175 \pm 0.021$ GeV along with the corresponding value of $\sin^2\theta_W = 0.2274$. They use $\sigma(W)/\sigma(Z) = 3.26 \pm 0.07 \pm 0.05$ and $\Gamma(Z) = 2.487 \pm 0.010$ GeV.
³² ALBAJAR 91 measured $R = 9.5 \pm 1.1 \pm 1.0$ (stat. + syst.). $\sigma(W)/\sigma(Z)$ is calculated in QCD at the parton level using $m_W = 80.18 \pm 0.28$ GeV and $m_Z = 91.172 \pm 0.031$ GeV along with $\sin^2\theta_W = 0.2322 \pm 0.0014$. They use $\sigma(W)/\sigma(Z) = 3.23 \pm 0.05$ and $\Gamma(Z) = 2.498 \pm 0.020$ GeV. This measurement is obtained combining both the electron and muon channels.

W⁺ DECAY MODES

W⁻ modes are charge conjugates of the modes below.

Mode	Fraction (Γ_i/Γ)	Confidence level
Γ_1 $\ell^+\nu$	[a] (10.80 ± 0.09) %	
Γ_2 $e^+\nu$	(10.75 ± 0.13) %	
Γ_3 $\mu^+\nu$	(10.57 ± 0.15) %	
Γ_4 $\tau^+\nu$	(11.25 ± 0.20) %	
Γ_5 hadrons	(67.60 ± 0.27) %	
Γ_6 $\pi^+\gamma$	< 8	× 10 ⁻⁵ 95%
Γ_7 $D_s^+\gamma$	< 1.3	× 10 ⁻³ 95%
Γ_8 cX	(33.4 ± 2.6) %	
Γ_9 c \bar{X}	(31 $^{+13}_{-11}$) %	
Γ_{10} invisible	[b] (1.4 ± 2.9) %	

[a] ℓ indicates each type of lepton (e, μ , and τ), not sum over them.

[b] This represents the width for the decay of the W boson into a charged particle with momentum below detectability, p < 200 MeV.

W PARTIAL WIDTHS

$\Gamma(\text{invisible})$ Γ_{10}
This represents the width for the decay of the W boson into a charged particle with momentum below detectability, p < 200 MeV.

VALUE (MeV)	DOCUMENT ID	TECN	COMMENT
30 $^{+52}_{-48}$ ± 33	³³ BARATE	99L ALEP	$E_{cm}^{ee} = 161+172+183$ GeV
• • • We do not use the following data for averages, fits, limits, etc. • • •			
	³⁴ BARATE	99L ALEP	$E_{cm}^{ee} = 161+172+183$ GeV

- ³³ BARATE 99L measure this quantity using the dependence of the total cross section σ_{WW} upon a change in the total width. The fit is performed to the WW measured cross sections at 161, 172, and 183 GeV. This partial width is < 139 MeV at 95%CL.
³⁴ BARATE 99L use W-pair production to search for effectively invisible W decays, tagging with the decay of the other W boson to Standard Model particles. The partial width for effectively invisible decay is < 27 MeV at 95%CL.

W BRANCHING RATIOS

Overall fits are performed to determine the branching ratios of the W. LEP averages on $W \rightarrow e\nu_e$, $W \rightarrow \mu\nu_\mu$, and $W \rightarrow \tau\nu_\tau$, and their correlations are first obtained by combining results from the four experiments taking properly into account the common systematics. The procedure is described in the note LEPEWWG/XSEC/2001-02, 30 March 2001, at <http://lepewwg.web.cern.ch/LEPEWWG/lepww/4f/PDG01>. The LEP average values so obtained, using published data, are given in the note LEPEWWG/XSEC/2005-01 accessible at <http://lepewwg.web.cern.ch/LEPEWWG/lepww/4f/PDG05/>. These results, together with results from the p \bar{p} colliders are then used in fits to obtain the world average W branching ratios. A first fit determines three individual leptonic branching ratios, B(W → eν_e), B(W → μν_μ), and B(W → τν_τ). This fit has a $\chi^2 = 4.7$ for 10 degrees of freedom. A second fit assumes lepton universality and determines the leptonic branching ratio B(W → ℓν_ℓ) and the hadronic branching ratio is derived as B(W → hadrons) = 1-3B(W → ℓν). This fit has a $\chi^2 = 11.3$ for 12 degrees of freedom.

The LEP $W \rightarrow \ell\nu$ data are obtained by the Collaborations using individual leptonic channels and are, therefore, not included in the overall fits to avoid double counting.

Note: The LEP combination including the new OPAL results, ABBIENDI 07A, could not be performed in time for this Review. Thus, the OUR FIT values quoted below use the previous OPAL results as in ABBIENDI, G 00.

See key on page 405

Gauge & Higgs Boson Particle Listings

W

 $\Gamma(\ell^+\nu)/\Gamma_{\text{total}}$ Γ_1/Γ ℓ indicates average over $e, \mu,$ and τ modes, not sum over modes.

VALUE (units 10^{-2})	EVTS	DOCUMENT ID	TECN	COMMENT
10.80 ± 0.09 OUR FIT				
10.86 ± 0.12 ± 0.08	16438	ABBIENDI	07A OPAL	$E_{\text{cm}}^{ee} = 161\text{--}209$ GeV
10.85 ± 0.14 ± 0.08	13600	ABDALLAH	04G DLPH	$E_{\text{cm}}^{ee} = 161\text{--}209$ GeV
10.83 ± 0.14 ± 0.10	11246	ACHARD	04J L3	$E_{\text{cm}}^{ee} = 161\text{--}209$ GeV
10.96 ± 0.12 ± 0.05	16116	SCHAELE	04A ALEP	$E_{\text{cm}}^{ee} = 183\text{--}209$ GeV
11.02 ± 0.52	11858	³⁵ ABBOTT	99H D0	$E_{\text{cm}}^{p\bar{p}} = 1.8$ TeV
10.4 ± 0.8	3642	³⁶ ABE	92I CDF	$E_{\text{cm}}^{p\bar{p}} = 1.8$ TeV

³⁵ ABBOTT 99H measure $R \equiv [\sigma_W B(W \rightarrow \ell\nu_\ell)]/[\sigma_Z B(Z \rightarrow \ell\ell)] = 10.90 \pm 0.52$ combining electron and muon channels. They use $M_W = 80.39 \pm 0.06$ GeV and the SM theoretical predictions for $\sigma(W)/\sigma(Z)$ and $B(Z \rightarrow \ell\ell)$.

³⁶ $121.6 \pm 38^{+27}_{-31}$ $W \rightarrow \mu\nu$ events from ABE 92I and $2426W \rightarrow e\nu$ events of ABE 91C. ABE 92I give the inverse quantity as 9.6 ± 0.7 and we have inverted.

 $\Gamma(e^+\nu)/\Gamma_{\text{total}}$ Γ_2/Γ

VALUE (units 10^{-2})	EVTS	DOCUMENT ID	TECN	COMMENT
10.75 ± 0.13 OUR FIT				
10.71 ± 0.25 ± 0.11	2374	ABBIENDI	07A OPAL	$E_{\text{cm}}^{ee} = 161\text{--}209$ GeV
10.55 ± 0.31 ± 0.14	1804	ABDALLAH	04G DLPH	$E_{\text{cm}}^{ee} = 161\text{--}209$ GeV
10.78 ± 0.29 ± 0.13	1576	ACHARD	04J L3	$E_{\text{cm}}^{ee} = 161\text{--}209$ GeV
10.78 ± 0.27 ± 0.10	2142	SCHAELE	04A ALEP	$E_{\text{cm}}^{ee} = 183\text{--}209$ GeV
• • • We do not use the following data for averages, fits, limits, etc. • • •				
10.61 ± 0.28		³⁷ ABAZOV	04D TEVA	$E_{\text{cm}}^{p\bar{p}} = 1.8$ TeV

³⁷ ABAZOV 04D take into account all correlations to properly combine the CDF (ABE 95W) and $D\bar{D}$ (ABBOTT 00B) measurements of the ratio R in the electron channel. The ratio R is defined as $[\sigma_W \cdot B(W \rightarrow e\nu_e)] / [\sigma_Z \cdot B(Z \rightarrow ee)]$. The combination gives $R^{\text{TeVatron}} = 10.59 \pm 0.23$. σ_W / σ_Z is calculated at next-to-next-to-leading order (3.360 ± 0.051). The branching fraction $B(Z \rightarrow ee)$ is taken from this Review as (3.363 ± 0.004)%.

 $\Gamma(\mu^+\nu)/\Gamma_{\text{total}}$ Γ_3/Γ

VALUE (units 10^{-2})	EVTS	DOCUMENT ID	TECN	COMMENT
10.57 ± 0.15 OUR FIT				
10.78 ± 0.24 ± 0.10	2397	ABBIENDI	07A OPAL	$E_{\text{cm}}^{ee} = 161\text{--}209$ GeV
10.65 ± 0.26 ± 0.08	1998	ABDALLAH	04G DLPH	$E_{\text{cm}}^{ee} = 161\text{--}209$ GeV
10.03 ± 0.29 ± 0.12	1423	ACHARD	04J L3	$E_{\text{cm}}^{ee} = 161\text{--}209$ GeV
10.87 ± 0.25 ± 0.08	2216	SCHAELE	04A ALEP	$E_{\text{cm}}^{ee} = 183\text{--}209$ GeV

 $\Gamma(\tau^+\nu)/\Gamma_{\text{total}}$ Γ_4/Γ

VALUE (units 10^{-2})	EVTS	DOCUMENT ID	TECN	COMMENT
11.25 ± 0.20 OUR FIT				
11.14 ± 0.31 ± 0.17	2177	ABBIENDI	07A OPAL	$E_{\text{cm}}^{ee} = 161\text{--}209$ GeV
11.46 ± 0.39 ± 0.19	2034	ABDALLAH	04G DLPH	$E_{\text{cm}}^{ee} = 161\text{--}209$ GeV
11.89 ± 0.40 ± 0.20	1375	ACHARD	04J L3	$E_{\text{cm}}^{ee} = 161\text{--}209$ GeV
11.25 ± 0.32 ± 0.20	2070	SCHAELE	04A ALEP	$E_{\text{cm}}^{ee} = 183\text{--}209$ GeV

 $\Gamma(\text{hadrons})/\Gamma_{\text{total}}$ Γ_5/Γ

OUR FIT value is obtained by a fit to the lepton branching ratio data assuming lepton universality.

VALUE (units 10^{-2})	EVTS	DOCUMENT ID	TECN	COMMENT
67.60 ± 0.27 OUR FIT				
67.41 ± 0.37 ± 0.23	16438	ABBIENDI	07A OPAL	$E_{\text{cm}}^{ee} = 161\text{--}209$ GeV
67.45 ± 0.41 ± 0.24	13600	ABDALLAH	04G DLPH	$E_{\text{cm}}^{ee} = 161\text{--}209$ GeV
67.50 ± 0.42 ± 0.30	11246	ACHARD	04J L3	$E_{\text{cm}}^{ee} = 161\text{--}209$ GeV
67.13 ± 0.37 ± 0.15	16116	SCHAELE	04A ALEP	$E_{\text{cm}}^{ee} = 183\text{--}209$ GeV

 $\Gamma(\mu^+\nu)/\Gamma(e^+\nu)$ Γ_3/Γ_2

VALUE	EVTS	DOCUMENT ID	TECN	COMMENT
0.983 ± 0.018 OUR FIT				
0.89 ± 0.10	13k	³⁸ ABACHI	95D D0	$E_{\text{cm}}^{p\bar{p}} = 1.8$ TeV
1.02 ± 0.08	1216	³⁹ ABE	92I CDF	$E_{\text{cm}}^{p\bar{p}} = 1.8$ TeV
1.00 ± 0.14 ± 0.08	67	ALBAJAR	89 UA1	$E_{\text{cm}}^{p\bar{p}} = 546,630$ GeV
• • • We do not use the following data for averages, fits, limits, etc. • • •				
1.24 \pm $\begin{smallmatrix} 0.6 \\ -0.4 \end{smallmatrix}$	14	ARNISON	84D UA1	Repl. by ALBAJAR 89

³⁸ ABACHI 95D obtain this result from the measured $\sigma_W B(W \rightarrow \mu\nu) = 2.09 \pm 0.23 \pm 0.11$ nb and $\sigma_W B(W \rightarrow e\nu) = 2.36 \pm 0.07 \pm 0.13$ nb in which the first error is the combined statistical and systematic uncertainty, the second reflects the uncertainty in the luminosity.

³⁹ ABE 92I obtain $\sigma_W B(W \rightarrow \mu\nu) = 2.21 \pm 0.07 \pm 0.21$ and combine with ABE 91C $\sigma_W B(W \rightarrow e\nu)$ to give a ratio of the couplings from which we derive this measurement.

 $\Gamma(\tau^+\nu)/\Gamma(e^+\nu)$ Γ_4/Γ_2

VALUE	EVTS	DOCUMENT ID	TECN	COMMENT
1.046 ± 0.023 OUR FIT				
0.961 ± 0.061	980	⁴⁰ ABBOTT	00D D0	$E_{\text{cm}}^{p\bar{p}} = 1.8$ TeV
0.94 ± 0.14	179	⁴¹ ABE	92E CDF	$E_{\text{cm}}^{p\bar{p}} = 1.8$ TeV
1.04 ± 0.08 ± 0.08	754	⁴² ALITTI	92F UA2	$E_{\text{cm}}^{p\bar{p}} = 630$ GeV
1.02 ± 0.20 ± 0.12	32	ALBAJAR	89 UA1	$E_{\text{cm}}^{p\bar{p}} = 546,630$ GeV
• • • We do not use the following data for averages, fits, limits, etc. • • •				
0.995 ± 0.112 ± 0.083	198	ALITTI	91C UA2	Repl. by ALITTI 92F
1.02 ± 0.20 ± 0.10	32	ALBAJAR	87 UA1	Repl. by ALBAJAR 89

⁴⁰ ABBOTT 00D measure $\sigma_W \times B(W \rightarrow \tau\nu_\tau) = 2.22 \pm 0.09 \pm 0.10 \pm 0.10$ nb. Using the ABBOTT 00B result $\sigma_W \times B(W \rightarrow e\nu_e) = 2.31 \pm 0.01 \pm 0.05 \pm 0.10$ nb, they quote the ratio of the couplings from which we derive this measurement.

⁴¹ ABE 92E use two procedures for selecting $W \rightarrow \tau\nu_\tau$ events. The missing E_T trigger leads to $132 \pm 14 \pm 8$ events and the τ trigger to $47 \pm 9 \pm 4$ events. Proper statistical and systematic correlations are taken into account to arrive at $\sigma_B(W \rightarrow \tau\nu) = 2.05 \pm 0.27$ nb. Combined with ABE 91C result on $\sigma_B(W \rightarrow e\nu)$, ABE 92E quote a ratio of the couplings from which we derive this measurement.

⁴² This measurement is derived by us from the ratio of the couplings of ALITTI 92F.

 $\Gamma(\pi^+\gamma)/\Gamma(e^+\nu)$ Γ_6/Γ_2

VALUE	CL%	DOCUMENT ID	TECN	COMMENT
< 7 × 10⁻⁴	95	ABE	98H CDF	$E_{\text{cm}}^{p\bar{p}} = 1.8$ TeV
< 4.9 × 10 ⁻³	95	⁴³ ALITTI	92D UA2	$E_{\text{cm}}^{p\bar{p}} = 630$ GeV
< 5.8 × 10 ⁻³	95	⁴⁴ ALBAJAR	90 UA1	$E_{\text{cm}}^{p\bar{p}} = 546, 630$ GeV

⁴³ ALITTI 92D limit is 3.8×10^{-3} at 90% CL.

⁴⁴ ALBAJAR 90 obtain < 0.048 at 90% CL.

 $\Gamma(D_s^+\gamma)/\Gamma(e^+\nu)$ Γ_7/Γ_2

VALUE	CL%	DOCUMENT ID	TECN	COMMENT
< 1.2 × 10⁻²	95	ABE	98P CDF	$E_{\text{cm}}^{p\bar{p}} = 1.8$ TeV

 $\Gamma(cX)/\Gamma(\text{hadrons})$ Γ_8/Γ_5

VALUE	EVTS	DOCUMENT ID	TECN	COMMENT
0.49 ± 0.04 OUR AVERAGE				
0.481 ± 0.042 ± 0.032	3005	⁴⁵ ABBIENDI	00V OPAL	$E_{\text{cm}}^{ee} = 183 + 189$ GeV
0.51 ± 0.05 ± 0.03	746	⁴⁶ BARATE	99M ALEP	$E_{\text{cm}}^{ee} = 172 + 183$ GeV

⁴⁵ ABBIENDI 00V tag $W \rightarrow cX$ decays using measured jet properties, lifetime information, and leptons produced in charm decays. From this result, and using the additional measurements of $\Gamma(W)$ and $B(W \rightarrow \text{hadrons})$, $|V_{cs}|$ is determined to be $0.969 \pm 0.045 \pm 0.036$.

⁴⁶ BARATE 99M tag c jets using a neural network algorithm. From this measurement $|V_{cs}|$ is determined to be $1.00 \pm 0.11 \pm 0.07$.

 $R_{cs} = \Gamma(c\bar{s})/\Gamma(\text{hadrons})$ Γ_9/Γ_5

VALUE	DOCUMENT ID	TECN	COMMENT
0.46 \pm $\begin{smallmatrix} 0.18 \\ 0.14 \end{smallmatrix} \pm 0.07$	⁴⁷ ABREU	98N DLPH	$E_{\text{cm}}^{ee} = 161 + 172$ GeV

⁴⁷ ABREU 98N tag c and s jets by identifying a charged kaon as the highest momentum particle in a hadronic jet. They also use a lifetime tag to independently identify a c jet, based on the impact parameter distribution of charged particles in a jet. From this measurement $|V_{cs}|$ is determined to be $0.94^{+0.32}_{-0.26} \pm 0.13$.

AVERAGE PARTICLE MULTIPLICITIES IN HADRONIC W DECAY

Summed over particle and antiparticle, when appropriate.

 $\langle N_{\pi^\pm} \rangle$

VALUE	DOCUMENT ID	TECN	COMMENT
15.70 ± 0.35	⁴⁸ ABREU,P	00F DLPH	$E_{\text{cm}}^{ee} = 189$ GeV

⁴⁸ ABREU,P 00F measure $\langle N_{\pi^\pm} \rangle = 31.65 \pm 0.48 \pm 0.76$ and $15.51 \pm 0.38 \pm 0.40$ in the fully hadronic and semileptonic final states respectively. The value quoted is a weighted average without assuming any correlations.

 $\langle N_{K^\pm} \rangle$

VALUE	DOCUMENT ID	TECN	COMMENT
2.20 ± 0.19	⁴⁹ ABREU,P	00F DLPH	$E_{\text{cm}}^{ee} = 189$ GeV

⁴⁹ ABREU,P 00F measure $\langle N_{K^\pm} \rangle = 4.38 \pm 0.42 \pm 0.12$ and $2.23 \pm 0.32 \pm 0.17$ in the fully hadronic and semileptonic final states respectively. The value quoted is a weighted average without assuming any correlations.

 $\langle N_p \rangle$

VALUE	DOCUMENT ID	TECN	COMMENT
0.92 ± 0.14	⁵⁰ ABREU,P	00F DLPH	$E_{\text{cm}}^{ee} = 189$ GeV

⁵⁰ ABREU,P 00F measure $\langle N_p \rangle = 1.82 \pm 0.29 \pm 0.16$ and $0.94 \pm 0.23 \pm 0.06$ in the fully hadronic and semileptonic final states respectively. The value quoted is a weighted average without assuming any correlations.

Gauge & Higgs Boson Particle Listings

W

 $\langle N_{\text{charged}} \rangle$

VALUE	DOCUMENT ID	TECN	COMMENT
19.39 ± 0.08 OUR AVERAGE			
19.38 ± 0.05 ± 0.08	⁵¹ ABBIENDI	06A OPAL	$E_{\text{cm}}^{\text{e}^+e^-} = 189\text{--}209$ GeV
19.44 ± 0.17	⁵² ABREU,P	00F DLPH	$E_{\text{cm}}^{\text{e}^+e^-} = 183\text{--}189$ GeV
19.3 ± 0.3 ± 0.3	⁵³ ABBIENDI	99N OPAL	$E_{\text{cm}}^{\text{e}^+e^-} = 183$ GeV
19.23 ± 0.74	⁵⁴ ABREU	98c DLPH	$E_{\text{cm}}^{\text{e}^+e^-} = 172$ GeV

⁵¹ ABBIENDI 06A measure $\langle N_{\text{charged}} \rangle = 38.74 \pm 0.12 \pm 0.26$ when both W bosons decay hadronically and $\langle N_{\text{charged}} \rangle = 19.39 \pm 0.11 \pm 0.09$ when one W boson decays semileptonically. The value quoted here is obtained under the assumption that there is no color reconnection between W bosons; the value is a weighted average taking into account correlations in the systematic uncertainties.

⁵² ABREU,P 00F measure $\langle N_{\text{charged}} \rangle = 39.12 \pm 0.33 \pm 0.36$ and $38.11 \pm 0.57 \pm 0.44$ in the fully hadronic final states at 189 and 183 GeV respectively, and $\langle N_{\text{charged}} \rangle = 19.49 \pm 0.31 \pm 0.27$ and $19.78 \pm 0.49 \pm 0.43$ in the semileptonic final states. The value quoted is a weighted average without assuming any correlations.

⁵³ ABBIENDI 99N use the final states $W^+ W^- \rightarrow q\bar{q}\ell\bar{\nu}_\ell$ to derive this value.

⁵⁴ ABREU 98c combine results from both the fully hadronic as well semileptonic WW final states after demonstrating that the W decay charged multiplicity is independent of the topology within errors.

TRIPLE GAUGE COUPLINGS (TGC'S)

Revised March 2009 by M.W. Grunewald (U. College Dublin and U. Ghent) and A. Gurtu (Tata Inst.).

Fourteen independent couplings, 7 each for ZWW and γWW , completely describe the VWW vertices within the most general framework of the electroweak Standard Model (SM) consistent with Lorentz invariance and $U(1)$ gauge invariance. Of each of the 7 TGC's, 3 conserve C and P individually, 3 violate CP , and one TGC violates C and P individually while conserving CP . Assumption of C and P conservation and electromagnetic gauge invariance reduces the independent VWW couplings to five: one common set [1,2] is $(\kappa_\gamma, \kappa_Z, \lambda_\gamma, \lambda_Z, g_1^Z)$, where $\kappa_\gamma = \kappa_Z = g_1^Z = 1$ and $\lambda_\gamma = \lambda_Z = 0$ in the Standard Model at the tree level. The parameters κ_Z and λ_Z are related to the other three due to constraints of gauge invariance as follows: $\kappa_Z = g_1^Z - (\kappa_\gamma - 1) \tan^2 \theta_W$ and $\lambda_Z = \lambda_\gamma$, where θ_W is the weak mixing angle. The W magnetic dipole moment, μ_W , and the W electric quadrupole moment, q_W , are expressed as $\mu_W = e(1 + \kappa_\gamma + \lambda_\gamma)/2M_W$ and $q_W = -e(\kappa_\gamma - \lambda_\gamma)/M_W^2$.

Precision measurements of suitable observables at LEP1 has already led to an exploration of much of the TGC parameter space. At LEP2, the VWW coupling arises in W -pair production via s -channel exchange, or in single W production via the radiation of a virtual photon off the incident e^+ or e^- . At the TEVATRON, hard-photon bremsstrahlung off a produced W or Z signals the presence of a triple-gauge vertex. In order to extract the value of one TGC, the others are generally kept fixed to their SM values.

While most analyses use the above gauge constraints in the extraction of TGCs, one analysis of W -pair events also determines the real and imaginary parts of all 14 couplings using unconstrained single-parameter fits [3]. The results are consistent.

References

1. K. Hagiwara *et al.*, Nucl. Phys. **B282**, 253 (1987).
2. G. Gounaris *et al.*, CERN 96-01 p. 525.
3. S. Schael *et al.* (ALEPH Collab.), Phys. Lett. **B614**, 7 (2005).

 g_1^Z

OUR FIT below is obtained by combining the measurements taking into account properly the common systematic errors (see LEPEWWG/TGC/2005-01 at <http://lepewwg.web.cern.ch/LEPEWWG/lepww/tgc>).

VALUE	EVTS	DOCUMENT ID	TECN	COMMENT
0.984 +0.022 -0.019 OUR FIT				
1.07 +0.08 -0.12	1880	⁵⁵ ABDALLAH	08c DLPH	$E_{\text{cm}}^{\text{e}^+e^-} = 189\text{--}209$ GeV
1.001 ± 0.027 ± 0.013	9310	⁵⁶ SCHAEEL	05A ALEP	$E_{\text{cm}}^{\text{e}^+e^-} = 183\text{--}209$ GeV
0.987 +0.034 -0.033	9800	⁵⁷ ABBIENDI	04D OPAL	$E_{\text{cm}}^{\text{e}^+e^-} = 183\text{--}209$ GeV
0.966 +0.034 -0.032 ± 0.015	8325	⁵⁸ ACHARD	04D L3	$E_{\text{cm}}^{\text{e}^+e^-} = 161\text{--}209$ GeV
• • • We do not use the following data for averages, fits, limits, etc. • • •				
1.04 ± 0.09		⁵⁹ ABAZOV	09AD D0	$E_{\text{cm}}^{\text{p}\bar{\text{p}}} = 1.96$ TeV
		⁶⁰ ABAZOV	09AJ D0	$E_{\text{cm}}^{\text{p}\bar{\text{p}}} = 1.96$ TeV
	13	⁶¹ ABAZOV	07Z D0	$E_{\text{cm}}^{\text{p}\bar{\text{p}}} = 1.96$ TeV
	2.3	⁶² ABAZOV	05s D0	$E_{\text{cm}}^{\text{p}\bar{\text{p}}} = 1.96$ TeV
0.98 ± 0.07 ± 0.01	2114	⁶³ ABREU	01i DLPH	$E_{\text{cm}}^{\text{e}^+e^-} = 183\text{--}189$ GeV
	331	⁶⁴ ABBOTT	99i D0	$E_{\text{cm}}^{\text{p}\bar{\text{p}}} = 1.8$ TeV

⁵⁵ ABDALLAH 08c determine this triple gauge coupling from the measurement of the spin density matrix elements in $e^+ e^- \rightarrow W^+ W^- \rightarrow (qq)(\ell\nu)$, where $\ell = e$ or μ . Values of all other couplings are fixed to their standard model values.

⁵⁶ SCHAEEL 05A study single-photon, single- W , and WW -pair production from 183 to 209 GeV. The result quoted here is derived from the WW -pair production sample. Each parameter is determined from a single-parameter fit in which the other parameters assume their Standard Model values.

⁵⁷ ABBIENDI 04D combine results from $W^+ W^-$ in all decay channels. Only CP -conserving couplings are considered and each parameter is determined from a single-parameter fit in which the other parameters assume their Standard Model values. The 95% confidence interval is $0.923 < g_1^Z < 1.054$.

⁵⁸ ACHARD 04D study WW -pair production, single- W production and single-photon production with missing energy from 189 to 209 GeV. The result quoted here is obtained from the WW -pair production sample including data from 161 to 183 GeV, ACCIARRI 99Q. Each parameter is determined from a single-parameter fit in which the other parameters assume their Standard Model values.

⁵⁹ ABAZOV 09AD study the $p\bar{p} \rightarrow \ell\nu 2\text{jet}$ process arising in WW and WZ production. They select 12,473 (14,392) events in the electron (muon) channel with an expected di-boson signal of 436 (527) events. The results on the anomalous couplings are derived from an analysis of the p_T spectrum of the 2-jet system and quoted at 68% C.L. and for a form factor of 2 TeV. This measurement is not used for obtaining the mean as it is for a specific form factor.

⁶⁰ ABAZOV 09AJ study the $p\bar{p} \rightarrow 2\ell 2\nu$ process arising in WW production. They select 100 events with an expected WW signal of 65 events. An analysis of the p_T spectrum of the two charged leptons leads to 95% C.L. limits of $0.86 < g_1^Z < 1.3$, for a form factor $\Lambda = 2$ TeV.

⁶¹ ABAZOV 07Z set limits on anomalous TGCs using the measured cross section and $p_T(Z)$ distribution in WZ production with both the W and the Z decaying leptonically into electrons and muons. Setting other couplings to their standard model values, the 95% C.L. limits for a form factor scale $\Lambda = 1.5$ TeV are $-0.15 < \Delta g_1^Z < 0.35$, and for $\Lambda = 2$ TeV are $-0.14 < \Delta g_1^Z < 0.34$.

⁶² ABAZOV 05s study $p\bar{p} \rightarrow WZ$ production with a subsequent trilepton decay to $\ell\nu\ell'\bar{\nu}'$ (ℓ and $\ell' = e$ or μ). Three events (estimated background 0.71 ± 0.08 events) with WZ decay characteristics are observed from which they derive limits on the anomalous WWZ couplings. The 95% CL limit for a form factor scale $\Lambda = 1.5$ TeV is $0.51 < g_1^Z < 1.66$, fixing λ_Z and κ_Z to their Standard Model values.

⁶³ ABREU 01i combine results from e^+e^- interactions at 189 GeV leading to $W^+ W^-$ and $W\nu_e$ final states with results from ABREU 99L at 183 GeV. The 95% confidence interval is $0.84 < g_1^Z < 1.13$.

⁶⁴ ABBOTT 99i perform a simultaneous fit to the $W\gamma$, $WW \rightarrow$ dilepton, $WW/WZ \rightarrow \nu jj$, $WW/WZ \rightarrow \mu\nu jj$, and $WZ \rightarrow$ trilepton data samples. For $\Lambda = 2.0$ TeV, the 95% CL limits are $0.63 < g_1^Z < 1.57$, fixing λ_Z and κ_Z to their Standard Model values, and assuming Standard Model values for the $WW\gamma$ couplings.

 κ_γ

OUR FIT below is obtained by combining the measurements taking into account properly the common systematic errors (see LEPEWWG/TGC/2005-01 at <http://lepewwg.web.cern.ch/LEPEWWG/lepww/tgc>).

VALUE	EVTS	DOCUMENT ID	TECN	COMMENT
0.973 +0.044 -0.045 OUR FIT				
0.68 +0.17 -0.15	1880	⁶⁵ ABDALLAH	08c DLPH	$E_{\text{cm}}^{\text{e}^+e^-} = 189\text{--}209$ GeV
0.971 ± 0.055 ± 0.030	10689	⁶⁶ SCHAEEL	05A ALEP	$E_{\text{cm}}^{\text{e}^+e^-} = 183\text{--}209$ GeV
0.88 +0.09 -0.08	9800	⁶⁷ ABBIENDI	04D OPAL	$E_{\text{cm}}^{\text{e}^+e^-} = 183\text{--}209$ GeV
1.013 +0.067 -0.064 ± 0.026	10575	⁶⁸ ACHARD	04D L3	$E_{\text{cm}}^{\text{e}^+e^-} = 161\text{--}209$ GeV
• • • We do not use the following data for averages, fits, limits, etc. • • •				
	53	⁶⁹ AARON	09B H1	$E_{\text{cm}}^{\text{p}\bar{\text{p}}} = 0.3$ TeV
1.07 +0.26 -0.29		⁷⁰ ABAZOV	09AD D0	$E_{\text{cm}}^{\text{p}\bar{\text{p}}} = 1.96$ TeV
		⁷¹ ABAZOV	09AJ D0	$E_{\text{cm}}^{\text{p}\bar{\text{p}}} = 1.96$ TeV

		72	ABAZOV	08R	D0	$E_{cm}^{pp} = 1.96$ TeV		
1617		73	AALTONEN	07L	CDF	$E_{cm}^{pp} = 1.96$ GeV		
17		74	ABAZOV	06H	D0	$E_{cm}^{pp} = 1.96$ TeV		
141		75	ABAZOV	05J	D0	$E_{cm}^{pp} = 1.96$ TeV		
1.25	$+0.21$ -0.20	± 0.06	2298	76	ABREU	01I	DLPH	$E_{cm}^{ee} = 183+189$ GeV
				77	BREITWEG	00	ZEUS	$e^+p \rightarrow e^+W^\pm X$, $\sqrt{s} \approx 300$ GeV
0.92	± 0.34		331	78	ABBOTT	99I	D0	$E_{cm}^{pp} = 1.8$ TeV

⁶⁵ ABDALLAH 08c determine this triple gauge coupling from the measurement of the spin density matrix elements in $e^+e^- \rightarrow W^+W^- \rightarrow (qq)(\ell\nu)$, where $\ell = e$ or μ . Values of all other couplings are fixed to their standard model values.

⁶⁶ SCHAEEL 05A study single-photon, single- W , and WW -pair production from 183 to 209 GeV. Each parameter is determined from a single-parameter fit in which the other parameters assume their Standard Model values.

⁶⁷ ABBIENDI 04D combine results from W^+W^- in all decay channels. Only CP -conserving couplings are considered and each parameter is determined from a single-parameter fit in which the other parameters assume their Standard Model values. The 95% confidence interval is $0.73 < \kappa_\gamma < 1.07$.

⁶⁸ ACHARD 04D study WW -pair production, single- W production and single-photon production with missing energy from 189 to 209 GeV. The result quoted here is obtained including data from 161 to 183 GeV, ACCIARRI 99q. Each parameter is determined from a single-parameter fit in which the other parameters assume their Standard Model values.

⁶⁹ AARON 09B study single- W production in ep collisions at 0.3 TeV C.M. energy. They select 53 $W \rightarrow e/\mu$ events with a standard model expectation of 54.1 ± 7.4 events. Fitting the transverse momentum spectrum of the hadronic recoil system they obtain a 95% C.L. limit of $-3.7 < \kappa_\gamma < -1.5$ or $0.3 < \kappa_\gamma < 1.5$, where the ambiguity is due to the quadratic dependence of the cross section to the coupling parameter.

⁷⁰ ABAZOV 09AD study the $p\bar{p} \rightarrow \ell\nu 2j$ et process arising in WW and WZ production. They select 12,473 (14,392) events in the electron (muon) channel with an expected di-boson signal of 436 (527) events. The results on the anomalous couplings are derived from an analysis of the p_T spectrum of the 2-jet system and quoted at 68% C.L. and for a form factor of 2 TeV. This measurement is not used for obtaining the mean as it is for a specific form factor.

⁷¹ ABAZOV 09AJ study the $p\bar{p} \rightarrow 2\ell 2\nu$ process arising in WW production. They select 100 events with an expected WW signal of 65 events. An analysis of the p_T spectrum of the two charged leptons leads to 95% C.L. limits of $0.46 < \kappa_\gamma < 1.83$, for a form factor $\Lambda = 2$ TeV.

⁷² ABAZOV 08R use $0.7 \text{ fb}^{-1} p\bar{p}$ data at 1.96 TeV to select 263 $W\gamma + X$ events, of which 187 constitute signal, with the W decaying into an electron or a muon, which is required to be well separated from a photon with $E_T > 9$ GeV. A likelihood fit to the photon E_T spectrum yields a 95% CL limit $0.49 < \kappa_\gamma < 1.51$ with other couplings fixed to their Standard Model values.

⁷³ AALTONEN 07L set limits on anomalous TGCs using the $p_T(W)$ distribution in WW and WZ production with the W decaying into an electron or muon and the Z to 2 jets. Setting other couplings to their standard model value, the 95% C.L. limits are $0.54 < \kappa_\gamma < 1.39$ for a form factor scale $\Lambda = 1.5$ TeV.

⁷⁴ ABAZOV 06H study $p\bar{p} \rightarrow WW$ production with a subsequent decay $WW \rightarrow e^+\nu_e e^-\bar{\nu}_e$, $WW \rightarrow e^\pm\nu_e\mu^\mp\nu_\mu$ or $WW \rightarrow \mu^\pm\nu_\mu\mu^\mp\nu_\mu$. The 95% C.L. limit for a form factor scale $\Lambda = 1$ TeV is $-0.05 < \kappa_\gamma < 2.29$, fixing $\lambda_\gamma = 0$. With the assumption that the $WW\gamma$ and WWZ couplings are equal the 95% C.L. one-dimensional limit ($\Lambda = 2$ TeV) is $0.68 < \kappa < 1.45$.

⁷⁵ ABAZOV 05J perform a likelihood fit to the photon E_T spectrum of $W\gamma + X$ events, where the W decays to an electron or muon which is required to be well separated from the photon. For $\Lambda = 2.0$ TeV the 95% CL limits are $0.12 < \kappa_\gamma < 1.96$. In the fit λ_γ is kept fixed to its Standard Model value.

⁷⁶ ABREU 01I combine results from e^+e^- interactions at 189 GeV leading to W^+W^- , $W\nu_e$, and $\nu\bar{\nu}\gamma$ final states with results from ABREU 99L at 183 GeV. The 95% confidence interval is $0.87 < \kappa_\gamma < 1.68$.

⁷⁷ BREITWEG 00 search for W production in events with large hadronic p_T . For $p_T > 20$ GeV, the upper limit on the cross section gives the 95%CL limit $-3.7 < \kappa_\gamma < 2.5$ (for $\lambda_\gamma = 0$).

⁷⁸ ABBOTT 99I perform a simultaneous fit to the $W\gamma$, $WW \rightarrow$ dilepton, $WW/WZ \rightarrow e\nu jj$, $WW/WZ \rightarrow \mu\nu jj$, and $WZ \rightarrow$ trilepton data samples. For $\Lambda = 2.0$ TeV, the 95%CL limits are $0.75 < \kappa_\gamma < 1.39$.

 λ_γ

OUR FIT below is obtained by combining the measurements taking into account properly the common systematic errors (see LEPEWWG/TGC/2005-01 at <http://lepewwg.web.cern.ch/LEPEWWG/lepww/tgc>).

VALUE	EVTS	DOCUMENT ID	TECN	COMMENT
-0.028 ± 0.020 -0.021				OUR FIT
0.16 ± 0.12 -0.13	1880	⁷⁹ ABDALLAH	08c	DLPH $E_{cm}^{ee} = 189-209$ GeV
$-0.012 \pm 0.027 \pm 0.011$	10689	⁸⁰ SCHAEEL	05A	ALEP $E_{cm}^{ee} = 183-209$ GeV
-0.060 ± 0.034 -0.033	9800	⁸¹ ABBIENDI	04D	OPAL $E_{cm}^{ee} = 183-209$ GeV
$-0.021 \pm 0.035 \pm 0.017$ -0.034	10575	⁸² ACHARD	04D	L3 $E_{cm}^{ee} = 161-209$ GeV
• • •				We do not use the following data for averages, fits, limits, etc. • • •
	53	⁸³ AARON	09B	H1 $E_{cm}^{ep} = 0.3$ TeV
0.00 ± 0.06		⁸⁴ ABAZOV	09AD	D0 $E_{cm}^{pp} = 1.96$ TeV
		⁸⁵ ABAZOV	09AJ	D0 $E_{cm}^{pp} = 1.96$ TeV

		86	ABAZOV	08R	D0	$E_{cm}^{pp} = 1.96$ TeV		
1617		87	AALTONEN	07L	CDF	$E_{cm}^{pp} = 1.96$ GeV		
17		88	ABAZOV	06H	D0	$E_{cm}^{pp} = 1.96$ TeV		
141		89	ABAZOV	05J	D0	$E_{cm}^{pp} = 1.96$ TeV		
0.05	± 0.09	± 0.01	2298	90	ABREU	01I	DLPH	$E_{cm}^{ee} = 183+189$ GeV
				91	BREITWEG	00	ZEUS	$e^+p \rightarrow e^+W^\pm X$, $\sqrt{s} \approx 300$ GeV
0.00	$+0.10$ -0.09		331	92	ABBOTT	99I	D0	$E_{cm}^{pp} = 1.8$ TeV

⁷⁹ ABDALLAH 08c determine this triple gauge coupling from the measurement of the spin density matrix elements in $e^+e^- \rightarrow W^+W^- \rightarrow (qq)(\ell\nu)$, where $\ell = e$ or μ . Values of all other couplings are fixed to their standard model values.

⁸⁰ SCHAEEL 05A study single-photon, single- W , and WW -pair production from 183 to 209 GeV. Each parameter is determined from a single-parameter fit in which the other parameters assume their Standard Model values.

⁸¹ ABBIENDI 04D combine results from W^+W^- in all decay channels. Only CP -conserving couplings are considered and each parameter is determined from a single-parameter fit in which the other parameters assume their Standard Model values. The 95% confidence interval is $-0.13 < \lambda_\gamma < 0.01$.

⁸² ACHARD 04D study WW -pair production, single- W production and single-photon production with missing energy from 189 to 209 GeV. The result quoted here is obtained including data from 161 to 183 GeV, ACCIARRI 99q. Each parameter is determined from a single-parameter fit in which the other parameters assume their Standard Model values.

⁸³ AARON 09B study single- W production in ep collisions at 0.3 TeV C.M. energy. They select 53 $W \rightarrow e/\mu$ events with a standard model expectation of 54.1 ± 7.4 events. Fitting the transverse momentum spectrum of the hadronic recoil system they obtain a 95% C.L. limit of $-2.5 < \lambda_\gamma < 2.5$.

⁸⁴ ABAZOV 09AD study the $p\bar{p} \rightarrow \ell\nu 2j$ et process arising in WW and WZ production. They select 12,473 (14,392) events in the electron (muon) channel with an expected di-boson signal of 436 (527) events. The results on the anomalous couplings are derived from an analysis of the p_T spectrum of the 2-jet system and quoted at 68% C.L. and for a form factor of 2 TeV. This measurement is not used for obtaining the mean as it is for a specific form factor.

⁸⁵ ABAZOV 09AJ study the $p\bar{p} \rightarrow 2\ell 2\nu$ process arising in WW production. They select 100 events with an expected WW signal of 65 events. An analysis of the p_T spectrum of the two charged leptons leads to 95% C.L. limits of $-0.14 < \lambda_\gamma < 0.18$, for a form factor $\Lambda = 2$ TeV.

⁸⁶ ABAZOV 08R use $0.7 \text{ fb}^{-1} p\bar{p}$ data at 1.96 TeV to select 263 $W\gamma + X$ events, of which 187 constitute signal, with the W decaying into an electron or a muon, which is required to be well separated from a photon with $E_T > 9$ GeV. A likelihood fit to the photon E_T spectrum yields a 95% CL limit $-0.12 < \lambda_\gamma < 0.13$ with other couplings fixed to their Standard Model values.

⁸⁷ AALTONEN 07L set limits on anomalous TGCs using the $p_T(W)$ distribution in WW and WZ production with the W decaying into an electron or muon and the Z to 2 jets. Setting other couplings to their standard model value, the 95% C.L. limits are $-0.18 < \lambda_\gamma < 0.17$ for a form factor scale $\Lambda = 1.5$ TeV.

⁸⁸ ABAZOV 06H study $p\bar{p} \rightarrow WW$ production with a subsequent decay $WW \rightarrow e^+\nu_e e^-\bar{\nu}_e$, $WW \rightarrow e^\pm\nu_e\mu^\mp\nu_\mu$ or $WW \rightarrow \mu^\pm\nu_\mu\mu^\mp\nu_\mu$. The 95% C.L. limit for a form factor scale $\Lambda = 1$ TeV is $-0.97 < \lambda_\gamma < 1.04$, fixing $\kappa_\gamma = 1$. With the assumption that the $WW\gamma$ and WWZ couplings are equal the 95% C.L. one-dimensional limit ($\Lambda = 2$ TeV) is $-0.29 < \lambda < 0.30$.

⁸⁹ ABAZOV 05J perform a likelihood fit to the photon E_T spectrum of $W\gamma + X$ events, where the W decays to an electron or muon which is required to be well separated from the photon. For $\Lambda = 2.0$ TeV the 95% CL limits are $-0.20 < \lambda_\gamma < 0.20$. In the fit κ_γ is kept fixed to its Standard Model value.

⁹⁰ ABREU 01I combine results from e^+e^- interactions at 189 GeV leading to W^+W^- , $W\nu_e$, and $\nu\bar{\nu}\gamma$ final states with results from ABREU 99L at 183 GeV. The 95% confidence interval is $-0.11 < \lambda_\gamma < 0.23$.

⁹¹ BREITWEG 00 search for W production in events with large hadronic p_T . For $p_T > 20$ GeV, the upper limit on the cross section gives the 95%CL limit $-3.2 < \lambda_\gamma < 3.2$ for κ_γ fixed to its Standard Model value.

⁹² ABBOTT 99I perform a simultaneous fit to the $W\gamma$, $WW \rightarrow$ dilepton, $WW/WZ \rightarrow e\nu jj$, $WW/WZ \rightarrow \mu\nu jj$, and $WZ \rightarrow$ trilepton data samples. For $\Lambda = 2.0$ TeV, the 95%CL limits are $-0.18 < \lambda_\gamma < 0.19$.

 κ_Z

This coupling is CP -conserving (C - and P - separately conserving).

VALUE	EVTS	DOCUMENT ID	TECN	COMMENT
0.924 ± 0.059 -0.056 ± 0.024	7171	93 ACHARD	04D	L3 $E_{cm}^{ee} = 189-209$ GeV
• • •				We do not use the following data for averages, fits, limits, etc. • • •
	17	⁹⁴ ABAZOV	06H	D0 $E_{cm}^{pp} = 1.96$ TeV
	2.3	⁹⁵ ABAZOV	05S	D0 $E_{cm}^{pp} = 1.96$ TeV

⁹³ ACHARD 04D study WW -pair production, single- W production and single-photon production with missing energy from 189 to 209 GeV. The result quoted here is obtained using the WW -pair production sample. Each parameter is determined from a single-parameter fit in which the other parameters assume their Standard Model values.

⁹⁴ ABAZOV 06H study $p\bar{p} \rightarrow WW$ production with a subsequent decay $WW \rightarrow e^+\nu_e e^-\bar{\nu}_e$, $WW \rightarrow e^\pm\nu_e\mu^\mp\nu_\mu$ or $WW \rightarrow \mu^\pm\nu_\mu\mu^\mp\nu_\mu$. The 95% C.L. limit for a form factor scale $\Lambda = 2$ TeV is $0.55 < \kappa_Z < 1.55$, fixing $\lambda_Z = 0$. With the assumption that the $WW\gamma$ and WWZ couplings are equal the 95% C.L. one-dimensional limit ($\Lambda = 2$ TeV) is $0.68 < \kappa < 1.45$.

⁹⁵ ABAZOV 05S study $p\bar{p} \rightarrow WZ$ production with a subsequent trilepton decay to $\ell\nu\ell'\bar{\ell}'$ (ℓ and $\ell' = e$ or μ). Three events (estimated background 0.71 ± 0.08 events) with WZ decay characteristics are observed from which they derive limits on the anomalous WWZ couplings. The 95% CL limit for a form factor scale $\Lambda = 1$ TeV is $-1.0 < \kappa_Z < 3.4$, fixing λ_Z and g_Z^T to their Standard Model values.

Gauge & Higgs Boson Particle Listings

W

 λ_Z

This coupling is CP-conserving (C- and P- separately conserving).

VALUE	EVTS	DOCUMENT ID	TECN	COMMENT
$-0.086 \pm 0.060 \pm 0.023$	7171	96 ACHARD	04D L3	$E_{cm}^{ee} = 189-209$ GeV
	13	97 ABAZOV	07Z D0	$E_{cm}^{pp} = 1.96$ TeV
	17	98 ABAZOV	06H D0	$E_{cm}^{pp} = 1.96$ TeV
	2.3	99 ABAZOV	05s D0	$E_{cm}^{pp} = 1.96$ TeV

- • • We do not use the following data for averages, fits, limits, etc. • • •
- 96 ACHARD 04D study W^+W^- pair production, single- W production and single-photon production with missing energy from 189 to 209 GeV. The result quoted here is obtained using the W^+W^- pair production sample. Each parameter is determined from a single-parameter fit in which the other parameters assume their Standard Model values.
- 97 ABAZOV 07Z set limits on anomalous TGCs using the measured cross section and $p_T(Z)$ distribution in WZ production with both the W and the Z decaying leptonically into electrons and muons. Setting other couplings to their standard model values, the 95% C.L. limits for a form factor scale $\Lambda = 1.5$ TeV are $-0.18 < \lambda_Z < 0.22$, and for $\Lambda = 2$ TeV are $-0.17 < \lambda_Z < 0.21$.
- 98 ABAZOV 06H study $\bar{p}p \rightarrow WW$ production with a subsequent decay $WW \rightarrow e^+ \nu_e e^- \bar{\nu}_e$, $WW \rightarrow e^\pm \nu_e \mu^\mp \nu_\mu$ or $WW \rightarrow \mu^+ \nu_\mu \mu^- \bar{\nu}_\mu$. The 95% C.L. limit for a form factor scale $\Lambda = 2$ TeV is $-0.39 < \lambda_Z < 0.39$, fixing $\kappa_Z = 1$. With the assumption that the $W\gamma$ and WWZ couplings are equal the 95% C.L. one-dimensional limit ($\Lambda = 2$ TeV) is $-0.29 < \lambda < 0.30$.
- 99 ABAZOV 05s study $\bar{p}p \rightarrow WZ$ production with a subsequent trilepton decay to $\ell\nu\ell'\bar{\nu}$ (ℓ and $\ell' = e$ or μ). Three events (estimated background 0.71 ± 0.08 events) with WZ decay characteristics are observed from which they derive limits on the anomalous WWZ couplings. The 95% CL limit for a form factor scale $\Lambda = 1.5$ TeV is $-0.48 < \lambda_Z < 0.48$, fixing g_Z^Z and κ_Z to their Standard Model values.

 g_Z^Z

This coupling is CP-conserving but C- and P-violating.

VALUE	EVTS	DOCUMENT ID	TECN	COMMENT
0.93 ± 0.09 OUR AVERAGE				Error includes scale factor of 1.1.
0.96 ± 0.13	9800	100 ABBIENDI	04D OPAL	$E_{cm}^{ee} = 183-209$ GeV
$1.00 \pm 0.13 \pm 0.05$	7171	101 ACHARD	04D L3	$E_{cm}^{ee} = 189-209$ GeV
$0.56 \pm 0.23 \pm 0.12$	1154	102 ACCIARRI	99Q L3	$E_{cm}^{ee} = 161+172+183$ GeV
0.84 ± 0.23	103	EBOLI	00 THEO LEP1, SLC+ Tevatron	

- • • We do not use the following data for averages, fits, limits, etc. • • •
- 100 ABBIENDI 04D combine results from W^+W^- in all decay channels. Only CP-conserving couplings are considered and each parameter is determined from a single-parameter fit in which the other parameters assume their Standard Model values. The 95% confidence interval is $0.72 < g_Z^Z < 1.21$.
- 101 ACHARD 04D study W^+W^- pair production, single- W production and single-photon production with missing energy from 189 to 209 GeV. The result quoted here is obtained using the W^+W^- pair production sample. Each parameter is determined from a single-parameter fit in which the other parameters assume their Standard Model values.
- 102 ACCIARRI 99Q study W -pair, single- W , and single photon events.
- 103 EBOLI 00 extract this indirect value of the coupling studying the non-universal one-loop contributions to the experimental value of the $Z \rightarrow b\bar{b}$ width ($\Lambda = 1$ TeV is assumed).

 g_Z^Z

This coupling is CP-violating (C-violating and P-conserving).

VALUE	EVTS	DOCUMENT ID	TECN	COMMENT
-0.30 ± 0.17 OUR AVERAGE				
-0.39 ± 0.19	1880	104 ABDALLAH	08c DLPH	$E_{cm}^{ee} = 189-209$ GeV
-0.02 ± 0.32	1065	105 ABBIENDI	01H OPAL	$E_{cm}^{ee} = 189$ GeV

- 104 ABDALLAH 08c determine this triple gauge coupling from the measurement of the spin density matrix elements in $e^+e^- \rightarrow W^+W^- \rightarrow (qq)(\ell\nu)$, where $\ell = e$ or μ . Values of all other couplings are fixed to their standard model values.
- 105 ABBIENDI 01H study W -pair events, with one leptonically and one hadronically decaying W . The coupling is extracted using information from the W production angle together with decay angles from the leptonically decaying W .

 $\tilde{\kappa}_Z$

This coupling is CP-conserving (C-conserving and P-violating).

VALUE	EVTS	DOCUMENT ID	TECN	COMMENT
-0.12 ± 0.06 OUR AVERAGE				
-0.09 ± 0.08	1880	106 ABDALLAH	08c DLPH	$E_{cm}^{ee} = 189-209$ GeV
-0.20 ± 0.10	1065	107 ABBIENDI	01H OPAL	$E_{cm}^{ee} = 189$ GeV

- 106 ABDALLAH 08c determine this triple gauge coupling from the measurement of the spin density matrix elements in $e^+e^- \rightarrow W^+W^- \rightarrow (qq)(\ell\nu)$, where $\ell = e$ or μ . Values of all other couplings are fixed to their standard model values.
- 107 ABBIENDI 01H study W -pair events, with one leptonically and one hadronically decaying W . The coupling is extracted using information from the W production angle together with decay angles from the leptonically decaying W .

 $\tilde{\lambda}_Z$

This coupling is CP-violating (C-conserving and P-violating).

VALUE	EVTS	DOCUMENT ID	TECN	COMMENT
-0.09 ± 0.07 OUR AVERAGE				
-0.08 ± 0.07	1880	108 ABDALLAH	08c DLPH	$E_{cm}^{ee} = 189-209$ GeV
-0.18 ± 0.24	1065	109 ABBIENDI	01H OPAL	$E_{cm}^{ee} = 189$ GeV

- 108 ABDALLAH 08c determine this triple gauge coupling from the measurement of the spin density matrix elements in $e^+e^- \rightarrow W^+W^- \rightarrow (qq)(\ell\nu)$, where $\ell = e$ or μ . Values of all other couplings are fixed to their standard model values.
- 109 ABBIENDI 01H study W -pair events, with one leptonically and one hadronically decaying W . The coupling is extracted using information from the W production angle together with decay angles from the leptonically decaying W .

W ANOMALOUS MAGNETIC MOMENT

The full magnetic moment is given by $\mu_W = e(1+\kappa+\lambda)/2m_W$. In the Standard Model, at tree level, $\kappa = 1$ and $\lambda = 0$. Some papers have defined $\Delta\kappa = 1-\kappa$ and assume that $\lambda = 0$. Note that the electric quadrupole moment is given by $-e(\kappa-\lambda)/m_W^2$. A description of the parameterization of these moments and additional references can be found in HAGIWARA 87 and BAUR 88. The parameter Λ appearing in the theoretical limits below is a regularization cutoff which roughly corresponds to the energy scale where the structure of the W boson becomes manifest.

VALUE ($e/2m_W$)	EVTS	DOCUMENT ID	TECN	COMMENT
2.22 ± 0.20	2298	110 ABREU	01I DLPH	$E_{cm}^{ee} = 183+189$ GeV

- • • We do not use the following data for averages, fits, limits, etc. • • •
- 111 ABE 95G report $-1.3 < \kappa < 3.2$ for $\lambda=0$ and $-0.7 < \lambda < 0.7$ for $\kappa=1$ in $\rho\bar{p} \rightarrow e\nu_e\gamma X$ and $\mu\nu_\mu\gamma X$ at $\sqrt{s} = 1.8$ TeV.
- 112 ALITTI 92c measure $\kappa = 1 + \frac{2.6}{2.2}$ and $\lambda = 0 + \frac{1.7}{-1.8}$ in $\rho\bar{p} \rightarrow e\nu\gamma + X$ at $\sqrt{s} = 630$ GeV. At 95%CL they report $-3.5 < \kappa < 5.9$ and $-3.6 < \lambda < 3.5$.
- 113 SAMUEL 92 use preliminary CDF and UA2 data and find $-2.4 < \kappa < 3.7$ at 96%CL and $-3.1 < \lambda < 4.2$ at 95%CL respectively. They use data for $W\gamma$ production and radiative W decay.
- 114 SAMUEL 91 use preliminary CDF data for $\rho\bar{p} \rightarrow W\gamma X$ to obtain $-11.3 \leq \Delta\kappa \leq 10.9$. Note that their $\kappa = 1 - \Delta\kappa$.
- 115 GRIFOLS 88 uses deviation from ρ parameter to set limit $\Delta\kappa \lesssim 65 (M_W^2/\Lambda^2)$.
- 116 GROTCHE 87 finds the limit $-37 < \Delta\kappa < 73.5$ (90% CL) from the experimental limits on $e^+e^- \rightarrow \nu\bar{\nu}\gamma$ assuming three neutrino generations and $-19.5 < \Delta\kappa < 56$ for four generations. Note their $\Delta\kappa$ has the opposite sign as our definition.
- 117 VANDERBIJ 87 uses existing limits to the photon structure to obtain $|\Delta\kappa| < 33 (m_W/\Lambda)$. In addition VANDERBIJ 87 discusses problems with using the ρ parameter of the Standard Model to determine $\Delta\kappa$.
- 118 GRAU 85 uses the muon anomaly to derive a coupled limit on the anomalous magnetic dipole and electric quadrupole (λ) moments $1.05 > \Delta\kappa \ln(\Lambda/m_W) + \lambda/2 > -2.77$. In the Standard Model $\lambda = 0$.
- 119 SUZUKI 85 uses partial-wave unitarity at high energies to obtain $|\Delta\kappa| \lesssim 190 (m_W/\Lambda)^2$. From the anomalous magnetic moment of the muon, SUZUKI 85 obtains $|\Delta\kappa| \lesssim 2.2/\ln(\Lambda/m_W)$. Finally SUZUKI 85 uses deviations from the ρ parameter and obtains a very qualitative, order-of-magnitude limit $|\Delta\kappa| \lesssim 150 (m_W/\Lambda)^4$ if $|\Delta\kappa| \ll 1$.
- 120 HERZOG 84 consider the contribution of W -boson to muon magnetic moment including anomalous coupling of $W\gamma$. Obtain a limit $-1 < \Delta\kappa < 3$ for $\Lambda \gtrsim 1$ TeV.

ANOMALOUS W/Z QUARTIC COUPLINGS

Revised March 2006 by C. Caso (University of Genova) and A. Gurtu (Tata Institute).

The Standard Model predictions for $WWWW$, $WWZZ$, $WWZ\gamma$, $WW\gamma\gamma$, and $ZZ\gamma\gamma$ couplings are small at LEP, but expected to become important at a TeV Linear Collider. Outside the Standard Model framework such possible couplings, a_0, a_c, a_n , are expressed in terms of the following dimension-6 operators [1,2];

$$L_6^0 = -\frac{e^2}{16\Lambda^2} a_0 F^{\mu\nu} F_{\mu\nu} \vec{W}^\alpha \cdot \vec{W}_\alpha$$

$$L_6^c = -\frac{e^2}{16\Lambda^2} a_c F^{\mu\alpha} F_{\mu\beta} \vec{W}^\beta \cdot \vec{W}_\alpha$$

$$L_6^n = -i\frac{e^2}{16\Lambda^2} a_n \epsilon_{ijk} W_{\mu\alpha}^{(i)} W_\nu^{(j)} W^{(k)\alpha} F^{\mu\nu}$$

$$\tilde{L}_6^0 = -\frac{e^2}{16\Lambda^2} \tilde{a}_0 F^{\mu\nu} \tilde{F}_{\mu\nu} \vec{W}^\alpha \cdot \vec{W}_\alpha$$

$$\tilde{L}_6^n = -i\frac{e^2}{16\Lambda^2} \tilde{a}_n \epsilon_{ijk} W_{\mu\alpha}^{(i)} W_\nu^{(j)} W^{(k)\alpha} \tilde{F}^{\mu\nu}$$

where F, W are photon and W fields, L_6^0 and L_6^C conserve C , P separately (\tilde{L}_6^0 conserves only C) and generate anomalous $W^+W^-\gamma\gamma$ and $ZZ\gamma\gamma$ couplings, L_6^n violates CP (\tilde{L}_6^n violates both C and P) and generates an anomalous $W^+W^-Z\gamma$ coupling, and Λ is an energy scale for new physics. For the $ZZ\gamma\gamma$ coupling the CP -violating term represented by L_6^n does not contribute. These couplings are assumed to be real and to vanish at tree level in the Standard Model.

Within the same framework as above, a more recent description of the quartic couplings [3] treats the anomalous parts of the $WW\gamma\gamma$ and $ZZ\gamma\gamma$ couplings separately leading to two sets parameterized as a_0^V/Λ^2 and a_c^V/Λ^2 , where $V = W$ or Z .

At LEP the processes studied in search of these quartic couplings are $e^+e^- \rightarrow WW\gamma$, $e^+e^- \rightarrow \gamma\gamma\nu\bar{\nu}$, and $e^+e^- \rightarrow Z\gamma\gamma$ and limits are set on the quantities a_0^W/Λ^2 , a_c^W/Λ^2 , a_n/Λ^2 . The characteristics of the first process depend on all the three couplings whereas those of the latter two depend only on the two CP -conserving couplings. The sensitive measured variables are the cross sections for these processes as well as the energy and angular distributions of the photon and recoil mass to the photon pair.

References

- G. Belanger and F. Boudjema, Phys. Lett. **B288**, 201 (1992).
- J.W. Stirling and A. Werthenbach, Eur. Phys. J. **C14**, 103 (2000);
J.W. Stirling and A. Werthenbach, Phys. Lett. **B466**, 369 (1999);
A. Denner *et al.*, Eur. Phys. J. **C20**, 201 (2001);
G. Montagna *et al.*, Phys. Lett. **B515**, 197 (2001).
- G. Belanger *et al.*, Eur. Phys. J. **C13**, 103 (2000).

a_0/Λ^2 , a_c/Λ^2 , a_n/Λ^2

Using the $WW\gamma$ final state, the LEP combined 95% CL limits on the anomalous contributions to the $WW\gamma\gamma$ and $WWZ\gamma$ vertices (as of summer 2003) are given below:

(See P. Wells, "Experimental Tests of the Standard Model," Int. Europhysics Conference on High-Energy Physics, Aachen, Germany, 17–23 July 2003)

$$\begin{aligned} -0.02 < a_0^W/\Lambda^2 < 0.02 \text{ GeV}^{-2}, \\ -0.05 < a_c^W/\Lambda^2 < 0.03 \text{ GeV}^{-2}, \\ -0.15 < a_n/\Lambda^2 < 0.15 \text{ GeV}^{-2}. \end{aligned}$$

VALUE	DOCUMENT ID	TECN
-------	-------------	------

• • • We do not use the following data for averages, fits, limits, etc. • • •

121	ABBIENDI 04B	OPAL
122	ABBIENDI 04L	OPAL
123	HEISTER 04A	ALEP
124	ABDALLAH 03I	DLPH
125	ACHARD 02F	L3
121	ABBIENDI 04B	select 187 $e^+e^- \rightarrow W^+W^-\gamma$ events in the C.M. energy range 180–209 GeV, where $E_\gamma > 2.5$ GeV, the photon has a polar angle $ \cos\theta_\gamma < 0.975$ and is well isolated from the nearest jet and charged lepton, and the effective masses of both fermion-antifermion systems agree with the W mass within $3\Gamma_W$. The measured differential cross section as a function of the photon energy and photon polar angle is used to extract the 95% CL limits: $-0.020 \text{ GeV}^{-2} < a_0/\Lambda^2 < 0.020 \text{ GeV}^{-2}$, $-0.053 \text{ GeV}^{-2} < a_c/\Lambda^2 < 0.037 \text{ GeV}^{-2}$ and $-0.16 \text{ GeV}^{-2} < a_n/\Lambda^2 < 0.15 \text{ GeV}^{-2}$.
122	ABBIENDI 04L	select 20 $e^+e^- \rightarrow \nu\bar{\nu}\gamma\gamma$ acoplanar events in the energy range 180–209 GeV and 176 $e^+e^- \rightarrow q\bar{q}\gamma\gamma$ events in the energy range 130–209 GeV. These samples are used to constrain possible anomalous $W^+W^-\gamma\gamma$ and $ZZ\gamma\gamma$ quartic couplings. Further combining with the $W^+W^-\gamma$ sample of ABBIENDI 04B the following one-parameter 95% CL limits are obtained: $-0.007 < a_0^Z/\Lambda^2 < 0.023 \text{ GeV}^{-2}$, $-0.029 < a_c^Z/\Lambda^2 < 0.029 \text{ GeV}^{-2}$, $-0.020 < a_0^W/\Lambda^2 < 0.020 \text{ GeV}^{-2}$, $-0.052 < a_c^W/\Lambda^2 < 0.037 \text{ GeV}^{-2}$.
123	In the CM energy range 183 to 209 GeV HEISTER 04A select 30 $e^+e^- \rightarrow \nu\bar{\nu}\gamma\gamma$ events with two acoplanar, high energy and high transverse momentum photons. The photon-photon acoplanarity is required to be $> 5^\circ$, $E_\gamma/\sqrt{s} > 0.025$ (the more energetic photon	

having energy $> 0.2\sqrt{s}$), $p_{T,\gamma}/E_{\text{beam}} > 0.05$ and $|\cos\theta_\gamma| < 0.94$. A likelihood fit to the photon energy and recoil missing mass yields the following one-parameter 95% CL limits: $-0.012 < a_0^Z/\Lambda^2 < 0.019 \text{ GeV}^{-2}$, $-0.041 < a_c^Z/\Lambda^2 < 0.044 \text{ GeV}^{-2}$, $-0.060 < a_0^W/\Lambda^2 < 0.055 \text{ GeV}^{-2}$, $-0.099 < a_c^W/\Lambda^2 < 0.093 \text{ GeV}^{-2}$.

- 124 ABDALLAH 03i select 122 $e^+e^- \rightarrow W^+W^-\gamma$ events in the C.M. energy range 189–209 GeV, where $E_\gamma > 5$ GeV, the photon has a polar angle $|\cos\theta_\gamma| < 0.95$ and is well isolated from the nearest charged fermion. A fit to the photon energy spectra yields $a_c^W/\Lambda^2 = 0.000^{+0.019}_{-0.040} \text{ GeV}^{-2}$, $a_0/\Lambda^2 = -0.004^{+0.018}_{-0.010} \text{ GeV}^{-2}$, $\tilde{a}_0/\Lambda^2 = -0.007^{+0.019}_{-0.008} \text{ GeV}^{-2}$, $a_n/\Lambda^2 = -0.09^{+0.16}_{-0.05} \text{ GeV}^{-2}$, and $\tilde{a}_n/\Lambda^2 = +0.05^{+0.07}_{-0.15} \text{ GeV}^{-2}$, keeping the other parameters fixed to their Standard Model values (0). The 95% CL limits are: $-0.063 \text{ GeV}^{-2} < a_c/\Lambda^2 < +0.032 \text{ GeV}^{-2}$, $-0.020 \text{ GeV}^{-2} < a_0/\Lambda^2 < +0.020 \text{ GeV}^{-2}$, $-0.020 \text{ GeV}^{-2} < \tilde{a}_0/\Lambda^2 < +0.020 \text{ GeV}^{-2}$, $-0.18 \text{ GeV}^{-2} < a_n/\Lambda^2 < +0.14 \text{ GeV}^{-2}$, $-0.16 \text{ GeV}^{-2} < \tilde{a}_n/\Lambda^2 < +0.17 \text{ GeV}^{-2}$.
- 125 ACHARD 02F select 86 $e^+e^- \rightarrow W^+W^-\gamma$ events at 192–207 GeV, where $E_\gamma > 5$ GeV and the photon is well isolated. They also select 43 acoplanar $e^+e^- \rightarrow \nu\bar{\nu}\gamma\gamma$ events in this energy range, where the photon energies are > 5 GeV and > 1 GeV and the photon polar angles are between 14° and 166° . All these 43 events are in the recoil mass region corresponding to the Z (75–110 GeV). Using the shape and normalization of the photon spectra in the $W^+W^-\gamma$ events, and combining with the 42 event sample from 189 GeV data (ACCIARRI 00T), they obtain: $a_0/\Lambda^2 = 0.000 \pm 0.010 \text{ GeV}^{-2}$, $a_c/\Lambda^2 = -0.013 \pm 0.023 \text{ GeV}^{-2}$, and $a_n/\Lambda^2 = -0.002 \pm 0.076 \text{ GeV}^{-2}$. Further combining the analyses of $W^+W^-\gamma$ events with the low recoil mass region of $\nu\bar{\nu}\gamma\gamma$ events (including samples collected at 183 + 189 GeV), they obtain the following one-parameter 95% CL limits: $-0.015 \text{ GeV}^{-2} < a_0/\Lambda^2 < 0.015 \text{ GeV}^{-2}$, $-0.048 \text{ GeV}^{-2} < a_c/\Lambda^2 < 0.026 \text{ GeV}^{-2}$, and $-0.14 \text{ GeV}^{-2} < a_n/\Lambda^2 < 0.13 \text{ GeV}^{-2}$.

W REFERENCES

AARON 09B	EPJ C64 251	F.D. Aaron <i>et al.</i>	(H1 Collab.)
ABAZOV 09AB	PRL 103 141801	V.M. Abazov <i>et al.</i>	(DO Collab.)
ABAZOV 09AD	PR D80 052012	V.M. Abazov <i>et al.</i>	(DO Collab.)
ABAZOV 09AJ	PRL 103 191801	V.M. Abazov <i>et al.</i>	(DO Collab.)
ABAZOV 09AK	PRL 103 231802	V.M. Abazov <i>et al.</i>	(DO Collab.)
AALTONEN 08B	PRL 100 071801	T. Aaltonen <i>et al.</i>	(CDF Collab.)
ABAZOV 08R	PRL 100 241805	V.M. Abazov <i>et al.</i>	(DO Collab.)
ABDALLAH 08A	EPJ C55 1	J. Abdallah <i>et al.</i>	(DELPHI Collab.)
ABDALLAH 08C	EPJ C54 345	J. Abdallah <i>et al.</i>	(DELPHI Collab.)
AALTONEN 07F	PRL 99 151801	T. Aaltonen <i>et al.</i>	(CDF Collab.)
Also	PR D77 112001	T. Aaltonen <i>et al.</i>	(CDF Collab.)
AALTONEN 07L	PR D76 111103R	T. Aaltonen <i>et al.</i>	(CDF Collab.)
ABAZOV 07Z	PR D76 111104R	V.M. Abazov <i>et al.</i>	(DO Collab.)
ABBIENDI 07A	EPJ C52 757	G. Abbiendi <i>et al.</i>	(OPAL Collab.)
ABAZOV 06H	PR D74 057101	V.M. Abazov <i>et al.</i>	(DO Collab.)
Also	PR D74 059904 (erratum)	V.M. Abazov <i>et al.</i>	(DO Collab.)
ABBIENDI 06E	EPJ C45 307	G. Abbiendi <i>et al.</i>	(OPAL Collab.)
ABBIENDI 06A	EPJ C45 291	G. Abbiendi <i>et al.</i>	(OPAL Collab.)
ACHARD 06	EPJ C45 569	P. Achard <i>et al.</i>	(L3 Collab.)
AKTAS 06	PL B632 35	A. Aktas <i>et al.</i>	(H1 Collab.)
SCHAEF 06	EPJ C47 309	S. Schaefer <i>et al.</i>	(ALEPH Collab.)
ABAZOV 05J	PR D71 091108R	V.M. Abazov <i>et al.</i>	(DO Collab.)
ABAZOV 05S	PRL 95 141802	V.M. Abazov <i>et al.</i>	(DO Collab.)
SCHAEF 05A	PL B614 7	S. Schaefer <i>et al.</i>	(ALEPH Collab.)
ABAZOV 04D	PR D70 092008	V.M. Abazov <i>et al.</i>	(CDF, DO Collab.)
ABBIENDI 04B	PL B580 17	G. Abbiendi <i>et al.</i>	(OPAL Collab.)
ABBIENDI 04D	EPJ C33 463	G. Abbiendi <i>et al.</i>	(OPAL Collab.)
ABBIENDI 04L	PR D70 032005	G. Abbiendi <i>et al.</i>	(OPAL Collab.)
ABDALLAH 04G	EPJ C34 127	J. Abdallah <i>et al.</i>	(DELPHI Collab.)
ACHARD 04D	PL B586 151	P. Achard <i>et al.</i>	(L3 Collab.)
ACHARD 04J	PL B600 22	P. Achard <i>et al.</i>	(L3 Collab.)
HEISTER 04A	PL B602 31	A. Heister <i>et al.</i>	(ALEPH Collab.)
SCHAEF 04A	EPJ C38 147	S. Schaefer <i>et al.</i>	(ALEPH Collab.)
ABBIENDI 03C	EPJ C26 321	G. Abbiendi <i>et al.</i>	(OPAL Collab.)
ABDALLAH 03E	EPJ C31 139	J. Abdallah <i>et al.</i>	(DELPHI Collab.)
ABAZOV 02D	PR D66 012001	V.M. Abazov <i>et al.</i>	(DO Collab.)
ABAZOV 02E	PR D66 032008	V.M. Abazov <i>et al.</i>	(DO Collab.)
ACHARD 02F	PL B527 29	P. Achard <i>et al.</i>	(L3 Collab.)
CHEKANOV 02C	PL B539 197	S. Chekanov <i>et al.</i>	(ZEUS Collab.)
ABBIENDI 01H	EPJ C19 229	G. Abbiendi <i>et al.</i>	(OPAL Collab.)
ABREU 01E	PL B502 9	P. Abreu <i>et al.</i>	(DELPHI Collab.)
AFFOLDER 01I	PR D64 052001	T. Affolder <i>et al.</i>	(CDF Collab.)
ABBIENDI 00V	PL B490 71	G. Abbiendi <i>et al.</i>	(OPAL Collab.)
ABBIENDI.G	00 PL B493 249	G. Abbiendi <i>et al.</i>	(OPAL Collab.)
ABBOTT 00B	PR D61 072001	B. Abbott <i>et al.</i>	(DO Collab.)
ABBOTT 00D	PRL 84 5710	B. Abbott <i>et al.</i>	(DO Collab.)
ABREU.P	00F EPJ C18 203	P. Abreu <i>et al.</i>	(DELPHI Collab.)
Also	EPJ C25 493 (erratum)	P. Abreu <i>et al.</i>	(DELPHI Collab.)
ACCIARRI 00T	PL B490 187	M. Acciarri <i>et al.</i>	(L3 Collab.)
AFFOLDER 00M	PRL 85 3347	T. Affolder <i>et al.</i>	(CDF Collab.)
BREITWEG 00	PL B471 411	J. Breitweg <i>et al.</i>	(ZEUS Collab.)
BREITWEG 00D	EPJ C12 411	J. Breitweg <i>et al.</i>	(ZEUS Collab.)
EBOLI 00	MPL A15 1	O. Eboli, M. Gonzalez-Garcia, S. Novaeas	(OPAL Collab.)
ABBIENDI 99N	PL B453 153	G. Abbiendi <i>et al.</i>	(OPAL Collab.)
ABBOTT 99H	PR D60 052003	B. Abbott <i>et al.</i>	(DO Collab.)
ABBOTT 99L	PR D60 072002	B. Abbott <i>et al.</i>	(DO Collab.)
ABREU 99I	PL B459 382	P. Abreu <i>et al.</i>	(DELPHI Collab.)
ACCIARRI 99	PL B454 386	M. Acciarri <i>et al.</i>	(L3 Collab.)
ACCIARRI 99Q	PL B467 171	M. Acciarri <i>et al.</i>	(L3 Collab.)
BARATE 99J	PL B453 107	R. Barate <i>et al.</i>	(ALEPH Collab.)
BARATE 99L	PL B462 389	R. Barate <i>et al.</i>	(ALEPH Collab.)
BARATE 99M	PL B465 349	R. Barate <i>et al.</i>	(ALEPH Collab.)
ABBOTT 98P	PR D58 092003	B. Abbott <i>et al.</i>	(DO Collab.)
ABBOTT 98N	PR D58 012002	B. Abbott <i>et al.</i>	(DO Collab.)
ABE 98P	PR D58 031101	F. Abe <i>et al.</i>	(CDF Collab.)
ABE 98B	PR D58 091101	F. Abe <i>et al.</i>	(CDF Collab.)
ABREU 98C	PL B416 233	P. Abreu <i>et al.</i>	(DELPHI Collab.)
ABREU 98N	PL B439 209	P. Abreu <i>et al.</i>	(DELPHI Collab.)
BARATE 97F	PL B401 347	R. Barate <i>et al.</i>	(ALEPH Collab.)
BARATE 97S	PL B415 435	R. Barate <i>et al.</i>	(ALEPH Collab.)
ABACHI 95D	PRL 75 1456	S. Abachi <i>et al.</i>	(DO Collab.)
ABE 95C	PRL 74 341	F. Abe <i>et al.</i>	(CDF Collab.)
ABE 95G	PRL 74 1936	F. Abe <i>et al.</i>	(CDF Collab.)
ABE 95P	PRL 75 11	F. Abe <i>et al.</i>	(CDF Collab.)
Also	PR D52 4784	F. Abe <i>et al.</i>	(CDF Collab.)
ABE 95W	PR D52 2624	F. Abe <i>et al.</i>	(CDF Collab.)
Also	PRL 73 220	F. Abe <i>et al.</i>	(CDF Collab.)
ABE 92E	PRL 68 3398	F. Abe <i>et al.</i>	(CDF Collab.)
ABE 92I	PRL 69 28	F. Abe <i>et al.</i>	(CDF Collab.)

Gauge & Higgs Boson Particle Listings

 W, Z

ALITTI	92	PL B276 365	J. Alitti <i>et al.</i>	(UA2 Collab.)
ALITTI	92B	PL B276 354	J. Alitti <i>et al.</i>	(UA2 Collab.)
ALITTI	92C	PL B277 194	J. Alitti <i>et al.</i>	(UA2 Collab.)
ALITTI	92D	PL B277 203	J. Alitti <i>et al.</i>	(UA2 Collab.)
ALITTI	92F	PL B280 137	J. Alitti <i>et al.</i>	(UA2 Collab.)
SAMUEL	92	PL B280 124	M.A. Samuel <i>et al.</i>	(OKSU, CARL)
ABE	91C	PR D44 29	F. Abe <i>et al.</i>	(CDF Collab.)
ALBAJAR	91	PL B253 503	C. Albajar <i>et al.</i>	(UA1 Collab.)
ALITTI	91C	ZPHY C52 209	J. Alitti <i>et al.</i>	(UA2 Collab.)
SAMUEL	91	PRL 67 9	M.A. Samuel <i>et al.</i>	(OKSU, CARL)
Also		PRL 67 2920 (erratum)	M.A. Samuel <i>et al.</i>	
ABE	90G	PRL 65 2243	F. Abe <i>et al.</i>	(CDF Collab.)
Also		PR D43 2070	F. Abe <i>et al.</i>	(CDF Collab.)
ALBAJAR	90	PL B241 283	C. Albajar <i>et al.</i>	(UA1 Collab.)
ALITTI	90B	PL B241 150	J. Alitti <i>et al.</i>	(UA2 Collab.)
ABE	89I	PRL 62 1005	F. Abe <i>et al.</i>	(CDF Collab.)
ALBAJAR	89	ZPHY C44 15	C. Albajar <i>et al.</i>	(UA1 Collab.)
BAUR	88	NP B308 127	U. Baur, D. Zeppenfeld	(FSU, WISC)
GRIFOLS	88	IJMP A3 225	J.A. Grifols, S. Peris, J. Sola	(BARC, DESY)
Also		PL B197 437	J.A. Grifols, S. Peris, J. Sola	(BARC, DESY)
ALBAJAR	87	PL B185 233	C. Albajar <i>et al.</i>	(UA1 Collab.)
ANSARI	87	PL B186 440	R. Ansari <i>et al.</i>	(UA2 Collab.)
GROTH	87	PR D36 2153	H. Grotch, R.W. Robinett	(PSU)
HAGIWARA	87	NP B282 253	K. Hagiwara <i>et al.</i>	(KEK, UCLA, FSU)
VANDERBIJ	87	PR D35 1088	J.J. van der Bij	(FNAL)
GRAU	85	PL 154B 283	A. Grau, J.A. Grifols	(BARC)
SUZUKI	85	PL 153B 289	M. Suzuki	(LBL)
ARNISON	84D	PL 134B 469	G.T.J. Arnison <i>et al.</i>	(UA1 Collab.)
HERZOG	84	PL 148B 355	F. Herzog	(WISC)
Also		PL 155B 468 (erratum)	F. Herzog	(WISC)
ARNISON	83	PL 122B 103	G.T.J. Arnison <i>et al.</i>	(UA1 Collab.)
BANNER	83B	PL 122B 476	M. Banner <i>et al.</i>	(UA2 Collab.)



$$J = 1$$

THE Z BOSON

Revised March 2009 by M. Grünewald (U. College Dublin and U. Ghent), and A. Gurtu (Tata Inst.).

Precision measurements at the Z -boson resonance using electron–positron colliding beams began in 1989 at the SLC and at LEP. During 1989–95, the four LEP experiments (ALEPH, DELPHI, L3, OPAL) made high-statistics studies of the production and decay properties of the Z . Although the SLD experiment at the SLC collected much lower statistics, it was able to match the precision of LEP experiments in determining the effective electroweak mixing angle $\sin^2\bar{\theta}_W$ and the rates of Z decay to b - and c -quarks, owing to availability of polarized electron beams, small beam size, and stable beam spot.

The Z -boson properties reported in this section may broadly be categorized as:

- The standard ‘lineshape’ parameters of the Z consisting of its mass, M_Z , its total width, Γ_Z , and its partial decay widths, $\Gamma(\text{hadrons})$, and $\Gamma(\ell\bar{\ell})$ where $\ell = e, \mu, \tau, \nu$;
- Z asymmetries in leptonic decays and extraction of Z couplings to charged and neutral leptons;
- The b - and c -quark-related partial widths and charge asymmetries which require special techniques;
- Determination of Z decay modes and the search for modes that violate known conservation laws;
- Average particle multiplicities in hadronic Z decay;
- Z anomalous couplings.

The effective vector and axial-vector coupling constants describing the Z -to-fermion coupling are also measured in $p\bar{p}$ and ep collisions at the Tevatron and at HERA. The corresponding cross-section formulae are given in Section 39 (Cross-section formulae for specific processes) and Section 16 (Structure Functions) in this *Review*. In this minireview, we concentrate on the measurements in e^+e^- collisions at LEP and SLC.

The standard ‘lineshape’ parameters of the Z are determined from an analysis of the production cross sections of these final states in e^+e^- collisions. The $Z \rightarrow \nu\bar{\nu}(\gamma)$ state is identified directly by detecting single photon production and indirectly by subtracting the visible partial widths from the total width. Inclusion in this analysis of the forward-backward asymmetry of charged leptons, $A_{FB}^{(0,\ell)}$, of the τ polarization, $P(\tau)$, and its forward-backward asymmetry, $P(\tau)^{fb}$, enables the separate determination of the effective vector (\bar{g}_V) and axial vector (\bar{g}_A) couplings of the Z to these leptons and the ratio (\bar{g}_V/\bar{g}_A), which is related to the effective electroweak mixing angle $\sin^2\bar{\theta}_W$ (see the ‘Electroweak Model and Constraints on New Physics’ review).

Determination of the b - and c -quark-related partial widths and charge asymmetries involves tagging the b and c quarks for which various methods are employed: requiring the presence of a high momentum prompt lepton in the event with high transverse momentum with respect to the accompanying jet; impact parameter and lifetime tagging using precision vertex measurement with high-resolution detectors; application of neural-network techniques to classify events as b or non- b on a statistical basis using event–shape variables; and using the presence of a charmed meson (D/D^*) or a kaon as a tag.

 Z -parameter determination

LEP was run at energy points on and around the Z mass (88–94 GeV) constituting an energy ‘scan.’ The shape of the cross-section variation around the Z peak can be described by a Breit-Wigner *ansatz* with an energy-dependent total width [1–3]. The **three** main properties of this distribution, viz., the **position** of the peak, the **width** of the distribution, and the **height** of the peak, determine respectively the values of M_Z , Γ_Z , and $\Gamma(e^+e^-) \times \Gamma(f\bar{f})$, where $\Gamma(e^+e^-)$ and $\Gamma(f\bar{f})$ are the electron and fermion partial widths of the Z . The quantitative determination of these parameters is done by writing analytic expressions for these cross sections in terms of the parameters, and fitting the calculated cross sections to the measured ones by varying these parameters, taking properly into account all the errors. Single-photon exchange (σ_γ^0) and γ - Z interference ($\sigma_{\gamma Z}^0$) are included, and the large ($\sim 25\%$) initial-state radiation (ISR) effects are taken into account by convoluting the analytic expressions over a ‘Radiator Function’ [1–5] $H(s, s')$. Thus for the process $e^+e^- \rightarrow f\bar{f}$:

$$\sigma_f(s) = \int H(s, s') \sigma_f^0(s') ds' \quad (1)$$

$$\sigma_f^0(s) = \sigma_Z^0 + \sigma_\gamma^0 + \sigma_{\gamma Z}^0 \quad (2)$$

$$\sigma_Z^0 = \frac{12\pi}{M_Z^2} \frac{\Gamma(e^+e^-)\Gamma(f\bar{f})}{\Gamma_Z^2} \frac{s \Gamma_Z^2}{(s - M_Z^2)^2 + s^2 \Gamma_Z^2 / M_Z^2} \quad (3)$$

$$\sigma_\gamma^0 = \frac{4\pi\alpha^2(s)}{3s} Q_f^2 N_c^f \quad (4)$$

$$\begin{aligned} \sigma_{\gamma Z}^0 = & -\frac{2\sqrt{2}\alpha(s)}{3} (Q_f G_F N_c^f \mathcal{G}_V^e \mathcal{G}_V^f) \\ & \times \frac{(s - M_Z^2) M_Z^2}{(s - M_Z^2)^2 + s^2 \Gamma_Z^2 / M_Z^2} \quad (5) \end{aligned}$$

where Q_f is the charge of the fermion, $N_c^f = 3$ for quarks and 1 for leptons, and \mathcal{G}_V^f is the vector coupling of the Z to the fermion-antifermion pair $f\bar{f}$.

Since $\sigma_{\gamma Z}^0$ is expected to be much less than σ_Z^0 , the LEP Collaborations have generally calculated the interference term in the framework of the Standard Model. This fixing of $\sigma_{\gamma Z}^0$ leads to a tighter constraint on M_Z , and consequently a smaller error on its fitted value. It is possible to relax this constraint and carry out the fit within the S-matrix framework, which is briefly described in the next section.

In the above framework, the QED radiative corrections have been explicitly taken into account by convoluting over the ISR and allowing the electromagnetic coupling constant to run [6]: $\alpha(s) = \alpha/(1 - \Delta\alpha)$. On the other hand, weak radiative corrections that depend upon the assumptions of the electroweak theory and on the values of M_{top} and M_{Higgs} are accounted for by **absorbing them into the couplings**, which are then called the *effective* couplings \mathcal{G}_V and \mathcal{G}_A (or alternatively the effective parameters of the \star scheme of Kennedy and Lynn [7].)

\mathcal{G}_V^f and \mathcal{G}_A^f are complex numbers with small imaginary parts. As experimental data does not allow simultaneous extraction of both real and imaginary parts of the effective couplings, the convention $g_A^f = \text{Re}(\mathcal{G}_A^f)$ and $g_V^f = \text{Re}(\mathcal{G}_V^f)$ is used and the imaginary parts are added in the fitting code [4].

Defining

$$A_f = 2 \frac{g_V^f \cdot g_A^f}{(g_V^f)^2 + (g_A^f)^2} \quad (6)$$

the lowest-order expressions for the various lepton-related asymmetries on the Z pole are [8–10] $A_{FB}^{(0,\ell)} = (3/4)A_e A_f$, $P(\tau) = -A_\tau$, $P(\tau)^{fb} = -(3/4)A_e$, $A_{LR} = A_e$. The full analysis takes into account the energy-dependence of the asymmetries. Experimentally A_{LR} is defined as $(\sigma_L - \sigma_R)/(\sigma_L + \sigma_R)$, where $\sigma_{L(R)}$ are the $e^+e^- \rightarrow Z$ production cross sections with left- (right)-handed electrons.

The definition of the partial decay width of the Z to $f\bar{f}$ includes the effects of QED and QCD final-state corrections, as well as the contribution due to the imaginary parts of the couplings:

$$\Gamma(f\bar{f}) = \frac{G_F M_Z^3}{6\sqrt{2}\pi} N_c^f (|\mathcal{G}_A^f|^2 R_A^f + |\mathcal{G}_V^f|^2 R_V^f) + \Delta_{ew/QCD} \quad (7)$$

where R_V^f and R_A^f are radiator factors to account for final state QED and QCD corrections, as well as effects due to nonzero fermion masses, and $\Delta_{ew/QCD}$ represents the non-factorizable electroweak/QCD corrections.

S-matrix approach to the Z

While most experimental analyses of LEP/SLC data have followed the ‘Breit-Wigner’ approach, an alternative S-matrix-based analysis is also possible. The Z , like all unstable particles, is associated with a complex pole in the S matrix. The pole position is process-independent and gauge-invariant. The mass, \bar{M}_Z , and width, $\bar{\Gamma}_Z$, can be defined in terms of the pole in the energy plane via [11–14]

$$\bar{s} = \bar{M}_Z^2 - i\bar{M}_Z \bar{\Gamma}_Z \quad (8)$$

leading to the relations

$$\begin{aligned} \bar{M}_Z &= M_Z / \sqrt{1 + \Gamma_Z^2 / M_Z^2} \\ &\approx M_Z - 34.1 \text{ MeV} \quad (9) \end{aligned}$$

$$\begin{aligned} \bar{\Gamma}_Z &= \Gamma_Z / \sqrt{1 + \Gamma_Z^2 / M_Z^2} \\ &\approx \Gamma_Z - 0.9 \text{ MeV} . \quad (10) \end{aligned}$$

The L3 and OPAL Collaborations at LEP (ACCIARRI 00Q and ABBIENDI 04G) have analyzed their data using the S-matrix approach as defined in Eq. (8), in addition to the conventional one. They observe a downward shift in the Z mass as expected.

Handling the large-angle e^+e^- final state

Unlike other $f\bar{f}$ decay final states of the Z , the e^+e^- final state has a contribution not only from the s -channel but also from the t -channel and s - t interference. The full amplitude is not amenable to fast calculation, which is essential if one has to carry out minimization fits within reasonable computer time. The usual procedure is to calculate the non- s channel part of the cross section separately using the Standard Model programs ALIBABA [15] or TOPAZO [16], with the measured value of M_{top} , and $M_{\text{Higgs}} = 150$ GeV, and add it to the s -channel cross section calculated as for other channels. This leads to two additional sources of error in the analysis: firstly, the theoretical calculation in ALIBABA itself is known to be accurate to $\sim 0.5\%$, and secondly, there is uncertainty due to the error on M_{top} and the unknown value of M_{Higgs} (100–1000 GeV). These errors are propagated into the analysis by including them in the systematic error on the e^+e^- final state. As these errors are common to the four LEP experiments, this is taken into account when performing the LEP average.

Errors due to uncertainty in LEP energy determination [17–22]

The systematic errors related to the LEP energy measurement can be classified as:

Gauge & Higgs Boson Particle Listings

Z

- The absolute energy scale error;
- Energy-point-to-energy-point errors due to the non-linear response of the magnets to the exciting currents;
- Energy-point-to-energy-point errors due to possible higher-order effects in the relationship between the dipole field and beam energy;
- Energy reproducibility errors due to various unknown uncertainties in temperatures, tidal effects, corrector settings, RF status, *etc.*

Precise energy calibration was done outside normal data-taking using the resonant depolarization technique. Run-time energies were determined every 10 minutes by measuring the relevant machine parameters and using a model which takes into account all the known effects, including leakage currents produced by trains in the Geneva area and the tidal effects due to gravitational forces of the Sun and the Moon. The LEP Energy Working Group has provided a covariance matrix from the determination of LEP energies for the different running periods during 1993–1995 [17].

Choice of fit parameters

The LEP Collaborations have chosen the following primary set of parameters for fitting: M_Z , Γ_Z , σ_{hadron}^0 , $R(\text{lepton})$, $A_{FB}^{(0,\ell)}$, where $R(\text{lepton}) = \Gamma(\text{hadrons})/\Gamma(\text{lepton})$, $\sigma_{\text{hadron}}^0 = 12\pi\Gamma(e^+e^-)\Gamma(\text{hadrons})/M_Z^2\Gamma_Z^2$. With a knowledge of these fitted parameters and their covariance matrix, any other parameter can be derived. The main advantage of these parameters is that they form a physics motivated set of parameters with much reduced correlations.

Thus, the most general fit carried out to cross section and asymmetry data determines the **nine parameters**: M_Z , Γ_Z , σ_{hadron}^0 , $R(e)$, $R(\mu)$, $R(\tau)$, $A_{FB}^{(0,e)}$, $A_{FB}^{(0,\mu)}$, $A_{FB}^{(0,\tau)}$. Assumption of lepton universality leads to a **five-parameter fit** determining M_Z , Γ_Z , σ_{hadron}^0 , $R(\text{lepton})$, $A_{FB}^{(0,\ell)}$.

Combining results from LEP and SLC experiments

With a steady increase in statistics over the years and improved understanding of the common systematic errors between LEP experiments, the procedures for combining results have evolved continuously [23]. The Line Shape Sub-group of the LEP Electroweak Working Group investigated the effects of these common errors, and devised a combination procedure for the precise determination of the Z parameters from LEP experiments. Using these procedures, this note also gives the results after combining the final parameter sets from the four experiments, and these are the results quoted as the fit results in the Z listings below. Transformation of variables leads to values of derived parameters like partial decay widths and branching ratios to hadrons and leptons. Finally, transforming the LEP combined nine parameter set to $(M_Z, \Gamma_Z, \sigma_{\text{hadron}}^0, g_A^f, g_V^f, f = e, \mu, \tau)$ using the average values of lepton asymmetry parameters (A_e, A_μ, A_τ) as constraints, leads to the best fitted values of the vector and axial-vector couplings (g_V, g_A) of the charged leptons to the Z .

Brief remarks on the handling of common errors and their magnitudes are given below. The identified common errors are those coming from

(a) LEP energy-calibration uncertainties, and

(b) the theoretical uncertainties in (i) the luminosity determination using small angle Bhabha scattering, (ii) estimating the non-s channel contribution to large angle Bhabha scattering, (iii) the calculation of QED radiative effects, and (iv) the parametrization of the cross section in terms of the parameter set used.

Common LEP energy errors

All the collaborations incorporate in their fit the full LEP energy error matrix as provided by the LEP energy group for their intersection region [17]. The effect of these errors is separated out from that of other errors by carrying out fits with energy errors scaled up and down by $\sim 10\%$ and redoing the fits. From the observed changes in the overall error matrix, the covariance matrix of the common energy errors is determined. Common LEP energy errors lead to uncertainties on M_Z , Γ_Z , and σ_{hadron}^0 of 1.7, 1.2 MeV, and 0.011 nb, respectively.

Common luminosity errors

BHLUMI 4.04 [24] is used by all LEP collaborations for small-angle Bhabha scattering leading to a common uncertainty in their measured cross sections of 0.061% [25]. BHLUMI does not include a correction for production of light fermion pairs. OPAL explicitly corrects for this effect and reduces their luminosity uncertainty to 0.054%, which is taken fully correlated with the other experiments. The other three experiments among themselves have a common uncertainty of 0.061%.

Common non-s channel uncertainties

The same standard model programs ALIBABA [15] and TOPAZ0 [16] are used to calculate the non-s channel contribution to the large angle Bhabha scattering [26]. As this contribution is a function of the Z mass, which itself is a variable in the fit, it is parametrized as a function of M_Z by each collaboration to properly track this contribution as M_Z varies in the fit. The common errors on R_e and $A_{FB}^{(0,e)}$ are 0.024 and 0.0014 respectively, and are correlated between them.

Common theoretical uncertainties: QED

There are large initial-state photon and fermion pair radiation effects near the Z resonance, for which the best currently available evaluations include contributions up to $\mathcal{O}(\alpha^3)$. To estimate the remaining uncertainties, different schemes are incorporated in the standard model programs ZFITTER [5], TOPAZ0 [16], and MIZA [27]. Comparing the different options leads to error estimates of 0.3 and 0.2 MeV on M_Z and Γ_Z respectively, and of 0.02% on σ_{hadron}^0 .

Common theoretical uncertainties: parametrization of lineshape and asymmetries

To estimate uncertainties arising from ambiguities in the model-independent parametrization of the differential cross-section near the Z resonance, results from TOPAZ0 and ZFITTER were compared by using ZFITTER to fit the cross sections

and asymmetries calculated using TOPAZ0. The resulting uncertainties on M_Z , Γ_Z , σ_{hadron}^0 , $R(\text{lepton})$, and $A_{FB}^{(0,\ell)}$ are 0.1 MeV, 0.1 MeV, 0.001 nb, 0.004, and 0.0001 respectively.

Thus, the overall theoretical errors on M_Z , Γ_Z , σ_{hadron}^0 are 0.3 MeV, 0.2 MeV, and 0.008 nb respectively; on each $R(\text{lepton})$ is 0.004 and on each $A_{FB}^{(0,\ell)}$ is 0.0001. Within the set of three $R(\text{lepton})$'s and the set of three $A_{FB}^{(0,\ell)}$'s, the respective errors are fully correlated.

All the theory-related errors mentioned above utilize Standard Model programs which need the Higgs mass and running electromagnetic coupling constant as inputs; uncertainties on these inputs will also lead to common errors. All LEP collaborations used the same set of inputs for Standard Model calculations: $M_Z = 91.187$ GeV, the Fermi constant $G_F = (1.16637 \pm 0.00001) \times 10^{-5}$ GeV⁻² [28], $\alpha^{(5)}(M_Z) = 1/128.877 \pm 0.090$ [29], $\alpha_s(M_Z) = 0.119$ [30], $M_{\text{top}} = 174.3 \pm 5.1$ GeV [30] and $M_{\text{Higgs}} = 150$ GeV. The only observable effect, on M_Z , is due to the variation of M_{Higgs} between 100–1000 GeV (due to the variation of the γ/Z interference term which is taken from the Standard Model): M_Z changes by +0.23 MeV per unit change in $\log_{10} M_{\text{Higgs}}/\text{GeV}$, which is not an error but a correction to be applied once M_{Higgs} is determined. The effect is much smaller than the error on M_Z (± 2.1 MeV).

Methodology of combining the LEP experimental results

The LEP experimental results actually used for combination are slightly modified from those published by the experiments (which are given in the Listings below). This has been done in order to facilitate the procedure by making the inputs more consistent. These modified results are given explicitly in [23]. The main differences compared to the published results are (a) consistent use of ZFITTER 6.23 and TOPAZ0 (the published ALEPH results used ZFITTER 6.10); (b) use of the combined energy-error matrix, which makes a difference of 0.1 MeV on the M_Z and Γ_Z for L3 only as at that intersection the RF modeling uncertainties are the largest.

Thus, nine-parameter sets from all four experiments with their covariance matrices are used together with all the common errors correlations. A grand covariance matrix, V , is constructed and a combined nine-parameter set is obtained by minimizing $\chi^2 = \Delta^T V^{-1} \Delta$, where Δ is the vector of residuals of the combined parameter set to the results of individual experiments. Imposing lepton universality in the combination results in the combined five parameter set.

Study of $Z \rightarrow b\bar{b}$ and $Z \rightarrow c\bar{c}$

In the sector of c - and b -physics, the LEP experiments have measured the ratios of partial widths $R_b = \Gamma(Z \rightarrow b\bar{b})/\Gamma(Z \rightarrow \text{hadrons})$, and $R_c = \Gamma(Z \rightarrow c\bar{c})/\Gamma(Z \rightarrow \text{hadrons})$, and the forward-backward (charge) asymmetries $A_{FB}^{b\bar{b}}$ and $A_{FB}^{c\bar{c}}$. The SLD experiment at SLC has measured the ratios R_c and R_b and, utilizing the polarization of the electron beam, was able to obtain the final state coupling parameters A_b and A_c from a measurement of the left-right forward-backward asymmetry of

b - and c -quarks. The high precision measurement of R_c at SLD was made possible owing to the small beam size and very stable beam spot at SLC, coupled with a highly precise CCD pixel detector. Several of the analyses have also determined other quantities, in particular the semileptonic branching ratios, $B(b \rightarrow \ell^-)$, $B(b \rightarrow c \rightarrow \ell^+)$, and $B(c \rightarrow \ell^+)$, the average time-integrated $B^0\bar{B}^0$ mixing parameter $\bar{\chi}$ and the probabilities for a c -quark to fragment into a D^+ , a D_s , a D^{*+} , or a charmed baryon. The latter measurements do not concern properties of the Z boson, and hence they do not appear in the Listing below. However, for completeness, we will report at the end of this minireview their values as obtained fitting the data contained in the Z section. All these quantities are correlated with the electroweak parameters, and since the mixture of b hadrons is different from the one at the $\Upsilon(4S)$, their values might differ from those measured at the $\Upsilon(4S)$.

All the above quantities are correlated to each other since:

- Several analyses (for example the lepton fits) determine more than one parameter simultaneously;
- Some of the electroweak parameters depend explicitly on the values of other parameters (for example R_b depends on R_c);
- Common tagging and analysis techniques produce common systematic uncertainties.

The LEP Electroweak Heavy Flavour Working Group has developed [31] a procedure for combining the measurements taking into account known sources of correlation. The combining procedure determines fourteen parameters: the six parameters of interest in the electroweak sector, R_b , R_c , $A_{FB}^{b\bar{b}}$, $A_{FB}^{c\bar{c}}$, A_b and A_c and, in addition, $B(b \rightarrow \ell^-)$, $B(b \rightarrow c \rightarrow \ell^+)$, $B(c \rightarrow \ell^+)$, $\bar{\chi}$, $f(D^+)$, $f(D_s)$, $f(c_{\text{baryon}})$ and $P(c \rightarrow D^{*+}) \times B(D^{*+} \rightarrow \pi^+ D^0)$, to take into account their correlations with the electroweak parameters. Before the fit both the peak and off-peak asymmetries are translated to the common energy $\sqrt{s} = 91.26$ GeV using the predicted energy-dependence from ZFITTER [5].

Summary of the measurements and of the various kinds of analysis

The measurements of R_b and R_c fall into two classes. In the first, named single-tag measurement, a method for selecting b and c events is applied and the number of tagged events is counted. A second technique, named double-tag measurement, has the advantage that the tagging efficiency is directly derived from the data thereby reducing the systematic error on the measurement.

The measurements in the b - and c -sector can be essentially grouped in the following categories:

- Lifetime (and lepton) double-tagging measurements of R_b . These are the most precise measurements of R_b and obviously dominate the combined result. The main sources of systematics come from the charm contamination and from estimating the hemisphere b -tagging efficiency correlation;
- Analyses with $D/D^{*\pm}$ to measure R_c . These measurements make use of several different tagging techniques (inclusive/exclusive double tag, exclusive double tag, reconstruction of all weakly decaying charmed states) and no assumptions are made on the energy-dependence of charm fragmentation;
- A measurement of R_c using single leptons and assuming $B(b \rightarrow c \rightarrow \ell^+)$;
- Lepton fits which use hadronic events with one or more leptons in the final state to measure the asymmetries $A_{FB}^{b\bar{b}}$ and $A_{FB}^{c\bar{c}}$. Each analysis usually gives several other electroweak parameters. The dominant sources of systematics are due to lepton identification, to other semileptonic branching ratios and to the modeling of the semileptonic decay;
- Measurements of $A_{FB}^{b\bar{b}}$ using lifetime tagged events with a hemisphere charge measurement. These measurements dominate the combined result;
- Analyses with $D/D^{*\pm}$ to measure $A_{FB}^{c\bar{c}}$ or simultaneously $A_{FB}^{b\bar{b}}$ and $A_{FB}^{c\bar{c}}$;
- Measurements of A_b and A_c from SLD, using several tagging methods (lepton, kaon, D/D^* , and vertex mass). These quantities are directly extracted from a measurement of the left–right forward–backward asymmetry in $c\bar{c}$ and $b\bar{b}$ production using a polarized electron beam.

Averaging procedure

All the measurements are provided by the LEP and SLD Collaborations in the form of tables with a detailed breakdown of the systematic errors of each measurement and its dependence on other electroweak parameters.

The averaging proceeds via the following steps:

- Define and propagate a consistent set of external inputs such as branching ratios, hadron lifetimes, fragmentation models *etc.* All the measurements are checked to ensure that all use a common set of assumptions (for instance, since the QCD corrections for the forward–backward asymmetries are strongly dependent on the experimental conditions, the data are corrected before combining);
- Form the full (statistical and systematic) covariance matrix of the measurements. The systematic correlations between different analyses are calculated from the detailed error breakdown in the measurement tables. The correlations relating several measurements made by the same analysis are also used;
- Take into account any explicit dependence of a measurement on the other electroweak parameters. As an example of this dependence, we illustrate the case of the double-tag measurement of R_b , where c -quarks constitute the main background. The normalization of the charm contribution is not usually fixed by the data and the measurement of R_b depends on the assumed value of R_c , which can be written as:

$$R_b = R_b^{\text{meas}} + a(R_c) \frac{(R_c - R_c^{\text{used}})}{R_c}, \quad (11)$$
 where R_b^{meas} is the result of the analysis which assumed a value of $R_c = R_c^{\text{used}}$ and $a(R_c)$ is the constant which gives the dependence on R_c ;
- Perform a χ^2 minimization with respect to the combined electroweak parameters.

After the fit the average peak asymmetries $A_{FB}^{c\bar{c}}$ and $A_{FB}^{b\bar{b}}$ are corrected for the energy shift from 91.26 GeV to M_Z and for QED (initial state radiation), γ exchange, and γZ interference effects, to obtain the corresponding pole asymmetries $A_{FB}^{0,c}$ and $A_{FB}^{0,b}$.

This averaging procedure, using the fourteen parameters described above, and applied to the data contained in the Z particle listing below, gives the following results (where the last 8 parameters do not depend directly on the Z):

$$R_b^0 = 0.21629 \pm 0.00066$$

$$R_c^0 = 0.1721 \pm 0.0030$$

$$A_{FB}^{0,b} = 0.0992 \pm 0.0016$$

$$A_{FB}^{0,c} = 0.0707 \pm 0.0035$$

$$A_b = 0.923 \pm 0.020$$

$$A_c = 0.670 \pm 0.027$$

$$B(b \rightarrow \ell^-) = 0.1071 \pm 0.0022$$

$$B(b \rightarrow c \rightarrow \ell^+) = 0.0801 \pm 0.0018$$

$$B(c \rightarrow \ell^+) = 0.0969 \pm 0.0031$$

$$\bar{\chi} = 0.1250 \pm 0.0039$$

$$f(D^+) = 0.235 \pm 0.016$$

$$f(D_s) = 0.126 \pm 0.026$$

$$f(c_{\text{baryon}}) = 0.093 \pm 0.022$$

$$P(c \rightarrow D^{*+}) \times B(D^{*+} \rightarrow \pi^+ D^0) = 0.1622 \pm 0.0048$$

Among the non–electroweak observables, the B semileptonic branching fraction $B(b \rightarrow \ell^-)$ is of special interest, since the dominant error source on this quantity is the dependence on the semileptonic decay model for $b \rightarrow \ell^-$, with $\Delta B(b \rightarrow$

$\ell^-)_{b \rightarrow \ell^-} - \text{model} = 0.0012$. Extensive studies have been made to understand the size of this error. Among the electroweak quantities, the quark asymmetries with leptons depend also on the semileptonic decay model, while the asymmetries using other methods usually do not. The fit implicitly requires that the different methods give consistent results and this effectively constrains the decay model, and thus reduces in principle the error from this source in the fit result.

To obtain a conservative estimate of the modelling error, the above fit has been repeated removing all asymmetry measurements. The results of the fit on B-decay related observables are [23]: $B(b \rightarrow \ell^-) = 0.1069 \pm 0.0022$, with $\Delta B(b \rightarrow \ell^-)_{b \rightarrow \ell^-} - \text{model} = 0.0013$, $B(b \rightarrow c \rightarrow \ell^+) = 0.0802 \pm 0.0019$ and $\bar{\chi} = 0.1259 \pm 0.0042$.

References

- R.N. Cahn, Phys. Rev. **D36**, 2666 (1987).
- F.A. Berends *et al.*, "Z Physics at LEP 1," CERN Report 89-08 (1989), Vol. 1, eds. G. Altarelli, R. Kleiss, and C. Verzegnassi, p. 89.
- A. Borrelli *et al.*, Nucl. Phys. **B333**, 357 (1990).
- D. Bardin and G. Passarino, "Upgrading of Precision Calculations for Electroweak Observables," hep-ph/9803425; D. Bardin, G. Passarino, and M. Grunewald, "Precision Calculation Project Report," hep-ph/9902452.
- D. Bardin *et al.*, Z. Phys. **C44**, 493 (1989); Comp. Phys. Comm. **59**, 303 (1990); D. Bardin *et al.*, Nucl. Phys. **B351**, 1 (1991); Phys. Lett. **B255**, 290 (1991), and CERN-TH/6443/92 (1992); Comp. Phys. Comm. **133**, 229 (2001).
- G. Burgers *et al.*, "Z Physics at LEP 1," CERN Report 89-08 (1989), Vol. 1, eds. G. Altarelli, R. Kleiss, and C. Verzegnassi, p. 55.
- D.C. Kennedy and B.W. Lynn, Nucl. Phys. **B322**, 1 (1989).
- M. Consoli *et al.*, "Z Physics at LEP 1," CERN Report 89-08 (1989), Vol. 1, eds. G. Altarelli, R. Kleiss, and C. Verzegnassi, p. 7.
- M. Bohm *et al.*, *ibid.*, p. 203.
- S. Jadach *et al.*, *ibid.*, p. 235.
- R. Stuart, Phys. Lett. **B262**, 113 (1991).
- A. Sirlin, Phys. Rev. Lett. **67**, 2127 (1991).
- A. Leike, T. Riemann, and J. Rose, Phys. Lett. **B273**, 513 (1991).
- See also D. Bardin *et al.*, Phys. Lett. **B206**, 539 (1988).
- W. Beenakker, F.A. Berends, and S.C. van der Marck, Nucl. Phys. **B349**, 323 (1991).
- G. Montagna *et al.*, Nucl. Phys. **B401**, 3 (1993); Comp. Phys. Comm. **76**, 328 (1993); Comp. Phys. Comm. **93**, 120 (1996); G. Montagna *et al.*, Comp. Phys. Comm. **117**, 278 (1999).
- R. Assmann *et al.*, (Working Group on LEP Energy), Eur. Phys. J. **C6**, 187 (1999).
- R. Assmann *et al.*, (Working Group on LEP Energy), Z. Phys. **C66**, 567 (1995).
- L. Arnaudon *et al.*, (Working Group on LEP Energy and LEP Collaborations), Phys. Lett. **B307**, 187 (1993).
- L. Arnaudon *et al.*, (Working Group on LEP Energy), CERN-PPE/92-125 (1992).
- L. Arnaudon *et al.*, Phys. Lett. **B284**, 431 (1992).
- R. Bailey *et al.*, 'LEP Energy Calibration' CERN-SL-90-95-AP, Proceedings of the "2nd European Particle Accelerator Conference," Nice, France, 12-16 June 1990, pp. 1765-1767.
- The LEP Collaborations: ALEPH, DELPHI, L3, OPAL, and the LEP Electroweak Working Group: CERN-PH-EP/2007-039 (2007); CERN-PH-EP/2006-042 (2006). The LEP Collaborations: ALEPH, DELPHI, L3, OPAL, the LEP Electroweak Working Group, and the SLD Heavy Flavour Group: Phys. Reports **427**, 257 (2006); CERN-PH-EP/2005-051 (2005); CERN-PH-EP/2004-069 (2004); CERN-EP/2003-091 (2003); CERN-EP/2002-091 (2002); CERN-EP/2001-098 (2001); CERN-EP/2001-021 (2001); CERN-EP/2000-016 (1999); CERN-EP/99-15 (1998); CERN-PPE/97-154 (1997); CERN-PPE/96-183 (1996); CERN-PPE/95-172 (1995); CERN-PPE/94-187 (1994); CERN-PPE/93-157 (1993).
- S. Jadach *et al.*, BHLUMI 4.04, Comp. Phys. Comm. **102**, 229 (1997); S. Jadach and O. Nicosini, Event generators for Bhabha scattering, in Physics at LEP2, CERN-96-01 Vol. 2, February 1996.
- B.F.L. Ward *et al.*, Phys. Lett. **B450**, 262 (1999).
- W. Beenakker and G. Passarino, Phys. Lett. **B425**, 199 (1998).
- M. Martinez *et al.*, Z. Phys. **C49**, 645 (1991); M. Martinez and F. Teubert, Z. Phys. **C65**, 267 (1995), updated with results summarized in S. Jadach, B. Pietrzyk, and M. Skrzypek, Phys. Lett. **B456**, 77 (1999) and Reports of the working group on precision calculations for the Z resonance, CERN 95-03, ed. D. Bardin, W. Hollik, and G. Passarino, and references therein.
- T. van Ritbergen and R. Stuart, Phys. Lett. **B437**, 201 (1998); Phys. Rev. Lett. **82**, 488 (1999).
- S. Eidelman and F. Jegerlehner, Z. Phys. **C67**, 585 (1995); M. Steinhauser, Phys. Lett. **B429**, 158 (1998).
- Particle Data Group (D.E. Groom *et al.*), Eur. Phys. J. **C15**, 1 (2000).
- The LEP Experiments: ALEPH, DELPHI, L3, and OPAL Nucl. Instrum. Methods **A378**, 101 (1996).

Z MASS

OUR FIT is obtained using the fit procedure and correlations as determined by the LEP Electroweak Working Group (see the note "The Z boson" and ref. LEP-SLC 06). The fit is performed using the Z mass and width, the Z hadronic pole cross section, the ratios of hadronic to leptonic partial widths, and the Z pole forward-backward lepton asymmetries. This set is believed to be most free of correlations.

The Z-boson mass listed here corresponds to the mass parameter in a Breit-Wigner distribution with mass dependent width. The value is 34 MeV greater than the real part of the position of the pole (in the energy-squared plane) in the Z-boson propagator. Also the LEP experiments have generally assumed a fixed value of the $\gamma - Z$ interferences term based on the standard model. Keeping this term as free parameter leads to a somewhat larger error on the fitted Z mass. See ACCIARRI 00q and ABBIENDI 04g for a detailed investigation of both these issues.

VALUE (GeV)	EVTS	DOCUMENT ID	TECN	COMMENT
91.1876 ± 0.0021 OUR FIT				
91.1852 ± 0.0030	4.57M	¹ ABBIENDI	01A OPAL	$E_{\text{cm}}^{\text{hc}} = 88-94$ GeV
91.1863 ± 0.0028	4.08M	² ABREU	00F DLPH	$E_{\text{cm}}^{\text{hc}} = 88-94$ GeV

Gauge & Higgs Boson Particle Listings

Z

91.1898 ± 0.0031	3.96M	³ ACCIARRI	00c L3	$E_{cm}^{ee} = 88-94$ GeV
91.1885 ± 0.0031	4.57M	⁴ BARATE	00c ALEP	$E_{cm}^{ee} = 88-94$ GeV
• • • We do not use the following data for averages, fits, limits, etc. • • •				
91.1872 ± 0.0033		⁵ ABBIENDI	04g OPAL	$E_{cm}^{ee} = \text{LEP1} +$ $130-209$ GeV
91.272 ± 0.032 ± 0.033		⁶ ACHARD	04c L3	$E_{cm}^{ee} = 183-209$ GeV
91.1875 ± 0.0039	3.97M	⁷ ACCIARRI	00q L3	$E_{cm}^{ee} = \text{LEP1} +$ $130-189$ GeV
91.151 ± 0.008		⁸ MIYABAYASHI	95 TOPZ	$E_{cm}^{ee} = 57.8$ GeV
91.74 ± 0.28 ± 0.93	156	⁹ ALITTI	92b UA2	$E_{cm}^{pp} = 630$ GeV
90.9 ± 0.3 ± 0.2	188	¹⁰ ABE	89c CDF	$E_{cm}^{pp} = 1.8$ TeV
91.14 ± 0.12	480	¹¹ ABRAMS	89b MRK2	$E_{cm}^{ee} = 89-93$ GeV
93.1 ± 1.0 ± 3.0	24	¹² ALBAJAR	89 UA1	$E_{cm}^{pp} = 546,630$ GeV

- ¹ ABBIENDI 01A error includes approximately 2.3 MeV due to statistics and 1.8 MeV due to LEP energy uncertainty.
- ² The error includes 1.6 MeV due to LEP energy uncertainty.
- ³ The error includes 1.8 MeV due to LEP energy uncertainty.
- ⁴ BARATE 00c error includes approximately 2.4 MeV due to statistics, 0.2 MeV due to experimental systematics, and 1.7 MeV due to LEP energy uncertainty.
- ⁵ ABBIENDI 04g obtain this result using the S-matrix formalism for a combined fit to their cross section and asymmetry data at the Z peak and their data at 130–209 GeV. The authors have corrected the measurement for the 34 MeV shift with respect to the Breit-Wigner fits.
- ⁶ ACHARD 04c select $e^+e^- \rightarrow Z\gamma$ events with hard initial-state radiation. Z decays to $q\bar{q}$ and muon pairs are considered. The fit results obtained in the two samples are found consistent to each other and combined considering the uncertainty due to ISR modelling as fully correlated.
- ⁷ ACCIARRI 00q interpret the s-dependence of the cross sections and lepton forward-backward asymmetries in the framework of the S-matrix formalism. They fit to their cross section and asymmetry data at high energies, using the results of S-matrix fits to Z-peak data (ACCIARRI 00c) as constraints. The 130–189 GeV data constrains the γ/Z interference term. The authors have corrected the measurement for the 34.1 MeV shift with respect to the Breit-Wigner fits. The error contains a contribution of ± 2.3 MeV due to the uncertainty on the γ/Z interference.
- ⁸ MIYABAYASHI 95 combine their low energy total hadronic cross-section measurement with the ACTON 93D data and perform a fit using an S-matrix formalism. As expected, this result is below the mass values obtained with the standard Breit-Wigner parametrization.
- ⁹ Enters fit through W/Z mass ratio given in the W Particle Listings. The ALITTI 92b systematic error (± 0.93) has two contributions: one (± 0.92) cancels in m_W/m_Z and one (± 0.12) is noncancelling. These were added in quadrature.
- ¹⁰ First error of ABE 89 is combination of statistical and systematic contributions; second is mass scale uncertainty.
- ¹¹ ABRAMS 89B uncertainty includes 35 MeV due to the absolute energy measurement.
- ¹² ALBAJAR 89 result is from a total sample of 33 $Z \rightarrow e^+e^-$ events.

Z WIDTH

OUR FIT is obtained using the fit procedure and correlations as determined by the LEP Electroweak Working Group (see the note "The Z boson" and ref. LEP-SLC 06).

VALUE (GeV)	EVTS	DOCUMENT ID	TECN	COMMENT
2.4952 ± 0.0023 OUR FIT				
2.4948 ± 0.0041	4.57M	¹³ ABBIENDI	01A OPAL	$E_{cm}^{ee} = 88-94$ GeV
2.4876 ± 0.0041	4.08M	¹⁴ ABREU	00f DLPH	$E_{cm}^{ee} = 88-94$ GeV
2.5024 ± 0.0042	3.96M	¹⁵ ACCIARRI	00c L3	$E_{cm}^{ee} = 88-94$ GeV
2.4951 ± 0.0043	4.57M	¹⁶ BARATE	00c ALEP	$E_{cm}^{ee} = 88-94$ GeV
• • • We do not use the following data for averages, fits, limits, etc. • • •				
2.4943 ± 0.0041		¹⁷ ABBIENDI	04g OPAL	$E_{cm}^{ee} = \text{LEP1} +$ $130-209$ GeV
2.5025 ± 0.0041	3.97M	¹⁸ ACCIARRI	00q L3	$E_{cm}^{ee} = \text{LEP1} +$ $130-189$ GeV
2.50 ± 0.21 ± 0.06		¹⁹ ABREU	96r DLPH	$E_{cm}^{ee} = 91.2$ GeV
3.8 ± 0.8 ± 1.0	188	ABE	89c CDF	$E_{cm}^{pp} = 1.8$ TeV
2.42 $\begin{smallmatrix} +0.45 \\ -0.35 \end{smallmatrix}$	480	²⁰ ABRAMS	89b MRK2	$E_{cm}^{ee} = 89-93$ GeV
2.7 $\begin{smallmatrix} +1.2 \\ -1.0 \end{smallmatrix}$ ± 1.3	24	²¹ ALBAJAR	89 UA1	$E_{cm}^{pp} = 546,630$ GeV
2.7 ± 2.0 ± 1.0	25	²² ANSARI	87 UA2	$E_{cm}^{pp} = 546,630$ GeV

- ¹³ ABBIENDI 01A error includes approximately 3.6 MeV due to statistics, 1 MeV due to event selection systematics, and 1.3 MeV due to LEP energy uncertainty.
- ¹⁴ The error includes 1.2 MeV due to LEP energy uncertainty.
- ¹⁵ The error includes 1.3 MeV due to LEP energy uncertainty.
- ¹⁶ BARATE 00c error includes approximately 3.8 MeV due to statistics, 0.9 MeV due to experimental systematics, and 1.3 MeV due to LEP energy uncertainty.
- ¹⁷ ABBIENDI 04g obtain this result using the S-matrix formalism for a combined fit to their cross section and asymmetry data at the Z peak and their data at 130–209 GeV. The authors have corrected the measurement for the 1 MeV shift with respect to the Breit-Wigner fits.
- ¹⁸ ACCIARRI 00q interpret the s-dependence of the cross sections and lepton forward-backward asymmetries in the framework of the S-matrix formalism. They fit to their cross section and asymmetry data at high energies, using the results of S-matrix fits to Z-peak data (ACCIARRI 00c) as constraints. The 130–189 GeV data constrains the γ/Z interference term. The authors have corrected the measurement for the 0.9 MeV shift with respect to the Breit-Wigner fits.
- ¹⁹ ABREU 96r obtain this value from a study of the interference between initial and final state radiation in the process $e^+e^- \rightarrow Z \rightarrow \mu^+\mu^-$.

- ²⁰ ABRAMS 89B uncertainty includes 50 MeV due to the miniSAM background subtraction error.
- ²¹ ALBAJAR 89 result is from a total sample of 33 $Z \rightarrow e^+e^-$ events.
- ²² Quoted values of ANSARI 87 are from direct fit. Ratio of Z and W production gives either $\Gamma(Z) < (1.09 \pm 0.07) \times \Gamma(W)$, CL = 90% or $\Gamma(Z) = (0.82^{+0.19}_{-0.14} \pm 0.06) \times \Gamma(W)$. Assuming Standard-Model value $\Gamma(W) = 2.65$ GeV then gives $\Gamma(Z) < 2.89 \pm 0.19$ or $= 2.17^{+0.50}_{-0.37} \pm 0.16$.

Z DECAY MODES

Mode	Fraction (Γ_i/Γ)	Scale factor/ Confidence level
Γ_1 e^+e^-	(3.363 ± 0.004) %	
Γ_2 $\mu^+\mu^-$	(3.366 ± 0.007) %	
Γ_3 $\tau^+\tau^-$	(3.367 ± 0.008) %	
Γ_4 $\ell^+\ell^-$	[a] (3.3658 ± 0.0023) %	
Γ_5 invisible	(20.00 ± 0.06) %	
Γ_6 hadrons	(69.91 ± 0.06) %	
Γ_7 $(u\bar{u} + c\bar{c})/2$	(11.6 ± 0.6) %	
Γ_8 $(d\bar{d} + s\bar{s} + b\bar{b})/3$	(15.6 ± 0.4) %	
Γ_9 $c\bar{c}$	(12.03 ± 0.21) %	
Γ_{10} $b\bar{b}$	(15.12 ± 0.05) %	
Γ_{11} $b\bar{b}b\bar{b}$	(3.6 ± 1.3) % × 10 ⁻⁴	
Γ_{12} $g\bar{g}g$	< 1.1	CL=95%
Γ_{13} $\pi^0\gamma$	< 5.2	× 10 ⁻⁵ CL=95%
Γ_{14} $\eta\gamma$	< 5.1	× 10 ⁻⁵ CL=95%
Γ_{15} $\omega\gamma$	< 6.5	× 10 ⁻⁴ CL=95%
Γ_{16} $\eta'(958)\gamma$	< 4.2	× 10 ⁻⁵ CL=95%
Γ_{17} $\gamma\gamma$	< 5.2	× 10 ⁻⁵ CL=95%
Γ_{18} $\gamma\gamma\gamma$	< 1.0	× 10 ⁻⁵ CL=95%
Γ_{19} $\pi^\pm W^\mp$	[b] < 7	× 10 ⁻⁵ CL=95%
Γ_{20} $\rho^\pm W^\mp$	[b] < 8.3	× 10 ⁻⁵ CL=95%
Γ_{21} $J/\psi(1S)X$	(3.51 $\begin{smallmatrix} +0.23 \\ -0.25 \end{smallmatrix}$) × 10 ⁻³	S=1.1
Γ_{22} $\psi(2S)X$	(1.60 ± 0.29) × 10 ⁻³	
Γ_{23} $\chi_{c1}(1P)X$	(2.9 ± 0.7) × 10 ⁻³	
Γ_{24} $\chi_{c2}(1P)X$	< 3.2	× 10 ⁻³ CL=90%
Γ_{25} $\Upsilon(1S)X + \Upsilon(2S)X$ $+ \Upsilon(3S)X$	(1.0 ± 0.5) × 10 ⁻⁴	
Γ_{26} $\Upsilon(1S)X$	< 4.4	× 10 ⁻⁵ CL=95%
Γ_{27} $\Upsilon(2S)X$	< 1.39	× 10 ⁻⁴ CL=95%
Γ_{28} $\Upsilon(3S)X$	< 9.4	× 10 ⁻⁵ CL=95%
Γ_{29} $(D^0/\bar{D}^0)X$	(20.7 ± 2.0) %	
Γ_{30} $D^\pm X$	(12.2 ± 1.7) %	
Γ_{31} $D^*(2010)^\pm X$	[b] (11.4 ± 1.3) %	
Γ_{32} $D_{s1}(2536)^\pm X$	(3.6 ± 0.8) × 10 ⁻³	
Γ_{33} $D_{sJ}(2573)^\pm X$	(5.8 ± 2.2) × 10 ⁻³	
Γ_{34} $D_{sJ}^*(2629)^\pm X$	searched for	
Γ_{35} BX		
Γ_{36} B^*X		
Γ_{37} B^+X	[c] (6.08 ± 0.13) %	
Γ_{38} B_s^0X	[c] (1.59 ± 0.13) %	
Γ_{39} $B_c^\pm X$	searched for	
Γ_{40} $A_c^\pm X$	(1.54 ± 0.33) %	
Γ_{41} $\Xi_c^0 X$	seen	
Γ_{42} $\Xi_b^- X$	seen	
Γ_{43} b-baryon X	[c] (1.38 ± 0.22) %	
Γ_{44} anomalous γ + hadrons	[d] < 3.2	× 10 ⁻³ CL=95%
Γ_{45} $e^+e^- \gamma$	[d] < 5.2	× 10 ⁻⁴ CL=95%
Γ_{46} $\mu^+\mu^- \gamma$	[d] < 5.6	× 10 ⁻⁴ CL=95%
Γ_{47} $\tau^+\tau^- \gamma$	[d] < 7.3	× 10 ⁻⁴ CL=95%
Γ_{48} $\ell^+\ell^- \gamma \gamma$	[e] < 6.8	× 10 ⁻⁶ CL=95%
Γ_{49} $q\bar{q}\gamma\gamma$	[e] < 5.5	× 10 ⁻⁶ CL=95%
Γ_{50} $\nu\bar{\nu}\gamma\gamma$	[e] < 3.1	× 10 ⁻⁶ CL=95%
Γ_{51} $e^\pm \mu^\mp$	LF [b] < 1.7	× 10 ⁻⁶ CL=95%
Γ_{52} $e^\pm \tau^\mp$	LF [b] < 9.8	× 10 ⁻⁶ CL=95%
Γ_{53} $\mu^\pm \tau^\mp$	LF [b] < 1.2	× 10 ⁻⁵ CL=95%
Γ_{54} pe	L,B < 1.8	× 10 ⁻⁶ CL=95%
Γ_{55} $p\mu$	L,B < 1.8	× 10 ⁻⁶ CL=95%

- [a] ℓ indicates each type of lepton ($e, \mu, \text{ and } \tau$), not sum over them.
- [b] The value is for the sum of the charge states or particle/antiparticle states indicated.
- [c] This value is updated using the product of (i) the $Z \rightarrow b\bar{b}$ fraction from this listing and (ii) the b-hadron fraction in an

unbiased sample of weakly decaying b -hadrons produced in Z -decays provided by the Heavy Flavor Averaging Group (HFAG, <http://www.slac.stanford.edu/xorg/hfag/osc/PDG2009/#FRACZ>).

[d] See the Particle Listings below for the γ energy range used in this measurement.

[e] For $m_{\gamma\gamma} = (60 \pm 5)$ GeV.

Z PARTIAL WIDTHS

$\Gamma(e^+e^-)$ Γ_1

For the LEP experiments, this parameter is not directly used in the overall fit but is derived using the fit results; see the note "The Z boson" and ref. LEP-SLC 06.

VALUE (MeV)	EVTS	DOCUMENT ID	TECN	COMMENT
83.91 ± 0.12 OUR FIT				
83.66 ± 0.20	137.0K	ABBIENDI	01A OPAL	$E_{cm}^{ee} = 88-94$ GeV
83.54 ± 0.27	117.8k	ABREU	00F DLPH	$E_{cm}^{ee} = 88-94$ GeV
84.16 ± 0.22	124.4k	ACCIARRI	00c L3	$E_{cm}^{ee} = 88-94$ GeV
83.88 ± 0.19		BARATE	00c ALEP	$E_{cm}^{ee} = 88-94$ GeV
82.89 ± 1.20 ± 0.89		²³ ABE	95J SLD	$E_{cm}^{ee} = 91.31$ GeV

²³ ABE 95J obtain this measurement from Bhabha events in a restricted fiducial region to improve systematics. They use the values 91.187 and 2.489 GeV for the Z mass and total decay width to extract this partial width.

$\Gamma(\mu^+\mu^-)$ Γ_2

This parameter is not directly used in the overall fit but is derived using the fit results; see the note "The Z boson" and ref. LEP-SLC 06.

VALUE (MeV)	EVTS	DOCUMENT ID	TECN	COMMENT
83.99 ± 0.18 OUR FIT				
84.03 ± 0.30	182.8K	ABBIENDI	01A OPAL	$E_{cm}^{ee} = 88-94$ GeV
84.48 ± 0.40	157.6k	ABREU	00F DLPH	$E_{cm}^{ee} = 88-94$ GeV
83.95 ± 0.44	113.4k	ACCIARRI	00c L3	$E_{cm}^{ee} = 88-94$ GeV
84.02 ± 0.28		BARATE	00c ALEP	$E_{cm}^{ee} = 88-94$ GeV

$\Gamma(\tau^+\tau^-)$ Γ_3

This parameter is not directly used in the overall fit but is derived using the fit results; see the note "The Z boson" and ref. LEP-SLC 06.

VALUE (MeV)	EVTS	DOCUMENT ID	TECN	COMMENT
84.08 ± 0.22 OUR FIT				
83.94 ± 0.41	151.5K	ABBIENDI	01A OPAL	$E_{cm}^{ee} = 88-94$ GeV
83.71 ± 0.58	104.0k	ABREU	00F DLPH	$E_{cm}^{ee} = 88-94$ GeV
84.23 ± 0.58	103.0k	ACCIARRI	00c L3	$E_{cm}^{ee} = 88-94$ GeV
84.38 ± 0.31		BARATE	00c ALEP	$E_{cm}^{ee} = 88-94$ GeV

$\Gamma(\ell^+\ell^-)$ Γ_4

In our fit $\Gamma(\ell^+\ell^-)$ is defined as the partial Z width for the decay into a pair of massless charged leptons. This parameter is not directly used in the 5-parameter fit assuming lepton universality but is derived using the fit results. See the note "The Z boson" and ref. LEP-SLC 06.

VALUE (MeV)	EVTS	DOCUMENT ID	TECN	COMMENT
83.984 ± 0.086 OUR FIT				
83.82 ± 0.15	471.3K	ABBIENDI	01A OPAL	$E_{cm}^{ee} = 88-94$ GeV
83.85 ± 0.17	379.4k	ABREU	00F DLPH	$E_{cm}^{ee} = 88-94$ GeV
84.14 ± 0.17	340.8k	ACCIARRI	00c L3	$E_{cm}^{ee} = 88-94$ GeV
84.02 ± 0.15	500k	BARATE	00c ALEP	$E_{cm}^{ee} = 88-94$ GeV

$\Gamma(\text{invisible})$ Γ_5

We use only direct measurements of the invisible partial width using the single photon channel to obtain the average value quoted below. OUR FIT value is obtained as a difference between the total and the observed partial widths assuming lepton universality.

VALUE (MeV)	EVTS	DOCUMENT ID	TECN	COMMENT
499.0 ± 1.5 OUR FIT				
503 ± 16 OUR AVERAGE				Error includes scale factor of 1.2.
498 ± 12 ± 12	1791	ACCIARRI	98G L3	$E_{cm}^{ee} = 88-94$ GeV
539 ± 26 ± 17	410	AKERS	95c OPAL	$E_{cm}^{ee} = 88-94$ GeV
450 ± 34 ± 34	258	BUSKULIC	93L ALEP	$E_{cm}^{ee} = 88-94$ GeV
540 ± 80 ± 40	52	ADEVA	92 L3	$E_{cm}^{ee} = 88-94$ GeV
• • • We do not use the following data for averages, fits, limits, etc. • • •				
498.1 ± 2.6		²⁴ ABBIENDI	01A OPAL	$E_{cm}^{ee} = 88-94$ GeV
498.1 ± 3.2		²⁴ ABREU	00F DLPH	$E_{cm}^{ee} = 88-94$ GeV
499.1 ± 2.9		²⁴ ACCIARRI	00c L3	$E_{cm}^{ee} = 88-94$ GeV
499.1 ± 2.5		²⁴ BARATE	00c ALEP	$E_{cm}^{ee} = 88-94$ GeV

²⁴ This is an indirect determination of $\Gamma(\text{invisible})$ from a fit to the visible Z decay modes.

$\Gamma(\text{hadrons})$ Γ_6

This parameter is not directly used in the 5-parameter fit assuming lepton universality, but is derived using the fit results. See the note "The Z boson" and ref. LEP-SLC 06.

VALUE (MeV)	EVTS	DOCUMENT ID	TECN	COMMENT
1744.4 ± 2.0 OUR FIT				
1745.4 ± 3.5	4.10M	ABBIENDI	01A OPAL	$E_{cm}^{ee} = 88-94$ GeV
1738.1 ± 4.0	3.70M	ABREU	00F DLPH	$E_{cm}^{ee} = 88-94$ GeV
1751.1 ± 3.8	3.54M	ACCIARRI	00c L3	$E_{cm}^{ee} = 88-94$ GeV
1744.0 ± 3.4	4.07M	BARATE	00c ALEP	$E_{cm}^{ee} = 88-94$ GeV

Z BRANCHING RATIOS

OUR FIT is obtained using the fit procedure and correlations as determined by the LEP Electroweak Working Group (see the note "The Z boson" and ref. LEP-SLC 06).

$\Gamma(\text{hadrons})/\Gamma(e^+e^-)$ Γ_6/Γ_1

VALUE	EVTS	DOCUMENT ID	TECN	COMMENT
20.804 ± 0.050 OUR FIT				
20.902 ± 0.084	137.0K	²⁵ ABBIENDI	01A OPAL	$E_{cm}^{ee} = 88-94$ GeV
20.88 ± 0.12	117.8k	ABREU	00F DLPH	$E_{cm}^{ee} = 88-94$ GeV
20.816 ± 0.089	124.4k	ACCIARRI	00c L3	$E_{cm}^{ee} = 88-94$ GeV
20.677 ± 0.075		²⁶ BARATE	00c ALEP	$E_{cm}^{ee} = 88-94$ GeV
• • • We do not use the following data for averages, fits, limits, etc. • • •				
27.0 +11.7 - 8.8	12	²⁷ ABRAMS	89D MRK2	$E_{cm}^{ee} = 89-93$ GeV

²⁵ ABBIENDI 01A error includes approximately 0.067 due to statistics, 0.040 due to event selection systematics, 0.027 due to the theoretical uncertainty in t -channel prediction, and 0.014 due to LEP energy uncertainty.

²⁶ BARATE 00c error includes approximately 0.062 due to statistics, 0.033 due to experimental systematics, and 0.026 due to the theoretical uncertainty in t -channel prediction.

²⁷ ABRAMS 89D have included both statistical and systematic uncertainties in their quoted errors.

$\Gamma(\text{hadrons})/\Gamma(\mu^+\mu^-)$ Γ_6/Γ_2

OUR FIT is obtained using the fit procedure and correlations as determined by the LEP Electroweak Working Group (see the note "The Z boson" and ref. LEP-SLC 06).

VALUE	EVTS	DOCUMENT ID	TECN	COMMENT
20.785 ± 0.033 OUR FIT				
20.811 ± 0.058	182.8K	²⁸ ABBIENDI	01A OPAL	$E_{cm}^{ee} = 88-94$ GeV
20.65 ± 0.08	157.6k	ABREU	00F DLPH	$E_{cm}^{ee} = 88-94$ GeV
20.861 ± 0.097	113.4k	ACCIARRI	00c L3	$E_{cm}^{ee} = 88-94$ GeV
20.799 ± 0.056		²⁹ BARATE	00c ALEP	$E_{cm}^{ee} = 88-94$ GeV
• • • We do not use the following data for averages, fits, limits, etc. • • •				
18.9 +7.1 -5.3	13	³⁰ ABRAMS	89D MRK2	$E_{cm}^{ee} = 89-93$ GeV

²⁸ ABBIENDI 01A error includes approximately 0.050 due to statistics and 0.027 due to event selection systematics.

²⁹ BARATE 00c error includes approximately 0.053 due to statistics and 0.021 due to experimental systematics.

³⁰ ABRAMS 89D have included both statistical and systematic uncertainties in their quoted errors.

$\Gamma(\text{hadrons})/\Gamma(\tau^+\tau^-)$ Γ_6/Γ_3

OUR FIT is obtained using the fit procedure and correlations as determined by the LEP Electroweak Working Group (see the note "The Z boson" and ref. LEP-SLC 06).

VALUE	EVTS	DOCUMENT ID	TECN	COMMENT
20.764 ± 0.045 OUR FIT				
20.832 ± 0.091	151.5K	³¹ ABBIENDI	01A OPAL	$E_{cm}^{ee} = 88-94$ GeV
20.84 ± 0.13	104.0k	ABREU	00F DLPH	$E_{cm}^{ee} = 88-94$ GeV
20.792 ± 0.133	103.0k	ACCIARRI	00c L3	$E_{cm}^{ee} = 88-94$ GeV
20.707 ± 0.062		³² BARATE	00c ALEP	$E_{cm}^{ee} = 88-94$ GeV
• • • We do not use the following data for averages, fits, limits, etc. • • •				
15.2 +4.8 -3.9	21	³³ ABRAMS	89D MRK2	$E_{cm}^{ee} = 89-93$ GeV

³¹ ABBIENDI 01A error includes approximately 0.055 due to statistics and 0.071 due to event selection systematics.

³² BARATE 00c error includes approximately 0.054 due to statistics and 0.033 due to experimental systematics.

³³ ABRAMS 89D have included both statistical and systematic uncertainties in their quoted errors.

$\Gamma(\text{hadrons})/\Gamma(\ell^+\ell^-)$ Γ_6/Γ_4

ℓ indicates each type of lepton (e , μ , and τ), not sum over them.

Our fit result is obtained requiring lepton universality.

VALUE	EVTS	DOCUMENT ID	TECN	COMMENT
20.767 ± 0.025 OUR FIT				
20.823 ± 0.044	471.3K	³⁴ ABBIENDI	01A OPAL	$E_{cm}^{ee} = 88-94$ GeV
20.730 ± 0.060	379.4k	ABREU	00F DLPH	$E_{cm}^{ee} = 88-94$ GeV
20.810 ± 0.060	340.8k	ACCIARRI	00c L3	$E_{cm}^{ee} = 88-94$ GeV
20.725 ± 0.039	500k	³⁵ BARATE	00c ALEP	$E_{cm}^{ee} = 88-94$ GeV
• • • We do not use the following data for averages, fits, limits, etc. • • •				
18.9 +3.6 -3.2	46	ABRAMS	89B MRK2	$E_{cm}^{ee} = 89-93$ GeV

Gauge & Higgs Boson Particle Listings

Z

³⁴ ABBIENDI 01A error includes approximately 0.034 due to statistics and 0.027 due to event selection systematics.

³⁵ BARATE 00C error includes approximately 0.033 due to statistics, 0.020 due to experimental systematics, and 0.005 due to the theoretical uncertainty in t -channel prediction.

$\Gamma(\text{hadrons})/\Gamma_{\text{total}}$ Γ_6/Γ

This parameter is not directly used in the overall fit but is derived using the fit results; see the note "The Z boson" and ref. LEP-SLC 06.

VALUE (%)	DOCUMENT ID
69.911 ± 0.056 OUR FIT	

$\Gamma(e^+e^-)/\Gamma_{\text{total}}$ Γ_1/Γ

This parameter is not directly used in the overall fit but is derived using the fit results; see the note "The Z boson" and ref. LEP-SLC 06.

VALUE (%)	DOCUMENT ID
3.3632 ± 0.0042 OUR FIT	

$\Gamma(\mu^+\mu^-)/\Gamma_{\text{total}}$ Γ_2/Γ

This parameter is not directly used in the overall fit but is derived using the fit results; see the note "The Z boson" and ref. LEP-SLC 06.

VALUE (%)	DOCUMENT ID
3.3662 ± 0.0066 OUR FIT	

$\Gamma(\mu^+\mu^-)/\Gamma(e^+e^-)$ Γ_2/Γ_1

This parameter is not directly used in the overall fit but is derived using the fit results; see the note "The Z boson" and ref. LEP-SLC 06.

VALUE	DOCUMENT ID
1.0009 ± 0.0028 OUR FIT	

$\Gamma(\tau^+\tau^-)/\Gamma_{\text{total}}$ Γ_3/Γ

This parameter is not directly used in the overall fit but is derived using the fit results; see the note "The Z boson" and ref. LEP-SLC 06.

VALUE (%)	DOCUMENT ID
3.3696 ± 0.0083 OUR FIT	

$\Gamma(\tau^+\tau^-)/\Gamma(e^+e^-)$ Γ_3/Γ_1

This parameter is not directly used in the overall fit but is derived using the fit results; see the note "The Z boson" and ref. LEP-SLC 06.

VALUE	DOCUMENT ID
1.0019 ± 0.0032 OUR FIT	

$\Gamma(\ell^+\ell^-)/\Gamma_{\text{total}}$ Γ_4/Γ

ℓ indicates each type of lepton (e , μ , and τ), not sum over them.

Our fit result assumes lepton universality.

This parameter is not directly used in the overall fit but is derived using the fit results; see the note "The Z boson" and ref. LEP-SLC 06.

VALUE (%)	DOCUMENT ID
3.3658 ± 0.0023 OUR FIT	

$\Gamma(\text{invisible})/\Gamma_{\text{total}}$ Γ_5/Γ

See the data, the note, and the fit result for the partial width, Γ_5 , above.

VALUE (%)	DOCUMENT ID
20.000 ± 0.055 OUR FIT	

$\Gamma((u\bar{u} + c\bar{c})/2)/\Gamma(\text{hadrons})$ Γ_7/Γ_6

This quantity is the branching ratio of $Z \rightarrow$ "up-type" quarks to $Z \rightarrow$ hadrons. Except ACKERSTAFF 97T the values of $Z \rightarrow$ "up-type" and $Z \rightarrow$ "down-type" branchings are extracted from measurements of $\Gamma(\text{hadrons})$, and $\Gamma(Z \rightarrow \gamma + \text{jets})$ where γ is a high-energy (>5 or 7 GeV) isolated photon. As the experiments use different procedures and slightly different values of M_Z , $\Gamma(\text{hadrons})$ and α_s in their extraction procedures, our average has to be taken with caution.

VALUE	DOCUMENT ID	TECN	COMMENT
0.166 ± 0.009 OUR AVERAGE			
0.172 + 0.011 - 0.010	36 ABBIENDI	04E OPAL	$E_{\text{cm}}^{\text{e}} = 91.2$ GeV
0.160 ± 0.019 ± 0.019	37 ACKERSTAFF	97T OPAL	$E_{\text{cm}}^{\text{e}} = 88-94$ GeV
0.137 + 0.038 - 0.054	38 ABREU	95X DLPH	$E_{\text{cm}}^{\text{e}} = 88-94$ GeV
0.137 ± 0.033	39 ADRIANI	93 L3	$E_{\text{cm}}^{\text{e}} = 91.2$ GeV

³⁶ ABBIENDI 04E select photons with energy > 7 GeV and use $\Gamma(\text{hadrons}) = 1744.4 \pm 2.0$ MeV and $\alpha_s = 0.1172 \pm 0.002$ to obtain $\Gamma_u = 300^{+19}_{-18}$ MeV.

³⁷ ACKERSTAFF 97T measure $\Gamma_{u\bar{u}}/\Gamma_{d\bar{d} + \Gamma_{u\bar{u}} + \Gamma_{s\bar{s}}} = 0.258 \pm 0.031 \pm 0.032$. To obtain this branching ratio authors use $R_c + R_b = 0.380 \pm 0.010$. This measurement is fully negatively correlated with the measurement of $\Gamma_{d\bar{d},s\bar{s}}/\Gamma_{d\bar{d} + \Gamma_{u\bar{u}} + \Gamma_{s\bar{s}}}$ given in the next data block.

³⁸ ABREU 95X use $M_Z = 91.187 \pm 0.009$ GeV, $\Gamma(\text{hadrons}) = 1725 \pm 12$ MeV and $\alpha_s = 0.123 \pm 0.005$. To obtain this branching ratio we divide their value of $C_{2/3} = 0.91^{+0.25}_{-0.36}$ by their value of $(3C_{1/3} + 2C_{2/3}) = 6.66 \pm 0.05$.

³⁹ ADRIANI 93 use $M_Z = 91.181 \pm 0.022$ GeV, $\Gamma(\text{hadrons}) = 1742 \pm 19$ MeV and $\alpha_s = 0.125 \pm 0.009$. To obtain this branching ratio we divide their value of $C_{2/3} = 0.92 \pm 0.22$ by their value of $(3C_{1/3} + 2C_{2/3}) = 6.720 \pm 0.076$.

$\Gamma((d\bar{d} + s\bar{s} + b\bar{b})/3)/\Gamma(\text{hadrons})$ Γ_8/Γ_6

This quantity is the branching ratio of $Z \rightarrow$ "down-type" quarks to $Z \rightarrow$ hadrons. Except ACKERSTAFF 97T the values of $Z \rightarrow$ "up-type" and $Z \rightarrow$ "down-type" branchings are extracted from measurements of $\Gamma(\text{hadrons})$, and $\Gamma(Z \rightarrow \gamma + \text{jets})$ where γ is a high-energy (>5 or 7 GeV) isolated photon. As the experiments use different procedures and slightly different values of M_Z , $\Gamma(\text{hadrons})$ and α_s in their extraction procedures, our average has to be taken with caution.

VALUE	DOCUMENT ID	TECN	COMMENT
0.223 ± 0.006 OUR AVERAGE			
0.218 ± 0.007	40 ABBIENDI	04E OPAL	$E_{\text{cm}}^{\text{e}} = 91.2$ GeV
0.230 ± 0.010 ± 0.010	41 ACKERSTAFF	97T OPAL	$E_{\text{cm}}^{\text{e}} = 88-94$ GeV
0.243 + 0.036 - 0.026	42 ABREU	95X DLPH	$E_{\text{cm}}^{\text{e}} = 88-94$ GeV
0.243 ± 0.022	43 ADRIANI	93 L3	$E_{\text{cm}}^{\text{e}} = 91.2$ GeV

⁴⁰ ABBIENDI 04E select photons with energy > 7 GeV and use $\Gamma(\text{hadrons}) = 1744.4 \pm 2.0$ MeV and $\alpha_s = 0.1172 \pm 0.002$ to obtain $\Gamma_d = 381 \pm 12$ MeV.

⁴¹ ACKERSTAFF 97T measure $\Gamma_{d\bar{d},s\bar{s}}/(\Gamma_{d\bar{d}} + \Gamma_{u\bar{u}} + \Gamma_{s\bar{s}}) = 0.371 \pm 0.016 \pm 0.016$. To obtain this branching ratio authors use $R_c + R_b = 0.380 \pm 0.010$. This measurement is fully negatively correlated with the measurement of $\Gamma_{u\bar{u}}/(\Gamma_{d\bar{d}} + \Gamma_{u\bar{u}} + \Gamma_{s\bar{s}})$ presented in the previous data block.

⁴² ABREU 95X use $M_Z = 91.187 \pm 0.009$ GeV, $\Gamma(\text{hadrons}) = 1725 \pm 12$ MeV and $\alpha_s = 0.123 \pm 0.005$. To obtain this branching ratio we divide their value of $C_{1/3} = 1.62^{+0.24}_{-0.17}$ by their value of $(3C_{1/3} + 2C_{2/3}) = 6.66 \pm 0.05$.

⁴³ ADRIANI 93 use $M_Z = 91.181 \pm 0.022$ GeV, $\Gamma(\text{hadrons}) = 1742 \pm 19$ MeV and $\alpha_s = 0.125 \pm 0.009$. To obtain this branching ratio we divide their value of $C_{1/3} = 1.63 \pm 0.15$ by their value of $(3C_{1/3} + 2C_{2/3}) = 6.720 \pm 0.076$.

$R_c = \Gamma(c\bar{c})/\Gamma(\text{hadrons})$ Γ_9/Γ_6

OUR FIT is obtained by a simultaneous fit to several c - and b -quark measurements as explained in the note "The Z boson" and ref. LEP-SLC 06.

The Standard Model predicts $R_c = 0.1723$ for $m_t = 174.3$ GeV and $M_H = 150$ GeV.

VALUE	DOCUMENT ID	TECN	COMMENT
0.1721 ± 0.0030 OUR FIT			
0.1744 ± 0.0031 ± 0.0021	44 ABE	05F SLD	$E_{\text{cm}}^{\text{e}} = 91.28$ GeV
0.1665 ± 0.0051 ± 0.0081	45 ABREU	00 DLPH	$E_{\text{cm}}^{\text{e}} = 88-94$ GeV
0.1698 ± 0.0069	46 BARATE	00B ALEP	$E_{\text{cm}}^{\text{e}} = 88-94$ GeV
0.180 ± 0.011 ± 0.013	47 ACKERSTAFF	98E OPAL	$E_{\text{cm}}^{\text{e}} = 88-94$ GeV
0.167 ± 0.011 ± 0.012	48 ALEXANDER	96R OPAL	$E_{\text{cm}}^{\text{e}} = 88-94$ GeV
• • • We do not use the following data for averages, fits, limits, etc. • • •			
0.1623 ± 0.0085 ± 0.0209	49 ABREU	95D DLPH	$E_{\text{cm}}^{\text{e}} = 88-94$ GeV

⁴⁴ ABE 05F use hadronic Z decays collected during 1996-98 to obtain an enriched sample of $c\bar{c}$ events using a double tag method. The single c -tag is obtained with a neural network trained to perform flavor discrimination using as input several signatures (corrected secondary vertex mass, vertex decay length, multiplicity and total momentum of the hemisphere). A multitag approach is used, defining 4 regions of the output value of the neural network and R_c is extracted from a simultaneous fit to the count rates of the 4 different tags. The quoted systematic error includes an uncertainty of ± 0.0006 due to the uncertainty on R_b .

⁴⁵ ABREU 00 obtain this result properly combining the measurement from the D^{*+} production rate ($R_c = 0.1610 \pm 0.0104 \pm 0.0077 \pm 0.0043$ (BR)) with that from the overall charm counting ($R_c = 0.1692 \pm 0.0047 \pm 0.0063 \pm 0.0074$ (BR)) in $c\bar{c}$ events. The systematic error includes an uncertainty of ± 0.0054 due to the uncertainty on the charmed hadron branching fractions.

⁴⁶ BARATE 00B use exclusive decay modes to independently determine the quantities $R_c \times f(c \rightarrow X)$, $X = D^0, D^+, D_s^+, \text{ and } \Lambda_c$. Estimating $R_c \times f(c \rightarrow \Xi_c^-/\Omega_c^-) = 0.0034$, they simply sum over all the charm decays to obtain $R_c = 0.1738 \pm 0.0047 \pm 0.0088 \pm 0.0075$ (BR). This is combined with all previous ALEPH measurements (BARATE 98T and BUSKULIC 94G, $R_c = 0.1681 \pm 0.0054 \pm 0.0062$) to obtain the quoted value.

⁴⁷ ACKERSTAFF 98E use an inclusive/exclusive double tag. In one jet $D^{*\pm}$ mesons are exclusively reconstructed in several decay channels and in the opposite jet a slow pion (opposite charge inclusive $D^{*\pm}$) tag is used. The b content of this sample is measured by the simultaneous detection of a lepton in one jet and an inclusively reconstructed $D^{*\pm}$ meson in the opposite jet. The systematic error includes an uncertainty of ± 0.006 due to the external branching ratios.

⁴⁸ ALEXANDER 96R obtain this value via direct charm counting, summing the partial contributions from $D^0, D^+, D_s^+, \text{ and } \Lambda_c^+$, and assuming that strange-charmed baryons account for the 15% of the Λ_c^+ production. An uncertainty of ± 0.005 due to the uncertainties in the charm hadron branching ratios is included in the overall systematics.

⁴⁹ ABREU 95D perform a maximum likelihood fit to the combined p and $p\bar{p}$ distributions of single and dilepton samples. The second error includes an uncertainty of ± 0.0124 due to models and branching ratios.

$R_b = \Gamma(b\bar{b})/\Gamma(\text{hadrons})$ Γ_{10}/Γ_6

OUR FIT is obtained by a simultaneous fit to several c - and b -quark measurements as explained in the note "The Z boson" and ref. LEP-SLC 06.

The Standard Model predicts $R_b = 0.21581$ for $m_t = 174.3$ GeV and $M_H = 150$ GeV.

VALUE	DOCUMENT ID	TECN	COMMENT
0.21629 ± 0.00066 OUR FIT			
0.21594 ± 0.00094 ± 0.00075	50 ABE	05F SLD	$E_{\text{cm}}^{\text{e}} = 91.28$ GeV
0.2174 ± 0.0015 ± 0.0028	51 ACCIARRI	00 L3	$E_{\text{cm}}^{\text{e}} = 89-93$ GeV
0.2178 ± 0.0011 ± 0.0013	52 ABBIENDI	99B OPAL	$E_{\text{cm}}^{\text{e}} = 88-94$ GeV
0.21634 ± 0.00067 ± 0.00060	53 ABREU	99B DLPH	$E_{\text{cm}}^{\text{e}} = 88-94$ GeV
0.2159 ± 0.0009 ± 0.0011	54 BARATE	97F ALEP	$E_{\text{cm}}^{\text{e}} = 88-94$ GeV

• • • We do not use the following data for averages, fits, limits, etc. • • •

$0.2145 \pm 0.0089 \pm 0.0067$	55	ABREU	95D	DLPH	$E_{cm}^{ee} = 88-94$ GeV
$0.219 \pm 0.006 \pm 0.005$	56	BUSKULIC	94G	ALEP	$E_{cm}^{ee} = 88-94$ GeV
$0.251 \pm 0.049 \pm 0.030$	57	JACOBSEN	91	MRK2	$E_{cm}^{ee} = 91$ GeV

⁵⁰ ABE 05F use hadronic Z decays collected during 1996–98 to obtain an enriched sample of $b\bar{b}$ events using a double tag method. The single b-tag is obtained with a neural network trained to perform flavor discrimination using as input several signatures (corrected secondary vertex mass, vertex decay length, multiplicity and total momentum of the hemisphere; the key tag is obtained requiring the secondary vertex corrected mass to be above the D-meson mass). ABE 05F obtain $R_b = 0.21604 \pm 0.00098 \pm 0.00074$ where the systematic error includes an uncertainty of ± 0.00012 due to the uncertainty on R_c . The value reported here is obtained properly combining with ABE 98D. The quoted systematic error includes an uncertainty of ± 0.00012 due to the uncertainty on R_c .

⁵¹ ACCIARRI 00 obtain this result using a double-tagging technique, with a high p_T lepton tag and an impact parameter tag in opposite hemispheres.

⁵² ABBIENDI 99b tag $Z \rightarrow b\bar{b}$ decays using leptons and/or separated decay vertices. The b-tagging efficiency is measured directly from the data using a double-tagging technique.

⁵³ ABREU 99b obtain this result combining in a multivariate analysis several tagging methods (impact parameter and secondary vertex reconstruction, complemented by event shape variables). For R_c different from its Standard Model value of 0.172, R_b varies as $-0.024 \times (R_c - 0.172)$.

⁵⁴ BARATE 97f combine the lifetime-mass hemisphere tag (BARATE 97E) with event shape information and lepton tag to identify $Z \rightarrow b\bar{b}$ candidates. They further use c- and u/d s-selection tags to identify the background. For R_c different from its Standard Model value of 0.172, R_b varies as $-0.019 \times (R_c - 0.172)$.

⁵⁵ ABREU 95D perform a maximum likelihood fit to the combined p and p_T distributions of single and dilepton samples. The second error includes an uncertainty of ± 0.0023 due to models and branching ratios.

⁵⁶ BUSKULIC 94G perform a simultaneous fit to the p and p_T spectra of both single and dilepton events.

⁵⁷ JACOBSEN 91 tagged $b\bar{b}$ events by requiring coincidence of ≥ 3 tracks with significant impact parameters using vertex detector. Systematic error includes lifetime and decay uncertainties (± 0.014).

$\Gamma(b\bar{b}b\bar{b})/\Gamma(\text{hadrons})$ Γ_{11}/Γ_6

VALUE (units 10^{-4})	DOCUMENT ID	TECN	COMMENT
5.2 ± 1.9 OUR AVERAGE			
$3.6 \pm 1.7 \pm 2.7$	58	ABBIENDI 01G	OPAL $E_{cm}^{ee} = 88-94$ GeV
$6.0 \pm 1.9 \pm 1.4$	59	ABREU 99U	DLPH $E_{cm}^{ee} = 88-94$ GeV

⁵⁸ ABBIENDI 01G use a sample of four-jet events from hadronic Z decays. To enhance the $b\bar{b}b\bar{b}$ signal, at least three of the four jets are required to have a significantly detached secondary vertex.

⁵⁹ ABREU 99U force hadronic Z decays into 3jets to use all the available phase space and require a b tag for every jet. This decay mode includes primary and secondary 4b production, e.g. from gluon splitting to $b\bar{b}$.

$\Gamma(ggg)/\Gamma(\text{hadrons})$ Γ_{12}/Γ_6

VALUE	CL%	DOCUMENT ID	TECN	COMMENT
$< 1.6 \times 10^{-2}$	95	60	ABREU 96S	DLPH $E_{cm}^{ee} = 88-94$ GeV

⁶⁰ This branching ratio is slightly dependent on the jet-finder algorithm. The value we quote is obtained using the JADE algorithm, while using the DURHAM algorithm ABREU 96S obtain an upper limit of 1.5×10^{-2} .

$\Gamma(\pi^0\gamma)/\Gamma_{total}$ Γ_{13}/Γ

VALUE	CL%	DOCUMENT ID	TECN	COMMENT
$< 5.2 \times 10^{-5}$	95	61	ACCIARRI 95G	L3 $E_{cm}^{ee} = 88-94$ GeV
$< 5.5 \times 10^{-5}$	95		ABREU 94B	DLPH $E_{cm}^{ee} = 88-94$ GeV
$< 2.1 \times 10^{-4}$	95		DECAMP 92	ALEP $E_{cm}^{ee} = 88-94$ GeV
$< 1.4 \times 10^{-4}$	95		AKRAWY 91F	OPAL $E_{cm}^{ee} = 88-94$ GeV

⁶¹ This limit is for both decay modes $Z \rightarrow \pi^0\gamma/\gamma\gamma$ which are indistinguishable in ACCIARRI 95G.

$\Gamma(\eta\gamma)/\Gamma_{total}$ Γ_{14}/Γ

VALUE	CL%	DOCUMENT ID	TECN	COMMENT
$< 7.6 \times 10^{-5}$	95		ACCIARRI 95G	L3 $E_{cm}^{ee} = 88-94$ GeV
$< 8.0 \times 10^{-5}$	95		ABREU 94B	DLPH $E_{cm}^{ee} = 88-94$ GeV
$< 5.1 \times 10^{-5}$	95		DECAMP 92	ALEP $E_{cm}^{ee} = 88-94$ GeV
$< 2.0 \times 10^{-4}$	95		AKRAWY 91F	OPAL $E_{cm}^{ee} = 88-94$ GeV

$\Gamma(\omega\gamma)/\Gamma_{total}$ Γ_{15}/Γ

VALUE	CL%	DOCUMENT ID	TECN	COMMENT
$< 6.5 \times 10^{-4}$	95		ABREU 94B	DLPH $E_{cm}^{ee} = 88-94$ GeV

$\Gamma(\eta'(958)\gamma)/\Gamma_{total}$ Γ_{16}/Γ

VALUE	CL%	DOCUMENT ID	TECN	COMMENT
$< 4.2 \times 10^{-5}$	95		DECAMP 92	ALEP $E_{cm}^{ee} = 88-94$ GeV

$\Gamma(\gamma\gamma)/\Gamma_{total}$ Γ_{17}/Γ

VALUE	CL%	DOCUMENT ID	TECN	COMMENT
$< 5.2 \times 10^{-5}$	95	62	ACCIARRI 95G	L3 $E_{cm}^{ee} = 88-94$ GeV
$< 5.5 \times 10^{-5}$	95		ABREU 94B	DLPH $E_{cm}^{ee} = 88-94$ GeV
$< 1.4 \times 10^{-4}$	95		AKRAWY 91F	OPAL $E_{cm}^{ee} = 88-94$ GeV

⁶² This limit is for both decay modes $Z \rightarrow \pi^0\gamma/\gamma\gamma$ which are indistinguishable in ACCIARRI 95G.

$\Gamma(\gamma\gamma)/\Gamma_{total}$ Γ_{18}/Γ

VALUE	CL%	DOCUMENT ID	TECN	COMMENT
$< 1.0 \times 10^{-5}$	95	63	ACCIARRI 95C	L3 $E_{cm}^{ee} = 88-94$ GeV
$< 1.7 \times 10^{-5}$	95	63	ABREU 94B	DLPH $E_{cm}^{ee} = 88-94$ GeV
$< 6.6 \times 10^{-5}$	95		AKRAWY 91F	OPAL $E_{cm}^{ee} = 88-94$ GeV

⁶³ Limit derived in the context of composite Z model.

$\Gamma(\pi^\pm W^\mp)/\Gamma_{total}$ Γ_{19}/Γ

The value is for the sum of the charge states indicated.

VALUE	CL%	DOCUMENT ID	TECN	COMMENT
$< 7 \times 10^{-5}$	95		DECAMP 92	ALEP $E_{cm}^{ee} = 88-94$ GeV

$\Gamma(\rho^\pm W^\mp)/\Gamma_{total}$ Γ_{20}/Γ

The value is for the sum of the charge states indicated.

VALUE	CL%	DOCUMENT ID	TECN	COMMENT
$< 8.3 \times 10^{-5}$	95		DECAMP 92	ALEP $E_{cm}^{ee} = 88-94$ GeV

$\Gamma(J/\psi(1S)X)/\Gamma_{total}$ Γ_{21}/Γ

VALUE (units 10^{-3})	EVTS	DOCUMENT ID	TECN	COMMENT
$3.51^{+0.23}_{-0.25}$ OUR AVERAGE				Error includes scale factor of 1.1.
$3.21 \pm 0.21 \pm 0.19$	553	64	ACCIARRI 99F	L3 $E_{cm}^{ee} = 88-94$ GeV
$3.9 \pm 0.2 \pm 0.3$	511	65	ALEXANDER 96B	OPAL $E_{cm}^{ee} = 88-94$ GeV
$3.73 \pm 0.39 \pm 0.36$	153	66	ABREU 94P	DLPH $E_{cm}^{ee} = 88-94$ GeV

⁶⁴ ACCIARRI 99F combine $\mu^+\mu^-$ and $e^+e^- J/\psi(1S)$ decay channels. The branching ratio for prompt $J/\psi(1S)$ production is measured to be $(2.1 \pm 0.6 \pm 0.4^{+0.4}_{-0.2}(\text{theor.})) \times 10^{-4}$.

⁶⁵ ALEXANDER 96B identify $J/\psi(1S)$ from the decays into lepton pairs. $(4.8 \pm 2.4)\%$ of this branching ratio is due to prompt $J/\psi(1S)$ production (ALEXANDER 96N).

⁶⁶ Combining $\mu^+\mu^-$ and e^+e^- channels and taking into account the common systematic errors. $(7.7^{+6.3}_{-5.4})\%$ of this branching ratio is due to prompt $J/\psi(1S)$ production.

$\Gamma(\psi(2S)X)/\Gamma_{total}$ Γ_{22}/Γ

VALUE (units 10^{-3})	EVTS	DOCUMENT ID	TECN	COMMENT
1.60 ± 0.29 OUR AVERAGE				
$1.6 \pm 0.5 \pm 0.3$	39	67	ACCIARRI 97J	L3 $E_{cm}^{ee} = 88-94$ GeV
$1.6 \pm 0.3 \pm 0.2$	46.9	68	ALEXANDER 96B	OPAL $E_{cm}^{ee} = 88-94$ GeV
$1.60 \pm 0.73 \pm 0.33$	5.4	69	ABREU 94P	DLPH $E_{cm}^{ee} = 88-94$ GeV

⁶⁷ ACCIARRI 97J measure this branching ratio via the decay channel $\psi(2S) \rightarrow \ell^+\ell^- (\ell = \mu, e)$.

⁶⁸ ALEXANDER 96B measure this branching ratio via the decay channel $\psi(2S) \rightarrow J/\psi\pi^+\pi^-$, with $J/\psi \rightarrow \ell^+\ell^-$.

⁶⁹ ABREU 94P measure this branching ratio via decay channel $\psi(2S) \rightarrow J/\psi\pi^+\pi^-$, with $J/\psi \rightarrow \mu^+\mu^-$.

$\Gamma(\chi_{c1}(1P)X)/\Gamma_{total}$ Γ_{23}/Γ

VALUE (units 10^{-3})	EVTS	DOCUMENT ID	TECN	COMMENT
2.9 ± 0.7 OUR AVERAGE				
$2.7 \pm 0.6 \pm 0.5$	33	70	ACCIARRI 97J	L3 $E_{cm}^{ee} = 88-94$ GeV
$5.0 \pm 2.1^{+1.5}_{-0.9}$	6.4	71	ABREU 94P	DLPH $E_{cm}^{ee} = 88-94$ GeV

⁷⁰ ACCIARRI 97J measure this branching ratio via the decay channel $\chi_{c1} \rightarrow J/\psi + \gamma$, with $J/\psi \rightarrow \ell^+\ell^- (\ell = \mu, e)$. The $M(\ell^+\ell^-) - M(\ell^+\ell^-)$ mass difference spectrum is fitted with two gaussian shapes for χ_{c1} and χ_{c2} .

⁷¹ This branching ratio is measured via the decay channel $\chi_{c1} \rightarrow J/\psi + \gamma$, with $J/\psi \rightarrow \mu^+\mu^-$.

$\Gamma(\chi_{c2}(1P)X)/\Gamma_{total}$ Γ_{24}/Γ

VALUE	CL%	DOCUMENT ID	TECN	COMMENT
$< 3.2 \times 10^{-3}$	90	72	ACCIARRI 97J	L3 $E_{cm}^{ee} = 88-94$ GeV

⁷² ACCIARRI 97J derive this limit via the decay channel $\chi_{c2} \rightarrow J/\psi + \gamma$, with $J/\psi \rightarrow \ell^+\ell^- (\ell = \mu, e)$. The $M(\ell^+\ell^-) - M(\ell^+\ell^-)$ mass difference spectrum is fitted with two gaussian shapes for χ_{c1} and χ_{c2} .

$\Gamma(\mathcal{T}(1S)X + \mathcal{T}(2S)X + \mathcal{T}(3S)X)/\Gamma_{total}$ $\Gamma_{25}/\Gamma = (\Gamma_{26} + \Gamma_{27} + \Gamma_{28})/\Gamma$

VALUE (units 10^{-4})	EVTS	DOCUMENT ID	TECN	COMMENT
$1.0 \pm 0.4 \pm 0.22$	6.4	73	ALEXANDER 96F	OPAL $E_{cm}^{ee} = 88-94$ GeV

⁷³ ALEXANDER 96F identify the \mathcal{T} (which refers to any of the three lowest bound states) through its decay into e^+e^- and $\mu^+\mu^-$. The systematic error includes an uncertainty of ± 0.2 due to the production mechanism.

$\Gamma(\mathcal{T}(1S)X)/\Gamma_{total}$ Γ_{26}/Γ

VALUE	CL%	DOCUMENT ID	TECN	COMMENT
$< 4.4 \times 10^{-5}$	95	74	ACCIARRI 99F	L3 $E_{cm}^{ee} = 88-94$ GeV

⁷⁴ ACCIARRI 99F search for $\mathcal{T}(1S)$ through its decay into $\ell^+\ell^- (\ell = e \text{ or } \mu)$.

$\Gamma(\mathcal{T}(2S)X)/\Gamma_{total}$ Γ_{27}/Γ

VALUE	CL%	DOCUMENT ID	TECN	COMMENT
$< 13.9 \times 10^{-5}$	95	75	ACCIARRI 97R	L3 $E_{cm}^{ee} = 88-94$ GeV

⁷⁵ ACCIARRI 97R search for $\mathcal{T}(2S)$ through its decay into $\ell^+\ell^- (\ell = e \text{ or } \mu)$.

Gauge & Higgs Boson Particle Listings

Z

 $\Gamma(\Upsilon(3S)X)/\Gamma_{\text{total}}$ Γ_{28}/Γ_6

VALUE	CL%	DOCUMENT ID	TECN	COMMENT
$<9.4 \times 10^{-5}$	95	⁷⁶ ACCIARRI	97R L3	$E_{\text{cm}}^{\text{ee}} = 88-94$ GeV

⁷⁶ ACCIARRI 97R search for $\Upsilon(3S)$ through its decay into $\ell^+ \ell^-$ ($\ell = e$ or μ).

 $\Gamma((D^0/\bar{D}^0)X)/\Gamma(\text{hadrons})$ Γ_{29}/Γ_6

VALUE	EVTS	DOCUMENT ID	TECN	COMMENT
$0.296 \pm 0.019 \pm 0.021$	369	⁷⁷ ABREU	93I DLPH	$E_{\text{cm}}^{\text{ee}} = 88-94$ GeV

⁷⁷ The (D^0/\bar{D}^0) states in ABREU 93I are detected by the $K\pi$ decay mode. This is a corrected result (see the erratum of ABREU 93I).

 $\Gamma(D^\pm X)/\Gamma(\text{hadrons})$ Γ_{30}/Γ_6

VALUE	EVTS	DOCUMENT ID	TECN	COMMENT
$0.174 \pm 0.016 \pm 0.018$	539	⁷⁸ ABREU	93I DLPH	$E_{\text{cm}}^{\text{ee}} = 88-94$ GeV

⁷⁸ The D^\pm states in ABREU 93I are detected by the $K\pi\pi$ decay mode. This is a corrected result (see the erratum of ABREU 93I).

 $\Gamma(D^*(2010)^\pm X)/\Gamma(\text{hadrons})$ Γ_{31}/Γ_6

VALUE	EVTS	DOCUMENT ID	TECN	COMMENT
0.163 ± 0.019 OUR AVERAGE	Error includes scale factor of 1.3.			
$0.155 \pm 0.010 \pm 0.013$	358	⁷⁹ ABREU	93I DLPH	$E_{\text{cm}}^{\text{ee}} = 88-94$ GeV
0.21 ± 0.04	362	⁸⁰ DECAMP	91J ALEP	$E_{\text{cm}}^{\text{ee}} = 88-94$ GeV

⁷⁹ $D^*(2010)^\pm$ in ABREU 93I are reconstructed from $D^0\pi^\pm$, with $D^0 \rightarrow K^-\pi^+$. The new CLEO II measurement of $B(D^{*\pm} \rightarrow D^0\pi^\pm) = (68.1 \pm 1.6)\%$ is used. This is a corrected result (see the erratum of ABREU 93I).

⁸⁰ DECAMP 91J report $B(D^*(2010)^+ \rightarrow D^0\pi^+) B(D^0 \rightarrow K^-\pi^+) \Gamma(D^*(2010)^\pm X) / \Gamma(\text{hadrons}) = (5.11 \pm 0.34) \times 10^{-3}$. They obtained the above number assuming $B(D^0 \rightarrow K^-\pi^+) = (3.62 \pm 0.34 \pm 0.44)\%$ and $B(D^*(2010)^+ \rightarrow D^0\pi^+) = (55 \pm 4)\%$. We have rescaled their original result of 0.26 ± 0.05 taking into account the new CLEO II branching ratio $B(D^*(2010)^+ \rightarrow D^0\pi^+) = (68.1 \pm 1.6)\%$.

 $\Gamma(D_{s1}(2536)^\pm X)/\Gamma(\text{hadrons})$ Γ_{32}/Γ_6

VALUE (%)	EVTS	DOCUMENT ID	TECN	COMMENT
$0.52 \pm 0.09 \pm 0.06$	92	⁸¹ HEISTER	02B ALEP	$E_{\text{cm}}^{\text{ee}} = 88-94$ GeV

⁸¹ HEISTER 02B reconstruct this meson in the decay modes $D_{s1}(2536)^\pm \rightarrow D^{*\pm} K^0$ and $D_{s1}(2536)^\pm \rightarrow D^{*0} K^\pm$. The quoted branching ratio assumes that the decay width of the $D_{s1}(2536)$ is saturated by the two measured decay modes.

 $\Gamma(D_{sJ}(2573)^\pm X)/\Gamma(\text{hadrons})$ Γ_{33}/Γ_6

VALUE (%)	EVTS	DOCUMENT ID	TECN	COMMENT
$0.83 \pm 0.29 \pm 0.07$ -0.13	64	⁸² HEISTER	02B ALEP	$E_{\text{cm}}^{\text{ee}} = 88-94$ GeV

⁸² HEISTER 02B reconstruct this meson in the decay mode $D_{s2}^*(2573)^\pm \rightarrow D^0 K^\pm$. The quoted branching ratio assumes that the detected decay mode represents 45% of the full decay width.

 $\Gamma(D^{*'}(2629)^\pm X)/\Gamma(\text{hadrons})$ Γ_{34}/Γ_6

VALUE	DOCUMENT ID	TECN	COMMENT
searched for	⁸³ ABBIENDI	01N OPAL	$E_{\text{cm}}^{\text{ee}} = 88-94$ GeV

⁸³ ABBIENDI 01N searched for the decay mode $D^{*'}(2629)^\pm \rightarrow D^{*\pm}\pi^+\pi^-$ with $D^{*+} \rightarrow D^0\pi^+$, and $D^0 \rightarrow K^-\pi^+$. They quote a 95% CL limit for $Z \rightarrow D^{*'}(2629)^\pm \times B(D^{*'}(2629)^\pm \rightarrow D^{*\pm}\pi^+\pi^-) < 3.1 \times 10^{-3}$.

 $\Gamma(B^*X)/[\Gamma(BX) + \Gamma(B^*X)]$ $\Gamma_{36}/(\Gamma_{35} + \Gamma_{36})$

As the experiments assume different values of the b -baryon contribution, our average should be taken with caution.

VALUE	EVTS	DOCUMENT ID	TECN	COMMENT
0.75 ± 0.04 OUR AVERAGE				
$0.760 \pm 0.036 \pm 0.083$		⁸⁴ ACKERSTAFF	97M OPAL	$E_{\text{cm}}^{\text{ee}} = 88-94$ GeV
$0.771 \pm 0.026 \pm 0.070$		⁸⁵ BUSKULIC	96D ALEP	$E_{\text{cm}}^{\text{ee}} = 88-94$ GeV
$0.72 \pm 0.03 \pm 0.06$		⁸⁶ ABREU	95R DLPH	$E_{\text{cm}}^{\text{ee}} = 88-94$ GeV
$0.76 \pm 0.08 \pm 0.06$	1378	⁸⁷ ACCIARRI	95B L3	$E_{\text{cm}}^{\text{ee}} = 88-94$ GeV

⁸⁴ ACKERSTAFF 97M use an inclusive B reconstruction method and assume a $(13.2 \pm 4.1)\%$ b -baryon contribution. The value refers to a b -flavored meson mixture of B_u, B_d , and B_s .

⁸⁵ BUSKULIC 96D use an inclusive reconstruction of B hadrons and assume a $(12.2 \pm 4.3)\%$ b -baryon contribution. The value refers to a b -flavored mixture of B_u, B_d , and B_s .

⁸⁶ ABREU 95R use an inclusive B -reconstruction method and assume a $(10 \pm 4)\%$ b -baryon contribution. The value refers to a b -flavored meson mixture of B_u, B_d , and B_s .

⁸⁷ ACCIARRI 95B assume a 9.4% b -baryon contribution. The value refers to a b -flavored mixture of B_u, B_d , and B_s .

 $\Gamma(B^+X)/\Gamma(\text{hadrons})$ Γ_{37}/Γ_6

"OUR EVALUATION" is obtained using our current values for $f(\bar{b} \rightarrow B^+)$ and $R_b = \Gamma(b\bar{b})/\Gamma(\text{hadrons})$. We calculate $\Gamma(B^+X)/\Gamma(\text{hadrons}) = R_b \times f(\bar{b} \rightarrow B^+)$. The decay fraction $f(\bar{b} \rightarrow B^+)$ was provided by the Heavy Flavor Averaging Group (HFAG, http://www.slac.stanford.edu/xorg/hfag/osc/PDG_2009/#FRACZ).

VALUE	DOCUMENT ID	TECN	COMMENT
0.0869 ± 0.0019 OUR EVALUATION			
0.0887 ± 0.0030	⁸⁸ ABDALLAH	03K DLPH	$E_{\text{cm}}^{\text{ee}} = 88-94$ GeV

⁸⁸ ABDALLAH 03K measure the production fraction of B^+ mesons in hadronic Z decays $f(B^+) = (40.99 \pm 0.82 \pm 1.11)\%$. The value quoted here is obtained multiplying this production fraction by our value of $R_b = \Gamma(b\bar{b})/\Gamma(\text{hadrons})$.

 $\Gamma(B_s^0 X)/\Gamma(\text{hadrons})$ Γ_{38}/Γ_6

"OUR EVALUATION" is obtained using our current values for $f(\bar{b} \rightarrow B_s^0)$ and $R_b = \Gamma(b\bar{b})/\Gamma(\text{hadrons})$. We calculate $\Gamma(B_s^0 X)/\Gamma(\text{hadrons}) = R_b \times f(\bar{b} \rightarrow B_s^0)$. The decay fraction $f(\bar{b} \rightarrow B_s^0)$ was provided by the Heavy Flavor Averaging Group (HFAG, http://www.slac.stanford.edu/xorg/hfag/osc/PDG_2009/#FRACZ).

VALUE	DOCUMENT ID	TECN	COMMENT
0.0227 ± 0.0019 OUR EVALUATION			
seen	⁸⁹ ABREU	92M DLPH	$E_{\text{cm}}^{\text{ee}} = 88-94$ GeV
seen	⁹⁰ ACTON	92N OPAL	$E_{\text{cm}}^{\text{ee}} = 88-94$ GeV
seen	⁹¹ BUSKULIC	92E ALEP	$E_{\text{cm}}^{\text{ee}} = 88-94$ GeV

⁸⁹ ABREU 92M reported value is $\Gamma(B_s^0 X) \times B(B_s^0 \rightarrow D_s \mu \nu_\mu X) \times B(D_s \rightarrow \phi\pi)/\Gamma(\text{hadrons}) = (18 \pm 8) \times 10^{-5}$.

⁹⁰ ACTON 92N find evidence for B_s^0 production using D_s - ℓ correlations, with $D_s^+ \rightarrow \phi\pi^+$ and $K^*(892) K^+$. Assuming R_b from the Standard Model and averaging over the e and μ channels, authors measure the product branching fraction to be $f(\bar{b} \rightarrow B_s^0) \times B(B_s^0 \rightarrow D_s^- \ell^+ \nu_\ell X) \times B(D_s^- \rightarrow \phi\pi^-) = (3.9 \pm 1.1 \pm 0.8) \times 10^{-4}$.

⁹¹ BUSKULIC 92E find evidence for B_s^0 production using D_s - ℓ correlations, with $D_s^+ \rightarrow \phi\pi^+$ and $K^*(892) K^+$. Using $B(D_s^+ \rightarrow \phi\pi^+) = (2.7 \pm 0.7)\%$ and summing up the e and μ channels, the weighted average product branching fraction is measured to be $B(\bar{b} \rightarrow B_s^0) \times B(B_s^0 \rightarrow D_s^- \ell^+ \nu_\ell X) = 0.040 \pm 0.011^{+0.010}_{-0.012}$.

 $\Gamma(B_c^\pm X)/\Gamma(\text{hadrons})$ Γ_{39}/Γ_6

VALUE	DOCUMENT ID	TECN	COMMENT
searched for	⁹² ACKERSTAFF	98o OPAL	$E_{\text{cm}}^{\text{ee}} = 88-94$ GeV
searched for	⁹³ ABREU	97E DLPH	$E_{\text{cm}}^{\text{ee}} = 88-94$ GeV
searched for	⁹⁴ BARATE	97H ALEP	$E_{\text{cm}}^{\text{ee}} = 88-94$ GeV

⁹² ACKERSTAFF 98o searched for the decay modes $B_c \rightarrow J/\psi\pi^+, J/\psi a_1^+$, and $J/\psi\ell^+ \nu_\ell$, with $J/\psi \rightarrow \ell^+ \ell^-, \ell = e, \mu$. The number of candidates (background) for the three decay modes is $2(0.63 \pm 0.2), 0(1.10 \pm 0.22)$, and $1(0.82 \pm 0.19)$ respectively. Interpreting the $2B_c \rightarrow J/\psi\pi^+$ candidates as signal, they report $\Gamma(B_c^+ X) \times B(B_c \rightarrow J/\psi\pi^+)/\Gamma(\text{hadrons}) = (3.8^{+5.0}_{-2.4} \pm 0.5) \times 10^{-5}$. Interpreted as background, the 90% CL bounds are $\Gamma(B_c^+ X) \times B(B_c \rightarrow J/\psi\pi^+)/\Gamma(\text{hadrons}) < 1.06 \times 10^{-4}$, $\Gamma(B_c^+ X) \times B(B_c \rightarrow J/\psi a_1^+)/\Gamma(\text{hadrons}) < 5.29 \times 10^{-4}$, $\Gamma(B_c^+ X) \times B(B_c \rightarrow J/\psi\ell^+ \nu_\ell)/\Gamma(\text{hadrons}) < 6.96 \times 10^{-5}$.

⁹³ ABREU 97E searched for the decay modes $B_c \rightarrow J/\psi\pi^+, J/\psi\ell^+ \nu_\ell$, and $J/\psi(3\pi^+)$, with $J/\psi \rightarrow \ell^+ \ell^-, \ell = e, \mu$. The number of candidates (background) for the three decay modes is $1(1.7), 0(0.3)$, and $1(2.3)$ respectively. They report the following 90% CL limits: $\Gamma(B_c^+ X) \times B(B_c \rightarrow J/\psi\pi^+)/\Gamma(\text{hadrons}) < (1.05-0.84) \times 10^{-4}$, $\Gamma(B_c^+ X) \times B(B_c \rightarrow J/\psi\ell^+ \nu_\ell)/\Gamma(\text{hadrons}) < (5.8-5.0) \times 10^{-5}$, $\Gamma(B_c^+ X) \times B(B_c \rightarrow J/\psi(3\pi^+))/\Gamma(\text{hadrons}) < 1.75 \times 10^{-4}$, where the ranges are due to the predicted B_c lifetime (0.4-1.4) ps.

⁹⁴ BARATE 97H searched for the decay modes $B_c \rightarrow J/\psi\pi^+$ and $J/\psi\ell^+ \nu_\ell$ with $J/\psi \rightarrow \ell^+ \ell^-, \ell = e, \mu$. The number of candidates (background) for the two decay modes is $0(0.44)$ and $2(0.81)$ respectively. They report the following 90% CL limits: $\Gamma(B_c^+ X) \times B(B_c \rightarrow J/\psi\pi^+)/\Gamma(\text{hadrons}) < 3.6 \times 10^{-5}$ and $\Gamma(B_c^+ X) \times B(B_c \rightarrow J/\psi\ell^+ \nu_\ell)/\Gamma(\text{hadrons}) < 5.2 \times 10^{-5}$.

 $\Gamma(\Lambda_c^+ X)/\Gamma(\text{hadrons})$ Γ_{40}/Γ_6

VALUE	DOCUMENT ID	TECN	COMMENT
0.022 ± 0.005 OUR AVERAGE			
$0.024 \pm 0.005 \pm 0.006$	⁹⁵ ALEXANDER	96R OPAL	$E_{\text{cm}}^{\text{ee}} = 88-94$ GeV
$0.021 \pm 0.003 \pm 0.005$	⁹⁶ BUSKULIC	96Y ALEP	$E_{\text{cm}}^{\text{ee}} = 88-94$ GeV

⁹⁵ ALEXANDER 96R measure $R_b \times f(b \rightarrow \Lambda_c^+ X) \times B(\Lambda_c^+ \rightarrow pK^-\pi^+) = (0.122 \pm 0.023 \pm 0.010)\%$ in hadronic Z decays; the value quoted here is obtained using our best value $B(\Lambda_c^+ \rightarrow pK^-\pi^+) = (5.0 \pm 1.3)\%$. The first error is the total experiment's error and the second error is the systematic error due to the branching fraction uncertainty.

⁹⁶ BUSKULIC 96Y obtain the production fraction of Λ_c^+ baryons in hadronic Z decays $f(b \rightarrow \Lambda_c^+ X) = 0.110 \pm 0.014 \pm 0.006$ using $B(\Lambda_c^+ \rightarrow pK^-\pi^+) = (4.4 \pm 0.6)\%$; we have rescaled using our best value $B(\Lambda_c^+ \rightarrow pK^-\pi^+) = (5.0 \pm 1.3)\%$ obtaining $f(b \rightarrow \Lambda_c^+ X) = 0.097 \pm 0.013 \pm 0.025$ where the first error is their total experiment's error and the second error is the systematic error due to the branching fraction uncertainty. The value quoted here is obtained multiplying this production fraction by our value of $R_b = \Gamma(b\bar{b})/\Gamma(\text{hadrons})$.

$\Gamma(\Xi_c^0 X)/\Gamma(\text{hadrons})$ Γ_{41}/Γ_6

VALUE	DOCUMENT ID	TECN	COMMENT
• • • We do not use the following data for averages, fits, limits, etc. • • •			
seen	97 ABDALLAH	05c DLPH	$E_{\text{cm}}^{\text{ee}} = 88\text{--}94$ GeV
97 ABDALLAH 05c searched for the charmed strange baryon Ξ_c^0 in the decay channel $\Xi_c^0 \rightarrow \Xi^- \pi^+$ ($\Xi^- \rightarrow \Lambda \pi^-$). The production rate is measured to be $f_{\Xi_c^0} \times B(\Xi_c^0 \rightarrow \Xi^- \pi^+) = (4.7 \pm 1.4 \pm 1.1) \times 10^{-4}$ per hadronic Z decay.			

 $\Gamma(\Xi_b X)/\Gamma(\text{hadrons})$ Γ_{42}/Γ_6

Here Ξ_b is used as a notation for the strange b -baryon states Ξ_b^- and Ξ_b^0 .

VALUE	DOCUMENT ID	TECN	COMMENT
• • • We do not use the following data for averages, fits, limits, etc. • • •			
seen	98 ABDALLAH	05c DLPH	$E_{\text{cm}}^{\text{ee}} = 88\text{--}94$ GeV
seen	99 BUSKULIC	96T ALEP	$E_{\text{cm}}^{\text{ee}} = 88\text{--}94$ GeV
seen	100 ABREU	95v DLPH	$E_{\text{cm}}^{\text{ee}} = 88\text{--}94$ GeV
98 ABDALLAH 05c searched for the beauty strange baryon Ξ_b in the inclusive semileptonic decay channel $\Xi_b \rightarrow \Xi^- \ell^- \bar{\nu}_\ell X$. Evidence for the Ξ_b production is seen from the observation of Ξ^\mp production accompanied by a lepton of the same sign. From the excess of "right-sign" pairs $\Xi^\mp \ell^\mp$ compared to "wrong-sign" pairs $\Xi^\mp \ell^\pm$ the production rate is measured to be $B(b \rightarrow \Xi_b) \times B(\Xi_b \rightarrow \Xi^- \ell^- X) = (3.0 \pm 1.0 \pm 0.3) \times 10^{-4}$ per lepton species, averaged over electrons and muons.			
99 BUSKULIC 96T investigate Ξ -lepton correlations and find a significant excess of "right-sign" pairs $\Xi^\mp \ell^\mp$ compared to "wrong-sign" pairs $\Xi^\mp \ell^\pm$. This excess is interpreted as evidence for Ξ_b semileptonic decay. The measured product branching ratio is $B(b \rightarrow \Xi_b) \times B(\Xi_b \rightarrow X_c X \ell^- \bar{\nu}_\ell) \times B(X_c \rightarrow \Xi^- X') = (5.4 \pm 1.1 \pm 0.8) \times 10^{-4}$ per lepton species, averaged over electrons and muons, with X_c a charmed baryon.			
100 ABREU 95v observe an excess of "right-sign" pairs $\Xi^\mp \ell^\mp$ compared to "wrong-sign" pairs $\Xi^\mp \ell^\pm$ in jets: this excess is interpreted as evidence for the beauty strange baryon Ξ_b production, with $\Xi_b \rightarrow \Xi^- \ell^- \bar{\nu}_\ell X$. They find that the probability for this signal to come from non b -baryon decays is less than 5×10^{-4} and that Λ_b decays can account for less than 10% of these events. The Ξ_b production rate is then measured to be $B(b \rightarrow \Xi_b) \times B(\Xi_b \rightarrow \Xi^- \ell^- X) = (5.9 \pm 2.1 \pm 1.0) \times 10^{-4}$ per lepton species, averaged over electrons and muons.			

 $\Gamma(b\text{-baryon } X)/\Gamma(\text{hadrons})$ Γ_{43}/Γ_6

"OUR EVALUATION" is obtained using our current values for $f(b \rightarrow b\text{-baryon})$ and $R_b = \Gamma(b\bar{b})/\Gamma(\text{hadrons})$. We calculate $\Gamma(b\text{-baryon } X)/\Gamma(\text{hadrons}) = R_b \times f(b \rightarrow b\text{-baryon})$. The decay fraction $f(b \rightarrow b\text{-baryon})$ was provided by the Heavy Flavor Averaging Group (HFAG, http://www.slac.stanford.edu/xorg/hfag/osc/PDG_2009).

VALUE	DOCUMENT ID	TECN	COMMENT
0.0197 ± 0.0032 OUR EVALUATION			
0.0221 ± 0.0015 ± 0.0058	101 BARATE	98v ALEP	$E_{\text{cm}}^{\text{ee}} = 88\text{--}94$ GeV
101 BARATE 98v use the overall number of identified protons in b -hadron decays to measure $f(b \rightarrow b\text{-baryon}) = 0.102 \pm 0.007 \pm 0.027$. They assume $\text{BR}(b\text{-baryon} \rightarrow pX) = (58 \pm 6)\%$ and $\text{BR}(B_s^0 \rightarrow pX) = (8.0 \pm 4.0)\%$. The value quoted here is obtained multiplying this production fraction by our value of $R_b = \Gamma(b\bar{b})/\Gamma(\text{hadrons})$.			

 $\Gamma(\text{anomalous } \gamma + \text{hadrons})/\Gamma_{\text{total}}$ Γ_{44}/Γ

Limits on additional sources of prompt photons beyond expectations for final-state bremsstrahlung.

VALUE	CL%	DOCUMENT ID	TECN	COMMENT
<3.2 × 10⁻³	95	102 AKRAWY	90J OPAL	$E_{\text{cm}}^{\text{ee}} = 88\text{--}94$ GeV
102 AKRAWY 90J report $\Gamma(\gamma X) < 8.2$ MeV at 95%CL. They assume a three-body $\gamma q \bar{q}$ distribution and use $E(\gamma) > 10$ GeV.				

 $\Gamma(e^+ e^- \gamma)/\Gamma_{\text{total}}$ Γ_{45}/Γ

VALUE	CL%	DOCUMENT ID	TECN	COMMENT
<5.2 × 10⁻⁴	95	103 ACTON	91B OPAL	$E_{\text{cm}}^{\text{ee}} = 91.2$ GeV
103 ACTON 91B looked for isolated photons with $E > 2\%$ of beam energy (> 0.9 GeV).				

 $\Gamma(\mu^+ \mu^- \gamma)/\Gamma_{\text{total}}$ Γ_{46}/Γ

VALUE	CL%	DOCUMENT ID	TECN	COMMENT
<5.6 × 10⁻⁴	95	104 ACTON	91B OPAL	$E_{\text{cm}}^{\text{ee}} = 91.2$ GeV
104 ACTON 91B looked for isolated photons with $E > 2\%$ of beam energy (> 0.9 GeV).				

 $\Gamma(\tau^+ \tau^- \gamma)/\Gamma_{\text{total}}$ Γ_{47}/Γ

VALUE	CL%	DOCUMENT ID	TECN	COMMENT
<7.3 × 10⁻⁴	95	105 ACTON	91B OPAL	$E_{\text{cm}}^{\text{ee}} = 91.2$ GeV
105 ACTON 91B looked for isolated photons with $E > 2\%$ of beam energy (> 0.9 GeV).				

 $\Gamma(\ell^+ \ell^- \gamma)/\Gamma_{\text{total}}$ Γ_{48}/Γ

The value is the sum over $\ell = e, \mu, \tau$.

VALUE	CL%	DOCUMENT ID	TECN	COMMENT
<6.8 × 10⁻⁶	95	106 ACTON	93E OPAL	$E_{\text{cm}}^{\text{ee}} = 88\text{--}94$ GeV
106 For $m_{\gamma\gamma} = 60 \pm 5$ GeV.				

 $\Gamma(q\bar{q}\gamma)/\Gamma_{\text{total}}$ Γ_{49}/Γ

VALUE	CL%	DOCUMENT ID	TECN	COMMENT
<5.5 × 10⁻⁶	95	107 ACTON	93E OPAL	$E_{\text{cm}}^{\text{ee}} = 88\text{--}94$ GeV
107 For $m_{\gamma\gamma} = 60 \pm 5$ GeV.				

 $\Gamma(\nu\bar{\nu}\gamma\gamma)/\Gamma_{\text{total}}$ Γ_{50}/Γ

VALUE	CL%	DOCUMENT ID	TECN	COMMENT
<3.1 × 10⁻⁶	95	108 ACTON	93E OPAL	$E_{\text{cm}}^{\text{ee}} = 88\text{--}94$ GeV
108 For $m_{\gamma\gamma} = 60 \pm 5$ GeV.				

 $\Gamma(e^\pm \mu^\mp)/\Gamma_{\text{total}}$ Γ_{51}/Γ

Test of lepton family number conservation. The value is for the sum of the charge states indicated.

VALUE	CL%	DOCUMENT ID	TECN	COMMENT
<2.5 × 10⁻⁶	95	ABREU	97c DLPH	$E_{\text{cm}}^{\text{ee}} = 88\text{--}94$ GeV
<1.7 × 10⁻⁶	95	AKERS	95w OPAL	$E_{\text{cm}}^{\text{ee}} = 88\text{--}94$ GeV
<0.6 × 10⁻⁵	95	ADRIANI	93i L3	$E_{\text{cm}}^{\text{ee}} = 88\text{--}94$ GeV
<2.6 × 10⁻⁵	95	DECAMP	92 ALEP	$E_{\text{cm}}^{\text{ee}} = 88\text{--}94$ GeV

 $\Gamma(e^\pm \mu^\mp)/\Gamma(e^+ e^-)$ Γ_{51}/Γ_1

Test of lepton family number conservation. The value is for the sum of the charge states indicated.

VALUE	CL%	DOCUMENT ID	TECN	COMMENT
<0.07	90	ALBAJAR	89 UA1	$E_{\text{cm}}^{\text{p}\bar{\text{p}}} = 546,630$ GeV

 $\Gamma(e^\pm \tau^\mp)/\Gamma_{\text{total}}$ Γ_{52}/Γ

Test of lepton family number conservation. The value is for the sum of the charge states indicated.

VALUE	CL%	DOCUMENT ID	TECN	COMMENT
<2.2 × 10⁻⁵	95	ABREU	97c DLPH	$E_{\text{cm}}^{\text{ee}} = 88\text{--}94$ GeV
<9.8 × 10⁻⁶	95	AKERS	95w OPAL	$E_{\text{cm}}^{\text{ee}} = 88\text{--}94$ GeV
<1.3 × 10⁻⁵	95	ADRIANI	93i L3	$E_{\text{cm}}^{\text{ee}} = 88\text{--}94$ GeV
<1.2 × 10⁻⁴	95	DECAMP	92 ALEP	$E_{\text{cm}}^{\text{ee}} = 88\text{--}94$ GeV

 $\Gamma(\mu^\pm \tau^\mp)/\Gamma_{\text{total}}$ Γ_{53}/Γ

Test of lepton family number conservation. The value is for the sum of the charge states indicated.

VALUE	CL%	DOCUMENT ID	TECN	COMMENT
<1.2 × 10⁻⁵	95	ABREU	97c DLPH	$E_{\text{cm}}^{\text{ee}} = 88\text{--}94$ GeV
<1.7 × 10⁻⁵	95	AKERS	95w OPAL	$E_{\text{cm}}^{\text{ee}} = 88\text{--}94$ GeV
<1.9 × 10⁻⁵	95	ADRIANI	93i L3	$E_{\text{cm}}^{\text{ee}} = 88\text{--}94$ GeV
<1.0 × 10⁻⁴	95	DECAMP	92 ALEP	$E_{\text{cm}}^{\text{ee}} = 88\text{--}94$ GeV

 $\Gamma(p e)/\Gamma_{\text{total}}$ Γ_{54}/Γ

Test of baryon number and lepton number conservations. Charge conjugate states are implied.

VALUE	CL%	DOCUMENT ID	TECN	COMMENT
<1.8 × 10⁻⁶	95	109 ABBIENDI	99i OPAL	$E_{\text{cm}}^{\text{ee}} = 88\text{--}94$ GeV

109 ABBIENDI 99i give the 95%CL limit on the partial width $\Gamma(Z^0 \rightarrow pe) < 4.6$ KeV and we have transformed it into a branching ratio.

 $\Gamma(p \mu)/\Gamma_{\text{total}}$ Γ_{55}/Γ

Test of baryon number and lepton number conservations. Charge conjugate states are implied.

VALUE	CL%	DOCUMENT ID	TECN	COMMENT
<1.8 × 10⁻⁶	95	110 ABBIENDI	99i OPAL	$E_{\text{cm}}^{\text{ee}} = 88\text{--}94$ GeV

110 ABBIENDI 99i give the 95%CL limit on the partial width $\Gamma(Z^0 \rightarrow p\mu) < 4.4$ KeV and we have transformed it into a branching ratio.

AVERAGE PARTICLE MULTIPLICITIES IN HADRONIC Z DECAY

Summed over particle and antiparticle, when appropriate.

 $\langle N_\gamma \rangle$

VALUE	DOCUMENT ID	TECN	COMMENT
20.97 ± 0.02 ± 1.15	ACKERSTAFF	98A OPAL	$E_{\text{cm}}^{\text{ee}} = 91.2$ GeV

 $\langle N_{\pi^\pm} \rangle$

VALUE	DOCUMENT ID	TECN	COMMENT
17.03 ± 0.16 OUR AVERAGE			
17.007 ± 0.209	ABE	04c SLD	$E_{\text{cm}}^{\text{ee}} = 91.2$ GeV
17.26 ± 0.10 ± 0.88	ABREU	98L DLPH	$E_{\text{cm}}^{\text{ee}} = 91.2$ GeV
17.04 ± 0.31	BARATE	98v ALEP	$E_{\text{cm}}^{\text{ee}} = 91.2$ GeV
17.05 ± 0.43	AKERS	94p OPAL	$E_{\text{cm}}^{\text{ee}} = 91.2$ GeV

 $\langle N_{\pi^0} \rangle$

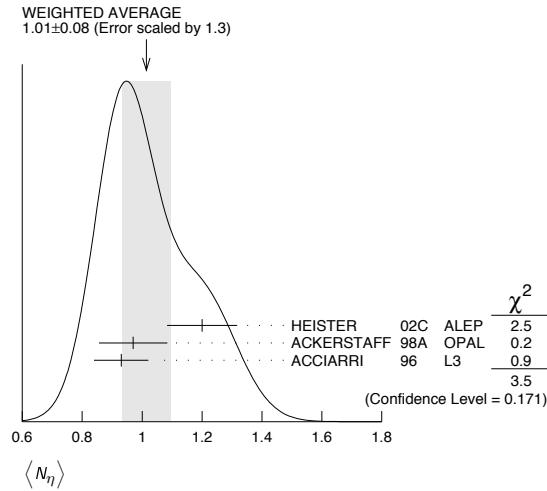
VALUE	DOCUMENT ID	TECN	COMMENT
9.76 ± 0.26 OUR AVERAGE			
9.55 ± 0.06 ± 0.75	ACKERSTAFF	98A OPAL	$E_{\text{cm}}^{\text{ee}} = 91.2$ GeV
9.63 ± 0.13 ± 0.63	BARATE	97J ALEP	$E_{\text{cm}}^{\text{ee}} = 91.2$ GeV
9.90 ± 0.02 ± 0.33	ACCIARRI	96 L3	$E_{\text{cm}}^{\text{ee}} = 91.2$ GeV
9.2 ± 0.2 ± 1.0	ADAM	96 DLPH	$E_{\text{cm}}^{\text{ee}} = 91.2$ GeV

Gauge & Higgs Boson Particle Listings

Z

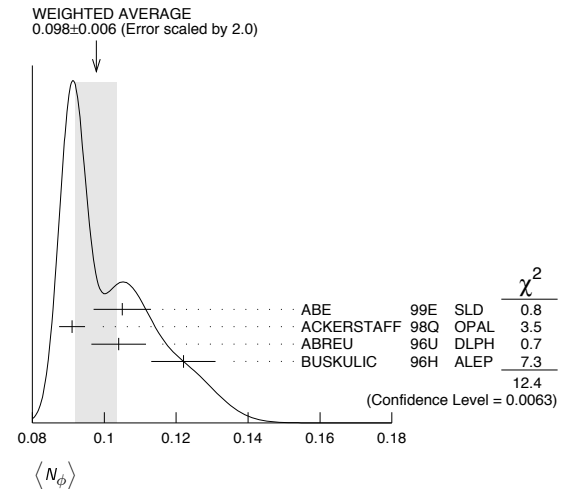
$\langle N_\eta \rangle$

VALUE	DOCUMENT ID	TECN	COMMENT
1.01 ± 0.08 OUR AVERAGE	Error includes scale factor of 1.3. See the ideogram below.		
1.20 ± 0.04 ± 0.11	HEISTER 02c	ALEP	$E_{cm}^{ee} = 91.2$ GeV
0.97 ± 0.03 ± 0.11	ACKERSTAFF 98A	OPAL	$E_{cm}^{ee} = 91.2$ GeV
0.93 ± 0.01 ± 0.09	ACCIARRI 96	L3	$E_{cm}^{ee} = 91.2$ GeV



$\langle N_\phi \rangle$

VALUE	DOCUMENT ID	TECN	COMMENT
0.098 ± 0.006 OUR AVERAGE	Error includes scale factor of 2.0. See the ideogram below.		
0.105 ± 0.008	ABE 99E	SLD	$E_{cm}^{ee} = 91.2$ GeV
0.091 ± 0.002 ± 0.003	ACKERSTAFF 98Q	OPAL	$E_{cm}^{ee} = 91.2$ GeV
0.104 ± 0.003 ± 0.007	ABREU 96U	DLPH	$E_{cm}^{ee} = 91.2$ GeV
0.122 ± 0.004 ± 0.008	BUSKULIC 96H	ALEP	$E_{cm}^{ee} = 91.2$ GeV



$\langle N_{\rho^\pm} \rangle$

VALUE	DOCUMENT ID	TECN	COMMENT
2.57 ± 0.15 OUR AVERAGE	Error includes scale factor of 1.1.		
2.59 ± 0.03 ± 0.16	111 BEDDALL 09	ALEPH	archive, $E_{cm}^{ee} = 91.2$ GeV
2.40 ± 0.06 ± 0.43	ACKERSTAFF 98A	OPAL	$E_{cm}^{ee} = 91.2$ GeV

111 BEDDALL 09 analyse 3.2 million hadronic Z decays as archived by ALEPH collaboration and report a value of $2.59 \pm 0.03 \pm 0.15 \pm 0.04$. The first error is statistical, the second systematic, and the third arises from extrapolation to full phase space. We combine the systematic errors in quadrature.

$\langle N_{\rho^0} \rangle$

VALUE	DOCUMENT ID	TECN	COMMENT
1.24 ± 0.10 OUR AVERAGE	Error includes scale factor of 1.1.		
1.19 ± 0.10	ABREU 99J	DLPH	$E_{cm}^{ee} = 91.2$ GeV
1.45 ± 0.06 ± 0.20	BUSKULIC 96H	ALEP	$E_{cm}^{ee} = 91.2$ GeV

$\langle N_\omega \rangle$

VALUE	DOCUMENT ID	TECN	COMMENT
1.02 ± 0.06 OUR AVERAGE	Error includes scale factor of 1.1.		
1.00 ± 0.03 ± 0.06	HEISTER 02c	ALEP	$E_{cm}^{ee} = 91.2$ GeV
1.04 ± 0.04 ± 0.14	ACKERSTAFF 98A	OPAL	$E_{cm}^{ee} = 91.2$ GeV
1.17 ± 0.09 ± 0.15	ACCIARRI 97D	L3	$E_{cm}^{ee} = 91.2$ GeV

$\langle N_{\eta'} \rangle$

VALUE	DOCUMENT ID	TECN	COMMENT
0.17 ± 0.05 OUR AVERAGE	Error includes scale factor of 2.4.		
0.14 ± 0.01 ± 0.02	ACKERSTAFF 98A	OPAL	$E_{cm}^{ee} = 91.2$ GeV
0.25 ± 0.04	112 ACCIARRI 97D	L3	$E_{cm}^{ee} = 91.2$ GeV

• • • We do not use the following data for averages, fits, limits, etc. • • •

0.068 ± 0.018 ± 0.016 113 BUSKULIC 92D ALEP $E_{cm}^{ee} = 91.2$ GeV

112 ACCIARRI 97D obtain this value averaging over the two decay channels $\eta' \rightarrow \pi^+ \pi^- \eta$ and $\eta' \rightarrow \rho^0 \gamma$.

113 BUSKULIC 92D obtain this value for $x > 0.1$.

$\langle N_{\eta(980)} \rangle$

VALUE	DOCUMENT ID	TECN	COMMENT
0.147 ± 0.011 OUR AVERAGE	Error includes scale factor of 1.1.		
0.164 ± 0.021	ABREU 99J	DLPH	$E_{cm}^{ee} = 91.2$ GeV
0.141 ± 0.007 ± 0.011	ACKERSTAFF 98Q	OPAL	$E_{cm}^{ee} = 91.2$ GeV

$\langle N_{\eta_0(980)^\pm} \rangle$

VALUE	DOCUMENT ID	TECN	COMMENT
0.27 ± 0.04 ± 0.10	ACKERSTAFF 98A	OPAL	$E_{cm}^{ee} = 91.2$ GeV

$\langle N_{f_2(1270)} \rangle$

VALUE	DOCUMENT ID	TECN	COMMENT
0.169 ± 0.025 OUR AVERAGE	Error includes scale factor of 1.4.		
0.214 ± 0.038	ABREU 99J	DLPH	$E_{cm}^{ee} = 91.2$ GeV
0.155 ± 0.011 ± 0.018	ACKERSTAFF 98Q	OPAL	$E_{cm}^{ee} = 91.2$ GeV

$\langle N_{f_1(1285)} \rangle$

VALUE	DOCUMENT ID	TECN	COMMENT
0.165 ± 0.051	114 ABDALLAH 03H	DLPH	$E_{cm}^{ee} = 91.2$ GeV

114 ABDALLAH 03H assume a $K\bar{K}\pi$ branching ratio of $(9.0 \pm 0.4)\%$.

$\langle N_{f_1(1420)} \rangle$

VALUE	DOCUMENT ID	TECN	COMMENT
0.056 ± 0.012	115 ABDALLAH 03H	DLPH	$E_{cm}^{ee} = 91.2$ GeV

115 ABDALLAH 03H assume a $K\bar{K}\pi$ branching ratio of 100%.

$\langle N_{f_2'(1525)} \rangle$

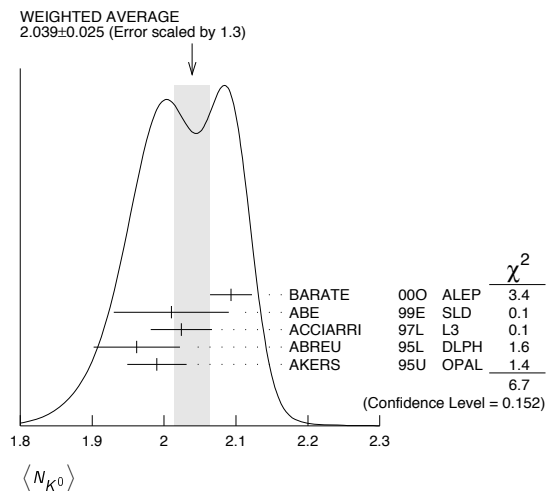
VALUE	DOCUMENT ID	TECN	COMMENT
0.012 ± 0.006	ABREU 99J	DLPH	$E_{cm}^{ee} = 91.2$ GeV

$\langle N_{K^\pm} \rangle$

VALUE	DOCUMENT ID	TECN	COMMENT
2.24 ± 0.04 OUR AVERAGE	Error includes scale factor of 1.1.		
2.203 ± 0.071	ABE 04c	SLD	$E_{cm}^{ee} = 91.2$ GeV
2.21 ± 0.05 ± 0.05	ABREU 98L	DLPH	$E_{cm}^{ee} = 91.2$ GeV
2.26 ± 0.12	BARATE 98V	ALEP	$E_{cm}^{ee} = 91.2$ GeV
2.42 ± 0.13	AKERS 94P	OPAL	$E_{cm}^{ee} = 91.2$ GeV

$\langle N_{K^0} \rangle$

VALUE	DOCUMENT ID	TECN	COMMENT
2.039 ± 0.025 OUR AVERAGE	Error includes scale factor of 1.3. See the ideogram below.		
2.093 ± 0.004 ± 0.029	BARATE 00O	ALEP	$E_{cm}^{ee} = 91.2$ GeV
2.01 ± 0.08	ABE 99E	SLD	$E_{cm}^{ee} = 91.2$ GeV
2.024 ± 0.006 ± 0.042	ACCIARRI 97L	L3	$E_{cm}^{ee} = 91.2$ GeV
1.962 ± 0.022 ± 0.056	ABREU 95L	DLPH	$E_{cm}^{ee} = 91.2$ GeV
1.99 ± 0.01 ± 0.04	AKERS 95U	OPAL	$E_{cm}^{ee} = 91.2$ GeV

 $\langle N_{K^*(892)^\pm} \rangle$

VALUE	DOCUMENT ID	TECN	COMMENT
0.72 ± 0.05 OUR AVERAGE			
0.712 ± 0.031 ± 0.059	ABREU 95L	DLPH	$E_{cm}^{ee} = 91.2$ GeV
0.72 ± 0.02 ± 0.08	ACTON 93	OPAL	$E_{cm}^{ee} = 91.2$ GeV

 $\langle N_{K^*(892)^0} \rangle$

VALUE	DOCUMENT ID	TECN	COMMENT
0.739 ± 0.022 OUR AVERAGE			
0.707 ± 0.041	ABE 99E	SLD	$E_{cm}^{ee} = 91.2$ GeV
0.74 ± 0.02 ± 0.02	ACKERSTAFF 97s	OPAL	$E_{cm}^{ee} = 91.2$ GeV
0.77 ± 0.02 ± 0.07	ABREU 96u	DLPH	$E_{cm}^{ee} = 91.2$ GeV
0.83 ± 0.01 ± 0.09	BUSKULIC 96h	ALEP	$E_{cm}^{ee} = 91.2$ GeV
0.97 ± 0.18 ± 0.31	ABREU 93	DLPH	$E_{cm}^{ee} = 91.2$ GeV

 $\langle N_{K_2^*(1430)} \rangle$

VALUE	DOCUMENT ID	TECN	COMMENT
0.073 ± 0.023	ABREU 99j	DLPH	$E_{cm}^{ee} = 91.2$ GeV
0.19 ± 0.04 ± 0.06	116 AKERS 95x	OPAL	$E_{cm}^{ee} = 91.2$ GeV

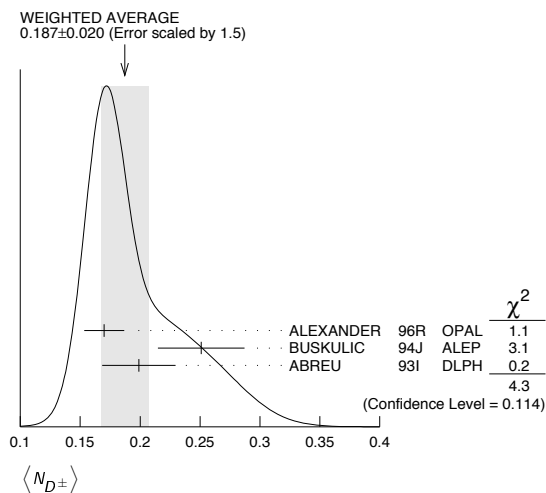
• • • We do not use the following data for averages, fits, limits, etc. • • •

116 AKERS 95x obtain this value for $x < 0.3$.

 $\langle N_{D^\pm} \rangle$

VALUE	DOCUMENT ID	TECN	COMMENT
0.187 ± 0.020 OUR AVERAGE	Error includes scale factor of 1.5. See the ideogram below.		
0.170 ± 0.009 ± 0.014	ALEXANDER 96R	OPAL	$E_{cm}^{ee} = 91.2$ GeV
0.251 ± 0.026 ± 0.025	BUSKULIC 94J	ALEP	$E_{cm}^{ee} = 91.2$ GeV
0.199 ± 0.019 ± 0.024	117 ABREU 93i	DLPH	$E_{cm}^{ee} = 91.2$ GeV

117 See ABREU 95 (erratum).

 $\langle N_{D^0} \rangle$

VALUE	DOCUMENT ID	TECN	COMMENT
0.462 ± 0.026 OUR AVERAGE			
0.465 ± 0.017 ± 0.027	ALEXANDER 96R	OPAL	$E_{cm}^{ee} = 91.2$ GeV
0.518 ± 0.052 ± 0.035	BUSKULIC 94J	ALEP	$E_{cm}^{ee} = 91.2$ GeV
0.403 ± 0.038 ± 0.044	118 ABREU 93i	DLPH	$E_{cm}^{ee} = 91.2$ GeV

118 See ABREU 95 (erratum).

 $\langle N_{D_s^\pm} \rangle$

VALUE	DOCUMENT ID	TECN	COMMENT
0.131 ± 0.010 ± 0.018	ALEXANDER 96R	OPAL	$E_{cm}^{ee} = 91.2$ GeV

 $\langle N_{D^*(2010)^\pm} \rangle$

VALUE	DOCUMENT ID	TECN	COMMENT
0.183 ± 0.008 OUR AVERAGE			
0.1854 ± 0.0041 ± 0.0091	119 ACKERSTAFF 98E	OPAL	$E_{cm}^{ee} = 91.2$ GeV
0.187 ± 0.015 ± 0.013	BUSKULIC 94J	ALEP	$E_{cm}^{ee} = 91.2$ GeV
0.171 ± 0.012 ± 0.016	120 ABREU 93i	DLPH	$E_{cm}^{ee} = 91.2$ GeV

119 ACKERSTAFF 98E systematic error includes an uncertainty of ± 0.0069 due to the branching ratios $B(D^{*+} \rightarrow D^0 \pi^+) = 0.683 \pm 0.014$ and $B(D^0 \rightarrow K^- \pi^+) = 0.0383 \pm 0.0012$.

120 See ABREU 95 (erratum).

 $\langle N_{D_{s1}(2536)^+} \rangle$

VALUE (units 10^{-3})	DOCUMENT ID	TECN	COMMENT
2.9^{+0.7}_{-0.6} ± 0.2	121 ACKERSTAFF 97w	OPAL	$E_{cm}^{ee} = 91.2$ GeV

121 ACKERSTAFF 97w obtain this value for $x > 0.6$ and with the assumption that its decay width is saturated by the $D^* K$ final states.

 $\langle N_{B^*} \rangle$

VALUE	DOCUMENT ID	TECN	COMMENT
0.28 ± 0.01 ± 0.03	122 ABREU 95R	DLPH	$E_{cm}^{ee} = 91.2$ GeV

122 ABREU 95R quote this value for a flavor-averaged excited state.

 $\langle N_{J/\psi(1S)} \rangle$

VALUE	DOCUMENT ID	TECN	COMMENT
0.0056 ± 0.0003 ± 0.0004	123 ALEXANDER 96b	OPAL	$E_{cm}^{ee} = 91.2$ GeV

123 ALEXANDER 96b identify $J/\psi(1S)$ from the decays into lepton pairs.

 $\langle N_{\psi(2S)} \rangle$

VALUE	DOCUMENT ID	TECN	COMMENT
0.0023 ± 0.0004 ± 0.0003	ALEXANDER 96b	OPAL	$E_{cm}^{ee} = 91.2$ GeV

 $\langle N_p \rangle$

VALUE	DOCUMENT ID	TECN	COMMENT
1.046 ± 0.026 OUR AVERAGE			
1.054 ± 0.035	ABE 04c	SLD	$E_{cm}^{ee} = 91.2$ GeV
1.08 ± 0.04 ± 0.03	ABREU 98L	DLPH	$E_{cm}^{ee} = 91.2$ GeV
1.00 ± 0.07	BARATE 98v	ALEP	$E_{cm}^{ee} = 91.2$ GeV
0.92 ± 0.11	AKERS 94p	OPAL	$E_{cm}^{ee} = 91.2$ GeV

 $\langle N_{\Delta(1232)^{++}} \rangle$

VALUE	DOCUMENT ID	TECN	COMMENT
0.087 ± 0.033 OUR AVERAGE	Error includes scale factor of 2.4.		
0.079 ± 0.009 ± 0.011	ABREU 95w	DLPH	$E_{cm}^{ee} = 91.2$ GeV
0.22 ± 0.04 ± 0.04	ALEXANDER 95D	OPAL	$E_{cm}^{ee} = 91.2$ GeV

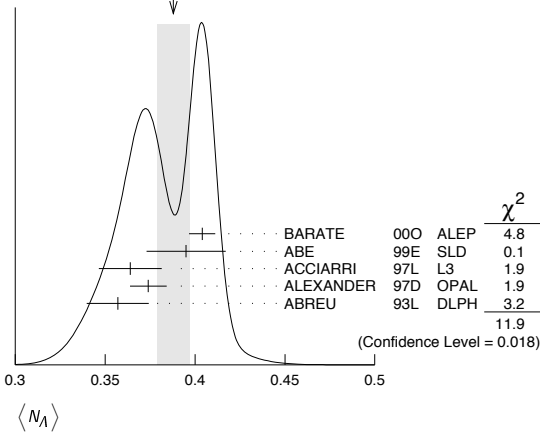
 $\langle N_\Lambda \rangle$

VALUE	DOCUMENT ID	TECN	COMMENT
0.388 ± 0.009 OUR AVERAGE	Error includes scale factor of 1.7. See the ideogram below.		
0.404 ± 0.002 ± 0.007	BARATE 00o	ALEP	$E_{cm}^{ee} = 91.2$ GeV
0.395 ± 0.022	ABE 99E	SLD	$E_{cm}^{ee} = 91.2$ GeV
0.364 ± 0.004 ± 0.017	ACCIARRI 97L	L3	$E_{cm}^{ee} = 91.2$ GeV
0.374 ± 0.002 ± 0.010	ALEXANDER 97D	OPAL	$E_{cm}^{ee} = 91.2$ GeV
0.357 ± 0.003 ± 0.017	ABREU 93L	DLPH	$E_{cm}^{ee} = 91.2$ GeV

Gauge & Higgs Boson Particle Listings

Z

WEIGHTED AVERAGE
0.388±0.009 (Error scaled by 1.7)



$\langle N_{\Lambda(1520)} \rangle$

VALUE	DOCUMENT ID	TECN	COMMENT
0.0224 ± 0.0027 OUR AVERAGE			
0.029 ± 0.005 ± 0.005	ABREU 00P	DLPH	$E_{cm}^{ee} = 91.2$ GeV
0.0213 ± 0.0021 ± 0.0019	ALEXANDER 97D	OPAL	$E_{cm}^{ee} = 91.2$ GeV

$\langle N_{\Sigma^+} \rangle$

VALUE	DOCUMENT ID	TECN	COMMENT
0.107 ± 0.010 OUR AVERAGE			
0.114 ± 0.011 ± 0.009	ACCIARRI 00J	L3	$E_{cm}^{ee} = 91.2$ GeV
0.099 ± 0.008 ± 0.013	ALEXANDER 97E	OPAL	$E_{cm}^{ee} = 91.2$ GeV

$\langle N_{\Sigma^-} \rangle$

VALUE	DOCUMENT ID	TECN	COMMENT
0.082 ± 0.007 OUR AVERAGE			
0.081 ± 0.002 ± 0.010	ABREU 00P	DLPH	$E_{cm}^{ee} = 91.2$ GeV
0.083 ± 0.006 ± 0.009	ALEXANDER 97E	OPAL	$E_{cm}^{ee} = 91.2$ GeV

$\langle N_{\Sigma^+ + \Sigma^-} \rangle$

VALUE	DOCUMENT ID	TECN	COMMENT
0.181 ± 0.018 OUR AVERAGE			
0.182 ± 0.010 ± 0.016	¹²⁴ ALEXANDER 97E	OPAL	$E_{cm}^{ee} = 91.2$ GeV
0.170 ± 0.014 ± 0.061	ABREU 95O	DLPH	$E_{cm}^{ee} = 91.2$ GeV

¹²⁴We have combined the values of $\langle N_{\Sigma^+} \rangle$ and $\langle N_{\Sigma^-} \rangle$ from ALEXANDER 97E adding the statistical and systematic errors of the two final states separately in quadrature. If isospin symmetry is assumed this value becomes $0.174 \pm 0.010 \pm 0.015$.

$\langle N_{\Sigma^0} \rangle$

VALUE	DOCUMENT ID	TECN	COMMENT
0.076 ± 0.010 OUR AVERAGE			
0.095 ± 0.015 ± 0.013	ACCIARRI 00J	L3	$E_{cm}^{ee} = 91.2$ GeV
0.071 ± 0.012 ± 0.013	ALEXANDER 97E	OPAL	$E_{cm}^{ee} = 91.2$ GeV
0.070 ± 0.010 ± 0.010	ADAM 96B	DLPH	$E_{cm}^{ee} = 91.2$ GeV

$\langle N_{(\Sigma^+ + \Sigma^- + \Sigma^0)/3} \rangle$

VALUE	DOCUMENT ID	TECN	COMMENT
0.084 ± 0.005 ± 0.008			
	ALEXANDER 97E	OPAL	$E_{cm}^{ee} = 91.2$ GeV

$\langle N_{\Sigma(1385)^+} \rangle$

VALUE	DOCUMENT ID	TECN	COMMENT
0.0239 ± 0.0009 ± 0.0012			
	ALEXANDER 97D	OPAL	$E_{cm}^{ee} = 91.2$ GeV

$\langle N_{\Sigma(1385)^-} \rangle$

VALUE	DOCUMENT ID	TECN	COMMENT
0.0240 ± 0.0010 ± 0.0014			
	ALEXANDER 97D	OPAL	$E_{cm}^{ee} = 91.2$ GeV

$\langle N_{\Sigma(1385)^+ + \Sigma(1385)^-} \rangle$

VALUE	DOCUMENT ID	TECN	COMMENT
0.046 ± 0.004 OUR AVERAGE			
0.0479 ± 0.0013 ± 0.0026	ALEXANDER 97D	OPAL	$E_{cm}^{ee} = 91.2$ GeV
0.0382 ± 0.0028 ± 0.0045	ABREU 95O	DLPH	$E_{cm}^{ee} = 91.2$ GeV

Error includes scale factor of 1.6.

$\langle N_{\Xi^-} \rangle$

VALUE	DOCUMENT ID	TECN	COMMENT
0.0258 ± 0.0009 OUR AVERAGE			
0.0247 ± 0.0009 ± 0.0025	ABDALLAH 06E	DLPH	$E_{cm}^{ee} = 91.2$ GeV
0.0259 ± 0.0004 ± 0.0009	ALEXANDER 97D	OPAL	$E_{cm}^{ee} = 91.2$ GeV

$\langle N_{\Xi(1530)^0} \rangle$

VALUE	DOCUMENT ID	TECN	COMMENT
0.0059 ± 0.0011 OUR AVERAGE			Error includes scale factor of 2.3.
0.0045 ± 0.0005 ± 0.0006	ABDALLAH 05C	DLPH	$E_{cm}^{ee} = 91.2$ GeV
0.0068 ± 0.0005 ± 0.0004	ALEXANDER 97D	OPAL	$E_{cm}^{ee} = 91.2$ GeV

$\langle N_{\Omega^-} \rangle$

VALUE	DOCUMENT ID	TECN	COMMENT
0.00164 ± 0.00028 OUR AVERAGE			
0.0018 ± 0.0003 ± 0.0002	ALEXANDER 97D	OPAL	$E_{cm}^{ee} = 91.2$ GeV
0.0014 ± 0.0002 ± 0.0004	ADAM 96B	DLPH	$E_{cm}^{ee} = 91.2$ GeV

$\langle N_{\Lambda_c^+} \rangle$

VALUE	DOCUMENT ID	TECN	COMMENT
0.078 ± 0.012 ± 0.012			
	ALEXANDER 96R	OPAL	$E_{cm}^{ee} = 91.2$ GeV

$\langle N_D \rangle$

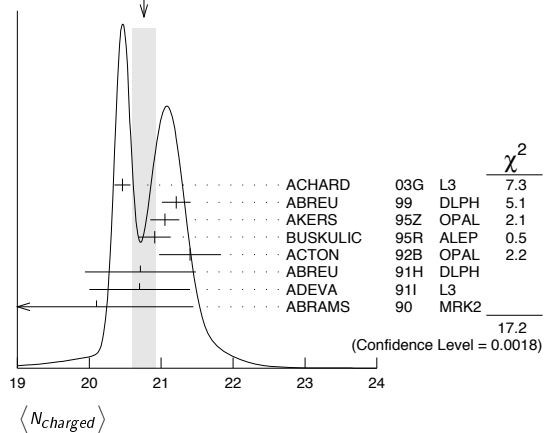
VALUE (units 10^{-6})	DOCUMENT ID	TECN	COMMENT
5.9 ± 1.8 ± 0.5			
	¹²⁵ SCHAEEL 06A	ALEP	$E_{cm}^{ee} = 91.2$ GeV

¹²⁵SCHAEEL 06A obtain this anti-deuteron production rate per hadronic Z decay in the anti-deuteron momentum range from 0.62 to 1.03 GeV/c.

$\langle N_{\text{charged}} \rangle$

VALUE	DOCUMENT ID	TECN	COMMENT
20.76 ± 0.16 OUR AVERAGE			Error includes scale factor of 2.1. See the ideogram below.
20.46 ± 0.01 ± 0.11	ACHARD 03G	L3	$E_{cm}^{ee} = 91.2$ GeV
21.21 ± 0.01 ± 0.20	ABREU 99	DLPH	$E_{cm}^{ee} = 91.2$ GeV
21.05 ± 0.20	AKERS 95Z	OPAL	$E_{cm}^{ee} = 91.2$ GeV
20.91 ± 0.03 ± 0.22	BUSKULIC 95R	ALEP	$E_{cm}^{ee} = 91.2$ GeV
21.40 ± 0.43	ACTON 92B	OPAL	$E_{cm}^{ee} = 91.2$ GeV
20.71 ± 0.04 ± 0.77	ABREU 91H	DLPH	$E_{cm}^{ee} = 91.2$ GeV
20.7 ± 0.7	ADEVA 91I	L3	$E_{cm}^{ee} = 91.2$ GeV
20.1 ± 1.0 ± 0.9	ABRAMS 90	MRK2	$E_{cm}^{ee} = 91.1$ GeV

WEIGHTED AVERAGE
20.76±0.16 (Error scaled by 2.1)



Z HADRONIC POLE CROSS SECTION

OUR FIT is obtained using the fit procedure and correlations as determined by the LEP Electroweak Working Group (see the note "The Z boson" and ref. LEP-SLC 06). This quantity is defined as

$$\sigma_h^0 = \frac{12\pi}{M_Z^2} \frac{\Gamma(e^+e^-)\Gamma(\text{hadrons})}{\Gamma_Z^2}$$

It is one of the parameters used in the Z lineshape fit.

VALUE (nb)	EVTS	DOCUMENT ID	TECN	COMMENT
41.541 ± 0.037 OUR FIT				
41.501 ± 0.055	4.10M	¹²⁶ ABBIENDI 01A	OPAL	$E_{cm}^{ee} = 88-94$ GeV
41.578 ± 0.069	3.70M	ABREU 00F	DLPH	$E_{cm}^{ee} = 88-94$ GeV
41.535 ± 0.055	3.54M	ACCIARRI 00C	L3	$E_{cm}^{ee} = 88-94$ GeV
41.559 ± 0.058	4.07M	¹²⁷ BARATE 00C	ALEP	$E_{cm}^{ee} = 88-94$ GeV
42 ± 4	450	ABRAMS 89B	MRK2	$E_{cm}^{ee} = 89.2-93.0$ GeV

¹²⁶ABBIENDI 01A error includes approximately 0.031 due to statistics, 0.033 due to event selection systematics, 0.029 due to uncertainty in luminosity measurement, and 0.011 due to LEP energy uncertainty.
¹²⁷BARATE 00C error includes approximately 0.030 due to statistics, 0.026 due to experimental systematics, and 0.025 due to uncertainty in luminosity measurement.

Z VECTOR COUPLINGS

These quantities are the effective vector couplings of the Z to charged leptons. Their magnitude is derived from a measurement of the Z lineshape and the forward-backward lepton asymmetries as a function of energy around the Z mass. The relative sign among the vector to axial-vector couplings is obtained from a measurement of the Z asymmetry parameters, A_e , A_μ , and A_τ . By convention the sign of g_A^e is fixed to be negative (and opposite to that of g_V^e obtained using ν_e scattering measurements). For the light quarks, the sign of the couplings is assigned consistently with this assumption. The fit values quoted below correspond to global nine- or five-parameter fits to lineshape, lepton forward-backward asymmetry, and A_e , A_μ , and A_τ measurements. See the note "The Z boson" and ref. LEP-SLC 06 for details. Where $p\bar{p}$ and $e p$ data is quoted, OUR FIT value corresponds to a weighted average of this with the LEP/SLD fit result.

g_V^e	VALUE	EVTS	DOCUMENT ID	TECN	COMMENT
-0.03817 ± 0.00047 OUR FIT					
$-0.058 \pm 0.016 \pm 0.007$	5026	128	ACOSTA	05M	CDF $E_{cm}^{p\bar{p}} = 1.96$ TeV
-0.0346 ± 0.0023	137.0K	129	ABBIENDI	01o	OPAL $E_{cm}^{ee} = 88-94$ GeV
-0.0412 ± 0.0027	124.4k	130	ACCIARRI	00c	L3 $E_{cm}^{ee} = 88-94$ GeV
-0.0400 ± 0.0037			BARATE	00c	ALEP $E_{cm}^{ee} = 88-94$ GeV
-0.0414 ± 0.0020		131	ABE	95j	SLD $E_{cm}^{ee} = 91.31$ GeV

- 128 ACOSTA 05M determine the forward-backward asymmetry of e^+e^- pairs produced via $q\bar{q} \rightarrow Z/\gamma^* \rightarrow e^+e^-$ in 15 M(e^+e^-) effective mass bins ranging from 40 GeV to 600 GeV. These results are used to obtain the vector and axial-vector couplings of the Z to e^+e^- , assuming the quark couplings are as predicted by the standard model. Higher order radiative corrections have not been taken into account.
- 129 ABBIENDI 01o use their measurement of the τ polarization in addition to the lineshape and forward-backward lepton asymmetries.
- 130 ACCIARRI 00c use their measurement of the τ polarization in addition to forward-backward lepton asymmetries.
- 131 ABE 95j obtain this result combining polarized Bhabha results with the A_{LR} measurement of ABE 94c. The Bhabha results alone give $-0.0507 \pm 0.0096 \pm 0.0020$.

g_V^μ	VALUE	EVTS	DOCUMENT ID	TECN	COMMENT
-0.0367 ± 0.0023 OUR FIT					
-0.0388 ± 0.0060 -0.0064	182.8K	132	ABBIENDI	01o	OPAL $E_{cm}^{ee} = 88-94$ GeV
-0.0386 ± 0.0073	113.4k	133	ACCIARRI	00c	L3 $E_{cm}^{ee} = 88-94$ GeV
-0.0362 ± 0.0061			BARATE	00c	ALEP $E_{cm}^{ee} = 88-94$ GeV
• • • We do not use the following data for averages, fits, limits, etc. • • •					
-0.0413 ± 0.0060	66143	134	ABBIENDI	01k	OPAL $E_{cm}^{ee} = 89-93$ GeV

- 132 ABBIENDI 01o use their measurement of the τ polarization in addition to the lineshape and forward-backward lepton asymmetries.
- 133 ACCIARRI 00c use their measurement of the τ polarization in addition to forward-backward lepton asymmetries.
- 134 ABBIENDI 01k obtain this from an angular analysis of the muon pair asymmetry which takes into account effects of initial state radiation on an event by event basis and of initial-final state interference.

g_V^τ	VALUE	EVTS	DOCUMENT ID	TECN	COMMENT
-0.0366 ± 0.0010 OUR FIT					
-0.0365 ± 0.0023	151.5K	135	ABBIENDI	01o	OPAL $E_{cm}^{ee} = 88-94$ GeV
-0.0384 ± 0.0026	103.0k	136	ACCIARRI	00c	L3 $E_{cm}^{ee} = 88-94$ GeV
-0.0361 ± 0.0068			BARATE	00c	ALEP $E_{cm}^{ee} = 88-94$ GeV

- 135 ABBIENDI 01o use their measurement of the τ polarization in addition to the lineshape and forward-backward lepton asymmetries.
- 136 ACCIARRI 00c use their measurement of the τ polarization in addition to forward-backward lepton asymmetries.

g_V^e	VALUE	EVTS	DOCUMENT ID	TECN	COMMENT
-0.03783 ± 0.00041 OUR FIT					
-0.0358 ± 0.0014	471.3K	137	ABBIENDI	01o	OPAL $E_{cm}^{ee} = 88-94$ GeV
-0.0397 ± 0.0020	379.4k	138	ABREU	00f	DLPH $E_{cm}^{ee} = 88-94$ GeV
-0.0397 ± 0.0017	340.8k	139	ACCIARRI	00c	L3 $E_{cm}^{ee} = 88-94$ GeV
-0.0383 ± 0.0018	500k		BARATE	00c	ALEP $E_{cm}^{ee} = 88-94$ GeV

- 137 ABBIENDI 01o use their measurement of the τ polarization in addition to the lineshape and forward-backward lepton asymmetries.
- 138 Using forward-backward lepton asymmetries.
- 139 ACCIARRI 00c use their measurement of the τ polarization in addition to forward-backward lepton asymmetries.

g_V^u	VALUE	EVTS	DOCUMENT ID	TECN	COMMENT
0.29 ± 0.10 -0.08 OUR AVERAGE					
0.27 ± 0.13	1500	140	AKTAS	06	H1 $e^\pm p \rightarrow \bar{\nu}_e(\nu_e)X$, $\sqrt{s} \approx 300$ GeV
0.24 ± 0.28 -0.11		141	LEP-SLC	06	$E_{cm}^{ee} = 88-94$ GeV
0.399 ± 0.152 -0.188	5026	142	ACOSTA	05M	CDF $E_{cm}^{p\bar{p}} = 1.96$ TeV

- 140 AKTAS 06 fit the neutral current ($1.5 \leq Q^2 \leq 30,000$ GeV²) and charged current ($1.5 \leq Q^2 \leq 15,000$ GeV²) differential cross sections. In the determination of the u -quark couplings the electron and d -quark couplings are fixed to their standard model values.
- 141 LEP-SLC 06 is a combination of the results from LEP and SLC experiments using light quark tagging. s - and d -quark couplings are assumed to be identical.
- 142 ACOSTA 05M determine the forward-backward asymmetry of e^+e^- pairs produced via $q\bar{q} \rightarrow Z/\gamma^* \rightarrow e^+e^-$ in 15 M(e^+e^-) effective mass bins ranging from 40 GeV to 600 GeV. These results are used to obtain the vector and axial-vector couplings of the Z to the light quarks, assuming the electron couplings are as predicted by the Standard Model. Higher order radiative corrections have not been taken into account.

g_V^d	VALUE	EVTS	DOCUMENT ID	TECN	COMMENT
-0.33 ± 0.05 -0.07 OUR AVERAGE					
-0.33 ± 0.33	1500	143	AKTAS	06	H1 $e^\pm p \rightarrow \bar{\nu}_e(\nu_e)X$, $\sqrt{s} \approx 300$ GeV
-0.33 ± 0.05 -0.07		144	LEP-SLC	06	$E_{cm}^{ee} = 88-94$ GeV
-0.226 ± 0.635 -0.290 ± 0.090	5026	145	ACOSTA	05M	CDF $E_{cm}^{p\bar{p}} = 1.96$ TeV

- 143 AKTAS 06 fit the neutral current ($1.5 \leq Q^2 \leq 30,000$ GeV²) and charged current ($1.5 \leq Q^2 \leq 15,000$ GeV²) differential cross sections. In the determination of the d -quark couplings the electron and u -quark couplings are fixed to their standard model values.
- 144 LEP-SLC 06 is a combination of the results from LEP and SLC experiments using light quark tagging. s - and d -quark couplings are assumed to be identical.
- 145 ACOSTA 05M determine the forward-backward asymmetry of e^+e^- pairs produced via $q\bar{q} \rightarrow Z/\gamma^* \rightarrow e^+e^-$ in 15 M(e^+e^-) effective mass bins ranging from 40 GeV to 600 GeV. These results are used to obtain the vector and axial-vector couplings of the Z to the light quarks, assuming the electron couplings are as predicted by the Standard Model. Higher order radiative corrections have not been taken into account.

Z AXIAL-VECTOR COUPLINGS

These quantities are the effective axial-vector couplings of the Z to charged leptons. Their magnitude is derived from a measurement of the Z lineshape and the forward-backward lepton asymmetries as a function of energy around the Z mass. The relative sign among the vector to axial-vector couplings is obtained from a measurement of the Z asymmetry parameters, A_e , A_μ , and A_τ . By convention the sign of g_A^e is fixed to be negative (and opposite to that of g_V^e obtained using ν_e scattering measurements). For the light quarks, the sign of the couplings is assigned consistently with this assumption. The fit values quoted below correspond to global nine- or five-parameter fits to lineshape, lepton forward-backward asymmetry, and A_e , A_μ , and A_τ measurements. See the note "The Z boson" and ref. LEP-SLC 06 for details. Where $p\bar{p}$ and $e p$ data is quoted, OUR FIT value corresponds to a weighted average of this with the LEP/SLD fit result.

g_A^e	VALUE	EVTS	DOCUMENT ID	TECN	COMMENT
-0.50111 ± 0.00035 OUR FIT					
$-0.528 \pm 0.123 \pm 0.059$	5026	146	ACOSTA	05M	CDF $E_{cm}^{p\bar{p}} = 1.96$ TeV
-0.50062 ± 0.00062	137.0K	147	ABBIENDI	01o	OPAL $E_{cm}^{ee} = 88-94$ GeV
-0.5015 ± 0.0007	124.4k	148	ACCIARRI	00c	L3 $E_{cm}^{ee} = 88-94$ GeV
-0.50166 ± 0.00057			BARATE	00c	ALEP $E_{cm}^{ee} = 88-94$ GeV
-0.4977 ± 0.0045		149	ABE	95j	SLD $E_{cm}^{ee} = 91.31$ GeV

- 146 ACOSTA 05M determine the forward-backward asymmetry of e^+e^- pairs produced via $q\bar{q} \rightarrow Z/\gamma^* \rightarrow e^+e^-$ in 15 M(e^+e^-) effective mass bins ranging from 40 GeV to 600 GeV. These results are used to obtain the vector and axial-vector couplings of the Z to e^+e^- , assuming the quark couplings are as predicted by the standard model. Higher order radiative corrections have not been taken into account.
- 147 ABBIENDI 01o use their measurement of the τ polarization in addition to the lineshape and forward-backward lepton asymmetries.
- 148 ACCIARRI 00c use their measurement of the τ polarization in addition to forward-backward lepton asymmetries.
- 149 ABE 95j obtain this result combining polarized Bhabha results with the A_{LR} measurement of ABE 94c. The Bhabha results alone give $-0.4968 \pm 0.0039 \pm 0.0027$.

g_A^μ	VALUE	EVTS	DOCUMENT ID	TECN	COMMENT
-0.50120 ± 0.00054 OUR FIT					
-0.50117 ± 0.00099	182.8K	150	ABBIENDI	01o	OPAL $E_{cm}^{ee} = 88-94$ GeV
-0.5009 ± 0.0014	113.4k	151	ACCIARRI	00c	L3 $E_{cm}^{ee} = 88-94$ GeV
-0.50046 ± 0.00093			BARATE	00c	ALEP $E_{cm}^{ee} = 88-94$ GeV
• • • We do not use the following data for averages, fits, limits, etc. • • •					
-0.520 ± 0.015	66143	152	ABBIENDI	01k	OPAL $E_{cm}^{ee} = 89-93$ GeV

- 150 ABBIENDI 01o use their measurement of the τ polarization in addition to the lineshape and forward-backward lepton asymmetries.
- 151 ACCIARRI 00c use their measurement of the τ polarization in addition to forward-backward lepton asymmetries.
- 152 ABBIENDI 01k obtain this from an angular analysis of the muon pair asymmetry which takes into account effects of initial state radiation on an event by event basis and of initial-final state interference.

Gauge & Higgs Boson Particle Listings

Z

g_A^{τ}	VALUE	EVTS	DOCUMENT ID	TECN	COMMENT
-0.50204 ± 0.00064 OUR FIT					
-0.50165 ± 0.00124	151.5K	153	ABBIENDI	01o	OPAL $E_{cm}^{ee} = 88-94$ GeV
-0.5023 ± 0.0017	103.0k	154	ACCIARRI	00c	L3 $E_{cm}^{ee} = 88-94$ GeV
-0.50216 ± 0.00100			BARATE	00c	ALEP $E_{cm}^{ee} = 88-94$ GeV

153 ABBIENDI 01o use their measurement of the τ polarization in addition to the lineshape and forward-backward lepton asymmetries.

154 ACCIARRI 00c use their measurement of the τ polarization in addition to forward-backward lepton asymmetries.

g_A^e	VALUE	EVTS	DOCUMENT ID	TECN	COMMENT
-0.50123 ± 0.00026 OUR FIT					
-0.50089 ± 0.00045	471.3K	155	ABBIENDI	01o	OPAL $E_{cm}^{ee} = 88-94$ GeV
-0.5007 ± 0.0005	379.4k		ABREU	00F	DLPH $E_{cm}^{ee} = 88-94$ GeV
-0.50153 ± 0.00053	340.8k	156	ACCIARRI	00c	L3 $E_{cm}^{ee} = 88-94$ GeV
-0.50150 ± 0.00046	500k		BARATE	00c	ALEP $E_{cm}^{ee} = 88-94$ GeV

155 ABBIENDI 01o use their measurement of the τ polarization in addition to the lineshape and forward-backward lepton asymmetries.

156 ACCIARRI 00c use their measurement of the τ polarization in addition to forward-backward lepton asymmetries.

g_A^u	VALUE	EVTS	DOCUMENT ID	TECN	COMMENT
0.50 ± 0.04 OUR AVERAGE					
0.57 ± 0.07	1500	157	AKTAS	06	H1 $e^{\pm} p \rightarrow \bar{\nu}_e(\nu_e) X$, $\sqrt{s} \approx 300$ GeV
0.47 ± 0.05 -0.33		158	LEP-SLC	06	$E_{cm}^{ee} = 88-94$ GeV
0.441 ± 0.207 -0.173	5026	159	ACOSTA	05M	CDF $E_{cm}^{pp} = 1.96$ TeV

157 AKTAS 06 fit the neutral current ($1.5 \leq Q^2 \leq 30,000$ GeV²) and charged current ($1.5 \leq Q^2 \leq 15,000$ GeV²) differential cross sections. In the determination of the u -quark couplings the electron and d -quark couplings are fixed to their standard model values.

158 LEP-SLC 06 is a combination of the results from LEP and SLC experiments using light quark tagging. s - and d -quark couplings are assumed to be identical.

159 ACOSTA 05M determine the forward-backward asymmetry of e^+e^- pairs produced via $q\bar{q} \rightarrow Z/\gamma^* \rightarrow e^+e^-$ in 15 M(e^+e^-) effective mass bins ranging from 40 GeV to 600 GeV. These results are used to obtain the vector and axial-vector couplings of the Z to the light quarks, assuming the electron couplings are as predicted by the Standard Model. Higher order radiative corrections have not been taken into account.

g_A^d	VALUE	EVTS	DOCUMENT ID	TECN	COMMENT
-0.524 ± 0.050 OUR AVERAGE					
-0.80 ± 0.24	1500	160	AKTAS	06	H1 $e^{\pm} p \rightarrow \bar{\nu}_e(\nu_e) X$, $\sqrt{s} \approx 300$ GeV
-0.52 ± 0.05 -0.03		161	LEP-SLC	06	$E_{cm}^{ee} = 88-94$ GeV
-0.016 ± 0.346 -0.536	5026	162	ACOSTA	05M	CDF $E_{cm}^{pp} = 1.96$ TeV

160 AKTAS 06 fit the neutral current ($1.5 \leq Q^2 \leq 30,000$ GeV²) and charged current ($1.5 \leq Q^2 \leq 15,000$ GeV²) differential cross sections. In the determination of the d -quark couplings the electron and u -quark couplings are fixed to their standard model values.

161 LEP-SLC 06 is a combination of the results from LEP and SLC experiments using light quark tagging. s - and d -quark couplings are assumed to be identical.

162 ACOSTA 05M determine the forward-backward asymmetry of e^+e^- pairs produced via $q\bar{q} \rightarrow Z/\gamma^* \rightarrow e^+e^-$ in 15 M(e^+e^-) effective mass bins ranging from 40 GeV to 600 GeV. These results are used to obtain the vector and axial-vector couplings of the Z to the light quarks, assuming the electron couplings are as predicted by the Standard Model. Higher order radiative corrections have not been taken into account.

Z COUPLINGS TO NEUTRAL LEPTONS

Averaging over neutrino species, the invisible Z decay width determines the effective neutrino coupling $g^{\nu e}$. For $g^{\nu e}$ and $g^{\nu \mu}$, $\nu_e e$ and $\nu_\mu e$ scattering results are combined with g_A^e and g_V^e measurements at the Z mass to obtain $g^{\nu e}$ and $g^{\nu \mu}$ following NOVIKOV 93c.

$g^{\nu e}$	VALUE	DOCUMENT ID	TECN	COMMENT
0.50076 ± 0.00076	163	LEP-SLC	06	$E_{cm}^{ee} = 88-94$ GeV

163 From invisible Z-decay width.

$g^{\nu \mu}$	VALUE	DOCUMENT ID	TECN	COMMENT
0.528 ± 0.085	164	VILAIN	94	CHM2 From $\nu_\mu e$ and $\nu_e e$ scattering

164 VILAIN 94 derive this value from their value of $g^{\nu \mu}$ and their ratio $g^{\nu e}/g^{\nu \mu} = 1.05 \pm 0.15$
 -0.18 .

$g^{\nu \mu}$	VALUE	DOCUMENT ID	TECN	COMMENT
0.502 ± 0.017	165	VILAIN	94	CHM2 From $\nu_\mu e$ scattering

165 VILAIN 94 derive this value from their measurement of the couplings $g_A^{\nu \mu} = -0.503 \pm 0.017$ and $g_V^{\nu \mu} = -0.035 \pm 0.017$ obtained from $\nu_\mu e$ scattering. We have re-evaluated this value using the current PDG values for g_A^e and g_V^e .

Z ASYMMETRY PARAMETERS

For each fermion-antifermion pair coupling to the Z these quantities are defined as

$$A_f = \frac{2g_V^f g_A^f}{(g_V^f)^2 + (g_A^f)^2}$$

where g_V^f and g_A^f are the effective vector and axial-vector couplings. For their relation to the various lepton asymmetries see the note "The Z boson" and ref. LEP-SLC 06.

 A_e

Using polarized beams, this quantity can also be measured as $(\sigma_L - \sigma_R)/(\sigma_L + \sigma_R)$, where σ_L and σ_R are the e^+e^- production cross sections for Z bosons produced with left-handed and right-handed electrons respectively.

A_e	VALUE	EVTS	DOCUMENT ID	TECN	COMMENT
0.1515 ± 0.0019 OUR AVERAGE					
$0.1454 \pm 0.0108 \pm 0.0036$	144810	166	ABBIENDI	01o	OPAL $E_{cm}^{ee} = 88-94$ GeV
0.1516 ± 0.0021	559000	167	ABE	01B	SLD $E_{cm}^{ee} = 91.24$ GeV
$0.1504 \pm 0.0068 \pm 0.0008$		168	HEISTER	01	ALEP $E_{cm}^{ee} = 88-94$ GeV
$0.1382 \pm 0.0116 \pm 0.0005$	105000	169	ABREU	00E	DLPH $E_{cm}^{ee} = 88-94$ GeV
$0.1678 \pm 0.0127 \pm 0.0030$	137092	170	ACCIARRI	98H	L3 $E_{cm}^{ee} = 88-94$ GeV
$0.162 \pm 0.041 \pm 0.014$	89838	171	ABE	97	SLD $E_{cm}^{ee} = 91.27$ GeV
$0.202 \pm 0.038 \pm 0.008$		172	ABE	95J	SLD $E_{cm}^{ee} = 91.31$ GeV

166 ABBIENDI 01o fit for A_e and A_τ from measurements of the τ polarization at varying τ production angles. The correlation between A_e and A_τ is less than 0.03.

167 ABE 01B use the left-right production and left-right forward-backward decay asymmetries in leptonic Z decays to obtain a value of 0.1544 ± 0.0060 . This is combined with left-right production asymmetry measurement using hadronic Z decays (ABE 00B) to obtain the quoted value.

168 HEISTER 01 obtain this result fitting the τ polarization as a function of the polar production angle of the τ .

169 ABREU 00E obtain this result fitting the τ polarization as a function of the polar τ production angle. This measurement is a combination of different analyses (exclusive τ decay modes, inclusive hadronic 1-prong reconstruction, and a neural network analysis).

170 Derived from the measurement of forward-backward τ polarization asymmetry.

171 ABE 97 obtain this result from a measurement of the observed left-right charge asymmetry, $A_Q^{\text{obs}} = 0.225 \pm 0.056 \pm 0.019$, in hadronic Z decays. If they combine this value of A_Q^{obs} with their earlier measurement of A_{LR}^{obs} they determine A_e to be $0.1574 \pm 0.0197 \pm 0.0067$ independent of the beam polarization.

172 ABE 95J obtain this result from polarized Bhabha scattering.

 A_μ

This quantity is directly extracted from a measurement of the left-right forward-backward asymmetry in $\mu^+\mu^-$ production at SLC using a polarized electron beam. This double asymmetry eliminates the dependence on the Z- e - e coupling parameter A_e .

A_μ	VALUE	EVTS	DOCUMENT ID	TECN	COMMENT
0.142 ± 0.015	16844	173	ABE	01B	SLD $E_{cm}^{ee} = 91.24$ GeV

173 ABE 01B obtain this direct measurement using the left-right production and left-right forward-backward polar angle asymmetries in $\mu^+\mu^-$ decays of the Z boson obtained with a polarized electron beam.

 A_τ

The LEP Collaborations derive this quantity from the measurement of the τ polarization in $Z \rightarrow \tau^+\tau^-$. The SLD Collaboration directly extracts this quantity from its measured left-right forward-backward asymmetry in $Z \rightarrow \tau^+\tau^-$ produced using a polarized e^- beam. This double asymmetry eliminates the dependence on the Z- e - e coupling parameter A_e .

A_τ	VALUE	EVTS	DOCUMENT ID	TECN	COMMENT
0.143 ± 0.004 OUR AVERAGE					
$0.1456 \pm 0.0076 \pm 0.0057$	144810	174	ABBIENDI	01o	OPAL $E_{cm}^{ee} = 88-94$ GeV
0.136 ± 0.015	16083	175	ABE	01B	SLD $E_{cm}^{ee} = 91.24$ GeV
$0.1451 \pm 0.0052 \pm 0.0029$		176	HEISTER	01	ALEP $E_{cm}^{ee} = 88-94$ GeV
$0.1359 \pm 0.0079 \pm 0.0055$	105000	177	ABREU	00E	DLPH $E_{cm}^{ee} = 88-94$ GeV
$0.1476 \pm 0.0088 \pm 0.0062$	137092		ACCIARRI	98H	L3 $E_{cm}^{ee} = 88-94$ GeV

174 ABBIENDI 01o fit for A_e and A_τ from measurements of the τ polarization at varying τ production angles. The correlation between A_e and A_τ is less than 0.03.

175 ABE 01B obtain this direct measurement using the left-right production and left-right forward-backward polar angle asymmetries in $\tau^+\tau^-$ decays of the Z boson obtained with a polarized electron beam.

176 HEISTER 01 obtain this result fitting the τ polarization as a function of the polar production angle of the τ .

177 ABREU 00E obtain this result fitting the τ polarization as a function of the polar τ production angle. This measurement is a combination of different analyses (exclusive τ decay modes, inclusive hadronic 1-prong reconstruction, and a neural network analysis).

A_S

The SLD Collaboration directly extracts this quantity by a simultaneous fit to four measured s -quark polar angle distributions corresponding to two states of e^- polarization (positive and negative) and to the $K^+ K^-$ and $K^\pm K_S^0$ strange particle tagging modes in the hadronic final states.

VALUE	EVTS	DOCUMENT ID	TECN	COMMENT
0.895 ± 0.066 ± 0.062	2870	178 ABE	00D	SLD $E_{\text{cm}}^e = 91.2$ GeV
178 ABE	00D	tag $Z \rightarrow s\bar{s}$ events by an absence of B or D hadrons and the presence in each hemisphere of a high momentum K^\pm or K_S^0 .		

A_C

This quantity is directly extracted from a measurement of the left-right forward-backward asymmetry in $c\bar{c}$ production at SLC using polarized electron beam. This double asymmetry eliminates the dependence on the Z - e - e coupling parameter A_e . OUR FIT is obtained by a simultaneous fit to several c - and b -quark measurements as explained in the note "The Z boson" and ref. LEP-SLC 06.

VALUE	EVTS	DOCUMENT ID	TECN	COMMENT
0.670 ± 0.027 OUR FIT				
0.6712 ± 0.0224 ± 0.0157	179	ABE	05	SLD $E_{\text{cm}}^e = 91.24$ GeV
• • • We do not use the following data for averages, fits, limits, etc. • • •				
0.583 ± 0.055 ± 0.055	180	ABE	02G	SLD $E_{\text{cm}}^e = 91.24$ GeV
0.688 ± 0.041	181	ABE	01c	SLD $E_{\text{cm}}^e = 91.25$ GeV

179 ABE 05 use hadronic Z decays collected during 1996–98 to obtain an enriched sample of $c\bar{c}$ events tagging on the invariant mass of reconstructed secondary decay vertices. The charge of the underlying c -quark is obtained with an algorithm that takes into account the net charge of the vertex as well as the charge of tracks emanating from the vertex and identified as kaons. This yields (9970 events) $A_C = 0.6747 \pm 0.0290 \pm 0.0233$. Taking into account all correlations with earlier results reported in ABE 02G and ABE 01c, they obtain the quoted overall SLD result.

180 ABE 02g tag b and c quarks through their semileptonic decays into electrons and muons. A maximum likelihood fit is performed to extract simultaneously A_b and A_c .

181 ABE 01c tag $Z \rightarrow c\bar{c}$ events using two techniques: exclusive reconstruction of D^{*+}, D^+ and D^0 mesons and the soft pion tag for $D^{*+} \rightarrow D^0 \pi^+$. The large background from D mesons produced in $b\bar{b}$ events is separated efficiently from the signal using precision vertex information. When combining the A_C values from these two samples, care is taken to avoid double counting of events common to the two samples, and common systematic errors are properly taken into account.

A_b

This quantity is directly extracted from a measurement of the left-right forward-backward asymmetry in $b\bar{b}$ production at SLC using polarized electron beam. This double asymmetry eliminates the dependence on the Z - e - e coupling parameter A_e . OUR FIT is obtained by a simultaneous fit to several c - and b -quark measurements as explained in the note "The Z boson" and ref. LEP-SLC 06.

VALUE	EVTS	DOCUMENT ID	TECN	COMMENT
0.923 ± 0.020 OUR FIT				
0.9170 ± 0.0147 ± 0.0145	182	ABE	05	SLD $E_{\text{cm}}^e = 91.24$ GeV
• • • We do not use the following data for averages, fits, limits, etc. • • •				
0.907 ± 0.020 ± 0.024	48028	183 ABE	03F	SLD $E_{\text{cm}}^e = 91.24$ GeV
0.919 ± 0.030 ± 0.024	184	ABE	02G	SLD $E_{\text{cm}}^e = 91.24$ GeV
0.855 ± 0.088 ± 0.102	7473	185 ABE	99L	SLD $E_{\text{cm}}^e = 91.27$ GeV

182 ABE 05 use hadronic Z decays collected during 1996–98 to obtain an enriched sample of $b\bar{b}$ events tagging on the invariant mass of reconstructed secondary decay vertices. The charge of the underlying b -quark is obtained with an algorithm that takes into account the net charge of the vertex as well as the charge of tracks emanating from the vertex and identified as kaons. This yields (25917 events) $A_b = 0.9173 \pm 0.0184 \pm 0.0173$. Taking into account all correlations with earlier results reported in ABE 03F, ABE 02G and ABE 99L, they obtain the quoted overall SLD result.

183 ABE 03F obtain an enriched sample of $b\bar{b}$ events tagging on the invariant mass of a 3-dimensional topologically reconstructed secondary decay. The charge of the underlying b quark is obtained using a self-calibrating track-charge method. For the 1996–1998 data sample they measure $A_b = 0.906 \pm 0.022 \pm 0.023$. The value quoted here is obtained combining the above with the result of ABE 981 (1993–1995 data sample).

184 ABE 02g tag b and c quarks through their semileptonic decays into electrons and muons. A maximum likelihood fit is performed to extract simultaneously A_b and A_c .

185 ABE 99L obtain an enriched sample of $b\bar{b}$ events tagging with an inclusive vertex mass cut. For distinguishing b and \bar{b} quarks they use the charge of identified K^\pm .

TRANSVERSE SPIN CORRELATIONS IN $Z \rightarrow \tau^+ \tau^-$

The correlations between the transverse spin components of $\tau^+ \tau^-$ produced in Z decays may be expressed in terms of the vector and axial-vector couplings:

$$C_{TT} = \frac{|g_A^\tau|^2 - |g_V^\tau|^2}{|g_A^\tau|^2 + |g_V^\tau|^2}$$

$$C_{TN} = -2 \frac{|g_A^\tau| |g_V^\tau|}{|g_A^\tau|^2 + |g_V^\tau|^2} \sin(\Phi_{g_V^\tau} - \Phi_{g_A^\tau})$$

C_{TT} refers to the transverse-transverse (within the collision plane) spin correlation and C_{TN} refers to the transverse-normal (to the collision plane) spin correlation.

The longitudinal τ polarization $P_\tau (= -A_\tau)$ is given by:

$$P_\tau = -2 \frac{|g_A^\tau| |g_V^\tau|}{|g_A^\tau|^2 + |g_V^\tau|^2} \cos(\Phi_{g_V^\tau} - \Phi_{g_A^\tau})$$

Here Φ is the phase and the phase difference $\Phi_{g_V^\tau} - \Phi_{g_A^\tau}$ can be obtained using both the measurements of C_{TN} and P_τ .

C_{TT}

VALUE	EVTS	DOCUMENT ID	TECN	COMMENT
1.01 ± 0.12 OUR AVERAGE				
0.87 ± 0.20 ^{+0.10} _{-0.12}	9.1k	ABREU	97G	DLPH $E_{\text{cm}}^e = 91.2$ GeV
1.06 ± 0.13 ± 0.05	120k	BARATE	97D	ALEP $E_{\text{cm}}^e = 91.2$ GeV

C_{TN}

VALUE	EVTS	DOCUMENT ID	TECN	COMMENT
0.08 ± 0.13 ± 0.04	120k	186 BARATE	97D	ALEP $E_{\text{cm}}^e = 91.2$ GeV
186 BARATE 97D combine their value of C_{TN} with the world average $P_\tau = -0.140 \pm 0.007$ to obtain $\tan(\Phi_{g_V^\tau} - \Phi_{g_A^\tau}) = -0.57 \pm 0.97$.				

FORWARD-BACKWARD $e^+ e^- \rightarrow f\bar{f}$ CHARGE ASYMMETRIES

These asymmetries are experimentally determined by tagging the respective lepton or quark flavor in $e^+ e^-$ interactions. Details of heavy flavor (c - or b -quark) tagging at LEP are described in the note on "The Z boson" and ref. LEP-SLC 06. The Standard Model predictions for LEP data have been (re)computed using the ZFITTER package (version 6.36) with input parameters $M_Z = 91.187$ GeV, $M_{\text{top}} = 174.3$ GeV, $M_{\text{Higgs}} = 150$ GeV, $\alpha_s = 0.119$, $\alpha^{(5)}(M_Z) = 1/128.877$ and the Fermi constant $G_F = 1.16637 \times 10^{-5} \text{ GeV}^{-2}$ (see the note on "The Z boson" for references). For non-LEP data the Standard Model predictions are as given by the authors of the respective publications.

 $A_{FB}^{(0,e)}$ CHARGE ASYMMETRY IN $e^+ e^- \rightarrow e^+ e^-$

OUR FIT is obtained using the fit procedure and correlations as determined by the LEP Electroweak Working Group (see the note "The Z boson" and ref. LEP-SLC 06). For the Z peak, we report the pole asymmetry defined by $(3/4)A_e^2$ as determined by the nine-parameter fit to cross-section and lepton forward-backward asymmetry data.

ASYMMETRY (%)	STD. MODEL	\sqrt{s} (GeV)	DOCUMENT ID	TECN
1.45 ± 0.25 OUR FIT				
0.89 ± 0.44	1.57	91.2	187 ABBIENDI	01A OPAL
1.71 ± 0.49	1.57	91.2	ABREU	00F DLPH
1.06 ± 0.58	1.57	91.2	ACCIARRI	00c L3
1.88 ± 0.34	1.57	91.2	188 BARATE	00c ALEP

187 ABBIENDI 01A error includes approximately 0.38 due to statistics, 0.16 due to event selection systematics, and 0.18 due to the theoretical uncertainty in t -channel prediction.

188 BARATE 00c error includes approximately 0.31 due to statistics, 0.06 due to experimental systematics, and 0.13 due to the theoretical uncertainty in t -channel prediction.

 $A_{FB}^{(0,\mu)}$ CHARGE ASYMMETRY IN $e^+ e^- \rightarrow \mu^+ \mu^-$

OUR FIT is obtained using the fit procedure and correlations as determined by the LEP Electroweak Working Group (see the note "The Z boson" and ref. LEP-SLC 06). For the Z peak, we report the pole asymmetry defined by $(3/4)A_e A_\mu$ as determined by the nine-parameter fit to cross-section and lepton forward-backward asymmetry data.

ASYMMETRY (%)	STD. MODEL	\sqrt{s} (GeV)	DOCUMENT ID	TECN
1.69 ± 0.13 OUR FIT				
1.59 ± 0.23	1.57	91.2	189 ABBIENDI	01A OPAL
1.65 ± 0.25	1.57	91.2	ABREU	00F DLPH
1.88 ± 0.33	1.57	91.2	ACCIARRI	00c L3
1.71 ± 0.24	1.57	91.2	190 BARATE	00c ALEP

• • • We do not use the following data for averages, fits, limits, etc. • • •

9 ± 30	-1.3	20	191 ABREU	95M DLPH
7 ± 26	-8.3	40	191 ABREU	95M DLPH
-11 ± 33	-24.1	57	191 ABREU	95M DLPH
-62 ± 17	-44.6	69	191 ABREU	95M DLPH
-56 ± 10	-63.5	79	191 ABREU	95M DLPH
-13 ± 5	-34.4	87.5	191 ABREU	95M DLPH
-29.0 ± 5.0	-32.1	56.9	192 ABE	90i VNS
- 9.9 ± 1.5 ± 0.5	-9.2	35	HEGNER	90 JADE
0.05 ± 0.22	0.026	91.14	193 ABRAMS	89D MRK2
-43.4 ± 17.0	-24.9	52.0	194 BACALA	89 AMY
-11.0 ± 16.5	-29.4	55.0	194 BACALA	89 AMY
-30.0 ± 12.4	-31.2	56.0	194 BACALA	89 AMY
-46.2 ± 14.9	-33.0	57.0	194 BACALA	89 AMY
-29 ± 13	-25.9	53.3	ADA CHI	88c TOPZ
+ 5.3 ± 5.0 ± 0.5	-1.2	14.0	ADEVA	88 MRKJ
-10.4 ± 1.3 ± 0.5	-8.6	34.8	ADEVA	88 MRKJ
-12.3 ± 5.3 ± 0.5	-10.7	38.3	ADEVA	88 MRKJ
-15.6 ± 3.0 ± 0.5	-14.9	43.8	ADEVA	88 MRKJ

Gauge & Higgs Boson Particle Listings

Z

-1.0 ± 6.0	-1.2	13.9	BRAUNSCH...	88D	TASS
-9.1 ± 2.3 ± 0.5	-8.6	34.5	BRAUNSCH...	88D	TASS
-10.6 ± 2.2 ± 0.5	-8.9	35.0	BRAUNSCH...	88D	TASS
-17.6 ± 4.4 ± 0.5	-15.2	43.6	BRAUNSCH...	88D	TASS
-4.8 ± 6.5 ± 1.0	-11.5	39	BEHREND	87C	CELL
-18.8 ± 4.5 ± 1.0	-15.5	44	BEHREND	87C	CELL
+2.7 ± 4.9	-1.2	13.9	BARTEL	86C	JADE
-11.1 ± 1.8 ± 1.0	-8.6	34.4	BARTEL	86C	JADE
-17.3 ± 4.8 ± 1.0	-13.7	41.5	BARTEL	86C	JADE
-22.8 ± 5.1 ± 1.0	-16.6	44.8	BARTEL	86C	JADE
-6.3 ± 0.8 ± 0.2	-6.3	29	ASH	85	MAC
-4.9 ± 1.5 ± 0.5	-5.9	29	DERRICK	85	HRS
-7.1 ± 1.7	-5.7	29	LEVI	83	MRK2
-16.1 ± 3.2	-9.2	34.2	BRANDELIK	82C	TASS

- 189 ABBIENDI 01A error is almost entirely on account of statistics.
 190 BARATE 00C error is almost entirely on account of statistics.
 191 ABREU 95M perform this measurement using radiative muon-pair events associated with high-energy isolated photons.
 192 ABE 90I measurements in the range $50 \leq \sqrt{s} \leq 60.8$ GeV.
 193 ABRAMS 89D asymmetry includes both $9 \mu^+ \mu^-$ and $15 \tau^+ \tau^-$ events.
 194 BACALA 89 systematic error is about 5%.

$A_{FB}^{(0,\tau)}$ CHARGE ASYMMETRY IN $e^+ e^- \rightarrow \tau^+ \tau^-$

OUR FIT is obtained using the fit procedure and correlations as determined by the LEP Electroweak Working Group (see the note "The Z boson" and ref. LEP-SLC 06). For the Z peak, we report the pole asymmetry defined by $(3/4)A_e A_\tau$ as determined by the nine-parameter fit to cross-section and lepton forward-backward asymmetry data.

ASYMMETRY (%)	STD. MODEL	\sqrt{s} (GeV)	DOCUMENT ID	TECN
1.88 ± 0.17 OUR FIT				
1.45 ± 0.30	1.57	91.2	195 ABBIENDI 01A	OPAL
2.41 ± 0.37	1.57	91.2	ABREU 00F	DLPH
2.60 ± 0.47	1.57	91.2	ACCIARRI 00C	L3
1.70 ± 0.28	1.57	91.2	196 BARATE 00C	ALEP

- We do not use the following data for averages, fits, limits, etc. •••
- | | | | | | |
|-------------------|--------|------|------------|-----|------|
| -32.8 ± 6.4 ± 1.5 | -32.1 | 56.9 | 197 ABE | 90I | VNS |
| -8.1 ± 2.0 ± 0.6 | -9.2 | 35 | HEGNER | 90 | JADE |
| -18.4 ± 19.2 | -24.9 | 52.0 | 198 BACALA | 89 | AMY |
| -17.7 ± 26.1 | -29.4 | 55.0 | 198 BACALA | 89 | AMY |
| -45.9 ± 16.6 | -31.2 | 56.0 | 198 BACALA | 89 | AMY |
| -49.5 ± 18.0 | -33.0 | 57.0 | 198 BACALA | 89 | AMY |
| -20 ± 14 | -25.9 | 53.3 | ADACHI | 88C | TOPZ |
| -10.6 ± 3.1 ± 1.5 | -8.5 | 34.7 | ADEVA | 88 | MRKJ |
| -8.5 ± 6.6 ± 1.5 | -15.4 | 43.8 | ADEVA | 88 | MRKJ |
| -6.0 ± 2.5 ± 1.0 | 8.8 | 34.6 | BARTEL | 85F | JADE |
| -11.8 ± 4.6 ± 1.0 | 14.8 | 43.0 | BARTEL | 85F | JADE |
| -5.5 ± 1.2 ± 0.5 | -0.063 | 29.0 | FERNANDEZ | 85 | MAC |
| -4.2 ± 2.0 | 0.057 | 29 | LEVI | 83 | MRK2 |
| -10.3 ± 5.2 | -9.2 | 34.2 | BEHREND | 82 | CELL |
| -0.4 ± 6.6 | -9.1 | 34.2 | BRANDELIK | 82C | TASS |
- 195 ABBIENDI 01A error includes approximately 0.26 due to statistics and 0.14 due to event selection systematics.
 196 BARATE 00C error includes approximately 0.26 due to statistics and 0.11 due to experimental systematics.
 197 ABE 90I measurements in the range $50 \leq \sqrt{s} \leq 60.8$ GeV.
 198 BACALA 89 systematic error is about 5%.

$A_{FB}^{(0,\ell)}$ CHARGE ASYMMETRY IN $e^+ e^- \rightarrow \ell^+ \ell^-$

For the Z peak, we report the pole asymmetry defined by $(3/4)A_\ell^2$ as determined by the five-parameter fit to cross-section and lepton forward-backward asymmetry data assuming lepton universality. For details see the note "The Z boson" and ref. LEP-SLC 06.

ASYMMETRY (%)	STD. MODEL	\sqrt{s} (GeV)	DOCUMENT ID	TECN
1.71 ± 0.10 OUR FIT				
1.45 ± 0.17	1.57	91.2	199 ABBIENDI 01A	OPAL
1.87 ± 0.19	1.57	91.2	ABREU 00F	DLPH
1.92 ± 0.24	1.57	91.2	ACCIARRI 00C	L3
1.73 ± 0.16	1.57	91.2	200 BARATE 00C	ALEP

- 199 ABBIENDI 01A error includes approximately 0.15 due to statistics, 0.06 due to event selection systematics, and 0.03 due to the theoretical uncertainty in t-channel prediction.
 200 BARATE 00C error includes approximately 0.15 due to statistics, 0.04 due to experimental systematics, and 0.02 due to the theoretical uncertainty in t-channel prediction.

$A_{FB}^{(0,u)}$ CHARGE ASYMMETRY IN $e^+ e^- \rightarrow u \bar{u}$

ASYMMETRY (%)	STD. MODEL	\sqrt{s} (GeV)	DOCUMENT ID	TECN
4.0 ± 6.7 ± 2.8	7.2	91.2	201 ACKERSTAFF 97T	OPAL

- 201 ACKERSTAFF 97T measure the forward-backward asymmetry of various fast hadrons made of light quarks. Then using SU(2) isospin symmetry and flavor independence for down and strange quarks authors solve for the different quark types.

$A_{FB}^{(0,s)}$ CHARGE ASYMMETRY IN $e^+ e^- \rightarrow s \bar{s}$

The s-quark asymmetry is derived from measurements of the forward-backward asymmetry of fast hadrons containing an s quark.

ASYMMETRY (%)	STD. MODEL	\sqrt{s} (GeV)	DOCUMENT ID	TECN
9.8 ± 1.1 OUR AVERAGE				
10.08 ± 1.13 ± 0.40	10.1	91.2	202 ABREU 00B	DLPH
6.8 ± 3.5 ± 1.1	10.1	91.2	203 ACKERSTAFF 97T	OPAL

- 202 ABREU 00B tag the presence of an s quark requiring a high-momentum-identified charged kaon. The s-quark pole asymmetry is extracted from the charged-kaon asymmetry taking the expected d- and u-quark asymmetries from the Standard Model and using the measured values for the c- and b-quark asymmetries.
 203 ACKERSTAFF 97T measure the forward-backward asymmetry of various fast hadrons made of light quarks. Then using SU(2) isospin symmetry and flavor independence for down and strange quarks authors solve for the different quark types. The value reported here corresponds then to the forward-backward asymmetry for "down-type" quarks.

$A_{FB}^{(0,c)}$ CHARGE ASYMMETRY IN $e^+ e^- \rightarrow c \bar{c}$

OUR FIT, which is obtained by a simultaneous fit to several c- and b-quark measurements as explained in the note "The Z boson" and ref. LEP-SLC 06, refers to the Z pole asymmetry. The experimental values, on the other hand, correspond to the measurements carried out at the respective energies.

ASYMMETRY (%)	STD. MODEL	\sqrt{s} (GeV)	DOCUMENT ID	TECN
7.07 ± 0.35 OUR FIT				
6.31 ± 0.93 ± 0.65	6.35	91.26	204 ABDALLAH 04F	DLPH
5.68 ± 0.54 ± 0.39	6.3	91.25	205 ABBIENDI 03P	OPAL
6.45 ± 0.57 ± 0.37	6.10	91.21	206 HEISTER 02H	ALEP
6.59 ± 0.94 ± 0.35	6.2	91.235	207 ABREU 99Y	DLPH
6.3 ± 0.9 ± 0.3	6.1	91.22	208 BARATE 98A	ALEP
6.3 ± 1.2 ± 0.6	6.1	91.22	209 ALEXANDER 97C	OPAL
8.3 ± 3.8 ± 2.7	6.2	91.24	210 ADRIANI 92D	L3

- We do not use the following data for averages, fits, limits, etc. •••
- | | | | | |
|---------------------|-------|--------|-------------------|------|
| 3.1 ± 3.5 ± 0.5 | -3.5 | 89.43 | 204 ABDALLAH 04F | DLPH |
| 11.0 ± 2.8 ± 0.7 | 12.3 | 92.99 | 204 ABDALLAH 04F | DLPH |
| -6.8 ± 2.5 ± 0.9 | -3.0 | 89.51 | 205 ABBIENDI 03P | OPAL |
| 14.6 ± 2.0 ± 0.8 | 12.2 | 92.95 | 205 ABBIENDI 03P | OPAL |
| -12.4 ± 15.9 ± 2.0 | -9.6 | 88.38 | 206 HEISTER 02H | ALEP |
| -2.3 ± 2.6 ± 0.2 | -3.8 | 89.38 | 206 HEISTER 02H | ALEP |
| -0.3 ± 8.3 ± 0.6 | 0.9 | 90.21 | 206 HEISTER 02H | ALEP |
| 10.6 ± 7.7 ± 0.7 | 9.6 | 92.05 | 206 HEISTER 02H | ALEP |
| 11.9 ± 2.1 ± 0.6 | 12.2 | 92.94 | 206 HEISTER 02H | ALEP |
| 12.1 ± 11.0 ± 1.0 | 14.2 | 93.90 | 206 HEISTER 02H | ALEP |
| -4.96 ± 3.68 ± 0.53 | -3.5 | 89.434 | 207 ABREU 99Y | DLPH |
| 11.80 ± 3.18 ± 0.62 | 12.3 | 92.990 | 207 ABREU 99Y | DLPH |
| -1.0 ± 4.3 ± 1.0 | -3.9 | 89.37 | 208 BARATE 98A | ALEP |
| 11.0 ± 3.3 ± 0.8 | 12.3 | 92.96 | 208 BARATE 98A | ALEP |
| 3.9 ± 5.1 ± 0.9 | -3.4 | 89.45 | 209 ALEXANDER 97C | OPAL |
| 15.8 ± 4.1 ± 1.1 | 12.4 | 93.00 | 209 ALEXANDER 97C | OPAL |
| -12.9 ± 7.8 ± 5.5 | -13.6 | 35 | BEHREND 90D | CELL |
| 7.7 ± 13.4 ± 5.0 | -22.1 | 43 | BEHREND 90D | CELL |
| -12.8 ± 4.4 ± 4.1 | -13.6 | 35 | ELSEN 90 | JADE |
| -10.9 ± 12.9 ± 4.6 | -23.2 | 44 | ELSEN 90 | JADE |
| -14.9 ± 6.7 | -13.3 | 35 | OULD-SAADA 89 | JADE |

- 204 ABDALLAH 04F tag b- and c-quarks using semileptonic decays combined with charge flow information from the hemisphere opposite to the lepton. Enriched samples of $c\bar{c}$ and $b\bar{b}$ events are obtained using lifetime information.
 205 ABBIENDI 03P tag heavy flavors using events with one or two identified leptons. This allows the simultaneous fitting of the b and c quark forward-backward asymmetries as well as the average $B^0-\bar{B}^0$ mixing.
 206 HEISTER 02H measure simultaneously b and c quark forward-backward asymmetries using their semileptonic decays to tag the quark charge. The flavor separation is obtained with a discriminating multivariate analysis.
 207 ABREU 99Y tag $Z \rightarrow b\bar{b}$ and $Z \rightarrow c\bar{c}$ events by an exclusive reconstruction of several D meson decay modes (D^{*+} , D^0 , and D^+ with their charge-conjugate states).
 208 BARATE 98A tag $Z \rightarrow c\bar{c}$ events requiring the presence of high-momentum reconstructed D^{*+} , D^+ , or D^0 mesons.
 209 ALEXANDER 97C identify the b and c events using a D/D^* tag.
 210 ADRIANI 92D use both electron and muon semileptonic decays.

$A_{FB}^{(0,b)}$ CHARGE ASYMMETRY IN $e^+ e^- \rightarrow b \bar{b}$

OUR FIT, which is obtained by a simultaneous fit to several c- and b-quark measurements as explained in the note "The Z boson" and ref. LEP-SLC 06, refers to the Z pole asymmetry. The experimental values, on the other hand, correspond to the measurements carried out at the respective energies.

ASYMMETRY (%)	STD. MODEL	\sqrt{s} (GeV)	DOCUMENT ID	TECN
9.92 ± 0.16 OUR FIT				
9.58 ± 0.32 ± 0.14	9.68	91.231	211 ABDALLAH 05	DLPH
10.04 ± 0.56 ± 0.25	9.69	91.26	212 ABDALLAH 04F	DLPH
9.72 ± 0.42 ± 0.15	9.67	91.25	213 ABBIENDI 03P	OPAL
9.77 ± 0.36 ± 0.18	9.69	91.26	214 ABBIENDI 02I	OPAL
9.52 ± 0.41 ± 0.17	9.59	91.21	215 HEISTER 02H	ALEP
10.00 ± 0.27 ± 0.11	9.63	91.232	216 HEISTER 01D	ALEP
7.62 ± 1.94 ± 0.85	9.64	91.235	217 ABREU 99Y	DLPH
9.60 ± 0.66 ± 0.33	9.69	91.26	218 ACCIARRI 99D	L3
9.31 ± 1.01 ± 0.55	9.65	91.24	219 ACCIARRI 98U	L3
9.4 ± 2.7 ± 2.2	9.61	91.22	220 ALEXANDER 97C	OPAL

• • • We do not use the following data for averages, fits, limits, etc. • • •

6.37 ± 1.43 ± 0.17	5.8	89.449	211 ABDALLAH 05	DLPH
10.41 ± 1.15 ± 0.24	12.1	92.990	211 ABDALLAH 05	DLPH
6.7 ± 2.2 ± 0.2	5.7	89.43	212 ABDALLAH 04F	DLPH
11.2 ± 1.8 ± 0.2	12.1	92.99	212 ABDALLAH 04F	DLPH
4.7 ± 1.8 ± 0.1	5.9	89.51	213 ABBIENDI 03P	OPAL
10.3 ± 1.5 ± 0.2	12.0	92.95	213 ABBIENDI 03P	OPAL
5.82 ± 1.53 ± 0.12	5.9	89.50	214 ABBIENDI 02I	OPAL
12.21 ± 1.23 ± 0.25	12.0	92.91	214 ABBIENDI 02I	OPAL
-13.1 ± 13.5 ± 1.0	3.2	88.38	215 HEISTER 02H	ALEP
5.5 ± 1.9 ± 0.1	5.6	89.38	215 HEISTER 02H	ALEP
-0.4 ± 6.7 ± 0.8	7.5	90.21	215 HEISTER 02H	ALEP
11.1 ± 6.4 ± 0.5	11.0	92.05	215 HEISTER 02H	ALEP
10.4 ± 1.5 ± 0.3	12.0	92.94	215 HEISTER 02H	ALEP
13.8 ± 9.3 ± 1.1	12.9	93.90	215 HEISTER 02H	ALEP
4.36 ± 1.19 ± 0.11	5.8	89.472	216 HEISTER 01D	ALEP
11.72 ± 0.97 ± 0.11	12.0	92.950	216 HEISTER 01D	ALEP
5.67 ± 7.56 ± 1.17	5.7	89.434	217 ABREU 99Y	DLPH
8.82 ± 6.33 ± 1.22	12.1	92.990	217 ABREU 99Y	DLPH
6.11 ± 2.93 ± 0.43	5.9	89.50	218 ACCIARRI 99D	L3
13.71 ± 2.40 ± 0.44	12.2	93.10	218 ACCIARRI 99D	L3
4.95 ± 5.23 ± 0.40	5.8	89.45	219 ACCIARRI 98U	L3
11.37 ± 3.99 ± 0.65	12.1	92.99	219 ACCIARRI 98U	L3
-8.6 ± 10.8 ± 2.9	5.8	89.45	220 ALEXANDER 97C	OPAL
-2.1 ± 9.0 ± 2.6	12.1	93.00	220 ALEXANDER 97C	OPAL
-71 ± 34 ± $\frac{7}{8}$	-58	58.3	SHIMONAKA 91	TOPZ
-22.2 ± 7.7 ± 3.5	-26.0	35	BEHREND 90D	CELL
-49.1 ± 16.0 ± 5.0	-39.7	43	BEHREND 90D	CELL
-28 ± 11	-23	35	BRAUNSCH... 90	TASS
-16.6 ± 7.7 ± 4.8	-24.3	35	ELSEN 90	JADE
-33.6 ± 22.2 ± 5.2	-39.9	44	ELSEN 90	JADE
3.4 ± 7.0 ± 3.5	-16.0	29.0	BAND 89	MAC
-72 ± 28 ± 13	-56	55.2	SAGAWA 89	AMY

211 ABDALLAH 05 obtain an enriched samples of $b\bar{b}$ events using lifetime information. The quark (or antiquark) charge is determined with a neural network using the secondary vertex charge, the jet charge and particle identification.

212 ABDALLAH 04F tag b^- and c^- quarks using semileptonic decays combined with charge flow information from the hemisphere opposite to the lepton. Enriched samples of $c\bar{c}$ and $b\bar{b}$ events are obtained using lifetime information.

213 ABBIENDI 03P tag heavy flavors using events with one or two identified leptons. This allows the simultaneous fitting of the b and c quark forward-backward asymmetries as well as the average $B^0-\bar{B}^0$ mixing.

214 ABBIENDI 02I tag $Z^0 \rightarrow b\bar{b}$ decays using a combination of secondary vertex and lepton tags. The sign of the b -quark charge is determined using an inclusive tag based on jet, vertex, and kaon charges.

215 HEISTER 02H measure simultaneously b and c quark forward-backward asymmetries using their semileptonic decays to tag the quark charge. The flavor separation is obtained with a discriminating multivariate analysis.

216 HEISTER 01D tag $Z \rightarrow b\bar{b}$ events using the impact parameters of charged tracks complemented with information from displaced vertices, event shape variables, and lepton identification. The b -quark direction and charge is determined using the hemisphere charge method along with information from fast kaon tagging and charge estimators of primary and secondary vertices. The change in the quoted value due to variation of A_{FB}^c and R_b is given as $+0.103 (A_{FB}^c - 0.0651) - 0.440 (R_b - 0.21585)$.

217 ABREU 99Y tag $Z \rightarrow b\bar{b}$ and $Z \rightarrow c\bar{c}$ events by an exclusive reconstruction of several D meson decay modes (D^{*+} , D^0 , and D^+ with their charge-conjugate states).

218 ACCIARRI 99D tag $Z \rightarrow b\bar{b}$ events using high p and p_T leptons. The analysis determines simultaneously a mixing parameter $\chi_b = 0.1192 \pm 0.0068 \pm 0.0051$ which is used to correct the observed asymmetry.

219 ACCIARRI 98U tag $Z \rightarrow b\bar{b}$ events using lifetime and measure the jet charge using the hemisphere charge.

220 ALEXANDER 97C identify the b and c events using a D/D^* tag.

CHARGE ASYMMETRY IN $e^+e^- \rightarrow q\bar{q}$

Summed over five lighter flavors.

Experimental and Standard Model values are somewhat event-selection dependent. Standard Model expectations contain some assumptions on $B^0-\bar{B}^0$ mixing and on other electroweak parameters.

ASYMMETRY (%)	STD. MODEL	\sqrt{s} (GeV)	DOCUMENT ID	TECN
---------------	------------	------------------	-------------	------

• • • We do not use the following data for averages, fits, limits, etc. • • •

-0.76 ± 0.12 ± 0.15			91.2	221 ABREU 92I	DLPH
4.0 ± 0.4 ± 0.63	4.0		91.3	222 ACTON 92L	OPAL
9.1 ± 1.4 ± 1.6	9.0		57.9	ADACHI 91B	TOPZ
-0.84 ± 0.15 ± 0.04			91	DECAMP 91B	ALEP
8.3 ± 2.9 ± 1.9	8.7		56.6	STUART 90	AMY
11.4 ± 2.2 ± 2.1	8.7		57.6	ABE 89L	VNS
6.0 ± 1.3	5.0		34.8	GREENSHAW 89	JADE
8.2 ± 2.9	8.5		43.6	GREENSHAW 89	JADE

221 ABREU 92I has 0.14 systematic error due to uncertainty of quark fragmentation.

222 ACTON 92L use the weight function method on 259k selected $Z \rightarrow$ hadrons events.

The systematic error includes a contribution of 0.2 due to $B^0-\bar{B}^0$ mixing effect, 0.4 due to Monte Carlo (MC) fragmentation uncertainties and 0.3 due to MC statistics. ACTON 92L derive a value of $\sin^2\theta_{W}^{\text{eff}}$ to be $0.2321 \pm 0.0017 \pm 0.0028$.

CHARGE ASYMMETRY IN $p\bar{p} \rightarrow Z \rightarrow e^+e^-$

ASYMMETRY (%)	STD. MODEL	\sqrt{s} (GeV)	DOCUMENT ID	TECN
5.2 ± 5.9 ± 0.4		91	ABE 91E	CDF

• • • We do not use the following data for averages, fits, limits, etc. • • •

ANOMALOUS $ZZ\gamma$, $Z\gamma\gamma$, AND ZZV COUPLINGS

Revised March 2006 by C. Caso (University of Genova) and A. Gurtu (Tata Institute).

In the reaction $e^+e^- \rightarrow Z\gamma$, deviations from the Standard Model for the $Z\gamma\gamma^*$ and $Z\gamma Z^*$ couplings may be described in terms of 8 parameters, h_i^V ($i = 1, 4; V = \gamma, Z$) [1]. The parameters h_i^Z describe the $Z\gamma\gamma^*$ couplings and the parameters h_i^V the $Z\gamma Z^*$ couplings. In this formalism h_1^V and h_2^V lead to CP -violating and h_3^V and h_4^V to CP -conserving effects. All these anomalous contributions to the cross section increase rapidly with center-of-mass energy. In order to ensure unitarity, these parameters are usually described by a form-factor representation, $h_i^V(s) = h_{i0}^V/(1 + s/\Lambda^2)^n$, where Λ is the energy scale for the manifestation of a new phenomenon and n is a sufficiently large power. By convention one uses $n = 3$ for $h_{1,3}^V$ and $n = 4$ for $h_{2,4}^V$. Usually limits on h_i^V 's are put assuming some value of Λ (sometimes ∞).

Above the $e^+e^- \rightarrow ZZ$ threshold, deviations from the Standard Model for the $ZZ\gamma^*$ and ZZZ^* couplings may be described by means of four anomalous couplings f_i^V ($i = 4, 5; V = \gamma, Z$) [2]. As above, the parameters f_i^γ describe the $Z\gamma\gamma^*$ couplings and the parameters f_i^Z the ZZZ^* couplings. The anomalous couplings f_5^V lead to violation of C and P symmetries while f_4^V introduces CP violation.

All these couplings h_i^V and f_i^V are zero at tree level in the Standard Model.

References

1. U. Baur and E.L. Berger Phys. Rev. **D47**, 4889 (1993).
2. K. Hagiwara *et al.*, Nucl. Phys. **B282**, 253 (1987).

h_i^V

Combining the LEP results properly taking into account the correlations the following 95% CL limits are derived (CERN-PH-EP/2005-051 or hep-ex/0511027):

$$\begin{aligned}
 -0.13 < h_1^Z < +0.13, & & -0.078 < h_2^Z < +0.071, \\
 -0.20 < h_3^Z < +0.07, & & -0.05 < h_4^Z < +0.12, \\
 -0.056 < h_1^\gamma < +0.055, & & -0.045 < h_2^\gamma < +0.025, \\
 -0.049 < h_3^\gamma < -0.008, & & -0.002 < h_4^\gamma < +0.034.
 \end{aligned}$$

VALUE	DOCUMENT ID	TECN	COMMENT
-------	-------------	------	---------

• • • We do not use the following data for averages, fits, limits, etc. • • •

223	ABAZOV	09L D0	$E_{\text{cm}}^{\overline{p\overline{p}}} = 1.96$ TeV
224	ABAZOV	07M D0	
225	ABDALLAH	07c DLPH	$E_{\text{cm}}^{\text{ee}} = 183\text{--}208$ GeV
226	ACHARD	04H L3	
227	ABBIENDI,G	00c OPAL	
228	ABBOTT	98M D0	
229	ABREU	98k DLPH	

- 223 ABAZOV 09L study $Z\gamma, Z \rightarrow \nu\overline{\nu}$ production in $p\overline{p}$ collisions at 1.96 TeV C.M. energy. They select 51 events with a photon of transverse energy E_T larger than 90 GeV, with an expected background of 17 events. Based on the photon E_T spectrum and including also Z decays to charged leptons (from ABAZOV 07M), the following 95% CL limits are reported: $|h_{30}^\gamma| < 0.033$, $|h_{40}^\gamma| < 0.0017$, $|h_{50}^\gamma| < 0.033$, $|h_{40}^Z| < 0.0017$.
- 224 ABAZOV 07M use 968 $p\overline{p} \rightarrow e^+e^-/\mu^+\mu^- \gamma X$ candidates, at 1.96 TeV center of mass energy, to tag $p\overline{p} \rightarrow Z\gamma$ events by requiring $E_T(\gamma) > 7$ GeV, lepton-gamma separation $\Delta R_{\ell\gamma} > 0.7$, and di-lepton invariant mass > 30 GeV. The cross section is in agreement with the SM prediction. Using these $Z\gamma$ events they obtain 95% C.L. limits on each h_i^Y , keeping all others fixed at their SM values. They report: $-0.083 < h_{30}^Z < 0.082$, $-0.0053 < h_{40}^Z < 0.0054$, $-0.085 < h_{50}^Z < 0.084$, $-0.0053 < h_{40}^Z < 0.0054$, for the form factor scale $\Lambda = 1.2$ TeV.
- 225 Using data collected at $\sqrt{s} = 183\text{--}208$ GeV, ABDALLAH 07c select 1,877 $e^+e^- \rightarrow Z\gamma$ events with $Z \rightarrow q\overline{q}$ or $\nu\overline{\nu}$, 171 $e^+e^- \rightarrow ZZZ$ events with $Z \rightarrow q\overline{q}$ or lepton pair (except an explicit τ pair), and 74 $e^+e^- \rightarrow Z\gamma^*$ events with a $q\overline{q}\mu^+\mu^-$ or $q\overline{q}e^+e^-$ signature, to derive 95% CL limits on h_i^Y . Each limit is derived with other parameters set to zero. They report: $-0.23 < h_1^Z < 0.23$, $-0.30 < h_2^Z < 0.16$, $-0.14 < h_1^C < 0.14$, $-0.049 < h_3^Z < 0.044$.
- 226 ACHARD 04H select 3515 $e^+e^- \rightarrow Z\gamma$ events with $Z \rightarrow q\overline{q}$ or $\nu\overline{\nu}$ at $\sqrt{s} = 189\text{--}209$ GeV to derive 95% CL limits on h_i^Y . For deriving each limit the other parameters are fixed at zero. They report: $-0.153 < h_1^Z < 0.141$, $-0.087 < h_2^Z < 0.079$, $-0.220 < h_3^Z < 0.112$, $-0.068 < h_4^Z < 0.148$, $-0.057 < h_1^C < 0.057$, $-0.050 < h_2^Z < 0.023$, $-0.059 < h_3^Z < 0.004$, $-0.004 < h_4^Z < 0.042$.
- 227 ABBIENDI,G 00c study $e^+e^- \rightarrow Z\gamma$ events (with $Z \rightarrow q\overline{q}$ and $Z \rightarrow \nu\overline{\nu}$) at 189 GeV to obtain the central values (and 95% CL limits) of these couplings: $h_1^Z = 0.000 \pm 0.100$ ($-0.190, 0.190$), $h_2^Z = 0.000 \pm 0.068$ ($-0.128, 0.128$), $h_3^Z = -0.074 \pm 0.102$ ($-0.269, 0.119$), $h_4^Z = 0.046 \pm 0.068$ ($-0.084, 0.175$), $h_1^C = 0.000 \pm 0.061$ ($-0.115, 0.115$), $h_2^Z = 0.000 \pm 0.041$ ($-0.077, 0.077$), $h_3^Z = -0.080 \pm 0.039$ ($-0.164, -0.006$), $h_4^Z = 0.064 \pm 0.033$ ($+0.007, +0.134$). The results are derived assuming that only one coupling at a time is different from zero.
- 228 ABBOTT 98M study $p\overline{p} \rightarrow Z\gamma + X$, with $Z \rightarrow e^+e^-, \mu^+\mu^-, \nu\overline{\nu}$ at 1.8 TeV, to obtain 95% CL limits at $\Lambda = 75.0$ GeV: $|h_{30}^\gamma| < 0.36$, $|h_{40}^\gamma| < 0.05$ (keeping $h_i^Z=0$), and $|h_{30}^\gamma| < 0.37$, $|h_{40}^\gamma| < 0.05$ (keeping $h_i^Z=0$). Limits on the CP -violating couplings are $|h_{10}^Z| < 0.36$, $|h_{20}^Z| < 0.05$ (keeping $h_i^Z=0$), and $|h_{10}^\gamma| < 0.37$, $|h_{20}^\gamma| < 0.05$ (keeping $h_i^Z=0$).
- 229 ABREU 98k determine a 95% CL upper limit on $\sigma(e^+e^- \rightarrow \gamma + \text{invisible particles}) < 2.5$ pb using 161 and 172 GeV data. This is used to set 95% CL limits on $|h_{30}^\gamma| < 0.8$ and $|h_{50}^\gamma| < 1.3$, derived at a scale $\Lambda=1$ TeV and with $n=3$ in the form factor representation.

 f_i^Y

Combining the LEP results properly taking into account the correlations the following 95% CL limits are derived (CERN-PH-EP/2005-051 or hep-ex/0511027):

$$\begin{aligned} -0.30 < f_4^Z < +0.30, & \quad -0.34 < f_5^Z < +0.38, \\ -0.17 < f_4^C < +0.19, & \quad -0.32 < f_5^C < +0.36. \end{aligned}$$

VALUE	DOCUMENT ID	TECN	COMMENT
••• We do not use the following data for averages, fits, limits, etc. •••			
	230	SCHAE	09 ALEP $E_{\text{cm}}^{\text{ee}} = 192\text{--}209$ GeV
	231	ABAZOV	08k D0 $E_{\text{cm}}^{\overline{p\overline{p}}} = 1.96$ TeV
	232	ABDALLAH	07c DLPH $E_{\text{cm}}^{\text{ee}} = 183\text{--}208$ GeV
	233	ABBIENDI	04c OPAL
	234	ACHARD	03D L3

- 230 Using data collected in the center of mass energy range 192–209 GeV, SCHAE 09 select 318 $e^+e^- \rightarrow ZZ$ events with 319.4 expected from the standard model. Using this data they derive the following 95% CL limits: $-0.321 < f_4^\gamma < 0.318$, $-0.534 < f_4^Z < 0.534$, $-0.724 < f_5^\gamma < 0.733$, $-1.194 < f_5^Z < 1.190$.
- 231 ABAZOV 08k search for ZZ and $Z\gamma^*$ events with 1 fb^{-1} $p\overline{p}$ data at 1.96 TeV in (e^+e^-) , $(\mu\mu)(\mu\mu)$, $(e^+e^-)(\mu\mu)$ final states requiring the lepton pair masses to be > 30 GeV. They observe 1 event, which is consistent with an expected signal of 1.71 ± 0.15 events and a background of 0.13 ± 0.03 events. From this they derive the following limits, for a form factor (Λ) value of 1.2 TeV: $-0.28 < f_{40}^Z < 0.28$, $-0.31 < f_{50}^Z < 0.29$, $-0.26 < f_{40}^\gamma < 0.26$, $-0.30 < f_{50}^\gamma < 0.28$.
- 232 Using data collected at $\sqrt{s} = 183\text{--}208$ GeV, ABDALLAH 07c select 171 $e^+e^- \rightarrow ZZ$ events with $Z \rightarrow q\overline{q}$ or lepton pair (except an explicit τ pair), and 74 $e^+e^- \rightarrow Z\gamma^*$ events with a $q\overline{q}\mu^+\mu^-$ or $q\overline{q}e^+e^-$ signature, to derive 95% CL limits on f_i^Y . Each limit is derived with other parameters set to zero. They report: $-0.40 < f_4^Z < 0.42$, $-0.38 < f_5^Z < 0.62$, $-0.23 < f_4^C < 0.25$, $-0.52 < f_5^C < 0.48$.

- 233 ABBIENDI 04c study ZZ production in e^+e^- collisions in the C.M. energy range 190–209 GeV. They select 340 events with an expected background of 180 events. Including the ABBIENDI 00N data at 183 and 189 GeV (118 events with an expected background of 65 events) they report the following 95% CL limits: $-0.45 < f_4^Z < 0.58$, $-0.94 < f_5^Z < 0.25$, $-0.32 < f_4^C < 0.33$, and $-0.71 < f_5^C < 0.59$.
- 234 ACHARD 03D study Z -boson pair production in e^+e^- collisions in the C.M. energy range 200–209 GeV. They select 549 events with an expected background of 432 events. Including the ACCIARRI 99G and ACCIARRI 99o data (183 and 189 GeV respectively, 286 events with an expected background of 241 events) and the 192–202 GeV ACCIARRI 01i results (656 events, expected background of 512 events), they report the following 95% CL limits: $-0.48 < f_4^Z < 0.46$, $-0.36 < f_5^Z < 1.03$, $-0.28 < f_4^C < 0.28$, and $-0.40 < f_5^C < 0.47$.

ANOMALOUS W/Z QUARTIC COUPLINGS

Revised March 2006 by C. Caso (University of Genova) and A. Gurtu (Tata Institute).

The Standard Model predictions for $WWWW$, $WWZZ$, $WWZ\gamma$, $WW\gamma\gamma$, and $ZZ\gamma\gamma$ couplings are small at LEP, but expected to become important at a TeV Linear Collider. Outside the Standard Model framework such possible couplings, a_0, a_c, a_n , are expressed in terms of the following dimension-6 operators [1,2];

$$\begin{aligned} L_6^0 &= -\frac{e^2}{16\Lambda^2} a_0 F^{\mu\nu} F_{\mu\nu} \vec{W}^\alpha \cdot \vec{W}_\alpha \\ L_6^c &= -\frac{e^2}{16\Lambda^2} a_c F^{\mu\alpha} F_{\mu\beta} \vec{W}^\beta \cdot \vec{W}_\alpha \\ L_6^n &= -i \frac{e^2}{16\Lambda^2} a_n \epsilon_{ijk} W_{\mu\alpha}^{(i)} W_\nu^{(j)} W^{(k)\alpha} F^{\mu\nu} \\ \tilde{L}_6^0 &= -\frac{e^2}{16\Lambda^2} \tilde{a}_0 F^{\mu\nu} \tilde{F}_{\mu\nu} \vec{W}^\alpha \cdot \vec{W}_\alpha \\ \tilde{L}_6^n &= -i \frac{e^2}{16\Lambda^2} \tilde{a}_n \epsilon_{ijk} W_{\mu\alpha}^{(i)} W_\nu^{(j)} W^{(k)\alpha} \tilde{F}^{\mu\nu} \end{aligned}$$

where F, W are photon and W fields, L_6^0 and L_6^c conserve C, P separately (\tilde{L}_6^0 conserves only C) and generate anomalous $W^+W^-\gamma\gamma$ and $ZZ\gamma\gamma$ couplings, L_6^n violates CP (\tilde{L}_6^n violates both C and P) and generates an anomalous $W^+W^-Z\gamma$ coupling, and Λ is an energy scale for new physics. For the $ZZ\gamma\gamma$ coupling the CP -violating term represented by L_6^n does not contribute. These couplings are assumed to be real and to vanish at tree level in the Standard Model.

Within the same framework as above, a more recent description of the quartic couplings [3] treats the anomalous parts of the $WW\gamma\gamma$ and $ZZ\gamma\gamma$ couplings separately leading to two sets parameterized as a_0^V/Λ^2 and a_c^V/Λ^2 , where $V = W$ or Z .

At LEP the processes studied in search of these quartic couplings are $e^+e^- \rightarrow WW\gamma$, $e^+e^- \rightarrow \gamma\gamma\nu\overline{\nu}$, and $e^+e^- \rightarrow Z\gamma\gamma$ and limits are set on the quantities $a_0^W/\Lambda^2, a_c^W/\Lambda^2, a_n/\Lambda^2$. The characteristics of the first process depend on all the three couplings whereas those of the latter two depend only on the two CP -conserving couplings. The sensitive measured variables are the cross sections for these processes as well as the energy and angular distributions of the photon and recoil mass to the photon pair.

References

- G. Belanger and F. Boudjema, Phys. Lett. **B288**, 201 (1992).
- J.W. Stirling and A. Werthenbach, Eur. Phys. J. **C14**, 103 (2000);
J.W. Stirling and A. Werthenbach, Phys. Lett. **B466**, 369 (1999);
A. Denner *et al.*, Eur. Phys. J. **C20**, 201 (2001);
G. Montagna *et al.*, Phys. Lett. **B515**, 197 (2001).
- G. Belanger *et al.*, Eur. Phys. J. **C13**, 103 (2000).

$a_0/\Lambda^2, a_c/\Lambda^2$

Combining published and unpublished preliminary LEP results the following 95% CL intervals for the QGCs associated with the ZZγγ vertex are derived (CERN-PH-EP/2005-051 or hep-ex/0511027):

-0.008 < a_0^Z/Λ^2 < +0.021
-0.029 < a_c^Z/Λ^2 < +0.039

VALUE DOCUMENT ID TECN
• • • We do not use the following data for averages, fits, limits, etc. • • •

235 ABBIENDI 04L select 20 e+e- -> nu nu gamma acoplanar events in the energy range 180-209 GeV and 176 e+e- -> q q gamma gamma events in the energy range 130-209 GeV. These samples are used to constrain possible anomalous W+ W- gamma gamma and ZZ gamma gamma quartic couplings. Further combining with the W+ W- gamma sample of ABBIENDI 04B the following one-parameter 95% CL limits are obtained: -0.007 < a_0^Z/Λ^2 < 0.023 GeV^-2, -0.029 < a_c^Z/Λ^2 < 0.029 GeV^-2, -0.020 < a_0^W/Λ^2 < 0.020 GeV^-2, -0.052 < a_c^W/Λ^2 < 0.037 GeV^-2.
236 In the CM energy range 183 to 209 GeV HEISTER 04A select 30 e+e- -> nu nu gamma gamma events with two acoplanar, high energy and high transverse momentum photons. The photon-photon acoplanarity is required to be > 5 degrees, E_gamma/sqrt(s) > 0.025 (the more energetic photon having energy > 0.2 sqrt(s)), p_T gamma/E_beam > 0.05 and |cos theta_gamma| < 0.94. A likelihood fit to the photon energy and recoil missing mass yields the following one-parameter 95% CL limits: -0.012 < a_0^Z/Λ^2 < 0.019 GeV^-2, -0.041 < a_c^Z/Λ^2 < 0.044 GeV^-2, -0.060 < a_0^W/Λ^2 < 0.055 GeV^-2, -0.099 < a_c^W/Λ^2 < 0.093 GeV^-2.
237 ACHARD 02g study e+e- -> Z gamma gamma -> q q gamma gamma events using data at center-of-mass energies from 200 to 209 GeV. The photons are required to be isolated, each with energy > 5 GeV and |cos theta| < 0.97, and the di-jet invariant mass to be compatible with that of the Z boson (74-111 GeV). Cuts on Z velocity (beta < 0.73) and on the energy of the most energetic photon reduce the backgrounds due to non-resonant production of the q q gamma gamma state and due to ISR respectively, yielding a total of 40 candidate events of which 8.6 are expected to be due to background. The energy spectra of the least energetic photon are fitted for all ten center-of-mass energy values from 130 GeV to 209 GeV (as obtained adding to the present analysis 130-202 GeV data of ACCIARRI 01E, for a total of 137 events with an expected background of 34.1 events) to obtain the fitted values a_0/Λ^2 = 0.00 +/- 0.02 GeV^-2 and a_c/Λ^2 = 0.03 +/- 0.02 GeV^-2, where the other parameter is kept fixed to its Standard Model value (0). A simultaneous fit to both parameters yields the 95% CL limits -0.02 GeV^-2 < a_0/Λ^2 < 0.03 GeV^-2 and -0.07 GeV^-2 < a_c/Λ^2 < 0.05 GeV^-2.

Z REFERENCES

ABAZOV 09L PRL 102 201802 V.M. Abazov et al. (DO Collab.)
BEDDALL 09 PL B670 300 A. Beddall, A. Beddall, A. Bingul (UGAZ)
SCHAEF 09 JHEP 0904 124 S. Schaefer et al. (ALEPH Collab.)
ABAZOV 08K PRL 100 131801 V.M. Abazov et al. (DO Collab.)
ABAZOV 07M PL B653 378 V.M. Abazov et al. (DO Collab.)
ABDALLAH 07C EPJ C31 525 J. Abdallah et al. (DELPHI Collab.)
ABDALLAH 05E PL B639 179 J. Abdallah et al. (DELPHI Collab.)
AKTAS 06 PL B632 35 A. Aktas et al. (H1 Collab.)
LEP-SLC 06 PRPL 427 257 ALEPH, DELPHI, L3, OPAL, SLD and working groups
SCHAEF 06A PL B639 192 S. Schaefer et al. (ALEPH Collab.)
ABDALLAH 05 EPJ C40 1 J. Abdallah et al. (DELPHI Collab.)
ABDALLAH 05C EPJ C44 299 J. Abdallah et al. (DELPHI Collab.)
ABE 05 PRL 94 091801 K. Abe et al. (SLD Collab.)
ABE 05F PR D71 112004 K. Abe et al. (SLD Collab.)
ACOSTA 05M PR D71 052002 D. Acosta et al. (CDF Collab.)
ABBIENDI 04B PL B580 17 G. Abbiendi et al. (OPAL Collab.)
ABBIENDI 04C EPJ C32 303 G. Abbiendi et al. (OPAL Collab.)
ABBIENDI 04D PL B586 167 G. Abbiendi et al. (OPAL Collab.)
ABBIENDI 04G EPJ C33 173 G. Abbiendi et al. (OPAL Collab.)
ABBIENDI 04L PR D70 032005 G. Abbiendi et al. (OPAL Collab.)
ABDALLAH 04F EPJ C34 109 J. Abdallah et al. (DELPHI Collab.)
ABE 04C PR D69 072003 K. Abe et al. (SLD Collab.)
ACHARD 04C PL B585 42 P. Achard et al. (L3 Collab.)
ACHARD 04H PL B597 119 P. Achard et al. (L3 Collab.)
HEISTER 04A PL B602 31 A. Heister et al. (ALEPH Collab.)
ABBIENDI 03P PL B577 18 G. Abbiendi et al. (OPAL Collab.)
ABDALLAH 03H PL B569 129 J. Abdallah et al. (DELPHI Collab.)
ABDALLAH 03K PL B576 29 J. Abdallah et al. (DELPHI Collab.)
ABE 03F PRL 90 141804 K. Abe et al. (SLD Collab.)
ACHARD 03D PL B572 133 P. Achard et al. (L3 Collab.)
ACHARD 03G PL B577 109 P. Achard et al. (L3 Collab.)
ABBIENDI 02I PL B546 29 G. Abbiendi et al. (OPAL Collab.)
ABE 02G PRL 88 151801 K. Abe et al. (SLD Collab.)
ACHARD 02G PL B540 43 P. Achard et al. (L3 Collab.)
HEISTER 02B PL B526 34 A. Heister et al. (ALEPH Collab.)
HEISTER 02C PL B528 19 A. Heister et al. (ALEPH Collab.)
HEISTER 02H EPJ C24 177 A. Heister et al. (ALEPH Collab.)
ABBIENDI 01A EPJ C19 587 G. Abbiendi et al. (OPAL Collab.)
ABBIENDI 01G EPJ C18 447 G. Abbiendi et al. (OPAL Collab.)
ABBIENDI 01K PL B516 1 G. Abbiendi et al. (OPAL Collab.)
ABBIENDI 01N EPJ C20 445 G. Abbiendi et al. (OPAL Collab.)
ABBIENDI 01O EPJ C21 1 G. Abbiendi et al. (OPAL Collab.)
ABE 01B PRL 86 1162 K. Abe et al. (SLD Collab.)
ABE 01C PR D63 032005 K. Abe et al. (SLD Collab.)
ACCIARRI 01E PL B505 47 M. Acciari et al. (L3 Collab.)
ACCIARRI 01I PL B497 23 M. Acciari et al. (L3 Collab.)
HEISTER 01 EPJ C20 401 A. Heister et al. (ALEPH Collab.)
HEISTER 01D EPJ C22 201 A. Heister et al. (ALEPH Collab.)
ABBIENDI 00N PL B476 256 G. Abbiendi et al. (OPAL Collab.)
ABBIENDI.G 00C EPJ C17 553 G. Abbiendi et al. (OPAL Collab.)
ABE 00B PRL 84 5945 K. Abe et al. (SLD Collab.)
ABE 00D PRL 85 5059 K. Abe et al. (SLD Collab.)
ABREU 00 EPJ C22 225 P. Abreu et al. (DELPHI Collab.)
ABREU 00B EPJ C14 613 P. Abreu et al. (DELPHI Collab.)
ABREU 00E EPJ C14 585 P. Abreu et al. (DELPHI Collab.)
ABREU 00F EPJ C16 371 P. Abreu et al. (DELPHI Collab.)
ABREU 00P PL B475 429 P. Abreu et al. (DELPHI Collab.)
ACCIARRI 00 EPJ C13 47 M. Acciari et al. (L3 Collab.)

ACCIARRI 00C EPJ C16 1 M. Acciari et al. (L3 Collab.)
ACCIARRI 00Q PL B479 79 M. Acciari et al. (L3 Collab.)
ACCIARRI 00J PL B489 93 M. Acciari et al. (L3 Collab.)
BARATE 00C EPJ C16 597 R. Barate et al. (ALEPH Collab.)
BARATE 00B EPJ C14 1 R. Barate et al. (ALEPH Collab.)
BARATE 00N EPJ C16 613 R. Barate et al. (ALEPH Collab.)
ABBIENDI 99B EPJ C8 217 G. Abbiendi et al. (OPAL Collab.)
ABBIENDI 99I PL B447 157 G. Abbiendi et al. (OPAL Collab.)
ABE 99E PR D59 052001 K. Abe et al. (SLD Collab.)
ABE 99L PRL 83 1902 K. Abe et al. (SLD Collab.)
ABREU 99 EPJ C6 19 P. Abreu et al. (DELPHI Collab.)
ABREU 99B EPJ C10 415 P. Abreu et al. (DELPHI Collab.)
ABREU 99J PL B449 364 P. Abreu et al. (DELPHI Collab.)
ABREU 99U PL B462 425 P. Abreu et al. (DELPHI Collab.)
ABREU 99Y EPJ C10 219 P. Abreu et al. (DELPHI Collab.)
ACCIARRI 99D PL B448 152 M. Acciari et al. (L3 Collab.)
ACCIARRI 99F PL B453 94 M. Acciari et al. (L3 Collab.)
ACCIARRI 99G PL B450 281 M. Acciari et al. (L3 Collab.)
ACCIARRI 99O PL B465 363 M. Acciari et al. (L3 Collab.)
ABBOTT 98M PR D57 R3817 D. B. Abbott et al. (DO Collab.)
ABE 98D PRL 80 660 K. Abe et al. (SLD Collab.)
ABE 98I PRL 81 942 K. Abe et al. (SLD Collab.)
ABREU 98K PL B423 194 P. Abreu et al. (DELPHI Collab.)
ABREU 98L EPJ C5 585 P. Abreu et al. (DELPHI Collab.)
ACCIARRI 98G PL B431 199 M. Acciari et al. (L3 Collab.)
ACCIARRI 98H PL B429 387 M. Acciari et al. (L3 Collab.)
ACCIARRI 98U PL B439 225 M. Acciari et al. (L3 Collab.)
ACKERSTAFF 98A EPJ C5 411 K. Ackerstaff et al. (OPAL Collab.)
ACKERSTAFF 98E EPJ C1 439 K. Ackerstaff et al. (OPAL Collab.)
ACKERSTAFF 98O PL B420 157 K. Ackerstaff et al. (OPAL Collab.)
ACKERSTAFF 98Q EPJ C4 19 K. Ackerstaff et al. (OPAL Collab.)
BARATE 98O PL B434 415 R. Barate et al. (ALEPH Collab.)
BARATE 98T EPJ C4 557 R. Barate et al. (ALEPH Collab.)
BARATE 98V EPJ C5 205 R. Barate et al. (ALEPH Collab.)
ABE 97 PRL 78 17 K. Abe et al. (SLD Collab.)
ABREU 97C ZPHY C73 243 P. Abreu et al. (DELPHI Collab.)
ABREU 97E PL B398 207 P. Abreu et al. (DELPHI Collab.)
ABREU 97F PL B404 194 P. Abreu et al. (DELPHI Collab.)
ACCIARRI 97D PL B393 465 M. Acciari et al. (L3 Collab.)
ACCIARRI 97J PL B407 351 M. Acciari et al. (L3 Collab.)
ACCIARRI 97L PL B407 389 M. Acciari et al. (L3 Collab.)
ACCIARRI 97M PL B413 167 M. Acciari et al. (L3 Collab.)
ACKERSTAFF 97N ZPHY C74 413 K. Ackerstaff et al. (OPAL Collab.)
ACKERSTAFF 97T PL B412 210 K. Ackerstaff et al. (OPAL Collab.)
ACKERSTAFF 97S ZPHY C76 387 K. Ackerstaff et al. (OPAL Collab.)
ACKERSTAFF 97W ZPHY C76 425 K. Ackerstaff et al. (OPAL Collab.)
ALEXANDER 97C ZPHY C73 379 G. Alexander et al. (OPAL Collab.)
ALEXANDER 97D ZPHY C73 569 G. Alexander et al. (OPAL Collab.)
ALEXANDER 97E ZPHY C73 587 G. Alexander et al. (OPAL Collab.)
BARATE 97E PL B405 191 R. Barate et al. (ALEPH Collab.)
BARATE 97F PL B401 150 R. Barate et al. (ALEPH Collab.)
BARATE 97G PL B401 163 R. Barate et al. (ALEPH Collab.)
BARATE 97H PL B401 213 R. Barate et al. (ALEPH Collab.)
BARATE 97J ZPHY C74 451 R. Barate et al. (ALEPH Collab.)
ABREU 96R ZPHY C72 31 P. Abreu et al. (DELPHI Collab.)
ABREU 96S PL B389 405 P. Abreu et al. (DELPHI Collab.)
ABREU 96U ZPHY C73 61 P. Abreu et al. (DELPHI Collab.)
ACCIARRI 96 PL B371 126 M. Acciari et al. (L3 Collab.)
ADAM 96 ZPHY C69 561 W. Adam et al. (DELPHI Collab.)
ADAM 96B ZPHY C70 371 W. Adam et al. (DELPHI Collab.)
ALEXANDER 96B ZPHY C70 197 G. Alexander et al. (OPAL Collab.)
ALEXANDER 96F PL B370 185 G. Alexander et al. (OPAL Collab.)
ALEXANDER 96N PL B384 343 G. Alexander et al. (OPAL Collab.)
ALEXANDER 96R ZPHY C72 1 G. Alexander et al. (OPAL Collab.)
BUSKULIC 96D ZPHY C69 393 D. Buskulic et al. (ALEPH Collab.)
BUSKULIC 96H ZPHY C69 379 D. Buskulic et al. (ALEPH Collab.)
BUSKULIC 96T PL B384 449 D. Buskulic et al. (ALEPH Collab.)
BUSKULIC 96Y PL B388 648 D. Buskulic et al. (ALEPH Collab.)
ABE 95J PRL 74 2880 K. Abe et al. (SLD Collab.)
ABREU 95 ZPHY C65 709 (erratum) P. Abreu et al. (DELPHI Collab.)
ABREU 95D ZPHY C66 323 P. Abreu et al. (DELPHI Collab.)
ABREU 95L ZPHY C65 587 P. Abreu et al. (DELPHI Collab.)
ABREU 95M ZPHY C65 603 P. Abreu et al. (DELPHI Collab.)
ABREU 95O ZPHY C67 543 P. Abreu et al. (DELPHI Collab.)
ABREU 95R ZPHY C68 353 P. Abreu et al. (DELPHI Collab.)
ABREU 95V ZPHY C68 541 P. Abreu et al. (DELPHI Collab.)
ABREU 95W PL B361 207 P. Abreu et al. (DELPHI Collab.)
ABREU 95X ZPHY C69 1 P. Abreu et al. (DELPHI Collab.)
ACCIARRI 95B PL B345 589 M. Acciari et al. (L3 Collab.)
ACCIARRI 95C PL B345 609 M. Acciari et al. (L3 Collab.)
ACCIARRI 95G PL B353 136 M. Acciari et al. (L3 Collab.)
AKERS 95C ZPHY C65 47 R. Akers et al. (OPAL Collab.)
AKERS 95U ZPHY C67 389 R. Akers et al. (OPAL Collab.)
AKERS 95W ZPHY C67 555 R. Akers et al. (OPAL Collab.)
AKERS 95Z ZPHY C68 203 R. Akers et al. (OPAL Collab.)
ALEXANDER 95D PL B358 162 G. Alexander et al. (OPAL Collab.)
BUSKULIC 95R ZPHY C69 15 D. Buskulic et al. (ALEPH Collab.)
MIYABAYASHI 95 PL B347 171 K. Miyabayashi et al. (TOPAZ Collab.)
ABE 04C PRL 73 25 K. Abe et al. (SLD Collab.)
ABREU 94B PL B327 386 P. Abreu et al. (DELPHI Collab.)
ABREU 94P PL B341 109 P. Abreu et al. (DELPHI Collab.)
AKERS 94P ZPHY C63 181 R. Akers et al. (OPAL Collab.)
BUSKULIC 94G ZPHY C62 179 D. Buskulic et al. (ALEPH Collab.)
BUSKULIC 94J ZPHY C62 1 D. Buskulic et al. (ALEPH Collab.)
VILAIN 94 PL B320 203 P. Vilain et al. (CHARM II Collab.)
ABREU 93Z ZPHY C62 236 P. Abreu et al. (DELPHI Collab.)
ABREU 93I ZPHY C59 533 P. Abreu et al. (DELPHI Collab.)
Also
ABREU 93L ZPHY C65 709 (erratum) P. Abreu et al. (DELPHI Collab.)
P. Abreu et al. (DELPHI Collab.)
ACTON 93 PL B305 407 P.D. Acton et al. (OPAL Collab.)
ACTON 93D ZPHY C58 219 P.D. Acton et al. (OPAL Collab.)
ACTON 93E PL B311 391 P.D. Acton et al. (OPAL Collab.)
ADRIANI 93 PL B301 136 O. Adriani et al. (L3 Collab.)
ADRIANI 93L PL B316 427 O. Adriani et al. (L3 Collab.)
BUSKULIC 93L PL B313 520 D. Buskulic et al. (ALEPH Collab.)
NOVIKOV 93C PL B298 453 V.A. Novikov, L.B. Okun, M.I. Vysotsky (ITEP)
ABREU 92T ZPHY C57 371 P. Abreu et al. (DELPHI Collab.)
ABREU 92M PL B289 199 P. Abreu et al. (DELPHI Collab.)
ACTON 92B ZPHY C53 539 D.P. Acton et al. (OPAL Collab.)
ACTON 92L PL B294 436 P.D. Acton et al. (OPAL Collab.)
ACTON 92N PL B295 357 P.D. Acton et al. (OPAL Collab.)
ADEVA 92 PL B275 209 B. Adeva et al. (L3 Collab.)
ADRIANI 92B PL B292 454 O. Adriani et al. (L3 Collab.)
ALITTI 92B PL B276 354 J. Alitti et al. (UA2 Collab.)
BUSKULIC 92D PL B292 210 D. Buskulic et al. (ALEPH Collab.)
BUSKULIC 92E PL B294 145 D. Buskulic et al. (ALEPH Collab.)
DECAMP 92 PRPL 216 253 D. Decamp et al. (ALEPH Collab.)
ABE 91E PRPL 67 1502 K. Abe et al. (OPAL Collab.)
ABREU 91H ZPHY C50 185 P. Abreu et al. (DELPHI Collab.)
ACTON 91B PL B273 338 D.P. Acton et al. (OPAL Collab.)
ADACHI 91 PL B255 613 I. Adachi et al. (TOPAZ Collab.)

Gauge & Higgs Boson Particle Listings

Z, Higgs Bosons — H^0 and H^\pm

ADEVA	91I	PL B259 199	B. Adeva et al.	(L3 Collab.)
AKRAWY	91F	PL B257 531	M.Z. Akrawy et al.	(OPAL Collab.)
DECAMP	91B	PL B259 377	D. Decamp et al.	(ALEPH Collab.)
DECAMP	91J	PL B266 218	D. Decamp et al.	(ALEPH Collab.)
JACOBSEN	91	PRL 67 3347	R.G. Jacobsen et al.	(Mark II Collab.)
SHIMONAKA	91	PL B268 457	A. Shimonaka et al.	(TOPAZ Collab.)
ABE	90I	ZPHY C48 13	K. Abe et al.	(VENUS Collab.)
ABRAMS	90	PRL 64 1334	G.S. Abrams et al.	(Mark II Collab.)
AKRAWY	90J	PL B246 285	M.Z. Akrawy et al.	(OPAL Collab.)
BEHREND	90D	ZPHY C47 333	H.J. Behrend et al.	(CELLO Collab.)
BRUNSCH...	90	ZPHY C48 433	W. Braunschweig et al.	(TASSO Collab.)
ELSEN	90	ZPHY C46 349	E. Elsen et al.	(JADE Collab.)
HEGNER	90	ZPHY C46 547	S. Hegner et al.	(JADE Collab.)
STUART	90	PRL 64 983	D. Stuart et al.	(AMY Collab.)
ABE	89	PRL 62 613	F. Abe et al.	(CDF Collab.)
ABE	89C	PRL 63 720	F. Abe et al.	(CDF Collab.)
ABE	89L	PL B232 425	K. Abe et al.	(VENUS Collab.)
ABRAMS	89B	PRL 63 2173	G.S. Abrams et al.	(Mark II Collab.)
ABRAMS	89D	PRL 63 2780	G.S. Abrams et al.	(Mark II Collab.)
ALBAJAR	89	ZPHY C44 15	C. Albajar et al.	(UA1 Collab.)
BACALA	89	PL B218 112	A. Bacala et al.	(AMY Collab.)
BAND	89	PL B218 369	H.R. Band et al.	(MAC Collab.)
GREENSHAW	89	ZPHY C42 1	T. Greenshaw et al.	(JADE Collab.)
OULD-SAADA	89	ZPHY C44 567	F. Ould-Saada et al.	(JADE Collab.)
SAGAWA	89	PRL 63 2341	H. Sagawa et al.	(AMY Collab.)
ADACHI	88C	PL B208 319	I. Adachi et al.	(TOPAZ Collab.)
ADEVA	88	PR D38 2665	B. Adeva et al.	(Mark-J Collab.)
BRUNSCH...	88D	ZPHY C40 163	W. Braunschweig et al.	(TASSO Collab.)
ANSARI	87	PL B186 440	R. Ansari et al.	(UA2 Collab.)
BEHREND	87C	PL B191 209	H.J. Behrend et al.	(CELLO Collab.)
BARTEL	86C	ZPHY C30 371	W. Bartel et al.	(JADE Collab.)
Also		ZPHY C26 507	W. Bartel et al.	(JADE Collab.)
Also		PL 108B 140	W. Bartel et al.	(JADE Collab.)
ASH	85	PRL 55 1831	W.W. Ash et al.	(MAC Collab.)
BARTEL	85F	PL 161B 188	W. Bartel et al.	(JADE Collab.)
DERRICK	85	PR D31 2352	M. Derrick et al.	(HRS Collab.)
FERNANDEZ	85	PRL 54 1624	E. Fernandez et al.	(MAC Collab.)
LEVI	83	PRL 51 1941	M.E. Levi et al.	(Mark II Collab.)
BEHREND	82	PL 114B 282	H.J. Behrend et al.	(CELLO Collab.)
BRANDELIK	82C	PL 110B 173	R. Brandelik et al.	(TASSO Collab.)

Higgs Bosons — H^0 and H^\pm , Searches for

HIGGS BOSONS: THEORY AND SEARCHES

Updated May 2010 by G. Bernardi (LPNHE, CNRS/IN2P3, U. of Paris VI & VII), M. Carena (Fermi National Accelerator Laboratory and the University of Chicago), and T. Junk (Fermi National Accelerator Laboratory).

I. Introduction

Understanding the mechanism that breaks electroweak symmetry and generates the masses of all known elementary particles is one of the most fundamental problems in particle physics. The Higgs mechanism [1] provides a general framework to explain the observed masses of the W^\pm and Z gauge bosons by means of charged and neutral Goldstone bosons that end up as the longitudinal components of the gauge bosons. These Goldstone bosons are generated by the underlying dynamics of electroweak symmetry breaking (EWSB). However, the fundamental dynamics of the electroweak symmetry breaking are unknown. There are two main classes of theories proposed in the literature, those with weakly coupled dynamics - such as in the Standard Model (SM) [2] - and those with strongly coupled dynamics.

In the SM, the electroweak interactions are described by a gauge field theory based on the $SU(2)_L \times U(1)_Y$ symmetry group. The Higgs mechanism posits a self-interacting complex doublet of scalar fields, and renormalizable interactions are arranged such that the neutral component of the scalar doublet acquires a vacuum expectation value $v \approx 246$ GeV, which sets the scale of EWSB. Three massless Goldstone bosons are generated, which are absorbed to give masses to the W^\pm and Z gauge bosons. The remaining component of the complex doublet becomes the Higgs boson - a new fundamental scalar particle. The masses of all fermions are also a consequence of EWSB since the Higgs doublet is postulated to couple to the

fermions through Yukawa interactions. If the Higgs boson mass m_H is below ~ 180 GeV, all fields remain weakly interacting up to the Planck scale, M_{Pl} .

The validity of the SM as an effective theory describing physics up to the Planck scale is questionable, however, because of the following “naturalness” argument. All fermion masses and dimensionless couplings are logarithmically sensitive to the scale Λ at which new physics becomes relevant. In contrast, scalar squared masses are quadratically sensitive to Λ . Thus, the observable SM Higgs mass has the following form:

$$m_H^2 = (m_H^2)_0 + \frac{kg^2\Lambda^2}{16\pi^2},$$

where $(m_H)_0$ is a fundamental parameter of the theory. The second term is a one-loop correction in which g is an electroweak coupling and k is a constant, presumably of $\mathcal{O}(1)$, that is calculable within the low-energy effective theory. The two contributions arise from independent sources and one would not expect that the observable Higgs boson mass is significantly smaller than either of the two terms. Hence, if the scale of new physics Λ is much larger than the electroweak scale, unnatural cancellations must occur to remove the quadratic dependence of the Higgs boson mass on this large energy scale and to give a Higgs boson mass of order of the electroweak scale, as required from unitarity constraints [3,4], and as preferred by precision measurements of electroweak observables [5]. Thus, the SM is expected to be embedded in a more fundamental theory which will stabilize the hierarchy between the electroweak scale and the Planck scale in a natural way. A theory of that type would usually predict the onset of new physics at scales of the order of, or just above, the electroweak scale. Theorists strive to construct models of new physics that keep the successful features of the SM while curing its shortcomings, including the absence of a dark matter candidate or an electroweak scale explanation of the observed baryon asymmetry of the universe.

In the weakly-coupled approach to electroweak symmetry breaking, supersymmetric (SUSY) extensions of the SM provide a possible explanation for the stability of the electroweak energy scale in the presence of quantum corrections [7]. These theories predict a spectrum of Higgs scalars [8]. The properties of the lightest Higgs scalar often resemble those of the SM Higgs boson, with a mass that is predicted to be less than 135 GeV [9] in the simplest supersymmetric model. Additional neutral and charged Higgs bosons with masses of order of the weak scale are also predicted. Moreover, low-energy supersymmetry with a supersymmetry breaking scale of order 1 TeV allows for grand unification of the electromagnetic, weak and strong gauge interactions in a consistent way, strongly supported by the prediction of the electroweak mixing angle at low energy scales, with an accuracy at the percent level [10,11].

Alternatively, new strong interactions near the TeV scale can induce strong breaking of the electroweak symmetry [12]. Recently, so-called “Little Higgs” models have been proposed in which the scale of the new strong interactions is pushed up

above 10 TeV [13], and the lightest Higgs scalar resembles the weakly-coupled SM Higgs boson.

Alternatively, a new approach to electroweak symmetry breaking has been explored in which extra space dimensions beyond the usual 3 + 1 dimensional space-time are introduced [14] with characteristic sizes of order $(1 \text{ TeV})^{-1}$. In such scenarios, the mechanisms for electroweak symmetry breaking are inherently extra-dimensional and the resulting Higgs phenomenology can depart significantly from the SM paradigm [15].

Prior to 1989, when the e^+e^- collider LEP at CERN came into operation, searches for Higgs bosons were sensitive only to Higgs bosons with masses of a few GeV and below [16]. In the LEP1 phase, the collider operated at center-of-mass energies close to M_Z . During the LEP2 phase, the energy was increased in steps, reaching 209 GeV in the year 2000 before the final shutdown. The combined data of the four LEP experiments, ALEPH, DELPHI, L3, and OPAL, was sensitive to neutral Higgs bosons with masses up to about 115 GeV and to charged Higgs bosons with masses up to about 90 GeV [17,18].

The search for the Higgs boson continues at the Tevatron $p\bar{p}$ collider, operating at a center-of-mass energy of 1.96 TeV. The sensitivity of the two experiments, CDF and DØ, is improving, and with the integrated luminosity collected so far, is already high enough to probe SM Higgs boson masses beyond the LEP reach [19]. Other neutral and charged Higgs particles postulated in most theories beyond the SM are also actively sought at the Tevatron. The searches for Higgs bosons will continue with significantly higher sensitivities in the coming years at the LHC pp collider and are expected to cover masses up to about 1 TeV for the SM Higgs boson [20,21]. Once evidence for the dynamics of electroweak symmetry breaking is obtained, a more complete understanding of the mechanism will require measurements at future e^+e^- [22] and perhaps $\mu^+\mu^-$ colliders [23].

In order to keep this review up to date, some unpublished results are quoted. LEP results are marked with (*) in the reference list and can be accessed conveniently from the public web page

lepiggs.web.cern.ch/LEPHIGGS/pdg2008/index.html.

Preliminary results from the CDF collaboration are marked with (**) and can be obtained from the public web page

<http://www-cdf.fnal.gov/physics/physics.html>;

those from DØ are marked with (***) and can be obtained at <http://www-d0.fnal.gov/Run2Physics/WWW/results.htm>.

II. The Standard Model Higgs Boson

In the SM, the Higgs boson mass is given by $m_H = \sqrt{\lambda/2} v$, where λ is the Higgs self-coupling parameter and v is the vacuum expectation value of the Higgs field, $v = (\sqrt{2}G_F)^{-1/2} \approx 246 \text{ GeV}$, fixed by the Fermi coupling G_F , which is determined precisely from muon decay measurements [24]. Since λ is presently unknown, the value of the SM Higgs boson mass m_H cannot be predicted. However, besides the upper

bound on the Higgs boson mass from unitarity constraints [3,4], additional theoretical arguments place approximate upper and lower bounds on m_H [25]. There is an upper bound based on the perturbativity of the theory up to the scale Λ at which the SM breaks down, and a lower bound derived from the stability of the Higgs potential. If m_H is too large, then the Higgs self-coupling diverges at some scale Λ below the Planck scale. If m_H is too small, then the Higgs potential develops a second (global) minimum at a large value of the scalar field of order Λ . New physics must enter at a scale Λ or below, so that the global minimum of the theory corresponds to the observed $SU(2)_L \times U(1)_Y$ broken vacuum with $v = 246 \text{ GeV}$. Given a value of Λ , one can compute the minimum and maximum allowed Higgs boson mass. Conversely, the value of m_H itself can provide an important constraint on the scale up to which the SM remains successful as an effective theory. In particular, a Higgs boson with mass in the range $130 \text{ GeV} \lesssim m_H \lesssim 180 \text{ GeV}$ is consistent with an effective SM description that survives all the way to the Planck scale, although the hierarchy problem between the electroweak scale and $\Lambda = M_{\text{Pl}}$ still persists. The lower bound on m_H can be reduced to about 115 GeV [26], if one allows for the electroweak vacuum to be metastable, with a lifetime greater than the age of the universe.

The SM Higgs couplings to fundamental fermions are proportional to the fermion masses, and the couplings to bosons are proportional to the squares of the boson masses. In particular, the SM Higgs boson is a CP -even scalar, and its couplings to gauge bosons, Higgs bosons and fermions are given by:

$$g_{Hf\bar{f}} = \frac{m_f}{v}, \quad g_{HVV} = \frac{2m_V^2}{v}, \quad g_{HHVV} = \frac{2m_V^2}{v^2}$$

$$g_{HHH} = \frac{3m_H^2}{v}, \quad g_{HHHH} = \frac{3m_H^2}{v^2}$$

where $V = W^\pm$ or Z . In Higgs boson production and decay processes, the dominant mechanisms involve the coupling of the H to the W^\pm , Z and/or the third generation quarks and leptons. The Higgs boson's coupling to gluons, Hgg , is induced at leading order by a one-loop graph in which the H couples to a virtual $t\bar{t}$ pair. Likewise, the Higgs boson's coupling to photons, $H\gamma\gamma$, is also generated via loops, although in this case the one-loop graph with a virtual W^+W^- pair provides the dominant contribution [8]. Reviews of the SM Higgs boson's properties and its phenomenology, with an emphasis on the impact of loop corrections to the Higgs boson decay rates and cross sections, can be found in Refs. [27,28].

The cross sections for the production of SM Higgs bosons are summarized in Fig. 1 for $p\bar{p}$ collisions at the Tevatron, and in Fig. 2 for pp collisions at the LHC [29]. The cross section for the $gg \rightarrow H + X$ process is known at next-to-next-to-leading order (NNLO) in QCD, in the large top-mass limit, and at NLO in QCD for arbitrary top mass [30]. The NLO QCD corrections approximately double the leading-order prediction, and the NNLO corrections add approximately 50% to the NLO prediction. NLO electroweak corrections (not included in the

Gauge & Higgs Boson Particle Listings

Higgs Bosons — H^0 and H^\pm

figures) range between 0 and 6% of the LO term [31]. Mixed QCD-electroweak corrections $O(\alpha\alpha_s)$ are computed in [32]. In addition, soft-gluon contributions to the cross sections have been resummed at next-to-next-to-leading logarithmic (NNLL) and NNNLL accuracy [33]. Updated predictions for the gluon fusion cross sections using the most recent parametrizations of parton distribution functions at next-to-next-to-leading order can be found in [32,34]. An additional enhancement of the cross section is obtained when a resummation of the kinematically enhanced terms in the time-like gluon form factor is performed [35]. At LHC and Tevatron energies, and for intermediate Higgs-boson masses, this increases the cross section by about 6% compared with that obtained using soft-gluon resummation alone, and by about 10% compared with the fixed-order results at NNLO. Certain search strategies look for Higgs boson production in association with jets. In the heavy top quark mass limit, Higgs boson production cross section in association with one jet is considered in Refs. [36–39] and in association with two jets in Refs. [40,41].

The cross sections for the associated production processes $q\bar{q} \rightarrow W^\pm H + X$ and $q\bar{q} \rightarrow ZH + X$ are known at NNLO for the QCD corrections and at NLO for the electroweak corrections [42,43]. The residual uncertainty is rather small, less than 5%. For the vector boson fusion processes $qq \rightarrow qqH + X$, corrections to the production cross section are known at NNLO in QCD and the remaining theoretical uncertainties are approximately 2% [44]. The cross section for the associated production process $t\bar{t}H$ has been calculated at NLO in QCD [45], while the bottom fusion Higgs boson production cross section is known at NNLO in the case of five quark flavors [42,46,47].

The branching ratios for the most relevant decay modes of the SM Higgs boson are shown in Fig. 3 as functions of m_H , and the total decay width is shown in Fig. 4, also as function of m_H [28,48]. For masses below 135 GeV, decays to fermion pairs dominate, of which the decay $H \rightarrow b\bar{b}$ has the largest branching ratio. Decays to $\tau^+\tau^-$, $c\bar{c}$ and gluon pairs together contribute less than 15%. For such low masses, the total decay width is less than 10 MeV. For Higgs boson masses above 135 GeV, the W^+W^- decay dominates (below the W^+W^- threshold, one of the W bosons is virtual) with an important contribution from $H \rightarrow ZZ$, and the decay width rises rapidly, reaching about 1 GeV at $m_H = 200$ GeV and 100 GeV at $m_H = 500$ GeV. Above the $t\bar{t}$ threshold, the branching ratio into top-quark pairs increases rapidly as a function of the Higgs boson mass, reaching a maximum of about 20% at $m_H \sim 450$ GeV.

Searches for the SM Higgs Boson at LEP

The principal mechanism for producing the SM Higgs boson in e^+e^- collisions at LEP energies is Higgs-strahlung in the s -channel, $e^+e^- \rightarrow HZ$ [49]. The Z boson in the final state is either virtual (LEP1), or on mass shell (LEP2). The SM

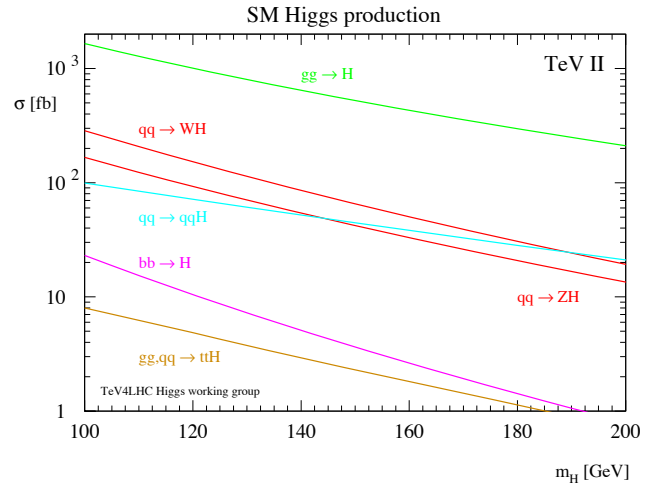


Figure 1: SM Higgs boson production cross sections for $p\bar{p}$ collisions at 1.96 TeV, from Ref. 29 and references therein. Color version at end of book.

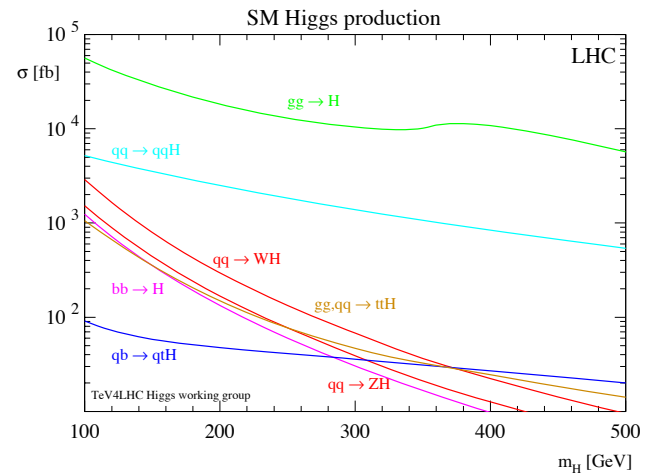


Figure 2: SM Higgs boson production cross sections for pp collisions at 14 TeV [29]. Color version at end of book.

Higgs boson can also be produced by W^+W^- and ZZ fusion in the t -channel [50], but at LEP these processes have small cross sections. The sensitivity of the LEP searches to the Higgs boson is primarily a function of the center-of-mass energy, E_{CM} . For $m_H < E_{CM} - M_Z$, the cross section is quite large, of order 1 pb or more, while for $m_H > E_{CM} - M_Z$, the cross section is smaller by an order of magnitude or more.

During the LEP1 phase, the ALEPH, DELPHI, L3 and OPAL collaborations analyzed over 17 million Z decays and set lower bounds of approximately 65 GeV on the mass of the SM Higgs boson [51]. At LEP2, substantial data samples were collected at center-of-mass energies up to 209 GeV.

Each production and decay mode was analyzed separately. Data recorded at each center-of-mass energy were studied independently and the results from the four LEP experiments were

Gauge & Higgs Boson Particle Listings

Higgs Bosons — H^0 and H^\pm

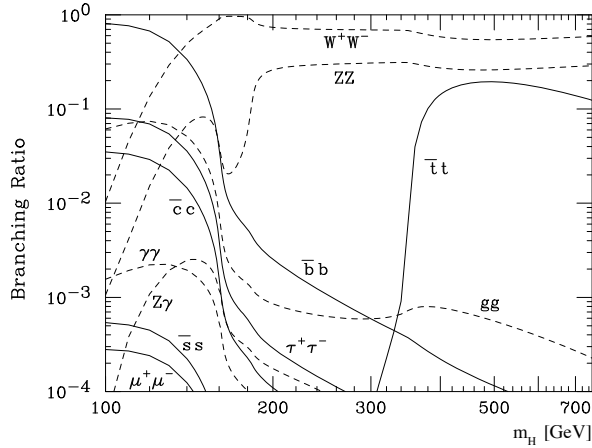


Figure 3: Branching ratios for the main decays of the SM Higgs boson [28,48].

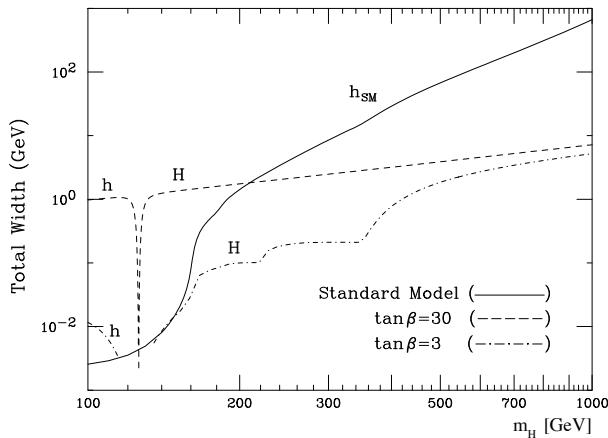


Figure 4: The total decay width of the SM Higgs boson, shown as a function of m_H [48]. Also shown are the decay widths for the CP-even neutral Higgs bosons, h and H , for two choices of $\tan\beta$, in the MSSM benchmark scenario $m_{h\text{-max}}$, described in Section III.

then combined. Distributions of neural network discriminants which are functions of reconstructed event quantities such as invariant masses and b -tagging discriminants were assembled for the data, and also for the signal and background predictions. The CL_s method [52] was used to compute the observed and expected limits on the Higgs boson production cross section as functions of the Higgs boson mass sought, and from that, a lower bound on m_H was derived. The p -value for the background-only hypothesis, which is the probability for the background model to produce a fluctuation as signal-like as that seen in the data or more, was also computed.

Higgs bosons were sought in four final state topologies: The four-jet topology in which $H \rightarrow b\bar{b}$ and $Z \rightarrow q\bar{q}$; the final states with tau leptons produced in the processes $H \rightarrow \tau^+\tau^-$ where $Z \rightarrow q\bar{q}$, together with the mode $H \rightarrow b\bar{b}$ with $Z \rightarrow \tau^+\tau^-$; the missing energy topology produced mainly in the process $H \rightarrow b\bar{b}$

with $Z \rightarrow \nu\bar{\nu}$, and finally the leptonic states $H \rightarrow b\bar{b}$ with $Z \rightarrow e^+e^-, \mu^+\mu^-$. At LEP1, only the modes with $Z \rightarrow \ell^+\ell^-$ and $Z \rightarrow \nu\bar{\nu}$ were used because the backgrounds in the other channels were prohibitive. For the data collected at LEP2, all decay modes were used.

For very light Higgs bosons, with $m_H < 2m_\tau$, the decay modes exploited above are not kinematically allowed, and decays to jets, muon pairs, pion pairs, and lighter particles dominate, depending sensitively on m_H . For very low masses, OPAL's decay-mode independent search [53] for the Bjorken process $e^+e^- \rightarrow S^0 Z$, where S^0 denotes a generic neutral, scalar particle, provides sensitivity. This search is based on studies of the recoil mass spectrum in events with $Z \rightarrow e^+e^-$ and $Z \rightarrow \mu^+\mu^-$ decays, and on the final states $Z \rightarrow \nu\bar{\nu}$ and $S^0 \rightarrow e^+e^-$ or photons. Upper bounds on the cross section are produced for scalar masses between 1 KeV and 100 GeV.

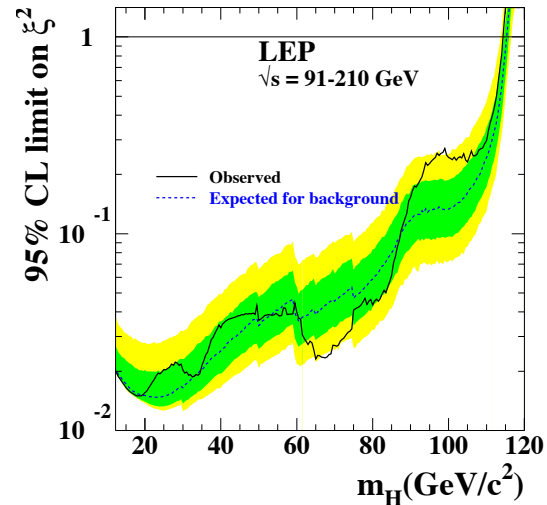


Figure 5: The 95% confidence level upper bound on the ratio $\xi^2 = (g_{HZZ}/g_{HZZ}^{\text{SM}})^2$ [17]. The solid line indicates the observed limit, and the dashed line indicates the median limit expected in the absence of a Higgs boson signal. The dark and light shaded bands around the expected limit line correspond to the 68% and 95% probability bands, indicating the range of statistical fluctuations of the expected outcomes. The horizontal line corresponds to the Standard Model coupling. Standard Model Higgs boson decay branching fractions are assumed. Color version at end of book.

The LEP searches did not show any conclusive evidence for the production of a SM Higgs boson. However, in the LEP2 data, ALEPH reported an excess of about three standard deviations, suggesting the production of a SM Higgs boson with mass ~ 115 GeV [54]. Analyses of the data from DELPHI [55], L3 [56], and OPAL [57] did not show evidence for such an excess, but could not, however, exclude a 115 GeV Higgs

Gauge & Higgs Boson Particle Listings

Higgs Bosons — H^0 and H^\pm

boson at the 95% C.L. When the data of the four experiments were combined, the overall significance of a possible signal at $m_H = 115$ GeV was low, as given by the background-only p -value of 0.09 [17]. The same combination of the LEP data yields a 95% C.L. lower bound of 114.4 GeV for the mass of the SM Higgs boson. The median limit one would expect to obtain in a large ensemble of identical experiments with no signal present is 115.3 GeV. Fig. 5 shows the observed production cross section limits, relative to the SM Higgs boson production rate (including vector-boson fusion), assuming SM Higgs boson branching ratios.

Indirect Constraints on the SM Higgs Boson

Indirect experimental bounds for the SM Higgs boson mass are obtained from fits to precision measurements of electroweak observables. The Higgs boson contributes to the W^\pm and Z vacuum polarization through loop effects, leading to a logarithmic sensitivity of the ratio of the W^\pm and Z gauge boson masses on the Higgs boson mass. A global fit to precision electroweak data, accumulated in the last two decades at LEP, SLC, the Tevatron, and elsewhere, gives $m_H = 87_{-26}^{+35}$ GeV, or $m_H < 157$ GeV at 95% C.L. [5]. The top quark contributes to the W^\pm boson vacuum polarization through loop effects that depend quadratically on the top mass, which plays an important role in the global fit. A top quark mass of 173.1 ± 1.3 GeV [58] and a W^\pm boson mass of 80.399 ± 0.023 GeV [59] were used. If the direct LEP search limit of $m_H > 114.4$ GeV is taken into account, an upper limit of $m_H < 186$ GeV at 95% C.L. is obtained.

Searches for the SM Higgs Boson at the Tevatron

At the Tevatron, the most important SM Higgs boson production processes are gluon fusion ($gg \rightarrow H$) and Higgs boson production in association with a vector boson ($W^\pm H$ or ZH) [60]. For masses less than about 135 GeV, the most promising discovery channels are $W^\pm H$ and ZH with $H \rightarrow b\bar{b}$. The contribution of $H \rightarrow W^*W$ is dominant at higher masses, $m_H > 135$ GeV. Using this decay mode, both the direct ($gg \rightarrow H$) and the associated production ($p\bar{p} \rightarrow W^\pm H$ or ZH) channels are explored, and the results of both Tevatron experiments are combined to maximize the sensitivity to the Higgs boson.

The signal-to-background ratio is much smaller in the Tevatron searches than in the LEP analyses, and the systematic uncertainties on the estimated background rates are typically larger than the signal rates. In order to estimate the background rates in the selected samples more accurately, auxiliary measurements are made in data samples which are expected to be depleted in Higgs boson signal. These auxiliary samples are chosen to maximize the sensitivity to each specific background in turn. Then, Monte Carlo simulations are used to extrapolate these measurements into the Higgs signal regions. The dominant physics backgrounds such as top-pair, diboson, $W^\pm b\bar{b}$, and single top production are estimated by Monte Carlo simulations in this way, i.e., after having been tuned or verified by

corresponding measurements in dedicated analyses, thereby reducing the uncertainty on the total background estimate. The uncertainties on the background rates diminish with increasing integrated luminosity because increasingly larger data samples are used to constrain them, and thus these uncertainties are not expected to be limiting factors in the sensitivity of the searches.

At Higgs boson masses of 150 GeV and below, the searches for associated production, $p\bar{p} \rightarrow W^\pm H, ZH$, are performed in different channels:

a) $p\bar{p} \rightarrow W^\pm H$, where the W^\pm decays leptonically and $H \rightarrow b\bar{b}$. These searches have been published by CDF using 2.7 fb^{-1} of data [61] and by DØ using 1.1 fb^{-1} of data [62]. The latest updates as of this review are based on 4.8 fb^{-1} of data from CDF [63] and 5.0 fb^{-1} from DØ [64]; the Higgs boson production cross section limits obtained by both collaborations are four to five times higher than the SM expectation in this channel for a Higgs boson mass of 115 GeV. These updates use advanced analysis techniques such as neural networks to separate a potential signal from the background processes, and also to separate correctly identified b -jets from jets originating from gluons or from u, d, s or c quarks, mistakenly identified as b -jets.

b) $p\bar{p} \rightarrow ZH$, where the Z decays into $\nu\bar{\nu}$, is also a sensitive channel, but, since the final state is characterized by missing transverse energy and two b -jets, multijet backgrounds without Z bosons require special care. The sensitivity of this search is enhanced by $W^\pm H$ events in which the charged lepton from the W^\pm decay escapes detection; these events have the same experimental signature as the $ZH \rightarrow \nu\bar{\nu}$ signal. The CDF Collaboration has published a result in this channel using 2.1 fb^{-1} of data [65] and the DØ Collaboration has published a result in this channel with 5.2 fb^{-1} of data [66] with optimized triggers and selection criteria which improve the signal acceptance, as well as refined analysis techniques. An update with 3.6 fb^{-1} (CDF [67]) was also released in 2009. The sensitivity of these channels is comparable to that obtained in the $W^\pm H$ channel.

c) $p\bar{p} \rightarrow ZH$, where the Z decays into charged leptons (e or μ), suffers from a smaller Z branching fraction, but it has a lower background rate. Both collaborations constrain the kinematics of the events to improve the reconstructed mass resolution. The sensitivity of these channels is not much lower than that of the previous two channels. The CDF Collaboration has published a result in this channel using 2.7 fb^{-1} of data [68] and the DØ Collaboration has published a result based on 0.45 fb^{-1} of data [69]. Preliminary updates with 4.2 fb^{-1} of data are available from both CDF and DØ [70,71].

d) Both Tevatron collaborations search for SM $H \rightarrow \tau^+\tau^-$, where the $gg \rightarrow H, WH, ZH$, and vector-boson fusion production processes are considered [72,73]. The DØ publication has been updated with a 4.9 fb^{-1} data sample [74]. DØ also includes a search for $WH \rightarrow \tau\nu b\bar{b}$, using a 4.0 fb^{-1} data sample [75]. This final state is partly covered by CDF in its

isolated-track selection [76], in a 4.3 fb^{-1} data sample. These analyses benefit from the more inclusive production mechanisms considered, but the $H \rightarrow \tau^+\tau^-$ decay branching fraction is significantly less than that to $b\bar{b}$, as shown in Fig. 3.

e) Both Tevatron collaborations search for the SM process $H \rightarrow \gamma\gamma$, making use of all production modes. Since $\text{BR}(H \rightarrow \gamma\gamma)$ is so small in the SM, they contribute little to the SM combined sensitivity. Nonetheless, they set strong constraints on extended models, and thus are discussed later in this review.

e) The CDF Collaboration has published a search in 2.0 fb^{-1} of data for $WH + ZH \rightarrow jjb\bar{b}$ [77], making use of signal events in which the vector boson decays to jets. While the expected signal yields are higher than in other modes due to the favorable branching fractions, the multijet backgrounds are also quite large.

When combining the low-mass channels of the two collaborations, the expected (observed) limit is 1.8 (2.7) times higher than the expected SM production cross section for $m_H = 115 \text{ GeV}$, as can be seen in Fig. 6 [78]. With the projected improvements in analysis sensitivity, and the accumulation of more integrated luminosity (12 fb^{-1} of data are expected by the end of 2011), the low-mass Higgs boson is expected to be probed at the Tevatron.

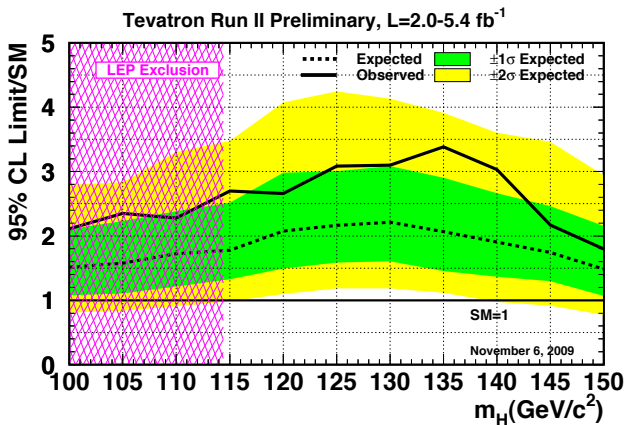


Figure 6: Upper bound on the SM Higgs boson cross section obtained by combining CDF and DØ search results, as a function of the mass of the Higgs boson sought [78]. The limits are shown as a multiple of the SM cross section. The ratios of the different production and decay modes are assumed to be as predicted by the SM. The solid curve is the observed upper bound, and the dashed black curve is the median expected upper bound assuming no signal is present. The shaded bands show the 68% and 95% probability bands around the expected upper bound. Color version at end of book.

Around $m_H = 135 \text{ GeV}$, where all branching fractions are below 50%, no channel is strongly dominant and the overall sensitivity is weaker. At these masses, the $WH \rightarrow WWW^*$ channel¹ brings further sensitivity [79,80,81] beyond the $b\bar{b}$ channel alone.

To probe masses above 135 GeV, the dominant $H \rightarrow WW^*$ decay mode is best exploited. The dominant production mode is $gg \rightarrow H$ which can be used in this channel since the leptonic W boson decays distinguish the signal from backgrounds containing jets. Nonetheless, WH production, ZH production, and vector-boson fusion qqH production contribute additional signal in this channel which is used in the searches. The WW pair issued from a Higgs boson decay has a spin correlation which is different from that of the dominant background, electroweak WW production. These spin correlations are transmitted to the distributions of observed leptons, providing a handle to separate the signal from the background. The invariant mass of the Higgs boson decay products cannot be reconstructed due to the undetected neutrinos, but the sensitivity is nevertheless significant. Results were published with 4.8 fb^{-1} by CDF [82] and 5.4 fb^{-1} by DØ [83], together with the combination of these results [19], which are reproduced in Fig. 7. An expected (observed) upper limit is set on the $gg \rightarrow H$ cross section 0.9 (0.9) times the SM prediction at $m_H = 165 \text{ GeV}$ [78], a SM Higgs boson with mass between 162 and 166 GeV is excluded at the 95% C.L.

Overall, the combined CDF and DØ analyses are expected to test, at the 95% C.L. or better, the SM Higgs boson predictions for masses between the LEP limit and about 185 GeV before the end of Run II. The channels used at the Tevatron for Higgs boson masses below 130 GeV are different from those dominantly used at the LHC, hence with the full Run II luminosity, they are expected to provide complementary information if a low mass Higgs boson exists.

The SM Higgs boson production processes and branching ratios presented above are limited to the case of three generations of quarks and leptons. The existence of a fourth generation of fermions is compatible with present experimental bounds and would have direct consequences on the SM Higgs boson production and decay branching ratios, and hence on Higgs searches at LEP, the Tevatron, and the LHC [84,85]. Current experimental searches bound the fourth generation quark masses to be above the top quark mass [86]. These additional heavy quarks lead to new contributions in the loop-induced couplings of the Higgs boson to gluons and photons, leading to a strong enhancement of the gluon fusion production rate and of the branching ratio of the Higgs boson decay into a pair of gluons. The branching ratios of Higgs boson decay to $b\bar{b}$, tau pairs, and pairs of W and Z bosons are reduced, although near $m_H \sim 2M_W$, the decay to a pair of W bosons still nearly saturates the decay width, even with the enhanced gluon decay. Due to a cancellation

¹ The star indicates that below the $H \rightarrow W^+W^-$ threshold, one of the W^\pm bosons is virtual.

Gauge & Higgs Boson Particle Listings

Higgs Bosons — H^0 and H^\pm

between the W and heavy fermion contributions, the photon decay channels may be further suppressed. The enhancement of the gluon fusion production rate makes the search channels using Higgs boson decays into tau leptons and W and Z bosons promising for a light Higgs boson. In addition, in the case of a fourth generation Majorana neutrino, exotic signals such as Higgs boson decay into same-sign dileptons may be possible.

The CDF and $D\bar{O}$ search results in the $H \rightarrow W^+W^-$ decay mode have been used to test an extension of the SM with four generations of quarks and leptons, using only the $gg \rightarrow H \rightarrow W^+W^-$ mechanism [87]. The production cross section is computed at NNLO [88], and the decay branching fractions are computed using a modified version of HDECAY [28,84]. The excluded ratio to the fourth-generation prediction is shown in Fig. 8, excluding such a Higgs boson with a mass between 131 and 204 GeV. These limits are robust against other choices of the heavy fermion masses.

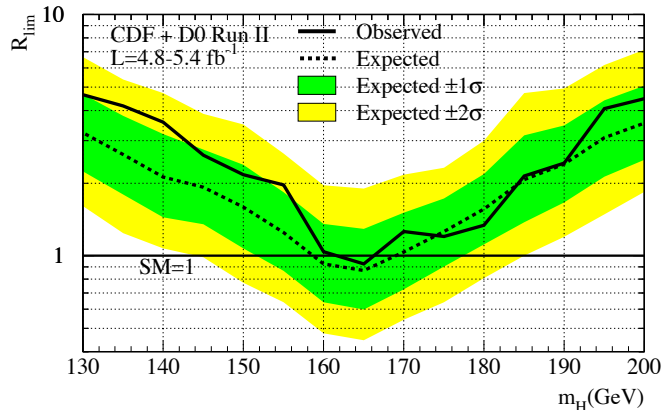


Figure 7: Upper bound on the SM Higgs boson cross section obtained by combining CDF and $D\bar{O}$ search results in the $H \rightarrow W^+W^-$ decay mode, as a function of the mass of the Higgs boson sought [19]. The limits are shown as a multiple of the SM cross section. The ratios of the different production and decay modes are assumed to be as predicted by the SM. The solid curve shows the observed upper bound, the dashed black curve shows the median expected upper bound assuming no signal is present. The shaded bands show the 68% and 95% probability bands around the expected upper bound. Color version at end of book.

Studies to assess the sensitivity to diffractive Higgs boson production at the Tevatron and the LHC are being pursued [89]. Three different diffractive production mechanisms can be considered: exclusive production, $p\bar{p}, pp \rightarrow p + H + \bar{p}, p$; inclusive production, $p\bar{p}, pp \rightarrow X + H + Y$; and central inelastic production, $p\bar{p}, pp \rightarrow p + (HX) + \bar{p}, p$, where a plus sign indicates the presence of a rapidity gap. Tests of the different production mechanisms using appropriate final states in the Tevatron data

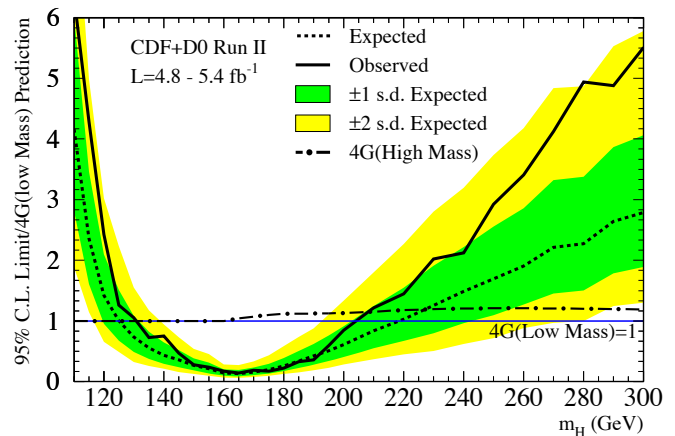


Figure 8: Upper bound on the Higgs boson cross section of the 4th generation sequential model obtained by combining CDF and $D\bar{O}$ search results in the $H \rightarrow W^+W^-$ decay mode, as a function of the mass of the Higgs boson sought [87]. The limits are shown as a multiple of the cross section obtained in this extended model. The solid curve shows the observed upper bound, the dashed black curve shows the median expected upper bound assuming no signal is present, and the colored bands show the 68% and 95% probability bands around the expected upper bound. Color version at end of book.

are important for improving predictions for diffractive Higgs boson production at the LHC.

Prospects for SM Higgs Boson Searches at the LHC

At the LHC, the main production processes are gluon fusion ($gg \rightarrow H$), Higgs boson production in association with a vector boson ($W^\pm H$ or ZH) or with a top-quark pair ($t\bar{t}H$), and the vector boson fusion process (qqH or $q\bar{q}H$) [60]. This array of production and decay modes, together with a large integrated luminosity, allows for a variety of search channels. Search strategies have been explored in many analyses over the last years [20,21]. The searches in the inclusive channels $H \rightarrow \gamma\gamma$ (for low mass) and $H \rightarrow ZZ^* \rightarrow 4l$ (for high mass) will be complemented with more exclusive searches in order to strengthen the discovery potential, particularly at low mass. Vector boson fusion processes, making use of forward jet tagging and the decay modes $H \rightarrow \tau^+\tau^-$, $H \rightarrow \gamma\gamma$ as well as $H \rightarrow W^+W^-$ [90] will provide additional sensitivity. Other analyses, expected to be relevant at higher integrated luminosities, select Higgs boson decays to $b\bar{b}$ or $\gamma\gamma$ in association with a lepton from the decay of an associated W^\pm boson, Z boson, or top quark.

The projections of the ATLAS and CMS collaborations show that, with an integrated luminosity of 10 - 30 fb^{-1} at a center-of-mass energy of 14 TeV, the SM Higgs boson is expected to be discovered if it exists and has a mass below 1 TeV. With a lower

See key on page 405

Gauge & Higgs Boson Particle Listings

Higgs Bosons — H^0 and H^\pm

integrated luminosity, the discovery of a Higgs boson with a mass below 130 GeV is challenging. If the Higgs boson's mass is in this range, a few years of running may be needed to discover it. However, the combination of the results in all channels of the two experiments could allow for a 5σ discovery with about 5 fb^{-1} of data, once the detectors and the composition of the selected event samples are understood [91,92].

If a SM Higgs boson is discovered, its properties could be studied at the LHC. Its mass could be measured by each experiment with a precision of $\sim 0.1\%$ in the 100–400 GeV mass range [21,93]. This projection is based on the invariant mass reconstruction from electromagnetic calorimeter objects, using the decays $H \rightarrow \gamma\gamma$ or $H \rightarrow ZZ^* \rightarrow 4\ell$. The precision would be degraded at higher masses because of the larger decay width, but even at $m_H \sim 700$ GeV a precision of 1% on m_H is expected to be achievable. The width of the SM Higgs boson would be too narrow to be measured directly for $m_H < 200$ GeV; nonetheless, it could be constrained indirectly using partial width measurements [94,95]. For $300 < m_H < 700$ GeV, a direct measurement of the decay width could be performed with a precision of about 6%. The possibilities for measuring other properties of the Higgs boson, such as its spin, its CP -eigenvalue, its couplings to bosons and fermions, and its self-coupling, have been investigated in numerous studies [21,93,96–98]. Given a sufficiently high integrated luminosity (300 fb^{-1}), most of these properties are expected to be accessible to analysis for some specific mass ranges. The measurement of Higgs self-couplings, however, appears to be impossible at the LHC, although a luminosity upgrade, the so-called Super-LHC, could allow for such a measurement. The results of these measurements could either firmly establish the Higgs mechanism, or point the way to new physics.

III. Higgs Bosons in the MSSM

Electroweak symmetry breaking driven by a weakly-coupled elementary scalar sector requires a mechanism to explain the smallness of the electroweak symmetry breaking scale compared with the Planck scale [99]. Within supersymmetric extensions of the SM, supersymmetry-breaking effects, whose origins may lie at energy scales much larger than 1 TeV, can induce a radiative breaking of the electroweak symmetry due to the effects of the large Higgs-top quark Yukawa coupling [100]. In this way, the electroweak symmetry breaking scale is intimately tied to the mechanism of supersymmetry breaking. Thus, supersymmetry provides an explanation for the stability of the hierarchy of scales, provided that the supersymmetry-breaking masses are of $\mathcal{O}(1 \text{ TeV})$ or less [99].

A fundamental theory of supersymmetry breaking is unknown at this time. Nevertheless, one can parameterize the low-energy theory in terms of the most general set of soft supersymmetry-breaking renormalizable operators [101]. The Minimal Supersymmetric extension of the Standard Model (MSSM) [102] associates a supersymmetric partner to each gauge boson and chiral fermion of the SM, and provides a

realistic model of physics at the weak scale. However, even in this minimal model with the most general set of soft supersymmetry-breaking terms, more than 100 new parameters are introduced [103]. Fortunately, only a small number of these parameters impact the Higgs phenomenology through tree level and quantum effects.

The MSSM contains the particle spectrum of a two-Higgs-doublet model (2HDM) extension of the SM and the corresponding supersymmetric partners. Two Higgs doublets, H_u and H_d , are required to ensure an anomaly-free SUSY extension of the SM and to generate mass for both “up”-type and “down”-type quarks and charged leptons [8]. After the spontaneous breaking of the electroweak symmetry, five physical Higgs particles are left in the spectrum: one charged Higgs pair, H^\pm , one CP -odd scalar, A , and two CP -even states, H and h .

The supersymmetric structure of the theory imposes constraints on the Higgs sector of the model. In particular, the parameters of the Higgs self-interaction are given by the gauge coupling constants. As a result, all Higgs sector parameters at tree level are determined by only two free parameters: the ratio of the H_u and H_d vacuum expectation values,

$$\tan\beta = v_u/v_d,$$

with $v_u^2 + v_d^2 \approx (246 \text{ GeV})^2$; and one Higgs boson mass, conventionally chosen to be m_A . The other tree-level Higgs boson masses are then given in terms of these parameters

$$m_{H^\pm}^2 = m_A^2 + M_W^2$$

$$m_{H,h}^2 = \frac{1}{2} \left[m_A^2 + M_Z^2 \pm \sqrt{(m_A^2 + M_Z^2)^2 - 4(M_Z m_A \cos 2\beta)^2} \right]$$

and α is the angle that diagonalizes the CP -even Higgs squared-mass matrix.

An important consequence of these mass formulae is that the mass of the lightest CP -even Higgs boson is bounded from above:

$$m_h \leq M_Z |\cos 2\beta|.$$

This contrasts sharply with the SM, in which this Higgs boson mass is only constrained by perturbativity and unitarity bounds. In the large m_A limit, also called the decoupling limit [104], one finds $m_h^2 \simeq (M_Z \cos 2\beta)^2$ and $m_A \simeq m_H \simeq m_{H^\pm}$, up to corrections of $\mathcal{O}(M_Z^2/m_A)$. Below the scale m_A , the effective Higgs sector consists only of h , which behaves very similarly to the SM Higgs boson.

The phenomenology of the Higgs sector depends on the couplings of the Higgs bosons to gauge bosons, and fermions. The couplings of the two CP -even Higgs bosons to W^\pm and Z bosons are given in terms of the angles α and β by

$$g_{hVV} = g_V m_V \sin(\beta - \alpha) \quad g_{HVV} = g_V m_V \cos(\beta - \alpha),$$

where $g_V \equiv 2m_V/v$. There are no tree-level couplings of A or H^\pm to VV . The couplings of the Z boson to two neutral Higgs

Gauge & Higgs Boson Particle Listings

Higgs Bosons — H^0 and H^\pm

bosons, which must have opposite CP -quantum numbers, are given by

$$g_{hAZ} = g_Z \cos(\beta - \alpha)/2$$

$$g_{HAZ} = -g_Z \sin(\beta - \alpha)/2.$$

Charged Higgs-W boson couplings to neutral Higgs bosons and four-point couplings of vector bosons and Higgs bosons can be found in Ref. 8.

The tree-level Higgs couplings to fermions obey the following property: the neutral components of one Higgs doublet couples exclusively to down-type fermion pairs while the neutral components of the other couples exclusively to up-type fermion pairs [8,105]. This pattern of Higgs-fermion couplings defines the Type-II (2HDM)². Fermion masses are generated when the neutral Higgs components acquire vacuum expectation values. The relations between Yukawa couplings and fermion masses are (in third-generation notation)

$$h_b = \sqrt{2} m_b/v_d = \sqrt{2} m_b/(v \cos \beta)$$

$$h_t = \sqrt{2} m_t/v_u = \sqrt{2} m_t/(v \sin \beta).$$

Similarly, one can define the Yukawa coupling of the Higgs boson to τ -leptons (the latter is a down-type fermion).

The couplings of the neutral Higgs bosons to $f\bar{f}$ relative to the SM value, $gm_f/2M_W$, are given by

$$h\bar{b}b: \quad -\sin \alpha / \cos \beta = \sin(\beta - \alpha) - \tan \beta \cos(\beta - \alpha),$$

$$h\bar{t}t: \quad \cos \alpha / \sin \beta = \sin(\beta - \alpha) + \cot \beta \cos(\beta - \alpha),$$

$$H\bar{b}b: \quad \cos \alpha / \cos \beta = \cos(\beta - \alpha) + \tan \beta \sin(\beta - \alpha),$$

$$H\bar{t}t: \quad \sin \alpha / \sin \beta = \cos(\beta - \alpha) - \cot \beta \sin(\beta - \alpha),$$

$$A\bar{b}b: \quad \gamma_5 \tan \beta, \quad A\bar{t}t: \quad \gamma_5 \cot \beta,$$

where the γ_5 indicates a pseudoscalar coupling. In each relation above, the factor listed for $\bar{b}b$ also pertains to $\tau^+\tau^-$. The charged Higgs boson couplings to fermion pairs are given by

$$g_{H^-t\bar{b}} = \frac{g}{\sqrt{2}M_W} [m_t \cot \beta P_R + m_b \tan \beta P_L],$$

$$g_{H^- \tau^+ \nu} = \frac{g}{\sqrt{2}M_W} [m_\tau \tan \beta P_L],$$

with $P_{L,R} = (1 \mp \gamma_5)/2$.

The Higgs couplings to down-type fermions can be significantly enhanced at large $\tan \beta$ in the following two cases: (i) If $m_A \gg M_Z$, then $|\cos(\beta - \alpha)| \ll 1$, $m_H \simeq m_A$, and the $\bar{b}bH$ and $\bar{b}bA$ couplings have equal strength and are significantly enhanced by a factor of $\tan \beta$ relative to the SM $\bar{b}bH$ coupling, whereas the VVH coupling is negligibly small. The values of the VVh and $\bar{b}b\bar{h}$ couplings are equal to the corresponding couplings of the SM Higgs boson. (ii) If $m_A < M_Z$ and $\tan \beta \gg 1$, then $|\cos(\beta - \alpha)| \approx 1$ and $m_h \simeq m_A$. In this case, the $\bar{b}b\bar{h}$ and $\bar{b}bA$ couplings have equal strength and are significantly enhanced by a factor of $\tan \beta$ relative to the SM $\bar{b}bH$ coupling,

² In the Type-I 2HDM, one field couples to all fermions while the other field is decoupled from them.

while the VVh coupling is negligibly small. In addition, the VVH coupling is equal in strength to the SM VVH coupling and one can refer to H as a SM-like Higgs boson, although the value of the $\bar{b}bH$ coupling can differ from the corresponding SM $\bar{b}bH$ coupling. Note that in both cases (i) and (ii) above, only two of the three neutral Higgs bosons have enhanced couplings to $\bar{b}b$.

Radiative Corrections to MSSM Higgs Masses and Couplings

Radiative corrections can have a significant impact on the values of Higgs boson masses and couplings in the MSSM. Important contributions come from loops of SM particles as well as their supersymmetric partners. The dominant effects arise from the incomplete cancellation between top and scalar-top (stop) loops. The stop and sbottom masses and mixing angles depend on the supersymmetric Higgsino mass parameter μ and on the soft-supersymmetry-breaking parameters [102]: M_Q , M_U , M_D , A_t and A_b , where the first three are the left-chiral and the two right-chiral top and bottom scalar quark mass parameters, respectively, and the last two are the trilinear parameters that enter the off-diagonal squark mixing elements: $X_t \equiv A_t - \mu \cot \beta$ and $X_b \equiv A_b - \mu \tan \beta$. The corrections affecting the Higgs boson masses, production, and decay properties depend on all of these parameters. For simplicity, we shall initially assume that A_t , A_b , and μ are real parameters. The impact of complex phases on MSSM parameters, which will induce CP -violation in the Higgs sector, is addressed below.

Radiative corrections to the Higgs boson masses have been computed using a number of techniques, with a variety of approximations; see Refs. [106] through [116]. They depend strongly on the top quark mass ($\sim m_t^4$) and the stop mixing parameter X_t , and there is also a logarithmic dependence on the stop masses. For large $\tan \beta$, effects from the bottom-sbottom sector are also relevant. One of the most striking effects is the increase of the upper bound of the light CP -even Higgs boson mass, as first noted in [106,107]. The value of m_h is maximized for large $m_A \gg M_Z$, when all other MSSM parameters are fixed. Moreover, $\tan \beta \gg 1$ also maximizes m_h , when all other parameters are held fixed. Taking m_A large (the decoupling limit) and $\tan \beta \gg 1$, the value of m_h can be further maximized at one-loop level for $X_t \simeq \sqrt{6}M_{\text{SUSY}}$, where $M_{\text{SUSY}} \simeq M_Q \simeq M_U \simeq M_D$ is an assumed common value of the soft SUSY-breaking squark mass parameters. This choice of X_t is called the “maximal-mixing scenario” which will be indicated by m_h -max. Instead, for $X_t = 0$, which is called the “no-mixing scenario,” the value of m_h has its lowest possible value, for fixed m_A and all other MSSM parameters. The value of m_h also depends on the specific value of M_{SUSY} and μ and more weakly on the electroweak gaugino mass as well as the gluino mass at two-loop level. For example, raising M_{SUSY} from 1 TeV to 2 TeV can increase m_h by 2-5 GeV. Variation of the value of m_t by 1 GeV changes the value of m_h by about the same amount. For any given scenario

See key on page 405

Gauge & Higgs Boson Particle Listings

Higgs Bosons — H^0 and H^\pm

defined by a full set of MSSM parameters, we will denote the maximum value of m_h by $m_h^{\max}(\tan\beta)$, for each value of $\tan\beta$. Allowing for the experimental uncertainty on m_t and for the uncertainty inherent in the theoretical analysis, one finds for $M_{\text{SUSY}} \lesssim 2$ TeV, large m_A and $\tan\beta \gg 1$, $m_h^{\max} = 135$ GeV in the m_h -max scenario, and $m_h^{\max} = 122$ GeV in the no-mixing scenario [117,118]. In practice, parameter values leading to maximal mixing are not obtained in most models of supersymmetry breaking, so typical upper limits on m_h will lie between these two extremes [119]. The relatively small mass of the lightest neutral scalar boson is a prediction for both the CP -conserving (CPC) and CP -violating (CPV) [120] scenarios, which emphasizes the importance of the searches at currently running and future accelerators.

Radiative corrections also modify significantly the values of the Higgs boson couplings to fermion pairs and to vector boson pairs. The tree-level Higgs couplings depend strongly on the value of $\cos(\beta - \alpha)$. In a first approximation, when radiative corrections of the Higgs squared-mass matrix are computed, the diagonalizing angle α is shifted from its tree-level value, and hence one may compute a “radiatively-corrected” value for $\cos(\beta - \alpha)$. This shift provides one important source of the radiative corrections to the Higgs couplings. In particular, depending on the sign of μX_t and the magnitude of X_t/M_{SUSY} , modifications of α can lead to important variations of the SM-like Higgs boson coupling to bottom quarks and tau leptons [115]. Additional contributions from the one-loop vertex corrections to tree-level Higgs couplings must also be considered [111,121–127]. These contributions alter significantly the Higgs-fermion Yukawa couplings at large $\tan\beta$, both in the neutral and charged Higgs sector. Moreover, these radiative corrections can modify the basic relationship $g_{h,H,A\bar{b}b}/g_{h,H,A\tau^+\tau^-} \propto m_b/m_\tau$, and change the main features of MSSM Higgs phenomenology.

Decay Properties of MSSM Higgs Bosons

In the MSSM, neglecting CP -violating effects, one must consider the decay properties of three neutral Higgs bosons and one charged Higgs pair. In the region of parameter space where $m_A \gg m_Z$ and the masses of supersymmetric particles are large, the decoupling limit applies, and the decay rates of h into SM particles are nearly indistinguishable from those of the SM Higgs boson. Hence, the h boson will decay mainly to fermion pairs, since the mass, less than about 135 GeV, is far below the W^+W^- threshold. The SM-like branching ratios of h are modified if decays into supersymmetric particles are kinematically allowed [128]. In addition, if light superpartners exist that can couple to photons and/or gluons, then the decay rates to gg and $\gamma\gamma$ could deviate from the corresponding SM rates. In the decoupling limit, the heavier Higgs states, H , A and H^\pm , are roughly mass degenerate, and their decay branching ratios strongly depend on $\tan\beta$ as shown below. The AWW and AZZ couplings vanish, and the HWW and HZZ couplings are very small. For values of $m_A \sim \mathcal{O}(M_Z)$,

all Higgs boson states lie below 200 GeV in mass. In this parameter regime, there is a significant area of the parameter space in which none of the neutral Higgs boson decay properties approximates that of the SM Higgs boson. For $\tan\beta \gg 1$, the resulting Higgs phenomenology shows marked differences from that of the SM Higgs boson [129] and significant modifications to the $b\bar{b}$ and/or the $\tau^+\tau^-$ decay rates may occur via radiative effects.

After incorporating the leading radiative corrections to Higgs couplings from both QCD and supersymmetry, the following decay features are relevant in the MSSM. The decay modes $h, H, A \rightarrow b\bar{b}, \tau^+\tau^-$ dominate the neutral Higgs boson decay modes when $\tan\beta$ is large for all values of the Higgs boson masses. For small $\tan\beta$, these modes are significant for neutral Higgs boson masses below $2m_t$ (although there are other competing modes in this mass range), whereas the $t\bar{t}$ decay mode dominates above its kinematic threshold. In contrast to the SM Higgs boson, the vector boson decay modes of H are strongly suppressed at large m_H due to the suppressed HVV couplings in the decoupling limit. For the charged Higgs boson, $H^+ \rightarrow \tau^+\nu_\tau$ dominates below $t\bar{b}$ threshold, while $H^+ \rightarrow t\bar{b}$ dominates for large values of m_{H^\pm} . For low values of $\tan\beta$ ($\lesssim 1$) and low values of the charged Higgs boson mass ($\lesssim 120$ GeV), the decay mode $H^+ \rightarrow c\bar{s}$ becomes relevant.

In addition to the decay modes of the neutral Higgs bosons into fermion and gauge boson final states, additional decay channels may be allowed which involve scalars of the extended Higgs sector, *e.g.*, $h \rightarrow AA$. Supersymmetric final states from Higgs boson decays into charginos, neutralinos and third-generation squarks and sleptons can be important if they are kinematically allowed [130]. One interesting possibility is a significant branching ratio for the decay of a neutral Higgs boson to the invisible mode $\tilde{\chi}_1^0\tilde{\chi}_1^0$ (where the lightest neutralino $\tilde{\chi}_1^0$ is the lightest supersymmetric particle) [131], which poses a significant challenge at hadron colliders.

Searches for Neutral Higgs Bosons (CPC Scenario)

Most of the experimental investigations carried out at LEP and the Tevatron assume CP -conservation (CPC) in the MSSM Higgs sector. In many cases the search results are interpreted in a number of specific benchmark models where a representative set of the relevant SUSY breaking parameters are specified [117]. Some of these parameter choices illustrate scenarios in which the detection of Higgs bosons at LEP or in hadron collisions is experimentally challenging due to the limited phase space or the suppression of the main discovery channels. For instance, the m_h -max scenario defined above maximizes the allowed values of m_h , for a given $\tan\beta$, M_{SUSY} , and m_t , leading to relatively conservative exclusion limits.

Searches for Neutral MSSM Higgs Bosons at LEP

In e^+e^- collisions at LEP energies, the main production mechanisms of the neutral MSSM Higgs bosons are the Higgsstrahlung processes $e^+e^- \rightarrow hZ, HZ$ and the pair production processes $e^+e^- \rightarrow hA, HA$, while the fusion processes play a

Gauge & Higgs Boson Particle Listings

Higgs Bosons — H^0 and H^\pm

marginal role. The cross sections can be expressed in terms of the SM cross section and the parameters α and β introduced above. For the light CP -even Higgs boson h the following expressions hold, in good approximation,

$$\sigma_{hZ} = \sin^2(\beta - \alpha)\sigma_{hZ}^{\text{SM}}, \quad \sigma_{hA} = \cos^2(\beta - \alpha)\bar{\lambda}\sigma_{hZ}^{\text{SM}}$$

where σ_{hZ}^{SM} stands for a SM cross section with a SM Higgs boson of mass equal to m_h . The phase space functions are

$$\bar{\lambda} = \lambda_{Ah}^{3/2} / \left[\lambda_{Zh}^{1/2} (12M_Z^2/s + \lambda_{Zh}) \right]$$

and $\lambda_{ij} = [1 - (m_i + m_j)^2/s][1 - (m_i - m_j)^2/s]$, where s is the square of the e^+e^- collision energy. These Higgs-strahlung and pair production cross sections are complementary since $\sin^2(\beta - \alpha) + \cos^2(\beta - \alpha) = 1$. The cross sections for the heavy scalar boson H are obtained by interchanging $\sin^2(\beta - \alpha)$ and $\cos^2(\beta - \alpha)$ and replacing the index h by H in the above expressions, and by defining σ_{HZ}^{SM} similarly to σ_{hZ}^{SM} . The Higgs-strahlung process $e^+e^- \rightarrow hZ$ is relevant for large $m_A > m_h^{\text{max}}(\tan\beta)$ or low $m_A < m_h^{\text{max}}(\tan\beta)$ and low $\tan\beta$; while the pair-production process $e^+e^- \rightarrow hA$ is relevant for low $m_A < m_h^{\text{max}}(\tan\beta)$.

The searches at LEP exploit the complementarity between the Higgs-strahlung process $e^+e^- \rightarrow hZ$, and the pair-production process $e^+e^- \rightarrow hA$. In addition, when $m_A < m_h^{\text{max}}(\tan\beta)$, the H boson has SM-like couplings to the Z boson, so if kinematically allowed, $e^+e^- \rightarrow HZ$ is also considered. For Higgs-strahlung, the searches for the SM Higgs boson are re-interpreted, taking into account the MSSM reduction factor $\sin^2(\beta - \alpha)$ for h ($\cos^2(\beta - \alpha)$ for H). For pair production, dedicated searches are performed for the $(b\bar{b})(b\bar{b})$ and $(\tau^+\tau^-)(q\bar{q})$ final states.

The limits from the four LEP experiments are described in Refs. [54,55,132,133]. The combined LEP data did not reveal any excess of events which would indicate the production of Higgs bosons, and combined limits were derived [18]. These limits are shown in Fig. 9 for the m_h -max scenario, in the $(m_h, \tan\beta)$ parameter plane (see Ref. 18 for other projections and other benchmark models). For values of $\tan\beta$ below ~ 5 or for $m_A \gg M_Z$ and high values of $\tan\beta$, the limit on m_h is nearly that of the SM searches, as $\sin^2(\beta - \alpha) \approx 1$. For higher values of $\tan\beta$, the $e^+e^- \rightarrow hA$ searches become the most important, and they do not set as stringent a limit on m_h . In this scenario, the 95% C.L. mass bounds are $m_h > 92.8$ GeV and $m_A > 93.4$ GeV, and values of $\tan\beta$ from 0.7 to 2.0 are excluded taking $m_t = 174.3$ GeV. This excluded $\tan\beta$ range depends on M_{SUSY} and m_t ; larger values of either of these masses increase the Higgs boson mass, and reduce the excluded range of $\tan\beta$. Furthermore, the uncertainty on the SM-like Higgs boson mass from higher-order corrections, which were not included in the current analysis, is about 3 GeV [118].

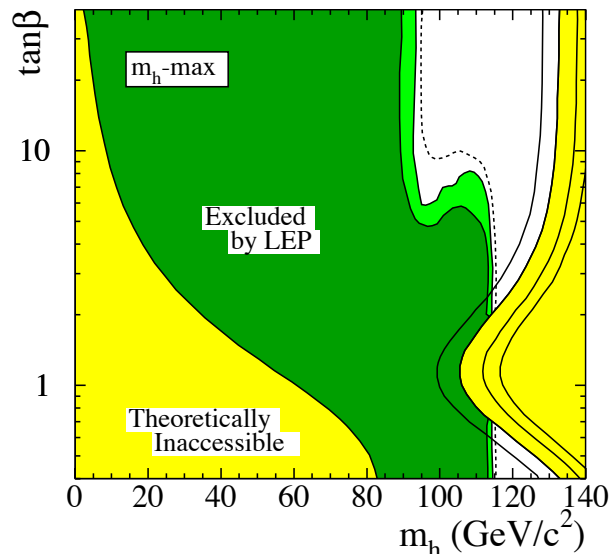


Figure 9: The MSSM exclusion contours, at 95% C.L. (light-green) and 99.7% CL (dark-green), obtained by LEP for the CPC m_h -max benchmark scenario, with $m_t = 174.3$ GeV. The figure shows the excluded and theoretically inaccessible regions in the $(m_h, \tan\beta)$ projection. The upper edge of the theoretically allowed region is sensitive to the top quark mass; it is indicated, from left to right, for $m_t = 169.3, 174.3, 179.3$ and 183.0 GeV. The dashed lines indicate the boundaries of the regions which are expected to be excluded on the basis of Monte Carlo simulations with no signal (from Ref. 18). Color version at end of book.

The neutral Higgs bosons may also be produced by Yukawa processes $e^+e^- \rightarrow f\bar{f}\phi$, where the Higgs particle $\phi \equiv h, H, A$, is radiated off a massive fermion ($f \equiv b$ or τ^\pm). These processes can be dominant at low masses, and whenever the $e^+e^- \rightarrow hZ$ and hA processes are suppressed. The corresponding ratios of the $f\bar{f}h$ and $f\bar{f}A$ couplings to the SM coupling are $\sin\alpha/\cos\beta$ and $\tan\beta$, respectively. The LEP data have been used to search for $b\bar{b}b\bar{b}$, $b\bar{b}\tau^+\tau^-$, and $\tau^+\tau^-\tau^+\tau^-$ final states [134,135]. Regions of low mass and high enhancement factors are excluded by these searches.

Searches for Neutral MSSM Higgs Bosons at Hadron Colliders

The production mechanisms for the SM Higgs boson at hadron colliders can also be relevant for the production of the MSSM neutral Higgs bosons. However, one must take into account the possibility of enhanced or suppressed couplings with respect to those of the Standard Model, since these can significantly modify the production cross sections of neutral Higgs bosons. The supersymmetric-QCD corrections due to the exchange of virtual squarks and gluinos may modify the

cross sections depending on the values of these supersymmetric particle masses. The MSSM neutral Higgs boson production cross sections at hadron colliders have been computed in Refs. [115,127,136].

Over a large fraction of the MSSM parameter space, one of the CP -even neutral Higgs bosons (h or H) couples to the vector bosons with SM-like strength and has a mass below 135 GeV. As shown in the SM Higgs section above (Fig. 6), the current searches for SM-like Higgs bosons at the Tevatron are not yet able to cover that mass range. However, if the expected improvements in sensitivity are achieved, the regions of MSSM parameter space in which one of these two scalars behaves like the SM Higgs will also be probed [137,138].

Scenarios with enhanced Higgs boson production cross sections are studied at the Tevatron. The best sensitivity is in the regime with low to moderate m_A and with large $\tan\beta$ which enhances the couplings of the Higgs bosons to down-type fermions. The corresponding limits on the Higgs boson production cross section times the branching ratio of the Higgs boson into down-type fermions can be interpreted in MSSM benchmark scenarios [139]. If $\phi = A, H$ for $m_A > m_h^{\max}$, and $\phi = A, h$ for $m_A < m_h^{\max}$, the most promising channels at the Tevatron are $b\bar{b}\phi, \phi \rightarrow b\bar{b}$ or $\phi \rightarrow \tau^+\tau^-$, with three tagged b -jets or $b\tau\tau$ in the final state, respectively, and the inclusive $p\bar{p} \rightarrow \phi \rightarrow \tau^+\tau^-$ process, with contributions from both $gg \rightarrow \phi$ and $b\bar{b}\phi$ production. Although Higgs boson production via gluon fusion has a higher cross section than via associated production, it cannot be used to study the $\phi \rightarrow b\bar{b}$ decay mode since the signal is overwhelmed by QCD background.

The CDF and $D\bar{O}$ collaborations have searched for neutral Higgs bosons produced in association with bottom quarks and which decay into $b\bar{b}$ [140–142], or into $\tau^+\tau^-$ [143]. The most recent searches in the $b\bar{b}\phi$ channel with $\phi \rightarrow b\bar{b}$ analyze approximately 2.5 fb^{-1} of data (CDF) and 2.6 fb^{-1} ($D\bar{O}$). Dedicated triggers are used to collect the data samples, but the multijet QCD background remains very large. These triggers require the presence of at least three jets, and also require tracks reconstructed with large impact parameters which point near calorimeter energy deposits. The data are analyzed by requiring three well-separated jets with reconstructed secondary vertices indicating the presence of B hadrons. The distribution of the invariant mass of the two leading jets would be more sharply peaked for the Higgs boson signal than for the background. The QCD background rates and shapes are inferred from data control samples, in particular, the sample with two b tagged jets and a third, untagged jet. Monte Carlo models are used to estimate the biases on the shapes of the background predictions due to the requirement of a third b tag. Separate signal hypotheses are tested and limits are placed on $\sigma(p\bar{p} \rightarrow b\bar{b}\phi) \times \text{BR}(\phi \rightarrow b\bar{b})$. Fig. 10 shows the upper limits from CDF and $D\bar{O}$ assuming that the decay widths of the Higgs bosons are small compared with the experimental resolution.

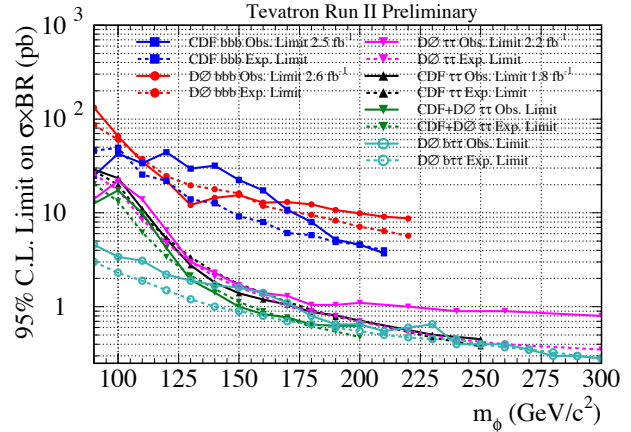


Figure 10: The 95% C.L. limits on $\sigma(b\bar{b}\phi) \times \text{BR}(\phi \rightarrow b\bar{b})$ and $\sigma(\phi + X) \times \text{BR}(\phi \rightarrow \tau^+\tau^-)$ from the Tevatron collaborations. The $D\bar{O}$ limit on $\sigma(b\bar{b}\phi) \times \text{BR}(\phi \rightarrow \tau^+\tau^-)$ and the Tevatron combined limit on $\sigma(\phi + X) \times \text{BR}(\phi \rightarrow \tau^+\tau^-)$ are also shown. The observed limits are indicated with solid lines, and the expected limits are indicated with dashed lines. The limits are to be compared with the sum of signal predictions for Higgs bosons with similar masses. The decay widths of the Higgs bosons are assumed to be much smaller than the experimental resolution. Color version at end of book.

CDF and $D\bar{O}$ have also performed searches for inclusive production of Higgs bosons with subsequent decays to $\tau^+\tau^-$ using dedicated triggers designed for these searches [144–146]. Tau leptons are more difficult to identify than jets containing B hadrons, as only some of the possible τ lepton decays are sufficiently distinct from the jet backgrounds. Both CDF and $D\bar{O}$ search for pairs of isolated tau leptons; one of the tau leptons is required to decay leptonically (either to an electron and two neutrinos, or a muon and two neutrinos), while the other tau may decay either leptonically or hadronically. Requirements placed on the energies and angles of the visible tau decay products help to reduce the background from W +jets processes, where a jet is falsely reconstructed as a tau lepton. The dominant remaining background process is $Z \rightarrow \tau^+\tau^-$, which can be separated from a Higgs boson signal by using the invariant mass of the observed decay products of the tau leptons. Fig. 10 shows the limits on $\sigma(p\bar{p} \rightarrow \phi + X) \times \text{BR}(\phi \rightarrow \tau^+\tau^-)$ for the CDF and $D\bar{O}$ searches, which use 1.8 and 2.2 fb^{-1} of data, respectively. Fig. 10 also shows the combination [147] of CDF and $D\bar{O}$'s search results in the tau-pair decay mode, for Higgs boson masses tested by both collaborations. The decay widths of the Higgs bosons are assumed to be small compared with the experimental resolution, which is much broader in the tau channels than in the $bbb(b)$ search, due to the presence of energetic neutrinos in the tau decay products.

Gauge & Higgs Boson Particle Listings

Higgs Bosons — H^0 and H^\pm

In order to interpret the experimental data in terms of MSSM benchmark scenarios, it is necessary to consider carefully the effect of radiative corrections on the production and decay processes. The bounds from the $b\bar{b}\phi, \phi \rightarrow b\bar{b}$ channel depend strongly on the radiative corrections affecting the relation between the bottom quark mass and the bottom Yukawa coupling. In the channels with $\tau^+\tau^-$ final states, however, compensations occur between large corrections in the Higgs boson production and decay. The total production rate of bottom quarks and τ pairs mediated by the production of a CP -odd Higgs boson in the large $\tan\beta$ regime is approximately given by

$$\sigma(b\bar{b}A) \times \text{BR}(A \rightarrow b\bar{b}) \simeq \sigma(b\bar{b}A)_{\text{SM}} \frac{\tan^2\beta}{(1+\Delta_b)^2} \frac{9}{(1+\Delta_b)^2+9},$$

and

$$\sigma(gg \rightarrow A, b\bar{b}A) \times \text{BR}(A \rightarrow \tau^+\tau^-) \simeq \sigma(gg \rightarrow A, b\bar{b}A)_{\text{SM}} \frac{\tan^2\beta}{(1+\Delta_b)^2+9},$$

where $\sigma(b\bar{b}A)_{\text{SM}}$ and $\sigma(gg \rightarrow A, b\bar{b}A)_{\text{SM}}$ denote the values of the corresponding SM Higgs boson cross sections for a SM Higgs boson mass equal to m_A . The function Δ_b includes the dominant effects of SUSY radiative corrections for large $\tan\beta$ [125,126]. The main radiative contributions in Δ_b depend strongly on $\tan\beta$ and on the SUSY mass parameters [115]. The $b\bar{b}A$ channel is more sensitive to the value of Δ_b through the factor $1/(1+\Delta_b)^2$ than the inclusive $\tau^+\tau^-$ channel, for which this leading dependence on Δ_b cancels out. As a consequence, the limits derived from the inclusive $\tau^+\tau^-$ channel depend less on the precise MSSM scenario chosen than those of the $b\bar{b}A$ channel.

The production and decay rates of the CP -even Higgs bosons with $\tan\beta$ -enhanced couplings to down-type fermions — H (or h) for m_A larger (or smaller) than m_h^{max} , respectively — are governed by formulae similar to the ones presented above. At high $\tan\beta$, one of the CP -even and the CP -odd Higgs bosons are nearly degenerate in mass, enhancing the signal cross section by roughly a factor of two, without complicating the experimental signature except in a small mass region in which the three neutral MSSM Higgs boson masses are close together and each boson contributes to the total production rate. A detailed discussion of the impact of radiative corrections in these search modes is presented in Ref. 139.

The excluded domain in the $(m_A, \tan\beta)$ projection for the combination of CDF and $D\phi$'s inclusive $\phi \rightarrow \tau^+\tau^-$ searches [147] are shown in Fig. 11. The searches consider the contribution of both the CP -odd and CP -even neutral Higgs bosons with enhanced couplings to bottom quarks. The excluded regions are shown in the m_h -max and no -mixing benchmark scenarios, with $\mu = 200$ GeV. The $bbb(b)$ searches are somewhat less sensitive, typically yielding expected upper

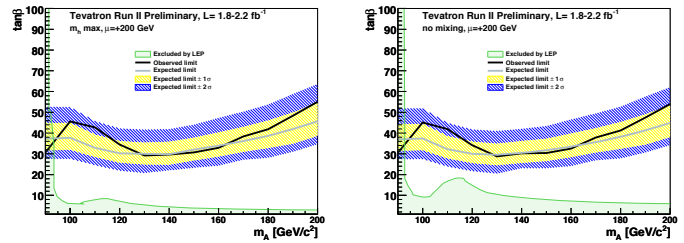


Figure 11: The 95% C.L. MSSM exclusion contours obtained by a combination of the CDF and $D\phi$ searches for $H \rightarrow \tau^+\tau^-$ in the m_h -max (left) and no -mixing (right) benchmark scenarios, both with $\mu = 200$ GeV, projected onto the $(m_A, \tan\beta)$ plane [147]. The regions above the solid black line are excluded, and the shaded and hatched bands centered on the lighter line show the distributions of expected exclusions in the absence of a signal. Also shown are the regions excluded by LEP searches [18], assuming a top quark mass of 174.3 GeV. The Tevatron results are not sensitive to the precise value of the top quark mass. Color version at end of book.

limits on $\tan\beta$ of 60 and above due to higher QCD backgrounds, sensitivity to the Higgs boson width, and the Δ_b corrections.

The sensitivity of the Tevatron searches will improve with the continuously growing data samples and with the combination of all channels of both experiments. The small backgrounds in the $\tau^+\tau^-$ channels, and the fact that better exclusions in the $bbb(b)$ channel imply narrower Higgs boson decay widths, which feeds back to improve the sensitivity of the searches, mean that the limits on the cross sections are expected to improve faster than $1/\sqrt{\mathcal{L}}$, where \mathcal{L} is the integrated luminosity. Eventually, $\tan\beta$ down to about 20 should be tested for values of m_A up to a few hundred GeV. By the end of Run II, the Tevatron searches for the associated production of a SM Higgs boson in $W^\pm H$ and ZH channels may have a strong impact on the excluded domains in Fig. 11. The combination of the LEP and Tevatron searches is expected to probe vast regions of the $(m_A, \tan\beta)$ plane.

Searches for charged Higgs bosons at the Tevatron are presented in Section IV, in the more general framework of the 2HDM.

Prospects for discovering the MSSM Higgs bosons at the LHC have been explored in detail at $\sqrt{s} = 14$ TeV; see Refs. [93,21] for reviews of these studies. They predict that the reach of the LHC experiments would be sufficient to discover MSSM Higgs bosons in many different channels. The main channels for the SM-like Higgs boson are expected to be $q\bar{q}\phi \rightarrow q\bar{q}\tau^+\tau^-$ and inclusive $\phi \rightarrow \gamma\gamma$, where $\phi = h$ or H , depending on m_A . The discovery of a light SM-like Higgs boson with $m_h < 130$ GeV would require a few years of running. With an integrated luminosity larger than 30 fb^{-1} , the $t\bar{t}\phi$ production process may become effective. For non-SM-like

See key on page 405

Gauge & Higgs Boson Particle Listings

Higgs Bosons — H^0 and H^\pm

MSSM Higgs bosons, the most relevant channels are expected to be $pp \rightarrow H/A + X$, with $H/A \rightarrow \tau^+\tau^-$ and $pp \rightarrow tH^\pm + X$ with $H^\pm \rightarrow \tau\nu_\tau$ [137]. After the inclusion of supersymmetric radiative corrections to the production cross sections and decay widths [139,148], the prospective discovery reach in these channels is robust, with mild dependence on the specific MSSM parameters.

Effects of CP Violation on the MSSM Higgs Spectrum

In the Standard Model, CP -violation (CPV) is induced by phases in the Yukawa couplings of the quarks to the Higgs field, which results in one non-trivial phase in the CKM mixing matrix. SUSY scenarios with new CPV phases are theoretically appealing, since additional CPV beyond that observed in the K and B meson systems is required to explain the observed cosmic matter-antimatter asymmetry [149,150]. In the MSSM, there are additional sources of CPV from phases in the various supersymmetric mass parameters. In particular, the gaugino mass parameters (M_i , $i = 1, 2, 3$), the Higgsino mass parameter, μ , the bilinear Higgs squared-mass parameter, m_{12}^2 , and the trilinear couplings of the squark and slepton fields (\tilde{f}) to the Higgs fields, A_f , may carry non-trivial phases. The two parameter combinations $\arg[\mu A_f(m_{12}^2)^*]$ and $\arg[\mu M_i(m_{12}^2)^*]$ are invariant under phase redefinitions of the MSSM fields [151,152]. Therefore, if one of these quantities is non-zero, there would be new sources of CP -violation, which affects the MSSM Higgs sector through radiative corrections [120,152–157]. The mixing of the neutral CP -odd and CP -even Higgs boson states is no longer forbidden. Hence, m_A is no longer a physical parameter. However, the charged Higgs boson mass m_{H^\pm} is still physical and can be used as an input for the computation of the neutral Higgs spectrum of the theory.

For large values of m_{H^\pm} , corresponding to the decoupling limit, the properties of the lightest neutral Higgs boson state approach those of the SM Higgs boson. That is, for $m_{H^\pm} \gg M_W$, the lightest neutral Higgs boson is approximately a CP -even state, with CPV couplings that are suppressed by terms of $\mathcal{O}(m_W^2/m_{H^\pm}^2)$. In particular, the upper bound on the lightest neutral Higgs boson mass, takes the same value as in the CP -conserving case [152]. Nevertheless, there still can be significant mixing between the two heavier neutral mass eigenstates. For a detailed study of the Higgs boson mass spectrum and parametric dependence of the Higgs boson mass radiative corrections, see Ref. [153,156].

Major variations to the MSSM Higgs phenomenology occur in the presence of explicit CPV phases. In the CPV case, vector boson pairs couple to all three neutral Higgs boson mass eigenstates, H_i ($i = 1, 2, 3$), with couplings

$$g_{H_i V V} = \cos \beta \mathcal{O}_{1i} + \sin \beta \mathcal{O}_{2i}$$

$$g_{H_i H_j Z} = \mathcal{O}_{3i}(\cos \beta \mathcal{O}_{2j} - \sin \beta \mathcal{O}_{1j}) - \mathcal{O}_{3j}(\cos \beta \mathcal{O}_{2i} - \sin \beta \mathcal{O}_{1i})$$

where the $g_{H_i V V}$ couplings are normalized to the analogous SM coupling and the $g_{H_i H_j Z}$ have been normalized to $g_Z^{\text{SM}}/2$. \mathcal{O}_{ij} is the orthogonal matrix relating the weak eigenstates to the

mass eigenstates. It has non-zero off-diagonal entries mixing the CP -even and CP -odd components of the weak eigenstates. The above couplings obey the relations

$$\sum_{i=1}^3 g_{H_i Z Z}^2 = 1 \quad \text{and} \quad g_{H_k Z Z} = \varepsilon_{ijk} g_{H_i H_j Z}$$

where ε_{ijk} is the Levi-Civita symbol.

Another consequence of CPV effects in the scalar sector is that all neutral Higgs bosons can couple to both scalar and pseudoscalar fermion bilinear densities. The couplings of the mass eigenstates H_i to fermions depend on the loop-corrected fermion Yukawa couplings (similarly to the CPC case), on $\tan \beta$ and on the \mathcal{O}_{ji} . The resulting expressions for the scalar and pseudoscalar components of the neutral Higgs boson mass eigenstates to fermions and the charged Higgs boson to fermions are given in Refs. [153,158].

Regarding their decay properties, the lightest mass eigenstate, H_1 , predominantly decays to $b\bar{b}$ if kinematically allowed, with a smaller fraction decaying to $\tau^+\tau^-$, similar to the CPC case. If kinematically allowed, a SM-like neutral Higgs boson, H_2 or H_3 can decay predominantly to $H_1 H_1$; otherwise it will decay preferentially to $b\bar{b}$.

Searches for Neutral Higgs Bosons in CPV Scenarios

In CPV MSSM scenarios, the three neutral Higgs eigenstates H_i do not have well-defined CP quantum numbers; they all could be produced by Higgs-strahlung, $e^+e^- \rightarrow H_i Z$, and in pairs, $e^+e^- \rightarrow H_i H_j$ ($i \neq j$), with rates which depend on the details of the CPV scenario. Possible cascade decays such as H_2 or $H_3 \rightarrow H_1 H_1$ can lead to interesting experimental signatures in the Higgs-strahlung processes, $e^+e^- \rightarrow H_2 Z$ or $H_3 Z$. For wide ranges of the model parameters, the lightest neutral Higgs boson H_1 has a predicted mass that would be accessible at LEP, if it would couple to the Z boson with SM-like strength. The second- and third-lightest Higgs bosons H_2 and H_3 may have been either out of reach, or may have had small cross sections. Altogether, the searches in the CPV MSSM scenario are experimentally more difficult, and hence have a weaker sensitivity.

The cross section for the Higgs-strahlung and pair production processes are given by [120,152,153,157]

$$\sigma_{H_i Z} = g_{H_i Z Z}^2 \sigma_{H_i Z}^{\text{SM}} \quad \sigma_{H_i H_j} = g_{H_i H_j Z}^2 \bar{\lambda} \sigma_{H_i Z}^{\text{SM}}$$

In the expression of $\bar{\lambda}$, defined for the CPC case, the indices h and A are to be replaced by H_i and H_j , respectively, $\sigma_{H_i Z}^{\text{SM}}$ stands for the SM cross section for a SM Higgs boson with a mass equal to m_{H_i} , and the couplings are defined above in term of the orthogonal matrix relating the weak eigenstates to the mass eigenstates.

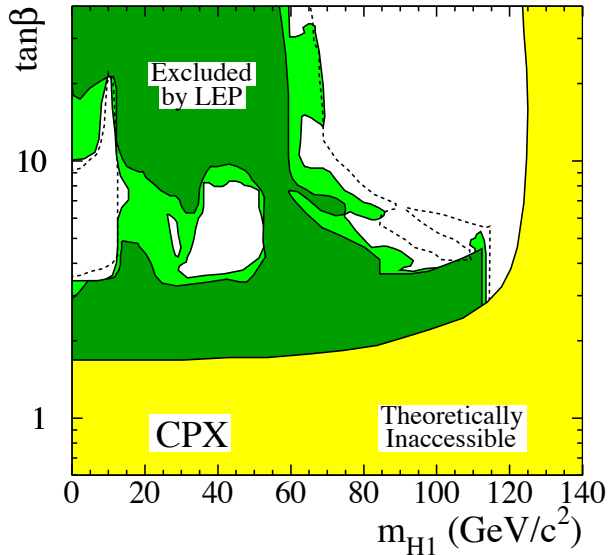


Figure 12: The MSSM exclusion contours, at the 95% C.L. (light-green) and the 99.7% CL (dark-green), obtained by LEP for the CPX scenario defined in the text. Here, $m_t = 174.3$ GeV. The figure shows the excluded and theoretically inaccessible regions in the $(m_{H_1}, \tan\beta)$ projection. The dashed lines indicate the boundary of the region which is expected to be excluded at the 95% C.L. in the absence of a signal. Color version at end of book.

The Higgs boson searches at LEP were interpreted [18] in a *CPV* benchmark scenario [120] for which the parameters were chosen so as to maximize the phenomenological differences with respect to the *CPC* scenario. This scenario, called CPX, is specified by $|A_t| = |A_b| = 1000$ GeV, $\phi_A = \phi_{m_{\tilde{g}}} = \pi/2$, $\mu = 2$ TeV, and $M_{\text{SUSY}} = 500$ GeV. Fig. 12 shows the exclusion limits of LEP in the $(m_{H_1}, \tan\beta)$ plane for $m_t = 174.3$ GeV. Values of $\tan\beta$ less than about 3 are excluded in this scenario. However, no absolute lower bound can be set for the mass of the lightest neutral Higgs boson H_1 , for an updated study see Ref. [159]. Similar exclusion plots, for other choices of model parameters, can be found in Ref. [18]. The Tevatron *CP*-conserving results and projection for MSSM Higgs searches, as well as the existing projections for LHC MSSM *CP*-conserving searches have been reinterpreted in the framework of *CP*-violating MSSM Higgs in Ref. 138. The CPX scenario was also studied by ATLAS and CMS collaborations.

Indirect Constraints from Electroweak and *B*-physics Observables and Dark Matter Searches

Indirect bounds from a global fit to precision measurements of electroweak observables can be derived in terms of MSSM parameters [160] in a way similar to what was done in the SM. The minimum χ^2 for the MSSM fit is slightly lower than what

is obtained for the SM, and the fit accommodates a low value of the lightest Higgs boson mass which is a prediction of the MSSM [161]. Given the MSSM and SM predictions for M_W as a function of m_t , and varying the Higgs boson mass and the SUSY spectrum, one finds that the MSSM overlaps with the SM when SUSY masses are large, of $\mathcal{O}(2 \text{ TeV})$, and the light SM-like Higgs boson has a mass close to the experimental bound of 114.4 GeV. The MSSM Higgs boson mass expectations are compatible with the constraints provided by the measurements of m_t and M_W [162].

Improvements in our understanding of *B*-physics observables put indirect constraints on MSSM scenarios in regions in which Higgs boson searches at the Tevatron and the LHC are sensitive. In particular, $\text{BR}(B_s \rightarrow \mu^+\mu^-)$, $\text{BR}(b \rightarrow s\gamma)$, and $\text{BR}(B_u \rightarrow \tau\nu)$ play an important role within minimal flavor-violating (MFV) models [163], in which flavor effects are induced by loop factors proportional to the CKM matrix elements, as in the SM. For example, see Refs. [137,164,165,166]. The supersymmetric contributions to these observables come both at the tree- and loop-level, and have a different parametric dependence, but share the property that they become significant for large values of $\tan\beta$, which is also the regime in which searches for non-standard MSSM Higgs bosons at hadron colliders become relevant. The recent measurement of ΔM_s and the CP-odd phase ϕ_s by the CDF and DØ collaborations [167,168,169] could also have implications for MSSM Higgs physics.

In the SM, the relevant contributions to the rare decay $B_s \rightarrow \mu^+\mu^-$ come through the *Z*-penguin and the W^\pm -box diagrams [172]. In supersymmetry with large $\tan\beta$, there are also significant contributions from Higgs-mediated neutral currents [173,174,175,176], which grow with the sixth power of $\tan\beta$ and decrease with the fourth power of the *CP*-odd Higgs boson mass m_A . Therefore, the upper limits from the Tevatron [170] put strong restrictions on possible flavor-changing neutral currents (FCNC) in the MSSM at large $\tan\beta$.

Further constraints are obtained from the rare decay $b \rightarrow s\gamma$. The SM rate is known up to NNLO corrections [177,179] and is in good agreement with measurements [178]. In the minimal flavor-violating MSSM, there are new contributions from charged Higgs and chargino-stop diagrams. The charged Higgs boson's contribution is enhanced for small values of its mass and can be partially canceled by the chargino contribution or by higher-order $\tan\beta$ -enhanced loop effects.

The branching ratio $B_u \rightarrow \tau\nu$, measured by the Belle [180] and BaBar [181] collaborations, also constrains the MSSM. The SM expectation is in slight tension with the latest experimental results [6]. In the MSSM, there is an extra tree-level contribution from the charged Higgs which interferes destructively with the SM contribution, and which increases for small values of the charged Higgs boson mass and large values of $\tan\beta$ [182]. Charged Higgs effects on $B \rightarrow D\tau\nu$ decays [183,184], constrain in an important way the parameter space region for small values

See key on page 405

Gauge & Higgs Boson Particle Listings

Higgs Bosons — H^0 and H^\pm

of the charged Higgs boson mass and large values of $\tan\beta$, that is compatible with measured values of $B_u \rightarrow \tau\nu$ [185,186,6].

Several studies [137,164–166,187] have shown that, in extended regions of parameter space, the combined B -physics measurements impose strong constraints on the MSSM models to which Higgs boson searches at the Tevatron and the LHC are sensitive. Consequently, the observation of a non-SM Higgs boson at the Tevatron or the LHC would point to a rather narrow, well-defined region of MSSM parameter space [137,188] or to something beyond the minimal flavor violation framework.

Another indirect constraint on the Higgs sector comes from the search for dark matter. If dark matter particles are weakly interacting and massive, then particle physics can provide models which predict the correct relic density of the universe. In particular, the lightest supersymmetric particle, typically the lightest neutralino, is an excellent dark matter particle candidate [189]. Within the MSSM, the measured relic density places constraints in the parameter space, which in turn have implications for Higgs searches at colliders, and also for experiments looking for direct evidence of dark matter particles in elastic scattering with atomic nuclei. Large values of $\tan\beta$ and small m_A are relevant for the $b\bar{b}A/H$ and $A/H \rightarrow \tau^+\tau^-$ searches at the Tevatron, and also provide a significant contribution from the CP -even Higgs H exchange to the spin-independent cross sections for direct detection experiments such as CDMS. Consequently, a positive signal at the Tevatron would raise prospects for a signal at CDMS, and vice-versa [187,188,190–192]. However, there are theoretical uncertainties in the calculation of dark matter scattering cross sections, and in the precise value of the local dark matter density, which are important.

IV. Charged Higgs Bosons

Charged Higgs bosons are predicted by models with an extended Higgs sector, for example, models with two Higgs field doublets (2HDM). The Higgs sector of the MSSM is a special Type-II 2HDM in which the mass of the charged Higgs boson is strongly correlated with the other Higgs boson masses. The charged Higgs boson mass in the MSSM is restricted at tree level by $m_{H^\pm} > M_W$. This restriction does not hold for some regions of parameter space after including radiative corrections. Due to the correlations among Higgs boson masses in the MSSM, the results of searches for charged Higgs bosons from LEP and the Tevatron do not significantly constrain the MSSM parameter space beyond what is already obtained from the searches for neutral Higgs bosons.

In e^+e^- collisions, charged Higgs bosons would be pair-produced via s -channel exchange of a photon or a Z boson [193]. In the 2HDM framework, the couplings are specified by the electric charge and the weak mixing angle θ_W , and the cross section at tree level depends only on the mass m_{H^\pm} . Charged Higgs bosons decay preferentially to heavy particles, but the branching ratios are model-dependent. In the Type-II 2HDM and for masses which are accessible at LEP energies,

the decays $H^\pm \rightarrow c\bar{s}$ and $\tau^+\nu_\tau$ dominate. The final states $H^+H^- \rightarrow (c\bar{s})(\bar{c}s)$, $(\tau^+\nu_\tau)(\tau^-\bar{\nu}_\tau)$, and $(c\bar{s})(\tau^-\bar{\nu}_\tau) + (\bar{c}s)(\tau^+\nu_\tau)$ were considered, and the search results are usually presented as a function of $\text{BR}(H^+ \rightarrow \tau^+\nu)$. The sensitivity of the LEP searches was limited to $m_{H^\pm} < 90$ GeV, due to the background from $e^+e^- \rightarrow W^+W^-$ [194], and the kinematic limitation on the production cross section. The combined LEP data constrain $m_{H^\pm} > 78.6$ GeV independently of $\text{BR}(H^+ \rightarrow \tau^+\nu)$ [195]. The excluded limits, translated to the $(\tan\beta, m_{H^\pm})$ plane using tree level calculations of Type-II 2HDM, are shown in Fig. 13.

In the Type-I 2HDM, and if the CP -odd neutral Higgs boson A is light (which is not excluded in the general 2HDM case), the decay $H^\pm \rightarrow W^\pm A$ may be dominant for masses accessible at LEP [196], a possibility that was investigated by the DELPHI collaboration [197].

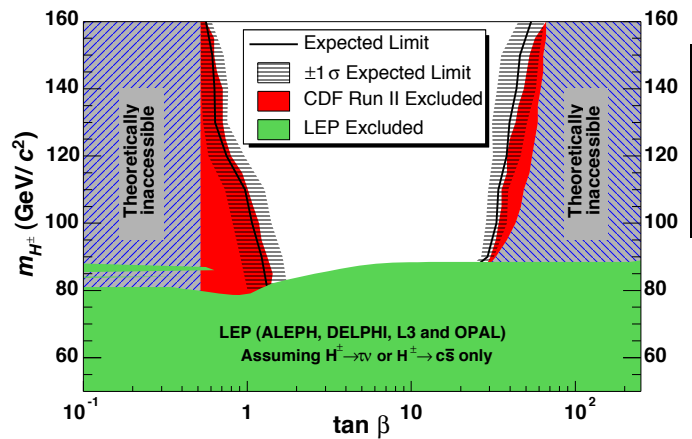


Figure 13: Summary of the 95% C.L. exclusions in the $(m_{H^\pm}, \tan\beta)$ plane obtained by LEP [195] and CDF [214]. The benchmark scenario parameters used to interpret the CDF results are very close to those of the m_h^{\max} scenario, and m_t is assumed to be 175 GeV. The full lines indicate the median limits expected in the absence of a H^\pm signal, and the horizontal hatching represents the $\pm 1\sigma$ bands about this expectation. Color version at end of book.

At hadron colliders, charged Higgs bosons can be produced in different modes. If $m_{H^\pm} < m_t - m_b$, the charged Higgs can be produced in the decays of the top quark via the decay $t \rightarrow bH^+$, which would compete with the SM process $t \rightarrow bW^+$. Relevant QCD and SUSY-QCD corrections to $\text{BR}(t \rightarrow H^+b)$ have been computed [198–201]. For $m_{H^\pm} < m_t - m_b$, the total cross section for charged Higgs boson production (in the narrow-width approximation) is given by ³

$$\sigma(p\bar{p} \rightarrow H^\pm + X) = (1 - [\text{BR}(t \rightarrow bW^+)]^2) \sigma(p\bar{p} \rightarrow t\bar{t} + X).$$

³ For values of m_{H^\pm} near m_t , the width effects are important. In addition, the full $2 \rightarrow 3$ processes $p\bar{p} \rightarrow H^\pm t\bar{b} + X$ and $p\bar{p} \rightarrow H^\pm t\bar{b} + X$ must be considered.

Gauge & Higgs Boson Particle Listings

Higgs Bosons — H^0 and H^\pm

In general, in the Type-II 2HDM, the H^+ may be observed in the decay $t \rightarrow bH^+$ at the Tevatron or at the LHC for $\tan\beta \lesssim 1$ or $\tan\beta \gg 1$.

If $m_{H^\pm} > m_t - m_b$, then charged Higgs boson production occurs mainly through radiation off a third generation quark. Single charged Higgs associated production proceeds via the $2 \rightarrow 3$ partonic processes $gg, q\bar{q} \rightarrow t\bar{b}H^-$ (and the charge conjugate final state). For charged Higgs boson production cross sections at the Tevatron and the LHC see [102,202–208].

Charged Higgs bosons can also be produced via associated production with W^\pm bosons through $b\bar{b}$ annihilation and gg -fusion [209]. They can also be produced in pairs via $q\bar{q}$ annihilation [210]. The inclusive H^+H^- cross section is less than the cross section for single charged Higgs associated production [210–212].

At the Tevatron, earlier searches by the $D\bar{O}$ and CDF collaborations are reported in [213], and more recent searches are presented in [214,215]. Fig. 13 shows the regions excluded by the CDF search, along with the regions excluded by the LEP searches, in the MSSM for a choice of parameters which is almost identical to the m_h -max benchmark scenario adopted by the LEP collaborations in their search for neutral MSSM Higgs bosons.

Indirect limits in the $(m_{H^\pm}, \tan\beta)$ plane have been obtained by comparing the measured rate of $b \rightarrow s\gamma$ to the SM prediction. In the Type-II 2HDM and in the absence of other sources of new physics at the electroweak scale, a bound $m_{H^\pm} > 295$ GeV has been derived [177]. Although this indirect bound appears much stronger than the results from direct searches, it can be invalidated by new physics contributions, such as those which can be present in the MSSM.

Doubly-Charged Higgs Bosons

Higgs bosons with double electric charge are predicted, for example, by models with additional triplet scalar fields or left-right symmetric models [216]. It has been emphasized that the see-saw mechanism could lead to doubly-charged Higgs bosons with masses which are accessible to current and future colliders [217]. Searches were performed at LEP for the pair-production process $e^+e^- \rightarrow H^{++}H^{--}$ with four prompt leptons in the final state [218–220]. Lower mass bounds between 95 GeV and 100 GeV were obtained for left-right symmetric models (the exact limits depend on the lepton flavors). Doubly-charged Higgs bosons were also searched for in single production [221]. Furthermore, such particles would modify the Bhabha scattering cross section and forward-backward asymmetry via t -channel exchange. The absence of a significant deviation from the SM prediction puts constraints on the Yukawa coupling of $H^{\pm\pm}$ to electrons for Higgs boson masses which reach into the TeV range [220,221].

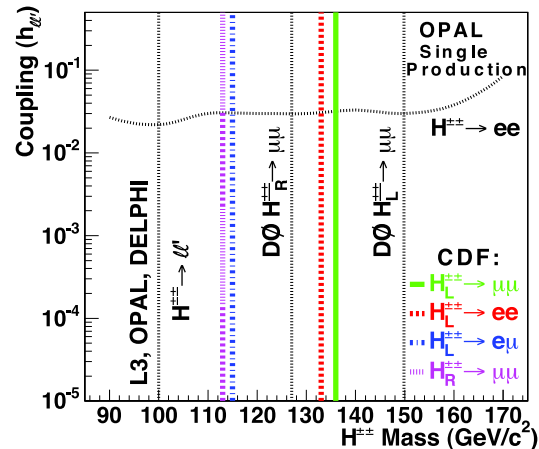


Figure 14: The 95% C.L. exclusion limits on the masses and couplings to leptons of right- and left-handed doubly-charged Higgs bosons, obtained by LEP and Tevatron experiments (from Ref. 223). Color version at end of book.

Searches have also been carried out at the Tevatron for the pair production process $p\bar{p} \rightarrow H^{++}H^{--}$. The $D\bar{O}$ search is performed in the $\mu^+\mu^+\mu^-\mu^-$ final state [222], while CDF also considers $e^+e^+e^-e^-$ and $e^+\mu^+e^-\mu^-$, and final states with τ leptons [223]. Lower bounds are obtained for left- and right-handed $H^{\pm\pm}$ bosons. For example, assuming $\text{BR}(H^{\pm\pm} \rightarrow \mu^\pm\mu^\pm) = 100\%$, the $D\bar{O}$ (CDF) data exclude a left- and a right-chiral doubly-charged Higgs boson with mass larger than 150 (136) GeV and 127 (113) GeV, respectively, at 95% C.L. A search of CDF for a long-lived $H^{\pm\pm}$ boson, which would decay outside the detector, is described in [224]. The current status of the mass and coupling limits, from direct searches at LEP and at the Tevatron, is summarized in Fig. 14.

V. Other Model Extensions

There are many ways to extend the minimal Higgs sector of the Standard Model. In the preceding sections we have considered the phenomenology of the MSSM Higgs sector, which at tree level is a constrained Type-II 2HDM (with restrictions on the Higgs boson masses and couplings), and also more general 2HDMS of Types I and II. Other extensions of the Higgs sector can include multiple copies of $SU(2)_L$ doublets, additional Higgs singlets, triplets or more complicated combinations of Higgs multiplets. It is also possible to enlarge the gauge symmetry beyond $SU(2)_L \times U(1)_Y$ along with the necessary Higgs structure to generate gauge boson and fermion masses. There are two main experimental constraints that govern these extensions: (i) precision measurements, which constrain $\rho = m_W^2/(m_Z^2 \cos^2\theta_W)$ to be very close to 1. In electroweak models based on the SM gauge group, the tree-level value of ρ is determined by the Higgs multiplet structure. By suitable choices for the hypercharges, and in some cases the

See key on page 405

Gauge & Higgs Boson Particle Listings

Higgs Bosons — H^0 and H^\pm

mass splitting between the charged and neutral Higgs sector or the vacuum expectation values of the Higgs fields, it is possible to obtain a richer combination of singlets, doublets, triplets and higher multiplets compatible with precision measurements [225]; (ii) the second important constraint comes from flavor changing neutral current (FCNC) effects. In the presence of multiple Higgs doublets, the Glashow-Weinberg theorem [226] states that tree-level FCNC's mediated by neutral Higgs bosons will be absent if all fermions of a given electric charge couple to no more than one Higgs doublet. The Higgs doublet models Type-I and Type-II are two different ways of satisfying this theorem. The coupling pattern of these two types can be arranged by imposing either a discrete symmetry or, in the case of Type-II, supersymmetry. The resulting phenomenology of extended Higgs sectors can differ significantly from that of the SM Higgs boson.

The most studied extension of the MSSM has a scalar singlet and its supersymmetric partner [227–229]. These models have an extended Higgs sector with two additional neutral scalar states (one CP -even and one CP -odd), beyond those present in the MSSM. In these models, the tree-level bound on the lightest Higgs boson, considering arguments of perturbativity of the theory up to the GUT scale, is about 100 GeV. The radiative corrections to the masses are similar to those in the MSSM, and yield an upper bound of about 145 GeV for the mass of the lightest neutral CP -even scalar [230,231]. The precise LEP II bounds on the Higgs boson masses depend on the couplings of the Higgs bosons to the gauge bosons and such couplings tend to be weakened somewhat from mixing with the singlet. The DELPHI Collaboration places constraints on such models [232], as does DØ [233].

Another extension of the MSSM which can raise the value of the lightest Higgs boson mass to a few hundred GeV is based on gauge extensions of the MSSM [234,237]. The addition of asymptotically-free gauge interactions naturally yields extra contributions to the quartic Higgs couplings. These extended gauge sector models can be combined with the presence of extra singlets or replace the singlet with a pair of triplets [236].

It is also possible that the MSSM is the low energy effective field theory of a more fundamental SUSY theory that includes additional particles with masses at or somewhat above the TeV range, and that couple significantly to the MSSM Higgs sector. A model-independent analysis of the spectrum and couplings of the MSSM Higgs fields, based on an effective theory of the MSSM degrees of freedom has been studied in the literature [237–240]. In these scenarios the tree-level mass of the lightest CP -even state can easily be above the LEP bound of 114 GeV, thus allowing for a relatively light spectrum of superpartners, restricted only by direct searches. The Higgs spectrum and couplings can be significantly modified compared to the MSSM ones, often allowing for interesting new decay modes. It is also possible to moderately enhance the gluon fusion production cross section of the SM-like Higgs with respect to both the Standard Model and the MSSM.

Many non-SUSY solutions to the problem of electroweak symmetry breaking and the hierarchy problem are being developed. For example, the so-called “Little Higgs” models propose additional sets of heavy vector-like quarks, gauge bosons, and scalar particles, with masses in the 100 GeV to a few TeV range. The couplings of the new particles are tuned in such a way that the quadratic divergences induced in the SM by the top, gauge-boson and Higgs loops are canceled at the one-loop level. If the Little Higgs mechanism successfully resolves the hierarchy problem, it should be possible to detect some of these new states at the LHC. For reviews of models and phenomenology, and a more complete list of references, see Refs. [241] and [242].

In Little Higgs models the production and decays of the Higgs boson are modified. For example, when the dominant production mode of the Higgs is through gluon fusion, the contribution of new fermions in the loop diagrams involved in the effective ϕgg vertex can reduce the production rate. The rate is generally suppressed relative to the SM rate due to the symmetries which protect the Higgs boson mass from quadratic divergences at the one-loop level. However, the branching ratio of the Higgs to photon pairs can be enhanced in these models [243]. By design, Little Higgs models are valid only up to a scale $\Lambda \sim 5$ -10 TeV. The new physics which would enter above Λ remains unspecified, and will impact the Higgs sector. In general, it can modify Higgs couplings to third-generation fermions and gauge bosons, though these modifications are suppressed by $1/\Lambda$ [244].

Distinctive features in the Higgs phenomenology of Little Higgs models may also stem from the fact that loop-level electroweak precision bounds on models with a tree-level custodial symmetry allows for a Higgs boson heavier than the one permitted by precision electroweak fits in the SM. This looser bound follows from a cancellation of the effects on the ρ parameter of a higher mass Higgs boson and the heavy partner of the top quark. The Higgs boson can have a mass as high as 800-1000 GeV in some Little Higgs models and still be consistent with electroweak precision data [245]. Lastly, the scalar content of a Little Higgs structure is model dependent. There could be two, or even more scalar doublets in a little Higgs model, or even different representations of the electroweak gauge group [246].

Models of extra space dimensions present an alternative way of avoiding the scale hierarchy problem [14]. New states, known as Kaluza-Klein (KK) excitations, can appear at the TeV scale, where gravity-mediated interactions may become relevant. They share the quantum numbers of the graviton and/or SM particles. In a particular realization of these models, based on warped extra dimensions, a light Higgs-like particle, the radion, may appear in the spectrum [247]. The mass of the radion, as well as its possible mixing with the light Higgs boson, depends strongly on the mechanism that stabilizes the extra dimension, and on the curvature-Higgs mixing.

The radion couples to the trace of the energy-momentum tensor of the SM particles, leading to effective interactions with

Gauge & Higgs Boson Particle Listings

Higgs Bosons — H^0 and H^\pm

quarks, leptons, and weak gauge bosons which are similar to the ones of the Higgs boson, although they are suppressed by the ratio of the weak scale to the characteristic mass of the new excitations. An important characteristic of the radion is its enhanced couplings to gluons. Therefore, if it is light and mixes with the Higgs boson, it may modify the standard Higgs phenomenology at lepton and hadron colliders. A search for the radion in LEP data, conducted by OPAL using both b -tagged and flavor-independent searches, gave negative results [248]. Radion masses below 58 GeV are excluded for the mass eigenstate which becomes the Higgs boson in the no-mixing limit, for all parameters of the Randall-Sundrum model.

In models of warped extra dimensions in which the SM particles propagate in the extra dimensions, the KK excitations of the vector-like fermions may be pair-produced at colliders and decay into combinations of two Higgs bosons and jets, or one Higgs boson, a gauge boson, and jets. KK excitations may also be singly-produced. Some of these interesting possible new signatures for SM-like Higgs bosons in association with top or bottom quarks have been studied [15].

If Higgs bosons are not discovered at the Tevatron or the LHC, other studies might be able to test alternative theories of dynamical electroweak symmetry breaking which do not involve a fundamental Higgs scalar [249].

VI. Other Searches for Higgs Bosons Beyond the SM

Decays of Higgs bosons into invisible (weakly-interacting and neutral) particles may occur in many models. For example, in the MSSM the Higgs can decay into pairs of neutralinos. In a different context, Higgs bosons might also decay into pairs of Goldstone bosons or Majorons [250]. In the process $e^+e^- \rightarrow hZ$, the mass of the invisible Higgs boson can be inferred from the kinematics of the reconstructed Z boson by using the beam energy constraint. Results from the LEP experiments can be found in Refs. [54,251]. A preliminary combination of LEP data yields a 95% C.L. lower bound of 114.4 GeV for the mass of a Higgs boson, if it is produced with SM production rate, and if it decays exclusively into invisible final states [252].

Hidden-valley models [253] predict a rich phenomenology of new particles, some of which can be long-lived and hadronize with SM particles to form exotic particles which decay at measurable distances in collider experiments. $D\bar{O}$ has searched for pair-produced long-lived particles produced resonantly and which decay to $b\bar{b}$ pairs, and sets limits on Higgs boson production in hidden-valley models [254].

Most of the searches for the processes $e^+e^- \rightarrow hZ$ and hA , which have been discussed in the context of the CPC-MSSM, rely on the assumption that the Higgs bosons have a sizable branching ratio to $b\bar{b}$. However, for specific parameters of the MSSM [255], the general 2HDM case, or composite models [115,117,256], decays to non- $b\bar{b}$ final states may be significantly enhanced. Some flavor-independent searches have

been reported at LEP which do not require the experimental signature of a b -jet [257], and a preliminary combination of LEP data has been performed [18,258]. If Higgs bosons are produced at the SM rate and decay only to jets of hadrons, then the 95% C.L. lower limit on the mass of the Higgs boson is 112.9 GeV, independent of the fractions of gluons and b , c , s , u and d -quarks in Higgs boson decay. In conjunction with b -flavor sensitive searches, large domains of the general Type-II 2HDM parameter space have been excluded [259].

Photonic final states from the processes $e^+e^- \rightarrow Z/\gamma^* \rightarrow H\gamma$ and from $H \rightarrow \gamma\gamma$, do not occur in the SM at tree level, but these they may proceed due to W^\pm and top quark loops [260]. Additional loops from SUSY particles would modify the rates only slightly [261], but models with anomalous couplings predict enhancements by orders of magnitude. Searches for the processes $e^+e^- \rightarrow (H \rightarrow b\bar{b})\gamma$, $(H \rightarrow \gamma\gamma)q\bar{q}$, and $(H \rightarrow \gamma\gamma)\gamma$ have been used to set limits on such anomalous couplings. These searches also contribute in the combinations of searches for the standard model Higgs boson, although the small predicted signal rates imply that they contribute less than other channels. These searches also constrain the Type-I “fermiophobic” 2HDM [262], which also predicts an enhanced $h \rightarrow \gamma\gamma$ rate. The LEP searches are described in [263,264]. In a preliminary combination of LEP data [265], a fermiophobic Higgs boson with mass less than 108.2 GeV (95% C.L.) has been excluded. Limits of about 80 GeV have been obtained at the Tevatron in Run I [266]. Run II results based on 2.7 fb^{-1} of $D\bar{O}$ data and 3.0 fb^{-1} of CDF data extend the exclusion to 106 GeV [267]. CDF has updated this analysis with 5.4 fb^{-1} of data [268]. Other production of fermiophobic Higgs bosons, leading to a 3-photons final state, have also been searched for [269]. The Type-I 2HDM also predicts an enhanced rate for the decays $h \rightarrow W^*W$ and Z^*Z , a possibility that has been addressed by L3 [264] and ALEPH [270].

The DELPHI collaboration has used the LEP 1 and LEP 2 data to search for Higgs bosons produced in pairs, in association with Z bosons, and in association with b quarks, and τ leptons. The decays considered are $\phi \rightarrow b\bar{b}, \tau^+\tau^-$, and to pairs of Higgs bosons, yielding four- b , four- b +jets, six- b and four- τ final states. No evidence for a Higgs boson was found [135], and DELPHI sets mass-dependent limits on a variety of processes, which apply to a large class of models. The limits on the cross sections of Yukawa production of Higgs bosons are typically more than 100 times larger than the SM predictions, while Higgs-strahlung limits for b and τ decays extend up to the kinematic limits of approximately 114 GeV. Limits on pair-produced Higgs bosons extend up to approximately $m_h + m_A = 140 \text{ GeV}$ for full-strength production, assuming $b\bar{b}$ and $\tau^+\tau^-$ decays.

OPAL’s decay-mode independent search for $e^+e^- \rightarrow S^0Z$ [53] provides sensitivity to arbitrarily-decaying scalar particles, as only the recoiling Z boson is required to be reconstructed. The energy and momentum constraints provided by the e^+e^- collisions allow the S^0 ’s four-vector to be reconstructed and

See key on page 405

Gauge & Higgs Boson Particle Listings

Higgs Bosons — H^0 and H^\pm

limits placed on its production independent of its decay characteristics, allowing sensitivity for very light scalar masses. The limits obtained in this search are less than one-tenth of the SM Higgs-strahlung production rate for $1 \text{ KeV} < m_{S0} < 19 \text{ GeV}$, and less than the SM Higgs-strahlung rate for $m_{S0} < 81 \text{ GeV}$.

VII. Outlook

At the Tevatron, Higgs boson searches performed in several channels with 2.0 to 5.4 fb^{-1} have achieved the necessary sensitivity to test for the presence of a SM Higgs boson with a mass near $2M_W$. With anticipated improvements in analysis sensitivity, the expected total analyzed integrated luminosity of about 10 fb^{-1} , and the combination of results from both experiments, the Tevatron should be able to exclude most of the SM Higgs boson mass range up to 185 GeV (at 95% C.L.), and could produce 3σ evidence for a Higgs boson with a mass close to 115 GeV or 160 GeV. The Tevatron searches are also sensitive to the neutral Higgs bosons of the MSSM for $m_A < 300 \text{ GeV}$ and $\tan\beta > 30$.

The LHC is planned to deliver proton-proton collisions at a center of mass energy of 7 TeV in 2010 and 2011, and it will produce a large data sample at the center of mass energy of 14 TeV starting in 2013. The ATLAS and CMS detectors have been optimized for Higgs boson searches. The discovery of a SM Higgs boson is expected to be possible over the mass range between 100 GeV and 1 TeV, given sufficient integrated luminosity. This broad range is covered by a variety of searches based on several production and decay processes. The LHC experiments are expected to provide full coverage of the MSSM parameter space by direct searches for the h , H , A , and H^\pm bosons, and by searching for h bosons in cascade decays of SUSY particles. The simultaneous discovery of several of the Higgs bosons is expected to be possible over extended domains of the MSSM parameter space.

A high-energy e^+e^- linear collider may start operation around the year 2020. According to present planning, it would run initially at a center-of-mass energy of 500 GeV, and an upgrade would allow running at 1 TeV later [22]. One of the primary goals is to extend precision measurements, which are typical of e^+e^- colliders, to the Higgs sector. According to several studies, the Higgs couplings to fermions and vector bosons could be measured with a precision of a few percent, and the parameters of the MSSM could be studied in great detail. At the highest collider energies and luminosities, the self-coupling of the Higgs fields could be measured directly through final states with two Higgs bosons [271].

Higgs boson production in the s -channel might be possible at a future $\mu^+\mu^-$ collider [23]. Mass measurements with a precision of a few MeV would be possible, and the total width could be obtained directly from Breit-Wigner scans. The heavy CP -even and CP -odd bosons, H and A , degenerate over most of the MSSM parameter space, could be directly disentangled from the line shape.

Higgs bosons enter calculations of electroweak observables through loop effects, so it has been possible to constrain the SM Higgs sector using a global fit to precision electroweak measurements. The fit favors Higgs bosons that are not heavy, a fact which is compatible with the predictions of the MSSM. B -physics observables explored at CLEO, BaBar, Belle and the Tevatron independently constrain the MSSM parameter space available for Higgs searches. These indirect limits derive in part from the specific effects on flavor physics of the supersymmetry-breaking mechanism. The combined information of direct and indirect SUSY Higgs searches together with the results from direct search for dark matter, could provide important information about supersymmetry.

In the theoretical landscape, several models are emerging with novel approaches to the problem of electroweak symmetry breaking. Many of them incorporate a Higgs sector with features distinctly different from the SM, and their phenomenology could be studied at the LHC.

There is uncertainty on the mass range for the scale of new physics. It arises from one side by the attempt to explain the hierarchy between the electroweak scale and the Planck scale in a natural way, which demands new physics at or below the TeV scale, and on the other side by the strong bounds at that same scale, of order of a TeV or larger, that come from the precise measurements delivered by the experiments in the last two decades. Supersymmetry remains a suggestive candidate for new physics. Models with no fundamental Higgs bosons are harder to accommodate with precision data, but the LHC and a future lepton collider will be able to make strong statements about the mechanism of electroweak symmetry breaking.

References

1. P.W. Higgs, Phys. Rev. Lett. **12**, 132 (1964); *idem*, Phys. Rev. **145**, 1156 (1966); F. Englert and R. Brout, Phys. Rev. Lett. **13**, 321 (1964); G.S. Guralnik, C.R. Hagen, and T.W. Kibble, Phys. Rev. Lett. **13**, 585 (1964).
2. S.L. Glashow, Nucl. Phys. **20**, 579 (1961); S. Weinberg, Phys. Rev. Lett. **19**, 1264 (1967); A. Salam, *Elementary Particle Theory*, eds.: Svartholm, Almqvist, and Wiksell, Stockholm, 1968; S. Glashow, J. Iliopoulos, and L. Maiani, Phys. Rev. **D2**, 1285 (1970).
3. J.M. Cornwall, D.N. Levin, and G. Tiktopoulos, Phys. Rev. Lett. **30**, 1286 (1973); Phys. Rev. **D10**, 1145 (1974); C.H. Llewellyn Smith, Phys. Lett. **B46**, 233 (1973).
4. B.W. Lee, C. Quigg, and H.B. Thacker, Phys. Rev. **D16**, 1519 (1977).
5. LEP Electroweak Working Group, status of August 2009, <http://lepewwg.web.cern.ch/LEPEWWG/>; The ALEPH, CDF, DØ, DELPHI, L3, OPAL, SLD Collabs., the LEP Electroweak Working Group, the Tevatron Electroweak Working Group, and the SLD Electroweak and Heavy Flavor groups, LEPEWWG/2009-01 (2009); J. Erler and P. Langacker, *Electroweak Model and Constraints on New Physics*, in this volume.

Gauge & Higgs Boson Particle Listings

Higgs Bosons — H^0 and H^\pm

6. M. Bona *et al.*, [UTfit Collab.], arXiv:0908.3470 [hep-ph]; http://ckmfitter.in2p3.fr/plots_Moriond09.
7. J. Wess and B. Zumino, Nucl. Phys. **B70**, 39 (1974); *idem.*, Phys. Lett. **49B**, 52 (1974); H.P. Nilles, Phys. Rev. **C110**, 1 (1984); H.E. Haber and G.L. Kane, Phys. Rev. **C117**, 75 (1985); S.P. Martin, arXiv:hep-ph/9709356 (1997); P. Fayet, Phys. Lett. **B69**, 489 (1977); *ibid.*, **B84**, 421 (1979); *ibid.*, **B86**, 272 (1979); *idem.*, Nucl. Phys. **B101**, 81 (2001).
8. J.F. Gunion *et al.*, *The Higgs Hunter's Guide* (Addison-Wesley) 1990; A. Djouadi, arXiv:hep-ph/0503172 (2005), arXiv:hep-ph/0503173 (2005).
9. A detailed discussion and list of references is given in subsection III.
10. L.E. Ibáñez and G.G. Ross, Phys. Lett. **B105**, 439 (1981); S. Dimopoulos, S. Raby, and F. Wilczek, Phys. Rev. **D24**, 1681 (1981); M.B. Einhorn and D.R.T. Jones, Nucl. Phys. **B196**, 475 (1982); W.J. Marciano and G. Senjanovic, Phys. Rev. **D25**, 3092 (1982).
11. J. Ellis, S. Kelley, and D.V. Nanopoulos, Phys. Lett. **B249**, 441 (1990); P. Langacker and M. Luo, Phys. Rev. **D44**, 817 (1991); U. Amaldi, W. de Boer, and H. Fürstenau, Phys. Lett. **B260**, 447 (1991); P. Langacker and N. Polonsky, Phys. Rev. **D52**, 3081 (1995); S. Pokorski, *Act. Phys. Pol.* **B30**, 1759 (1999); For a recent review, see: R.N. Mohapatra, in *Particle Physics 1999, Proceedings of the ICTP Summer School in Particle Physics*, Trieste, Italy, 21 June–9 July, 1999, eds. G. Senjanovic and A.Yu. Smirnov. (World Scientific, Singapore, 2000) pp. 336–394.
12. S. Weinberg, Phys. Rev. **D13**, 974 (1979); Phys. Rev. **D19**, 1277 (1979); L. Susskind, Phys. Rev. **D20**, 2619 (1979); E. Farhi and L. Susskind, Phys. Rev. **74**, 277 (1981); R.K. Kaul, Rev. Mod. Phys. **55**, 449 (1983); C.T. Hill and E.H. Simmons, Phys. Reports **381**, 235 (2003) [E: *ibid.*, **390**, 553 (2004)].
13. N. Arkani-Hamed, A.G. Cohen, and H. Georgi, Phys. Lett. **B513**, 232 (2001); N. Arkani-Hamed *et al.*, JHEP **0207**, 034 (2002); N. Arkani-Hamed *et al.*, JHEP **0208**, 020 (2002); N. Arkani-Hamed *et al.*, JHEP **0208**, 021 (2002); I. Low, W. Skiba, and D. Smith, Phys. Rev. **D66**, 072001 (2002).
14. I. Antoniadis, Phys. Lett. **B246**, 377 (1990); N. Arkani-Hamed, S. Dimopoulos, and G.R. Dvali, Phys. Lett. **B429**, 263 (1998); L. Randall and R. Sundrum, Phys. Rev. Lett. **83**, 3370 (1999) *idem.*, **84**, 4690 (1999); G.F. Giudice *et al.*, Nucl. Phys. **B544**, 3 (1999); C. Csáki *et al.*, Phys. Rev. **D63**, 065002 (2001).
15. J. A. Aguilar-Saavedra, JHEP **0612**, 033 (2006); M. Carena *et al.*, Phys. Rev. **D76**, 035006 (2007); A.D. Medina, N.R. Shah, and C.E.M. Wagner, arXiv:0706.1281 (2007); A. Djouadi and G. Moreau, arXiv:0707.3800 (2007); H. Davoudiasl, B. Lillie, and T. G. Rizzo, JHEP **0608**, 042 (2006); A. Falkowski, arXiv:0711.0828 (2007).
16. P.J. Franzini and P. Taxil, in *Z physics at LEP 1*, CERN 89-08 (1989).
17. ALEPH, DELPHI, L3, and OPAL Collabs., The LEP Working Group for Higgs Boson Searches, Phys. Lett. **B565**, 61 (2003).
18. ALEPH, DELPHI, L3, and OPAL Collabs., The LEP Working Group for Higgs Boson Searches, Eur. Phys. J. **C47**, 547 (2006).
19. The CDF and DØ Collabs., Phys. Rev. Lett. **104**, 061802 (2010).
20. ATLAS Collab., arXiv:0901.0512 [hep-ex].
21. CMS Collab., J. Phys. **G34**, 995 (2007).
22. E. Accomando *et al.*, Physics Reports **299**, 1–78 (1998); TESLA Technical Design Report, Part 3: *Physics at an e^+e^- Linear Collider*, arXiv:hep-ph/0106315 (2001); ACFA Linear Collider Working Group, *Particle Physics Experiments at JLC*, arXiv:hep-ph/0109166 (2001); A. Djouadi *et al.*, *ILC Global Design Effort and World Wide Study*, arXiv:0709.1893 [hep-ph] (2007); E. Accomando *et al.*, CLIC Physics Working Group, arXiv:hep-ph/0412251 (2004); J. Brau *et al.*, [ILC Collab.], arXiv:0712.1950 [physics.acc-ph] (2007); G. Aarons *et al.*, [ILC Collab.], arXiv:0709.1893 [hep-ph] (2007).
23. B. Autin *et al.*, (eds.), CERN 99-02; C.M. Ankenbrandt *et al.*, Phys. Rev. ST Acc. Beams **2**, 081001 (1999); C. Blochinger *et al.*, *Physics Opportunities at $\mu^+\mu^-$ Higgs Factories*, arXiv:hep-ph/0202199 (2002).
24. T. van Ritbergen and R. G. Stuart, Phys. Rev. Lett. **82**, 488 (1999); T. van Ritbergen and R. G. Stuart, Nucl. Phys. **B564**, 343 (2000); M. Steinhauser and T. Seidensticker, Phys. Lett. **B467**, 271 (1999).
25. N. Cabibbo *et al.*, Nucl. Phys. **B158**, 295 (1979); See, *e.g.*, G. Altarelli and G. Isidori, Phys. Lett. **B337**, 141 (1994); J.A. Casas, J.R. Espinosa, and M. Quirós, Phys. Lett. **B342**, 171 (1995) *idem.*, Phys. Lett. **B382**, 374 (1996); T. Hambye and K. Riesselmann, Phys. Rev. **D55**, 7255 (1997).
26. J. R. Espinosa and M. Quiros, Phys. Lett. **B353**, 257 (1995); G. Isidori *et al.*, Nucl. Phys. **B609**, 387 (2001).
27. B.A. Kniehl, Phys. Rept. **240**, 211 (1994).
28. E. Gross *et al.*, Z. Phys. **C63**, 417 (1994); [E: *ibid.*, **C66**, 32 (1995)]; E. Braaten and J.P. Leveille, Phys. Rev. **D22**, 715 (1980); N. Sakai, Phys. Rev. **D22**, 2220 (1980); T. Inami and T. Kubota, Nucl. Phys. **B179**, 171 (1981); S.G. Gorishniĭ, A.L. Kataev, and S.A. Larin, Sov. J. Nucl. Phys. **40**, 329 (1984) [*Yad. Fiz.* **40**, 517 (1984)]; M. Drees and K. Hikasa, Phys. Lett. **B240**, 455 (1990) [E: **B262**, 497 (1991)];

- A. Djouadi, M. Spira, and P.M. Zerwas, *Z. Phys.* **C70**, 675 (1996);
A. Djouadi, J. Kalinowski, and M. Spira, *Comput. Phys. Commun.* **108**, 56 (1998);
B.A. Kniehl, *Nucl. Phys.* **B376**, 3 (1992);
A.L. Kataev, *Sov. Phys. JETP Lett.* **66**, 327 (1997) [*Pis'ma Zh. Éksp. Teor. Fiz.* **66**, 308 (1997)].
29. For a compilation of theoretical results for SM and MSSM Higgs cross sections at the Tevatron and the LHC see: <http://maltoni.home.cern.ch/maltoni/TeV4LHC/>. The text of this review describes recent updates.
 30. R.V. Harlander and W.B. Kilgore, *Phys. Rev. Lett.* **88**, 201801 (2002);
C. Anastasiou and K. Melnikov, *Nucl. Phys.* **B646**, 220 (2002);
V. Ravindran, J. Smith, and W.L. van Neerven, *Nucl. Phys.* **B665**, 325 (2003);
M. Spira *et al.*, *Nucl. Phys.* **B453**, 17 (1995).
 31. S. Actis *et al.*, *Phys. Lett.* **B670**, 12 (2008);
U. Aglietti *et al.*, *Phys. Lett.* **B595**, 432 (2004);
G. Degross and F. Maltoni, *Phys. Lett.* **B600**, 255 (2004).
 32. C. Anastasiou, R. Boughezal, and F. Petriello, *JHEP* **0904**, 003 (2009).
 33. S. Catani *et al.*, *JHEP* **0307**, 028 (2003);
S. Moch and A. Vogt, *Phys. Lett.* **B631**, 48 (2005);
E. Laenen and L. Magnea, *Phys. Lett.* **B632**, 270 (2006);
A. Idilbi *et al.*, *Phys. Rev.* **D73**, 077501 (2006).
 34. D. de Florian and M. Grazzini, *Phys. Lett.* **B674**, 291 (2009).
 35. V. Ahrens *et al.*, *Eur. Phys. J.* **C62**, 333 (2009).
 36. C.R. Schmidt, *Phys. Lett.* **B413**, 391 (1997).
 37. D. de Florian, M. Grazzini, and Z. Kunszt, *Phys. Rev. Lett.* **82**, 5209 (1999).
 38. *Nucl. Phys.* **B634**, 247 (2002).
 39. C.J. Glosser and C.R. Schmidt, *JHEP* **0212**, 016 (2002).
 40. J.M. Campbell, R.K. Ellis, and G. Zanderighi, *JHEP* **0610**, 028 (2006).
 41. J.M. Campbell, R.K. Ellis, and C. Williams, [arXiv:1001.4495 \[hep-ph\]](https://arxiv.org/abs/1001.4495).
 42. K.A. Assamagan *et al.*, [arXiv:hep-ph/0406152](https://arxiv.org/abs/hep-ph/0406152) (2004).
 43. O. Brein, A. Djouadi, and R. Harlander, *Phys. Lett.* **B579**, 149 (2004);
M.L. Ciccolini, S. Dittmaier, and M. Krämer, *Phys. Rev.* **D68**, 073003 (2003).
 44. P. Bolzoni *et al.*, [arXiv:1003.4451 \[hep-ph\]](https://arxiv.org/abs/1003.4451) (2010);
T. Han, G. Valencia, and S. Willenbrock, *Phys. Rev. Lett.* **69**, 3274 (1992);
E.L. Berger and J. Campbell, *Phys. Rev.* **D70**, 073011 (2004);
T. Figy, C. Oleari, and D. Zeppenfeld, *Phys. Rev.* **D68**, 073005 (2003).
 45. W. Beenakker *et al.*, *Phys. Rev. Lett.* **87**, 201805 (2001);
L. Reina and S. Dawson, *Phys. Rev. Lett.* **87**, 201804 (2001);
S. Dawson *et al.*, *Phys. Rev.* **D67**, 071503 (2003).
 46. R.V. Harlander and W.B. Kilgore, *Phys. Rev.* **D68**, 013001 (2003);
J. Campbell *et al.*, *Phys. Rev.* **D67**, 095002 (2003);
S. Dawson *et al.*, *Phys. Rev. Lett.* **94**, 031802 (2005);
S. Dittmaier, M. Krämer, and M. Spira, *Phys. Rev.* **D70**, 074010 (2004);
S. Dawson *et al.*, *Phys. Rev.* **D69**, 074027 (2004).
 47. W.J. Stirling and D.J. Summers, *Phys. Lett.* **B283**, 411 (1992);
F. Maltoni *et al.*, *Phys. Rev.* **D64**, 094023 (2001).
 48. M. Carena and H.E. Haber, *Prog. in Part. Nucl. Phys.* **50**, 152 (2003).
 49. J. Ellis *et al.*, *Nucl. Phys.* **B106**, 292 (1976);
B.L. Ioffe and V.A. Khoze, *Sov. J. Nucl. Phys.* **9**, 50 (1978).
 50. D.R.T. Jones and S.T. Petcov, *Phys. Lett.* **84B**, 440 (1979);
R.N. Cahn and S. Dawson, *Phys. Lett.* **136B**, 96 (1984);
ibid., **138B**, 464 (1984);
W. Kilian *et al.*, *Phys. Lett.* **B373**, 135 (1996).
 51. P. Janot, *Searching for Higgs Bosons at LEP 1 and LEP 2*, in *Perspectives in Higgs Physics II*, World Scientific, ed. G.L. Kane (1998).
 52. See the Review on *Statistics* in this volume.
 53. OPAL Collab., *Eur. Phys. J.* **C27**, 311 (2003).
 54. ALEPH Collab., *Phys. Lett.* **B526**, 191 (2002).
 55. DELPHI Collab., *Eur. Phys. J.* **C32**, 145 (2004).
 56. L3 Collab., *Phys. Lett.* **B517**, 319 (2001).
 57. OPAL Collab., *Eur. Phys. J.* **C26**, 479 (2003).
 58. The CDF and DØ Collabs. and the Tevatron Electroweak Working Group, *Combination of the CDF and DØ Results on the Mass of the Top Quark*, [arXiv:0903.2503 \[hep-ex\]](https://arxiv.org/abs/0903.2503) (2009).
 59. The CDF and DØ Collabs. and the Tevatron Electroweak Working Group, *Updated Combination of CDF and DØ Results for the Mass of the W Boson*, [arXiv:0908.1374 \[hep-ex\]](https://arxiv.org/abs/0908.1374) (2009);
The ALEPH, DELPHI, L3, and OPAL Collabs. and the LEP Electroweak Working Group, [arXiv:hep-ex/0612034](https://arxiv.org/abs/hep-ex/0612034) (2006).
 60. S.L. Glashow, D.V. Nanopoulos, and A. Yildiz, *Phys. Rev.* **D18**, 1724 (1978);
A. Stange, W. Marciano, and S. Willenbrock, *Phys. Rev.* **D49**, 1354 (1994); *ibid.*, **D50**, 4491 (1994).
 61. CDF Collab., *Phys. Rev. Lett.* **103**, 101802 (2009).
 62. DØ Collab., *Phys. Rev. Lett.* **102**, 051803 (2009).
 63. (***) CDF Collab., CDF Note 10068, “Search for Standard Model Higgs Boson Production in Association with W Boson Using Matrix Element Techniques with 4.8 fb^{-1} of CDF Data” (2010).
 64. (***) DØ Collab., DØ Note 5972-CONF, “Search for WH associated production using neural networks with 5.0 fb^{-1} of Tevatron data” (2009).
 65. CDF Collab., *Phys. Rev. Lett.* **104**, 141801 (2010).
 66. DØ Collab., *Phys. Rev. Lett.* **104**, 071801 (2010).
 67. (***) CDF Collab., CDF Note 9642, “Search for the Standard Model Higgs Boson in the \cancel{E}_T plus jets sample” (2009).
 68. CDF Collab., *Phys. Rev.* **D80**, 071101 (2009).
 69. DØ Collab., *Phys. Lett.* **B655**, 209 (2007).
 70. (***) CDF Collab., CDF Note 9889, “A Search for the Standard Model Higgs Boson in the Process $ZH \rightarrow \ell^+ \ell^- b\bar{b}$ Using 4.1 fb^{-1} of CDF II Data” (2009).
 71. (***) DØ Collab., DØ Note 5876-CONF, “Search for $ZH(\rightarrow e^+e^-b\bar{b})$ and $ZH(\rightarrow \mu^+\mu^-b\bar{b})$ Production in

Gauge & Higgs Boson Particle Listings

Higgs Bosons — H^0 and H^\pm

- 4.2 fb⁻¹ of data with the DØ Detector in $p\bar{p}$ collisions at $\sqrt{s} = 1.96$ TeV” (2009).
72. (**) CDF Collab., CDF Note 9248, “Search for the Standard Model Higgs Boson in the $H \rightarrow \tau^+\tau^-$ Channel at CDF Run II” (2008).
 73. DØ Collab., Phys. Rev. Lett. **102**, 251801 (2009).
 74. (***) DØ Collab., DØ Note 5845-CONF, “Search for the SM Higgs boson in the $\tau^+\tau^-q\bar{q}$ final state” (2009).
 75. (***) DØ Collab., DØ Note 5977-CONF, “Search for the standard model Higgs boson in the $WH \rightarrow \tau\nu b\bar{b}$ channel with 4.0 fb⁻¹ of $p\bar{p}$ collisions at $\sqrt{s} = 1.96$ TeV” (2009).
 76. (**) CDF Collab., CDF Note 9997, “Search for Standard Model Higgs Boson Production in Association with W Boson using 4.3 fb⁻¹ of CDF Data” (2009);
(**) CDF Collab., CDF Note 9985, “Search for Standard Model Higgs Boson Production in Association with W Boson Using Matrix Element Techniques with 4.3 fb⁻¹ of CDF Data” (2009).
 77. CDF Collab., Phys. Rev. Lett. **103**, 221801 (2009).
 78. The CDF and DØ Collabs. and the Tevatron New Physics and Higgs Working Group, arXiv:0911.3930 [hep-ex] (2009).
 79. DØ Collab., Phys. Rev. Lett. **97**, 151804 (2006).
 80. (**) CDF Collab., CDF Note 7307, “Search for the WH Production Using High- p_T Isolated Like-Sign Dilepton Events in Run II” (2004).
 81. (***) DØ Collab., DØ Note 5873-CONF, “Search for the Associated Higgs Boson Production with Like Sign Leptons in $p\bar{p}$ Collisions $\sqrt{s} = 1.96$ TeV” (2009).
 82. CDF Collab., Phys. Rev. Lett. **104**, 061803 (2010).
 83. DØ Collab., Phys. Rev. Lett. **104**, 061804 (2010).
 84. G.D. Kribs *et al.*, Phys. Rev. **D76**, 075016 (2007).
 85. P. Bechtle *et al.*, Comput. Phys. Commun. **181**, 138 (2010).
 86. C.J. Flacco *et al.*, arXiv:1005.1077 [hep-ph] (2010).
 87. The CDF and DØ Collabs., arXiv:1005.3216 [hep-ex] (2010).
 88. C. Anastasiou, R. Boughezal, and E. Furlan, arXiv:1003.4677 [hep-ph] (2010).
 89. A. Schafer, O. Nachtmann, and R. Schopf, Phys. Lett. **B249**, 331 (1990);
A. Bialas and P.V. Landshoff, Phys. Lett. **B256**, 540 (1991);
M. Heyssler, Z. Kunszt, and W.J. Stirling Phys. Lett. **B406**, 95 (1997);
R. Enberg *et al.*, Phys. Rev. Lett. **89**, 081801 (2002);
V.A. Khoze, A.D. Martin, and M.G. Ryskin, Phys. Lett. **B401**, 330 (1997); Eur. Phys. J. **C14**, 525 (2000);
Eur. Phys. J. **C25**, 391 (2002); Eur. Phys. J. **C26**, 229 (2002);
A.B. Kaidalov *et al.*, Eur. Phys. J. **C33**, 261 (2004);
C. Royon, Mod. Phys. Lett. **A18**, 2169 (2003).
 90. E. Yazgan *et al.*, CMS-NOTE-2007-011 and arXiv:0706.1898 [hep-ex] (2007).
 91. J.-J. Blaising *et al.*, “Potential LHC contributions to Europe’s future Strategy at the high energy frontier,” input number 54 to the CERN Council Strategy Group, <http://council-strategygroup.web.cern.ch/council-strategygroup/>.
 92. G. Azuelos *et al.*, Eur. Phys. J. **C66**, 525 (2010).
 93. V. Buescher and K. Jakobs, Int. J. Mod. Phys. **A20**, 2523 (2005).
 94. D. Zeppenfeld *et al.*, Phys. Rev. **D62**, 013009 (2000);
D. Zeppenfeld, “Higgs Couplings at the LHC,” in *Proceedings of the APS/DPF/DPB Summer Study on the Future of Particle Physics* (Snowmass 2001), eds. R. Davidson and C. Quigg, SNOWMASS-2001-P123, arXiv:hep-ph/0203123 (2002).
 95. M. Dührssen *et al.*, Phys. Rev. **D70**, 113009 (2004).
 96. T. Plehn, D.L. Rainwater, and D. Zeppenfeld, Phys. Rev. Lett. **88**, 051801 (2002).
 97. V. Hankele *et al.*, Phys. Rev. **D74**, 095001 (2006).
 98. C. Ruwiedel, N. Wermes, and M. Schumacher, Eur. Phys. J. **C51**, 385 (2007).
 99. E. Witten, Nucl. Phys. **B188**, 513 (1981);
R.K. Kaul, Phys. Lett. **B109**, 19 (1982);
Pramana **19**, 183 (1982);
L. Susskind, Phys. Rev. **104**, 181 (1984).
 100. L.E. Ibáñez and G.G. Ross, Phys. Lett. **B110**, 215 (1982);
L.E. Ibáñez, Phys. Lett. **B118**, 73 (1982);
J. Ellis, D.V. Nanopoulos, and K. Tamvakis, Phys. Lett. **B121**, 123 (1983);
L. Alvarez-Gaumé, J. Polchinski, and M.B. Wise, Nucl. Phys. **B221**, 495 (1983).
 101. S. Dimopoulos and H. Georgi, Nucl. Phys. **B193**, 150 (1981);
K. Harada and N. Sakai, Prog. Theor. Phys. **67**, 1877 (1982);
K. Inoue *et al.*, Prog. Theor. Phys. **67**, 1889 (1982);
L. Girardello and M.T. Grisaru, Nucl. Phys. **B194**, 65 (1982);
L.J. Hall and L. Randall, Phys. Rev. Lett. **65**, 2939 (1990);
I. Jack and D.R.T. Jones, Phys. Lett. **B457**, 101 (1999).
 102. H.E. Haber and G.L. Kane, Phys. Rev. **C117**, 75 (1985);
H.E. Haber, *Supersymmetry*, in this volume.
 103. S. Dimopoulos and D.W. Sutter, Nucl. Phys. **B452**, 496 (1995);
D.W. Sutter, Stanford Ph. D. thesis, hep-ph/9704390 (1997);
H.E. Haber, Nucl. Phys. B (Proc. Suppl.) **62A-C**, 469 (1998).
 104. H.E. Haber and Y. Nir, Nucl. Phys. **B335**, 363 (1990);
A. Dobado, M.J. Herrero, and S. Penaranda, Eur. Phys. J. **C17**, 487 (2000);
J.F. Gunion and H.E. Haber, Phys. Rev. **D67**, 075019 (2003).
 105. L.J. Hall and M.B. Wise, Nucl. Phys. **B187**, 397 (1981).
 106. Y. Okada, M. Yamaguchi, and T. Yanagida, Prog. Theor. Phys. **85**, 1 (1991);
J. Ellis, G. Ridolfi, and F. Zwirner, Phys. Lett. **B257**, 83 (1991).
 107. H.E. Haber and R. Hempfling, Phys. Rev. Lett. **66**, 1815 (1991).
 108. S.P. Li and M. Sher, Phys. Lett. **B140**, 339 (1984);
R. Barbieri and M. Frigeni, Phys. Lett. **B258**, 395 (1991);
M. Drees and M.M. Nojiri, Phys. Rev. **D45**, 2482 (1992);
J.A. Casas *et al.*, Nucl. Phys. **B436**, 3 (1995) [E: **B439**, 466 (1995)];

- J. Ellis, G. Ridolfi, and F. Zwirner, Phys. Lett. **B262**, 477 (1991);
A. Brignole *et al.*, Phys. Lett. **B271**, 123 (1991) [E: **B273**, 550 (1991)].
109. R.-J. Zhang, Phys. Lett. **B447**, 89 (1999);
J.R. Espinosa and R.-J. Zhang, JHEP **0003**, 026 (2000);
J.R. Espinosa and R.-J. Zhang, Nucl. Phys. **B586**, 3 (2000);
A. Brignole *et al.*, Nucl. Phys. **B631**, 195 (2002), Nucl. Phys. **B643**, 79 (2002);
A. Dedes, G. Degrassi, and P. Slavich, Nucl. Phys. **B672**, 144 (2003).
110. H.E. Haber and R. Hempfling, Phys. Rev. Lett. **66**, 1815 (1991);
J.F. Gunion and A. Turski, Phys. Rev. **D39**, 2701 (1989), Phys. Rev. **D40**, 2333 (1989);
M.S. Berger, Phys. Rev. **D41**, 225 (1990);
A. Brignole, Phys. Lett. **B277**, 313 (1992); Phys. Lett. **B281**, 284 (1992);
M.A. Diaz and H.E. Haber, Phys. Rev. **D45**, 4246 (1992);
P.H. Chankowski, S. Pokorski, and J. Rosiek; Phys. Lett. **B274**, 191 (1992); Nucl. Phys. **B423**, 437 (1994);
A. Yamada, Phys. Lett. **B263**, 233 (1991); Z. Phys. **C61**, 247 (1994);
A. Dabelstein, Z. Phys. **C67**, 496 (1995);
R. Hempfling and A.H. Hoang, Phys. Lett. **B331**, 99 (1994);
S. Heinemeyer, W. Hollik, and G. Weiglein, Phys. Rev. **D58**, 091701 (1998); Phys. Lett. **B440**, 296 (1998); Eur. Phys. J. **C9**, 343 (1999).
111. D.M. Pierce *et al.*, Nucl. Phys. **B491**, 3 (1997).
112. R. Barbieri, M. Frigeni, and F. Caravaglios, Phys. Lett. **B258**, 167 (1991);
Y. Okada, M. Yamaguchi, and T. Yanagida, Phys. Lett. **B262**, 45 (1991);
J.R. Espinosa and M. Quirós, Phys. Lett. **B266**, 389 (1991);
D.M. Pierce, A. Papadopoulos, and S. Johnson, Phys. Rev. Lett. **68**, 3678 (1992);
K. Sasaki, M. Carena, and C.E.M. Wagner, Nucl. Phys. **B381**, 66 (1992);
R. Hempfling, in *Phenomenological Aspects of Supersymmetry*, eds. W. Hollik, R. Rückl, and J. Wess (Springer-Verlag, Berlin, 1992) pp. 260–279;
J. Kodaira, Y. Yasui, and K. Sasaki, Phys. Rev. **D50**, 7035 (1994);
H.E. Haber and R. Hempfling, Phys. Rev. **D48**, 4280 (1993);
M. Carena *et al.*, Phys. Lett. **B355**, 209 (1995);
M. Carena, M. Quirós, and C.E.M. Wagner, Nucl. Phys. **B461**, 407 (1996).
113. H.E. Haber, R. Hempfling, and A.H. Hoang, Z. Phys. **C75**, 539 (1997);
M. Carena *et al.*, Nucl. Phys. **B580**, 29 (2000).
114. S. Martin, Phys. Rev. **D67**, 095012 (2003); Phys. Rev. **D71**, 016012 (2005); Phys. Rev. **D75**, 055005 (2007).
115. M. Carena, S. Mrenna, and C.E.M. Wagner, Phys. Rev. **D60**, 075010 (1999); *ibid.*, Phys. Rev. **D62**, 055008 (2000).
116. S. Heinemeyer, W. Hollik, and G. Weiglein, Phys. Lett. **B455**, 179 (1999);
J.R. Espinosa and I. Navarro, Nucl. Phys. **B615**, 82 (2001);
G. Degrassi, P. Slavich, and F. Zwirner, Nucl. Phys. **B611**, 403 (2001);
S. Heinemeyer *et al.*, Eur. Phys. J. **C39**, 465 (2005).
117. M. Carena *et al.*, hep-ph/9912223 (1999); *idem*, Eur. Phys. J. **C26**, 601 (2003).
118. G. Degrassi *et al.*, Eur. Phys. J. **C28**, 133 (2003).
119. S. Heinemeyer *et al.*, J. High Energy Phys. **0808**, 087 (2008).
120. M. Carena *et al.*, Phys. Lett. **B495**, 155 (2000);
M. Carena *et al.*, Nucl. Phys. **B625**, 345 (2002).
121. A. Dabelstein, Nucl. Phys. **B456**, 25 (1995);
F. Borzumati *et al.*, Nucl. Phys. **B555**, 53 (1999);
H. Eberl *et al.*, Phys. Rev. **D62**, 055006 (2000).
122. J.A. Coarasa, R.A. Jiménez, and J. Solà, Phys. Lett. **B389**, 312 (1996);
R.A. Jiménez and J. Solà, Phys. Lett. **B389**, 53 (1996);
A. Bartl *et al.*, Phys. Lett. **B378**, 167 (1996).
123. S. Heinemeyer, W. Hollik and G. Weiglein, Eur. Phys. J. **C16**, 139 (2000).
124. H.E. Haber *et al.*, Phys. Rev. **D63**, 055004 (2001).
125. L. Hall, R. Rattazzi, and U. Sarid, Phys. Rev. **D50**, 7048 (1994);
R. Hempfling, Phys. Rev. **D49**, 6168 (1994).
126. M. Carena *et al.*, Nucl. Phys. **B426**, 269 (1994).
127. M. Carena *et al.*, Phys. Lett. **B499**, 141 (2001).
128. E. Berger *et al.*, Phys. Rev. **D66**, 095001 (2002).
129. E. Boos *et al.*, Phys. Rev. **D66**, 055004 (2002).
130. A. Djouadi, J. Kalinowski, and P.M. Zerwas, Z. Phys. **C57**, 569 (1993);
H. Baer *et al.*, Phys. Rev. **D47**, 1062 (1993);
A. Djouadi *et al.*, Phys. Lett. **B376**, 220 (1996);
A. Djouadi *et al.*, Z. Phys. **C74**, 93 (1997);
S. Heinemeyer and W. Hollik, Nucl. Phys. **B474**, 32 (1996).
131. J.F. Gunion, Phys. Rev. Lett. **72**, 199 (1994);
D. Choudhury and D.P. Roy, Phys. Lett. **B322**, 368 (1994);
O.J. Eboli and D. Zeppenfeld, Phys. Lett. **B495**, 147 (2000);
B.P. Kersevan, M. Malawski, and E. Richter-Was, Eur. Phys. J. **C29**, 541 (2003).
132. OPAL Collab., Eur. Phys. J. **C37**, 49 (2004).
133. L3 Collab., Phys. Lett. **B545**, 30 (2002).
134. OPAL Collab., Eur. Phys. J. **C23**, 397 (2002).
135. DELPHI Collab., Eur. Phys. J. **C38**, 1 (2004).
136. J.F. Gunion and H.E. Haber, Nucl. Phys. **B278**, 449 (1986) [E: **B402**, 567 (1993)];
S. Dawson, A. Djouadi, and M. Spira, Phys. Rev. Lett. **77**, 16 (1996);
A. Djouadi, Phys. Lett. **B435**, 101 (1998);
A. Djouadi *et al.*, Phys. Lett. **B318**, 347 (1993);
R.V. Harlander and W.B. Kilgore, JHEP **0210**, 017 (2002);
C. Anastasiou and K. Melnikov, Phys. Rev. **D67**, 037501 (2003);
J. Guasch, P. Hafliger, and M. Spira, Phys. Rev. **D68**, 115001 (2003);
R.V. Harlander and M. Steinhauser, JHEP **0409**, 066 (2004);
S. Dawson *et al.*, Mod. Phys. Lett. **A21**, 89 (2006);
A. Djouadi and M. Spira, Phys. Rev. **D62**, 014004

Gauge & Higgs Boson Particle Listings

Higgs Bosons — H^0 and H^\pm

- (2000);
M. Muhlleitner and M. Spira, Nucl. Phys. **B790**, 1 (2008);
T. Hahn *et al.*, arXiv:hep-ph/0607308 (2006).
137. M. Carena, A. Menon, and C.E.M. Wagner, Phys. Rev. **D76**, 035004 (2007);
P. Draper, T. Liu, and C.E.M. Wagner, Phys. Rev. **D80**, 035025 (2009).
138. P. Draper, T. Liu, and C.E.M. Wagner, arXiv:0911.0034 [hep-ph].
139. M. Carena *et al.*, Eur. Phys. J. **C45**, 797 (2006).
140. DØ Collab., Phys. Rev. Lett. **101**, 221802 (2008).
141. (***) DØ Collab., DØ Note 5726-CONF, "Search for Neutral Higgs Bosons in Multi- b -jet events in $p\bar{p}$ Collisions at $\sqrt{s} = 1.96$ TeV" (2008).
142. (***) CDF Collab., CDF Note 10105, "Search for Higgs Bosons Produced in Association with b -Quarks" (2010).
143. DØ Collab., Phys. Rev. Lett. **104**, 151801 (2010).
144. CDF Collab., Phys. Rev. Lett. **103**, 201801 (2009).
145. DØ Collab., Phys. Rev. Lett. **101**, 071804 (2008).
146. (***) DØ Collab., DØ Note 5740-CONF, "Search for MSSM Higgs Boson Production in Di-tau Final States with $\mathcal{L} = 2.2$ fb $^{-1}$ at the DØ Detector" (2008).
147. CDF and DØ Collaborations and the Tevatron New Physics and Higgs Working Group, arXiv:1003.3363 [hep-ex].
148. S. Gennai *et al.*, Eur. Phys. J. **C52**, 383 (2007).
149. A.D. Sakharov, JETP Lett. **5**, 24 (1967).
150. M. Carena *et al.*, Nucl. Phys. **B599**, 158 (2001).
151. S. Dimopoulos and S. Thomas, Nucl. Phys. **B465**, 23, (1996);
S. Thomas, Int. J. Mod. Phys. **A13**, 2307 (1998).
152. A. Pilaftsis and C.E.M. Wagner, Nucl. Phys. **B553**, 3 (1999).
153. M. Carena *et al.*, Nucl. Phys. **B586**, 92 (2000).
154. A. Pilaftsis, Phys. Rev. **D58**, 096010 (1998); Phys. Lett. **B435**, 88 (1998);
K.S. Babu *et al.*, Phys. Rev. **D59**, 016004 (1999).
155. G.L. Kane and L.-T. Wang, Phys. Lett. **B488**, 383 (2000);
S.Y. Choi, M. Drees, and J.S. Lee, Phys. Lett. **B481**, 57 (2000);
S.Y. Choi and J.S. Lee, Phys. Rev. **D61**, 015003 (2000);
S.Y. Choi, K. Hagiwara, and J.S. Lee, Phys. Rev. **D64**, 032004 (2001); Phys. Lett. **B529**, 212 (2002);
T. Ibrahim and P. Nath, Phys. Rev. **D63**, 035009 (2001);
T. Ibrahim, Phys. Rev. **D64**, 035009 (2001);
S. Heinemeyer, Eur. Phys. J. **C22**, 521 (2001);
S.W. Ham *et al.*, Phys. Rev. **D68**, 055003 (2003).
156. M. Frank *et al.*, JHEP **0702**, 047 (2007);
S. Heinemeyer *et al.*, Phys. Lett. **B652**, 300 (2007);
T. Hahn *et al.*, arXiv:0710.4891 (2007).
157. D.A. Demir, Phys. Rev. **D60**, 055006 (1999);
S. Y. Choi *et al.*, Phys. Lett. **B481**, 57 (2000).
158. E. Christova *et al.*, Nucl. Phys. **B639**, 263 (2002) [E: Nucl. Phys. **B647**, 359 (2002)].
159. K. E. Williams and G. Weiglein, arXiv:0710.5320 (2007).
160. W. de Boer and C. Sander, Phys. Lett. **B585**, 276 (2004);
S. Heinemeyer *et al.*, JHEP **0608**, 052 (2006);
A. Djouadi *et al.*, Phys. Rev. Lett. **78**, 3626 (1997); Phys. Rev. **D 57** (1998) 4179;
S. Heinemeyer and G. Weiglein, JHEP **10** (2002) 072;
J. Haestier *et al.*, JHEP **0512**, 027, (2005);
S. Heinemeyer, W. Hollik, and G. Weiglein, Phys. Rept. **425**, 265 (2006);
S. Heinemeyer *et al.*, arXiv:0710.2972 (2007).
161. O. Buchmueller *et al.*, Eur. Phys. J. **C64**, 391 (2009).
162. O. Buchmueller *et al.*, Phys. Rev. **D81**, 035009 (2010).
163. G. D'Ambrosio *et al.*, Nucl. Phys. **B645**, 155 (2002).
164. J.R. Ellis *et al.*, JHEP **0708**, 083 (2007).
165. E. Lunghi, W. Porod, and O. Vives, Phys. Rev. **D74**, 075003 (2006).
166. M. Carena *et al.*, Phys. Rev. **D74**, 015009 (2006).
167. DØ Collab., Phys. Rev. Lett. **97**, 021802 (2006);
CDF Collab., Phys. Rev. Lett. **97**, 062003 (2006);
idem., Phys. Rev. Lett. **97**, 242004 (2006).
168. (**, ***) CDF and DØ Collaborations, CDF Note 9787, DØ Note 5928-CONF, "Combination of DØ and CDF Results on $\Delta\Gamma_s$ and the CP-Violating Phase $\beta_s^{J/\psi\phi}$ " (2009).
169. DØ Collab., arXiv:1005.2757 [hep-ex] (2010).
170. CDF Collab., Phys. Rev. Lett. **95**, 221805 (2005);
DØ Collab., Phys. Rev. **D74**, 031107 (2006);
(**) CDF Collab., CDF Note 9892, "Search for $B_s^0 \rightarrow \mu^+\mu^-$ and $B_d^0 \rightarrow \mu^+\mu^-$ Decays in 3.7 fb $^{-1}$ of $p\bar{p}$ Collisions with CDF II" (2009);
(***) DØ Collab., DØ Note 5906-CONF, "A new expected upper limit on $B_s \rightarrow \mu^+\mu^-$ using 5 fb $^{-1}$ of Run II data" (2009).
171. J. Foster, K.i. Okumura, and L. Roszkowski, JHEP **0508**, 094 (2005); L. Roszkowski, R. Ruiz de Austri, and R. Trotta, JHEP **0707**, 075 (2007); Phys. Lett. **B641**, 452 (2006).
172. G. Buchalla, A.J. Buras, and M.E. Lautenbacher, Rev. Mod. Phys. **68**, 1125 (1996).
173. A. Dedes and A. Pilaftsis, Phys. Rev. **D67**, 015012 (2003).
174. A.J. Buras *et al.*, Phys. Lett. **B546**, 96 (2002).
175. A.J. Buras *et al.*, Nucl. Phys. **B659**, 2 (2003).
176. K.S. Babu and C.F. Kolda, Phys. Rev. Lett. **84**, 228 (2000).
177. M. Misiak *et al.*, Phys. Rev. Lett. **98**, 022002 (2007), and references therein.
178. Heavy Flavor Averaging Group (HFAG), <http://www.slac.stanford.edu/xorg/hfag/rare/lep-pho09/rad11/btosg.pdf>.
179. T. Becher and M. Neubert, Phys. Rev. Lett. **98**, 022003 (2007).
180. I. Adachi *et al.*, [Belle Collab.], arXiv:0809.3834 [hep-ex] (2008).
181. B. Aubert *et al.*, [BABAR Collab.], arXiv:0809.4027 [hep-ex] (2008).
182. G. Isidori and P. Paradisi, Phys. Lett. **B639**, 499 (2006).
183. B. Aubert *et al.*, [BABAR Collab.], Phys. Rev. Lett. **100**, 021801 (2008).
184. I. Adachi *et al.*, arXiv:0910.4301 [hep-ex] (2009).
185. U. Nierste, S. Trine, and S. Westhoff, Phys. Rev. **D78**, 015006 (2008).

186. S. Trine, arXiv:0810.3633 [hep-ph] (2008).
187. M. Carena, A. Menon, and C.E.M. Wagner, Phys. Rev. **D79**, 075025 (2009).
188. J. Ellis *et al.*, Phys. Lett. **B653**, 292 (2007).
189. N. Cabibbo, G. R. Farrar, and L. Maiani, Phys. Lett. **B105**, 155 (1981);
H. Goldberg, Phys. Rev. Lett. **50**, 1419 (1983);
J.R. Ellis *et al.*, Nucl. Phys. **B238**, 453 (1984);
G. Bertone, D. Hooper, and J. Silk, Phys. Reports **405**, 279 (2005).
190. M. Carena, D. Hooper, and A. Vallinotto, Phys. Rev. **D75**, 055010 (2007);
M. Carena, D. Hooper, and P. Skands, Phys. Rev. Lett. **97**, 051801 (2006).
191. A. Djouadi and Y. Mambrini, JHEP **0612**, 001 (2006).
192. J. Ellis, K.A. Olive, and Y. Santoso, Phys. Rev. **D71**, 095007 (2005).
193. A. Djouadi, M. Spira, and P.M. Zerwas, Z. Phys. **C70**, 675 (1996).
194. ALEPH Collab., Phys. Lett. **B543**, 1 (2002);
DELPHI Collab., Phys. Lett. **B525**, 17 (2002);
L3 Collab., Phys. Lett. **B575**, 208 (2003);
OPAL Collab., Eur. Phys. J. **C7**, 407 (1999).
195. (*) ALEPH, DELPHI, L3 and OPAL Collaborations, The LEP Working Group for Higgs Boson Searches, *Search for Charged Higgs Bosons: Preliminary ...*, LHWG-Note/2001-05.
196. A. G. Akeroyd *et al.*, Eur. Phys. J. **C20**, 51 (2001).
197. DELPHI Collab., Eur. Phys. J. **C34**, 399 (2004).
198. J.A. Coarasa *et al.*, Eur. Phys. J. **C2**, 373 (1998).
199. C.S. Li and T.C. Yuan, Phys. Rev. **D42**, 3088 (1990);
[E: Phys. Rev. **D47**, 2156 (1993);
A. Czarnecki and S. Davidson, Phys. Rev. **D47**, 3063 (1993);
C.S. Li, Y.-S. Wei, and J.-M. Yang, Phys. Lett. **B285**, 137 (1992).
200. J. Guasch, R.A. Jiménez, and J. Solà, Phys. Lett. **B360**, 47 (1995).
201. M. Carena *et al.*, Nucl. Phys. **B577**, 88 (2000).
202. M. Guchait and S. Moretti, JHEP **0201**, 001 (2002).
203. R.M. Barnett, H.E. Haber, and D.E. Soper, Nucl. Phys. **B306**, 697 (1988).
204. F. Olness and W.-K. Tung, Nucl. Phys. **B308**, 813 (1988).
205. F. Borzumati, J.-L. Kneur, and N. Polonsky, Phys. Rev. **D60**, 115011 (1999).
206. A. Belyaev *et al.*, JHEP **0206**, 059 (2002).
207. L.G. Jin *et al.*, Eur. Phys. J. **C14**, 91 (2000); Phys. Rev. **D62**, 053008 (2000);
A. Belyaev *et al.*, Phys. Rev. **D65**, 031701 (2002);
G. Gao *et al.*, Phys. Rev. **D66**, 015007 (2002).
208. S.-H. Zhu, Phys. Rev. **D67**, 075006 (2005);
T. Plehn, Phys. Rev. **D67**, 014018 (2003).
209. A.A. Barrientos Bendejú, and B.A. Kniehl, Phys. Rev. **D59**, 015009 (1999); Phys. Rev. **D61**, 015009 (2000);
Phys. Rev. **D63**, 015009 (2001).
210. A.A. Barrientos Bendejú and B.A. Kniehl, Nucl. Phys. **B568**, 305 (2000).
211. A. Krause *et al.*, Nucl. Phys. **B519**, 85 (1998).
212. O. Brein and W. Hollik, Eur. Phys. J. **C13**, 175 (2000).
213. DØ Collab., Phys. Rev. Lett. **82**, 4975 (1999);
idem, **88**, 151803 (2002);
CDF Collab., Phys. Rev. **D62**, 012004 (2000);
idem, Phys. Rev. Lett. **79**, 357 (1997).
214. CDF Collab., Phys. Rev. Lett. **96**, 042003 (2006).
215. DØ Collab., Phys. Lett. **B682**, 278 (2009).
216. G.B. Gelmini and M. Roncadelli, Phys. Lett. **B99**, 411 (1981);
R.N. Mohapatra and J.D. Vergados, Phys. Rev. Lett. **47**, 1713 (1981);
V. Barger *et al.*, Phys. Rev. **D26**, 218 (1982).
217. B. Dutta and R.N. Mohapatra, Phys. Rev. **D59**, 015018 (1998);
C. S. Aulakh *et al.*, Phys. Rev. **D58**, 115007 (1998);
C. S. Aulakh, A. Melfo, and G. Senjanovic, Phys. Rev. **D57**, 4174 (1998).
218. DELPHI Collab., Phys. Lett. **B552**, 127 (2003).
219. OPAL Collab., Phys. Lett. **B295**, 347 (1992);
idem, **B526**, 221 (2002).
220. L3 Collab., Phys. Lett. **B576**, 18 (2003).
221. OPAL Collab., Phys. Lett. **B577**, 93 (2003).
222. DØ Collab., Phys. Rev. Lett. **93**, 141801 (2004);
DØ Collab., Phys. Rev. Lett. **101**, 071803 (2008).
223. CDF Collab., Phys. Rev. Lett. **93**, 221802 (2004);
CDF Collab., Phys. Rev. Lett. **101**, 121801 (2008).
224. CDF Collab., Phys. Rev. Lett. **95**, 071801 (2005).
225. H.E. Haber, *Proceedings of the 1990 Theoretical Advanced Study Institute in Elementary Particle Physics*, eds. M. Cvetič and Paul Langacker (World Scientific, Singapore, 1991) pp. 340–475, and references therein.
226. S. Glashow and S. Weinberg, Phys. Rev. **D15**, 1958 (1977).
227. P. Fayet, Phys. Lett. **B90**, 104 (1975);
H.-P. Nilles, M. Srednicki, and D. Wyler, Phys. Lett. **B120**, 346 (1983);
J.-M. Frere, D.R.T. Jones, and S. Raby, Nucl. Phys. **B222**, 11 (1983);
J.-P. Derendinger and C.A. Savoy, Nucl. Phys. **B237**, 307 (1984);
B.R. Greene and P.J. Miron, Phys. Lett. **B168**, 226 (1986);
J. Ellis *et al.*, Phys. Lett. **B176**, 403 (1986);
L. Durand and J.L. Lopez, Phys. Lett. **B217**, 463 (1989);
M. Drees, Int. J. Mod. Phys. **A4**, 3635 (1989);
U. Ellwanger, Phys. Lett. **B303**, 271 (1993);
U. Ellwanger, M. Rausch de Taubenberg, and C.A. Savoy, Phys. Lett. **B315**, 331 (1993); Z. Phys. **C67**, 665 (1995);
Phys. Lett. **B492**, 21 (1997);
P.N. Pandita, Phys. Lett. **B318**, 338 (1993); Z. Phys. **C59**, 575 (1993);
T. Elliott, S.F. King, and P.L. White, Phys. Lett. **B305**, 71 (1993); Phys. Lett. **B314**, 56 (1993); Phys. Rev. **D49**, 2435 (1994); Phys. Lett. **B351**, 213 (1995);
K.S. Babu and S.M. Barr, Phys. Rev. **D49**, R2156 (1994);
S.F. King and P.L. White, Phys. Rev. **D52**, 4183 (1995);
N. Haba, M. Matsuda, and M. Tanimoto, Phys. Rev. **D54**, 6928 (1996);
F. Franke and H. Fraas, Int. J. Mod. Phys. **A12**, 479 (1997);
S.W. Ham, S.K. Oh, and H.S. Song, Phys. Rev. **D61**, 055010 (2000);

Gauge & Higgs Boson Particle Listings

Higgs Bosons — H^0 and H^\pm

- D.A. Demir, E. Ma, and U. Sarkar, *J. Phys.* **G26**, L117 (2000);
 R. B. Nevzorov and M. A. Trusov, *Phys. Atom. Nucl.* **64**, 1299 (2001);
 U. Ellwanger and C. Hugonie, *Eur. Phys. J.* **C25**, 297 (2002);
 U. Ellwanger *et al.*, [arXiv:hep-ph/0305109](https://arxiv.org/abs/hep-ph/0305109) (2003);
 D. J. Miller and S. Moretti, [arXiv:hep-ph/0403137](https://arxiv.org/abs/hep-ph/0403137) (2004).
228. A. Dedes *et al.*, *Phys. Rev.* **D63**, 055009 (2001);
 A. Menon, D. Morrissey, and C.E.M. Wagner, *Phys. Rev.* **D70**, 035005, (2004).
229. R. Dermisek and J. F. Gunion, *Phys. Rev.* **D76**, 095006 (2007);
 R. Dermisek and J. F. Gunion, *Phys. Rev.* **D81**, 075003 (2010).
230. J. R. Espinosa and M. Quiros, *Phys. Lett.* **B279**, 92 (1992).
231. U. Ellwanger and C. Hugonie, *Mod. Phys. Lett.* **A22**, 1581 (2007).
232. (*) DELPHI Collab., *Interpretation of the searches for Higgs bosons in the MSSM with an additional scalar singlet*, DELPHI 1999-97 CONF 284.
233. DØ Collab., *Phys. Rev. Lett.* **103**, 061801 (2009).
234. P. Batra *et al.*, *JHEP* **0402**, 043 (2004);
 P. Batra *et al.*, *JHEP* **0406**, 032 (2004).
235. M. Dine, N. Seiberg, and S. Thomas, *Phys. Rev.* **D76**, 095004 (2007) and references therein.
236. J. R. Espinosa and M. Quiros, *Phys. Rev. Lett.* **81**, 516 (1998).
237. M. Dine, N. Seiberg, and S. Thomas, *Phys. Rev.* **D76**, 095004 (2007).
238. P. Batra and E. Ponton, *Phys. Rev.* **D79**, 035001 (2009).
239. M. Carena *et al.*, *Phys. Rev.* **D81**, 015001 (2010).
240. I. Antoniadis *et al.*, *Nucl. Phys.* **B831**, 133 (2010).
241. M. Perelstein, *Prog. Part. Nucl. Phys.* **58**, 247 (2007).
242. M. Schmaltz and D. Tucker-Smith, *Ann. Rev. Nucl. Part. Sci.* **55**, 229 (2005).
243. C. R. Chen, K. Tobe, and C. P. Yuan, *Phys. Lett.* **B640**, 263 (2006).
244. G. F. Giudice *et al.*, *JHEP* **0706**, 045 (2007).
245. J. Hubisz *et al.*, *JHEP* **0601**, 135 (2006).
246. I. Low, W. Skiba, and D. Smith, *Phys. Rev.* **D66**, 072001 (2002).
247. G. F. Giudice, R. Rattazzi, and J. D. Wells, *Nucl. Phys.* **B595**, 250 (2001);
 M. Chaichian *et al.*, *Phys. Lett.* **B524**, 161 (2002);
 D. Dominici *et al.*, *Acta Phys. Polon.* **B33**, 2507 (2002);
 J. L. Hewett and T. G. Rizzo, *JHEP* **0308**, 028 (2003).
248. OPAL Collab., *Phys. Lett.* **B609**, 20 (2005).
249. S. Chivukula *et al.*, *Dynamical Electroweak Symmetry Breaking*, in this volume.
250. Y. Chikashige *et al.*, *Phys. Lett.* **B98**, 265 (1981);
 A.S. Joshipura and S.D. Rindani, *Phys. Rev. Lett.* **69**, 3269 (1992);
 F. de Campos *et al.*, *Phys. Rev.* **D55**, 1316 (1997).
251. DELPHI Collab., *Eur. Phys. J.* **C32**, 475 (2004);
 L3 Collab., *Phys. Lett.* **B609**, 35 (2005);
 OPAL Collab., *Phys. Lett.* **B377**, 273 (1996).
252. (*) ALEPH, DELPHI, L3 and OPAL Collaborations, The LEP Working Group for Higgs Boson Searches, *Search for Invisible Higgs Bosons: Preliminary ...*, LHWG-Note/2001-06.
253. M. J. Strassler and K. M. Zureck, *Phys. Lett.* **B651**, 374 (2007).
254. DØ Collab., *Phys. Rev. Lett.* **103**, 071801 (2009).
255. E.L. Berger *et al.*, *Phys. Rev.* **D66**, 095001 (2002).
256. W. Loinaz and J. Wells, *Phys. Lett.* **B445**, 178 (1998);
 X. Calmet and H. Fritzsch, *Phys. Lett.* **B496**, 190 (2000).
257. ALEPH Collab., *Phys. Lett.* **B544**, 25 (2002);
 DELPHI Collab., *Eur. Phys. J.* **C44**, 147 (2005);
 L3 Collab., *Phys. Lett.* **B583**, 14 (2004);
 OPAL Collab., *Eur. Phys. J.* **C18**, 425 (2001).
258. (*) The LEP Working Group for Higgs Boson Searches, *Flavour Independent Search for Hadronically Decaying Neutral Higgs Bosons at LEP*, LHWG Note 2001-07.
259. OPAL Collab., *Eur. Phys. J.* **C18**, 425 (2001);
 DELPHI Collab., *Eur. Phys. J.* **C38**, 1 (2004).
260. J. Ellis *et al.*, *Nucl. Phys.* **B106**, 292 (1976);
 A. Abbasabadi *et al.*, *Phys. Rev.* **D52**, 3919 (1995);
 R.N. Cahn *et al.*, *Phys. Lett.* **B82**, 113 (1997).
261. G. Gamberini *et al.*, *Nucl. Phys.* **B292**, 237 (1987);
 R. Bates *et al.*, *Phys. Rev.* **D34**, 172 (1986);
 K. Hagiwara *et al.*, *Phys. Lett.* **B318**, 155 (1993);
 O.J.P. Éboli *et al.*, *Phys. Lett.* **B434**, 340 (1998).
262. A. G. Akeroyd, *Phys. Lett.* **B368**, 89 (1996);
 H. Haber *et al.*, *Nucl. Phys.* **B161**, 493 (1979).
263. ALEPH Collab., *Phys. Lett.* **B544**, 16 (2002);
 DELPHI Collab., *Eur. Phys. J.* **C35**, 313 (2004);
 OPAL Collab., *Phys. Lett.* **B544**, 44 (2002).
264. L3 Collab., *Phys. Lett.* **B534**, 28 (2002).
265. (*) ALEPH, DELPHI, L3, and OPAL Collabs., The LEP Working Group for Higgs Boson Searches, *Search for Higgs Bosons Decaying into Photons: Combined ...*, LHWG Note/2002-02.
266. DØ Collab., *Phys. Rev. Lett.* **82**, 2244 (1999);
 CDF Collab., *Phys. Rev.* **D64**, 092002 (2001).
267. DØ Collab., *Phys. Rev. Lett.* **102**, 231801 (2009);
 CDF Collab., *Phys. Rev. Lett.* **103**, 061803 (2009).
268. (***) CDF Collab., “Search for a SM Higgs Boson with the Diphoton Final State at CDF,” CDF Note 10065 (2010).
269. (***) DØ Collab., DØ Note 5067-CONF, “Search for Fermiophobic Higgs Boson in $3\gamma + X$ Events” (2007).
270. ALEPH Collab., *Eur. Phys. J.* **C49**, 439 (2007).
271. G.J. Gounaris *et al.*, *Phys. Lett.* **B83**, 191 (1979);
 V. Barger *et al.*, *Phys. Rev.* **D38**, 2766 (1988);
 F. Boudjema and E. Chopin, *Z. Phys.* **C37**, 85 (1996);
 A. Djouadi *et al.*, *Eur. Phys. J.* **C10**, 27 (1999).

STANDARD MODEL H^0 (Higgs Boson) MASS LIMITS

These limits apply to the Higgs boson of the three-generation Standard Model with the minimal Higgs sector. For a review and a bibliography, see the Note above on “Searches for Higgs Bosons.”

 H^0 Direct Search Limits

Limits on the Standard Model Higgs obtained from the study of Z^0 decays rule out conclusively its existence in the whole mass region $m_{H^0} \lesssim 60$ GeV. These limits, as well as stronger limits obtained from e^+e^- collisions at LEP at energies up to 202 GeV, and weaker limits obtained from other sources, have been superseded by the more recent data of LEP. They have been removed from this compilation, and are documented in previous editions of this Review of Particle Physics. The same holds

for limits obtained from $p\bar{p}$ collisions at the Tevatron that have been superseded by more recent results incorporating a larger integrated luminosity.

In this Section, unless otherwise stated, limits from the four LEP experiments (ALEPH, DELPHI, L3, and OPAL) are obtained from the study of the $e^+e^- \rightarrow H^0 Z$ process, at center-of-mass energies reported in the comment lines.

VALUE (GeV)	CL%	DOCUMENT ID	TECN	COMMENT
>114.1	95	1 ABDALLAH	04 DLPH	$E_{cm} \leq 209$ GeV
>112.7	95	1 ABBIENDI	03B OPAL	$E_{cm} \leq 209$ GeV
>114.4	95	1,2 HEISTER	03D LEP	$E_{cm} \leq 209$ GeV
>111.5	95	1,3 HEISTER	02 ALEP	$E_{cm} \leq 209$ GeV
>112.0	95	1 ACHARD	01C L3	$E_{cm} \leq 209$ GeV
• • • We do not use the following data for averages, fits, limits, etc. • • •				
		4 AALTONEN	09A CDF	$p\bar{p} \rightarrow H^0 X, H^0 \rightarrow WW^*$
		5 AALTONEN	09AG CDF	$p\bar{p} \rightarrow H^0 WX$
		6 AALTONEN	09AI CDF	$p\bar{p} \rightarrow H^0 WX$
		7 AALTONEN	09AO CDF	$p\bar{p} \rightarrow H^0 ZX$
		8 AALTONEN	09AS CDF	$p\bar{p} \rightarrow H^0 WX, H^0 ZX$
		9 ABAZOV	09C D0	$p\bar{p} \rightarrow H^0 WX$
		10 ABAZOV	09Q D0	$H^0 \rightarrow \gamma\gamma$
		11 ABAZOV	09U D0	$H^0 \rightarrow \tau^+\tau^-$
		12 AALTONEN	08AF CDF	$p\bar{p} \rightarrow H^0 ZX$
		13 AALTONEN	08V CDF	$p\bar{p} \rightarrow H^0 WX$
		14 AALTONEN	08X CDF	$p\bar{p} \rightarrow H^0 ZX, H^0 WX$
		15 ABAZOV	08AO D0	$p\bar{p} \rightarrow H^0 ZX, H^0 WX$
		16 ABAZOV	08Y D0	$p\bar{p} \rightarrow H^0 WX$
		17 ABAZOV	07X D0	$p\bar{p} \rightarrow H^0 ZX$
		18 ABAZOV	06 D0	$p\bar{p} \rightarrow H^0 X, H^0 \rightarrow WW^*$
		19 ABAZOV	06O D0	$p\bar{p} \rightarrow H^0 WX, H^0 \rightarrow WW^*$

1 Search for $e^+e^- \rightarrow H^0 Z$ in the final states $H^0 \rightarrow b\bar{b}$ with $Z \rightarrow \ell\bar{\ell}, \nu\bar{\nu}, q\bar{q}, \tau^+\tau^-$ and $H^0 \rightarrow \tau^+\tau^-$ with $Z \rightarrow q\bar{q}$.

2 Combination of the results of all LEP experiments.

3 A 3 σ excess of candidate events compatible with m_{H^0} near 114 GeV is observed in the combined channels $q\bar{q}q\bar{q}, q\bar{q}\ell\bar{\ell}, q\bar{q}\tau^+\tau^-$.

4 AALTONEN 09A search for H^0 production in $p\bar{p}$ collisions at $E_{cm} = 1.96$ TeV in the decay mode $H^0 \rightarrow WW^*$ ($\rightarrow \ell^+\ell^-\nu\bar{\nu}$). A limit on $\sigma(H^0) \cdot B(H^0 \rightarrow WW^*)$ between 0.7 and 2.5 pb (95% CL) is given for $m_{H^0} = 110$ –200 GeV, which is 1.7–45 times larger than the expected Standard Model cross section. The best limit is obtained for $m_{H^0} = 160$ GeV.

5 AALTONEN 09AG search for associated $H^0 W$ production in 1.9 fb $^{-1}$ of $p\bar{p}$ collisions at $E_{cm} = 1.96$ TeV in the decay mode $H^0 \rightarrow b\bar{b}, W \rightarrow \ell\nu$. A limit on $\sigma(H^0 W) \cdot B(H^0 \rightarrow b\bar{b})$ (95% CL) is given for $m_{H^0} = 110$ –150 GeV, which is 7.5–101.9 times larger than the expected Standard Model cross section. The limit for $m_{H^0} = 115$ GeV is 9.0 times larger than the expected Standard Model cross section. Superseded by AALTONEN 09AI.

6 AALTONEN 09AI search for associated $H^0 W$ production in 2.7 fb $^{-1}$ of $p\bar{p}$ collisions at $E_{cm} = 1.96$ TeV in the decay mode $H^0 \rightarrow b\bar{b}, W \rightarrow \ell\nu$. A limit on $\sigma(H^0 W) \cdot B(H^0 \rightarrow b\bar{b})$ (95% CL) is given for $m_{H^0} = 100$ –150 GeV, which is 3.3–75.5 times larger than the expected Standard Model cross section. The limit for $m_{H^0} = 115$ GeV is 5.6 times larger than the expected Standard Model cross section.

7 AALTONEN 09AO search for associated $H^0 Z$ production in 2.7 fb $^{-1}$ of $p\bar{p}$ collisions at $E_{cm} = 1.96$ TeV in the decay mode $H^0 \rightarrow b\bar{b}, Z \rightarrow \ell^+\ell^-$. A limit on $\sigma(H^0 Z) \cdot B(H^0 \rightarrow b\bar{b})$ (95% CL) is given for $m_{H^0} = 100$ –150 GeV, which is 7.0–71.3 times larger than the expected Standard Model cross section. The limit for $m_{H^0} = 115$ GeV is 8.2 times larger than the expected Standard Model cross section.

8 AALTONEN 09AS search for associated $H^0 W$ and $H^0 Z$ production in 2.0 fb $^{-1}$ of $p\bar{p}$ collisions at $E_{cm} = 1.96$ TeV in the decay mode $H^0 \rightarrow b\bar{b}, W/Z \rightarrow q\bar{q}$. A limit (95% CL) is given for $m_{H^0} = 100$ –150 GeV, which is 29.4–263 times larger than the expected Standard Model cross section. The limit for $m_{H^0} = 120$ GeV is 37.5 times larger than the expected Standard Model cross section.

9 ABAZOV 09C search for associated $H^0 W$ production in 1 fb $^{-1}$ of $p\bar{p}$ collisions at $E_{cm} = 1.96$ TeV in the decay mode $H^0 \rightarrow b\bar{b}, W \rightarrow \ell\nu$. A limit $\sigma(H^0 W) \cdot B(H^0 \rightarrow b\bar{b}) < (2.1-0.95)$ pb (95% CL) is given for $m_{H^0} = 100$ –150 GeV, which is 9.1–84 times larger than the expected Standard Model cross section.

10 ABAZOV 09Q search for $H^0 \rightarrow \gamma\gamma$ in 2.7 fb $^{-1}$ of $p\bar{p}$ collisions at $E_{cm} = 1.96$ TeV in the mass range $m_{H^0} = 100$ –150 GeV. A limit (95% CL) is given for $m_{H^0} = 115$ –130 GeV, which is about 20 times larger than the expected Standard Model cross section.

11 ABAZOV 09U search for $H^0 \rightarrow \tau^+\tau^-$ with $\tau \rightarrow$ hadrons in 1 fb $^{-1}$ of $p\bar{p}$ collisions at $E_{cm} = 1.96$ TeV. The production mechanisms include associated $W/Z+H^0$ production, weak boson fusion, and gluon fusion. A limit (95% CL) is given for $m_{H^0} = 105$ –145 GeV, which is 20–82 times larger than the expected Standard Model cross section. The limit for $m_{H^0} = 115$ GeV is 29 times larger than the expected Standard Model cross section.

12 AALTONEN 08AF search for associated $H^0 Z$ production in $p\bar{p}$ collisions at $E_{cm} = 1.96$ TeV in the decay mode $H^0 \rightarrow b\bar{b}, Z \rightarrow \ell^+\ell^-$. A limit $\sigma(H^0 Z) \cdot B(H^0 \rightarrow b\bar{b}) < (1.5-1.2)$ pb (95% CL) is given for $m_{H^0} = 110$ –150 GeV, which is 15–160 times larger than the expected Standard Model cross section. Superseded by AALTONEN 09AO.

13 AALTONEN 08V search for associated $H^0 W$ production in $p\bar{p}$ collisions at $E_{cm} = 1.96$ TeV in the decay mode $H^0 \rightarrow b\bar{b}, W \rightarrow \ell\nu$. A limit $\sigma(H^0 W) \cdot B(H^0 \rightarrow b\bar{b}) < (3.9-1.3)$ pb (95% CL) is given for $m_{H^0} = 110$ –150 GeV, which is 25–120 times larger than the expected Standard Model cross section. Superseded by AALTONEN 09AI.

14 AALTONEN 08X search for associated $H^0 Z$ and $H^0 W$ production in $p\bar{p}$ collisions at $E_{cm} = 1.96$ TeV in the decay mode $H^0 \rightarrow b\bar{b}, Z \rightarrow \nu\bar{\nu}$ and $W \rightarrow (\ell)\nu$, where ℓ is not detected. A limit $\sigma \cdot B(H^0 \rightarrow b\bar{b}) < (4.7-3.3)$ pb (95% CL) is given for $m_{H^0} = 110$ –140 GeV, which is 18–66 times larger than the expected Standard Model cross section.

15 ABAZOV 08AO search for associated $H^0 Z$ and $H^0 W$ production in 0.9 fb $^{-1}$ of $p\bar{p}$ collisions at $E_{cm} = 1.96$ TeV in the decay mode $H^0 \rightarrow b\bar{b}, Z \rightarrow \nu\bar{\nu}$ and $W \rightarrow (\ell)\nu$, where ℓ is not detected. A limit $\sigma \cdot B(H^0 \rightarrow b\bar{b}) < (2.6-2.3)$ pb (95% CL) is given for $m_{H^0} = 105$ –135 GeV, which is 8.7–34 times larger than the expected Standard Model cross section.

16 ABAZOV 08Y search for associated $H^0 W$ production in $p\bar{p}$ collisions at $E_{cm} = 1.96$ TeV in the decay mode $H^0 \rightarrow b\bar{b}, W \rightarrow \ell\nu$. A limit $\sigma(H^0 W) \cdot B(H^0 \rightarrow b\bar{b}) < (1.9-1.6)$ pb (95% CL) is given for $m_{H^0} = 105$ –145 GeV, which is 10–93 times larger than the expected Standard Model cross section. These results are combined with ABAZOV 06, ABAZOV 06O, ABAZOV 06Q, and ABAZOV 07X to give cross section limits for $m_{H^0} = 100$ –200 GeV which are 6–24 times larger than the Standard Model expectation.

17 ABAZOV 07X search for associated $H^0 Z$ production in $p\bar{p}$ collisions at $E_{cm} = 1.96$ TeV in the final state $Z \rightarrow e^+e^-$ or $\mu^+\mu^-$; $H^0 \rightarrow b\bar{b}$. A limit $\sigma(ZH^0) \cdot B(H^0 \rightarrow b\bar{b}) < (4.4-3.1)$ pb (95%CL) is given for $m_{H^0} = 105$ –145 GeV, which is more than 40 times larger than the expected Standard Model cross section.

18 ABAZOV 06 search for Higgs boson production in $p\bar{p}$ collisions at $E_{cm} = 1.96$ TeV with the decay chain $H^0 \rightarrow WW^* \rightarrow \ell^\pm\nu\ell'^\mp\nu'$. A limit $\sigma(H^0) \cdot B(H^0 \rightarrow WW^*) < (5.6-3.2)$ pb (95% CL) is given for $m_{H^0} = 120$ –200 GeV, which far exceeds the expected Standard Model cross section.

19 ABAZOV 06O search for associated $H^0 W$ production in $p\bar{p}$ collisions at $E_{cm} = 1.96$ TeV with the decay $H^0 \rightarrow WW^*$, in the final states $\ell^\pm\ell'^\mp\nu\nu'X$ where $\ell = e, \mu$. A limit $\sigma(H^0 W) \cdot B(H^0 \rightarrow WW^*) < (3.2-2.8)$ pb (95% CL) is given for $m_{H^0} = 115$ –175 GeV, which far exceeds the expected Standard Model cross section.

H^0 Indirect Mass Limits from Electroweak Analysis

For limits obtained before the direct measurement of the top quark mass, see the 1996 (Physical Review **D54** 1 (1996)) Edition of this Review. Other studies based on data available prior to 1996 can be found in the 1998 Edition (The European Physical Journal **C3** 1 (1998)) of this Review. For indirect limits obtained from other considerations of theoretical nature, see the Note on “Searches for Higgs Bosons.”

VALUE (GeV)	DOCUMENT ID	TECN
80$^{+30}_{-23}$	20 FLACHER	09 RVUE
• • • We do not use the following data for averages, fits, limits, etc. • • •		
129 $^{+74}_{-49}$	21 LEP-SLC	06 RVUE
20 FLACHER 09 make Standard Model fits to Z and neutral current parameters, $m_t, m_W,$ and Γ_W measurements available in 2008 (using also preliminary data). The 2σ (3σ) interval is 39–155 (26–209) GeV. The quoted results are obtained from a fit that does not include the limit from the direct Higgs searches.		
21 LEP-SLC 06 make Standard Model fits to Z parameters from LEP/SLC and $m_t, m_W,$ and Γ_W measurements available in 2005 with $\Delta\alpha_{had}^{(5)}(m_Z) = 0.02758 \pm 0.00035$. The 95% CL limit is 285 GeV.		

MASS LIMITS FOR NEUTRAL HIGGS BOSONS IN SUPERSYMMETRIC MODELS

The minimal supersymmetric model has two complex doublets of Higgs bosons. The resulting physical states are two scalars [H_1^0 and H_2^0], where we define $m_{H_1^0} < m_{H_2^0}$, a pseudoscalar (A^0), and a charged Higgs pair

(H^\pm). H_1^0 and H_2^0 are also called h and H in the literature. There are two free parameters in the theory which can be chosen to be m_{A^0} and $\tan\beta = v_2/v_1$, the ratio of vacuum expectation values of the two Higgs doublets. Tree-level Higgs masses are constrained by the model to be $m_{H_1^0} \leq$

$m_Z, m_{H_2^0} \geq m_Z, m_{A^0} \geq m_{H_1^0}$, and $m_{H^\pm} \geq m_W$. However, as described in the review on “Searches for Higgs Bosons” in this Volume these relations are violated by radiative corrections.

Unless otherwise noted, the experiments in e^+e^- collisions search for the processes $e^+e^- \rightarrow H_1^0 Z^0$ in the channels used for the Standard Model Higgs searches and $e^+e^- \rightarrow H_1^0 A^0$ in the final states $b\bar{b}b\bar{b}$ and $b\bar{b}\tau^+\tau^-$. In $p\bar{p}$ collisions the experiments search for a variety of processes, as explicitly specified for each entry. Limits on the A^0 mass arise from these direct searches, as well as from the relations valid in the minimal supersymmetric model between m_{A^0} and $m_{H_1^0}$. As discussed in

the review on “Searches for Higgs Bosons” in this Volume, these relations depend, via potentially large radiative corrections, on the mass of the t quark and on the supersymmetric parameters, in particular those of the stop sector. The limits are weaker for larger t and τ masses. To include the radiative corrections to the Higgs masses, unless otherwise stated, the listed papers use theoretical predictions incorporating two-loop corrections and examine the two scenarios of no scalar top mixing and the m_h^{\max} benchmark scenario (which gives rise to the most conservative upper bound on the mass of H_1^0 for given values of m_{A^0} and $\tan\beta$), see CARENA 99b and CARENA 03.

Limits in the low-mass region of H_1^0 , as well as other by now obsolete limits from different techniques, have been removed from this compilation, and can be found in earlier editions of this Review. Unless otherwise stated, the following results assume no invisible H_1^0 or A^0 decays.

Gauge & Higgs Boson Particle Listings

Higgs Bosons — H^0 and H^\pm H_1^0 (Higgs Boson) MASS LIMITS in Supersymmetric Models

VALUE (GeV)	CL%	DOCUMENT ID	TECN	COMMENT
>89.7		22 ABDALLAH 08B	DLPH	$E_{cm} \leq 209$ GeV
>92.8	95	23 SCHAEEL 06B	LEP	$E_{cm} \leq 209$ GeV
>84.5	95	24,25 ABBIENDI 04M	OPAL	$E_{cm} \leq 209$ GeV
>86.0	95	24,26 ACHARD 02H	L3	$E_{cm} \leq 209$ GeV, $\tan\beta > 0.4$

• • • We do not use the following data for averages, fits, limits, etc. • • •

- 27 AALTONEN 09AR CDF $p\bar{p} \rightarrow H_{1,2}^0/A^0 + X$,
 $H_{1,2}^0/A^0 \rightarrow \tau^+\tau^-$
- 28 ABAZOV 09F D0 $p\bar{p} \rightarrow H_{1,2}^0/A^0 + b + X$,
 $H_{1,2}^0/A^0 \rightarrow \tau^+\tau^-$
- 29 ABAZOV 08AJ D0 $p\bar{p} \rightarrow H_{1,2}^0/A^0 + b + X$,
 $H_{1,2}^0/A^0 \rightarrow b\bar{b}$
- 30 ABAZOV 08W D0 $p\bar{p} \rightarrow H_{1,2}^0/A^0 + X$,
 $H_{1,2}^0/A^0 \rightarrow \tau^+\tau^-$
- >89.7 95 24,31 ABDALLAH 04 DLPH $E_{cm} \leq 209$ GeV, $\tan\beta > 0.4$
- 32 ABBIENDI 03G OPAL $H_1^0 \rightarrow A^0 A^0$
- >89.8 95 24,33 HEISTER 02 ALEP $E_{cm} \leq 209$ GeV, $\tan\beta > 0.5$
- 22 ABDALLAH 08B give limits in eight CP -conserving benchmark scenarios and some CP -violating scenarios. See paper for excluded regions for each scenario. Supersedes ABDALLAH 04.
- 23 SCHAEEL 06B make a combined analysis of the LEP data. The quoted limit is for the m_h^{\max} scenario with $m_t = 174.3$ GeV. In the CP -violating CPX scenario no lower bound on $m_{H_1^0}$ can be set at 95% CL. See paper for excluded regions in various scenarios. See Figs. 2-6 and Tabs. 14-21 for limits on $\sigma(ZH^0) \cdot B(H^0 \rightarrow b\bar{b}, \tau^+\tau^-)$ and $\sigma(H_1^0 H_2^0) \cdot B(H_1^0 H_2^0 \rightarrow b\bar{b}, \tau^+\tau^-)$.
- 24 Search for $e^+e^- \rightarrow H_1^0 A^0$ in the final states $b\bar{b}b\bar{b}$ and $b\bar{b}\tau^+\tau^-$, and $e^+e^- \rightarrow H_1^0 Z$. Universal scalar mass of 1 TeV, SU(2) gaugino mass of 200 GeV, and $\mu = -200$ GeV are assumed, and two-loop radiative corrections incorporated. The limits hold for $m_t = 175$ GeV, and for the m_h^{\max} scenario.
- 25 ABBIENDI 04M exclude $0.7 < \tan\beta < 1.9$, assuming $m_t = 174.3$ GeV. Limits for other MSSM benchmark scenarios, as well as for CP violating cases, are also given.
- 26 ACHARD 02H also search for the final state $H_1^0 Z \rightarrow 2A^0 q\bar{q}, A^0 \rightarrow q\bar{q}$. In addition, the MSSM parameter set in the “large- μ ” and “no-mixing” scenarios are examined.
- 27 AALTONEN 09AR search for Higgs bosons decaying to $\tau^+\tau^-$ in two doublet models in 1.8 fb^{-1} of $p\bar{p}$ collisions at $E_{cm} = 1.96$ TeV. See their Fig. 2 for the limit on $\sigma \cdot B(H_{1,2}^0/A^0 \rightarrow \tau^+\tau^-)$ for different Higgs masses, and see their Fig. 3 for the excluded region in the MSSM parameter space.
- 28 ABAZOV 09F search for associated production of a Higgs boson and a b quark in $p\bar{p}$ collisions at $E_{cm} = 1.96$ TeV with the decay $H_{1,2}^0/A^0 \rightarrow \tau^+\tau^-$. See their Fig. 2 for the limit on $\sigma \cdot B(H_{1,2}^0/A^0 \rightarrow \tau^+\tau^-)$ (for different Higgs masses) and for the excluded region in the MSSM parameter space for $\mu = \pm 200$ GeV.
- 29 ABAZOV 08AJ search for associated production of a Higgs boson and a b quark in $p\bar{p}$ collisions at $E_{cm} = 1.96$ TeV with the decay $H_{1,2}^0/A^0 \rightarrow b\bar{b}$. See their Tab. 3 for the limit on $\sigma \cdot B(H_{1,2}^0/A^0 \rightarrow b\bar{b})$ for different Higgs masses, and see their Fig. 3 for the excluded region in the MSSM parameter space for $\mu = \pm 200$ GeV.
- 30 ABAZOV 08W search for Higgs boson production in $p\bar{p}$ collisions at $E_{cm} = 1.96$ TeV with the decay $H_{1,2}^0/A^0 \rightarrow \tau^+\tau^-$. See their Fig. 3 for the limit on $\sigma \cdot B(H_{1,2}^0/A^0 \rightarrow \tau^+\tau^-)$ for different Higgs masses, and see their Fig. 4 for the excluded region in the MSSM parameter space.
- 31 This limit applies also in the no-mixing scenario. Furthermore, ABDALLAH 04 excludes the range $0.54 < \tan\beta < 2.36$. The limit improves in the region $\tan\beta < 6$ (see Fig. 28). Limits for $\mu = 1$ TeV are given in Fig. 30.
- 32 ABBIENDI 03G search for $e^+e^- \rightarrow H_1^0 Z$ followed by $H_1^0 \rightarrow A^0 A^0, A^0 \rightarrow c\bar{c}, g\bar{g}$, or $\tau^+\tau^-$. In the no-mixing scenario, the region $m_{H_1^0} = 45\text{--}85$ GeV and $m_{A^0} = 2\text{--}9.5$ GeV is excluded at 95% CL.
- 33 HEISTER 02 excludes the range $0.7 < \tan\beta < 2.3$. A wider range is excluded with different stop mixing assumptions. Updates BARATE 01c.

 A^0 (Pseudoscalar Higgs Boson) MASS LIMITS in Supersymmetric Models

VALUE (GeV)	CL%	DOCUMENT ID	TECN	COMMENT
>90.4		34 ABDALLAH 08B	DLPH	$E_{cm} \leq 209$ GeV
>93.4	95	35 SCHAEEL 06B	LEP	$E_{cm} \leq 209$ GeV
>85.0	95	36,37 ABBIENDI 04M	OPAL	$E_{cm} \leq 209$ GeV
>86.5	95	36,38 ACHARD 02H	L3	$E_{cm} \leq 209$ GeV, $\tan\beta > 0.4$
>90.1	95	36,39 HEISTER 02	ALEP	$E_{cm} \leq 209$ GeV, $\tan\beta > 0.5$

• • • We do not use the following data for averages, fits, limits, etc. • • •

- 40 AALTONEN 09AR CDF $p\bar{p} \rightarrow H_{1,2}^0/A^0 + X$,
 $H_{1,2}^0/A^0 \rightarrow \tau^+\tau^-$
- 41 ABAZOV 09F D0 $p\bar{p} \rightarrow H_{1,2}^0/A^0 + b + X$,
 $H_{1,2}^0/A^0 \rightarrow \tau^+\tau^-$
- 42 ABAZOV 08AJ D0 $p\bar{p} \rightarrow H_{1,2}^0/A^0 + b + X$,
 $H_{1,2}^0/A^0 \rightarrow b\bar{b}$

		43 ABAZOV 08W	D0	$p\bar{p} \rightarrow H_{1,2}^0/A^0 + X$, $H_{1,2}^0/A^0 \rightarrow \tau^+\tau^-$
		44 ACOSTA 05Q	CDF	$p\bar{p} \rightarrow H_{1,2}^0/A^0 + X$
>90.4	95	36,45 ABDALLAH 04	DLPH	$E_{cm} \leq 209$ GeV, $\tan\beta > 0.4$
		46 ABBIENDI 03G	OPAL	$H_1^0 \rightarrow A^0 A^0$
		47 AKEROYD 02	RVUE	

- 34 ABDALLAH 08B give limits in eight CP -conserving benchmark scenarios and some CP -violating scenarios. See paper for excluded regions for each scenario. Supersedes ABDALLAH 04.
- 35 SCHAEEL 06B make a combined analysis of the LEP data. The quoted limit is for the m_h^{\max} scenario with $m_t = 174.3$ GeV. In the CP -violating CPX scenario no lower bound on $m_{H_1^0}$ can be set at 95% CL. See paper for excluded regions in various scenarios. See Figs. 2-6 and Tabs. 14-21 for limits on $\sigma(ZH^0) \cdot B(H^0 \rightarrow b\bar{b}, \tau^+\tau^-)$ and $\sigma(H_1^0 H_2^0) \cdot B(H_1^0 H_2^0 \rightarrow b\bar{b}, \tau^+\tau^-)$.
- 36 Search for $e^+e^- \rightarrow H_1^0 A^0$ in the final states $b\bar{b}b\bar{b}$ and $b\bar{b}\tau^+\tau^-$, and $e^+e^- \rightarrow H_1^0 Z$. Universal scalar mass of 1 TeV, SU(2) gaugino mass of 200 GeV, and $\mu = -200$ GeV are assumed, and two-loop radiative corrections incorporated. The limits hold for $m_t = 175$ GeV, and for the m_h^{\max} scenario.
- 37 ABBIENDI 04M exclude $0.7 < \tan\beta < 1.9$, assuming $m_t = 174.3$ GeV. Limits for other MSSM benchmark scenarios, as well as for CP violating cases, are also given.
- 38 ACHARD 02H also search for the final state $H_1^0 Z \rightarrow 2A^0 q\bar{q}, A^0 \rightarrow q\bar{q}$. In addition, the MSSM parameter set in the “large- μ ” and “no-mixing” scenarios are examined.
- 39 HEISTER 02 excludes the range $0.7 < \tan\beta < 2.3$. A wider range is excluded with different stop mixing assumptions. Updates BARATE 01c.
- 40 AALTONEN 09AR search for Higgs bosons decaying to $\tau^+\tau^-$ in two doublet models in 1.8 fb^{-1} of $p\bar{p}$ collisions at $E_{cm} = 1.96$ TeV. See their Fig. 2 for the limit on $\sigma \cdot B(H_{1,2}^0/A^0 \rightarrow \tau^+\tau^-)$ for different Higgs masses, and see their Fig. 3 for the excluded region in the MSSM parameter space.
- 41 ABAZOV 09F search for associated production of a Higgs boson and a b quark in $p\bar{p}$ collisions at $E_{cm} = 1.96$ TeV with the decay $H_{1,2}^0/A^0 \rightarrow \tau^+\tau^-$. See their Fig. 2 for the limit on $\sigma \cdot B(H_{1,2}^0/A^0 \rightarrow \tau^+\tau^-)$ (for different Higgs masses) and for the excluded region in the MSSM parameter space for $\mu = \pm 200$ GeV.
- 42 ABAZOV 08AJ search for associated production of a Higgs boson and a b quark in $p\bar{p}$ collisions at $E_{cm} = 1.96$ TeV with the decay $H_{1,2}^0/A^0 \rightarrow b\bar{b}$. See their Tab. 3 for the limit on $\sigma \cdot B(H_{1,2}^0/A^0 \rightarrow b\bar{b})$ for different Higgs masses, and see their Fig. 3 for the excluded region in the MSSM parameter space for $\mu = \pm 200$ GeV.
- 43 ABAZOV 08W search for Higgs boson production in $p\bar{p}$ collisions at $E_{cm} = 1.96$ TeV with the decay $H_{1,2}^0/A^0 \rightarrow \tau^+\tau^-$. See their Fig. 3 for the limit on $\sigma \cdot B(H_{1,2}^0/A^0 \rightarrow \tau^+\tau^-)$ for different Higgs masses, and see their Fig. 4 for the excluded region in the MSSM parameter space.
- 44 ACOSTA 05Q search for $H_{1,2}^0/A^0$ production in $p\bar{p}$ collisions at $E_{cm} = 1.8$ TeV with $H_{1,2}^0/A^0 \rightarrow \tau^+\tau^-$. At $m_{A^0} = 100$ GeV, the obtained cross section upper limit is above theoretical expectation.
- 45 This limit applies also in the no-mixing scenario. Furthermore, ABDALLAH 04 excludes the range $0.54 < \tan\beta < 2.36$. The limit improves in the region $\tan\beta < 6$ (see Fig. 28). Limits for $\mu = 1$ TeV are given in Fig. 30.
- 46 ABBIENDI 03G search for $e^+e^- \rightarrow H_1^0 Z$ followed by $H_1^0 \rightarrow A^0 A^0, A^0 \rightarrow c\bar{c}, g\bar{g}$, or $\tau^+\tau^-$. In the no-mixing scenario, the region $m_{H_1^0} = 45\text{--}85$ GeV and $m_{A^0} = 2\text{--}9.5$ GeV is excluded at 95% CL.
- 47 AKEROYD 02 examine the possibility of a light A^0 with $\tan\beta < 1$. Electroweak measurements are found to be inconsistent with such a scenario.

 H^0 (Higgs Boson) MASS LIMITS in Extended Higgs Models

This Section covers models which do not fit into either the Standard Model or its simplest minimal Supersymmetric extension (MSSM), leading to anomalous production rates, or nonstandard final states and branching ratios. In particular, this Section covers limits which may apply to generic two-Higgs-doublet models (2HDM), or to special regions of the MSSM parameter space where decays to invisible particles or to photon pairs are dominant (see the Note on ‘Searches for Higgs Bosons’ at the beginning of this Chapter). See the footnotes or the comment lines for details on the nature of the models to which the limits apply.

VALUE (GeV)	CL%	DOCUMENT ID	TECN	COMMENT
• • •		We do not use the following data for averages, fits, limits, etc. • • •		
>108.2	95	48 ABBIENDI 10	OPAL	invisible H^0
		49 ABBIENDI 10	OPAL	$H^0 \rightarrow \tilde{\chi}_1^0 \tilde{\chi}_2^0$
>106	95	50 AALTONEN 09AB	CDF	$H^0 \rightarrow \gamma\gamma$
		51 AALTONEN 09AR	CDF	$p\bar{p} \rightarrow H_{1,2}^0/A^0 + X$, $H_{1,2}^0/A^0 \rightarrow \tau^+\tau^-$
>101	95	52 ABAZOV 09Q	D0	$H^0 \rightarrow \gamma\gamma$
		53 ABAZOV 09V	D0	$H^0 \rightarrow A^0 A^0$
		54 AUBERT 09P	BABR	$\Upsilon(3S) \rightarrow A^0 \gamma$
		55 AUBERT 09Z	BABR	$\Upsilon(2S) \rightarrow A^0 \gamma$
		56 AUBERT 09Z	BABR	$\Upsilon(3S) \rightarrow A^0 \gamma$
		57 ABAZOV 08U	D0	$H^0 \rightarrow \gamma\gamma$
		58 LOVE 08	CLEO	$\Upsilon(1S) \rightarrow A^0 \gamma$
		59 ABBIENDI 07	OPAL	invisible H^0 , large width

See key on page 405

Gauge & Higgs Boson Particle Listings
Higgs Bosons — H^0 and H^\pm

>105.8	95	60	BESSON	07	CLEO	$\Upsilon(1S) \rightarrow \eta_b \gamma$
		61	SCHAEF	07	ALEP	$e^+e^- \rightarrow H^0 Z, H^0 \rightarrow WW^*$
none 1–55	95	62	ABBIENDI	05A	OPAL	H_1^0 , Type II model
none 3–63	95	62	ABBIENDI	05A	OPAL	A^0 , Type II model
>110.6	95	63	ABDALLAH	05D	DLPH	$H^0 \rightarrow 2$ jets
>112.3	95	64	ACHARD	05	L3	invisible H^0
>104	95	65	ABBIENDI	04K	OPAL	$H^0 \rightarrow 2$ jets
		66	ABDALLAH	04	DLPH	$H^0 VV$ couplings
>112.1	95	64	ABDALLAH	04B	DLPH	Invisible H^0
>104.1	95	67,68	ABDALLAH	04L	DLPH	$e^+e^- \rightarrow H^0 Z, H^0 \rightarrow \gamma\gamma$
		69	ABDALLAH	04O	DLPH	$Z \rightarrow f\bar{f}H$
		70	ABDALLAH	04O	DLPH	$e^+e^- \rightarrow H^0 Z, H^0 A^0$
>110.3	95	71	ACHARD	04B	L3	$H^0 \rightarrow 2$ jets
		72	ACHARD	04F	L3	Anomalous coupling
		73	ABBIENDI	03F	OPAL	$e^+e^- \rightarrow H^0 Z, H^0 \rightarrow \text{any}$
		74	ABBIENDI	03G	OPAL	$H^0 \rightarrow A^0 A^0$
>107	95	75	ACHARD	03C	L3	$H^0 \rightarrow WW^*, ZZ^*, \gamma\gamma$
		76	ABBIENDI	02D	OPAL	$e^+e^- \rightarrow b\bar{b}H$
>105.5	95	67,77	ABBIENDI	02F	OPAL	$H^0 \rightarrow \gamma\gamma$
>105.4	95	78	ACHARD	02C	L3	$H_1^0 \rightarrow \gamma\gamma$
>114.1	95	64	HEISTER	02	ALEP	Invisible $H^0, E_{cm} \leq 209$ GeV
>105.4	95	67,79	HEISTER	02L	ALEP	$H^0 \rightarrow \gamma\gamma$
>109.1	95	80	HEISTER	02M	ALEP	$H^0 \rightarrow 2$ jets or $\tau^+\tau^-$
none 1–44	95	81	ABBIENDI	01E	OPAL	H_1^0 , Type-II model
none 12–56	95	81	ABBIENDI	01E	OPAL	A^0 , Type-II model
> 98	95	82	AFFOLDER	01H	CDF	$p\bar{p} \rightarrow H^0 W/Z, H^0 \rightarrow \gamma\gamma$
>106.4	95	64	BARATE	01C	ALEP	Invisible $H^0, E_{cm} \leq 202$ GeV
> 89.2	95	83	ACCIARRI	00M	L3	Invisible H^0
		84	ACCIARRI	00R	L3	$e^+e^- \rightarrow H^0 \gamma$ and/or $H^0 \rightarrow \gamma\gamma$
		85	ACCIARRI	00R	L3	$e^+e^- \rightarrow e^+e^- H^0$
> 94.9	95	86	ACCIARRI	00S	L3	$e^+e^- \rightarrow H^0 Z, H^0 \rightarrow \gamma\gamma$
>100.7	95	87	BARATE	00L	ALEP	$e^+e^- \rightarrow H^0 Z, H^0 \rightarrow \gamma\gamma$
> 68.0	95	88	ABBIENDI	99E	OPAL	$\tan\beta > 1$
> 96.2	95	89	ABBIENDI	99O	OPAL	$e^+e^- \rightarrow H^0 Z, H^0 \rightarrow \gamma\gamma$
> 78.5	95	90	ABBOTT	99B	D0	$p\bar{p} \rightarrow H^0 W/Z, H^0 \rightarrow \gamma\gamma$
		91	ABREU	99P	DLPH	$e^+e^- \rightarrow H^0 \gamma$ and/or $H^0 \rightarrow \gamma\gamma$
		92	GONZALEZ-G.	98B	RVUE	Anomalous coupling
		93	KRAWCZYK	97	RVUE	$(g-2)_\mu$
		94	ALEXANDER	96H	OPAL	$Z \rightarrow H^0 \gamma$
		95	ABREU	95H	DLPH	$Z \rightarrow H^0 Z^*, H^0 A^0$
		96	PICH	92	RVUE	Very light Higgs

48 ABBIENDI 10 search for $e^+e^- \rightarrow H^0 Z$ with H^0 decaying invisibly. The limit assumes SM production cross section and $B(H^0 \rightarrow \text{invisible}) = 1$.

49 ABBIENDI 10 search for $e^+e^- \rightarrow ZH^0$ with the decay chain $H^0 \rightarrow \tilde{\chi}_1^0 \tilde{\chi}_2^0, \tilde{\chi}_2^0 \rightarrow \tilde{\chi}_1^0 + (\gamma \text{ or } Z^*)$, when $\tilde{\chi}_1^0$ and $\tilde{\chi}_2^0$ are nearly degenerate. For a mass difference of 2 (4) GeV, a lower limit on m_{H^0} of 108.4 (107.0) GeV (95% CL) is obtained for SM ZH^0 cross section and $B(H^0 \rightarrow \tilde{\chi}_1^0 \tilde{\chi}_2^0) = 1$.

50 AALTONEN 09AB search for $H^0 \rightarrow \gamma\gamma$ in 3.0 fb $^{-1}$ of $p\bar{p}$ collisions at $E_{cm} = 1.96$ TeV in the mass range $m_{H^0} = 70$ –150 GeV. Associated $H^0 W, H^0 Z$ production and WW, ZZ fusion are considered. The limit assumes that all fermion Yukawa couplings vanish.

51 AALTONEN 09AR search for Higgs bosons decaying to $\tau^+\tau^-$ in two doublet models in 1.8 fb $^{-1}$ of $p\bar{p}$ collisions at $E_{cm} = 1.96$ TeV. See their Fig. 2 for the limit on $\sigma \cdot B(H_{1,2}^0/A^0 \rightarrow \tau^+\tau^-)$ for different Higgs masses, and see their Fig. 3 for the excluded region in the MSSM parameter space.

52 ABAZOV 09Q search for $H^0 \rightarrow \gamma\gamma$ in 2.7 fb $^{-1}$ of $p\bar{p}$ collisions at $E_{cm} = 1.96$ TeV in the mass range $m_{H^0} = 100$ –150 GeV. The limit assumes that all fermion Yukawa couplings vanish.

53 ABAZOV 09V search for H^0 production followed by the decay chain $H^0 \rightarrow A^0 A^0 \rightarrow \mu^+\mu^- \mu^+\mu^-$ or $\mu^+\mu^- \tau^+\tau^-$ in 4.2 fb $^{-1}$ of $p\bar{p}$ collisions at $E_{cm} = 1.96$ TeV. See their Fig. 3 for limits on $\sigma(H^0) \cdot B(H^0 \rightarrow A^0 A^0)$ for $m_{A^0} = 3.6$ –19 GeV.

54 AUBERT 09P search for the process $\Upsilon(3S) \rightarrow A^0 \gamma$ with $A^0 \rightarrow \tau^+\tau^-$ for $4.03 < m_{A^0} < 9.52$ and $9.61 < m_{A^0} < 10.10$ GeV, and give limits on $B(\Upsilon(3S) \rightarrow A^0 \gamma) \cdot B(A^0 \rightarrow \tau^+\tau^-)$ in the range $(1.5$ – $16) \times 10^{-5}$ (90% CL).

55 AUBERT 09Z search for the process $\Upsilon(2S) \rightarrow A^0 \gamma$ with $A^0 \rightarrow \mu^+\mu^-$ for $0.212 < m_{A^0} < 9.3$ GeV and give limits on $B(\Upsilon(2S) \rightarrow A^0 \gamma) \cdot B(A^0 \rightarrow \mu^+\mu^-)$ in the range $(0.3$ – $8) \times 10^{-6}$ (90% CL).

56 AUBERT 09Z search for the process $\Upsilon(3S) \rightarrow A^0 \gamma$ with $A^0 \rightarrow \mu^+\mu^-$ for $0.212 < m_{A^0} < 9.3$ GeV and give limits on $B(\Upsilon(3S) \rightarrow A^0 \gamma) \cdot B(A^0 \rightarrow \mu^+\mu^-)$ in the range $(0.3$ – $5) \times 10^{-6}$ (90% CL).

57 ABAZOV 08U search for $H^0 \rightarrow \gamma\gamma$ in $p\bar{p}$ collisions at $E_{cm} = 1.96$ TeV in the mass range $m_{H^0} = 70$ –150 GeV. Associated $H^0 W, H^0 Z$ production and WW, ZZ fusion are considered. See their Tab. 1 for the limit on $\sigma \cdot B(H^0 \rightarrow \gamma\gamma)$, and see their Fig. 3 for the excluded region in the $m_{H^0} - B(H^0 \rightarrow \gamma\gamma)$ plane.

58 LOVE 08 search for the process $\Upsilon(1S) \rightarrow A^0 \gamma$ with $A^0 \rightarrow \mu^+\mu^-$ (for $m_{A^0} < 2m_\tau$) and $A^0 \rightarrow \tau^+\tau^-$. Limits on $B(\Upsilon(1S) \rightarrow A^0 \gamma) \cdot B(A^0 \rightarrow \ell^+\ell^-)$ in the range 10^{-6} – 10^{-4} (90% CL) are given.

59 ABBIENDI 07 search for $e^+e^- \rightarrow H^0 Z$ with $Z \rightarrow q\bar{q}$ and H^0 decaying to invisible final states. The H^0 width is varied between 1 GeV and 3 TeV. A limit $\sigma \cdot B(H^0 \rightarrow \text{invisible}) < (0.07$ – $0.57)$ pb (95% CL) is obtained at $E_{cm} = 206$ GeV for $m_{H^0} = 60$ –114 GeV.

60 BESSON 07 give a limit $B(\Upsilon(1S) \rightarrow \eta_b \gamma) \cdot B(\eta_b \rightarrow \tau^+\tau^-) < 0.27\%$ (95% CL), which constrains a possible A^0 exchange contribution to the η_b decay.

61 SCHAEF 07 search for Higgs bosons in association with a fermion pair and decaying to WW^* . The limit is from this search and HEISTER 02L for a H^0 with SM production cross section and $B(H^0 \rightarrow f\bar{f}) = 0$ for all fermions f .

62 ABBIENDI 05A search for $e^+e^- \rightarrow H_1^0 A^0$ in general Type-II two-doublet models, with decays $H_1^0, A^0 \rightarrow q\bar{q}, gg, \tau^+\tau^-$, and $H_1^0 \rightarrow A^0 A^0$.

63 ABDALLAH 05D search for $e^+e^- \rightarrow H^0 Z$ and $H^0 A^0$ with H^0, A^0 decaying to two jets of any flavor including gg . The limit is for SM $H^0 Z$ production cross section with $B(H^0 \rightarrow jj) = 1$.

64 Search for $e^+e^- \rightarrow H^0 Z$ with H^0 decaying invisibly. The limit assumes SM production cross section and $B(H^0 \rightarrow \text{invisible}) = 1$.

65 ABBIENDI 04K search for $e^+e^- \rightarrow H^0 Z$ with H^0 decaying to two jets of any flavor including gg . The limit is for SM production cross section with $B(H^0 \rightarrow jj) = 1$.

66 ABDALLAH 04 consider the full combined LEP and LEP2 datasets to set limits on the Higgs coupling to W or Z bosons, assuming SM decays of the Higgs. Results in Fig. 26.

67 Search for associated production of a $\gamma\gamma$ resonance with a Z boson, followed by $Z \rightarrow q\bar{q}, \ell^+\ell^-$, or $\nu\bar{\nu}$, at $E_{cm} \leq 209$ GeV. The limit is for a H^0 with SM production cross section and $B(H^0 \rightarrow f\bar{f})=0$ for all fermions f .

68 Updates ABREU 01F.

69 ABDALLAH 04O search for $Z \rightarrow b\bar{b}H^0, b\bar{b}A^0, \tau^+\tau^-H^0$ and $\tau^+\tau^-A^0$ in the final states $4b, b\bar{b}\tau^+\tau^-$, and 4τ . See paper for limits on Yukawa couplings.

70 ABDALLAH 04O search for $e^+e^- \rightarrow H^0 Z$ and $H^0 A^0$ with H^0, A^0 decaying to $b\bar{b}, \tau^+\tau^-$, or $H^0 \rightarrow A^0 A^0$ at $E_{cm} = 189$ –208 GeV. See paper for limits on couplings.

71 ACHARD 04B search for $e^+e^- \rightarrow H^0 Z$ with H^0 decaying to $b\bar{b}, c\bar{c}$, or gg . The limit is for SM production cross section with $B(H^0 \rightarrow jj) = 1$.

72 ACHARD 04F search for H^0 with anomalous coupling to gauge boson pairs in the processes $e^+e^- \rightarrow H^0 \gamma, e^+e^- H^0, H^0 Z$ with decays $H^0 \rightarrow f\bar{f}, \gamma\gamma, Z\gamma$, and WW^*W at $E_{cm} = 189$ –209 GeV. See paper for limits.

73 ABBIENDI 03F search for $H^0 \rightarrow \text{anything}$ in $e^+e^- \rightarrow H^0 Z$, using the recoil mass spectrum of $Z \rightarrow e^+e^-$ or $\mu^+\mu^-$. In addition, it searched for $Z \rightarrow \nu\bar{\nu}$ and $H^0 \rightarrow e^+e^-$ or photons. Scenarios with large width or continuum H^0 mass distribution are considered. See their Figs. 11–14 for the results.

74 ABBIENDI 03G search for $e^+e^- \rightarrow H_1^0 Z$ followed by $H_1^0 \rightarrow A^0 A^0, A^0 \rightarrow c\bar{c}, gg$, or $\tau^+\tau^-$ in the region $m_{H_1^0} = 45$ –86 GeV and $m_{A^0} = 2$ –11 GeV. See their Fig. 7 for the limits.

75 ACHARD 03C search for $e^+e^- \rightarrow ZH^0$ followed by $H^0 \rightarrow WW^*$ or ZZ^* at $E_{cm} = 200$ –209 GeV and combine with the ACHARD 02C result. The limit is for a H^0 with SM production cross section and $B(H^0 \rightarrow f\bar{f}) = 0$ for all f . For $B(H^0 \rightarrow WW^*) + B(H^0 \rightarrow ZZ^*) = 1, m_{H^0} > 108.1$ GeV is obtained. See fig. 6 for the limits under different BR assumptions.

76 ABBIENDI 02D search for $Z \rightarrow b\bar{b}H_1^0$ and $b\bar{b}A^0$ with $H_1^0/A^0 \rightarrow \tau^+\tau^-$, in the range $4 < m_H < 12$ GeV. See their Fig. 8 for limits on the Yukawa coupling.

77 For $B(H^0 \rightarrow \gamma\gamma)=1, m_{H^0} > 117$ GeV is obtained.

78 ACHARD 02C search for associated production of a $\gamma\gamma$ resonance with a Z boson, followed by $Z \rightarrow q\bar{q}, \ell^+\ell^-$, or $\nu\bar{\nu}$, at $E_{cm} \leq 209$ GeV. The limit is for a H^0 with SM production cross section and $B(H^0 \rightarrow f\bar{f})=0$ for all fermions f . For $B(H^0 \rightarrow \gamma\gamma)=1, m_{H^0} > 114$ GeV is obtained.

79 For $B(H^0 \rightarrow \gamma\gamma)=1, m_{H^0} > 113.1$ GeV is obtained.

80 HEISTER 02M search for $e^+e^- \rightarrow H^0 Z$, assuming that H^0 decays to $q\bar{q}, gg$, or $\tau^+\tau^-$ only. The limit assumes SM production cross section.

81 ABBIENDI 01E search for neutral Higgs bosons in general Type-II two-doublet models, at $E_{cm} \leq 189$ GeV. In addition to usual final states, the decays $H_1^0, A^0 \rightarrow q\bar{q}, gg$ are searched for. See their Figs. 15,16 for excluded regions.

82 AFFOLDER 01H search for associated production of a $\gamma\gamma$ resonance and a W or Z (tagged by two jets, an isolated lepton, or missing E_T). The limit assumes Standard Model values for the production cross section and for the couplings of the H^0 to W and Z bosons. See their Fig. 11 for limits with $B(H^0 \rightarrow \gamma\gamma) < 1$.

83 ACCIARRI 00M search for $e^+e^- \rightarrow ZH^0$ with H^0 decaying invisibly at $E_{cm}=183$ –189 GeV. The limit assumes SM production cross section and $B(H^0 \rightarrow \text{invisible})=1$. See their Fig. 6 for limits for smaller branching ratios.

84 ACCIARRI 00R search for $e^+e^- \rightarrow H^0 \gamma$ with $H^0 \rightarrow b\bar{b}, Z\gamma$, or $\gamma\gamma$. See their Fig. 3 for limits on $\sigma \cdot B$. Explicit limits within an effective interaction framework are also given, for which the Standard Model Higgs search results are used in addition.

85 ACCIARRI 00R search for the two-photon type processes $e^+e^- \rightarrow e^+e^- H^0$ with $H^0 \rightarrow b\bar{b}$ or $\gamma\gamma$. See their Fig. 4 for limits on $\Gamma(H^0 \rightarrow \gamma\gamma) \cdot B(H^0 \rightarrow \gamma\gamma \text{ or } b\bar{b})$ for $m_{H^0}=70$ –170 GeV.

86 ACCIARRI 00S search for associated production of a $\gamma\gamma$ resonance with a $q\bar{q}, \nu\bar{\nu}$, or $\ell^+\ell^-$ pair in e^+e^- collisions at $E_{cm} = 189$ GeV. The limit is for a H^0 with SM production cross section and $B(H^0 \rightarrow f\bar{f})=0$ for all fermions f . For $B(H^0 \rightarrow \gamma\gamma)=1, m_{H^0} > 98$ GeV is obtained. See their Fig. 5 for limits on $B(H^0 \rightarrow \gamma\gamma) \cdot \sigma(e^+e^- \rightarrow Hf\bar{f})/\sigma(e^+e^- \rightarrow Hf\bar{f})$ (SM).

87 BARATE 00L search for associated production of a $\gamma\gamma$ resonance with a $q\bar{q}, \nu\bar{\nu}$, or $\ell^+\ell^-$ pair in e^+e^- collisions at $E_{cm} = 88$ –202 GeV. The limit is for a H^0 with SM production cross section and $B(H^0 \rightarrow f\bar{f})=0$ for all fermions f . For $B(H^0 \rightarrow \gamma\gamma)=1, m_{H^0} > 109$ GeV is obtained. See their Fig. 3 for limits on $B(H^0 \rightarrow \gamma\gamma) \cdot \sigma(e^+e^- \rightarrow Hf\bar{f})/\sigma(e^+e^- \rightarrow Hf\bar{f})$ (SM).

88 ABBIENDI 99E search for $e^+e^- \rightarrow H^0 A^0$ and $H^0 Z$ at $E_{cm} = 183$ GeV. The limit is with $m_H=m_A$ in general two Higgs-doublet models. See their Fig. 18 for the exclusion limit in the m_H-m_A plane. Updates the results of ACKERSTAFF 98S.

Gauge & Higgs Boson Particle Listings

Higgs Bosons — H^0 and H^\pm

- 89 ABBIENDI 99o search for associated production of a $\gamma\gamma$ resonance with a $q\bar{q}, \nu\bar{\nu}$, or $\ell^+ \ell^-$ pair in e^+e^- collisions at 189 GeV. The limit is for a H^0 with SM production cross section and $B(H^0 \rightarrow f\bar{f})=0$, for all fermions f . See their Fig. 4 for limits on $\sigma(e^+e^- \rightarrow H^0 Z^0) \times B(H^0 \rightarrow \gamma\gamma) \times B(X^0 \rightarrow f\bar{f})$ for various masses. Updates the results of ACKERSTAFF 98Y.
- 90 ABBOTT 99B search for associated production of a $\gamma\gamma$ resonance and a dijet pair. The limit assumes Standard Model values for the production cross section and for the couplings of the H^0 to W and Z bosons. Limits in the range of $\sigma(H^0 + Z/W) \times B(H^0 \rightarrow \gamma\gamma) = 0.80\text{--}0.34$ pb are obtained in the mass range $m_{H^0} = 65\text{--}150$ GeV.
- 91 ABREU 99P search for $e^+e^- \rightarrow H^0\gamma$ with $H^0 \rightarrow b\bar{b}$ or $\gamma\gamma$, and $e^+e^- \rightarrow H^0 q\bar{q}$ with $H^0 \rightarrow \gamma\gamma$. See their Fig. 4 for limits on $\sigma \times B$. Explicit limits within an effective interaction framework are also given.
- 92 GONZALEZ-GARCIA 98B use $D\bar{D}$ limit for $\gamma\gamma$ events with missing E_T in $p\bar{p}$ collisions (ABBOTT 98) to constrain possible ZH or WH production followed by unconventional $H \rightarrow \gamma\gamma$ decay which is induced by higher-dimensional operators. See their Figs. 1 and 2 for limits on the anomalous couplings.
- 93 KRAWCZYK 97 analyse the muon anomalous magnetic moment in a two-doublet Higgs model (with type II Yukawa couplings) assuming no $H_1^0 ZZ$ coupling and obtain $m_{H_1^0} \gtrsim 5$ GeV or $m_{A^0} \gtrsim 5$ GeV for $\tan\beta > 50$. Other Higgs bosons are assumed to be much heavier.
- 94 ALEXANDER 96H give $B(Z \rightarrow H^0\gamma) \times B(H^0 \rightarrow q\bar{q}) < 1.4 \times 10^{-5}$ (95%CL) and $B(Z \rightarrow H^0\gamma) \times B(H^0 \rightarrow b\bar{b}) < 0.7\text{--}2 \times 10^{-5}$ (95%CL) in the range $20 < m_{H^0} < 80$ GeV.
- 95 See Fig. 4 of ABREU 95H for the excluded region in the $m_{H^0} - m_{A^0}$ plane for general two-doublet models. For $\tan\beta > 1$, the region $m_{H^0} + m_{A^0} \lesssim 87$ GeV, $m_{H^0} < 47$ GeV is excluded at 95% CL.
- 96 PICH 92 analyse H^0 with $m_{H^0} < 2m_\mu$ in general two-doublet models. Excluded regions in the space of mass-mixing angles from LEP, beam dump, and π^\pm, η rare decays are shown in Figs. 3,4. The considered mass region is not totally excluded.

 H^\pm (Charged Higgs) MASS LIMITS

Unless otherwise stated, the limits below assume $B(H^+ \rightarrow \tau^+\nu) + B(H^+ \rightarrow c\bar{s}) = 1$, and hold for all values of $B(H^+ \rightarrow \tau^+\nu_\tau)$, and assume H^+ weak isospin of $T_3 = +1/2$. In the following, $\tan\beta$ is the ratio of the two vacuum expectation values in two-doublet models (2HDM).

The limits are also applicable to point-like technipions. For a discussion of techniparticles, see the Review of Dynamical Electroweak Symmetry Breaking in this Review.

For limits obtained in hadronic collisions before the observation of the top quark, and based on the top mass values inconsistent with the current measurements, see the 1996 (Physical Review **D54** 1 (1996)) Edition of this Review.

Searches in e^+e^- collisions at and above the Z pole have conclusively ruled out the existence of a charged Higgs in the region $m_{H^\pm} \lesssim 45$ GeV, and are now superseded by the most recent searches in higher energy e^+e^- collisions at LEP. Results by now obsolete are therefore not included in this compilation, and can be found in the previous Edition (The European Physical Journal **C15** 1 (2000)) of this Review.

In the following, and unless otherwise stated, results from the LEP experiments (ALEPH, DELPHI, L3, and OPAL) are assumed to derive from the study of the $e^+e^- \rightarrow H^+H^-$ process. Limits from $b \rightarrow s\gamma$ decays are usually stronger in generic 2HDM models than in Supersymmetric models.

VALUE (GeV)	CL%	DOCUMENT ID	TECN	COMMENT
> 74.4	95	ABDALLAH 04I	DLPH	$E_{cm} \leq 209$ GeV
> 76.5	95	ACHARD 03E	L3	$E_{cm} \leq 209$ GeV
> 79.3	95	HEISTER 02P	ALEP	$E_{cm} \leq 209$ GeV

••• We do not use the following data for averages, fits, limits, etc. •••

		97 AALTONEN 09AJ	CDF	$t \rightarrow bH^+$
		98 ABAZOV 09AC	D0	$t \rightarrow bH^+$
		99 ABAZOV 09AG	D0	$t \rightarrow bH^+$
		100 ABAZOV 09AI	D0	$t \rightarrow bH^+$
		101 ABAZOV 09P	D0	$H^+ \rightarrow t\bar{b}$
		102 ABULENCIA 06E	CDF	$t \rightarrow bH^+$
> 92.0	95	ABBIENDI 04	OPAL	$B(\tau\nu) = 1$
> 76.7	95	103 ABDALLAH 04I	DLPH	Type I
		104 ABBIENDI 03	OPAL	$\tau \rightarrow \mu\nu_\nu, e\nu_\nu$
		105 ABAZOV 02B	D0	$t \rightarrow bH^+, H \rightarrow \tau\nu$
		106 BORZUMATI 02	RVUE	
		107 ABBIENDI 01Q	OPAL	$B \rightarrow \tau\nu_\tau X$
		108 BARATE 01E	ALEP	$B \rightarrow \tau\nu_\tau$
> 315	99	109 GAMBINO 01	RVUE	$b \rightarrow s\gamma$
		110 AFFOLDER 00I	CDF	$t \rightarrow bH^+, H \rightarrow \tau\nu$
> 59.5	95	ABBIENDI 99E	OPAL	$E_{cm} \leq 183$ GeV
		111 ABBOTT 99E	D0	$t \rightarrow bH^+$
		112 ACKERSTAFF 99D	OPAL	$\tau \rightarrow e\nu\nu, \mu\nu\nu$
		113 ACCIARRI 97F	L3	$B \rightarrow \tau\nu_\tau$
		114 AMMAR 97B	CLEO	$\tau \rightarrow \mu\nu\nu$
		115 COARASA 97	RVUE	$B \rightarrow \tau\nu_\tau X$
		116 GUCHAIT 97	RVUE	$t \rightarrow bH^+, H \rightarrow \tau\nu$
		117 MANGANO 97	RVUE	$B_{u(c)} \rightarrow \tau\nu_\tau$
		118 STAHL 97	RVUE	$\tau \rightarrow \mu\nu\nu$
> 244	95	119 ALAM 95	CLE2	$b \rightarrow s\gamma$
		120 BUSKULIC 95	ALEP	$b \rightarrow \tau\nu_\tau X$

- 97 AALTONEN 09AJ search for $t \rightarrow bH^+, H^+ \rightarrow c\bar{s}$ in $t\bar{t}$ events in 2.2 fb^{-1} of $p\bar{p}$ collisions at $E_{cm} = 1.96$ TeV. Upper limits on $B(t \rightarrow bH^+)$ between 0.08 and 0.32 (95% CL) are given for $m_{H^+} = 60\text{--}150$ GeV and $B(H^+ \rightarrow c\bar{s}) = 1$.
- 98 ABAZOV 09AC search for $t \rightarrow bH^+, H^+ \rightarrow \tau^+\nu$ in $t\bar{t}$ events in 0.9 fb^{-1} of $p\bar{p}$ collisions at $E_{cm} = 1.96$ TeV. Upper limits on $B(t \rightarrow bH^+)$ between 0.19 and 0.25 (95% CL) are given for $m_{H^+} = 80\text{--}155$ GeV and $B(H^+ \rightarrow \tau^+\nu) = 1$. See their Fig. 4 for an excluded region in a MSSM scenario.
- 99 ABAZOV 09AG measure $t\bar{t}$ cross sections in final states with $\ell + \text{jets}$ ($\ell = e, \mu$), $\ell\ell$, and $\tau\ell$ in 1 fb^{-1} of $p\bar{p}$ collisions at $E_{cm} = 1.96$ TeV, which constrains possible $t \rightarrow bH^+$ branching fractions. Upper limits (95% CL) on $B(t \rightarrow bH^+)$ between 0.15 and 0.40 (0.48 and 0.57) are given for $B(H^+ \rightarrow \tau^+\nu) = 1$ ($B(H^+ \rightarrow c\bar{s}) = 1$) for $m_{H^+} = 80\text{--}155$ GeV.
- 100 ABAZOV 09AI search for $t \rightarrow bH^+$ in $t\bar{t}$ events in 1 fb^{-1} of $p\bar{p}$ collisions at $E_{cm} = 1.96$ TeV. Final states with $\ell + \text{jets}$ ($\ell = e, \mu$), $\ell\ell$, and $\tau\ell$ are examined. Upper limits on $B(t \rightarrow bH^+)$ (95% CL) between 0.15 and 0.19 (0.19 and 0.22) are given for $B(H^+ \rightarrow \tau^+\nu) = 1$ ($B(H^+ \rightarrow c\bar{s}) = 1$) for $m_{H^+} = 80\text{--}155$ GeV. For $B(H^+ \rightarrow \tau^+\nu) = 1$ also a simultaneous extraction of $B(t \rightarrow bH^+)$ and the $t\bar{t}$ cross section is performed, yielding a limit on $B(t \rightarrow bH^+)$ between 0.12 and 0.26 for $m_{H^+} = 80\text{--}155$ GeV. See their Figs. 5–8 for excluded regions in several MSSM scenarios.
- 101 ABAZOV 09P search for H^+ production by $q\bar{q}'$ annihilation followed by $H^+ \rightarrow t\bar{b}$ decay in 0.9 fb^{-1} of $p\bar{p}$ collisions at $E_{cm} = 1.96$ TeV. Cross section limits in several two-doublet models are given for $m_{H^+} = 180\text{--}300$ GeV. A region with $20 \lesssim \tan\beta \lesssim 70$ is excluded (95% CL) for $180 \text{ GeV} \lesssim m_{H^+} \lesssim 184$ GeV in type-I models.
- 102 ABULENCIA 06E search for associated $H^0 W$ production in $p\bar{p}$ collisions at $E_{cm} = 1.96$ TeV. A fit is made for $t\bar{t}$ production processes in dilepton, lepton + jets, and lepton + τ final states, with the decays $t \rightarrow W^+b$ and $t \rightarrow H^+b$ followed by $H^+ \rightarrow \tau^+\nu, c\bar{s}, t^*\bar{b}$, or W^+H^0 . Within the MSSM the search is sensitive to the region $\tan\beta < 1$ or > 30 in the mass range $m_{H^+} = 80\text{--}160$ GeV. See Fig. 2 for the excluded region in a certain MSSM scenario.
- 103 ABDALLAH 04I search for $e^+e^- \rightarrow H^+H^-$ with H^\pm decaying to $\tau\nu, c\bar{s}$, or W^*A^0 in Type-I two-Higgs-doublet models.
- 104 ABBIENDI 03 give a limit $m_{H^+} > 1.28 \tan\beta$ GeV (95%CL) in Type II two-doublet models.
- 105 ABAZOV 02B search for a charged Higgs boson in top decays with $H^+ \rightarrow \tau^+\nu$ at $E_{cm} = 1.8$ TeV. For $m_{H^+} = 75$ GeV, the region $\tan\beta > 32.0$ is excluded at 95%CL. The excluded mass region extends to over 140 GeV for $\tan\beta$ values above 100.
- 106 BORZUMATI 02 point out that the decay modes such as $b\bar{b}W, A^0W$, and supersymmetric ones can have substantial branching fractions in the mass range explored at LEP II and Tevatron.
- 107 ABBIENDI 01Q give a limit $\tan\beta/m_{H^+} < 0.53 \text{ GeV}^{-1}$ (95%CL) in Type II two-doublet models.
- 108 BARATE 01E give a limit $\tan\beta/m_{H^+} < 0.40 \text{ GeV}^{-1}$ (90% CL) in Type II two-doublet models. An independent measurement of $B \rightarrow \tau\nu_\tau X$ gives $\tan\beta/m_{H^+} < 0.49 \text{ GeV}^{-1}$ (90% CL).
- 109 GAMBINO 01 use the world average data in the summer of 2001 $B(b \rightarrow s\gamma) = (3.23 \pm 0.42) \times 10^{-4}$. The limit applies for Type-II two-doublet models.
- 110 AFFOLDER 00I search for a charged Higgs boson in top decays with $H^+ \rightarrow \tau^+\nu$ in $p\bar{p}$ collisions at $E_{cm} = 1.8$ TeV. The excluded mass region extends to over 120 GeV for $\tan\beta$ values above 100 and $B(\tau\nu) = 1$. If $B(t \rightarrow bH^+) \gtrsim 0.6$, m_{H^+} up to 160 GeV is excluded. Updates ABE 97L.
- 111 ABBOTT 99E search for a charged Higgs boson in top decays in $p\bar{p}$ collisions at $E_{cm} = 1.8$ TeV, by comparing the observed $t\bar{t}$ cross section (extracted from the data assuming the dominant decay $t \rightarrow bW^+$) with theoretical expectation. The search is sensitive to regions of the domains $\tan\beta \lesssim 1$, $50 < m_{H^+}(\text{GeV}) \lesssim 120$ and $\tan\beta \gtrsim 40$, $50 < m_{H^+}(\text{GeV}) \lesssim 160$. See Fig. 3 for the details of the excluded region.
- 112 ACKERSTAFF 99D measure the Michel parameters ρ, ξ, η , and $\xi\delta$ in leptonic τ decays from $Z \rightarrow \tau\tau$. Assuming $e\text{-}\mu$ universality, the limit $m_{H^+} > 0.97 \tan\beta$ GeV (95% CL) is obtained for two-doublet models in which only one doublet couples to leptons.
- 113 ACCIARRI 97F give a limit $m_{H^+} > 2.6 \tan\beta$ GeV (90% CL) from their limit on the exclusive $B \rightarrow \tau\nu_\tau$ branching ratio.
- 114 AMMAR 97B measure the Michel parameter ρ from $\tau \rightarrow e\nu\nu$ decays and assumes e/μ universality to extract the Michel η parameter from $\tau \rightarrow \mu\nu\nu$ decays. The measurement is translated to a lower limit on m_{H^+} in a two-doublet model $m_{H^+} > 0.97 \tan\beta$ GeV (90% CL).
- 115 COARASA 97 reanalyzed the constraint on the $(m_{H^\pm}, \tan\beta)$ plane derived from the inclusive $B \rightarrow \tau\nu_\tau X$ branching ratio in GROSSMAN 95B and BUSKULIC 95. They show that the constraint is quite sensitive to supersymmetric one-loop effects.
- 116 GUCHAIT 97 studies the constraints on m_{H^\pm} set by Tevatron data on $\ell\tau$ final states in $t\bar{t} \rightarrow (Wb)(Hb), W \rightarrow \ell\nu, H \rightarrow \tau\nu_\tau$. See Fig. 2 for the excluded region.
- 117 MANGANO 97 reconsiders the limit in ACCIARRI 97F including the effect of the potentially large $B_c \rightarrow \tau\nu_\tau$ background to $B_H \rightarrow \tau\nu_\tau$ decays. Stronger limits are obtained.
- 118 STAHL 97 fit τ lifetime, leptonic branching ratios, and the Michel parameters and derive limit $m_{H^+} > 1.5 \tan\beta$ GeV (90% CL) for a two-doublet model. See also STAHL 94.
- 119 ALAM 95 measure the inclusive $b \rightarrow s\gamma$ branching ratio at $T(4S)$ and give $B(b \rightarrow s\gamma) < 4.2 \times 10^{-4}$ (95% CL), which translates to the limit $m_{H^+} > [244 + 63/(\tan\beta)^{1.3}]$ GeV in the Type II two-doublet model. Light supersymmetric particles can invalidate this bound.
- 120 BUSKULIC 95 give a limit $m_{H^+} > 1.9 \tan\beta$ GeV (90% CL) for Type-II models from $b \rightarrow \tau\nu_\tau X$ branching ratio, as proposed in GROSSMAN 94.

MASS LIMITS for $H^{\pm\pm}$ (doubly-charged Higgs boson)

This section covers searches for a doubly-charged Higgs boson with couplings to lepton pairs. Its weak isospin T_3 is thus restricted to two possibilities depending on lepton chiralities: $T_3(H^{\pm\pm}) = \pm 1$, with the coupling $g_{\ell\ell}$ to $\ell_L^-\ell_L^-$ and $\ell_R^+\ell_R^+$ ("left-handed") and $T_3(H^{\pm\pm}) = 0$, with the coupling to $\ell_R^-\ell_R^-$ and $\ell_L^+\ell_L^+$ ("right-handed"). These Higgs bosons appear in some left-right symmetric models based on the gauge group $SU(2)_L \times SU(2)_R \times U(1)$. These two cases are listed separately in the following. Unless noted, one of the lepton flavor combinations is assumed to be dominant in the decay.

LIMITS for $H^{\pm\pm}$ with $T_3 = \pm 1$

VALUE	CL%	DOCUMENT ID	TECN	COMMENT
>114	95	121 AALTONEN	08AA CDF	$e\tau$
>112	95	121 AALTONEN	08AA CDF	$\mu\tau$
>150	95	122 ABAZOV	08V D0	$\mu\mu$
>136	95	123 ACOSTA	04G CDF	$\mu\mu$
> 98.1	95	124 ABDALLAH	03 DLPH	$\tau\tau$
> 99.0	95	125 ABBIENDI	02C OPAL	$\tau\tau$
• • •				We do not use the following data for averages, fits, limits, etc. • • •
>133	95	126 AKTAS	06A H1	single $H^{\pm\pm}$
>118.4	95	127 ACOSTA	05L CDF	stable
		128 ABAZOV	04E D0	$\mu\mu$
		129 ABBIENDI	03Q OPAL	$E_{cm} \leq 209$ GeV, single $H^{\pm\pm}$
		130 GORDEEV	97 SPEC	muonium conversion
		131 ASAKA	95 THEO	
> 45.6	95	132 ACTON	92M OPAL	
> 30.4	95	133 ACTON	92M OPAL	
none 6.5–36.6	95	134 SWARTZ	90 MRK2	

- 121 AALTONEN 08AA search for $H^{++}H^{--}$ production in $p\bar{p}$ collisions at $E_{cm} = 1.96$ TeV. The limit assumes 100% branching ratio to the specified final state.
- 122 ABAZOV 08v search for $H^{++}H^{--}$ production in $p\bar{p}$ collisions at $E_{cm} = 1.96$ TeV. The limit is for $B(H \rightarrow \mu\mu) = 1$.
- 123 ACOSTA 04G search for $H^{++}H^{--}$ pair production in $p\bar{p}$ collisions with muon and electron final states. The limit holds for $\mu\mu$. For ee and $e\mu$ modes, the limits are 133 and 115 GeV, respectively. The limits are valid for $g_{\ell\ell} \gtrsim 10^{-5}$.
- 124 ABDALLAH 03 search for $H^{++}H^{--}$ pair production either followed by $H^{++} \rightarrow \tau^+\tau^+$, or decaying outside the detector.
- 125 ABBIENDI 02c searches for pair production of $H^{++}H^{--}$, with $H^{\pm\pm} \rightarrow \ell^\pm\ell^\pm$ ($\ell, \ell' = e, \mu, \tau$). The limit holds for $\ell = \ell' = \tau$, and becomes stronger for other combinations of leptonic final states. To ensure the decay within the detector, the limit only applies for $g(H\ell\ell) \gtrsim 10^{-7}$.
- 126 AKTAS 06a search for single $H^{\pm\pm}$ production in ep collisions at HERA. Assuming that H^{++} only couples to $e^+\mu^+$ with $g_{e\mu} = 0.3$ (electromagnetic strength), a limit $m_{H^{++}} > 141$ GeV (95% CL) is derived. For the case where H^{++} couples to $e\tau$ only the limit is 112 GeV.
- 127 ACOSTA 05l search for $H^{++}H^{--}$ pair production in $p\bar{p}$ collisions. The limit is valid for $g_{\ell\ell} < 10^{-8}$ so that the Higgs decays outside the detector.
- 128 ABAZOV 04e search for $H^{++}H^{--}$ pair production in $H^{\pm\pm} \rightarrow \mu^\pm\mu^\pm$. The limit is valid for $g_{\mu\mu} \gtrsim 10^{-7}$.
- 129 ABBIENDI 03q searches for single $H^{\pm\pm}$ via direct production in $e^+e^- \rightarrow e^\mp e^\mp H^{\pm\pm}$, and via t -channel exchange in $e^+e^- \rightarrow e^+e^-$. In the direct case, and assuming $B(H^{\pm\pm} \rightarrow \ell^\pm\ell^\pm) = 1$, a 95% CL limit on $h_{ee} < 0.071$ is set for $m_{H^{\pm\pm}} < 160$ GeV (see Fig. 6). In the second case, indirect limits on h_{ee} are set for $m_{H^{\pm\pm}} < 2$ TeV (see Fig. 8).
- 130 GORDEEV 97 search for muonium-antimuonium conversion and find $G_{M\bar{M}}/G_F < 0.14$ (90% CL), where $G_{M\bar{M}}$ is the lepton-flavor violating effective four-fermion coupling. This limit may be converted to $m_{H^{++}} > 210$ GeV if the Yukawa couplings of H^{++} to ee and $\mu\mu$ are as large as the weak gauge coupling. For similar limits on muonium-antimuonium conversion, see the muon Particle Listings.
- 131 ASAKA 95 point out that H^{++} decays dominantly to four fermions in a large region of parameter space where the limit of ACTON 92m from the search of dilepton modes does not apply.
- 132 ACTON 92m limit assumes $H^{\pm\pm} \rightarrow \ell^\pm\ell^\pm$ or $H^{\pm\pm}$ does not decay in the detector. Thus the region $g_{\ell\ell} \approx 10^{-7}$ is not excluded.
- 133 ACTON 92m from $\Delta Z < 40$ MeV.
- 134 SWARTZ 90 assume $H^{\pm\pm} \rightarrow \ell^\pm\ell^\pm$ (any flavor). The limits are valid for the Higgs-lepton coupling $g(H\ell\ell) \gtrsim 7.4 \times 10^{-7} [m_H/\text{GeV}]^{1/2}$. The limits improve somewhat for ee and $\mu\mu$ decay modes.

LIMITS for $H^{\pm\pm}$ with $T_3 = 0$

VALUE	CL%	DOCUMENT ID	TECN	COMMENT
>127	95	135 ABAZOV	08V D0	$\mu\mu$
>113	95	136 ACOSTA	04G CDF	$\mu\mu$
> 97.3	95	137 ABDALLAH	03 DLPH	$\tau\tau$
> 97.3	95	138 ACHARD	03F L3	$\tau\tau$
> 98.5	95	139 ABBIENDI	02C OPAL	$\tau\tau$
• • •				We do not use the following data for averages, fits, limits, etc. • • •
>109	95	140 AKTAS	06A H1	single $H^{\pm\pm}$
> 98.2	95	141 ACOSTA	05L CDF	stable
		142 ABAZOV	04E D0	$\mu\mu$
		143 ABBIENDI	03Q OPAL	$E_{cm} \leq 209$ GeV, single $H^{\pm\pm}$
		144 GORDEEV	97 SPEC	muonium conversion
> 45.6	95	145 ACTON	92M OPAL	
> 25.5	95	146 ACTON	92M OPAL	
none 7.3–34.3	95	147 SWARTZ	90 MRK2	

- 135 ABAZOV 08v search for $H^{++}H^{--}$ production in $p\bar{p}$ collisions at $E_{cm} = 1.96$ TeV. The limit is for $B(H \rightarrow \mu\mu) = 1$.
- 136 ACOSTA 04g search for $H^{++}H^{--}$ pair production in $p\bar{p}$ collisions with muon and electron final states. The limit holds for $\mu\mu$.
- 137 ABDALLAH 03 search for $H^{++}H^{--}$ pair production either followed by $H^{++} \rightarrow \tau^+\tau^+$, or decaying outside the detector.
- 138 ACHARD 03f search for $e^+e^- \rightarrow H^{++}H^{--}$ with $H^{\pm\pm} \rightarrow \ell^\pm\ell^\pm$. The limit holds for $\ell = \ell' = \tau$, and slightly different limits apply for other flavor combinations. The limit is valid for $g_{\ell\ell} \gtrsim 10^{-7}$.
- 139 ABBIENDI 02c searches for pair production of $H^{++}H^{--}$, with $H^{\pm\pm} \rightarrow \ell^\pm\ell^\pm$ ($\ell, \ell' = e, \mu, \tau$). The limit holds for $\ell = \ell' = \tau$, and becomes stronger for other combinations of leptonic final states. To ensure the decay within the detector, the limit only applies for $g(H\ell\ell) \gtrsim 10^{-7}$.
- 140 AKTAS 06a search for single $H^{\pm\pm}$ production in ep collisions at HERA. Assuming that H^{++} only couples to $e^+\mu^+$ with $g_{e\mu} = 0.3$ (electromagnetic strength), a limit $m_{H^{++}} > 141$ GeV (95% CL) is derived. For the case where H^{++} couples to $e\tau$ only the limit is 112 GeV.
- 141 ACOSTA 05l search for $H^{++}H^{--}$ pair production in $p\bar{p}$ collisions. The limit is valid for $g_{\ell\ell} < 10^{-8}$ so that the Higgs decays outside the detector.
- 142 ABAZOV 04e search for $H^{++}H^{--}$ pair production in $H^{\pm\pm} \rightarrow \mu^\pm\mu^\pm$. The limit is valid for $g_{\mu\mu} \gtrsim 10^{-7}$.
- 143 ABBIENDI 03q searches for single $H^{\pm\pm}$ via direct production in $e^+e^- \rightarrow e^\mp e^\mp H^{\pm\pm}$, and via t -channel exchange in $e^+e^- \rightarrow e^+e^-$. In the direct case, and assuming $B(H^{\pm\pm} \rightarrow \ell^\pm\ell^\pm) = 1$, a 95% CL limit on $h_{ee} < 0.071$ is set for $m_{H^{\pm\pm}} < 160$ GeV (see Fig. 6). In the second case, indirect limits on h_{ee} are set for $m_{H^{\pm\pm}} < 2$ TeV (see Fig. 8).
- 144 GORDEEV 97 search for muonium-antimuonium conversion and find $G_{M\bar{M}}/G_F < 0.14$ (90% CL), where $G_{M\bar{M}}$ is the lepton-flavor violating effective four-fermion coupling. This limit may be converted to $m_{H^{++}} > 210$ GeV if the Yukawa couplings of H^{++} to ee and $\mu\mu$ are as large as the weak gauge coupling. For similar limits on muonium-antimuonium conversion, see the muon Particle Listings.
- 145 ACTON 92m limit assumes $H^{\pm\pm} \rightarrow \ell^\pm\ell^\pm$ or $H^{\pm\pm}$ does not decay in the detector. Thus the region $g_{\ell\ell} \approx 10^{-7}$ is not excluded.
- 146 ACTON 92m from $\Delta Z < 40$ MeV.
- 147 SWARTZ 90 assume $H^{\pm\pm} \rightarrow \ell^\pm\ell^\pm$ (any flavor). The limits are valid for the Higgs-lepton coupling $g(H\ell\ell) \gtrsim 7.4 \times 10^{-7} [m_H/\text{GeV}]^{1/2}$. The limits improve somewhat for ee and $\mu\mu$ decay modes.

H^0 and H^\pm REFERENCES

ABBIENDI	10	PL B682 381	G. Abbiendi et al.	(OPAL Collab.)
AALTONEN	09A	PRL 102 021802	T. Aaltonen et al.	(CDF Collab.)
AALTONEN	09AB	PRL 103 061803	T. Aaltonen et al.	(CDF Collab.)
AALTONEN	09AG	PR D80 012002	T. Aaltonen et al.	(CDF Collab.)
AALTONEN	09AJ	PRL 103 101802	T. Aaltonen et al.	(CDF Collab.)
AALTONEN	09AJ	PRL 103 101803	T. Aaltonen et al.	(CDF Collab.)
AALTONEN	09AO	PR D80 071101R	T. Aaltonen et al.	(CDF Collab.)
AALTONEN	09AR	PRL 103 201801	T. Aaltonen et al.	(CDF Collab.)
AALTONEN	09AS	PRL 103 221801	T. Aaltonen et al.	(CDF Collab.)
ABAZOV	09AC	PR D80 051107R	V.M. Abazov et al.	(D0 Collab.)
ABAZOV	09AG	PR D80 071102R	V.M. Abazov et al.	(D0 Collab.)
ABAZOV	09AI	PL B682 278	V.M. Abazov et al.	(D0 Collab.)
ABAZOV	09C	PRL 102 051803	V.M. Abazov et al.	(D0 Collab.)
ABAZOV	09F	PRL 102 051804	V.M. Abazov et al.	(D0 Collab.)
ABAZOV	09P	PRL 102 191802	V.M. Abazov et al.	(D0 Collab.)
ABAZOV	09Q	PRL 102 231801	V.M. Abazov et al.	(D0 Collab.)
ABAZOV	09U	PRL 102 251801	V.M. Abazov et al.	(D0 Collab.)
ABAZOV	09V	PRL 103 061801	V.M. Abazov et al.	(D0 Collab.)
AUBERT	09P	PRL 103 181801	B. Aubert et al.	(BABAR Collab.)
AUBERT	09Z	PRL 103 081803	B. Aubert et al.	(BABAR Collab.)
FLACHER	09	EPJ C60 543	H. Flacher et al.	(CERN, DESY, HAMB)
AALTONEN	08AA	PRL 101 121801	T. Aaltonen et al.	(CDF Collab.)
AALTONEN	08AF	PRL 101 251803	T. Aaltonen et al.	(CDF Collab.)
AALTONEN	08AV	PRL 100 041801	T. Aaltonen et al.	(CDF Collab.)
Also		PR D78 032008	T. Aaltonen et al.	(CDF Collab.)
AALTONEN	08X	PRL 100 211801	T. Aaltonen et al.	(CDF Collab.)
ABAZOV	08AJ	PRL 101 221802	V.M. Abazov et al.	(D0 Collab.)
ABAZOV	08AO	PRL 101 251802	V.M. Abazov et al.	(D0 Collab.)
ABAZOV	08U	PRL 101 051801	V.M. Abazov et al.	(D0 Collab.)
ABAZOV	08V	PRL 101 071803	V.M. Abazov et al.	(D0 Collab.)
ABAZOV	08W	PRL 101 071804	V.M. Abazov et al.	(D0 Collab.)
ABAZOV	08Y	PL B663 26	V.M. Abazov et al.	(D0 Collab.)
ABDALLAH	08B	EPJ C54 1	J. Abdallah et al.	(DELPHI Collab.)
Also		EPJ C56 165 (erratum)	J. Abdallah et al.	(DELPHI Collab.)
LOVE	08	PRL 101 151802	W. Love et al.	(CLEO Collab.)
ABAZOV	07X	PL B655 209	V.M. Abazov et al.	(D0 Collab.)
ABBIENDI	07	EPJ C49 457	G. Abbiendi et al.	(OPAL Collab.)
BESSION	07	PRL 98 052002	D. Besson et al.	(CLEO Collab.)
SCHAEEL	07	EPJ C49 439	S. Schaeel et al.	(ALEPH Collab.)
ABAZOV	06	PRL 96 011801	V.M. Abazov et al.	(D0 Collab.)
ABAZOV	06O	PRL 97 151804	V.M. Abazov et al.	(D0 Collab.)
ABAZOV	06Q	PRL 97 161803	V.M. Abazov et al.	(D0 Collab.)
ABULENCIA	06E	PRL 96 042003	A. Abulencia et al.	(CDF Collab.)
AKTAS	05A	PL B638 432	A. Aktas et al.	(H1 Collab.)
LEP-SLC	06	PRPL 427 257	ALEPH, DELPHI, L3, OPAL, SLD and working groups	
SCHAEEL	06B	EPJ C47 547	S. Schaeel et al.	(LEP Collab.)
ABBIENDI	05A	EPJ C40 317	G. Abbiendi et al.	(OPAL Collab.)
ABDALLAH	05D	EPJ C44 147	J. Abdallah et al.	(DELPHI Collab.)
ACHARD	05	PL B609 35	P. Achard et al.	(L3 Collab.)
ACOSTA	05L	PRL 95 071801	D. Acosta et al.	(CDF Collab.)
ACOSTA	05Q	PR D72 072004	D. Acosta et al.	(CDF Collab.)
ABAZOV	04E	PRL 93 141801	V.M. Abazov et al.	(D0 Collab.)
ABBIENDI	04	EPJ C32 453	G. Abbiendi et al.	(OPAL Collab.)
ABBIENDI	04M	PL B597 11	G. Abbiendi et al.	(OPAL Collab.)
ABBIENDI	04K	EPJ C37 49	G. Abbiendi et al.	(OPAL Collab.)
ABDALLAH	04	EPJ C32 145	J. Abdallah et al.	(DELPHI Collab.)
ABDALLAH	04B	EPJ C32 475	J. Abdallah et al.	(DELPHI Collab.)
ABDALLAH	04I	EPJ C34 399	J. Abdallah et al.	(DELPHI Collab.)
ABDALLAH	04L	EPJ C35 313	J. Abdallah et al.	(DELPHI Collab.)
ABDALLAH	04O	EPJ C38 1	J. Abdallah et al.	(DELPHI Collab.)
ACHARD	04B	PL B583 14	P. Achard et al.	(L3 Collab.)
ACHARD	04F	PL B589 89	P. Achard et al.	(L3 Collab.)
ACOSTA	04G	PRL 93 221802	D. Acosta et al.	(CDF Collab.)
ABBIENDI	03	PL B551 35	G. Abbiendi et al.	(OPAL Collab.)

Gauge & Higgs Boson Particle Listings

Higgs Bosons — H^0 and H^\pm , Heavy Bosons Other than Higgs Bosons

ABBIENDI	03B	EPJ C26 479	G. Abbiendi et al.	(OPAL Collab.)
ABBIENDI	03F	EPJ C27 311	G. Abbiendi et al.	(OPAL Collab.)
ABBIENDI	03G	EPJ C27 483	G. Abbiendi et al.	(OPAL Collab.)
ABBIENDI	03Q	PL B577 93	G. Abbiendi et al.	(OPAL Collab.)
ABDALLAH	03	PL B552 127	J. Abdallah et al.	(DELPHI Collab.)
ACHARD	03C	PL B568 191	P. Achard et al.	(L3 Collab.)
ACHARD	03E	PL B575 208	P. Achard et al.	(L3 Collab.)
ACHARD	03F	PL B576 18	P. Achard et al.	(L3 Collab.)
CARENA	03	EPJ C26 601	M.S. Carena et al.	(L3 Collab.)
HEISTER	03D	PL B565 61	A. Heister et al.	(ALEPH, DELPHI, L3+)
ALEPH, DELPHI, L3, OPAL, LEP Higgs Working Group				
ABAZOV	02B	PRL 88 151803	V.M. Abazov et al.	(D0 Collab.)
ABBIENDI	02C	PL B526 221	G. Abbiendi et al.	(OPAL Collab.)
ABBIENDI	02D	EPJ C23 397	G. Abbiendi et al.	(OPAL Collab.)
ABBIENDI	02F	PL B544 44	G. Abbiendi et al.	(OPAL Collab.)
ACHARD	02C	PL B534 28	P. Achard et al.	(L3 Collab.)
ACHARD	02H	PL B545 30	P. Achard et al.	(L3 Collab.)
AKERROYD	02	PR D66 037702	A.G. Akeroyd et al.	
BORZUMATI	02	PL B549 170	F.M. Borzumati, A. Djouadi	
HEISTER	02	PL B526 191	A. Heister et al.	(ALEPH Collab.)
HEISTER	02L	PL B544 16	A. Heister et al.	(ALEPH Collab.)
HEISTER	02M	PL B544 25	A. Heister et al.	(ALEPH Collab.)
HEISTER	02P	PL B543 1	A. Heister et al.	(ALEPH Collab.)
ABBIENDI	01E	EPJ C18 425	G. Abbiendi et al.	(OPAL Collab.)
ABBIENDI	01Q	PL B520 1	G. Abbiendi et al.	(OPAL Collab.)
ABREU	01F	PL B507 89	P. Abreu et al.	(DELPHI Collab.)
ACHARD	01C	PL B517 319	P. Achard et al.	(L3 Collab.)
AFFOLDER	01H	PR D64 092002	T. Affolder et al.	(CDF Collab.)
BARATE	01C	PL B499 53	R. Barate et al.	(ALEPH Collab.)
BARATE	01E	EPJ C19 213	R. Barate et al.	(ALEPH Collab.)
GAMBINO	01	NP B611 338	P. Gambino, M. Misiak	(ALEPH Collab.)
ACCIARRI	00M	PL B485 85	M. Acciari et al.	(L3 Collab.)
ACCIARRI	00R	PL B489 102	M. Acciari et al.	(L3 Collab.)
ACCIARRI	00S	PL B489 115	M. Acciari et al.	(L3 Collab.)
AFFOLDER	00I	PR D62 012004	T. Affolder et al.	(CDF Collab.)
BARATE	00L	PL B487 241	R. Barate et al.	(ALEPH Collab.)
PDG	00	EPJ C15 1	D.E. Groom et al.	
ABBIENDI	99E	EPJ C7 407	G. Abbiendi et al.	(OPAL Collab.)
ABBIENDI	99O	PL B464 311	G. Abbiendi et al.	(OPAL Collab.)
ABBOTT	99B	PRL 82 2244	B. Abbott et al.	(D0 Collab.)
ABBOTT	99E	PRL 82 4975	B. Abbott et al.	(D0 Collab.)
ABREU	99P	PL B458 431	P. Abreu et al.	(DELPHI Collab.)
ACKERSTAFF	99D	EPJ C8 3	K. Akerstaff et al.	(OPAL Collab.)
CARENA	99B	hep-ph/9912223	M.S. Carena et al.	
CERN-TH/99-374				
ABBOTT	98	PRL 80 442	B. Abbott et al.	(D0 Collab.)
ACKERSTAFF	98S	EPJ C5 19	K. Akerstaff et al.	(OPAL Collab.)
ACKERSTAFF	98Y	PL B437 218	K. Akerstaff et al.	(OPAL Collab.)
GONZALEZ-G.	98B	PR D57 7045	M.C. Gonzalez-Garcia, S.M. Lietti, S.F. Novae	
PDG	98	EPJ C3 1	C. Caso et al.	
ABE	97L	PRL 79 357	F. Abe et al.	(CDF Collab.)
ACCIARRI	97F	PL B396 327	M. Acciari et al.	(L3 Collab.)
AMMAR	97B	PRL 78 4686	J. Ammar et al.	(CLEO Collab.)
COARASA	97	PL B406 337	J.A. Coarasa, R.A. Jimenez, J. Sola	
GORDEEV	97	PAN 60 1164	V.A. Gordeev et al.	(PNPI)
Translated from YAF 60 1291.				
GUCHAIT	97	PR D55 7263	M. Guchait, D.P. Roy	(TATA)
KRAWCZYK	97	PR D55 6968	M. Krawczyk, J. Zochowski	(WARS)
MANGANO	97	PL B410 299	M. Mangano, S. Slabospitsky	
STAHL	97	ZPHY C74 73	A. Stahl, H. Voss	(BONN)
ALEXANDER	96H	ZPHY C71 1	G. Alexander et al.	(OPAL Collab.)
PDG	96	PR D54 1	R.M. Barnett et al.	
ABREU	95H	ZPHY C67 69	P. Abreu et al.	(DELPHI Collab.)
ALAM	95	PRL 74 2885	M.S. Alam et al.	(CLEO Collab.)
ASAKA	95	PL B345 36	T. Asaka, K.I. Hikasa	(TOHOK)
BUSKULIC	95	PL B343 444	D. Buskulic et al.	(ALEPH Collab.)
GROSSMAN	95B	PL B357 630	Y. Grossman, H. Haber, Y. Nir	
GROSSMAN	94	PL B332 373	Y. Grossman, Z. Ligeti	
STAHL	94	PL B324 121	A. Stahl	(BONN)
ACTON	92M	PL B295 347	P.D. Acton et al.	(OPAL Collab.)
PICH	92	NP B388 31	A. Pich, J. Prades, P. Yepes	(CERN, CPPM)
SWARTZ	90	PRL 64 2877	M.L. Swartz et al.	(Mark II Collab.)

Heavy Bosons Other Than Higgs Bosons, Searches for

We list here various limits on charged and neutral heavy vector bosons (other than W 's and Z 's), heavy scalar bosons (other than Higgs bosons), vector or scalar leptoquarks, and axiglons.

 W' -BOSON SEARCHES

Revised September 2009 by M.-C. Chen (UC Irvine) and B.A. Dobrescu (Fermilab).

The W' boson is a hypothetical massive particle of electric charge ± 1 and spin 1, which is predicted in various extensions of the Standard Model.

W' couplings to quarks and leptons. The Lagrangian terms describing couplings of a W' boson to fermions are given by

$$W'_\mu \left[\bar{u}_i (C_{qij}^R P_R + C_{qij}^L P_L) \gamma^\mu d_j + \bar{\nu}_i (C_{lij}^R P_R + C_{lij}^L P_L) \gamma^\mu e_j \right] + \text{h.c.} \quad (1)$$

Here u, d, ν and e are the Standard Model fermions in the mass eigenstate basis, $i, j = 1, 2, 3$ label the fermion generation, and $P_{R,L} = (1 \pm \gamma_5)/2$. The coefficients $C_{qij}^L, C_{qij}^R, C_{lij}^L, C_{lij}^R$ are complex dimensionless parameters. If $C_{lij}^R \neq 0$, then the i th

generation includes a right-handed neutrino. It is often assumed that there are correlations between the left- and right-handed couplings [1]. Although this is true in some of the original models that include a W' [2], there exist theories where all the left- and right-handed couplings are free parameters.

Unitarity considerations imply that the W' is a gauge boson associated with a spontaneously broken-gauge symmetry. This is true even when it is a composite particle (*e.g.*, the charged techni- ρ in technicolor theories [3]), or a Kaluza-Klein mode in theories where the W boson propagates in extra dimensions [4]. The simplest extension of the electroweak gauge group that includes a W' is $SU(2)_1 \times SU(2)_2 \times U(1)$, but larger groups are also encountered in some theories. A generic property of all these gauge theories is that besides a W' they contain at least a Z' boson, whose mass is typically comparable or smaller than $M_{W'}$. Despite the severe limits on Z' bosons [5], theories where the properties of the new gauge bosons would allow the W' to be discovered before the Z' are quite common (for example, a leptophobic W' decaying to $t\bar{b}$ may be observed easier than a Z' in the $t\bar{t}$ final state which has higher backgrounds).

The renormalizable photon- W' coupling is completely fixed by electromagnetic gauge invariance. By contrast, the renormalizable $W'WZ$ and $W'W'Z$ couplings are model-dependent, and the same is true for the W' couplings to Z' or Higgs bosons.

Depending on the symmetry-breaking sector, a tree-level mass mixing may be induced between the electrically-charged gauge bosons. Upon diagonalization of their mass matrix, the $W - Z$ mass ratio and the couplings of the observed W are shifted from the Standard Model values. Given that these are well measured, the mixing angle between the two gauge bosons must be smaller than about 10^{-2} . Similarly, a $Z - Z'$ mixing is induced in generic theories, leading to even tighter constraints. There are, however, theories in which these mixings are negligible even when the W' and Z' masses are below the electroweak scale (for example, this is a consequence of a new parity, as in Ref. 6).

A popular model [2] is based on the “left-right symmetric” gauge group, $SU(2)_L \times SU(2)_R \times U(1)_{B-L}$, with the Standard Model fermions that couple to W transforming as doublets under $SU(2)_L$, and the other ones transforming as doublets under $SU(2)_R$. In this model the W' couples primarily to the right-handed fermions, and its coupling to left-handed fermions arises solely due to $W-W'$ mixing. As a result, C_q^L is proportional to the CKM matrix, and its elements are much smaller than the diagonal elements of C_q^R .

There are many other models based on the $SU(2)_1 \times SU(2)_2 \times U(1)$ gauge symmetry. In the “alternate left-right” model [7], all the couplings shown in Eq. (1) vanish, but there are some new fermions such that the W' couples to pairs involving a Standard Model fermion and a new fermion. In the “unified Standard Model” [8], the left-handed quarks are doublets under one $SU(2)$, and the left-handed leptons are doublets under a different $SU(2)$, leading to a mostly leptophobic W' : $C_{lij}^L \ll C_{qij}^L$ and $C_{qij}^R = C_{lij}^R = 0$. Fermions

See key on page 405

Gauge & Higgs Boson Particle Listings

Heavy Bosons Other than Higgs Bosons

of different generations may also transform as doublets under different $SU(2)$ gauge groups [9]. In particular, the couplings to third generation quarks may be enhanced [10].

The W' couplings to Standard Model fermions may be highly suppressed if the quarks and leptons are singlets under one $SU(2)$ [11], or if there are some vectorlike fermions that mix with the Standard Model ones [12]. Gauge groups that embed the electroweak symmetry, such as $SU(3)_W \times U(1)$ or $SU(4)_W \times U(1)$, also include one or more W' bosons [13].

Collider searches. At LEP-II, W' bosons could have been produced in pairs via their photon and Z couplings. The production cross section depends only on the W' mass, and is large enough for $M_{W'} \leq \sqrt{s}/2 \approx 105$ GeV so that W' bosons are ruled out for most patterns of decay modes.

Searches for W' bosons in the Run II at the Tevatron have been performed so far by the DØ and CDF Collaborations for W' decays into $e\nu$ [14,15] or $t\bar{b}$ [16,17]. Assuming that the W' boson has a narrow width, the contribution of the s -channel W' exchange to the total rate for $p\bar{p} \rightarrow f\bar{f}'X$, where f and f' are fermions and X is any final state of charge ± 1 , may be approximated by the branching fraction $B(W' \rightarrow f\bar{f}')$ times the production cross section

$$\sigma(p\bar{p} \rightarrow W'X) \approx \frac{\pi}{48s} \sum_{i,j} \left[(C_{q_{ij}}^L)^2 + (C_{q_{ij}}^R)^2 \right] w_{ij}(s, M_{W'}^2), \quad (2)$$

where the i, j indices label the fermion generations. The functions w_{ij} include the information about proton structure, and are given to leading order in α_s by

$$w_{ij}(z) = \int_z^1 \frac{dx}{x} [u_i(x) d_j(z/x) + \bar{u}_i(x) \bar{d}_j(z/x)], \quad (3)$$

where $u_i(x)$ and $d_i(x)$ are the parton distributions inside the proton for the up- and down-type quark of the i th generation, respectively. QCD corrections to W' production are sizable, but preserve the above factorization of couplings at next-to-leading order [18].

Similar considerations apply at the LHC, except that the $q\bar{q}$ initial state involves a sea parton in pp collisions. Nevertheless, the energy and luminosity will be higher than at the Tevatron, so that W' bosons with masses in the several TeV range will be probed. Preliminary studies of the discovery potential in the $e\nu$ and $\mu\nu$ channels have been presented by the CMS and ATLAS Collaborations in Ref. 19. If a W' boson will be discovered and the final state fermions have left-handed helicity, then the effects of $W - W'$ interference could be observed at the LHC [20] (and perhaps at the Tevatron [21]), providing useful information about the W' couplings.

In the $e\nu$ channel, the signal consists of a high-energy electron and a large missing transverse energy, with the invariant mass distribution forming a peak at $M_{W'}$. The best upper limit to date on the production cross-section $\sigma(p\bar{p} \rightarrow W'X)$ times the branching fraction $B(W' \rightarrow e\nu)$ has been set by DØ at around 10 – 40 fb for $M_{W'}$ in the 0.5 – 1.2 TeV range [15].

This limit at 95% CL, based on 1 fb^{-1} of data, applies only if the right-handed neutrino of the first generation is light compared to $M_{W'}/2$ and escapes the detector. In the particular case where the W' couplings to right-handed fermions are equal to the Standard-Model W couplings to left-handed fermions ($C_q^R = g_{\text{CKM}}, C_l^R = g, C_q^L = C_l^L = 0$), the limit corresponds to $M_{W'} > 1.0$ TeV.

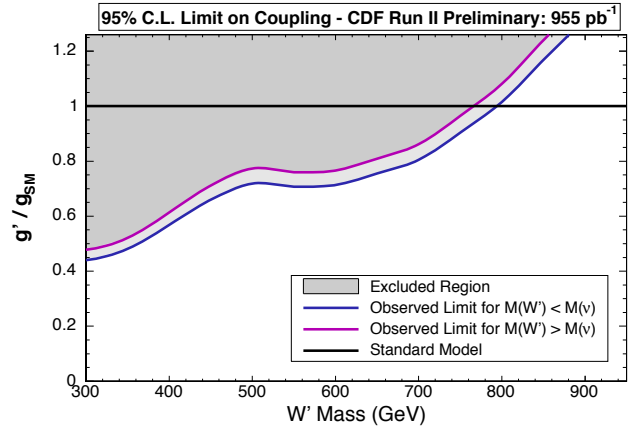


Figure 1: 95% CL exclusion limit from CDF [17] in the gauge coupling versus $M_{W'}$ plane, using the $t\bar{b}$ and $t\bar{b}$ final states. Color version at end of book.

In the $t\bar{b}$ channel, the signal consists of a W decaying leptonically and two b -jets. The current best upper limit on the W' coupling to quarks ($C_{q_{11}}^R$ normalized to the Standard Model W coupling) set by CDF with 1.9 fb^{-1} [17], is shown in Fig. 1.

In some theories (e.g., [6]), the W' couplings to Standard Model fermions are suppressed by discrete symmetries. W' production then occurs in pairs, through a photon or Z . The decay modes are model-dependent and often involve other new particles. The ensuing collider signals arise from cascade decays and typically include missing transverse energy.

A fermiophobic W' which couples to WZ may be produced at hadron colliders in association with a Z , or via WW fusion. This would give rise to $(WZ)Z$ and $(WZ)jj$ final states (the parantheses represent a resonance) at the LHC [22]. The study of these processes would be important for understanding the origin of electroweak symmetry-breaking.

Low-energy constraints. The properties of W' bosons are also constrained by measurements of processes at energies much below $M_{W'}$. The bounds on the tree-level $W - W'$ mixing [23] are mostly due to the change in the properties of the W compared to the Standard Model. Limits on the deviation in the ZWW coupling provide a leading constraint for fermiophobic W' bosons [12].

Constraints arising from low-energy effects of W' exchange are strongly model-dependent. If the W' couplings to quarks are not suppressed, then box diagrams involving a W and a W' contribute to neutral meson-mixing. In the case of W' couplings

Gauge & Higgs Boson Particle Listings

Heavy Bosons Other than Higgs Bosons

to right-handed quarks as in the left-right symmetric model, the limit from $K_L - K_s$ mixing is severe: $M_{W'} > 2.5$ TeV [24]. However, if no correlation between C_{qij}^R and C_{lij}^R is assumed, then the limit on $M_{W'}$ may be significantly relaxed [1]. There are also W' contributions to the neutron electric dipole moment, muon decays, and other processes.

If right-handed neutrinos have Majorana masses, then there are tree-level contributions to neutrinoless double-beta decay, and a limit on $M_{W'}$ versus the ν_R mass may be derived [25]. For ν_R masses below a few GeV, the W' contributes to leptonic and semileptonic B meson decays, so that limits may be placed on various combinations of W' parameters [1]. For right-handed neutrino masses below ~ 30 MeV, most stringent constraints on $M_{W'}$ are due to the limits on ν_R emission from supernova.

References

- P. Langacker and S.U. Sankar, Phys. Rev. D**40**, 1569 (1989).
- R.N. Mohapatra and J.C. Pati, Phys. Rev. D**11**, 566 (1975). G. Senjanovic and R.N. Mohapatra, Phys. Rev. D**12**, 1502 (1975).
- M. Bando, T. Kugo, and K. Yamawaki, Phys. Rept. **164**, 217 (1988).
- H.C. Cheng *et al*, Phys. Rev. D**64**, 065007 (2001).
- See the Section on “ Z' searches” in this *Review*.
- H.C. Cheng and I. Low, JHEP **0309**, 051 (2003).
- K.S. Babu, X.G. He, and E. Ma, Phys. Rev. D**36**, 878 (1987).
- H. Georgi, E.E. Jenkins, and E.H. Simmons, Nucl. Phys. B**331**, 541 (1990).
- See, *e.g.*, X.y. Li and E. Ma, J. Phys. G**19**, 1265 (1993).
- D.J. Muller and S. Nandi, Phys. Lett. B**383**, 345 (1996). E. Malkawi, T. Tait, and C.P. Yuan, Phys. Lett. B**385**, 304 (1996).
- A. Donini *et al*, Nucl. Phys. B**507**, 51 (1997).
- R.S. Chivukula *et al*, Phys. Rev. D**74**, 075011 (2006). H.J. He, T. Tait, and C.P. Yuan, Phys. Rev. D**62**, 011702 (2000).
- F. Pisano and V. Pleitez, Phys. Rev. D**46**, 410 (1992); **51**, 3865 (1995).
- A. Abulencia *et al*. [CDF Collaboration], Phys. Rev. D**75**, 091101 (2007).
- V.M. Abazov *et al*. [D0 Collaboration], Phys. Rev. Lett. **100**, 031804 (2008).
- V.M. Abazov *et al*. [D0 Collaboration], Phys. Rev. Lett. **100**, 211803 (2008).
- T. Aaltonen *et al*. [CDF Collaboration], Phys. Rev. Lett. **103**, 041801 (2009).
- Z. Sullivan, Phys. Rev. D**66**, 075011 (2002).
- G. Aad *et al*. [ATLAS Collaboration], arXiv:0901.0512, p. 1726-1749; CMS Collaboration, report EXO-08-004 (July 2008).
- T.G. Rizzo, JHEP **0705**, 037 (2007).
- E. Boos *et al*, Phys. Lett. B**655**, 245 (2007).
- H.J. He *et al*, Phys. Rev. D**78**, 031701 (2008).
- See the particle listings for W' in this *Review*.
- Y. Zhang *et al*, Phys. Rev. D**76**, 091301 (2007).

- See Fig. 5 of G. Prezeau, M. Ramsey-Musolf, and P. Vogel, Phys. Rev. D**68**, 034016 (2003).

MASS LIMITS for W' (Heavy Charged Vector Boson Other Than W) in Hadron Collider Experiments

Couplings of W' to quarks and leptons are taken to be identical with those of W . The following limits are obtained from $p\bar{p} \rightarrow W'X$ with W' decaying to the mode indicated in the comments. New decay channels (*e.g.*, $W' \rightarrow WZ$) are assumed to be suppressed. UA1 and UA2 experiments assume that the $t\bar{b}$ channel is not open.

VALUE (GeV)	CL%	DOCUMENT ID	TECN	COMMENT
>1000	95	ABAZOV 08c	D0	$W' \rightarrow e\nu$
••• We do not use the following data for averages, fits, limits, etc. •••				
> 800	95	¹ AALTONEN	09AA	CDF $W' \rightarrow t\bar{b}$
none 280–840	95	² AALTONEN	09AC	CDF $W' \rightarrow q\bar{q}$
> 731	95	³ ABAZOV	08P	D0 $W' \rightarrow t\bar{b}$
> 788	95	ABULENCIA	07K	CDF $W' \rightarrow e\nu$
none 200–610	95	⁴ ABAZOV	06N	D0 $W' \rightarrow t\bar{b}$
> 800	95	ABAZOV	04C	D0 $W' \rightarrow q\bar{q}$
225–536	95	⁵ ACOSTA	03B	CDF $W' \rightarrow t\bar{b}$
none 200–480	95	⁶ AFFOLDER	02c	CDF $W' \rightarrow WZ$
> 786	95	⁷ AFFOLDER	01i	CDF $W' \rightarrow e\nu, \mu\nu$
> 660	95	⁸ ABE	00	CDF $W' \rightarrow \mu\nu$
none 300–420	95	⁹ ABE	97G	CDF $W' \rightarrow q\bar{q}$
> 720	95	¹⁰ ABACHI	96C	D0 $W' \rightarrow e\nu$
> 610	95	¹¹ ABACHI	95E	D0 $W' \rightarrow e\nu, \tau\nu$
> 652	95	¹² ABE	95M	CDF $W' \rightarrow e\nu$
> 251	90	¹³ ALITTI	93	UA2 $W' \rightarrow q\bar{q}$
none 260–600	95	¹⁴ RIZZO	93	RVUE $W' \rightarrow q\bar{q}$
> 220	90	¹⁵ ALBAJAR	89	UA1 $W' \rightarrow e\nu$
> 209	90	¹⁶ ANSARI	87D	UA2 $W' \rightarrow e\nu$

¹ The AALTONEN 09AA quoted limit is for a right-handed W' with SM-like coupling allowing $W' \rightarrow \ell\nu$ decays.

² AALTONEN 09AC search for new particle decaying to dijets.

³ The ABAZOV 08P quoted limit is for W' with SM-like coupling which interferes with the SM W boson. For W' with right-handed coupling, the bound becomes >739 GeV (>768 GeV) if W' decays to both leptons and quarks (only to quarks).

⁴ The ABAZOV 06N quoted limit is for W' with SM-like coupling which interferes with the SM W boson. For W' with right-handed coupling, $M_{W'}$ between 200 and 630 (670) GeV is excluded for $M_{\nu_R} \ll M_{W'}$ ($M_{\nu_R} > M_{W'}$).

⁵ The ACOSTA 03B quoted limit is for $M_{W'} \gg M_{\nu_R}$. For $M_{W'} < M_{\nu_R}$, $M_{W'}$ between 225 and 566 GeV is excluded.

⁶ The quoted limit is obtained assuming $W'WZ$ coupling strength is the same as the ordinary WWZ coupling strength in the Standard Model. See their Fig. 2 for the limits on the production cross sections as a function of the W' width.

⁷ AFFOLDER 01i combine a new bound on $W' \rightarrow e\nu$ of 754 GeV with the bound of ABE 00 on $W' \rightarrow \mu\nu$ to obtain quoted bound.

⁸ ABE 00 assume that the neutrino from W' decay is stable and has a mass significantly less than $m_{W'}$.

⁹ ABE 97G search for new particle decaying to dijets.

¹⁰ For bounds on W_R with nonzero right-handed mass, see Fig. 5 from ABACHI 96C.

¹¹ ABACHI 95E assume that the decay $W' \rightarrow WZ$ is suppressed and that the neutrino from W' decay is stable and has a mass significantly less $m_{W'}$.

¹² ABE 95M assume that the decay $W' \rightarrow WZ$ is suppressed and the (right-handed) neutrino is light, noninteracting, and stable. If $m_{\nu} = 60$ GeV, for example, the effect on the mass limit is negligible.

¹³ ALITTI 93 search for resonances in the two-jet invariant mass. The limit assumes $\Gamma(W')/m_{W'} = \Gamma(W)/m_W$ and $B(W' \rightarrow jj) = 2/3$. This corresponds to W_R with $m_{\nu_R} > m_{W_R}$ (no leptonic decay) and $W_R \rightarrow t\bar{b}$ allowed. See their Fig. 4 for limits in the $m_{W'} - B(q\bar{q})$ plane.

¹⁴ RIZZO 93 analyses CDF limit on possible two-jet resonances. The limit is sensitive to the inclusion of the assumed K factor.

¹⁵ ALBAJAR 89 cross section limit at 630 GeV is $\sigma(W') B(e\nu) < 4.1$ pb (90% CL).

¹⁶ See Fig. 5 of ANSARI 87D for the excluded region in the $m_{W'} - [(g_{W'q})^2 B(W' \rightarrow e\bar{\nu})]$ plane. Note that the quantity $(g_{W'q})^2 B(W' \rightarrow e\bar{\nu})$ is normalized to unity for the standard W couplings.

W_R (Right-Handed W Boson) MASS LIMITS

Assuming a light right-handed neutrino, except for BEALL 82, LANGACKER 89B, and COLANGELO 91. $g_R = g_L$ assumed. [Limits in the section MASS LIMITS for W' below are also valid for W_R if $m_{\nu_R} \ll m_{W_R}$.] Some limits assume manifest left-right symmetry, *i.e.*, the equality of left- and right Cabibbo-Kobayashi-Maskawa matrices. For a comprehensive review, see LANGACKER 89B. Limits on the $W_L - W_R$ mixing angle ζ are found in the next section. Values in brackets are from cosmological and astrophysical considerations and assume a light right-handed neutrino.

VALUE (GeV)	CL%	DOCUMENT ID	TECN	COMMENT
> 715	90	¹⁷ CZAKON	99	RVUE Electroweak

See key on page 405

Gauge & Higgs Boson Particle Listings Heavy Bosons Other than Higgs Bosons

• • • We do not use the following data for averages, fits, limits, etc. • • •

> 180	90	18	MELCONIAN	07	CNTR	^{37}K	β^+ decay
> 290.7	90	19	SCHUMANN	07	CNTR		Polarized neutron decay
[> 3300]	95	20	CYBURT	05	COSM		Nucleosynthesis; light ν_R
> 310	90	21	THOMAS	01	CNTR		β^+ decay
> 137	95	22	ACKERSTAFF	99D	OPAL		τ decay
>1400	68	23	BARENBOIM	98	RVUE		Electroweak, Z-Z' mixing
> 549	68	24	BARENBOIM	97	RVUE		μ decay
> 220	95	25	STAHL	97	RVUE		τ decay
> 220	90	26	ALLET	96	CNTR		β^+ decay
> 281	90	27	KUZNETSOV	95	CNTR		Polarized neutron decay
> 282	90	28	KUZNETSOV	94B	CNTR		Polarized neutron decay
> 439	90	29	BHATTACH...	93	RVUE		Z-Z' mixing
> 250	90	30	SEVERIJNS	93	CNTR		β^+ decay
		31	IMAZATO	92	CNTR		K^+ decay
> 475	90	32	POLAK	92B	RVUE		μ decay
> 240	90	33	AQUINO	91	RVUE		Neutron decay
> 496	90	33	AQUINO	91	RVUE		Neutron and muon decay
> 700		34	COLANGELO	91	THEO		$m_{K_L^0} - m_{K_S^0}$
> 477	90	35	POLAK	91	RVUE		μ decay
[none 540-23000]		36	BARBIERI	89B	ASTR	SN 1987A;	light ν_R
> 300	90	37	LANGACKER	89B	RVUE		General
> 160	90	38	BALKE	88	CNTR		$\mu \rightarrow e\nu\bar{\nu}$
> 406	90	39	JODIDIO	86	ELEC		Any ζ
> 482	90	39	JODIDIO	86	ELEC		$\zeta = 0$
> 800			MOHAPATRA	86	RVUE	SU(2) _L × SU(2) _R × U(1)	
> 400	95	40	STOKER	85	ELEC		Any ζ
> 475	95	40	STOKER	85	ELEC		$\zeta < 0.041$
		41	BERGSMA	83	CHRM		$\nu_\mu e \rightarrow \mu\nu e$
> 380	90	42	CARR	83	ELEC		μ^+ decay
>1600		43	BEALL	82	THEO		$m_{K_L^0} - m_{K_S^0}$

- 17 CZAKON 99 perform a simultaneous fit to charged and neutral sectors.
- 18 MELCONIAN 07 measure the neutrino angular asymmetry in β^+ -decays of polarized ^{37}K , stored in a magneto-optical trap. Result is consistent with SM prediction and does not constrain the $W_L - W_R$ mixing angle appreciably.
- 19 SCHUMANN 07 limit is from measurements of the asymmetry $\langle \bar{p}_\nu \cdot \sigma_n \rangle$ in the β decay of polarized neutrons. Zero mixing is assumed.
- 20 CYBURT 05 limit follows by requiring that three light ν_R 's decouple when $T_{dec} > 140$ MeV. For different T_{dec} , the bound becomes $M_{W_R} > 3.3 \text{ TeV} (T_{dec} / 140 \text{ MeV})^{3/4}$.
- 21 THOMAS 01 limit is from measurement of β^+ polarization in decay of polarized ^{12}N . The listed limit assumes no mixing.
- 22 ACKERSTAFF 99D limit is from τ decay parameters. Limit increase to 145 GeV for zero mixing.
- 23 BARENBOIM 98 assumes minimal left-right model with Higgs of SU(2)_R in SU(2)_L doublet. For Higgs in SU(2)_L triplet, $m_{W_R} > 1100$ GeV. Bound calculated from effect of corresponding Z_{LR} on electroweak data through Z-Z_{LR} mixing.
- 24 The quoted limit is from μ decay parameters. BARENBOIM 97 also evaluate limit from $K_L - K_S$ mass difference.
- 25 STAHL 97 limit is from fit to τ -decay parameters.
- 26 ALLET 96 measured polarization-asymmetry correlation in ^{12}N β^+ decay. The listed limit assumes zero L-R mixing.
- 27 KUZNETSOV 95 limit is from measurements of the asymmetry $\langle \bar{p}_\nu \cdot \sigma_n \rangle$ in the β decay of polarized neutrons. Zero mixing assumed. See also KUZNETSOV 94B.
- 28 KUZNETSOV 94B limit is from measurements of the asymmetry $\langle \bar{p}_\nu \cdot \sigma_n \rangle$ in the β decay of polarized neutrons. Zero mixing assumed.
- 29 BHATTACHARYA 93 uses Z-Z' mixing limit from LEP '90 data, assuming a specific Higgs sector of SU(2)_L × SU(2)_R × U(1) gauge model. The limit is for $m_t = 200$ GeV and slightly improves for smaller m_t .
- 30 SEVERIJNS 93 measured polarization-asymmetry correlation in ^{107}In β^+ decay. The listed limit assumes zero L-R mixing. Value quoted here is from SEVERIJNS 94 erratum.
- 31 IMAZATO 92 measure positron asymmetry in $K^+ \rightarrow \mu^+ \nu_\mu$ decay and obtain $\xi_{P_\mu} > 0.990$ (90% CL). If W_R couples to $u\bar{s}$ with full weak strength ($V_{us}^R = 1$), the result corresponds to $m_{W_R} > 653$ GeV. See their Fig. 4 for m_{W_R} limits for general $|V_{us}^R|^2 = 1 - |V_{ud}^R|^2$.
- 32 POLAK 92B limit is from fit to muon decay parameters and is essentially determined by JODIDIO 86 data assuming $\zeta = 0$. Supersedes POLAK 91.
- 33 AQUINO 91 limits obtained from neutron lifetime and asymmetries together with unitarity of the CKM matrix. Manifest left-right symmetry assumed. Stronger of the two limits also includes muon decay results.
- 34 COLANGELO 91 limit uses hadronic matrix elements evaluated by QCD sum rule and is less restrictive than BEALL 82 limit which uses vacuum saturation approximation. Manifest left-right symmetry assumed.
- 35 POLAK 91 limit is from fit to muon decay parameters and is essentially determined by JODIDIO 86 data assuming $\zeta = 0$. Superseded by POLAK 92B.
- 36 BARBIERI 89B limit holds for $m_{\nu_R} \leq 10$ MeV.
- 37 LANGACKER 89B limit is for any ν_R mass (either Dirac or Majorana) and for a general class of right-handed quark mixing matrices.
- 38 BALKE 88 limit is for $m_{\nu_e R} = 0$ and $m_{\nu_\mu R} \leq 50$ MeV. Limits come from precise measurements of the muon decay asymmetry as a function of the positron energy.
- 39 JODIDIO 86 is the same TRIUMF experiment as STOKER 85 (and CARR 83); however, it uses a different technique. The results given here are combined results of the two techniques. The technique here involves precise measurement of the end-point e^+ spectrum in the decay of the highly polarized μ^+ .
- 40 STOKER 85 is same TRIUMF experiment as CARR 83. Here they measure the decay e^+ spectrum asymmetry above 46 MeV/c using a muon-spin-rotation technique. Assumed a light right-handed neutrino. Quoted limits are from combining with CARR 83.

41 BERGSMA 83 set limit $m_{W_2}/m_{W_1} > 1.9$ at CL = 90%.

42 CARR 83 is TRIUMF experiment with a highly polarized μ^+ beam. Looked for deviation from V-A at the high momentum end of the decay e^+ energy spectrum. Limit from previous world-average muon polarization parameter is $m_{W_R} > 240$ GeV. Assumes a light right-handed neutrino.

43 BEALL 82 limit is obtained assuming that W_R contribution to $K_L^0 - K_S^0$ mass difference is smaller than the standard one, neglecting the top quark contributions. Manifest left-right symmetry assumed.

Limit on $W_L - W_R$ Mixing Angle ζ

Lighter mass eigenstate $W_1 = W_L \cos \zeta - W_R \sin \zeta$. Light ν_R assumed unless noted. Values in brackets are from cosmological and astrophysical considerations.

VALUE	CL%	DOCUMENT ID	TECN	COMMENT
< 0.022	90	MACDONALD 08	TWST	$\mu \rightarrow e\nu\bar{\nu}$
< 0.12	95	44 ACKERSTAFF 99D	OPAL	τ decay
< 0.013	90	45 CZAKON 99	RVUE	Electroweak
< 0.0333		46 BARENBOIM 97	RVUE	μ decay
< 0.04	90	47 MISHRA 92	CCFR	νN scattering
-0.0006 to 0.0028	90	48 AQUINO 91	RVUE	
[none 0.00001-0.02]		49 BARBIERI 89B	ASTR	SN 1987A
< 0.040	90	50 JODIDIO 86	ELEC	μ decay
-0.056 to 0.040	90	50 JODIDIO 86	ELEC	μ decay

- • • We do not use the following data for averages, fits, limits, etc. • • •
- 44 ACKERSTAFF 99D limit is from τ decay parameters.
- 45 CZAKON 99 perform a simultaneous fit to charged and neutral sectors.
- 46 The quoted limit is from μ decay parameters. BARENBOIM 97 also evaluate limit from $K_L - K_S$ mass difference.
- 47 MISHRA 92 limit is from the absence of extra large- x , large- y $\bar{\nu}_\mu N \rightarrow \bar{\nu}_\mu X$ events at Tevatron, assuming left-handed ν and right-handed $\bar{\nu}$ in the neutrino beam. The result gives $\zeta^2(1 - 2m_{W_1}^2/m_{W_2}^2) < 0.0015$. The limit is independent of ν_R mass.
- 48 AQUINO 91 limits obtained from neutron lifetime and asymmetries together with unitarity of the CKM matrix. Manifest left-right asymmetry is assumed.
- 49 BARBIERI 89B limit holds for $m_{\nu_R} \leq 10$ MeV.
- 50 First JODIDIO 86 result assumes $m_{W_R} = \infty$, second is for unconstrained m_{W_R} .

Z'-BOSON SEARCHES

Revised September 2009 by M.-C. Chen (UC Irvine) and B.A. Dobrescu (Fermilab).

The Z' boson is a hypothetical massive, electrically-neutral and color-singlet particle of spin 1. This particle is predicted in many extensions of the standard model, and has been the object of extensive phenomenological studies [1].

Z' couplings to quarks and leptons. The couplings of a Z' boson to the first-generation fermions are given by

$$Z'_\mu (g_u^L \bar{u}_L \gamma^\mu u_L + g_d^L \bar{d}_L \gamma^\mu d_L + g_u^R \bar{u}_R \gamma^\mu u_R + g_d^R \bar{d}_R \gamma^\mu d_R + g_\nu^L \bar{\nu}_L \gamma^\mu \nu_L + g_e^L \bar{e}_L \gamma^\mu e_L + g_e^R \bar{e}_R \gamma^\mu e_R) \quad (1)$$

where u, d, ν and e are the quark and lepton fields in the mass eigenstate basis, and the coefficients $g_u^L, g_d^L, g_u^R, g_d^R, g_\nu^L, g_e^L, g_e^R$ are real dimensionless parameters. If the Z' couplings to quarks and leptons are generation-independent, then these seven parameters describe the couplings of the Z' to all standard-model fermions. More generally, however, the Z' couplings to fermions are generation-dependent, in which case Eq. (1) may be written with some generation indices $i, j = 1, 2, 3$ labelling the quark and lepton fields, and with the seven coefficients promoted to 3×3 Hermitian matrices.

These parameters describing the Z' interactions with quarks and leptons are subject to some theoretical constraints. Quantum field theories that include a heavy spin-1 particle are well behaved at high energies only if that particle is a gauge boson associated with a spontaneously broken gauge symmetry. Quantum effects preserve the gauge symmetry only if the couplings

Gauge & Higgs Boson Particle Listings

Heavy Bosons Other than Higgs Bosons

of the gauge boson to fermions satisfy a certain set of equations called anomaly cancellation conditions. Furthermore, the fermion charges under the new gauge symmetry are constrained by the requirement that the quarks and leptons get masses from gauge-invariant interactions with Higgs doublets or whatever else breaks the electroweak symmetry.

The relation between the couplings displayed in Eq. (1) and the gauge charges z_f^L and z_f^R of the fermions $f = u, d, \nu, e$ involves the unitary 3×3 matrices V_f^L and V_f^R that transform the gauge eigenstate fermions f_{Li} and f_{Ri} , respectively, into the mass eigenstate ones. In addition, the Z' couplings are modified if the new gauge boson \tilde{Z}'_μ (in the gauge eigenstate basis) has a kinetic mixing $(-\chi/2)B^{\mu\nu}\tilde{Z}'_{\mu\nu}$ with the hypercharge gauge boson B^μ , or a mass mixing $\delta M^2\tilde{Z}'^\mu\tilde{Z}'_\mu$ with the linear combination (\tilde{Z}'_μ) of neutral bosons which has same couplings as the Z^0 in the standard model [2]. Both the kinetic and mass mixings shift the mass and couplings of the Z boson, such that the electroweak measurements impose upper limits on χ and $\delta M^2/(M_{Z'}^2 - M_Z^2)$ of the order of 10^{-3} [3]. Keeping only linear terms in these two small quantities, the couplings of the mass-eigenstate Z' boson are given by

$$g_f^L = g_z V_f^L z_f^L (V_f^L)^\dagger + \frac{e}{c_W} \left(\frac{s_W \chi M_{Z'}^2 + \delta M^2}{2s_W (M_{Z'}^2 - M_Z^2)} \sigma_f^3 - \epsilon Q_f \right),$$

$$g_f^R = g_z V_f^R z_f^R (V_f^R)^\dagger - \frac{e}{c_W} \epsilon Q_f, \quad (2)$$

where g_z is the new gauge coupling, Q_f is the electric charge of f , e is the electromagnetic gauge coupling, s_W and c_W are the sine and cosine of the weak mixing angle, $\sigma_f^3 = +1$ for $f = u, \nu$ and $\sigma_f^3 = -1$ for $f = d, e$, and

$$\epsilon = \frac{\chi (M_{Z'}^2 - c_W^2 M_Z^2) + s_W \delta M^2}{M_{Z'}^2 - M_Z^2}. \quad (3)$$

$U(1)$ gauge groups. A simple origin of a Z' is a new $U(1)'$ gauge symmetry. In that case, the matricial equalities $z_u^L = z_d^L$ and $z_\nu^L = z_e^L$ are required by the $SU(2)_W$ gauge symmetry. Given that the $U(1)'$ interaction is not asymptotically free, the theory may be well-behaved at high energies (for example, by embedding $U(1)'$ in a non-Abelian gauge group) only if the Z' couplings are commensurate numbers, *i.e.*, any ratio of couplings is a rational number. Satisfying the anomaly cancellation conditions (which include an equation cubic in charges) with rational numbers is highly nontrivial, and in general new fermions charged under $U(1)'$ are necessary. Even then, one should make sure that some anomaly-free set of fermions exists before assuming specific couplings of the Z' to quarks and leptons.

Consider first the case where the couplings are generation-independent (the V_f matrices then disappear from Eq. (2)), so that there are five commensurate couplings: $g_q^L, g_u^R, g_d^R, g_l^L, g_e^R$. Four sets of charges are displayed in Table 1, each of them spanned by one free parameter, x [4]. The first set, labelled $B - xL$, has charges proportional to the baryon number minus

Table 1: Examples of generation-independent $U(1)'$ charges for quarks and leptons. The parameter x is an arbitrary rational number. Anomaly cancellation requires certain new fermions [4].

fermion	$U(1)_{B-xL}$	$U(1)_{10+5\bar{5}}$	$U(1)_{d-xu}$	$U(1)_{q+xu}$
(u_L, d_L)	1/3	1/3	0	1/3
u_R	1/3	-1/3	$-x/3$	$x/3$
d_R	1/3	$-x/3$	1/3	$(2-x)/3$
(ν_L, e_L)	$-x$	$x/3$	$(-1+x)/3$	-1
e_R	$-x$	-1/3	$x/3$	$-(2+x)/3$

x times the lepton number. These charges allow all standard model Yukawa couplings to a Higgs doublet which is neutral under $U(1)_{B-xL}$, so that there is no tree-level $\tilde{Z}-\tilde{Z}'$ mixing. For $x = 1$ one recovers the $U(1)_{B-L}$ group, which is non-anomalous in the presence of one “right-handed neutrino” (a chiral fermion that is a singlet under the standard model gauge group) per generation. For $x \neq 1$, it is necessary to include some fermions that are vectorlike (*i.e.*, their mass terms are gauge invariant) with respect to the electroweak gauge group and chiral with respect to $U(1)_{B-xL}$. In the particular cases $x = 0$ or $x \gg 1$ the Z' is leptophobic or quark-phobic, respectively.

The second set, $U(1)_{10+5\bar{5}}$, has charges that commute with the representations of the $SU(5)$ grand unified group. Here x is related to the mixing angle between the two $U(1)$ bosons encountered in the $E_6 \rightarrow SU(5) \times U(1) \times U(1)$ symmetry breaking patterns of grand unified theories [1,5]. This set leads to $\tilde{Z}-\tilde{Z}'$ mass mixing at tree level, such that for a Z' mass close to the electroweak scale, the measurements at the Z -pole require some fine tuning between the charges and VEVs of two Higgs doublets. Vectorlike fermions charged under the electroweak gauge group and also carrying color are required (except for $x = -3$) to make this set anomaly free. The particular cases $x = -3, 1, -1/2$ are usually labelled $U(1)_\chi$, $U(1)_\psi$, and $U(1)_\eta$, respectively. Under the third set, $U(1)_{d-xu}$, the weak-doublet quarks are neutral, and the ratio of u_R and d_R charges is $-x$. For $x = 1$ this is the “right-handed” group $U(1)_R$. For $x = 0$, the charges are those of the E_6 -inspired $U(1)_I$ group, which requires new quarks and leptons.

In the absence of new fermions charged under the standard model group, the most general generation-independent charge assignment is $U(1)_{q+xu}$, which is a linear combination of hypercharge and $B - L$. Many other anomaly-free solutions exist if generation-dependent charges are allowed. Table 2 shows such solutions that depend on two free parameters, x and y , with generation dependence only in the lepton sector, which includes one right-handed neutrino per generation. The charged-lepton masses may be generated by Yukawa couplings to a single Higgs doublet. These are forced to be flavor diagonal by the generation-dependent $U(1)'$ charges, so that there are no tree-level flavor-changing neutral current (FCNC) processes involving electrically-charged leptons. For the “leptocratic” set,

Gauge & Higgs Boson Particle Listings

Heavy Bosons Other than Higgs Bosons

Table 2: Lepton-flavor dependent charges under various $U(1)$ gauge groups. No new fermions other than right-handed neutrinos are required.

fermion	$B - xL_e - yL_\mu$	2+1 leptocratic
q_{1L}, q_{2L}, q_{3L}	1/3	1/3
u_R, c_R, t_R	1/3	$x/3$
d_R, s_R, b_R	1/3	$(2-x)/3$
(ν_L^e, e_L)	$-x$	$-1 - 2y$
(ν_L^μ, μ_L)	$-y$	$-1 + y$
(ν_L^τ, τ_L)	$x + y - 3$	$-1 + y$
e_R	$-x$	$-(2+x)/3 - 2y$
μ_R	$-y$	$-(2+x)/3 + y$
τ_R	$x + y - 3$	$-(2+x)/3 + y$

neutrino masses are induced by operators of high dimensionality that may explain their smallness [6].

If the $SU(2)_W$ -doublet quarks have generation-dependent $U(1)'$ charges, then the mass eigenstate quarks have flavor off-diagonal couplings to the Z' (see Eq. (1), and note that $V_u^L (V_d^L)^\dagger$ is the CKM matrix). These are severely constrained by measurements of FCNC processes, which in this case are mediated at tree-level by Z' exchange [7]. The constraints are relaxed if the first and second generation charges are the same, although they are increasingly tightened by the measurements of B meson properties. If only the $SU(2)_W$ -singlet quarks have generation-dependent $U(1)'$ charges, there is more freedom in adjusting the flavor off-diagonal couplings because the $V_{u,d}^R$ matrices are not observable in the standard model.

The anomaly cancellation conditions for $U(1)'$ could be relaxed only if at scales above $\sim 4\pi M_{Z'}/g_z$ there is an axion which has certain dimension-5 couplings to the gauge bosons. However, such a scenario violates unitarity unless the quantum field theory description breaks down at a scale near $M_{Z'}$.

Other models. Z' bosons may also arise from larger gauge groups. These may be orthogonal to the electroweak group, as in $SU(2)_W \times U(1)_Y \times SU(2)'$, or may embed the electroweak group, as in $SU(3)_W \times U(1)$. If the larger group is spontaneously broken down to $SU(2)_W \times U(1)_Y \times U(1)'$ at a scale v' larger than the electroweak scale v , then the above discussion applies up to corrections of order $(v/v')^2$. In some cases, though, the larger gauge group may break together with the electroweak symmetry directly to the electromagnetic $U(1)_{em}$. Consequently, the left-handed fermion charges are no longer correlated, *i.e.*, $z_u^L \neq z_d^L$ and $z_\nu^L \neq z_e^L$. Furthermore, additional gauge bosons are present at the electroweak scale, including at least a W' boson [8], and the Z' couples to a pair of W bosons.

If the electroweak gauge bosons propagate in extra dimensions, then their Kaluza-Klein excitations include a series of Z' boson pairs. Each of these pairs can be associated with a different $SU(2) \times U(1)$ gauge group in four dimensions. The properties of the Kaluza-Klein particles depend strongly on the

extra-dimensional theory [9]. For example, in universal extra dimensions there is a parity that forces all couplings of Eq. (1) to vanish in the case of the lightest Kaluza-Klein bosons, while allowing couplings to pairs of fermions involving a standard model one and a heavy vectorlike fermion. There are also 4-dimensional gauge theories (*e.g.*, little Higgs with T parity) with Z' bosons exhibiting similar properties. By contrast, in a warped extra dimension, the couplings of Eq. (1) may be sizable even when standard model fields propagate along the extra dimension.

Z' bosons may also be composite particles. For example, in technicolor theories, the techni- ρ is a spin-1 boson that may be interpreted as arising from a spontaneously broken gauge symmetry [10].

Resonances versus cascade decays. In the presence of the couplings shown in Eq. (1), the Z' boson may be produced in the s -channel at hadron or lepton colliders, and would decay to pairs of fermions. The decay width into a pair of electrons is given by

$$\Gamma(Z' \rightarrow e^+e^-) \approx \left[(g_e^L)^2 + (g_e^R)^2 \right] \frac{M_{Z'}}{24\pi}, \quad (4)$$

where small corrections from electroweak loops are not included. The decay width into $q\bar{q}$ is similar, except for an additional color factor of 3, QCD radiative corrections, and fermion mass corrections. Thus, one may compute the Z' branching fractions in terms of the couplings of Eq. (1). However, other decay channels, such as WW or a pair of new particles, could have large widths and need to be added to the total decay width.

As mentioned above, there are interesting theories in which the Z' couplings are controlled by a discrete symmetry which does not allow its decay into a pair of standard model particles. Typically, such theories involve several new particles, which may be produced only in pairs and undergo cascade decays through Z' 's, leading to signals involving some missing transverse energy. Given that the cascade decays depend on the properties of new particles other than Z' , this case is not discussed further here.

LEP-II limits. The Z' contribution to the cross sections for $e^+e^- \rightarrow f\bar{f}$ proceeds through an s -channel Z' exchange (when $f = e$, there are also t - and u -channel exchanges). For $M_{Z'} < \sqrt{s}$, the Z' appears as an $f\bar{f}$ resonance in the radiative return process where photon emission tunes the effective center-of-mass energy to $M_{Z'}$. The agreement between the LEP-II measurements and the standard model predictions implies that either the Z' couplings are smaller than or of order 10^{-2} , or else $M_{Z'}$ is above 209 GeV, the maximum energy of LEP-II. In the latter case, the Z' effects may be approximated up to corrections of order $s/M_{Z'}^2$ by the contact interactions

$$\frac{g_z^2}{M_{Z'}^2 - s} [\bar{e}\gamma_\mu (z_e^L P_L + z_e^R P_R) e] [\bar{f}\gamma^\mu (z_f^L P_L + z_f^R P_R) f], \quad (5)$$

where $P_{L,R}$ are chirality projection operators, and the relation between Z' couplings and charges (see Eq. (2) in the

Gauge & Higgs Boson Particle Listings

Heavy Bosons Other than Higgs Bosons

limit where the mass and kinetic mixings are neglected) was used assuming generation-independent charges. The four LEP collaborations have set limits on the coefficients of such operators for all possible chiral structures and for various combinations of fermions [11]. Thus, one may derive bounds on $(M_{Z'}/g_z)|z_e^L z_f^L|^{-1/2}$ and the analogous combinations of LR , RL and RR charges, which are typically on the order of a few TeV. Fig. 1 shows the LEP-II limits derived in [4] on the four sets of charges shown in Table 1.

Somewhat stronger bounds could be set on $M_{Z'}/g_z$ for specific sets of Z' couplings if the combined effects of several operators from Eq. (5) are taken into account. Even better limits on Z' bosons having various couplings could be set by dedicated analyses by the LEP collaborations. Such analyses have so far been performed only for fixed values of the gauge coupling (see section 3.5.2 of [11]).

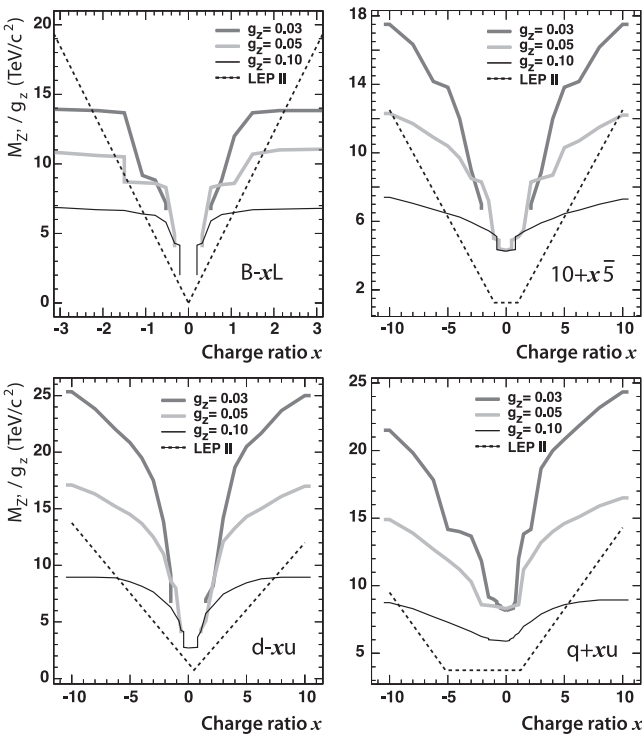


Figure 1: Exclusion limits on the sets of $U(1)$ charges shown in Table 1, from CDF (for different values of the gauge coupling g_z) and the LEP-II experiments (adapted from Ref. 13). The CDF analysis combined the invariant mass and angular distributions of the e^+e^- final state.

Tevatron searches. At hadron colliders, Z' bosons with couplings to quarks (see Eq. (1)) may be produced in the s channel, and would show up as resonances in the invariant mass distribution of the decay products. Searches for Z' bosons in the Run II at the Tevatron have been performed by the CDF and $D\bar{O}$ Collaborations in e^+e^- [12,13], $\mu^+\mu^-$ [14], $e\mu$ [15],

$\tau^+\tau^-$ [16], $t\bar{t}$ [17] and WW [18] final states. In addition to the invariant mass distribution for each of these pairs, the angular distribution can be used to set limits on (or measure, after discovery) several combinations of Z' parameters.

The Z' decay into e^+e^- is interesting due to relatively good mass resolution and large acceptance. Fig. 1 shows the limits on the sets of $U(1)$ charges from Table 1 obtained by CDF with 450 pb^{-1} in the e^+e^- final state [13]. The Z' decay into $\mu^+\mu^-$, $e\mu$ and $\tau^+\tau^-$, along with $t\bar{t}$ which suffers from larger backgrounds, are also important as they probe various combinations of Z' couplings to fermions. Furthermore, these channels are sensitive to Z' bosons with suppressed couplings to the electrons (see Table 2), which are not constrained by the LEP searches. The $Z' \rightarrow WW$ channel may probe the gauge origin of the new spin-1 particle.

The total cross section is the observable that typically is most sensitive to a Z' . For a narrow s -channel resonance, the interference of Z' with the Z or photon may be neglected, and the total cross section in the dilepton channel takes the form

$$\sigma(p\bar{p} \rightarrow Z'X \rightarrow \ell^+\ell^-X) = \frac{\pi}{48s} \sum_q c_q w_q(s, M_{Z'}^2) \quad (6)$$

for flavor-diagonal couplings to quarks. The coefficients

$$c_q = \left[(g_q^L)^2 + (g_q^R)^2 \right] B(Z' \rightarrow \ell^+\ell^-) \quad (7)$$

contain all the dependence on the couplings of quarks and leptons to the Z' , while the functions w_q include all the information about parton distributions and QCD corrections [4]. This factorization holds exactly to NLO, and the deviations from it induced at NNLO are very small. Note that only the w_u and w_d functions are likely to be sizable.

The results are often presented as an exclusion limit in the $\sigma(p\bar{p} \rightarrow Z'X \rightarrow \ell^+\ell^-X)$ versus $M_{Z'}$ plane; the current limit for the $\mu^+\mu^-$ channel, based on 2.3 fb^{-1} of data, is 10 fb for $M_{Z'} \approx 400$ GeV, decreasing to about 3 fb for $M_{Z'} > 700$ GeV [14]. An alternative is to plot exclusion curves for fixed $M_{Z'}$ values in the $c_u - c_d$ plane, allowing a simple derivation of the mass limit within any Z' model.

LHC discovery potential. Z' bosons may be discovered at the LHC through their decays into e^+e^- , $\mu^+\mu^-$ and other fermion pairs. The factorization given in Eq. (6) is also applicable to the LHC, with different w_q functions, which now depend on the PDF's for the two incoming protons. Assuming that the couplings to fermions are of order 0.1 or larger, search for e^+e^- resonances at the CMS experiment will probe Z' masses in the 1 – 2 TeV range with 300 pb^{-1} of data at a center-of-mass energy of 10 TeV [19]. The $\mu^+\mu^-$ channel has lower resolution, but can be competitive with the e^+e^- one due to lower backgrounds; the reach of the ATLAS experiment in both these channels (and also in $\tau^+\tau^-$) has been estimated in [20], assuming 14 TeV center-of-mass energy.

The observation of a dilepton resonance at the LHC would determine the mass and width of the Z' . A measurement of the

See key on page 405

Gauge & Higgs Boson Particle Listings

Heavy Bosons Other than Higgs Bosons

total cross section would define a narrow band in the $c_u - c_d$ plane. Even though the original quark direction in a pp collider is unknown, the leptonic forward-backward asymmetry A_{FB}^l can be extracted from the kinematics of the dilepton system, and is sensitive to parity-violating couplings. A fit to the Z' rapidity distribution can distinguish between the couplings to up and down quarks. These measurements, combined with off-peak observables, have the potential to differentiate among various Z' models [21]. For example, the couplings of a Z' with mass below 1.5 TeV can be well determined with 100 fb^{-1} of data at a center-of-mass energy of 14 TeV. The spin of the Z' may be determined with this amount of data for a Z' mass up to 3 TeV [22].

The $pp \rightarrow Z'X \rightarrow W^+W^-X$ process may also be explored at the LHC, and is important for disentangling the origin of electroweak symmetry breaking. The Z' may be produced in this process through its couplings to either quarks [23] or W bosons [24].

Low-energy constraints. Z' properties are also constrained by a variety of low-energy experiments [25]. Polarized electron-nucleon scattering and atomic parity violation are sensitive to electron-quark contact interactions, which get contributions from Z' exchange that can be expressed in terms of the couplings introduced in Eq. (1) and $M'_{Z'}$. Further corrections to the electron-quark contact interactions are induced in the presence of $\tilde{Z} - \tilde{Z}'$ mixing because of the shifts in the Z couplings to quarks and leptons [2]. Deep-inelastic neutrino-nucleon scattering is similarly affected by Z' bosons. Other low-energy observables are discussed in Ref. 3. Interestingly, due to the $\tilde{Z} - \tilde{Z}'$ mixing, the global fit in Z' models often prefers a higher Higgs mass than in the standard model [26].

Although the LEP and Tevatron data are most constraining for many Z' models, one should be careful in assessing the relative reach of various experiments given the freedom in Z' couplings. For example, a Z' associated with the $U(1)_{B-xL_e-yL_\mu}$ model (see Table 2) for $x = 0$ and $y \gg 1$ couples only to leptons of the second and third generations, with implications for the muon $g - 2$, neutrino oscillations or τ decays, and would be hard to see in processes involving first-generation fermions.

References

- For reviews, see P. Langacker, [arXiv:0801.1345](#);
A. Leike, Phys. Rept. **317**, 143 (1999);
J. Hewett and T. Rizzo, Phys. Rept. **183**, 193 (1989).
- K.S. Babu, C. Kolda, and J. March-Russell, Phys. Rev. **D57**, 6788 (1998);
B. Holdom, Phys. Lett. **B259**, 329 (1991).
- J. Erler and P. Langacker, “Electroweak model and constraints on new physics” in this *Review*.
- M.S. Carena *et al.*, Phys. Rev. **D70**, 093009 (2004).
- See, *e.g.*, F. Del Aguila, M. Cvetič, and P. Langacker, Phys. Rev. **D52**, 37 (1995).
- M.-C. Chen, A. de Gouvêa, and B.A. Dobrescu, Phys. Rev. **D75**, 055009 (2007).

- P. Langacker and M. Plumacher, Phys. Rev. **D62**, 013006 (2000);
R.S. Chivukula and E.H. Simmons, Phys. Rev. **D66**, 015006 (2002).
- See the Section on “ W' searches” in this *Review*.
- G.F. Giudice and J.D. Wells, “Extra dimensions” in this *Review*.
- M. Bando, T. Kugo, and K. Yamawaki, Phys. Rept. **164**, 217 (1988).
- J. Alcaraz *et al.* [ALEPH, DELPHI, L3, OPAL Collaborations, LEP Electroweak Working Group], [hep-ex/0612034](#).
- DØ Collaboration, note 5923-Conf, July 2009;
T. Aaltonen *et al.* [CDF Collaboration], Phys. Rev. Lett. **102**, 031801 (2009).
- A. Abulencia *et al.* [CDF Collaboration], Phys. Rev. Lett. **96**, 211801 (2006).
- T. Aaltonen *et al.* [CDF Collaboration], Phys. Rev. Lett. **102**, 091805 (2009);
DØ Collaboration, note 4577-Conf (2004).
- A. Abulencia *et al.* [CDF Collaboration], Phys. Rev. Lett. **96**, 211802 (2006).
- D. Acosta *et al.* [CDF Collaboration], Phys. Rev. Lett. **95**, 131801 (2005).
- DØ Collaboration, note 5882, March 2009;
CDF Collaboration, note 9844, July 2009.
- CDF Collaboration, note 9730, April 2009.
- CMS note EXO-09-006, July 2009.
- G. Aad *et al.* [ATLAS Collaboration], [arXiv:0901.0512](#), p. 1696-1725.
- F. Petriello and S. Quackenbush, Phys. Rev. **D77**, 115004 (2008).
- P. Osland *et al.*, Phys. Rev. **D79**, 115021 (2009).
- A. Alves *et al.*, [arXiv:0907.2915](#).
- H. J. He *et al.*, Phys. Rev. **D78**, 031701 (2008).
- See, *e.g.*, V.D. Barger *et al.*, Phys. Rev. **D57**, 391 (1998).
- M. S. Chanowitz, [arXiv:0806.0890](#).

MASS LIMITS for Z' (Heavy Neutral Vector Boson Other Than Z)

Limits for Z'_{SM}

Z'_{SM} is assumed to have couplings with quarks and leptons which are identical to those of Z , and decays only to known fermions.

VALUE (GeV)	CL%	DOCUMENT ID	TECN	COMMENT
>1030	95	51 AALTONEN	09v CDF	$p\bar{p}; Z'_{SM} \rightarrow \mu^+ \mu^-$
>1305	95	52 ABDALLAH	06c DLPH	$e^+ e^-$
>1500	95	53 CHEUNG	01B RVUE	Electroweak
• • • We do not use the following data for averages, fits, limits, etc. • • •				
none 320–740	95	54 AALTONEN	09Ac CDF	$Z' \rightarrow q\bar{q}$
> 963	95	55 AALTONEN	09T CDF	$p\bar{p}; Z'_{SM} \rightarrow e^+ e^-$
>1403	95	56 ERLER	09 RVUE	Electroweak
> 923	95	55 AALTONEN	07H CDF	Repl. by AALTONEN 09T
> 850	95	55 ABULENCIA	06L CDF	Repl. by AALTONEN 07H
> 825	95	57 ABULENCIA	05A CDF	$p\bar{p}; Z'_{SM} \rightarrow e^+ e^-, \mu^+ \mu^-$
> 399	95	58 ACOSTA	05R CDF	$p\bar{p}; Z'_{SM} \rightarrow \tau^+ \tau^-$
none 400–640	95	ABAZOV	04c D0	$p\bar{p}; Z'_{SM} \rightarrow q\bar{q}$
>1018	95	59 ABBIENDI	04G OPAL	$e^+ e^-$
> 670	95	60 ABAZOV	01B D0	$p\bar{p}; Z'_{SM} \rightarrow e^+ e^-$
> 710	95	61 ABREU	00s DLPH	$e^+ e^-$
> 898	95	62 BARATE	00i ALEP	$e^+ e^-$
> 809	95	63 ERLER	99 RVUE	Electroweak
> 690	95	64 ABE	97s CDF	$p\bar{p}; Z'_{SM} \rightarrow e^+ e^-, \mu^+ \mu^-$
> 490	95	ABACHI	96D D0	$p\bar{p}; Z'_{SM} \rightarrow e^+ e^-$
> 398	95	65 VILAIN	94B CHM2	$\nu_\mu e \rightarrow \nu_\mu e$ and $\bar{\nu}_\mu e \rightarrow \bar{\nu}_\mu e$
> 237	90	66 ALITTI	93 UA2	$p\bar{p}; Z'_{SM} \rightarrow q\bar{q}$
none 260–600	95	67 RIZZO	93 RVUE	$p\bar{p}; Z'_{SM} \rightarrow q\bar{q}$
> 426	90	68 ABE	90F VNS	$e^+ e^-$

Gauge & Higgs Boson Particle Listings

Heavy Bosons Other than Higgs Bosons

- 51 AALTONEN 09v search for resonances decaying to $\mu^+\mu^-$ in $p\bar{p}$ collisions at $\sqrt{s} = 1.96$ TeV.
- 52 ABDALLAH 06c use data $\sqrt{s} = 130\text{--}207$ GeV.
- 53 CHEUNG 01B limit is derived from bounds on contact interactions in a global electroweak analysis.
- 54 AALTONEN 09AC search for new particle decaying to dijets.
- 55 AALTONEN 09T, AALTONEN 07H, and ABULENCIA 06L search for resonances decaying to e^+e^- in $p\bar{p}$ collisions at $\sqrt{s} = 1.96$ TeV.
- 56 ERLER 09 give 95% CL limit on the Z - Z' mixing $-0.0026 < \theta < 0.0006$.
- 57 ABULENCIA 05A search for resonances decaying to electron or muon pairs in $p\bar{p}$ collisions at $\sqrt{s} = 1.96$ TeV.
- 58 ACOSTA 05R search for resonances decaying to tau lepton pairs in $p\bar{p}$ collisions at $\sqrt{s} = 1.96$ TeV.
- 59 ABBIENDI 04G give 95% CL limit on Z - Z' mixing $-0.00422 < \theta < 0.00091$. $\sqrt{s} = 91$ to 207 GeV.
- 60 ABAZOV 01B search for resonances in $p\bar{p} \rightarrow e^+e^-$ at $\sqrt{s}=1.8$ TeV. They find $\sigma \cdot B(Z' \rightarrow ee) < 0.06$ pb for $M_{Z'} > 500$ GeV.
- 61 ABREU 00s uses LEP data at $\sqrt{s}=90$ to 189 GeV.
- 62 BARATE 00i search for deviations in cross section and asymmetries in $e^+e^- \rightarrow$ fermions at $\sqrt{s}=90$ to 183 GeV. Assume $\theta=0$. Bounds in the mass-mixing plane are shown in their Figure 18.
- 63 ERLER 99 give 90%CL limit on the Z - Z' mixing $-0.0041 < \theta < 0.0003$. $\rho_0=1$ is assumed.
- 64 ABE 97s find $\sigma(Z') \times B(e^+e^-, \mu^+\mu^-) < 40$ fb for $m_{Z'} > 600$ GeV at $\sqrt{s}=1.8$ TeV.
- 65 VILAIN 94B assume $m_t = 150$ GeV.
- 66 ALITTI 93 search for resonances in the two-jet invariant mass. The limit assumes $B(Z' \rightarrow q\bar{q})=0.7$. See their Fig. 5 for limits in the $m_{Z'}-B(q\bar{q})$ plane.
- 67 RIZZO 93 analyses CDF limit on possible two-jet resonances.
- 68 ABE 90f use data for $R, R_{\ell\ell}$, and $A_{\ell\ell}$. They fix $m_W = 80.49 \pm 0.43 \pm 0.24$ GeV and $m_Z = 91.13 \pm 0.03$ GeV.

Limits for Z_{LR}

Z_{LR} is the extra neutral boson in left-right symmetric models. $g_L = g_R$ is assumed unless noted. Values in parentheses assume stronger constraint on the Higgs sector, usually motivated by specific left-right symmetric models (see the Note on the W'). Values in brackets are from cosmological and astrophysical considerations and assume a light right-handed neutrino. Direct search bounds assume decays to Standard Model fermions only, unless noted.

VALUE (GeV)	CL%	DOCUMENT ID	TECN	COMMENT
>998	95	69 ERLER	09 RVUE	Electroweak
>600	95	SCHAEL 07A	ALEP	e^+e^-
>630	95	70 ABE	97s CDF	$p\bar{p}; Z'_{LR} \rightarrow e^+e^-, \mu^+\mu^-$
••• We do not use the following data for averages, fits, limits, etc. •••				
>455	95	71 ABDALLAH	06c DLPH	e^+e^-
>518	95	72 ABBIENDI	04g OPAL	e^+e^-
>860	95	73 CHEUNG	01B RVUE	Electroweak
>380	95	74 ABREU	00s DLPH	e^+e^-
>436	95	75 BARATE	00i ALEP	Repl. by SCHAEL 07A
>550	95	76 CHAY	00 RVUE	Electroweak
		77 ERLER	00 RVUE	Cs
		78 CASALBUONI	99 RVUE	Cs
(> 1205)	90	79 CZAKON	99 RVUE	Electroweak
>564	95	80 ERLER	99 RVUE	Electroweak
(> 1673)	95	81 ERLER	99 RVUE	Electroweak
(> 1700)	68	82 BARENBOIM	98 RVUE	Electroweak
>244	95	83 CONRAD	98 RVUE	$\nu_\mu N$ scattering
>253	95	84 VILAIN	94B CHM2	$\nu_\mu e \rightarrow \nu_\mu e$ and $\bar{\nu}_\mu e \rightarrow \bar{\nu}_\mu e$
none 200–600	95	85 RIZZO	93 RVUE	$p\bar{p}; Z_{LR} \rightarrow q\bar{q}$
[> 2000]		WALKER	91 COSM	Nucleosynthesis; light ν_R
none 200–500		86 GRIFOLS	90 ASTR	SN 1987A; light ν_R
none 350–2400		87 BARBIERI	89B ASTR	SN 1987A; light ν_R

- 69 ERLER 09 give 95% CL limit on the Z - Z' mixing $-0.0013 < \theta < 0.0006$.
- 70 ABE 97s find $\sigma(Z') \times B(e^+e^-, \mu^+\mu^-) < 40$ fb for $m_{Z'} > 600$ GeV at $\sqrt{s}=1.8$ TeV.
- 71 ABDALLAH 06c give 95% CL limit $|\theta| < 0.0028$. See their Fig. 14 for limit contours in the mass-mixing plane.
- 72 ABBIENDI 04G give 95% CL limit on Z - Z' mixing $-0.00098 < \theta < 0.00190$. See their Fig. 20 for the limit contour in the mass-mixing plane. $\sqrt{s} = 91$ to 207 GeV.
- 73 CHEUNG 01B limit is derived from bounds on contact interactions in a global electroweak analysis.
- 74 ABREU 00s give 95% CL limit on Z - Z' mixing $|\theta| < 0.0018$. See their Fig. 6 for the limit contour in the mass-mixing plane. $\sqrt{s}=90$ to 189 GeV.
- 75 BARATE 00i search for deviations in cross section and asymmetries in $e^+e^- \rightarrow$ fermions at $\sqrt{s}=90$ to 183 GeV. Assume $\theta=0$. Bounds in the mass-mixing plane are shown in their Figure 18.
- 76 CHAY 00 also find $-0.0003 < \theta < 0.0019$. For g_R free, $m_{Z'} > 430$ GeV.
- 77 ERLER 00 discuss the possibility that a discrepancy between the observed and predicted values of $Q_W(\text{Cs})$ is due to the exchange of Z' . The data are better described in a certain class of the Z' models including Z_{LR} and Z_χ .
- 78 CASALBUONI 99 discuss the discrepancy between the observed and predicted values of $Q_W(\text{Cs})$. It is shown that the data are better described in a class of models including the Z_{LR} model.
- 79 CZAKON 99 perform a simultaneous fit to charged and neutral sectors. Assumes manifest left-right symmetric model. Finds $|\theta| < 0.0042$.
- 80 ERLER 99 give 90% CL limit on the Z - Z' mixing $-0.0009 < \theta < 0.0017$.
- 81 ERLER 99 assumes 2 Higgs doublets, transforming as 10 of $SO(10)$, embedded in E_6 .
- 82 BARENBOIM 98 also gives 68% CL limits on the Z - Z' mixing $-0.0005 < \theta < 0.0033$. Assumes Higgs sector of minimal left-right model.

- 83 CONRAD 98 limit is from measurements at CCFR, assuming no Z - Z' mixing.
- 84 VILAIN 94B assume $m_t = 150$ GeV and $\theta=0$. See Fig. 2 for limit contours in the mass-mixing plane.
- 85 RIZZO 93 analyses CDF limit on possible two-jet resonances.
- 86 GRIFOLS 90 limit holds for $m_{\nu_R} \lesssim 1$ MeV. A specific Higgs sector is assumed. See also GRIFOLS 90D, RIZZO 91.
- 87 BARBIERI 89B limit holds for $m_{\nu_R} \leq 10$ MeV. Bounds depend on assumed supernova core temperature.

Limits for Z_χ

Z_χ is the extra neutral boson in $SO(10) \rightarrow SU(5) \times U(1)_\chi$. $g_\chi = e/\cos\theta_W$ is assumed unless otherwise stated. We list limits with the assumption $\rho=1$ but with no further constraints on the Higgs sector. Values in parentheses assume stronger constraint on the Higgs sector motivated by superstring models. Values in brackets are from cosmological and astrophysical considerations and assume a light right-handed neutrino.

VALUE (GeV)	CL%	DOCUMENT ID	TECN	COMMENT
> 892	95	88 AALTONEN	09v CDF	$p\bar{p}; Z'_\chi \rightarrow \mu^+\mu^-$
>1143	95	89 ERLER	09 RVUE	Electroweak
> 781	95	90 ABBIENDI	04g OPAL	e^+e^-
••• We do not use the following data for averages, fits, limits, etc. •••				
> 862	95	91 AALTONEN	09T CDF	$p\bar{p}; Z'_\chi \rightarrow e^+e^-$
> 822	95	91 AALTONEN	07H CDF	Repl. by AALTONEN 09T
> 680	95	SCHAEL 07A	ALEP	e^+e^-
> 545	95	92 ABDALLAH	06c DLPH	e^+e^-
> 740	95	91 ABULENCIA	06L CDF	Repl. by AALTONEN 07H
> 690	95	93 ABULENCIA	05A CDF	$p\bar{p}; Z'_\chi \rightarrow e^+e^-, \mu^+\mu^-$
>2100		94 BARGER	03b COSM	Nucleosynthesis; light ν_R
> 680	95	95 CHEUNG	01B RVUE	Electroweak
> 440	95	96 ABREU	00s DLPH	e^+e^-
> 533	95	97 BARATE	00i ALEP	Repl. by SCHAEL 07A
> 554	95	98 CHO	00 RVUE	Electroweak
		99 ERLER	00 RVUE	Cs
		100 ROSNER	00 RVUE	Cs
> 545	95	101 ERLER	99 RVUE	Electroweak
(> 1368)	95	102 ERLER	99 RVUE	Electroweak
> 215	95	103 CONRAD	98 RVUE	$\nu_\mu N$ scattering
> 595	95	104 ABE	97s CDF	$p\bar{p}; Z'_\chi \rightarrow e^+e^-, \mu^+\mu^-$
> 190	95	105 ARIMA	97 VNS	Bhabha scattering
> 262	95	106 VILAIN	94B CHM2	$\nu_\mu e \rightarrow \nu_\mu e; \bar{\nu}_\mu e \rightarrow \bar{\nu}_\mu e$
[>1470]		107 FARAGGI	91 COSM	Nucleosynthesis; light ν_R
> 231	90	108 ABE	90f VNS	e^+e^-
[> 1140]		109 GONZALEZ-G.	90b COSM	Nucleosynthesis; light ν_R
[> 2100]		110 GRIFOLS	90 ASTR	SN 1987A; light ν_R

- 88 AALTONEN 09v search for resonances decaying to $\mu^+\mu^-$ in $p\bar{p}$ collisions at $\sqrt{s} = 1.96$ TeV.
- 89 ERLER 09 give 95% CL limit on the Z - Z' mixing $-0.0016 < \theta < 0.0006$.
- 90 ABBIENDI 04G give 95% CL limit on Z - Z' mixing $-0.00099 < \theta < 0.00194$. See their Fig. 20 for the limit contour in the mass-mixing plane. $\sqrt{s} = 91$ to 207 GeV.
- 91 AALTONEN 09T, AALTONEN 07H, and ABULENCIA 06L search for resonances decaying to e^+e^- in $p\bar{p}$ collisions at $\sqrt{s} = 1.96$ TeV.
- 92 ABDALLAH 06c give 95% CL limit $|\theta| < 0.0031$. See their Fig. 14 for limit contours in the mass-mixing plane.
- 93 ABULENCIA 05A search for resonances decaying to electron or muon pairs in $p\bar{p}$ collisions at $\sqrt{s} = 1.96$ TeV.
- 94 BARGER 03b limit is from the nucleosynthesis bound on the effective number of light neutrinos $\delta N_\nu < 1$. The quark-hadron transition temperature $T_C=150$ MeV is assumed. The limit with $T_C=400$ MeV is >4300 GeV.
- 95 CHEUNG 01B limit is derived from bounds on contact interactions in a global electroweak analysis.
- 96 ABREU 00s give 95% CL limit on Z - Z' mixing $|\theta| < 0.0017$. See their Fig. 6 for the limit contour in the mass-mixing plane. $\sqrt{s}=90$ to 189 GeV.
- 97 BARATE 00i search for deviations in cross section and asymmetries in $e^+e^- \rightarrow$ fermions at $\sqrt{s}=90$ to 183 GeV. Assume $\theta=0$. Bounds in the mass-mixing plane are shown in their Figure 18.
- 98 CHO 00 use various electroweak data to constrain Z' models assuming $m_H=100$ GeV. See Fig. 3 for limits in the mass-mixing plane.
- 99 ERLER 00 discuss the possibility that a discrepancy between the observed and predicted values of $Q_W(\text{Cs})$ is due to the exchange of Z' . The data are better described in a certain class of the Z' models including Z_{LR} and Z_χ .
- 100 ROSNER 00 discusses the possibility that a discrepancy between the observed and predicted values of $Q_W(\text{Cs})$ is due to the exchange of Z' . The data are better described in a certain class of the Z' models including Z_χ .
- 101 ERLER 99 give 90% CL limit on the Z - Z' mixing $-0.0020 < \theta < 0.0015$.
- 102 ERLER 99 assumes 2 Higgs doublets, transforming as 10 of $SO(10)$, embedded in E_6 .
- 103 CONRAD 98 limit is from measurements at CCFR, assuming no Z - Z' mixing.
- 104 ABE 97s find $\sigma(Z') \times B(e^+e^-, \mu^+\mu^-) < 40$ fb for $m_{Z'} > 600$ GeV at $\sqrt{s}=1.8$ TeV.
- 105 Z - Z' mixing is assumed to be zero. $\sqrt{s} = 57.77$ GeV.
- 106 VILAIN 94B assume $m_t = 150$ GeV and $\theta=0$. See Fig. 2 for limit contours in the mass-mixing plane.
- 107 FARAGGI 91 limit assumes the nucleosynthesis bound on the effective number of neutrinos $\delta N_\nu < 0.5$ and is valid for $m_{\nu_R} < 1$ MeV.
- 108 ABE 90f use data for $R, R_{\ell\ell}$, and $A_{\ell\ell}$. ABE 90f fix $m_W = 80.49 \pm 0.43 \pm 0.24$ GeV and $m_Z = 91.13 \pm 0.03$ GeV.
- 109 Assumes the nucleosynthesis bound on the effective number of light neutrinos ($\delta N_\nu < 1$) and that ν_R is light ($\lesssim 1$ MeV).
- 110 GRIFOLS 90 limit holds for $m_{\nu_R} \lesssim 1$ MeV. See also GRIFOLS 90D, RIZZO 91.

See key on page 405

Gauge & Higgs Boson Particle Listings

Heavy Bosons Other than Higgs Bosons

Limits for Z_ψ

Z_ψ is the extra neutral boson in $E_6 \rightarrow SO(10) \times U(1)_\psi$. $g_\psi = e/\cos\theta_{WW}$ is assumed unless otherwise stated. We list limits with the assumption $\rho=1$ but with no further constraints on the Higgs sector. Values in brackets are from cosmological and astrophysical considerations and assume a light right-handed neutrino.

VALUE (GeV)	CL%	DOCUMENT ID	TECN	COMMENT
>878	95	111 AALTONEN	09v CDF	$p\bar{p}; Z'_\psi \rightarrow \mu^+ \mu^-$
>475	95	112 ABDALLAH	06c DLPH	$e^+ e^-$
• • • We do not use the following data for averages, fits, limits, etc. • • •				
>851	95	113 AALTONEN	09t CDF	$p\bar{p}; Z'_\psi \rightarrow e^+ e^-$
>147	95	114 ERLER	09 RVUE	Electroweak
>822	95	113 AALTONEN	07h CDF	Repl. by AALTONEN 09t
>410	95	SCHAEEL	07A ALEP	$e^+ e^-$
>725	95	113 ABULENCIA	06L CDF	Repl. by AALTONEN 07h
>675	95	115 ABULENCIA	05A CDF	$p\bar{p}; Z'_\psi \rightarrow e^+ e^-, \mu^+ \mu^-$
>366	95	116 ABBIENDI	04g OPAL	$e^+ e^-$
>600	95	117 BARGER	03b COSM	Nucleosynthesis; light ν_R
>350	95	118 ABREU	00s DLPH	$e^+ e^-$
>294	95	119 BARATE	00i ALEP	Repl. by SCHAEEL 07A
>137	95	120 CHO	00 RVUE	Electroweak
>146	95	121 ERLER	99 RVUE	Electroweak
> 54	95	122 CONRAD	98 RVUE	$\nu_\mu N$ scattering
>590	95	123 ABE	97s CDF	$p\bar{p}; Z'_\psi \rightarrow e^+ e^-, \mu^+ \mu^-$
>135	95	124 VILAIN	94b CHM2	$\nu_\mu e \rightarrow \nu_\mu e; \bar{\nu}_\mu e \rightarrow \bar{\nu}_\mu e$
>105	90	125 ABE	90f VNS	$e^+ e^-$
[> 160]		126 GONZALEZ-G.	90d COSM	Nucleosynthesis; light ν_R
[> 2000]		127 GRIFOLS	90d ASTR	SN 1987A; light ν_R

- 111 AALTONEN 09v search for resonances decaying to $\mu^+ \mu^-$ in $p\bar{p}$ collisions at $\sqrt{s} = 1.96$ TeV.
- 112 ABDALLAH 06c give 95% CL limit $|\theta| < 0.0027$. See their Fig. 14 for limit contours in the mass-mixing plane.
- 113 AALTONEN 09t, AALTONEN 07h, and ABULENCIA 06L search for resonances decaying to $e^+ e^-$ in $p\bar{p}$ collisions at $\sqrt{s} = 1.96$ TeV.
- 114 ERLER 09 give 95% CL limit on the Z - Z' mixing $-0.0018 < \theta < 0.0009$.
- 115 ABULENCIA 05A search for resonances decaying to electron or muon pairs in $p\bar{p}$ collisions at $\sqrt{s} = 1.96$ TeV.
- 116 ABBIENDI 04g give 95% CL limit on Z - Z' mixing $-0.00129 < \theta < 0.00258$. See their Fig. 20 for the limit contour in the mass-mixing plane. $\sqrt{s} = 91$ to 207 GeV.
- 117 BARGER 03b limit is from the nucleosynthesis bound on the effective number of light neutrino $\delta N_\nu < 1$. The quark-hadron transition temperature $T_C = 150$ MeV is assumed. The limit with $T_C = 400$ MeV is > 1100 GeV.
- 118 ABREU 00s give 95% CL limit on Z - Z' mixing $|\theta| < 0.0018$. See their Fig. 6 for the limit contour in the mass-mixing plane. $\sqrt{s} = 90$ to 189 GeV.
- 119 BARATE 00i search for deviations in cross section and asymmetries in $e^+ e^- \rightarrow$ fermions at $\sqrt{s} = 90$ to 183 GeV. Assume $\theta = 0$. Bounds in the mass-mixing plane are shown in their Figure 18.
- 120 CHO 00 use various electroweak data to constrain Z' models assuming $m_H = 100$ GeV. See Fig. 3 for limits in the mass-mixing plane.
- 121 ERLER 99 give 90% CL limit on the Z - Z' mixing $-0.0013 < \theta < 0.0024$.
- 122 CONRAD 98 limit is from measurements at CCFR, assuming no Z - Z' mixing.
- 123 ABE 97s find $\sigma(Z') \times B(e^+ e^-, \mu^+ \mu^-) < 40$ fb for $m_{Z'} > 600$ GeV at $\sqrt{s} = 1.8$ TeV.
- 124 VILAIN 94b assume $m_t = 150$ GeV and $\theta = 0$. See Fig. 2 for limit contours in the mass-mixing plane.
- 125 ABE 90f use data for $R, R_{\ell\ell}$, and $A_{\ell\ell}$. ABE 90f fix $m_W = 80.49 \pm 0.43 \pm 0.24$ GeV and $m_Z = 91.13 \pm 0.03$ GeV.
- 126 Assumes the nucleosynthesis bound on the effective number of light neutrinos ($\delta N_\nu < 1$) and that ν_R is light ($\lesssim 1$ MeV).
- 127 GRIFOLS 90d limit holds for $m_{\nu_R} \lesssim 1$ MeV. See also RIZZO 91.

Limits for Z_η

Z_η is the extra neutral boson in E_6 models, corresponding to $Q_\eta = \sqrt{3/8} Q_\chi - \sqrt{5/8} Q_\psi$. $g_\eta = e/\cos\theta_{WW}$ is assumed unless otherwise stated. We list limits with the assumption $\rho=1$ but with no further constraints on the Higgs sector. Values in parentheses assume stronger constraint on the Higgs sector motivated by superstring models. Values in brackets are from cosmological and astrophysical considerations and assume a light right-handed neutrino.

VALUE (GeV)	CL%	DOCUMENT ID	TECN	COMMENT
> 904	95	128 AALTONEN	09v CDF	$p\bar{p}; Z'_\eta \rightarrow \mu^+ \mu^-$
> 515	95	129 ABBIENDI	04g OPAL	$e^+ e^-$
> 619	95	130 CHO	00 RVUE	Electroweak
• • • We do not use the following data for averages, fits, limits, etc. • • •				
> 877	95	131 AALTONEN	09t CDF	$p\bar{p}; Z'_\eta \rightarrow e^+ e^-$
> 427	95	132 ERLER	09 RVUE	Electroweak
> 891	95	131 AALTONEN	07h CDF	Repl. by AALTONEN 09t
> 350	95	SCHAEEL	07A ALEP	$e^+ e^-$
> 360	95	133 ABDALLAH	06c DLPH	$e^+ e^-$
> 745	95	131 ABULENCIA	06L CDF	Repl. by AALTONEN 07h
> 720	95	134 ABULENCIA	05A CDF	$p\bar{p}; Z'_\eta \rightarrow e^+ e^-, \mu^+ \mu^-$
>1600		135 BARGER	03b COSM	Nucleosynthesis; light ν_R
> 310	95	136 ABREU	00s DLPH	$e^+ e^-$

> 329	95	137 BARATE	00i ALEP	Repl. by SCHAEEL 07A
> 365	95	138 ERLER	99 RVUE	Electroweak
> 87	95	139 CONRAD	98 RVUE	$\nu_\mu N$ scattering
> 620	95	140 ABE	97s CDF	$p\bar{p}; Z'_\eta \rightarrow e^+ e^-, \mu^+ \mu^-$
> 100	95	141 VILAIN	94b CHM2	$\nu_\mu e \rightarrow \nu_\mu e; \bar{\nu}_\mu e \rightarrow \bar{\nu}_\mu e$
> 125	90	142 ABE	90f VNS	$e^+ e^-$
[> 820]		143 GONZALEZ-G.	90d COSM	Nucleosynthesis; light ν_R
[> 3300]		144 GRIFOLS	90 ASTR	SN 1987A; light ν_R
[> 1040]		143 LOPEZ	90 COSM	Nucleosynthesis; light ν_R

- 128 AALTONEN 09v search for resonances decaying to $\mu^+ \mu^-$ in $p\bar{p}$ collisions at $\sqrt{s} = 1.96$ TeV.
- 129 ABBIENDI 04g give 95% CL limit on Z - Z' mixing $-0.00447 < \theta < 0.00331$. See their Fig. 20 for the limit contour in the mass-mixing plane. $\sqrt{s} = 91$ to 207 GeV.
- 130 CHO 00 use various electroweak data to constrain Z' models assuming $m_H = 100$ GeV. See Fig. 3 for limits in the mass-mixing plane.
- 131 AALTONEN 09t, AALTONEN 07h, and ABULENCIA 06L search for resonances decaying to $e^+ e^-$ in $p\bar{p}$ collisions at $\sqrt{s} = 1.96$ TeV.
- 132 ERLER 09 give 95% CL limit on the Z - Z' mixing $-0.0047 < \theta < 0.0021$.
- 133 ABDALLAH 06c give 95% CL limit $|\theta| < 0.0092$. See their Fig. 14 for limit contours in the mass-mixing plane.
- 134 ABULENCIA 05A search for resonances decaying to electron or muon pairs in $p\bar{p}$ collisions at $\sqrt{s} = 1.96$ TeV.
- 135 BARGER 03b limit is from the nucleosynthesis bound on the effective number of light neutrino $\delta N_\nu < 1$. The quark-hadron transition temperature $T_C = 150$ MeV is assumed. The limit with $T_C = 400$ MeV is > 3300 GeV.
- 136 ABREU 00s give 95% CL limit on Z - Z' mixing $|\theta| < 0.0024$. See their Fig. 6 for the limit contour in the mass-mixing plane. $\sqrt{s} = 90$ to 189 GeV.
- 137 BARATE 00i search for deviations in cross section and asymmetries in $e^+ e^- \rightarrow$ fermions at $\sqrt{s} = 90$ to 183 GeV. Assume $\theta = 0$. Bounds in the mass-mixing plane are shown in their Figure 18.
- 138 ERLER 99 give 90% CL limit on the Z - Z' mixing $-0.0062 < \theta < 0.0011$.
- 139 CONRAD 98 limit is from measurements at CCFR, assuming no Z - Z' mixing.
- 140 ABE 97s find $\sigma(Z') \times B(e^+ e^-, \mu^+ \mu^-) < 40$ fb for $m_{Z'} > 600$ GeV at $\sqrt{s} = 1.8$ TeV.
- 141 VILAIN 94b assume $m_t = 150$ GeV and $\theta = 0$. See Fig. 2 for limit contours in the mass-mixing plane.
- 142 ABE 90f use data for $R, R_{\ell\ell}$, and $A_{\ell\ell}$. ABE 90f fix $m_W = 80.49 \pm 0.43 \pm 0.24$ GeV and $m_Z = 91.13 \pm 0.03$ GeV.
- 143 These authors claim that the nucleosynthesis bound on the effective number of light neutrinos ($\delta N_\nu < 1$) constrains Z' masses if ν_R is light ($\lesssim 1$ MeV).
- 144 GRIFOLS 90 limit holds for $m_{\nu_R} \lesssim 1$ MeV. See also GRIFOLS 90d, RIZZO 91.

Limits for other Z'

VALUE (GeV)	DOCUMENT ID	TECN	COMMENT
• • • We do not use the following data for averages, fits, limits, etc. • • •			
145	AALTONEN 08d	CDF	$Z' \rightarrow t\bar{t}$
145	AALTONEN 08y	CDF	$Z' \rightarrow t\bar{t}$
145	ABAZOV 08AA	D0	$Z' \rightarrow t\bar{t}$
146	ABULENCIA 06m	CDF	$Z' \rightarrow e\mu$
147	ABAZOV 04A	D0	Repl. by ABAZOV 08AA
148	BARGER 03b	COSM	Nucleosynthesis; light ν_R
149	CHO 00	RVUE	E_6 -motivated
150	CHO 98	RVUE	E_6 -motivated
151	ABE 97g	CDF	$Z' \rightarrow \bar{q}q$

- 145 Search for narrow resonance decaying to $t\bar{t}$. See their Fig. 3 for limit on $\sigma \cdot B$.
- 146 ABULENCIA 06m search for new particle with lepton flavor violating decay at $\sqrt{s} = 1.96$ TeV. See their Fig. 4 for an exclusion plot on a mass-coupling plane.
- 147 Search for narrow resonance decaying to $t\bar{t}$. See their Fig. 2 for limit on $\sigma \cdot B$.
- 148 BARGER 03b use the nucleosynthesis bound on the effective number of light neutrino δN_ν . See their Figs. 4-5 for limits in general E_6 motivated models.
- 149 CHO 00 use various electroweak data to constrain Z' models assuming $m_H = 100$ GeV. See Fig. 2 for limits in general E_6 -motivated models.
- 150 CHO 98 study constraints on four-Fermi contact interactions obtained from low-energy electroweak experiments, assuming no Z - Z' mixing.
- 151 Search for Z' decaying to dijets at $\sqrt{s} = 1.8$ TeV. For Z' with electromagnetic strength coupling, no bound is obtained.

Indirect Constraints on Kaluza-Klein Gauge Bosons

Bounds on a Kaluza-Klein excitation of the Z boson or photon in $d=1$ extra dimension. These bounds can also be interpreted as a lower bound on $1/R$, the size of the extra dimension. Unless otherwise stated, bounds assume all fermions live on a single brane and all gauge fields occupy the $4+d$ -dimensional bulk. See also the section on "Extra Dimensions" in the "Searches" Listings in this Review.

VALUE (TeV)	CL%	DOCUMENT ID	TECN	COMMENT
• • • We do not use the following data for averages, fits, limits, etc. • • •				
> 4.7		152 MUECK	02 RVUE	Electroweak
> 3.3	95	153 CORNET	00 RVUE	$e\nu q q'$
>5000		154 DELGADO	00 RVUE	$e\chi$
> 2.6	95	155 DELGADO	00 RVUE	Electroweak
> 3.3	95	156 RIZZO	00 RVUE	Electroweak
> 2.9	95	157 MARCIANO	99 RVUE	Electroweak
> 2.5	95	158 MASIP	99 RVUE	Electroweak
> 1.6	90	159 NATH	99 RVUE	Electroweak
> 3.4	95	160 STRUMIA	99 RVUE	Electroweak

Gauge & Higgs Boson Particle Listings

Heavy Bosons Other than Higgs Bosons

- ¹⁵²MUECK 02 limit is 2σ and is from global electroweak fit ignoring correlations among observables. Higgs is assumed to be confined on the brane and its mass is fixed. For scenarios of bulk Higgs, of brane- $SU(2)_L$, bulk- $U(1)_Y$, and of bulk- $SU(2)_L$, brane- $U(1)_Y$, the corresponding limits are > 4.6 TeV, > 4.3 TeV and > 3.0 TeV, respectively.
- ¹⁵³Bound is derived from limits on $e\nu q q'$ contact interaction, using data from HERA and the Tevatron.
- ¹⁵⁴Bound holds only if first two generations of quarks lives on separate branes. If quark mixing is not complex, then bound lowers to 400 TeV from Δm_K .
- ¹⁵⁵See Figs. 1 and 2 of DELGADO 00 for several model variations. Special boundary conditions can be found which permit KK states down to 950 GeV and that agree with the measurement of $Q_{WW}(Cs)$. Quoted bound assumes all Higgs bosons confined to brane; placing one Higgs doublet in the bulk lowers bound to 2.3 TeV.
- ¹⁵⁶Bound is derived from global electroweak analysis assuming the Higgs field is trapped on the matter brane. If the Higgs propagates in the bulk, the bound increases to 3.8 TeV.
- ¹⁵⁷Bound is derived from global electroweak analysis but considering only presence of the KK W bosons.
- ¹⁵⁸Global electroweak analysis used to obtain bound independent of position of Higgs on brane or in bulk.
- ¹⁵⁹Bounds from effect of KK states on G_F , α , M_{WZ} , and M_Z . Hard cutoff at string scale determined using gauge coupling unification. Limits for $d=2,3,4$ rise to 3.5, 5.7, and 7.8 TeV.
- ¹⁶⁰Bound obtained for Higgs confined to the matter brane with $m_H=500$ GeV. For Higgs in the bulk, the bound increases to 3.5 TeV.

LEPTOQUARKS

Written November 2007 by S. Rolli (Tufts U.) and M. Tanabashi (Nagoya U.)

Leptoquarks are hypothetical particles carrying both baryon number (B) and lepton number (L). The possible quantum numbers of leptoquark states can be restricted by assuming that their direct interactions with the ordinary SM fermions are dimensionless and invariant under the standard model (SM) gauge group. Table 1 shows the list of all possible quantum numbers with this assumption [1]. The columns of $SU(3)_C$, $SU(2)_W$, and $U(1)_Y$ in Table 1 indicate the QCD representation, the weak isospin representation, and the weak hypercharge, respectively. The spin of a leptoquark state is taken to be 1 (vector leptoquark) or 0 (scalar leptoquark).

Table 1: Possible leptoquarks and their quantum numbers.

Spin	$3B+L$	$SU(3)_c$	$SU(2)_W$	$U(1)_Y$	Allowed coupling
0	-2	$\bar{3}$	1	1/3	$\bar{q}_L^c \ell_L$ or $\bar{u}_R^c e_R$
0	-2	$\bar{3}$	1	4/3	$\bar{d}_R^c e_R$
0	-2	$\bar{3}$	3	1/3	$\bar{q}_L^c \ell_L$
1	-2	$\bar{3}$	2	5/6	$\bar{q}_L^c \gamma^\mu e_R$ or $\bar{d}_R^c \gamma^\mu \ell_L$
1	-2	$\bar{3}$	2	-1/6	$\bar{u}_R^c \gamma^\mu \ell_L$
0	0	3	2	7/6	$\bar{q}_L e_R$ or $\bar{u}_R \ell_L$
0	0	3	2	1/6	$\bar{d}_R \ell_L$
1	0	3	1	2/3	$\bar{q}_L \gamma^\mu \ell_L$ or $\bar{d}_R \gamma^\mu e_R$
1	0	3	1	5/3	$\bar{u}_R \gamma^\mu e_R$
1	0	3	3	2/3	$\bar{q}_L \gamma^\mu \ell_L$

If we do not require leptoquark states to couple directly with SM fermions, different assignments of quantum numbers become possible [2,3].

Leptoquark states are expected to exist in various extensions of SM. The Pati-Salam model [4] is an example predicting the existence of a leptoquark state. Vector leptoquark states also exist in grand unification theories based on $SU(5)$ [5], $SO(10)$ [6], which includes Pati-Salam color $SU(4)$, and larger gauge groups. Scalar quarks in supersymmetric models with R-parity violation may also have leptoquark-type Yukawa

couplings. The bounds on the leptoquark states can therefore be applied to constraining R-parity-violating supersymmetric models. Scalar leptoquarks are expected to exist at TeV scale in extended technicolor models [7,8] where leptoquark states appear as the bound states of techni-fermions. Compositeness of quarks and leptons also provides examples of models which may have light leptoquark states [9].

Bounds on leptoquark states are obtained both directly and indirectly. Direct limits are from their production cross sections at colliders, while indirect limits are calculated from the bounds on the leptoquark-induced four-fermion interactions, which are obtained from low-energy experiments, or from collider experiments below threshold.

If a leptoquark couples to fermions more than a single generation in the mass eigenbasis of the SM fermions, it can induce four-fermion interactions causing flavor-changing neutral currents and lepton-family-number violations. The quantum number assignment of Table 1 allows several leptoquark states to couple to both left- and right-handed quarks simultaneously. Such leptoquark states are called non-chiral and may cause four-fermion interactions affecting the $(\pi \rightarrow e\nu)/(\pi \rightarrow \mu\nu)$ ratio [10]. Non-chiral scalar leptoquarks also contribute to the muon anomalous magnetic moment [11,12]. Indirect limits provide stringent constraints on these leptoquarks.

It is therefore often assumed that a leptoquark state couples only to a single generation in a chiral interaction, where indirect limits become much weaker. This assumption gives strong constraints on concrete models of leptoquarks, however. Leptoquark states which couple only to left- or right-handed quarks are called chiral leptoquarks. Leptoquark states which couple only to the first (second, third) generation are referred as the first- (second-, third-) generation leptoquarks. Refs. [13,14] give extensive lists of the bounds on the leptoquark-induced four-fermion interactions. For the isoscalar and vector leptoquarks S_0 and V_0 , for example, which couple with the first- (second-) generation left-handed quark, and the first-generation left-handed lepton, the bounds of Ref. 13 read $\lambda^2 < 0.03 \times (M_{LQ}/300 \text{ GeV})^2$ for S_0 , and $\lambda^2 < 0.02 \times (M_{LQ}/300 \text{ GeV})^2$ for V_0 ($\lambda^2 < 5 \times (M_{LQ}/300 \text{ GeV})^2$ for S_0 , and $\lambda^2 < 3 \times (M_{LQ}/300 \text{ GeV})^2$ for V_0) with λ being the leptoquark coupling strength. The e^+e^- experiments are sensitive to the indirect effects coming from t - and u -channel exchanges of leptoquarks in the $e^+e^- \rightarrow q\bar{q}$ process. The HERA experiments give bounds on the leptoquark-induced four-fermion interaction. For detailed bounds obtained in this way, see the Boson Particle Listings for “Indirect Limits for Leptoquarks” and its references.

Collider experiments provide direct limits on the leptoquark states through limits on the pair- and single-production cross sections. The leading-order cross sections of the parton processes

$$q + \bar{q} \rightarrow LQ + \overline{LQ}$$

$$g + g \rightarrow LQ + \overline{LQ}$$

See key on page 405

Gauge & Higgs Boson Particle Listings Heavy Bosons Other than Higgs Bosons

$$e + q \rightarrow LQ \quad (1)$$

may be written as [15]

$$\begin{aligned} \hat{\sigma}_{\text{LO}}[q\bar{q} \rightarrow LQ + \overline{LQ}] &= \frac{2\alpha_s^2\pi}{27\hat{s}}\beta^3, \\ \hat{\sigma}_{\text{LO}}[gg \rightarrow LQ + \overline{LQ}] &= \frac{\alpha_s^2\pi}{96\hat{s}} \\ &\times \left[\beta(41 - 31\beta^2) + (18\beta^2 - \beta^4 - 17) \log \frac{1+\beta}{1-\beta} \right], \\ \hat{\sigma}_{\text{LO}}[eq \rightarrow LQ] &= \frac{\pi\lambda^2}{4}\delta(\hat{s} - M_{LQ}^2) \end{aligned} \quad (2)$$

for a scalar leptoquark. Here $\sqrt{\hat{s}}$ is the invariant energy of the parton subprocess, and $\beta \equiv \sqrt{1 - 4M_{LQ}^2/\hat{s}}$. The leptoquark Yukawa coupling is given by λ . Leptoquarks are also produced singly at hadron colliders through $g + q \rightarrow LQ + \ell$ [16], which allows extending the collider reach in the leptoquark search [17], depending on the leptoquark Yukawa coupling.

The Tevatron and LEP experiments search for pair production of the leptoquark states, which arises from the leptoquark gauge interaction. The gauge couplings of a scalar leptoquark are determined uniquely according to its quantum numbers in Table 1. Since all of the leptoquark states belong to color-triplet representation, the scalar leptoquark pair-production cross section at Tevatron can be determined solely as a function of the leptoquark mass without making further assumptions. This is in contrast to the indirect or single-production limits, which give constraints in the leptoquark mass-coupling plane. For the first- and second-generation scalar leptoquark states with decaying branching fraction $B(eq) = 1$ and $B(\mu q) = 1$, the CDF and D0 experiments obtain the lower bounds on the leptoquark mass > 236 GeV (first generation, CDF) [18], > 256 GeV (first generation, D0) [19], > 226 GeV (second generation, CDF) [20], and > 251 GeV (second generation, D0) [21] at 95% CL. On the other hand, the magnetic-dipole-type and the electric-quadrupole-type interactions of a vector leptoquark are not determined even if we fix its gauge quantum numbers as listed in the Table [22]. The production of vector leptoquarks depends in general on additional assumptions that the leptoquark couplings and their pair-production cross sections are enhanced relative to the scalar leptoquark contributions. At the Tevatron for instance, since the acceptance for vector and scalar leptoquark detection is similar, limits on the vector leptoquark mass will be more stringent. The leptoquark pair-production cross sections in e^+e^- collisions depend on the leptoquark $SU(2) \times U(1)$ quantum numbers and Yukawa coupling with electron [23]. The OPAL experiment gives mass bounds on various leptoquark states from the pair-production cross sections [24]. For a second-generation weak-isosinglet weak-hypercharge $-4/3$ scalar-leptoquark state, for example, the OPAL pair-production bound is $M_{LQ} > 100$ GeV at 95% CL.

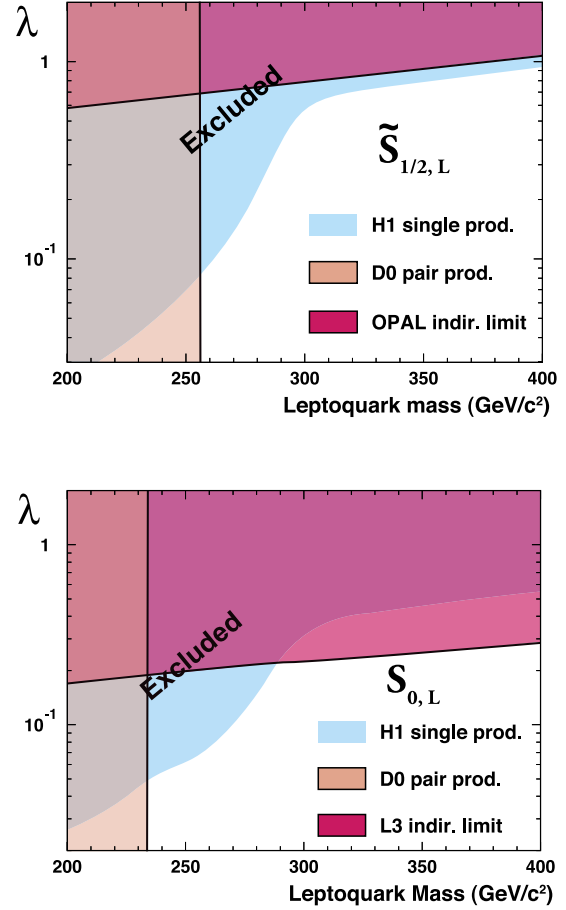


Figure 1: Limits on two typical first-generation scalar leptoquark states in the mass-coupling plane. The upper figure is for a weak-isodoublet, weak-hypercharge $7/6$, $3B + L = 0$ leptoquark state, while the lower figure for a weak-isosinglet, weak-hypercharge $-1/3$, $3B + L = 2$ state. Color version at end of book.

The searches for the leptoquark single production are performed by the HERA experiments. Since the leptoquark single-production cross section depends on the leptoquark Yukawa coupling, the leptoquark limits from HERA are usually displayed in the mass-coupling plane. For leptoquark Yukawa coupling $\lambda = 0.1$, the ZEUS bounds on the first-generation leptoquarks range from 248 to 290 GeV, depending on the leptoquark species [25]. Similar bounds are obtained by H1 [26]. The LEP experiments also search for the single production of the leptoquark states from the process $e\gamma \rightarrow LQ + q$.

Fig. 1 summarizes D0, LEP, and H1 limits on two typical first-generation scalar-leptoquark states in the mass-coupling plane [26].

The search for LQ will be continued soon at the CERN LHC. Preliminary feasibility studies by the LHC experiments ATLAS [27] and CMS [28] indicate that clear signals can be established for masses up to about $M(LQ) 1.3$ to 1.4 TeV for

Gauge & Higgs Boson Particle Listings

Heavy Bosons Other than Higgs Bosons

first- and second-generation scalar LQ, with a final reach of presumably 1.5 TeV.

Reference

1. W. Buchmüller, R. Rückl, and D. Wyler, Phys. Lett. **B191**, 442 (1987).
2. K. S. Babu, C. F. Kolda, and J. March-Russell, Phys. Lett. **B408**, 261 (1997).
3. J. L. Hewett and T. G. Rizzo, Phys. Rev. **D58**, 055005 (1998).
4. J.C. Pati and A. Salam, Phys. Rev. **D10**, 275 (1974).
5. H. Georgi and S.L. Glashow, Phys. Rev. Lett. **32**, 438 (1974).
6. H. Georgi, AIP Conf. Proc. **23**, 575 (1975);
H. Fritzsch and P. Minkowski, Ann. Phys. **93**, 193 (1975).
7. For a review, see, E. Farhi and L. Susskind, Phys. Reports **74**, 277 (1981).
8. K. Lane and M. Ramana, Phys. Rev. **D44**, 2678 (1991).
9. See, for example, B. Schrepf and F. Schrepf, Phys. Lett. **153B**, 101 (1985).
10. O. Shanker, Nucl. Phys. **B204**, 375, (1982).
11. U. Mahanta, Eur. Phys. J. **C21**, 171 (2001) [Phys. Lett. **B515**, 111 (2001)].
12. K. Cheung, Phys. Rev. **D64**, 033001 (2001).
13. S. Davidson, D.C. Bailey, and B.A. Campbell, Z. Phys. **C61**, 613 (1994).
14. M. Leurer, Phys. Rev. **D49**, 333 (1994);
Phys. Rev. **D50**, 536 (1994).
15. T. Plehn *et al.*, Z. Phys. **C74**, 611 (1997);
M. Kramer *et al.*, Phys. Rev. Lett. **79**, 341 (1997); and references therein.
16. J.L. Hewett and S. Pakvasa, Phys. Rev. **D37**, 3165 (1988);
O.J.P. Eboli and A.V. Olinto, Phys. Rev. **D38**, 3461 (1988);
A. Dobado, M.J. Herrero, and C. Muñoz, Phys. Lett. **207B**, 97 (1988);
V.D. Barger *et al.*, Phys. Lett. **B220**, 464 (1989);
M. De Montigny and L. Marleau, Phys. Rev. **D40**, 2869 (1989) [Erratum-*ibid.* **D56**, 3156 (1997)].
17. A. Belyaev *et al.*, JHEP **0509**, 005 (2005).
18. D. Acosta *et al.*, [CDF Collaboration], Phys. Rev. **D72**, 051107 (2005).
19. V.M. Abazov *et al.*, [D0 Collaboration], Phys. Rev. **D71**, 071104 (2005).
20. A. Abulencia *et al.*, [CDF Collaboration], Phys. Rev. **D73**, 051102 (2006).
21. V.M. Abazov *et al.*, [D0 Collaboration], Phys. Lett. **B636**, 183 (2006).
22. J. Blümlein, E. Boos, and A. Kryukov, Z. Phys. **C76**, 137 (1997).
23. J. Blümlein and R. Rückl, Phys. Lett. **B304**, 337 (1993).
24. G. Abbiendi *et al.*, [OPAL Collaboration], Eur. Phys. J. **C31**, 281 (2003).
25. S. Chekanov *et al.*, [ZEUS Collaboration], Phys. Rev. **D68**, 052004 (2003).
26. A. Aktas *et al.*, [H1 Collaboration], Phys. Lett. **B629**, 9 (2005).
27. V.A. Mitsou *et al.*, hep-ph/0411189.

28. S. Abdulin and F. Charles, Phys. Lett. **B464**, 223 (1999).

MASS LIMITS for Leptoquarks from Pair Production

These limits rely only on the color or electroweak charge of the leptoquark.

VALUE (GeV)	CL%	DOCUMENT ID	TECN	COMMENT
>316	95	161 ABAZOV	09 D0	Second generation
>299	95	162 ABAZOV	09AF D0	First generation
>229	95	163 ABAZOV	07J D0	Third generation
>226	95	164 ABULENCIA	06T CDF	Second generation
>236	95	165 ACOSTA	05P CDF	First generation
••• We do not use the following data for averages, fits, limits, etc. •••				
		166 AALTONEN	08P CDF	Third generation
>153	95	167 AALTONEN	08Z CDF	Third generation
>205	95	168 ABAZOV	08AD D0	All generations
>210	95	167 ABAZOV	08AN D0	Third generation
>251	95	169 ABAZOV	06A D0	Superseded by ABAZOV 09
>136	95	170 ABAZOV	06L D0	Superseded by ABAZOV 08AD
>256	95	171 ABAZOV	05H D0	First generation
>117	95	168 ACOSTA	05I CDF	First generation
> 99	95	172 ABBIENDI	03R OPAL	First generation
>100	95	172 ABBIENDI	03R OPAL	Second generation
> 98	95	172 ABBIENDI	03R OPAL	Third generation
> 98	95	173 ABAZOV	02 D0	All generations
>225	95	174 ABAZOV	01D D0	First generation
> 85.8	95	175 ABBIENDI	00M OPAL	Superseded by ABBIENDI 03R
> 85.5	95	175 ABBIENDI	00M OPAL	Superseded by ABBIENDI 03R
> 82.7	95	175 ABBIENDI	00M OPAL	Superseded by ABBIENDI 03R
>200	95	176 ABBOTT	00C D0	Second generation
>123	95	177 AFFOLDER	00K CDF	Second generation
>148	95	178 AFFOLDER	00K CDF	Third generation
>160	95	179 ABBOTT	99J D0	Second generation
>225	95	180 ABBOTT	98E D0	First generation
> 94	95	181 ABBOTT	98J D0	Third generation
>202	95	182 ABE	98S CDF	Second generation
>242	95	183 GROSS-PILCH.	98	First generation
> 99	95	184 ABE	97F CDF	Third generation
>213	95	185 ABE	97X CDF	First generation
> 45.5	95	186,187 ABREU	93J DLPH	First + second generation
> 44.4	95	188 ADRIANI	93M L3	First generation
> 44.5	95	188 ADRIANI	93M L3	Second generation
> 45	95	188 DECAMP	92 ALEP	Third generation
none 8.9–22.6	95	189 KIM	90 AMY	First generation
none 10.2–23.2	95	189 KIM	90 AMY	Second generation
none 5–20.8	95	190 BARTEL	87B JADE	
none 7–20.5	95	191 BEHREND	86B CELL	
161 ABAZOV 09 search for scalar leptoquarks using $\mu\mu jj$ and $\mu\nu jj$ events in $p\bar{p}$ collisions at $E_{cm} = 1.96$ TeV. The limit above assumes $B(\mu q) = 1$. For $B(\mu q) = 0.5$, the limit becomes 270 GeV.				
162 ABAZOV 09AF search for scalar leptoquarks using $e\bar{e} jj$ and $e\nu jj$ events in $p\bar{p}$ collisions at $E_{cm} = 1.96$ TeV. The limit above assumes $B(e q) = 1$. For $B(e q) = 0.5$ the bound becomes 284 GeV.				
163 ABAZOV 07J search for pair productions of scalar leptoquark state decaying to νb in $p\bar{p}$ collisions at $E_{cm} = 1.96$ TeV. The limit above assumes $B(\nu b) = 1$.				
164 ABULENCIA 06T search for scalar leptoquarks using $\mu\mu jj$, $\mu\nu jj$, and $\nu\nu jj$ events in $p\bar{p}$ collisions at $E_{cm} = 1.96$ TeV. The quoted limit assumes $B(\mu q) = 1$. For $B(\mu q) = 0.5$ or 0.1, the bound becomes 208 GeV or 143 GeV, respectively. See their Fig. 4 for the exclusion limit as a function of $B(\mu q)$.				
165 ACOSTA 05P search for scalar leptoquarks using $e\bar{e} jj$, $e\nu jj$ events in $p\bar{p}$ collisions at $E_{cm} = 1.96$ TeV. The limit above assumes $B(e q) = 1$. For $B(e q) = 0.5$ and 0.1, the bound becomes 205 GeV and 145 GeV, respectively.				
166 AALTONEN 08P search for vector leptoquarks using $\tau^+\tau^- b\bar{b}$ events in $p\bar{p}$ collisions at $E_{cm} = 1.96$ TeV. Assuming Yang-Mills (minimal) couplings, the mass limit is >317 GeV (251 GeV) at 95% CL for $B(\tau b) = 1$.				
167 Search for pair production of scalar leptoquark state decaying to τb in $p\bar{p}$ collisions at $E_{cm} = 1.96$ TeV. The limit above assumes $B(\tau b) = 1$.				
168 Search for scalar leptoquarks using $\nu\nu jj$ events in $p\bar{p}$ collisions at $E_{cm} = 1.96$ TeV. The limit above assumes $B(\nu q) = 1$.				
169 ABAZOV 06A search for scalar leptoquarks using $\mu\mu jj$ events in $p\bar{p}$ collisions at $E_{cm} = 1.8$ TeV and at 1.96 TeV. The limit above assumes $B(\mu q) = 1$. For $B(\mu q) = 0.5$ and 0.1, the limit becomes 204 GeV.				
170 ABAZOV 06L search for scalar leptoquarks using $\nu\nu jj$ events in $p\bar{p}$ collisions at $E_{cm} = 1.8$ TeV and at 1.96 TeV. The limit above assumes $B(\nu q) = 1$.				
171 ABAZOV 05H search for scalar leptoquarks using $e\bar{e} jj$ and $e\nu jj$ events in $p\bar{p}$ collisions at $E_{cm} = 1.8$ TeV and 1.96 TeV. The limit above assumes $B(e q) = 1$. For $B(e q) = 0.5$ the bound becomes 234 GeV.				
172 ABBIENDI 03R search for scalar/vector leptoquarks in e^+e^- collisions at $\sqrt{s} = 189$ –209 GeV. The quoted limits are for charge $-4/3$ isospin 0 scalar-leptoquark with $B(\ell q) = 1$. See their table 12 for other cases.				
173 ABAZOV 02 search for scalar leptoquarks using $\nu\nu jj$ events in $p\bar{p}$ collisions at $E_{cm} = 1.8$ TeV. The bound holds for all leptoquark generations. Vector leptoquarks are likewise constrained to lie above 200 GeV.				
174 ABAZOV 01D search for scalar leptoquarks using $e\nu jj$, $e\bar{e} jj$, and $\nu\nu jj$ events in $p\bar{p}$ collisions at $E_{cm} = 1.8$ TeV. The limit above assumes $B(e q) = 1$. For $B(e q) = 0.5$ and 0, the bound becomes 204 and 79 GeV, respectively. Bounds for vector leptoquarks are also given. Supersedes ABBOTT 98E.				
175 ABBIENDI 00M search for scalar/vector leptoquarks in e^+e^- collisions at $\sqrt{s} = 183$ GeV. The quoted limits are for charge $-4/3$ isospin 0 scalar-leptoquarks with $B(\ell q) = 1$. See their Table 8 and Figs. 6–9 for other cases.				
176 ABBOTT 00C search for scalar leptoquarks using $\mu\mu jj$, $\mu\nu jj$, and $\nu\nu jj$ events in $p\bar{p}$ collisions at $E_{cm} = 1.8$ TeV. The limit above assumes $B(\mu q) = 1$. For $B(\mu q) = 0.5$ and 0,				

See key on page 405

Gauge & Higgs Boson Particle Listings

Heavy Bosons Other than Higgs Bosons

- the bound becomes 180 and 79 GeV respectively. Bounds for vector leptoquarks are also given.
- 177 AFFOLDER 00k search for scalar leptoquark using $\nu\nu cc$ events in $p\bar{p}$ collisions at $E_{cm}=1.8$ TeV. The quoted limit assumes $B(\nu c)=1$. Bounds for vector leptoquarks are also given.
- 178 AFFOLDER 00k search for scalar leptoquark using $\nu\nu bb$ events in $p\bar{p}$ collisions at $E_{cm}=1.8$ TeV. The quoted limit assumes $B(\nu b)=1$. Bounds for vector leptoquarks are also given.
- 179 ABBOTT 99j search for leptoquarks using $\mu\nu jj$ events in $p\bar{p}$ collisions at $E_{cm}=1.8$ TeV. The quoted limit is for a scalar leptoquark with $B(\mu q)=B(\nu q)=0.5$. Limits on vector leptoquarks range from 240 to 290 GeV.
- 180 ABBOTT 98E search for scalar leptoquarks using $e\nu jj$, $e\bar{e}jj$, and $\nu\nu jj$ events in $p\bar{p}$ collisions at $E_{cm}=1.8$ TeV. The limit above assumes $B(eq)=1$. For $B(eq)=0.5$ and 0, the bound becomes 204 and 79 GeV, respectively.
- 181 ABBOTT 98j search for charge $-1/3$ third generation scalar and vector leptoquarks in $p\bar{p}$ collisions at $E_{cm}=1.8$ TeV. The quoted limit is for scalar leptoquark with $B(\nu b)=1$.
- 182 ABE 98s search for scalar leptoquarks using $\mu\nu jj$ events in $p\bar{p}$ collisions at $E_{cm}=1.8$ TeV. The limit is for $B(\mu q)=1$. For $B(\mu q)=B(\nu q)=0.5$, the limit is >160 GeV.
- 183 GROSS-PILCHER 98 is the combined limit of the CDF and DØ Collaborations as determined by a joint CDF/DØ working group and reported in this FNAL Technical Memo. Original data published in ABE 97x and ABBOTT 98E.
- 184 ABE 97f search for third generation scalar and vector leptoquarks in $p\bar{p}$ collisions at $E_{cm}=1.8$ TeV. The quoted limit is for scalar leptoquark with $B(\tau b)=1$.
- 185 ABE 97x search for scalar leptoquarks using $e\bar{e}jj$ events in $p\bar{p}$ collisions at $E_{cm}=1.8$ TeV. The limit is for $B(eq)=1$.
- 186 Limit is for charge $-1/3$ isospin-0 leptoquark with $B(\ell q)=2/3$.
- 187 First and second generation leptoquarks are assumed to be degenerate. The limit is slightly lower for each generation.
- 188 Limits are for charge $-1/3$, isospin-0 scalar leptoquarks decaying to $\ell^- q$ or νq with any branching ratio. See paper for limits for other charge-isospin assignments of leptoquarks.
- 189 KIM 90 assume pair production of charge 2/3 scalar-leptoquark via photon exchange. The decay of the first (second) generation leptoquark is assumed to be any mixture of $d e^+$ and $u \bar{\nu}$ ($s \mu^+$ and $c \bar{\nu}$). See paper for limits for specific branching ratios.
- 190 BARTEL 87B limit is valid when a pair of charge 2/3 spinless leptoquarks X is produced with point coupling, and when they decay under the constraint $B(X \rightarrow c \bar{\nu}_\mu) + B(X \rightarrow s \mu^+) = 1$.
- 191 BEHREND 86B assumed that a charge 2/3 spinless leptoquark, χ , decays either into $s \mu^+$ or $c \bar{\nu}$: $B(\chi \rightarrow s \mu^+) + B(\chi \rightarrow c \bar{\nu}) = 1$.

MASS LIMITS for Leptoquarks from Single Production

These limits depend on the q - ℓ -leptoquark coupling g_{LQ} . It is often assumed that $g_{LQ}^2/4\pi=1/137$. Limits shown are for a scalar, weak isoscalar, charge $-1/3$ leptoquark.

VALUE (GeV)	CL%	DOCUMENT ID	TECN	COMMENT
>298	95	192 CHEKANOV	03B ZEUS	First generation
> 73	95	193 ABREU	93J DLPH	Second generation
••• We do not use the following data for averages, fits, limits, etc. •••				
>295	95	194 ABAZOV	07E D0	Second generation
		195 AKTAS	05B H1	First generation
		196 CHEKANOV	05A ZEUS	Lepton-flavor violation
>197	95	197 ABBIENDI	02B OPAL	First generation
		198 CHEKANOV	02 ZEUS	Repl. by CHEKANOV 05A
>290	95	199 ADLOFF	01C H1	First generation
>204	95	200 BREITWEG	01 ZEUS	First generation
		201 BREITWEG	00E ZEUS	First generation
>161	95	202 ABREU	99G DLPH	First generation
>200	95	203 ADLOFF	99 H1	First generation
		204 DERRICK	97 ZEUS	Lepton-flavor violation
>168	95	205 DERRICK	93 ZEUS	First generation
192 CHEKANOV 03B limit is for a scalar, weak isoscalar, charge $-1/3$ leptoquark coupled with $e\bar{\nu}$. See their Figs. 11–12 and Table 5 for limits on states with different quantum numbers.				
193 Limit from single production in Z decay. The limit is for a leptoquark coupling of electromagnetic strength and assumes $B(\ell q)=2/3$. The limit is 77 GeV if first and second leptoquarks are degenerate.				
194 ABAZOV 07E search for leptoquark single production through $q\bar{q}$ fusion process in $p\bar{p}$ collisions. See their Fig. 4 for exclusion plot in mass-coupling plane.				
195 AKTAS 05B limit is for a scalar, weak isoscalar, charge $-1/3$ leptoquark coupled with $e\bar{\nu}$. See their Fig. 3 for limits on states with different quantum numbers.				
196 CHEKANOV 05 search for various leptoquarks with lepton-flavor violating couplings. See their Figs. 6–10 and Tables 1–8 for detailed limits.				
197 For limits on states with different quantum numbers and the limits in the mass-coupling plane, see their Fig. 4 and Fig. 5.				
198 CHEKANOV 02 search for various leptoquarks with lepton-flavor violating couplings. See their Figs. 6–7 and Tables 5–6 for detailed limits.				
199 For limits on states with different quantum numbers and the limits in the mass-coupling plane, see their Fig. 3.				
200 See their Fig. 14 for limits in the mass-coupling plane.				
201 BREITWEG 00E search for $F=0$ leptoquarks in e^+p collisions. For limits in mass-coupling plane, see their Fig. 11.				
202 ABREU 99G limit obtained from process $e\gamma \rightarrow LQ+q$. For limits on vector and scalar states with different quantum numbers and the limits in the coupling-mass plane, see their Fig. 4 and Table 2.				
203 For limits on states with different quantum numbers and the limits in the mass-coupling plane, see their Fig. 13 and Fig. 14. ADLOFF 99 also search for leptoquarks with lepton-flavor violating couplings. ADLOFF 99 supersedes AID 96B.				
204 DERRICK 97 search for various leptoquarks with lepton-flavor violating couplings. See their Figs. 5–8 and Table 1 for detailed limits.				
205 DERRICK 93 search for single leptoquark production in $e p$ collisions with the decay $e q$ and νq . The limit is for leptoquark coupling of electromagnetic strength and assumes				

$B(eq)=B(\nu q)=1/2$. The limit for $B(eq)=1$ is 176 GeV. For limits on states with different quantum numbers, see their Table 3.

Indirect Limits for Leptoquarks

VALUE (TeV)	CL%	DOCUMENT ID	TECN	COMMENT
••• We do not use the following data for averages, fits, limits, etc. •••				
>	0.49	206 AKTAS	07A H1	Lepton-flavor violation
		207 SCHAEEL	07A ALEP	$e^+ e^- \rightarrow q\bar{q}$
		208 SMIRNOV	07 RVUE	$K \rightarrow e\mu, B \rightarrow e\tau$
		209 CHEKANOV	05A ZEUS	Lepton-flavor violation
>	1.7	210 ADLOFF	03 H1	First generation
>	46	211 CHANG	03 BELL	Pati-Salam type
		212 CHEKANOV	02 ZEUS	Repl. by CHEKANOV 05A
		213 CHEUNG	01B RVUE	First generation
>	1.7	214 ACCIARRI	00P L3	$e^+ e^- \rightarrow q\bar{q}$
>	0.39	215 ADLOFF	00 H1	First generation
>	1.5	216 BARATE	00I ALEP	Repl. by SCHAEEL 07A
>	0.2	217 BARGER	00 RVUE	Cs
		218 GABRIELLI	00 RVUE	Lepton flavor violation
>	0.74	219 ZARNECKI	00 RVUE	S_1 leptoquark
		220 ABBIENDI	99 OPAL	
		221 ABE	98V CDF	$B_s \rightarrow e^\pm \mu^\mp$, Pati-Salam type
		222 ACCIARRI	98J L3	$e^+ e^- \rightarrow q\bar{q}$
		223 ACKERSTAFF	98V OPAL	$e^+ e^- \rightarrow q\bar{q}, e^+ e^- \rightarrow b\bar{b}$
>	0.76	224 DEANDREA	97 RVUE	\bar{R}_2 leptoquark
		225 DERRICK	97 ZEUS	Lepton-flavor violation
		226 GROSSMAN	97 RVUE	$B \rightarrow \tau^+ \tau^- (X)$
		227 JADACH	97 RVUE	$e^+ e^- \rightarrow q\bar{q}$
>1200		228 KUZNETSOV	95B RVUE	Pati-Salam type
		229 MIZUKOSHI	95 RVUE	Third generation scalar leptoquark
>	0.3	230 BHATTACH...	94 RVUE	Spin-0 leptoquark coupled to $\bar{\nu}_R t_L$
		231 DAVIDSON	94 RVUE	
>	18	232 KUZNETSOV	94 RVUE	Pati-Salam type
>	0.43	233 LEURER	94 RVUE	First generation spin-1 leptoquark
>	0.44	233 LEURER	94B RVUE	First generation spin-0 leptoquark
		234 MAHANTA	94 RVUE	P and T violation
>	1	235 SHANKER	82 RVUE	Nonchiral spin-0 leptoquark
>	125	235 SHANKER	82 RVUE	Nonchiral spin-1 leptoquark
206 AKTAS 07A search for lepton-flavor violation in $e p$ collision. See their Tables 4–7 for limits on lepton-flavor violating four-fermion interactions induced by various leptoquarks.				
207 SCHAEEL 07A limit is for the weak-isoscalar spin-0 left-handed leptoquark with the coupling of electromagnetic strength. For the limits of leptoquarks with different quantum numbers, see their Table 35.				
208 SMIRNOV 07 obtains mass limits for the vector and scalar chiral leptoquark states from $K \rightarrow e\mu, B \rightarrow e\tau$ decays.				
209 CHEKANOV 05 search for various leptoquarks with lepton-flavor violating couplings. See their Figs. 6–10 and Tables 1–8 for detailed limits.				
210 ADLOFF 03 limit is for the weak isotriplet spin-0 leptoquark at strong coupling $\lambda=\sqrt{4\pi}$. For the limits of leptoquarks with different quantum numbers, see their Table 3. Limits are derived from bounds on $e^\pm q$ contact interactions.				
211 The bound is derived from $B(B^0 \rightarrow e^\pm \mu^\mp) < 1.7 \times 10^{-7}$.				
212 CHEKANOV 02 search for lepton-flavor violation in $e p$ collisions. See their Tables 1–4 for limits on lepton-flavor violating and four-fermion interactions induced by various leptoquarks.				
213 CHEUNG 01B quoted limit is for a scalar, weak isoscalar, charge $-1/3$ leptoquark with a coupling of electromagnetic strength. The limit is derived from bounds on contact interactions in a global electroweak analysis. For the limits of leptoquarks with different quantum numbers, see Table 5.				
214 ACCIARRI 00P limit is for the weak isoscalar spin-0 leptoquark with the coupling of electromagnetic strength. For the limits of leptoquarks with different quantum numbers, see their Table 4.				
215 ADLOFF 00 limit is for the weak isotriplet spin-0 leptoquark at strong coupling, $\lambda=\sqrt{4\pi}$. For the limits of leptoquarks with different quantum numbers, see their Table 2.				
ADLOFF 00 limits are from the Q^2 spectrum measurement of $e^+ p \rightarrow e^+ X$.				
216 BARATE 00i search for deviations in cross section and jet-charge asymmetry in $e^+ e^- \rightarrow \bar{q}q$ due to t -channel exchange of a leptoquark at $\sqrt{s}=130$ to 183 GeV. Limits for other scalar and vector leptoquarks are also given in their Table 22.				
217 BARGER 00 explain the deviation of atomic parity violation in cesium atoms from prediction is explained by scalar leptoquark exchange.				
218 GABRIELLI 00 calculate various process with lepton flavor violation in leptoquark models.				
219 ZARNECKI 00 limit is derived from data of HERA, LEP, and Tevatron and from various low-energy data including atomic parity violation. Leptoquark coupling with electromagnetic strength is assumed.				
220 ABBIENDI 99 limits are from $e^+ e^- \rightarrow q\bar{q}$ cross section at 130–136, 161–172, 183 GeV. See their Fig. 8 and Fig. 9 for limits in mass-coupling plane.				
221 ABE 98v quoted limit is from $B(B_s \rightarrow e^\pm \mu^\mp) < 8.2 \times 10^{-6}$. ABE 98v also obtain a similar limit on $M_{LQ} > 20.4$ TeV from $B(B_d \rightarrow e^\pm \mu^\mp) < 4.5 \times 10^{-6}$. Both bounds assume the non-canonical association of the b quark with electrons or muons under SU(4).				
222 ACCIARRI 98J limit is from $e^+ e^- \rightarrow q\bar{q}$ cross section at $\sqrt{s}=130$ –172 GeV which can be affected by the t - and u -channel exchanges of leptoquarks. See their Fig. 4 and Fig. 5 for limits in the mass-coupling plane.				
223 ACKERSTAFF 98V limits are from $e^+ e^- \rightarrow q\bar{q}$ and $e^+ e^- \rightarrow b\bar{b}$ cross sections at $\sqrt{s}=130$ –172 GeV, which can be affected by the t - and u -channel exchanges of leptoquarks. See their Fig. 21 and Fig. 22 for limits of leptoquarks in mass-coupling plane.				
224 DEANDREA 97 limit is for \bar{R}_2 leptoquark obtained from atomic parity violation (APV). The coupling of leptoquark is assumed to be electromagnetic strength. See Table 2 for limits of the four-fermion interactions induced by various scalar leptoquark exchange. DEANDREA 97 combines APV limit and limits from Tevatron and HERA. See Fig. 1–4 for combined limits of leptoquark in mass-coupling plane.				

Gauge & Higgs Boson Particle Listings

Heavy Bosons Other than Higgs Bosons

- 225 DERRICK 97 search for lepton-flavor violation in ep collision. See their Tables 2–5 for limits on lepton-flavor violating four-fermion interactions induced by various leptoquarks.
- 226 GROSSMAN 97 estimate the upper bounds on the branching fraction $B \rightarrow \tau^+ \tau^- (X)$ from the absence of the B decay with large missing energy. These bounds can be used to constrain leptoquark induced four-fermion interactions.
- 227 JADACH 97 limit is from $e^+ e^- \rightarrow q\bar{q}$ cross section at $\sqrt{s}=172.3$ GeV which can be affected by the t - and u -channel exchanges of leptoquarks. See their Fig. 1 for limits on vector leptoquarks in mass-coupling plane.
- 228 KUZNETSOV 95b use π, K, B, τ decays and μe conversion and give a list of bounds on the leptoquark mass and the fermion mixing matrix in the Pati-Salam model. The quoted limit is from $K_L \rightarrow \mu e$ decay assuming zero mixing.
- 229 MIZUKOSHI 95 calculate the one-loop radiative correction to the Z-physics parameters in various scalar leptoquark models. See their Fig. 4 for the exclusion plot of third generation leptoquark models in mass-coupling plane.
- 230 BHATTACHARYYA 94 limit is from one-loop radiative correction to the leptonic decay width of the Z. $m_H=250$ GeV, $\alpha_s(m_Z)=0.12$, $m_t=180$ GeV, and the electroweak strength of leptoquark coupling are assumed. For leptoquark coupled to $\bar{e}_L, \bar{\mu}_L, \bar{\tau}_L$, and $\bar{\nu}_\tau$, see Fig. 2 in BHATTACHARYYA 94b erratum and Fig. 3.
- 231 DAVIDSON 94 gives an extensive list of the bounds on leptoquark-induced four-fermion interactions from π, K, D, B, μ, τ decays and meson mixings, etc. See Table 15 of DAVIDSON 94 for detail.
- 232 KUZNETSOV 94 gives mixing independent bound of the Pati-Salam leptoquark from the cosmological limit on $\pi^0 \rightarrow \bar{\nu}\nu$.
- 233 LEURER 94, LEURER 94b limits are obtained from atomic parity violation and apply to any chiral leptoquark which couples to the first generation with electromagnetic strength. For a nonchiral leptoquark, universality in π_{e2} decay provides a much more stringent bound.
- 234 MAHANTA 94 gives bounds of P - and T -violating scalar-leptoquark couplings from atomic and molecular experiments.
- 235 From $(\pi \rightarrow e\nu)/(\pi \rightarrow \mu\nu)$ ratio. SHANKER 82 assumes the leptoquark induced four-fermion coupling $4g^2/M^2 (\bar{\nu}_{eL} u_R) (\bar{d}_L e_R)$ with $g=0.004$ for spin-0 leptoquark and $g^2/M^2 (\bar{\nu}_{eL} \gamma_\mu u_L) (\bar{d}_R \gamma^\mu e_R)$ with $g \approx 0.6$ for spin-1 leptoquark.

MASS LIMITS for Diquarks

VALUE (GeV)	CL%	DOCUMENT ID	TECN	COMMENT
none 290–630	95	236 AALTONEN	09AC CDF	E_6 diquark
none 290–420	95	237 ABE	97G CDF	E_6 diquark
none 15–31.7	95	238 ABREU	94D DLPH SUSY	E_6 diquark
236 AALTONEN 09AC				search for new narrow resonance decaying to dijets.
237 ABE 97G				search for new particle decaying to dijets.
238 ABREU 94D				limit is from $e^+ e^- \rightarrow \tau^+ \tau^- c$. Range extends up to 43 GeV if diquarks are degenerate in mass.

MASS LIMITS for g_A (axigluon)

Axigluons are massive color-octet gauge bosons in chiral color models and have axial-vector coupling to quarks with the same coupling strength as gluons.

VALUE (GeV)	CL%	DOCUMENT ID	TECN	COMMENT
none 260–1250	95	239 AALTONEN	09AC CDF	$p\bar{p} \rightarrow g_A X, g_A \rightarrow 2$ jets
>910	95	240 CHOUDHURY	07 RVUE	$p\bar{p} \rightarrow t\bar{t} X$
>365	95	241 DONCHESKI	98 RVUE	$\Gamma(Z \rightarrow \text{hadron})$
none 200–980	95	242 ABE	97G CDF	$p\bar{p} \rightarrow g_A X, g_A \rightarrow 2$ jets
none 200–870	95	243 ABE	95N CDF	$p\bar{p} \rightarrow g_A X, g_A \rightarrow q\bar{q}$
none 240–640	95	244 ABE	93G CDF	$p\bar{p} \rightarrow g_A X, g_A \rightarrow 2$ jets
> 50	95	245 CUYPERS	91 RVUE	$\sigma(e^+ e^- \rightarrow \text{hadrons})$
none 120–210	95	246 ABE	90H CDF	$p\bar{p} \rightarrow g_A X, g_A \rightarrow 2$ jets
> 29	95	247 ROBINETT	89 THEO	Partial-wave unitarity
none 150–310	95	248 ALBAJAR	88B UA1	$p\bar{p} \rightarrow g_A X, g_A \rightarrow 2$ jets
> 20		BERGSTROM	88 RVUE	$p\bar{p} \rightarrow \gamma X$ via $g_A g$
> 9		CUYPERS	88 RVUE	τ decay
> 25		DONCHESKI	88B RVUE	τ decay
239 AALTONEN 09AC				search for new narrow resonance decaying to dijets.
240 CHOUDHURY 07				limit is from the $t\bar{t}$ production cross section measured at CDF.
241 DONCHESKI 98				compare α_s derived from low-energy data and that from $\Gamma(Z \rightarrow \text{hadrons})/\Gamma(Z \rightarrow \text{leptons})$.
242 ABE 97G				search for new particle decaying to dijets.
243 ABE 95N				assume axigluons decaying to quarks in the Standard Model only.
244 ABE 93G				assume $\Gamma(g_A) = N\alpha_s m_{g_A}/6$ with $N = 10$.
245 CUYPERS 91				compare α_s measured in τ decay and that from R at PEP/PETRA energies.
246 ABE 90H				assumes $\Gamma(g_A) = N\alpha_s m_{g_A}/6$ with $N = 5$ ($\Gamma(g_A) = 0.09 m_{g_A}$). For $N = 10$, the excluded region is reduced to 120–150 GeV.
247 ROBINETT 89				result demands partial-wave unitarity of $J = 0$ $t\bar{t} \rightarrow t\bar{t}$ scattering amplitude and derives a limit $m_{g_A} > 0.5 m_t$. Assumes $m_t > 56$ GeV.
248 ALBAJAR 88B				result is from the nonobservation of a peak in two-jet invariant mass distribution. $\Gamma(g_A) < 0.4 m_{g_A}$ assumed. See also BAGGER 88.
249 CUYPERS 88				requires $\Gamma(\tau \rightarrow g g_A) < \Gamma(\tau \rightarrow g g g)$. A similar result is obtained by DONCHESKI 88.
250 DONCHESKI 88B				requires $\Gamma(\tau \rightarrow g q\bar{q})/\Gamma(\tau \rightarrow g g g) < 0.25$, where the former decay proceeds via axigluon exchange. A more conservative estimate of < 0.5 leads to $m_{g_A} > 21$ GeV.

X^0 (Heavy Boson) Searches in Z Decays

Searches for radiative transition of Z to a lighter spin-0 state X^0 decaying to hadrons, a lepton pair, a photon pair, or invisible particles as shown in the comments. The limits are for the product of branching ratios.

VALUE	CL%	DOCUMENT ID	TECN	COMMENT
•••				We do not use the following data for averages, fits, limits, etc. •••
251 BARATE	98U	ALEP	$X^0 \rightarrow \ell\bar{\ell}, q\bar{q}, gg, \gamma\gamma, \nu\bar{\nu}$	
252 ACCIARRI	97Q	L3	$X^0 \rightarrow$ invisible particle(s)	
253 ACTON	93E	OPAL	$X^0 \rightarrow \gamma\gamma$	
254 ABREU	92D	DLPH	$X^0 \rightarrow$ hadrons	
255 ADRIANI	92F	L3	$X^0 \rightarrow$ hadrons	
256 ACTON	91B	OPAL	$X^0 \rightarrow$ anything	
$< 1.1 \times 10^{-4}$	95	257 ACTON	91B	OPAL $X^0 \rightarrow e^+ e^-$
$< 9 \times 10^{-5}$	95	257 ACTON	91B	OPAL $X^0 \rightarrow \mu^+ \mu^-$
$< 1.1 \times 10^{-4}$	95	257 ACTON	91B	OPAL $X^0 \rightarrow \tau^+ \tau^-$
$< 2.8 \times 10^{-4}$	95	258 ADEVA	91D	L3 $X^0 \rightarrow e^+ e^-$
$< 2.3 \times 10^{-4}$	95	258 ADEVA	91D	L3 $X^0 \rightarrow \mu^+ \mu^-$
$< 4.7 \times 10^{-4}$	95	259 ADEVA	91D	L3 $X^0 \rightarrow$ hadrons
$< 8 \times 10^{-4}$	95	260 AKRAWY	90J	OPAL $X^0 \rightarrow$ hadrons
251 BARATE 98U				obtain limits on $B(Z \rightarrow \gamma X^0)B(X^0 \rightarrow \ell\bar{\ell}, q\bar{q}, gg, \gamma\gamma, \nu\bar{\nu})$. See their Fig. 17.
252		ACCIARRI 97Q		See Fig. 4 of ACCIARRI 97Q for the upper limit on $B(Z \rightarrow \gamma X^0; E_\gamma > E_{\min})$ as a function of E_{\min} .
253 ACTON 93E				give $\sigma(e^+ e^- \rightarrow X^0 \gamma) \cdot B(X^0 \rightarrow \gamma\gamma) < 0.4$ pb (95%CL) for $m_{X^0}=60 \pm 2.5$ GeV. If the process occurs via s-channel γ exchange, the limit translates to $\Gamma(X^0) \cdot B(X^0 \rightarrow \gamma\gamma)^2 < 20$ MeV for $m_{X^0} = 60 \pm 1$ GeV.
254 ABREU 92D				give $\sigma_Z \cdot B(Z \rightarrow \gamma X^0) \cdot B(X^0 \rightarrow \text{hadrons}) < (3-10)$ pb for $m_{X^0} = 10-78$ GeV. A very similar limit is obtained for spin-1 X^0 .
255 ADRIANI 92F				search for isolated γ in hadronic Z decays. The limit $\sigma_Z \cdot B(Z \rightarrow \gamma X^0) \cdot B(X^0 \rightarrow \text{hadrons}) < (2-10)$ pb (95%CL) is given for $m_{X^0} = 25-85$ GeV.
256 ACTON 91				searches for $Z \rightarrow Z^* X^0, Z^* \rightarrow e^+ e^-, \mu^+ \mu^-$, or $\nu\bar{\nu}$. Excludes any new scalar X^0 with $m_{X^0} < 9.5$ GeV/c if it has the same coupling to ZZ^* as the MSM Higgs boson.
257 ACTON 91B				limits are for $m_{X^0} = 60-85$ GeV.
258 ADEVA 91D				limits are for $m_{X^0} = 30-89$ GeV.
259 ADEVA 91D				limits are for $m_{X^0} = 30-86$ GeV.
260 AKRAWY 90J				give $\Gamma(Z \rightarrow \gamma X^0) \cdot B(X^0 \rightarrow \text{hadrons}) < 1.9$ MeV (95%CL) for $m_{X^0} = 32-80$ GeV. We divide by $\Gamma(Z) = 2.5$ GeV to get product of branching ratios. For nonresonant transitions, the limit is $B(Z \rightarrow \gamma q\bar{q}) < 8.2$ MeV assuming three-body phase space distribution.

MASS LIMITS for a Heavy Neutral Boson Coupling to $e^+ e^-$

VALUE (GeV)	CL%	DOCUMENT ID	TECN	COMMENT
•••				We do not use the following data for averages, fits, limits, etc. •••
none 55–61		261 ODAKA	89 VNS	$\Gamma(X^0 \rightarrow e^+ e^-) \cdot B(X^0 \rightarrow \text{had.}) \gtrsim 0.2$ MeV
>45	95	262 DERRICK	86 HRS	$\Gamma(X^0 \rightarrow e^+ e^-) = 6$ MeV
>46.6	95	263 ADEVA	85 MRKJ	$\Gamma(X^0 \rightarrow e^+ e^-) = 10$ keV
>48	95	263 ADEVA	85 MRKJ	$\Gamma(X^0 \rightarrow e^+ e^-) = 4$ MeV
		264 BERGER	85B PLUT	
none 39.8–45.5		265 ADEVA	84 MRKJ	$\Gamma(X^0 \rightarrow e^+ e^-) = 10$ keV
>47.8	95	265 ADEVA	84 MRKJ	$\Gamma(X^0 \rightarrow e^+ e^-) = 4$ MeV
none 39.8–45.2		265 BEHREND	84C CELL	
>47	95	265 BEHREND	84C CELL	$\Gamma(X^0 \rightarrow e^+ e^-) = 4$ MeV
261 ODAKA 89				looked for a narrow or wide scalar resonance in $e^+ e^- \rightarrow \text{hadrons}$ at $E_{\text{cm}} = 55.0-60.8$ GeV.
262 DERRICK 86				found no deviation from the Standard Model Bhabha scattering at $E_{\text{cm}} = 29$ GeV and set limits on the possible scalar boson $e^+ e^-$ coupling. See their figure 4 for excluded region in the $\Gamma(X^0 \rightarrow e^+ e^-) \cdot m_{X^0}$ plane. Electronic chiral invariance requires a parity doublet of X^0 , in which case the limit applies for $\Gamma(X^0 \rightarrow e^+ e^-) = 3$ MeV.
263 ADEVA 85				first limit is from $2\gamma, \mu^+ \mu^-,$ hadrons assuming X^0 is a scalar. Second limit is from $e^+ e^-$ channel. $E_{\text{cm}} = 40-47$ GeV. Supersedes ADEVA 84.
264 BERGER 85B				looked for effect of spin-0 boson exchange in $e^+ e^- \rightarrow e^+ e^-$ and $\mu^+ \mu^-$ at $E_{\text{cm}} = 34.7$ GeV. See Fig. 5 for excluded region in the $m_{X^0} - \Gamma(X^0)$ plane.
265 ADEVA 84 and BEHREND 84C				have $E_{\text{cm}} = 39.8-45.5$ GeV. MARK-J searched X^0 in $e^+ e^- \rightarrow \text{hadrons}, 2\gamma, \mu^+ \mu^-, e^+ e^-$ and CELLO in the same channels plus τ pair. No narrow or broad X^0 is found in the energy range. They also searched for the effect of X^0 with $m_X > E_{\text{cm}}$. The second limits are from Bhabha data and for spin-0 singlet. The same limits apply for $\Gamma(X^0 \rightarrow e^+ e^-) = 2$ MeV if X^0 is a spin-0 doublet. The second limit of BEHREND 84C was read off from their figure 2. The original papers also list limits in other channels.

Search for X^0 Resonance in $e^+ e^-$ Collisions

The limit is for $\Gamma(X^0 \rightarrow e^+ e^-) \cdot B(X^0 \rightarrow f)$, where f is the specified final state. Spin 0 is assumed for X^0 .

VALUE (keV)	CL%	DOCUMENT ID	TECN	COMMENT
•••				We do not use the following data for averages, fits, limits, etc. •••

Gauge & Higgs Boson Particle Listings

Heavy Bosons Other than Higgs Bosons, Axions (A^0) and Other Very Light Bosons

RIZZO	00	PR D61 016007	T. G. Rizzo, J.D. Wells
ROSNER	00	PR D61 016006	J.L. Rosner
ZARNECKI	00	EPJ C17 695	A. Zarnecki
ABBIENDI	99	EPJ C6 1	G. Abbiendi et al. (OPAL Collab.)
ABBOTT	99J	PRL 83 2896	B. Abbott et al. (DO Collab.)
ABREU	99G	PL B446 62	P. Abreu et al. (DELPHI Collab.)
ACKERSTAFF	99D	EPJ C8 3	K. Ackerstaff et al. (OPAL Collab.)
ADLOFF	99	EPJ C11 447	C. Adloff et al. (HI Collab.)
Also			
CASALBUONI	99	PL B460 135	R. Casalbuoni et al.
CZAKON	99	PL B458 355	M. Czakon, J. Gluza, M. Zralek
ERLER	99	PL B456 68	J. Erler, P. Langacker
MARCIANO	99	PR D60 093006	W. Marciano
MASIP	99	PR D60 096005	M. Masip, A. Pomarol
NATH	99	PR D60 116004	P. Nath, M. Yamaguchi
STRUMIA	99	PL B466 107	A. Strumia
ABBOTT	98E	PRL 80 2051	B. Abbott et al. (DO Collab.)
ABBOTT	98J	PRL 81 38	B. Abbott et al. (DO Collab.)
ABE	98S	PRL 81 4806	F. Abe et al. (CDF Collab.)
ABE	98V	PRL 81 5742	F. Abe et al. (CDF Collab.)
ACCIARRI	98J	PL B433 163	M. Acciari et al. (CDF Collab.)
ACKERSTAFF	98U	EPJ C2 441	K. Ackerstaff et al. (OPAL Collab.)
BARATE	98U	EPJ C4 571	R. Barate et al. (ALEPH Collab.)
BARENBOIM	98	EPJ C1 369	G. Barenboim
CHO	98	EPJ C5 155	G. Cho, K. Hagiwara, S. Matsumoto
CONRAD	98	RMP 70 1341	J.M. Conrad, M.H. Shaevitz, T. Bolton
DONCHESKI	98	PR D58 097702	M.A. Doncheski, R.W. Robinett
GROSS-PILCHER	98	hep-ex/9810015	C. Grosso-Pilcher, G. Landsberg, M. Paterno
ABE	97F	PRL 78 2906	F. Abe et al. (CDF Collab.)
ABE	97G	PR D95 R5263	F. Abe et al. (CDF Collab.)
ABE	97S	PRL 79 2192	F. Abe et al. (CDF Collab.)
ABE	97W	PRL 79 3819	F. Abe et al. (CDF Collab.)
ABE	97X	PRL 79 4327	F. Abe et al. (CDF Collab.)
ACCIARRI	97Q	PL B412 201	M. Acciari et al. (L3 Collab.)
ARIMA	97	PR D55 19	T. Arima et al. (VENUS Collab.)
BARENBOIM	97	PR D55 4213	G. Barenboim et al. (VALE, IFIC)
DEANDREA	97	PL B409 277	A. Deandrea (MARS)
DERRICK	97	ZPHY C73 613	M. Derrick et al. (ZEUS Collab.)
GROSSMAN	97	PR D55 2768	Y. Grossman, Z. Ligeti, E. Nardi
JADACH	97	PL B408 281	S. Jadach, B.F.L. Ward, Z. Was (CERN, INPK+)
STAHL	97	ZPHY C74 73	A. Stahl, H. Voss (BOHN)
ABACHI	96C	PRL 76 3271	S. Abachi et al. (DO Collab.)
ABACHI	96D	PL B395 471	S. Abachi et al. (DO Collab.)
ABREU	96T	ZPHY C72 179	P. Abreu et al. (DELPHI Collab.)
ADAM	96C	PL B380 471	W. Adam et al. (DELPHI Collab.)
AID	96B	PL B369 173	S. Aid et al. (HI Collab.)
ALLET	96	PL B383 139	M. Allet et al. (VILL, LEUV, LOUV, WIS C)
ABACHI	95E	PL B358 405	S. Abachi et al. (DO Collab.)
ABE	95M	PRL 74 2900	F. Abe et al. (CDF Collab.)
ABE	95N	PRL 74 3538	F. Abe et al. (CDF Collab.)
BALEST	95	PR D51 2053	R. Balest et al. (CLEO Collab.)
KUZNETSOV	95	PR 75 794	I.A. Kuznetsov et al. (PNPI, KIAE, HARV+)
KUZNETSOV	95B	PAN 58 2113	A.V. Kuznetsov, N.V. Mikheev (YARO)
Also			
MIZUKOSHI	95	NP B443 20	J.K. Mizukoshi, O.J.P. Eboli, M.C. Gonzalez-Garcia
ABREU	94O	ZPHY C64 183	P. Abreu et al. (DELPHI Collab.)
BHATTACH...	94	PL B336 100	G. Bhattacharyya, J. Ellis, K. Sridhar (CERN)
Also			
BHATTACH...	94B	PL B338 522 (erratum)	G. Bhattacharyya, J. Ellis, K. Sridhar (CERN)
BHATTACH...	94B	PL B338 522 (erratum)	G. Bhattacharyya, J. Ellis, K. Sridhar (CERN)
DAVIDSON	94	ZPHY C61 613	S. Davidson, D. Bailey, B.A. Campbell (CPA+)
KUZNETSOV	94	PL B329 295	A.V. Kuznetsov, N.V. Mikheev (YARO)
KUZNETSOV	94B	JETPL 60 315	I.A. Kuznetsov et al. (PNPI, KIAE, HARV+)
Also			
LEURER	94	PR D50 536	M. Leurer (REHO)
LEURER	94B	PR D49 333	M. Leurer (REHO)
Also			
MAHANTA	94	PRL 71 1324	U. Mahanta (REHO)
SEVERIJNS	94	PRL 73 611 (erratum)	N. Severijns et al. (LOUV, WIS C, LEUV+)
VILAIN	94B	PL B332 465	P. Vilain et al. (CHARM II Collab.)
ABE	93C	PL B302 119	K. Abe et al. (VENUS Collab.)
ABE	93D	PL B304 373	T. Abe et al. (TOPAZ Collab.)
ABE	93G	PRL 71 2542	F. Abe et al. (CDF Collab.)
ABREU	93J	PL B316 620	P. Abreu et al. (DELPHI Collab.)
ACTON	93E	PL B311 391	P.D. Acton et al. (OPAL Collab.)
ADRIANI	93M	PRPL 236 1	O. Adriani et al. (L3 Collab.)
ALITTI	93	NP B400 3	J. Alitti et al. (UA2 Collab.)
BHATTACH...	93	PR D47 R3693	G. Bhattacharyya et al. (CALC, JADA, ICTP+)
BUSKULIC	93F	PL B308 425	D. Buskulic et al. (ALEPH Collab.)
DERRICK	93	PL B306 173	M. Derrick et al. (ZEUS Collab.)
RIZZO	93	PR D48 4470	T. G. Rizzo (ANL)
SEVERIJNS	93	PRL 70 4047	N. Severijns et al. (LOUV, WIS C, LEUV+)
Also			
STERNER	93	PRL 73 611 (erratum)	N. Severijns et al. (LOUV, WIS C, LEUV+)
ABREU	92D	ZPHY C53 555	K.L. Sterner et al. (AMY Collab.)
ADRIANI	92F	PL B292 472	P. Abreu et al. (DELPHI Collab.)
DECAMP	92	PRPL 216 253	O. Adriani et al. (L3 Collab.)
IMAZATO	92	PRL 69 877	D. Decamp et al. (ALEPH Collab.)
MISHRA	92B	PRL 68 3499	J. Imazato et al. (KEK, INUS, TOKY+)
POLAK	92	PR D46 3871	S.R. Mishra et al. (COLU, CHIC, FNAL+)
ACTON	91	PL B268 122	J. Polak, M. Zralek (SILES)
ACTON	91B	PL B273 338	D.P. Acton et al. (OPAL Collab.)
ADEVA	91D	PL B262 155	D.P. Acton et al. (OPAL Collab.)
AQUINO	91	PL B261 280	B. Adeva et al. (L3 Collab.)
COLANGELO	91	PL B253 154	M. Aquino, A. Fernandez, A. Garcia (CINV, PUEB)
CUNYERS	91	PL B259 173	P. Colangelo, G. Nardulli (BARI)
FARAGGI	91	MPL A6 61	F. Cuypers, A.F. Falk, P.H. Frampton (DURH, HARV+)
POLAK	91	NP B343 395	A.E. Faraggi, D.A.E. Nanopoulos (TAMU)
RIZZO	91	PR D44 202	J. Polak, M. Zralek (SILES)
WALKER	91	APJ 376 51	T. G. Rizzo (WIS C, ISU)
ABE	90F	PL B246 297	T.P. Walker et al. (HSCA, OSU, CHIC+)
ABE	90H	PR D41 1722	K. Abe et al. (VENUS Collab.)
AKRAWY	90J	PL B246 285	F. Abe et al. (CDF Collab.)
ANTREAS YAN	90C	PL B251 204	M.Z. Akrawy et al. (OPAL Collab.)
GONZALEZ-G...	90D	PL B240 163	D. Antreasyan et al. (Crystal Ball Collab.)
GRIFOLS	90	NP B331 244	M.C. Gonzalez-Garcia, J.W.F. Valle (VALE)
GRIFOLS	90D	PR D42 3293	J.A. Griffols, E. Maso (BARC)
KIM	90	PL B240 243	J.A. Griffols, E. Maso, T.G. Rizzo (BARC, CERN+)
LOPEZ	90	PL B241 392	G.H. Kim et al. (AMY Collab.)
ALBAJAR	89	ZPHY C44 15	J.L. Lopez, D.V. Nanopoulos (TAMU)
ALBRECHT	89	ZPHY C42 349	C. Albajar et al. (UA1 Collab.)
BARBIERI	89B	PR D39 1229	H. Albrecht et al. (ARGUS Collab.)
LANGACKER	89B	PR D40 1569	R. Barbieri, R.N. Mohapatra (PISA, UMD)
ODAKA	89	JPSJ 58 3037	P. Langacker, S. Uma Sankar (PENN)
ROBINETT	89	PR D39 834	S. Otake et al. (VENUS Collab.)
ALBAJAR	88B	PL B209 127	R.W. Robinett (PSU)
BAGGER	88	PR D37 1188	C. Albajar et al. (UA1 Collab.)
BALKE	88	PR D37 587	J. Bagger, C. Schmidt, S. King (HARV, BOST)
BERGSTROM	88	PL B212 386	B. Balke et al. (LBL, UC, COLO, NWES+)
CUNYERS	88	PRL 60 1237	L. Bergstrom (STOH)
DONCHESKI	88	PL B206 137	F. Cuypers, P.H. Frampton (UNICB)
DONCHESKI	88B	PR D38 412	M.A. Doncheski, H. Grotch, R. Robinett (PSU)
ANSARI	87D	PL B195 613	M.A. Doncheski, H. Grotch, R.W. Robinett (PSU)
			R. Ansari et al. (UA2 Collab.)

BARTEL	87B	ZPHY C36 15	W. Bartel et al. (JADE Collab.)
BEHREND	86B	PL B178 452	H.J. Behrend et al. (CELLO Collab.)
DERRICK	86	PL 166B 463	M. Derrick et al. (HRS Collab.)
Also			
JODIDIO	86	PR D34 3286	M. Derrick et al. (HRS Collab.)
Also			
MOHAPATRA	86	PR D34 1967	A. Jodidio et al. (LBL, NWES, TRIU)
Also			
ADEVA	85	PR D37 237 (erratum)	A. Jodidio et al. (LBL, NWES, TRIU)
BERGER	85B	PL 152B 439	R.N. Mohapatra (UMD)
STOKER	85	ZPHY C27 341	B. Adeva et al. (Mark-J Collab.)
ADEVA	84C	PRL 54 1887	C. Berger et al. (PLUTO Collab.)
ADEVA	84	PRL 53 134	D.P. Stoker et al. (LBL, NWES, TRIU)
BEHREND	84C	PL 140B 130	B. Adeva et al. (Mark-J Collab.)
BERGSMAS	83	PL 122B 465	H.J. Behrend et al. (CELLO Collab.)
CARR	83	PRL 51 627	F. Bergsma et al. (CHARM Collab.)
BEALL	82	PRL 48 848	J. Carr et al. (LBL, NWES, TRIU)
SHANKER	82	NP B204 375	G. Beall, M. Bander, A. Soni (UCI, UCLA)
			O. Shanker (TRIU)

Axions (A^0) and Other Very Light Bosons, Searches for

AXIONS AND OTHER SIMILAR PARTICLES

Revised January 2010 by C. Hagmann (LLNL), H. Murayama (UC Berkeley), G.G. Raffelt (MPI Physics), L.J. Rosenberg (U. of Washington), and K. van Bibber (LLNL).

Introduction

In this section, we list coupling-strength and mass limits for light neutral scalar or pseudoscalar bosons that couple weakly to normal matter and radiation. Such bosons may arise from a global spontaneously broken U(1) symmetry, resulting in a massless Nambu-Goldstone (NG) boson. If there is a small explicit symmetry breaking, either already in the Lagrangian or due to quantum effects such as anomalies, the boson acquires a mass and is called a pseudo-NG boson. Typical examples are axions (A^0) [1,2], familons [3] and Majorons [4], associated, respectively, with a spontaneously broken Peccei-Quinn, family and lepton-number symmetry.

A common characteristic among these light bosons ϕ is that their coupling to Standard-Model particles is suppressed by the energy scale that characterizes the symmetry breaking, *i.e.*, the decay constant f . The interaction Lagrangian is

$$\mathcal{L} = f^{-1} J^\mu \partial_\mu \phi, \quad (1)$$

where J^μ is the Noether current of the spontaneously broken global symmetry. If f is very large, these new particles interact very weakly. Detecting them would provide a window to physics far beyond what can be probed at accelerators.

Axions remain of particular interest because the Peccei-Quinn (PQ) mechanism remains perhaps the most credible scheme to preserve CP in QCD. Moreover, the cold dark matter of the universe may well consist of axions and they are searched for in dedicated experiments with a realistic chance of discovery.

Originally it was assumed that the PQ scale f_A was related to the electroweak symmetry-breaking scale $v_{\text{weak}} = (\sqrt{2}G_F)^{-1/2} = 247$ GeV. However, the associated “standard” and “variant” axions were quickly excluded—we refer to the Listings for detailed limits. Here we focus on “invisible axions” with $f_A \gg v_{\text{weak}}$ as the main possibility.

Axions have a characteristic two-photon vertex, inherited from their mixing with π^0 and η . It allows for the main search strategy based on axion-photon conversion in external magnetic fields [5], an effect that also can be of astrophysical interest. While for axions the product “ $A\gamma\gamma$ interaction strength \times mass”

See key on page 405

Gauge & Higgs Boson Particle Listings Axions (A^0) and Other Very Light Bosons

is essentially fixed by the corresponding π^0 properties, one may consider more general axion-like particles (ALPs) where the two parameters are independent. Several experiments have recently explored this more general parameter space.

I. THEORY

I.1 Peccei-Quinn mechanism and axions

The QCD Lagrangian includes a CP-violating term $\mathcal{L}_\Theta = \bar{\Theta} (\alpha_s/8\pi) G^{\mu\nu a} \tilde{G}_{\mu\nu}^a$, where $-\pi \leq \bar{\Theta} \leq +\pi$ is the effective Θ parameter after diagonalizing quark masses, G is the color field strength tensor, and \tilde{G} its dual. Limits on the neutron electric dipole moment [6] imply $|\bar{\Theta}| \lesssim 10^{-10}$ even though $\bar{\Theta} = \mathcal{O}(1)$ is otherwise completely satisfactory. The spontaneously broken global Peccei-Quinn symmetry $U(1)_{\text{PQ}}$ was introduced to solve this “strong CP problem” [1], an axion being the pseudo-NG boson of $U(1)_{\text{PQ}}$ [2]. This symmetry is broken due to the axion’s anomalous triangle coupling to gluons,

$$\mathcal{L} = \left(\bar{\Theta} - \frac{\phi_A}{f_A} \right) \frac{\alpha_s}{8\pi} G^{\mu\nu a} \tilde{G}_{\mu\nu}^a, \quad (2)$$

where ϕ_A is the axion field and f_A the axion decay constant. Color anomaly factors have been absorbed in the normalization of f_A which is defined by this Lagrangian. Thus normalized, f_A is the quantity that enters all low-energy phenomena [7]. Non-perturbative effects induce a potential for ϕ_A whose minimum is at $\phi_A = \bar{\Theta} f_A$, thereby canceling the $\bar{\Theta}$ term in the QCD Lagrangian and thus restoring CP symmetry.

The resulting axion mass is given by $m_A f_A \approx m_\pi f_\pi$ where $m_\pi = 135$ MeV and $f_\pi \approx 92$ MeV. In more detail one finds

$$m_A = \frac{z^{1/2}}{1+z} \frac{f_\pi m_\pi}{f_A} = \frac{0.60 \text{ meV}}{f_A/10^{10} \text{ GeV}}, \quad (3)$$

where $z = m_u/m_d$. We have used the canonical value $z = 0.56$ [8], although the range $z = 0.35\text{--}0.60$ is plausible [9].

Originally one assumed $f_A \sim v_{\text{weak}}$ [1,2]. Tree-level flavor conservation fixes the axion properties in terms of a single parameter $\tan\beta$, the ratio of the vacuum expectation values of two Higgs fields that appear as a minimal ingredient. This “standard axion” is excluded after extensive searches [10]. A narrow peak structure observed in positron spectra from heavy ion collisions [11] suggested an axion-like particle of mass 1.8 MeV that decays into e^+e^- , but extensive follow-up searches were negative. “Variant axion models” were proposed which keep $f_A \sim v_{\text{weak}}$ while dropping the constraint of tree-level flavor conservation [12], but these models are also excluded [13].

Axions with $f_A \gg v_{\text{weak}}$ evade all current experimental limits. One generic class of models invokes “hadronic axions” where new heavy quarks carry $U(1)_{\text{PQ}}$ charges, leaving ordinary quarks and leptons without tree-level axion couplings. The prototype is the KSVZ model [14], where in addition the heavy quarks are electrically neutral. Another generic class requires at least two Higgs doublets and ordinary quarks and leptons carry PQ charges, the prototype being the DFSZ model [15]. All of these models contain at least one electroweak singlet

scalar that acquires a vacuum expectation value and thereby breaks the PQ symmetry. The KSVZ and DFSZ models are frequently used as generic examples, but other models exist where both heavy quarks and Higgs doublets carry PQ charges.

I.2 Model-dependent axion couplings

Although the generic axion interactions scale approximately with f_π/f_A from the corresponding π^0 couplings, there are non-negligible model-dependent factors and uncertainties. The axion’s two-photon interaction plays a key role for many searches,

$$\mathcal{L}_{A\gamma\gamma} = \frac{G_{A\gamma\gamma}}{4} F_{\mu\nu} \tilde{F}^{\mu\nu} \phi_A = -G_{A\gamma\gamma} \mathbf{E} \cdot \mathbf{B} \phi_A, \quad (4)$$

where F is the electromagnetic field-strength tensor and \tilde{F} its dual. The coupling constant is

$$G_{A\gamma\gamma} = \frac{\alpha}{2\pi f_A} \left(\frac{E}{N} - \frac{2}{3} \frac{4+z}{1+z} \right) = \frac{\alpha}{2\pi} \left(\frac{E}{N} - \frac{2}{3} \frac{4+z}{1+z} \right) \frac{1+z}{z^{1/2}} \frac{m_A}{m_\pi f_\pi}, \quad (5)$$

where E and N are the electromagnetic and color anomalies of the axial current associated with the axion. In grand unified models, and notably for DFSZ [15], $E/N = 8/3$, whereas for KSVZ [14] $E/N = 0$ if the electric charge of the new heavy quark is taken to vanish. In general, a broad range of E/N values is possible [16]. The two-photon decay width is

$$\Gamma_{A \rightarrow \gamma\gamma} = \frac{G_{A\gamma\gamma}^2 m_A^3}{64\pi} = 1.1 \times 10^{-24} \text{ s}^{-1} \left(\frac{m_A}{\text{eV}} \right)^5. \quad (6)$$

The second expression uses Eq. (5) with $z = 0.56$ and $E/N = 0$. Axions decay faster than the age of the universe if $m_A \gtrsim 20$ eV.

The interaction with fermions f has derivative form and is invariant under a shift $\phi_A \rightarrow \phi_A + \phi_0$ as behoves a NG boson,

$$\mathcal{L}_{Aff} = \frac{C_f}{2f_A} \bar{\Psi}_f \gamma^\mu \gamma_5 \Psi_f \partial_\mu \phi_A. \quad (7)$$

Here, Ψ_f is the fermion field, m_f its mass, and C_f a model-dependent coefficient. The dimensionless combination $g_{Aff} \equiv C_f m_f / f_A$ plays the role of a Yukawa coupling and $\alpha_{Aff} \equiv g_{Aff}^2 / 4\pi$ of a “fine-structure constant.” The often-used pseudoscalar form $\mathcal{L}_{Aff} = -i(C_f m_f / f_A) \bar{\Psi}_f \gamma_5 \Psi_f \phi_A$ need not be equivalent to the appropriate derivative structure, for example when two NG bosons are attached to one fermion line as in axion emission by nucleon bremsstrahlung [17].

In the DFSZ model [15], the tree-level coupling coefficient to electrons is

$$C_e = \frac{\cos^2 \beta}{3}, \quad (8)$$

where $\tan\beta$ is the ratio of two Higgs vacuum expectation values that are generic to this and similar models.

For nucleons, $C_{n,p}$ are related to axial-vector current matrix elements by generalized Goldberger-Treiman relations,

$$C_p = (C_u - \eta) \Delta u + (C_d - \eta z) \Delta d + (C_s - \eta w) \Delta s, \quad (9)$$

$$C_n = (C_u - \eta) \Delta d + (C_d - \eta z) \Delta u + (C_s - \eta w) \Delta s.$$

Gauge & Higgs Boson Particle Listings

Axions (A^0) and Other Very Light Bosons

Here, $\eta = (1 + z + w)^{-1}$ with $z = m_u/m_d$ and $w = m_u/m_s \ll z$ and the Δq are given by the axial vector current matrix element $\Delta q S_\mu = \langle p | \bar{q} \gamma_\mu \gamma_5 q | p \rangle$ with S_μ the proton spin.

Neutron beta decay and strong isospin symmetry considerations imply $\Delta u - \Delta d = F + D = 1.269 \pm 0.003$, whereas hyperon decays and flavor SU(3) symmetry imply $\Delta u + \Delta d - 2\Delta s = 3F - D = 0.586 \pm 0.031$ [19]. The strange-quark contribution is $\Delta s = -0.08 \pm 0.01_{\text{stat}} \pm 0.05_{\text{sys}}$ from the COMPASS experiment [18], and $\Delta s = -0.085 \pm 0.008_{\text{exp}} \pm 0.013_{\text{theor}} \pm 0.009_{\text{evol}}$ from HERMES [19], in agreement with each other and with an early estimate of $\Delta s = -0.11 \pm 0.03$ [20]. We thus adopt $\Delta u = 0.84 \pm 0.02$, $\Delta d = -0.43 \pm 0.02$ and $\Delta s = -0.09 \pm 0.02$, very similar to what was used in the axion literature.

The uncertainty of the axion-nucleon couplings is dominated by the uncertainty $z = m_u/m_d = 0.35\text{--}0.60$ that we mentioned earlier. For hadronic axions $C_{u,d,s} = 0$ so that $-0.51 < C_p < -0.36$ and $0.10 > C_n > -0.05$. Therefore it is well possible that $C_n = 0$ whereas C_p does not vanish within the plausible z range. In the DFSZ model, $C_u = \frac{1}{3} \sin^2 \beta$ and $C_d = \frac{1}{3} \cos^2 \beta$ and C_n and C_p as functions of β and z do not vanish simultaneously.

The axion-pion interaction is given by the Lagrangian [21]

$$\mathcal{L}_{A\pi} = \frac{C_{A\pi}}{f_\pi f_A} (\pi^0 \pi^+ \partial_\mu \pi^- + \pi^0 \pi^- \partial_\mu \pi^+ - 2\pi^+ \pi^- \partial_\mu \pi^0) \partial_\mu \phi_A, \quad (10)$$

where $C_{A\pi} = (1 - z)/[3(1 + z)]$ in hadronic models. The chiral symmetry-breaking Lagrangian provides an additional term $\mathcal{L}'_{A\pi} \propto (m_\pi^2/f_\pi f_A) (\pi^0 \pi^0 + 2\pi^- \pi^+) \pi^0 \phi_A$. For hadronic axions it vanishes identically, in contrast to the DFSZ model (Roberto Peccei, private communication).

II. LABORATORY SEARCHES

II.1 Photon regeneration

Searching for “invisible axions” is extremely challenging. The most promising approaches rely on the axion-two-photon vertex, allowing for axion-photon conversion in external electric or magnetic fields [5]. For the Coulomb field of a charged particle, the conversion is best viewed as a scattering process, $\gamma + Ze \leftrightarrow Ze + A$, called Primakoff effect [22]. In the other extreme of a macroscopic field, usually a large-scale B -field, the momentum transfer is small, the interaction coherent over a large distance, and the conversion is best viewed as an axion-photon oscillation phenomenon in analogy to neutrino flavor oscillations [23].

Photons propagating through a transverse magnetic field, with incident \mathbf{E}_γ and magnet \mathbf{B} parallel, may convert into axions. For $m_A^2 L/2\omega \ll 2\pi$, where L is the length of the B field region and ω the photon energy, the resultant axion beam is coherent with the incident photon beam and the conversion probability is $\Pi \sim (1/4)(G_{A\gamma\gamma} BL)^2$. A practical realization uses a laser beam propagating down the bore of a superconducting dipole magnet (like the bending magnets in high-energy accelerators). If another magnet is in line with the first, but shielded by an optical barrier, then photons may

be regenerated from the pure axion beam [24]. The overall probability $P(\gamma \rightarrow A \rightarrow \gamma) = \Pi^2$.

The first such experiment utilized two magnets of length $L = 4.4$ m and $B = 3.7$ T and found $G_{A\gamma\gamma} < 6.7 \times 10^{-7}$ GeV $^{-1}$ at 95% CL for $m_A < 1$ meV [25]. More recently, several such experiments were performed (see Listings), improving the limit to $G_{A\gamma\gamma} < 3.5 \times 10^{-7}$ GeV $^{-1}$ at 3σ in the massless limit [26]. Some of these experiments have also reported limits for scalar bosons where the photon \mathbf{E}_γ must be chosen perpendicular to the magnet \mathbf{B} .

A new concept, resonantly-enhanced photon regeneration, may open unexplored regions of coupling strength [27]. In this scheme, both the production and detection magnets are within Fabry-Perot optical cavities and actively locked in frequency. The $\gamma \rightarrow A \rightarrow \gamma$ rate is enhanced by a factor $2\mathcal{F}\mathcal{F}'/\pi^2$ relative to a single-pass experiment, where \mathcal{F} and \mathcal{F}' are the finesses of the two cavities. The resonant enhancement could be of order $10^{(10-12)}$, improving the $G_{A\gamma\gamma}$ sensitivity by $10^{(2.5-3)}$. Another new concept involves axion absorption and emission between electromagnetic fields within a high finesse optical cavity [28]. A signal appears as resonant sidebands on the carrier. This technique could be sensitive in the mass range $10^{-6}\text{--}10^{-4}$ eV and reach the KSVZ line after one year of operation.

II.2 Photon polarization

An alternative to regenerating the lost photons is to use the beam itself to detect conversion: the polarization of light propagating through a transverse B field suffers dichroism and birefringence [29]. Dichroism: The E_\parallel component, but not E_\perp , is depleted by axion production, causing a small rotation of linearly polarized light. For $m_A^2 L/2\omega \ll 2\pi$ the effect is independent of m_A , for heavier axions it oscillates and diminishes as m_A increases, and it vanishes for $m_A > \omega$. Birefringence: This rotation occurs because there is mixing of virtual axions in the E_\parallel state, but not for E_\perp . Hence, linearly polarized light will develop elliptical polarization. Higher-order QED also induces vacuum birefringence. A search for these effects was performed on the same dipole magnets in the early experiment above [30]. The dichroic rotation gave a stronger limit than the ellipticity rotation: $G_{A\gamma\gamma} < 3.6 \times 10^{-7}$ GeV $^{-1}$ at 95% CL for $m_A < 5 \times 10^{-4}$ eV. The ellipticity limits are better at higher masses, as they fall off smoothly and do not terminate at m_A .

In 2006 the PVLAS collaboration reported a signature of magnetically induced vacuum dichroism that could be interpreted as the effect of a pseudoscalar with $m_A = 1\text{--}1.5$ meV and $G_{A\gamma\gamma} = (1.6\text{--}5) \times 10^{-6}$ GeV $^{-1}$ [31]. Since then, these findings are attributed to instrumental artifacts [32]. This particle interpretation is also excluded by the above photon regeneration searches that were triggered by the original PVLAS result.

II.3 Long-range forces

New bosons would mediate long-range forces, which are severely constrained by “fifth force” experiments [33]. Those

See key on page 405

Gauge & Higgs Boson Particle Listings Axions (A^0) and Other Very Light Bosons

looking for new mass-spin couplings provide significant constraints on pseudoscalar bosons [34]. However, they do not yet cover realistic parameters for invisible axion models because they are only sensitive for small m_A . The corresponding coupling strengths scale with $f_A^{-1} \approx m_A/m_\pi f_\pi$ and are too small to be detected. Still, these efforts provide constraints on more general low-mass bosons.

III. AXIONS FROM ASTROPHYSICAL SOURCES

III.1 Stellar energy-loss limits:

Low-mass weakly-interacting particles (neutrinos, gravitons, axions, baryonic or leptonic gauge bosons, *etc.*) are produced in hot astrophysical plasmas, and can thus transport energy out of stars. The coupling strength of these particles with normal matter and radiation is bounded by the constraint that stellar lifetimes or energy-loss rates not conflict with observation [35–37].

We begin this discussion with our Sun and concentrate on hadronic axions. They are produced predominantly by the Primakoff process $\gamma + Ze \rightarrow Ze + A$. Integrating over a standard solar model yields the axion luminosity [49]

$$L_A = G_{10}^2 1.85 \times 10^{-3} L_\odot, \quad (11)$$

where $G_{10} = G_{A\gamma\gamma} \times 10^{10}$ GeV. The maximum of the spectrum is at 3.0 keV, the average at 4.2 keV, and the number flux at Earth is $G_{10}^2 3.75 \times 10^{11}$ cm⁻² s⁻¹. The solar photon luminosity is fixed, so axion losses require enhanced nuclear energy production and thus enhanced neutrino fluxes. The all-flavor measurements by SNO together with a standard solar model imply $L_A \lesssim 0.10 L_\odot$, corresponding to $G_{10} \lesssim 7$ [38], mildly superseding a similar limit from helioseismology [39].

A more restrictive limit derives from globular-cluster (GC) stars that allow for detailed tests of stellar-evolution theory. The stars on the horizontal branch (HB) in the color-magnitude diagram have reached helium burning with a core-averaged energy release of about 80 erg g⁻¹ s⁻¹, compared to Primakoff axion losses of $G_{10}^2 30$ erg g⁻¹ s⁻¹. The accelerated consumption of helium reduces the HB lifetime by about 80/(80+30 G_{10}^2). Number counts of HB stars in 15 GCs compared with the number of red giants (that are not much affected by Primakoff losses) reveal agreement with expectations within 20–40% in any one GC and overall on the 10% level [36]. Therefore, a reasonably conservative limit is

$$G_{A\gamma\gamma} \lesssim 1 \times 10^{-10} \text{ GeV}^{-1}, \quad (12)$$

although a detailed error budget is not available.

We translate this constraint on $G_{A\gamma\gamma}$ to $f_A > 2.3 \times 10^7$ GeV ($m_A < 0.3$ eV), using $z = 0.56$ and $E/N = 0$ as in the KSVZ model, and show the excluded range in Figure 1. For the DFSZ model with $E/N = 8/3$, the corresponding limits are slightly less restrictive, $f_A > 0.8 \times 10^7$ GeV ($m_A < 0.7$ eV). The exact high-mass end of the exclusion range has not been determined. The relevant temperature is around 10 keV and the average photon energy is therefore around 30 keV. The excluded m_A range thus certainly extends beyond the shown 100 keV.

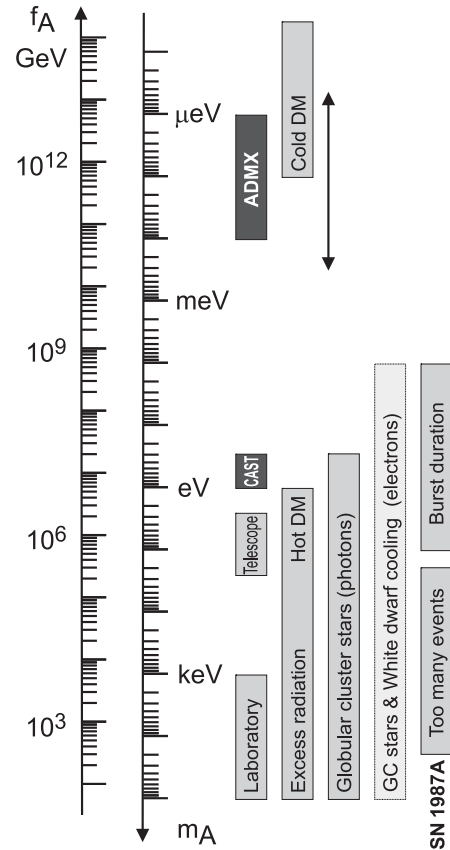


Figure 1: Exclusion ranges as described in the text. The dark intervals are the approximate CAST and ADMX search ranges. Limits on coupling strengths are translated into limits on m_A and f_A using $z = 0.56$ and the KSVZ values for the coupling strengths. The “Laboratory” bar is a rough representation of the exclusion range for standard or variant axions. The “GC stars and white-dwarf cooling” range uses the DFSZ model with an axion-electron coupling corresponding to $\cos^2 \beta = 1/2$. The Cold Dark Matter exclusion range is particularly uncertain. We show the benchmark case from the misalignment mechanism.

If axions couple directly to electrons, the dominant emission processes are $\gamma + e^- \rightarrow e^- + A$ and $e^- + Ze \rightarrow Ze + e^- + A$. Moreover, bremsstrahlung is efficient in white dwarfs (WDs), where the Primakoff and Compton processes are suppressed by the large plasma frequency. The enhanced energy losses would delay helium ignition in GC stars, implying $\alpha_{Aee} \lesssim 0.5 \times 10^{-26}$ [40]. Enhanced WD cooling leads to a similar limit from the WD luminosity function [41]. For pulsationally unstable WDs (ZZ Ceti stars), the period decrease \dot{P}/P is a measure of the cooling speed. A well-studied case is the star G117–B15A, where the measured \dot{P}/P implies [42]

$$\alpha_{Aee} < 1.3 \times 10^{-27} \quad (13)$$

Gauge & Higgs Boson Particle Listings

Axions (A^0) and Other Very Light Bosons

at a statistical 95% CL. (We have corrected the published limit for an apparent misprint.) This result is equivalent to $g_{Aee} < 1.3 \times 10^{-13}$ or in the DFSZ model to $f_A > 1.3 \times 10^9 \text{ GeV} \cos^2 \beta$ and $m_A < 4.5 \text{ meV}/\cos^2 \beta$. We show these constraints in Figure 1 for $\cos^2 \beta = 1/2$.

Similar constraints derive from the measured duration of the neutrino signal of the supernova SN 1987A. Numerical simulations for a variety of cases, including axions and Kaluza-Klein gravitons, reveal that the energy-loss rate of a nuclear medium at the density $3 \times 10^{14} \text{ g cm}^{-3}$ and temperature 30 MeV should not exceed about $1 \times 10^{19} \text{ erg g}^{-1} \text{ s}^{-1}$ [36]. The energy-loss rate from nucleon bremsstrahlung, $N + N \rightarrow N + N + A$, is $(C_N/2f_A)^2 (T^4/\pi^2 m_N) F$. Here F is a numerical factor that represents an integral over the dynamical spin-density structure function because axions couple to the nucleon spin. For realistic conditions, even after considerable effort, one is limited to a heuristic estimate leading to $F \approx 1$ [37].

The SN 1987A limits are of particular interest for hadronic axions where the bounds on α_{Aee} are moot. Within uncertainties of $z = m_u/m_d$ a reasonable choice for the coupling constants is then $C_p = -0.4$ and $C_n = 0$. Using a proton fraction of 0.3, $F = 1$, and $T = 30 \text{ MeV}$ one finds [37]

$$f_A \gtrsim 4 \times 10^8 \text{ GeV} \quad \text{and} \quad m_A \lesssim 16 \text{ meV}. \quad (14)$$

If axions interact sufficiently strongly they are trapped. Only about three orders of magnitude in g_{ANN} or m_A are excluded, a range shown somewhat schematically in Figure 1. For even larger couplings, the axion flux would have been negligible, yet it would have triggered additional events in the detectors, excluding a further range [43]. A possible gap between these two SN 1987A arguments was discussed as the ‘‘hadronic axion window’’ under the assumption that $G_{A\gamma\gamma}$ was anomalously small [44]. This range is now excluded by hot dark matter bounds (see below).

III.2 Searches for solar axions

Instead of using stellar energy losses to derive axion limits, one can also search directly for these fluxes, notably from the Sun. The main focus has been on axion-like particles with a two-photon vertex. They are produced by the Primakoff process with a flux given by Equation 11 and can be detected at Earth with the reverse process in a macroscopic B -field (‘‘axion helioscope’’) [5]. The average energy of solar axions of 4.2 keV implies a photon-axion oscillation length in vacuum of $2\pi(2\omega/m_A^2) \sim \mathcal{O}(1 \text{ mm})$, precluding the vacuum mixing from achieving its theoretical maximum in any practical magnet. However, one can endow the photon with an effective mass in a gas, $m_\gamma = \omega_{\text{plas}}$, thus matching the axion and photon dispersion relations [45].

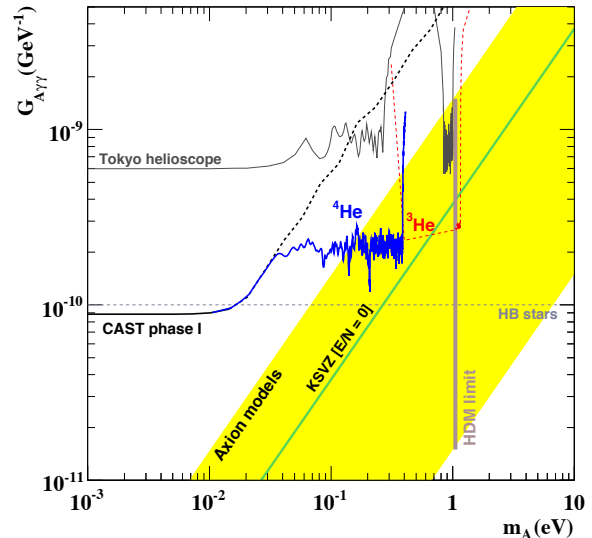


Figure 2: Solar exclusion plot for axion-like particles [50]. The red dashed line is the sensitivity of the ongoing ${}^3\text{He}$ phase of CAST. The vertical line (HDM) is the hot dark-matter limit [59]. The yellow band represents models with $0.07 < |E/N - 1.92| < 0.7$, the green solid line corresponds to KSVZ axions.

An early implementation of these ideas used a conventional dipole magnet, with a conversion volume of variable-pressure gas with a xenon proportional chamber as x-ray detector [46]. The conversion magnet was fixed in orientation and collected data for about 1000 s/day. Axions were excluded for $G_{A\gamma\gamma} < 3.6 \times 10^{-9} \text{ GeV}^{-1}$ for $m_A < 0.03 \text{ eV}$, and $G_{A\gamma\gamma} < 7.7 \times 10^{-9} \text{ GeV}^{-1}$ for $0.03 < m_A < 0.11 \text{ eV}$ at 95% CL.

Later, the Tokyo axion helioscope used a superconducting magnet on a tracking mount, viewing the Sun continuously. They reported $G_{A\gamma\gamma} < 6 \times 10^{-10} \text{ GeV}^{-1}$ for $m_A < 0.3 \text{ eV}$ [47]. Recently this experiment was recommissioned and a similar limit for masses around 1 eV was reported [48]. These exclusion ranges are shown in Figure 2.

The most recent helioscope CAST (CERN Axion Solar Telescope) uses a decommissioned LHC dipole magnet on a tracking mount. The hardware includes grazing-incidence x-ray optics with solid-state x-ray detectors, as well as a novel x-ray Micromegas position-sensitive gaseous detector. CAST has established a 95% CL limit $G_{A\gamma\gamma} < 8.8 \times 10^{-11} \text{ GeV}^{-1}$ for $m_A < 0.02 \text{ eV}$ [49]. To cover larger masses and to ‘‘cross the axion line,’’ the magnet bores are filled with a gas at varying pressure. The runs with ${}^4\text{He}$ cover masses up to about 0.4 eV [50], providing the limits shown in Figure 2. Ongoing runs with ${}^3\text{He}$ gas have explored masses up to 0.85 eV, aiming to about 1.16 eV, but final results are not yet available.

Other Primakoff searches for solar axions have been carried out using crystal detectors, exploiting the coherent conversion of axions into photons when the axion angle of incidence satisfies

See key on page 405

Gauge & Higgs Boson Particle Listings Axions (A^0) and Other Very Light Bosons

a Bragg condition with a crystal plane [51]. However, none of these limits is more restrictive than the one derived from solar neutrinos that was discussed earlier.

Another idea is to look at the Sun with an x-ray satellite when the Earth is in between. Solar axions would convert in the Earth magnetic field on the far side and could be detected [52]. The sensitivity to $G_{A\gamma\gamma}$ could be comparable to CAST, but only for much smaller m_A .

III.3 Conversion of astrophysical photon fluxes

Large-scale B fields exist in astrophysics that can induce axion-photon oscillations. In practical cases, B is much smaller than in the laboratory, whereas the conversion region L is much larger. Therefore, while the product BL can be large, realistic sensitivities are usually restricted to very low-mass particles, far away from the “axion line” in a plot like Figure 2.

One example is SN 1987A, which would have emitted a burst of axion-like particles due to the Primakoff production in its core. They would have partially converted into γ -rays in the galactic B -field. The absence of a γ -ray burst in coincidence with SN 1987A neutrinos provides a limit $G_{A\gamma\gamma} \lesssim 1 \times 10^{-11} \text{ GeV}^{-1}$ for $m_A \lesssim 10^{-9} \text{ eV}$ [53], the most restrictive limit for very small m_A . Axion-like particles from other stars can be converted to photons, but no tangible new limits or signatures seem to have appeared.

Conversely, photons from distant sources could transform to axion-like particles, depleting the original flux. This mechanism was proposed as an alternative to cosmic acceleration for explaining the apparent dimming of distant SNe Ia [54]. However, this effect would apply to all distant sources, including quasars and the cosmic microwave background and would depend on energy. All things considered, this mechanism can only play a subdominant role [55]. On the other hand, very recently the observed scatter of x/ γ -ray fluxes from active galactic nuclei was interpreted in terms of very low-mass ALPs [56].

High-energy γ -rays are typically produced in magnetized environments where cosmic rays are accelerated. The conversion into axion-like particles can then, in principle, imprint observable features on the spectrum for a range of coupling constants not excluded by other arguments [57].

IV. COSMIC AXIONS

IV.1 Cosmic axion populations

In the early universe, axions are produced by processes involving quarks and gluons [58]. After color confinement, the dominant thermalization process is $\pi + \pi \leftrightarrow \pi + A$ [21]. The resulting axion population would contribute a hot dark matter component in analogy to massive neutrinos. Cosmological precision data provide restrictive constraints on a possible hot dark-matter fraction that translate into $m_A < 0.4\text{--}1.0 \text{ eV}$ at the 95% statistical CL [59]. The spread of published limits reflects the use of different cosmological data sets.

For $m_A \gtrsim 20 \text{ eV}$, axions decay fast on a cosmic time scale, removing the axion population while injecting photons. This

excess radiation provides additional limits up to very large axion masses [60]. An anomalously small $G_{A\gamma\gamma}$ provides no loophole because suppressing decays leads to thermal axions overdominating the mass density of the universe.

The main cosmological interest in axions derives from their possible role as cold dark matter (CDM). In addition to thermal processes, axions are abundantly produced by the “misalignment mechanism” [61]. After the breakdown of the PQ symmetry, the axion field relaxes somewhere in the “bottom of the wine bottle” potential. Near the QCD epoch, instanton effects explicitly break the PQ symmetry, the very effect that causes dynamical PQ symmetry restoration. This “tilting of the wine bottle” drives the axion field toward the CP-conserving minimum, thereby exciting coherent oscillations of the axion field that ultimately represent a condensate of CDM. The cosmic mass density in this homogeneous field mode is [62]

$$\Omega_A h^2 \approx 0.7 \left(\frac{f_A}{10^{12} \text{ GeV}} \right)^{7/6} \left(\frac{\bar{\Theta}_i}{\pi} \right)^2, \quad (15)$$

where h is the present-day Hubble expansion parameter in units of $100 \text{ km s}^{-1} \text{ Mpc}^{-1}$, and $-\pi \leq \bar{\Theta}_i \leq \pi$ is the initial “misalignment angle” relative to the CP-conserving position. If the PQ symmetry breakdown takes place after inflation, $\bar{\Theta}_i$ will take on different values in different patches of the universe. The average contribution is [62]

$$\Omega_A h^2 \approx 0.3 \left(\frac{f_A}{10^{12} \text{ GeV}} \right)^{7/6}. \quad (16)$$

Comparing with the measured CDM density of $\Omega_{\text{CDM}} h^2 \approx 0.13$ implies that axions with $m_A \approx 10 \text{ } \mu\text{eV}$ provide the dark matter, whereas smaller masses are excluded (Figure 1).

This density sets only a rough scale for the expected m_A . The mass of CDM axions could be significantly smaller or larger than $10 \text{ } \mu\text{eV}$. Apart from the overall particle physics uncertainties, the cosmological sequence of events is crucial. Assuming axions make up CDM, much smaller masses are possible if inflation took place after the PQ transition and the initial value $\bar{\Theta}_i$ was small (“anthropic axion window” [63]). Conversely, if the PQ transition took place after inflation, there are additional sources for nonthermal axions, notably the decay of cosmic strings and domain walls, although these populations are comparable to the misalignment contribution [62].

If the reheat temperature after inflation is too small to restore PQ symmetry, the axion field is present during inflation. It is subject to quantum fluctuations, leading to isocurvature fluctuations that are severely constrained [64].

In the opposite case without inflation after the PQ transition, the spatial axion density variations are large at the QCD transition and they are not erased by free streaming. When matter begins to dominate the universe, gravitationally bound “axion mini clusters” form promptly [65]. A significant fraction of CDM axions can reside in these bound objects.

Gauge & Higgs Boson Particle Listings

Axions (A^0) and Other Very Light Bosons

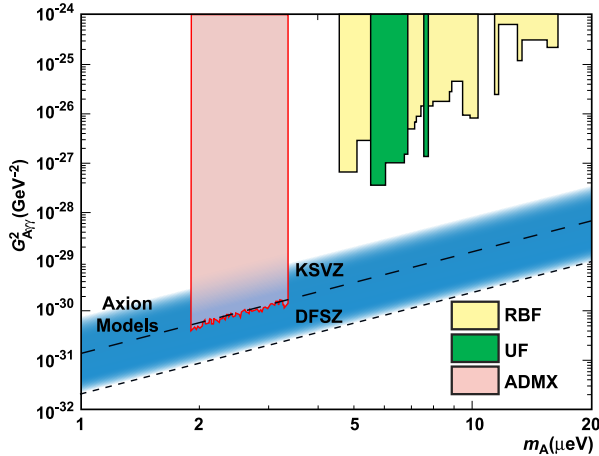


Figure 3: Exclusion region reported from the microwave cavity experiments RBF and UF [71] and ADMX [72]. A local dark-matter density of 450 MeV cm^{-3} is assumed.

IV.2 Telescope searches

The two-photon decay is extremely slow for axions with masses in the CDM regime, but could be detectable for eV masses. The signature would be a quasi-monochromatic emission line from galaxies and galaxy clusters. The expected optical line intensity for DFSZ axions is similar to the continuum night emission. An early search in three rich Abell clusters [66], and a recent search in two rich Abell clusters [67], exclude the “Telescope” range in Figure 1 unless the axion-photon coupling is strongly suppressed. Of course, axions in this mass range would anyway provide an excessive hot DM contribution.

Very-mass axions in halos produce a weak quasi-monochromatic radio line. Virial velocities in undisrupted dwarf galaxies are very low, and the axion decay line would therefore be extremely narrow. A search with the Haystack radio telescope on three nearby dwarf galaxies provided a limit $G_{A\gamma\gamma} < 1.0 \times 10^{-9} \text{ GeV}^{-1}$ at 96% CL for $298 < m_A < 363 \text{ } \mu\text{eV}$ [68]. However, this combination of m_A and $G_{A\gamma\gamma}$ does not exclude plausible axion models.

IV.3 Microwave cavity experiments

The limits of Figure 1 suggest that axions, if they exist, provide a significant fraction or even perhaps all of the cosmic CDM. In a broad range of the plausible m_A range for CDM, galactic halo axions may be detected by their resonant conversion into a quasi-monochromatic microwave signal in a high-Q electromagnetic cavity permeated by a strong static B field [5,69]. The cavity frequency is tunable, and the signal is maximized when the frequency is the total axion energy, rest mass plus kinetic energy, of $\nu = (m_A/2\pi) [1 + \mathcal{O}(10^{-6})]$, the width above the rest mass representing the virial distribution in the galaxy. The frequency spectrum may also contain finer structure from axions more recently fallen into the galactic potential and not yet completely virialized [70].

The feasibility of this technique was established in early experiments of relatively small sensitive volume, $\mathcal{O}(1 \text{ liter})$, with HFET-based amplifiers, setting limits in the range $4.5 < m_A < 16.3 \text{ } \mu\text{eV}$ [71], but lacking by 2–3 orders of magnitude the sensitivity required to detect realistic axions. Later, ADMX ($B \sim 8 \text{ T}$, $V \sim 200 \text{ liters}$) has achieved sensitivity to KSVZ axions, assuming they saturate the local dark matter density and are well virialized, over the mass range $1.9\text{--}3.3 \text{ } \mu\text{eV}$ [72]. Should halo axions have a component not yet virialized, ADMX is sensitive to DFSZ axions [73]. The corresponding 90% CL exclusion regions shown in Figure 3 are normalized to an assumed local CDM density of $7.5 \times 10^{-25} \text{ g cm}^{-3}$ (450 MeV cm^{-3}). Very recently the ADMX experiment has commissioned an upgrade [74] that replaces the microwave HFET amplifiers by near quantum-limited low-noise dc SQUID microwave amplifiers [75], allowing for a significantly improved sensitivity. Alternatively, a Rydberg atom single-photon detector [76] can in principle evade the standard quantum limit for coherent photon detection. Efforts are underway to incorporate Rydberg atom systems in RF cavity axion searches [77].

Conclusions

Experimental, astrophysical, and cosmological limits have been refined and indicate that axions, if they exist, very likely have very low mass, $m_A \lesssim 10 \text{ meV}$, suggesting that axions are a non-negligible fraction of the cosmic CDM. The upgraded versions of the ADMX experiment will ultimately cover the range $1\text{--}100 \text{ } \mu\text{eV}$ with a sensitivity allowing one to detect such axions, unless the local DM density is unexpectedly small or the axion-photon coupling anomalously weak. Other experimental techniques remain of interest to search for axion-like particles, although at present no method besides the DM search is known that could detect realistic axions obeying the astrophysical and cosmological limits, and fulfilling the QCD-implied relationship between mass and coupling strength.

References

1. R.D. Peccei and H. Quinn, Phys. Rev. Lett. **38**, 1440 (1977), Phys. Rev. **D16**, 1791 (1977).
2. S. Weinberg, Phys. Rev. Lett. **40**, 223 (1978); F. Wilczek, Phys. Rev. Lett. **40**, 279 (1978).
3. F. Wilczek, Phys. Rev. Lett. **49**, 1549 (1982).
4. Y. Chikashige, R.N. Mohapatra, and R.D. Peccei, Phys. Lett. **98B**, 265 (1981); G.B. Gelmini and M. Roncadelli, Phys. Lett. **99B**, 411 (1981).
5. P. Sikivie, Phys. Rev. Lett. **51**, 1415 (1983) and Erratum *ibid.*, **52**, 695 (1984).
6. C.A. Baker *et al.*, Phys. Rev. Lett. **97**, 131801 (2006).
7. H. Georgi, D.B. Kaplan, and L. Randall, Phys. Lett. **B169**, 73 (1986).
8. H. Leutwyler, Phys. Lett. **B378**, 313 (1996).
9. Mini review on Quark Masses in: C. Amsler *et al.* (Particle Data Group), Phys. Lett. **B667**, 1 (2008).
10. T.W. Donnelly *et al.*, Phys. Rev. **D18**, 1607 (1978); S. Barshay *et al.*, Phys. Rev. Lett. **46**, 1361 (1981);

See key on page 405

Gauge & Higgs Boson Particle Listings Axions (A^0) and Other Very Light Bosons

- A. Barroso and N.C. Mukhopadhyay, Phys. Lett. **B106**, 91 (1981);
R.D. Peccei, in *Proceedings of Neutrino '81*, Honolulu, Hawaii, Vol. 1, p. 149 (1981);
L.M. Krauss and F. Wilczek, Phys. Lett. **B173**, 189 (1986).
11. J. Schweppe *et al.*, Phys. Rev. Lett. **51**, 2261 (1983);
T. Cowan *et al.*, Phys. Rev. Lett. **54**, 1761 (1985).
 12. R.D. Peccei, T.T. Wu, and T. Yanagida, Phys. Lett. **B172**, 435 (1986).
 13. W.A. Bardeen, R.D. Peccei, and T. Yanagida, Nucl. Phys. **B279**, 401 (1987).
 14. J.E. Kim, Phys. Rev. Lett. **43**, 103 (1979);
M.A. Shifman, A.I. Vainstein, and V.I. Zakharov, Nucl. Phys. **B166**, 493 (1980).
 15. M. Dine, W. Fischler, and M. Srednicki, Phys. Lett. **B104**, 199 (1981);
A.R. Zhitnitsky, Sov. J. Nucl. Phys. **31**, 260 (1980).
 16. S.L. Cheng, C.Q. Geng, and W.T. Ni, Phys. Rev. **D52**, 3132 (1995).
 17. G. Raffelt and D. Seckel, Phys. Rev. Lett. **60**, 1793 (1988);
M. Carena and R.D. Peccei, Phys. Rev. **D40**, 652 (1989);
K. Choi, K. Kang, and J.E. Kim, Phys. Rev. Lett. **62**, 849 (1989).
 18. V.Y. Alexakhin *et al.* (COMPASS Collab.), Phys. Lett. **B647**, 8 (2007).
 19. A. Airapetian *et al.* (HERMES Collab.), Phys. Rev. **D75**, 012007 (2007) and Erratum *ibid.*, **D76**, 039901 (2007).
 20. J.R. Ellis and M. Karliner, in: *The spin structure of the nucleon: International school of nucleon structure* (3–10 August 1995, Erice, Italy), ed. by B. Frois, V.W. Hughes, and N. De Groot (World Scientific, Singapore, 1997) [hep-ph/9601280].
 21. S. Chang and K. Choi, Phys. Lett. **B316**, 51 (1993).
 22. D.A. Dicus *et al.*, Phys. Rev. **D18**, 1829 (1978).
 23. G. Raffelt and L. Stodolsky, Phys. Rev. **D37**, 1237 (1988).
 24. K. van Bibber *et al.*, Phys. Rev. Lett. **59**, 759 (1987).
 25. G. Ruoso *et al.*, Z. Phys. **C56**, 505 (1992);
R. Cameron *et al.*, Phys. Rev. **D47**, 3707 (1993).
 26. M. Fouche *et al.*, Phys. Rev. **D78**, 032013 (2008);
A.S. Chou *et al.* (GammeV Collab.), Phys. Rev. Lett. **100**, 080402 (2008);
A. Afanasev *et al.*, Phys. Rev. Lett. **101**, 120401 (2008);
K. Ehret *et al.* (ALPS Collab.), Nucl. Instrum. Methods **A612**, 83 (2009).
 27. P. Sikivie, D. Tanner, and K. van Bibber, Phys. Rev. Lett. **98**, 172002 (2007);
G. Mueller *et al.*, Phys. Rev. **D80**, 072004 (2009).
 28. A. Melissinos, Phys. Rev. Lett. **102**, 202001 (2009).
 29. L. Maiani *et al.*, Phys. Lett. **B175**, 359 (1986).
 30. Y. Semertzidis *et al.*, Phys. Rev. Lett. **64**, 2988 (1990).
 31. E. Zavattini *et al.* (PVLAS Collab.), Phys. Rev. Lett. **96**, 110406 (2006).
 32. E. Zavattini *et al.* (PVLAS Collab.), Phys. Rev. **D77**, 032006 (2008).
 33. E. Fischbach and C. Talmadge, Nature **356**, 207 (1992).
 34. J.E. Moody and F. Wilczek, Phys. Rev. D **30**, 130 (1984);
A.N. Youdin *et al.*, Phys. Rev. Lett. **77**, 2170 (1996);
Wei-Tou Ni *et al.*, Phys. Rev. Lett. **82**, 2439 (1999);
D.F. Phillips *et al.*, Phys. Rev. **D63**, 111101 (R) (2001);
B.R. Heckel *et al.* (Eöt-Wash Collab.), Phys. Rev. Lett. **97**, 021603 (2006).
 35. M.S. Turner, Phys. Reports **197**, 67 (1990);
G.G. Raffelt, Phys. Reports **198**, 1 (1990).
 36. G.G. Raffelt, *Stars as Laboratories for Fundamental Physics*, (Univ. of Chicago Press, Chicago, 1996).
 37. G.G. Raffelt, Lect. Notes Phys. **741**, 51 (2008).
 38. P. Gondolo and G. Raffelt, Phys. Rev. **D79**, 107301 (2009).
 39. H. Schlattl, A. Weiss, and G. Raffelt, Astropart. Phys. **10**, 353 (1999).
 40. G. Raffelt and A. Weiss, Phys. Rev. **D51**, 1495 (1995);
M. Catelan, J.A. de Freitas Pacheco, and J.E. Horvath, Astrophys. J. **461**, 231 (1996).
 41. G.G. Raffelt, Phys. Lett. **B166**, 402 (1986);
S.I. Blinnikov and N.V. Dunina-Barkovskaya, Mon. Not. R. Astron. Soc. **266**, 289 (1994);
J. Isern *et al.*, J. Phys. Conf. Ser. **172**, 012005 (2009).
 42. A.H. Córdoba *et al.*, New Astron. **6**, 197 (2001);
J. Isern and E. García-Berro, Nucl. Phys. B Proc. Suppl. **114**, 107 (2003).
 43. J. Engel, D. Seckel, and A.C. Hayes, Phys. Rev. Lett. **65**, 960 (1990).
 44. T. Moroi and H. Murayama, Phys. Lett. **B440**, 69 (1998).
 45. K. van Bibber *et al.*, Phys. Rev. **D39**, 2089 (1989).
 46. D. Lazarus *et al.*, Phys. Rev. Lett. **69**, 2333 (1992).
 47. S. Moriyama *et al.*, Phys. Lett. **B434**, 147 (1998);
Y. Inoue *et al.*, Phys. Lett. **B536**, 18 (2002).
 48. M. Minowa *et al.*, Phys. Lett. **B668**, 93 (2008).
 49. S. Andriamonje *et al.* (CAST Collab.), JCAP **0704**, 010 (2007).
 50. E. Arik *et al.* (CAST Collab.), JCAP **0902**, 008 (2009).
 51. F.T. Avignone III *et al.*, Phys. Rev. Lett. **81**, 5068 (1998);
A. Morales *et al.* (COSME Collab.), Astropart. Phys. **16**, 325 (2002);
R. Bernabei *et al.*, Phys. Lett. **B515**, 6 (2001);
Z. Ahmed *et al.* (CDMS Collab.), Phys. Rev. Lett. **103**, 141802 (2009).
 52. H. Davoudiasl and P. Huber, Phys. Rev. Lett. **97**, 141302 (2006).
 53. J.W. Brockway, E.D. Carlson, and G.G. Raffelt, Phys. Lett. **B383**, 439 (1996);
J.A. Grifols, E. Massó, and R. Toldrà, Phys. Rev. Lett. **77**, 2372 (1996).
 54. C. Csaki, N. Kaloper, and J. Terning, Phys. Rev. Lett. **88**, 161302 (2002).
 55. A. Mirizzi, G.G. Raffelt, and P.D. Serpico, Lect. Notes Phys. **741**, 115 (2008).
 56. C. Burrage, A.C. Davis and D.J. Shaw, Phys. Rev. Lett. **102**, 201101 (2009).
 57. D. Hooper and P.D. Serpico, Phys. Rev. Lett. **99**, 231102 (2007);
K.A. Hochmuth and G. Sigl, Phys. Rev. **D76**, 123011 (2007);
A. De Angelis, O. Mansutti and M. Roncadelli, Phys. Rev. **D76**, 121301 (2007);
A. Mirizzi and D. Montanino, JCAP **0912**, 004 (2009).
 58. M.S. Turner, Phys. Rev. Lett. **59**, 2489 (1987) and Erratum *ibid.*, **60**, 1101 (1988);
E. Massó, F. Rota, and G. Zsembinszki, Phys. Rev. **D66**, 023004 (2002).

Gauge & Higgs Boson Particle Listings

Axions (A^0) and Other Very Light Bosons

59. A. Melchiorri, O. Mena, and A. Slosar, Phys. Rev. **D76**, 041303 (2007);
S. Hannestad *et al.*, JCAP **0804**, 019 (2008).
60. E. Massó and R. Toldra, Phys. Rev. **D55**, 7967 (1997).
61. J. Preskill, M.B. Wise, and F. Wilczek, Phys. Lett. **B120**, 127 (1983);
L.F. Abbott and P. Sikivie, Phys. Lett. **B120**, 133 (1983);
M. Dine and W. Fischler, Phys. Lett. **B120**, 137 (1983).
62. P. Sikivie, Lect. Notes Phys. **741**, 19 (2008).
63. M. Tegmark *et al.*, Phys. Rev. **D73**, 023505 (2006).
64. M. Beltrán, J. García-Bellido, and J. Lesgourgues, Phys. Rev. **D75**, 103507 (2007);
M.P. Hertzberg, M. Tegmark and F. Wilczek, Phys. Rev. **D78**, 083507 (2008);
J. Hamann *et al.*, JCAP **0906**, 022 (2009).
65. E.W. Kolb and I.I. Tkachev, Phys. Rev. Lett. **71**, 3051 (1993), Astrophys. J. **460**, L25 (1996).
66. M. Bershadsky *et al.*, Phys. Rev. Lett. **66**, 1398 (1991);
M. Ressel, Phys. Rev. **D44**, 3001 (1991).
67. D. Grin *et al.*, Phys. Rev. **D75**, 105018 (2007).
68. B.D. Blout *et al.*, Astrophys. J. **546**, 825 (2001).
69. P. Sikivie, Phys. Rev. **D32**, 2988 (1985);
L. Krauss *et al.*, Phys. Rev. Lett. **55**, 1797 (1985);
R. Bradley *et al.*, Rev. Mod. Phys. **75**, 777 (2003).
70. P. Sikivie and J. Ipser, Phys. Lett. **B291**, 288 (1992);
P. Sikivie *et al.*, Phys. Rev. Lett. **75**, 2911 (1995).
71. S. DePañfilis *et al.*, Phys. Rev. Lett. **59**, 839 (1987);
W. Wuensch *et al.*, Phys. Rev. **D40**, 3153 (1989);
C. Hagmann *et al.*, Phys. Rev. **D42**, 1297 (1990).
72. S. Asztalos *et al.*, Phys. Rev. **D69**, 011101 (2004).
73. L. Duffy *et al.*, Phys. Rev. Lett. **95**, 091304 (2005).
74. S. J. Asztalos *et al.* (ADMX Collab.), arXiv:0910.5914.
75. M. Mück, J.B. Kycia, and J. Clarke, Appl. Phys. Lett. **78**, 967 (2001).
76. I. Ogawa, S. Matsuki, and K. Yamamoto, Phys. Rev. **D53**, 1740 (1996).
77. S. Matsuki *et al.*, Nucl. Phys. B (Proc. Suppl.) **51**, 213 (1996);
Y. Kishimoto *et al.*, Phys. Lett. **A303**, 279 (2002);
M. Tada *et al.*, Phys. Lett. **A303**, 285 (2002).

A^0 (Axion) MASS LIMITS from Astrophysics and Cosmology

These bounds depend on model-dependent assumptions (i.e. — on a combination of axion parameters).

VALUE (MeV)	DOCUMENT ID	TECN	COMMENT
•••	We do not use the following data for averages, fits, limits, etc. •••		
>0.2	BARROSO 82	ASTR	Standard Axion
>0.25	1 RAFFELT 82	ASTR	Standard Axion
>0.2	2 DICUS 78c	ASTR	Standard Axion
	MIKHAELIAN 78	ASTR	Stellar emission
>0.3	2 SATO 78	ASTR	Standard Axion
>0.2	VYSOTSKII 78	ASTR	Standard Axion

¹ Lower bound from 5.5 MeV γ -ray line from the sun.

² Lower bound from requiring the red giants' stellar evolution not be disrupted by axion emission.

A^0 (Axion) and Other Light Boson (X^0) Searches in Hadron Decays

Limits are for branching ratios.

VALUE	CL%	DOCUMENT ID	TECN	COMMENT
•••	We do not use the following data for averages, fits, limits, etc. •••			

$<2.4 \times 10^{-7}$	90	³ TUNG 09	K391	$K_L^0 \rightarrow \pi^0 \pi^0 A^0, A^0 \rightarrow \gamma\gamma$
		⁴ PARK 05	HYCP	$\Sigma^+ \rightarrow p A^0, A^0 \rightarrow \mu^+ \mu^-$
$<7 \times 10^{-10}$	90	⁵ ADLER 04	B787	$K^+ \rightarrow \pi^+ X^0$
$<7.3 \times 10^{-11}$	90	⁶ ANISIMOVSK..04	B949	$K^+ \rightarrow \pi^+ X^0$
$<4.5 \times 10^{-11}$	90	⁷ ADLER 02c	B787	$K^+ \rightarrow \pi^+ X^0$
$<4 \times 10^{-5}$	90	⁸ ADLER 01	B787	$K^+ \rightarrow \pi^+ \pi^0 A^0$
$<4.9 \times 10^{-5}$	90	AMMAR 01b	CLEO	$B^\pm \rightarrow \pi^\pm (K^\pm) X^0$
$<5.3 \times 10^{-5}$	90	AMMAR 01b	CLEO	$B^0 \rightarrow K_S^0 X^0$
$<3.3 \times 10^{-5}$	90	⁹ ALTEGOER 98	NOMD	$\pi^0 \rightarrow \gamma X^0, m_{X^0} < 120$ MeV
$<5.0 \times 10^{-8}$	90	¹⁰ KITCHING 97	B787	$K^+ \rightarrow \pi^+ X^0 (X^0 \rightarrow \gamma\gamma)$
$<5.2 \times 10^{-10}$	90	¹¹ ADLER 96	B787	$K^+ \rightarrow \pi^+ X^0$
$<2.8 \times 10^{-4}$	90	¹² AMSLER 96b	CBAR	$\pi^0 \rightarrow \gamma X^0, m_{X^0} < 65$ MeV
$<3 \times 10^{-4}$	90	¹² AMSLER 96b	CBAR	$\eta \rightarrow \gamma X^0, m_{X^0} = 50-200$ MeV
$<4 \times 10^{-5}$	90	¹² AMSLER 96b	CBAR	$\eta' \rightarrow \gamma X^0, m_{X^0} = 50-925$ MeV
$<6 \times 10^{-5}$	90	¹² AMSLER 94b	CBAR	$\pi^0 \rightarrow \gamma X^0, m_{X^0} = 65-125$ MeV
$<6 \times 10^{-5}$	90	¹² AMSLER 94b	CBAR	$\eta \rightarrow \gamma X^0, m_{X^0} = 200-525$ MeV
$<7 \times 10^{-3}$	90	¹³ MEIJERDREES 94	CNTR	$\pi^0 \rightarrow \gamma X^0, m_{X^0} = 20$ MeV
$<2 \times 10^{-3}$	90	¹³ MEIJERDREES 94	CNTR	$\pi^0 \rightarrow \gamma X^0, m_{X^0} = 100$ MeV
$<2 \times 10^{-7}$	90	¹⁴ ATIYA 93b	B787	Sup. by ADLER 04
$<3 \times 10^{-13}$	90	¹⁵ NG 93	COSM	$\pi^0 \rightarrow \gamma X^0$
$<1.1 \times 10^{-8}$	90	¹⁶ ALLIEGRO 92	SPEC	$K^+ \rightarrow \pi^+ X^0 (X^0 \rightarrow e^+ e^-)$
$<5 \times 10^{-4}$	90	¹⁷ ATIYA 92	B787	$\pi^0 \rightarrow \gamma X^0$
$<4 \times 10^{-6}$	90	¹⁸ MEIJERDREES 92	SPEC	$\pi^0 \rightarrow \gamma X^0, X^0 \rightarrow e^+ e^-, m_{X^0} = 100$ MeV
$<1 \times 10^{-7}$	90	¹⁹ ATIYA 90b	B787	Sup. by KITCHING 97
$<1.3 \times 10^{-8}$	90	²⁰ KORENCHENKO 87	SPEC	$\pi^+ \rightarrow e^+ \nu A^0 (A^0 \rightarrow e^+ e^-)$
$<1 \times 10^{-9}$	90	²¹ EICHLER 86	SPEC	Stopped $\pi^+ \rightarrow e^+ \nu A^0$
$<2 \times 10^{-5}$	90	²² YAMAZAKI 84	SPEC	For $160 < m < 260$ MeV
$<(1.5-4) \times 10^{-6}$	90	²² YAMAZAKI 84	SPEC	K decay, $m_{X^0} \ll 100$ MeV
		²³ ASANO 82	CNTR	Stopped $K^+ \rightarrow \pi^+ X^0$
		²⁴ ASANO 81b	CNTR	Stopped $K^+ \rightarrow \pi^+ X^0$
		²⁵ ZHITNITSKII 79		Heavy axion

³ The limit applies at $m_{A^0} = 214.3$ MeV, motivated by PARK 05. TUNG 09 show mass-dependent limits in their Fig. 5.

⁴ PARK 05 found three candidate events for $\Sigma^+ \rightarrow p A^0$ in the HyperCP experiment. Due to a narrow spread in dimuon mass, they hypothesize the events as a possible signal of a new boson. It can be interpreted as an axion-like particle with $m_{A^0} = 214.3 \pm 0.5$ MeV and the branching fraction $B(\Sigma^+ \rightarrow p A^0) \times B(A^0 \rightarrow \mu^+ \mu^-) = (3.1^{+2.4}_{-1.9} \times 1.5) \times 10^{-8}$.

⁵ This limit applies for a mass near 180 MeV. For other masses in the range $m_{X^0} = 150-250$ MeV the limit is less restrictive, but still improves ADLER 02c and ATIYA 93b.

⁶ ANISIMOVSKY 04 bound is for $m_{X^0} = 0$.

⁷ ADLER 02c bound is for $m_{X^0} < 60$ MeV. See Fig. 2 for limits at higher masses.

⁸ The quoted limit is for $m_{X^0} = 0-80$ MeV. See their Fig. 5 for the limit at higher mass. The branching fraction limit assumes pure phase space decay distributions.

⁹ ALTEGOER 98 looked for X^0 from π^0 decay which penetrate the shielding and convert to π^0 in the external Coulomb field of a nucleus.

¹⁰ KITCHING 97 limit is for $B(K^+ \rightarrow \pi^+ X^0) \cdot B(X^0 \rightarrow \gamma\gamma)$ and applies for $m_{X^0} \approx 50$ MeV, $\tau_{X^0} < 10^{-10}$ s. Limits are provided for $0 < m_{X^0} < 100$ MeV, $\tau_{X^0} < 10^{-8}$ s.

¹¹ ADLER 96 looked for a peak in missing-mass distribution. This work is an update of ATIYA 93. The limit is for massless stable X^0 particles and extends to $m_{X^0} = 80$ MeV at the same level. See paper for dependence on finite lifetime.

¹² AMSLER 94b and AMSLER 96b looked for a peak in missing-mass distribution.

¹³ The MEIJERDREES 94 limit is based on inclusive photon spectrum and is independent of X^0 decay modes. It applies to $\tau(X^0) > 10^{-23}$ sec.

¹⁴ ATIYA 93b looked for a peak in missing mass distribution. The bound applies for stable X^0 of $m_{X^0} = 150-250$ MeV, and the limit becomes stronger (10^{-8}) for $m_{X^0} = 180-240$ MeV.

¹⁵ NG 93 studied the production of X^0 via $\gamma\gamma \rightarrow \pi^0 \rightarrow \gamma X^0$ in the early universe at $T \approx 1$ MeV. The bound on extra neutrinos from nucleosynthesis $\Delta N_\nu < 0.3$ (WALKER 91) is employed. It applies to $m_{X^0} \ll 1$ MeV in order to be relativistic down to nucleosynthesis temperature. See paper for heavier X^0 .

¹⁶ ALLIEGRO 92 limit applies for $m_{X^0} = 150-340$ MeV and is the branching ratio times the decay probability. Limit is $< 1.5 \times 10^{-8}$ at 99% CL.

¹⁷ ATIYA 92 looked for a peak in missing mass distribution. The limit applies to $m_{X^0} = 0-130$ MeV in the narrow resonance limit. See paper for the dependence on lifetime. Covariance requires X^0 to be a vector particle.

¹⁸ MEIJERDREES 92 limit applies for $\tau_{X^0} = 10^{-23}-10^{-11}$ sec. Limits between 2×10^{-4} and 4×10^{-6} are obtained for $m_{X^0} = 25-120$ MeV. Angular momentum conservation requires that X^0 has spin ≥ 1 .

¹⁹ ATIYA 90b limit is for $B(K^+ \rightarrow \pi^+ X^0) \cdot B(X^0 \rightarrow \gamma\gamma)$ and applies for $m_{X^0} = 50$ MeV, $\tau_{X^0} < 10^{-10}$ s. Limits are also provided for $0 < m_{X^0} < 100$ MeV, $\tau_{X^0} < 10^{-8}$ s.

²⁰ KORENCHENKO 87 limit assumes $m_{A^0} = 1.7$ MeV, $\tau_{A^0} \lesssim 10^{-12}$ s, and $B(A^0 \rightarrow e^+ e^-) = 1$.

²¹ EICHLER 86 looked for $\pi^+ \rightarrow e^+ \nu A^0$ followed by $A^0 \rightarrow e^+ e^-$. Limits on the branching fraction depend on the mass and lifetime of A^0 . The quoted limits are valid when $\tau(A^0) \gtrsim 3 \times 10^{-10}$ s if the decays are kinematically allowed.

²² YAMAZAKI 84 looked for a discrete line in $K^+ \rightarrow \pi^+ X$. Sensitive to wide mass range (5-300 MeV), independent of whether X decays promptly or not.

See key on page 405

Gauge & Higgs Boson Particle Listings

Axions (A^0) and Other Very Light Bosons

²³ASANO 82 at KEK set limits for $B(K^+ \rightarrow \pi^+ X^0)$ for $m_{X^0} < 100$ MeV as BR $< 4. \times 10^{-8}$ for $\tau(X^0 \rightarrow n\gamma\text{'s}) > 1. \times 10^{-9}$ s, BR $< 1.4 \times 10^{-6}$ for $\tau < 1. \times 10^{-9}$ s.
²⁴ASANO 81B is KEK experiment. Set $B(K^+ \rightarrow \pi^+ X^0) < 3.8 \times 10^{-8}$ at CL = 90%.
²⁵ZHITNITSKII 79 argue that a heavy axion predicted by YANG 78 ($3 < m < 40$ MeV) contradicts experimental muon anomalous magnetic moments.

A^0 (Axion) Searches in Quarkonium Decays

Decay or transition of quarkonium. Limits are for branching ratio.

VALUE	CL%	DOCUMENT ID	TECN	COMMENT
● ● ● We do not use the following data for averages, fits, limits, etc. ● ● ●				
		²⁶ AUBERT 09Z	BABR	$\Upsilon(2S, 3S) \rightarrow \gamma A^0, A^0 \rightarrow \mu^+ \mu^-$
		²⁷ LOVE 08	CLEO	$\Upsilon(1S) \rightarrow \gamma A^0, A^0 \rightarrow \mu^+ \mu^-$, or $\tau^+ \tau^-$
$< 1.3 \times 10^{-5}$	90	²⁸ BALEST 95	CLEO	$\Upsilon(1S) \rightarrow A^0 \gamma$
$< 4.0 \times 10^{-5}$	90	ANTREASYAN 90C	CBAL	$\Upsilon(1S) \rightarrow A^0 \gamma$
		ANTREASYAN 90C	RVUE	
$< 5 \times 10^{-5}$	90	³⁰ DRUZHININ 87	ND	$\phi \rightarrow A^0 \gamma (A^0 \rightarrow e^+ e^-)$
$< 2 \times 10^{-3}$	90	³¹ DRUZHININ 87	ND	$\phi \rightarrow A^0 \gamma (A^0 \rightarrow \gamma \gamma)$
$< 7 \times 10^{-6}$	90	³² DRUZHININ 87	ND	$\phi \rightarrow A^0 \gamma (A^0 \rightarrow \text{missing})$
$< 3.1 \times 10^{-4}$	90	³³ ALBRECHT 86D	ARG	$\Upsilon(1S) \rightarrow A^0 \gamma (A^0 \rightarrow e^+ e^-)$
$< 4 \times 10^{-4}$	90	³³ ALBRECHT 86D	ARG	$\Upsilon(1S) \rightarrow A^0 \gamma (A^0 \rightarrow \mu^+ \mu^-$, $\pi^+ \pi^-$, $K^+ K^-)$
$< 8 \times 10^{-4}$	90	³⁴ ALBRECHT 86D	ARG	$\Upsilon(1S) \rightarrow A^0 \gamma$
$< 1.3 \times 10^{-3}$	90	³⁵ ALBRECHT 86D	ARG	$\Upsilon(1S) \rightarrow A^0 \gamma (A^0 \rightarrow e^+ e^-$, $\gamma \gamma)$
$< 2. \times 10^{-3}$	90	³⁶ BOWCOCK 86	CLEO	$\Upsilon(2S) \rightarrow \Upsilon(1S) \rightarrow A^0$
$< 5. \times 10^{-3}$	90	³⁷ MAGERAS 86	CUSB	$\Upsilon(1S) \rightarrow A^0 \gamma$
$< 3. \times 10^{-4}$	90	³⁸ ALAM 83	CLEO	$\Upsilon(1S) \rightarrow A^0 \gamma$
$< 9.1 \times 10^{-4}$	90	³⁹ NICZYPORUK 83	LENA	$\Upsilon(1S) \rightarrow A^0 \gamma$
$< 1.4 \times 10^{-5}$	90	⁴⁰ EDWARDS 82	CBAL	$J/\psi \rightarrow A^0 \gamma$
$< 3.5 \times 10^{-4}$	90	⁴¹ SIVERTZ 82	CUSB	$\Upsilon(1S) \rightarrow A^0 \gamma$
$< 1.2 \times 10^{-4}$	90	⁴¹ SIVERTZ 82	CUSB	$\Upsilon(3S) \rightarrow A^0 \gamma$

²⁶AUBERT 09Z show mass-dependent limits on $B(\Upsilon \rightarrow \gamma A^0) B(A^0 \rightarrow \mu^+ \mu^-)$ in their Fig. 2.
²⁷LOVE 08 show mass-dependent limits on $B(\Upsilon \rightarrow \gamma A^0) B(A^0 \rightarrow \mu^+ \mu^-)$ or $\tau^+ \tau^-$ on their Fig. 3.

²⁸BALEST 95 looked for a monochromatic γ from $\Upsilon(1S)$ decay. The bound is for $m_{A^0} < 5.0$ GeV. See Fig. 7 in the paper for bounds for heavier m_{A^0} . They also quote a bound on branching ratios $10^{-3}-10^{-5}$ of three-body decay $\gamma X \bar{X}$ for $0 < m_X < 3.1$ GeV.

²⁹The combined limit of ANTREASYAN 90C and EDWARDS 82 excludes standard axion with $m_{A^0} < 2m_e$ at 90% CL as long as $C_{\Upsilon} C_{J/\psi} > 0.09$, where $C_V (V = \Upsilon, J/\psi)$ is the reduction factor for $\Gamma(V \rightarrow A^0 \gamma)$ due to QCD and/or relativistic corrections. The same data excludes $0.02 < x < 260$ (90% CL) if $C_{\Upsilon} = C_{J/\psi} = 0.5$, and further combining with ALBRECHT 86D result excludes $5 \times 10^{-5} < x < 260$. x is the ratio of the vacuum expectation values of the two Higgs fields. These limits use conventional assumption $\Gamma(A^0 \rightarrow ee) \propto x^{-2}$. The alternative assumption $\Gamma(A^0 \rightarrow ee) \propto x^2$ gives a somewhat different excluded region $0.00075 < x < 44$.

³⁰The first DRUZHININ 87 limit is valid when $\tau_{A^0}/m_{A^0} < 3 \times 10^{-13}$ s/MeV and $m_{A^0} < 20$ MeV.

³¹The second DRUZHININ 87 limit is valid when $\tau_{A^0}/m_{A^0} < 5 \times 10^{-13}$ s/MeV and $m_{A^0} < 20$ MeV.

³²The third DRUZHININ 87 limit is valid when $\tau_{A^0}/m_{A^0} > 7 \times 10^{-12}$ s/MeV and $m_{A^0} < 200$ MeV.

³³ $\tau_{A^0} < 1 \times 10^{-13}$ s and $m_{A^0} < 1.5$ GeV. Applies for $A^0 \rightarrow \gamma \gamma$ when $m_{A^0} < 100$ MeV.

³⁴ $\tau_{A^0} > 1 \times 10^{-7}$ s.

³⁵Independent of τ_{A^0} .

³⁶BOWCOCK 86 looked for A^0 that decays into $e^+ e^-$ in the cascade decay $\Upsilon(2S) \rightarrow \Upsilon(1S) \pi^+ \pi^-$ followed by $\Upsilon(1S) \rightarrow A^0 \gamma$. The limit for $B(\Upsilon(1S) \rightarrow A^0 \gamma) B(A^0 \rightarrow e^+ e^-)$ depends on m_{A^0} and τ_{A^0} . The quoted limit for $m_{A^0} = 1.8$ MeV is at $\tau_{A^0} \sim 2. \times 10^{-12}$ s, where the limit is the worst. The same limit $2. \times 10^{-3}$ applies for all lifetimes for masses $2m_e < m_{A^0} < 2m_\mu$ when the results of this experiment are combined with the results of ALAM 83.

³⁷MAGERAS 86 looked for $\Upsilon(1S) \rightarrow \gamma A^0 (A^0 \rightarrow e^+ e^-)$. The quoted branching fraction limit is for $m_{A^0} = 1.7$ MeV, at $\tau(A^0) \sim 4. \times 10^{-13}$ s where the limit is the worst.

³⁸ALAM 83 is at CESR. This limit combined with limit for $B(J/\psi \rightarrow A^0 \gamma)$ (EDWARDS 82) excludes standard axion.

³⁹NICZYPORUK 83 is DESY-DORIS experiment. This limit together with lower limit 9.2×10^{-4} of $B(\Upsilon \rightarrow A^0 \gamma)$ derived from $B(J/\psi(1S) \rightarrow A^0 \gamma)$ limit (EDWARDS 82) excludes standard axion.

⁴⁰EDWARDS 82 looked for $J/\psi \rightarrow \gamma A^0$ decays by looking for events with a single γ [of energy $\sim 1/2$ the $J/\psi(1S)$ mass], plus nothing else in the detector. The limit is inconsistent with the axion interpretation of the FAISSNER 81B result.

⁴¹SIVERTZ 82 is CESR experiment. Looked for $\Upsilon \rightarrow \gamma A^0, A^0$ undetected. Limit for $1S$ (3S) is valid for $m_{A^0} < 7$ GeV (4 GeV).

$< 4.4 \times 10^{-5}$	90	⁴² BADERT...	02	CNTR	$\alpha\text{-Ps} \rightarrow \gamma X_1 X_2, m_{X_1} + m_{X_2} \leq 900$ keV
$< 2 \times 10^{-4}$	90	MAENO	95	CNTR	$\alpha\text{-Ps} \rightarrow A^0 \gamma, m_{A^0} = 850-1013$ keV
$< 3.0 \times 10^{-3}$	90	⁴³ ASAI	94	CNTR	$\alpha\text{-Ps} \rightarrow A^0 \gamma, m_{A^0} = 30-500$ keV
$< 2.8 \times 10^{-5}$	90	⁴⁴ AKOPYAN	91	CNTR	$\alpha\text{-Ps} \rightarrow A^0 \gamma (A^0 \rightarrow \gamma \gamma)$, $m_{A^0} < 30$ keV
$< 1.1 \times 10^{-6}$	90	⁴⁵ ASAI	91	CNTR	$\alpha\text{-Ps} \rightarrow A^0 \gamma, m_{A^0} < 800$ keV
$< 3.8 \times 10^{-4}$	90	GNINENKO	90	CNTR	$\alpha\text{-Ps} \rightarrow A^0 \gamma, m_{A^0} < 30$ keV
$< (1-5) \times 10^{-4}$	95	⁴⁶ TSUCHIAKI	90	CNTR	$\alpha\text{-Ps} \rightarrow A^0 \gamma, m_{A^0} = 300-900$ keV
$< 6.4 \times 10^{-5}$	90	⁴⁷ ORITO	89	CNTR	$\alpha\text{-Ps} \rightarrow A^0 \gamma, m_{A^0} < 30$ keV
		⁴⁸ AMALDI	85	CNTR	Ortho-positronium
		⁴⁹ CARBONI	83	CNTR	Ortho-positronium

⁴²BADERTSCHER 02 looked for a three-body decay of ortho-positronium into a photon and two penetrating (neutral or milli-charged) particles.

⁴³The ASAI 94 limit is based on inclusive photon spectrum and is independent of A^0 decay modes.

⁴⁴The AKOPYAN 91 limit applies for a short-lived A^0 with $\tau_{A^0} < 10^{-13}$ s m_{A^0} [keV].

⁴⁵ASAI 91 limit translates to $g_{A^0 e^+ e^-}^2 / 4\pi < 1.1 \times 10^{-11}$ (90% CL) for $m_{A^0} < 800$ keV.

⁴⁶The TSUCHIAKI 90 limit is based on inclusive photon spectrum and is independent of A^0 decay modes.

⁴⁷ORITO 89 limit translates to $g_{A^0 e^+ e^-}^2 / 4\pi < 6.2 \times 10^{-10}$. Somewhat more sensitive limits are obtained for larger m_{A^0} : $B < 7.6 \times 10^{-6}$ at 100 keV.

⁴⁸AMALDI 85 set limits $B(A^0 \gamma) / B(\gamma \gamma) < (1-5) \times 10^{-6}$ for $m_{A^0} = 900-100$ keV which are about 1/10 of the CARBONI 83 limits.

⁴⁹CARBONI 83 looked for ortho-positronium $\rightarrow A^0 \gamma$. Set limit for A^0 electron coupling squared, $g(e e A^0)^2 / (4\pi) < 6. \times 10^{-10} - 7. \times 10^{-9}$ for m_{A^0} from 150-900 keV (CL = 99.7%). This is about 1/10 of the bound from $g-2$ experiments.

A^0 (Axion) Search in Photoproduction

VALUE	CL%	DOCUMENT ID	TECN	COMMENT
● ● ● We do not use the following data for averages, fits, limits, etc. ● ● ●				
		⁵⁰ BASSOMPIERRE...	95	$m_{A^0} = 1.8 \pm 0.2$ MeV

⁵⁰BASSOMPIERRE 95 is an extension of BASSOMPIERRE 93. They looked for a peak in the invariant mass of $e^+ e^-$ pairs in the region $m_{e^+ e^-} = 1.8 \pm 0.2$ MeV. They obtained bounds on the production rate A^0 for $\tau(A^0) = 10^{-18}-10^{-9}$ sec. They also found an excess of events in the range $m_{e^+ e^-} = 2.1-3.5$ MeV.

A^0 (Axion) Production in Hadron Collisions

Limits are for $\sigma(A^0) / \sigma(\pi^0)$.

VALUE	CL%	EVTS	DOCUMENT ID	TECN	COMMENT	
● ● ● We do not use the following data for averages, fits, limits, etc. ● ● ●						
			⁵¹ JAIN	07	CNTR	$A^0 \rightarrow e^+ e^-$
			⁵² AHMAD	97	SPEC	e^+ production
			⁵³ LEINBERGER	97	SPEC	$A^0 \rightarrow e^+ e^-$
			⁵⁴ GANZ	96	SPEC	$A^0 \rightarrow e^+ e^-$
			⁵⁵ KAMEL	96	EMUL	^{32}S emulsion, $A^0 \rightarrow e^+ e^-$
			⁵⁶ BLUEMLEIN	92	BDMP	$A^0 N_Z \rightarrow \ell^+ \ell^- N_Z$
			⁵⁷ MEIJERDREES	92	SPEC	$\pi^- p \rightarrow n A^0, A^0 \rightarrow e^+ e^-$
			⁵⁸ BLUEMLEIN	91	BDMP	$A^0 \rightarrow e^+ e^-, 2\gamma$
			⁵⁹ FAISSNER	89	OSPK	Beam dump, $A^0 \rightarrow e^+ e^-$
			⁶⁰ DEBOER	88	RVUE	$A^0 \rightarrow e^+ e^-$
			⁶¹ EL-NADI	88	EMUL	$A^0 \rightarrow e^+ e^-$
			⁶² FAISSNER	88	OSPK	Beam dump, $A^0 \rightarrow 2\gamma$
			⁶³ BADIER	86	BDMP	$A^0 \rightarrow e^+ e^-$
$< 2. \times 10^{-11}$	90	0	⁶⁴ BERGSMA	85	CHRM	CERN beam dump
$< 1. \times 10^{-13}$	90	0	⁶⁴ BERGSMA	85	CHRM	CERN beam dump
		24	⁶⁵ FAISSNER	83	OSPK	Beam dump, $A^0 \rightarrow 2\gamma$
			⁶⁶ FAISSNER	83B	RVUE	LAMPF beam dump
			⁶⁷ FRANK	83B	RVUE	LAMPF beam dump
			⁶⁸ HOFFMAN	83	CNTR	$\pi p \rightarrow n A^0 (A^0 \rightarrow e^+ e^-)$
			⁶⁹ FETSCHER	82	RVUE	See FAISSNER 81B
		12	⁷⁰ FAISSNER	81	OSPK	CERN PS ν wideband
		15	⁷¹ FAISSNER	81B	OSPK	Beam dump, $A^0 \rightarrow 2\gamma$
		8	⁷² KIM	81	OSPK	26 GeV $pN \rightarrow A^0 X$
		0	⁷³ FAISSNER	80	OSPK	Beam dump, $A^0 \rightarrow e^+ e^-$
$< 1. \times 10^{-8}$	90		⁷⁴ JACQUES	80	HLBC	28 GeV protons
$< 1. \times 10^{-14}$	90		⁷⁴ JACQUES	80	HLBC	Beam dump
			⁷⁵ SOUKAS	80	CALO	28 GeV p beam dump
			⁷⁶ BECHIS	79	CNTR	
$< 1. \times 10^{-8}$	90		⁷⁷ COTEUS	79	OSPK	Beam dump
$< 1. \times 10^{-3}$	95		⁷⁸ DISHAW	79	CALO	400 GeV pp
$< 1. \times 10^{-8}$	90		ALIBRAN	78	HYBR	Beam dump
$< 6. \times 10^{-9}$	95		ASRATYAN	78B	CALO	Beam dump

A^0 (Axion) Searches in Positronium Decays

Decay or transition of positronium. Limits are for branching ratio.

VALUE	CL%	DOCUMENT ID	TECN	COMMENT
● ● ● We do not use the following data for averages, fits, limits, etc. ● ● ●				

Gauge & Higgs Boson Particle Listings

Axions (A^0) and Other Very Light Bosons

- $<1.5 \times 10^{-8}$ 90 79 BELLOTTI 78 HLBC Beam dump
 $<5.4 \times 10^{-14}$ 90 79 BELLOTTI 78 HLBC $m_{A^0}=1.5$ MeV
 $<4.1 \times 10^{-9}$ 90 79 BELLOTTI 78 HLBC $m_{A^0}=1$ MeV
 $<1. \times 10^{-8}$ 90 80 BOSETTI 78B HYBR Beam dump
 81 DONNELLY 78
 $<0.5 \times 10^{-8}$ 90 HANSL 78D WIRE Beam dump
 82 MICELMAC... 78
 83 VYSOTSKII 78
- 51 JAIN 07 claims evidence for $A^0 \rightarrow e^+e^-$ produced in ^{207}Pb collision on nuclear emulsion (Ag/Br) for $m(A^0) = 7 \pm 1$ or 19 ± 1 MeV and $\tau(A^0) \leq 10^{-13}$ s.
 52 AHMAD 97 reports a result of APEX Collaboration which studied positron production in $^{238}\text{U} \rightarrow ^{232}\text{Ta}$ and $^{238}\text{U} \rightarrow ^{181}\text{Ta}$ collisions, without requiring a coincident electron. No narrow lines were found for $250 < E_{e^+} < 750$ keV.
 53 LEINBERGER 97 (ORANGE Collaboration) at GSI looked for a narrow sum-energy e^+e^- line at ~ 635 keV in $^{238}\text{U} \rightarrow ^{181}\text{Ta}$ collision. Limits on the production probability for a narrow sum-energy e^+e^- line are set. See their Table 2.
 54 GANZ 96 (EPOS II Collaboration) has placed upper bounds on the production cross section of e^+e^- pairs from $^{238}\text{U} \rightarrow ^{181}\text{Ta}$ and $^{238}\text{U} \rightarrow ^{232}\text{Th}$ collisions at GSI. See Table 2 for limits both for back-to-back and isotropic configurations of e^+e^- pairs. These limits rule out the existence of peaks in the e^+e^- sum-energy distribution, reported by an earlier version of this experiment.
 55 KAMEL 96 looked for e^+e^- pairs from the collision of ^{32}S (200 GeV/nucleon) and emulsion. No evidence of mass peaks is found in the region of sensitivity $m_{ee} > 2$ MeV.
 56 BLUEMLEIN 92 is a proton beam dump experiment at Serpukhov with a secondary target to induce Bethe-Heitler production of e^+e^- or $\mu^+\mu^-$ from the produce A^0 . See Fig. 5 for the excluded region in m_{A^0} - x plane. For the standard axion, $0.3 < x < 25$ is excluded at 95% CL. If combined with BLUEMLEIN 91, $0.008 < x < 32$ is excluded.
 57 MEIJERDREES 92 give $\Gamma(\pi^+p \rightarrow nA^0) \cdot \text{B}(A^0 \rightarrow e^+e^-) / \Gamma(\pi^+p \rightarrow \text{all}) < 10^{-5}$ (90% CL) for $m_{A^0} = 100$ MeV, $\tau_{A^0} = 10^{-11} - 10^{-23}$ sec. Limits ranging from 2.5×10^{-3} to 10^{-7} are given for $m_{A^0} = 25 - 136$ MeV.
 58 BLUEMLEIN 91 is a proton beam dump experiment at Serpukhov. No candidate event for $A^0 \rightarrow e^+e^-$, 2γ are found. Fig. 6 gives the excluded region in m_{A^0} - x plane ($x = \tan\beta = v_2/v_1$). Standard axion is excluded for $0.2 < m_{A^0} < 3.2$ MeV for most $x > 1$, $0.2 - 11$ MeV for most $x < 1$.
 59 FAISSNER 89 searched for $A^0 \rightarrow e^+e^-$ in a proton beam dump experiment at SIN. No excess of events was observed over the background. A standard axion with mass $2m_e - 20$ MeV is excluded. Lower limit on f_{A^0} of $\approx 10^4$ GeV is given for $m_{A^0} = 2m_e - 20$ MeV.
 60 DEBOER 88 reanalyze EL-NADI 88 data and claim evidence for three distinct states with mass ~ 1.1 , ~ 2.1 , and ~ 9 MeV, lifetimes $10^{-16} - 10^{-15}$ s decaying to e^+e^- and note the similarity of the data with those of a cosmic-ray experiment by Bristol group (B.M. Anand, Proc. of the Royal Society of London, Section A **A22** 183 (1953)). For a criticism see PERKINS 89, who suggests that the events are compatible with π^0 Dalitz decay. DEBOER 89b is a reply which contests the criticism.
 61 EL-NADI 88 claim the existence of a neutral particle decaying into e^+e^- with mass 1.60 ± 0.59 MeV, lifetime $(0.15 \pm 0.01) \times 10^{-14}$ s, which is produced in heavy ion interactions with emulsion nuclei at ~ 4 GeV/c/nucleon.
 62 FAISSNER 88 is a proton beam dump experiment at SIN. They found no candidate event for $A^0 \rightarrow \gamma\gamma$. A standard axion decaying to 2γ is excluded except for a region $x \approx 1$. Lower limit on f_{A^0} of $10^2 - 10^3$ GeV is given for $m_{A^0} = 0.1 - 1$ MeV.
 63 BADIER 86 did not find long-lived A^0 in 300 GeV π^- Beam Dump Experiment that decays into e^+e^- in the mass range $m_{A^0} = (20 - 200)$ MeV, which excludes the A^0 decay constant $f(A^0)$ in the interval (60-600) GeV. See their figure 6 for excluded region on $f(A^0) - m_{A^0}$ plane.
 64 BERGSMAN 85 look for $A^0 \rightarrow 2\gamma, e^+e^-, \mu^+\mu^-$. First limit above is for $m_{A^0} = 1$ MeV; second is for 200 MeV. See their figure 4 for excluded region on $f_{A^0} - m_{A^0}$ plane, where f_{A^0} is A^0 decay constant. For Peccei-Quinn PECCCI 77 $A^0, m_{A^0} < 180$ keV and $\tau > 0.037$ s. (CL = 90%). For the axion of FAISSNER 81b at 250 keV, BERGSMAN 85 expect 15 events but observe zero.
 65 FAISSNER 83 observed 19 $1-\gamma$ and 12 $2-\gamma$ events where a background of 4.8 and 2.3 respectively is expected. A small-angle peak is observed even if iron wall is set in front of the decay region.
 66 FAISSNER 83b extrapolate SIN γ signal to LAMPF ν experimental condition. Resulting 370γ 's are not at variance with LAMPF upper limit of 450 γ 's. Derived from LAMPF limit that $[d\sigma(A^0)/d\omega \text{ at } 90^\circ] m_{A^0} / \tau_{A^0} < 14 \times 10^{-35} \text{ cm}^2 \text{ sr}^{-1} \text{ MeV ms}^{-1}$. See comment on FRANK 83b.
 67 FRANK 83b stress the importance of LAMPF data bins with negative net signal. By statistical analysis say that LAMPF and SIN-A0 are at variance when extrapolation by phase-space model is done. They find LAMPF upper limit is 248 not 450 γ 's. See comment on FAISSNER 83b.
 68 HOFFMAN 83 set CL = 90% limit $d\sigma/dt \text{ B}(e^+e^-) < 3.5 \times 10^{-32} \text{ cm}^2/\text{GeV}^2$ for $140 < m_{A^0} < 160$ MeV. Limit assumes $\tau(A^0) < 10^{-9}$ s.
 69 FETSCHER 82 reanalyzes SIN beam-dump data of FAISSNER 81. Claims no evidence for axion since $2-\gamma$ peak rate remarkably decreases if iron wall is set in front of the decay region.
 70 FAISSNER 81 see excess μe events. Suggest axion interactions.
 71 FAISSNER 81b is SIN 590 MeV proton beam dump. Observed 14.5 ± 5.0 events of 2γ decay of long-lived neutral penetrating particle with $m_{2\gamma} \lesssim 1$ MeV. Axion interpretation with $\eta-A^0$ mixing gives $m_{A^0} = 250 \pm 25$ keV, $\tau_{(2\gamma)} = (7.3 \pm 3.7) \times 10^{-3}$ s from above rate. See critical remarks below in comments of FETSCHER 82, FAISSNER 83, FAISSNER 83b, FRANK 83b, and BERGSMAN 85. Also see in the next subsection ALEKSEEV 82b, CAVAIIGNAC 83, and ANANEV 85.
 72 KIM 81 analyzed 8 candidates for $A^0 \rightarrow 2\gamma$ obtained by Aachen-Padova experiment at CERN with 26 GeV protons on Be. Estimated axion mass is about 300 keV and lifetime is $(0.86 - 5.6) \times 10^{-3}$ s depending on models. Faissner (private communication), says axion production underestimated and mass overestimated. Correct value around 200 keV.

- 73 FAISSNER 80 is SIN beam dump experiment with 590 MeV protons looking for $A^0 \rightarrow e^+e^-$ decay. Assuming $A^0/\pi^0 = 5.5 \times 10^{-7}$, obtained decay rate limit $20/(A^0 \text{ mass}) \text{ MeV/s}$ (CL = 90%), which is about 10^{-7} below theory and interpreted as upper limit to $m_{A^0} < 2m_{e^-}$.
 74 JACQUES 80 is a BNL beam dump experiment. First limit above comes from nonobservation of excess neutral-current-type events $[\sigma(\text{production})\sigma(\text{interaction}) < 7. \times 10^{-68} \text{ cm}^4, \text{ CL} = 90\%]$. Second limit is from nonobservation of axion decays into 2γ 's or e^+e^- , and for axion mass a few MeV.
 75 SOUKAS 80 at BNL observed no excess of neutral-current-type events in beam dump.
 76 BECHIS 79 looked for the axion production in low energy electron Bremsstrahlung and the subsequent decay into either 2γ or e^+e^- . No signal found. CL = 90% limits for model parameter(s) are given.
 77 COTEUS 79 is a beam dump experiment at BNL.
 78 DISHAW 79 is a calorimetric experiment and looks for low energy tail of energy distributions due to energy lost to weakly interacting particles.
 79 BELLOTTI 78 first value comes from search for $A^0 \rightarrow e^+e^-$. Second value comes from search for $A^0 \rightarrow 2\gamma$, assuming mass $< 2m_{e^-}$. For any mass satisfying this, limit is above value $\times (\text{mass}^{-4})$. Third value uses data of PL 60B 401 and quotes $\sigma(\text{production})\sigma(\text{interaction}) < 10^{-67} \text{ cm}^4$.
 80 BOSETTI 78B quotes $\sigma(\text{production})\sigma(\text{interaction}) < 2. \times 10^{-67} \text{ cm}^4$.
 81 DONNELLY 78 examines data from reactor neutrino experiments of REINES 76 and GURR 74 as well as SLAC beam dump experiment. Evidence is negative.
 82 MICELMACHER 78 finds no evidence of axion existence in reactor experiments of REINES 76 and GURR 74. (See reference under DONNELLY 78 below).
 83 VYSOTSKII 78 derived lower limit for the axion mass 25 keV from luminosity of the sun and 200 keV from red supergiants.

A^0 (Axion) Searches in Reactor Experiments

VALUE	DOCUMENT ID	TECN	COMMENT
• • • We do not use the following data for averages, fits, limits, etc. • • •			
	84 CHANG 07		Primakoff or Compton
	85 ALTMANN 95	CNTR	Reactor; $A^0 \rightarrow e^+e^-$
	86 KETOV 86	SPEC	Reactor; $A^0 \rightarrow \gamma\gamma$
	87 KOCH 86	SPEC	Reactor; $A^0 \rightarrow \gamma\gamma$
	88 DATAR 82	CNTR	Light water reactor
	89 VUILLEUMIER 81	CNTR	Reactor; $A^0 \rightarrow 2\gamma$
84 CHANG 07 looked for monochromatic photons from Primakoff or Compton conversion of axions from the Kuo-Sheng reactor due to axion coupling to photon or electron, respectively. The search places model-independent limits on the products $G_{A\gamma\gamma} G_{ANN}$ and $G_{Aee} G_{ANN}$ for $m(A^0)$ less than the MeV range.			
85 ALTMANN 95 looked for A^0 decaying into e^+e^- from the Bugey5 nuclear reactor. They obtain an upper limit on the A^0 production rate of $\omega(A^0)/\omega(\gamma) \times \text{B}(A^0 \rightarrow e^+e^-) < 10^{-16}$ for $m_{A^0} = 1.5$ MeV at 90% CL. The limit is weaker for heavier A^0 . In the case of a standard axion, this limit excludes a mass in the range $2m_e < m_{A^0} < 4.8$ MeV at 90% CL. See Fig. 5 of their paper for exclusion limits of axion-like resonances Z^0 in the (m_{X^0}, f_{X^0}) plane.			
86 KETOV 86 searched for A^0 at the Rovno nuclear power plant. They found an upper limit on the A^0 production probability of $0.8 [100 \text{ keV}/m_{A^0}]^6 \times 10^{-6}$ per fission. In the standard axion model, this corresponds to $m_{A^0} > 150$ keV. Not valid for $m_{A^0} \gtrsim 1$ MeV.			
87 KOCH 86 searched for $A^0 \rightarrow \gamma\gamma$ at nuclear power reactor Biblis A. They found an upper limit on the A^0 production rate of $\omega(A^0)/\omega(\gamma(M1)) < 1.5 \times 10^{-10}$ (CL=95%). Standard axion with $m_{A^0} = 250$ keV gives 10^{-5} for the ratio. Not valid for $m_{A^0} > 1022$ keV.			
88 DATAR 82 looked for $A^0 \rightarrow 2\gamma$ in neutron capture ($np \rightarrow dA^0$) at Tarapur 500 MW reactor. Sensitive to sum of $l = 0$ and $l = 1$ amplitudes. With ZEHNDER 81 [$(l = 0) - (l = 1)$] result, assert nonexistence of standard A^0 .			
89 VUILLEUMIER 81 is at Grenoble reactor. Set limit $m_{A^0} < 280$ keV.			

A^0 (Axion) and Other Light Boson (X^0) Searches in Nuclear Transitions

Limits are for branching ratio.

VALUE	CL%	DOCUMENT ID	TECN	COMMENT
• • • We do not use the following data for averages, fits, limits, etc. • • •				
$< 8.5 \times 10^{-6}$	90	90 DERBIN 02	CNTR	^{125}mTe decay
		91 DEBOER 97c	RVUE	M1 transitions
		92 TSUNODA 95	CNTR	^{252}Cf fission, $A^0 \rightarrow ee$
$< 5.5 \times 10^{-10}$	95	93 MINOWA 93	CNTR	$^{139}\text{La}^* \rightarrow ^{139}\text{La}A^0$
$< 1.2 \times 10^{-6}$	95	94 HICKS 92	CNTR	^{35}S decay, $A^0 \rightarrow \gamma\gamma$
$< 2 \times 10^{-4}$	90	95 ASANUMA 90	CNTR	^{241}Am decay
$< 1.5 \times 10^{-9}$	95	96 DEBOER 90	CNTR	$^8\text{Be}^* \rightarrow ^8\text{Be}A^0$
$< (0.4-10) \times 10^{-3}$	95			$A^0 \rightarrow e^+e^-$
$< (0.2-1) \times 10^{-3}$	90	97 BINI 89	CNTR	$^{16}\text{O}^* \rightarrow ^{16}\text{O}X^0$
		98 AVIGNONE 88	CNTR	$\text{Cu}^* \rightarrow \text{Cu}A^0 (A^0 \rightarrow 2\gamma, A^0 \rightarrow \gamma e, A^0 Z \rightarrow \gamma Z)$
$< 1.5 \times 10^{-4}$	90	99 DATAR 88	CNTR	$^{12}\text{C}^* \rightarrow ^{12}\text{C}A^0$
$< 5 \times 10^{-3}$	90	100 DEBOER 88c	CNTR	$^{16}\text{O}^* \rightarrow ^{16}\text{O}X^0$
				$A^0 \rightarrow e^+e^-$
$< 3.4 \times 10^{-5}$	95	101 DOEHNER 88	SPEC	$^2\text{H}^*, A^0 \rightarrow e^+e^-$
$< 4 \times 10^{-4}$	95	102 SAVAGE 88	CNTR	Nuclear decay (isovector)

See key on page 405

Gauge & Higgs Boson Particle Listings
Axions (A^0) and Other Very Light Bosons

< 3×10^{-3}	95	102 SAVAGE	88	CNTR	Nuclear decay (isoscalar)
< 10.6×10^{-2}	90	103 HALLIN	86	SPEC	${}^6\text{Li}$ isovector decay
< 10.8	90	103 HALLIN	86	SPEC	${}^{10}\text{B}$ isoscalar decays
< 2.2	90	103 HALLIN	86	SPEC	${}^{14}\text{N}$ isoscalar decays
< 4×10^{-4}	90	104 SAVAGE	86B	CNTR	${}^{14}\text{N}^*$
		105 ANANEV	85	CNTR	Li^* , deut* $A^0 \rightarrow 2\gamma$
		106 CAVAIGNAC	83	CNTR	${}^{97}\text{Nb}^*$, deut* transition $A^0 \rightarrow 2\gamma$
		107 ALEKSEEV	82B	CNTR	Li^* , deut* transition $A^0 \rightarrow 2\gamma$
		108 LEHMANN	82	CNTR	$\text{Cu}^* \rightarrow \text{Cu}A^0$ ($A^0 \rightarrow 2\gamma$)
		109 ZEHNDER	82	CNTR	Li^* , Nb* decay, n -capt.
		110 ZEHNDER	81	CNTR	$\text{Ba}^* \rightarrow \text{Ba}A^0$ ($A^0 \rightarrow 2\gamma$)
		111 CALAPRICE	79		Carbon

⁹⁰DERBIN 02 looked for the axion emission in an M1 transition in ${}^{125}\text{mTe}$ decay. They looked for a possible presence of a shifted energy spectrum in gamma rays due to the undetected axion.

⁹¹DEBOER 97C reanalyzed the existent data on Nuclear M1 transitions and find that a 9 MeV boson decaying into e^+e^- would explain the excess of events with large opening angles. See also DEBOER 01 for follow-up experiments.

⁹²TUNODA 95 looked for axion emission when ${}^{252}\text{Cf}$ undergoes a spontaneous fission, with the axion decaying into e^+e^- . The bound is for $m_{A^0}=40$ MeV. It improves to 2.5×10^{-5} for $m_{A^0}=200$ MeV.

⁹³MINOWA 93 studied chain process, ${}^{139}\text{Ce} \rightarrow {}^{139}\text{La}^*$ by electron capture and M1 transition of ${}^{139}\text{La}^*$ to the ground state. It does not assume decay modes of A^0 . The bound applies for $m_{A^0} < 166$ keV.

⁹⁴HICKS 92 bound is applicable for $\tau_{X^0} < 4 \times 10^{-11}$ sec.

⁹⁵The ASANUMA 90 limit is for the branching fraction of X^0 emission per ${}^{241}\text{Am}$ α decay and valid for $\tau_{X^0} < 3 \times 10^{-11}$ s.

⁹⁶The DEBOER 90 limit is for the branching ratio ${}^8\text{Be}^*$ (18.15 MeV, 1^+) \rightarrow ${}^8\text{Be}A^0$, $A^0 \rightarrow e^+e^-$ for the mass range $m_{A^0} = 4\text{--}15$ MeV.

⁹⁷The BINI 89 limit is for the branching fraction of ${}^{16}\text{O}^*$ (6.05 MeV, 0^+) \rightarrow ${}^{16}\text{O}X^0$, $X^0 \rightarrow e^+e^-$ for $m_{X^0} = 1.5\text{--}3.1$ MeV. $\tau_{X^0} \lesssim 10^{-11}$ s is assumed. The spin-parity of X is restricted to 0^+ or 1^- .

⁹⁸AVIGNONE 88 looked for the 1115 keV transition $\text{C}^* \rightarrow \text{Cu}A^0$, either from $A^0 \rightarrow 2\gamma$ in-flight decay or from the secondary A^0 interactions by Compton and by Primakoff processes. Limits for axion parameters are obtained for $m_{A^0} < 1.1$ MeV.

⁹⁹DATAR 88 rule out light pseudoscalar particle emission through its decay $A^0 \rightarrow e^+e^-$ in the mass range 1.02–2.5 MeV and lifetime range $10^{-13}\text{--}10^{-8}$ s. The above limit is for $\tau = 5 \times 10^{-13}$ s and $m = 1.7$ MeV; see the paper for the τ - m dependence of the limit.

¹⁰⁰The limit is for the branching fraction of ${}^{16}\text{O}^*$ (6.05 MeV, 0^+) \rightarrow ${}^{16}\text{O}X^0$, $X^0 \rightarrow e^+e^-$ against internal pair conversion for $m_{X^0} = 1.7$ MeV and $\tau_{X^0} < 10^{-11}$ s. Similar limits are obtained for $m_{X^0} = 1.3\text{--}3.2$ MeV. The spin parity of X^0 must be either 0^+ or 1^- . The limit at 1.7 MeV is translated into a limit for the X^0 -nucleon coupling constant: $g_{X^0 N N}^2/4\pi < 2.3 \times 10^{-9}$.

¹⁰¹The DOEHNER 88 limit is for $m_{A^0} = 1.7$ MeV, $\tau(A^0) < 10^{-10}$ s. Limits less than 10^{-4} are obtained for $m_{A^0} = 1.2\text{--}2.2$ MeV.

¹⁰²SAVAGE 88 looked for A^0 that decays into e^+e^- in the decay of the 9.17 MeV $J^P = 2^+$ state in ${}^{14}\text{N}$, 17.64 MeV state $J^P = 1^+$ in ${}^8\text{Be}$, and the 18.15 MeV state $J^P = 1^+$ in ${}^8\text{Be}$. This experiment constrains the isovector coupling of A^0 to hadrons, if $m_{A^0} = (1.1 \rightarrow 2.2)$ MeV and the isoscalar coupling of A^0 to hadrons, if $m_{A^0} = (1.1 \rightarrow 2.6)$ MeV. Both limits are valid only if $\tau(A^0) \lesssim 1 \times 10^{-11}$ s.

¹⁰³Limits are for $\Gamma(A^0(1.8 \text{ MeV}))/\Gamma(\pi\text{M1})$; i.e., for 1.8 MeV axion emission normalized to the rate for internal emission of e^+e^- pairs. Valid for $\tau_{A^0} < 2 \times 10^{-11}$ s. ${}^6\text{Li}$ isovector decay data strongly disfavor PECCEI 86 model I, whereas the ${}^{10}\text{B}$ and ${}^{14}\text{N}$ isoscalar decay data strongly reject PECCEI 86 model II and III.

¹⁰⁴SAVAGE 86B looked for A^0 that decays into e^+e^- in the decay of the 9.17 MeV $J^P = 2^+$ state in ${}^{14}\text{N}$. Limit on the branching fraction is valid if $\tau_{A^0} \lesssim 1 \times 10^{-11}$ s for $m_{A^0} = (1.1\text{--}1.7)$ MeV. This experiment constrains the iso-vector coupling of A^0 to hadrons.

¹⁰⁵ANANEV 85 with IBR-2 pulsed reactor exclude standard A^0 at CL = 95% masses below 470 keV (Li^* decay) and below $2m_d$ for deuteron* decay.

¹⁰⁶CAVAIGNAC 83 at Bugey reactor exclude axion at any $m_{97\text{Nb}^*}$ decay and axion with m_{A^0} between 275 and 288 keV (deuteron* decay).

¹⁰⁷ALEKSEEV 82 with IBR-2 pulsed reactor exclude standard A^0 at CL = 95% mass-ranges $m_{A^0} < 400$ keV (Li^* decay) and $330 \text{ keV} < m_{A^0} < 2.2$ MeV. (deuteron* decay).

¹⁰⁸LEHMANN 82 obtained $A^0 \rightarrow 2\gamma$ rate $< 6.2 \times 10^{-5}/\text{s}$ (CL = 95%) excluding m_{A^0} between 100 and 1000 keV.

¹⁰⁹ZEHNDER 82 used Gosgen 2.8GW light-water reactor to check A^0 production. No 2γ peak in Li^* , Nb* decay (both single p transition) nor in n capture (combined with previous Ba^* negative result) rules out standard A^0 . Set limit $m_{A^0} < 60$ keV for any A^0 .

¹¹⁰ZEHNDER 81 looked for $\text{Ba}^* \rightarrow A^0\text{Ba}$ transition with $A^0 \rightarrow 2\gamma$. Obtained 2γ coincidence rate $< 2.2 \times 10^{-5}/\text{s}$ (CL = 95%) excluding $m_{A^0} > 160$ keV (or 200 keV depending on Higgs mixing). However, see BARROSO 81.

¹¹¹CALAPRICE 79 saw no axion emission from excited states of carbon. Sensitive to axion mass between 1 and 15 MeV.

none $4 \times 10^{-16}\text{--}4.5 \times 10^{-12}$	90	112 BROSS	91	BDMP	$eN \rightarrow eA^0$ ($A^0 \rightarrow ee$)
		113 GUO	90	BDMP	$eN \rightarrow eA^0$ ($A^0 \rightarrow ee$)
		114 BJORKEN	88	CALO	$A \rightarrow e^+e^-$ or 2γ
		115 BLINOV	88	MD1	$ee \rightarrow eeA^0$ ($A^0 \rightarrow ee$)
none $1 \times 10^{-14}\text{--}1 \times 10^{-10}$	90	116 RIORDAN	87	BDMP	$eN \rightarrow eA^0$ ($A^0 \rightarrow ee$)
none $1 \times 10^{-14}\text{--}1 \times 10^{-11}$	90	117 BROWN	86	BDMP	$eN \rightarrow eA^0$ ($A^0 \rightarrow ee$)
none $6 \times 10^{-14}\text{--}9 \times 10^{-11}$	95	118 DAVIER	86	BDMP	$eN \rightarrow eA^0$ ($A^0 \rightarrow ee$)
none $3 \times 10^{-13}\text{--}1 \times 10^{-7}$	90	119 KONAKA	86	BDMP	$eN \rightarrow eA^0$ ($A^0 \rightarrow ee$)

¹¹²The listed BROSS 91 limit is for $m_{A^0} = 1.14$ MeV. $B(A^0 \rightarrow e^+e^-) = 1$ assumed. Excluded domain in the $\tau_{A^0}\text{--}m_{A^0}$ plane extends up to $m_{A^0} \approx 7$ MeV (see Fig. 5).

Combining with electron $g\text{--}2$ constraint, axions coupling only to e^+e^- ruled out for $m_{A^0} < 4.8$ MeV (90% CL).

¹¹³GUO 90 use the same apparatus as BROWN 86 and improve the previous limit in the shorter lifetime region. Combined with $g\text{--}2$ constraint, axions coupling only to e^+e^- are ruled out for $m_{A^0} < 2.7$ MeV (90% CL).

¹¹⁴BJORKEN 88 reports limits on axion parameters (f_A , m_A , τ_A) for $m_{A^0} < 200$ MeV from electron beam-dump experiment with production via Primakoff photoproduction, bremsstrahlung from electrons, and resonant annihilation of positrons on atomic electrons.

¹¹⁵BLINOV 88 assume zero spin, $m = 1.8$ MeV and lifetime $< 5 \times 10^{-12}$ s and find $\Gamma(A^0 \rightarrow \gamma\gamma)B(A^0 \rightarrow e^+e^-) < 2$ eV (CL=90%).

¹¹⁶Assumes $A^0\gamma\gamma$ coupling is small and hence Primakoff production is small. Their figure 2 shows limits on axions for $m_{A^0} < 15$ MeV.

¹¹⁷Uses electrons in hadronic showers from an incident 800 GeV proton beam. Limits for $m_{A^0} < 15$ MeV are shown in their figure 3.

¹¹⁸ $m_{A^0} = 1.8$ MeV assumed. The excluded domain in the $\tau_{A^0}\text{--}m_{A^0}$ plane extends up to $m_{A^0} \approx 14$ MeV, see their figure 4.

¹¹⁹The limits are obtained from their figure 3. Also given is the limit on the $A^0\gamma\gamma\text{--}A^0e^+e^-$ coupling plane by assuming Primakoff production.

Search for A^0 (Axion) Resonance in Bhabha Scattering

The limit is for $\Gamma(A^0)[B(A^0 \rightarrow e^+e^-)]^2$.

VALUE (10^{-3} eV)	CL%	DOCUMENT ID	TECN	COMMENT	
• • • We do not use the following data for averages, fits, limits, etc. • • •					
< 1.3	97	120 HALLIN	92	CNTR	$m_{A^0} = 1.75\text{--}1.88$ MeV
none 0.0016–0.47	90	121 HENDERSON	92C	CNTR	$m_{A^0} = 1.5\text{--}1.86$ MeV
< 2.0	90	122 WU	92	CNTR	$m_{A^0} = 1.56\text{--}1.86$ MeV
< 0.013	95	TSERTOS	91	CNTR	$m_{A^0} = 1.832$ MeV
none 0.19–3.3	95	123 WIDMANN	91	CNTR	$m_{A^0} = 1.78\text{--}1.92$ MeV
< 5	97	BAUER	90	CNTR	$m_{A^0} = 1.832$ MeV
none 0.09–1.5	95	124 JUDGE	90	CNTR	$m_{A^0} = 1.832$ MeV, elastic
< 1.9	97	125 TSERTOS	89	CNTR	$m_{A^0} = 1.82$ MeV
<(10–40)	97	125 TSERTOS	89	CNTR	$m_{A^0} = 1.51\text{--}1.65$ MeV
<(1–2.5)	97	125 TSERTOS	89	CNTR	$m_{A^0} = 1.80\text{--}1.86$ MeV
< 31	95	LORENZ	88	CNTR	$m_{A^0} = 1.646$ MeV
< 94	95	LORENZ	88	CNTR	$m_{A^0} = 1.726$ MeV
< 23	95	LORENZ	88	CNTR	$m_{A^0} = 1.782$ MeV
< 19	95	LORENZ	88	CNTR	$m_{A^0} = 1.837$ MeV
< 3.8	97	126 TSERTOS	88	CNTR	$m_{A^0} = 1.832$ MeV
		127 VANKLINKEN	88	CNTR	
		128 MAIER	87	CNTR	
<2500	90	MILLS	87	CNTR	$m_{A^0} = 1.8$ MeV
		129 VONWIMMER	.87	CNTR	

¹²⁰HALLIN 92 quote limits on lifetime, $8 \times 10^{-14}\text{--}5 \times 10^{-13}$ sec depending on mass, assuming $B(A^0 \rightarrow e^+e^-) = 100\%$. They say that TSERTOS 91 overstated their sensitivity by a factor of 3.

¹²¹HENDERSON 92C exclude axion with lifetime $\tau_{A^0} = 1.4 \times 10^{-12}\text{--}4.0 \times 10^{-10}$ s, assuming $B(A^0 \rightarrow e^+e^-) = 100\%$. HENDERSON 92C also exclude a vector boson with $\tau = 1.4 \times 10^{-12}\text{--}6.0 \times 10^{-10}$ s.

¹²²WU 92 quote limits on lifetime $> 3.3 \times 10^{-13}$ s assuming $B(A^0 \rightarrow e^+e^-) = 100\%$. They say that TSERTOS 89 overestimate the limit by a factor of $\pi/2$. WU 92 also quote a bound for vector boson, $\tau > 8.2 \times 10^{-13}$ s.

¹²³WIDMANN 91 bound applies exclusively to the case $B(A^0 \rightarrow e^+e^-) = 1$, since the detection efficiency varies substantially as $\Gamma(A^0)_{\text{total}}$ changes. See their Fig. 6.

¹²⁴JUDGE 90 excludes an elastic pseudoscalar e^+e^- resonance for 4.5×10^{-13} s $< \tau(A^0) < 7.5 \times 10^{-12}$ s (95% CL) at $m_{A^0} = 1.832$ MeV. Comparable limits can be set for $m_{A^0} = 1.776\text{--}1.856$ MeV.

¹²⁵See also TSERTOS 88B in references.

¹²⁶The upper limit listed in TSERTOS 88 is too large by a factor of 4. See TSERTOS 88B, footnote 3.

¹²⁷VANKLINKEN 88 looked for relatively long-lived resonance ($\tau = 10^{-10}\text{--}10^{-12}$ s). The sensitivity is not sufficient to exclude such a narrow resonance.

¹²⁸MAIER 87 obtained limits $R\Gamma \lesssim 60$ eV (100 eV) at $m_{A^0} \approx 1.64$ MeV (1.83 MeV) for energy resolution $\Delta E_{\text{cm}} \approx 3$ keV, where R is the resonance cross section normalized

 A^0 (Axion) Limits from Its Electron Coupling

Limits are for $\tau(A^0 \rightarrow e^+e^-)$.

VALUE (s)	CL%	DOCUMENT ID	TECN	COMMENT
• • • We do not use the following data for averages, fits, limits, etc. • • •				

Gauge & Higgs Boson Particle Listings

Axions (A^0) and Other Very Light Bosons

to that of Bhabha scattering, and $\Gamma = \Gamma_{e^+e^-}^2/\Gamma_{\text{total}}$. For a discussion implying that $\Delta E_{\text{cm}} \approx 10$ keV, see TSERTOS 89.

¹²⁹VONWIMMERSPERG 87 measured Bhabha scattering for $E_{\text{cm}} = 1.37\text{--}1.86$ MeV and found a possible peak at 1.73 with $\int \sigma dE_{\text{cm}} = 14.5 \pm 6.8$ keV-b. For a comment and a reply, see VANKLINKEN 88b and VONWIMMERSPERG 88. Also see CONNELL 88.

Search for A^0 (Axion) Resonance in $e^+e^- \rightarrow \gamma\gamma$

The limit is for $\Gamma(A^0 \rightarrow e^+e^-)\Gamma(A^0 \rightarrow \gamma\gamma)/\Gamma_{\text{total}}$

VALUE (10^{-3} eV)	CL%	DOCUMENT ID	TECN	COMMENT
••• We do not use the following data for averages, fits, limits, etc. •••				
< 0.18	95	VO	94 CNTR	$m_{A^0} = 1.1$ MeV
< 1.5	95	VO	94 CNTR	$m_{A^0} = 1.4$ MeV
< 12	95	VO	94 CNTR	$m_{A^0} = 1.7$ MeV
< 6.6	95	¹³⁰ TRZASKA	91 CNTR	$m_{A^0} = 1.8$ MeV
< 4.4	95	WIDMANN	91 CNTR	$m_{A^0} = 1.78\text{--}1.92$ MeV
		¹³¹ FOX	89 CNTR	
< 0.11	95	¹³² MINOWA	89 CNTR	$m_{A^0} = 1.062$ MeV
< 33	97	CONNELL	88 CNTR	$m_{A^0} = 1.580$ MeV
< 42	97	CONNELL	88 CNTR	$m_{A^0} = 1.642$ MeV
< 73	97	CONNELL	88 CNTR	$m_{A^0} = 1.782$ MeV
< 79	97	CONNELL	88 CNTR	$m_{A^0} = 1.832$ MeV
¹³⁰ TRZASKA 91 also give limits in the range $(6.6\text{--}30) \times 10^{-3}$ eV (95%CL) for $m_{A^0} = 1.6\text{--}2.0$ MeV.				
¹³¹ FOX 89 measured positron annihilation with an electron in the source material into two photons and found no signal at 1.062 MeV ($< 9 \times 10^{-5}$ of two-photon annihilation at rest).				
¹³² Similar limits are obtained for $m_{A^0} = 1.045\text{--}1.085$ MeV.				

Search for X^0 (Light Boson) Resonance in $e^+e^- \rightarrow \gamma\gamma\gamma$

The limit is for $\Gamma(X^0 \rightarrow e^+e^-)\Gamma(X^0 \rightarrow \gamma\gamma\gamma)/\Gamma_{\text{total}}$. C invariance forbids spin-0 X^0 coupling to both e^+e^- and $\gamma\gamma\gamma$.

VALUE (10^{-3} eV)	CL%	DOCUMENT ID	TECN	COMMENT
••• We do not use the following data for averages, fits, limits, etc. •••				
< 0.2	95	¹³³ VO	94 CNTR	$m_{X^0} = 1.1\text{--}1.9$ MeV
< 1.0	95	¹³⁴ VO	94 CNTR	$m_{X^0} = 1.1$ MeV
< 2.5	95	¹³⁴ VO	94 CNTR	$m_{X^0} = 1.4$ MeV
< 120	95	¹³⁴ VO	94 CNTR	$m_{X^0} = 1.7$ MeV
< 3.8	95	¹³⁵ SKALSEY	92 CNTR	$m_{X^0} = 1.5$ MeV
¹³³ VO 94 looked for $X^0 \rightarrow \gamma\gamma\gamma$ decaying at rest. The precise limits depend on m_{X^0} . See Fig. 2(b) in paper.				
¹³⁴ VO 94 looked for $X^0 \rightarrow \gamma\gamma\gamma$ decaying in flight.				
¹³⁵ SKALSEY 92 also give limits 4.3 for $m_{X^0} = 1.54$ and 7.5 for 1.64 MeV. The spin of X^0 is assumed to be one.				

Light Boson (X^0) Search in Nonresonant e^+e^- Annihilation at Rest

Limits are for the ratio of $n\gamma + X^0$ production relative to $\gamma\gamma$.

VALUE (units 10^{-6})	CL%	DOCUMENT ID	TECN	COMMENT
••• We do not use the following data for averages, fits, limits, etc. •••				
< 4.2	90	¹³⁶ MITSUMI	96 CNTR	γX^0
< 4	68	¹³⁷ SKALSEY	95 CNTR	γX^0
< 40	68	¹³⁸ SKALSEY	95 RVUE	γX^0
< 0.18	90	¹³⁹ ADACHI	94 CNTR	$\gamma\gamma X^0, X^0 \rightarrow \gamma\gamma$
< 0.26	90	¹⁴⁰ ADACHI	94 CNTR	$\gamma\gamma X^0, X^0 \rightarrow \gamma\gamma$
< 0.33	90	¹⁴¹ ADACHI	94 CNTR	$\gamma X^0, X^0 \rightarrow \gamma\gamma\gamma$
¹³⁶ MITSUMI 96 looked for a monochromatic γ . The bound applies for a vector X^0 with $C = -1$ and $m_{X^0} < 200$ keV. They derive an upper bound on eeX^0 coupling and hence on the branching ratio $B(\alpha\text{-Ps} \rightarrow \gamma\gamma X^0) < 6.2 \times 10^{-6}$. The bounds weaken for heavier X^0 .				
¹³⁷ SKALSEY 95 looked for a monochromatic γ without an accompanying γ in e^+e^- annihilation. The bound applies for scalar and vector X^0 with $C = -1$ and $m_{X^0} = 100\text{--}1000$ keV.				
¹³⁸ SKALSEY 95 reinterpreted the bound on γA^0 decay of $\alpha\text{-Ps}$ by ASAI 91 where 3% of delayed annihilations are not from 3S_1 states. The bound applies for scalar and vector X^0 with $C = -1$ and $m_{X^0} = 0\text{--}800$ keV.				
¹³⁹ ADACHI 94 looked for a peak in the $\gamma\gamma$ invariant mass distribution in $\gamma\gamma\gamma\gamma$ production from e^+e^- annihilation. The bound applies for $m_{X^0} = 70\text{--}800$ keV.				
¹⁴⁰ ADACHI 94 looked for a peak in the missing-mass mass distribution in $\gamma\gamma$ channel, using $\gamma\gamma\gamma\gamma$ production from e^+e^- annihilation. The bound applies for $m_{X^0} < 800$ keV.				
¹⁴¹ ADACHI 94 looked for a peak in the missing mass distribution in $\gamma\gamma\gamma$ channel, using $\gamma\gamma\gamma\gamma$ production from e^+e^- annihilation. The bound applies for $m_{X^0} = 200\text{--}900$ keV.				

Searches for Goldstone Bosons (X^0)

(Including Horizontal Bosons and Majorons.) Limits are for branching ratios.

VALUE	CL%	DOCUMENT ID	TECN	COMMENT
••• We do not use the following data for averages, fits, limits, etc. •••				

142	LESSA	07	RVUE	Meson, ℓ decays to Majoron
143	DIAZ	98	THEO	$H^0 \rightarrow X^0 X^0, A^0 \rightarrow X^0 X^0 X^0$, Majoron
144	BOBRAKOV	91		Electron quasi-magnetic interaction
< 3.3×10^{-2}	95	¹⁴⁵ ALBRECHT	90E ARG	$\tau \rightarrow \mu X^0$. Familon
< 1.8×10^{-2}	95	¹⁴⁵ ALBRECHT	90E ARG	$\tau \rightarrow e X^0$. Familon
< 6.4×10^{-9}	90	¹⁴⁶ ATIYA	90 B787	$K^+ \rightarrow \pi^+ X^0$. Familon
< 1.1×10^{-9}	90	¹⁴⁷ BOLTON	88 CBOX	$\mu^+ \rightarrow e^+ \gamma X^0$. Familon
		¹⁴⁸ CHANDA	88 ASTR	Sun, Majoron
		¹⁴⁹ CHOI	88 ASTR	Majoron, SN 1987A
< 5×10^{-6}	90	¹⁵⁰ PICCIOTTO	88 CNTR	$\pi \rightarrow e \nu X^0$, Majoron
< 1.3×10^{-9}	90	¹⁵¹ GOLDMAN	87 CNTR	$\mu \rightarrow e \gamma X^0$. Familon
< 3×10^{-4}	90	¹⁵² BRYMAN	86B RVUE	$\mu \rightarrow e X^0$. Familon
< 1×10^{-10}	90	¹⁵³ EICHLER	86 SPEC	$\mu^+ \rightarrow e^+ X^0$. Familon
< 2.6×10^{-6}	90	¹⁵⁴ JODIDIO	86 SPEC	$\mu^+ \rightarrow e^+ X^0$. Familon
		¹⁵⁵ BALTRUSAITIS	85 MRK3	$\tau \rightarrow \ell X^0$. Familon
		¹⁵⁶ DICUS	83 COSM	$\nu(\text{hvy}) \rightarrow \nu(\text{light}) X^0$

¹⁴²LESSA 07 consider decays of the form Meson $\rightarrow \ell\nu$ Majoron and $\ell \rightarrow \ell'\nu$ Majoron and use existing data to derive limits on the neutrino-Majoron Yukawa couplings $g_{\alpha\beta}$ ($\alpha, \beta = e, \mu, \tau$). Their best limits are $|g_{e\alpha}|^2 < 5.5 \times 10^{-6}$, $|g_{\mu\alpha}|^2 < 4.5 \times 10^{-5}$, $|g_{\tau\alpha}|^2 < 5.5 \times 10^{-2}$ at CL = 90%.

¹⁴³DIAZ 98 studied models of spontaneously broken lepton number with both singlet and triplet Higgses. They obtain limits on the parameter space from invisible decay $Z \rightarrow H^0 A^0 \rightarrow X^0 X^0 X^0 X^0$ and $e^+e^- \rightarrow Z H^0$ with $H^0 \rightarrow X^0 X^0$.

¹⁴⁴BOBRAKOV 91 searched for anomalous magnetic interactions between polarized electrons expected from the exchange of a massless pseudoscalar boson (axion). A limit $x_e^2 < 2 \times 10^{-4}$ (95%CL) is found for the effective anomalous magneton parametrized as $x_e(G_F/8\pi\sqrt{2})^{1/2}$.

¹⁴⁵ALBRECHT 90E limits are for $B(\tau \rightarrow \ell X^0)/B(\tau \rightarrow \ell\nu\bar{\nu})$. Valid for $m_{X^0} < 100$ MeV. The limits rise to 7.1% (for μ), 5.0% (for e) for $m_{X^0} = 500$ MeV.

¹⁴⁶ATIYA 90 limit is for $m_{X^0} = 0$. The limit $B < 1 \times 10^{-8}$ holds for $m_{X^0} < 95$ MeV. For the reduction of the limit due to finite lifetime of X^0 , see their Fig. 3.

¹⁴⁷BOLTON 88 limit corresponds to $F > 3.1 \times 10^9$ GeV, which does not depend on the chirality property of the coupling.

¹⁴⁸CHANDA 88 find $v_T < 10$ MeV for the weak-triplet Higgs vacuum expectation value in Gelmini-Roncadelli model, and $v_S > 5.8 \times 10^6$ GeV in the singlet Majoron model.

¹⁴⁹CHOI 88 used the observed neutrino flux from the supernova SN1987A to exclude the neutrino Majoron Yukawa coupling h in the range $2 \times 10^{-5} < h < 3 \times 10^{-4}$ for the interaction $L_{\text{int}} = \frac{1}{2} h \bar{\nu}_\nu \gamma_5 \psi_\nu \phi_X$. For several families of neutrinos, the limit applies for $(\Sigma h_i^2)^{1/4}$.

¹⁵⁰PICCIOTTO 88 limit applies when $m_{X^0} < 55$ MeV and $\tau_{X^0} > 2$ ns, and it decreases to 4×10^{-7} at $m_{X^0} = 125$ MeV, beyond which no limit is obtained.

¹⁵¹GOLDMAN 87 limit corresponds to $F > 2.9 \times 10^9$ GeV for the family symmetry breaking scale from the Lagrangian $L_{\text{int}} = (1/F) \bar{\psi}_\mu \gamma^\mu (a + b\gamma_5) \psi_e \phi_\mu \phi_{X^0}$ with $a^2 + b^2 = 1$.

This is not as sensitive as the limit $F > 9.9 \times 10^9$ GeV derived from the search for $\mu^+ \rightarrow e^+ X^0$ by JODIDIO 86, but does not depend on the chirality property of the coupling.

¹⁵²Limits are for $\Gamma(\mu \rightarrow e X^0)/\Gamma(\mu \rightarrow e\nu\bar{\nu})$. Valid when $m_{X^0} = 0\text{--}93.4, 98.1\text{--}103.5$ MeV.

¹⁵³EICHLER 86 looked for $\mu^+ \rightarrow e^+ X^0$ followed by $X^0 \rightarrow e^+e^-$. Limits on the branching fraction depend on the mass and and lifetime of X^0 . The quoted limits are valid when $\tau_{X^0} \lesssim 3 \times 10^{-10}$ s if the decays are kinematically allowed.

¹⁵⁴JODIDIO 86 corresponds to $F > 9.9 \times 10^9$ GeV for the family symmetry breaking scale with the parity-conserving effective Lagrangian $L_{\text{int}} = (1/F) \bar{\psi}_\mu \gamma^\mu \psi_e \phi_\mu \phi_{X^0}$.

¹⁵⁵BALTRUSAITIS 85 search for light Goldstone boson (X^0) of broken U(1). CL = 95% limits are $B(\tau \rightarrow \mu^+ X^0)/B(\tau \rightarrow \mu^+ \nu\bar{\nu}) < 0.125$ and $B(\tau \rightarrow e^+ X^0)/B(\tau \rightarrow e^+ \nu\bar{\nu}) < 0.04$. Inferred limit for the symmetry breaking scale is $m > 3000$ TeV.

¹⁵⁶The primordial heavy neutrino must decay into ν and familon, f_A , early so that the red-shifted decay products are below critical density, see their table. In addition, $K \rightarrow \pi f_A$ and $\mu \rightarrow e f_A$ are unseen. Combining these excludes $m_{\text{heavy}\nu}$ between 5×10^{-5} and 5×10^{-4} MeV (μ decay) and $m_{\text{heavy}\nu}$ between 5×10^{-5} and 0.1 MeV (K -decay).

Majoron Searches in Neutrinoless Double β Decay

Limits are for the half-life of neutrinoless $\beta\beta$ decay with a Majoron emission.

No experiment currently claims any such evidence. Only the best or comparable limits for each isotope are reported. Also see the reviews ZUBER 98 and FAESSLER 98b.

$t_{1/2}$ (10^{21} yr)	CL%	ISOTOPE	TRANSITION	METHOD	DOCUMENT ID
••• We do not use the following data for averages, fits, limits, etc. •••					
> 7200	90	¹²⁸ Te	CNTR		157 BERNATOW... 92
> 1.52	90	¹⁵⁰ Nd	$0\nu 1\chi$	NEMO-3	158 ARGYRIADES 09
> 27	90	¹⁰⁰ Mo	$0\nu 1\chi$	NEMO-3	159 ARNOLD 06
> 15	90	⁸² Se	$0\nu 1\chi$	NEMO-3	160 ARNOLD 06
> 14	90	¹⁰⁰ Mo	$0\nu 1\chi$	NEMO-3	161 ARNOLD 04
> 12	90	⁸² Se	$0\nu 1\chi$	NEMO-3	162 ARNOLD 04
> 2.2	90	¹³⁰ Te	$0\nu 1\chi$	Cryog. det.	163 ARNABOLDI 03
> 0.9	90	¹³⁰ Te	$0\nu 2\chi$	Cryog. det.	164 ARNABOLDI 03
> 8	90	¹¹⁶ Cd	$0\nu 1\chi$	CdWO ₄ scint.	165 DANEVICH 03
> 0.8	90	¹¹⁶ Cd	$0\nu 2\chi$	CdWO ₄ scint.	166 DANEVICH 03
> 500	90	¹³⁶ Xe	$0\nu \chi$	Liquid Xe Scint.	167 BERNABEI 02b
> 5.8	90	¹⁰⁰ Mo	$0\nu \chi$	ELEGANT V	168 FUSHIMI 02
> 0.32	90	¹⁰⁰ Mo	$0\nu \chi$	Liq. Ar ioniz.	169 ASHITKOV 01

Gauge & Higgs Boson Particle Listings

Axions (A^0) and Other Very Light Bosons

- ¹⁹⁸ The region $m_{A^0} \gtrsim 2$ eV is also allowed.
- ¹⁹⁹ ERICSON 89 considered various nuclear corrections to axion emission in a supernova core, and found a reduction of the previous limit (MAYLE 88) by a large factor.
- ²⁰⁰ MAYLE 89 limit based on naive quark model couplings of axion to nucleons. Limit based on couplings motivated by EMC measurements is 2–4 times weaker. The limit from axion-electron coupling is weak: see HATSUDA 88B.
- ²⁰¹ RAFFELT 88B derives a limit for the energy generation rate by exotic processes in helium-burning stars $\epsilon < 100$ erg $g^{-1} s^{-1}$, which gives a firmer basis for the axion limits based on red giant cooling.
- ²⁰² RAFFELT 87 also gives a limit $g_{A\gamma} < 1 \times 10^{-10}$ GeV^{-1} .
- ²⁰³ DEARBORN 86 also gives a limit $g_{A\gamma} < 1.4 \times 10^{-11}$ GeV^{-1} .
- ²⁰⁴ RAFFELT 86 gives a limit $g_{A\gamma} < 1.1 \times 10^{-10}$ GeV^{-1} from red giants and $< 2.4 \times 10^{-9}$ GeV^{-1} from the sun.
- ²⁰⁵ KAPLAN 85 says $m_{A^0} < 23$ eV is allowed for a special choice of model parameters.
- ²⁰⁶ FUKUGITA 82 gives a limit $g_{A\gamma} < 2.3 \times 10^{-10}$ GeV^{-1} .

Search for Relic Invisible Axions

Limits are for $[G_{A\gamma\gamma}/m_{A^0}^2] \rho_A$ where $G_{A\gamma\gamma}$ denotes the axion two-photon coupling,

$$L_{int} = \frac{G_{A\gamma\gamma}}{4} \phi_A F_{\mu\nu} \tilde{F}^{\mu\nu} = G_{A\gamma\gamma} \phi_A \mathbf{E} \cdot \mathbf{B}, \text{ and } \rho_A \text{ is the axion energy density near the earth.}$$

VALUE	CL%	DOCUMENT ID	TECN	COMMENT
• • • We do not use the following data for averages, fits, limits, etc. • • •				
$< 1.9 \times 10^{-43}$	97.7	207 DUFFY	06 CNTR	$m_{A^0} = 1.98\text{--}2.17 \times 10^{-6}$ eV
$< 5.5 \times 10^{-43}$	90	208 ASZTALOS	04 CNTR	$m_{A^0} = 1.9\text{--}3.3 \times 10^{-6}$ eV
		209 KIM	98 THEO	
$< 2 \times 10^{-41}$		210 HAGMANN	90 CNTR	$m_{A^0} = (5.4\text{--}5.9)10^{-6}$ eV
$< 1.3 \times 10^{-42}$	95	211 WUENSCH	89 CNTR	$m_{A^0} = (4.5\text{--}10.2)10^{-6}$ eV
$< 2 \times 10^{-41}$	95	211 WUENSCH	89 CNTR	$m_{A^0} = (11.3\text{--}16.3)10^{-6}$ eV
²⁰⁷ DUFFY 06 used the upgraded detector of ASZTALOS 04, while assuming a smaller velocity dispersion than the isothermal model as in Eq. (8) of their paper. See Fig. 10 of their paper on the axion mass dependence of the limit.				
²⁰⁸ ASZTALOS 04 looked for a conversion of halo axions to microwave photons in magnetic field. At 90% CL, the KSVZ axion cannot have a local halo density more than 0.45 GeV/cm^3 in the quoted mass range. See Fig. 7 of their paper on the axion mass dependence of the limit.				
²⁰⁹ KIM 98 calculated the axion-to-photon couplings for various axion models and compared them to the HAGMANN 90 bounds. This analysis demonstrates a strong model dependence of $G_{A\gamma\gamma}$ and hence the bound from relic axion search.				
²¹⁰ HAGMANN 90 experiment is based on the proposal of SIKIVIE 83.				
²¹¹ WUENSCH 89 looks for condensed axions near the earth that could be converted to photons in the presence of an intense electromagnetic field via the Primakoff effect, following the proposal of SIKIVIE 83. The theoretical prediction with $[G_{A\gamma\gamma}/m_{A^0}^2]^2 = 2 \times 10^{-14}$ MeV^{-4} (the three generation DFSZ model) and $\rho_A = 300$ MeV/cm^3 that makes up galactic halos gives $(G_{A\gamma\gamma}/m_{A^0}^2) \rho_A = 4 \times 10^{-44}$. Note that our definition of $G_{A\gamma\gamma}$ is $(1/4\pi)$ smaller than that of WUENSCH 89.				

Invisible A^0 (Axion) Limits from Photon Coupling

Limits are for the axion-two-photon coupling $G_{A\gamma\gamma}$ defined by $L = G_{A\gamma\gamma} \phi_A \mathbf{E} \cdot \mathbf{B}$.

For scalars S^0 the limit is on the coupling constant in $L = G_{S\gamma\gamma} \phi_S (\mathbf{E}^2 - \mathbf{B}^2)$.

VALUE (GeV^{-1})	CL%	DOCUMENT ID	TECN	COMMENT
• • • We do not use the following data for averages, fits, limits, etc. • • •				
$< 2.4 \times 10^{-9}$	95	212 AHMED	09A CDMS	$m_{A^0} < 100$ eV
$< 1.2\text{--}2.8 \times 10^{-10}$	95	213 ARIK	09 CAST	$m_{A^0} = 0.02\text{--}0.39$ eV
		214 CHOU	09	Chameleons
$< 7 \times 10^{-10}$		215 GONDOLO	09 ASTR	$m_{A^0} < \text{few keV}$
$< 1.3 \times 10^{-6}$	95	216 AFANASEV	08	$m_{S^0} < 1$ MeV
$< 3.5 \times 10^{-7}$	99.7	217 CHOU	08	$m_{A^0} < 0.5$ MeV
$< 1.1 \times 10^{-6}$	99.7	218 FOUICHE	08	$m_{A^0} < 1$ MeV
$< 5.6\text{--}13.4 \times 10^{-10}$	95	219 INOUE	08	$m_{A^0} = 0.84\text{--}1.00$ eV
$< 5 \times 10^{-7}$		220 ZAVATTINI	08	$m_{A^0} < 1$ MeV
$< 8.8 \times 10^{-11}$	95	221 ANDRIAMON..07	CAST	$m_{A^0} < 0.02$ eV
$< 1.25 \times 10^{-6}$	95	222 ROBILLIARD	07	$m_{A^0} < 1$ MeV
$2\text{--}5 \times 10^{-6}$		223 ZAVATTINI	06	$m_{A^0} = 1\text{--}1.5$ MeV
$< 1.1 \times 10^{-9}$	95	224 INOUE	02	$m_{A^0} = 0.05\text{--}0.27$ eV
$< 2.78 \times 10^{-9}$	95	225 MORALES	02B	$m_{A^0} < 1$ keV
$< 1.7 \times 10^{-9}$	90	226 BERNABEI	01B	$m_{A^0} < 100$ eV
$< 1.5 \times 10^{-4}$	90	227 ASTIER	00B NOMD	$m_{A^0} < 40$ eV
		228 MASSO	00 THEO	induced γ coupling
$< 2.7 \times 10^{-9}$	95	229 AVIGNONE	98 SLAX	$m_{A^0} < 1$ keV
$< 6.0 \times 10^{-10}$	95	230 MORIYAMA	98	$m_{A^0} < 0.03$ eV
$< 3.6 \times 10^{-7}$	95	231 CAMERON	93	$m_{A^0} < 10^{-3}$ eV, optical rotation
$< 6.7 \times 10^{-7}$	95	232 CAMERON	93	$m_{A^0} < 10^{-3}$ eV, photon regeneration
$< 3.6 \times 10^{-9}$	99.7	233 LAZARUS	92	$m_{A^0} < 0.03$ eV
$< 7.7 \times 10^{-9}$	99.7	233 LAZARUS	92	$m_{A^0} = 0.03\text{--}0.11$ eV
$< 7.7 \times 10^{-7}$	99	234 RUOSO	92	$m_{A^0} < 10^{-3}$ eV
$< 2.5 \times 10^{-6}$		235 SEMERTZIDIS	90	$m_{A^0} < 7 \times 10^{-4}$ eV

- ²¹² AHMED 09A is analogous to AVIGNONE 98.
- ²¹³ ARIK 09 is the ^4He filling version of the CAST axion helioscope in analogy to INOUE 02 and INOUE 08. See their Fig. 7 for mass-dependent limits.
- ²¹⁴ CHOU 09 use the GammeV apparatus in the afterglow mode to search for chameleons, (pseudo)scalar bosons with a mass depending on the environment. For pseudoscalars they exclude at 3σ the range $2.6 \times 10^{-7} \text{ GeV}^{-1} < G_{A\gamma\gamma} < 4.2 \times 10^{-6} \text{ GeV}^{-1}$ for vacuum m_{A^0} roughly below 6 meV for density scaling index exceeding 0.8.
- ²¹⁵ GONDOLO 09 use the all-flavor measured solar neutrino flux to constrain solar interior temperature and thus energy losses.
- ²¹⁶ LIPSS photon regeneration experiment, assuming scalar particle S^0 . See Fig. 4 for mass-dependent limits.
- ²¹⁷ CHOU 08 perform a variable-baseline photon regeneration experiment. See their Fig. 3 for mass-dependent limits. Excludes the PVLAS result of ZAVATTINI 06.
- ²¹⁸ FOUICHE 08 is an update of ROBILLIARD 07. See their Fig. 12 for mass-dependent limits.
- ²¹⁹ INOUE 08 is an extension of INOUE 02 to larger axion masses, using the Tokyo axion helioscope. See their Fig. 4 for mass-dependent limits.
- ²²⁰ ZAVATTINI 08 is an upgrade of ZAVATTINI 06, see their Fig. 8 for mass-dependent limits. They now exclude the parameter range where ZAVATTINI 06 had seen a positive signature.
- ²²¹ ANDRIAMONJE 07 looked for Primakoff conversion of solar axions in 9T superconducting magnet into X-rays. Supersedes ZIOUTAS 05.
- ²²² ROBILLIARD 07 perform a photon regeneration experiment with a pulsed laser and pseudomagnetic field. See their Fig. 4 for mass-dependent limits. Excludes the PVLAS result of ZAVATTINI 06 with a CL exceeding 99.9%.
- ²²³ ZAVATTINI 06 propagate a laser beam in a magnetic field and observe dichroism and birefringence effects that could be attributed to an axion-like particle. This result is now excluded by ROBILLIARD 07, ZAVATTINI 08, and CHOU 08.
- ²²⁴ INOUE 02 looked for Primakoff conversion of solar axions in 4T superconducting magnet into X ray.
- ²²⁵ MORALES 02B looked for the coherent conversion of solar axions to photons via the Primakoff effect in Germanium detector.
- ²²⁶ BERNABEI 01B looked for Primakoff coherent conversion of solar axions into photons via Bragg scattering in NaI crystal in DAMA dark matter detector.
- ²²⁷ ASTIER 00B looked for production of axions from the interaction of high-energy photons with the horn magnetic field and their subsequent re-conversion to photons via the interaction with the NOMAD dipole magnetic field.
- ²²⁸ MASSO 00 studied limits on axion-proton coupling using the induced axion-photon coupling through the proton loop and CAMERON 93 bound on the axion-photon coupling using optical rotation. They obtained the bound $g_P^2/4\pi < 1.7 \times 10^{-9}$ for the coupling $g_P \vec{p} \cdot \vec{\gamma} \rho \phi_A$.
- ²²⁹ AVIGNONE 98 result is based on the coherent conversion of solar axions to photons via the Primakoff effect in a single crystal germanium detector.
- ²³⁰ Based on the conversion of solar axions to X-rays in a strong laboratory magnetic field.
- ²³¹ Experiment based on proposal by MAIANI 86.
- ²³² Experiment based on proposal by VANBIBBER 87.
- ²³³ LAZARUS 92 experiment is based on proposal found in VANBIBBER 89.
- ²³⁴ RUOSO 92 experiment is based on the proposal by VANBIBBER 87.
- ²³⁵ SEMERTZIDIS 90 experiment is based on the proposal of MAIANI 86. The limit is obtained by taking the noise amplitude as the upper limit. Limits extend to $m_{A^0} = 4 \times 10^{-3}$ where $G_{A\gamma\gamma} < 1 \times 10^{-4} \text{ GeV}^{-1}$.

Limit on Invisible A^0 (Axion) Electron Coupling

The limit is for $G_{Aee} \partial_\mu \phi_A \vec{\tau} \cdot \vec{\mu} \gamma_5 e$ in GeV^{-1} , or equivalently, the dipole-dipole

$$\text{potential } \frac{G_{Aee}^2}{4\pi} ((\boldsymbol{\sigma}_1 \cdot \boldsymbol{\sigma}_2) - 3(\boldsymbol{\sigma}_1 \cdot \mathbf{n})(\boldsymbol{\sigma}_2 \cdot \mathbf{n}))/r^3 \text{ where } \mathbf{n} = \mathbf{r}/r.$$

VALUE (GeV^{-1})	CL%	DOCUMENT ID	TECN	COMMENT
• • • We do not use the following data for averages, fits, limits, etc. • • •				
$< 1.4 \times 10^{-9}$	90	236 AHMED	09A CDMS	$m_{A^0} = 2.5$ keV
$< 3 \times 10^{-6}$		237 DAVOUDIALL	09 ASTR	Earth cooling
$< 0.6\text{--}2 \times 10^{-8}$	90	238 AALSETH	08 CNTR	$m_{A^0} = 0.3\text{--}7$ keV
$< 5.3 \times 10^{-5}$	66	239 NI	94	Induced magnetism
$< 6.7 \times 10^{-5}$	66	239 CHUI	93	Induced magnetism
$< 3.6 \times 10^{-4}$	66	240 PAN	92	Torsion pendulum
$< 2.7 \times 10^{-5}$	95	239 BOBRAKOV	91	Induced magnetism
$< 1.9 \times 10^{-3}$	66	241 WINELAND	91	NMR
$< 8.9 \times 10^{-4}$	66	240 RITTER	90	Torsion pendulum
$< 6.6 \times 10^{-5}$	95	239 VOROBYOV	88	Induced magnetism
²³⁶ AHMED 09A is analogous to AALSETH 08, using the CDMS detector. See their Fig. 5 for mass-dependent limits.				
²³⁷ DAVOUDIALL 09 use geophysical constraints on Earth cooling by axion emission.				
²³⁸ AALSETH 08 assume keV-mass pseudoscalars are the local dark matter and constrain the axio-electric effect in the CoGeNT detector. See their Fig. 3 for mass-dependent limits.				
²³⁹ These experiments measured induced magnetization of a bulk material by the spin-dependent potential generated from other bulk material with aligned electron spins, where the magnetic field is shielded with superconductor.				
²⁴⁰ These experiments used a torsion pendulum to measure the potential between two bulk matter objects where the spins are polarized but without a net magnetic field in either of them.				
²⁴¹ WINELAND 91 looked for an effect of bulk matter with aligned electron spins on atomic hyperfine splitting using nuclear magnetic resonance.				

See key on page 405

Gauge & Higgs Boson Particle Listings
Axions (A0) and Other Very Light Bosons

Invisible A0 (Axion) Limits from Nucleon Coupling

Limits are for the axion mass in eV.

Table with columns: VALUE (eV), CL%, DOCUMENT ID, TECN, COMMENT. Includes entries for DERBIN 09, BELLINI 08A, ADELBERGER 07, etc.

We do not use the following data for averages, fits, limits, etc.

- DERBIN 09 is analogous to KRCMAR 98.
BELLINI 08A is analogous to KRCMAR 01 and DERBIN 05.
BELLINI 08 consider solar axions emitted in the M1 transition of 7Li*...
ADELBERGER 07 use precision tests of Newton's law to constrain a force contribution...
DERBIN 07 is analogous to KRCMAR 98.
NAMBA 07 is analogous to KRCMAR 98.
DERBIN 05 bound is based on the same principle as KRCMAR 01.
LJUBICIC 04 looked for ejection of K-shell electrons by the axioelectric effect...
KRCMAR 01 looked for solar axions emitted by the M1 transition of 7Li...
KRCMAR 98 looked for solar axions emitted by the M1 transition of thermally excited 57Fe nuclei...

Axion Limits from T-violating Medium-Range Forces

The limit is for the coupling g = gp gs in a T-violating potential between nucleons or nucleon and electron of the form V = g/hbar^2 (sigma dot pi) (1/r2 + 1/lambda) e^-r/lambda...

Table with columns: VALUE, DOCUMENT ID, TECN, COMMENT. Includes entries for SEREBROV 10, IGNATOVICH 09, BAESSLER 07, HECKEL 06, NI 99, POSPELOV 98, YODIN 96, RITTER 93, VENEMA 92, WINELAND 91.

- SEREBROV 10 use spin precession of ultracold neutrons close to bulk matter and find g < 2 x 10^-21 (cm/lambda)^2 at 95% CL for the force range lambda = 10^-4-1 cm.
IGNATOVICH 09 use data on depolarization of ultracold neutrons in material traps. They show lambda-dependent limits in their Fig. 1.
SEREBROV 09 uses data on depolarization of ultracold neutrons stored in material traps and finds g < 2.96 x 10^-21 (cm/lambda)^2 for the force range lambda = 10^-3-1 cm and g < 3.9 x 10^-22 (cm/lambda)^2 for lambda = 10^-4-10^-3 cm, each time at 95% CL, significantly improving on BAESSLER 07.
BAESSLER 07 use the observation of quantum states of ultracold neutrons in the Earth's gravitational field to constrain g for an interaction range 1 microm - a few mm. See their Fig. 3 for results.
HECKEL 06 studied the influence of unpolarized bulk matter, including the laboratory's surroundings or the Sun, on a torsion pendulum containing about 9 x 10^22 polarized electrons. See their Fig. 4 for limits on g as a function of interaction range.
NI 99 searched for a T-violating medium-range force acting on paramagnetic Tb F3 salt. See their Fig. 1 for the result.
POSPELOV 98 studied the possible contribution of T-violating Medium-Range Force to the neutron electric dipole moment, which is possible when axion interactions violate CP. The size of the force among nucleons must be smaller than gravity by a factor of 2 x 10^-10 (1 cm/lambda_A), where lambda_A = hbar/m_A c.
YODIN 96 compared the precession frequencies of atomic 199Hg and Cs when a large mass is positioned near the cells, relative to an applied magnetic field. See Fig. 3 for their limits.
RITTER 93 studied the influence of bulk mass with polarized electrons on an unpolarized torsion pendulum, providing limits in the interaction range from 1 to 100 cm.
VENEMA 92 looked for an effect of Earth's gravity on nuclear spin-precession frequencies of 199Hg and 201Hg atoms.
WINELAND 91 looked for an effect of bulk matter with aligned electron spins on atomic hyperfine resonances in stored 9Be+ ions using nuclear magnetic resonance.

REFERENCES FOR Searches for Axions (A0) and Other Very Light Bosons

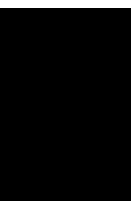
SEREBROV 10 JETPL 91 6
AHMED 09A PRL 103 141802
ANDRIAMONJON 09 JCAP 0912 002
ARGYRADES 09 PR C80 032501R
ARIK 09 JCAP 0902 008
AUBERT 09Z PRL 103 081803
CHOU 09 PRL 102 030402
DAVOUDIASH 09 PR D79 095024
DERBIN 09 EPJ C62 755
DERBIN 09A PL B678 181
GONDULO 09 PR D79 107301
IGNATOVICH 09 EPJ C64 19
KEKEZ 09 PL B671 345
SEREBROV 09 PL B680 423
TUNG 09 PRL 102 051802
AALSETH 08 PRL 101 251301
AFANASEV 08 PRL 101 120401
BELLI 08A NP A806 388
BELLINI 08 EPJ C54 61
CHOU 08 PRL 100 080402
FOUCHE 08 PR D78 032013
HANNESTAD 08 JCAP 0804 019
INOUE 08 PL B668 93
LOVE 08 PRL 101 151802
ZAVATTINI 08 PR D77 032006
ADELBERGER 07 PRL 98 131104
ANDRIAMONJON 07 JCAP 0704 010
BAESSLER 07 PR D75 075006
CHANG 07 PR D75 052004
DERBIN 07 JETPL 85 12
HANNESTAD 07 JCAP 0708 015
JAIN 07 JPG 34 129
LESSA 07 PR D75 094001
MELCHIORRI 07A PR D76 041303R
NAMBA 07 PL B645 398
ROBILLIARD 07 PR 99 190403
ARNOLD 06 NP A765 483
DUFFY 06 PR D74 012006
HECKEL 06 PRL 97 021603
ZAVATTINI 06 PRL 96 110406
DERBIN 05 JETPL 81 365
Translated from ZETFP 81 453.
HANNESTAD 05A JCAP 0507 002
PARK 05 PRL 94 021801
ZIOUTAS 05 PRL 94 121301
ADLER 04 PR D70 037102
ANISIMOVSKY... 04 PRL 93 031801
ARNOLD 04 JETPL 80 377
Translated from ZETFP 80 429.
ASZTALOS 04 PR D69 011101R
LJUBICIC 04 PL B599 143
ARNABOLDI 03 PL B557 167
CIVITARESE 03 NP A729 867
DANEVICH 03 PR C68 035501
ADLER 02C PL B537 211
BADERT... 02 PL B542 29
BERNABELI 02D PL B546 23
DERBIN 02 PAN 65 1302
Translated from YAF 65 1335.
FUSHIMI 02 PL B531 190
INOUE 02 PL B536 18
MORALES 02B ASP 16 325
ADLER 01 PR D63 032004
AMMAR 01B PRL 87 271801
ASHITKOV 01 JETPL 74 529
Translated from ZETFP 74 601.
BERNABELI 01B PL B515 6
DANEVICH 01 NP A694 375
DEBOER 01 JPG 27 L29
KRCMAR 01 PR D64 115016
STOICA 01 NP A694 269
ALESSAND... 00 PL B466 13
ARNOLD 00 NP A678 341
ASTIER 00B PL B479 371
DANEVICH 00 PR C62 045501
MASSO 00 PR D61 011701R
ARNOLD 99 NP A658 299
NI 99 PRL 82 2439
SIMKOVIC 99 PR C60 055502
ALTEGOER 98 PL B428 197
ARNOLD 98 NP A636 209
AVIGNONE 98 PRL 81 5068
DIAZ 98 NP B527 44
FAESSLER 98B JPG 24 2139
KIM 98 PR D58 055006
KRCMAR 98 PL B442 38
LUESCHER 98 PL B434 407
MORIYAMA 98 PL B434 147
MORO 98 PL B440 69
POSPELOV 98 PR D58 097703
ZUBER 98 PRPL 305 295
AHMAD 97 PRL 78 618
BORISOV 97 JETP 83 868
DEBOER 97C JPG 23 1385
KACHELRIESS 97 PR D56 1313
KEL 97 PR D56 2419
KITCHING 97 PRL 79 4079
LEINBERGER 97 PL B394 16
ADLER 96 PRL 76 1421
AMSLER 96B ZPHY C70 219
GANZ 96 PL B389 4
GUNTHER 96 PR D54 3641
KAMEL 96 PL B368 291
MITSUI 96 EPL 33 111
YODIN 96 PRL 77 2170
ALTMANN 95 ZPHY C68 221
BALEST 95 PR D51 2053
BASSOMPIERE... 95 PL B355 584
MAENO 95 PL B351 574
MORIYAMA 95B PRL 75 3222
RAFFELT 95 PR D51 1495
SKALSEY 95 PR D51 6292
TSUNODA 95 EPL 30 273
ADACHI 94 PR A49 3201
ALTHERR 94 ASP 2 175
AMSLER 94B PL B333 271
ASA 94 PL B323 90
MEUDERDRES 94 PR D49 4937
NI 94 Physica B194 153
VO 94 PR C49 1551
A. Serbrev et al. (CDMS Collab.)
S. Andriamonje et al. (NEMO-3 Collab.)
E. Arik et al. (CAST Collab.)
B. Aubert et al. (BABAR Collab.)
A.S. Chou et al. (GammeV Collab.)
H. Davoudiasl, P. Huber
A.V. Derbin et al.
A.V. Derbin et al.
P. Gondolo, G. Raffelt (UTAH, MPIM)
V.K. Ignatovich, Y.N. Pokotilovski (JINR)
D. Kekez et al.
A. Serbrev (PNPI)
Y.C. Tung et al. (KEK E391a Collab.)
C.E. Aalseth et al. (CoGeNT Collab.)
A. Afanasev et al.
P. Belli et al.
G. Bellini et al. (Borexino Collab.)
A.S. Chou et al. (GammeV Collab.)
M. Fouche et al.
S. Hannestad et al.
Y. Inoue et al.
W. Love et al. (CLEO Collab.)
E. Zavattini et al. (PVLAS Collab.)
E.G. Adelberger et al.
S. Andriamonje et al. (CAST Collab.)
S. Baessler et al.
H.M. Chang et al. (TEXONO Collab.)
A.V. Derbin et al.
S. Hannestad et al.
P.L. Jain, G. Singh
A.P. Lessa, O.L.G. Peres
A. Melchiorri, O. Menz, A. Slosar
T. Namba
C. Robilliard et al.
R. Arnold et al. (NEMO-3 Collab.)
L.D. Duffy et al.
B.R. Heckel et al.
E. Zavattini et al. (PVLAS Collab.)
A.V. Derbin et al.
Translated from ZETFP 81 453.
S. Hannestad, A. Mirizzi, G. Raffelt (FNAL HyperCP Collab.)
K. Zioutas et al. (CAST Collab.)
S. Adler et al. (BNL E787 Collab.)
V.V. Anisimovskiy et al. (BNL E949 Collab.)
R. Arnold et al. (NEMO3 Detector Collab.)
S.J. Asztalos et al.
A. Ljubcic et al.
C. Arnaboldi et al.
O. Civitarese, J. Suhonen
F.A. Danevich et al.
S. Adler et al. (BNL E787 Collab.)
A. Badertscher et al.
R. Bernabei et al. (DAMA Collab.)
A.V. Derbin et al.
Translated from YAF 65 1335.
K. Fushimi et al. (ELEGANT V Collab.)
Y. Inoue et al. (COSME Collab.)
S. Adler et al. (BNL E787 Collab.)
R. Ammar et al. (CLEO Collab.)
V.D. Ashitkov et al.
R. Bernabei et al. (DAMA Collab.)
F.A. Danevich et al.
F.W.N. de Boer et al.
M. Krcmar et al.
S. Stoica, H.V. Klapprod-Kleingrothous
A. Alessandrello et al.
R. Arnold et al.
P. Astier et al. (NOMAD Collab.)
F.A. Danevich et al.
E. Masso
R. Arnold et al. (NEMO Collab.)
W.-T. Ni et al.
F. Simkovic et al.
J. Altegoer et al. (NEMO-2 Collab.)
R. Arnold et al.
F.T. Avignone et al. (Solar Axion Experiment)
M.A. Diaz et al.
A. Faessler, F. Simkovic
J.E. Kim
M. Krcmar et al.
R. Luescher et al.
S. Moriyama et al.
T. Moroi, H. Murayama
M. Pospelov
K. Zuber
I. Ahmad et al. (APEX Collab.)
A.V. Borisov, V.Y. Grishinia (MOSU)
F.W.N. de Boer et al.
H. Kachelriess, C. Wilke, G. Wunner (BOCH)
W. Keil et al.
P. Kitching et al. (BNL E787 Collab.)
U. Leinberger et al. (ORANGE Collab.)
S. Adler et al. (BNL E787 Collab.)
C. AMSLER et al. (Crystal Barrel Collab.)
R. Ganz et al. (GSI, HEID, FRAN, JAGL+)
M. Gunther et al. (MPH, SASSO)
S. Kamel (SHAMS)
T. Mitsui et al. (TOKY)
A.M. Yudin et al. (AMHT, WASH)
M. Altmann et al. (MUNT, LAPP, CPPM)
R. Balest et al. (CLEO Collab.)
G. Bassompierre et al. (LAPP, LGCT, LYON)
T. Maeno et al. (TOKY)
S. Moriyama
G. Raffelt, A. Weiss (MPIM, MPJA)
M. Skalsey, R.S. Conti (MICH)
T. Tsunoda et al. (TOKY)
S. Adachi et al. (TMU)
T. Altherr, E. Petitgirard, T. del Rio Gaztelurrutia
C. AMSLER et al. (Crystal Barrel Collab.)
S. Asai et al. (TOKY)
M.R. Dres et al. (BRCO, OREG, TRIU)
W.T. Ni et al. (NTHU)
D.T. Vo et al. (ISU, LBL, LLNL, UCD)

LEPTONS

e	515
μ	516
τ	525
Heavy Charged Lepton Searches	553
Neutrino Properties	554
Number of Neutrino Types	561
Double- β Decay	562
Neutrino Mixing	567
Heavy Neutral Leptons, Searches for	577

Notes in the Lepton Listings

Muon Anomalous Magnetic Moment (rev.)	517
Muon Decay Parameters (rev.)	521
τ Branching Fractions (rev.)	529
τ -Lepton Decay Parameters	548
Number of Light Neutrino Types from Collider Experiments	561
Neutrinoless Double- β Decay (rev.)	562





LEPTONS

e

$$J = \frac{1}{2}$$

e MASS (atomic mass units u)

The primary determination of an electron's mass comes from measuring the ratio of the mass to that of a nucleus, so that the result is obtained in u (atomic mass units). The conversion factor to MeV is more uncertain than the mass of the electron in u; indeed, the recent improvements in the mass determination are not evident when the result is given in MeV. In this datablock we give the result in u, and in the following datablock in MeV.

VALUE (10^{-6} u)	DOCUMENT ID	TECN	COMMENT
548.5799043 ± 0.0000023	MOHR 08	RVUE	2006 CODATA value
• • • We do not use the following data for averages, fits, limits, etc. • • •			
548.5799045 ± 0.0000024	MOHR 05	RVUE	2002 CODATA value
548.5799092 ± 0.0000004	¹ BEIER 02	CNTR	Penning trap
548.5799110 ± 0.0000012	MOHR 99	RVUE	1998 CODATA value
548.5799111 ± 0.0000012	² FARNHAM 95	CNTR	Penning trap
548.579903 ± 0.000013	COHEN 87	RVUE	1986 CODATA value

¹BEIER 02 compares Larmor frequency of the electron bound in a $^{12}\text{C}^{5+}$ ion with the cyclotron frequency of a single trapped $^{12}\text{C}^{5+}$ ion.

²FARNHAM 95 compares cyclotron frequency of trapped electrons with that of a single trapped $^{12}\text{C}^{6+}$ ion.

e MASS

2006 CODATA (MOHR 08) gives the conversion factor from u (atomic mass units, see the above datablock) to MeV as 931.494 028 (23). Earlier values use the then-current conversion factor. The conversion error dominates the uncertainty of the masses given below.

VALUE (MeV)	DOCUMENT ID	TECN	COMMENT
0.510998910 ± 0.00000013	MOHR 08	RVUE	2006 CODATA value
• • • We do not use the following data for averages, fits, limits, etc. • • •			
0.510998918 ± 0.00000044	MOHR 05	RVUE	2002 CODATA value
0.510998901 ± 0.000000020	^{3,4} BEIER 02	CNTR	Penning trap
0.510998902 ± 0.000000021	MOHR 99	RVUE	1998 CODATA value
0.510998903 ± 0.000000020	^{3,5} FARNHAM 95	CNTR	Penning trap
0.510998895 ± 0.000000024	³ COHEN 87	RVUE	1986 CODATA value
0.5110034 ± 0.0000014	COHEN 73	RVUE	1973 CODATA value

³Converted to MeV using the 1998 CODATA value of the conversion constant, 931.494013 ± 0.000037 MeV/u.

⁴BEIER 02 compares Larmor frequency of the electron bound in a $^{12}\text{C}^{5+}$ ion with the cyclotron frequency of a single trapped $^{12}\text{C}^{5+}$ ion.

⁵FARNHAM 95 compares cyclotron frequency of trapped electrons with that of a single trapped $^{12}\text{C}^{6+}$ ion.

$$(m_{e^+} - m_{e^-}) / m_{\text{average}}$$

A test of *CPT* invariance.

VALUE	CL%	DOCUMENT ID	TECN	COMMENT
< 8 × 10⁻⁹	90	⁶ FEE 93	CNTR	Positronium spectroscopy
• • • We do not use the following data for averages, fits, limits, etc. • • •				
< 4 × 10 ⁻⁸	90	CHU 84	CNTR	Positronium spectroscopy

⁶FEE 93 value is obtained under the assumption that the positronium Rydberg constant is exactly half the hydrogen one.

$$|q_{e^+} + q_{e^-}|/e$$

A test of *CPT* invariance. See also similar tests involving the proton.

VALUE	DOCUMENT ID	TECN	COMMENT
< 4 × 10⁻⁸	⁷ HUGHES 92	RVUE	
• • • We do not use the following data for averages, fits, limits, etc. • • •			
< 2 × 10 ⁻¹⁸	⁸ SCHAEFER 95	THEO	Vacuum polarization
< 1 × 10 ⁻¹⁸	⁹ MUELLER 92	THEO	Vacuum polarization

⁷HUGHES 92 uses recent measurements of Rydberg-energy and cyclotron-frequency ratios.

⁸SCHAEFER 95 removes model dependency of MUELLER 92.

⁹MUELLER 92 argues that an inequality of the charge magnitudes would, through higher-order vacuum polarization, contribute to the net charge of atoms.

e MAGNETIC MOMENT ANOMALY

$$\mu_e/\mu_B - 1 = (g-2)/2$$

VALUE (units 10^{-6})	DOCUMENT ID	TECN	CHG	COMMENT
1159.65218073 ± 0.00000028	HANNEKE 08	MRS		Single electron
• • • We do not use the following data for averages, fits, limits, etc. • • •				
1159.65218111 ± 0.00000074	¹⁰ MOHR 08	RVUE		2006 CODATA value
1159.65218085 ± 0.00000076	¹¹ ODOM 06	MRS	-	Single electron
1159.6521859 ± 0.00000038	MOHR 05	RVUE		2002 CODATA value
1159.6521869 ± 0.00000041	MOHR 99	RVUE		1998 CODATA value
1159.652193 ± 0.000010	COHEN 87	RVUE		1986 CODATA value
1159.6521884 ± 0.0000043	VANDYCK 87	MRS	-	Single electron
1159.6521879 ± 0.0000043	VANDYCK 87	MRS	+	Single positron

¹⁰MOHR 08 average is dominated by ODOM 06.

¹¹Superseded by HANNEKE 08 per private communication with Gerald Gabrielse.

$$(g_{e^+} - g_{e^-}) / g_{\text{average}}$$

A test of *CPT* invariance.

VALUE (units 10^{-12})	CL%	DOCUMENT ID	TECN	COMMENT
- 0.5 ± 2.1		¹² VANDYCK 87	MRS	Penning trap
• • • We do not use the following data for averages, fits, limits, etc. • • •				
< 12	95	¹³ VASSERMAN 87	CNTR	Assumes $m_{e^+} = m_{e^-}$
22 ± 64		SCHWINBERG 81	MRS	Penning trap

¹²VANDYCK 87 measured $(g_-/g_+) - 1$ and we converted it.

¹³VASSERMAN 87 measured $(g_+ - g_-)/(g-2)$. We multiplied by $(g-2)/g = 1.2 \times 10^{-3}$.

e ELECTRIC DIPOLE MOMENT (d)

A nonzero value is forbidden by both *T* invariance and *P* invariance.

VALUE (10^{-26} ecm)	CL%	DOCUMENT ID	TECN	COMMENT
0.069 ± 0.074		REGAN 02	MRS	²⁰⁵ Tl beams
• • • We do not use the following data for averages, fits, limits, etc. • • •				
0.18 ± 0.12 ± 0.10		¹⁴ COMMINS 94	MRS	²⁰⁵ Tl beams
- 0.27 ± 0.83		¹⁴ ABDULLAH 90	MRS	²⁰⁵ Tl beams
- 14 ± 24		CHO 89	NMR	Tl F molecules
- 1.5 ± 5.5 ± 1.5		MURTHY 89		Cesium, no B field
- 50 ± 110		LAMOREAUX 87	NMR	¹⁹⁹ Hg
190 ± 340	90	SANDARS 75	MRS	Thallium
70 ± 220	90	PLAYER 70	MRS	Xenon
< 300	90	WEISSKOPF 68	MRS	Cesium

¹⁴ABDULLAH 90, COMMINS 94, and REGAN 02 use the relativistic enhancement of a valence electron's electric dipole moment in a high-Z atom.

e⁻ MEAN LIFE / BRANCHING FRACTION

A test of charge conservation. See the "Note on Testing Charge Conservation and the Pauli Exclusion Principle" following this section in our 1992 edition (Physical Review **D45** S1 (1992), p. VI.10).

Most of these experiments are one of three kinds: Attempts to observe (a) the 25.5 keV gamma ray produced in $e^- \rightarrow \nu_e \gamma$, (b) the (K) shell x-ray produced when an electron decays without additional energy deposit, e.g., $e^- \rightarrow \nu_e \bar{\nu}_e \nu_e$ ("disappearance" experiments), and (c) nuclear de-excitation gamma rays after the electron disappears from an atomic shell and the nucleus is left in an excited state. The last can include both weak boson and photon mediating processes. We use the best $e^- \rightarrow \nu_e \gamma$ limit for the Summary Tables.

Note that we use the mean life rather than the half life, which is often reported.

e → ν_e γ and astrophysical limits

VALUE (yr)	CL%	DOCUMENT ID	TECN	COMMENT
> 4.6 × 10²⁶	90	BACK 02	BORX	$e^- \rightarrow \nu \gamma$
• • • We do not use the following data for averages, fits, limits, etc. • • •				
> 1.22 × 10 ²⁶	68	¹⁵ KLAPDOR-K...07	CNTR	$e^- \rightarrow \nu \gamma$
> 3.4 × 10 ²⁶	68	BELLI 00b	DAMA	$e^- \rightarrow \nu \gamma$, liquid Xe
> 3.7 × 10 ²⁵	68	AHARONOV 95b	CNTR	$e^- \rightarrow \nu \gamma$
> 2.35 × 10 ²⁵	68	BALYSH 93	CNTR	$e^- \rightarrow \nu \gamma$, ⁷⁶ Ge detector
> 1.5 × 10 ²⁵	68	AVIGNONE 86	CNTR	$e^- \rightarrow \nu \gamma$
> 1 × 10 ³⁹		¹⁶ ORITO 85	ASTR	Astrophysical argument
> 3 × 10 ²³	68	BELLOTTI 83b	CNTR	$e^- \rightarrow \nu \gamma$

¹⁵The authors of A. Derbin et al, arXiv:0704.2047v1 argue that this limit is overestimated by at least a factor of 5.

¹⁶ORITO 85 assumes that electromagnetic forces extend out to large enough distances and that the age of our galaxy is 10^{10} years.

Lepton Particle Listings

e, μ

Disappearance and nuclear-de-excitation experiments

VALUE (yr)	CL%	DOCUMENT ID	TECN	COMMENT
$>6.4 \times 10^{24}$	68	17 BELLI	99B	DAMA De-excitation of ^{129}Xe
$>4.2 \times 10^{24}$	68	BELLI	99	DAMA Iodine L-shell disappearance
$>2.4 \times 10^{23}$	90	18 BELLI	99D	DAMA De-excitation of ^{127}I (in NaI)
$>4.3 \times 10^{23}$	68	AHARONOV	95B	CNTR Ge K-shell disappearance
$>2.7 \times 10^{23}$	68	REUSSER	91	CNTR Ge K-shell disappearance
$>2 \times 10^{22}$	68	BELLOTTI	83B	CNTR Ge K-shell disappearance

¹⁷BELLI 99B limit on charge nonconserving e^- capture involving excitation of the 236.1 keV nuclear state of ^{129}Xe ; the 90% CL limit is 3.7×10^{24} yr. Less stringent limits for other states are also given.

¹⁸BELLI 99D limit on charge nonconserving e^- capture involving excitation of the 57.6 keV nuclear state of ^{127}I . Less stringent limits for the other states and for the state of ^{23}Na are also given.

LIMITS ON LEPTON-FLAVOR VIOLATION IN PRODUCTION

Forbidden by lepton family number conservation.

This section was added for the 2008 edition of this Review and is not complete. For a list of further measurements see references in the papers listed below.

$\sigma(e^+e^- \rightarrow e^\pm\tau^\mp) / \sigma(e^+e^- \rightarrow \mu^\pm\mu^-)$

VALUE	CL%	DOCUMENT ID	TECN	COMMENT
$<8.9 \times 10^{-6}$	95	AUBERT	07P	BABR e^+e^- at $E_{\text{cm}} = 10.58$ GeV
$<1.8 \times 10^{-3}$	95	GOMEZ-CAD...	91	MRK2 e^+e^- at $E_{\text{cm}} = 29$ GeV

$\sigma(e^+e^- \rightarrow \mu^\pm\tau^\mp) / \sigma(e^+e^- \rightarrow \mu^\pm\mu^-)$

VALUE	CL%	DOCUMENT ID	TECN	COMMENT
$<4.0 \times 10^{-6}$	95	AUBERT	07P	BABR e^+e^- at $E_{\text{cm}} = 10.58$ GeV
$<6.1 \times 10^{-3}$	95	GOMEZ-CAD...	91	MRK2 e^+e^- at $E_{\text{cm}} = 29$ GeV

e REFERENCES

HANNEKE 08	PRL 100 120801	D. Hanneke, S. Fogwell, G. Gabrielse (HARV)
MOHR 08	RMP 80 633	P.J. Mohr, B.N. Taylor, D.B. Newell (NIST)
AUBERT 07P	PL D75 031103R	B. Aubert et al. (BABAR Collab.)
KLADOR-K... 07	PL B644 109	H.V. Klador-Kleingrothaus, I.V. Krivosheina, I.V. Titkova (HARV)
ODOM 06	PRL 97 030801	B. Odom et al. (HARV)
MOHR 05	RMP 77 1	P.J. Mohr, B.N. Taylor (NIST)
BACK 02	PL B525 29	H.O. Back et al. (BOREXINO/SASSO Collab.)
BEIER 02	PRL 88 011603	T. Beier et al. (DAMA Collab.)
REGAN 02	PRL 88 071805	B.C. Regan et al. (DAMA Collab.)
BELLI 00B	PR D61 117301	P. Belli et al. (DAMA Collab.)
BELLI 99	PL B460 236	P. Belli et al. (DAMA Collab.)
BELLI 99B	PL B465 315	P. Belli et al. (DAMA Collab.)
BELLI 99D	PR C60 065001	P. Belli et al. (DAMA Collab.)
MOHR 99	JPCRD 28 1713	P.J. Mohr, B.N. Taylor (NIST)
Also	RMP 72 351	P.J. Mohr, B.N. Taylor (NIST)
AHARONOV 95B	PR D52 3785	Y. Aharonov et al. (SCUC, PNL, ZARA+)
Also	PL B353 168	Y. Aharonov et al. (SCUC, PNL, ZARA+)
FARNHAM 95	PRL 75 3598	D.L. Farnham, R.S. van Dyck, P.B. Schwinberg (WASH)
SCHAEFER 95	PR A51 838	A. Schaefer, J. Reinhardt (FRAN)
COMMINS 94	PR A50 2960	E.D. Commins et al. (KIAE, MPIH, SASSO)
BALYSH 93	PL B298 278	A. Balysh et al. (M.S. Fei et al.)
FEE 93	PR A48 192	R.S. Fee et al. (LANL, AARH)
HUGHES 92	PRL 69 578	R.J. Hughes, B.I. Deutch (LANL, AARH)
MUELLER 92	PRL 69 3432	B. Mueller, M.H. Thoma (DUKE)
PDG 92	PR D45 51	K. Hikasa et al. (KEK, LBL, BOST+)
GOMEZ-CAD... 91	PRL 66 1007	J.J. Gomez-Cadenas et al. (SLAC MARK-2 Collab.)
REUSSER 91	PL B255 143	D. Reusser et al. (NEUC, CIT, PSI)
ABDULLAH 90	PRL 65 2347	K. Abdullah et al. (LBL, UCB)
CHO 89	PRL 63 2559	D. Cho, K. Sangster, E.A. Hinds (YALE)
MURTHY 89	PRL 63 965	S.A. Murthy et al. (AMHT)
COHEN 87	RMP 59 1121	E.R. Cohen, B.N. Taylor (RIS, NBS)
LAMOREAUX 87	PRL 59 2275	S.K. Lamoreaux et al. (WASH)
VANDYCK 87	PRL 59 26	R.S. van Dyck, P.B. Schwinberg, H.G. Dehmelt (WASH)
VASSERMAN 87	PL B198 302	I.B. Vasserman et al. (NOVO)
Also	PL B187 172	I.B. Vasserman et al. (NOVO)
AVIGNONE 86	PR D34 97	F.T. Avignone et al. (PNL, SCUC)
ORITO 85	PRL 54 2457	S. Orito, M. Yoshimura (TOKY, KEK)
CHU 84	PRL 52 1689	S. Chu, A.P. Mills, J.L. Hall (BELL, NBS, COLO)
BELLOTTI 83B	PL 124B 435	E. Bellotti et al. (MILA)
SCHWINBERG 81	PRL 47 1679	P.B. Schwinberg, R.S. van Dyck, H.G. Dehmelt (WASH)
SANDARS 75	PR A11 473	P.G.H. Sandars, D.M. Sternheimer (OXF, BNL)
COHEN 73	JPCRD 2 664	E.R. Cohen, B.N. Taylor (RIS, NBS)
PLAYER 70	JPB 3 1620	M.A. Player, P.G.H. Sandars (OXF)
WEISSKOPF 68	PRL 21 1645	M.C. Weisskopf et al. (BRAN)



$$J = \frac{1}{2}$$

μ MASS (atomic mass units u)

The muon's mass is obtained from the muon-electron mass ratio as determined from the measurement of Zeeman transition frequencies in muonium ($\mu^+\text{e}^-$ atom). Since the electron's mass is most accurately known in u, the muon's mass is also most accurately known in u. The conversion factor to MeV has approximately the same relative uncertainty as the mass of the muon in u. In this datablock we give the result in u, and in the following datablock in MeV.

VALUE (u)	DOCUMENT ID	TECN	CHG	COMMENT
$0.1134289256 \pm 0.000000029$	MOHR	08	RVUE	2006 CODATA value

• • • We do not use the following data for averages, fits, limits, etc. • • •

$0.1134289264 \pm 0.000000030$	MOHR	05	RVUE	2002 CODATA value
$0.1134289168 \pm 0.000000034$	¹ MOHR	99	RVUE	1998 CODATA value
$0.113428913 \pm 0.000000017$	² COHEN	87	RVUE	1986 CODATA value

¹ MOHR 99 make use of other 1998 CODATA entries below.
² COHEN 87 make use of other 1986 CODATA entries below.

μ MASS

2006 CODATA (MOHR 08) gives the conversion factor from u (atomic mass units, see the above datablock) to MeV as 931.494 028 (23). Earlier values use the then-current conversion factor. The conversion error contributes significantly to the uncertainty of the masses given below.

VALUE (MeV)	DOCUMENT ID	TECN	CHG	COMMENT
$105.6583668 \pm 0.0000038$	MOHR	08	RVUE	2006 CODATA value
• • • We do not use the following data for averages, fits, limits, etc. • • •				
$105.6583692 \pm 0.0000094$	MOHR	05	RVUE	2002 CODATA value
$105.6583568 \pm 0.0000052$	MOHR	99	RVUE	1998 CODATA value
105.658353 ± 0.000016	³ COHEN	87	RVUE	1986 CODATA value
105.658386 ± 0.000044	⁴ MARIAM	82	CNTR +	
105.65836 ± 0.00026	⁵ CROWE	72	CNTR	
105.65865 ± 0.00044	⁶ CRANE	71	CNTR	

³ Converted to MeV using the 1998 CODATA value of the conversion constant, 931.494013 ± 0.000037 MeV/u.

⁴ MARIAM 82 give $m_\mu/m_e = 206.768259(62)$.

⁵ CROWE 72 give $m_\mu/m_e = 206.7682(5)$.

⁶ CRANE 71 give $m_\mu/m_e = 206.76878(85)$.

μ MEAN LIFE τ

Measurements with an error $> 0.001 \times 10^{-6}$ s have been omitted.

VALUE (10^{-6} s)	DOCUMENT ID	TECN	CHG	COMMENT
2.197034 ± 0.000021	OUR AVERAGE			Error includes scale factor of 1.2.
$2.197083 \pm 0.000032 \pm 0.000015$	BARCZYK	08	CNTR +	Muons from π^+ decay at rest
$2.197013 \pm 0.000021 \pm 0.000011$	CHITWOOD	07	CNTR +	Surface μ^+ at PSI
2.197078 ± 0.000073	BARDIN	84	CNTR +	
2.197025 ± 0.000155	BARDIN	84	CNTR -	
2.19695 ± 0.000006	GIOVANNETTI	84	CNTR +	
2.19711 ± 0.000008	BALANDIN	74	CNTR +	
2.1973 ± 0.0003	DUCLOS	73	CNTR +	

$\tau_{\mu^+}/\tau_{\mu^-}$ MEAN LIFE RATIO

A test of CPT invariance.

VALUE	DOCUMENT ID	TECN	COMMENT	
1.000024 ± 0.000078	BARDIN	84	CNTR	
• • • We do not use the following data for averages, fits, limits, etc. • • •				
1.0008 ± 0.0010	BAILEY	79	CNTR	Storage ring
1.000 ± 0.001	MEYER	63	CNTR	Mean life μ^+/μ^-

$(\tau_{\mu^+} - \tau_{\mu^-}) / \tau_{\text{average}}$

A test of CPT invariance. Calculated from the mean-life ratio, above.

VALUE	DOCUMENT ID
$(2 \pm 8) \times 10^{-5}$	OUR EVALUATION

μ/p MAGNETIC MOMENT RATIO

This ratio is used to obtain a precise value of the muon mass and to reduce experimental muon Larmor frequency measurements to the muon magnetic moment anomaly. Measurements with an error > 0.00001 have been omitted. By convention, the minus sign on this ratio is omitted. CODATA values were fitted using their selection of data, plus other data from multiparameter fits.

VALUE	DOCUMENT ID	TECN	CHG	COMMENT
$3.183345137 \pm 0.000000085$	MOHR	08	RVUE	2006 CODATA value
• • • We do not use the following data for averages, fits, limits, etc. • • •				
$3.183345118 \pm 0.000000089$	MOHR	05	RVUE	2002 CODATA value
$3.18334513 \pm 0.000000039$	LIU	99	CNTR +	HFS in muonium
$3.18334539 \pm 0.000000010$	MOHR	99	RVUE	1998 CODATA value
$3.18334547 \pm 0.000000047$	COHEN	87	RVUE	1986 CODATA value
3.1833441 ± 0.00000017	KLEMPPT	82	CNTR +	Precession strob
3.1833461 ± 0.00000011	MARIAM	82	CNTR +	HFS splitting
3.1833448 ± 0.00000029	CAMANI	78	CNTR +	See KLEMPPT 82
3.1833403 ± 0.00000044	CASPERSON	77	CNTR +	HFS splitting
3.1833402 ± 0.00000072	COHEN	73	RVUE	1973 CODATA value
3.1833467 ± 0.00000082	CROWE	72	CNTR +	Precession phase

THE MUON ANOMALOUS MAGNETIC MOMENT

Updated July 2009 by A. Höcker (CERN), and W.J. Marciano (BNL).

The Dirac equation predicts a muon magnetic moment, $\vec{M} = g_\mu \frac{e}{2m_\mu} \vec{S}$, with gyromagnetic ratio $g_\mu = 2$. Quantum loop effects lead to a small calculable deviation from $g_\mu = 2$, parameterized by the anomalous magnetic moment

$$a_\mu \equiv \frac{g_\mu - 2}{2}. \quad (1)$$

That quantity can be accurately measured and, within the Standard Model (SM) framework, precisely predicted. Hence, comparison of experiment and theory tests the SM at its quantum loop level. A deviation in a_μ^{exp} from the SM expectation would signal effects of new physics, with current sensitivity reaching up to mass scales of $\mathcal{O}(\text{TeV})$ [1,2]. For recent and very thorough muon $g - 2$ reviews, see Refs. [3,4].

The E821 experiment at Brookhaven National Lab (BNL) studied the precession of μ^+ and μ^- in a constant external magnetic field as they circulated in a confining storage ring. It found [6]¹

$$\begin{aligned} a_{\mu^+}^{\text{exp}} &= 11\,659\,204(6)(5) \times 10^{-10}, \\ a_{\mu^-}^{\text{exp}} &= 11\,659\,215(8)(3) \times 10^{-10}, \end{aligned} \quad (2)$$

where the first errors are statistical and the second systematic. Assuming CPT invariance and taking into account correlations between systematic errors, one finds for their average [6]

$$a_\mu^{\text{exp}} = 11\,659\,208.9(5.4)(3.3) \times 10^{-10}. \quad (3)$$

These results represent about a factor of 14 improvement over the classic CERN experiments of the 1970's [7].

The SM prediction for a_μ^{SM} is generally divided into three parts (see Fig. 1 for representative Feynman diagrams)

$$a_\mu^{\text{SM}} = a_\mu^{\text{QED}} + a_\mu^{\text{EW}} + a_\mu^{\text{Had}}. \quad (4)$$

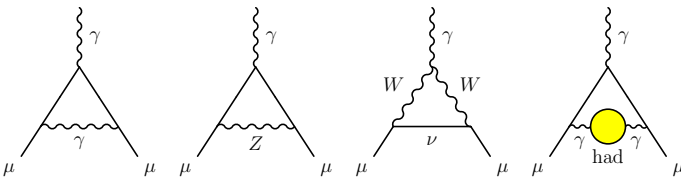


Figure 1: Representative diagrams contributing to a_μ^{SM} . From left to right: first order QED (Schwinger term), lowest-order weak, lowest-order hadronic.

¹ The original results reported by the experiment have been updated in Eqs. (2) and (3) to the newest value for the absolute muon-to-proton magnetic ratio $\lambda = 3.183345137(85)$ [5]. The change induced in a_μ^{exp} with respect to the value of $\lambda = 3.18334539(10)$ used in Ref. [6] amounts to $+0.92 \times 10^{-10}$.

The QED part includes all photonic and leptonic (e, μ, τ) loops starting with the classic $\alpha/2\pi$ Schwinger contribution. It has been computed through 4 loops and estimated at the 5-loop level [8]

$$\begin{aligned} a_\mu^{\text{QED}} &= \frac{\alpha}{2\pi} + 0.765857410(27) \left(\frac{\alpha}{\pi}\right)^2 + 24.05050964(43) \left(\frac{\alpha}{\pi}\right)^3 \\ &\quad + 130.8055(80) \left(\frac{\alpha}{\pi}\right)^4 + 663(20) \left(\frac{\alpha}{\pi}\right)^5 + \dots \end{aligned} \quad (5)$$

Employing $\alpha^{-1} = 137.035999084(51)$, determined [8,9] from the electron a_e measurement, leads to

$$a_\mu^{\text{QED}} = 116\,584\,718.09(0.15) \times 10^{-11}, \quad (6)$$

where the error results from uncertainties in the coefficients of Eq. (5) and in α .

Loop contributions involving heavy W^\pm, Z or Higgs particles are collectively labeled as a_μ^{EW} . They are suppressed by at least a factor of $\frac{\alpha}{\pi} \frac{m_\mu^2}{m_W^2} \simeq 4 \times 10^{-9}$. At 1-loop order [10]

$$\begin{aligned} a_\mu^{\text{EW}}[\text{1-loop}] &= \frac{G_\mu m_\mu^2}{8\sqrt{2}\pi^2} \left[\frac{5}{3} + \frac{1}{3} (1 - 4\sin^2\theta_W)^2 \right. \\ &\quad \left. + \mathcal{O}\left(\frac{m_\mu^2}{M_W^2}\right) + \mathcal{O}\left(\frac{m_\mu^2}{m_H^2}\right) \right], \\ &= 194.8 \times 10^{-11}, \end{aligned} \quad (7)$$

for $\sin^2\theta_W \equiv 1 - M_W^2/M_Z^2 \simeq 0.223$, and where $G_\mu \simeq 1.166 \times 10^{-5} \text{ GeV}^{-2}$ is the Fermi coupling constant. Two-loop corrections are relatively large and negative [11]

$$a_\mu^{\text{EW}}[\text{2-loop}] = -40.7(1.0)(1.8) \times 10^{-11}, \quad (8)$$

where the errors stem from quark triangle loops and the assumed Higgs mass range between 100 and 500 GeV. The 3-loop leading logarithms are negligible [11,12], $\mathcal{O}(10^{-12})$, implying in total

$$a_\mu^{\text{EW}} = 154(1)(2) \times 10^{-11}. \quad (9)$$

Hadronic (quark and gluon) loop contributions to a_μ^{SM} give rise to its main theoretical uncertainties. At present, those effects are not calculable from first principles, but such an approach, at least partially, may become possible as lattice QCD matures. Instead, one currently relies on a dispersion relation approach to evaluate the lowest-order (*i.e.*, $\mathcal{O}(\alpha^2)$) hadronic vacuum polarization contribution $a_\mu^{\text{Had}}[\text{LO}]$ from corresponding cross section measurements [13]

$$a_\mu^{\text{Had}}[\text{LO}] = \frac{1}{3} \left(\frac{\alpha}{\pi}\right)^2 \int_{m_\pi^2}^{\infty} ds \frac{K(s)}{s} R^{(0)}(s), \quad (10)$$

where $K(s)$ is a QED kernel function [14], and where $R^{(0)}(s)$ denotes the ratio of the bare² cross section for e^+e^- annihilation

² The bare cross section is defined as the measured cross section corrected for initial-state radiation, electron-vertex loop contributions and vacuum-polarization effects in the photon propagator. However, QED effects in the hadron vertex and final state, as photon radiation, are included.

Lepton Particle Listings

 μ

into hadrons to the pointlike muon-pair cross section at center-of-mass energy \sqrt{s} . The function $K(s) \sim 1/s$ in Eq. (10) gives a strong weight to the low-energy part of the integral. Hence, $a_\mu^{\text{Had}}[\text{LO}]$ is dominated by the $\rho(770)$ resonance.

Currently, the available $\sigma(e^+e^- \rightarrow \text{hadrons})$ data give a leading-order hadronic vacuum polarization (representative) contribution of [15]

$$a_\mu^{\text{Had}}[\text{LO}] = 6\,955(40)(7) \times 10^{-11}, \quad (11)$$

where the first error is experimental (dominated by systematic uncertainties), and the second due to perturbative QCD, which is used at intermediate and large energies to predict the contribution from the quark-antiquark continuum.

Alternatively, one can use precise vector spectral functions from $\tau \rightarrow \nu_\tau + \text{hadrons}$ decays [16] that can be related to isovector $e^+e^- \rightarrow \text{hadrons}$ cross sections by isospin symmetry. When isospin-violating corrections (from QED and $m_d - m_u \neq 0$) are applied, one finds [17]

$$a_\mu^{\text{Had}}[\text{LO}] = 7\,053(40)(19)(7) \times 10^{-11} (\tau), \quad (12)$$

where the first error is experimental, the second estimates the uncertainty in the isospin-breaking corrections applied to the τ data, and the third error is due to perturbative QCD. The discrepancy between the e^+e^- and τ -based determinations of $a_\mu^{\text{Had}}[\text{LO}]$ has been reduced with respect to earlier evaluations. New e^+e^- and τ data from the B -factory experiments BABAR and Belle have increased the experimental information. Reevaluated isospin-breaking corrections have also contributed to this improvement [17]. The remaining discrepancy may be indicative of problems with one or both data sets. It may also suggest the need for additional isospin-violating corrections to the τ data.

Higher order, $\mathcal{O}(\alpha^3)$, hadronic contributions are obtained from dispersion relations using the same $e^+e^- \rightarrow \text{hadrons}$ data [16,18,21], giving $a_\mu^{\text{Had,Disp}}[\text{NLO}] = (-98 \pm 1) \times 10^{-11}$, along with model-dependent estimates of the hadronic light-by-light scattering contribution, $a_\mu^{\text{Had,LBL}}[\text{NLO}]$, motivated by large- N_C QCD [22–28].³ Following [26], one finds for the sum of the two terms

$$a_\mu^{\text{Had}}[\text{NLO}] = 7(26) \times 10^{-11}, \quad (13)$$

where the error is dominated by hadronic light-by-light uncertainties.

Adding Eqs. (6), (9), (11) and (13) gives the representative e^+e^- data-based SM prediction

$$a_\mu^{\text{SM}} = 116\,591\,834(2)(41)(26) \times 10^{-11}, \quad (14)$$

where the errors are due to the electroweak, lowest-order hadronic, and higher-order hadronic contributions, respectively. The difference between experiment and theory

$$\Delta a_\mu = a_\mu^{\text{exp}} - a_\mu^{\text{SM}} = 255(63)(49) \times 10^{-11}, \quad (15)$$

³ Some representative recent estimates of the hadronic light-by-light scattering contribution, $a_\mu^{\text{Had,LBL}}[\text{NLO}]$, that followed after the sign correction of [24], are: $105(26) \times 10^{-11}$ [26], $110(40) \times 10^{-11}$ [22], $136(25) \times 10^{-11}$ [23].

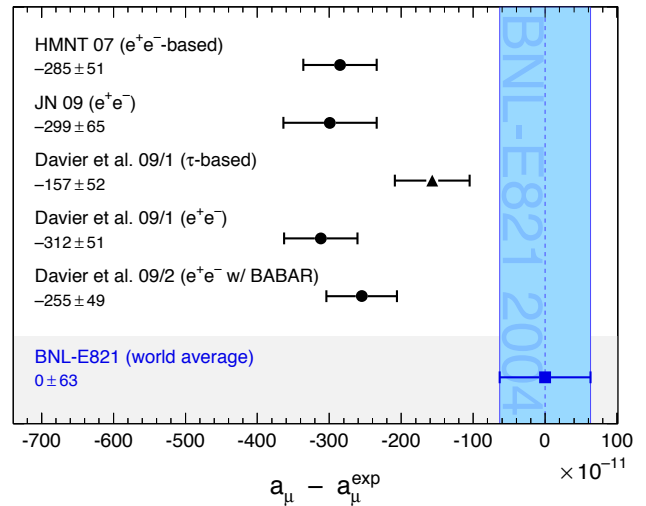


Figure 2: Compilation of recently published results for a_μ (in units of 10^{-11}), subtracted by the central value of the experimental average (3). The shaded band indicates the experimental error. The SM predictions are taken from: HMNT [18], JN [4], Davier *et al.*, 09/1 [17], and Davier *et al.*, 09/2 [15]. Note that the quoted errors do not include the uncertainty on the subtracted experimental value. To obtain for each theory calculation a result equivalent to Eq. (15), the errors from theory and experiment must be added in quadrature.

(with all errors combined in quadrature) represents an interesting but not yet conclusive discrepancy of 3.2 times the estimated 1σ error. All the recent estimates for the hadronic contribution compiled in Fig. 2 exhibit similar discrepancies. Switching to τ data reduces the discrepancy to 1.9σ , assuming the isospin-violating corrections are under control within the estimated uncertainties.

An alternate interpretation is that Δa_μ may be a new physics signal with supersymmetric particle loops as the leading candidate explanation. Such a scenario is quite natural, since generically, supersymmetric models predict [1] an additional contribution to a_μ^{SM}

$$a_\mu^{\text{SUSY}} \simeq \pm 130 \times 10^{-11} \cdot \left(\frac{100 \text{ GeV}}{m_{\text{SUSY}}} \right)^2 \tan\beta, \quad (16)$$

where m_{SUSY} is a representative supersymmetric mass scale, and $\tan\beta \simeq 3\text{--}40$ is a potential enhancement factor. Supersymmetric particles in the mass range 100–500 GeV could be the source of the deviation Δa_μ . If so, those particles could be directly observed at the next generation of high energy colliders. New physics effects [1] other than supersymmetry could also explain a non-vanishing Δa_μ .

References

1. A. Czarnecki and W.J. Marciano, Phys. Rev. **D64**, 013014 (2001).

2. M. Davier and W.J. Marciano, *Ann. Rev. Nucl. and Part. Sci.* **54**, 115 (2004).
3. J. Miller, E. de Rafael, and B. Lee Roberts, *Rep. Progress Phys.* **70**, 75 (2007).
4. F. Jegerlehner and A. Nyffeler, *Phys. Reports* **477**, 1 (2009).
5. P.J. Mohr, B.N. Taylor, and D.B. Newell, CODATA Group, *Rev. Mod. Phys.* **80**, 633 (2008).
6. G.W. Bennett *et al.*, *Phys. Rev. Lett.* **89**, 101804 (2002); Erratum *ibid.* *Phys. Rev. Lett.* **89**, 129903 (2002); G.W. Bennett *et al.*, *Phys. Rev. Lett.* **92**, 161802 (2004); G.W. Bennett *et al.*, *Phys. Rev.* **D73**, 072003 (2006).
7. J. Bailey *et al.*, *Nucl. Phys.* **B150**, 1 (1979).
8. T. Kinoshita and M. Nio, *Phys. Rev.* **D73**, 013003 (2006); T. Aoyama *et al.*, *Phys. Rev. Lett.* **99**, 110406 (2007); T. Kinoshita and M. Nio, *Phys. Rev.* **D70**, 113001 (2004); T. Kinoshita, *Nucl. Phys.* **B144**, 206 (2005)(Proc. Suppl.); T. Kinoshita and M. Nio, *Phys. Rev.* **D73**, 053007 (2006); A.L. Kataev, [arXiv:hep-ph/0602098](https://arxiv.org/abs/hep-ph/0602098) (2006); M. Passera, *J. Phys.* **G31**, 75 (2005).
9. G. Gabrielse *et al.*, *Phys. Rev. Lett.* **97**, 030802 (2006); Erratum *ibid.* *Phys. Rev. Lett.* **99**, 039902 (2007); D. Hanneke, S. Fogwell, and G. Gabrielse, *Phys. Rev. Lett.* **100**, 120801 (2008).
10. R. Jackiw and S. Weinberg, *Phys. Rev.* **D5**, 2396 (1972); G. Altarelli *et al.*, *Phys. Lett.* **B40**, 415 (1972); I. Bars and M. Yoshimura, *Phys. Rev.* **D6**, 374 (1972); K. Fujikawa, B.W. Lee, and A.I. Sanda, *Phys. Rev.* **D6**, 2923 (1972).
11. A. Czarnecki *et al.*, *Phys. Rev.* **D67**, 073006 (2003); S. Heinemeyer, D. Stockinger, and G. Weiglein, *Nucl. Phys.* **B699**, 103 (2004); T. Gribouk and A. Czarnecki, *Phys. Rev.* **D72**, 053016 (2005); A. Czarnecki, B. Krause, and W.J. Marciano, *Phys. Rev. Lett.* **76**, 3267 (1996); A. Czarnecki, B. Krause and W.J. Marciano, *Phys. Rev.* **D52**, 2619, (1995); S. Peris, M. Perrottet, and E. de Rafael, *Phys. Lett.* **B355**, 523 (1995); T. Kukhto *et al.*, *Nucl. Phys.* **B371**, 567 (1992).
12. G. Degrossi and G.F. Giudice, *Phys. Rev.* **D58**, 053007 (1998).
13. C. Bouchiat and L. Michel, *J. Phys. Radium* **22**, 121 (1961); M. Gourdin and E. de Rafael, *Nucl. Phys.* **B10**, 667 (1969).
14. S.J. Brodsky and E. de Rafael, *Phys. Rev.* **168**, 1620 (1968).
15. M. Davier *et al.*, [arXiv:0908.4300](https://arxiv.org/abs/0908.4300) [hep-ph] (2009).
16. R. Alemany *et al.*, *Eur. Phys. J.* **C2**, 123 (1998).
17. M. Davier *et al.*, [arXiv:0906.5443](https://arxiv.org/abs/0906.5443) [hep-ph] (2009).
18. K. Hagiwara *et al.*, *Phys. Lett.* **B649**, 173 (2007).
19. M. Davier, *Nucl. Phys.* (Proc. Suppl.), **B169**, 288 (2007).
20. M. Davier *et al.*, *Eur. Phys. J.* **C31**, 503 (2003); M. Davier *et al.*, *Eur. Phys. J.* **C27**, 497 (2003).
21. B. Krause, *Phys. Lett.* **B390**, 392 (1997).
22. J. Bijnens and J. Prades, *Mod. Phys. Lett.* **A22**, 767 (2007).
23. K. Melnikov and A. Vainshtein, *Phys. Rev.* **D70**, 113006 (2004).

24. M. Knecht and A. Nyffeler, *Phys. Rev.* **D65**, 073034 (2002); M. Knecht *et al.*, *Phys. Rev. Lett.* **88**, 071802 (2002).
25. J. Bijnens *et al.*, *Nucl. Phys.* **B626**, 410 (2002).
26. J. Prades, E. de Rafael, and A. Vainshtein, [arXiv:0901.0306](https://arxiv.org/abs/0901.0306) [hep-ph] (2009).
27. J. Hayakawa and T. Kinoshita, *Erratum Phys. Rev.* **D66**, 019902 (2002).
28. E. de Rafael, *Phys. Lett.* **B322**, 239 (1994).

 μ MAGNETIC MOMENT ANOMALY

The parity-violating decay of muons in a storage ring is observed. The difference frequency ω_a between the muon spin precession and the orbital angular frequency ($e/m_\mu c$)(B) is measured, as is the free proton NMR frequency ω_p , thus determining the ratio $R = \omega_a/\omega_p$. Given the magnetic moment ratio $\lambda = \mu_\mu/\mu_p$ (from hyperfine structure in muonium), $(g-2)/2 = R/(\lambda-R)$.

$$\mu_\mu/(e\hbar/2m_\mu) - 1 = (g_\mu - 2)/2$$

VALUE (units 10^{-10})	DOCUMENT ID	TECN	CHG	COMMENT
11659208.9 ± 5.4 ± 3.3	⁷ BENNETT	06	MUG2	Average μ^+ and μ^-
••• We do not use the following data for averages, fits, limits, etc. •••				
11659208 ± 6	BENNETT	04	MUG2	Average μ^+ and μ^-
11659214 ± 8 ± 3	BENNETT	04	MUG2	Storage ring
11659203 ± 6 ± 5	BENNETT	04	MUG2	Storage ring
11659204 ± 7 ± 5	BENNETT	02	MUG2	Storage ring
11659202 ± 14 ± 6	BROWN	01	MUG2	Storage ring
11659191 ± 59	BROWN	00	MUG2	+
11659100 ± 110	⁸ BAILEY	79	CNTR	Storage ring
11659360 ± 120	⁸ BAILEY	79	CNTR	Storage ring
11659230 ± 85	⁸ BAILEY	79	CNTR	Storage ring
11620000 ± 5000	CHARPAK	62	CNTR	+

⁷ BENNETT 06 reports $(g_\mu - 2)/2 = (11659208.0 \pm 5.4 \pm 3.3) \times 10^{-10}$. We rescaled this value using μ/p magnetic moment ratio of 3.183345137(85) from MOHR 08.

⁸ BAILEY 79 values recalculated by HUGHES 99 using the COHEN 87 μ/p magnetic moment. The improved MOHR 99 value does not change the result.

$$(g_{\mu^+} - g_{\mu^-}) / g_{\text{average}}$$

A test of CPT invariance.

VALUE (units 10^{-8})	DOCUMENT ID	TECN
-0.11 ± 0.12	BENNETT	04 MUG2
••• We do not use the following data for averages, fits, limits, etc. •••		
-2.6 ± 1.6	BAILEY	79 CNTR

 μ ELECTRIC DIPOLE MOMENT (d)

A nonzero value is forbidden by both T invariance and P invariance.

VALUE (10^{-19} ecm)	DOCUMENT ID	TECN	CHG	COMMENT
-0.1 ± 0.9	⁹ BENNETT	09	MUG2	Storage ring
••• We do not use the following data for averages, fits, limits, etc. •••				
-0.1 ± 1.0	BENNETT	09	MUG2	Storage ring
-0.1 ± 0.7	BENNETT	09	MUG2	Storage ring
-3.7 ± 3.4	¹⁰ BAILEY	78	CNTR	Storage ring
8.6 ± 4.5	BAILEY	78	CNTR	Storage ring
0.8 ± 4.3	BAILEY	78	CNTR	Storage ring

⁹ This is the combination of the two BENNETT 09 results quoted here separately for μ^+ and μ^- . BENNETT 09 uses the convention $d = 1/2 \cdot (d_{\mu^-} - d_{\mu^+})$.

¹⁰ This is the combination of the two BAILEY 78 results quoted here separately for μ^+ and μ^- . BAILEY 78 uses the convention $d = 1/2 \cdot (d_{\mu^+} - d_{\mu^-})$ and reports 3.7 ± 3.4 . We convert their result to use the same convention as BENNETT 09.

MUON-ELECTRON CHARGE RATIO ANOMALY $q_{\mu^+}/q_{e^-} + 1$

VALUE	DOCUMENT ID	TECN	CHG	COMMENT
(1.1 ± 2.1) × 10⁻⁹	¹¹ MEYER	00	CNTR	1s-2s muonium interval

¹¹ MEYER 00 measure the 1s-2s muonium interval, and then interpret the result in terms of muon-electron charge ratio q_{μ^+}/q_{e^-} .

Lepton Particle Listings

 μ μ^- DECAY MODES μ^+ modes are charge conjugates of the modes below.

Mode	Fraction (Γ_i/Γ)	Confidence level
Γ_1 $e^- \bar{\nu}_e \nu_\mu$	$\approx 100\%$	
Γ_2 $e^- \bar{\nu}_e \nu_\mu \gamma$	[a] $(1.4 \pm 0.4)\%$	
Γ_3 $e^- \bar{\nu}_e \nu_\mu e^+ e^-$	[b] $(3.4 \pm 0.4) \times 10^{-5}$	
Lepton Family number (LF) violating modes		
Γ_4 $e^- \nu_e \bar{\nu}_\mu$	LF [c] < 1.2	90%
Γ_5 $e^- \gamma$	LF < 1.2	$\times 10^{-11}$ 90%
Γ_6 $e^- e^+ e^-$	LF < 1.0	$\times 10^{-12}$ 90%
Γ_7 $e^- 2\gamma$	LF < 7.2	$\times 10^{-11}$ 90%

[a] This only includes events with the γ energy > 10 MeV. Since the $e^- \bar{\nu}_e \nu_\mu$ and $e^- \bar{\nu}_e \nu_\mu \gamma$ modes cannot be clearly separated, we regard the latter mode as a subset of the former.

[b] See the Particle Listings below for the energy limits used in this measurement.

[c] A test of additive vs. multiplicative lepton family number conservation.

 μ^- BRANCHING RATIOS

$\Gamma(e^- \bar{\nu}_e \nu_\mu \gamma)/\Gamma_{\text{total}}$	VALUE	EVTS	DOCUMENT ID	TECN	CHG	COMMENT	Γ_2/Γ
0.014 ± 0.004			CRITTENDEN 61	CNTR		γ KE > 10 MeV	
••• We do not use the following data for averages, fits, limits, etc. •••							
	862		BOGART 67	CNTR		γ KE > 14.5 MeV	
0.0033 ± 0.0013			CRITTENDEN 61	CNTR		γ KE > 20 MeV	
	27		ASHKIN 59	CNTR			

$\Gamma(e^- \bar{\nu}_e \nu_\mu e^+ e^-)/\Gamma_{\text{total}}$	VALUE	EVTS	DOCUMENT ID	TECN	CHG	COMMENT	Γ_3/Γ
$3.4 \pm 0.2 \pm 0.3$		7443	12 BERTL 85	SPEC	+	SINDRUM	
••• We do not use the following data for averages, fits, limits, etc. •••							
2.2 ± 1.5		7	13 CRITTENDEN 61	HLBC	+	$E(e^+ e^-) > 10$ MeV	
2		1	14 GUREVICH 60	EMUL	+		
1.5 ± 1.0		3	15 LEE 59	HBC	+		

¹² BERTL 85 has transverse momentum cut $p_T > 17$ MeV/c. Systematic error was increased by us.

¹³ CRITTENDEN 61 count only those decays where total energy of either (e^+ , e^-) combination is > 10 MeV.

¹⁴ GUREVICH 60 interpret their event as either virtual or real photon conversion. e^+ and e^- energies not measured.

¹⁵ In the three LEE 59 events, the sum of energies $E(e^+) + E(e^-) + E(e^+)$ was 51 MeV, 55 MeV, and 33 MeV.

$\Gamma(e^- \nu_e \bar{\nu}_\mu)/\Gamma_{\text{total}}$	VALUE	CL%	DOCUMENT ID	TECN	CHG	COMMENT	Γ_4/Γ
< 0.012	90	16	FREEDMAN 93	CNTR	+	ν oscillation search	
••• We do not use the following data for averages, fits, limits, etc. •••							
< 0.018	90		KRAKAUER 91B	CALO	+		
< 0.05	90	17	BERGSMA 83	CALO		$\bar{\nu}_\mu e \rightarrow \mu^- \bar{\nu}_e$	
< 0.09	90		JONKER 80	CALO		See BERGSMA 83	
-0.001 ± 0.061			WILLIS 80	CNTR	+		
0.13 ± 0.15			BLIETSCHAU 78	HLBC	\pm	Avg. of 4 values	
< 0.25	90		EICHTEN 73	HLBC	+		
¹⁶ FREEDMAN 93 limit on $\bar{\nu}_e$ observation is here interpreted as a limit on lepton family number violation.							
¹⁷ BERGSMA 83 gives a limit on the inverse muon decay cross-section ratio $\sigma(\bar{\nu}_\mu e^- \rightarrow \mu^- \bar{\nu}_e)/\sigma(\nu_\mu e^- \rightarrow \mu^- \nu_e)$, which is essentially equivalent to $\Gamma(e^- \nu_e \bar{\nu}_\mu)/\Gamma_{\text{total}}$ for small values like that quoted.							

$\Gamma(e^- \gamma)/\Gamma_{\text{total}}$	VALUE	CL%	DOCUMENT ID	TECN	CHG	COMMENT	Γ_5/Γ
< 1.2	90		BROOKS 99	SPEC	+	LAMPF	
••• We do not use the following data for averages, fits, limits, etc. •••							
< 1.2	90		AHMED 02	SPEC	+	MEGA	
< 4.9	90		BOLTON 88	CBOX	+	LAMPF	
< 100	90		AZUELOS 83	CNTR	+	TRIUMF	
< 17	90		KINNISON 82	SPEC	+	LAMPF	
< 100	90		SCHAAF 80	ELEC	+	SIN	

 $\Gamma(e^- e^+ e^-)/\Gamma_{\text{total}}$

Forbidden by lepton family number conservation.

VALUE (units 10^{-12})	CL%	DOCUMENT ID	TECN	CHG	COMMENT
< 1.0	90	¹⁸ BELLGARDT 88	SPEC	+	SINDRUM
••• We do not use the following data for averages, fits, limits, etc. •••					
< 36	90	BARANOV 91	SPEC	+	ARES
< 35	90	BOLTON 88	CBOX	+	LAMPF
< 2.4	90	¹⁸ BERTL 85	SPEC	+	SINDRUM
< 160	90	¹⁸ BERTL 84	SPEC	+	SINDRUM
< 130	90	¹⁸ BOLTON 84	CNTR	+	LAMPF

¹⁸ These experiments assume a constant matrix element. $\Gamma(e^- 2\gamma)/\Gamma_{\text{total}}$

Forbidden by lepton family number conservation.

VALUE (units 10^{-11})	CL%	DOCUMENT ID	TECN	CHG	COMMENT
< 7.2	90	BOLTON 88	CBOX	+	LAMPF
••• We do not use the following data for averages, fits, limits, etc. •••					
< 840	90	¹⁹ AZUELOS 83	CNTR	+	TRIUMF
< 5000	90	²⁰ BOWMAN 78	CNTR	+	DEPOMMIER 77 data

¹⁹ AZUELOS 83 uses the phase space distribution of BOWMAN 78.²⁰ BOWMAN 78 assumes an interaction Lagrangian local on the scale of the inverse μ mass.LIMIT ON $\mu^- \rightarrow e^-$ CONVERSION

Forbidden by lepton family number conservation.

$\sigma(\mu^- 32\text{S} \rightarrow e^- 32\text{S}) / \sigma(\mu^- 32\text{S} \rightarrow \nu_\mu 32\text{P}^*)$	VALUE	CL%	DOCUMENT ID	TECN	COMMENT
$< 7 \times 10^{-11}$	90		BADERT...	80	STRC SIN
••• We do not use the following data for averages, fits, limits, etc. •••					
$< 4 \times 10^{-10}$	90		BADERT...	77	STRC SIN

$\sigma(\mu^- \text{Cu} \rightarrow e^- \text{Cu}) / \sigma(\mu^- \text{Cu} \rightarrow \text{capture})$	VALUE	CL%	DOCUMENT ID	TECN	COMMENT
$< 1.6 \times 10^{-8}$	90		BRYMAN 72	SPEC	
••• We do not use the following data for averages, fits, limits, etc. •••					

$\sigma(\mu^- \text{Ti} \rightarrow e^- \text{Ti}) / \sigma(\mu^- \text{Ti} \rightarrow \text{capture})$	VALUE	CL%	DOCUMENT ID	TECN	COMMENT
$< 4.3 \times 10^{-12}$	90	²¹	DOHMEN 93	SPEC	SINDRUM II
••• We do not use the following data for averages, fits, limits, etc. •••					
$< 4.6 \times 10^{-12}$	90		AHMAD 88	TPC	TRIUMF
$< 1.6 \times 10^{-11}$	90		BRYMAN 85	TPC	TRIUMF

²¹ DOHMEN 93 assumes $\mu^- \rightarrow e^-$ conversion leaves the nucleus in its ground state, a process enhanced by coherence and expected to dominate.

$\sigma(\mu^- \text{Pb} \rightarrow e^- \text{Pb}) / \sigma(\mu^- \text{Pb} \rightarrow \text{capture})$	VALUE	CL%	DOCUMENT ID	TECN	COMMENT
$< 4.6 \times 10^{-11}$	90		HONECKER 96	SPEC	SINDRUM II
••• We do not use the following data for averages, fits, limits, etc. •••					
$< 4.9 \times 10^{-10}$	90		AHMAD 88	TPC	TRIUMF

$\sigma(\mu^- \text{Au} \rightarrow e^- \text{Au}) / \sigma(\mu^- \text{Au} \rightarrow \text{capture})$	VALUE	CL%	DOCUMENT ID	TECN	CHG	COMMENT
$< 7 \times 10^{-13}$	90		BERTL 06	SPEC	-	SINDRUM II

LIMIT ON $\mu^- \rightarrow e^+$ CONVERSION

Forbidden by total lepton number conservation.

$\sigma(\mu^- 32\text{S} \rightarrow e^+ 32\text{S}^*) / \sigma(\mu^- 32\text{S} \rightarrow \nu_\mu 32\text{P}^*)$	VALUE	CL%	DOCUMENT ID	TECN	COMMENT
$< 9 \times 10^{-10}$	90		BADERT...	80	STRC SIN
••• We do not use the following data for averages, fits, limits, etc. •••					
$< 1.5 \times 10^{-9}$	90		BADERT...	78	STRC SIN

$\sigma(\mu^- 127\text{I} \rightarrow e^+ 127\text{Sb}^*) / \sigma(\mu^- 127\text{I} \rightarrow \text{anything})$	VALUE	CL%	DOCUMENT ID	TECN	COMMENT
$< 3 \times 10^{-10}$	90	²²	ABELA 80	CNTR	Radiochemical tech.
²² ABELA 80 is upper limit for $\mu^- e^+$ conversion leading to particle-stable states of ¹²⁷ Sb. Limit for total conversion rate is higher by a factor less than 4 (G. Backenstoss, private communication).					

$\sigma(\mu^- \text{Cu} \rightarrow e^+ \text{Co}) / \sigma(\mu^- \text{Cu} \rightarrow \nu_\mu \text{Ni})$	VALUE	CL%	DOCUMENT ID	TECN	COMMENT
$< 2.6 \times 10^{-8}$	90		BRYMAN 72	SPEC	
$< 2.2 \times 10^{-7}$	90		CONFORTO 62	OSPK	
••• We do not use the following data for averages, fits, limits, etc. •••					

$\sigma(\mu^- \text{Ti} \rightarrow e^+ \text{Ca}) / \sigma(\mu^- \text{Ti} \rightarrow \text{capture})$

VALUE	CL%	EVTS	DOCUMENT ID	TECN	CHG	COMMENT
$< 3.6 \times 10^{-11}$	90	1	23,24 KAULARD	98	SPEC	– SINDRUM II
$< 1.7 \times 10^{-12}$	90	1	24,25 KAULARD	98	SPEC	– SINDRUM II
$< 4.3 \times 10^{-12}$	90		25 DOHMEN	93	SPEC	SINDRUM II
$< 8.9 \times 10^{-11}$	90		23 DOHMEN	93	SPEC	SINDRUM II
$< 1.7 \times 10^{-10}$	90		26 AHMAD	88	TPC	TRIUMF

²³This limit assumes a giant resonance excitation of the daughter Ca nucleus (mean energy and width both 20 MeV).

²⁴KAULARD 98 obtained these same limits using the unified classical analysis of FELDMAN 98.

²⁵This limit assumes the daughter Ca nucleus is left in the ground state. However, the probability of this is unknown.

²⁶Assuming a giant-resonance-excitation model.

LIMIT ON MUONIUM \rightarrow ANTIMUONIUM CONVERSION

Forbidden by lepton family number conservation.

 $R_g = G_C / G_F$

The effective Lagrangian for the $\mu^+ e^- \rightarrow \mu^- e^+$ conversion is assumed to be

$$\mathcal{L} = 2^{-1/2} G_C [\bar{\psi}_\mu \gamma_\lambda (1 - \gamma_5) \psi_e] [\bar{\psi}_\mu \gamma_\lambda (1 - \gamma_5) \psi_e] + \text{h.c.}$$

The experimental result is then an upper limit on G_C/G_F , where G_F is the Fermi coupling constant.

VALUE	CL%	EVTS	DOCUMENT ID	TECN	CHG	COMMENT
< 0.0030	90	1	27 WILLMANN	99	SPEC	+ μ^+ at 26 GeV/c
< 0.14	90	1	28 GORDEEV	97	SPEC	+ JINR phasotron
< 0.018	90	0	29 ABELA	96	SPEC	+ μ^+ at 24 MeV
< 6.9	90		NI	93	CBOX	LAMPF
< 0.16	90		MATTHIAS	91	SPEC	LAMPF
< 0.29	90		HUBER	90B	CNTR	TRIUMF
< 20	95		BEER	86	CNTR	TRIUMF
< 42	95		MARSHALL	82	CNTR	

²⁷WILLMANN 99 quote both probability $P_{M\bar{M}} < 8.3 \times 10^{-11}$ at 90%CL in a 0.1 T field and $R_g = G_C/G_F$.

²⁸GORDEEV 97 quote limits on both $f = G_{MM}/G_F$ and the probability $W_{MM} < 4.7 \times 10^{-7}$ (90% CL).

²⁹ABELA 96 quote both probability $P_{M\bar{M}} < 8 \times 10^{-9}$ at 90% CL and $R_g = G_C/G_F$.

MUON DECAY PARAMETERS

Revised August 2009 by W. Fetscher and H.-J. Gerber (ETH Zürich).

Introduction: All measurements in direct muon decay, $\mu^- \rightarrow e^- + 2$ neutrals, and its inverse, $\nu_\mu + e^- \rightarrow \mu^- +$ neutral, are successfully described by the “ V - A interaction,” which is a particular case of a local, derivative-free, lepton-number-conserving, four-fermion interaction [1]. As shown below, within this framework, the Standard Model assumptions, such as the V - A form and the nature of the neutrals (ν_μ and $\bar{\nu}_e$), and hence the doublet assignments ($\nu_e e^-$) $_L$ and ($\nu_\mu \mu^-$) $_L$, have been determined from experiments [2,3]. All considerations on muon decay are valid for the leptonic tau decays $\tau \rightarrow \ell + \nu_\tau + \bar{\nu}_e$ with the replacements $m_\mu \rightarrow m_\tau$, $m_e \rightarrow m_\ell$.

Parameters: The differential decay probability to obtain an e^\pm with (reduced) energy between x and $x + dx$, emitted in the direction $\hat{\mathbf{x}}_3$ at an angle between ϑ and $\vartheta + d\vartheta$ with respect to the muon polarization vector \mathbf{P}_μ , and with its spin parallel to the arbitrary direction $\hat{\boldsymbol{\zeta}}$, neglecting radiative corrections, is given by

$$\begin{aligned} \frac{d^2\Gamma}{dx d\cos\vartheta} &= \frac{m_\mu}{4\pi^3} W_{e\mu}^4 G_F^2 \sqrt{x^2 - x_0^2} \\ &\times (F_{\text{IS}}(x) \pm P_\mu \cos\vartheta F_{\text{AS}}(x)) \\ &\times \left[1 + \hat{\boldsymbol{\zeta}} \cdot \mathbf{P}_e(x, \vartheta) \right]. \end{aligned} \quad (1)$$

Here, $W_{e\mu} = \max(E_e) = (m_\mu^2 + m_e^2)/2m_\mu$ is the maximum e^\pm energy, $x = E_e/W_{e\mu}$ is the reduced energy, $x_0 = m_e/W_{e\mu} = 9.67 \times 10^{-3}$, and $P_\mu = |\mathbf{P}_\mu|$ is the degree of muon polarization. $\hat{\boldsymbol{\zeta}}$ is the direction in which a perfect polarization-sensitive electron detector is most sensitive. The isotropic part of the spectrum, $F_{\text{IS}}(x)$, the anisotropic part $F_{\text{AS}}(x)$, and the electron polarization, $\mathbf{P}_e(x, \vartheta)$, may be parametrized by the Michel parameter ρ [1], by η [4], by ξ and δ [5,6], *etc.* These are bilinear combinations of the coupling constants $g_{e\mu}^\gamma$, which occur in the matrix element (given below).

If the masses of the neutrinos as well as x_0^2 are neglected, the energy and angular distribution of the electron in the rest frame of a muon (μ^\pm) measured by a polarization insensitive detector, is given by

$$\begin{aligned} \frac{d^2\Gamma}{dx d\cos\vartheta} &\sim x^2 \cdot \left\{ 3(1-x) + \frac{2\rho}{3}(4x-3) + 3\eta x_0(1-x)/x \right. \\ &\left. \pm P_\mu \cdot \xi \cdot \cos\vartheta \left[1-x + \frac{2\delta}{3}(4x-3) \right] \right\}. \end{aligned} \quad (2)$$

Here, ϑ is the angle between the electron momentum and the muon spin, and $x \equiv 2E_e/m_\mu$. For the Standard Model coupling, we obtain $\rho = \xi\delta = 3/4$, $\xi = 1$, $\eta = 0$ and the differential decay rate is

$$\frac{d^2\Gamma}{dx d\cos\vartheta} = \frac{G_F^2 m_\mu^5}{192\pi^3} [3 - 2x \pm P_\mu \cos\vartheta(2x-1)] x^2. \quad (3)$$

The coefficient in front of the square bracket is the total decay rate.

If only the neutrino masses are neglected, and if the e^\pm polarization is detected, then the functions in Eq. (1) become

$$\begin{aligned} F_{\text{IS}}(x) &= x(1-x) + \frac{2}{9}\rho(4x^2 - 3x - x_0^2) + \eta \cdot x_0(1-x) \\ F_{\text{AS}}(x) &= \frac{1}{3}\xi \sqrt{x^2 - x_0^2} \\ &\times [1 - x + \frac{2}{3}\delta(4x-3) + (\sqrt{1-x_0^2} - 1)] \\ \mathbf{P}_e(x, \vartheta) &= P_{T_1} \cdot \hat{\mathbf{x}}_1 + P_{T_2} \cdot \hat{\mathbf{x}}_2 + P_L \cdot \hat{\mathbf{x}}_3. \end{aligned} \quad (4)$$

Here $\hat{\mathbf{x}}_1$, $\hat{\mathbf{x}}_2$, and $\hat{\mathbf{x}}_3$ are orthogonal unit vectors defined as follows:

$$\begin{aligned} \hat{\mathbf{x}}_3 &\text{ is along the } e \text{ momentum } \mathbf{p}_e \\ \frac{\hat{\mathbf{x}}_3 \times \mathbf{P}_\mu}{|\hat{\mathbf{x}}_3 \times \mathbf{P}_\mu|} &= \hat{\mathbf{x}}_2 \text{ is transverse to } \mathbf{p}_e \text{ and perpendicular} \\ &\text{ to the “decay plane”} \\ \hat{\mathbf{x}}_2 \times \hat{\mathbf{x}}_3 &= \hat{\mathbf{x}}_1 \text{ is transverse to the } \mathbf{p}_e \text{ and in the} \\ &\text{ “decay plane.”} \end{aligned}$$

The components of \mathbf{P}_e then are given by

$$\begin{aligned} P_{T_1}(x, \vartheta) &= P_\mu \sin\vartheta \cdot F_{T_1}(x) / (F_{\text{IS}}(x) \pm P_\mu \cos\vartheta \cdot F_{\text{AS}}(x)) \\ P_{T_2}(x, \vartheta) &= P_\mu \sin\vartheta \cdot F_{T_2}(x) / (F_{\text{IS}}(x) \pm P_\mu \cos\vartheta \cdot F_{\text{AS}}(x)) \\ P_L(x, \vartheta) &= \left(\pm F_{\text{IP}}(x) + P_\mu \cos\vartheta \right. \\ &\left. \times F_{\text{AP}}(x) \right) / (F_{\text{IS}}(x) \pm P_\mu \cos\vartheta \cdot F_{\text{AS}}(x)), \end{aligned}$$

Lepton Particle Listings

μ

where

$$\begin{aligned}
F_{T_1}(x) &= \frac{1}{12} \left\{ -2 \left[\xi'' + 12(\rho - \frac{3}{4}) \right] (1-x)x_0 \right. \\
&\quad \left. - 3\eta(x^2 - x_0^2) + \eta''(-3x^2 + 4x - x_0^2) \right\} \\
F_{T_2}(x) &= \frac{1}{3} \sqrt{x^2 - x_0^2} \left\{ 3\frac{\alpha'}{A}(1-x) + 2\frac{\beta'}{A}\sqrt{1-x_0^2} \right\} \\
F_{IP}(x) &= \frac{1}{54} \sqrt{x^2 - x_0^2} \left\{ 9\xi' \left(-2x + 2 + \sqrt{1-x_0^2} \right) \right. \\
&\quad \left. + 4\xi(\delta - \frac{3}{4})(4x - 4 + \sqrt{1-x_0^2}) \right\} \\
F_{AP}(x) &= \frac{1}{6} \left\{ \xi''(2x^2 - x - x_0^2) + 4(\rho - \frac{3}{4})(4x^2 - 3x - x_0^2) \right. \\
&\quad \left. + 2\eta''(1-x)x_0 \right\}. \tag{5}
\end{aligned}$$

For the experimental values of the parameters ρ , ξ , ξ' , ξ'' , δ , η , η'' , α/A , β/A , α'/A , β'/A , which are not all independent, see the Data Listings below. Experiments in the past have also been analyzed using the parameters a , b , c , a' , b' , c' , α/A , β/A , α'/A , β'/A (and $\eta = (\alpha - 2\beta)/2A$), as defined by Kinoshita and Sirlin [5,6]. They serve as a model-independent summary of all possible measurements on the decay electron (see Listings below). The relations between the two sets of parameters are

$$\begin{aligned}
\rho - \frac{3}{4} &= \frac{3}{4}(-a + 2c)/A, \\
\eta &= (\alpha - 2\beta)/A, \\
\eta'' &= (3\alpha + 2\beta)/A, \\
\delta - \frac{3}{4} &= \frac{9}{4} \cdot \frac{(a' - 2c')/A}{1 - [a + 3a' + 4(b + b') + 6c - 14c']/A}, \\
1 - \xi \frac{\delta}{\rho} &= 4 \frac{[(b + b') + 2(c - c')]/A}{1 - (a - 2c)/A}, \\
1 - \xi' &= [(a + a') + 4(b + b') + 6(c + c')]/A, \\
1 - \xi'' &= (-2a + 20c)/A,
\end{aligned}$$

where

$$A = a + 4b + 6c. \tag{6}$$

The differential decay probability to obtain a *left-handed* ν_e with (reduced) energy between y and $y + dy$, neglecting radiative corrections as well as the masses of the electron and of the neutrinos, is given by [7]

$$\frac{d\Gamma}{dy} = \frac{m_\mu^5 G_F^2}{16\pi^3} \cdot Q_L^{\nu_e} \cdot y^2 \left\{ (1-y) - \omega_L \cdot (y - \frac{3}{4}) \right\}. \tag{7}$$

Here, $y = 2 E_{\nu_e}/m_\mu$. $Q_L^{\nu_e}$ and ω_L are parameters. ω_L is the neutrino analog of the spectral shape parameter ρ of Michel. Since in the Standard Model, $Q_L^{\nu_e} = 1$, $\omega_L = 0$, the measurement of $d\Gamma/dy$ has allowed a null-test of the Standard Model (see Listings below).

Matrix element: All results in direct muon decay (energy spectra of the electron and of the neutrinos, polarizations, and angular distributions), and in inverse muon decay (the reaction cross section) at energies well below $m_W c^2$, may be parametrized in terms of amplitudes $g_{\varepsilon\mu}^\gamma$ and the Fermi coupling constant G_F , using the matrix element

$$\frac{4G_F}{\sqrt{2}} \sum_{\substack{\gamma=S,V,T \\ \varepsilon,\mu=R,L}} g_{\varepsilon\mu}^\gamma \langle \bar{e}_\varepsilon | \Gamma^\gamma | (\nu_e)_n \rangle \langle (\bar{\nu}_\mu)_m | \Gamma_\gamma | \mu_\mu \rangle. \tag{8}$$

We use the notation of Fetscher *et al.* [2], who in turn use the sign conventions and definitions of Scheck [8]. Here, $\gamma = S, V, T$ indicates a scalar, vector, or tensor interaction; and $\varepsilon, \mu = R, L$ indicate a right- or left-handed chirality of the electron or muon. The chiralities n and m of the ν_e and $\bar{\nu}_\mu$ are then determined by the values of γ, ε , and μ . The particles are represented by fields of definite chirality [9].

As shown by Langacker and London [10], explicit lepton-number nonconservation still leads to a matrix element equivalent to Eq. (8). They conclude that it is not possible, even in principle, to test lepton-number conservation in (leptonic) muon decay if the final neutrinos are massless and are not observed.

The ten complex amplitudes $g_{\varepsilon\mu}^\gamma$ (g_{RR}^T and g_{LL}^T are identically zero) and G_F constitute 19 independent (real) parameters to be determined by experiment. The Standard Model interaction corresponds to one single amplitude g_{LL}^V being unity and all the others being zero.

The (direct) muon decay experiments are compatible with an arbitrary mix of the scalar and vector amplitudes g_{LL}^S and g_{LL}^V – in the extreme even with purely scalar $g_{LL}^S = 2$, $g_{LL}^V = 0$. The decision in favour of the Standard Model comes from the quantitative observation of inverse muon decay, which would be forbidden for pure g_{LL}^S [2].

Experimental determination of V–A: In order to determine the amplitudes $g_{\varepsilon\mu}^\gamma$ uniquely from experiment, the following set of equations, where the left-hand sides represent experimental results, has to be solved.

$$\begin{aligned}
a &= 16(|g_{RL}^V|^2 + |g_{LR}^V|^2) + |g_{RL}^S + 6g_{RL}^T|^2 + |g_{LR}^S + 6g_{LR}^T|^2 \\
a' &= 16(|g_{RL}^V|^2 - |g_{LR}^V|^2) + |g_{RL}^S + 6g_{RL}^T|^2 - |g_{LR}^S + 6g_{LR}^T|^2 \\
\alpha &= 8\text{Re} \left\{ g_{RL}^V (g_{LR}^{S*} + 6g_{LR}^{T*}) + g_{LR}^V (g_{RL}^{S*} + 6g_{RL}^{T*}) \right\} \\
\alpha' &= 8\text{Im} \left\{ g_{LR}^V (g_{RL}^{S*} + 6g_{RL}^{T*}) - g_{RL}^V (g_{LR}^{S*} + 6g_{LR}^{T*}) \right\} \\
b &= 4(|g_{RR}^V|^2 + |g_{LL}^V|^2) + |g_{RR}^S|^2 + |g_{LL}^S|^2 \\
b' &= 4(|g_{RR}^V|^2 - |g_{LL}^V|^2) + |g_{RR}^S|^2 - |g_{LL}^S|^2 \\
\beta &= -4\text{Re} \left\{ g_{RR}^V g_{LL}^{S*} + g_{LL}^V g_{RR}^{S*} \right\} \\
\beta' &= 4\text{Im} \left\{ g_{RR}^V g_{LL}^{S*} - g_{LL}^V g_{RR}^{S*} \right\} \\
c &= \frac{1}{2} \left\{ |g_{RL}^S - 2g_{RL}^T|^2 + |g_{LR}^S - 2g_{LR}^T|^2 \right\} \\
c' &= \frac{1}{2} \left\{ |g_{RL}^S - 2g_{RL}^T|^2 - |g_{LR}^S - 2g_{LR}^T|^2 \right\}
\end{aligned}$$

and

$$\begin{aligned}
Q_L^{\nu_e} &= 1 - \left\{ \frac{1}{4}|g_{LR}^S|^2 + \frac{1}{4}|g_{LL}^S|^2 + |g_{RR}^V|^2 + |g_{RL}^V|^2 + 3|g_{LR}^T|^2 \right\} \\
\omega_L &= \frac{3}{4} \frac{\{|g_{RR}^S|^2 + 4|g_{LR}^V|^2 + |g_{RL}^S + 2g_{RL}^T|^2\}}{|g_{RL}^S|^2 + |g_{RR}^S|^2 + 4|g_{LL}^V|^2 + 4|g_{LR}^V|^2 + 12|g_{RL}^T|^2}.
\end{aligned}$$

It has been noted earlier by C. Jarlskog [11], that certain experiments observing the decay electron are especially informative if they yield the V - A values. The complete solution is now found as follows. Fetscher *et al.* [2] introduced four probabilities $Q_{\varepsilon\mu}(\varepsilon, \mu = R, L)$ for the decay of a μ -handed muon into an ε -handed electron, and showed that there exist upper bounds

on Q_{RR} , Q_{LR} , and Q_{RL} , and a lower bound on Q_{LL} . These probabilities are given in terms of the $g_{\varepsilon\mu}^\gamma$'s by

$$Q_{\varepsilon\mu} = \frac{1}{4}|g_{\varepsilon\mu}^S|^2 + |g_{\varepsilon\mu}^V|^2 + 3(1 - \delta_{\varepsilon\mu})|g_{\varepsilon\mu}^T|^2, \quad (9)$$

where $\delta_{\varepsilon\mu} = 1$ for $\varepsilon = \mu$, and $\delta_{\varepsilon\mu} = 0$ for $\varepsilon \neq \mu$. They are related to the parameters a , b , c , a' , b' , and c' by

$$\begin{aligned} Q_{RR} &= 2(b + b')/A, \\ Q_{LR} &= [(a - a') + 6(c - c')]/2A, \\ Q_{RL} &= [(a + a') + 6(c + c')]/2A, \\ Q_{LL} &= 2(b - b')/A, \end{aligned} \quad (10)$$

with $A = 16$. In the Standard Model, $Q_{LL} = 1$ and the others are zero.

Since the upper bounds on Q_{RR} , Q_{LR} , and Q_{RL} are found to be small, and since the helicity of the ν_μ in pion decay is known from experiment [12,13] to very high precision to be -1 [14], the cross section S of *inverse* muon decay, normalized to the V - A value, yields [2]

$$|g_{LL}^S|^2 \leq 4(1 - S) \quad (11)$$

and

$$|g_{LL}^V|^2 = S. \quad (12)$$

Thus the Standard Model assumption of a pure V - A leptonic charged weak interaction of e and μ is derived (within errors) from experiments at energies far below mass of the W^\pm : Eq. (12) gives a lower limit for V - A , and Eqs. (9) and (11) give upper limits for the other four-fermion interactions. The existence of such upper limits may also be seen from $Q_{RR} + Q_{RL} = (1 - \xi')/2$ and $Q_{RR} + Q_{LR} = \frac{1}{2}(1 + \xi/3 - 16 \xi\delta/9)$. Table 1 gives the current experimental limits on the magnitudes of the $g_{\varepsilon\mu}^\gamma$'s. More stringent limits on the six coupling constants g_{LR}^S , g_{LR}^V , g_{LR}^T , g_{RL}^S , g_{RL}^V , and g_{RL}^T have been derived from upper limits on the neutrino mass [18]. Limits on the ‘‘charge retention’’ coordinates, as used in the older literature (*e.g.*, Ref. 19), are given by Burkard *et al.* [20].

Table 1. Coupling constants $g_{\varepsilon\mu}^\gamma$. Ninety-percent confidence level experimental limits. The limits on $|g_{LL}^S|$ and $|g_{LL}^V|$ are from Ref. 15, and the others from a general analysis of muon decay measurements. Top three rows: Ref. 16, bottom three rows: Ref. 17. The experimental uncertainty on the muon polarization in pion decay is included. Note that, by definition, $|g_{\varepsilon\mu}^S| \leq 2$, $|g_{\varepsilon\mu}^V| \leq 1$ and $|g_{\varepsilon\mu}^T| \leq 1/\sqrt{3}$.

$ g_{LR}^S < 0.062$	$ g_{RR}^V < 0.031$	$ g_{RR}^T \equiv 0$
$ g_{LR}^S < 0.074$	$ g_{LR}^V < 0.025$	$ g_{LR}^T < 0.021$
$ g_{RL}^S < 0.412$	$ g_{RL}^V < 0.104$	$ g_{RL}^T < 0.103$
$ g_{LL}^S < 0.550$	$ g_{LL}^V > 0.960$	$ g_{LL}^T \equiv 0$
$ g_{LR}^S + 6g_{LR}^T < 0.143$	$ g_{RL}^S + 6g_{RL}^T < 0.418$	
$ g_{LR}^S + 2g_{LR}^T < 0.108$	$ g_{RL}^S + 2g_{RL}^T < 0.417$	
$ g_{LR}^S - 2g_{LR}^T < 0.070$	$ g_{RL}^S - 2g_{RL}^T < 0.418$	

References

1. L. Michel, Proc. Phys. Soc. **A63**, 514 (1950).
2. W. Fetscher, H.-J. Gerber, and K.F. Johnson, Phys. Lett. **B173**, 102 (1986).
3. P. Langacker, Comm. Nucl. Part. Phys. **19**, 1 (1989).
4. C. Bouchiat and L. Michel, Phys. Rev. **106**, 170 (1957).
5. T. Kinoshita and A. Sirlin, Phys. Rev. **107**, 593 (1957).
6. T. Kinoshita and A. Sirlin, Phys. Rev. **108**, 844 (1957).
7. W. Fetscher, Phys. Rev. **D49**, 5945 (1994).
8. F. Scheck, in *Electroweak and Strong Interactions* (Springer Verlag, 1996).
9. K. Mursula and F. Scheck, Nucl. Phys. **B253**, 189 (1985).
10. P. Langacker and D. London, Phys. Rev. **D39**, 266 (1989).
11. C. Jarlskog, Nucl. Phys. **75**, 659 (1966).
12. A. Jodidio *et al.*, Phys. Rev. **D34**, 1967 (1986); A. Jodidio *et al.*, Phys. Rev. **D37**, 237 (1988).
13. L.Ph. Roesch *et al.*, Helv. Phys. Acta **55**, 74 (1982).
14. W. Fetscher, Phys. Lett. **140B**, 117 (1984).
15. S.R. Mishra *et al.*, Phys. Lett. **B252**, 170 (1990); S.R. Mishra, private communication; See also P. Vilain *et al.*, Phys. Lett. **B364**, 121 (1995).
16. R.P. MacDonald *et al.*, Phys. Rev. **D78**, 032010 (2008).
17. C.A. Gagliardi, R.E. Tribble, and N.J. Williams, Phys. Rev. **D72**, 073002 (2005).
18. G. Pr ezeau and A. Kurylov, Phys. Rev. Lett. **95**, 101802 (2005).
19. S.E. Derenzo, Phys. Rev. **181**, 1854 (1969).
20. H. Burkard *et al.*, Phys. Lett. **160B**, 343 (1985).

μ DECAY PARAMETERS

ρ PARAMETER

(V - A) theory predicts $\rho = 0.75$.

VALUE	EVTS	DOCUMENT ID	TECN	CHG	COMMENT
0.7503 ± 0.0004 OUR AVERAGE					
0.75014 ± 0.00017 ± 0.00045		30	MACDONALD	08	TWST + Surface μ^+
0.75080 ± 0.00032 ± 0.00100	6G	31	MUSSER	05	TWST + Surface μ^+
0.7518 ± 0.00026			DERENZO	69	RVUE
••• We do not use the following data for averages, fits, limits, etc. •••					
0.72 ± 0.06 ± 0.08			AMORUSO	04	ICAR Liquid Ar TPC
0.762 ± 0.008	170k	32	FRYBERGER	68	ASPK + 25–53 MeV e^+
0.760 ± 0.009	280k	32	SHERWOOD	67	ASPK + 25–53 MeV e^+
0.7503 ± 0.0026	800k	32	PEOPLES	66	ASPK + 20–53 MeV e^+

³⁰ The quoted systematic error includes a contribution of 0.00011 (added in quadrature) from the dependence on the Michel parameter η .

³¹ The quoted systematic error includes a contribution of 0.00023 (added in quadrature) from the dependence on the Michel parameter η .

³² η constrained = 0. These values incorporated into a two parameter fit to ρ and η by DERENZO 69.

η PARAMETER

(V - A) theory predicts $\eta = 0$.

VALUE	EVTS	DOCUMENT ID	TECN	CHG	COMMENT
0.057 ± 0.034 OUR AVERAGE					
0.071 ± 0.037 ± 0.005	30M		DANNEBERG	05	CNTR + 7–53 MeV e^+
0.011 ± 0.081 ± 0.026	5.3M	33	BURKARD	85B	CNTR + 9–53 MeV e^+
-0.12 ± 0.21	6346		DERENZO	69	HBC + 1.6–6.8 MeV e^+
••• We do not use the following data for averages, fits, limits, etc. •••					
-0.0021 ± 0.0070 ± 0.0010	30M	34	DANNEBERG	05	CNTR + 7–53 MeV e^+
-0.012 ± 0.015 ± 0.003	5.3M	34	BURKARD	85B	CNTR + 9–53 MeV e^+
-0.007 ± 0.013	5.3M	35	BURKARD	85B	FT + 9–53 MeV e^+
-0.7 ± 0.5	170k	36	FRYBERGER	68	ASPK + 25–53 MeV e^+
-0.7 ± 0.6	280k	36	SHERWOOD	67	ASPK + 25–53 MeV e^+
0.05 ± 0.5	800k	36	PEOPLES	66	ASPK + 20–53 MeV e^+
-2.0 ± 0.9	9213	37	PLANO	60	HBC + Whole spectrum

³³ Previously we used the global fit result from BURKARD 85B in OUR AVERAGE, we now only include their actual measurement.

³⁴ $\alpha = \alpha' = 0$ assumed.

³⁵ Global fit to all measured parameters. The fit correlation coefficients are given in BURKARD 85B.

³⁶ ρ constrained = 0.75.

³⁷ Two parameter fit to ρ and η ; PLANO 60 discounts value for η .

Lepton Particle Listings

 μ δ PARAMETER $(V-A)$ theory predicts $\delta = 0.75$.

VALUE	EVTS	DOCUMENT ID	TECN	CHG	COMMENT
0.7504 ± 0.0006	OUR AVERAGE				
0.75067 ± 0.00030 ± 0.00067		MACDONALD 08	TWST	+	Surface μ^+
0.74964 ± 0.00066 ± 0.00112	6G	GAPONENKO 05	TWST	+	surface μ^+
0.7486 ± 0.0026 ± 0.0028		³⁸ BALKE 88	SPEC	+	Surface μ^+ 's
• • •					We do not use the following data for averages, fits, limits, etc. • • •
0.752 ± 0.009	490k	³⁹ VOSSLER 69			
0.782 ± 0.031		FRYBERGER 68	ASPK	+	25–53 MeV e^+
0.78 ± 0.05	8354	KRUGER 61			
		PLANO 60	HBC	+	Whole spectrum

³⁸BALKE 88 uses $\rho = 0.752 \pm 0.003$.³⁹VOSSLER 69 has measured the asymmetry below 10 MeV. See comments about radiative corrections in VOSSLER 69. $(\xi \text{ PARAMETER}) \times (\mu \text{ LONGITUDINAL POLARIZATION})$ $(V-A)$ theory predicts $\xi = 1$, longitudinal polarization = 1.

VALUE	EVTS	DOCUMENT ID	TECN	CHG	COMMENT
1.0007 ± 0.0035	OUR AVERAGE				
1.0003 ± 0.0006 ± 0.0038		JAMIESON 06	TWST	+	surface μ^+ beam
1.0027 ± 0.0079 ± 0.0030		BELTRAMI 87	CNTR		SIN, π decay in flight
• • •					We do not use the following data for averages, fits, limits, etc. • • •
1.0013 ± 0.0030 ± 0.0053		⁴⁰ IMAZATO 92	SPEC	+	$K^+ \rightarrow \mu^+ \nu_\mu$
0.975 ± 0.015		AKHMANOV 68	EMUL		140 kg
0.975 ± 0.030	66k	GUREVICH 64	EMUL		See AKHMANOV 68
0.903 ± 0.027		⁴¹ ALI-ZADE 61	EMUL	+	27 kg
0.93 ± 0.06	8354	PLANO 60	HBC	+	8.8 kg
0.97 ± 0.05	9k	BARDON 59	CNTR		Bromofom target

⁴⁰The corresponding 90% confidence limit from IMAZATO 92 is $|\xi P_\mu| > 0.990$. This measurement is of K^+ decay, not π^+ decay, so we do not include it in an average, nor do we yet set up a separate data block for K results.⁴¹Depolarization by medium not known sufficiently well. $\xi \times (\mu \text{ LONGITUDINAL POLARIZATION}) \times \delta / \rho$

VALUE	CL%	DOCUMENT ID	TECN	CHG	COMMENT
>0.99682	90	⁴² JODIDIO 86	SPEC	+	TRIUMF
• • •					We do not use the following data for averages, fits, limits, etc. • • •
>0.9966	90	⁴³ STOKER 85	SPEC	+	μ -spin rotation
>0.9959	90	CARR 83	SPEC	+	11 kg
⁴² JODIDIO 86 includes data from CARR 83 and STOKER 85. The value here is from the erratum.					
⁴³ STOKER 85 find $(\xi P_\mu \delta / \rho) > 0.9955$ and > 0.9966 , where the first limit is from new μ spin-rotation data and the second is from combination with CARR 83 data. In $V-A$ theory, $(\delta / \rho) = 1.0$.					

 $\xi' = \text{LONGITUDINAL POLARIZATION OF } e^+$ $(V-A)$ theory predicts the longitudinal polarization = ± 1 for e^\pm , respectively. We have flipped the sign for e^- so our programs can average.

VALUE	EVTS	DOCUMENT ID	TECN	CHG	COMMENT
1.00 ± 0.04	OUR AVERAGE				
0.998 ± 0.045	1M	BURKARD 85	CNTR	+	Bhabha + annihl
0.89 ± 0.28	29k	SCHWARTZ 67	OSPK	-	Moller scattering
0.94 ± 0.38		BLOOM 64	CNTR	+	Brems. transmiss.
1.04 ± 0.18		DUCCLOS 64	CNTR	+	Bhabha scattering
1.05 ± 0.30		BUHLER 63	CNTR	+	Annihilation

 ξ'' PARAMETER

VALUE	EVTS	DOCUMENT ID	TECN	CHG	COMMENT
0.65 ± 0.36	326k	⁴⁴ BURKARD 85	CNTR	+	Bhabha + annihl

⁴⁴BURKARD 85 measure $(\xi'' - \xi \xi') / \xi$ and ξ' and set $\xi = 1$.TRANSVERSE e^+ POLARIZATION IN PLANE OF μ SPIN, e^+ MOMENTUM

VALUE (units 10^{-3})	EVTS	DOCUMENT ID	TECN	CHG	COMMENT
7 ± 8	OUR AVERAGE				
6.3 ± 7.7 ± 3.4	30M	DANNEBERG 05	CNTR	+	7–53 MeV e^+
16 ± 21 ± 10	5.3M	BURKARD 85B	CNTR	+	Annihil 9–53 MeV

TRANSVERSE e^+ POLARIZATION NORMAL TO PLANE OF μ SPIN, e^+ MOMENTUMZero if T invariance holds.

VALUE (units 10^{-3})	EVTS	DOCUMENT ID	TECN	CHG	COMMENT
-2 ± 8	OUR AVERAGE				
-3.7 ± 7.7 ± 3.4	30M	DANNEBERG 05	CNTR	+	7–53 MeV e^+
7 ± 22 ± 7	5.3M	BURKARD 85B	CNTR	+	Annihil 9–53 MeV

 α/A

VALUE (units 10^{-3})	EVTS	DOCUMENT ID	TECN	CHG	COMMENT
0.4 ± 4.3		⁴⁵ BURKARD 85B	FIT		

• • • We do not use the following data for averages, fits, limits, etc. • • •

15 ± 50 ± 14 5.3M BURKARD 85B CNTR + 9–53 MeV e^+ ⁴⁵Global fit to all measured parameters. Correlation coefficients are given in BURKARD 85B. α'/A Zero if T invariance holds.

VALUE (units 10^{-3})	EVTS	DOCUMENT ID	TECN	CHG	COMMENT
-10 ± 20	OUR AVERAGE				
-3.4 ± 21.3 ± 4.9	30M	DANNEBERG 05	CNTR	+	7–53 MeV e^+
-47 ± 50 ± 14	5.3M	⁴⁶ BURKARD 85B	CNTR	+	9–53 MeV e^+
• • •					We do not use the following data for averages, fits, limits, etc. • • •
-0.2 ± 4.3		⁴⁷ BURKARD 85B	FIT		

⁴⁶Previously we used the global fit result from BURKARD 85B in OUR AVERAGE, we now only include their actual measurement. BURKARD 85B measure e^+ polarizations P_{T_1} and P_{T_2} versus e^+ energy.⁴⁷Global fit to all measured parameters. The fit correlation coefficients are given in BURKARD 85B. β/A

VALUE (units 10^{-3})	EVTS	DOCUMENT ID	TECN	CHG	COMMENT
3.9 ± 6.2		⁴⁸ BURKARD 85B	FIT		

• • • We do not use the following data for averages, fits, limits, etc. • • •

2 ± 17 ± 6 5.3M BURKARD 85B CNTR + 9–53 MeV e^+ ⁴⁸Global fit to all measured parameters. The fit correlation coefficients are given in BURKARD 85B. β'/A Zero if T invariance holds.

VALUE (units 10^{-3})	EVTS	DOCUMENT ID	TECN	CHG	COMMENT
2 ± 7	OUR AVERAGE				
-0.5 ± 7.8 ± 1.8	30M	DANNEBERG 05	CNTR	+	7–53 MeV e^+
17 ± 17 ± 6	5.3M	⁴⁹ BURKARD 85B	CNTR	+	9–53 MeV e^+
• • •					We do not use the following data for averages, fits, limits, etc. • • •
-1.3 ± 3.5 ± 0.6	30M	⁵⁰ DANNEBERG 05	CNTR	+	7–53 MeV e^+
1.5 ± 6.3		⁵¹ BURKARD 85B	FIT		

⁴⁹Previously we used the global fit result from BURKARD 85B in OUR AVERAGE, we now only include their actual measurement. BURKARD 85B measure e^+ polarizations P_{T_1} and P_{T_2} versus e^+ energy.⁵⁰ $\alpha = \alpha' = 0$ assumed.⁵¹Global fit to all measured parameters. The fit correlation coefficients are given in BURKARD 85B. a/A

This comes from an alternative parameterization to that used in the Summary Table (see the "Note on Muon Decay Parameters" above).

VALUE (units 10^{-3})	CL%	DOCUMENT ID	TECN
• • •			
<15.9	90	⁵² BURKARD 85B	FIT
⁵² Global fit to all measured parameters. Correlation coefficients are given in BURKARD 85B.			

 a'/A

This comes from an alternative parameterization to that used in the Summary Table (see the "Note on Muon Decay Parameters" above).

VALUE (units 10^{-3})	CL%	DOCUMENT ID	TECN
• • •			
5.3 ± 4.1		⁵³ BURKARD 85B	FIT
⁵³ Global fit to all measured parameters. Correlation coefficients are given in BURKARD 85B.			

 $(b'+b)/A$

This comes from an alternative parameterization to that used in the Summary Table (see the "Note on Muon Decay Parameters" above).

VALUE (units 10^{-3})	CL%	DOCUMENT ID	TECN
• • •			
<1.04	90	⁵⁴ BURKARD 85B	FIT
⁵⁴ Global fit to all measured parameters. Correlation coefficients are given in BURKARD 85B.			

 c/A

This comes from an alternative parameterization to that used in the Summary Table (see the "Note on Muon Decay Parameters" above).

VALUE (units 10^{-3})	CL%	DOCUMENT ID	TECN
• • •			
<6.4	90	⁵⁵ BURKARD 85B	FIT
⁵⁵ Global fit to all measured parameters. Correlation coefficients are given in BURKARD 85B.			

 c'/A

This comes from an alternative parameterization to that used in the Summary Table (see the "Note on Muon Decay Parameters" above).

VALUE (units 10^{-3})	CL%	DOCUMENT ID	TECN
• • •			
3.5 ± 2.0		⁵⁶ BURKARD 85B	FIT
⁵⁶ Global fit to all measured parameters. Correlation coefficients are given in BURKARD 85B.			

7 PARAMETER

(V-A) theory predicts $\overline{\eta} = 0$. $\overline{\eta}$ affects spectrum of radiative muon decay.

Table with columns: VALUE, DOCUMENT ID, TECN, CHG, COMMENT. Includes entries for EICHENBER... 84 ELEC + rho free, BOGART 67 CNTR +, and EICHENBER... 84 ELEC + rho=0.75 assumed.

mu REFERENCES

Extensive table of muon references with columns: NAME, YEAR, DOCUMENT ID, TECN, CHG, COMMENT. Lists numerous experiments like BENNETT 09, BARCZYK 08, MACDONALD 08, etc.

Table of tau mass references with columns: NAME, YEAR, DOCUMENT ID, TECN, COMMENT. Lists experiments like FRYBERGER 68, BOGART 67, SCHWARTZ 67, etc.

T

J = 1/2

tau discovery paper was PERL 75. e+e- -> tau+tau- cross-section threshold behavior and magnitude are consistent with pointlike spin-1/2 Dirac particle. BRANDELIK 78 ruled out pointlike spin-0 or spin-1 particle. FELDMAN 78 ruled out J = 3/2. KIRKBY 79 also ruled out J=integer, J = 3/2.

tau MASS

Table of tau mass measurements with columns: VALUE (MeV), EVTS, DOCUMENT ID, TECN, COMMENT. Includes entries like 1776.82 +/- 0.16 OUR AVERAGE, 1776.68 +/- 0.12 +/- 0.41, etc.

... We do not use the following data for averages, fits, limits, etc. ...

- 1 AUBERT 09AK and BELOUS 07 fit tau pseudomass spectrum in tau -> pi+pi-pi- nu_tau decays. Result assumes m_nu_tau = 0.
2 ABBIENDI 00A fit tau pseudomass spectrum in tau -> pi+ pi- pi+ pi- decays. Result assumes m_nu_tau = 0.
3 BAI 96 fit sigma(e+e- -> tau+tau-) at different energies near threshold.
4 ALBRECHT 92M fit tau pseudomass spectrum in tau -> 2pi-pi+ nu_tau decays. Result assumes m_nu_tau = 0.
5 BACINO 78B value comes from e+X threshold. Published mass 1782 MeV increased by 1 MeV using the high precision psi(2S) mass measurement of ZHOLENTZ 80 to eliminate the absolute SPEAR energy calibration uncertainty.
6 BALEST 93 fit spectra of minimum kinematically allowed tau mass in events of the type e+e- -> tau+tau- -> (pi+n pi0 nu_tau)(pi-m pi0 nu_tau) n <= 2, m <= 2, 1 <= n+m <= 3. If m_nu_tau != 0, result increases by (m2_nu_tau/1100 MeV).
7 BAI 92 fit sigma(e+e- -> tau+tau-) near threshold using e mu events.

(m_tau+ - m_tau-)/m_average

A test of CPT invariance.

Table of (m_tau+ - m_tau-)/m_average with columns: VALUE, CL%, DOCUMENT ID, TECN, COMMENT. Includes entries like <2.8 x 10^-4, 90, BELOUS 07, etc.

tau MEAN LIFE

Table of tau mean life measurements with columns: VALUE (10^-15 s), EVTS, DOCUMENT ID, TECN, COMMENT. Includes entries like 290.6 +/- 1.0 OUR AVERAGE, 290.9 +/- 1.4 +/- 1.0, etc.

Lepton Particle Listings

 τ

• • • We do not use the following data for averages, fits, limits, etc. • • •

291.2 ± 2.0 ± 1.2		BARATE	97i	ALEP	Repl. by BARATE 97R
291.4 ± 3.0		ABREU	96B	DLPH	Repl. by ABDAL-LAH 04T
290.1 ± 4.0	34k	ACCIARRI	96k	L3	Repl. by ACCIARRI 00B
297 ± 9 ± 5	1671	ABE	95Y	SLD	1992-1993 SLC runs
304 ± 14 ± 7	4100	BATTLE	92	CLEO	$E_{cm}^{ee} = 10.6$ GeV
301 ± 29	3780	KLEINWORT	89	JADE	$E_{cm}^{ee} = 35-46$ GeV
288 ± 16 ± 17	807	AMIDEI	88	MRK2	$E_{cm}^{ee} = 29$ GeV
306 ± 20 ± 14	695	BRAUNSCH...	88c	TASS	$E_{cm}^{ee} = 36$ GeV
299 ± 15 ± 10	1311	ABACHI	87c	HRS	$E_{cm}^{ee} = 29$ GeV
295 ± 14 ± 11	5696	ALBRECHT	87P	ARG	$E_{cm}^{ee} = 9.3-10.6$ GeV
309 ± 17 ± 7	3788	BAND	87B	MAC	$E_{cm}^{ee} = 29$ GeV
325 ± 14 ± 18	8470	BEBEK	87C	CLEO	$E_{cm}^{ee} = 10.5$ GeV
460 ± 190	102	FELDMAN	82	MRK2	$E_{cm}^{ee} = 29$ GeV

 τ MAGNETIC MOMENT ANOMALY

The q^2 dependence is expected to be small providing no thresholds are nearby.

$$\mu_{\tau}/(e\hbar/2m_{\tau}) - 1 = (g_{\tau} - 2)/2$$

For a theoretical calculation $[(g_{\tau} - 2)/2 = 117 721(5) \times 10^{-8}]$, see EIDELMAN 07.

VALUE	CL%	DOCUMENT ID	TECN	COMMENT
> -0.052 and < 0.013 (CL = 95%) OUR LIMIT				
> -0.052 and < 0.013	95	¹ ABDALLAH	04k	DLPH $e^+e^- \rightarrow e^+e^-\tau^+\tau^-$ at LEP2
< 0.107	95	² ACHARD	04g	L3 $e^+e^- \rightarrow e^+e^-\tau^+\tau^-$ at LEP2
> -0.007 and < 0.005	95	³ GONZALEZ-S..00	RVUE	$e^+e^- \rightarrow \tau^+\tau^-$ and $W \rightarrow \tau\nu_{\tau}$
> -0.052 and < 0.058	95	⁴ ACCIARRI	98e	L3 1991-1995 LEP runs
> -0.068 and < 0.065	95	⁵ ACKERSTAFF	98N	OPAL 1990-1995 LEP runs
> -0.004 and < 0.006	95	⁶ ESCRIBANO	97	RVUE $Z \rightarrow \tau^+\tau^-$ at LEP
< 0.01	95	⁷ ESCRIBANO	93	RVUE $Z \rightarrow \tau^+\tau^-$ at LEP
< 0.12	90	GRIFOLS	91	RVUE $Z \rightarrow \tau\tau\gamma$ at LEP
< 0.023	95	⁸ SILVERMAN	83	RVUE $e^+e^- \rightarrow \tau^+\tau^-$ at PETRA

- • • We do not use the following data for averages, fits, limits, etc. • • •
- ¹ ABDALLAH 04k limit is derived from $e^+e^- \rightarrow e^+e^-\tau^+\tau^-$ total cross-section measurements at \sqrt{s} between 183 and 208 GeV. In addition to the limits, the authors also quote a value of -0.018 ± 0.017 .
- ² ACHARD 04g limit is derived from $e^+e^- \rightarrow e^+e^-\tau^+\tau^-$ total cross-section measurements at \sqrt{s} between 189 and 206 GeV, and is on the absolute value of the magnetic moment anomaly.
- ³ GONZALEZ-SPRINBERG 00 use data on tau lepton production at LEP1, SLC, and LEP2, and data from colliders and LEP2 to determine limits. Assume imaginary component is zero.
- ⁴ ACCIARRI 98e use $Z \rightarrow \tau^+\tau^-\gamma$ events. In addition to the limits, the authors also quote a value of $0.004 \pm 0.027 \pm 0.023$.
- ⁵ ACKERSTAFF 98N use $Z \rightarrow \tau^+\tau^-\gamma$ events. The limit applies to an average of the form factor for off-shell τ 's having p^2 ranging from m_{τ}^2 to $(M_Z - m_{\tau})^2$.
- ⁶ ESCRIBANO 97 use preliminary experimental results.
- ⁷ ESCRIBANO 93 limit derived from $\Gamma(Z \rightarrow \tau^+\tau^-)$, and is on the absolute value of the magnetic moment anomaly.
- ⁸ SILVERMAN 83 limit is derived from $e^+e^- \rightarrow \tau^+\tau^-$ total cross-section measurements for q^2 up to $(37 \text{ GeV})^2$.

 τ ELECTRIC DIPOLE MOMENT (d_{τ})

A nonzero value is forbidden by both T invariance and P invariance.

The q^2 dependence is expected to be small providing no thresholds are nearby.

Re(d_{τ})

VALUE (10^{-16} e cm)	CL%	DOCUMENT ID	TECN	COMMENT
- 0.22 to 0.45	95	¹ INAMI	03	BELL $E_{cm}^{ee} = 10.6$ GeV
< 2.3	90	² GROZIN	09A	RVUE From e EDM limit
< 3.7	95	³ ABDALLAH	04k	DLPH $e^+e^- \rightarrow e^+e^-\tau^+\tau^-$ at LEP2
< 11.4	95	⁴ ACHARD	04g	L3 $e^+e^- \rightarrow e^+e^-\tau^+\tau^-$ at LEP2
< 4.6	95	⁵ ALBRECHT	00	ARG $E_{cm}^{ee} = 10.4$ GeV
> -3.1 and < 3.1	95	ACCIARRI	98e	L3 1991-1995 LEP runs
> -3.8 and < 3.6	95	⁶ ACKERSTAFF	98N	OPAL 1990-1995 LEP runs
< 0.11	95	^{7,8} ESCRIBANO	97	RVUE $Z \rightarrow \tau^+\tau^-$ at LEP
< 0.5	95	⁹ ESCRIBANO	93	RVUE $Z \rightarrow \tau^+\tau^-$ at LEP
< 7	90	GRIFOLS	91	RVUE $Z \rightarrow \tau\tau\gamma$ at LEP
< 1.6	90	DELAGUILA	90	RVUE $e^+e^- \rightarrow \tau^+\tau^-$ $E_{cm}^{ee} = 35$ GeV

• • • We do not use the following data for averages, fits, limits, etc. • • •

- ¹ INAMI 03 use $e^+e^- \rightarrow \tau^+\tau^-$ events.
- ² GROZIN 09A calculate the contribution to the electron electric dipole moment from the τ electric dipole moment appearing in loops, which is $\Delta d_e = 6.9 \times 10^{-12} d_{\tau}$. Dividing the REGAN 02 upper limit $|d_e| \leq 1.6 \times 10^{-27}$ e cm at CL=90% by 6.9×10^{-12} gives this limit.
- ³ ABDALLAH 04k limit is derived from $e^+e^- \rightarrow e^+e^-\tau^+\tau^-$ total cross-section measurements at \sqrt{s} between 183 and 208 GeV and is on the absolute value of d_{τ} .
- ⁴ ACHARD 04g limit is derived from $e^+e^- \rightarrow e^+e^-\tau^+\tau^-$ total cross-section measurements at \sqrt{s} between 189 and 206 GeV, and is on the absolute value of d_{τ} .
- ⁵ ALBRECHT 00 use $e^+e^- \rightarrow \tau^+\tau^-$ events. Limit is on the absolute value of $\text{Re}(d_{\tau})$.
- ⁶ ACKERSTAFF 98N use $Z \rightarrow \tau^+\tau^-\gamma$ events. The limit applies to an average of the form factor for off-shell τ 's having p^2 ranging from m_{τ}^2 to $(M_Z - m_{\tau})^2$.
- ⁷ ESCRIBANO 97 derive the relationship $|d_{\tau}| = \cot \theta_W |d_{\tau}^W|$ using effective Lagrangian methods, and use a conference result $|d_{\tau}^W| < 5.8 \times 10^{-18}$ e cm at 95% CL (L. Silvestris, ICHEP96) to obtain this result.
- ⁸ ESCRIBANO 97 use preliminary experimental results.
- ⁹ ESCRIBANO 93 limit derived from $\Gamma(Z \rightarrow \tau^+\tau^-)$, and is on the absolute value of the electric dipole moment.

Im(d_{τ})

VALUE (10^{-16} e cm)	CL%	DOCUMENT ID	TECN	COMMENT
- 0.25 to 0.008	95	¹ INAMI	03	BELL $E_{cm}^{ee} = 10.6$ GeV
< 1.8	95	² ALBRECHT	00	ARG $E_{cm}^{ee} = 10.4$ GeV

• • • We do not use the following data for averages, fits, limits, etc. • • •

- ¹ INAMI 03 use $e^+e^- \rightarrow \tau^+\tau^-$ events.
- ² ALBRECHT 00 use $e^+e^- \rightarrow \tau^+\tau^-$ events. Limit is on the absolute value of $\text{Im}(d_{\tau})$.

 τ WEAK DIPOLE MOMENT (d_{τ}^W)

A nonzero value is forbidden by CP invariance.

The q^2 dependence is expected to be small providing no thresholds are nearby.

Re(d_{τ}^W)

VALUE (10^{-17} e cm)	CL%	DOCUMENT ID	TECN	COMMENT
< 0.50	95	¹ HEISTER	03F	ALEP 1990-1995 LEP runs
< 3.0	90	¹ ACCIARRI	98c	L3 1991-1995 LEP runs
< 0.56	95	ACKERSTAFF	97L	OPAL 1991-1995 LEP runs
< 0.78	95	² AKERS	95F	OPAL Repl. by ACKERSTAFF 97L
< 1.5	95	² BUSKULIC	95c	ALEP Repl. by HEISTER 03F
< 7.0	95	² ACTON	92F	OPAL $Z \rightarrow \tau^+\tau^-$ at LEP
< 3.7	95	² BUSKULIC	92J	ALEP Repl. by BUSKULIC 95c

- • • We do not use the following data for averages, fits, limits, etc. • • •
- ¹ Limit is on the absolute value of the real part of the weak dipole moment.
- ² Limit is on the absolute value of the real part of the weak dipole moment, and applies for $q^2 = m_Z^2$.

Im(d_{τ}^W)

VALUE (10^{-17} e cm)	CL%	DOCUMENT ID	TECN	COMMENT
< 1.1	95	¹ HEISTER	03F	ALEP 1990-1995 LEP runs
< 1.5	95	ACKERSTAFF	97L	OPAL 1991-1995 LEP runs
< 4.5	95	² AKERS	95F	OPAL Repl. by ACKERSTAFF 97L

- ¹ HEISTER 03F limit is on the absolute value of the imaginary part of the weak dipole moment.
- ² Limit is on the absolute value of the imaginary part of the weak dipole moment, and applies for $q^2 = m_Z^2$.

 τ WEAK ANOMALOUS MAGNETIC DIPOLE MOMENT (α_{τ}^W)

Electroweak radiative corrections are expected to contribute at the 10^{-6} level. See BERNABEU 95.

The q^2 dependence is expected to be small providing no thresholds are nearby.

Re(α_{τ}^W)

VALUE	CL%	DOCUMENT ID	TECN	COMMENT
< 1.1 × 10⁻³	95	¹ HEISTER	03F	ALEP 1990-1995 LEP runs
> -0.0024 and < 0.0025	95	² GONZALEZ-S..00	RVUE	$e^+e^- \rightarrow \tau^+\tau^-$ and $W \rightarrow \tau\nu_{\tau}$
< 4.5 × 10 ⁻³	90	¹ ACCIARRI	98c	L3 1991-1995 LEP runs

• • • We do not use the following data for averages, fits, limits, etc. • • •

- ¹ Limit is on the absolute value of the real part of the weak anomalous magnetic dipole moment.
- ² GONZALEZ-SPRINBERG 00 use data on tau lepton production at LEP1, SLC, and LEP2, and data from colliders and LEP2 to determine limits. Assume imaginary component is zero.

$\text{Im}(\alpha_W^{\prime\prime})$

VALUE	CL%	DOCUMENT ID	TECN	COMMENT
$<2.7 \times 10^{-3}$	95	¹ HEISTER	03F ALEP	1990-1995 LEP runs
••• We do not use the following data for averages, fits, limits, etc. •••				
$<9.9 \times 10^{-3}$	90	¹ ACCIARRI	98c L3	1991-1995 LEP runs

¹Limit is on the absolute value of the imaginary part of the weak anomalous magnetic dipole moment.

 τ^- DECAY MODES

τ^+ modes are charge conjugates of the modes below. "h \pm " stands for π^\pm or K^\pm . "e μ " stands for e or μ . "Neutrals" stands for γ 's and/or π^0 's.

Mode	Fraction (Γ_i/Γ)	Scale factor/ Confidence level
Modes with one charged particle		
Γ_1 particle $^- \geq 0$ neutrals $\geq 0K^0 \nu_\tau$ ("1-prong")	(85.36 \pm 0.08) %	S=1.3
Γ_2 particle $^- \geq 0$ neutrals $\geq 0K_L^0 \nu_\tau$	(84.72 \pm 0.08) %	S=1.4
Γ_3 $\mu^- \bar{\nu}_\mu \nu_\tau$	[a] (17.36 \pm 0.05) %	
Γ_4 $\mu^- \bar{\nu}_\mu \nu_\tau \gamma$	[b] (3.6 \pm 0.4) $\times 10^{-3}$	
Γ_5 $e^- \bar{\nu}_e \nu_\tau$	[a] (17.85 \pm 0.05) %	
Γ_6 $e^- \bar{\nu}_e \nu_\tau \gamma$	[b] (1.75 \pm 0.18) %	
Γ_7 $h^- \geq 0K_L^0 \nu_\tau$	(12.13 \pm 0.07) %	S=1.1
Γ_8 $h^- \nu_\tau$	(11.61 \pm 0.06) %	S=1.1
Γ_9 $\pi^- \nu_\tau$	[a] (10.91 \pm 0.07) %	S=1.1
Γ_{10} $K^- \nu_\tau$	[a] (6.96 \pm 0.23) $\times 10^{-3}$	S=1.1
Γ_{11} $h^- \geq 1$ neutrals ν_τ	(37.06 \pm 0.10) %	S=1.2
Γ_{12} $h^- \geq 1\pi^0 \nu_\tau$ (ex. K^0)	(36.54 \pm 0.11) %	S=1.2
Γ_{13} $h^- \pi^0 \nu_\tau$	(25.94 \pm 0.09) %	S=1.1
Γ_{14} $\pi^- \pi^0 \nu_\tau$	[a] (25.51 \pm 0.09) %	S=1.1
Γ_{15} $\pi^- \pi^0$ non- $\rho(770) \nu_\tau$	(3.0 \pm 3.2) $\times 10^{-3}$	
Γ_{16} $K^- \pi^0 \nu_\tau$	[a] (4.29 \pm 0.15) $\times 10^{-3}$	
Γ_{17} $h^- \geq 2\pi^0 \nu_\tau$	(10.85 \pm 0.12) %	S=1.3
Γ_{18} $h^- 2\pi^0 \nu_\tau$	(9.51 \pm 0.11) %	S=1.2
Γ_{19} $h^- 2\pi^0 \nu_\tau$ (ex. K^0)	(9.35 \pm 0.11) %	S=1.2
Γ_{20} $\pi^- 2\pi^0 \nu_\tau$ (ex. K^0)	[a] (9.29 \pm 0.11) %	S=1.2
Γ_{21} $\pi^- 2\pi^0 \nu_\tau$ (ex. K^0), sclar	< 9 $\times 10^{-3}$	CL=95%
Γ_{22} $\pi^- 2\pi^0 \nu_\tau$ (ex. K^0), vector	< 7 $\times 10^{-3}$	CL=95%
Γ_{23} $K^- 2\pi^0 \nu_\tau$ (ex. K^0)	[a] (6.5 \pm 2.3) $\times 10^{-4}$	
Γ_{24} $h^- \geq 3\pi^0 \nu_\tau$	(1.34 \pm 0.07) %	S=1.1
Γ_{25} $h^- \geq 3\pi^0 \nu_\tau$ (ex. K^0)	(1.25 \pm 0.07) %	S=1.1
Γ_{26} $h^- 3\pi^0 \nu_\tau$	(1.18 \pm 0.08) %	
Γ_{27} $\pi^- 3\pi^0 \nu_\tau$ (ex. K^0)	[a] (1.04 \pm 0.07) %	
Γ_{28} $K^- 3\pi^0 \nu_\tau$ (ex. K^0, η)	[a] (4.9 \pm 2.3) $\times 10^{-4}$	S=1.1
Γ_{29} $h^- 4\pi^0 \nu_\tau$ (ex. K^0)	(1.5 \pm 0.4) $\times 10^{-3}$	
Γ_{30} $h^- 4\pi^0 \nu_\tau$ (ex. K^0, η)	[a] (1.1 \pm 0.4) $\times 10^{-3}$	
Γ_{31} $K^- \geq 0\pi^0 \geq 0K^0 \geq 0\gamma \nu_\tau$	(1.57 \pm 0.04) %	S=1.1
Γ_{32} $K^- \geq 1$ (π^0 or K^0 or γ) ν_τ	(8.72 \pm 0.32) $\times 10^{-3}$	S=1.1
Modes with K^0's		
Γ_{33} K_S^0 (particles) $^- \nu_\tau$	(9.2 \pm 0.4) $\times 10^{-3}$	S=1.5
Γ_{34} $h^- \bar{K}^0 \nu_\tau$	(1.00 \pm 0.05) %	S=1.8
Γ_{35} $\pi^- \bar{K}^0 \nu_\tau$	[a] (8.4 \pm 0.4) $\times 10^{-3}$	S=2.1
Γ_{36} $\pi^- \bar{K}^0$ (non- $K^*(892)^-$) ν_τ	(5.4 \pm 2.1) $\times 10^{-4}$	
Γ_{37} $K^- K^0 \nu_\tau$	[a] (1.59 \pm 0.16) $\times 10^{-3}$	
Γ_{38} $K^- K^0 \geq 0\pi^0 \nu_\tau$	(3.18 \pm 0.24) $\times 10^{-3}$	
Γ_{39} $h^- \bar{K}^0 \pi^0 \nu_\tau$	(5.5 \pm 0.4) $\times 10^{-3}$	
Γ_{40} $\pi^- \bar{K}^0 \pi^0 \nu_\tau$	[a] (4.0 \pm 0.4) $\times 10^{-3}$	
Γ_{41} $\bar{K}^0 \rho^- \nu_\tau$	(2.2 \pm 0.5) $\times 10^{-3}$	
Γ_{42} $K^- K^0 \pi^0 \nu_\tau$	[a] (1.59 \pm 0.20) $\times 10^{-3}$	
Γ_{43} $\pi^- \bar{K}^0 \geq 1\pi^0 \nu_\tau$	(3.2 \pm 1.0) $\times 10^{-3}$	
Γ_{44} $\pi^- \bar{K}^0 \pi^0 \pi^0 \nu_\tau$	(2.6 \pm 2.4) $\times 10^{-4}$	
Γ_{45} $K^- K^0 \pi^0 \pi^0 \nu_\tau$	< 1.6 $\times 10^{-4}$	CL=95%
Γ_{46} $\pi^- K^0 \bar{K}^0 \nu_\tau$	(1.7 \pm 0.4) $\times 10^{-3}$	S=1.6
Γ_{47} $\pi^- K_S^0 K_S^0 \nu_\tau$	[a] (2.4 \pm 0.5) $\times 10^{-4}$	
Γ_{48} $\pi^- K_S^0 K_L^0 \nu_\tau$	[a] (1.2 \pm 0.4) $\times 10^{-3}$	S=1.7
Γ_{49} $\pi^- K^0 \bar{K}^0 \pi^0 \nu_\tau$	(3.1 \pm 2.3) $\times 10^{-4}$	
Γ_{50} $\pi^- K_S^0 K_S^0 \pi^0 \nu_\tau$	< 2.0 $\times 10^{-4}$	CL=95%
Γ_{51} $\pi^- K_S^0 K_L^0 \pi^0 \nu_\tau$	(3.1 \pm 1.2) $\times 10^{-4}$	
Γ_{52} $K^0 h^+ h^- h^- \geq 0$ neutrals ν_τ	< 1.7 $\times 10^{-3}$	CL=95%
Γ_{53} $K^0 h^+ h^- h^- \nu_\tau$	(2.3 \pm 2.0) $\times 10^{-4}$	

Modes with three charged particles

Γ_{54} $h^- h^- h^+ \geq 0$ neutrals $\geq 0K_L^0 \nu_\tau$	(15.19 \pm 0.08) %	S=1.4
Γ_{55} $h^- h^- h^+ \geq 0$ neutrals ν_τ (ex. $K_S^0 \rightarrow \pi^+ \pi^-$) ("3-prong")	(14.56 \pm 0.08) %	S=1.3
Γ_{56} $h^- h^- h^+ \nu_\tau$	(9.80 \pm 0.08) %	S=1.4
Γ_{57} $h^- h^- h^+ \nu_\tau$ (ex. K^0)	(9.46 \pm 0.07) %	S=1.3
Γ_{58} $h^- h^- h^+ \nu_\tau$ (ex. K^0, ω)	(9.42 \pm 0.07) %	S=1.3
Γ_{59} $\pi^- \pi^+ \pi^- \nu_\tau$	(9.32 \pm 0.07) %	S=1.2
Γ_{60} $\pi^- \pi^+ \pi^- \nu_\tau$ (ex. K^0)	(9.03 \pm 0.06) %	S=1.2
Γ_{61} $\pi^- \pi^+ \pi^- \nu_\tau$ (ex. K^0), non-axial vector	< 2.4 %	CL=95%
Γ_{62} $\pi^- \pi^+ \pi^- \nu_\tau$ (ex. K^0, ω)	[a] (9.00 \pm 0.06) %	S=1.2
Γ_{63} $h^- h^- h^+ \geq 1$ neutrals ν_τ	(5.38 \pm 0.07) %	S=1.2
Γ_{64} $h^- h^- h^+ \geq 1\pi^0 \nu_\tau$ (ex. K^0)	(5.08 \pm 0.06) %	S=1.1
Γ_{65} $h^- h^- h^+ \pi^0 \nu_\tau$	(4.75 \pm 0.06) %	S=1.2
Γ_{66} $h^- h^- h^+ \pi^0 \nu_\tau$ (ex. K^0)	(4.56 \pm 0.06) %	S=1.2
Γ_{67} $h^- h^- h^+ \pi^0 \nu_\tau$ (ex. K^0, ω)	(2.79 \pm 0.08) %	S=1.2
Γ_{68} $\pi^- \pi^+ \pi^- \pi^0 \nu_\tau$	(4.61 \pm 0.06) %	S=1.1
Γ_{69} $\pi^- \pi^+ \pi^- \pi^0 \nu_\tau$ (ex. K^0)	(4.48 \pm 0.06) %	S=1.2
Γ_{70} $\pi^- \pi^+ \pi^- \pi^0 \nu_\tau$ (ex. K^0, ω)	[a] (2.70 \pm 0.08) %	S=1.2
Γ_{71} $h^- \rho^+ \nu_\tau$		
Γ_{72} $h^- \rho^+ h^- \nu_\tau$		
Γ_{73} $h^- \rho^- h^+ \nu_\tau$		
Γ_{74} $h^- h^- h^+ \geq 2\pi^0 \nu_\tau$ (ex. K^0)	(5.18 \pm 0.33) $\times 10^{-3}$	
Γ_{75} $h^- h^- h^+ 2\pi^0 \nu_\tau$	(5.06 \pm 0.32) $\times 10^{-3}$	
Γ_{76} $h^- h^- h^+ 2\pi^0 \nu_\tau$ (ex. K^0)	(4.95 \pm 0.32) $\times 10^{-3}$	
Γ_{77} $h^- h^- h^+ 2\pi^0 \nu_\tau$ (ex. K^0, ω, η)	[a] (10 \pm 4) $\times 10^{-4}$	
Γ_{78} $h^- h^- h^+ 3\pi^0 \nu_\tau$	[a] (2.3 \pm 0.7) $\times 10^{-4}$	S=1.3
Γ_{79} $K^- h^+ h^- \geq 0$ neutrals ν_τ	(6.24 \pm 0.24) $\times 10^{-3}$	S=1.5
Γ_{80} $K^- h^+ \pi^- \nu_\tau$ (ex. K^0)	(4.27 \pm 0.20) $\times 10^{-3}$	S=2.4
Γ_{81} $K^- h^+ \pi^- \pi^0 \nu_\tau$ (ex. K^0)	(8.7 \pm 1.2) $\times 10^{-4}$	S=1.1
Γ_{82} $K^- \pi^+ \pi^- \geq 0$ neutrals ν_τ	(4.78 \pm 0.21) $\times 10^{-3}$	S=1.3
Γ_{83} $K^- \pi^+ \pi^- \geq 0\pi^0 \nu_\tau$ (ex. K^0)	(3.68 \pm 0.20) $\times 10^{-3}$	S=1.4
Γ_{84} $K^- \pi^+ \pi^- \nu_\tau$	(3.42 \pm 0.17) $\times 10^{-3}$	S=1.8
Γ_{85} $K^- \pi^+ \pi^- \nu_\tau$ (ex. K^0)	[a] (2.87 \pm 0.16) $\times 10^{-3}$	S=2.1
Γ_{86} $K^- \rho^+ \nu_\tau \rightarrow$ $K^- \pi^+ \pi^- \nu_\tau$	(1.4 \pm 0.5) $\times 10^{-3}$	
Γ_{87} $K^- \pi^+ \pi^- \pi^0 \nu_\tau$	(1.36 \pm 0.14) $\times 10^{-3}$	
Γ_{88} $K^- \pi^+ \pi^- \pi^0 \nu_\tau$ (ex. K^0)	(8.1 \pm 1.2) $\times 10^{-4}$	
Γ_{89} $K^- \pi^+ \pi^- \pi^0 \nu_\tau$ (ex. K^0, η)	[a] (7.7 \pm 1.2) $\times 10^{-4}$	
Γ_{90} $K^- \pi^+ \pi^- \pi^0 \nu_\tau$ (ex. K^0, ω)	(3.7 \pm 0.9) $\times 10^{-4}$	
Γ_{91} $K^- \pi^+ K^- \geq 0$ neut. ν_τ	< 9 $\times 10^{-4}$	CL=95%
Γ_{92} $K^- K^+ \pi^- \geq 0$ neut. ν_τ	(1.46 \pm 0.06) $\times 10^{-3}$	S=1.6
Γ_{93} $K^- K^+ \pi^- \nu_\tau$	[a] (1.40 \pm 0.05) $\times 10^{-3}$	S=1.7
Γ_{94} $K^- K^+ \pi^- \pi^0 \nu_\tau$	[a] (6.1 \pm 2.5) $\times 10^{-5}$	S=1.4
Γ_{95} $K^- K^+ K^- \geq 0$ neut. ν_τ	< 2.1 $\times 10^{-3}$	CL=95%
Γ_{96} $K^- K^+ K^- \nu_\tau$	(1.58 \pm 0.18) $\times 10^{-5}$	
Γ_{97} $K^- K^+ K^- \nu_\tau$ (ex. ϕ)	< 2.5 $\times 10^{-6}$	CL=90%
Γ_{98} $K^- K^+ K^- \pi^0 \nu_\tau$	< 4.8 $\times 10^{-6}$	CL=90%
Γ_{99} $\pi^- K^+ \pi^- \geq 0$ neut. ν_τ	< 2.5 $\times 10^{-3}$	CL=95%
Γ_{100} $e^- e^- e^+ \bar{\nu}_e \nu_\tau$	(2.8 \pm 1.5) $\times 10^{-5}$	
Γ_{101} $\mu^- e^- e^+ \bar{\nu}_\mu \nu_\tau$	< 3.6 $\times 10^{-5}$	CL=90%

Modes with five charged particles

Γ_{102} $3h^- 2h^+ \geq 0$ neutrals ν_τ (ex. $K_S^0 \rightarrow \pi^- \pi^+$) ("5-prong")	(1.02 \pm 0.04) $\times 10^{-3}$	S=1.1
Γ_{103} $3h^- 2h^+ \nu_\tau$ (ex. K^0)	[a] (8.39 \pm 0.35) $\times 10^{-4}$	S=1.1
Γ_{104} $3h^- 2h^+ \pi^0 \nu_\tau$ (ex. K^0)	[a] (1.78 \pm 0.27) $\times 10^{-4}$	
Γ_{105} $3h^- 2h^+ 2\pi^0 \nu_\tau$	< 3.4 $\times 10^{-6}$	CL=90%

Lepton Particle Listings

 τ

Miscellaneous other allowed modes			
Γ_{106}	$(5\pi)^- \nu_\tau$	$(7.6 \pm 0.5) \times 10^{-3}$	
Γ_{107}	$4h^- 3h^+ \geq 0$ neutrals ν_τ	< 3.0	$\times 10^{-7}$ CL=90%
	("7-prong")		
Γ_{108}	$4h^- 3h^+ \nu_\tau$	< 4.3	$\times 10^{-7}$ CL=90%
Γ_{109}	$4h^- 3h^+ \pi^0 \nu_\tau$	< 2.5	$\times 10^{-7}$ CL=90%
Γ_{110}	$X^-(S=-1) \nu_\tau$	$(2.86 \pm 0.07) \%$	S=1.3
Γ_{111}	$K^*(892)^- \geq 0$ neutrals \geq	$(1.42 \pm 0.18) \%$	S=1.4
	$0K_L^0 \nu_\tau$		
Γ_{112}	$K^*(892)^- \nu_\tau$	$(1.20 \pm 0.07) \%$	S=1.8
Γ_{113}	$K^*(892)^- \nu_\tau \rightarrow \pi^- \bar{K}^0 \nu_\tau$	$(7.8 \pm 0.5) \times 10^{-3}$	
Γ_{114}	$K^*(892)^0 K^- \geq 0$ neutrals ν_τ	$(3.2 \pm 1.4) \times 10^{-3}$	
Γ_{115}	$K^*(892)^0 K^- \nu_\tau$	$(2.1 \pm 0.4) \times 10^{-3}$	
Γ_{116}	$\bar{K}^*(892)^0 \pi^- \geq 0$ neutrals ν_τ	$(3.8 \pm 1.7) \times 10^{-3}$	
Γ_{117}	$\bar{K}^*(892)^0 \pi^- \nu_\tau$	$(2.2 \pm 0.5) \times 10^{-3}$	
Γ_{118}	$(\bar{K}^*(892) \pi)^- \nu_\tau \rightarrow$	$(1.0 \pm 0.4) \times 10^{-3}$	
	$\pi^- \bar{K}^0 \pi^0 \nu_\tau$		
Γ_{119}	$K_1(1270)^- \nu_\tau$	$(4.7 \pm 1.1) \times 10^{-3}$	
Γ_{120}	$K_1(1400)^- \nu_\tau$	$(1.7 \pm 2.6) \times 10^{-3}$	S=1.7
Γ_{121}	$K^*(1410)^- \nu_\tau$	$(1.5 \pm 1.4) \times 10^{-3}$	
		(-1.0)	
Γ_{122}	$K_0^*(1430)^- \nu_\tau$	< 5	$\times 10^{-4}$ CL=95%
Γ_{123}	$K_2^*(1430)^- \nu_\tau$	< 3	$\times 10^{-3}$ CL=95%
Γ_{124}	$a_0(980)^- \geq 0$ neutrals ν_τ		
Γ_{125}	$\eta \pi^- \nu_\tau$	< 1.4	$\times 10^{-4}$ CL=95%
Γ_{126}	$\eta \pi^- \pi^0 \nu_\tau$	[a] $(1.39 \pm 0.10) \times 10^{-3}$	S=1.4
Γ_{127}	$\eta \pi^- \pi^0 \pi^0 \nu_\tau$	$(1.5 \pm 0.5) \times 10^{-4}$	
Γ_{128}	$\eta K^- \nu_\tau$	[a] $(1.61 \pm 0.11) \times 10^{-4}$	S=1.1
Γ_{129}	$\eta K^*(892)^- \nu_\tau$	$(1.38 \pm 0.15) \times 10^{-4}$	
Γ_{130}	$\eta K^- \pi^0 \nu_\tau$	$(4.8 \pm 1.2) \times 10^{-5}$	
Γ_{131}	$\eta K^- \pi^0$ (non- $K^*(892)$) ν_τ	< 3.5	$\times 10^{-5}$ CL=90%
Γ_{132}	$\eta \bar{K}^0 \pi^- \nu_\tau$	$(9.3 \pm 1.5) \times 10^{-5}$	
Γ_{133}	$\eta \bar{K}^0 \pi^- \pi^0 \nu_\tau$	< 5.0	$\times 10^{-5}$ CL=90%
Γ_{134}	$\eta K^- K^0 \nu_\tau$	< 9.0	$\times 10^{-6}$ CL=90%
Γ_{135}	$\eta \pi^+ \pi^- \pi^- \geq 0$ neutrals ν_τ	< 3	$\times 10^{-3}$ CL=90%
Γ_{136}	$\eta \pi^- \pi^+ \pi^- \nu_\tau$ (ex. K^0)	$(1.64 \pm 0.12) \times 10^{-4}$	
Γ_{137}	$\eta a_1(1260)^- \nu_\tau \rightarrow$	< 3.9	$\times 10^{-4}$ CL=90%
	$\eta \pi^- \nu_\tau$	< 7.4	$\times 10^{-6}$ CL=90%
Γ_{138}	$\eta \eta \pi^- \nu_\tau$	< 2.0	$\times 10^{-4}$ CL=95%
Γ_{139}	$\eta \eta \pi^- \pi^0 \nu_\tau$	< 3.0	$\times 10^{-6}$ CL=90%
Γ_{140}	$\eta \eta K^- \nu_\tau$	< 7.2	$\times 10^{-6}$ CL=90%
Γ_{141}	$\eta'(958) \pi^- \nu_\tau$	< 8.0	$\times 10^{-5}$ CL=90%
Γ_{142}	$\eta'(958) \pi^- \pi^0 \nu_\tau$		
Γ_{143}	$\phi \pi^- \nu_\tau$	$(3.4 \pm 0.6) \times 10^{-5}$	
Γ_{144}	$\phi K^- \nu_\tau$	$(3.70 \pm 0.33) \times 10^{-5}$	S=1.3
Γ_{145}	$f_1(1285) \pi^- \nu_\tau$	$(3.6 \pm 0.7) \times 10^{-4}$	
Γ_{146}	$f_1(1285) \pi^- \nu_\tau \rightarrow$	$(1.11 \pm 0.08) \times 10^{-4}$	
	$\eta \pi^- \pi^+ \pi^- \nu_\tau$		
Γ_{147}	$\pi(1300)^- \nu_\tau \rightarrow (\rho \pi)^- \nu_\tau \rightarrow$	< 1.0	$\times 10^{-4}$ CL=90%
	$(3\pi)^- \nu_\tau$		
Γ_{148}	$\pi(1300)^- \nu_\tau \rightarrow$	< 1.9	$\times 10^{-4}$ CL=90%
	$((\pi \pi)_S\text{-wave } \pi)^- \nu_\tau \rightarrow$		
	$(3\pi)^- \nu_\tau$		
Γ_{149}	$h^- \omega \geq 0$ neutrals ν_τ	$(2.41 \pm 0.09) \%$	S=1.2
Γ_{150}	$h^- \omega \nu_\tau$	[a] $(1.99 \pm 0.08) \%$	S=1.3
Γ_{151}	$K^- \omega \nu_\tau$	$(4.1 \pm 0.9) \times 10^{-4}$	
Γ_{152}	$h^- \omega \pi^0 \nu_\tau$	[a] $(4.1 \pm 0.4) \times 10^{-3}$	
Γ_{153}	$h^- \omega 2\pi^0 \nu_\tau$	$(1.4 \pm 0.5) \times 10^{-4}$	
Γ_{154}	$h^- 2\omega \nu_\tau$	< 5.4	$\times 10^{-7}$ CL=90%
Γ_{155}	$2h^- h^+ \omega \nu_\tau$	$(1.20 \pm 0.22) \times 10^{-4}$	

Lepton Family number (LF), Lepton number (L), or Baryon number (B) violating modes

L means lepton number violation (e.g. $\tau^- \rightarrow e^+ \pi^- \pi^-$). Following common usage, LF means lepton family violation and not lepton number violation (e.g. $\tau^- \rightarrow e^- \pi^+ \pi^-$). B means baryon number violation.

Γ_{156}	$e^- \gamma$	LF	< 3.3	$\times 10^{-8}$	CL=90%
Γ_{157}	$\mu^- \gamma$	LF	< 4.4	$\times 10^{-8}$	CL=90%
Γ_{158}	$e^- \pi^0$	LF	< 8.0	$\times 10^{-8}$	CL=90%
Γ_{159}	$\mu^- \pi^0$	LF	< 1.1	$\times 10^{-7}$	CL=90%
Γ_{160}	$e^- K_S^0$	LF	< 3.3	$\times 10^{-8}$	CL=90%
Γ_{161}	$\mu^- K_S^0$	LF	< 4.0	$\times 10^{-8}$	CL=90%
Γ_{162}	$e^- \eta$	LF	< 9.2	$\times 10^{-8}$	CL=90%
Γ_{163}	$\mu^- \eta$	LF	< 6.5	$\times 10^{-8}$	CL=90%
Γ_{164}	$e^- \rho^0$	LF	< 4.6	$\times 10^{-8}$	CL=90%
Γ_{165}	$\mu^- \rho^0$	LF	< 2.6	$\times 10^{-8}$	CL=90%
Γ_{166}	$e^- \omega$	LF	< 1.1	$\times 10^{-7}$	CL=90%
Γ_{167}	$\mu^- \omega$	LF	< 8.9	$\times 10^{-8}$	CL=90%
Γ_{168}	$e^- K^*(892)^0$	LF	< 5.9	$\times 10^{-8}$	CL=90%
Γ_{169}	$\mu^- K^*(892)^0$	LF	< 5.9	$\times 10^{-8}$	CL=90%
Γ_{170}	$e^- \bar{K}^*(892)^0$	LF	< 4.6	$\times 10^{-8}$	CL=90%
Γ_{171}	$\mu^- \bar{K}^*(892)^0$	LF	< 7.3	$\times 10^{-8}$	CL=90%
Γ_{172}	$e^- \eta'(958)$	LF	< 1.6	$\times 10^{-7}$	CL=90%
Γ_{173}	$\mu^- \eta'(958)$	LF	< 1.3	$\times 10^{-7}$	CL=90%
Γ_{174}	$e^- f_0(980) \rightarrow e^- \pi^+ \pi^-$	LF	< 3.2	$\times 10^{-8}$	CL=90%
Γ_{175}	$\mu^- f_0(980) \rightarrow \mu^- \pi^+ \pi^-$	LF	< 3.4	$\times 10^{-8}$	CL=90%
Γ_{176}	$e^- \phi$	LF	< 3.1	$\times 10^{-8}$	CL=90%
Γ_{177}	$\mu^- \phi$	LF	< 1.3	$\times 10^{-7}$	CL=90%
Γ_{178}	$e^- e^+ e^-$	LF	< 3.6	$\times 10^{-8}$	CL=90%
Γ_{179}	$e^- \mu^+ \mu^-$	LF	< 3.7	$\times 10^{-8}$	CL=90%
Γ_{180}	$e^+ \mu^- \mu^-$	LF	< 2.3	$\times 10^{-8}$	CL=90%
Γ_{181}	$\mu^- e^+ e^-$	LF	< 2.7	$\times 10^{-8}$	CL=90%
Γ_{182}	$\mu^+ e^- e^-$	LF	< 2.0	$\times 10^{-8}$	CL=90%
Γ_{183}	$\mu^- \mu^+ \mu^-$	LF	< 3.2	$\times 10^{-8}$	CL=90%
Γ_{184}	$e^- \pi^+ \pi^-$	LF	< 4.4	$\times 10^{-8}$	CL=90%
Γ_{185}	$e^+ \pi^- \pi^-$	L	< 8.8	$\times 10^{-8}$	CL=90%
Γ_{186}	$\mu^- \pi^+ \pi^-$	L	< 3.3	$\times 10^{-8}$	CL=90%
Γ_{187}	$\mu^+ \pi^- \pi^-$	L	< 3.7	$\times 10^{-8}$	CL=90%
Γ_{188}	$e^- \pi^+ K^-$	LF	< 5.8	$\times 10^{-8}$	CL=90%
Γ_{189}	$e^- \pi^- K^+$	LF	< 5.2	$\times 10^{-8}$	CL=90%
Γ_{190}	$e^+ \pi^- K^-$	L	< 6.7	$\times 10^{-8}$	CL=90%
Γ_{191}	$e^- K_S^0 K_S^0$	LF	< 2.2	$\times 10^{-6}$	CL=90%
Γ_{192}	$e^+ K^+ K^-$	LF	< 5.4	$\times 10^{-8}$	CL=90%
Γ_{193}	$e^+ K^- K^-$	L	< 6.0	$\times 10^{-8}$	CL=90%
Γ_{194}	$\mu^- \pi^+ K^-$	LF	< 1.6	$\times 10^{-7}$	CL=90%
Γ_{195}	$\mu^- \pi^- K^+$	LF	< 1.0	$\times 10^{-7}$	CL=90%
Γ_{196}	$\mu^+ \pi^- K^-$	L	< 9.4	$\times 10^{-8}$	CL=90%
Γ_{197}	$\mu^- K_S^0 K_S^0$	LF	< 3.4	$\times 10^{-6}$	CL=90%
Γ_{198}	$\mu^- K^+ K^-$	LF	< 6.8	$\times 10^{-8}$	CL=90%
Γ_{199}	$\mu^+ K^- K^-$	L	< 9.6	$\times 10^{-8}$	CL=90%
Γ_{200}	$e^- \pi^0 \pi^0$	LF	< 6.5	$\times 10^{-6}$	CL=90%
Γ_{201}	$\mu^- \pi^0 \pi^0$	LF	< 1.4	$\times 10^{-5}$	CL=90%
Γ_{202}	$e^- \eta \eta$	LF	< 3.5	$\times 10^{-5}$	CL=90%
Γ_{203}	$\mu^- \eta \eta$	LF	< 6.0	$\times 10^{-5}$	CL=90%
Γ_{204}	$e^- \pi^0 \eta$	LF	< 2.4	$\times 10^{-5}$	CL=90%
Γ_{205}	$\mu^- \pi^0 \eta$	LF	< 2.2	$\times 10^{-5}$	CL=90%
Γ_{206}	$\bar{p} \gamma$	L,B	< 3.5	$\times 10^{-6}$	CL=90%
Γ_{207}	$\bar{p} \pi^0$	L,B	< 1.5	$\times 10^{-5}$	CL=90%
Γ_{208}	$\bar{p} 2\pi^0$	L,B	< 3.3	$\times 10^{-5}$	CL=90%
Γ_{209}	$\bar{p} \eta$	L,B	< 8.9	$\times 10^{-6}$	CL=90%
Γ_{210}	$\bar{p} \pi^0 \eta$	L,B	< 2.7	$\times 10^{-5}$	CL=90%
Γ_{211}	$\Lambda \pi^-$	L,B	< 7.2	$\times 10^{-8}$	CL=90%
Γ_{212}	$\Lambda \pi^-$	L,B	< 1.4	$\times 10^{-7}$	CL=90%
Γ_{213}	e^- light boson	LF	< 2.7	$\times 10^{-3}$	CL=95%
Γ_{214}	μ^- light boson	LF	< 5	$\times 10^{-3}$	CL=95%

[a] Basis mode for the τ .

[b] See the Particle Listings below for the energy limits used in this measurement.

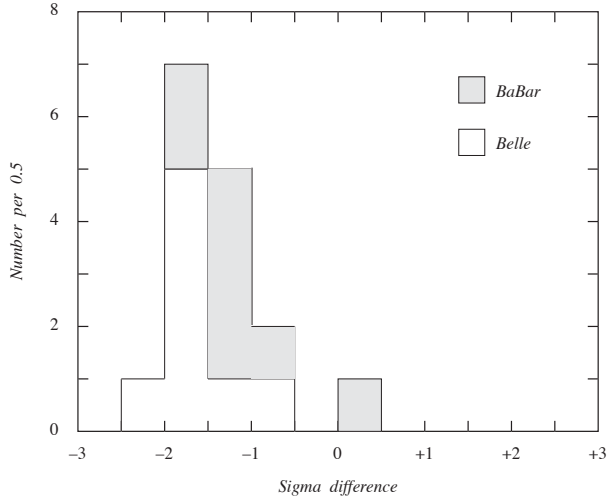


Figure 1: Distribution of the normalized difference between the 16 B -factory measurements of conventional τ -decay branching fractions and non- B -factory measurements. The Belle and BaBar collaborations have each published 8 measurements.

The cause of this discrepancy remains to be understood.

The constrained fit to τ branching fractions: The Lepton Summary Table and the List of τ -Decay Modes contain branching fractions for 119 conventional τ -decay modes and upper limits on the branching fractions for 32 other conventional τ -decay modes. Of the 119 modes with branching fractions, 82 are derived from a constrained fit to τ branching fraction data. The goal of the constrained fit is to make optimal use of the experimental data to determine τ branching fractions. For example, the branching fractions for the decay mode $\tau^- \rightarrow \pi^- \pi^+ \pi^- \pi^0 \nu_\tau$ is determined mostly from experimental measurements of the branching fraction for $\tau^- \rightarrow h^- h^- h^+ \pi^0 \nu_\tau$ and measurements of exclusive branching fractions for 3-prong modes containing charged kaons and 1 π^0 .

Branching fractions from the constrained fit are derived from a set of basis modes. The basis modes form an exclusive set whose branching fractions are constrained to sum exactly to one. The set of selected basis modes expands as branching fraction measurements for new τ -decay modes are published. The number of basis modes has expanded from 12 in the year 1994 fit to 31 in the 2002 through 2010 fits. The 31 basis modes selected for the 2010 fit are listed in Table 1. See the 1996 edition of this *Review* [1] for a complete description of our notation for naming τ -decay modes and the selection of the basis modes. For each edition since the 1996 edition, the changes in the selected basis modes from the previous edition are described in the τ Branching Fractions Review. Figure 2 illustrates the basis mode branching fractions from the 2010 fit.

Table 1: Basis modes and fit values(%) for the 2010 fit to τ branching fraction data.

$e^- \bar{\nu}_e \nu_\tau$	17.85 ± 0.05
$\mu^- \bar{\nu}_\mu \nu_\tau$	17.36 ± 0.05
$\pi^- \nu_\tau$	10.91 ± 0.07
$\pi^- \pi^0 \nu_\tau$	25.51 ± 0.09
$\pi^- 2\pi^0 \nu_\tau$ (ex. K^0)	9.29 ± 0.11
$\pi^- 3\pi^0 \nu_\tau$ (ex. K^0)	1.04 ± 0.07
$h^- 4\pi^0 \nu_\tau$ (ex. K^0, η)	0.11 ± 0.04
$K^- \nu_\tau$	0.696 ± 0.023
$K^- \pi^0 \nu_\tau$	0.429 ± 0.015
$K^- 2\pi^0 \nu_\tau$ (ex. K^0)	0.065 ± 0.023
$K^- 3\pi^0 \nu_\tau$ (ex. K^0, η)	0.049 ± 0.023
$\pi^- \bar{K}^0 \nu_\tau$	0.84 ± 0.04
$\pi^- \bar{K}^0 \pi^0 \nu_\tau$	0.40 ± 0.04
$\pi^- K_S^0 K_S^0 \nu_\tau$	0.024 ± 0.005
$\pi^- K_S^0 K_L^0 \nu_\tau$	0.12 ± 0.04
$K^- K^0 \nu_\tau$	0.159 ± 0.016
$K^- K^0 \pi^0 \nu_\tau$	0.159 ± 0.020
$\pi^- \pi^+ \pi^- \nu_\tau$ (ex. K^0, ω)	9.00 ± 0.06
$\pi^- \pi^+ \pi^- \pi^0 \nu_\tau$ (ex. K^0, ω)	2.70 ± 0.08
$K^- \pi^+ \pi^- \nu_\tau$ (ex. K^0)	0.287 ± 0.016
$K^- \pi^+ \pi^- \pi^0 \nu_\tau$ (ex. K^0, η)	0.077 ± 0.012
$K^- K^+ \pi^- \nu_\tau$	0.140 ± 0.005
$K^- K^+ \pi^- \pi^0 \nu_\tau$	0.0061 ± 0.0025
$h^- h^- h^+ 2\pi^0 \nu_\tau$ (ex. K^0, ω, η)	0.10 ± 0.04
$h^- h^- h^+ 3\pi^0 \nu_\tau$	0.023 ± 0.007
$3h^- 2h^+ \nu_\tau$ (ex. K^0)	0.0839 ± 0.0035
$3h^- 2h^+ \pi^0 \nu_\tau$ (ex. K^0)	0.0178 ± 0.0027
$h^- \omega \nu_\tau$	1.99 ± 0.08
$h^- \omega \pi^0 \nu_\tau$	0.41 ± 0.04
$\eta \pi^- \pi^0 \nu_\tau$	0.139 ± 0.010
$\eta K^- \nu_\tau$	0.0161 ± 0.0011

In selecting the basis modes, assumptions and choices must be made. For example, we assume the decays $\tau^- \rightarrow \pi^- K^+ \pi^- \geq 0\pi^0 \nu_\tau$ and $\tau^- \rightarrow \pi^+ K^- K^- \geq 0\pi^0 \nu_\tau$ have negligible branching fractions. This is consistent with standard model predictions for τ decay, although the experimental limits for these branching fractions are not very stringent. The 95% confidence level upper limits for these branching fractions in the current Listings are $B(\tau^- \rightarrow \pi^- K^+ \pi^- \geq 0\pi^0 \nu_\tau) < 0.25\%$ and $B(\tau^- \rightarrow \pi^+ K^- K^- \geq 0\pi^0 \nu_\tau) < 0.09\%$, values not so different from measured branching fractions for allowed 3-prong modes containing charged kaons. Although our usual goal is to impose as few theoretical constraints as possible so that the world averages and fit results can be used to test the theoretical constraints (*i.e.*, we do not make use of the theoretical constraint from lepton universality on the ratio of the τ -leptonic branching fractions $B(\tau^- \rightarrow \mu^- \bar{\nu}_\mu \nu_\tau) / B(\tau^- \rightarrow e^- \bar{\nu}_e \nu_\tau) = 0.9726$), the experimental challenge to identify charged prongs in 3-prong τ decays is sufficiently difficult that experimenters have been

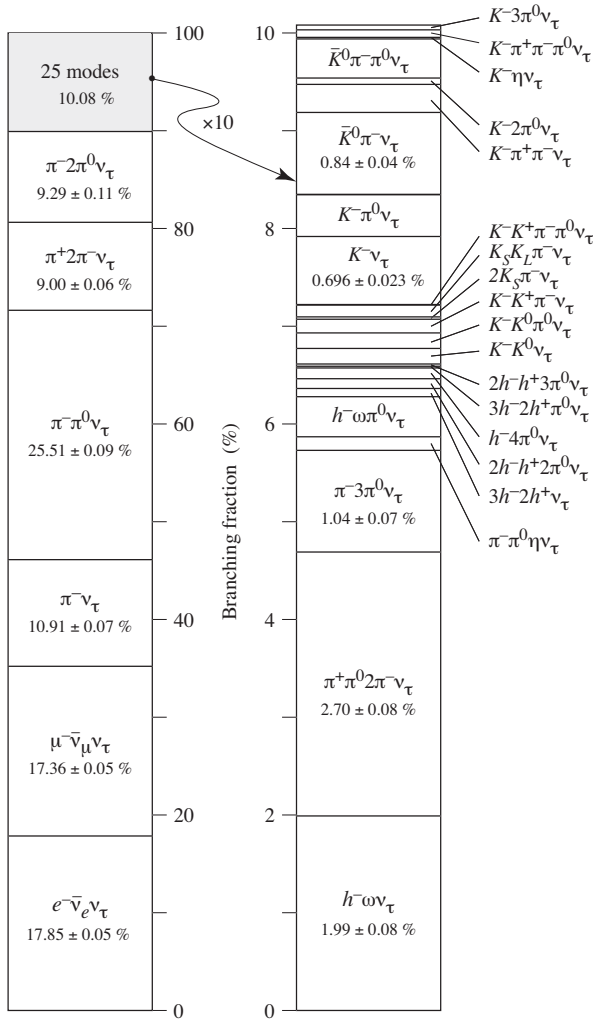


Figure 2: Basis mode branching fractions of the τ . Six modes account for 90% of the decays, 25 modes account for the last 10%. The list of excluded intermediate states for each basis mode has been suppressed.

forced to make these assumptions when measuring the branching fractions of the allowed decays. We are constrained by the assumptions made by the experimenters.

There are several τ -decay modes with small but well-measured (> 2.5 sigma from zero) branching fractions [2] which cannot be expressed in terms of the selected basis modes and are therefore left out of the fit:

$$\begin{aligned} B(\tau^- \rightarrow \pi^- K_S^0 K_L^0 \pi^0 \nu_\tau) &= (3.1 \pm 1.2) \times 10^{-4} \\ B(\tau^- \rightarrow 2K^- K^+ \nu_\tau) &= (0.158 \pm 0.018) \times 10^{-4} \\ B(\tau^- \rightarrow \eta K^- \pi^0 \nu_\tau) &= (0.48 \pm 0.12) \times 10^{-4} \\ B(\tau^- \rightarrow \eta \bar{K}^0 \pi^- \nu_\tau) &= (0.93 \pm 0.15) \times 10^{-4}. \end{aligned}$$

Certain components of other small but well-measured τ -decay modes cannot be expressed in terms of the selected basis modes and therefore are also left out of the fit:

$$B(\tau^- \rightarrow \eta \pi^- \pi^0 \pi^0 \nu_\tau) \times$$

$$B(\eta \rightarrow \gamma\gamma \text{ or } \eta \rightarrow \pi^+ \pi^- \gamma \text{ or } \eta \rightarrow 3\pi^0) = (1.1 \pm 0.4) \times 10^{-4},$$

$$B(\tau^- \rightarrow \eta \pi^- \pi^+ \pi^- \nu_\tau) \times$$

$$B(\eta \rightarrow \gamma\gamma \text{ or } \eta \rightarrow \pi^+ \pi^- \gamma) = (0.72 \pm 0.05) \times 10^{-4},$$

$$B(\tau^- \rightarrow \phi K^- \nu_\tau) \times$$

$$B(\phi \rightarrow K_S^0 K_L^0 \text{ or } \phi \rightarrow \eta\gamma) = (0.13 \pm 0.01) \times 10^{-4},$$

$$B(\tau^- \rightarrow f_1(1285) \pi^- \nu_\tau) B(f_1(1285) \rightarrow \rho^0 \gamma) = (0.20 \pm 0.06) \times 10^{-4},$$

$$B(\tau^- \rightarrow h^- \omega \pi^0 \pi^0 \nu_\tau) B(\omega \rightarrow \pi^0 \gamma) = (0.12 \pm 0.04) \times 10^{-4},$$

$$B(\tau^- \rightarrow 2h^- h^+ \omega \nu_\tau) B(\omega \rightarrow \pi^0 \gamma) = (0.10 \pm 0.02) \times 10^{-4}.$$

The sum of these excluded branching fractions is $(0.07 \pm 0.01)\%$. This is near our goal of 0.1% for the internal consistency of the τ Listings for this edition, and thus for simplicity we do not include these small branching fraction decay modes in the basis set.

Beginning with the 2002 edition, the fit algorithm has been improved to allow for correlations between branching fraction measurements used in the fit. If only a few measurements are correlated, the correlation coefficients are listed in the footnote for each measurement. If a large number of measurements are correlated, then the full correlation matrix is listed in the footnote to the measurement that first appears in the τ Listings. Footnotes to the other measurements refer to the first measurement. For example, the large correlation matrices for the branching fraction measurements contained in Refs. [3,4] are listed in Footnotes to the $\Gamma(e^- \bar{\nu}_e \nu_\tau) / \Gamma_{\text{total}}$ and $\Gamma(h^- \nu_\tau) / \Gamma_{\text{total}}$ measurements respectively. Sometimes experimental papers contain correlation coefficients between measurements using only statistical errors without including systematic errors. We usually cannot make use of these correlation coefficients.

The 2010 constrained fit has a χ^2 of 102.9 for 103 degrees of freedom up from 95.7 for 100 degrees of freedom in the 2008 fit. Two basis-mode branching fractions changed by more than 1.0σ from their 2008 values, $B(\eta \pi^- \pi^0 \nu_\tau)$ and $B(\eta K^- \nu_\tau)$, due to new measurements by the Belle Collaboration [5] of τ -decay modes containing η 's.

Overconsistency of Leptonic Branching Fraction Measurements:

To minimize the effects of older experiments which often have larger systematic errors and sometimes make assumptions that have later been shown to be invalid, we exclude old measurements in decay modes which contain at least several newer data of much higher precision. As a rule, we exclude those experiments with large errors which together would contribute no more than 5% of the weight in the average. This procedure leaves five measurements for $B_e \equiv B(\tau^- \rightarrow e^- \bar{\nu}_e \nu_\tau)$ and five measurements for $B_\mu \equiv B(\tau^- \rightarrow \mu^- \bar{\nu}_\mu \nu_\tau)$. For both B_e and B_μ , the selected measurements are considerably more consistent with each other than should be expected from the quoted errors on the individual measurements. The χ^2 from the calculation of the average of the selected measurements is 0.34 for B_e and 0.08 for B_μ . Assuming normal errors, the probability of a smaller χ^2 is 1.3% for B_e and 0.08% for B_μ .

Lepton Particle Listings

 τ

References

1. R.M. Barnett *et al.* (Particle Data Group), *Review of Particle Physics*, Phys. Rev. **D54**, 1 (1996).
2. See the τ Listings for references.
3. S. Schael *et al.* (Alep Collab.), Phys. Rep. **421**, 191 (2005).
4. J. Abdallah *et al.* (Delphi Collab.), Eur. Phys. J. **C46**, 1 (2006).
5. K. Inami *et al.* (Belle Collab.), Phys. Lett. **B672**, 209 (2009).

 τ^- BRANCHING RATIOS

$$\Gamma(\text{particle}^- \geq 0 \text{ neutrals} \geq 0K^0 \nu_\tau (\text{"1-prong"})) / \Gamma_{\text{total}} \quad \Gamma_1 / \Gamma$$

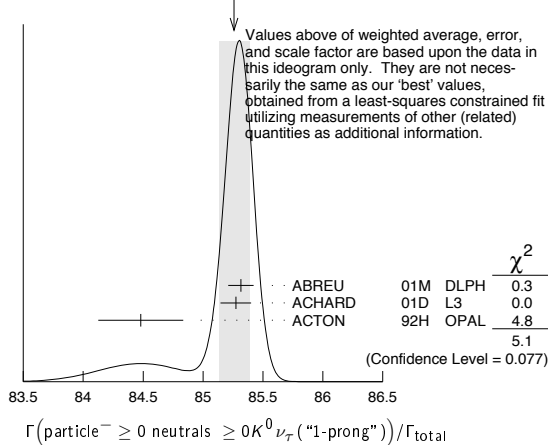
$$\Gamma_1 / \Gamma = (\Gamma_3 + \Gamma_5 + \Gamma_9 + \Gamma_{10} + \Gamma_{14} + \Gamma_{16} + \Gamma_{20} + \Gamma_{23} + \Gamma_{27} + \Gamma_{28} + \Gamma_{30} + \Gamma_{35} + \Gamma_{37} + \Gamma_{40} + \Gamma_{42} + 2\Gamma_{47} + \Gamma_{48} + 0.708\Gamma_{126} + 0.715\Gamma_{128} + 0.09\Gamma_{150} + 0.09\Gamma_{152}) / \Gamma$$

The charged particle here can be e , μ , or hadron. In many analyses, the sum of the topological branching fractions (1, 3, and 5 prongs) is constrained to be unity. Since the 5-prong fraction is very small, the measured 1-prong and 3-prong fractions are highly correlated and cannot be treated as independent quantities in our overall fit. We arbitrarily choose to use the 3-prong fraction in our fit, and leave the 1-prong fraction out. We do, however, use these 1-prong measurements in our average below. The measurements used only for the average are marked "avg," whereas "f&a" marks a result used for the fit and the average.

VALUE (%)	EVTS	DOCUMENT ID	TECN	COMMENT
85.36 ± 0.08 OUR FIT	Error includes scale factor of 1.3.			
85.26 ± 0.13 OUR AVERAGE	Error includes scale factor of 1.6. See the ideogram below.			
85.316 ± 0.093 ± 0.049	avg 78k	¹ ABREU	01M DLPH	1992-1995 LEP runs
85.274 ± 0.105 ± 0.073	avg	² ACHARD	01D L3	1992-1995 LEP runs
84.48 ± 0.27 ± 0.23	avg	ACTON	92H OPAL	1990-1991 LEP runs
••• We do not use the following data for averages, fits, limits, etc. •••				
85.45 ± 0.69		DECAMP	92c ALEP	Repl. by SCHAEEL 05c
-0.73 ± 0.65				

- 1 The correlation coefficients between this measurement and the ABREU 01M measurements of $B(\tau \rightarrow 3\text{-prong})$ and $B(\tau \rightarrow 5\text{-prong})$ are -0.98 and -0.08 respectively.
- 2 The correlation coefficients between this measurement and the ACHARD 01D measurements of $B(\tau \rightarrow 3\text{-prong})$ and $B(\tau \rightarrow 5\text{-prong})$ are -0.978 and -0.082 respectively.

WEIGHTED AVERAGE
85.26 ± 0.13 (Error scaled by 1.6)



$$\Gamma(\text{particle}^- \geq 0 \text{ neutrals} \geq 0K^0 \nu_\tau) / \Gamma_{\text{total}} \quad \Gamma_2 / \Gamma$$

$$\Gamma_2 / \Gamma = (\Gamma_3 + \Gamma_5 + \Gamma_9 + \Gamma_{10} + \Gamma_{14} + \Gamma_{16} + \Gamma_{20} + \Gamma_{23} + \Gamma_{27} + \Gamma_{28} + \Gamma_{30} + 0.6569\Gamma_{35} + 0.6569\Gamma_{37} + 0.6569\Gamma_{40} + 0.6569\Gamma_{42} + 1.0985\Gamma_{47} + 0.3139\Gamma_{48} + 0.708\Gamma_{126} + 0.715\Gamma_{128} + 0.09\Gamma_{150} + 0.09\Gamma_{152}) / \Gamma$$

VALUE (%)	EVTS	DOCUMENT ID	TECN	COMMENT
84.72 ± 0.08 OUR FIT	Error includes scale factor of 1.4.			
85.1 ± 0.4 OUR AVERAGE				
85.6 ± 0.6 ± 0.3	avg 3300	¹ ADEVA	91F L3	$E_{\text{cm}}^{\text{ee}} = 88.3\text{--}94.3$ GeV
84.9 ± 0.4 ± 0.3	avg	BEHREND	89B CELL	$E_{\text{cm}}^{\text{ee}} = 14\text{--}47$ GeV
84.7 ± 0.8 ± 0.6	avg	² AIHARA	87B TPC	$E_{\text{cm}}^{\text{ee}} = 29$ GeV
••• We do not use the following data for averages, fits, limits, etc. •••				
86.4 ± 0.3 ± 0.3		ABACHI	89B HRS	$E_{\text{cm}}^{\text{ee}} = 29$ GeV
87.1 ± 1.0 ± 0.7		³ BURCHAT	87 MRK2	$E_{\text{cm}}^{\text{ee}} = 29$ GeV
87.2 ± 0.5 ± 0.8		SCHMIDKE	86 MRK2	$E_{\text{cm}}^{\text{ee}} = 29$ GeV
84.7 ± 1.1 ± 1.6	169	⁴ ALTHOFF	85 TASS	$E_{\text{cm}}^{\text{ee}} = 34.5$ GeV
-1.3 ± 0.9		BARTEL	85F JADE	$E_{\text{cm}}^{\text{ee}} = 34.6$ GeV
86.1 ± 0.5 ± 0.9		⁵ BERGER	85 PLUT	$E_{\text{cm}}^{\text{ee}} = 34.6$ GeV
87.8 ± 1.3 ± 3.9		FERNANDEZ	85 MAC	$E_{\text{cm}}^{\text{ee}} = 29$ GeV
86.7 ± 0.3 ± 0.6				

- 1 Not independent of ADEVA 91F $\Gamma(h^- h^- h^+ \geq 0 \text{ neutrals} \geq 0K^0 \nu_\tau) / \Gamma_{\text{total}}$ value.
- 2 Not independent of AIHARA 87B $\Gamma(\mu^- \bar{\nu}_\mu \nu_\tau) / \Gamma_{\text{total}}$, $\Gamma(e^- \bar{\nu}_e \nu_\tau) / \Gamma_{\text{total}}$, and $\Gamma(h^- \geq 0 \text{ neutrals} \geq 0K^0 \nu_\tau) / \Gamma_{\text{total}}$ values.
- 3 Not independent of SCHMIDKE 86 value (also not independent of BURCHAT 87 value for $\Gamma(h^- h^- h^+ \geq 0 \text{ neutrals} \geq 0K^0 \nu_\tau) / \Gamma_{\text{total}}$).
- 4 Not independent of ALTHOFF 85 $\Gamma(\mu^- \bar{\nu}_\mu \nu_\tau) / \Gamma_{\text{total}}$, $\Gamma(e^- \bar{\nu}_e \nu_\tau) / \Gamma_{\text{total}}$, $\Gamma(h^- \geq 0 \text{ neutrals} \geq 0K^0 \nu_\tau) / \Gamma_{\text{total}}$, and $\Gamma(h^- h^- h^+ \geq 0 \text{ neutrals} \geq 0K^0 \nu_\tau) / \Gamma_{\text{total}}$ values.
- 5 Not independent of (1-prong + $0\pi^0$) and (1-prong + $\geq 1\pi^0$) values.

$\Gamma(\mu^- \bar{\nu}_\mu \nu_\tau) / \Gamma_{\text{total}} \quad \Gamma_3 / \Gamma$
Data marked "avg" are highly correlated with data appearing elsewhere in the Listings, and are therefore used for the average given below but not in the overall fits. "f&a" marks results used for the fit and the average.

To minimize the effect of experiments with large systematic errors, we exclude experiments which together would contribute 5% of the weight in the average.

VALUE (%)	EVTS	DOCUMENT ID	TECN	COMMENT
17.36 ± 0.05 OUR FIT				
17.33 ± 0.05 OUR AVERAGE				
17.319 ± 0.070 ± 0.032 f&a	54k	¹ SCHAEEL	05c ALEP	1991-1995 LEP runs
17.34 ± 0.09 ± 0.06 f&a	31.4k	ABBIENDI	03 OPAL	1990-1995 LEP runs
17.342 ± 0.110 ± 0.067 f&a	21.5k	² ACCIARRI	01F L3	1991-1995 LEP runs
17.325 ± 0.095 ± 0.077 f&a	27.7k	ABREU	99x DLPH	1991-1995 LEP runs
17.37 ± 0.08 ± 0.18 avg		³ ANASTASSOV	97 CLEO	$E_{\text{cm}}^{\text{ee}} = 10.6$ GeV
••• We do not use the following data for averages, fits, limits, etc. •••				
17.31 ± 0.11 ± 0.05	20.7k	BUSKULIC	96c ALEP	Repl. by SCHAEEL 05c
17.02 ± 0.19 ± 0.24	6586	ABREU	95T DLPH	Repl. by ABREU 99x
17.36 ± 0.27	7941	AKERS	95i OPAL	Repl. by ABBI-ENDDI 03
17.6 ± 0.4 ± 0.4	2148	ADRIANI	93M L3	Repl. by ACCIA-RRI 01F
17.4 ± 0.3 ± 0.5		⁴ ALBRECHT	93G ARG	$E_{\text{cm}}^{\text{ee}} = 9.4\text{--}10.6$ GeV
17.35 ± 0.41 ± 0.37		DECAMP	92c ALEP	1989-1990 LEP runs
17.7 ± 0.8 ± 0.4	568	BEHREND	90 CELL	$E_{\text{cm}}^{\text{ee}} = 35$ GeV
17.4 ± 1.0	2197	ADEVA	88 MRKJ	$E_{\text{cm}}^{\text{ee}} = 14\text{--}16$ GeV
17.7 ± 1.2 ± 0.7		AIHARA	87B TPC	$E_{\text{cm}}^{\text{ee}} = 29$ GeV
18.3 ± 0.9 ± 0.8		BURCHAT	87 MRK2	$E_{\text{cm}}^{\text{ee}} = 29$ GeV
18.6 ± 0.8 ± 0.7	558	⁵ BARTEL	86D JADE	$E_{\text{cm}}^{\text{ee}} = 34.6$ GeV
12.9 ± 1.7 ± 0.7		ALTHOFF	85 TASS	$E_{\text{cm}}^{\text{ee}} = 34.5$ GeV
18.0 ± 0.9 ± 0.5	473	⁵ ASH	85B MAC	$E_{\text{cm}}^{\text{ee}} = 29$ GeV
18.0 ± 1.0 ± 0.6		⁶ BALTRUSAITIS	85 MRK3	$E_{\text{cm}}^{\text{ee}} = 3.77$ GeV
19.4 ± 1.6 ± 1.7	153	BERGER	85 PLUT	$E_{\text{cm}}^{\text{ee}} = 34.6$ GeV
17.6 ± 2.6 ± 2.1	47	BEHREND	83c CELL	$E_{\text{cm}}^{\text{ee}} = 34$ GeV
17.8 ± 2.0 ± 1.8		BERGER	81B PLUT	$E_{\text{cm}}^{\text{ee}} = 9\text{--}32$ GeV

- 1 See footnote to SCHAEEL 05c $\Gamma(\tau^- \rightarrow e^- \bar{\nu}_e \nu_\tau) / \Gamma_{\text{total}}$ measurement for correlations with other measurements.
- 2 The correlation coefficient between this measurement and the ACCIARRI 01F measurement of $B(\tau^- \rightarrow e^- \bar{\nu}_e \nu_\tau)$ is 0.08.
- 3 The correlation coefficients between this measurement and the ANASTASSOV 97 measurements of $B(e \bar{\nu}_e \nu_\tau)$, $B(\mu^- \bar{\nu}_\mu \nu_\tau) / B(e \bar{\nu}_e \nu_\tau)$, $B(h^- \nu_\tau)$, and $B(h^- \nu_\tau) / B(e \bar{\nu}_e \nu_\tau)$ are 0.50, 0.58, 0.50, and 0.08 respectively.
- 4 Not independent of ALBRECHT 92D $\Gamma(\mu^- \bar{\nu}_\mu \nu_\tau) / \Gamma(e^- \bar{\nu}_e \nu_\tau)$ and ALBRECHT 93G $\Gamma(\mu^- \bar{\nu}_\mu \nu_\tau) \times \Gamma(e^- \bar{\nu}_e \nu_\tau) / \Gamma_{\text{total}}^2$ values.
- 5 Modified using $B(e^- \bar{\nu}_e \nu_\tau) / B(1 \text{ prong})$ and $B(1 \text{ prong}) = 0.855$.
- 6 Error correlated with BALTRUSAITIS 85 $e \nu \nu_\tau$ value.

VALUE (%)	EVTS	DOCUMENT ID	TECN	COMMENT
0.361 ± 0.016 ± 0.035				
0.30 ± 0.04 ± 0.05	116	¹ BERGFELD	00 CLEO	$E_{\text{cm}}^{\text{ee}} = 10.6$ GeV
0.23 ± 0.10	10	² ALEXANDER	96s OPAL	1991-1994 LEP runs
		³ WU	90 MRK2	$E_{\text{cm}}^{\text{ee}} = 29$ GeV

- 1 BERGFELD 00 impose requirements on detected γ 's corresponding to a τ -rest-frame energy cutoff $E_\gamma^* > 10$ MeV. For $E_\gamma^* > 20$ MeV, they quote $(3.04 \pm 0.14 \pm 0.30) \times 10^{-3}$.
- 2 ALEXANDER 96s impose requirements on detected γ 's corresponding to a τ -rest-frame energy cutoff $E_\gamma > 20$ MeV.
- 3 WU 90 reports $\Gamma(\mu^- \bar{\nu}_\mu \nu_\tau \gamma) / \Gamma(\mu^- \bar{\nu}_\mu \nu_\tau) = 0.013 \pm 0.006$, which is converted to $\Gamma(\mu^- \bar{\nu}_\mu \nu_\tau \gamma) / \Gamma_{\text{total}}$ using $\Gamma(\mu^- \bar{\nu}_\mu \nu_\tau \gamma) / \Gamma_{\text{total}} = 1.735\%$. Requirements on detected γ 's correspond to a τ rest frame energy cutoff $E_\gamma > 37$ MeV.

$\Gamma(e^- \bar{\nu}_e \nu_\tau) / \Gamma_{\text{total}} \quad \Gamma_5 / \Gamma$
To minimize the effect of experiments with large systematic errors, we exclude experiments which together would contribute 5% of the weight in the average.

VALUE (%)	EVTS	DOCUMENT ID	TECN	COMMENT
17.85 ± 0.05 OUR FIT				
17.82 ± 0.05 OUR AVERAGE				
17.837 ± 0.072 ± 0.036	56k	¹ SCHAEEL	05c ALEP	1991-1995 LEP runs
17.806 ± 0.104 ± 0.076	24.7k	² ACCIARRI	01F L3	1991-1995 LEP runs
17.81 ± 0.09 ± 0.06	33.1k	ABBIENDI	99H OPAL	1991-1995 LEP runs
17.877 ± 0.109 ± 0.110	23.3k	ABREU	99x DLPH	1991-1995 LEP runs
17.76 ± 0.06 ± 0.17		³ ANASTASSOV	97 CLEO	$E_{\text{cm}}^{\text{ee}} = 10.6$ GeV

• • • We do not use the following data for averages, fits, limits, etc. • • •

17.78 ± 0.10 ± 0.09	25.3k	ALEXANDER	96D	OPAL	Repl. by ABBI-ENDI ^{99H}
17.79 ± 0.12 ± 0.06	20.6k	BUSKULIC	96C	ALEP	Repl. by SCHAEEL 05c
17.51 ± 0.23 ± 0.31	5059	ABREU	95T	DLPH	Repl. by ABREU 99x
17.9 ± 0.4 ± 0.4	2892	ADRIANI	93M	L3	Repl. by ACCIARRI 01F
17.5 ± 0.3 ± 0.5		4 ALBRECHT	93G	ARG	$E_{cm}^{ee} = 9.4-10.6$ GeV
17.97 ± 0.14 ± 0.23	3970	AKERIB	92	CLEO	Repl. by ANASTASSOV 97
19.1 ± 0.4 ± 0.6	2960	5 AMMAR	92	CLEO	$E_{cm}^{ee} = 10.5-10.9$ GeV
18.09 ± 0.45 ± 0.45		DECAMP	92C	ALEP	Repl. by SCHAEEL 05c
17.0 ± 0.5 ± 0.6	1.7k	ABACHI	90	HRS	$E_{cm}^{ee} = 29$ GeV
18.4 ± 0.8 ± 0.4	644	BEHREND	90	CELL	$E_{cm}^{ee} = 35$ GeV
16.3 ± 0.3 ± 3.2		JANSSEN	89	CBAL	$E_{cm}^{ee} = 9.4-10.6$ GeV
18.4 ± 1.2 ± 1.0		AIHARA	87B	TPC	$E_{cm}^{ee} = 29$ GeV
19.1 ± 0.8 ± 1.1		BURCHAT	87	MRK2	$E_{cm}^{ee} = 29$ GeV
16.8 ± 0.7 ± 0.9	515	5 BARTEL	86D	JADE	$E_{cm}^{ee} = 34.6$ GeV
20.4 ± 3.0 ± 1.4		ALTHOFF	85	TASS	$E_{cm}^{ee} = 34.5$ GeV
17.8 ± 0.9 ± 0.6	390	5 ASH	85B	MAC	$E_{cm}^{ee} = 29$ GeV
18.2 ± 0.7 ± 0.5		6 BALTRUSAITIS	85	MRK3	$E_{cm}^{ee} = 3.77$ GeV
13.0 ± 1.9 ± 2.9		BERGER	85	PLUT	$E_{cm}^{ee} = 34.6$ GeV
18.3 ± 2.4 ± 1.9	60	BEHREND	83C	CELL	$E_{cm}^{ee} = 34$ GeV
16.0 ± 1.3	459	7 BACINO	78B	DLCO	$E_{cm}^{ee} = 3.1-7.4$ GeV

¹ Correlation matrix for SCHAEEL 05c branching fractions, in percent:

- (1) $\Gamma(\tau^- \rightarrow e^- \bar{\nu}_e \nu_\tau) / \Gamma_{total}$
- (2) $\Gamma(\tau^- \rightarrow \mu^- \bar{\nu}_\mu \nu_\tau) / \Gamma_{total}$
- (3) $\Gamma(\tau^- \rightarrow \pi^- \nu_\tau) / \Gamma_{total}$
- (4) $\Gamma(\tau^- \rightarrow \pi^- \pi^0 \nu_\tau) / \Gamma_{total}$
- (5) $\Gamma(\tau^- \rightarrow \pi^- 2\pi^0 \nu_\tau (ex. K^0)) / \Gamma_{total}$
- (6) $\Gamma(\tau^- \rightarrow \pi^- 3\pi^0 \nu_\tau (ex. K^0)) / \Gamma_{total}$
- (7) $\Gamma(\tau^- \rightarrow h^- 4\pi^0 \nu_\tau (ex. K^0, \eta)) / \Gamma_{total}$
- (8) $\Gamma(\tau^- \rightarrow \pi^- \pi^+ \pi^- \nu_\tau (ex. K^0, \omega)) / \Gamma_{total}$
- (9) $\Gamma(\tau^- \rightarrow \pi^- \pi^+ \pi^- \pi^0 \nu_\tau (ex. K^0)) / \Gamma_{total}$
- (10) $\Gamma(\tau^- \rightarrow h^- h^- h^+ 2\pi^0 \nu_\tau (ex. K^0)) / \Gamma_{total}$
- (11) $\Gamma(\tau^- \rightarrow h^- h^- h^+ 3\pi^0 \nu_\tau) / \Gamma_{total}$
- (12) $\Gamma(\tau^- \rightarrow 3h^- 2h^+ \nu_\tau (ex. K^0)) / \Gamma_{total}$
- (13) $\Gamma(\tau^- \rightarrow 3h^- 2h^+ \pi^0 \nu_\tau (ex. K^0)) / \Gamma_{total}$

(1)	(2)	(3)	(4)	(5)	(6)	(7)	(8)	(9)	(10)	(11)	(12)	(13)
(2)	-20											
(3)	-9	-6										
(4)	-16	-12	2									
(5)	-5	-5	-17	-37								
(6)	0	-4	-15	2	-27							
(7)	-2	-4	-24	-15	20	-47						
(8)	-14	-9	15	-5	-17	-14	-8					
(9)	-13	-12	-25	-30	4	-2	16	-15				
(10)	0	-2	-23	-14	4	10	13	-6	-17			
(11)	1	0	-5	1	4	6	0	-9	-2	-11		
(12)	0	1	9	4	-8	-4	-6	9	-5	-4	-2	
(13)	1	-4	-3	-5	3	2	-4	-3	-1	4	-24	

² The correlation coefficient between this measurement and the ACCIARRI 01F measurement of $B(\tau^- \rightarrow \mu^- \bar{\nu}_\mu \nu_\tau)$ is 0.08.

³ The correlation coefficients between this measurement and the ANASTASSOV 97 measurements of $B(\mu^- \bar{\nu}_\mu \nu_\tau)$, $B(\mu^- \bar{\nu}_\mu \nu_\tau) / B(e^- \bar{\nu}_e \nu_\tau)$, $B(h^- \nu_\tau)$, and $B(h^- \nu_\tau) / B(e^- \bar{\nu}_e \nu_\tau)$ are 0.50, -0.42, 0.48, and -0.39 respectively.

⁴ Not independent of ALBRECHT 92D $\Gamma(\mu^- \bar{\nu}_\mu \nu_\tau) / \Gamma(e^- \bar{\nu}_e \nu_\tau)$ and ALBRECHT 93G $\Gamma(\mu^- \bar{\nu}_\mu \nu_\tau) \times \Gamma(e^- \bar{\nu}_e \nu_\tau) / \Gamma_{total}^2$ values.

⁵ Modified using $B(e^- \bar{\nu}_e \nu_\tau) / B(\pi^- \nu_\tau)$ and $B(\pi^- \nu_\tau) / B(e^- \bar{\nu}_e \nu_\tau)$ = 0.855.

⁶ Error correlated with BALTRUSAITIS 85 $\Gamma(\mu^- \bar{\nu}_\mu \nu_\tau) / \Gamma_{total}$.

⁷ BACINO 78B value comes from fit to events with e^\pm and one other nonelectron charged prong.

$\Gamma(\mu^- \bar{\nu}_\mu \nu_\tau) / \Gamma(e^- \bar{\nu}_e \nu_\tau)$ Γ_3 / Γ_5

Standard Model prediction including mass effects is 0.9726.

Data marked "avg" are highly correlated with data appearing elsewhere in the Listings, and are therefore used for the average given below but not in the overall fits. "f&a" marks results used for the fit and the average.

VALUE	DOCUMENT ID	TECN	COMMENT
0.973 ± 0.004 OUR FIT			
0.978 ± 0.011 OUR AVERAGE			
0.9777 ± 0.0063 ± 0.0087	f&a	1 ANASTASSOV 97	CLEO $E_{cm}^{ee} = 10.6$ GeV
0.997 ± 0.035 ± 0.040	f&a	ALBRECHT 92D	ARG $E_{cm}^{ee} = 9.4-10.6$ GeV

¹ The correlation coefficients between this measurement and the ANASTASSOV 97 measurements of $B(\mu^- \bar{\nu}_\mu \nu_\tau)$, $B(e^- \bar{\nu}_e \nu_\tau)$, $B(h^- \nu_\tau)$, and $B(h^- \nu_\tau) / B(e^- \bar{\nu}_e \nu_\tau)$ are 0.58, -0.42, 0.07, and 0.45 respectively.

$\Gamma(e^- \bar{\nu}_e \nu_\tau \gamma) / \Gamma_{total}$ Γ_6 / Γ

VALUE (%)	DOCUMENT ID	TECN	COMMENT
1.75 ± 0.06 ± 0.17	1 BERGFELD	00	CLEO $E_{cm}^{ee} = 10.6$ GeV

¹ BERGFELD 00 impose requirements on detected γ 's corresponding to a τ -rest-frame energy cutoff $E_\gamma^* > 10$ MeV.

$\Gamma(h^- \geq 0K_L^0 \nu_\tau) / \Gamma_{total}$ Γ_7 / Γ

$\Gamma_7 / \Gamma = (\Gamma_9 + \Gamma_{10} + \frac{1}{2}\Gamma_{35} + \frac{1}{2}\Gamma_{37} + \Gamma_{47}) / \Gamma$

Data marked "avg" are highly correlated with data appearing elsewhere in the Listings, and are therefore used for the average given below but not in the overall fits. "f&a" marks results used for the fit and the average.

VALUE (%)	EVTS	DOCUMENT ID	TECN	COMMENT
12.13 ± 0.07 OUR FIT				Error includes scale factor of 1.1.
12.2 ± 0.4 OUR AVERAGE				
12.47 ± 0.26 ± 0.43	f&a 2967	1 ACCIARRI 95	L3	1992 LEP run
12.4 ± 0.7 ± 0.7	f&a 283	2 ABREU 92N	DLPH	1990 LEP run
12.1 ± 0.7 ± 0.5	f&a 309	ALEXANDER 91D	OPAL	1990 LEP run
11.3 ± 0.5 ± 0.8	avg 798	3 FORD 87	MAC	$E_{cm}^{ee} = 29$ GeV

• • • We do not use the following data for averages, fits, limits, etc. • • •

12.44 ± 0.11 ± 0.11	15k	4 BUSKULIC 96	ALEP	Repl. by SCHAEEL 05c
11.7 ± 0.6 ± 0.8		5 ALBRECHT 92D	ARG	$E_{cm}^{ee} = 9.4-10.6$ GeV
12.98 ± 0.44 ± 0.33		6 DECAMP 92C	ALEP	Repl. by SCHAEEL 05c
12.3 ± 0.9 ± 0.5	1338	BEHREND 90	CELL	$E_{cm}^{ee} = 35$ GeV
11.1 ± 1.1 ± 1.4		7 BURCHAT 87	MRK2	$E_{cm}^{ee} = 29$ GeV
12.3 ± 0.6 ± 1.1	328	8 BARTEL 86D	JADE	$E_{cm}^{ee} = 34.6$ GeV
13.0 ± 2.0 ± 4.0		BERGER 85	PLUT	$E_{cm}^{ee} = 34.6$ GeV
11.2 ± 1.7 ± 1.2	34	9 BEHREND 83C	CELL	$E_{cm}^{ee} = 34$ GeV

¹ ACCIARRI 95 with 0.65% added to remove their correction for $\pi^- K_L^0$ backgrounds.

² ABREU 92N with 0.5% added to remove their correction for $K^*(892)^-$ backgrounds.

³ FORD 87 result for $B(\pi^- \nu_\tau)$ with 0.67% added to remove their K^- correction and adjusted for 1992 B("1 prong").

⁴ BUSKULIC 96 quote $11.78 \pm 0.11 \pm 0.13$ We add 0.66 to undo their correction for unseen K_L^0 and modify the systematic error accordingly.

⁵ Not independent of ALBRECHT 92D $\Gamma(\mu^- \bar{\nu}_\mu \nu_\tau) / \Gamma(e^- \bar{\nu}_e \nu_\tau)$, $\Gamma(\mu^- \bar{\nu}_\mu \nu_\tau) \times \Gamma(e^- \bar{\nu}_e \nu_\tau)$, and $\Gamma(h^- \geq 0K_L^0 \nu_\tau) / \Gamma(e^- \bar{\nu}_e \nu_\tau)$ values.

⁶ DECAMP 92C quote $B(h^- \geq 0K_L^0 \nu_\tau) \geq 0 (K_S^0 \rightarrow \pi^+ \pi^-) / \Gamma_{total} = 13.32 \pm 0.44 \pm 0.33$. We subtract 0.35 to correct for their inclusion of the K_S^0 decays.

⁷ BURCHAT 87 with 1.1% added to remove their correction for K^- and $K^*(892)^-$ backgrounds.

⁸ BARTEL 86D result for $B(\pi^- \nu_\tau)$ with 0.59% added to remove their K^- correction and adjusted for 1992 B("1 prong").

⁹ BEHREND 83C quote $B(\pi^- \nu_\tau) = 9.9 \pm 1.7 \pm 1.3$ after subtracting 1.3 ± 0.5 to correct for $B(K^- \nu_\tau)$.

$\Gamma(h^- \nu_\tau) / \Gamma_{total}$ $\Gamma_8 / \Gamma = (\Gamma_9 + \Gamma_{10}) / \Gamma$

Data marked "avg" are highly correlated with data appearing elsewhere in the Listings, and are therefore used for the average given below but not in the overall fits. "f&a" marks results used for the fit and the average.

VALUE (%)	EVTS	DOCUMENT ID	TECN	COMMENT
11.61 ± 0.06 OUR FIT				Error includes scale factor of 1.1.
11.63 ± 0.12 OUR AVERAGE				Error includes scale factor of 1.4. See the ideogram below.
11.571 ± 0.120 ± 0.114	f&a 19k	1 ABDALLAH 06A	DLPH	1992-1995 LEP runs
11.98 ± 0.13 ± 0.16	f&a	ACKERSTAFF 98M	OPAL	1991-1995 LEP runs
11.52 ± 0.05 ± 0.12	f&a	2 ANASTASSOV 97	CLEO	$E_{cm}^{ee} = 10.6$ GeV

¹ Correlation matrix for ABDALLAH 06A branching fractions, in percent:

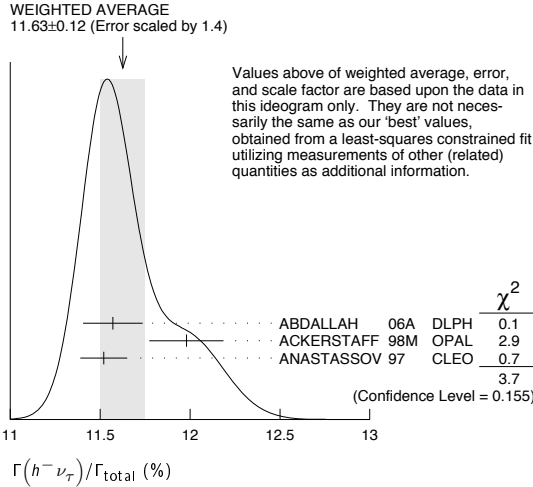
- (1) $\Gamma(\tau^- \rightarrow h^- \nu_\tau) / \Gamma_{total}$
- (2) $\Gamma(\tau^- \rightarrow h^- \pi^0 \nu_\tau) / \Gamma_{total}$
- (3) $\Gamma(\tau^- \rightarrow h^- \geq 1\pi^0 \nu_\tau (ex. K^0)) / \Gamma_{total}$
- (4) $\Gamma(\tau^- \rightarrow h^- 2\pi^0 \nu_\tau (ex. K^0)) / \Gamma_{total}$
- (5) $\Gamma(\tau^- \rightarrow h^- \geq 3\pi^0 \nu_\tau (ex. K^0)) / \Gamma_{total}$
- (6) $\Gamma(\tau^- \rightarrow h^- h^- h^+ \nu_\tau (ex. K^0)) / \Gamma_{total}$
- (7) $\Gamma(\tau^- \rightarrow h^- h^- h^+ \pi^0 \nu_\tau (ex. K^0)) / \Gamma_{total}$
- (8) $\Gamma(\tau^- \rightarrow h^- h^- h^+ \geq 1\pi^0 \nu_\tau (ex. K^0)) / \Gamma_{total}$
- (9) $\Gamma(\tau^- \rightarrow h^- h^- h^+ \geq 2\pi^0 \nu_\tau (ex. K^0)) / \Gamma_{total}$
- (10) $\Gamma(\tau^- \rightarrow 3h^- 2h^+ \nu_\tau (ex. K^0)) / \Gamma_{total}$
- (11) $\Gamma(\tau^- \rightarrow 3h^- 2h^+ \pi^0 \nu_\tau (ex. K^0)) / \Gamma_{total}$

(1)	(2)	(3)	(4)	(5)	(6)	(7)	(8)	(9)	(10)	(11)
(2)	-34									
(3)	-47	56								
(4)	6	-66	15							
(5)	-6	38	11	-86						
(6)	-7	-8	15	0	-2					
(7)	-2	-1	-5	-3	3	-53				
(8)	-4	-4	-13	-4	-2	-56	75			
(9)	-1	-1	-4	3	-6	26	-78	-16		
(10)	-1	-1	1	0	0	-2	-3	-1	3	
(11)	0	0	0	0	0	1	0	-5	5	-57

Lepton Particle Listings

 τ

²The correlation coefficients between this measurement and the ANASTASSOV 97 measurements of $B(\mu\bar{\nu}_\mu\nu_\tau)$, $B(e\bar{\nu}_e\nu_\tau)$, $B(\mu\bar{\nu}_\mu\nu_\tau)/B(e\bar{\nu}_e\nu_\tau)$, and $B(h^-\nu_\tau)/B(e\bar{\nu}_e\nu_\tau)$ are 0.50, 0.48, 0.07, and 0.63 respectively.


 $\Gamma(h^-\nu_\tau)/\Gamma(e^-\bar{\nu}_e\nu_\tau)$ $\Gamma_8/\Gamma_5 = (\Gamma_9+\Gamma_{10})/\Gamma_5$

Data marked "avg" are highly correlated with data appearing elsewhere in the Listings, and are therefore used for the average given below but not in the overall fits. "f&a" marks results used for the fit and the average.

VALUE	DOCUMENT ID	TECN	COMMENT
0.650 ± 0.004 OUR FIT			Error includes scale factor of 1.1.
0.6484 ± 0.0041 ± 0.0060 avg	¹ ANASTASSOV 97	CLEO	$E_{cm}^{ee} = 10.6$ GeV

¹The correlation coefficients between this measurement and the ANASTASSOV 97 measurements of $B(\mu\bar{\nu}_\mu\nu_\tau)$, $B(e\bar{\nu}_e\nu_\tau)$, $B(\mu\bar{\nu}_\mu\nu_\tau)/B(e\bar{\nu}_e\nu_\tau)$, and $B(h^-\nu_\tau)$ are 0.08, -0.39, 0.45, and 0.63 respectively.

 $\Gamma(\pi^-\nu_\tau)/\Gamma_{total}$ Γ_9/Γ

Data marked "avg" are highly correlated with data appearing elsewhere in the Listings, and are therefore used for the average given below but not in the overall fits. "f&a" marks results used for the fit and the average.

VALUE (%)	EVTs	DOCUMENT ID	TECN	COMMENT
10.91 ± 0.07 OUR FIT				Error includes scale factor of 1.1.
10.828 ± 0.070 ± 0.078 f&a	38k	¹ SCHAEL 05c	ALEP	1991-1995 LEP runs
•••				We do not use the following data for averages, fits, limits, etc. •••
11.06 ± 0.11 ± 0.14		² BUSKULIC 96	ALEP	Repl. by SCHAEL 05c
11.7 ± 0.4 ± 1.8	1138	BLOCKER 82d	MRK2	$E_{cm}^{ee} = 3.5-6.7$ GeV

¹See footnote to SCHAEL 05c $\Gamma(\tau^- \rightarrow e^-\bar{\nu}_e\nu_\tau)/\Gamma_{total}$ measurement for correlations with other measurements.

²Not independent of BUSKULIC 96 $B(h^-\nu_\tau)$ and $B(K^-\nu_\tau)$ values.

 $\Gamma(K^-\nu_\tau)/\Gamma_{total}$ Γ_{10}/Γ

VALUE (%)	EVTs	DOCUMENT ID	TECN	COMMENT
0.696 ± 0.023 OUR FIT				Error includes scale factor of 1.1.
0.685 ± 0.023 OUR AVERAGE				
0.658 ± 0.027 ± 0.029		¹ ABBIENDI 01j	OPAL	1990-1995 LEP runs
0.696 ± 0.025 ± 0.014	2032	BARATE 99k	ALEP	1991-1995 LEP runs
0.85 ± 0.18	27	ABREU 94k	DLPH	LEP 1992 Z data
0.66 ± 0.07 ± 0.09	99	BATTLE 94	CLEO	$E_{cm}^{ee} \approx 10.6$ GeV
•••				We do not use the following data for averages, fits, limits, etc. •••
0.72 ± 0.04 ± 0.04	728	BUSKULIC 96	ALEP	Repl. by BARATE 99k
0.59 ± 0.18	16	MILLS 84	DLCO	$E_{cm}^{ee} = 29$ GeV
1.3 ± 0.5	15	BLOCKER 82b	MRK2	$E_{cm}^{ee} = 3.9-6.7$ GeV

¹The correlation coefficient between this measurement and the ABBIENDI 01j $B(\tau^- \rightarrow K^- \geq 0\pi^0 \geq 0K^0 \geq 0\gamma\nu_\tau)$ is 0.60.

 $\Gamma(h^- \geq 1 \text{ neutrals } \nu_\tau)/\Gamma_{total}$ Γ_{11}/Γ

VALUE (%)	DOCUMENT ID	TECN	COMMENT
37.06 ± 0.10 OUR FIT			Error includes scale factor of 1.2.
•••			We do not use the following data for averages, fits, limits, etc. •••
36.14 ± 0.33 ± 0.58	¹ AKERS 94E	OPAL	1991-1992 LEP runs
38.4 ± 1.2 ± 1.0	² BURCHAT 87	MRK2	$E_{cm}^{ee} = 29$ GeV
42.7 ± 2.0 ± 2.9	BERGER 85	PLUT	$E_{cm}^{ee} = 34.6$ GeV

¹Not independent of ACKERSTAFF 98M $B(h^-\pi^0\nu_\tau)$ and $B(h^-\geq 2\pi^0\nu_\tau)$ values.

²BURCHAT 87 quote for $B(\pi^\pm \geq 1 \text{ neutral } \nu_\tau) = 0.378 \pm 0.012 \pm 0.010$. We add 0.006 to account for contribution from $(K^*\nu_\tau)$ which they fixed at BR = 0.013.

 $\Gamma(h^- \geq 1\pi^0\nu_\tau(\text{ex. } K^0))/\Gamma_{total}$ $\Gamma_{12}/\Gamma = (\Gamma_{14}+\Gamma_{16}+\Gamma_{20}+\Gamma_{23}+\Gamma_{27}+\Gamma_{28}+\Gamma_{30}+0.325\Gamma_{126}+0.325\Gamma_{128})/\Gamma$

VALUE (%)	EVTs	DOCUMENT ID	TECN	COMMENT
36.54 ± 0.11 OUR FIT				Error includes scale factor of 1.2.
36.641 ± 0.155 ± 0.127 avg	45k	¹ ABDALLAH 06A	DLPH	1992-1995 LEP runs

¹See footnote to ABDALLAH 06A $\Gamma(\tau^- \rightarrow h^-\nu_\tau)/\Gamma_{total}$ measurement for correlations with other measurements.

 $\Gamma(h^-\pi^0\nu_\tau)/\Gamma_{total}$ $\Gamma_{13}/\Gamma = (\Gamma_{14}+\Gamma_{16})/\Gamma$

VALUE (%)	EVTs	DOCUMENT ID	TECN	COMMENT
25.94 ± 0.09 OUR FIT				Error includes scale factor of 1.1.
25.73 ± 0.16 OUR AVERAGE				
25.67 ± 0.01 ± 0.39	5.4M	FUJIKAWA 08	BELL	$72 \text{ fb}^{-1} E_{cm}^{ee} = 10.6$ GeV
25.740 ± 0.201 ± 0.138	35k	¹ ABDALLAH 06A	DLPH	1992-1995 LEP runs
25.89 ± 0.17 ± 0.29		ACKERSTAFF 98M	OPAL	1991-1995 LEP runs
25.05 ± 0.35 ± 0.50	6613	ACCARI 95	L3	1992 LEP run
25.87 ± 0.12 ± 0.42	51k	² ARTUSO 94	CLEO	$E_{cm}^{ee} = 10.6$ GeV
•••				We do not use the following data for averages, fits, limits, etc. •••
25.76 ± 0.15 ± 0.13	31k	BUSKULIC 96	ALEP	Repl. by SCHAEL 05c
25.98 ± 0.36 ± 0.52		³ AKERS 94E	OPAL	Repl. by ACKERSTAFF 98M
22.9 ± 0.8 ± 1.3	283	⁴ ABREU 92N	DLPH	$E_{cm}^{ee} = 88.2-94.2$ GeV
23.1 ± 0.4 ± 0.9	1249	⁵ ALBRECHT 92Q	ARG	$E_{cm}^{ee} = 10$ GeV
25.02 ± 0.64 ± 0.88	1849	DECAMP 92c	ALEP	1989-1990 LEP runs
22.0 ± 0.8 ± 1.9	779	ANTREASYAN 91	CBAL	$E_{cm}^{ee} = 9.4-10.6$ GeV
22.6 ± 1.5 ± 0.7	1101	BEHREND 90	CELL	$E_{cm}^{ee} = 35$ GeV
23.1 ± 1.9 ± 1.6		BEHREND 84	CELL	$E_{cm}^{ee} = 14,22$ GeV

¹See footnote to ABDALLAH 06A $\Gamma(\tau^- \rightarrow h^-\nu_\tau)/\Gamma_{total}$ measurement for correlations with other measurements.

²ARTUSO 94 reports the combined result from three independent methods, one of which (23% of the $\tau^- \rightarrow h^-\pi^0\nu_\tau$) is normalized to the inclusive one-prong branching fraction, taken as 0.854 ± 0.004 . Renormalization to the present value causes negligible change.

³AKERS 94E quote $(26.25 \pm 0.36 \pm 0.52) \times 10^{-2}$; we subtract 0.27% from their number to correct for $\tau^- \rightarrow h^-K_L^0\nu_\tau$.

⁴ABREU 92N with 0.5% added to remove their correction for $K^*(892)^-$ backgrounds.

⁵ALBRECHT 92Q with 0.5% added to remove their correction for $\tau^- \rightarrow K^*(892)^-\nu_\tau$ background.

 $\Gamma(\pi^-\pi^0\nu_\tau)/\Gamma_{total}$ Γ_{14}/Γ

Data marked "avg" are highly correlated with data appearing elsewhere in the Listings, and are therefore used for the average given below but not in the overall fits. "f&a" marks results used for the fit and the average.

VALUE (%)	EVTs	DOCUMENT ID	TECN	COMMENT
25.51 ± 0.09 OUR FIT				Error includes scale factor of 1.1.
25.46 ± 0.12 OUR AVERAGE				
25.471 ± 0.097 ± 0.085 f&a	81k	¹ SCHAEL 05c	ALEP	1991-1995 LEP runs
25.36 ± 0.44 avg		² ARTUSO 94	CLEO	$E_{cm}^{ee} = 10.6$ GeV
•••				We do not use the following data for averages, fits, limits, etc. •••
25.30 ± 0.15 ± 0.13		³ BUSKULIC 96	ALEP	Repl. by SCHAEL 05c
21.5 ± 0.4 ± 1.9	4400	^{4,5} ALBRECHT 88L	ARG	$E_{cm}^{ee} = 10$ GeV
23.0 ± 1.3 ± 1.7	582	ADLER 87b	MRK3	$E_{cm}^{ee} = 3.77$ GeV
25.8 ± 1.7 ± 2.5		⁶ BURCHAT 87	MRK2	$E_{cm}^{ee} = 29$ GeV
22.3 ± 0.6 ± 1.4	629	⁵ YELTON 86	MRK2	$E_{cm}^{ee} = 29$ GeV

¹See footnote to SCHAEL 05c $\Gamma(\tau^- \rightarrow e^-\bar{\nu}_e\nu_\tau)/\Gamma_{total}$ measurement for correlations with other measurements.

²Not independent of ARTUSO 94 $B(h^-\pi^0\nu_\tau)$ and BATTLE 94 $B(K^-\pi^0\nu_\tau)$ values.

³Not independent of BUSKULIC 96 $B(h^-\pi^0\nu_\tau)$ and $B(K^-\pi^0\nu_\tau)$ values.

⁴The authors divide by $(\Gamma_3 + \Gamma_5 + \Gamma_9 + \Gamma_{10})/\Gamma = 0.467$ to obtain this result.

⁵Experiment had no hadron identification. Kaon corrections were made, but insufficient information is given to permit their removal.

⁶BURCHAT 87 value is not independent of YELTON 86 value. Nonresonant decays included.

 $\Gamma(\pi^-\pi^0 \text{ non-}\rho(770)\nu_\tau)/\Gamma_{total}$ Γ_{15}/Γ

VALUE (%)	DOCUMENT ID	TECN	COMMENT
0.3 ± 0.1 ± 0.3	¹ BEHREND 84	CELL	$E_{cm}^{ee} = 14,22$ GeV

¹BEHREND 84 assume a flat nonresonant mass distribution down to the $\rho(770)$ mass, using events with mass above 1300 to set the level.

 $\Gamma(K^-\pi^0\nu_\tau)/\Gamma_{total}$ Γ_{16}/Γ

VALUE (%)	EVTs	DOCUMENT ID	TECN	COMMENT
0.429 ± 0.015 OUR FIT				
0.426 ± 0.016 OUR AVERAGE				
0.416 ± 0.003 ± 0.018	78k	AUBERT 07AP	BABR	$230 \text{ fb}^{-1} E_{cm}^{ee} = 10.6$ GeV
0.471 ± 0.059 ± 0.023	360	ABBIENDI 04j	OPAL	1991-1995 LEP runs
0.444 ± 0.026 ± 0.024	923	BARATE 99k	ALEP	1991-1995 LEP runs
0.51 ± 0.10 ± 0.07	37	BATTLE 94	CLEO	$E_{cm}^{ee} \approx 10.6$ GeV

••• We do not use the following data for averages, fits, limits, etc. •••

0.52 ± 0.04 ± 0.05 395 BUSKULIC 96 ALEP Repl. by BARATE 99k

$$\Gamma(h^- \geq 2\pi^0 \nu_\tau) / \Gamma_{\text{total}} \quad \Gamma_{17} / \Gamma$$

$$\Gamma_{17} / \Gamma = (\Gamma_{20} + \Gamma_{23} + \Gamma_{27} + \Gamma_{30} + 0.157\Gamma_{35} + 0.157\Gamma_{37} + 0.157\Gamma_{40} + 0.157\Gamma_{42} + 0.0985\Gamma_{47} + 0.319\Gamma_{126} + 0.322\Gamma_{128}) / \Gamma$$

Data marked "avg" are highly correlated with data appearing elsewhere in the Listings, and are therefore used for the average given below but not in the overall fits. "f&a" marks results used for the fit and the average.

VALUE (%)	EVTs	DOCUMENT ID	TECN	COMMENT
10.85 ± 0.12 OUR FIT	Error includes scale factor of 1.3.			
9.91 ± 0.31 ± 0.27 f&a		ACKERSTAFF 98M	OPAL	1991-1995 LEP runs
• • • We do not use the following data for averages, fits, limits, etc. • • •				
9.89 ± 0.34 ± 0.55		1 AKERS 94E	OPAL	Repl. by ACKER-STAFF 98M
14.0 ± 1.2 ± 0.6	938	2 BEHREND 90	CELL	$E_{\text{cm}}^{\text{ee}} = 35$ GeV
12.0 ± 1.4 ± 2.5		3 BURCHAT 87	MRK2	$E_{\text{cm}}^{\text{ee}} = 29$ GeV
13.9 ± 2.0 $\pm \frac{+1.9}{-2.2}$		4 AIHARA 86E	TPC	$E_{\text{cm}}^{\text{ee}} = 29$ GeV

1 AKERS 94E not independent of AKERS 94E $B(h^- \geq 1\pi^0 \nu_\tau)$ and $B(h^- \pi^0 \nu_\tau)$ measurements.

2 No independent of BEHREND 90 $\Gamma(h^- 2\pi^0 \nu_\tau \text{ (ex. } K^0))$ and $\Gamma(h^- \geq 3\pi^0 \nu_\tau)$.

3 Error correlated with BURCHAT 87 $\Gamma(\rho^- \nu_e) / \Gamma(\text{total})$ value.

4 AIHARA 86E (TPC) quote $B(2\pi^0 \pi^- \nu_\tau) + 1.6B(3\pi^0 \pi^- \nu_\tau) + 1.1B(\pi^0 \eta \pi^- \nu_\tau)$.

$$\Gamma(h^- 2\pi^0 \nu_\tau) / \Gamma_{\text{total}} \quad \Gamma_{18} / \Gamma$$

$$\Gamma_{18} / \Gamma = (\Gamma_{20} + \Gamma_{23} + 0.157\Gamma_{35} + 0.157\Gamma_{37}) / \Gamma$$

VALUE (%)	EVTs	DOCUMENT ID	TECN	COMMENT
9.51 ± 0.11 OUR FIT	Error includes scale factor of 1.2.			
• • • We do not use the following data for averages, fits, limits, etc. • • •				
9.48 ± 0.13 ± 0.10	12k	1 BUSKULIC 96	ALEP	Repl. by SCHAEEL 05c
1 BUSKULIC 96 quote $9.29 \pm 0.13 \pm 0.10$. We add 0.19 to undo their correction for $\tau^- \rightarrow h^- K^0 \nu_\tau$.				

$$\Gamma(h^- 2\pi^0 \nu_\tau \text{ (ex. } K^0)) / \Gamma_{\text{total}} \quad \Gamma_{19} / \Gamma$$

$$\Gamma_{19} / \Gamma = (\Gamma_{20} + \Gamma_{23}) / \Gamma$$

Data marked "avg" are highly correlated with data appearing elsewhere in the Listings, and are therefore used for the average given below but not in the overall fits. f&a marks results used for the fit and the average.

VALUE (%)	EVTs	DOCUMENT ID	TECN	COMMENT
9.35 ± 0.11 OUR FIT	Error includes scale factor of 1.2.			
9.17 ± 0.27 OUR AVERAGE				
9.498 ± 0.320 ± 0.275 f&a	9.5k	1 ABDALLAH 06A	DLPH	1992-1995 LEP runs
8.88 ± 0.37 ± 0.42 f&a	1060	ACCARIARI 95	L3	1992 LEP run
8.96 ± 0.16 ± 0.44 avg		2 PROCARIO 93	CLEO	$E_{\text{cm}}^{\text{ee}} \approx 10.6$ GeV
• • • We do not use the following data for averages, fits, limits, etc. • • •				
10.38 ± 0.66 ± 0.82	809	3 DECAMP 92c	ALEP	Repl. by SCHAEEL 05c
5.7 ± 0.5 $\pm \frac{+1.7}{-1.0}$	133	4 ANTREASIAN 91	CBAL	$E_{\text{cm}}^{\text{ee}} = 9.4-10.6$ GeV
10.0 ± 1.5 ± 1.1	333	5 BEHREND 90	CELL	$E_{\text{cm}}^{\text{ee}} = 35$ GeV
8.7 ± 0.4 ± 1.1	815	6 BAND 87	MAC	$E_{\text{cm}}^{\text{ee}} = 29$ GeV
6.2 ± 0.6 ± 1.2		7 GAN 87	MRK2	$E_{\text{cm}}^{\text{ee}} = 29$ GeV
6.0 ± 3.0 ± 1.8		BEHREND 84	CELL	$E_{\text{cm}}^{\text{ee}} = 14,22$ GeV

1 See footnote to ABDALLAH 06A $\Gamma(\tau^- \rightarrow h^- \nu_\tau) / \Gamma_{\text{total}}$ measurement for correlations with other measurements.

2 PROCARIO 93 entry is obtained from $B(h^- 2\pi^0 \nu_\tau) / B(h^- \pi^0 \nu_\tau)$ using ARTUSO 94 result for $B(h^- \pi^0 \nu_\tau)$.

3 We subtract 0.0015 to account for $\tau^- \rightarrow K^*(892)^- \nu_\tau$ contribution.

4 ANTREASIAN 91 subtract 0.001 to account for the $\tau^- \rightarrow K^*(892)^- \nu_\tau$ contribution.

5 BEHREND 90 subtract 0.002 to account for the $\tau^- \rightarrow K^*(892)^- \nu_\tau$ contribution.

6 BAND 87 assume $B(\pi^- 3\pi^0 \nu_\tau) = 0.01$ and $B(\pi^- \pi^0 \eta \nu_\tau) = 0.005$.

7 GAN 87 analysis use photon multiplicity distribution.

$$\Gamma(h^- 2\pi^0 \nu_\tau \text{ (ex. } K^0)) / \Gamma(h^- \pi^0 \nu_\tau) \quad \Gamma_{19} / \Gamma_{13}$$

$$\Gamma_{19} / \Gamma_{13} = (\Gamma_{20} + \Gamma_{23}) / (\Gamma_{14} + \Gamma_{16})$$

VALUE	DOCUMENT ID	TECN	COMMENT
0.361 ± 0.005 OUR FIT	Error includes scale factor of 1.2.		
0.342 ± 0.006 ± 0.016	1 PROCARIO 93	CLEO	$E_{\text{cm}}^{\text{ee}} \approx 10.6$ GeV
1 PROCARIO 93 quote $0.345 \pm 0.006 \pm 0.016$ after correction for 2 kaon backgrounds assuming $B(K^{*-} \nu_\tau) = 1.42 \pm 0.18\%$ and $B(h^- K^0 \pi^0 \nu_\tau) = 0.48 \pm 0.48\%$. We multiply by 0.990 ± 0.010 to remove these corrections to $B(h^- \pi^0 \nu_\tau)$.			

$$\Gamma(\pi^- 2\pi^0 \nu_\tau \text{ (ex. } K^0)) / \Gamma_{\text{total}} \quad \Gamma_{20} / \Gamma$$

Data marked "avg" are highly correlated with data appearing elsewhere in the Listings, and are therefore used for the average given below but not in the overall fits. "f&a" marks results used for the fit and the average.

VALUE (%)	EVTs	DOCUMENT ID	TECN	COMMENT
9.29 ± 0.11 OUR FIT	Error includes scale factor of 1.2.			
9.239 ± 0.086 ± 0.090 f&a	31k	1 SCHAEEL 05c	ALEP	1991-1995 LEP runs
• • • We do not use the following data for averages, fits, limits, etc. • • •				
9.21 ± 0.13 ± 0.11		2 BUSKULIC 96	ALEP	Repl. by SCHAEEL 05c

1 See footnote to SCHAEEL 05c $\Gamma(\tau^- \rightarrow e^- \bar{\nu}_e \nu_\tau) / \Gamma_{\text{total}}$ measurement for correlations with other measurements.

2 Not independent of BUSKULIC 96 $B(h^- 2\pi^0 \nu_\tau \text{ (ex. } K^0))$ and $B(K^- 2\pi^0 \nu_\tau \text{ (ex. } K^0))$ values.

$$\Gamma(\pi^- 2\pi^0 \nu_\tau \text{ (ex. } K^0), \text{ scalar}) / \Gamma(\pi^- 2\pi^0 \nu_\tau \text{ (ex. } K^0)) \quad \Gamma_{21} / \Gamma_{20}$$

VALUE	CL%	DOCUMENT ID	TECN	COMMENT
<0.094	95	1 BROWDER 00	CLEO	$4.7 \text{ fb}^{-1} E_{\text{cm}}^{\text{ee}} = 10.6$ GeV
1 Model-independent limit from structure function analysis on contribution to $B(\tau^- \rightarrow \pi^- 2\pi^0 \nu_\tau \text{ (ex. } K^0))$ from scalars.				

$$\Gamma(\pi^- 2\pi^0 \nu_\tau \text{ (ex. } K^0), \text{ vector}) / \Gamma(\pi^- 2\pi^0 \nu_\tau \text{ (ex. } K^0)) \quad \Gamma_{22} / \Gamma_{20}$$

VALUE	CL%	DOCUMENT ID	TECN	COMMENT
<0.073	95	1 BROWDER 00	CLEO	$4.7 \text{ fb}^{-1} E_{\text{cm}}^{\text{ee}} = 10.6$ GeV
1 Model-independent limit from structure function analysis on contribution to $B(\tau^- \rightarrow \pi^- 2\pi^0 \nu_\tau \text{ (ex. } K^0))$ from vectors.				

$$\Gamma(K^- 2\pi^0 \nu_\tau \text{ (ex. } K^0)) / \Gamma_{\text{total}} \quad \Gamma_{23} / \Gamma$$

VALUE (units 10^{-4})	EVTs	DOCUMENT ID	TECN	COMMENT
6.5 ± 2.3 OUR FIT				
5.8 ± 2.4 OUR AVERAGE				
5.6 ± 2.0 ± 1.5	131	BARATE 99k	ALEP	1991-1995 LEP runs
9 ± 10 ± 3	3	1 BATTLE 94	CLEO	$E_{\text{cm}}^{\text{ee}} \approx 10.6$ GeV
• • • We do not use the following data for averages, fits, limits, etc. • • •				
8 ± 2 ± 2	59	BUSKULIC 96	ALEP	Repl. by BARATE 99k

1 BATTLE 94 quote $(14 \pm 10 \pm 3) \times 10^{-4}$ or $< 30 \times 10^{-4}$ at 90% CL. We subtract $(5 \pm 2) \times 10^{-4}$ to account for $\tau^- \rightarrow K^-(K^0 \rightarrow \pi^0 \pi^0) \nu_\tau$ background.

$$\Gamma(h^- \geq 3\pi^0 \nu_\tau) / \Gamma_{\text{total}} \quad \Gamma_{24} / \Gamma$$

$$\Gamma_{24} / \Gamma = (\Gamma_{27} + \Gamma_{28} + \Gamma_{30} + 0.157\Gamma_{40} + 0.157\Gamma_{42} + 0.0985\Gamma_{47} + 0.319\Gamma_{126} + 0.322\Gamma_{128}) / \Gamma$$

VALUE (%)	EVTs	DOCUMENT ID	TECN	COMMENT
1.34 ± 0.07 OUR FIT	Error includes scale factor of 1.1.			
• • • We do not use the following data for averages, fits, limits, etc. • • •				
1.53 ± 0.40 ± 0.46	186	DECAMP 92c	ALEP	Repl. by SCHAEEL 05c
3.2 ± 1.0 ± 1.0		BEHREND 90	CELL	$E_{\text{cm}}^{\text{ee}} = 35$ GeV

$$\Gamma(h^- \geq 3\pi^0 \nu_\tau \text{ (ex. } K^0)) / \Gamma_{\text{total}} \quad \Gamma_{25} / \Gamma$$

$$\Gamma_{25} / \Gamma = (\Gamma_{27} + \Gamma_{28} + \Gamma_{30} + 0.325\Gamma_{126} + 0.325\Gamma_{128}) / \Gamma$$

VALUE (%)	EVTs	DOCUMENT ID	TECN	COMMENT
1.25 ± 0.07 OUR FIT	Error includes scale factor of 1.1.			
1.403 ± 0.214 ± 0.224	1.1k	1 ABDALLAH 06A	DLPH	1992-1995 LEP runs
1 See footnote to ABDALLAH 06A $\Gamma(\tau^- \rightarrow h^- \nu_\tau) / \Gamma_{\text{total}}$ measurement for correlations with other measurements.				

$$\Gamma(h^- 3\pi^0 \nu_\tau) / \Gamma_{\text{total}} \quad \Gamma_{26} / \Gamma$$

$$\Gamma_{26} / \Gamma = (\Gamma_{27} + \Gamma_{28} + 0.157\Gamma_{40} + 0.157\Gamma_{42} + 0.322\Gamma_{128}) / \Gamma$$

Data marked "avg" are highly correlated with data appearing elsewhere in the Listings, and are therefore used for the average given below but not in the overall fits. "f&a" marks results used for the fit and the average.

VALUE (%)	EVTs	DOCUMENT ID	TECN	COMMENT
1.18 ± 0.08 OUR FIT	Error includes scale factor of 1.2.			
1.21 ± 0.17 OUR AVERAGE				
1.70 ± 0.24 ± 0.38 f&a	293	ACCARIARI 95	L3	1992 LEP run
1.15 ± 0.08 ± 0.13 avg		1 PROCARIO 93	CLEO	$E_{\text{cm}}^{\text{ee}} \approx 10.6$ GeV
• • • We do not use the following data for averages, fits, limits, etc. • • •				
1.24 ± 0.09 ± 0.11	2.3k	2 BUSKULIC 96	ALEP	Repl. by SCHAEEL 05c
0.0 $\pm \frac{+1.4}{-0.1} \pm \frac{+1.1}{-0.1}$		3 GAN 87	MRK2	$E_{\text{cm}}^{\text{ee}} = 29$ GeV

1 PROCARIO 93 entry is obtained from $B(h^- 3\pi^0 \nu_\tau) / B(h^- \pi^0 \nu_\tau)$ using ARTUSO 94 result for $B(h^- \pi^0 \nu_\tau)$.

2 BUSKULIC 96 quote $B(h^- 3\pi^0 \nu_\tau \text{ (ex. } K^0)) = 1.17 \pm 0.09 \pm 0.11$. We add 0.07 to remove their correction for K^0 backgrounds.

3 Highly correlated with GAN 87 $\Gamma(\eta \pi^- \pi^0 \nu_\tau) / \Gamma_{\text{total}}$ value. Authors quote $B(\pi^\pm 3\pi^0 \nu_\tau) + 0.67B(\pi^\pm \eta \pi^0 \nu_\tau) = 0.047 \pm 0.010 \pm 0.011$.

$$\Gamma(h^- 3\pi^0 \nu_\tau) / \Gamma(h^- \pi^0 \nu_\tau) \quad \Gamma_{26} / \Gamma_{13}$$

$$\Gamma_{26} / \Gamma_{13} = (\Gamma_{27} + \Gamma_{28} + 0.157\Gamma_{40} + 0.157\Gamma_{42} + 0.322\Gamma_{128}) / (\Gamma_{14} + \Gamma_{16})$$

VALUE	DOCUMENT ID	TECN	COMMENT
0.0456 ± 0.0029 OUR FIT	Error includes scale factor of 1.2.		
0.044 ± 0.003 ± 0.005	1 PROCARIO 93	CLEO	$E_{\text{cm}}^{\text{ee}} \approx 10.6$ GeV
1 PROCARIO 93 quote $0.041 \pm 0.003 \pm 0.005$ after correction for 2 kaon backgrounds assuming $B(K^{*-} \nu_\tau) = 1.42 \pm 0.18\%$ and $B(h^- K^0 \pi^0 \nu_\tau) = 0.48 \pm 0.48\%$. We add 0.003 ± 0.003 and multiply the sum by 0.990 ± 0.010 to remove these corrections.			

$$\Gamma(\pi^- 3\pi^0 \nu_\tau \text{ (ex. } K^0)) / \Gamma_{\text{total}} \quad \Gamma_{27} / \Gamma$$

VALUE (%)	EVTs	DOCUMENT ID	TECN	COMMENT
1.04 ± 0.07 OUR FIT				
0.977 ± 0.069 ± 0.058	6.1k	1 SCHAEEL 05c	ALEP	1991-1995 LEP runs

1 See footnote to SCHAEEL 05c $\Gamma(\tau^- \rightarrow e^- \bar{\nu}_e \nu_\tau) / \Gamma_{\text{total}}$ measurement for correlations with other measurements.

Lepton Particle Listings

 τ $\Gamma(K^- 3\pi^0 \nu_\tau (\text{ex. } K^0, \eta))/\Gamma_{\text{total}}$ Γ_{28}/Γ

VALUE (units 10^{-4})	EVTS	DOCUMENT ID	TECN	COMMENT
4.9 ± 2.3 OUR FIT				Error includes scale factor of 1.1.
3.7 ± 2.1 ± 1.1	22	BARATE	99K	ALEP 1991-1995 LEP runs
• • •				We do not use the following data for averages, fits, limits, etc. • • •
5 ± 13		¹ BUSKULIC	94E	ALEP Repl. by BARATE 99K
		¹ BUSKULIC	94E	quote $B(K^- \geq 0\pi^0 \geq 0K^0 \nu_\tau) - [B(K^- \nu_\tau) + B(K^- \pi^0 \nu_\tau) + B(K^- K^0 \nu_\tau) + B(K^- \pi^0 \pi^0 \nu_\tau) + B(K^- \pi^0 K^0 \nu_\tau)] = (5 \pm 13) \times 10^{-4}$ accounting for common systematic errors in BUSKULIC 94E and BUSKULIC 94F measurements of these modes. We assume $B(K^- \geq 2K^0 \nu_\tau)$ and $B(K^- \geq 4\pi^0 \nu_\tau)$ are negligible.

 $\Gamma(h^- 4\pi^0 \nu_\tau (\text{ex. } K^0))/\Gamma_{\text{total}}$ $\Gamma_{29}/\Gamma = (\Gamma_{30} + 0.319\Gamma_{126})/\Gamma$

VALUE (%)	EVTS	DOCUMENT ID	TECN	COMMENT
0.15 ± 0.04 OUR FIT				
0.16 ± 0.05 ± 0.05		¹ PROCARIO	93	CLEO $E_{\text{cm}}^{\text{ee}} \approx 10.6$ GeV
• • •				We do not use the following data for averages, fits, limits, etc. • • •
0.16 ± 0.04 ± 0.09	232	² BUSKULIC	96	ALEP Repl. by SCHAEEL 05c
		¹ PROCARIO	93	quotes $B(h^- 4\pi^0 \nu_\tau)/B(h^- \pi^0 \nu_\tau) = 0.006 \pm 0.002 \pm 0.002$. We multiply by the ARTUSO 94 result for $B(h^- \pi^0 \nu_\tau)$ to obtain $B(h^- 4\pi^0 \nu_\tau)$. PROCARIO 93 assume $B(h^- \geq 5\pi^0 \nu_\tau)$ is small and do not correct for it.
		² BUSKULIC	96	quote result for $\tau^- \rightarrow h^- \geq 4\pi^0 \nu_\tau$. We assume $B(h^- \geq 5\pi^0 \nu_\tau)$ is negligible.

 $\Gamma(h^- 4\pi^0 \nu_\tau (\text{ex. } K^0, \eta))/\Gamma_{\text{total}}$ Γ_{30}/Γ

VALUE (%)	EVTS	DOCUMENT ID	TECN	COMMENT
0.11 ± 0.04 OUR FIT				
0.112 ± 0.037 ± 0.035	957	¹ SCHAEEL	05c	ALEP 1991-1995 LEP runs
				¹ See footnote to SCHAEEL 05c $\Gamma(\tau^- \rightarrow e^- \bar{\nu}_e \nu_\tau)/\Gamma_{\text{total}}$ measurement for correlations with other measurements.

 $\Gamma(K^- \geq 0\pi^0 \geq 0K^0 \geq 0\gamma \nu_\tau)/\Gamma_{\text{total}}$ $\Gamma_{31}/\Gamma = (\Gamma_{10} + \Gamma_{16} + \Gamma_{23} + \Gamma_{28} + \Gamma_{37} + \Gamma_{42} + 0.715\Gamma_{128})/\Gamma$

Data marked "avg" are highly correlated with data appearing elsewhere in the Listings, and are therefore used for the average given below but not in the overall fits. "f&a" marks results used for the fit and the average.

VALUE (%)	EVTS	DOCUMENT ID	TECN	COMMENT
1.57 ± 0.04 OUR FIT				Error includes scale factor of 1.1.
1.53 ± 0.04 OUR AVERAGE				
1.528 ± 0.039 ± 0.040	f&a	¹ ABBIENDI	01J	OPAL 1990-1995 LEP runs
1.520 ± 0.040 ± 0.041	avg	² BARATE	99K	ALEP 1991-1995 LEP runs
1.54 ± 0.24	f&a	ABREU	94K	DLPH LEP 1992 Z data
1.70 ± 0.12 ± 0.19	f&a	³ BATTLE	94	CLEO $E_{\text{cm}}^{\text{ee}} \approx 10.6$ GeV
• • •				We do not use the following data for averages, fits, limits, etc. • • •
1.70 ± 0.05 ± 0.06	1610	⁴ BUSKULIC	96	ALEP Repl. by BARATE 99K
1.6 ± 0.4 ± 0.2	35	AIHARA	87B	TPC $E_{\text{cm}}^{\text{ee}} = 29$ GeV
1.71 ± 0.29	53	MILLS	84	DLCO $E_{\text{cm}}^{\text{ee}} = 29$ GeV

¹ The correlation coefficient between this measurement and the ABBIENDI 01J $B(\tau^- \rightarrow K^- \nu_\tau)$ is 0.60.

² Not independent of BARATE 99K $B(K^- \nu_\tau)$, $B(K^- \pi^0 \nu_\tau)$, $B(K^- 2\pi^0 \nu_\tau (\text{ex. } K^0))$, $B(K^- 3\pi^0 \nu_\tau (\text{ex. } K^0))$, $B(K^- K^0 \nu_\tau)$, and $B(K^- K^0 \pi^0 \nu_\tau)$ values.

³ BATTLE 94 quote $1.60 \pm 0.12 \pm 0.19$. We add 0.10 ± 0.02 to correct for their rejection of $K_S^0 \rightarrow \pi^+ \pi^-$ decays.

⁴ Not independent of BUSKULIC 96 $B(K^- \nu_\tau)$, $B(K^- \pi^0 \nu_\tau)$, $B(K^- 2\pi^0 \nu_\tau)$, $B(K^- K^0 \nu_\tau)$, and $B(K^- K^0 \pi^0 \nu_\tau)$ values.

 $\Gamma(K^- \geq 1(\pi^0 \text{ or } K^0 \text{ or } \gamma) \nu_\tau)/\Gamma_{\text{total}}$ $\Gamma_{32}/\Gamma = (\Gamma_{16} + \Gamma_{23} + \Gamma_{28} + \Gamma_{37} + \Gamma_{42} + 0.715\Gamma_{128})/\Gamma$

Data marked "avg" are highly correlated with data appearing elsewhere in the Listings, and are therefore used for the average given below but not in the overall fits. "f&a" marks results used for the fit and the average.

VALUE (%)	EVTS	DOCUMENT ID	TECN	COMMENT
0.872 ± 0.032 OUR FIT				Error includes scale factor of 1.1.
0.86 ± 0.05 OUR AVERAGE				
0.869 ± 0.031 ± 0.034	avg	¹ ABBIENDI	01J	OPAL 1990-1995 LEP runs
0.69 ± 0.25	avg	² ABREU	94K	DLPH LEP 1992 Z data
• • •				We do not use the following data for averages, fits, limits, etc. • • •
1.2 ± 0.5 $^{+0.2}_{-0.4}$	9	AIHARA	87B	TPC $E_{\text{cm}}^{\text{ee}} = 29$ GeV
		¹ Not independent of ABBIENDI 01J $B(\tau^- \rightarrow K^- \nu_\tau)$ and $B(\tau^- \rightarrow K^- \geq 0\pi^0 \geq 0K^0 \geq 0\gamma \nu_\tau)$ values.		
		² Not independent of ABREU 94K $B(K^- \nu_\tau)$ and $B(K^- \geq 0$ neutrals $\nu_\tau)$ measurements.		

 $\Gamma(K_S^0 (\text{particles})^- \nu_\tau)/\Gamma_{\text{total}}$ $\Gamma_{33}/\Gamma = (\frac{1}{2}\Gamma_{35} + \frac{1}{2}\Gamma_{37} + \frac{1}{2}\Gamma_{40} + \frac{1}{2}\Gamma_{42} + \frac{1}{2}\Gamma_{47} + \Gamma_{48})/\Gamma$

VALUE (%)	EVTS	DOCUMENT ID	TECN	COMMENT
0.92 ± 0.04 OUR FIT				Error includes scale factor of 1.5.
0.97 ± 0.07 OUR AVERAGE				
0.970 ± 0.058 ± 0.062	929	BARATE	98E	ALEP 1991-1995 LEP runs
0.97 ± 0.09 ± 0.06	141	AKERS	96	OPAL $E_{\text{cm}}^{\text{ee}} = 88-94$ GeV

 $\Gamma(h^- \bar{K}^0 \nu_\tau)/\Gamma_{\text{total}}$ $\Gamma_{34}/\Gamma = (\Gamma_{35} + \Gamma_{37})/\Gamma$

Data marked "avg" are highly correlated with data appearing elsewhere in the Listings, and are therefore used for the average given below but not in the overall fits. "f&a" marks results used for the fit and the average.

VALUE (%)	EVTS	DOCUMENT ID	TECN	COMMENT	
1.00 ± 0.05 OUR FIT				Error includes scale factor of 1.8.	
0.90 ± 0.07 OUR AVERAGE					
1.01 ± 0.11 ± 0.07	avg	555	¹ BARATE	98E	ALEP 1991-1995 LEP runs
0.855 ± 0.036 ± 0.073	f&a	1242	COAN	96	CLEO $E_{\text{cm}}^{\text{ee}} \approx 10.6$ GeV
				¹ Not independent of BARATE 98E $B(\tau^- \rightarrow \pi^- \bar{K}^0 \nu_\tau)$ and $B(\tau^- \rightarrow K^- K^0 \nu_\tau)$ values.	

 $\Gamma(\pi^- \bar{K}^0 \nu_\tau)/\Gamma_{\text{total}}$ Γ_{35}/Γ

Data marked "avg" are highly correlated with data appearing elsewhere in the Listings, and are therefore used for the average given below but not in the overall fits. "f&a" marks results used for the fit and the average.

VALUE (%)	EVTS	DOCUMENT ID	TECN	COMMENT	
0.84 ± 0.04 OUR FIT				Error includes scale factor of 2.1.	
0.831 ± 0.030 OUR AVERAGE				Error includes scale factor of 1.4. See the ideogram below.	
0.808 ± 0.004 ± 0.026	f&a	53k	EPIFANOV	07	BELL 351 fb ⁻¹ $E_{\text{cm}}^{\text{ee}} = 10.6$ GeV
0.933 ± 0.068 ± 0.049	f&a	377	ABBIENDI	00c	OPAL 1991-1995 LEP runs
0.928 ± 0.045 ± 0.034	f&a	937	¹ BARATE	99K	ALEP 1991-1995 LEP runs
0.855 ± 0.117 ± 0.066	avg	509	² BARATE	98E	ALEP 1991-1995 LEP runs
0.704 ± 0.041 ± 0.072	avg		³ COAN	96	CLEO $E_{\text{cm}}^{\text{ee}} \approx 10.6$ GeV
0.95 ± 0.15 ± 0.06	f&a		⁴ ACCIARRI	95F	L3 1991-1993 LEP runs
• • •				We do not use the following data for averages, fits, limits, etc. • • •	
0.79 ± 0.10 ± 0.09		98	⁵ BUSKULIC	96	ALEP Repl. by BARATE 99K

¹ BARATE 99K measure K^0 's by detecting K_L^0 's in their hadron calorimeter.

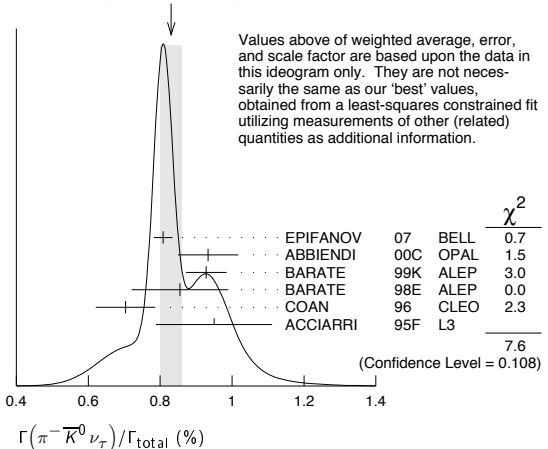
² BARATE 98E reconstruct K^0 's using $K_S^0 \rightarrow \pi^+ \pi^-$ decays. Not independent of BARATE 98E $B(K^0 \text{ particles}^- \nu_\tau)$ value.

³ Not independent of COAN 96 $B(h^- K^0 \nu_\tau)$ and $B(K^- K^0 \nu_\tau)$ measurements.

⁴ ACCIARRI 95F do not identify π^-/K^- and assume $B(K^- K^0 \nu_\tau) = (0.29 \pm 0.12)\%$.

⁵ BUSKULIC 96 measure K^0 's by detecting K_L^0 's in their hadron calorimeter.

WEIGHTED AVERAGE
0.831 ± 0.030 (Error scaled by 1.4)

 $\Gamma(\pi^- \bar{K}^0 (\text{non-} K^*(892)^- \nu_\tau)/\Gamma_{\text{total}}$ Γ_{36}/Γ

VALUE (units 10^{-4})	CL%	DOCUMENT ID	TECN	COMMENT
5.4 ± 2.1		¹ EPIFANOV	07	BELL 351 fb ⁻¹ $E_{\text{cm}}^{\text{ee}} = 10.6$ GeV
• • •				We do not use the following data for averages, fits, limits, etc. • • •
<17	95	ACCIARRI	95F	L3 1991-1993 LEP runs

¹ EPIFANOV 07 quote $B(\tau^- \rightarrow K^*(892)^- \nu_\tau) B(K^*(892)^- \rightarrow K_S^0 \pi^-) / B(\tau^- \rightarrow K_S^0 \pi^- \nu_\tau) = 0.933 \pm 0.027$. We multiply their $B(\tau^- \rightarrow \bar{K}^0 \pi^- \nu_\tau)$ by $[1 - (0.933 \pm 0.027)]$ to obtain this result.

 $\Gamma(K^- K^0 \nu_\tau)/\Gamma_{\text{total}}$ Γ_{37}/Γ

VALUE (%)	EVTS	DOCUMENT ID	TECN	COMMENT
0.159 ± 0.016 OUR FIT				
0.158 ± 0.017 OUR AVERAGE				
0.162 ± 0.021 ± 0.011	150	¹ BARATE	99K	ALEP 1991-1995 LEP runs
0.158 ± 0.042 ± 0.017	46	² BARATE	98E	ALEP 1991-1995 LEP runs
0.151 ± 0.021 ± 0.022	111	COAN	96	CLEO $E_{\text{cm}}^{\text{ee}} \approx 10.6$ GeV
• • •				We do not use the following data for averages, fits, limits, etc. • • •
0.26 ± 0.09 ± 0.02	13	³ BUSKULIC	96	ALEP Repl. by BARATE 99K

¹ BARATE 99K measure K^0 's by detecting K_L^0 's in their hadron calorimeter.

² BARATE 98E reconstruct K^0 's using $K_S^0 \rightarrow \pi^+ \pi^-$ decays.

³ BUSKULIC 96 measure K^0 's by detecting K_L^0 's in their hadron calorimeter.

$\Gamma(K^- K^0 \geq 0\pi^0 \nu_\tau)/\Gamma_{\text{total}}$		$\Gamma_{38}/\Gamma = (\Gamma_{37} + \Gamma_{42})/\Gamma$		
VALUE (%)	EVTS	DOCUMENT ID	TECN	COMMENT
0.318 ± 0.024 OUR FIT				
0.330 ± 0.055 ± 0.039	124	ABBIENDI	00C	OPAL 1991–1995 LEP runs

$\Gamma(h^- \bar{K}^0 \pi^0 \nu_\tau)/\Gamma_{\text{total}}$		$\Gamma_{39}/\Gamma = (\Gamma_{40} + \Gamma_{42})/\Gamma$		
Data marked "avg" are highly correlated with data appearing elsewhere in the Listings, and are therefore used for the average given below but not in the overall fits. "f&a" marks results used for the fit and the average.				
VALUE (%)	EVTS	DOCUMENT ID	TECN	COMMENT
0.55 ± 0.04 OUR FIT				
0.50 ± 0.06 OUR AVERAGE	Error includes scale factor of 1.2.			
0.446 ± 0.052 ± 0.046	avg 157	¹ BARATE	98E	ALEP 1991–1995 LEP runs
0.562 ± 0.050 ± 0.048	f&a 264	COAN	96	CLEO $E_{\text{cm}}^e \approx 10.6$ GeV

$\Gamma(\pi^- \bar{K}^0 \pi^0 \nu_\tau)/\Gamma_{\text{total}}$		Γ_{40}/Γ		
Data marked "avg" are highly correlated with data appearing elsewhere in the Listings, and are therefore used for the average given below but not in the overall fits. "f&a" marks results used for the fit and the average.				
VALUE (%)	EVTS	DOCUMENT ID	TECN	COMMENT
0.40 ± 0.04 OUR FIT				
0.36 ± 0.04 OUR AVERAGE				
0.347 ± 0.053 ± 0.037	f&a 299	¹ BARATE	99K	ALEP 1991–1995 LEP runs
0.294 ± 0.073 ± 0.037	f&a 142	² BARATE	98E	ALEP 1991–1995 LEP runs
0.417 ± 0.058 ± 0.044	avg	³ COAN	96	CLEO $E_{\text{cm}}^e \approx 10.6$ GeV
0.41 ± 0.12 ± 0.03	f&a	⁴ ACCIARRI	95F	L3 1991–1993 LEP runs

$\Gamma(\pi^- \bar{K}^0 \pi^0 \nu_\tau)/\Gamma_{\text{total}}$		Γ_{40}/Γ		
Data marked "avg" are highly correlated with data appearing elsewhere in the Listings, and are therefore used for the average given below but not in the overall fits. "f&a" marks results used for the fit and the average.				
VALUE (%)	EVTS	DOCUMENT ID	TECN	COMMENT
0.40 ± 0.04 OUR FIT				
0.36 ± 0.04 OUR AVERAGE				
0.347 ± 0.053 ± 0.037	f&a 299	¹ BARATE	99K	ALEP 1991–1995 LEP runs
0.294 ± 0.073 ± 0.037	f&a 142	² BARATE	98E	ALEP 1991–1995 LEP runs
0.417 ± 0.058 ± 0.044	avg	³ COAN	96	CLEO $E_{\text{cm}}^e \approx 10.6$ GeV
0.41 ± 0.12 ± 0.03	f&a	⁴ ACCIARRI	95F	L3 1991–1993 LEP runs
• • • We do not use the following data for averages, fits, limits, etc. • • •				
0.32 ± 0.11 ± 0.05	23	⁵ BUSKULIC	96	ALEP Repl. by BARATE 99K
¹ BARATE 99K measure K^0 's by detecting K_L^0 's in their hadron calorimeter.				
² BARATE 98E reconstruct K^0 's using $K_S^0 \rightarrow \pi^+ \pi^-$ decays.				
³ Not independent of COAN 96 $B(h^- \bar{K}^0 \pi^0 \nu_\tau)$ and $B(K^- K^0 \pi^0 \nu_\tau)$ measurements.				
⁴ ACCIARRI 95F do not identify π^-/K^- and assume $B(K^- K^0 \pi^0 \nu_\tau) = (0.05 \pm 0.05)\%$.				
⁵ BUSKULIC 96 measure K^0 's by detecting K_L^0 's in their hadron calorimeter.				

$\Gamma(\bar{K}^0 \rho^- \nu_\tau)/\Gamma_{\text{total}}$		Γ_{41}/Γ		
VALUE (%)	EVTS	DOCUMENT ID	TECN	COMMENT
0.22 ± 0.05 OUR AVERAGE				
0.250 ± 0.057 ± 0.044		¹ BARATE	99K	ALEP 1991–1995 LEP runs
0.188 ± 0.054 ± 0.038		² BARATE	98E	ALEP 1991–1995 LEP runs

¹ BARATE 99K measure K^0 's by detecting K_L^0 's in hadron calorimeter. They determine the $\bar{K}^0 \rho^-$ fraction in $\tau^- \rightarrow \pi^- \bar{K}^0 \pi^0 \nu_\tau$ decays to be $(0.72 \pm 0.12 \pm 0.10)$ and multiply their $B(\pi^- \bar{K}^0 \pi^0 \nu_\tau)$ measurement by this fraction to obtain the quoted result.				
² BARATE 98E reconstruct K^0 's using $K_S^0 \rightarrow \pi^+ \pi^-$ decays. They determine the $\bar{K}^0 \rho^-$ fraction in $\tau^- \rightarrow \pi^- \bar{K}^0 \pi^0 \nu_\tau$ decays to be $(0.64 \pm 0.09 \pm 0.10)$ and multiply their $B(\pi^- \bar{K}^0 \pi^0 \nu_\tau)$ measurement by this fraction to obtain the quoted result.				

$\Gamma(K^- K^0 \pi^0 \nu_\tau)/\Gamma_{\text{total}}$		Γ_{42}/Γ		
VALUE (%)	EVTS	DOCUMENT ID	TECN	COMMENT
0.159 ± 0.020 OUR FIT				
0.144 ± 0.023 OUR AVERAGE				
0.143 ± 0.025 ± 0.015	78	¹ BARATE	99K	ALEP 1991–1995 LEP runs
0.152 ± 0.076 ± 0.021	15	² BARATE	98E	ALEP 1991–1995 LEP runs
0.145 ± 0.036 ± 0.020	32	COAN	96	CLEO $E_{\text{cm}}^e \approx 10.6$ GeV

• • • We do not use the following data for averages, fits, limits, etc. • • •				
0.10 ± 0.05 ± 0.03	5	³ BUSKULIC	96	ALEP Repl. by BARATE 99K
¹ BARATE 99K measure K^0 's by detecting K_L^0 's in their hadron calorimeter.				
² BARATE 98E reconstruct K^0 's using $K_S^0 \rightarrow \pi^+ \pi^-$ decays.				
³ BUSKULIC 96 measure K^0 's by detecting K_L^0 's in their hadron calorimeter.				

$\Gamma(\pi^- \bar{K}^0 \geq 1\pi^0 \nu_\tau)/\Gamma_{\text{total}}$		$\Gamma_{43}/\Gamma = (\Gamma_{40} + \Gamma_{44})/\Gamma$		
VALUE (%)	EVTS	DOCUMENT ID	TECN	COMMENT
0.324 ± 0.074 ± 0.066	148	ABBIENDI	00C	OPAL 1991–1995 LEP runs

$\Gamma(\pi^- \bar{K}^0 \pi^0 \pi^0 \nu_\tau)/\Gamma_{\text{total}}$		Γ_{44}/Γ			
VALUE (units 10^{-3})	CL%	EVTS	DOCUMENT ID	TECN	COMMENT
0.26 ± 0.24			¹ BARATE	99R	ALEP 1991–1995 LEP runs

• • • We do not use the following data for averages, fits, limits, etc. • • •					
<0.66	95	17	² BARATE	99K	ALEP 1991–1995 LEP runs
0.58 ± 0.33 ± 0.14		5	³ BARATE	98E	ALEP 1991–1995 LEP runs
¹ BARATE 99R combine the BARATE 98E and BARATE 99K measurements to obtain this value.					
² BARATE 99K measure K^0 's by detecting K_L^0 's in their hadron calorimeter.					
³ BARATE 98E reconstruct K^0 's using $K_S^0 \rightarrow \pi^+ \pi^-$ decays.					

$\Gamma(K^- K^0 \pi^0 \pi^0 \nu_\tau)/\Gamma_{\text{total}}$		Γ_{45}/Γ		
VALUE	CL%	DOCUMENT ID	TECN	COMMENT
<0.16 × 10⁻³	95	¹ BARATE	99R	ALEP 1991–1995 LEP runs
• • • We do not use the following data for averages, fits, limits, etc. • • •				
<0.18 × 10 ⁻³	95	² BARATE	99K	ALEP 1991–1995 LEP runs
<0.39 × 10 ⁻³	95	³ BARATE	98E	ALEP 1991–1995 LEP runs

¹ BARATE 99R combine the BARATE 98E and BARATE 99K bounds to obtain this value.				
² BARATE 99K measure K^0 's by detecting K_L^0 's in hadron calorimeter.				
³ BARATE 98E reconstruct K^0 's by using $K_S^0 \rightarrow \pi^+ \pi^-$ decays.				

$\Gamma(\pi^- K^0 \bar{K}^0 \nu_\tau)/\Gamma_{\text{total}}$		$\Gamma_{46}/\Gamma = (2\Gamma_{47} + \Gamma_{48})/\Gamma$		
Data marked "avg" are highly correlated with data appearing elsewhere in the Listings, and are therefore used for the average given below but not in the overall fits. "f&a" marks results used for the fit and the average.				
VALUE (%)	EVTS	DOCUMENT ID	TECN	COMMENT
0.17 ± 0.04 OUR FIT	Error includes scale factor of 1.6.			
0.153 ± 0.030 ± 0.016 avg	74	¹ BARATE	98E	ALEP 1991–1995 LEP runs

• • • We do not use the following data for averages, fits, limits, etc. • • •				
0.31 ± 0.12 ± 0.04		² ACCIARRI	95F	L3 1991–1993 LEP runs
¹ BARATE 98E obtain this value by adding twice their $B(\pi^- K_S^0 K_L^0 \nu_\tau)$ value to their $B(\pi^- K_S^0 K_L^0 \nu_\tau)$ value.				
² ACCIARRI 95F assume $B(\pi^- K_S^0 K_S^0 \nu) = B(\pi^- K_S^0 K_L^0 \nu) = 1/2B(\pi^- K_S^0 K_L^0 \nu)$.				

$\Gamma(\pi^- K_S^0 K_L^0 \nu_\tau)/\Gamma_{\text{total}}$		Γ_{47}/Γ		
Bose-Einstein correlations might make the mixing fraction different than 1/4.				
VALUE (units 10^{-4})	EVTS	DOCUMENT ID	TECN	COMMENT
2.4 ± 0.5 OUR FIT				
2.4 ± 0.5 OUR AVERAGE				

2.6 ± 1.0 ± 0.5	6	BARATE	98E	ALEP 1991–1995 LEP runs
2.3 ± 0.5 ± 0.3	42	COAN	96	CLEO $E_{\text{cm}}^e \approx 10.6$ GeV

$\Gamma(\pi^- K_S^0 K_L^0 \nu_\tau)/\Gamma_{\text{total}}$		Γ_{48}/Γ		
VALUE (units 10^{-4})	EVTS	DOCUMENT ID	TECN	COMMENT
12 ± 4 OUR FIT	Error includes scale factor of 1.7.			
10.1 ± 2.3 ± 1.3	68	BARATE	98E	ALEP 1991–1995 LEP runs

$\Gamma(\pi^- K^0 \bar{K}^0 \pi^0 \nu_\tau)/\Gamma_{\text{total}}$		Γ_{49}/Γ		
VALUE	DOCUMENT ID	TECN	COMMENT	
(0.31 ± 0.23) × 10⁻³	¹ BARATE	99R	ALEP	1991–1995 LEP runs
¹ BARATE 99R combine $\Gamma(\pi^- K_S^0 K_S^0 \pi^0 \nu_\tau)/\Gamma_{\text{total}}$ and $\Gamma(\pi^- K_S^0 K_L^0 \pi^0 \nu_\tau)/\Gamma_{\text{total}}$ measurements to obtain this value.				

$\Gamma(\pi^- K_S^0 K_S^0 \pi^0 \nu_\tau)/\Gamma_{\text{total}}$		Γ_{50}/Γ		
VALUE (units 10^{-4})	CL%	DOCUMENT ID	TECN	COMMENT
<2.0	95	BARATE	98E	ALEP 1991–1995 LEP runs

$\Gamma(\pi^- K_S^0 K_L^0 \pi^0 \nu_\tau)/\Gamma_{\text{total}}$		Γ_{51}/Γ		
VALUE (units 10^{-4})	EVTS	DOCUMENT ID	TECN	COMMENT
3.1 ± 1.1 ± 0.5	11	BARATE	98E	ALEP 1991–1995 LEP runs

$\Gamma(K^0 h^+ h^- h^- \geq 0 \text{ neutrals } \nu_\tau)/\Gamma_{\text{total}}$		Γ_{52}/Γ		
VALUE (%)	CL%	DOCUMENT ID	TECN	COMMENT
<0.17	95	TSCHIRHART	88	HRS $E_{\text{cm}}^e = 29$ GeV
• • • We do not use the following data for averages, fits, limits, etc. • • •				
<0.27	90	BELTRAMI	85	HRS $E_{\text{cm}}^e = 29$ GeV

$\Gamma(K^0 h^+ h^- h^- \nu_\tau)/\Gamma_{\text{total}}$		Γ_{53}/Γ		
VALUE (units 10^{-4})	EVTS	DOCUMENT ID	TECN	COMMENT
2.3 ± 1.9 ± 0.7	6	¹ BARATE	98E	ALEP 1991–1995 LEP runs
¹ BARATE 98E reconstruct K^0 's using $K_S^0 \rightarrow \pi^+ \pi^-$ decays.				

$\Gamma(h^- h^- h^+ \geq 0 \text{ neutrals } \geq 0 K_L^0 \nu_\tau)/\Gamma_{\text{total}}$		Γ_{54}/Γ		
$\Gamma_{54}/\Gamma = (0.3431\Gamma_{35} + 0.3431\Gamma_{37} + 0.3431\Gamma_{40} + 0.3431\Gamma_{42} + 0.4307\Gamma_{47} + 0.6861\Gamma_{48} + \Gamma_{62} + \Gamma_{70} + \Gamma_{77} + \Gamma_{78} + \Gamma_{85} + \Gamma_{89} + \Gamma_{93} + \Gamma_{94} + 0.285\Gamma_{126} + 0.285\Gamma_{128} + 0.9101\Gamma_{150} + 0.9101\Gamma_{152})/\Gamma$				
VALUE (%)	EVTS	DOCUMENT ID	TECN	COMMENT
15.19 ± 0.08 OUR FIT	Error includes scale factor of 1.4.			
14.8 ± 0.4 OUR AVERAGE				

14.4 ± 0.6 ± 0.3		ADEVA	91F	L3 $E_{\text{cm}}^e = 88.3\text{--}94.3$ GeV
15.0 ± 0.4 ± 0.3		BEHREND	89B	CELL $E_{\text{cm}}^e = 14\text{--}47$ GeV
15.1 ± 0.8 ± 0.6		AIHARA	87B	TPC $E_{\text{cm}}^e = 29$ GeV

Lepton Particle Listings

τ

• • • We do not use the following data for averages, fits, limits, etc. • • •

13.5 ± 0.3 ± 0.3	ABACHI	89B	HRS	$E_{cm}^{ee} = 29$ GeV
12.8 ± 1.0 ± 0.7	¹ BURCHAT	87	MRK2	$E_{cm}^{ee} = 29$ GeV
12.1 ± 0.5 ± 1.2	RUCKSTUHL	86	DLCO	$E_{cm}^{ee} = 29$ GeV
12.8 ± 0.5 ± 0.8	1420	86	MRK2	$E_{cm}^{ee} = 29$ GeV
15.3 ± 1.1 ^{+1.3} / _{-1.6}	367	ALTHOFF	85	TASS $E_{cm}^{ee} = 34.5$ GeV
13.6 ± 0.5 ± 0.8	BARTEL	85F	JADE	$E_{cm}^{ee} = 34.6$ GeV
12.2 ± 1.3 ± 3.9	² BERGER	85	PLUT	$E_{cm}^{ee} = 34.6$ GeV
13.3 ± 0.3 ± 0.6	FERNANDEZ	85	MAC	$E_{cm}^{ee} = 29$ GeV
24 ± 6	35	BRANDELIK	80	TASS $E_{cm}^{ee} = 30$ GeV
32 ± 5	692	³ BACINO	78B	DLCO $E_{cm}^{ee} = 3.1-7.4$ GeV
35 ± 11	³ BRANDELIK	78	DASP	Assumes $V-A$ decay
18 ± 6.5	33	³ JAROS	78	LGW $E_{cm}^{ee} > 6$ GeV

- ¹BURCHAT 87 value is not independent of SCHMIDKE 86 value.
- ²Not independent of BERGER 85 $\Gamma(\mu^- \bar{\nu}_\mu \nu_\tau)/\Gamma_{total}$, $\Gamma(e^- \bar{\nu}_e \nu_\tau)/\Gamma_{total}$, $\Gamma(h^- \geq 1 \text{ neutrals } \nu_\tau)/\Gamma_{total}$, and $\Gamma(h^- \geq 0 K_L^0 \nu_\tau)/\Gamma_{total}$, and therefore not used in the fit.
- ³Low energy experiments are not in average or fit because the systematic errors in background subtraction are judged to be large.

$$\Gamma(h^- h^- h^+ \geq 0 \text{ neutrals } \nu_\tau \text{ (ex. } K_S^0 \rightarrow \pi^+ \pi^- \text{ ("3-prong"))})/\Gamma_{total} \quad \Gamma_{55}/\Gamma$$

$$\Gamma_{55}/\Gamma = (\Gamma_{62} + \Gamma_{70} + \Gamma_{77} + \Gamma_{78} + \Gamma_{85} + \Gamma_{89} + \Gamma_{93} + \Gamma_{94} + 0.285\Gamma_{126} + 0.285\Gamma_{128} + 0.9101\Gamma_{150} + 0.9101\Gamma_{152})/\Gamma$$

Data marked "avg" are highly correlated with data appearing elsewhere in the Listings, and are therefore used for the average given below but not in the overall fits. "f&a" marks results used for the fit and the average.

VALUE (%)	EVTs	DOCUMENT ID	TECN	COMMENT
14.56 ± 0.08 OUR FIT	Error includes scale factor of 1.3.			
14.61 ± 0.06 OUR AVERAGE				
14.652 ± 0.067 ± 0.086	avg	SCHAEEL	05c	ALEP 1991-1995 LEP runs
14.569 ± 0.093 ± 0.048	avg	¹ ABREU	01M	DLPH 1992-1995 LEP runs
14.556 ± 0.105 ± 0.076	f&a	² ACHARD	01D	L3 1992-1995 LEP runs
14.96 ± 0.09 ± 0.22	f&a	10.4k	AKERS	95Y OPAL 1991-1994 LEP runs
14.22 ± 0.10 ± 0.37	avg	³ BALEST	95c	CLEO $E_{cm}^{ee} \approx 10.6$ GeV
• • • We do not use the following data for averages, fits, limits, etc. • • •				
15.26 ± 0.26 ± 0.22		ACTON	92H	OPAL Repl. by AKERS 95Y
13.3 ± 0.3 ± 0.8		⁴ ALBRECHT	92D	ARG $E_{cm}^{ee} = 9.4-10.6$ GeV
14.35 ^{+0.40} / _{-0.45} ± 0.24		DECAMP	92c	ALEP 1989-1990 LEP runs

- ¹The correlation coefficients between this measurement and the ABREU 01M measurements of $B(\tau \rightarrow 1\text{-prong})$ and $B(\tau \rightarrow 5\text{-prong})$ are -0.98 and -0.08 respectively.
- ²The correlation coefficients between this measurement and the ACHARD 01D measurements of $B(\tau \rightarrow "1\text{-prong}")$ and $B(\tau \rightarrow "5\text{-prong}")$ are -0.978 and -0.19 respectively.
- ³Not independent of BALEST 95c $B(h^- h^- h^+ \nu_\tau)$ and $B(h^- h^- h^+ \pi^0 \nu_\tau)$ values, and BORTOLETTO 93 $B(h^- h^- h^+ 2\pi^0 \nu_\tau)/B(h^- h^- h^+ \geq 0 \text{ neutrals } \nu_\tau)$ value.
- ⁴This ALBRECHT 92D value is not independent of their $\Gamma(\mu^- \bar{\nu}_\mu \nu_\tau)\Gamma(e^- \bar{\nu}_e \nu_\tau)/\Gamma_{total}^2$ value.

$$\Gamma(h^- h^- h^+ \nu_\tau)/\Gamma_{total} \quad \Gamma_{56}/\Gamma$$

$$\Gamma_{56}/\Gamma = (0.3431\Gamma_{35} + 0.3431\Gamma_{37} + \Gamma_{62} + \Gamma_{85} + \Gamma_{93} + 0.017\Gamma_{150})/\Gamma$$

Data marked "avg" are highly correlated with data appearing elsewhere in the Listings, and are therefore used for the average given below but not in the overall fits. "f&a" marks results used for the fit and the average.

VALUE (%)	EVTs	DOCUMENT ID	TECN	COMMENT
9.80 ± 0.08 OUR FIT	Error includes scale factor of 1.4.			
7.6 ± 0.1 ± 0.5 avg	7.5k	¹ ALBRECHT	96E	ARG $E_{cm}^{ee} = 9.4-10.6$ GeV
• • • We do not use the following data for averages, fits, limits, etc. • • •				
9.92 ± 0.10 ± 0.09	11.2k	² BUSKULIC	96	ALEP Repl. by SCHAEEL 05c
9.49 ± 0.36 ± 0.63		DECAMP	92c	ALEP Repl. by SCHAEEL 05c
8.7 ± 0.7 ± 0.3	694	³ BEHREND	90	CELL $E_{cm}^{ee} = 35$ GeV
7.0 ± 0.3 ± 0.7	1566	⁴ BAND	87	MAC $E_{cm}^{ee} = 29$ GeV
6.7 ± 0.8 ± 0.9		⁵ BURCHAT	87	MRK2 $E_{cm}^{ee} = 29$ GeV
6.4 ± 0.4 ± 0.9		⁶ RUCKSTUHL	86	DLCO $E_{cm}^{ee} = 29$ GeV
7.8 ± 0.5 ± 0.8	890	SCHMIDKE	86	MRK2 $E_{cm}^{ee} = 29$ GeV
8.4 ± 0.4 ± 0.7	1255	⁶ FERNANDEZ	85	MAC $E_{cm}^{ee} = 29$ GeV
9.7 ± 2.0 ± 1.3		BEHREND	84	CELL $E_{cm}^{ee} = 14,22$ GeV

- ¹ALBRECHT 96E not independent of ALBRECHT 93c $\Gamma(h^- h^- h^+ \nu_\tau \text{ (ex. } K^0) \times \Gamma(\text{particle}^- \geq 0 \text{ neutrals } \geq 0 K_L^0 \nu_\tau)/\Gamma_{total}^2$ value.
- ²BUSKULIC 96 quote $B(h^- h^- h^+ \nu_\tau \text{ (ex. } K^0)) = 9.50 \pm 0.10 \pm 0.11$. We add 0.42 to remove their K^0 correction and reduce the systematic error accordingly.
- ³BEHREND 90 subtract 0.3% to account for the $\tau^- \rightarrow K^*(892)^- \nu_\tau$ contribution to measured events.
- ⁴BAND 87 subtract for charged kaon modes; not independent of FERNANDEZ 85 value.
- ⁵BURCHAT 87 value is not independent of SCHMIDKE 86 value.
- ⁶Value obtained by multiplying paper's $R = B(h^- h^- h^+ \nu_\tau)/B(3\text{-prong})$ by $B(3\text{-prong}) = 0.143$ and subtracting 0.3% for $K^*(892)$ background.

$$\Gamma(h^- h^- h^+ \nu_\tau \text{ (ex. } K^0))/\Gamma_{total} \quad \Gamma_{57}/\Gamma$$

$$\Gamma_{57}/\Gamma = (\Gamma_{62} + \Gamma_{85} + \Gamma_{93} + 0.017\Gamma_{150})/\Gamma$$

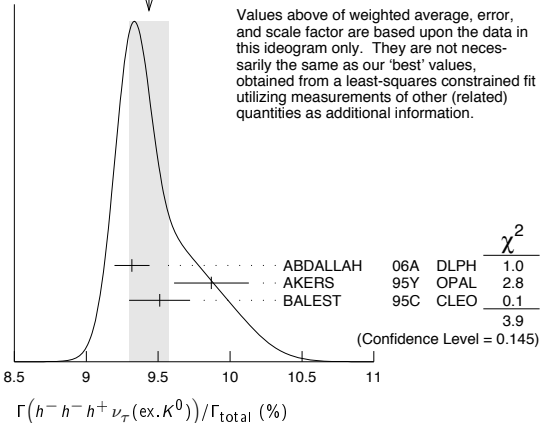
Data marked "avg" are highly correlated with data appearing elsewhere in the Listings, and are therefore used for the average given below but not in the overall fits. "f&a" marks results used for the fit and the average.

VALUE (%)	EVTs	DOCUMENT ID	TECN	COMMENT
9.46 ± 0.07 OUR FIT	Error includes scale factor of 1.3.			
9.44 ± 0.14 OUR AVERAGE	Error includes scale factor of 1.4. See the ideogram below.			
9.317 ± 0.090 ± 0.082	f&a	12.2k	¹ ABDALLAH	06A DLPH 1992-1995 LEP runs
9.87 ± 0.10 ± 0.24	avg		² AKERS	95Y OPAL 1991-1994 LEP runs
9.51 ± 0.07 ± 0.20	f&a	37.7k	BALEST	95c CLEO $E_{cm}^{ee} \approx 10.6$ GeV

• • • We do not use the following data for averages, fits, limits, etc. • • •

- ¹See footnote to ABDALLAH 06A $\Gamma(\tau^- \rightarrow h^- \nu_\tau)/\Gamma_{total}$ measurement for correlations with other measurements.
- ²Not independent of AKERS 95Y $B(h^- h^- h^+ \geq 0 \text{ neutrals } \nu_\tau \text{ (ex. } K_S^0 \rightarrow \pi^+ \pi^-))$ and $B(h^- h^- h^+ \nu_\tau \text{ (ex. } K^0))/B(h^- h^- h^+ \geq 0 \text{ neutrals } \nu_\tau \text{ (ex. } K_S^0 \rightarrow \pi^+ \pi^-))$ values.
- ³Not independent of BUSKULIC 96 $B(h^- h^- h^+ \nu_\tau)$ value.

WEIGHTED AVERAGE
9.44 ± 0.14 (Error scaled by 1.4)



$$\Gamma(h^- h^- h^+ \nu_\tau \text{ (ex. } K^0))/\Gamma_{total} \quad \Gamma_{58}/\Gamma = (\Gamma_{62} + \Gamma_{85} + \Gamma_{93})/\Gamma$$

$$\Gamma(h^- h^- h^+ \nu_\tau \text{ (ex. } K^0))/\Gamma_{total} \quad \Gamma_{59}/\Gamma = (0.3431\Gamma_{35} + \Gamma_{62} + 0.017\Gamma_{150})/\Gamma$$

VALUE (%)	DOCUMENT ID	TECN	COMMENT
0.650 ± 0.004 OUR FIT	Error includes scale factor of 1.2.		
0.660 ± 0.004 ± 0.014	AKERS	95Y	OPAL 1991-1994 LEP runs

$$\Gamma(h^- h^- h^+ \nu_\tau \text{ (ex. } K^0 \mu))/\Gamma_{total} \quad \Gamma_{58}/\Gamma = (\Gamma_{62} + \Gamma_{85} + \Gamma_{93})/\Gamma$$

VALUE (%)	DOCUMENT ID	TECN	COMMENT
9.42 ± 0.07 OUR FIT	Error includes scale factor of 1.3.		

$$\Gamma(\pi^- \pi^+ \pi^- \nu_\tau)/\Gamma_{total} \quad \Gamma_{59}/\Gamma = (0.3431\Gamma_{35} + \Gamma_{62} + 0.017\Gamma_{150})/\Gamma$$

VALUE (%)	DOCUMENT ID	TECN	COMMENT
9.32 ± 0.07 OUR FIT	Error includes scale factor of 1.2.		

$$\Gamma(\pi^- \pi^+ \pi^- \nu_\tau \text{ (ex. } K^0))/\Gamma_{total} \quad \Gamma_{60}/\Gamma = (\Gamma_{62} + 0.017\Gamma_{150})/\Gamma$$

VALUE (%)	EVTs	DOCUMENT ID	TECN	COMMENT
9.03 ± 0.06 OUR FIT	Error includes scale factor of 1.2.			
8.85 ± 0.13 OUR AVERAGE				
8.83 ± 0.01 ± 0.13	1.6M	¹ AUBERT	08	BABR 342 fb ⁻¹ $E_{cm}^{ee} = 10.6$ GeV
9.13 ± 0.05 ± 0.46	43k	² BRIERE	03	CLE3 $E_{cm}^{ee} = 10.6$ GeV

- ¹Correlation matrix for AUBERT 08 branching fractions:

(1)	(2)	(3)	
(2)	0.544		
(3)	0.390	0.177	
(4)	0.031	0.093	0.087

- ²47% correlated with BRIERE 03 $\tau^- \rightarrow K^- \pi^+ \pi^- \nu_\tau$ and 71% correlated with $\tau^- \rightarrow K^- K^+ \pi^- \nu_\tau$ because of a common 5% normalization error.

$$\Gamma(\pi^- \pi^+ \pi^- \nu_\tau \text{ (ex. } K^0, \text{ non-axial vector)})/\Gamma(\pi^- \pi^+ \pi^- \nu_\tau \text{ (ex. } K^0)) \quad \Gamma_{61}/\Gamma_{60} = \Gamma_{61}/(\Gamma_{62} + 0.017\Gamma_{150})$$

VALUE	CL%	DOCUMENT ID	TECN	COMMENT
<0.261	95	¹ ACKERSTAFF	97R	OPAL 1992-1994 LEP runs

- ¹Model-independent limit from structure function analysis on contribution to $B(\tau^- \rightarrow \pi^- \pi^+ \pi^- \nu_\tau \text{ (ex. } K^0))$ from non-axial vectors.

$\Gamma(\pi^-\pi^+\pi^-\nu_\tau(\text{ex. } K^0, \omega))/\Gamma_{\text{total}}$ Γ_{62}/Γ

VALUE (%)	EVTS	DOCUMENT ID	TECN	COMMENT
9.00 ± 0.06 OUR FIT				Error includes scale factor of 1.2.
9.041 ± 0.060 ± 0.076	29k	¹ SCHAE1	05c ALEP	1991-1995 LEP runs

¹ See footnote to SCHAE1 05c $\Gamma(\tau^- \rightarrow e^- \bar{\nu}_e \nu_\tau)/\Gamma_{\text{total}}$ measurement for correlations with other measurements.

 $\Gamma(h^- h^- h^+ \geq 1 \text{ neutrals } \nu_\tau)/\Gamma_{\text{total}}$ Γ_{63}/Γ

VALUE (%)	EVTS	DOCUMENT ID	TECN	COMMENT
5.38 ± 0.07 OUR FIT				Error includes scale factor of 1.2.
5.6 ± 0.7 ± 0.3	352	¹ BEHREND	90 CELL	$E_{\text{cm}}^{\text{ex}} = 35 \text{ GeV}$
4.2 ± 0.5 ± 0.9	203	² ALBRECHT	87L ARG	$E_{\text{cm}}^{\text{ex}} = 10 \text{ GeV}$
6.1 ± 0.8 ± 0.9		³ BURCHAT	87 MRK2	$E_{\text{cm}}^{\text{ex}} = 29 \text{ GeV}$
7.6 ± 0.4 ± 0.9		^{4,5} RUCKSTUHL	86 DLCO	$E_{\text{cm}}^{\text{ex}} = 29 \text{ GeV}$
4.7 ± 0.5 ± 0.8	530	⁶ SCHMIDKE	86 MRK2	$E_{\text{cm}}^{\text{ex}} = 29 \text{ GeV}$
5.6 ± 0.4 ± 0.7		⁵ FERNANDEZ	85 MAC	$E_{\text{cm}}^{\text{ex}} = 29 \text{ GeV}$
6.2 ± 2.3 ± 1.7		BEHREND	84 CELL	$E_{\text{cm}}^{\text{ex}} = 14, 22 \text{ GeV}$

• • • We do not use the following data for averages, fits, limits, etc. **• • •**

¹ BEHREND 90 value is not independent of BEHREND 90 $B(h^- h^- h^+ \geq 1 \text{ neutrals}) + B(5\text{-prong})$.

² ALBRECHT 87L measure the product of branching ratios $B(3\pi^+ \pi^0 \nu_\tau) B((e\bar{\nu}_e \mu\bar{\nu}_\mu \text{ or } \pi^0 \text{ or } K^0 \text{ or } \rho) \nu_\tau) = 0.029$ and use the PDG 86 values for the second branching ratio which sum to 0.69 ± 0.03 to get the quoted value.

³ BURCHAT 87 value is not independent of SCHMIDKE 86 value.

⁴ Contributions from kaons and from $>1\pi^0$ are subtracted. Not independent of (3-prong + $0\pi^0$) and (3-prong + $\geq 0\pi^0$) values.

⁵ Value obtained using paper's $R = B(h^- h^- h^+ \nu_\tau)/B(3\text{-prong})$ and current $B(3\text{-prong}) = 0.143$.

⁶ Not independent of SCHMIDKE 86 $h^- h^- h^+ \nu_\tau$ and $h^- h^- h^+ (\geq 0\pi^0) \nu_\tau$ values.

Data marked "avg" are highly correlated with data appearing elsewhere in the Listings, and are therefore used for the average given below but not in the overall fits. "f&a" marks results used for the fit and the average.

VALUE (%)	EVTS	DOCUMENT ID	TECN	COMMENT
5.08 ± 0.06 OUR FIT				Error includes scale factor of 1.1.
5.10 ± 0.12 OUR AVERAGE				
5.106 ± 0.083 ± 0.103	10.1k	¹ ABDALLAH	06A DLPH	1992-1995 LEP runs
5.09 ± 0.10 ± 0.23	avg	² AKERS	95Y OPAL	1991-1994 LEP runs

• • • We do not use the following data for averages, fits, limits, etc. **• • •**

VALUE (%)	EVTS	DOCUMENT ID	TECN	COMMENT
4.95 ± 0.29 ± 0.65	570	DECAMP	92c ALEP	Repl. by SCHAE1 05c

¹ See footnote to ABDALLAH 06A $\Gamma(\tau^- \rightarrow h^- \nu_\tau)/\Gamma_{\text{total}}$ measurement for correlations with other measurements.

² Not independent of AKERS 95Y $B(h^- h^- h^+ \geq 0 \text{ neutrals } \nu_\tau(\text{ex. } K_S^0 \rightarrow \pi^+ \pi^-))$ and $B(h^- h^- h^+ \geq 0 \text{ neutrals } \nu_\tau(\text{ex. } K_S^0)/B(h^- h^- h^+ \geq 0 \text{ neutrals } \nu_\tau(\text{ex. } K_S^0 \rightarrow \pi^+ \pi^-))$ values.

 $\Gamma(h^- h^- h^+ \pi^0 \nu_\tau)/\Gamma_{\text{total}}$ Γ_{65}/Γ

VALUE (%)	EVTS	DOCUMENT ID	TECN	COMMENT
4.75 ± 0.06 OUR FIT				Error includes scale factor of 1.2.
4.45 ± 0.09 ± 0.07	6.1k	¹ BUSKULIC	96 ALEP	Repl. by SCHAE1 05c

¹ BUSKULIC 96 quote $B(h^- h^- h^+ \pi^0 \nu_\tau(\text{ex. } K^0)) = 4.30 \pm 0.09 \pm 0.09$. We add 0.15 to remove their K^0 correction and reduce the systematic error accordingly.

 $\Gamma(h^- h^- h^+ \pi^0 \nu_\tau(\text{ex. } K^0, \omega))/\Gamma_{\text{total}}$ Γ_{66}/Γ

VALUE (%)	EVTS	DOCUMENT ID	TECN	COMMENT
4.56 ± 0.06 OUR FIT				Error includes scale factor of 1.2.
4.45 ± 0.14 OUR AVERAGE				Error includes scale factor of 1.2.
4.545 ± 0.106 ± 0.103	8.9k	¹ ABDALLAH	06A DLPH	1992-1995 LEP runs
4.23 ± 0.06 ± 0.22	7.2k	BALEST	95c CLEO	$E_{\text{cm}}^{\text{ex}} \approx 10.6 \text{ GeV}$

¹ See footnote to ABDALLAH 06A $\Gamma(\tau^- \rightarrow h^- \nu_\tau)/\Gamma_{\text{total}}$ measurement for correlations with other measurements.

 $\Gamma(h^- h^- h^+ \pi^0 \nu_\tau(\text{ex. } K^0, \omega))/\Gamma_{\text{total}}$ $\Gamma_{67}/\Gamma = (\Gamma_{70} + \Gamma_{89} + \Gamma_{94} + 0.226\Gamma_{128})/\Gamma$

VALUE (%)	EVTS	DOCUMENT ID	TECN	COMMENT
2.79 ± 0.08 OUR FIT				Error includes scale factor of 1.2.

 $\Gamma(\pi^-\pi^+\pi^-\pi^0 \nu_\tau)/\Gamma_{\text{total}}$ $\Gamma_{68}/\Gamma = (0.3431\Gamma_{40} + \Gamma_{70} + 0.888\Gamma_{150} + 0.017\Gamma_{152})/\Gamma$

VALUE (%)	EVTS	DOCUMENT ID	TECN	COMMENT
4.61 ± 0.06 OUR FIT				Error includes scale factor of 1.1.

 $\Gamma(\pi^-\pi^+\pi^-\pi^0 \nu_\tau(\text{ex. } K^0))/\Gamma_{\text{total}}$ $\Gamma_{69}/\Gamma = (\Gamma_{70} + 0.888\Gamma_{150} + 0.017\Gamma_{152})/\Gamma$

VALUE (%)	EVTS	DOCUMENT ID	TECN	COMMENT
4.48 ± 0.06 OUR FIT				Error includes scale factor of 1.2.
4.55 ± 0.13 OUR AVERAGE				Error includes scale factor of 1.6.
4.598 ± 0.057 ± 0.064	16k	¹ SCHAE1	05c ALEP	1991-1995 LEP runs
4.19 ± 0.10 ± 0.21		² EDWARDS	00A CLEO	$4.7 \text{ fb}^{-1} E_{\text{cm}}^{\text{ex}} = 10.6 \text{ GeV}$

¹ SCHAE1 05c quote $(4.590 \pm 0.057 \pm 0.064)\%$. We add 0.008% to remove their correction for $\tau^- \rightarrow \pi^- \pi^0 \omega \nu_\tau \rightarrow \pi^- \pi^0 \pi^+ \pi^- \nu_\tau$ decays. See footnote to SCHAE1 05c $\Gamma(\tau^- \rightarrow e^- \bar{\nu}_e \nu_\tau)/\Gamma_{\text{total}}$ measurement for correlations with other measurements.

² EDWARDS 00A quote $(4.19 \pm 0.10) \times 10^{-2}$ with a 5% systematic error.

 $\Gamma(\pi^-\pi^+\pi^-\pi^0 \nu_\tau(\text{ex. } K^0, \omega))/\Gamma_{\text{total}}$ Γ_{70}/Γ

VALUE (%)	EVTS	DOCUMENT ID	TECN	COMMENT
2.70 ± 0.08 OUR FIT				Error includes scale factor of 1.2.

 $\Gamma(h^- \rho \pi^0 \nu_\tau)/\Gamma(h^- h^- h^+ \pi^0 \nu_\tau)$ Γ_{71}/Γ_{65}

VALUE (%)	EVTS	DOCUMENT ID	TECN	COMMENT
0.30 ± 0.04 ± 0.02	393	ALBRECHT	91D ARG	$E_{\text{cm}}^{\text{ex}} = 9.4\text{--}10.6 \text{ GeV}$

• • • We do not use the following data for averages, fits, limits, etc. **• • •**

 $\Gamma(h^- \rho^+ h^- \nu_\tau)/\Gamma(h^- h^- h^+ \pi^0 \nu_\tau)$ Γ_{72}/Γ_{65}

VALUE (%)	EVTS	DOCUMENT ID	TECN	COMMENT
0.10 ± 0.03 ± 0.04	142	ALBRECHT	91D ARG	$E_{\text{cm}}^{\text{ex}} = 9.4\text{--}10.6 \text{ GeV}$

• • • We do not use the following data for averages, fits, limits, etc. **• • •**

 $\Gamma(h^- \rho^- h^+ \nu_\tau)/\Gamma(h^- h^- h^+ \pi^0 \nu_\tau)$ Γ_{73}/Γ_{65}

VALUE (%)	EVTS	DOCUMENT ID	TECN	COMMENT
0.26 ± 0.05 ± 0.01	370	ALBRECHT	91D ARG	$E_{\text{cm}}^{\text{ex}} = 9.4\text{--}10.6 \text{ GeV}$

• • • We do not use the following data for averages, fits, limits, etc. **• • •**

 $\Gamma(h^- h^- h^+ \geq 2\pi^0 \nu_\tau(\text{ex. } K^0))/\Gamma_{\text{total}}$ $\Gamma_{74}/\Gamma = (\Gamma_{77} + \Gamma_{78} + 0.226\Gamma_{126} + 0.888\Gamma_{152})/\Gamma$

VALUE (%)	EVTS	DOCUMENT ID	TECN	COMMENT
0.518 ± 0.033 OUR FIT				
0.561 ± 0.068 ± 0.095	1.3k	¹ ABDALLAH	06A DLPH	1992-1995 LEP runs

¹ See footnote to ABDALLAH 06A $\Gamma(\tau^- \rightarrow h^- \nu_\tau)/\Gamma_{\text{total}}$ measurement for correlations with other measurements.

 $\Gamma(h^- h^- h^+ 2\pi^0 \nu_\tau)/\Gamma_{\text{total}}$ $\Gamma_{75}/\Gamma = (0.4307\Gamma_{47} + \Gamma_{77} + 0.226\Gamma_{126} + 0.888\Gamma_{152})/\Gamma$

VALUE (%)	EVTS	DOCUMENT ID	TECN	COMMENT
0.518 ± 0.033 OUR FIT				
0.506 ± 0.032 OUR FIT				

 $\Gamma(h^- h^- h^+ 2\pi^0 \nu_\tau(\text{ex. } K^0))/\Gamma_{\text{total}}$ $\Gamma_{76}/\Gamma = (\Gamma_{77} + 0.226\Gamma_{126} + 0.888\Gamma_{152})/\Gamma$

VALUE (%)	EVTS	DOCUMENT ID	TECN	COMMENT
0.495 ± 0.032 OUR FIT				
0.435 ± 0.030 ± 0.035	2.6k	¹ SCHAE1	05c ALEP	1991-1995 LEP runs

• • • We do not use the following data for averages, fits, limits, etc. **• • •**

¹ SCHAE1 05c quote $(0.392 \pm 0.030 \pm 0.035)\%$. We add 0.043% to remove their correction for $\tau^- \rightarrow \pi^- \eta \pi^0 \nu_\tau \rightarrow \pi^- \pi^+ \pi^- 2\pi^0 \nu_\tau$ and $\tau^- \rightarrow K^*(892) \eta \nu_\tau \rightarrow K^- \pi^+ \pi^- 2\pi^0 \nu_\tau$ decays. See footnote to SCHAE1 05c $\Gamma(\tau^- \rightarrow e^- \bar{\nu}_e \nu_\tau)/\Gamma_{\text{total}}$ measurement for correlations with other measurements.

 $\Gamma(h^- h^- h^+ 2\pi^0 \nu_\tau(\text{ex. } K^0))/\Gamma(h^- h^- h^+ \geq 0 \text{ neutrals } \geq 0 K_L^0 \nu_\tau)$ $\Gamma_{76}/\Gamma_{54} = (\Gamma_{77} + 0.226\Gamma_{126} + 0.888\Gamma_{152})/(0.3431\Gamma_{35} + 0.3431\Gamma_{37} + 0.3431\Gamma_{40} + 0.3431\Gamma_{42} + 0.4307\Gamma_{47} + 0.6861\Gamma_{48} + \Gamma_{62} + \Gamma_{70} + \Gamma_{77} + \Gamma_{78} + \Gamma_{85} + \Gamma_{89} + \Gamma_{93} + \Gamma_{94} + 0.285\Gamma_{126} + 0.285\Gamma_{128} + 0.9101\Gamma_{150} + 0.9101\Gamma_{152})$

VALUE (%)	EVTS	DOCUMENT ID	TECN	COMMENT
0.326 ± 0.0021 OUR FIT				
0.034 ± 0.002 ± 0.003	668	BORTOLETTO	093 CLEO	$E_{\text{cm}}^{\text{ex}} \approx 10.6 \text{ GeV}$

• • • We do not use the following data for averages, fits, limits, etc. **• • •**

 $\Gamma(h^- h^- h^+ 2\pi^0 \nu_\tau(\text{ex. } K^0, \omega, \eta))/\Gamma_{\text{total}}$ Γ_{77}/Γ

VALUE (units 10^{-4})	EVTS	DOCUMENT ID	TECN	COMMENT
10 ± 4 OUR FIT				

 $\Gamma(h^- h^- h^+ 3\pi^0 \nu_\tau)/\Gamma_{\text{total}}$ Γ_{78}/Γ

VALUE (units 10^{-4})	CL%	EVTS	DOCUMENT ID	TECN	COMMENT
2.3 ± 0.7 OUR FIT					Error includes scale factor of 1.3.
2.2 ± 0.3 ± 0.4	139	ANASTASSOV	01 CLEO	$E_{\text{cm}}^{\text{ex}} = 10.6 \text{ GeV}$	

• • • We do not use the following data for averages, fits, limits, etc. **• • •**

VALUE (%)	EVTS	DOCUMENT ID	TECN	COMMENT
< 4.9	95	SCHAE1	05c ALEP	1991-1995 LEP runs
2.85 ± 0.56 ± 0.51	57	ANDERSON	97 CLEO	Repl. by ANAS-TASSOV 01

¹ BUSKULIC 96 state their measurement is for $B(h^- h^- h^+ \geq 3\pi^0 \nu_\tau)$. We assume that $B(h^- h^- h^+ \geq 4\pi^0 \nu_\tau)$ is very small.

Lepton Particle Listings

T

$$\Gamma(K^- h^+ h^- \geq 0 \text{ neutrals } \nu_\tau) / \Gamma_{\text{total}} \\ \Gamma_{79} / \Gamma = (0.3431\Gamma_{37} + 0.3431\Gamma_{42} + \Gamma_{85} + \Gamma_{89} + \Gamma_{93} + \Gamma_{94} + 0.285\Gamma_{128}) / \Gamma$$

VALUE (%)	CL%	DOCUMENT ID	TECN	COMMENT
0.624 ± 0.024 OUR FIT				Error includes scale factor of 1.5.
<0.6	90	AIHARA	84c	TPC $E_{\text{cm}}^{\text{ee}} = 29 \text{ GeV}$

$$\Gamma(K^- h^+ \pi^- \nu_\tau (\text{ex. } K^0)) / \Gamma_{\text{total}} \quad \Gamma_{80} / \Gamma = (\Gamma_{85} + \Gamma_{93}) / \Gamma$$

VALUE (%)	DOCUMENT ID
0.427 ± 0.020 OUR FIT	Error includes scale factor of 2.4.

$$\Gamma(K^- h^+ \pi^- \nu_\tau (\text{ex. } K^0)) / \Gamma(\pi^- \pi^+ \pi^- \nu_\tau (\text{ex. } K^0)) \\ \Gamma_{80} / \Gamma_{60} = (\Gamma_{85} + \Gamma_{93}) / (\Gamma_{62} + 0.017\Gamma_{150})$$

VALUE (%)	EVTS	DOCUMENT ID	TECN	COMMENT
4.73 ± 0.21 OUR FIT				Error includes scale factor of 2.4.
5.44 ± 0.21 ± 0.53	7.9k	RICHICHI	99	CLEO $E_{\text{cm}}^{\text{ee}} = 10.6 \text{ GeV}$

$$\Gamma(K^- h^+ \pi^- \pi^0 \nu_\tau (\text{ex. } K^0)) / \Gamma_{\text{total}} \quad \Gamma_{81} / \Gamma = (\Gamma_{89} + \Gamma_{94} + 0.226\Gamma_{128}) / \Gamma$$

VALUE (units 10^{-4})	DOCUMENT ID
8.7 ± 1.2 OUR FIT	Error includes scale factor of 1.1.

$$\Gamma(K^- h^+ \pi^- \pi^0 \nu_\tau (\text{ex. } K^0)) / \Gamma(\pi^- \pi^+ \pi^- \pi^0 \nu_\tau (\text{ex. } K^0)) \\ \Gamma_{81} / \Gamma_{69} = (\Gamma_{89} + \Gamma_{94} + 0.226\Gamma_{128}) / (\Gamma_{70} + 0.888\Gamma_{150} + 0.017\Gamma_{152})$$

VALUE (%)	EVTS	DOCUMENT ID	TECN	COMMENT
1.95 ± 0.27 OUR FIT				
2.61 ± 0.45 ± 0.42	719	RICHICHI	99	CLEO $E_{\text{cm}}^{\text{ee}} = 10.6 \text{ GeV}$

$$\Gamma(K^- \pi^+ \pi^- \geq 0 \text{ neutrals } \nu_\tau) / \Gamma_{\text{total}} \\ \Gamma_{82} / \Gamma = (0.3431\Gamma_{37} + 0.3431\Gamma_{42} + \Gamma_{85} + \Gamma_{89} + 0.285\Gamma_{128}) / \Gamma$$

VALUE (%)	EVTS	DOCUMENT ID	TECN	COMMENT
0.478 ± 0.021 OUR FIT				Error includes scale factor of 1.3.
0.58 ± 0.15 -0.13 ± 0.12	20	¹ BAUER	94	TPC $E_{\text{cm}}^{\text{ee}} = 29 \text{ GeV}$

• • • We do not use the following data for averages, fits, limits, etc. • • •

0.22 ± 0.16 -0.13 ± 0.05	9	² MILLS	85	DLCO $E_{\text{cm}}^{\text{ee}} = 29 \text{ GeV}$
----------------------------------	---	--------------------	----	---

¹ We multiply 0.58% by 0.20, the relative systematic error quoted by BAUER 94, to obtain the systematic error.

² Error correlated with MILLS 85 ($K K \pi \nu$) value. We multiply 0.22% by 0.23, the relative systematic error quoted by MILLS 85, to obtain the systematic error.

$$\Gamma(K^- \pi^+ \pi^- \geq 0 \pi^0 \nu_\tau (\text{ex. } K^0)) / \Gamma_{\text{total}} \quad \Gamma_{83} / \Gamma = (\Gamma_{85} + \Gamma_{89} + 0.226\Gamma_{128}) / \Gamma$$

Data marked "avg" are highly correlated with data appearing elsewhere in the Listings, and are therefore used for the average given below but not in the overall fits. "f&a" marks results used for the fit and the average.

VALUE (%)	DOCUMENT ID	TECN	COMMENT
0.368 ± 0.020 OUR FIT			Error includes scale factor of 1.4.
0.30 ± 0.05 OUR AVERAGE			

0.343 ± 0.073 ± 0.031	avg	ABBIENDI	00d	OPAL 1990-1995 LEP runs
0.275 ± 0.064	avg	¹ BARATE	98	ALEP 1991-1995 LEP runs

¹ Not independent of BARATE 98 $\Gamma(\tau^- \rightarrow K^- \pi^+ \pi^- \nu_\tau) / \Gamma_{\text{total}}$ and $\Gamma(\tau^- \rightarrow K^- \pi^+ \pi^- \pi^0 \nu_\tau) / \Gamma_{\text{total}}$ values.

$$\Gamma(K^- \pi^+ \pi^- \nu_\tau) / \Gamma_{\text{total}} \quad \Gamma_{84} / \Gamma = (0.3431\Gamma_{37} + \Gamma_{85}) / \Gamma$$

VALUE (%)	DOCUMENT ID
0.342 ± 0.017 OUR FIT	Error includes scale factor of 1.8.

$$\Gamma(K^- \pi^+ \pi^- \nu_\tau (\text{ex. } K^0)) / \Gamma_{\text{total}} \quad \Gamma_{85} / \Gamma$$

Data marked "avg" are highly correlated with data appearing elsewhere in the Listings, and are therefore used for the average given below but not in the overall fits. "f&a" marks results used for the fit and the average.

VALUE (%)	EVTS	DOCUMENT ID	TECN	COMMENT
0.287 ± 0.016 OUR FIT				Error includes scale factor of 2.1.
0.280 ± 0.019 OUR AVERAGE				Error includes scale factor of 2.1. See the ideogram below.

0.273 ± 0.002 ± 0.009 f&a	70k	¹ AUBERT	08	BABR 342 fb ⁻¹ $E_{\text{cm}}^{\text{ee}} = 10.6 \text{ GeV}$
0.415 ± 0.053 ± 0.040 f&a	269	ABBIENDI	04j	OPAL 1991-1995 LEP runs
0.384 ± 0.014 ± 0.038 f&a	3.5k	² BRIERE	03	CLE3 $E_{\text{cm}}^{\text{ee}} = 10.6 \text{ GeV}$
0.346 ± 0.023 ± 0.056 avg	158	³ RICHICHI	99	CLEO $E_{\text{cm}}^{\text{ee}} = 10.6 \text{ GeV}$
0.214 ± 0.037 ± 0.029 f&a		BARATE	98	ALEP 1991-1995 LEP runs

• • • We do not use the following data for averages, fits, limits, etc. • • •

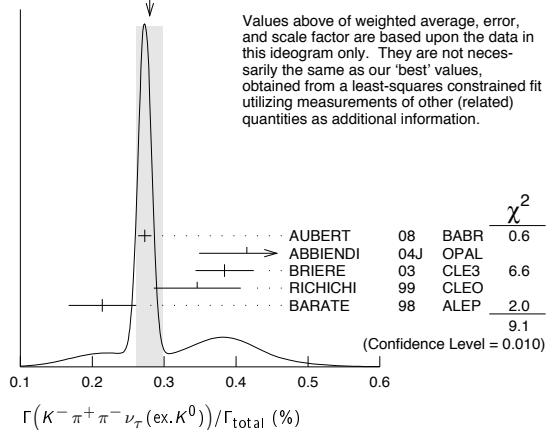
0.360 ± 0.082 ± 0.048		ABBIENDI	00d	OPAL 1990-1995 LEP runs
-----------------------	--	----------	-----	-------------------------

¹ See footnote to AUBERT 08 $\Gamma(\tau^- \rightarrow \pi^- \pi^+ \pi^- \nu_\tau (\text{ex. } K^0)) / \Gamma_{\text{total}}$ measurement for correlations with other measurements.

² 47% correlated with BRIERE 03 $\tau^- \rightarrow \pi^- \pi^+ \pi^- \nu_\tau$ and 34% correlated with $\tau^- \rightarrow K^- K^+ \pi^- \nu_\tau$ because of a common 5% normalization error.

³ Not independent of RICHICHI 99 $\Gamma(\tau^- \rightarrow K^- h^+ \pi^- \nu_\tau (\text{ex. } K^0)) / \Gamma_{\text{total}}$, $\Gamma(\tau^- \rightarrow K^- K^+ \pi^- \nu_\tau) / \Gamma_{\text{total}}$, $\Gamma(\tau^- \rightarrow \pi^- \pi^+ \pi^- \nu_\tau (\text{ex. } K^0)) / \Gamma_{\text{total}}$ and BALEST 95c $\Gamma(\tau^- \rightarrow h^- h^- h^+ \pi^- \nu_\tau (\text{ex. } K^0)) / \Gamma_{\text{total}}$ values.

WEIGHTED AVERAGE
0.280 ± 0.019 (Error scaled by 2.1)



Values above of weighted average, error, and scale factor are based upon the data in this ideogram only. They are not necessarily the same as our "best" values, obtained from a least-squares constrained fit utilizing measurements of other (related) quantities as additional information.

$$\Gamma(K^- \rho^0 \nu_\tau \rightarrow K^- \pi^+ \pi^- \nu_\tau) / \Gamma(K^- \pi^+ \pi^- \nu_\tau (\text{ex. } K^0)) \quad \Gamma_{86} / \Gamma_{85}$$

VALUE	DOCUMENT ID	TECN	COMMENT
0.48 ± 0.14 ± 0.10	¹ ASNER	00b	CLEO $E_{\text{cm}}^{\text{ee}} = 10.6 \text{ GeV}$

• • • We do not use the following data for averages, fits, limits, etc. • • •

0.39 ± 0.14	² BARATE	99r	ALEP 1991-1995 LEP runs
-------------	---------------------	-----	-------------------------

¹ ASNER 00b assume $\tau^- \rightarrow K^- \pi^+ \pi^- \nu_\tau (\text{ex. } K^0)$ decays proceed only through $K \rho$ and $K^* \pi$ intermediate states. They assume the resonance structure of $\tau^- \rightarrow K^- \pi^+ \pi^- \nu_\tau (\text{ex. } K^0)$ decays is dominated by $K_1(1270)^-$ and $K_1(1400)^-$ resonances, and assume $B(K_1(1270) \rightarrow K^*(892) \pi) = (16 \pm 5)\%$, $B(K_1(1270) \rightarrow K \rho) = (42 \pm 6)\%$, and $B(K_1(1400) \rightarrow K \rho) = 0$.

² BARATE 99r assume $\tau^- \rightarrow K^- \pi^+ \pi^- \nu_\tau (\text{ex. } K^0)$ decays proceed only through $K \rho$ and $K^* \pi$ intermediate states. The quoted error is statistical only.

$$\Gamma(K^- \pi^+ \pi^- \pi^0 \nu_\tau) / \Gamma_{\text{total}} \quad \Gamma_{87} / \Gamma = (0.3431\Gamma_{42} + \Gamma_{89} + 0.226\Gamma_{128}) / \Gamma$$

VALUE (units 10^{-4})	DOCUMENT ID
13.6 ± 1.4 OUR FIT	

$$\Gamma(K^- \pi^+ \pi^- \pi^0 \nu_\tau (\text{ex. } K^0)) / \Gamma_{\text{total}} \quad \Gamma_{88} / \Gamma = (\Gamma_{89} + 0.226\Gamma_{128}) / \Gamma$$

Data marked "avg" are highly correlated with data appearing elsewhere in the Listings, and are therefore used for the average given below but not in the overall fits. "f&a" marks results used for the fit and the average.

VALUE (units 10^{-4})	CL%	DOCUMENT ID	TECN	COMMENT
8.1 ± 1.2 OUR FIT				
7.3 ± 1.2 OUR AVERAGE				

7.4 ± 0.8 ± 1.1 f&a		¹ ARMS	05	CLE3 7.6 fb ⁻¹ , $E_{\text{cm}}^{\text{ee}} = 10.6 \text{ GeV}$
7.5 ± 2.6 ± 1.8 avg		² RICHICHI	99	CLEO $E_{\text{cm}}^{\text{ee}} = 10.6 \text{ GeV}$
6.1 ± 3.9 ± 1.8 f&a		BARATE	98	ALEP 1991-1995 LEP runs

• • • We do not use the following data for averages, fits, limits, etc. • • •

<17	95	ABBIENDI	00d	OPAL 1990-1995 LEP runs
-----	----	----------	-----	-------------------------

¹ Not independent of ARMS 05 $\Gamma(\tau^- \rightarrow K^- \pi^+ \pi^- \pi^0 \nu_\tau (\text{ex. } K^0, \omega)) / \Gamma_{\text{total}}$ and $\Gamma(\tau^- \rightarrow K^- \omega \nu_\tau) / \Gamma_{\text{total}}$ values.

² Not independent of RICHICHI 99

$\Gamma(\tau^- \rightarrow K^- h^+ \pi^- \nu_\tau (\text{ex. } K^0)) / \Gamma(\tau^- \rightarrow \pi^- \pi^+ \pi^- \nu_\tau (\text{ex. } K^0))$, $\Gamma(\tau^- \rightarrow K^- K^+ \pi^- \nu_\tau) / \Gamma(\tau^- \rightarrow \pi^- \pi^+ \pi^- \nu_\tau (\text{ex. } K^0))$ and BALEST 95c $\Gamma(\tau^- \rightarrow h^- h^- h^+ \pi^- \nu_\tau (\text{ex. } K^0)) / \Gamma_{\text{total}}$ values.

$$\Gamma(K^- \pi^+ \pi^- \pi^0 \nu_\tau (\text{ex. } K^0, \eta)) / \Gamma_{\text{total}} \quad \Gamma_{89} / \Gamma$$

VALUE (units 10^{-4})	DOCUMENT ID
7.7 ± 1.2 OUR FIT	

$$\Gamma(K^- \pi^+ \pi^- \pi^0 \nu_\tau (\text{ex. } K^0, \omega)) / \Gamma_{\text{total}} \quad \Gamma_{90} / \Gamma$$

VALUE (units 10^{-4})	EVTS	DOCUMENT ID	TECN	COMMENT
3.7 ± 0.5 ± 0.8	833	ARMS	05	CLE3 7.6 fb ⁻¹ , $E_{\text{cm}}^{\text{ee}} = 10.6 \text{ GeV}$

$$\Gamma(K^- \pi^+ K^- \geq 0 \text{ neut. } \nu_\tau) / \Gamma_{\text{total}} \quad \Gamma_{91} / \Gamma$$

VALUE (%)	CL%	DOCUMENT ID	TECN	COMMENT
<0.09	95	BAUER	94	TPC $E_{\text{cm}}^{\text{ee}} = 29 \text{ GeV}$

$$\Gamma(K^- K^+ \pi^- \geq 0 \text{ neut. } \nu_\tau) / \Gamma_{\text{total}} \quad \Gamma_{92} / \Gamma = (\Gamma_{93} + \Gamma_{94}) / \Gamma$$

Data marked "avg" are highly correlated with data appearing elsewhere in the Listings, and are therefore used for the average given below but not in the overall fits. "f&a" marks results used for the fit and the average.

VALUE (%)	EVTS	DOCUMENT ID	TECN	COMMENT
0.146 ± 0.006 OUR FIT				Error includes scale factor of 1.6.
0.203 ± 0.031 OUR AVERAGE				

0.159 ± 0.053 ± 0.020 f&a		ABBIENDI	00d	OPAL 1990-1995 LEP runs
0.238 ± 0.042 avg		¹ BARATE	98	ALEP 1991-1995 LEP runs
0.15 ± 0.09 ± 0.03 f&a	4	² BAUER	94	TPC $E_{\text{cm}}^{\text{ee}} = 29 \text{ GeV}$

Lepton Particle Listings

τ

$\Gamma((5\pi^-)\nu_\tau)/\Gamma_{total}$ Γ_{106}/Γ
 $\Gamma_{106}/\Gamma = (\Gamma_{30} + \Gamma_{47} + \Gamma_{77} + \Gamma_{103} + 0.553\Gamma_{126} + 0.888\Gamma_{152})/\Gamma$

Data marked "avg" are highly correlated with data appearing elsewhere in the Listings, and are therefore used for the average given below but not in the overall fits. "f&a" marks results used for the fit and the average.

VALUE (%)	DOCUMENT ID	TECN	COMMENT
0.76 ± 0.05 OUR FIT			
0.61 ± 0.06 ± 0.08 avg	¹ GIBAUT 94B	CLEO	$E_{cm}^{ee} = 10.6$ GeV

¹ Not independent of GIBAUT 94B $B(3h^-2h^+\nu_\tau)$, PROCARIO 93 $B(h^-4\pi^0\nu_\tau)$, and BORTOLETTO 93 $B(2h^-h^+2\pi^0\nu_\tau)/B("3prong")$ measurements. Result is corrected for η contributions.

$\Gamma(4h^-3h^+ \geq 0 \text{ neutrals } \nu_\tau ("7\text{-prong"}))/\Gamma_{total}$ Γ_{107}/Γ

VALUE	CL%	DOCUMENT ID	TECN	COMMENT
< 3.0 × 10⁻⁷	90	AUBERT,B	05F BABR	232 fb^{-1} , $E_{cm}^{ee} = 10.6$ GeV

• • • We do not use the following data for averages, fits, limits, etc. • • •

< 1.8 × 10 ⁻⁵	95	ACKERSTAFF 97J	OPAL	1990-1995 LEP runs
< 2.4 × 10 ⁻⁶	90	EDWARDS 97B	CLEO	$E_{cm}^{ee} = 10.6$ GeV
< 2.9 × 10 ⁻⁴	90	BYLSMA 87	HRS	$E_{cm}^{ee} = 29$ GeV

$\Gamma(4h^-3h^+\nu_\tau)/\Gamma_{total}$ Γ_{108}/Γ

VALUE	CL%	DOCUMENT ID	TECN	COMMENT
< 4.3 × 10⁻⁷	90	AUBERT,B	05F BABR	232 fb^{-1} , $E_{cm}^{ee} = 10.6$ GeV

$\Gamma(4h^-3h^+\pi^0\nu_\tau)/\Gamma_{total}$ Γ_{109}/Γ

VALUE	CL%	DOCUMENT ID	TECN	COMMENT
< 2.5 × 10⁻⁷	90	AUBERT,B	05F BABR	232 fb^{-1} , $E_{cm}^{ee} = 10.6$ GeV

$\Gamma(X^-(S=-1)\nu_\tau)/\Gamma_{total}$ $\Gamma_{110}/\Gamma = (\Gamma_{10} + \Gamma_{16} + \Gamma_{23} + \Gamma_{28} + \Gamma_{35} + \Gamma_{40} + \Gamma_{85} + \Gamma_{89} + \Gamma_{128})/\Gamma$

Data marked "avg" are highly correlated with data appearing elsewhere in the Listings, and are therefore used for the average given below but not in the overall fits. "f&a" marks results used for the fit and the average.

VALUE (%)	DOCUMENT ID	TECN	COMMENT
2.86 ± 0.07 OUR FIT	Error includes scale factor of 1.3.		
2.87 ± 0.12 avg	¹ BARATE 99R	ALEP	1991-1995 LEP runs

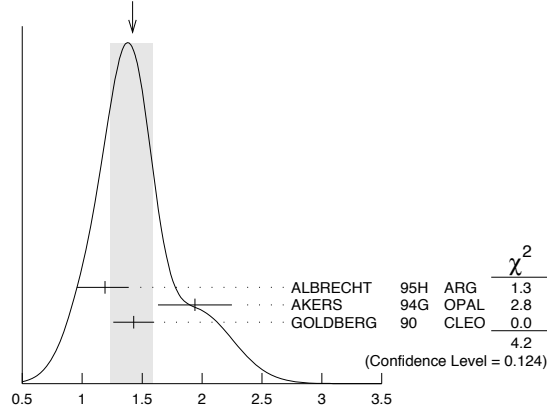
¹ BARATE 99R perform a combined analysis of all ALEPH LEP 1 data on τ branching fraction measurements for decay modes having total strangeness equal to -1.

$\Gamma(K^*(892)^- \geq 0 \text{ neutrals } \geq 0K_L^0\nu_\tau)/\Gamma_{total}$ Γ_{111}/Γ

VALUE (%)	EVTS	DOCUMENT ID	TECN	COMMENT
1.42 ± 0.18 OUR AVERAGE	Error includes scale factor of 1.4. See the ideogram below.			
1.19 ± 0.15 +0.13 -0.18	104	ALBRECHT 95H	ARG	$E_{cm}^{ee} = 9.4-10.6$ GeV
1.94 ± 0.27 ± 0.15	74	¹ AKERS 94G	OPAL	$E_{cm}^{ee} = 88-94$ GeV
1.43 ± 0.11 ± 0.13	475	² GOLDBERG 90	CLEO	$E_{cm}^{ee} = 9.4-10.9$ GeV

¹ AKERS 94G reject events in which a K_S^0 accompanies the $K^*(892)^-$. We do not correct for them.
² GOLDBERG 90 estimates that 10% of observed $K^*(892)^-$ are accompanied by a π^0 .

WEIGHTED AVERAGE
1.42 ± 0.18 (Error scaled by 1.4)



$\Gamma(K^*(892)^- \geq 0 \text{ neutrals } \geq 0K_L^0\nu_\tau)/\Gamma_{total}$ Γ_{111}/Γ

$\Gamma(K^*(892)^-\nu_\tau)/\Gamma_{total}$ Γ_{112}/Γ

VALUE (%)	EVTS	DOCUMENT ID	TECN	COMMENT
1.20 ± 0.07 OUR AVERAGE	Error includes scale factor of 1.8. See the ideogram below.			
1.131 ± 0.006 ± 0.051	49k	¹ EPIFANOV 07	BELL	351 fb^{-1} $E_{cm}^{ee} = 10.6$ GeV
1.326 ± 0.063		BARATE 99R	ALEP	1991-1995 LEP runs
1.11 ± 0.12		² COAN 96	CLEO	$E_{cm}^{ee} \approx 10.6$ GeV
1.42 ± 0.22 ± 0.09		³ ACCIARRI 95F	L3	1991-1993 LEP runs

• • • We do not use the following data for averages, fits, limits, etc. • • •

1.39 ± 0.09 ± 0.10		⁴ BUSKULIC 96	ALEP	Repl. by BARATE 99R
1.45 ± 0.13 ± 0.11	273	⁵ BUSKULIC 94F	ALEP	Repl. by BUSKULIC 96
1.23 ± 0.21 +0.11 -0.21	54	⁶ ALBRECHT 88L	ARG	$E_{cm}^{ee} = 10$ GeV
1.9 ± 0.3 ± 0.4	44	⁷ TSCHIRHART 88	HRS	$E_{cm}^{ee} = 29$ GeV
1.5 ± 0.4 ± 0.4	15	⁸ AIHARA 87C	TPC	$E_{cm}^{ee} = 29$ GeV
1.3 ± 0.3 ± 0.3	31	YELTON 86	MRK2	$E_{cm}^{ee} = 29$ GeV
1.7 ± 0.7	11	DORFAN 81	MRK2	$E_{cm}^{ee} = 4.2-6.7$ GeV

¹ EPIFANOV 07 quote $B(\tau^- \rightarrow K^*(892)^-\nu_\tau) B(K^*(892)^- \rightarrow K_S^0\pi^-) = (3.77 \pm 0.02(\text{stat}) \pm 0.12(\text{syst}) \pm 0.12(\text{mod})) \times 10^{-3}$. We add the systematic and model uncertainties in quadrature and divide by $B(K^*(892)^- \rightarrow K_S^0\pi^-) = 0.3333$.

² Not independent of COAN 96 $B(\pi^-\bar{K}^0\nu_\tau)$ and BATTLE 94 $B(K^-\pi^0\nu_\tau)$ measurements. K final states are consistent with and assumed to originate from $K^*(892)^-$ production.

³ This result is obtained from their $B(\pi^-\bar{K}^0\nu_\tau)$ assuming all those decays originate in $K^*(892)^-$ decays.

⁴ Not independent of BUSKULIC 96 $B(\pi^-\bar{K}^0\nu_\tau)$ and $B(K^-\pi^0\nu_\tau)$ measurements.

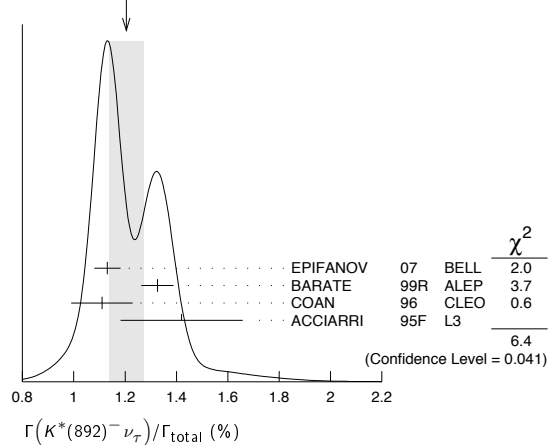
⁵ BUSKULIC 94F obtain this result from BUSKULIC 94F $B(\bar{K}^0\pi^-\nu_\tau)$ and BUSKULIC 94E $B(K^-\pi^0\nu_\tau)$ assuming all of those decays originate in $K^*(892)^-$ decays.

⁶ The authors divide by $\Gamma_2/\Gamma = 0.865$ to obtain this result.

⁷ Not independent of TSCHIRHART 88 $\Gamma(\tau^- \rightarrow h^-\bar{K}^0 \geq 0 \text{ neutrals } \geq 0K_L^0\nu_\tau) / \Gamma$.

⁸ Decay π^- identified in this experiment, is assumed in the others.

WEIGHTED AVERAGE
1.20 ± 0.07 (Error scaled by 1.8)



$\Gamma(K^*(892)^-\nu_\tau)/\Gamma(\pi^-\pi^0\nu_\tau)$ Γ_{112}/Γ_{14}

VALUE	DOCUMENT ID	TECN	COMMENT
0.075 ± 0.027	¹ ABREU 94K	DLPH	LEP 1992 Z data

¹ ABREU 94K quote $B(\tau^- \rightarrow K^*(892)^-\nu_\tau) B(K^*(892)^- \rightarrow K^-\pi^0) / B(\tau^- \rightarrow \rho^-\nu_\tau) = 0.025 \pm 0.009$. We divide by $B(K^*(892)^- \rightarrow K^-\pi^0) = 0.333$ to obtain this result.

$\Gamma(K^*(892)^-\nu_\tau \rightarrow \pi^-\bar{K}^0\nu_\tau)/\Gamma(\pi^-\bar{K}^0\nu_\tau)$ Γ_{113}/Γ_{35}

VALUE	EVTS	DOCUMENT ID	TECN	COMMENT
0.933 ± 0.027	49k	EPIFANOV 07	BELL	351 fb^{-1} $E_{cm}^{ee} = 10.6$ GeV

$\Gamma(K^*(892)^0K^- \geq 0 \text{ neutrals } \nu_\tau)/\Gamma_{total}$ Γ_{114}/Γ

VALUE (%)	EVTS	DOCUMENT ID	TECN	COMMENT
0.32 ± 0.08 ± 0.12	119	GOLDBERG 90	CLEO	$E_{cm}^{ee} = 9.4-10.9$ GeV

$\Gamma(K^*(892)^0K^-\nu_\tau)/\Gamma_{total}$ Γ_{115}/Γ

VALUE (%)	EVTS	DOCUMENT ID	TECN	COMMENT
0.21 ± 0.04 OUR AVERAGE				
0.213 ± 0.048		¹ BARATE 98	ALEP	1991-1995 LEP runs
0.20 ± 0.05 ± 0.04	47	ALBRECHT 95H	ARG	$E_{cm}^{ee} = 9.4-10.6$ GeV

¹ BARATE 98 measure the $K^-(\rho^0 \rightarrow \pi^+\pi^-)$ fraction in $\tau^- \rightarrow K^-\pi^+\pi^-\nu_\tau$ decays to be $(35 \pm 11)\%$ and derive this result from their measurement of $\Gamma(\tau^- \rightarrow K^-\pi^+\pi^-\nu_\tau)/\Gamma_{total}$ assuming the intermediate states are all $K^-\rho$ and $K^*K^*(892)^0$.

$\Gamma(K^*(892)^0\pi^- \geq 0 \text{ neutrals } \nu_\tau)/\Gamma_{total}$ Γ_{116}/Γ

VALUE (%)	EVTS	DOCUMENT ID	TECN	COMMENT
0.38 ± 0.11 ± 0.13	105	GOLDBERG 90	CLEO	$E_{cm}^{ee} = 9.4-10.9$ GeV

$\Gamma(K^*(892)^0\pi^-\nu_\tau)/\Gamma_{total}$ Γ_{117}/Γ

VALUE (%)	EVTS	DOCUMENT ID	TECN	COMMENT
0.22 ± 0.05 OUR AVERAGE				
0.209 ± 0.058		¹ BARATE 98	ALEP	1991-1995 LEP runs
0.25 ± 0.10 ± 0.05	27	ALBRECHT 95H	ARG	$E_{cm}^{ee} = 9.4-10.6$ GeV

¹ BARATE 98 measure the $K^-K^*(892)^0$ fraction in $\tau^- \rightarrow K^-K^+\pi^-\nu_\tau$ decays to be $(87 \pm 13)\%$ and derive this result from their measurement of $\Gamma(\tau^- \rightarrow K^-K^+\pi^-\nu_\tau)/\Gamma_{total}$.

$\Gamma(h^- \omega \pi^0 \nu_\tau) / \Gamma(h^- h^+ 2\pi^0 \nu_\tau (\text{ex. } K^0))$ Γ_{152}/Γ_{76}
 $\Gamma_{152}/\Gamma_{76} = \Gamma_{152}/(\Gamma_{77} + 0.226\Gamma_{126} + 0.888\Gamma_{152})$

Table with columns: VALUE, DOCUMENT ID, TECN, COMMENT. Row 1: $0.83 \pm 0.08 \text{ OUR FIT}$, BORTOLETTO93, CLEO, $E_{\text{cm}}^{ee} \approx 10.6 \text{ GeV}$

$\Gamma(h^- \omega 2\pi^0 \nu_\tau) / \Gamma_{\text{total}}$ Γ_{153}/Γ

Table with columns: VALUE (units 10^{-4}), EVTS, DOCUMENT ID, TECN, COMMENT. Row 1: $1.4 \pm 0.4 \pm 0.3$, 53, ANASTASSOV 01, CLEO, $E_{\text{cm}}^{ee} = 10.6 \text{ GeV}$

$\Gamma(h^- 2\omega \nu_\tau) / \Gamma_{\text{total}}$ Γ_{154}/Γ

Table with columns: VALUE, CL%, DOCUMENT ID, TECN, COMMENT. Row 1: $< 5.4 \times 10^{-7}$, 90, AUBERT,B 06, BABR, 232 fb^{-1} , $E_{\text{cm}}^{ee} = 10.6 \text{ GeV}$

$\Gamma(2h^- h^+ \omega \nu_\tau) / \Gamma_{\text{total}}$ Γ_{155}/Γ

Table with columns: VALUE (units 10^{-4}), EVTS, DOCUMENT ID, TECN, COMMENT. Row 1: $1.2 \pm 0.2 \pm 0.1$, 110, ANASTASSOV 01, CLEO, $E_{\text{cm}}^{ee} = 10.6 \text{ GeV}$

$\Gamma(e^- \gamma) / \Gamma_{\text{total}}$ Γ_{156}/Γ
Test of lepton family number conservation.

Table with columns: VALUE, CL%, DOCUMENT ID, TECN, COMMENT. Rows include <math>< 3.3 \times 10^{-8}</math>, <math>< 1.2 \times 10^{-7}</math>, <math>< 1.1 \times 10^{-7}</math>, <math>< 3.9 \times 10^{-7}</math>, <math>< 2.7 \times 10^{-6}</math>, <math>< 1.1 \times 10^{-4}</math>, <math>< 1.2 \times 10^{-4}</math>, <math>< 2.0 \times 10^{-4}</math>, <math>< 6.4 \times 10^{-4}</math>

$\Gamma(\mu^- \gamma) / \Gamma_{\text{total}}$ Γ_{157}/Γ
Test of lepton family number conservation.

Table with columns: VALUE, CL%, DOCUMENT ID, TECN, COMMENT. Rows include <math>< 4.4 \times 10^{-8}</math>, <math>< 4.5 \times 10^{-8}</math>, <math>< 6.8 \times 10^{-8}</math>, <math>< 3.1 \times 10^{-7}</math>, <math>< 1.1 \times 10^{-6}</math>, <math>< 3.0 \times 10^{-6}</math>, <math>< 6.2 \times 10^{-5}</math>, <math>< 0.42 \times 10^{-5}</math>, <math>< 3.4 \times 10^{-5}</math>, <math>< 55 \times 10^{-5}</math>

$\Gamma(e^- \pi^0) / \Gamma_{\text{total}}$ Γ_{158}/Γ
Test of lepton family number conservation.

Table with columns: VALUE, CL%, DOCUMENT ID, TECN, COMMENT. Rows include <math>< 8.0 \times 10^{-8}</math>, <math>< 1.3 \times 10^{-7}</math>, <math>< 1.9 \times 10^{-7}</math>, <math>< 3.7 \times 10^{-6}</math>, <math>< 17 \times 10^{-5}</math>, <math>< 14 \times 10^{-5}</math>, <math>< 210 \times 10^{-5}</math>

$\Gamma(\mu^- \pi^0) / \Gamma_{\text{total}}$ Γ_{159}/Γ
Test of lepton family number conservation.

Table with columns: VALUE, CL%, DOCUMENT ID, TECN, COMMENT. Rows include <math>< 1.1 \times 10^{-7}</math>, <math>< 1.2 \times 10^{-7}</math>, <math>< 4.1 \times 10^{-7}</math>, <math>< 4.0 \times 10^{-6}</math>, <math>< 4.4 \times 10^{-5}</math>, <math>< 82 \times 10^{-5}</math>

$\Gamma(e^- K_S^0) / \Gamma_{\text{total}}$ Γ_{160}/Γ
Test of lepton family number conservation.

Table with columns: VALUE, CL%, DOCUMENT ID, TECN, COMMENT. Rows include <math>< 3.3 \times 10^{-8}</math>, <math>< 5.6 \times 10^{-8}</math>, <math>< 9.1 \times 10^{-7}</math>, <math>< 1.3 \times 10^{-3}</math>

$\Gamma(\mu^- K_S^0) / \Gamma_{\text{total}}$ Γ_{161}/Γ
Test of lepton family number conservation.

Table with columns: VALUE, CL%, DOCUMENT ID, TECN, COMMENT. Rows include <math>< 4.0 \times 10^{-8}</math>, <math>< 4.9 \times 10^{-8}</math>, <math>< 9.5 \times 10^{-7}</math>, <math>< 1.0 \times 10^{-3}</math>

$\Gamma(e^- \eta) / \Gamma_{\text{total}}$ Γ_{162}/Γ
Test of lepton family number conservation.

Table with columns: VALUE, CL%, DOCUMENT ID, TECN, COMMENT. Rows include <math>< 9.2 \times 10^{-8}</math>, <math>< 1.6 \times 10^{-7}</math>, <math>< 2.4 \times 10^{-7}</math>, <math>< 8.2 \times 10^{-6}</math>, <math>< 6.3 \times 10^{-5}</math>, <math>< 24 \times 10^{-5}</math>

$\Gamma(\mu^- \eta) / \Gamma_{\text{total}}$ Γ_{163}/Γ
Test of lepton family number conservation.

Table with columns: VALUE, CL%, DOCUMENT ID, TECN, COMMENT. Rows include <math>< 6.5 \times 10^{-8}</math>, <math>< 1.5 \times 10^{-7}</math>, <math>< 1.5 \times 10^{-7}</math>, <math>< 3.4 \times 10^{-7}</math>, <math>< 9.6 \times 10^{-6}</math>, <math>< 7.3 \times 10^{-5}</math>

$\Gamma(e^- \rho^0) / \Gamma_{\text{total}}$ Γ_{164}/Γ
Test of lepton family number conservation.

Table with columns: VALUE, CL%, DOCUMENT ID, TECN, COMMENT. Rows include <math>< 4.6 \times 10^{-8}</math>, <math>< 6.3 \times 10^{-8}</math>, <math>< 6.5 \times 10^{-7}</math>, <math>< 2.0 \times 10^{-6}</math>, <math>< 4.2 \times 10^{-6}</math>, <math>< 1.9 \times 10^{-5}</math>, <math>< 37 \times 10^{-5}</math>

$\Gamma(\mu^- \rho^0) / \Gamma_{\text{total}}$ Γ_{165}/Γ
Test of lepton family number conservation.

Table with columns: VALUE, CL%, DOCUMENT ID, TECN, COMMENT. Rows include <math>< 2.6 \times 10^{-8}</math>, <math>< 6.8 \times 10^{-8}</math>, <math>< 2.0 \times 10^{-7}</math>, <math>< 6.3 \times 10^{-6}</math>, <math>< 5.7 \times 10^{-6}</math>, <math>< 2.9 \times 10^{-5}</math>, <math>< 44 \times 10^{-5}</math>

$\Gamma(e^- \omega) / \Gamma_{\text{total}}$ Γ_{166}/Γ

Table with columns: VALUE, CL%, DOCUMENT ID, TECN, COMMENT. Rows include <math>< 1.1 \times 10^{-7}</math>, <math>< 1.8 \times 10^{-7}</math>

$\Gamma(\mu^- \omega) / \Gamma_{\text{total}}$ Γ_{167}/Γ

Table with columns: VALUE, CL%, DOCUMENT ID, TECN, COMMENT. Rows include <math>< 8.9 \times 10^{-8}</math>, <math>< 1.0 \times 10^{-7}</math>

$\Gamma(e^- K^*(892)^0) / \Gamma_{\text{total}}$ Γ_{168}/Γ
Test of lepton family number conservation.

Table with columns: VALUE, CL%, DOCUMENT ID, TECN, COMMENT. Rows include <math>< 5.9 \times 10^{-8}</math>, <math>< 7.8 \times 10^{-8}</math>, <math>< 3.0 \times 10^{-7}</math>, <math>< 5.1 \times 10^{-6}</math>, <math>< 6.3 \times 10^{-6}</math>, <math>< 3.8 \times 10^{-5}</math>

Lepton Particle Listings

T

 $\Gamma(\mu^- K^*(892)^0)/\Gamma_{\text{total}}$ Γ_{169}/Γ

Test of lepton family number conservation.

VALUE	CL%	DOCUMENT ID	TECN	COMMENT
$<5.9 \times 10^{-8}$	90	NISHIO	08 BELL	543 fb $^{-1}$ $E_{\text{cm}}^{ee} = 10.6$ GeV
••• We do not use the following data for averages, fits, limits, etc. •••				
$<1.7 \times 10^{-7}$	90	AUBERT	09w BABR	451 fb $^{-1}$ $E_{\text{cm}}^{ee} = 10.6$ GeV
$<3.9 \times 10^{-7}$	90	YUSA	06 BELL	158 fb $^{-1}$ $E_{\text{cm}}^{ee} = 10.6$ GeV
$<7.5 \times 10^{-6}$	90	BLISS	98 CLEO	$E_{\text{cm}}^{ee} = 10.6$ GeV
$<9.4 \times 10^{-6}$	90	¹ BARTELT	94 CLEO	Repl. by BLISS 98
$<4.5 \times 10^{-5}$	90	ALBRECHT	92k ARG	$E_{\text{cm}}^{ee} = 10$ GeV

¹ BARTELT 94 assume phase space decays.
 $\Gamma(e^- \bar{K}^*(892)^0)/\Gamma_{\text{total}}$ Γ_{170}/Γ

Test of lepton family number conservation.

VALUE	CL%	DOCUMENT ID	TECN	COMMENT
$<4.6 \times 10^{-8}$	90	AUBERT	09w BABR	451 fb $^{-1}$ $E_{\text{cm}}^{ee} = 10.6$ GeV
••• We do not use the following data for averages, fits, limits, etc. •••				
$<7.7 \times 10^{-8}$	90	NISHIO	08 BELL	543 fb $^{-1}$ $E_{\text{cm}}^{ee} = 10.6$ GeV
$<4.0 \times 10^{-7}$	90	YUSA	06 BELL	158 fb $^{-1}$ $E_{\text{cm}}^{ee} = 10.6$ GeV
$<7.4 \times 10^{-6}$	90	BLISS	98 CLEO	$E_{\text{cm}}^{ee} = 10.6$ GeV
$<1.1 \times 10^{-5}$	90	¹ BARTELT	94 CLEO	Repl. by BLISS 98

¹ BARTELT 94 assume phase space decays.
 $\Gamma(\mu^- \bar{K}^*(892)^0)/\Gamma_{\text{total}}$ Γ_{171}/Γ

Test of lepton family number conservation.

VALUE	CL%	DOCUMENT ID	TECN	COMMENT
$<7.3 \times 10^{-8}$	90	AUBERT	09w BABR	451 fb $^{-1}$ $E_{\text{cm}}^{ee} = 10.6$ GeV
••• We do not use the following data for averages, fits, limits, etc. •••				
$<1.0 \times 10^{-7}$	90	NISHIO	08 BELL	543 fb $^{-1}$ $E_{\text{cm}}^{ee} = 10.6$ GeV
$<4.0 \times 10^{-7}$	90	YUSA	06 BELL	158 fb $^{-1}$ $E_{\text{cm}}^{ee} = 10.6$ GeV
$<7.5 \times 10^{-6}$	90	BLISS	98 CLEO	$E_{\text{cm}}^{ee} = 10.6$ GeV
$<8.7 \times 10^{-6}$	90	¹ BARTELT	94 CLEO	Repl. by BLISS 98

¹ BARTELT 94 assume phase space decays.
 $\Gamma(e^- \eta(958))/\Gamma_{\text{total}}$ Γ_{172}/Γ

Test of lepton family number conservation.

VALUE	CL%	DOCUMENT ID	TECN	COMMENT
$<1.6 \times 10^{-7}$	90	MIYAZAKI	07 BELL	401 fb $^{-1}$, $E_{\text{cm}}^{ee} = 10.6$ GeV
••• We do not use the following data for averages, fits, limits, etc. •••				
$<2.4 \times 10^{-7}$	90	AUBERT	07i BABR	339 fb $^{-1}$, $E_{\text{cm}}^{ee} = 10.6$ GeV
$<1.0 \times 10^{-7}$	90	ENARI	05 BELL	154 fb $^{-1}$, $E_{\text{cm}}^{ee} = 10.6$ GeV

 $\Gamma(\mu^- \eta(958))/\Gamma_{\text{total}}$ Γ_{173}/Γ

Test of lepton family number conservation.

VALUE	CL%	DOCUMENT ID	TECN	COMMENT
$<1.3 \times 10^{-7}$	90	MIYAZAKI	07 BELL	401 fb $^{-1}$, $E_{\text{cm}}^{ee} = 10.6$ GeV
••• We do not use the following data for averages, fits, limits, etc. •••				
$<1.4 \times 10^{-7}$	90	AUBERT	07i BABR	339 fb $^{-1}$, $E_{\text{cm}}^{ee} = 10.6$ GeV
$<4.7 \times 10^{-7}$	90	ENARI	05 BELL	154 fb $^{-1}$, $E_{\text{cm}}^{ee} = 10.6$ GeV

 $\Gamma(e^- f_0(980) \rightarrow e^- \pi^+ \pi^-)/\Gamma_{\text{total}}$ Γ_{174}/Γ

Test of lepton family number conservation.

VALUE	CL%	DOCUMENT ID	TECN	COMMENT
$<3.2 \times 10^{-8}$	90	MIYAZAKI	09 BELL	671 fb $^{-1}$ $E_{\text{cm}}^{ee} = 10.6$ GeV

 $\Gamma(\mu^- f_0(980) \rightarrow \mu^- \pi^+ \pi^-)/\Gamma_{\text{total}}$ Γ_{175}/Γ

Test of lepton family number conservation.

VALUE	CL%	DOCUMENT ID	TECN	COMMENT
$<3.4 \times 10^{-8}$	90	MIYAZAKI	09 BELL	671 fb $^{-1}$ $E_{\text{cm}}^{ee} = 10.6$ GeV

 $\Gamma(e^- \phi)/\Gamma_{\text{total}}$ Γ_{176}/Γ

Test of lepton family number conservation.

VALUE	CL%	DOCUMENT ID	TECN	COMMENT
$<3.1 \times 10^{-8}$	90	AUBERT	09w BABR	451 fb $^{-1}$ $E_{\text{cm}}^{ee} = 10.6$ GeV
••• We do not use the following data for averages, fits, limits, etc. •••				
$<7.3 \times 10^{-8}$	90	NISHIO	08 BELL	543 fb $^{-1}$ $E_{\text{cm}}^{ee} = 10.6$ GeV
$<7.3 \times 10^{-7}$	90	YUSA	06 BELL	158 fb $^{-1}$ $E_{\text{cm}}^{ee} = 10.6$ GeV
$<6.9 \times 10^{-6}$	90	BLISS	98 CLEO	$E_{\text{cm}}^{ee} = 10.6$ GeV

 $\Gamma(\mu^- \phi)/\Gamma_{\text{total}}$ Γ_{177}/Γ

Test of lepton family number conservation.

VALUE	CL%	DOCUMENT ID	TECN	COMMENT
$<1.3 \times 10^{-7}$	90	NISHIO	08 BELL	543 fb $^{-1}$ $E_{\text{cm}}^{ee} = 10.6$ GeV
••• We do not use the following data for averages, fits, limits, etc. •••				
$<1.9 \times 10^{-7}$	90	AUBERT	09w BABR	451 fb $^{-1}$ $E_{\text{cm}}^{ee} = 10.6$ GeV
$<7.7 \times 10^{-7}$	90	YUSA	06 BELL	158 fb $^{-1}$ $E_{\text{cm}}^{ee} = 10.6$ GeV
$<7.0 \times 10^{-6}$	90	BLISS	98 CLEO	$E_{\text{cm}}^{ee} = 10.6$ GeV

 $\Gamma(e^- e^+ e^-)/\Gamma_{\text{total}}$ Γ_{178}/Γ

Test of lepton family number conservation.

VALUE	CL%	DOCUMENT ID	TECN	COMMENT
$<3.6 \times 10^{-8}$	90	MIYAZAKI	08 BELL	535 fb $^{-1}$ $E_{\text{cm}}^{ee} = 10.6$ GeV
••• We do not use the following data for averages, fits, limits, etc. •••				
$<4.3 \times 10^{-8}$	90	AUBERT	07BK BABR	376 fb $^{-1}$ $E_{\text{cm}}^{ee} = 10.6$ GeV
$<2.0 \times 10^{-7}$	90	AUBERT	04J BABR	91.5 fb $^{-1}$ $E_{\text{cm}}^{ee} = 10.6$ GeV
$<3.5 \times 10^{-7}$	90	YUSA	04 BELL	87.1 fb $^{-1}$ $E_{\text{cm}}^{ee} = 10.6$ GeV
$<2.9 \times 10^{-6}$	90	BLISS	98 CLEO	$E_{\text{cm}}^{ee} = 10.6$ GeV
$<0.33 \times 10^{-5}$	90	¹ BARTELT	94 CLEO	Repl. by BLISS 98
$<1.3 \times 10^{-5}$	90	ALBRECHT	92k ARG	$E_{\text{cm}}^{ee} = 10$ GeV
$<2.7 \times 10^{-5}$	90	BOWCOCK	90 CLEO	$E_{\text{cm}}^{ee} = 10.4-10.9$
$<40 \times 10^{-5}$	90	HAYES	82 MRK2	$E_{\text{cm}}^{ee} = 3.8-6.8$ GeV

¹ BARTELT 94 assume phase space decays.
 $\Gamma(e^- \mu^+ \mu^-)/\Gamma_{\text{total}}$ Γ_{179}/Γ

Test of lepton family number conservation.

VALUE	CL%	DOCUMENT ID	TECN	COMMENT
$<3.7 \times 10^{-8}$	90	AUBERT	07BK BABR	376 fb $^{-1}$ $E_{\text{cm}}^{ee} = 10.6$ GeV
••• We do not use the following data for averages, fits, limits, etc. •••				
$<4.1 \times 10^{-8}$	90	MIYAZAKI	08 BELL	535 fb $^{-1}$ $E_{\text{cm}}^{ee} = 10.6$ GeV
$<3.3 \times 10^{-7}$	90	AUBERT	04J BABR	91.5 fb $^{-1}$ $E_{\text{cm}}^{ee} = 10.6$ GeV
$<2.0 \times 10^{-7}$	90	YUSA	04 BELL	87.1 fb $^{-1}$ $E_{\text{cm}}^{ee} = 10.6$ GeV
$<1.8 \times 10^{-6}$	90	BLISS	98 CLEO	$E_{\text{cm}}^{ee} = 10.6$ GeV
$<0.36 \times 10^{-5}$	90	¹ BARTELT	94 CLEO	Repl. by BLISS 98
$<1.9 \times 10^{-5}$	90	ALBRECHT	92k ARG	$E_{\text{cm}}^{ee} = 10$ GeV
$<2.7 \times 10^{-5}$	90	BOWCOCK	90 CLEO	$E_{\text{cm}}^{ee} = 10.4-10.9$
$<33 \times 10^{-5}$	90	HAYES	82 MRK2	$E_{\text{cm}}^{ee} = 3.8-6.8$ GeV

¹ BARTELT 94 assume phase space decays.
 $\Gamma(e^+ \mu^- \mu^-)/\Gamma_{\text{total}}$ Γ_{180}/Γ

Test of lepton family number conservation.

VALUE	CL%	DOCUMENT ID	TECN	COMMENT
$<2.3 \times 10^{-8}$	90	MIYAZAKI	08 BELL	535 fb $^{-1}$ $E_{\text{cm}}^{ee} = 10.6$ GeV
••• We do not use the following data for averages, fits, limits, etc. •••				
$<5.6 \times 10^{-8}$	90	AUBERT	07BK BABR	376 fb $^{-1}$ $E_{\text{cm}}^{ee} = 10.6$ GeV
$<1.3 \times 10^{-7}$	90	AUBERT	04J BABR	91.5 fb $^{-1}$ $E_{\text{cm}}^{ee} = 10.6$ GeV
$<2.0 \times 10^{-7}$	90	YUSA	04 BELL	87.1 fb $^{-1}$ $E_{\text{cm}}^{ee} = 10.6$ GeV
$<1.5 \times 10^{-6}$	90	BLISS	98 CLEO	$E_{\text{cm}}^{ee} = 10.6$ GeV
$<0.35 \times 10^{-5}$	90	¹ BARTELT	94 CLEO	Repl. by BLISS 98
$<1.8 \times 10^{-5}$	90	ALBRECHT	92k ARG	$E_{\text{cm}}^{ee} = 10$ GeV
$<1.6 \times 10^{-5}$	90	BOWCOCK	90 CLEO	$E_{\text{cm}}^{ee} = 10.4-10.9$

¹ BARTELT 94 assume phase space decays.
 $\Gamma(\mu^- e^+ e^-)/\Gamma_{\text{total}}$ Γ_{181}/Γ

Test of lepton family number conservation.

VALUE	CL%	DOCUMENT ID	TECN	COMMENT
$<2.7 \times 10^{-8}$	90	MIYAZAKI	08 BELL	535 fb $^{-1}$ $E_{\text{cm}}^{ee} = 10.6$ GeV
••• We do not use the following data for averages, fits, limits, etc. •••				
$<8.0 \times 10^{-8}$	90	AUBERT	07BK BABR	376 fb $^{-1}$ $E_{\text{cm}}^{ee} = 10.6$ GeV
$<2.7 \times 10^{-7}$	90	AUBERT	04J BABR	91.5 fb $^{-1}$ $E_{\text{cm}}^{ee} = 10.6$ GeV
$<1.9 \times 10^{-7}$	90	YUSA	04 BELL	87.1 fb $^{-1}$ $E_{\text{cm}}^{ee} = 10.6$ GeV
$<1.7 \times 10^{-6}$	90	BLISS	98 CLEO	$E_{\text{cm}}^{ee} = 10.6$ GeV
$<0.34 \times 10^{-5}$	90	¹ BARTELT	94 CLEO	Repl. by BLISS 98
$<1.4 \times 10^{-5}$	90	ALBRECHT	92k ARG	$E_{\text{cm}}^{ee} = 10$ GeV
$<2.7 \times 10^{-5}$	90	BOWCOCK	90 CLEO	$E_{\text{cm}}^{ee} = 10.4-10.9$
$<44 \times 10^{-5}$	90	HAYES	82 MRK2	$E_{\text{cm}}^{ee} = 3.8-6.8$ GeV

¹ BARTELT 94 assume phase space decays.
 $\Gamma(\mu^+ e^- e^-)/\Gamma_{\text{total}}$ Γ_{182}/Γ

Test of lepton family number conservation.

VALUE	CL%	DOCUMENT ID	TECN	COMMENT
$<2.0 \times 10^{-8}$	90	MIYAZAKI	08 BELL	535 fb $^{-1}$ $E_{\text{cm}}^{ee} = 10.6$ GeV
••• We do not use the following data for averages, fits, limits, etc. •••				
$<5.8 \times 10^{-8}$	90	AUBERT	07BK BABR	376 fb $^{-1}$ $E_{\text{cm}}^{ee} = 10.6$ GeV
$<1.1 \times 10^{-7}$	90	AUBERT	04J BABR	91.5 fb $^{-1}$ $E_{\text{cm}}^{ee} = 10.6$ GeV
$<2.0 \times 10^{-7}$	90	YUSA	04 BELL	87.1 fb $^{-1}$ $E_{\text{cm}}^{ee} = 10.6$ GeV
$<1.5 \times 10^{-6}$	90	BLISS	98 CLEO	$E_{\text{cm}}^{ee} = 10.6$ GeV
$<0.34 \times 10^{-5}$	90	¹ BARTELT	94 CLEO	Repl. by BLISS 98
$<1.4 \times 10^{-5}$	90	ALBRECHT	92k ARG	$E_{\text{cm}}^{ee} = 10$ GeV
$<1.6 \times 10^{-5}$	90	BOWCOCK	90 CLEO	$E_{\text{cm}}^{ee} = 10.4-10.9$

¹ BARTELT 94 assume phase space decays.

Lepton Particle Listings

 τ $\Gamma(\mu^+ \pi^- K^-)/\Gamma_{\text{total}}$ Γ_{196}/Γ

Test of lepton number conservation.

VALUE	CL%	DOCUMENT ID	TECN	COMMENT
$<9.4 \times 10^{-8}$	90	MIYAZAKI	10 BELL	671 fb^{-1} , $E_{\text{cm}}^{\text{ee}} = 10.6 \text{ GeV}$

• • • We do not use the following data for averages, fits, limits, etc. • • •

$<2.9 \times 10^{-7}$	90	YUSA	06 BELL	158 fb^{-1} , $E_{\text{cm}}^{\text{ee}} = 10.6 \text{ GeV}$
$<2.2 \times 10^{-7}$	90	AUBERT,BE	05D BABR	221 fb^{-1} , $E_{\text{cm}}^{\text{ee}} = 10.6 \text{ GeV}$
$<7.0 \times 10^{-6}$	90	BLISS	98 CLEO	$E_{\text{cm}}^{\text{ee}} = 10.6 \text{ GeV}$
$<2.0 \times 10^{-5}$	90	¹ BARTELT	94 CLEO	Repl. by BLISS 98
$<5.8 \times 10^{-5}$	90	ALBRECHT	92K ARG	$E_{\text{cm}}^{\text{ee}} = 10 \text{ GeV}$
$<4.0 \times 10^{-5}$	90	BOWCOCK	90 CLEO	$E_{\text{cm}}^{\text{ee}} = 10.4\text{--}10.9$

¹BARTELT 94 assume phase space decays.

 $\Gamma(\mu^- K_S^0 K_S^0)/\Gamma_{\text{total}}$ Γ_{197}/Γ

Test of lepton family number conservation.

VALUE	CL%	DOCUMENT ID	TECN	COMMENT
$<3.4 \times 10^{-6}$	90	CHEN	02C CLEO	$E_{\text{cm}}^{\text{ee}} = 10.6 \text{ GeV}$

 $\Gamma(\mu^- K^+ K^-)/\Gamma_{\text{total}}$ Γ_{198}/Γ

Test of lepton family number conservation.

VALUE	CL%	DOCUMENT ID	TECN	COMMENT
$<6.8 \times 10^{-8}$	90	MIYAZAKI	10 BELL	671 fb^{-1} , $E_{\text{cm}}^{\text{ee}} = 10.6 \text{ GeV}$

• • • We do not use the following data for averages, fits, limits, etc. • • •

$<8.0 \times 10^{-7}$	90	YUSA	06 BELL	158 fb^{-1} , $E_{\text{cm}}^{\text{ee}} = 10.6 \text{ GeV}$
$<2.5 \times 10^{-7}$	90	AUBERT,BE	05D BABR	221 fb^{-1} , $E_{\text{cm}}^{\text{ee}} = 10.6 \text{ GeV}$
$<15 \times 10^{-6}$	90	BLISS	98 CLEO	$E_{\text{cm}}^{\text{ee}} = 10.6 \text{ GeV}$

 $\Gamma(\mu^+ K^- K^-)/\Gamma_{\text{total}}$ Γ_{199}/Γ

Test of lepton number conservation.

VALUE	CL%	DOCUMENT ID	TECN	COMMENT
$<9.6 \times 10^{-8}$	90	MIYAZAKI	10 BELL	671 fb^{-1} , $E_{\text{cm}}^{\text{ee}} = 10.6 \text{ GeV}$

• • • We do not use the following data for averages, fits, limits, etc. • • •

$<4.4 \times 10^{-7}$	90	YUSA	06 BELL	158 fb^{-1} , $E_{\text{cm}}^{\text{ee}} = 10.6 \text{ GeV}$
$<4.8 \times 10^{-7}$	90	AUBERT,BE	05D BABR	221 fb^{-1} , $E_{\text{cm}}^{\text{ee}} = 10.6 \text{ GeV}$
$<6.0 \times 10^{-6}$	90	BLISS	98 CLEO	$E_{\text{cm}}^{\text{ee}} = 10.6 \text{ GeV}$

 $\Gamma(e^- \pi^0 \pi^0)/\Gamma_{\text{total}}$ Γ_{200}/Γ

Test of lepton family number conservation.

VALUE	CL%	DOCUMENT ID	TECN	COMMENT
$<6.5 \times 10^{-6}$	90	BONVICINI	97 CLEO	$E_{\text{cm}}^{\text{ee}} = 10.6 \text{ GeV}$

 $\Gamma(\mu^- \pi^0 \pi^0)/\Gamma_{\text{total}}$ Γ_{201}/Γ

Test of lepton family number conservation.

VALUE	CL%	DOCUMENT ID	TECN	COMMENT
$<14 \times 10^{-6}$	90	BONVICINI	97 CLEO	$E_{\text{cm}}^{\text{ee}} = 10.6 \text{ GeV}$

 $\Gamma(e^- \eta \eta)/\Gamma_{\text{total}}$ Γ_{202}/Γ

Test of lepton family number conservation.

VALUE	CL%	DOCUMENT ID	TECN	COMMENT
$<35 \times 10^{-6}$	90	BONVICINI	97 CLEO	$E_{\text{cm}}^{\text{ee}} = 10.6 \text{ GeV}$

 $\Gamma(\mu^- \eta \eta)/\Gamma_{\text{total}}$ Γ_{203}/Γ

Test of lepton family number conservation.

VALUE	CL%	DOCUMENT ID	TECN	COMMENT
$<60 \times 10^{-6}$	90	BONVICINI	97 CLEO	$E_{\text{cm}}^{\text{ee}} = 10.6 \text{ GeV}$

 $\Gamma(e^- \pi^0 \eta)/\Gamma_{\text{total}}$ Γ_{204}/Γ

Test of lepton family number conservation.

VALUE	CL%	DOCUMENT ID	TECN	COMMENT
$<24 \times 10^{-6}$	90	BONVICINI	97 CLEO	$E_{\text{cm}}^{\text{ee}} = 10.6 \text{ GeV}$

 $\Gamma(\mu^- \pi^0 \eta)/\Gamma_{\text{total}}$ Γ_{205}/Γ

Test of lepton family number conservation.

VALUE	CL%	DOCUMENT ID	TECN	COMMENT
$<22 \times 10^{-6}$	90	BONVICINI	97 CLEO	$E_{\text{cm}}^{\text{ee}} = 10.6 \text{ GeV}$

 $\Gamma(\bar{p} \gamma)/\Gamma_{\text{total}}$ Γ_{206}/Γ

Test of lepton number and baryon number conservation.

VALUE	CL%	DOCUMENT ID	TECN	COMMENT
$<3.5 \times 10^{-6}$	90	GODANG	99 CLEO	$E_{\text{cm}}^{\text{ee}} = 10.6 \text{ GeV}$

• • • We do not use the following data for averages, fits, limits, etc. • • •

$<29 \times 10^{-5}$	90	ALBRECHT	92K ARG	$E_{\text{cm}}^{\text{ee}} = 10 \text{ GeV}$
----------------------	----	----------	---------	--

 $\Gamma(\bar{p} \pi^0)/\Gamma_{\text{total}}$ Γ_{207}/Γ

Test of lepton number and baryon number conservation.

VALUE	CL%	DOCUMENT ID	TECN	COMMENT
$<15 \times 10^{-6}$	90	GODANG	99 CLEO	$E_{\text{cm}}^{\text{ee}} = 10.6 \text{ GeV}$

• • • We do not use the following data for averages, fits, limits, etc. • • •

$<66 \times 10^{-5}$	90	ALBRECHT	92K ARG	$E_{\text{cm}}^{\text{ee}} = 10 \text{ GeV}$
----------------------	----	----------	---------	--

 $\Gamma(\bar{p} 2\pi^0)/\Gamma_{\text{total}}$ Γ_{208}/Γ

Test of lepton number and baryon number conservation.

VALUE	CL%	DOCUMENT ID	TECN	COMMENT
$<33 \times 10^{-6}$	90	GODANG	99 CLEO	$E_{\text{cm}}^{\text{ee}} = 10.6 \text{ GeV}$

 $\Gamma(\bar{p} \eta)/\Gamma_{\text{total}}$ Γ_{209}/Γ

Test of lepton number and baryon number conservation.

VALUE	CL%	DOCUMENT ID	TECN	COMMENT
$<8.9 \times 10^{-6}$	90	GODANG	99 CLEO	$E_{\text{cm}}^{\text{ee}} = 10.6 \text{ GeV}$

• • • We do not use the following data for averages, fits, limits, etc. • • •

$<130 \times 10^{-5}$	90	ALBRECHT	92K ARG	$E_{\text{cm}}^{\text{ee}} = 10 \text{ GeV}$
-----------------------	----	----------	---------	--

 $\Gamma(\bar{p} \pi^0 \eta)/\Gamma_{\text{total}}$ Γ_{210}/Γ

Test of lepton number and baryon number conservation.

VALUE	CL%	DOCUMENT ID	TECN	COMMENT
$<27 \times 10^{-6}$	90	GODANG	99 CLEO	$E_{\text{cm}}^{\text{ee}} = 10.6 \text{ GeV}$

 $\Gamma(\Lambda \pi^-)/\Gamma_{\text{total}}$ Γ_{211}/Γ

Test of lepton number and baryon number conservation.

VALUE	CL%	DOCUMENT ID	TECN	COMMENT
$<0.72 \times 10^{-7}$	90	MIYAZAKI	06 BELL	154 fb^{-1} , $E_{\text{cm}}^{\text{ee}} = 10.6 \text{ GeV}$

 $\Gamma(\bar{\Lambda} \pi^-)/\Gamma_{\text{total}}$ Γ_{212}/Γ

Test of lepton number and baryon number conservation.

VALUE	CL%	DOCUMENT ID	TECN	COMMENT
$<1.4 \times 10^{-7}$	90	MIYAZAKI	06 BELL	154 fb^{-1} , $E_{\text{cm}}^{\text{ee}} = 10.6 \text{ GeV}$

 $\Gamma(e^- \text{light boson})/\Gamma(e^- \bar{\nu}_e \nu_\tau)$ Γ_{213}/Γ_5

Test of lepton family number conservation.

VALUE	CL%	DOCUMENT ID	TECN	COMMENT
<0.015	95	¹ ALBRECHT	95G ARG	$E_{\text{cm}}^{\text{ee}} = 9.4\text{--}10.6 \text{ GeV}$

• • • We do not use the following data for averages, fits, limits, etc. • • •

<0.018	95	² ALBRECHT	90E ARG	$E_{\text{cm}}^{\text{ee}} = 9.4\text{--}10.6 \text{ GeV}$
<0.040	95	³ BALTRUSAITIS...	85 MRK3	$E_{\text{cm}}^{\text{ee}} = 3.77 \text{ GeV}$

¹ALBRECHT 95G limit holds for bosons with mass $< 0.4 \text{ GeV}$. The limit rises to 0.036 for a mass of 1.0 GeV, then falls to 0.006 at the upper mass limit of 1.6 GeV.

²ALBRECHT 90E limit applies for spinless boson with mass $< 100 \text{ MeV}$, and rises to 0.050 for mass = 500 MeV.

³BALTRUSAITIS 85 limit applies for spinless boson with mass $< 100 \text{ MeV}$.

 $\Gamma(\mu^- \text{light boson})/\Gamma(e^- \bar{\nu}_e \nu_\tau)$ Γ_{214}/Γ_5

Test of lepton family number conservation.

VALUE	CL%	DOCUMENT ID	TECN	COMMENT
<0.026	95	¹ ALBRECHT	95G ARG	$E_{\text{cm}}^{\text{ee}} = 9.4\text{--}10.6 \text{ GeV}$

• • • We do not use the following data for averages, fits, limits, etc. • • •

<0.033	95	² ALBRECHT	90E ARG	$E_{\text{cm}}^{\text{ee}} = 9.4\text{--}10.6 \text{ GeV}$
<0.125	95	³ BALTRUSAITIS...	85 MRK3	$E_{\text{cm}}^{\text{ee}} = 3.77 \text{ GeV}$

¹ALBRECHT 95G limit holds for bosons with mass $< 1.3 \text{ GeV}$. The limit rises to 0.034 for a mass of 1.4 GeV, then falls to 0.003 at the upper mass limit of 1.6 GeV.

²ALBRECHT 90E limit applies for spinless boson with mass $< 100 \text{ MeV}$, and rises to 0.071 for mass = 500 MeV.

³BALTRUSAITIS 85 limit applies for spinless boson with mass $< 100 \text{ MeV}$.

 τ -DECAY PARAMETERS τ -LEPTON DECAY PARAMETERS

Updated July 2007 by A. Stahl (RWTH Aachen).

The purpose of the measurements of the decay parameters (*i.e.*, Michel parameters) of the τ is to determine the structure (spin and chirality) of the current mediating its decays.

Leptonic Decays: The Michel parameters are extracted from the energy spectrum of the charged daughter lepton $\ell = e, \mu$ in the decays $\tau \rightarrow \ell \nu_\ell \nu_\tau$. Ignoring radiative corrections, neglecting terms of order $(m_\ell/m_\tau)^2$ and $(m_\tau/\sqrt{s})^2$, and setting the neutrino masses to zero, the spectrum in the laboratory frame reads

$$\frac{d\Gamma}{dx} = \frac{G_{\tau\ell}^2 m_\tau^5}{192 \pi^3} \times$$

$$\left\{ f_0(x) + \rho f_1(x) + \eta \frac{m_\ell}{m_\tau} f_2(x) - P_\tau [\xi g_1(x) + \xi \delta g_2(x)] \right\}, \quad (1)$$

with

$$\begin{aligned} f_0(x) &= 2 - 6x^2 + 4x^3 \\ f_1(x) &= -\frac{4}{9} + 4x^2 - \frac{32}{9}x^3 & g_1(x) &= -\frac{2}{3} + 4x - 6x^2 + \frac{8}{3}x^3 \\ f_2(x) &= 12(1-x)^2 & g_2(x) &= \frac{4}{9} - \frac{16}{3}x + 12x^2 - \frac{64}{9}x^3. \end{aligned}$$

The quantity x is the fractional energy of the daughter lepton ℓ , *i.e.*, $x = E_\ell/E_{\ell,max} \approx E_\ell/(\sqrt{s}/2)$ and P_τ is the polarization of the tau leptons. The integrated decay width is given by

$$\Gamma = \frac{G_{\tau\ell}^2 m_\tau^5}{192 \pi^3} \left(1 + 4\eta \frac{m_\ell}{m_\tau} \right). \quad (2)$$

The situation is similar to muon decays $\mu \rightarrow e\nu_e\nu_\mu$. The generalized matrix element with the couplings $g_{\varepsilon\mu}^\gamma$ and their relations to the Michel parameters ρ , η , ξ , and δ have been described in the “Note on Muon Decay Parameters.” The Standard Model expectations are 3/4, 0, 1, and 3/4, respectively. For more details, see Ref. 1.

Hadronic Decays: In the case of hadronic decays $\tau \rightarrow h\nu_\tau$, with $h = \pi, \rho$, or a_1 , the ansatz is restricted to purely vectorial currents. The matrix element is

$$\frac{G_{\tau h}}{\sqrt{2}} \sum_{\lambda=R,L} g_\lambda \langle \bar{\Psi}_\omega(\nu_\tau) | \gamma^\mu | \Psi_\lambda(\tau) \rangle J_\mu^h \quad (3)$$

with the hadronic current J_μ^h . The neutrino chirality ω is uniquely determined from λ . The spectrum depends only on a single parameter ξ_h

$$\frac{d^n\Gamma}{dx_1 dx_2 \dots dx_n} = f(\vec{x}) + \xi_h P_\tau g(\vec{x}), \quad (4)$$

with f and g being channel-dependent functions of the n observables $\vec{x} = (x_1, x_2, \dots, x_n)$ (see Ref. 2). The parameter ξ_h is related to the couplings through

$$\xi_h = |g_L|^2 - |g_R|^2. \quad (5)$$

ξ_h is the negative of the chirality of the τ neutrino in these decays. In the Standard Model, $\xi_h = 1$. Also included in the Data Listings for ξ_h are measurements of the neutrino helicity which coincide with ξ_h , if the neutrino is massless (ASNER 00, ACKERSTAFF 97R, AKERS 95P, ALBRECHT 93C, and ALBRECHT 90I).

Combination of Measurements: The individual measurements are combined, taking into account the correlations between the parameters. In a first fit, universality between the two leptonic decays, and between all hadronic decays, is assumed. A second fit is made without these assumptions. The results of the two fits are provided as OUR FIT in the Data Listings below in the tables whose title includes “(e or mu)” or “(all hadronic modes),” and “(e),” “(mu)” *etc.*, respectively. The measurements show good agreement with the Standard Model. The χ^2 values with respect to the Standard model predictions are 24.1 for 41 degrees of freedom and 26.8 for 56 degrees of freedom, respectively. The correlations are reduced through this combination to less than 20%, with the exception of ρ and η

which are correlated by +23%, for the fit with universality and by +70% for $\tau \rightarrow \mu\nu_\mu\nu_\tau$.

Model-independent Analysis: From the Michel parameters, limits can be derived on the couplings $g_{\varepsilon\lambda}^\kappa$ without further module assumptions. In the Standard model $g_{LL}^V = 1$ (leptonic decays), and $g_L = 1$ (hadronic decays) and all other couplings vanish. First, the partial decay widths have to be compared to the Standard Model predictions to derive limits on the normalization of the couplings $A_x = G_{\tau x}^2/G_F^2$ with Fermi’s constant G_F :

$$\begin{aligned} A_e &= 1.0012 \pm 0.0053, \\ A_\mu &= 0.981 \pm 0.018, \\ A_\pi &= 1.018 \pm 0.012. \end{aligned} \quad (6)$$

Then limits on the couplings (95% CL) can be extracted (see Ref. 3 and Ref. 4). Without the assumption of universality, the limits given in Table 1 are derived.

Table 1: Coupling constants $g_{\varepsilon\mu}^\gamma$. 95% confidence level experimental limits. The limits include the quoted values of A_e , A_μ , and A_π and assume $A_\rho = A_{a_1} = 1$.

$\tau \rightarrow e\nu_e\nu_\tau$		
$ g_{RR}^S < 0.70$	$ g_{RR}^V < 0.17$	$ g_{RR}^T \equiv 0$
$ g_{LR}^S < 0.99$	$ g_{LR}^V < 0.13$	$ g_{LR}^T < 0.082$
$ g_{RL}^S < 2.01$	$ g_{RL}^V < 0.52$	$ g_{RL}^T < 0.51$
$ g_{LL}^S < 2.01$	$ g_{LL}^V < 1.005$	$ g_{LL}^T \equiv 0$
$\tau \rightarrow \mu\nu_\mu\nu_\tau$		
$ g_{RR}^S < 0.72$	$ g_{RR}^V < 0.18$	$ g_{RR}^T \equiv 0$
$ g_{LR}^S < 0.95$	$ g_{LR}^V < 0.12$	$ g_{LR}^T < 0.079$
$ g_{RL}^S < 2.01$	$ g_{RL}^V < 0.52$	$ g_{RL}^T < 0.51$
$ g_{LL}^S < 2.01$	$ g_{LL}^V < 1.005$	$ g_{LL}^T \equiv 0$
$\tau \rightarrow \pi\nu_\tau$		
$ g_R^V < 0.15$	$ g_L^V > 0.992$	
$\tau \rightarrow \rho\nu_\tau$		
$ g_R^V < 0.10$	$ g_L^V > 0.995$	
$\tau \rightarrow a_1\nu_\tau$		
$ g_R^V < 0.16$	$ g_L^V > 0.987$	

Model-dependent Interpretation: More stringent limits can be derived assuming specific models. For example, in the framework of a two Higgs doublet model, the measurements correspond to a limit of $m_{H^\pm} > 1.9 \text{ GeV} \times \tan\beta$ on the mass of the charged Higgs boson, or a limit of 253 GeV on the mass of the

Lepton Particle Listings

 τ

second W boson in left-right symmetric models for arbitrary mixing (both 95% CL). See Ref. 4 and Ref. 5.

Footnotes and References

1. F. Scheck, Phys. Reports **44**, 187 (1978);
W. Fetscher and H.J. Gerber in *Precision Tests of the Standard Model*, edited by P. Langacker, World Scientific, 1993;
A. Stahl, *Physics with τ Leptons*, Springer Tracts in Modern Physics.
2. M. Davier *et al.*, Phys. Lett. **B306**, 411 (1993).
3. OPAL Collab., K. Ackerstaff *et al.*, Eur. Phys. J. **C8**, 3 (1999).
4. A. Stahl, Nucl. Phys. (Proc. Supp.) **B76**, 173 (1999).
5. M.-T. Dova *et al.*, Phys. Rev. **D58**, 015005 (1998);
T. Hebbeker and W. Lohmann, Z. Phys. **C74**, 399 (1997);
A. Pich and J.P. Silva, Phys. Rev. **D52**, 4006 (1995).

 $\rho(e \text{ or } \mu)$ PARAMETER $(V-A)$ theory predicts $\rho = 0.75$.

VALUE	EVTs	DOCUMENT ID	TECN	COMMENT
0.745 ± 0.008 OUR FIT				
0.749 ± 0.008 OUR AVERAGE				
0.742 ± 0.014 ± 0.006	81k	HEISTER	01E ALEP	1991–1995 LEP runs
0.775 ± 0.023 ± 0.020	36k	ABREU	00L DLPH	1992–1995 runs
0.781 ± 0.028 ± 0.018	46k	ACKERSTAFF	99D OPAL	1990–1995 LEP runs
0.762 ± 0.035	54k	ACCIARRI	98R L3	1991–1995 LEP runs
0.731 ± 0.031		¹ ALBRECHT	98 ARG	$E_{cm}^{ee} = 9.5\text{--}10.6$ GeV
0.72 ± 0.09 ± 0.03		² ABE	97o SLD	1993–1995 SLC runs
0.747 ± 0.010 ± 0.006	55k	ALEXANDER	97F CLEO	$E_{cm}^{ee} = 10.6$ GeV
0.79 ± 0.10 ± 0.10	3732	FORD	87B MAC	$E_{cm}^{ee} = 29$ GeV
0.71 ± 0.09 ± 0.03	1426	BEHREND	85 CLEO	e^+e^- near $\mathcal{T}(4S)$
••• We do not use the following data for averages, fits, limits, etc. •••				
0.735 ± 0.013 ± 0.008	31k	AMMAR	97B CLEO	Repl. by ALEXANDER 97F
0.794 ± 0.039 ± 0.031	18k	ACCIARRI	96H L3	Repl. by ACCIARRI 98R
0.732 ± 0.034 ± 0.020	8.2k	³ ALBRECHT	95 ARG	$E_{cm}^{ee} = 9.5\text{--}10.6$ GeV
0.738 ± 0.038		⁴ ALBRECHT	95C ARG	Repl. by ALBRECHT 98
0.751 ± 0.039 ± 0.022		BUSKULIC	95D ALEP	Repl. by HEISTER 01E
0.742 ± 0.035 ± 0.020	8000	ALBRECHT	90E ARG	$E_{cm}^{ee} = 9.4\text{--}10.6$ GeV

¹ Combined fit to ARGUS tau decay parameter measurements in ALBRECHT 98, ALBRECHT 95c, ALBRECHT 93g, and ALBRECHT 94e. ALBRECHT 98 use tau pair events of the type $\tau^-\tau^+ \rightarrow (\ell^-\bar{\nu}_\ell\nu_\tau)(\pi^+\pi^0\bar{\nu}_\tau)$, and their charged conjugates.

² ABE 97o assume $\eta = 0$ in their fit. Letting η vary in the fit gives a ρ value of $0.69 \pm 0.13 \pm 0.05$.

³ Value is from a simultaneous fit for the ρ and η decay parameters to the lepton energy spectrum. Not independent of ALBRECHT 90E $\rho(e \text{ or } \mu)$ value which assumes $\eta = 0$. Result is strongly correlated with ALBRECHT 95c.

⁴ Combined fit to ARGUS tau decay parameter measurements in ALBRECHT 95c, ALBRECHT 93g, and ALBRECHT 94e.

 $\rho(e)$ PARAMETER $(V-A)$ theory predicts $\rho = 0.75$.

VALUE	EVTs	DOCUMENT ID	TECN	COMMENT
0.747 ± 0.010 OUR FIT				
0.744 ± 0.010 OUR AVERAGE				
0.747 ± 0.019 ± 0.014	44k	HEISTER	01E ALEP	1991–1995 LEP runs
0.744 ± 0.036 ± 0.037	17k	ABREU	00L DLPH	1992–1995 runs
0.779 ± 0.047 ± 0.029	25k	ACKERSTAFF	99D OPAL	1990–1995 LEP runs
0.68 ± 0.04 ± 0.07		¹ ALBRECHT	98 ARG	$E_{cm}^{ee} = 9.5\text{--}10.6$ GeV
0.71 ± 0.14 ± 0.05		ABE	97o SLD	1993–1995 SLC runs
0.747 ± 0.012 ± 0.004	34k	ALEXANDER	97F CLEO	$E_{cm}^{ee} = 10.6$ GeV
0.735 ± 0.036 ± 0.020	4.7k	² ALBRECHT	95 ARG	$E_{cm}^{ee} = 9.5\text{--}10.6$ GeV
0.79 ± 0.08 ± 0.06	3230	³ ALBRECHT	93G ARG	$E_{cm}^{ee} = 9.4\text{--}10.6$ GeV
0.64 ± 0.06 ± 0.07	2753	JANSSSEN	89 CBAL	$E_{cm}^{ee} = 9.4\text{--}10.6$ GeV
0.62 ± 0.17 ± 0.14	1823	FORD	87B MAC	$E_{cm}^{ee} = 29$ GeV
0.60 ± 0.13	699	BEHREND	85 CLEO	e^+e^- near $\mathcal{T}(4S)$
0.72 ± 0.10 ± 0.11	594	BACINO	79B DLCO	$E_{cm}^{ee} = 3.5\text{--}7.4$ GeV
••• We do not use the following data for averages, fits, limits, etc. •••				
0.732 ± 0.014 ± 0.009	19k	AMMAR	97B CLEO	Repl. by ALEXANDER 97F
0.793 ± 0.050 ± 0.025		BUSKULIC	95D ALEP	Repl. by HEISTER 01E
0.747 ± 0.045 ± 0.028	5106	ALBRECHT	90E ARG	Repl. by ALBRECHT 95

¹ ALBRECHT 98 use tau pair events of the type $\tau^-\tau^+ \rightarrow (\ell^-\bar{\nu}_\ell\nu_\tau)(\pi^+\pi^0\bar{\nu}_\tau)$, and their charged conjugates.

² ALBRECHT 95 use tau pair events of the type $\tau^-\tau^+ \rightarrow (\ell^-\bar{\nu}_\ell\nu_\tau)(h^+h^-(\pi^0)\bar{\nu}_\tau)$ and their charged conjugates.

³ ALBRECHT 93g use tau pair events of the type $\tau^-\tau^+ \rightarrow (\mu^-\bar{\nu}_\mu\nu_\tau)(e^+\nu_e\bar{\nu}_\tau)$ and their charged conjugates.

 $\rho(\mu)$ PARAMETER $(V-A)$ theory predicts $\rho = 0.75$.

VALUE	EVTs	DOCUMENT ID	TECN	COMMENT
0.763 ± 0.020 OUR FIT				
0.770 ± 0.022 OUR AVERAGE				
0.776 ± 0.045 ± 0.019	46k	HEISTER	01E ALEP	1991–1995 LEP runs
0.999 ± 0.098 ± 0.045	22k	ABREU	00L DLPH	1992–1995 runs
0.777 ± 0.044 ± 0.016	27k	ACKERSTAFF	99D OPAL	1990–1995 LEP runs
0.69 ± 0.06 ± 0.06		¹ ALBRECHT	98 ARG	$E_{cm}^{ee} = 9.5\text{--}10.6$ GeV
0.54 ± 0.28 ± 0.14		ABE	97o SLD	1993–1995 SLC runs
0.750 ± 0.017 ± 0.045	22k	ALEXANDER	97F CLEO	$E_{cm}^{ee} = 10.6$ GeV
0.76 ± 0.07 ± 0.08	3230	ALBRECHT	93G ARG	$E_{cm}^{ee} = 9.4\text{--}10.6$ GeV
0.734 ± 0.055 ± 0.027	3041	ALBRECHT	90E ARG	$E_{cm}^{ee} = 9.4\text{--}10.6$ GeV
0.89 ± 0.14 ± 0.08	1909	FORD	87B MAC	$E_{cm}^{ee} = 29$ GeV
0.81 ± 0.13	727	BEHREND	85 CLEO	e^+e^- near $\mathcal{T}(4S)$
••• We do not use the following data for averages, fits, limits, etc. •••				
0.747 ± 0.048 ± 0.044	13k	AMMAR	97B CLEO	Repl. by ALEXANDER 97F
0.693 ± 0.057 ± 0.028		BUSKULIC	95D ALEP	Repl. by HEISTER 01E

¹ ALBRECHT 98 use tau pair events of the type $\tau^-\tau^+ \rightarrow (\ell^-\bar{\nu}_\ell\nu_\tau)(\pi^+\pi^0\bar{\nu}_\tau)$, and their charged conjugates.

 $\xi(e \text{ or } \mu)$ PARAMETER $(V-A)$ theory predicts $\xi = 1$.

VALUE	EVTs	DOCUMENT ID	TECN	COMMENT
0.985 ± 0.030 OUR FIT				
0.981 ± 0.031 OUR AVERAGE				
0.986 ± 0.068 ± 0.031	81k	HEISTER	01E ALEP	1991–1995 LEP runs
0.929 ± 0.070 ± 0.030	36k	ABREU	00L DLPH	1992–1995 runs
0.98 ± 0.22 ± 0.10	46k	ACKERSTAFF	99D OPAL	1990–1995 LEP runs
0.70 ± 0.16	54k	ACCIARRI	98R L3	1991–1995 LEP runs
1.03 ± 0.11		¹ ALBRECHT	98 ARG	$E_{cm}^{ee} = 9.5\text{--}10.6$ GeV
1.05 ± 0.35 ± 0.04		² ABE	97o SLD	1993–1995 SLC runs
1.007 ± 0.040 ± 0.015	55k	ALEXANDER	97F CLEO	$E_{cm}^{ee} = 10.6$ GeV
••• We do not use the following data for averages, fits, limits, etc. •••				
0.94 ± 0.21 ± 0.07	18k	ACCIARRI	96H L3	Repl. by ACCIARRI 98R
0.97 ± 0.14		³ ALBRECHT	95C ARG	Repl. by ALBRECHT 98
1.18 ± 0.15 ± 0.16		BUSKULIC	95D ALEP	Repl. by HEISTER 01E
0.90 ± 0.15 ± 0.10	3230	⁴ ALBRECHT	93G ARG	$E_{cm}^{ee} = 9.4\text{--}10.6$ GeV

¹ Combined fit to ARGUS tau decay parameter measurements in ALBRECHT 98, ALBRECHT 95c, ALBRECHT 93g, and ALBRECHT 94e. ALBRECHT 98 use tau pair events of the type $\tau^-\tau^+ \rightarrow (\ell^-\bar{\nu}_\ell\nu_\tau)(\pi^+\pi^0\bar{\nu}_\tau)$, and their charged conjugates.

² ABE 97o assume $\eta = 0$ in their fit. Letting η vary in the fit gives a ξ value of $1.02 \pm 0.36 \pm 0.05$.

³ Combined fit to ARGUS tau decay parameter measurements in ALBRECHT 95c, ALBRECHT 93g, and ALBRECHT 94e. ALBRECHT 95c uses events of the type $\tau^-\tau^+ \rightarrow (\ell^-\bar{\nu}_\ell\nu_\tau)(h^+h^-(\pi^0)\bar{\nu}_\tau)$ and their charged conjugates.

⁴ ALBRECHT 93g measurement determines $|\xi|$ for the case $\xi(e) = \xi(\mu)$, but the authors point out that other LEP experiments determine the sign to be positive.

 $\xi(e)$ PARAMETER $(V-A)$ theory predicts $\xi = 1$.

VALUE	EVTs	DOCUMENT ID	TECN	COMMENT
0.994 ± 0.040 OUR FIT				
1.00 ± 0.04 OUR AVERAGE				
1.011 ± 0.094 ± 0.038	44k	HEISTER	01E ALEP	1991–1995 LEP runs
1.01 ± 0.12 ± 0.05	17k	ABREU	00L DLPH	1992–1995 runs
1.13 ± 0.39 ± 0.14	25k	ACKERSTAFF	99D OPAL	1990–1995 LEP runs
1.11 ± 0.20 ± 0.08		¹ ALBRECHT	98 ARG	$E_{cm}^{ee} = 9.5\text{--}10.6$ GeV
1.16 ± 0.52 ± 0.06		ABE	97o SLD	1993–1995 SLC runs
0.979 ± 0.048 ± 0.016	34k	ALEXANDER	97F CLEO	$E_{cm}^{ee} = 10.6$ GeV
••• We do not use the following data for averages, fits, limits, etc. •••				
1.03 ± 0.23 ± 0.09		BUSKULIC	95D ALEP	Repl. by HEISTER 01E

¹ ALBRECHT 98 use tau pair events of the type $\tau^-\tau^+ \rightarrow (\ell^-\bar{\nu}_\ell\nu_\tau)(\pi^+\pi^0\bar{\nu}_\tau)$, and their charged conjugates.

 $\xi(\mu)$ PARAMETER $(V-A)$ theory predicts $\xi = 1$.

VALUE	EVTs	DOCUMENT ID	TECN	COMMENT
1.030 ± 0.059 OUR FIT				
1.06 ± 0.06 OUR AVERAGE				
1.030 ± 0.120 ± 0.050	46k	HEISTER	01E ALEP	1991–1995 LEP runs
1.16 ± 0.19 ± 0.06	22k	ABREU	00L DLPH	1992–1995 runs
0.79 ± 0.41 ± 0.09	27k	ACKERSTAFF	99D OPAL	1990–1995 LEP runs
1.26 ± 0.27 ± 0.14		¹ ALBRECHT	98 ARG	$E_{cm}^{ee} = 9.5\text{--}10.6$ GeV
0.75 ± 0.50 ± 0.14		ABE	97o SLD	1993–1995 SLC runs
1.054 ± 0.069 ± 0.047	22k	ALEXANDER	97F CLEO	$E_{cm}^{ee} = 10.6$ GeV
••• We do not use the following data for averages, fits, limits, etc. •••				
1.23 ± 0.22 ± 0.10		BUSKULIC	95D ALEP	Repl. by HEISTER 01E

¹ ALBRECHT 98 use tau pair events of the type $\tau^-\tau^+ \rightarrow (\ell^-\bar{\nu}_\ell\nu_\tau)(\pi^+\pi^0\bar{\nu}_\tau)$, and their charged conjugates.

$\eta(e \text{ or } \mu)$ PARAMETER(V-A) theory predicts $\eta = 0$.

VALUE	EVTS	DOCUMENT ID	TECN	COMMENT
0.013 ± 0.020 OUR FIT				
0.015 ± 0.021 OUR AVERAGE				
0.012 ± 0.026 ± 0.004	81k	HEISTER	01E ALEP	1991-1995 LEP runs
-0.005 ± 0.036 ± 0.037		ABREU	00L DLPH	1992-1995 runs
0.027 ± 0.055 ± 0.005	46k	ACKERSTAFF	99D OPAL	1990-1995 LEP runs
0.27 ± 0.14	54k	ACCIARRI	98R L3	1991-1995 LEP runs
-0.13 ± 0.47 ± 0.15		ABE	97O SLD	1993-1995 SLC runs
-0.015 ± 0.061 ± 0.062	31k	AMMAR	97B CLEO	$E_{cm}^{ee} = 10.6$ GeV
0.03 ± 0.18 ± 0.12	8.2k	ALBRECHT	95 ARG	$E_{cm}^{ee} = 9.5-10.6$ GeV
• • • We do not use the following data for averages, fits, limits, etc. • • •				
0.25 ± 0.17 ± 0.11	18k	ACCIARRI	96H L3	Repl. by ACCIARRI 98R
-0.04 ± 0.15 ± 0.11		BUSKULIC	95D ALEP	Repl. by HEISTER 01E

 $\eta(\mu)$ PARAMETER(V-A) theory predicts $\eta = 0$.

VALUE	EVTS	DOCUMENT ID	TECN	COMMENT
0.094 ± 0.073 OUR FIT				
0.17 ± 0.15 OUR AVERAGE				Error includes scale factor of 1.2.
0.160 ± 0.150 ± 0.060	46k	HEISTER	01E ALEP	1991-1995 LEP runs
0.72 ± 0.32 ± 0.15		ABREU	00L DLPH	1992-1995 runs
-0.59 ± 0.82 ± 0.45		¹ ABE	97O SLD	1993-1995 SLC runs
0.010 ± 0.149 ± 0.171	13k	² AMMAR	97B CLEO	$E_{cm}^{ee} = 10.6$ GeV
• • • We do not use the following data for averages, fits, limits, etc. • • •				
0.010 ± 0.065 ± 0.001	27k	³ ACKERSTAFF	99D OPAL	1990-1995 LEP runs
-0.24 ± 0.23 ± 0.18		BUSKULIC	95D ALEP	Repl. by HEISTER 01E
¹ Highly correlated (corr. = 0.92) with ABE 97O $\rho(\mu)$ measurement.				
² Highly correlated (corr. = 0.949) with AMMAR 97B $\rho(\mu)$ value.				
³ ACKERSTAFF 99D result is dominated by a constraint on η from the OPAL measurements of the τ lifetime and $B(\tau^- \rightarrow \mu^- \bar{\nu}_\mu \nu_\tau)$ assuming lepton universality for the total coupling strength.				

 $(\delta\xi)(e \text{ or } \mu)$ PARAMETER(V-A) theory predicts $(\delta\xi) = 0.75$.

VALUE	EVTS	DOCUMENT ID	TECN	COMMENT
0.746 ± 0.021 OUR FIT				
0.744 ± 0.022 OUR AVERAGE				
0.776 ± 0.045 ± 0.024	81k	HEISTER	01E ALEP	1991-1995 LEP runs
0.779 ± 0.070 ± 0.028	36k	ABREU	00L DLPH	1992-1995 runs
0.65 ± 0.14 ± 0.07	46k	ACKERSTAFF	99D OPAL	1990-1995 LEP runs
0.70 ± 0.11	54k	ACCIARRI	98R L3	1991-1995 LEP runs
0.63 ± 0.09		¹ ALBRECHT	98 ARG	$E_{cm}^{ee} = 9.5-10.6$ GeV
0.88 ± 0.27 ± 0.04		² ABE	97O SLD	1993-1995 SLC runs
0.745 ± 0.026 ± 0.009	55k	ALEXANDER	97F CLEO	$E_{cm}^{ee} = 10.6$ GeV
• • • We do not use the following data for averages, fits, limits, etc. • • •				
0.81 ± 0.14 ± 0.06	18k	ACCIARRI	96H L3	Repl. by ACCIARRI 98R
0.65 ± 0.12		³ ALBRECHT	95C ARG	Repl. by ALBRECHT 98
0.88 ± 0.11 ± 0.07		BUSKULIC	95D ALEP	Repl. by HEISTER 01E
¹ Combined fit to ARGUS tau decay parameter measurements in ALBRECHT 98, ALBRECHT 95C, ALBRECHT 93G, and ALBRECHT 94E. ALBRECHT 98 use tau pair events of the type $\tau^- \tau^+ \rightarrow (\ell^- \bar{\nu}_\ell \nu_\tau)(\pi^+ \pi^0 \bar{\nu}_\tau)$, and their charged conjugates.				
² ABE 97O assume $\eta = 0$ in their fit. Letting η vary in the fit gives a $(\delta\xi)$ value of $0.87 \pm 0.27 \pm 0.04$.				
³ Combined fit to ARGUS tau decay parameter measurements in ALBRECHT 95C, ALBRECHT 93G, and ALBRECHT 94E. ALBRECHT 95C uses events of the type $\tau^- \tau^+ \rightarrow (\ell^- \bar{\nu}_\ell \nu_\tau)(h^+ h^- h^+ \bar{\nu}_\tau)$ and their charged conjugates.				

 $(\delta\xi)(e)$ PARAMETER(V-A) theory predicts $(\delta\xi) = 0.75$.

VALUE	EVTS	DOCUMENT ID	TECN	COMMENT
0.734 ± 0.028 OUR FIT				
0.731 ± 0.029 OUR AVERAGE				
0.778 ± 0.066 ± 0.024	44k	HEISTER	01E ALEP	1991-1995 LEP runs
0.85 ± 0.12 ± 0.04	17k	ABREU	00L DLPH	1992-1995 runs
0.72 ± 0.31 ± 0.14	25k	ACKERSTAFF	99D OPAL	1990-1995 LEP runs
0.56 ± 0.14 ± 0.06		¹ ALBRECHT	98 ARG	$E_{cm}^{ee} = 9.5-10.6$ GeV
0.85 ± 0.43 ± 0.08		ABE	97O SLD	1993-1995 SLC runs
0.720 ± 0.032 ± 0.010	34k	ALEXANDER	97F CLEO	$E_{cm}^{ee} = 10.6$ GeV
• • • We do not use the following data for averages, fits, limits, etc. • • •				
1.11 ± 0.17 ± 0.07		BUSKULIC	95D ALEP	Repl. by HEISTER 01E
¹ ALBRECHT 98 use tau pair events of the type $\tau^- \tau^+ \rightarrow (\ell^- \bar{\nu}_\ell \nu_\tau)(\pi^+ \pi^0 \bar{\nu}_\tau)$, and their charged conjugates.				

 $(\delta\xi)(\mu)$ PARAMETER(V-A) theory predicts $(\delta\xi) = 0.75$.

VALUE	EVTS	DOCUMENT ID	TECN	COMMENT
0.778 ± 0.037 OUR FIT				
0.79 ± 0.04 OUR AVERAGE				
0.786 ± 0.066 ± 0.028	46k	HEISTER	01E ALEP	1991-1995 LEP runs
0.86 ± 0.13 ± 0.04	22k	ABREU	00L DLPH	1992-1995 runs
0.63 ± 0.23 ± 0.05	27k	ACKERSTAFF	99D OPAL	1990-1995 LEP runs
0.73 ± 0.18 ± 0.10		¹ ALBRECHT	98 ARG	$E_{cm}^{ee} = 9.5-10.6$ GeV
0.82 ± 0.32 ± 0.07		ABE	97O SLD	1993-1995 SLC runs
0.786 ± 0.041 ± 0.032	22k	ALEXANDER	97F CLEO	$E_{cm}^{ee} = 10.6$ GeV
• • • We do not use the following data for averages, fits, limits, etc. • • •				
0.71 ± 0.14 ± 0.06		BUSKULIC	95D ALEP	Repl. by HEISTER 01E

¹ ALBRECHT 98 use tau pair events of the type $\tau^- \tau^+ \rightarrow (\ell^- \bar{\nu}_\ell \nu_\tau)(\pi^+ \pi^0 \bar{\nu}_\tau)$, and their charged conjugates. **$\xi(\pi)$ PARAMETER**(V-A) theory predicts $\xi(\pi) = 1$.

VALUE	EVTS	DOCUMENT ID	TECN	COMMENT
0.993 ± 0.022 OUR FIT				
0.994 ± 0.023 OUR AVERAGE				
0.994 ± 0.020 ± 0.014	27k	HEISTER	01E ALEP	1991-1995 LEP runs
0.81 ± 0.17 ± 0.02		ABE	97O SLD	1993-1995 SLC runs
1.03 ± 0.06 ± 0.04	2.0k	COAN	97 CLEO	$E_{cm}^{ee} = 10.6$ GeV
• • • We do not use the following data for averages, fits, limits, etc. • • •				
0.987 ± 0.057 ± 0.027		BUSKULIC	95D ALEP	Repl. by HEISTER 01E
0.95 ± 0.11 ± 0.05		¹ BUSKULIC	94D ALEP	1990+1991 LEP run
¹ Superseded by BUSKULIC 95D.				

 $\xi(\rho)$ PARAMETER(V-A) theory predicts $\xi(\rho) = 1$.

VALUE	EVTS	DOCUMENT ID	TECN	COMMENT
0.994 ± 0.008 OUR FIT				
0.994 ± 0.009 OUR AVERAGE				
0.987 ± 0.012 ± 0.011	59k	HEISTER	01E ALEP	1991-1995 LEP runs
0.99 ± 0.12 ± 0.04		ABE	97O SLD	1993-1995 SLC runs
0.995 ± 0.010 ± 0.003	66k	ALEXANDER	97F CLEO	$E_{cm}^{ee} = 10.6$ GeV
1.022 ± 0.028 ± 0.030	1.7k	¹ ALBRECHT	94E ARG	$E_{cm}^{ee} = 9.4-10.6$ GeV
• • • We do not use the following data for averages, fits, limits, etc. • • •				
1.045 ± 0.058 ± 0.032		BUSKULIC	95D ALEP	Repl. by HEISTER 01E
1.03 ± 0.11 ± 0.05		² BUSKULIC	94D ALEP	1990+1991 LEP run
¹ ALBRECHT 94E measure the square of this quantity and use the sign determined by ALBRECHT 90I to obtain the quoted result.				
² Superseded by BUSKULIC 95D.				

 $\xi(a_1)$ PARAMETER(V-A) theory predicts $\xi(a_1) = 1$.

VALUE	EVTS	DOCUMENT ID	TECN	COMMENT
1.001 ± 0.027 OUR FIT				
1.002 ± 0.028 OUR AVERAGE				
1.000 ± 0.016 ± 0.024	35k	¹ HEISTER	01E ALEP	1991-1995 LEP runs
1.02 ± 0.13 ± 0.03	17.2k	ASNER	00 CLEO	$E_{cm}^{ee} = 10.6$ GeV
1.29 ± 0.26 ± 0.11	7.4k	² ACKERSTAFF	97R OPAL	1992-1994 LEP runs
0.85 ± 0.15 ± 0.05		ALBRECHT	95C ARG	$E_{cm}^{ee} = 9.5-10.6$ GeV
1.25 ± 0.23 ± 0.08	7.5k	ALBRECHT	93C ARG	$E_{cm}^{ee} = 9.4-10.6$ GeV
• • • We do not use the following data for averages, fits, limits, etc. • • •				
1.08 ± 0.46 ± 0.14 ± 0.41 ± 0.25	2.6k	³ AKERS	95P OPAL	Repl. by ACKERSTAFF 97R
0.937 ± 0.116 ± 0.064		BUSKULIC	95D ALEP	Repl. by HEISTER 01E
¹ HEISTER 01E quote $1.000 \pm 0.016 \pm 0.013 \pm 0.020$ where the errors are statistical, systematic, and an uncertainty due to the final state model. We combine the systematic error and model uncertainty.				
² ACKERSTAFF 97R obtain this result with a model independent fit to the hadronic structure functions. Fitting with the model of Kuhn and Santamaria (ZPHY C48, 445 (1990)) gives $0.87 \pm 0.16 \pm 0.04$, and with the model of Isgur et al. (PR D39,1357 (1989)) they obtain $1.20 \pm 0.21 \pm 0.14$.				
³ AKERS 95P obtain this result with a model independent fit to the hadronic structure functions. Fitting with the model of Kuhn and Santamaria (ZPHY C48, 445 (1990)) gives $0.87 \pm 0.27 \pm 0.05 \pm 0.06$, and with the model of Isgur et al. (PR D39,1357 (1989)) they obtain $1.10 \pm 0.31 \pm 0.13 \pm 0.14$.				

 $\xi(\text{all hadronic modes})$ PARAMETER(V-A) theory predicts $\xi = 1$.

VALUE	EVTS	DOCUMENT ID	TECN	COMMENT
0.995 ± 0.007 OUR FIT				
0.997 ± 0.007 OUR AVERAGE				
0.992 ± 0.007 ± 0.008	102k	¹ HEISTER	01E ALEP	1991-1995 LEP runs
0.997 ± 0.027 ± 0.011	39k	² ABREU	00L DLPH	1992-1995 runs
1.02 ± 0.13 ± 0.03	17.2k	³ ASNER	00 CLEO	$E_{cm}^{ee} = 10.6$ GeV
1.032 ± 0.031	37k	⁴ ACCIARRI	98R L3	1991-1995 LEP runs
0.93 ± 0.10 ± 0.04		ABE	97O SLD	1993-1995 SLC runs
1.29 ± 0.26 ± 0.11	7.4k	⁵ ACKERSTAFF	97R OPAL	1992-1994 LEP runs
0.995 ± 0.010 ± 0.003	66k	⁶ ALEXANDER	97F CLEO	$E_{cm}^{ee} = 10.6$ GeV
1.03 ± 0.06 ± 0.04	2.0k	⁷ COAN	97 CLEO	$E_{cm}^{ee} = 10.6$ GeV
1.017 ± 0.039		⁸ ALBRECHT	95C ARG	$E_{cm}^{ee} = 9.5-10.6$ GeV
1.25 ± 0.23 ± 0.15 ± 0.08	7.5k	⁹ ALBRECHT	93C ARG	$E_{cm}^{ee} = 9.4-10.6$ GeV
• • • We do not use the following data for averages, fits, limits, etc. • • •				
0.970 ± 0.053 ± 0.011	14k	¹⁰ ACCIARRI	96H L3	Repl. by ACCIARRI 98R
1.08 ± 0.46 ± 0.14 ± 0.41 ± 0.25	2.6k	¹¹ AKERS	95P OPAL	Repl. by ACKERSTAFF 97R
1.006 ± 0.032 ± 0.019		¹² BUSKULIC	95D ALEP	Repl. by HEISTER 01E
1.022 ± 0.028 ± 0.030	1.7k	¹³ ALBRECHT	94E ARG	$E_{cm}^{ee} = 9.4-10.6$ GeV
0.99 ± 0.07 ± 0.04		¹⁴ BUSKULIC	94D ALEP	1990+1991 LEP run

Lepton Particle Listings

τ , Heavy Charged Lepton Searches

BAND	87B	PRL 59 415	H.R. Band et al.	(MAC Collab.)
BARINGER	87	PRL 59 1993	P. Baringer et al.	(CLEO Collab.)
BEBEK	87C	PR D36 690	C. Bebek et al.	(CLEO Collab.)
BURCHAT	87	PR D35 27	P.R. Burchat et al.	(Mark II Collab.)
BYLSMA	87	PR D35 2269	B.G. Bylsma et al.	(HRS Collab.)
COFFMAN	87	PR D36 2185	D.M. Coffman et al.	(Mark III Collab.)
DERRICK	87	PL B189 260	M. Derrick et al.	(HRS Collab.)
FORD	87	PR D35 408	W.T. Ford et al.	(MAC Collab.)
FORD	87B	PR D36 1971	W.T. Ford et al.	(MAC Collab.)
GAN	87	PRL 59 411	K.K. Gan et al.	(Mark II Collab.)
GAN	87B	PL B197 561	K.K. Gan et al.	(Mark II Collab.)
AIHARA	86E	PRL 57 1836	H. Aihara et al.	(TPC Collab.)
BARTEL	86D	PL B182 216	W. Bartel et al.	(JADE Collab.)
PDG	86	PL 170B 1	M. Aguilar-Benitez et al.	(CERN, CIT+)
RUCKSTUHL	86	PRL 56 2132	W. Ruckstuhl et al.	(DELCO Collab.)
SCHMIDKE	86	PRL 57 527	W.B. Schmidke et al.	(Mark II Collab.)
YELTON	86	PRL 56 812	J.M. Yelton et al.	(Mark II Collab.)
ALTHOFF	85	ZPHY C26 521	M. Althoff et al.	(TASSO Collab.)
ASH	85B	PRL 55 2118	W.W. Ash et al.	(MAC Collab.)
BALTUSAITIS...	85	PRL 55 1842	R.M. Baltusaitis et al.	(Mark III Collab.)
BARTEL	85F	PL 161B 188	W. Bartel et al.	(JADE Collab.)
BEHRENDIS	85	PR D32 2468	S. Behrendis et al.	(CLEO Collab.)
BELTRAMI	85	PRL 54 1775	I. Beltrami et al.	(HRS Collab.)
BERGER	85	ZPHY C28 1	C. Berger et al.	(PLUTO Collab.)
BURCHAT	85	PRL 54 2489	P.R. Burchat et al.	(Mark II Collab.)
FERNANDEZ	85	PRL 54 1624	E. Fernandez et al.	(MAC Collab.)
MILLS	85	PRL 54 624	G.B. Mills et al.	(DELCO Collab.)
AIHARA	84C	PR D30 2436	H. Aihara et al.	(TPC Collab.)
BEHREND	84	ZPHY C23 103	H.J. Behrend et al.	(CELLO Collab.)
MILLS	84	PRL 52 1944	G.B. Mills et al.	(DELCO Collab.)
BEHREND	83C	PL 127B 270	H.J. Behrend et al.	(CELLO Collab.)
SILVERMAN	83	PR D27 1196	D.J. Silverman, G.L. Shaw	(UCI)
BEHREND	82	PL 114B 282	H.J. Behrend et al.	(CELLO Collab.)
BLOCKER	82B	PRL 48 1586	C.A. Blocker et al.	(Mark II Collab.)
BLOCKER	82D	PL 109B 119	C.A. Blocker et al.	(Mark II Collab.)
FELDMAN	82	PL 48 66	G.J. Feldman et al.	(Mark II Collab.)
HAYES	82	PR D25 2869	K.G. Hayes et al.	(Mark II Collab.)
BERGER	81B	PL 99B 489	C. Berger et al.	(PLUTO Collab.)
DORFAN	81	PRL 46 215	J.M. Dorfan et al.	(Mark II Collab.)
BRANDELIK	80	PL 92B 199	R. Brandelik et al.	(TASSO Collab.)
ZHOLENTZ	80	PL 96B 214	A.A. Zholents et al.	(NOVO)
Also		SJNP 34 814	A.A. Zholents et al.	(NOVO)
Also		Translated from YAF 34 1471		
BACINO	79B	SLAC 22 749	W.J. Bacino et al.	(DELCO Collab.)
KIRKBY	79	SLAC-PUB-2419	J. Kirkby	(SLAC) J
Also		Batavia Lepton Photon Conference.		
BACINO	78B	PRL 41 13	W.J. Bacino et al.	(DELCO Collab.) J
Also		Tokyo Conf. 249	J. Kirz	(STON)
Also		PL 96B 214	A.A. Zholents et al.	(NOVO)
BRANDELIK	78	PL 73B 109	R. Brandelik et al.	(DASP Collab.) J
FELDMAN	78	Tokyo Conf. 777	G.J. Feldman	(SLAC) J
JAROS	78	PRL 40 1120	J. Jaros et al.	(LGW Collab.)
PERL	75	PRL 35 1489	M.L. Perl et al.	(LBL, SLAC)

OTHER RELATED PAPERS

DAVIER	06	RMP 78 1043	M. Davier, A. Hocker, Z. Zhang	(LALO, PARIN+)
RAHAL-CAL...	98	JMP A13 8495	G. Rahal-Calbi	(ETH)
GENTILE	96	PRPL 274 287	S. Gentile, M. Pohl	(ROMAL, ETH)
WEINSTEIN	93	ARNPS 43 457	A.J. Weinstein, R. Stroynowski	(CIT, STMU)
PERL	92	RPP 55 653	M.L. Perl	(SLAC)
PICH	90	MPL A5 1995	A. Pich	(VALE)
BARISH	88	PRPL 157 1	B.C. Barish, R. Stroynowski	(CIT)
GAN	88	JMP A3 531	K.K. Gan, M.L. Perl	(SLAC)
HAYES	88	PR D38 3351	K.G. Hayes, M.L. Perl	(SLAC)
PERL	80	ARNPS 30 299	M.L. Perl	(SLAC)

Heavy Charged Lepton Searches

Charged Heavy Lepton MASS LIMITS

Sequential Charged Heavy Lepton (L^\pm) MASS LIMITS

These experiments assumed that a fourth generation L^\pm decayed to a fourth generation ν_L (or L^0) where ν_L was stable, or that L^\pm decays to a light ν_ℓ via mixing.

See the "Quark and Lepton Compositeness, Searches for" Listings for limits on radiatively decaying excited leptons, i.e. $L^* \rightarrow \ell\gamma$. See the "WIMPs and other Particle Searches" section for heavy charged particle search limits in which the charged particle could be a lepton.

VALUE (GeV)	CL%	DOCUMENT ID	TECN	COMMENT
>100.8	95	ACHARD 01B L3		Decay to νW
>101.9	95	ACHARD 01B L3		$m_L - m_{L^0} > 15$ GeV
• • • We do not use the following data for averages, fits, limits, etc. • • •				
> 81.5	95	ACKERSTAFF 98c OPAL		Assumed $m_{L^\pm} - m_{L^0} > 8.4$ GeV
> 80.2	95	ACKERSTAFF 98c OPAL		$m_{L^0} > m_{L^\pm}$ and $L^\pm \rightarrow \nu W$
< 48 or > 61	95	¹ ACCIARRI 96G L3		
> 63.9	95	ALEXANDER 96P OPAL		Decay to massless ν 's
> 63.5	95	BUSKULIC 96s ALEP		$m_L - m_{L^0} > 7$ GeV
> 65	95	BUSKULIC 96s ALEP		Decay to massless ν 's
none 10-225		² AHMED 94 CNTR		H1 Collab. at HERA
none 12.6-29.6	95	KIM 91B AMY		Massless ν assumed
> 44.3	95	AKRAWY 90G OPAL		
none 0.5-10	95	³ RILES 90 MRK2		For $(m_{L^0} - m_{L^0}) > 0.25-0.4$ GeV
> 8		⁴ STOKER 89 MRK2		For $(m_{L^+} - m_{L^0}) = 0.4$ GeV
> 12		⁴ STOKER 89 MRK2		For $m_{L^0} = 0.9$ GeV
none 18.4-27.6	95	⁵ ABE 88 VNS		
> 25.5	95	⁶ ADACHI 88B TOPZ		
none 1.5-22.0	95	BEHREND 88c CELL		
> 41	90	⁷ ALBAJAR 87B UAI		

> 22.5	95	⁸ ADEVA 85 MRKJ		
> 18.0	95	⁹ BARTEL 83 JADE		
none 4-14.5	95	¹⁰ BERGER 81B PLUT		
> 15.5	95	¹¹ BRANDELIK 81 TASS		
> 13.		¹² AZIMOV 80		
> 16.	95	¹³ BARBER 80B CNTR		
> 0.490		¹⁴ ROTHE 69 RVUE		
¹ ACCIARRI 96G assumes LEP result that the associated neutral heavy lepton mass > 40 GeV.				
² The AHMED 94 limits are from a search for neutral and charged sequential heavy leptons at HERA via the decay channels $L^- \rightarrow e\gamma$, $L^- \rightarrow \nu W^-$, $L^- \rightarrow eZ$; and $L^0 \rightarrow \nu\gamma$, $L^0 \rightarrow e^- W^+$, $L^- \rightarrow \nu Z$, where the W decays to $\ell\nu_\ell$, or to jets, and Z decays to $\ell^+ \ell^-$ or jets.				
³ RILES 90 limits were the result of a special analysis of the data in the case where the mass difference $m_{L^\pm} - m_{L^0}$ was allowed to be quite small, where L^0 denotes the neutrino into which the sequential charged lepton decays. With a slightly reduced m_{L^\pm} range, the mass difference extends to about 4 GeV.				
⁴ STOKER 89 (Mark II at PEP) gives bounds on charged heavy lepton (L^+) mass for the generalized case in which the corresponding neutral heavy lepton (L^0) in the SU(2) doublet is not of negligible mass.				
⁵ ABE 88 search for L^+ and $L^- \rightarrow$ hadrons looking for acoplanar jets. The bound is valid for $m_{\nu} < 10$ GeV.				
⁶ ADACHI 88B search for hadronic decays giving acoplanar events with large missing energy. $E_{cm}^{ee} = 52$ GeV.				
⁷ Assumes associated neutrino is approximately massless.				
⁸ ADEVA 85 analyze one-isolated-muon data and sensitive to $\tau < 10$ nanosec. Assume $B(\text{lepton}) = 0.30$. $E_{cm} = 40-47$ GeV.				
⁹ BARTEL 83 limit is from PETRA e^+e^- experiment with average $E_{cm} = 34.2$ GeV.				
¹⁰ BERGER 81B is DESY DORIS and PETRA experiment. Looking for $e^+e^- \rightarrow L^+L^-$.				
¹¹ BRANDELIK 81 is DESY-PETRA experiment. Looking for $e^+e^- \rightarrow L^+L^-$.				
¹² AZIMOV 80 estimated probabilities for $M+N$ type events in $e^+e^- \rightarrow L^+L^-$ deducing semi-hadronic decay multiplicities of L from e^+e^- annihilation data at $E_{cm} = (2/3)m_L$. Obtained above limit comparing these with e^+e^- data (BRANDELIK 80).				
¹³ BARBER 80B looked for $e^+e^- \rightarrow L^+L^-$, $L \rightarrow \nu^+ X$ with MARK-J at DESY-PETRA.				
¹⁴ ROTHE 69 examines previous data on μ pair production and π and K decays.				

Stable Charged Heavy Lepton (L^\pm) MASS LIMITS

VALUE (GeV)	CL%	DOCUMENT ID	TECN
>102.6	95	ACHARD 01B L3	
• • • We do not use the following data for averages, fits, limits, etc. • • •			
> 28.2	95	¹⁵ ADACHI 90c TOPZ	
none 18.5-42.8	95	AKRAWY 90a OPAL	
> 26.5	95	DECAMP 90f ALEP	
none $m_{\mu} - 36.3$	95	SODERSTROM90 MRK2	
¹⁵ ADACHI 90c put lower limits on the mass of stable charged particles with electric charge Q satisfying $2/3 < Q/e < 4/3$ and with spin 0 or 1/2. We list here the special case for a stable charged heavy lepton.			

Charged Long-Lived Heavy Lepton MASS LIMITS

VALUE (GeV)	CL%	EVTS	DOCUMENT ID	TECN	CHG	COMMENT
>102.0	95		ABBIENDI 03L OPAL			pair produced in e^+e^-
> 0.1	0	¹⁶ ANSORGE 73B	HBC			Long-lived
none 0.55-4.5		¹⁷ BUSHNIN 73	CNTR			Long-lived
none 0.2-0.92		¹⁸ BARNA 68	CNTR			Long-lived
none 0.97-1.03		¹⁸ BARNA 68	CNTR			Long-lived
¹⁶ ANSORGE 73B looks for electron pair production and electron-like Bremsstrahlung.						
¹⁷ BUSHNIN 73 is SERPUKHOV 70 GeV p experiment. Masses assume mean life above 7×10^{-10} and 3×10^{-8} respectively. Calculated from cross section (see "Charged Quasi-Stable Lepton Production Differential Cross Section" below) and 30 GeV muon pair production data.						
¹⁸ BARNA 68 is SLAC photoproduction experiment.						

Doubly-Charged Heavy Lepton MASS LIMITS

VALUE (GeV)	CL%	DOCUMENT ID	TECN	CHG
• • • We do not use the following data for averages, fits, limits, etc. • • •				
none 1-9 GeV	90	¹⁹ CLARK 81	SPEC	++
¹⁹ CLARK 81 is FNAL experiment with 209 GeV muons. Bounds apply to μp which couples with full weak strength to muon. See also section on "Doubly-Charged Lepton Production Cross Section."				

Doubly-Charged Lepton Production Cross Section (μN Scattering)

VALUE (cm ²)	EVTS	DOCUMENT ID	TECN	CHG
• • • We do not use the following data for averages, fits, limits, etc. • • •				
< 6×10^{-38}	0	²⁰ CLARK 81	SPEC	++
²⁰ CLARK 81 is FNAL experiment with 209 GeV muon. Looked for μ^+ nucleon $\rightarrow \bar{p}^0 X$, $\bar{p}^0 \rightarrow \mu^+ \mu^- \bar{\nu}_\mu$ and $\mu^+ n \rightarrow \mu^+ p^+ X$, $\mu^+ p^+ \rightarrow 2\mu^+ \nu_\mu$. Above limits are for $\sigma \times BR$ taken from their mass-dependence plot figure 2.				

Lepton Particle Listings

Heavy Charged Lepton Searches, Neutrino Properties

REFERENCES FOR Heavy Charged Lepton Searches

ABBIENDI	03L	PL B572 8	G. Abbiendi <i>et al.</i>	(OPAL Collab.)
ACHARD	01B	PL B517 75	P. Achard <i>et al.</i>	(L3 Collab.)
ACKERSTAFF	98C	EPJ C1 45	K. Ackerstaff <i>et al.</i>	(OPAL Collab.)
ACCIARRI	96G	PL B377 304	M. Acciarri <i>et al.</i>	(L3 Collab.)
ALEXANDER	96P	PL B385 433	G. Alexander <i>et al.</i>	(OPAL Collab.)
BUSKULIC	96S	PL B384 439	D. Buskulic <i>et al.</i>	(ALEPH Collab.)
AHMED	94	PL B340 205	T. Ahmed <i>et al.</i>	(H1 Collab.)
KIM	91B	JMP A6 2583	G.N. Kim <i>et al.</i>	(AMY Collab.)
ADACHI	90C	PL B244 352	I. Adachi <i>et al.</i>	(TOPAZ Collab.)
AKRAWY	90G	PL B240 250	M.Z. Akrawy <i>et al.</i>	(OPAL Collab.)
AKRAWY	90D	B252 290	M.Z. Akrawy <i>et al.</i>	(OPAL Collab.)
DECAMP	90F	PL B236 511	D. Decamp <i>et al.</i>	(ALEPH Collab.)
RILES	90	PR D42 1	K. Riles <i>et al.</i>	(Mark II Collab.)
SODERSTROM	90	PRL 64 2980	E. Soderstrom <i>et al.</i>	(Mark II Collab.)
STOKER	89	PR D39 1811	D.P. Stoker <i>et al.</i>	(Mark II Collab.)
ABE	88	PRL 61 915	K. Abe <i>et al.</i>	(VENUS Collab.)
ADACHI	88B	PR D37 1339	I. Adachi <i>et al.</i>	(TOPAZ Collab.)
BEHREND	88C	ZPHY C41 7	H.J. Behrend <i>et al.</i>	(CELLO Collab.)
ALBAJAR	87B	PL B185 241	C. Albajar <i>et al.</i>	(UA1 Collab.)
ADEVA	85	PL 152B 439	B. Adeva <i>et al.</i>	(Mark-J Collab.)
		PRPL 109 131	B. Adeva <i>et al.</i>	(Mark-J Collab.)
BARTEL	83	PL 122B 353	W. Bartel <i>et al.</i>	(JADE Collab.)
BERGER	81B	PL 99B 489	C. Berger <i>et al.</i>	(PLUTO Collab.)
BRANDELIK	81	PL 99B 163	R. Brandelik <i>et al.</i>	(TASSO Collab.)
CLARK	81	PRL 46 299	A.R. Clark <i>et al.</i>	(UCB, LBL, FNAL+)
		PR D25 2762	W.H. Smith <i>et al.</i>	(LBL, FNAL, PRIN)
AZIMOV	80	JETPL 32 664	Y.I. Azimov, V.A. Khoze	(PNPI)
		Translated from ZETFP 32 677		
BARBER	80B	PRL 45 1904	D.P. Barber <i>et al.</i>	(Mark-J Collab.)
BRANDELIK	80	PL 92B 199	R. Brandelik <i>et al.</i>	(TASSO Collab.)
ANSORGE	75B	PR DT 26	R.E. Ansorge <i>et al.</i>	(CAVE)
BUSHNIN	73	NP B58 476	Y.B. Bushnin <i>et al.</i>	(SERP)
		PL 42B 136	S.V. Golovkin <i>et al.</i>	(SERP)
ROTHE	69	NP B10 241	K.W. Rothe, A.M. Wolsky	(PENN)
BARNA	68	PR 173 1391	A. Barna <i>et al.</i>	(SLAC, STAN)

OTHER RELATED PAPERS

PERL	81	SLAC-PUB-2752	M.L. Perl	(SLAC)
		Physics in Collision Conference.		

Neutrino Properties

INTRODUCTION TO THE NEUTRINO PROPERTIES LISTINGS

Revised August 2009 by P. Vogel (Caltech) and A. Piepke (University of Alabama).

The following Listings concern measurements of various properties of neutrinos. Nearly all of the measurements, all of which so far are limits, actually concern superpositions of the mass eigenstates ν_i , which are in turn related to the weak eigenstates ν_ℓ , via the neutrino mixing matrix

$$|\nu_\ell\rangle = \sum_i U_{\ell i} |\nu_i\rangle.$$

In the analogous case of quark mixing via the CKM matrix, the smallness of the off-diagonal terms (small mixing angles) permits a “dominant eigenstate” approximation. However, the present results of neutrino oscillation searches show that the mixing matrix contains two large mixing angles. We cannot, therefore, associate any particular state $|\nu_i\rangle$ with any particular lepton label e, μ or τ . Nevertheless, neutrinos are produced in weak decays with a definite lepton flavor, and are typically detected by the charged current weak interaction again associated with a specific lepton flavor. Hence, the listings for the neutrino mass that follow are separated into the three associated charged-lepton categories. Other properties (mean lifetime, magnetic moment, charge, and charge radius) are no longer separated this way. If needed, the associated lepton flavor is reported in the footnotes.

Measured quantities (mass-squared, magnetic moments, mean lifetimes, *etc.*) all depend upon the mixing parameters $|U_{\ell i}|^2$, but to some extent also on experimental conditions (*e.g.*,

on energy resolution). Most of these observables, in particular mass-squared, cannot distinguish between Dirac and Majorana neutrinos, and are unaffected by CP phases.

Direct neutrino mass measurements are usually based on the analysis of the kinematics of charged particles (leptons, pions) emitted together with neutrinos (flavor states) in various weak decays. The most sensitive neutrino mass measurement to date, involving electron type antineutrinos, is based on fitting the shape of the beta spectrum. The quantity $\langle m_\beta^2 \rangle = \sum_i |U_{ei}|^2 m_{\nu_i}^2$ is determined or constrained, where the sum is over all mass eigenvalues m_{ν_i} that are too close together to be resolved experimentally. If the energy resolution is better than $\Delta m_{ij}^2 \equiv m_{\nu_i}^2 - m_{\nu_j}^2$, the corresponding heavier m_{ν_i} and mixing parameter could be determined by fitting the resulting spectral anomaly (step or kink).

A limit on $\langle m_\beta^2 \rangle$ implies an *upper* limit on the *minimum* value m_{\min}^2 of $m_{\nu_i}^2$, independent of the mixing parameters U_{ei} : $m_{\min}^2 \leq \langle m_\beta^2 \rangle$. However, if and when the value of $\langle m_\beta^2 \rangle$ is determined and the study of neutrino oscillations provides us with the values of *all* neutrino mass-squared differences $\Delta m_{ij}^2 \equiv m_i^2 - m_j^2$ and the mixing parameters $|U_{ei}|^2$, then the individual neutrino mass squares $m_{\nu_j}^2 = \langle m_\beta^2 \rangle - \sum_i |U_{ei}|^2 \Delta m_{ij}^2$ can be determined.

All confirmed neutrino oscillation experiments using solar, reactor, atmospheric and accelerator neutrinos can be described using three active neutrino flavors, *i.e.*, two mass splittings and three mixing angles. Combined three neutrino analyses determine the squared mass differences and two of the mixing angles to within reasonable accuracy. For given $|\Delta m_{ij}^2|$, a limit on $\langle m_\beta^2 \rangle$ from beta decay defines an *upper* limit on the *maximum* value m_{\max} of m_{ν_i} : $m_{\max}^2 \leq \langle m_\beta^2 \rangle + \sum_{i < j} |\Delta m_{ij}^2|$. The analysis of the low energy beta decay of tritium, combined with the oscillation results, thus limits *all* active neutrino masses. Traditionally experimental neutrino mass limits obtained from pion decay $\pi^+ \rightarrow \mu^+ + \nu_\mu$, or the shape of the spectrum of decay products of the τ lepton, did not distinguish between flavor and mass eigenstates. These results are reported as limits of the μ and τ based neutrino mass. After the determination of the $|\Delta m_{ij}^2|$'s, the corresponding neutrino mass limits are no longer competitive with those derived from low energy beta decays, with the proviso, however, that the oscillation searches, reported below, can be regarded as a reliable source of *all* $|\Delta m_{ij}^2|$ values.

The spread of arrival times of the neutrinos from SN1987A, coupled with the measured neutrino energies, provided a time-of-flight limit on a quantity similar to $\langle m_\beta \rangle \equiv \sqrt{\langle m_\beta^2 \rangle}$. This statement, clothed in various degrees of sophistication, has been the basis for a very large number of papers. The resulting limits, however, are no longer comparable with the limits from tritium beta decay.

Constraint on the sum of the neutrino masses can be obtained from the analysis of the cosmic microwave background anisotropy, combined with the galaxy redshift surveys and

See key on page 405

Lepton Particle Listings

Neutrino Properties

other data. These limits are reported in a separate table (Sum of Neutrino Masses, m_{tot}). Discussion concerning the model dependence of this limit is continuing.

$\bar{\nu}$ MASS (electron based)

Those limits given below are for the square root of $m_{\nu_e}^{2(\text{eff})} \equiv \sum_i |U_{ei}|^2 m_{\nu_i}^2$. Limits that come from the kinematics of ${}^3\text{H}\beta^- \bar{\nu}$ decay are the square roots of the limits for $m_{\nu_e}^{2(\text{eff})}$. Obtained from the measurements reported in the Listings for “ $\bar{\nu}$ Mass Squared,” below.

VALUE (eV)	CL%	DOCUMENT ID	TECN	COMMENT
< 2 OUR EVALUATION				
< 2.3	95	1 KRAUS	05 SPEC	${}^3\text{H}\beta$ decay
< 2.5	95	2 LOBASHEV	99 SPEC	${}^3\text{H}\beta$ decay
• • • We do not use the following data for averages, fits, limits, etc. • • •				
<21.7	90	3 ARNABOLDI	03A BOLO	${}^{187}\text{Re}\beta$ decay
< 5.7	95	4 LOREDO	02 ASTR	SN1987A
< 2.8	95	5 WEINHEIMER	99 SPEC	${}^3\text{H}\beta$ decay
< 4.35	95	6 BELESEV	95 SPEC	${}^3\text{H}\beta$ decay
<12.4	95	7 CHING	95 SPEC	${}^3\text{H}\beta$ decay
<92	95	8 HIDDEMANN	95 SPEC	${}^3\text{H}\beta$ decay
15 $\begin{smallmatrix} +32 \\ -15 \end{smallmatrix}$		HIDDEMANN	95 SPEC	${}^3\text{H}\beta$ decay
<19.6	95	9 KERNAN	95 ASTR	SN 1987A
< 7.0	95	10 STOEFFL	95 SPEC	${}^3\text{H}\beta$ decay
< 7.2	95	11 WEINHEIMER	93 SPEC	${}^3\text{H}\beta$ decay
<11.7	95	12 HOLZSCHUH	92B SPEC	${}^3\text{H}\beta$ decay
<13.1	95	13 KAWAKAMI	91 SPEC	${}^3\text{H}\beta$ decay
< 9.3	95	14 ROBERTSON	91 SPEC	${}^3\text{H}\beta$ decay
<14	95	AVIGNONE	90 ASTR	SN 1987A
<16		SPERGEL	88 ASTR	SN 1987A
17 to 40		15 BORIS	87 SPEC	${}^3\text{H}\beta$ decay

1 KRAUS 05 is a continuation of the work reported in WEINHEIMER 99. This result represents the final analysis of data taken from 1997 to 2001. Various sources of systematic uncertainties have been identified and quantified. The background has been reduced compared to the initial running period. A spectral anomaly at the endpoint, reported in LOBASHEV 99, was not observed.

2 LOBASHEV 99 report a new measurement which continues the work reported in BELESEV 95. This limit depends on phenomenological fit parameters used to derive their best fit to $m_{\nu_e}^2$, making an unambiguous interpretation difficult. See the footnote under “ $\bar{\nu}$ Mass Squared.”

3 ARNABOLDI 03A *et al.* report kinematical neutrino mass limit using β -decay of ${}^{187}\text{Re}$. Bolometric AgReO₄ micro-calorimeters are used. Mass bound is substantially weaker than those derived from tritium β -decays but has different systematic uncertainties.

4 LOREDO 02 updates LOREDO 89.

5 WEINHEIMER 99 presents two analyses which exclude the spectral anomaly and result in an acceptable $m_{\nu_e}^2$. We report the most conservative limit, but the other is nearly the same. See the footnote under “ $\bar{\nu}$ Mass Squared.”

6 BELESEV 95 (Moscow) use an integral electrostatic spectrometer with adiabatic magnetic collimation and a gaseous tritium sources. A fit to a normal Kurie plot above 18300–18350 eV (to avoid a low-energy anomaly) plus a monochromatic line 7–15 eV below the endpoint yields $m_{\nu_e}^2 = -4.1 \pm 10.9 \text{ eV}^2$, leading to this Bayesian limit.

7 CHING 95 quotes results previously given by SUN 93; no experimental details are given. A possible explanation for consistently negative values of $m_{\nu_e}^2$ is given.

8 HIDDEMANN 95 (Munich) experiment uses atomic tritium embedded in a metal-dioxide lattice. Bayesian limit calculated from the weighted mean $m_{\nu_e}^2 = 221 \pm 4244 \text{ eV}^2$ from the two runs listed below.

9 STOEFFL 95 (LLNL) result is the Bayesian limit obtained from the $m_{\nu_e}^2$ errors given below but with $m_{\nu_e}^2$ set equal to 0. The anomalous endpoint accumulation leads to a value of $m_{\nu_e}^2$ which is negative by more than 5 standard deviations.

10 WEINHEIMER 93 (Mainz) is a measurement of the endpoint of the tritium β spectrum using an electrostatic spectrometer with a magnetic guiding field. The source is molecular tritium frozen onto an aluminum substrate.

11 HOLZSCHUH 92B (Zurich) result is obtained from the measurement $m_{\nu_e}^2 = -24 \pm 48 \pm 61$ (1σ errors), in eV^2 , using the PDG prescription for conversion to a limit in m_{ν_e} .

12 KAWAKAMI 91 (Tokyo) experiment uses tritium-labeled arachidic acid. This result is the Bayesian limit obtained from the $m_{\nu_e}^2$ limit with the errors combined in quadrature. This was also done in ROBERTSON 91, although the authors report a different procedure.

13 ROBERTSON 91 (LANL) experiment uses gaseous molecular tritium. The result is in strong disagreement with the earlier claims by the ITP group [LUBIMOV 80, BORIS 87 (+ BORIS 88 erratum)] that m_{ν_e} lies between 17 and 40 eV. However, the probability of a positive $m_{\nu_e}^2$ is only 3% if statistical and systematic error are combined in quadrature.

14 See also comment in BORIS 87B and erratum in BORIS 88.

$\bar{\nu}$ MASS SQUARED (electron based)

Given troubling systematics which result in improbably negative estimators of $m_{\nu_e}^{2(\text{eff})} \equiv \sum_i |U_{ei}|^2 m_{\nu_i}^2$, in many experiments, we use only KRAUS 05 and LOBASHEV 99 for our average.

VALUE (eV ²)	CL%	DOCUMENT ID	TECN	COMMENT
– 1.1 ± 2.4 OUR AVERAGE				
– 0.6 ± 2.2 ± 2.1		15 KRAUS	05 SPEC	${}^3\text{H}\beta$ decay
– 1.9 ± 3.4 ± 2.2		16 LOBASHEV	99 SPEC	${}^3\text{H}\beta$ decay
• • • We do not use the following data for averages, fits, limits, etc. • • •				
– 3.7 ± 5.3 ± 2.1		17 WEINHEIMER	99 SPEC	${}^3\text{H}\beta$ decay
– 22 ± 4.8		18 BELESEV	95 SPEC	${}^3\text{H}\beta$ decay
129 ± 6010		19 HIDDEMANN	95 SPEC	${}^3\text{H}\beta$ decay
313 ± 5994		19 HIDDEMANN	95 SPEC	${}^3\text{H}\beta$ decay
–130 ± 20 ± 15	95	20 STOEFFL	95 SPEC	${}^3\text{H}\beta$ decay
– 31 ± 75 ± 48		21 SUN	93 SPEC	${}^3\text{H}\beta$ decay
– 39 ± 34 ± 15		22 WEINHEIMER	93 SPEC	${}^3\text{H}\beta$ decay
– 24 ± 48 ± 61		23 HOLZSCHUH	92B SPEC	${}^3\text{H}\beta$ decay
– 65 ± 85 ± 65		24 KAWAKAMI	91 SPEC	${}^3\text{H}\beta$ decay
–147 ± 68 ± 41		25 ROBERTSON	91 SPEC	${}^3\text{H}\beta$ decay

15 KRAUS 05 is a continuation of the work reported in WEINHEIMER 99. This result represents the final analysis of data taken from 1997 to 2001. Problems with significantly negative squared neutrino masses, observed in some earlier experiments, have been resolved in this work.

16 LOBASHEV 99 report a new measurement which continues the work reported in BELESEV 95. The data were corrected for electron trapping effects in the source, eliminating the dependence of the fitted neutrino mass on the fit interval. The analysis assuming a pure beta spectrum yields significantly negative fitted $m_{\nu_e}^2 \approx -(20-10) \text{ eV}^2$. This problem is attributed to a discrete spectral anomaly of about 6×10^{-11} intensity with a time-dependent energy of 5–15 eV below the endpoint. The data analysis accounts for this anomaly by introducing two extra phenomenological fit parameters resulting in a best fit of $m_{\nu_e}^2 = -1.9 \pm 3.4 \pm 2.2 \text{ eV}^2$ which is used to derive a neutrino mass limit. However, the introduction of phenomenological fit parameters which are correlated with the derived $m_{\nu_e}^2$ limit makes unambiguous interpretation of this result difficult.

17 WEINHEIMER 99 is a continuation of the work reported in WEINHEIMER 93. Using a lower temperature of the frozen tritium source eliminated the dewetting of the T_2 film, which introduced a dependence of the fitted neutrino mass on the fit interval in the earlier work. An indication for a spectral anomaly reported in LOBASHEV 99 has been seen, but its time dependence does not agree with LOBASHEV 99. Two analyses, which exclude the spectral anomaly either by choice of the analysis interval or by using a particular data set which does not exhibit the anomaly, result in acceptable $m_{\nu_e}^2$ fits and are used to derive the neutrino mass limit published by the authors. We list the most conservative of the two.

18 BELESEV 95 (Moscow) use an integral electrostatic spectrometer with adiabatic magnetic collimation and a gaseous tritium sources. This value comes from a fit to a normal Kurie plot above 18300–18350 eV (to avoid a low-energy anomaly), including the effects of an apparent peak 7–15 eV below the endpoint.

19 HIDDEMANN 95 (Munich) experiment uses atomic tritium embedded in a metal-dioxide lattice. They quote measurements from two data sets.

20 STOEFFL 95 (LLNL) uses a gaseous source of molecular tritium. An anomalous pileup of events at the endpoint leads to the negative value for $m_{\nu_e}^2$. The authors acknowledge that “the negative value for the best fit of $m_{\nu_e}^2$ has no physical meaning” and discuss possible explanations for this effect.

21 SUN 93 uses a tritiated hydrocarbon source. See also CHING 95.

22 WEINHEIMER 93 (Mainz) is a measurement of the endpoint of the tritium β spectrum using an electrostatic spectrometer with a magnetic guiding field. The source is molecular tritium frozen onto an aluminum substrate.

23 HOLZSCHUH 92B (Zurich) source is a monolayer of tritiated hydrocarbon.

24 KAWAKAMI 91 (Tokyo) experiment uses tritium-labeled arachidic acid.

25 ROBERTSON 91 (LANL) experiment uses gaseous molecular tritium. The result is in strong disagreement with the earlier claims by the ITP group [LUBIMOV 80, BORIS 87 (+ BORIS 88 erratum)] that m_{ν_e} lies between 17 and 40 eV. However, the probability of a positive $m_{\nu_e}^2$ is only 3% if statistical and systematic error are combined in quadrature.

ν MASS (electron based)

These are measurement of m_{ν_e} (in contrast to $m_{\bar{\nu}_e}$ given above). The masses can be different for a Dirac neutrino in the absence of *CPT* invariance. The possible distinction between ν and $\bar{\nu}$ properties is usually ignored elsewhere in these Listings.

VALUE (eV)	CL%	DOCUMENT ID	TECN	COMMENT
<460	68	YASUMI	94 CNTR	${}^{163}\text{Ho}$ decay
<225	95	SPRINGER	87 CNTR	${}^{163}\text{Ho}$ decay

ν MASS (muon based)

Limits given below are for the square root of $m_{\nu_\mu}^{2(\text{eff})} \equiv \sum_i |U_{\mu i}|^2 m_{\nu_i}^2$.

In some of the COSM papers listed below, the authors did not distinguish between weak and mass eigenstates.

Lepton Particle Listings

Neutrino Properties

OUR EVALUATION is based on OUR AVERAGE for the π^\pm mass and the ASSAMAGAN 96 value for the muon momentum for the π^\pm decay at rest. The limit is calculated using the unified classical analysis of FELDMAN 98 for a Gaussian distribution near a physical boundary. WARNING: since $m_{\nu_\mu}^{2(\text{eff})}$ is calculated from the differences of large numbers, it and the corresponding limits are extraordinarily sensitive to small changes in the pion mass, the decay muon momentum, and their errors. For example, the limits obtained using JECKELMANN 94, LENZ 98, and the weighted averages are 0.15, 0.29, and 0.19 MeV, respectively.

VALUE (MeV)	CL%	DOCUMENT ID	TECN	COMMENT
<0.19 (CL = 90%) OUR EVALUATION				
<0.17	90	26 ASSAMAGAN 96	SPEC	$m_{\nu_\mu}^2 = -0.016 \pm 0.023$

• • • We do not use the following data for averages, fits, limits, etc. • • •

<0.15		27 DOLGOV	95	COSM	Nucleosynthesis
<0.48		28 ENQVIST	93	COSM	Nucleosynthesis
<0.3		29 FULLER	91	COSM	Nucleosynthesis
<0.42		29 LAM	91	COSM	Nucleosynthesis
<0.50	90	30 ANDERHUB	82	SPEC	$m_{\nu_\mu}^2 = -0.14 \pm 0.20$
<0.65	90	CLARK	74	ASPK	$K_{\mu 3}$ decay

26 ASSAMAGAN 96 measurement of p_μ from $\pi^\pm \rightarrow \mu^\pm \nu$ at rest combined with JECKELMANN 94 Solution B pion mass yields $m_{\nu_\mu}^2 = -0.016 \pm 0.023$ with corresponding Bayesian limit listed above. If Solution A is used, $m_{\nu_\mu}^2 = -0.143 \pm 0.024$ MeV². Replaces ASSAMAGAN 94.

27 DOLGOV 95 removes earlier assumptions (DOLGOV 93) about thermal equilibrium below T_{QCD} for wrong-helicity Dirac neutrinos (ENQVIST 93, FULLER 91) to set more stringent limits.

28 ENQVIST 93 bases limit on the fact that thermalized wrong-helicity Dirac neutrinos would speed up expansion of early universe, thus reducing the primordial abundance. FULLER 91 exploits the same mechanism but in the older calculation obtains a larger production rate for these states, and hence a lower limit. Neutrino lifetime assumed to exceed nucleosynthesis time, ~ 1 s.

29 Assumes neutrino lifetime >1 s. For Dirac neutrinos only. See also ENQVIST 93.

30 ANDERHUB 82 kinematics is insensitive to the pion mass.

ν MASS (tau based)

The limits given below are the square roots of limits for $m_{\nu_\tau}^{2(\text{eff})} \equiv \sum_i |U_{\tau i}|^2 m_{\nu_i}^2$.

In some of the ASTR and COSM papers listed below, the authors did not distinguish between weak and mass eigenstates.

VALUE (MeV)	CL%	EVTS	DOCUMENT ID	TECN	COMMENT
< 18.2					
	95		31 BARATE	98F	ALEP 1991-1995 LEP runs

• • • We do not use the following data for averages, fits, limits, etc. • • •

< 28	95		32 ATHANAS	00	CLEO $E_{\text{cm}}^{\text{eff}} = 10.6$ GeV
< 27.6	95		33 ACKERSTAFF	98T	OPAL 1990-1995 LEP runs
< 30	95	473	34 AMMAR	98	CLEO $E_{\text{cm}}^{\text{eff}} = 10.6$ GeV
< 60	95		35 ANASTASSOV	97	CLEO $E_{\text{cm}}^{\text{eff}} = 10.6$ GeV
< 0.37 or > 22			36 FIELDS	97	COSM Nucleosynthesis
< 68	95		37 SWAIN	97	THEO m_τ, τ_τ, τ partial widths
< 29.9	95		38 ALEXANDER	96M	OPAL 1990-1994 LEP runs
< 149			39 BOTTINO	96	THEO π, μ, τ leptonic decays
< 1 or > 25			40 HANNESTAD	96C	COSM Nucleosynthesis
< 71	95		41 SOBIE	96	THEO $m_\tau, \tau_\tau, B(\tau^- \rightarrow e^- \bar{\nu}_e \nu_\tau)$
< 24	95	25	42 BUSKULIC	95H	ALEP 1991-1993 LEP runs
< 0.19			43 DOLGOV	95	COSM Nucleosynthesis
< 3			44 SIGL	95	ASTR SN 1987A
< 0.4 or > 30			45 DODELSON	94	COSM Nucleosynthesis
< 0.1 or > 50			46 KAWASAKI	94	COSM Nucleosynthesis
155-225			47 PERES	94	THEO π, K, μ, τ weak decays
< 32.6	95	113	48 CINABRO	93	CLEO $E_{\text{cm}}^{\text{eff}} \approx 10.6$ GeV
< 0.3 or > 35			49 DOLGOV	93	COSM Nucleosynthesis
< 0.74			50 ENQVIST	93	COSM Nucleosynthesis
< 31	95	19	51 ALBRECHT	92M	ARG $E_{\text{cm}}^{\text{eff}} = 9.4-10.6$ GeV
< 0.3			52 FULLER	91	COSM Nucleosynthesis
< 0.5 or > 25			53 KOLB	91	COSM Nucleosynthesis
< 0.42			52 LAM	91	COSM Nucleosynthesis

31 BARATE 98F result based on kinematics of 2939 $\tau^- \rightarrow 2\pi^- \pi^+ \nu_\tau$ and 52 $\tau^- \rightarrow 3\pi^- 2\pi^+ (\pi^0) \nu_\tau$ decays. If possible 2.5% excited a_1 decay is included in 3-prong sample analysis, limit increases to 19.2 MeV.

32 ATHANAS 00 bound comes from analysis of $\tau^- \rightarrow \pi^- \pi^+ \pi^- \pi^0 \nu_\tau$ decays.

33 ACKERSTAFF 98T use $\tau \rightarrow 5\pi^\pm \nu_\tau$ decays to obtain a limit of 43.2 MeV (95%CL). They combine this with ALEXANDER 96M value using $\tau \rightarrow 3h^\pm \nu_\tau$ decays to obtain quoted limit.

34 AMMAR 98 limit comes from analysis of $\tau^- \rightarrow 3\pi^- 2\pi^+ \nu_\tau$ and $\tau^- \rightarrow 2\pi^- \pi^+ 2\pi^0 \nu_\tau$ decay modes.

35 ANASTASSOV 97 derive limit by comparing their m_τ measurement (which depends on m_{ν_τ}) to BAI 96 m_τ threshold measurement.

36 FIELDS 97 limit for a Dirac neutrino. For a Majorana neutrino the mass region < 0.93 or > 31 MeV is excluded. These bounds assume $N_{\nu_\nu} < 4$ from nucleosynthesis; a wider excluded region occurs with a smaller N_{ν_ν} upper limit.

37 SWAIN 97 derive their limit from the Standard Model relationships between the tau mass, lifetime, branching fractions for $\tau^- \rightarrow e^- \bar{\nu}_e \nu_\tau, \tau^- \rightarrow \mu^- \bar{\nu}_\mu \nu_\tau, \tau^- \rightarrow \pi^- \nu_\tau$, and $\tau^- \rightarrow K^- \nu_\tau$, and the muon mass and lifetime by assuming lepton universality and using world average values. Limit is reduced to 48 MeV when the CLEO τ mass measurement (BALEST 93) is included; see CLEO's more recent m_{ν_τ} limit (ANASTASSOV 97).

Consideration of mixing with a fourth generation heavy neutrino yields $\sin^2 \theta_L < 0.016$ (95%CL).

38 ALEXANDER 96M bound comes from analyses of $\tau^- \rightarrow 3\pi^- 2\pi^+ \nu_\tau$ and $\tau^- \rightarrow h^- h^+ \nu_\tau$ decays.

39 BOTTINO 96 assumes three generations of neutrinos with mixing, finds consistency with massless neutrinos with no mixing based on 1995 data for masses, lifetimes, and leptonic partial widths.

40 HANNESTAD 96C limit is on the mass of a Majorana neutrino. This bound assumes $N_{\nu_\nu} < 4$ from nucleosynthesis. A wider excluded region occurs with a smaller N_{ν_ν} upper limit. This paper is the corrected version of HANNESTAD 96; see the erratum: HANNESTAD 96B.

41 SOBIE 96 derive their limit from the Standard Model relationship between the tau mass, lifetime, and leptonic branching fraction, and the muon mass and lifetime, by assuming lepton universality and using world average values.

42 BUSKULIC 95H bound comes from a two-dimensional fit of the visible energy and invariant mass distribution of $\tau \rightarrow 5\pi(\pi^0) \nu_\tau$ decays. Replaced by BARATE 98F.

43 DOLGOV 95 removes earlier assumptions (DOLGOV 93) about thermal equilibrium below T_{QCD} for wrong-helicity Dirac neutrinos (ENQVIST 93, FULLER 91) to set more stringent limits. DOLGOV 96 argues that a possible window near 20 MeV is excluded.

44 SIGL 95 exclude massive Dirac or Majorana neutrinos with lifetimes between 10^{-3} and 10^8 seconds if the decay products are predominantly γ or $e^+ e^-$.

45 DODELSON 94 calculate constraints on ν_τ mass and lifetime from nucleosynthesis for 4 generic decay modes. Limits depend strongly on decay mode. Quoted limit is valid for all decay modes of Majorana neutrinos with lifetime greater than about 300s. For Dirac neutrinos limits change to < 0.3 or > 33 .

46 KAWASAKI 94 excluded region is for Majorana neutrino with lifetime >1000 s. Other limits are given as a function of ν_τ lifetime for decays of the type $\nu_\tau \rightarrow \nu_\mu \phi$ where ϕ is a Nambu-Goldstone boson.

47 PERES 94 used PDG 92 values for parameters to obtain a value consistent with mixing. Reexamination by BOTTINO 96 which included radiative corrections and 1995 PDG parameters resulted in two allowed regions, $m_3 < 70$ MeV and 140 MeV $m_3 < 149$ MeV.

48 CINABRO 93 bound comes from analysis of $\tau^- \rightarrow 3\pi^- 2\pi^+ \nu_\tau$ and $\tau^- \rightarrow 2\pi^- \pi^+ 2\pi^0 \nu_\tau$ decay modes.

49 DOLGOV 93 assumes neutrino lifetime >100 s. For Majorana neutrinos, the low mass limit is 0.5 MeV. KAWANO 92 points out that these bounds can be overcome for a Dirac neutrino if it possesses a magnetic moment. See also DOLGOV 96.

50 ENQVIST 93 bases limit on the fact that thermalized wrong-helicity Dirac neutrinos would speed up expansion of early universe, thus reducing the primordial abundance. FULLER 91 exploits the same mechanism but in the older calculation obtains a larger production rate for these states, and hence a lower limit. Neutrino lifetime assumed to exceed nucleosynthesis time, ~ 1 s.

51 ALBRECHT 92M reports measurement of a slightly lower τ mass, which has the effect of reducing the ν_τ mass reported in ALBRECHT 88B. Bound is from analysis of $\tau^- \rightarrow 3\pi^- 2\pi^+ \nu_\tau$ mode.

52 Assumes neutrino lifetime >1 s. For Dirac neutrinos. See also ENQVIST 93.

53 KOLB 91 exclusion region is for Dirac neutrino with lifetime >1 s; other limits are given.

Revised August 2009 by K.A. Olive (University of Minnesota).

The limits on low mass ($m_\nu \lesssim 1$ MeV) neutrinos apply to m_{tot} given by

$$m_{\text{tot}} = \sum_\nu (g_\nu/2) m_\nu,$$

where g_ν is the number of spin degrees of freedom for ν plus $\bar{\nu}$: $g_\nu = 4$ for neutrinos with Dirac masses; $g_\nu = 2$ for Majorana neutrinos. Stable neutrinos in this mass range make a contribution to the total energy density of the Universe which is given by

$$\rho_\nu = m_{\text{tot}} n_\nu = m_{\text{tot}} (3/11) n_\gamma,$$

where the factor 3/11 is the ratio of (light) neutrinos to photons. Writing $\Omega_\nu = \rho_\nu / \rho_c$, where ρ_c is the critical energy density of the Universe, and using $n_\gamma = 412 \text{ cm}^{-3}$, we have

$$\Omega_\nu h^2 = m_{\text{tot}} / (94 \text{ eV}).$$

While an upper limit to the matter density of $\Omega_m h^2 < 0.12$ would constrain $m_{\text{tot}} < 11$ eV, much stronger constraints are obtained from a combination of observations of the CMB and the amplitude of density fluctuations on smaller scales from the clustering of galaxies and the Lyman- α forest. These combine to give an upper limit around 0.5 eV.

SUM OF THE NEUTRINO MASSES, m_{tot}

(Defined in the above note), of effectively stable neutrinos (i.e., those with mean lives greater than or equal to the age of the universe). These papers assumed Dirac neutrinos. When necessary, we have generalized the results reported so they apply to m_{tot} . For other limits, see SZALAY 76, VYSOTSKY 77, BERNSTEIN 81, FREESE 84, SCHRAMM 84, and COWSIK 85.

VALUE (eV)	CL%	DOCUMENT ID	TECN	COMMENT
• • • We do not use the following data for averages, fits, limits, etc. • • •				
< 1.1		54 ICHIKI	09	COSM
< 1.3		55 KOMATSU	09	COSM WMAP
< 1.2		56 TERENO	09	COSM
< 0.33		57 VIKHLININ	09	COSM
< 0.28		58 BERNARDIS	08	COSM
< 0.17–2.3		59 FOGLI	07	COSM
< 0.42	95	60 KRISTIANSEN	07	COSM
< 0.63–2.2		61 ZUNCKEL	07	COSM
< 0.24	95	62 CIRELLI	06	COSM
< 0.62	95	63 HANNESTAD	06	COSM
< 1.2		64 SANCHEZ	06	COSM
< 0.17	95	62 SELJAK	06	COSM
< 2.0	95	65 ICHIKAWA	05	COSM
< 0.75		66 BARGER	04	COSM
< 1.0		67 CROTTY	04	COSM
< 0.7		68 SPERGEL	03	COSM WMAP
< 0.9		69 LEWIS	02	COSM
< 4.2		70 WANG	02	COSM CMB
< 2.7		71 FUKUGITA	00	COSM
< 5.5		72 CROFT	99	ASTR Ly α power spec
<180		SZALAY	74	COSM
<132		COWSIK	72	COSM
<280		MARX	72	COSM
<400		GERSHTEIN	66	COSM
54	Constrains the total mass of neutrinos from weak lensing measurements when combined with CMB. Limit improves to 0.54 eV when supernovae and baryon acoustic oscillation observations are included. Assumes Λ CDM model.			
55	Constrains the total mass of neutrinos from five-year WMAP data. Limit improves to 0.67 eV when supernovae and baryon acoustic oscillation observations are included. Limits quoted assume the Λ CDM model. Supersedes SPERGEL 07.			
56	Constrains the total mass of neutrinos from weak lensing measurements when combined with CMB. Limit improves to $0.03 < \Sigma m_\nu < 0.54$ eV when supernovae and baryon acoustic oscillation observations are included. The slight preference for massive neutrinos at the two-sigma level disappears when systematic errors are taken into account. Assumes Λ CDM model.			
57	Constrains the total mass of neutrinos from recent Chandra X-ray observations of galaxy clusters when combined with CMB, supernovae, and baryon acoustic oscillation measurements. Assumes flat universe and constant dark-energy equation of state, w .			
58	Constrains the total mass of neutrinos from recent CMB and SOSS LRG power spectrum data along with bias mass relations from SDSS, DEEP2, and Lyman-Break Galaxies. It assumes Λ CDM model. Limit degrades to 0.59 eV in a more general w CDM model.			
59	Constrains the total mass of neutrinos from neutrino oscillation experiments and cosmological data. The most conservative limit uses only WMAP three-year data, while the most stringent limit includes CMB, large-scale structure, supernova, and Lyman-alpha data.			
60	Constrains the total mass of neutrinos from recent CMB, large scale structure, SNIa, and baryon acoustic oscillation data. The limit relaxes to 1.75 when WMAP data alone is used with no prior. Paper shows results with several combinations of data sets. Supersedes KRISTIANSEN 06.			
61	Constrains the total mass of neutrinos from the CMB and the large scale structure data. The most conservative limit is obtained when generic initial conditions are allowed.			
62	Constrains the total mass of neutrinos from recent CMB, large scale structure, Lyman-alpha forest, and SNIa data.			
63	Constrains the total mass of neutrinos from recent CMB and large scale structure data. See also GOOBAR 06.			
64	Constrains the total mass of neutrinos from the CMB and the final 2dF Galaxy Redshift Survey.			
65	Constrains the total mass of neutrinos from the CMB experiments alone, assuming Λ CDM Universe. FUKUGITA 06 show that this result is unchanged by the 3-year WMAP data.			
66	Constrains the total mass of neutrinos from the power spectrum of fluctuations derived from the Sloan Digital Sky Survey and the 2dF galaxy redshift survey, WMAP and 27 other CMB experiments and measurements by the HST Key project.			
67	Constrains the total mass of neutrinos from the power spectrum of fluctuations derived from the Sloan Digital Sky Survey, the 2dF galaxy redshift survey, WMAP and ACBAR. The limit is strengthened to 0.6 eV when measurements by the HST Key project and supernovae data are included.			

- 68 Constrains the fractional contribution of neutrinos to the total matter density in the Universe from WMAP data combined with other CMB measurements, the 2dFGRS data, and Lyman α data. The limit does not noticeably change if the Lyman α data are not used.
- 69 LEWIS 02 constrains the total mass of neutrinos from the power spectrum of fluctuations derived from the CMB, HST Key project, 2dF galaxy redshift survey, supernovae type Ia, and BBN.
- 70 WANG 02 constrains the total mass of neutrinos from the power spectrum of fluctuations derived from the CMB and other cosmological data sets such as galaxy clustering and the Lyman α forest.
- 71 FUKUGITA 00 is a limit on neutrino masses from structure formation. The constraint is based on the clustering scale σ_8 and the COBE normalization and leads to a conservative limit of 0.9 eV assuming 3 nearly degenerate neutrinos. The quoted limit is on the sum of the light neutrino masses.
- 72 CROFT 99 result based on the power spectrum of the Ly α forest. If $\Omega_{\text{matter}} < 0.5$, the limit is improved to $m_\nu < 2.4 (\Omega_{\text{matter}}/0.17-1)$ eV.

Limits on MASSES of Light Stable Right-Handed ν (with necessarily suppressed interaction strengths)

VALUE (eV)	DOCUMENT ID	TECN	COMMENT
• • • We do not use the following data for averages, fits, limits, etc. • • •			
<100–200	73 OLIVE	82	COSM Dirac ν
<200–2000	73 OLIVE	82	COSM Majorana ν
73 Depending on interaction strength G_R where $G_R < G_F$.			

Limits on MASSES of Heavy Stable Right-Handed ν (with necessarily suppressed interaction strengths)

VALUE (GeV)	DOCUMENT ID	TECN	COMMENT
• • • We do not use the following data for averages, fits, limits, etc. • • •			
> 10	74 OLIVE	82	COSM $G_R/G_F < 0.1$
>100	74 OLIVE	82	COSM $G_R/G_F < 0.01$
74 These results apply to heavy Majorana neutrinos and are summarized by the equation: $m_\nu > 1.2 \text{ GeV } (G_F/G_R)$. The bound saturates, and if G_R is too small no mass range is allowed.			

ν CHARGE

VALUE (units: electron charge)	CL%	DOCUMENT ID	TECN	COMMENT
• • • We do not use the following data for averages, fits, limits, etc. • • •				
$< 3.7 \times 10^{-12}$	90	75 GNINENKO	07	RVUE Nuclear reactor
$< 2 \times 10^{-14}$		76 RAFFELT	99	ASTR Red giant luminosity
$< 6 \times 10^{-14}$		77 RAFFELT	99	ASTR Solar cooling
$< 4 \times 10^{-4}$		78 BABU	94	RVUE BEBC beam dump
$< 3 \times 10^{-4}$		79 DAVIDSON	91	RVUE SLAC e^- beam dump
$< 2 \times 10^{-15}$		80 BARBIELLINI	87	ASTR SN 1987A
$< 1 \times 10^{-13}$		81 BERNSTEIN	63	ASTR Solar energy losses

- 75 GNINENKO 07 use limit on \mathcal{P}_e magnetic moment from LI 03B to derive this result. The limit is considerably weaker than the limits on the charge of ν_e and $\bar{\nu}_e$ from various astrophysics considerations.
- 76 This RAFFELT 99 limit applies to all neutrino flavors which are light enough (< 5 keV) to be emitted from globular-cluster red giants.
- 77 This RAFFELT 99 limit is derived from the helioseismological limit on a new energy-loss channel of the Sun, and applies to all neutrino flavors which are light enough (< 1 keV) to be emitted from the sun.
- 78 BABU 94 use COOPER-SARKAR 92 limit on ν magnetic moment to derive quoted result. It applies to ν_τ .
- 79 DAVIDSON 91 use data from early SLAC electron beam dump experiment to derive charge limit as a function of neutrino mass. It applies to ν_τ .
- 80 Exact BARBIELLINI 87 limit depends on assumptions about the intergalactic or galactic magnetic fields and about the direct distance and time through the field. It applies to ν_e .
- 81 The limit applies to all flavors.

ν (MEAN LIFE) / MASS

Measures $[\sum |U_{ej}|^2 \Gamma_j m_j]^{-1}$, where the sum is over mass eigenstates which cannot be resolved experimentally. Some of the limits constrain the radiative decay and are based on the limit of the corresponding photon flux. Other apply to the decay of a heavier neutrino into the lighter one and a Majoron or other invisible particle. Many of these limits apply to any ν within the indicated mass range.

Limits on the radiative decay are either directly based on the limits of the corresponding photon flux, or are derived from the limits on the neutrino magnetic moments. In the later case the transition rate for $\nu_i \rightarrow \nu_j + \gamma$ is constrained by $\Gamma_{ij} = \frac{1}{\tau_{ij}} = \frac{(m_i^2 - m_j^2)^3}{m_j^3} \mu_{ij}^2$ where μ_{ij} is the neutrino transition moment in the mass eigenstates basis. Typically, the limits on lifetime based on the magnetic moments are many orders of magnitude more restrictive than limits based on the nonobservation of photons.

Lepton Particle Listings

Neutrino Properties

VALUE (s/eV)	CL%	DOCUMENT ID	TECN	COMMENT
> 15.4	90	82 KRAKAUER	91 CNTR	$\nu_\mu, \bar{\nu}_\mu$ at LAMPF
> 7 $\times 10^9$		83 RAFFELT	85 ASTR	
> 300	90	84 REINES	74 CNTR	$\bar{\nu}_e$
• • • We do not use the following data for averages, fits, limits, etc. • • •				
	90	85 MIRIZZI	07 CMB	radiative decay
	90	86 MIRIZZI	07 CIB	radiative decay
	90	87 WONG	07 CNTR	Reactor $\bar{\nu}_e$
> 0.11	90	88 XIN	05 CNTR	Reactor ν_e
	90	89 XIN	05 CNTR	Reactor ν_e
> 0.004	90	90 AHARMIM	04 SNO	quasidegen. ν masses
> 4.4 $\times 10^{-5}$	90	90 AHARMIM	04 SNO	hierarchical ν masses
$\gtrsim 100$	95	91 CECCHINI	04 ASTR	Radiative decay for ν mass > 0.01 eV
> 0.067	90	92 EGUCHI	04 KLND	quasidegen. ν masses
> 1.1 $\times 10^{-3}$	90	92 EGUCHI	04 KLND	hierarchical ν masses
> 8.7 $\times 10^{-5}$	99	93 BANDYOPA...	03 FIT	nonradiative decay
≥ 4200	90	94 DERBIN	02B CNTR	Solar $p\bar{p}$ and Be ν
> 2.8 $\times 10^{-5}$	99	95 JOSHIPURA	02B FIT	nonradiative decay
		96 DOLGOV	99 COSM	
		97 BILLER	98 ASTR	$m_\nu = 0.05-1$ eV
> 2.8 $\times 10^{15}$	98,99	98,99 BLUDMAN	92 ASTR	$m_\nu < 50$ eV
none $10^{-12} - 5 \times 10^4$		100 DODELSON	92 ASTR	$m_\nu = 1-300$ keV
< 10^{-12} or $> 5 \times 10^4$		100 DODELSON	92 ASTR	$m_\nu = 1-300$ keV
		101 GRANEK	91 COSM	Decaying L^0
> 6.4	90	102 KRAKAUER	91 CNTR	ν_e at LAMPF
> 1.1 $\times 10^{15}$		103 WALKER	90 ASTR	$m_\nu = 0.03 - \sim 2$ MeV
> 6.3 $\times 10^{15}$	99,104	99,104 CHUPP	89 ASTR	$m_\nu < 20$ eV
> 1.7 $\times 10^{15}$		99 KOLB	89 ASTR	$m_\nu < 20$ eV
		105 RAFFELT	89 RVUE	$\bar{\nu}$ (Dirac, Majorana)
		106 RAFFELT	89B ASTR	
> 8.3 $\times 10^{14}$		107 VONFEILIT...	88 ASTR	
> 22	68	108 OBERAUER	87	$\bar{\nu}_R$ (Dirac)
> 38	68	108 OBERAUER	87	$\bar{\nu}$ (Majorana)
> 59	68	108 OBERAUER	87	$\bar{\nu}_L$ (Dirac)
> 30	68	KETOV	86 CNTR	$\bar{\nu}$ (Dirac)
> 20	68	KETOV	86 CNTR	$\bar{\nu}$ (Majorana)
		109 BINETRUY	84 COSM	$m_\nu \sim 1$ MeV
> 0.11	90	110 FRANK	81 CNTR	$\nu\bar{\nu}$ LAMPF
> 2 $\times 10^{21}$		111 STECKER	80 ASTR	$m_\nu = 10-100$ eV
> 1.0 $\times 10^{-2}$	90	110 BLIETSCHAU	78 HLBC	ν_μ , CERN GGM
> 1.7 $\times 10^{-2}$	90	110 BLIETSCHAU	78 HLBC	$\bar{\nu}_\mu$, CERN GGM
< 3 $\times 10^{-11}$		112 FALK	78 ASTR	$m_\nu < 10$ MeV
> 2.2 $\times 10^{-3}$	90	110 BARNES	77 DBC	ν , ANL 12-ft
		113 COWSIK	77 ASTR	
> 3. $\times 10^{-3}$	90	110 BELLOTTI	76 HLBC	ν , CERN GGM
> 1.3 $\times 10^{-2}$	90	110 BELLOTTI	76 HLBC	$\bar{\nu}$, CERN GGM

82 KRAKAUER 91 quotes the limit $\tau/m_{\nu_1} > (0.75a^2 + 21.65a + 26.3) \text{ s/eV}$, where a is a parameter describing the asymmetry in the neutrino decay defined as $dN_{\nu_1}/d\cos\theta = (1/2)(1 + a\cos\theta)$. The parameter $a = 0$ for a Majorana neutrino, but can vary from -1 to 1 for a Dirac neutrino. The bound given by the authors is the most conservative (which applies for $a = -1$).

83 RAFFELT 85 limit on the radiative decay is from solar x - and γ -ray fluxes. Limit depends on ν flux from $p\bar{p}$, now established from GALLEX and SAGE to be > 0.5 of expectation.

84 REINES 74 looked for ν of nonzero mass decaying radiatively to a neutral of lesser mass $+ \gamma$. Used liquid scintillator detector near fission reactor. Finds lab lifetime 6×10^7 s or more. Above value of (mean life)/mass assumes average effective neutrino energy of 0.2 MeV. To obtain the limit 6×10^7 s REINES 74 assumed that the full $\bar{\nu}_e$ reactor flux could be responsible for yielding decays with photon energies in the interval 0.1 MeV $- 0.5$ MeV. This represents some overestimate so their lower limit is an over-estimate of the lab lifetime (VOGEL 84). If so, OBERAUER 87 may be comparable or better.

85 MIRIZZI 07 determine a limit on the neutrino radiative decay from analysis of the maximum allowed distortion of the CMB spectrum as measured by the COBE/FIRAS. For the decay $\nu_2 \rightarrow \nu_1$ the lifetime limit is $\lesssim 4 \times 10^{20}$ s for $m_{\min} \lesssim 0.14$ eV. For transition with the $|\Delta m_{31}|$ mass difference the lifetime limit is $\sim 2 \times 10^{19}$ s for $m_{\min} \lesssim 0.14$ eV and $\sim 5 \times 10^{20}$ s for $m_{\min} \gtrsim 0.14$ eV.

86 MIRIZZI 07 determine a limit on the neutrino radiative decay from analysis of the cosmic infrared background (CIB) using the Spitzer Observatory data. For transition with the $|\Delta m_{31}|$ mass difference they obtain the lifetime limit $\sim 10^{20}$ s for $m_{\min} \lesssim 0.14$ eV.

87 WONG 07 use their limit on the neutrino magnetic moment together with the assumed experimental value of $\Delta m_{13}^2 \sim 2 \times 10^{-3} \text{ eV}^2$ to obtain $\tau_{13}/m_1^3 > 3.2 \times 10^{27} \text{ s/eV}^3$ for the radiative decay in the case of the inverted mass hierarchy. Similarly to RAFFELT 89 this limit can be violated if electric and magnetic moments are equal to each other. Analogous, but numerically somewhat different limits are obtained for τ_{23} and τ_{21} .

88 XIN 05 search for the γ from radiative decay of ν_e produced by the electron capture on ^{51}Cr . No events were seen and the limit on τ/m_ν was derived. This is a weaker limit on the decay of ν_e than KRAKAUER 91.

89 XIN 05 use their limit on the neutrino magnetic moment of ν_e together with the assumed experimental value of $\Delta m_{1,3}^2 \sim 2 \times 10^{-3} \text{ eV}^2$ to obtain $\tau_{13}/m_1^3 > 1 \times 10^{23} \text{ s/eV}^3$ for the radiative decay in the case of the inverted mass hierarchy. Similarly to RAFFELT 89 this limit can be violated if electric and magnetic moments are equal to each other.

Analogous, but numerically somewhat different limits are obtained for τ_{23} and τ_{21} . Again, this limit is specific for ν_e .

90 AHARMIM 04 obtained these results from the solar $\bar{\nu}_e$ flux limit set by the SNO measurement assuming ν_2 decay through nonradiative process $\nu_2 \rightarrow \bar{\nu}_1 X$, where X is a Majoron or other invisible particle. Limits are given for the cases of quasidegenerate and hierarchical neutrino masses.

91 CECCHINI 04 obtained this bound through the observations performed on the occasion of the 21 June 2001 total solar eclipse, looking for visible photons from radiative decays of solar neutrinos. Limit is a τ/m_{ν_2} in $\nu_2 \rightarrow \nu_1 \gamma$. Limit ranges from ~ 100 to 10^7 s/eV for $0.01 < m_{\nu_1} < 0.1 \text{ eV}$.

92 EGUCHI 04 obtained these results from the solar $\bar{\nu}_e$ flux limit set by the KamLAND measurement assuming ν_2 decay through nonradiative process $\nu_2 \rightarrow \bar{\nu}_1 X$, where X is a Majoron or other invisible particle. Limits are given for the cases of quasidegenerate and hierarchical neutrino masses.

93 The ratio of the lifetime over the mass derived by BANDYOPADHYAY 03 is for ν_2 . They obtained this result using the following solar-neutrino data: total rates measured in Cl and Ga experiments, the Super-Kamiokande's zenith-angle spectra, and SNO's day and night spectra. They assumed that ν_1 is the lowest mass, stable or nearly stable neutrino state and ν_2 decays through nonradiative Majoron emission process, $\nu_2 \rightarrow \bar{\nu}_1 + J$, or through nonradiative process with all the final state particles being sterile. The best fit is obtained in the region of the LMA solution.

94 DERBIN 02b (also BACK 03b) obtained this bound for the radiative decay from the results of background measurements with Counting Test Facility (the prototype of the Borexino detector). The laboratory gamma spectrum is given as $dN_\gamma/d\cos\theta = (1/2)(1 + \alpha\cos\theta)$ with $\alpha=0$ for a Majorana neutrino, and α varying to -1 to 1 for a Dirac neutrino. The listed bound is for the case of $\alpha=0$. The most conservative bound $1.5 \times 10^3 \text{ s eV}^{-1}$ is obtained for the case of $\alpha=-1$.

95 The ratio of the lifetime over the mass derived by JOSHIPURA 02b is for ν_2 . They obtained this result from the total rates measured in all solar neutrino experiments. They assumed that ν_1 is the lowest mass, stable or nearly stable neutrino state and ν_2 decays through nonradiative process like Majoron emission decay, $\nu_2 \rightarrow \nu'_1 + J$ where ν'_1 state is sterile. The exact limit depends on the specific solution of the solar neutrino problem. The quoted limit is for the LMA solution.

96 DOLGOV 99 places limits in the (Majorana) τ -associated ν mass-lifetime plane based on nucleosynthesis. Results would be considerably modified if neutrino oscillations exist.

97 BILLER 98 use the observed TeV γ -ray spectra to set limits on the mean life of any radiatively decaying neutrino between 0.05 and 1 eV . Curve shows $\tau_\nu/B_\gamma > 0.15 \times 10^{21} \text{ s}$ at 0.05 eV , $> 1.2 \times 10^{21} \text{ s}$ at 0.17 eV , $> 3 \times 10^{21} \text{ s}$ at 1 eV , where B_γ is the branching ratio to photons.

98 BLUDMAN 92 sets additional limits by this method for higher mass ranges. Cosmological limits are also obtained.

99 Limit on the radiative decay based on nonobservation of γ 's in coincidence with ν 's from SN 1987A.

100 DODELSON 92 range is for wrong-helicity keV mass Dirac ν 's from the core of neutron star in SN 1987A decaying to ν 's that would have interacted in KAM2 or LMB detectors.

101 GRANEK 91 considers heavy neutrino decays to $\gamma\nu_L$ and $3\nu_L$, where $m_{\nu_L} < 100 \text{ keV}$. Lifetime is calculated as a function of heavy neutrino mass, branching ratio into $\gamma\nu_L$, and m_{ν_L} .

102 KRAKAUER 91 quotes the limit for ν_e , $\tau/m_{\nu_e} > (0.3a^2 + 9.8a + 15.9) \text{ s/eV}$, where a is a parameter describing the asymmetry in the radiative neutrino decay defined as $dN_{\nu_e}/d\cos\theta = (1/2)(1 + a\cos\theta)$ $a=0$ for a Majorana neutrino, but can vary from -1 to 1 for a Dirac neutrino. The bound given by the authors is the most conservative (which applies for $a = -1$).

103 WALKER 90 uses SN 1987A γ flux limits after 289 days.

104 CHUPP 89 should be multiplied by a branching ratio (about 1) and a detection efficiency (about 1/4), and pertains to radiative decay of any neutrino to a lighter or sterile neutrino.

105 RAFFELT 89 uses KYULDJIEV 84 to obtain $\tau m^3 > 3 \times 10^{18} \text{ s eV}^3$ (based on $\bar{\nu}_e e^-$ cross sections). The bound for the radiative decay is not valid if electric and magnetic transition moments are equal for Dirac neutrinos.

106 RAFFELT 89b analyze stellar evolution and exclude the region $3 \times 10^{12} < \tau m^3 < 3 \times 10^{21} \text{ s eV}^3$.

107 Model-dependent theoretical analysis of SN 1987A neutrinos. Quoted limit is for $[\sum_j |U_{ej}|^2 \Gamma_j m_j]^{-1}$, where $\ell = \mu, \tau$. Limit is $3.3 \times 10^{14} \text{ s/eV}$ for $\ell = e$.

108 OBERAUER 87 looks for photons and e^+e^- pairs from radiative decays of reactor neutrinos.

109 BINETRUY 84 finds $\tau < 10^8 \text{ s}$ for neutrinos in a radiation-dominated universe.

110 These experiments look for $\nu_k \rightarrow \nu_j \gamma$ or $\bar{\nu}_k \rightarrow \bar{\nu}_j \gamma$.

111 STECKER 80 limit based on UV background; result given is $\tau > 4 \times 10^{22} \text{ s}$ at $m_\nu = 20 \text{ eV}$.

112 FALK 78 finds lifetime constraints based on supernova energetics.

113 COWSIK 77 considers variety of scenarios. For neutrinos produced in the big bang, present limits on optical photon flux require $\tau > 10^{23} \text{ s}$ for $m_\nu \sim 1 \text{ eV}$. See also COWSIK 79 and GOLDMAN 79.

ν MAGNETIC MOMENT

The coupling of neutrinos to an electromagnetic field is characterized by a 3×3 matrix λ of the magnetic (μ) and electric (d) dipole moments ($\lambda = \mu - id$). For Majorana neutrinos the matrix λ is antisymmetric and only transition moments are allowed, while for Dirac neutrinos λ is a general 3×3 matrix. In the standard electroweak theory extended to include neutrino masses (see FUJIKAWA 80) $\mu_\nu = 3eG_F m_\nu / (8\pi^2 \sqrt{2}) = 3.2 \times 10^{-19} (m_\nu/\text{eV}) \mu_B$, i.e. it is unobservably small given the known

See key on page 405

Lepton Particle Listings Neutrino Properties

small neutrino masses. In more general models there is no longer a proportionality between neutrino mass and its magnetic moment, even though only massive neutrinos have nonvanishing magnetic moments without fine tuning.

Laboratory bounds on λ are obtained via elastic ν - e scattering, where the scattered neutrino is not observed. The combinations of matrix elements of λ that are constrained by various experiments depend on the initial neutrino flavor and on its propagation between source and detector (e.g., solar ν_e and reactor $\bar{\nu}_e$ do not constrain the same combinations). The listings below therefore identify the initial neutrino flavor.

Other limits, e.g. from various stellar cooling processes, apply to all neutrino flavors. Analogous flavor independent, but weaker, limits are obtained from the analysis of $e^+e^- \rightarrow \nu\bar{\nu}\gamma$ collider experiments.

VALUE ($10^{-10} \mu_B$)	CL%	DOCUMENT ID	TECN	COMMENT
< 0.54	90	114 ARPESELLA 08A	BORX	Solar ν spectrum shape
< 6.8	90	115 AUERBACH 01	LSND	$\nu_e e$, $\nu_\mu e$ scattering
< 3900	90	116 SCHWIENHO...01	DONU	$\nu_\tau e^- \rightarrow \nu_\tau e^-$
• • • We do not use the following data for averages, fits, limits, etc. • • •				
< 0.011–0.027		117 KUZNETSOV 09	ASTR	$\nu_L \rightarrow \nu_R$ in SN1987A
< 0.58	90	118 BEDA 07	CNTR	Reactor $\bar{\nu}_e$
< 0.74	90	119 WONG 07	CNTR	Reactor $\bar{\nu}_e$
< 0.9	90	120 DARAKTCH... 05		Reactor $\bar{\nu}_e$
< 130	90	121 XIN 05	CNTR	Reactor ν_e
< 37	95	122 GRIFOLS 04	FIT	Solar ^8B ν (SNO NC)
< 3.6	90	123 LIU 04	SKAM	Solar ν spectrum shape
< 1.1	90	124 LIU 04	SKAM	Solar ν spectrum shape (LMA region)
< 5.5	90	125 BACK 03b	CNTR	Solar pp and Be ν
< 1.0	90	126 DARAKTCH... 03		Reactor $\bar{\nu}_e$
< 1.3	90	127 LI 03b	CNTR	Reactor $\bar{\nu}_e$
< 2	90	128 GRIMUS 02	FIT	solar + reactor (Majorana ν)
< 80000	90	129 TANIMOTO 00	RVUE	$e^+e^- \rightarrow \nu\bar{\nu}\gamma$
< 0.01–0.04		130 AYALA 99	ASTR	$\nu_L \rightarrow \nu_R$ in SN1987A
< 1.5	90	131 BEACOM 99	SKAM	ν spectrum shape
< 0.03		132 RAFFELT 99	ASTR	Red giant luminosity
< 4		133 RAFFELT 99	ASTR	Solar cooling
< 44000	90	134 ABREU 97j	DLPH	$e^+e^- \rightarrow \nu\bar{\nu}\gamma$ at LEP
< 33000	90	135 ACCIARRI 97Q	L3	$e^+e^- \rightarrow \nu\bar{\nu}\gamma$ at LEP
< 0.62		135 ELMFORS 97	COSM	Depolarization in early universe plasma
< 27000	95	136 ESCRIBANO 97	RVUE	$\Gamma(Z \rightarrow \nu\nu)$ at LEP
< 30	90	137 VILAIN 95b	CHM2	$\nu_\mu e \rightarrow \nu_\mu e$
< 55000	90	138 GOULD 94	RVUE	$e^+e^- \rightarrow \nu\bar{\nu}\gamma$ at LEP
< 1.9	95	137 DERBIN 93	CNTR	Reactor $\bar{\nu}_e \rightarrow \bar{\nu}_e$
< 5400	90	138 COOPER... 92	BEBC	$\nu_\tau e^- \rightarrow \nu_\tau e^-$
< 2.4	90	139 VIDYAKIN 92	CNTR	Reactor $\bar{\nu}_e \rightarrow \bar{\nu}_e$
< 56000	90	140 DESHPANDE 91	RVUE	$e^+e^- \rightarrow \nu\bar{\nu}\gamma$
< 100	95	140 DORENBOS... 91	CHRM	$\nu_\mu e \rightarrow \nu_\mu e$
< 8.5	90	141 AHRENS 90	CNTR	$\nu_\mu e \rightarrow \nu_\mu e$
< 10.8	90	141 KRAKAUER 90	CNTR	LAMPF $\nu e \rightarrow \nu e$
< 7.4	90	141 KRAKAUER 90	CNTR	LAMPF $(\nu_\mu, \bar{\nu}_\mu)e$ elast.
< 0.02		142 RAFFELT 90	ASTR	Red giant luminosity
< 0.1		143 RAFFELT 89b	ASTR	Cooling helium stars
		144 FUKUGITA 88	COSM	Primordial magn. fields
< 40000	90	145 GROTC 88	RVUE	$e^+e^- \rightarrow \nu\bar{\nu}\gamma$
$\leq .3$		143 RAFFELT 88b	ASTR	He burning stars
< 0.11		143 FUKUGITA 87	ASTR	Cooling helium stars
< 0.0006		146 NUSSINOV 87	ASTR	Cosmic EM backgrounds
< 0.1–0.2		MORGAN 81	COSM	^4He abundance
< 0.85		BEG 78	ASTR	Stellar plasmons
< 0.6		147 SUTHERLAND 76	ASTR	Red giants + degenerate dwarfs
< 81		148 KIM 74	RVUE	$\bar{\nu}_\mu e \rightarrow \bar{\nu}_\mu e$
< 1		BERNSTEIN 63	ASTR	Solar cooling
< 14		COWAN 57	CNTR	Reactor $\bar{\nu}$

114 ARPESELLA 08A obtained this limit using the shape of the recoil electron energy spectrum from the Borexino 192 live days of solar neutrino data.

115 AUERBACH 01 limit is based on the LSND ν_e and ν_μ electron scattering measurements. The limit is slightly more stringent than KRAKAUER 90.

116 SCHWIENHORST 01 quote an experimental sensitivity of 4.9×10^{-7} .

117 KUZNETSOV 09 obtain a limit on the flavor averaged magnetic moment of Dirac neutrinos from the time averaged neutrino signal of SN1987A. Improves and supersedes the analysis of BARBIERI 88 and AYALA 99.

118 BEDA 07 performed search for electromagnetic $\bar{\nu}_e$ - e scattering at Kalininskaya nuclear reactor. A Ge detector with active and passive shield was used and the electron recoil spectrum between 3.0 and 61.3 keV analyzed. This is the most stringent limit on magnetic moment of reactor $\bar{\nu}_e$.

119 WONG 07 performed search for non-standard $\bar{\nu}_e$ - e scattering at the Kuo-Sheng nuclear reactor. Ge detector equipped with active anti-Compton shield is used. Most stringent laboratory limit on magnetic moment of reactor $\bar{\nu}_e$. Supersedes LI 03b.

120 DARAKTCHIEVA 05 present the final analysis of the search for non-standard $\bar{\nu}_e$ - e scattering component at Bugey nuclear reactor. Full kinematical event reconstruction of both the kinetic energy above 700 keV and scattering angle of the recoil electron, by use of TPC. Most stringent laboratory limit on magnetic moment. Supersedes DARAKTCHIEVA 03.

121 XIN 05 evaluated the ν_e flux at the Kuo-Sheng nuclear reactor and searched for non-standard ν_e - e scattering. Ge detector equipped with active anti-Compton shield was used. This laboratory limit on magnetic moment is considerably less stringent than the limits for reactor $\bar{\nu}_e$, but is specific to ν_e .

122 GRIFOLS 04 obtained this bound using the SNO data of the solar ^8B neutrino flux measured with deuteron breakup. This bound applies to $\mu_{\text{eff}} = (\mu_{21}^2 + \mu_{22}^2 + \mu_{23}^2)^{1/2}$.

123 LIU 04 obtained this limit using the shape of the recoil electron energy spectrum from the Super-Kamiokande-I 1496 days of solar neutrino data. Neutrinos are assumed to have only diagonal magnetic moments, $\mu_{\nu 1} = \mu_{\nu 2}$. This limit corresponds to the oscillation parameters in the vacuum oscillation region.

124 LIU 04 obtained this limit using the shape of the recoil electron energy spectrum from the Super-Kamiokande-I 1496 live-day solar neutrino data, by limiting the oscillation parameter region in the LMA region allowed by solar neutrino experiments plus KamLAND. $\mu_{\nu 1} = \mu_{\nu 2}$ is assumed. In the LMA region, the same limit would be obtained even if neutrinos have off-diagonal magnetic moments.

125 BACK 03b obtained this bound from the results of background measurements with Counting Test Facility (the prototype of the Borexino detector). Standard Solar Model flux was assumed. This μ_ν can be different from the reactor μ_ν in certain oscillation scenarios (see BEACOM 99).

126 DARAKTCHIEVA 03 searched for non-standard $\bar{\nu}_e$ - e scattering component at Bugey nuclear reactor. Full kinematical event reconstruction by use of TPC. Superseded by DARAKTCHIEVA 05.

127 LI 03b used Ge detector in active shield near nuclear reactor to test for nonstandard $\bar{\nu}_e$ - e scattering.

128 GRIMUS 02 obtain stringent bounds on all Majorana neutrino transition moments from a simultaneous fit of LMA-MSW oscillation parameters and transition moments to global solar neutrino data + reactor data. Using only solar neutrino data, a 90% CL bound of $6.3 \times 10^{-10} \mu_B$ is obtained.

129 TANIMOTO 00 combined $e^+e^- \rightarrow \nu\bar{\nu}\gamma$ data from VENUS, TOPAZ, and AMY.

130 AYALA 99 improves the limit of BARBIERI 88.

131 BEACOM 99 obtain the limit using the shape, but not the absolute magnitude which is affected by oscillations, of the solar neutrino spectrum obtained by Superkamiokande (825 days). This μ_ν can be different from the reactor μ_ν in certain oscillation scenarios.

132 RAFFELT 99 is an update of RAFFELT 90. This limit applies to all neutrino flavors which are light enough (< 5 keV) to be emitted from globular-cluster red giants. This limit pertains equally to electric dipole moments and magnetic transition moments, and it applies to both Dirac and Majorana neutrinos.

133 RAFFELT 99 is essentially an update of BERNSTEIN 63, but is derived from the helioseismological limit on a new energy-loss channel of the Sun. This limit applies to all neutrino flavors which are light enough (< 1 keV) to be emitted from the Sun. This limit pertains equally to electric dipole and magnetic transition moments, and it applies to both Dirac and Majorana neutrinos.

134 ACCIARRI 97Q result applies to both direct and transition magnetic moments and for $q^2=0$.

135 ELMFORS 97 calculate the rate of depolarization in a plasma for neutrinos with a magnetic moment and use the constraints from a big-bang nucleosynthesis on additional degrees of freedom.

136 Applies to absolute value of magnetic moment.

137 DERBIN 93 determine the cross section for 0.6–2.0 MeV electron energy as $(1.28 \pm 0.63) \times \sigma_{\text{weak}}$. However, the (reactor on - reactor off)/(reactor off) is only $\sim 1/100$.

138 COOPER-SARKAR 92 assume $f_{D_S}/f_\pi = 2$ and D_S, \bar{D}_S production cross section = $2.6 \mu\text{b}$ to calculate ν flux.

139 VIDYAKIN 92 limit is from a $e\bar{\nu}_e$ elastic scattering experiment. No experimental details are given except for the cross section from which this limit is derived. Signal/noise was $1/10$. The limit uses $\sin^2\theta_W = 0.23$ as input.

140 DORENBOSCH 91 corrects an incorrect statement in DORENBOSCH 89 that the ν magnetic moment is $< 1 \times 10^{-9}$ at the 95%CL. DORENBOSCH 89 measures both $\nu_\mu e$ and $\bar{\nu}_e$ elastic scattering and assume $\mu(\nu) = \mu(\bar{\nu})$.

141 KRAKAUER 90 experiment fully reported in ALLEN 93.

142 RAFFELT 90 limit applies for a diagonal magnetic moment of a Dirac neutrino, or for a transition magnetic moment of a Majorana neutrino. In the latter case, the same analysis gives $< 1.4 \times 10^{-12}$. Limit at 95%CL obtained from δM_C .

143 Significant dependence on details of stellar models.

144 FUKUGITA 88 find magnetic dipole moments of any two neutrino species are bounded by $\mu < 10^{-16} [10^{-9} G/B_0]$ where B_0 is the present-day intergalactic field strength.

145 GROTC 88 combined data from MAC, ASP, CELLO, and Mark J.

146 For $m_\nu = 8$ –200 eV. NUSSINOV 87 examines transition magnetic moments for $\nu_\mu \rightarrow \nu_e$ and obtain $< 3 \times 10^{-15}$ for $m_\nu > 16$ eV and $< 6 \times 10^{-14}$ for $m_\nu > 4$ eV.

147 We obtain above limit from SUTHERLAND 76 using their limit $f < 1/3$.

148 KIM 74 is a theoretical analysis of $\bar{\nu}_\mu$ reaction data.

NEUTRINO CHARGE RADIUS SQUARED

We report limits on the so-called neutrino charge radius squared. While the straight-forward definition of a neutrino charge radius has been proven to be gauge-dependent and, hence, unphysical (LEE 77c), there have been recent attempts to define a physically observable neutrino charge radius

Lepton Particle Listings

Neutrino Properties, Number of Neutrino Types

BEG	78	PR D17 1395	M.A.B. Beg, W.J. Marciano, M. Ruderman (ROCK+)
BLIETSCHAU	78	NP B133 205	J. Blietschau <i>et al.</i> (Gargamelle Collab.)
FALK	78	PL 79B 511	S.W. Falk, D.N. Schramm (CHIC)
BARNES	77	PRL 38 1049	V.E. Barnes <i>et al.</i> (PURD, ANL)
COWSIK	77	PRL 39 784	R. Cowsik (MPIM, TATA)
LEE	77C	PR D16 1444	B.W. Lee, R.E. Shrock (STON)
VYSOTSKY	77	JETPL 26 188	M.I. Vysocky, A.D. Dolgov, Y.B. Zeldovich (ITEP)
Translated from ZETFP 26 200.			
BELLOTTI	76	LNC 17 553	E. Bellotti <i>et al.</i> (MILA)
SUTHERLAND	76	PR D13 2700	P. Sutherland <i>et al.</i> (PENN, COLL, NYU)
SZALAY	76	AA 49 437	A.S. Szalay, G. Marx (EOTV)
CLARK	74	PR D9 533	A.R. Clark <i>et al.</i> (LBL)
KIM	74	PR D9 3050	J.E. Kim, V.S. Mathur, S. Okubo (ROCH)
REINES	74	PRL 32 180	F. Reines, H.W. Sobel, H.S. Gurr (UCI)
SZALAY	74	APAH 35 8	A.S. Szalay, G. Marx (EOTV)
COWSIK	72	PRL 29 669	R. Cowsik, J. McClelland (UCB)
MARX	72	Nu Conf. Budapest	G. Marx, A.S. Szalay (EOTV)
GERSHTEIN	66	JETPL 4 120	S.S. Gershtein, Y.B. Zeldovich (KIAM)
Translated from ZETFP 4 189.			
BERNSTEIN	63	PR 132 1227	J. Bernstein, M. Ruderman, G. Feinberg (NYU+)
COWAN	57	PR 107 528	C.L. Cowan, F. Reines (LANL)

Number of Neutrino Types

The neutrinos referred to in this section are those of the Standard $SU(2) \times U(1)$ Electroweak Model possibly extended to allow nonzero neutrino masses. Light neutrinos are those with $m < m_Z/2$. The limits are on the number of neutrino mass eigenstates, including ν_1 , ν_2 , and ν_3 .

THE NUMBER OF LIGHT NEUTRINO TYPES FROM COLLIDER EXPERIMENTS

Revised March 2008 by D. Karlen (University of Victoria and TRIUMF).

The most precise measurements of the number of light neutrino types, N_ν , come from studies of Z production in e^+e^- collisions. The invisible partial width, Γ_{inv} , is determined by subtracting the measured visible partial widths, corresponding to Z decays into quarks and charged leptons, from the total Z width. The invisible width is assumed to be due to N_ν light neutrino species each contributing the neutrino partial width Γ_ν as given by the Standard Model. In order to reduce the model dependence, the Standard Model value for the ratio of the neutrino to charged leptonic partial widths, $(\Gamma_\nu/\Gamma_\ell)_{\text{SM}} = 1.991 \pm 0.001$, is used instead of $(\Gamma_\nu)_{\text{SM}}$ to determine the number of light neutrino types:

$$N_\nu = \frac{\Gamma_{\text{inv}}}{\Gamma_\ell} \left(\frac{\Gamma_\ell}{\Gamma_\nu} \right)_{\text{SM}}. \quad (1)$$

The combined result from the four LEP experiments is $N_\nu = 2.984 \pm 0.008$ [1].

In the past, when only small samples of Z decays had been recorded by the LEP experiments and by the Mark II at SLC, the uncertainty in N_ν was reduced by using Standard Model fits to the measured hadronic cross sections at several center-of-mass energies near the Z resonance. Since this method is much more dependent on the Standard Model, the approach described above is favored.

Before the advent of the SLC and LEP, limits on the number of neutrino generations were placed by experiments at lower-energy e^+e^- colliders by measuring the cross section of the process $e^+e^- \rightarrow \nu\bar{\nu}\gamma$. The ASP, CELLO, MAC, MARK J, and VENUS experiments observed a total of 3.9 events above background [2], leading to a 95% CL limit of $N_\nu < 4.8$. This process has a much larger cross section at center-of-mass energies near the Z mass and has been measured at LEP by the ALEPH, DELPHI, L3, and OPAL experiments [3]. These

experiments have observed several thousand such events, and the combined result is $N_\nu = 3.00 \pm 0.08$. The same process has also been measured by the LEP experiments at much higher center-of-mass energies, between 130 and 208 GeV, in searches for new physics [4]. Combined with the lower energy data, the result is $N_\nu = 2.92 \pm 0.05$.

Experiments at $p\bar{p}$ colliders also placed limits on N_ν by determining the total Z width from the observed ratio of $W^\pm \rightarrow \ell^\pm\nu$ to $Z \rightarrow \ell^+\ell^-$ events [5]. This involved a calculation that assumed Standard Model values for the total W width and the ratio of W and Z leptonic partial widths, and used an estimate of the ratio of Z to W production cross sections. Now that the Z width is very precisely known from the LEP experiments, the approach is now one of those used to determine the W width.

References

1. ALEPH, DELPHI, L3, OPAL, and SLD Collaborations, and LEP Electroweak Working Group, and SLD Electroweak Group, and SLD Heavy Flavour Group, Phys. Reports **427**, 257 (2006).
2. VENUS: K. Abe *et al.*, Phys. Lett. **B232**, 431 (1989); ASP: C. Hearty *et al.*, Phys. Rev. **D39**, 3207 (1989); CELLO: H.J. Behrend *et al.*, Phys. Lett. **B215**, 186 (1988); MAC: W.T. Ford *et al.*, Phys. Rev. **D33**, 3472 (1986); MARK J: H. Wu, Ph.D. Thesis, Univ. Hamburg (1986).
3. L3: M. Acciarri *et al.*, Phys. Lett. **B431**, 199 (1998); DELPHI: P. Abreu *et al.*, Z. Phys. **C74**, 577 (1997); OPAL: R. Akers *et al.*, Z. Phys. **C65**, 47 (1995); ALEPH: D. Buskulic *et al.*, Phys. Lett. **B313**, 520 (1993).
4. DELPHI: J. Abdallah *et al.*, Eur. Phys. J. **C38**, 395 (2005); L3: P. Achard *et al.*, Phys. Lett. **B587**, 16 (2004); ALEPH: A. Heister *et al.*, Eur. Phys. J. **C28**, 1 (2003); OPAL: G. Abbiendi *et al.*, Eur. Phys. J. **C18**, 253 (2000).
5. UA1: C. Albajar *et al.*, Phys. Lett. **B198**, 271 (1987); UA2: R. Ansari *et al.*, Phys. Lett. **B186**, 440 (1987).

Number from e^+e^- Colliders

Number of Light ν Types

VALUE	DOCUMENT ID	TECN
2.9840 ± 0.0082	¹ LEP-SLC	06 RVUE

• • • We do not use the following data for averages, fits, limits, etc. • • •

3.00 ± 0.05	² LEP	92 RVUE
-------------	------------------	---------

¹ Combined fit from ALEPH, DELPHI, L3 and OPAL Experiments.

² Simultaneous fits to all measured cross section data from all four LEP experiments.

Number of Light ν Types from Direct Measurement of Invisible Z Width

In the following, the invisible Z width is obtained from studies of single-photon events from the reaction $e^+e^- \rightarrow \nu\bar{\nu}\gamma$. All are obtained from LEP runs in the $E_{\text{cm}}^{\text{eff}}$ range 88–209 GeV.

VALUE	DOCUMENT ID	TECN	COMMENT
2.92 ± 0.05 OUR AVERAGE	Error includes scale factor of 1.2.		
2.84 ± 0.10 ± 0.14	ABDALLAH	05B DLPH	$\sqrt{s} = 180\text{--}209$ GeV
2.98 ± 0.05 ± 0.04	ACHARD	04E L3	1990–2000 LEP runs
2.86 ± 0.09	HEISTER	03C ALEP	$\sqrt{s} = 189\text{--}209$ GeV
2.69 ± 0.13 ± 0.11	ABBIENDI,G	00D OPAL	1998 LEP run
2.89 ± 0.32 ± 0.19	ABREU	97J DLPH	1993–1994 LEP runs
3.23 ± 0.16 ± 0.10	AKERS	95C OPAL	1990–1992 LEP runs
2.68 ± 0.20 ± 0.20	BUSKULIC	93L ALEP	1990–1991 LEP runs

• • • We do not use the following data for averages, fits, limits, etc. • • •

2.84 ± 0.15 ± 0.14	ABREU	00Z DLPH	1997–1998 LEP runs
3.01 ± 0.08	ACCIARRI	99R L3	1991–1998 LEP runs
3.1 ± 0.6 ± 0.1	ADAM	96C DLPH	$\sqrt{s} = 130, 136$ GeV

Lepton Particle Listings

Number of Neutrino Types, Double- β Decay

Limits from Astrophysics and Cosmology

Number of Light ν Types

("light" means $<$ about 1 MeV). See also OLIVE 81. For a review of limits based on Nucleosynthesis, Supernovae, and also on terrestrial experiments, see DENEGRI 90. Also see "Big-Bang Nucleosynthesis" in this Review.

VALUE	CL%	DOCUMENT ID	TECN	COMMENT
$0.9 < N_\nu < 8.2$		3 ICHIKAWA	07	COSM
$3 < N_\nu < 7$	95	4 CIRELLI	06	COSM
$2.7 < N_\nu < 4.6$	95	5 HANNESSTAD	06	COSM
$3.6 < N_\nu < 7.4$	95	4 SELJAK	06	COSM
< 4.4		6 CYBURT	05	COSM
< 3.3		7 BARGER	03c	COSM
$1.4 < N_\nu < 6.8$		8 CROTTY	03	COSM
$1.9 < N_\nu < 6.6$		8 PIERPAOLI	03	COSM
$2 < N_\nu < 4$		LISI	99	BBN
< 4.3		OLIVE	99	BBN
< 4.9		COPI	97	Cosmology
< 3.6		HATA	97b	High D/H quasar abs.
< 4.0		OLIVE	97	BBN; high ^4He and ^7Li
< 4.7		CARDALL	96b	COSM High D/H quasar abs.
< 3.9		FIELDS	96	COSM BBN; high ^4He and ^7Li
< 4.5		KERNAN	96	COSM High D/H quasar abs.
< 3.6		OLIVE	95	BBN; ≥ 3 massless ν
< 3.3		WALKER	91	Cosmology
< 3.4		OLIVE	90	Cosmology
< 4		YANG	84	Cosmology
< 4		YANG	79	Cosmology
< 7		STEIGMAN	77	Cosmology
		PEEBLES	71	Cosmology
< 16		9 SHVARTSMAN	69	Cosmology
		HOYLE	64	Cosmology

³ Constrains the number of neutrino types from recent CMB and large scale structure data. No priors on other cosmological parameters are used.

⁴ Constrains the number of neutrino types from recent CMB, large scale structure, Lyman-alpha forest, and SNIa data. The slight preference for $N_\nu > 3$ comes mostly from the Lyman-alpha forest data.

⁵ Constrains the number of neutrino types from recent CMB and large scale structure data. See also HAMANN 07.

⁶ Limit on the number of neutrino types based on ^4He and D/H abundance assuming a baryon density fixed to the WMAP data. Limit relaxes to 4.6 if D/H is not used or to 5.8 if only D/H and the CMB are used. See also CYBURT 01 and CYBURT 03.

⁷ Limit on the number of neutrino types based on combination of WMAP data and big-bang nucleosynthesis. The limit from WMAP data alone is 8.3. See also KNELLER 01. $N_\nu \geq 3$ is assumed to compute the limit.

⁸ 95% confidence level range on the number of neutrino flavors from WMAP data combined with other CMB measurements, the 2dFGRS data, and HST data.

⁹ SHVARTSMAN 69 limit inferred from his equations.

Number Coupling with Less Than Full Weak Strength

VALUE	DOCUMENT ID	TECN	COMMENT
< 20	10 OLIVE	81c	COSM
< 20	10 STEIGMAN	79	COSM

¹⁰ Limit varies with strength of coupling. See also WALKER 91.

REFERENCES FOR Limits on Number of Neutrino Types

HAMANN 07	JCAP 0708 021	J. Hamann et al.
ICHIKAWA 07	JCAP 0705 007	K. Ichikawa, M. Kawasaki, F. Takahashi
CIRELLI 06	JCAP 0612 013	M. Cirelli et al.
HANNESSTAD 06	JCAP 0611 016	S. Hannestad, G. Raffelt
LEP-SLC 06	PRPL 427 257	ALEPH, DELPHI, L3, OPAL, SLD and working groups
SELJAK 06	JCAP 0610 014	U. Seljak, A. Slosar, P. McDonald
ABDALLAH 05b	EPJ C38 395	J. Abdallah et al. (DELPHI Collab.)
CYBURT 05	ASP 23 313	R.H. Cyburt et al.
ACHARD 04e	PL B587 16	P. Achard et al. (L3 Collab.)
BARGER 03c	PL B566 8	V. Barger et al.
CROTTY 03	PR D67 123005	P. Crotty, J. Lesgourgues, S. Pastor
CYBURT 03	PL B567 227	R.H. Cyburt, B.D. Fields, K.A. Olive
HEISTER 03c	EPJ C28 1	A. Heister et al. (ALEPH Collab.)
PIERPAOLI 03	MNRAS 342 L63	E. Pierpaoli
CYBURT 01	ASP 17 97	R.H. Cyburt, B.D. Fields, K.A. Olive
KNELLER 01	PR D64 123506	J.P. Kneller et al.
ABBIENDI, G. 00d	EPJ C18 253	G. Abbiendi et al. (OPAL Collab.)
ABREU 00z	EPJ C17 53	P. Abreu et al. (DELPHI Collab.)
ACCIARRI 99r	PL B470 268	M. Acciarri et al. (L3 Collab.)
LISI 99	PR D59 123520	E. Lisi, S. Sarkar, F.L. Villante
OLIVE 99	ASP 11 403	K.A. Olive, D. Thomas
ABREU 97j	ZPHY C74 577	P. Abreu et al. (DELPHI Collab.)
COPI 97	PR D55 3389	C.J. Copi, D.N. Schramm, M.S. Turner (CHIC)
HATA 97b	PR D55 540	N. Hata et al. (OSU, PENN)
OLIVE 97	ASP 7 27	K.A. Olive, D. Thomas (MINN, FLOR)
ADAM 96c	PL B380 471	W. Adam et al. (DELPHI Collab.)
CARDALL 96b	APJ 472 435	C.Y. Cardall, G.M. Fuller (UCSD)
FIELDS 96	New Ast 1 77	B.D. Fields et al. (NDAM, CERN, MINN+)
KERNAN 96	PR D54 3681	P.S. Kernan, S. Sarkar (CASE, OXFTP)
AKERS 95c	ZPHY C65 47	R. Akers et al. (OPAL Collab.)
OLIVE 95	PL B354 357	K.A. Olive, G. Steigman (MINN, OSU)
BUSKULIC 93l	PL B313 520	D. Buskulic et al. (ALEPH Collab.)

LEP 92	PL B276 247	LEP Collabs. (LEP, ALEPH, DELPHI, L3, OPAL)
WALKER 91	APJ 376 51	T.P. Walker et al. (HSCA, OSU, CHIC+)
DENEGRI 90	RMP 62 1	D. Denegri, B. Sadoulet, M. Spiro (CERN, UCB+)
OLIVE 90	PL B236 454	K.A. Olive et al. (MINN, CHIC, OSU+)
YANG 84	APJ 281 493	J. Yang et al. (CHIC, BART)
OLIVE 81	APJ 246 557	K.A. Olive et al. (CHIC, BART)
OLIVE 81c	NP B180 497	K.A. Olive, D.N. Schramm, G. Steigman (EFI+)
STEIGMAN 79	PRL 43 239	G. Steigman, K.A. Olive, D.N. Schramm (BART+)
YANG 79	APJ 227 697	J. Yang et al. (CHIC, YALE, UVA)
STEIGMAN 77	PL 65B 202	G. Steigman, D.N. Schramm, J.E. Gunn (YALE, CHIC+)
PEEBLES 71	Physical Cosmology	P.Z. Peebles (PRIN)
Princeton Univ. Press (1971)		
SHVARTSMAN 69	JETPL 9 184	V.F. Shvartsman (MOSU)
Translated from ZETFP 9 315.		
HOYLE 64	NAT 203 1108	F. Hoyle, R.J. Tayler (CAMB)

Double- β Decay

OMITTED FROM SUMMARY TABLE

NEUTRINOLESS DOUBLE- β DECAY

Revised August 2009 by P. Vogel (Caltech) and A. Piepke (University of Alabama).

Neutrinoless double-beta ($0\nu\beta\beta$) decay would signal violation of total lepton number conservation. The process can be mediated by an exchange of a light Majorana neutrino, or by an exchange of other particles. However, the existence of $0\nu\beta\beta$ -decay requires Majorana neutrino mass, no matter what the actual mechanism is. As long as only a limit on the lifetime is available, limits on the effective Majorana neutrino mass, on the lepton-number violating right-handed current or other possible mechanisms mediating $0\nu\beta\beta$ -decay can be obtained, independently of the actual mechanism. These limits are listed in the next three tables, together with a claimed $0\nu\beta\beta$ -decay signal reported by part of the Heidelberg-Moscow collaboration. A 6σ excess of counts at the decay energy is used for a determination of the Majorana neutrino mass. This signal has not yet been independently confirmed. In the following we assume that the exchange of light Majorana neutrinos ($m_{\nu_i} \leq 10$ MeV) contributes dominantly to the decay rate.

Besides a dependence on the phase space ($G^{0\nu}$) and the nuclear matrix element ($M^{0\nu}$), the observable $0\nu\beta\beta$ -decay rate is proportional to the square of the effective Majorana mass $\langle m_{\beta\beta} \rangle$, $(T_{1/2}^{0\nu})^{-1} = G^{0\nu} \cdot |M^{0\nu}|^2 \cdot \langle m_{\beta\beta} \rangle^2$, with $\langle m_{\beta\beta} \rangle^2 = |\sum_i U_{ei}^2 m_{\nu_i}|^2$. The sum contains, in general, complex CP -phases in U_{ei}^2 , i.e., cancellations may occur. For three neutrino flavors, there are three physical phases for Majorana neutrinos and one for Dirac neutrinos. The two additional Majorana phase differences affect only processes to which lepton-number-changing amplitudes contribute. Given the general 3×3 mixing matrix for Majorana neutrinos, one can construct other analogous lepton number violating quantities, $\langle m_{\ell\ell} \rangle = \sum_i U_{ei} U_{\ell i} m_{\nu_i}$. However, these are currently much less constrained than $\langle m_{\beta\beta} \rangle$.

Nuclear structure calculations are needed to deduce $\langle m_{\beta\beta} \rangle$ from the decay rate. While $G^{0\nu}$ can be calculated reliably, the computation of $M^{0\nu}$ is subject to uncertainty. Indiscriminate averaging over all published matrix element values would result, for any given nuclide, in a factor of ~ 3 uncertainty in the derived $\langle m_{\beta\beta} \rangle$ values. More recent evaluations, insisting that the known $2\nu\beta\beta$ rate is correctly reproduced, result in a considerable reduction in the spread of the $M^{0\nu}$ values. E.g.

in [1] the spread appears to be as low as $\pm 30\%$. The particle physics quantities to be determined are thus nuclear model-dependent, so the half-life measurements are listed first. Where possible, we reference the nuclear matrix elements used in the subsequent analysis. Since rates for the more conventional $2\nu\beta\beta$ decay serve to calibrate the nuclear theory, results for this process are also given.

Oscillation experiments utilizing atmospheric-, accelerator-, solar-, and reactor-produced neutrinos and anti-neutrinos yield strong evidence that at least some neutrinos are massive. However, these findings shed no light on the mass hierarchy (*i.e.*, on the sign of Δm_{atm}^2), the absolute neutrino mass values or the properties of neutrinos under CPT-conjugation (Dirac or Majorana).

All confirmed oscillation experiments can be consistently described using three interacting neutrino species with two mass splittings and three mixing angles. Full three flavor analyses such as *e.g.* [2] yield: $|\Delta m_{atm}^2| \equiv |m_3^2 - (m_2^2 + m_1^2)/2| = (2.39_{-0.20}^{+0.27}) \times 10^{-3} \text{ eV}^2$ and $\sin^2 \theta_{atm} \equiv \sin^2 \theta_{23} = 0.466_{-0.100}^{+0.136}$ for the parameters observed in atmospheric and accelerator experiments. Oscillations of solar ν_e and reactor $\bar{\nu}_e$ lead to $\Delta m_{\odot}^2 \equiv m_2^2 - m_1^2 = (7.67_{-0.36}^{+0.34}) \times 10^{-5} \text{ eV}^2$ and $\sin^2 \theta_{\odot} \equiv \sin^2 \theta_{12} = 0.312_{-0.034}^{+0.040}$. (All errors correspond to 95% CL) The investigation of reactor $\bar{\nu}_e$ at ~ 1 km baseline, combined with solar neutrino and long baseline reactor experiments, indicates that electron type neutrinos couple only weakly to the third mass eigenstate with $\sin^2 \theta_{13} < 0.036$.

Based on the 3-neutrino analysis: $\langle m_{\beta\beta} \rangle^2 \approx |\cos^2 \theta_{\odot} m_1 + e^{i\Delta\alpha_{21}} \sin^2 \theta_{\odot} m_2 + e^{i\Delta\alpha_{31}} \sin^2 \theta_{13} m_3|^2$, with $\Delta\alpha_{21}, \Delta\alpha_{31}$ denoting the physically relevant Majorana CP -phase differences (possible Dirac phase δ is absorbed in these $\Delta\alpha$). Given the present knowledge of the neutrino oscillation parameters one can derive the relation between the effective Majorana mass and the mass of the lightest neutrino, as illustrated in the left panel of Fig. 1. The three mass hierarchies allowed by the oscillation data: normal ($m_1 < m_2 < m_3$), inverted ($m_3 < m_1 < m_2$), and degenerate ($m_1 \approx m_2 \approx m_3$), result in different projections. The width of the innermost hatched bands reflects the uncertainty introduced by the unknown Majorana phases. If the experimental errors of the oscillation parameters are taken into account, then the allowed areas are widened as shown by the outer bands of Fig. 1. Because of the overlap of the different mass scenarios a measurement of $\langle m_{\beta\beta} \rangle$ in the degenerate or inversely hierarchical ranges would not determine the hierarchy. The middle panel of Fig. 1 depicts the relation of $\langle m_{\beta\beta} \rangle$ with the summed neutrino mass $M = m_1 + m_2 + m_3$, constrained by observational cosmology. The oscillation data thus allow to test whether observed values of $\langle m_{\beta\beta} \rangle$ and M are consistent within the 3 neutrino framework. The right hand panel of Fig. 1, finally, shows $\langle m_{\beta\beta} \rangle$ as a function of the average mass $\langle m_{\beta} \rangle = [\sum |U_{ei}|^2 m_{\nu_i}^2]^{1/2}$ determined through the analysis of low energy beta decays. The rather large intrinsic width of the $\beta\beta$ -decay constraint essentially does not allow to positively

identify the inverted hierarchy, and thus the sign of Δm_{atm}^2 , even in combination with these other observables. Naturally, if the value of $\langle m_{\beta\beta} \rangle \leq 0.01 \text{ eV}$ is ever established then normal hierarchy becomes the only possible scenario.

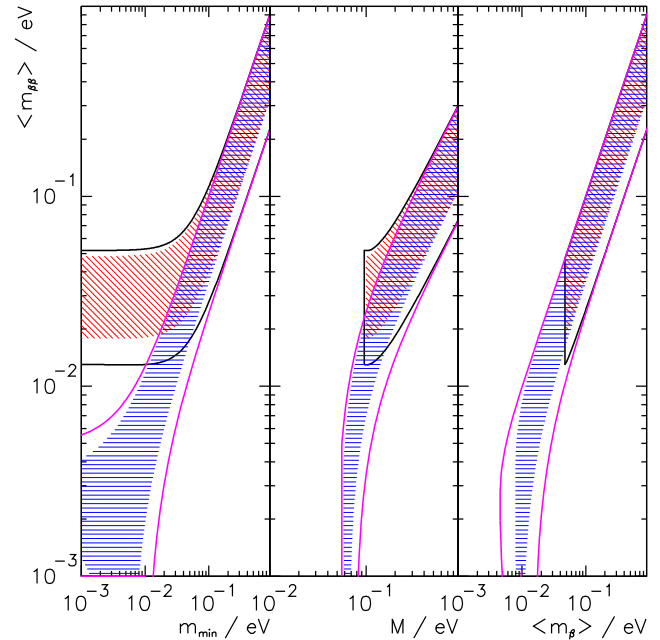


Figure 1: The left panel shows the dependence of $\langle m_{\beta\beta} \rangle$ on the absolute mass of the lightest neutrino m_{min} . The middle panel shows $\langle m_{\beta\beta} \rangle$ as a function of the summed neutrino mass M , while the right panel depicts $\langle m_{\beta\beta} \rangle$ as a function of the mass $\langle m_{\beta} \rangle$. In all panels, the width of the hatched areas is due to the unknown Majorana phases and thus irreducible. The allowed areas given by the solid lines are obtained by taking into account the errors of the oscillation parameters. The two sets of solid lines correspond to the normal and inverted hierarchies. These sets merge into each other for $\langle m_{\beta\beta} \rangle \geq 0.1 \text{ eV}$, which corresponds to the degenerate mass pattern.

It should be noted that systematic uncertainties of the nuclear matrix elements are not folded into the mass limits reported by $\beta\beta$ -decay experiments. Taking this additional uncertainty into account would further widen the projections. The uncertainties in oscillation parameters affect the width of the allowed bands in an asymmetric manner, as shown in Fig. 1. For example, for the degenerate mass pattern ($\langle m_{\beta\beta} \rangle \geq 0.1 \text{ eV}$) the upper edge is simply $\langle m_{\beta\beta} \rangle \sim m$, where m is the common mass of the degenerate multiplet, independent of the oscillation parameters, while the lower edge is $m \cos(2\theta_{\odot})$. Similar arguments explain the other features of Fig. 1.

If the neutrinoless double-beta decay is observed, it will be possible to fix a *range* of absolute values of the masses m_{ν_i} . Unlike the direct neutrino mass measurements, however, a limit

Lepton Particle Listings

Double- β Decay

on $\langle m_{\beta\beta} \rangle$ does not allow one to constrain the individual mass values m_{ν_i} even when the mass differences Δm^2 are known.

Neutrino oscillation data imply, for the first time, the existence of a *lower limit* ~ 0.013 eV for the Majorana neutrino mass for the inverted hierarchy mass pattern while $\langle m_{\beta\beta} \rangle$ could, by fine tuning, vanish in the case of the normal mass hierarchy. Several new double-beta searches have been proposed to probe the interesting $\langle m_{\beta\beta} \rangle$ mass range.

If lepton-number-violating right-handed current weak interactions exist, their strength can be characterized by the phenomenological coupling constants η and λ (η describes the coupling between the right-handed lepton current and left-handed quark current while λ describes the coupling when both currents are right-handed). The $0\nu\beta\beta$ decay rate then depends on $\langle \eta \rangle = \eta \sum_i U_{ei} V_{ei}$ and $\langle \lambda \rangle = \lambda \sum_i U_{ei} V_{ei}$ that vanish for massless or unmixed neutrinos (V_{ej} is a matrix analogous to U_{ej} but describing the mixing with the hypothetical right-handed neutrinos). This mechanism of the $0\nu\beta\beta$ decay could be, in principle, distinguished from the light Majorana neutrino exchange by the observation of the single electron spectra. The limits on $\langle \eta \rangle$ and $\langle \lambda \rangle$ are listed in a separate table. The reader is cautioned that a number of earlier experiments did not distinguish between η and λ . In addition, see the section on Majoron searches for additional limits set by these experiments.

References

1. F. Šimković *et al.*, Phys. Rev. **C77**, 045503 (2008).
2. G.L. Fogli *et al.*, Phys. Rev. **D78**, 033010 (2008).

Half-life Measurements and Limits for Double- β Decay

In most cases the transitions $(Z,A) \rightarrow (Z-2,A) + 2e^- + (0 \text{ or } 2) \bar{\nu}_e$ to the 0^+ ground state of the final nucleus are listed. However, we also list transitions that increase the nuclear charge ($2e^+$, e^+ /EC and ECEC) and transitions to excited states of the final nuclei (0^+_k , 2^+ , and 2^+_k). In the following Listings, only best or comparable limits or lifetimes for each isotope are reported. For 2ν decay, which is well established, only measured half-lives are reported.

$t_{1/2}$ (10^{21} yr)	CL% ISOTOPE	TRANSITION	METHOD	DOCUMENT ID
• • • We do not use the following data for averages, fits, limits, etc. • • •				
> 18.0	90 ¹⁵⁰ Nd 0ν		NEMO-3	1 ARGYRADES 09
$(9.11^{+0.25}_{-0.22} \pm 0.63)$ E-3	¹⁵⁰ Nd 2ν		NEMO-3	2 ARGYRADES 09
> 0.43	90 ⁶⁴ Zn 0ν	β^+ EC	ZnWO ₄ scint.	3 BELLI 09A
> 0.11	90 ⁶⁴ Zn 0ν	ECEC	ZnWO ₄ scint.	4 BELLI 09A
> 4.1×10^{-4}	90 ¹²⁰ Te 0ν	β^+ EC	CdZnTe det.	5 DAWSON 09
> 0.02	90 ¹²⁴ Sn 0ν	$\beta\beta$	tin liq. scint.	6 HWANG 09
$0.55^{+0.12}_{-0.09}$	100 Mo $2\nu+0\nu$	$0^+ \rightarrow 0^+_1$	Ge coincidence	7 KIDD 09
> 3000	90 ¹³⁰ Te 0ν		TeO ₂ bolometer	8 ARNABOLDI 08
> 0.004	90 ⁶⁴ Zn 0ν	2K	ZnWO ₄ scint.	9 BELLI 08
> 0.22	90 ⁶⁴ Zn 0ν		ZnWO ₄ scint.	10 BELLI 08
> 0.001	90 ¹⁰⁸ Cd 0ν	2K	CdWO ₄ scint.	11 BELLI 08B
> 0.0013	90 ¹¹⁴ Cd 2ν	$\beta\beta$	CdWO ₄ scint.	12 BELLI 08B
> 1.1	90 ¹¹⁴ Cd 0ν	$\beta\beta$	CdWO ₄ scint.	13 BELLI 08B
> 58	90 ⁴⁸ Ca 0ν		CaF ₂ scint.	14 UMEHARA 08
$0.57^{+0.13}_{-0.09} \pm 0.08$	68 ¹⁰⁰ Mo 2ν	$0^+ \rightarrow 0^+_1$	NEMO-3	15 ARNOLD 07
> 89	90 ¹⁰⁰ Mo 0ν	$0^+ \rightarrow 0^+_1$	NEMO-3	16 ARNOLD 07
> 1.1	90 ¹⁰⁰ Mo 2ν	$0^+ \rightarrow 2^+$	NEMO-3	17 ARNOLD 07
> 160	90 ¹⁰⁰ Mo 0ν	$0^+ \rightarrow 2^+$	NEMO-3	18 ARNOLD 07
> 0.0019	90 ⁷⁴ Se $0\nu+2\nu$		γ in Ge det.	19 BARABASH 07
> 0.0055	90 ⁷⁴ Se $0\nu+2\nu$	$0^+ \rightarrow 2^+_1$	γ in Ge det.	20 BARABASH 07
> $(1.9-6.0) 10^{-4}$	90 ¹²⁰ Te 0ν		γ in Ge det.	21 BARABASH 07B
> 1.9×10^{-4}	90 ¹²⁰ Te $0\nu+2\nu$		γ in Ge det.	22 BARABASH 07B

> 7.5×10^{-4}	90 ¹²⁰ Te $0\nu+2\nu$	$0^+ \rightarrow 2^+$	γ in Ge det.	23 BARABASH 07B
> 1.19×10^{-4}	90 ⁶⁴ Zn 0ν		CdZnTe calorim.	24 BLOXHAM 07
> 1.21×10^{-4}	90 ¹²⁰ Te 0ν		CdZnTe calorim.	25 BLOXHAM 07
> 2.68×10^{-6}	90 ¹²⁰ Te 0ν		CdZnTe calorim.	26 BLOXHAM 07
> 9.72×10^{-6}	90 ¹²⁰ Te 0ν	$0^+ \rightarrow 2^+_1$	CdZnTe calorim.	27 BLOXHAM 07
22300^{+4400}_{-3100}	68 ⁷⁶ Ge 0ν		Enriched HPGe	28 KLAPDOR-K... 06A
> 1800	90 ¹³⁰ Te 0ν		Cryog. det.	29 ARNABOLDI 05
> 460	90 ¹⁰⁰ Mo 0ν		NEMO-3	30 ARNOLD 05A
> 100	90 ⁸² Se 0ν		NEMO-3	31 ARNOLD 05A
$(7.11 \pm 0.02 \pm 0.54)$ E-3	¹⁰⁰ Mo 2ν		NEMO-3	32 ARNOLD 05A
$(9.6 \pm 0.3 \pm 1.0)$ E-2	⁸² Se 2ν		NEMO-3	33 ARNOLD 05A
> 550	90 ¹³⁰ Te 0ν		Cryog. det.	34 ARNABOLDI 04
> 310	90 ¹⁰⁰ Mo 0ν		NEMO-3	35 ARNOLD 04
> 140	90 ⁸² Se 0ν		NEMO-3	36 ARNOLD 04
$(7.68 \pm 0.02 \pm 0.54)$ E-3	¹⁰⁰ Mo 2ν		NEMO-3	37 ARNOLD 04
$(10.3 \pm 0.3 \pm 0.7)$ E-2	⁸² Se 2ν		NEMO-3	38 ARNOLD 04
$0.14^{+0.04}_{-0.02} \pm 0.03$	68 ¹⁵⁰ Nd $0\nu+2\nu$	$0^+ \rightarrow 0^+_1$	γ in Ge det.	39 BARABASH 04
11900^{+25900}_{-5000}	99.7 ⁷⁶ Ge 0ν		Enriched HPGe	40 KLAPDOR-K... 04A
> 14	90 ⁴⁸ Ca 0ν		CaF ₂ scint.	41 OGAWA 04
> 210	90 ¹³⁰ Te 0ν		Cryog. det.	42 ARNABOLDI 03
> 31	90 ¹³⁰ Te 0ν	$0^+ \rightarrow 2^+$	Cryog. det.	43 ARNABOLDI 03
$0.61 \pm 0.14^{+0.29}_{-0.35}$	90 ¹³⁰ Te 2ν		Cryog. det.	44 ARNABOLDI 03
> 110	90 ¹²⁸ Te 0ν		Cryog. det.	45 ARNABOLDI 03
$(0.029^{+0.004}_{-0.003})$	116 Cd 2ν		¹¹⁶ CdWO ₄ scint.	46 DANEVICH 03
> 170	90 ¹¹⁶ Cd 0ν		¹¹⁶ CdWO ₄ scint.	47 DANEVICH 03
> 29	90 ¹¹⁶ Cd 0ν	$0^+ \rightarrow 2^+$	¹¹⁶ CdWO ₄ scint.	48 DANEVICH 03
> 14	90 ¹¹⁶ Cd 0ν	$0^+ \rightarrow 0^+_1$	¹¹⁶ CdWO ₄ scint.	49 DANEVICH 03
> 6	90 ¹¹⁶ Cd 0ν	$0^+ \rightarrow 0^+_2$	¹¹⁶ CdWO ₄ scint.	50 DANEVICH 03
$1.74 \pm 0.01^{+0.18}_{-0.16}$	76 Ge 2ν		Enriched HPGe	51 DOERR 03
> 15700	90 ⁷⁶ Ge 0ν		Enriched HPGe	52 AALSETH 02B
> 58	90 ¹³⁴ Xe 0ν		Liquid Xe Scint.	53 BERNABEI 02D
> 1200	90 ¹³⁶ Xe 0ν		Liquid Xe Scint.	54 BERNABEI 02D
$15000^{+168000}_{-7500}$	76 Ge 0ν		Enriched HPGe	55 KLAPDOR-K... 02D
$(7.2 \pm 0.9 \pm 1.8)$ E-3	100 Mo 2ν		Liq. Ar ioniz.	56 ASHITKOV 01
> 4.9	90 ¹⁰⁰ Mo 0ν		Liq. Ar ioniz.	57 ASHITKOV 01
> 1.3	90 ¹⁶⁰ Gd 0ν		Gd ₂ SiO ₅ :Ce	58 DANEVICH 01
> 1.3	90 ¹⁶⁰ Gd 0ν	$0^+ \rightarrow 2^+$	Gd ₂ SiO ₅ :Ce	59 DANEVICH 01
$0.59^{+0.17}_{-0.11} \pm 0.06$	100 Mo $0\nu+2\nu$	$0^+ \rightarrow 0^+_1$	Ge coinc.	60 DEBRAECKEL 01
> 55	90 ¹⁰⁰ Mo $0\nu, \langle m_{\nu} \rangle$		ELEGANT V	61 EJIRI 01
> 42	90 ¹⁰⁰ Mo $0\nu, \langle \lambda \rangle$		ELEGANT V	61 EJIRI 01
> 49	90 ¹⁰⁰ Mo $0\nu, \langle \eta \rangle$		ELEGANT V	61 EJIRI 01
> 19000	90 ⁷⁶ Ge 0ν		Enriched HPGe	62 KLAPDOR-K... 01
$1.55 \pm 0.001^{+0.19}_{-0.15}$	76 Ge 2ν		Enriched HPGe	63 KLAPDOR-K... 01
(9.4 ± 3.2) E-3	90 ⁹⁶ Zr $0\nu+2\nu$		Geochem	64 WIESER 01
$0.042^{+0.033}_{-0.013}$	48 Ca 2ν		Ge spectrometer	65 BRUDANIN 00
$0.021^{+0.008}_{-0.004} \pm 0.002$	96 Zr 2ν		NEMO-2	66 ARNOLD 99
> 1.0	90 ⁹⁶ Zr 0ν		NEMO-2	66 ARNOLD 99
$(8.3 \pm 1.0 \pm 0.7)$ E-2	⁸² Se 2ν		NEMO-2	67 ARNOLD 98
> 9.5	90 ⁸² Se 0ν		NEMO-2	68 ARNOLD 98
> 2.8	90 ⁸² Se 0ν	$0^+ \rightarrow 2^+$	NEMO-2	69 ARNOLD 98
$(7.6^{+2.2}_{-1.4})$ E-3	100 Mo 2ν		Si(Li)	70 ALSTON... 97
$(6.82^{+0.38}_{-0.53} \pm 0.68)$ E-3	100 Mo 2ν		TPC	71 DESILVA 97
$(6.75^{+0.37}_{-0.42} \pm 0.68)$ E-3	150 Nd 2ν		TPC	72 DESILVA 97
> 1.2	90 ¹⁵⁰ Nd 0ν		TPC	73 DESILVA 97
$(3.75 \pm 0.35 \pm 0.21)$ E-2	¹¹⁶ Cd 2ν	$0^+ \rightarrow 0^+$	NEMO 2	74 ARNOLD 96
$0.043^{+0.024}_{-0.011} \pm 0.014$	48 Ca 2ν		TPC	75 BALLYSH 96
0.79 ± 0.10	130 Te $0\nu+2\nu$		Geochem	76 TAKAOKA 96
$0.61^{+0.18}_{-0.11}$	100 Mo $0\nu+2\nu$	$0^+ \rightarrow 0^+_1$	γ in HPGe	77 BARABASH 95
$(9.5 \pm 0.4 \pm 0.9)$ E-3	100 Mo 2ν		NEMO 2	DASSIE 95
> 0.6	90 ¹⁰⁰ Mo 0ν	$0^+ \rightarrow 0^+_1$	NEMO 2	DASSIE 95
$0.026^{+0.009}_{-0.005} \pm 0.0035$	116 Cd 2ν	$0^+ \rightarrow 0^+$	ELEGANT IV	EJIRI 95
$0.017^{+0.010}_{-0.005} \pm 0.0035$	150 Nd 2ν	$0^+ \rightarrow 0^+$	TPC	ARTEMEV 93
0.039 ± 0.009	96 Zr $0\nu+2\nu$		Geochem	KAWASHIMA 93
2.7 ± 0.1	130 Te $0\nu+2\nu$		Geochem	BERNATOW... 92
7200 ± 400	128 Te $0\nu+2\nu$		Geochem	78 BERNATOW... 92
> 27	68 ⁸² Se 0ν	$0^+ \rightarrow 0^+$	TPC	ELLIOTT 92
$0.108^{+0.026}_{-0.006}$	82 Se 2ν	$0^+ \rightarrow 0^+$	TPC	ELLIOTT 92
2.0 ± 0.6	238 U $0\nu+2\nu$		Radiochem	79 TURKEVICH 91
> 9.5	76 Ca 0ν		CaF ₂ scint.	YOU 91
$0.12 \pm 0.01 \pm 0.04$	68 ⁸² Se $0\nu+2\nu$		Geochem.	80 LIN 88
$0.75 \pm 0.03 \pm 0.23$	68 ¹³⁰ Te $0\nu+2\nu$		Geochem.	81 LIN 88
1800 ± 700	68 ¹²⁸ Te $0\nu+2\nu$		Geochem.	82 LIN 88B
2.60 ± 0.28	130 Te $0\nu+2\nu$		Geochem	83 KIRSTEN 83

¹ ARGYRADES 09 use the NEMO-3 tracking calorimeter containing 36.5 g of ¹⁵⁰Nd, a total exposure of 924.7 days, to derive a limit for the $0\nu\beta\beta$ half-life. Supersedes DESILVA 97.

See key on page 405

Lepton Particle Listings

Double- β Decay

- 2 ARGYRIADES 09 use the NEMO-3 tracking calorimeter containing 36.5 g of ^{150}Nd , a total exposure of 924.7 days, to determine the value of the $2\nu\beta\beta$ half-life. This result is in marginal agreement, but has somewhat smaller error bars, than DESILVA 97.
- 3 BELLI 09A use ZnWO_4 scintillating crystals to search for various modes of $\beta\beta$ decay. This work improves the limits for different modes of ^{64}Zn decay into the ground state of ^{64}Ni , in this case for the $0\nu\beta^+\text{EC}$ mode. Supersedes BELLI 08.
- 4 BELLI 09A use ZnWO_4 scintillating crystals to search for various modes of $\beta\beta$ decay. This work improves the limits for different modes of ^{64}Zn decay into the ground state of ^{64}Ni , in this case for the $0\nu\text{ECC}$ mode. Supersedes BELLI 08.
- 5 DAWSON 09 use an array of $^{16}\text{CdZnTe}$ detectors that contain nine $\beta\beta$ -decay candidate nuclei. Several lifetime limits were obtained, of which the $\beta^+\text{EC}$ decay of ^{120}Te exceeds the previous best limit. Supersedes BARABASH 07B and BLOXHAM 07.
- 6 HWANG 09 use a tin loaded liquid scintillator to search for the $0\nu\beta\beta$ -decay of ^{124}Sn . They report the most stringent limit for this nuclide.
- 7 KIDD 09 combine past and new data with an improved coincidence detection efficiency determination. The result agrees with ARNOLD 95. Supersedes DEBRAECKELEER 01 and BARABASH 95.
- 8 ARNABOLDI 08 use high resolution TeO_2 bolometric calorimeter to search for double beta decay of ^{130}Te . Supersedes ARNABOLDI 05.
- 9 BELLI 08 use ZnWO_4 scintillation calorimeter to search for neutrinoless double K-shell electron capture decay of ^{64}Zn . Slightly weaker limit is obtained for capture from other shells. The half-life limit for the 2ν mode is 6.2×10^{18} years.
- 10 BELLI 08 use ZnWO_4 scintillation calorimeter to search for neutrinoless β^+ plus electron capture decay of ^{64}Zn . The half-life limit for the 2ν mode is 2.1×10^{20} years.
- 11 BELLI 08B use CdWO_4 scintillation calorimeter to search for 0ν and 2ν decay with 2K electron captures of ^{108}Cd . The absence of signal at $2 \times K$ electron binding energy (4.8 keV) is used to derive the half-life limit. Search for γ at 223 keV gives half-life limit for the 0ν mode of 1.0×10^{18} years.
- 12 BELLI 08B use CdWO_4 scintillation calorimeter to search for $2\nu\beta\beta$ decay of ^{114}Cd .
- 13 BELLI 08B use CdWO_4 scintillation calorimeter to search for $0\nu\beta\beta$ decay of ^{114}Cd .
- 14 UMEHARA 08 use CaF_2 scintillation calorimeter to search for double beta decay of ^{48}Ca . Limit is significantly more stringent than quoted sensitivity: 18×10^{21} years.
- 15 First exclusive measurement of 2ν -decay to the first excited 0_1^+ -state of daughter nucleus. ARNOLD 07 use the NEMO-3 tracking calorimeter to detect all particles emitted in decay. Result agrees with the inclusive ($0\nu + 2\nu$) measurement of DEBRAECKELEER 01.
- 16 Limit on 0ν -decay to the first excited 0_1^+ -state of daughter nucleus using NEMO-3 tracking calorimeter. Supersedes DASSIE 95.
- 17 Limit on 2ν -decay to the first excited 2^+ -state of daughter nucleus using NEMO-3 tracking calorimeter.
- 18 Limit on 0ν -decay to the first excited 2^+ -state of daughter nucleus using NEMO-3 tracking calorimeter.
- 19 BARABASH 07 use Ge calorimeter to search for γ -radiation following double electron capture or β^+ plus electron capture decays of ^{74}Sr to the ground state of ^{74}Ge . This limit is based on the search for the 511 keV annihilation radiation. Various other limits, for the capture from different atomic shells and also to the excited states, are reported in the paper.
- 20 BARABASH 07 use Ge calorimeter to search for γ -radiation following double electron capture decay of ^{74}Sr into the second excited 2^+ -state of ^{74}Ge . That transition has been considered due to a possible resonance enhancement. The 2ν mode would be suppressed for this decay by its extremely small phase space factor.
- 21 BARABASH 07B use Ge calorimeter to search for γ -radiation following the double electron capture decay of ^{120}Te . This limit is based on the search for the bremsstrahlung radiation. Various limits, for the capture from different atomic shells, are reported that cover the range of half-lives shown.
- 22 BARABASH 07B use Ge calorimeter to search for the 511 keV positron annihilation radiation following the β^+ plus electron capture decay of ^{120}Te .
- 23 BARABASH 07B use Ge calorimeter to search for γ -radiation following the double electron capture decay of ^{120}Te into the excited 2^+ state of ^{120}Sn . This limit is based on the search for the γ -radiation from the excited 2^+ state.
- 24 BLOXHAM 07 use CdZnTe solid state detectors to search for the decays of the various double beta detector components, here for double electron capture ^{64}Zn decay.
- 25 BLOXHAM 07 use CdZnTe solid state detectors to search for the decays of the various double beta detector components, here for β^+ plus electron capture ^{120}Te decay.
- 26 BLOXHAM 07 use CdZnTe solid state detectors to search for the decays of the various double beta detector components, here for double electron capture ^{120}Te decay.
- 27 BLOXHAM 07 use CdZnTe solid state detectors to search for the decays of the various double beta detector components, here for double electron capture ^{120}Te decay to the first excited 2^+ -state.
- 28 KLAPDOR-KLEINGROTHAUS 06A present re-analysis of data originally published in KLAPDOR-KLEINGROTHAUS 04A. Modified pulse shape analysis leads the authors to claim improved 6σ statistical evidence for observation of 0ν -decay, compared to 4.2σ in KLAPDOR-KLEINGROTHAUS 04A. Analysis of the systematic uncertainty is not presented. Supersedes KLAPDOR-KLEINGROTHAUS 04A.
- 29 Supersedes ARNABOLDI 04. Bolometric TeO_2 detector array CUORICINO is used for high resolution search for $0\nu\beta\beta$ decay. The half-life limit is derived from 3.09 kg yr ^{130}Te exposure.
- 30 NEMO-3 tracking calorimeter containing 6.9 kg of enriched ^{100}Mo is used in ARNOLD 05A. A limit for $0\nu\beta\beta$ half-life of ^{100}Mo is reported. Supersedes ARNOLD 04.
- 31 NEMO-3 tracking calorimeter is used in ARNOLD 05A to place limit on $0\nu\beta\beta$ half-life of ^{82}Se . Detector contains 0.93 kg of enriched ^{82}Se . Supersedes ARNOLD 04.
- 32 ARNOLD 05A use the NEMO-3 tracking calorimeter to determine the $2\nu\beta\beta$ half-life of ^{100}Mo with high statistics and low background (389 days of data taking). Supersedes ARNOLD 04.
- 33 ARNOLD 05A use the NEMO-3 tracking detector to determine the $2\nu\beta\beta$ half-life of ^{82}Se with high statistics and low background (389 days of data taking). Supersedes ARNOLD 04.
- 34 Supersedes ARNABOLDI 03. Bolometric TeO_2 detector array Cuoricino used for high resolution search for $0\nu\beta\beta$ decay.
- 35 ARNOLD 04 use the NEMO-3 tracking detector to determine the limit for $0\nu\beta\beta$ half-life of ^{100}Mo . This represents an improvement, by a factor of ~ 6 , when compared with EJIRI 01.
- 36 ARNOLD 04 use the NEMO-3 tracking detector to determine the limit for $0\nu\beta\beta$ half-life of ^{82}Se . This represents an improvement, by a factor of ~ 10 , when compared with ELLIOTT 92. It supersedes the limit of ARNOLD 98 for this decay using NEMO-2.
- 37 ARNOLD 04 use the NEMO-3 tracking detector to determine the $2\nu\beta\beta$ half-life of ^{100}Mo with high statistics and low background. The half-life is determined assuming the Single State Dominance. It is in agreement with, and more accurate than, previous determinations. Supersedes DASSIE 95 determination of this quantity with NEMO-2.
- 38 ARNOLD 04 use the NEMO-3 tracking detector to determine the $2\nu\beta\beta$ half-life of ^{82}Se . The half-life is in agreement with ARNOLD 98 with NEMO-2 which it supersedes.
- 39 BARABASH 04 perform an inclusive measurement of the $\beta\beta$ decay of ^{150}Nd into the first excited (0_1^+) state of ^{150}Sm . Gamma radiation emitted in decay of the excited state is detected.
- 40 Supersedes KLAPDOR-KLEINGROTHAUS 02D. Authors present new analysis of event excess seen in Heidelberg-Moscow experiment at $\beta\beta$ -decay energy. Enhanced statistics leads to a 4.2σ evidence for observation of $0\nu\beta\beta$ -decay and a finite Majorana neutrino mass. Stated error is purely statistical. No systematic errors are mentioned in the paper. More details can be found in KLAPDOR-KLEINGROTHAUS 04C.
- 41 CaF_2 scintillation calorimeter ELEGANT VI used to set limit on $0\nu\beta\beta$ -decay rate of ^{48}Ca . The stated half-life limit benefits from a downward fluctuation on the number of background events. The experimental sensitivity is 5.9×10^{21} yr. at 90% CL. Replaces YOU 91 as the most stringent experiment using ^{48}Ca .
- 42 Supersedes ALESSANDRELLO 00. Array of TeO_2 crystals in high resolution cryogenic calorimeter. Some enriched in ^{130}Te . Ground state to ground state decay.
- 43 Decay into first excited state of daughter nucleus.
- 44 Two neutrino decay into ground state. Relatively large error mainly due to uncertainties in background determination. Reported value is shorter than the geochemical measurements of KIRSTEN 83 and BERNATOWICZ 92 but in agreement with LIN 88 and TAKAOKA 96.
- 45 Supersedes ALESSANDRELLO 00. Array of TeO_2 crystals in high resolution cryogenic calorimeter. Some enriched in ^{128}Te . Ground state to ground state decay.
- 46 Calorimetric measurement of 2ν ground state decay of ^{116}Cd using enriched CdWO_4 scintillators. Agrees with EJIRI 95 and ARNOLD 96. Supersedes DANEVICH 00.
- 47 Limit on 0ν decay of ^{116}Cd using enriched CdWO_4 scintillators. Supersedes DANEVICH 00.
- 48 Limit on 0ν decay of ^{116}Cd into first excited 2^+ state of daughter nucleus using enriched CdWO_4 scintillators. Supersedes DANEVICH 00.
- 49 Limit on 0ν decay of ^{116}Cd into first excited 0^+ state of daughter nucleus using enriched CdWO_4 scintillators. Supersedes DANEVICH 00.
- 50 Limit on 0ν decay of ^{116}Cd into second excited 0^+ state of daughter nucleus using enriched CdWO_4 scintillators. Supersedes DANEVICH 00.
- 51 Results of the Heidelberg-Moscow experiment (KLAPDOR-KLEINGROTHAUS 01 and GUENTHER 97) are reanalyzed using a new simulation of the complete background spectrum. The $\beta\beta 2\nu$ -decay rate is deduced from a 41.57 kg-y exposure. The result is in agreement and supersedes the above referenced half-lives with similar statistical and systematic errors.
- 52 AALSETH 02B limit is based on 117 mol-yr of data using enriched Ge detectors. Background reduction by means of pulse shape analysis is applied to part of the data set. Reported limit is slightly less restrictive than that in KLAPDOR-KLEINGROTHAUS 01 However, it excludes part of the allowed half-life range reported in KLAPDOR-KLEINGROTHAUS 01B for the same nuclide. The analysis has been criticized in KLAPDOR-KLEINGROTHAUS 04B. The criticism was addressed and disputed in AALSETH 04.
- 53 BERNABEI 02D report a limit for the $0\nu, 0^+ \rightarrow 0^+$ decay of ^{134}Xe , present in the source at 17%, by considering the maximum number of events for this mode compatible with the fitted smooth background.
- 54 BERNABEI 02D report a limit for the $0\nu, 0^+ \rightarrow 0^+$ decay of ^{136}Xe , by considering the maximum number of events for this mode compatible with the fitted smooth background. The quoted sensitivity is 450×10^{21} yr. The Feldman and Cousins method is used to obtain the quoted limit.
- 55 KLAPDOR-KLEINGROTHAUS 02D is an expanded version of KLAPDOR-KLEINGROTHAUS 01B. The authors re-evaluate the data collected by the Heidelberg-Moscow experiment (KLAPDOR-KLEINGROTHAUS 01) and present a more detailed description of their analysis of an excess of counts at the energy expected for neutrinoless double-beta decay. They interpret this excess, which has a significance of 2.2 to 3.1 σ depending on the data analysis, as evidence for the observation of Lepton Number violation and violation of Baryon minus Lepton Number. The analysis has been criticized by AALSETH 02 and others. The criticisms have been addressed in KLAPDOR-KLEINGROTHAUS 02. See also KLAPDOR-KLEINGROTHAUS 02B. GROMOV 06 analysis of the background supports the assignment of the weak γ transitions near 2040 keV to the decay of ^{214}Bi as claimed in KLAPDOR-KLEINGROTHAUS 04A and KLAPDOR-KLEINGROTHAUS 04C, and in earlier works.
- 56 ASHITKOV 01 result for 2ν of ^{100}Mo is in agreement with other determinations of that half-life.
- 57 ASHITKOV 01 result for 0ν of ^{100}Mo is less stringent than EJIRI 01.
- 58 DANEVICH 01 place limit on 0ν decay of ^{160}Gd using $\text{Gd}_2\text{SiO}_5:\text{Ce}$ crystal scintillators. The limit is more stringent than KOBAYASHI 95.
- 59 DANEVICH 01 place limits on 0ν decay of ^{160}Gd into excited 2^+ state of daughter nucleus using $\text{Gd}_2\text{SiO}_5:\text{Ce}$ crystal scintillators.

Lepton Particle Listings

Double- β Decay

- ⁶⁰ DEBRAECKELEER 01 performed an inclusive measurement of the $\beta\beta$ decay into the second excited state of the daughter nucleus. A novel coincidence technique counting the de-excitation photons is employed. The result agrees with BARABASH 95.
- ⁶¹ EJIRI 01 uses tracking calorimeter and isotopically enriched passive source. Efficiencies were calculated assuming $\langle m_{\nu} \rangle$, $\langle \lambda \rangle$, or $\langle \eta \rangle$ driven decay. This is a continuation of EJIRI 96 which it supersedes.
- ⁶² KLAPDOR-KLEINGROTHAUS 01 is a continuation of the work published in BAUDIS 99. Isotopically enriched Ge detectors are used in calorimetric measurement. The most stringent bound is derived from the data set in which pulse-shape analysis has been used to reduce background. Exposure time is 35.5 kg y. Supersedes BAUDIS 99 as most stringent result.
- ⁶³ KLAPDOR-KLEINGROTHAUS 01 is a measurement of the $\beta\beta 2\nu$ -decay rate with higher statistics than GUENTHER 97. The reported value has a larger systematic error than their previous result.
- ⁶⁴ WIESER 01 reports an inclusive geochemical measurement of ⁹⁶Zr $\beta\beta$ half life. Their result agrees within 2σ with ARNOLD 99 but only marginally, within 3σ , with KAWASHIMA 93.
- ⁶⁵ BRUDANIN 00 determine the 2ν half-life of ⁴⁸Ca. Their value is less accurate than BALYSH 96.
- ⁶⁶ ARNOLD 99 measure directly the 2ν decay of Zr for the first time, using the NEMO-2 tracking detector and an isotopically enriched source. The lifetime is more accurate than the geochemical result of KAWASHIMA 93.
- ⁶⁷ ARNOLD 98 measure the 2ν decay of ⁸²Se by comparing the spectra in an enriched and natural selenium source using the NEMO-2 tracking detector. The measured half-life is in agreement, perhaps slightly shorter, than ELLIOTT 92.
- ⁶⁸ ARNOLD 98 determine the limit for 0ν decay to the ground state of ⁸²Se using the NEMO-2 tracking detector. The half-life limit is in agreement, but less stringent, than ELLIOTT 92.
- ⁶⁹ ARNOLD 98 determine the limit for 0ν decay to the excited 2^+ state of ⁸²Se using the NEMO-2 tracking detector.
- ⁷⁰ ALSTON-GARNJOST 97 report evidence for 2ν decay of ¹⁰⁰Mo. This decay has been also observed by EJIRI 91, DASSIE 95, and DESILVA 97.
- ⁷¹ DESILVA 97 result for 2ν decay of ¹⁰⁰Mo is in agreement with ALSTON-GARNJOST 97 and DASSIE 95. This measurement has the smallest errors.
- ⁷² DESILVA 97 result for 2ν decay of ¹⁵⁰Nd is in marginal agreement with ARTEMEV 93. It has smaller errors.
- ⁷³ DESILVA 97 do not explain whether their efficiency for 0ν decay of ¹⁵⁰Nd was calculated under the assumption of a $\langle m_{\nu} \rangle$, $\langle \lambda \rangle$, or $\langle \eta \rangle$ driven decay.
- ⁷⁴ ARNOLD 96 measure the 2ν decay of ¹¹⁶Cd. This result is in agreement with EJIRI 95, but has smaller errors. Supersedes ARNOLD 95.
- ⁷⁵ BALYSH 96 measure the 2ν decay of ⁴⁸Ca, using a passive source of enriched ⁴⁸Ca in a TPC.
- ⁷⁶ TAKAOKA 96 measure the geochemical half-life of ¹³⁰Te. Their value is in disagreement with the quoted values of BERNATOWICZ 92 and KIRSTEN 83; but agrees with several other unquoted determinations, e.g., MANUEL 91.
- ⁷⁷ BARABASH 95 cannot distinguish 0ν and 2ν , but it is inferred indirectly that the 0ν mode accounts for less than 0.026% of their event sample. They also note that their result disagrees with the previous experiment by the NEMO group (BLUM 92).
- ⁷⁸ BERNATOWICZ 92 finds ¹²⁸Te/¹³⁰Te activity ratio from slope of ¹²⁸Xe/¹³²Xe vs ¹³⁰Xe/¹³²Xe ratios during extraction, and normalizes to lead-dated ages for the ¹³⁰Te lifetime. The authors state that their results imply that "(a) the double beta decay of ¹²⁸Te has been firmly established and its half-life has been determined ... without any ambiguity due to trapped Xe interferences... (b) Theoretical calculations ... underestimate the [long half-lives of ¹²⁸Te ¹³⁰Te] by 1 or 2 orders of magnitude, pointing to a real suppression in the 2ν decay rate of these isotopes. (c) Despite [this], most $\beta\beta$ -models predict a ratio of 2ν decay widths ... in fair agreement with observation." Further details of the experiment are given in BERNATOWICZ 93. Our listed half-life has been revised downward from the published value by the authors, on the basis of reevaluated cosmic-ray ¹²⁸Xe production corrections.
- ⁷⁹ TURKEVICH 91 observes activity in old U sample. The authors compare their results with theoretical calculations. They state "Using the phase-space factors of Boehm and Vogel (BOEHM 87) leads to matrix element values for the ²³⁸U transition in the same range as deduced for ¹³⁰Te and ⁷⁶Ge. On the other hand, the latest theoretical estimates (STAUDT 90) give an upper limit that is 10 times lower. This large discrepancy implies either a defect in the calculations or the presence of a faster path than the standard two-neutrino mode in this case." See BOEHM 87 and STAUDT 90.
- ⁸⁰ Result agrees with direct determination of ELLIOTT 92.
- ⁸¹ Inclusive half life inferred from mass spectroscopic determination of abundance of $\beta\beta$ -decay product ¹³⁰Te in mineral kirkite (NiTeSe). Systematic uncertainty reflects variations in U-Xe gas-retention-age derived from different uranite samples. Agrees with geochemical determination of TAKAOKA 96 and direct measurement of ARNOLDI 03. Inconsistent with results of KIRSTEN 83 and BERNATOWICZ 92.
- ⁸² Ratio of inclusive double beta half lives of ¹²⁸Te and ¹³⁰Te determined from minerals melonite (NiTe₂) and altaite (PbTe) by means of mass spectroscopic measurement of abundance of $\beta\beta$ -decay products. As gas-retention-age could not be determined the authors use half life of ¹³⁰Te (LIN 88) to infer the half life of ¹²⁸Te. No estimate of the systematic uncertainty of this method is given. The directly determined half life ratio agrees with BERNATOWICZ 92. However, the inferred ¹²⁸Te half life disagrees with KIRSTEN 83 and BERNATOWICZ 92.
- ⁸³ KIRSTEN 83 reports "2 σ " error. References are given to earlier determinations of the ¹³⁰Te lifetime.

$\langle m_{\nu} \rangle$, The Effective Weighted Sum of Majorana Neutrino Masses Contributing to Neutrinoless Double- β Decay

$\langle m_{\nu} \rangle = |\sum U_{1j}^2 m_{\nu_j}|$, where the sum goes from 1 to n and where n = number of neutrino generations, and ν_j is a Majorana neutrino. Note that U_{ej}^2 , not $|U_{ej}|^2$,

occurs in the sum. The possibility of cancellations has been stressed. In the following Listings, only best or comparable limits or lifetimes for each isotope are reported.

VALUE (eV)	CL% ISOTOPE	TRANSITION	METHOD	DOCUMENT ID
• • • We do not use the following data for averages, fits, limits, etc. • • •				
< 4.0–6.8	90 ¹⁵⁰ Nd	0ν	NEMO-3	⁸⁴ ARGYRIADES 09
< 0.19–0.68	90 ¹³⁰ Te	0ν	TeO ₂ bolometer	⁸⁵ ARNABOLDI 08
< 3.5–22	90 ⁴⁸ Ca	0ν	CaF ₂ scint.	⁸⁶ UMEHARA 08
< 9.3–60	90 ¹⁰⁰ Mo	$0^+ \rightarrow 0^+$	NEMO-3	⁸⁷ ARNOLD 07
< 6500	90 ¹⁰⁰ Mo	$0^+ \rightarrow 2^+$	NEMO-3	⁸⁸ ARNOLD 07
0.32±0.03	68 ⁷⁶ Ge	0ν	Enriched HPGe	⁸⁹ KLAPDOR-K... 06A
< 0.2–1.1	90 ¹³⁰ Te		Cryog. det.	⁹⁰ ARNABOLDI 05
< 0.7–2.8	90 ¹⁰⁰ Mo	0ν	NEMO-3	⁹¹ ARNOLD 05A
< 1.7–4.9	90 ⁸² Se	0ν	NEMO-3	⁹² ARNOLD 05A
< 0.37–1.9	90 ¹³⁰ Te		Cryog. det.	⁹³ ARNABOLDI 04
< 0.8–1.2	90 ¹⁰⁰ Mo	0ν	NEMO-3	⁹⁴ ARNOLD 04
< 1.5–3.1	90 ⁸² Se	0ν	NEMO-3	⁹⁴ ARNOLD 04
0.1–0.9	99.7 ⁷⁶ Ge		Enriched HP Ge	⁹⁵ KLAPDOR-K... 04A
< 7.2–44.7	90 ⁴⁸ Ca		CaF ₂ scint.	⁹⁶ OGAWA 04
< 1.1–2.6	90 ¹³⁰ Te		Cryog. det.	⁹⁷ ARNABOLDI 03
< 1.5–1.7	90 ¹¹⁶ Cd	0ν	¹¹⁶ CdWO ₄ scint.	⁹⁸ DANEVICH 03
< 0.33–1.35	90		Enriched HPGe	⁹⁹ AALSETH 02B
< 2.9	90 ¹³⁶ Xe	0ν	Liquid Xe Scint.	¹⁰⁰ BERNABEI 02D
0.39 ^{+0.17} _{-0.28}	76 ⁷⁶ Ge	0ν	Enriched HPGe	¹⁰¹ KLAPDOR-K... 02D
< 2.1–4.8	90 ¹⁰⁰ Mo	0ν	ELEGANT V	¹⁰² EJIRI 01
< 0.35	90 ⁷⁶ Ge		Enriched HPGe	¹⁰³ KLAPDOR-K... 01
< 23	90 ⁹⁶ Zr		NEMO-2	¹⁰⁴ ARNOLD 99
< 1.1–1.5	¹²⁸ Te		Geochem	¹⁰⁵ BERNATOW... 92
< 5	68 ⁸² Se		TPC	¹⁰⁶ ELLIOTT 92
< 8.3	76 ⁴⁸ Ca	0ν	CaF ₂ scint.	YOU 91

- ⁸⁴ ARGYRIADES 09 limit is based on data taken with the NEMO-3 detector and ¹⁵⁰Nd. A range of nuclear matrix elements that include the effect of nuclear deformation have been used.
- ⁸⁵ Limit was obtained using high resolution TeO₂ bolometer calorimeter to search for double beta decay of ¹³⁰Te. Reported range of limits reflects spread of matrix element calculations used. Supersedes ARNABOLDI 05.
- ⁸⁶ Limit was obtained using CaF₂ scintillation calorimeter to search for double beta decay of ⁴⁸Ca. Reported range of limits reflects spread of QRPA and SM matrix element calculations used. Supersedes OGAWA 04.
- ⁸⁷ ARNOLD 07 use NEMO-3 half life limit for 0ν -decay of ¹⁰⁰Mo to the first excited 0^+ -state of daughter nucleus to obtain neutrino mass limit. The spread reflects the choice of two different nuclear matrix elements. This limit is not competitive when compared to the decay to the ground state.
- ⁸⁸ ARNOLD 07 use NEMO-3 half life limit for 0ν -decay of ¹⁰⁰Mo to the first excited 2^+ -state of daughter nucleus to obtain neutrino mass limit. This limit is not competitive when compared to the decay to the ground state.
- ⁸⁹ Re-analysis of data originally published in KLAPDOR-KLEINGROTHAUS 04A. Modified pulse shape analysis leads the authors to claim 6σ statistical evidence for observation of 0ν -decay. Authors use matrix element of STAUDT 90. Uncertainty of nuclear matrix element is not reflected in stated error. Supersedes KLAPDOR-KLEINGROTHAUS 04A.
- ⁹⁰ Supersedes ARNABOLDI 04. Reported range of limits due to use of different nuclear matrix element calculations.
- ⁹¹ Mass limits reported in ARNOLD 05A are derived from ¹⁰⁰Mo data, obtained by the NEMO-3 collaboration. The range reflects the spread of matrix element calculations considered in this work. Supersedes ARNOLD 04.
- ⁹² Neutrino mass limits based on ⁸²Se data utilizing the NEMO-3 detector. The range reported in ARNOLD 05A reflects the spread of matrix element calculations considered in this work. Supersedes ARNOLD 04.
- ⁹³ Supersedes ARNABOLDI 03. Reported range of limits due to use of different nuclear matrix element calculations.
- ⁹⁴ ARNOLD 04 limit is based on the nuclear matrix elements of SIMKOVIC 99, STOICA 01 and CIVITARESE 03.
- ⁹⁵ Supersedes KLAPDOR-KLEINGROTHAUS 02D. Event excess at $\beta\beta$ -decay energy is used to derive Majorana neutrino mass using the nuclear matrix elements of STAUDT 90. The mass range shown is based on the authors evaluation of the uncertainties of the STAUDT 90 matrix element calculation. If this uncertainty is neglected, and only statistical errors are considered, the range in $\langle m_{\nu} \rangle$ becomes (0.2–0.6) eV at the 3σ level.
- ⁹⁶ Calorimetric CaF₂ scintillator. Range of limits reflects authors' estimate of the uncertainty of the nuclear matrix elements. Replaces YOU 91 as the most stringent limit based on ⁴⁸Ca.
- ⁹⁷ Supersedes ALESSANDRELLO 00. Cryogenic calorimeter search. Reported a range reflecting uncertainty in nuclear matrix element calculations.
- ⁹⁸ Limit for $\langle m_{\nu} \rangle$ is based on the nuclear matrix elements of STAUDT 90 and ARNOLD 96. Supersedes DANEVICH 00.
- ⁹⁹ AALSETH 02B reported range of limits on $\langle m_{\nu} \rangle$ reflects the spread of theoretical nuclear matrix elements. Excludes part of allowed mass range reported in KLAPDOR-KLEINGROTHAUS 01B.
- ¹⁰⁰ BERNABEI 02D limit is based on the matrix elements of SIMKOVIC 02. The range of neutrino masses based on a variety of matrix elements is 1.1–2.9 eV.
- ¹⁰¹ KLAPDOR-KLEINGROTHAUS 02D is a detailed description of the analysis of the data collected by the Heidelberg-Moscow experiment, previously presented in KLAPDOR-KLEINGROTHAUS 01B. Matrix elements in STAUDT 90 have been used. See the footnote in the preceding table for further details. See also KLAPDOR-KLEINGROTHAUS 02B.

See key on page 405

Lepton Particle Listings

Double- β Decay, Neutrino Mixing

- ¹⁰² The range of the reported $\langle m_{\nu} \rangle$ values reflects the spread of the nuclear matrix elements. On axis value assuming $\langle \lambda \rangle = \langle \eta \rangle = 0$.
- ¹⁰³ KLAPDOR-KLEINGROTHAUS 01 uses the calculation by STAUDT 90. Using several other models in the literature could worsen the limit up to 1.2eV. This is the most stringent experimental bound on m_{ν} . It supersedes BAUDIS 99b.
- ¹⁰⁴ ARNOLD 99 limit based on the nuclear matrix elements of STAUDT 90.
- ¹⁰⁵ BERNATOWICZ 92 finds these majorana neutrino mass limits assuming that the measured geochemical decay width is a limit on the 0ν decay width. The range is the range found using matrix elements from HAXTON 84, TOMODA 87, and SUHONEN 91. Further details of the experiment are given in BERNATOWICZ 93.
- ¹⁰⁶ ELLIOTT 92 uses the matrix elements of HAXTON 84.

Limits on Lepton-Number Violating ($V+A$) Current Admixture

For reasons given in the discussion at the beginning of this section, we list only results from 1989 and later. $\langle \lambda \rangle = \lambda \sum U_{ej} V_{ej}$ and $\langle \eta \rangle = \eta \sum U_{ej} V_{ej}$, where the sum is over the number of neutrino generations. This sum vanishes for massless or unmixed neutrinos. In the following Listings, only best or comparable limits or lifetimes for each isotope are reported.

$\langle \lambda \rangle$ (10^{-6})	CL%	$\langle \eta \rangle$ (10^{-8})	CL%	ISOTOPE	METHOD	DOCUMENT ID
<120	90			100Mo	$0^+ \rightarrow 2^+$	107 ARNOLD 07
$0.692^{+0.058}_{-0.056}$	68	$0.305^{+0.026}_{-0.025}$	68	⁷⁶ Ge	Enriched HPGe	108 KLAPDOR-K...06A
< 2.5	90			100Mo	0ν , NEMO-3	109 ARNOLD 05A
< 3.8	90			⁸² Se	0ν , NEMO-3	110 ARNOLD 05A
< 1.5-2.0	90			100Mo	0ν , NEMO-3	111 ARNOLD 04
< 3.2-3.8	90			⁸² Se	0ν , NEMO-3	112 ARNOLD 04
< 1.6-2.4	90	< 0.9-5.3	90	¹³⁰ Te	Cryog. det.	113 ARNABOLDI 03
< 2.2	90	< 2.5	90	¹¹⁶ Cd	¹¹⁶ CdWO ₄ scint.	114 DANEVICH 03
< 3.2-4.7	90	< 2.4-2.7	90	100Mo	ELEGANT V	115 EJIRI 01
< 1.1	90	< 0.64	90	⁷⁶ Ge	Enriched HPGe	116 GUENTHER 97
< 4.4	90	< 2.3	90	¹³⁶ Xe	TPC	117 VUILLEUMIER 93
		< 5.3		¹²⁸ Te	Geochem	118 BERNATOW... 92

- ¹⁰⁷ ARNOLD 07 use NEMO-3 half life limit for 0ν -decay of ¹⁰⁰Mo to the first excited 2^+ -state of daughter nucleus to limit the right-right handed admixture of weak currents $\langle \lambda \rangle$. This limit is not competitive when compared to the decay to the ground state.
- ¹⁰⁸ Re-analysis of data originally published in KLAPDOR-KLEINGROTHAUS 04a. Modified pulse shape analysis leads the authors to claim 6σ statistical evidence for observation of 0ν -decay. Authors use matrix element of MUTO 89 to determine $\langle \lambda \rangle$ and $\langle \eta \rangle$. Uncertainty of nuclear matrix element is not reflected in stated errors.
- ¹⁰⁹ ARNOLD 05a derive limit for $\langle \lambda \rangle$ based on ¹⁰⁰Mo data collected with NEMO-3 detector. No limit for $\langle \eta \rangle$ is given. Supersedes ARNOLD 04.
- ¹¹⁰ ARNOLD 05a derive limit for $\langle \lambda \rangle$ based on ⁸²Se data collected with NEMO-3 detector. No limit for $\langle \eta \rangle$ is given. Supersedes ARNOLD 04.
- ¹¹¹ ARNOLD 04 use the matrix elements of SUHONEN 94 to obtain a limit for $\langle \lambda \rangle$, no limit for $\langle \eta \rangle$ is given. This limit is more stringent than the limit in EJIRI 01 for the same nucleus.
- ¹¹² ARNOLD 04 use the matrix elements of TOMODA 91 and SUHONEN 91 to obtain a limit for $\langle \lambda \rangle$, no limit for $\langle \eta \rangle$ is given.
- ¹¹³ Supersedes ALESSANDRELLO 00. Cryogenic calorimeter search. Reported a range reflecting uncertainty in nuclear matrix element calculations.
- ¹¹⁴ Limits for $\langle \lambda \rangle$ and $\langle \eta \rangle$ are based on nuclear matrix elements of STAUDT 90. Supersedes DANEVICH 00.
- ¹¹⁵ The range of the reported $\langle \lambda \rangle$ and $\langle \eta \rangle$ values reflects the spread of the nuclear matrix elements. On axis value assuming $\langle m_{\nu} \rangle = 0$ and $\langle \lambda \rangle = \langle \eta \rangle = 0$, respectively.
- ¹¹⁶ GUENTHER 97 limits use the matrix elements of STAUDT 90. Supersedes BALYSH 95 and BALYSH 92.
- ¹¹⁷ VUILLEUMIER 93 uses the matrix elements of MUTO 89. Based on a half-life limit 2.6×10^{23} y at 90%CL.
- ¹¹⁸ BERNATOWICZ 92 takes the measured geochemical decay width as a limit on the 0ν width, and uses the SUHONEN 91 coefficients to obtain the least restrictive limit on η . Further details of the experiment are given in BERNATOWICZ 93.

Double- β Decay REFERENCES

ARGYRIADES 09	PR C00 032501R	J. Argyriades et al.	(NEMO-3 Collab.)
BELLI 09a	NP A826 256	P. Belli et al.	
DAWSON 09	PR C00 025502	J.V. Dawson et al.	
HWANG 09	ASP 31 412	M.J. Hwang et al.	
KIDD 09	NP A821 251	M. Kidd et al.	
ARNABOLDI 08	PR C78 035502	C. Arnaboldi et al.	
BELLI 08	PL B658 193	P. Belli et al.	(INFN Gran Sasso)
BELLI 08b	EPJ A36 167	P. Belli et al.	
UMEHARA 08	PR C78 058501	S. Umehara et al.	
ARNOLD 07	NP A781 209	R. Arnold et al.	(NEMO-3 Collab.)
BARABASH 07	NP A785 371	A.S. Barabash et al.	
BARABASH 07b	JPG 34 1721	A.S. Barabash et al.	
BLOXHAM 07	PR C76 025501	T. Bloxham et al.	(COBRA Collab.)
GROMOV 06	PPNL 3 157	K. Gromov et al.	
KLAPDOR-K... 06a	MPL A21 1547	H.V. Klapdor-Kleingrothaus, I.V. Krivosheina	
ARNABOLDI 05	PRL 95 142501	C. Arnaboldi et al.	(CUORICINO Collab.)
ARNOLD 05a	PRL 95 182302	R. Arnold et al.	(NEMO-3 Collab.)
AALSETH 04	PR D70 078302	C.E. Aalseth et al.	
ARNABOLDI 04	PL B584 260	C. Arnaboldi et al.	
ARNOLD 04	JETPL 80 377	R. Arnold et al.	(NEMO3 Detector Collab.)

Translated from ZETFP 80 429.

BARABASH 04	JETPL 79 10	A.S. Barabash et al.
KLAPDOR-K... 04a	PL B586 198	H.V. Klapdor-Kleingrothaus et al.
KLAPDOR-K... 04b	PR D70 078301	H.V. Klapdor-Kleingrothaus, A. Dietz, I.V. Krivosheina
KLAPDOR-K... 04c	NIM A522 371	H.V. Klapdor-Kleingrothaus et al.
OGAWA 04	NP A730 215	I. Ogawa et al.
ARNABOLDI 03	PL B557 167	C. Arnaboldi et al.
CIVITARESE 03	NP A729 867	O. Civitarese, J. Suhonen
DANEVICH 03	PR C68 035501	F.A. Danevich et al.
DOERR 03	NIM A513 596	C. Doerr, H.V. Klapdor-Kleingrothaus
AALSETH 02	MPL A17 1475	C.E. Aalseth et al.
AALSETH 02b	PR D65 092007	C.E. Aalseth et al.
BERNABEI 02D	PL B546 23	R. Bernabei et al.
KLAPDOR-K... 02	hep-ph/0205228	H.V. Klapdor-Kleingrothaus
KLAPDOR-K... 02B	PPNL 110 57	H.V. Klapdor-Kleingrothaus, A. Dietz, I.V. Krivosheina
KLAPDOR-K... 02D	FP 32 1181	H.V. Klapdor-Kleingrothaus, A. Dietz, I.V. Krivosheina
SIMKOVIC 02	hep-ph/0204278	F. Simkovic, P. Domin, A. Faessler
ASHITKOV 01	JETPL 74 529	V.D. Ashitkov et al.

DANEVICH 01	NP A694 375	F.A. Danevich et al.
DEBRAECKEL... 01	PRL 86 3510	L. De Braeckeleer et al.
EJIRI 01	PR C63 065501	H. Ejiri et al.
KLAPDOR-K... 01	EPJ A15 147	H.V. Klapdor-Kleingrothaus et al.
KLAPDOR-K... 01B	MPL A16 2409	H.V. Klapdor-Kleingrothaus et al.
STOICA 01	NP A694 269	S. Stoica, H.V. Klapdor-Kleingrothaus
WIESER 01	PR C64 024308	M.E. Wieser, J.R. De Laeter
ALESSAND... 00	PL B486 13	A. Alessandrello et al.
BRUDANIN 00	PL B495 63	V.B. Brudanin et al.
DANEVICH 00	PR C62 045501	F.A. Danevich et al.
ARNOLD 99	NP A658 299	R. Arnold et al.
BAUDIS 99	PR D59 022001	L. Baudis et al.
BAUDIS 99b	PRL 83 41	L. Baudis et al.
SIMKOVIC 99	PR C60 055502	F. Simkovic et al.
ARNOLD 98	NP A636 209	R. Arnold et al.
ALSTON... 97	PR C55 474	M. Alston-Garnjost et al.
DESILVA 97	PR C56 2451	A. de Silva et al.
GUENTHER 97	PR D55 54	M. Gunther et al.
ARNOLD 96	ZPHY C72 239	R. Arnold et al.
BALYSH 96	PRL 77 5186	A. Balysh et al.
EJIRI 96	NP A611 85	H. Ejiri et al.
TAKAOKA 96	PR C53 1557	N. Takaoka, Y. Motomura, K. Nagao
ARNOLD 95	JETPL 61 170	R.G. Arnold et al.

BALYSH 95	PL B356 450	A. Balysh et al.
BARABASH 95	PL B345 408	A.S. Barabash et al.
DASSIE 95	PR D51 2090	D. Dassie et al.
EJIRI 95	JPS J 64 339	H. Ejiri et al.
KOBAYASHI 95	NP A586 457	M. Kobayashi, M. Kobayashi
SUHONEN 94	PR C49 3055	J. Suhonen, O. Civitarese
ARTEMIEV 93	JETPL 58 262	V.A. Artemiev et al.
BERNATOW... 93	PR C47 806	T. Bernatowicz et al.
KAWASHIMA 93	PR C47 R2452	A. Kawashima, K. Takahashi, A. Masuda
VUILLEUMIER 93	PR D48 1009	J.C. Vuilleumier et al.
BALYSH 92	PL B283 32	A. Balysh et al.
BERNATOW... 92	PRL 69 2341	T. Bernatowicz et al.
BLUM 92	PL B275 506	D. Blum et al.
ELLIOTT 92	PR C46 1535	S.R. Elliott et al.
EJIRI 91	PL B258 17	H. Ejiri et al.
MANUEL 91	JPG 17 S221	O.K. Manuel
SUHONEN 91	NP A535 509	J. Suhonen, S.B. Khadkikar, A. Faessler
TOMODA 91	RPP 54 53	T. Tomoda
TURKEVICH 91	PRL 67 3211	A. Turkevich, T.E. Economou, G.A. Cowan
YOU 91	PL B265 53	K. You et al.
STAUDT 90	EPL 13 31	A. Staudt, K. Muto, H.V. Klapdor-Kleingrothaus
MUTO 89	ZPHY A334 187	K. Muto, E. Bender, H.V. Klapdor
LIN 88	NP A481 477	W.J. Lin et al.
LIN 88b	NP A481 484	W.J. Lin et al.
BOEHM 87	Massive Neutrinos	F. Bohm, P. Vogel
Cambridge Univ. Press, Cambridge		
TOMODA 87	PL B199 475	T. Tomoda, A. Faessler
HAXTON 84	PPNP 12 409	W.C. Haxton, G.J. Stevenson
KIRSTEN 83	PRL 50 474	T. Kirsten, H. Richter, E. Jessberger

Neutrino Mixing

With the exception of the LSND anomaly, current neutrino data can be described within the framework of a 3×3 mixing matrix between the flavor eigenstates ν_e , ν_μ , and ν_τ and the mass eigenstates ν_1 , ν_2 , and ν_3 . (See Eq. (13.77) of the review "Neutrino Mass, Mixing, and Oscillations" by K. Nakamura and S.T. Petcov.) The Listings are divided into the following sections:

(A) **Neutrino fluxes and event ratios:** shows measurements which correspond to various oscillation tests for Accelerator, Reactor, Atmospheric, and Solar neutrino experiments. Typically ratios involve a measurement in a realm sensitive to oscillations compared to one for which no oscillation effect is expected.

(B) **Three neutrino mixing parameters:** shows measurements of $\sin^2(2\theta_{12})$, $\sin^2(2\theta_{23})$, Δm_{21}^2 , Δm_{32}^2 , and limits for $\sin^2(2\theta_{13})$ which are all interpretations of data based on the three neutrino mixing scheme described in the review "Neutrino Mass, Mixing, and Oscillations."

Lepton Particle Listings

Neutrino Mixing

(C) **Other neutrino mixing results:** shows measurements and limits for the probability of oscillation for experiments which might be relevant to the LSND oscillation claim. Included are experiments which are sensitive to $\nu_\mu \rightarrow \nu_e$, $\bar{\nu}_\mu \rightarrow \bar{\nu}_e$, sterile neutrinos, and CPT tests.

(A) Neutrino fluxes and event ratios

Events (observed/expected) from accelerator ν_μ experiments.

Some neutrino oscillation experiments compare the flux in two or more detectors. This is usually quoted as the ratio of the event rate in the far detector to the expected rate based on an extrapolation from the near detector in the absence of oscillations.

VALUE	DOCUMENT ID	TECN	COMMENT
• • • We do not use the following data for averages, fits, limits, etc. • • •			
0.71 ± 0.08	1 AHN	06A	K2K K2K to Super-K
0.64 ± 0.05	2 MICHAEL	06	MINS All charged current events
0.71 ± 0.08 -0.09	3 ALIU	05	K2K KEK to Super-K
0.70 ± 0.10 -0.11	4 AHN	03	K2K KEK to Super-K

¹ Based on the observation of 112 events when $158.1^{+9.2}_{-8.6}$ were expected without oscillations. Including not only the number of events but also the shape of the energy distribution, the evidence for oscillation is at the level of about 4.3 σ . Supersedes ALIU 05.

² This ratio is based on the observation of 215 events compared to an expectation of 336 ± 14 without oscillations. See also ADAMSON 08.

³ This ratio is based on the observation of 107 events at the far detector 250 km away from KEK, and an expectation of 151^{+12}_{-10} .

⁴ This ratio is based on the observation of 56 events with an expectation of $80.1^{+6.2}_{-5.4}$.

Events (observed/expected) from reactor $\bar{\nu}_e$ experiments.

The quoted values are the ratios of the measured reactor $\bar{\nu}_e$ event rate at the quoted distances, and the rate expected without oscillations. The expected rate is based on the experimental data for the most significant reactor fuels (^{235}U , ^{239}Pu , ^{241}Pu) and on calculations for ^{238}U .

VALUE	DOCUMENT ID	TECN	COMMENT
• • • We do not use the following data for averages, fits, limits, etc. • • •			
0.658 ± 0.044 ± 0.047	5 ARAKI	05	KLND Japanese react. ~ 180 km
0.611 ± 0.085 ± 0.041	6 EGUCHI	03	KLND Japanese react. ~ 180 km
1.01 ± 0.024 ± 0.053	7 BOEHM	01	Palo Verde react. 0.75–0.89 km
1.01 ± 0.028 ± 0.027	8 APOLLONIO	99	CHOOZ reactors 1 km
0.987 ± 0.006 ± 0.037	9 GREENWOOD	96	Savannah River, 18.2 m
0.988 ± 0.004 ± 0.05	ACHKAR	95	CNTR Bugey reactor, 15 m
0.994 ± 0.010 ± 0.05	ACHKAR	95	CNTR Bugey reactor, 40 m
0.915 ± 0.132 ± 0.05	ACHKAR	95	CNTR Bugey reactor, 95 m
0.987 ± 0.014 ± 0.027	10 DECLAIS	94	CNTR Bugey reactor, 15 m
0.985 ± 0.018 ± 0.034	KUVSHIN...	91	CNTR Rovno reactor
1.05 ± 0.02 ± 0.05	VUILLEUMIER	82	Gösgen reactor
0.955 ± 0.035 ± 0.110	11 KWON	81	$\bar{\nu}_e p \rightarrow e^+ n$
0.89 ± 0.15	11 BOEHM	80	$\bar{\nu}_e p \rightarrow e^+ n$

⁵ Updated result of KamLAND, including the data used in EGUCHI 03. Note that the survival probabilities for different periods are not directly comparable because the effective baseline varies with power output of the reactor sources involved, and there were large variations in the reactor power production in Japan in 2003.

⁶ EGUCHI 03 observe reactor neutrino disappearance at ~ 180 km baseline to various Japanese nuclear power reactors.

⁷ BOEHM 01 search for neutrino oscillations at 0.75 and 0.89 km distance from the Palo Verde reactors.

⁸ APOLLONIO 99, APOLLONIO 98 search for neutrino oscillations at 1.1 km fixed distance from Chooz reactors. They use $\bar{\nu}_e p \rightarrow e^+ n$ in Gd-loaded scintillator target. APOLLONIO 99 supersedes APOLLONIO 98. See also APOLLONIO 03 for detailed description.

⁹ GREENWOOD 96 search for neutrino oscillations at 18 m and 24 m from the reactor at Savannah River.

¹⁰ DECLAIS 94 result based on integral measurement of neutrons only. Result is ratio of measured cross section to that expected in standard V-A theory. Replaced by ACHKAR 95.

¹¹ KWON 81 represents an analysis of a larger set of data from the same experiment as BOEHM 80.

Atmospheric neutrinos

Neutrinos and antineutrinos produced in the atmosphere induce μ -like and e -like events in underground detectors. The ratio of the numbers of the two kinds of events is defined as μ/e . It has the advantage that systematic effects, such as flux uncertainty, tend to cancel, for both experimental and theoretical values of the ratio. The "ratio of the ratios" of experimental to theoretical μ/e , $R(\mu/e)$, or that of experimental to theoretical μ/total , $R(\mu/\text{total})$ with $\text{total} = \mu + e$, is reported below. If the actual value is

not unity, the value obtained in a given experiment may depend on the experimental conditions. In addition, the measured "up-down asymmetry" for μ ($N_{\text{up}}(\mu)/N_{\text{down}}(\mu)$) or e ($N_{\text{up}}(e)/N_{\text{down}}(e)$) is reported. The expected "up-down asymmetry" is nearly unity if there is no neutrino oscillation.

$R(\mu/e) = (\text{Measured Ratio } \mu/e) / (\text{Expected Ratio } \mu/e)$

VALUE	DOCUMENT ID	TECN	COMMENT
• • • We do not use the following data for averages, fits, limits, etc. • • •			
0.658 ± 0.016 ± 0.035	12 ASHIE	05	SKAM sub-GeV
0.702 ± 0.032 -0.036 ± 0.101	13 ASHIE	05	SKAM multi-GeV
0.69 ± 0.10 ± 0.06	14 SANCHEZ	03	SOU2 Calorimeter raw data
	15 FUKUDA	96B	KAMI Water Cherenkov
	16 DAUM	95	FREJ Calorimeter
1.00 ± 0.15 ± 0.08	17 FUKUDA	94	KAMI sub-GeV
0.60 ± 0.06 -0.05 ± 0.05	18 FUKUDA	94	KAMI multi-GeV
0.57 ± 0.08 -0.07 ± 0.07	19 BECKER-SZ...	92B	IMB Water Cherenkov

¹² ASHIE 05 results are based on an exposure of 92 kton yr during the complete Super-Kamiokande I running period. The analyzed data sample consists of fully-contained single-ring e -like events with $0.1 \text{ GeV}/c < p_e$ and μ -like events $0.2 \text{ GeV}/c < p_\mu$, both having a visible energy $< 1.33 \text{ GeV}$. These criteria match the definition used by FUKUDA 94.

¹³ ASHIE 05 results are based on an exposure of 92 kton yr during the complete Super-Kamiokande I running period. The analyzed data sample consists of fully-contained single-ring events with visible energy $> 1.33 \text{ GeV}$ and partially-contained events. All partially-contained events are classified as μ -like.

¹⁴ SANCHEZ 03 result is based on an exposure of 5.9 kton yr, and updates ALLISON 99 result. The analyzed data sample consists of fully-contained e -flavor and μ -flavor events having lepton momentum $> 0.3 \text{ GeV}/c$.

¹⁵ FUKUDA 96B studied neutron background in the atmospheric neutrino sample observed in the Kamiokande detector. No evidence for the background contamination was found.

¹⁶ DAUM 95 results are based on an exposure of 2.0 kton yr which includes the data used by BERGER 90B. This ratio is for the contained and semicontained events. DAUM 95 also report $R(\mu/e) = 0.99 \pm 0.13 \pm 0.08$ for the total neutrino induced data sample which includes upward going stopping muons and horizontal muons in addition to the contained and semicontained events.

¹⁷ FUKUDA 94 result is based on an exposure of 7.7 kton yr and updates the HIRATA 92 result. The analyzed data sample consists of fully-contained e -like events with $0.1 < p_e < 1.33 \text{ GeV}/c$ and fully-contained μ -like events with $0.2 < p_\mu < 1.5 \text{ GeV}/c$.

¹⁸ FUKUDA 94 result is based on the data sample consisting of fully contained events with visible energy $> 1.33 \text{ GeV}$ and partially contained μ -like events.

¹⁹ BECKER-SZENDY 92B reports the fraction of nonshowing events (mostly muons from atmospheric neutrinos) as $0.36 \pm 0.02 \pm 0.02$, as compared with expected fraction $0.51 \pm 0.01 \pm 0.05$. After cutting the energy range to the Kamiokande limits, BEIER 92 finds $R(\mu/e)$ very close to the Kamiokande value.

$R(\nu_\mu) = (\text{Measured Flux of } \nu_\mu) / (\text{Expected Flux of } \nu_\mu)$

VALUE	DOCUMENT ID	TECN	COMMENT
• • • We do not use the following data for averages, fits, limits, etc. • • •			
0.84 ± 0.12	20 ADAMSON	06	MINS MINOS atmospheric
0.72 ± 0.026 ± 0.13	21 AMBROSIO	01	MCRO upward through-going
0.57 ± 0.05 ± 0.15	22 AMBROSIO	00	MCRO upgoing partially contained
0.71 ± 0.05 ± 0.19	23 AMBROSIO	00	MCRO downgoing partially contained + upgoing stopping
0.74 ± 0.036 ± 0.046	24 AMBROSIO	98	MCRO Streamer tubes
	25 CASPER	91	IMB Water Cherenkov
	26 AGLIETTA	89	NUSX
0.95 ± 0.22	27 BOLIEV	81	Baksan
0.62 ± 0.17	CROUCH	78	Case Western/UCI

²⁰ ADAMSON 06 uses a measurement of 107 total neutrinos compared to an expected rate of 127 ± 13 without oscillations.

²¹ AMBROSIO 01 result is based on the upward through-going muon tracks with $E_\mu > 1 \text{ GeV}$. The data came from three different detector configurations, but the statistics is largely dominated by the full detector run, from May 1994 to December 2000. The total live time, normalized to the full detector configuration, is 6.17 years. The first error is the statistical error, the second is the systematic error, dominated by the theoretical error in the predicted flux.

²² AMBROSIO 00 result is based on the upgoing partially contained event sample. It came from 4.1 live years of data taking with the full detector, from April 1994 to February 1999. The average energy of atmospheric muon neutrinos corresponding to this sample is 4 GeV. The first error is statistical, the second is the systematic error, dominated by the 25% theoretical error in the rate (20% in the flux and 15% in the cross section, added in quadrature). Within statistics, the observed deficit is uniform over the zenith angle.

²³ AMBROSIO 00 result is based on the combined samples of downgoing partially contained events and upgoing stopping events. These two subsamples could not be distinguished due to the lack of timing information. The result came from 4.1 live years of data taking with the full detector, from April 1994 to February 1999. The average energy of atmospheric muon neutrinos corresponding to this sample is 4 GeV. The first error is statistical, the second is the systematic error, dominated by the 25% theoretical error in the rate (20% in the flux and 15% in the cross section, added in quadrature). Within statistics, the observed deficit is uniform over the zenith angle.

²⁴ AMBROSIO 98 result is for all nadir angles and updates AHLEN 95 result. The lower cutoff on the muon energy is 1 GeV. In addition to the statistical and systematic errors,

See key on page 405

Lepton Particle Listings

Neutrino Mixing

there is a Monte Carlo flux error (theoretical error) of ± 0.13 . With a neutrino oscillation hypothesis, the fit either to the flux or zenith distribution independently yields $\sin^2 2\theta = 1.0$ and $\Delta(m^2) \sim$ a few times 10^{-3} eV^2 . However, the fit to the observed zenith distribution gives a maximum probability for χ^2 of only 5% for the best oscillation hypothesis.

²⁵ CASPER 91 correlates showering/nonshowering signature of single-ring events with parent atmospheric-neutrino flavor. They find nonshowering ($\approx \nu_\mu$ induced) fraction is $0.41 \pm 0.03 \pm 0.02$, as compared with expected 0.51 ± 0.05 (syst).

²⁶ AGLIETTA 89 finds no evidence for any anomaly in the neutrino flux. They define $\rho = (\text{measured number of } \nu_e\text{'s})/(\text{measured number of } \nu_\mu\text{'s})$. They report $\rho(\text{measured}) = \rho(\text{expected}) = 0.96^{+0.32}_{-0.28}$.

²⁷ From this data BOLIEV 81 obtain the limit $\Delta(m^2) \leq 6 \times 10^{-3} \text{ eV}^2$ for maximal mixing, $\nu_\mu \leftrightarrow \nu_\mu$ type oscillation.

$R(\mu/\text{total}) = (\text{Measured Ratio } \mu/\text{total}) / (\text{Expected Ratio } \mu/\text{total})$

VALUE	DOCUMENT ID	TECN	COMMENT
-------	-------------	------	---------

• • • We do not use the following data for averages, fits, limits, etc. • • •

$1.1^{+0.07}_{-0.12} \pm 0.11$	²⁸ CLARK	97	IMB multi-GeV
--------------------------------	---------------------	----	---------------

²⁸ CLARK 97 obtained this result by an analysis of fully contained and partially contained events in the IMB water-Cherenkov detector with visible energy $> 0.95 \text{ GeV}$.

$N_{\text{up}}(\mu)/N_{\text{down}}(\mu)$

VALUE	DOCUMENT ID	TECN	COMMENT
-------	-------------	------	---------

• • • We do not use the following data for averages, fits, limits, etc. • • •

$0.551^{+0.035}_{-0.033} \pm 0.004$	²⁹ ASHIE	05	SKAM multi-GeV
-------------------------------------	---------------------	----	----------------

²⁹ ASHIE 05 results are based on an exposure of 92 kton yr during the complete Super-Kamiokande I running period. The analyzed data sample consists of fully-contained single-ring μ -like events with visible energy $> 1.33 \text{ GeV}$ and partially-contained events. All partially-contained events are classified as μ -like. Upward-going events are those with $-1 < \cos(\text{zenith angle}) < -0.2$ and downward-going events are those with $0.2 < \cos(\text{zenith angle}) < 1$. The μ -like up-down ratio for the multi-GeV data deviates from 1 (the expectation for no atmospheric ν_μ oscillations) by more than 12 standard deviations.

$N_{\text{up}}(e)/N_{\text{down}}(e)$

VALUE	DOCUMENT ID	TECN	COMMENT
-------	-------------	------	---------

• • • We do not use the following data for averages, fits, limits, etc. • • •

$0.961^{+0.086}_{-0.079} \pm 0.016$	³⁰ ASHIE	05	SKAM multi-GeV
-------------------------------------	---------------------	----	----------------

³⁰ ASHIE 05 results are based on an exposure of 92 kton yr during the complete Super-Kamiokande I running period. The analyzed data sample consists of fully-contained single-ring e -like events with visible energy $> 1.33 \text{ GeV}$. Upward-going events are those with $-1 < \cos(\text{zenith angle}) < -0.2$ and downward-going events are those with $0.2 < \cos(\text{zenith angle}) < 1$. The e -like up-down ratio for the multi-GeV data is consistent with 1 (the expectation for no atmospheric ν_e oscillations).

$R(\text{up/down}; \mu) = (\text{Measured up/down}; \mu) / (\text{Expected up/down}; \mu)$

VALUE	DOCUMENT ID	TECN	COMMENT
-------	-------------	------	---------

• • • We do not use the following data for averages, fits, limits, etc. • • •

$0.62^{+0.19}_{-0.14} \pm 0.02$	³¹ ADAMSON	06	MINS atmospheric ν with far detector
---------------------------------	-----------------------	----	--

³¹ ADAMSON 06 result is obtained with the MINOS far detector with an exposure of 4.54 kton yr. The expected ratio is calculated with no neutrino oscillation.

$R(\mu^+/\mu^-) = (\text{Measured } N(\mu^+)/N(\mu^-)) / (\text{Expected } N(\mu^+)/N(\mu^-))$

VALUE	DOCUMENT ID	TECN	COMMENT
-------	-------------	------	---------

• • • We do not use the following data for averages, fits, limits, etc. • • •

$1.39^{+0.35}_{-0.46} \pm 0.14$	³² ADAMSON	07	MINS Upward and horizontal μ with far detector
---------------------------------	-----------------------	----	--

$0.96^{+0.38}_{-0.27} \pm 0.15$	³³ ADAMSON	06	MINS atmospheric ν with far detector
---------------------------------	-----------------------	----	--

³² ADAMSON 07 result is obtained with the MINOS far detector in 854.24 live days, based on neutrino-induced upward-going and horizontal muons. This result is consistent with $CP T$ conservation.

³³ ADAMSON 06 result is obtained with the MINOS far detector with an exposure of 4.54 kton yr, based on contained events. The expected ratio is calculated by assuming the same oscillation parameters for neutrinos and antineutrinos.

Solar neutrinos

Solar neutrinos are produced by thermonuclear fusion reactions in the Sun. Radiochemical experiments measure particular combinations of fluxes from various neutrino-producing reactions, whereas water-Cherenkov experiments mainly measure a flux of neutrinos from decay of ${}^8\text{B}$. Solar neutrino fluxes are composed of all active neutrino species, ν_e , ν_μ , and ν_τ . In addition, some other mechanisms may cause antineutrino components in solar neutrino fluxes. Each measurement method is sensitive to a particular component or a combination of components of solar neutrino fluxes. For details, see Section 13.4 of Reviews, Tables, and Plots.

ν_e Capture Rates from Radiochemical Experiments

1 SNU (Solar Neutrino Unit) = 10^{-36} captures per atom per second.

VALUE (SNU)	DOCUMENT ID	TECN	COMMENT
-------------	-------------	------	---------

• • • We do not use the following data for averages, fits, limits, etc. • • •

$65.4^{+3.1}_{-3.0} +2.6_{-2.8}$	³⁴ ABDURASHI...	09	SAGE ${}^{71}\text{Ga} \rightarrow {}^{71}\text{Ge}$
----------------------------------	----------------------------	----	--

$62.9^{+5.5}_{-5.3} \pm 2.5$	³⁵ ALTMANN	05	GNO ${}^{71}\text{Ga} \rightarrow {}^{71}\text{Ge}$
------------------------------	-----------------------	----	---

$69.3 \pm 4.1 \pm 3.6$	³⁶ ALTMANN	05	GNO + GALX combined
------------------------	-----------------------	----	---------------------

$77.5 \pm 6.2^{+4.3}_{-4.7}$	³⁷ HAMPEL	99	GALX ${}^{71}\text{Ga} \rightarrow {}^{71}\text{Ge}$
------------------------------	----------------------	----	--

$2.56 \pm 0.16 \pm 0.16$	³⁸ CLEVELAND	98	HOME ${}^{37}\text{Cl} \rightarrow {}^{37}\text{Ar}$
--------------------------	-------------------------	----	--

³⁴ ABDURASHITOV 09 reports a combined analysis of 168 extractions of the SAGE solar neutrino experiment during the period January 1990 through December 2007, and updates the ABDURASHITOV 02 result. The data are consistent with the assumption that the solar neutrino production rate is constant in time. Note that a $\sim 15\%$ systematic uncertainty in the overall normalization may be added to the ABDURASHITOV 09 result, because calibration experiments for gallium solar neutrino measurements using intense ${}^{51}\text{Cr}$ (twice by GALLEX and once by SAGE) and ${}^{37}\text{Ar}$ (by SAGE) result in an average ratio of 0.87 ± 0.05 of the observed to calculated rates.

³⁵ ALTMANN 05 reports the complete result from the GNO solar neutrino experiment (GNO I+II+III), which is the successor project of GALLEX. Experimental technique of GNO is essentially the same as that of GALLEX. The run data cover the period 20 May 1998 through 9 April 2003.

³⁶ Combined result of GALLEX I+II+III+IV (HAMPEL 99) and GNO I+II+III.

³⁷ HAMPEL 99 report the combined result for GALLEX I+II+III+IV (65 runs in total), which update the HAMPEL 96 result. The GALLEX IV result (12 runs) is $118.4 \pm 17.8 \pm 6.6$ SNU. (HAMPEL 99 discuss the consistency of partial results with the mean.) The GALLEX experimental program has been completed with these runs. The total run data cover the period 14 May 1991 through 23 January 1997. A total of 300 ${}^{71}\text{Ge}$ events were observed. Note that a $\sim 15\%$ systematic uncertainty in the overall normalization may be added to the HAMPEL 99 result, because calibration experiments for gallium solar neutrino measurements using intense ${}^{51}\text{Cr}$ (twice by GALLEX and once by SAGE) and ${}^{37}\text{Ar}$ (by SAGE) result in an average ratio of 0.87 ± 0.05 of the observed to calculated rates.

³⁸ CLEVELAND 98 is a detailed report of the ${}^{37}\text{Cl}$ experiment at the Homestake Mine. The average solar neutrino-induced ${}^{37}\text{Ar}$ production rate from 108 runs between 1970 and 1994 updates the DAVIS 89 result.

$\phi_{\text{ES}}({}^8\text{B})$

${}^8\text{B}$ solar-neutrino flux measured via νe elastic scattering. This process is sensitive to all active neutrino flavors, but with reduced sensitivity to ν_μ , ν_τ due to the cross-section difference, $\sigma(\nu_{\mu,\tau} e) \sim 0.16\sigma(\nu_e e)$. If the ${}^8\text{B}$ solar-neutrino flux involves nonelectron flavor active neutrinos, their contribution to the flux is ~ 0.16 times of ν_e .

VALUE ($10^6 \text{ cm}^{-2} \text{ s}^{-1}$)	DOCUMENT ID	TECN	COMMENT
---	-------------	------	---------

• • • We do not use the following data for averages, fits, limits, etc. • • •

$1.77^{+0.24}_{-0.21} +0.09_{-0.10}$	³⁹ AHARMIM	08	SNO Phase III
--------------------------------------	-----------------------	----	---------------

$2.38 \pm 0.05^{+0.16}_{-0.15}$	⁴⁰ CRAVENS	08	SKAM average flux
---------------------------------	-----------------------	----	-------------------

$2.35 \pm 0.02 \pm 0.08$	⁴¹ HOSAKA	06	SKAM average flux
--------------------------	----------------------	----	-------------------

$2.35 \pm 0.22 \pm 0.15$	⁴² AHARMIM	05A	SNO Salty D_2O ; ${}^8\text{B}$ shape not constrained
--------------------------	-----------------------	-----	---

$2.34 \pm 0.23^{+0.15}_{-0.14}$	⁴² AHARMIM	05A	SNO Salty D_2O ; ${}^8\text{B}$ shape constrained
---------------------------------	-----------------------	-----	---

$2.39^{+0.24}_{-0.23} \pm 0.12$	⁴³ AHMAD	02	SNO average flux
---------------------------------	---------------------	----	------------------

$2.39 \pm 0.34^{+0.16}_{-0.14}$	⁴⁴ AHMAD	01	SNO average flux
---------------------------------	---------------------	----	------------------

$2.80 \pm 0.19 \pm 0.33$	⁴⁵ FUKUDA	96	KAMI average flux
--------------------------	----------------------	----	-------------------

2.70 ± 0.27	⁴⁹ FUKUDA	96	KAMI day flux
-----------------	----------------------	----	---------------

$2.87^{+0.27}_{-0.26}$	⁴⁵ FUKUDA	96	KAMI night flux
------------------------	----------------------	----	-----------------

³⁹ AHARMIM 08 reports the results from SNO Phase III measurement using an array of ${}^3\text{He}$ proportional counters to measure the rate of NC interactions in heavy water, over the period between November 27, 2004 and November 28, 2006, corresponding to 385.17 live days. A simultaneous fit was made for the number of NC events detected by the proportional counters and the numbers of NC, CC, and ES events detected by the PMTs, where the spectral distributions of the ES and CC events were not constrained to the ${}^8\text{B}$ shape.

⁴⁰ CRAVENS 08 reports the Super-Kamiokande-II results for 791 live days from December 2002 to October 2005. The photocathode coverage of the detector is 19% (reduced from 40% of that of Super-Kamiokande-I due to an accident in 2001). The analysis threshold for the average flux is 7 MeV.

⁴¹ HOSAKA 06 reports the final results for 1496 live days with Super-Kamiokande-I between May 31, 1996 and July 15, 2001, and replace FUKUDA 02 results. The analysis threshold is 5 MeV except for the first 280 live days (6.5 MeV).

⁴² AHARMIM 05A measurements were made with dissolved NaCl (0.195% by weight) in heavy water over the period between July 26, 2001 and August 28, 2003, corresponding to 391.4 live days, and update AHMED 04A. The CC, ES, and NC events were statistically separated. In one method, the ${}^8\text{B}$ energy spectrum was not constrained. In the other method, the constraint of an undistorted ${}^8\text{B}$ energy spectrum was added for comparison with AHMAD 02 results.

⁴³ AHMAD 02 reports the ${}^8\text{B}$ solar-neutrino flux measured via νe elastic scattering above the kinetic energy threshold of 5 MeV. The data correspond to 306.4 live days with SNO between November 2, 1999 and May 28, 2001, and updates AHMAD 01 results.

Lepton Particle Listings

Neutrino Mixing

⁴⁴AHMAD 01 reports the ⁸B solar-neutrino flux measured via νe elastic scattering above the kinetic energy threshold of 6.75 MeV. The data correspond to 241 live days with SNO between November 2, 1999 and January 15, 2001.

⁴⁵FUKUDA 96 results are for a total of 2079 live days with Kamiokande II and III from January 1987 through February 1995, covering the entire solar cycle 22, with threshold $E_e > 9.3$ MeV (first 449 days), > 7.5 MeV (middle 794 days), and > 7.0 MeV (last 836 days). These results update the HIRATA 90 result for the average ⁸B solar-neutrino flux and HIRATA 91 result for the day-night variation in the ⁸B solar-neutrino flux. The total data sample was also analyzed for short-term variations: within experimental errors, no strong correlation of the solar-neutrino flux with the sunspot numbers was found.

ϕ_{CC} (⁸B)

⁸B solar-neutrino flux measured with charged-current reaction which is sensitive exclusively to ν_e .

VALUE ($10^6 \text{ cm}^{-2}\text{s}^{-1}$)	DOCUMENT ID	TECN	COMMENT
---	-------------	------	---------

• • • We do not use the following data for averages, fits, limits, etc. • • •

$1.67 \pm 0.05 \pm 0.07$ $-0.04 - 0.08$	46 AHARMIM	08	SNO Phase III
$1.68 \pm 0.06 \pm 0.08$ -0.09	47 AHARMIM	05A	SNO Salty D ₂ O; ⁸ B shape not const.
$1.72 \pm 0.05 \pm 0.11$	47 AHARMIM	05A	SNO Salty D ₂ O; ⁸ B shape constrained
$1.76 \pm 0.06 \pm 0.09$ -0.05	48 AHMAD	02	SNO average flux
$1.75 \pm 0.07 \pm 0.12 \pm 0.05$ -0.11	49 AHMAD	01	SNO average flux

⁴⁶AHARMIM 08 reports the results from SNO Phase III measurement using an array of ³He proportional counters to measure the rate of NC interactions in heavy water, over the period between November 27, 2004 and November 28, 2006, corresponding to 385.17 live days. A simultaneous fit was made for the number of NC events detected by the proportional counters and the numbers of NC, CC, and ES events detected by the PMTs, where the spectral distributions of the ES and CC events were not constrained to the ⁸B shape.

⁴⁷AHARMIM 05A measurements were made with dissolved NaCl (0.195% by weight) in heavy water over the period between July 26, 2001 and August 28, 2003, corresponding to 391.4 live days, and update AHMED 04A. The CC, ES, and NC events were statistically separated. In one method, the ⁸B energy spectrum was not constrained. In the other method, the constraint of an undistorted ⁸B energy spectrum was added for comparison with AHMAD 02 results.

⁴⁸AHMAD 02 reports the SNO result of the ⁸B solar-neutrino flux measured with charged-current reaction on deuterium, $\nu_e d \rightarrow ppe^-$, above the kinetic energy threshold of 5 MeV. The data correspond to 306.4 live days with SNO between November 2, 1999 and May 28, 2001, and updates AHMAD 01 results. The complete description of the SNO Phase I data set is given in AHARMIM 07.

⁴⁹AHMAD 01 reports the first SNO result of the ⁸B solar-neutrino flux measured with the charged-current reaction on deuterium, $\nu_e d \rightarrow ppe^-$, above the kinetic energy threshold of 6.75 MeV. The data correspond to 241 live days with SNO between November 2, 1999 and January 15, 2001.

ϕ_{NC} (⁸B)

⁸B solar neutrino flux measured with neutral-current reaction, which is equally sensitive to ν_e , ν_μ , and ν_τ .

VALUE ($10^6 \text{ cm}^{-2}\text{s}^{-1}$)	DOCUMENT ID	TECN	COMMENT
---	-------------	------	---------

• • • We do not use the following data for averages, fits, limits, etc. • • •

$5.54 \pm 0.33 \pm 0.36$ $-0.31 - 0.34$	50 AHARMIM	08	SNO Phase III, prop. counter + PMT
$4.94 \pm 0.21 \pm 0.38$ -0.34	51 AHARMIM	05A	SNO Salty D ₂ O; ⁸ B shape not const.
$4.81 \pm 0.19 \pm 0.28$ -0.27	51 AHARMIM	05A	SNO Salty D ₂ O; ⁸ B shape constrained
$5.09 \pm 0.44 \pm 0.46$ $-0.43 - 0.43$	52 AHMAD	02	SNO average flux; ⁸ B shape const.
$6.42 \pm 1.57 \pm 0.55$ -0.58	52 AHMAD	02	SNO average flux; ⁸ B shape not const.

⁵⁰AHARMIM 08 reports the results from SNO Phase III measurement using an array of ³He proportional counters to measure the rate of NC interactions in heavy water, over the period between November 27, 2004 and November 28, 2006, corresponding to 385.17 live days. A simultaneous fit was made for the number of NC events detected by the proportional counters and the numbers of NC, CC, and ES events detected by the PMTs, where the spectral distributions of the ES and CC events were not constrained to the ⁸B shape.

⁵¹AHARMIM 05A measurements were made with dissolved NaCl (0.195% by weight) in heavy water over the period between July 26, 2001 and August 28, 2003, corresponding to 391.4 live days, and update AHMED 04A. The CC, ES, and NC events were statistically separated. In one method, the ⁸B energy spectrum was not constrained. In the other method, the constraint of an undistorted ⁸B energy spectrum was added for comparison with AHMAD 02 results.

⁵²AHMAD 02 reports the first SNO result of the ⁸B solar-neutrino flux measured with the neutral-current reaction on deuterium, $\nu_e d \rightarrow np\nu_e$, above the neutral-current reaction threshold of 2.2 MeV. The data correspond to 306.4 live days with SNO between November 2, 1999 and May 28, 2001. The complete description of the SNO Phase I data set is given in AHARMIM 07.

$\phi_{\nu_\mu + \nu_\tau}$ (⁸B)

Nonelectron-flavor active neutrino component (ν_μ and ν_τ) in the ⁸B solar-neutrino flux.

VALUE ($10^6 \text{ cm}^{-2}\text{s}^{-1}$)	DOCUMENT ID	TECN	COMMENT
---	-------------	------	---------

• • • We do not use the following data for averages, fits, limits, etc. • • •

$3.26 \pm 0.25 \pm 0.40$ -0.35	53 AHARMIM	05A	SNO From ϕ_{NC} , ϕ_{CC} , and ϕ_{ES} ; ⁸ B shape not const.
$3.09 \pm 0.22 \pm 0.30$ -0.27	53 AHARMIM	05A	SNO From ϕ_{NC} , ϕ_{CC} , and ϕ_{ES} ; ⁸ B shape constrained
$3.41 \pm 0.45 \pm 0.48$ -0.45	54 AHMAD	02	SNO From ϕ_{NC} , ϕ_{CC} , and ϕ_{ES}
3.69 ± 1.13	55 AHMAD	01	Derived from SNO+SuperKam, water Cherenkov

⁵³AHARMIM 05A measurements were made with dissolved NaCl (0.195% by weight) in heavy water over the period between July 26, 2001 and August 28, 2003, corresponding to 391.4 live days, and update AHMED 04A. The CC, ES, and NC events were statistically separated. In one method, the ⁸B energy spectrum was not constrained. In the other method, the constraint of an undistorted ⁸B energy spectrum was added for comparison with AHMAD 02 results.

⁵⁴AHMAD 02 deduced the nonelectron-flavor active neutrino component (ν_μ and ν_τ) in the ⁸B solar-neutrino flux, by combining the charged-current result, the νe elastic-scattering result and the neutral-current result. The complete description of the SNO Phase I data set is given in AHARMIM 07.

⁵⁵AHMAD 01 deduced the nonelectron-flavor active neutrino component (ν_μ and ν_τ) in the ⁸B solar-neutrino flux, by combining the SNO charged-current result (AHMAD 01) and the Super-Kamiokande νe elastic-scattering result (FUKUDA 01).

Total Flux of Active ⁸B Solar Neutrinos

Total flux of active neutrinos (ν_e , ν_μ , and ν_τ).

VALUE ($10^6 \text{ cm}^{-2}\text{s}^{-1}$)	DOCUMENT ID	TECN	COMMENT
---	-------------	------	---------

• • • We do not use the following data for averages, fits, limits, etc. • • •

$5.54 \pm 0.33 \pm 0.36$ $-0.31 - 0.34$	56 AHARMIM	08	SNO ϕ_{NC} in Phase III
$4.94 \pm 0.21 \pm 0.38$ -0.34	57 AHARMIM	05A	SNO From ϕ_{NC} ; ⁸ B shape not const.
$4.81 \pm 0.19 \pm 0.28$ -0.27	57 AHARMIM	05A	SNO From ϕ_{NC} ; ⁸ B shape constrained
$5.09 \pm 0.44 \pm 0.46$ $-0.43 - 0.43$	58 AHMAD	02	SNO Direct measurement from ϕ_{NC}
5.44 ± 0.99	59 AHMAD	01	Derived from SNO+SuperKam, water Cherenkov

⁵⁶AHARMIM 08 reports the results from SNO Phase III measurement using an array of ³He proportional counters to measure the rate of NC interactions in heavy water, over the period between November 27, 2004 and November 28, 2006, corresponding to 385.17 live days. A simultaneous fit was made for the number of NC events detected by the proportional counters and the numbers of NC, CC, and ES events detected by the PMTs, where the spectral distributions of the ES and CC events were not constrained to the ⁸B shape.

⁵⁷AHARMIM 05A measurements were made with dissolved NaCl (0.195% by weight) in heavy water over the period between July 26, 2001 and August 28, 2003, corresponding to 391.4 live days, and update AHMED 04A. The CC, ES, and NC events were statistically separated. In one method, the ⁸B energy spectrum was not constrained. In the other method, the constraint of an undistorted ⁸B energy spectrum was added for comparison with AHMAD 02 results.

⁵⁸AHMAD 02 determined the total flux of active ⁸B solar neutrinos by directly measuring the neutral-current reaction, $\nu_e d \rightarrow np\nu_e$, which is equally sensitive to ν_e , ν_μ , and ν_τ . The complete description of the SNO Phase I data set is given in AHARMIM 07.

⁵⁹AHMAD 01 deduced the total flux of active ⁸B solar neutrinos by combining the SNO charged-current result (AHMAD 01) and the Super-Kamiokande νe elastic-scattering result (FUKUDA 01).

Day-Night Asymmetry (⁸B)

$A = (\phi_{\text{night}} - \phi_{\text{day}}) / \phi_{\text{average}}$

VALUE	DOCUMENT ID	TECN	COMMENT
-------	-------------	------	---------

• • • We do not use the following data for averages, fits, limits, etc. • • •

$0.063 \pm 0.042 \pm 0.037$	60 CRAVENS	08	SKAM Based on ϕ_{ES}
$0.021 \pm 0.020 \pm 0.012$ -0.013	61 HOSAKA	06	SKAM Based on ϕ_{ES}
$0.017 \pm 0.016 \pm 0.012$ -0.013	62 HOSAKA	06	SKAM Fitted in the LMA region
$-0.056 \pm 0.074 \pm 0.053$	63 AHARMIM	05A	SNO From salty SNO ϕ_{CC}
$-0.037 \pm 0.063 \pm 0.032$	63 AHARMIM	05A	SNO From salty SNO ϕ_{CC} ; const. of no ϕ_{NC} asymmetry
$0.14 \pm 0.063 \pm 0.015$ -0.014	64 AHMAD	02B	SNO Derived from SNO ϕ_{CC}
$0.07 \pm 0.049 \pm 0.013$ -0.012	65 AHMAD	02B	SNO Const. of no ϕ_{NC} asymmetry

⁶⁰CRAVENS 08 reports the Super-Kamiokande-II results for 791 live days from December 2002 to October 2005. The photocathode coverage of the detector is 19% (reduced from 40% of that of Super-Kamiokande-I due to an accident in 2001). The analysis threshold for the day and night fluxes is 7.5 MeV.

⁶¹ HOSAKA 06 reports the final results for 1496 live days with Super-Kamiokande-I between May 31, 1996 and July 15, 2001, and replace FUKUDA 02 results. The analysis threshold is 5 MeV except for the first 280 live days (6.5 MeV).

⁶² This result with reduced statistical uncertainty is obtained by assuming two-neutrino oscillations within the LMA (large mixing angle) region and by fitting the time variation of the solar neutrino flux measured via ν_e elastic scattering to the variations expected from neutrino oscillations. For details, see SMY 04. There is an additional small systematic error of ± 0.0004 coming from uncertainty of oscillation parameters.

⁶³ AHARMIM 05A measurements were made with dissolved NaCl (0.195% by weight) in heavy water over the period between July 26, 2001 and August 28, 2003, with 176.5 days of the live time recorded during the day and 214.9 days during the night. This result is obtained with the spectral distribution of the CC events not constrained to the ^8B shape.

⁶⁴ AHMAD 02b results are based on the charged-current interactions recorded between November 2, 1999 and May 28, 2001, with the day and night live times of 128.5 and 177.9 days, respectively. The complete description of the SNO Phase I data set is given in AHARMIM 07.

⁶⁵ AHMAD 02b results are derived from the charged-current interactions, neutral-current interactions, and νe elastic scattering, with the total flux of active neutrinos constrained to have no asymmetry. The data were recorded between November 2, 1999 and May 28, 2001, with the day and night live times of 128.5 and 177.9 days, respectively. The complete description of the SNO Phase I data set is given in AHARMIM 07.

$\phi_{\text{ES}} (^7\text{Be})$

^7Be solar-neutrino flux measured via ν_e elastic scattering. This process is sensitive to all active neutrino flavors, but with reduced sensitivity to ν_μ, ν_τ due to the cross-section difference, $\sigma(\nu_{\mu,\tau}e) \sim 0.2 \sigma(\nu_e e)$. If the ^7Be solar-neutrino flux involves nonelectron flavor active neutrinos, their contribution to the flux is ~ 0.2 times that of ν_e .

VALUE ($10^9 \text{ cm}^{-2} \text{ s}^{-1}$)	DOCUMENT ID	TECN
---	-------------	------

• • • We do not use the following data for averages, fits, limits, etc. • • •

3.36 ± 0.34	⁶⁶ ARPESELLA 08A	BORX
-------------	-----------------------------	------

⁶⁶ ARPESELLA 08A reports the 0.862 MeV ^7Be solar-neutrino flux measured via ν elastic scattering. The data correspond to 192 live days with BOREXINO (41.3 ton-yr fiducial exposure) between May 16, 2007 and April 12, 2008. The measured flux is calculated from the ratio of the measured rate to the rate expected from the non-oscillated solar ν in the high metallicity SSM PENA-GARAY 09.

$\phi_{\text{CC}} (pp)$

pp solar-neutrino flux measured with charged-current reaction which is sensitive exclusively to ν_e .

VALUE ($10^{10} \text{ cm}^{-2} \text{ s}^{-1}$)	DOCUMENT ID	TECN	COMMENT
--	-------------	------	---------

• • • We do not use the following data for averages, fits, limits, etc. • • •

3.38 ± 0.47	⁶⁷ ABDURASHI... 09	FIT	Fit existing solar- ν data
-------------	-------------------------------	-----	--------------------------------

⁶⁷ ABDURASHITOV 09 reports the pp solar-neutrino flux derived from the Ga solar neutrino capture rate by subtracting contributions from $^8\text{B}, ^7\text{Be}, pep$ and CNO solar neutrino fluxes determined by other solar neutrino experiments as well as neutrino oscillation parameters determined from available world neutrino oscillation data.

$\phi_{\text{ES}} (\text{hep})$

hep solar-neutrino flux measured via νe elastic scattering. This process is sensitive to all active neutrino flavors, but with reduced sensitivity to ν_μ, ν_τ due to the cross-section difference, $\sigma(\nu_{\mu,\tau}e) \sim 0.16 \sigma(\nu_e e)$. If the hep solar-neutrino flux involves nonelectron flavor active neutrinos, their contribution to the flux is ~ 0.16 times of ν_e .

VALUE ($10^3 \text{ cm}^{-2} \text{ s}^{-1}$)	CL%	DOCUMENT ID	TECN
---	-----	-------------	------

• • • We do not use the following data for averages, fits, limits, etc. • • •

<73	90	⁶⁸ HOSAKA 06	SKAM
-----	----	-------------------------	------

⁶⁸ HOSAKA 06 result is obtained from the recoil electron energy window of 18–21 MeV, and updates FUKUDA 01 result.

$\phi_{\overline{\nu}_e} (^8\text{B})$

Searches are made for electron antineutrino flux from the Sun. Flux limits listed here are derived relative to the BS05(OP) Standard Solar Model ^8B solar neutrino flux, with an assumption that solar $\overline{\nu}_e$ s follow an unoscillated ^8B neutrino spectrum.

VALUE (%)	CL%	DOCUMENT ID	TECN	COMMENT
-----------	-----	-------------	------	---------

• • • We do not use the following data for averages, fits, limits, etc. • • •

<1.9	90	⁶⁹ BALATA 06	CNTR	$1.8 < E_{\overline{\nu}_e} < 20.0 \text{ MeV}$
<0.72	90	AHARMIM 04	SNO	$4.0 < E_{\overline{\nu}_e} < 14.8 \text{ MeV}$
<0.025	90	EGUCHI 04	KLND	$8.3 < E_{\overline{\nu}_e} < 14.8 \text{ MeV}$
<0.7	90	GANDO 03	SKAM	$8.0 < E_{\overline{\nu}_e} < 20.0 \text{ MeV}$
<1.7	90	AGLIETTA 96	LSD	$7 < E_{\overline{\nu}_e} < 17 \text{ MeV}$

⁶⁹ BALATA 06 obtained this result from the search for $\overline{\nu}_e$ interactions with Counting Test Facility (the prototype of the Borexino detector).

(B) Three-neutrino mixing parameters

INTRODUCTION TO THREE-NEUTRINO MIXING PARAMETERS LISTINGS

Updated April 2010 by M. Goodman (ANL).

Introduction and Notation:

With the exception of the LSND anomaly, current accelerator, reactor, solar and atmospheric neutrino data can be described within the framework of a 3×3 mixing matrix between the flavor eigenstates ν_e, ν_μ and ν_τ and mass eigenstates ν_1, ν_2 and ν_3 . (See equation 13.77 of the review “Neutrino Mass, Mixing and Oscillations” by K. Nakamura and S.T. Petcov.) Whether or not this is the ultimately correct framework, it is currently widely used to parametrize neutrino mixing data and to plan new experiments.

The mass differences are called $\Delta m_{21}^2 \equiv m_2^2 - m_1^2$ and $\Delta m_{32}^2 \equiv m_3^2 - m_2^2$. In these listings, we assume

$$\Delta m_{32}^2 \sim \Delta m_{31}^2 \quad (1)$$

although in the future, experiments may be precise enough to measure these separately. The angle are labeled θ_{12}, θ_{23} and θ_{13} . The CP violating phase is called δ , but that does not yet appear in the listings. The familiar two neutrino form for oscillations is

$$P(\nu_a \rightarrow \nu_b) = \sin^2(2\theta) \sin^2(\Delta m^2 L/4E). \quad (2)$$

Despite the fact that the mixing angles have been measured to be much larger than in the quark sector, the two neutrino form is often a very good approximation and is used in many situations.

The angles appear in the equations below in many forms. They most often appear as $\sin^2(2\theta)$. The listings currently use this convention.

Accelerator neutrino experiments:

Ignoring the small Δm_{21}^2 scale, CP violation, and matter effects, the equations for the probability of appearance in an accelerator oscillation experiment are:

$$P(\nu_\mu \rightarrow \nu_\tau) = \sin^2(2\theta_{23}) \cos^4(\theta_{13}) \sin^2(\Delta m_{32}^2 L/4E) \quad (3)$$

$$P(\nu_\mu \rightarrow \nu_e) = \sin^2(2\theta_{13}) \sin^2(\theta_{23}) \sin^2(\Delta m_{32}^2 L/4E) \quad (4)$$

$$P(\nu_e \rightarrow \nu_\mu) = \sin^2(2\theta_{13}) \sin^2(\theta_{23}) \sin^2(\Delta m_{32}^2 L/4E) \quad (5)$$

$$P(\nu_e \rightarrow \nu_\tau) = \sin^2(2\theta_{13}) \cos^2(\theta_{23}) \sin^2(\Delta m_{32}^2 L/4E) \quad (6)$$

For the case of negligible θ_{13} , these probabilities vanish except for $P(\nu_\mu \rightarrow \nu_\tau)$, which then takes the familiar two-neutrino form.

New long-baseline experiments are being planned to search for non-zero θ_{13} through $P(\nu_\mu \rightarrow \nu_e)$. Including the CP violating terms and low mass scale, the equation for neutrino

Lepton Particle Listings

Neutrino Mixing

oscillation in vacuum is:

$$\begin{aligned}
 P(\nu_\mu \rightarrow \nu_e) &= P1 + P2 + P3 + P4 \\
 P1 &= \sin^2(\theta_{23}) \sin^2(2\theta_{13}) \sin^2(\Delta m_{32}^2 L/4E) \\
 P2 &= \cos^2(\theta_{23}) \sin^2(2\theta_{13}) \sin^2(\Delta m_{21}^2 L/4E) \\
 P3 &= -/+ J \sin(\delta) \sin(\Delta m_{32}^2 L/4E) \\
 P4 &= J \cos(\delta) \cos(\Delta m_{32}^2 L/4E)
 \end{aligned} \tag{7}$$

where

$$\begin{aligned}
 J &= \cos(\theta_{13}) \sin(2\theta_{12}) \sin(2\theta_{13}) \sin(2\theta_{23}) \times \\
 &\quad \sin(\Delta m_{32}^2 L/4E) \sin(\Delta m_{21}^2 L/4E)
 \end{aligned} \tag{8}$$

and the sign in P3 is negative for neutrinos and positive for anti-neutrinos. For most new proposed long-baseline accelerator experiments, P2 can safely be neglected, but depending on the values of θ_{13} and δ , the other three terms could be comparable. Also, depending on the distance and the mass hierarchy, matter effects will need to be included.

Reactor neutrino experiments:

Nuclear reactors are prolific sources of $\bar{\nu}_e$ with an energy near 4 MeV. The oscillation probability can be expressed

$$\begin{aligned}
 P(\bar{\nu}_e \rightarrow \bar{\nu}_e) &= 1 - \cos^4(\theta_{13}) \sin^2(2\theta_{12}) \sin^2(\Delta m_{21}^2 L/4E) \\
 &\quad - \cos^2(\theta_{12}) \sin^2(2\theta_{13}) \sin^2(\Delta m_{31}^2 L/4E) \\
 &\quad - \sin^2(\theta_{12}) \sin^2(2\theta_{13}) \sin^2(\Delta m_{32}^2 L/4E)
 \end{aligned} \tag{9}$$

not using the approximation in Eq. (1). For short distances ($L < 5$ km) we can ignore the second term on the right and can reimpose approximation Eq. (1). This takes the familiar two neutrino form with θ_{13} and Δm_{32}^2 :

$$P(\bar{\nu}_e \rightarrow \bar{\nu}_e) = 1 - \sin^2(2\theta_{13}) \sin^2(\Delta m_{32}^2 L/4E). \tag{10}$$

For long distances and small θ_{13} , the last two terms in Eq. (9) oscillate rapidly and average to zero for an experiment with finite energy resolution, leading to the familiar two neutrino form but with θ_{12} and Δm_{21}^2 .

Solar and Atmospheric neutrino experiments:

Solar neutrino experiments are sensitive to ν_e disappearance and have allowed the measurement of θ_{12} and Δm_{21}^2 . They are also sensitive to θ_{13} . We identify $\Delta m_{\odot}^2 = \Delta m_{21}^2$ and $\theta_{\odot} = \theta_{12}$.

Atmospheric neutrino experiments are primarily sensitive to ν_μ disappearance through $\nu_\mu \rightarrow \nu_\tau$ oscillations, and have allowed the measurement of θ_{23} and Δm_{32}^2 . We identify $\Delta m_A^2 = \Delta m_{32}^2$ and $\theta_A = \theta_{23}$. Despite the large ν_e component of the atmospheric neutrino flux, it is difficult to measure Δm_{21}^2 effects. This is because of a cancellation between $\nu_\mu \rightarrow \nu_e$ and $\nu_e \rightarrow \nu_\mu$ together with the fact that the ratio of ν_μ and ν_e atmospheric fluxes, which arise from sequential π and μ decay, is near 2.

Oscillation Parameter Listings:

In Section (B) we encode the three mixing angles θ_{12} , θ_{23} , θ_{13} and two mass squared differences Δm_{21}^2 and Δm_{32}^2 . Our

knowledge of θ_{12} and Δm_{21}^2 comes from the KamLAND reactor neutrino experiment together with solar neutrino experiments. Our knowledge of θ_{23} and Δm_{32}^2 comes from atmospheric neutrino experiments and long-baseline accelerator experiments. Searches for a non-zero value of θ_{13} are proceeding at reactor experiments looking for $\bar{\nu}_e$ disappearance and at long-baseline accelerator experiments looking for ν_e appearance. The interpretation of both kinds of results depends on Δm_{32}^2 , and the accelerator results also depend on the mass hierarchy, θ_{23} and the CP violating phase δ . We present 90%CL limit on θ_{13} at the current best fit value of Δm_{32}^2 , but that limit is asymmetric around that best fit value. There is a 50% chance that the upper limit is higher. A true 90%CL upper limit cannot be calculated without a global fit (we note that the union of two Confidence Levels is not a Confidence Level). A more conservative approach would be to quote the reactor 90% CL at the one sigma low value for Δm_{32}^2 and that is done in the footnote when possible.

$\sin^2(2\theta_{12})$

VALUE	DOCUMENT ID	TECN	COMMENT
0.87±0.03	⁷⁰ AHARMIM	08	FIT KamLAND + global solar
•••	We do not use the following data for averages, fits, limits, etc. •••		
0.92±0.05	⁷¹ ABE	08A	FIT KamLAND
0.87±0.04	⁷² ABE	08A	FIT KamLAND + global fit
0.85 ^{+0.04} _{-0.06}	⁷³ HOSAKA	06	FIT KamLAND + global solar
0.85 ^{+0.06} _{-0.05}	⁷⁴ HOSAKA	06	FIT SKAM+SNO+KamLAND
0.86 ^{+0.05} _{-0.07}	⁷⁵ HOSAKA	06	FIT SKAM+SNO
0.86 ^{+0.03} _{-0.04}	⁷⁶ AHARMIM	05A	FIT KamLAND + global solar
0.75-0.95	⁷⁷ AHARMIM	05A	FIT global solar
0.82±0.05	⁷⁸ ARAKI	05	FIT KamLAND + global solar
0.82±0.04	⁷⁹ AHMED	04A	FIT KamLAND + global solar
0.71-0.93	⁸⁰ AHMED	04A	FIT global solar
0.85 ^{+0.05} _{-0.07}	⁸¹ SMY	04	FIT KamLAND + global solar
0.83 ^{+0.06} _{-0.08}	⁸² SMY	04	FIT global solar
0.87 ^{+0.07} _{-0.08}	⁸³ SMY	04	FIT SKAM + SNO
0.62-0.88	⁸⁴ AHMAD	02B	FIT global solar
0.62-0.95	⁸⁵ FUKUDA	02	FIT global solar

⁷⁰The result given by AHARMIM 08 is $\theta = (34.4^{+1.3}_{-1.2})^\circ$. This result is obtained by a two-neutrino oscillation analysis using solar neutrino data including those of Borexino (ARPESELLA 08A) and Super-Kamiokande-I (HOSAKA 06), and KamLAND data (ABE 08A). *CPT* invariance is assumed.

⁷¹ABE 08A obtained this result by a rate + shape + time combined geoneutrino and reactor two-neutrino fit for Δm_{21}^2 and $\tan^2\theta_{12}$, using KamLAND data only.

⁷²ABE 08A obtained this result by means of a two-neutrino fit using KamLAND, Homestake, SAGE, GALLEX, GNO, SK (zenith angle and E-spectrum), the SNO χ^2 -map, and solar flux data. *CPT* invariance is assumed.

⁷³HOSAKA 06 obtained this result by a two-neutrino oscillation analysis using SK ν_e data, CC data from other solar neutrino experiments, and KamLAND data (ARAKI 05). *CPT* invariance is assumed.

⁷⁴HOSAKA 06 obtained this result by a two-neutrino oscillation analysis using the data from Super-Kamiokande, SNO (AHMAD 02 and AHMAD 02B), and KamLAND (ARAKI 05) experiments. *CPT* invariance is assumed.

⁷⁵HOSAKA 06 obtained this result by a two-neutrino oscillation analysis using the Super-Kamiokande and SNO (AHMAD 02 and AHMAD 02B) solar neutrino data.

⁷⁶The result given by AHARMIM 05A is $\theta = (33.9 \pm 1.6)^\circ$. This result is obtained by a two-neutrino oscillation analysis using SNO pure deuterium and salt phase data, SK ν_e data, Cl and Ga CC data, and KamLAND data (ARAKI 05). *CPT* invariance is assumed. AHARMIM 05A also quotes $\theta = (33.9^{+2.4}_{-2.2})^\circ$ as the error enveloping the 68% CL two-dimensional region. This translates into $\sin^2 2\theta = 0.86^{+0.05}_{-0.06}$.

⁷⁷AHARMIM 05A obtained this result by a two-neutrino oscillation analysis using the data from all solar neutrino experiments. The listed range of the parameter envelops the 95% CL two-dimensional region shown in figure 35a of AHARMIM 05A. AHARMIM 05A also quotes $\tan^2\theta = 0.45^{+0.09}_{-0.08}$ as the error enveloping the 68% CL two-dimensional region. This translates into $\sin^2 2\theta = 0.86^{+0.05}_{-0.07}$.

⁷⁸ARAKI 05 obtained this result by a two-neutrino oscillation analysis using KamLAND and solar neutrino data. *CPT* invariance is assumed. The 1σ error shown here is translated

Lepton Particle Listings

Neutrino Mixing

See key on page 405

from the number provided by the KamLAND collaboration, $\tan^2\theta = 0.40^{+0.07}_{-0.05}$. The corresponding number quoted in ARAKI 05 is $\tan^2\theta = 0.40^{+0.10}_{-0.07}$ ($\sin^2 2\theta = 0.82 \pm 0.07$), which envelops the 68% CL two-dimensional region.

⁷⁹The result given by AHMED 04A is $\theta = (32.5^{+1.7}_{-1.6})^\circ$. This result is obtained by a two-neutrino oscillation analysis using solar neutrino and KamLAND data (EGUCHI 03). *CPT* invariance is assumed. AHMED 04A also quotes $\theta = (32.5^{+2.4}_{-2.3})^\circ$ as the error enveloping the 68% CL two-dimensional region. This translates into $\sin^2 2\theta = 0.82 \pm 0.06$.

⁸⁰AHMED 04A obtained this result by a two-neutrino oscillation analysis using the data from all solar neutrino experiments. The listed range of the parameter envelops the 95% CL two-dimensional region shown in Fig. 5(a) of AHMED 04A. The best-fit point is $\Delta(m^2) = 6.5 \times 10^{-5} \text{ eV}^2$, $\tan^2\theta = 0.40$ ($\sin^2 2\theta = 0.82$).

⁸¹The result given by SMY 04 is $\tan^2\theta = 0.44 \pm 0.08$. This result is obtained by a two-neutrino oscillation analysis using solar neutrino and KamLAND data (ANNI 03). *CPT* invariance is assumed.

⁸²SMY 04 obtained this result by a two-neutrino oscillation analysis using the data from all solar neutrino experiments. The 1σ errors are read from Fig. 6(a) of SMY 04.

⁸³SMY 04 obtained this result by a two-neutrino oscillation analysis using the Super-Kamiokande and SNO (AHMAD 02 and AHMAD 02b) solar neutrino data. The 1σ errors are read from Fig. 6(a) of SMY 04.

⁸⁴AHMAD 02b obtained this result by a two-neutrino oscillation analysis using the data from all solar neutrino experiments. The listed range of the parameter envelops the 95% CL two-dimensional region shown in Fig. 4(b) of AHMAD 02b. The best fit point is $\Delta(m^2) = 5.0 \times 10^{-5} \text{ eV}^2$ and $\tan\theta = 0.34$ ($\sin^2 2\theta = 0.76$).

⁸⁵FUKUDA 02 obtained this result by a two-neutrino oscillation analysis using the data from all solar neutrino experiments. The listed range of the parameter envelops the 95% CL two-dimensional region shown in Fig. 4 of FUKUDA 02. The best fit point is $\Delta(m^2) = 6.9 \times 10^{-5} \text{ eV}^2$ and $\tan^2\theta = 0.38$ ($\sin^2 2\theta = 0.80$).

Δm_{21}^2

VALUE (10^{-5} eV^2)	DOCUMENT ID	TECN	COMMENT
$7.59^{+0.19}_{-0.21}$	86 AHARMIM	08 FIT	KamLAND + global solar

• • • We do not use the following data for averages, fits, limits, etc. • • •

$7.58^{+0.14}_{-0.13} \pm 0.15$	87 ABE	08A FIT	KamLAND
7.59 ± 0.21	88 ABE	08A FIT	KamLAND + global solar
8.0 ± 0.3	89 HOSAKA	06 FIT	KamLAND + global solar
8.0 ± 0.3	90 HOSAKA	06 FIT	SKAM+SNO+KamLAND
$6.3^{+3.7}_{-1.5}$	91 HOSAKA	06 FIT	SKAM+SNO
5-12	92 HOSAKA	06 FIT	SKAM day/night in the LMA region
$8.0^{+0.4}_{-0.3}$	93 AHARMIM	05A FIT	KamLAND + global solar LMA
3.3-14.4	94 AHARMIM	05A FIT	global solar
$7.9^{+0.4}_{-0.3}$	95 ARAKI	05 FIT	KamLAND + global solar
$7.1^{+1.0}_{-0.3}$	96 AHMED	04A FIT	KamLAND + global solar
3.2-13.7	97 AHMED	04A FIT	global solar
$7.1^{+0.6}_{-0.5}$	98 SMY	04 FIT	KamLAND + global solar
$6.0^{+1.7}_{-1.6}$	99 SMY	04 FIT	global solar
$6.0^{+2.5}_{-1.6}$	100 SMY	04 FIT	SKAM + SNO
2.8-12.0	101 AHMAD	02B FIT	global solar
3.2-19.1	102 FUKUDA	02 FIT	global solar

⁸⁶AHARMIM 08 obtained this result by a two-neutrino oscillation analysis using all solar neutrino data including those of Borexino (ARPESELLA 08a) and Super-Kamiokande-I (HOSAKA 06), and KamLAND data (ABE 08a). *CPT* invariance is assumed.

⁸⁷ABE 08a obtained this result by a rate + shape + time combined geoneutrino and reactor two-neutrino fit for Δm_{21}^2 and $\tan^2\theta_{12}$, using KamLAND data only.

⁸⁸ABE 08a obtained this result by means of a two-neutrino fit using KamLAND, Homestake, SAGE, GALLEX, GNO, SK (zenith angle and E-spectrum), the SNO χ^2 -map, and solar flux data. *CPT* invariance is assumed.

⁸⁹HOSAKA 06 obtained this result by a two-neutrino oscillation analysis using solar neutrino and KamLAND data (ARAKI 05). *CPT* invariance is assumed.

⁹⁰HOSAKA 06 obtained this result by a two-neutrino oscillation analysis using the data from Super-Kamiokande, SNO (AHMAD 02 and AHMAD 02b), and KamLAND (ARAKI 05) experiments. *CPT* invariance is assumed.

⁹¹HOSAKA 06 obtained this result by a two-neutrino oscillation analysis using the Super-Kamiokande and SNO (AHMAD 02 and AHMAD 02b) solar neutrino data.

⁹²HOSAKA 06 obtained this result from the consistency between the observed and expected day-night flux asymmetry amplitude. The listed 68% CL range is derived from the 1σ boundary of the amplitude fit to the data. Oscillation parameters are constrained to be in the LMA region. The mixing angle is fixed at $\tan^2\theta = 0.44$ because the fit depends only very weakly on it.

⁹³AHARMIM 05a obtained this result by a two-neutrino oscillation analysis using solar neutrino and KamLAND data (ARAKI 05). *CPT* invariance is assumed. AHARMIM 05a also quotes $\Delta(m^2) = (8.0^{+0.6}_{-0.4}) \times 10^{-5} \text{ eV}^2$ as the error enveloping the 68% CL two-dimensional region.

⁹⁴AHARMIM 05a obtained this result by a two-neutrino oscillation analysis using the data from all solar neutrino experiments. The listed range of the parameter envelops the 95% CL two-dimensional region shown in figure 35a of AHARMIM 05a. AHARMIM 05a

also quotes $\Delta(m^2) = (6.5^{+4.4}_{-2.3}) \times 10^{-5} \text{ eV}^2$ as the error enveloping the 68% CL two-dimensional region.

⁹⁵ARAKI 05 obtained this result by a two-neutrino oscillation analysis using KamLAND and solar neutrino data. *CPT* invariance is assumed. The 1σ error shown here is provided by the KamLAND collaboration. The error quoted in ARAKI 05, $\Delta(m^2) = (7.9^{+0.6}_{-0.5}) \times 10^{-5}$, envelops the 68% CL two-dimensional region.

⁹⁶AHMED 04A obtained this result by a two-neutrino oscillation analysis using solar neutrino and KamLAND data (EGUCHI 03). *CPT* invariance is assumed. AHMED 04A also quotes $\Delta(m^2) = (7.1^{+1.2}_{-0.6}) \times 10^{-5} \text{ eV}^2$ as the error enveloping the 68% CL two-dimensional region.

⁹⁷AHMED 04A obtained this result by a two-neutrino oscillation analysis using the data from all solar neutrino experiments. The listed range of the parameter envelops the 95% CL two-dimensional region shown in Fig. 5(a) of AHMED 04A. The best-fit point is $\Delta(m^2) = 6.5 \times 10^{-5} \text{ eV}^2$, $\tan^2\theta = 0.40$ ($\sin^2 2\theta = 0.82$).

⁹⁸SMY 04 obtained this result by a two-neutrino oscillation analysis using solar neutrino and KamLAND data (ANNI 03). *CPT* invariance is assumed.

⁹⁹SMY 04 obtained this result by a two-neutrino oscillation analysis using the data from all solar neutrino experiments. The 1σ errors are read from Fig. 6(a) of SMY 04.

¹⁰⁰SMY 04 obtained this result by a two-neutrino oscillation analysis using the Super-Kamiokande and SNO (AHMAD 02 and AHMAD 02b) solar neutrino data. The 1σ errors are read from Fig. 6(a) of SMY 04.

¹⁰¹AHMAD 02b obtained this result by a two-neutrino oscillation analysis using the data from all solar neutrino experiments. The listed range of the parameter envelops the 95% CL two-dimensional region shown in Fig. 4(b) of AHMAD 02b. The best fit point is $\Delta(m^2) = 5.0 \times 10^{-5} \text{ eV}^2$ and $\tan\theta = 0.34$ ($\sin^2 2\theta = 0.76$).

¹⁰²FUKUDA 02 obtained this result by a two-neutrino oscillation analysis using the data from all solar neutrino experiments. The listed range of the parameter envelops the 95% CL two-dimensional region shown in Fig. 4 of FUKUDA 02. The best fit point is $\Delta(m^2) = 6.9 \times 10^{-5} \text{ eV}^2$ and $\tan^2\theta = 0.38$ ($\sin^2 2\theta = 0.80$).

$\sin^2(2\theta_{23})$

The ranges below correspond to the projection onto the $\sin^2(2\theta_{23})$ axis of the 90% CL contours in the $\sin^2(2\theta_{23}) - \Delta m_{32}^2$ plane presented by the authors.

VALUE	DOCUMENT ID	TECN	COMMENT
>0.92	103 ASHIE	05 SKAM	Super-Kamiokande

• • • We do not use the following data for averages, fits, limits, etc. • • •

>0.85	ADAMSON	08A MINS	MINOS
>0.2	104 ADAMSON	06 MINS	atmospheric ν with far detector
>0.59	105 AHN	06A K2K	KEK to Super-K
>0.91	106 HOSAKA	06A SKAM	3ν oscillation; normal mass hierarchy
>0.86	107 HOSAKA	06A SKAM	3ν oscillation; inverted mass hierarchy
>0.7	108 MICHAEL	06 MINS	MINOS
>0.58	109 ALIU	05 K2K	KEK to Super-K
>0.6	110 ALLISON	05 SOU2	
>0.80	111 AMBROSIO	04 MCRO	MACRO
>0.90	112 ASHIE	04 SKAM	L/E distribution
>0.30	113 AHN	03 K2K	KEK to Super-K
>0.45	114 AMBROSIO	03 MCRO	MACRO
>0.77	115 AMBROSIO	03 MCRO	MACRO
>0.50	116 SANCHEZ	03 SOU2	Soudan-2 Atmospheric
>0.80	117 AMBROSIO	01 MCRO	upward μ
>0.82	118 AMBROSIO	01 MCRO	upward μ
>0.45	119 FUKUDA	99c	SKAM upward μ
>0.70	120 FUKUDA	99d	SKAM upward μ
>0.30	121 FUKUDA	99d	SKAM stop μ / through
>0.82	122 FUKUDA	98c	SKAM Super-Kamiokande
>0.30	123 HATAKEYA MA98	KAMI	Kamiokande
>0.73	124 HATAKEYA MA98	KAMI	Kamiokande
>0.65	125 FUKUDA	94 KAMI	Kamiokande

¹⁰³ASHIE 05 obtained this result by a two-neutrino oscillation analysis using 92 kton yr atmospheric neutrino data from the complete Super-Kamiokande I running period.

¹⁰⁴ADAMSON 06 obtained this result by a two-neutrino oscillation analysis of the L/E distribution using 4.54 kton yr atmospheric neutrino data with the MINOS far detector.

¹⁰⁵Supercedes ALIU 05.

¹⁰⁶HOSAKA 06a obtained this result ($\sin^2\theta_{23} = 0.37-0.65$) by a three-neutrino oscillation analysis with one mass scale dominance ($\Delta m_{21}^2 = 0$) using the Super-Kamiokande-I atmospheric neutrino data. The normal mass hierarchy is assumed.

¹⁰⁷HOSAKA 06a obtained this result ($\sin^2\theta_{23} = 0.37-0.69$) by a three-neutrino oscillation analysis with one mass scale dominance ($\Delta m_{21}^2 = 0$) using the Super-Kamiokande-I atmospheric neutrino data. The inverted mass hierarchy is assumed.

¹⁰⁸MICHAEL 06 best fit is for maximal mixing. See also ADAMSON 08.

¹⁰⁹The best fit is for maximal mixing.

¹¹⁰ALLISON 05 result is based upon atmospheric neutrino interactions including upward-stopping muons, with an exposure of 5.9 kton yr. From a two-flavor oscillation analysis the best-fit point is $\Delta m^2 = 0.0017 \text{ eV}^2$ and $\sin^2(2\theta) = 0.97$.

¹¹¹AMBROSIO 04 obtained this result, without using the absolute normalization of the neutrino flux, by combining the angular distribution of upward through-going muon tracks with $E_\mu > 1 \text{ GeV}$, N_{low} and N_{high} , and the numbers of InDown + UpStop and InUp events. Here, N_{low} and N_{high} are the number of events with reconstructed neutrino energies $< 30 \text{ GeV}$ and $> 130 \text{ GeV}$, respectively. InDown and InUp represent events with downward and upward-going tracks starting inside the detector due to neutrino

Lepton Particle Listings

Neutrino Mixing

- interactions, while UpStop represents entering upward-going tracks which stop in the detector. The best fit is for maximal mixing.
- 112 ASHIE 04 obtained this result from the $L(\text{flight length})/E(\text{estimated neutrino energy})$ distribution of ν_μ disappearance probability, using the Super-Kamiokande-I 1489 live-day atmospheric neutrino data.
- 113 There are several islands of allowed region from this K2K analysis, extending to high values of Δm^2 . We only include the one that overlaps atmospheric neutrino analyses. The best fit is for maximal mixing.
- 114 AMBROSIO 03 obtained this result on the basis of the ratio $R = N_{\text{low}}/N_{\text{high}}$, where N_{low} and N_{high} are the number of upward through-going muon events with reconstructed neutrino energy < 30 GeV and > 130 GeV, respectively. The data came from the full detector run started in 1994. The method of FELDMAN 98 is used to obtain the limits.
- 115 AMBROSIO 03 obtained this result by using the ratio R and the angular distribution of the upward through-going muons. R is given in the previous note and the angular distribution is reported in AMBROSIO 01. The method of FELDMAN 98 is used to obtain the limits. The best fit is to maximal mixing.
- 116 SANCHEZ 03 is based on an exposure of 5.9 kton yr. The result is obtained using a likelihood analysis of the neutrino L/E distribution for a selection μ flavor sample while the e -flavor sample provides flux normalization. The method of FELDMAN 98 is used to obtain the allowed region. The best fit is $\sin^2(2\theta) = 0.97$.
- 117 AMBROSIO 01 result is based on the angular distribution of upward through-going muon tracks with $E_\mu > 1$ GeV. The data came from three different detector configurations, but the statistics is largely dominated by the full detector run, from May 1994 to December 2000. The total live time, normalized to the full detector configuration is 6.17 years. The best fit is obtained outside the physical region. The method of FELDMAN 98 is used to obtain the limits. The best fit is for maximal mixing.
- 118 AMBROSIO 01 result is based on the angular distribution and normalization of upward through-going muon tracks with $E_\mu > 1$ GeV. See the previous footnote.
- 119 FUKUDA 99c obtained this result from a total of 537 live days of upward through-going muon data in Super-Kamiokande between April 1996 to January 1998. With a threshold of $E_\mu > 1.6$ GeV, the observed flux is $(1.74 \pm 0.07 \pm 0.02) \times 10^{-13} \text{ cm}^{-2}\text{s}^{-1}\text{sr}^{-1}$. The best fit is $\sin^2(2\theta) = 0.95$.
- 120 FUKUDA 99d obtained this result from a simultaneous fitting to zenith angle distributions of upward-stopping and through-going muons. The flux of upward-stopping muons of minimum energy of 1.6 GeV measured between April 1996 and January 1998 is $(0.39 \pm 0.04 \pm 0.02) \times 10^{-13} \text{ cm}^{-2}\text{s}^{-1}\text{sr}^{-1}$. This is compared to the expected flux of $(0.73 \pm 0.16 \text{ (theoretical error)}) \times 10^{-13} \text{ cm}^{-2}\text{s}^{-1}\text{sr}^{-1}$. The best fit is to maximal mixing.
- 121 FUKUDA 99d obtained this result from the zenith dependence of the upward-stopping/through-going flux ratio. The best fit is to maximal mixing.
- 122 FUKUDA 98c obtained this result by an analysis of 33.0 kton yr atmospheric neutrino data. The best fit is for maximal mixing.
- 123 HATAKEYAMA 98 obtained this result from a total of 2456 live days of upward-going muon data in Kamiokande between December 1985 and May 1995. With a threshold of $E_\mu > 1.6$ GeV, the observed flux of upward through-going muons is $(1.94 \pm 0.10^{+0.07}_{-0.06}) \times 10^{-13} \text{ cm}^{-2}\text{s}^{-1}\text{sr}^{-1}$. This is compared to the expected flux of $(2.46 \pm 0.54 \text{ (theoretical error)}) \times 10^{-13} \text{ cm}^{-2}\text{s}^{-1}\text{sr}^{-1}$. The best fit is for maximal mixing.
- 124 HATAKEYAMA 98 obtained this result from a combined analysis of Kamiokande contained events (FUKUDA 94) and upward going muon events. The best fit is $\sin^2(2\theta) = 0.95$.
- 125 FUKUDA 94 obtained the result by a combined analysis of sub- and multi-GeV atmospheric neutrino events in Kamiokande. The best fit is for maximal mixing.

Δm_{32}^2

The sign of Δm_{32}^2 is not known at this time. Only the absolute value is quoted below. Unless otherwise specified, the ranges below correspond to the projection onto the Δm_{32}^2 axis of the 90% CL contours in the $\sin^2(2\theta_{23}) - \Delta m_{32}^2$ plane presented by the authors.

VALUE (10^{-3} eV^2)	CL%	DOCUMENT ID	TECN	COMMENT
2.43 ± 0.13	68	ADAMSON	08A	MINS MINOS
• • • We do not use the following data for averages, fits, limits, etc. • • •				
0.07–5.0		126 ADAMSON	06	MINS atmospheric ν with far detector
1.9–4.0		127,128 AHN	06A	K2K KEK to Super-K
1.8–3.1		129 HOSAKA	06A	SKAM 3ν oscillation; normal mass hierarchy
1.8–3.7		130 HOSAKA	06A	SKAM 3ν oscillation; inverted mass hierarchy
2.2–3.8		131 MICHAEL	06	MINS MINOS
1.9–3.6		127 ALIU	05	K2K KEK to Super-K
0.3–1.2		132 ALLISON	05	SOU2
1.5–3.4		133 ASHIE	05	SKAM atmospheric neutrino
0.6–8.0		134 AMBROSIO	04	MCRO MACRO
1.9 to 3.0		135 ASHIE	04	SKAM L/E distribution
1.5–3.9		136 AHN	03	K2K KEK to Super-K
0.25–9.0		137 AMBROSIO	03	MCRO MACRO
0.6–7.0		138 AMBROSIO	03	MCRO MACRO
0.15–15		139 SANCHEZ	03	SOU2 Soudan-2 Atmospheric
0.6–15		140 AMBROSIO	01	MCRO upward μ
1.0–6.0		141 AMBROSIO	01	MCRO upward μ
1.0–5.0		142 FUKUDA	99C	SKAM upward μ
1.5–15.0		143 FUKUDA	99D	SKAM upward μ
0.7–18		144 FUKUDA	99D	SKAM stop μ / through

- 0.5–6.0 145 FUKUDA 98c SKAM Super-Kamiokande
- 0.55–5.0 146 HATAKEYAMA 98 KAMI Kamiokande
- 4–23 147 HATAKEYAMA 98 KAMI Kamiokande
- 5–25 148 FUKUDA 94 KAMI Kamiokande
- 126 ADAMSON 06 obtained this result by a two-neutrino oscillation analysis of the L/E distribution using 4.54 kton yr atmospheric neutrino data with the MINOS far detector.
- 127 The best fit in the physical region is for $\Delta m^2 = 2.8 \times 10^{-3} \text{ eV}^2$.
- 128 Supercedes ALIU 05.
- 129 HOSAKA 06A obtained this result by a three-neutrino oscillation analysis with one mass scale dominance ($\Delta m_{21}^2 = 0$) using the Super-Kamiokande-I atmospheric neutrino data. The normal mass hierarchy is assumed.
- 130 HOSAKA 06A obtained this result by a three-neutrino oscillation analysis with one mass scale dominance ($\Delta m_{21}^2 = 0$) using the Super-Kamiokande-I atmospheric neutrino data. The inverted mass hierarchy is assumed.
- 131 MICHAEL 06 best fit is $2.74 \times 10^{-3} \text{ eV}^2$. See also ADAMSON 08.
- 132 ALLISON 05 result is based on an atmospheric neutrino observation with an exposure of 5.9 kton yr. From a two-flavor oscillation analysis the best-fit point is $\Delta m^2 = 0.0017 \text{ eV}^2$ and $\sin^2 2\theta = 0.97$.
- 133 ASHIE 05 obtained this result by a two-neutrino oscillation analysis using 92 kton yr atmospheric neutrino data from the complete Super-Kamiokande I running period. The best fit is for $\Delta m^2 = 2.1 \times 10^{-3} \text{ eV}^2$.
- 134 AMBROSIO 04 obtained this result, without using the absolute normalization of the neutrino flux, by combining the angular distribution of upward through-going muon tracks with $E_\mu > 1$ GeV, N_{low} and N_{high} , and the numbers of InDown + UpStop and InUp events. Here, N_{low} and N_{high} are the number of events with reconstructed neutrino energies < 30 GeV and > 130 GeV, respectively. InDown and InUp represent events with downward and upward-going tracks starting inside the detector due to neutrino interactions, while UpStop represents entering upward-going tracks which stop in the detector. The best fit is for $\Delta m^2 = 2.3 \times 10^{-3} \text{ eV}^2$.
- 135 ASHIE 04 obtained this result from the $L(\text{flight length})/E(\text{estimated neutrino energy})$ distribution of ν_μ disappearance probability, using the Super-Kamiokande-I 1489 live-day atmospheric neutrino data. The best fit is for $\Delta m^2 = 2.4 \times 10^{-3} \text{ eV}^2$.
- 136 There are several islands of allowed region from this K2K analysis, extending to high values of Δm^2 . We only include the one that overlaps atmospheric neutrino analyses. The best fit is for $\Delta m^2 = 2.8 \times 10^{-3} \text{ eV}^2$.
- 137 AMBROSIO 03 obtained this result on the basis of the ratio $R = N_{\text{low}}/N_{\text{high}}$, where N_{low} and N_{high} are the number of upward through-going muon events with reconstructed neutrino energy < 30 GeV and > 130 GeV, respectively. The data came from the full detector run started in 1994. The method of FELDMAN 98 is used to obtain the limits. The best fit is for $\Delta m^2 = 2.5 \times 10^{-3} \text{ eV}^2$.
- 138 AMBROSIO 03 obtained this result by using the ratio R and the angular distribution of the upward through-going muons. R is given in the previous note and the angular distribution is reported in AMBROSIO 01. The method of FELDMAN 98 is used to obtain the limits. The best fit is for $\Delta m^2 = 2.5 \times 10^{-3} \text{ eV}^2$.
- 139 SANCHEZ 03 is based on an exposure of 5.9 kton yr. The result is obtained using a likelihood analysis of the neutrino L/E distribution for a selection μ flavor sample while the e -flavor sample provides flux normalization. The method of FELDMAN 98 is used to obtain the allowed region. The best fit is for $\Delta m^2 = 5.2 \times 10^{-3} \text{ eV}^2$.
- 140 AMBROSIO 01 result is based on the angular distribution of upward through-going muon tracks with $E_\mu > 1$ GeV. The data came from three different detector configurations, but the statistics is largely dominated by the full detector run, from May 1994 to December 2000. The total live time, normalized to the full detector configuration is 6.17 years. The best fit is obtained outside the physical region. The method of FELDMAN 98 is used to obtain the limits.
- 141 AMBROSIO 01 result is based on the angular distribution and normalization of upward through-going muon tracks with $E_\mu > 1$ GeV. See the previous footnote.
- 142 FUKUDA 99c obtained this result from a total of 537 live days of upward through-going muon data in Super-Kamiokande between April 1996 to January 1998. With a threshold of $E_\mu > 1.6$ GeV, the observed flux is $(1.74 \pm 0.07 \pm 0.02) \times 10^{-13} \text{ cm}^{-2}\text{s}^{-1}\text{sr}^{-1}$. The best fit is for $\Delta m^2 = 5.9 \times 10^{-3} \text{ eV}^2$.
- 143 FUKUDA 99d obtained this result from a simultaneous fitting to zenith angle distributions of upward-stopping and through-going muons. The flux of upward-stopping muons of minimum energy of 1.6 GeV measured between April 1996 and January 1998 is $(0.39 \pm 0.04 \pm 0.02) \times 10^{-13} \text{ cm}^{-2}\text{s}^{-1}\text{sr}^{-1}$. This is compared to the expected flux of $(0.73 \pm 0.16 \text{ (theoretical error)}) \times 10^{-13} \text{ cm}^{-2}\text{s}^{-1}\text{sr}^{-1}$. The best fit is for $\Delta m^2 = 3.9 \times 10^{-3} \text{ eV}^2$.
- 144 FUKUDA 99d obtained this result from the zenith dependence of the upward-stopping/through-going flux ratio. The best fit is for $\Delta m^2 = 3.1 \times 10^{-3} \text{ eV}^2$.
- 145 FUKUDA 98c obtained this result by an analysis of 33.0 kton yr atmospheric neutrino data. The best fit is for $\Delta m^2 = 2.2 \times 10^{-3} \text{ eV}^2$.
- 146 HATAKEYAMA 98 obtained this result from a total of 2456 live days of upward-going muon data in Kamiokande between December 1985 and May 1995. With a threshold of $E_\mu > 1.6$ GeV, the observed flux of upward through-going muons is $(1.94 \pm 0.10^{+0.07}_{-0.06}) \times 10^{-13} \text{ cm}^{-2}\text{s}^{-1}\text{sr}^{-1}$. This is compared to the expected flux of $(2.46 \pm 0.54 \text{ (theoretical error)}) \times 10^{-13} \text{ cm}^{-2}\text{s}^{-1}\text{sr}^{-1}$. The best fit is for $\Delta m^2 = 2.2 \times 10^{-3} \text{ eV}^2$.
- 147 HATAKEYAMA 98 obtained this result from a combined analysis of Kamiokande contained events (FUKUDA 94) and upward going muon events. The best fit is for $\Delta m^2 = 13 \times 10^{-3} \text{ eV}^2$.
- 148 FUKUDA 94 obtained the result by a combined analysis of sub- and multi-GeV atmospheric neutrino events in Kamiokande. The best fit is for $\Delta m^2 = 16 \times 10^{-3} \text{ eV}^2$.

See key on page 405

Lepton Particle Listings

Neutrino Mixing

$\sin^2(2\theta_{13})$

At present time, limits of $\sin^2(2\theta_{13})$ are derived from the search for the reactor $\bar{\nu}_e$ disappearance at distances corresponding to the Δm_{32}^2 value, i.e. $L \sim 1$ km. Alternatively, somewhat weaker limits can be obtained from the analysis of the solar neutrino data.

VALUE	CL%	DOCUMENT ID	TECN	COMMENT
<0.15	90	149 APOLLONIO	99	CHOZ Reactor Experiment
• • • We do not use the following data for averages, fits, limits, etc. • • •				
$0.11^{+0.11}_{-0.08}$	68	150 ADAMSON	09	MINS Normal mass hierarchy
$0.18^{+0.15}_{-0.11}$	68	151 ADAMSON	09	MINS Inverted mass hierarchy
0.06 ± 0.04		152 FOGLI	08	FIT Global neutrino data
0.08 ± 0.07		153 FOGLI	08	FIT Solar + KamLAND data
0.05 ± 0.05		154 FOGLI	08	FIT Atmospheric + LBL + CHOOZ data
< 0.48	90	155 HOSAKA	06A	SKAM 3ν oscillation; normal mass hierarchy
< 0.79	90	156 HOSAKA	06A	SKAM 3ν oscillation; inverted mass hierarchy
< 0.36		157 YAMAMOTO	06	K2K Accelerator experiment
< 0.48	90	158 AHN	04	K2K Accelerator experiment
< 0.36	90	159 BOEHM	01	Palo Verde react.
< 0.45	90	160 BOEHM	00	Palo Verde react.

149 The quoted limit is for $\Delta m_{32}^2 = 2.43 \times 10^{-3} \text{ eV}^2$. That value of Δm_{32}^2 is the central value for ADAMSON 08. For the ADAMSON 08 $1-\sigma$ low value of $2.30 \times 10^{-3} \text{ eV}^2$, the $\sin^2 2\theta_{13}$ limit is < 0.16. See also APOLLONIO 03 for a detailed description of the experiment.

150 The quoted limit is for $\Delta m_{32}^2 = 2.43 \times 10^{-3} \text{ eV}^2$, $\theta_{13} = \pi/2$, and $\delta = 0$. For other values of δ , the 68% CL region spans from 0.02 to 0.26.

151 The quoted limit is for $\Delta m_{32}^2 = 2.43 \times 10^{-3} \text{ eV}^2$, $\theta_{13} = \pi/2$, and $\delta = 0$. For other values of δ , the 68% CL region spans from 0.04 to 0.34.

152 FOGLI 08 obtained this result from a global analysis of all neutrino oscillation data, that is, solar + KamLAND + atmospheric + accelerator long baseline + CHOOZ.

153 FOGLI 08 obtained this result from an analysis using the solar and KamLAND neutrino oscillation data.

154 FOGLI 08 obtained this result from an analysis using the atmospheric, accelerator long baseline, and CHOOZ neutrino oscillation data.

155 HOSAKA 06A obtained this result by a three-neutrino oscillation analysis with one mass scale dominance ($\Delta m_{21}^2 = 0$) using the Super-Kamiokande-I atmospheric neutrino data. The normal mass hierarchy is assumed.

156 HOSAKA 06A obtained this result by a three-neutrino oscillation analysis with one mass scale dominance ($\Delta m_{21}^2 = 0$) using the Super-Kamiokande-I atmospheric neutrino data. The inverted mass hierarchy is assumed.

157 YAMAMOTO 06 searched for $\nu_\mu \rightarrow \nu_e$ appearance. Assumes $2 \sin^2(2\theta_{\mu e}) = \sin^2(2\theta_{13})$. The quoted limit is for $\Delta m_{32}^2 = 1.9 \times 10^{-3} \text{ eV}^2$. That value of Δm_{32}^2 is the one- σ low value for AHN 06A. For the AHN 06A best fit value of $2.8 \times 10^{-3} \text{ eV}^2$, the $\sin^2(2\theta_{13})$ limit is < 0.26. Supersedes AHN 04.

158 AHN 04 searched for $\nu_\mu \rightarrow \nu_e$ appearance. Assuming $2 \sin^2(2\theta_{\mu e}) = \sin^2(2\theta_{13})$, a limit on $\sin^2(2\theta_{\mu e})$ is converted to a limit on $\sin^2(2\theta_{13})$. The quoted limit is for $\Delta m_{32}^2 = 1.9 \times 10^{-3} \text{ eV}^2$. That value of Δm_{32}^2 is the one- σ low value for ALIU 05. For the ALIU 05 best fit value of $2.8 \times 10^{-3} \text{ eV}^2$, the $\sin^2(2\theta_{13})$ limit is < 0.30.

159 The quoted limit is for $\Delta m_{32}^2 = 1.9 \times 10^{-3} \text{ eV}^2$. That value of Δm_{32}^2 is the $1-\sigma$ low value for ALIU 05. For the ALIU 05 best fit value of $2.8 \times 10^{-3} \text{ eV}^2$, the $\sin^2 2\theta_{13}$ limit is < 0.19. In this range, the θ_{13} limit is larger for lower values of Δm_{32}^2 , and smaller for higher values of Δm_{32}^2 .

160 The quoted limit is for $\Delta m_{32}^2 = 1.9 \times 10^{-3} \text{ eV}^2$. That value of Δm_{32}^2 is the $1-\sigma$ low value for ALIU 05. For the ALIU 05 best fit value of $2.8 \times 10^{-3} \text{ eV}^2$, the $\sin^2 2\theta_{13}$ limit is < 0.23.

(C) Other neutrino mixing results

The LSND collaboration reported in AGUILAR 01 a signal which is consistent with $\bar{\nu}_\mu \rightarrow \bar{\nu}_e$ oscillations. In a three neutrino framework, this would be a measurement of θ_{12} and Δm_{21}^2 . This does not appear to be consistent with the interpretation of other neutrino data. The MiniBooNE experiment, reported in AGUILAR-AREVALO 07, does a two-neutrino analysis which, assuming CPT conservation, rules out AGUILAR 01. The following listings include results which might be relevant towards understanding these observations. They include searches for $\nu_\mu \rightarrow \nu_e$, $\bar{\nu}_\mu \rightarrow \bar{\nu}_e$, sterile neutrino oscillations, and CPT violation.

$\Delta(m^2)$ for $\sin^2(2\theta) = 1$ ($\nu_\mu \rightarrow \nu_e$)

VALUE (eV^2)	CL%	DOCUMENT ID	TECN	COMMENT
• • • We do not use the following data for averages, fits, limits, etc. • • •				
<0.034	90	AGUILAR-AR...07	MBOO	MiniBooNE
<0.0008	90	AHN	04	K2K Water Cherenkov
<0.4	90	ASTIER	03	NOMD CERN SPS
<2.4	90	AVVAKUMOV	02	NTEV NUTEV FNAL
		161 AGUILAR	01	LSND $\nu_\mu \rightarrow \nu_e$ osc.prob.

0.03 to 0.3	95	162 ATHANASSO...98	LSND	$\nu_\mu \rightarrow \nu_e$
<2.3	90	163 LOVERRE	96	CHARM/CDHS
<0.9	90	VILAIN	94c	CHM2 CERN SPS
<0.09	90	ANGELINI	86	HLCB BEBC CERN PS

161 AGUILAR 01 is the final analysis of the LSND full data set. Search is made for the $\nu_\mu \rightarrow \nu_e$ oscillations using ν_μ from π^+ decay in flight by observing beam-on electron events from $\nu_e C \rightarrow e^- X$. Present analysis results in $8.1 \pm 12.2 \pm 1.7$ excess events in the $60 < E_e < 200$ MeV energy range, corresponding to oscillation probability of $0.10 \pm 0.16 \pm 0.04\%$. This is consistent, though less significant, with the previous result of ATHANASSOPOULOS 98, which it supersedes. The present analysis uses selection criteria developed for the decay at rest region, and is less effective in removing the background above 60 MeV than ATHANASSOPOULOS 98.

162 ATHANASSOPOULOS 98 is a search for the $\nu_\mu \rightarrow \nu_e$ oscillations using ν_μ from π^+ decay in flight. The 40 observed beam-on electron events are consistent with $\nu_e C \rightarrow e^- X$; the expected background is 21.9 ± 2.1 . Authors interpret this excess as evidence for an oscillation signal corresponding to oscillations with probability $(0.26 \pm 0.10 \pm 0.05)\%$. Although the significance is only 2.3σ , this measurement is an important and consistent cross check of ATHANASSOPOULOS 96 who reported evidence for $\bar{\nu}_\mu \rightarrow \bar{\nu}_e$ oscillations from μ^+ decay at rest. See also ATHANASSOPOULOS 98b.

163 LOVERRE 96 uses the charged-current to neutral-current ratio from the combined CHARM (ALLABY 86) and CDHS (ABRAMOWICZ 86) data from 1986.

$\sin^2(2\theta)$ for "Large" $\Delta(m^2)$ ($\nu_\mu \rightarrow \nu_e$)

VALUE (units 10^{-3})	CL%	DOCUMENT ID	TECN	COMMENT
• • • We do not use the following data for averages, fits, limits, etc. • • •				
< 1.8	90	164 AGUILAR-AR...07	MBOO	MiniBooNE
<110	90	165 AHN	04	K2K Water Cherenkov
< 1.4	90	ASTIER	03	NOMD CERN SPS
< 1.6	90	AVVAKUMOV	02	NTEV NUTEV FNAL
		166 AGUILAR	01	LSND $\nu_\mu \rightarrow \nu_e$ osc.prob.
0.5 to 30	95	167 ATHANASSO...98	LSND	$\nu_\mu \rightarrow \nu_e$
< 3.0	90	168 LOVERRE	96	CHARM/CDHS
< 9.4	90	VILAIN	94c	CHM2 CERN SPS
< 5.6	90	169 VILAIN	94c	CHM2 CERN SPS

164 The limit is $\sin^2 2\theta < 0.9 \times 10^{-3}$ at $\Delta m^2 = 2 \text{ eV}^2$. That value of Δm^2 corresponds to the smallest mixing angle consistent with the reported signal from LSND in AGUILAR 01.

165 The limit becomes $\sin^2 2\theta < 0.15$ at $\Delta m^2 = 2.8 \times 10^{-3} \text{ eV}^2$, the best-fit value of the ν_μ disappearance analysis in K2K.

166 AGUILAR 01 is the final analysis of the LSND full data set of the search for the $\nu_\mu \rightarrow \nu_e$ oscillations. See footnote in preceding table for further details.

167 ATHANASSOPOULOS 98 report $(0.26 \pm 0.10 \pm 0.05)\%$ for the oscillation probability; the value of $\sin^2 2\theta$ for large Δm^2 is deduced from this probability. See footnote in preceding table for further details, and see the paper for a plot showing allowed regions. If effect is due to oscillation, it is most likely to be intermediate $\sin^2 2\theta$ and Δm^2 . See also ATHANASSOPOULOS 98b.

168 LOVERRE 96 uses the charged-current to neutral-current ratio from the combined CHARM (ALLABY 86) and CDHS (ABRAMOWICZ 86) data from 1986.

169 VILAIN 94c limit derived by combining the ν_μ and $\bar{\nu}_\mu$ data assuming CP conservation.

$\Delta(m^2)$ for $\sin^2(2\theta) = 1$ ($\bar{\nu}_\mu \rightarrow \bar{\nu}_e$)

VALUE (eV^2)	CL%	DOCUMENT ID	TECN	COMMENT
• • • We do not use the following data for averages, fits, limits, etc. • • •				
<0.06	90	AGUILAR-AR...09b	MBOO	MiniBooNE
<0.055	90	170 ARMBRUSTER02	KAR2	Liquid Sci. calor.
<2.6	90	AVVAKUMOV	02	NTEV NUTEV FNAL
0.03-0.05		171 AGUILAR	01	LSND LAMPF
0.05-0.08	90	172 ATHANASSO...96	LSND	LAMPF
0.048-0.090	80	173 ATHANASSO...95		
<0.07	90	174 HILL	95	
<0.9	90	VILAIN	94c	CHM2 CERN SPS
<0.14	90	175 FREEDMAN	93	CNTR LAMPF

170 ARMBRUSTER 02 is the final analysis of the KARMEN 2 data for 17.7 m distance from the ISIS stopped pion and muon neutrino source. It is a search for $\bar{\nu}_e$ detected by the inverse β -decay reaction on protons and ^{12}C . 15 candidate events are observed, and 15.8 ± 0.5 background events are expected, hence no oscillation signal is detected. The results exclude large regions of the parameter area favored by the LSND experiment.

171 AGUILAR 01 is the final analysis of the LSND full data set. It is a search for $\bar{\nu}_e$ 30 m from LAMPF beam stop. Neutrinos originate mainly for π^+ decay at rest. $\bar{\nu}_e$ are detected through $\bar{\nu}_e p \rightarrow e^+ n$ ($20 < E_{e^+} < 60$ MeV) in delayed coincidence with $np \rightarrow d\gamma$. Authors observe $87.9 \pm 22.4 \pm 6.0$ total excess events. The observation is attributed to $\bar{\nu}_\mu \rightarrow \bar{\nu}_e$ oscillations with the oscillation probability of $0.264 \pm 0.067 \pm 0.045\%$, consistent with the previously published result. Taking into account all constraints, the most favored allowed region of oscillation parameters is a band of $\Delta(m^2)$ from $0.2-2.0 \text{ eV}^2$. Supersedes ATHANASSOPOULOS 95, ATHANASSOPOULOS 96, and ATHANASSOPOULOS 98.

172 ATHANASSOPOULOS 96 is a search for $\bar{\nu}_e$ 30 m from LAMPF beam stop. Neutrinos originate mainly from π^+ decay at rest. $\bar{\nu}_e$ could come from either $\bar{\nu}_\mu \rightarrow \bar{\nu}_e$ or $\nu_e \rightarrow \bar{\nu}_e$; our entry assumes the first interpretation. They are detected through $\bar{\nu}_e p \rightarrow e^+ n$ ($20 \text{ MeV} < E_{e^+} < 60 \text{ MeV}$) in delayed coincidence with $np \rightarrow d\gamma$. Authors

Lepton Particle Listings

Neutrino Mixing

observe $51 \pm 20 \pm 8$ total excess events over an estimated background 12.5 ± 2.9 . ATHANASSOPOULOS 96b is a shorter version of this paper.

- 173 ATHANASSOPOULOS 95 error corresponds to the 1.6σ band in the plot. The expected background is 2.7 ± 0.4 events. Corresponds to an oscillation probability of $(0.34^{+0.20}_{-0.18} \pm 0.07)\%$. For a different interpretation, see HILL 95. Replaced by ATHANASSOPOULOS 96.
- 174 HILL 95 is a report by one member of the LSND Collaboration, reporting a different conclusion from the analysis of the data of this experiment (see ATHANASSOPOULOS 95). Contrary to the rest of the LSND Collaboration, Hill finds no evidence for the neutrino oscillation $\bar{\nu}_\mu \rightarrow \bar{\nu}_e$ and obtains only upper limits.
- 175 FREEDMAN 93 is a search at LAMPF for $\bar{\nu}_e$ generated from any of the three neutrino types $\nu_\mu, \bar{\nu}_\mu$, and ν_e which come from the beam stop. The $\bar{\nu}_e$'s would be detected by the reaction $\bar{\nu}_e p \rightarrow e^+ n$. FREEDMAN 93 replaces DURKIN 88.

$\sin^2(2\theta)$ for "Large" $\Delta(m^2)$ ($\bar{\nu}_\mu \rightarrow \bar{\nu}_e$)

VALUE (units 10^{-3})	CL%	DOCUMENT ID	TECN	COMMENT
• • • We do not use the following data for averages, fits, limits, etc. • • •				
<3.3	90	176 AGUILAR-AR...09b	MBOO	MiniBooNE
<1.7	90	177 ARMBRUSTER02	KAR2	Liquid Sci. calor.
<1.1	90	AVVAKUMOV 02	NTEV	NUTEV FNAL
$5.3 \pm 1.3 \pm 9.0$		178 AGUILAR 01	LSND	LAMPF
$6.2 \pm 2.4 \pm 1.0$		179 ATHANASSO...96	LSND	LAMPF
3-12	80	180 ATHANASSO...95		
<6	90	181 HILL 95		

- 176 This result is inconclusive with respect to small amplitude mixing suggested by LSND.
- 177 ARMBRUSTER 02 is the final analysis of the KARMEN 2 data. See footnote in the preceding table for further details, and the paper for the exclusion plot.
- 178 AGUILAR 01 is the final analysis of the LSND full data set. The deduced oscillation probability is $0.264 \pm 0.067 \pm 0.045\%$; the value of $\sin^2 2\theta$ for large $\Delta(m^2)$ is twice this probability (although these values are excluded by other constraints). See footnote in preceding table for further details, and the paper for a plot showing allowed regions. Supersedes ATHANASSOPOULOS 95, ATHANASSOPOULOS 96, and ATHANASSOPOULOS 98.
- 179 ATHANASSOPOULOS 96 reports $(0.31 \pm 0.12 \pm 0.05)\%$ for the oscillation probability; the value of $\sin^2 2\theta$ for large $\Delta(m^2)$ should be twice this probability. See footnote in preceding table for further details, and see the paper for a plot showing allowed regions.
- 180 ATHANASSOPOULOS 95 error corresponds to the 1.6σ band in the plot. The expected background is 2.7 ± 0.4 events. Corresponds to an oscillation probability of $(0.34^{+0.20}_{-0.18} \pm 0.07)\%$. For a different interpretation, see HILL 95. Replaced by ATHANASSOPOULOS 96.
- 181 HILL 95 is a report by one member of the LSND Collaboration, reporting a different conclusion from the analysis of the data of this experiment (see ATHANASSOPOULOS 95). Contrary to the rest of the LSND Collaboration, Hill finds no evidence for the neutrino oscillation $\bar{\nu}_\mu \rightarrow \bar{\nu}_e$ and obtains only upper limits.

$\Delta(m^2)$ for $\sin^2(2\theta) = 1$ ($\nu_\mu(\bar{\nu}_\mu) \rightarrow \nu_e(\bar{\nu}_e)$)

VALUE (eV ²)	CL%	DOCUMENT ID	TECN	COMMENT
<0.075	90	BORODOV... 92	CNTR	BNL E776

- • • We do not use the following data for averages, fits, limits, etc. • • •
- <1.6 90 182 ROMOSAN 97 CCFR FNAL
- 182 ROMOSAN 97 uses wideband beam with a 0.5 km decay region.
- ### $\sin^2(2\theta)$ for "Large" $\Delta(m^2)$ ($\nu_\mu(\bar{\nu}_\mu) \rightarrow \nu_e(\bar{\nu}_e)$)
- | VALUE (units 10^{-3}) | CL% | DOCUMENT ID | TECN | COMMENT |
|--------------------------|-----|----------------|------|---------|
| <1.8 | 90 | 183 ROMOSAN 97 | CCFR | FNAL |
- • • We do not use the following data for averages, fits, limits, etc. • • •
- <3.8 90 184 MCFARLAND 95 CCFR FNAL
- <3 90 BORODOV... 92 CNTR BNL E776
- 183 ROMOSAN 97 uses wideband beam with a 0.5 km decay region.
- 184 MCFARLAND 95 state that "This result is the most stringent to date for $250 < \Delta(m^2) < 450$ eV² and also excludes at 90%CL much of the high $\Delta(m^2)$ region favored by the recent LSND observation." See ATHANASSOPOULOS 95 and ATHANASSOPOULOS 96.

$\Delta(m^2)$ for $\sin^2(2\theta) = 1$ ($\bar{\nu}_e \not\rightarrow \bar{\nu}_e$)

VALUE (eV ²)	CL%	DOCUMENT ID	TECN	COMMENT
<0.01	90	185 ACHKAR 95	CNTR	Bugey reactor

- • • We do not use the following data for averages, fits, limits, etc. • • •
- 185 ACHKAR 95 bound is for $L=15, 40$, and 95 m.

$\sin^2(2\theta)$ for "Large" $\Delta(m^2)$ ($\bar{\nu}_e \not\rightarrow \bar{\nu}_e$)

VALUE	CL%	DOCUMENT ID	TECN	COMMENT
<0.02	90	186 ACHKAR 95	CNTR	For $\Delta(m^2) = 0.6$ eV ²

- • • We do not use the following data for averages, fits, limits, etc. • • •
- 186 ACHKAR 95 bound is from data for $L=15, 40$, and 95 m distance from the Bugey reactor.

Sterile neutrino limits from atmospheric neutrino studies

$\Delta(m^2)$ for $\sin^2(2\theta) = 1$ ($\nu_\mu \rightarrow \nu_s$)

ν_s means ν_τ or any sterile (noninteracting) ν .

VALUE (10^{-5} eV ²)	CL%	DOCUMENT ID	TECN	COMMENT
• • • We do not use the following data for averages, fits, limits, etc. • • •				
<3000 (or <550)	90	187 OYAMA 89	KAMI	Water Cherenkov
<4.2 (or >54)	90	BIONTA 88	IMB	Flux has $\nu_\mu, \bar{\nu}_\mu, \nu_e$, and $\bar{\nu}_e$

- 187 OYAMA 89 gives a range of limits, depending on assumptions in their analysis. They argue that the region $\Delta(m^2) = (100-1000) \times 10^{-5}$ eV² is not ruled out by any data for large mixing.

Search for $\nu_\mu \rightarrow \nu_s$

VALUE	DOCUMENT ID	TECN	COMMENT
• • • We do not use the following data for averages, fits, limits, etc. • • •			
188	AMBROSIO 01	MCRO	matter effects
189	FUKUDA 00	SKAM	neutral currents + matter effects

- 188 AMBROSIO 01 tested the pure 2-flavor $\nu_\mu \rightarrow \nu_s$ hypothesis using matter effects which change the shape of the zenith-angle distribution of upward through-going muons. With maximum mixing and $\Delta(m^2)$ around 0.0024 eV², the $\nu_\mu \rightarrow \nu_s$ oscillation is disfavored with 99% confidence level with respect to the $\nu_\mu \rightarrow \nu_\tau$ hypothesis.
- 189 FUKUDA 00 tested the pure 2-flavor $\nu_\mu \rightarrow \nu_s$ hypothesis using three complementary atmospheric-neutrino data samples. With this hypothesis, zenith-angle distributions are expected to show characteristic behavior due to neutral currents and matter effects. In the $\Delta(m^2)$ and $\sin^2 2\theta$ region preferred by the Super-Kamiokande data, the $\nu_\mu \rightarrow \nu_s$ hypothesis is rejected at the 99% confidence level, while the $\nu_\mu \rightarrow \nu_\tau$ hypothesis consistently fits all of the data sample.

CPT tests

$\langle \Delta m_{21}^2 - \Delta m_{21}^2 \rangle$

VALUE (10^{-4} eV ²)	CL%	DOCUMENT ID	TECN	COMMENT
• • • We do not use the following data for averages, fits, limits, etc. • • •				
<1.1	99.7	190 DEGOUVEA 05	FIT	solar vs. reactor

- 190 DEGOUVEA 05 obtained this bound at the 3σ CL from the KamLAND (ARAKI 05) and solar neutrino data.

REFERENCES FOR Neutrino Mixing

ABDURASHI... 09	PR C80 015807	J.N. Abdurashitov et al.	(SAGE Collab.)
ADAMS ON 09	PRL 103 261802	P. Adamson et al.	(MINOS Collab.)
AGUILAR-AR... 09B	PRL 103 111801	A.A. Aguilar-Arevalo et al.	(MiniBooNE Collab.)
PENA-GARAY 09	arXiv:0811.2424v1	C. Pena-Garay, A. Serenelli	
ABE 08A	PRL 100 221803	S. Abe et al.	(KamLAND Collab.)
Also	PRL 101 119904E	S. Abe et al.	(KamLAND Collab.)
ADAMS ON 08	PR D77 072002	P. Adamson et al.	(MINOS Collab.)
ADAMS ON 08A	PRL 101 131802	P. Adamson et al.	(MINOS Collab.)
AHARMIM 08	PRL 101 111301	B. Aharmim et al.	(SNO Collab.)
ARPESELLA 08A	PRL 101 091302	C. Arpesella et al.	(Borexino Collab.)
CRAVENS 08	PR D78 032002	J.P. Cravens et al.	(Super-Kamiokande Collab.)
FOGLI 08	PRL 101 141801	G.L. Fogli, et al.	
ADAMS ON 07	PR D75 092003	P. Adamson et al.	(MINOS Collab.)
AGUILAR-AR... 07	PRL 98 231801	A.A. Aguilar-Arevalo et al.	(MiniBooNE Collab.)
AHARMIM 07	PR C75 045502	B. Aharmim et al.	(SNO Collab.)
ADAMS ON 06	PR D73 072002	P. Adamson et al.	(MINOS Collab.)
AHN 06A	PR D74 072003	M.H. Ahn et al.	(K2K Collab.)
BALATA 06	EPJ C47 21	M. Balata et al.	(Borexino Collab.)
HOSAKA 06	PR D73 112001	J. Hosaka et al.	(Super-Kamiokande Collab.)
HOSAKA 06A	PR D74 032002	J. Hosaka et al.	(Super-Kamiokande Collab.)
MICHAEL 06	PRL 97 191801	D. Michael et al.	(MINOS Collab.)
YAMAMOTO 06	PRL 96 181801	S. Yamamoto et al.	(K2K Collab.)
AHARMIM 05A	PR C72 055502	B. Aharmim et al.	(SNO Collab.)
ALIU 05	PR 94 081802	E. Aliu et al.	(K2K Collab.)
ALLISON 05	PR D72 052005	W.W.M. Allison et al.	(SOUDAN-2 Collab.)
ALTMANN 05	PL B616 174	M. Altmann et al.	(GNO Collab.)
ARAKI 05	PRL 94 081801	T. Araki et al.	(KamLAND Collab.)
ASHIE 05	PR D71 112005	Y. Ashie et al.	(Super-Kamiokande Collab.)
DEGOUVEA 05	PR D71 093002	A. de Gouvea, C. Pena-Garay	
AHARMIM 04	PR D70 093014	B. Aharmim et al.	(SNO Collab.)
AHMED 04A	PRL 92 181301	S.N. Ahmed et al.	(SNO Collab.)
AHN 04	PRL 93 051801	M.H. Ahn et al.	(K2K Collab.)
AMBROSIO 04	EPJ C36 323	M. Ambrosio et al.	(MACRO Collab.)
ASHIE 04	PRL 93 101801	Y. Ashie et al.	(Super-Kamiokande Collab.)
EGUCHI 04	PRL 92 071301	K. Eguchi et al.	(KamLAND Collab.)
SMY 04	PR D69 011104R	M.B. Smy et al.	(Super-Kamiokande Collab.)
AHN 03	PRL 90 041801	M.H. Ahn et al.	(K2K Collab.)
AMBROSIO 03	PL B566 35	M. Ambrosio et al.	(MACRO Collab.)
APOLLONIO 03	EPJ C27 331	M. Apollonio et al.	(CHOOZ Collab.)
ASTIER 03	PL B570 19	P. Astier et al.	(NOMAD Collab.)
EGUCHI 03	PRL 90 021802	K. Eguchi et al.	(KamLAND Collab.)
GANDO 03	PRL 90 171302	Y. Gando et al.	(Super-Kamiokande Collab.)
IANNI 03	JPG 29 2107	A. Ianni	(INFN Gran Sasso)
SANCHEZ 03	PR D68 113004	M. Sanchez et al.	(Soudan 2 Collab.)
ABDURASHI... 02	JETP 95 181	J.N. Abdurashitov et al.	(SAGE Collab.)
Translated from ZETF 122 211.			
AHMAD 02	PRL 89 011301	Q.R. Ahmad et al.	(SNO Collab.)
AHMAD 02B	PRL 89 011302	Q.R. Ahmad et al.	(SNO Collab.)
ARMBRUSTER 02	PR D65 112001	B. Armbuster et al.	(KARMEN 2 Collab.)
AVVAKUMOV 02	PRL 89 011804	S. Avvakumov et al.	(NuTeV Collab.)
FUKUDA 02	PL B539 179	S. Fukuda et al.	(Super-Kamiokande Collab.)
AGUILAR 01	PR D64 112007	A. Aguilar et al.	(LSND Collab.)
AHMAD 01	PRL 87 071301	Q.R. Ahmad et al.	(SNO Collab.)
AMBROSIO 01	PL B517 59	M. Ambrosio et al.	(MACRO Collab.)
BOEHM 01	PR D64 112001	F. Boehm et al.	
FUKUDA 01	PRL 86 5651	S. Fukuda et al.	(Super-Kamiokande Collab.)

See key on page 405

Lepton Particle Listings

Neutrino Mixing, Heavy Neutral Leptons, Searches for

AMBROSIO	00	PL B478 5	M. Ambrosio <i>et al.</i>	(MACRO Collab.)
BOEHM	00	PRL 84 3764	F. Boehm <i>et al.</i>	
FUKUDA	00	PRL 85 3999	S. Fukuda <i>et al.</i>	(Super-Kamiokande Collab.)
ALLISON	99	PL B449 137	W.W.M. Allison <i>et al.</i>	(Soudan 2 Collab.)
APOLLONIO	99	PL B466 415	M. Apollonio <i>et al.</i>	(CHOOZ Collab.)
Also		PL B472 434 (erratum)	M. Apollonio <i>et al.</i>	(CHOOZ Collab.)
FUKUDA	99C	PRL 82 2644	Y. Fukuda <i>et al.</i>	(Super-Kamiokande Collab.)
FUKUDA	99D	PL B467 185	Y. Fukuda <i>et al.</i>	(Super-Kamiokande Collab.)
HAMPEL	99	PL B447 127	W. Hampel <i>et al.</i>	(GALLEX Collab.)
AMBROSIO	98	PL B434 451	M. Ambrosio <i>et al.</i>	(MACRO Collab.)
APOLLONIO	98	PL B420 397	M. Apollonio <i>et al.</i>	(CHOOZ Collab.)
ATHANASSO...	98	PRL 81 1774	C. Athanassopoulos <i>et al.</i>	(LSND Collab.)
ATHANASSO...	98B	PR C58 2489	C. Athanassopoulos <i>et al.</i>	(LSND Collab.)
CLEVELAND	98	APJ 496 505	B.T. Cleveland <i>et al.</i>	(Homestake Collab.)
FELDMAN	98	PR D57 3873	G.J. Feldman, R.D. Cousins	
FUKUDA	98C	PRL 81 1562	Y. Fukuda <i>et al.</i>	(Super-Kamiokande Collab.)
HATAKEYAMA	98	PRL 81 2016	S. Hatakeyama <i>et al.</i>	(Kamiokande Collab.)
CLARK	97	PRL 79 345	R. Clark <i>et al.</i>	(IMB Collab.)
ROMOSAN	97	PRL 78 2912	A. Romosan <i>et al.</i>	(CCFR Collab.)
AGLIETTA	96	JETPL 63 791	M. Aglietta <i>et al.</i>	(LSD Collab.)
Translated from ZETFP 63 753.				
ATHANASSO...	96	PR C54 2685	C. Athanassopoulos <i>et al.</i>	(LSND Collab.)
ATHANASSO...	96B	PRL 77 3082	C. Athanassopoulos <i>et al.</i>	(LSND Collab.)
FUKUDA	96	PRL 77 1683	Y. Fukuda <i>et al.</i>	(Kamiokande Collab.)
FUKUDA	96B	PL B388 397	Y. Fukuda <i>et al.</i>	(Kamiokande Collab.)
GREENWOOD	96	PR D53 6054	Z.D. Greenwood <i>et al.</i>	(UCI, SVR, SUCU)
HAMPEL	96	PL B388 384	W. Hampel <i>et al.</i>	(GALLEX Collab.)
LOVERRE	96	PL B370 156	P.F. Loverre	
ACHKAR	95	NP B434 503	B. Achkar <i>et al.</i>	(SING, SACLD, CPPM, CDEF+)
AHLEN	95	PL B357 481	S.P. Ahlen <i>et al.</i>	(MACRO Collab.)
ATHANASSO...	95	PRL 75 2650	C. Athanassopoulos <i>et al.</i>	(LSND Collab.)
DAUM	95	ZPHY C66 417	K. Daum <i>et al.</i>	(FREJUS Collab.)
HILL	95	PRL 75 2654	J.E. Hill	(PENN)
MCFARLAND	95	PRL 75 3993	K.S. McFarland <i>et al.</i>	(CCFR Collab.)
DECLAIS	94	PL B338 383	Y. Declais <i>et al.</i>	
FUKUDA	94	PL B335 237	Y. Fukuda <i>et al.</i>	(Kamiokande Collab.)
VILAIN	94C	ZPHY C64 539	P. Vilain <i>et al.</i>	(CHARM II Collab.)
FREEDMAN	93	PR D47 811	S.J. Freedman <i>et al.</i>	(LAMPF E645 Collab.)
BECKER-SZ...	92B	PR D46 3720	R.A. Becker-Szendy <i>et al.</i>	(IMB Collab.)
BEIER	92	PL B283 446	E.W. Beier <i>et al.</i>	(KAM2 Collab.)
Also		PTRSL A346 63	L.W. Beier, E.D. Frank	(PENN)
BORODOV...	92	PRL 68 274	L. Borodovsky <i>et al.</i>	(COLU, JHU, ILL)
HIRATA	92	PL B280 146	K.S. Hirata <i>et al.</i>	(Kamiokande II Collab.)
CASPER	91	PRL 66 2561	D. Casper <i>et al.</i>	(IMB Collab.)
HIRATA	91	PRL 66 9	K.S. Hirata <i>et al.</i>	(Kamiokande II Collab.)
KUVSHININ...	91	JETPL 54 253	A.A. Kuvshinnikov <i>et al.</i>	(KIAE)
BERGER	90B	PL B245 305	C. Berger <i>et al.</i>	(FREJUS Collab.)
HIRATA	90	PRL 65 1297	K.S. Hirata <i>et al.</i>	(Kamiokande II Collab.)
AGLIETTA	89	EPL 8 611	M. Aglietta <i>et al.</i>	(FREJUS Collab.)
DAVIS	89	ARNPS 39 467	R. Davis, A.K. Mann, L. Wolfenstein	(BNL, PENN+)
OYAMA	89	PR D39 1481	Y. Oyama <i>et al.</i>	(Kamiokande II Collab.)
BIONTA	88	PR D38 768	R.M. Bionta <i>et al.</i>	(IMB Collab.)
DURKIN	88	PRL 61 1811	L.S. Durkin <i>et al.</i>	(OSU, ANL, CIT+)
ABRAMOWICZ	86	PRL 57 298	H. Abramowicz <i>et al.</i>	(CDHS Collab.)
ALLABY	86	PL B177 446	J.V. Allaby <i>et al.</i>	(CHARM Collab.)
ANGELINI	86	PL B179 307	C. Angelini <i>et al.</i>	(PISA, ATHU, PADO+)
VUILLEUMIER	82	PL 114B 298	J.L. Vuilleumier <i>et al.</i>	(CIT, SIN, MUNI)
BOLIEV	81	SJNP 34 787	M.M. Boliev <i>et al.</i>	(INRM)
Translated from YAF 34 1418.				
KWON	81	PR D24 1097	H. Kwon <i>et al.</i>	(CIT, ISNG, MUNI)
BOEHM	80	PL 97B 310	F. Boehm <i>et al.</i>	(ILLG, CIT, ISNG, MUNI)
CROUCH	78	PR D18 2239	M.F. Crouch <i>et al.</i>	(CASE, UCI, WITW)

• • • We do not use the following data for averages, fits, limits, etc. • • •

> 76.0	95	ABBIENDI	00I	OPAL	Majorana, coupling to e
> 88.0	95	ABBIENDI	00I	OPAL	Dirac, coupling to e
> 76.0	95	ABBIENDI	00I	OPAL	Majorana, coupling to μ
> 88.1	95	ABBIENDI	00I	OPAL	Dirac, coupling to μ
> 53.8	95	ABBIENDI	00I	OPAL	Majorana, coupling to τ
> 71.1	95	ABBIENDI	00I	OPAL	Dirac, coupling to τ
> 76.5	95	ABREU	990	DLPH	Dirac coupling to e
> 79.5	95	ABREU	990	DLPH	Dirac coupling to μ
> 60.5	95	ABREU	990	DLPH	Dirac coupling to τ
> 63	95	2,3 BUSKULIC	96S	ALEP	Dirac
> 54.3	95	2,4 BUSKULIC	96S	ALEP	Majorana

²BUSKULIC 96S requires the decay length of the heavy lepton to be < 1 cm, limiting the square of the mixing angle $|U_{\ell j}|^2$ to 10^{-10} .

³BUSKULIC 96S limit for mixing with τ . Mass is > 63.6 GeV for mixing with e or μ .

⁴BUSKULIC 96S limit for mixing with τ . Mass is > 55.2 GeV for mixing with e or μ .

Astrophysical Limits on Neutrino MASS for $m_\nu > 1$ GeV

VALUE (GeV)	CL%	DOCUMENT ID	TECN	COMMENT
none 60-115		⁵ FARGION	95	ASTR Dirac
none 9.2-2000		⁶ GARCIA	95	COSM Nucleosynthesis
none 26-4700		⁶ BECK	94	COSM Dirac
none 6 - hundreds		^{7,8} MORI	92B	KAM2 Dirac neutrino
none 24 - hundreds		^{7,8} MORI	92B	KAM2 Majorana neutrino
none 10-2400	90	⁹ REUSSER	91	CNTR HPGe search
none 3-100	90	SATO	91	KAM2 Kamiokande II
none 12-1400		¹⁰ ENQVIST	89	COSM
none 4-16	90	^{6,7} CALDWELL	88	COSM Dirac ν
none 4-35	90	OLIVE	88	COSM Majorana ν
>4.2 to 4.7		SREDNICKI	88	COSM Dirac ν
>5.3 to 7.4		SREDNICKI	88	COSM Majorana ν
none 20-1000	95	⁶ AHLEN	87	COSM Dirac ν
>4.1		GRIEST	87	COSM Dirac ν

⁵FARGION 95 bound is sensitive to assumed ν concentration in the Galaxy. See also KONOPLICH 94.

⁶These results assume that neutrinos make up dark matter in the galactic halo.

⁷Limits based on annihilations in the sun and are due to an absence of high energy neutrinos detected in underground experiments.

⁸MORI 92B results assume that neutrinos make up dark matter in the galactic halo. Limits based on annihilations in earth are also given.

⁹REUSSER 91 uses existing $\beta\beta$ detector (see FISHER 89) to search for CDM Dirac neutrinos.

¹⁰ENQVIST 89 argue that there is no cosmological upper bound on heavy neutrinos.

Heavy Neutral Leptons, Searches for

(A) Heavy Neutral Leptons

Stable Neutral Heavy Lepton MASS LIMITS

Note that LEP results in combination with REUSSER 91 exclude a fourth stable neutrino with $m < 2400$ GeV.

VALUE (GeV)	CL%	DOCUMENT ID	TECN	COMMENT
>45.0	95	ABREU	92B	DLPH Dirac
>39.5	95	ABREU	92B	DLPH Majorana
>44.1	95	ALEXANDER	91F	OPAL Dirac
>37.2	95	ALEXANDER	91F	OPAL Majorana
none 3-100	90	SATO	91	KAM2 Kamiokande II
>42.8	95	¹ ADEVA	90S	L3 Dirac
>34.8	95	¹ ADEVA	90S	L3 Majorana
>42.7	95	DECAMP	90F	ALEP Dirac

¹ADEVA 90S limits for the heavy neutrino apply if the mixing with the charged leptons satisfies $|U_{1j}|^2 + |U_{2j}|^2 + |U_{3j}|^2 > 6.2 \times 10^{-8}$ at $m_{L0} = 20$ GeV and $> 5.1 \times 10^{-10}$ for $m_{L0} = 40$ GeV.

Heavy Neutral Lepton MASS LIMITS

Limits apply only to heavy lepton type given in comment at right of data Listings.

See the "Quark and Lepton Compositeness, Searches for" Listings for limits on radiatively decaying excited neutral leptons, i.e. $\nu^* \rightarrow \nu\gamma$.

VALUE (GeV)	CL%	DOCUMENT ID	TECN	COMMENT
>101.3	95	ACHARD	01B	L3 Dirac coupling to e
>101.5	95	ACHARD	01B	L3 Dirac coupling to μ
> 90.3	95	ACHARD	01B	L3 Dirac coupling to τ
> 89.5	95	ACHARD	01B	L3 Majorana coupling to e
> 90.7	95	ACHARD	01B	L3 Majorana coupling to μ
> 80.5	95	ACHARD	01B	L3 Majorana coupling to τ

(B) Other Bounds from Nuclear and Particle Decays

Limits on $|U_{eX}|^2$ as Function of m_{ν_X}

Peak and kink search tests

Limits on $|U_{eX}|^2$ as function of m_{ν_X}

VALUE	CL%	DOCUMENT ID	TECN	COMMENT
<1 $\times 10^{-7}$	90	¹¹ BRITTON	92B	CNTR 50 MeV < m_{ν_X} < 130 MeV

• • • We do not use the following data for averages, fits, limits, etc. • • •

<5 $\times 10^{-6}$	90	DELEENER...	91	$m_{\nu_X} = 20$ MeV
<5 $\times 10^{-7}$	90	DELEENER...	91	$m_{\nu_X} = 40$ MeV
<3 $\times 10^{-7}$	90	DELEENER...	91	$m_{\nu_X} = 60$ MeV
<1 $\times 10^{-6}$	90	DELEENER...	91	$m_{\nu_X} = 80$ MeV
<1 $\times 10^{-6}$	90	DELEENER...	91	$m_{\nu_X} = 100$ MeV
<5 $\times 10^{-7}$	90	AZUELOS	86	CNTR $m_{\nu_X} = 60$ MeV
<2 $\times 10^{-7}$	90	AZUELOS	86	CNTR $m_{\nu_X} = 80$ MeV
<3 $\times 10^{-7}$	90	AZUELOS	86	CNTR $m_{\nu_X} = 100$ MeV
<1 $\times 10^{-6}$	90	AZUELOS	86	CNTR $m_{\nu_X} = 120$ MeV
<2 $\times 10^{-7}$	90	AZUELOS	86	CNTR $m_{\nu_X} = 130$ MeV
<1 $\times 10^{-4}$	90	¹² BRYMAN	83B	CNTR $m_{\nu_X} = 5$ MeV
<1.5 $\times 10^{-6}$	90	BRYMAN	83B	CNTR $m_{\nu_X} = 53$ MeV
<1 $\times 10^{-5}$	90	BRYMAN	83B	CNTR $m_{\nu_X} = 70$ MeV
<1 $\times 10^{-4}$	90	BRYMAN	83B	CNTR $m_{\nu_X} = 130$ MeV
<1 $\times 10^{-4}$	68	¹³ SHROCK	81	THEO $m_{\nu_X} = 10$ MeV
<5 $\times 10^{-6}$	68	¹³ SHROCK	81	THEO $m_{\nu_X} = 60$ MeV
<1 $\times 10^{-5}$	68	¹⁴ SHROCK	80	THEO $m_{\nu_X} = 80$ MeV
<3 $\times 10^{-6}$	68	¹⁴ SHROCK	80	THEO $m_{\nu_X} = 160$ MeV

Lepton Particle Listings

Heavy Neutral Leptons, Searches for

- ¹¹ BRITTON 92B is from a search for additional peaks in the e^+ spectrum from $\pi^+ \rightarrow e^+ \nu_e$ decay at TRIUMF. See also BRITTON 92.
- ¹² BRYMAN 83B obtain upper limits from both direct peak search and analysis of $B(\pi \rightarrow e\nu)/B(\pi \rightarrow \mu\nu)$. Latter limits are not listed, except for this entry (i.e. — we list the most stringent limits for given mass).
- ¹³ Analysis of $(\pi^+ \rightarrow e^+ \nu_e)/(\pi^+ \rightarrow \mu^+ \nu_\mu)$ and $(K^+ \rightarrow e^+ \nu_e)/(K^+ \rightarrow \mu^+ \nu_\mu)$ decay ratios.
- ¹⁴ Analysis of $(K^+ \rightarrow e^+ \nu_e)$ spectrum.

Kink search in nuclear β decay

High-sensitivity follow-up experiments show that indications for a neutrino with mass 17 keV (Simpson, Hime, and others) were not valid. Accordingly, we no longer list the experiments by these authors and some others which made positive claims of 17 keV neutrino emission. Complete listings are given in the 1994 edition (Physical Review **D50** 1173 (1994)) and in the 1998 edition (The European Physical Journal **C3** 1 (1998)). We list below only the best limits on $|U_{eX}|^2$ for each m_{ν_X} . See WIETFELDT 96 for a comprehensive review.

VALUE (units 10^{-3})	CL%	m_{ν_i} (keV)	ISOTOPE	METHOD	DOCUMENT ID
• • • We do not use the following data for averages, fits, limits, etc. • • •					
< 4–20	90	700–3500	^{38m} K	Trap	15 TRINCZEK 03
< 9–116	95	1–0.1	¹⁸⁷ Re	cryog.	16 GALEAZZI 01
< 1	95	10–90	³⁵ S	Mag spect	17 HOLZSCHUH 00
< 4	95	14–17	²⁴¹ Pu	Electrostatic spec	18 DRAGOUN 99
< 1	95	4–30	⁶³ Ni	Mag spect	19 HOLZSCHUH 99
< 10–40	90	370–640	³⁷ Ar	EC ion recoil	20 HINDI 98
< 10	95	1	³ H	SPEC	21 HIDDEMANN 95
< 6	95	2	³ H	SPEC	21 HIDDEMANN 95
< 2	95	3	³ H	SPEC	21 HIDDEMANN 95
< 0.7	99	16.3–16.6	³ H	Prop chamber	22 KALBFLEISCH 93
< 2	95	13–40	³⁵ S	Si(Li)	23 MORTARA 93
< 0.73	95	17	⁶³ Ni	Mag spect	OHSHIMA 93
< 1.0	95	10–24	⁶³ Ni	Mag spect	KAWAKAMI 92
< 0.9–2.5	90	1200–6800	²⁰ F	beta spectrum	24 DEUTSCH 90
< 8	90	80	³⁵ S	Mag spect	25 APALIKOV 85
< 1.5	90	60	³⁵ S	Mag spect	APALIKOV 85
< 3.0	90	5–50		Mag spect	MARKET 85
< 0.62	90	48	³⁵ S	Si(Li)	OHI 85
< 0.90	90	30	³⁵ S	Si(Li)	OHI 85
< 4	90	140	⁶⁴ Cu	Mag spect	26 SCHRECK... 83
< 8	90	440	⁶⁴ Cu	Mag spect	26 SCHRECK... 83
< 100	90	0.1–3000		THEO	27 SHROCK 80
< 0.1	68	80		THEO	28 SHROCK 80

- ¹⁵ TRINCZEK 03 is a search for admixture of heavy neutrino ν_e , in contrast to $\bar{\nu}_e$ used in many other searches. Full kinematic reconstruction of the neutrino momentum by use of a magneto optical trap.
- ¹⁶ GALEAZZI 01 use an cryogenic microcalorimeter to search for mass 50–1000 eV neutrino admixtures using the ¹⁸⁷Re beta spectrum with 2.4 keV endpoint. They derive limits for the admixture of heavy neutrinos, ranging from 9×10^{-3} for mass 1 keV to 0.116 for mass 100 eV. This is a significant improvement with respect to HIDDEMANN 95, especially for masses below ~ 500 MeV, where the limit is about a factor of ~ 2 higher.
- ¹⁷ HOLZSCHUH 00 use an iron-free β spectrometer to measure the ³⁵S β decay spectrum. An analysis of the spectrum in the energy range 56–173 keV is used to derive limits for the admixture of heavy neutrinos. This extends the range of neutrino masses explored in HOLZSCHUH 99.
- ¹⁸ DRAGOUN 99 analyze the β decay spectrum of ²⁴¹Pu in the energy range 0.2–9.2 keV to derive limits for the admixture of heavy neutrinos. It is not competitive with HOLZSCHUH 99.
- ¹⁹ HOLZSCHUH 99 use an iron-free β spectrometer to measure the ⁶³Ni β decay spectrum. An analysis of the spectrum in the energy range 33–67.8 keV is used to derive limits for the admixture of heavy neutrinos.
- ²⁰ HINDI 98 obtain a limit on heavy neutrino admixture from EC decay of ³⁷Ar by measuring the time-of-flight distribution of the recoiling ions in coincidence with x-rays or Auger electrons. The authors report upper limit for $|U_{eX}|^2$ of $\approx 3\%$ for $m_{\nu_X} = 500$ keV, 1% for $m_{\nu_X} = 550$ keV, 2% for $m_{\nu_X} = 600$ keV, and 4% for $m_{\nu_X} = 650$ keV. Their reported limits for $m_{\nu_X} \leq 450$ keV are inferior to the limits of SCHRECKENBACH 83.

- ²¹ In the beta spectrum from tritium β decay nonvanishing or mixed $m_{\bar{\nu}_1}$ state in the mass region 0.01–4 keV. For $m_{\nu_X} < 1$ keV, their upper limit on $|U_{eX}|^2$ becomes less
- ²² KALBFLEISCH 93 extends the 17 keV neutrino search of BAHRAN 92, using an improved proportional chamber to which a small amount of ³H is added. Systematics are significantly reduced, allowing for an improved upper limit. The authors give a 99% confidence limit on $|U_{eX}|^2$ as a function of m_{ν_X} in the range from 13.5 keV to 17.5 keV. See also the related papers BAHRAN 93, BAHRAN 93B, and BAHRAN 95 on theoretical aspects of beta spectra and fitting methods for heavy neutrinos.
- ²³ MORTARA 93 limit is from study using a high-resolution solid-state detector with a superconducting solenoid. The authors note that “The sensitivity to neutrino mass is verified by measurement with a mixed source of ³⁵S and ¹⁴C, which artificially produces a distortion in the beta spectrum similar to that expected from the massive neutrino.”
- ²⁴ DEUTSCH 90 search for emission of heavy $\bar{\nu}_e$ in super-allowed beta decay of ²⁰F by spectral analysis of the electrons.
- ²⁵ This limit was taken from the figure 3 of APALIKOV 85; the text gives a more restrictive limit of 1.7×10^{-3} at CL = 90%.

- ²⁶ SCHRECKENBACH 83 is a combined measurement of the β^+ and β^- spectrum.
- ²⁷ SHROCK 80 was a retroactive analysis of data on several superallowed β decays to search for kinks in the Kurie plot.
- ²⁸ Application of test to search for kinks in β decay Kurie plots.

Searches for Decays of Massive ν

Limits on $|U_{eX}|^2$ as function of m_{ν_X}

VALUE	CL%	DOCUMENT ID	TECN	COMMENT
• • • We do not use the following data for averages, fits, limits, etc. • • •				
$< 1.6 \times 10^{-4}$	90	²⁹ BACK	03A CNTR	$m_{\nu_X} = 4$ MeV
$< 4.5 \times 10^{-5}$	90	²⁹ BACK	03A CNTR	$m_{\nu_X} = 7$ MeV
$< 3.8 \times 10^{-5}$	90	²⁹ BACK	03A CNTR	$m_{\nu_X} = 10$ MeV
$< 1.5 \times 10^{-3}$	95	ACHARD	01 L3	$m_{\nu_X} = 80$ GeV
$< 2 \times 10^{-2}$	95	ACHARD	01 L3	$m_{\nu_X} = 175$ GeV
< 0.3	95	ACHARD	01 L3	$m_{\nu_X} = 200$ GeV
$< 4 \times 10^{-3}$	95	ACCIARRI	99K L3	$m_{\nu_X} = 80$ GeV
$< 5 \times 10^{-2}$	95	ACCIARRI	99K L3	$m_{\nu_X} = 175$ GeV
$< 2 \times 10^{-5}$	95	³⁰ ABREU	97I DLPH	$m_{\nu_X} = 6$ GeV
$< 3 \times 10^{-5}$	95	³⁰ ABREU	97I DLPH	$m_{\nu_X} = 50$ GeV
$< 1.8 \times 10^{-3}$	90	³¹ HAGNER	95 MWPC	$m_{\nu_h} = 1.5$ MeV
$< 2.5 \times 10^{-4}$	90	³¹ HAGNER	95 MWPC	$m_{\nu_h} = 4$ MeV
$< 4.2 \times 10^{-3}$	90	³¹ HAGNER	95 MWPC	$m_{\nu_h} = 9$ MeV
$< 1 \times 10^{-5}$	90	³² BARANOV	93	$m_{\nu_X} = 100$ MeV
$< 1 \times 10^{-6}$	90	³² BARANOV	93	$m_{\nu_X} = 200$ MeV
$< 3 \times 10^{-7}$	90	³² BARANOV	93	$m_{\nu_X} = 300$ MeV
$< 2 \times 10^{-7}$	90	³² BARANOV	93	$m_{\nu_X} = 400$ MeV
$< 6.2 \times 10^{-8}$	95	ADEVA	90S L3	$m_{\nu_X} = 20$ GeV
$< 5.1 \times 10^{-10}$	95	ADEVA	90S L3	$m_{\nu_X} = 40$ GeV
all values ruled out	95	³³ BURCHAT	90 MRK2	$m_{\nu_X} < 19.6$ GeV
$< 1 \times 10^{-10}$	95	³³ BURCHAT	90 MRK2	$m_{\nu_X} = 22$ GeV
$< 1 \times 10^{-11}$	95	³³ BURCHAT	90 MRK2	$m_{\nu_X} = 41$ GeV
all values ruled out	95	DECAMP	90F ALEP	$m_{\nu_X} = 25.0$ – 42.7 GeV
$< 1 \times 10^{-13}$	95	DECAMP	90F ALEP	$m_{\nu_X} = 42.7$ – 45.7 GeV
$< 5 \times 10^{-3}$	90	AKERLOF	88 HRS	$m_{\nu_X} = 1.8$ GeV
$< 2 \times 10^{-5}$	90	AKERLOF	88 HRS	$m_{\nu_X} = 4$ GeV
$< 3 \times 10^{-6}$	90	AKERLOF	88 HRS	$m_{\nu_X} = 6$ GeV
$< 1.2 \times 10^{-7}$	90	BERNARDI	88 CNTR	$m_{\nu_X} = 100$ MeV
$< 1 \times 10^{-8}$	90	BERNARDI	88 CNTR	$m_{\nu_X} = 200$ MeV
$< 2.4 \times 10^{-9}$	90	BERNARDI	88 CNTR	$m_{\nu_X} = 300$ MeV
$< 2.1 \times 10^{-9}$	90	BERNARDI	88 CNTR	$m_{\nu_X} = 400$ MeV
$< 2 \times 10^{-2}$	68	³⁴ OBERAUER	87	$m_{\nu_X} = 1.5$ MeV
$< 8 \times 10^{-4}$	68	³⁴ OBERAUER	87	$m_{\nu_X} = 4.0$ MeV
$< 8 \times 10^{-3}$	90	BADIER	86 CNTR	$m_{\nu_X} = 400$ MeV
$< 8 \times 10^{-5}$	90	BADIER	86 CNTR	$m_{\nu_X} = 1.7$ GeV
$< 8 \times 10^{-8}$	90	BERNARDI	86 CNTR	$m_{\nu_X} = 100$ MeV
$< 4 \times 10^{-8}$	90	BERNARDI	86 CNTR	$m_{\nu_X} = 200$ MeV
$< 6 \times 10^{-9}$	90	BERNARDI	86 CNTR	$m_{\nu_X} = 400$ MeV
$< 3 \times 10^{-5}$	90	DORENBOS...	86 CNTR	$m_{\nu_X} = 150$ MeV
$< 1 \times 10^{-6}$	90	DORENBOS...	86 CNTR	$m_{\nu_X} = 500$ MeV
$< 1 \times 10^{-7}$	90	DORENBOS...	86 CNTR	$m_{\nu_X} = 1.6$ GeV
$< 7 \times 10^{-7}$	90	³⁵ COOPER...	85 HLBC	$m_{\nu_X} = 0.4$ GeV
$< 8 \times 10^{-8}$	90	³⁵ COOPER...	85 HLBC	$m_{\nu_X} = 1.5$ GeV
$< 1 \times 10^{-2}$	90	³⁶ BERGSMÄ	83B CNTR	$m_{\nu_X} = 10$ MeV
$< 1 \times 10^{-5}$	90	³⁶ BERGSMÄ	83B CNTR	$m_{\nu_X} = 110$ MeV
$< 6 \times 10^{-7}$	90	³⁶ BERGSMÄ	83B CNTR	$m_{\nu_X} = 410$ MeV
$< 1 \times 10^{-5}$	90	GRONAU	83	$m_{\nu_X} = 160$ MeV
$< 1 \times 10^{-6}$	90	GRONAU	83	$m_{\nu_X} = 480$ MeV

- ²⁹ BACK 03A searched for heavy neutrinos emitted from ⁸B decay in the Sun using the decay $\nu_h \rightarrow \nu_e e^+ e^-$ in the Counting Test Facility (the prototype of theorexino detector) and obtained limits on heavy neutrino admixture for the ν_h mass range 1.1–12 MeV.
- ³⁰ ABREU 97I long-lived ν_X analysis. Short-lived analysis extends limit to lower masses with decreasing sensitivity except at 3.5 GeV, where the limit is the same as at 6 GeV.
- ³¹ HAGNER 95 obtain limits on heavy neutrino admixture from the decay $\nu_h \rightarrow \nu_e e^+ e^-$ at a nuclear reactor for the ν_h mass range 2–9 MeV.
- ³² BARANOV 93 is a search for neutrino decays into $e^+ e^- \nu_e$ using a beam dump experiment at the 70 GeV Serpukhov proton synchrotron. The limits are not as good as those achieved earlier by BERGSMÄ 83 and BERNARDI 86, BERNARDI 88.
- ³³ BURCHAT 90 includes the analyses reported in JUNG 90, ABRAMS 89c, and WENDT 87.
- ³⁴ OBERAUER 87 bounds from search for $\nu \rightarrow \nu' e e$ decay mode using reactor (anti)neutrinos.

See key on page 405

Lepton Particle Listings

Heavy Neutral Leptons, Searches for

³⁵ COOPER-SARKAR 85 also give limits based on model-dependent assumptions for ν_τ flux. We do not list these. Note that for this bound to be nontrivial, x is not equal to 3, i.e. ν_X cannot be the dominant mass eigenstate in ν_τ since $m_{\nu_3} < 70$ MeV (ALBRECHT 85i). Also, of course, x is not equal to 1 or 2, so a fourth generation would be required for this bound to be nontrivial.

³⁶ BERGSMAN 83B also quote limits on $|U_{e3}|^2$ where the index 3 refers to the mass eigenstate dominantly coupled to the τ . Those limits were based on assumptions about the D_S mass and $D_S \rightarrow \tau \nu_\tau$ branching ratio which are no longer valid. See COOPER-SARKAR 85.

Limits on Coupling of μ to ν_X as Function of m_{ν_X}

Peak search test

Limits on $B(\pi \text{ (or } K) \rightarrow \mu \nu_X)$.

VALUE	CL%	DOCUMENT ID	TECN	COMMENT
• • • We do not use the following data for averages, fits, limits, etc. • • •				
		37 ASTIER	02	NOMD $\pi \rightarrow \mu X$ for $m_X = 33.9$ MeV
$< 6.0 \times 10^{-10}$	95	38 DAUM	00	CNTR $\pi \rightarrow \mu X$ for $m_X = 33.9$ MeV
		39 FORMAGGIO	00	CNTR $\pi \rightarrow \mu X$ for $m_X = 33.9$ MeV
< 0.22	90	40 ASSAMAGAN	98	SILI $m_{\nu_X} = 0.53$ MeV
< 0.029	90	40 ASSAMAGAN	98	SILI $m_{\nu_X} = 0.75$ MeV
< 0.016	90	40 ASSAMAGAN	98	SILI $m_{\nu_X} = 1.0$ MeV
$< 4-6 \times 10^{-5}$		41 BRYMAN	96	CNTR $m_{\nu_X} = 30-33.91$ MeV
$\sim 1 \times 10^{-16}$		42 ARMBRUSTER	95	KARM $m_{\nu_X} = 33.9$ MeV
$< 4 \times 10^{-7}$	95	43 BILGER	95	LEPS $m_{\nu_X} = 33.9$ MeV
$< 7 \times 10^{-8}$	95	43 BILGER	95	LEPS $m_{\nu_X} = 33.9$ MeV
$< 2.6 \times 10^{-8}$	95	43 DAUM	95B	TOF $m_{\nu_X} = 33.9$ MeV
$< 2 \times 10^{-2}$	90	DAUM	87	$m_{\nu_X} = 1$ MeV
$< 1 \times 10^{-3}$	90	DAUM	87	$m_{\nu_X} = 2$ MeV
$< 6 \times 10^{-5}$	90	DAUM	87	$3 \text{ MeV} < m_{\nu_X} < 19.5 \text{ MeV}$
$< 3 \times 10^{-2}$	90	44 MINEHART	84	$m_{\nu_X} = 2$ MeV
$< 1 \times 10^{-3}$	90	44 MINEHART	84	$m_{\nu_X} = 4$ MeV
$< 3 \times 10^{-4}$	90	44 MINEHART	84	$m_{\nu_X} = 10$ GeV
$< 5 \times 10^{-6}$	90	45 HAYANO	82	$m_{\nu_X} = 330$ MeV
$< 1 \times 10^{-4}$	90	45 HAYANO	82	$m_{\nu_X} = 70$ MeV
$< 9 \times 10^{-7}$	90	45 HAYANO	82	$m_{\nu_X} = 250$ MeV
$< 1 \times 10^{-1}$	90	44 ABELA	81	$m_{\nu_X} = 4$ MeV
$< 7 \times 10^{-5}$	90	44 ABELA	81	$m_{\nu_X} = 10.5$ MeV
$< 2 \times 10^{-4}$	90	44 ABELA	81	$m_{\nu_X} = 11.5$ MeV
$< 2 \times 10^{-5}$	90	44 ABELA	81	$m_{\nu_X} = 16-30$ MeV

³⁷ ASTIER 02 search for anomalous pion decay into a 33.9 MeV neutral particle. No evidence was found and the sensitivity to the branching ratio $B(\pi \rightarrow \mu X) \cdot B(X \rightarrow \nu e^+ e^-)$ is as low as 3.7×10^{-15} , depending on the X lifetime.

³⁸ DAUM 00 search for anomalous pion decay into a 33.9 MeV neutral particle that might be responsible for the time-distribution anomaly observed by the KARMEN Collaboration.

³⁹ FORMAGGIO 00 search for anomalous pion decay into a 33.9 MeV neutral particle Q^0 that might be responsible for the time-distribution anomaly observed by the KARMEN Collaboration. In the E815 (NuTeV) experiment at Fermilab no evidence was found, with sensitivity for the pion branching ratio $B(\pi \rightarrow \mu Q^0) \cdot B(Q^0 \rightarrow \text{visible})$ as low as 10^{-13} .

⁴⁰ ASSAMAGAN 98 obtain a limit on heavy neutrino admixture from π^+ decay essentially at rest, by measuring with good resolution the momentum distribution of the muons. However, the search uses an ad hoc shape correction. The authors report upper limit for $|U_{\mu X}|^2$ of 0.22 for $m_{\nu} = 0.53$ MeV, 0.029 for $m_{\nu} = 0.75$ MeV, and 0.016 for $m_{\nu} = 1.0$ MeV at 90% CL.

⁴¹ BRYMAN 96 search for massive unconventional neutrinos of mass m_{ν_X} in π^+ decay.

⁴² ARMBRUSTER 95 study the reactions $^{12}C(\nu_e, e^-)^{12}N$ and $^{12}C(\nu, \nu')^{12}C^*$ induced by neutrinos from π^+ and μ^+ decay at the ISIS neutron spallation source at the Rutherford-Appleton laboratory. An anomaly in the time distribution can be interpreted as the decay $\pi^+ \rightarrow \mu^+ \nu_X$, where ν_X is a neutral weakly interacting particle with mass ≈ 33.9 MeV and spin 1/2. The lower limit to the branching ratio is a function of the lifetime of the new massive neutral particle, and reaches a minimum of a few $\times 10^{-16}$ for $\tau_X \sim 5$ s.

⁴³ From experiments of π^+ and π^- decay in flight at PSI, to check the claim of the KARMEN Collaboration quoted above (ARMBRUSTER 95).

⁴⁴ $\pi^+ \rightarrow \mu^+ \nu_\mu$ peak search experiment.

⁴⁵ $K^+ \rightarrow \mu^+ \nu_\mu$ peak search experiment.

Peak search test

Limits on $|U_{\mu X}|^2$ as function of m_{ν_X} .

VALUE	CL%	DOCUMENT ID	TECN	COMMENT
• • • We do not use the following data for averages, fits, limits, etc. • • •				
$< 1-10 \times 10^{-4}$		46 BRYMAN	96	CNTR $m_{\nu_X} = 30-33.91$ MeV
$< 2 \times 10^{-5}$	95	47 ASANO	81	$m_{\nu_X} = 70$ MeV
$< 3 \times 10^{-6}$	95	47 ASANO	81	$m_{\nu_X} = 210$ MeV

$< 3 \times 10^{-6}$	95	47 ASANO	81	$m_{\nu_X} = 230$ MeV
$< 6 \times 10^{-6}$	95	48 ASANO	81	$m_{\nu_X} = 240$ MeV
$< 5 \times 10^{-7}$	95	48 ASANO	81	$m_{\nu_X} = 280$ MeV
$< 6 \times 10^{-6}$	95	48 ASANO	81	$m_{\nu_X} = 300$ MeV
$< 1 \times 10^{-2}$	95	CALAPRICE	81	$m_{\nu_X} = 7$ MeV
$< 3 \times 10^{-3}$	95	49 CALAPRICE	81	$m_{\nu_X} = 33$ MeV
$< 1 \times 10^{-4}$	68	50 SHROCK	81	THEO $m_{\nu_X} = 13$ MeV
$< 3 \times 10^{-5}$	68	50 SHROCK	81	THEO $m_{\nu_X} = 33$ MeV
$< 6 \times 10^{-3}$	68	51 SHROCK	81	THEO $m_{\nu_X} = 80$ MeV
$< 5 \times 10^{-3}$	68	51 SHROCK	81	THEO $m_{\nu_X} = 120$ MeV

⁴⁶ BRYMAN 96 search for massive unconventional neutrinos of mass m_{ν_X} in π^+ decay. They interpret the result as an upper limit for the admixture of a heavy sterile or otherwise

⁴⁷ $K^+ \rightarrow \mu^+ \nu_\mu$ peak search experiment.

⁴⁸ Analysis of experiment on $K^+ \rightarrow \mu^+ \nu_\mu \nu_X \bar{\nu}_X$ decay.

⁴⁹ $\pi^+ \rightarrow \mu^+ \nu_\mu$ peak search experiment.

⁵⁰ Analysis of magnetic spectrometer experiment, bubble chamber experiment, and emulsion experiment on $\pi^+ \rightarrow \mu^+ \nu_\mu$ decay.

⁵¹ Analysis of magnetic spectrometer experiment on $K \rightarrow \mu, \nu_\mu$ decay.

Peak Search in Muon Capture

Limits on $|U_{\mu X}|^2$ as function of m_{ν_X} .

VALUE	DOCUMENT ID	COMMENT
• • • We do not use the following data for averages, fits, limits, etc. • • •		
$< 1 \times 10^{-1}$	DEUTSCH 83	$m_{\nu_X} = 45$ MeV
$< 7 \times 10^{-3}$	DEUTSCH 83	$m_{\nu_X} = 70$ MeV
$< 1 \times 10^{-1}$	DEUTSCH 83	$m_{\nu_X} = 85$ MeV

Searches for Decays of Massive ν

Limits on $|U_{\mu X}|^2$ as function of m_{ν_X} .

VALUE	CL%	DOCUMENT ID	TECN	COMMENT
• • • We do not use the following data for averages, fits, limits, etc. • • •				
$< 5 \times 10^{-7}$	90	52 VAITAITIS	99	CCFR $m_{\nu_X} = 0.28$ GeV
$< 8 \times 10^{-8}$	90	52 VAITAITIS	99	CCFR $m_{\nu_X} = 0.37$ GeV
$< 5 \times 10^{-7}$	90	52 VAITAITIS	99	CCFR $m_{\nu_X} = 0.50$ GeV
$< 6 \times 10^{-8}$	90	52 VAITAITIS	99	CCFR $m_{\nu_X} = 1.50$ GeV
$< 2 \times 10^{-5}$	95	53 ABREU	97i	DLPH $m_{\nu_X} = 6$ GeV
$< 3 \times 10^{-5}$	95	53 ABREU	97i	DLPH $m_{\nu_X} = 50$ GeV
$< 3 \times 10^{-6}$	90	GALLAS	95	CNTR $m_{\nu_X} = 1$ GeV
$< 3 \times 10^{-5}$	90	54 VILAIN	95c	CHM2 $m_{\nu_X} = 2$ GeV
$< 6.2 \times 10^{-8}$	95	ADEVA	90s	L3 $m_{\nu_X} = 20$ GeV
$< 5.1 \times 10^{-10}$	95	ADEVA	90s	L3 $m_{\nu_X} = 40$ GeV
all values ruled out	95	55 BURCHAT	90	MRK2 $m_{\nu_X} < 19.6$ GeV
$< 1 \times 10^{-10}$	95	55 BURCHAT	90	MRK2 $m_{\nu_X} = 22$ GeV
$< 1 \times 10^{-11}$	95	55 BURCHAT	90	MRK2 $m_{\nu_X} = 41$ GeV
all values ruled out	95	DECAMP	90f	ALEP $m_{\nu_X} = 25.0-42.7$ GeV
$< 1 \times 10^{-13}$	95	DECAMP	90f	ALEP $m_{\nu_X} = 42.7-45.7$ GeV
$< 5 \times 10^{-3}$	90	AKERLOF	88	HRS $m_{\nu_X} = 1.8$ GeV
$< 2 \times 10^{-5}$	90	AKERLOF	88	HRS $m_{\nu_X} = 4$ GeV
$< 3 \times 10^{-6}$	90	AKERLOF	88	HRS $m_{\nu_X} = 6$ GeV
$< 1 \times 10^{-7}$	90	BERNARDI	88	CNTR $m_{\nu_X} = 200$ MeV
$< 3 \times 10^{-9}$	90	BERNARDI	88	CNTR $m_{\nu_X} = 300$ MeV
$< 4 \times 10^{-4}$	90	56 MISHRA	87	CNTR $m_{\nu_X} = 1.5$ GeV
$< 4 \times 10^{-3}$	90	56 MISHRA	87	CNTR $m_{\nu_X} = 2.5$ GeV
$< 0.9 \times 10^{-2}$	90	56 MISHRA	87	CNTR $m_{\nu_X} = 5$ GeV
< 0.1	90	56 MISHRA	87	CNTR $m_{\nu_X} = 10$ GeV
$< 8 \times 10^{-4}$	90	BADIER	86	CNTR $m_{\nu_X} = 600$ MeV
$< 1.2 \times 10^{-5}$	90	BADIER	86	CNTR $m_{\nu_X} = 1.7$ GeV
$< 3 \times 10^{-8}$	90	BERNARDI	86	CNTR $m_{\nu_X} = 200$ MeV
$< 6 \times 10^{-9}$	90	BERNARDI	86	CNTR $m_{\nu_X} = 350$ MeV
$< 1 \times 10^{-6}$	90	DORENBOS...	86	CNTR $m_{\nu_X} = 500$ MeV
$< 1 \times 10^{-7}$	90	DORENBOS...	86	CNTR $m_{\nu_X} = 1600$ MeV
$< 0.8 \times 10^{-5}$	90	57 COOPER-...	85	HLBC $m_{\nu_X} = 0.4$ GeV
$< 1.0 \times 10^{-7}$	90	57 COOPER-...	85	HLBC $m_{\nu_X} = 1.5$ GeV

⁵² VAITAITIS 99 search for $L_\mu^0 \rightarrow \mu X$. See paper for rather complicated limit as function of m_{ν_X} .

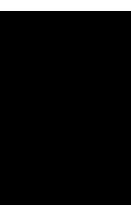
⁵³ ABREU 97i long-lived ν_X analysis. Short-lived analysis extends limit to lower masses with decreasing sensitivity except at 3.5 GeV, where the limit is the same as at 6 GeV.

QUARKS

<i>u</i>	590
<i>d</i>	590
<i>s</i>	590
<i>c</i>	594
<i>b</i>	595
<i>t</i>	596
<i>b'</i> (Fourth Generation) Quark	612
<i>t'</i> (Fourth Generation) Quark	613
Free Quark Searches	613

Notes in the Quark Listings

Quark Masses (rev.)	583
The Top Quark (rev.)	596
Free Quark Searches	613





QUARKS

QUARK MASSES

Updated Jan 2010 by A.V. Manohar (University of California, San Diego) and C.T. Sachrajda (University of Southampton)

A. Introduction

This note discusses some of the theoretical issues relevant for the determination of quark masses, which are fundamental parameters of the Standard Model of particle physics. Unlike the leptons, quarks are confined inside hadrons and are not observed as physical particles. Quark masses therefore cannot be measured directly, but must be determined indirectly through their influence on hadronic properties. Although one often speaks loosely of quark masses as one would of the mass of the electron or muon, any quantitative statement about the value of a quark mass must make careful reference to the particular theoretical framework that is used to define it. It is important to keep this *scheme dependence* in mind when using the quark mass values tabulated in the data listings.

Historically, the first determinations of quark masses were performed using quark models. The resulting masses only make sense in the limited context of a particular quark model, and cannot be related to the quark mass parameters of the Standard Model. In order to discuss quark masses at a fundamental level, definitions based on quantum field theory be used, and the purpose of this note is to discuss these definitions and the corresponding determinations of the values of the masses.

B. Mass parameters and the QCD Lagrangian

The QCD [1] Lagrangian for N_F quark flavors is

$$\mathcal{L} = \sum_{k=1}^{N_F} \bar{q}_k (i\mathcal{D} - m_k) q_k - \frac{1}{4} G_{\mu\nu} G^{\mu\nu}, \quad (1)$$

where $\mathcal{D} = (\partial_\mu - igA_\mu) \gamma^\mu$ is the gauge covariant derivative, A_μ is the gluon field, $G_{\mu\nu}$ is the gluon field strength, m_k is the mass parameter of the k^{th} quark, and q_k is the quark Dirac field. After renormalization, the QCD Lagrangian Eq. (1) gives finite values for physical quantities, such as scattering amplitudes. Renormalization is a procedure that invokes a subtraction scheme to render the amplitudes finite, and requires the introduction of a dimensionful scale parameter μ . The mass parameters in the QCD Lagrangian Eq. (1) depend on the renormalization scheme used to define the theory, and also on the scale parameter μ . The most commonly used renormalization scheme for QCD perturbation theory is the $\overline{\text{MS}}$ scheme.

The QCD Lagrangian has a chiral symmetry in the limit that the quark masses vanish. This symmetry is spontaneously broken by dynamical chiral symmetry breaking, and explicitly broken by the quark masses. The nonperturbative scale of dynamical chiral symmetry breaking, Λ_χ , is around 1 GeV [2]. It is conventional to call quarks heavy if $m > \Lambda_\chi$, so that explicit

chiral symmetry breaking dominates (c , b , and t quarks are heavy), and light if $m < \Lambda_\chi$, so that spontaneous chiral symmetry breaking dominates (u , d and s quarks are light). The determination of light- and heavy-quark masses is considered separately in sections D and E below.

At high energies or short distances, nonperturbative effects, such as chiral symmetry breaking, become small and one can, in principle, determine quark masses by analyzing mass-dependent effects using QCD perturbation theory. Such computations are conventionally performed using the $\overline{\text{MS}}$ scheme at a scale $\mu \gg \Lambda_\chi$, and give the $\overline{\text{MS}}$ “running” mass $\overline{m}(\mu)$. We use the $\overline{\text{MS}}$ scheme when reporting quark masses; one can readily convert these values into other schemes using perturbation theory.

The μ dependence of $\overline{m}(\mu)$ at short distances can be calculated using the renormalization group equation,

$$\mu^2 \frac{d\overline{m}(\mu)}{d\mu^2} = -\gamma(\overline{\alpha}_s(\mu)) \overline{m}(\mu), \quad (2)$$

where γ is the anomalous dimension which is now known to four-loop order in perturbation theory [3,4]. $\overline{\alpha}_s$ is the coupling constant in the $\overline{\text{MS}}$ scheme. Defining the expansion coefficients γ_r by

$$\gamma(\overline{\alpha}_s) \equiv \sum_{r=1}^{\infty} \gamma_r \left(\frac{\overline{\alpha}_s}{4\pi} \right)^r,$$

the first four coefficients are given by

$$\begin{aligned} \gamma_1 &= 4, \\ \gamma_2 &= \frac{202}{3} - \frac{20N_L}{9}, \\ \gamma_3 &= 1249 + \left(-\frac{2216}{27} - \frac{160}{3}\zeta(3) \right) N_L - \frac{140}{81} N_L^2, \\ \gamma_4 &= \frac{4603055}{162} + \frac{135680}{27}\zeta(3) - 8800\zeta(5) \\ &\quad + \left(-\frac{91723}{27} - \frac{34192}{9}\zeta(3) + 880\zeta(4) + \frac{18400}{9}\zeta(5) \right) N_L \\ &\quad + \left(\frac{5242}{243} + \frac{800}{9}\zeta(3) - \frac{160}{3}\zeta(4) \right) N_L^2 \\ &\quad + \left(-\frac{332}{243} + \frac{64}{27}\zeta(3) \right) N_L^3, \end{aligned}$$

where N_L is the number of active light quark flavors at the scale μ , i.e. flavors with masses $< \mu$, and ζ is the Riemann zeta function ($\zeta(3) \simeq 1.2020569$, $\zeta(4) \simeq 1.0823232$, and $\zeta(5) \simeq 1.0369278$). In addition, as the renormalization scale crosses quark mass thresholds one needs to match the scale dependence of m below and above the threshold. There are finite threshold corrections; the necessary formulae can be found in Ref. [5].

C. Lattice Gauge Theory

The use of the lattice simulations for *ab initio* determinations of the fundamental parameters of QCD, including the coupling constant and quark masses (except for the top-quark

Quark Particle Listings

Quarks

mass) is a very active area of research, with the current emphasis being on the reduction and control of the systematic uncertainties. We now briefly review some of the features of lattice QCD. In this approach space-time is approximated by a finite, discrete *lattice* of points and multi-local correlation functions are computed by the numerical evaluation of the corresponding functional integrals. To determine quark masses, one computes a convenient and appropriate set of physical quantities (frequently chosen to be a set of hadronic masses) using lattice QCD for a variety of input values of the quark masses. The true (physical) values of the quark masses are those which correctly reproduce the set of physical quantities being used for calibration.

The values of the quark masses obtained directly in lattice simulations are bare quark masses, with the lattice spacing a (i.e. the distance between neighboring points of the lattice) as the ultraviolet cut-off. In order for the lattice results to be useful in phenomenology, it is therefore necessary to relate the bare quark masses in a lattice formulation of QCD to renormalized masses in some standard renormalization scheme such as $\overline{\text{MS}}$. Provided that both the ultraviolet cut-off a^{-1} and the renormalization scale are much greater than Λ_{QCD} , the bare and renormalized masses can be related in perturbation theory (this is frequently facilitated by the use of chiral Ward identities). However, the coefficients in lattice perturbation theory are often found to be large, and our ignorance of higher order terms is generally a significant source of systematic uncertainty. Increasingly, non-perturbative renormalization is used to calculate the relation between the bare and renormalized masses, circumventing the need for lattice perturbation theory.

The precision with which quark masses can be determined in lattice simulations is limited by the available computing resources. There are a number of sources of systematic uncertainty and there has been considerable progress in recent years in reducing these. It remains true that the main source of uncertainty arises from the *chiral extrapolation*, the extrapolation of results from the up and down quark masses at which the simulations are performed to the physical masses. Recent developments in algorithms, together with improved computing power are allowing the computations to be performed at ever smaller masses which are in the chiral regime where chiral perturbation theory (see section D) is expected to be valid. This is in marked contrast with the situation of just a few years ago, when many computations were being performed without including sea quarks at all (i.e. in the so-called *quenched approximation*), in which effectively the sea quarks are infinitely heavy.

In addition one has to consider the uncertainties due to the fact that the lattice spacing is non-zero (lattice artefacts) and that the volume is not infinite. The former are studied by observing the stability of the results as a is varied or by using "improved" formulations of lattice QCD (or both). The dominant source of finite-volume error arises from the long-distance propagation of pions, the lightest hadrons. This can

be studied theoretically using chiral perturbation theory and/or numerically by varying the volume of the lattice.

D. Light quarks

For light quarks, one can use the techniques of chiral perturbation theory [6,7,8] to extract quark mass ratios. The mass term for light quarks in the QCD Lagrangian is

$$\overline{\Psi}M\Psi = \overline{\Psi}_L M \Psi_R + \overline{\Psi}_R M^\dagger \Psi_L, \quad (3)$$

where M is the light quark mass matrix M ,

$$M = \begin{pmatrix} m_u & 0 & 0 \\ 0 & m_d & 0 \\ 0 & 0 & m_s \end{pmatrix}, \quad (4)$$

and $\Psi = (u, d, s)$. The mass term is the only term in the QCD Lagrangian that mixes left- and right-handed quarks. In the limit $M \rightarrow 0$, there is an independent $SU(3) \times U(1)$ flavor symmetry for the left- and right-handed quarks. The vector $U(1)$ symmetry is baryon number; the axial $U(1)$ symmetry of the classical theory is broken in the quantum theory due to the anomaly. The remaining $G_\chi = SU(3)_L \times SU(3)_R$ chiral symmetry of the QCD Lagrangian is spontaneously broken to $SU(3)_V$, which, in the limit $M \rightarrow 0$, leads to eight massless Goldstone bosons, the π 's, K 's, and η .

The symmetry G_χ is only an approximate symmetry, since it is explicitly broken by the quark mass matrix M . The Goldstone bosons acquire masses which can be computed in a systematic expansion in M , in terms of low-energy constants, which are unknown nonperturbative parameters of the theory, and are not fixed by the symmetries. One treats the quark mass matrix M as an external field that transforms under G_χ as $M \rightarrow LMR^\dagger$, where $\Psi_L \rightarrow L\Psi_L$ and $\Psi_R \rightarrow R\Psi_R$ are the $SU(3)_L$ and $SU(3)_R$ transformations, and writes down the most general Lagrangian invariant under G_χ . Then one sets M to its given constant value Eq. (4), which implements the symmetry breaking. To first order in M one finds that [9]

$$\begin{aligned} m_{\pi^0}^2 &= B(m_u + m_d), \\ m_{\pi^\pm}^2 &= B(m_u + m_d) + \Delta_{\text{em}}, \\ m_{K^0}^2 &= m_{K^\pm}^2 = B(m_d + m_s), \\ m_{K^\pm}^2 &= B(m_u + m_s) + \Delta_{\text{em}}, \\ m_\eta^2 &= \frac{1}{3}B(m_u + m_d + 4m_s), \end{aligned} \quad (5)$$

with two unknown constants B and Δ_{em} , the electromagnetic mass difference. From Eq. (5), one can determine the quark mass ratios [9]

$$\begin{aligned} \frac{m_u}{m_d} &= \frac{2m_{\pi^0}^2 - m_{\pi^\pm}^2 + m_{K^\pm}^2 - m_{K^0}^2}{m_{K^0}^2 - m_{K^\pm}^2 + m_{\pi^\pm}^2} = 0.56, \\ \frac{m_s}{m_d} &= \frac{m_{K^0}^2 + m_{K^\pm}^2 - m_{\pi^\pm}^2}{m_{K^0}^2 + m_{\pi^\pm}^2 - m_{K^\pm}^2} = 20.1, \end{aligned} \quad (6)$$

to lowest order in chiral perturbation theory, with an error which will be estimated below. Since the mass ratios extracted using

chiral perturbation theory use the symmetry transformation property of M under the chiral symmetry G_χ , it is important to use a renormalization scheme for QCD that does not change this transformation law. Any mass independent subtraction scheme such as $\overline{\text{MS}}$ is suitable. The ratios of quark masses are scale independent in such a scheme, and Eq. (6) can be taken to be the ratio of $\overline{\text{MS}}$ masses. Chiral perturbation theory cannot determine the overall scale of the quark masses, since it uses only the symmetry properties of M , and any multiple of M has the same G_χ transformation law as M .

Chiral perturbation theory is a systematic expansion in powers of the light quark masses. The typical expansion parameter is $m_K^2/\Lambda_\chi^2 \sim 0.25$ if one uses $SU(3)$ chiral symmetry, and $m_\pi^2/\Lambda_\chi^2 \sim 0.02$ if one uses $SU(2)$ chiral symmetry. Electromagnetic effects at the few percent level also break $SU(2)$ and $SU(3)$ symmetry. The mass formulæ Eq. (5) were derived using $SU(3)$ chiral symmetry, and are expected to have a 25% uncertainty due to second order corrections.

There is a subtlety which arises when one tries to determine quark mass ratios at second order in chiral perturbation theory. The second order quark mass term [10]

$$\left(M^\dagger\right)^{-1} \det M^\dagger \quad (7)$$

(which can be generated by instantons) transforms in the same way under G_χ as M . Chiral perturbation theory cannot distinguish between M and $\left(M^\dagger\right)^{-1} \det M^\dagger$; one can make the replacement $M \rightarrow M(\lambda) = M + \lambda M \left(M^\dagger M\right)^{-1} \det M^\dagger$ in the chiral Lagrangian,

$$\begin{aligned} M(\lambda) &= \text{diag}(m_u(\lambda), m_d(\lambda), m_s(\lambda)) \\ &= \text{diag}(m_u + \lambda m_d m_s, m_d + \lambda m_u m_s, m_s + \lambda m_u m_d), \end{aligned} \quad (8)$$

and leave all observables unchanged.

The combination

$$\left(\frac{m_u}{m_d}\right)^2 + \frac{1}{Q^2} \left(\frac{m_s}{m_d}\right)^2 = 1 \quad (9)$$

where

$$Q^2 = \frac{m_s^2 - \hat{m}^2}{m_d^2 - m_u^2}, \quad \hat{m} = \frac{1}{2}(m_u + m_d),$$

is insensitive to the transformation in Eq. (8). Eq. (9) gives an ellipse in the $m_u/m_d - m_s/m_d$ plane. The ellipse is well-determined by chiral perturbation theory, but the exact location on the ellipse, and the absolute normalization of the quark masses, has larger uncertainties. Q is determined to be in the range 21–25 from $\eta \rightarrow 3\pi$ decay and the electromagnetic contribution to the $K^+ - K^0$ and $\pi^+ - \pi^0$ mass differences [11].

It is particularly important to determine the quark mass ratio m_u/m_d , since there is no strong CP problem if $m_u = 0$. The chiral symmetry G_χ of the QCD Lagrangian is not enhanced even if $m_u = 0$. [The possible additional axial u -quark number symmetry is anomalous. The only additional symmetry when $m_u = 0$ is CP .] As a result $m_u = 0$ is not a special value for chiral perturbation theory.

The absolute normalization of the quark masses can be determined by using methods that go beyond chiral perturbation theory, such as spectral function sum rules [12,13] for hadronic correlation functions or lattice simulations.

Sum Rules: Sum rule methods have been extensively used to determine quark masses and for illustration we briefly discuss here their application to hadronic τ decays [14]. Other applications involve very similar techniques.

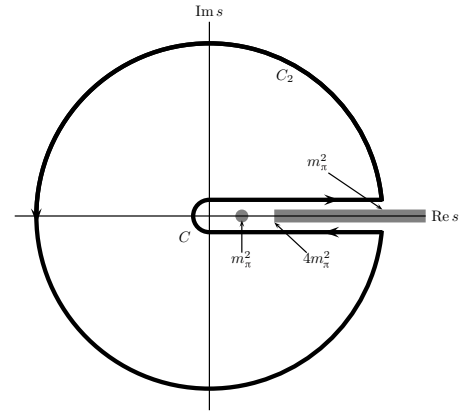


Figure 1: The analytic structure of $\Pi(s)$ in the complex s -plane. The contours C_1 and C_2 are the integration contours discussed in the text.

The experimentally measured quantity is R_τ ,

$$\frac{dR_\tau}{ds} = \frac{d\Gamma/ds(\tau^- \rightarrow \text{hadrons} + \nu_\tau(\gamma))}{\Gamma(\tau^- \rightarrow e^- \bar{\nu}_e \nu_\tau(\gamma))} \quad (10)$$

the hadronic invariant mass spectrum in semihadronic τ decay, normalized to the leptonic τ decay rate. It is useful to define q as the total momentum of the hadronic final state, so $s = q^2$ is the hadronic invariant mass. The total hadronic τ decay rate R_τ is then given by integrating dR_τ/ds over the kinematically allowed range $0 \leq s \leq M_\tau^2$.

R_τ can be written as

$$\begin{aligned} R_\tau &= 12\pi \int_0^{M_\tau^2} \frac{ds}{M_\tau^2} \left(1 - \frac{s}{M_\tau^2}\right)^2 \\ &\quad \times \left[\left(1 + 2\frac{s}{M_\tau^2}\right) \text{Im} \Pi^T(s) + \text{Im} \Pi^L(s) \right] \end{aligned} \quad (11)$$

where $s = q^2$, and the hadronic spectral functions $\Pi^{L,T}$ are defined from the time-ordered correlation function of two weak currents is the time-ordered correlator of the weak interaction current ($j^\mu(x)$ and $j^\nu(0)$) by

$$\Pi^{\mu\nu}(q) = i \int d^4x e^{iq \cdot x} \langle 0 | T \left(j^\mu(x) j^\nu(0)^\dagger \right) | 0 \rangle, \quad (12)$$

$$\Pi^{\mu\nu}(q) = (-g^{\mu\nu} + q^\mu q^\nu) \Pi^T(s) + q^\mu q^\nu \Pi^L(s), \quad (13)$$

and the decomposition Eq. (13) is the most general possible structure consistent with Lorentz invariance.

Quark Particle Listings

Quarks

By the optical theorem, the imaginary part of $\Pi^{\mu\nu}$ is proportional to the total cross-section for the current to produce all possible states. A detailed analysis including the phase space factors leads to Eq. (11). The spectral functions $\Pi^{L,T}(s)$ are analytic in the complex s plane, with singularities along the real axis. There is an isolated pole at $s = m_\pi^2$, and single- and multi-particle singularities for $s \geq 4m_\pi^2$, the two-particle threshold. The discontinuity along the real axis is $\Pi^{L,T}(s + i0^+) - \Pi^{L,T}(s - i0^+) = 2i\text{Im} \Pi^{L,T}(s)$. As a result, Eq. (11) can be rewritten with the replacement $\text{Im} \Pi^{L,T}(s) \rightarrow -i\Pi^{L,T}(s)/2$, and the integration being over the contour C_1 . Finally, the contour C_1 can be deformed to C_2 without crossing any singularities, and so leaving the integral unchanged. One can derive a series of sum rules analogous to Eq. (11) by weighting the differential τ hadronic decay rate by different powers of the hadronic invariant mass,

$$R_\tau^{kl} = \int_0^{M_\tau^2} ds \left(1 - \frac{s}{M_\tau^2}\right)^k \left(\frac{s}{M_\tau^2}\right)^l \frac{dR_\tau}{ds} \quad (14)$$

where dR_τ/ds is the hadronic invariant mass distribution in τ decay normalized to the leptonic decay rate. This leads to the final form of the sum rule(s),

$$R_\tau^{kl} = -6\pi i \int_{C_2} \frac{ds}{M_\tau^2} \left(1 - \frac{s}{M_\tau^2}\right)^{2+k} \left(\frac{s}{M_\tau^2}\right)^l \times \left[\left(1 + 2\frac{s}{M_\tau^2}\right) \Pi^T(s) + \Pi^L(s) \right]. \quad (15)$$

The manipulations so far are completely rigorous and exact, relying only on the general analytic structure of quantum field theory. The left-hand side of the sum rule Eq. (15) is obtained from experiment. The right hand-side can be computed for s far away from any physical cuts using the operator product expansion (OPE) for the time-ordered product of currents in Eq. (12), and QCD perturbation theory. The OPE is an expansion for the time-ordered product Eq. (12) in a series of local operators, and is an expansion about the $q \rightarrow \infty$ limit. It gives $\Pi(s)$ as an expansion in powers of $\alpha_s(s)$ and Λ_{QCD}^2/s , and is valid when s is far (in units of Λ_{QCD}^2) from any singularities in the complex s -plane.

The OPE gives $\Pi(s)$ as a series in α_s , quark masses, and various non-perturbative vacuum matrix element. By computing $\Pi(s)$ theoretically, and comparing with the experimental values of R_τ^{kl} , one determines various parameters such as α_s and the quark masses. The theoretical uncertainties in using Eq. (15) arise from neglected higher order corrections (both perturbative and non-perturbative), and because the OPE is no longer valid near the real axis, where Π has singularities. The contribution of neglected higher order corrections can be estimated as for any other perturbative computation. The error due to the failure of the OPE is more difficult to estimate. In Eq. (15), the OPE fails on the endpoints of C_2 that touch the real axis at $s = M_\tau^2$. The weight factor $(1 - s/M_\tau^2)$ in Eq. (15) vanishes at this point, so the importance of the endpoint can be reduced by choosing larger values of k .

Lattice Gauge Theory: Lattice simulations allow for detailed studies of the behaviour of hadronic masses and matrix elements as functions of the quark masses. Moreover, the quark masses do not have to take their physical values, but can be varied freely and chiral perturbation theory applies also for unphysical masses, provided that they are sufficiently light. There are now a significant number of simulations with $N_f = 2 + 1$ or $N_f = 2$ flavours of sea quarks, some of which are sufficiently light to be considered in the chiral regime, and it is now appropriate to ignore results from quenched calculations. Thus *quenching*, an uncontrolled systematic error present in earlier calculations, is now eliminated.

Recent unquenched determinations of the masses of the light quarks were obtained using a variety of formulations of lattice QCD (see, for example, the set of results in refs. [15] – [20]). Some of the simulations have been performed with two flavours of sea quarks and some with three flavours. The lattice systematic uncertainties in these determinations are different (e.g. due to the different lattice formulations of QCD, the use of perturbative or non-perturbative renormalization, the different chiral and continuum extrapolations and the treatment of finite-volume effects). Taking these into consideration, we give below our current estimates for the quark masses determined from lattice simulations.

Current lattice simulations are performed in the isospin symmetry limit, i.e. with the masses of the up and down quarks equal, $m_u = m_d \equiv m_{ud}$ and, apart from ref. [19], electromagnetic effects are not included in the simulation. It is average of the physical up and down quark masses which is determined directly. In order to estimate m_u and m_d separately, further experimental and theoretical inputs have to be included. Recently this has been done by the MILC collaboration [15,16,17,18] and by the RBC collaboration [19]; the latter include (quenched) electromagnetic effects. One important conclusion from these and earlier studies is that $m_u \neq 0$.

The quark masses for light quarks discussed so far are often referred to as current quark masses. Nonrelativistic quark models use constituent quark masses, which are of order 350 MeV for the u and d quarks. Constituent quark masses model the effects of dynamical chiral symmetry breaking, and are not related to the quark mass parameters m_k of the QCD Lagrangian Eq. (1). Constituent masses are only defined in the context of a particular hadronic model.

E. Heavy quarks

The masses and decay rates of hadrons containing a single heavy quark, such as the B and D mesons can be determined using the heavy quark effective theory (HQET) [21]. The theoretical calculations involve radiative corrections computed in perturbation theory with an expansion in $\alpha_s(m_Q)$ and non-perturbative corrections with an expansion in powers of Λ_{QCD}/m_Q . Due to the asymptotic nature of the QCD perturbation series, the two kinds of corrections are intimately

related; an example of this are renormalon effects in the perturbative expansion which are associated with non-perturbative corrections.

Systems containing two heavy quarks such as the Υ or J/Ψ are treated using NRQCD [22]. The typical momentum and energy transfers in these systems are $\alpha_s m_Q$, and $\alpha_s^2 m_Q$, respectively, so these bound states are sensitive to scales much smaller than m_Q . However, smeared observables, such as the cross-section for $e^+e^- \rightarrow \bar{b}b$ averaged over some range of s that includes several bound state energy levels, are better behaved and only sensitive to scales near m_Q . For this reason, most determinations of the b quark mass using perturbative calculations compare smeared observables with experiment [23,24,25].

Lattice simulations of QCD requires the quark mass to be much smaller than a^{-1} , where a is the lattice spacing, in order to avoid large errors due to the granularity of the lattice. Since computing resources limit a^{-1} in current simulations to be typically in the range 1.5–2.5 GeV, this is not possible for the b -quark and is marginal for the c -quark. For this reason, particularly for the b -quark, simulations are performed using effective theories, including HQET and NRQCD. Using effective theories, m_b is obtained from what is essentially a computation of the difference of $M_{H_b} - m_b$, where M_{H_b} is the mass of a hadron H_b containing a b -quark. The relative error on m_b is therefore much smaller than that for $M_{H_b} - m_b$, and this is the reason for the small errors quoted in section F. The principal systematic errors are the matching of the effective theories to QCD and the presence of power divergences in a^{-1} in the $1/m_b$ corrections which have to be subtracted numerically. The use of HQET or NRQCD is less precise for the charm quark, and in this case *improved* formulations of QCD, in which the errors to the finite lattice spacing are formally reduced are being used (see in particular refs. [26,27]).

For an observable particle such as the electron, the position of the pole in the propagator is the definition of the particle mass. In QCD this definition of the quark mass is known as the pole mass. It is known that the on-shell quark propagator has no infrared divergences in perturbation theory [28,29], so this provides a perturbative definition of the quark mass. The pole mass cannot be used to arbitrarily high accuracy because of nonperturbative infrared effects in QCD. The full quark propagator has no pole because the quarks are confined, so that the pole mass cannot be defined outside of perturbation theory. The relation between the pole mass m_Q and the $\overline{\text{MS}}$ mass \overline{m}_Q is known to three loops [30,31,32,33]

$$m_Q = \overline{m}_Q(\overline{m}_Q) \left\{ 1 + \frac{4\overline{\alpha}_s(\overline{m}_Q)}{3\pi} + \left[-1.0414 \sum_k \left(1 - \frac{4\overline{m}_{Q_k}}{3\overline{m}_Q} \right) + 13.4434 \right] \left[\frac{\overline{\alpha}_s(\overline{m}_Q)}{\pi} \right]^2 + [0.6527N_L^2 - 26.655N_L + 190.595] \left[\frac{\overline{\alpha}_s(\overline{m}_Q)}{\pi} \right]^3 \right\}, \quad (16)$$

where $\overline{\alpha}_s(\mu)$ is the strong interaction coupling constants in the $\overline{\text{MS}}$ scheme, and the sum over k extends over the N_L flavors Q_k lighter than Q . The complete mass dependence of the α_s^2 term can be found in [30]; the mass dependence of the α_s^3 term is not known. For the b -quark, Eq. (16) reads

$$m_b = \overline{m}_b(\overline{m}_b) [1 + 0.09 + 0.05 + 0.03], \quad (17)$$

where the contributions from the different orders in α_s are shown explicitly. The two and three loop corrections are comparable in size and have the same sign as the one loop term. This is a signal of the asymptotic nature of the perturbation series [there is a renormalon in the pole mass]. Such a badly behaved perturbation expansion can be avoided by directly extracting the $\overline{\text{MS}}$ mass from data without extracting the pole mass as an intermediate step.

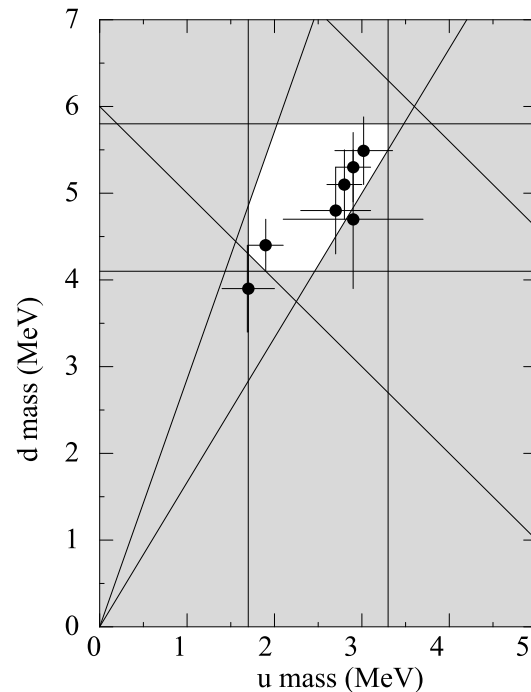


Figure 2: The allowed region (shown in white) for up quark and down quark masses. This region was determined in part from papers reporting values for m_u and m_d (data points shown) and in part from analysis of the allowed ranges of other mass parameters (see Fig. 3). The parameter $(m_u + m_d)/2$ yields the two downward-sloping lines, while m_u/m_d yields the two rising lines originating at $(0,0)$. The grey point is from a paper giving no error bars.

Quark Particle Listings

Quarks

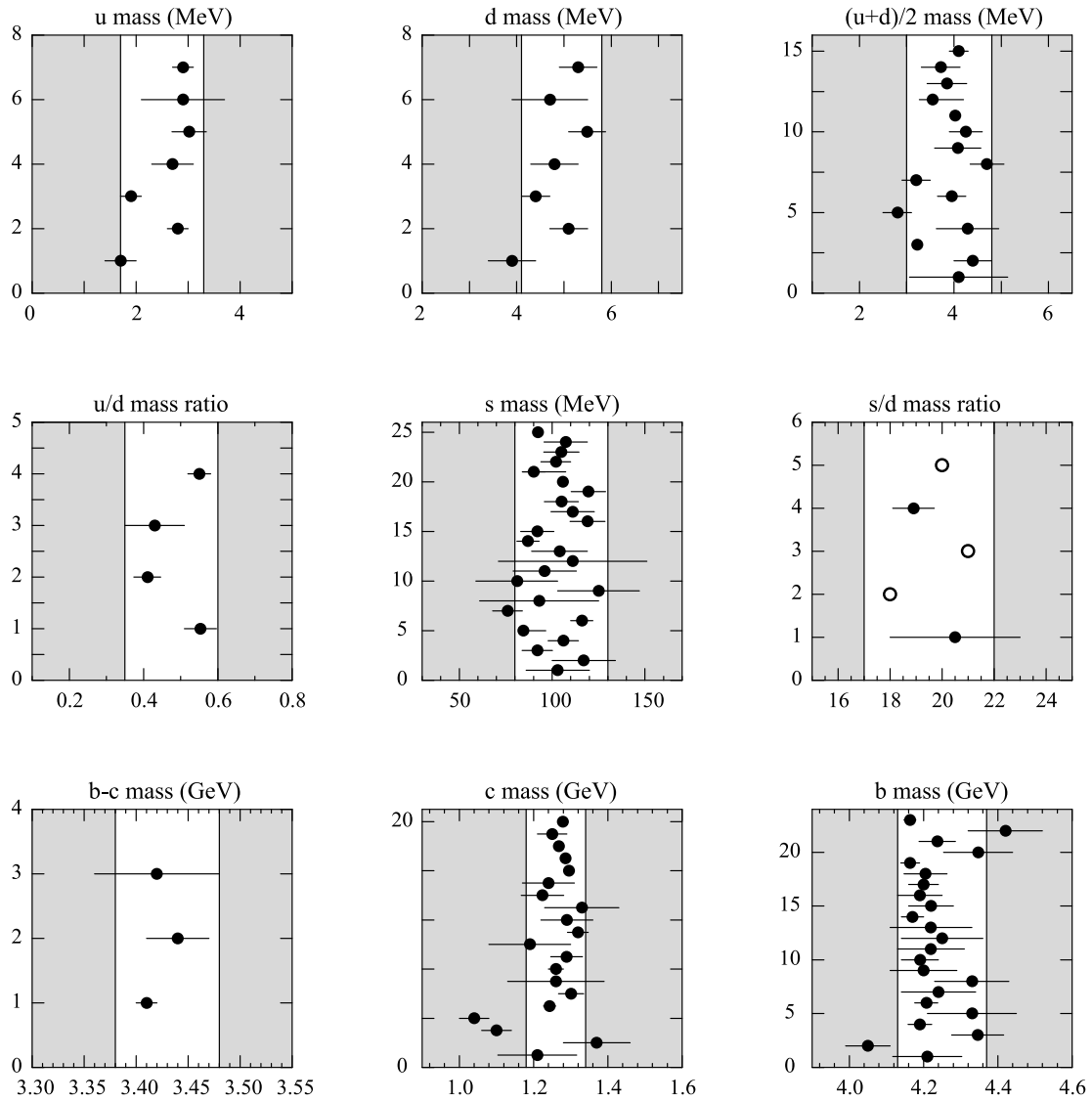


Figure 3. The values of each quark mass parameter taken from the Data Listings. Points from papers reporting no error bars are colored grey. Arrows indicate limits reported. The grey regions indicate values excluded by our evaluations; some regions were determined in part though examination of Fig. 2.

See key on page 405

F. Numerical values and caveats

The quark masses in the particle data listings have been obtained by using a wide variety of methods. Each method involves its own set of approximations and errors. In most cases, the errors are a best guess at the size of neglected higher-order corrections or other uncertainties. The expansion parameters for some of the approximations are not very small (for example, they are $m_K^2/\Lambda_\chi^2 \sim 0.25$ for the chiral expansion and $\Lambda_{\text{QCD}}/m_b \sim 0.1$ for the heavy-quark expansion), so an unexpectedly large coefficient in a neglected higher-order term could significantly alter the results. It is also important to note that the quark mass values can be significantly different in the different schemes.

The heavy quark masses obtained using HQET, QCD sum rules, or lattice gauge theory are consistent with each other if they are all converted into the same scheme and scale. We have specified all masses in the $\overline{\text{MS}}$ scheme. For light quarks, the renormalization scale has been chosen to be $\mu = 2 \text{ GeV}$. The light quark masses at 1 GeV are significantly different from those at 2 GeV, $\overline{m}(1 \text{ GeV})/\overline{m}(2 \text{ GeV}) \sim 1.35$. It is conventional to choose the renormalization scale equal to the quark mass for a heavy quark, so we have quoted $\overline{m}_Q(\mu)$ at $\mu = \overline{m}_Q$ for the c and b quarks. Recent analyses of inclusive B meson decays have shown that recently proposed mass definitions lead to a better behaved perturbation series than for the $\overline{\text{MS}}$ mass, and hence to more accurate mass values. We have chosen to also give values for one of these, the b quark mass in the 1S-scheme [34,35]. Other schemes that have been proposed are the PS-scheme [36] and the kinetic scheme [37].

If necessary, we have converted values in the original papers to our chosen scheme using two-loop formulæ. It is important to realize that our conversions introduce significant additional errors. In converting to the $\overline{\text{MS}}$ b -quark mass, for example, the three-loop conversions from the 1S and pole masses give values about 40 MeV and 135 MeV lower than the two-loop conversions. The uncertainty in $\alpha_s(M_Z) = 0.1187(20)$ gives an uncertainty of ± 20 MeV and ± 35 MeV respectively in the same conversions. We have not added these additional errors when we do our conversions.

References

1. See the review of QCD in this volume..
2. A.V. Manohar and H. Georgi, Nucl. Phys. **B234**, 189 (1984).
3. K.G. Chetyrkin, Phys. Lett. **B404**, 161 (1997).
4. J.A.M. Vermaseren, S.A. Larin, and T. van Ritbergen, Phys. Lett. **B405**, 327 (1997).
5. K.G. Chetyrkin, B.A. Kniehl, and M. Steinhauser, Nucl. Phys. **B510**, 61 (1998).
6. S. Weinberg, Physica **96A**, 327 (1979).
7. J. Gasser and H. Leutwyler, Ann. Phys. **158**, 142 (184).
8. For a review, see A. Pich, Rept. Prog. Phys. **58**, 563 (1995).
9. S. Weinberg, Trans. N.Y. Acad. Sci. **38**, 185 (1977).
10. D.B. Kaplan and A.V. Manohar, Phys. Rev. Lett. **56**, 2004 (1986).
11. H. Leutwyler, Phys. Lett. **B374**, 163 (1996).
12. S. Weinberg, Phys. Rev. Lett. **18**, 507 (1967)..
13. M.A. Shifman, A.I. Vainshtein, V.I. Zakharov, Nucl. Phys. **B147**, 385 (1979).
14. E. Braaten, S. Narison, and A. Pich, Nucl. Phys. **B373**, 581 (1992).
15. C. Bernard *et al.*, PoS **LAT2007** (2007) 090[arXiv:0710.1118 [hep-lat]].
16. A. Bazavov *et al.*, arXiv:0903.3598 [hep-lat].
17. C. Aubin *et al.* [HPQCD Collab.], Phys. Rev. **D70**, 031504 (2004).
18. C. Aubin *et al.* [MILC Collab.], Phys. Rev. D **70** (2004) 114501 [arXiv:hep-lat/0407028].
19. T. Blum, T. Doi, M. Hayakawa, T. Izubuchi and N. Yamada, Phys. Rev. D **76** (2007) 114508 [arXiv:0708.0484 [hep-lat]].
20. A. Ali Khan *et al.* [CP-PACS Collab.], Phys. Rev. D **65** (2002) 054505 [Erratum-ibid. D **67** (2003) 059901] [arXiv:hep-lat/0105015].
21. N. Isgur and M.B. Wise, Phys. Lett. **B232**, 113 (1989), *ibid* **B237**, 527 (1990).
22. G.T. Bodwin, E. Braaten, and G.P. Lepage, Phys. Rev. **D51**, 1125 (1995).
23. A.H. Hoang, Phys. Rev. **D61**, 034005 (2000).
24. K. Melnikov and A. Yelkhovsky, Phys. Rev. **D59**, 114009 (1999).
25. M. Beneke and A. Signer, Phys. Lett. **B471**, 233 (1999).
26. A.X. El-Khadra, A.S. Kronfeld, and P.B. Mackenzie, Phys. Rev. **D55**, 3933 (1997).
27. S. Aoki, Y. Kuramashi, and S.i. Tominaga, Prog. Theor. Phys. **109**, 383 (2003).
28. R. Tarrach, Nucl. Phys. **B183**, 384 (1981).
29. A. Kronfeld, Phys. Rev. **D58**, 051501 (1998).
30. N. Gray *et al.*, Z. Phys. **C48**, 673 (1990).
31. D.J. Broadhurst, N. Gray, and K. Schilcher, Z. Phys. **C52**, 111 (1991).
32. K.G. Chetyrkin and M. Steinhauser, Phys. Rev. Lett. **83**, 4001 (1999).
33. K. Melnikov and T. van Ritbergen, Phys. Lett. **B482**, 99 (2000).
34. A.H. Hoang, Z. Ligeti, A.V. Manohar, Phys. Rev. Lett. **82**, 277 (1999).
35. A.H. Hoang, Z. Ligeti, A.V. Manohar, Phys. Rev. **D59**, 074017 (1999).
36. M. Beneke, Phys. Lett. **B434**, 115 (1998).
37. P. Gambino and N. Uraltsev, Eur. Phys. J. **C34**, 181 (2004).

Quark Particle Listings

Quarks, u, d, s , Light Quarks (u, d, s)

u $I(J^P) = \frac{1}{2}(\frac{1}{2}^+)$
 Mass $m = 1.7\text{--}3.3$ MeV Charge = $\frac{2}{3} e$ $I_z = +\frac{1}{2}$
 $m_u/m_d = 0.35\text{--}0.60$

d $I(J^P) = \frac{1}{2}(\frac{1}{2}^+)$
 Mass $m = 4.1\text{--}5.8$ MeV Charge = $-\frac{1}{3} e$ $I_z = -\frac{1}{2}$
 $m_s/m_d = 17$ to 22
 $\bar{m} = (m_u + m_d)/2 = 3.0\text{--}4.8$ MeV

s $I(J^P) = 0(\frac{1}{2}^+)$
 Mass $m = 101^{+29}_{-21}$ MeV Charge = $-\frac{1}{3} e$ Strangeness = -1
 $(m_s - (m_u + m_d)/2)/(m_d - m_u) = 22$ to 30

LIGHT QUARKS (u, d, s)

OMITTED FROM SUMMARY TABLE

u-QUARK MASS

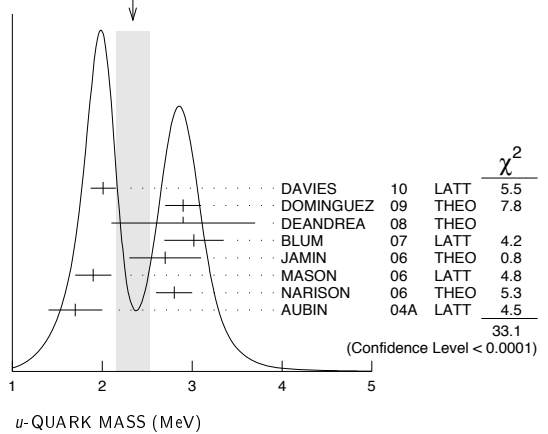
The u -, d -, and s -quark masses are estimates of so-called “current-quark masses,” in a mass-independent subtraction scheme such as \overline{MS} . The ratios m_u/m_d and m_s/m_d are extracted from pion and kaon masses using chiral symmetry. The estimates of d and u masses are not without controversy and remain under active investigation. Within the literature there are even suggestions that the u quark could be essentially massless. The s -quark mass is estimated from SU(3) splittings in hadron masses.

We have normalized the \overline{MS} masses at a renormalization scale of $\mu = 2$ GeV. Results quoted in the literature at $\mu = 1$ GeV have been rescaled by dividing by 1.35. The values of “Our Evaluation” were determined in part via Figures 1 and 2.

VALUE (MeV)	DOCUMENT ID	TECN	COMMENT
$2.49^{+0.81}_{-0.79}$ (1.7–3.3) OUR EVALUATION	See the ideogram below.		
2.01 ± 0.14	1 DAVIES	10 LATT	\overline{MS} scheme
2.9 ± 0.2	2 DOMINGUEZ	09 THEO	\overline{MS} scheme
2.9 ± 0.8	3 DEANDREA	08 THEO	\overline{MS} scheme
3.02 ± 0.33	4 BLUM	07 LATT	\overline{MS} scheme
2.7 ± 0.4	5 JAMIN	06 THEO	\overline{MS} scheme
1.9 ± 0.2	6 MASON	06 LATT	\overline{MS} scheme
2.8 ± 0.2	7 NARISON	06 THEO	\overline{MS} scheme
1.7 ± 0.3	8 AUBIN	04A LATT	\overline{MS} scheme
• • • We do not use the following data for averages, fits, limits, etc. • • •			
2.9 ± 0.6	9 JAMIN	02 THEO	\overline{MS} scheme
2.3 ± 0.4	10 NARISON	99 THEO	\overline{MS} scheme
3.9 ± 1.1	11 JAMIN	95 THEO	\overline{MS} scheme
3.0 ± 0.7	12 NARISON	95c THEO	\overline{MS} scheme

- DAVIES 10 determine $\bar{m}_c(\mu)/\bar{m}_s(\mu) = 11.85 \pm 0.16$ using a lattice computation with dynamical fermions of the pseudoscalar meson masses. Mass m_d is obtained from this using the value of m_c from ALLISON 08 and the BAZAVOV 10 values for the light quark mass ratios, m_s/\bar{m} and m_u/m_d .
- DOMINGUEZ 09 use QCD finite energy sum rules for the two-point function of the divergence of the axial vector current computed to order α_s^4 .
- DEANDREA 08 determine $m_u - m_d$ from $\eta \rightarrow 3\pi^0$, and combine with the PDG 06 lattice average value of $m_u + m_d = 7.6 \pm 1.6$ to determine m_u and m_d .
- BLUM 07 determine quark mass using a QED plus QCD lattice computation with two dynamical flavors of the pseudoscalar meson masses.
- JAMIN 06 determine $m_d(2 \text{ GeV})$ by combining the value of m_s obtained from the spectral function for the scalar $K\pi$ form factor with other determinations of the quark mass ratios.
- MASON 06 extract light quark masses from a lattice simulation using staggered fermions with an improved action, and three dynamical light quark flavors with degenerate u and d quarks. Perturbative corrections were included at NNLO order. The quark masses m_u and m_d were determined from their $(m_u + m_d)/2$ measurement and AUBIN 04A m_u/m_d value.
- NARISON 06 uses sum rules for $e^+e^- \rightarrow$ hadrons to order α_s^3 to determine m_s combined with other determinations of the quark mass ratios.
- AUBIN 04A employ a partially quenched lattice calculation of the pseudoscalar meson masses.
- JAMIN 02 first calculates the strange quark mass from QCD sum rules using the scalar channel, and then combines with the quark mass ratios obtained from chiral perturbation theory to obtain m_u .
- NARISON 99 uses sum rules to order α_s^3 for ϕ meson decays to get m_s , and finds m_d by combining with sum rule estimates of $m_u + m_d$ and Dashen's formula.
- JAMIN 95 uses QCD sum rules at next-to-leading order. We have rescaled $m_d(1 \text{ GeV}) = 5.3 \pm 1.5$ to $\mu = 2 \text{ GeV}$.
- For NARISON 95c, we have rescaled $m_u(1 \text{ GeV}) = 4 \pm 1$ to $\mu = 2 \text{ GeV}$.

WEIGHTED AVERAGE
 2.34 ± 0.19 (Error scaled by 2.3)



			χ^2
DAVIES	10	LATT	5.5
DOMINGUEZ	09	THEO	7.8
DEANDREA	08	THEO	
BLUM	07	LATT	4.2
JAMIN	06	THEO	0.8
MASON	06	LATT	4.8
NARISON	06	THEO	5.3
AUBIN	04A	LATT	4.5
			33.1

(Confidence Level < 0.0001)

d-QUARK MASS

See the comment for the u quark above.

We have normalized the \overline{MS} masses at a renormalization scale of $\mu = 2$ GeV. Results quoted in the literature at $\mu = 1$ GeV have been rescaled by dividing by 1.35. The values of “Our Evaluation” were determined in part via Figures 1 and 2.

VALUE (MeV)	DOCUMENT ID	TECN	COMMENT
$5.05^{+0.75}_{-0.95}$ (4.1–5.8) OUR EVALUATION	See the ideogram below.		
4.79 ± 0.16	13 DAVIES	10 LATT	\overline{MS} scheme
5.3 ± 0.4	14 DOMINGUEZ	09 THEO	\overline{MS} scheme
4.7 ± 0.8	15 DEANDREA	08 THEO	\overline{MS} scheme
5.49 ± 0.39	16 BLUM	07 LATT	\overline{MS} scheme
4.8 ± 0.5	17 JAMIN	06 THEO	\overline{MS} scheme
4.4 ± 0.3	18 MASON	06 LATT	\overline{MS} scheme
5.1 ± 0.4	19 NARISON	06 THEO	\overline{MS} scheme
3.9 ± 0.5	20 AUBIN	04A LATT	\overline{MS} scheme
• • • We do not use the following data for averages, fits, limits, etc. • • •			
5.2 ± 0.9	21 JAMIN	02 THEO	\overline{MS} scheme
6.4 ± 1.1	22 NARISON	99 THEO	\overline{MS} scheme
7.0 ± 1.1	23 JAMIN	95 THEO	\overline{MS} scheme
7.4 ± 0.7	24 NARISON	95c THEO	\overline{MS} scheme

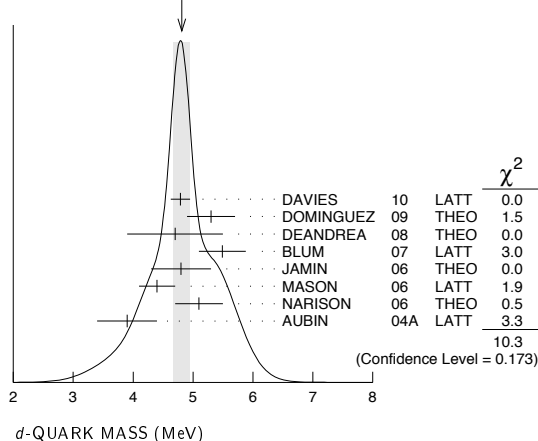
- DAVIES 10 determine $\bar{m}_c(\mu)/\bar{m}_s(\mu) = 11.85 \pm 0.16$ using a lattice computation with dynamical fermions of the pseudoscalar meson masses. Mass m_d is obtained from this using the value of m_c from ALLISON 08 and the BAZAVOV 10 values for the light quark mass ratios, m_s/\bar{m} and m_u/m_d .
- DOMINGUEZ 09 use QCD finite energy sum rules for the two-point function of the divergence of the axial vector current computed to order α_s^4 .
- DEANDREA 08 determine $m_u - m_d$ from $\eta \rightarrow 3\pi^0$, and combine with the PDG 06 lattice average value of $m_u + m_d = 7.6 \pm 1.6$ to determine m_u and m_d .
- BLUM 07 determine quark mass using a QED plus QCD lattice computation with two dynamical flavors of the pseudoscalar meson masses.
- JAMIN 06 determine $m_d(2 \text{ GeV})$ by combining the value of m_s obtained from the spectral function for the scalar $K\pi$ form factor with other determinations of the quark mass ratios.
- MASON 06 extract light quark masses from a lattice simulation using staggered fermions with an improved action, and three dynamical light quark flavors with degenerate u and d quarks. Perturbative corrections were included at NNLO order. The quark masses m_u and m_d were determined from their $(m_u + m_d)/2$ measurement and AUBIN 04A m_u/m_d value.
- NARISON 06 uses sum rules for $e^+e^- \rightarrow$ hadrons to order α_s^3 to determine m_s combined with other determinations of the quark mass ratios.
- AUBIN 04A perform three flavor dynamical lattice calculation of pseudoscalar meson masses, with continuum estimate of electromagnetic effects in the kaon masses, and one-loop perturbative renormalization constant.
- JAMIN 02 first calculates the strange quark mass from QCD sum rules using the scalar channel, and then combines with the quark mass ratios obtained from chiral perturbation theory to obtain m_d .
- NARISON 99 uses sum rules to order α_s^3 for ϕ meson decays to get m_s , and finds m_d by combining with sum rule estimates of $m_u + m_d$ and Dashen's formula.
- JAMIN 95 uses QCD sum rules at next-to-leading order. We have rescaled $m_d(1 \text{ GeV}) = 9.4 \pm 1.5$ to $\mu = 2 \text{ GeV}$.
- For NARISON 95c, we have rescaled $m_d(1 \text{ GeV}) = 10 \pm 1$ to $\mu = 2 \text{ GeV}$.

See key on page 405

Quark Particle Listings

Light Quarks (u, d, s)

WEIGHTED AVERAGE
4.81±0.14 (Error scaled by 1.2)



$$\bar{m} = (m_u + m_d)/2$$

See the comments for the u quark above.

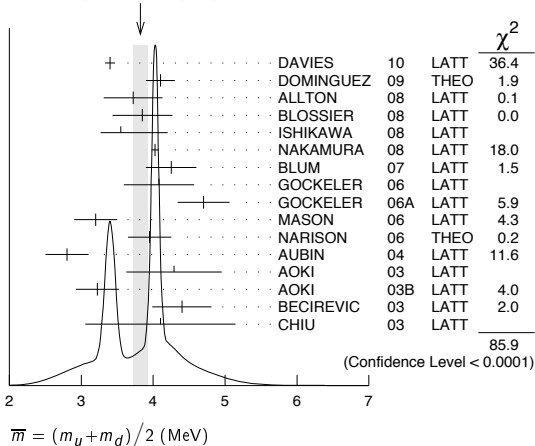
We have normalized the \bar{m} masses at a renormalization scale of $\mu = 2$ GeV. Results quoted in the literature at $\mu = 1$ GeV have been rescaled by dividing by 1.35. The values of "Our Evaluation" were determined in part via Figures 1 and 2.

VALUE (MeV)	DOCUMENT ID	TECN	COMMENT
3.77^{+1.03}_{-0.77} (3.0-4.8) OUR EVALUATION	See the ideogram below.		
3.40 ± 0.07	25 DAVIES	10 LATT	\overline{MS} scheme
4.1 ± 0.2	26 DOMINGUEZ	09 THEO	\overline{MS} scheme
3.72 ± 0.41	27 ALLTON	08 LATT	\overline{MS} scheme
3.85 ± 0.12 ± 0.4	28 BLOSSIER	08 LATT	\overline{MS} scheme
3.55 ^{+0.65} _{-0.28}	29 ISHIKAWA	08 LATT	\overline{MS} scheme
4.026 ± 0.048	30 NAKAMURA	08 LATT	\overline{MS} scheme
4.25 ± 0.35	31 BLUM	07 LATT	\overline{MS} scheme
4.08 ± 0.25 ± 0.42	32 GOCKELER	06 LATT	\overline{MS} scheme
4.7 ± 0.2 ± 0.3	33 GOCKELER	06A LATT	\overline{MS} scheme
3.2 ± 0.3	34 MASON	06 LATT	\overline{MS} scheme
3.95 ± 0.3	35 NARISON	06 THEO	\overline{MS} scheme
2.8 ± 0.3	36 AUBIN	04 LATT	\overline{MS} scheme
4.29 ± 0.14 ± 0.65	37 AOKI	03 LATT	\overline{MS} scheme
3.223 ± 0.3	38 AOKI	03B LATT	\overline{MS} scheme
4.4 ± 0.1 ± 0.4	39 BECIREVIC	03 LATT	\overline{MS} scheme
4.1 ± 0.3 ± 1.0	40 CHIU	03 LATT	\overline{MS} scheme
• • • We do not use the following data for averages, fits, limits, etc. • • •			
≥ 4.85 ± 0.20	41 DOMINGUEZ...08b	THEO	\overline{MS} scheme
3.45 ^{+0.14} _{-0.20}	42 ALIKHAN	02 LATT	\overline{MS} scheme
5.3 ± 0.3	43 CHIU	02 LATT	\overline{MS} scheme
3.9 ± 0.6	44 MALTMAN	02 THEO	\overline{MS} scheme
3.9 ± 0.6	45 MALTMAN	01 THEO	\overline{MS} scheme
4.57 ± 0.18	46 AOKI	00 LATT	\overline{MS} scheme
4.4 ± 2	47 GOCKELER	00 LATT	\overline{MS} scheme
4.23 ± 0.29	48 AOKI	99 LATT	\overline{MS} scheme
≥ 2.1	49 STEELE	99 THEO	\overline{MS} scheme
4.5 ± 0.4	50 BECIREVIC	98 LATT	\overline{MS} scheme
4.6 ± 1.2	51 DOSCH	98 THEO	\overline{MS} scheme
4.7 ± 0.9	52 PRADES	98 THEO	\overline{MS} scheme
2.7 ± 0.2	53 EICKER	97 LATT	\overline{MS} scheme
3.6 ± 0.6	54 GOUGH	97 LATT	\overline{MS} scheme
3.4 ± 0.4 ± 0.3	55 GUPTA	97 LATT	\overline{MS} scheme
> 3.8	56 LELLOUCH	97 THEO	\overline{MS} scheme
4.5 ± 1.0	57 BIJNENS	95 THEO	\overline{MS} scheme

- 25 DAVIES 10 determine $\bar{m}_c(\mu)/\bar{m}_s(\mu) = 11.85 \pm 0.16$ using a lattice computation with dynamical fermions of the pseudoscalar meson masses. Mass \bar{m} is obtained from this using the value of m_c from ALLISON 08 and the BAZAVOV 10 values for the light quark mass ratio, m_s/\bar{m} .
- 26 DOMINGUEZ 09 use QCD finite energy sum rules for the two-point function of the divergence of the axial vector current computed to order α_s^4 .
- 27 ALLTON 08 use a lattice computation of the π , K , and Ω masses with 2+1 dynamical flavors of domain wall quarks, and non-perturbative renormalization.
- 28 BLOSSIER 08 use a lattice computation of pseudoscalar meson masses and decay constants with 2 dynamical flavors and non-perturbative renormalization.
- 29 ISHIKAWA 08 use a lattice computation of the light meson spectrum with 2+1 dynamical flavors of $\mathcal{O}(a)$ improved Wilson quarks, and one-loop perturbative renormalization.
- 30 NAKAMURA 08 do a lattice computation using quenched domain wall fermions and non-perturbative renormalization.
- 31 BLUM 07 determine quark mass using a QED plus QCD lattice computation with two dynamical flavors of the pseudoscalar meson masses.

- 32 GOCKELER 06 use an unquenched lattice computation of the axial Ward Identity with $N_f = 2$ dynamical light quark flavors, and non-perturbative renormalization, to obtain $\bar{m}(2 \text{ GeV}) = 4.08 \pm 0.25 \pm 0.19 \pm 0.23 \text{ MeV}$, where the first error is statistical, the second and third are systematic due to the fit range and force scale uncertainties, respectively. We have combined the systematic errors linearly.
- 33 GOCKELER 06A use an unquenched lattice computation of the pseudoscalar meson masses with $N_f = 2$ dynamical light quark flavors, and non-perturbative renormalization.
- 34 MASON 06 extract light quark masses from a lattice simulation using staggered fermions with an improved action, and three dynamical light quark flavors with degenerate u and d quarks. Perturbative corrections were included at NNLO order.
- 35 NARISON 06 uses sum rules for $e^+e^- \rightarrow$ hadrons to order α_s^3 to determine m_s combined with other determinations of the quark mass ratios.
- 36 AUBIN 04 perform three flavor dynamical lattice calculation of pseudoscalar meson masses, with one-loop perturbative renormalization constant.
- 37 AOKI 03 uses quenched lattice simulation of the meson and baryon masses with degenerate light quarks. The extrapolations are done using quenched chiral perturbation theory.
- 38 The errors given in AOKI 03B were ± 0.046 . We changed them to ± 0.3 for calculating the overall best values. AOKI 03B uses lattice simulation of the meson and baryon masses with two dynamical light quarks. Simulations are performed using the $\mathcal{O}(a)$ improved Wilson action.
- 39 BECIREVIC 03 perform quenched lattice computation using the vector and axial Ward identities. Uses $\mathcal{O}(a)$ improved Wilson action and nonperturbative renormalization.
- 40 CHIU 03 determines quark masses from the pion and kaon masses using a lattice simulation with a chiral fermion action in quenched approximation.
- 41 DOMINGUEZ-CLARIMON 08b obtain an inequality from sum rules for the scalar two-point correlator.
- 42 ALIKHAN 02 uses lattice simulation of the meson and baryon masses with two dynamical flavors and degenerate light quarks.
- 43 CHIU 02 extracts the average light quark mass from quenched lattice simulations using quenched chiral perturbation theory.
- 44 MALTMAN 02 uses finite energy sum rules in the ud and us pseudoscalar channels. Other mass values are also obtained by similar methods.
- 45 MALTMAN 01 uses Borel transformed and finite energy sum rules.
- 46 AOKI 00 obtain the light quark masses from a quenched lattice simulation of the meson and baryon spectrum with the Wilson quark action.
- 47 GOCKELER 00 obtained from a quenched lattice computation of the pseudoscalar meson masses using $\mathcal{O}(a)$ improved Wilson fermions and nonperturbative renormalization.
- 48 AOKI 99 obtain the light quark masses from a quenched lattice simulation of the meson spectrum with the staggered quark action employing the regularization independent scheme.
- 49 STEELE 99 obtain a bound on the light quark masses by applying the Holder inequality to a sum rule. We have converted their bound of $(m_u+m_d)/2 \geq 3 \text{ MeV}$ at $\mu=1 \text{ GeV}$ to $\mu=2 \text{ GeV}$.
- 50 BECIREVIC 98 compute the quark mass using the Alpha action in the quenched approximation. The conversion from the regularization independent scheme to the \overline{MS} scheme is at NNLO.
- 51 DOSCH 98 use sum rule determinations of the quark condensate and chiral perturbation theory to obtain $9.4 \leq (m_u+m_d)(1 \text{ GeV}) \leq 15.7 \text{ MeV}$. We have converted to result to $\mu=2 \text{ GeV}$.
- 52 PRADES 98 uses finite energy sum rules for the axial current correlator.
- 53 EICKER 97 use lattice gauge computations with two dynamical light flavors.
- 54 GOUGH 97 use lattice gauge computations in the quenched approximation. Correcting for quenching gives $2.1 < \bar{m} < 3.5 \text{ MeV}$ at $\mu=2 \text{ GeV}$.
- 55 GUPTA 97 use Lattice Monte Carlo computations in the quenched approximation. The value for two light dynamic flavors at $\mu = 2 \text{ GeV}$ is $2.7 \pm 0.3 \pm 0.3 \text{ MeV}$.
- 56 LELLOUCH 97 obtain lower bounds on quark masses using hadronic spectral functions.
- 57 BIJNENS 95 determines $m_u+m_d(1 \text{ GeV}) = 12 \pm 2.5 \text{ MeV}$ using finite energy sum rules. We have rescaled this to 2 GeV.

WEIGHTED AVERAGE
3.82±0.10 (Error scaled by 2.8)



$$m_u/m_d \text{ MASS RATIO}$$

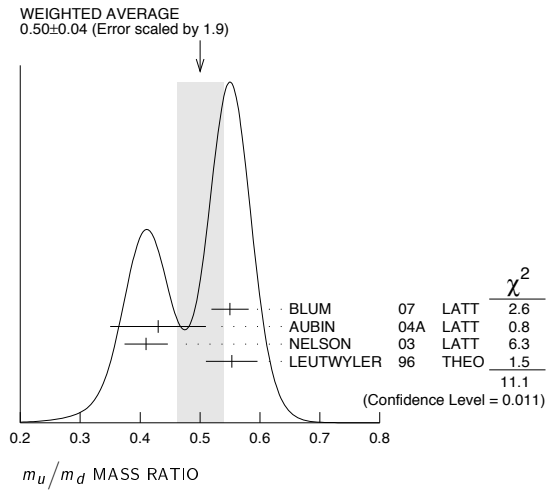
VALUE	DOCUMENT ID	TECN	COMMENT
4.94^{+0.106}_{-0.144} (0.35-0.60) OUR EVALUATION	See the ideogram below.		
0.550 ± 0.031	58 BLUM	07 LATT	\overline{MS} scheme
0.43 ± 0.08	59 AUBIN	04A LATT	\overline{MS} scheme
0.410 ± 0.036	60 NELSON	03 LATT	\overline{MS} scheme
0.553 ± 0.043	61 LEUTWYLER	96 THEO	Compilation

Quark Particle Listings

Light Quarks (*u, d, s*)

• • • We do not use the following data for averages, fits, limits, etc. • • •

- | | | | |
|--------------|--------------|----------|------------------------|
| 0.44 | 62 GAO | 97 THEO | \overline{MS} scheme |
| <0.3 | 63 CHOI | 92 THEO | |
| 0.26 | 64 DONOGHUE | 92 THEO | |
| 0.30 ± 0.07 | 65 DONOGHUE | 92B THEO | |
| 0.66 | 66 GERARD | 90 THEO | |
| 0.4 to 0.65 | 67 LEUTWYLER | 90B THEO | |
| 0.05 to 0.78 | 68 MALTMAN | 90 THEO | |
- 58 BLUM 07 determine quark mass using a QED plus QCD lattice computation with two dynamical flavors of the pseudoscalar meson masses.
- 59 AUBIN 04A perform three flavor dynamical lattice calculation of pseudoscalar meson masses, with continuum estimate of electromagnetic effects in the kaon masses.
- 60 NELSON 03 computes coefficients in the order p^4 chiral Lagrangian using a lattice calculation with three dynamical flavors. The ratio m_u/m_d is obtained by combining this with the chiral perturbation theory computation of the meson masses to order p^4 .
- 61 LEUTWYLER 96 uses a combined fit to $\eta \rightarrow 3\pi$ and $\psi' \rightarrow J/\psi(\pi, \eta)$ decay rates, and the electromagnetic mass differences of the π and K .
- 62 GAO 97 uses electromagnetic mass splittings of light mesons.
- 63 CHOI 92 result obtained from the decays $\psi(2S) \rightarrow J/\psi(1S)\pi$ and $\psi(2S) \rightarrow J/\psi(1S)\eta$, and a dilute instanton gas estimate of some unknown matrix elements.
- 64 DONOGHUE 92 result is from a combined analysis of meson masses, $\eta \rightarrow 3\pi$ using second-order chiral perturbation theory including nonanalytic terms, and $(\psi(2S) \rightarrow J/\psi(1S)\pi)/(\psi(2S) \rightarrow J/\psi(1S)\eta)$.
- 65 DONOGHUE 92B computes quark mass ratios using $(\psi(2S) \rightarrow J/\psi(1S)\pi)/(\psi(2S) \rightarrow J/\psi(1S)\eta)$, and an estimate of L_{14} using Weinberg sum rules.
- 66 GERARD 90 uses large N and η - η' mixing.
- 67 LEUTWYLER 90B determines quark mass ratios using second-order chiral perturbation theory for the meson and baryon masses, including nonanalytic corrections. Also uses Weinberg sum rules to determine L_7 .
- 68 MALTMAN 90 uses second-order chiral perturbation theory including nonanalytic terms for the meson masses. Uses a criterion of "maximum reasonableness" that certain coefficients which are expected to be of order one are ≤ 3 .



s-QUARK MASS

See the comment for the *u* quark above.

We have normalized the \overline{MS} masses at a renormalization scale of $\mu = 2$ GeV. Results quoted in the literature at $\mu = 1$ GeV have been rescaled by dividing by 1.35.

VALUE (MeV)	DOCUMENT ID	TECN	COMMENT
101⁺²⁹₋₂₁ (80-130) OUR EVALUATION	See the ideogram below.		
92.4 ± 1.5	69 DAVIES	10 LATT	\overline{MS} scheme
107.3 ± 11.7	70 ALLTON	08 LATT	\overline{MS} scheme
105 ± 3 ± 9	71 BLOSSIER	08 LATT	\overline{MS} scheme
102 ± 8	72 DOMINGUEZ	08A THEO	\overline{MS} scheme
90.1 ^{+17.2} _{-6.1}	73 ISHIKAWA	08 LATT	\overline{MS} scheme
105.6 ± 1.2	74 NAKAMURA	08 LATT	\overline{MS} scheme
119.5 ± 9.3	75 BLUM	07 LATT	\overline{MS} scheme
105 ± 6 ± 7	76 CHETYSKIN	06 THEO	\overline{MS} scheme
111 ± 6 ± 10	77 GOCKELER	06 LATT	\overline{MS} scheme
119 ± 5 ± 8	78 GOCKELER	06A LATT	\overline{MS} scheme
92 ± 9	79 JAMIN	06 THEO	\overline{MS} scheme
87 ± 6	80 MASON	06 LATT	\overline{MS} scheme
104 ± 15	81 NARISON	06 THEO	\overline{MS} scheme
≥ 71 ± 4, ≤ 151 ± 14	82 NARISON	06 THEO	\overline{MS} scheme
96 ⁺⁵ ₋₃ ± 16 ₋₁₈	83 BAIKOV	05 THEO	\overline{MS} scheme
81 ± 22	84 GAMIZ	05 THEO	\overline{MS} scheme

125 ± 28	85 GORBUNOV	05 THEO	\overline{MS} scheme
93 ± 32	86 NARISON	05 THEO	\overline{MS} scheme
76 ± 8	87 AUBIN	04 LATT	\overline{MS} scheme
116 ± 6 ± 0.65	88 AOKI	03 LATT	\overline{MS} scheme
84.5 ⁺¹² _{-1.7}	89 AOKI	03B LATT	\overline{MS} scheme
106 ± 2 ± 8	90 BECIREVIC	03 LATT	\overline{MS} scheme
92 ± 9 ± 16	91 CHIU	03 LATT	\overline{MS} scheme
117 ± 17	92 GAMIZ	03 THEO	\overline{MS} scheme
103 ± 17	93 GAMIZ	03 THEO	\overline{MS} scheme

• • • We do not use the following data for averages, fits, limits, etc. • • •

88 ⁺³ ₋₆	94 ALIKHAN	02 LATT	\overline{MS} scheme
115 ± 8	95 CHIU	02 LATT	\overline{MS} scheme
99 ± 16	96 JAMIN	02 THEO	\overline{MS} scheme
100 ± 12	97 MALTMAN	02 THEO	\overline{MS} scheme
116 ± 20 ₋₂₅	98 CHEN	01B THEO	\overline{MS} scheme
125 ± 27	99 KOERNER	01 THEO	\overline{MS} scheme
130 ± 15	100 AOKI	00 LATT	\overline{MS} scheme
97 ± 4	101 GARDEN	00 LATT	\overline{MS} scheme
105 ± 4	102 GOCKELER	00 LATT	\overline{MS} scheme
118 ± 14	103 AOKI	99 LATT	\overline{MS} scheme
170 ± 44 ₋₅₅	104 BARATE	99R ALEP	\overline{MS} scheme
115 ± 8	105 MALTMAN	99 THEO	\overline{MS} scheme
129 ± 24	106 NARISON	99 THEO	\overline{MS} scheme
114 ± 23	107 PICH	99 THEO	\overline{MS} scheme
111 ± 12	108 BECIREVIC	98 LATT	\overline{MS} scheme
148 ± 48	109 CHETYSKIN	98 THEO	\overline{MS} scheme
103 ± 10	110 CUCCHIERI	98 LATT	\overline{MS} scheme
115 ± 19	111 DOMINGUEZ	98 THEO	\overline{MS} scheme
152.4 ± 14.1	112 CHETYSKIN	97 THEO	\overline{MS} scheme
≥ 89	113 COLANGELO	97 THEO	\overline{MS} scheme
140 ± 20	114 EICKER	97 LATT	\overline{MS} scheme
95 ± 16	115 GOUGH	97 LATT	\overline{MS} scheme
100 ± 21 ± 10	116 GUPTA	97 LATT	\overline{MS} scheme
>100	117 LELLOUCH	97 THEO	\overline{MS} scheme
140 ± 24	118 JAMIN	95 THEO	\overline{MS} scheme

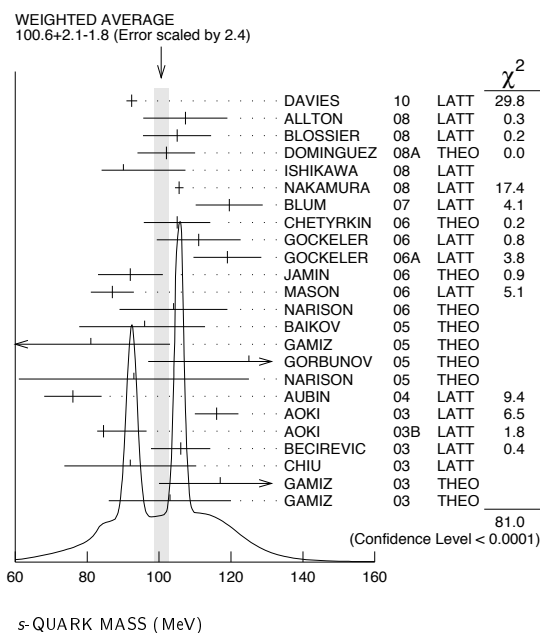
- 69 DAVIES 10 determine $\overline{m}_c(\mu)/\overline{m}_s(\mu) = 11.85 \pm 0.16$ using a lattice computation with dynamical fermions of the pseudoscalar meson masses. Mass m_s is obtained from this using the value of m_c from ALLISON 08.
- 70 ALLTON 08 use a lattice computation of the π , K , and Ω masses with 2+1 dynamical flavors of domain wall quarks, and non-perturbative renormalization.
- 71 BLOSSIER 08 use a lattice computation of pseudoscalar meson masses and decay constants with 2 dynamical flavors and non-perturbative renormalization.
- 72 DOMINGUEZ 08A make determination from QCD finite energy sum rules for the pseudoscalar two-point function computed to order α_s^4 .
- 73 ISHIKAWA 08 use a lattice computation of the light meson spectrum with 2+1 dynamical flavors of $\mathcal{O}(a)$ improved Wilson quarks, and one-loop perturbative renormalization.
- 74 NAKAMURA 08 do a lattice computation using quenched domain wall fermions and non-perturbative renormalization.
- 75 BLUM 07 determine quark mass using a QED plus QCD lattice computation with two dynamical flavors of the pseudoscalar meson masses.
- 76 CHETYSKIN 06 use QCD sum rules in the pseudoscalar channel to order α_s^4 .
- 77 GOCKELER 06 use an unquenched lattice computation of the axial Ward Identity with $N_f = 2$ dynamical light quark flavors, and non-perturbative renormalization, to obtain $\overline{m}_s(2 \text{ GeV}) = 111 \pm 6 \pm 4 \pm 6 \text{ MeV}$, where the first error is statistical, the second and third are systematic due to the fit range and force scale uncertainties, respectively. We have combined the systematic errors linearly.
- 78 GOCKELER 06A use an unquenched lattice computation of the pseudoscalar meson masses with $N_f = 2$ dynamical light quark flavors, and non-perturbative renormalization.
- 79 JAMIN 06 determine $\overline{m}_s(2 \text{ GeV})$ from the spectral function for the scalar $K\pi$ form factor.
- 80 MASON 06 extract light quark masses from a lattice simulation using staggered fermions with an improved action, and three dynamical light quark flavors with degenerate u and d quarks. Perturbative corrections were included at NNLO order.
- 81 NARISON 06 uses sum rules for $e^+e^- \rightarrow \text{hadrons}$ to order α_s^3 .
- 82 NARISON 06 obtains the quoted range from positivity of the spectral functions.
- 83 BAIKOV 05 determines $\overline{m}_s(M_\tau) = 100^{+5}_{-3} \pm 17$ from sum rules using the strange spectral function in τ decay. The computations were done to order α_s^3 , with an estimate of the α_s^4 terms. We have converted the result to $\mu = 2 \text{ GeV}$.
- 84 GAMIZ 05 determines $\overline{m}_s(2 \text{ GeV})$ from sum rules using the strange spectral function in τ decay. The computations were done to order α_s^2 , with an estimate of the α_s^3 terms.
- 85 GORBUNOV 05 use hadronic tau decays to N³LO, including power corrections.
- 86 NARISON 05 determines $\overline{m}_s(2 \text{ GeV})$ from sum rules using the strange spectral function in τ decay. The computations were done to order α_s^3 .
- 87 AUBIN 04 perform three flavor dynamical lattice calculation of pseudoscalar meson masses, with one-loop perturbative renormalization constant.
- 88 AOKI 03 uses quenched lattice simulation of the meson and baryon masses with degenerate light quarks. The extrapolations are done using quenched chiral perturbation theory. Determines $m_s = 113.8 \pm 2.3 \pm 5.8$ using K mass as input and $m_s = 142.3 \pm 5.8 \pm 22$ using ϕ mass as input. We have performed a weighted average of these values.
- 89 AOKI 03B uses lattice simulation of the meson and baryon masses with two dynamical light quarks. Simulations are performed using the $\mathcal{O}(a)$ improved Wilson action.
- 90 BECIREVIC 03 perform quenched lattice computation using the vector and axial Ward identities. Uses $\mathcal{O}(a)$ improved Wilson action and nonperturbative renormalization. They also quote $\overline{m}_m = 24.3 \pm 0.2 \pm 0.6$.

See key on page 405

Quark Particle Listings

Light Quarks (u, d, s)

- 91 CHIU 03 determines quark masses from the pion and kaon masses using a lattice simulation with a chiral fermion action in quenched approximation.
- 92 GAMIZ 03 determines m_s from SU(3) breaking in the τ hadronic width. The value of V_{us} is chosen to satisfy CKM unitarity.
- 93 GAMIZ 03 determines m_s from SU(3) breaking in the τ hadronic width. The value of V_{us} is taken from the PDG.
- 94 ALIKHAN 02 uses lattice simulation of the meson and baryon masses with two dynamical flavors and degenerate light quarks. The above value uses the K -meson mass to determine m_s . If the ϕ meson is used, the number changes to 90^{+5}_{-10} .
- 95 CHIU 02 extracts the strange quark mass from quenched lattice simulations using quenched chiral perturbation theory.
- 96 JAMIN 02 calculates the strange quark mass from QCD sum rules using the scalar channel.
- 97 MALTMAN 02 uses finite energy sum rules in the ud and us pseudoscalar channels. Other mass values are also obtained by similar methods.
- 98 CHEN 01B uses an analysis of the hadronic spectral function in τ decay.
- 99 KOERNER 01 obtain the s quark mass of $m_s(m_\tau) = 130 \pm 27(\text{exp}) \pm 9(\text{thy})$ MeV from an analysis of Cabibbo suppressed τ decays. We have converted this to $\mu = 2$ GeV.
- 100 AOKI 00 obtain the light quark masses from a quenched lattice simulation of the meson and baryon spectrum with the Wilson quark action. We have averaged their results of $m_s = 115.6 \pm 2.3$ and $m_s = 143.7 \pm 5.8$ obtained using m_K and m_ϕ , respectively, to normalize the spectrum.
- 101 GARDEN 00 use a quenched lattice computation of the hadron spectrum.
- 102 GOCKELER 00 obtained from a quenched lattice computation of the pseudoscalar meson masses using $\mathcal{O}(a)$ improved Wilson fermions and nonperturbative renormalization.
- 103 AOKI 99 obtain the light quark masses from a quenched lattice simulation of the meson spectrum with the Staggered quark action employing the regularization independent scheme. We have averaged their results of $m_s = 106.0 \pm 7.1$ and $m_s = 129 \pm 12$ obtained using m_K and m_ϕ , respectively, to normalize the spectrum.
- 104 BARATE 99r obtain the strange quark mass from an analysis of the observed mass spectra in τ decay. We have converted their value of $m_s(m_\tau) = 176^{+46}_{-57}$ MeV to $\mu = 2$ GeV.
- 105 MALTMAN 99 determines the strange quark mass using finite energy sum rules.
- 106 NARISON 99 uses sum rules to order α_s^3 for ϕ meson decays.
- 107 PICH 99 obtain the s -quark mass from an analysis of the moments of the invariant mass distribution in τ decays.
- 108 BECIREVIC 98 compute the quark mass using the Alpha action in the quenched approximation. The conversion from the regularization independent scheme to the \overline{MS} scheme is at NNLO.
- 109 CHETYRKIN 98 uses spectral moments of hadronic τ decays to determine $m_s(1 \text{ GeV}) = 200 \pm 70$ MeV. We have rescaled the result to $\mu = 2$ GeV.
- 110 CUCCIERI 98 obtains the quark mass using a quenched lattice computation of the hadronic spectrum.
- 111 DOMINGUEZ 98 uses hadronic spectral function sum rules (to four loops, and including dimension six operators) to determine $m_s(1 \text{ GeV}) < 155 \pm 25$ MeV. We have rescaled the result to $\mu = 2$ GeV.
- 112 CHETYRKIN 97 obtains 205.5 ± 19.1 MeV at $\mu = 1$ GeV from QCD sum rules including fourth-order QCD corrections. We have rescaled the result to 2 GeV.
- 113 COLANGELO 97 is QCD sum rule computation. We have rescaled $m_s(1 \text{ GeV}) > 120$ to $\mu = 2$ GeV.
- 114 EICKER 97 use lattice gauge computations with two dynamical light flavors.
- 115 GOUGH 97 use lattice gauge computations in the quenched approximation. Correcting for quenching gives $54 < m_s < 92$ MeV at $\mu = 2$ GeV.
- 116 GUPTA 97 use Lattice Monte Carlo computations in the quenched approximation. The value for two light dynamical flavors at $\mu = 2$ GeV is $68 \pm 12 \pm 7$ MeV.
- 117 LELLOUCH 97 obtain lower bounds on quark masses using hadronic spectral functions.
- 118 JAMIN 95 uses QCD sum rules at next-to-leading order. We have rescaled $m_s(1 \text{ GeV}) = 189 \pm 32$ to $\mu = 2$ GeV.



OTHER LIGHT QUARK MASS RATIOS

 m_s/m_d MASS RATIO

VALUE	DOCUMENT ID	TECN	COMMENT
17 to 22 OUR EVALUATION			
• • • We do not use the following data for averages, fits, limits, etc. • • •			
20.0	119 GAO	97	THEO \overline{MS} scheme
18.9 \pm 0.8	120 LEUTWYLER	96	THEO Compilation
21	121 DONOGHUE	92	THEO
18	122 GERARD	90	THEO
18 to 23	123 LEUTWYLER	90B	THEO

- 119 GAO 97 uses electromagnetic mass splittings of light mesons.
- 120 LEUTWYLER 96 uses a combined fit to $\eta \rightarrow 3\pi$ and $\psi' \rightarrow J/\psi(\pi, \eta)$ decay rates, and the electromagnetic mass differences of the π and K .
- 121 DONOGHUE 92 result is from a combined analysis of meson masses, $\eta \rightarrow 3\pi$ using second-order chiral perturbation theory including nonanalytic terms, and $(\psi(2S) \rightarrow J/\psi(1S)\pi)/(\psi(2S) \rightarrow J/\psi(1S)\eta)$.
- 122 GERARD 90 uses large N and η - η' mixing.
- 123 LEUTWYLER 90B determines quark mass ratios using second-order chiral perturbation theory for the meson and baryon masses, including nonanalytic corrections. Also uses Weinberg sum rules to determine L_7 .

 m_s/\overline{m} MASS RATIO

VALUE	DOCUMENT ID	TECN	COMMENT
22 to 30 OUR EVALUATION			
• • • We do not use the following data for averages, fits, limits, etc. • • •			
28.8 \pm 1.65	124 ALLTON	08	LATT \overline{MS} scheme
27.3 \pm 0.3 \pm 1.2	125 BLOSSIER	08	LATT \overline{MS} scheme
23.5 \pm 1.5	126 OLLER	07A	THEO
27.4 \pm 0.4	127 AUBIN	04	LATT

- 124 ALLTON 08 use a lattice computation of the π , K , and Ω masses with 2+1 dynamical flavors of domain wall quarks, and non-perturbative renormalization.
- 125 BLOSSIER 08 use a lattice computation of pseudoscalar meson masses and decay constants with 2 dynamical flavors and non-perturbative renormalization.
- 126 OLLER 07A use unitarized chiral perturbation theory to order β^4 .
- 127 Three flavor dynamical lattice calculation of pseudoscalar meson masses.

Q MASS RATIO

VALUE	DOCUMENT ID	TECN	COMMENT
Q			
$Q \equiv \sqrt{(m_s^2 - \overline{m}^2)/(m_d^2 - m_u^2)}$; $\overline{m} \equiv (m_u + m_d)/2$			
• • • We do not use the following data for averages, fits, limits, etc. • • •			
22.8 \pm 0.4	128 MARTEMYA...	05	THEO
22.7 \pm 0.8	129 ANISOVICH	96	THEO

- 128 MARTEMYANOV 05 determine Q from $\eta \rightarrow 3\pi$ decay.
- 129 ANISOVICH 96 find Q from $\eta \rightarrow \pi^+ \pi^- \pi^0$ decay using dispersion relations and chiral perturbation theory.

LIGHT QUARKS (u, d, s) REFERENCES

BAZAVOV 10	arXiv:0903.3598	A. Bazavov et al.	(MILC Collab.)
DAVIES 10	PRL 104 132003	C.T.H. Davies et al.	(HPQCD Collab.)
DOMINGUEZ 09	PR D79 014009	C.A. Dominguez et al.	
ALLISON 08	PR D78 054513	I. Allison et al.	(HPQCD Collab.)
ALLTON 08	PR D78 114509	C. Allton et al.	(RBC and UKQCD Collab.)
BLOSSIER 08	JHEP 0804 020	B. Blossier et al.	(ETM Collab.)
DEANDREA 08	PR D78 034032	A. Deandrea, A. Nehme, P. Talavera	
DOMINGUEZ 08A	JHEP 0805 020	C.A. Dominguez et al.	
DOMINGUEZ... 08B	PL B660 49	A. Dominguez-Clarimon, E. de Rafael, J. Taron	
ISHIKAWA 08	PR D78 011502R	T. Ishikawa et al.	(CP-PACS and JLQCD Collab.)
NAKAMURA 08	PR D78 034502	Y. Nakamura et al.	(CP-PACS Collab.)
BLUM 07	PR D76 114508	T. Blum et al.	(RBC Collab.)
OLLER 07A	EPJ A34 371	J.A. Oller, L. Roca	
CHETYRKIN 06	EPJ C46 721	K.G. Chetyrkin, A. Khodjamirian	
GOCKELER 06	PR D73 054508	M. Gockeler et al.	(QCDSF, UKQCD Collabs)
GOCKELER 06A	PL B639 307	M. Gockeler et al.	(QCDSF, UKQCD Collabs)
JAMIN 06	PR D74 074009	M. Jamin, J.A. Oller, A. Pich	
MASON 06	PR D73 114501	Q. Mason et al.	(HPQCD Collab.)
NARISON 06	PR D74 034013	S. Narison	
PDG 06	JPG 33 1	W.-M. Yao et al.	(PDG Collab.)
BAIKOV 05	PRL 95 012003	P.A. Baikov, K.G. Chetyrkin, J.H. Kühn	
GAMIZ 05	PRL 94 011803	E. Gamiz et al.	
GORBUNOV 05	PR D71 013002	D.S. Gorbunov, A.A. Pivovarov	
MARTEMYA... 05	PR D71 017501	B.V. Martemyanov, V.S. Sopoov	
NARISON 05	PL B626 101	S. Narison	
AUBIN 04	PR D70 031504R	C. Aubin et al.	(HPQCD, MILC, UKQCD Collabs.)
AUBIN 04A	PR D70 114501	C. Aubin et al.	(MILC Collab.)
AOKI 03	PR D67 034503	S. Aoki et al.	(CP-PACS Collab.)
AOKI 03B	PR D68 054502	S. Aoki et al.	(CP-PACS Collab.)
BECIREVIC 03	PL B558 69	D. Becirevic, V. Lubitz, C. Tarantino	
CHIU 03	NP B873 217	T.-W. Chiu, T.-H. Hsieh	
GAMIZ 03	JHEP 0301 060	E. Gamiz et al.	
NELSON 03	PRL 90 021601	D. Nelson, G.T. Fleming, G.W. Kilcup	
ALIKHAN 02	PR D65 054505	A. Ali Khan et al.	(CP-PACS Collab.)
Also	PR D67 059901 (erratum)	A. Ali Khan et al.	(CP-PACS Collab.)
CHIU 02	PL B538 298	T.-W. Chiu, T.-H. Hsieh	
JAMIN 02	EPJ C24 237	M. Jamin, J.A. Oller, A. Pich	
MALTMAN 02	PR D65 074013	K. Maltman, J. Kambor	
CHEN 01B	EPJ C22 31	S. Chen et al.	
KOERNER 01	EPJ C20 259	J.G. Koerner, F. Krajewski, A.A. Pivovarov	
MALTMAN 01	PL B517 332	K. Maltman, J. Kambor	
AOKI 00	PRL 84 238	S. Aoki et al.	(CP-PACS Collab.)
GARDEN 00	NP B571 237	J. Garden et al.	(ALPHA, UKQCD Collabs)
GOCKELER 00	PR D62 054504	M. Gockeler et al.	
AOKI 99	PRL 82 4392	S. Aoki et al.	(JLQCD Collab.)
BARATE 99r	EPJ C11 599	R. Barate et al.	(ALEPH Collab.)
MALTMAN 99	PL B462 195	K. Maltman	
NARISON 99	PL B466 345	S. Narison	
PICH 99	JHEP 9910 004	A. Pich, J. Prades	

Quark Particle Listings

Light Quarks (u, d, s, c)

STEELE	99	PL B451 201	T.G. Steele, K. Kostiuk, J. Kwan
BECIREVIC	98	PL B444 401	D. Becirevic <i>et al.</i>
CHETYRKIN	98	NP B533 473	K.G. Chetyrkin, J.H. Kuehn, A.A. Pivovarov
CUCCHIERI	98	PL B422 212	A. Chucchieri <i>et al.</i>
DOMINGUEZ	98	PL B425 193	C.A. Dominguez, L. Pirovano, K. Schilcher
DOSCH	98	PL B417 173	H.G. Dosch, S. Narison
PRADES	98	NPBPS 64 253	J. Prades
CHETYRKIN	97	PL B404 337	K.G. Chetyrkin, D. Pirjol, K. Schilcher
COLANGELO	97	PL B408 340	P. Colangelo <i>et al.</i>
EICKER	97	PL B407 290	N. Eicker <i>et al.</i>
GAO	97	PR D56 4115	D.-N. Gao, B.A. Li, M.-L. Yan (SESAM Collab.)
GOUGH	97	PRL 79 1622	B. Gough <i>et al.</i>
GUPTA	97	PR D55 7203	R. Gupta, T. Bhattacharya
LELLOUCH	97	PL B414 195	L. Lellouch, E. de Rafael, J. Taron
ANISOVICH	96	PL B375 335	A.V. Anisovich, H. Leutwyler
LEUTWYLER	96	PL B378 313	H. Leutwyler
BIJNENS	95	PL B348 226	J. Bijnens, J. Prades, E. de Rafael (NORD, BOHR+)
JAMIN	95	ZPHY C66 633	M. Jamin, M. Munz (HEIDT, MUNT)
NARISON	95C	PL B358 113	S. Narison (MONP)
CHOI	92	PL B292 159	K.W. Choi (UCSD)
DONOGHUE	92	PRL 69 3444	J.F. Donoghue, B.R. Holstein, D. Wyler (MASA+)
DONOGHUE	92B	PR D45 892	J.F. Donoghue, D. Wyler (MASA, ZURI, UCSBT)
GERARD	90	MPL A5 391	J.M. Gerard (MPIM)
LEUTWYLER	90B	NP B337 108	H. Leutwyler (BERN)
MALTMAN	90	PL B234 158	K. Maltman, T. Goldman, Stephenson Jr. (YORKC+)



$$I(J^P) = 0(\frac{1}{2}^+)$$

$$\text{Charge} = \frac{2}{3} e \quad \text{Charm} = +1$$

c-QUARK MASS

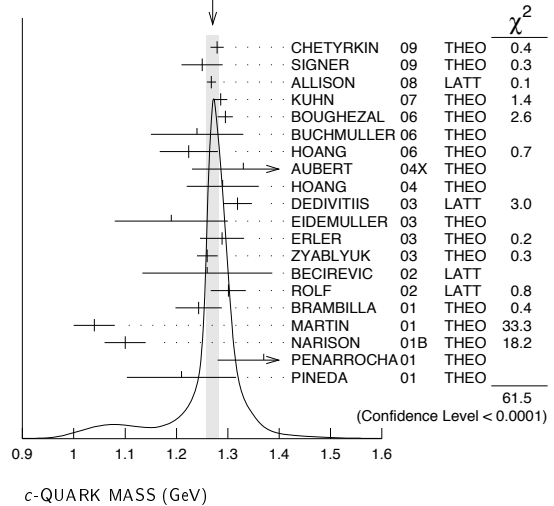
The c -quark mass corresponds to the “running” mass $m_c(\mu = m_c)$ in the $\overline{\text{MS}}$ scheme. We have converted masses in other schemes to the $\overline{\text{MS}}$ scheme using two-loop QCD perturbation theory with $\alpha_s(\mu = m_c) = 0.39$. The range 1.0–1.4 GeV for the $\overline{\text{MS}}$ mass corresponds to 1.47–1.83 GeV for the pole mass (see the “Note on Quark Masses”).

VALUE (GeV)	DOCUMENT ID	TECN	COMMENT
1.27\pm0.07\pm0.09 (1.18–1.34) OUR EVALUATION	See the ideogram below.		
1.279 \pm 0.013	1 CHETYRKIN 09	THEO	$\overline{\text{MS}}$ scheme
1.25 \pm 0.04	2 SIGNER 09	THEO	$\overline{\text{MS}}$ scheme
1.268 \pm 0.009	3 ALLISON 08	LATT	$\overline{\text{MS}}$ scheme
1.286 \pm 0.013	4 KUHN 07	THEO	$\overline{\text{MS}}$ scheme
1.295 \pm 0.015	5 BOUGHEZAL 06	THEO	$\overline{\text{MS}}$ scheme
1.24 \pm 0.09	6 BUCHMULLER 06	THEO	$\overline{\text{MS}}$ scheme
1.224 \pm 0.017 \pm 0.054	7 HOANG 06	THEO	$\overline{\text{MS}}$ scheme
1.33 \pm 0.10	8 AUBERT 04x	THEO	$\overline{\text{MS}}$ scheme
1.29 \pm 0.07	9 HOANG 04	THEO	$\overline{\text{MS}}$ scheme
1.319 \pm 0.028	10 DEDIVITIIS 03	LATT	$\overline{\text{MS}}$ scheme
1.19 \pm 0.11	11 EIDEMULLER 03	THEO	$\overline{\text{MS}}$ scheme
1.289 \pm 0.043	12 ERLER 03	THEO	$\overline{\text{MS}}$ scheme
1.26 \pm 0.02	13 ZYABLYUK 03	THEO	$\overline{\text{MS}}$ scheme
1.26 \pm 0.04 \pm 0.12	14 BECIREVIC 02	LATT	$\overline{\text{MS}}$ scheme
1.301 \pm 0.034	15 ROLF 02	LATT	$\overline{\text{MS}}$ scheme
1.243 \pm 0.045	16 BRAMBILLA 01	THEO	$\overline{\text{MS}}$ scheme
1.04 \pm 0.04	17 MARTIN 01	THEO	$\overline{\text{MS}}$ scheme
1.1 \pm 0.04	18 NARISON 01B	THEO	$\overline{\text{MS}}$ scheme
1.37 \pm 0.09	19 PENARROCHA 01	THEO	$\overline{\text{MS}}$ scheme
1.210 \pm 0.070 \pm 0.080	20 PINEDA 01	THEO	$\overline{\text{MS}}$ scheme
• • • We do not use the following data for averages, fits, limits, etc. • • •			
1.23 \pm 0.09	21 EIDEMULLER 01	THEO	$\overline{\text{MS}}$ scheme
1.304 \pm 0.027	22 KUHN 01	THEO	$\overline{\text{MS}}$ scheme
1.3 \pm 0.3 \pm 0.3	23 ASTIER 00D	NOMD	
1.79 \pm 0.38	24 VILAIN 99	THEO	$\overline{\text{MS}}$ scheme

- CHETYRKIN 09 determine m_c and m_b from the $e^+e^- \rightarrow Q\bar{Q}$ cross-section and sum rules, using a four-loop computation of the heavy quark vacuum polarization. They also determine $m_c(3\text{ GeV}) = 0.986 \pm 0.013\text{ GeV}$.
- SIGNER 09 determines the c -quark mass using non-relativistic sum rules to analyze the $e^+e^- \rightarrow c\bar{c}$ cross-section near threshold. Also determine the PS mass $m_{PS}(\mu_F = 0.7\text{ GeV}) = 1.50 \pm 0.04\text{ GeV}$.
- ALLISON 08 determine m_c by comparing four-loop perturbative results for the pseudoscalar current correlator to lattice simulations by the HPQCD collaboration.
- KUHN 07 determine $\overline{m}_c(\mu = 3\text{ GeV}) = 0.986 \pm 0.013\text{ GeV}$ and $\overline{m}_c(\overline{m}_c)$ from a four-loop sum-rule computation of the cross-section for $e^+e^- \rightarrow$ hadrons in the charm threshold region.
- BOUGHEZAL 06 result comes from the first moment of the hadronic production cross-section to order α_s^3 .
- BUCHMULLER 06 determine m_b and m_c by a global fit to inclusive B decay spectra.
- HOANG 06 determines $\overline{m}_c(\overline{m}_c)$ from a global fit to inclusive B decay data. The B decay distributions were computed to order $\alpha_s^2\beta_0$, and the conversion between different m_c mass schemes to order α_s^3 .
- AUBERT 04x obtain m_c from a fit to the hadron mass and lepton energy distributions in semileptonic B decay. The paper quotes values in the kinetic scheme. The $\overline{\text{MS}}$ value has been provided by the BABAR collaboration.
- HOANG 04 determines $\overline{m}_c(\overline{m}_c)$ from moments at order α_s^2 of the charm production cross-section in e^+e^- annihilation.
- DEDIVITIIS 03 use a quenched lattice computation of heavy-heavy and heavy-light meson masses.
- EIDEMULLER 03 determines m_b and m_c using QCD sum rules.
- ERLER 03 determines m_b and m_c using QCD sum rules. Includes recent BES data.

- ZYABLYUK 03 determines m_c by using QCD sum rules in the pseudoscalar channel and comparing with the η_c mass.
- BECIREVIC 02 uses Monte-Carlo calculations of lattice Ward identities and the D_S mass. The authors estimate an error of about 5% for use of the quenched approximation, not included in systematic error of 0.12.
- ROLF 02 determines m_c from a quenched lattice calculation of the D_S mass. The error estimate is for all systematics except the quenched approximation, including lattice spacing effects, finite volume effects, excited states contamination, rounding errors, and the scale uncertainty. The authors estimate the uncertainty due to the quenched approximation may be about 3%.
- BRAMBILLA 01 determine $\overline{m}_c(\overline{m}_c)$ from a computation of the J/ψ mass.
- MARTIN 01 obtain a pole mass of 1.33–1.4 GeV from an analysis of R , the rate for $e^+e^- \rightarrow$ hadrons. We have converted this to the $\overline{\text{MS}}$ scheme using the two-loop formula.
- NARISON 01B uses pseudoscalar sum rules in the B and D meson channels.
- PENARROCHA 01 result is from an analysis of the BES-II e^+e^- data using finite energy sum rules.
- PINEDA 01 uses the $\Upsilon(1S)$ system and the B - D mass difference to determine m_c . The errors are due to theory, and the uncertainty in λ_1 and m_b .
- EIDEMULLER 01 result is QCD sum rule analysis of charmonium using NRQCD at next-to-next-to-leading order.
- KUHN 01 uses an analysis of the e^+e^- total cross section to hadrons.
- Study of opposite sign dimuon events.
- VILAIN 99 obtain the charm quark mass from an analysis of charm production in neutrino scattering.

WEIGHTED AVERAGE
1.271 \pm 0.012 (Error scaled by 2.3)



$m_b - m_c$ QUARK MASS DIFFERENCE

VALUE (GeV)	DOCUMENT ID	TECN
-------------	-------------	------

3.38 to 3.48 OUR EVALUATION

• • • We do not use the following data for averages, fits, limits, etc. • • •

3.42 \pm 0.06	25 ABDALLAH 06B	DLPH
3.44 \pm 0.03	26 AUBERT 04x	BABR
3.41 \pm 0.01	26 BAUER 04	THEO

- ABDALLAH 06B determine $m_b - m_c$ from moments of the hadron invariant mass and lepton energy spectra in semileptonic inclusive B decays.
- Determine $m_b - m_c$ from a global fit to inclusive B decay spectra.

c-QUARK REFERENCES

CHETYRKIN 09	PR D80 074010	K.G. Chetyrkin <i>et al.</i>	(KARL, BNL)
SIGNER 09	PL B672 333	A. Signer	(DURH)
ALLISON 08	PR D78 054513	I. Allison <i>et al.</i>	(HPQCD Collab.)
KUHN 07	NP B778 192	J.H. Kuhn, M. Steinhauser, C. Sturm	(DELPHI Collab.)
ABDALLAH 06B	EPJ C45 35	J. Abdallah <i>et al.</i>	
BOUGHEZAL 06	PR D74 074006	R. Boughezal, M. Czakon, T. Schutzmeier	
BUCHMULLER 06	PR D73 073008	O.L. Buchmuller, H.U. Flacher	
HOANG 06	PL B633 526	A.H. Hoang, A.V. Manohar	(BABAR Collab.)
AUBERT 04x	PRL 93 011803	B. Aubert <i>et al.</i>	
BAUER 04	PR D70 094017	C. Bauer <i>et al.</i>	
HOANG 04	PL B594 127	A.H. Hoang, M. Jamin	
DEDIVITIIS 03	NP B675 309	G.M. de Divitiis <i>et al.</i>	
EIDEMULLER 03	PR D67 113002	M. Eidemuller	
ERLER 03	PL B558 125	J. Erler, M. Luo	(ITEP)
ZYABLYUK 03	JHEP 0301 081	K.N. Zybalyuk	
BECIREVIC 02	PL B524 115	D. Becirevic, V. Lubitz, G. Martinelli	
ROLF 02	JHEP 0212 007	J. Rolf, S. Sint	
BRAMBILLA 01	PL B513 381	N. Brambilla, Y. Sumino, A. Vairo	
EIDEMULLER 01	PL B498 203	M. Eidemuller, M. Jamin	
KUHN 01	NP B619 588	J.H. Kuhn, M. Steinhauser	
MARTIN 01	EPJ C19 681	A.D. Martin, J. Outhwaite, M.G. Ryskin	
NARISON 01B	PL B520 115	S. Narison	
PENARROCHA 01	PL B515 291	J. Penarrocha, K. Schilcher	
PINEDA 01	JHEP 0106 022	A. Pineda	
ASTIER 00D	PL B486 35	P. Astier <i>et al.</i>	(CERN NOMAD Collab.)
VILAIN 99	EPJ C11 19	P. Vilain <i>et al.</i>	(CHARM II Collab.)

b

$$I(J^P) = 0(\frac{1}{2}^+)$$

$$\text{Charge} = -\frac{1}{3} e \quad \text{Bottom} = -1$$

b-QUARK MASS

The first value is the “running mass” $\overline{m}_b(\mu = \overline{m}_b)$ in the $\overline{\text{MS}}$ scheme, and the second value is the 1S mass, which is half the mass of the $\Upsilon(1S)$ in perturbation theory. For a review of different quark mass definitions and their properties, see EL-KHADRA 02. The 1S mass is better suited for use in analyzing B decays than the $\overline{\text{MS}}$ mass because it gives a stable perturbative expansion. We have converted masses in other schemes to the $\overline{\text{MS}}$ mass and 1S mass using two-loop QCD perturbation theory with $\alpha_s(\mu = \overline{m}_b) = 0.22$. The values $4.20^{+0.17}_{-0.07}$ GeV for the $\overline{\text{MS}}$ mass and $4.68^{+0.17}_{-0.07}$ GeV for the 1S mass correspond to $4.79^{+0.19}_{-0.08}$ GeV for the pole mass, using the two-loop conversion formula. A discussion of masses in different schemes can be found in the “Note on Quark Masses.”

$\overline{\text{MS}}$ MASS (GeV)	1S MASS (GeV)	DOCUMENT ID	TECN
4.19 $^{+0.18}_{-0.06}$	OUR EVALUATION	of $\overline{\text{MS}}$ Mass. See the ideogram below.	
4.67 $^{+0.18}_{-0.06}$	OUR EVALUATION	of 1S Mass. See the ideogram below.	
4.163±0.016	4.640 ± 0.018	1	CHETYRKIN 09 THEO
5.26 ± 1.2	5.86 ± 1.3	2	ABDALLAH 08D DLPH
4.42 ± 0.06 ± 0.08	4.98 ± 0.07 ± 0.09	3	GUAZZINI 08 LATT
4.237±0.049	4.723 ± 0.055	4	SCHWANDA 08 BELL
4.347±0.048±0.08	4.838 ± 0.053 ± 0.09	5	DELLA-MOR... 07 LATT
4.164±0.025	4.635 ± 0.028	6	KUHN 07 THEO
4.19 ± 0.40	4.66 ± 0.45	7	ABDALLAH 06D DLPH
4.205±0.058	4.68 ± 0.06	8	BOUGHEZAL 06 THEO
4.20 ± 0.04	4.67 ± 0.04	9	BUCHMULLER 06 THEO
4.19 ± 0.06	4.66 ± 0.07	10	PINEDA 06 THEO
4.4 ± 0.3	4.9 ± 0.3	11,12	GRAY 05 LATT
4.22 ± 0.06	4.72 ± 0.07	13	AUBERT 04x THEO
4.17 ± 0.03	4.68 ± 0.03	14	BAUER 04 THEO
4.22 ± 0.11	4.72 ± 0.12	12,15	HOANG 04 THEO
4.25 ± 0.11	4.76 ± 0.12	12,16	MCNEILE 04 LATT
4.22 ± 0.09	4.74 ± 0.10	17	BAUER 03 THEO
4.19 ± 0.05	4.66 ± 0.05	18	BORDES 03 THEO
4.20 ± 0.09	4.67 ± 0.10	19	CORCELLA 03 THEO
4.33 ± 0.10	4.84 ± 0.11	12,20	DEDIVITIIS 03 LATT
4.24 ± 0.10	4.72 ± 0.11	21	EIDEMULLER 03 THEO
4.207±0.031	4.682 ± 0.035	22	ERLER 03 THEO
4.33 ± 0.06 ± 0.10	4.82 ± 0.07 ± 0.11	23	MAHMOOD 03 THEO
4.190±0.032	4.663 ± 0.036	24	BRAMBILLA 02 THEO
4.346±0.070	4.837 ± 0.078	25	PENIN 02 THEO
4.05 ± 0.06	4.51 ± 0.07	26	NARISON 01B THEO
4.210±0.090±0.025	4.69 ± 0.100 ± 0.028	27	PINEDA 01 THEO
• • • We do not use the following data for averages, fits, limits, etc. • • •			
3.95 ± 0.57	4.40 ± 0.63	28	ABBIENDI 01S OPAL
4.203±0.026	4.678 ± 0.029	29	BRAMBILLA 01 THEO
4.21 ± 0.05	4.69 ± 0.06	30	KUHN 01 THEO
4.7 ± 0.74	5.23 ± 0.82	31	BARATE 00v ALEP
4.20 ± 0.06	4.71 ± 0.03	32	HOANG 00 THEO
4.437 $^{+0.045}_{-0.029}$	4.938 $^{+0.050}_{-0.032}$	33	LUCHA 00 THEO
4.454 $^{+0.045}_{-0.029}$	4.957 $^{+0.050}_{-0.032}$	33	PINEDA 00 THEO
4.25 ± 0.08	4.73 ± 0.09	34	BENEKE 99 THEO
3.8 $^{+0.77}_{-2.0}$	4.23 $^{+0.86}_{-2.0}$	35	BRANDENB... 99
4.25 ± 0.09	4.73 ± 0.10	36	HOANG 99 THEO
4.2 ± 0.1	4.67 ± 0.11	37	MELNIKOV 99 THEO
4.21 ± 0.11	4.69 ± 0.12	38	PENIN 99 THEO
3.91 ± 0.67	4.35 ± 0.75	39	ABREU 98i DLPH
4.14 ± 0.04	4.61 ± 0.05	40	KUEHN 98 THEO
4.15 ± 0.05 ± 0.20	4.62 ± 0.06 ± 0.22	41	GIMENEZ 97 LATT
4.19 ± 0.06	4.66 ± 0.07	42	JAMIN 97 THEO
4.16 ± 0.32 ± 0.60	4.63 ± 0.36 ± 0.67	43	RODRIGO 97 THEO

1 CHETYRKIN 09 determine m_c and m_b from the $e^+e^- \rightarrow Q\overline{Q}$ cross-section and sum rules, using a four-loop computation of the heavy quark vacuum polarization. We have converted their m_b to the 1S scheme.

2 ABDALLAH 08D determine $\overline{m}_b(M_Z) = 3.76 \pm 1.0$ GeV from a leading order study of four-jet rates at LEP. We have converted this to $\overline{m}_b(\overline{m}_b)$ and m_b^{1S} .

3 GUAZZINI 08 determine $m_b(m_b)$ from a quenched lattice simulation of heavy meson masses. The ± 0.08 is an estimate of the quenching error. We have converted these values to the 1S scheme.

4 SCHWANDA 08 measure moments of the inclusive photon spectrum in $B \rightarrow X_S \gamma$ decay to determine m_b^{1S} . We have converted this to $\overline{\text{MS}}$ scheme.

5 DELLA-MORTE 07 determine $\overline{m}_b(\overline{m}_b)$ from a computation of the spin-averaged B meson mass using quenched lattice HQET at order $1/m$. The ± 0.08 is an estimate of the quenching error.

6 KUHN 07 determine $\overline{m}_b(\mu = 10 \text{ GeV}) = 3.609 \pm 0.025$ GeV and $\overline{m}_b(\overline{m}_b)$ from a four-loop sum-rule computation of the cross-section for $e^+e^- \rightarrow$ hadrons in the bottom threshold region. We have converted this to the 1S scheme.

7 ABDALLAH 06D determine $m_b(M_Z) = 2.85 \pm 0.32$ GeV from Z -decay three-jet events containing a b -quark. We have converted this to $\overline{m}_b(\overline{m}_b)$ and m_b^{1S} .

8 BOUGHEZAL 06 $\overline{\text{MS}}$ scheme result comes from the first moment of the hadronic production cross-section to order α_s^3 . We have converted it to the 1S scheme.

9 BUCHMULLER 06 determine m_b and m_c by a global fit to inclusive B decay spectra. We have converted this to the 1S scheme.

10 PINEDA 06 $\overline{\text{MS}}$ scheme result comes from a partial NNLL evaluation (complete at NNLO) of sum rules of the bottom production cross-section in e^+e^- annihilation. We have converted it to the 1S scheme.

11 GRAY 05 determines $\overline{m}_b(\overline{m}_b)$ from a lattice computation of the Υ spectrum. The simulations have 2+1 dynamical light flavors. The b quark is implemented using NRQCD. We have converted m_b to the 1S scheme.

12 AUBERT 04x obtain m_b from a fit to the hadron mass and lepton energy distributions in semileptonic B decay. The paper quotes values in the kinetic scheme. The $\overline{\text{MS}}$ value has been provided by the BABAR collaboration, and we have converted this to the 1S scheme.

13 BAUER 04 determine m_b , m_c and $m_b - m_c$ by a global fit to inclusive B decay spectra. HOANG 04 determines $m_b(\overline{m}_b)$ from moments at order α_s^2 of the bottom production cross-section in e^+e^- annihilation.

14 MCNEILE 04 use lattice QCD with dynamical light quarks and a static heavy quark to compute the masses of heavy-light mesons.

15 BAUER 03 determine the b quark mass by a global fit to B decay observables. The experimental data includes lepton energy and hadron invariant mass moments in semileptonic $B \rightarrow X_c \ell \nu_\ell$ decay, and the inclusive photon spectrum in $B \rightarrow X_S \gamma$ decay. The theoretical expressions used are of order $1/m^3$, and $\alpha_s^2 \beta_0$.

16 BORDES 03 determines m_b using QCD finite energy sum rules to order α_s^2 .

17 CORCELLA 03 determines \overline{m}_b using sum rules computed to order α_s^2 . Includes charm quark mass effects.

18 DEDIVITIIS 03 use a quenched lattice computation of heavy-heavy and heavy-light meson masses.

19 EIDEMULLER 03 determines \overline{m}_b and \overline{m}_c using QCD sum rules.

20 ERLER 03 determines \overline{m}_b and \overline{m}_c using QCD sum rules. Includes recent BES data.

21 MAHMOOD 03 determines m_b^{1S} by a fit to the lepton energy moments in $B \rightarrow X_c \ell \nu_\ell$ decay. The theoretical expressions used are of order $1/m^3$ and $\alpha_s^2 \beta_0$. We have converted their result to the $\overline{\text{MS}}$ scheme.

22 BRAMBILLA 02 determine $\overline{m}_b(\overline{m}_b)$ from a computation of the $\Upsilon(1S)$ mass to order α_s^4 , including finite m_c corrections. We have converted this to the 1S scheme.

23 PENIN 02 determines \overline{m}_b from the spectrum of the Υ system.

24 NARISON 01b uses pseudoscalar sum rules in the B and D meson channels.

25 PINEDA 01 uses the $\Upsilon(1S)$ system to determine the quark mass. The errors are due to theory, and the uncertainty in α_s .

26 ABBIENDI 01s find $\overline{m}_b(M_Z)$ to be 2.67 ± 0.4 GeV from an analysis of $Z \rightarrow b$ decays.

27 BRAMBILLA 01 determine $\overline{m}_b(\overline{m}_b)$ from a computation of the J/ψ mass. We have converted this to the 1S scheme.

28 KUHN 01 uses an analysis of the e^+e^- total cross section to hadrons.

29 BARATE 00v obtain the b quark mass $\overline{m}_b(M_Z) = 3.27 \pm 0.22(\text{stat}) \pm 0.22(\text{exp}) \pm 0.38(\text{had}) \pm 0.16(\text{thy})$ from an analysis of event shape variables in Z decays. We have converted this to $\mu = \overline{m}_b$.

30 HOANG 00 uses a NNLO calculation of the vacuum polarization function to determine spectral moments of the masses and electronic decay widths of the Υ mesons.

31 LUCHA 00, PINEDA 00 obtain the b -quark mass from a perturbative calculation of the Υ spectrum and decay widths to order α_s^4 .

32 BENEKE 99 uses a calculation of the $b\overline{b}$ production cross section and the mass of the Υ meson at NNLO.

33 BRANDENBURG 99 obtain a b -quark mass of $\overline{m}_b(M_Z) = 2.56 \pm 0.27 + 0.28 + 0.49$ from a study of three-jet events at the Z . We have converted this to $\mu = \overline{m}_b$.

34 HOANG 99 uses a NNLO calculation of the vacuum polarization function to determine spectral moments of the masses and electronic decay widths of the Υ mesons.

35 MELNIKOV 99 compute the quark mass using Υ sum rules at NNLO.

36 PENIN 99 compute the quark mass using Υ sum rules at NNLO.

37 ABREU 98i determines the $\overline{\text{MS}}$ mass $\overline{m}_b = 2.67 \pm 0.25 \pm 0.34 \pm 0.27$ GeV at $\mu = M_Z$ from three jet heavy quark production at LEP. ABREU 98i have rescaled the result to $\mu = \overline{m}_b$ using $\alpha_s = 0.118 \pm 0.003$.

38 KUEHN 98 uses a calculation of the vacuum polarization function, including resumming threshold effects, to determine spectral moments of the masses of the Υ mesons. We have converted their extracted value of 4.75 ± 0.04 for the pole mass to the $\overline{\text{MS}}$ scheme.

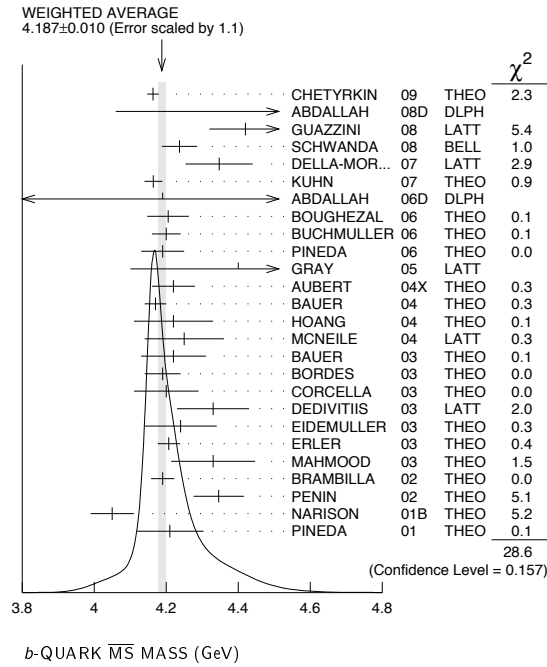
39 GIMENEZ 97 uses lattice computations of the B -meson propagator and the B -meson binding energy $\overline{\Lambda}$ in the HQET. Their systematic (second) error for the $\overline{\text{MS}}$ mass is an estimate of the effects of higher-order corrections in the matching of the HQET operators (renormalon effects).

40 JAMIN 97 apply the QCD moment method to the Υ system. They also find a pole mass of 4.60 ± 0.02 .

41 RODRIGO 97 determines the $\overline{\text{MS}}$ mass $\overline{m}_b = 2.85 \pm 0.22 \pm 0.20 \pm 0.36$ GeV at $\mu = M_Z$ from three jet heavy quark production at LEP. We have rescaled the result.

Quark Particle Listings

b, t



b-QUARK REFERENCES

CHETYRKIN	09	PR D80 074010	K.G. Chetyrkin <i>et al.</i>	(KARL, BNL)
ABDALLAH	08D	EPJ C55 525	J. Abdallah <i>et al.</i>	(DELPHI Collab.)
GUZZINI	08	JHEP 0801 076	D. Guazzini, R. Sommer, N. Tantalo	
SCHWANDA	08	PR D78 032016	C. Schwanda <i>et al.</i>	(BELLE Collab.)
DELLA-MOR...	07	JHEP 0701 007	M. Della Morte <i>et al.</i>	
KUHN	07	NP B776 192	J.H. Kuhn, M. Steinhauser, C. Sturm	
ABDALLAH	06D	EPJ C46 569	J. Abdallah <i>et al.</i>	(DELPHI Collab.)
BOUGHEZAL	06	PR D74 074006	R. Boughezal, M. Czakon, T. Schutzmeier	
BUCHMULLER	06	PR D73 073008	O.L. Buchmuller, H.U. Flaecher	
PINEDA	06	PR D73 111501R	A. Pineda, A. Signer	
GRAY	05	PR D72 094507	A. Gray <i>et al.</i>	(HPQCD, UKQCD Collab.)
AUBERT	04X	PRL 93 011803	B. Aubert <i>et al.</i>	(BABAR Collab.)
BAUER	04	PR D70 094017	C. Bauer <i>et al.</i>	
HOANG	04	PL B594 127	A.H. Hoang, M. Jamin	
MCNEILE	04	PL B600 77	C. McNeile, C. Michael, G. Thompson	(UKQCD Collab.)
BAUER	03	PR D67 054012	C.W. Bauer <i>et al.</i>	
BORDES	03	PL B562 81	J. Bordes, J. Penarrocha, K. Schilcher	
CORCELLA	03	PL B554 133	G. Corcella, A.H. Hoang	
DEDIVITIIS	03	NP B675 309	G.M. de Divitiis <i>et al.</i>	
EIDEMULLER	03	PR D67 113002	M. Eidemuller	
ERLER	03	PL B558 125	J. Erler, M. Luo	
MAHMOOD	03	PR D67 072001	A.H. Mahmood <i>et al.</i>	(CLEO Collab.)
BRAMBILLA	02	PR D65 034001	N. Brambilla, Y. Sumino, A. Vairo	
EL-KHADRA	02	ARNPS 52 201	A.X. El-Khadra, M. Luke	
PENIN	02	PL B538 335	A. Penin, M. Steinhauser	
ABBIENDI	01S	EPJ C21 411	G. Abbiendi <i>et al.</i>	(OPAL Collab.)
BRAMBILLA	01	PL B513 381	N. Brambilla, Y. Sumino, A. Vairo	
KUHN	01	NP B619 598	J.H. Kuhn, M. Steinhauser	
NARISON	01B	PL B520 115	S. Narison	
PINEDA	01	JHEP 0106 022	A. Pineda	
BARATE	00V	EPJ C18 1	R. Barate <i>et al.</i>	(ALEPH Collab.)
HOANG	00	PR D61 034005	A.H. Hoang	
LUCHA	00	PR D62 097501	W. Lucha, F.F. Schoeberl	
PINEDA	00	PR D61 077505	A. Pineda, F.J. Yndurain	
BENEKE	99	PL B471 233	M. Beneke, A. Signer	
BRANDENB...	99	PL B468 168	A. Brandenburg <i>et al.</i>	
HOANG	99	PR D59 014039	A.H. Hoang	
MELNIKOV	99	PR D59 114009	K. Melnikov, A. Yelkhovsky	
PENIN	99	NP B549 217	A.A. Penin, A.A. Pivovarov	
ABREU	98I	PL B418 430	P. Abreu <i>et al.</i>	(DELPHI Collab.)
KUEHN	98	NP B534 356	J.H. Kuehn, A.A. Penin, A.A. Pivovarov	
GIMENEZ	97	PL B393 124	V. Gimenez, G. Martinelli, C.T. Sachrajda	
JAMIN	97	NP B507 334	M. Jamin, A. Pich	
RODRIGO	97	PRL 79 193	C. Rodrigo, A. Santamaria, M.S. Bilenky	

t

$$I(J^P) = 0(\frac{1}{2}^+)$$

$$\text{Charge} = \frac{2}{3} e \quad \text{Top} = +1$$

THE TOP QUARK

Updated April 2010 by T.M. Liss (Univ. Illinois) and A. Quadri (Univ. Göttingen).

A. Introduction: The top quark is the $Q = 2/3$, $T_3 = +1/2$ member of the weak-isospin doublet containing the bottom quark (see the review on the “Standard Model of Electroweak Interactions” for more information). This note summarizes the properties of the top quark (mass, production cross section,

decay branching ratios, *etc.*), and provides a discussion of the experimental and theoretical issues involved in their determination

B. Top quark production at the Tevatron: All direct measurements of production and decay of the top quark have been made by the CDF and DØ experiments in $p\bar{p}$ collisions at the Fermilab Tevatron collider. The first studies were performed during Run I, at $\sqrt{s} = 1.8$ TeV, which was completed in 1996. The most recent, and most precise, measurements are from Run II, which started in 2001 at $\sqrt{s} = 1.96$ TeV. This note will discuss primarily results from Run II.

In hadron collisions, top quarks are produced dominantly in pairs through the QCD processes $q\bar{q} \rightarrow t\bar{t}$ and $gg \rightarrow t\bar{t}$. At $\sqrt{s} = 1.96$ TeV the most recent calculations are at NLO with next-to-leading-log soft gluon resummation [1]. Cacciari *et al.* gives a production cross section of 7.61 pb for $m_t = 171$ GeV/ c^2 with CTEQ6.5 PDFs. Over the range 150 GeV/ $c^2 \leq m_t \leq 190$ GeV/ c^2 the calculated cross section decreases (increases) by approximately 0.24 pb/GeV for m_t greater (less) than 171 GeV/ c^2 . A similar calculation by Kidonakis and Vogt yields a production cross section of 7.62 pb for $m_t = 171$ GeV/ c^2 using CTEQ6.6M, with nearly the same mass-dependence. The difference in the central value obtained using different PDFs is typically a few tenths of a pb or less. A detailed comparison of the most recent calculations is ongoing between the authors of the calculations. Approximately 85% of the production cross section at the Tevatron is from $q\bar{q}$ annihilation, with the remainder from gluon-gluon fusion [2]. Somewhat smaller cross sections are expected from electroweak single-top production mechanisms, namely from $q\bar{q}' \rightarrow t\bar{b}$ [3] and $qb \rightarrow q't$ [4], mediated by virtual s -channel and t -channel W bosons, respectively. The cross sections are calculated for $m_{top} = 175$ GeV/ c^2 to be 0.88 ± 0.11 pb for the s -channel, and 1.98 ± 0.25 pb for the t -channel [5], a little less than half of the $t\bar{t}$ production rate. The identification of top quarks in the electroweak single-top channel is much more difficult than in the QCD $t\bar{t}$ channel, due to a less distinctive signature and significantly larger backgrounds.

In top decay, the Ws and Wd final states are expected to be suppressed relative to Wb by the square of the CKM matrix elements V_{ts} and V_{td} . Assuming unitarity of the three-generation CKM matrix, these matrix element values are estimated to be less than 0.043 and 0.014, respectively, implying a value of $V_{tb} > 0.999$ (see the review “The CKM Quark-Mixing Matrix” for more information). With a mass above the Wb threshold, and V_{tb} close to unity, the decay width of the top quark is expected to be dominated by the two-body channel $t \rightarrow Wb$. Neglecting terms of order m_b^2/m_t^2 , α_s^2 , and $(\alpha_s/\pi)M_W^2/m_t^2$, the width predicted in the Standard Model (SM) at next-to-leading-order is [6]:

$$\Gamma_t = \frac{G_F m_t^3}{8\pi\sqrt{2}} \left(1 - \frac{M_W^2}{m_t^2}\right)^2 \left(1 + 2\frac{M_W^2}{m_t^2}\right) \left[1 - \frac{2\alpha_s}{3\pi} \left(\frac{2\pi^2}{3} - \frac{5}{2}\right)\right], \quad (1)$$

where m_t refers to the top quark pole mass. The width for a value of $m_t = 171 \text{ GeV}/c^2$, close to the world average, is $1.29 \text{ GeV}/c^2$ (we use $\alpha_s(M_Z) = 0.118$) and increases with mass. With its correspondingly short lifetime of $\approx 0.5 \times 10^{-24} \text{ s}$, the top quark is expected to decay before top-flavored hadrons or $t\bar{t}$ -quarkonium-bound states can form [7]. The order α_s^2 QCD corrections to Γ_t are also available [8], thereby improving the overall theoretical accuracy to better than 1%.

The final states for the leading pair-production process can be divided into three classes:

- A. $t\bar{t} \rightarrow W^+ b W^- \bar{b} \rightarrow q \bar{q}' b q'' \bar{q}''' \bar{b}$, (46.2%)
- B. $t\bar{t} \rightarrow W^+ b W^- \bar{b} \rightarrow q \bar{q}' b \ell \bar{\nu}_\ell \bar{b} + \bar{\ell} \nu_\ell b q \bar{q}' \bar{b}$, (43.5%)
- C. $t\bar{t} \rightarrow W^+ b W^- \bar{b} \rightarrow \bar{\ell} \nu_\ell b \ell' \bar{\nu}_{\ell'} \bar{b}$. (10.3%)

The quarks in the final state evolve into jets of hadrons. A, B, and C are referred to as the all-jets, lepton+jets (ℓ +jets), and dilepton ($\ell\ell$) channels, respectively. Their relative contributions, including hadronic corrections, are given in parentheses. While ℓ in the above processes refers to e , μ , or τ , most of the results to date rely on the e and μ channels. Therefore, in what follows, we will use ℓ to refer to e or μ , unless otherwise noted.

The initial and final-state quarks can radiate gluons that can be detected as additional jets. The number of jets reconstructed in the detectors depends on the decay kinematics, as well as on the algorithm for reconstructing jets used by the analysis. The transverse momenta of neutrinos are reconstructed from the imbalance in transverse momentum measured in each event (missing p_T , which is here also missing E_T).

The observation of $t\bar{t}$ pairs has been reported in all of the above decay classes. As discussed below, the production and decay properties of the top quark extracted from the three decay classes are consistent within their experimental uncertainty. In particular, the $t \rightarrow Wb$ decay mode is supported through the reconstruction of the $W \rightarrow jj$ invariant mass in events with two identified b -jets in the $\ell\nu_\ell b\bar{b}jj$ final state [9] and in the all-jets final state [10]. Also the CDF and DØ measurements of the top quark mass in lepton+jets events, where the jet energy scale is calibrated *in situ* using the invariant mass of the hadronically decaying W boson [11,12], support this decay mode.

The extraction of top-quark properties from Tevatron data relies on a good understanding of the production and decay mechanisms of the top quark, as well as of the background processes. For the background, the jets are expected to have a steeply falling E_T spectrum, to have an angular distribution peaked at small angles with respect to the beam, and to contain b - and c -quarks at the few-percent level. On the contrary, for the top signal, the fraction of events containing b jets is expected to be $\approx 100\%$, and the jets to be rather energetic, since they come from the decay of a massive object. It is therefore possible to improve the S/B ratio by requiring the presence of a b quark, or by selecting very energetic and central kinematic configurations, or both.

Background estimates can be checked using control samples with fewer jets, where there is little top contamination (0 or 1

jet for dilepton channels, 1 or 2 jets for lepton+jets channels, and ≤ 4 jets for multijets).

The cross sections for single-top production are proportional to $|V_{tb}|^2$, and no assumption is needed on the number of families or on the unitarity of the CKM matrix in extracting $|V_{tb}|$. Separate measurements of the s - and t -channel processes provide sensitivity to physics beyond the SM [13]. The single-top process has recently been observed by both DØ [14] and CDF [15]. These results are discussed in a separate section below.

Next-to-leading-order Monte-Carlo programs are now available for the $t\bar{t}$ production processes [16]. Theoretical estimates of the background processes (W or Z bosons+jets and dibosons+jets) using LO calculations have large uncertainties. While this limitation affects estimates of the overall production rates, it is believed that the LO determination of event kinematics, and of the fraction of W +multi-jet events that contain b - or c -quarks, are relatively accurate [17]. Comparison to CDF and DØ data, however, indicates the b - and c -quark fractions to be underestimated by the LO generators.

C. Measured top properties: Current measurements of top properties by CDF and DØ are based on Run-II data with integrated luminosities up to 5.3 fb^{-1} .

C.1 $t\bar{t}$ Production Cross Section: Both experiments determine the $t\bar{t}$ -production cross section, $\sigma_{t\bar{t}}$, from the observed or estimated number of top candidates, estimated background, $t\bar{t}$ acceptance, and integrated luminosity. The cross section has been measured in the dilepton, lepton+jets, and all-jets decay modes. To separate signal from background, the experiments use identification of jets likely to contain b -quarks (“ b -tagging”) and/or discriminating kinematic observables. Techniques used for b -tagging include identification of a secondary vertex (“ $\text{vtx } b\text{-tag}$ ”), a probability that a jet contains a secondary vertex based on the measured impact parameter of tracks (“jet probability”), or identification of a muon (electron) from a semileptonic b decay (“soft μ (e) $b\text{-tag}$ ”). CDF and DØ also use artificial neural network-based b -tagging algorithms that combine the properties of displaced tracks and secondary vertex information.

Due to the lepton identification (ID) requirements in the ℓ +jets and $\ell\ell$ modes, in particular the p_T requirement, the sensitivity is primarily to e and μ decays of the W , with only a small contribution from $W \rightarrow \tau\nu$ due to secondary $\tau \rightarrow (e, \mu)\nu X$ decays. In the $\ell\ell$ mode, when only one lepton is required to satisfy lepton ID criteria (ℓ +track), there is greater sensitivity to $W \rightarrow \tau\nu$. CDF uses a missing- E_T +jets selection in the ℓ +jets mode that does not require specific lepton-ID, and therefore has significant acceptance to $W \rightarrow \tau\nu$ decays, including hadronic τ decays, in addition to $W \rightarrow e\nu, \mu\nu$ decays. In a direct search for the τ decay mode of $t\bar{t}$ pairs in the lepton+hadronic τ channel, the ratio $r_\tau \equiv B(t \rightarrow b\tau\nu)/B_{SM}(t \rightarrow b\tau\nu)$ is found to be $r_\tau < 5.2$ at 95% C.L. [18]. DØ finds the production cross section (and visible cross section $\sigma \cdot Br$) to be consistent with SM expectations in

Quark Particle Listings

t

the lepton+hadronic τ channel [19], as well as in the τ +jets channel [20] and in the $\ell\tau$ channel [39]. In the most recent results from CDF, using more than 4 fb^{-1} , the measurement is done as a ratio to the Z -boson production cross section measured using the same dataset and triggers. This removes the uncertainty due to the integrated luminosity measurement and much of the uncertainties due to trigger and lepton ID efficiencies. Table 1 shows the measured cross sections from $D\emptyset$ and CDF. These should be compared to the theoretical calculations that yield $7.9 - 6.7 \text{ pb}$ for top masses from 170 to $175 \text{ GeV}/c^2$ respectively [1] (see Listings).

Next-to-leading-order calculations predict a forward-backward asymmetry of $(5 \pm 1.5)\%$ in $t\bar{t}$ production [21]. The CDF measurement in 3.2 fb^{-1} yields $19.3 \pm 6.9\%$ [22], while the $D\emptyset$ measurement of this asymmetry yields $12 \pm 8\%$ at the detector level [23] using 0.9 fb^{-1} . Though intriguingly larger, both results are presently consistent with the NLO prediction, in view of the large experimental systematics. The asymmetry arises due to interference between production diagrams with initial-state gluon radiation and diagrams with final-state gluon radiation. The discrepancy between the measurements and theoretical predictions has generated an interest in comparisons between $t\bar{t}$ +jet production cross section calculations and measurements. A recent measurement from CDF [24] in 4.1 fb^{-1} of integrated luminosity yields a cross section of $1.6 \pm 0.5 \text{ pb}$, in good agreement with the theoretical value of $1.79^{+0.16}_{-0.31} \text{ pb}$ [25].

The theory calculations at next-to-leading-order, including soft-gluon resummation [1], are in good agreement with all the measurements. The increased precision of combined measurements from larger Run-II samples can serve to constrain, or probe, exotic production mechanisms or decay channels that are predicted by some models [26–29]. Such non-SM effects would yield discrepancies between theory and data. New sources of top could also modify kinematic distributions, such as the invariant mass of the $t\bar{t}$ pair or the transverse momentum (p_T) of the top quark. Run-I studies of the $t\bar{t}$ invariant mass by CDF and $D\emptyset$ [30,31], and of p_T distributions by CDF [32], show no deviation from expected behavior. $D\emptyset$ [33] also found these kinematic distributions to be consistent with expectations of the SM in Run I. In Run II, distributions of primary kinematic variables such as the lepton p_T , missing E_T , and angular variables have been investigated [34–50] and found to be consistent with the SM. Recently, CDF has measured the differential production cross section $d\sigma/dM_{t\bar{t}}$ in 2.7 fb^{-1} [51]. Comparing the shape to the SM expectation, they find a p -value of 0.28 (for a definition of the p -value, see the section on hypothesis testing in the review on “STATISTICS” in this *Review*). The $t\bar{t}$ invariant mass distributions have been studied by both CDF [52] and $D\emptyset$ [53] for direct evidence of narrow resonances, with limits placed on putative Z' mass of 805 and 820 GeV/c^2 , respectively. CDF has also used the $M_{t\bar{t}}$ distribution to place limits on the coupling strength of a massive gluon as a function of its mass [54].

Table 1: Cross section for $t\bar{t}$ production in $p\bar{p}$ collisions at $\sqrt{s} = 1.96 \text{ TeV}$ from CDF and $D\emptyset$. The cross sections are evaluated using an acceptance for $m_t = 175 \text{ GeV}/c^2$ unless marked with ‘ \ddagger ’ or ‘ \star ’, in which case they are evaluated using an acceptance at $m_t = 172.5 \text{ GeV}/c^2$ and $m_t = 170.9 \text{ GeV}/c^2$, respectively. Only preliminary results (not yet submitted for publication as of April 2010) are shown; for published results see the Listings. Uncertainties given are the quadrature sum of statistical and systematic uncertainties of each measurement.

$\sigma_{t\bar{t}}(\text{pb})$	Source	$\int \mathcal{L} dt$ (fb^{-1})	Ref.	Method
7.3 ± 1.9	$D\emptyset$	2.1	[19]	$\ell\tau$ + b-jets
6.2 ± 1.2	$D\emptyset$	1.0	[36]	$\ell\ell$ + ℓ +track
$5.2 \pm 1.8\star$	$D\emptyset$	1.0	[37]	ℓ +track
5.1 ± 4.4	$D\emptyset$	0.4	[20]	τ +jet
8.4 ± 1.2	$D\emptyset$	0.4	[35]	$\ell\ell$
$7.0 \pm 0.8\ddagger$	CDF	4.3	[40]	ℓ + jets/vtx b -tag
$7.1 \pm 0.7\ddagger$	CDF	4.3	[40]	As above w/ ratio to $\sigma(Z)$
7.8 ± 2.9	CDF	1.7	[42]	ℓ + jets/soft e b -tag
$7.5 \pm 0.7\ddagger$	CDF	4.6	[43]	ℓ + jets/kinematics
$7.6 \pm 0.5\ddagger$	CDF	4.6	[43]	Above w/ ratio to $\sigma(Z)$
$6.9 \pm 1.0\ddagger$	CDF	4.3	[44]	ℓ + jets/NN b -tag
$8.0 \pm 0.9\ddagger$	CDF	2.2	[45]	Missing E_T + jets/ b -tag
$6.6 \pm 0.9\ddagger$	CDF	4.5	[46]	$\ell\ell$
$7.3 \pm 0.9\ddagger$	CDF	4.5	[46]	$\ell\ell$ /vtx b -tag
7.2 ± 1.3	CDF	2.9	[47]	All-jets/kin+vtx b -tags
$7.5 \pm 0.5\ddagger$	CDF	4.6	[41]	Combined

C.2 Electroweak Single-Top Quark Production: $D\emptyset$ [14] and CDF [15] have recently announced the discovery of electroweak production of single top quarks. The announcement is the culmination of a multi-year effort that required the use of many advanced analysis techniques to separate the signal from an overwhelming background. In s-channel single-top production, the top quark is accompanied by a bottom quark and the final state is therefore a W boson and two bottom jets. In t-channel production, the top is accompanied by both a bottom quark and a light quark jet, but the accompanying bottom quark is typically at large pseudorapidity and low transverse energy and hence escapes detection. The t-channel final state results also dominantly in W +2 jets, with just one of the jets coming from a bottom quark. Event selection therefore requires a high p_T electron or muon, two to four jets, one of which must be identified as originating from a bottom quark, and missing E_T . In addition, CDF uses events selected with large missing E_T and two or three energetic jets. The expected signal-to-background ratio in these samples is about 5%, and the challenge is to separate the signal not just from QCD-produced W +jets events, but also from $t\bar{t}$ events which end up in the signal region.

To overcome this challenge, both experiments have used a variety of multivariate techniques, including neural networks, boosted decision trees, multivariate likelihood functions and matrix elements. With the exception of the CDF missing E_T plus jets analysis, all the analyses use nearly the same datasets. Nevertheless, they are not completely correlated and the final results come from a combination of all analyses. Both experiments use a neural-network technique to combine the individual results into a final result. DØ reports a combined s- plus t-channel cross section of 3.94 ± 0.88 pb (for $m_t = 170$ GeV/ c^2), with a corresponding p -value of 2.5×10^{-7} (5.0σ), based on 2.3 fb $^{-1}$ of integrated luminosity [14]. CDF reports a combined cross section of $2.3_{-0.5}^{+0.6}$ pb for $m_t = 175$ GeV/ c^2 with a corresponding p -value of 3.1×10^{-7} (5.0σ), based on 3.2 fb $^{-1}$ of integrated luminosity [15]. A Bayesian analysis yields a combined single-top production cross section of $2.76_{-0.47}^{+0.58}$ pb [55].

The CKM matrix element V_{tb} is extracted from the measured cross sections using the ratio to the theoretical values, which assume $V_{tb} = 1.0$. The results are summarized in Table 2.

Table 2: Measurements of $|V_{tb}|$ from CDF and DØ single-top results.

$ V_{tb} $ or $ V_{tb}f_1^T $	Source	$\int \mathcal{L} dt$ (fb $^{-1}$)	Ref.
$ V_{tb}f_1^T = 1.07 \pm 0.12$	DØ	Run II 2.3	[14]
$ V_{tb} > 0.78$	DØ	Run II 2.3	[14]
$ V_{tb} = 0.91 \pm 0.13$	CDF	Run II 3.2	[15]
$ V_{tb} = 0.88 \pm 0.07$	CDF + DØ	Run II 3.2	[55]
$ V_{tb} > 0.77$	CDF + DØ	Run II 3.2	[55]

Both experiments have done separate measurements of the s- and t-channel cross sections by reoptimizing the analysis for one or both of the channels separately. In a simultaneous measurement of s- and t-channel cross sections, CDF measures $2.0_{-0.6}^{+0.7}$ pb and 0.7 ± 0.5 pb, respectively, in 3.2 fb $^{-1}$ of data [56], while DØ measures 1.05 ± 0.81 pb and $3.14_{-0.80}^{+0.94}$ pb, respectively in 2.3 fb $^{-1}$ of integrated luminosity [57]. In a separate analysis, optimized for the s-channel alone, CDF measures $1.49_{-0.75}^{+0.92}$ pb in 3.2 fb $^{-1}$ of data [58].

In the SM single-top-quark production yields a nearly 100% polarization of the top-quark spin along the direction, in the top rest frame, of the down-type quark or charged lepton from the W boson decay. This corresponds to the fact that single top quarks produced at the V-A Wtb vertex are left-handed. Recently CDF has searched for a small right-handed (V+A) component in 3.2 fb $^{-1}$ of integrated luminosity [59]. To discriminate between the SM V-A and a V+A component, the sample is split into a $\cos\theta < 0$ piece and a $\cos\theta > 0$ piece, where θ is the angle between the lepton and the down-type quark in the top-quark rest frame. The single-top production cross section in the two samples is measured separately, using the multivariate likelihood technique. The result is consistent with no V+A component and a polarization of $-1_{-0}^{+0.5}$.

C.3 Top Quark Mass Measurements: The top mass has been measured in the lepton+jets, dilepton, and the all-jets channel by both CDF and DØ. At present, the most precise measurements come from the lepton+jets channel containing four or more jets, and large missing E_T . The samples for the mass measurement are selected using topological or b -tagging methods. In this channel, four basic techniques are employed to extract the top mass. In the first, the so-called “template method” (TM) [60], an over-constrained (2C) kinematic fit is performed to the hypothesis $t\bar{t} \rightarrow W^+ b W^- \bar{b} \rightarrow \ell \bar{\nu}_\ell b q \bar{q}' \bar{b}$ for each event, assuming that the four jets of highest E_T originate from the four quarks in $t\bar{t}$ decay. There are 24 possible solutions, reflecting the allowed assignment of the final-state quarks to jets, and the two possible solutions for the longitudinal momentum, p_z , of the neutrino when the W -mass constraint is imposed on the leptonic W decay. The number of solutions is reduced to 12 when a jet is b -tagged and assigned as one of the b quarks, and to 4 when the event has two such b -tags. A χ^2 variable describes the agreement of the measurements with each possible solution under the $t\bar{t}$ hypothesis given jet-energy resolutions. The solution with the lowest χ^2 is defined as the best choice, resulting in one value for the reconstructed top quark mass per event. The distribution of reconstructed top-quark mass from the data events is then compared to templates modeled from a combination of signal and background distributions for a series of assumed top masses. The best fit value for the top quark mass and its uncertainty are obtained from a maximum-likelihood fit. In the second method, the “Matrix Element/Dynamic Likelihood Method” (ME/DLM), similar to that originally suggested by Kondo *et al.* [61] and Dalitz and Goldstein [62], a probability for each event is calculated as a function of the top mass, using an LO matrix element for the production and decay of $t\bar{t}$ pairs. All possible assignments of reconstructed jets to final-state quarks are used, each weighted by a probability determined from the matrix element. The correspondence between measured four-vectors and parton-level four-vectors is taken into account using probabilistic transfer functions. In a third method, the “Ideogram Method” [63,64], which combines some of the features of the above two techniques, each event is compared to the signal and background mass spectrum, weighted by the χ^2 probability of the kinematic fit for all 24 jet-quark combinations and an event probability. The latter is determined from the signal fraction in the sample and the event-by-event purity, as determined from a topological discriminant in Monte Carlo events. An additional variation on these techniques is the “Multivariate Likelihood” (ML) technique, where an integral over the matrix element is performed for each permutation, and then summed with weights determined by the b -tagging information on each jet. Backgrounds are handled in the ML technique by “deweighting” events according to a background probability calculated using variables based on the topology of the event.

Quark Particle Listings

t

With at least four jets in the final state, the dominant systematic uncertainty on the top quark mass is from the uncertainty on the jet-energy scale. CDF (TM, ME, ML) and DØ (ME) have reduced the jet-energy scale uncertainty by performing a simultaneous, *in situ*, fit to the $W \rightarrow jj$ hypothesis.

There are several techniques that rely solely on tracking, and thus avoid the jet-energy scale uncertainty. One method [65] exploits the fact that, in the rest frame of the top quark, the boost given to the bottom quark has a Lorentz factor $\gamma_b \approx 0.4 m_t/m_b$. The measurement of the transverse decay length L_{xy} of the b -hadrons from the top quark decay is therefore sensitive to the mass of the top quark. Another uses the correlation between the p_T spectrum of the leptons from the W -boson decay and m_t [67,66]. Finally, a recent measurement [68] uses the invariant mass of the lepton from the W -boson decay and the muon from a semileptonic decay of the associated B hadron to measure m_t .

mass from direct reconstruction without adding additional information. Assuming a value for m_t , the $t\bar{t}$ system can be reconstructed up to an eight-fold ambiguity from the choice of associating leptons and quarks to jets, and due to the two solutions for the p_z of each neutrino. Recently, an analytic solution to the problem has been proposed [69]. At the Tevatron, two basic techniques are employed: one based on templates, and one using matrix elements. The first class of techniques incorporates additional information to render the kinematic system solvable. In this class, there are two techniques that assign a weight as a function of top mass for each event based on solving for either the azimuth, ϕ , of each neutrino given an assumed pseudorapidity, η , ($\eta(\nu)$) [70,71], or for η of each neutrino given an assumed ϕ , ($\phi(\nu)$) [72]. An alternative approach, (MWT) [70], solves for η of each neutrino requiring the sum of the neutrino \vec{p}_T 's to equal the measured missing E_T vector. In another technique,

Table 3: Measurements of top quark mass from CDF and DØ. $\int \mathcal{L} dt$ is given in fb^{-1} . Only preliminary results (not yet submitted for publication as of April 2010) are shown; for published results see the Listings. Statistical uncertainties are listed first, followed by systematic uncertainties.

m_t (GeV/ c^2)	Source	$\int \mathcal{L} dt$	Ref.	Method
$173.7 \pm 0.8 \pm 1.6$	DØ Run II	3.6	[73]	ℓ +jets/ b -tag, ME($W \rightarrow jj$)
$174.7 \pm 2.9 \pm 2.4$	DØ Run II	3.6	[74]	$\ell\ell$, $\eta(\nu)$ +ME+MWT
$174.2 \pm 0.9 \pm 1.5$	DØ Run I+II	0.1-3.6	[75]	DØ combined selected measurements
$172.8 \pm 0.9 \pm 0.8$	CDF Run II	4.8	[76]	ℓ +jets/ b -tag, ML($W \rightarrow jj$)
$172.2 \pm 1.2 \pm 1.0$	CDF Run II	4.8	[77]	ℓ +jets/ b -tag, TM($W \rightarrow jj$)
$172.1 \pm 1.1 \pm 1.0$	CDF Run II	4.8	[77]	ℓ +jets TM($W \rightarrow jj$) & $\ell\ell$ $\eta(\nu)$ + m_{T2}
$172.4 \pm 1.4 \pm 1.3$	CDF Run II	3.2	[78]	ℓ +jets, ME ($W \rightarrow jj$)
$176.9 \pm 8.0 \pm 2.7$	CDF Run II	2.7	[66]	ℓ +jets, $P_T(\ell)$
$170.6 \pm 2.2 \pm 3.1$	CDF Run II	4.8	[77]	$\ell\ell$, $\eta(\nu)$
$154.6 \pm 13.3 \pm 2.3$	CDF Run II	2.8	[67]	$\ell\ell$, $P_T(\ell)$
$172.8 \pm 7.2 \pm 2.3$	CDF Run II	2.8	[79]	$\ell\ell$, ℓ +jets, $P_T(\ell)$
$174.8 \pm 2.4^{+1.2}_{-1.0}$	CDF Run II	2.9	[80]	all jets, TM($W \rightarrow jj$)
$165.2 \pm 4.4 \pm 1.9$	CDF Run II	1.9	[81]	all jets, Ideogram ($W \rightarrow jj$)
$172.6 \pm 0.9 \pm 1.2$	CDF Run I+II	0.110-3.2	[82]	CDF Combined selected measurements
$172.0 \pm 0.9 \pm 1.3^*$	CDF, DØ (I+II)	0.110-2.0		publ. results, PDG best
$173.1 \pm 0.6 \pm 1.1^{**}$	CDF, DØ (I+II)	0.110-3.6	[83]	publ. or prelim. results

* PDG uses this TEVEWWG result as its best value. It is a combination of published Run I + II measurements, yielding a χ^2 of 5.8 for 10 deg. of freedom.

**The TEVEWWG world average is a combination of published Run I and preliminary or pub. Run-II meas., yielding a χ^2 of 6.3 for 10 deg. of freedom.

Additional determinations of the top mass come from the dilepton channel with two or more jets and large missing E_T , and from the all-jets channel. The dilepton channel, with two unmeasured neutrinos, is under-constrained by one measurement. It is not possible to extract a value for the top-quark

($p_z(t\bar{t})$) [72], the kinematic system is rendered solvable by the addition of the requirement that the p_z of the $t\bar{t}$ system, equal to the sum of the p_z of the t and \bar{t} , be zero within a Gaussian uncertainty of 180 GeV/ c . In a variation of the $p_z(t\bar{t})$ technique, the theoretical relation between the top mass and its production cross section is used as an additional constraint. In most of the

techniques in this class, a single mass per event is extracted and a top-mass value found using a Monte Carlo template fit to the single-event masses, in a manner similar to that employed in the lepton+jets TM technique. The $D\bar{O}$ ($\eta(\nu)$) analysis uses the shape of the weight distribution as a function of m_{top} in the template fit. The second class, ME/DLM, uses weights based on the LO matrix element for an assumed mass, given the measured four-vectors (and integrating over the unknowns) to form a joint likelihood as a function of the top mass for the ensemble of fitted events.

The P_T spectrum of the leptons in the dilepton channel has also been used to extract a top mass measurement [67]. The resulting statistical uncertainty of the measurement is large, but as with the L_{xy} technique, it is almost free of the systematic uncertainty due to the jet-energy scale.

In the most recent set of CDF results (see Table 3), a measurement has been done using the lepton+jets and dilepton channels simultaneously. In the lepton+jets channel, the TM is used together with an *in situ* $W \rightarrow jj$ fit. In the dilepton channel, $\eta(\nu)$ is used plus a fit to the scalar sum of transverse energies (H_T), which is sensitive to the top mass.

In the all-jets channel, there is no unknown neutrino momentum to deal with, but the S/B is the poorest. Both CDF and $D\bar{O}$ use events with 6 or more jets, of which at least one is b -tagged. In addition, both experiments have employed a neural network selection, based on an array of kinematic variables to improve the S/B. At $D\bar{O}$, a top-quark mass is reconstructed from the jet-quark combination that best fits the hadronic W -mass constraint and the equal-mass constraint for the two top quarks. At CDF, the top-quark mass for each event was reconstructed applying the same fitting technique used in the ℓ +jets mode. In the most recent analysis, the *in situ* jet-energy scale calibration from the $W \rightarrow jj$ fit is also used. At both CDF and $D\bar{O}$, the resulting mass distribution is compared to Monte Carlo templates for various top-quark masses and the background distribution, and a maximum likelihood technique is used to extract the final measured value of m_t and its uncertainty.

$D\bar{O}$ also measures the top-quark mass via comparison of the $t\bar{t}$ production cross section with the SM expectation [38]. This method has the advantage that it is very simple and sensitive to the top quark pole mass, which is a very well defined concept. The fully-inclusive cross-section calculation, used for comparison, contains current best theoretical knowledge with reduced scheme- or scale-dependence.

Recent results are shown in Table 3. See the Top Quark Listings for a complete set of published results. The systematic uncertainty (second uncertainty shown) is comparable to the statistical uncertainty, and is primarily due to uncertainties in the jet-energy scale and in the Monte Carlo modeling. In the Run-II analyses, CDF and $D\bar{O}$ have controlled the jet-energy scale uncertainty via *in situ* $W \rightarrow jj$ calibration using the same $t\bar{t}$ events, as mentioned above.

The Tevatron Electroweak Working Group (TEVEWWG), responsible for the combined CDF/ $D\bar{O}$ average top mass in Table 3, took account of correlations between systematic uncertainties in the different measurements in a sophisticated manner [83]. The Particle Data Group (PDG) uses their combination of published Run-I and Run-II top-mass measurements, $m_t = 172.0 \pm 1.6 \text{ GeV}/c^2$ (statistical and systematic uncertainties combined in quadrature), as the PDG best value. The latest TEVEWWG world average [83], also including published and some preliminary Run-II results, yields $m_t = 173.1 \pm 1.3 \text{ GeV}/c^2$ (statistical and systematic uncertainties combined in quadrature).

Given the experimental technique used to extract the top mass, these mass values should be taken as representing the top *pole mass* (see the review “Note on Quark Masses” in this *Review* for more information). The top pole mass, like any quark mass, is defined up to an intrinsic ambiguity of order $\Lambda_{QCD} \sim 200 \text{ MeV}$ [84]. Ultimately, the precision of the mass measurements will be limited by the theoretical understanding of the relation between the observables and the theoretical definition of the mass.

Recently, $D\bar{O}$ has tested CPT invariance in the top sector. They measured the mass difference between t and \bar{t} quarks in lepton+jets final states of $t\bar{t}$ events in 1 fb^{-1} . The measured mass difference of $3.8 \pm 3.7 \text{ GeV}$ is consistent with the equality of t and \bar{t} masses [85].

Current global fits performed within the SM or its minimal supersymmetric extension, in which the top-mass measurements play a crucial role, provide indications for a relatively light Higgs (see “ H^0 Indirect Mass Limits” in the Particle Listings of this *Review* for more information). Such fits, including Z -pole data [86] and direct measurements of the mass and width of the W -boson, yield $m_t = 179_{-9}^{+12} \text{ GeV}/c^2$ [87]. A fit including additional electroweak precision data (see the review “Electroweak Model and Constraints on New Physics” in this *Review*) yields $m_t = 174.7_{-7.8}^{+10.0} \text{ GeV}/c^2$ (OUR EVALUATION). Both indirect evaluations are in good agreement with the direct top-quark mass measurements.

C.4 Top Quark Electric Charge: The top quark is the only quark whose electric charge has not been measured through production at threshold in e^+e^- collisions. Since the CDF and $D\bar{O}$ analyses on top quark production do not associate the b , \bar{b} , and W^\pm uniquely to the top or antitop, decays such as $t \rightarrow W^+\bar{b}$, $\bar{t} \rightarrow W^-b$ are not excluded. A charge $4/3$ quark of this kind would be consistent with current electroweak precision data. The $Z \rightarrow \ell^+\ell^-$ and $Z \rightarrow b\bar{b}$ data, in particular the discrepancy between A_{LR} from SLC at SLAC and $A_{FB}^{0,b}$ of b -quarks and $A_{FB}^{0,\ell}$ of leptons from LEP at CERN, can be fitted with a top quark of mass $m_t = 270 \text{ GeV}/c^2$, provided that the right-handed b quark mixes with the isospin $+1/2$ component of an exotic doublet of charge $-1/3$ and $-4/3$ quarks, $(Q_1, Q_4)_R$ [29,88].

CDF and $D\bar{O}$ study the top quark charge in double-tagged lepton+jets events and (CDF) single-tagged dilepton events.

Quark Particle Listings

t

Assuming the top and antitop quarks have equal but opposite electric charge, then reconstructing the charge of the b -quark through jet charge discrimination techniques, the $|Q_{top}| = 4/3$ and $|Q_{top}| = 2/3$ scenarios can be differentiated. For the exotic model of Chang *et al.* [88] with a top-quark charge $|Q_{top}| = 4/3$, DØ yields a p -value, corresponding to the probability of consistency with the exotic model, of 7.8% [89]. CDF excludes the model at 87% C.L. [90]. While these two results are not directly comparable, they both indicate that the observed particle is indeed consistent with being a SM $|Q_{top}| = 2/3$ quark. More recently CDF has measured the top quark charge using the soft e or μ from semileptonic b -decays in $t\bar{t}$ events [91]. The soft lepton carries the flavor information of the bottom quark (with a dilution factor) and a kinematic fitter is used to associate the soft-lepton-tagged jet with either the W^+ or W^- from the top decay. The result excludes a charge 4/3 top quark at the 95% C.L. and strongly favors the Standard Model charge 2/3 top quark.

C.5 Top Branching Ratio: CDF and DØ report direct measurements of the $t \rightarrow Wb$ branching ratio [34,92–93]. Comparing the number of events with 0, 1 and 2 tagged b jets in the lepton+jets channel, and for CDF also in the dilepton channel, and using the known b -tagging efficiency, the ratio $R = B(t \rightarrow Wb) / \sum_{q=d,s,b} B(t \rightarrow Wq)$ can be extracted. DØ performs a simultaneous fit for the number of $t\bar{t}$ events and the ratio R . A deviation of R from unity would imply either non-SM top decay, a non-SM background to $t\bar{t}$ production, or a fourth generation of quarks. The results are summarized in Table 4.

Table 4: Measurements and 95% C.L. lower limits of $R = B(t \rightarrow Wb) / B(t \rightarrow Wq)$ from CDF and DØ. A complete set of published results can be found in the Listings.

R	Source	$\int \mathcal{L} dt$ (pb $^{-1}$)	Ref.
$R = 0.97^{+0.09}_{-0.08}$	DØ Run II	900	[34]
$R > 0.79$	DØ Run II	900	[34]

C.6 W -Boson Helicity: Studies of decay angular distributions provide a direct check of the V - A nature of the Wtb coupling and information on the relative coupling of longitudinal and transverse W bosons to the top quark. In the SM, the fraction of decays to longitudinally polarized W bosons is expected to be [94] $\mathcal{F}_0^{\text{SM}} \approx x / (1 + x)$, $x = m_t^2 / 2M_W^2$ ($\mathcal{F}_0^{\text{SM}} \sim 70\%$ for $m_t = 175$ GeV/ c^2). Fractions of left-handed, right-handed, and longitudinal W bosons are denoted as \mathcal{F}_- , \mathcal{F}_+ , and \mathcal{F}_0 respectively. In the SM, \mathcal{F}_- is expected to be $\approx 30\%$ and $\mathcal{F}_+ \approx 0\%$. CDF and DØ use various techniques to measure the helicity of the W boson in top quark decays, in both the lepton+jets events and dilepton channels. The first method uses a kinematic fit, similar to that used in the lepton+jets mass analyses, but with the top quark mass constrained to 175 GeV/ c^2 ,

to improve the reconstruction of final-state observables, and render the under-constrained dilepton channel solvable. The distribution of the helicity angle ($\cos\theta^*$) between the lepton and the b quark in the W rest frame provides the most direct measure of the W helicity. The second method (p_T^ℓ) uses the different lepton p_T spectra from longitudinally or transversely polarized W -decays to determine the relative contributions. A third method uses the invariant mass of the lepton and the b -quark in top decays ($M_{b\ell}^2$) as an observable, which is directly related to $\cos\theta^*$. Finally, the Matrix Element method (ME) has also been used, in which a likelihood is formed from a product of event probabilities calculated from the ME for a given set of measured kinematic variables and assumed W -helicity fractions. The results of recent CDF and DØ analyses are summarized in Table 5. The datasets are now large enough to allow for a simultaneous fit of \mathcal{F}_0 and \mathcal{F}_+ , which we denote by ‘2-param’ in the table. Results with either \mathcal{F}_0 or \mathcal{F}_+ fixed at its SM value are denoted ‘1-param’. For the simultaneous fits the correlation coefficient between the two values is about -0.8 for both experiments. A complete set of published results can be found in the Listings. All results are in agreement with the SM expectation.

Table 5: Measurement and 95% C.L. upper limits of the W helicity in top quark decays. Published results are given in the Listings. Results listed are preliminary and not yet submitted for publication, as of April 2010.

W Helicity	Source	$\int \mathcal{L} dt$ (fb $^{-1}$)	Ref.	Method
$\mathcal{F}_0 = 0.70 \pm 0.08$	CDF Run II	2.7	[95]	ME 1-param
$\mathcal{F}_0 = 0.88 \pm 0.13$	CDF Run II	2.7	[95]	ME 2-param
$\mathcal{F}_0 = 0.49 \pm 0.14$	DØ Run II	2.7	[96]	$\cos\theta^*$ 2-param
$\mathcal{F}_+ = -0.01 \pm 0.05$	CDF Run II	2.7	[95]	ME 1-param
$\mathcal{F}_+ = -0.15 \pm 0.09$	CDF Run II	2.7	[95]	ME 2-param
$\mathcal{F}_+ = 0.110 \pm 0.079$	DØ Run II	2.7	[96]	$\cos\theta^*$ 2-param

C.7 $t\bar{t}$ Spin Correlations & Top Width: The t and \bar{t} are expected to be unpolarized, but to be correlated in their spins. Since top quarks decay before hadronizing, their spins at production are transmitted to their decay-daughter particles. Spin correlation is studied by analyzing the joint decay angular distribution of one t daughter and one \bar{t} daughter. The sensitivity to top spin is greatest when the daughters are down-type fermions (charged leptons or d -type quarks), in which case, the joint distribution is [97–99]

$$\frac{1}{\sigma} \frac{d^2\sigma}{d(\cos\theta_+)d(\cos\theta_-)} = \frac{1 + \kappa \cdot \cos\theta_+ \cdot \cos\theta_-}{4}, \quad (2)$$

where θ_+ and θ_- are the angles of the daughters in the top rest frames with respect to a particular spin quantization axis. The maximum value for κ , 0.782 at NLO at the Tevatron [100], is

found in the off-diagonal basis [97]. An alternative basis is the beam direction, which yields $\kappa = 0.777$ at the Tevatron.

DØ has measured κ in the dilepton sample using the neutrino weighting technique to reconstruct the t and \bar{t} rest frames, in which the angles θ_+ and θ_- are measured. Using an integrated luminosity of 4.2 fb^{-1} they measure $\kappa = -0.17^{+0.64}_{-0.53}$ [101]. Using 2.8 fb^{-1} of integrated luminosity, CDF measures κ in the dilepton sample using a full-reconstruction method similar to the $p_z(t\bar{t})$ technique used in the mass measurement in dileptons, but with the inclusion of $p_T(t\bar{t})$ and $M_{(t\bar{t})}$ probability distribution functions. The result is a 68% confidence interval of $-0.455 < \kappa < 0.865$ corresponding to a central value of $\kappa = 0.320^{+0.545}_{-0.775}$ [102]. Recently CDF has measured κ in lepton plus jets events using an integrated luminosity of 4.3 fb^{-1} . A χ^2 adapted from the TM mass measurement is used to assign observed objects to the W^+b and W^-b from t and \bar{t} , while constraining the top mass at $172.5 \text{ GeV}/c^2$, allowing reconstruction of the respective rest frames. With this technique a value of $\kappa = 0.60 \pm 0.52$ is measured [103].

Because production through gluon fusion produces predominantly like-helicity $t\bar{t}$ pairs, whereas production through $q\bar{q}$ annihilation produces predominantly opposite-helicity pairs [99], the putative spin correlations can be used to extract the fraction of $t\bar{t}$ pairs produced through each of these mechanisms. In 2 fb^{-1} of integrated luminosity, CDF has used the azimuthal correlation of the charged leptons in the dilepton decay channel to measure the fraction of $t\bar{t}$ production from gluon fusion, F_{gg} , and find $F_{gg} = 0.53^{+0.36}_{-0.38}$ [104], to be compared with the expectation of approximately 0.15 in the SM.

Related to the measurement of top-spin correlations, which requires a top lifetime less than the hadronization timescale, is the measurement of the top width. The top width is expected to be of order $1 \text{ GeV}/c^2$ (Eq. 1). The sensitivity of current experiments does not approach this level in direct measurements. CDF has made the first direct measurement of the top width using the mass fitting template method in lepton+jets events, fixing the top mass at $175 \text{ GeV}/c^2$ and varying the top width in constructing the Monte Carlo templates. The top width is found to be less than $7.5 \text{ GeV}/c^2$ at the 95% C.L. [105].

DØ extracts the total width of the top quark from the partial decay width $\Gamma(t \rightarrow Wb)$ and the branching fraction $B(t \rightarrow Wb)$. $\Gamma(t \rightarrow Wb)$ is obtained from the measured t -channel cross section for single top quark production in 2.3 fb^{-1} , and $B(t \rightarrow Wb)$ is extracted from a measurement of the ratio $R = B(t \rightarrow Wb)/B(t \rightarrow Wq)$ in $t\bar{t}$ events in lepton+jets channels with 0, 1 and 2 b-tags in 1 fb^{-1} of integrated luminosity. Assuming $B(t \rightarrow Wq) = 1$, where q includes any kinematically accessible quark, the result is: $\Gamma_t = 2.1 \pm 0.6 \text{ GeV}$ which translates to a top quark lifetime of $\tau_t = (3 \pm 1) \times 10^{-25} \text{ s}$. The use of the partial width measurement alone yields the limits $\Gamma_t > 1.2 \text{ GeV}$ and $\tau_t < 5 \times 10^{-25} \text{ s}$, at 95% C.L. [106].

C.8 Non-SM $t\bar{t}$ Production: Motivated by the large mass of the top quark, several models suggest that the top quark

plays a role in the dynamics of electroweak symmetry breaking. One example is topcolor [26], where a large top quark mass can be generated through the formation of a dynamic $t\bar{t}$ condensate, X , which is formed by a new strong gauge force coupling preferentially to the third generation. Another example is topcolor-assisted technicolor [27], predicting a heavy Z' boson that couples preferentially to the third generation of quarks with cross sections expected to be visible at the Tevatron. CDF and DØ have searched for $t\bar{t}$ production via intermediate, narrow-width, heavy-vector bosons X in the lepton+jets channels. The possible $t\bar{t}$ production via an intermediate resonance X is sought for as a peak in the spectrum of the invariant $t\bar{t}$ mass. CDF and DØ exclude narrow-width heavy-vector bosons X in the top-assisted technicolor model [107], with mass $M_X < 480 \text{ GeV}/c^2$ and $M_X < 560 \text{ GeV}/c^2$, respectively, in Run I [30,31], and $M_X < 805 \text{ GeV}/c^2$ and $M_X < 820 \text{ GeV}/c^2$ in Run II [52,53]. With 955 pb^{-1} of Run-II data, CDF has produced a less model-dependent limit for a narrow-width Z' , ruling out at the 95% C.L. a contribution greater than 0.64 pb for a Z' heavier than $700 \text{ GeV}/c^2$ decaying to $t\bar{t}$ [108]. Using a measurement of the forward-backward asymmetry in $t\bar{t}$ production, DØ extracts a 95% C.L. limit on the fraction of $t\bar{t}$ pairs produced by a Z' resonance as a function of the Z' mass [23]. A recent CDF analysis has placed limits on the coupling strength of a massive gluon to $t\bar{t}$ [54]. In 0.9 fb^{-1} and 3.1 fb^{-1} , DØ has set limits on scalar top-quark pair production, with subsequent decays to top quarks in the lepton+jets and the dilepton channel, respectively [50,109].

The existence of flavor-changing neutral-currents (FCNC) couplings can enhance the rate of single-top quark production, and both experiments have used upper limits on the observed rate to place limits on these couplings. In 230 pb^{-1} of Run-II data, DØ uses their single-top analysis to place limits on anomalous production via the FCNC coupling of a gluon to the top quark and a charm ($t c g$) or up quark ($t u g$) [110]. The observed limits are at 95% C.L.: $\kappa_{gtc}/\Lambda < 0.15 \text{ TeV}^{-1}$ and $\kappa_{gtu}/\Lambda < 0.037 \text{ TeV}^{-1}$. CDF has searched for FCNC in the s -channel Wtb production vertex. In 2.2 fb^{-1} of integrated luminosity, CDF sets limits on the couplings of $\kappa_{gtc}/\Lambda < 0.105 \text{ TeV}^{-1}$ and $\kappa_{gtu}/\Lambda < 0.025 \text{ TeV}^{-1}$ [111].

C.9 Non-SM Top Decays: Both CDF and DØ have searched for non-SM top decays [112–116], particularly those expected in supersymmetric models, such as $t \rightarrow H^+b$, followed by $H^+ \rightarrow \tau^+\bar{\nu}$ or $c\bar{s}$. The $t \rightarrow H^+b$ branching ratio has a minimum at $\tan\beta = \sqrt{m_t/m_b} \simeq 6$, and is large in the region of either $\tan\beta \ll 6$ or $\tan\beta \gg 6$. In the former range, $H^+ \rightarrow c\bar{s}$ is dominant, while $H^+ \rightarrow \tau^+\bar{\nu}$ dominates in the latter range. These studies are based either on direct searches for these final states, or on top “disappearance.” In the standard lepton+jets or dilepton cross-section analyses, any charged-Higgs decays are not detected as efficiently as $t \rightarrow W^\pm b$, primarily because the selection criteria are optimized for the standard decays, and because of the absence of energetic isolated leptons in Higgs

Quark Particle Listings

t

decays. A significant $t \rightarrow H^+b$ contribution would give rise to measured $t\bar{t}$ cross sections that would be lower than the prediction from the SM (assuming that non-SM contributions to $t\bar{t}$ production are negligible), and the measured cross-section ratio $\sigma_{t\bar{t}}^{\ell^+\ell^-j\ell^+j\ell^-}/\sigma_{t\bar{t}}^{\ell\ell}$ would differ from unity.

In Run II, CDF has searched for charged-Higgs production in dilepton, lepton+jets, and lepton+hadronic tau final states, considering possible H^+ decays to $c\bar{s}$, $\tau\bar{\nu}$, t^*b , or W^+h^0 , in addition to the SM decay $t \rightarrow W^+b$ [114,115]. Depending on the top and Higgs-decay branching ratios, which are scanned in a particular 2-Higgs doublet benchmark model, the number of expected events in these decay channels can show an excess or deficit when compared to SM expectations. A model-independent interpretation yields a limit of $B(t \rightarrow H^\pm b) < 0.91$ at 95% C.L. for $m_{H^\pm} \approx 100$ GeV, and $B(t \rightarrow H^\pm b) < 0.4$ in the tauonic model with $B(H^\pm \rightarrow \tau\nu) = 100\%$. In a more recent search, the dijet invariant mass in lepton+jets events has been used to search for a charged Higgs decaying to $c\bar{s}$ with mass above the W boson mass. The absence of a signal leads to a 95% C.L. limit of $B(t \rightarrow H^\pm b) < 0.1$ to 0.3 for masses between 60 and 150 GeV/ c^2 [115]. In 1 fb $^{-1}$ of integrated luminosity, the DØ collaboration has used the $t\bar{t}$ dilepton and lepton+jets events, including τ lepton channels, to search for evidence of charged-Higgs decays into τ leptons via the ratio of events with τ leptons to those with e and μ [38], global fits [117] and topological searches [118]. They exclude regions of $B(t \rightarrow H^\pm b)$ as a function of Higgs mass, ranging from $B(t \rightarrow H^\pm b) > 0.12$ at low mass to $B(t \rightarrow H^\pm b) > 0.2$ at high mass. In a companion analysis they look for evidence of leptophobic charged Higgs production in top decays in which the Higgs decays purely hadronically, leading to a suppression of the measured $t\bar{t}$ rate in all leptonic channels. They exclude $B(t \rightarrow H^\pm b) > 0.2$ for charged-Higgs masses between 80 and 155 GeV/ c^2 .

More details, and the results of these studies for the exclusion in the $m_{H^\pm}, \tan\beta$ plane, can be found in the review “Search for Higgs bosons” and in the “ H^+ Mass Limits” section of the Higgs Particle Listings of the current edition.

In the SM, the top-quark lifetime is expected to be about 0.5×10^{-24} s ($c\tau_t \approx 1.5 \times 10^{-10}$ μm), while additional quark generations, non-standard top-quark decays, or other extensions of the SM could yield long-lived top quarks in the data. CDF has studied the top-quark lifetime by measuring the distance between the initial $p\bar{p}$ scattering and the leptonic W^\pm decay vertex in lepton+jets events [119]. The measured lifetime is consistent with zero, and an upper limit $c\tau_t < 52.5$ μm is found at 95% C.L. DØ extracts the lifetime to be $\tau_t = (3 \pm 1) \times 10^{-25}$ s from the t -channel cross section for single top quark production and the measurement of the ratio $R = B(t \rightarrow Wb)/B(t \rightarrow Wq)$ [106].

Using up to 2.7 fb $^{-1}$ of data, DØ has measured the Wtb coupling form factors by combining information from the W boson helicity in top quark decays in $t\bar{t}$ events and single-top

quark production, allowing to place limits on the left-handed and right-handed vector and tensor couplings [120,121].

DØ excludes the production of W' bosons with masses below 731 GeV for a W' boson with standard-model-like couplings, below 739 GeV for a W' boson with right-handed couplings that is allowed to decay to both leptons and quarks, and below 768 GeV for a W' boson with right-handed couplings that is only allowed to decay to quarks [122]. CDF has recently released W' limits also using the single-top analysis [123]. In 1.9 fb $^{-1}$ of Run-II data, a W' with Standard-Model couplings is searched for in the $t\bar{t}$ decay mode. Masses below 800 GeV are excluded, assuming that any right-handed neutrino is lighter than the W' , and below 825 GeV if the right-handed neutrino is heavier than the W' .

CDF reported a search for flavor-changing neutral-current (FCNC) decays of the top quark $t \rightarrow q\gamma$ and $t \rightarrow qZ$ in the Run-I data [124], and recently with enhanced sensitivity in Run II [125]. The SM predicts such small rates that any observation would be a sign of new physics. CDF assumes that one top decays via FCNC, while the other decays via Wb . The Run-I analysis included a $t \rightarrow q\gamma$ search in which two signatures are examined, depending on whether the W decays leptonically or hadronically. For leptonic W decay, the signature is $\gamma\ell$ and missing E_T and two or more jets, while for hadronic W decay, it is $\gamma + \geq 4$ jets. In either case, one of the jets must have a secondary vertex b tag. One event is observed ($\mu\gamma$) with an expected background of less than half an event, giving an upper limit on the top branching ratio of $B(t \rightarrow q\gamma) < 3.2\%$ at 95% C.L. In the search for $t \rightarrow qZ$, CDF considers $Z \rightarrow \mu\mu$ or ee and $W \rightarrow qq'$, giving a $Z +$ four jets signature. A Run-II dataset of 1.9 fb $^{-1}$ is found consistent with background expectations and a 95% C.L. on the $t \rightarrow qZ$ branching fraction of $< 3.7\%$ (for $M_{\text{top}}=175$ GeV/ c^2) is set. By comparison to the number expected from the theoretical production cross section, CDF has used the observed number of double b -tagged lepton+jets candidate events to place limits on a variety of decay modes, ranging from $B(t \rightarrow Zc) < 13\%$ to $B(t \rightarrow \text{invisible}) < 9\%$ [126].

Constraints on FCNC couplings of the top quark can also be obtained from searches for anomalous single-top production in e^+e^- collisions, via the process $e^+e^- \rightarrow \gamma, Z^* \rightarrow t\bar{q}$ and its charge-conjugate ($q = u, c$), or in $e^\pm p$ collisions, via the process $e^\pm u \rightarrow e^\pm t$. For a leptonic W decay, the topology is at least a high- p_T lepton, a high- p_T jet and missing E_T , while for a hadronic W -decay, the topology is three high- p_T jets. Limits on the cross section for this reaction have been obtained by the LEP collaborations [127] in e^+e^- collisions, and by H1 [128] and ZEUS [129] in $e^\pm p$ collisions. When interpreted in terms of branching ratios in top decay [130,131], the LEP limits lead to typical 95% C.L. upper bounds of $B(t \rightarrow qZ) < 0.137$. Assuming no coupling to the Z boson, the 95% C.L. limits on the anomalous FCNC coupling $\kappa_\gamma < 0.17$ and < 0.27 by ZEUS and H1, respectively, are stronger than the CDF limit of $\kappa_\gamma < 0.42$, and improve over LEP sensitivity in that domain. The H1 limit is slightly weaker than the ZEUS limit due to

See key on page 405

an observed excess of five-candidate events over an expected background of 3.2 ± 0.4 . If this excess is attributed to FCNC top-quark production, this leads to a total cross section of $\sigma(ep \rightarrow e + t + X, \sqrt{s} = 319 \text{ GeV}) < 0.25 \text{ pb}$ [128,132].

Appendix. Expected Sensitivity at the LHC:

The top pair-production cross section at the LHC at $\sqrt{s} = 14 \text{ TeV}$ is predicted at NLO to be about 800 pb [133]. In the first years, the LHC will operate at $\sqrt{s} = 7 \text{ TeV}$, yielding an expected cross section of about 170 pb [134]. At $\sqrt{s} = 14 \text{ TeV}$ there will be 8 million $t\bar{t}$ pairs produced per year at a luminosity of $10^{33} \text{ cm}^{-2} \text{ s}^{-1}$. Such large event samples will permit precision measurements of the top-quark parameters. The statistical uncertainties on m_t will become negligible, and will allow to monitor the systematic uncertainties at a level at least comparable to the current Tevatron uncertainty on m_{top} [135–137].

Precision measurements of the top pair-production cross section are expected to be limited by the estimated 3–10% accuracy on the luminosity determination [135,136], but far more accurate measurements would be available from the ratio of the $t\bar{t}$ production to inclusive W or Z production.

Single-top production will also be of keen interest at the LHC, where a $|V_{tb}|$ measurement at the 5% level per experiment is projected with 10 fb^{-1} [135,136].

Tests of the $V - A$ nature of the tWb vertex through a measurement of the W helicity will be extended from the Tevatron to the LHC. Current estimates are that the longitudinal fraction can be measured with a precision of about 5% [136] with 10 fb^{-1} of data.

Top-antitop spin correlations should be relatively easy to observe and measure at the LHC, where the preferred dilepton mode will have large event samples, despite the small branching fraction. At the LHC, where $t\bar{t}$ is dominantly produced through gluon fusion, the correlation is such that the top quarks are mainly either both left- or both right-handed. The CMS collaboration [136] estimates that the relative asymmetry (defined as the difference in the fraction of like-handed and the fraction of oppositely-handed $t\bar{t}$ pairs) can be measured to about 17% accuracy with 10 fb^{-1} of data.

In addition to these SM measurements, the large-event samples will allow sensitive searches for new physics. The search for heavy resonances that decay to $t\bar{t}$, already begun at the Tevatron, will acquire enhanced reach both in mass and $\sigma \cdot B$. The ATLAS collaboration [135] has studied the reach for a 5σ discovery of a narrow resonance decaying to $t\bar{t}$. With 30 fb^{-1} , it is estimated that a resonance can be discovered at $4 \text{ TeV}/c^2$ for $\sigma \cdot B = 10 \text{ fb}$, and at $1 \text{ TeV}/c^2$ for $\sigma \cdot B = 1000 \text{ fb}$. FCNC decays, $t \rightarrow Zq, \gamma q, gq$, can take place in the SM, or in the MSSM, but at rates too small to be observed even at the LHC. As such, searches for these decay modes can provide sensitive tests of other extensions of the SM [135,136]. Updated sensitivity studies at $\sqrt{s} = 10 \text{ TeV}$ by the ATLAS Collaboration are available at [138]. Recently, the CERN management decided

to start proton-proton collisions in late 2009 at $\sqrt{s} = 7 \text{ TeV}$. The production rates and the estimated sensitivities change accordingly.

References

CDF note references can be retrieved from www-cdf.fnal.gov/physics/new/top/top.html, and DØ note references from www-d0.fnal.gov/Run2Physics/WWW/documents/Run2Results.htm.

1. M. Cacciari *et al.*, J. High Energy Phys.09, 127 (2008); N. Kidonakis and R. Vogt, Phys. Rev. **D78**, 074005 (2008); S. Moch and P. Uwer, Phys. Rev. **D78**, 034003 (2008); S. Moch and P. Uwer, Nucl. Phys. (Proc. Supp.) **B183**, 75 (2008).
2. M. Cacciari *et al.*, Sov. Phys. JETP **04**, 068 (2004).
3. S. Cortese and R. Petronzio, Phys. Lett. **B253**, 494 (1991).
4. S. Willenbrock and D. Dicus, Phys. Rev. **D34**, 155 (1986).
5. B.W. Harris *et al.*, Phys. Rev. **D66**, 054024 (2002); Z. Sullivan, Phys. Rev. **D70**, 114012 (2004); N. Kidonakis Phys. Rev. **D74**, 114012 (2006).
6. M. Jeżabek and J.H. Kühn, Nucl. Phys. **B314**, 1 (1989).
7. I.I.Y. Bigi *et al.*, Phys. Lett. **B181**, 157 (1986).
8. A. Czarnecki and K. Melnikov, Nucl. Phys. **B544**, 520 (1999); K.G. Chetyrkin *et al.*, Phys. Rev. **D60**, 114015 (1999).
9. F. Abe *et al.* (CDF Collab.), Phys. Rev. Lett. **80**, 5720 (1998).
10. V.M. Abazov *et al.* (DØ Collab.), Phys. Rev. **D76**, 072007 (2007).
11. A. Abulencia *et al.* (CDF Collab.), Phys. Rev. Lett. **96**, 022004 (2006); Phys. Rev. **D73**, 032003 (2006); Phys. Rev. **D73**, 092002 (2006).
12. V.M. Abazov *et al.* (DØ Collab.), Phys. Rev. **D79**, 092005 (2006); V.M. Abazov *et al.* (DØ Collab.), Phys. Rev. **D79**, 092001 (2007).
13. T. Tait and C.-P. Yuan, Phys. Rev. **D63**, 014018 (2001).
14. V.M. Abazov *et al.* (DØ Collab.), Phys. Rev. Lett. **103**, 092001 (2009); V.M. Abazov *et al.* (DØ Collab.), Phys. Rev. **D78**, 12005 (2008); V.M. Abazov *et al.* (DØ Collab.), Phys. Rev. Lett. **98**, 181802 (2007).
15. T. Aaltonen *et al.* (CDF Collab.), Phys. Rev. Lett. **103**, 092002 (2009).
16. S. Frixione and B. Webber, hep-ph/0402116; S. Frixione and B. Webber, J. High Energy Phys.06, 029 (2002); S. Frixione, P. Nason and B. Webber, J. High Energy Phys.08,007 (2003); S. Frixione, P. Nason and G. Ridolfi, hep-ph/07073088.
17. J.M. Campbell and R.K. Ellis, Phys. Rev. **D62**, 114012 (2000), Phys. Rev. **D65**, 113007 (2002); J.M. Campbell and J. Huston, Phys. Rev. **D70**, 094021 (2004).
18. A. Abulencia *et al.* (CDF Collab.), Phys. Lett. **B639**, 172 (2006).
19. DØ Collab., DØ conference note 5607 (2008).
20. DØ Collab., DØ conference note 5234 (2006).
21. O. Antunano, J.H. Kühn and G. Rodrigo, Phys. Rev. **D77**, 014003 (2008); M.T. Bowen, S. Ellis and D. Rainwater, Phys. Rev. **D73**, 014008 (2006); S. Dittmaier, P. Uwer and S. Weinzierl, Phys. Rev. Lett. **98**, 262002

Quark Particle Listings

t

- (2007); L.G. Almeida, G. Sterman, and W. Vogelsang, Phys. Rev. **D78**, 014008 (2008).
22. CDF Collab., CDF conference note 9724 (2009).
 23. V.M. Abazov *et al.* (DØ Collab.), Phys. Rev. Lett. **100**, 142002 (2008).
 24. CDF Collab., CDF conference note 9850 (2009).
 25. S. Dittmaier, P. Uwer, and S. Weinzierl, arXiv:0810.0452v2.
 26. C.T. Hill, Phys. Lett. **B266**, 419 (1991).
 27. C.T. Hill, Phys. Lett. **B345**, 483 (1995).
 28. C.T. Hill and S.J. Park, Phys. Rev. **D49**, 4454 (1994); H.P. Nilles, Phys. Reports **110**, 1 (1984); H.E. Haber and G.L. Kane, Phys. Reports **117**, 75 (1985); E.H. Simmons, Thinking About Top: Looking Outside The Standard Model, hep-ph/9908511, and references therein; E.H. Simmons, The Top Quark: Experimental Roots and Branches of Theory, hep-ph/0211335, and references therein.
 29. D. Choudhury, T.M.P. Tait, and C.E.M. Wagner, Phys. Rev. **D65**, 053002 (2002).
 30. T. Affolder *et al.* (CDF Collab.), Phys. Rev. Lett. **85**, 2062 (2000).
 31. V.M. Abazov *et al.* (DØ Collab.), Phys. Rev. Lett. **92**, 221801 (2004).
 32. T. Affolder *et al.* (CDF Collab.), Phys. Rev. Lett. **87**, 102001 (2001).
 33. B. Abbott *et al.* (DØ Collab.), Phys. Rev. **D58**, 052001 (1998); S. Abachi *et al.* (DØ Collab.), Phys. Rev. Lett. **79**, 1197 (1997).
 34. V.M. Abazov *et al.* (DØ Collab.), Phys. Rev. Lett. **100**, 192003 (2008).
 35. DØ Collab., DØ conference note 6038 (2010).
 36. DØ Collab., DØ conference note 5477 (2007).
 37. DØ Collab., DØ conference note 5465 (2007).
 38. V.M. Abazov *et al.* (DØ Collab.), Phys. Rev. **D80**, 071102 (2009).
 39. V.M. Abazov *et al.* (DØ Collab.), Phys. Lett. **B679**, 177 (2009).
 40. CDF Collab., CDF conference note 9878 (2009).
 41. CDF Collab., CDF conference note 9913 (2009).
 42. CDF Collab., CDF conference note 9348 (2008).
 43. CDF Collab., CDF conference note 9950 (2009).
 44. CDF Collab., CDF conference note 10049 (2010).
 45. CDF Collab., CDF conference note 9988 (2009).
 46. CDF Collab., CDF conference note 9890 (2009).
 47. CDF Collab., CDF conference note 9841 (2009).
 48. CDF Collab., CDF conference note 9448 (2008).
 49. D. Acosta *et al.* (CDF Collab.), Phys. Rev. Lett. **95**, 022001 (2005).
 50. V.M. Abazov *et al.* (DØ Collab.), Phys. Lett. **B674**, 4 (2009).
 51. T. Aaltonen *et al.* (CDF Collab.), Phys. Rev. Lett. **102**, 222003 (2009).
 52. CDF Collab., CDF conference note 9844 (2009).
 53. DØ Collab., DØ conference note 5882 (2009).
 54. T. Aaltonen *et al.* (CDF Collab.), arXiv:0911.3112.
 55. The Tevatron Electroweak Working Group, For the CDF and DØ Collaborations, FERMILAB-TM-2440-E, arXiv: 0908.2171.
 56. CDF collab., CDF conference note 9716 (2009).
 57. V.A. Abazov *et al.* (DØ Collab.), Phys. Lett. **B682**, 363 (2010).
 58. CDF collab., CDF conference note 9712 (2009).
 59. CDF collab., CDF conference note 9920 (2009).
 60. F. Abe *et al.* (CDF Collab.), Phys. Rev. **D50**, 2966 (1994); F. Abe *et al.* (DØ Collab.), Phys. Rev. Lett. **74**, 2626 (1995); S. Abachi *et al.* (DØ Collab.), Phys. Rev. Lett. **74**, 2632 (1995).
 61. K. Kondo *et al.*, J. Phys. Soc. Jpn. **G62**, 1177 (1993).
 62. R.H. Dalitz and G.R. Goldstein, Phys. Rev. **D45**, 1531 (1992); Phys. Lett. **B287**, 225 (1992); Proc. Royal Soc. London **A445**, 2803 (1999).
 63. P. Abreu *et al.* (DELPHI Collab.), Eur. Phys. J. **C2**, 581 (1998).
 64. V.M. Abazov *et al.* (DØ Collab.), Phys. Rev. **D75**, 092001 (2007).
 65. A. Abulencia *et al.* (CDF Collab.), Phys. Rev. **D75**, 071102 (2007).
 66. CDF Collab., conference note 9683 (2009).
 67. CDF Collab., conference note 9831 (2009).
 68. T. Aaltonen *et al.* (CDF Collab.), Phys. Rev. **D80**, 051104 (2009).
 69. L. Sonnenschein, Phys. Rev. **D73**, 054015 (2006).
 70. B. Abbott *et al.* (DØ Collab.), Phys. Rev. Lett. **80**, 2063 (1998); B. Abbott *et al.* (DØ Collab.), Phys. Rev. **D60**, 052001 (1999).
 71. F. Abe *et al.* (CDF Collab.), Phys. Rev. Lett. **82**, 271 (1999).
 72. A. Abulencia *et al.* (CDF Collab.), Phys. Rev. **D73**, 112006 (2006).
 73. DØ Collab., DØ conference note 5877 (2009).
 74. DØ Collab., DØ conference note 5897 (2009).
 75. DØ Collab., DØ conference note 5900 (2009).
 76. CDF Collab., CDF conference note 10077 (2010).
 77. CDF Collab., CDF conference note 10033 (2010).
 78. CDF Collab., CDF conference note 9725 (2009).
 79. CDF Collab., CDF conference note 9881 (2009).
 80. CDF Collab., CDF conference note 9694 (2009).
 81. CDF Collab., CDF conference note 9265 (2008).
 82. CDF Collab., CDF conference note 9714 (2009).
 83. The Tevatron Electroweak Working Group, For the CDF and DØ Collaborations, arXiv:0903.2503.
 84. M. Smith and S. Willenbrock, Phys. Rev. Lett. **79**, 3825 (1997).
 85. V.M. Abazov *et al.* (DØ Collab.), Phys. Rev. Lett. **103**, 132001 (2009).
 86. ALEPH, DELPHI, L3, OPAL, SLD and Working Groups, Phys. Reports **427**, 257 (2006).
 87. The LEP Collaborations: ALEPH, DELPHI, L3, OPAL, SLD, CDF, and DØ Collaborations, and the LEP, Tevatron and SLD Electroweak Working Groups, arXiv:0911.2604v2.
 88. D. Chang, W.F. Chang, and E. Ma, Phys. Rev. **D59**, 091503 (1999), Phys. Rev. **D61**, 037301 (2000).

89. V.M. Abazov *et al.* (DØ Collab.), Phys. Rev. Lett. **98**, 04181 (2007).
90. CDF Collab., CDF conference note 8967 (2007).
91. CDF Collab., CDF conference note 9939 (2010).
92. T. Affolder *et al.* (CDF Collab.), Phys. Rev. Lett. **86**, 3233 (2001).
93. V.M. Abazov *et al.* (DØ Collab.), Phys. Lett. **B639**, 616 (2006).
94. G.L. Kane, G.A. Ladinsky, and C.P. Yuan, Phys. Rev. **D45**, 124 (1992).
95. CDF Collab., CDF conference note 10004 (2009).
96. DØ Collab., DØ conference note 5722 (2008).
97. G. Mahlon and S. Parke, Phys. Rev. **D53**, 4886 (1996); G. Mahlon and S. Parke, Phys. Lett. **B411**, 173 (1997).
98. G.R. Goldstein, in *Spin 96: Proceedings of the 12th International Symposium on High Energy Spin Physics*, Amsterdam, 1996, ed. C.W. Jager (World Scientific, Singapore, 1997), p. 328.
99. T. Stelzer and S. Willenbrock, Phys. Lett. **B374**, 169 (1996).
100. W. Bernreuther *et al.* Nucl. Phys. **B690**, 81 (2004).
101. DØ Collab., DØ conference note 5950 (2009).
102. CDF Collab., CDF conference note 9824 (2009).
103. CDF Collab., CDF conference note 10048 (2010).
104. CDF Collab., CDF conference note 9432 (2008).
105. CDF Collab., CDF conference note 10035 (2010); CDF Collab., T. Aaltonen *et al.*, Phys. Rev. Lett. **102**, 042001 (2009).
106. DØ Collab., DØ conference note 6034 (2010).
107. R.M. Harris, C.T. Hill, and S.J. Parke, hep-ph/9911288 (1995).
108. T. Aaltonen *et al.* (CDF Collaboration), Phys. Rev. **D77**, 051102 (R) (2008).
109. DØ Collab., DØ conference note 5937 (2009).
110. V.M. Abazov *et al.* (DØ Collab.), Phys. Rev. Lett. **99**, 191802 (2007).
111. T. Aaltonen *et al.* (CDF Collab.), Phys. Rev. Lett. **102**, 151801 (2009)..
112. F. Abe *et al.* (CDF Collab.), Phys. Rev. Lett. **79**, 357 (1997); T. Affolder *et al.* (CDF Collab.), Phys. Rev. **D62**, 012004 (2000).
113. B. Abbott *et al.* (DØ Collab.), Phys. Rev. Lett. **82**, 4975 (1999); V.M. Abazov *et al.* (DØ Collab.), Phys. Rev. Lett. **88**, 151803 (2002).
114. A. Abulencia *et al.* (CDF Collab.), Phys. Rev. Lett. **96**, 042003 (2006).
115. T. Aaltonen *et al.* (CDF Collab.), Phys. Rev. Lett. **103**, 101803 (2009).
116. DØ Collab., DØ conference note 5715 (2008).
117. V.M. Abazov *et al.* (DØ Collab.), Phys. Lett. **B682**, 278 (2009).
118. V.M. Abazov *et al.* (DØ Collab.), Phys. Rev. **D80**, 051107 (2009).
119. CDF Collab., CDF conference note 8104 (2006).
120. V.M. Abazov *et al.* (DØ Collab.), Phys. Rev. Lett. **102**, 092002 (2009).
121. V.M. Abazov *et al.* (DØ Collab.), DØ conference note 5838 (2009).
122. V.M. Abazov *et al.* (DØ Collab.), Phys. Rev. Lett. **100**, 211803 (2008).
123. T. Aaltonen *et al.* (CDF Collab.), Phys. Rev. Lett. **103**, 041801 (2009).
124. F. Abe *et al.* (CDF Collab.), Phys. Rev. Lett. **80**, 2525 (1998).
125. T. Aaltonen *et al.* (CDF Collab.), Phys. Rev. Lett. **101**, 192002 (2008).
126. CDF Collab., CDF conference note 9496 (2008).
127. A. Heister *et al.* (ALEPH Collab.), Phys. Lett. **B543**, 173 (2002); J. Abdallah *et al.* (DELPHI Collab.), Phys. Lett. **B590**, 21 (2004); P. Achard *et al.* (L3 Collab.), Phys. Lett. **B549**, 290 (2002); G. Abbiendi *et al.* (OPAL Collab.), Phys. Lett. **B521**, 181 (2001).
128. F.D. Aaron *et al.* (H1 Collab.), Phys. Lett. **B678**, 450 (2009).
129. S. Chekanov *et al.* (ZEUS Collab.), Phys. Lett. **B559**, 153 (2003).
130. M. Beneke *et al.*, hep-ph/0003033, in *Proceedings of 1999 CERN Workshop on Standard Model Physics (and more) at the LHC*, G. Altarelli and M.L. Mangano eds.
131. V.F. Obraztsov, S.R. Slabospitsky, and O.P. Yushchenko, Phys. Lett. **B426**, 393 (1998).
132. T. Carli, D. Dannheim, and L. Bellagamba, Mod. Phys. Lett. **A19**, 1881 (2004).
133. R. Bonciani *et al.*, Nucl. Phys. **B529** 424 (1998).
134. N. Kidonakis, arXiv:0909.0037.
135. The ATLAS Collaboration, *ATLAS Detector and Physics Performance TDR, Volume II*, CERN/LHCC 99-14/15.
136. The CMS Collaboration, *CMS Detector and Physics Performance TDR, Volume II*, CERN/LHCC 2006/021.
137. I. Borjanovic *et al.*, Eur. Phys. J. **C39S2**, 63 (2005).
138. The ATLAS Collaboration, *Expected Performance of the ATLAS Experiment - Detector, Trigger and Physics*, arXiv:0901.0512.

t-Quark Mass in $p\bar{p}$ Collisions

OUR EVALUATION OF $172.0 \pm 0.9 \pm 1.3$ GeV (TEVEWWG 10) is an average of top mass measurements from Tevatron Run-I (1992–1996) and Run-II (2001–present) that were published at the time of preparing this Review. This average was provided by the Tevatron Electroweak Working Group (TEVEWWG). It takes correlated uncertainties properly into account and has a χ^2 of 5.8 for 10 degrees of freedom.

For earlier search limits see PDG 96, Physical Review **D54** 1 (1996). We no longer include a compilation of indirect top mass determinations from Standard Model Electroweak fits in the Listings (our last compilation can be found in the Listings of the 2007 partial update). For a discussion of current results see the reviews "The Top Quark" and "Electroweak Model and Constraints on New Physics."

VALUE (GeV)	DOCUMENT ID	TECN	COMMENT
172.0 ± 0.9 ± 1.3 OUR EVALUATION			See comments in the header above.
172.7 ± 1.8 ± 1.2	¹ AALTONEN	09J CDF	$\ell + \cancel{E}_T + 4$ jets(b -tag)
171.1 ± 3.7 ± 2.1	² AALTONEN	09K CDF	6 jets, vtx b -tag
171.2 ± 2.7 ± 2.9	³ AALTONEN	09o CDF	dilepton
174.7 ± 4.4 ± 2.0	⁴ ABAZOV	09AH D0	dilepton + b -tag (ν WT+MWT)
171.5 ± 1.8 ± 1.1	⁵ ABAZOV	08AH D0	$\ell + \cancel{E}_T + 4$ jets
180.7 ^{+15.5} _{-13.4} ± 8.6	⁶ ABULENCIA	07J CDF	lepton + jets
180.1 ± 3.6 ± 3.9	^{7,8} ABAZOV	04G D0	lepton + jets
176.1 ± 5.1 ± 5.3	⁹ AFFOLDER	01 CDF	lepton + jets
167.4 ± 10.3 ± 4.8	^{10,11} ABE	99B CDF	dilepton
168.4 ± 12.3 ± 3.6	⁸ ABBOTT	98D D0	dilepton
186 ± 10 ± 5.7	^{10,12} ABE	97R CDF	6 or more jets

Quark Particle Listings

 t

• • • We do not use the following data for averages, fits, limits, etc. • • •

180.5 ± 12.0 ± 3.6	13	AALTONEN	09AK	CDF	$\ell + \cancel{E}_T + \text{jets}$ (soft μ b -tag)
171.9 ± 1.7 ± 1.1	14	AALTONEN	09L	CDF	$\ell + \text{jets}$, $\ell\ell + \text{jets}$
165.5 ± 3.4 ± 3.3 ± 3.1	15	AALTONEN	09X	CDF	$\ell\ell + \cancel{E}_T$ ($\nu\phi$ weighting)
169.1 ± 5.9 ± 5.2	16	ABAZOV	09AG	D0	cross sects, theory + exp
171.5 ± 9.9 ± 9.8	17	ABAZOV	09R	D0	cross sects, theory + exp
170.7 ± 4.2 ± 3.9 ± 3.5	18,19	AALTONEN	08C	CDF	dilepton, $\sigma_{t\bar{t}}$ constrained
177.1 ± 4.9 ± 4.7	20,21	AALTONEN	07	CDF	6 jets with ≥ 1 b vtx
172.3 ± 10.8 ± 9.6 ± 10.8	22	AALTONEN	07B	CDF	≥ 4 jets (b -tag)
174.0 ± 2.2 ± 4.8	23	AALTONEN	07D	CDF	≥ 6 jets, vtx b -tag
170.8 ± 2.2 ± 1.4	24,25	AALTONEN	07I	CDF	lepton + jets (b -tag)
173.7 ± 4.4 ± 2.1 ± 2.0	21,26	ABAZOV	07F	D0	lepton + jets
176.2 ± 9.2 ± 3.9	27	ABAZOV	07W	D0	dilepton (MWT)
179.5 ± 7.4 ± 5.6	27	ABAZOV	07W	D0	dilepton (ν WWT)
164.5 ± 3.9 ± 3.9	25,28	ABULENCIA	07D	CDF	dilepton
170.3 ± 4.1 ± 1.2 ± 4.5 ± 1.8	25,29	ABAZOV	06U	D0	lepton + jets (b -tag)
173.2 ± 2.6 ± 2.4 ± 3.2	30,31	ABULENCIA	06D	CDF	lepton + jets
173.5 ± 3.7 ± 3.6 ± 1.3	19,30	ABULENCIA	06D	CDF	lepton + jets
165.2 ± 6.1 ± 3.4	25,32	ABULENCIA	06G	CDF	dilepton
170.1 ± 6.0 ± 4.1	19,33	ABULENCIA	06V	CDF	dilepton
178.5 ± 13.7 ± 7.7	34,35	ABAZOV	05	D0	6 or more jets
176.1 ± 6.6	36	AFFOLDER	01	CDF	dilepton, lepton+jets, all-jets
172.1 ± 5.2 ± 4.9	37	ABBOTT	99G	D0	di-lepton, lepton+jets
176.0 ± 6.5	11,38	ABE	99B	CDF	dilepton, lepton+jets, all-jets
173.3 ± 5.6 ± 5.5	8,39	ABBOTT	98F	D0	lepton + jets
175.9 ± 4.8 ± 5.3	10,40	ABE	98E	CDF	lepton + jets
161 ± 17 ± 10	10	ABE	98F	CDF	dilepton
172.1 ± 5.2 ± 4.9	41	BHAT	98B	RVUE	dilepton and lepton+jets
173.8 ± 5.0	42	BHAT	98B	RVUE	dilepton, lepton+jets, all-jets
173.3 ± 5.6 ± 6.2	8	ABACHI	97E	D0	lepton + jets
199 ± 19 ± 21 ± 22		ABACHI	95	D0	lepton + jets
176 ± 8 ± 10		ABE	95F	CDF	lepton + b -jet
174 ± 10 ± 13 ± 12		ABE	94E	CDF	lepton + b -jet

¹ Based on 1.9 fb⁻¹ of data at $\sqrt{s} = 1.96$ TeV. The first error is from statistics and jet energy scale uncertainty, and the latter is from the other systematics. Matrix element method with effective propagators.

² Based on 943 pb⁻¹ of data at $\sqrt{s} = 1.96$ TeV. The first error is from statistical and jet-energy-scale uncertainties, and the latter is from other systematics. AALTONEN 09k selected 6 jet events with one or more vertex b -tags and used the tree-level matrix element to construct template models of signal and background.

³ Based on 2 fb⁻¹ of data at $\sqrt{s} = 1.96$ TeV. Matrix Element method. Optimal selection criteria for candidate events with two high p_T leptons, high \cancel{E}_T , and two or more jets with and without b -tag are obtained by neural network with neuroevolution technique to minimize the statistical error of m_t .

⁴ Based on 1 fb⁻¹ of data at $\sqrt{s} = 1.96$ TeV. Events with two identified leptons, and those with one lepton plus one isolated track and a b -tag were used to constrain m_t . The result is a combination of the ν WT (ν Weighting Technique) result of $176.2 \pm 4.8 \pm 2.1$ GeV and the MWT (Matrix-element Weighting Technique) result of $173.2 \pm 4.9 \pm 2.0$ GeV.

⁵ Result is based on 1 fb⁻¹ of data at 1.96 TeV. The first error is from statistics and jet energy scale uncertainty, and the latter is from the other systematics.

⁶ Based on 695 pb⁻¹ of data at $\sqrt{s} = 1.96$ TeV. The transverse decay length of the b hadron is used to determine m_t , and the result is free from the JES (jet energy scale) uncertainty.

⁷ Obtained by re-analysis of the lepton + jets candidate events that led to ABBOTT 98F. It is based upon the maximum likelihood method which makes use of the leading order matrix elements.

⁸ Based on 125 ± 7 pb⁻¹ of data at $\sqrt{s} = 1.8$ TeV.

⁹ Based on ~106 pb⁻¹ of data at $\sqrt{s} = 1.8$ TeV.

¹⁰ Based on 109 ± 7 pb⁻¹ of data at $\sqrt{s} = 1.8$ TeV.

¹¹ See AFFOLDER 01 for details of systematic error re-evaluation.

¹² Based on the first observation of all hadronic decays of $t\bar{t}$ pairs. Single b -quark tagging with jet-shape variable constraints was used to select signal enriched multi-jet events. The updated systematic error is listed. See AFFOLDER 01, appendix C.

¹³ Based on 2 fb⁻¹ of data at $\sqrt{s} = 1.96$ TeV. The top mass is obtained from the measurement of the invariant mass of the lepton (e or μ) from W decays and the soft μ in b -jet. The result is insensitive to jet energy scaling.

¹⁴ Based on 1.9 fb⁻¹ of data at $\sqrt{s} = 1.96$ TeV. The first error is from statistical and jet-energy-scale (JES) uncertainties, and the second is from other systematics. Events with lepton + jets and those with dilepton + jets were simultaneously fit to constrain m_t and JES. Lepton + jets data only give $m_t = 171.8 \pm 2.2$ GeV, and dilepton data only give $m_t = 171.2^{+5.3}_{-5.1}$ GeV.

¹⁵ Based on 2.9 fb⁻¹ of data at $\sqrt{s} = 1.96$ TeV. Mass m_t is estimated from the likelihood for the eight-fold kinematical solutions in the plane of the azimuthal angles of the two neutrino momenta.

¹⁶ Based on 1 fb⁻¹ of data at $\sqrt{s} = 1.96$ TeV. Uses $\ell + \text{jets}$, $\ell\ell$ and $\ell\tau + \text{jets}$. Compares the measured $t\bar{t}$ cross section to an approx. NNLO theoretical prediction - see their Table IV.

¹⁷ Based on 1 fb⁻¹ of data at $\sqrt{s} = 1.96$ TeV. Uses $\ell\ell$ and $\ell\tau + \text{jets}$. Compares the measured $t\bar{t}$ cross section to a partial NNLO theoretical prediction.

¹⁸ Reports measurement of $170.7^{+4.2}_{-3.9} \pm 2.6 \pm 2.4$ GeV based on 1.2 fb⁻¹ of data at $\sqrt{s} = 1.96$ TeV. The last error is due to the theoretical uncertainty on $\sigma_{t\bar{t}}$. Without the cross-section constraint a top mass of $169.7^{+5.2}_{-4.9} \pm 3.1$ GeV is obtained.

¹⁹ Template method.

²⁰ Based on 310 pb⁻¹ of data at $\sqrt{s} = 1.96$ TeV.

²¹ Ideogram method.

²² Based on 311 pb⁻¹ of data at $\sqrt{s} = 1.96$ TeV. Events with 4 or more jets with $E_T > 15$ GeV, significant missing E_T , and secondary vertex b -tag are used in the fit. About 44% of the signal acceptance is from $\tau\nu + 4$ jets. Events with identified e or μ are vetoed to provide a statistically independent measurement.

²³ Based on 1.02 fb⁻¹ of data at $\sqrt{s} = 1.96$ TeV.

²⁴ Based on 955 pb⁻¹ of data at $\sqrt{s} = 1.96$ TeV. m_t and JES (Jet Energy Scale) are fitted simultaneously, and the first error contains the JES contribution of 1.5 GeV.

²⁵ Matrix element method.

²⁶ Based on 425 pb⁻¹ of data at $\sqrt{s} = 1.96$ TeV. The first error is a combination of statistics and JES (Jet Energy Scale) uncertainty, which has been measured simultaneously to give JES = 0.989 ± 0.029 (stat).

²⁷ Based on 370 pb⁻¹ of data at $\sqrt{s} = 1.96$ TeV. Combined result of MWT (Matrix-element Weighting Technique) and ν WWT (ν Weighting Technique) analyses is $178.1 \pm 6.7 \pm 4.8$ GeV.

²⁸ Based on 1.0 fb⁻¹ of data at $\sqrt{s} = 1.96$ TeV. ABULENCIA 07D improves the matrix element description by including the effects of initial-state radiation.

²⁹ Based on ~400 pb⁻¹ of data at $\sqrt{s} = 1.96$ TeV. The first error includes statistical and systematic jet energy scale uncertainties, the second error is from the other systematics. The result is obtained with the b -tagging information. The result without b -tagging is $169.2^{+5.0+1.5}_{-7.4-1.4}$ GeV. Superseded by ABAZOV 08AH.

³⁰ Based on 318 pb⁻¹ of data at $\sqrt{s} = 1.96$ TeV.

³¹ Dynamical likelihood method.

³² Based on 340 pb⁻¹ of data at $\sqrt{s} = 1.96$ TeV.

³³ Based on 360 pb⁻¹ of data at $\sqrt{s} = 1.96$ TeV.

³⁴ Based on 110.2 ± 5.8 pb⁻¹ at $\sqrt{s} = 1.8$ TeV.

³⁵ Based on the all hadronic decays of $t\bar{t}$ pairs. Single b -quark tagging via the decay chain $b \rightarrow c \rightarrow \mu$ was used to select signal enriched multijet events. The result was obtained by the maximum likelihood method after bias correction.

³⁶ Obtained by combining the measurements in the lepton + jets [AFFOLDER 01], all-jets [ABE 97R, ABE 99B], and dilepton [ABE 99B] decay topologies.

³⁷ Obtained by combining the D0 result m_t (GeV) = $168.4 \pm 12.3 \pm 3.6$ from 6 di-lepton events (see also ABBOTT 98D) and m_t (GeV) = $173.3 \pm 5.6 \pm 5.5$ from lepton+jet events (ABBOTT 98F).

³⁸ Obtained by combining the CDF results of m_t (GeV) = $167.4 \pm 10.3 \pm 4.8$ from 8 dilepton events, m_t (GeV) = $175.9 \pm 4.8 \pm 5.3$ from lepton+jet events (ABE 98E), and m_t (GeV) = $186.0 \pm 10.0 \pm 5.7$ from all-jet events (ABE 97R). The systematic errors in the latter two measurements are changed in this paper.

³⁹ See ABAZOV 04c.

⁴⁰ The updated systematic error is listed. See AFFOLDER 01, appendix C.

⁴¹ Obtained by combining the D0 results of m_t (GeV) = $168.4 \pm 12.3 \pm 3.6$ from 6 dilepton events and m_t (GeV) = $173.3 \pm 5.6 \pm 5.5$ from 77 lepton+jet events.

⁴² Obtained by combining the D0 results from dilepton and lepton+jet events, and the CDF results (ABE 99B) from dilepton, lepton+jet events, and all-jet events.

 $2(m_t - m_{\bar{t}}) / (m_t + m_{\bar{t}})$ Test of CPT conservation.

VALUE	DOCUMENT ID	TECN	COMMENT
0.022 ± 0.022	¹ ABAZOV	09AA D0	$\ell + \cancel{E}_T + 4$ jets (≥ 1 b -tag)

¹ Based on 1 fb⁻¹ of data in $p\bar{p}$ collisions at $\sqrt{s} = 1.96$ TeV. $m_t - m_{\bar{t}} = 3.8 \pm 3.7$ GeV.

 t -quark DECAY WIDTH

VALUE (GeV)	CL%	DOCUMENT ID	TECN	COMMENT
<13.1	95	¹ AALTONEN	09M	CDF $m_t(\text{rec})$ distribution

¹ Based on 955 pb⁻¹ of $p\bar{p}$ collision data at $\sqrt{s} = 1.96$ TeV. AALTONEN 09M selected $t\bar{t}$ candidate events for the $\ell + \cancel{E}_T + \text{jets}$ channel with one or two b -tags, and examine the decay width dependence of the reconstructed m_t distribution. The result is for $m_t = 175$ GeV, whereas the upper limit is lower for smaller m_t .

 t DECAY MODES

Mode	Fraction (Γ_i/Γ)	Confidence level
Γ_1 Wq ($q = b, s, d$)		
Γ_2 Wb		
Γ_3 $\ell\nu_\ell$ anything	[a,b] (9.4 ± 2.4) %	
Γ_4 $\tau\nu_\tau b$		
Γ_5 γq ($q = u, c$)	[c] < 5.9 × 10 ⁻³	95%

 $\Delta T = 1$ weak neutral current (T_1) modes

Γ_6 Zq ($q = u, c$)	T_1 [d] < 3.7 %	95%
--------------------------------	-------------------	-----

[a] ℓ means e or μ decay mode, not the sum over them.

[b] Assumes lepton universality and W -decay acceptance.

[c] This limit is for $\Gamma(t \rightarrow \gamma q)/\Gamma(t \rightarrow Wb)$.

[d] This limit is for $\Gamma(t \rightarrow Zq)/\Gamma(t \rightarrow Wb)$.

Quark Particle Listings

 t

- ¹ Results are based on 1.9 fb^{-1} of data in $p\bar{p}$ collisions at 1.96 TeV. F_0 result is obtained assuming $F_{\pm} = 0$, while F_{\pm} result is obtained for $F_0 = 0.70$, the SM values. Model independent fits for the two fractions give $F_0 = 0.66 \pm 0.16 \pm 0.05$ and $F_{\pm} = -0.03 \pm 0.06 \pm 0.03$.
- ² Based on 1 fb^{-1} of data at $p\bar{p}$ collisions $\sqrt{s} = 1.96 \text{ TeV}$. Combined result of the W helicity measurement in $t\bar{t}$ events (ABAZOV 08b) and the search for anomalous tbW couplings in the single top production (ABAZOV 08a). Constraints when t_1^L and one of the anomalous couplings are simultaneously allowed to vary are given in their Fig. 1 and Table 1.
- ³ Result is based on 0.9 fb^{-1} of data at 1.96 TeV. Single top quark production events are used to measure the Lorentz structure of the tbW coupling. The upper bounds on the non-standard couplings are obtained when only one non-standard coupling is allowed to be present together with the SM one, $t_1^L = V_{tb}^*$.
- ⁴ Based on 1 fb^{-1} at $\sqrt{s} = 1.96 \text{ TeV}$.
- ⁵ Based on 370 pb^{-1} of data at $\sqrt{s} = 1.96 \text{ TeV}$, using the ℓ + jets and dilepton decay channels. The result assumes $F_0 = 0.70$, and it gives $F_{\pm} < 0.23$ at 95% CL.
- ⁶ Based on 700 pb^{-1} of data at $\sqrt{s} = 1.96 \text{ TeV}$.
- ⁷ Based on 318 pb^{-1} of data at $\sqrt{s} = 1.96 \text{ TeV}$.
- ⁸ Based on 200 pb^{-1} of data at $\sqrt{s} = 1.96 \text{ TeV}$. $t \rightarrow Wb \rightarrow \ell\nu b$ ($\ell = e$ or μ). The errors are stat + syst.
- ⁹ ABAZOV 05g studied the angular distribution of leptonic decays of W bosons in $t\bar{t}$ candidate events with lepton + jets final states, and obtained the fraction of longitudinally polarized W under the constraint of no right-handed current, $F_{\pm} = 0$. Based on 125 pb^{-1} of data at $\sqrt{s} = 1.8 \text{ TeV}$.
- ¹⁰ ABAZOV 05L studied the angular distribution of leptonic decays of W bosons in $t\bar{t}$ events, where one of the W 's from t or \bar{t} decays into e or μ and the other decays hadronically. The fraction of the "+" helicity W boson is obtained by assuming $F_0 = 0.7$, which is the generic prediction for any linear combination of V and A currents. Based on $230 \pm 15 \text{ pb}^{-1}$ of data at $\sqrt{s} = 1.96 \text{ TeV}$.
- ¹¹ ACOSTA 05d measures the $m_{\ell}^2 + b$ distribution in $t\bar{t}$ production events where one or both W 's decay leptonically to $\ell = e$ or μ , and finds a bound on the V+A coupling of the tbW vertex. By assuming the SM value of the longitudinal W fraction $F_0 = \text{B}(t \rightarrow W_0 b) = 0.70$, the bound on F_{\pm} is obtained. If the results are combined with those of AFFOLDER 00b, the bounds become $F_{V+A} < 0.61$ (95% CL) and $F_{\pm} < 0.18$ (95% CL), respectively. Based on $109 \pm 7 \text{ pb}^{-1}$ of data at $\sqrt{s} = 1.8 \text{ TeV}$ (run I).
- ¹² AFFOLDER 00b studied the angular distribution of leptonic decays of W bosons in $t \rightarrow Wb$ events. The ratio F_0 is the fraction of the helicity zero (longitudinal) W bosons in the decaying top quark rest frame. $\text{B}(t \rightarrow W_{\pm} b)$ is the fraction of positive helicity (right-handed) positive charge W bosons in the top quark decays. It is obtained by assuming the Standard Model value of F_0 .

 t -quark FCNC couplings κ^{utg}/Λ and κ^{ctg}/Λ

VALUE (TeV ⁻¹)	CL%	DOCUMENT ID	TECN	COMMENT
<0.018	95	¹ AALTONEN 09N CDF		κ^{utg}/Λ ($\kappa^{ctg} = 0$)
<0.069	95	¹ AALTONEN 09N CDF		κ^{ctg}/Λ ($\kappa^{utg} = 0$)
<0.037	95	² ABAZOV 07V D0		κ^{utg}/Λ
<0.15	95	² ABAZOV 07V D0		κ^{ctg}/Λ

- ¹ Based on 2.2 fb^{-1} of data in $p\bar{p}$ collisions at $\sqrt{s} = 1.96 \text{ TeV}$. Upper limit of single top quark production cross section $\sigma(u(c) + g \rightarrow t) < 1.8 \text{ pb}$ (95% CL) via FCNC t - u - g and t - c - g couplings lead to the bounds. $\text{B}(t \rightarrow u + g) < 3.9 \times 10^{-4}$ and $\text{B}(t \rightarrow c + g) < 5.7 \times 10^{-3}$ follow.
- ² Result is based on 230 pb^{-1} of data at $\sqrt{s} = 1.96 \text{ TeV}$. Absence of single top quark production events via FCNC t - u - g and t - c - g couplings lead to the upper bounds on the dimensioned couplings, κ^{utg}/Λ and κ^{ctg}/Λ , respectively.

Single t -Quark Production Cross Section in $p\bar{p}$ Collisions at $\sqrt{s} = 1.8 \text{ TeV}$ Direct probes of the tbW coupling and possible new physics at $\sqrt{s} = 1.8 \text{ TeV}$.

VALUE (pb)	CL%	DOCUMENT ID	TECN	COMMENT
<24	95	¹ ACOSTA 04H CDF		$p\bar{p} \rightarrow tb + X, tqb + X$
<18	95	² ACOSTA 02 CDF		$p\bar{p} \rightarrow tb + X$
<13	95	³ ACOSTA 02 CDF		$p\bar{p} \rightarrow tqb + X$

- ¹ ACOSTA 04H bounds single top-quark production from the s -channel W -exchange process, $q'\bar{q} \rightarrow t\bar{b}$, and the t -channel W -exchange process, $q'g \rightarrow qt\bar{b}$. Based on $\sim 106 \text{ pb}^{-1}$ of data.
- ² ACOSTA 02 bounds the cross section for single top-quark production via the s -channel W -exchange process, $q'\bar{q} \rightarrow t\bar{b}$. Based on $\sim 106 \text{ pb}^{-1}$ of data.
- ³ ACOSTA 02 bounds the cross section for single top-quark production via the t -channel W -exchange process, $q'g \rightarrow qt\bar{b}$. Based on $\sim 106 \text{ pb}^{-1}$ of data.

Single t -Quark Production Cross Section in $p\bar{p}$ Collisions at $\sqrt{s} = 1.96 \text{ TeV}$ Direct probes of the tbW coupling and possible new physics at $\sqrt{s} = 1.96 \text{ TeV}$.OUR EVALUATION is an average of two results below that is provided by the Tevatron Electroweak Working Group (TEVEWWG 09B). It takes correlated uncertainties into account and assumes $m_t = 170 \text{ GeV}$.

VALUE (pb)	CL%	DOCUMENT ID	TECN	COMMENT
$2.76^{+0.58}_{-0.47}$				OUR EVALUATION See comments in the header above.
$2.3^{+0.6}_{-0.5}$		¹ AALTONEN 09AT CDF		s - + t -channel
3.94 ± 0.88		² ABAZOV 09Z D0		s - + t -channel

• • • We do not use the following data for averages, fits, limits, etc. • • •

$3.14^{+0.94}_{-0.80}$		³ ABAZOV 10 D0		t -channel
1.05 ± 0.81		³ ABAZOV 10 D0		s -channel
$2.2^{+0.7}_{-0.6}$		⁴ AALTONEN 08AH CDF		s - + t -channel
4.7 ± 1.3		⁵ ABAZOV 08I D0		s - + t -channel
4.9 ± 1.4		⁶ ABAZOV 07H D0		s - + t -channel
< 6.4	95	⁷ ABAZOV 05P D0		$p\bar{p} \rightarrow tb + X$
< 5.0	95	⁷ ABAZOV 05P D0		$p\bar{p} \rightarrow tqb + X$
< 10.1	95	⁸ ACOSTA 05N CDF		$p\bar{p} \rightarrow tqb + X$
< 13.6	95	⁸ ACOSTA 05N CDF		$p\bar{p} \rightarrow tb + X$
< 17.8	95	⁸ ACOSTA 05N CDF		$p\bar{p} \rightarrow tb + X, tqb + X$

- ¹ Based on 3.2 fb^{-1} of data. Events with isolated ℓ + E_T + jets with at least one b -tag are analyzed and s - and t -channel single top events are selected by using the likelihood function, matrix element, neural-network, boosted decision tree, likelihood function optimized for s -channel process, and neural-network based analysis of events with E_T that has sensitivity for $W \rightarrow \tau\nu$ decays. The result is for $m_t = 175 \text{ GeV}$, and the mean value decreases by 0.02 pb/GeV for smaller m_t . The signal has 5.0 sigma significance. The result gives $|V_{tb}| = 0.91 \pm 0.11$ (stat+syst) ± 0.07 (theory), or $|V_{tb}| > 0.71$ at 95% CL.
- ² Based on 2.3 fb^{-1} of data. Events with isolated ℓ + E_T + ≥ 2 jets with 1 or 2 b -tags are analyzed and s - and t -channel single top events are selected by using boosted decision tree, Bayesian neural networks and the matrix element method. The signal has 5.0 sigma significance. The result gives $|V_{tb}| = 1.07 \pm 0.12$, or $|V_{tb}| > 0.78$ at 95% CL. The analysis assumes $m_t = 170 \text{ GeV}$.
- ³ Result is based on 2.3 fb^{-1} of data. Events with isolated ℓ + E_T + 2, 3, 4 jets with one or two b -tags are selected. The analysis assumes $m_t = 170 \text{ GeV}$.
- ⁴ Result is based on 2.2 fb^{-1} of data. Events with isolated ℓ + E_T + 2, 3 jets with at least one b -tag are selected, and s - and t -channel single top events are selected by using likelihood, matrix element, and neural network discriminants. The result can be interpreted as $|V_{tb}| = 0.88^{+0.13}_{-0.12}$ (stat + syst) ± 0.07 (theory), and $|V_{tb}| > 0.66$ (95% CL) under the $|V_{tb}| < 1$ constraint.
- ⁵ Result is based on 0.9 fb^{-1} of data. Events with isolated ℓ + E_T + 2, 3, 4 jets with one or two b -vertex-tag are selected, and contributions from W + jets, $t\bar{t}$, s - and t -channel single top events are identified by using boosted decision trees, Bayesian neural networks, and matrix element analysis. The result can be interpreted as the measurement of the CKM matrix element $|V_{tb}| = 1.31^{+0.25}_{-0.21}$, or $|V_{tb}| > 0.68$ (95% CL) under the $|V_{tb}| < 1$ constraint.
- ⁶ Result is based on 0.9 fb^{-1} of data. This result constrains V_{tb} to $0.68 < |V_{tb}| \leq 1$ at 95% CL.
- ⁷ ABAZOV 05P bounds single top-quark production from either the s -channel W -exchange process, $q'\bar{q} \rightarrow t\bar{b}$, or the t -channel W -exchange process, $q'g \rightarrow qt\bar{b}$, based on $\sim 230 \text{ pb}^{-1}$ of data.
- ⁸ ACOSTA 05N bounds single top-quark production from the t -channel W -exchange process ($q'g \rightarrow qt\bar{b}$), the s -channel W -exchange process ($q'\bar{q} \rightarrow t\bar{b}$), and from the combined cross section of t - and s -channel. Based on $\sim 162 \text{ pb}^{-1}$ of data.

Single t -Quark Production Cross Section in ep Collisions

VALUE (pb)	CL%	DOCUMENT ID	TECN	COMMENT
<0.25	95	¹ AARON 09A H1		$e^{\pm}p \rightarrow e^{\pm}tX$
<0.55	95	² AKTAS 04 H1		$e^{\pm}p \rightarrow e^{\pm}tX$
<0.225	95	³ CHEKANOV 03 ZEUS		$e^{\pm}p \rightarrow e^{\pm}tX$

- ¹ AARON 09A looked for single top production via FCNC in $e^{\pm}p$ collisions at HERA with 474 pb^{-1} of data at $\sqrt{s} = 301$ - 319 GeV . The result supersedes that of AKTAS 04.
- ² AKTAS 04 looked for single top production via FCNC in e^{\pm} collisions at HERA with 118.3 pb^{-1} , and found 5 events in the e or μ channels while 1.31 ± 0.22 events are expected from the Standard Model background. No excess was found for the hadronic channel. The observed cross section of $\sigma(ep \rightarrow e tX) = 0.29^{+0.15}_{-0.14} \text{ pb}$ at $\sqrt{s} = 319 \text{ GeV}$ gives the quoted upper bound if the observed events are due to statistical fluctuation.
- ³ CHEKANOV 03 looked in 130.1 pb^{-1} of data at $\sqrt{s} = 301$ and 318 GeV . The limit is for $\sqrt{s} = 318 \text{ GeV}$ and assumes $m_t = 175 \text{ GeV}$.

 $t\bar{t}$ production cross section in $p\bar{p}$ collisions at $\sqrt{s} = 1.8 \text{ TeV}$ Only the final combined $t\bar{t}$ production cross sections obtained from Tevatron Run I by the CDF and D0 experiments are quoted below.

VALUE (pb)	DOCUMENT ID	TECN	COMMENT
$5.69 \pm 1.21 \pm 1.04$	¹ ABAZOV 03A D0		Combined Run I data
$6.5^{+1.7}_{-1.4}$	² AFFOLDER 01A CDF		Combined Run I data

- ¹ Combined result from 110 pb^{-1} of Tevatron Run I data. Assume $m_t = 172.1 \text{ GeV}$.
- ² Combined result from 105 pb^{-1} of Tevatron Run I data. Assume $m_t = 175 \text{ GeV}$.

 $t\bar{t}$ production cross section in $p\bar{p}$ collisions at $\sqrt{s} = 1.96 \text{ TeV}$

VALUE (pb)	DOCUMENT ID	TECN	COMMENT
$9.6 \pm 1.2^{+0.6}_{-0.5} \pm 0.6$	¹ AALTONEN 09AD CDF		$\ell\ell + E_T$ / vtx b -tag
$9.1 \pm 1.1^{+1.0}_{-0.9} \pm 0.6$	² AALTONEN 09H CDF		$\ell + \geq 3$ jets + E_T / soft μ b -tag
$8.18^{+0.98}_{-0.87}$	³ ABAZOV 09AG D0		ℓ + jets, $\ell\ell$ and $\ell\tau$ + jets
$7.5 \pm 1.0^{+0.7}_{-0.6} \pm 0.6$	⁴ ABAZOV 09R D0		$\ell\ell$ and $\ell\tau$ + jets
$8.18^{+0.90}_{-0.84} \pm 0.50$	⁵ ABAZOV 08M D0		ℓ + n jets with 0,1,2 b -tag

• • • We do not use the following data for averages, fits, limits, etc. • • •

See key on page 405

Quark Particle Listings

 b' (Fourth Generation) Quark, t' (Fourth Generation) Quark, Free Quark Searches

>27.2	95	27,28	ENO	89	AMY	any decay; event shape
>29.0	95	27	ENO	89	AMY	$B(b' \rightarrow bg) > 65\%$ $b' \rightarrow b\gamma$ for $B(b' \rightarrow b\gamma)$ > 5% are excluded. Charged Higgs decay were not discussed.
>24.4	95	29	IGARASHI	88	AMY	μ, e
>23.8	95	30	SAGAWA	88	AMY	event shape
>22.7	95	31	ADEVA	86	MRKJ	μ
>21		32	ALTHOFF	84c	TASS	R , event shape
>19		33	ALTHOFF	84i	TASS	Aplanarity

- ¹⁵ DECAMP 90F looked for isolated charged particles, for isolated photons, and for four-jet final states. The modes $b' \rightarrow bg$ for $B(b' \rightarrow bg) > 65\%$ $b' \rightarrow b\gamma$ for $B(b' \rightarrow b\gamma)$ > 5% are excluded. Charged Higgs decay were not discussed.
- ¹⁶ ABDALLAH 07 searched for b' pair production at $E_{cm}=196-209$ GeV, with 420 pb⁻¹. No signal leads to the 95% CL upper limits on $B(b' \rightarrow bZ)$ and $B(b' \rightarrow cW)$ for $m_{b'}$ = 96 to 103 GeV.
- ¹⁷ ADRIANI 93G search for vector quarkonium states near Z and give limit on quarkonium-Z mixing parameter $\delta m^2 < (10-30)$ GeV² (95%CL) for the mass 88-94.5 GeV. Using Richardson potential, a 1S ($b'\bar{b}'$) state is excluded for the mass range 87.7-94.7 GeV. This range depends on the potential choice.
- ¹⁸ ABREU 90D assumed $m_{H^-} < m_{b'} - 3$ GeV.
- ¹⁹ Superseded by ABREU 91F.
- ²⁰ AKRAWY 90B search was restricted to data near the Z peak at $E_{cm} = 91.26$ GeV at LEP. The excluded region is between 23.6 and 41.4 GeV if no H^+ decays exist. For charged Higgs decays the excluded regions are between $(m_{H^+} + 1.5 \text{ GeV})$ and 45.5 GeV.
- ²¹ AKRAWY 90J search for isolated photons in hadronic Z decay and derive $B(Z \rightarrow b'\bar{b}') \cdot B(b' \rightarrow \gamma X) / B(Z \rightarrow \text{hadrons}) < 2.2 \times 10^{-3}$. Mass limit assumes $B(b' \rightarrow \gamma X) > 10\%$.
- ²² ABE 89E search at $E_{cm} = 56-57$ GeV at TRISTAN for multihadron events with a spherical shape (using thrust and acoplanarity) or containing isolated leptons.
- ²³ ABE 89G search was at $E_{cm} = 55-60.8$ GeV at TRISTAN.
- ²⁴ If the photonic decay mode is large ($B(b' \rightarrow b\gamma) > 25\%$), the ABRAMS 89c limit is 45.4 GeV. The limit for Higgs decay ($b' \rightarrow cH^-, H^- \rightarrow \bar{c}s$) is 45.2 GeV.
- ²⁵ ADACHI 89c search was at $E_{cm} = 56.5-60.8$ GeV at TRISTAN using multi-hadron events accompanying muons.
- ²⁶ ADACHI 89c also gives limits for any mixture of CC and bg decays.
- ²⁷ ENO 89 search at $E_{cm} = 50-60.8$ at TRISTAN.
- ²⁸ ENO 89 considers arbitrary mixture of the charged current, bg , and $b\gamma$ decays.
- ²⁹ IGARASHI 88 searches for leptons in low-thrust events and gives $\Delta R(b') < 0.26$ (95% CL) assuming charged current decay, which translates to $m_{b'} > 24.4$ GeV.
- ³⁰ SAGAWA 88 set limit $\sigma(\text{top}) < 6.1$ pb at CL=95% for top-flavored hadron production from event shape analyses at $E_{cm} = 52$ GeV. By using the quark parton model cross-section formula near threshold, the above limit leads to lower mass bounds of 23.8 GeV for charge $-1/3$ quarks.
- ³¹ ADEVA 86 give 95%CL upper bound on an excess of the normalized cross section, ΔR , as a function of the minimum c.m. energy (see their figure 3). Production of a pair of $1/3$ charge quarks is excluded up to $E_{cm} = 45.4$ GeV.
- ³² ALTHOFF 84c narrow state search sets limit $\Gamma(e^+e^-)B(\text{hadrons}) < 2.4$ keV CL = 95% and heavy charge $1/3$ quark pair production $m > 21$ GeV, CL = 95%.
- ³³ ALTHOFF 84i exclude heavy quark pair production for $7 < m < 19$ GeV ($1/3$ charge) using aplanarity distributions (CL = 95%).

REFERENCES FOR Searches for (Fourth Generation) b' Quark

ABAZOV	08X	PRL 101 111802	V.M. Abazov et al.	(DO Collab.)
HUANG	08	PR D77 037302	P.Q. Hung, M. Sher	(UVA, WILL)
AALTONEN	07C	PR D76 072006	T. Aaltonen et al.	(CDF Collab.)
ABDALLAH	07	EPJ C50 507	J. Abdallah et al.	(DELPHI Collab.)
ACOSTA	03	PRL 90 131801	D. Acosta et al.	(CDF Collab.)
AFFOLDER	00	PRL 84 835	A. Affolder et al.	(CDF Collab.)
ABE	95N	PR D58 051102	F. Abe et al.	(CDF Collab.)
ABACHI	97D	PRL 78 3818	S. Abachi et al.	(DO Collab.)
FROGGATT	97	ZPHY C73 333	C.D. Froggatt, D.J. Smith, H.B. Nielsen	(GLAS+)
ABACHI	95F	PR D52 4877	S. Abachi et al.	(DO Collab.)
ADRIANI	93G	PL B313 326	O. Adriani et al.	(L3 Collab.)
ADRIANI	93M	PRPL 236 1	O. Adriani et al.	(L3 Collab.)
MUKHOPAD...	93	PR D48 2105	B. Mukhopadhyaya, D.P. Roy	(TATA)
ABE	92	PRL 68 447	F. Abe et al.	(CDF Collab.)
Also				
ABE	92G	PR D45 3921	F. Abe et al.	(CDF Collab.)
ABREU	91F	NP B367 511	F. Abe et al.	(CDF Collab.)
ABE	90B	PRL 64 147	P. Abreu et al.	(DELPHI Collab.)
ABE	90D	PL B234 382	K. Abe et al.	(CDF Collab.)
ABREU	90D	PL B242 536	P. Abreu et al.	(DELPHI Collab.)
ADACHI	90	PL B234 197	I. Adachi et al.	(TOPAZ Collab.)
AKESSON	90	ZPHY C46 179	T. Akesson et al.	(UA2 Collab.)
AKRAWY	90B	PL B236 364	M.Z. Akrawy et al.	(OPAL Collab.)
AKRAWY	90J	PL B246 285	M.Z. Akrawy et al.	(OPAL Collab.)
ALBAJAR	90B	ZPHY C48 1	C. Albajar et al.	(UA1 Collab.)
DECAMP	90F	PL B236 511	D. Decamp et al.	(ALEPH Collab.)
ABE	89E	PR D39 3524	K. Abe et al.	(VENUS Collab.)
ABE	89G	PRL 63 1776	K. Abe et al.	(VENUS Collab.)
ABRAMS	89C	PRL 63 2447	G.S. Abrams et al.	(Mark II Collab.)
ADACHI	89C	PL B229 427	I. Adachi et al.	(TOPAZ Collab.)
ENO	89	PRL 63 1910	S. Eno et al.	(AMY Collab.)
ALBAJAR	88	ZPHY C37 505	C. Albajar et al.	(UA1 Collab.)
ALTARELLI	88	NP B308 724	G. Altarelli et al.	(CERN, ROMA, ETH)
IGARASHI	88	PRL 60 2359	S. Igarashi et al.	(AMY Collab.)
SAGAWA	88	PRL 60 93	H. Sagawa et al.	(AMY Collab.)
ADEVA	86	PR D34 681	M. Adeva et al.	(Mark-J Collab.)
ALTHOFF	84C	PL 138B 441	M. Althoff et al.	(TASSO Collab.)
ALTHOFF	84I	ZPHY C22 307	M. Althoff et al.	(TASSO Collab.)

 t' (4th Generation) Quark, Searches forMASS LIMITS for t' (4th Generation) Quark or Hadron in $p\bar{p}$ Collisions

VALUE (GeV)	CL%	DOCUMENT ID	TECN	COMMENT
>256	95	1,2 AALTONEN	08H CDF	$p\bar{p}$ at 1.96 GeV

¹ Searches for pair production of a new heavy top-like quark t' decaying to a W boson and another quark by fitting the observed spectrum of total transverse energy and reconstructed t' mass in the lepton + jets events.

² HUANG 08 reexamined the t' mass lower bound of 256 GeV obtained in AALTONEN 08H that assumes $B(b' \rightarrow qZ) = 1$ for $q = u, c$ which does not hold when $m_{b'} < m_{t'} - m_W$ or the mixing $\sin^2(\theta_{bt'})$ is so tiny that the decay occurs outside of the vertex detector.

Fig. 1 gives that lower bound on $m_{t'}$ in the plane of $\sin^2(\theta_{bt'})$ and $m_{b'}$.

REFERENCES FOR Searches for (Fourth Generation) t' Quark

AALTONEN	08H	PRL 100 161803	T. Aaltonen et al.	(CDF Collab.)
HUANG	08	PR D77 037302	P.Q. Hung, M. Sher	(UVA, WILL)

Free Quark Searches

FREE QUARK SEARCHES

The basis for much of the theory of particle scattering and hadron spectroscopy is the construction of the hadrons from a set of fractionally charged constituents (quarks). A central but unproven hypothesis of this theory, Quantum Chromodynamics, is that quarks cannot be observed as free particles but are confined to mesons and baryons.

Experiments show that it is at best difficult to “unglue” quarks. Accelerator searches at increasing energies have produced no evidence for free quarks, while only a few cosmic-ray and matter searches have produced uncorroborated events.

This compilation is only a guide to the literature, since the quoted experimental limits are often only indicative. Reviews can be found in Refs. 1-4.

References

1. M.L. Perl, E.R. Lee, and D. Lomba, Mod. Phys. Lett. **A19**, 2595 (2004).
2. P.F. Smith, Ann. Rev. Nucl. and Part. Sci. **39**, 73 (1989).
3. L. Lyons, Phys. Reports **129**, 225 (1985).
4. M. Marinelli and G. Morpurgo, Phys. Reports **85**, 161 (1982).

Quark Production Cross Section — Accelerator Searches

X-SECT (cm ²)	CHG (e/3)	MASS (GeV)	ENERGY (GeV)	BEAM	EVTS	DOCUMENT ID	TECN
<1.3E-36	±2	45-84	130-172	e^+e^-	0	ABREU	97D DLPH
<2.E-35	+2	250	1800	$p\bar{p}$	0	¹ ABE	92J CDF
<1.E-35	+4	250	1800	$p\bar{p}$	0	¹ ABE	92J CDF
<3.8E-28		14.5A	28	Sj-Pb	0	² HE	91 PLAS
<3.2E-28		14.5A	28	Sj-Cu	0	² HE	91 PLAS
<1.E-40	±1,2	<10		$p, \nu, \bar{\nu}$	0	BERGSMA	84B CHRM
<1.E-36	±1,2	<9	200	μ	0	AUBERT	83C SPEC
<2.E-10	±2,4	1-3	200	p	0	³ BUSSIERE	80 CNTR
<5.E-38	+1,2	>5	300	p	0	^{4,5} STEVENSON	79 CNTR
<1.E-33	±1	<20	52	pp	0	BASILE	78 SPEC
<9.E-39	±1,2	<6	400	p	0	⁴ ANTREASYAN	77 SPEC
<8.E-35	+1,2	<20	52	pp	0	⁶ FABJAN	75 CNTR
<5.E-38	-1,2	4-9	200	p	0	NASH	74 CNTR
<1.E-32	+2,4	4-24	52	pp	0	ALPER	73 SPEC
<5.E-31	+1,2,4	<12	300	p	0	LEIPUNER	73 CNTR
<6.E-34	±1,2	<13	52	pp	0	BOTT	72 CNTR
<1.E-36	-4	4	70	p	0	ANTIPOV	71 CNTR
<1.E-35	±1,2	2	28	p	0	⁷ ALLABY	69B CNTR
<4.E-37	-2	<5	70	p	0	³ ANTIPOV	69 CNTR

Quark Particle Listings

Free Quark Searches

GALLINARO	77	PRL 38 1255	G. Gallinaro, M. Marinelli, G. Morpurgo	(GENO)	BELLAMY	68	PR 166 1391	E.H. Bellamy <i>et al.</i>	(STAN, SLAC)
JONES	77B	RMP 49 717	L.W. Jones		BJORNBOE	68	NC B53 241	J. Bjornboe <i>et al.</i>	(BOHR, TATA, BERN+)
LARUE	77	PRL 38 1011	G.S. Larue, W.M. Fairbank, A.F. Hebard	(STAN)	BRAGINSK	68	JETP 27 51	V.B. Braginsky <i>et al.</i>	(MOSU)
MULLER	77	SCI 196 521	R.A. Muller <i>et al.</i>	(LBL)			Translated from ZETF 54 91.		
OGOROD...	77	JETP 45 857	D.D. Ogorodnikov, I.M. Samoilo, A.M. Soltsev		BRIATORE	68	NC 57A 850	L. Briatore <i>et al.</i>	(TORI, CERN, BGNA)
		Translated from ZETF 72 1633.			FRANZINI	68	PRL 21 1013	P. Franzini, S. Shulman	(COLU)
BALDIN	76	SJNP 22 264	B.Y. Baldin <i>et al.</i>	(JINR)	GARMIRE	68	PR 166 1280	G. Garmire, C. Leong, V. Sreekantan	(MIT)
		Translated from YAF 22 512.			HANAYAMA	68	CJP 46 5734	Y. Hanayama <i>et al.</i>	(OSAK)
BRIATORE	76	NC 31A 553	L. Briatore <i>et al.</i>	(LCGT, FRAS, FREIB)	KASHA	68	PR 172 1297	H. Kasha, R.J. Stefanski	(BNL, YALE)
STEVENS	76	PR D14 716	C.M. Stevens, J.P. Schiffer, W. Chupka	(ANL)	KASHA	68B	PRL 20 217	H. Kasha <i>et al.</i>	(BNL, YALE)
ALBROW	75	NP B97 189	M.G. Albrow <i>et al.</i>	(CERN, DARE, FOM+)	KASHA	68C	CJP 46 5730	H. Kasha <i>et al.</i>	(BNL, YALE)
FABJAN	75	NP B101 349	C.W. Fabjan <i>et al.</i>	(CERN, MPIM)	RANK	68	PR 176 1635	D. Rank	(MICH)
HAZEN	75	NP B95 189	W.E. Hazen <i>et al.</i>	(MICH, LEED)	BARTON	67	PRSL 90 87	J.C. Barton	(NPOL)
JOVANOV...	75	PL 56B 105	J.V. Jovanovich <i>et al.</i>	(MANI, AACH, CERN+)	BATHOW	67	PL 25B 163	G. Bathow <i>et al.</i>	(DESY)
KRISOR	75	NC 27A 132	K. Krisor	(AACH3)	BUHLER	67	NC 49A 209	A. Buhler-Broglin <i>et al.</i>	(CERN, BGNA)
CLARK	74B	PR D10 2721	A.F. Clark <i>et al.</i>	(LLL)	BUHLER	67B	NC 51A 837	A. Buhler-Broglin <i>et al.</i>	(CERN, BGNA+)
GALIK	74	PR D9 1856	R.S. Galik <i>et al.</i>	(SLAC, FNAL)	FOSS	67	PL 25B 166	J. Foss <i>et al.</i>	(MIT)
KIFUNE	74	JPSJ 36 629	T. Kifune <i>et al.</i>	(TOKY, KEK)	GOMEZ	67	PRL 18 1022	R. Gomez <i>et al.</i>	(CIT)
NASH	74	PRL 32 858	T. Nash <i>et al.</i>	(FNAL, CORN, NYU)	KASHA	67	PR 154 1263	H. Kasha <i>et al.</i>	(BNL, YALE)
ALPER	73	PL 46B 265	B. Alper <i>et al.</i>	(CERN, LVP, LUND, BOHR+)	STOVER	67	PR 164 1599	R.W. Stover, T.J. Moran, J.W. Trischka	(SYRA)
ASHTON	73	JPA 6 577	F. Ashton <i>et al.</i>	(DURH)	BARTON	66	PL 21 360	J.C. Barton, C.T. Stockel	(NPOL)
HICKS	73B	NC 14A 65	R.B. Hicks, R.W. Flint, S. Standil	(MANI)	BENNETT	66	PRL 17 1196	W.R. Bennett	(YALE)
LEIPUNER	73	PRL 31 1226	L.B. Leipuner <i>et al.</i>	(BNL, YALE)	BUHLER	66	NC 45A 520	A. Buhler-Broglin <i>et al.</i>	(CERN, BGNA+)
BEAUCHAMP	72	PR D6 1211	W.T. Beauchamp <i>et al.</i>	(ARIZ)	CHUPKA	66	PRL 17 60	W.A. Chupka, J.P. Schiffer, C.M. Stevens	(ANL)
BOHM	72B	PRL 28 326	A. Bohm <i>et al.</i>	(AACH)	GALLINARO	66	PL 23 609	G. Gallinaro, G. Morpurgo	(GENO)
BOTT	72	PL 40B 633	M. Bott-Bodenhausen <i>et al.</i>	(CERN, MPIM)	KASHA	66	PR 150 1140	H. Kasha, L.B. Leipuner, R.K. Adair	(BNL, YALE)
COX	72	PR D6 1203	A.J. Cox <i>et al.</i>	(ARIZ)	LAMB	66	PRL 17 1068	R.C. Lamb <i>et al.</i>	(ANL)
CROUCH	72	PR D5 2667	M.F. Crouch, K. Mori, G.R. Smith	(CASE)	DELISE	65	PR 140B 458	D.A. de Lise, T. Bowen	(ARIZ)
DARDO	72	NC 9A 319	M. Dardo <i>et al.</i>	(TORI)	DORFAN	65	PRL 14 999	D.E. Dorfán <i>et al.</i>	(COLU)
EVANS	72	PRSE A70 143	G.R. Evans <i>et al.</i>	(EDIN, LEED)	FRANZINI	65B	PRL 14 196	P. Franzini <i>et al.</i>	(BNL, COLU)
TONWAR	72	JPA 5 569	S.C. Tonwar, S. Naranan, B.V. Sreekantan	(TATA)	MASSAM	65	NC 40A 589	T. Massam, T. Muller, A. Zichichi	(CERN)
ANTIPOV	71	NP B29 374	Y.M. Antipov <i>et al.</i>	(SERP)	BINGHAM	64	PL 9 201	H.H. Bingham <i>et al.</i>	(CERN, EPOL)
CHIN	71	NC 2A 419	S. Chin <i>et al.</i>	(OSAK)	BLUM	64	PRL 13 353A	W. Blum <i>et al.</i>	(CERN)
CLARK	71B	PRL 27 51	A.F. Clark <i>et al.</i>	(LLL, LBL)	BOWEN	64	PRL 13 728	T. Bowen <i>et al.</i>	(ARIZ)
HAZEN	71	PRL 26 582	W.E. Hazen	(MICH)	HAGOPIAN	64	PRL 13 280	V. Hagopian <i>et al.</i>	(PENN, BNL)
BOSIA	70	NC 66A 167	G.F. Bosia, L. Briatore	(TORI)	LEIPUNER	64	PRL 12 423	L.B. Leipuner <i>et al.</i>	(BNL, YALE)
CHU	70	PRL 24 917	W.T. Chu <i>et al.</i>	(OSU, ROSE, KANS)	MORRISON	64	PL 9 199	D.R.O. Morrison	(CERN)
	Also	PRL 25 550	W.W.M. Allison <i>et al.</i>	(ANL)	SUNYAR	64	PR 136 B1157	A.W. Sunyar, A.Z. Schwarzschild, P.I. Connors	(BNL)
ELBERT	70	NP B20 217	J.W. Elbert <i>et al.</i>	(WISC)	HILLAS	59	NAT 184 B92	A.M. Hillas, T.E. Cranshaw	(AERE)
FAISSNER	70B	PRL 24 1357	H. Faissner <i>et al.</i>	(AACH3)	MILLIKAN	10	Phil Mag 19 209	R.A. Millikan	(CHIC)
KRIDER	70	PR D1 835	E.P. Krider, T. Bowen, R.M. Kalbach	(ARIZ)					
MORPURGO	70	NIM 79 95	G. Morpurgo, G. Gallinaro, G. Palmieri	(GENO)					
ALLABY	69B	NC 64A 75	J.V. Allaby <i>et al.</i>	(CERN)					
ANTIPOV	69	PL 29B 245	Y.M. Antipov <i>et al.</i>	(SERP)					
ANTIPOV	69B	PL 30B 576	Y.M. Antipov <i>et al.</i>	(SERP)					
CAIRNS	69	PR 186 1394	I. Cairns <i>et al.</i>	(SYDN)					
COOK	69	PR 188 2092	D.D. Cook <i>et al.</i>	(ILL)					
FUKUSHIMA	69	PR 178 2058	Y. Fukushima <i>et al.</i>	(TOKY)					
MCCUSKER	69	PRL 23 658	C.B.A. McCusker, I. Cairns	(SYDN)					

OTHER RELATED PAPERS

LYONS	85	PRPL C129 225	L. Lyons	(OXF)
Review				
MARINELLI	82	PRPL 85 161	M. Marinelli, G. Morpurgo	(GENO)
Review				

LIGHT UNFLAVORED MESONS ($S = C = B = 0$)

- π^\pm 619
- π^0 623
- η 625
- $f_0(600)$ 630
- $\rho(770)$ 637
- $\omega(782)$ 643
- $\eta'(958)$ 648
- $f_0(980)$ 652
- $a_0(980)$ 655
- $\phi(1020)$ 656
- $h_1(1170)$ 663
- $b_1(1235)$ 663
- $a_1(1260)$ 664
- $f_2(1270)$ 666
- $f_1(1285)$ 669
- $\eta(1295)$ 672
- $\pi(1300)$ 672
- $a_2(1320)$ 673
- $f_0(1370)$ 676
- $h_1(1380)$ 679
- $\pi_1(1400)$ 679
- $\eta(1405)$ 680
- $f_1(1420)$ 684
- $\omega(1420)$ 686
- $f_2(1430)$ 687
- $a_0(1450)$ 687
- $\rho(1450)$ 688
- $\eta(1475)$ 690
- $f_0(1500)$ 691
- $f_1(1510)$ 694
- $f_2'(1525)$ 694
- $f_2(1565)$ 697
- $\rho(1570)$ 698
- $h_1(1595)$ 698
- $\pi_1(1600)$ 698
- $a_1(1640)$ 699
- $f_2(1640)$ 700
- $\eta_2(1645)$ 700
- $\omega(1650)$ 701
- $\omega_3(1670)$ 702
- $\pi_2(1670)$ 702
- $\phi(1680)$ 704
- $\rho_3(1690)$ 705
- $\rho(1700)$ 709
- $a_2(1700)$ 713
- $f_0(1710)$ 714
- $\eta(1760)$ 716
- $\pi(1800)$ 716
- $f_2(1810)$ 718
- $X(1835)$ 719
- $\phi_3(1850)$ 719
- $\eta_2(1870)$ 719
- $\pi_2(1880)$ 720
- $\rho(1900)$ 720
- $f_2(1910)$ 721
- $f_2(1950)$ 722

- $\rho_3(1990)$ 723
- $f_2(2010)$ 723
- $f_0(2020)$ 723
- $a_4(2040)$ 724
- $f_4(2050)$ 724
- $\pi_2(2100)$ 726
- $f_0(2100)$ 726
- $f_2(2150)$ 726
- $\rho(2150)$ 728
- $\phi(2170)$ 729
- $f_0(2200)$ 730
- $f_J(2220)$ 730
- $\eta(2225)$ 731
- $\rho_3(2250)$ 731
- $f_2(2300)$ 732
- $f_4(2300)$ 732
- $f_0(2330)$ 733
- $f_2(2340)$ 733
- $\rho_5(2350)$ 733
- $a_6(2450)$ 734
- $f_6(2510)$ 734

OTHER LIGHT UNFLAVORED ($S = C = B = 0$)

- Further States 735

STRANGE MESONS ($S = \pm 1, C = B = 0$)

- K^\pm 740
- K^0 758
- K_S^0 762
- K_L^0 766
- $K_0^*(800)$ 787
- $K^*(892)$ 788
- $K_1(1270)$ 790
- $K_1(1400)$ 792
- $K^*(1410)$ 792
- $K_0^*(1430)$ 793
- $K_2^*(1430)$ 794
- $K(1460)$ 796
- $K_2(1580)$ 796
- $K(1630)$ 796
- $K_1(1650)$ 797
- $K^*(1680)$ 797
- $K_2(1770)$ 797
- $K_3^*(1780)$ 798
- $K_2(1820)$ 799
- $K(1830)$ 800
- $K_0^*(1950)$ 800
- $K_2^*(1980)$ 800
- $K_4^*(2045)$ 800
- $K_2(2250)$ 801
- $K_3(2320)$ 801
- $K_5^*(2380)$ 802
- $K_4(2500)$ 802
- $K(3100)$ 802

• Indicates the particle is in the Meson Summary Table

(continued on the next page)

CHARMED MESONS ($C = \pm 1$)

• D^\pm	803
• D^0	819
• $D^*(2007)^0$	849
• $D^*(2010)^\pm$	850
• $D_0^*(2400)^0$	851
• $D_0^*(2400)^\pm$	851
• $D_1(2420)^0$	852
• $D_1(2420)^\pm$	852
• $D_1(2430)^0$	853
• $D_2^*(2460)^0$	853
• $D_2^*(2460)^\pm$	854
• $D^*(2640)^\pm$	855

CHARMED, STRANGE MESONS ($C = S = \pm 1$)

• D_s^\pm	856
• $D_s^{*\pm}$	871
• $D_{s0}^*(2317)^\pm$	872
• $D_{s1}(2460)^\pm$	872
• $D_{s1}(2536)^\pm$	874
• $D_{s2}(2573)$	875
• $D_{s1}^*(2700)^\pm$	875
• $D_{sJ}^*(2860)^\pm$	876
• $D_{sJ}^*(3040)^\pm$	876

BOTTOM MESONS ($B = \pm 1$)

B -particle organization	877
• B^\pm	887
• B^0	930
• B^\pm/B^0 ADMIXTURE	993
• $B^\pm/B^0/B_s^0/b$ -baryon ADMIXTURE	1007
• V_{cb} and V_{ub} CKM Matrix Elements	1014
• B^*	1029
• $B_1(5721)^0$	1030
• $B_J^*(5732)$	1029
• $B_2^*(5747)^0$	1030

BOTTOM, STRANGE MESONS ($B = \pm 1, S = \mp 1$)

• B_s^0	1031
• B_s^*	1037
• $B_{s1}(5830)^0$	1038
• $B_{s2}^*(5840)^0$	1038
• $B_{sJ}^*(5850)$	1038

BOTTOM, CHARMED MESONS ($B = C = \pm 1$)

• B_c^\pm	1039
-------------	------

$c\bar{c}$ MESONS

Charmonium system	1040
• $\eta_c(1S)$	1040
• $J/\psi(1S)$	1044
• $\chi_{c0}(1P)$	1061
• $\chi_{c1}(1P)$	1068
• $h_c(1P)$	1073
• $\chi_{c2}(1P)$	1074
• $\eta_c(2S)$	1081
• $\psi(2S)$	1082
• $\psi(3770)$	1094

• Indicates the particle is in the Meson Summary Table

• $X(3872)$	1099
• $\chi_{c2}(2P)$	1101
• $X(3940)$	1101
• $X(3945)$	1101
• $\psi(4040)$	1102
• $X(4050)^\pm$	1103
• $X(4140)$	1103
• $\psi(4160)$	1103
• $X(4160)$	1104
• $X(4250)^\pm$	1105
• $X(4260)$	1105
• $X(4350)$	1106
• $X(4360)$	1107
• $\psi(4415)$	1107
• $X(4430)^\pm$	1108
• $X(4660)$	1108

$b\bar{b}$ MESONS

Bottomonium system	1109
• $\eta_b(1S)$	1110
• $\Upsilon(1S)$	1110
• $\chi_{b0}(1P)$	1114
• $\chi_{b1}(1P)$	1115
• $\chi_{b2}(1P)$	1116
• $\Upsilon(2S)$	1117
• $\Upsilon(1D)$	1120
• $\chi_{b0}(2P)$	1120
• $\chi_{b1}(2P)$	1121
• $\chi_{b2}(2P)$	1123
• $\Upsilon(3S)$	1124
• $\Upsilon(4S)$	1127
• $\Upsilon(10860)$	1129
• $\Upsilon(11020)$	1130

NON- $q\bar{q}$ CANDIDATES

Non- $q\bar{q}$ Candidates	1131
----------------------------	------

Notes in the Meson Listings

Form Factors for Radiative Pion & Kaon Decays (rev.)	620
Note on Scalar Mesons (rev.)	630
The $\rho(770)$ (rev.)	637
The $\eta(1405)$, $\eta(1475)$, $f_1(1420)$, and $f_1(1510)$ (rev.)	680
The $\rho(1450)$ and the $\rho(1700)$ (rev.)	709
Rare Kaon Decays (rev.)	742
Dalitz Plot Parameters for $K \rightarrow 3\pi$ Decays	752
$K_{\ell 3}^\pm$ and $K_{\ell 3}^0$ Form Factors (rev.)	753
CPT Invariance Tests in Neutral Kaon Decay (rev.)	759
CP Violation in $K_S \rightarrow 3\pi$	764
V_{ud} , V_{us} , Cabibbo Angle, and CKM Unitarity (rev.)	771
CP -Violation in K_L Decays (rev.)	779
Dalitz-Plot Analysis Formalism	807
Review of Charm Dalitz-Plot Analyses (rev.)	811
$D^0-\bar{D}^0$ Mixing (rev.)	820
D_s^+ Branching Fractions (new)	858
Decay Constants of Charged Pseudoscalar Mesons (rev.)	860
Production and Decay of b -flavored Hadrons (rev.)	877
Polarization in B Decays (rev.)	967
$B^0-\bar{B}^0$ Mixing (rev.)	973
Determination of V_{cb} and V_{ub} (rev.)	1014
Branching Ratios of $\psi(2S)$ and $\chi_{c0,1,2}$ (rev.)	1060

LIGHT UNFLAVORED MESONS ($S = C = B = 0$)

For $l = 1$ (π, b, ρ, a): $u\bar{d}, (u\bar{u}-d\bar{d})/\sqrt{2}, d\bar{u}$;
for $l = 0$ ($\eta, \eta', h, h', \omega, \phi, f, f'$): $c_1(u\bar{u} + d\bar{d}) + c_2(s\bar{s})$

 π^\pm

$$I^G(J^P) = 1^-(0^-)$$

We have omitted some results that have been superseded by later experiments. The omitted results may be found in our 1988 edition Physics Letters **B204** 1 (1988).

π^\pm MASS

The most accurate charged pion mass measurements are based upon x-ray wavelength measurements for transitions in π^- -mesonic atoms. The observed line is the blend of three components, corresponding to different K-shell occupancies. JECKELMANN 94 revisits the occupancy question, with the conclusion that two sets of occupancy ratios, resulting in two different pion masses (Solutions A and B), are equally probable. We choose the higher Solution B since only this solution is consistent with a positive mass-squared for the muon neutrino, given the precise muon momentum measurements now available (DAUM 91, ASSAMAGAN 94, and ASSAMAGAN 96) for the decay of pions at rest. Earlier mass determinations with π -mesonic atoms may have used incorrect K-shell screening corrections.

Measurements with an error of > 0.005 MeV have been omitted from this Listing.

VALUE (MeV)	DOCUMENT ID	TECN	CHG	COMMENT	
139.57018 ± 0.00035 OUR FIT	Error includes scale factor of 1.2.				
139.57018 ± 0.00035 OUR AVERAGE	Error includes scale factor of 1.2.				
139.57071 ± 0.00053	¹ LENZ	98	CNTR	— pionic N2-atoms gas target	
139.56995 ± 0.00035	² JECKELMANN 94	CNTR	—	π^- atom, Soln. B	
• • • We do not use the following data for averages, fits, limits, etc. • • •					
139.57022 ± 0.00014	³ ASSAMAGAN 96	SPEC	+	$\pi^+ \rightarrow \mu^+ \nu_\mu$	
139.56782 ± 0.00037	⁴ JECKELMANN 94	CNTR	—	π^- atom, Soln. A	
139.56996 ± 0.00067	⁵ DAUM	91	SPEC	+	$\pi^+ \rightarrow \mu^+ \nu$
139.56752 ± 0.00037	⁶ JECKELMANN 86b	CNTR	—	Mesonic atoms	
139.5704 ± 0.0011	⁵ ABELA	84	SPEC	+	See DAUM 91
139.5664 ± 0.0009	⁷ LU	80	CNTR	—	Mesonic atoms
139.5686 ± 0.0020	CARTER	76	CNTR	—	Mesonic atoms
139.5660 ± 0.0024	^{7,8} MARUSHEN..	76	CNTR	—	Mesonic atoms

¹ LENZ 98 result does not suffer K-electron configuration uncertainties as does JECKELMANN 94.

² JECKELMANN 94 Solution B (dominant 2-electron K-shell occupancy), chosen for consistency with positive $m_{\nu_\mu}^2$.

³ ASSAMAGAN 96 measures the μ^+ momentum p_μ in $\pi^+ \rightarrow \mu^+ \nu_\mu$ decay at rest to be 29.79200 ± 0.00011 MeV/c. Combined with the μ^+ mass and the assumption $m_{\nu_\mu} = 0$, this gives the π^+ mass above; if $m_{\nu_\mu} > 0$, m_{π^+} given above is a lower limit. Combined instead with m_μ and (assuming *CPT*) the π^- mass of JECKELMANN 94, p_μ gives an upper limit on m_{ν_μ} (see the ν_μ).

⁴ JECKELMANN 94 Solution A (small 2-electron K-shell occupancy) in combination with either the DAUM 91 or ASSAMAGAN 94 pion decay muon momentum measurement yields a significantly negative $m_{\nu_\mu}^2$. It is accordingly not used in our fits.

⁵ The DAUM 91 value includes the ABELA 84 result. The value is based on a measurement of the μ^+ momentum for π^+ decay at rest, $p_\mu = 29.79179 \pm 0.00053$ MeV, uses $m_\mu = 105.658389 \pm 0.000034$ MeV, and assumes that $m_{\nu_\mu} = 0$. The last assumption means that in fact the value is a lower limit.

⁶ JECKELMANN 86b gives $m_\pi/m_e = 273.12677(71)$. We use $m_e = 0.51099906(15)$ MeV from COHEN 87. The authors note that two solutions for the probability distribution of K-shell occupancy fit equally well, and use other data to choose the lower of the two possible π^\pm masses.

⁷ These values are scaled with a new wavelength-energy conversion factor $\lambda E = 1.23984244(37) \times 10^{-6}$ eV m from COHEN 87. The LU 80 screening correction relies upon a theoretical calculation of inner-shell refilling rates.

⁸ This MARUSHENKO 76 value used at the authors' request to use the accepted set of calibration γ energies. Error increased from 0.0017 MeV to include QED calculation error of 0.0017 MeV (12 ppm).

$$m_{\pi^+} - m_{\mu^+}$$

Measurements with an error > 0.05 MeV have been omitted from this Listing.

VALUE (MeV)	EVTS	DOCUMENT ID	TECN	CHG	COMMENT	
• • • We do not use the following data for averages, fits, limits, etc. • • •						
33.91157 ± 0.00067	⁹	DAUM	91	SPEC	+	$\pi^+ \rightarrow \mu^+ \nu$
33.9111 ± 0.0011		ABELA	84	SPEC	—	See DAUM 91
33.925 ± 0.025		BOOTH	70	CNTR	+	Magnetic spect.
33.881 ± 0.035	145	HYMAN	67	HEBC	+	K^- He

⁹ The DAUM 91 value assumes that $m_{\nu_\mu} = 0$ and uses our $m_\mu = 105.658389 \pm 0.000034$ MeV.

$$(m_{\pi^+} - m_{\pi^-}) / m_{\text{average}}$$

A test of *CPT* invariance.

VALUE (units 10^{-4})	DOCUMENT ID	TECN
2 ± 5	AYRES	71 CNTR

π^\pm MEAN LIFE

Measurements with an error $> 0.02 \times 10^{-8}$ s have been omitted.

VALUE (10^{-8} s)	DOCUMENT ID	TECN	CHG	COMMENT	
2.6033 ± 0.0005 OUR AVERAGE	Error includes scale factor of 1.2.				
2.60361 ± 0.00052	¹⁰ KOPTEV	95	SPEC	+	Surface μ^+ 's
2.60231 ± 0.00050 ± 0.00084	NUMAO	95	SPEC	+	Surface μ^+ 's
2.609 ± 0.008	DUNAITSEV	73	CNTR	+	
2.602 ± 0.004	AYRES	71	CNTR	±	
2.604 ± 0.005	NORDBERG	67	CNTR	+	
2.602 ± 0.004	ECKHAUSE	65	CNTR	+	
• • • We do not use the following data for averages, fits, limits, etc. • • •					
2.640 ± 0.008	¹¹ KINSEY	66	CNTR	+	

¹⁰ KOPTEV 95 combines the statistical and systematic errors; the statistical error dominates.

¹¹ Systematic errors in the calibration of this experiment are discussed by NORDBERG 67.

$$(\tau_{\pi^+} - \tau_{\pi^-}) / \tau_{\text{average}}$$

A test of *CPT* invariance.

VALUE (units 10^{-4})	DOCUMENT ID	TECN
5.5 ± 7.1	AYRES	71 CNTR
• • • We do not use the following data for averages, fits, limits, etc. • • •		
-14 ± 29	PETRUKHIN	68 CNTR
40 ± 70	BARDON	66 CNTR
23 ± 40	¹² LOBKOWICZ	66 CNTR

¹² This is the most conservative value given by LOBKOWICZ 66.

π^+ DECAY MODES

π^- modes are charge conjugates of the modes below.

For decay limits to particles which are not established, see the section on Searches for Axions and Other Very Light Bosons.

Mode	Fraction (Γ_i/Γ)	Confidence level
Γ_1 $\mu^+ \nu_\mu$	[a] (99.98770 ± 0.00004) %	
Γ_2 $\mu^+ \nu_\mu \gamma$	[b] (2.00 ± 0.25) × 10^{-4}	
Γ_3 $e^+ \nu_e$	[a] (1.230 ± 0.004) × 10^{-4}	
Γ_4 $e^+ \nu_e \gamma$	[b] (7.39 ± 0.05) × 10^{-7}	
Γ_5 $e^+ \nu_e \pi^0$	(1.036 ± 0.006) × 10^{-8}	
Γ_6 $e^+ \nu_e e^+ e^-$	(3.2 ± 0.5) × 10^{-9}	
Γ_7 $e^+ \nu_e \nu \bar{\nu}$	< 5	× 10^{-6} 90%

Lepton Family number (*LF*) or Lepton number (*L*) violating modes

Γ_8 $\mu^+ \bar{\nu}_e$	<i>L</i>	[c] < 1.5	× 10^{-3} 90%
Γ_9 $\mu^+ \nu_e$	<i>LF</i>	[c] < 8.0	× 10^{-3} 90%
Γ_{10} $\mu^- e^+ e^+ \nu$	<i>LF</i>	< 1.6	× 10^{-6} 90%

[a] Measurements of $\Gamma(e^+ \nu_e)/\Gamma(\mu^+ \nu_\mu)$ always include decays with γ 's, and measurements of $\Gamma(e^+ \nu_e \gamma)$ and $\Gamma(\mu^+ \nu_\mu \gamma)$ never include low-energy γ 's. Therefore, since no clean separation is possible, we consider the modes with γ 's to be subreactions of the modes without them, and let $[\Gamma(e^+ \nu_e) + \Gamma(\mu^+ \nu_\mu)]/\Gamma_{\text{total}} = 100\%$.

[b] See the Particle Listings below for the energy limits used in this measurement; low-energy γ 's are not included.

[c] Derived from an analysis of neutrino-oscillation experiments.

π^+ BRANCHING RATIOS

$\Gamma(e^+ \nu_e)/\Gamma_{\text{total}}$ See note [a] in the list of π^+ decay modes just above, and see also the next block of data. See also the note on "Decay Constants of Charged Pseudoscalar Mesons" in the D_s^\pm Listings.

VALUE (units 10^{-4})	DOCUMENT ID
1.230 ± 0.004 OUR EVALUATION	

Meson Particle Listings

 π^\pm

$$\frac{\Gamma(e^+\nu_e) + \Gamma(e^+\nu_e\gamma)}{\Gamma(\mu^+\nu_\mu) + \Gamma(\mu^+\nu_\mu\gamma)} \quad (\Gamma_3 + \Gamma_4) / (\Gamma_1 + \Gamma_2)$$

See note [a] in the list of π^\pm decay modes above. See NUMAO 92 for a discussion of $e\text{-}\mu$ universality. See also the note on “Decay Constants of Charged Pseudoscalar Mesons” in the D_s^\pm Listings.

VALUE (units 10^{-4})	EVTS	DOCUMENT ID	TECN	COMMENT
1.230 ± 0.004 OUR AVERAGE				
1.2346 ± 0.0035 ± 0.0036	120k	CZAPEK	93	CALO Stopping π^+
1.2265 ± 0.0034 ± 0.0044	190k	BRITTON	92	CNTR Stopping π^+
1.218 ± 0.014	32k	BRYMAN	86	CNTR Stopping π^+
• • • We do not use the following data for averages, fits, limits, etc. • • •				
1.273 ± 0.028	11k	¹³ DICAPUA	64	CNTR
1.21 ± 0.07		ANDERSON	60	SPEC
¹³ DICAPUA 64 has been updated using the current mean life.				

$$\Gamma(\mu^+\nu_\mu\gamma) / \Gamma_{\text{total}} \quad \Gamma_2 / \Gamma$$

Note that measurements here do not cover the full kinematic range.

VALUE (units 10^{-4})	EVTS	DOCUMENT ID	TECN	CHG	COMMENT
2.0 ± 0.24 ± 0.08		¹⁴ BRESSI	98	CALO +	Stopping π^+
• • • We do not use the following data for averages, fits, limits, etc. • • •					
1.24 ± 0.25	26	CASTAGNOLI	58	EMUL	$KE_\mu < 3.38$ MeV
¹⁴ BRESSI 98 result is given for $E_\gamma > 1$ MeV only. Result agrees with QED expectation, 2.283×10^{-4} and does not confirm discrepancy of earlier experiment CASTAGNOLI 58.					

$$\Gamma(e^+\nu_e\gamma) / \Gamma_{\text{total}} \quad \Gamma_4 / \Gamma$$

The very different values reflect the very different kinematic ranges covered (bigger range, bigger value). And none of them covers the whole kinematic range.

VALUE (units 10^{-8})	EVTS	DOCUMENT ID	TECN	CHG	COMMENT
73.86 ± 0.54		¹⁵ BYCHKOV	09	PIBE	$e^+\nu\gamma$ at rest
• • • We do not use the following data for averages, fits, limits, etc. • • •					
16.1 ± 2.3		¹⁶ BOLOTOV	90B	SPEC	17 GeV $\pi^- \rightarrow e^- \bar{\nu}_e \gamma$
5.6 ± 0.7	226	¹⁷ STETZ	78	SPEC	$P_e > 56$ MeV/c
3.0	143	DEPOMMIER	63B	CNTR	(KE) $_{e^+\gamma} > 48$ MeV
¹⁵ This BYCHKOV 09 value is for $E_\gamma > 10$ MeV and $\Theta_{e^+\gamma} > 40^\circ$.					
¹⁶ BOLOTOV 90B is for $E_\gamma > 21$ MeV, $E_e > 70 - 0.8 E_\gamma$.					
¹⁷ STETZ 78 is for an $e^- \gamma$ opening angle $> 132^\circ$. Obtains 3.7 when using same cutoffs as DEPOMMIER 63B.					

$$\Gamma(e^+\nu_e\pi^0) / \Gamma_{\text{total}} \quad \Gamma_5 / \Gamma$$

VALUE (units 10^{-8})	EVTS	DOCUMENT ID	TECN	CHG	COMMENT
1.036 ± 0.006 OUR AVERAGE					
1.036 ± 0.006	64k ^{18,19}	POCANIC	04	PIBE +	π decay at rest
1.026 ± 0.039	1224	²⁰ MCFARLANE	85	CNTR +	Decay in flight
1.00 $^{+0.08}_{-0.10}$	332	DEPOMMIER	68	CNTR +	
1.07 ± 0.21	38	²¹ BACASTOW	65	OSPK +	
1.10 ± 0.26		²¹ BERTRAM	65	OSPK +	
1.1 ± 0.2	43	²¹ DUNAITSEV	65	CNTR +	
0.97 ± 0.20	36	²¹ BARTLETT	64	OSPK +	
• • • We do not use the following data for averages, fits, limits, etc. • • •					
1.15 ± 0.22	52	²¹ DEPOMMIER	63	CNTR +	See DEPOMMIER 68
¹⁸ POCANIC 04 normalizes to $e^+\nu_e$ decays, using the PDG 2004 value $B(\pi^+ \rightarrow e^+\nu_e) = (1.230 \pm 0.004) \times 10^{-4}$. We add their statistical (0.004×10^{-8}) , systematic (0.004×10^{-8}) and systematic error due to the uncertainty of $B(\pi^+ \rightarrow e^+\nu_e)$ (0.003×10^{-8}) in quadrature.					
¹⁹ This result can be used to calculate V_{ud} from pion beta decay: $V_{ud}^{PIBETA} = 0.9728 \pm 0.0030$.					
²⁰ MCFARLANE 85 combines a measured rate $(0.394 \pm 0.015)/s$ with 1982 PDG mean life.					
²¹ DEPOMMIER 68 says the result of DEPOMMIER 63 is at least 10% too large because of a systematic error in the π^0 detection efficiency, and that this may be true of all the previous measurements (also V. Soergel, private communication, 1972).					

$$\Gamma(e^+\nu_e e^+) / \Gamma(\mu^+\nu_\mu) \quad \Gamma_6 / \Gamma_1$$

VALUE (units 10^{-3})	CL%	EVTS	DOCUMENT ID	TECN	COMMENT
3.2 ± 0.5 ± 0.2		98	EGLI	89	SPEC Uses $R_{PCAC} = 0.068 \pm 0.004$
• • • We do not use the following data for averages, fits, limits, etc. • • •					
0.46 ± 0.16 ± 0.07		7	²² BARANOV	92	SPEC Stopped π^+
< 4.8	90		KORENCHE...	76B	SPEC
< 34	90		KORENCHE...	71	OSPK
²² This measurement by BARANOV 92 is of the structure-dependent part of the decay. The value depends on values assumed for ratios of form factors.					

$$\Gamma(e^+\nu_e \bar{\nu}) / \Gamma_{\text{total}} \quad \Gamma_7 / \Gamma$$

VALUE (units 10^{-6})	CL%	DOCUMENT ID	TECN	COMMENT
< 5	90	PICCIOTTO	88	SPEC

$$\Gamma(\mu^+\bar{\nu}_e) / \Gamma_{\text{total}} \quad \Gamma_8 / \Gamma$$

Forbidden by total lepton number conservation. See the note on “Decay Constants of Charged Pseudoscalar Mesons” in the D_s^\pm Listings.

VALUE (units 10^{-3})	CL%	DOCUMENT ID	TECN	COMMENT
< 1.5	90	²³ COOPER	82	HLBC Wideband ν beam
²³ COOPER 82 limit on $\bar{\nu}_e$ observation is here interpreted as a limit on lepton number violation.				

$$\Gamma(\mu^+\nu_e) / \Gamma_{\text{total}} \quad \Gamma_9 / \Gamma$$

Forbidden by lepton family number conservation.

VALUE (units 10^{-3})	CL%	DOCUMENT ID	TECN	COMMENT
< 8.0	90	²⁴ COOPER	82	HLBC Wideband ν beam
²⁴ COOPER 82 limit on ν_e observation is here interpreted as a limit on lepton family number violation.				

$$\Gamma(\mu^- e^+ e^+) / \Gamma_{\text{total}} \quad \Gamma_{10} / \Gamma$$

Forbidden by lepton family number conservation.

VALUE (units 10^{-6})	CL%	DOCUMENT ID	TECN	CHG	COMMENT
< 1.6	90	BARANOV	91B	SPEC +	
• • • We do not use the following data for averages, fits, limits, etc. • • •					
< 7.7	90	KORENCHE...	87	SPEC +	

 π^\pm — POLARIZATION OF EMITTED μ^\pm $\pi^\pm \rightarrow \mu^\pm \nu$

Tests the Lorentz structure of leptonic charged weak interactions.

VALUE	CL%	DOCUMENT ID	TECN	CHG	COMMENT
• • • We do not use the following data for averages, fits, limits, etc. • • •					
< (-0.9959)	90	²⁵ FETSCHER	84	RVUE +	
-0.99 ± 0.16		²⁶ ABELA	83	SPEC -	μ X-rays
²⁵ FETSCHER 84 uses only the measurement of CARR 83.					
²⁶ Sign of measurement reversed in ABELA 83 to compare with μ^\pm measurements.					

FORM FACTORS FOR RADIATIVE PION AND KAON DECAYS

Updated August 2009 by W. Bertl (Paul Scherrer Inst.)

The radiative decays, $\pi^\pm \rightarrow l^\pm \nu \gamma$ and $K^\pm \rightarrow l^\pm \nu \gamma$, with l standing for an e or a μ , and γ for a real or virtual photon (e^+e^- pair), provide a powerful tool to investigate the hadronic structure of pions and kaons. The structure-dependent part SD_i of the amplitude describes the emission of photons from virtual hadronic states, and is parametrized in terms of form factors F_i , with $i = V, A$ (vector, axial vector), in the standard description [1,2]. Exotic, non-standard contributions like $i = T, S$ (tensor, scalar) have also been considered, and we shall discuss them below. Apart from the SD terms, the decay amplitude depends also on Inner Bremsstrahlung IB from the weak decay $\pi^\pm(K^\pm) \rightarrow l^\pm \nu$ accompanied by the photon radiated from the external charged particles. Naturally, experiments try to optimize their kinematics so as to minimize the “trivial” IB part of the amplitude.

The SD amplitude in its standard form is given as

$$M(SD_V) = \frac{-eG_F V_{qq'}}{\sqrt{2}m_P} \epsilon^\mu \ell^\nu F_V^P \epsilon_{\mu\nu\sigma\tau} k^\sigma q^\tau \quad (1)$$

$$M(SD_A) = \frac{-ieG_F V_{qq'}}{\sqrt{2}m_P} \epsilon^\mu \ell^\nu \{F_A^P [(qk - k^2)g_{\mu\nu} - q_\mu k_\nu] + R^P k^2 g_{\mu\nu}\}, \quad (2)$$

which contains an additional axial form factor R^P which only can be accessed if the photon remains virtual. $V_{qq'}$ is the Cabibbo-Kobayashi-Maskawa mixing-matrix element; ϵ^μ is the polarization vector of the photon (or the effective vertex, $\epsilon^\mu = (e/k^2)\bar{u}(p_-)\gamma^\mu v(p_+)$, of the e^+e^- pair); $\ell^\nu = \bar{u}(p_\nu)\gamma^\nu(1 - \gamma_5)v(p_l)$ is the lepton-neutrino current; q and k are the meson

and photon four-momenta ($k = p_+ + p_-$ for virtual photons); and P stands for π or K .

The pion vector form factor, F_V^π , is related via CVC (Conserved Vector Current) to the $\pi^0 \rightarrow \gamma\gamma$ decay width by $|F_V^\pi| = (1/\alpha)\sqrt{2\Gamma_{\pi^0 \rightarrow \gamma\gamma}/\pi m_{\pi^0}}$ [3]. The resulting value, $F_V^\pi(0) = 0.0259(9)$, has been confirmed by calculations based on chiral perturbation theory (χPT) [4], and by two experiments given in the Listings below. A recent experiment by the PIBETA collaboration [5] obtained an F_V that is in excellent agreement with the CVC hypothesis. It also measured the slope parameter a in $F_V^\pi(s) = F_V^\pi(0)(1 + a \cdot s)$, where $s = (1 - 2E_\gamma/m_\pi)$, and E_γ is the gamma energy in the pion rest frame: $a = 0.095 \pm 0.058$. A functional dependence on s is expected for all form factors. It becomes non-negligible in the case of $F_V^\pi(s)$ when a wide range of photon momenta is recorded; proper treatment in the analysis of K decays is mandatory.

The form factor, R^P , can be related to the electromagnetic radius, r_P , of the meson [2]: $R^P = \frac{1}{3}m_P f_P \langle r_P^2 \rangle$ using PCAC (Partial Conserved Axial vector Current; f_P is the meson decay constant). In lowest order χPT , the ratio F_A/F_V is related to the pion electric polarizability $\alpha_E = [\alpha/(8\pi^2 m_\pi f_\pi^2)] \times F_A/F_V$ [6]. The calculation of the other form factors, F_A^π, F_V^K , and F_A^K , is model-dependent [1,2,4].

For decay processes where the photon is real, the partial decay width can be written in analytical form as a sum of IB, SD, and IB/SD interference terms INT [1,4]:

$$\begin{aligned} \frac{d^2\Gamma_{P \rightarrow \ell\nu\gamma}}{dx dy} &= \frac{d^2(\Gamma_{\text{IB}} + \Gamma_{\text{SD}} + \Gamma_{\text{INT}})}{dx dy} \\ &= \frac{\alpha}{2\pi} \Gamma_{P \rightarrow \ell\nu} \frac{1}{(1-r)^2} \left\{ \text{IB}(x, y) \right. \\ &+ \frac{1}{r} \left(\frac{m_P}{2f_P} \right)^2 \left[(F_V + F_A)^2 \text{SD}^+(x, y) + (F_V - F_A)^2 \text{SD}^-(x, y) \right] \\ &\left. + \frac{m_P}{f_P} \left[(F_V + F_A) \text{S}_{\text{INT}}^+(x, y) + (F_V - F_A) \text{S}_{\text{INT}}^-(x, y) \right] \right\}. \quad (3) \end{aligned}$$

Here

$$\begin{aligned} \text{IB}(x, y) &= \left[\frac{1-y+r}{x^2(x+y-1-r)} \right] \\ &\left[x^2 + 2(1-x)(1-r) - \frac{2xr(1-r)}{x+y-1-r} \right] \\ \text{SD}^+(x, y) &= (x+y-1-r) \left[(x+y-1)(1-x) - r \right] \\ \text{SD}^-(x, y) &= (1-y+r) \left[(1-x)(1-y) + r \right] \\ \text{S}_{\text{INT}}^+(x, y) &= \left[\frac{1-y+r}{x(x+y-1-r)} \right] \left[(1-x)(1-x-y) + r \right] \\ \text{S}_{\text{INT}}^-(x, y) &= \left[\frac{1-y+r}{x(x+y-1-r)} \right] \left[x^2 - (1-x)(1-x-y) - r \right] \end{aligned} \quad (4)$$

where $x = 2E_\gamma/m_P$, $y = 2E_\ell/m_P$, and $r = (m_\ell/m_P)^2$. Recently, formulas (3) and (4) have been extended to describe polarized distributions in radiative meson and muon decays [7].

The ‘‘helicity’’ factor r is responsible for the enhancement of the SD over the IB amplitude in the decays $\pi^\pm \rightarrow e^\pm \nu \gamma$, while $\pi^\pm \rightarrow \mu^\pm \nu \gamma$ is dominated by IB. Interference terms are important for the decay $K^\pm \rightarrow \mu^\pm \nu \gamma$ [8], but contribute only a few percent correction to pion decays. However, they provide the basis for determining the signs of F_V and F_A . Radiative corrections to the decay $\pi^+ \rightarrow e^+ \nu \gamma$ have to be taken into account in the analysis of the precision experiments. They make up to 4% corrections in the total decay rate [9]. In $\pi^\pm \rightarrow e^\pm \nu e^+ e^-$ and $K^\pm \rightarrow \ell^\pm \nu e^+ e^-$ decays, all three form factors, F_V^P, F_A^P , and R^P , can be determined [10,11].

We give the experimental π^\pm form factors F_V^π, F_A^π , and R^π in the Listings below. In the K^\pm Listings, we give the extracted sum $F_A^K + F_V^K$ and difference $F_A^K - F_V^K$, as well as F_V^K, F_A^K and R^K .

Several searches for the exotic form factors F_T^K, F_T^K (tensor), and F_S^K (scalar) have been pursued in the past, some of them claiming non-zero results [12,13]. In particular, F_T^K has been brought into focus by experimental as well as theoretical work. It was shown that a tensor contribution could destructively interfere with the inner bremsstrahlung amplitude, leading to a substantial reduction of the branching ratio as compared with standard V–A calculations [14]. In addition, a tensor contribution as large as $F_T = -(5.6 \pm 1.7) \times 10^{-3}$ could not be completely ruled out by constraints from other measurements [15]. New high-statistics data from the PIBETA collaboration have been re-analyzed together with an additional data set optimized for low backgrounds in the radiative pion decay. In particular, lower beam rates have been used in order to reduce the accidental background, thereby making the treatment of systematic uncertainties easier and more reliable. The PIBETA analysis now restricts F_T to the range $-5.2 \times 10^{-4} < F_T < 4.0 \times 10^{-4}$ at a 90% confidence limit [5]. This result is in excellent agreement with the most recent theoretical work [4].

Precision measurements of radiative pion and kaon decays are effective tools to study QCD in the non-perturbative region. The structure-dependent form factors have direct relations to (renormalized) coupling constants of chiral perturbation theories. Therefore, they are of interest beyond the scope of radiative decays. On the other hand, the interest in searching for new physics manifesting in exotic form factors F_T or F_S has weakened over the last years mainly for two reasons: (i) on the experimental side, the lack of results confirming the non-zero findings; (ii) on the theoretical side, numerical uncertainties are still too large to allow a clear distinction of exotic and standard contributions at the currently required level. Likely this will change in the future, but meanwhile other processes such as $\pi^+ \rightarrow e^+ \nu$ seem to be better suited to search for new physics at the precision frontier, because of the very accurate and reliable theoretical predictions and the more straightforward experimental analysis.

Meson Particle Listings

 π^\pm

References

- D.A. Bryman *et al.*, Phys. Reports **88**, 151 (1982). See our note on “Decay Constants of Charged Pseudoscalar Mesons” elsewhere in this *Review*;
S.G. Brown and S.A. Bludman, Phys. Rev. **136**, B1160 (1964);
P. DeBaenst and J. Pestieau, Nuovo Cim. **A53**, 137 (1968).
- W.T. Chu *et al.*, Phys. Rev. **166**, 1577 (1968);
D.Yu. Bardin and E.A. Ivanov, Sov. J. Part. Nucl. **7**, 286 (1976);
A. Kersch and F. Scheck, Nucl. Phys. **B263**, 475 (1986).
- V.G. Vaks and B.L. Ioffe, Nuovo Cim. **10**, 342 (1958);
V.F. Muller, Z. Phys. **173**, 438 (1963).
- C.Q. Geng, I-Lin Ho, and T.H. Wu, Nucl. Phys. **B684**, 281 (2004);
J. Bijnens and P. Talavera, Nucl. Phys. **B489**, 387 (1997);
V. Mateu and J. Portoles, Eur. Phys. J. **C52**, 325 (2007);
R. Unterdorfer, H. Pichl, Eur. Phys. J. **C55**, 273 (2008).
- D. Počanić *et al.*, Phys. Rev. Lett. **93**, 181803 (2004);
E. Frlež *et al.*, Phys. Rev. Lett. **93**, 181804 (2004);
M. Bychkov *et al.*, Phys. Rev. Lett. **103**, 051802 (2009).
- J.F. Donoghue and B.R. Holstein, Phys. Rev. **D40**, 2378 (1989).
- E. Gabrielli and L. Trentadue, Nucl. Phys. **B792**, 48 (2008).
- S. Adler *et al.*, Phys. Rev. Lett. **85**, 2256 (2000).
- Yu.M. Bystritsky, E.A. Kuraev, and E.P. Velicheva, Phys. Rev. **D69**, 114004 (2004);
R. Unterdorfer and H. Pichl have treated radiative corrections of the structure terms to lowest order within χPT for the first time. See the reference under [4].
- S. Egli *et al.*, Phys. Lett. **B175**, 97 (1986).
- A.A. Poblaguev *et al.*, Phys. Rev. Lett. **89**, 061803 (2002).
- V.N. Bolotov *et al.*, Phys. Lett. **B243**, 308 (1990).
- S.A. Akimenko *et al.*, Phys. Lett. **B259**, 225 (1991).
- A.A. Poblaguev, Phys. Lett. **B238**, 108 (1990);
V.M. Belyaev and I.I. Kogan, Phys. Lett. **B280**, 238 (1992);
A.V. Chernyshev *et al.*, Mod. Phys. Lett. **A12**, 1669 (1997);
A.A. Poblaguev, Phys. Rev. **D68**, 054020 (2003);
M.V. Chizhov, Phys. Part. Nucl. Lett. **2**, 193 (2005).
- P. Herzceg, Phys. Rev. **D49**, 247 (1994).

 π^\pm FORM FACTORS F_V , VECTOR FORM FACTOR

VALUE	EVTS	DOCUMENT ID	TECN	COMMENT
0.0254 ± 0.0017 OUR AVERAGE				
0.0258 ± 0.0017	65k	27 BYCHKOV	09 PIBE	$e^+ \nu \gamma$ at rest
0.014 ± 0.009		28 BOLOTOV	90B SPEC	17 GeV $\pi^- \rightarrow e^- \bar{\nu}_e \gamma$
0.023 ± 0.015 -0.013	98	EGLI	89 SPEC	$\pi^+ \rightarrow e^+ \nu_e e^+ e^-$

²⁷The BYCHKOV 09 F_A and F_V results are highly (anti-)correlated: $F_A + 1.0286 F_V = 0.03853 \pm 0.00014$.

²⁸BOLOTOV 90B only determines the absolute value.

 F_A , AXIAL-VECTOR FORM FACTOR

VALUE	EVTS	DOCUMENT ID	TECN	COMMENT
0.0119 ± 0.0001	65k	29,30 BYCHKOV	09 PIBE	$e^+ \nu \gamma$ at rest
• • • We do not use the following data for averages, fits, limits, etc. • • •				
0.0115 ± 0.0004	41k	29,31 FRLEZ	04 PIBE	$\pi^+ \rightarrow e^+ \nu \gamma$ at rest
0.0106 ± 0.0060		29,32 BOLOTOV	90B SPEC	17 GeV $\pi^- \rightarrow e^- \bar{\nu}_e \gamma$
0.021 ± 0.011 -0.013	98	EGLI	89 SPEC	$\pi^+ \rightarrow e^+ \nu_e e^+ e^-$
0.0135 ± 0.0016		29,32 BAY	86 SPEC	$\pi^+ \rightarrow e^+ \nu \gamma$
0.006 ± 0.003		29,32 PIILONEN	86 SPEC	$\pi^+ \rightarrow e^+ \nu \gamma$
0.011 ± 0.003		29,32,33 STETZ	78 SPEC	$\pi^+ \rightarrow e^+ \nu \gamma$

²⁹These values come from fixing the vector form factor at the CVC prediction, $F_V = 0.0259 \pm 0.0005$.

³⁰When F_V is released, the BYCHKOV 09 F_A is 0.0117 ± 0.0017 , and F_A and F_V results are highly (anti-)correlated: $F_A + 1.0286 F_V = 0.03853 \pm 0.00014$.

³¹The sign of $\gamma = F_A / F_V$ is determined to be positive.

³²Only the absolute value of F_A is determined.

³³The result of STETZ 78 has a two-fold ambiguity. We take the solution compatible with later determinations.

VECTOR FORM FACTOR SLOPE PARAMETER a

This is a in $F_V(q^2) = F_V(0) (1 + a q^2)$

VALUE	EVTS	DOCUMENT ID	TECN	COMMENT
0.10 ± 0.06	65k	BYCHKOV	09 PIBE	$e^+ \nu \gamma$ at rest

 R , SECOND AXIAL-VECTOR FORM FACTOR

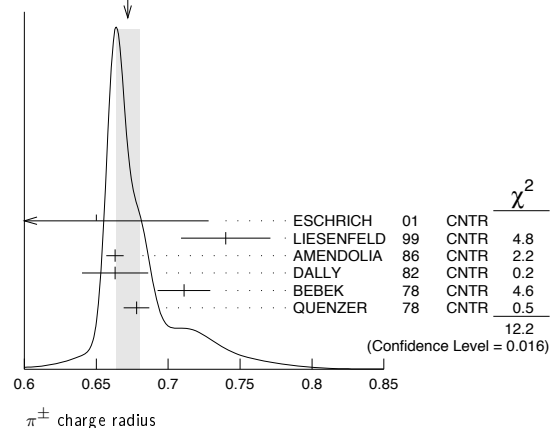
VALUE	EVTS	DOCUMENT ID	TECN	COMMENT
0.059 + 0.009 - 0.008	98	EGLI	89 SPEC	$\pi^+ \rightarrow e^+ \nu_e e^+ e^-$

 π^\pm CHARGE RADIUS

VALUE (fm)	DOCUMENT ID	TECN	COMMENT
0.672 ± 0.008 OUR AVERAGE			Error includes scale factor of 1.7. See the ideogram below.
0.65 ± 0.05 ± 0.06	ESCHRICH 01	CNTR	$\pi e \rightarrow \pi e$
0.740 ± 0.031	LIESENFELD 99	CNTR	$e p \rightarrow e \pi^+ n$
0.663 ± 0.006	AMENDOLIA 86	CNTR	$\pi e \rightarrow \pi e$
0.663 ± 0.023	DALLY 82	CNTR	$\pi e \rightarrow \pi e$
0.711 ± 0.009 ± 0.016	BEBEK 78	CNTR	$e N \rightarrow e \pi N$
0.678 ± 0.004 ± 0.008	QUENZER 78	CNTR	$e^+ e^- \rightarrow \pi^+ \pi^-$
• • • We do not use the following data for averages, fits, limits, etc. • • •			
0.661 ± 0.012	³⁴ BIJNENS 98	CNTR	χPT extraction
0.660 ± 0.024	AMENDOLIA 84	CNTR	$\pi e \rightarrow \pi e$
0.78 ± 0.09 - 0.10	ADYLOV 77	CNTR	$\pi e \rightarrow \pi e$
0.74 ± 0.11 - 0.13	BARDIN 77	CNTR	$e p \rightarrow e \pi^+ n$
0.56 ± 0.04	DALLY 77	CNTR	$\pi e \rightarrow \pi e$

³⁴BIJNENS 98 fits existing data.

WEIGHTED AVERAGE
0.672 ± 0.008 (Error scaled by 1.7)

 π^\pm REFERENCES

We have omitted some papers that have been superseded by later experiments. The omitted papers may be found in our 1988 edition Physics Letters **B204** 1 (1988).

BYCHKOV 09	PRL 103 051802	M. Bychkov <i>et al.</i>	(PSI PIBETA Collab.)
FRLEZ 04	PRL 93 181804	E. Frlež <i>et al.</i>	(PSI PIBETA Collab.)
POČANIĆ 04	PRL 93 181803	D. Počanić <i>et al.</i>	(PSI PIBETA Collab.)
ESCHRICH 01	PL B522 233	I. Eschrich <i>et al.</i>	(FNAL SELEX Collab.)
LIESENFELD 99	PL B468 20	A. Liesenfeld <i>et al.</i>	
BIJNENS 98	JHEP 9805 014	J. Bijnens <i>et al.</i>	
BRESSI 98	NP B513 555	G. Bressi <i>et al.</i>	
LENZ 98	PL B416 50	S. Lenz <i>et al.</i>	
ASSAMAGAN 96	PR D53 6065	K.A. Assamagan <i>et al.</i>	(PSI, ZURI, VILL+)
KOPTEV 95	JETPL 61 877	V.P. Koptev <i>et al.</i>	(PNPI)
NUMAO 95	PR D52 4655	T. Numao <i>et al.</i>	(TRIU, BRCO)
ASSAMAGAN 94	PL B335 231	K.A. Assamagan <i>et al.</i>	(PSI, ZURI, VILL+)
JECKELMANN 94	PL B335 326	B. Jäckelmann, P.F.A. Goudsmit, H.J. Leisi	(PSI PIBETA Collab.)
CZAPEK 93	PRL 70 17	G. Czapek <i>et al.</i>	(BERN, VILL)
BARANOV 92	SJNP 55 1644	V.A. Baranov <i>et al.</i>	(JINR)
Translated from YAF 55 2940.			
BRITTON 92	PRL 68 3000	D.I. Britton <i>et al.</i>	(TRIU, CARL)
Also	PR D49 28	D.I. Britton <i>et al.</i>	(TRIU, CARL)
NUMAO 92	MPL A7 3357	T. Numao	(TRIU)
BARANOV 91B	SJNP 54 790	V.A. Baranov <i>et al.</i>	(JINR)
Translated from YAF 54 1298.			

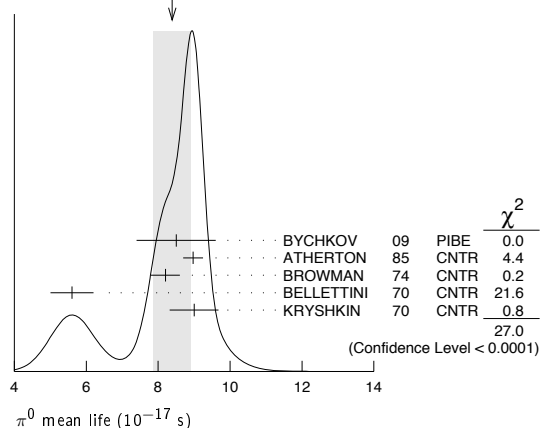
DAUM	91	PL B265 425	M. Daum <i>et al.</i>	(VILL)
BOLOTOV	90B	PL B243 308	V.N. Bolotov <i>et al.</i>	(INRM)
EGLI	89	PL B222 533	S. Egli <i>et al.</i>	(SINDRUM Collab.)
Also		PL B175 97	S. Egli <i>et al.</i>	(AACH3, ETH, SIN, ZURI)
PDG	88	PL B204 1	G.P. Yost <i>et al.</i>	(LBL+)
PICCIOTTO	88	PR D37 1131	C.E. Picciotto <i>et al.</i>	(TRIU, CNRC)
COHEN	87	RMP 59 1121	E.R. Cohen, B.N. Taylor	(RIS C, NBS)
KORENCHEN...	87	SJNP 46 192	S.M. Korenchenko <i>et al.</i>	(JINR)
Translated from YAF 46 313.				
AMENDOLIA	86	NP B277 168	S.R. Amendolia <i>et al.</i>	(CERN NA7 Collab.)
BAY	86	PL B174 445	A. Bay <i>et al.</i>	(LAUS, ZURI)
BRYMAN	86	PR D33 1211	D.A. Bryman <i>et al.</i>	(TRIU, CNRC)
Also		PRL 50 7	D.A. Bryman <i>et al.</i>	(TRIU, CNRC)
JECKELMANN	86B	NP A457 709	B. Jeckelmann <i>et al.</i>	(ETH, FRIB)
Also		PRL 56 1444	B. Jeckelmann <i>et al.</i>	(ETH, FRIB)
PILONEN	86	PRL 57 1402	L.E. Pilonen <i>et al.</i>	(LANL, TEMP, CHIC)
MC FARLANE	85	PR D32 547	W.K. McFarlane <i>et al.</i>	(TEMP, LANL)
ABELA	84	PL 146B 431	R. Abela <i>et al.</i>	(SIN)
Also		PL 74B 126	M. Daum <i>et al.</i>	(SIN)
Also		PR D20 2692	M. Daum <i>et al.</i>	(SIN)
AMENDOLIA	84	PL 146B 116	S.R. Amendolia <i>et al.</i>	(CERN NA7 Collab.)
FETSCHER	84	PL 140B 117	W. Fetscher	(ETH)
ABELA	83	NP A395 413	R. Abela <i>et al.</i>	(BASL, KARLK, KARLE)
CARR	83	PRL 51 627	J. Carr <i>et al.</i>	(LBL, NWES, TRIU)
COOPER	82	PL 112B 97	A.M. Cooper <i>et al.</i>	(RL)
DALLY	82	PRL 48 375	E.B. Dally <i>et al.</i>	
LU	80	PRL 45 1066	D.C. Lu <i>et al.</i>	(YALE, COLU, JHU)
BEBEK	78	PR D17 1693	C.J. Bebek <i>et al.</i>	
QUENZER	78	PL 74B 512	A. Quenzler <i>et al.</i>	(LALO)
STETZ	78	NP B138 285	A.W. Stetz <i>et al.</i>	(LBL, UCLA)
ADYLOV	77	NP B128 461	G.T. Adylov <i>et al.</i>	
BARDIN	77	NP B120 45	G. Bardin <i>et al.</i>	
DALLY	77	PRL 39 1176	E.B. Dally <i>et al.</i>	
CARTER	76	PRL 37 1380	A.L. Carter <i>et al.</i>	(CARL, CNRC, CHIC+)
KORENCHEN...	76B	JETP 44 35	S.M. Korenchenko <i>et al.</i>	(JINR)
Translated from ZETF 71 69.				
MARUSHEN...	76	JETPL 23 72	V.I. Marushenko <i>et al.</i>	(PNPI)
Translated from ZETFP 23 80.				
Also		Private Comm.	R.E. Shafer	(FNAL)
Also		Private Comm.	A. Smirnov	(PNPI)
DUNAITSEV	73	SJNP 16 292	A.F. Dunaitsev <i>et al.</i>	(SERP)
Translated from YAF 16 524.				
AYRES	71	PR D3 1061	D.S. Ayres <i>et al.</i>	(LRL, UCSB)
Also		PR 157 1288	D.S. Ayres <i>et al.</i>	(LRL)
Also		PRL 21 261	D.S. Ayres <i>et al.</i>	(LRL, UCSB)
Also		Thesis UCRL 18369	D.S. Ayres	(LRL)
KORENCHEN...	71	PRL 23 1267	A.J. Greenberg <i>et al.</i>	(LRL, UCSB)
Also		SJNP 13 189	S.M. Korenchenko <i>et al.</i>	(JINR)
Translated from YAF 13 339.				
BOOTH	70	PL 32B 723	P.S.L. Booth <i>et al.</i>	(LIVP)
DEPOMMIER	68	NP B4 189	P. Depommier <i>et al.</i>	(CERN)
PETRUKHIN	68	JINR P1 3862	V.I. Petrukhin <i>et al.</i>	(JINR)
HYMAN	67	PL 25B 376	L.G. Hyman <i>et al.</i>	(ANL, CMU, NWES)
NORDBERG	67	PL 24B 594	M.E. Nordberg, F. Lobkowicz, R.L. Burman	(ROCH)
BARDON	66	PRL 16 775	M. Bardon <i>et al.</i>	(COLU)
KINSEY	66	PR 144 1132	K.F. Kinsey, F. Lobkowicz, M.E. Nordberg	(ROCH)
LOBKOWICZ	66	PRL 17 548	F. Lobkowicz <i>et al.</i>	(ROCH, BNL)
BACASTOW	65	PR 139 B407	R.B. Bacastow <i>et al.</i>	(LRL, SLAC)
BERTRAM	65	PR 139 B617	W.K. Bertram <i>et al.</i>	(MICH, CMU)
DUNAITSEV	65	JETP 20 58	A.F. Dunaitsev <i>et al.</i>	(JINR)
Translated from ZETF 47 84.				
ECKHAUSE	65	PL 19 348	M. Eckhause <i>et al.</i>	(WILL)
BARTLETT	64	PR 136 B1452	D. Bartlett <i>et al.</i>	(COLU)
DICAPUA	64	PR 133 B1333	M. di Capua <i>et al.</i>	(COLU)
Also		Private Comm.	L. Pondrom	(WISC)
DEPOMMIER	63	PL 5 61	P. Depommier <i>et al.</i>	(CERN)
DEPOMMIER	63B	PL 7 285	P. Depommier <i>et al.</i>	(CERN)
ANDERSON	60	PR 119 2050	H.L. Anderson <i>et al.</i>	(EFI)
CASTAGNOLI	58	PR 112 1779	C. Castagnoli, M. Muchnik	(ROMA)

Some measurements with larger errors have been omitted.

VALUE (10^{-17} s)	EVTS	DOCUMENT ID	TECN	COMMENT
8.4 ± 0.5 OUR AVERAGE				Error includes scale factor of 2.6. See the ideogram below.
8.5 ± 1.1		1 BYCHKOV 09	PIBE	$\pi^+ \rightarrow e^+ \nu \gamma$ at rest
8.97 ± 0.22 ± 0.17		ATHERTON 85	CNTR	
8.2 ± 0.4		2 BROWMAN 74	CNTR	Primakoff effect
5.6 ± 0.6		BELLETTINI 70	CNTR	Primakoff effect
9 ± 0.68		KRYSHKIN 70	CNTR	Primakoff effect
••• We do not use the following data for averages, fits, limits, etc. •••				
8.4 ± 0.5 ± 0.5	1182	3 WILLIAMS 88	CBAL	$e^+ e^- \rightarrow e^+ e^- \pi^0$

1 BYCHKOV 09 obtains this using the conserved-vector-current relation between the vector form factor F_V and the π^0 lifetime.
 2 BROWMAN 74 gives a π^0 width $\Gamma = 8.02 \pm 0.42$ eV. The mean life is \hbar/Γ .
 3 WILLIAMS 88 gives $\Gamma(\gamma\gamma) = 7.7 \pm 0.5 \pm 0.5$ eV. We give here $\tau = \hbar/\Gamma(\text{total})$.

WEIGHTED AVERAGE
8.4±0.5 (Error scaled by 2.6)



π^0 DECAY MODES

For decay limits to particles which are not established, see the appropriate Search sections (A^0 (axion) and Other Light Boson (X^0) Searches, etc.).

Mode	Fraction (Γ_i/Γ)	Scale factor/ Confidence level
Γ_1 2γ	(98.823 ± 0.034) %	S=1.5
Γ_2 $e^+ e^- \gamma$	(1.174 ± 0.035) %	S=1.5
Γ_3 γ positronium	(1.82 ± 0.29) × 10 ⁻⁹	
Γ_4 $e^+ e^- e^- e^-$	(3.34 ± 0.16) × 10 ⁻⁵	
Γ_5 $e^+ e^-$	(6.46 ± 0.33) × 10 ⁻⁸	
Γ_6 4γ	< 2 × 10 ⁻⁸	CL=90%
Γ_7 $\nu \bar{\nu}$	[a] < 2.7 × 10 ⁻⁷	CL=90%
Γ_8 $\nu_e \bar{\nu}_e$	< 1.7 × 10 ⁻⁶	CL=90%
Γ_9 $\nu_\mu \bar{\nu}_\mu$	< 1.6 × 10 ⁻⁶	CL=90%
Γ_{10} $\nu_\tau \bar{\nu}_\tau$	< 2.1 × 10 ⁻⁶	CL=90%
Γ_{11} $\gamma \nu \bar{\nu}$	< 6 × 10 ⁻⁴	CL=90%

Charge conjugation (C) or Lepton Family number (LF) violating modes

Γ_{12} 3γ	C	< 3.1 × 10 ⁻⁸	CL=90%
Γ_{13} $\mu^+ e^-$	LF	< 3.8 × 10 ⁻¹⁰	CL=90%
Γ_{14} $\mu^- e^+$	LF	< 3.4 × 10 ⁻⁹	CL=90%
Γ_{15} $\mu^+ e^- + \mu^- e^+$	LF	< 3.6 × 10 ⁻¹⁰	CL=90%

[a] Astrophysical and cosmological arguments give limits of order 10⁻¹³; see the Particle Listings below.

CONSTRAINED FIT INFORMATION

An overall fit to 2 branching ratios uses 6 measurements and one constraint to determine 3 parameters. The overall fit has a $\chi^2 = 4.6$ for 4 degrees of freedom.

The following off-diagonal array elements are the correlation coefficients $\langle \delta x_i \delta x_j \rangle / (\delta x_i \delta x_j)$, in percent, from the fit to the branching fractions, $x_i \equiv \Gamma_i/\Gamma_{\text{total}}$. The fit constrains the x_i whose labels appear in this array to sum to one.

x_2	-100	
x_4	0	-1
	x_1	x_2



$I^G(J^{PC}) = 1^-(0^-+)$

We have omitted some results that have been superseded by later experiments. The omitted results may be found in our 1988 edition Physics Letters **B204** 1 (1988).

π^0 MASS

The value is calculated from m_{π^\pm} and $(m_{\pi^\pm} - m_{\pi^0})$. See also the notes under the π^\pm Mass Listings.

VALUE (MeV)	DOCUMENT ID
134.9766 ± 0.0006 OUR FIT	Error includes scale factor of 1.1.

$m_{\pi^\pm} - m_{\pi^0}$

Measurements with an error > 0.01 MeV have been omitted.

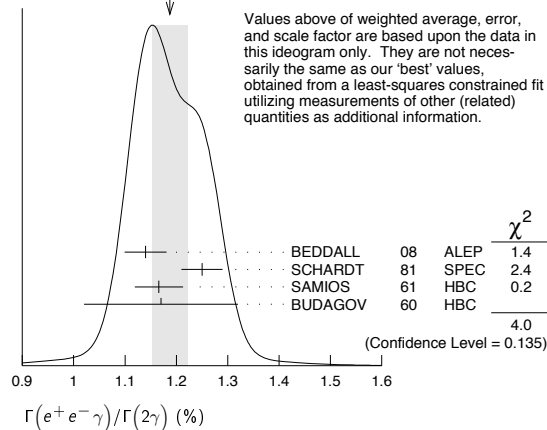
VALUE (MeV)	DOCUMENT ID	TECN	COMMENT
4.5936 ± 0.0005 OUR FIT			
4.5936 ± 0.0005 OUR AVERAGE			
4.59364 ± 0.00048	CRAWFORD 91	CNTR	$\pi^- p \rightarrow \pi^0 n, n$ TOF
4.5930 ± 0.0013	CRAWFORD 86	CNTR	$\pi^- p \rightarrow \pi^0 n, n$ TOF
••• We do not use the following data for averages, fits, limits, etc. •••			
4.59366 ± 0.00048	CRAWFORD 88B	CNTR	See CRAWFORD 91
4.6034 ± 0.0052	VASILEVSKY 66	CNTR	
4.6056 ± 0.0055	CZIRN 63	CNTR	

π^0 MEAN LIFE

Meson Particle Listings

 π^0 π^0 BRANCHING RATIOS $\Gamma(e^+e^-\gamma)/\Gamma(2\gamma)$

VALUE (%)	EVTS	DOCUMENT ID	TECN	COMMENT	Γ_2/Γ_1
1.188 ± 0.035 OUR FIT	Error	includes scale factor of 1.5.			
1.188 ± 0.034 OUR AVERAGE	Error	includes scale factor of 1.4. See the ideogram below.			
1.140 ± 0.024 ± 0.033	12.5k	⁴ BEDDALL	08 ALEP	$e^+e^- \rightarrow Z \rightarrow$ hadrons	
1.25 ± 0.04		SCHARDT	81 SPEC	$\pi^- p \rightarrow n\pi^0$	
1.166 ± 0.047	3071	⁵ SAMIOS	61 HBC	$\pi^- p \rightarrow n\pi^0$	
1.17 ± 0.15	27	BUDAGOV	60 HBC		
• • • We do not use the following data for averages, fits, limits, etc. • • •					
1.196		JOSEPH	60 THEO	QED calculation	

⁴This BEDDALL 08 value is obtained from ALEPH archived data.⁵SAMIOS 61 value uses a Panofsky ratio = 1.62.WEIGHTED AVERAGE
1.188 ± 0.034 (Error scaled by 1.4) $\Gamma(\gamma\text{positronium})/\Gamma(2\gamma)$

VALUE (units 10^{-3})	EVTS	DOCUMENT ID	TECN	COMMENT	Γ_3/Γ_1
1.84 ± 0.29	277	AFANASYEV	90 CNTR	pC 70 GeV	

 $\Gamma(e^+e^+e^-e^-)/\Gamma(2\gamma)$

VALUE (units 10^{-5})	EVTS	DOCUMENT ID	TECN	COMMENT	Γ_4/Γ_1
3.38 ± 0.16 OUR FIT					
3.38 ± 0.16 OUR AVERAGE					
3.46 ± 0.19	30.5k	⁶ ABOUZAID	08D KTEV	$K_L^0 \rightarrow \pi^0\pi^0\pi_{DD}^0$	
3.18 ± 0.30	146	⁷ SAMIOS	62B HBC		

⁶This ABOUZAID 08D value includes all radiative final states. The error includes both statistical and systematic errors. The correlation between the Dalitz-pair planes gives a direct measurement of the π^0 parity. The $\pi^0 2\gamma^*$ form factor is measured and limits are placed on a scalar contribution to the decay.⁷SAMIOS 62B value uses a Panofsky ratio = 1.62. $\Gamma(e^+e^-)/\Gamma_{\text{total}}$ Experimental results are listed; branching ratios corrected for radiative effects are given in the footnotes. BERMAN 60 found $B(\pi^0 \rightarrow e^+e^-) \geq 4.69 \times 10^{-8}$ via an exact QED calculation.

VALUE (units 10^{-8})	EVTS	DOCUMENT ID	TECN	CHG	COMMENT	Γ_5/Γ
6.4 ± 0.33 OUR AVERAGE						
6.44 ± 0.25 ± 0.22	794	⁸ ABOUZAID	07 KTEV		$K_L^0 \rightarrow 3\pi^0$ in flight	
6.9 ± 2.3 ± 0.6	21	⁹ DESHPANDE	93 SPEC		$K^+ \rightarrow \pi^+\pi^0$	
7.6 $\begin{smallmatrix} +2.9 \\ -2.8 \end{smallmatrix}$ ± 0.5	8	¹⁰ MCFARLAND	93 SPEC		$K_L^0 \rightarrow 3\pi^0$ in flight	

• • • We do not use the following data for averages, fits, limits, etc. • • •

6.09 ± 0.40 ± 0.24 275 ¹¹ ALAVI-HARATI 99c SPEC 0 Repl. by ABOUZAID 07⁸ABOUZAID 07 result is for $m_{e^+e^-}/m_{\pi^0} > 0.95$. With radiative corrections the result becomes $(7.48 \pm 0.29 \pm 0.25) \times 10^{-8}$.⁹The DESHPANDE 93 result with bremsstrahlung radiative corrections is $(8.0 \pm 2.6 \pm 0.6) \times 10^{-8}$.¹⁰The MCFARLAND 93 result is for $B[\pi^0 \rightarrow e^+e^-]$, $(m_{e^+e^-}/m_{\pi^0})^2 > 0.95$. With radiative corrections it becomes $(8.8^{+4.5}_{-3.2} \pm 0.6) \times 10^{-8}$.¹¹ALAVI-HARATI 99c quote result for $B[\pi^0 \rightarrow e^+e^-]$, $(m_{e^+e^-}/m_{\pi^0})^2 > 0.95$ to minimize radiative contributions from $\pi^0 \rightarrow e^+e^-\gamma$. After radiative corrections they obtain $(7.04 \pm 0.46 \pm 0.28) \times 10^{-8}$. $\Gamma(e^+e^-)/\Gamma(2\gamma)$

VALUE (units 10^{-7})	CL%	EVTS	DOCUMENT ID	TECN	COMMENT	Γ_5/Γ_1
• • • We do not use the following data for averages, fits, limits, etc. • • •						
<1.3	90		NIEBUHR	89 SPEC	$\pi^- p \rightarrow \pi^0 n$ at rest	
<5.3	90		ZEPHAT	87 SPEC	$\pi^- p \rightarrow \pi^0 n$ 0.3 GeV/c	
1.7 ± 0.6 ± 0.3		59	FRANK	83 SPEC	$\pi^- p \rightarrow n\pi^0$	
1.8 ± 0.6		58	MISCHKE	82 SPEC	See FRANK 83	
2.23 $\begin{smallmatrix} +2.40 \\ -1.10 \end{smallmatrix}$	90	8	FISCHER	78B SPRK	$K^+ \rightarrow \pi^+\pi^0$	

 $\Gamma(4\gamma)/\Gamma_{\text{total}}$

VALUE (units 10^{-8})	CL%	EVTS	DOCUMENT ID	TECN	COMMENT	Γ_6/Γ
< 2	90		MCDONOUGH	88 CBOX	$\pi^- p$ at rest	
• • • We do not use the following data for averages, fits, limits, etc. • • •						
<160	90		BOLOTOV	86c CALO		
<440	90	0	AUERBACH	80 CNTR		

 $\Gamma(\nu\bar{\nu})/\Gamma_{\text{total}}$

The astrophysical and cosmological limits are many orders of magnitude lower, but we use the best laboratory limit for the Summary Tables.

VALUE (units 10^{-6})	CL%	EVTS	DOCUMENT ID	TECN	COMMENT	Γ_7/Γ
< 0.27	90		12 ARTAMONOV	05A B949	$K^+ \rightarrow \pi^+\pi^0$	
• • • We do not use the following data for averages, fits, limits, etc. • • •						
< 0.83	90		12 ATIYA	91 B787	$K^+ \rightarrow \pi^+\nu\nu'$	
< 2.9 × 10 ⁻⁷			13 LAM	91	Cosmological limit	
< 3.2 × 10 ⁻⁷			14 NATALE	91	SN 1987A	
< 6.5	90		DORENBOS..	88 CHR M	Beam dump, prompt ν	

¹²This limit applies to all possible $\nu\nu'$ states as well as to other massless, weakly interacting states.¹³LAM 91 considers the production of right-handed neutrinos produced from the cosmic thermal background at the temperature of about the pion mass through the reaction $\gamma\gamma \rightarrow \pi^0 \rightarrow \nu\bar{\nu}$.¹⁴NATALE 91 considers the excess energy-loss rate from SN1987A if the process $\gamma\gamma \rightarrow \pi^0 \rightarrow \nu\bar{\nu}$ occurs, permitted if the neutrinos have a right-handed component. As pointed out in LAM 91 (and confirmed by Natale), there is a factor 4 error in the NATALE 91 published result (0.8×10^{-7}). $\Gamma(\nu_e\bar{\nu}_e)/\Gamma_{\text{total}}$

VALUE (units 10^{-6})	CL%	DOCUMENT ID	TECN	COMMENT	Γ_8/Γ
<1.7	90	DORENBOS..	88 CHR M	Beam dump, prompt ν	
• • • We do not use the following data for averages, fits, limits, etc. • • •					
<3.1	90	¹⁵ HOFFMAN	88 RVUE	Beam dump, prompt ν	
¹⁵ HOFFMAN 88 analyzes data from a 400-GeV BEBC beam-dump experiment.					

 $\Gamma(\nu_\mu\bar{\nu}_\mu)/\Gamma_{\text{total}}$

VALUE (units 10^{-6})	CL%	EVTS	DOCUMENT ID	TECN	COMMENT	Γ_9/Γ
<1.6	90	8.7	AUERBACH	04 LSND	800 MeV p on Cu	
<3.1	90		¹⁶ HOFFMAN	88 RVUE	Beam dump, prompt ν	
• • • We do not use the following data for averages, fits, limits, etc. • • •						
<7.8	90		DORENBOS..	88 CHR M	Beam dump, prompt ν	
¹⁶ HOFFMAN 88 analyzes data from a 400-GeV BEBC beam-dump experiment.						

 $\Gamma(\nu_\tau\bar{\nu}_\tau)/\Gamma_{\text{total}}$

VALUE (units 10^{-6})	CL%	DOCUMENT ID	TECN	COMMENT	Γ_{10}/Γ
<2.1	90	¹⁷ HOFFMAN	88 RVUE	Beam dump, prompt ν	
• • • We do not use the following data for averages, fits, limits, etc. • • •					
<4.1	90	DORENBOS..	88 CHR M	Beam dump, prompt ν	
¹⁷ HOFFMAN 88 analyzes data from a 400-GeV BEBC beam-dump experiment.					

 $\Gamma(\gamma\nu\bar{\nu})/\Gamma_{\text{total}}$

VALUE	CL%	DOCUMENT ID	TECN	COMMENT	Γ_{11}/Γ
Standard Model prediction is 6×10^{-18}					
<6 × 10 ⁻⁴	90	ATIYA	92 CNTR	$K^+ \rightarrow \gamma\nu\bar{\nu}\pi^+$	

 $\Gamma(3\gamma)/\Gamma_{\text{total}}$

VALUE (units 10^{-8})	CL%	EVTS	DOCUMENT ID	TECN	COMMENT	Γ_{12}/Γ
< 3.1	90		MCDONOUGH	88 CBOX	$\pi^- p$ at rest	
• • • We do not use the following data for averages, fits, limits, etc. • • •						
< 38	90	0	HIGHLAND	80 CNTR		
<150	90	0	AUERBACH	78 CNTR		
<490	90	0	¹⁸ DUCLOS	65 CNTR		
<490	90		¹⁸ KUTIN	65 CNTR		

¹⁸These experiments give $B(3\gamma/2\gamma) < 5.0 \times 10^{-6}$.

Meson Particle Listings

 η

Charged modes

Γ_8	charged modes	(28.10±0.34) %	S=1.2
Γ_9	$\pi^+\pi^-\pi^0$	(22.74±0.28) %	S=1.2
Γ_{10}	$\pi^+\pi^-\gamma$	(4.60±0.16) %	S=2.1
Γ_{11}	$e^+e^-\gamma$	(7.0 ± 0.7) × 10 ⁻³	S=1.5
Γ_{12}	$\mu^+\mu^-\gamma$	(3.1 ± 0.4) × 10 ⁻⁴	
Γ_{13}	e^+e^-	< 2.7 × 10 ⁻⁵	CL=90%
Γ_{14}	$\mu^+\mu^-$	(5.8 ± 0.8) × 10 ⁻⁶	
Γ_{15}	$2e^+2e^-$	< 6.9 × 10 ⁻⁵	CL=90%
Γ_{16}	$\pi^+\pi^-e^+e^-(\gamma)$	(2.68±0.11) × 10 ⁻⁴	
Γ_{17}	$e^+e^-\mu^+\mu^-$	< 1.6 × 10 ⁻⁴	CL=90%
Γ_{18}	$2\mu^+2\mu^-$	< 3.6 × 10 ⁻⁴	CL=90%
Γ_{19}	$\mu^+\mu^-\pi^+\pi^-$	< 3.6 × 10 ⁻⁴	CL=90%
Γ_{20}	$\pi^+\pi^-2\gamma$	< 2.0 × 10 ⁻³	
Γ_{21}	$\pi^+\pi^-\pi^0\gamma$	< 5 × 10 ⁻⁴	CL=90%
Γ_{22}	$\pi^0\mu^+\mu^-\gamma$	< 3 × 10 ⁻⁶	CL=90%

Charge conjugation (C), Parity (P),
Charge conjugation × Parity (CP), or
Lepton Family number (LF) violating modes

Γ_{23}	$\pi^0\gamma$	C	< 9 × 10 ⁻⁵	CL=90%
Γ_{24}	$\pi^+\pi^-$	P,CP	< 1.3 × 10 ⁻⁵	CL=90%
Γ_{25}	$2\pi^0$	P,CP	< 3.5 × 10 ⁻⁴	CL=90%
Γ_{26}	$2\pi^0\gamma$	C	< 5 × 10 ⁻⁴	CL=90%
Γ_{27}	$3\pi^0\gamma$	C	< 6 × 10 ⁻⁵	CL=90%
Γ_{28}	3γ	C	< 1.6 × 10 ⁻⁵	CL=90%
Γ_{29}	$4\pi^0$	P,CP	< 6.9 × 10 ⁻⁷	CL=90%
Γ_{30}	$\pi^0e^+e^-$	C	[a] < 4 × 10 ⁻⁵	CL=90%
Γ_{31}	$\pi^0\mu^+\mu^-$	C	[a] < 5 × 10 ⁻⁶	CL=90%
Γ_{32}	$\mu^+e^- + \mu^-e^+$	LF	< 6 × 10 ⁻⁶	CL=90%

[a] C parity forbids this to occur as a single-photon process.

CONSTRAINED FIT INFORMATION

An overall fit to a decay rate and 19 branching ratios uses 48 measurements and one constraint to determine 9 parameters. The overall fit has a $\chi^2 = 56.0$ for 40 degrees of freedom.

The following *off-diagonal* array elements are the correlation coefficients $\langle \delta x_i \delta x_j \rangle / (\delta x_i \delta x_j)$, in percent, from the fit to the branching fractions, $x_i \equiv \Gamma_i / \Gamma_{\text{total}}$. The fit constrains the x_i whose labels appear in this array to sum to one.

x_3	26								
x_4	-1	-1							
x_9	-64	-71	-1						
x_{10}	-44	-45	0	11					
x_{11}	-9	-9	0	-8	-3				
x_{12}	0	0	0	-1	0	0			
x_{16}	0	0	0	0	0	0	0		
Γ	-10	-3	0	6	4	1	0	0	
	x_2	x_3	x_4	x_9	x_{10}	x_{11}	x_{12}	x_{16}	

Mode	Rate (keV)	Scale factor	
Γ_2	2γ	0.510 ± 0.026	
Γ_3	$3\pi^0$	0.423 ± 0.022	
Γ_4	$\pi^0 2\gamma$	(3.5 ± 0.7) × 10 ⁻⁴	
Γ_9	$\pi^+\pi^-\pi^0$	0.295 ± 0.016	
Γ_{10}	$\pi^+\pi^-\gamma$	0.060 ± 0.004	1.2
Γ_{11}	$e^+e^-\gamma$	0.0091 ± 0.0010	1.3
Γ_{12}	$\mu^+\mu^-\gamma$	(4.0 ± 0.6) × 10 ⁻⁴	
Γ_{16}	$\pi^+\pi^-e^+e^-(\gamma)$	(3.48 ± 0.23) × 10 ⁻⁴	

 η DECAY RATES $\Gamma(2\gamma)$ Γ_2

See the table immediately above giving the fitted decay rates. Following the advice of NEFKENS 02, we have removed the Primakoff-effect measurement from the average. See also the "Note on the Decay Width $\Gamma(\eta \rightarrow \gamma\gamma)$," in our 1994 edition, Phys. Rev. D50, 1 August 1994, Part I, p. 1451, for a discussion of the various measurements.

VALUE (keV)	EVTS	DOCUMENT ID	TECN	COMMENT
0.510±0.026 OUR FIT				
0.510±0.026 OUR AVERAGE				
0.51 ± 0.12 ± 0.05	36	BARU	90 MD1	$e^+e^- \rightarrow e^+e^-\eta$
0.490±0.010±0.048	2287	ROE	90 ASP	$e^+e^- \rightarrow e^+e^-\eta$
0.514±0.017±0.035	1295	WILLIAMS	88 CBAL	$e^+e^- \rightarrow e^+e^-\eta$
0.53 ± 0.04 ± 0.04		BARTEL	85E JADE	$e^+e^- \rightarrow e^+e^-\eta$

• • • We do not use the following data for averages, fits, limits, etc. • • •

0.476±0.062		² RODRIGUES	08 CNTR	Reanalysis
0.64 ± 0.14 ± 0.13		AIHARA	86 TPC	$e^+e^- \rightarrow e^+e^-\eta$
0.56 ± 0.16	56	WEINSTEIN	83 CBAL	$e^+e^- \rightarrow e^+e^-\eta$
0.324±0.046		BROWMAN	74B CNTR	Primakoff effect
1.00 ± 0.22		³ BEMPORAD	67 CNTR	Primakoff effect

² RODRIGUES 08 uses a more sophisticated calculation for the inelastic background due to incoherent photoproduction to reanalyze the η photoproduction data on Be and Cu at 9 GeV from BROWMAN 74B. This brings the value of $\Gamma(\eta \rightarrow 2\gamma)$ in line with direct measurements of the width. The error here is only statistical.

³ BEMPORAD 67 gives $\Gamma(2\gamma) = 1.21 \pm 0.26$ keV assuming $\Gamma(2\gamma)/\Gamma(\text{total}) = 0.314$. Bemporad private communication gives $\Gamma(2\gamma)/\Gamma(\text{total}) = 0.380 \pm 0.083$. We evaluate this using $\Gamma(2\gamma)/\Gamma(\text{total}) = 0.38 \pm 0.01$. Not included in average because the uncertainty resulting from the separation of the coulomb and nuclear amplitudes has apparently been underestimated.

 η BRANCHING RATIOS

Neutral modes

$\Gamma(\text{neutral modes})/\Gamma_{\text{total}}$		$\Gamma_1/\Gamma = (\Gamma_2+\Gamma_3+\Gamma_4)/\Gamma$	
VALUE	EVTS	DOCUMENT ID	TECN COMMENT
0.7190±0.0034 OUR FIT			Error includes scale factor of 1.2.
0.705 ± 0.008	16k	BASILE	71D CNTR MM spectrometer
• • • We do not use the following data for averages, fits, limits, etc. • • •			
0.79 ± 0.08		BUNIATOV	67 OSPK

$\Gamma(2\gamma)/\Gamma_{\text{total}}$ Γ_2/Γ

VALUE (units 10 ⁻²)	EVTS	DOCUMENT ID	TECN	COMMENT
39.31±0.20 OUR FIT				Error includes scale factor of 1.1.
39.49±0.17±0.30	65k	ABEGG	96 SPEC	$pd \rightarrow {}^3\text{He}\eta$
• • • We do not use the following data for averages, fits, limits, etc. • • •				
38.45±0.40±0.36	14k	⁴ LOPEZ	07 CLEO	$\psi(2S) \rightarrow J/\psi\eta$

⁴ Not independent of other results listed for LOPEZ 07. Assuming decays of $\eta \rightarrow \gamma\gamma$, $3\pi^0$, $\pi^+\pi^-\pi^0$, $\pi^+\pi^-\gamma$, and $e^+e^-\gamma$ account for all η decays within a contribution of 0.3% to the systematic error.

$\Gamma(2\gamma)/\Gamma(\text{neutral modes})$ $\Gamma_2/\Gamma_1 = \Gamma_2/(\Gamma_2+\Gamma_3+\Gamma_4)$

VALUE	EVTS	DOCUMENT ID	TECN	COMMENT
0.5467±0.0019 OUR FIT				Error includes scale factor of 1.5.
0.548 ± 0.023 OUR AVERAGE				
0.535 ± 0.018		BUTTRAM	70 OSPK	
0.59 ± 0.033		BUNIATOV	67 OSPK	
• • • We do not use the following data for averages, fits, limits, etc. • • •				
0.52 ± 0.09	88	ABROSIMOV	80 HLBC	
0.60 ± 0.14	113	KENDALL	74 OSPK	
0.57 ± 0.09		STRUGALSKI	71 HLBC	
0.579 ± 0.052		FELDMAN	67 OSPK	
0.416 ± 0.044		DIGIUGNO	66 CNTR	Error doubled
0.44 ± 0.07		GRUNHAUS	66 OSPK	
0.39 ± 0.06		⁵ JONES	66 CNTR	

⁵ This result from combining cross sections from two different experiments.

$\Gamma(3\pi^0)/\Gamma_{\text{total}}$ Γ_3/Γ

VALUE (units 10 ⁻²)	EVTS	DOCUMENT ID	TECN	COMMENT
32.57±0.23 OUR FIT				Error includes scale factor of 1.1.
• • • We do not use the following data for averages, fits, limits, etc. • • •				
34.03±0.56±0.49	1821	⁶ LOPEZ	07 CLEO	$\psi(2S) \rightarrow J/\psi\eta$

⁶ Not independent of other results listed for LOPEZ 07. Assuming decays of $\eta \rightarrow \gamma\gamma$, $3\pi^0$, $\pi^+\pi^-\pi^0$, $\pi^+\pi^-\gamma$, and $e^+e^-\gamma$ account for all η decays within a contribution of 0.3% to the systematic error.

$\Gamma(3\pi^0)/\Gamma(\text{neutral modes})$ $\Gamma_3/\Gamma_1 = \Gamma_3/(\Gamma_2+\Gamma_3+\Gamma_4)$

VALUE	EVTS	DOCUMENT ID	TECN	COMMENT
0.4529±0.0019 OUR FIT				
0.439 ± 0.024				
• • • We do not use the following data for averages, fits, limits, etc. • • •				
0.44 ± 0.08	75	ABROSIMOV	80 HLBC	
0.32 ± 0.09		STRUGALSKI	71 HLBC	
0.41 ± 0.033		BUNIATOV	67 OSPK	Not indep. of $\Gamma(2\gamma)/\Gamma(\text{neutral modes})$
0.177 ± 0.035		FELDMAN	67 OSPK	
0.209 ± 0.054		DIGIUGNO	66 CNTR	Error doubled
0.29 ± 0.10		GRUNHAUS	66 OSPK	

$\Gamma(3\pi^0)/\Gamma(2\gamma)$ Γ_3/Γ_2

VALUE	EVTS	DOCUMENT ID	TECN	COMMENT
0.828±0.006 OUR FIT				
0.829±0.007 OUR AVERAGE				
0.884±0.022±0.019	1821	LOPEZ	07 CLEO	$\psi(2S) \rightarrow J/\psi\eta$
0.817±0.012±0.032	17.4k	⁷ AKHMESHIN	05 CMD2	$e^+e^- \rightarrow \phi \rightarrow \eta\gamma$
0.826±0.024		ACHASOV	00D SND	$e^+e^- \rightarrow \phi \rightarrow \eta\gamma$
0.832±0.005±0.012		KRUSCHE	95D SPEC	$\gamma p \rightarrow \eta p$, threshold
0.841±0.034		AMSLER	93 CBAR	$\bar{p}p \rightarrow \pi^+\pi^-\eta$ at rest
0.822±0.009		ALDE	84 GAM2	

• • • We do not use the following data for averages, fits, limits, etc. • • •

0.796 ± 0.016 ± 0.016	ACHASOV	00	SND	See ACHASOV 00D
0.91 ± 0.14	COX	70B	HBC	
0.75 ± 0.09	DEVONS	70	OSPK	
0.88 ± 0.16	BALTAY	67D	DBC	
1.1 ± 0.2	CENCE	67	OSPK	
1.25 ± 0.39	BACCI	63	CNTR	Inverse BR reported

⁷ Uses result from AKHMETSHIN 01B.

$\Gamma(\pi^0 2\gamma)/\Gamma_{total}$ Γ_4/Γ

Early results are summarized in the review by LANDSBERG 85.

VALUE (units 10^{-4})	CL%	EVTS	DOCUMENT ID	TECN	COMMENT
2.7 ± 0.5 OUR FIT					Error includes scale factor of 1.1.
2.21 ± 0.24 ± 0.47	≈ 500	⁸ PRAKHOV	08	CRYB	$\pi^- \rho \rightarrow \eta n \approx$ threshold

• • • We do not use the following data for averages, fits, limits, etc. • • •

3.5 ± 0.7 ± 0.6	1.6k	^{9,10} PRAKHOV	05	CRYB	See PRAKHOV 08
<8.4	90	7	ACHASOV	01D	SND $e^+ e^- \rightarrow \phi \rightarrow \eta \gamma$
<30	90	0	DAVYDOV	81	GAM2 $\pi^- \rho \rightarrow \eta n$

⁸ PRAKHOV 08 is a reanalysis of the data of PRAKHOV 05, using for the first time the invariant-mass spectrum of the two photons.

⁹ Normalized using $\Gamma(\eta \rightarrow 2\gamma)/\Gamma = 0.3943 \pm 0.0026$.

¹⁰ This measurement and the independent analysis of the same data by KNECHT 04 both imply a lower value of $\Gamma(\pi^0 2\gamma)$ than the one obtained by ALDE 84 from $\Gamma(\pi^0 2\gamma)/\Gamma(2\gamma)$.

$\Gamma(\pi^0 2\gamma)/\Gamma(2\gamma)$ Γ_4/Γ_2

VALUE (units 10^{-3})	EVTS	DOCUMENT ID	TECN	CHG	COMMENT
0.69 ± 0.13 OUR FIT					Error includes scale factor of 1.1.
1.8 ± 0.4		ALDE	84	GAM2	0

• • • We do not use the following data for averages, fits, limits, etc. • • •

2.5 ± 0.6	70	BINON	82	GAM2	See ALDE 84
-----------	----	-------	----	------	-------------

$\Gamma(\pi^0 2\gamma)/\Gamma(3\pi^0)$ Γ_4/Γ_3

VALUE (units 10^{-4})	DOCUMENT ID	TECN	COMMENT
8.3 ± 1.6 OUR FIT			Error includes scale factor of 1.1.

• • • We do not use the following data for averages, fits, limits, etc. • • •

8.3 ± 2.8 ± 1.4	¹¹ KNECHT	04	CRYB	$\pi^- \rho \rightarrow n \eta$
-----------------	----------------------	----	------	---------------------------------

¹¹ Independent analysis of same data as PRAKHOV 05.

$\Gamma(2\pi^0 2\gamma)/\Gamma_{total}$ Γ_5/Γ

VALUE	CL%	DOCUMENT ID	TECN	COMMENT
<1.2 × 10⁻³	90	¹² NEFKENS	05A	CRYB $p(720 \text{ MeV}/c) \pi^- \rightarrow n \eta$

• • • We do not use the following data for averages, fits, limits, etc. • • •

<4.0 × 10 ⁻³	90	BLIK	07	GAM4 $\pi^- \rho \rightarrow \eta n$
-------------------------	----	------	----	--------------------------------------

¹² Measurement is done in limited $\gamma\gamma$ energy range.

$\Gamma(4\gamma)/\Gamma_{total}$ Γ_6/Γ

VALUE	CL%	DOCUMENT ID	TECN	COMMENT
<2.8 × 10⁻⁴	90	BLIK	07	GAM4 $\pi^- \rho \rightarrow \eta n$

$\Gamma(\text{invisible})/\Gamma(2\gamma)$ Γ_7/Γ_2

VALUE	CL%	DOCUMENT ID	TECN	COMMENT
<1.65 × 10⁻³	90	¹³ ABLIKIM	06Q	BES2 $J/\psi \rightarrow \phi \eta$

¹³ Based on 58M J/ψ decays.

Charged modes

$\Gamma(\pi^+ \pi^- \pi^0)/\Gamma_{total}$ Γ_9/Γ

VALUE (units 10^{-2})	EVTS	DOCUMENT ID	TECN	COMMENT
22.74 ± 0.28 OUR FIT				Error includes scale factor of 1.2.

• • • We do not use the following data for averages, fits, limits, etc. • • •

22.60 ± 0.35 ± 0.29	3915	¹⁴ LOPEZ	07	CLEO $\psi(2S) \rightarrow J/\psi \eta$
---------------------	------	---------------------	----	---

¹⁴ Not independent of other results listed for LOPEZ 07. Assuming decays of $\eta \rightarrow \gamma \gamma$, $3\pi^0$, $\pi^+ \pi^- \pi^0$, $\pi^+ \pi^- \gamma$, and $e^+ e^- \gamma$ account for all η decays within a contribution of 0.3% to the systematic error.

$\Gamma(\text{neutral modes})/\Gamma(\pi^+ \pi^- \pi^0)$ $\Gamma_1/\Gamma_9 = (\Gamma_2 + \Gamma_3 + \Gamma_4)/\Gamma_9$

VALUE	EVTS	DOCUMENT ID	TECN	
3.16 ± 0.05 OUR FIT			Error includes scale factor of 1.2.	
3.26 ± 0.30 OUR AVERAGE				
2.54 ± 1.89	74	KENDALL	74	OSPK
3.4 ± 1.1	29	AGUILAR...	72B	HBC
2.83 ± 0.80	70	BLOODWORTH...	72B	HBC
3.6 ± 0.6	244	FLATTE	67B	HBC
2.89 ± 0.56		ALFF...	66	HBC
3.6 ± 0.8	50	KRAEMER	64	DBC
3.8 ± 1.1		PAULI	64	DBC

¹⁵ Error increased from published value 0.5 by Bloodworth (private communication).

$\Gamma(2\gamma)/\Gamma(\pi^+ \pi^- \pi^0)$ Γ_2/Γ_9

VALUE	EVTS	DOCUMENT ID	TECN	COMMENT
1.728 ± 0.028 OUR FIT				Error includes scale factor of 1.2.
1.70 ± 0.04 OUR AVERAGE				
1.704 ± 0.032 ± 0.026	3915	¹⁶ LOPEZ	07	CLEO $\psi(2S) \rightarrow J/\psi \eta$
1.61 ± 0.14		ABLIKIM	06E	BES2 $e^+ e^- \rightarrow J/\psi \rightarrow \eta \gamma$
1.78 ± 0.10 ± 0.13	1077	AMSLER	95	CBAR $\bar{p} p \rightarrow \pi^+ \pi^- \eta$ at rest
1.72 ± 0.25	401	BAGLIN	69	HLBC
1.61 ± 0.39		FOSTER	65	HBC

¹⁶ LOPEZ 07 reports $\Gamma(\eta \rightarrow \pi^+ \pi^- \pi^0) / \Gamma(\eta \rightarrow 2\gamma) = \Gamma_9/\Gamma_2 = 0.587 \pm 0.011 \pm 0.009$.

$\Gamma(3\pi^0)/\Gamma(\pi^+ \pi^- \pi^0)$ Γ_3/Γ_9

VALUE	EVTS	DOCUMENT ID	TECN	COMMENT
1.432 ± 0.026 OUR FIT				Error includes scale factor of 1.2.
1.48 ± 0.05 OUR AVERAGE				
1.46 ± 0.03 ± 0.09		ACHASOV	06A	SND $e^+ e^- \rightarrow \eta \gamma$
1.52 ± 0.04 ± 0.08	23k	¹⁷ AKHMETSHIN	01B	CMD2 $e^+ e^- \rightarrow \phi \rightarrow \eta \gamma$
1.44 ± 0.09 ± 0.10	1627	AMSLER	95	CBAR $\bar{p} p \rightarrow \pi^+ \pi^- \eta$ at rest
1.50 ^{+0.15} _{-0.29}	199	BAGLIN	69	HLBC
1.47 ^{+0.20} _{-0.17}		BULLOCK	68	HLBC

• • • We do not use the following data for averages, fits, limits, etc. • • •

1.3 ± 0.4		BAGLIN	67B	HLBC
0.90 ± 0.24		FOSTER	65	HBC
2.0 ± 1.0		FOELSCH	64	HBC
0.83 ± 0.32		CRAWFORD	63	HBC

¹⁷ AKHMETSHIN 01B uses results from AKHMETSHIN 99F.

$\Gamma(\pi^+ \pi^- \pi^0)/[\Gamma(2\gamma) + \Gamma(3\pi^0)]$ $\Gamma_9/(\Gamma_2 + \Gamma_3)$

VALUE	DOCUMENT ID	TECN	COMMENT
0.316 ± 0.005 OUR FIT			Error includes scale factor of 1.2.
0.304 ± 0.012			
	ACHASOV	00D	SND $e^+ e^- \rightarrow \phi \rightarrow \eta \gamma$

• • • We do not use the following data for averages, fits, limits, etc. • • •

0.3141 ± 0.0081 ± 0.0058	ACHASOV	00B	SND See ACHASOV 00D
--------------------------	---------	-----	---------------------

$\Gamma(\pi^+ \pi^- \gamma)/\Gamma_{total}$ Γ_{10}/Γ

VALUE (units 10^{-2})	EVTS	DOCUMENT ID	TECN	COMMENT
4.60 ± 0.16 OUR FIT				Error includes scale factor of 2.1.

• • • We do not use the following data for averages, fits, limits, etc. • • •

3.96 ± 0.14 ± 0.14	859	¹⁸ LOPEZ	07	CLEO $\psi(2S) \rightarrow J/\psi \eta$
--------------------	-----	---------------------	----	---

¹⁸ Not independent of other results listed for LOPEZ 07. Assuming decays of $\eta \rightarrow \gamma \gamma$, $3\pi^0$, $\pi^+ \pi^- \pi^0$, $\pi^+ \pi^- \gamma$, and $e^+ e^- \gamma$ account for all η decays within a contribution of 0.3% to the systematic error.

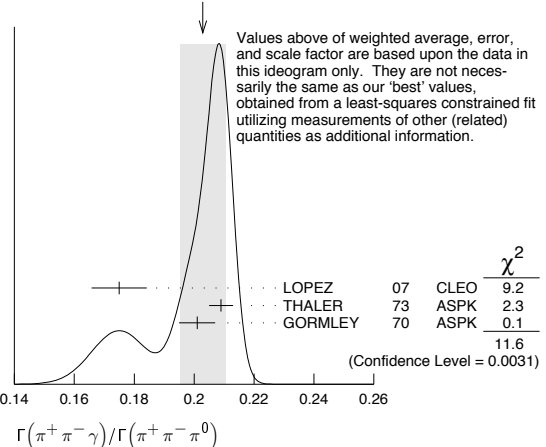
$\Gamma(\pi^+ \pi^- \gamma)/\Gamma(\pi^+ \pi^- \pi^0)$ Γ_{10}/Γ_9

VALUE	EVTS	DOCUMENT ID	TECN	COMMENT
0.202 ± 0.007 OUR FIT				Error includes scale factor of 2.4.
0.203 ± 0.008 OUR AVERAGE				Error includes scale factor of 2.4. See the ideogram below.
0.175 ± 0.007 ± 0.006	859	LOPEZ	07	CLEO $\psi(2S) \rightarrow J/\psi \eta$
0.209 ± 0.004	18k	THALER	73	ASPK
0.201 ± 0.006	7250	GORMLEY	70	ASPK

• • • We do not use the following data for averages, fits, limits, etc. • • •

0.28 ± 0.04		BALTAY	67B	DBC
0.25 ± 0.035		LITCHFIELD	67	DBC
0.30 ± 0.06		CRAWFORD	66	HBC
0.196 ± 0.041		FOSTER	65c	HBC

WEIGHTED AVERAGE
0.203 ± 0.008 (Error scaled by 2.4)



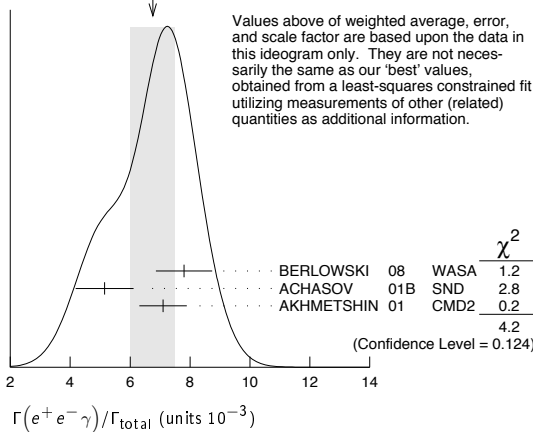
Meson Particle Listings

 η

$\Gamma(e^+e^-\gamma)/\Gamma_{\text{total}}$		Γ_{11}/Γ		
VALUE (units 10^{-3})	EVTS	DOCUMENT ID	TECN	COMMENT
7.0 ± 0.7 OUR FIT				Error includes scale factor of 1.5.
6.8 ± 0.7 OUR AVERAGE				Error includes scale factor of 1.4. See the ideogram below.
7.8 ± 0.5 ± 0.8	435 ± 31	BERLOWSKI 08	WASA	$p d \rightarrow {}^3\text{He } \eta$
5.15 ± 0.62 ± 0.74	283	ACHASOV 01B	SND	$e^+e^- \rightarrow \phi \rightarrow \eta\gamma$
7.10 ± 0.64 ± 0.46	323	AKHMETSHIN 01	CMD2	$e^+e^- \rightarrow \phi \rightarrow \eta\gamma$
• • • We do not use the following data for averages, fits, limits, etc. • • •				
9.4 ± 0.7 ± 0.5	172	¹⁹ LOPEZ 07	CLEO	$\psi(2S) \rightarrow J/\psi\eta$

¹⁹Not independent of other results listed for LOPEZ 07. Assuming decays of $\eta \rightarrow \gamma\gamma$, $3\pi^0$, $\pi^+\pi^-\pi^0$, $\pi^+\pi^-\gamma$, and $e^+e^-\gamma$ account for all η decays within a contribution of 0.3% to the systematic error.

WEIGHTED AVERAGE
6.8±0.7 (Error scaled by 1.4)



$\Gamma(e^+e^-\gamma)/\Gamma(\pi^+\pi^-\gamma)$		Γ_{11}/Γ_{10}		
VALUE	EVTS	DOCUMENT ID	TECN	COMMENT
0.153 ± 0.016 OUR FIT				Error includes scale factor of 1.6.
0.237 ± 0.021 ± 0.015	172	LOPEZ 07	CLEO	$\psi(2S) \rightarrow J/\psi\eta$

$\Gamma(e^+e^-\gamma)/\Gamma(\pi^+\pi^-\pi^0)$		Γ_{11}/Γ_9		
VALUE (units 10^{-2})	EVTS	DOCUMENT ID	TECN	COMMENT
3.10 ± 0.30 OUR FIT				Error includes scale factor of 1.5.
2.1 ± 0.5	80	JANE 75B	OSPK	See the erratum

$\Gamma(\text{neutral modes})/[\Gamma(\pi^+\pi^-\pi^0) + \Gamma(\pi^+\pi^-\gamma) + \Gamma(e^+e^-\gamma)]$		$\Gamma_1/(\Gamma_9 + \Gamma_{10} + \Gamma_{11}) = (\Gamma_2 + \Gamma_3 + \Gamma_4)/(\Gamma_9 + \Gamma_{10} + \Gamma_{11})$		
VALUE	EVTS	DOCUMENT ID	TECN	COMMENT
2.56 ± 0.04 OUR FIT				Error includes scale factor of 1.2.
2.64 ± 0.23		BALTAY 67B	DBC	
• • • We do not use the following data for averages, fits, limits, etc. • • •				
4.5 ± 1.0	280	²⁰ JAMES 66	HBC	
3.20 ± 1.26	53	²⁰ BASTIEN 62	HBC	
2.5 ± 1.0	10	²⁰ PICKUP 62	HBC	

²⁰These experiments are not used in the averages as they do not separate clearly $\eta \rightarrow \pi^+\pi^-\pi^0$ and $\eta \rightarrow \pi^+\pi^-\gamma$ from each other. The reported values thus probably contain some unknown fraction of $\eta \rightarrow \pi^+\pi^-\gamma$.

$\Gamma(2\gamma)/[\Gamma(\pi^+\pi^-\pi^0) + \Gamma(\pi^+\pi^-\gamma) + \Gamma(e^+e^-\gamma)]$		$\Gamma_2/(\Gamma_9 + \Gamma_{10} + \Gamma_{11})$		
VALUE	EVTS	DOCUMENT ID	TECN	COMMENT
1.402 ± 0.023 OUR FIT				Error includes scale factor of 1.2.
1.1 ± 0.4 OUR AVERAGE				
1.51 ± 0.93	75	KENDALL 74	OSPK	
0.99 ± 0.48		CRAWFORD 63	HBC	

$\Gamma(\mu^+\mu^-\gamma)/\Gamma_{\text{total}}$		Γ_{12}/Γ		
VALUE (units 10^{-4})	EVTS	DOCUMENT ID	TECN	COMMENT
3.1 ± 0.4 OUR FIT				
3.1 ± 0.4	600	DZHELADIN 80	SPEC	$\pi^- p \rightarrow \eta n$
• • • We do not use the following data for averages, fits, limits, etc. • • •				
1.5 ± 0.75	100	BUSHNIN 78	SPEC	See DZHELADIN 80

$\Gamma(e^+e^-)/\Gamma_{\text{total}}$		Γ_{13}/Γ		
VALUE	CL%	DOCUMENT ID	TECN	COMMENT
< 2.7 × 10⁻⁵	90	BERLOWSKI 08	WASA	$p d \rightarrow {}^3\text{He } \eta$
• • • We do not use the following data for averages, fits, limits, etc. • • •				
< 0.77 × 10 ⁻⁴	90	BROWDER 97B	CLE2	$e^+e^- \sim 10.5 \text{ GeV}$
< 2 × 10 ⁻⁴	90	WHITE 96	SPEC	$p d \rightarrow \eta^3\text{He}$
< 3 × 10 ⁻⁴	90	DAVIES 74	RVUE	Uses ESTEN 67

$\Gamma(\mu^+\mu^-)/\Gamma_{\text{total}}$		Γ_{14}/Γ			
VALUE (units 10^{-6})	CL%	EVTS	DOCUMENT ID	TECN	COMMENT
5.8 ± 0.8 OUR AVERAGE					
5.7 ± 0.7 ± 0.5	114		ABEGG 94	SPEC	$p d \rightarrow \eta^3\text{He}$
6.5 ± 2.1	27		DZHELADIN 80B	SPEC	$\pi^- p \rightarrow \eta n$
• • • We do not use the following data for averages, fits, limits, etc. • • •					
5.6 ^{+0.6} _{-0.7} ± 0.5	100		KESSLER 93	SPEC	See ABEGG 94
< 20	95	0	WEHMANN 68	OSPK	

$\Gamma(\mu^+\mu^-)/\Gamma(2\gamma)$		Γ_{14}/Γ_2		
VALUE (units 10^{-5})	CL%	DOCUMENT ID	TECN	COMMENT
• • • We do not use the following data for averages, fits, limits, etc. • • •				
5.9 ± 2.2		HYAMS 69	OSPK	

$\Gamma(2e^+2e^-)/\Gamma_{\text{total}}$		Γ_{15}/Γ		
VALUE	CL%	DOCUMENT ID	TECN	COMMENT
< 6.9 × 10⁻⁵	90	AKHMETSHIN 01	CMD2	$e^+e^- \rightarrow \phi \rightarrow \eta\gamma$
• • • We do not use the following data for averages, fits, limits, etc. • • •				
< 9.7 × 10 ⁻⁵	90	BERLOWSKI 08	WASA	$p d \rightarrow {}^3\text{He } \eta$

$\Gamma(\pi^+\pi^-e^+e^-(\gamma))/\Gamma_{\text{total}}$		Γ_{16}/Γ		
VALUE (units 10^{-4})	EVTS	DOCUMENT ID	TECN	COMMENT
2.68 ± 0.11 OUR FIT				
2.68 ± 0.09 ± 0.07	1555 ± 52	²¹ AMBROSINO 09B	KLOE	$e^+e^- \rightarrow \phi \rightarrow \eta\gamma$
• • • We do not use the following data for averages, fits, limits, etc. • • •				
4.3 ^{+2.0} _{-1.6} ± 0.4	16	BERLOWSKI 08	WASA	$p d \rightarrow {}^3\text{He } \eta$
4.3 ± 1.3 ± 0.4	16	BARGHOLTZ 07	CNTR	See BERLOWSKI 08
3.7 ^{+2.5} _{-1.8} ± 0.3	4	AKHMETSHIN 01	CMD2	$e^+e^- \rightarrow \phi \rightarrow \eta\gamma$

²¹This AMBROSINO 09B value includes radiative events.

$\Gamma(e^+e^-\mu^+\mu^-)/\Gamma_{\text{total}}$		Γ_{17}/Γ		
VALUE	CL%	DOCUMENT ID	TECN	COMMENT
< 1.6 × 10⁻⁴	90	BERLOWSKI 08	WASA	$p d \rightarrow {}^3\text{He } \eta$

$\Gamma(2\mu^+2\mu^-)/\Gamma_{\text{total}}$		Γ_{18}/Γ		
VALUE	CL%	DOCUMENT ID	TECN	COMMENT
< 3.6 × 10⁻⁴	90	BERLOWSKI 08	WASA	$p d \rightarrow {}^3\text{He } \eta$

$\Gamma(\mu^+\mu^-\pi^+\pi^-)/\Gamma_{\text{total}}$		Γ_{19}/Γ		
VALUE	CL%	DOCUMENT ID	TECN	COMMENT
< 3.6 × 10⁻⁴	90	BERLOWSKI 08	WASA	$p d \rightarrow {}^3\text{He } \eta$

$\Gamma(\pi^+\pi^-2\gamma)/\Gamma(\pi^+\pi^-\pi^0)$		Γ_{20}/Γ_9		
VALUE	CL%	DOCUMENT ID	TECN	COMMENT
< 9 × 10⁻³		PRICE 67	HBC	
• • • We do not use the following data for averages, fits, limits, etc. • • •				
< 16 × 10 ⁻³	95	BALTAY 67B	DBC	

$\Gamma(\pi^+\pi^-\pi^0\gamma)/\Gamma(\pi^+\pi^-\pi^0)$		Γ_{21}/Γ_9			
VALUE	CL%	EVTS	DOCUMENT ID	TECN	COMMENT
< 0.24 × 10⁻²	90	0	THALER 73	ASPK	
• • • We do not use the following data for averages, fits, limits, etc. • • •					
< 1.7 × 10 ⁻²	90		ARNOLD 68	HLBC	
< 1.6 × 10 ⁻²	95		BALTAY 67B	DBC	
< 7.0 × 10 ⁻²			FLATTE 67	HBC	
< 0.9 × 10 ⁻²			PRICE 67	HBC	

$\Gamma(\pi^0\mu^+\mu^-)/\Gamma_{\text{total}}$		Γ_{22}/Γ		
VALUE	CL%	DOCUMENT ID	TECN	COMMENT
< 3 × 10⁻⁶	90	DZHELADIN 81	SPEC	$\pi^- p \rightarrow \eta n$

Forbidden modes

$\Gamma(\pi^0\gamma)/\Gamma_{\text{total}}$		Γ_{23}/Γ		
Forbidden by angular momentum conservation.				
VALUE	CL%	DOCUMENT ID	TECN	COMMENT
< 9 × 10⁻⁵	90	NEFKENS 05A	CRYB	$p(720 \text{ MeV}/c) \pi^- \rightarrow n\eta$

$\Gamma(\pi^+\pi^-)/\Gamma_{\text{total}}$		Γ_{24}/Γ			
Forbidden by P and CP invariance.					
VALUE	CL%	EVTS	DOCUMENT ID	TECN	COMMENT
< 0.13 × 10⁻⁴	90	16M	AMBROSINO 05A	KLOE	$e^+e^- \rightarrow \phi \rightarrow \eta\gamma$
• • • We do not use the following data for averages, fits, limits, etc. • • •					
< 3.3 × 10 ⁻⁴	90		AKHMETSHIN 99B	CMD2	$e^+e^- \rightarrow \phi \rightarrow \eta\gamma$
< 9 × 10 ⁻⁴	90		AKHMETSHIN 97C	CMD2	See AKHMETSHIN 99B
< 15 × 10 ⁻⁴	0		THALER 73	ASPK	

$\Gamma(2\pi^0)/\Gamma_{\text{total}}$ Γ_{25}/Γ Forbidden by P and CP invariance.

VALUE	CL%	DOCUMENT ID	TECN	COMMENT
$<3.5 \times 10^{-4}$	90	BLIK	07	GAM4 $\pi^- p \rightarrow \eta n$
$<4.3 \times 10^{-4}$	90	AKHMETSHIN 99c	CMD2	$e^+ e^- \rightarrow \phi \rightarrow \eta \gamma$
$<6 \times 10^{-4}$	90	22 ACHASOV	98	SND $e^+ e^- \rightarrow \phi \rightarrow \eta \gamma$

22 ACHASOV 98 observes one event in a $\pm 3\sigma$ region around the η mass, while a Monte Carlo calculation gives 10 ± 5 events. The limit here is the Poisson upper limit for one observed event and no background.

 $\Gamma(2\pi^0\gamma)/\Gamma_{\text{total}}$ Γ_{26}/Γ Forbidden by C invariance.

VALUE	CL%	DOCUMENT ID	TECN	CHG	COMMENT
$<5 \times 10^{-4}$	90	NEFKENS	05	CRYB	0 $p(720 \text{ MeV}/c) \pi^- \rightarrow n \eta$
$<17 \times 10^{-4}$	90	BLIK	07	GAM4	$\pi^- p \rightarrow \eta n$

 $\Gamma(3\pi^0\gamma)/\Gamma_{\text{total}}$ Γ_{27}/Γ Forbidden by C invariance.

VALUE	CL%	DOCUMENT ID	TECN	CHG	COMMENT
$<6 \times 10^{-5}$	90	NEFKENS	05	CRYB	0 $p(720 \text{ MeV}/c) \pi^- \rightarrow n \eta$
$<24 \times 10^{-5}$	90	BLIK	07	GAM4	$\pi^- p \rightarrow \eta n$

 $\Gamma(3\gamma)/\Gamma_{\text{total}}$ Γ_{28}/Γ Forbidden by C invariance.

VALUE	CL%	DOCUMENT ID	TECN	COMMENT
$<16 \times 10^{-5}$	90	BLIK	07	GAM4 $\pi^- p \rightarrow \eta n$
$<4 \times 10^{-5}$	90	NEFKENS	05A	CRYB $p(720 \text{ MeV}/c) \pi^- \rightarrow n \eta$

 $\Gamma(3\gamma)/\Gamma(2\gamma)$ Γ_{28}/Γ_2

VALUE	CL%	DOCUMENT ID	TECN	CHG	
$<1.2 \times 10^{-3}$	95	ALDE	84	GAM2	0

 $\Gamma(3\gamma)/\Gamma(3\pi^0)$ Γ_{28}/Γ_3

VALUE	CL%	DOCUMENT ID	TECN	COMMENT
$<4.9 \times 10^{-5}$	90	ALOISIO	04	KLOE $\phi \rightarrow \eta \gamma$

 $\Gamma(4\pi^0)/\Gamma_{\text{total}}$ Γ_{29}/Γ Forbidden by P and CP invariance.

VALUE	CL%	DOCUMENT ID	TECN	COMMENT
$<6.9 \times 10^{-7}$	90	PRAKHOV	00	CRYB $\pi^- p \rightarrow n \eta$, 720 MeV/c
$<200 \times 10^{-7}$	90	BLIK	07	GAM4 $\pi^- p \rightarrow \eta n$

 $\Gamma(\pi^0 e^+ e^-)/\Gamma_{\text{total}}$ Γ_{30}/Γ C parity forbids this to occur as a single-photon process.

VALUE	CL%	DOCUMENT ID	TECN	COMMENT
$<1.6 \times 10^{-4}$	90	MARTYNOV	76	HLBC
$<8.4 \times 10^{-4}$	90	BAZIN	68	DBC
$<70 \times 10^{-4}$		RITTENBERG	65	HBC

 $\Gamma(\pi^0 e^+ e^-)/\Gamma(\pi^+ \pi^- \pi^0)$ Γ_{30}/Γ_9 C parity forbids this to occur as a single-photon process.

VALUE	CL%	EVTS	DOCUMENT ID	TECN	COMMENT
$<1.9 \times 10^{-4}$	90		JANE	75	OSPK
$<42 \times 10^{-4}$	90		BAGLIN	67	HLBC
$<16 \times 10^{-4}$	90	0	BILLING	67	HLBC
$<77 \times 10^{-4}$		0	FOSTER	65B	HBC
$<110 \times 10^{-4}$			PRICE	65	HBC

 $\Gamma(\pi^0 \mu^+ \mu^-)/\Gamma_{\text{total}}$ Γ_{31}/Γ C parity forbids this to occur as a single-photon process.

VALUE	CL%	DOCUMENT ID	TECN	COMMENT
$<5 \times 10^{-6}$	90	DZHEL'YADIN	81	SPEC $\pi^- p \rightarrow \eta n$
$<500 \times 10^{-6}$		WEHMANN	68	OSPK

 $[\Gamma(\mu^+ e^-) + \Gamma(\mu^- e^+)]/\Gamma_{\text{total}}$ Γ_{32}/Γ

Forbidden by lepton family number conservation.

VALUE	CL%	DOCUMENT ID	TECN	COMMENT
$<6 \times 10^{-6}$	90	WHITE	96	SPEC $p d \rightarrow \eta \text{ } ^3\text{He}$

 η C -NONCONSERVING DECAY PARAMETERS $\pi^+ \pi^- \pi^0$ LEFT-RIGHT ASYMMETRY PARAMETERMeasurements with an error $> 1.0 \times 10^{-2}$ have been omitted.

VALUE (units 10^{-2})	EVTS	DOCUMENT ID	TECN
--------------------------	------	-------------	------

**0.09 \pm 0.11
-0.12 OUR AVERAGE**

$+0.09 \pm 0.10$	$^{+0.09}_{-0.14}$	1.34M	AMBROSINO 08D KLOE
0.28 \pm 0.26	165k	JANE	74 OSPK
-0.05 ± 0.22	220k	LAYTER	72 ASPK

• • • We do not use the following data for averages, fits, limits, etc. • • •

1.5 \pm 0.5	37k	23 GORMLEY	68c ASPK
---------------	-----	------------	----------

23 The GORMLEY 68c asymmetry is probably due to unmeasured ($\mathbf{E} \times \mathbf{B}$) spark chamber effects. New experiments with ($\mathbf{E} \times \mathbf{B}$) controls don't observe an asymmetry.

 $\pi^+ \pi^- \pi^0$ SEXTANT ASYMMETRY PARAMETERMeasurements with an error $> 2.0 \times 10^{-2}$ have been omitted.

VALUE (units 10^{-2})	EVTS	DOCUMENT ID	TECN
--------------------------	------	-------------	------

**0.12 \pm 0.10
-0.11 OUR AVERAGE**

$+0.08 \pm 0.10$	$^{+0.08}_{-0.13}$	1.34M	AMBROSINO 08D KLOE
0.20 \pm 0.25	165k	JANE	74 OSPK
0.10 \pm 0.22	220k	LAYTER	72 ASPK
0.5 \pm 0.5	37k	GORMLEY	68c WIRE

 $\pi^+ \pi^- \pi^0$ QUADRANT ASYMMETRY PARAMETER

VALUE (units 10^{-2})	EVTS	DOCUMENT ID	TECN
--------------------------	------	-------------	------

-0.09 \pm 0.09 OUR AVERAGE

-0.05 ± 0.10	$^{+0.03}_{-0.05}$	1.34M	AMBROSINO 08D KLOE
-0.30 ± 0.25	165k	JANE	74 OSPK
-0.07 ± 0.22	220k	LAYTER	72 ASPK

 $\pi^+ \pi^- \gamma$ LEFT-RIGHT ASYMMETRY PARAMETERMeasurements with an error $> 2.0 \times 10^{-2}$ have been omitted.

VALUE (units 10^{-2})	EVTS	DOCUMENT ID	TECN
--------------------------	------	-------------	------

0.9 \pm 0.4 OUR AVERAGE

1.2 \pm 0.6	35k	JANE	74B OSPK
0.5 \pm 0.6	36k	THALER	72 ASPK
1.22 \pm 1.56	7257	GORMLEY	70 ASPK

 $\pi^+ \pi^- \gamma$ PARAMETER β (D -wave)Sensitive to a D -wave contribution: $dN/d\cos\theta = \sin^2\theta (1 + \beta \cos^2\theta)$.

VALUE	EVTS	DOCUMENT ID	TECN
-------	------	-------------	------

-0.02 \pm 0.07 OUR AVERAGE

0.11 \pm 0.11	35k	JANE	74B OSPK
-0.060 ± 0.065	7250	GORMLEY	70 WIRE
0.12 \pm 0.06	24	THALER	72 ASPK

24 The authors don't believe this indicates D -wave because the dependence of β on the γ energy is inconsistent with the theoretical prediction. A $\cos^2\theta$ dependence can also come from P - and F -wave interference.

 η CP -NONCONSERVING DECAY PARAMETER $\pi^+ \pi^- e^+ e^-$ DECAY-PLANE ASYMMETRY PARAMETER A_ϕ

In the η rest frame, the total momentum of the $e^+ e^-$ pair is equal and opposite to that of the $\pi^+ \pi^-$ pair. Let \hat{z} be the unit vector along the momentum of the $e^+ e^-$ pair; let \hat{n}_{ee} and $\hat{n}_{\pi\pi}$ be the unit vectors normal to the $e^+ e^-$ and $\pi^+ \pi^-$ planes; and let ϕ be the angle between the two normals. Then

$$\sin\phi \cos\phi = [(\hat{n}_{ee} \times \hat{n}_{\pi\pi}) \cdot \hat{z}] (\hat{n}_{ee} \cdot \hat{n}_{\pi\pi}),$$

and

$$A_\phi \equiv \frac{N_{\sin\phi \cos\phi > 0} - N_{\sin\phi \cos\phi < 0}}{N_{\sin\phi \cos\phi > 0} + N_{\sin\phi \cos\phi < 0}}.$$

VALUE (units 10^{-2})	EVTS	DOCUMENT ID	TECN	COMMENT
--------------------------	------	-------------	------	---------

$-0.6 \pm 2.5 \pm 1.8$	1555 \pm 52	AMBROSINO 09B	KLOE	$e^+ e^- \rightarrow \phi \rightarrow \eta \gamma$
------------------------	---------------	---------------	------	--

ENERGY DEPENDENCE OF $\eta \rightarrow 3\pi$ DALITZ PLOTSPARAMETERS FOR $\eta \rightarrow \pi^+ \pi^- \pi^0$

See the "Note on η Decay Parameters" in our 1994 edition, Phys. Rev. **D50**, 1 August 1994, Part 1, p. 1454. The following experiments fit to one or more of the coefficients a , b , c , d , or e for $|\text{matrix element}|^2 = 1 + ay + by^2 + cx + dx^2 + exy$.

VALUE	EVTS	DOCUMENT ID	TECN	COMMENT
-------	------	-------------	------	---------

• • • We do not use the following data for averages, fits, limits, etc. • • •

1.34M		AMBROSINO 08D	KLOE	
3230	25	ABELE	98D	$\bar{p} p \rightarrow \pi^0 \pi^0 \eta$ at rest
1077	26	AMSLER	95	$\bar{p} p \rightarrow \pi^+ \pi^- \eta$ at rest
81k		LAYTER	73	ASPK
220k		LAYTER	72	ASPK
1138		CARPENTER	70	HBC
349		DANBURG	70	DBC

resonances are difficult to resolve because of their large decay widths which cause a strong overlap between resonances and background, and also because several decay channels open up within a short mass interval. In addition, the $K\bar{K}$ and $\eta\eta$ thresholds produce sharp cusps in the energy dependence of the resonant amplitude. Furthermore, one expects non- $q\bar{q}$ scalar objects, like glueballs and multiquark states in the mass range below 1800 MeV. For some recent reviews see Ref. [1–4].

Scalars are produced, for example, in πN scattering on polarized/unpolarized targets, $p\bar{p}$ annihilation, central hadronic production, J/Ψ , B^- , D^- and K -meson decays, $\gamma\gamma$ formation, and ϕ radiative decays. Experiments are accompanied by the development of theoretical models for the reaction amplitudes, which are based on common fundamental principles of two-body unitarity, analyticity, Lorentz invariance, and chiral- and flavor-symmetry using different techniques (K -matrix formalism, N/D -method, Dalitz Tuan ansatz, unitarized quark models with coupled channels, effective chiral field theories such as the linear sigma model, *etc.*). Dynamics near the lowest two-body thresholds in some analyses is described by crossed channel (t , u) meson exchange or with an effective range parameterization instead of or in addition to resonant features in the s -channel, only. Furthermore, elastic S -wave scattering amplitudes involving soft pions have zeros close to threshold [5–6], which may be shifted or removed in associated production processes.

The mass and width of a resonance are found from the position of the nearest pole in the process amplitude (T -matrix or S -matrix) at an unphysical sheet of the complex energy plane: $(E - i\Gamma/2)$. It is important to note that only in the case of narrow well-separated resonances, far away from the opening of decay channels, does the naive Breit-Wigner parameterization (or K -matrix pole parameterization) agree with this pole position.

In this note, we discuss all light scalars organized in the listings under the entries ($I = 1/2$) $K_0^*(800)$ (or κ), $K_0^*(1430)$, ($I = 1$) $a_0(980)$, $a_0(1450)$, and ($I = 0$) $f_0(600)$ (or σ), $f_0(980)$, $f_0(1370)$, and $f_0(1500)$. This list is minimal and does not necessarily exhaust the list of actual resonances. The ($I = 2$) $\pi\pi$ and ($I = 3/2$) $K\pi$ phase shifts do not exhibit any resonant behavior. See also our notes in previous issues for further comments on *e.g.*, scattering lengths and older papers.

II. The $I = 1/2$ States: The $K_0^*(1430)$ [7] is perhaps the least controversial of the light scalar mesons. The $K\pi$ S -wave scattering has two possible isospin channels, $I = 1/2$ and $I = 3/2$. The $I = 3/2$ wave is elastic and repulsive up to 1.7 GeV [8] and contains no known resonances. The $I = 1/2$ $K\pi$ phase shift, measured from about 100 MeV above threshold in Kp production, rises smoothly, passes 90° at 1350 MeV, and continues to rise to about 170° at 1600 MeV. The first important inelastic threshold is $K\eta'(958)$. In the inelastic region the continuation of the amplitude is uncertain since the partial-wave decomposition has several solutions. The data are extrapolated towards the $K\pi$ threshold using effective range type formulas [7,9], or chiral perturbation predictions [10–12].

In analyses using unitarized amplitudes there is agreement on the presence of a resonance pole around 1410 MeV having a width of about 300 MeV. With reduced model dependence [13] finds a larger width of 500 MeV.

The presence and properties of the light $K^*(800)$ or “ κ ” meson in the 700-900 MeV region are difficult to establish since it appears to have a very large width ($\Gamma \approx 500$ MeV) and resides close to the $K\pi$ threshold. Hadronic D -meson decays provide additional data points in the vicinity of the $K\pi$ threshold - experimental results from E791 *e.g.* Ref. [14,15], FOCUS [13,16], CLEO [17], and BaBar [18] are discussed in the *Review of Charm Dalitz Plot Analyses*. Precision information from semileptonic D decays avoiding theoretically ambiguous three-body final state interactions is not available. BES II [19] (re-analyzed by [20]) finds a κ like structure in J/ψ decays to $\bar{K}^{*0}(892)K^+\pi^-$ where κ recoils against the $K^*(892)$. Also clean with respect to final state interaction is the decay $\tau^- \rightarrow K_S^0\pi^-\nu_\tau$ studied by Belle [21], with $K^*(800)$ parameters fixed to Ref. [19].

Some authors find a κ pole in their phenomenological analysis (see *e.g.* [11,17,22–34]), while others do not (see *e.g.* [12,18,35–37]). The pole position for the κ was found in a theoretical analysis [38] in the $K\pi \rightarrow K\pi$ amplitude on the second sheet. This analysis involves the Mandelstam representation, which includes unitarity, analyticity and crossing symmetry.

III. The $I = 1$ States: Two isovector states are known, the established $a_0(980)$ and the $a_0(1450)$. Independent of any model, the $K\bar{K}$ component in the $a_0(980)$ wave function must be large: it lies just below the opening of the $K\bar{K}$ channel to which it strongly couples. This generates an important cusp-like behavior in the resonant amplitude. Hence, its mass and width parameters are strongly distorted. To reveal its true coupling constants, a coupled channel model with energy-dependent widths and mass shift contributions is necessary. All listed $a_0(980)$ measurements agree on a mass position value near 980 MeV, but the width takes values between 50 and 100 MeV, mostly due to the different models. For example, the analysis of the $p\bar{p}$ -annihilation data [9] using an unitary K -matrix description finds a width as determined from the T -matrix pole of 92 ± 8 MeV, while the observed width of the peak in the $\pi\eta$ mass spectrum is about 45 MeV.

The relative coupling $K\bar{K}/\pi\eta$ is determined indirectly from $f_1(1285)$ [39–41] or $\eta(1410)$ decays [42–44], from the line shape observed in the $\pi\eta$ decay mode [45–48], or from the coupled-channel analysis of $\pi\pi\eta$ and $K\bar{K}\pi$ final states of $p\bar{p}$ annihilation at rest [9].

The $a_0(1450)$ is seen in $p\bar{p}$ annihilation experiments with stopped and higher momenta \bar{p} , with a mass of about 1450 MeV or close to the $a_2(1320)$ meson which is typically a dominant feature. A contribution from $a_0(1450)$ is also found in the analysis of the $D^\pm \rightarrow K^+K^-\pi^\pm$ decay [49]. The broad structure at about 1300 MeV observed in $\pi N \rightarrow K\bar{K}N$ reactions [50] needs further confirmation in its existence and isospin assignment.

Meson Particle Listings

$f_0(600)$

IV. The $I = 0$ States: The $I = 0 J^{PC} = 0^{++}$ sector is the most complex one, both experimentally and theoretically. The data have been obtained from $\pi\pi$, $K\bar{K}$, $\eta\eta$, 4π , and $\eta\eta'(958)$ systems produced in S -wave. Analyses based on several different production processes conclude that probably four poles are needed in the mass range from $\pi\pi$ threshold to about 1600 MeV. The claimed isoscalar resonances are found under separate entries σ or $f_0(600)$, $f_0(980)$, $f_0(1370)$, and $f_0(1500)$.

For discussions of the $\pi\pi$ S wave below the $K\bar{K}$ threshold and on the long history of the $\sigma(600)$, which was suggested in linear sigma models more than 50 years ago, see our reviews in previous editions and the conference proceedings [51].

Information on the $\pi\pi$ S -wave phase shift $\delta_J^0 = \delta_0^0$ was already extracted 35 years ago from the πN scattering [52,53], and near threshold from the K_{e4} -decay [54]. The reported $\pi\pi \rightarrow K\bar{K}$ cross sections [55–58] have large uncertainties. The πN data have been analyzed in combination with high-statistics data (see entries labeled as RVUE for re-analyses of the data). The $2\pi^0$ invariant mass spectra of the $p\bar{p}$ annihilation at rest [59,60] and the central collision [61] do not show a distinct resonance structure below 900 MeV, but these data are consistently described with the standard solution for πN data [52,62], which allows for the existence of the broad σ . An enhancement is observed in the $\pi^+\pi^-$ invariant mass near threshold in the decays $D^+ \rightarrow \pi^+\pi^-\pi^+$ [63–65] and $J/\psi \rightarrow \omega\pi^+\pi^-$ [66,67], and in $\psi(2S) \rightarrow J/\psi\pi^+\pi^-$ with very limited phase space [68,69].

The precise σ pole is difficult to establish because of its large width, and because it can certainly not be modelled by a naive Breit-Wigner resonance. It is distorted by background as required by chiral symmetry, and from crossed channel exchanges, the $f_0(1370)$, and other dynamical features. However, most of the analyzes under $f_0(600)$ listed in our previous issues agree on a pole position near $(500 - i250)$ MeV. In particular, analyses of $\pi\pi$ data that include unitarity, $\pi\pi$ threshold behavior and the chiral symmetry constraints from Adler zeroes and scattering lengths need the σ .

A precise pole position with an uncertainty of less than 20 MeV (see our table for T -matrix pole) is derived by Ref. [70]. An important ingredient is the use of Roy-Steiner equations derived from crossing symmetry, analyticity and unitarity. With these constraints [70] find that their position of the σ pole depends, almost exclusively, only on the value of the isosinglet S -wave phase shift at 800 MeV and the S -wave scattering lengths a_0^0 and a_0^2 . Using analyticity and unitarity only to describe data from $K_{2\pi}$ and K_{e4} decays [71] find comparable pole position and scattering length a_0^0 . A similar determination in a fit by [72] to K_{e4} decay data and to higher energy $\pi\pi$ phase shifts also results in a σ pole position consistent with the result of [70].

According to Ref. [73,74] the data for $\sigma \rightarrow \gamma\gamma$ are consistent with what is expected for a two step process of $\gamma\gamma \rightarrow \pi^+\pi^-$ via pion exchange in the t - and u -channel, followed by a final state interaction $\pi^+\pi^- \rightarrow \pi^0\pi^0$. The same conclusion is drawn

in Ref. [75] where the bulk part of the $\sigma \rightarrow \gamma\gamma$ decay width is dominated by rescattering. Therefore it may be difficult to learn anything new about the nature of the σ from its $\gamma\gamma$ coupling. There are theoretical indications (e.g. [76–79]) that the σ pole behaves differently from a $q\bar{q}$ -state.

The $f_0(980)$ overlaps strongly with the σ and background represented by a very slowly varying phase extending to higher masses and/or the $f_0(1370)$. This can lead to a dip in the $\pi\pi$ spectrum at the $K\bar{K}$ threshold. It changes from a dip into a peak structure in the $\pi^0\pi^0$ invariant mass spectrum of the reaction $\pi^-p \rightarrow \pi^0\pi^0n$ [80], with increasing four-momentum transfer to the $\pi^0\pi^0$ system, which means increasing the a_1 -exchange contribution in the amplitude, while the π -exchange decreases. The σ , and the $f_0(980)$, are also observed in data for radiative decays ($\phi \rightarrow f_0\gamma$) from SND [81,82], CMD2 [83], and KLOE [84,85]. Analyses of $\gamma\gamma \rightarrow \pi\pi$ data [86–88] underline the importance of the $K\bar{K}$ coupling of $f_0(980)$, while the resulting two-photon width of the $f_0(980)$ cannot be determined precisely [89]. A reliable interpretation of the $f_0(980)$ based on these observations is not possible at present.

The f_0 's above 1 GeV. A meson resonance that is very well studied experimentally, is the $f_0(1500)$ seen by the Crystal Barrel experiment in five decay modes: $\pi\pi$, $K\bar{K}$, $\eta\eta$, $\eta\eta'(958)$, and 4π [9,59,60]. Due to its interference with the $f_0(1370)$ (and $f_0(1710)$), the peak attributed to $f_0(1500)$ can appear shifted in invariant mass spectra. Therefore, the application of simple Breit-Wigner forms arrive at slightly different resonance masses for $f_0(1500)$. Analyses of central-production data of the likewise five decay modes Ref. [90,91] agree on the description of the S -wave with the one above. The $p\bar{p}$, $p\bar{n}/n\bar{p}$ measurements [92–94,60] show a single enhancement at 1400 MeV in the invariant 4π mass spectra, which is resolved into $f_0(1370)$ and $f_0(1500)$ [95,96]. The data on 4π from central production [97] require both resonances, too, but disagree on the relative content of $\rho\rho$ and $\sigma\sigma$ in 4π . All investigations agree that the 4π decay mode represents about half of the $f_0(1500)$ decay width and is dominant for $f_0(1370)$.

The determination of the $\pi\pi$ coupling of $f_0(1370)$ is aggravated by the strong overlap with the broad $f_0(600)$ and $f_0(1500)$. Since it does not show up prominently in the 2π spectra, its mass and width are difficult to determine. Multi-channel analyses of hadronically produced two- and three-body final states agree on a mass between 1300 MeV and 1400 MeV and a narrow $f_0(1500)$, but arrive at a somewhat smaller width for $f_0(1370)$.

Both Belle and BaBar have observed scalars in B and D meson decays. They observe broad or narrow structures between 1 and 1.6 GeV in K^+K^- and $\pi^+\pi^-$ decays [98–102] (see also [103]). It could be a result of interference of several resonances in this mass range, but lack of statistics prevents an unambiguous identification of this effect.

V. Interpretation of the scalars below 1 GeV: In the literature, many suggestions are discussed, such as conventional $q\bar{q}$ mesons, $qq\bar{q}\bar{q}$ or meson-meson bound states mixed with a

scalar glueball. In reality, they can be superpositions of these components, and one depends on models to determine the dominant one. Although we have seen progress in recent years, this question remains open. Here, we mention some of the present conclusions.

The $f_0(980)$ and $a_0(980)$ are often interpreted as multi-quark states [104–108] or $K\bar{K}$ bound states [109]. The insight into their internal structure using two-photon widths [82,110–115] is not conclusive. The $f_0(980)$ appears as a peak structure in $J/\psi \rightarrow \phi\pi^+\pi^-$ and in D_s decays without $f_0(600)$ background. Based on that observation it is suggested that $f_0(980)$ has a large $s\bar{s}$ component, which according to Ref. [116] is surrounded by a virtual $K\bar{K}$ cloud (see also [117]). Data on radiative decays ($\phi \rightarrow f_0\gamma$ and $\phi \rightarrow a_0\gamma$) from SND, CMD2, and KLOE (see above) favor a 4-quark picture of the $f_0(980)$ and $a_0(980)$. The underlying model for this conclusion [118,119] however may be oversimplified. But it remains quite possible that the states $f_0(980)$ and $a_0(980)$, together with the $f_0(600)$ and the $K_0^*(800)$, form a new low-mass state nonet of predominantly four-quark states, where at larger distances the quarks recombine into a pair of pseudoscalar mesons creating a meson cloud (see e.g. Ref. [120]). Different QCD sum rule studies [121–125] do not agree on a tetraquark configuration for the same particle group.

Attempts have been made to start directly from chiral Lagrangians [24,119,126–130] which predict the existence of the σ meson near 500 MeV. Hence, e.g., in the chiral linear sigma model with 3 flavors, the σ , $a_0(980)$, $f_0(980)$, and κ (or $K_0^*(1430)$) would form a nonet (not necessarily $q\bar{q}$), while the lightest pseudoscalars would be their chiral partners.

In such models inspired by the linear sigma model the light $\sigma(600)$ is often referred to as the "Higgs boson of strong interactions", since the σ plays a role similar to the Higgs particle in electro-weak symmetry breaking. It is important for chiral symmetry breaking which generates most of the proton and η' mass, and what is referred to as the constituent quark mass.

In the approach of Ref. [24] the above resonances are generated starting from chiral perturbation theory predictions near the first open channel, and then by extending the predictions to the resonance regions using unitarity.

In the unitarized quark model with coupled $q\bar{q}$ and meson-meson channels, the light scalars can be understood as additional manifestations of bare $q\bar{q}$ confinement states, strongly mass shifted from the 1.3 - 1.5 GeV region and very distorted due to the strong 3P_0 coupling to S -wave two-meson decay channels [131–135]. Thus, the light scalar nonet comprising the $f_0(600)$, $f_0(980)$, $K_0^*(800)$, and $a_0(980)$, as well as the regular nonet consisting of the $f_0(1370)$, $f_0(1500)$ (or $f_0(1700)$), $K_0^*(1430)$, and $a_0(1450)$, respectively, are two manifestations of the same bare input states (see also Ref. [136]).

Other models with different groupings of the observed resonances exist and may e.g. be found in earlier versions of this review and papers listed as other related papers below.

VI. Interpretation of the f_0 's above 1 GeV:

The $f_0(1370)$ and $f_0(1500)$ decay mostly into pions (2π and 4π) while the $f_0(1710)$ decays mainly into $K\bar{K}$ final states. The $K\bar{K}$ decay branching ratio of the $f_0(1500)$ is small [90,137].

If one uses the naive quark model it is natural to assume that the $f_0(1370)$, $a_0(1450)$, and the $K_0^*(1430)$ are in the same SU(3) flavor nonet, being the $(u\bar{u} + d\bar{d})$, $u\bar{d}$ and $u\bar{s}$ states, respectively, while the $f_0(1710)$ is the $s\bar{s}$ state. Indeed, the production of $f_0(1710)$ (and $f_2'(1525)$) is observed in $p\bar{p}$ annihilation [138] but the rate is suppressed compared to $f_0(1500)$ (respectively $f_2(1270)$), as would be expected from the OZI rule for $s\bar{s}$ states. The $f_0(1500)$ would also qualify as $(u\bar{u} + d\bar{d})$ state, although it is very narrow compared to the other states and too light to be the first radial excitation.

However, in $\gamma\gamma$ collisions leading to $K_S^0 K_S^0$ [139] a spin 0 signal is observed at the $f_0(1710)$ mass (together with a dominant spin 2 component), while the $f_0(1500)$ is not observed in $\gamma\gamma \rightarrow K\bar{K}$ nor $\pi^+\pi^-$ [140]. In $\gamma\gamma$ collisions leading to $\pi^0\pi^0$ Ref. [141] reports the observation of a scalar around 1470 MeV albeit with large uncertainties on the mass and $\gamma\gamma$ couplings. This state could be the $f_0(1370)$ or the $f_0(1500)$. The upper limit from $\pi^+\pi^-$ [140] excludes a large $n\bar{n}$ content for the $f_0(1500)$ and hence points to a mainly $s\bar{s}$ state [142]. This appears to contradict the small $K\bar{K}$ decay branching ratio of the $f_0(1500)$ and makes a $q\bar{q}$ assignment difficult for this state. Hence the $f_0(1500)$ could be mainly glue due the absence of a 2γ -coupling, while the $f_0(1710)$ coupling to 2γ would be compatible with an $s\bar{s}$ state. However, the 2γ -couplings are sensitive to glue mixing with $q\bar{q}$ [143].

Note that an isovector scalar, possibly the $a_0(1450)$ (albeit at a lower mass of 1317 MeV) is observed in $\gamma\gamma$ collisions leading to $\eta\pi^0$ [144]. The state interferes destructively with the non-resonant background, but its $\gamma\gamma$ coupling is comparable to that of the $a_2(1320)$, in accord with simple predictions (see e.g. Ref. [142]).

The narrow width of $f_0(1500)$, and its enhanced production at low transverse momentum transfer in central collisions [145–147] also favor $f_0(1500)$ to be non- $q\bar{q}$. In the mixing scheme of Ref. [143], which uses central production data from WA102 and the recent hadronic J/ψ decay data from BES [148,149], glue is shared between $f_0(1370)$, $f_0(1500)$ and $f_0(1710)$. The $f_0(1370)$ is mainly $n\bar{n}$, the $f_0(1500)$ mainly glue and the $f_0(1710)$ dominantly $s\bar{s}$. This agrees with previous analyses [150,151].

However, alternative schemes have been proposed (e.g. in Ref. [152,153]; for a review see e.g. Ref. [1]) . In particular, for a scalar glueball, the two-gluon coupling to $n\bar{n}$ appears to be suppressed by chiral symmetry [154] and therefore the $K\bar{K}$ decay could be enhanced. This mechanism would imply that the $f_0(1710)$ can possibly be interpreted as an unmixed glueball [155]. In Ref. [156] the large K^+K^- scalar signal reported by Belle in B decays into $KK\bar{K}$ [157], compatible with the $f_0(1500)$, is explained as due to constructive interference with a broad glueball background. However, the Belle data

Meson Particle Listings

 $f_0(600)$

are inconsistent with the BaBar measurements which show instead a broad scalar at this mass for B decays into both $K^\pm K^\pm K^\mp$ [101] and $K^+ K^- \pi^0$ [158].

Whether the $f_0(1500)$ is observed in 'gluon rich' radiative J/ψ decays is debatable [159] because of the limited amount of data - more data for this and the $\gamma\gamma$ mode are needed.

References

1. C. Amsler and N.A. Tornqvist, Phys. Reports **389**, 61 (2004).
2. D.V. Bugg, Phys. Reports **397**, 257 (2004).
3. F.E. Close and N.A. Tornqvist, J. Phys. **G28**, R249 (2002).
4. E. Klempt and A. Zaitsev, Phys. Reports **454**, 1 (2007).
5. J.L. Adler, Phys. Rev. **137**, B1022 (1965).
6. J.L. Adler, Phys. Rev. **139**, B1638 (1965).
7. D. Aston *et al.*, Nucl. Phys. **B296**, 493 (1988).
8. P.G. Estabrooks *et al.*, Nucl. Phys. **B133**, 490 (1978).
9. A. Abele *et al.*, Phys. Rev. **D57**, 3860 (1998).
10. V. Bernard, N. Kaiser, and U.G. Meissner, Phys. Rev. **D43**, 2757 (1991).
11. M. Jamin *et al.*, Nucl. Phys. **B587**, 331 (2000).
12. S.N. Cherry and M.R. Pennington, Nucl. Phys. **A688**, 823 (2001).
13. J.M. Link *et al.*, Phys. Lett. **B648**, 156 (2007).
14. E.M. Aitala *et al.*, Phys. Rev. Lett. **89**, 121801 (2002).
15. E.M. Aitala *et al.*, Phys. Rev. **D73**, 032004 (2006).
16. J.M. Link *et al.*, Phys. Lett. **B525**, 205 (2002).
17. C. Cawfield *et al.*, Phys. Rev. **D74**, 031108R (2006).
18. B. Aubert *et al.*, Phys. Rev. **D76**, 011102R (2007).
19. M. Ablikim *et al.*, Phys. Lett. **B633**, 681 (2006).
20. F.K. Guo *et al.*, Nucl. Phys. **A773**, 78 (2006).
21. D. Epifanov *et al.*, Phys. Lett. **B654**, 65 (2007).
22. A.V. Anisovich and A.V. Sarantsev, Phys. Lett. **B413**, 137 (1997).
23. R. Delbourgo *et al.*, Int. J. Mod. Phys. **A13**, 657 (1998).
24. J.A. Oller *et al.*, Phys. Rev. **D60**, 099906E (1999).
25. J.A. Oller and E. Oset, Phys. Rev. **D60**, 074023 (1999).
26. C.M. Shakin and H. Wang, Phys. Rev. **D63**, 014019 (2001).
27. M.D. Scadron *et al.*, Nucl. Phys. **A724**, 391 (2003).
28. D. Black *et al.*, Phys. Rev. **D64**, 014031 (2001).
29. D.V. Bugg, Phys. Lett. **B572**, 1 (2003).
30. M. Ishida, Prog. Theor. Phys. Supp. **149**, 190 (2003).
31. H.Q. Zheng *et al.*, Nucl. Phys. **A733**, 235 (2004).
32. J.R. Pelaez, Mod. Phys. Lett. **A19**, 2879 (2004).
33. Z.Y. Zhou and H.Q. Zheng, Nucl. Phys. **A775**, 212 (2006).
34. J.M. Link *et al.*, Phys. Lett. **B653**, 1 (2007).
35. S. Kopp *et al.*, Phys. Rev. **D63**, 092001 (2001).
36. J.M. Link *et al.*, Phys. Lett. **B535**, 43 (2002).
37. J.M. Link *et al.*, Phys. Lett. **B621**, 72 (2005).
38. S. Descotes-Genon and B. Moussallam, Eur. Phys. J. **C48**, 553 (2006).
39. D. Barberis *et al.*, Phys. Lett. **B440**, 225 (1998).
40. M.J. Corden *et al.*, Nucl. Phys. **B144**, 253 (1978).
41. C. Defoix *et al.*, Nucl. Phys. **B44**, 125 (1972).
42. Z. Bai *et al.*, Phys. Rev. Lett. **65**, 2507 (1990).
43. T. Bolton *et al.*, Phys. Rev. Lett. **69**, 1328 (1992).
44. C. Amsler *et al.*, Phys. Lett. **B353**, 571 (1995).
45. S.M. Flatte, Phys. Lett. **63B**, 224 (1976).
46. C. Amsler *et al.*, Phys. Lett. **B333**, 277 (1994).
47. G. Janssen *et al.*, Phys. Rev. **D52**, 2690 (1995).
48. D.V. Bugg, Phys. Rev. **D78**, 074023 (2008).
49. P. Rubin *et al.*, Phys. Rev. **D78**, 072003 (2008).
50. A.D. Martin and E.N. Ozmutlu, Nucl. Phys. **B158**, 520 (1979).
51. S. Ishida ed. *et al.*, *KEK-Proceedings 2000-4*.
52. G. Grayer *et al.*, Nucl. Phys. **B75**, 189 (1974).
53. H. Becker *et al.*, Nucl. Phys. **B151**, 46 (1979).
54. L. Rosselet *et al.*, Phys. Rev. **D15**, 574 (1977).
55. W. Wetzel *et al.*, Nucl. Phys. **B115**, 208 (1976).
56. V.A. Polychronakos *et al.*, Phys. Rev. **D19**, 1317 (1979).
57. D. Cohen *et al.*, Phys. Rev. **D22**, 2595 (1980).
58. A. Etkin *et al.*, Phys. Rev. **D25**, 1786 (1982).
59. C. Amsler *et al.*, Phys. Lett. **B355**, 425 (1995).
60. A. Abele *et al.*, Phys. Lett. **B380**, 453 (1996).
61. D.M. Alde *et al.*, Phys. Lett. **B397**, 250 (1997).
62. R. Kaminski, L. Lesniak, and K. Rybicki, Z. Phys. **C74**, 79 (1997).
63. E.M. Aitala *et al.*, Phys. Rev. Lett. **86**, 770 (2001).
64. J.M. Link *et al.*, Phys. Lett. **B585**, 200 (2004).
65. G. Bonvicini *et al.*, Phys. Rev. **D76**, 012001 (2007).
66. J.E. Augustin and G. Cosme, Nucl. Phys. **B320**, 1 (1989).
67. M. Ablikim *et al.*, Phys. Lett. **B598**, 149 (2004).
68. A. Gallegos *et al.*, Phys. Rev. **D69**, 074033 (2004).
69. M. Ablikim *et al.*, Phys. Lett. **B645**, 19 (2007).
70. I. Caprini, G. Colangelo, and H. Leutwyler, Phys. Rev. Lett. **96**, 132001 (2006).
71. R. Garcia-Martin, J.R. Pelaez, and F.J. Yndurain, Phys. Rev. **D76**, 074034 (2007).
72. I. Caprini, Phys. Rev. **D77**, 114019 (2008).
73. M.R. Pennington, Phys. Rev. Lett. **97**, 011601 (2006).
74. M.R. Pennington, Mod. Phys. Lett. **A22**, 1439 (2007).
75. G. Mennessier, S. Narison, W. Ochs, Phys. Lett. **B665**, 205 (2008).
76. J.R. Pelaez and G. Rios, Phys. Rev. Lett. **97**, 242002 (2006).
77. H.-X. Chen, A. Hosaka, and S.-L. Zhu, Phys. Lett. **B650**, 369 (2007).
78. F. Giacosa, Phys. Rev. **D75**, 054007 (2007).
79. L. Maiani *et al.*, Eur. Phys. J. **C50**, 609 (2007).
80. N.N. Achasov and G.N. Shestakov, Phys. Rev. **D58**, 054011 (1998).
81. N.N. Achasov *et al.*, Phys. Lett. **B479**, 53 (2000).
82. N.N. Achasov *et al.*, Phys. Lett. **B485**, 349 (2000).
83. R.R. Akhmetshin *et al.*, Phys. Lett. **B462**, 371 (1999).
84. A. Aloisio *et al.*, Phys. Lett. **B536**, 209 (2002).
85. F. Ambrosino *et al.*, Eur. Phys. J. **C49**, 473 (2007).
86. M. Boggione and M.R. Pennington, Eur. Phys. J. **C9**, 11 (1999).
87. T. Mori *et al.*, Phys. Rev. **D75**, 051101R (2007).

88. N.N. Achasov and G.N. Shestakov, Phys. Rev. **D77**, 074020 (2008).
89. M.R. Pennington *et al.*, Eur. Phys. J. **C56**, 1 (2008).
90. D. Barberis *et al.*, Phys. Lett. **B462**, 462 (1999).
91. D. Barberis *et al.*, Phys. Lett. **B479**, 59 (2000).
92. M. Gaspero, Nucl. Phys. **A562**, 407 (1993).
93. A. Adamo *et al.*, Nucl. Phys. **A558**, 13C (1993).
94. C. Amsler *et al.*, Phys. Lett. **B322**, 431 (1994).
95. A. Abele *et al.*, Eur. Phys. J. **C19**, 667 (2001).
96. A. Abele *et al.*, Eur. Phys. J. **C21**, 261 (2001).
97. D. Barberis *et al.*, Phys. Lett. **B471**, 440 (2000).
98. A. Garmash *et al.*, Phys. Rev. **D65**, 092005 (2002).
99. A. Garmash *et al.*, Phys. Rev. Lett. **96**, 251803 (2006).
100. A. Garmash *et al.*, Phys. Rev. **D75**, 012006 (2007).
101. B. Aubert *et al.*, Phys. Rev. **D74**, 032003 (2006).
102. B. Aubert *et al.*, Phys. Rev. Lett. **99**, 221801 (2007).
103. E. Klempt, M. Matveev, A.V. Sarantsev, Eur. Phys. J. **C55**, 39 (2008).
104. R. Jaffe, Phys. Rev. **D15**, 267,281 (1977).
105. M. Alford and R.L. Jaffe, Nucl. Phys. **B578**, 367 (2000).
106. L. Maiani *et al.*, Phys. Rev. Lett. **93**, 212002 (2004).
107. L. Maiani, A.D. Polosa, V. Riquer, Phys. Lett. **B651**, 129 (2007).
108. G. 'tHooft *et al.*, Phys. Lett. **B662**, 424 (2008).
109. J. Weinstein and N. Isgur, Phys. Rev. **D41**, 2236 (1990).
110. T. Barnes, Phys. Lett. **B165**, 434 (1985).
111. Z.P. Li *et al.*, Phys. Rev. **D43**, 2161 (1991).
112. R. Delbourgo, D. Lui, and M. Scadron, Phys. Lett. **B446**, 332 (1999).
113. J.L. Lucio and M. Napsuciale, Phys. Lett. **B454**, 365 (1999).
114. R.H. Lemmer, Phys. Lett. **B650**, 152 (2007).
115. T. Branz, T. Gutsche and V. Lyubovitskij, Eur. Phys. J. **A37**, 303 (2008).
116. A. Deandrea *et al.*, Phys. Lett. **B502**, 79 (2001).
117. K.M. Ecklund *et al.*, Phys. Rev. **D80**, 052009 (2010).
118. M. Boglione and M.R. Pennington, Eur. Phys. J. **C30**, 503 (2003).
119. J.A. Oller *et al.*, Nucl. Phys. **A714**, 161 (2003).
120. F. Giacosa and G. Pagliara, Phys. Rev. **C76**, 065204 (2007).
121. S. Narison, Nucl. Phys. **B96**, 244 (2001).
122. H.J. Lee, Eur. Phys. J. **A30**, 423 (2006).
123. H.X. Chen, A. Hosaka, S.L. Zhu, Phys. Rev. **D76**, 094025 (2007).
124. J. Sugiyama *et al.*, Phys. Rev. **D76**, 114010 (2007).
125. T. Kojo, D. Jido, Phys. Rev. **D78**, 114005 (2008).
126. M. Scadron, Eur. Phys. J. **C6**, 141 (1999).
127. M. Ishida, Prog. Theor. Phys. **101**, 661 (1999).
128. N. Tornqvist, Eur. Phys. J. **C11**, 359 (1999).
129. M. Napsuciale and S. Rodriguez, Phys. Lett. **B603**, 195 (2004).
130. M. Napsuciale and S. Rodriguez, Phys. Rev. **D70**, 094043 (2004).
131. N.A. Tornqvist, Z. Phys. **C68**, 647 (1995).
132. N.A. Tornqvist and M. Roos, Phys. Rev. Lett. **76**, 1575 (1996).
133. E. Van Beveren *et al.*, Z. Phys. **C30**, 615 (1986).
134. E. Van Beveren and G. Rupp, Eur. Phys. J. **C10**, 469 (1999).
135. E. Van Beveren, Eur. Phys. J. **C22**, 493 (2001).
136. M. Boglione and M.R. Pennington, Phys. Rev. **D65**, 114010 (2002).
137. A. Abele *et al.*, Phys. Lett. **B385**, 425 (1996).
138. C. Amsler *et al.*, Phys. Lett. **B639**, 165 (2006).
139. M. Acciarri *et al.*, Phys. Lett. **B501**, 173 (2001).
140. R. Barate *et al.*, Phys. Lett. **B472**, 189 (2000).
141. S. Uehara *et al.*, Phys. Rev. **D78**, 052004 (2008).
142. C. Amsler *et al.*, Phys. Lett. **B541**, 22 (2002).
143. F.E. Close and Q. Zhao, Phys. Rev. **D71**, 094022 (2005).
144. S. Uehara *et al.*, Phys. Rev. **D80**, 032001 (2009).
145. F.E. Close *et al.*, Phys. Lett. **B397**, 333 (1997).
146. F.E. Close, Phys. Lett. **B419**, 387 (1998).
147. A. Kirk, Phys. Lett. **B489**, 29 (2000).
148. M. Ablikim *et al.*, Phys. Lett. **B603**, 138 (2004).
149. M. Ablikim *et al.*, Phys. Lett. **B607**, 243 (2005).
150. C. Amsler and F.E. Close, Phys. Rev. **D53**, 295 (1996).
151. F.E. Close and A. Kirk, Eur. Phys. J. **C21**, 531 (2001).
152. P. Minkowski and W. Ochs, Eur. Phys. J. **C9**, 283 (1999).
153. W. Lee and D. Weingarten, Phys. Rev. **D61**, 014015 (2000).
154. M. Chanowitz, Phys. Rev. Lett. **95**, 172001 (2005).
155. M. Albaladejo and J.A. Oller, Phys. Rev. Lett. **101**, 252002 (2008).
156. P. Minkowski, W. Ochs, Eur. Phys. J. **C39**, 71 (2005).
157. A. Garmash *et al.*, Phys. Rev. **D71**, 092003 (2005).
158. B. Aubert *et al.*, Phys. Rev. Lett. **99**, 161802 (2007).
159. M. Ablikim *et al.*, Phys. Lett. **B642**, 441 (2006).

 $f_0(600)$ T-MATRIX POLE \sqrt{s} Note that $\Gamma \approx 2 \text{Im}(\sqrt{s_{\text{pole}}})$.

VALUE (MeV)	DOCUMENT ID	TECN	COMMENT
(400-1200)-i(250-500) OUR ESTIMATE			
• • • We do not use the following data for averages, fits, limits, etc. • • •			
$(455 \pm 6 +^{31}_{-13}) - i(556 \pm 12 +^{68}_{-86})$	1 CAPRINI	08	RVUE Compilation
$(463 \pm 6 +^{31}_{-13}) - i(518 \pm 12 +^{66}_{-68})$	2 CAPRINI	08	RVUE Compilation
$(552 \pm^{84}_{-106}) - i(232 \pm^{81}_{-72})$	3 ABLIKIM	07A	BES2 $\psi(2S) \rightarrow \pi^+ \pi^- J/\psi$
$(466 \pm 18) - i(223 \pm 28)$	4 BONVICINI	07	CLEO $D^+ \rightarrow \pi^- \pi^+ \pi^+$
$(472 \pm 30) - i(271 \pm 30)$	5 BUGG	07A	RVUE Compilation
$(484 \pm 17) - i(255 \pm 10)$	GARCIA-MAR.	07	RVUE $K^* e 4$
$(441 \pm^{16}_{-27}) - i(272 \pm^9_{-12.5})$	6 CAPRINI	06	RVUE $\pi\pi \rightarrow \pi\pi$
$(470 \pm 50) - i(285 \pm 25)$	7 ZHOU	05	RVUE
$(541 \pm 39) - i(252 \pm 42)$	8 ABLIKIM	04A	BES2 $J/\psi \rightarrow \omega \pi^+ \pi^-$
$(528 \pm 32) - i(207 \pm 23)$	9 GALLEGOS	04	RVUE Compilation
$(440 \pm 8) - i(212 \pm 15)$	10 PELAEZ	04A	RVUE $\pi\pi \rightarrow \pi\pi$
$(533 \pm 25) - i(247 \pm 25)$	11 BUGG	03	RVUE
$532 - i272$	BLACK	01	RVUE $\pi^0 \pi^0 \rightarrow \pi^0 \pi^0$
$(470 \pm 30) - i(295 \pm 20)$	6 COLANGELO	01	RVUE $\pi\pi \rightarrow \pi\pi$
$(535 \pm^{48}_{-36}) - i(155 \pm^{76}_{-53})$	12 ISHIDA	01	$\mathcal{T}(3S) \rightarrow \mathcal{T}\pi\pi$
$610 \pm 14 - i620 \pm 26$	13 SUROVTSOV	01	RVUE $\pi\pi \rightarrow \pi\pi, K\bar{K}$
$(558 \pm^{34}_{-27}) - i(196 \pm^{32}_{-41})$	ISHIDA	00B	$\rho\bar{\rho} \rightarrow \pi^0 \pi^0 \pi^0$
$445 - i235$	HANNAH	99	RVUE π scalar form factor
$(523 \pm 12) - i(259 \pm 7)$	KAMINSKI	99	RVUE $\pi\pi \rightarrow \pi\pi, K\bar{K}, \sigma\sigma$
$442 - i227$	OLLER	99	RVUE $\pi\pi \rightarrow \pi\pi, K\bar{K}$
$469 - i203$	OLLER	99B	RVUE $\pi\pi \rightarrow \pi\pi, K\bar{K}$
$445 - i221$	OLLER	99C	RVUE $\pi\pi \rightarrow \pi\pi, K\bar{K}, \eta\eta$
$(1530 \pm^{90}_{-250}) - i(560 \pm 40)$	ANISOVICH	98B	RVUE Compilation

Meson Particle Listings

 $f_0(600)$

420 - i 212	LOCHER	98	RVUE	$\pi\pi \rightarrow \pi\pi, K\bar{K}$
(602 \pm 26) - i (196 \pm 27)	14 ISHIDA	97		$\pi\pi \rightarrow \pi\pi$
(537 \pm 20) - i (250 \pm 17)	15 KAMINSKI	97B	RVUE	$\pi\pi \rightarrow \pi\pi, K\bar{K}, 4\pi$
470 - i 250	16,17 TORNQVIST	96	RVUE	$\pi\pi \rightarrow \pi\pi, K\bar{K}, K\pi,$ $\eta\pi$
\sim (1100 - i 300)	AMSLER	95B	CBAR	$\bar{p}p \rightarrow 3\pi^0$
400 - i 500	17,18 AMSLER	95D	CBAR	$\bar{p}p \rightarrow 3\pi^0$
1100 - i 137	17,19 AMSLER	95D	CBAR	$\bar{p}p \rightarrow 3\pi^0$
387 - i 305	17,20 JANSSEN	95	RVUE	$\pi\pi \rightarrow \pi\pi, K\bar{K}$
525 - i 269	21 ACHASOV	94	RVUE	$\pi\pi \rightarrow \pi\pi$
(506 \pm 10) - i (247 \pm 3)	KAMINSKI	94	RVUE	$\pi\pi \rightarrow \pi\pi, K\bar{K}$
370 - i 356	22 ZOU	94B	RVUE	$\pi\pi \rightarrow \pi\pi, K\bar{K}$
408 - i 342	17,22 ZOU	93	RVUE	$\pi\pi \rightarrow \pi\pi, K\bar{K}$
870 - i 370	17,23 AU	87	RVUE	$\pi\pi \rightarrow \pi\pi, K\bar{K}$
470 - i 208	24 VANBEVEREN	86	RVUE	$\pi\pi \rightarrow \pi\pi, K\bar{K}, \eta\eta,$ \dots
(750 \pm 50) - i (450 \pm 50)	25 ESTABROOKS	79	RVUE	$\pi\pi \rightarrow \pi\pi, K\bar{K}$
(660 \pm 100) - i (320 \pm 70)	PROPOPO... 73	HBC	$\pi\pi \rightarrow \pi\pi, K\bar{K}$	
650 - i 370	26 BASDEVANT	72	RVUE	$\pi\pi \rightarrow \pi\pi$

- From the K_{e4} data of BATLEY 08A and $\pi N \rightarrow \pi\pi N$ data of HYAMS 73.
- From the K_{e4} data of BATLEY 08A and $\pi N \rightarrow \pi\pi N$ data of PROTOPOESCU 73, GRAYER 74, and ESTABROOKS 74.
- From a mean of three different $f_0(600)$ parametrizations. Uses 40k events.
- From an isobar model using 2.6k events.
- Reanalysis of ABLIKIM 04A, PISLAK 01, and HYAMS 73 data.
- From the solution of the Roy equation (ROY 71) for the isoscalar S-wave and using a phase-shift analysis of HYAMS 73 and PROTOPOESCU 73 data.
- Reanalysis of the data from PROTOPOESCU 73, ESTABROOKS 74, GRAYER 74, ROSSELET 77, PISLAK 03, and AKHMETSHIN 04.
- From a mean of six different analyses and $f_0(600)$ parameterizations.
- Using data on $\psi(2S) \rightarrow J/\psi\pi\pi$ from BAI 00E and on $\Upsilon(nS) \rightarrow \Upsilon(mS)\pi\pi$ from BUTLER 94B and ALEXANDER 98.
- Reanalysis of data from PROTOPOESCU 73, ESTABROOKS 74, GRAYER 74, and COHEN 80 in the unitarized ChPT model.
- From a combined analysis of HYAMS 73, AUGUSTIN 89, AITALA 01B, and PISLAK 01.
- A similar analysis (KOMADA 01) finds $(580^{+79}_{-30}) - i(190^{+107}_{-49})$ MeV.
- Coupled channel reanalysis of BATON 70, BENSINGER 71, BAILLON 72, HYAMS 73, HYAMS 75, ROSSELET 77, COHEN 80, and ETKIN 82B using the uniformizing variable.
- Reanalysis of data from HYAMS 73, GRAYER 74, SRINIVASAN 75, and ROSSELET 77 using the interfering amplitude method.
- Average and spread of 4 variants ("up" and "down") of KAMINSKI 97B 3-channel model.
- Uses data from BEIER 72B, OCHS 73, HYAMS 73, GRAYER 74, ROSSELET 77, CASON 83, ASTON 88, and ARMSTRONG 91B. Coupled channel analysis with flavor symmetry and all light two-pseudoscalars systems.
- Demonstrates explicitly that $f_0(600)$ and $f_0(1370)$ are two different poles.
- Coupled channel analysis of $\bar{p}p \rightarrow 3\pi^0, \pi^0\eta\eta$ and $\pi^0\pi^0\eta$ on sheet II.
- Coupled channel analysis of $\bar{p}p \rightarrow 3\pi^0, \pi^0\eta\eta$ and $\pi^0\pi^0\eta$ on sheet III.
- Analysis of data from FALVARD 88.
- Analysis of data from OCHS 73, ESTABROOKS 75, ROSSELET 77, and MUKHIN 80.
- Analysis of data from OCHS 73, GRAYER 74, and ROSSELET 77.
- Analysis of data from OCHS 73, GRAYER 74, BECKER 79, and CASON 83.
- Coupled-channel analysis using data from PROTOPOESCU 73, HYAMS 73, HYAMS 75, GRAYER 74, ESTABROOKS 74, ESTABROOKS 75, FROGGATT 77, CORDEEN 79, BISWAS 81.
- Analysis of data from APEL 73, GRAYER 74, CASON 76, PAWLICKI 77. Includes spread and errors of 4 solutions.
- Analysis of data from BATON 70, BENSINGER 71, COLTON 71, BAILLON 72, PROTOPOESCU 73, and WALKER 67.

 $f_0(600)$ BREIT-WIGNER MASS OR K-MATRIX POLE PARAMETERS

VALUE (MeV)	DOCUMENT ID	TECN	COMMENT
(400-1200) OUR ESTIMATE			
513 \pm 32	27 MURAMATSU 02	CLEO	$e^+e^- \approx 10$ GeV
• • • We do not use the following data for averages, fits, limits, etc. • • •			
478 \pm $^{+24}_{-23}$ \pm 17	AITALA	01B E791	$D^+ \rightarrow \pi^-\pi^+\pi^+$
563 \pm $^{+58}_{-29}$	28 ISHIDA	01	$\Upsilon(3S) \rightarrow \Upsilon\pi\pi$
555	29 ASNER	00 CLE2	$\tau^- \rightarrow \pi^-\pi^0\pi^0\nu_\tau$
540 \pm 36	ISHIDA	00B	$p\bar{p} \rightarrow \pi^0\pi^0\pi^0$
750 \pm 4	ALEKSEEV	99 SPEC	$1.78\pi^-\rho^{\text{polar}} \rightarrow \pi^-\pi^+n$
744 \pm 5	ALEKSEEV	98 SPEC	$1.78\pi^-\rho^{\text{polar}} \rightarrow \pi^-\pi^+n$
759 \pm 5	30 TROYAN	98	$5.2np \rightarrow np\pi^+\pi^-$
780 \pm 30	ALDE	97 GAM2	$450pp \rightarrow pp\pi^0\pi^0$
585 \pm 20	31 ISHIDA	97	$\pi\pi \rightarrow \pi\pi$
761 \pm 12	32 SVEC	96 RVUE	$6-17\pi N^{\text{polar}} \rightarrow \pi^+\pi^-N$
\sim 860	33,34 TORNQVIST	96 RVUE	$\pi\pi \rightarrow \pi\pi, K\bar{K}, K\pi, \eta\pi$
1165 \pm 50	35,36 ANISOVICH	95 RVUE	$\pi^-\rho \rightarrow \pi^0\pi^0n,$ $\bar{p}p \rightarrow \pi^0\pi^0\pi^0, \pi^0\pi^0\eta,$ $\pi^0\eta\eta$
\sim 1000	37 ACHASOV	94 RVUE	$\pi\pi \rightarrow \pi\pi$
414 \pm 20	32 AUGUSTIN	89 DM2	

- Statistical uncertainty only.
- A similar analysis (KOMADA 01) finds 526^{+48}_{-37} MeV.
- From the best fit of the Dalitz plot.
- 6 σ effect, no PWA.
- Reanalysis of data from HYAMS 73, GRAYER 74, SRINIVASAN 75, and ROSSELET 77 using the interfering amplitude method.
- Breit-Wigner fit to S-wave intensity measured in $\pi N \rightarrow \pi^-\pi^+N$ on polarized targets. The fit does not include $f_0(980)$.
- Uses data from ASTON 88, OCHS 73, HYAMS 73, ARMSTRONG 91B, GRAYER 74, CASON 83, ROSSELET 77, and BEIER 72B. Coupled channel analysis with flavor symmetry and all light two-pseudoscalars systems.
- Also observed by ASNER 00 in $\tau^- \rightarrow \pi^-\pi^0\pi^0\nu_\tau$ decays.
- Uses $\pi^0\pi^0$ data from ANISOVICH 94, AMSLER 94D, and ALDE 95B, $\pi^+\pi^-$ data from OCHS 73, GRAYER 74 and ROSSELET 77, and $\eta\eta$ data from ANISOVICH 94.
- The pole is on Sheet III. Demonstrates explicitly that $f_0(600)$ and $f_0(1370)$ are two different poles.
- Analysis of data from OCHS 73, ESTABROOKS 75, ROSSELET 77, and MUKHIN 80.

 $f_0(600)$ BREIT-WIGNER WIDTH

VALUE (MeV)	DOCUMENT ID	TECN	COMMENT
(600-1000) OUR ESTIMATE			
335 \pm 67	38 MURAMATSU 02	CLEO	$e^+e^- \approx 10$ GeV
• • • We do not use the following data for averages, fits, limits, etc. • • •			
324 \pm $^{+42}_{-40}$ \pm 21	AITALA	01B E791	$D^+ \rightarrow \pi^-\pi^+\pi^+$
372 \pm $^{+229}_{-95}$	39 ISHIDA	01	$\Upsilon(3S) \rightarrow \Upsilon\pi\pi$
540	40 ASNER	00 CLE2	$\tau^- \rightarrow \pi^-\pi^0\pi^0\nu_\tau$
372 \pm 80	ISHIDA	00B	$p\bar{p} \rightarrow \pi^0\pi^0\pi^0$
119 \pm 13	ALEKSEEV	99 SPEC	$1.78\pi^-\rho^{\text{polar}} \rightarrow \pi^-\pi^+n$
77 \pm 22	ALEKSEEV	98 SPEC	$1.78\pi^-\rho^{\text{polar}} \rightarrow \pi^-\pi^+n$
35 \pm 12	41 TROYAN	98	$5.2np \rightarrow np\pi^+\pi^-$
780 \pm 60	ALDE	97 GAM2	$450pp \rightarrow pp\pi^0\pi^0$
385 \pm 70	42 ISHIDA	97	$\pi\pi \rightarrow \pi\pi$
290 \pm 54	43 SVEC	96 RVUE	$6-17\pi N^{\text{polar}} \rightarrow \pi^+\pi^-N$
\sim 880	44,45 TORNQVIST	96 RVUE	$\pi\pi \rightarrow \pi\pi, K\bar{K}, K\pi, \eta\pi$
460 \pm 40	46,47 ANISOVICH	95 RVUE	$\pi^-\rho \rightarrow \pi^0\pi^0n,$ $\bar{p}p \rightarrow \pi^0\pi^0\pi^0, \pi^0\pi^0\eta,$ $\pi^0\eta\eta$
\sim 3200	48 ACHASOV	94 RVUE	$\pi\pi \rightarrow \pi\pi$
494 \pm 58	43 AUGUSTIN	89 DM2	

- Statistical uncertainty only.
- A similar analysis (KOMADA 01) finds 301^{+145}_{-100} MeV.
- From the best fit of the Dalitz plot.
- 6 σ effect, no PWA.
- Reanalysis of data from HYAMS 73, GRAYER 74, SRINIVASAN 75, and ROSSELET 77 using the interfering amplitude method.
- Breit-Wigner fit to S-wave intensity measured in $\pi N \rightarrow \pi^-\pi^+N$ on polarized targets. The fit does not include $f_0(980)$.
- Uses data from ASTON 88, OCHS 73, HYAMS 73, ARMSTRONG 91B, GRAYER 74, CASON 83, ROSSELET 77, and BEIER 72B. Coupled channel analysis with flavor symmetry and all light two-pseudoscalars systems.
- Also observed by ASNER 00 in $\tau^- \rightarrow \pi^-\pi^0\pi^0\nu_\tau$ decays.
- Uses $\pi^0\pi^0$ data from ANISOVICH 94, AMSLER 94D, and ALDE 95B, $\pi^+\pi^-$ data from OCHS 73, GRAYER 74 and ROSSELET 77, and $\eta\eta$ data from ANISOVICH 94.
- The pole is on Sheet III. Demonstrates explicitly that $f_0(600)$ and $f_0(1370)$ are two different poles.
- Analysis of data from OCHS 73, ESTABROOKS 75, ROSSELET 77, and MUKHIN 80.

 $f_0(600)$ DECAY MODES

Mode	Fraction (Γ_i/Γ)
Γ_1 $\pi\pi$	dominant
Γ_2 $\gamma\gamma$	seen

 $f_0(600)$ PARTIAL WIDTHS

VALUE (keV)	DOCUMENT ID	TECN	COMMENT	Γ_2
• • • We do not use the following data for averages, fits, limits, etc. • • •				
1.2 \pm 0.4	49 BERNABEU 08	RVUE		
3.9 \pm 0.6	50 MENNESSIER 08	RVUE	$\gamma\gamma \rightarrow \pi^+\pi^-, \pi^0\pi^0$	
4.1 \pm 0.3	51 PENNINGTON 06	RVUE	$\gamma\gamma \rightarrow \pi^0\pi^0$	
3.8 \pm 1.5	52,53 BOGLIONE 99	RVUE	$\gamma\gamma \rightarrow \pi^+\pi^-, \pi^0\pi^0$	
5.4 \pm 2.3	52 MORGAN 90	RVUE	$\gamma\gamma \rightarrow \pi^+\pi^-, \pi^0\pi^0$	
10 \pm 6	COURAU 86	DM1	$e^+e^- \rightarrow \pi^+\pi^-\pi^+\pi^-$	
49 Using p, n polarizabilities from PDG 06 and fitting to $\pi\pi$ phase motion from GARCIA-MARTIN 07 and σ -poles from GARCIA-MARTIN 07 and CAPRINI 06.				
50 Using an analytic K-matrix model.				
51 Using unitarity and the σ pole position from CAPRINI 06.				
52 This width could equally well be assigned to the $f_0(1370)$. The authors analyse data from BOYER 90 and MARSISKE 90 and report strong correlation with $\gamma\gamma$ width of $f_2(1270)$.				
53 Supersedes MORGAN 90.				

$f_0(600)$ REFERENCES

BATLEY	08A	EPJ C54 411	J.R. Batley <i>et al.</i>	(CERN NA48/2 Collab.)
BERNABEU	08	PRL 100 241804	J. Bernabeu, J. Prades	(IFIC, GRAN)
CAPRINI	08	PR D77 114019	I. Caprini	
MENNESSIER	08	PL B645 205	G. Mennessier, S. Narison, W. Ochs	
ABLIKIM	07A	PL B645 19	M. Ablikim <i>et al.</i>	(BES Collab.)
BONVICINI	07	PR D76 012001	G. Bonvicini <i>et al.</i>	(CLEO Collab.)
BUGG	07A	JPG 34 151	D.V. Bugg <i>et al.</i>	
GARCIA-MAR...	07	PR D76 074034	R. Garcia-Martin, J.R. Pelaez, F.J. Yndurain	
CAPRINI	06	PRL 96 132001	I. Caprini, G. Colangelo, H. Leutwyler	(BCIP+)
PDG	06	JPG 33 1	W.-M. Yao <i>et al.</i>	(PDG Collab.)
PENNINGTON	06	PRL 97 011601	M.R. Pennington	
ZHOU	05	JHEP 0502 043	Z.Y. Zhou <i>et al.</i>	
ABLIKIM	04A	PL B598 149	M. Ablikim <i>et al.</i>	(BES Collab.)
AKHMETSHIN	04	PL B578 285	R.R. Akhmetshin <i>et al.</i>	(Novosibirsk CMD-2 Collab.)
GALLEGOS	04	PR D69 074033	A. Gallegos <i>et al.</i>	
PELAEZ	04A	MPL A19 2879	J.R. Pelaez	
BUGG	03	PL B572 1	D.V. Bugg	
PISLAK	03	PR D67 072004	S. Pislak <i>et al.</i>	(BNL E865 Collab.)
MURAMATSU	02	PRL 89 251802	H. Muramatsu <i>et al.</i>	(CLEO Collab.)
Also		PRL 90 059901 (erratum)	H. Muramatsu <i>et al.</i>	(CLEO Collab.)
AITALA	01B	PRL 86 770	E.M. Aitala <i>et al.</i>	(FNAL E791 Collab.)
BLACK	01	PR D64 014031	D. Black <i>et al.</i>	
COLANGELO	01	NP B603 125	G. Colangelo, J. Gasser, H. Leutwyler	
ISHIDA	01	PL B518 47	M. Ishida <i>et al.</i>	
KOMADA	01	PL B508 31	T. Komada <i>et al.</i>	
PISLAK	01	PRL 87 221801	S. Pislak <i>et al.</i>	(BNL E865 Collab.)
Also		PR D67 072004	S. Pislak <i>et al.</i>	(BNL E865 Collab.)
SUROVTSVET	01	PR D63 054024	Y.S. Surovtsev, D. Krupa, M. Nagy	
ASNER	00	PR D61 012002	D.M. Asner <i>et al.</i>	(CLEO Collab.)
BAI	00E	PR D62 032002	J. Bai <i>et al.</i>	(BES Collab.)
ISHIDA	00B	PTP 104 203	M. Ishida <i>et al.</i>	
ALEKSEEV	99	NP B541 3	I.G. Alekseev <i>et al.</i>	
BGIOLIONE	99	EPJ C9 11	M. Boglione, M.R. Pennington	
HANNAH	99	PR D60 017502	T. Hannah	
KAMINSKI	99	EPJ C9 141	R. Kaminski, L. Lesniak, B. Loiseau	(CRAC, PARIN)
OLLER	99	PR D60 099906 (erratum)	J.A. Oller <i>et al.</i>	
OLLER	99B	NP A652 407 (erratum)	J.A. Oller, E. Oset	
OLLER	99C	PR D60 074023	J.A. Oller, E. Oset	
ALEKSEEV	98	PAN 61 174	I.G. Alekseev <i>et al.</i>	
ALEXANDER	98	PR D58 052004	J.P. Alexander <i>et al.</i>	(CLEO Collab.)
ANISOVICH	98B	SPU 41 419	V.V. Anisovich <i>et al.</i>	
Translated from		UFN 168 481.		
LOCHER	98	EPJ C4 317	M.P. Locher <i>et al.</i>	(PSI)
TROYAN	98	JINRRC 5-91 33	Yu. Troyan <i>et al.</i>	
ALDE	97	PL B397 350	D.M. Alde <i>et al.</i>	(GAMS Collab.)
ISHIDA	97	PTP 98 1005	S. Ishida <i>et al.</i>	(TOKY, MINA, KEK)
KAMINSKI	97B	PL B413 130	R. Kaminski, L. Lesniak, B. Loiseau	(CRAC, IPN)
Also		PTP 95 745	S. Ishida <i>et al.</i>	(TOKY, MINA, KEK)
SVEC	96	PR D53 2343	M. Svec	(MCGI)
TORNQVIST	96	PRL 76 1575	N.A. Tornqvist, M. Roos	(HELS)
ALDE	95B	ZPHY C66 375	D.M. Alde <i>et al.</i>	(GAMS Collab.)
AMSLER	95B	PL B342 433	C. Amstler <i>et al.</i>	(Crystal Barrel Collab.)
AMSLER	95D	PL B355 425	C. Amstler <i>et al.</i>	(Crystal Barrel Collab.)
ANISOVICH	95	PL B355 363	V.V. Anisovich <i>et al.</i>	(PNPI, SERP)
JANSSSEN	95	PR D52 2690	G. Janssen <i>et al.</i>	(STON, ADLD, JULI)
ACHASOV	94	PR D49 5779	N.M. Achasov, G.N. Shestakov	(NOVA)
AMSLER	94D	PL B333 277	C. Amstler <i>et al.</i>	(Crystal Barrel Collab.)
ANISOVICH	94	PL B323 233	V.V. Anisovich <i>et al.</i>	(Crystal Barrel Collab.)
BUTLER	94B	PR D49 40	F. Butler <i>et al.</i>	(CLEO Collab.)
KAMINSKI	94	PR D50 3145	R. Kaminski, L. Lesniak, J.P. Maillet	(CRAC+)
ZOU	94B	PR D50 591	B.S. Zou, D.V. Bugg	(LOQM)
ZOU	93	PR D48 R3948	B.S. Zou, D.V. Bugg	(LOQM)
ARMSTRONG	91B	ZPHY C52 389	T.A. Armstrong <i>et al.</i>	(ATHU, BARI, BIRM+)
BOYER	90	PR D42 1350	J. Boyer <i>et al.</i>	(Mark II Collab.)
MARISISKE	90	PR D41 3324	H. Marislike <i>et al.</i>	(Crystal Ball Collab.)
MORGAN	90	ZPHY C48 623	D. Morgan, M.R. Pennington	(BAL, DIRH)
AUGUSTIN	89	PR D39 5779	D. Augustin, G. Cosme	(DM2 Collab.)
ASTON	88	NP B296 493	D. Aston <i>et al.</i>	(SLAC, NAGO, CINC, INUS)
FALVARD	88	PR D38 2706	A. Falvard <i>et al.</i>	(CLER, FRAS, LALO+)
AU	87	PR D35 1633	K.L. Au, D. Morgan, M.R. Pennington	(DURH, RAL)
COURAU	86	NP B271 1	A. Courau <i>et al.</i>	(CLER, LALO)
VANBEVEREN	86	ZPHY C30 615	E. van Beveren <i>et al.</i>	(NUM, BIEL)
CASON	83	PR D28 1586	N.M. Cason <i>et al.</i>	(NDAM, ANL)
ETKIN	82B	PR D25 1786	A. Etkin <i>et al.</i>	(BNL, CUNY, TUFTS, VAND)
BISWAS	81	PRL 47 1378	N.N. Biswas <i>et al.</i>	(NDAM, ANL)
COHEN	80	PR D22 2595	D. Cohen <i>et al.</i>	(ANL) IJP
MUKHIN	80	JETPL 32 601	K.N. Mukhin <i>et al.</i>	(KAE)
Translated from		ZETFP 32 636.		
BECKER	79	NP B151 46	H. Becker <i>et al.</i>	(MPIM, CERN, ZEEM, CRAC)
CORDEN	79	NP B157 250	M.J. Corden <i>et al.</i>	(BIRM, RHEL, TELA+ JIP)
ESTABROOKS	79	PR D19 2678	P. Estabrooks <i>et al.</i>	(CARL)
FROGGATT	77	NP B129 89	C.D. Froggatt, J.L. Petersen	(GLAS, NORD)
PAWLICKI	77	PR D15 3196	A.J. Pawlicki <i>et al.</i>	(ANL) IJ
ROSSELET	77	PR D15 574	L. Rosselet <i>et al.</i>	(GEVA, SAEL)
CASON	76	PRL 36 1485	N.M. Cason <i>et al.</i>	(NDAM, ANL) IJ
ESTABROOKS	75	NP B95 322	P.G. Estabrooks, A.D. Martin	(DURH)
HYAMS	75	NP B100 205	B.D. Hyams <i>et al.</i>	(CERN, MPIM)
SRINIVASAN	75	PR D12 681	V. Srinivasan <i>et al.</i>	(NDAM, ANL)
ESTABROOKS	74	NP B79 301	P.G. Estabrooks, A.D. Martin	(DURH)
GRAYER	74	NP B75 189	G. Grayer <i>et al.</i>	(CERN, MPIM)
APEL	73	PL 41B 542	W.D. Apel <i>et al.</i>	(KARL, PISA)
HYAMS	73	NP B64 134	B.D. Hyams <i>et al.</i>	(CERN, MPIM)
OCHS	73	Thesis	W. Ochs	(MPIM, MUNI)
PROTOPOP...	73	PR D7 1279	S.D. Protopopescu <i>et al.</i>	(LBL)
BAILLON	72	PL 38B 555	P.H. Baillon <i>et al.</i>	(SLAC)
BASDEVANT	72	PL 41B 178	J.W. Basdevant, C.D. Froggatt, J.L. Petersen	(CERN)
BEIER	72B	PRL 29 511	E.W. Beier <i>et al.</i>	(PENN)
BENSINGER	71	PL 36B 134	J.R. Bensingier <i>et al.</i>	(WIS C)
COLTON	71	PR D3 2028	E.P. Colton <i>et al.</i>	(LBL, FNAL, UCLA+)
ROY	71	PL 36B 353	S.M. Roy	
BATON	70	PL 38B 528	J.P. Baton, G. Laurens, J. Reigner	(SAEL)
WALKER	67	RMP 39 695	W.D. Walker	(WIS C)

 $\rho(770)$

$$I^G(J^{PC}) = 1^+(1^-)$$

THE $\rho(770)$

Updated May 2010 by S. Eidelman (Novosibirsk) and G. Venanzoni (Frascati).

The determination of the parameters of the $\rho(770)$ is beset with many difficulties because of its large width. In physical region fits for hadroproduced ρ mesons, the line shape does not correspond to a relativistic Breit-Wigner function with a P -wave width, but requires some additional shape parameter. This dependence on parameterization was demonstrated long ago [1]. Bose-Einstein correlations are another source of shifts in the $\rho(770)$ line shape, particularly in multiparticle final state systems [2].

The same model dependence afflicts any other source of resonance parameters, such as the energy-dependence of the phase shift δ_1^1 , or the pole position. It is, therefore, not surprising that a study of $\rho(770)$ dominance in the decays of the η and η' reveals the need for specific dynamical effects, in addition to the $\rho(770)$ pole [3,4].

The cleanest determination of the $\rho(770)$ mass and width comes from e^+e^- annihilation and τ -lepton decays. Barate *et al.* [5] shows that the charged $\rho(770)$ parameters measured in τ -lepton decays are consistent with those of the neutral one determined from e^+e^- data [6]. This conclusion is qualitatively supported by the high-statistics study of Anderson *et al.* [7]. However, model-independent comparison of the two-pion mass spectrum in τ decays, and the $e^+e^- \rightarrow \pi^+\pi^-$ cross section, gives indications of discrepancies between the overall normalization: τ data are about 3% higher than e^+e^- data [7,8]. A detailed analysis using such two-pion mass spectra from τ decays measured by OPAL [9], CLEO [7], and ALEPH [10], as well as recent pion form factor measurements in e^+e^- annihilation by CMD-2 [11,12], show that the discrepancy can be as high as 10% above the ρ meson [13,14]. This discrepancy remains after recent measurements of the two-pion cross section in e^+e^- annihilation at KLOE [15,16] and SND [17,18]. The effect is not accounted for by isospin breaking [19-21], but the accuracy of its calculation may be overestimated [22,23]. Ghozzi [24] suggests that this effect can be explained if the charged ρ mass were higher than that of the neutral one by a few MeV. Existing theoretical models of the possible mass difference predict either a much smaller value [25], or a heavier neutral ρ meson [26]. Experimental accuracy is not yet sufficient for unambiguous conclusions. The size of the effect is also sensitive to the possible width difference [27,28]. The discrepancy between e^+e^- and τ becomes smaller after a new measurement of the pion form factor using radiative return at BaBar [29], a high-statistics study of τ decays into two pions at Belle [30] and reanalysis of isospin breaking effects [31]. Benayoun *et al.* [32,33] performs a detailed analysis of the whole set of the ρ , ω , and ϕ decays, consistently taking into account mixing effects in the hidden local symmetry model, and claims

Meson Particle Listings

 $\rho(770)$

that in this approach τ decays to two pions can be naturally accounted for.

References

- J. Pisut and M. Roos, Nucl. Phys. **B6**, 325 (1968).
- G.D. Lafferty, Z. Phys. **C60**, 659 (1993).
- A. Abele *et al.*, Phys. Lett. **B402**, 195 (1997).
- M. Benayoun *et al.*, Eur. Phys. J. **C31**, 525 (2003).
- R. Barate *et al.*, Z. Phys. **C76**, 15 (1997).
- L.M. Barkov *et al.*, Nucl. Phys. **B256**, 365 (1985).
- S. Anderson *et al.*, Phys. Rev. **D61**, 112002 (2000).
- S. Eidelman and V. Ivanchenko, Nucl. Phys. (Proc. Supp.) **B76**, 319 (1999).
- K. Ackerstaff *et al.*, Eur. Phys. J. **C7**, 571 (1999).
- S. Schael *et al.*, Phys. Reports **421**, 191 (2005).
- R.R. Akhmetshin *et al.*, Phys. Lett. **B527**, 161 (2002).
- R.R. Akhmetshin *et al.*, Phys. Lett. **B578**, 285 (2004).
- M. Davier *et al.*, Eur. Phys. J. **C27**, 497 (2003).
- M. Davier *et al.*, Eur. Phys. J. **C31**, 503 (2003).
- A. Aloisio *et al.*, Phys. Lett. **B606**, 12 (2005).
- F. Ambrosino *et al.*, Phys. Lett. **B670**, 285 (2009).
- M.N. Achasov *et al.*, Sov. Phys. JETP **101**, 1053 (2005).
- M.N. Achasov *et al.*, Sov. Phys. JETP **103**, 380 (2006).
- R. Alemany *et al.*, Eur. Phys. J. **C2**, 123 (1998).
- V. Cirigliano *et al.*, Phys. Lett. **B513**, 361 (2001).
- V. Cirigliano *et al.*, Eur. Phys. J. **C23**, 121 (2002).
- K. Maltman and C.E. Wolfe, Phys. Rev. **D73**, 013004 (2006).
- C.E. Wolfe and K. Maltman, Phys. Rev. **D80**, 114024 (2009).
- S. Ghozzi and F. Jegerlehner, Phys. Lett. **B583**, 222 (2004).
- J. Bijnens *et al.*, Phys. Lett. **B374**, 210 (1996).
- M.N. Achasov *et al.*, Sov. Phys. JETP Lett. **69**, 7 (1999).
- G. Toledo Sanchez, J.L. Garcia-Luna, and V. Gonzalez-Enciso, Phys. Rev. **D76**, 033001 (2007).
- F.V. Florez-Baez *et al.*, Phys. Rev. **D76**, 096010 (2007).
- B. Aubert *et al.*, Phys. Rev. Lett. **103**, 231801 (2009).
- M. Fujikawa *et al.*, Phys. Rev. **D78**, 072006 (2008).
- M. Davier *et al.*, Eur. Phys. J. **C66**, 127 (2010).
- M. Benayoun *et al.*, Eur. Phys. J. **C55**, 199 (2008).
- M. Benayoun *et al.*, Eur. Phys. J. **C65**, 211 (2010).

 $\rho(770)$ MASS

We no longer list S -wave Breit-Wigner fits, or data with high combinatorial background.

NEUTRAL ONLY, e^+e^-

VALUE (MeV)	EVTS	DOCUMENT ID	TECN	COMMENT
775.49 ± 0.34 OUR AVERAGE				
775.97 ± 0.46 ± 0.70	900k	1 AKHMETSHIN 07		$e^+e^- \rightarrow \pi^+\pi^-$
774.6 ± 0.4 ± 0.5	800k	2,3 ACHASOV 06	SND	$e^+e^- \rightarrow \pi^+\pi^-$
775.65 ± 0.64 ± 0.50	114k	4,5 AKHMETSHIN 04	CMD2	$e^+e^- \rightarrow \pi^+\pi^-$
775.9 ± 0.5 ± 0.5	1.98M	6 ALOISIO 03	KLOE	$1.02 e^+e^- \rightarrow \pi^+\pi^-$
				$\pi^+\pi^-\pi^0$
775.8 ± 0.9 ± 2.0	500k	6 ACHASOV 02	SND	$1.02 e^+e^- \rightarrow \pi^+\pi^-$
				$\pi^+\pi^-\pi^0$
775.9 ± 1.1		7 BARKOV 85	OLYA	$e^+e^- \rightarrow \pi^+\pi^-$

••• We do not use the following data for averages, fits, limits, etc. •••

775.8 ± 0.5 ± 0.3	1.98M	8 ALOISIO 03	KLOE	$1.02 e^+e^- \rightarrow \pi^+\pi^-\pi^0$
775.9 ± 0.6 ± 0.5	1.98M	9 ALOISIO 03	KLOE	$1.02 e^+e^- \rightarrow \pi^+\pi^-\pi^0$
775.0 ± 0.6 ± 1.1	500k	10 ACHASOV 02	SND	$1.02 e^+e^- \rightarrow \pi^+\pi^-\pi^0$
775.1 ± 0.7 ± 5.3		11 BENAYOUN 98	RVUE	$e^+e^- \rightarrow \pi^+\pi^-$, $\mu^+\mu^-$
770.5 ± 1.9 ± 5.1		12 GARDNER 98	RVUE	$0.28-0.92 e^+e^- \rightarrow \pi^+\pi^-$
764.1 ± 0.7		13 O'CONNELL 97	RVUE	$e^+e^- \rightarrow \pi^+\pi^-$
757.5 ± 1.5		14 BERNICHA 94	RVUE	$e^+e^- \rightarrow \pi^+\pi^-$
768 ± 1		15 GESHKEN... 89	RVUE	$e^+e^- \rightarrow \pi^+\pi^-$

CHARGED ONLY, τ DECAYS and e^+e^-

VALUE (MeV)	EVTS	DOCUMENT ID	TECN	CHG	COMMENT
775.11 ± 0.34 OUR AVERAGE					
774.6 ± 0.2 ± 0.5	5.4M	16,17 FUJIKAWA 08	BELL	±	$\tau^- \rightarrow \pi^-\pi^0\nu_\tau$
775.5 ± 0.7		17,18 SCHAEEL 05c	ALEP		$\tau^- \rightarrow \pi^-\pi^0\nu_\tau$
775.5 ± 0.5 ± 0.4	1.98M	6 ALOISIO 03	KLOE		$1.02 e^+e^- \rightarrow \pi^+\pi^-\pi^0$
775.1 ± 1.1 ± 0.5	87k	19,20 ANDERSON 00A	CLE2		$\tau^- \rightarrow \pi^-\pi^0\nu_\tau$

••• We do not use the following data for averages, fits, limits, etc. •••

774.8 ± 0.6 ± 0.4	1.98M	9 ALOISIO 03	KLOE	-	$1.02 e^+e^- \rightarrow \pi^+\pi^-\pi^0$
776.3 ± 0.6 ± 0.7	1.98M	9 ALOISIO 03	KLOE	+	$1.02 e^+e^- \rightarrow \pi^+\pi^-\pi^0$
773.9 ± 2.0 ± 0.3		21 SANZ-CILLERO03	RVUE		$\tau^- \rightarrow \pi^-\pi^0\nu_\tau$
774.5 ± 0.7 ± 1.5	500k	6 ACHASOV 02	SND	±	$1.02 e^+e^- \rightarrow \pi^+\pi^-\pi^0$
775.1 ± 0.5		22 PICH 01	RVUE		$\tau^- \rightarrow \pi^-\pi^0\nu_\tau$

MIXED CHARGES, OTHER REACTIONS

VALUE (MeV)	EVTS	DOCUMENT ID	TECN	CHG	COMMENT
763.0 ± 0.3 ± 1.2	600k	23 ABELE 99E	CBAR	0±	$0.0 \bar{p}p \rightarrow \pi^+\pi^-\pi^0$

CHARGED ONLY, HADROPRODUCED

VALUE (MeV)	EVTS	DOCUMENT ID	TECN	CHG	COMMENT
766.5 ± 1.1 OUR AVERAGE					
763.7 ± 3.2		ABELE 97	CBAR		$\bar{p}n \rightarrow \pi^-\pi^0\pi^0$
768 ± 9		AGUILAR... 91	EHS		400 pp
767 ± 3	2935	24 CAPRARO 87	SPEC	-	200 $\pi^- \text{Cu} \rightarrow \pi^-\pi^0\text{Cu}$
761 ± 5	967	24 CAPRARO 87	SPEC	-	200 $\pi^- \text{Pb} \rightarrow \pi^-\pi^0\text{Pb}$
771 ± 4		HUSTON 86	SPEC	+	202 $\pi^+ \text{A} \rightarrow \pi^+\pi^0\text{A}$
766 ± 7	6500	25 BYERLY 73	OSPK	-	5 π^-p
766.8 ± 1.5	9650	26 PISUT 68	RVUE	-	1.7-3.2 π^-p , $t < 10$
767 ± 6	900	24 EISNER 67	HBC	-	4.2 π^-p , $t < 10$

NEUTRAL ONLY, PHOTOPRODUCED

VALUE (MeV)	EVTS	DOCUMENT ID	TECN	CHG	COMMENT
768.5 ± 1.1 OUR AVERAGE					
770 ± 2 ± 1	79k	27 BREITWEG 98B	ZEUS	0	50-100 γp
767.6 ± 2.7		BARTALUCCI 78	CNTR	0	$\gamma p \rightarrow e^+e^-p$
775 ± 5		GLADDING 73	CNTR	0	2.9-4.7 γp
767 ± 4	1930	BALLAM 72	HBC	0	2.8 γp
770 ± 4	2430	BALLAM 72	HBC	0	4.7 γp
765 ± 10		ALVENSLEB... 70	CNTR	0	γA , $t < 0.01$
767.7 ± 1.9	140k	BIGGS 70	CNTR	0	<4.1 $\gamma C \rightarrow \pi^+\pi^-C$
765 ± 5	4000	ASBURY 67B	CNTR	0	$\gamma + \text{Pb}$

••• We do not use the following data for averages, fits, limits, etc. •••

771 ± 2	79k	28 BREITWEG 98B	ZEUS	0	50-100 γp
---------	-----	-----------------	------	---	-------------------

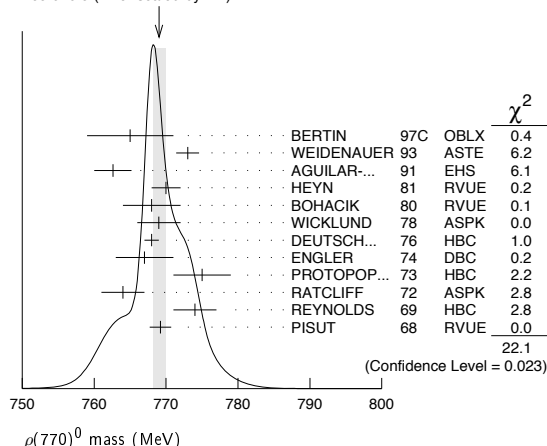
NEUTRAL ONLY, OTHER REACTIONS

VALUE (MeV)	EVTS	DOCUMENT ID	TECN	CHG	COMMENT
769.0 ± 0.9 OUR AVERAGE Error includes scale factor of 1.4. See the ideogram below.					
765 ± 6		BERTIN 97c	OBLX		0.0 $\bar{p}p \rightarrow \pi^+\pi^-\pi^0$
773 ± 1.6		WEIDENAUER 93	ASTE		$\bar{p}p \rightarrow \pi^+\pi^-\omega$
762.6 ± 2.6		AGUILAR... 91	EHS		400 pp
770 ± 2		29 HEYN 81	RVUE		Pion form factor
768 ± 4		30,31 BOHACIK 80	RVUE	0	
769 ± 3		25 WICKLUND 78	ASPK	0	3.4,6 $\pi^\pm N$
768 ± 1	76000	DEUTSCH... 76	HBC	0	16 π^+p
767 ± 4	4100	ENGLER 74	DBC	0	6 $\pi^+n \rightarrow \pi^+\pi^-\pi^0$
775 ± 4	32000	30 PROTOPOP... 73	HBC	0	7.1 π^+p , $t < 0.4$
764 ± 3	6800	RATCLIFF 72	ASPK	0	15 π^-p , $t < 0.3$
774 ± 3	1700	REYNOLDS 69	HBC	0	2.26 π^-p
769.2 ± 1.5	13300	32 PISUT 68	RVUE	0	1.7-3.2 π^-p , $t < 10$

• • • We do not use the following data for averages, fits, limits, etc. • • •

773.5 ± 2.5		33 COLANGELO	01 RVUE	$\pi\pi \rightarrow \pi\pi$
762.3 ± 0.5 ± 1.2	600k	34 ABELE	99E CBAR	0 0.0 $\bar{p}p \rightarrow \pi^+\pi^-\pi^0$
777 ± 2	4943	35 ADAMS	97 E665	470 $\mu p \rightarrow \mu X B$
770 ± 2		36 BOGOLYUB...	97 MIRA	32 $\bar{p}p \rightarrow \pi^+\pi^-\pi^0 X$
768 ± 8		36 BOGOLYUB...	97 MIRA	32 $p p \rightarrow \pi^+\pi^-\pi^0 X$
761.1 ± 2.9		DUBNICKA	89 RVUE	π form factor
777.4 ± 2.0		37 CHABAUD	83 ASPK	0 17 $\pi^- p$ polarized
769.5 ± 0.7		30,31 LANG	79 RVUE	0
770 ± 9		31 ESTABROOKS	74 RVUE	0 17 $\pi^- p \rightarrow \pi^+\pi^-\pi^0$
773.5 ± 1.7	11200	24 JACOBS	72 HBC	0 2.8 $\pi^- p$
775 ± 3	2250	HYAMS	68 OSPK	0 11.2 $\pi^- p$

WEIGHTED AVERAGE
769.0 ± 0.9 (Error scaled by 1.4)



- 1 A combined fit of AKHMETSHIN 07, AULCHENKO 06, and AULCHENKO 05.
- 2 Supersedes ACHASOV 05A.
- 3 A fit of the SND data from 400 to 1000 MeV using parameters of the $\rho(1450)$ and $\rho(1700)$ from a fit of the data of BARKOV 85, BISELLO 89 and ANDERSON 00A.
- 4 Using the GOUNARIS 68 parametrization with the complex phase of the $\rho\omega$ interference.
- 5 Update of AKHMETSHIN 02.
- 6 Assuming $m_{\rho^+} = m_{\rho^-}$, $\Gamma_{\rho^+} = \Gamma_{\rho^-}$.
- 7 From the GOUNARIS 68 parametrization of the pion form factor.
- 8 Assuming $m_{\rho^+} = m_{\rho^-} = m_{\rho^0}$, $\Gamma_{\rho^+} = \Gamma_{\rho^-} = \Gamma_{\rho^0}$.
- 9 Without limitations on masses and widths.
- 10 Assuming $m_{\rho^0} = m_{\rho^\pm}$, $g_{\rho^0\pi\pi} = g_{\rho^\pm\pi\pi}$.
- 11 Using the data of BARKOV 85 in the hidden local symmetry model.
- 12 From the fit to $e^+e^- \rightarrow \pi^+\pi^-$ data from the compilations of HEYN 81 and BARKOV 85, including the GOUNARIS 68 parametrization of the pion form factor.
- 13 A fit of BARKOV 85 data assuming the direct $\omega\pi\pi$ coupling.
- 14 Applying the S-matrix formalism to the BARKOV 85 data.
- 15 Includes BARKOV 85 data. Model-dependent width definition.
- 16 $|F_\pi(0)|^2$ fixed to 1.
- 17 From the GOUNARIS 68 parametrization of the pion form factor.
- 18 The error combines statistical and systematic uncertainties. Supersedes BARATE 97M.
- 19 $\rho(1700)$ mass and width fixed at 1700 MeV and 235 MeV respectively.
- 20 From the GOUNARIS 68 parametrization of the pion form factor. The second error is a model error taking into account different parametrizations of the pion form factor.
- 21 Using the data of BARATE 97M and the effective chiral Lagrangian.
- 22 From a fit of the model-independent parametrization of the pion form factor to the data of BARATE 97M.
- 23 Assuming the equality of ρ^+ and ρ^- masses and widths.
- 24 Mass errors enlarged by us to Γ/\sqrt{N} ; see the note with the $K^*(892)$ mass.
- 25 Phase shift analysis. Systematic errors added corresponding to spread of different fits.
- 26 From fit of 3-parameter relativistic P-wave Breit-Wigner to total mass distribution. Includes BATON 68, MILLER 67B, ALFF-STEINBERGER 66, HAGOPIAN 66, HAGOPIAN 66B, JACOBS 66B, JAMES 66, WEST 66, BLIEDEN 65 and CARMONY 64.
- 27 From the parametrization according to SOEDING 66.
- 28 From the parametrization according to ROSS 66.
- 29 HEYN 81 includes all spacelike and timelike F_π values until 1978.
- 30 From pole extrapolation.
- 31 From phase shift analysis of GRAYER 74 data.
- 32 Includes MALAMUD 69, ARMENISE 68, BACON 67, HUWE 67, MILLER 67B, ALFF-STEINBERGER 66, HAGOPIAN 66, HAGOPIAN 66B, JACOBS 66B, JAMES 66, WEST 66, GOLDHABER 64, ABOLINS 63.
- 33 Breit-Wigner mass from a phase-shift analysis of HYAMS 73 and PROTOPOPESCU 73 data.
- 34 Using relativistic Breit-Wigner and taking into account $\rho\omega$ interference.
- 35 Systematic errors not evaluated.
- 36 Systematic effects not studied.
- 37 From fit of 3-parameter relativistic Breit-Wigner to helicity-zero part of P-wave intensity. CHABAUD 83 includes data of GRAYER 74.

$m_{\rho(770)^0} - m_{\rho(770)^\pm}$

VALUE (MeV)	EVTs	DOCUMENT ID	TECN	CHG	COMMENT
-0.7 ± 0.8 OUR AVERAGE					Error includes scale factor of 1.5. See the ideogram below.
-2.4 ± 0.8		38 SCHAEEL	05c	ALEP	$\tau^- \rightarrow \pi^- \pi^0 \nu_\tau$
0.4 ± 0.7 ± 0.6	1.98M	39 ALOISIO	03	KLOE	1.02 $e^+e^- \rightarrow \pi^+\pi^-\pi^0$
1.3 ± 1.1 ± 2.0	500k	39 ACHASOV	02	SND	1.02 $e^+e^- \rightarrow \pi^+\pi^-\pi^0$
1.6 ± 0.6 ± 1.7	600k	ABELE	99E	CBAR	0 ± 0.0 $\bar{p}p \rightarrow \pi^+\pi^-\pi^0$
-4 ± 4	3000	40 REYNOLDS	69	HBC	-0 2.26 $\pi^- p$
-5 ± 5	3600	40 FOSTER	68	HBC	± 0.0 $\bar{p}p$
2.4 ± 2.1	22950	41 PISUT	68	RVUE	$\pi N \rightarrow \rho N$

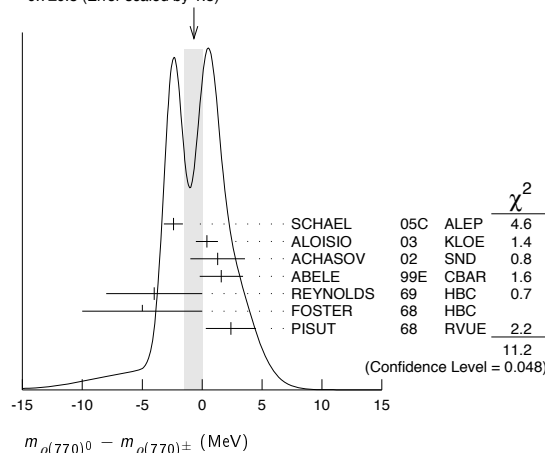
38 From the combined fit of the τ^- data from ANDERSON 00A and SCHAEEL 05c and e^+e^- data from the compilation of BARKOV 85, AKHMETSHIN 04, and ALOISIO 05. Supersedes BARATE 97M.

39 Assuming $m_{\rho^+} = m_{\rho^-}$, $\Gamma_{\rho^+} = \Gamma_{\rho^-}$.

40 From quoted masses of charged and neutral modes.

41 Includes MALAMUD 69, ARMENISE 68, BATON 68, BACON 67, HUWE 67, MILLER 67B, ALFF-STEINBERGER 66, HAGOPIAN 66, HAGOPIAN 66B, JACOBS 66B, JAMES 66, WEST 66, BLIEDEN 65, CARMONY 64, GOLDHABER 64, ABOLINS 63.

WEIGHTED AVERAGE
-0.7 ± 0.8 (Error scaled by 1.5)



$m_{\rho(770)^+} - m_{\rho(770)^-}$

VALUE (MeV)	EVTs	DOCUMENT ID	TECN	CHG	COMMENT
1.5 ± 0.8 ± 0.7	1.98M	42 ALOISIO	03	KLOE	1.02 $e^+e^- \rightarrow \pi^+\pi^-\pi^0$

42 Without limitations on masses and widths.

$\rho(770)$ RANGE PARAMETER

The range parameter R enters an energy-dependent correction to the width, of the form $(1 + q_r^2 R^2) / (1 + q^2 R^2)$, where q is the momentum of one of the pions in the $\pi\pi$ rest system. At resonance, $q = q_r$.

VALUE (GeV ⁻¹)	DOCUMENT ID	TECN	CHG	COMMENT
5.3 ± 0.9 -0.7	CHABAUD	83	ASPK	0 17 $\pi^- p$ polarized

$\rho(770)$ WIDTH

We no longer list S-wave Breit-Wigner fits, or data with high combinatorial background.

NEUTRAL ONLY, e^+e^-

VALUE (MeV)	EVTs	DOCUMENT ID	TECN	CHG	COMMENT
146.2 ± 0.7 OUR AVERAGE					Error includes scale factor of 1.1.
145.98 ± 0.75 ± 0.50	900k	43 AKHMETSHIN	07		$e^+e^- \rightarrow \pi^+\pi^-$
146.1 ± 0.8 ± 1.5	800k	44,45 ACHASOV	06	SND	$e^+e^- \rightarrow \pi^+\pi^-$
143.85 ± 1.33 ± 0.80	114k	46,47 AKHMETSHIN	04	CMD2	$e^+e^- \rightarrow \pi^+\pi^-$
147.3 ± 1.5 ± 0.7	1.98M	48 ALOISIO	03	KLOE	1.02 $e^+e^- \rightarrow \pi^+\pi^-\pi^0$
151.1 ± 2.6 ± 3.0	500k	48 ACHASOV	02	SND	0 1.02 $e^+e^- \rightarrow \pi^+\pi^-\pi^0$
150.5 ± 3.0		49 BARKOV	85	OLYA	0 $e^+e^- \rightarrow \pi^+\pi^-$

Meson Particle Listings

 $\rho(770)$

••• We do not use the following data for averages, fits, limits, etc. •••

143.9 ± 1.3 ± 1.1	1.98M	50	ALOISIO	03	KLOE	1.02 $e^+e^- \rightarrow \pi^+\pi^-\pi^0$
147.4 ± 1.5 ± 0.7	1.98M	51	ALOISIO	03	KLOE	1.02 $e^+e^- \rightarrow \pi^+\pi^-\pi^0$
149.8 ± 2.2 ± 2.0	500k	52	ACHASOV	02	SND	1.02 $e^+e^- \rightarrow \pi^+\pi^-\pi^0$
147.9 ± 1.5 ± 7.5		53	BENAYOUN	98	RVUE	$e^+e^- \rightarrow \pi^+\pi^-$, $\mu^+\mu^-$
153.5 ± 1.3 ± 4.6		54	GARDNER	98	RVUE	$0.28-0.92 e^+e^- \rightarrow \pi^+\pi^-$
145.0 ± 1.7		55	O'CONNELL	97	RVUE	$e^+e^- \rightarrow \pi^+\pi^-$
142.5 ± 3.5		56	BERNICA	94	RVUE	$e^+e^- \rightarrow \pi^+\pi^-$
138 ± 1		57	GESHKEN...	89	RVUE	$e^+e^- \rightarrow \pi^+\pi^-$

CHARGED ONLY, τ DECAYS and e^+e^-

VALUE (MeV)	EVTS	DOCUMENT ID	TECN	CHG	COMMENT
149.1 ± 0.8 OUR FIT					
149.1 ± 0.8 OUR AVERAGE					
148.1 ± 0.4 ± 1.7	5.4M	58,59	FUJIKAWA	08	BELL ± $\tau^- \rightarrow \pi^-\pi^0\nu_\tau$
149.0 ± 1.2		59,60	SCHAEEL	05c	ALEP $\tau^- \rightarrow \pi^-\pi^0\nu_\tau$
149.9 ± 2.3 ± 2.0	500k	48	ACHASOV	02	SND ± $1.02 e^+e^- \rightarrow \pi^+\pi^-\pi^0$
150.4 ± 1.4 ± 1.4	87k	61,62	ANDERSON	00A	CLE2 $\tau^- \rightarrow \pi^-\pi^0\nu_\tau$
••• We do not use the following data for averages, fits, limits, etc. •••					
143.7 ± 1.3 ± 1.2	1.98M	48	ALOISIO	03	KLOE ± $1.02 e^+e^- \rightarrow \pi^+\pi^-\pi^0$
142.9 ± 1.3 ± 1.4	1.98M	51	ALOISIO	03	KLOE - $1.02 e^+e^- \rightarrow \pi^+\pi^-\pi^0$
144.7 ± 1.4 ± 1.2	1.98M	51	ALOISIO	03	KLOE + $1.02 e^+e^- \rightarrow \pi^+\pi^-\pi^0$
150.2 ± 2.0 ± 0.7		63	SANZ-CILLERO	03	RVUE $\tau^- \rightarrow \pi^-\pi^0\nu_\tau$
150.9 ± 2.2 ± 2.0	500k	52	ACHASOV	02	SND $1.02 e^+e^- \rightarrow \pi^+\pi^-\pi^0$

MIXED CHARGES, OTHER REACTIONS

VALUE (MeV)	EVTS	DOCUMENT ID	TECN	CHG	COMMENT
149.5 ± 1.3	600k	64	ABELE	99E	CBAR $0 \pm 0.0 \bar{p}p \rightarrow \pi^+\pi^-\pi^0$

CHARGED ONLY, HADROPRODUCED

VALUE (MeV)	EVTS	DOCUMENT ID	TECN	CHG	COMMENT
150.2 ± 2.4 OUR FIT					
150.2 ± 2.4 OUR AVERAGE					
152.8 ± 4.3		ABELE	97	CBAR	$\bar{p}n \rightarrow \pi^-\pi^0\pi^0$
155 ± 11	2935	65	CAPRARO	87	SPEC - $200 \pi^-\text{Cu} \rightarrow \pi^-\pi^0\text{Cu}$
154 ± 20	967	65	CAPRARO	87	SPEC - $200 \pi^-\text{Pb} \rightarrow \pi^-\pi^0\text{Pb}$
150 ± 5		HUSTON	86	SPEC +	$202 \pi^+\text{A} \rightarrow \pi^+\pi^0\text{A}$
146 ± 12	6500	66	BYERLY	73	OSPK - $5 \pi^-p$
148.2 ± 4.1	9650	67	PISUT	68	RVUE - $1.7-3.2 \pi^-p, t < 10$
146 ± 13	900	EISNER	67	HBC -	$4.2 \pi^-p, t < 10$

NEUTRAL ONLY, PHOTOPRODUCED

VALUE (MeV)	EVTS	DOCUMENT ID	TECN	CHG	COMMENT
150.7 ± 2.9 OUR AVERAGE					
146 ± 3 ± 13	79k	68	BREITWEG	98B	ZEUS 0 $50-100 \gamma p$
150.9 ± 3.0		BARTALUCCI	78	CNTR 0	$\gamma p \rightarrow e^+e^-p$
••• We do not use the following data for averages, fits, limits, etc. •••					
138 ± 3	79k	69	BREITWEG	98B	ZEUS 0 $50-100 \gamma p$
147 ± 11		GLADDING	73	CNTR 0	$2.9-4.7 \gamma p$
155 ± 12	2430	BALLAM	72	HBC 0	$4.7 \gamma p$
145 ± 13	1930	BALLAM	72	HBC 0	$2.8 \gamma p$
140 ± 5		ALVENSLEB...	70	CNTR 0	$\gamma A, t < 0.01$
146.1 ± 2.9	140k	BIGGS	70	CNTR 0	$< 4.1 \gamma C \rightarrow \pi^+\pi^-C$
160 ± 10		LANZEROTTI	68	CNTR 0	γp
130 ± 5	4000	ASBURY	67B	CNTR 0	$\gamma + \text{Pb}$

NEUTRAL ONLY, OTHER REACTIONS

VALUE (MeV)	EVTS	DOCUMENT ID	TECN	CHG	COMMENT
150.9 ± 1.7 OUR AVERAGE					
Error includes scale factor of 1.1.					
122 ± 20		BERTIN	97c	OBLX	$0.0 \bar{p}p \rightarrow \pi^+\pi^-\pi^0$
145.7 ± 5.3		WEIDENAUER	93	ASTE	$\bar{p}p \rightarrow \pi^+\pi^-\omega$
144.9 ± 3.7		DUBNICKA	89	RVUE	π form factor
148 ± 6		70,71	BOHACIK	80	RVUE 0
152 ± 9		66	WICKLUND	78	ASPK 0 $3.4, 6 \pi^\pm p N$
154 ± 2	76000	DEUTSCH...	76	HBC 0	$16 \pi^+p$
157 ± 8	6800	RATCLIFF	72	ASPK 0	$15 \pi^-p, t < 0.3$
143 ± 8	1700	REYNOLDS	69	HBC 0	$2.26 \pi^-p$
••• We do not use the following data for averages, fits, limits, etc. •••					
147.0 ± 2.5	600k	72	ABELE	99E	CBAR 0 $0.0 \bar{p}p \rightarrow \pi^+\pi^-\pi^0$
146 ± 3	4943	73	ADAMS	97	E665 $470 \mu p \rightarrow \mu X B$
160.0 ± 4.1		74	CHABAUD	83	ASPK 0 $17 \pi^-p$ polarized
155 ± 1		75	HEYN	81	RVUE 0 π form factor
148.0 ± 1.3		70,71	LANG	79	RVUE 0

146 ± 14	4100	ENGLER	74	DBC 0	$6 \pi^+n \rightarrow \pi^+\pi^-p$
143 ± 13		71	ESTABROOKS	74	RVUE 0 $17 \pi^-p \rightarrow \pi^+\pi^-n$
160 ± 10	32000	70	PROTOPOPO...	73	HBC 0 $7.1 \pi^+p, t < 0.4$
145 ± 12	2250	65	HYAMS	68	OSPK 0 $11.2 \pi^-p$
163 ± 15	13300	76	PISUT	68	RVUE 0 $1.7-3.2 \pi^-p, t < 10$

- 43 A combined fit of AKHMETSHIN 07, AULCHENKO 06, and AULCHENKO 05.
 44 Supersedes ACHASOV 05A.
 45 A fit of the SND data from 400 to 1000 MeV using parameters of the $\rho(1450)$ and $\rho(1700)$ from a fit of the data of BARKOV 85, BISELLO 89 and ANDERSON 00A.
 46 Using the GOUNARIS 68 parametrization with the complex phase of the $\rho\omega$ interference.
 47 From a fit in the energy range 0.61 to 0.96 GeV. Update of AKHMETSHIN 02.
 48 Assuming $m_{\rho^+} = m_{\rho^-}$, $\Gamma_{\rho^+} = \Gamma_{\rho^-}$.
 49 From the GOUNARIS 68 parametrization of the pion form factor.
 50 Assuming $m_{\rho^+} = m_{\rho^-} = m_{\rho^0}$, $\Gamma_{\rho^+} = \Gamma_{\rho^-} = \Gamma_{\rho^0}$.
 51 Without limitations on masses and widths.
 52 Assuming $m_{\rho^0} = m_{\rho^\pm}$, $g_{\rho^0\pi\pi} = g_{\rho^\pm\pi\pi}$.
 53 Using the data of BARKOV 85 in the hidden local symmetry model.
 54 From the fit to $e^+e^- \rightarrow \pi^+\pi^-$ data from the compilations of HEYN 81 and BARKOV 85, including the GOUNARIS 68 parametrization of the pion form factor.
 55 A fit of BARKOV 85 data assuming the direct $\omega\pi\pi$ coupling.
 56 Applying the S-matrix formalism to the BARKOV 85 data.
 57 Includes BARKOV 85 data. Model-dependent width definition.
 58 $|F_\pi(0)|^2$ fixed to 1.
 59 From the GOUNARIS 68 parametrization of the pion form factor.
 60 The error combines statistical and systematic uncertainties. Supersedes BARATE 97M.
 61 $\rho(1700)$ mass and width fixed at 1700 MeV and 235 MeV respectively.
 62 From the GOUNARIS 68 parametrization of the pion form factor. The second error is a model error taking into account different parametrizations of the pion form factor.
 63 Using the data of BARATE 97M and the effective chiral Lagrangian.
 64 Assuming the equality of ρ^+ and ρ^- masses and widths.
 65 Width errors enlarged by us to $4\Gamma/\sqrt{N}$; see the note with the $K^*(892)$ mass.
 66 Phase shift analysis. Systematic errors added corresponding to spread of different fits.
 67 From fit of 3-parameter relativistic P -wave Breit-Wigner to total mass distribution. Includes BATON 68, MILLER 67B, ALFF-STEINBERGER 66, HAGOPIAN 66, HAGOPIAN 66B, JACOBS 66B, JAMES 66, WEST 66, BLIEDEN 65 and CARMONY 64.
 68 From the parametrization according to SOEDING 66.
 69 From the parametrization according to ROSS 66.
 70 From pole extrapolation.
 71 From phase shift analysis of GRAYER 74 data.
 72 Using relativistic Breit-Wigner and taking into account $\rho\omega$ interference.
 73 Systematic errors not evaluated.
 74 From fit of 3-parameter relativistic Breit-Wigner to helicity-zero part of P -wave intensity. CHABAUD 83 includes data of GRAYER 74.
 75 HEYN 81 includes all spacelike and timelike F_π values until 1978.
 76 Includes MALAMUD 69, ARMENISE 68, BACON 67, HUWE 67, MILLER 67B, ALFF-STEINBERGER 66, HAGOPIAN 66, HAGOPIAN 66B, JACOBS 66B, JAMES 66, WEST 66, GOLDHABER 64, ABOLINS 63.

 $\Gamma_{\rho(770)^0} - \Gamma_{\rho(770)^\pm}$

VALUE	EVTS	DOCUMENT ID	TECN	COMMENT
0.3 ± 1.3 OUR AVERAGE Error includes scale factor of 1.4.				
-0.2 ± 1.0		77	SCHAEEL	05c ALEP $\tau^- \rightarrow \pi^-\pi^0\nu_\tau$
3.6 ± 1.8 ± 1.7	1.98M	78	ALOISIO	03 KLOE $1.02 e^+e^- \rightarrow \pi^+\pi^-\pi^0$

 $\Gamma_{\rho(770)^+} - \Gamma_{\rho(770)^-}$

VALUE	EVTS	DOCUMENT ID	TECN	COMMENT
1.8 ± 2.0 ± 0.5	1.98M	79	ALOISIO	03 KLOE $1.02 e^+e^- \rightarrow \pi^+\pi^-\pi^0$

77 From the combined fit of the τ^- data from ANDERSON 00A and SCHAEEL 05c and e^+e^- data from the compilation of BARKOV 85, AKHMETSHIN 04, and ALOISIO 05. Supersedes BARATE 97M.
 78 Assuming $m_{\rho^+} = m_{\rho^-}$, $\Gamma_{\rho^+} = \Gamma_{\rho^-}$.
 79 Without limitations on masses and widths.

 $\rho(770)$ DECAY MODES

Mode	Fraction (Γ_i/Γ)	Scale factor/ Confidence level
Γ_1 $\pi\pi$	~ 100	%
$\rho(770)^\pm$ decays		
Γ_2 $\pi^\pm\pi^0$	~ 100	%
Γ_3 $\pi^\pm\gamma$	(4.5 ± 0.5)	$\times 10^{-4} \text{ S} = 2.2$
Γ_4 $\pi^\pm\eta$	< 6	$\times 10^{-4} \text{ S} = 84\%$
Γ_5 $\pi^\pm\pi^+\pi^-\pi^0$	< 2.0	$\times 10^{-4} \text{ S} = 84\%$

$\rho(770)^0$ decays

Γ_i	Decay	Value	Unit	%
Γ_6	$\pi^+\pi^-$	~ 100		
Γ_7	$\pi^+\pi^-\gamma$	(9.9 ± 1.6)	$\times 10^{-3}$	
Γ_8	$\pi^0\gamma$	(6.0 ± 0.8)	$\times 10^{-4}$	
Γ_9	$\eta\gamma$	(3.00 ± 0.20)	$\times 10^{-4}$	
Γ_{10}	$\pi^0\pi^0\gamma$	(4.5 ± 0.8)	$\times 10^{-5}$	
Γ_{11}	$\mu^+\mu^-$	$[a]$ (4.55 ± 0.28)	$\times 10^{-5}$	
Γ_{12}	e^+e^-	$[a]$ (4.72 ± 0.05)	$\times 10^{-5}$	
Γ_{13}	$\pi^+\pi^-\pi^0$	$(1.01^{+0.54}_{-0.36} \pm 0.34)$	$\times 10^{-4}$	
Γ_{14}	$\pi^+\pi^-\pi^+\pi^-$	(1.8 ± 0.9)	$\times 10^{-5}$	
Γ_{15}	$\pi^+\pi^-\pi^0\pi^0$	(1.6 ± 0.8)	$\times 10^{-5}$	
Γ_{16}	$\pi^0e^+e^-$	< 1.2	$\times 10^{-5}$	
Γ_{17}	ηe^+e^-			$\sim 90\%$

[a] The $\omega\rho$ interference is then due to $\omega\rho$ mixing only, and is expected to be small. If $e\mu$ universality holds, $\Gamma(\rho^0 \rightarrow \mu^+\mu^-) = \Gamma(\rho^0 \rightarrow e^+e^-) \times 0.99785$.

CONSTRAINED FIT INFORMATION

An overall fit to the total width and a partial width uses 10 measurements and one constraint to determine 3 parameters. The overall fit has a $\chi^2 = 10.7$ for 8 degrees of freedom.

The following *off-diagonal* array elements are the correlation coefficients $\langle \delta p_i \delta p_j \rangle / (\delta p_i \delta p_j)$, in percent, from the fit to parameters p_i , including the branching fractions, $x_i \equiv \Gamma_i / \Gamma_{\text{total}}$. The fit constrains the x_i whose labels appear in this array to sum to one.

x_3	-100	
Γ	15	-15
	x_2	x_3

Mode	Rate (MeV)	Scale factor
Γ_2 $\pi^+\pi^0$	150.2 ± 2.4	
Γ_3 $\pi^+\pi^-\gamma$	0.068 ± 0.007	2.3

CONSTRAINED FIT INFORMATION

An overall fit to the total width, a partial width, and 7 branching ratios uses 21 measurements and one constraint to determine 9 parameters. The overall fit has a $\chi^2 = 6.0$ for 13 degrees of freedom.

The following *off-diagonal* array elements are the correlation coefficients $\langle \delta p_i \delta p_j \rangle / (\delta p_i \delta p_j)$, in percent, from the fit to parameters p_i , including the branching fractions, $x_i \equiv \Gamma_i / \Gamma_{\text{total}}$. The fit constrains the x_i whose labels appear in this array to sum to one.

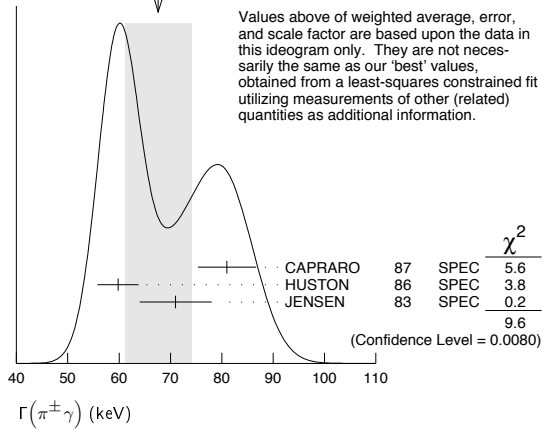
x_7	-100							
x_8	-5	0						
x_9	-1	0	1					
x_{10}	-1	0	0	0				
x_{11}	2	-3	0	0	0			
x_{12}	0	0	-8	-9	0	0		
x_{14}	-1	0	0	0	0	0	0	
Γ	0	0	4	5	0	0	-54	
	x_6	x_7	x_8	x_9	x_{10}	x_{11}	x_{12}	x_{14}

Mode	Rate (MeV)
Γ_6 $\pi^+\pi^-$	147.5 ± 0.9
Γ_7 $\pi^+\pi^-\gamma$	1.48 ± 0.24
Γ_8 $\pi^0\gamma$	0.089 ± 0.012
Γ_9 $\eta\gamma$	0.0447 ± 0.0031
Γ_{10} $\pi^0\pi^0\gamma$	0.0066 ± 0.0012
Γ_{11} $\mu^+\mu^-$	$[a]$ 0.0068 ± 0.0004
Γ_{12} e^+e^-	$[a]$ 0.00704 ± 0.00006
Γ_{14} $\pi^+\pi^-\pi^+\pi^-$	0.0027 ± 0.0014

$\rho(770)$ PARTIAL WIDTHS

$\Gamma(\pi^{\pm}\gamma)$	Value (keV)	Document ID	TECN	CHG	Comment
68 ± 7 OUR FIT					Error includes scale factor of 2.3.
81 ± 4 OUR AVERAGE					Error includes scale factor of 2.2. See the ideogram below.
68 $\pm 4 \pm 4$	CAPRARO	87	SPEC	-	200 $\pi^-A \rightarrow \pi^-\pi^0A$
59.8 ± 4.0	HUSTON	86	SPEC	+	202 $\pi^+A \rightarrow \pi^+\pi^0A$
71 ± 7	JENSEN	83	SPEC	-	156-260 $\pi^-A \rightarrow \pi^-\pi^0A$

WEIGHTED AVERAGE
68 \pm 7 (Error scaled by 2.2)



$\Gamma(e^+e^-)$	Value (keV)	EVTS	Document ID	TECN	Comment
7.04 ± 0.06 OUR FIT					
7.04 ± 0.06 OUR AVERAGE					
7.048 $\pm 0.057 \pm 0.050$	900k	80	AKHMETSHIN 07		$e^+e^- \rightarrow \pi^+\pi^-$
7.06 $\pm 0.11 \pm 0.05$	114k	81,82	AKHMETSHIN 04	CMD2	$e^+e^- \rightarrow \pi^+\pi^-$
6.77 $\pm 0.10 \pm 0.30$			BARKOV 85	OLYA	$e^+e^- \rightarrow \pi^+\pi^-$
• • • We do not use the following data for averages, fits, limits, etc. • • •					
7.12 $\pm 0.02 \pm 0.11$	800k	83	ACHASOV 06	SND	$e^+e^- \rightarrow \pi^+\pi^-$
6.3 ± 0.1		84	BENAYOUN 98	RVUE	$e^+e^- \rightarrow \pi^+\pi^-, \mu^+\mu^-$

$\Gamma(\pi^0\gamma)$	Value (keV)	EVTS	Document ID	TECN	Comment
• • • We do not use the following data for averages, fits, limits, etc. • • •					
77 $\pm 17 \pm 11$	36500	85	ACHASOV 03	SND	0.60-0.97 $e^+e^- \rightarrow \pi^0\gamma$
121 ± 31			DOLINSKY 89	ND	$e^+e^- \rightarrow \pi^0\gamma$

$\Gamma(\eta\gamma)$	Value (keV)	Document ID	TECN	Comment	
• • • We do not use the following data for averages, fits, limits, etc. • • •					
62 ± 17		86	DOLINSKY 89	ND	$e^+e^- \rightarrow \eta\gamma$

$\Gamma(\pi^+\pi^-\pi^+\pi^-)$	Value (keV)	EVTS	Document ID	TECN	Comment
• • • We do not use the following data for averages, fits, limits, etc. • • •					
2.8 $\pm 1.4 \pm 0.5$	153		AKHMETSHIN 00	CMD2	0.6-0.97 $e^+e^- \rightarrow \pi^+\pi^-\pi^+\pi^-$

80 A combined fit of AKHMETSHIN 07, AULCHENKO 06, and AULCHENKO 05.
 81 Using the GOUNARIS 68 parametrization with the complex phase of the $\rho\omega$ interference.
 82 From a fit in the energy range 0.61 to 0.96 GeV. Update of AKHMETSHIN 02.
 83 Supersedes ACHASOV 05A.
 84 Using the data of BARKOV 85 in the hidden local symmetry model.
 85 Using $\Gamma_{\text{total}} = 147.9 \pm 1.3$ MeV and $B(\rho \rightarrow \pi^0\gamma)$ from ACHASOV 03.
 86 Solution corresponding to constructive $\omega\rho$ interference.

$\rho(770) \Gamma(e^+e^-) \Gamma(i) / \Gamma^2(\text{total})$

$\Gamma(e^+e^-) / \Gamma_{\text{total}} \times \Gamma(\pi^+\pi^-) / \Gamma_{\text{total}}$	Value (units 10^{-5})	EVTS	Document ID	TECN	Comment	
4.876 $\pm 0.023 \pm 0.064$		800k	87,88	ACHASOV 06	SND	$e^+e^- \rightarrow \pi^+\pi^-$
87 Supersedes ACHASOV 05A.						

88 A fit of the SND data from 400 to 1000 MeV using parameters of the $\rho(1450)$ and $\rho(1700)$ from a fit of the data of BARKOV 85, BISELLO 89 and ANDERSON 00A.

$\Gamma(e^+e^-) / \Gamma_{\text{total}} \times \Gamma(\eta\gamma) / \Gamma_{\text{total}}$	Value (units 10^{-8})	EVTS	Document ID	TECN	Comment
1.42 ± 0.10 OUR FIT					
1.45 ± 0.12 OUR AVERAGE					
1.32 $\pm 0.14 \pm 0.08$	33k	89	ACHASOV 07B	SND	0.6-1.38 $e^+e^- \rightarrow \eta\gamma$
1.50 $\pm 0.65 \pm 0.09$	17.4k	90	AKHMETSHIN 05	CMD2	0.60-1.38 $e^+e^- \rightarrow \eta\gamma$
1.61 $\pm 0.20 \pm 0.11$	23k	91,92	AKHMETSHIN 01B	CMD2	$e^+e^- \rightarrow \eta\gamma$
1.85 ± 0.49		93	DOLINSKY 89	ND	$e^+e^- \rightarrow \eta\gamma$

89 From a combined fit of $\sigma(e^+e^- \rightarrow \eta\gamma)$ with $\eta \rightarrow 3\pi^0$ and $\eta \rightarrow \pi^+\pi^-\pi^0$, and fixing $B(\eta \rightarrow 3\pi^0) / B(\eta \rightarrow \pi^+\pi^-\pi^0) = 1.44 \pm 0.04$. Recalculated by us from the cross section at the peak. Supersedes ACHASOV 00B and ACHASOV 06A.
 90 From the $\eta \rightarrow 2\gamma$ decay and using $B(\eta \rightarrow \gamma\gamma) = 39.43 \pm 0.26\%$.
 91 From the $\eta \rightarrow 3\pi^0$ decay and using $B(\eta \rightarrow 3\pi^0) = (32.24 \pm 0.29) \times 10^{-2}$.
 92 The combined fit from 600 to 1380 MeV taking into account $\rho(770)$, $\omega(782)$, $\phi(1020)$, and $\rho(1450)$ (mass and width fixed at 1450 MeV and 310 MeV respectively).
 93 Recalculated by us from the cross section in the peak.

Meson Particle Listings

 $\rho(770)$ $\Gamma(e^+e^-)/\Gamma_{\text{total}} \times \Gamma(\pi^0\gamma)/\Gamma_{\text{total}}$

VALUE (units 10^{-8})	EVTS	DOCUMENT ID	TECN	COMMENT
2.8 ± 0.4 OUR FIT				
2.8 ± 0.4 OUR AVERAGE				
$2.90^{+0.60}_{-0.55} \pm 0.18$	18680	AKHMETSHIN 05	CMD2	$0.60-1.38 e^+e^- \rightarrow \pi^0\gamma$
$2.37 \pm 0.53 \pm 0.33$	36500	⁹⁴ ACHASOV	03	SND $0.60-0.97 e^+e^- \rightarrow \pi^0\gamma$
$3.61 \pm 0.74 \pm 0.49$	10625	⁹⁵ DOLINSKY	89	ND $e^+e^- \rightarrow \pi^0\gamma$

⁹⁴ Using $\sigma_\phi \rightarrow \pi^0\gamma$ from ACHASOV 00 and $m_\rho = 775.97$ MeV in the model with the energy-independent phase of ρ - ω interference equal to $(-10.2 \pm 7.0)^\circ$.

⁹⁵ Recalculated by us from the cross section in the peak.

 $\Gamma(e^+e^-)/\Gamma_{\text{total}} \times \Gamma(\pi^+\pi^-\pi^0)/\Gamma_{\text{total}}$

VALUE (units 10^{-9})	EVTS	DOCUMENT ID	TECN	COMMENT
4.58 ± 2.46 ± 1.56	1.2M	⁹⁶ ACHASOV	03D	RVUE $0.44-2.00 e^+e^- \rightarrow \pi^+\pi^-\pi^0$

• • • We do not use the following data for averages, fits, limits, etc. • • •

⁹⁶ Statistical significance in less than 3 σ .

 $\rho(770)$ BRANCHING RATIOS $\Gamma(\pi^\pm\eta)/\Gamma(\pi\pi)$

VALUE (units 10^{-4})	CL%	DOCUMENT ID	TECN	CHG	COMMENT
<60	84	FERBEL	66	HBC	\pm $\pi^\pm p$ above 2.5

 $\Gamma(\pi^\pm\pi^+\pi^-\pi^0)/\Gamma(\pi\pi)$

VALUE (units 10^{-4})	CL%	DOCUMENT ID	TECN	CHG	COMMENT
<20	84	FERBEL	66	HBC	\pm $\pi^\pm p$ above 2.5

• • • We do not use the following data for averages, fits, limits, etc. • • •

35 ± 40		JAMES	66	HBC	$+$ $2.1 \pi^+ p$
-------------	--	-------	----	-----	-------------------

 $\Gamma(\mu^+\mu^-)/\Gamma(\pi^+\pi^-)$

VALUE (units 10^{-5})	DOCUMENT ID	TECN	COMMENT
4.60 ± 0.28 OUR FIT			
4.6 ± 0.2 ± 0.2	ANTIPOV	89	SIGM $\pi^- \text{Cu} \rightarrow \mu^+\mu^-\pi^- \text{Cu}$

• • • We do not use the following data for averages, fits, limits, etc. • • •

$8.2^{+1.6}_{-3.6}$	⁹⁷ ROTHWELL	69	CNTR	Photoproduction
5.6 ± 1.5	⁹⁸ WEHMANN	69	OSPK	$12 \pi^- \text{C, Fe}$
$9.7^{+3.1}_{-3.3}$	⁹⁹ HYAMS	67	OSPK	$11 \pi^- \text{Li, H}$

 $\Gamma(e^+e^-)/\Gamma(\pi\pi)$

VALUE (units 10^{-4})	DOCUMENT ID	TECN	COMMENT
0.40 ± 0.05	¹⁰⁰ BENAKSAS	72	OSPK $e^+e^- \rightarrow \pi^+\pi^-$

• • • We do not use the following data for averages, fits, limits, etc. • • •

 $\Gamma(\eta\gamma)/\Gamma_{\text{total}}$

VALUE (units 10^{-4})	EVTS	DOCUMENT ID	TECN	CHG	COMMENT
3.00 ± 0.21 OUR FIT					
2.90 ± 0.32 OUR AVERAGE					
$2.79 \pm 0.34 \pm 0.03$	33k	¹⁰¹ ACHASOV	07B	SND	$0.6-1.38 e^+e^- \rightarrow \eta\gamma$
3.6 ± 0.9		¹⁰² ANDREWS	77	CNTR	$0.6-1.38 e^+e^- \rightarrow \eta\gamma$

• • • We do not use the following data for averages, fits, limits, etc. • • •

$3.21 \pm 1.39 \pm 0.20$	17.4k	^{103,104} AKHMETSHIN	05	CMD2	$0.60-1.38 e^+e^- \rightarrow \eta\gamma$
$3.39 \pm 0.42 \pm 0.23$	102,105,106	AKHMETSHIN	01B	CMD2	$e^+e^- \rightarrow \eta\gamma$
$1.9^{+0.6}_{-0.8}$		¹⁰⁷ BENAYOUN	96	RVUE	$0.54-1.04 e^+e^- \rightarrow \eta\gamma$
4.0 ± 1.1	102,104	DOLINSKY	89	ND	$e^+e^- \rightarrow \eta\gamma$

 $\Gamma(\pi^+\pi^-\pi^+\pi^-)/\Gamma_{\text{total}}$

VALUE (units 10^{-5})	CL%	EVTS	DOCUMENT ID	TECN	COMMENT
1.8 ± 0.9 OUR FIT					
1.8 ± 0.9 ± 0.3	153		AKHMETSHIN 00	CMD2	$0.6-0.97 e^+e^- \rightarrow \pi^+\pi^-\pi^+\pi^-$

• • • We do not use the following data for averages, fits, limits, etc. • • •

<20	90	KURDADZE	88	OLYA	$e^+e^- \rightarrow \pi^+\pi^-\pi^+\pi^-$
-----	----	----------	----	------	---

 $\Gamma(\pi^+\pi^-\pi^+\pi^-)/\Gamma(\pi\pi)$

VALUE (units 10^{-4})	CL%	DOCUMENT ID	TECN	CHG	COMMENT
<15	90	ERBE	69	HBC	$0.25-5.8 \gamma p$
<20		CHUNG	68	HBC	$0.3, 2.4, 2 \pi^- p$
<20	90	HUSON	68	HLBC	$0.16, 0 \pi^- p$
<80		JAMES	66	HBC	$0.2, 1 \pi^+ p$

• • • We do not use the following data for averages, fits, limits, etc. • • •

 $\Gamma(\pi^+\pi^-\pi^0)/\Gamma_{\text{total}}$

VALUE (units 10^{-4})	CL%	EVTS	DOCUMENT ID	TECN	COMMENT
1.01 ± 0.54 ± 0.34		1.2M	¹⁰⁸ ACHASOV	03D	RVUE $0.44-2.00 e^+e^- \rightarrow \pi^+\pi^-\pi^0$
<1.2	90		VASSERMAN	88B	ND $e^+e^- \rightarrow \pi^+\pi^-\pi^0$

• • • We do not use the following data for averages, fits, limits, etc. • • •

 $\Gamma(\pi^+\pi^-\pi^0)/\Gamma(\pi\pi)$

VALUE	CL%	DOCUMENT ID	TECN	CHG	COMMENT
<0.01	84	¹⁰⁹ BRAMON	86	RVUE	$0 J/\psi \rightarrow \omega\pi^0$
<0.01		ABRAMS	71	HBC	$0.3, 7 \pi^+ p$

• • • We do not use the following data for averages, fits, limits, etc. • • •

 $\Gamma(\pi^+\pi^-\pi^0\pi^0)/\Gamma_{\text{total}}$

VALUE (units 10^{-5})	CL%	DOCUMENT ID	TECN	COMMENT
1.60 ± 0.74 ± 0.18		¹¹⁰ ACHASOV	09A	SND $e^+e^- \rightarrow \pi^+\pi^-\pi^0\pi^0$

• • • We do not use the following data for averages, fits, limits, etc. • • •

<4	90	AULCHENKO	87C	ND	$e^+e^- \rightarrow \pi^+\pi^-\pi^0\pi^0$
<20	90	KURDADZE	86	OLYA	$e^+e^- \rightarrow \pi^+\pi^-\pi^0\pi^0$

 $\Gamma(\pi^+\pi^-\gamma)/\Gamma_{\text{total}}$

VALUE	CL%	DOCUMENT ID	TECN	COMMENT	
0.0099 ± 0.0016 OUR FIT					
0.0099 ± 0.0016		¹¹¹ DOLINSKY	91	ND	$e^+e^- \rightarrow \pi^+\pi^-\gamma$

• • • We do not use the following data for averages, fits, limits, etc. • • •

0.0111 ± 0.0014		¹¹² VASSERMAN	88	ND	$e^+e^- \rightarrow \pi^+\pi^-\gamma$
<0.005	90	¹¹³ VASSERMAN	88	ND	$e^+e^- \rightarrow \pi^+\pi^-\gamma$

 $\Gamma(\pi^0\gamma)/\Gamma_{\text{total}}$

VALUE (units 10^{-4})	EVTS	DOCUMENT ID	TECN	COMMENT	
$6.21^{+1.28}_{-1.18} \pm 0.39$	18680	^{114,115} AKHMETSHIN	05	CMD2	$0.60-1.38 e^+e^- \rightarrow \pi^0\gamma$
$5.22 \pm 1.17 \pm 0.75$	36500	^{115,116} ACHASOV	03	SND	$0.60-0.97 e^+e^- \rightarrow \pi^0\gamma$
6.8 ± 1.7		¹¹⁷ BENAYOUN	96	RVUE	$0.54-1.04 e^+e^- \rightarrow \pi^0\gamma$
7.9 ± 2.0		¹¹⁵ DOLINSKY	89	ND	$e^+e^- \rightarrow \pi^0\gamma$

• • • We do not use the following data for averages, fits, limits, etc. • • •

 $\Gamma(\pi^0e^+e^-)/\Gamma_{\text{total}}$

VALUE (units 10^{-5})	CL%	DOCUMENT ID	TECN	COMMENT	
<1.2	90	ACHASOV	08	SND	$0.36-0.97 e^+e^- \rightarrow \pi^0e^+e^-$

• • • We do not use the following data for averages, fits, limits, etc. • • •

<1.6		AKHMETSHIN 05A	CMD2	$0.72-0.84 e^+e^-$
------	--	----------------	------	--------------------

 $\Gamma(\eta e^+e^-)/\Gamma_{\text{total}}$

VALUE (units 10^{-5})	DOCUMENT ID	TECN	COMMENT
<0.7	AKHMETSHIN 05A	CMD2	$0.72-0.84 e^+e^-$

• • • We do not use the following data for averages, fits, limits, etc. • • •

 $\Gamma(\pi^0\pi^0\gamma)/\Gamma_{\text{total}}$

VALUE (units 10^{-5})	EVTS	DOCUMENT ID	TECN	COMMENT	
4.5 ± 0.8 OUR FIT					
4.5 ± 0.9 OUR AVERAGE					
$5.2^{+1.5}_{-1.3} \pm 0.6$	190	¹¹⁸ AKHMETSHIN	04B	CMD2	$0.6-0.97 e^+e^- \rightarrow \pi^0\pi^0\gamma$
$4.1^{+1.0}_{-0.9} \pm 0.3$	295	¹¹⁹ ACHASOV	02F	SND	$0.36-0.97 e^+e^- \rightarrow \pi^0\pi^0\gamma$

• • • We do not use the following data for averages, fits, limits, etc. • • •

$4.8^{+3.4}_{-1.8} \pm 0.5$	63	¹²⁰ ACHASOV	00G	SND	$e^+e^- \rightarrow \pi^0\pi^0\gamma$
-----------------------------	----	------------------------	-----	-----	---------------------------------------

⁹⁷ Possibly large ρ - ω interference leads us to increase the minus error.

⁹⁸ Result contains 11 ± 11% correction using SU(3) for central value. The error on the correction takes account of possible ρ - ω interference and the upper limit agrees with the upper limit of $\omega \rightarrow \mu^+\mu^-$ from this experiment.

⁹⁹ HYAMS 67's mass resolution is 20 MeV. The ω region was excluded.

¹⁰⁰ The ρ' contribution is not taken into account.

¹⁰¹ ACHASOV 07B reports $[\Gamma(\rho(770) \rightarrow \eta\gamma)/\Gamma_{\text{total}}] \times [B(\rho(770) \rightarrow e^+e^-)] = (1.32 \pm 0.14 \pm 0.08) \times 10^{-8}$ which we divide by our best value $B(\rho(770) \rightarrow e^+e^-) = (4.72 \pm 0.05) \times 10^{-5}$. Our first error is their experiment's error and our second error is the systematic error from using our best value. Supersedes ACHASOV 00D and ACHASOV 06A.

¹⁰² Solution corresponding to constructive ω - ρ interference.

¹⁰³ Using $B(\rho \rightarrow e^+e^-) = (4.67 \pm 0.09) \times 10^{-5}$ and $B(\eta \rightarrow \gamma\gamma) = 39.43 \pm 0.26\%$.

¹⁰⁴ Not independent of the corresponding $\Gamma(e^+e^-) \times \Gamma(\eta\gamma)/\Gamma_{\text{total}}^2$.

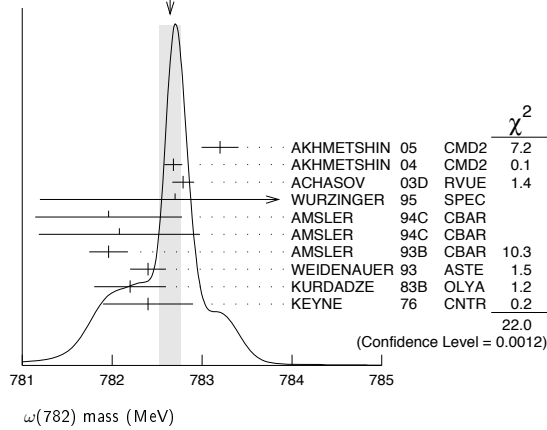
¹⁰⁵ The combined fit from 600 to 1380 MeV taking into account $\rho(770)$, $\omega(782)$, $\phi(1020)$, and $\rho(1450)$ (mass and width fixed at 1450 MeV and 310 MeV respectively).

¹⁰⁶ Using $B(\rho \rightarrow e^+e^-) = (4.75 \pm 0.10) \times 10^{-5}$ from AKHMETSHIN 02 and $B(\eta \rightarrow 3\pi^0) = (32.24 \pm 0.29) \times 10^{-2}$.

Meson Particle Listings

$\omega(782)$

WEIGHTED AVERAGE
782.65±0.12 (Error scaled by 1.9)



$\omega(782)$ WIDTH

VALUE (MeV)	EVTS	DOCUMENT ID	TECN	COMMENT
8.49±0.08 OUR AVERAGE				
8.68±0.23±0.10	11200	9 AKHMETSHIN 04	CMD2	$e^+e^- \rightarrow \pi^+\pi^-\pi^0$
8.68±0.04±0.15	1.2M	10 ACHASOV 03D	RVUE	0.44-2.00 $e^+e^- \rightarrow \pi^+\pi^-\pi^0$
8.2 ± 0.3	19500	WURZINGER 95	SPEC	1.33 $p\bar{d} \rightarrow {}^3\text{He}\omega$
8.4 ± 0.1		11 AULCHENKO 87	ND	$e^+e^- \rightarrow \pi^+\pi^-\pi^0$
8.30±0.40		BARKOV 87	CMD	$e^+e^- \rightarrow \pi^+\pi^-\pi^0$
9.8 ± 0.9	1488	KURDADZE 83B	OLYA	$e^+e^- \rightarrow \pi^+\pi^-\pi^0$
9.0 ± 0.8	433	CORDIER 80	DM1	$e^+e^- \rightarrow \pi^+\pi^-\pi^0$
9.1 ± 0.8	451	BENAKSAS 72B	OSPK	$e^+e^- \rightarrow \pi^+\pi^-\pi^0$
••• We do not use the following data for averages, fits, limits, etc. •••				
12 ± 2	1430	COOPER 78B	HBC	0.7-0.8 $p\bar{p} \rightarrow 5\pi$
9.4 ± 2.5	2100	GESSAROLI 77	HBC	11 $\pi^-p \rightarrow \omega n$
10.22±0.43	20000	12 KEYNE 76	CNTR	$\pi^-p \rightarrow \omega n$
13.3 ± 2	418	AGUILAR-... 72B	HBC	3,9,4,6 K^-p
10.5 ± 1.5		BORENSTEIN 72	HBC	2.18 K^-p
7.70±0.9 ±1.15	940	BROWN 72	MMS	2.5 $\pi^-p \rightarrow nMM$
10.3 ± 1.4	510	BIZZARRI 71	HBC	0.0 $p\bar{p} \rightarrow K_1^0 K_1^0 \omega$
12.8 ± 3.0	248	BIZZARRI 71	HBC	0.0 $p\bar{p} \rightarrow K^+ K^- \omega$
9.5 ± 1.0	3583	COYNE 71	HBC	3.7 $\pi^+p \rightarrow \pi^+\pi^-\pi^0$

9 Update of AKHMETSHIN 00c.
 10 From the combined fit of ANTONELLI 92, ACHASOV 01E, ACHASOV 02E, and ACHASOV 03D data on the $\pi^+\pi^-\pi^0$ and ANTONELLI 92 on the $\omega\pi^+\pi^-$ final states. Supersedes ACHASOV 99E and ACHASOV 02E.
 11 Relativistic Breit-Wigner includes radiative corrections.
 12 Observed by threshold-crossing technique. Mass resolution = 4.8 MeV FWHM.

$\omega(782)$ DECAY MODES

Mode	Fraction (Γ_i/Γ)	Scale factor/ Confidence level
Γ_1 $\pi^+\pi^-\pi^0$	(89.2 ± 0.7) %	
Γ_2 $\pi^0\gamma$	(8.28±0.28) %	S=2.1
Γ_3 $\pi^+\pi^-$	(1.53 $^{+0.11}_{-0.13}$) %	S=1.2
Γ_4 neutrals (excluding $\pi^0\gamma$)	(8 $^{+8}_{-5}$) × 10 ⁻³	S=1.1
Γ_5 $\eta\gamma$	(4.6 ± 0.4) × 10 ⁻⁴	S=1.1
Γ_6 $\pi^0 e^+ e^-$	(7.7 ± 0.6) × 10 ⁻⁴	
Γ_7 $\pi^0 \mu^+ \mu^-$	(1.3 ± 0.4) × 10 ⁻⁴	S=2.1
Γ_8 $\eta e^+ e^-$		
Γ_9 $e^+ e^-$	(7.28±0.14) × 10 ⁻⁵	S=1.3
Γ_{10} $\pi^+\pi^-\pi^0\pi^0$	< 2 × 10 ⁻⁴	CL=90%
Γ_{11} $\pi^+\pi^-\gamma$	< 3.6 × 10 ⁻³	CL=95%
Γ_{12} $\pi^+\pi^-\pi^+\pi^-$	< 1 × 10 ⁻³	CL=90%
Γ_{13} $\pi^0\pi^0\gamma$	(6.6 ± 1.1) × 10 ⁻⁵	
Γ_{14} $\eta\pi^0\gamma$	< 3.3 × 10 ⁻⁵	CL=90%
Γ_{15} $\mu^+\mu^-$	(9.0 ± 3.1) × 10 ⁻⁵	
Γ_{16} 3γ	< 1.9 × 10 ⁻⁴	CL=95%

Charge conjugation (C) violating modes

Γ_{17} $\eta\pi^0$	C	< 2.1 × 10 ⁻⁴	CL=90%
Γ_{18} $2\pi^0$	C	< 2.1 × 10 ⁻⁴	CL=90%
Γ_{19} $3\pi^0$	C	< 2.3 × 10 ⁻⁴	CL=90%

CONSTRAINED FIT INFORMATION

An overall fit to 15 branching ratios uses 51 measurements and one constraint to determine 10 parameters. The overall fit has a $\chi^2 = 51.8$ for 42 degrees of freedom.

The following off-diagonal array elements are the correlation coefficients $\langle \delta x_i \delta x_j \rangle / (\delta x_i \delta x_j)$, in percent, from the fit to the branching fractions, $x_i \equiv \Gamma_i/\Gamma_{\text{total}}$. The fit constrains the x_i whose labels appear in this array to sum to one.

x_2	22													
x_3	-18	-4												
x_4	-92	-56	1											
x_5	7	7	-1	-9										
x_6	-1	0	0	0	0									
x_7	-1	0	0	0	0	0								
x_9	-38	-33	7	44	-21	0	0							
x_{13}	1	4	0	-2	0	0	0	-1						
x_{15}	0	0	0	0	0	0	0	0	0					
x_1	x_2	x_3	x_4	x_5	x_6	x_7	x_9	x_{13}						

$\omega(782)$ PARTIAL WIDTHS

$\Gamma(\pi^0\gamma)$ Γ_2

VALUE (keV)	EVTS	DOCUMENT ID	TECN	COMMENT
••• We do not use the following data for averages, fits, limits, etc. •••				
788±12±27	36500	13 ACHASOV 03	SND	0.60-0.97 $e^+e^- \rightarrow \pi^0\gamma$
764±51	10625	DOLINSKY 89	ND	$e^+e^- \rightarrow \pi^0\gamma$

13 Using $\Gamma_\omega = 8.44 \pm 0.09$ MeV and $B(\omega \rightarrow \pi^0\gamma)$ from ACHASOV 03.

$\Gamma(\eta\gamma)$ Γ_5

VALUE (keV)	DOCUMENT ID	TECN	COMMENT
••• We do not use the following data for averages, fits, limits, etc. •••			
6.1±2.5	14 DOLINSKY 89	ND	$e^+e^- \rightarrow \eta\gamma$

14 Using $\Gamma_\omega = 8.4 \pm 0.1$ MeV and $B(\omega \rightarrow \eta\gamma)$ from DOLINSKY 89.

$\Gamma(e^+e^-)$ Γ_9

VALUE (keV)	EVTS	DOCUMENT ID	TECN	COMMENT
0.60 ± 0.02 OUR EVALUATION				
••• We do not use the following data for averages, fits, limits, etc. •••				
0.591±0.015	11200	15,16 AKHMETSHIN 04	CMD2	$e^+e^- \rightarrow \pi^+\pi^-\pi^0$
0.653±0.003±0.021	1.2M	17 ACHASOV 03D	RVUE	0.44-2.00 $e^+e^- \rightarrow \pi^+\pi^-\pi^0$
0.600±0.031	10625	DOLINSKY 89	ND	$e^+e^- \rightarrow \pi^+\pi^-\pi^0\gamma$

15 Using $B(\omega \rightarrow \pi^+\pi^-\pi^0) = 0.891 \pm 0.007$ and $\Gamma_{\text{total}} = 8.44 \pm 0.09$ MeV.
 16 Update of AKHMETSHIN 00c.
 17 Using ACHASOV 03, ACHASOV 03D and $B(\omega \rightarrow \pi^+\pi^-) = (1.70 \pm 0.28)\%$.

$\omega(782)$ $\Gamma(e^+e^-)\Gamma(i)/\Gamma^2(\text{total})$

$\Gamma(e^+e^-)/\Gamma_{\text{total}} \times \Gamma(\pi^+\pi^-\pi^0)/\Gamma_{\text{total}}$ $\Gamma_9/\Gamma \times \Gamma_1/\Gamma$

VALUE (units 10 ⁻⁵)	EVTS	DOCUMENT ID	TECN	COMMENT
6.49±0.11 OUR FIT				Error includes scale factor of 1.3.
6.38±0.10 OUR AVERAGE				Error includes scale factor of 1.1.
6.24±0.11±0.08	11.2k	18 AKHMETSHIN 04	CMD2	$e^+e^- \rightarrow \pi^+\pi^-\pi^0$
6.70±0.06±0.27		AUBERT,B 04N	BABR	10.6 $e^+e^- \rightarrow \pi^+\pi^-\pi^0\gamma$
6.74±0.04±0.24	1.2M	19,20 ACHASOV 03D	RVUE	0.44-2.00 $e^+e^- \rightarrow \pi^+\pi^-\pi^0$
6.37±0.35		19 DOLINSKY 89	ND	$e^+e^- \rightarrow \pi^+\pi^-\pi^0$
6.45±0.24		19 BARKOV 87	CMD	$e^+e^- \rightarrow \pi^+\pi^-\pi^0$
5.79±0.42	1488	19 KURDADZE 83B	OLYA	$e^+e^- \rightarrow \pi^+\pi^-\pi^0$
5.89±0.54	433	19 CORDIER 80	DM1	$e^+e^- \rightarrow \pi^+\pi^-\pi^0$
7.54±0.84	451	19 BENAKSAS 72B	OSPK	$e^+e^- \rightarrow \pi^+\pi^-\pi^0$

18 Update of AKHMETSHIN 00c.
 19 Recalculated by us from the cross section in the peak.
 20 From the combined fit of ANTONELLI 92, ACHASOV 01E, ACHASOV 02E, and ACHASOV 03D data on the $\pi^+\pi^-\pi^0$ and ANTONELLI 92 on the $\omega\pi^+\pi^-$ final states. Supersedes ACHASOV 99E and ACHASOV 02E.

$\Gamma(e^+e^-)/\Gamma_{\text{total}} \times \Gamma(\pi^0\gamma)/\Gamma_{\text{total}}$ $\Gamma_9/\Gamma \times \Gamma_2/\Gamma$

VALUE (units 10 ⁻⁶)	EVTS	DOCUMENT ID	TECN	COMMENT
6.02±0.20 OUR FIT				Error includes scale factor of 1.9.
6.45±0.17 OUR AVERAGE				
6.47±0.14±0.39	18680	AKHMETSHIN 05	CMD2	0.60-1.38 $e^+e^- \rightarrow \pi^0\gamma$
6.50±0.11±0.20	36500	21 ACHASOV 03	SND	0.60-0.97 $e^+e^- \rightarrow \pi^0\gamma$
6.34±0.21±0.21	10625	22 DOLINSKY 89	ND	$e^+e^- \rightarrow \pi^0\gamma$

21 Using $\sigma_{\phi \rightarrow \pi^0\gamma}$ from ACHASOV 00 and $m_\omega = 782.57$ MeV in the model with the energy-independent phase of $\rho\omega$ interference equal to $(-10.2 \pm 7.0)^\circ$.
 22 Recalculated by us from the cross section in the peak.

$\Gamma(e^+e^-)/\Gamma_{\text{total}} \times \Gamma(\pi^+\pi^-)/\Gamma_{\text{total}}$ $\Gamma_9/\Gamma \times \Gamma_3/\Gamma$

VALUE (units 10^{-8})	EVTS	DOCUMENT ID	TECN	COMMENT
$1.225 \pm 0.058 \pm 0.041$	800k	23 ACHASOV	06	SND $e^+e^- \rightarrow \pi^+\pi^-$

²³ Supersedes ACHASOV 05A.

 $\Gamma(e^+e^-)/\Gamma_{\text{total}} \times \Gamma(\eta\gamma)/\Gamma_{\text{total}}$ $\Gamma_9/\Gamma \times \Gamma_5/\Gamma$

VALUE (units 10^{-8})	EVTS	DOCUMENT ID	TECN	COMMENT
3.32 ± 0.28 OUR FIT				Error includes scale factor of 1.1.
3.18 ± 0.28 OUR AVERAGE				

3.10 ± 0.31 ± 0.11	33k	24 ACHASOV	07B	SND 0.6–1.38 $e^+e^- \rightarrow \eta\gamma$
3.17 $^{+1.85}_{-1.31}$ ± 0.21	17.4k	25 AKHMETSHIN 05	CMD2	0.60–1.38 $e^+e^- \rightarrow \eta\gamma$
3.41 ± 0.52 ± 0.21	23k	26,27 AKHMETSHIN 01B	CMD2	$e^+e^- \rightarrow \eta\gamma$

²⁴ From a combined fit of $\sigma(e^+e^- \rightarrow \eta\gamma)$ with $\eta \rightarrow 3\pi^0$ and $\eta \rightarrow \pi^+\pi^-\pi^0$, and fixing $B(\eta \rightarrow 3\pi^0) / B(\eta \rightarrow \pi^+\pi^-\pi^0) = 1.44 \pm 0.04$. Recalculated by us from the cross section at the peak. Supersedes ACHASOV 00D and ACHASOV 06A.

²⁵ From the $\eta \rightarrow 2\gamma$ decay and using $B(\eta \rightarrow \gamma\gamma) = 39.43 \pm 0.26\%$.

²⁶ From the $\eta \rightarrow 3\pi^0$ decay and using $B(\eta \rightarrow 3\pi^0) = (32.24 \pm 0.29) \times 10^{-2}$.

²⁷ The combined fit from 600 to 1380 MeV taking into account $\rho(770)$, $\omega(782)$, $\phi(1020)$, and $\rho(1450)$ (mass and width fixed at 1450 MeV and 310 MeV respectively).

 $\omega(782)$ BRANCHING RATIOS $\Gamma(\pi^+\pi^-\pi^0)/\Gamma_{\text{total}}$ Γ_1/Γ

VALUE	EVTS	DOCUMENT ID	TECN	COMMENT
0.9024 ± 0.0019		28 AMBROSINO	08G	KLOE 1.0–1.03 $e^+e^- \rightarrow \pi^+\pi^-\pi^0, 2\pi^0\gamma$
0.8965 ± 0.0016 ± 0.0048	1.2M	29,30 ACHASOV	03D	RVUE 0.44–2.00 $e^+e^- \rightarrow \pi^+\pi^-\pi^0$
0.880 ± 0.020 ± 0.032	11200	30,31 AKHMETSHIN 00C	CMD2	$e^+e^- \rightarrow \pi^+\pi^-\pi^0$
0.8942 ± 0.0062		30 DOLINSKY	89	ND $e^+e^- \rightarrow \pi^+\pi^-\pi^0$

²⁸ Not independent of $\Gamma(\pi^0\gamma) / \Gamma(\pi^+\pi^-\pi^0)$ from AMBROSINO 08G.

²⁹ Using ACHASOV 03, ACHASOV 03D and $B(\omega \rightarrow \pi^+\pi^-) = (1.70 \pm 0.28)\%$.

³⁰ Not independent of the corresponding $\Gamma(e^+e^-) \times \Gamma(\pi^+\pi^-\pi^0)/\Gamma_{\text{total}}^2$.

³¹ Using $\Gamma(e^+e^-) = 0.60 \pm 0.02$ keV.

 $\Gamma(\pi^0\gamma)/\Gamma_{\text{total}}$ Γ_2/Γ

VALUE (units 10^{-2})	EVTS	DOCUMENT ID	TECN	COMMENT
8.09 ± 0.14		32 AMBROSINO	08G	KLOE $e^+e^- \rightarrow \pi^+\pi^-\pi^0, 2\pi^0\gamma$
9.06 ± 0.20 ± 0.57	18680	33,34 AKHMETSHIN 05	CMD2	0.60–1.38 $e^+e^- \rightarrow \pi^0\gamma$
9.34 ± 0.15 ± 0.31	36500	34 ACHASOV	03	SND 0.60–0.97 $e^+e^- \rightarrow \pi^0\gamma$
8.65 ± 0.16 ± 0.42	1.2M	35,36 ACHASOV	03D	RVUE 0.44–2.00 $e^+e^- \rightarrow \pi^+\pi^-\pi^0$
8.39 ± 0.24	9975	37 BENAYOUN	96	RVUE $e^+e^- \rightarrow \pi^0\gamma$
8.88 ± 0.62	10625	34 DOLINSKY	89	ND $e^+e^- \rightarrow \pi^0\gamma$

³² Not independent of $\Gamma(\pi^0\gamma) / \Gamma(\pi^+\pi^-\pi^0)$ from AMBROSINO 08G.

³³ Using $B(\omega \rightarrow e^+e^-) = (7.14 \pm 0.13) \times 10^{-5}$.

³⁴ Not independent of the corresponding $\Gamma(e^+e^-) \times \Gamma(\pi^0\gamma)/\Gamma_{\text{total}}^2$.

³⁵ Using ACHASOV 03, ACHASOV 03D and $B(\omega \rightarrow \pi^+\pi^-) = (1.70 \pm 0.28)\%$.

³⁶ Not independent of the corresponding $\Gamma(e^+e^-) \times \Gamma(\pi^+\pi^-\pi^0)/\Gamma_{\text{total}}^2$.

³⁷ Reanalysis of DRUZHININ 84, DOLINSKY 89, DOLINSKY 91 taking into account the triangle anomaly contributions.

 $\Gamma(\pi^0\gamma)/\Gamma(\pi^+\pi^-\pi^0)$ Γ_2/Γ_1

VALUE (units 10^{-2})	DOCUMENT ID	TECN	COMMENT
9.28 ± 0.31 OUR FIT			Error includes scale factor of 2.3.
9.05 ± 0.27 OUR AVERAGE			Error includes scale factor of 1.8.
8.97 ± 0.16	AMBROSINO 08G	KLOE	$e^+e^- \rightarrow \pi^+\pi^-\pi^0, 2\pi^0\gamma$
9.94 ± 0.36 ± 0.38	38 AULCHENKO	00A	SND $e^+e^- \rightarrow \pi^+\pi^-\pi^0, 2\pi^0\gamma$
8.4 ± 1.3	KEYNE	76	CNTR $\pi^-p \rightarrow \omega n$
10.9 ± 2.5	BENAKSAS	72C	OSPK $e^+e^- \rightarrow \pi^0\gamma$
8.1 ± 2.0	BALDIN	71	HLBC 2.9 $\pi^+\pi^-$
13 ± 4	JACQUET	69B	HLBC 2.05 $\pi^+\pi^- \rightarrow \pi^+\pi^0$
9.7 ± 0.2 ± 0.5	39,40 ACHASOV	03D	RVUE 0.44–2.00 $e^+e^- \rightarrow \pi^+\pi^-\pi^0$
9.9 ± 0.7	39 DOLINSKY	89	ND $e^+e^- \rightarrow \pi^0\gamma$

³⁸ From $\sigma_0^{\omega\pi^0} \rightarrow \pi^0\pi^0\gamma(m_\phi)/\sigma_0^{\omega\pi^0} \rightarrow \pi^+\pi^-\pi^0\pi^0(m_\phi)$ with a phase-space correction factor of 1/1.023.

³⁹ Not independent of the corresponding $\Gamma(e^+e^-) \times \Gamma(\pi^0\gamma)/\Gamma_{\text{total}}^2$.

⁴⁰ Using ACHASOV 03. Based on 1.2M events.

 $\Gamma(\pi^+\pi^-)/\Gamma_{\text{total}}$ Γ_3/Γ

See also $\Gamma(\pi^+\pi^-)/\Gamma(\pi^+\pi^-\pi^0)$.

VALUE (units 10^{-2})	EVTS	DOCUMENT ID	TECN	COMMENT
--------------------------	------	-------------	------	---------

1.53 $^{+0.11}_{-0.13}$ OUR FIT Error includes scale factor of 1.2.

1.49 ± 0.13 OUR AVERAGE Error includes scale factor of 1.3. See the ideogram below.

1.46 ± 0.12 ± 0.02	900k	41 AKHMETSHIN 07		$e^+e^- \rightarrow \pi^+\pi^-$
1.30 ± 0.24 ± 0.05	11.2k	42 AKHMETSHIN 04	CMD2	$e^+e^- \rightarrow \pi^+\pi^-$
2.38 $^{+1.77}_{-0.90}$ ± 0.18	5.4k	43 ACHASOV	02E	SND 1.1–1.38 $e^+e^- \rightarrow \pi^+\pi^-$
2.3 ± 0.5		BARKOV	85	OLYA $e^+e^- \rightarrow \pi^+\pi^-$
1.6 $^{+0.9}_{-0.7}$		QUENZER	78	DMI $e^+e^- \rightarrow \pi^+\pi^-$
3.6 ± 1.9		BENAKSAS	72	OSPK $e^+e^- \rightarrow \pi^+\pi^-$
1.75 ± 0.11	4.5M	44 ACHASOV	05A	SND $e^+e^- \rightarrow \pi^+\pi^-$
2.01 ± 0.29		45 BENAYOUN	03	RVUE $e^+e^- \rightarrow \pi^+\pi^-$
1.9 ± 0.3		46 GARDNER	99	RVUE $e^+e^- \rightarrow \pi^+\pi^-$
2.3 ± 0.4		47 BENAYOUN	98	RVUE $e^+e^- \rightarrow \pi^+\pi^-, \mu^+\mu^-$
1.0 ± 0.11		48 WICKLUND	78	ASPK 3,4,6 $\pi^\pm N$
1.22 ± 0.30		ALVENSLEB...	71C	CNTR Photoproduction
1.3 $^{+1.2}_{-0.9}$		MOFFEIT	71	HBC 2,8,4,7 γp
0.80 $^{+0.28}_{-0.20}$		49 BIGGS	70B	CNTR 4,2 $\gamma C \rightarrow \pi^+\pi^- C$

⁴¹ A combined fit of AKHMETSHIN 07, AULCHENKO 06, and AULCHENKO 05.

⁴² Update of AKHMETSHIN 02.

⁴³ From the $m_{\pi^+\pi^-}$ spectrum taking into account the interference of the $\rho\pi$ and $\omega\pi$ amplitudes.

⁴⁴ Using $\Gamma(\omega \rightarrow e^+e^-)$ from the 2004 Edition of this Review (PDG 04).

⁴⁵ Using the data of AKHMETSHIN 02 in the hidden local symmetry model.

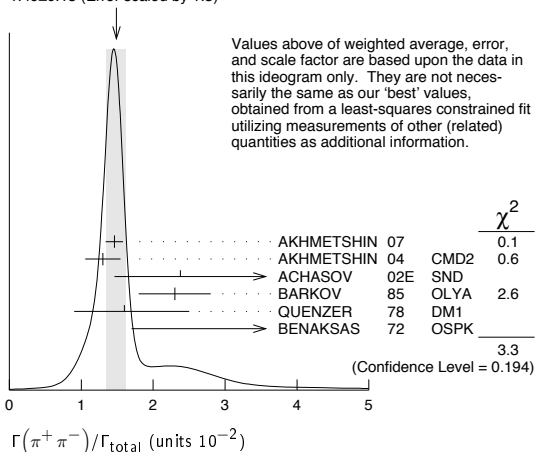
⁴⁶ Using the data of BARKOV 85.

⁴⁷ Using the data of BARKOV 85 in the hidden local symmetry model.

⁴⁸ From a model-dependent analysis assuming complete coherence.

⁴⁹ Re-evaluated under $\Gamma(\pi^+\pi^-)/\Gamma(\pi^+\pi^-\pi^0)$ by BEHREND 71 using more accurate $\omega \rightarrow \rho$ photoproduction cross-section ratio.

WEIGHTED AVERAGE
1.49 ± 0.13 (Error scaled by 1.3)

 $\Gamma(\pi^+\pi^-)/\Gamma(\pi^+\pi^-\pi^0)$ Γ_3/Γ_1

See also $\Gamma(\pi^+\pi^-)/\Gamma_{\text{total}}$.

VALUE	DOCUMENT ID	TECN	COMMENT
-------	-------------	------	---------

0.0172 ± 0.0014 OUR FIT Error includes scale factor of 1.2.

0.026 ± 0.005 OUR AVERAGE

0.021 $^{+0.028}_{-0.009}$	50,51 RATCLIFF	72	ASPK 15 $\pi^-p \rightarrow n2\pi$
0.028 ± 0.006	50 BEHREND	71	ASPK Photoproduction
0.022 $^{+0.009}_{-0.01}$	52 ROOS	70	RVUE

⁵⁰ The fitted width of these data is 160 MeV in agreement with present average, thus the ω contribution is overestimated. Assuming ρ width 145 MeV.

⁵¹ Significant interference effect observed. NB of $\omega \rightarrow 3\pi$ comes from an extrapolation.

⁵² ROOS 70 combines ABRAMOVICH 70 and BIZZARRI 70.

 $\Gamma(\pi^+\pi^-)/\Gamma(\pi^0\gamma)$ Γ_3/Γ_2

VALUE	EVTS	DOCUMENT ID	TECN	COMMENT
0.20 ± 0.04	1.98M	53 ALOISIO	03	KLOE 1.02 $e^+e^- \rightarrow \pi^+\pi^-\pi^0$

⁵³ Using the data of ALOISIO 02D.

Meson Particle Listings

 $\omega(782)$

$\Gamma(\text{neutrals})/\Gamma_{\text{total}}$		$(\Gamma_2+\Gamma_4)/\Gamma$			
VALUE	EVTS	DOCUMENT ID	TECN	COMMENT	
0.091±0.006 OUR FIT					
0.081±0.011 OUR AVERAGE					
0.075±0.025		BIZZARRI	71	HBC	0.0 $\rho\bar{p}$
0.079±0.019		DEINET	69B	OSPK	1.5 π^-p
0.084±0.015		BOLLINI	68c	CNTR	2.1 π^-p
••• We do not use the following data for averages, fits, limits, etc. •••					
0.073±0.018	42	BASILE	72B	CNTR	1.67 π^-p

$\Gamma(\text{neutrals})/\Gamma(\pi^+\pi^-\pi^0)$		$(\Gamma_2+\Gamma_4)/\Gamma_1$			
VALUE	EVTS	DOCUMENT ID	TECN	COMMENT	
0.102±0.008 OUR FIT					
0.103±0.011 OUR AVERAGE					
0.15±0.04	46	AGUILAR...	72B	HBC	3.9,4.6 K^-p
0.10±0.03	19	BARASH	67B	HBC	0.0 $\bar{p}p$
0.134±0.026	850	DIGIUGNO	66B	CNTR	1.4 π^-p
0.097±0.016	348	FLATTE	66	HBC	1.4-1.7 $K^-p \rightarrow \Lambda MM$
0.06 ^{+0.05} _{-0.02}		JAMES	66	HBC	2.1 π^+p
0.08±0.03	35	KRAEMER	64	DBC	1.2 π^+d
••• We do not use the following data for averages, fits, limits, etc. •••					
0.11±0.02	20	BUSCHBECK	63	HBC	1.5 K^-p

$\Gamma(\pi^0\gamma)/\Gamma(\text{neutrals})$		$\Gamma_2/(\Gamma_2+\Gamma_4)$			
VALUE	CL%	DOCUMENT ID	TECN	COMMENT	
••• We do not use the following data for averages, fits, limits, etc. •••					
0.78±0.07	54	DAKIN	72	OSPK	1.4 $\pi^-p \rightarrow nMM$
>0.81	90	DEINET	69B	OSPK	
54 Error statistical only. Authors obtain good fit also assuming $\pi^0\gamma$ as the only neutral decay.					

$\Gamma(\text{neutrals})/\Gamma(\text{charged particles})$		$(\Gamma_2+\Gamma_4)/(\Gamma_1+\Gamma_3)$			
VALUE		DOCUMENT ID	TECN	COMMENT	
0.100±0.008 OUR FIT					
0.124±0.021		FELDMAN	67c	OSPK	1.2 π^-p

$\Gamma(\eta\gamma)/\Gamma_{\text{total}}$		Γ_5/Γ			
VALUE (units 10^{-4})	EVTS	DOCUMENT ID	TECN	COMMENT	
4.6±0.4 OUR FIT					Error includes scale factor of 1.1.
6.3±1.3 OUR AVERAGE					Error includes scale factor of 1.2.
6.6±1.7	55	ABELE	97E	CBAR	0.0 $\bar{p}p \rightarrow 5\gamma$
8.3±2.1		ALDE	93	GAM2	38 $\pi^-p \rightarrow \omega n$
3.0 ^{+2.5} _{-1.8}	56	ANDREWS	77	CNTR	6.7-10 γCu
••• We do not use the following data for averages, fits, limits, etc. •••					
4.3±0.5±0.1	33k	57 ACHASOV	07B	SND	0.6-1.38 $e^+e^- \rightarrow \eta\gamma$
4.4 ^{+2.59} _{-1.83} ±0.28	17.4k	58,59 AKHMETSHIN	05	CMD2	0.60-1.38 $e^+e^- \rightarrow \eta\gamma$
5.10±0.72±0.34	23k	60 AKHMETSHIN	01B	CMD2	$e^+e^- \rightarrow \eta\gamma$
0.7 to 5.5		61 CASE	00	CBAR	0.0 $\bar{p}p \rightarrow \eta\eta\gamma$
6.56 ^{+2.41} _{-2.55}	3525	56,62 BENAYOUN	96	RVUE	$e^+e^- \rightarrow \eta\gamma$
7.3±2.9		56,58 DOLINSKY	89	ND	$e^+e^- \rightarrow \eta\gamma$

- 55 No flat $\eta\eta\gamma$ background assumed.
56 Solution corresponding to constructive $\omega\rho$ interference.
57 ACHASOV 07B reports $[\Gamma(\omega(782) \rightarrow \eta\gamma)/\Gamma_{\text{total}}] \times [B(\omega(782) \rightarrow e^+e^-)] = (3.10 \pm 0.31 \pm 0.11) \times 10^{-8}$ which we divide by our best value $B(\omega(782) \rightarrow e^+e^-) = (7.28 \pm 0.14) \times 10^{-5}$. Our first error is their experiment's error and our second error is the systematic error from using our best value. Supersedes ACHASOV 00D and ACHASOV 06A.
58 Not independent of the corresponding $\Gamma(e^+e^-) \times \Gamma(\eta\gamma)/\Gamma_{\text{total}}^2$.
59 Using $B(\omega \rightarrow e^+e^-) = (7.14 \pm 0.13) \times 10^{-5}$ and $B(\eta \rightarrow \gamma\gamma) = 39.43 \pm 0.26\%$.
60 Using $B(\omega \rightarrow e^+e^-) = (7.07 \pm 0.19) \times 10^{-5}$ and using $B(\eta \rightarrow 3\pi^0) = (32.24 \pm 0.29) \times 10^{-2}$. Solution corresponding to constructive $\omega\rho$ interference. The combined fit from 600 to 1380 MeV taking into account $\rho(770)$, $\omega(782)$, $\phi(1020)$, and $\rho(1450)$ (mass and width fixed at 1450 MeV and 310 MeV respectively). Not independent of the corresponding $\Gamma(e^+e^-) \times \Gamma(\eta\gamma)/\Gamma_{\text{total}}^2$.
61 Depending on the degree of coherence with the flat $\eta\eta\gamma$ background and using $B(\omega \rightarrow \pi^0\gamma) = (8.5 \pm 0.5) \times 10^{-2}$.
62 Reanalysis of DRUZHININ 84, DOLINSKY 89, DOLINSKY 91 taking into account the triangle anomaly contributions.

$\Gamma(\eta\gamma)/\Gamma(\pi^0\gamma)$		Γ_5/Γ_2			
VALUE		DOCUMENT ID	TECN	COMMENT	
••• We do not use the following data for averages, fits, limits, etc. •••					
0.0098±0.0024	63	ALDE	93	GAM2	38 $\pi^-p \rightarrow \omega n$
0.0082±0.0033	64	DOLINSKY	89	ND	$e^+e^- \rightarrow \eta\gamma$
0.010±0.045		APEL	72B	OSPK	4-8 $\pi^-p \rightarrow n3\gamma$
63 Model independent determination. 64 Solution corresponding to constructive $\omega\rho$ interference.					

$\Gamma(\pi^0 e^+ e^-)/\Gamma_{\text{total}}$		Γ_6/Γ			
VALUE (units 10^{-4})	EVTS	DOCUMENT ID	TECN	COMMENT	
7.7±0.6 OUR FIT					
7.7±0.6 OUR AVERAGE					
7.61±0.53±0.64		ACHASOV	08	SND	0.36-0.97 $e^+e^- \rightarrow \pi^0 e^+ e^-$
8.19±0.71±0.62		AKHMETSHIN	05A	CMD2	0.72-0.84 e^+e^-
5.9±1.9	43	DOLINSKY	88	ND	$e^+e^- \rightarrow \pi^0 e^+ e^-$

$\Gamma(\pi^0 \mu^+ \mu^-)/\Gamma_{\text{total}}$		Γ_7/Γ			
VALUE (units 10^{-4})	EVTS	DOCUMENT ID	TECN	COMMENT	
1.3±0.4 OUR FIT					Error includes scale factor of 2.1.
1.3±0.4 OUR AVERAGE					Error includes scale factor of 2.1.
1.72±0.25±0.14	3k	ARNALDI	09	NA60	158A In-In collisions
0.96±0.23		DZHELADIN	81B	CNTR	25-33 $\pi^-p \rightarrow \omega n$

$\Gamma(\eta e^+ e^-)/\Gamma_{\text{total}}$		Γ_8/Γ			
VALUE (units 10^{-5})		DOCUMENT ID	TECN	COMMENT	
••• We do not use the following data for averages, fits, limits, etc. •••					
<1.1		AKHMETSHIN	05A	CMD2	0.72-0.84 e^+e^-

$\Gamma(e^+ e^-)/\Gamma_{\text{total}}$		Γ_9/Γ			
VALUE (units 10^{-4})	EVTS	DOCUMENT ID	TECN	COMMENT	
0.728±0.014 OUR FIT					Error includes scale factor of 1.3.
••• We do not use the following data for averages, fits, limits, etc. •••					
0.700±0.016	11200	65,66 AKHMETSHIN	04	CMD2	$e^+e^- \rightarrow \pi^+\pi^-\pi^0$
0.752±0.004±0.024	1.2M	66,67 ACHASOV	03D	RVUE	0.44-2.00 $e^+e^- \rightarrow \pi^+\pi^-\pi^0$
0.714±0.036		66 DOLINSKY	89	ND	$e^+e^- \rightarrow \pi^+\pi^-\pi^0$
0.72±0.03		66 BARKOV	87	CMD	$e^+e^- \rightarrow \pi^+\pi^-\pi^0$
0.64±0.04	1488	66 KURDADZE	83B	OLYA	$e^+e^- \rightarrow \pi^+\pi^-\pi^0$
0.675±0.069	433	66 CORDIER	80	DM1	$e^+e^- \rightarrow \pi^+\pi^-\pi^0$
0.83±0.10	451	66 BENAKSAS	72B	OSPK	$e^+e^- \rightarrow \pi^+\pi^-\pi^0$
0.77±0.06		68 AUGUSTIN	69D	OSPK	$e^+e^- \rightarrow \pi^+\pi^-\pi^0$
0.65±0.13	33	69 ASTVACAT...	68	OSPK	Assume SU(3)+mixing
65 Using $B(\omega \rightarrow \pi^+\pi^-\pi^0) = 0.891 \pm 0.007$. Update of AKHMETSHIN 00c. 66 Not independent of the corresponding $\Gamma(e^+e^-) \times \Gamma(\pi^+\pi^-\pi^0)/\Gamma_{\text{total}}^2$. 67 Using ACHASOV 03, ACHASOV 03D and $B(\omega \rightarrow \pi^+\pi^-) = (1.70 \pm 0.28)\%$. 68 Rescaled by us to correspond to ω width 8.4 MeV. Systematic errors underestimated. 69 Not resolved from ρ decay. Error statistical only.					

$\Gamma(\pi^+\pi^-\pi^0\pi^0)/\Gamma_{\text{total}}$		Γ_{10}/Γ			
VALUE (units 10^{-4})	CL%	DOCUMENT ID	TECN	COMMENT	
< 2	90	ACHASOV	09A	SND	$e^+e^- \rightarrow \pi^+\pi^-\pi^0\pi^0$
••• We do not use the following data for averages, fits, limits, etc. •••					
<200	90	KURDADZE	86	OLYA	$e^+e^- \rightarrow \pi^+\pi^-\pi^0\pi^0$

$\Gamma(\pi^+\pi^-\gamma)/\Gamma_{\text{total}}$		Γ_{11}/Γ			
VALUE	CL%	DOCUMENT ID	TECN	COMMENT	
<0.0036	95	WEIDENAUER	90	ASTE	$\bar{p}p \rightarrow \pi^+\pi^-\pi^+\pi^-\gamma$
••• We do not use the following data for averages, fits, limits, etc. •••					
<0.004	95	BITYUKOV	88B	SPEC	32 $\pi^-p \rightarrow \pi^+\pi^-\gamma X$

$\Gamma(\pi^+\pi^-\gamma)/\Gamma(\pi^+\pi^-\pi^0)$		Γ_{11}/Γ_1			
VALUE	CL%	DOCUMENT ID	TECN	COMMENT	
••• We do not use the following data for averages, fits, limits, etc. •••					
<0.066	90	KALBFLEISCH	75	HBC	2.18 $K^-p \rightarrow \Lambda^+\pi^-\gamma$
<0.05	90	FLATTE	66	HBC	1.2-1.7 $K^-p \rightarrow \Lambda^+\pi^-\gamma$

$\Gamma(\pi^+\pi^-\pi^+\pi^-)/\Gamma_{\text{total}}$		Γ_{12}/Γ			
VALUE	CL%	DOCUMENT ID	TECN	COMMENT	
<1×10 ⁻³	90	KURDADZE	88	OLYA	$e^+e^- \rightarrow \pi^+\pi^-\pi^+\pi^-$

$\Gamma(\pi^0\pi^0\gamma)/\Gamma_{\text{total}}$		Γ_{13}/Γ			
VALUE (units 10^{-5})	EVTS	DOCUMENT ID	TECN	COMMENT	
6.6±1.1 OUR FIT					
6.5±1.2 OUR AVERAGE					
6.4 ^{+2.4} _{-2.0} ±0.8	190	70 AKHMETSHIN	04B	CMD2	0.6-0.97 $e^+e^- \rightarrow \pi^0\pi^0\gamma$
6.6 ^{+1.4} _{-1.3} ±0.6	295	ACHASOV	02F	SND	0.36-0.97 $e^+e^- \rightarrow \pi^0\pi^0\gamma$
••• We do not use the following data for averages, fits, limits, etc. •••					

11.8 ^{+2.1} _{-1.9} ±1.4	190	71 AKHMETSHIN	04B	CMD2	0.6-0.97 $e^+e^- \rightarrow \pi^0\pi^0\gamma$
7.8±2.7±2.0	63	70,72 ACHASOV	00G	SND	$e^+e^- \rightarrow \pi^0\pi^0\gamma$
12.7±2.3±2.5	63	71,72 ACHASOV	00G	SND	$e^+e^- \rightarrow \pi^0\pi^0\gamma$
70 In the model assuming the $\rho \rightarrow \pi^0\pi^0\gamma$ decay via the $\omega\pi$ and $f_0(600)\gamma$ mechanisms. 71 In the model assuming the $\rho \rightarrow \pi^0\pi^0\gamma$ decay via the $\omega\pi$ mechanism only. 72 Superseded by ACHASOV 02F.					

See key on page 405

Meson Particle Listings

 $\eta'(958)$ $\eta'(958)$ PARTIAL WIDTHS

$\Gamma(\gamma\gamma)$								Γ_5	
VALUE (keV)	EVTS	DOCUMENT ID	TECN	COMMENT					
4.29±0.14 OUR FIT									
4.28±0.19 OUR AVERAGE									
4.17±0.10±0.27	2000	4 ACCIARRI	98Q L3	$e^+e^- \rightarrow e^+e^-\pi^+\pi^-\gamma$					
4.53±0.29±0.51	266	KARCH	92 CBAL	$e^+e^- \rightarrow e^+e^-\eta\pi^0\pi^0$					
3.61±0.13±0.48		5 BEHREND	91 CELL	$e^+e^- \rightarrow e^+e^-\eta'(958)$					
4.6±1.1±0.6	23	BARU	90 MD1	$e^+e^- \rightarrow e^+e^-\pi^+\pi^-\gamma$					
4.57±0.25±0.44		BUTLER	90 MRK2	$e^+e^- \rightarrow e^+e^-\eta'(958)$					
5.08±0.24±0.71	547	6 ROE	90 ASP	$e^+e^- \rightarrow e^+e^-2\gamma$					
3.8±0.7±0.6	34	AIHARA	88c TPC	$e^+e^- \rightarrow e^+e^-\eta\pi^+\pi^-$					
4.9±0.5±0.5	136	7 WILLIAMS	88 CBAL	$e^+e^- \rightarrow e^+e^-2\gamma$					
••• We do not use the following data for averages, fits, limits, etc. •••									
4.7±0.6±0.9	143	8 GIDAL	87 MRK2	$e^+e^- \rightarrow e^+e^-\eta\pi^+\pi^-$					
4.0±0.9		9 BARTEL	85E JADE	$e^+e^- \rightarrow e^+e^-2\gamma$					
<p>4 No non-resonant $\pi^+\pi^-$ contribution found. 5 Reevaluated by us using $B(\eta' \rightarrow \rho(770)\gamma) = (30.2 \pm 1.3)\%$. 6 Reevaluated by us using $B(\eta' \rightarrow \gamma\gamma) = (2.11 \pm 0.13)\%$. 7 Reevaluated by us using $B(\eta' \rightarrow \gamma\gamma) = (2.11 \pm 0.13)\%$. 8 Superseded by BUTLER 90. 9 Systematic error not evaluated.</p>									

 $\eta'(958)$ $\Gamma(i)\Gamma(\gamma\gamma)/\Gamma(\text{total})$

This combination of a partial width with the partial width into $\gamma\gamma$ and with the total width is obtained from the integrated cross section into channel(i) in the $\gamma\gamma$ annihilation.

$\Gamma(\gamma\gamma) \times \Gamma(\rho^0\gamma(\text{including non-resonant } \pi^+\pi^-\gamma))/\Gamma_{\text{total}}$								$\Gamma_5\Gamma_2/\Gamma$	
VALUE (keV)	EVTS	DOCUMENT ID	TECN	COMMENT					
1.26±0.04 OUR FIT									
1.26±0.07 OUR AVERAGE									
1.09±0.04±0.13		BEHREND	91 CELL	$e^+e^- \rightarrow e^+e^-\rho(770)^0\gamma$					
1.35±0.09±0.21		AIHARA	87 TPC	$e^+e^- \rightarrow e^+e^-\rho\gamma$					
1.13±0.04±0.13	867	ALBRECHT	87B ARG	$e^+e^- \rightarrow e^+e^-\rho\gamma$					
1.53±0.09±0.21		ALTHOFF	84E TASS	$e^+e^- \rightarrow e^+e^-\rho\gamma$					
1.14±0.08±0.11	243	BERGER	84B PLUT	$e^+e^- \rightarrow e^+e^-\rho\gamma$					
1.73±0.34±0.35	95	JENNI	83 MRK2	$e^+e^- \rightarrow e^+e^-\rho\gamma$					
1.49±0.13±0.027	213	BARTEL	82B JADE	$e^+e^- \rightarrow e^+e^-\rho\gamma$					
••• We do not use the following data for averages, fits, limits, etc. •••									
1.85±0.31±0.24	43	BEHREND	83B CELL	$e^+e^- \rightarrow e^+e^-\rho\gamma$					

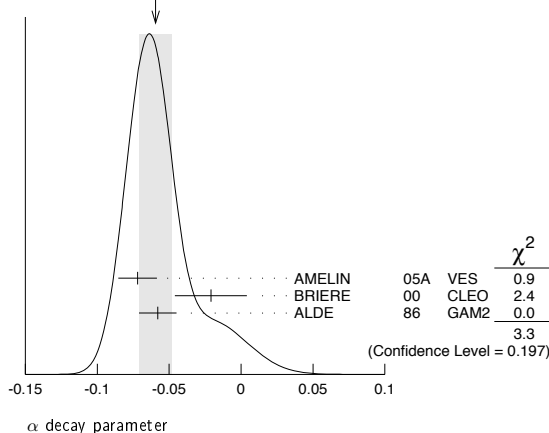
$\Gamma(\gamma\gamma) \times \Gamma(\pi^0\eta)/\Gamma_{\text{total}}$								$\Gamma_5\Gamma_3/\Gamma$	
VALUE (keV)	EVTS	DOCUMENT ID	TECN	COMMENT					
0.93±0.05 OUR FIT									
0.92±0.06±0.11									
••• We do not use the following data for averages, fits, limits, etc. •••									
0.95±0.05±0.08		11 KARCH	90 CBAL	$e^+e^- \rightarrow e^+e^-\eta\pi^0\pi^0$					
1.00±0.08±0.10		11,12 ANTREASNYAN	87 CBAL	$e^+e^- \rightarrow e^+e^-\eta\pi^0\pi^0$					
<p>10 Reevaluated by us using $B(\eta \rightarrow \gamma\gamma) = (39.21 \pm 0.34)\%$. Supersedes ANTREASNYAN 87 and KARCH 90. 11 Superseded by KARCH 90. 12 Using $BR(\eta \rightarrow 2\gamma) = (38.9 \pm 0.5)\%$.</p>									

 $\eta'(958)$ DECAY PARAMETERS

$$|\text{MATRIX ELEMENT}|^2 = |1 + \alpha y|^2 + cx + dx^2$$

 α decay parameter

VALUE	EVTS	DOCUMENT ID	TECN	COMMENT
-0.059±0.011 OUR AVERAGE				Error includes scale factor of 1.3. See the ideogram below.
-0.072±0.012±0.006	7k	13 AMELIN	05A VES	$28 \pi^- A \rightarrow \eta' \pi^- A^*$
-0.021±0.025	6.7k	14 BRIERE	00 CLEO	$10.6 e^+e^- \rightarrow \text{hadrons}$
-0.058±0.013	15,16	ALDE	86 GAM2	$38 \pi^- p \rightarrow n\eta 2\pi^0$
••• We do not use the following data for averages, fits, limits, etc. •••				
-0.08 ± 0.03	15,16	KALBFLEISCH	74 RVUE	$\eta' \rightarrow \eta\pi^+\pi^-$
<p>13 This is a real part of α while $\text{Im}(\alpha) = 0.0 \pm 0.1 \pm 0.0$. 14 Assuming $\text{Im}(\alpha) = 0$, $c = 0$, and $d = 0$. 15 May not necessarily be the same for $\eta' \rightarrow \eta\pi^+\pi^-$ and $\eta' \rightarrow \eta\pi^0\pi^0$. 16 Assuming $\text{Im}(\alpha) = 0$, $c = 0$.</p>				

WEIGHTED AVERAGE
-0.059±0.011 (Error scaled by 1.3) $\eta'(958) \rightarrow \eta\pi\pi$ DECAY PARAMETERS

$$|\text{MATRIX ELEMENT}|^2 \propto 1 + aY + bY^2 + cX + dX^2$$

X and Y are Dalitz variables and a, b, c, and d are real-valued parameters. May be different for $\eta'(958) \rightarrow \eta\pi^+\pi^-$ and $\eta'(958) \rightarrow \eta\pi^0\pi^0$ decays.

 a decay parameter

VALUE	EVTS	DOCUMENT ID	TECN	COMMENT
••• We do not use the following data for averages, fits, limits, etc. •••				
-0.066±0.016±0.003	15k	17 BLIK	09 GAM4	$32.5 \pi^- p \rightarrow \eta' n$
-0.127±0.016±0.008	20k	18 DOROFEEV	07 VES	$27 \pi^- p \rightarrow \eta' n$ $\pi^- A \rightarrow \eta' \pi^- A^*$
<p>17 From $\eta' \rightarrow \eta\pi^0\pi^0$ decay. Parameters a, b, c, d are strongly correlated. 18 From $\eta' \rightarrow \eta\pi^+\pi^-$ decay.</p>				

 b decay parameter

VALUE	EVTS	DOCUMENT ID	TECN	COMMENT
••• We do not use the following data for averages, fits, limits, etc. •••				
-0.063±0.028±0.004	15k	19 BLIK	09 GAM4	$32.5 \pi^- p \rightarrow \eta' n$
-0.106±0.028±0.014	20k	20 DOROFEEV	07 VES	$27 \pi^- p \rightarrow \eta' n$ $\pi^- A \rightarrow \eta' \pi^- A^*$
<p>19 From $\eta' \rightarrow \eta\pi^0\pi^0$ decay. Parameters a, b, c, d are strongly correlated. 20 From $\eta' \rightarrow \eta\pi^+\pi^-$ decay.</p>				

 c decay parameter

VALUE	EVTS	DOCUMENT ID	TECN	COMMENT
••• We do not use the following data for averages, fits, limits, etc. •••				
-0.107±0.096±0.003	15k	21 BLIK	09 GAM4	$32.5 \pi^- p \rightarrow \eta' n$
0.015±0.011±0.014	20k	22 DOROFEEV	07 VES	$27 \pi^- p \rightarrow \eta' n$ $\pi^- A \rightarrow \eta' \pi^- A^*$
<p>21 From $\eta' \rightarrow \eta\pi^0\pi^0$ decay. Parameters a, b, c, d are strongly correlated. 22 From $\eta' \rightarrow \eta\pi^+\pi^-$ decay.</p>				

 d decay parameter

VALUE	EVTS	DOCUMENT ID	TECN	COMMENT
••• We do not use the following data for averages, fits, limits, etc. •••				
0.018±0.078±0.006	15k	23 BLIK	09 GAM4	$32.5 \pi^- p \rightarrow \eta' n$
-0.082±0.017±0.008	20k	24 DOROFEEV	07 VES	$27 \pi^- p \rightarrow \eta' n$ $\pi^- A \rightarrow \eta' \pi^- A^*$
<p>23 From $\eta' \rightarrow \eta\pi^0\pi^0$ decay. Parameters a, b, c, d are strongly correlated. If $c \equiv 0$ from Bose-Einstein symmetry, $d = -0.067 \pm 0.020 \pm 0.003$. 24 From $\eta' \rightarrow \eta\pi^+\pi^-$ decay.</p>				

 $\eta'(958)$ β PARAMETER

$$|\text{MATRIX ELEMENT}|^2 = (1 + 2\beta Z)$$

See the "Note on η Decay Parameters" in our 1994 edition Physical Review D50 1173 (1994), p. 1454.

 β decay parameter

VALUE	EVTS	DOCUMENT ID	TECN	COMMENT
-0.46±0.22 OUR AVERAGE				Error includes scale factor of 1.4.
-0.59±0.18	235	BLIK	08 GAMS	$32 \pi^- p \rightarrow \eta' n$
-0.1 ± 0.3		ALDE	87B GAM2	$38 \pi^- p \rightarrow n3\pi^0$

Meson Particle Listings

 $\eta'(958)$ $\eta'(958)$ BRANCHING RATIOS

$\Gamma(\pi^+\pi^-\eta)/\Gamma_{\text{total}}$ Γ_1/Γ
0.432 ± 0.007 OUR FIT

• • • We do not use the following data for averages, fits, limits, etc. • • •

0.424 ± 0.011 ± 0.004 1.2k 25 PEDLAR 09 CLEO $J/\psi \rightarrow \gamma\eta'$
 25 Not independent of other η' branching fractions and ratios in PEDLAR 09.

$\Gamma(\pi^+\pi^-\eta(\text{charged decay}))/\Gamma_{\text{total}}$ **0.286 Γ_1/Γ**
0.1237 ± 0.0020 OUR FIT

• • • We do not use the following data for averages, fits, limits, etc. • • •

0.123 ± 0.014 107 RITTENBERG 69 HBC 1.7–2.7 K^-p
 0.10 ± 0.04 10 LONDON 66 HBC 2.24 $K^-p \rightarrow \Lambda 2\pi^+ 2\pi^- \pi^0$
 0.07 ± 0.04 7 BADIER 65B HBC 3 K^-p

$\Gamma(\pi^+\pi^-\eta(\text{neutral decay}))/\Gamma_{\text{total}}$ **0.714 Γ_1/Γ**
0.309 ± 0.005 OUR FIT

• • • We do not use the following data for averages, fits, limits, etc. • • •

0.314 ± 0.026 281 RITTENBERG 69 HBC 1.7–2.7 K^-p

$\Gamma(\rho^0\gamma(\text{including non-resonant } \pi^+\pi^-\gamma))/\Gamma_{\text{total}}$ Γ_2/Γ
0.293 ± 0.006 OUR FIT

• • • We do not use the following data for averages, fits, limits, etc. • • •

0.287 ± 0.007 ± 0.004 0.2k 26 PEDLAR 09 CLEO $J/\psi \rightarrow \gamma\eta'$
 0.329 ± 0.033 298 RITTENBERG 69 HBC 1.7–2.7 K^-p
 0.2 ± 0.1 20 LONDON 66 HBC 2.24 $K^-p \rightarrow \Lambda \pi^+ \pi^- \gamma$
 0.34 ± 0.09 35 BADIER 65B HBC 3 K^-p

26 Not independent of other η' branching fractions and ratios in PEDLAR 09.

$\Gamma(\rho^0\gamma(\text{including non-resonant } \pi^+\pi^-\gamma))/\Gamma(\pi^+\pi^-\eta)$ Γ_2/Γ_1
0.678 ± 0.017 OUR FIT
0.683 ± 0.020 OUR AVERAGE

0.677 ± 0.024 ± 0.011 PEDLAR 09 CLE3 $J/\psi \rightarrow \eta'\gamma$

0.69 ± 0.03 ABLIKIM 06E BES2 $J/\psi \rightarrow \eta'\gamma$

$\Gamma(\rho^0\gamma(\text{including non-resonant } \pi^+\pi^-\gamma))/\Gamma(\pi^+\pi^-\eta(\text{neutral decay}))$ $\Gamma_2/0.714\Gamma_1$
0.949 ± 0.024 OUR FIT
0.97 ± 0.09 OUR AVERAGE

0.70 ± 0.22 AMSLER 04B CBAR 0 $\bar{p}p \rightarrow \pi^+\pi^-\eta$

1.07 ± 0.17 BELADIDZE 92C VES 36 $\pi^- \text{Be} \rightarrow \pi^- \eta' \eta \text{Be}$

0.92 ± 0.14 473 DANBURG 73 HBC 2.2 $K^-p \rightarrow \Lambda X^0$

1.11 ± 0.18 192 JACOBS 73 HBC 2.9 $K^-p \rightarrow \Lambda X^0$

$\Gamma(\pi^0\pi^0\eta)/\Gamma_{\text{total}}$ Γ_3/Γ
0.217 ± 0.008 OUR FIT

• • • We do not use the following data for averages, fits, limits, etc. • • •

0.235 ± 0.013 ± 0.004 3.2k 27 PEDLAR 09 CLEO $J/\psi \rightarrow \gamma\eta'$

27 Not independent of other η' branching fractions and ratios in PEDLAR 09.

$\Gamma(\pi^0\pi^0\eta(3\pi^0\text{ decay}))/\Gamma_{\text{total}}$ **0.321 Γ_3/Γ**
0.0697 ± 0.0026 OUR FIT

• • • We do not use the following data for averages, fits, limits, etc. • • •

0.11 ± 0.06 4 BENSINGER 70 DBC 2.2 $\pi^+ d$

$\Gamma(\pi^0\pi^0\eta)/\Gamma(\pi^+\pi^-\eta)$ Γ_3/Γ_1
0.502 ± 0.026 OUR FIT
0.555 ± 0.043 ± 0.013

PEDLAR 09 CLE3 $J/\psi \rightarrow \eta'\gamma$

$\Gamma(\rho^0\gamma(\text{including non-resonant } \pi^+\pi^-\gamma))/\Gamma(\pi\pi\eta)$ $\Gamma_2/(\Gamma_1+\Gamma_3)$
0.451 ± 0.012 OUR FIT
0.43 ± 0.02 ± 0.02

• • • We do not use the following data for averages, fits, limits, etc. • • •

0.31 ± 0.15 DAVIS 68 HBC 5.5 K^-p

$\Gamma(\omega\gamma)/\Gamma_{\text{total}}$ Γ_4/Γ
0.0275 ± 0.0023 OUR FIT

• • • We do not use the following data for averages, fits, limits, etc. • • •

0.0234 ± 0.0030 ± 0.0004 70 28 PEDLAR 09 CLEO $J/\psi \rightarrow \gamma\eta'$

28 Not independent of other η' branching fractions and ratios in PEDLAR 09.

$\Gamma(\omega\gamma)/\Gamma(\pi^+\pi^-\eta)$ Γ_4/Γ_1
0.064 ± 0.005 OUR FIT
0.055 ± 0.007 ± 0.001

PEDLAR 09 CLE3 $J/\psi \rightarrow \eta'\gamma$

• • • We do not use the following data for averages, fits, limits, etc. • • •

0.068 ± 0.013 68 ZANFINO 77 ASPK 8.4 $\pi^- p$

$\Gamma(\omega\gamma)/\Gamma(\pi^0\pi^0\eta)$ Γ_4/Γ_3
0.126 ± 0.011 OUR FIT
0.147 ± 0.016

ALDE 87B GAM2 38 $\pi^- p \rightarrow n 4\gamma$

$\Gamma(\rho^0\gamma(\text{including non-resonant } \pi^+\pi^-\gamma))/[\Gamma(\pi^+\pi^-\eta) + \Gamma(\pi^0\pi^0\eta) + \Gamma(\omega\gamma)]$ $\Gamma_2/(\Gamma_1+\Gamma_3+\Gamma_4)$
0.433 ± 0.012 OUR FIT

• • • We do not use the following data for averages, fits, limits, etc. • • •

0.25 ± 0.14 DAUBER 64 HBC 1.95 K^-p

$[\Gamma(\pi^0\pi^0\eta(\text{charged decay})) + \Gamma(\omega(\text{charged decay})\gamma)]/\Gamma_{\text{total}}$ **(0.286 $\Gamma_3 + 0.89\Gamma_4)/\Gamma$**
0.0865 ± 0.0032 OUR FIT

• • • We do not use the following data for averages, fits, limits, etc. • • •

0.045 ± 0.029 42 RITTENBERG 69 HBC 1.7–2.7 K^-p

$\Gamma(\pi^+\pi^-\text{ neutrals})/\Gamma_{\text{total}}$ **(0.714 $\Gamma_1 + 0.286\Gamma_3 + 0.89\Gamma_4)/\Gamma$**
0.395 ± 0.004 OUR FIT

• • • We do not use the following data for averages, fits, limits, etc. • • •

0.4 ± 0.1 39 LONDON 66 HBC 2.24 $K^-p \rightarrow \Lambda \pi^+ \pi^- \text{ neutrals}$

0.35 ± 0.06 33 BADIER 65B HBC 3 K^-p

$\Gamma(\gamma\gamma)/\Gamma_{\text{total}}$ Γ_5/Γ
2.22 ± 0.08 OUR FIT
2.00 ± 0.15 OUR AVERAGE

1.98 $^{+0.31}_{-0.27}$ ± 0.07 114 29 WICHT 08 BELL $B^\pm \rightarrow K^\pm \gamma\gamma$

2.00 ± 0.18 30 STANTON 80 SPEC 8.45 $\pi^- p \rightarrow n \pi^+ \pi^- 2\gamma$

• • • We do not use the following data for averages, fits, limits, etc. • • •

2.25 ± 0.16 ± 0.03 0.3k 31 PEDLAR 09 CLEO $J/\psi \rightarrow \gamma\eta'$

1.8 ± 0.2 6000 32 APEL 79 NICE 15–40 $\pi^- p \rightarrow n 2\gamma$

2.5 ± 0.7 DUANE 74 MMS $\pi^- p \rightarrow n \text{MM}$

1.71 ± 0.33 68 DALPIAZ 72 CNTR 1.6 $\pi^- p \rightarrow n X^0$

2.0 $^{+0.8}_{-0.6}$ 31 HARVEY 71 OSPK 3.65 $\pi^- p \rightarrow n X^0$

29 WICHT 08 reports $[\Gamma(\eta'(958) \rightarrow \gamma\gamma)/\Gamma_{\text{total}}] \times [B(B^+ \rightarrow \eta' K^+)] = (1.40^{+0.16+0.15}_{-0.15-0.12}) \times 10^{-6}$ which we divide by our best value $B(B^+ \rightarrow \eta' K^+) = (7.06 \pm 0.25) \times 10^{-5}$. Our first error is their experiment's error and our second error is the systematic error from using our best value.

30 Includes APEL 79 result.

31 Not independent of other η' branching fractions and ratios in PEDLAR 09.

32 Data is included in STANTON 80 evaluation.

$\Gamma(\gamma\gamma)/\Gamma(\pi^+\pi^-\eta)$ Γ_5/Γ_1
0.0512 ± 0.0023 OUR FIT
0.053 ± 0.004 ± 0.001

PEDLAR 09 CLE3 $J/\psi \rightarrow \eta'\gamma$

$\Gamma(\gamma\gamma)/\Gamma(\rho^0\gamma(\text{including non-resonant } \pi^+\pi^-\gamma))$ Γ_5/Γ_2
0.0756 ± 0.0034 OUR FIT
0.080 ± 0.008

ABL IKIM 06E BES2 $J/\psi \rightarrow \eta'\gamma$

$\Gamma(\gamma\gamma)/\Gamma(\pi^0\pi^0\eta)$ Γ_5/Γ_3
0.102 ± 0.004 OUR FIT
0.105 ± 0.010 OUR AVERAGE Error includes scale factor of 1.9.

0.091 ± 0.009 AMSLER 93 CBAR 0.0 $\bar{p}p$

0.112 ± 0.002 ± 0.006 ALDE 87B GAM2 38 $\pi^- p \rightarrow n 2\gamma$

$\Gamma(\gamma\gamma)/\Gamma(\pi^0\pi^0\eta(\text{neutral decay}))$ $\Gamma_5/0.714\Gamma_3$
0.143 ± 0.006 OUR FIT

• • • We do not use the following data for averages, fits, limits, etc. • • •

0.188 ± 0.058 16 APEL 72 OSPK 3.8 $\pi^- p \rightarrow n X^0$

$\Gamma(\text{neutrals})/\Gamma_{\text{total}}$ **(0.714 $\Gamma_3 + 0.09\Gamma_4 + \Gamma_5)/\Gamma$**
0.180 ± 0.006 OUR FIT

• • • We do not use the following data for averages, fits, limits, etc. • • •

0.185 ± 0.022 535 BASILE 71 CNTR 1.6 $\pi^- p \rightarrow n X^0$

0.189 ± 0.026 123 RITTENBERG 69 HBC 1.7–2.7 K^-p

$\Gamma(3\pi^0)/\Gamma(\pi^0\pi^0\eta)$ Γ_6/Γ_3

VALUE (units 10^{-4})	EVTS	DOCUMENT ID	TECN	COMMENT
78 ± 10 OUR FIT				
78 ± 10 OUR AVERAGE				
86 ± 19	235	BLIK	08	GAMS 32 $\pi^- p \rightarrow \eta' n$
74 ± 15		ALDE	87B	GAM2 38 $\pi^- p \rightarrow n6\gamma$
75 ± 18		BINON	84	GAM2 30-40 $\pi^- p \rightarrow n6\gamma$

 $\Gamma(\mu^+\mu^-\gamma)/\Gamma(\gamma\gamma)$ Γ_7/Γ_5

VALUE (units 10^{-3})	EVTS	DOCUMENT ID	TECN	COMMENT
4.9 ± 1.2	33	VIKTOROV	80	CNTR 25,33 $\pi^- p \rightarrow 2\mu\gamma$

 $\Gamma(\pi^+\pi^-\mu^+\mu^-)/\Gamma_{total}$ Γ_8/Γ

VALUE (units 10^{-4})	CL%	DOCUMENT ID	TECN	COMMENT
< 2.4	90	33 NAIK	09	CLEO $J/\psi \rightarrow \gamma\eta'$
33 Not independent of measured value of Γ_8/Γ_1 from NAIK 09.				

 $\Gamma(\pi^+\pi^-\mu^+\mu^-)/\Gamma(\pi^+\pi^-\eta)$ Γ_8/Γ_1

VALUE (units 10^{-3})	CL%	DOCUMENT ID	TECN	COMMENT
< 0.5	90	34 NAIK	09	CLEO $J/\psi \rightarrow \gamma\eta'$
34 NAIK 09 reports $[\Gamma(\eta'(958) \rightarrow \pi^+\pi^-\mu^+\mu^-)/\Gamma(\eta'(958) \rightarrow \pi^+\pi^-\eta)] / [B(\eta \rightarrow 2\gamma)] < 1.3 \times 10^{-3}$ which we multiply by our best value $B(\eta \rightarrow 2\gamma) = 39.31 \times 10^{-2}$.				

 $\Gamma(\pi^+\pi^-\pi^0)/\Gamma_{total}$ Γ_9/Γ

VALUE (units 10^{-2})	CL%	DOCUMENT ID	TECN	COMMENT
0.36 ± 0.11 OUR FIT				
0.36 ± 0.11 OUR AVERAGE				
$0.37 \pm 0.11 \pm 0.04$		35 NAIK	09	CLEO $J/\psi \rightarrow \gamma\eta'$
< 9	95	DANBURG	73	HBC 2.2 $K^- p \rightarrow \Lambda X^0$
< 5	90	RITTENBERG	69	HBC 1.7-2.7 $K^- p$
35 Not independent of measured value of Γ_9/Γ_1 from NAIK 09.				

 $\Gamma(\pi^+\pi^-\pi^0)/\Gamma(\pi^+\pi^-\eta)$ Γ_9/Γ_1

VALUE (units 10^{-3})	EVTS	DOCUMENT ID	TECN	COMMENT
8.3 ± 2.5 OUR FIT				
$8.25 \pm 2.49 \pm 0.04$	20	36 NAIK	09	CLEO $J/\psi \rightarrow \gamma\eta'$
36 NAIK 09 reports $[\Gamma(\eta'(958) \rightarrow \pi^+\pi^-\pi^0)/\Gamma(\eta'(958) \rightarrow \pi^+\pi^-\eta)] / [B(\eta \rightarrow 2\gamma)] = (21 \pm 6 \pm 2) \times 10^{-3}$ which we multiply by our best value $B(\eta \rightarrow 2\gamma) = (39.31 \pm 0.20) \times 10^{-2}$. Our first error is their experiment's error and our second error is the systematic error from using our best value.				

 $\Gamma(\pi^0\rho^0)/\Gamma_{total}$ Γ_{10}/Γ

VALUE	CL%	DOCUMENT ID	TECN	COMMENT
< 0.04	90	RITTENBERG	65	HBC 2.7 $K^- p$

 $\Gamma(2(\pi^+\pi^-))/\Gamma_{total}$ Γ_{11}/Γ

VALUE (units 10^{-4})	CL%	DOCUMENT ID	TECN	COMMENT
< 2.4	90	37 NAIK	09	CLEO $J/\psi \rightarrow \gamma\eta'$
< 100	90	RITTENBERG	69	HBC 1.7-2.7 $K^- p$
37 Not independent of measured value of Γ_{11}/Γ_1 from NAIK 09.				

 $\Gamma(2(\pi^+\pi^-))/\Gamma(\pi^+\pi^-\eta)$ Γ_{11}/Γ_1

VALUE (units 10^{-3})	CL%	DOCUMENT ID	TECN	COMMENT
< 0.6	90	38 NAIK	09	CLEO $J/\psi \rightarrow \gamma\eta'$
38 NAIK 09 reports $[\Gamma(\eta'(958) \rightarrow 2(\pi^+\pi^-))/\Gamma(\eta'(958) \rightarrow \pi^+\pi^-\eta)] / [B(\eta \rightarrow 2\gamma)] < 1.4 \times 10^{-3}$ which we multiply by our best value $B(\eta \rightarrow 2\gamma) = 39.31 \times 10^{-2}$.				

 $\Gamma(\pi^+\pi^-\pi^0)/\Gamma_{total}$ Γ_{12}/Γ

VALUE (units 10^{-4})	CL%	DOCUMENT ID	TECN	COMMENT
< 27	90	39 NAIK	09	CLEO $J/\psi \rightarrow \gamma\eta'$
39 Not independent of measured value of Γ_{12}/Γ_1 from NAIK 09.				

 $\Gamma(\pi^+\pi^-\pi^0)/\Gamma(\pi^+\pi^-\eta)$ Γ_{12}/Γ_1

VALUE (units 10^{-3})	CL%	DOCUMENT ID	TECN	COMMENT
< 6	90	40 NAIK	09	CLEO $J/\psi \rightarrow \gamma\eta'$
40 NAIK 09 reports $[\Gamma(\eta'(958) \rightarrow \pi^+\pi^-\pi^0)/\Gamma(\eta'(958) \rightarrow \pi^+\pi^-\eta)] / [B(\eta \rightarrow 2\gamma)] < 15 \times 10^{-3}$ which we multiply by our best value $B(\eta \rightarrow 2\gamma) = 39.31 \times 10^{-2}$.				

 $\Gamma(2(\pi^+\pi^-) neutrals)/\Gamma_{total}$ Γ_{13}/Γ

VALUE	CL%	DOCUMENT ID	TECN	COMMENT
< 0.01	95	DANBURG	73	HBC 2.2 $K^- p \rightarrow \Lambda X^0$
• • • We do not use the following data for averages, fits, limits, etc. • • •				
< 0.01	90	RITTENBERG	69	HBC 1.7-2.7 $K^- p$

 $\Gamma(2(\pi^+\pi^-)\pi^0)/\Gamma_{total}$ Γ_{14}/Γ

VALUE	CL%	DOCUMENT ID	TECN	COMMENT
< 0.002	90	41 NAIK	09	CLEO $J/\psi \rightarrow \gamma\eta'$
< 0.01	90	RITTENBERG	69	HBC 1.7-2.7 $K^- p$
41 Not independent of measured value of Γ_{14}/Γ_1 from NAIK 09.				

 $\Gamma(2(\pi^+\pi^-)\pi^0)/\Gamma(\pi^+\pi^-\eta)$ Γ_{14}/Γ_1

VALUE (units 10^{-3})	CL%	DOCUMENT ID	TECN	COMMENT
< 4	90	42 NAIK	09	CLEO $J/\psi \rightarrow \gamma\eta'$
42 NAIK 09 reports $[\Gamma(\eta'(958) \rightarrow 2(\pi^+\pi^-)\pi^0)/\Gamma(\eta'(958) \rightarrow \pi^+\pi^-\eta)] / [B(\eta \rightarrow 2\gamma)] < 11 \times 10^{-3}$ which we multiply by our best value $B(\eta \rightarrow 2\gamma) = 39.31 \times 10^{-2}$.				

 $\Gamma(2(\pi^+\pi^-)2\pi^0)/\Gamma_{total}$ Γ_{15}/Γ

VALUE	CL%	DOCUMENT ID	TECN	COMMENT
< 0.01	95	KALBFLEISCH	64B	HBC $K^- p \rightarrow \Lambda 2(\pi^+\pi^-) + MM$
• • • We do not use the following data for averages, fits, limits, etc. • • •				
< 0.01	90	LONDON	66	HBC Compilation

 $\Gamma(3(\pi^+\pi^-))/\Gamma_{total}$ Γ_{16}/Γ

VALUE (units 10^{-3})	CL%	DOCUMENT ID	TECN	COMMENT
< 0.53	90	43 NAIK	09	CLEO $J/\psi \rightarrow \gamma\eta'$
< 5	95	KALBFLEISCH	64B	HBC $K^- p \rightarrow \Lambda 2(\pi^+\pi^-)$
43 Not independent of measured value of Γ_{16}/Γ_1 from NAIK 09.				

 $\Gamma(3(\pi^+\pi^-))/\Gamma(\pi^+\pi^-\eta)$ Γ_{16}/Γ_1

VALUE (units 10^{-3})	CL%	DOCUMENT ID	TECN	COMMENT
< 1.2	90	44 NAIK	09	CLEO $J/\psi \rightarrow \gamma\eta'$
44 NAIK 09 reports $[\Gamma(\eta'(958) \rightarrow 3(\pi^+\pi^-))/\Gamma(\eta'(958) \rightarrow \pi^+\pi^-\eta)] / [B(\eta \rightarrow 2\gamma)] < 3.0 \times 10^{-3}$ which we multiply by our best value $B(\eta \rightarrow 2\gamma) = 39.31 \times 10^{-2}$.				

 $\Gamma(\pi^+\pi^-\pi^0)/\Gamma_{total}$ Γ_{17}/Γ

VALUE (units 10^{-3})	CL%	DOCUMENT ID	TECN	COMMENT
2.4 ± 1.3 OUR FIT				
2.4 ± 1.3 OUR AVERAGE				
$2.5 \pm 1.2 \pm 0.5$		45 NAIK	09	CLEO $J/\psi \rightarrow \gamma\eta'$
< 6	90	RITTENBERG	65	HBC 2.7 $K^- p$
45 Not independent of measured value of Γ_{17}/Γ_1 from NAIK 09.				

 $\Gamma(\pi^+\pi^-\pi^0)/\Gamma(\pi^+\pi^-\eta)$ Γ_{17}/Γ_1

VALUE (units 10^{-3})	EVTS	DOCUMENT ID	TECN	COMMENT
5.6 ± 3.0 OUR FIT				
$5.50 \pm 2.99 \pm 0.03$	8	46 NAIK	09	CLEO $J/\psi \rightarrow \gamma\eta'$
46 NAIK 09 reports $[\Gamma(\eta'(958) \rightarrow \pi^+\pi^-\pi^0)/\Gamma(\eta'(958) \rightarrow \pi^+\pi^-\eta)] / [B(\eta \rightarrow 2\gamma)] = (14 \pm 7 \pm 3) \times 10^{-3}$ which we multiply by our best value $B(\eta \rightarrow 2\gamma) = (39.31 \pm 0.20) \times 10^{-2}$. Our first error is their experiment's error and our second error is the systematic error from using our best value.				

 $\Gamma(\gamma e^+ e^-)/\Gamma_{total}$ Γ_{18}/Γ

VALUE (units 10^{-3})	CL%	DOCUMENT ID	TECN	COMMENT
< 0.9	90	BRIERE	00	CLEO 10.6 $e^+ e^-$

 $\Gamma(\pi^0\gamma\gamma)/\Gamma(\pi^0\pi^0\eta)$ Γ_{19}/Γ_3

VALUE (units 10^{-4})	CL%	DOCUMENT ID	TECN	COMMENT
< 37	90	ALDE	87B	GAM2 38 $\pi^- p \rightarrow n4\gamma$

 $\Gamma(4\pi^0)/\Gamma(\pi^0\pi^0\eta)$ Γ_{20}/Γ_3

VALUE (units 10^{-4})	CL%	DOCUMENT ID	TECN	COMMENT
< 23	90	ALDE	87B	GAM2 38 $\pi^- p \rightarrow n8\gamma$

 $\Gamma(e^+ e^-)/\Gamma_{total}$ Γ_{21}/Γ

VALUE (units 10^{-7})	CL%	DOCUMENT ID	TECN	COMMENT
< 2.1	90	VOROBYEV	88	ND $e^+ e^- \rightarrow \pi^+\pi^-\eta$

Meson Particle Listings

$f_0(980)$

26 ± 10 ~ 112	AMSLER 95B 60 AMSLER 95D	CBAR 0.0 $\overline{p}p \rightarrow 3\pi^0$ CBAR 0.0 $\overline{p}p \rightarrow \pi^0 \pi^0 \pi^0$, $\pi^0 \eta \eta, \pi^0 \pi^0 \eta$
80 ± 12 30 74	61 ANISOVICH 95 JANSSEN 95	RVUE $\pi\pi \rightarrow \pi\pi, K\overline{K}$ RVUE $\overline{p}p \rightarrow \eta 2\pi^0$
29 ± 2 46	63 KAMINSKI 94 64 ZOU 94B	RVUE $\pi\pi \rightarrow \pi\pi, K\overline{K}$ RVUE
48 ± 12	65 MORGAN 93	RVUE $\pi\pi(K\overline{K}) \rightarrow \pi\pi(K\overline{K}), J/\psi \rightarrow \phi\pi\pi(K\overline{K}), D_S \rightarrow \pi(\pi\pi)$
37.4 ± 10.6 72 ± 8	55 AGUILAR... 91 66 ARMSTRONG 91	EHS 400 pp OMEG 300 $pp \rightarrow pp\pi\pi$, $ppK\overline{K}$
110 ± 30 29 ± 13	BREAKSTONE 90 55 ABACHI 86B	SFM $pp \rightarrow pp\pi^+\pi^-$ HRS $e^+e^- \rightarrow \pi^+\pi^-X$
120 ± 281 ± 20	ETKIN 82B	MPS 23 $\pi^-p \rightarrow n 2K_S^0$
28 ± 10 70 to 300	66 GIDAL 81 67 ACHASOV 80	MRK2 $J/\psi \rightarrow \pi^+\pi^-X$ RVUE
100 ± 80 30 ± 8	68 AGUILAR... 78 66 LEEPER 77	HBC 0.7 $\overline{p}p \rightarrow K_S^0 K_S^0$ ASPK 2-2.4 $\pi^-p \rightarrow \pi^+\pi^-n, K^+K^-n$
48 ± 14 32 ± 10 30 ± 10 54 ± 16	66 BINNIE 73 69 GRAYR 73 69 HYAMS 73 69 PROTOPOP... 73	CNTR $\pi^-p \rightarrow nMM$ ASPK 17 $\pi^-p \rightarrow \pi^+\pi^-n$ ASPK 17 $\pi^-p \rightarrow \pi^+\pi^-n$ HBC 7 $\pi^+p \rightarrow \pi^+\pi^+\pi^-$

$f_0(980)$ DECAY MODES

Mode	Fraction (Γ_i/Γ)
Γ_1 $\pi\pi$	dominant
Γ_2 $K\overline{K}$	seen
Γ_3 $\gamma\gamma$	seen
Γ_4 e^+e^-	

$f_0(980)$ PARTIAL WIDTHS

$\Gamma(\gamma\gamma)$	VALUE (keV)	DOCUMENT ID	TECN	COMMENT
Γ_3	0.29 ± 0.07 -0.06	OUR AVERAGE		
	0.286 ± 0.017 ± 0.211 -0.070	70 UEHARA	08A BELL	10.6 $e^+e^- \rightarrow e^+e^-\pi^0\pi^0$
	0.205 ± 0.095 ± 0.147 -0.083 -0.117	71 MORI	07 BELL	10.6 $e^+e^- \rightarrow e^+e^-\pi^+\pi^-$
	0.28 ± 0.09 -0.13	72 BOGLIONE	99 RVUE	$\gamma\gamma \rightarrow \pi^+\pi^-, \pi^0\pi^0$
	0.42 ± 0.06 ± 0.18	73 OEST	90 JADE	$e^+e^- \rightarrow e^+e^-\pi^0\pi^0$
	0.29 ± 0.07 ± 0.12	74,75 BOYER	90 MRK2	$e^+e^- \rightarrow e^+e^-\pi^+\pi^-$
	0.31 ± 0.14 ± 0.09	74,75 MARSISKE	90 CBAL	$e^+e^- \rightarrow e^+e^-\pi^0\pi^0$
	0.63 ± 0.14	76 MORGAN	90 RVUE	$\gamma\gamma \rightarrow \pi^+\pi^-, \pi^0\pi^0$

• • • We do not use the following data for averages, fits, limits, etc. • • •

70 Using finite width corrections according to FLATTE 76 and ACHASOV 05, and the ratio $g_{f_0}^2 K K / g_{f_0}^2 \pi\pi = 0$.

71 Using finite width corrections according to FLATTE 76 and ACHASOV 05, and the ratio $g_{f_0}^2 K K / g_{f_0}^2 \pi\pi = 4.21 \pm 0.25 \pm 0.21$ from ABLIKIM 05.

72 Supersedes MORGAN 90.

73 OEST 90 quote systematic errors $+0.08$
 -0.18 . We use ± 0.18 . Observed 60 events.

74 From analysis allowing arbitrary background unconstrained by unitarity.

75 Data included in MORGAN 90, BOGLIONE 99 analyses.

76 From amplitude analysis of BOYER 90 and MARSISKE 90, data corresponds to resonance parameters $m = 989$ MeV, $\Gamma = 61$ MeV.

$\Gamma(e^+e^-)$

VALUE (eV)	CL%	DOCUMENT ID	TECN	COMMENT
<8.4	90	VOROBYEV 88	ND	$e^+e^- \rightarrow \pi^0\pi^0$

$f_0(980)$ BRANCHING RATIOS

$\Gamma(\pi\pi) / [\Gamma(\pi\pi) + \Gamma(K\overline{K})]$	VALUE	EVTS	DOCUMENT ID	TECN	COMMENT
$\Gamma_1 / (\Gamma_1 + \Gamma_2)$	0.52 ± 0.12	9.9k	77 AUBERT	06o BABR	$B^\pm \rightarrow K^\pm \pi^\pm \pi^\mp$
	0.75 ± 0.11 -0.13		78 ABLIKIM	05q BES2	$\chi_{c0} \rightarrow 2\pi^+ 2\pi^-$, $\pi^+\pi^- K^+K^-$
	0.84 ± 0.02		79 ANISOVICH	02b SPEC	Combined fit
~ 0.68			OLLER	99B RVUE	$\pi\pi \rightarrow \pi\pi, K\overline{K}$
	0.67 ± 0.09		80 LOVERRE	80 HBC	$4\pi^-p \rightarrow n 2K_S^0$
	0.81 ± 0.09 0.04		80 CASON	78 STRC	$7\pi^-p \rightarrow n 2K_S^0$
	0.78 ± 0.03		80 WETZEL	76 OSPK	$8.9\pi^-p \rightarrow n 2K_S^0$

77 Recalculated by us using $\Gamma(K^+K^-) / \Gamma(\pi^+\pi^-) = 0.69 \pm 0.32$ from AUBERT 06o and isospin relations.

78 Using data from ABLIKIM 04g.

79 From a combined K-matrix analysis of Crystal Barrel ($0. p\overline{p} \rightarrow \pi^0\pi^0\pi^0, \pi^0\eta\eta, \pi^0\pi^0\eta$), GAMS ($\pi p \rightarrow \pi^0\pi^0 n, \eta\eta n, \eta\eta' n$), and BNL ($\pi p \rightarrow K\overline{K} n$) data.

80 Measure $\pi\pi$ elasticity assuming two resonances coupled to the $\pi\pi$ and $K\overline{K}$ channels only.

$f_0(980)$ REFERENCES

ANISOVICH 09	IJMP A24 2481	V.V. Anisovich, A.V. Sarantsev	
ECKLUND 09	PR D80 052009	K.M. Ecklund et al.	(CLEO Collab.)
UEHARA 08A	PR D78 052004	S. Uehara et al.	(BELLE Collab.)
AMBROSINO 07	EPJ C49 473	F. Ambrosino et al.	(KLOE Collab.)
AUBERT 07AK	PR D76 012008	B. Aubert et al.	(BABAR Collab.)
BONVICINI 07	PR D76 012001	G. Bonvicini et al.	(CLEO Collab.)
MORI 07	PR D75 051101R	T. Mori et al.	(BELLE Collab.)
AMBROSINO 06B	PL B634 148	F. Ambrosino et al.	(KLOE Collab.)
AUBERT 06O	PR D74 032003	B. Aubert et al.	(BABAR Collab.)
GARMASH 06	PL 96 251803	A. Garmash et al.	(BELLE Collab.)
ABLIKIM 05	PL B607 243	M. Ablikim et al.	(BES Collab.)
ABLIKIM 05Q	PR D72 092002	M. Ablikim et al.	(BES Collab.)
ACHASOV 05	PR D72 013006	N.N. Achasov, G.N. Shestakov	
GARMASH 05	PR D71 092003	A. Garmash et al.	(BELLE Collab.)
ABLIKIM 04G	PR D70 092002	M. Ablikim et al.	(BES Collab.)
ANISOVICH 03	EPJ A16 229	V.V. Anisovich et al.	
TIKHOMIROV 03	PAN 66 828	G.D. Tikhomirov et al.	
ALOSIO 02D	Translated from YAF 66 860.	A. Aloisio et al.	(KLOE Collab.)
ANISOVICH 02D	PL B537 21	V.V. Anisovich et al.	
BRAMON 02	PAN 65 1545	V.V. Anisovich et al.	
ACHASOV 01F	EPJ C26 253	A. Bramon et al.	
AITALA 01A	PR D63 094007	N.N. Achasov, V.V. Gubin	(Novosibirsk SND Collab.)
AITALA 01B	PRL 86 765	E.M. Aitala et al.	(FNAL E791 Collab.)
ACHASOV 00H	PRL 86 770	E.M. Aitala et al.	(FNAL E791 Collab.)
AKHMETSHIN 99B	PL B485 349	M.N. Achasov et al.	(Novosibirsk SND Collab.)
AKHMETSHIN 99C	PL B462 371	R.R. Akhmetshin et al.	(Novosibirsk CMD-2 Collab.)
BARBERIS 99	PL B462 380	R.R. Akhmetshin et al.	(Novosibirsk CMD-2 Collab.)
BARBERIS 99B	PL B453 305	D. Barberis et al.	(Omega Expt.)
BARBERIS 99C	PL B453 316	D. Barberis et al.	(Omega Expt.)
BARBERIS 99D	PL B453 325	D. Barberis et al.	(Omega Expt.)
BELLAZZINI 99	PL B462 462	D. Barberis et al.	(Omega Expt.)
BOGLIONE 99	PL B467 296	R. Bellazzini et al.	
KAMINSKI 99	EPJ C9 11	M. Boglione, M.R. Pennington	
OLLER 99B	NP A652 407 (erratum)	R. Kaminski, L. Lesniak, B. Loiseau	(CRAC, PARIN)
OLLER 99C	PR D60 099906 (erratum)	J.A. Oller et al.	
ACHASOV 98I	PL B440 442	J.A. Oller, E. Oset	
ACKERSTAFF 90Q	EPJ C4 19	J.A. Oller, E. Oset	
		M.N. Achasov et al.	(OPAL Collab.)
		K. Ackerstaff et al.	

Table listing meson decays and production methods, including ALDE, ANISOVICH, LOCHER, etc. with associated reference codes and production techniques like YAF, UFN, etc.

Table listing meson decays and production methods, including GRASSLER, WELLS, DEFOIX, BARNES, etc. with associated reference codes and production techniques like HBC, DBC, etc.

Table listing meson decays and production methods, including OLLER, ABELE, BERTIN, DEBILLY, etc. with associated reference codes and production techniques like RVUE, CBAR, etc.

Section for $a_0(980)$ with the equation $I^G(J^{PC}) = 1^-(0^{++})$ and a reference to a minireview on scalar mesons under $f_0(600)$.

Table for $a_0(980)$ MASS, showing VALUE (MeV) and DOCUMENT ID with a note: '980±20 OUR ESTIMATE Mass determination very model dependent'

Table for $\eta\pi$ FINAL STATE ONLY, showing VALUE (MeV), EVTS, DOCUMENT ID, TECN, CHG, and COMMENT. Includes entries for AMBROSINO, ANISOVICH, UEHARA, BUGG, ACHARD, ACHASOV, BARBERIS, OLLER, TEIGE, ANISOVICH, TORNOVIST, JANSSEN, AMSLER, ARMSTRONG, ATKINSON, EVANGELIS, GURTU, CONFORTO, and CORDEN.

Table for $a_0(980)$ WIDTH, showing VALUE (MeV), EVTS, DOCUMENT ID, TECN, CHG, and COMMENT. Includes entries for UEHARA, BUGG, ACHARD, BARBERIS, OLLER, TEIGE, ANISOVICH, BERTIN, TORNOVIST, JANSSEN, AMSLER, ARMSTRONG, EVANGELIS, GURTU, CONFORTO, CORDEN, GRASSLER, FLATTE, WELLS, DEFQIX, CAMPBELL, MILLER, and AMMAR.

Meson Particle Listings

a0(980), phi(1020)

K-K ONLY

Table with columns: VALUE (MeV), EVTS, DOCUMENT ID, TECN, CHG, COMMENT. Contains data for a0(980) decays into K-pi and K-eta.

a0(980) DECAY MODES

Table with columns: Mode, Fraction (Gamma_i/Gamma). Lists decay modes like eta pi, KK, rho pi, gamma gamma, and e+e-.

a0(980) PARTIAL WIDTHS

Table with columns: Gamma(gamma), VALUE (keV), DOCUMENT ID, TECN. Includes the value 0.30 +/- 0.10 keV.

a0(980) Gamma(i)Gamma(gamma)/Gamma(total)

Table with columns: Gamma(eta pi) x Gamma(gamma)/Gamma(total), VALUE (keV), EVTS, DOCUMENT ID, TECN, COMMENT. Includes the value 0.21 +/- 0.08/-0.04.

28 From a fit with the S-wave amplitude including two interfering Breit-Wigners plus a background term.

Table with columns: Gamma(eta pi) x Gamma(e+e-)/Gamma(total), VALUE (eV), CL%, DOCUMENT ID, TECN, COMMENT. Includes the value < 1.5.

a0(980) BRANCHING RATIOS

Table with columns: Gamma(KK)/Gamma(eta pi), VALUE, DOCUMENT ID, TECN, CHG, COMMENT. Includes the value 0.183 +/- 0.024.

Table with columns: Gamma(rho pi)/Gamma(eta pi), VALUE, CL%, DOCUMENT ID, TECN, CHG, COMMENT. Includes the value < 0.25.

a0(980) REFERENCES

List of references for a0(980) decays and branching ratios, including authors like Ambrosino, Anisovich, Uehara, Bugg, Achasov, Barberis, Oller, Teige, Abele, Amsler, Vorobyev, Antreasyan, Atkinson, Evangelista, Debilly, Gurtu, Conforto, Corden, Grassler, Jaffe, Flatte, Gay, Wells, Defoix, Ammar, Barnes, Campbell, Miller, Astier, Barlow, Conforto, Armenteros, and Rosenfeld.

phi(1020)

I^G(J^PC) = 0^-(1^-^-)

phi(1020) MASS

Table with columns: VALUE (MeV), EVTS, DOCUMENT ID, TECN, COMMENT. Contains mass measurements for phi(1020) with values like 1019.45 +/- 0.020 and 1019.30 +/- 0.02 +/- 0.10.

1019.8 ± 0.2 ± 0.5	766	IVANOV	81	OLYA	1-1.4 $e^+e^- \rightarrow K^+K^-$
1019.4 ± 0.5	337	COOPER	78B	HBC	0.7-0.8 $\bar{p}p \rightarrow K_S^0 K_L^0 \pi^+ \pi^-$
1020 ± 1	383	7 BALDI	77	CNTR	10 $\pi^- p \rightarrow \pi^- \phi p$
1018.9 ± 0.6	800	COHEN	77	ASPK	6 $\pi^\pm N \rightarrow K^+ K^- N$
1019.7 ± 0.5	454	KALBFLEISCH	76	HBC	2.18 $K^- p \rightarrow \Lambda K \bar{K}$
1019.4 ± 0.8	984	BESCH	74	CNTR	2 $\gamma p \rightarrow p K^+ K^-$
1020.3 ± 0.4	100	BALLAM	73	HBC	2.8-9.3 γp
1019.4 ± 0.7	120	BINNIE	73B	CNTR	$\pi^- p \rightarrow \phi n$
1019.6 ± 0.5	120	9 AGUILAR-...	72B	HBC	3.9, 4.6 $K^- p \rightarrow \Lambda K^+ K^-$
1019.9 ± 0.5	100	9 AGUILAR-...	72B	HBC	3.9, 4.6 $K^- p \rightarrow K^- p K^+ K^-$
1020.4 ± 0.5	131	COLLEY	72	HBC	10 $K^+ p \rightarrow K^+ p \phi$
1019.9 ± 0.3	410	STOTTLE...	71	HBC	2.9 $K^- p \rightarrow \Sigma / \Lambda K \bar{K}$

¹ Update of AKHMETSHIN 99d

² From the combined fit assuming that the total $\phi(1020)$ production cross section is saturated by those of K^+K^- , $K_S^0 K_L^0$, $\pi^+\pi^-\pi^0$, and $\eta\gamma$ decays modes and using ACHASOV 00b for the $\eta\gamma$ decay mode.

³ Using a total width of 4.43 ± 0.05 MeV. Systematic uncertainty included.

⁴ Using a total width of 4.43 ± 0.05 MeV.

⁵ PELLINEN 82 review includes AKERLOF 77, DAUM 81, BALDI 77, AYRES 74, DE-GROOT 74.

⁶ Strongly correlated with AKHMETSHIN 04.

⁷ Systematic errors not evaluated.

⁸ Weighted and scaled average of 12 measurements of DIJKSTRA 86.

⁹ Mass errors enlarged by us to Γ/\sqrt{N} ; see the note with the $K^*(892)$ mass.

$\phi(1020)$ WIDTH

VALUE (MeV)	EVTS	DOCUMENT ID	TECN	COMMENT
4.26 ± 0.04 OUR AVERAGE		Error includes scale factor of 1.4. See the ideogram below.		
4.30 ± 0.06 ± 0.17	105k	AKHMETSHIN 06	CMD2	0.98-1.06 $e^+e^- \rightarrow \pi^+\pi^-\pi^0$
4.280 ± 0.033 ± 0.025	272k	10 AKHMETSHIN 04	CMD2	$e^+e^- \rightarrow K_L^0 K_S^0$
4.21 ± 0.04	1900k	11 ACHASOV 01E	SND	$e^+e^- \rightarrow K^+K^-, K_S^0 K_L^0, \pi^+\pi^-\pi^0$
4.44 ± 0.09	55 600	AKHMETSHIN 95	CMD2	$e^+e^- \rightarrow$ hadrons
4.5 ± 0.7	1500	ARENTON 82	AEMS	11.8 polar. $pp \rightarrow K K$
4.2 ± 0.6	766	12 IVANOV 81	OLYA	1-1.4 $e^+e^- \rightarrow K^+K^-$
4.3 ± 0.6		12 CORDIER 80	DM1	$e^+e^- \rightarrow \pi^+\pi^-\pi^0$
4.36 ± 0.29	3681	12 BUKIN 78C	OLYA	$e^+e^- \rightarrow$ hadrons
4.4 ± 0.6	984	12 BESCH 74	CNTR	2 $\gamma p \rightarrow p K^+ K^-$
4.67 ± 0.72	681	12 BALAKIN 71	OSPK	$e^+e^- \rightarrow$ hadrons
4.09 ± 0.29		BIZOT 70	OSPK	$e^+e^- \rightarrow$ hadrons
4.24 ± 0.02 ± 0.03	542k	13 AKHMETSHIN 08	CMD2	1.02 $e^+e^- \rightarrow K^+K^-$
4.28 ± 0.13	12540	14 AUBERT,B 05J	BABR	$D^0 \rightarrow \bar{K}^0 K^+ K^-$
4.45 ± 0.06	271k	DIJKSTRA 86	SPEC	100 $\pi^- Be$
3.6 ± 0.8	337	12 COOPER 78B	HBC	0.7-0.8 $\bar{p}p \rightarrow K_S^0 K_L^0 \pi^+ \pi^-$
4.5 ± 0.50	1300	12,14 AKERLOF 77	SPEC	400 $pA \rightarrow K^+ K^- X$
4.5 ± 0.8	500	12,14 AYRES 74	ASPK	3-6 $\pi^- p \rightarrow K^+ K^- n, K^- p \rightarrow K^+ K^- \Lambda / \Sigma^0$
3.81 ± 0.37		COSME 74B	OSPK	$e^+e^- \rightarrow K_L^0 K_S^0$
3.8 ± 0.7	454	12 BORENSTEIN 72	HBC	2.18 $K^- p \rightarrow K \bar{K} n$

• • • We do not use the following data for averages, fits, limits, etc. • • •

4.24 ± 0.02 ± 0.03	542k	13 AKHMETSHIN 08	CMD2	1.02 $e^+e^- \rightarrow K^+K^-$
4.28 ± 0.13	12540	14 AUBERT,B 05J	BABR	$D^0 \rightarrow \bar{K}^0 K^+ K^-$
4.45 ± 0.06	271k	DIJKSTRA 86	SPEC	100 $\pi^- Be$
3.6 ± 0.8	337	12 COOPER 78B	HBC	0.7-0.8 $\bar{p}p \rightarrow K_S^0 K_L^0 \pi^+ \pi^-$

¹⁰ Update of AKHMETSHIN 99d

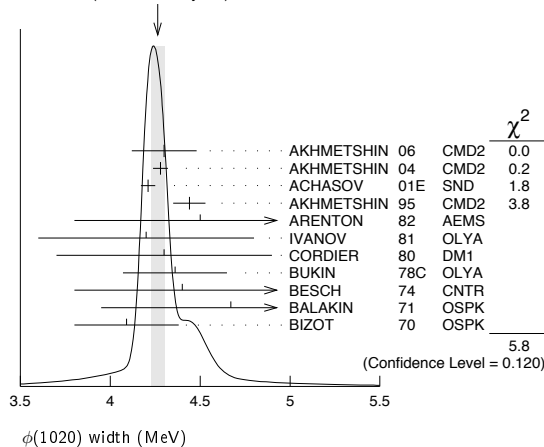
¹¹ From the combined fit assuming that the total $\phi(1020)$ production cross section is saturated by those of K^+K^- , $K_S^0 K_L^0$, $\pi^+\pi^-\pi^0$, and $\eta\gamma$ decays modes and using ACHASOV 00b for the $\eta\gamma$ decay mode.

¹² Width errors enlarged by us to $4\Gamma/\sqrt{N}$; see the note with the $K^*(892)$ mass.

¹³ Strongly correlated with AKHMETSHIN 04.

¹⁴ Systematic errors not evaluated.

WEIGHTED AVERAGE
4.26±0.04 (Error scaled by 1.4)



$\phi(1020)$ DECAY MODES

Mode	Fraction (Γ_i/Γ)	Scale factor/ Confidence level
Γ_1 $K^+ K^-$	(48.9 ± 0.5) %	S=1.1
Γ_2 $K_L^0 K_S^0$	(34.2 ± 0.4) %	S=1.1
Γ_3 $\rho\pi^+ + \pi^+\pi^-\pi^0$	(15.32 ± 0.32) %	S=1.1
Γ_4 $\rho\pi^-$		
Γ_5 $\pi^+\pi^-\pi^0$		
Γ_6 $\eta\gamma$	(1.309 ± 0.024) %	S=1.2
Γ_7 $\pi^0\gamma$	(1.27 ± 0.06) × 10 ⁻³	
Γ_8 $\ell^+\ell^-$	—	
Γ_9 e^+e^-	(2.954 ± 0.030) × 10 ⁻⁴	S=1.1
Γ_{10} $\mu^+\mu^-$	(2.87 ± 0.19) × 10 ⁻⁴	
Γ_{11} ηe^+e^-	(1.15 ± 0.10) × 10 ⁻⁴	
Γ_{12} $\pi^+\pi^-$	(7.4 ± 1.3) × 10 ⁻⁵	
Γ_{13} $\omega\pi^0$	(4.7 ± 0.5) × 10 ⁻⁵	
Γ_{14} $\omega\gamma$	< 5 %	CL=84%
Γ_{15} $\rho\gamma$	< 1.2 × 10 ⁻⁵	CL=90%
Γ_{16} $\pi^+\pi^-\gamma$	(4.1 ± 1.3) × 10 ⁻⁵	
Γ_{17} $f_0(980)\gamma$	(3.22 ± 0.19) × 10 ⁻⁴	S=1.1
Γ_{18} $\pi^0\pi^0\gamma$	(1.13 ± 0.06) × 10 ⁻⁴	
Γ_{19} $\pi^+\pi^-\pi^+\pi^-$	(4.0 ± 2.8) × 10 ⁻⁶	
Γ_{20} $\pi^+\pi^+\pi^-\pi^-\pi^0$	< 4.6 × 10 ⁻⁶	CL=90%
Γ_{21} $\pi^0 e^+e^-$	(1.12 ± 0.28) × 10 ⁻⁵	
Γ_{22} $\pi^0\eta\gamma$	(7.27 ± 0.30) × 10 ⁻⁵	S=1.5
Γ_{23} $a_0(980)\gamma$	(7.6 ± 0.6) × 10 ⁻⁵	
Γ_{24} $K^0 \bar{K}^0 \gamma$	< 1.9 × 10 ⁻⁸	CL=90%
Γ_{25} $\eta'(958)\gamma$	(6.25 ± 0.21) × 10 ⁻⁵	
Γ_{26} $\eta\pi^0\pi^0\gamma$	< 2 × 10 ⁻⁵	CL=90%
Γ_{27} $\mu^+\mu^-\gamma$	(1.4 ± 0.5) × 10 ⁻⁵	
Γ_{28} $\rho\gamma\gamma$	< 1.2 × 10 ⁻⁴	CL=90%
Γ_{29} $\eta\pi^+\pi^-$	< 1.8 × 10 ⁻⁵	CL=90%
Γ_{30} $\eta\mu^+\mu^-$	< 9.4 × 10 ⁻⁶	CL=90%

See key on page 405

Meson Particle Listings

$\phi(1020)$, $h_1(1170)$, $b_1(1235)$

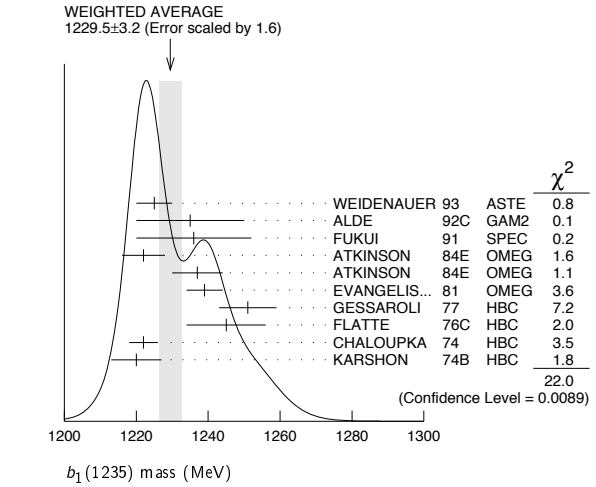
PARROUR	76	PL 63B 357	G. Parour <i>et al.</i>	(ORSAY)
PARROUR	76B	PL 63B 362	G. Parour <i>et al.</i>	(ORSAY)
KALBFLEISCH	75	PR D11 987	G.R. Kalbfleisch, R.C. Strand, J.W. Chapman	(BNL+)
AYRES	74	PRL 32 1463	D.S. Ayres <i>et al.</i>	(ANL)
BESCH	74	NP B70 257	H.J. Besch <i>et al.</i>	(BONN)
COSME	74	PL 48B 155	G. Cosme <i>et al.</i>	(ORSAY)
COSME	74B	PL 48B 159	G. Cosme <i>et al.</i>	(ORSAY)
DEGROOT	74	NP B74 77	A.J. de Groot <i>et al.</i>	(AMST, NIJM)
AUGUSTIN	73	PRL 30 462	J.E. Augustin <i>et al.</i>	(ORSAY)
BALLAM	73	PR D7 3150	J. Ballam <i>et al.</i>	(SLAC, LBL)
BINNIE	73B	PR D8 2789	D.M. Binnie <i>et al.</i>	(LOIC, SHMP)
AGUILAR...	72B	PR D6 29	M. Aguilar-Benitez <i>et al.</i>	(BNL)
ALVENSLEB...	72	PRL 28 66	H. Alvensleben <i>et al.</i>	(MIT, DESY)
BORENSTEIN	72	PR D5 1559	S.R. Borenstein <i>et al.</i>	(BNL, MICH)
COLLEY	72	NP B50 1	D.C. Colley <i>et al.</i>	(BIRM, GLAS)
BALAKIN	71	PL 34B 328	V.E. Balakin <i>et al.</i>	(NOVO)
CHATELUS	71	Thesis LAL 1247	Y. Chatelus	(STRB)
Also		PL 32B 416	J.C. Bizot <i>et al.</i>	(ORSAY)
HAYES	71	PR D4 899	S. Hayes <i>et al.</i>	(CORN)
STOTTLE...	71	Thesis ORO 2504 170	A.R. Stottlemeyer	(UMD)
BIZOT	70	PL 32B 416	J.C. Bizot <i>et al.</i>	(ORSAY)
Also		Liverpool Sym. 69	J.P. Perez-Y-Jorba	
EARLES	70	PRL 25 1312	D.R. Earles <i>et al.</i>	(NEAS)
LINDSEY	66	PL 147 913	J.S. Lindsey, G. Smith	(LRL)
LONDON	66	PR 143 1034	G.W. London <i>et al.</i>	(BNL, SYRA) IGJPC
BADIER	65B	PL 17 337	J. Badier <i>et al.</i>	(EPOL, SACL, AMST)
LINDSEY	65	PRL 15 221	J.S. Lindsey, G.A. Smith	(LRL)
LINDSEY	65	data included in LINDSEY 66.		
SCHLEIN	63	PRL 10 368	P.E. Schlein <i>et al.</i>	(UCLA) IGJP

$b_1(1235)$

$$I^G(J^{PC}) = 1^+(1^{+-})$$

$b_1(1235)$ MASS

VALUE (MeV)	EVTS	DOCUMENT ID	TECN	CHG	COMMENT
1229.5 ± 3.2	OUR AVERAGE				Error includes scale factor of 1.6. See the ideogram below.
1225 ± 5		WEIDENAUER 93	ASTE		$\bar{p}p \rightarrow 2\pi^+2\pi^-\pi^0$
1235 ± 15		ALDE 92c	GAM2		$38,100 \pi^-\rho \rightarrow \omega\pi^0 n$
1236 ± 16		FUKUI 91	SPEC		$8.95 \pi^-\rho \rightarrow \omega\pi^0 n$
1222 ± 6		ATKINSON 84E	OMEG ±		$25-55 \gamma\rho \rightarrow \omega\pi X$
1237 ± 7		ATKINSON 84E	OMEG 0		$25-55 \gamma\rho \rightarrow \omega\pi X$
1239 ± 5		EVANGELIS... 81	OMEG -		$12 \pi^-\rho \rightarrow \omega\pi\rho$
1251 ± 8	450	GESSAROLI 77	HBC -		$11 \pi^-\rho \rightarrow \pi^-\omega\rho$
1245 ± 11	890	FLATTE 76C	HBC -		$4.2 K^-\rho \rightarrow \pi^-\omega\Sigma^+$
1222 ± 4	1400	CHALOUPKA 74	HBC -		$3.9 \pi^-\rho$
1220 ± 7	600	KARSHON 74B	HBC +		$4.9 \pi^+\rho$
1190 ± 10		AUGUSTIN 89	DM2 ±		$e^+e^- \rightarrow 5\pi$
1213 ± 5		ATKINSON 84c	OMEG 0		$20-70 \gamma\rho$
1271 ± 11		COLLICK 84	SPEC +		$200 \pi^+Z \rightarrow Z\pi\omega$



$h_1(1170)$

$$I^G(J^{PC}) = 0^-(1^{+-})$$

$h_1(1170)$ MASS

VALUE (MeV)	DOCUMENT ID	TECN	CHG	COMMENT
1170 ± 20	OUR ESTIMATE			
1168 ± 4	ANDO 92	SPEC		$8 \pi^-\rho \rightarrow \pi^+\pi^-\pi^0 n$
1166 ± 5 ± 3	1 ANDO 92	SPEC		$8 \pi^-\rho \rightarrow \pi^+\pi^-\pi^0 n$
1190 ± 60	2 DANKOWY... 81	SPEC 0		$8 \pi p \rightarrow 3\pi n$
1 Average and spread of values using 2 variants of the model of BOWLER 75.				
2 Uses the model of BOWLER 75.				

$h_1(1170)$ WIDTH

VALUE (MeV)	DOCUMENT ID	TECN	CHG	COMMENT
360 ± 40	OUR ESTIMATE			
345 ± 6	ANDO 92	SPEC		$8 \pi^-\rho \rightarrow \pi^+\pi^-\pi^0 n$
375 ± 6 ± 34	3 ANDO 92	SPEC		$8 \pi^-\rho \rightarrow \pi^+\pi^-\pi^0 n$
320 ± 50	4 DANKOWY... 81	SPEC 0		$8 \pi p \rightarrow 3\pi n$
3 Average and spread of values using 2 variants of the model of BOWLER 75.				
4 Uses the model of BOWLER 75.				

$h_1(1170)$ DECAY MODES

Mode	Fraction (Γ_i/Γ)
$\Gamma_1 \rho\pi$	seen

$h_1(1170)$ BRANCHING RATIOS

$\Gamma(\rho\pi)/\Gamma_{\text{total}}$	DOCUMENT ID	TECN	COMMENT	Γ_1/Γ
seen	ANDO 92	SPEC	$8 \pi^-\rho \rightarrow \pi^+\pi^-\pi^0 n$	
seen	ATKINSON 84	OMEG	$20-70 \gamma\rho \rightarrow \pi^+\pi^-\pi^0\rho$	
seen	DANKOWY... 81	SPEC	$8 \pi p \rightarrow 3\pi n$	

$h_1(1170)$ REFERENCES

ANDO 92	PL B291 496	A. Ando <i>et al.</i>	(KEK, KYOT, NIRS, SAGA+)
ATKINSON 84	NP B231 15	M. Atkinson <i>et al.</i>	(BONN, CERN, GLAS+)
DANKOWY... 81	PRL 46 580	J.A. Dankowyc <i>et al.</i>	(TNT0, BNL, CARL+)
BOWLER 75	NP B97 227	M.G. Bowler <i>et al.</i>	(OXFPT, DARE)

$b_1(1235)$ WIDTH

VALUE (MeV)	EVTS	DOCUMENT ID	TECN	CHG	COMMENT
142 ± 9	OUR AVERAGE				Error includes scale factor of 1.2.
113 ± 12		WEIDENAUER 93	ASTE		$\bar{p}p \rightarrow 2\pi^+2\pi^-\pi^0$
160 ± 30		ALDE 92c	GAM2		$38,100 \pi^-\rho \rightarrow \omega\pi^0 n$
151 ± 31		FUKUI 91	SPEC		$8.95 \pi^-\rho \rightarrow \omega\pi^0 n$
170 ± 15		EVANGELIS... 81	OMEG -		$12 \pi^-\rho \rightarrow \omega\pi\rho$
170 ± 50	225	BALTAY 78B	HBC +		$15 \pi^+\rho \rightarrow p4\pi$
155 ± 32	450	GESSAROLI 77	HBC -		$11 \pi^-\rho \rightarrow \pi^-\omega\rho$
182 ± 45	890	FLATTE 76C	HBC -		$4.2 K^-\rho \rightarrow \pi^-\omega\Sigma^+$
135 ± 20	1400	CHALOUPKA 74	HBC -		$3.9 \pi^-\rho$
156 ± 22	600	KARSHON 74B	HBC +		$4.9 \pi^+\rho$
210 ± 19		AUGUSTIN 89	DM2 ±		$e^+e^- \rightarrow 5\pi$
231 ± 14		ATKINSON 84c	OMEG 0		$20-70 \gamma\rho$
232 ± 29		COLLICK 84	SPEC +		$200 \pi^+Z \rightarrow Z\pi\omega$

$b_1(1235)$ DECAY MODES

Mode	Fraction (Γ_i/Γ)	Confidence level
$\Gamma_1 \omega\pi$	dominant	
$[D/S \text{ amplitude ratio} = 0.277 \pm 0.027]$		
$\Gamma_2 \pi^\pm\gamma$	$(1.6 \pm 0.4) \times 10^{-3}$	
$\Gamma_3 \eta\rho$	seen	
$\Gamma_4 \pi^+\pi^+\pi^-\pi^0$	< 50 %	84%
$\Gamma_5 (K\bar{K})^\pm\pi^0$	< 8 %	90%
$\Gamma_6 K_S^0 K_S^0 \pi^\pm$	< 6 %	90%
$\Gamma_7 K_S^0 K_S^0 \pi^\pm$	< 2 %	90%
$\Gamma_8 \phi\pi$	< 1.5 %	84%

Meson Particle Listings

$b_1(1235)$, $a_1(1260)$

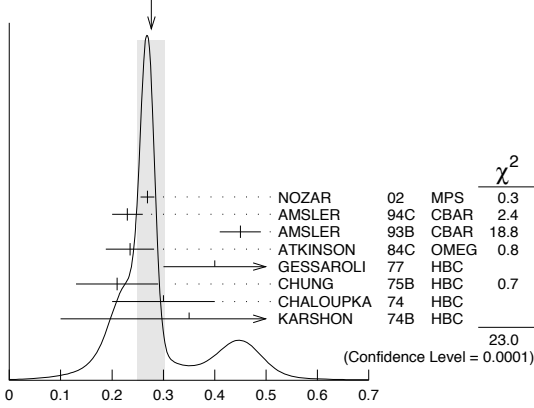
$b_1(1235)$ PARTIAL WIDTHS

$\Gamma(\pi^\pm \gamma)$	DOCUMENT ID	TECN	CHG	COMMENT	Γ_2
VALUE (keV)					
230 ± 60	COLLICK	84	SPEC	+ 200 $\pi^+ Z \rightarrow Z \pi \omega$	

$b_1(1235)$ D-wave/S-wave AMPLITUDE RATIO IN DECAY OF $b_1(1235) \rightarrow \omega \pi$

VALUE	EVTS	DOCUMENT ID	TECN	CHG	COMMENT
0.277 ± 0.027 OUR AVERAGE		Error includes scale factor of 2.4. See the ideogram below.			
0.269 ± 0.009 ± 0.010		NOZAR	02	MPS	- 18 $\pi^- p \rightarrow \omega \pi^- p$
0.23 ± 0.03		AMSLER	94c	CBAR	0.0 $\bar{p} p \rightarrow \omega \eta \pi^0$
0.45 ± 0.04		AMSLER	93b	CBAR	0.0 $\bar{p} p \rightarrow \omega \pi^0 \pi^0$
0.235 ± 0.047		ATKINSON	84c	OMEG	20-70 γp
0.4 $^{+0.1}_{-0.1}$		GESSAROLI	77	HBC	- 11 $\pi^- p \rightarrow \pi^- \omega p$
0.21 ± 0.08		CHUNG	75b	HBC	+ 7.1 $\pi^+ p$
0.3 ± 0.1		CHALOU PKA	74	HBC	- 3.9-7.5 $\pi^- p$
0.35 ± 0.25	600	KARSHON	74b	HBC	+ 4.9 $\pi^+ p$

WEIGHTED AVERAGE
0.277±0.027 (Error scaled by 2.4)



$b_1(1235)$ D-wave/S-wave amplitude ratio in decay of $b_1(1235) \rightarrow \omega \pi$

$b_1(1235)$ D-wave/S-wave AMPLITUDE PHASE DIFFERENCE IN DECAY OF $b_1(1235) \rightarrow \omega \pi$

VALUE (°)	DOCUMENT ID	TECN	CHG	COMMENT
10.5 ± 2.4 ± 3.9	NOZAR	02	MPS	- 18 $\pi^- p \rightarrow \omega \pi^- p$

$b_1(1235)$ BRANCHING RATIOS

$\Gamma(\eta p)/\Gamma(\omega \pi)$	DOCUMENT ID	TECN	CHG	COMMENT	Γ_3/Γ_1
VALUE					
<0.10	ATKINSON	84d	OMEG	20-70 γp	
$\Gamma(\pi^+ \pi^- \pi^0)/\Gamma(\omega \pi)$	DOCUMENT ID	TECN	CHG	COMMENT	Γ_4/Γ_1
VALUE					
<0.5	ABOLINS	63	HBC	+ 3.5 $\pi^+ p$	
$\Gamma((K\bar{K})^\pm \pi^0)/\Gamma(\omega \pi)$	DOCUMENT ID	TECN	CHG	COMMENT	Γ_5/Γ_1
VALUE					
<0.08	BALTAY	67	HBC	± 0.0 $\bar{p} p$	
$\Gamma(K_S^0 K_L^0 \pi^\pm)/\Gamma(\omega \pi)$	DOCUMENT ID	TECN	CHG	COMMENT	Γ_6/Γ_1
VALUE					
<0.06	BALTAY	67	HBC	± 0.0 $\bar{p} p$	
$\Gamma(K_S^0 K_S^0 \pi^\pm)/\Gamma(\omega \pi)$	DOCUMENT ID	TECN	CHG	COMMENT	Γ_7/Γ_1
VALUE					
<0.02	BALTAY	67	HBC	± 0.0 $\bar{p} p$	
$\Gamma(\phi \pi)/\Gamma(\omega \pi)$	DOCUMENT ID	TECN	CHG	COMMENT	Γ_8/Γ_1
VALUE					
<0.004	VIKTOROV	96	SPEC	0 32.5 $\pi^- p \rightarrow K^+ K^- \pi^0 n$	

• • • We do not use the following data for averages, fits, limits, etc. • • •

<0.04	95	BIZZARRI	69	HBC	± 0.0 $\bar{p} p$
<0.015		DAHL	67	HBC	1.6-4.2 $\pi^- p$

$b_1(1235)$ REFERENCES

NOZAR	02	PL B541 35	M. Nozar et al.
VIKTOROV	96	PAN 59 1184 Translated from YAF 59 1239	V.A. Viktorov et al. (SERP)
AMSLER	94c	PL B327 425	C. AMSler et al. (Crystal Barrel Collab.)
AMSLER	93b	PL B311 362	C. AMSler et al. (Crystal Barrel Collab.)
WEIDENAUER	93	ZPHY C59 387	P. Weidenauer et al. (ASTERIX Collab.)
ALDE	92c	ZPHY C54 553	D.M. Alde et al. (BELG, SERP, KEK, LANL+)
FUKUI	91	PL B257 241	S. Fukui et al. (SUGI, NAGO, KEK, KYOT+)
AUGUSTIN	89	NP B320 1	J.E. Augustin, G. Cosme (DM2 Collab.)
ATKINSON	84c	NP B243 1	M. Atkinson et al. (BONN, CERN, GLAS+)
ATKINSON	84d	NP B242 269	M. Atkinson et al. (BONN, CERN, GLAS+)
ATKINSON	84e	PL 138B 459	M. Atkinson et al. (BONN, CERN, GLAS+)
COLLICK	84	PRL 53 2374	B. Collick et al. (MINN, ROCH, FNAL)
EVANGELIS...	81	NP B178 197	C. Evangelista et al. (BARI, BONN, CERN+)
BALTAY	78b	PR D17 62	C. Baltay et al. (COLU, BING)
GESSAROLI	77	NP B126 382	R. Gessaroli et al. (BGNA, FIRZ, GENO+)
FLATTE	76c	PL 64B 225	S.M. Flatte et al. (CERN, AMST, NIJM+)
CHUNG	75b	PR D11 2426	S.U. Chung et al. (BNL, LBL, UCS C)
CHALOU PKA	74	PL 51B 407	V. Chaloupka et al. (CERN) JP
KARSHON	74b	PR D10 3608	U. Karshon et al. (REHO) JP
BIZZARRI	69	NP B14 169	R. Bizzarri et al. (CERN, CDEF)
BALTAY	67	PRL 18 93	C. Baltay et al. (COLU)
DAHL	67	PR 163 1377	O.I. Dahl et al. (LRL)
ABOLINS	63	PRL 11 381	M.A. Abolins et al. (UCSD)

$a_1(1260)$

$$I^G(J^{PC}) = 1^-(1^{++})$$

See also our review under the $a_1(1260)$ in PDG 06, Journal of Physics, G 33 1 (2006).

$a_1(1260)$ MASS

VALUE (MeV)	EVTS	DOCUMENT ID	TECN	COMMENT
1230 ± 40 OUR ESTIMATE				
• • • We do not use the following data for averages, fits, limits, etc. • • •				
1243 ± 12 ± 20		1 AUBERT	07AU BABR	10.6 $e^+ e^- \rightarrow \rho^0 p^+ \pi^- \pi^- \gamma$
1230-1270	6360	2 LINK	07A FOCS	$D^0 \rightarrow \pi^- \pi^+ \pi^- \pi^+$
1203 ± 3		3 GOMEZ-DUM...	04 RVUE	$\tau^+ \rightarrow \pi^+ \pi^+ \pi^- \nu_\tau$
1330 ± 24	90k	SALVINI	04 OBLX	$\bar{p} p \rightarrow 2\pi^+ 2\pi^-$
1331 ± 10 ± 3	37k	4 ASNER	00 CLE2	10.6 $e^+ e^- \rightarrow \tau^+ \tau^-$, $\tau^- \rightarrow \pi^- \pi^0 \pi^0 \nu_\tau$
1255 ± 7 ± 6	5904	5 ABREU	98G DLPH	$e^+ e^-$
1207 ± 5 ± 8	5904	6 ABREU	98G DLPH	$e^+ e^-$
1196 ± 4 ± 5	5904	7,8 ABREU	98G DLPH	$e^+ e^-$
1240 ± 10		BARBERIS	98B	45.0 $pp \rightarrow p_f \pi^+ \pi^- \pi^0 p_S$
1262 ± 9 ± 7		5,9 ACKERSTAFF	97R OPAL	$E_{cm}^{e^+e^-} = 88-94$, $\tau \rightarrow 3\pi\nu$
1210 ± 7 ± 2		6,9 ACKERSTAFF	97R OPAL	$E_{cm}^{e^+e^-} = 88-94$, $\tau \rightarrow 3\pi\nu$
1211 ± 7 $^{+50}_{-0}$		6 ALBRECHT	93c ARG	$\tau^+ \rightarrow \pi^+ \pi^+ \pi^- \nu$
1121 ± 8		10 ANDO	92 SPEC	8 $\pi^- p \rightarrow \pi^+ \pi^- \pi^0 n$
1242 ± 37		11 IVANOV	91 RVUE	$\tau \rightarrow \pi^+ \pi^+ \pi^- \nu$
1260 ± 14		12 IVANOV	91 RVUE	$\tau \rightarrow \pi^+ \pi^+ \pi^- \nu$
1250 ± 9		13 IVANOV	91 RVUE	$\tau \rightarrow \pi^+ \pi^+ \pi^- \nu$
1208 ± 15		ARMSTRONG	90 OMEG	300.0 $pp \rightarrow pp \pi^+ \pi^- \pi^0$
1220 ± 15		14 ISGUR	89 RVUE	$\tau^+ \rightarrow \pi^+ \pi^+ \pi^- \nu$
1260 ± 25		15 BOWLER	88 RVUE	$\tau^+ \rightarrow \pi^+ \pi^+ \pi^- \nu$
1166 ± 18 ± 11		BAND	87 MAC	$\tau^+ \rightarrow \pi^+ \pi^+ \pi^- \nu$
1164 ± 41 ± 23		BAND	87 MAC	$\tau^+ \rightarrow \pi^+ \pi^0 \pi^0 \nu$
1250 ± 40		14 TORNQVIST	87 RVUE	$\tau^+ \rightarrow \pi^+ \pi^+ \pi^- \nu$
1046 ± 11		ALBRECHT	86B ARG	$\tau^+ \rightarrow \pi^+ \pi^+ \pi^- \nu$
1056 ± 20 ± 15		RUCKSTUHL	86 DLCO	$\tau^+ \rightarrow \pi^+ \pi^+ \pi^- \nu$
1194 ± 14 ± 10		SCHMIDKE	86 MRK2	$\tau^+ \rightarrow \pi^+ \pi^+ \pi^- \nu$
1255 ± 23		BELLINI	85 SPEC	40 $\pi^- A \rightarrow \pi^- \pi^+ \pi^- A$
1240 ± 80		16 DANKOWY...	81 SPEC	8.45 $\pi^- p \rightarrow n 3\pi$
1280 ± 30		16 DAUM	81B CNTR	63.94 $\pi^- p \rightarrow p 3\pi$
1041 ± 13		17 GAVILLET	77 HBC	4.2 $K^- p \rightarrow \Sigma 3\pi$

1 The $\rho^\pm \pi^\mp$ state can be also due to the $\pi(1300)$.
 2 Using the Breit-Wigner parameterization; strong correlation between mass and width.
 3 Using the data of BARATE 98R.
 4 From a fit to the 3π mass spectrum including the $K\bar{K}^*(892)$ threshold.
 5 Uses the model of KUHN 90.
 6 Uses the model of ISGUR 89.
 7 Includes the effect of a possible a_1' state.
 8 Uses the model of FEINDT 90.
 9 Supersedes AKERS 95P.
 10 Average and spread of values using 2 variants of the model of BOWLER 75.
 11 Reanalysis of RUCKSTUHL 86.
 12 Reanalysis of SCHMIDKE 86.
 13 Reanalysis of ALBRECHT 86B.
 14 From a combined reanalysis of ALBRECHT 86B, SCHMIDKE 86, and RUCKSTUHL 86.
 15 From a combined reanalysis of ALBRECHT 86B and DAUM 81B.
 16 Uses the model of BOWLER 75.
 17 Produced in K^- backward scattering.

$a_1(1260)$ WIDTH

VALUE (MeV)	EVTS	DOCUMENT ID	TECN	COMMENT
250 to 600 OUR ESTIMATE				
• • • We do not use the following data for averages, fits, limits, etc. • • •				
410 ± 31 ± 30		18 AUBERT 07AU	BABR	10.6 $e^+e^- \rightarrow \rho^0 \rho^\pm \pi^\mp \gamma$
520-680	6360	19 LINK 07A	FOCS	$D^0 \rightarrow \pi^- \pi^+ \pi^- \pi^+$
480 ± 20		20 GOMEZ-DUM.04	RVUE	$\tau^+ \rightarrow \pi^+ \pi^+ \pi^- \nu_\tau$
580 ± 41	90k	SALVINI 04	OBLX	$\bar{p}p \rightarrow 2\pi^+ 2\pi^-$
460 ± 85	205	21 DRUTSKOY 02	BELL	$B \rightarrow D^{(*)} K^* 0$
814 ± 36 ± 13	37k	22 ASNER 00	CLE2	10.6 $e^+e^- \rightarrow \tau^+ \tau^-$, $\tau^- \rightarrow \pi^- \pi^0 \pi^0 \nu_\tau$
450 ± 50	22k	23 AKHMETSHIN 99E	CMD2	1.05-1.38 $e^+e^- \rightarrow$ $\pi^+ \pi^- \pi^0 \pi^0$
570 ± 10		24 BONDAR 99	RVUE	$e^+e^- \rightarrow 4\pi, \tau \rightarrow 3\pi \nu_\tau$
587 ± 27 ± 21	5904	25 ABREU 98G	DLPH	e^+e^-
478 ± 3 ± 15	5904	26 ABREU 98G	DLPH	e^+e^-
425 ± 14 ± 8	5904	27,28 ABREU 98G	DLPH	e^+e^-
400 ± 35		BARBERIS 98B		450 $pp \rightarrow p_f \pi^+ \pi^- \pi^0 p_s$
621 ± 32 ± 58		25,29 ACKERSTAFF 97R	OPAL	$E_{cm}^{e^+e^-} = 88-94, \tau \rightarrow 3\pi \nu$
457 ± 15 ± 17		26,29 ACKERSTAFF 97R	OPAL	$E_{cm}^{e^+e^-} = 88-94, \tau \rightarrow 3\pi \nu$
446 ± 21 $^{+140}_{-0}$		26 ALBRECHT 93C	ARG	$\tau^+ \rightarrow \pi^+ \pi^+ \pi^- \nu$
239 ± 11		ANDO 92	SPEC	$8 \pi^- p \rightarrow \pi^+ \pi^- \pi^0 n$
266 ± 13 ± 4		30 ANDO 92	SPEC	$8 \pi^- p \rightarrow \pi^+ \pi^- \pi^0 n$
465 $^{+228}_{-143}$		31 IVANOV 91	RVUE	$\tau \rightarrow \pi^+ \pi^+ \pi^- \nu$
298 $^{+40}_{-34}$		32 IVANOV 91	RVUE	$\tau \rightarrow \pi^+ \pi^+ \pi^- \nu$
488 ± 32		33 IVANOV 91	RVUE	$\tau \rightarrow \pi^+ \pi^+ \pi^- \nu$
430 ± 50		ARMSTRONG 90	OMEG	300.0 $pp \rightarrow p p \pi^+ \pi^- \pi^0$
420 ± 40		34 ISGUR 89	RVUE	$\tau^+ \rightarrow \pi^+ \pi^+ \pi^- \nu$
396 ± 43		35 BOWLER 88	RVUE	
405 ± 75 ± 25		BAND 87	MAC	$\tau^+ \rightarrow \pi^+ \pi^+ \pi^- \nu$
419 ± 108 ± 57		BAND 87	MAC	$\tau^+ \rightarrow \pi^+ \pi^0 \pi^0 \nu$
521 ± 27		ALBRECHT 86B	ARG	$\tau^+ \rightarrow \pi^+ \pi^+ \pi^- \nu$
476 $^{+132}_{-120} \pm 54$		RUCKSTUHL 86	DLCO	$\tau^+ \rightarrow \pi^+ \pi^+ \pi^- \nu$
462 ± 56 ± 30		SCHMIDKE 86	MRK2	$\tau^+ \rightarrow \pi^+ \pi^+ \pi^- \nu$
292 ± 40		BELLINI 85	SPEC	40 $\pi^- A \rightarrow \pi^- \pi^+ \pi^- A$
380 ± 100		36 DANKOWY... 81	SPEC	8.45 $\pi^- p \rightarrow n 3\pi$
300 ± 50		36 DAUM 81B	CNTR	63,94 $\pi^- p \rightarrow p 3\pi$
230 ± 50		37 GAVILLET 77	HBC	4.2 $K^- p \rightarrow \Sigma 3\pi$

18 The $\rho^\pm \pi^\mp$ state can be also due to the $\pi(1300)$.
 19 Using the Breit-Wigner parameterization; strong correlation between mass and width.
 20 Using the data of BARATE 98R.
 21 From a fit of the $K^- K^* 0$ distribution assuming $m_{a_1} = 1230$ MeV and purely resonant production of the $K^- K^* 0$ system.
 22 From a fit to the 3π mass spectrum including the $K \bar{K}^*(892)$ threshold.
 23 Using the $a_1(1260)$ mass of 1230 MeV.
 24 From AKHMETSHIN 99E and ASNER 00 data using the $a_1(1260)$ mass of 1230 MeV.
 25 Uses the model of KUHN 90.
 26 Uses the model of ISGUR 89.
 27 Includes the effect of a possible a_1' state.
 28 Uses the model of FEINDT 90.
 29 Supersedes AKERS 95P.
 30 Average and spread of values using 2 variants of the model of BOWLER 75.
 31 Reanalysis of RUCKSTUHL 86.
 32 Reanalysis of SCHMIDKE 86.
 33 Reanalysis of ALBRECHT 86B.
 34 From a combined reanalysis of ALBRECHT 86B, SCHMIDKE 86, and RUCKSTUHL 86.
 35 From a combined reanalysis of ALBRECHT 86B and DAUM 81B.
 36 Uses the model of BOWLER 75.
 37 Produced in K^- backward scattering.

$a_1(1260)$ DECAY MODES

Mode	Fraction (Γ_i/Γ)
Γ_1 $\pi^+ \pi^- \pi^0$	
Γ_2 $\pi^0 \pi^0 \pi^0$	
Γ_3 $(\rho\pi)S$ -wave	seen
Γ_4 $(\rho\pi)D$ -wave	seen
Γ_5 $(\rho(1450)\pi)S$ -wave	seen
Γ_6 $(\rho(1450)\pi)D$ -wave	seen
Γ_7 $\sigma\pi$	seen
Γ_8 $f_0(980)\pi$	not seen
Γ_9 $f_0(1370)\pi$	seen
Γ_{10} $f_2(1270)\pi$	seen
Γ_{11} $K \bar{K}^*(892) + c.c.$	seen
Γ_{12} $\pi\gamma$	seen

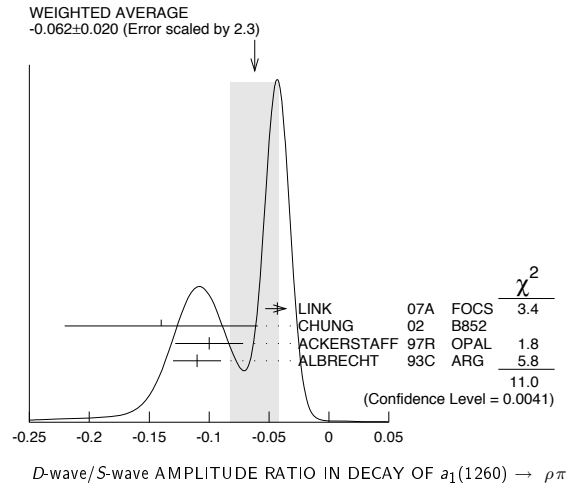
$a_1(1260)$ PARTIAL WIDTHS

$\Gamma(\pi\gamma)$	VALUE (keV)	DOCUMENT ID	TECN	COMMENT	Γ_{12}
	640 ± 246	ZIELINSKI	84C	SPEC	200 $\pi^+ Z \rightarrow Z 3\pi$

D-wave/S-wave AMPLITUDE RATIO IN DECAY OF $a_1(1260) \rightarrow \rho\pi$

VALUE	DOCUMENT ID	TECN	COMMENT
-0.062 ± 0.020 OUR AVERAGE			Error includes scale factor of 2.3. See the ideogram below.
-0.043 ± 0.009 ± 0.005	LINK 07A	FOCS	$D^0 \rightarrow \pi^- \pi^+ \pi^- \pi^+$
-0.14 ± 0.04 ± 0.07	38 CHUNG 02	B852	18.3 $\pi^- p \rightarrow \pi^+ \pi^- \pi^- p$
-0.10 ± 0.02 ± 0.02	39,40 ACKERSTAFF 97R	OPAL	$E_{cm}^{e^+e^-} = 88-94, \tau \rightarrow 3\pi \nu$
-0.11 ± 0.02	39 ALBRECHT 93C	ARG	$\tau^+ \rightarrow \pi^+ \pi^+ \pi^- \nu$

38 Deck-type background not subtracted.
 39 Uses the model of ISGUR 89.
 40 Supersedes AKERS 95P.



$a_1(1260)$ BRANCHING RATIOS

$\Gamma((\rho\pi)S\text{-wave})/\Gamma_{total}$	VALUE (units 10^{-2})	EVTS	DOCUMENT ID	TECN	COMMENT	Γ_3/Γ
					• • • We do not use the following data for averages, fits, limits, etc. • • •	
	60.19	37k	41 ASNER 00	CLE2	10.6 $e^+e^- \rightarrow \tau^+ \tau^-$, $\tau^- \rightarrow \pi^- \pi^0 \pi^0 \nu_\tau$	

$\Gamma((\rho\pi)D\text{-wave})/\Gamma_{total}$	VALUE (units 10^{-2})	EVTS	DOCUMENT ID	TECN	COMMENT	Γ_4/Γ
					• • • We do not use the following data for averages, fits, limits, etc. • • •	
	1.30 ± 0.60 ± 0.22	37k	41 ASNER 00	CLE2	10.6 $e^+e^- \rightarrow \tau^+ \tau^-$, $\tau^- \rightarrow \pi^- \pi^0 \pi^0 \nu_\tau$	

$\Gamma((\rho(1450)\pi)S\text{-wave})/\Gamma_{total}$	VALUE (units 10^{-2})	EVTS	DOCUMENT ID	TECN	COMMENT	Γ_5/Γ
					• • • We do not use the following data for averages, fits, limits, etc. • • •	
	0.56 ± 0.84 ± 0.32	37k	41,42 ASNER 00	CLE2	10.6 $e^+e^- \rightarrow \tau^+ \tau^-$, $\tau^- \rightarrow \pi^- \pi^0 \pi^0 \nu_\tau$	

$\Gamma((\rho(1450)\pi)D\text{-wave})/\Gamma_{total}$	VALUE (units 10^{-2})	EVTS	DOCUMENT ID	TECN	COMMENT	Γ_6/Γ
					• • • We do not use the following data for averages, fits, limits, etc. • • •	
	2.04 ± 1.20 ± 0.28	37k	41,42 ASNER 00	CLE2	10.6 $e^+e^- \rightarrow \tau^+ \tau^-$, $\tau^- \rightarrow \pi^- \pi^0 \pi^0 \nu_\tau$	

$\Gamma(\sigma\pi)/\Gamma_{total}$	VALUE (units 10^{-2})	EVTS	DOCUMENT ID	TECN	COMMENT	Γ_7/Γ
					• • • We do not use the following data for averages, fits, limits, etc. • • •	
	seen		CHUNG 02	B852	18.3 $\pi^- p \rightarrow$ $\pi^+ \pi^- \pi^- p$	
	18.76 ± 4.29 ± 1.48	37k	41,43 ASNER 00	CLE2	10.6 $e^+e^- \rightarrow \tau^+ \tau^-$, $\tau^- \rightarrow \pi^- \pi^0 \pi^0 \nu_\tau$	

$\Gamma(f_0(980)\pi)/\Gamma_{total}$	VALUE (units 10^{-2})	EVTS	DOCUMENT ID	TECN	COMMENT	Γ_8/Γ
					• • • We do not use the following data for averages, fits, limits, etc. • • •	
	not seen	37k	ASNER 00	CLE2	10.6 $e^+e^- \rightarrow \tau^+ \tau^-$, $\tau^- \rightarrow \pi^- \pi^0 \pi^0 \nu_\tau$	

Meson Particle Listings

a1(1260), f2(1270)

Gamma(f0(1370) pi) / Gamma total, Gamma9 / Gamma

Table with 5 columns: VALUE (units 10^-2), EVTS, DOCUMENT ID, TECN, COMMENT. Row 1: 7.40 ± 2.71 ± 1.26, 37k, 41.44, ASNER, 00, CLE2, 10.6 e+ e- -> tau+ tau-, tau- -> pi- pi0 pi0 nu tau.

Gamma(f2(1270) pi) / Gamma total, Gamma10 / Gamma

Table with 5 columns: VALUE (units 10^-2), EVTS, DOCUMENT ID, TECN, COMMENT. Row 1: 1.19 ± 0.49 ± 0.17, 37k, 41.45, ASNER, 00, CLE2, 10.6 e+ e- -> tau+ tau-, tau- -> pi- pi0 pi0 nu tau.

Gamma(K K* (892) + c.c.) / Gamma total, Gamma11 / Gamma

Table with 5 columns: VALUE (units 10^-2), EVTS, DOCUMENT ID, TECN, COMMENT. Row 1: 2.2 ± 0.5, 2255, 46, COAN, 04, CLEO, tau- -> K- pi- K+ nu tau.

Gamma(sigma pi) / Gamma((rho pi) S-wave), Gamma7 / Gamma3

Table with 5 columns: VALUE, EVTS, DOCUMENT ID, TECN, COMMENT. Row 1: 0.06 ± 0.05, 90k, SALVINI, 04, OBLX, p p -> 2 pi+ 2 pi-.

Gamma(pi0 pi0 pi0) / Gamma(pi+ pi- pi0), Gamma2 / Gamma1

Table with 5 columns: VALUE, CL%, DOCUMENT ID, COMMENT. Row 1: <0.008, 90, 51, BARBERIS, 01, 450 p p -> p p 3 pi0 p s.

- 41 From a fit to the Dalitz plot.
42 Assuming for rho(1450) mass and width of 1370 and 386 MeV respectively.
43 Assuming for sigma mass and width of 860 and 880 MeV respectively.
44 Assuming for f0(1370) mass and width of 1186 and 350 MeV respectively.
45 Assuming for f2(1270) mass and width of 1275 and 185 MeV respectively.
46 Using structure functions from KUHN 92 and DECKER 93a and B(tau- -> K- pi- K+ nu tau) = (0.155 ± 0.006 ± 0.009)% from BRIERE 03.
47 From a comparison to ALAM 94 assuming purely resonant production of the K- K*0 system.
48 From a fit to the 3 pi mass spectrum including the K K* (892) threshold.
49 Assuming a1(1260) dominance and taking B(tau- -> a1(1260) nu tau) from BUSKULIC 96.
50 Uses multichannel Aitchison-Bowler model (BOWLER 75). Uses data from GAVILLET 77, DAUM 80, and DANKOWYCH 81.
51 Inconsistent with observations of sigma pi, f0(1370) pi, and f2(1270) pi decay modes.

a1(1260) REFERENCES

AUBERT 07AU PR D76 092005 B. Aubert et al. (BABAR Collab.)
LINK 07A PR D75 052003 J.M. Link et al. (FNAL FOCUS Collab.)
PDG 06 JPG 33 1 W.-M. Yao et al. (PDG Collab.)
COAN 04 PRL 92 232001 T.E. Coan et al. (CLEO Collab.)
GOMEZ-DUMM... 04 PR D69 073002 D. Gomez Dumm, A. Pich, J. Portoles (OBELIX Collab.)
SALVINI 04 EPJ C35 21 P. Salvini et al. (CLEO Collab.)
BRIERE 03 PRL 90 181802 R. A. Briere et al. (CLEO Collab.)
CHUNG 02 PR D65 072001 S.U. Chung et al. (BNL E852 Collab.)
DRUTSKOY 02 PL B542 171 A. Drutskoy et al. (BELLE Collab.)
BARBERIS 01 PL B507 14 D. Barberis et al. (CLEO Collab.)
ASNER 00 PR D61 012002 D.M. Asner et al. (CLEO Collab.)
AKHMETSHIN 99E PL B466 392 R.R. Akhmetshin et al. (Novosibirsk CMD-2 Collab.)
BARATE 99R EPJ C11 599 R. Barate et al. (ALEPH Collab.)
BONDAR 99 PL B466 403 A.E. Bondar et al. (Novosibirsk CMD-2 Collab.)
ABREU 98G PL B426 411 P. Abreu et al. (DELPHI Collab.)
BARATE 98R EPJ C4 409 R. Barate et al. (ALEPH Collab.)
BARBERIS 98B PL B422 399 D. Barberis et al. (WA 102 Collab.)
ACKERSTAFF 97R ZPHY C75 593 K. Ackerstaff et al. (OPAL Collab.)
BUSKULIC 96 ZPHY C70 579 D. Buskulic et al. (ALEPH Collab.)
AKERS 95P ZPHY C67 45 R. Akers et al. (OPAL Collab.)
ALAM 94 PR D50 43 M.S. Alam et al. (CLEO Collab.)
ALBRECHT 93C ZPHY C58 61 H. Albrecht et al. (ARGUS Collab.)
DECKER 93A ZPHY C58 445 R. Decker et al. (ARGUS Collab.)
ANDO 92 PL B291 496 A. Ando et al. (KEK, KYOT, NIRS, SAGA+)
KUHN 92 ZPHY C56 661 J.H. Kuhn, E. Mirkes
IVANOV 91 ZPHY C49 563 Y.P. Ivanov, A.A. Osipov, M.K. Volkov (JINR)
ARMSTRONG 90 ZPHY C48 213 T.A. Armstrong, M. Benayoun, W. Busch (WA76 Coll.)
FEINDT 90 ZPHY C48 681 M. Feindt (HAMB)
KUHN 90 ZPHY C48 445 J.H. Kuhn et al. (MPIM)
ISGUR 89 PR D39 1357 N. Isgur, C. Morningstar, C. Reader (TNTO)
BOWLER 88 PL B209 99 M.G. Bowler (OXF)
BAND 87 PL B198 297 H.R. Band et al. (MAC Collab.)
TORRQVIST 87 ZPHY C36 695 N.A. Torrkvist (HELS)
ALBRECHT 86B ZPHY C33 7 H. Albrecht et al. (ARGUS Collab.)
RUCKSTUHL 86 PRL 56 2132 W. Ruckstuhl et al. (DELCO Collab.)
SCHMIDKE 86 PRL 57 527 W.B. Schmidke et al. (Mark II Collab.)
BELLINI 85 SJNP 41 781 D. Bellini et al.
Translated from YAF 41 1223.
ZIELINSKI 84C PRL 52 1195 M. Zielinski et al. (ROCH, MINN, FNAL)
LONGACRE 82 PR D26 82 R.S. Longacre (BNL)
DANKOWYCH... 81 PRL 46 500 J.A. Dankowycz et al. (TNTO, BNL, CARL+)
DAUM 81B NP B182 269 C. Daum et al. (AMST, CERN, CRAC, MPIM+)
DAUM 80 PL 89B 281 C. Daum et al. (AMST, CERN, CRAC, MPIM+)
GAVILLET 77 PL 69B 119 P. Gavillet et al. (AMST, CERN, NUM+ JIP)
BOWLER 75 NP B97 227 M.G. Bowler et al. (OXFPT, DARE)

f2(1270)

I(G JPC) = 0+ (2++)

f2(1270) MASS

Table with 5 columns: VALUE (MeV), EVTS, DOCUMENT ID, TECN, COMMENT. Row 1: 1275.1 ± 1.2 OUR AVERAGE, Error includes scale factor of 1.1.
1262 ± 1/2 ± 8, ABLIKIM, 06v, BES2, e+ e- -> J/psi -> gamma pi+ pi-
1275 ± 15, ABLIKIM, 05, BES2, J/psi -> phi pi+ pi-
1283 ± 5, ALDE, 98, GAM4, 100 pi- p -> pi0 pi0 n
1278 ± 5, BERTIN, 97c, OBLX, 0.0 p p -> pi+ pi- pi0
1272 ± 8, 200k, PROKOSHKIN, 94, GAM2, 38 pi- p -> pi0 pi0 n
1269.7 ± 5.2, 5730, AUGUSTIN, 89, DM2, e+ e- -> 5 pi
1283 ± 8, 400, ALDE, 87, GAM4, 100 pi- p -> 4 pi0 n
1274 ± 5, 2, AUGUSTIN, 87, DM2, J/psi -> gamma pi+ pi-
1283 ± 6, 3, LONGACRE, 86, MPS, 22 pi- p -> n 2 K_S^0
1276 ± 7, COURAU, 84, DLCO, e+ e- -> e+ e- pi+ pi-
1273.3 ± 2.3, 4, CHABAUD, 83, ASPK, 17 pi- p polarized
1280 ± 4, 5, CASON, 82, STRC, 8 pi+ p -> Delta++ pi0 pi0
1281 ± 7, 11600, GIDAL, 81, MRK2, J/psi decay
1282 ± 5, 6, CORDEN, 79, OMEG, 12-15 pi- p -> n 2 pi
1269 ± 4, 10k, APEL, 75, NICE, 40 pi- p -> n 2 pi0
1272 ± 4, 4600, ENGLER, 74, DBC, 6 pi+ n -> pi+ pi- p
1277 ± 4, 5300, FLATTE, 71, HBC, 7.0 pi+ p
1273 ± 8, 2, STUNTEBECK, 70, HBC, 8 pi- p, 5.4 pi+ d
1265 ± 8, BOESEBECK, 68, HBC, 8 pi+ p
... 1270 ± 8, 7, ANISOVICH, 09, RVUE, 0.0 p p, pi N
1277 ± 6, 870, 8, SCHEGELSKY, 06A, RVUE, gamma gamma -> K_S^0 K_S^0
1251 ± 10, TIKHOMIROV, 03, SPEC, 40.0 pi- C -> K_S^0 K_S^0 K_L^0 X
1260 ± 10, 9, ALDE, 97, GAM2, 450 p p -> p p pi0 pi0
1278 ± 6, 9, GRYGOREV, 96, SPEC, 40 pi- N -> K_S^0 K_S^0 X
1262 ± 11, AGUILAR..., 91, EHS, 400 p p
1275 ± 10, AKER, 91, CBF, 0.0 p p -> 3 pi0
1220 ± 10, BREAKSTONE, 90, SFM, p p -> p p pi+ pi-
1288 ± 12, ABACHI, 86B, HRS, e+ e- -> pi+ pi- X
1284 ± 30, 3k, BINON, 83, GAM2, 38 pi- p -> n 2 eta
1280 ± 20, 3k, APEL, 82, CNTR, 25 pi- p -> n 2 pi0
1284 ± 10, 16000, DEUTSCH..., 76, HBC, 16 pi+ p
1258 ± 10, 600, TAKAHASHI, 72, HBC, 8 pi- p -> n 2 pi
1275 ± 13, ARMENISE, 70, HBC, 9 pi+ n -> p pi+ pi-
1261 ± 5, 1960, 2, ARMENISE, 68, DBC, 5.1 pi+ n -> p pi+ MM-
1270 ± 10, 360, 2, ARMENISE, 68, DBC, 5.1 pi+ n -> p pi0 MM
1268 ± 6, 10, JOHNSON, 68, HBC, 3.7-4.2 pi- p

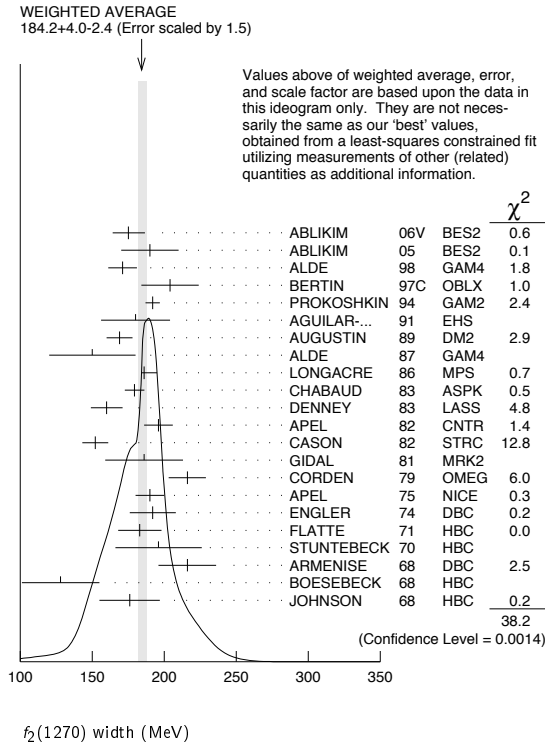
- 1 T-matrix pole.
2 Mass errors enlarged by us to Gamma/sqrt(N); see the note with the K*(892) mass.
3 From a partial-wave analysis of data using a K-matrix formalism with 5 poles.
4 From an energy-independent partial-wave analysis.
5 From an amplitude analysis of the reaction pi+ pi- -> 2 pi0.
6 From an amplitude analysis of pi+ pi- -> pi+ pi- scattering data.
7 4-poles, 5-channel K matrix fit.
8 From analysis of L3 data at 91 and 183-209 GeV.
9 Systematic uncertainties not estimated.
10 JOHNSON 68 includes BONDAR 63, LEE 64, DERADO 65, EISNER 67.

f2(1270) WIDTH

Table with 5 columns: VALUE (MeV), EVTS, DOCUMENT ID, TECN, COMMENT. Row 1: 185.1 ± 2.9 OUR FIT, Error includes scale factor of 1.5.
184.2 ± 4.0 OUR AVERAGE, Error includes scale factor of 1.5. See the ideogram below.
175 ± 6 ± 10, ABLIKIM, 06v, BES2, e+ e- -> J/psi -> gamma pi+ pi-
190 ± 20, ABLIKIM, 05, BES2, J/psi -> phi pi+ pi-
171 ± 10, ALDE, 98, GAM4, 100 pi- p -> pi0 pi0 n
204 ± 20, BERTIN, 97c, OBLX, 0.0 p p -> pi+ pi- pi0
192 ± 5, 200k, PROKOSHKIN, 94, GAM2, 38 pi- p -> pi0 pi0 n
180 ± 24, AGUILAR..., 91, EHS, 400 p p
169 ± 9, 5730, AUGUSTIN, 89, DM2, e+ e- -> 5 pi
150 ± 30, 400, 12, ALDE, 87, GAM4, 100 pi- p -> 4 pi0 n
186 ± 9 - 2, 13, LONGACRE, 86, MPS, 22 pi- p -> n 2 K_S^0
179.2 ± 6.9 - 6.6, 14, CHABAUD, 83, ASPK, 17 pi- p polarized
160 ± 11, DENNEY, 83, LASS, 10 pi+ N
196 ± 10, 3k, APEL, 82, CNTR, 25 pi- p -> n 2 pi0
152 ± 9, 15, CASON, 82, STRC, 8 pi+ p -> Delta++ pi0 pi0
186 ± 27, 11600, GIDAL, 81, MRK2, J/psi decay
216 ± 13, 16, CORDEN, 79, OMEG, 12-15 pi- p -> n 2 pi

190 ±10	10k	APEL	75	NICE	40 $\pi^- p \rightarrow n2\pi^0$
192 ±16	4600	ENGLER	74	DBC	6 $\pi^+ n \rightarrow \pi^+ \pi^- p$
183 ±15	5300	FLATTE	71	HBC	7 $\pi^+ p \rightarrow \Delta^{++} f_2$
196 ±30		12 STUNTEBECK	70	HBC	8 $\pi^- p, 5.4 \pi^+ d$
216 ±20	1960	12 ARMENISE	68	DBC	5.1 $\pi^+ n \rightarrow p\pi^+ MM^-$
128 ±27		12 BOESEBECK	68	HBC	8 $\pi^+ p$
176 ±21		12,17 JOHNSON	68	HBC	3.7-4.2 $\pi^- p$
194 ±36		18 ANISOVICH	09	RVUE	0.0 $\bar{p} p, \pi N$
195 ±15	870	19 SCHEGELSKY	06A	RVUE	$\gamma\gamma \rightarrow K_S^0 K_S^0$
121 ±26		TIKHOMIROV	03	SPEC	40.0 $\pi^- C \rightarrow K_S^0 K_S^0 K_L^0 X$
187 ±20		20 ALDE	97	GAM2	450 $pp \rightarrow pp\pi^0\pi^0$
184 ±10		20 GRYGOREV	96	SPEC	40 $\pi^- N \rightarrow K_S^0 K_S^0 X$
200 ±10		AKER	91	CBAR	0.0 $\bar{p} p \rightarrow 3\pi^0$
240 ±40	3k	BINON	83	GAM2	38 $\pi^- p \rightarrow n2\eta$
187 ±30	650	12 ANTIPOV	77	CIBS	25 $\pi^- p \rightarrow p3\pi$
225 ±38	16000	DEUTSCH...	76	HBC	16 $\pi^+ p$
166 ±28	600	12 TAKAHASHI	72	HBC	8 $\pi^- p \rightarrow n2\pi$
173 ±53		12 ARMENISE	70	HBC	9 $\pi^+ n \rightarrow p\pi^+ \pi^-$

- • • We do not use the following data for averages, fits, limits, etc. • • •
- 11 T-matrix pole.
- 12 Width errors enlarged by us to $4\Gamma/\sqrt{N}$; see the note with the $K^*(892)$ mass.
- 13 From a partial-wave analysis of data using a K-matrix formalism with 5 poles.
- 14 From an energy-independent partial-wave analysis.
- 15 From an amplitude analysis of the reaction $\pi^+ \pi^- \rightarrow 2\pi^0$.
- 16 From an amplitude analysis of $\pi^+ \pi^- \rightarrow \pi^+ \pi^-$ scattering data.
- 17 JOHNSON 68 includes BONDAR 63, LEE 64, DERADO 65, EISNER 67.
- 18 4-poles, 5-channel K matrix fit.
- 19 From analysis of L3 data at 91 and 183-209 GeV.
- 20 Systematic uncertainties not estimated.



$f_2(1270)$ DECAY MODES

Mode	Fraction (Γ_i/Γ)	Scale factor/ Confidence level
Γ_1 $\pi\pi$	(84.8 $^{+2.4}_{-1.2}$) %	S=1.2
Γ_2 $\pi^+ \pi^- 2\pi^0$	(7.1 $^{+1.4}_{-2.7}$) %	S=1.3
Γ_3 $K\bar{K}$	(4.6 ± 0.4) %	S=2.8
Γ_4 $2\pi^+ 2\pi^-$	(2.8 ± 0.4) %	S=1.2
Γ_5 $\eta\eta$	(4.0 ± 0.8) × 10 ⁻³	S=2.1
Γ_6 $4\pi^0$	(3.0 ± 1.0) × 10 ⁻³	
Γ_7 $\gamma\gamma$	(1.64 ± 0.19) × 10 ⁻⁵	S=1.9
Γ_8 $\eta\pi\pi$	< 8 × 10 ⁻³	CL=95%
Γ_9 $K^0 K^- \pi^+ + c.c.$	< 3.4 × 10 ⁻³	CL=95%
Γ_{10} $e^+ e^-$	< 6 × 10 ⁻¹⁰	CL=90%

CONSTRAINED FIT INFORMATION

An overall fit to the total width, 4 partial widths, a combination of partial widths obtained from integrated cross sections, and 6 branching ratios uses 44 measurements and one constraint to determine 8 parameters. The overall fit has a $\chi^2 = 81.8$ for 37 degrees of freedom.

The following off-diagonal array elements are the correlation coefficients $\langle \delta p_i \delta p_j \rangle / (\delta p_i \delta p_j)$, in percent, from the fit to parameters p_i , including the branching fractions, $x_i \equiv \Gamma_i / \Gamma_{total}$. The fit constrains the x_i whose labels appear in this array to sum to one.

x_2	-91						
x_3	11	-39					
x_4	10	-37	1				
x_5	1	-6	0	0			
x_6	0	-7	0	0	0		
x_7	8	-5	-6	1	0	0	
Γ	-78	71	-11	-8	-1	0	-11
	x_1	x_2	x_3	x_4	x_5	x_6	x_7

Mode	Rate (MeV)	Scale factor
Γ_1 $\pi\pi$	156.9 $^{+4.0}_{-1.2}$	
Γ_2 $\pi^+ \pi^- 2\pi^0$	13.2 $^{+2.8}_{-5.0}$	1.3
Γ_3 $K\bar{K}$	8.5 ± 0.8	2.9
Γ_4 $2\pi^+ 2\pi^-$	5.2 ± 0.7	1.2
Γ_5 $\eta\eta$	0.74 ± 0.14	2.1
Γ_6 $4\pi^0$	0.55 ± 0.18	
Γ_7 $\gamma\gamma$	0.00303 ± 0.00035	1.9

$f_2(1270)$ PARTIAL WIDTHS

$\Gamma(\pi\pi)$	VALUE (MeV)	EVTS	DOCUMENT ID	TECN	COMMENT	Γ_1
------------------	-------------	------	-------------	------	---------	------------

156.9 $^{+4.0}_{-1.2}$ OUR FIT

157.0 $^{+6.0}_{-1.0}$ 21 LONGACRE 86 MPS 22 $\pi^- p \rightarrow n2K_S^0$

• • • We do not use the following data for averages, fits, limits, etc. • • •

152 ± 8 870 22 SCHEGELSKY 06A RVUE $\gamma\gamma \rightarrow K_S^0 K_S^0$

$\Gamma(K\bar{K})$	VALUE (MeV)	EVTS	DOCUMENT ID	TECN	COMMENT	Γ_3
--------------------	-------------	------	-------------	------	---------	------------

8.5 ± 0.8 OUR FIT Error includes scale factor of 2.9.

9.0 $^{+0.7}_{-0.3}$ 21 LONGACRE 86 MPS 22 $\pi^- p \rightarrow n2K_S^0$

• • • We do not use the following data for averages, fits, limits, etc. • • •

7.5 ± 2.0 870 22 SCHEGELSKY 06A RVUE $\gamma\gamma \rightarrow K_S^0 K_S^0$

$\Gamma(\eta\eta)$	VALUE (MeV)	EVTS	DOCUMENT ID	TECN	COMMENT	Γ_5
--------------------	-------------	------	-------------	------	---------	------------

0.74 ± 0.14 OUR FIT Error includes scale factor of 2.1.

1.0 ± 0.1 21 LONGACRE 86 MPS 22 $\pi^- p \rightarrow n2K_S^0$

• • • We do not use the following data for averages, fits, limits, etc. • • •

1.8 ± 0.4 870 22 SCHEGELSKY 06A RVUE $\gamma\gamma \rightarrow K_S^0 K_S^0$

$\Gamma(\gamma\gamma)$	VALUE (keV)	EVTS	DOCUMENT ID	TECN	COMMENT	Γ_7
------------------------	-------------	------	-------------	------	---------	------------

The value of this width depends on the theoretical model used. Unitarised models with scalars give values clustering around ≈ 2.6 keV; without an S-wave contribution, values are systematically higher (typically around 3 keV).

3.03 ± 0.35 OUR FIT Error includes scale factor of 1.9.

3.14 ± 0.20 23 PENNINGTON 08 RVUE $\gamma\gamma \rightarrow \pi^+ \pi^-, \pi^0 \pi^0$

• • • We do not use the following data for averages, fits, limits, etc. • • •

2.55 ± 0.15 870 22 SCHEGELSKY 06A RVUE $\gamma\gamma \rightarrow K_S^0 K_S^0$

2.84 ± 0.35 99 BOGLIONE 99 RVUE $\gamma\gamma \rightarrow \pi^+ \pi^-, \pi^0 \pi^0$

2.93 ± 0.23 ± 0.32 24 YABUKI 95 VNS

2.58 ± 0.13 $^{+0.36}_{-0.27}$ 25 BEHREND 92 CELL $e^+ e^- \rightarrow e^+ e^- \pi^+ \pi^-$

3.10 ± 0.35 ± 0.35 26 BLINOV 92 MD1 $e^+ e^- \rightarrow e^+ e^- \pi^+ \pi^-$

2.27 ± 0.47 ± 0.11 90 ADACHI 90 TOPZ $e^+ e^- \rightarrow e^+ e^- \pi^+ \pi^-$

3.15 ± 0.04 ± 0.39 90 BOYER 90 MRK2 $e^+ e^- \rightarrow e^+ e^- \pi^+ \pi^-$

3.19 ± 0.16 $^{+0.29}_{-0.28}$ 90 MARSISKE 90 CBAL $e^+ e^- \rightarrow e^+ e^- \pi^0 \pi^0$

2.35 ± 0.65 27 MORGAN 90 RVUE $\gamma\gamma \rightarrow \pi^+ \pi^-, \pi^0 \pi^0$

3.19 ± 0.09 $^{+0.22}_{-0.38}$ 2177 OEST 90 JADE $e^+ e^- \rightarrow e^+ e^- \pi^0 \pi^0$

Meson Particle Listings

 $f_1(1285)$ $f_1(1285)$ WIDTH

Only experiments giving width error less than 20 MeV are kept for averaging.

VALUE (MeV)	EVTs	DOCUMENT ID	TECN	COMMENT
24.3 ± 1.1 OUR AVERAGE		Error includes scale factor of 1.4. See the ideogram below.		
35 ± 6 ± 4		AUBERT	07AU BABR	10.6 $e^+e^- \rightarrow f_1(1285)\pi^+\pi^-\gamma$
40.0 ± 8.6 ± 9.3	203	BAI	04J BES2	$J/\psi \rightarrow \gamma\gamma\pi^+\pi^-$
29 ± 12	237	ABDALLAH	03H DLPH	91.2 $e^+e^- \rightarrow K_S^0 K^\pm \pi^\mp + X$
45 ± 9 ± 7	20k	ADAMS	01B B852	18 GeV $\pi^-p \rightarrow K^+K^-n$
55 ± 18	1400	ALDE	97B GAM4	100 $\pi^-p \rightarrow \eta\pi^0\pi^0n$
24 ± 3		BARBERIS	97B OMEG	450 $pp \rightarrow pp2(\pi^+\pi^-)$
20 ± 2		BARBERIS	97C OMEG	450 $pp \rightarrow ppK_S^0 K^\pm \pi^\mp$
36 ± 5		ANTINORI	95 OMEG	300,450 $pp \rightarrow pp2(\pi^+\pi^-)$
29.0 ± 4.1		LEE	94 MPS2	18 $\pi^-p \rightarrow K^+\bar{K}^0 2\pi^-p$
25 ± 4	140	ARMSTRONG	89 OMEG	300 $pp \rightarrow K\bar{K}\pi pp$
22 ± 2	4750	BIRMAN	88 MPS	8 $\pi^-p \rightarrow K^+\bar{K}^0\pi^-n$
25 ± 4	504	BITYUKOV	88 SPEC	32.5 $\pi^-p \rightarrow K^+K^-\pi^0n$
19 ± 5		ANDO	86 SPEC	8 $\pi^-p \rightarrow \eta\pi^+\pi^-n$
32 ± 8	420	REEVES	86 SPEC	6.6 $p\bar{p} \rightarrow K K \pi X$
22 ± 2		CHUNG	85 SPEC	8 $\pi^-p \rightarrow N K \bar{K} \pi$
32 ± 3	604	ARMSTRONG	84 OMEG	85 $\pi^+p \rightarrow K\bar{K}\pi pp$, $pp \rightarrow K\bar{K}\pi pp$
24 ± 3		CHAUVAT	84 SPEC	ISR 31.5 pp
29 ± 10	103	DIONISI	80 HBC	4 $\pi^-p \rightarrow K\bar{K}\pi n$
28.3 ± 6.7	320	NACASCH	78 HBC	0.7, 0.76 $p\bar{p} \rightarrow K\bar{K}3\pi$
18.2 ± 1.2		SOSA	99 SPEC	$pp \rightarrow p_{slow} (K_S^0 K^+\pi^-)$
19.4 ± 1.5		SOSA	99 SPEC	$pp \rightarrow p_{slow} (K_S^0 K^-\pi^+)$
40 ± 5		ABATZIS	94 OMEG	450 $pp \rightarrow pp2(\pi^+\pi^-)$
31 ± 5		ARMSTRONG	89E OMEG	300 $pp \rightarrow pp2(\pi^+\pi^-)$
41 ± 12		ARMSTRONG	89G OMEG	85 $\pi^+p \rightarrow 4\pi pp$, $pp \rightarrow 4\pi pp$
17.9 ± 10.9	60	RATH	89 MPS	21.4 $\pi^-p \rightarrow K_S^0 K_S^0 \pi^0 n$
14 ± 20 ± 14 ± 10	16	BECKER	87 MRK3	$e^+e^- \rightarrow \phi K\bar{K}\pi$
26 ± 12		EVANGELIS...	81 OMEG	12 $\pi^-p \rightarrow \eta\pi^+\pi^-\pi^-p$
25 ± 15	200	GURTU	79 HBC	4.2 $K^-p \rightarrow \eta\eta 2\pi$
~10		STANTON	79 CNTR	8.5 $\pi^-p \rightarrow n2\gamma 2\pi$
24 ± 18	210	GRASSLER	77 HBC	16 π^+p
28 ± 5	150	DEFOIX	72 HBC	0.7 $p\bar{p} \rightarrow 7\pi$
46 ± 9	180	DUBOC	72 HBC	1.2 $p\bar{p} \rightarrow 2K4\pi$
37 ± 5	500	THUN	72 MMS	13.4 π^-p
10 ± 10		BOESEBECK	71 HBC	16.0 $\pi p \rightarrow p5\pi$
30 ± 15		CAMPBELL	69 DBC	2.7 π^+d
60 ± 15		LORSTAD	69 HBC	0.7 $p\bar{p}$, 4,5-body
35 ± 10		DAHL	67 HBC	1.6-4.2 π^-p

⁷Supersedes ABATZIS 94, ARMSTRONG 89E.

⁸From partial wave analysis of $K^+\bar{K}^0\pi^-$ system.

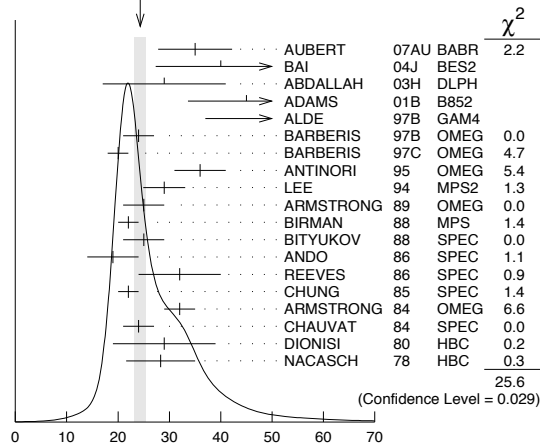
⁹No systematic error given.

¹⁰From phase shift analysis of $\eta\pi^+\pi^-$ system.

¹¹Resolution is not unfolded.

¹²Seen in the missing mass spectrum.

WEIGHTED AVERAGE
24.3 ± 1.1 (Error scaled by 1.4)

 $f_1(1285)$ DECAY MODES

Mode	Fraction (Γ_i/Γ)	Scale factor/ Confidence level
Γ_1 4π	$(33.1^{+2.1}_{-1.8})\%$	S=1.3
Γ_2 $\pi^0\pi^0\pi^+\pi^-$	$(22.0^{+1.4}_{-1.2})\%$	S=1.3
Γ_3 $2\pi^+2\pi^-$	$(11.0^{+0.7}_{-0.6})\%$	S=1.3
Γ_4 $\rho^0\pi^+\pi^-$	$(11.0^{+0.7}_{-0.6})\%$	S=1.3
Γ_5 $\rho^0\rho^0$	seen	
Γ_6 $4\pi^0$	$< 7 \times 10^{-4}$	CL=90%
Γ_7 $\eta\pi\pi$	$(52 \pm 5)\%$	
Γ_8 $a_0(980)\pi$ [ignoring $a_0(980) \rightarrow K\bar{K}$]	$(36 \pm 7)\%$	
Γ_9 $\eta\pi\pi$ [excluding $a_0(980)\pi$]	$(16 \pm 7)\%$	
Γ_{10} $K\bar{K}\pi$	$(9.0 \pm 0.4)\%$	S=1.1
Γ_{11} $K\bar{K}^*(892)$	not seen	
Γ_{12} $\gamma\rho^0$	$(5.5 \pm 1.3)\%$	S=2.8
Γ_{13} $\phi\gamma$	$(7.4 \pm 2.6) \times 10^{-4}$	
Γ_{14} $\gamma\gamma^*$		
Γ_{15} $\gamma\gamma$		

CONSTRAINED FIT INFORMATION

An overall fit to 7 branching ratios uses 16 measurements and one constraint to determine 5 parameters. The overall fit has a $\chi^2 = 24.7$ for 12 degrees of freedom.

The following off-diagonal array elements are the correlation coefficients $\langle \delta x_i \delta x_j \rangle / (\delta x_i \delta x_j)$, in percent, from the fit to the branching fractions, $x_i \equiv \Gamma_i/\Gamma_{\text{total}}$. The fit constrains the x_i whose labels appear in this array to sum to one.

x_8	-17			
x_9	-8	-95		
x_{10}	46	-9	-4	
x_{12}	-36	-4	-2	-34
x_1	x_8	x_9	x_{10}	

 $f_1(1285)$ $\Gamma(i)\Gamma(\gamma\gamma)/\Gamma(\text{total})$

VALUE (keV)	CL%	DOCUMENT ID	TECN	COMMENT
<0.62	95	GIDAL	87	MRK2 $e^+e^- \rightarrow e^+e^-\eta\pi^+\pi^-$

 $f_1(1285)$ $\Gamma(\gamma\gamma^*)/\Gamma(\text{total})$

VALUE (keV)	EVTs	DOCUMENT ID	TECN	COMMENT
1.4 ± 0.4 OUR AVERAGE		Error includes scale factor of 1.4.		
1.18 ± 0.25 ± 0.20	26	^{13,14} AIHARA	88B TPC	$e^+e^- \rightarrow e^+e^-\eta\pi^+\pi^-$
2.30 ± 0.61 ± 0.42		^{13,15} GIDAL	87	MRK2 $e^+e^- \rightarrow e^+e^-\eta\pi^+\pi^-$

• • • We do not use the following data for averages, fits, limits, etc. • • •

1.8 ± 0.3 ± 0.3	420	¹⁶ ACHARD	02B L3	183-209 $e^+e^- \rightarrow e^+e^-\eta\pi^+\pi^-$
-----------------	-----	----------------------	--------	---

¹³Assuming a ρ -pole form factor.

¹⁴Published value multiplied by $\eta\pi\pi$ branching ratio 0.49.

¹⁵Published value divided by 2 and multiplied by the $\eta\pi\pi$ branching ratio 0.49.

¹⁶Published value multiplied by the $\eta\pi\pi$ branching ratio 0.52.

 $f_1(1285)$ BRANCHING RATIOS

MODE	VALUE	DOCUMENT ID	TECN	COMMENT	Γ_{10}/Γ_1	
$\Gamma(K\bar{K}\pi)/\Gamma(4\pi)$	0.271 ± 0.016 OUR FIT	Error includes scale factor of 1.3.				
	0.271 ± 0.016 OUR AVERAGE	Error includes scale factor of 1.2.				
	0.265 ± 0.014	¹⁷ BARBERIS	97C OMEG	450 $pp \rightarrow ppK_S^0 K^\pm \pi^\mp$		
	0.28 ± 0.05	¹⁸ ARMSTRONG	89E OMEG	300 $pp \rightarrow pp f_1(1285)$		
	0.37 ± 0.03 ± 0.05	¹⁹ ARMSTRONG	89G OMEG	85 $\pi p \rightarrow 4\pi X$		

¹⁷Using $2(\pi^+\pi^-)$ data from BARBERIS 97B.

¹⁸Assuming $\rho\pi\pi$ and $a_0(980)\pi$ intermediate states.

¹⁹ 4π consistent with being entirely $\rho\pi\pi$.

MODE	VALUE	DOCUMENT ID
$\Gamma(\pi^0\pi^0\pi^+\pi^-)/\Gamma_{\text{total}}$	0.220 ± 0.014 ± 0.012 OUR FIT	

Error includes scale factor of 1.3.

MODE	VALUE	DOCUMENT ID
$\Gamma(2\pi^+2\pi^-)/\Gamma_{\text{total}}$	0.110 ± 0.007 ± 0.006 OUR FIT	

Error includes scale factor of 1.3.

$\Gamma(\rho^0\pi^+\pi^-)/\Gamma_{\text{total}}$ $\Gamma_4/\Gamma = \frac{1}{3}\Gamma_1/\Gamma$

VALUE DOCUMENT ID COMMENT
0.110 ± 0.007 OUR FIT Error includes scale factor of 1.1.
 -0.006

 $\Gamma(\rho^0\rho^0)/\Gamma_{\text{total}}$ Γ_5/Γ

VALUE DOCUMENT ID COMMENT
 • • • We do not use the following data for averages, fits, limits, etc. • • •
 seen BARBERIS 00c 450 $p\bar{p} \rightarrow p_f 4\pi p_S$

 $\Gamma(4\pi^0)/\Gamma_{\text{total}}$ Γ_6/Γ

VALUE (units 10^{-4}) CL% DOCUMENT ID TECN COMMENT
 <7 90 ALDE 87 GAM4 100 $\pi^- p \rightarrow 4\pi^0 n$

 $\Gamma(K\bar{K}\pi)/\Gamma(\eta\pi\pi)$ $\Gamma_{10}/\Gamma_7 = \Gamma_{10}/(\Gamma_8 + \Gamma_9)$

VALUE DOCUMENT ID TECN COMMENT
0.171 ± 0.013 OUR FIT Error includes scale factor of 1.1.
0.170 ± 0.012 OUR AVERAGE
 0.166 ± 0.01 ± 0.008 BARBERIS 98c OMEG 450 $p\bar{p} \rightarrow p_f f_1(1285) p_S$
 0.42 ± 0.15 GURTU 79 HBC 4.2 $K^- p$
 0.5 ± 0.2 20 CORDEN 78 OMEG 12-15 $\pi^- p$
 0.20 ± 0.08 21 DEFOIX 72 HBC 0.7 $\bar{p}p \rightarrow 7\pi$
 0.16 ± 0.08 CAMPBELL 69 DBC 2.7 $\pi^+ d$

20 CORDEN 78 assumes low-mass $\eta\pi\pi$ region is dominantly 1^{++} . See BARBERIS 98c and MANAK 00a for discussion.
 21 $K\bar{K}$ system characterized by the $l = 1$ threshold enhancement. (See under $a_0(980)$).

 $\Gamma(a_0(980)\pi [\text{ignoring } a_0(980) \rightarrow K\bar{K}])/ \Gamma(\eta\pi\pi)$ $\Gamma_8/\Gamma_7 = \Gamma_8/(\Gamma_8 + \Gamma_9)$

VALUE CL% EVTS DOCUMENT ID TECN COMMENT
0.69 ± 0.13 OUR FIT
0.69 ± 0.12 OUR AVERAGE
 0.72 ± 0.15 GURTU 79 HBC 4.2 $K^- p$
 0.6 ± 0.3 CORDEN 78 OMEG 12-15 $\pi^- p$
 -0.2
 • • • We do not use the following data for averages, fits, limits, etc. • • •
 >0.69 95 318 ACHARD 02b L3 183-209 $e^+e^- \rightarrow e^+e^-\eta\pi^+\pi^-$
 0.28 ± 0.07 1400 ALDE 97b GAM4 100 $\pi^- p \rightarrow \eta\pi^0\pi^0 n$
 1.0 ± 0.3 GRASSLER 77 HBC 16 $\pi^{\mp} p$

 $\Gamma(4\pi)/\Gamma(\eta\pi\pi)$ $\Gamma_1/\Gamma_7 = \Gamma_1/(\Gamma_8 + \Gamma_9)$

VALUE DOCUMENT ID TECN COMMENT
0.63 ± 0.06 OUR FIT Error includes scale factor of 1.2.
0.41 ± 0.14 OUR AVERAGE
 0.37 ± 0.11 ± 0.11 BOLTON 92 MRK3 $J/\psi \rightarrow \gamma f_1(1285)$
 0.64 ± 0.40 GURTU 79 HBC 4.2 $K^- p$
 • • • We do not use the following data for averages, fits, limits, etc. • • •
 0.93 ± 0.30 22 GRASSLER 77 HBC 16 $\pi^{\mp} p$
 22 Assuming $\rho\pi\pi$ and $a_0(980)\pi$ intermediate states.

 $\Gamma(K\bar{K}^*(892))/\Gamma_{\text{total}}$ Γ_{11}/Γ

VALUE DOCUMENT ID TECN COMMENT
not seen NACASCH 78 HBC 0.7, 0.76 $\bar{p}p \rightarrow K\bar{K}^3\pi$
 • • • We do not use the following data for averages, fits, limits, etc. • • •
 seen 23 ACHARD 07 L3 183-209 $e^+e^- \rightarrow e^+e^-K_S^0 K_{\pm}^{\pm}\pi^{\mp}$
 23 A clear signal of 19.8 ± 4.4 events observed at high Q^2 .

 $\Gamma(\rho^0\pi^+\pi^-)/\Gamma(2\pi^+2\pi^-)$ Γ_4/Γ_3

VALUE DOCUMENT ID TECN COMMENT
 • • • We do not use the following data for averages, fits, limits, etc. • • •
 1.0 ± 0.4 GRASSLER 77 HBC 16 GeV $\pi^{\pm} p$

 $\Gamma(\phi\gamma)/\Gamma(K\bar{K}\pi)$ Γ_{13}/Γ_{10}

VALUE (units 10^{-2}) CL% EVTS DOCUMENT ID TECN COMMENT
0.82 ± 0.21 ± 0.20 19 BITYUKOV 88 SPEC 32.5 $\pi^- p \rightarrow K^+ K^- \pi^0 n$
 • • • We do not use the following data for averages, fits, limits, etc. • • •
 <0.50 95 BARBERIS 98c OMEG 450 $p\bar{p} \rightarrow p_f f_1(1285) p_S$
 <0.93 95 AMELIN 95 VES 37 $\pi^- N \rightarrow \pi^- \pi^+ \pi^- \gamma N$

 $\Gamma(\gamma\rho^0)/\Gamma(K\bar{K}\pi)$ Γ_{12}/Γ_{10}

VALUE CL% DOCUMENT ID TECN COMMENT
 • • • We do not use the following data for averages, fits, limits, etc. • • •
 >0.035 90 24 COFFMAN 90 MRK3 $J/\psi \rightarrow \gamma\gamma\pi^+\pi^-$
 24 Using $B(J/\psi \rightarrow \gamma f_1(1285) \rightarrow \gamma\gamma\rho^0) = 0.25 \times 10^{-4}$ and $B(J/\psi \rightarrow \gamma f_1(1285) \rightarrow \gamma K\bar{K}\pi) < 0.72 \times 10^{-3}$.

 $\Gamma(\gamma\rho^0)/\Gamma(2\pi^+2\pi^-)$ $\Gamma_{12}/\Gamma_3 = \Gamma_{12}/\frac{1}{3}\Gamma_1$

VALUE DOCUMENT ID TECN COMMENT
0.50 ± 0.13 OUR FIT Error includes scale factor of 2.5.
0.45 ± 0.18 25 COFFMAN 90 MRK3 $J/\psi \rightarrow \gamma\gamma\pi^+\pi^-$
 25 Using $B(J/\psi \rightarrow \gamma f_1(1285) \rightarrow \gamma\gamma\rho^0) = 0.25 \times 10^{-4}$ and $B(J/\psi \rightarrow \gamma f_1(1285) \rightarrow \gamma 2\pi^+ 2\pi^-) = 0.55 \times 10^{-4}$ given by MIR 88.

 $\Gamma(\gamma\rho^0)/\Gamma_{\text{total}}$ Γ_{12}/Γ

VALUE (units 10^{-2}) CL% DOCUMENT ID TECN COMMENT
5.5 ± 1.3 OUR FIT Error includes scale factor of 2.8.
2.8 ± 0.7 ± 0.6 AMELIN 95 VES 37 $\pi^- N \rightarrow \pi^- \pi^+ \pi^- \gamma N$
 • • • We do not use the following data for averages, fits, limits, etc. • • •
 <5 95 BITYUKOV 91b SPEC 32 $\pi^- p \rightarrow \pi^+ \pi^- \gamma n$

 $\Gamma(\eta\pi\pi)/\Gamma(\gamma\rho^0)$ $\Gamma_7/\Gamma_{12} = (\Gamma_8 + \Gamma_9)/\Gamma_{12}$

VALUE DOCUMENT ID TECN COMMENT
9.5 ± 2.0 OUR FIT Error includes scale factor of 2.5.
7.9 ± 0.9 OUR AVERAGE
 10.0 ± 1.0 ± 2.0 BARBERIS 98c OMEG 450 $p\bar{p} \rightarrow p_f f_1(1285) p_S$
 7.5 ± 1.0 26 ARMSTRONG 92c OMEG 300 $p\bar{p} \rightarrow p\bar{p}\pi^+\pi^- \gamma, p\bar{p}\eta\pi^+\pi^-$
 26 Published value multiplied by 1.5.

 $f_1(1285)$ REFERENCES

ACHARD	07	JHEP	0703	018	P. Achard et al.	(L3 Collab.)
AUBERT	07AU	PR	D76	092005	B. Aubert et al.	(BABAR Collab.)
BAI	04J	PL	B594	47	J.Z. Bai et al.	(BES Collab.)
ABDALLAH	03H	PL	B569	129	J. Abdallah et al.	(DELPHI Collab.)
ACHARD	02B	PL	B526	269	P. Achard et al.	(L3 Collab.)
ACCIARRI	01G	PL	B501	1	M. Acciari et al.	(L3 Collab.)
ADAMS	01B	PL	B516	264	G.S. Adams et al.	(BNL E852 Collab.)
BARBERIS	00C	PL	B471	440	D. Barberis et al.	(WA 102 Collab.)
MANAK	00A	PR	D62	012003	J.J. Manak et al.	(BNL E852 Collab.)
SOSA	99	PRL	83	913	M. Sosa et al.	
BARBERIS	98C	PL	B440	225	D. Barberis et al.	(WA 102 Collab.)
ALDE	97B	PAN	60	386	D. Alde et al.	(GAMS Collab.)
BARBERIS	97B	PL	B413	217	D. Barberis et al.	(WA 102 Collab.)
BARBERIS	97C	PL	B413	225	D. Barberis et al.	(WA 102 Collab.)
AMELIN	95	ZPHY	C66	71	D.V. Amelin et al.	(VES Collab.)
ANTINORI	95	PL	B353	589	F. Antinori et al.	(ATHU, BARI, BIRM+)
ABATZIS	94	PL	B324	509	S. Abatzis et al.	(ATHU, BARI, BIRM+)
LEE	94	PL	B323	227	J.H. Lee et al.	(BNL, IND, KYUN, MASD+)
ARMSTRONG	93C	PL	B307	394	T.A. Armstrong et al.	(FNAL, FERR, GENO+)
ARMSTRONG	92C	ZPHY	C54	371	T.A. Armstrong et al.	(ATHU, BARI, BIRM+)
BOLTON	92C	PL	B278	495	T. Bolton et al.	(Mark III Collab.)
BITYUKOV	91B	SJNP	54	318	S.I. Bitiyukov et al.	(SERP)
FUKUI	91C	PL	B267	293	S. Fukui et al.	(SUGI, NAGO, KEK, KYOT+)
COFFMAN	90	PR	D41	1410	D.M. Coffman et al.	(Mark III Collab.)
ARMSTRONG	89	PL	B221	216	T.A. Armstrong et al.	(CERN, CDEF, BIRM+)
ARMSTRONG	89E	PL	B228	536	T.A. Armstrong, M. Benayoun	(ATHU, BARI, BIRM+)
ARMSTRONG	89G	ZPHY	C43	55	T.A. Armstrong et al.	(CERN, BIRM, BARI+)
RATH	89	PR	D40	693	M.G. Rath et al.	(NDAM, BRAN, BNL, CUNY+)
AIHARA	88B	PL	B209	107	H. Aihara et al.	(TPC-2 Collab.)
BIRMAN	88	PRL	61	1557	A. Birman et al.	(BNL, FSU, IND, MASD) JP
BITYUKOV	88	PL	B203	327	S.I. Bitiyukov et al.	(SERP)
MIR	88	Photon-Photon	88,	126	R. Mir	(Mark III Collab.)
ALDE	87	PL	B198	286	D.M. Alde et al.	(LANL, BRUX, SERP, LAPP)
BECKER	87	PRL	59	186	J.J. Becker et al.	(Mark III Collab.)
GIDAL	87	PRL	59	2012	G. Gidal et al.	(LBL, SLAC, HARV)
ANDO	86	PRL	57	1296	A. Ando et al.	(KEK, KYOT, NIRS, SAGA+)
REEVES	86	PR	D34	1960	D.F. Reeves et al.	(FLOR, BNL, IND+)
CHUNG	85	PRL	55	779	S.U. Chung et al.	(BNL, FLOR, IND+)
ARMSTRONG	84	PL	146B	273	T.A. Armstrong et al.	(ATHU, BARI, BIRM+)
BITYUKOV	84B	PL	144B	133	S.I. Bitiyukov et al.	(SERP)
CHAUVAT	84	PL	148B	382	P. Chauvat et al.	(CERN, CLER, UCLA+)
TORNQVIST	82B	NP	B203	268	N.A. Tornqvist	(HELS)
EVANGELISTA	81	NP	B178	197	C. Evangelista et al.	(BARI, BONN, CERN+)
BROMBERG	80	PR	D22	1513	C.M. Bromberg et al.	(CIT, FNAL, ILLC+)
DIONIISI	80	NP	B169	1	C. Dionisi et al.	(CERN, MADR, CDEF+)
GURTU	79	NP	B151	181	A. Gurtu et al.	(CERN, ZEEM, NIJ, OXF)
STANTON	79	PRL	42	346	N.R. Stanton et al.	(OSU, CARL, MCGI+)
CORDEN	78	NP	B144	253	M.J. Corden et al.	(BIRM, RHEL, TELA+)
NACASCH	78	NP	B135	203	R. Nacasch et al.	(PARIS, MADR, CERN)
GRASSLER	77	NP	B121	189	H. Grassler et al.	(AACH3, BERL, BONN+)
DEFOIX	72	NP	B44	125	C. Defoix et al.	(CDEF, CERN)
DUBOC	72	NP	B46	429	J. Duboc et al.	(PARIS, LIPP)
THUN	72	PRL	28	1733	R. Thun et al.	(STON, NEAS)
BARDADIN...	71	PR	D4	2711	M. Bardadin-Otwinowska et al.	(Wars)
BOESEBECK	71	PL	34B	659	K. Boesebeck (AACH, BERL, BONN, CERN, CRAC+)	
CAMPBELL	69	PRL	22	1204	J.H. Campbell et al.	(PURD)
LORSTAD	69	NP	B14	63	B. Lorstad et al.	(CDEF, CERN) JP
D'ANDLAU	68	NP	B5	693	C. d'Andlau et al.	(CDEF, CERN, IRAD+)
DAHL	67	PR	163	1377	O.I. Dahl et al.	(LRL) IJP

Meson Particle Listings

$\eta(1295), \pi(1300)$

$\eta(1295)$

$$J^G(J^{PC}) = 0^+(0^{-+})$$

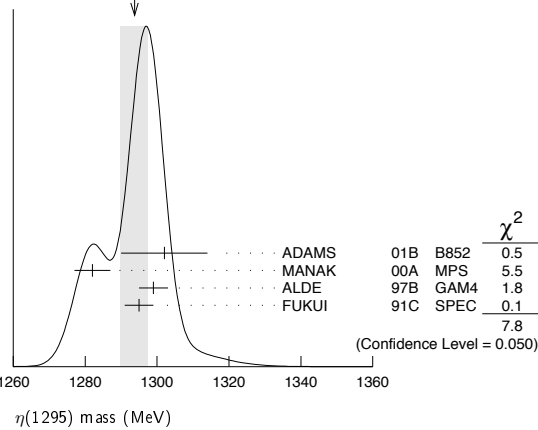
See also the mini-review under $\eta(1405)$

$\eta(1295)$ MASS

VALUE (MeV)	EVTS	DOCUMENT ID	TECN	COMMENT
1294 ± 4 OUR AVERAGE	Error includes scale factor of 1.6. See the ideogram below.			
1302 ± 9 ± 8	20k	ADAMS	01B B852	18 GeV $\pi^- p \rightarrow K^+ K^- \pi^0 n$
1282 ± 5	9082	MANAK	00A MPS	18 $\pi^- p \rightarrow \eta \pi^+ \pi^- n$
1299 ± 4	2100	ALDE	97B GAM4	100 $\pi^- p \rightarrow \eta \pi^0 \pi^0 n$
1295 ± 4		FUKUI	91C SPEC	8.95 $\pi^- p \rightarrow \eta \pi^+ \pi^- n$

- • • We do not use the following data for averages, fits, limits, etc. • • •
- 1264 ± 8 1 AUGUSTIN 90 DM2 $J/\psi \rightarrow \gamma \eta \pi^+ \pi^-$
- ~ 1275 STANTON 79 CNTR $8.4 \pi^- p \rightarrow n \eta 2\pi$

WEIGHTED AVERAGE
1294 ± 4 (Error scaled by 1.6)



1 PWA analysis of AUGUSTIN 92 assigns 0^{-+} quantum numbers to this state rather than 1^{++} as before.

$\eta(1295)$ WIDTH

VALUE (MeV)	EVTS	DOCUMENT ID	TECN	COMMENT
55 ± 5 OUR AVERAGE				
57 ± 23 ± 21	20k	ADAMS	01B B852	18 GeV $\pi^- p \rightarrow K^+ K^- \pi^0 n$
66 ± 13	9082	MANAK	00A MPS	18 $\pi^- p \rightarrow \eta \pi^+ \pi^- n$
53 ± 6		FUKUI	91C SPEC	8.95 $\pi^- p \rightarrow \eta \pi^+ \pi^- n$

- • • We do not use the following data for averages, fits, limits, etc. • • •
 - < 40 2100 ALDE 97B GAM4 100 $\pi^- p \rightarrow \eta \pi^0 \pi^0 n$
 - 44 ± 20 2 AUGUSTIN 90 DM2 $J/\psi \rightarrow \gamma \eta \pi^+ \pi^-$
 - ~ 70 STANTON 79 CNTR $8.4 \pi^- p \rightarrow n \eta 2\pi$
- 2 PWA analysis of AUGUSTIN 92 assigns 0^{-+} quantum numbers to this state rather than 1^{++} as before.

$\eta(1295)$ DECAY MODES

Mode	Fraction (Γ_i/Γ)
Γ_1 $\eta \pi^+ \pi^-$	seen
Γ_2 $a_0(980) \pi$	seen
Γ_3 $\gamma \gamma$	
Γ_4 $\eta \pi^0 \pi^0$	seen
Γ_5 $\eta(\pi\pi)S$ -wave	seen
Γ_6 $\sigma \eta$	
Γ_7 $K \bar{K} \pi$	

$\eta(1295)$ $\Gamma(i)\Gamma(\gamma\gamma)/\Gamma(\text{total})$

$\Gamma(\eta \pi^+ \pi^-) \times \Gamma(\gamma\gamma)/\Gamma_{\text{total}}$	$\Gamma_1 \Gamma_3/\Gamma$			
VALUE (keV)	CL%	DOCUMENT ID	TECN	COMMENT
< 0.066	95	ACCIARRI	01G L3	183-202 $e^+ e^- \rightarrow e^+ e^- \eta \pi^+ \pi^-$
• • • We do not use the following data for averages, fits, limits, etc. • • •				
< 0.6	90	AIHARA	88C TPC	$e^+ e^- \rightarrow e^+ e^- \eta \pi^+ \pi^-$
< 0.3		ANTREASIAN	87 CBAL	$e^+ e^- \rightarrow e^+ e^- \eta \pi \pi$

$\Gamma(K \bar{K} \pi) \times \Gamma(\gamma\gamma)/\Gamma_{\text{total}}$

VALUE (keV)	CL%	DOCUMENT ID	TECN	COMMENT
• • • We do not use the following data for averages, fits, limits, etc. • • •				
< 0.014	90	3,4 AHOHE	05 CLE2	10.6 $e^+ e^- \rightarrow e^+ e^- K_S^0 K^\pm \pi^\mp$

3 Using $\eta(1295)$ mass and width 1294 MeV and 55 MeV, respectively.

4 Assuming three-body phase-space decay to $K_S^0 K^\pm \pi^\mp$.

$\eta(1295)$ BRANCHING RATIOS

$\Gamma(a_0(980)\pi)/\Gamma_{\text{total}}$	Γ_2/Γ		
VALUE	DOCUMENT ID	TECN	COMMENT
• • • We do not use the following data for averages, fits, limits, etc. • • •			
not seen	BERTIN	97 OBLX	0.0 $\bar{p} p \rightarrow K^\pm(K^0) \pi^\mp \pi^+ \pi^-$
seen	BIRMAN	88 MPS	8 $\pi^- p \rightarrow K^+ \bar{K}^0 \pi^- n$
large	ANDO	86 SPEC	8 $\pi^- p \rightarrow \eta \pi^+ \pi^- n$
large	STANTON	79 CNTR	8.4 $\pi^- p \rightarrow n \eta 2\pi$

$\Gamma(a_0(980)\pi)/\Gamma(\eta \pi^0 \pi^0)$

VALUE	DOCUMENT ID	TECN	COMMENT
0.65 ± 0.10	5 ALDE	97B GAM4	100 $\pi^- p \rightarrow \eta \pi^0 \pi^0 n$

5 Assuming that $a_0(980)$ decays only to $\eta \pi$.

$\Gamma(\eta(\pi\pi)S\text{-wave})/\Gamma(\eta \pi^0 \pi^0)$

VALUE	DOCUMENT ID	TECN	COMMENT
0.35 ± 0.10	ALDE	97B GAM4	100 $\pi^- p \rightarrow \eta \pi^0 \pi^0 n$

$\Gamma(a_0(980)\pi)/\Gamma(\sigma\eta)$

VALUE	EVTS	DOCUMENT ID	TECN	COMMENT
0.48 ± 0.22	9082	MANAK	00A MPS	18 $\pi^- p \rightarrow \eta \pi^+ \pi^- n$

$\eta(1295)$ REFERENCES

AHOHE 05	PR D71 072001	R. Ahohe et al.	(CLEO Collab.)
ACCIARRI 01G	PL B501 1	M. Acciari et al.	(L3 Collab.)
ADAMS 01B	PL B516 264	G.S. Adams et al.	(BNL E852 Collab.)
MANAK 00A	PR D62 012003	J.J. Manak et al.	(BNL E852 Collab.)
ALDE 97B	PAN 60 386	D. Alde et al.	(GAMS Collab.)
	Translated from YAF 60 458.		
BERTIN 97	PL B400 226	A. Bertin et al.	(OBELIX Collab.)
AUGUSTIN 92	PR D46 1951	J.E. Augustin, G. Cosme	(DM2 Collab.)
FUKUI 91C	PL B267 293	S. Fukui et al.	(SUGI, NAGO, KEK, KYOT+)
AUGUSTIN 90	PR D42 10	J.E. Augustin et al.	(DM2 Collab.)
AIHARA 88C	PR D38 1	H. Aihara et al.	(TPC-2 Collab.)
BIRMAN 88	PRL 61 1557	A. Birman et al.	(BNL, FSU, IND, MASD)JP
ANTREASIAN 87	PR D36 2633	D. Antreasian et al.	(Crystal Ball Collab.)
ANDO 86	PRL 57 1296	A. Ando et al.	(KEK, KYOT, NIRS, SAGA+IJP)
STANTON 79	PRL 42 346	N.R. Stanton et al.	(OSU, CARL, MCGI+JP)

$\pi(1300)$

$$J^G(J^{PC}) = 1^-(0^{-+})$$

$\pi(1300)$ MASS

VALUE (MeV)	EVTS	DOCUMENT ID	TECN	COMMENT
1300 ± 100 OUR ESTIMATE				

- • • We do not use the following data for averages, fits, limits, etc. • • •
- 1345 ± 8 ± 10 18k 1 SCHEGELSKY 06 RVUE $\gamma \gamma \rightarrow \pi^+ \pi^- \pi^0$
- 1200 ± 40 90k SALVINI 04 OBLX $\bar{p} p \rightarrow 2\pi^+ 2\pi^-$
- 1343 ± 15 ± 24 CHUNG 02 B852 18.3 $\pi^- p \rightarrow \pi^+ \pi^- \pi^- p$
- 1375 ± 40 ABELE 01 CBAR 0.0 $\bar{p} d \rightarrow \pi^- 4\pi^0 p$
- 1275 ± 15 BERTIN 97D OBLX 0.05 $\bar{p} p \rightarrow 2\pi^+ 2\pi^-$
- ~ 1114 ABELE 96 CBAR 0.0 $\bar{p} p \rightarrow 5\pi^0$
- 1190 ± 30 ZIELINSKI 84 SPEC 200 $\pi^+ Z \rightarrow Z 3\pi$
- 1240 ± 30 BELLINI 82 SPEC 40 $\pi^- A \rightarrow A 3\pi$
- 1273 ± 50 2 AARON 81 RVUE
- 1342 ± 20 BONESINI 81 OMEG 12 $\pi^- p \rightarrow p 3\pi$
- ~ 1400 DAUM 81B SPEC 63,94 $\pi^- p$

1 From analysis of L3 data at 183-209 GeV.

2 Uses multichannel Aitchison-Bowler model (BOWLER 75). Uses data from DAUM 80 and DANKOWYCH 81.

$\pi(1300)$ WIDTH

VALUE (MeV)	EVTS	DOCUMENT ID	TECN	COMMENT
200 to 600 OUR ESTIMATE				
• • • We do not use the following data for averages, fits, limits, etc. • • •				
260 ± 20 ± 30 18k 3 SCHEGELSKY 06 RVUE $\gamma \gamma \rightarrow \pi^+ \pi^- \pi^0$				

See key on page 405

Meson Particle Listings

$\pi(1300), a_2(1320)$

Table with columns: mass, document ID, author, technique, decay mode. Includes entries for 470±120, 449±39±47, 268±50, 218±100, ~340, 440±80, 360±120, 580±100, 220±70, ~600.

3 From analysis of L3 data at 183-209 GeV.
4 Uses multichannel Aitchison-Bowler model (BOWLER 75). Uses data from DAUM 80 and DANKOWYCH 81.

$\pi(1300)$ DECAY MODES

Table with columns: Mode, Fraction (Γ_i/Γ). Includes modes $\rho\pi$, $\pi(\pi\pi)s$ -wave, $\gamma\gamma$.

$\pi(1300)$ $\Gamma(i)\Gamma(\gamma\gamma)/\Gamma(\text{total})$

Table with columns: $\Gamma(\rho\pi) \times \Gamma(\gamma\gamma)/\Gamma(\text{total})$, VALUE (keV), CL%, DOCUMENT ID, TECN, COMMENT, $\Gamma_1\Gamma_3/\Gamma$. Includes entries for <0.085, <0.8, <0.54.

5 From analysis of L3 data at 183-209 GeV.

$\pi(1300)$ BRANCHING RATIOS

Table with columns: $\Gamma(\pi(\pi\pi)s\text{-wave})/\Gamma(\rho\pi)$, VALUE, CL%, EVTS, DOCUMENT ID, TECN, COMMENT, Γ_2/Γ_1 . Includes entries for 2.2 ± 0.4, <0.15, 2.12.

6 Uses multichannel Aitchison-Bowler model (BOWLER 75). Uses data from DAUM 80 and DANKOWYCH 81.

$\pi(1300)$ REFERENCES

Table with columns: author, document ID, year, technique, comment. Lists references for SCHEGELSKY, SALVINI, CHUNG, ABELE, ACCIARRI, ALBRECHT, BERTIN, ZIELINSKI, BELLINI, AARON, BONESINI, DANKOWYCH, DAUM, BOWLER.

$a_2(1320)$

$I^G(J^{PC}) = 1^-(2^{++})$

$a_2(1320)$ MASS

Table with columns: VALUE (MeV), DOCUMENT ID. Includes entry 1318.3 ± 0.6 OUR AVERAGE.

3π MODE

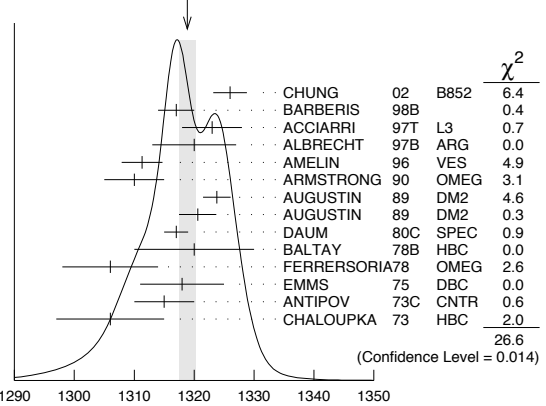
The data in this block is included in the average printed for a previous datablock.

Table with columns: mass, document ID, author, technique, decay mode. Includes entries for 1318.9 ± 1.4 OUR AVERAGE, 1326 ± 2 ± 2, 1317 ± 3, 1323 ± 4 ± 3, 1320 ± 7, 1311.3 ± 1.6 ± 3.0, 1310 ± 5.

Table with columns: mass, document ID, author, technique, decay mode. Includes entries for 1323.8 ± 2.3, 1320.6 ± 3.1, 1317 ± 2, 1320 ± 10, 1306 ± 8, 1318 ± 7, 1315 ± 5, 1306 ± 9, 1300 ± 2 ± 4, 1305 ± 14, 1310 ± 2, 1343 ± 11, 1309 ± 5, 1299 ± 6, 1300 ± 6, 1309 ± 4, 1306 ± 4.

1 From a fit to $J^P = 2^+ \rho\pi$ partial wave.
2 From analysis of L3 data at 183-209 GeV.

WEIGHTED AVERAGE
1318.9±1.4 (Error scaled by 1.4)



$K\bar{K}$ MODE

The data in this block is included in the average printed for a previous datablock.

1318.1 ± 0.7 OUR AVERAGE

Table with columns: mass, document ID, author, technique, decay mode. Includes entries for 1319 ± 5, 1324 ± 6, 1320 ± 2, 1312 ± 4, 1316 ± 2, 1318 ± 1, 1320 ± 2, 1313 ± 4, 1319 ± 3.

• • • We do not use the following data for averages, fits, limits, etc. • • •

Table with columns: mass, document ID, author, technique, decay mode. Includes entries for 1304 ± 10, 1330 ± 11, 1324 ± 5.

3 From a fit to $J^P = 2^+$ partial wave.
4 Number of events evaluated by us.
5 Systematic error in mass scale subtracted.
6 From analysis of L3 data at 91 and 183-209 GeV.

$\eta\pi$ MODE

The data in this block is included in the average printed for a previous datablock.

1317.7 ± 1.4 OUR AVERAGE

Table with columns: mass, document ID, author, technique, decay mode. Includes entries for 1308 ± 9, 1316 ± 9, 1317 ± 1 ± 2, 1315 ± 5 ± 2, 1325.1 ± 5.1, 1317.7 ± 1.4 ± 2.0, 1323 ± 8.

$\Gamma(\pi^\pm\gamma)$ Γ_9

VALUE (keV)	EVTs	DOCUMENT ID	TECN	CHG	COMMENT
287 ± 30 OUR AVERAGE					
284 ± 25 ± 25	7100	MOLCHANOV 01	SELX		600 $\pi^- A \rightarrow \pi^+ \pi^- \pi^- A$
295 ± 60		CIHANGIR 82	SPEC	+	200 $\pi^+ A$
461 ± 110		22 MAY 77	SPEC	±	9.7 γA

• • • We do not use the following data for averages, fits, limits, etc. • • •

22 Assuming one-pion exchange.

$\Gamma(\gamma\gamma)$ Γ_{10}

VALUE (keV)	EVTs	DOCUMENT ID	TECN	CHG	COMMENT
1.00 ± 0.06 OUR AVERAGE					
0.98 ± 0.05 ± 0.09		ACCIARRI 97T	L3		$e^+ e^- \rightarrow e^+ e^- \pi^+ \pi^- \pi^0$
0.96 ± 0.03 ± 0.13		ALBRECHT 97B	ARG		$e^+ e^- \rightarrow e^+ e^- \pi^+ \pi^- \pi^0$
1.26 ± 0.26 ± 0.18	36	BARU 90	MD1		$e^+ e^- \rightarrow e^+ e^- \pi^+ \pi^- \pi^0$
1.00 ± 0.07 ± 0.15	415	BEHREND 90c	CELL	0	$e^+ e^- \rightarrow e^+ e^- \pi^+ \pi^- \pi^0$
1.03 ± 0.13 ± 0.21		BUTLER 90	MRK2		$e^+ e^- \rightarrow e^+ e^- \pi^+ \pi^- \pi^0$
1.01 ± 0.14 ± 0.22	85	OEST 90	JADE		$e^+ e^- \rightarrow e^+ e^- \pi^+ \pi^- \pi^0 \eta$
0.90 ± 0.27 ± 0.15	56	23 ALTHOFF 86	TASS	0	$e^+ e^- \rightarrow e^+ e^- 3\pi$
1.14 ± 0.20 ± 0.26		24 ANTREASIAN 86	CBAL	0	$e^+ e^- \rightarrow e^+ e^- \pi^0 \eta$
1.06 ± 0.18 ± 0.19		BERGER 84c	PLUT	0	$e^+ e^- \rightarrow e^+ e^- 3\pi$
0.81 ± 0.19 ± 0.42	35	23 BEHREND 83b	CELL	0	$e^+ e^- \rightarrow e^+ e^- 3\pi$
0.77 ± 0.18 ± 0.27	22	24 EDWARDS 82f	CBAL	0	$e^+ e^- \rightarrow e^+ e^- \pi^0 \eta$

• • • We do not use the following data for averages, fits, limits, etc. • • •

23 From $\rho\pi$ decay mode.
24 From $\eta\pi^0$ decay mode.

$\Gamma(e^+ e^-)$ Γ_{11}

VALUE (eV)	CL%	DOCUMENT ID	TECN	CHG	COMMENT
< 0.56					
< 25	90	ACHASOV 00k	SND		$e^+ e^- \rightarrow \pi^0 \pi^0$
< 25	90	VOROBYEV 88	ND		$e^+ e^- \rightarrow \pi^0 \eta$

• • • We do not use the following data for averages, fits, limits, etc. • • •

$a_2(1320) \Gamma(i)\Gamma(\gamma\gamma)/\Gamma(\text{total})$

$\Gamma(3\pi) \times \Gamma(\gamma\gamma)/\Gamma_{\text{total}}$ $\Gamma_1 \Gamma_{10}/\Gamma$

VALUE (keV)	EVTs	DOCUMENT ID	TECN	CHG	COMMENT
0.75 ± 0.02 ± 0.02					
0.65 ± 0.02 ± 0.02	18k	25 SCHEGELSKY 06	RVUE		$\gamma\gamma \rightarrow \pi^+ \pi^- \pi^0$

• • • We do not use the following data for averages, fits, limits, etc. • • •

25 From analysis of L3 data at 183–209 GeV.

$\Gamma(\eta\pi) \times \Gamma(\gamma\gamma)/\Gamma_{\text{total}}$ $\Gamma_5 \Gamma_{10}/\Gamma$

VALUE (keV)	DOCUMENT ID	TECN	CHG	COMMENT
0.145 ± 0.097				
0.145 ± 0.097	26 UEHARA 09a	BELL		$e^+ e^- \rightarrow e^+ e^- \eta \pi^0$

• • • We do not use the following data for averages, fits, limits, etc. • • •

26 From the D_2 -wave. The fraction of the D_0 -wave is $3.4 \pm 2.3\%$.

$\Gamma(K\bar{K}) \times \Gamma(\gamma\gamma)/\Gamma_{\text{total}}$ $\Gamma_7 \Gamma_{10}/\Gamma$

VALUE (keV)	DOCUMENT ID	TECN	CHG	COMMENT
0.126 ± 0.007 ± 0.028				
0.081 ± 0.006 ± 0.027	27 ALBRECHT 90g	ARG		$e^+ e^- \rightarrow e^+ e^- K^+ K^-$
0.081 ± 0.006 ± 0.027	28 ALBRECHT 90g	ARG		$e^+ e^- \rightarrow e^+ e^- K^+ K^-$

• • • We do not use the following data for averages, fits, limits, etc. • • •

27 Using an incoherent background.
28 Using a coherent background.

$a_2(1320)$ BRANCHING RATIOS

$[\Gamma(\rho_2(1270)\pi) + \Gamma(\rho(1450)\pi)]/\Gamma(\rho(770)\pi)$ $(\Gamma_3 + \Gamma_4)/\Gamma_2$

VALUE	CL%	DOCUMENT ID	TECN	CHG	COMMENT
< 0.12					
< 0.12	90	ABRAMOV... 70b	HBC	-	3.93 $\pi^- \rho$

$\Gamma(\eta\pi)/\Gamma(3\pi)$ Γ_5/Γ_1

VALUE	EVTs	DOCUMENT ID	TECN	CHG	COMMENT
0.207 ± 0.018 OUR FIT					
0.213 ± 0.020 OUR AVERAGE					
0.18 ± 0.05		FORINO 76	HBC		11 $\pi^- \rho$
0.22 ± 0.05	52	ANTIPOV 73	CNTR	-	40 $\pi^- \rho$
0.211 ± 0.044	149	CHALOUKKA 73	HBC	-	3.9 $\pi^- \rho$
0.246 ± 0.042	167	ALSTON... 71	HBC	+	7.0 $\pi^+ \rho$
0.25 ± 0.09	15	BOECKMANN 70	HBC	+	5.0 $\pi^+ \rho$
0.23 ± 0.08	22	ASCOLI 68	HBC	-	5 $\pi^- \rho$
0.12 ± 0.08		CHUNG 68	HBC	-	3.2 $\pi^- \rho$
0.22 ± 0.09		CONTE 67	HBC	-	11.0 $\pi^- \rho$

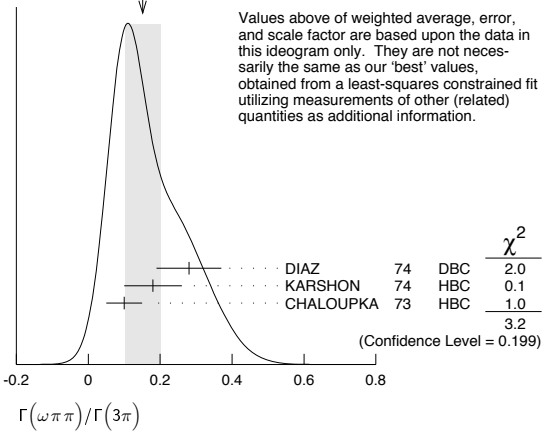
$\Gamma(\omega\pi\pi)/\Gamma(3\pi)$ Γ_6/Γ_1

VALUE	EVTs	DOCUMENT ID	TECN	CHG	COMMENT
0.15 ± 0.05 OUR FIT					
0.15 ± 0.05 OUR AVERAGE					
0.28 ± 0.09	60	DIAZ 74	DBC	0	6 $\pi^+ n$
0.18 ± 0.08		29 KARSHON 74	HBC		Avg. of above two
0.10 ± 0.05	279	CHALOUKKA 73	HBC	-	3.9 $\pi^- \rho$
0.29 ± 0.08	140	29 KARSHON 74	HBC	0	4.9 $\pi^+ \rho$
0.10 ± 0.04	60	29 KARSHON 74	HBC	+	4.9 $\pi^+ \rho$
0.19 ± 0.08		DEFOIX 73	HBC	0	0.7 $\bar{p} p$

• • • We do not use the following data for averages, fits, limits, etc. • • •

29 KARSHON 74 suggest an additional $l = 0$ state strongly coupled to $\omega\pi\pi$ which could explain discrepancies in branching ratios and masses. We use a central value and a systematic spread.

WEIGHTED AVERAGE
0.15±0.05 (Error scaled by 1.3)



$\Gamma(K\bar{K})/\Gamma(3\pi)$ Γ_7/Γ_1

VALUE	EVTs	DOCUMENT ID	TECN	CHG	COMMENT
0.070 ± 0.012 OUR FIT					
0.078 ± 0.017					
0.011 ± 0.003		30 BERTIN 98b	OBLX		0.0 $\bar{p} p \rightarrow K^\pm K_S \pi^\mp$
0.056 ± 0.014	50	31 CHALOUKKA 73	HBC	-	3.9 $\pi^- \rho$
0.097 ± 0.018	113	31 ALSTON... 71	HBC	+	7.0 $\pi^+ \rho$
0.06 ± 0.03		31 ABRAMOV... 70b	HBC	-	3.93 $\pi^- \rho$
0.054 ± 0.022		31 CHUNG 68	HBC	-	3.2 $\pi^- \rho$

• • • We do not use the following data for averages, fits, limits, etc. • • •

30 Using 4π data from BERTIN 97D.
31 Included in CHABAUD 78 review.

$\Gamma(K\bar{K})/\Gamma(\eta\pi)$ Γ_7/Γ_5

VALUE	DOCUMENT ID	TECN	CHG	COMMENT
0.08 ± 0.02				
0.08 ± 0.02	32 BERTIN 98b	OBLX		0.0 $\bar{p} p \rightarrow K^\pm K_S \pi^\mp$

• • • We do not use the following data for averages, fits, limits, etc. • • •

32 Using $\eta\pi\pi$ data from AMSLER 94D.

$\Gamma(\eta\pi)/[\Gamma(3\pi) + \Gamma(\eta\pi) + \Gamma(K\bar{K})]$ $\Gamma_5/(\Gamma_1 + \Gamma_5 + \Gamma_7)$

VALUE	EVTs	DOCUMENT ID	TECN	CHG	COMMENT
0.162 ± 0.012 OUR FIT					
0.140 ± 0.028 OUR AVERAGE					
0.13 ± 0.04		ESPIGAT 72	HBC	±	0.0 $\bar{p} p$
0.15 ± 0.04	34	BARNHAM 71	HBC	+	3.7 $\pi^+ \rho$

$\Gamma(K\bar{K})/[\Gamma(3\pi) + \Gamma(\eta\pi) + \Gamma(K\bar{K})]$ $\Gamma_7/(\Gamma_1 + \Gamma_5 + \Gamma_7)$

VALUE	EVTs	DOCUMENT ID	TECN	CHG	COMMENT
0.054 ± 0.009 OUR FIT					
0.048 ± 0.012 OUR AVERAGE					
0.05 ± 0.02		TOET 73	HBC	+	5 $\pi^+ \rho$
0.09 ± 0.04		TOET 73	HBC	0	5 $\pi^+ \rho$
0.03 ± 0.02	8	DAMERI 72	HBC	-	11 $\pi^- \rho$
0.06 ± 0.03	17	BARNHAM 71	HBC	+	3.7 $\pi^+ \rho$
0.020 ± 0.004		33 ESPIGAT 72	HBC	±	0.0 $\bar{p} p$

• • • We do not use the following data for averages, fits, limits, etc. • • •

33 Not averaged because of discrepancy between masses from $K\bar{K}$ and $\rho\pi$ modes.

$\Gamma(\eta'(958)\pi)/\Gamma_{\text{total}}$ Γ_8/Γ

VALUE	CL%	DOCUMENT ID	TECN	CHG	COMMENT
< 0.006					
< 0.006	95	ALDE 92b	GAM2		38,100 $\pi^- \rho \rightarrow \eta' \pi^0 n$
< 0.02	97	BARNHAM 71	HBC	+	3.7 $\pi^+ \rho$
0.004 ± 0.004		BOESEBECK 68	HBC	+	8 $\pi^+ \rho$

• • • We do not use the following data for averages, fits, limits, etc. • • •

- ¹³Breit-Wigner mass.
- ¹⁴Breit-Wigner mass. May also be the $f_0(1500)$.
- ¹⁵Reanalysis of ABELE 96C data.
- ¹⁶Also observed by GARMASH 07 in $B^0 \rightarrow K_S^0 \pi^+ \pi^-$ decays. Supersedes GARMASH 05.
- ¹⁷Uses data from BEIER 72b, OCHS 73, HYAMS 73, GRAYER 74, ROSSELET 77, CA-SON 83, ASTON 88, and ARMSTRONG 91b. Coupled channel analysis with flavor symmetry and all light two-pseudoscalars systems.
- ¹⁸Also observed by ASNER 00 in $\tau^- \rightarrow \pi^- \pi^0 \pi^0 \nu_\tau$ decays

$K\bar{K}$ MODE

VALUE (MeV)	DOCUMENT ID	TECN	COMMENT
• • • We do not use the following data for averages, fits, limits, etc. • • •			
1440 ± 6	VLADIMIRSK...06	SPEC	40 $\pi^- p \rightarrow K_S^0 K_S^0 n$
1391 ± 10	TIKHOMIROV 03	SPEC	40.0 $\pi^- C \rightarrow K_S^0 K_S^0 K_L^0 X$
1440 ± 5.0	BOLONKIN 88	SPEC	40 $\pi^- p \rightarrow K_S^0 K_S^0 n$
1463 ± 9	ETKIN 82b	MPS	23 $\pi^- p \rightarrow n 2K_S^0$
1425 ± 15	WICKLUND 80	SPEC	6 $\pi N \rightarrow K^+ K^- N$
~ 1300	POLYCHRO... 79	STRC	7 $\pi^- p \rightarrow n 2K_S^0$

4π MODE $2(\pi\pi)_S + \rho\rho$

VALUE (MeV)	EVTS	DOCUMENT ID	TECN	COMMENT
• • • We do not use the following data for averages, fits, limits, etc. • • •				
1395 ± 4.0		ABELE 01	CBAR	0.0 $\bar{p} d \rightarrow \pi^- 4\pi^0 p$
1374 ± 3.8		AMSLER 94	CBAR	0.0 $\bar{p} p \rightarrow \pi^+ \pi^- 3\pi^0$
1345 ± 1.2		ADAMO 93	OBLX	$\bar{p} p \rightarrow 3\pi^+ 2\pi^-$
1386 ± 3.0		GASPERO 93	DBC	0.0 $\bar{p} n \rightarrow 2\pi^+ 3\pi^-$
~ 1410	5751	¹⁹ BETTINI 66	DBC	0.0 $\bar{p} n \rightarrow 2\pi^+ 3\pi^-$
¹⁹ $\rho\rho$ dominant.				

$\eta\eta$ MODE

VALUE (MeV)	DOCUMENT ID	TECN	COMMENT
• • • We do not use the following data for averages, fits, limits, etc. • • •			
1430	AMSLER 92	CBAR	0.0 $\bar{p} p \rightarrow \pi^0 \eta\eta$
1220 ± 4.0	ALDE 86d	GAM4	100 $\pi^- p \rightarrow n 2\eta$

COUPLED CHANNEL MODE

VALUE (MeV)	DOCUMENT ID	TECN
• • • We do not use the following data for averages, fits, limits, etc. • • •		
1306 ± 2.0	²⁰ ANISOVICH 03	RVUE
²⁰ K-matrix pole from combined analysis of $\pi^- p \rightarrow \pi^0 \pi^0 n$, $\pi^- p \rightarrow K\bar{K}n$, $\pi^+ \pi^- \rightarrow \pi^+ \pi^-$, $\bar{p} p \rightarrow \pi^0 \pi^0 \pi^0$, $\pi^0 \eta\eta$, $\pi^0 \pi^0 \eta$, $\pi^+ \pi^- \pi^0$, $K^+ K^- \pi^0$, $K_S^0 K_S^0 \pi^0$, $K^+ K_S^0 \pi^-$ at rest, $\bar{p} n \rightarrow \pi^- \pi^- \pi^+$, $K_S^0 K^- \pi^0$, $K_S^0 K_S^0 \pi^-$ at rest.		

$f_0(1370)$ BREIT-WIGNER WIDTH

VALUE (MeV)	DOCUMENT ID
200 to 500 OUR ESTIMATE	

$\pi\pi$ MODE

VALUE (MeV)	EVTS	DOCUMENT ID	TECN	COMMENT
• • • We do not use the following data for averages, fits, limits, etc. • • •				
300 ± 80		²¹ AUBERT 09L	BABR	$B^\pm \rightarrow \pi^\pm \pi^\pm \pi^\mp$
$90 \pm \frac{2+5}{1-22}$		²² UEHARA 08A	BELL	10.6 $e^+ e^- \rightarrow e^+ e^- \pi^0 \pi^0$
298 ± 21	2.6k	BONVICINI 07	CLEO	$D^+ \rightarrow \pi^- \pi^+ \pi^+$
126 ± 25	4286	²³ GARMASH 06	BELL	$B^+ \rightarrow K^+ \pi^+ \pi^-$
265 ± 40		ABLIKIM 05	BES2	$J/\psi \rightarrow \phi \pi^+ \pi^-$
$350 \pm 100 \pm \frac{105}{60}$		ABLIKIM 05Q	BES2	$\psi(2S) \rightarrow \gamma \pi^+ \pi^- K^+ K^-$
173 ± 32 ± 6	848	AITALA 01A	E791	$D_s^\pm \rightarrow \pi^- \pi^+ \pi^+$
222 ± 20		BARBERIS 99b	OMEG	450 $pp \rightarrow p_S p_f \pi^+ \pi^-$
255 ± 60		BELLAZZINI 99	GAM4	450 $pp \rightarrow p p \pi^0 \pi^0$
190 ± 50		ALDE 98	GAM4	100 $\pi^- p \rightarrow \pi^0 \pi^0 n$
323 ± 13		BERTIN 98	OBLX	0.05-0.405 $\bar{p} p \rightarrow \pi^+ \pi^+ \pi^-$
350		^{24,25} TORNQVIST 95	RVUE	$\pi\pi \rightarrow \pi\pi, K\bar{K}, K\pi, \eta\pi$
195 ± 33		ARMSTRONG 91	OMEG	300 $pp \rightarrow p p \pi\pi, p p K\bar{K}$
285 ± 60		BREAKSTONE 90	SFM	62 $pp \rightarrow p p \pi^+ \pi^-$
460 ± 50		AKESSON 86	SPEC	63 $pp \rightarrow p p \pi^+ \pi^-$
~ 400		²⁶ FROGGATT 77	RVUE	$\pi^+ \pi^-$ channel

- ²¹The systematic errors are not reported.
- ²²Breit-Wigner width. May also be the $f_0(1500)$.
- ²³Also observed by GARMASH 07 in $B^0 \rightarrow K_S^0 \pi^+ \pi^-$ decays. Supersedes GARMASH 05.
- ²⁴Uses data from BEIER 72b, OCHS 73, HYAMS 73, GRAYER 74, ROSSELET 77, CA-SON 83, ASTON 88, and ARMSTRONG 91b. Coupled channel analysis with flavor symmetry and all light two-pseudoscalars systems.
- ²⁵Also observed by ASNER 00 in $\tau^- \rightarrow \pi^- \pi^0 \pi^0 \nu_\tau$ decays
- ²⁶Width defined as distance between 45 and 135° phase shift.

$K\bar{K}$ MODE

VALUE (MeV)	DOCUMENT ID	TECN	COMMENT
• • • We do not use the following data for averages, fits, limits, etc. • • •			
121 ± 15	VLADIMIRSK...06	SPEC	40 $\pi^- p \rightarrow K_S^0 K_S^0 n$
55 ± 26	TIKHOMIROV 03	SPEC	40.0 $\pi^- C \rightarrow K_S^0 K_S^0 K_L^0 X$
250 ± 80	BOLONKIN 88	SPEC	40 $\pi^- p \rightarrow K_S^0 K_S^0 n$
$118 \pm \frac{138}{16}$	ETKIN 82b	MPS	23 $\pi^- p \rightarrow n 2K_S^0$
160 ± 30	WICKLUND 80	SPEC	6 $\pi N \rightarrow K^+ K^- N$
~ 150	POLYCHRO... 79	STRC	7 $\pi^- p \rightarrow n 2K_S^0$

4π MODE $2(\pi\pi)_S + \rho\rho$

VALUE (MeV)	EVTS	DOCUMENT ID	TECN	COMMENT
• • • We do not use the following data for averages, fits, limits, etc. • • •				
275 ± 5.5		ABELE 01	CBAR	0.0 $\bar{p} d \rightarrow \pi^- 4\pi^0 p$
375 ± 6.1		AMSLER 94	CBAR	0.0 $\bar{p} p \rightarrow \pi^+ \pi^- 3\pi^0$
398 ± 2.6		ADAMO 93	OBLX	$\bar{p} p \rightarrow 3\pi^+ 2\pi^-$
310 ± 5.0		GASPERO 93	DBC	0.0 $\bar{p} n \rightarrow 2\pi^+ 3\pi^-$
~ 90	5751	²⁷ BETTINI 66	DBC	0.0 $\bar{p} n \rightarrow 2\pi^+ 3\pi^-$
²⁷ $\rho\rho$ dominant.				

$\eta\eta$ MODE

VALUE (MeV)	DOCUMENT ID	TECN	COMMENT
• • • We do not use the following data for averages, fits, limits, etc. • • •			
250	AMSLER 92	CBAR	0.0 $\bar{p} p \rightarrow \pi^0 \eta\eta$
320 ± 4.0	ALDE 86d	GAM4	100 $\pi^- p \rightarrow n 2\eta$

COUPLED CHANNEL MODE

VALUE (MeV)	DOCUMENT ID	TECN
• • • We do not use the following data for averages, fits, limits, etc. • • •		
$147 \pm \frac{30}{-5.0}$	²⁸ ANISOVICH 03	RVUE
²⁸ K-matrix pole from combined analysis of $\pi^- p \rightarrow \pi^0 \pi^0 n$, $\pi^- p \rightarrow K\bar{K}n$, $\pi^+ \pi^- \rightarrow \pi^+ \pi^-$, $\bar{p} p \rightarrow \pi^0 \pi^0 \pi^0$, $\pi^0 \eta\eta$, $\pi^0 \pi^0 \eta$, $\pi^+ \pi^- \pi^0$, $K^+ K^- \pi^0$, $K_S^0 K_S^0 \pi^0$, $K^+ K_S^0 \pi^-$ at rest, $\bar{p} n \rightarrow \pi^- \pi^- \pi^+$, $K_S^0 K^- \pi^0$, $K_S^0 K_S^0 \pi^-$ at rest.		

$f_0(1370)$ DECAY MODES

Mode	Fraction (Γ_i/Γ)
Γ_1 $\pi\pi$	seen
Γ_2 4π	seen
Γ_3 $4\pi^0$	seen
Γ_4 $2\pi^+ 2\pi^-$	seen
Γ_5 $\pi^+ \pi^- 2\pi^0$	seen
Γ_6 $\rho\rho$	dominant
Γ_7 $2(\pi\pi)_S$ -wave	seen
Γ_8 $\pi(1300)\pi$	seen
Γ_9 $a_1(1260)\pi$	seen
Γ_{10} $\eta\eta$	seen
Γ_{11} $K\bar{K}$	seen
Γ_{12} $K\bar{K}n\pi$	not seen
Γ_{13} 6π	not seen
Γ_{14} $\omega\omega$	not seen
Γ_{15} $\gamma\gamma$	seen
Γ_{16} $e^+ e^-$	not seen

$f_0(1370)$ PARTIAL WIDTHS

$\Gamma(\gamma\gamma)$	Γ_{15}
See $\gamma\gamma$ widths under $f_0(600)$ and MORGAN 90.	

$\Gamma(e^+ e^-)$	Γ_{16}
VALUE (eV) CL% DOCUMENT ID TECN COMMENT	
<20 90 VOROBYEV 88 ND	$e^+ e^- \rightarrow \pi^0 \pi^0$

$f_0(1370)$ BRANCHING RATIOS

$\Gamma(\pi\pi)/\Gamma_{total}$	Γ_1/Γ
• • • We do not use the following data for averages, fits, limits, etc. • • •	
0.26 ± 0.09	BUGG 96 RVUE
<0.15	²⁹ AMSLER 94 CBAR $\bar{p} p \rightarrow \pi^+ \pi^- 3\pi^0$
<0.06	GASPERO 93 DBC 0.0 $\bar{p} n \rightarrow$ hadrons
²⁹ Using AMSLER 95B (3 π^0).	
$\Gamma(4\pi)/\Gamma_{total}$	$\Gamma_2/\Gamma = (\Gamma_3 + \Gamma_4 + \Gamma_5)/\Gamma$
• • • We do not use the following data for averages, fits, limits, etc. • • •	
>0.72	GASPERO 93 DBC 0.0 $\bar{p} n \rightarrow$ hadrons

Meson Particle Listings

f₀(1370)

Γ(4π⁰)/Γ(4π) Γ₃/Γ₂

Table with columns: VALUE, DOCUMENT ID, TECN, COMMENT. Includes values like 0.068 ± 0.005 and document IDs like ABELE 96, GASPERO 93.

Γ(2π⁺2π⁻)/Γ(4π) Γ₄/Γ₂ = Γ₄/(Γ₃+Γ₄+Γ₅)

Table with columns: VALUE, DOCUMENT ID, TECN, COMMENT. Includes value 0.420 ± 0.014 and document IDs like GASPERO 93.

Γ(π⁺π⁻2π⁰)/Γ(4π) Γ₅/Γ₂ = Γ₅/(Γ₃+Γ₄+Γ₅)

Table with columns: VALUE, DOCUMENT ID, TECN, COMMENT. Includes value 0.512 ± 0.019 and document IDs like GASPERO 93.

Γ(ρρ)/Γ(4π) Γ₆/Γ₂

Table with columns: VALUE, DOCUMENT ID, TECN, COMMENT. Includes value 0.26 ± 0.07 and document IDs like ABELE 01B.

Γ(2(ππ)_{S-wave})/Γ(ππ) Γ₇/Γ₁

Table with columns: VALUE, DOCUMENT ID, TECN, COMMENT. Includes value 5.6 ± 2.6 and document IDs like ABELE 01.

Γ(2(ππ)_{S-wave})/Γ(4π) Γ₇/Γ₂

Table with columns: VALUE, DOCUMENT ID, TECN, COMMENT. Includes value 0.51 ± 0.09 and document IDs like ABELE 01B.

Γ(ρρ)/Γ(2(ππ)_{S-wave}) Γ₆/Γ₇

Table with columns: VALUE, DOCUMENT ID, TECN, COMMENT. Includes values like 1.6 ± 0.2 and document IDs like BARBERIS 00C, AMSLER 94, GASPERO 93.

Γ(π(1300)π)/Γ(4π) Γ₈/Γ₂

Table with columns: VALUE, DOCUMENT ID, TECN, COMMENT. Includes value 0.17 ± 0.06 and document IDs like ABELE 01B.

Γ(a₁(1260)π)/Γ(4π) Γ₉/Γ₂

Table with columns: VALUE, DOCUMENT ID, TECN, COMMENT. Includes value 0.06 ± 0.02 and document IDs like ABELE 01B.

Γ(ηη)/Γ(4π) Γ₁₀/Γ₂ = Γ₁₀/(Γ₃+Γ₄+Γ₅)

Table with columns: VALUE, DOCUMENT ID, TECN, COMMENT. Includes values like (28 ± 11) × 10⁻³ and document IDs like ANISOVICH 02D.

Γ(KK̄)/Γ_{total} Γ₁₁/Γ

Table with columns: VALUE, DOCUMENT ID, TECN, COMMENT. Includes value 0.35 ± 0.13 and document IDs like BUGG 96, RVUE.

Γ(KK̄π)/Γ(ππ) Γ₁₁/Γ₁

Table with columns: VALUE, DOCUMENT ID, TECN, COMMENT. Includes values like 0.08 ± 0.08 and document IDs like ABLIKIM 05, BARGIOTTI 03, ANISOVICH 02D, BARBERIS 99D.

Γ(KK̄nπ)/Γ_{total} Γ₁₂/Γ

Table with columns: VALUE, DOCUMENT ID, TECN, COMMENT. Includes value < 0.03 and document IDs like GASPERO 93.

Γ(6π)/Γ_{total} Γ₁₃/Γ

Table with columns: VALUE, DOCUMENT ID, TECN, COMMENT. Includes value < 0.22 and document IDs like GASPERO 93.

Γ(ωω)/Γ_{total} Γ₁₄/Γ

Table with columns: VALUE, DOCUMENT ID, TECN, COMMENT. Includes value < 0.13 and document IDs like GASPERO 93.

f₀(1370) REFERENCES

ANISOVICH 09 IJMP A24 2481 V.V. Anisovich, A.V. Sarantsev
AUBERT 09L PR D79 072006 B. Aubert et al. (BABAR Collab.)
UEHARA 08A PR D78 052004 S. Uehara et al. (BELLE Collab.)
BONVICINI 07 PR D76 012001 G. Bonvicini et al. (CLEO Collab.)
BUGG 07A JPG 34 151 D.V. Bugg et al. (BELLE Collab.)
GARMASH 07 PR D75 012006 A. Garmash et al. (BELLE Collab.)
GARMASH 06 PRL 96 251803 A. Garmash et al. (BELLE Collab.)
PDC 06 JPG 33 1 W.-M. Yao et al. (PDG Collab.)
VLADIMIRSK... 06 PAN 69 493 V.V. Vladimirov et al. (ITEP, Moscow)
ABLIKIM 05 PL B607 243 M. Ablikim et al. (BES Collab.)
ABLIKIM 05Q PR D72 092002 M. Ablikim et al. (BES Collab.)
GARMASH 05 PR D71 092003 A. Garmash et al. (BELLE Collab.)
ANISOVICH 03 EPJ A16 229 V.V. Anisovich et al. (OBELIX Collab.)
BARGIOTTI 03 EPJ C26 371 M. Bargiotti et al. (OBELIX Collab.)
TIKHOMIROV 03 PAN 66 828 G.D. Tikhomirov et al. (OBELIX Collab.)
ANISOVICH 02D PAN 65 1545 V.V. Anisovich et al.
ABELE 01 EPJ C19 667 A. Abele et al. (Crystal Barrel Collab.)
ABELE 01B EPJ C21 261 A. Abele et al. (Crystal Barrel Collab.)
AITALA 01A PRL 86 765 E.M. Aitala et al. (FNAL E791 Collab.)
ASNER 00 PR D61 012002 D.M. Asner et al. (CLEO Collab.)
BARBERIS 00C PL B471 440 D. Barberis et al. (WA 102 Collab.)
BARBERIS 00E PL B479 59 D. Barberis et al. (WA 102 Collab.)
BARBERIS 99B PL B453 316 D. Barberis et al. (Omega Expt.)
BARBERIS 99D PL B462 462 D. Barberis et al. (Omega Expt.)
BELLAZZINI 99 PL B467 296 R. Bellazzini et al.
KAMINSKI 99 EPJ C9 141 R. Kaminski, L. Lesniak, B. Loiseau (CRAC, PARIN)
ALDE 98 EPJ A3 361 D. Alde et al. (GAM4 Collab.)
Also PAN 62 405 D. Alde et al. (GAMS Collab.)
ANISOVICH 90B SPU 411 419 V.V. Anisovich et al.
BERTIN 98 PR D57 55 A. Bertin et al. (OBELIX Collab.)
BARBERIS 97B PL B413 217 D. Barberis et al. (WA 102 Collab.)
BERTIN 97C PL B408 476 A. Bertin et al. (OBELIX Collab.)
ABELE 96 PL B380 453 A. Abele et al. (Crystal Barrel Collab.)
ABELE 96B PL B385 425 A. Abele et al. (Crystal Barrel Collab.)
ABELE 96C NP A609 562 A. Abele et al. (Crystal Barrel Collab.)
BUGG 96 NP B471 59 D.V. Bugg, A.V. Sarantsev, B.S. Zou (LOQM, PNPI)
AMSLER 95B PL B342 433 C. AMSler et al. (Crystal Barrel Collab.)
AMSLER 95C PL B352 571 C. AMSler et al. (Crystal Barrel Collab.)
AMSLER 95D PL B355 425 C. AMSler et al. (Crystal Barrel Collab.)
JANSSEN 95 PR D52 2690 G. Janssen et al. (STON, ADDL, JULI)
TORNVQUIST 95 ZPHY C68 647 N.A. Tornqvist (HELS)
AMSLER 94 PL B322 431 C. AMSler et al. (Crystal Barrel Collab.) JPC
AMSLER 94D PL B333 277 C. AMSler et al. (Crystal Barrel Collab.)
ANISOVICH 94 PL B323 233 V.V. Anisovich et al. (Crystal Barrel Collab.) JPC
BUGG 94 PR D50 4412 D.V. Bugg et al. (LOQM)
KAMINSKI 94 PR D50 3145 R. Kaminski, L. Lesniak, J.P. Maillet (CRA+)
ADAMO 93 NP A558 13C A. Adamo et al. (OBELIX Collab.) JPC
GASPERO 93 NP A562 407 M. Gaspero (ROMA1) JPC
AMSLER 92 PL B291 347 C. AMSler et al. (Crystal Barrel Collab.)
ARMSTRONG 91 ZPHY C51 351 T.A. Armstrong et al. (ATHU, BARI, BIRM+)
ARMSTRONG 91B ZPHY C52 389 T.A. Armstrong et al. (ATHU, BARI, BIRM+)
BREAKSTONE 90 ZPHY C48 569 A.M. Breakstone et al. (ISU, BGN, CERN+)
MORGAN 90 ZPHY C48 623 D. Morgan, M.R. Pennington (RAL, DURH)
ASTON 88 NP B296 493 D. Aston et al. (SLAC, NAGO, CINC, INUS)
BOLONKIN 88 NP B309 426 B.V. Bolonkin et al. (ITEP, SERP)
FALVARD 88 PR D38 2706 A. Falvard et al. (CLER, FRAS, LALO+)
VOROBYEV 88 SJNP 48 273 P.V. Vorobyev et al. (NOVO)
AU 87 Translated from YAF 48 436 K.L. Au, D. Morgan, M.R. Pennington (DURH, RAL)
AKESSON 86 NP B264 154 T. Akeesson et al. (Axial Field Spec. Collab.)
ALDE 86D NP B269 485 D.M. Alde et al. (BELG, LAPP, SERP, CERN+)
CASON 83 PR D28 1586 N.M. Cason et al. (NDAM, ANL)
ETKIN 82B PR D25 1786 A. Etkin et al. (BNL, CUNY, TUFTS, VAND)
WICKLUND 80 PRL 45 1469 A.B. Wicklund et al. (ANL)
BECKER 79 NP B151 46 H. Becker et al. (MPIM, CERN, ZEEM, CRAC)
POLYCHRONAKOS 79 PR D19 1317 V.A. Polychronakos et al. (NDAM, ANL)
FROGGATT 77 NP B129 89 C.D. Froggatt, J.L. Petersen (GLAS, NORD)
ROSSELET 77 PR D15 574 L. Rosselet et al. (GEVA, SAACL)
GRAYEY 74 NP B75 189 G. Grayey et al. (CERN, MPIM)
HYAMS 73 NP B64 134 B.D. Hyams et al. (CERN, MPIM)
OCHS 73 Thesis W. Ochs (MPIM, MUNI)
BEIER 72B PRL 29 511 E.W. Beier et al. (PENN)
BETTINI 66 NC 42A 695 A. Bettini et al. (PADO, PISA)

See key on page 405

Meson Particle Listings

$h_1(1380)$, $\pi_1(1400)$

$h_1(1380)$ $I^G(J^{PC}) = ?^-(1^{+-})$

OMITTED FROM SUMMARY TABLE
Seen in partial-wave analysis of the $K\bar{K}\pi$ system. Needs confirmation.

$h_1(1380)$ MASS

VALUE (MeV)	DOCUMENT ID	TECN	COMMENT
1386 ± 19 OUR AVERAGE			
1440 ± 60	ABELE 97H	CBAR	$\bar{p}p \rightarrow K_L^0 K_S^0 \pi^0 \pi^0$
1380 ± 20	ASTON 88c	LASS	11 $K^- p \rightarrow K_S^0 K^\pm \pi^\mp \Lambda$

$h_1(1380)$ WIDTH

VALUE (MeV)	DOCUMENT ID	TECN	COMMENT
91 ± 30 OUR AVERAGE	Error includes scale factor of 1.1.		
170 ± 80	ABELE 97H	CBAR	$\bar{p}p \rightarrow K_L^0 K_S^0 \pi^0 \pi^0$
80 ± 30	ASTON 88c	LASS	11 $K^- p \rightarrow K_S^0 K^\pm \pi^\mp \Lambda$

$h_1(1380)$ DECAY MODES

Mode	Γ_1
$K\bar{K}^*(892) + c.c.$	

$h_1(1380)$ REFERENCES

ABELE 97H PL B415 280	A. Abele et al.	(Crystal Barrel Collab.)
ASTON 88C PL B201 573	D. Aston et al.	(SLAC, NAGO, CINC, INUS)

$\pi_1(1400)$ $I^G(J^{PC}) = 1^-(1^{-+})$

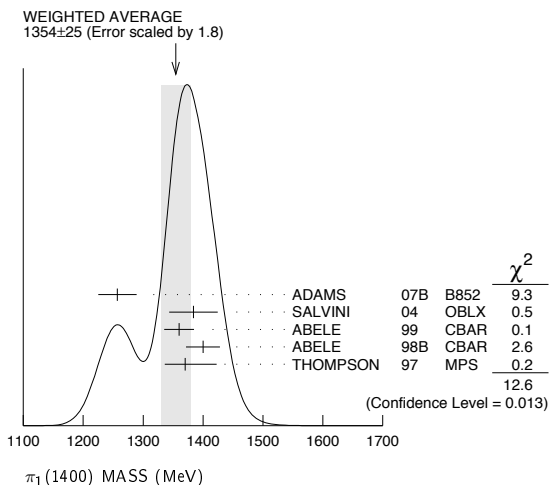
See also the mini-review under non- $q\bar{q}$ candidates in PDG 06, Journal of Physics, G **33** 1 (2006).

$\pi_1(1400)$ MASS

VALUE (MeV)	EVTS	DOCUMENT ID	TECN	CHG	COMMENT
1354 ± 25 OUR AVERAGE					Error includes scale factor of 1.8. See the ideogram below.
1257 ± 20 ± 25	23.5k	ADAMS 07B	B852		18 $\pi^- p \rightarrow \eta \pi^0 n$
1384 ± 20 ± 35	90k	SALVINI 04	OBLX		$\bar{p}p \rightarrow 2\pi^+ 2\pi^-$
1360 ± 25		ABELE 99	CBAR		0.0 $\bar{p}p \rightarrow \pi^0 \pi^0 \eta$
1400 ± 20 ± 20		ABELE 98B	CBAR		0.0 $\bar{p}n \rightarrow \pi^- \pi^0 \eta$
1370 ± 16 ± 50		1 THOMPSON 97	MPS		18 $\pi^- p \rightarrow \eta \pi^- p$
-30					

- • • We do not use the following data for averages, fits, limits, etc. • • •
- 1323.1 ± 4.6 ² AOYAGI 93 BKEI $\pi^- p \rightarrow \eta \pi^- p$
- 1406 ± 20 ³ ALDE 88B GAM4 0 100 $\pi^- p \rightarrow \eta \pi^0 n$

¹ Natural parity exchange, questioned by DZIERBA 03.
² Unnatural parity exchange.
³ Seen in the P_0 -wave intensity of the $\eta \pi^0$ system, unnatural parity exchange.



$\pi_1(1400)$ WIDTH

VALUE (MeV)	EVTS	DOCUMENT ID	TECN	CHG	COMMENT
330 ± 35 OUR AVERAGE					
354 ± 64 ± 58	23.5k	ADAMS 07B	B852		18 $\pi^- p \rightarrow \eta \pi^0 n$
378 ± 50 ± 50	90k	SALVINI 04	OBLX		$\bar{p}p \rightarrow 2\pi^+ 2\pi^-$
220 ± 90		ABELE 99	CBAR		0.0 $\bar{p}p \rightarrow \pi^0 \pi^0 \eta$
310 ± 50 ± 50		ABELE 98B	CBAR		0.0 $\bar{p}n \rightarrow \pi^- \pi^0 \eta$
-30					
385 ± 40 ± 65		⁴ THOMPSON 97	MPS		18 $\pi^- p \rightarrow \eta \pi^- p$
-105					

- • • We do not use the following data for averages, fits, limits, etc. • • •
 - 143.2 ± 12.5 ⁵ AOYAGI 93 BKEI $\pi^- p \rightarrow \eta \pi^- p$
 - 180 ± 20 ⁶ ALDE 88B GAM4 0 100 $\pi^- p \rightarrow \eta \pi^0 n$
- ⁴ Resolution is not unfolded, natural parity exchange, questioned by DZIERBA 03.
⁵ Unnatural parity exchange.
⁶ Seen in the P_0 -wave intensity of the $\eta \pi^0$ system, unnatural parity exchange.

$\pi_1(1400)$ DECAY MODES

Mode	Fraction (Γ_i/Γ)
$\Gamma_1 \eta \pi^0$	seen
$\Gamma_2 \eta \pi^-$	seen
$\Gamma_3 \eta' \pi$	

$\pi_1(1400)$ BRANCHING RATIOS

$\Gamma(\eta \pi^0)/\Gamma_{total}$	DOCUMENT ID	TECN	CHG	COMMENT	Γ_i/Γ
• • •	We do not use the following data for averages, fits, limits, etc. • • •				
not seen	PROKOSHKIN 95B	GAM4		100 $\pi^- p \rightarrow \eta \pi^0 n$	
not seen	⁷ BUGG 94	RVUE		$\bar{p}p \rightarrow \eta 2\pi^0$	
not seen	⁸ APEL 81	NICE 0		40 $\pi^- p \rightarrow \eta \pi^0 n$	

⁷ Using Crystal Barrel data.
⁸ A general fit allowing S, D, and P waves (including $m=0$) is not done because of limited statistics.

$\Gamma(\eta \pi^-)/\Gamma_{total}$	DOCUMENT ID	TECN	COMMENT	Γ_2/Γ
• • •	We do not use the following data for averages, fits, limits, etc. • • •			
possibly seen	BELADIDZE 93	VES	37 $\pi^- N \rightarrow \eta \pi^- N$	

$\Gamma(\eta' \pi)/\Gamma(\eta \pi^0)$	CL%	DOCUMENT ID	TECN	COMMENT	Γ_3/Γ_1
• • •	We do not use the following data for averages, fits, limits, etc. • • •				
< 0.80	95	BOUTEMEUR 90	GAM4	100 $\pi^- p \rightarrow 4\eta n$	

$\pi_1(1400)$ REFERENCES

ADAMS 07B PL B657 27	G.S. Adams et al.	(BNL E852 Collab.)
PDG 06 JPG 33 1	W.-M. Yao et al.	(PDG Collab.)
SALVINI 04 EPJ C35 21	P. Salvini et al.	(OBELIX Collab.)
DZIERBA 03 PR D67 094015	A.R. Dzierba et al.	
ABELE 99 PL B446 349	A. Abele et al.	(Crystal Barrel Collab.)
ABELE 98B PL B423 175	A. Abele et al.	(Crystal Barrel Collab.)
THOMPSON 97 PRL 79 1630	D.R. Thompson et al.	(BNL E852 Collab.)
PROKOSHKIN 95B PAN 58 506	Y.D. Prokoshkin, S.A. Sadovsky	(SERP)
Translated from YAF 58 662.		
BUGG 94 PR D50 4412	D.V. Bugg et al.	(LOQM)
AOYAGI 93 PL B314 246	H. Aoyagi et al.	(BKEI Collab.)
BELADIDZE 93 PL B313 276	G.M. Beladidze et al.	(VES Collab.)
BOUTEMEUR 90 Hadron 89 Conf. p 119	M. Boutemeur, M. Poulet	(SERP, BELG, LANL+)
ALDE 88B PL B205 397	D.M. Alde et al.	(SERP, BELG, LANL, LAPP) IGJPC
APEL 81 NP B193 269	W.D. Apel et al.	(SERP, CERN)

Meson Particle Listings

 $\eta(1405)$ **$\eta(1405)$**

$$J^{G(J^{PC})} = 0^{+(0^{-+})}$$

THE $\eta(1405)$, $\eta(1475)$, $f_1(1420)$, AND $f_1(1510)$

Revised February 2010 by C. Amsler (Zürich) and A. Masoni (INFN Cagliari).

The first observation of the $\eta(1440)$ was made in $p\bar{p}$ annihilation at rest into $\eta(1440)\pi^+\pi^-$, $\eta(1440) \rightarrow K\bar{K}\pi$ [1]. This state was reported to decay through $a_0(980)\pi$ and $K^*(892)\bar{K}$ with roughly equal contributions. The $\eta(1440)$ was also observed in radiative $J/\psi(1S)$ decay into $K\bar{K}\pi$ [2–4] and $\gamma\rho$ [5]. There is now evidence for the existence of two pseudoscalars in this mass region, the $\eta(1405)$ and $\eta(1475)$. The former decays mainly through $a_0(980)\pi$ (or direct $K\bar{K}\pi$) and the latter mainly to $K^*(892)\bar{K}$.

The simultaneous observation of two pseudoscalars is reported in three production mechanisms: π^-p [6,7]; radiative $J/\psi(1S)$ decay [8,9]; and $p\bar{p}$ annihilation at rest [11–14]. All of them give values for the masses, widths, and decay modes in reasonable agreement. However, Ref. [9] favors a state decaying into $K^*(892)\bar{K}$ at a lower mass than the state decaying into $a_0(980)\pi$, although agreement with MARK-III is not excluded. In $J/\psi(1S)$ radiative decay, the $\eta(1405)$ decays into $K\bar{K}\pi$ through $a_0(980)\pi$, and hence a signal is also expected in the $\eta\pi\pi$ mass spectrum. This was indeed observed by MARK III in $\eta\pi^+\pi^-$ [15], which reports a mass of 1400 MeV, in line with the existence of the $\eta(1405)$ decaying into $a_0(980)\pi$. BES [10] reports an enhancement in $K^+K^-\pi^0$ around 1.44 GeV in $J/\psi(1S)$ decay, recoiling against an ω (but not a ϕ) without resolving the presence of two states nor performing a spin-parity analysis, due to low statistics. This state could also be the $f_1(1420)$ (see below).

The $\eta(1405)$ is also observed in $p\bar{p}$ annihilation at rest into $\eta\pi^+\pi^-\pi^0\pi^0$, where it decays into $\eta\pi\pi$ [16]. The intermediate $a_0(980)\pi$ accounts for roughly half of the $\eta\pi\pi$ signal, in agreement with MARK III [15] and DM2 [4].

The $\eta(1295)$ has been observed by four π^-p experiments [7,17–19], and evidence is reported in $p\bar{p}$ annihilation [23–25]. In $J/\psi(1S)$ radiative decay, an $\eta(1295)$ signal is evident in the 0^{-+} $\eta\pi\pi$ wave of the DM2 data [9]. Also BaBar [20] reports evidence for a signal around 1295 MeV in B decays into $\eta\pi\pi K$. However, the existence of the $\eta(1295)$ is questioned in Refs. [21] and [22]. The authors claim a single pseudoscalar meson in the 1400 MeV region. This conclusion is based on properties of the wave functions in the 3P_0 model (and on an unpublished analysis of the annihilation $p\bar{p} \rightarrow 4\pi\eta$). The pseudoscalar signal around 1400 MeV is then attributed to the first radial excitation of the η .

Assuming establishment of the $\eta(1295)$, the $\eta(1475)$ could be the first radial excitation of the η' , with the $\eta(1295)$ being the first radial excitation of the η . Ideal mixing, suggested by the $\eta(1295)$ and $\pi(1300)$ mass degeneracy, would then imply that the second isoscalar in the nonet is mainly $s\bar{s}$, and hence couples to $K^*\bar{K}$, in agreement with properties of the $\eta(1475)$.

Also, its width matches the expected width for the radially excited $s\bar{s}$ state [26,27]. A study of radial excitations of pseudoscalar mesons [28] favors the $s\bar{s}$ interpretation of the $\eta(1475)$. However, due to the strong kinematical suppression the data are not sufficient to exclude a sizeable $s\bar{s}$ admixture also in the $\eta(1405)$.

The $K\bar{K}\pi$ and $\eta\pi\pi$ channels were studied in $\gamma\gamma$ collisions by L3 [29]. The analysis leads to a clear $\eta(1475)$ signal in $K\bar{K}\pi$, decaying into $K^*\bar{K}$, very well identified in the untagged data sample, where contamination from spin 1 resonances is not allowed. At the same time, L3 [29] did not observe the $\eta(1405)$, neither in $K\bar{K}\pi$ nor in $\eta\pi\pi$. The observation of the $\eta(1475)$, combined with the absence of an $\eta(1405)$ signal, strengthens the two-resonances hypothesis. Since gluonium production is presumably suppressed in $\gamma\gamma$ collisions, the L3 results [29] suggest that $\eta(1405)$ has a large gluonic content (see also Refs. [30] and [31]).

The L3 result is somewhat in disagreement with that of CLEO-II, which did not observe any pseudoscalar signal in $\gamma\gamma \rightarrow \eta(1475) \rightarrow K_S^0 K^\pm \pi^\mp$ [32]. However, more data are required. Moreover, after the CLEO-II result, L3 performed a further analysis with full statistics [33], confirming the evidence of the $\eta(1475)$ observed by L3. The CLEO upper limit [32] for $\Gamma_{\gamma\gamma}(\eta(1475))$, and the L3 results [33], are consistent with the world average for the $\eta(1475)$ width.

BaBar [20] also reports the $\eta(1475)$ in B decays into $K\bar{K}\pi$ (and possibly $\eta\pi\pi$). Upper limits are given for $\eta(1405)$ decay into $K\bar{K}^*$. The data sample is not sufficient to identify a possible $\eta(1405)$ contribution into $\eta\pi\pi$.

The gluonium interpretation for the $\eta(1405)$ is not favored by lattice gauge theories which predict the 0^{-+} state above 2 GeV [34]. However, the $\eta(1405)$ is an excellent candidate for the 0^{-+} glueball in the fluxtube model [35]. In this model, the 0^{++} $f_0(1500)$ glueball is also naturally related to a 0^{-+} glueball with mass degeneracy broken in QCD. Also, Ref. [36] shows that the pseudoscalar glueball could lie at a lower mass than predicted from lattice calculation. In this model the $\eta(1405)$ appears as the natural glueball candidate (see also Refs. [37] and [38]). A detailed review of the experimental situation is available in Ref. [39].

Let us now deal with 1^{++} isoscalars. The $f_1(1420)$, decaying into $K^*\bar{K}$, was first reported in π^-p reactions at 4 GeV/c [40]. However, later analyses found that the 1400–1500 MeV region was far more complex [41–43]. A reanalysis of the MARK III data in radiative $J/\psi(1S)$ decay into $K\bar{K}\pi$ [8] shows the $f_1(1420)$ decaying into $K^*\bar{K}$. Also, a $C=+1$ state is observed in tagged $\gamma\gamma$ collisions (*e.g.*, Ref. [44]).

In $\pi^-p \rightarrow \eta\pi\pi n$ charge-exchange reactions at 8–9 GeV/c the $\eta\pi\pi$ mass spectrum is dominated by the $\eta(1440)$ and $\eta(1295)$ [17,45], and at 100 GeV/c Ref. [18] reports the $\eta(1295)$ and $\eta(1440)$ decaying into $\eta\pi^0\pi^0$ with a weak $f_1(1285)$ signal, and no evidence for the $f_1(1420)$.

Axial (1^{++}) mesons are not observed in $\bar{p}p$ annihilation at rest in liquid hydrogen, which proceeds dominantly through S -wave annihilation. However, in gaseous hydrogen, P -wave annihilation is enhanced and, indeed, Ref. [12] reports $f_1(1420)$ decaying into $K^*\bar{K}$. The $f_1(1420)$, decaying into $K\bar{K}\pi$, is also seen in pp central production, together with the $f_1(1285)$. The latter decays via $a_0(980)\pi$, and the former only via $K^*\bar{K}$, while the $\eta(1440)$ is absent [46,47]. The $K_S K_S \pi^0$ decay mode of the $f_1(1420)$ establishes unambiguously $C=+1$. On the other hand, there is no evidence for any state decaying into $\eta\pi\pi$ around 1400 MeV, and hence the $\eta\pi\pi$ mode of the $f_1(1420)$ must be suppressed [48].

We now turn to the experimental evidence for the $f_1(1510)$. Two states, the $f_1(1420)$ and $f_1(1510)$, decaying into $K^*\bar{K}$, compete for the $s\bar{s}$ assignment in the 1^{++} nonet. The $f_1(1510)$ was seen in $K^-p \rightarrow \Lambda K\bar{K}\pi$ at 4 GeV/c [49], and at 11 GeV/c [50]. Evidence is also reported in π^-p at 8 GeV/c, based on the phase motion of the 1^{++} $K^*\bar{K}$ wave [43]. A somewhat broader 1^{++} signal is also observed in $J/\psi(1S)$ radiative decay into $\eta\pi^+\pi^-$ [51].

The absence of $f_1(1420)$ in K^-p [50] argues against the $f_1(1420)$ being the $s\bar{s}$ member of the 1^{++} nonet. However, the $f_1(1420)$ was reported in K^-p but not in π^-p [52], while two experiments do not observe the $f_1(1510)$ in K^-p [52,53]. The latter is also not seen in radiative $J/\psi(1S)$ decay [8,9] and possibly [10], central collisions [47], or $\gamma\gamma$ collisions [54], although, surprisingly for an $s\bar{s}$ state, a signal is reported in 4π decays [55]. These facts lead to the conclusion that $f_1(1510)$ is not well established [56].

Assigning the $f_1(1420)$ to the 1^{++} nonet, one finds a nonet mixing angle of $\sim 50^\circ$ [56]. However, arguments favoring the $f_1(1420)$ being a hybrid $q\bar{q}g$ meson, or a four-quark state, were put forward in Refs. [57] and [58], respectively, while Ref. [59] argued for a molecular state formed by the π orbiting in a P -wave around an S -wave $K\bar{K}$ state.

Summarizing, there is convincing evidence for the $f_1(1420)$ decaying into $K^*\bar{K}$, and for two pseudoscalars in the $\eta(1440)$ region, the $\eta(1405)$ and $\eta(1475)$, decaying into $a_0(980)\pi$ and $K^*\bar{K}$, respectively. The $f_1(1510)$ is not well established.

References

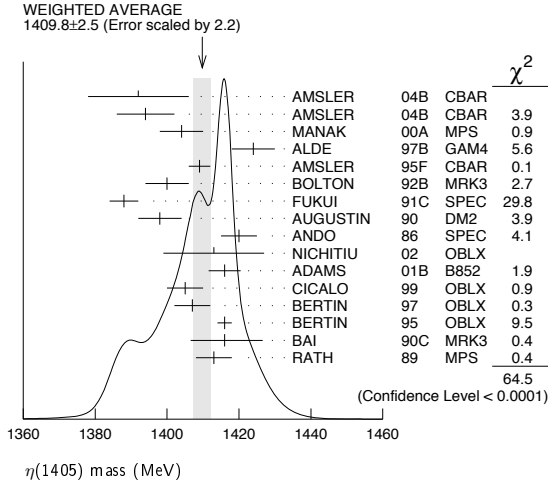
1. P.H. Baillon *et al.*, Nuovo Cimento **50A**, 393 (1967).
2. D.L. Scharre *et al.*, Phys. Lett. **97B**, 329 (1980).
3. C. Edwards *et al.*, Phys. Rev. Lett. **49**, 259 (1982).
4. J.E. Augustin *et al.*, Phys. Rev. **D42**, 10 (1990).
5. J.Z. Bai *et al.*, Phys. Lett. **B594**, 47 (2004).
6. M.G. Rath *et al.*, Phys. Rev. **D40**, 693 (1989).
7. T. Adams *et al.*, Phys. Rev. Lett. **87**, 041801 (2001).
8. J.Z. Bai *et al.*, Phys. Rev. Lett. **65**, 2507 (1990).
9. J.E. Augustin and G. Cosme, Phys. Rev. **D46**, 1951 (1992).
10. M. Ablikim *et al.*, Phys. Rev. **D77**, 032005 (2008).
11. A. Bertin *et al.*, Phys. Lett. **B361**, 187 (1995).
12. A. Bertin *et al.*, Phys. Lett. **B400**, 226 (1997).
13. C. Cicalo *et al.*, Phys. Lett. **B462**, 453 (1999).
14. F. Nichitiu *et al.*, Phys. Lett. **B545**, 261 (2002).
15. T. Bolton *et al.*, Phys. Rev. Lett. **69**, 1328 (1992).
16. C. Amsler *et al.*, Phys. Lett. **B358**, 389 (1995).
17. S. Fukui *et al.*, Phys. Lett. **B267**, 293 (1991).
18. D. Alde *et al.*, Phys. Atom. Nucl. **60**, 386 (1997).
19. J.J. Manak *et al.*, Phys. Rev. **D62**, 012003 (2000).
20. B. Aubert *et al.*, Phys. Rev. Lett. **101**, 091801 (2008).
21. E. Klempt, Int. J. Mod. Phys. **A21**, 739 (2006).
22. E. Klempt and A. Zaitsev, Phys. Reports **454**, 1 (2007).
23. A.V. Anisovich *et al.*, Nucl. Phys. **A690**, 567 (2001).
24. A. Abele *et al.*, Phys. Rev. **D57**, 3860 (1998).
25. C. Amsler *et al.*, Eur. Phys. J. **C33**, 23 (2004).
26. F. Close *et al.*, Phys. Lett. **B397**, 333 (1997).
27. T. Barnes *et al.*, Phys. Rev. **D55**, 4157 (1997).
28. T. Gutsche *et al.*, Phys. Rev. **D79**, 014036 (2009).
29. M. Acciarri *et al.*, Phys. Lett. **B501**, 1 (2001).
30. F. Close *et al.*, Phys. Rev. **D55**, 5749 (1997).
31. D.M. Li *et al.*, Eur. Phys. J. **C28**, 335 (2003).
32. R. Ahohe *et al.*, Phys. Rev. **D71**, 072001 (2005).
33. P. Achard *et al.*, JHEP **0703**, 018 (2007).
34. G.S. Bali *et al.*, Phys. Lett. **B309**, 378 (1993).
35. L. Faddeev *et al.*, Phys. Rev. **D70**, 114033 (2004).
36. H.-Y. Cheng *et al.*, Phys. Rev. **D79**, 014024 (2009).
37. G. Li *et al.*, J. Phys. G: Nucl. Part. Phys. **35**, 055002 (2008).
38. T. Gutsche *et al.*, Phys. Rev. **D80**, 014014 (2009).
39. A. Masoni, C. Cicalo, and G.L. Usai, J. Phys. **G32**, R293 (2006).
40. C. Dionisi *et al.*, Nucl. Phys. **B169**, 1 (1980).
41. S.U. Chung *et al.*, Phys. Rev. Lett. **55**, 779 (1985).
42. D.F. Reeves *et al.*, Phys. Rev. **D34**, 1960 (1986).
43. A. Birman *et al.*, Phys. Rev. Lett. **61**, 1557 (1988).
44. H.J. Behrend *et al.*, Z. Phys. **C42**, 367 (1989).
45. A. Ando *et al.*, Phys. Rev. Lett. **57**, 1296 (1986).
46. T.A. Armstrong *et al.*, Phys. Lett. **B221**, 216 (1989).
47. D. Barberis *et al.*, Phys. Lett. **B413**, 225 (1997).
48. T.A. Armstrong *et al.*, Z. Phys. **C52**, 389 (1991).
49. P. Gavillet *et al.*, Z. Phys. **C16**, 119 (1982).
50. D. Aston *et al.*, Phys. Lett. **B201**, 573 (1988).
51. J.Z. Bai *et al.*, Phys. Lett. **B446**, 356 (1999).
52. S. Bitukov *et al.*, Sov. J. Nucl. Phys. **39**, 738 (1984).
53. E. King *et al.*, Nucl. Phys. (Proc. Supp.) **B21**, 11 (1991).
54. H. Aihara *et al.*, Phys. Rev. **D38**, 1 (1988).
55. D.A. Bauer *et al.*, Phys. Rev. **D48**, 3976 (1993).
56. F.E. Close and A. Kirk, Z. Phys. **C76**, 469 (1997).
57. S. Ishida *et al.*, Prog. Theor. Phys. **82**, 119 (1989).
58. D.O. Caldwell, *Hadron 89 Conf.*, p. 127.
59. R.S. Longacre, Phys. Rev. **D42**, 874 (1990).

Meson Particle Listings

$\eta(1405)$

$\eta(1405)$ MASS

1409.8 ± 2.5 OUR AVERAGE Includes data from the 2 datablocks that follow this one. Error includes scale factor of 2.2. See the ideogram below.

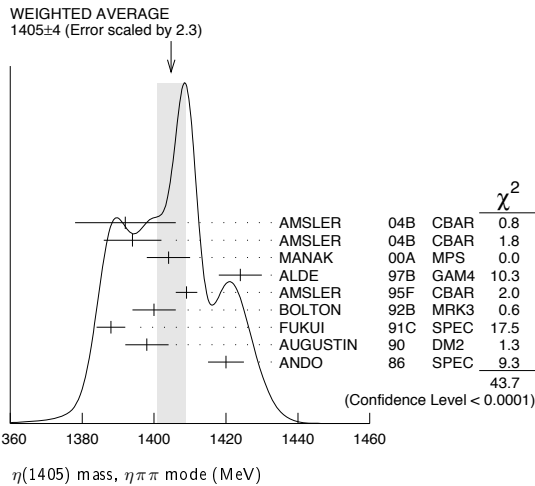


$\eta\pi\pi$ MODE

The data in this block is included in the average printed for a previous datablock.

1405 ± 4 OUR AVERAGE Error includes scale factor of 2.3. See the ideogram below.

VALUE (MeV)	EVTs	DOCUMENT ID	TECN	COMMENT
1392 ± 14	900 ± 375	AMSLER 04B CBAR	04B CBAR	$0 \bar{p}p \rightarrow \pi^+\pi^-\pi^+\pi^- \eta$
1394 ± 8	6.6 ± 2.0k	AMSLER 04B CBAR	04B CBAR	$0 \bar{p}p \rightarrow \pi^+\pi^-\pi^0\pi^0 \eta$
1404 ± 6	9082	MANAK 00A MPS	00A MPS	$18 \pi^-p \rightarrow \eta\pi^+\pi^- n$
1424 ± 6	2200	ALDE 97B GAM4	97B GAM4	$100 \pi^-p \rightarrow \eta\pi^0\pi^0 n$
1409 ± 3		AMSLER 95F CBAR	95F CBAR	$0 \bar{p}p \rightarrow \pi^+\pi^-\pi^0\pi^0 \eta$
1400 ± 6		1 BOLTON 92B MRK3	92B MRK3	$J/\psi \rightarrow \gamma\eta\pi^+\pi^-$
1388 ± 4		FUKUI 91C SPEC	91C SPEC	$8.95 \pi^-p \rightarrow \eta\pi^+\pi^- n$
1398 ± 6	261	2 AUGUSTIN 90 DM2	90 DM2	$J/\psi \rightarrow \gamma\eta\pi^+\pi^-$
1420 ± 5		ANDO 86 SPEC	86 SPEC	$8 \pi^-p \rightarrow \eta\pi^+\pi^- n$
• • • We do not use the following data for averages, fits, limits, etc. • • •				
1385 ± 7		BAI 99 BES	99 BES	$J/\psi \rightarrow \gamma\eta\pi^+\pi^-$



$K\bar{K}\pi$ MODE ($a_0(980)\pi$ or direct $K\bar{K}\pi$)

The data in this block is included in the average printed for a previous datablock.

1413.9 ± 1.7 OUR AVERAGE Error includes scale factor of 1.1.

VALUE (MeV)	EVTs	DOCUMENT ID	TECN	COMMENT
1413 ± 14	3651	3 NICHITIU 02 OBLX	02 OBLX	
1416 ± 4 ± 2	20k	ADAMS 01B B852	01B B852	$18 \text{ GeV } \pi^-p \rightarrow K^+K^-\pi^0 n$
1405 ± 5		4 CICALO 99 OBLX	99 OBLX	$0 \bar{p}p \rightarrow K^\pm K_S^0 \pi^\mp \pi^+\pi^-$
1407 ± 5		4 BERTIN 97 OBLX	97 OBLX	$0 \bar{p}p \rightarrow K^\pm(K^0)\pi^\mp \pi^+\pi^-$
1416 ± 2		4 BERTIN 95 OBLX	95 OBLX	$0 \bar{p}p \rightarrow K\bar{K}\pi\pi\pi$
1416 ± 8 $\frac{+7}{-5}$	700	5 BAI 90C MRK3	90C MRK3	$J/\psi \rightarrow \gamma K_S^0 K^\pm \pi^\mp$
1413 ± 5		5 RATH 89 MPS	89 MPS	$21.4 \pi^-p \rightarrow n K_S^0 K_S^0 \pi^0$
• • • We do not use the following data for averages, fits, limits, etc. • • •				
1459 ± 5		6 AUGUSTIN 92 DM2	92 DM2	$J/\psi \rightarrow \gamma K\bar{K}\pi$

$\pi\pi\gamma$ MODE

VALUE (MeV)	EVTs	DOCUMENT ID	TECN	COMMENT
1390 ± 12	235 ± 91	AMSLER 04B CBAR	04B CBAR	$0 \bar{p}p \rightarrow \pi^+\pi^-\pi^+\pi^-\gamma$
• • • We do not use the following data for averages, fits, limits, etc. • • •				
1424 ± 10 ± 11	547	BAI 04J BES2	04J BES2	$J/\psi \rightarrow \gamma\gamma\pi^+\pi^-$
1401 ± 18		7,8 AUGUSTIN 90 DM2	90 DM2	$J/\psi \rightarrow \pi^+\pi^-\gamma\gamma$
1432 ± 8		8 COFFMAN 90 MRK3	90 MRK3	$J/\psi \rightarrow \pi^+\pi^-\gamma\gamma$

4π MODE

VALUE (MeV)	EVTs	DOCUMENT ID	TECN	COMMENT
1420 ± 20		BUGG 95 MRK3	95 MRK3	$J/\psi \rightarrow \gamma\pi^+\pi^-\pi^+\pi^-$
1489 ± 12	3270	9 BISELLO 89B DM2	89B DM2	$J/\psi \rightarrow 4\pi\gamma$

$K\bar{K}\pi$ MODE (unresolved)

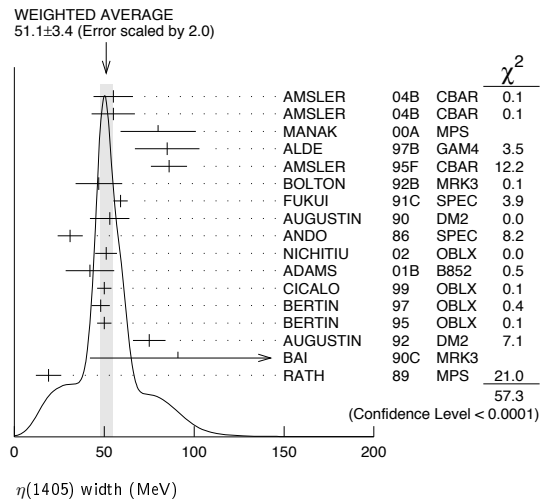
• • • We do not use the following data for averages, fits, limits, etc. • • •

VALUE (MeV)	EVTs	DOCUMENT ID	TECN	COMMENT
1437.6 ± 3.2	249 ± 35	10,11 ABLIKIM 08E BES2	08E BES2	$J/\psi \rightarrow \omega K_S^0 K^+\pi^- + c.c.$
1445.9 ± 5.7	62 ± 18	10,11 ABLIKIM 08E BES2	08E BES2	$J/\psi \rightarrow \omega K^+K^-\pi^0$
1442 ± 10	410	10 BAI 98C BES	98C BES	$J/\psi \rightarrow \gamma K^+K^-\pi^0$
1445 ± 8	693	10 AUGUSTIN 90 DM2	90 DM2	$J/\psi \rightarrow \gamma K_S^0 K^\pm \pi^\mp$
1433 ± 8	296	10 AUGUSTIN 90 DM2	90 DM2	$J/\psi \rightarrow \gamma K^+K^-\pi^0$
1413 ± 8	500	10 DUCH 89 ASTE	89 ASTE	$\bar{p}p \rightarrow \pi^+\pi^-\pi^\pm \pi^\mp K^0$
1453 ± 7	170	10 RATH 89 MPS	89 MPS	$21.4 \pi^-p \rightarrow K_S^0 K_S^0 \pi^0 n$
1419 ± 1	8800	10 BIRMAN 88 MPS	88 MPS	$8 \pi^-p \rightarrow K^+K^0 \pi^- n$
1424 ± 3	620	10 REEVES 86 SPEC	86 SPEC	$6.6 p\bar{p} \rightarrow K\bar{K}\pi X$
1421 ± 2		10 CHUNG 85 SPEC	85 SPEC	$8 \pi^-p \rightarrow K\bar{K}\pi n$
1440 $\frac{+20}{-15}$	174	10 EDWARDS 82E CBAL	82E CBAL	$J/\psi \rightarrow \gamma K^+K^-\pi^0$
1440 $\frac{+10}{-15}$		10 SCHARRE 80 MRK2	80 MRK2	$J/\psi \rightarrow \gamma K_S^0 K^\pm \pi^\mp$
1425 ± 7	800	10,12 BAILLON 67 HBC	67 HBC	$0 \bar{p}p \rightarrow K\bar{K}\pi\pi\pi$

- From fit to the $a_0(980)\pi^0$ partial wave.
- Best fit with a single Breit Wigner.
- Decaying dominantly directly to $K^+K^-\pi^0$.
- Decaying into $(K\bar{K})_S\pi$, $(K\pi)_S\bar{K}$, and $a_0(980)\pi$.
- From fit to the $a_0(980)\pi^0$ partial wave. Cannot rule out a $a_0(980)\pi^1$ partial wave.
- Excluded from averaging because averaging would be meaningless.
- Best fit with a single Breit Wigner.
- This peak in the $\gamma\rho$ channel may not be related to the $\eta(1405)$.
- Estimated by us from various fits.
- These experiments identify only one pseudoscalar in the 1400–1500 range. Data could also refer to $\eta(1475)$.
- Systematic uncertainty not evaluated.
- From best fit of $0^-\pi^+$ partial wave, 50% $K^*(892)K$, 50% $a_0(980)\pi$.

$\eta(1405)$ WIDTH

51.1 ± 3.4 OUR AVERAGE Includes data from the 2 datablocks that follow this one. Error includes scale factor of 2.0. See the ideogram below.



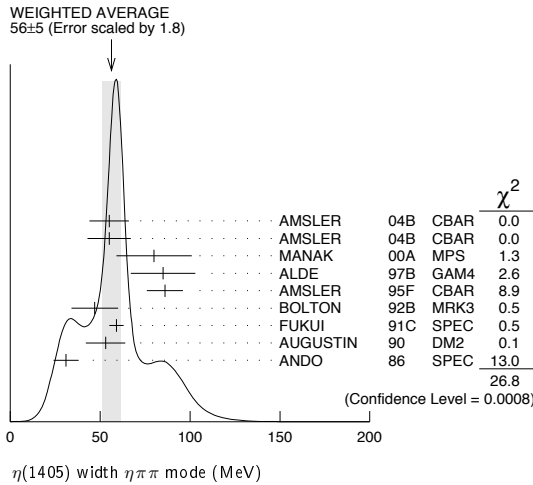
$\eta\pi\pi$ MODE

VALUE (MeV)	EVTs	DOCUMENT ID	TECN	COMMENT
-------------	------	-------------	------	---------

The data in this block is included in the average printed for a previous datablock.

56 ± 5 OUR AVERAGE Error includes scale factor of 1.8. See the ideogram below.

55 ± 11	900 ± 375	AMSLER	04B CBAR	$0 \bar{p}p \rightarrow \pi^+\pi^-\pi^+\pi^-\eta$
55 ± 12	6.6 ± 2.0k	AMSLER	04B CBAR	$0 \bar{p}p \rightarrow \pi^+\pi^-\pi^0\pi^0\gamma$
80 ± 21	9082	MANAK	00A MPS	$18 \pi^-\rho \rightarrow \eta\pi^+\pi^-\eta$
85 ± 18	2200	ALDE	97B GAM4	$100 \pi^-\rho \rightarrow \eta\pi^0\pi^0\eta$
86 ± 10		AMSLER	95F CBAR	$0 \bar{p}p \rightarrow \pi^+\pi^-\pi^0\pi^0\eta$
47 ± 13		13 BOLTON	92B MRK3	$J/\psi \rightarrow \gamma\eta\pi^+\pi^-$
59 ± 4		FUKUI	91C SPEC	$8.95 \pi^-\rho \rightarrow \eta\pi^+\pi^-\eta$
53 ± 11		14 AUGUSTIN	90 DM2	$J/\psi \rightarrow \gamma\eta\pi^+\pi^-$
31 ± 7		ANDO	86 SPEC	$8 \pi^-\rho \rightarrow \eta\pi^+\pi^-\eta$



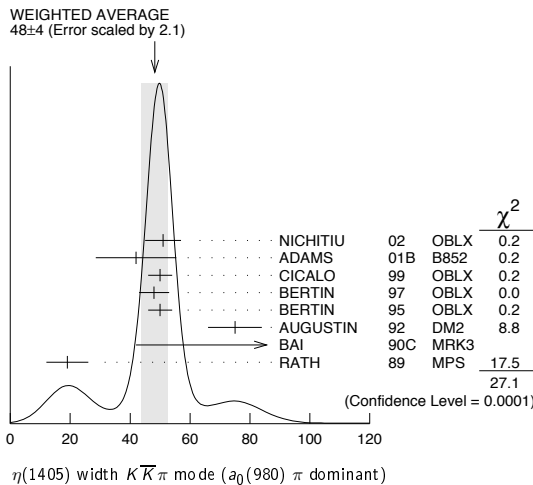
$K\bar{K}\pi$ MODE ($a_0(980)\pi$ or direct $K\bar{K}\pi$)

VALUE (MeV)	EVTs	DOCUMENT ID	TECN	COMMENT
-------------	------	-------------	------	---------

The data in this block is included in the average printed for a previous datablock.

48 ± 4 OUR AVERAGE Error includes scale factor of 2.1. See the ideogram below.

51 ± 6	3651	15 NICHITIU	02 OBLX	
42 ± 10 ± 9	20k	ADAMS 01B	B852	$18 \text{ GeV } \pi^-\rho \rightarrow K^+K^-\pi^0\eta$
50 ± 4		CICALO 99	OBLX	$0 \bar{p}p \rightarrow K^\pm K_S^0 \pi^\mp \pi^+\pi^-$
48 ± 5		16 BERTIN 97	OBLX	$0.0 \bar{p}p \rightarrow K^\pm(K^0)\pi^\mp \pi^+\pi^-$
50 ± 4		16 BERTIN 95	OBLX	$0 \bar{p}p \rightarrow K\bar{K}\pi\pi\pi$
75 ± 9		AUGUSTIN 92	DM2	$J/\psi \rightarrow \gamma K\bar{K}\pi$
91 ± $\frac{67}{31} \pm \frac{15}{38}$		17 BAI 90C	MRK3	$J/\psi \rightarrow \gamma K_S^0 K^\pm \pi^\mp$
19 ± 7		17 RATH 89	MPS	$21.4 \pi^-\rho \rightarrow \eta K_S^0 K_S^0 \pi^0$



$\pi\pi\gamma$ MODE

VALUE (MeV)	EVTs	DOCUMENT ID	TECN	COMMENT
-------------	------	-------------	------	---------

64 ± 18 235 ± 91 AMSLER 04B CBAR $0 \bar{p}p \rightarrow \pi^+\pi^-\pi^+\pi^-\gamma$

• • • We do not use the following data for averages, fits, limits, etc. • • •

101.0 ± 8.8 ± 8.8	547	BAI	04J BES2	$J/\psi \rightarrow \gamma\gamma\pi^+\pi^-$
174 ± 44		AUGUSTIN 90	DM2	$J/\psi \rightarrow \pi^+\pi^-\gamma\gamma$
90 ± 26		18 COFFMAN 90	MRK3	$J/\psi \rightarrow \pi^+\pi^-\gamma\gamma$

4 π MODE

VALUE (MeV)	EVTs	DOCUMENT ID	TECN	COMMENT
-------------	------	-------------	------	---------

• • • We do not use the following data for averages, fits, limits, etc. • • •

160 ± 30		BUGG 95	MRK3	$J/\psi \rightarrow \gamma\pi^+\pi^-\pi^+\pi^-$
144 ± 13	3270	19 BISELLO 89B	DM2	$J/\psi \rightarrow 4\pi\gamma$

$K\bar{K}\pi$ MODE (unresolved)

VALUE (MeV)	EVTs	DOCUMENT ID	TECN	COMMENT
-------------	------	-------------	------	---------

• • • We do not use the following data for averages, fits, limits, etc. • • •

48.9 ± 9.0	249 ± 35	20,21 ABLIKIM 08E	BES2	$J/\psi \rightarrow \omega K_S^0 K^+\pi^- + c.c.$
34.2 ± 18.5	62 ± 18	20,21 ABLIKIM 08E	BES2	$J/\psi \rightarrow \omega K^+K^-\pi^0$
93 ± 14	296	20 AUGUSTIN 90	DM2	$J/\psi \rightarrow \gamma K^+K^-\pi^0$
105 ± 10	693	20 AUGUSTIN 90	DM2	$J/\psi \rightarrow \gamma K_S^0 K^\pm \pi^\mp$
62 ± 16	500	20 DUCH 89	ASTE	$\bar{p}p \rightarrow K\bar{K}\pi\pi\pi$
100 ± 11	170	20 RATH 89	MPS	$21.4 \pi^-\rho \rightarrow K_S^0 K_S^0 \pi^0\eta$
66 ± 2	8800	20 BIRMAN 88	MPS	$8 \pi^-\rho \rightarrow K^+\bar{K}^0\pi^-\eta$
60 ± 10	620	20 REEVES 86	SPEC	$6.6 p\bar{p} \rightarrow K K \pi X$
60 ± 10		20 CHUNG 85	SPEC	$8 \pi^-\rho \rightarrow K\bar{K}\pi\eta$
55 +20 -30	174	20 EDWARDS 82E	CBAL	$J/\psi \rightarrow \gamma K^+K^-\pi^0$
50 +30 -20		20 SCHARRE 80	MRK2	$J/\psi \rightarrow \gamma K_S^0 K^\pm \pi^\mp$
80 ± 10	800	20,22 BAILLON 67	HBC	$0.0 \bar{p}p \rightarrow K\bar{K}\pi\pi\pi$

- 13 From fit to the $a_0(980)\pi 0^+$ partial wave.
- 14 From $\eta\pi^+\pi^-$ mass distribution - mainly $a_0(980)\pi$ - no spin-parity determination available.
- 15 Decaying dominantly directly to $K^+K^-\pi^0$.
- 16 Decaying into $(K\bar{K})_S\pi$, $(K\pi)_S\bar{K}$, and $a_0(980)\pi$.
- 17 From fit to the $a_0(980)\pi 0^+$ partial wave, but $a_0(980)\pi 1^+$ cannot be excluded.
- 18 This peak in the $\gamma\rho$ channel may not be related to the $\eta(1405)$.
- 19 Estimated by us from various fits.
- 20 These experiments identify only one pseudoscalar in the 1400-1500 range. Data could also refer to $\eta(1475)$.
- 21 Systematic uncertainty not evaluated.
- 22 From best fit to 0^+ partial wave, 50% $K^*(892)K$, 50% $a_0(980)\pi$.

$\eta(1405)$ DECAY MODES

Mode	Fraction (Γ_i/Γ)	Confidence level
Γ_1 $K\bar{K}\pi$	seen	
Γ_2 $\eta\pi\pi$	seen	
Γ_3 $a_0(980)\pi$	seen	
Γ_4 $\eta(\pi\pi)_S$ -wave	seen	
Γ_5 $f_0(980)\eta$	seen	
Γ_6 4π	seen	
Γ_7 $\rho\rho$	<58 %	99.85%
Γ_8 $\gamma\gamma$		
Γ_9 $\rho^0\gamma$	seen	
Γ_{10} $\phi\gamma$		
Γ_{11} $K^*(892)K$	seen	

$\eta(1405)$ $\Gamma(i)\Gamma(\gamma\gamma)/\Gamma(\text{total})$

VALUE (keV)	CL%	DOCUMENT ID	TECN	COMMENT
-------------	-----	-------------	------	---------

• • • We do not use the following data for averages, fits, limits, etc. • • •

<0.035	90	23,24 AHOHE 05	CLE2	$10.6 e^+e^- \rightarrow e^+e^- K_S^0 K^\pm \pi^\mp$
--------	----	----------------	------	--

VALUE (keV)	CL%	DOCUMENT ID	TECN	COMMENT
-------------	-----	-------------	------	---------

$\Gamma(\eta\pi\pi) \times \Gamma(\gamma\gamma)/\Gamma(\text{total})$ $\Gamma_2\Gamma_8/\Gamma$

<0.095	95	ACCIARRI 01G	L3	$183-202 e^+e^- \rightarrow e^+e^-\eta\pi^+\pi^-$
--------	----	--------------	----	---

VALUE (keV)	CL%	DOCUMENT ID	TECN	COMMENT
-------------	-----	-------------	------	---------

$\Gamma(\rho^0\gamma) \times \Gamma(\gamma\gamma)/\Gamma(\text{total})$ $\Gamma_9\Gamma_8/\Gamma$

• • • We do not use the following data for averages, fits, limits, etc. • • •

<1.5	95	ALTHOFF 84E	TASS	$e^+e^- \rightarrow e^+e^-\pi^+\pi^-\gamma$
------	----	-------------	------	---

23 Using $\eta(1405)$ mass and width 1410 MeV and 51 MeV, respectively.
24 Assuming three-body phase-space decay to $K_S^0 K^\pm \pi^\mp$.

$\eta(1405)$ BRANCHING RATIOS

VALUE	CL%	DOCUMENT ID	TECN	COMMENT
-------	-----	-------------	------	---------

• • • We do not use the following data for averages, fits, limits, etc. • • •

1.09 ± 0.48		25 AMSLER 04B	CBAR	$0 \bar{p}p \rightarrow \pi^+\pi^-\pi^+\pi^-\eta$
<0.5	90	EDWARDS 83B	CBAL	$J/\psi \rightarrow \eta\pi\pi\gamma$
<1.1	90	SCHARRE 80	MRK2	$J/\psi \rightarrow \eta\pi\pi\gamma$
<1.5	95	FOSTER 68B	HBC	$0.0 \bar{p}p$

Meson Particle Listings

 $\omega(1420)$ $\omega(1420)$

$$J^{PC} = 0^{-}(1^{-}-)$$

 $\omega(1420)$ MASS

VALUE (MeV)	EVTS	DOCUMENT ID	TECN	COMMENT
(1400-1450) OUR ESTIMATE				
• • •	We do not use the following data for averages, fits, limits, etc. • • •			
1382 ± 23 ± 70		AUBERT	07AU BABR	10.6 e ⁺ e ⁻ → ωπ ⁺ π ⁻ γ
1350 ± 20 ± 20		AUBERT,B	04N BABR	10.6 e ⁺ e ⁻ → π ⁺ π ⁻ π ⁰ γ
1400 ± 50 ± 130	1.2M	¹ ACHASOV	03D RVUE	0.44-2.00 e ⁺ e ⁻ → π ⁺ π ⁻ π ⁰
1450 ± 10		² HENNER	02 RVUE	1.2-2.0 e ⁺ e ⁻ → ρπ, ωππ
1373 ± 70	177	³ AKHMETSHIN	00D CMD2	1.2-1.38 e ⁺ e ⁻ → ωπ ⁺ π ⁻
1370 ± 25	5095	ANISOVICH	00H SPEC	0.0 p \bar{p} → ωπ ⁰ π ⁰ π ⁰
1400 ⁺¹⁰⁰ ₋₂₀₀		⁴ ACHASOV	98H RVUE	e ⁺ e ⁻ → π ⁺ π ⁻ π ⁰
~ 1400		⁵ ACHASOV	98H RVUE	e ⁺ e ⁻ → ωπ ⁺ π ⁻
~ 1460		⁶ ACHASOV	98H RVUE	e ⁺ e ⁻ → K ⁺ K ⁻
1440 ± 70		⁷ CLEGG	94 RVUE	
1419 ± 31	315	⁸ ANTONELLI	92 DM2	1.34-2.4e ⁺ e ⁻ → ρπ

¹ From the combined fit of ANTONELLI 92, ACHASOV 01E, ACHASOV 02E, and ACHASOV 03D data on the π⁺π⁻π⁰ and ANTONELLI 92 on the ωπ⁺π⁻ final states. Supersedes ACHASOV 99E and ACHASOV 02E.

² Using results of CORDIER 81 and preliminary data of DOLINSKY 91 and ANTONELLI 92.

³ Using the data of AKHMETSHIN 00D and ANTONELLI 92. The ρπ dominance for the energy dependence of the ω(1420) and ω(1650) width assumed.

⁴ Using data from BARKOV 87, DOLINSKY 91, and ANTONELLI 92.

⁵ Using the data from ANTONELLI 92.

⁶ Using the data from IVANOV 81 and BISELLO 88b.

⁷ From a fit to two Breit-Wigner functions and using the data of DOLINSKY 91 and ANTONELLI 92.

⁸ From a fit to two Breit-Wigner functions interfering between them and with the ω,φ tails with fixed (+,-,+) phases.

 $\omega(1420)$ WIDTH

VALUE (MeV)	EVTS	DOCUMENT ID	TECN	COMMENT
(180-250) OUR ESTIMATE				
• • •	We do not use the following data for averages, fits, limits, etc. • • •			
130 ± 50 ± 100		AUBERT	07AU BABR	10.6 e ⁺ e ⁻ → ωπ ⁺ π ⁻ γ
450 ± 70 ± 70		AUBERT,B	04N BABR	10.6 e ⁺ e ⁻ → π ⁺ π ⁻ π ⁰ γ
870 ⁺⁵⁰⁰ ₋₃₀₀ ± 450	1.2M	⁹ ACHASOV	03D RVUE	0.44-2.00 e ⁺ e ⁻ → π ⁺ π ⁻ π ⁰
199 ± 15		¹⁰ HENNER	02 RVUE	1.2-2.0 e ⁺ e ⁻ → ρπ, ωππ
188 ± 45	177	¹¹ AKHMETSHIN	00D CMD2	1.2-1.38 e ⁺ e ⁻ → ωπ ⁺ π ⁻
360 ⁺¹⁰⁰ ₋₆₀	5095	ANISOVICH	00H SPEC	0.0 p \bar{p} → ωπ ⁰ π ⁰ π ⁰
240 ± 70		¹² CLEGG	94 RVUE	
174 ± 59	315	¹³ ANTONELLI	92 DM2	1.34-2.4e ⁺ e ⁻ → ρπ

⁹ From the combined fit of ANTONELLI 92, ACHASOV 01E, ACHASOV 02E, and ACHASOV 03D data on the π⁺π⁻π⁰ and ANTONELLI 92 on the ωπ⁺π⁻ final states. Supersedes ACHASOV 99E and ACHASOV 02E.

¹⁰ Using results of CORDIER 81 and preliminary data of DOLINSKY 91 and ANTONELLI 92.

¹¹ Using the data of AKHMETSHIN 00D and ANTONELLI 92. The ρπ dominance for the energy dependence of the ω(1420) and ω(1650) width assumed.

¹² From a fit to two Breit-Wigner functions and using the data of DOLINSKY 91 and ANTONELLI 92.

¹³ From a fit to two Breit-Wigner functions interfering between them and with the ω,φ tails with fixed (+,-,+) phases.

 $\omega(1420)$ DECAY MODES

Mode	Fraction (Γ _i /Γ)
Γ ₁ ρπ	dominant
Γ ₂ ωππ	seen
Γ ₃ b ₁ (1235)π	seen
Γ ₄ e ⁺ e ⁻	seen
Γ ₅ π ⁰ γ	

 $\omega(1420)$ Γ(i)Γ(e⁺e⁻)/Γ²(total)

Γ(ρπ)/Γ _{total} × Γ(e ⁺ e ⁻)/Γ _{total}	Γ ₁ /Γ × Γ ₄ /Γ			
VALUE (units 10 ⁻⁶)	EVTS	DOCUMENT ID	TECN	COMMENT
• • •	We do not use the following data for averages, fits, limits, etc. • • •			
0.82 ± 0.05 ± 0.06		AUBERT,B	04N BABR	10.6 e ⁺ e ⁻ → π ⁺ π ⁻ π ⁰ γ
0.65 ± 0.13 ± 0.21	1.2M	^{14,15} ACHASOV	03D RVUE	0.44-2.00 e ⁺ e ⁻ → π ⁺ π ⁻ π ⁰
0.625 ± 0.160		^{16,17} CLEGG	94 RVUE	
0.466 ± 0.178	18,19	ANTONELLI	92 DM2	1.34-2.4e ⁺ e ⁻ → ρπ

¹⁴ Calculated by us from the cross section at the peak.

¹⁵ From the combined fit of ANTONELLI 92, ACHASOV 01E, ACHASOV 02E, and ACHASOV 03D data on the π⁺π⁻π⁰ and ANTONELLI 92 on the ωπ⁺π⁻ final states. Supersedes ACHASOV 99E and ACHASOV 02E.

¹⁶ From a fit to two Breit-Wigner functions and using the data of DOLINSKY 91 and ANTONELLI 92.

¹⁷ From the partial and leptonic width given by the authors.

¹⁸ From a fit to two Breit-Wigner functions interfering between them and with the ω,φ tails with fixed (+,-,+) phases.

¹⁹ From the product of the leptonic width and partial branching ratio given by the authors.

 $\Gamma(\omega\pi\pi)/\Gamma_{total} \times \Gamma(e^+e^-)/\Gamma_{total}$ Γ₂/Γ × Γ₄/Γ

VALUE (units 10 ⁻⁸)	DOCUMENT ID	TECN	COMMENT
• • •	We do not use the following data for averages, fits, limits, etc. • • •		
19.7 ± 5.7	AUBERT	07AU BABR	10.6 e ⁺ e ⁻ → ωπ ⁺ π ⁻ γ
1.9 ± 1.9	²⁰ AKHMETSHIN	00D CMD2	1.2-2.4 e ⁺ e ⁻ → ωπ ⁺ π ⁻

²⁰ Using the data of AKHMETSHIN 00D and ANTONELLI 92. The ρπ dominance for the energy dependence of the ω(1420) and ω(1650) width assumed.

 $\Gamma(\omega\pi\gamma)/\Gamma_{total} \times \Gamma(e^+e^-)/\Gamma_{total}$ Γ₅/Γ × Γ₄/Γ

VALUE (units 10 ⁻⁸)	DOCUMENT ID	TECN	COMMENT
• • •	We do not use the following data for averages, fits, limits, etc. • • •		
2.03 ^{+0.70} _{-0.75}	²¹ AKHMETSHIN	05 CMD2	0.60-1.38 e ⁺ e ⁻ → π ⁰ γ

²¹ Using 1420 MeV and 220 MeV for the ω(1420) mass and width.

 $\omega(1420)$ BRANCHING RATIOS $\Gamma(\omega\pi\pi)/\Gamma_{total}$ Γ₂/Γ

VALUE	DOCUMENT ID	TECN	COMMENT
• • •	We do not use the following data for averages, fits, limits, etc. • • •		
0.301 ± 0.029	²² HENNER	02 RVUE	1.2-2.0 e ⁺ e ⁻ → ρπ, ωππ possibly seen
	AKHMETSHIN	00D CMD2	e ⁺ e ⁻ → ωπ ⁺ π ⁻

 $\Gamma(\omega\pi\pi)/\Gamma(b_1(1235)\pi)$ Γ₂/Γ₃

VALUE	EVTS	DOCUMENT ID	TECN	COMMENT
• • •	We do not use the following data for averages, fits, limits, etc. • • •			
0.60 ± 0.16	5095	ANISOVICH	00H SPEC	0.0 p \bar{p} → ωπ ⁰ π ⁰ π ⁰

 $\Gamma(\rho\pi)/\Gamma_{total}$ Γ₁/Γ

VALUE	DOCUMENT ID	TECN	COMMENT
• • •	We do not use the following data for averages, fits, limits, etc. • • •		
0.699 ± 0.029	²² HENNER	02 RVUE	1.2-2.0 e ⁺ e ⁻ → ρπ, ωππ

 $\Gamma(e^+e^-)/\Gamma_{total}$ Γ₄/Γ

VALUE (units 10 ⁻⁷)	EVTS	DOCUMENT ID	TECN	COMMENT
• • •	We do not use the following data for averages, fits, limits, etc. • • •			
~ 6.6	1.2M	^{23,24} ACHASOV	03D RVUE	0.44-2.00 e ⁺ e ⁻ → π ⁺ π ⁻ π ⁰
23 ± 1		²² HENNER	02 RVUE	1.2-2.0 e ⁺ e ⁻ → ρπ, ωππ

²² Assuming that the ω(1420) decays into ρπ and ωππ only.

²³ Calculated by us from the cross section at the peak.

²⁴ Assuming that the ω(1420) decays into ρπ only.

 $\omega(1420)$ REFERENCES

AUBERT	07AU	PR D76 092005	B. Aubert <i>et al.</i>	(BABAR Collab.)
AKHMETSHIN	05	PL B605 26	R.R. Akhmetshin <i>et al.</i>	(Novosibirsk CMD-2 Collab.)
AUBERT,B	04N	PR D70 072004	B. Aubert <i>et al.</i>	(BABAR Collab.)
ACHASOV	03D	PR D68 052006	M.N. Achasov <i>et al.</i>	(Novosibirsk SND Collab.)
ACHASOV	02E	PR D66 032001	M.N. Achasov <i>et al.</i>	(Novosibirsk SND Collab.)
HENNER	02	EPJ C26 3	V.K. Henner <i>et al.</i>	
ACHASOV	01E	PR D63 072002	M.N. Achasov <i>et al.</i>	(Novosibirsk SND Collab.)
AKHMETSHIN	00D	PL B489 125	R.R. Akhmetshin <i>et al.</i>	(Novosibirsk CMD-2 Collab.)
ANISOVICH	00H	PL B485 341	A.V. Anisovich <i>et al.</i>	
ACHASOV	99E	PL B462 365	M.N. Achasov <i>et al.</i>	(Novosibirsk SND Collab.)
ACHASOV	98H	PR D57 1334	M.N. Achasov, A.A. Kozevnikov	
CLEGG	94	ZPHY C62 455	A.B. Clegg, A. Donnachie	(LANC, MCHS)
ANTONELLI	92	ZPHY C56 15	A. Antonelli <i>et al.</i>	(DM2 Collab.)
DOLINSKY	91	PRPL 202 99	S.I. Dolinsky <i>et al.</i>	(NOVO)
BISELLO	88B	ZPHY C39 13	D. Bisello <i>et al.</i>	(PADO, CLER, FRAS+)
BARKOV	87	JETPL 46 164	L.M. Barkov <i>et al.</i>	(NOVO)
		Translated from ZETFP 46 132.		
CORDIER	81	PL 106B 155	A. Cordier <i>et al.</i>	(ORSAY)
IVANOV	81	PL 107B 297	P.M. Ivanov <i>et al.</i>	(NOVO)

See key on page 405

Meson Particle Listings

$f_2(1430)$, $a_0(1450)$

$f_2(1430)$

$$I^G(J^{PC}) = 0^+(2^{++})$$

OMITTED FROM SUMMARY TABLE

This entry lists nearby peaks observed in the D wave of the $K\bar{K}$ and $\pi^+\pi^-$ systems. Needs confirmation.

$f_2(1430)$ MASS

VALUE (MeV)	DOCUMENT ID	TECN	COMMENT
≈ 1430 OUR ESTIMATE			
• • • We do not use the following data for averages, fits, limits, etc. • • •			
1453 ± 4	¹ VLADIMIRSK...01	SPEC	40 $\pi^-p \rightarrow K_S^0 K_S^0 n$
1421 ± 5	AUGUSTIN	87 DM2	$J/\psi \rightarrow \gamma\pi^+\pi^-$
1480 ± 5.0	AKESSON	86 SPEC	$pp \rightarrow pp\pi^+\pi^-$
1436 ⁺²⁶ ₋₁₆	DAUM	84 CNTR	17-18 $\pi^-p \rightarrow K^+K^-n$
1412 ± 3	DAUM	84 CNTR	63 $\pi^-p \rightarrow K_S^0 K_S^0 n, K^+K^-n$
1439 ⁺⁵ ₋₆	² BEUSCH	67 OSPK	5,7,12 $\pi^-p \rightarrow K_S^0 K_S^0 n$

¹ $J^{PC} = 0^{++}$ or 2^{++} .
² Not seen by WETZEL 76.

$f_2(1430)$ WIDTH

VALUE (MeV)	DOCUMENT ID	TECN	COMMENT
• • • We do not use the following data for averages, fits, limits, etc. • • •			
13 ± 5	³ VLADIMIRSK...01	SPEC	40 $\pi^-p \rightarrow K_S^0 K_S^0 n$
30 ± 9	AUGUSTIN	87 DM2	$J/\psi \rightarrow \gamma\pi^+\pi^-$
150 ± 5.0	AKESSON	86 SPEC	$pp \rightarrow pp\pi^+\pi^-$
81 ⁺⁵⁶ ₋₂₉	DAUM	84 CNTR	17-18 $\pi^-p \rightarrow K^+K^-n$
14 ± 6	DAUM	84 CNTR	63 $\pi^-p \rightarrow K_S^0 K_S^0 n, K^+K^-n$
43 ⁺¹⁷ ₋₁₈	⁴ BEUSCH	67 OSPK	5,7,12 $\pi^-p \rightarrow K_S^0 K_S^0 n$

³ $J^{PC} = 0^{++}$ or 2^{++} .
⁴ Not seen by WETZEL 76.

$f_2(1430)$ DECAY MODES

Mode	Fraction (Γ_i/Γ)
Γ_1 $K\bar{K}$	seen
Γ_2 $\pi\pi$	seen

$f_2(1430)$ REFERENCES

VLADIMIRSK...01	PAN 64 1895	V.V. Vladimirov et al.
AUGUSTIN	87 ZPHY C36 369	J.E. Augustin et al.
AKESSON	86 NP B364 154	T. Akeesson et al.
DAUM	84 ZPHY C23 339	C. Daum et al.
WETZEL	76 NP B115 208	W. Wetzel et al.
BEUSCH	67 PL 25B 357	W. Beusch et al.

$a_0(1450)$

$$I^G(J^{PC}) = 1^-(0^{++})$$

See minireview on scalar mesons under $f_0(600)$.

$a_0(1450)$ MASS

VALUE (MeV)	EVTS	DOCUMENT ID	TECN	COMMENT
1474 ± 19 OUR AVERAGE				
1480 ± 30		ABELE	98 CBAR	0.0 $\bar{p}p \rightarrow K_L^0 K^{\pm}\pi^{\mp}$
1470 ± 25		¹ AMSLER	95D CBAR	0.0 $\bar{p}p \rightarrow \pi^0\pi^0\pi^0, \pi^0\eta\eta, \pi^0\pi^0\eta$
• • • We do not use the following data for averages, fits, limits, etc. • • •				
1515 ± 30		² ANISOVICH	09 RVUE	0.0 $\bar{p}p, \pi N$
1316.8 ^{+1.0} _{-1.0} ± 4.6		³ UEHARA	09A BELL	$\gamma\gamma \rightarrow \pi^0\eta$
1432 ± 13 ± 25		⁴ BUGG	08A RVUE	$\bar{p}p$
1477 ± 10	80k	⁵ UMAN	06 E835	5.2 $\bar{p}p \rightarrow \eta\eta\pi^0$
1441 ⁺⁴⁰ ₋₁₅	35280	² BAKER	03 SPEC	$\bar{p}p \rightarrow \omega\pi^+\pi^-\pi^0$
1303 ± 16		⁶ BARGIOTTI	03 OBLX	$\bar{p}p$
1296 ± 10		⁷ AMSLER	02 CBAR	0.9 $\bar{p}p \rightarrow \pi^0\pi^0\eta$
1565 ± 30		⁷ ANISOVICH	98B RVUE	Compilation
1290 ± 10		⁸ BERTIN	98B OBLX	0.0 $\bar{p}p \rightarrow K^{\pm}K_S^0\pi^{\mp}$
1450 ± 40		AMSLER	94D CBAR	0.0 $\bar{p}p \rightarrow \pi^0\pi^0\eta$
1410 ± 25		ETKIN	82C MPS	23 $\pi^-p \rightarrow n2K_S^0$
~ 1300		MARTIN	78 SPEC	10 $K^{\pm}p \rightarrow K_S^0\pi p$
1255 ± 5		⁹ CASON	76	

¹ Coupled-channel analysis of AMSLER 95B, AMSLER 95C, and AMSLER 94D.
² From the pole position.
³ May be a different state.
⁴ Using data from AMSLER 94D, ABELE 98, and BAKER 03. Supersedes BUGG 94.
⁵ Statistical error only.
⁶ Coupled channel analysis of $\pi^+\pi^-\pi^0, K^+K^-\pi^0$, and $K^{\pm}K_S^0\pi^{\mp}$.
⁷ T-matrix pole.
⁸ Not confirmed by BUGG 08A.
⁹ Isospin 0 not excluded.

$a_0(1450)$ WIDTH

VALUE (MeV)	EVTS	DOCUMENT ID	TECN	COMMENT
265 ± 13 OUR AVERAGE				
265 ± 15		ABELE	98 CBAR	0.0 $\bar{p}p \rightarrow K_L^0 K^{\pm}\pi^{\mp}$
265 ± 30		¹⁰ AMSLER	95D CBAR	0.0 $\bar{p}p \rightarrow \pi^0\pi^0\pi^0, \pi^0\eta\eta, \pi^0\pi^0\eta$
• • • We do not use the following data for averages, fits, limits, etc. • • •				
230 ± 36		¹¹ ANISOVICH	09 RVUE	0.0 $\bar{p}p, \pi N$
65.0 ^{+2.1+99.1} _{-5.4-32.6}		¹² UEHARA	09A BELL	$\gamma\gamma \rightarrow \pi^0\eta$
196 ± 10 ± 10		¹³ BUGG	08A RVUE	$\bar{p}p$
267 ± 11	80k	¹⁴ UMAN	06 E835	5.2 $\bar{p}p \rightarrow \eta\eta\pi^0$
110 ± 14	35280	¹¹ BAKER	03 SPEC	$\bar{p}p \rightarrow \omega\pi^+\pi^-\pi^0$
92 ± 16		¹⁵ BARGIOTTI	03 OBLX	$\bar{p}p$
81 ± 21		¹⁶ AMSLER	02 CBAR	0.9 $\bar{p}p \rightarrow \pi^0\pi^0\eta$
292 ± 40		¹⁶ ANISOVICH	98B RVUE	Compilation
80 ± 5		¹⁷ BERTIN	98B OBLX	0.0 $\bar{p}p \rightarrow K^{\pm}K_S^0\pi^{\mp}$
270 ± 40		AMSLER	94D CBAR	0.0 $\bar{p}p \rightarrow \pi^0\pi^0\eta$
230 ± 30		ETKIN	82C MPS	23 $\pi^-p \rightarrow n2K_S^0$
~ 250		MARTIN	78 SPEC	10 $K^{\pm}p \rightarrow K_S^0\pi p$
79 ± 10		¹⁸ CASON	76	

¹⁰ Coupled-channel analysis of AMSLER 95B, AMSLER 95C, and AMSLER 94D.
¹¹ From the pole position.
¹² May be a different state.
¹³ Using data from AMSLER 94D, ABELE 98, and BAKER 03. Supersedes BUGG 94.
¹⁴ Statistical error only.
¹⁵ Coupled channel analysis of $\pi^+\pi^-\pi^0, K^+K^-\pi^0$, and $K^{\pm}K_S^0\pi^{\mp}$.
¹⁶ T-matrix pole.
¹⁷ Not confirmed by BUGG 08A.
¹⁸ Isospin 0 not excluded.

$a_0(1450)$ DECAY MODES

Mode	Fraction (Γ_i/Γ)
Γ_1 $\pi\eta$	seen
Γ_2 $\pi\eta'(958)$	seen
Γ_3 $K\bar{K}$	seen
Γ_4 $\omega\pi\pi$	seen
Γ_5 $a_0(980)\pi\pi$	seen
Γ_6 $\gamma\gamma$	seen

$a_0(1450)$ $\Gamma(i)\Gamma(\gamma\gamma)/\Gamma(\text{total})$

VALUE (eV)	DOCUMENT ID	TECN	COMMENT	$\Gamma_1\Gamma_6/\Gamma$
• • • We do not use the following data for averages, fits, limits, etc. • • •				
432 ± 6 ⁺¹⁰⁷³ ₋₂₅₆	¹⁹ UEHARA	09A BELL	$\gamma\gamma \rightarrow \pi^0\eta$	
¹⁹ May be a different state.				

$a_0(1450)$ BRANCHING RATIOS

$\Gamma(\pi\eta'(958))/\Gamma(\pi\eta)$	Γ_2/Γ_1			
VALUE	DOCUMENT ID	TECN	COMMENT	
0.35 ± 0.16	²⁰ ABELE	98 CBAR	0.0 $\bar{p}p \rightarrow K_L^0 K^{\pm}\pi^{\mp}$	
• • • We do not use the following data for averages, fits, limits, etc. • • •				
0.43 ± 0.19	ABELE	97C CBAR	0.0 $\bar{p}p \rightarrow \pi^0\pi^0\eta'$	
²⁰ Using $\pi^0\eta$ from AMSLER 94D.				
$\Gamma(K\bar{K})/\Gamma(\pi\eta)$	Γ_3/Γ_1			
VALUE	DOCUMENT ID	TECN	COMMENT	
0.88 ± 0.23	²¹ ABELE	98 CBAR	0.0 $\bar{p}p \rightarrow K_L^0 K^{\pm}\pi^{\mp}$	
²¹ Using $\pi^0\eta$ from AMSLER 94D.				
$\Gamma(\omega\pi\pi)/\Gamma(\pi\eta)$	Γ_4/Γ_1			
VALUE	EVTS	DOCUMENT ID	TECN	COMMENT
• • • We do not use the following data for averages, fits, limits, etc. • • •				
10.7 ± 2.3	35280	²² BAKER	03 SPEC	$\bar{p}p \rightarrow \omega\pi^+\pi^-\pi^0$
²² Using results on $\bar{p}p \rightarrow a_0(1450)^0\pi^0, a_0(1450) \rightarrow \eta\pi^0$ from ABELE 96C and assuming the $\omega\rho$ mechanism for the $\omega\pi\pi$ state.				

See key on page 405

Meson Particle Listings

 $\rho(1450)$ $\pi\pi$ MODE

VALUE (MeV)	EVTS	DOCUMENT ID	TECN	COMMENT
•••				We do not use the following data for averages, fits, limits, etc. •••
434±16±60	5.4M	24,25 FUJIKAWA	08 BELL	$\tau^- \rightarrow \pi^- \pi^0 \nu_\tau$
468±41		26 SCHAEEL	05C ALEP	$\tau^- \rightarrow \pi^- \pi^0 \nu_\tau$
455±41	87k	24,27 ANDERSON	00A CLE2	$\tau^- \rightarrow \pi^- \pi^0 \nu_\tau$
~374		28 ABELE	99C CBAR	$0.0 \bar{p}d \rightarrow \pi^+ \pi^- \pi^- p$
275±10		BERTIN	98 OBLX	$0.05-0.405 \bar{p}p \rightarrow \pi^+ \pi^+ \pi^-$
343±20		29 ABELE	97 CBAR	$\bar{p}n \rightarrow \pi^- \pi^0 \pi^0$
310±40		27 BERTIN	97C OBLX	$0.0 \bar{p}p \rightarrow \pi^+ \pi^- \pi^0$
236±36		BERTIN	97D OBLX	$0.05 \bar{p}p \rightarrow 2\pi^+ 2\pi^-$
269±31		BISELLO	89 DM2	$e^+ e^- \rightarrow \pi^+ \pi^-$
391±70		DUBNICKA	89 RVUE	$e^+ e^- \rightarrow \pi^+ \pi^-$
218±46		30 KURDADZE	83 OLYA	$0.64-1.4 e^+ e^- \rightarrow \pi^+ \pi^-$

²⁴ From the GOUNARIS 68 parametrization of the pion form factor.

²⁵ $|F_\pi(0)|^2$ fixed to 1.

²⁶ From the combined fit of the τ^- data from ANDERSON 00A and SCHAEEL 05C and $e^+ e^-$ data from the compilation of BARKOV 85, AKHMETSHIN 04, and ALOISIO 05. $\rho(1700)$ mass and width fixed at 1713 MeV and 235 MeV, respectively. Supersedes BARATE 97M.

²⁷ $\rho(1700)$ mass and width fixed at 1700 MeV and 235 MeV, respectively.

²⁸ $\rho(1700)$ mass and width fixed at 1780 MeV and 275 MeV respectively.

²⁹ T-matrix pole.

³⁰ Using for $\rho(1700)$ mass and width 1600 ± 20 and 300 ± 10 MeV respectively.

 $K\bar{K}$ MODE

VALUE (MeV)	EVTS	DOCUMENT ID	TECN	CHG	COMMENT
•••					We do not use the following data for averages, fits, limits, etc. •••
146.5±10.5	27k	31 ABELE	99D CBAR	±	$0.0 \bar{p}p \rightarrow K^+ K^- \pi^0$

³¹ K-matrix pole. Isospin not determined, could be $\omega(1420)$.

 $K\bar{K}^*(892) + c.c.$ MODE

VALUE (MeV)	DOCUMENT ID	TECN	COMMENT
•••			We do not use the following data for averages, fits, limits, etc. •••
418±25±4	AUBERT	08s BABR	$10.6 e^+ e^- \rightarrow K\bar{K}^*(892)\gamma$

 $\rho(1450)$ DECAY MODES

Mode	Fraction (Γ_i/Γ)
Γ_1 $\pi\pi$	seen
Γ_2 4π	seen
Γ_3 $\omega\pi$	
Γ_4 $a_1(1260)\pi$	
Γ_5 $h_1(1170)\pi$	
Γ_6 $\pi(1300)\pi$	
Γ_7 $\rho\rho$	
Γ_8 $\rho(\pi\pi)$ s-wave	
Γ_9 $e^+ e^-$	seen
Γ_{10} $\eta\rho$	possibly seen
Γ_{11} $a_2(1320)\pi$	not seen
Γ_{12} $K\bar{K}$	not seen
Γ_{13} $K\bar{K}^*(892) + c.c.$	possibly seen
Γ_{14} $\eta\gamma$	possibly seen

 $\rho(1450)$ $\Gamma(i)\Gamma(e^+e^-)/\Gamma(\text{total})$ $\Gamma(\pi\pi) \times \Gamma(e^+e^-)/\Gamma(\text{total})$ $\Gamma_1\Gamma_9/\Gamma$

VALUE (keV)	DOCUMENT ID	TECN	COMMENT
•••			We do not use the following data for averages, fits, limits, etc. •••
0.12	32 DIEKMAN	88 RVUE	$e^+ e^- \rightarrow \pi^+ \pi^-$
$0.027^{+0.015}_{-0.010}$	33 KURDADZE	83 OLYA	$0.64-1.4 e^+ e^- \rightarrow \pi^+ \pi^-$

 $\Gamma(\eta\rho) \times \Gamma(e^+e^-)/\Gamma(\text{total})$ $\Gamma_{10}\Gamma_9/\Gamma$

VALUE (eV)	DOCUMENT ID	TECN	COMMENT
•••			We do not use the following data for averages, fits, limits, etc. •••
74±20	34 AKHMETSHIN 00D	CMD2	$e^+ e^- \rightarrow \eta\pi^+\pi^-$
91±19	ANTONELLI	88 DM2	$e^+ e^- \rightarrow \eta\pi^+\pi^-$

 $\Gamma(\eta\gamma) \times \Gamma(e^+e^-)/\Gamma(\text{total})$ $\Gamma_{14}\Gamma_9/\Gamma$

VALUE (eV)	DOCUMENT ID	TECN	COMMENT
•••			We do not use the following data for averages, fits, limits, etc. •••
<16.4	35 AKHMETSHIN 05	CMD2	$0.60-1.38 e^+ e^- \rightarrow \eta\gamma$
$2.2 \pm 0.5 \pm 0.3$	36 AKHMETSHIN 01B	CMD2	$e^+ e^- \rightarrow \eta\gamma$

 $\Gamma(K\bar{K}^*(892) + c.c.) \times \Gamma(e^+e^-)/\Gamma(\text{total})$ $\Gamma_{13}\Gamma_9/\Gamma$

VALUE (eV)	DOCUMENT ID	TECN	COMMENT
•••			We do not use the following data for averages, fits, limits, etc. •••
127±15±6	AUBERT	08s BABR	$10.6 e^+ e^- \rightarrow K\bar{K}^*(892)\gamma$

³² Using total width = 235 MeV.
³³ Using for $\rho(1700)$ mass and width 1600 ± 20 and 300 ± 10 MeV respectively.
³⁴ Using the data of ANTONELLI 88, DOLINSKY 91, and AKHMETSHIN 00D. The energy-independent width of the $\rho(1450)$ and $\rho(1700)$ mesons assumed.
³⁵ From 2γ decay mode of η using 1465 MeV and 310 MeV for the $\rho(1450)$ mass and width. Recalculated by us.
³⁶ Using the data of AKHMETSHIN 01B on $e^+ e^- \rightarrow \eta\gamma$, AKHMETSHIN 00D and ANTONELLI 88 on $e^+ e^- \rightarrow \eta\pi^+\pi^-$. Recalculated by us using width of 226 MeV.

 $\rho(1450)$ BRANCHING RATIOS $\Gamma(\pi\pi)/\Gamma(4\pi)$ Γ_1/Γ_2

VALUE	DOCUMENT ID	TECN	COMMENT
•••			We do not use the following data for averages, fits, limits, etc. •••
0.37 ± 0.10	37,38 ABELE	01B CBAR	$0.0 \bar{p}n \rightarrow 5\pi$

 $\Gamma(\omega\pi)/\Gamma(\text{total})$ Γ_3/Γ

VALUE	DOCUMENT ID	TECN	COMMENT
•••			We do not use the following data for averages, fits, limits, etc. •••
~0.21	CLEGG	94 RVUE	

 $\Gamma(\pi\pi)/\Gamma(\omega\pi)$ Γ_1/Γ_3

VALUE	DOCUMENT ID	TECN	COMMENT
•••			We do not use the following data for averages, fits, limits, etc. •••
~0.32	CLEGG	94 RVUE	

 $\Gamma(\omega\pi)/\Gamma(4\pi)$ Γ_3/Γ_2

VALUE	DOCUMENT ID	TECN	COMMENT
•••			We do not use the following data for averages, fits, limits, etc. •••
<0.14	CLEGG	88 RVUE	

 $\Gamma(a_1(1260)\pi)/\Gamma(4\pi)$ Γ_4/Γ_2

VALUE	DOCUMENT ID	TECN	COMMENT
•••			We do not use the following data for averages, fits, limits, etc. •••
0.27 ± 0.08	37 ABELE	01B CBAR	$0.0 \bar{p}n \rightarrow 5\pi$

 $\Gamma(h_1(1170)\pi)/\Gamma(4\pi)$ Γ_5/Γ_2

VALUE	DOCUMENT ID	TECN	COMMENT
•••			We do not use the following data for averages, fits, limits, etc. •••
0.08 ± 0.04	37 ABELE	01B CBAR	$0.0 \bar{p}n \rightarrow 5\pi$

 $\Gamma(\pi(1300)\pi)/\Gamma(4\pi)$ Γ_6/Γ_2

VALUE	DOCUMENT ID	TECN	COMMENT
•••			We do not use the following data for averages, fits, limits, etc. •••
0.37 ± 0.13	37 ABELE	01B CBAR	$0.0 \bar{p}n \rightarrow 5\pi$

 $\Gamma(\rho\rho)/\Gamma(4\pi)$ Γ_7/Γ_2

VALUE	DOCUMENT ID	TECN	COMMENT
•••			We do not use the following data for averages, fits, limits, etc. •••
0.11 ± 0.05	37 ABELE	01B CBAR	$0.0 \bar{p}n \rightarrow 5\pi$

 $\Gamma(\rho(\pi\pi)\text{s-wave})/\Gamma(4\pi)$ Γ_8/Γ_2

VALUE	DOCUMENT ID	TECN	COMMENT
•••			We do not use the following data for averages, fits, limits, etc. •••
0.17 ± 0.09	37 ABELE	01B CBAR	$0.0 \bar{p}n \rightarrow 5\pi$

 $\Gamma(\eta\rho)/\Gamma(\text{total})$ Γ_{10}/Γ

VALUE	DOCUMENT ID	TECN	COMMENT
•••			We do not use the following data for averages, fits, limits, etc. •••
<0.04	DONNACHIE	87B RVUE	

 $\Gamma(\eta\rho)/\Gamma(\omega\pi)$ Γ_{10}/Γ_3

VALUE	DOCUMENT ID	TECN	COMMENT
•••			We do not use the following data for averages, fits, limits, etc. •••
~0.24	39 DONNACHIE	91 RVUE	
>2	FUKUI	91 SPEC	$8.95 \pi^- p \rightarrow \omega\pi^0 n$

 $\Gamma(a_2(1320)\pi)/\Gamma(\text{total})$ Γ_{11}/Γ

VALUE	DOCUMENT ID	TECN	COMMENT
•••			We do not use the following data for averages, fits, limits, etc. •••
not seen	AMELIN	00 VES	$37 \pi^- p \rightarrow \eta\pi^+\pi^- n$

 $\Gamma(K\bar{K})/\Gamma(\omega\pi)$ Γ_{12}/Γ_3

VALUE	DOCUMENT ID	TECN	COMMENT
•••			We do not use the following data for averages, fits, limits, etc. •••
<0.08	39 DONNACHIE	91 RVUE	

Meson Particle Listings

$\rho(1450), \eta(1475)$

$\Gamma(K\bar{K}^*(892) + c.c.)/\Gamma_{total}$ Γ_{13}/Γ

VALUE DOCUMENT ID TECN COMMENT

••• We do not use the following data for averages, fits, limits, etc. •••

possibly seen COAN 04 CLEO $\tau^- \rightarrow K^- \pi^- K^+ \nu_\tau$

³⁷ $\omega\pi$ not included.

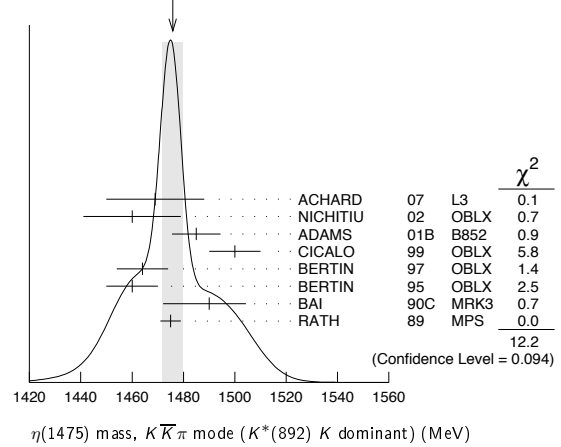
³⁸ Using ABELE 97.

³⁹ Using data from BISELLO 91B, DOLINSKY 86 and ALBRECHT 87L.

$\rho(1450)$ REFERENCES

AUBERT 08S PR D77 092002	B. Aubert et al. (BABAR Collab.)
FUJIKAWA 08 PR D78 072006	M. Fujikawa et al. (BELLE Collab.)
AKHMETSHIN 05 PL B605 26	R.R. Akhmetshin et al. (Novosibirsk CMD-2 Collab.)
ALOISIO 05 PL B606 12	A. Aloisio et al. (KLOE Collab.)
SCHAEEL 05C PRPL 421 191	S. Schaeel et al. (ALEPH Collab.)
AKHMETSHIN 04 PL B578 285	R.R. Akhmetshin et al. (Novosibirsk CMD-2 Collab.)
COAN 04 PRL 92 232001	T.E. Coan et al. (CLEO Collab.)
AKHMETSHIN 03B PL B562 173	R.R. Akhmetshin et al. (Novosibirsk CMD-2 Collab.)
ABELE 01B EPJ C21 261	A. Abele et al. (Crystal Barrel Collab.)
AKHMETSHIN 01B PL B509 217	R.R. Akhmetshin et al. (Novosibirsk CMD-2 Collab.)
ALEXANDER 01B PR D64 092001	J.P. Alexander et al. (CLEO Collab.)
AKHMETSHIN 00D PL B489 125	R.R. Akhmetshin et al. (Novosibirsk CMD-2 Collab.)
AMELIN 00 NP A668 83	D. Amelin et al. (VES Collab.)
ANDERSON 00A PR D61 112002	S. Anderson et al. (CLEO Collab.)
EDWARDS 00A PR D61 072003	K.W. Edwards et al. (CLEO Collab.)
ABELE 99C PL B450 275	A. Abele et al. (Crystal Barrel Collab.)
ABELE 99D PL B468 178	A. Abele et al. (Crystal Barrel Collab.)
BERTIN 96 PR D57 55	A. Bertin et al. (OBELIX Collab.)
ABELE 97 PL B391 191	A. Abele et al. (Crystal Barrel Collab.)
ACHASOV 97 PR D55 2663	N.N. Achasov et al. (NOVM Collab.)
BARATE 97M ZPHY C76 15	R. Barate et al. (ALEPH Collab.)
BERTIN 97C PL B408 476	A. Bertin et al. (OBELIX Collab.)
BERTIN 97D PL B414 220	A. Bertin et al. (OBELIX Collab.)
CLEGG 94 ZPHY C62 455	A.B. Clegg, A. Donnachie (LANC, MCHS)
BISELLO 91B NPBPS B21 111	D. Bisello (DM2 Collab.)
DOLINSKY 91 PRPL 202 99	S.I. Dolinsky et al. (NOVO Collab.)
DONNACHIE 91 ZPHY C51 689	A. Donnachie, A.B. Clegg (MCHS, LANC)
FUKUI 91 PL B257 241	S. Fukui et al. (SUGI, NAGO, KEK, KYOT+)
ARMSTRONG 89E PL B228 536	T.A. Armstrong, M. Benayoun (ATHU, BARI, BIRM+)
BISELLO 89 PL B220 321	D. Bisello et al. (DM2 Collab.)
DUBNICKA 89 JPG 15 1349	S. Dubnicka et al. (JINR, SLOV)
ANTONELLI 88 PL B212 133	A. Antonelli et al. (DM2 Collab.)
CLEGG 88 ZPHY C40 313	A.B. Clegg, A. Donnachie (MCHS, LANC)
DIEKMANN 88 PRPL 159 99	B. Diekmann (BONN)
FUKUI 88 PL B202 441	S. Fukui et al. (SUGI, NAGO, KEK, KYOT+)
ALBRECHT 87L PL B185 223	H. Albrecht et al. (ARGUS Collab.)
DONNACHIE 87B ZPHY C34 257	A. Donnachie, A.B. Clegg (MCHS, LANC)
DOLINSKY 86 PL B174 453	S.I. Dolinsky et al. (NOVO Collab.)
BARKOV 85 NP B256 365	L.M. Barkov et al. (NOVO Collab.)
KURDADZE 83 JETPL 37 733	L.M. Kurdadze et al. (NOVO Collab.)
Translated from ZETFP 37 613	
ASTON 80C PL 92B 211	D. Aston (BONN, CERN, EPOL, GLAS, LANC+)
BARBER 80C ZPHY C4 169	D.P. Barber et al. (DARE, LANC, SHEF)
GOUNARIS 68 PRL 21 244	G.J. Gounaris, J.J. Sakurai

WEIGHTED AVERAGE
1476±4 (Error scaled by 1.3)



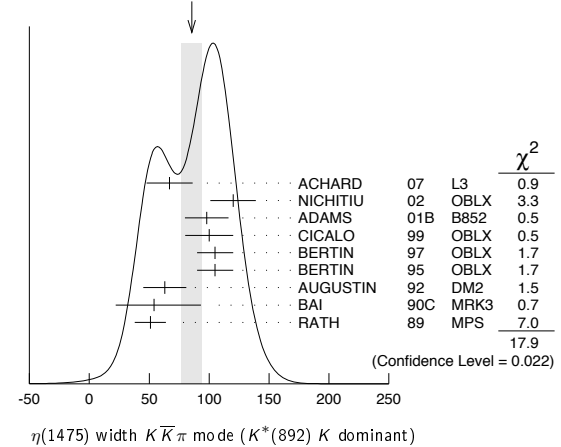
$\eta(1475)$ mass, $K\bar{K}\pi$ mode ($K^*(892)$ K dominant) (MeV)

$\eta(1475)$ WIDTH

$K\bar{K}\pi$ MODE ($K^*(892)$ K dominant)

VALUE (MeV)	EVTS	DOCUMENT ID	TECN	COMMENT
85 ± 9 OUR AVERAGE		Error includes scale factor of 1.5. See the ideogram below.		
67 ± 18 ± 7	74	ACHARD 07 L3		$183-209 e^+e^- \rightarrow e^+e^- K_S^0 K^\pm \pi^\mp$
120 ± 19	3651	NICHITIU 02 OBLX		
98 ± 18 ± 3	20k	ADAMS 01B B852	18 GeV $\pi^- p \rightarrow K^+ K^- \pi^0 n$	
100 ± 20		CICALO 99 OBLX	$0 \bar{p} p \rightarrow K^\pm K_S^0 \pi^\mp \pi^+ \pi^-$	
105 ± 15		BERTIN 97 OBLX	$0 \bar{p} p \rightarrow K^\pm (K^0) \pi^\mp \pi^+ \pi^-$	
105 ± 15		BERTIN 95 OBLX	$0 \bar{p} p \rightarrow K\bar{K}\pi\pi\pi$	
63 ± 18		AUGUSTIN 92 DM2	$J/\psi \rightarrow \gamma K\bar{K}\pi$	
54 + 37 + 13 - 21 - 24		BAI 90C MRK3	$J/\psi \rightarrow \gamma K_S^0 K^\pm \pi^\mp$	
51 ± 13		RATH 89 MPS	$21.4 \pi^- p \rightarrow n K_S^0 K_S^0 \pi^0$	

WEIGHTED AVERAGE
85±9 (Error scaled by 1.5)



$\eta(1475)$ width $K\bar{K}\pi$ mode ($K^*(892)$ K dominant)

$\eta(1475)$ DECAY MODES

Mode	Fraction (Γ_i/Γ)
Γ_1 $K\bar{K}\pi$	dominant
Γ_2 $K\bar{K}^*(892) + c.c.$	seen
Γ_3 $a_0(980)\pi$	seen
Γ_4 $\gamma\gamma$	seen

$\eta(1475)$ $\Gamma(i)\Gamma(\gamma\gamma)/\Gamma(total)$

VALUE (keV)	CL%	EVTS	DOCUMENT ID	TECN	COMMENT
0.23 ± 0.05 ± 0.05		74	1 ACHARD 07 L3		$183-209 e^+e^- \rightarrow e^+e^- K_S^0 K^\pm \pi^\mp$
••• We do not use the following data for averages, fits, limits, etc. •••					
< 0.089	90	2,3	AHOHE 05 CLE2		$10.6 e^+e^- \rightarrow e^+e^- K_S^0 K^\pm \pi^\mp$

$\eta(1475)$

$$I^G(J^{PC}) = 0^+(0^{-+})$$

See also the $\eta(1405)$.

$\eta(1475)$ MASS

$K\bar{K}\pi$ MODE ($K^*(892)$ K dominant)

VALUE (MeV)	EVTS	DOCUMENT ID	TECN	COMMENT
1476 ± 4 OUR AVERAGE		Error includes scale factor of 1.3. See the ideogram below.		
1469 ± 14 ± 13	74	ACHARD 07 L3		$183-209 e^+e^- \rightarrow e^+e^- K_S^0 K^\pm \pi^\mp$
1460 ± 19	3651	NICHITIU 02 OBLX		
1485 ± 8 ± 5	20k	ADAMS 01B B852	18 GeV $\pi^- p \rightarrow K^+ K^- \pi^0 n$	
1500 ± 10		CICALO 99 OBLX	$0 \bar{p} p \rightarrow K^\pm K_S^0 \pi^\mp \pi^+ \pi^-$	
1464 ± 10		BERTIN 97 OBLX	$0 \bar{p} p \rightarrow K^\pm (K^0) \pi^\mp \pi^+ \pi^-$	
1460 ± 10		BERTIN 95 OBLX	$0 \bar{p} p \rightarrow K\bar{K}\pi\pi\pi$	
1490 + 14 + 3 - 8 - 16	1100	BAI 90C MRK3	$J/\psi \rightarrow \gamma K_S^0 K^\pm \pi^\mp$	
1475 ± 4		RATH 89 MPS	$21.4 \pi^- p \rightarrow n K_S^0 K_S^0 \pi^0$	
••• We do not use the following data for averages, fits, limits, etc. •••				
1421 ± 14		AUGUSTIN 92 DM2	$J/\psi \rightarrow \gamma K\bar{K}\pi$	

- ¹ Supersedes ACCIARRI 01g. Compatible with K^*K decay. Using $B(K_S^0 \rightarrow \pi^+\pi^-) = 0.6895$.
- ² Using $\eta(1475)$ mass of 1481 MeV and width of 48 MeV. The upper limit increases to 0.140 keV if the world average value, 87 MeV, of the width is used.
- ³ Assuming three-body phase-space decay to $K_S^0 K^\pm \pi^\mp$.

$\eta(1475)$ BRANCHING RATIOS

$\Gamma(K\bar{K}^*(892) + c.c.) / \Gamma(K\bar{K}\pi)$		Γ_2 / Γ_1	
VALUE	DOCUMENT ID	TECN	COMMENT
•••	We do not use the following data for averages, fits, limits, etc.	•••	
0.50 ± 0.10	⁴ BAILLON	67	HBC 0.0 $\bar{p}p \rightarrow K\bar{K}\pi\pi$

$\Gamma(K\bar{K}^*(892) + c.c.) / [\Gamma(K\bar{K}^*(892) + c.c.) + \Gamma(a_0(980)\pi)]$		$\Gamma_2 / (\Gamma_2 + \Gamma_3)$		
VALUE	CL%	DOCUMENT ID	TECN	COMMENT
•••	We do not use the following data for averages, fits, limits, etc.	•••		
<0.25	90	EDWARDS	82E	CBAL $J/\psi \rightarrow K^+K^-\pi^0\gamma$

⁴ Data could also refer to $\eta(1405)$.

$\eta(1475)$ REFERENCES

ACHARD	07	JHEP 0703 018	P. Achard et al.	(L3 Collab.)
AHOHE	05	PR D71 072001	R. Ahohe et al.	(CLEO Collab.)
NICHITIU	02	PL B545 261	F. Nichitiu et al.	(OBELIX Collab.)
ACCIARRI	01G	PL B501 1	M. Acciari et al.	(L3 Collab.)
ADAMS	01B	PL B516 264	G.S. Adams et al.	(BNL E852 Collab.)
CICALO	99	PL B462 453	C. Cicalo et al.	(OBELIX Collab.)
BERTIN	97	PL B400 226	A. Bertin et al.	(OBELIX Collab.)
BERTIN	95	PL B361 187	A. Bertin et al.	(OBELIX Collab.)
AUGUSTIN	92	PR D46 1951	J.E. Augustin, G. Cosme	(DM2 Collab.)
BAI	90C	PRL 65 2507	Z. Bai et al.	(Mark III Collab.)
RATH	89	PR D40 633	M.G. Rath et al.	(NDAM, BRAN, BNL, CUNY+)
EDWARDS	82E	PRL 49 259	C. Edwards et al.	(CIT, HARV, PRIN+)
BAILLON	67	NC 50A 393	P.H. Baillon et al.	(CERN, CDEF, IRAD)

$f_0(1500)$

$J^{PC} = 0^+(0^{++})$

See also the mini-reviews on scalar mesons under $f_0(600)$ (see the index for the page number) and on non- $q\bar{q}$ candidates in PDG 06, Journal of Physics, G **33** 1 (2006).

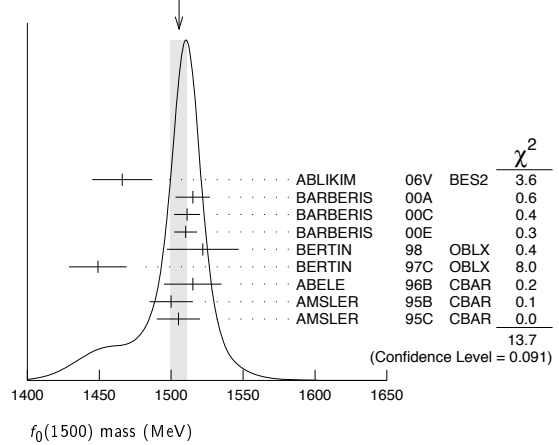
$f_0(1500)$ MASS

VALUE (MeV)	EVTS	DOCUMENT ID	TECN	COMMENT
1505 ± 6 OUR AVERAGE		Error includes scale factor of 1.3. See the ideogram below.		
1466 ± 6 ± 20		ABLIKIM	06V	BES2 $e^+e^- \rightarrow J/\psi \rightarrow \gamma\pi^+\pi^-$
1515 ± 12		¹ BARBERIS	00A	450 $pp \rightarrow p_f\eta\eta p_S$
1511 ± 9		^{1,2} BARBERIS	00C	450 $pp \rightarrow p_f 4\pi p_S$
1510 ± 8		¹ BARBERIS	00E	450 $pp \rightarrow p_f\eta\eta p_S$
1522 ± 25		BERTIN	98	OBLX 0.05-0.405 $\bar{p}p \rightarrow \pi^+\pi^+\pi^-$
1449 ± 20		¹ BERTIN	97C	OBLX 0.0 $\bar{p}p \rightarrow \pi^+\pi^-\pi^0$
1515 ± 20		ABELE	96B	CBAR 0.0 $\bar{p}p \rightarrow \pi^0 K_L^0 K_L^0$
1500 ± 15		³ AMSLER	95B	CBAR 0.0 $\bar{p}p \rightarrow 3\pi^0$
1505 ± 15		⁴ AMSLER	95C	CBAR 0.0 $\bar{p}p \rightarrow \eta\eta\pi^0$
•••	We do not use the following data for averages, fits, limits, etc.	•••		
1486 ± 10		¹ ANISOVICH	09	RVUE 0.0 $\bar{p}p \rightarrow \pi N$
1470 ± 60	568	⁵ KLEMP	08	E791 $D_s^+ \rightarrow \pi^-\pi^+\pi^+$
1470 ⁺⁶ ₋₇ ⁺⁷² ₋₂₅₅		⁶ UEHARA	08A	BELL 10.6 $e^+e^- \rightarrow e^+e^-\pi^0\pi^0$
1495 ± 4		AMSLER	06	CBAR 0.9 $\bar{p}p \rightarrow K^+K^-\pi^0$
1539 ± 20	9.9k	AUBERT	06O	BABR $B^+ \rightarrow K^+K^+K^-$
1473 ± 5	80k	^{7,8} UMAN	06	E835 5.2 $\bar{p}p \rightarrow \eta\eta\pi^0$
1478 ± 6		VLADIMIRSK...	06	SPEC 40 $\pi^-\pi^- \rightarrow K_S^0 K_S^0 n$
1493 ± 7		⁷ BINON	05	GAMS 33 $\pi^-\pi^- \rightarrow \eta\eta n$
1524 ± 14	1400	⁹ GARMASH	05	BELL $B^+ \rightarrow K^+K^+K^-$
1489 ⁺⁸ ₋₄		¹⁰ ANISOVICH	03	RVUE
1490 ± 30		⁷ ABELE	01	CBAR 0.0 $\bar{p}d \rightarrow \pi^- 4\pi^0 p$
1497 ± 10		⁷ BARBERIS	99	OMEG 450 $pp \rightarrow p_S p_f K^+ K^-$
1502 ± 10		⁷ BARBERIS	99B	OMEG 450 $pp \rightarrow p_S p_f \pi^+\pi^-$
1502 ± 12 ± 10		¹¹ BARBERIS	99D	OMEG 450 $pp \rightarrow K^+K^-, \pi^+\pi^-$
1530 ± 45		⁷ BELLAZZINI	99	GAM4 450 $pp \rightarrow p p \pi^0 \pi^0$
1505 ± 18		⁷ FRENCH	99	300 $pp \rightarrow p_f(K^+K^-)p_S$
1447 ± 27		¹² KAMINSKI	99	RVUE $\pi\pi \rightarrow \pi\pi, K\bar{K}, \sigma\sigma$
1580 ± 80		⁷ ALDE	98	GAM4 100 $\pi^-\pi^- \rightarrow \pi^0\pi^0 n$
1499 ± 8		¹ ANISOVICH	98B	RVUE Compilation
~ 1520		REYES	98	SPEC 800 $pp \rightarrow p_S p_f K_S^0 K_S^0$
1510 ± 20		¹ BARBERIS	97B	OMEG 450 $pp \rightarrow p p 2(\pi^+\pi^-)$
~ 1475		FRABETTI	97D	E687 $D_s^\pm \rightarrow \pi^\mp \pi^\pm \pi^\pm$
~ 1505		ABELE	96	CBAR 0.0 $\bar{p}p \rightarrow 5\pi^0$
1500 ± 8		¹ ABELE	96C	RVUE Compilation
1460 ± 20	120	⁷ AMELIN	96B	VES 37 $\pi^- A \rightarrow \eta\eta\pi^- A$
1500 ± 8		BUGG	96	RVUE

1500 ± 10	¹³ AMSLER	95D	CBAR 0.0 $\bar{p}p \rightarrow \pi^0\pi^0\pi^0, \pi^0\eta\eta, \pi^0\pi^0\eta$
1445 ± 5	¹⁴ ANTINORI	95	OMEG 300,450 $pp \rightarrow p p 2(\pi^+\pi^-)$
1497 ± 30	⁷ ANTINORI	95	OMEG 300,450 $pp \rightarrow p p \pi^+\pi^-$
~ 1505	BUGG	95	MRK3 $J/\psi \rightarrow \gamma\pi^+\pi^-\pi^+\pi^-$
1446 ± 5	⁷ ABATZIS	94	OMEG 450 $pp \rightarrow p p 2(\pi^+\pi^-)$
1545 ± 25	⁷ AMSLER	94E	CBAR 0.0 $\bar{p}p \rightarrow \pi^0\eta\eta'$
1520 ± 25	^{1,15} ANISOVICH	94	CBAR 0.0 $\bar{p}p \rightarrow 3\pi^0, \pi^0\eta\eta$
1505 ± 20	^{1,16} BUGG	94	RVUE $\bar{p}p \rightarrow 3\pi^0, \eta\eta\pi^0, \eta\pi^0\pi^0$
1560 ± 25	⁷ AMSLER	92	CBAR 0.0 $\bar{p}p \rightarrow \pi^0\eta\eta$
1550 ± 45 ± 30	⁷ BELADIDZE	92C	VES 36 $\pi^- Be \rightarrow \pi^- \eta' \eta Be$
1449 ± 4	⁷ ARMSTRONG	89E	OMEG 300 $pp \rightarrow p p 2(\pi^+\pi^-)$
1610 ± 20	⁷ ALDE	88	GAM4 300 $\pi^- N \rightarrow \pi^- N 2\eta$
~ 1525	ASTON	88D	LASS 11 $K^- p \rightarrow K_S^0 K_S^0 \Lambda$
1570 ± 20	⁷ ALDE	87	GAM4 100 $\pi^- p \rightarrow 4\pi^0 n$
1575 ± 45	¹⁷ ALDE	86D	GAM4 100 $\pi^- p \rightarrow 2\eta n$
1568 ± 33	⁷ BINON	84C	GAM2 38 $\pi^- p \rightarrow \eta\eta' n$
1592 ± 25	⁷ BINON	83	GAM2 38 $\pi^- p \rightarrow 2\eta n$
1525 ± 5	⁷ GRAY	83	DBC 0.0 $\bar{p}N \rightarrow 3\pi$

- ¹ T-matrix pole.
- ² Average between $\pi^+\pi^-2\pi^0$ and $2(\pi^+\pi^-)$.
- ³ T-matrix pole, supersedes ANISOVICH 94.
- ⁴ T-matrix pole, supersedes ANISOVICH 94 and AMSLER 92.
- ⁵ Reanalysis of AITALA 01A data. This state could also be $f_0(1370)$.
- ⁶ Breit-Wigner mass. May also be the $f_0(1370)$.
- ⁷ Breit-Wigner mass.
- ⁸ Statistical error only.
- ⁹ Breit-Wigner, solution 1, PWA ambiguous.
- ¹⁰ K-matrix pole from combined analysis of $\pi^-p \rightarrow \pi^0\pi^0 n, \pi^-p \rightarrow K\bar{K}n, \pi^+\pi^- \rightarrow \pi^+\pi^-, \bar{p}p \rightarrow \pi^0\pi^0\pi^0, \pi^0\eta\eta, \pi^0\pi^0\eta, \pi^+\pi^-\pi^0, K^+K^-\pi^0, K_S^0 K_S^0 \pi^0, K^+K_S^0 \pi^-$ at rest, $\bar{p}n \rightarrow \pi^-\pi^-\pi^+, K_S^0 K^-\pi^0, K_S^0 K_S^0 \pi^-$ at rest.
- ¹¹ Supersedes BARBERIS 99 and BARBERIS 99B.
- ¹² T-matrix pole on sheet --+.
- ¹³ T-matrix pole. Coupled-channel analysis of AMSLER 95B, AMSLER 95C, and AMSLER 94D.
- ¹⁴ Supersedes ABATZIS 94, ARMSTRONG 89E. Breit-Wigner mass.
- ¹⁵ From a simultaneous analysis of the annihilations $\bar{p}p \rightarrow 3\pi^0, \pi^0\eta\eta$.
- ¹⁶ Reanalysis of ANISOVICH 94 data.
- ¹⁷ From central value and spread of two solutions. Breit-Wigner mass.

WEIGHTED AVERAGE
1505±6 (Error scaled by 1.3)



$f_0(1500)$ WIDTH

VALUE (MeV)	EVTS	DOCUMENT ID	TECN	COMMENT
109 ± 7 OUR AVERAGE				
108 ⁺¹⁴ ₋₁₁ ± 25		ABLIKIM	06V	BES2 $e^+e^- \rightarrow J/\psi \rightarrow \gamma\pi^+\pi^-$
110 ± 24		¹⁸ BARBERIS	00A	450 $pp \rightarrow p_f\eta\eta p_S$
102 ± 18		^{18,19} BARBERIS	00C	450 $pp \rightarrow p_f 4\pi p_S$
110 ± 16		¹⁸ BARBERIS	00E	450 $pp \rightarrow p_f\eta\eta p_S$
108 ± 33		BERTIN	98	OBLX 0.05-0.405 $\bar{p}p \rightarrow \pi^+\pi^+\pi^-$
114 ± 30		¹⁸ BERTIN	97C	OBLX 0.0 $\bar{p}p \rightarrow \pi^+\pi^-\pi^0$
105 ± 15		ABELE	96B	CBAR 0.0 $\bar{p}p \rightarrow \pi^0 K_L^0 K_L^0$
120 ± 25		²⁰ AMSLER	95B	CBAR 0.0 $\bar{p}p \rightarrow 3\pi^0$
120 ± 30		²¹ AMSLER	95C	CBAR 0.0 $\bar{p}p \rightarrow \eta\eta\pi^0$

Meson Particle Listings

 $f_0(1500)$

••• We do not use the following data for averages, fits, limits, etc. •••

114 ± 10	18	ANISOVICH	09	RVUE	0.0 $\bar{p}p, \pi N$
90 ⁺ ₁₋₂₂	22	UEHARA	08A	BELL	10.6 $e^+e^- \rightarrow e^+e^-\pi^0\pi^0$
121 ± 8		AMSLER	06	CBAR	0.9 $\bar{p}p \rightarrow K^+K^-\pi^0$
257 ± 33	9.9k	AUBERT	06o	BABR	$B^+ \rightarrow K^+K^+K^-$
108 ± 9	80k	23,24	UMAN	06	E835 5.2 $\bar{p}p \rightarrow \eta\eta\pi^0$
119 ± 10		VLADIMIRSK...	06	SPEC	40 $\pi^-p \rightarrow K_S^0 K_S^0 n$
90 ± 15		23	BINON	05	GAMS 33 $\pi^-p \rightarrow \eta\eta n$
136 ± 23	1400	25	GARMASH	05	BELL $B^+ \rightarrow K^+K^+K^-$
102 ± 10		26	ANISOVICH	03	RVUE
140 ± 40		23	ABELE	01	CBAR 0.0 $\bar{p}d \rightarrow \pi^-4\pi^0 p$
104 ± 25		23	BARBERIS	99	OMEG 450 $pp \rightarrow p_S p_f K^+ K^-$
131 ± 15		23	BARBERIS	99B	OMEG 450 $pp \rightarrow p_S p_f \pi^+ \pi^-$
98 ± 18 ± 16		27	BARBERIS	99D	OMEG 450 $pp \rightarrow K^+ K^-, \pi^+ \pi^-$
160 ± 50		23	BELLAZZINI	99	GAM4 450 $pp \rightarrow p p \pi^0 \pi^0$
100 ± 33		23	FRENCH	99	300 $pp \rightarrow p_f(K^+K^-)p_S$
108 ± 46		28	KAMINSKI	99	RVUE $\pi\pi \rightarrow \pi\pi, K\bar{K}, \sigma\sigma$
280 ± 100		23	ALDE	98	GAM4 100 $\pi^-p \rightarrow \pi^0\pi^0 n$
130 ± 20		18	ANISOVICH	98B	RVUE Compilation
120 ± 35		18	BARBERIS	97B	OMEG 450 $pp \rightarrow p p 2(\pi^+ \pi^-)$
~ 100			FRABETTI	97D	E687 $D_S^\pm \rightarrow \pi^\mp \pi^\pm \pi^\pm$
~ 169			ABELE	96	CBAR 0.0 $\bar{p}p \rightarrow 5\pi^0$
100 ± 30	120	23	AMELIN	96B	VES 37 $\pi^-A \rightarrow \eta\eta\pi^-A$
132 ± 15		96	BUGG	RVUE	
154 ± 30		29	AMSLER	95D	CBAR 0.0 $\bar{p}p \rightarrow \pi^0\pi^0\pi^0, \pi^0\eta\eta, \pi^0\pi^0\eta$
65 ± 10		30	ANTINORI	95	OMEG 300,450 $pp \rightarrow p p 2(\pi^+ \pi^-)$
199 ± 30		23	ANTINORI	95	OMEG 300,450 $pp \rightarrow p p \pi^+ \pi^-$
56 ± 12		23	ABATZIS	94	OMEG 450 $pp \rightarrow p p 2(\pi^+ \pi^-)$
100 ± 40		23	AMSLER	94E	CBAR 0.0 $\bar{p}p \rightarrow \pi^0\eta\eta'$
148 ± 20	18,31	ANISOVICH	94	CBAR	0.0 $\bar{p}p \rightarrow 3\pi^0, \pi^0\eta\eta$
150 ± 20	18,32	BUGG	94	RVUE	$\bar{p}p \rightarrow 3\pi^0, \eta\eta\pi^0, \eta\pi^0\pi^0$
245 ± 50		23	AMSLER	92	CBAR 0.0 $\bar{p}p \rightarrow \pi^0\eta\eta$
153 ± 67 ± 50		23	BELADIDZE	92C	VES 36 $\pi^-Be \rightarrow \pi^-\eta'\eta Be$
78 ± 18		23	ARMSTRONG	89E	OMEG 300 $pp \rightarrow p p 2(\pi^+ \pi^-)$
170 ± 40		23	ALDE	88	GAM4 300 $\pi^-N \rightarrow \pi^-N2\eta$
150 ± 20	600	23	ALDE	87	GAM4 100 $\pi^-p \rightarrow 4\pi^0 n$
265 ± 65		33	ALDE	86D	GAM4 100 $\pi^-p \rightarrow 2\eta n$
260 ± 60		23	BINON	84C	GAM2 38 $\pi^-p \rightarrow \eta\eta' n$
210 ± 40		23	BINON	83	GAM2 38 $\pi^-p \rightarrow 2\eta n$
101 ± 13		23	GRAY	83	DBC 0.0 $\bar{p}N \rightarrow 3\pi$

¹⁸ T-matrix pole.

¹⁹ Average between $\pi^+\pi^-2\pi^0$ and $2(\pi^+\pi^-)$.

²⁰ T-matrix pole, supersedes ANISOVICH 94.

²¹ T-matrix pole, supersedes ANISOVICH 94 and AMSLER 92.

²² Breit-Wigner width. May also be the $f_0(1370)$.

²³ Breit-Wigner width.

²⁴ Statistical error only.

²⁵ Breit-Wigner, solution 1, PWA ambiguous.

²⁶ K-matrix pole from combined analysis of $\pi^-p \rightarrow \pi^0\pi^0 n, \pi^-p \rightarrow K\bar{K}n, \pi^+\pi^- \rightarrow \pi^+\pi^-, \bar{p}p \rightarrow \pi^0\pi^0\pi^0, \pi^0\eta\eta, \pi^0\pi^0\eta, \pi^+\pi^-\pi^0, K^+K^-\pi^0, K_S^0 K_S^0 \pi^0, K^+K_S^0 \pi^-$ at rest, $\bar{p}n \rightarrow \pi^-\pi^-\pi^+, K_S^0 K^-\pi^0, K_S^0 K_S^0 \pi^-$ at rest.

²⁷ Supersedes BARBERIS 99 and BARBERIS 99B.

²⁸ T-matrix pole on sheet --+.

²⁹ T-matrix pole. Coupled-channel analysis of AMSLER 95B, AMSLER 95C, and AMSLER 94d.

³⁰ Supersedes ABATZIS 94, ARMSTRONG 89E. Breit-Wigner mass.

³¹ From a simultaneous analysis of the annihilations $\bar{p}p \rightarrow 3\pi^0, \pi^0\eta\eta$.

³² Reanalysis of ANISOVICH 94 data.

³³ From central value and spread of two solutions. Breit-Wigner mass.

 $f_0(1500)$ DECAY MODES

Mode	Fraction (Γ_i/Γ)	Scale factor
Γ_1 $\pi\pi$	(34.9 ± 2.3) %	1.2
Γ_2 $\pi^+\pi^-$	seen	
Γ_3 $2\pi^0$	seen	
Γ_4 4π	(49.5 ± 3.3) %	1.2
Γ_5 $4\pi^0$	seen	
Γ_6 $2\pi^+2\pi^-$	seen	
Γ_7 $2(\pi\pi)s$ -wave	seen	
Γ_8 $\rho\rho$	seen	
Γ_9 $\pi(1300)\pi$	seen	
Γ_{10} $a_1(1260)\pi$	seen	
Γ_{11} $\eta\eta$	(5.1 ± 0.9) %	1.4
Γ_{12} $\eta\eta'(958)$	(1.9 ± 0.8) %	1.7
Γ_{13} $K\bar{K}$	(8.6 ± 1.0) %	1.1
Γ_{14} $\gamma\gamma$	not seen	

CONSTRAINED FIT INFORMATION

An overall fit to 6 branching ratios uses 10 measurements and one constraint to determine 5 parameters. The overall fit has a $\chi^2 = 11.4$ for 6 degrees of freedom.

The following *off-diagonal* array elements are the correlation coefficients $\langle \delta x_i \delta x_j \rangle / (\delta x_i \delta x_j)$, in percent, from the fit to the branching fractions, $x_i \equiv \Gamma_i/\Gamma_{\text{total}}$. The fit constrains the x_i whose labels appear in this array to sum to one.

x_4	-83			
x_{11}	11	-52		
x_{12}	-5	-31	29	
x_{13}	39	-67	33	6
	x_1	x_4	x_{11}	x_{12}

 $f_0(1500)$ $\Gamma(i)\Gamma(\gamma\gamma)/\Gamma(\text{total})$

$\Gamma(\pi\pi) \times \Gamma(\gamma\gamma)/\Gamma_{\text{total}}$ $\Gamma_1/\Gamma_{14}/\Gamma$

VALUE (eV) CL% DOCUMENT ID TECN COMMENT

••• We do not use the following data for averages, fits, limits, etc. •••

33⁺₆₋₂₁ 12+1809 21 34 UEHARA 08A BELL 10.6 $e^+e^- \rightarrow e^+e^-\pi^0\pi^0$

not seen ACCIARRI 01H L3 $\gamma\gamma \rightarrow K_S^0 K_S^0, E_{\text{cm}}^{\text{eff}} = 91, 183-209 \text{ GeV}$

<460 95 BARATE 00E ALEP $\gamma\gamma \rightarrow \pi^+\pi^-$

34 May also be the $f_0(1370)$. Multiplied by us by 3 to obtain the $\pi\pi$ value.

 $f_0(1500)$ BRANCHING RATIOS

$\Gamma(\pi\pi)/\Gamma_{\text{total}}$ Γ_1/Γ

VALUE DOCUMENT ID TECN COMMENT

••• We do not use the following data for averages, fits, limits, etc. •••

0.454 ± 0.104 BUGG 96 RVUE

$\Gamma(\pi^+\pi^-)/\Gamma_{\text{total}}$ Γ_2/Γ

VALUE DOCUMENT ID TECN COMMENT

seen BERTIN 98 OBLX 0.05-0.405 $\bar{p}p \rightarrow \pi^+\pi^+\pi^-$

••• We do not use the following data for averages, fits, limits, etc. •••

possibly seen FRABETTI 97D E687 $D_S^\pm \rightarrow \pi^\mp \pi^\pm \pi^\pm$

$\Gamma(4\pi)/\Gamma(\pi\pi)$ Γ_4/Γ_1

VALUE DOCUMENT ID TECN COMMENT

1.42 ± 0.18 OUR FIT Error includes scale factor of 1.2.

1.42 ± 0.18 OUR AVERAGE Error includes scale factor of 1.2.

1.37 ± 0.16 BARBERIS 00D 450 $pp \rightarrow p_f 4\pi p_S$

2.1 ± 0.6 35 AMSLER 98 RVUE

••• We do not use the following data for averages, fits, limits, etc. •••

2.1 ± 0.2 36 ANISOVICH 02D SPEC Combined fit

3.4 ± 0.8 35 ABELE 96 CBAR 0.0 $\bar{p}p \rightarrow 5\pi^0$

$\Gamma(2(\pi\pi)s\text{-wave})/\Gamma(\pi\pi)$ Γ_7/Γ_1

VALUE DOCUMENT ID TECN COMMENT

••• We do not use the following data for averages, fits, limits, etc. •••

0.42 ± 0.26 37 ABELE 01 CBAR 0.0 $\bar{p}d \rightarrow \pi^-4\pi^0 p$

$\Gamma(2(\pi\pi)s\text{-wave})/\Gamma(4\pi)$ Γ_7/Γ_4

VALUE DOCUMENT ID TECN COMMENT

••• We do not use the following data for averages, fits, limits, etc. •••

0.26 ± 0.07 ABELE 01B CBAR 0.0 $\bar{p}d \rightarrow 5\pi p$

$\Gamma(\rho\rho)/\Gamma(4\pi)$ Γ_8/Γ_4

VALUE DOCUMENT ID TECN COMMENT

••• We do not use the following data for averages, fits, limits, etc. •••

0.13 ± 0.08 ABELE 01B CBAR 0.0 $\bar{p}d \rightarrow 5\pi p$

$\Gamma(\rho\rho)/\Gamma(2(\pi\pi)s\text{-wave})$ Γ_8/Γ_7

VALUE DOCUMENT ID COMMENT

••• We do not use the following data for averages, fits, limits, etc. •••

3.3 ± 0.5 BARBERIS 00C 450 $pp \rightarrow p_f \pi^+ \pi^- 2\pi^0 p_S$

2.6 ± 0.4 BARBERIS 00C 450 $pp \rightarrow p_f 2(\pi^+ \pi^-) p_S$

$\Gamma(\pi(1300)\pi)/\Gamma(4\pi)$ Γ_9/Γ_4

VALUE DOCUMENT ID TECN COMMENT

••• We do not use the following data for averages, fits, limits, etc. •••

0.50 ± 0.25 ABELE 01B CBAR 0.0 $\bar{p}d \rightarrow 5\pi p$

$\Gamma(a_1(1260)\pi)/\Gamma(4\pi)$ Γ_{10}/Γ_4

VALUE DOCUMENT ID TECN COMMENT

••• We do not use the following data for averages, fits, limits, etc. •••

0.12 ± 0.05 ABELE 01B CBAR 0.0 $\bar{p}d \rightarrow 5\pi p$

Meson Particle Listings

 $f_1(1510), f_2'(1525)$ $f_1(1510)$

$$J^{PC} = 0^+(1^{++})$$

OMITTED FROM SUMMARY TABLE
See the minireview under $\eta(1405)$.

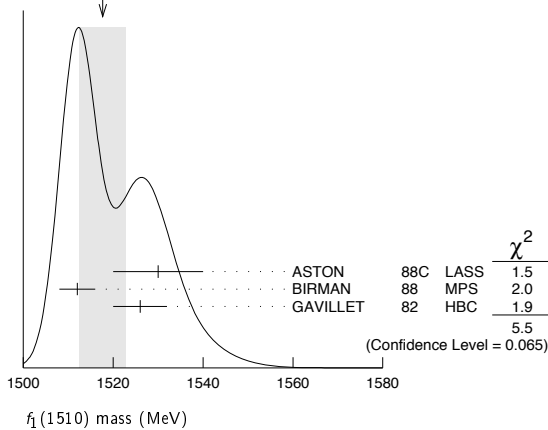
 $f_1(1510)$ MASS

VALUE (MeV)	EVTs	DOCUMENT ID	TECN	COMMENT
1518 ± 5 OUR AVERAGE				Error includes scale factor of 1.7. See the ideogram below.
1530 ± 10		ASTON	88c LASS	11 $K^- p \rightarrow K_S^0 K^\pm \pi^\mp \Lambda$
1512 ± 4	600	¹ BIRMAN	88 MPS	8 $\pi^- p \rightarrow K^+ \bar{K}^0 \pi^- n$
1526 ± 6	271	GAVILLET	82 HBC	4.2 $K^- p \rightarrow \Lambda K K \pi$
~ 1525		² BAUER	93B	$\gamma\gamma^* \rightarrow \pi^+ \pi^- \pi^0 \pi^0$

• • • We do not use the following data for averages, fits, limits, etc. • • •

¹ From partial wave analysis of $K^+ \bar{K}^0 \pi^-$ state.
² Not seen by AIHARA 88c in the $K_S^0 K^\pm \pi^\mp$ final state.

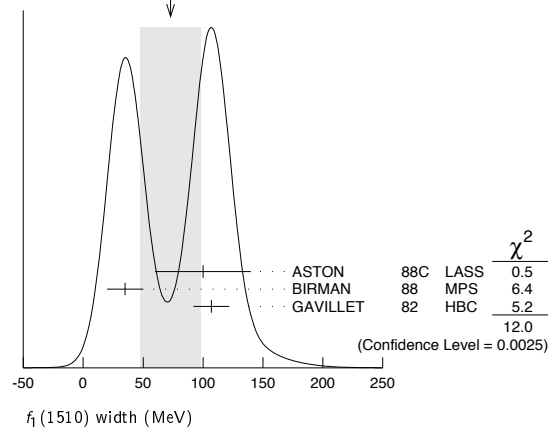
WEIGHTED AVERAGE
1518 ± 5 (Error scaled by 1.7)

 $f_1(1510)$ WIDTH

VALUE (MeV)	EVTs	DOCUMENT ID	TECN	COMMENT
73 ± 25 OUR AVERAGE				Error includes scale factor of 2.5. See the ideogram below.
100 ± 40		ASTON	88c LASS	11 $K^- p \rightarrow K_S^0 K^\pm \pi^\mp \Lambda$
35 ± 15	600	³ BIRMAN	88 MPS	8 $\pi^- p \rightarrow K^+ \bar{K}^0 \pi^- n$
107 ± 15	271	GAVILLET	82 HBC	4.2 $K^- p \rightarrow \Lambda K K \pi$

³ From partial wave analysis of $K^+ \bar{K}^0 \pi^-$ state.

WEIGHTED AVERAGE
73 ± 25 (Error scaled by 2.5)

 $f_1(1510)$ DECAY MODES

Mode	Fraction (Γ_i/Γ)
Γ_1 $K \bar{K}^*(892) + c.c.$	seen

 $f_1(1510)$ REFERENCES

BAUER	93B	PR D48 3976	D.A. Bauer <i>et al.</i>	(SLAC)
AIHARA	88C	PR D38 1	H. Aihara <i>et al.</i>	(TPC-2 γ Collab.)
ASTON	88C	PL B201 573	D. Aston <i>et al.</i>	(SLAC, MAGO, CINC, INUS) JP
BIRMAN	88	PRL 61 1557	A. Birman <i>et al.</i>	(BNL, FSU, IND, MASD) JP
GAVILLET	82	ZPHY C16 119	P. Gavillet <i>et al.</i>	(CERN, CDEF, PADO+)

 $f_2'(1525)$

$$J^{PC} = 0^+(2^{++})$$

 $f_2'(1525)$ MASS

VALUE (MeV) DOCUMENT ID
1525 ± 5 OUR ESTIMATE This is only an educated guess; the error given is larger than the error on the average of the published values.

PRODUCED BY PION BEAM

VALUE (MeV)	EVTs	DOCUMENT ID	TECN	COMMENT
1525 ± 5 OUR ESTIMATE				This is only an educated guess; the error given is larger than the error on the average of the published values.
• • • We do not use the following data for averages, fits, limits, etc. • • •				
1521 ± 13		TIKHOMIROV 03	SPEC	40.0 $\pi^- C \rightarrow K_S^0 K_S^0 K_L^0 X$
1547 \pm 2		¹ LONGACRE 86	MPS	22 $\pi^- p \rightarrow K_S^0 K_S^0 n$
1496 \pm 9		² CHABAUD 81	ASPK	6 $\pi^- p \rightarrow K^+ K^- n$
1497 \pm 8		CHABAUD 81	ASPK	18.4 $\pi^- p \rightarrow K^+ K^- n$
1492 ± 29		GORLICH 80	ASPK	17 $\pi^- p$ polarized $\rightarrow K^+ K^- n$
1502 ± 25		³ CORDEN 79	OMEG	12-15 $\pi^- p \rightarrow \pi^+ \pi^- n$
1480	14	CRENNELL 66	HBC	6.0 $\pi^- p \rightarrow K_S^0 K_S^0 n$

PRODUCED BY K^\pm BEAM

VALUE (MeV)	EVTs	DOCUMENT ID	TECN	COMMENT
1523.4 ± 1.3 OUR AVERAGE				Includes data from the datablock that follows this one. Error includes scale factor of 1.1.
1526.8 ± 4.3		ASTON	88d LASS	11 $K^- p \rightarrow K_S^0 K_S^0 \Lambda$
1504 ± 12		BOLONKIN 86	SPEC	40 $K^- p \rightarrow K_S^0 K_S^0 Y$
1529 ± 3		ARMSTRONG 83B	OMEG	18.5 $K^- p \rightarrow K^- K^+ \Lambda$
1521 ± 6	650	AGUILAR...	81B HBC	4.2 $K^- p \rightarrow \Lambda K^+ K^-$
1521 ± 3	572	ALHARRAN 81	HBC	8.25 $K^- p \rightarrow \Lambda K \bar{K}^0$
1522 ± 6	123	BARREIRO 77	HBC	4.15 $K^- p \rightarrow \Lambda K_S^0 K_S^0$
1528 ± 7	166	EVA NGELIS...	77 OMEG	10 $K^- p \rightarrow K^+ K^- (\Lambda, \Sigma)$
1527 ± 3	120	BRANDENB...	76c ASPK	13 $K^- p \rightarrow K^+ K^- (\Lambda, \Sigma)$
1519 ± 7	100	AGUILAR...	72B HBC	3.9, 4.6 $K^- p \rightarrow K \bar{K} (\Lambda, \Sigma)$
• • • We do not use the following data for averages, fits, limits, etc. • • •				
1514 ± 8	61	BINON 07	GAMS	32.5 $K^- p \rightarrow \eta \eta (\Lambda/\Sigma^0)$
1513 ± 10		⁴ BARKOV 99	SPEC	40 $K^- p \rightarrow K_S^0 K_S^0 Y$

PRODUCED IN $e^+ e^-$ ANNIHILATION

VALUE (MeV)	EVTs	DOCUMENT ID	TECN	COMMENT
1520.7 ± 2.0 OUR AVERAGE				The data in this block is included in the average printed for a previous datablock.
1521 ± 5		ABLIKIM 05	BES2	$J/\psi \rightarrow \phi K^+ K^-$
1518 ± 1 ± 3		ABE 04	BELL	10.6 $e^+ e^- \rightarrow e^+ e^- K^+ K^-$
1519 ± 2 \pm 15		BAI 03g	BES	$J/\psi \rightarrow \gamma K \bar{K}$
1523 ± 6	331	⁵ ACCIARRI 01H	L3	91, 183-209 $e^+ e^- \rightarrow e^+ e^- K_S^0 K_S^0$
1535 ± 5 ± 4		ABREU 96c	DLPH	$Z^0 \rightarrow K^+ K^- + X$
1516 ± 5 \pm 9		BAI 96c	BES	$J/\psi \rightarrow \gamma K^+ K^-$
1531.6 ± 10.0		AUGUSTIN 88	DM2	$J/\psi \rightarrow \gamma K^+ K^-$
1515 ± 5		⁶ FALVARD 88	DM2	$J/\psi \rightarrow \phi K^+ K^-$
1525 ± 10 ± 10		BALTRUSAIT...87	MRK3	$J/\psi \rightarrow \gamma K^+ K^-$
• • • We do not use the following data for averages, fits, limits, etc. • • •				
1523 ± 5	870	⁷ SHEGELSKY 06A	RVUE	$\gamma\gamma \rightarrow K_S^0 K_S^0$
1496 ± 2		⁸ FALVARD 88	DM2	$J/\psi \rightarrow \phi K^+ K^-$

PRODUCED IN $\bar{p}p$ ANNIHILATION

VALUE (MeV)	DOCUMENT ID	TECN	COMMENT
• • • We do not use the following data for averages, fits, limits, etc. • • •			
1530 ± 12	⁹ ANISOVICH 09	RVUE	0.0 $\bar{p}p, \pi N$
1513 ± 4	AMSLER 06	CBAR	0.9 $\bar{p}p \rightarrow K^+ K^- \pi^0$
1508 ± 9	¹⁰ AMSLER 02	CBAR	0.9 $\bar{p}p \rightarrow \pi^0 \eta \eta, \pi^0 \pi^0 \pi^0$

CENTRAL PRODUCTION

VALUE (MeV)	DOCUMENT ID	TECN	COMMENT
1515 ± 15	BARBERIS 99	OMEG	450 $pp \rightarrow p_s p_f K^+ K^-$

PRODUCED IN ep COLLISIONS

VALUE (MeV)	EVTs	DOCUMENT ID	TECN	COMMENT
$1512 \pm 3 \begin{smallmatrix} +1.4 \\ -0.5 \end{smallmatrix}$		11 CHEKANOV	08	ZEUS $ep \rightarrow K_S^0 K_S^0 X$
1537 ± 9	84	12 CHEKANOV	04	ZEUS $ep \rightarrow K_S^0 K_S^0 X$

- • • We do not use the following data for averages, fits, limits, etc. • • •
- ¹ From a partial-wave analysis of data using a K-matrix formalism with 5 poles.
- ² CHABAUD 81 is a reanalysis of PAWLICKI 77 data.
- ³ From an amplitude analysis where the $f'_2(1525)$ width and elasticity are in complete disagreement with the values obtained from $K\bar{K}$ channel, making the solution dubious.
- ⁴ Systematic errors not estimated.
- ⁵ Supersedes ACCIARRI 95J.
- ⁶ From an analysis ignoring interference with $f_0(1710)$.
- ⁷ From analysis of L3 data at 91 and 183–209 GeV.
- ⁸ From an analysis including interference with $f_0(1710)$.
- ⁹ 4-poles, 5-channel K matrix fit.
- ¹⁰ T-matrix pole.
- ¹¹ In the SU(3) based model with a specific interference pattern of the $f_2(1270)$, $a_2^0(1320)$, and $f'_2(1525)$ mesons incoherently added to the $f_0(1710)$ and non-resonant background.
- ¹² Systematic errors not estimated.

 $f'_2(1525)$ WIDTH

VALUE (MeV)	DOCUMENT ID	COMMENT
$73 \pm \frac{6}{5}$ OUR FIT		
76 ± 10	PDG	90 For fitting

PRODUCED BY PION BEAM

VALUE (MeV)	DOCUMENT ID	TECN	COMMENT
102 ± 42	TIKHOMIROV 03	SPEC	$40.0 \pi^- C \rightarrow K_S^0 K_S^0 K_L^0 X$
$108 \pm \frac{5}{2}$	13 LONGACRE 86	MPS	$22 \pi^- p \rightarrow K_S^0 K_S^0 n$
$69 \pm \frac{22}{-16}$	14 CHABAUD 81	ASPK	$6 \pi^- p \rightarrow K^+ K^- n$
$137 \pm \frac{23}{-21}$	CHABAUD 81	ASPK	$18.4 \pi^- p \rightarrow K^+ K^- n$
$150 \pm \frac{83}{-50}$	GORLICH 80	ASPK	$17 \pi^- p \text{ polarized} \rightarrow K^+ K^- n$
165 ± 42	15 CORDEN 79	OMEG	$12\text{--}15 \pi^- p \rightarrow \pi^+ \pi^- n$
$92 \pm \frac{39}{-22}$	16 POLYCHRO... 79	STRC	$7 \pi^- p \rightarrow n K_S^0 K_S^0$

PRODUCED BY K^\pm BEAM

VALUE (MeV)	EVTs	DOCUMENT ID	TECN	COMMENT
80.2 ± 2.6 OUR AVERAGE		Includes data from the datablock that follows this one.		
90 ± 12		ASTON 88D	LASS	$11 K^- p \rightarrow K_S^0 K_S^0 \Lambda$
73 ± 18		BOLONKIN 86	SPEC	$40 K^- p \rightarrow K_S^0 K_S^0 Y$
83 ± 15		ARMSTRONG 83B	OMEG	$18.5 K^- p \rightarrow K^- K^+ \Lambda$
85 ± 16	650	AGUILAR...	81B	HBC $4.2 K^- p \rightarrow \Lambda K^+ K^-$
$80 \pm \frac{14}{-11}$	572	ALHARRAN 81	HBC	$8.25 K^- p \rightarrow \Lambda K\bar{K}$
72 ± 25	166	EVANGELIS...	77	OMEG $10 K^- p \rightarrow K^+ K^- (\Lambda, \Sigma)$
69 ± 22	100	AGUILAR...	72B	HBC $3.9, 4.6 K^- p \rightarrow K\bar{K}(\Lambda, \Sigma)$
• • • We do not use the following data for averages, fits, limits, etc. • • •				
92 ± 25	61	BINON 07	GAMS	$32.5 K^- p \rightarrow \eta \eta (\Lambda / \Sigma^0)$
75 ± 20	17	BARKOV 09	SPEC	$40 K^- p \rightarrow K_S^0 K_S^0 Y$
$62 \pm \frac{19}{-14}$	123	BARREIRO 77	HBC	$4.15 K^- p \rightarrow \Lambda K_S^0 K_S^0$
61 ± 8	120	BRANDENB... 76C	ASPK	$13 K^- p \rightarrow K^+ K^- (\Lambda, \Sigma)$

PRODUCED IN e^+e^- ANNIHILATION

VALUE (MeV)	EVTs	DOCUMENT ID	TECN	COMMENT
The data in this block is included in the average printed for a previous datablock.				
79.9 ± 3.3 OUR AVERAGE		Error includes scale factor of 1.1.		
77 ± 15		ABLIKIM 05	BES2	$J/\psi \rightarrow \phi K^+ K^-$
$82 \pm 2 \pm 3$		ABE 04	BELL	$10.6 e^+ e^- \rightarrow e^+ e^- K^+ K^-$
$75 \pm 4 \pm \frac{15}{-5}$		BAI 03G	BES	$J/\psi \rightarrow \gamma K\bar{K}$
100 ± 15	331	18 ACCIARRI 01H	L3	$91, 183\text{--}209 e^+ e^- \rightarrow e^+ e^- K_S^0 K_S^0$
$60 \pm 20 \pm 19$		ABREU 96C	DLPH	$Z^0 \rightarrow K^+ K^- + X$
$60 \pm 23 \pm \frac{13}{-20}$		BAI 96C	BES	$J/\psi \rightarrow \gamma K^+ K^-$
103 ± 30		AUGUSTIN 88	DM2	$J/\psi \rightarrow \gamma K^+ K^-$
62 ± 10		19 FALVARD 88	DM2	$J/\psi \rightarrow \phi K^+ K^-$
85 ± 35		BALTRUSAIT..87	MRK3	$J/\psi \rightarrow \gamma K^+ K^-$
• • • We do not use the following data for averages, fits, limits, etc. • • •				
104 ± 10	870	20 SCHEGELSKY 06A	RVUE	$\gamma\gamma \rightarrow K_S^0 K_S^0$
100 ± 3		21 FALVARD 88	DM2	$J/\psi \rightarrow \phi K^+ K^-$

PRODUCED IN $\bar{p}p$ ANNIHILATION

VALUE (MeV)	DOCUMENT ID	TECN	COMMENT
79 ± 8	22 AMSLER 02	CBAR	$0.9 \bar{p}p \rightarrow \pi^0 \eta \eta, \pi^0 \pi^0 \pi^0$
• • • We do not use the following data for averages, fits, limits, etc. • • •			
128 ± 20	23 ANISOVICH 09	RVUE	$0.0 \bar{p}p, \pi N$
76 ± 6	AMSLER 06	CBAR	$0.9 \bar{p}p \rightarrow K^+ K^- \pi^0$

CENTRAL PRODUCTION

VALUE (MeV)	DOCUMENT ID	TECN	COMMENT
70 ± 25	BARBERIS 99	OMEG	$450 p\bar{p} \rightarrow p_S p_f K^+ K^-$

PRODUCED IN ep COLLISIONS

VALUE (MeV)	EVTs	DOCUMENT ID	TECN	COMMENT
$83 \pm 9 \pm \frac{5}{-4}$		24 CHEKANOV 08	ZEUS	$ep \rightarrow K_S^0 K_S^0 X$
• • • We do not use the following data for averages, fits, limits, etc. • • •				
$50 \pm \frac{34}{-22}$	84	25 CHEKANOV 04	ZEUS	$ep \rightarrow K_S^0 K_S^0 X$

- ¹³ From a partial-wave analysis of data using a K-matrix formalism with 5 poles.
- ¹⁴ CHABAUD 81 is a reanalysis of PAWLICKI 77 data.
- ¹⁵ From an amplitude analysis where the $f'_2(1525)$ width and elasticity are in complete disagreement with the values obtained from $K\bar{K}$ channel, making the solution dubious.
- ¹⁶ From a fit to the D with $f_2(1270)$ - $f'_2(1525)$ interference. Mass fixed at 1516 MeV.
- ¹⁷ Systematic errors not estimated.
- ¹⁸ Supersedes ACCIARRI 95J.
- ¹⁹ From an analysis ignoring interference with $f_0(1710)$.
- ²⁰ From analysis of L3 data at 91 and 183–209 GeV.
- ²¹ From an analysis including interference with $f_0(1710)$.
- ²² T-matrix pole.
- ²³ 4-poles, 5-channel K matrix fit.
- ²⁴ In the SU(3) based model with a specific interference pattern of the $f_2(1270)$, $a_2^0(1320)$, and $f'_2(1525)$ mesons incoherently added to the $f_0(1710)$ and non-resonant background.
- ²⁵ Systematic errors not estimated.

 $f'_2(1525)$ DECAY MODES

Mode	Fraction (Γ_i/Γ)
Γ_1 $K\bar{K}$	(88.7 \pm 2.2) %
Γ_2 $\eta\eta$	(10.4 \pm 2.2) %
Γ_3 $\pi\pi$	(8.2 \pm 1.5) $\times 10^{-3}$
Γ_4 $K\bar{K}^*(892) + \text{c.c.}$	
Γ_5 $\pi K\bar{K}$	
Γ_6 $\pi\pi\eta$	
Γ_7 $\pi^+ \pi^+ \pi^- \pi^-$	
Γ_8 $\gamma\gamma$	(1.11 \pm 0.14) $\times 10^{-6}$

CONSTRAINED FIT INFORMATION

An overall fit to the total width, 2 partial widths, a combination of partial widths obtained from integrated cross sections, and 3 branching ratios uses 16 measurements and one constraint to determine 5 parameters. The overall fit has a $\chi^2 = 14.0$ for 12 degrees of freedom.

The following *off-diagonal* array elements are the correlation coefficients $\langle \delta p_i \delta p_j \rangle / (\delta p_i \delta p_j)$, in percent, from the fit to parameters p_i , including the branching fractions, $x_i \equiv \Gamma_i/\Gamma_{\text{total}}$. The fit constrains the x_i whose labels appear in this array to sum to one.

x_2	-100			
x_3	-6	-1		
x_8	-6	6	1	
Γ	-23	23	-1	-55
	x_1	x_2	x_3	x_8

Mode	Rate (MeV)
Γ_1 $K\bar{K}$	65 $\pm \frac{5}{-4}$
Γ_2 $\eta\eta$	7.6 ± 1.8
Γ_3 $\pi\pi$	0.60 ± 0.12
Γ_8 $\gamma\gamma$	(8.1 \pm 0.9) $\times 10^{-5}$

 $f'_2(1525)$ PARTIAL WIDTHS

VALUE (MeV)	DOCUMENT ID	TECN	COMMENT
$65 \pm \frac{5}{-4}$ OUR FIT			
$63 \pm \frac{6}{-5}$	26 LONGACRE 86	MPS	$22 \pi^- p \rightarrow K_S^0 K_S^0 n$

$f_2(1565)$

$$J^{PC} = 0^+(2^{++})$$

OMITTED FROM SUMMARY TABLE

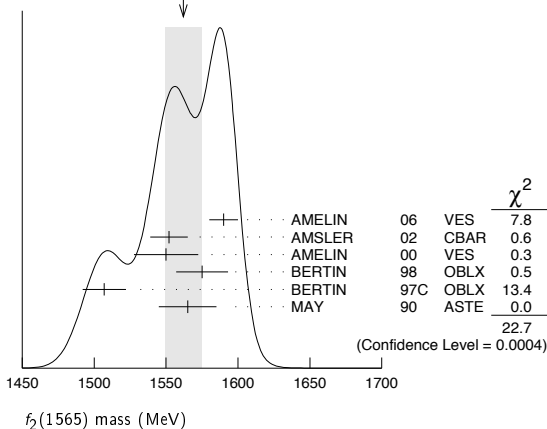
Seen mostly in antinucleon-nucleon annihilation. Needs confirmation in other channels.

$f_2(1565)$ MASS

VALUE (MeV)	DOCUMENT ID	TECN	COMMENT
1562±13 OUR AVERAGE	Error includes scale factor of 2.1. See the ideogram below.		
1590±10	1 AMELIN 06	VES	$36 \pi^- p \rightarrow \omega \omega n$
1552±13	2 AMSLER 02	CBAR	$0.9 \bar{p} p \rightarrow \pi^0 \eta \eta, \pi^0 \pi^0 \pi^0$
1550±10±20	AMELIN 00	VES	$37 \pi^- p \rightarrow \eta \pi^+ \pi^- n$
1575±18	BERTIN 98	OBLX	$0.05-0.405 \bar{n} p \rightarrow \pi^+ \pi^+ \pi^-$
1507±15	2 BERTIN 97c	OBLX	$0.0 \bar{p} p \rightarrow \pi^+ \pi^- \pi^0$
1565±20	MAY 90	ASTE	$0.0 \bar{p} p \rightarrow \pi^+ \pi^- \pi^0$
1560±15	3 ANISOVICH 09	RVUE	$0.0 \bar{p} p, \pi N$
1598±11±9	BAKER 99b	SPEC	$0 \bar{p} p \rightarrow \omega \omega \pi^0$
1534±20	4 ABELE 96c	RVUE	Compilation
~1552	5 AMSLER 95d	CBAR	$0.0 \bar{p} p \rightarrow \pi^0 \pi^0 \pi^0, \pi^0 \eta \eta, \pi^0 \pi^0 \eta$
1598±72	BALOSHIN 95	SPEC	$40 \pi^- C \rightarrow K_S^0 K_S^0 X$
1566+80-50	6 ANISOVICH 94	CBAR	$0.0 \bar{p} p \rightarrow 3\pi^0, \eta \eta \pi^0$
1502±9	ADAMO 93	OBLX	$\bar{n} p \rightarrow \pi^+ \pi^+ \pi^-$
1488±10	7 ARMSTRONG 93c	E760	$\bar{p} p \rightarrow \pi^0 \eta \eta \rightarrow 6\gamma$
1508±10	7 ARMSTRONG 93d	E760	$\bar{p} p \rightarrow 3\pi^0 \rightarrow 6\gamma$
1525±10	7 ARMSTRONG 93d	E760	$\bar{p} p \rightarrow \eta \pi^0 \pi^0 \rightarrow 6\gamma$
~1504	8 WEIDENAUER 93	ASTE	$0.0 \bar{p} N \rightarrow 3\pi^- 2\pi^+$
1540±15	7 ADAMO 92	OBLX	$\bar{n} p \rightarrow \pi^+ \pi^+ \pi^-$
1515±10	9 AKER 91	CBAR	$0.0 \bar{p} p \rightarrow 3\pi^0$
1477±5	BRIDGES 86c	DBC	$0.0 \bar{p} N \rightarrow 3\pi^- 2\pi^+$

- 1 Supersedes the $\omega\omega$ state of BELADIDZE 92b earlier assigned to the $f_2(1640)$.
- 2 T-matrix pole.
- 3 On sheet II in a two-pole solution.
- 4 T-matrix pole, large coupling to $\rho\rho$ and $\omega\omega$, could be $f_2(1640)$.
- 5 Coupled-channel analysis of AMSLER 95b, AMSLER 95c, and AMSLER 94d.
- 6 From a simultaneous analysis of the annihilations $\bar{p} p \rightarrow 3\pi^0, \pi^0 \eta \eta$ including AKER 91 data.
- 7 J^P not determined, could be partly $f_0(1500)$.
- 8 J^P not determined.
- 9 Superseded by AMSLER 95b.

WEIGHTED AVERAGE 1562±13 (Error scaled by 2.1)



$f_2(1565)$ WIDTH

VALUE (MeV)	DOCUMENT ID	TECN	COMMENT
134±8 OUR AVERAGE			
140±11	10 AMELIN 06	VES	$36 \pi^- p \rightarrow \omega \omega n$
113±23	11 AMSLER 02	CBAR	$0.9 \bar{p} p \rightarrow \pi^0 \eta \eta, \pi^0 \pi^0 \pi^0$
130±20±40	AMELIN 00	VES	$37 \pi^- p \rightarrow \eta \pi^+ \pi^- n$
119±24	BERTIN 98	OBLX	$0.05-0.405 \bar{n} p \rightarrow \pi^+ \pi^+ \pi^-$
130±20	11 BERTIN 97c	OBLX	$0.0 \bar{p} p \rightarrow \pi^+ \pi^- \pi^0$
170±40	MAY 90	ASTE	$0.0 \bar{p} p \rightarrow \pi^+ \pi^- \pi^0$

••• We do not use the following data for averages, fits, limits, etc. •••

280±40	12 ANISOVICH 09	RVUE	$0.0 \bar{p} p, \pi N$
180±60	13 ABELE 96c	RVUE	Compilation
~142	14 AMSLER 95d	CBAR	$0.0 \bar{p} p \rightarrow \pi^0 \pi^0 \pi^0, \pi^0 \eta \eta, \pi^0 \pi^0 \eta$
263±101	BALOSHIN 95	SPEC	$40 \pi^- C \rightarrow K_S^0 K_S^0 X$
166+80-20	15 ANISOVICH 94	CBAR	$0.0 \bar{p} p \rightarrow 3\pi^0, \eta \eta \pi^0$
130±10	16 ADAMO 93	OBLX	$\bar{n} p \rightarrow \pi^+ \pi^+ \pi^-$
148±27	17 ARMSTRONG 93c	E760	$\bar{p} p \rightarrow \pi^0 \eta \eta \rightarrow 6\gamma$
103±15	17 ARMSTRONG 93d	E760	$\bar{p} p \rightarrow 3\pi^0 \rightarrow 6\gamma$
111±10	17 ARMSTRONG 93d	E760	$\bar{p} p \rightarrow \eta \pi^0 \pi^0 \rightarrow 6\gamma$
~206	18 WEIDENAUER 93	ASTE	$0.0 \bar{p} N \rightarrow 3\pi^- 2\pi^+$
132±37	17 ADAMO 92	OBLX	$\bar{n} p \rightarrow \pi^+ \pi^+ \pi^-$
120±10	19 AKER 91	CBAR	$0.0 \bar{p} p \rightarrow 3\pi^0$
116±9	BRIDGES 86c	DBC	$0.0 \bar{p} N \rightarrow 3\pi^- 2\pi^+$
10 Supersedes the $\omega\omega$ state of BELADIDZE 92b earlier assigned to the $f_2(1640)$.			
11 T-matrix pole.			
12 On sheet II in a two-pole solution.			
13 T-matrix pole, large coupling to $\rho\rho$ and $\omega\omega$, could be $f_2(1640)$.			
14 Coupled-channel analysis of AMSLER 95b, AMSLER 95c, and AMSLER 94d.			
15 From a simultaneous analysis of the annihilations $\bar{p} p \rightarrow 3\pi^0, \pi^0 \eta \eta$ including AKER 91 data.			
16 Supersedes ADAMO 92.			
17 J^P not determined, could be partly $f_0(1500)$.			
18 J^P not determined.			
19 Superseded by AMSLER 95b.			

$f_2(1565)$ DECAY MODES

Mode	Fraction (Γ_i/Γ)
$\Gamma_1 \pi\pi$	seen
$\Gamma_2 \pi^+\pi^-$	seen
$\Gamma_3 \pi^0\pi^0$	seen
$\Gamma_4 \rho^0\rho^0$	seen
$\Gamma_5 2\pi^+2\pi^-$	seen
$\Gamma_6 \eta\eta$	seen
$\Gamma_7 a_2(1320)\pi$	
$\Gamma_8 \omega\omega$	seen
$\Gamma_9 K\bar{K}$	
$\Gamma_{10} \gamma\gamma$	

$f_2(1565)$ PARTIAL WIDTHS

VALUE (MeV)	EVTS	DOCUMENT ID	TECN	COMMENT	Γ_6
••• We do not use the following data for averages, fits, limits, etc. •••					
1.2±0.3	870	20 SCHEGELSKY 06a	RVUE	$\gamma\gamma \rightarrow K_S^0 K_S^0$	
VALUE (MeV)	EVTS	DOCUMENT ID	TECN	COMMENT	Γ_9
••• We do not use the following data for averages, fits, limits, etc. •••					
2.0±1.0	870	20 SCHEGELSKY 06a	RVUE	$\gamma\gamma \rightarrow K_S^0 K_S^0$	
VALUE (keV)	EVTS	DOCUMENT ID	TECN	COMMENT	Γ_{10}
••• We do not use the following data for averages, fits, limits, etc. •••					
0.70±0.14	870	20 SCHEGELSKY 06a	RVUE	$\gamma\gamma \rightarrow K_S^0 K_S^0$	
20 From analysis of L3 data at 91 and 183–209 GeV, using $f_2(1565)$ mass of 1570 MeV, width of 160 MeV, $\Gamma(\pi\pi) = 25$ MeV, and SU(3) relations.					

$f_2(1565)$ BRANCHING RATIOS

$\Gamma(\pi\pi)/\Gamma_{total}$	DOCUMENT ID	TECN	COMMENT	Γ_1/Γ
••• We do not use the following data for averages, fits, limits, etc. •••				
seen	BAKER 99b	SPEC	$0 \bar{p} p \rightarrow \omega \omega \pi^0$	
$\Gamma(\pi^+\pi^-)/\Gamma_{total}$	DOCUMENT ID	TECN	COMMENT	Γ_2/Γ
••• We do not use the following data for averages, fits, limits, etc. •••				
seen	BERTIN 98	OBLX	$0.05-0.405 \bar{n} p \rightarrow \pi^+ \pi^+ \pi^-$	
not seen	21 ANISOVICH 94b	RVUE	$\bar{p} p \rightarrow \pi^+ \pi^- \pi^0$	
seen	MAY 89	ASTE	$\bar{p} p \rightarrow \pi^+ \pi^- \pi^0$	
21 ANISOVICH 94b is from a reanalysis of MAY 90.				
$\Gamma(\pi^0\pi^0)/\Gamma_{total}$	DOCUMENT ID	TECN	COMMENT	Γ_3/Γ
seen	AMSLER 95b	CBAR	$0.0 \bar{p} p \rightarrow 3\pi^0$	

Meson Particle Listings

 $f_2(1565)$, $\rho(1570)$, $h_1(1595)$, $\pi_1(1600)$ $\Gamma(\pi^+\pi^-)/\Gamma(\rho^0\rho^0)$ Γ_2/Γ_4

VALUE	DOCUMENT ID	TECN	COMMENT
0.042 ± 0.013	BRIDGES	86B	DBC $\bar{p}n \rightarrow 3\pi^- 2\pi^+$

 $\Gamma(\eta)/\Gamma(\pi^0\pi^0)$ Γ_6/Γ_3

VALUE	DOCUMENT ID	TECN	COMMENT
0.024 ± 0.005 ± 0.012	22 ARMSTRONG	93C	E760 $\bar{p}p \rightarrow \pi^0\eta\eta \rightarrow 6\gamma$ 22 J^P not determined, could be partly $f_0(1500)$.

 $\Gamma(\omega\omega)/\Gamma_{total}$ Γ_8/Γ

VALUE	DOCUMENT ID	TECN	COMMENT
seen	BAKER	99B	SPEC $0\bar{p}p \rightarrow \omega\pi^0$

 $f_2(1565)$ REFERENCES

ANISOVICH	09	JUMP A24 2481	V.V. Anisovich, A.V. Sarantsev	
AMELIN	06	PAN 69 690	D.V. Amelin et al.	(VES Collab.)
Translated from YAF 69 715.				
SCHEGELSKY	06A	EPJ A27 207	V.A. Schegelsky et al.	
AMSLER	02	EPJ C23 229	C. Amstler et al.	
AMELIN	00	NP A668 83	D. Amelin et al.	(VES Collab.)
BAKER	99B	PL B467 147	C.A. Baker et al.	
BERTIN	98	PR D57 55	A. Bertin et al.	(OBELIX Collab.)
BERTIN	97C	PL B408 476	A. Bertin et al.	(OBELIX Collab.)
ABELE	96C	NP A609 562	A. Abele et al.	(Crystal Barrel Collab.)
AMSLER	95B	PL B342 433	C. Amstler et al.	(Crystal Barrel Collab.)
AMSLER	95C	PL B353 571	C. Amstler et al.	(Crystal Barrel Collab.)
AMSLER	95D	PL B355 425	C. Amstler et al.	(Crystal Barrel Collab.)
BALOSHIN	95	PAN 58 46	O.N. Baloshin et al.	(ITEP)
Translated from YAF 58 50.				
AMSLER	94D	PL B333 277	C. Amstler et al.	(Crystal Barrel Collab.)
ANISOVICH	94	PL B323 233	V.V. Anisovich et al.	(Crystal Barrel Collab.)
ANISOVICH	94B	PR D50 1972	V.V. Anisovich et al.	(LOQM)
ADAMO	93	NP A558 13C	A. Adamo et al.	(OBELIX Collab.)
ARMSTRONG	93C	PL B307 394	T.A. Armstrong et al.	(FNAL, FERR, GENO+)
ARMSTRONG	93D	PL B307 399	T.A. Armstrong et al.	(FNAL, FERR, GENO+)
WEIDENAUER	93	ZPHY C59 387	P. Weidenauer et al.	(ASTERIX Collab.)
ADAMO	92	PL B287 368	A. Adamo et al.	(OBELIX Collab.)
BELADIDZE	92B	ZPHY C54 367	G.M. Beladidze et al.	(VES Collab.)
AKER	91	PL B260 249	E. Aker et al.	(Crystal Barrel Collab.)
MAY	90	ZPHY C46 203	B. May et al.	(ASTERIX Collab.)
MAY	89	PL B225 450	B. May et al.	(ASTERIX Collab.)
BRIDGES	86B	PRL 56 215	D.L. Bridges et al.	(SYRA, CASE)
BRIDGES	86C	PRL 57 1534	D.L. Bridges et al.	(SYRA)

 $\rho(1570)$

$$I^G(J^{PC}) = 1^+(1^{--})$$

OMITTED FROM SUMMARY TABLE

May be an OZI-violating decay mode of $\rho(1700)$. See our mini-review under the $\rho(1700)$. $\rho(1570)$ MASS

VALUE (MeV)	EVTS	DOCUMENT ID	TECN	COMMENT
1570 ± 36 ± 62	54	1 AUBERT	08S	BABR $10.6 e^+e^- \rightarrow \phi\pi^0\gamma$
1480 ± 40		2 BITYUKOV	87	SPEC $32.5 \pi^-p \rightarrow \phi\pi^0 n$

¹ From the fit with two resonances.
² Systematic errors not estimated.

 $\rho(1570)$ WIDTH

VALUE (MeV)	EVTS	DOCUMENT ID	TECN	COMMENT
144 ± 75 ± 43	54	3 AUBERT	08S	BABR $10.6 e^+e^- \rightarrow \phi\pi^0\gamma$
130 ± 60		4 BITYUKOV	87	SPEC $32.5 \pi^-p \rightarrow \phi\pi^0 n$

³ From the fit with two resonances.
⁴ Systematic errors not estimated.

 $\rho(1570)$ DECAY MODES

Mode	Fraction (Γ_i/Γ)
Γ_1 e^+e^-	seen
Γ_2 $\phi\pi$	not seen
Γ_3 $\omega\pi$	

 $\rho(1570)$ $\Gamma(i)\Gamma(e^+e^-)/\Gamma_{total}$

VALUE (eV)	CL%	EVTS	DOCUMENT ID	TECN	COMMENT
3.5 ± 0.9 ± 0.3		54	5 AUBERT	08S	BABR $10.6 e^+e^- \rightarrow \phi\pi^0\gamma$

• • • We do not use the following data for averages, fits, limits, etc. • • •

< 70 90 6 AULCHENKO 87B ND $e^+e^- \rightarrow K_S^0 K_L^0 \pi^0$

⁵ From the fit with two resonances.
⁶ Using mass and width of BITYUKOV 87.

 $\rho(1570)$ BRANCHING RATIOS $\Gamma(\phi\pi)/\Gamma_{total}$ Γ_2/Γ

VALUE	DOCUMENT ID	TECN	COMMENT
not seen	ABELE	97H	CBAR $\bar{p}p \rightarrow K_L^0 K_S^0 \pi^0 \pi^0$
< 0.01	7 DONNACHIE	91	RVUE

⁷ Using data from BISELLO 91B, DOLINSKY 86, and ALBRECHT 87L.

 $\Gamma(\phi\pi)/\Gamma(\omega\pi)$ Γ_2/Γ_3

VALUE	CL%	DOCUMENT ID	TECN	COMMENT
> 0.5	95	BITYUKOV	87	SPEC $32.5 \pi^-p \rightarrow \phi\pi^0 n$

 $\rho(1570)$ REFERENCES

AUBERT	08S	PR D77 092002	B. Aubert et al.	(BABAR Collab.)
ABELE	97H	PL B415 280	A. Abele et al.	(Crystal Barrel Collab.)
BISELLO	91B	NPBPS B21 111	D. Bisello	(DM2 Collab.)
DONNACHIE	91	ZPHY C51 689	A. Donnachie, A.B. Clegg	(MCHS, LANC)
ALBRECHT	87L	PL B185 223	H. Albrecht et al.	(ARGUS Collab.)
AULCHENKO	87B	JETPL 45 145	V.M. Aukchenko et al.	(NOVO)
Translated from ZETFP 45 118.				
BITYUKOV	87B	PL B188 383	S.I. Bitiyukov et al.	(SERP)
DOLINSKY	86	PL B174 453	S.I. Dolinsky et al.	(NOVO)

 $h_1(1595)$

$$I^G(J^{PC}) = 0^-(1^{+-})$$

OMITTED FROM SUMMARY TABLE

Seen in a partial-wave analysis of the $\omega\eta$ system produced in the reaction $\pi^-p \rightarrow \omega\eta n$ at 18 GeV/c. $h_1(1595)$ MASS

VALUE (MeV)	DOCUMENT ID	TECN	COMMENT
1594 ± 15 ± 10 - 60	EUGENIO	01	SPEC $18 \pi^-p \rightarrow \omega\eta n$

 $h_1(1595)$ WIDTH

VALUE (MeV)	DOCUMENT ID	TECN	COMMENT
384 ± 60 ± 70 - 100	EUGENIO	01	SPEC $18 \pi^-p \rightarrow \omega\eta n$

 $h_1(1595)$ DECAY MODES

Mode	Fraction (Γ_i/Γ)
Γ_1 $\omega\eta$	seen

 $h_1(1595)$ REFERENCES

EUGENIO	01	PL B497 190	P. Eugenio et al.
---------	----	-------------	-------------------

 $\pi_1(1600)$

$$I^G(J^{PC}) = 1^-(1^{+-})$$

 $\pi_1(1600)$ MASS

VALUE (MeV)	EVTS	DOCUMENT ID	TECN	COMMENT
1662 ± 15 - 11		OUR AVERAGE Error includes scale factor of 1.2.		

1664 ± 8 ± 10	145k	1 LU	05	B852 $18 \pi^-p \rightarrow \omega\pi^- \pi^0 p$
1709 ± 24 ± 41	69k	2 KUHN	04	B852 $18 \pi^-p \rightarrow \eta\pi^+ \pi^- \pi^- p$
1597 ± 10 ± 45 - 10		2 IVANOV	01	B852 $18 \pi^-p \rightarrow \eta' \pi^- p$

• • • We do not use the following data for averages, fits, limits, etc. • • •

1593 ± 8 ± 29 - 47 2,3 ADAMS 98B B852 $18.3 \pi^-p \rightarrow \pi^+ \pi^- \pi^- p$

¹ May be a different state: natural and unnatural parity exchanges.

² Natural parity exchange.

³ Superseded by DZIERBA 06 excluding this state in a more refined PWA analysis, with 2.6 M events of $\pi^-p \rightarrow \pi^- \pi^- \pi^+ p$ and 3 M events of $\pi^-p \rightarrow \pi^- \pi^0 \pi^0 p$ of E852 data.

 $\pi_1(1600)$ WIDTH

VALUE (MeV)	EVTS	DOCUMENT ID	TECN	COMMENT
234 ± 50 OUR AVERAGE		Error includes scale factor of 1.7. See the ideogram below.		

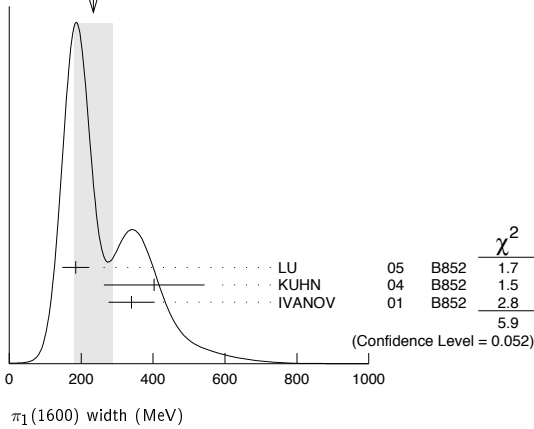
185 ± 25 ± 28	145k	4 LU	05	B852 $18 \pi^-p \rightarrow \omega\pi^- \pi^0 p$
403 ± 80 ± 115	69k	5 KUHN	04	B852 $18 \pi^-p \rightarrow \eta\pi^+ \pi^- \pi^- p$
340 ± 40 ± 50		5 IVANOV	01	B852 $18 \pi^-p \rightarrow \eta' \pi^- p$

• • • We do not use the following data for averages, fits, limits, etc. • • •

168 ± 20 ± 150 - 12 5,6 ADAMS 98B B852 $18.3 \pi^-p \rightarrow \pi^+ \pi^- \pi^- p$

⁴ May be a different state: natural and unnatural parity exchanges.
⁵ Natural parity exchange.
⁶ Superseded by DZIERBA 06 excluding this state in a more refined PWA analysis, with 2.6 M events of $\pi^- p \rightarrow \pi^- \pi^- \pi^+ p$ and 3 M events of $\pi^- p \rightarrow \pi^- \pi^0 \pi^0 p$ of E852 data.

WEIGHTED AVERAGE
234±50 (Error scaled by 1.7)



$\pi_1(1600)$ DECAY MODES

Mode	Fraction (Γ_i/Γ)
Γ_1 $\pi \pi \pi$	not seen
Γ_2 $\rho^0 \pi^-$	not seen
Γ_3 $f_2(1270) \pi^-$	not seen
Γ_4 $b_1(1235) \pi$	seen
Γ_5 $\eta'(958) \pi^-$	seen
Γ_6 $f_1(1285) \pi$	seen

$\pi_1(1600)$ BRANCHING RATIOS

$\Gamma(\rho^0 \pi^-)/\Gamma_{total}$	DOCUMENT ID	TECN	COMMENT	Γ_2/Γ
not seen	NOZAR 09	CLAS	$\gamma p \rightarrow 2\pi^+ \pi^- n$	
not seen	7 DZIERBA 06	B852	$18 \pi^- p$	

⁷ From the PWA analysis of 2.6 M $\pi^- p \rightarrow \pi^- \pi^- \pi^+ p$ and 3 M events of $\pi^- p \rightarrow \pi^- \pi^0 \pi^0 p$ of E852 data. Supersedes ADAMS 98B.

$\Gamma(f_2(1270) \pi^-)/\Gamma_{total}$	DOCUMENT ID	TECN	COMMENT	Γ_3/Γ
not seen	8 DZIERBA 06	B852	$18 \pi^- p$	

⁸ From the PWA analysis of 2.6 M $\pi^- p \rightarrow \pi^- \pi^- \pi^+ p$ and 3 M events of $\pi^- p \rightarrow \pi^- \pi^0 \pi^0 p$ of E852 data. Supersedes CHUNG 02.

$\Gamma(b_1(1235) \pi)/\Gamma_{total}$	EVTS	DOCUMENT ID	TECN	COMMENT	Γ_4/Γ
seen	35280	9 BAKER 03	SPEC	$\bar{p} p \rightarrow \omega \pi^+ \pi^- \pi^0$	
seen	145k	LU 05	B852	$18 \pi^- p \rightarrow \omega \pi^- \pi^0 p$	

• • • We do not use the following data for averages, fits, limits, etc. • • •

⁹ $B((b_1 \pi)_{D-wave})/B((b_1 \pi)_{S-wave}) = 0.3 \pm 0.1$.

$\Gamma(\eta'(958) \pi^-)/\Gamma_{total}$	DOCUMENT ID	TECN	COMMENT	Γ_5/Γ
seen	IVANOV 01	B852	$18 \pi^- p \rightarrow \eta' \pi^- p$	

$\Gamma(f_1(1285) \pi)/\Gamma(\eta'(958) \pi^-)$	EVTS	DOCUMENT ID	TECN	COMMENT	Γ_6/Γ_5
3.80±0.78	69k	10 KUHN 04	B852	$18 \pi^- p \rightarrow \eta \pi^+ \pi^- \pi^- p$	

¹⁰ Using $\eta'(958) \pi$ data from IVANOV 01.

$\pi_1(1600)$ REFERENCES

NOZAR 09	PRL 102 102002	M. Nozar et al.	(CLAS Collab.)
DZIERBA 06	PR D73 072001	A.R. Dzierba et al.	(BNL E852 Collab.)
LU 05	PRL 94 032002	M. Lu et al.	(BNL E852 Collab.)
KUHN 04	PL B595 109	J. Kuhn et al.	(BNL E852 Collab.)
BAKER 03	PL B563 140	C.A. Baker et al.	
CHUNG 02	PR D65 072001	S.U. Chung et al.	(BNL E852 Collab.)
IVANOV 01	PRL 86 3977	E.I. Ivanov et al.	(BNL E852 Collab.)
ADAMS 98B	PRL 81 5760	G.S. Adams et al.	(BNL E852 Collab.)

$a_1(1640)$

$I^G(JPC) = 1^-(1^{++})$

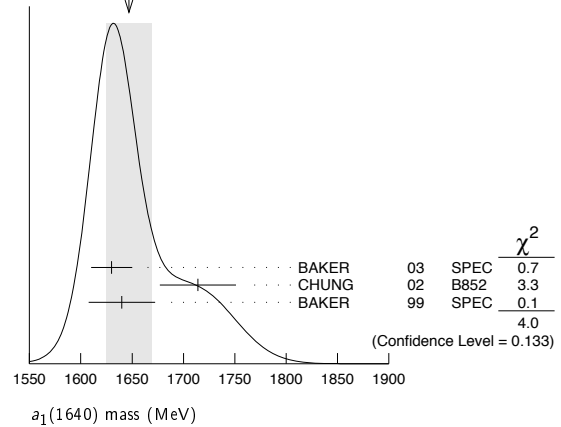
OMITTED FROM SUMMARY TABLE

Seen in the amplitude analysis of the $3\pi^0$ system produced in $\bar{p} p \rightarrow 4\pi^0$. Possibly seen in the study of the hadronic structure in decay $\tau \rightarrow 3\pi \nu_\tau$ (ABREU 98G and ASNER 00). Needs confirmation.

$a_1(1640)$ MASS

VALUE (MeV)	EVTS	DOCUMENT ID	TECN	COMMENT
1647±22 OUR AVERAGE				Error includes scale factor of 1.4. See the ideogram below.
1630±20	35280	1 BAKER 03	SPEC	$\bar{p} p \rightarrow \omega \pi^+ \pi^- \pi^0$
1714±9±36		CHUNG 02	B852	$18.3 \pi^- p \rightarrow \pi^+ \pi^- \pi^- p$
1640±12±30		BAKER 99	SPEC	$1.94 \bar{p} p \rightarrow 4\pi^0$
• • •				We do not use the following data for averages, fits, limits, etc. • • •
1670±90		BELLINI 85	SPEC	$40 \pi^- A \rightarrow \pi^- \pi^+ \pi^- A$

WEIGHTED AVERAGE
1647±22 (Error scaled by 1.4)



¹ Using the $a_1(1260)$ mass and width results of BOWLER 88.

$a_1(1640)$ WIDTH

VALUE (MeV)	EVTS	DOCUMENT ID	TECN	COMMENT
254±27 OUR AVERAGE				Error includes scale factor of 1.1.
225±30	35280	2 BAKER 03	SPEC	$\bar{p} p \rightarrow \omega \pi^+ \pi^- \pi^0$
308±37±62		CHUNG 02	B852	$18.3 \pi^- p \rightarrow \pi^+ \pi^- \pi^- p$
300±22±40		BAKER 99	SPEC	$1.94 \bar{p} p \rightarrow 4\pi^0$
• • •				We do not use the following data for averages, fits, limits, etc. • • •
300±100		BELLINI 85	SPEC	$40 \pi^- A \rightarrow \pi^- \pi^+ \pi^- A$

² Using the $a_1(1260)$ mass and width results of BOWLER 88.

$a_1(1640)$ DECAY MODES

Mode	Fraction (Γ_i/Γ)
Γ_1 $\pi \pi \pi$	seen
Γ_2 $f_2(1270) \pi$	seen
Γ_3 $\sigma \pi$	seen
Γ_4 $\rho \pi S$ -wave	seen
Γ_5 $\rho \pi D$ -wave	seen
Γ_6 $\omega \pi \pi$	seen
Γ_7 $f_1(1285) \pi$	seen
Γ_8 $a_1(1260) \eta$	not seen

$a_1(1640)$ BRANCHING RATIOS

$\Gamma(f_2(1270) \pi)/\Gamma(\sigma \pi)$	DOCUMENT ID	TECN	COMMENT	Γ_2/Γ_3
0.24±0.07	BAKER 99	SPEC	$1.94 \bar{p} p \rightarrow 4\pi^0$	

• • • We do not use the following data for averages, fits, limits, etc. • • •

$\Gamma(\rho \pi D$ -wave)/ Γ_{total}	DOCUMENT ID	TECN	COMMENT	Γ_5/Γ
seen	CHUNG 02	B852	$18.3 \pi^- p \rightarrow \pi^+ \pi^- \pi^- p$	
seen	AMELIN 95B	VES	$36 \pi^- A \rightarrow \pi^+ \pi^- \pi^- A$	

Meson Particle Listings

 $a_1(1640)$, $f_2(1640)$, $\eta_2(1645)$

$\Gamma(\omega\pi\pi)/\Gamma_{\text{total}}$ Γ_6/Γ

VALUE	EVTS	DOCUMENT ID	TECN	COMMENT
••• We do not use the following data for averages, fits, limits, etc. •••				
seen	35280	³ BAKER	03	SPEC $\bar{p}p \rightarrow \omega\pi^+\pi^-\pi^0$

$\Gamma(f_1(1285)\pi)/\Gamma_{\text{total}}$ Γ_7/Γ

VALUE	DOCUMENT ID	TECN	COMMENT
••• We do not use the following data for averages, fits, limits, etc. •••			
not seen	KUHN	04	B852 $18\pi^-\rho \rightarrow \eta\pi^+\pi^-\pi^-\rho$
seen	LEE	94	MPS2 $18\pi^-\rho \rightarrow K^+\bar{K}^0\pi^-\pi^-\rho$

$\Gamma(a_1(1260)\eta)/\Gamma_{\text{total}}$ Γ_8/Γ

VALUE	DOCUMENT ID	TECN	COMMENT
not seen	KUHN	04	B852 $18\pi^-\rho \rightarrow \eta\pi^+\pi^-\pi^-\rho$

³ Assuming the $\omega\rho$ mechanism for the $\omega\pi\pi$ state.

 $a_1(1640)$ REFERENCES

KUHN	04	PL B595 109	J. Kuhn et al.	(BNL E852 Collab.)
BAKER	03	PL B563 140	C.A. Baker et al.	
CHUNG	02	PR D65 072001	S.U. Chung et al.	(BNL E852 Collab.)
ASNER	00	PR D61 012002	D.M. Asner et al.	(CLEO Collab.)
BAKER	99	PL B449 114	C.A. Baker et al.	
ABREU	98G	PL B426 411	P. Abreu et al.	(DELPHI Collab.)
AMELIN	95B	PL B356 595	D.V. Amelin et al.	(SERP, TBIL)
LEE	94	PL B323 227	J.H. Lee et al.	(BNL, IND, KYUN, MASD+)
BOWLER	88	PL B209 99	M.G. Bowler	(OXF)
BELLINI	85	SJNP 41 781	D. Bellini et al.	
		Translated from YAF 41 1223.		

 $f_2(1640)$

$$J^{PC} = 0^+(2^{++})$$

OMITTED FROM SUMMARY TABLE

 $f_2(1640)$ MASS

VALUE (MeV)	DOCUMENT ID	TECN	COMMENT
1639 ± 6 OUR AVERAGE	Error includes scale factor of 1.2.		
1620 ± 16	BUGG	95	MRK3 $J/\psi \rightarrow \gamma\pi^+\pi^-\pi^+\pi^-$
1647 ± 7	ADAMO	92	OBLX $\bar{\pi}\rho \rightarrow 3\pi^+2\pi^-$
1635 ± 7	ALDE	90	GAM2 $38\pi^-\rho \rightarrow \omega\omega\pi$
••• We do not use the following data for averages, fits, limits, etc. •••			
1640 ± 5	AMSLER	06	CBAR $0.9\bar{p}\rho \rightarrow K^+K^-\pi^0$
1659 ± 6	VLADIMIRSK...	06	SPEC $40\pi^-\rho \rightarrow K_S^0 K_S^0 \eta$
1643 ± 7	¹ ALDE	89B	GAM2 $38\pi^-\rho \rightarrow \omega\omega\pi$

¹ Superseded by ALDE 90.

 $f_2(1640)$ WIDTH

VALUE (MeV)	CL%	DOCUMENT ID	TECN	COMMENT
99⁺⁶⁰₋₄₀ OUR AVERAGE		Error includes scale factor of 2.9.		
140 ⁺⁶⁰ ₋₂₀		BUGG	95	MRK3 $J/\psi \rightarrow \gamma\pi^+\pi^-\pi^+\pi^-$
58 ± 20		ADAMO	92	OBLX $\bar{\pi}\rho \rightarrow 3\pi^+2\pi^-$
••• We do not use the following data for averages, fits, limits, etc. •••				
44 ± 9		AMSLER	06	CBAR $0.9\bar{p}\rho \rightarrow K^+K^-\pi^0$
152 ± 18		VLADIMIRSK...	06	SPEC $40\pi^-\rho \rightarrow K_S^0 K_S^0 \eta$
< 70	90	ALDE	90	GAM2 $38\pi^-\rho \rightarrow \omega\omega\pi$

 $f_2(1640)$ DECAY MODES

Mode	Fraction (Γ_i/Γ)
Γ_1 $\omega\omega$	seen
Γ_2 4π	seen
Γ_3 $K\bar{K}$	seen

 $f_2(1640)$ BRANCHING RATIOS

$\Gamma(K\bar{K})/\Gamma_{\text{total}}$ Γ_3/Γ

VALUE	DOCUMENT ID	TECN	COMMENT
seen	AMSLER	06	CBAR $0.9\bar{p}\rho \rightarrow K^+K^-\pi^0$

 $f_2(1640)$ REFERENCES

AMSLER	06	PL B639 165	C. Amstler et al.	(CBAR Collab.)
VLADIMIRSK...	06	PAN 69 493	V.V. Vladimirov et al.	(ITEP, Moscow)
		Translated from YAF 69 515.		
BUGG	95	PL B353 378	D.V. Bugg et al.	(LOQM, PNPI, WASH)JP
ADAMO	92	PL B287 368	A. Adamo et al.	(OBELIX Collab.)
ALDE	90	PL B241 600	D.M. Alde et al.	(SERP, BELG, LANL, LAPP+)
ALDE	89B	PL B216 451	D.M. Alde et al.	(SERP, BELG, LANL, LAPP+)IGJPC

 $\eta_2(1645)$

$$J^{PC} = 0^+(2^{-+})$$

 $\eta_2(1645)$ MASS

VALUE (MeV)	DOCUMENT ID	TECN	CHG	COMMENT
1617 ± 5 OUR AVERAGE				
1613 ± 8	BARBERIS	00B		450 $pp \rightarrow p_f \eta \pi^+ \pi^- \rho_S$
1617 ± 8	BARBERIS	00C		450 $pp \rightarrow p_f 4\pi \rho_S$
1620 ± 20	BARBERIS	97B	OMEG	450 $pp \rightarrow pp2(\pi^+ \pi^-)$
1645 ± 14 ± 15	ADOMEIT	96	CBAR 0	1.94 $\bar{p}\rho \rightarrow \eta 3\pi^0$
••• We do not use the following data for averages, fits, limits, etc. •••				
1645 ± 6 ± 20	ANISOVICH	00E	SPEC	0.9-1.94 $\bar{p}\rho \rightarrow \eta 3\pi^0$

 $\eta_2(1645)$ WIDTH

VALUE (MeV)	DOCUMENT ID	TECN	CHG	COMMENT
181 ± 11 OUR AVERAGE				
185 ± 17	BARBERIS	00B		450 $pp \rightarrow p_f \eta \pi^+ \pi^- \rho_S$
177 ± 18	BARBERIS	00C		450 $pp \rightarrow p_f 4\pi \rho_S$
180 ± 25	BARBERIS	97B	OMEG	450 $pp \rightarrow pp2(\pi^+ \pi^-)$
180 ⁺⁴⁰ ₋₂₁ ± 25	ADOMEIT	96	CBAR 0	1.94 $\bar{p}\rho \rightarrow \eta 3\pi^0$
••• We do not use the following data for averages, fits, limits, etc. •••				
200 ± 25	ANISOVICH	00E	SPEC	0.9-1.94 $\bar{p}\rho \rightarrow \eta 3\pi^0$

 $\eta_2(1645)$ DECAY MODES

Mode	Fraction (Γ_i/Γ)
Γ_1 $a_2(1320)\pi$	seen
Γ_2 $K\bar{K}\pi$	seen
Γ_3 $K^*\bar{K}$	seen
Γ_4 $\eta\pi^+\pi^-$	seen
Γ_5 $a_0(980)\pi$	seen
Γ_6 $f_2(1270)\eta$	not seen

 $\eta_2(1645)$ BRANCHING RATIOS

$\Gamma(K\bar{K}\pi)/\Gamma(a_2(1320)\pi)$ Γ_2/Γ_1

VALUE	DOCUMENT ID	TECN	COMMENT
0.07 ± 0.03	¹ BARBERIS	97C	OMEG 450 $pp \rightarrow ppK\bar{K}\pi$

¹ Using $2(\pi^+ \pi^-)$ data from BARBERIS 97B.

$\Gamma(a_2(1320)\pi)/\Gamma(a_0(980)\pi)$ Γ_1/Γ_5

VALUE	DOCUMENT ID	COMMENT
13.0 ± 2.7	BARBERIS	00B 450 $pp \rightarrow p_f \eta \pi^+ \pi^- \rho_S$

$\Gamma(f_2(1270)\eta)/\Gamma_{\text{total}}$ Γ_6/Γ

VALUE	DOCUMENT ID	COMMENT
••• We do not use the following data for averages, fits, limits, etc. •••		
not seen	BARBERIS	00B 450 $pp \rightarrow p_f \eta \pi^+ \pi^- \rho_S$

 $\eta_2(1645)$ REFERENCES

ANISOVICH	00E	PL B477 19	A.V. Anisovich et al.	
BARBERIS	00B	PL B471 435	D. Barberis et al.	(WA 102 Collab.)
BARBERIS	00C	PL B471 440	D. Barberis et al.	(WA 102 Collab.)
BARBERIS	97B	PL B413 217	D. Barberis et al.	(WA 102 Collab.)
BARBERIS	97C	PL B413 225	D. Barberis et al.	(WA 102 Collab.)
ADOMEIT	96	ZPHY C71 227	J. Adomeit et al.	(Crystal Barrel Collab.)

See key on page 405

Meson Particle Listings

$\omega(1650)$

$\omega(1650)$

$I^G(J^{PC}) = 0^-(1^{--})$

$\omega(1650) \Gamma(i)\Gamma(e^+e^-)/\Gamma^2(\text{total})$

$\Gamma(\rho\pi)/\Gamma_{\text{total}} \times \Gamma(e^+e^-)/\Gamma_{\text{total}} \quad \Gamma_1/\Gamma \times \Gamma_4/\Gamma$

Table with columns: VALUE (units 10^-6), EVTS, DOCUMENT ID, TECN, COMMENT. Includes entries for AUBERT, B, ACHASOV, CLEGG, ANTONELLI.

$\Gamma(\omega\pi\pi)/\Gamma_{\text{total}} \times \Gamma(e^+e^-)/\Gamma_{\text{total}} \quad \Gamma_2/\Gamma \times \Gamma_4/\Gamma$

Table with columns: VALUE (units 10^-7), EVTS, DOCUMENT ID, TECN, COMMENT. Includes entries for AUBERT, ACHASOV, AKHMETSHIN, CLEGG, ANTONELLI.

$\Gamma(\omega\eta)/\Gamma_{\text{total}} \times \Gamma(e^+e^-)/\Gamma_{\text{total}} \quad \Gamma_3/\Gamma \times \Gamma_4/\Gamma$

Table with columns: VALUE (units 10^-6), CL%, EVTS, DOCUMENT ID, TECN, COMMENT. Includes entries for AUBERT, AKHMETSHIN.

$\omega(1650)$ MASS
Table with columns: VALUE (MeV), EVTS, DOCUMENT ID, TECN, COMMENT. Includes 'OUR ESTIMATE' and various experimental data points.

1 From the combined fit of ANTONELLI 92, ACHASOV 01E, ACHASOV 02E, and ACHASOV 03D data on the $\pi^+\pi^-\pi^0$ and ANTONELLI 92 on the $\omega\pi^+\pi^-$ final states. Supersedes ACHASOV 99E and ACHASOV 02E.
2 Using results of CORDIER 81 and preliminary data of DOLINSKY 91 and ANTONELLI 92.

$\omega(1650)$ BRANCHING RATIOS

$\Gamma(\omega\pi\pi)/\Gamma_{\text{total}} \quad \Gamma_2/\Gamma$

Table with columns: VALUE, EVTS, DOCUMENT ID, TECN, COMMENT. Includes entries for ACHASOV, HENNER.

$\Gamma(\rho\pi)/\Gamma_{\text{total}} \quad \Gamma_1/\Gamma$

Table with columns: VALUE, EVTS, DOCUMENT ID, TECN, COMMENT. Includes entries for ACHASOV, HENNER.

$\Gamma(e^+e^-)/\Gamma_{\text{total}} \quad \Gamma_4/\Gamma$

Table with columns: VALUE (units 10^-7), EVTS, DOCUMENT ID, TECN, COMMENT. Includes entries for ACHASOV, HENNER.

$\omega(1650)$ REFERENCES

AUBERT 07AU PR D76 092005 B. Aubert et al. (BABAR Collab.)
AUBERT 06D PR D73 052003 B. Aubert et al. (BABAR Collab.)
AUBERT.B 04N PR D70 072004 B. Aubert et al. (BABAR Collab.)
ACHASOV 03D PR D68 052006 M.N. Achasov et al. (Novosibirsk SND Collab.)

$\omega(1650)$ WIDTH

OUR ESTIMATE

Table with columns: VALUE (MeV), EVTS, DOCUMENT ID, TECN, COMMENT. Includes various experimental data points for the width.

10 From the combined fit of ANTONELLI 92, ACHASOV 01E, ACHASOV 02E, and ACHASOV 03D data on the $\pi^+\pi^-\pi^0$ and ANTONELLI 92 on the $\omega\pi^+\pi^-$ final states. Supersedes ACHASOV 99E and ACHASOV 02E.
11 Using results of CORDIER 81 and preliminary data of DOLINSKY 91 and ANTONELLI 92.

$\omega(1650)$ DECAY MODES

Table with columns: Mode, Fraction (Γ_i/Γ). Lists decay modes like $\rho\pi$, $\omega\pi\pi$, $\omega\eta$, e^+e^- and their relative fractions.

Meson Particle Listings

$\omega_3(1670), \pi_2(1670)$

$\omega_3(1670)$		$I^G(J^{PC}) = 0^-(3^{--})$				
VALUE (MeV)	EVTS	DOCUMENT ID	TECN	COMMENT		
1667 ± 4 OUR AVERAGE						
1665.3 ± 5.2 ± 4.5	23400	AMELIN	96	VES	36 $\pi^- p \rightarrow \pi^+ \pi^- \pi^0 n$	
1685 ± 20	60	BAUBILLIER	79	HBC	8.2 $K^- p$ backward	
1673 ± 12	430	1,2 BALTAY	78E	HBC	15 $\pi^+ p \rightarrow \Delta 3\pi$	
1650 ± 12		CORDEN	78B	OMEG	8-12 $\pi^- p \rightarrow N 3\pi$	
1669 ± 11	600	2 WAGNER	75	HBC	7 $\pi^+ p \rightarrow \Delta^{++} 3\pi$	
1678 ± 14	500	DIAZ	74	DBC	6 $\pi^+ n \rightarrow \rho 3\pi^0$	
1660 ± 13	200	DIAZ	74	DBC	6 $\pi^+ n \rightarrow \rho \omega \pi^0 \pi^0$	
1679 ± 17	200	MATTHEWS	71D	DBC	7.0 $\pi^+ n \rightarrow \rho 3\pi^0$	
1670 ± 20		KENYON	69	DBC	8 $\pi^+ n \rightarrow \rho 3\pi^0$	
• • • We do not use the following data for averages, fits, limits, etc. • • •						
~1700	110	1 CERRADA	77B	HBC	4.2 $K^- p \rightarrow \Lambda 3\pi$	
1695 ± 20		BARNES	69B	HBC	4.6 $K^- p \rightarrow \omega 2\pi X$	
1636 ± 20		ARMENISE	68B	DBC	5.1 $\pi^+ n \rightarrow \rho 3\pi^0$	
1 Phase rotation seen for $J^P = 3^- \rho \pi$ wave. 2 From a fit to $I(J^P) = 0(3^-) \rho \pi$ partial wave.						

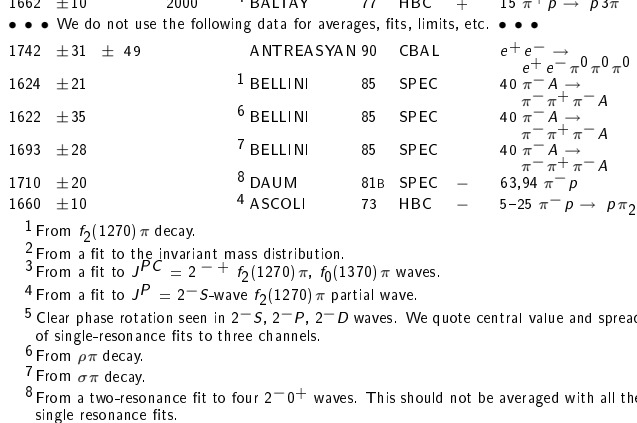
$\omega_3(1670)$ WIDTH						
VALUE (MeV)	EVTS	DOCUMENT ID	TECN	COMMENT		
168 ± 10 OUR AVERAGE						
149 ± 19 ± 7	23400	AMELIN	96	VES	36 $\pi^- p \rightarrow \pi^+ \pi^- \pi^0 n$	
160 ± 80	60	3 BAUBILLIER	79	HBC	8.2 $K^- p$ backward	
173 ± 16	430	4,5 BALTAY	78E	HBC	15 $\pi^+ p \rightarrow \Delta 3\pi$	
253 ± 39		CORDEN	78B	OMEG	8-12 $\pi^- p \rightarrow N 3\pi$	
173 ± 28	600	3,5 WAGNER	75	HBC	7 $\pi^+ p \rightarrow \Delta^{++} 3\pi$	
167 ± 40	500	DIAZ	74	DBC	6 $\pi^+ n \rightarrow \rho 3\pi^0$	
122 ± 39	200	DIAZ	74	DBC	6 $\pi^+ n \rightarrow \rho \omega \pi^0 \pi^0$	
155 ± 40	200	3 MATTHEWS	71D	DBC	7.0 $\pi^+ n \rightarrow \rho 3\pi^0$	
• • • We do not use the following data for averages, fits, limits, etc. • • •						
90 ± 20		BARNES	69B	HBC	4.6 $K^- p \rightarrow \omega 2\pi$	
100 ± 40		KENYON	69	DBC	8 $\pi^+ n \rightarrow \rho 3\pi^0$	
112 ± 60		ARMENISE	68B	DBC	5.1 $\pi^+ n \rightarrow \rho 3\pi^0$	
3 Width errors enlarged by us to $4\Gamma/\sqrt{N}$; see the note with the $K^*(892)$ mass. 4 Phase rotation seen for $J^P = 3^- \rho \pi$ wave. 5 From a fit to $I(J^P) = 0(3^-) \rho \pi$ partial wave.						

$\omega_3(1670)$ DECAY MODES		
Mode	Fraction (Γ_i/Γ)	
Γ_1 $\rho \pi$	seen	
Γ_2 $\omega \pi \pi$	seen	
Γ_3 $b_1(1235) \pi$	possibly seen	

$\omega_3(1670)$ BRANCHING RATIOS				
$\Gamma(\omega \pi \pi)/\Gamma(\rho \pi)$		Γ_2/Γ_1		
VALUE	EVTS	DOCUMENT ID	TECN	COMMENT
• • • We do not use the following data for averages, fits, limits, etc. • • •				
0.71 ± 0.27	100	DIAZ	74	DBC 6 $\pi^+ n \rightarrow \rho 5\pi^0$
$\Gamma(b_1(1235) \pi)/\Gamma(\rho \pi)$		Γ_3/Γ_1		
VALUE		DOCUMENT ID	TECN	COMMENT
possibly seen		DIAZ	74	DBC 6 $\pi^+ n \rightarrow \rho 5\pi^0$
$\Gamma(b_1(1235) \pi)/\Gamma(\omega \pi \pi)$		Γ_3/Γ_2		
VALUE	CL%	DOCUMENT ID	TECN	COMMENT
• • • We do not use the following data for averages, fits, limits, etc. • • •				
>0.75	68	BAUBILLIER	79	HBC 8.2 $K^- p$ backward

$\omega_3(1670)$ REFERENCES					
AMELIN	96	ZPHY C70 71	D.V. Amelin et al.	(SERP, TBIL)	
BAUBILLIER	79	PL 89B 131	M. Baubillier et al.	(BIRM, CERN, GLAS+)	
BALTAY	78E	PL 40 87	C. Baltay, C.V. Cautis, M. Kalelkar	(COLU) JP	
CORDEN	78B	NP B138 235	M.J. Corden et al.	(BIRM, RHEL, TELA+)	
CERRADA	77B	NP B126 241	F. Cerrada et al.	(AMST, CERN, NIJM+)	JP
WAGNER	75	PL 58B 201	J. Diaz et al.	(LBL) JP	
DIAZ	74	PL 32 260	F. Wagner, M. Tabak, D.M. Chew	(CASE, GMU)	
MATTHEWS	71D	PR D3 2561	J.A.J. Matthews et al.	(TNTO, WIS C)	
BARNES	69B	PL 23 142	V.E. Barnes et al.	(BNL)	
KENYON	69	PL 23 146	I.R. Kenyon et al.	(BNL, UCND, ORNL)	
ARMENISE	68B	PL 26B 336	N. Armenise et al.	(BARI, BGNA, FIRZ+)	

$\pi_2(1670)$		$I^G(J^{PC}) = 1^-(2^{-+})$				
VALUE (MeV)	EVTS	DOCUMENT ID	TECN	CHG	COMMENT	
1672.4 ± 3.2 OUR AVERAGE						
1749 ± 10 ± 100	145 k	LU	05	B852	18 $\pi^- p \rightarrow \omega \pi^- \pi^0 \rho$	
1676 ± 3 ± 8		1 CHUNG	02	B852	18.3 $\pi^- p \rightarrow \pi^+ \pi^- \pi^- \pi^0$	
1685 ± 10 ± 30		2 BARBERIS	01		450 $p p \rightarrow \rho_f 3\pi^0 \rho_S$	
1687 ± 9 ± 15		AMELIN	99	VES	37 $\pi^- A \rightarrow \omega \pi^- \pi^0 A^*$	
1669 ± 4		BARBERIS	98B		450 $p p \rightarrow \rho_f \rho \pi \rho_S$	
1670 ± 4		BARBERIS	98B		450 $p p \rightarrow \rho_f f_2(1270) \pi \rho_S$	
1730 ± 20		3 AMELIN	95B	VES	36 $\pi^- A \rightarrow \pi^+ \pi^- \pi^- A$	
1690 ± 14		4 BERDNIKOV	94	VES	37 $\pi^- A \rightarrow K^+ K^- \pi^- A$	
1710 ± 20	700	ANTIPOV	87	SIGM	50 $\pi^- Cu \rightarrow \mu^+ \mu^- \pi^- Cu$	
1676 ± 6		4 EVANGELIS...	81	OMEG	12 $\pi^- p \rightarrow 3\pi p$	
1657 ± 14		4,5 DAUM	80D	SPEC	63-94 $\pi p \rightarrow 3\pi X$	
1662 ± 10	2000	4 BALTAY	77	HBC	+ 15 $\pi^+ p \rightarrow \rho 3\pi$	
• • • We do not use the following data for averages, fits, limits, etc. • • •						
1742 ± 31 ± 49		ANTREASYAN	90	CBAL	$e^+ e^- \rightarrow e^+ e^- \pi^0 \pi^0 \pi^0$	
1624 ± 21		1 BELLINI	85	SPEC	40 $\pi^- A \rightarrow \pi^- \pi^+ \pi^- A$	
1622 ± 35		6 BELLINI	85	SPEC	40 $\pi^- A \rightarrow \pi^- \pi^+ \pi^- A$	
1693 ± 28		7 BELLINI	85	SPEC	40 $\pi^- A \rightarrow \pi^- \pi^+ \pi^- A$	
1710 ± 20		8 DAUM	81B	SPEC	63.94 $\pi^- p$	
1660 ± 10		4 ASCOLI	73	HBC	- 5-25 $\pi^- p \rightarrow \rho \pi_2$	
1 From $f_2(1270) \pi$ decay. 2 From a fit to the invariant mass distribution. 3 From a fit to $J^{PC} = 2^- + f_2(1270) \pi, f_0(1370) \pi$ waves. 4 From a fit to $J^P = 2^- S$ -wave $f_2(1270) \pi$ partial wave. 5 Clear phase rotation seen in $2^- S, 2^- D$ waves. We quote central value and spread of single-resonance fits to three channels. 6 From $\rho \pi$ decay. 7 From $\sigma \pi$ decay. 8 From a two-resonance fit to four $2^- 0^+$ waves. This should not be averaged with all the single resonance fits.						



$\pi_2(1670)$ WIDTH						
VALUE (MeV)	EVTS	DOCUMENT ID	TECN	CHG	COMMENT	
259 ± 9 OUR AVERAGE						
408 ± 60 ± 250	145 k	LU	05	B852	18 $\pi^- p \rightarrow \omega \pi^- \pi^0 \rho$	
254 ± 3 ± 31		9 CHUNG	02	B852	18.3 $\pi^- p \rightarrow \pi^+ \pi^- \pi^- \pi^0$	
265 ± 30 ± 40		10 BARBERIS	01		450 $p p \rightarrow \rho_f 3\pi^0 \rho_S$	
168 ± 43 ± 53		AMELIN	99	VES	37 $\pi^- A \rightarrow \omega \pi^- \pi^0 A^*$	
268 ± 15		BARBERIS	98B		450 $p p \rightarrow \rho_f \rho \pi \rho_S$	
256 ± 15		BARBERIS	98B		450 $p p \rightarrow \rho_f f_2(1270) \pi \rho_S$	

$\pi_2(1670)$ WIDTH						
VALUE (MeV)	EVTS	DOCUMENT ID	TECN	CHG	COMMENT	
259 ± 9 OUR AVERAGE						
408 ± 60 ± 250	145 k	LU	05	B852	18 $\pi^- p \rightarrow \omega \pi^- \pi^0 \rho$	
254 ± 3 ± 31		9 CHUNG	02	B852	18.3 $\pi^- p \rightarrow \pi^+ \pi^- \pi^- \pi^0$	
265 ± 30 ± 40		10 BARBERIS	01		450 $p p \rightarrow \rho_f 3\pi^0 \rho_S$	
168 ± 43 ± 53		AMELIN	99	VES	37 $\pi^- A \rightarrow \omega \pi^- \pi^0 A^*$	
268 ± 15		BARBERIS	98B		450 $p p \rightarrow \rho_f \rho \pi \rho_S$	
256 ± 15		BARBERIS	98B		450 $p p \rightarrow \rho_f f_2(1270) \pi \rho_S$	

See key on page 405

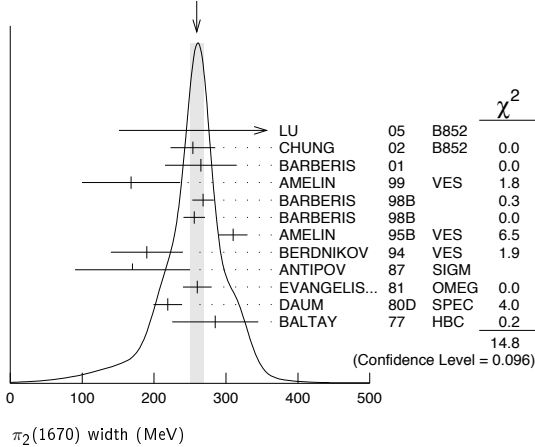
Meson Particle Listings

 $\pi_2(1670)$

310 ± 20	11 AMELIN	95B VES	36 $\pi^- A \rightarrow \pi^+ \pi^- \pi^- A$
190 ± 50	12 BERDNIKOV	94 VES	37 $\pi^- A \rightarrow K^+ K^- \pi^- A$
170 ± 80	700 ANTIPOV	87 SIGM	50 $\pi^- \text{Cu} \rightarrow \mu^+ \mu^- \pi^- \text{Cu}$
260 ± 20	12 EVANGELIS...	81 OMEG	12 $\pi^- p \rightarrow 3\pi p$
219 ± 20	12,13 DAUM	80D SPEC	63-94 $\pi p \rightarrow 3\pi X$
285 ± 60	2000 12 BALTAY	77 HBC	15 $\pi^+ p \rightarrow \rho 3\pi$
• • • We do not use the following data for averages, fits, limits, etc. • • •			
236 ± 49 ± 36	ANTREASNYAN	90 CBAL	$e^+ e^- \rightarrow e^+ e^- \pi^0 \pi^0$
304 ± 22	9 BELLINI	85 SPEC	40 $\pi^- A \rightarrow \pi^- \pi^+ \pi^- A$
404 ± 108	14 BELLINI	85 SPEC	40 $\pi^- A \rightarrow \pi^- \pi^+ \pi^- A$
330 ± 90	15 BELLINI	85 SPEC	40 $\pi^- A \rightarrow \pi^- \pi^+ \pi^- A$
312 ± 50	16 DAUM	81B SPEC	63,94 $\pi^- p$
270 ± 60	12 ASCOLI	73 HBC	5-25 $\pi^- p \rightarrow \rho \pi_2$

9 From $f_2(1270)\pi$ decay.

10 From a fit to the invariant mass distribution.

11 From a fit to $J^{PC} = 2^- 2^- f_2(1270)\pi, f_0(1370)\pi$ waves.12 From a fit to $J^P = 2^- f_2(1270)\pi$ partial wave.13 Clear phase rotation seen in $2^- S, 2^- P, 2^- D$ waves. We quote central value and spread of single-resonance fits to three channels.14 From $\rho\pi$ decay.15 From $\sigma\pi$ decay.16 From a two-resonance fit to four $2^- 0^+$ waves. This should not be averaged with all the single resonance fits.WEIGHTED AVERAGE
259±9 (Error scaled by 1.3) $\pi_2(1670)$ DECAY MODES

Mode	Fraction (Γ_i/Γ)	Confidence level
Γ_1 3π	(95.8 ± 1.4) %	
Γ_2 $\pi^+ \pi^- \pi^0$		
Γ_3 $\pi^0 \pi^0 \pi^0$		
Γ_4 $f_2(1270)\pi$	(56.3 ± 3.2) %	
Γ_5 $\rho\pi$	(31 ± 4) %	
Γ_6 $\sigma\pi$	(10.9 ± 3.4) %	
Γ_7 $(\pi\pi)s$ -wave	(8.7 ± 3.4) %	
Γ_8 $K \bar{K}^*(892) + \text{c.c.}$	(4.2 ± 1.4) %	
Γ_9 $\omega\rho$	(2.7 ± 1.1) %	
Γ_{10} $\gamma\gamma$	< 2.8 × 10 ⁻⁷	90%
Γ_{11} $\eta\pi$		
Γ_{12} $\pi^\pm 2\pi^+ 2\pi^-$		
Γ_{13} $\rho(1450)\pi$	< 3.6 × 10 ⁻³	97.7%
Γ_{14} $b_1(1235)\pi$	< 1.9 × 10 ⁻³	97.7%
Γ_{15} $\eta 3\pi$		
Γ_{16} $f_1(1285)\pi$	possibly seen	
Γ_{17} $a_2(1320)\pi$	not seen	

CONSTRAINED FIT INFORMATION

An overall fit to 4 branching ratios uses 6 measurements and one constraint to determine 4 parameters. The overall fit has a $\chi^2 = 1.9$ for 3 degrees of freedom.

The following *off-diagonal* array elements are the correlation coefficients $\langle \delta x_i \delta x_j \rangle / (\delta x_i \delta x_j)$, in percent, from the fit to the branching fractions, $x_i \equiv \Gamma_i/\Gamma_{\text{total}}$. The fit constrains the x_i whose labels appear in this array to sum to one.

x_5	-53		
x_7	-29	-59	
x_8	-8	-21	-9
	x_4	x_5	x_7

 $\pi_2(1670)$ PARTIAL WIDTHS

$\Gamma(\gamma\gamma)$	CL%	DOCUMENT ID	TECN	CHG	COMMENT	Γ_{10}
<0.072	90	17 ACCIARRI	97T L3		$e^+ e^- \rightarrow e^+ e^- \pi^+ \pi^- \pi^0$	
• • • We do not use the following data for averages, fits, limits, etc. • • •						
<0.19	90	17 ALBRECHT	97B ARG		$e^+ e^- \rightarrow e^+ e^- \pi^+ \pi^- \pi^0$	
1.41 ± 0.23 ± 0.28		ANTREASNYAN	90 CBAL	0	$e^+ e^- \rightarrow e^+ e^- \pi^0 \pi^0 \pi^0$	
0.8 ± 0.3 ± 0.12		18 BEHREND	90c CELL	0	$e^+ e^- \rightarrow e^+ e^- \pi^+ \pi^- \pi^0$	
1.3 ± 0.3 ± 0.2		19 BEHREND	90c CELL	0	$e^+ e^- \rightarrow e^+ e^- \pi^+ \pi^- \pi^0$	
17 Decaying into $f_2(1270)\pi$ and $\rho\pi$.						
18 Constructive interference between $f_2(1270)\pi, \rho\pi$ and background.						
19 Incoherent Ansatz.						

 $\pi_2(1670)$ $\Gamma(i)\Gamma(\gamma\gamma)/\Gamma(\text{total})$

$\Gamma(\pi^+ \pi^- \pi^0) \times \Gamma(\gamma\gamma)/\Gamma_{\text{total}}$	CL%	DOCUMENT ID	TECN	COMMENT	Γ_2/Γ_{10}
<0.1	95	20 SCHEGELSKY	06 RVUE	$\gamma\gamma \rightarrow \pi^+ \pi^- \pi^0$	
20 From analysis of L3 data at 183-209 GeV.					

 $\pi_2(1670)$ BRANCHING RATIOS

$\Gamma(3\pi)/\Gamma_{\text{total}}$	DOCUMENT ID	$\Gamma_1/\Gamma = (\Gamma_4 + \Gamma_5 + \Gamma_7)/\Gamma$
0.958 ± 0.014 OUR FIT		
$\Gamma(\pi^0 \pi^0 \pi^0)/\Gamma(\pi^+ \pi^- \pi^0)$	DOCUMENT ID	COMMENT
0.29 ± 0.03 ± 0.05	21 BARBERIS 01	450 $\rho\rho \rightarrow \rho_f 3\pi^0 \rho_s$

$\Gamma(\rho\pi)/0.565\Gamma(f_2(1270)\pi)$	DOCUMENT ID	TECN	COMMENT	$\Gamma_5/0.565\Gamma_4$
0.97 ± 0.09 OUR AVERAGE			Error includes scale factor of 1.9.	
0.76 ± 0.07 ± 0.10	CHUNG 02	B852	18.3 $\pi^- p \rightarrow \pi^+ \pi^- \pi^- p$	
1.01 ± 0.05	BARBERIS 98B		450 $\rho\rho \rightarrow \rho_f \pi^+ \pi^- \pi^0 \rho_s$	

$\Gamma(\sigma\pi)/\Gamma(f_2(1270)\pi)$	DOCUMENT ID	TECN	COMMENT	Γ_6/Γ_4
0.19 ± 0.06 OUR AVERAGE				
0.17 ± 0.02 ± 0.07	CHUNG 02	B852	18.3 $\pi^- p \rightarrow \pi^+ \pi^- \pi^- p$	
0.24 ± 0.10	22,23 BAKER	99 SPEC	1.94 $\bar{p}p \rightarrow 4\pi^0$	

$\frac{1}{2}\Gamma(\rho\pi)/\Gamma(\pi^\pm \pi^+ \pi^-)$	DOCUMENT ID	TECN	CHG	COMMENT	$\frac{1}{2}\Gamma_5/(0.565\Gamma_4 + \frac{1}{2}\Gamma_5 + 0.624\Gamma_7)$
0.29 ± 0.04 OUR FIT					
0.29 ± 0.05	24 DAUM	81B SPEC		63,94 $\pi^- p$	

$0.565\Gamma(f_2(1270)\pi)/\Gamma(\pi^\pm \pi^+ \pi^-)$	DOCUMENT ID	TECN	CHG	COMMENT	$0.565\Gamma_4/(0.565\Gamma_4 + \frac{1}{2}\Gamma_5 + 0.624\Gamma_7)$
0.60 ± 0.05 OUR FIT					
0.61 ± 0.04	24 DAUM	81B SPEC		63,94 $\pi^- p$	
0.76 +0.24 -0.34	ARMENISE 69	DBC	+	5.1 $\pi^+ d \rightarrow d 3\pi$	
0.35 ± 0.20	BALTAY 68	HBC	+	7-8.5 $\pi^+ p$	

$0.565\Gamma(f_2(1270)\pi)/\Gamma(\pi^\pm \pi^+ \pi^-)$	DOCUMENT ID	TECN	CHG	COMMENT	$0.565\Gamma_4/(0.565\Gamma_4 + \frac{1}{2}\Gamma_5 + 0.624\Gamma_7)$
<0.3	BARTSCH 68	HBC	+	8 $\pi^+ p \rightarrow 3\pi p$	

$0.565\Gamma(f_2(1270)\pi)/\Gamma(\pi^\pm \pi^+ \pi^-)$	DOCUMENT ID	TECN	CHG	COMMENT	$0.565\Gamma_4/(0.565\Gamma_4 + \frac{1}{2}\Gamma_5 + 0.624\Gamma_7)$
0.61 ± 0.04	24 DAUM	81B SPEC		63,94 $\pi^- p$	

$0.565\Gamma(f_2(1270)\pi)/\Gamma(\pi^\pm \pi^+ \pi^-)$	DOCUMENT ID	TECN	CHG	COMMENT	$0.565\Gamma_4/(0.565\Gamma_4 + \frac{1}{2}\Gamma_5 + 0.624\Gamma_7)$
0.76 +0.24 -0.34	ARMENISE 69	DBC	+	5.1 $\pi^+ d \rightarrow d 3\pi$	
0.35 ± 0.20	BALTAY 68	HBC	+	7-8.5 $\pi^+ p$	

$0.565\Gamma(f_2(1270)\pi)/\Gamma(\pi^\pm \pi^+ \pi^-)$	DOCUMENT ID	TECN	CHG	COMMENT	$0.565\Gamma_4/(0.565\Gamma_4 + \frac{1}{2}\Gamma_5 + 0.624\Gamma_7)$
<0.3	BARTSCH 68	HBC	+	8 $\pi^+ p \rightarrow 3\pi p$	

$0.565\Gamma(f_2(1270)\pi)/\Gamma(\pi^\pm \pi^+ \pi^-)$	DOCUMENT ID	TECN	CHG	COMMENT	$0.565\Gamma_4/(0.565\Gamma_4 + \frac{1}{2}\Gamma_5 + 0.624\Gamma_7)$
0.61 ± 0.04	24 DAUM	81B SPEC		63,94 $\pi^- p$	

$0.565\Gamma(f_2(1270)\pi)/\Gamma(\pi^\pm \pi^+ \pi^-)$	DOCUMENT ID	TECN	CHG	COMMENT	$0.565\Gamma_4/(0.565\Gamma_4 + \frac{1}{2}\Gamma_5 + 0.624\Gamma_7)$
0.76 +0.24 -0.34	ARMENISE 69	DBC	+	5.1 $\pi^+ d \rightarrow d 3\pi$	
0.35 ± 0.20	BALTAY 68	HBC	+	7-8.5 $\pi^+ p$	

$0.565\Gamma(f_2(1270)\pi)/\Gamma(\pi^\pm \pi^+ \pi^-)$	DOCUMENT ID	TECN	CHG	COMMENT	$0.565\Gamma_4/(0.565\Gamma_4 + \frac{1}{2}\Gamma_5 + 0.624\Gamma_7)$
<0.3	BARTSCH 68	HBC	+	8 $\pi^+ p \rightarrow 3\pi p$	

See key on page 405

Meson Particle Listings

φ(1680), ρ₃(1690)

PHOTOPRODUCTION

Table with 4 columns: VALUE (MeV), DOCUMENT ID, TECN, COMMENT. Lists photoproduction data for φ(1680).

ρπ ANNIHILATION

Table with 4 columns: VALUE (MeV), DOCUMENT ID, TECN, COMMENT. Lists ρπ annihilation data.

φ(1680) DECAY MODES

Table with 3 columns: Mode, Fraction (Γ_i/Γ), and Comment. Lists various decay modes for φ(1680).

φ(1680) Γ(i)Γ(e⁺e⁻)/Γ²(total)

This combination of a branching ratio into channel (i) and branching ratio into e⁺e⁻ is directly measured and obtained from the cross section at the peak.

Γ(K_L⁰K_S⁰)/Γ_{total} × Γ(e⁺e⁻)/Γ_{total} Γ₄/Γ × Γ₅/Γ

Table with 4 columns: VALUE (units 10⁻⁶), EVTS, DOCUMENT ID, TECN, COMMENT. Lists data for KLKS and ee branching ratios.

Γ(K⁺K⁻(892) + c.c.)/Γ_{total} × Γ(e⁺e⁻)/Γ_{total} Γ₁/Γ × Γ₅/Γ

Table with 4 columns: VALUE (units 10⁻⁶), EVTS, DOCUMENT ID, TECN, COMMENT. Lists data for KK(892) and ee branching ratios.

Γ(φππ)/Γ_{total} × Γ(e⁺e⁻)/Γ_{total} Γ₇/Γ × Γ₅/Γ

Table with 4 columns: VALUE (units 10⁻⁷), EVTS, DOCUMENT ID, TECN, COMMENT. Lists φππ and ee branching ratios.

Γ(φη)/Γ_{total} × Γ(e⁺e⁻)/Γ_{total} Γ₉/Γ × Γ₅/Γ

Table with 4 columns: VALUE (units 10⁻⁶), DOCUMENT ID, TECN, COMMENT. Lists φη and ee branching ratios.

φ(1680) BRANCHING RATIOS

Table with 4 columns: VALUE, DOCUMENT ID, TECN, COMMENT. Lists branching ratios for φ(1680) to KK(892) and KSπ.

Γ(K⁺K⁻)/Γ(K⁺K⁻(892) + c.c.) Γ₃/Γ₁

Table with 4 columns: VALUE, DOCUMENT ID, TECN, COMMENT. Lists ratio of KK to KK(892) + c.c. branching ratios.

Γ(ωππ)/Γ(K⁺K⁻(892) + c.c.)

Table with 4 columns: VALUE, DOCUMENT ID, TECN, COMMENT. Lists ωππ and KK(892) + c.c. ratios.

Γ(φη)/Γ(K⁺K⁻(892) + c.c.)

Table with 4 columns: VALUE, DOCUMENT ID, TECN, COMMENT. Lists φη and KK(892) + c.c. ratios.

φ(1680) REFERENCES

Bibliography table listing references for φ(1680) with columns for author, document ID, year, and journal.

ρ₃(1690)

J^{PC} = 1⁺(3⁻)

ρ₃(1690) MASS

Table with 4 columns: VALUE (MeV), DOCUMENT ID, TECN, COMMENT. Lists mass values for ρ₃(1690).

2π MODE

Table with 4 columns: VALUE (MeV), EVTS, DOCUMENT ID, TECN, COMMENT. Lists 2π mode data.

1686 ± 4 OUR AVERAGE

Table with 4 columns: VALUE, DOCUMENT ID, TECN, COMMENT. Lists 2π mode data for the 1686 ± 4 average.

- Footnotes explaining mass errors and phase shift analysis for the 2π mode.

K⁺K⁻ AND K⁺K⁰ π DECS

Table with 4 columns: VALUE (MeV), EVTS, DOCUMENT ID, TECN, COMMENT. Lists K⁺K⁻ and K⁺K⁰π decays.

1696 ± 4 OUR AVERAGE

Table with 4 columns: VALUE, DOCUMENT ID, TECN, COMMENT. Lists K⁺K⁻ and K⁺K⁰π decays for the 1696 ± 4 average.

- Footnotes explaining partial waves and systematic errors for the K⁺K⁻ and K⁺K⁰π decays.

Meson Particle Listings

$\rho_3(1690)$

$(4\pi)^\pm$ MODE

VALUE (MeV) EVTS DOCUMENT ID TECN CHG COMMENT
The data in this block is included in the average printed for a previous datablock.

1686 ± 5 OUR AVERAGE Error includes scale factor of 1.1.

1694 ± 6		⁸ EVANGELIS...	81	OMEG	-	12 $\pi^- \rho \rightarrow p4\pi$
1665 ± 15	177	BALTAY	78B	HBC	+	15 $\pi^+ \rho \rightarrow p4\pi$
1670 ± 10		THOMPSON	74	HBC	+	13 $\pi^+ \rho$
1687 ± 20		CASON	73	HBC	-	8,18.5 $\pi^- \rho$
1685 ± 14		⁹ CASON	73	HBC	-	8,18.5 $\pi^- \rho$
1680 ± 40	144	BARTSCH	70B	HBC	+	8 $\pi^+ \rho \rightarrow N4\pi$
1689 ± 20	102	⁹ BARTSCH	70B	HBC	+	8 $\pi^+ \rho \rightarrow N2\rho$
1705 ± 21		CASO	70	HBC	-	11.2 $\pi^- \rho \rightarrow n\rho2\pi$

• • • We do not use the following data for averages, fits, limits, etc. • • •

1718 ± 10		¹⁰ EVANGELIS...	81	OMEG	-	12 $\pi^- \rho \rightarrow p4\pi$
1673 ± 9		¹¹ EVANGELIS...	81	OMEG	-	12 $\pi^- \rho \rightarrow p4\pi$
1733 ± 9	66	⁹ KLIGER	74	HBC	-	4.5 $\pi^- \rho \rightarrow p4\pi$
1630 ± 15		HOLMES	72	HBC	+	10-12 $K^+ \rho$
1720 ± 15		BALTAY	68	HBC	+	7, 8.5 $\pi^+ \rho$

⁸ From $\rho^- \rho^0$ mode, not independent of the other two EVANGELISTA 81 entries.
⁹ From $\rho^\pm \rho^0$ mode.
¹⁰ From $a_2(1320)^- \pi^0$ mode, not independent of the other two EVANGELISTA 81 entries.
¹¹ From $a_2(1320)^0 \pi^-$ mode, not independent of the other two EVANGELISTA 81 entries.

$\omega\pi$ MODE

VALUE (MeV) DOCUMENT ID TECN CHG COMMENT
The data in this block is included in the average printed for a previous datablock.

1681 ± 7 OUR AVERAGE

1670 ± 25		¹² ALDE	95	GAM2		38 $\pi^- \rho \rightarrow \omega\pi^0 n$
1690 ± 15		EVANGELIS...	81	OMEG	-	12 $\pi^- \rho \rightarrow \omega\pi p$
1666 ± 14		GESSAROLI	77	HBC		11 $\pi^- \rho \rightarrow \omega\pi p$
1686 ± 9		THOMPSON	74	HBC	+	13 $\pi^+ \rho$
1654 ± 24		BARNHAM	70	HBC	+	10 $K^+ \rho \rightarrow \omega\pi X$

¹² Supersedes ALDE 92c.
 $\eta\pi^+ \pi^-$ MODE
 (For difficulties with MMS experiments, see the $a_2(1320)$ mini-review in the 1973 edition.)

VALUE (MeV) DOCUMENT ID TECN CHG COMMENT
The data in this block is included in the average printed for a previous datablock.

1682 ± 12 OUR AVERAGE

1685 ± 10 ± 20		AMELIN	00	VES		37 $\pi^- \rho \rightarrow \eta\pi^+ \pi^- n$
1680 ± 15		FUKUI	88	SPEC	0	8.95 $\pi^- \rho \rightarrow \eta\pi^+ \pi^- n$
1700 ± 47		¹³ ANDERSON	69	MMS	-	16 $\pi^- \rho$ backward
1632 ± 15		^{13,14} FOCACCI	66	MMS	-	7-12 $\pi^- \rho \rightarrow \rho MM$
1700 ± 15		^{13,14} FOCACCI	66	MMS	-	7-12 $\pi^- \rho \rightarrow \rho MM$
1748 ± 15		^{13,14} FOCACCI	66	MMS	-	7-12 $\pi^- \rho \rightarrow \rho MM$

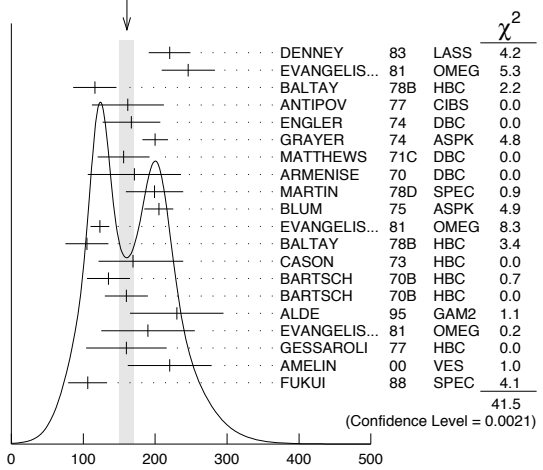
¹³ Seen in 2.5-3 GeV/c $\bar{p}p$. $2\pi^+ 2\pi^-$, with 0, 1, 2 $\pi^+ \pi^-$ pairs in ρ band not seen by OREN 74 (2.3 GeV/c $\bar{p}p$) with more statistics. (Jan. 1976)
¹⁴ Not seen by BOWEN 72.

$\rho_3(1690)$ WIDTH

$2\pi, K\bar{K},$ AND $K\bar{K}\pi$ MODES

VALUE (MeV) DOCUMENT ID
161 ± 10 OUR AVERAGE Includes data from the 5 datablocks that follow this one. Error includes scale factor of 1.5. See the ideogram below.

WEIGHTED AVERAGE
161 ± 10 (Error scaled by 1.5)



$\rho_3(1690)$ width, $2\pi, K\bar{K},$ and $K\bar{K}\pi$ modes (MeV)

2π MODE

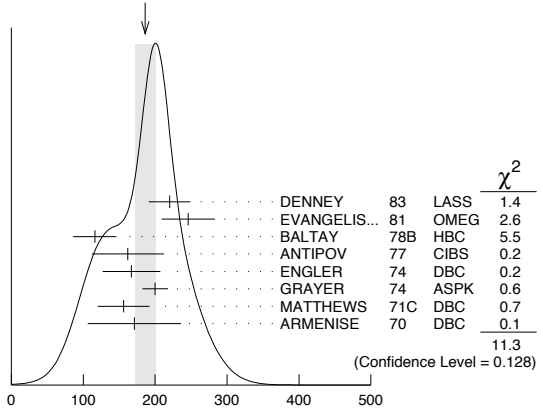
VALUE (MeV) EVTS DOCUMENT ID TECN CHG COMMENT
The data in this block is included in the average printed for a previous datablock.

186 ± 14 OUR AVERAGE Error includes scale factor of 1.3. See the ideogram below.

220 ± 29		DENNEY	83	LASS		10 $\pi^+ N$
246 ± 37		EVANGELIS...	81	OMEG	-	12 $\pi^- \rho \rightarrow 2\pi p$
116 ± 30	476	BALTAY	78B	HBC	0	15 $\pi^+ \rho \rightarrow \pi^+ \pi^- n$
162 ± 50	175	¹⁵ ANTIPOV	77	CIBS	0	25 $\pi^- \rho \rightarrow p3\pi$
167 ± 40	600	ENGLER	74	DBC	0	6 $\pi^+ n \rightarrow \pi^+ \pi^- p$
200 ± 18		¹⁶ GRAY	74	ASPK	0	17 $\pi^- \rho \rightarrow \pi^+ \pi^- n$
156 ± 36		MATTHEWS	71C	DBC	0	7 $\pi^+ N$
171 ± 65		ARMENISE	70	DBC	0	9 $\pi^+ d$
322 ± 35		¹⁷ CORDEN	79	OMEG		12-15 $\pi^- \rho \rightarrow n2\pi$
240 ± 30		^{16,18} ESTABROOKS	75	RVUE		17 $\pi^- \rho \rightarrow \pi^+ \pi^- n$
180 ± 30	122	BARTSCH	70B	HBC	+	8 $\pi^+ \rho \rightarrow N2\pi$
267 ± 72 - 46		STUNTEBECK 70	HDHC	0		8 $\pi^- p, 5.4 \pi^+ d$
188 ± 49		ARMENISE	68	DBC	0	5.1 $\pi^+ d$
180 ± 40		GOLDBERG	65	HBC	0	6 $\pi^+ d, 8 \pi^- p$

¹⁵ Width errors enlarged by us to $4\Gamma/\sqrt{N}$; see the note with the $K^*(892)$ mass.
¹⁶ Uses same data as HYAMS 75 and BECKER 79.
¹⁷ From a phase shift solution containing a $f_2'(1525)$ width two times larger than the $K\bar{K}$ result.
¹⁸ From phase-shift analysis. Error takes account of spread of different phase-shift solutions.

WEIGHTED AVERAGE
186 ± 14 (Error scaled by 1.3)



$\rho_3(1690)$ width, 2π mode (MeV)

$K\bar{K}$ AND $K\bar{K}\pi$ MODES

VALUE (MeV)	EVTS	DOCUMENT ID	TECN	CHG	COMMENT
-------------	------	-------------	------	-----	---------

The data in this block is included in the average printed for a previous datablock.

204±18 OUR AVERAGE

199±40	6000	19 MARTIN	78D	SPEC	10 $\pi^- \rho \rightarrow K_S^0 K^- \rho$
205±20		BLUM	75	ASPK 0	18.4 $\pi^- \rho \rightarrow n K^+ K^-$

••• We do not use the following data for averages, fits, limits, etc. •••

219±4		ALPER	80	CNTR 0	62 $\pi^- \rho \rightarrow K^+ K^- n$
186±11		20 COSTA...	80	OMEG	10 $\pi^- \rho \rightarrow K^+ K^- n$
112±60		ADERHOLZ	69	HBC +	8 $\pi^+ \rho \rightarrow K\bar{K}\pi$

¹⁹ From a fit to $J^P = 3^-$ partial wave.

²⁰ They cannot distinguish between $\rho_3(1690)$ and $\omega_3(1670)$.

 $(4\pi)^\pm$ MODE

VALUE (MeV)	EVTS	DOCUMENT ID	TECN	CHG	COMMENT
-------------	------	-------------	------	-----	---------

The data in this block is included in the average printed for a previous datablock.

129±10 OUR AVERAGE

123±13		21 EVANGELIS...	81	OMEG -	12 $\pi^- \rho \rightarrow p 4\pi$
105±30		BALTAY	78B	HBC +	15 $\pi^+ \rho \rightarrow p 4\pi$
169 ⁺⁷⁰ ₋₄₈		CASON	73	HBC -	8,18.5 $\pi^- \rho$
135±30		144 BARTSCH	70B	HBC +	8 $\pi^+ \rho \rightarrow N 4\pi$
160±30		102 BARTSCH	70B	HBC +	8 $\pi^+ \rho \rightarrow N 2\rho$

••• We do not use the following data for averages, fits, limits, etc. •••

230±28		22 EVANGELIS...	81	OMEG -	12 $\pi^- \rho \rightarrow p 4\pi$
184±33		23 EVANGELIS...	81	OMEG -	12 $\pi^- \rho \rightarrow p 4\pi$
150		66 24 KLIGER	74	HBC -	4.5 $\pi^- \rho \rightarrow p 4\pi$
106±25		THOMPSON	74	HBC +	13 $\pi^+ \rho$
125 ⁺⁸³ ₋₃₅		24 CASON	73	HBC -	8,18.5 $\pi^- \rho$
130±30		HOLMES	72	HBC +	10-12 $K^+ \rho$
180±30		24 BARTSCH	70B	HBC +	8 $\pi^+ \rho \rightarrow N a_2 \pi$

²¹ From $\rho^- \rho^0$ mode, not independent of the other two EVANGELISTA 81 entries.

²² From $a_2(1320) \pi^0$ mode, not independent of the other two EVANGELISTA 81 entries.

²³ From $a_2(1320) \pi^-$ mode, not independent of the other two EVANGELISTA 81 entries.

²⁴ From $\rho^\pm \rho^0$ mode.

 $\omega\pi$ MODE

VALUE (MeV)	DOCUMENT ID	TECN	CHG	COMMENT
-------------	-------------	------	-----	---------

The data in this block is included in the average printed for a previous datablock.

190±40 OUR AVERAGE

230±65		25 ALDE	95	GAM2	38 $\pi^- \rho \rightarrow \omega \pi^0 n$
190±65		EVANGELIS...	81	OMEG -	12 $\pi^- \rho \rightarrow \omega \pi p$
160±56		GESSAROLI	77	HBC	11 $\pi^- \rho \rightarrow \omega \pi p$

••• We do not use the following data for averages, fits, limits, etc. •••

89±25		THOMPSON	74	HBC +	13 $\pi^+ \rho$
130 ⁺⁷³ ₋₄₃		BARNHAM	70	HBC +	10 $K^+ \rho \rightarrow \omega \pi X$

²⁵ Supersedes ALDE 92c.

 $\eta\pi^+\pi^-$ MODE

(For difficulties with MMS experiments, see the $a_2(1320)$ mini-review in the 1973 edition.)

VALUE (MeV)	DOCUMENT ID	TECN	CHG	COMMENT
-------------	-------------	------	-----	---------

The data in this block is included in the average printed for a previous datablock.

126±40 OUR AVERAGE Error includes scale factor of 1.8.

220±30±50		AMELIN	00	VES	37 $\pi^- \rho \rightarrow \eta \pi^+ \pi^- n$
106±27		FUKUI	88	SPEC 0	8.95 $\pi^- \rho \rightarrow \eta \pi^+ \pi^- n$

••• We do not use the following data for averages, fits, limits, etc. •••

195		26 ANDERSON	69	MMS -	16 $\pi^- \rho$ back-ward
< 21		26,27 FOCACCI	66	MMS -	7-12 $\pi^- \rho \rightarrow \rho MM$
< 30		26,27 FOCACCI	66	MMS -	7-12 $\pi^- \rho \rightarrow \rho MM$
< 38		26,27 FOCACCI	66	MMS -	7-12 $\pi^- \rho \rightarrow \rho MM$

²⁶ Seen in 2.5-3 GeV/c $\bar{p} p$. $2\pi^+ 2\pi^-$, with 0, 1, 2 $\pi^+ \pi^-$ pairs in ρ^0 band not seen by OREN 74 (2.3 GeV/c $\bar{p} p$) with more statistics. (Jan. 1979)

²⁷ Not seen by BOWEN 72.

 $\rho_3(1690)$ DECAY MODES

Mode	Fraction (Γ_i/Γ)	Scale factor
Γ_1 4π	(71.1 ± 1.9) %	
Γ_2 $\pi^\pm \pi^+ \pi^- \pi^0$	(67 ± 22) %	
Γ_3 $\omega \pi$	(16 ± 6) %	
Γ_4 $\pi \pi$	(23.6 ± 1.3) %	
Γ_5 $K\bar{K}\pi$	(3.8 ± 1.2) %	
Γ_6 $K\bar{K}$	(1.58 ± 0.26) %	1.2
Γ_7 $\eta \pi^+ \pi^-$	seen	
Γ_8 $\rho(770) \eta$	seen	
Γ_9 $\pi \pi \rho$	seen	
Excluding 2ρ and $a_2(1320)\pi$.		
Γ_{10} $a_2(1320)\pi$	seen	
Γ_{11} $\rho \rho$	seen	
Γ_{12} $\phi \pi$		
Γ_{13} $\eta \pi$		
Γ_{14} $\pi^\pm 2\pi^+ 2\pi^- \pi^0$		

CONSTRAINED FIT INFORMATION

An overall fit to 5 branching ratios uses 10 measurements and one constraint to determine 4 parameters. The overall fit has a $\chi^2 = 14.7$ for 7 degrees of freedom.

The following off-diagonal array elements are the correlation coefficients $\langle \delta x_i \delta x_j \rangle / (\delta x_i \delta x_j)$, in percent, from the fit to the branching fractions, $x_i \equiv \Gamma_i/\Gamma_{\text{total}}$. The fit constrains the x_i whose labels appear in this array to sum to one.

x_4	-77		
x_5	-74	17	
x_6	-15	2	0
	x_1	x_4	x_5

 $\rho_3(1690)$ BRANCHING RATIOS

$\Gamma(\pi\pi)/\Gamma_{\text{total}}$	DOCUMENT ID	TECN	CHG	COMMENT	Γ_4/Γ_1
0.236±0.013 OUR FIT					
0.243±0.013 OUR AVERAGE					
0.259 ^{+0.018} _{-0.019}	BECKER	79	ASPK 0	17 $\pi^- \rho$ polarized	
0.23 ± 0.02	CORDEN	79	OMEG	12-15 $\pi^- \rho \rightarrow n 2\pi$	
0.22 ± 0.04	28 MATTHEWS	71C	HDBC 0	7 $\pi^+ n \rightarrow \pi^- \rho$	
0.245 ± 0.006	29 ESTABROOKS	75	RVUE	17 $\pi^- \rho \rightarrow \pi^+ \pi^- n$	

••• We do not use the following data for averages, fits, limits, etc. •••

²⁸ One-pion-exchange model used in this estimation.

²⁹ From phase-shift analysis of HYAMS 75 data.

$\Gamma(\pi\pi)/\Gamma(\pi^\pm \pi^+ \pi^- \pi^0)$	DOCUMENT ID	TECN	CHG	COMMENT	Γ_4/Γ_2
0.35±0.11	CASON	73	HBC -	8,18.5 $\pi^- \rho$	
< 0.2	HOLMES	72	HBC +	10-12 $K^+ \rho$	
< 0.12	BALLAM	71B	HBC -	16 $\pi^- \rho$	

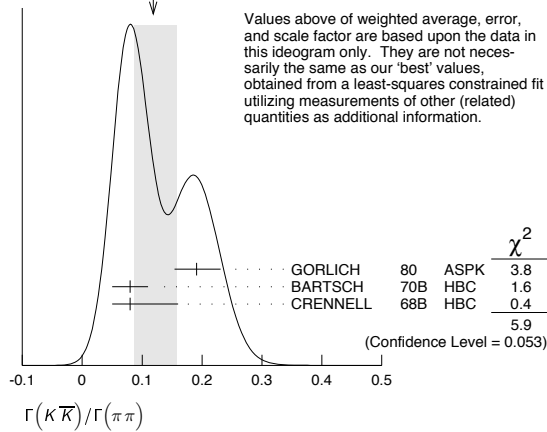
$\Gamma(\pi\pi)/\Gamma(4\pi)$	DOCUMENT ID	TECN	CHG	COMMENT	Γ_4/Γ_1
0.332±0.026 OUR FIT				Error includes scale factor of 1.1.	
0.30 ± 0.10	BALTAY	78B	HBC 0	15 $\pi^+ \rho \rightarrow p 4\pi$	

$\Gamma(K\bar{K})/\Gamma(\pi\pi)$	DOCUMENT ID	TECN	CHG	COMMENT	Γ_6/Γ_4
0.067±0.011 OUR FIT				Error includes scale factor of 1.2.	
0.118^{+0.040}_{-0.032} OUR AVERAGE				Error includes scale factor of 1.7. See the ideogram below.	
0.191 ^{+0.040} _{-0.037}	GORLICH	80	ASPK 0	17,18 $\pi^- \rho$ polarized	
0.08 ± 0.03	BARTSCH	70B	HBC +	8 $\pi^+ \rho$	
0.08 ^{+0.08} _{-0.03}	CRENNELL	68B	HBC	6.0 $\pi^- \rho$	

Meson Particle Listings

$\rho_3(1690)$

WEIGHTED AVERAGE
0.118±0.040-0.032 (Error scaled by 1.7)



$\Gamma(K\bar{K})/\Gamma(\pi\pi)$ Γ_5/Γ_4

VALUE	DOCUMENT ID	TECN	CHG	COMMENT
0.16±0.05 OUR FIT				
0.16±0.05	30 BARTSCH	70B	HBC	+ 8 $\pi^+\rho$
	30 Increased by us to correspond to $B(\rho_3(1690) \rightarrow \pi\pi)=0.24$.			

$[\Gamma(\pi\pi\rho) + \Gamma(a_2(1320)\pi) + \Gamma(\rho\rho)]/\Gamma(\pi^\pm\pi^+\pi^-\pi^0)$ $(\Gamma_9+\Gamma_{10}+\Gamma_{11})/\Gamma_2$

VALUE	DOCUMENT ID	TECN	CHG	COMMENT
0.94±0.09 OUR AVERAGE				
0.96±0.21	BALTAY	78B	HBC	+ 15 $\pi^+\rho \rightarrow p4\pi$
0.88±0.15	BALLAM	71B	HBC	- 16 $\pi^-\rho$
1 ±0.15	BARTSCH	70B	HBC	+ 8 $\pi^+\rho$
consistent with 1	CASO	68	HBC	- 11 $\pi^-\rho$

$\Gamma(\rho\rho)/\Gamma(\pi^\pm\pi^+\pi^-\pi^0)$ Γ_{11}/Γ_2

VALUE	EVTS	DOCUMENT ID	TECN	CHG	COMMENT
0.12±0.11		BALTAY	78B	HBC	+ 15 $\pi^+\rho \rightarrow p4\pi$
0.56	66	KLIGER	74	HBC	- 4.5 $\pi^-\rho \rightarrow p4\pi$
0.13±0.09		31 THOMPSON	74	HBC	+ 13 $\pi^+\rho$
0.7 ±0.15		BARTSCH	70B	HBC	+ 8 $\pi^+\rho$
		31 $\rho\rho$ and $a_2(1320)\pi$ modes are indistinguishable.			

$\Gamma(\rho\rho)/[\Gamma(\pi\pi\rho) + \Gamma(a_2(1320)\pi) + \Gamma(\rho\rho)]$ $\Gamma_{11}/(\Gamma_9+\Gamma_{10}+\Gamma_{11})$

VALUE	DOCUMENT ID	TECN	CHG	COMMENT
0.48±0.16	CASO	68	HBC	- 11 $\pi^-\rho$

$\Gamma(a_2(1320)\pi)/\Gamma(\pi^\pm\pi^+\pi^-\pi^0)$ Γ_{10}/Γ_2

VALUE	DOCUMENT ID	TECN	CHG	COMMENT
0.66±0.08	BALTAY	78B	HBC	+ 15 $\pi^+\rho \rightarrow p4\pi$
0.36±0.14	32 THOMPSON	74	HBC	+ 13 $\pi^+\rho$
not seen	CASON	73	HBC	- 8,18.5 $\pi^-\rho$
0.6 ±0.15	BARTSCH	70B	HBC	+ 8 $\pi^+\rho$
0.6	BALTAY	68	HBC	+ 7,8.5 $\pi^+\rho$
	32 $\rho\rho$ and $a_2(1320)\pi$ modes are indistinguishable.			

$\Gamma(\omega\pi)/\Gamma(\pi^\pm\pi^+\pi^-\pi^0)$ Γ_3/Γ_2

VALUE	CL%	DOCUMENT ID	TECN	CHG	COMMENT
0.23±0.05 OUR AVERAGE		Error includes scale factor of 1.2.			
0.33±0.07		THOMPSON	74	HBC	+ 13 $\pi^+\rho$
0.12±0.07		BALLAM	71B	HBC	- 16 $\pi^-\rho$
0.25±0.10		BALTAY	68	HBC	+ 7,8.5 $\pi^+\rho$
0.25±0.10		JOHNSTON	68	HBC	- 7.0 $\pi^-\rho$
<0.11	95	BALTAY	78B	HBC	+ 15 $\pi^+\rho \rightarrow p4\pi$
<0.09		KLIGER	74	HBC	- 4.5 $\pi^-\rho \rightarrow p4\pi$

$\Gamma(\phi\pi)/\Gamma(\pi^\pm\pi^+\pi^-\pi^0)$ Γ_{12}/Γ_2

VALUE	DOCUMENT ID	TECN	CHG	COMMENT
<0.11	BALTAY	68	HBC	+ 7,8.5 $\pi^+\rho$

$\Gamma(\pi^\pm 2\pi^+ 2\pi^-\pi^0)/\Gamma(\pi^\pm\pi^+\pi^-\pi^0)$ Γ_{14}/Γ_2

VALUE	DOCUMENT ID	TECN	CHG	COMMENT
<0.15	BALTAY	68	HBC	+ 7,8.5 $\pi^+\rho$

$\Gamma(\eta\pi)/\Gamma(\pi^\pm\pi^+\pi^-\pi^0)$ Γ_{13}/Γ_2

VALUE	DOCUMENT ID	TECN	CHG	COMMENT
<0.02	THOMPSON	74	HBC	+ 13 $\pi^+\rho$

• • • We do not use the following data for averages, fits, limits, etc. • • •

$\Gamma(K\bar{K}^*)/\Gamma_{total}$ Γ_6/Γ

VALUE	DOCUMENT ID	TECN	CHG	COMMENT
0.0158±0.0026 OUR FIT	Error includes scale factor of 1.2.			
0.0130±0.0024 OUR AVERAGE				
0.013 ±0.003	COSTA...	80	OMEG 0	10 $\pi^-\rho \rightarrow K^+K^-\eta$
0.013 ±0.004	33 MARTIN	78B	SPEC	- 10 $\pi\rho \rightarrow K_S^0K^-\rho$

33 From $(\Gamma_4\Gamma_6)^{1/2} = 0.056 \pm 0.034$ assuming $B(\rho_3(1690) \rightarrow \pi\pi) = 0.24$.

$\Gamma(\omega\pi)/[\Gamma(\omega\pi) + \Gamma(\rho\rho)]$ $\Gamma_3/(\Gamma_3+\Gamma_{11})$

VALUE	DOCUMENT ID	TECN	CHG	COMMENT
0.22±0.08	CASON	73	HBC	- 8,18.5 $\pi^-\rho$

• • • We do not use the following data for averages, fits, limits, etc. • • •

$\Gamma(\eta\pi^+\pi^-)/\Gamma_{total}$ Γ_7/Γ

VALUE	DOCUMENT ID	TECN	COMMENT
seen	FUKUI	88	SPEC 8.95 $\pi^-\rho \rightarrow \eta\pi^+\pi^-\eta$

$\Gamma(a_2(1320)\pi)/\Gamma(\rho(770)\eta)$ Γ_{10}/Γ_8

VALUE	DOCUMENT ID	TECN	COMMENT
5.5±2.0	AMELIN	00	VES 37 $\pi^-\rho \rightarrow \eta\pi^+\pi^-\eta$

$\rho_3(1690)$ REFERENCES

AMELIN	00	NP A668 83	D. Amelin et al.	(VES Collab.)
ALDE	95	ZPHY C66 379	D.M. Alde et al.	(GAMS Collab.) JP
ALDE	92C	ZPHY C54 553	D.M. Alde et al.	(BELG, SERP, KEK, LANL+)
FUKUI	88	PL B202 441	S. Fukui et al.	(SUGI, NAGO, KEK, KYOT+)
DENNEY	83	PR D28 2726	D.L. Denney et al.	(IOWA, MICH)
EVANGELIS...	81	NP B178 197	C. Evangelista et al.	(BARI, BONN, CERN+)
ALPER	80	PL 94B 422	B. Alper et al.	(AMST, CERN, CRAC, MPIM+)
COSTA...	80	NP B175 402	G. Costa de Beauregard et al.	(BARI, BONN+)
GORLICH	80	NP B174 16	L. Gorlich et al.	(CRAC, MPIM, CERN+)
BECKER	79	NP B151 46	H. Becker et al.	(MPIM, CERN, ZEEM, CRAC)
CORDEN	79	NP B157 250	M.J. Corden et al.	(BIRM, RHEL, TEL+)
BALTAY	78B	PR D17 62	C. Baltay et al.	(COLU, BINC)
MARTIN	78B	NP B140 158	A.D. Martin et al.	(DURH, GEVA)
MARTIN	78D	PL 74B 417	A.D. Martin et al.	(DURH, GEVA)
ANTIPOV	77	NP B119 45	Y.M. Antipov et al.	(SERP, GEVA)
GESSAROLI	77	NP B126 382	R. Gessaroli et al.	(BGNA, FIRZ, GENO+)
BLUM	75	PL 57B 403	W. Blum et al.	(CERN, MPIM) JP
ESTABROOKS	75	NP B95 322	P.G. Estabrooks, A.D. Martin	(DURH)
HYAMS	75	NP B100 205	B.D. Hyams et al.	(CERN, MPIM)
ENGLER	74	PR D10 2070	A. Engler et al.	(CMU, CASE)
GRAYER	74	NP B75 189	G. Grayer et al.	(CERN, MPIM)
KLIGER	74	SJNP 19 428	G.K. Kliger et al.	(ITEP)
Translated from YAF 19 839.				
OREN	74	NP B71 189	Y. Oren et al.	(ANL, OXF)
THOMPSON	74	NP B69 220	G. Thompson et al.	(PURD)
CASON	73	PR D7 1971	N.M. Cason et al.	(NDAM)
BOWEN	72	PRL 29 890	D.R. Bowen et al.	(NEAS, STON)
HOLMES	72	PR D6 3336	R. Holmes et al.	(ROCH)
BALLAM	71B	PR D3 2606	J. Ballam et al.	(SLAC)
MATTHEWS	71C	NP B33 1	J.A.J. Matthews et al.	(TNTO, WISC) JP
ARMENISE	70	LNC 4 199	N. Armenise et al.	(BARI, BGNA, FIRZ)
BARNHAM	70	PRL 24 1083	K.W.J. Barnham et al.	(BIRM)
BARTSCH	70B	NP B22 109	J. Bartsch et al.	(AACH, BERL, CERN)
CASO	70	LNC 3 707	C. Caso et al.	(GENO, HAMB, MILA, SA CL)
STUNTEBECK	70	PL 32B 391	P.H. Stuntebeck et al.	(NDAM)
ADERHOLZ	69	NP B11 259	M. Aderholz et al.	(AACH3, BERL, CERN+)
ANDERSON	69	PRL 22 1390	E.W. Anderson et al.	(BNL, CMU)
ARMENISE	68	NC 54A 999	N. Armenise et al.	(BARI, BGNA, FIRZ+)
BALTAY	68	PRL 20 887	C. Baltay et al.	(COLU, ROCH, RUTG, YALE)
CASO	68	NC 54A 983	C. Caso et al.	(GENO, HAMB, MILA, SA CL)
CRENNELL	68B	PL 28B 136	D.J. Crennell et al.	(BNL)
JOHNSTON	68	PRL 20 3414	T.F. Johnston et al.	(CERN)
FOCACCI	66	PRL 17 990	M.M. Focacci et al.	(TNTO, WISC) IJP
GOLDBERG	65	PL 17 354	M. Goldberg et al.	(CERN, EPOL, ORSAY+)

$\rho(1700)$

$$I^G(J^{PC}) = 1^+(1^{--})$$

THE $\rho(1450)$ AND THE $\rho(1700)$

Updated May 2010 by S. Eidelman (Novosibirsk) and G. Venanzoni (Frascati).

In our 1988 edition, we replaced the $\rho(1600)$ entry with two new ones, the $\rho(1450)$ and the $\rho(1700)$, because there was emerging evidence that the 1600-MeV region actually contains two ρ -like resonances. Erkal [1] had pointed out this possibility with a theoretical analysis on the consistency of 2π and 4π electromagnetic form factors and the $\pi\pi$ scattering length. Donnachie [2], with a full analysis of data on the 2π and 4π final states in e^+e^- annihilation and photoproduction reactions, had also argued that in order to obtain a consistent picture, two resonances were necessary. The existence of $\rho(1450)$ was supported by the analysis of $\eta\rho^0$ mass spectra obtained in photoproduction and e^+e^- annihilation [3], as well as that of $e^+e^- \rightarrow \omega\pi$ [4].

The analysis of [2] was further extended by [5,6] to include new data on 4π -systems produced in e^+e^- annihilation, and in τ -decays (τ decays to 4π , and e^+e^- annihilation to 4π can be related by the Conserved Vector Current assumption). These systems were successfully analyzed using interfering contributions from two ρ -like states, and from the tail of the $\rho(770)$ decaying into two-body states. While specific conclusions on $\rho(1450) \rightarrow 4\pi$ were obtained, little could be said about the $\rho(1700)$.

Independent evidence for two 1^- states is provided by [7] in 4π electroproduction at $\langle Q^2 \rangle = 1$ (GeV/c)², and by [8] in a high-statistics sample of the $\eta\pi\pi$ system in π^-p charge exchange.

This scenario with two overlapping resonances is supported by other data. Bisello [9] measured the pion form factor in the interval 1.35–2.4 GeV, and observed a deep minimum around 1.6 GeV. The best fit was obtained with the hypothesis of ρ -like resonances at 1420 and 1770 MeV, with widths of about 250 MeV. Antonelli [10] found that the $e^+e^- \rightarrow \eta\pi^+\pi^-$ cross section is better fitted with two fully interfering Breit-Wigners, with parameters in fair agreement with those of [2] and [9]. These results can be considered as a confirmation of the $\rho(1450)$.

Decisive evidence for the $\pi\pi$ decay mode of both $\rho(1450)$ and $\rho(1700)$ comes from $\bar{p}p$ annihilation at rest [11]. It has been shown that these resonances also possess a $K\bar{K}$ decay mode [12–14]. High-statistics studies of the decays $\tau \rightarrow \pi\pi\nu_\tau$ [15,16], and $\tau \rightarrow 4\pi\nu_\tau$ [17] also require the $\rho(1450)$, but are not sensitive to the $\rho(1700)$, because it is too close to the τ mass. A recent very-high-statistics study of the $\tau \rightarrow \pi\pi\nu_\tau$ decay performed at Belle [18] reports the first observation of both $\rho(1450)$ and $\rho(1700)$ in τ decays.

The structure of these ρ states is not yet completely clear. Barnes [19] and Close [20] claim that $\rho(1450)$ has a mass consistent with radial $2S$, but its decays show characteristics of hybrids, and suggest that this state may be a $2S$ -hybrid

mixture. Donnachie [21] argues that hybrid states could have a 4π decay mode dominated by the $a_1\pi$. Such behavior has been observed by [22] in $e^+e^- \rightarrow 4\pi$ in the energy range 1.05–1.38 GeV, and by [17] in $\tau \rightarrow 4\pi$ decays. Alexander [23] observes the $\rho(1450) \rightarrow \omega\pi$ decay mode in B -meson decays, however, does not find $\rho(1700) \rightarrow \omega\pi^0$. A similar conclusion is made by [24], who studied the process $e^+e^- \rightarrow \omega\pi^0$. Various decay modes of the $\rho(1450)$ and $\rho(1700)$ are observed in $\bar{p}n$ and $\bar{p}p$ annihilation [25,26], but no definite conclusions can be drawn. More data should be collected to clarify the nature of the ρ states, particularly in the energy range above 1.6 GeV.

We now list under a separate entry the $\rho(1570)$, the $\phi\pi$ state with $J^{PC} = 1^{--}$ earlier observed by [27] (referred to as $C(1480)$) and recently confirmed by [28]. While [29] shows that it may be a threshold effect, [5] and [30] suggest two independent vector states with this decay mode. The $C(1480)$ has not been seen in the $\bar{p}p$ [31] and e^+e^- [32,33] experiments. However, the sensitivity of the two latter is an order of magnitude lower than that of [28]. Note that [28] can not exclude that their observation is due to an OZI-suppressed decay mode of the $\rho(1700)$.

Several observations on the $\omega\pi$ system in the 1200-MeV region [34–40] may be interpreted in terms of either $J^P = 1^-$ $\rho(770) \rightarrow \omega\pi$ production [41], or $J^P = 1^+$ $b_1(1235)$ production [39,40]. We argue that no special entry for a $\rho(1250)$ is needed. The LASS amplitude analysis [42] showing evidence for $\rho(1270)$ is preliminary and needs confirmation. For completeness, the relevant observations are listed under the $\rho(1450)$.

Recently [43] reported a very broad 1^{--} resonance-like K^+K^- state in $J/\psi \rightarrow K^+K^-\pi^0$ decays. Its pole position corresponds to mass of 1576 MeV and width of 818 MeV. [44–46] suggest its exotic structure (molecular or multiquark), while [47] and [48] explain it by the interference between the $\rho(1450)$ and $\rho(1700)$. We quote [43] as $X(1575)$ in the section “Further States.”

Evidence for ρ -like mesons decaying into 6π states was first noted by [49] in the analysis of 6π mass spectra from e^+e^- annihilation [50,51] and diffractive photoproduction [52]. Clegg [49] argued that two states at about 2.1 and 1.8 GeV exist: while the former is a candidate for the $\rho(2150)$, the latter could be a manifestation of the $\rho(1700)$ distorted by threshold effects. BaBar reported observations of the new decay modes of the $\rho(2150)$ in the channels $\eta'(958)\pi^+\pi^-$ and $f_1(1285)\pi^+\pi^-$ [53]. The relativistic quark model [54] predicts the 2^3D_1 state with $J^{PC} = 1^{--}$ at 2.15 GeV which can be identified with the $\rho(2150)$.

The E687 Collaboration at Fermilab reported an observation of a narrow-dip structure at 1.9 GeV in the $3\pi^+3\pi^-$ diffractive photoproduction [55]. A similar effect of the dip in the cross section of $e^+e^- \rightarrow 6\pi$ around 1.9 GeV has been earlier reported by DM2 [51], where 6π included both $3\pi^+3\pi^-$ and $2\pi^+2\pi^-\pi^0$. Later the dip in the R value (the total cross section of $e^+e^- \rightarrow$ hadrons divided by the cross section of $e^+e^- \rightarrow \mu^+\mu^-$) was

Meson Particle Listings

 $\rho(1700)$

observed by [56], again around 1.9 GeV. This energy is close to the $N\bar{N}$ threshold, which hints at the possible relation between the dip and $N\bar{N}$, *e.g.*, the frequently discussed narrow $N\bar{N}$ resonance or just a threshold effect. Such behaviour is also characteristic of exotic objects like vector $q\bar{q}$ hybrids. Note that [57] failed to find this state in the reaction $\bar{n}p \rightarrow 3\pi^+2\pi^-\pi^0$. A reanalysis of the E687 data by [58] shows that a dip may arise due to interference of a narrow object with a broad $\rho(1700)$ independently of the nature of the former. BaBar studied the processes $e^+e^- \rightarrow 3\pi^+3\pi^-$ and $e^+e^- \rightarrow 2\pi^+2\pi^-2\pi^0$ using the radiative return, and observed a structure around 1.9 GeV in both final states [59]. The data are not well described by a single Breit-Wigner state, and a good fit is achieved while taking into account the interference of such a structure with a Jacob-Slansky amplitude for continuum. The mass of this state obtained by BaBar is consistent with [56] and [55], but the width is substantially larger. Recently [28] observed a structure at 1.9 GeV in the radiative return to the $\phi\pi$ final state, with a much smaller width of 48 ± 17 MeV consistent with that of [56,58]. We list these observations under a separate particle $\rho(1900)$, which needs confirmation.

References

1. C. Erkal, Z. Phys. **C31**, 615 (1986).
2. A. Donnachie and H. Mirzaie, Z. Phys. **C33**, 407 (1987).
3. A. Donnachie and A.B. Clegg, Z. Phys. **C34**, 257 (1987).
4. A. Donnachie and A.B. Clegg, Z. Phys. **C51**, 689 (1991).
5. A.B. Clegg and A. Donnachie, Z. Phys. **C40**, 313 (1988).
6. A.B. Clegg and A. Donnachie, Z. Phys. **C62**, 455 (1994).
7. T.J. Killian *et al.*, Phys. Rev. **D21**, 3005 (1980).
8. S. Fukui *et al.*, Phys. Lett. **B202**, 441 (1988).
9. D. Bisello *et al.*, Phys. Lett. **B220**, 321 (1989).
10. A. Antonelli *et al.*, Phys. Lett. **B212**, 133 (1988).
11. A. Abele *et al.*, Phys. Lett. **B391**, 191 (1997).
12. A. Abele *et al.*, Phys. Rev. **D57**, 3860 (1998).
13. A. Bertin *et al.*, Phys. Lett. **B434**, 180 (1998).
14. A. Abele *et al.*, Phys. Lett. **B468**, 178 (1999).
15. R. Barate *et al.*, Z. Phys. **C76**, 15 (1997).
16. S. Anderson, Phys. Rev. **D61**, 112002 (2000).
17. K.W. Edwards *et al.*, Phys. Rev. **D61**, 072003 (2000).
18. M. Fujikawa *et al.*, Phys. Rev. **D78**, 072006 (2008).
19. T. Barnes *et al.*, Phys. Rev. **D55**, 4157 (1997).
20. F.E. Close *et al.*, Phys. Rev. **D56**, 1584 (1997).
21. A. Donnachie and Yu.S. Katashnikova, Phys. Rev. **D60**, 114011 (1999).
22. R.R. Akhmetshin *et al.*, Phys. Lett. **B466**, 392 (1999).
23. J.P. Alexander *et al.*, Phys. Rev. **D64**, 092001 (2001).
24. R.R. Akhmetshin *et al.*, Phys. Lett. **B562**, 173 (2003).
25. A. Abele *et al.*, Eur. Phys. J. **C21**, 261 (2001).
26. M. Bargiotti *et al.*, Phys. Lett. **B561**, 233 (2003).
27. S.I. Bitukov *et al.*, Phys. Lett. **B188**, 383 (1987).
28. B. Aubert *et al.*, Phys. Rev. **D77**, 092002 (2008).
29. N.N. Achasov and G.N. Shestakov, Phys. Atom. Nucl. **59**, 1262 (1996).
30. L.G. Landsberg, Sov. J. Nucl. Phys. **55**, 1051 (1992).
31. A. Abele *et al.*, Phys. Lett. **B415**, 280 (1997).
32. V.M. Aulchenko *et al.*, Sov. Phys. JETP Lett. **45**, 145 (1987).
33. D. Bisello *et al.*, Z. Phys. **C52**, 227 (1991).
34. P. Frenkiel *et al.*, Nucl. Phys. **B47**, 61 (1972).
35. G. Cosme *et al.*, Phys. Lett. **B63**, 352 (1976).
36. D.P. Barber *et al.*, Z. Phys. **C4**, 169 (1980).
37. D. Aston, Phys. Lett. **B92**, 211 (1980).
38. M. Atkinson *et al.*, Nucl. Phys. **B243**, 1 (1984).
39. J.E. Brau *et al.*, Phys. Rev. **D37**, 2379 (1988).
40. C. Amsler *et al.*, Phys. Lett. **B311**, 362 (1993).
41. J. Layssac and F.M. Renard, Nuovo Cimento **6A**, 134 (1971).
42. D. Aston *et al.*, Nucl. Phys. (Proc. Supp.) **B21**, 105 (1991).
43. M. Ablikim *et al.*, Phys. Rev. Lett. **97**, 142002 (2006).
44. G.-J. Ding and M.-L. Yan, Phys. Lett. **B643**, 33 (2006).
45. F.K. Guo *et al.*, Nucl. Phys. **A773**, 78 (2006).
46. A. Zhang *et al.*, Phys. Rev. **D76**, 036004 (2007).
47. B.A. Li, Phys. Rev. **D76**, 094016 (2007).
48. X. Liu *et al.*, Phys. Rev. **D75**, 074017 (2007).
49. A.B. Clegg and A. Donnachie, Z. Phys. **C45**, 677 (1990).
50. D. Bisello *et al.*, Phys. Lett. **107B**, 145 (1981).
51. A. Castro *et al.*, LAL-88-58(1988).
52. M. Atkinson *et al.*, Z. Phys. **C29**, 333 (1985).
53. B. Aubert *et al.*, Phys. Rev. **D76**, 092005 (2007).
54. S. Godfrey and N. Isgur, Phys. Rev. **D32**, 189 (1985).
55. P.L. Frabetti *et al.*, Phys. Lett. **B514**, 240 (2001).
56. A. Antonelli *et al.*, Phys. Lett. **B365**, 427 (1996).
57. M. Agnello *et al.*, Phys. Lett. **B527**, 39 (2002).
58. P.L. Frabetti *et al.*, Phys. Lett. **B578**, 290 (2004).
59. B. Aubert *et al.*, Phys. Rev. **D73**, 052003 (2006).

 $\rho(1700)$ MASS $\eta\rho^0$ AND $\pi^+\pi^-$ MODES

VALUE (MeV)	DOCUMENT ID
1720 ± 20 OUR ESTIMATE	

 $\eta\rho^0$ MODE

VALUE (MeV)	DOCUMENT ID	TECN	COMMENT
The data in this block is included in the average printed for a previous datablock.			

••• We do not use the following data for averages, fits, limits, etc. •••

1740 ± 20	ANTONELLI 88	DM2	$e^+e^- \rightarrow \eta\pi^+\pi^-$
1701 ± 15	FUKUI 88	SPEC	$8.95 \pi^-p \rightarrow \eta\pi^+\pi^-n$

¹ Assuming $\rho^+ f_0(1370)$ decay mode interferes with $a_1(1260)^+\pi$ background. From a two Breit-Wigner fit.

 $\pi\pi$ MODE

VALUE (MeV)	EVTS	DOCUMENT ID	TECN	COMMENT
The data in this block is included in the average printed for a previous datablock.				

••• We do not use the following data for averages, fits, limits, etc. •••

1728 ± 17 ± 89	5.4M	2,3 FUJIKAWA	08	BELL	$\tau^- \rightarrow \pi^-\pi^0\nu_\tau$
1780 $\begin{smallmatrix} +37 \\ -29 \end{smallmatrix}$		4 ABELE	97	CBAR	$\bar{p}n \rightarrow \pi^-\pi^0\pi^0$
1719 ± 15		4 BERTIN	97c	OBLX	$0.0 \bar{p}p \rightarrow \pi^+\pi^-\pi^0$
1730 ± 30		CLEGG	94	RVUE	$e^+e^- \rightarrow \pi^+\pi^-$
1768 ± 21		BISELLO	89	DM2	$e^+e^- \rightarrow \pi^+\pi^-$
1745.7 ± 91.9		DUBNICKA	89	RVUE	$e^+e^- \rightarrow \pi^+\pi^-$
1546 ± 26		GESHKEN...	89	RVUE	
1650		5 ERKAL	85	RVUE	20-70 $\gamma p \rightarrow \gamma\pi$
1550 ± 70		ABE	84B	HYBR	20 $\gamma p \rightarrow \pi^+\pi^-\pi^0$
1590 ± 20		6 ASTON	80	OMEG	20-70 $\gamma p \rightarrow \rho 2\pi$
1600 ± 10		7 ATIYA	79B	SPEC	50 $\gamma C \rightarrow C 2\pi$
1598 $\begin{smallmatrix} +24 \\ -22 \end{smallmatrix}$		BECKER	79	ASPK	17 π^-p polarized
1659 ± 25		5 LANG	79	RVUE	
1575		5 MARTIN	78c	RVUE	17 $\pi^-p \rightarrow \pi^+\pi^-n$
1610 ± 30		5 FROGGATT	77	RVUE	17 $\pi^-p \rightarrow \pi^+\pi^-n$
1590 ± 20		8 HYAMS	73	ASPK	17 $\pi^-p \rightarrow \pi^+\pi^-n$

Meson Particle Listings

 $\rho(1700)$ $\rho(1700)$ DECAY MODES

Mode	Fraction (Γ_i/Γ)
Γ_1 4π	
Γ_2 $2(\pi^+\pi^-)$	large
Γ_3 $\rho\pi\pi$	dominant
Γ_4 $\rho^0\pi^+\pi^-$	large
Γ_5 $\rho^0\pi^0\pi^0$	
Γ_6 $\rho^\pm\pi^\mp\pi^0$	large
Γ_7 $a_1(1260)\pi$	seen
Γ_8 $h_1(1170)\pi$	seen
Γ_9 $\pi(1300)\pi$	seen
Γ_{10} $\rho\rho$	seen
Γ_{11} $\pi^+\pi^-$	seen
Γ_{12} $\pi\pi$	seen
Γ_{13} $K\bar{K}^*(892) + c.c.$	seen
Γ_{14} $\eta\rho$	seen
Γ_{15} $a_2(1320)\pi$	not seen
Γ_{16} KK	seen
Γ_{17} e^+e^-	seen
Γ_{18} $\pi^0\omega$	seen

 $\rho(1700)$ $\Gamma(i)\Gamma(e^+e^-)/\Gamma(\text{total})$

This combination of a partial width with the partial width into e^+e^- and with the total width is obtained from the cross-section into channel i in e^+e^- annihilation.

 $\Gamma(2(\pi^+\pi^-)) \times \Gamma(e^+e^-)/\Gamma_{\text{total}}$ $\Gamma_2\Gamma_{17}/\Gamma$

VALUE (keV)	DOCUMENT ID	TECN	COMMENT
••• We do not use the following data for averages, fits, limits, etc. •••			
2.6 ± 0.2	DEL COURT	81B	DM1 $e^+e^- \rightarrow 2(\pi^+\pi^-)$
2.83 ± 0.42	BACCI	80	FRAG $e^+e^- \rightarrow 2(\pi^+\pi^-)$

 $\Gamma(\pi^+\pi^-) \times \Gamma(e^+e^-)/\Gamma_{\text{total}}$ $\Gamma_{11}\Gamma_{17}/\Gamma$

VALUE (keV)	DOCUMENT ID	TECN	COMMENT
••• We do not use the following data for averages, fits, limits, etc. •••			
0.13	³⁶ DIEKMAN	88	RVUE $e^+e^- \rightarrow \pi^+\pi^-$
$0.029^{+0.016}_{-0.012}$	KURDADZE	83	OLYA $0.64-1.4 e^+e^- \rightarrow \pi^+\pi^-$

³⁶ Using total width = 220 MeV.

 $\Gamma(K\bar{K}^*(892) + c.c.) \times \Gamma(e^+e^-)/\Gamma_{\text{total}}$ $\Gamma_{13}\Gamma_{17}/\Gamma$

VALUE (keV)	DOCUMENT ID	TECN	COMMENT
••• We do not use the following data for averages, fits, limits, etc. •••			
0.305 ± 0.071	³⁷ BIZOT	80	DM1 e^+e^-

³⁷ Model dependent.

 $\Gamma(\eta\rho) \times \Gamma(e^+e^-)/\Gamma_{\text{total}}$ $\Gamma_{14}\Gamma_{17}/\Gamma$

VALUE (eV)	DOCUMENT ID	TECN	COMMENT
••• We do not use the following data for averages, fits, limits, etc. •••			
7 ± 3	ANTONELLI	88	DM2 $e^+e^- \rightarrow \eta\pi^+\pi^-$

 $\Gamma(K\bar{K}) \times \Gamma(e^+e^-)/\Gamma_{\text{total}}$ $\Gamma_{16}\Gamma_{17}/\Gamma$

VALUE (keV)	DOCUMENT ID	TECN	COMMENT
••• We do not use the following data for averages, fits, limits, etc. •••			
0.035 ± 0.029	³⁸ BIZOT	80	DM1 e^+e^-

³⁸ Model dependent.

 $\Gamma(\rho\pi\pi) \times \Gamma(e^+e^-)/\Gamma_{\text{total}}$ $\Gamma_3\Gamma_{17}/\Gamma$

VALUE (keV)	DOCUMENT ID	TECN	COMMENT
••• We do not use the following data for averages, fits, limits, etc. •••			
3.510 ± 0.090	³⁹ BIZOT	80	DM1 e^+e^-

³⁹ Model dependent.

 $\rho(1700)$ BRANCHING RATIOS $\Gamma(\rho\pi\pi)/\Gamma(4\pi)$ Γ_3/Γ_1

VALUE	DOCUMENT ID	TECN	COMMENT
••• We do not use the following data for averages, fits, limits, etc. •••			
0.28 ± 0.06	⁴⁰ ABELE	01B	CBAR $0.0 \bar{p}n \rightarrow 5\pi$

⁴⁰ $\omega\pi$ not included.

 $\Gamma(\rho^0\pi^+\pi^-)/\Gamma(2(\pi^+\pi^-))$ Γ_4/Γ_2

VALUE	EVTs	DOCUMENT ID	TECN	COMMENT
••• We do not use the following data for averages, fits, limits, etc. •••				
~ 1.0		DEL COURT	81B	DM1 $e^+e^- \rightarrow 2(\pi^+\pi^-)$
0.7 ± 0.1	500	SCHACHT	74	STRC $5.5-18 \gamma\rho \rightarrow p4\pi$
0.80		⁴¹ BINGHAM	72B	HBC $9.3 \gamma\rho \rightarrow p4\pi$

⁴¹ The $\pi\pi$ system is in S-wave.

 $\Gamma(\rho^0\pi^0\pi^0)/\Gamma(\rho^\pm\pi^\mp\pi^0)$ Γ_5/Γ_6

VALUE	DOCUMENT ID	TECN	CHG	COMMENT
••• We do not use the following data for averages, fits, limits, etc. •••				
<0.10	ATKINSON	85B	OMEG	$20-70 \gamma\rho$
<0.15	ATKINSON	82	OMEG 0	$20-70 \gamma\rho \rightarrow p4\pi$

 $\Gamma(a_1(1260)\pi)/\Gamma(4\pi)$ Γ_7/Γ_1

VALUE	DOCUMENT ID	TECN	COMMENT
••• We do not use the following data for averages, fits, limits, etc. •••			
0.16 ± 0.05	⁴² ABELE	01B	CBAR $0.0 \bar{p}n \rightarrow 5\pi$

⁴² $\omega\pi$ not included.

 $\Gamma(h_1(1170)\pi)/\Gamma(4\pi)$ Γ_8/Γ_1

VALUE	DOCUMENT ID	TECN	COMMENT
••• We do not use the following data for averages, fits, limits, etc. •••			
0.17 ± 0.06	⁴³ ABELE	01B	CBAR $0.0 \bar{p}n \rightarrow 5\pi$

⁴³ $\omega\pi$ not included.

 $\Gamma(\pi(1300)\pi)/\Gamma(4\pi)$ Γ_9/Γ_1

VALUE	DOCUMENT ID	TECN	COMMENT
••• We do not use the following data for averages, fits, limits, etc. •••			
0.30 ± 0.10	⁴⁴ ABELE	01B	CBAR $0.0 \bar{p}n \rightarrow 5\pi$

⁴⁴ $\omega\pi$ not included.

 $\Gamma(\rho\rho)/\Gamma(4\pi)$ Γ_{10}/Γ_1

VALUE	DOCUMENT ID	TECN	COMMENT
••• We do not use the following data for averages, fits, limits, etc. •••			
0.09 ± 0.03	⁴⁵ ABELE	01B	CBAR $0.0 \bar{p}n \rightarrow 5\pi$

⁴⁵ $\omega\pi$ not included.

 $\Gamma(\pi^+\pi^-)/\Gamma_{\text{total}}$ Γ_{11}/Γ

VALUE	DOCUMENT ID	TECN	COMMENT
••• We do not use the following data for averages, fits, limits, etc. •••			
$0.287^{+0.043}_{-0.042}$	BECKER	79	ASPK $17 \pi^- p$ polarized
0.15 to 0.30	⁴⁶ MARTIN	78C	RVUE $17 \pi^- p \rightarrow \pi^+\pi^- n$
<0.20	⁴⁷ COSTA...	77B	RVUE $e^+e^- \rightarrow 2\pi, 4\pi$
0.30 ± 0.05	⁴⁶ FROGGATT	77	RVUE $17 \pi^- p \rightarrow \pi^+\pi^- n$
<0.15	⁴⁸ EISENBERG	73	HBC $5 \pi^+ p \rightarrow \Delta^{++} 2\pi$
0.25 ± 0.05	⁴⁹ HYAMS	73	ASPK $17 \pi^- p \rightarrow \pi^+\pi^- n$

⁴⁶ From phase shift analysis of HYAMS 73 data.

⁴⁷ Estimate using unitarity, time reversal invariance, Breit-Wigner.

⁴⁸ Estimated using one-pion-exchange model.

⁴⁹ Included in BECKER 79 analysis.

 $\Gamma(\pi^+\pi^-)/\Gamma(2(\pi^+\pi^-))$ Γ_{11}/Γ_2

VALUE	DOCUMENT ID	TECN	COMMENT
••• We do not use the following data for averages, fits, limits, etc. •••			
0.13 ± 0.05	ASTON	80	OMEG $20-70 \gamma\rho \rightarrow p2\pi$
<0.14	⁵⁰ DAVIER	73	STRC $6-18 \gamma\rho \rightarrow p4\pi$
<0.2	⁵¹ BINGHAM	72B	HBC $9.3 \gamma\rho \rightarrow p2\pi$

⁵⁰ Upper limit is estimate.

⁵¹ 2σ upper limit.

 $\Gamma(\pi\pi)/\Gamma(4\pi)$ Γ_{12}/Γ_1

VALUE	DOCUMENT ID	TECN	COMMENT
••• We do not use the following data for averages, fits, limits, etc. •••			
0.16 ± 0.04	^{52,53} ABELE	01B	CBAR $0.0 \bar{p}n \rightarrow 5\pi$

⁵² Using ABELE 97.

⁵³ $\omega\pi$ not included.

 $\Gamma(K\bar{K}^*(892) + c.c.)/\Gamma_{\text{total}}$ Γ_{13}/Γ

VALUE	DOCUMENT ID	TECN	COMMENT
••• We do not use the following data for averages, fits, limits, etc. •••			
possibly seen	COAN	04	CLEO $\tau^- \rightarrow K^- \pi^- K^+ \nu_\tau$

 $\Gamma(K\bar{K}^*(892) + c.c.)/\Gamma(2(\pi^+\pi^-))$ Γ_{13}/Γ_2

VALUE	DOCUMENT ID	TECN	COMMENT
••• We do not use the following data for averages, fits, limits, etc. •••			
0.15 ± 0.03	⁵⁴ DEL COURT	81B	DM1 $e^+e^- \rightarrow \bar{K} K \pi$

⁵⁴ Assuming $\rho(1700)$ and ω radial excitations to be degenerate in mass.

 $\Gamma(\eta\rho)/\Gamma_{\text{total}}$ Γ_{14}/Γ

VALUE	CL%	DOCUMENT ID	TECN	COMMENT
••• We do not use the following data for averages, fits, limits, etc. •••				
possibly seen		AKHMETSHIN	00D	CMD2 $e^+e^- \rightarrow \eta\pi^+\pi^-$
<0.04		DONNACHIE	87B	RVUE
<0.02	58	ATKINSON	86B	OMEG $20-70 \gamma\rho$

See key on page 405

Meson Particle Listings

$\rho(1700)$, $a_2(1700)$

$\Gamma(\eta\rho)/\Gamma(2(\pi^+\pi^-))$ Γ_{14}/Γ_2

Table with columns: VALUE, DOCUMENT ID, TECN, COMMENT. Row 1: 0.123±0.027, DELCOURT 82, DM1, $e^+e^- \rightarrow \pi^+\pi^-MM$. Row 2: ~0.1, ASTON 80, OMEG 20-70, $\gamma\rho$.

$\Gamma(\pi^+\pi^-\text{ neutrals})/\Gamma(2(\pi^+\pi^-))$ $(\Gamma_5+\Gamma_6+0.714\Gamma_{14})/\Gamma_2$

Table with columns: VALUE, DOCUMENT ID, TECN, COMMENT. Row 1: 2.6±0.4, BALLAM 74, HBC, 9.3 $\gamma\rho$. Row 2: 55, Upper limit. Background not subtracted.

$\Gamma(a_2(1320)\pi)/\Gamma_{\text{total}}$ Γ_{15}/Γ

Table with columns: VALUE, DOCUMENT ID, TECN, COMMENT. Row 1: not seen, AMELIN 00, VES, 37 $\pi^-p \rightarrow \eta\pi^+\pi^-n$.

$\Gamma(K\bar{K})/\Gamma(2(\pi^+\pi^-))$ Γ_{16}/Γ_2

Table with columns: VALUE, CL%, DOCUMENT ID, TECN, CHG, COMMENT. Row 1: 0.015±0.010, DELCOURT 81B, DM1, $e^+e^- \rightarrow K\bar{K}$. Row 2: <0.04, 95, BINGHAM 72B, HBC, 0, 9.3 $\gamma\rho$. Row 3: 56, Assuming $\rho(1700)$ and ω radial excitations to be degenerate in mass.

$\Gamma(K\bar{K})/\Gamma(K\bar{K}^*(892)+c.c.)$ Γ_{16}/Γ_{13}

Table with columns: VALUE, DOCUMENT ID, TECN, COMMENT. Row 1: 0.052±0.026, BUON 82, DM1, $e^+e^- \rightarrow \text{hadrons}$.

$\Gamma(\pi^0\omega)/\Gamma_{\text{total}}$ Γ_{18}/Γ

Table with columns: VALUE, EVTS, DOCUMENT ID, TECN, COMMENT. Row 1: not seen, 2382, AKHMETSHIN 03B, CMD2, $e^+e^- \rightarrow \pi^0\pi^0\gamma$. Row 2: seen, ACHASOV 97, RVUE, $e^+e^- \rightarrow \omega\pi^0$.

$\rho(1700)$ REFERENCES

List of references for rho(1700) with columns: Author, Document ID, Journal, Year, and Collaboration. Includes entries from Fujikawa et al., Coan et al., Frabetti et al., etc.

$a_2(1700)$

$J^{PC} = 1^-(2^+)$

OMITTED FROM SUMMARY TABLE

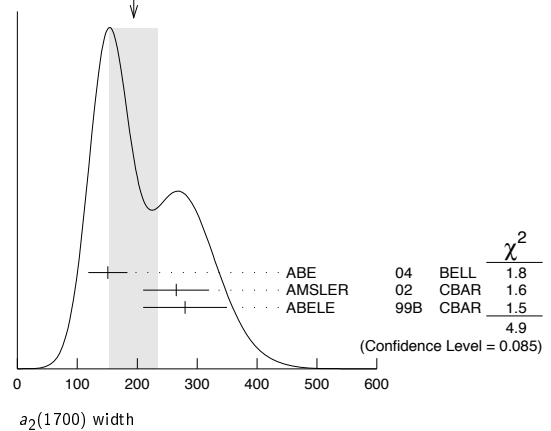
$a_2(1700)$ MASS

Table with columns: VALUE (MeV), EVTS, DOCUMENT ID, TECN, CHG, COMMENT. Row 1: 1732±16 OUR AVERAGE. Row 2: 1737±5±7, ABE 04, BELL, 10.6 $e^+e^- \rightarrow e^+e^-K^+K^-$. Row 3: 1698±44, 1, AMSLER 02, CBAR, 0.9 $\bar{p}p \rightarrow \pi^0\eta\eta$. Row 4: 1660±40, ABELE 99B, CBAR, 1.94 $\bar{p}p \rightarrow \pi^0\eta\eta$. Row 5: 1675±25, ANISOVICH 09, RVUE, 0.0 $\bar{p}p, \pi N$. Row 6: 1722±9±15, 18k, 2, SCHEGELSKY 06, RVUE, 0, $\gamma\gamma \rightarrow \pi^+\pi^-\pi^0$. Row 7: 1702±7, 80k, 3, UMAH 06, E835, 5.2 $\bar{p}p \rightarrow \eta\eta\pi^0$. Row 8: 1721±13±44, 145k, LU, 05, B852, 1.8 $\pi^-p \rightarrow \omega\pi^-\pi^0\rho$. Row 9: 1767±14, 221, 4, ACCIARRI 01H, L3, $\gamma\gamma \rightarrow K_S^0 K_S^0, E_{cm}^{ee} = 91, 183-209 \text{ GeV}$. Row 10: ~1775, 5, GRYGOREV 99, SPEC, 40 $\pi^-p \rightarrow K_S^0 K_S^0 n$. Row 11: 1752±21±4, ACCIARRI 97T, L3, $\gamma\gamma \rightarrow \pi^+\pi^-\pi^0$.

$a_2(1700)$ WIDTH

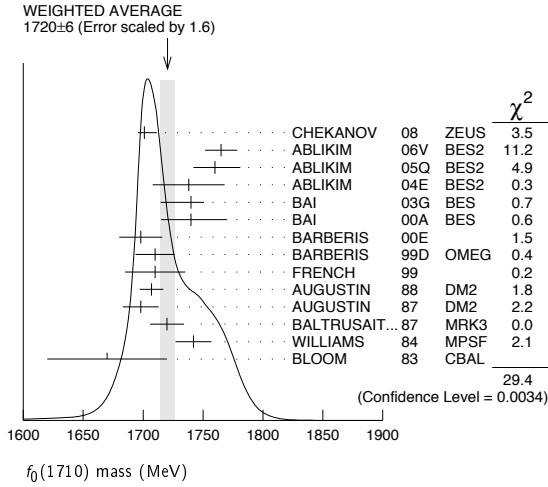
Table with columns: VALUE (MeV), EVTS, DOCUMENT ID, TECN, CHG, COMMENT. Row 1: 194±40 OUR AVERAGE. Row 2: 151±22±24, ABE 04, BELL, 10.6 $e^+e^- \rightarrow e^+e^-K^+K^-$. Row 3: 265±55, 6, AMSLER 02, CBAR, 0.9 $\bar{p}p \rightarrow \pi^0\eta\eta$. Row 4: 280±70, ABELE 99B, CBAR, 1.94 $\bar{p}p \rightarrow \pi^0\eta\eta$. Row 5: 270±50, 20, ANISOVICH 09, RVUE, 0.0 $\bar{p}p, \pi N$. Row 6: 336±20±20, 18k, 7, SCHEGELSKY 06, RVUE, 0, $\gamma\gamma \rightarrow \pi^+\pi^-\pi^0$. Row 7: 417±19, 80k, 8, UMAH 06, E835, 5.2 $\bar{p}p \rightarrow \eta\eta\pi^0$. Row 8: 279±49±66, 145k, LU, 05, B852, 1.8 $\pi^-p \rightarrow \omega\pi^-\pi^0\rho$. Row 9: 187±60, 221, 9, ACCIARRI 01H, L3, $\gamma\gamma \rightarrow K_S^0 K_S^0, E_{cm}^{ee} = 91, 183-209 \text{ GeV}$. Row 10: 150±110±34, ACCIARRI 97T, L3, $\gamma\gamma \rightarrow \pi^+\pi^-\pi^0$.

WEIGHTED AVERAGE 194 ± 40 (Error scaled by 1.6)



$a_2(1700)$ DECAY MODES

Table with columns: Mode, Fraction (Γ_i/Γ). Row 1: Γ_1 $\eta\pi$, seen. Row 2: Γ_2 $\gamma\gamma$. Row 3: Γ_3 $\rho\pi$. Row 4: Γ_4 $f_2(1270)\pi$. Row 5: Γ_5 $K\bar{K}$, seen. Row 6: Γ_6 $\omega\pi^-\pi^0$, seen. Row 7: Γ_7 $\omega\rho$, seen.



$f_0(1710)$ WIDTH

VALUE (MeV)	EVTs	DOCUMENT ID	TECN	COMMENT
135 ± 8	OUR AVERAGE	Error includes scale factor of 1.1.		
100 ± 24	± 7 -22	4k	28	CHEKANOV 08 ZEUS $e p \rightarrow K_S^0 K_S^0 X$
145 ± 8	± 69		29	ABLIKIM 06V BES2 $e^+ e^- \rightarrow J/\psi \rightarrow \gamma \pi^+ \pi^-$
125 ± 25	± 10 -15		29	ABLIKIM 05Q BES2 $\psi(2S) \rightarrow \gamma \pi^+ \pi^- K^+ K^-$
125 ± 20			29	ABLIKIM 04E BES2 $J/\psi \rightarrow \omega K^+ K^-$
166 ± 5	± 15 -8		30	BAI 03G BES $J/\psi \rightarrow \gamma K \bar{K}$
120 ± 50	-40		30	BAI 00A BES $J/\psi \rightarrow \gamma(\pi^+ \pi^- \pi^+ \pi^-)$
120 ± 26			31	BARBERIS 00E $450 pp \rightarrow p_f \eta \eta p_S$
126 ± 16	± 18		32	BARBERIS 99D OMEG $450 pp \rightarrow K^+ K^-, \pi^+ \pi^-$
105 ± 34			33	FRENCH 99 $300 pp \rightarrow p_f(K^+ K^-) p_S$
166.4 ± 33.2			34	AUGUSTIN 88 DM2 $J/\psi \rightarrow \gamma K^+ K^-, K_S^0 K_S^0$
136 ± 28			34	AUGUSTIN 87 DM2 $J/\psi \rightarrow \gamma \pi^+ \pi^-$
130 ± 20			35	BALTRUSAIT...87 MRK3 $J/\psi \rightarrow \gamma K^+ K^-$
57 ± 38			36	WILLIAMS 84 MP SF $200 \pi^- N \rightarrow 2K_S^0 X$
160 ± 80				BLOOM 83 CBAL $J/\psi \rightarrow \gamma 2\eta$
• • • We do not use the following data for averages, fits, limits, etc. • • •				
148 ± 40	-30			AMSLER 06 CBAR 1.64 $\bar{p} p \rightarrow K^+ K^- \pi^0$
188 ± 13		80k	29,37	UMAN 06 E835 $5.2 \bar{p} p \rightarrow \eta \eta \pi^0$
250 ± 30				VLADIMIRSK...06 SPEC $40 \pi^- p \rightarrow K_S^0 K_S^0 n$
270 ± 60	-30		38	ABLIKIM 05 BES2 $J/\psi \rightarrow \phi \pi^+ \pi^-$
260 ± 50			29	BINON 05 GAMS $33 \pi^- p \rightarrow \eta \eta n$
38 ± 20	-14	74	37	CHEKANOV 04 ZEUS $e p \rightarrow K_S^0 K_S^0 X$
144 ± 30		39,40		ANISOVICH 03 RVUE
320 ± 50	-20	40,41		ANISOVICH 03 RVUE
102 ± 26				TIKHOMIROV 03 SPEC $40.0 \pi^- C \rightarrow K_S^0 K_S^0 K_L^0 X$
267 ± 44		3651	30,42	NICHITIU 02 OBLX
220 ± 40		43,44		ANISOVICH 99B SPEC $0.6-1.2 p \bar{p} \rightarrow \eta \eta \pi^0$
100 ± 25		30		BARBERIS 99 OMEG $450 pp \rightarrow p_S p_f K^+ K^-$
160 ± 30		30		BARBERIS 99B OMEG $450 pp \rightarrow p_S p_f \pi^+ \pi^-$
250 ± 140		45		ANISOVICH 98B RVUE Compilation
30 ± 7		57	46	BARKOV 98 $\pi^- p \rightarrow K_S^0 K_S^0 n$
103 ± 18	± 30 -11		35	BAI 96C BES $J/\psi \rightarrow \gamma K^+ K^-$
85 ± 24	± 22 -19		30	BAI 96C BES $J/\psi \rightarrow \gamma K^+ K^-$
56 ± 19				BALOSHIN 95 SPEC $40 \pi^- C \rightarrow K_S^0 K_S^0 X$
160 ± 40			47	BUGG 95 MRK3 $J/\psi \rightarrow \gamma \pi^+ \pi^- \pi^+ \pi^-$
160 ± 60	-20		35	BUGG 95 MRK3 $J/\psi \rightarrow \gamma \pi^+ \pi^- \pi^+ \pi^-$
264 ± 25			34	ARMSTRONG 93C E760 $\bar{p} p \rightarrow \pi^0 \eta \eta \rightarrow 6\gamma$
200 to 300				BREAKSTONE 93 SFM $pp \rightarrow pp \pi^+ \pi^- \pi^+ \pi^-$
< 80 90% CL			48	ALDE 92D GAM2 $38 \pi^- p \rightarrow \eta \eta N^*$
181 ± 30			49	ARMSTRONG 89D OMEG $300 pp \rightarrow pp K^+ K^-$
104 ± 30			49	ARMSTRONG 89D OMEG $300 pp \rightarrow pp K_S^0 K_S^0$
30 ± 20			35	BOLONKIN 88 SPEC $40 \pi^- p \rightarrow K_S^0 K_S^0 n$
350 ± 150			30	BOLONKIN 88 SPEC $40 \pi^- p \rightarrow K_S^0 K_S^0 n$
148 ± 17			50	FALVARD 88 DM2 $J/\psi \rightarrow \phi K^+ K^-, K_S^0 K_S^0$
184 ± 6			51	FALVARD 88 DM2 $J/\psi \rightarrow \phi K^+ K^-, K_S^0 K_S^0$
122 ± 74	-15		52	LONGACRE 86 RVUE $22 \pi^- p \rightarrow n 2K_S^0$
200 ± 100				BURKE 82 MRK2 $J/\psi \rightarrow \gamma 2p$

- 220 ± 100
 -70 53,54 EDWARDS 82D CBAL $J/\psi \rightarrow \gamma 2\eta$
- 200 ± 156
 -9 55 ETKIN 82B MPS 23 $\pi^- p \rightarrow n 2K_S^0$
- 28 In the SU(3) based model with a specific interference pattern of the $f_2(1270)$, $a_2^0(1320)$, and $f_2'(1525)$ mesons incoherently added to the $f_0(1710)$ and non-resonant background.
- 29 Breit-Wigner width.
- 30 $J^P = 0^+$.
- 31 T-matrix pole.
- 32 Supersedes BARBERIS 99 and BARBERIS 99b.
- 33 $J^P = 0^+$, superseded by ARMSTRONG 89D.
- 34 No J^{PC} determination.
- 35 $J^P = 2^+$.
- 36 No J^{PC} determination.
- 37 Systematic errors not estimated.
- 38 This state may be different from $f_0(1710)$, see CLOSE 05.
- 39 (Solution 1)
- 40 K-matrix pole, assuming $J^P = 0^+$, from combined analysis of $\pi^- p \rightarrow \pi^0 \pi^0 n$, $\pi^- p \rightarrow K \bar{K} n$, $\pi^+ \pi^- \rightarrow \pi^+ \pi^-$, $\bar{p} p \rightarrow \pi^0 \pi^0 \pi^0$, $\pi^0 \eta \eta$, $\pi^0 \pi^0 \eta$, $\pi^+ \pi^- \pi^0$, $K^+ K^- \pi^0$, $K_S^0 K_S^0 \pi^0$, $K^+ K_S^0 \pi^-$ at rest, $\bar{p} n \rightarrow \pi^- \pi^- \pi^+$, $K_S^0 K^- \pi^0$, $K_S^0 K_S^0 \pi^-$ at rest.
- 41 (Solution 1)
- 42 Decaying to $f_0(1370) \pi \pi$.
- 43 $J^P = 0^+$.
- 44 Not seen by AMSLER 02.
- 45 T-matrix pole, assuming $J^P = 0^+$
- 46 No J^{PC} determination.
- 47 From a fit to the 0^+ partial wave.
- 48 ALDE 92D combines all the GAMS-2000 data.
- 49 $J^P = 2^+$, (0^+ excluded).
- 50 From an analysis ignoring interference with $f_2'(1525)$.
- 51 From an analysis including interference with $f_2'(1525)$.
- 52 Uses MRK3 data. From a partial-wave analysis of data using a K-matrix formalism with 5 poles, but assuming spin 2. Fit with constrained inelasticity.
- 53 $J^P = 2^+$ preferred.
- 54 From fit neglecting nearby $f_2'(1525)$. Replaced by BLOOM 83.
- 55 From an amplitude analysis of the $K_S^0 K_S^0$ system, superseded by LONGACRE 86.

$f_0(1710)$ DECAY MODES

Mode	Fraction (Γ_i/Γ)
Γ_1 $K \bar{K}$	seen
Γ_2 $\eta \eta$	seen
Γ_3 $\pi \pi$	seen
Γ_4 $\gamma \gamma$	
Γ_5 $\omega \omega$	seen

$f_0(1710)$ $\Gamma(i)/\Gamma(\gamma\gamma)/\Gamma(\text{total})$

VALUE (eV)	CL%	DOCUMENT ID	TECN	COMMENT	$\Gamma_1 \Gamma_4 / \Gamma$
<110	95	56	BEHREND 89C	CELL $\gamma \gamma \rightarrow K_S^0 K_S^0$	
• • • We do not use the following data for averages, fits, limits, etc. • • •					
<480	95		ALBRECHT 90G	ARG $\gamma \gamma \rightarrow K^+ K^-$	
<280	95	56	ALTHOFF 85B	TASS $\gamma \gamma \rightarrow K \bar{K} \pi$	
56 Assuming helicity 2.					

VALUE (keV)	CL%	DOCUMENT ID	TECN	COMMENT	$\Gamma_3 \Gamma_4 / \Gamma$
<0.82	95	57	BARATE 00E	ALEP $\gamma \gamma \rightarrow \pi^+ \pi^-$	
57 Assuming spin 0.					

$f_0(1710)$ BRANCHING RATIOS

VALUE	DOCUMENT ID	TECN	COMMENT	Γ_1/Γ
• • • We do not use the following data for averages, fits, limits, etc. • • •				
0.36 ± 0.12	ALBALADEJO 08	RVUE		
0.38 ± 0.09 -0.19	58,59	LONGACRE 86	MPS 22 $\pi^- p \rightarrow n 2K_S^0$	
$\Gamma(\eta\eta)/\Gamma_{\text{total}}$				Γ_2/Γ
VALUE	DOCUMENT ID	TECN	COMMENT	
• • • We do not use the following data for averages, fits, limits, etc. • • •				
0.22 ± 0.12	ALBALADEJO 08	RVUE		
0.18 ± 0.03 -0.13	58,59	LONGACRE 86	RVUE	
$\Gamma(\pi\pi)/\Gamma_{\text{total}}$				Γ_3/Γ
VALUE	DOCUMENT ID	TECN	COMMENT	
• • • We do not use the following data for averages, fits, limits, etc. • • •				
not seen	AMSLER 02	CBAR	0.9 $\bar{p} p \rightarrow \pi^0 \eta \eta$, $\pi^0 \pi^0 \pi^0$	
0.039 ± 0.002 -0.024	58,59	LONGACRE 86	RVUE	

Meson Particle Listings

$f_0(1710), \eta(1760), \pi(1800)$

$\Gamma(\pi\pi)/\Gamma(K\bar{K})$				Γ_3/Γ_1
VALUE	CL%	DOCUMENT ID	TECN COMMENT	
$0.41 \pm^{+0.11}_{-0.17}$		ABLIKIM 06v	BES2 $e^+e^- \rightarrow J/\psi \rightarrow \gamma\pi^+\pi^-$	
••• We do not use the following data for averages, fits, limits, etc. •••				
0.32±0.14		ALBALADEJO 08	RVUE	
< 0.11	95	60 ABLIKIM 04E	BES2 $J/\psi \rightarrow \omega K^+K^-$	
5.8 $^{+9.1}_{-5.5}$		61 ANISOVICH 02D	SPEC Combined fit	
0.2 ± 0.024 ± 0.036		BARBERIS 99D	OMEG 450 $p\bar{p} \rightarrow K^+K^-, \pi^+\pi^-$	
0.39±0.14		ARMSTRONG 91	OMEG 300 $p\bar{p} \rightarrow p\bar{p}\pi\pi, p\bar{p}K\bar{K}$	

$\Gamma(\eta\eta)/\Gamma(K\bar{K})$				Γ_2/Γ_1
VALUE	CL%	DOCUMENT ID	TECN COMMENT	
0.48 ± 0.15		BARBERIS 00E	450 $p\bar{p} \rightarrow p_f\eta\eta p_s$	
••• We do not use the following data for averages, fits, limits, etc. •••				
0.46 $^{+0.70}_{-0.38}$		61 ANISOVICH 02D	SPEC Combined fit	
< 0.02	90	62 PROKOSHKIN 91	GA24 300 $\pi^-\rho \rightarrow \pi^-\rho\eta\eta$	

$\Gamma(\omega\omega)/\Gamma_{total}$				Γ_5/Γ
VALUE	EVTS	DOCUMENT ID	TECN COMMENT	
seen	180	ABLIKIM 06H	BES $J/\psi \rightarrow \gamma\omega\omega$	
58 From a partial-wave analysis of data using a K-matrix formalism with 5 poles, but assuming spin 2.				
59 Fit with constrained inelasticity.				
60 Using data from ABLIKIM 04A.				
61 From a combined K-matrix analysis of Crystal Barrel ($0. p\bar{p} \rightarrow \pi^0\pi^0\pi^0, \pi^0\eta\eta, \pi^0\pi^0\eta$), GAMS ($\pi p \rightarrow \pi^0\pi^0 n, \eta\eta n, \eta\eta' n$), and BNL ($\pi p \rightarrow K\bar{K}n$) data.				
62 Combining results of GAM4 with those of ARMSTRONG 89D.				

$f_0(1710)$ REFERENCES

ALBALADEJO 08	PRL 101 252002	M. Albaladejo, J.A. Oller	
CHEKANOV 08	PRL 101 112003	S. Chekanov et al.	(ZEUS Collab.)
ABLIKIM 06H	PR D73 112007	M. Ablikim et al.	(BES Collab.)
ABLIKIM 06V	PL B642 441	M. Ablikim et al.	(BES Collab.)
AMSLER 06	PL B639 165	C. Amisler et al.	(CBAR Collab.)
UMAN 06	PR D73 052009	I. Uman et al.	(FNAL E835)
VLADIMIRSK... 06	PAN 69 493	V.V. Vladimirov et al.	(ITEP, Moscow)
ABLIKIM 05	Translated from YAF 69 515.	M. Ablikim et al.	(BES Collab.)
ABLIKIM 05Q	PL B607 243	M. Ablikim et al.	(BES Collab.)
ABLIKIM 05Q	PR D72 092002	M. Ablikim et al.	(BES Collab.)
BINON 05	PAN 68 960	F. Binon et al.	
ABLIKIM 05	Translated from YAF 68 998.	M. Ablikim et al.	
CLOSE 05	PR D71 094022	F.E. Close, Q. Zhao	
ABLIKIM 04A	PL B598 149	M. Ablikim et al.	(BES Collab.)
ABLIKIM 04E	PL B603 138	M. Ablikim et al.	(BES Collab.)
CHEKANOV 04	PL B578 33	S. Chekanov et al.	(ZEUS Collab.)
PDG 04	PL B592 1	S. Eidelman et al.	(PDG Collab.)
ANISOVICH 03	EPL A16 229	V.V. Anisovich et al.	
BAI 03G	PR D68 052003	J.Z. Bai et al.	(BES Collab.)
TIKHOMIROV 03	PAN 66 828	G.D. Tikhomirov et al.	
AMSLER 02	EPJ C23 29	C. Amisler et al.	
ANISOVICH 02D	PAN 65 1545	V.V. Anisovich et al.	
NICHTIU 02	PL B545 261	F. Nichtigiu et al.	(OBELIX Collab.)
BAI 00A	PL B472 207	J.Z. Bai et al.	(BES Collab.)
BARATE 00E	PL B472 189	R. Barate et al.	(ALEPH Collab.)
BARBERIS 00E	PL B479 59	D. Barberis et al.	(WA 102 Collab.)
ANISOVICH 99B	PL B449 154	A.V. Anisovich et al.	
BARBERIS 99	PL B453 305	D. Barberis et al.	(Omega Expt.)
BARBERIS 99B	PL B453 316	D. Barberis et al.	(Omega Expt.)
BARBERIS 99D	PL B462 462	D. Barberis et al.	(Omega Expt.)
FRENCH 99	PL B460 213	B. French et al.	(WA76 Collab.)
ANISOVICH 98B	SPU 41 419	V.V. Anisovich et al.	
BAI 98H	PRL 81 1179	J.Z. Bai et al.	(BES Collab.)
BARKOV 98	JETPL 68 764	B.P. Barkov et al.	
ABREU 96C	PL B379 309	P. Abreu et al.	(DELPHI Collab.)
BAI 96C	PRL 77 3959	J.Z. Bai et al.	(BES Collab.)
BALOSHIN 95	PAN 58 46	O.N. Baloshin et al.	(ITEP)
BUGG 95	Translated from YAF 58 50.	D.V. Bugg et al.	(LOQM, PNPI, WASH)
ARMSTRONG 93C	PL B307 394	T.A. Armstrong et al.	(FNAL, FERR, GENO+)
BREAKSTONE 93	ZPHY C58 251	A.M. Breakstone et al.	(IOWA, CERN, DORT+)
ALDE 92D	PL B284 457	D.M. Alde et al.	(GAM2 Collab.)
Also	SJNP 54 451	D.M. Alde et al.	(GAM2 Collab.)
ARMSTRONG 91	ZPHY C51 351	T.A. Armstrong et al.	(ATHU, BARI, BIRM+)
PROKOSHKIN 91	SPD 36 155	Y.D. Prokoshkin	(GAM2, GAM4 Collab.)
ALBRECHT 90G	ZPHY C48 183	H. Albrecht et al.	(ARGUS Collab.)
ARMSTRONG 89D	PL B227 186	T.A. Armstrong, M. Benayoun	(ATHU, BARI, BIRM+)
BEHREND 89C	ZPHY C43 91	H.J. Behrend et al.	(CELLO Collab.)
AUGUSTIN 88	PRL 60 2238	J.E. Augustin et al.	(DM2 Collab.)
BOLONKIN 88	NP B309 426	B.V. Bolonkin et al.	(ITEP, SERP)
FALVARD 88	PR D38 2706	A. Falvard et al.	(CLER, FRAS, LALO+)
AUGUSTIN 87	ZPHY C36 369	J.E. Augustin et al.	(LALO, CLER, FRAS+)
BALTRUSAIT... 87	PR D35 2077	R.M. Baltrusaitis et al.	(Mark III Collab.)
ALDE 86C	PL B182 105	D.M. Alde et al.	(SERP, BELG, LANL, LAPP)
LONGACRE 86	PL B177 223	R.S. Longacre et al.	(BNL, BRAN, CUNY+)
ALTHOFF 85B	ZPHY C29 189	M. Althoff et al.	(TASSO Collab.)
WILLIAMS 84	PR D30 877	E.G.H. Williams et al.	(VAND, NDAM, TUFTS+)
BLOOM 83	ARNIS 33 143	E.D. Bloom, C. Peck	(SLAC, CIT)
BURKE 82	PRL 49 632	D.L. Burke et al.	(LBL, SLAC)
EDWARDS 82D	PRL 48 458	C. Edwards et al.	(CIT, HARV, PRIN+)
ETKIN 82B	PR D25 1786	A. Etkin et al.	(BNL, CUNY, TUFTS, VAND)
ETKIN 82C	PR D25 2446	A. Etkin et al.	(BNL, CUNY, TUFTS, VAND)

$\eta(1760)$

$$J^G(JPC) = 0^+(0^{-+})$$

OMITTED FROM SUMMARY TABLE

Seen by DM2 in the $\rho\rho$ system (BISELLO 89B). Structure in this region has been reported before in the same system (BALTRUSAITIS 86B) and in the $\omega\omega$ system (BALTRUSAITIS 85C, BISELLO 87).

$\eta(1760)$ MASS

VALUE (MeV)	EVTS	DOCUMENT ID	TECN	COMMENT
1756 ± 9 OUR AVERAGE				
1744±10±15	1045	1 ABLIKIM 06H	BES	$J/\psi \rightarrow \gamma\omega\omega$
1760±11	320	2 BISELLO 89B	DM2	$J/\psi \rightarrow 4\pi\gamma$
1 From a partial wave analysis including $\eta(1760)$, $f_0(1710)$, $f_2(1640)$, and $f_2(1910)$.				
2 Estimated by us from various fits.				

$\eta(1760)$ WIDTH

VALUE (MeV)	EVTS	DOCUMENT ID	TECN	COMMENT
96 ± 70 OUR AVERAGE				Error includes scale factor of 5.1.
244 $^{+24}_{-21}$ ± 25	1045	3 ABLIKIM 06H	BES	$J/\psi \rightarrow \gamma\omega\omega$
60±16	320	4 BISELLO 89B	DM2	$J/\psi \rightarrow 4\pi\gamma$
3 From a partial wave analysis including $\eta(1760)$, $f_0(1710)$, $f_2(1640)$, and $f_2(1910)$.				
4 Estimated by us from various fits.				

$\eta(1760)$ REFERENCES

ABLIKIM 06H	PR D73 112007	M. Ablikim et al.	(BES Collab.)
BISELLO 89B	PR D39 701	G. Busetto et al.	(DM2 Collab.)
BISELLO 87	PL B192 239	D. Bisello et al.	(PADO, CLER, FRAS+)
BALTRUSAIT... 86B	PR D33 1222	R.M. Baltrusaitis et al.	(Mark III Collab.)
BALTRUSAIT... 85C	PRL 55 1723	R.M. Baltrusaitis et al.	(CIT, UCS C+)

$\pi(1800)$

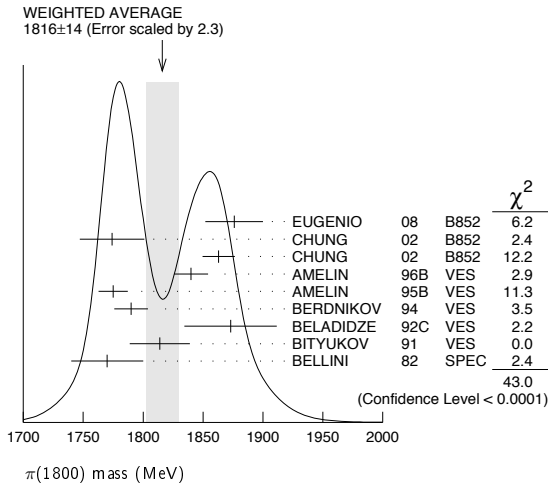
$$J^G(JPC) = 1^-(0^{-+})$$

See also minireview under non- $q\bar{q}$ candidates in PDG 06, Journal of Physics, G **33** 1 (2006).

$\pi(1800)$ MASS

VALUE (MeV)	EVTS	DOCUMENT ID	TECN	CHG	COMMENT
1816 ± 14 OUR AVERAGE					Error includes scale factor of 2.3. See the ideogram below.
1876±18±16	4k	1 EUGENIO 08	B852 -	18	$\pi^-\rho \rightarrow \eta\eta\pi^-\rho$
1774±18±20		2 CHUNG 02	B852	18.3	$\pi^-\rho \rightarrow \pi^+\pi^-\pi^-\rho$
1863± 9±10		3 CHUNG 02	B852	18.3	$\pi^-\rho \rightarrow \pi^+\pi^-\pi^-\rho$
1840±10±10	1200	AMELIN 96B	VES -	37	$\pi^-\rho \rightarrow \eta\eta\pi^-\rho$
1775 ± 7±10		4 AMELIN 95B	VES -	36	$\pi^-\rho \rightarrow \pi^+\pi^-\pi^-\rho$
1790±14		5 BERDNIKOV 94	VES -	37	$\pi^-\rho \rightarrow \pi^+\pi^-\pi^-\rho$
1873±33±20		BELADIDZE 92C	VES -	36	$\pi^-\rho \rightarrow \pi^-\eta'\eta\text{Be}$
1814±10±23	426 ± 57	BITYUKOV 91	VES -	36	$\pi^-\rho \rightarrow \pi^-\eta\eta\text{C}$
1770±30	1100	BELLINI 82	SPEC -	40	$\pi^-\rho \rightarrow 3\pi A$
1737± 5±15		AMELIN 99	VES	37	$\pi^-\rho \rightarrow \omega\pi^-\pi^0 A^*$
••• We do not use the following data for averages, fits, limits, etc. •••					
1 From a single-pole fit.					
2 In the $f_0(980)\pi$ wave.					
3 In the $f_0(600)\pi$ wave.					
4 From a fit to $JPC = 0^{-+}$ $f_0(980)\pi$, $f_0(1370)\pi$ waves.					
5 From a fit to $JPC = 0^{-+}$ $K_0^*(1430)K^-$ and $f_0(980)\pi^-$ waves.					

$\pi(1800)$



$\pi(1800)$ WIDTH

VALUE (MeV)	EVTs	DOCUMENT ID	TECN	CHG	COMMENT
208 ± 12 OUR AVERAGE					
221 ± 26 ± 38	4k	⁶ EUGENIO	08	B852	18 $\pi^- p \rightarrow \eta\eta\pi^- p$
223 ± 48 ± 50		⁷ CHUNG	02	B852	18.3 $\pi^- p \rightarrow \pi^+\pi^-\pi^- p$
191 ± 21 ± 20		⁸ CHUNG	02	B852	18.3 $\pi^- p \rightarrow \pi^+\pi^-\pi^- p$
210 ± 30 ± 30	1200	AMELIN	96B	VES	37 $\pi^- A \rightarrow \eta\eta\pi^- A$
190 ± 15 ± 15		⁹ AMELIN	95B	VES	36 $\pi^- A \rightarrow \pi^+\pi^-\pi^- A$
210 ± 70		¹⁰ BERDNIKOV	94	VES	37 $\pi^- A \rightarrow K^+K^-\pi^- A$
225 ± 35 ± 20		BELADIDZE	92C	VES	36 $\pi^- Be \rightarrow \pi^- \eta' \eta Be$
205 ± 18 ± 32	426 ± 57	BITYUKOV	91	VES	36 $\pi^- C \rightarrow \pi^- \eta \eta C$
310 ± 50	1100	BELLINI	82	SPEC	40 $\pi^- A \rightarrow 3\pi A$
259 ± 19 ± 6		AMELIN	99	VES	37 $\pi^- A \rightarrow \omega\pi^-\pi^0 A^*$

• • • We do not use the following data for averages, fits, limits, etc. • • •
⁶ From a single-pole fit.
⁷ In the $f_0(980)\pi$ wave.
⁸ In the $f_0(600)\pi$ wave.
⁹ From a fit to $J^{PC} = 0^{-+} f_0(980)\pi, f_0(1370)\pi$ waves.
¹⁰ From a fit to $J^{PC} = 0^{-+} K_0^*(1430)K^-$ and $f_0(980)\pi^-$ waves.

$\pi(1800)$ DECAY MODES

Mode	Fraction (Γ_i/Γ)
Γ_1 $\pi^+\pi^-\pi^-$	seen
Γ_2 $f_0(600)\pi^-$	seen
Γ_3 $f_0(980)\pi^-$	seen
Γ_4 $f_0(1370)\pi^-$	seen
Γ_5 $f_0(1500)\pi^-$	not seen
Γ_6 $\rho\pi^-$	not seen
Γ_7 $\eta\eta\pi^-$	seen
Γ_8 $a_0(980)\eta$	seen
Γ_9 $a_2(1320)\eta$	not seen
Γ_{10} $f_2'(1270)\pi$	not seen
Γ_{11} $f_0(1370)\pi^-$	not seen
Γ_{12} $f_0(1500)\pi^-$	seen
Γ_{13} $\eta\eta'(958)\pi^-$	seen
Γ_{14} $K_0^*(1430)K^-$	seen
Γ_{15} $K^*(892)K^-$	not seen

$\pi(1800)$ BRANCHING RATIOS

$\Gamma(f_0(980)\pi^-)/\Gamma(f_0(600)\pi^-)$	Γ_3/Γ_2
0.44 ± 0.08 ± 0.38	
	¹¹ CHUNG 02 B852 18.3 $\pi^- p \rightarrow \pi^+\pi^-\pi^- p$
$\Gamma(f_0(980)\pi^-)/\Gamma(f_0(1370)\pi^-)$	Γ_3/Γ_4
1.7 ± 1.3	
	¹² AMELIN 95B VES - 36 $\pi^- A \rightarrow \pi^+\pi^-\pi^- A$
$\Gamma(f_0(1370)\pi^-)/\Gamma_{total}$	Γ_4/Γ
seen	BELLINI 82 SPEC - 40 $\pi^- A \rightarrow 3\pi A$

$\Gamma(f_0(1500)\pi^-)/\Gamma_{total}$	Γ_5/Γ
not seen	CHUNG 02 B852 18.3 $\pi^- p \rightarrow \pi^+\pi^-\pi^- p$

$\Gamma(\rho\pi^-)/\Gamma_{total}$	Γ_6/Γ
not seen	BELLINI 82 SPEC - 40 $\pi^- A \rightarrow 3\pi A$

$\Gamma(\rho\pi^-)/\Gamma(f_0(980)\pi^-)$	Γ_6/Γ_3
• • • We do not use the following data for averages, fits, limits, etc. • • •	
< 0.25	CHUNG 02 B852 18.3 $\pi^- p \rightarrow \pi^+\pi^-\pi^- p$
< 0.14	90 AMELIN 95B VES - 36 $\pi^- A \rightarrow \pi^+\pi^-\pi^- A$

$\Gamma(\eta\eta\pi^-)/\Gamma(\pi^+\pi^-\pi^-)$	Γ_7/Γ_1
• • • We do not use the following data for averages, fits, limits, etc. • • •	
0.5 ± 0.1	1200 ¹² AMELIN 96B VES - 37 $\pi^- A \rightarrow \eta\eta\pi^- A$

$\Gamma(a_2(1320)\eta)/\Gamma_{total}$	Γ_9/Γ
not seen	EUGENIO 08 B852 18 $\pi^- p \rightarrow \eta\eta\pi^- p$

$\Gamma(f_2'(1270)\pi)/\Gamma_{total}$	Γ_{10}/Γ
not seen	EUGENIO 08 B852 18 $\pi^- p \rightarrow \eta\eta\pi^- p$

$\Gamma(f_0(1370)\pi^-)/\Gamma_{total}$	Γ_{11}/Γ
not seen	EUGENIO 08 B852 18 $\pi^- p \rightarrow \eta\eta\pi^- p$

$\Gamma(f_0(1500)\pi^-)/\Gamma(a_0(980)\eta)$	Γ_{12}/Γ_8
• • • We do not use the following data for averages, fits, limits, etc. • • •	
0.48 ± 0.17	4k ^{12,13} EUGENIO 08 B852 - 18 $\pi^- p \rightarrow \eta\eta\pi^- p$
0.030 +0.014 -0.011	¹² ANISOVICH 01B SPEC 0 0.6-1.94 $\rho\bar{p} \rightarrow \eta\eta\pi^0 \rho^0$
0.08 ± 0.03	1200 ^{12,14} AMELIN 96B VES - 37 $\pi^- A \rightarrow \eta\eta\pi^- A$

$\Gamma(\eta\eta'(958)\pi^-)/\Gamma(\eta\eta\pi^-)$	Γ_{13}/Γ_7
• • • We do not use the following data for averages, fits, limits, etc. • • •	
0.29 ± 0.07	¹² BELADIDZE 92C VES - 36 $\pi^- Be \rightarrow \pi^- \eta' \eta Be$
0.3 ± 0.1	426 ± 57 ¹² BITYUKOV 91 VES - 36 $\pi^- C \rightarrow \pi^- \eta \eta C$

$\Gamma(K_0^*(1430)K^-)/\Gamma_{total}$	Γ_{14}/Γ
seen	BERDNIKOV 94 VES - 37 $\pi^- A \rightarrow K^+K^-\pi^- A$

$\Gamma(K^*(892)K^-)/\Gamma_{total}$	Γ_{15}/Γ
not seen	BERDNIKOV 94 VES - 37 $\pi^- A \rightarrow K^+K^-\pi^- A$

¹¹ Assuming that $f_0(980)$ decays only to $\pi\pi$.
¹² Systematic errors not estimated.
¹³ From a single-pole fit.
¹⁴ Assuming that $f_0(1500)$ decays only to $\eta\eta$ and $a_0(980)$ decays only to $\eta\pi$.

$\pi(1800)$ REFERENCES

EUGENIO	08	PL B660 466	P. Eugenio et al.	(BNL E852 Collab.)
PDG	06	JPG 33 1	W.-M. Yao et al.	(PDG Collab.)
CHUNG	02	PR D65 072001	S.-U. Chung et al.	(BNL E852 Collab.)
ANISOVICH	01B	PL B500 222	A.V. Anisovich et al.	
AMELIN	99	PAN 62 445	D.V. Amelin et al.	(VES Collab.)
		Translated from YAF 62 487.		
AMELIN	96B	PAN 59 976	D.V. Amelin et al.	(SERP, TBIL)IGJPC
		Translated from YAF 59 1021.		
AMELIN	95B	PL B356 595	D.V. Amelin et al.	(SERP, TBIL)
BERDNIKOV	94	PL B337 219	E.B. Berdnikov et al.	(SERP, TBIL)
BELADIDZE	92C	SJNP 55 1535	G.M. Beladidze, S.I. Bityukov, G.V. Borisov	(SERP+)
		Translated from YAF 55 2748.		
BITYUKOV	91	PL B268 137	S.I. Bityukov et al.	(SERP, TBIL)
BELLINI	82	PRL 48 1697	G. Bellini et al.	(MILA, BGNA, JINR)

Meson Particle Listings

$f_2(1810)$

$f_2(1810)$

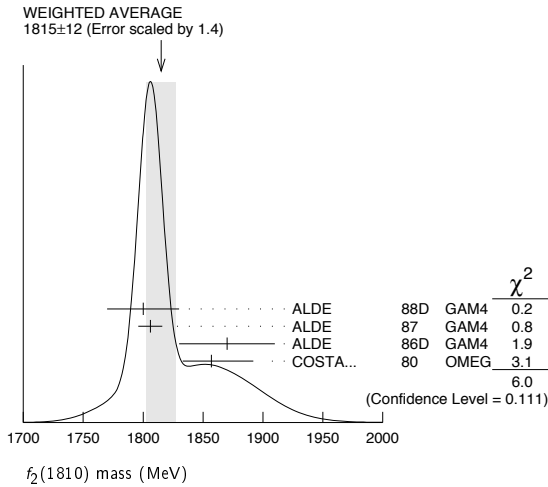
$$I^G(J^{PC}) = 0^+(2^{++})$$

OMITTED FROM SUMMARY TABLE
Needs confirmation.

$f_2(1810)$ MASS

VALUE (MeV)	EVTS	DOCUMENT ID	TECN	COMMENT
1815 ± 12 OUR AVERAGE				Error includes scale factor of 1.4. See the ideogram below.
1800 ± 30	40	ALDE	88D	GAM4 300 $\pi^- p \rightarrow \pi^- p 4\pi^0$
1806 ± 10	1600	ALDE	87	GAM4 100 $\pi^- p \rightarrow 4\pi^0 n$
1870 ± 40		¹ ALDE	86D	GAM4 100 $\pi^- p \rightarrow \eta\eta n$
1857 ⁺³⁵ ₋₂₄		² COSTA...	80	OMEG 10 $\pi^- p \rightarrow K^+ K^- n$
1858 ⁺¹⁸ ₋₇₁		³ LONGACRE	86	RVUE Compilation
1799 ± 15		⁴ CASON	82	STRC 8 $\pi^+ p \rightarrow \Delta^{++} \pi^0 \pi^0$

- • • We do not use the following data for averages, fits, limits, etc. • • •
- ¹ Seen in only one solution.
- ² Error increased by spread of two solutions. Included in LONGACRE 86 global analysis.
- ³ From a partial-wave analysis of data using a K-matrix formalism with 5 poles. Includes compilation of several other experiments.
- ⁴ From an amplitude analysis of the reaction $\pi^+ \pi^- \rightarrow 2\pi^0$. The resonance in the $2\pi^0$ final state is not confirmed by PROKOSHKIN 97.

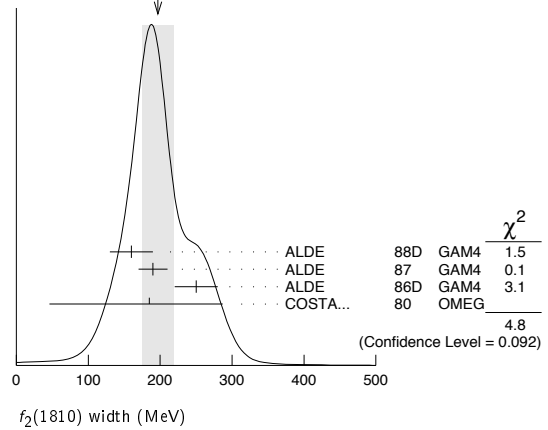


$f_2(1810)$ WIDTH

VALUE (MeV)	EVTS	DOCUMENT ID	TECN	COMMENT
197 ± 22 OUR AVERAGE				Error includes scale factor of 1.5. See the ideogram below.
160 ± 30	40	ALDE	88D	GAM4 300 $\pi^- p \rightarrow \pi^- p 4\pi^0$
190 ± 20	1600	ALDE	87	GAM4 100 $\pi^- p \rightarrow 4\pi^0 n$
250 ± 30		⁵ ALDE	86D	GAM4 100 $\pi^- p \rightarrow \eta\eta n$
185 ⁺¹⁰² ₋₁₃₉		⁶ COSTA...	80	OMEG 10 $\pi^- p \rightarrow K^+ K^- n$
388 ⁺¹⁵ ₋₂₁		⁷ LONGACRE	86	RVUE Compilation
280 ⁺⁴² ₋₃₅		⁸ CASON	82	STRC 8 $\pi^+ p \rightarrow \Delta^{++} \pi^0 \pi^0$

- • • We do not use the following data for averages, fits, limits, etc. • • •
- ⁵ Seen in only one solution.
- ⁶ Error increased by spread of two solutions. Included in LONGACRE 86 global analysis.
- ⁷ From a partial-wave analysis of data using a K-matrix formalism with 5 poles. Includes compilation of several other experiments.
- ⁸ From an amplitude analysis of the reaction $\pi^+ \pi^- \rightarrow 2\pi^0$. The resonance in the $2\pi^0$ final state is not confirmed by PROKOSHKIN 97.

WEIGHTED AVERAGE
197±22 (Error scaled by 1.5)



$f_2(1810)$ DECAY MODES

Mode	Fraction (Γ_i/Γ)
Γ_1 $\pi\pi$	
Γ_2 $\eta\eta$	
Γ_3 $4\pi^0$	seen
Γ_4 $K^+ K^-$	

$f_2(1810)$ BRANCHING RATIOS

$\Gamma(\pi\pi)/\Gamma_{total}$	DOCUMENT ID	TECN	COMMENT	Γ_1/Γ
not seen	AMSLER 02	CBAR	0.9 $\bar{p}p \rightarrow \pi^0 \eta\eta, \pi^0 \pi^0 \pi^0$	
not seen	PROKOSHKIN 97	GAM2	38 $\pi^- p \rightarrow \pi^0 \pi^0 n$	
0.21 ^{+0.02} _{-0.03}	⁹ LONGACRE	86	RVUE Compilation	
0.44 ± 0.03	¹⁰ CASON	82	STRC 8 $\pi^+ p \rightarrow \Delta^{++} \pi^0 \pi^0$	

⁹ From a partial-wave analysis of data using a K-matrix formalism with 5 poles. Includes compilation of several other experiments.
¹⁰ Included in LONGACRE 86 global analysis.

$\Gamma(\eta\eta)/\Gamma_{total}$	DOCUMENT ID	TECN	COMMENT	Γ_2/Γ
0.008 ^{+0.028} _{-0.003}	¹¹ LONGACRE	86	RVUE Compilation	

¹¹ From a partial-wave analysis of data using a K-matrix formalism with 5 poles. Includes compilation of several other experiments.

$\Gamma(\pi\pi)/\Gamma(4\pi^0)$	DOCUMENT ID	TECN	COMMENT	Γ_1/Γ_3
<0.75	ALDE	87	GAM4 100 $\pi^- p \rightarrow 4\pi^0 n$	

$\Gamma(4\pi^0)/\Gamma(\eta\eta)$	DOCUMENT ID	TECN	COMMENT	Γ_3/Γ_2
0.8 ± 0.3	ALDE	87	GAM4 100 $\pi^- p \rightarrow 4\pi^0 n$	

$\Gamma(K^+ K^-)/\Gamma_{total}$	DOCUMENT ID	TECN	COMMENT	Γ_4/Γ
0.003 ^{+0.019} _{-0.002}	¹² LONGACRE	86	RVUE Compilation	
seen	COSTA...	80	OMEG 10 $\pi^- p \rightarrow K^+ K^- n$	

¹² From a partial-wave analysis of data using a K-matrix formalism with 5 poles. Includes compilation of several other experiments.

$f_2(1810)$ REFERENCES

AMSLER 02	EPJ C23 29	C. Amstler et al.	
PROKOSHKIN 97	SPD 42 117	Y.D. Prokoshkin et al.	(SERP)
	Translated from DANS 353 323.		
ALDE 88D	SJNP 47 810	D.M. Alde et al.	(SERP, BELG, LANL, LAPP+)
	Translated from YAF 47 1273.		
ALDE 87	PL B198 286	D.M. Alde et al.	(LANL, BRUX, SERP, LAPP)
ALDE 86D	NP B219 485	D.M. Alde et al.	(BELG, LAPP, SERP, CERN+)
LONGACRE 86	PL B177 223	R.S. Longacre et al.	(BNL, BRAN, CUNY+)
CASON 82	PRL 48 1316	N.M. Cason et al.	(NDAM, ANL)
COSTA... 80	NP B175 402	G. Costa de Beaugard et al.	(BARI, BONN+)

See key on page 405

Meson Particle Listings
 $X(1835)$, $\phi_3(1850)$, $\eta_2(1870)$ **X(1835)**

$$I^G(J^{PC}) = ?^?(? - +)$$

OMITTED FROM SUMMARY TABLE

Needs confirmation. Seen by BA1 03F and ABLIKIM 05R in radiative decays of the J/ψ . Evidence for a threshold enhancement in the $p\bar{p}$ mass spectrum was also reported by ABE 02K, AUBERT, B 05L, and WANG 05A in $B^+ \rightarrow p\bar{p}K^+$, WANG 05A in $B^0 \rightarrow p\bar{p}K_S^0$, ABE 02W in $\bar{B}^0 \rightarrow p\bar{p}D^0$, and WEI 08 in $B^+ \rightarrow p\bar{p}\pi^+$ decays. Not seen by ATHAR 06 in $T(1S) \rightarrow p\bar{p}\gamma$.

X(1835) MASS

VALUE (MeV)	EVTS	DOCUMENT ID	TECN	COMMENT
1833.7 ± 6.1 ± 2.7	264	ABLIKIM	05R	BES2 $J/\psi \rightarrow \gamma\pi^+\pi^-\eta'$
••• We do not use the following data for averages, fits, limits, etc. •••				
1812 $^{+19}_{-26}$ ± 18	95	¹ ABLIKIM	06J	BES2 $J/\psi \rightarrow \gamma\omega\phi$
1831 ± 7		² ABLIKIM	05R	BES2 $J/\psi \rightarrow \gamma\rho\bar{p}$

¹ Favors $J^{PC} = 0^{++}$ quantum numbers assignment.² From the fit including final state interaction effects in isospin 0 S -wave according to SIBIRTSEV 05A. Systematic errors not estimated.**X(1835) WIDTH**

VALUE (MeV)	CL%	EVTS	DOCUMENT ID	TECN	COMMENT
67.7 ± 20.3 ± 7.7		264	ABLIKIM	05R	BES2 $J/\psi \rightarrow \gamma\pi^+\pi^-\eta'$
••• We do not use the following data for averages, fits, limits, etc. •••					
105 ± 20 ± 28		95	³ ABLIKIM	06J	BES2 $J/\psi \rightarrow \gamma\omega\phi$
< 153		90	⁴ ABLIKIM	05R	BES2 $J/\psi \rightarrow \gamma\rho\bar{p}$

³ Favors $J^{PC} = 0^{++}$ quantum numbers assignment.⁴ From the fit including final state interaction effects in isospin 0 S -wave according to SIBIRTSEV 05A. Systematic errors not estimated.**X(1835) DECAY MODES**

Mode	Fraction (Γ_i/Γ)
Γ_1 $p\bar{p}$	seen
Γ_2 $\pi^+\pi^-\eta'$	seen
Γ_3 $\omega\phi$	seen

X(1835) BRANCHING RATIOS

$\Gamma(p\bar{p})/\Gamma(\pi^+\pi^-\eta')$	DOCUMENT ID	TECN	COMMENT	Γ_1/Γ_2
0.333	ABLIKIM	05R	BES2 $J/\psi \rightarrow \gamma\pi^+\pi^-\eta'$	

$\Gamma(\omega\phi)/\Gamma_{\text{total}}$	DOCUMENT ID	TECN	COMMENT	Γ_3/Γ
seen	ABLIKIM	06J	BES2 $J/\psi \rightarrow \gamma\omega\phi$	

••• We do not use the following data for averages, fits, limits, etc. •••

not seen ⁵ LIU 09 BELL $B^\pm \rightarrow K^\pm\omega\phi$ ⁵ Reported $B(B^\pm \rightarrow K^\pm X(1812)) \times B(X \rightarrow \omega\phi) < 3.2 \times 10^{-7}$ at 90% CL.**X(1835) REFERENCES**

LIU	09	PR D79 071102R	C. Liu <i>et al.</i>	(BELLE Collab.)
WEI	08	PL B659 80	J.-T. Wei <i>et al.</i>	(BELLE Collab.)
ABLIKIM	06J	PRL 96 162002	M. Ablikim <i>et al.</i>	(BES Collab.)
ATHAR	06	PR D73 032001	S.B. Athar <i>et al.</i>	(CLEO Collab.)
ABLIKIM	05R	PRL 95 262001	M. Ablikim <i>et al.</i>	(BES Collab.)
AUBERT.B	05L	PR D72 051101R	B. Aubert <i>et al.</i>	(BABAR Collab.)
SIBIRTSEV	05A	PR D71 054010	A. Sibirtsev, J. Haidenbauer	
WANG	05A	PL B617 141	M.-Z. Wang <i>et al.</i>	(BELLE Collab.)
BAI	03F	PRL 91 022001	J.Z. Bai <i>et al.</i>	(BES Collab.)
ABE	02K	PRL 88 181803	K. Abe <i>et al.</i>	(BELLE Collab.)
ABE	02W	PRL 89 151802	K. Abe <i>et al.</i>	(BELLE Collab.)

 $\phi_3(1850)$

$$I^G(J^{PC}) = 0^-(3^{--})$$

 $\phi_3(1850)$ MASS

VALUE (MeV)	EVTS	DOCUMENT ID	TECN	COMMENT
1854 ± 7 OUR AVERAGE				
1855 ± 10		ASTON	88E	LASS 11 $K^-\rho \rightarrow K^-K^+\Lambda$, $K_S^0 K^\pm\pi^\mp\Lambda$
1870 $^{+30}_{-20}$	430	ARMSTRONG	82	OMEG 18.5 $K^-\rho \rightarrow K^-K^+\Lambda$
1850 ± 10	123	ALHARRAN	81B	HBC 8.25 $K^-\rho \rightarrow K\bar{K}\Lambda$

 $\phi_3(1850)$ WIDTH

VALUE (MeV)	EVTS	DOCUMENT ID	TECN	COMMENT
87 $^{+28}_{-23}$ OUR AVERAGE				Error includes scale factor of 1.2.
64 ± 31		ASTON	88E	LASS 11 $K^-\rho \rightarrow K^-K^+\Lambda$, $K_S^0 K^\pm\pi^\mp\Lambda$
160 $^{+90}_{-50}$	430	ARMSTRONG	82	OMEG 18.5 $K^-\rho \rightarrow K^-K^+\Lambda$
80 $^{+40}_{-30}$	123	ALHARRAN	81B	HBC 8.25 $K^-\rho \rightarrow K\bar{K}\Lambda$

 $\phi_3(1850)$ DECAY MODES

Mode	Fraction (Γ_i/Γ)
Γ_1 $K\bar{K}$	seen
Γ_2 $K\bar{K}^*(892) + \text{c.c.}$	seen

 $\phi_3(1850)$ BRANCHING RATIOS

$\Gamma(K\bar{K}^*(892) + \text{c.c.})/\Gamma(K\bar{K})$	DOCUMENT ID	TECN	COMMENT	Γ_2/Γ_1
0.55 $^{+0.85}_{-0.45}$	ASTON	88E	LASS 11 $K^-\rho \rightarrow K^-K^+\Lambda$, $K_S^0 K^\pm\pi^\mp\Lambda$	
••• We do not use the following data for averages, fits, limits, etc. •••				
0.8 ± 0.4	ALHARRAN	81B	HBC 8.25 $K^-\rho \rightarrow K\bar{K}\Lambda$	

 $\phi_3(1850)$ REFERENCES

ASTON	88E	PL B208 324	D. Aston <i>et al.</i>	(SLAC, NAGO, CINC, INUS)IGJPC
ARMSTRONG	82	PL 110B 77	T.A. Armstrong <i>et al.</i>	(BARI, BIRM, CERN+)JP
ALHARRAN	81B	PL 101B 357	S. Al-Harran <i>et al.</i>	(BIRM, CERN, GLAS+)

 $\eta_2(1870)$

$$I^G(J^{PC}) = 0^+(2^{--})$$

OMITTED FROM SUMMARY TABLE

Needs confirmation.

 $\eta_2(1870)$ MASS

VALUE (MeV)	EVTS	DOCUMENT ID	TECN	CHG	COMMENT
1842 ± 8 OUR AVERAGE					
1835 ± 12		BARBERIS	00B		450 $p\rho \rightarrow p_f\eta\pi^+\pi^-\rho_S$
1844 ± 13		BARBERIS	00C		450 $p\rho \rightarrow p_f4\pi\rho_S$
1840 ± 25		BARBERIS	97B	OMEG	450 $p\rho \rightarrow p\rho2(\pi^+\pi^-)$
1875 ± 20 ± 35		ADOMEIT	96	CBAR 0	1.94 $\bar{p}\rho \rightarrow \eta3\pi^0$
1881 ± 32 ± 40	26	KARCH	92	CBAL	$e^+e^- \rightarrow e^+e^-\eta\pi^0\pi^0$
••• We do not use the following data for averages, fits, limits, etc. •••					
1860 ± 5 ± 15		ANISOVICH	00E	SPEC	0.9-1.94 $\bar{p}\rho \rightarrow \eta3\pi^0$
1840 ± 15		BAI	99	BES	$J/\psi \rightarrow \gamma\eta\pi^+\pi^-$

 $\eta_2(1870)$ WIDTH

VALUE (MeV)	EVTS	DOCUMENT ID	TECN	CHG	COMMENT
225 ± 14 OUR AVERAGE					
235 ± 22		BARBERIS	00B		450 $p\rho \rightarrow p_f\eta\pi^+\pi^-\rho_S$
228 ± 23		BARBERIS	00C		450 $p\rho \rightarrow p_f4\pi\rho_S$
200 ± 40		BARBERIS	97B	OMEG	450 $p\rho \rightarrow p\rho2(\pi^+\pi^-)$
200 ± 25 ± 45		ADOMEIT	96	CBAR 0	1.94 $\bar{p}\rho \rightarrow \eta3\pi^0$
221 ± 92 ± 44	26	KARCH	92	CBAL	$e^+e^- \rightarrow e^+e^-\eta\pi^0\pi^0$
••• We do not use the following data for averages, fits, limits, etc. •••					
250 ± 25 $^{+50}_{-35}$		ANISOVICH	00E	SPEC	0.9-1.94 $\bar{p}\rho \rightarrow \eta3\pi^0$
170 ± 40		BAI	99	BES	$J/\psi \rightarrow \gamma\eta\pi^+\pi^-$

Meson Particle Listings

 $\eta_2(1870)$, $\pi_2(1880)$, $\rho(1900)$ $\eta_2(1870)$ DECAY MODES

Mode	
Γ_1	$\eta\pi\pi$
Γ_2	$a_2(1320)\pi$
Γ_3	$f_2(1270)\eta$
Γ_4	$a_0(980)\pi$

 $\eta_2(1870)$ BRANCHING RATIOS

$\Gamma(a_2(1320)\pi)/\Gamma(f_2(1270)\eta)$					Γ_2/Γ_3
VALUE	DOCUMENT ID	TECN	CHG	COMMENT	
6 ± 5 OUR AVERAGE	Error includes scale factor of 2.3.				
20.4 ± 6.6	BARBERIS	00B		450 $p\bar{p} \rightarrow \rho_f \eta \pi^+ \pi^- \rho_5$	
4.1 ± 2.3	ADOMEIT	96	CBAR 0	1.94 $\bar{p}p \rightarrow \eta 3\pi^0$	

$\Gamma(a_2(1320)\pi)/\Gamma(a_0(980)\pi)$					Γ_2/Γ_4
VALUE	DOCUMENT ID	TECN	CHG	COMMENT	
32.6 ± 12.6	BARBERIS	00B	450	$p\bar{p} \rightarrow \rho_f \eta \pi^+ \pi^- \rho_5$	

 $\eta_2(1870)$ REFERENCES

ANISOVICH	00E	PL B477 19	A.V. Anisovich <i>et al.</i>	
BARBERIS	00B	PL B471 435	D. Barberis <i>et al.</i>	(WA 102 Collab.)
BARBERIS	00C	PL B471 440	D. Barberis <i>et al.</i>	(WA 102 Collab.)
BAI	99	PL B446 356	J.Z. Bai <i>et al.</i>	(BES Collab.)
BARBERIS	97B	PL B413 217	D. Barberis <i>et al.</i>	(WA 102 Collab.)
ADOMEIT	96	ZPHY C71 227	J. Adomeit <i>et al.</i>	(Crystal Barrel Collab.)
KARCH	92	ZPHY C54 33	K. Karch <i>et al.</i>	(Crystal Ball Collab.)

 $\pi_2(1880)$

$$I^G(J^{PC}) = 1^-(2^{-+})$$

 $\pi(1880)$ MASS

VALUE (MeV)	EVTS	DOCUMENT ID	TECN	CHG	COMMENT
1895 ± 16 OUR AVERAGE					
1929 ± 24 ± 18	4k	EUGENIO	08	B852	— 18 $\pi^- \rho \rightarrow \eta \eta \pi^- \rho$
1876 ± 11 ± 67	145k	LU	05	B852	— 18 $\pi^- \rho \rightarrow \omega \pi^- \pi^0 \rho$
2003 ± 88 ± 148	69k	KUHN	04	B852	— 18 $\pi^- \rho \rightarrow \eta \pi^+ \pi^- \pi^- \pi^0$
1880 ± 20		ANISOVICH	01B	SPEC 0	0.6-1.94 $\bar{p}p \rightarrow \eta \eta \pi^0 \pi^0$

 $\pi(1880)$ WIDTH

VALUE (MeV)	EVTS	DOCUMENT ID	TECN	CHG	COMMENT
235 ± 34 OUR AVERAGE					
323 ± 87 ± 43	4k	EUGENIO	08	B852	— 18 $\pi^- \rho \rightarrow \eta \eta \pi^- \rho$
146 ± 17 ± 62	145k	LU	05	B852	— 18 $\pi^- \rho \rightarrow \omega \pi^- \pi^0 \rho$
306 ± 132 ± 121	69k	KUHN	04	B852	— 18 $\pi^- \rho \rightarrow \eta \pi^+ \pi^- \pi^- \pi^0$
255 ± 45		ANISOVICH	01B	SPEC 0	0.6-1.94 $\bar{p}p \rightarrow \eta \eta \pi^0 \pi^0$

 $\pi_2(1880)$ DECAY MODES

Mode	
Γ_1	$\eta\eta\pi^-$
Γ_2	$a_0(980)\eta$
Γ_3	$a_2(1320)\eta$
Γ_4	$f_0(1500)\pi$
Γ_5	$f_1(1285)\pi$
Γ_6	$\omega\pi^-\pi^0$

$\Gamma(a_2(1320)\eta)/\Gamma(f_1(1285)\pi)$					Γ_3/Γ_5
VALUE	EVTS	DOCUMENT ID	TECN	CHG	COMMENT
• • • We do not use the following data for averages, fits, limits, etc. • • •					
22.7 ± 7.3	69k	KUHN	04	B852	— 18 $\pi^- \rho \rightarrow \eta \pi^+ \pi^- \pi^- \pi^0$

$\Gamma(f_0(1500)\pi)/\Gamma(a_0(980)\pi)$					Γ_4/Γ_2
VALUE	DOCUMENT ID	TECN	CHG	COMMENT	
• • • We do not use the following data for averages, fits, limits, etc. • • •					
0.28 ^{+0.20} _{-0.15}	¹ ANISOVICH	01B	SPEC 0	0.6-1.94 $\bar{p}p \rightarrow \eta \eta \pi^0 \pi^0$	

¹ Systematic errors not estimated. $\pi_2(1880)$ REFERENCES

EUGENIO	08	PL B660 466	P. Eugenio <i>et al.</i>	(BNL E852 Collab.)
LU	05	PRL 94 032002	M. Lu <i>et al.</i>	(BNL E852 Collab.)
KUHN	04	PL B595 109	J. Kuhn <i>et al.</i>	(BNL E852 Collab.)
ANISOVICH	01B	PL B500 222	A.V. Anisovich <i>et al.</i>	

 $\rho(1900)$

$$I^G(J^{PC}) = 1^+(1^{-})$$

OMITTED FROM SUMMARY TABLE

See our mini-review under the $\rho(1700)$. $\rho(1900)$ MASS

VALUE (MeV)	EVTS	DOCUMENT ID	TECN	COMMENT
• • • We do not use the following data for averages, fits, limits, etc. • • •				
1909 ± 17 ± 25	54	¹ AUBERT	08S	BABR 10.6 $e^+e^- \rightarrow \phi\pi^0\gamma$
1880 ± 30		AUBERT	06D	BABR 10.6 $e^+e^- \rightarrow 3\pi^+3\pi^-\gamma$
1860 ± 20		AUBERT	06D	BABR 10.6 $e^+e^- \rightarrow 2(\pi^+\pi^-\pi^0)\gamma$
1910 ± 10		^{2,3} FRABETTI	04	E687 $\gamma p \rightarrow 3\pi^+3\pi^-p$
1870 ± 10		ANTONELLI	96	SPEC $e^+e^- \rightarrow$ hadrons

¹ From the fit with two resonances.² From a fit with two resonances with the JACOB 72 continuum.³ Supersedes FRABETTI 01. $\rho(1900)$ WIDTH

VALUE (MeV)	EVTS	DOCUMENT ID	TECN	COMMENT
• • • We do not use the following data for averages, fits, limits, etc. • • •				
48 ± 17 ± 2	54	⁴ AUBERT	08S	BABR 10.6 $e^+e^- \rightarrow \phi\pi^0\gamma$
130 ± 30		AUBERT	06D	BABR 10.6 $e^+e^- \rightarrow 3\pi^+3\pi^-\gamma$
160 ± 20		AUBERT	06D	BABR 10.6 $e^+e^- \rightarrow 2(\pi^+\pi^-\pi^0)\gamma$
37 ± 13		^{5,6} FRABETTI	04	E687 $\gamma p \rightarrow 3\pi^+3\pi^-p$
10 ± 5		ANTONELLI	96	SPEC $e^+e^- \rightarrow$ hadrons

⁴ From the fit with two resonances.⁵ From a fit with two resonances with the JACOB 72 continuum.⁶ Supersedes FRABETTI 01. $\rho(1900)$ $\Gamma(i)\Gamma(e^+e^-)/\Gamma^2(\text{total})$

$\Gamma(\phi\pi)/\Gamma_{\text{total}} \times \Gamma(e^+e^-)/\Gamma_{\text{total}}$					$\Gamma_4/\Gamma \times \Gamma_6/\Gamma$
VALUE (units 10^{-8})	EVTS	DOCUMENT ID	TECN	COMMENT	
• • • We do not use the following data for averages, fits, limits, etc. • • •					
4.2 ± 1.2 ± 0.8	54	⁷ AUBERT	08S	BABR 10.6 $e^+e^- \rightarrow \phi\pi^0\gamma$	

⁷ From the fit with two resonances. $\rho(1900)$ DECAY MODES

Mode	Fraction (Γ_i/Γ)	
Γ_1	6 π	seen
Γ_2	3 $\pi^+3\pi^-$	seen
Γ_3	2 $\pi^+2\pi^-2\pi^0$	
Γ_4	$\phi\pi$	
Γ_5	hadrons	seen
Γ_6	e^+e^-	seen
Γ_7	$\bar{N}N$	not seen

 $\rho(1900)$ BRANCHING RATIOS

$\Gamma(6\pi)/\Gamma_{\text{total}}$					Γ_1/Γ
VALUE	DOCUMENT ID	TECN	COMMENT		
not seen	AGNELLO	02	OBLX $\bar{\pi}p \rightarrow 3\pi^+2\pi^-\pi^0$		
seen	FRABETTI	01	E687 $\gamma p \rightarrow 3\pi^+3\pi^-p$		
seen	ANTONELLI	96	SPEC $e^+e^- \rightarrow$ hadrons		

 $\rho(1900)$ REFERENCES

AUBERT	08S	PR D77 092002	B. Aubert <i>et al.</i>	(BABAR Collab.)
AUBERT	06D	PR D73 052003	B. Aubert <i>et al.</i>	(BABAR Collab.)
FRABETTI	04	PL B578 290	P.L. Frabetti <i>et al.</i>	(FNAL E687 Collab.)
AGNELLO	02	PL B527 39	M. Agnello <i>et al.</i>	(OBELIX Collab.)
FRABETTI	01	PL B514 240	P.L. Frabetti <i>et al.</i>	(FNAL E687 Collab.)
ANTONELLI	96	PL B365 427	A. Antonelli <i>et al.</i>	(FENICE Collab.)
JACOB	72	PR D5 1847	M. Jacob, R. Slansky	

$f_2(1910)$

$I^G(J^{PC}) = 0^+(2^{++})$

OMITTED FROM SUMMARY TABLE

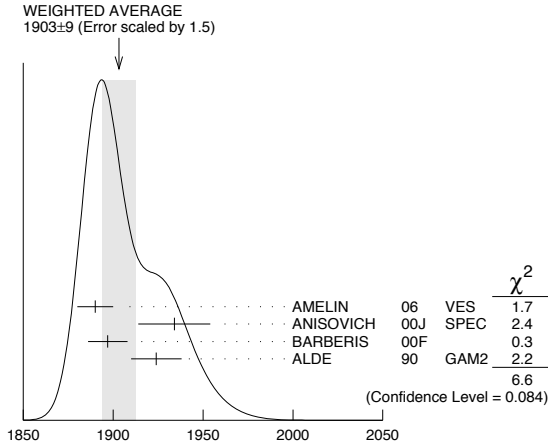
We list here three different peaks with close masses and widths seen in the mass distributions of $\omega\omega$, $\eta\eta'$, and K^+K^- final states. ALDE 91B argues that they are of different nature.

$f_2(1910)$ MASS

$f_2(1910)$ $\omega\omega$ MODE

VALUE (MeV)	DOCUMENT ID	TECN	COMMENT
1903 ± 9 OUR AVERAGE	Error includes scale factor of 1.5. See the ideogram below.		
1890 ± 10	¹ AMELIN 06	VES	36 $\pi^- p \rightarrow \omega\omega n$
1934 ± 20	ANISOVICH 00J	SPEC	
1897 ± 11	BARBERIS 00F		450 $pp \rightarrow p_f \omega\omega p_S$
1924 ± 14	ALDE 90	GAM2	38 $\pi^- p \rightarrow \omega\omega n$

¹ Supersedes BELADIDZE 92b.



$f_2(1910)$ $\omega\omega$ MODE MASS (MeV)

$f_2(1910)$ $\eta\eta'$ MODE

VALUE (MeV)	DOCUMENT ID	TECN	COMMENT
1934 ± 16	Error includes scale factor of 1.5. See the ideogram below.		
	² BARBERIS 00A		450 $pp \rightarrow p_f \eta\eta' p_S$
1911 ± 10	ALDE 91B	GAM2	38 $\pi^- p \rightarrow \eta\eta' n$

² Also compatible with $J^{PC}=1^-+$.

$f_2(1910)$ K^+K^- MODE

VALUE (MeV)	DOCUMENT ID	TECN	COMMENT
1941 ± 18	AMSLER 06	CBAR	1.64 $\bar{p}p \rightarrow K^+K^-\pi^0$

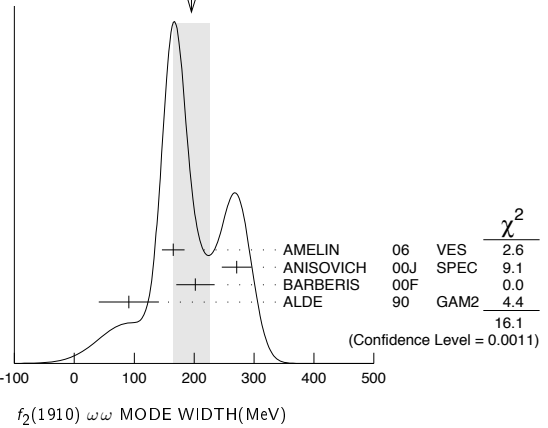
$f_2(1910)$ WIDTH

$f_2(1910)$ $\omega\omega$ MODE

VALUE (MeV)	DOCUMENT ID	TECN	COMMENT
196 ± 31 OUR AVERAGE	Error includes scale factor of 2.3. See the ideogram below.		
165 ± 19	³ AMELIN 06	VES	36 $\pi^- p \rightarrow \omega\omega n$
271 ± 25	ANISOVICH 00J	SPEC	
202 ± 32	BARBERIS 00F		450 $pp \rightarrow p_f \omega\omega p_S$
91 ± 50	ALDE 90	GAM2	38 $\pi^- p \rightarrow \omega\omega n$

³ Supersedes BELADIDZE 92b.

WEIGHTED AVERAGE
196 ± 31 (Error scaled by 2.3)



$f_2(1910)$ $\eta\eta'$ MODE

VALUE (MeV)	DOCUMENT ID	TECN	COMMENT
141 ± 41	Error includes scale factor of 1.5. See the ideogram below.		
	⁴ BARBERIS 00A		450 $pp \rightarrow p_f \eta\eta' p_S$
90 ± 35	ALDE 91B	GAM2	38 $\pi^- p \rightarrow \eta\eta' n$

⁴ Also compatible with $J^{PC}=1^-+$.

$f_2(1910)$ K^+K^- MODE

VALUE (MeV)	DOCUMENT ID	TECN	COMMENT
120 ± 40	AMSLER 06	CBAR	1.64 $\bar{p}p \rightarrow K^+K^-\pi^0$

$f_2(1910)$ DECAY MODES

Mode	Fraction (Γ_i/Γ)
Γ_1 $\pi^0\pi^0$	
Γ_2 K^+K^-	seen
Γ_3 $K_S^0 K_S^0$	
Γ_4 $\eta\eta$	seen
Γ_5 $\omega\omega$	seen
Γ_6 $\eta\eta'$	seen
Γ_7 $\eta'\eta'$	
Γ_8 $\rho\rho$	seen

$f_2(1910)$ BRANCHING RATIOS

$\Gamma(K^+K^-)/\Gamma_{total}$	DOCUMENT ID	TECN	COMMENT	Γ_2/Γ
seen	AMSLER 06	CBAR	1.64 $\bar{p}p \rightarrow K^+K^-\pi^0$	

$\Gamma(\pi^0\pi^0)/\Gamma(\eta\eta')$	DOCUMENT ID	TECN	COMMENT	Γ_1/Γ_6
<0.1	ALDE 89	GAM2	38 $\pi^- p \rightarrow \eta\eta' n$	

$\Gamma(K_S^0 K_S^0)/\Gamma(\eta\eta')$	DOCUMENT ID	TECN	COMMENT	Γ_3/Γ_6
<0.066	90	BALOSHIN 86	SPEC 40 $\pi p \rightarrow K_S^0 K_S^0 n$	

$\Gamma(\eta\eta)/\Gamma(\eta\eta')$	DOCUMENT ID	TECN	COMMENT	Γ_4/Γ_6
<0.05	90	ALDE 91B	GAM2 38 $\pi^- p \rightarrow \eta\eta' n$	

$\Gamma(\omega\omega)/\Gamma(\eta\eta')$	DOCUMENT ID	COMMENT	Γ_5/Γ_6
2.6 ± 0.6	BARBERIS 00F	450 $pp \rightarrow p_f \omega\omega p_S$	

$\Gamma(\eta'\eta')/\Gamma_{total}$	DOCUMENT ID	TECN	COMMENT	Γ_7/Γ
probably not seen	BARBERIS 00A		450 $pp \rightarrow p_f \eta'\eta' p_S$	
possibly seen	BELADIDZE 92D	VES	37 $\pi^- p \rightarrow \eta'\eta' n$	

Meson Particle Listings

$f_2(1910), f_2(1950)$

$\Gamma(\rho\rho)/\Gamma(\omega\omega)$	DOCUMENT ID	COMMENT	Γ_8/Γ_5
VALUE			
••• We do not use the following data for averages, fits, limits, etc. •••			
2.6 ± 0.4	BARBERIS 00F	450 $pp \rightarrow p_f \omega p_s$	

$f_2(1910)$ REFERENCES

AMELIN	06	PAN 69 690	D.V. Amelin et al.	(VES Collab.)
AMSLER	06	PL B639 165	C. Amster et al.	(CBAR Collab.)
ANISOVICH	00J	PL B491 47	A.V. Anisovich et al.	
BARBERIS	00A	PL B471 429	D. Barberis et al.	(WA 102 Collab.)
BARBERIS	00F	PL B484 198	D. Barberis et al.	(WA 102 Collab.)
BELADIDZE	92B	ZPHY C54 367	G.M. Beladidze et al.	(VES Collab.)
BELADIDZE	92D	ZPHY C57 13	G.M. Beladidze et al.	(VES Collab.)
ALDE	91B	SJNP 54 455	D.M. Alde et al.	(SERP, BELG, LANL, LAPP+)
		Translated from YAF 54 751.		
		Also		
		PL B276 375	D.M. Alde et al.	(BELG, SERP, KEK, LANL+)
ALDE	90	PL B241 600	D.M. Alde et al.	(SERP, BELG, LANL, LAPP+)
ALDE	89	PL B216 447	D.M. Alde et al.	(SERP, BELG, LANL, LAPP)
		Also		
		SJNP 48 1035	D.M. Alde et al.	(BELG, SERP, LANL, LAPP)
		Translated from YAF 48 1724.		
BALOSHIN	86	SJNP 43 959	O.N. Baloshin et al.	(ITEP)
		Translated from YAF 43 1487.		

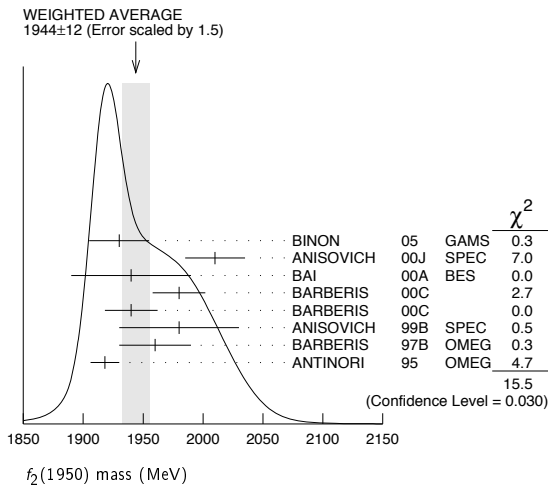
$f_2(1950)$

$$I^G(J^{PC}) = 0^+(2^{++})$$

$f_2(1950)$ MASS

VALUE (MeV)	DOCUMENT ID	TECN	COMMENT
1944 ± 12 OUR AVERAGE	Error includes scale factor of 1.5. See the ideogram below.		
1930 ± 25	¹ BINON 05	GAMS	33 $\pi^- p \rightarrow \eta\eta n$
2010 ± 25	ANISOVICH 00J	SPEC	
1940 ± 50	BAI 00A	BES	$J/\psi \rightarrow \gamma(\pi^+ \pi^- \pi^+ \pi^-)$
1980 ± 22	² BARBERIS 00C		450 $pp \rightarrow pp4\pi$
1940 ± 22	³ BARBERIS 00C		450 $pp \rightarrow pp2\pi2\pi^0$
1980 ± 50	ANISOVICH 99B	SPEC	1.35-1.94 $p\bar{p} \rightarrow \eta\eta\pi^0$
1960 ± 30	BARBERIS 97B	OMEG	450 $pp \rightarrow pp2(\pi^+ \pi^-)$
1918 ± 12	ANTINORI 95	OMEG	300,450 $pp \rightarrow pp2(\pi^+ \pi^-)$
••• We do not use the following data for averages, fits, limits, etc. •••			
2038 ⁺¹³⁺¹² / ₋₁₁₋₇₃	⁴ UEHARA 09	BELL	10.6 $e^+ e^- \rightarrow e^+ e^- \pi^0 \pi^0$
1980 ± 2 ± 14	ABE 04	BELL	10.6 $e^+ e^- \rightarrow e^+ e^- K^+ K^-$
1867 ± 46	⁵ AMSLER 02	CBAR	0.9 $\bar{p}p \rightarrow \pi^0 \eta\eta, \pi^0 \pi^0 \pi^0$
~ 1990	⁶ OAKDEN 94	RVUE	0.36-1.55 $\bar{p}p \rightarrow \pi\pi$
1950 ± 15	⁷ ASTON 91	LASS	11 $K^- p \rightarrow \Lambda K \bar{K} \pi\pi$

- ¹ First solution, PWA is ambiguous.
- ² Decaying into $\pi^+ \pi^- 2\pi^0$.
- ³ Decaying into $2(\pi^+ \pi^-)$.
- ⁴ Taking into account $f_4(2050)$.
- ⁵ T-matrix pole.
- ⁶ From solution B of amplitude analysis of data on $\bar{p}p \rightarrow \pi\pi$. See however KLOET 96 who fit $\pi^+ \pi^-$ only and find waves only up to $J = 3$ to be important but not significantly resonant.
- ⁷ Cannot determine spin to be 2.



$f_2(1950)$ WIDTH

VALUE (MeV)	DOCUMENT ID	TECN	COMMENT
472 ± 18 OUR AVERAGE			
450 ± 50	⁸ BINON 05	GAMS	33 $\pi^- p \rightarrow \eta\eta n$
495 ± 35	ANISOVICH 00J	SPEC	
380 ⁺¹²⁰ / ₋₉₀	BAI 00A	BES	$J/\psi \rightarrow \gamma(\pi^+ \pi^- \pi^+ \pi^-)$
520 ± 50	⁹ BARBERIS 00C		450 $pp \rightarrow pp4\pi$

485 ± 55	¹⁰ BARBERIS 00C		450 $pp \rightarrow pp4\pi$
500 ± 100	ANISOVICH 99B	SPEC	1.35-1.94 $p\bar{p} \rightarrow \eta\eta\pi^0$
460 ± 40	BARBERIS 97B	OMEG	450 $pp \rightarrow pp2(\pi^+ \pi^-)$
390 ± 60	ANTINORI 95	OMEG	300,450 $pp \rightarrow pp2(\pi^+ \pi^-)$
••• We do not use the following data for averages, fits, limits, etc. •••			

441 ⁺²⁷⁺²⁸ / ₋₂₅₋₁₉₂	¹¹ UEHARA 09	BELL	10.6 $e^+ e^- \rightarrow e^+ e^- \pi^0 \pi^0$
297 ± 12 ± 6	ABE 04	BELL	10.6 $e^+ e^- \rightarrow e^+ e^- K^+ K^-$
385 ± 58	¹² AMSLER 02	CBAR	0.9 $\bar{p}p \rightarrow \pi^0 \eta\eta, \pi^0 \pi^0 \pi^0$
~ 100	¹³ OAKDEN 94	RVUE	0.36-1.55 $\bar{p}p \rightarrow \pi\pi$
250 ± 50	¹⁴ ASTON 91	LASS	11 $K^- p \rightarrow \Lambda K \bar{K} \pi\pi$
⁸ First solution, PWA is ambiguous.			
⁹ Decaying into $\pi^+ \pi^- 2\pi^0$.			
¹⁰ Decaying into $2(\pi^+ \pi^-)$.			
¹¹ Taking into account $f_4(2050)$.			
¹² T-matrix pole.			
¹³ From solution B of amplitude analysis of data on $\bar{p}p \rightarrow \pi\pi$. See however KLOET 96 who fit $\pi^+ \pi^-$ only and find waves only up to $J = 3$ to be important but not significantly resonant.			
¹⁴ Cannot determine spin to be 2.			

$f_2(1950)$ DECAY MODES

Mode	Fraction (Γ_i/Γ)
Γ_1 $K^*(892)\bar{K}^*(892)$	seen
Γ_2 $\pi\pi$	
Γ_3 $\pi^+ \pi^-$	seen
Γ_4 $\pi^0 \pi^0$	seen
Γ_5 4π	seen
Γ_6 $\pi^+ \pi^- \pi^+ \pi^-$	
Γ_7 $a_2(1320)\pi$	
Γ_8 $f_2(1270)\pi\pi$	
Γ_9 $\eta\eta$	seen
Γ_{10} $K\bar{K}$	seen
Γ_{11} $\gamma\gamma$	seen

$f_2(1950)$ $\Gamma(i)\Gamma(\gamma\gamma)/\Gamma(\text{total})$

VALUE (eV)	DOCUMENT ID	TECN	COMMENT	$\Gamma_{10}\Gamma_{11}/\Gamma_{\text{total}}$
••• We do not use the following data for averages, fits, limits, etc. •••				
122 ± 4 ± 26	¹⁵ ABE 04	BELL	10.6 $e^+ e^- \rightarrow e^+ e^- K^+ K^-$	
¹⁵ Assuming spin 2.				

$\Gamma(\pi\pi) \times \Gamma(\gamma\gamma)/\Gamma_{\text{total}}$

VALUE	DOCUMENT ID	TECN	COMMENT	$\Gamma_{11}/\Gamma_{\text{total}}$
••• We do not use the following data for averages, fits, limits, etc. •••				
162 ⁺⁶⁹⁺¹¹³⁷ / ₋₄₂₋₂₀₄	¹⁶ UEHARA 09	BELL	10.6 $e^+ e^- \rightarrow e^+ e^- \pi^0 \pi^0$	
¹⁶ Taking into account $f_4(2050)$.				

$f_2(1950)$ BRANCHING RATIOS

$\Gamma(K^*(892)\bar{K}^*(892))/\Gamma_{\text{total}}$	$\Gamma_1/\Gamma_{\text{total}}$
VALUE	
seen	ASTON 91 LASS 0 11 $K^- p \rightarrow \Lambda K \bar{K} \pi\pi$

$\Gamma(a_2(1320)\pi)/\Gamma_{\text{total}}$	$\Gamma_7/\Gamma_{\text{total}}$
VALUE	
••• We do not use the following data for averages, fits, limits, etc. •••	
not seen	BARBERIS 00B 450 $pp \rightarrow p_f \eta \pi^+ \pi^- p_s$
not seen	BARBERIS 00C 450 $pp \rightarrow p_f 4\pi p_s$
possibly seen	BARBERIS 97B OMEG 450 $pp \rightarrow pp2(\pi^+ \pi^-)$

$\Gamma(\eta\eta)/\Gamma(4\pi)$	Γ_9/Γ_5
VALUE	
CL%	
DOCUMENT ID	
COMMENT	
••• We do not use the following data for averages, fits, limits, etc. •••	
< 5.0 × 10 ⁻³	90 BARBERIS 00E 450 $pp \rightarrow p_f \eta\eta p_s$

$\Gamma(\eta\eta)/\Gamma(\pi^+ \pi^-)$	Γ_9/Γ_3
VALUE	
DOCUMENT ID	
TECN	
COMMENT	
0.14 ± 0.05	AMSLER 02 CBAR 0.9 $\bar{p}p \rightarrow \pi^0 \eta\eta, \pi^0 \pi^0 \pi^0$

See key on page 405

Meson Particle Listings

$f_2(1950)$, $\rho_3(1990)$, $f_2(2010)$, $f_0(2020)$

 $f_2(1950)$ REFERENCES

UEHARA BINON	09 05	PR D79 052009 PAN 68 960 Translated from YAF 68 998	S. Uehara <i>et al.</i> F. Binon <i>et al.</i>	(BELLE Collab.)
ABE	04	EPJ C32 323	K. Abe <i>et al.</i>	(BELLE Collab.)
AMSLER	02	EPJ C23 29	C. Amisler <i>et al.</i>	
ANISOVICH	00J	PL B491 47	A.V. Anisovich <i>et al.</i>	
BAI	00A	PL B472 207	J.Z. Bai <i>et al.</i>	(BES Collab.)
BARBERIS	00B	PL B471 435	D. Barberis <i>et al.</i>	(WA 102 Collab.)
BARBERIS	00C	PL B471 440	D. Barberis <i>et al.</i>	(WA 102 Collab.)
BARBERIS	00E	PL B479 59	D. Barberis <i>et al.</i>	(WA 102 Collab.)
ANISOVICH	99B	PL B449 154	A.V. Anisovich <i>et al.</i>	
BARBERIS	97B	PL B413 217	D. Barberis <i>et al.</i>	(WA 102 Collab.)
KLOET	96	PR D53 6120	W.M. Kloet, F. Myhrer	(RUTG, NORD)
ANTINORI	95	PL B353 589	F. Antinori <i>et al.</i>	(ATHU, BARI, BIRM+JIP)
OAKDEN	94	NP A574 731	M.N. Oakden, M.R. Pennington	(DURH)
ASTON	91	NPBPS B21 5	D. Aston <i>et al.</i>	(LASS Collab.)

 $f_2(2010)$ DECAY MODES

Mode	Fraction (Γ_i/Γ)
Γ_1 $\phi\phi$	seen
Γ_2 $K\bar{K}$	seen

 $f_2(2010)$ BRANCHING RATIOS

$\Gamma(K\bar{K})/\Gamma_{\text{total}}$	Γ_2/Γ		
VALUE	DOCUMENT ID	TECN	COMMENT
seen	VLADIMIRSK...06	SPEC	$40\pi^-p \rightarrow K_S^0 K_S^0 n$

 $f_2(2010)$ REFERENCES

VLADIMIRSK...06	PAN 69 493 Translated from YAF 69 515	V.V. Vladimirov <i>et al.</i>	(ITEP, Moscow)
BOLONKIN	88 NP B309 426	B.V. Bolonkin <i>et al.</i>	(ITEP, SERP)
ETKIN	88 PL B201 568	A. Etkin <i>et al.</i>	(BNL, CUNY)
ETKIN	85 PL 165B 217	A. Etkin <i>et al.</i>	(BNL, CUNY)
LINDENBAUM	84 CNPP 13 285	S.J. Lindenbaum	(CUNY)
ETKIN	82 PRL 49 1620	A. Etkin <i>et al.</i>	(BNL, CUNY)
Also	Brighton Conf. 351	S.J. Lindenbaum	(BNL, CUNY)

 $\rho_3(1990)$

$$I^G(J^{PC}) = 1^+(3^{--})$$

OMITTED FROM SUMMARY TABLE

 $\rho_3(1990)$ MASS

VALUE (MeV)	DOCUMENT ID	TECN	COMMENT
• • • We do not use the following data for averages, fits, limits, etc. • • •			
1982 ± 14	¹ ANISOVICH 02	SPEC	$0.6-1.9 p\bar{p} \rightarrow \omega\pi^0,$ $\omega\eta\pi^0, \pi^+\pi^-$
~ 2007	HASAN 94	RVUE	$\bar{p}p \rightarrow \pi\pi$
¹ From the combined analysis of ANISOVICH 00J, ANISOVICH 01D, ANISOVICH 01E, and ANISOVICH 02.			

 $\rho_3(1990)$ WIDTH

VALUE (MeV)	DOCUMENT ID	TECN	COMMENT
• • • We do not use the following data for averages, fits, limits, etc. • • •			
188 ± 24	² ANISOVICH 02	SPEC	$0.6-1.9 p\bar{p} \rightarrow \omega\pi^0,$ $\omega\eta\pi^0, \pi^+\pi^-$
~ 287	HASAN 94	RVUE	$\bar{p}p \rightarrow \pi\pi$
² From the combined analysis of ANISOVICH 00J, ANISOVICH 01D, ANISOVICH 01E, and ANISOVICH 02.			

 $\rho_3(1990)$ REFERENCES

ANISOVICH 02	PL B542 8	A.V. Anisovich <i>et al.</i>	
ANISOVICH 01D	PL B508 6	A.V. Anisovich <i>et al.</i>	
ANISOVICH 01E	PL B513 281	A.V. Anisovich <i>et al.</i>	
ANISOVICH 00J	PL B491 47	A.V. Anisovich <i>et al.</i>	
HASAN 94	PL B334 215	A. Hasan, D.V. Bugg	(LOQM)

 $f_2(2010)$

$$I^G(J^{PC}) = 0^+(2^{++})$$

 $f_2(2010)$ MASS

VALUE (MeV)	DOCUMENT ID	TECN	COMMENT
2011 ± 62 ± 76	¹ ETKIN 88	MPS	$22\pi^-p \rightarrow \phi\phi n$
• • • We do not use the following data for averages, fits, limits, etc. • • •			
2005 ± 12	VLADIMIRSK...06	SPEC	$40\pi^-p \rightarrow K_S^0 K_S^0 n$
1980 ± 20	² BOLONKIN 88	SPEC	$40\pi^-p \rightarrow K_S^0 K_S^0 n$
2050 ± 90 ± 50	ETKIN 85	MPS	$22\pi^-p \rightarrow 2\phi n$
2120 ± 20 ± 120	LINDENBAUM 84	RVUE	
2160 ± 50	ETKIN 82	MPS	$22\pi^-p \rightarrow 2\phi n$
¹ Includes data of ETKIN 85. The percentage of the resonance going into $\phi\phi 2^{++} D_2$, D_2 , and D_0 is 98 ± 1 , 0 ± 1 , and 2 ± 1 , respectively.			
² Statistically very weak, only 1.4 s.d.			

 $f_2(2010)$ WIDTH

VALUE (MeV)	DOCUMENT ID	TECN	COMMENT
202 ± 67 ± 62	³ ETKIN 88	MPS	$22\pi^-p \rightarrow \phi\phi n$
• • • We do not use the following data for averages, fits, limits, etc. • • •			
209 ± 32	VLADIMIRSK...06	SPEC	$40\pi^-p \rightarrow K_S^0 K_S^0 n$
145 ± 50	⁴ BOLONKIN 88	SPEC	$40\pi^-p \rightarrow K_S^0 K_S^0 n$
200 ± 160 ± 50	ETKIN 85	MPS	$22\pi^-p \rightarrow 2\phi n$
300 ± 150 ± 50	LINDENBAUM 84	RVUE	
310 ± 70	ETKIN 82	MPS	$22\pi^-p \rightarrow 2\phi n$
³ Includes data of ETKIN 85.			
⁴ Statistically very weak, only 1.4 s.d.			

$$I^G(J^{PC}) = 0^+(0^{++})$$

OMITTED FROM SUMMARY TABLE

Needs confirmation.

 $f_0(2020)$ MASS

VALUE (MeV)	EVTs	DOCUMENT ID	TECN	COMMENT
1992 ± 16	^{1,2} BARBERIS 00c			$450 p\bar{p} \rightarrow p_f 4\pi p_S$
• • • We do not use the following data for averages, fits, limits, etc. • • •				
2037 ± 8	80k	³ UMAN 06	E835	$5.2 \bar{p}p \rightarrow \eta\eta\pi^0$
2040 ± 38		ANISOVICH 00J	SPEC	
2010 ± 60		ALDE 98	GAM4	$100\pi^-p \rightarrow \pi^0\pi^0 n$
2020 ± 35		BARBERIS 97B	OMEG	$450 p\bar{p} \rightarrow p\rho 2(\pi^+\pi^-)$
¹ Average between $\pi^+\pi^-2\pi^0$ and $2(\pi^+\pi^-)$.				
² T-matrix pole.				
³ Statistical error only.				

 $f_0(2020)$ WIDTH

VALUE (MeV)	EVTs	DOCUMENT ID	TECN	COMMENT
442 ± 60	^{4,5} BARBERIS 00c			$450 p\bar{p} \rightarrow p_f 4\pi p_S$
• • • We do not use the following data for averages, fits, limits, etc. • • •				
296 ± 17	80k	⁶ UMAN 06	E835	$5.2 \bar{p}p \rightarrow \eta\eta\pi^0$
405 ± 40		ANISOVICH 00J	SPEC	
240 ± 100		ALDE 98	GAM4	$100\pi^-p \rightarrow \pi^0\pi^0 n$
410 ± 50		BARBERIS 97B	OMEG	$450 p\bar{p} \rightarrow p\rho 2(\pi^+\pi^-)$
⁴ Average between $\pi^+\pi^-2\pi^0$ and $2(\pi^+\pi^-)$.				
⁵ T-matrix pole.				
⁶ Statistical error only.				

 $f_0(2020)$ DECAY MODES

Mode	Fraction (Γ_i/Γ)
Γ_1 $\rho\pi\pi$	seen
Γ_2 $\pi^0\pi^0$	seen
Γ_3 $\rho\rho$	seen
Γ_4 $\omega\omega$	seen
Γ_5 $\eta\eta$	seen

 $f_0(2020)$ BRANCHING RATIOS

$\Gamma(\rho\rho)/\Gamma(\omega\omega)$	Γ_3/Γ_4		
VALUE	DOCUMENT ID	COMMENT	
• • • We do not use the following data for averages, fits, limits, etc. • • •			
~ 3	BARBERIS 00F	$450 p\bar{p} \rightarrow p_f \omega \omega p_S$	
$\Gamma(\eta\eta)/\Gamma_{\text{total}}$	Γ_5/Γ		
VALUE	DOCUMENT ID	TECN	COMMENT
seen	UMAN 06	E835	$5.2 \bar{p}p \rightarrow \eta\eta\pi^0$

 $f_0(2020)$ REFERENCES

UMAN 06	PR D73 052009	I. Uman <i>et al.</i>	(FNAL E835)
ANISOVICH 00J	PL B491 47	A.V. Anisovich <i>et al.</i>	
BARBERIS 00C	PL B471 440	D. Barberis <i>et al.</i>	(WA 102 Collab.)
BARBERIS 00F	PL B484 198	D. Barberis <i>et al.</i>	(WA 102 Collab.)
ALDE 98	EPJ A3 361	D. Alde <i>et al.</i>	(GAMMA Collab.)
Also	PAN 62 405 Translated from YAF 62 446	D. Alde <i>et al.</i>	(GAMS Collab.)
BARBERIS 97B	PL B413 217	D. Barberis <i>et al.</i>	(WA 102 Collab.)

Meson Particle Listings

$a_4(2040)$, $f_4(2050)$

$a_4(2040)$

$$J^G(J^{PC}) = 1^-(4^{++})$$

$a_4(2040)$ MASS

VALUE (MeV)	EVTS	DOCUMENT ID	TECN	CHG	COMMENT
2001 ± 10	OUR AVERAGE				
1985 ± 10 ± 13	145k	LU	05	B852	18 $\pi^- \rho \rightarrow \omega \pi^- \pi^0 \rho$
1996 ± 25 ± 43		CHUNG	02	B852	18.3 $\pi^- \rho \rightarrow 3\pi \rho$
2005 ± 25 -45		1 ANISOVICH	01F	SPEC	2.0 $\bar{p} \rho \rightarrow 3\pi^0, \pi^0 \eta, \pi^0 \eta'$
2000 ± 40 ± 60 20		IVANOV	01	B852	18 $\pi^- \rho \rightarrow \eta' \pi^- \rho$
1944 ± 8 ± 50		2 AMELIN	99	VES	37 $\pi^- A \rightarrow \omega \pi^- \pi^0 A^*$
2010 ± 20		3 DONSKOV	96	GAM2 0	38 $\pi^- \rho \rightarrow \eta \pi^0 n$
2040 ± 30		4 CLELAND	82B	SPEC ±	50 $\pi \rho \rightarrow K_S^0 K^\pm \rho$
2030 ± 50		5 CORDEN	78C	OMEG 0	15 $\pi^- \rho \rightarrow 3\pi n$
2004 ± 6	80k	6 UMAN	06	E835	5.2 $\bar{p} \rho \rightarrow \eta \eta \pi^0$
1903 ± 10		7 BALDI	78	SPEC -	10 $\pi^- \rho \rightarrow \rho K_S^0 K^-$

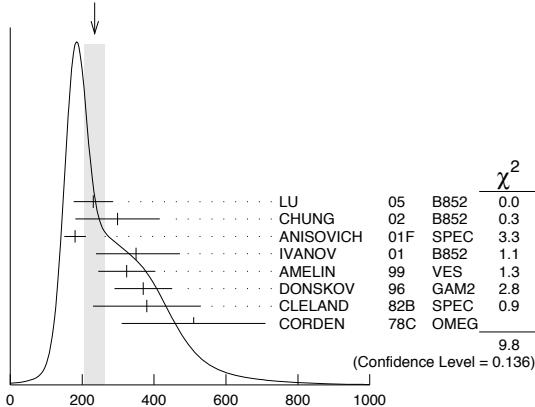
- • • We do not use the following data for averages, fits, limits, etc. • • •
- 1 From the combined analysis of ANISOVICH 99C, ANISOVICH 99E, and ANISOVICH 01F.
- 2 May be a different state.
- 3 From a simultaneous fit to the G_+ and G_0 wave intensities.
- 4 From an amplitude analysis.
- 5 $J^P = 4^+$ is favored, though $J^P = 2^+$ cannot be excluded.
- 6 Statistical error only.
- 7 From a fit to the Y_8^0 moment. Limited by phase space.

$a_4(2040)$ WIDTH

VALUE (MeV)	EVTS	DOCUMENT ID	TECN	CHG	COMMENT
235 ± 29	OUR AVERAGE				Error includes scale factor of 1.3. See the ideogram below.
231 ± 30 ± 46	145k	LU	05	B852	18 $\pi^- \rho \rightarrow \omega \pi^- \pi^0 \rho$
298 ± 81 ± 85		CHUNG	02	B852	18.3 $\pi^- \rho \rightarrow 3\pi \rho$
180 ± 30		8 ANISOVICH	01F	SPEC	2.0 $\bar{p} \rho \rightarrow 3\pi^0, \pi^0 \eta, \pi^0 \eta'$
350 ± 100 ± 70 50		IVANOV	01	B852	18 $\pi^- \rho \rightarrow \eta' \pi^- \rho$
324 ± 26 ± 75		9 AMELIN	99	VES	37 $\pi^- A \rightarrow \omega \pi^- \pi^0 A^*$
370 ± 80		10 DONSKOV	96	GAM2 0	38 $\pi^- \rho \rightarrow \eta \pi^0 n$
380 ± 150		11 CLELAND	82B	SPEC ±	50 $\pi \rho \rightarrow K_S^0 K^\pm \rho$
510 ± 200		12 CORDEN	78C	OMEG 0	15 $\pi^- \rho \rightarrow 3\pi n$
401 ± 16	80k	13 UMAN	06	E835	5.2 $\bar{p} \rho \rightarrow \eta \eta \pi^0$
166 ± 43		14 BALDI	78	SPEC -	10 $\pi^- \rho \rightarrow \rho K_S^0 K^-$

- • • We do not use the following data for averages, fits, limits, etc. • • •
- 8 From the combined analysis of ANISOVICH 99C, ANISOVICH 99E, and ANISOVICH 01F.
- 9 May be a different state.
- 10 From a simultaneous fit to the G_+ and G_0 wave intensities.
- 11 From an amplitude analysis.
- 12 $J^P = 4^+$ is favored, though $J^P = 2^+$ cannot be excluded.
- 13 Statistical error only.
- 14 From a fit to the Y_8^0 moment. Limited by phase space.

WEIGHTED AVERAGE
235 ± 29 (Error scaled by 1.3)



$a_4(2040)$ DECAY MODES

Mode	Fraction (Γ_i/Γ)
Γ_1 $K\bar{K}$	seen
Γ_2 $\pi^+ \pi^- \pi^0$	seen
Γ_3 $\rho \pi$	seen
Γ_4 $f_2(1270) \pi$	seen
Γ_5 $\omega \pi^- \pi^0$	seen
Γ_6 $\omega \rho$	seen
Γ_7 $\eta \pi^0$	seen
Γ_8 $\eta'(958) \pi$	seen

$a_4(2040)$ BRANCHING RATIOS

$\Gamma(K\bar{K})/\Gamma_{total}$	Γ_1/Γ
VALUE	DOCUMENT ID TECN CHG COMMENT
seen	BALDI 78 SPEC ± 10 $\pi^- \rho \rightarrow K_S^0 K^- \rho$

$\Gamma(\pi^+ \pi^- \pi^0)/\Gamma_{total}$	Γ_2/Γ
VALUE	DOCUMENT ID TECN CHG COMMENT
seen	CORDEN 78C OMEG 0 15 $\pi^- \rho \rightarrow 3\pi n$

$\Gamma(\rho \pi)/\Gamma(f_2(1270) \pi)$	Γ_3/Γ_4
VALUE	DOCUMENT ID TECN COMMENT
1.1 ± 0.2 ± 0.2	CHUNG 02 B852 18.3 $\pi^- \rho \rightarrow 3\pi \rho$

$\Gamma(\eta \pi^0)/\Gamma_{total}$	Γ_7/Γ
VALUE	DOCUMENT ID TECN CHG COMMENT
seen	DONSKOV 96 GAM2 0 38 $\pi^- \rho \rightarrow \eta \pi^0 n$

$\Gamma(\omega \rho)/\Gamma_{total}$	Γ_6/Γ
VALUE	EVTS DOCUMENT ID TECN COMMENT
seen	145k LU 05 B852 18 $\pi^- \rho \rightarrow \omega \pi^- \pi^0 \rho$

$a_4(2040)$ REFERENCES

UMAN 06 PR D73 052009	I. Uman et al.	(FNAL E835)
LU 05 PRL 94 032002	M. Lu et al.	(BNL E852 Collab.)
CHUNG 02 PR D65 072001	S.U. Chung et al.	(BNL E852 Collab.)
ANISOVICH 01F PL B517 261	A.V. Anisovich et al.	
IVANOV 01 PRL 86 3977	E.I. Ivanov et al.	(BNL E852 Collab.)
AMELIN 99 PAN 62 445	D.V. Amelin et al.	(VES Collab.)
ANISOVICH 99C PL B452 173	A.V. Anisovich et al.	
ANISOVICH 99E PL B452 187	A.V. Anisovich et al.	
DONSKOV 96 PAN 59 982	S.V. Donskov et al.	(GAMS Collab.) IGJPC
CLELAND 82B NP B208 228	W.E. Cleland et al.	(DURH, GEVA, LAUS+)
BALDI 78 PL 74B 413	R. Baldi et al.	(GEVA)JP
CORDEN 78C NP B136 77	M.J. Corden et al.	(BIRM, RHEL, TELA+)JP

$f_4(2050)$

$$J^G(J^{PC}) = 0^+(4^{++})$$

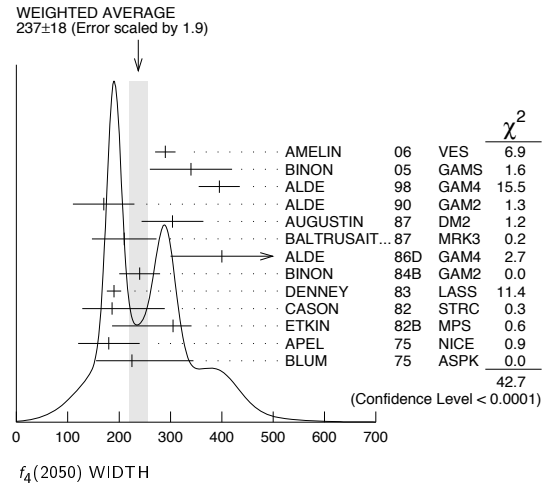
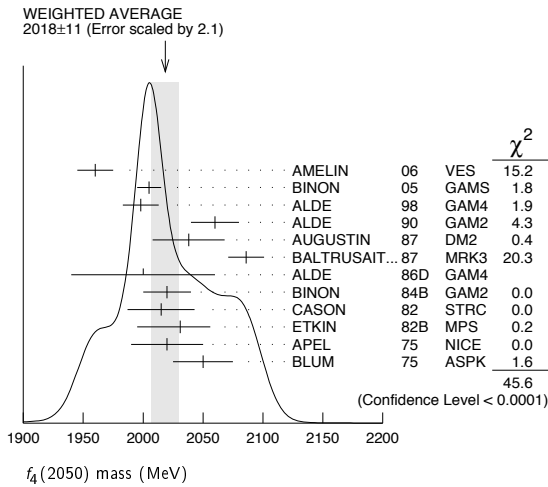
$f_4(2050)$ MASS

VALUE (MeV)	EVTS	DOCUMENT ID	TECN	COMMENT
2018 ± 11	OUR AVERAGE			Error includes scale factor of 2.1. See the ideogram below.
1960 ± 15		AMELIN	06	VES 36 $\pi^- \rho \rightarrow \omega \omega n$
2005 ± 10		1 BINON	05	GAMS 33 $\pi^- \rho \rightarrow \eta \eta n$
1998 ± 15		ALDE	98	GAM4 100 $\pi^- \rho \rightarrow \pi^0 \pi^0 n$
2060 ± 20		ALDE	90	GAM2 38 $\pi^- \rho \rightarrow \omega \omega n$
2038 ± 30		AUGUSTIN	87	DM2 $J/\psi \rightarrow \gamma \pi^+ \pi^-$
2086 ± 15		BALTRUSAIT..87	MRK3	$J/\psi \rightarrow \gamma \pi^+ \pi^-$
2000 ± 60		ALDE	86D	GAM4 100 $\pi^- \rho \rightarrow n 2\eta$
2020 ± 20	40k	2 BINON	84B	GAM2 38 $\pi^- \rho \rightarrow n 2\pi^0$
2015 ± 28		3 CASON	82	STRC 8 $\pi^+ \rho \rightarrow \Delta^+ + \pi^0 \pi^0$
2031 ± 25 -36		ETKIN	82B	MPS 23 $\pi^- \rho \rightarrow n 2K_S^0$
2020 ± 30	700	APEL	75	NICE 40 $\pi^- \rho \rightarrow n 2\pi^0$
2050 ± 25		BLUM	75	ASPK 18.4 $\pi^- \rho \rightarrow n K^+ K^-$

- • • We do not use the following data for averages, fits, limits, etc. • • •
- 4 ANISOVICH 09 RVUE 0.0 $\bar{p} \rho, \pi N$
- 5 UEHARA 09 BELL 10.6 $e^+ e^- \rightarrow e^+ e^- \pi^0 \pi^0$
- 2018 ± 6 ANISOVICH 00J SPEC 2.0 $\bar{p} \rho \rightarrow \eta \pi^0 \pi^0, \pi^0 \pi^0, \eta \eta, \eta \eta', \pi \pi$
- ~ 2000 6 MARTIN 98 RVUE $N\bar{N} \rightarrow \pi \pi$
- ~ 2010 7 MARTIN 97 RVUE $N\bar{N} \rightarrow \pi \pi$
- ~ 2040 8 OAKDEN 94 RVUE 0.36-1.55 $\bar{p} \rho \rightarrow \pi \pi$
- ~ 1990 9 OAKDEN 94 RVUE 0.36-1.55 $\bar{p} \rho \rightarrow \pi \pi$
- 1978 ± 5 10 ALPER 80 CNTR 62 $\pi^- \rho \rightarrow K^+ K^- n$
- 2040 ± 10 10 ROZANSKA 80 SPRK 18 $\pi^- \rho \rightarrow \rho \bar{p} n$
- 1935 ± 13 10 CORDEN 79 OMEG 12-15 $\pi^- \rho \rightarrow n 2\pi$
- 1988 ± 7 EVANGELIS... 79B OMEG 10 $\pi^- \rho \rightarrow K^+ K^- n$
- 1922 ± 14 11 ANTIPOV 77 CIBS 25 $\pi^- \rho \rightarrow \rho 3\pi$

- 1 From the first PWA solution.
- 2 From a partial-wave analysis of the data.
- 3 From an amplitude analysis of the reaction $\pi^+\pi^- \rightarrow 2\pi^0$.
- 4 K matrix pole.
- 5 Taking into account the $f_2(1950)$. Helicity-2 production favored.
- 6 Energy-dependent analysis.
- 7 Single energy analysis.
- 8 From solution A of amplitude analysis of data on $\bar{p}p \rightarrow \pi\pi$. See however KLOET 96 who fit $\pi^+\pi^-$ only and find waves only up to $J = 3$ to be important but not significantly resonant.
- 9 From solution B of amplitude analysis of data on $\bar{p}p \rightarrow \pi\pi$. See however KLOET 96 who fit $\pi^+\pi^-$ only and find waves only up to $J = 3$ to be important but not significantly resonant.
- 10 $I(J^P) = 0(4^+)$ from amplitude analysis assuming one-pion exchange.
- 11 Width errors enlarged by us to $4\Gamma/\sqrt{N}$; see the note with the $K^*(892)$ mass.

- 21 $I(J^P) = 0(4^+)$ from amplitude analysis assuming one-pion exchange.
- 22 Width errors enlarged by us to $4\Gamma/\sqrt{N}$; see the note with the $K^*(892)$ mass.



$f_4(2050)$ WIDTH

VALUE (MeV)	EVTS	DOCUMENT ID	TECN	COMMENT
237 ± 18 OUR AVERAGE		Error includes scale factor of 1.9. See the ideogram below.		
290 ± 20		AMELIN	06	VES $36 \pi^- p \rightarrow \omega \omega n$
340 ± 80	12	BINON	05	GAMS $33 \pi^- p \rightarrow \eta \eta n$
395 ± 40		ALDE	98	GAM4 $100 \pi^- p \rightarrow \pi^0 \pi^0 n$
170 ± 60		ALDE	90	GAM2 $38 \pi^- p \rightarrow \omega \omega n$
304 ± 60		AUGUSTIN	87	DM2 $J/\psi \rightarrow \gamma \pi^+ \pi^-$
210 ± 63		BALTRUSAIT...	87	MRK3 $J/\psi \rightarrow \gamma \pi^+ \pi^-$
400 ± 100		ALDE	86D	GAM4 $100 \pi^- p \rightarrow n 2\eta$
240 ± 40	40k	BINON	84B	GAM2 $38 \pi^- p \rightarrow n 2\pi^0$
190 ± 14		DENNEY	83	LASS $10 \pi^+ n / \pi^+ p$
186 ⁺¹⁰³ ₋₅₈		CASON	82	STRC $8 \pi^+ p \rightarrow \Delta^{++} \pi^0 \pi^0$
305 ⁺³⁶ ₋₁₁₉		ETKIN	82B	MPS $23 \pi^- p \rightarrow n 2K_S^0$
180 ± 60	700	APEL	75	NICE $40 \pi^- p \rightarrow n 2\pi^0$
225 ⁺¹²⁰ ₋₇₀		BLUM	75	ASPK $18.4 \pi^- p \rightarrow n K^+ K^-$
••• We do not use the following data for averages, fits, limits, etc. •••				
260 ± 40		15 ANISOVICH	09	RVUE $0.0 \bar{p} p, \pi N$
453 ± 20 ⁺³¹ ₋₁₂₉		16 UEHARA	09	BELL $10.6 e^+ e^- \rightarrow e^+ e^- \pi^0 \pi^0$
182 ± 7		ANISOVICH	00j	SPEC $2.0 \bar{p} p \rightarrow \eta \pi^0 \pi^0, \pi^0 \pi^0,$ $\eta \eta, \eta \eta', \pi \pi$
~ 170		17 MARTIN	98	RVUE $N \bar{N} \rightarrow \pi \pi$
~ 200		18 MARTIN	97	RVUE $N \bar{N} \rightarrow \pi \pi$
~ 60		19 OAKDEN	94	RVUE $0.36-1.55 \bar{p} p \rightarrow \pi \pi$
~ 80		20 OAKDEN	94	RVUE $0.36-1.55 \bar{p} p \rightarrow \pi \pi$
243 ± 16		21 ALPER	80	CNTR $62 \pi^- p \rightarrow K^+ K^- n$
140 ± 15		21 ROZANSKA	80	SPRK $18 \pi^- p \rightarrow p \bar{p} n$
263 ± 57		21 CORDEN	79	OMEG $12-15 \pi^- p \rightarrow n 2\pi$
100 ± 28		EVANGELIS...	79B	OMEG $10 \pi^- p \rightarrow K^+ K^- n$
107 ± 56		22 ANTIPOV	77	CIBS $25 \pi^- p \rightarrow p 3\pi$

- 12 From the first PWA solution.
- 13 From a partial-wave analysis of the data.
- 14 From an amplitude analysis of the reaction $\pi^+\pi^- \rightarrow 2\pi^0$.
- 15 K matrix pole.
- 16 Taking into account the $f_2(1950)$. Helicity-2 production favored.
- 17 Energy-dependent analysis.
- 18 Single energy analysis.
- 19 From solution A of amplitude analysis of data on $\bar{p}p \rightarrow \pi\pi$. See however KLOET 96 who fit $\pi^+\pi^-$ only and find waves only up to $J = 3$ to be important but not significantly resonant.
- 20 From solution B of amplitude analysis of data on $\bar{p}p \rightarrow \pi\pi$. See however KLOET 96 who fit $\pi^+\pi^-$ only and find waves only up to $J = 3$ to be important but not significantly resonant.

$f_4(2050)$ DECAY MODES

Mode	Fraction (Γ_i/Γ)
Γ_1 $\omega \omega$	seen
Γ_2 $\pi \pi$	(17.0 ± 1.5) %
Γ_3 $K \bar{K}$	(6.8 ^{+3.4} _{-1.8}) × 10 ⁻³
Γ_4 $\eta \eta$	(2.1 ± 0.8) × 10 ⁻³
Γ_5 $4\pi^0$	< 1.2 %
Γ_6 $\gamma \gamma$	
Γ_7 $a_2(1320) \pi$	seen

$f_4(2050)$ $\Gamma(i)\Gamma(\gamma\gamma)/\Gamma(\text{total})$

VALUE (keV)	CL%	DOCUMENT ID	TECN	COMMENT
••• We do not use the following data for averages, fits, limits, etc. •••				
< 0.29	95	ALTHOFF	85B	TASS $\gamma \gamma \rightarrow K \bar{K} \pi$
••• We do not use the following data for averages, fits, limits, etc. •••				
23.1 ^{+3.6+70.5} _{-3.3-15.6}		23 UEHARA	09	BELL $10.6 e^+ e^- \rightarrow e^+ e^- \pi^0 \pi^0$
< 1100	95	13 ± 4	OEST	90 JADE $e^+ e^- \rightarrow e^+ e^- \pi^0 \pi^0$

23 Taking into account the $f_2(1950)$. Helicity-2 production favored.

$f_4(2050)$ BRANCHING RATIOS

$\Gamma(\omega\omega)/\Gamma_{\text{total}}$	DOCUMENT ID	TECN	COMMENT	Γ_1/Γ
VALUE				
seen	AMELIN	06	VES $36 \pi^- p \rightarrow \omega \omega n$	
••• We do not use the following data for averages, fits, limits, etc. •••				
not seen	BARBERIS	00F	450 $pp \rightarrow p_f \omega p_S$	
••• We do not use the following data for averages, fits, limits, etc. •••				
$\Gamma(\omega\omega)/\Gamma(\pi\pi)$				Γ_1/Γ_2
VALUE				
1.5 ± 0.3	ALDE	90	GAM2 $38 \pi^- p \rightarrow \omega \omega n$	
••• We do not use the following data for averages, fits, limits, etc. •••				
$\Gamma(\pi\pi)/\Gamma_{\text{total}}$				Γ_2/Γ
VALUE				
0.170 ± 0.015 OUR AVERAGE				
0.18 ± 0.03	24 BINON	83C	GAM2 $38 \pi^- p \rightarrow n 4\gamma$	
0.16 ± 0.03	24 CASON	82	STRC $8 \pi^+ p \rightarrow \Delta^{++} \pi^0 \pi^0$	
0.17 ± 0.02	24 CORDEN	79	OMEG $12-15 \pi^- p \rightarrow n 2\pi$	
24 Assuming one pion exchange.				
$\Gamma(K\bar{K})/\Gamma(\pi\pi)$				Γ_3/Γ_2
VALUE				
0.04 ^{+0.02} _{-0.01}	ETKIN	82B	MPS $23 \pi^- p \rightarrow n 2K_S^0$	
••• We do not use the following data for averages, fits, limits, etc. •••				
$\Gamma(\eta\eta)/\Gamma_{\text{total}}$				Γ_4/Γ
VALUE (units 10 ⁻³)				
2.1 ± 0.8	ALDE	86D	GAM4 $100 \pi^- p \rightarrow n 4\gamma$	

$\eta\pi\pi$ MODE

VALUE (MeV)	DOCUMENT ID	TECN	CHG	COMMENT
The data in this block is included in the average printed for a previous datablock.				

- • • We do not use the following data for averages, fits, limits, etc. • • •
- 2135 ± 20 ± 45 ⁵ADOMEIT 96 CBAR 0 1.94 $\bar{p}p \rightarrow \eta 3\pi^0$
- ⁵ANISOVICH 00E recommends to withdraw ADOMEIT 96 that assumed a single $J^P = 2^+$ resonance.

 $\bar{p}p \rightarrow \pi\pi$

VALUE (MeV)	DOCUMENT ID	TECN	COMMENT
• • • We do not use the following data for averages, fits, limits, etc. • • •			

- • • We do not use the following data for averages, fits, limits, etc. • • •
- ~ 2226 HASAN 94 RVUE $\bar{p}p \rightarrow \pi\pi$
- ~ 2090 ⁶OAKDEN 94 RVUE 0.36-1.55 $\bar{p}p \rightarrow \pi\pi$
- ~ 2120 ⁷OAKDEN 94 RVUE 0.36-1.55 $\bar{p}p \rightarrow \pi\pi$
- ~ 2170 ⁸MARTIN 80B RVUE
- ~ 2150 ⁸MARTIN 80C RVUE
- ~ 2150 ⁹DULUDE 78B OSPK 1-2 $\bar{p}p \rightarrow \pi^0\pi^0$
- ⁶OAKDEN 94 makes an amplitude analysis of LEAR data on $\bar{p}p \rightarrow \pi\pi$ using a method based on Barrelet zeros. This is solution A. The amplitude analysis of HASAN 94 includes earlier data as well, and assume that the data can be parametrized in terms of towers of nearly degenerate resonances on the leading Regge trajectory. See also KLOET 96 and MARTIN 97 who make related analyses.
- ⁷From solution B of amplitude analysis of data on $\bar{p}p \rightarrow \pi\pi$.
- ⁸ $I(J^P) = 0(2^+)$ from simultaneous analysis of $p\bar{p} \rightarrow \pi^-\pi^+$ and $\pi^0\pi^0$.
- ⁹ $I^G(J^P) = 0^+(2^+)$ from partial-wave amplitude analysis.

S-CHANNEL $\bar{p}p$, $\bar{N}N$ or $\bar{K}K$

VALUE (MeV)	DOCUMENT ID	TECN	CHG	COMMENT
• • • We do not use the following data for averages, fits, limits, etc. • • •				

- • • We do not use the following data for averages, fits, limits, etc. • • •
- 2139 ± $\frac{8}{9}$ ¹⁰EVANGELIS... 97 SPEC 0.6-2.4 $\bar{p}p \rightarrow K_S^0 K_S^0$
- ~ 2190 ¹⁰CUTTS 78B CNTR 0.97-3 $\bar{p}p \rightarrow \bar{N}N$
- 2155 ± 15 ^{10,11}COUPLAND 77 CNTR 0 0.7-2.4 $\bar{p}p \rightarrow \bar{p}p$
- 2193 ± 2 ^{10,12}ALSPECTOR 73 CNTR $\bar{p}p$ S channel
- ¹⁰Isospins 0 and 1 not separated.
- ¹¹From a fit to the total elastic cross section.
- ¹²Referred to as T or T region by ALSPECTOR 73.

 $K\bar{K}$ MODE

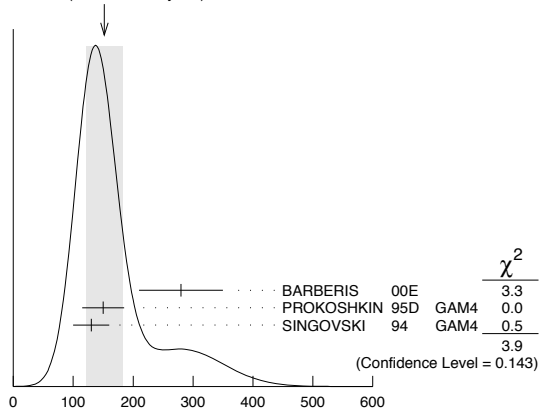
VALUE (MeV)	DOCUMENT ID	TECN	COMMENT
• • • We do not use the following data for averages, fits, limits, etc. • • •			

- • • We do not use the following data for averages, fits, limits, etc. • • •
- 2200 ± 13 VLADIMIRSK...06 SPEC 40 $\pi^-p \rightarrow K_S^0 K_S^0 n$
- 2150 ± 20 ABLIKIM 04E BES2 $J/\psi \rightarrow \omega K^+ K^-$
- 2130 ± 35 BARBERIS 99 OMEG 450 $pp \rightarrow p_S p_f K^+ K^-$

 $f_2(2150)$ WIDTH $f_2(2150)$ WIDTH, COMBINED MODES (MeV)

VALUE (MeV)	EVTS	DOCUMENT ID	TECN	COMMENT
152 ± 30 OUR AVERAGE Includes data from the 2 datablocks that follow this one. Error includes scale factor of 1.4. See the ideogram below.				

- • • We do not use the following data for averages, fits, limits, etc. • • •
- 182 ± 11 80k ¹³UMAN 06 E835 5.2 $\bar{p}p \rightarrow \eta\eta\pi^0$
- ¹³Statistical error only.

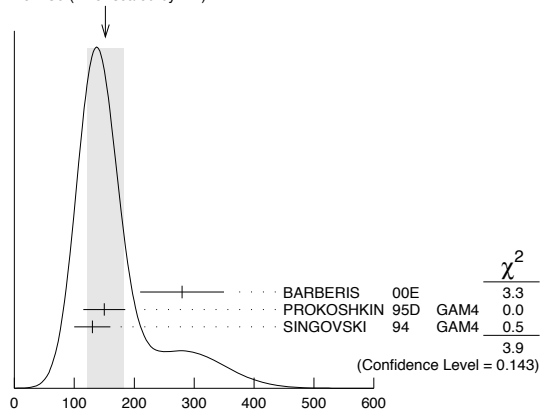
WEIGHTED AVERAGE
152 ± 30 (Error scaled by 1.4) $f_2(2150)$ WIDTH, COMBINED MODES (MeV) $\eta\eta$ MODE

VALUE (MeV)	DOCUMENT ID	TECN	COMMENT
The data in this block is included in the average printed for a previous datablock.			

152 ± 30 OUR AVERAGE Error includes scale factor of 1.4. See the ideogram below.

- 280 ± 70 BARBERIS 00E 450 $pp \rightarrow p_f \eta\eta p_S$
- 150 ± 35 PROKOSHKIN 95D GAM4 300 $\pi^- N \rightarrow \pi^- N 2\eta$,
450 $pp \rightarrow p p 2\eta$
- 130 ± 30 SINGOVSKI 94 GAM4 450 $pp \rightarrow p p 2\eta$
- • • We do not use the following data for averages, fits, limits, etc. • • •
- 310 ± 50 ¹⁴ABELE 99B CBAR
- seen ¹⁵ANISOVICH 99B SPEC 1.35-1.94 $\bar{p}p \rightarrow \eta\eta\pi^0$
- 200 ± 25 ¹⁶ANISOVICH 99K RVUE 0.6-1.94 $\bar{p}p \rightarrow \eta\eta, \eta\eta'$
- 203 ± 10 ¹⁷ARMSTRONG 93C E760 $\bar{p}p \rightarrow \pi^0\eta\eta \rightarrow 6\gamma$

- ¹⁴Spin not determined.
- ¹⁵ $J^PC = 0^{++}$
- ¹⁶PWA gives $J^PC = 0^{++}$.
- ¹⁷No J^PC determination.

WEIGHTED AVERAGE
152 ± 30 (Error scaled by 1.4) $f_2(2150)$ WIDTH, $\eta\eta$ MODE (MeV) $\eta\pi\pi$ MODE

VALUE (MeV)	DOCUMENT ID	TECN	CHG	COMMENT
The data in this block is included in the average printed for a previous datablock.				

- • • We do not use the following data for averages, fits, limits, etc. • • •
- 250 ± 25 ± 45 ¹⁸ADOMEIT 96 CBAR 0 1.94 $\bar{p}p \rightarrow \eta 3\pi^0$
- ¹⁸ANISOVICH 00E recommends to withdraw ADOMEIT 96 that assumed a single $J^P = 2^+$ resonance.

 $\bar{p}p \rightarrow \pi\pi$

VALUE (MeV)	DOCUMENT ID	TECN	COMMENT
250 OUR ESTIMATE			

- • • We do not use the following data for averages, fits, limits, etc. • • •
- ~ 226 HASAN 94 RVUE $\bar{p}p \rightarrow \pi\pi$
- ~ 70 ¹⁹OAKDEN 94 RVUE 0.36-1.55 $\bar{p}p \rightarrow \pi\pi$
- ~ 250 ²⁰MARTIN 80B RVUE
- ~ 250 ²⁰MARTIN 80C RVUE
- ~ 250 ²¹DULUDE 78B OSPK 1-2 $\bar{p}p \rightarrow \pi^0\pi^0$
- ¹⁹See however KLOET 96 who fit $\pi^+\pi^-$ only and find waves only up to $J = 3$ to be important but not significantly resonant.
- ²⁰ $I(J^P) = 0(2^+)$ from simultaneous analysis of $p\bar{p} \rightarrow \pi^-\pi^+$ and $\pi^0\pi^0$.
- ²¹ $I^G(J^P) = 0^+(2^+)$ from partial-wave amplitude analysis.

S-CHANNEL $\bar{p}p$, $\bar{N}N$ or $\bar{K}K$

VALUE (MeV)	DOCUMENT ID	TECN	CHG	COMMENT
• • • We do not use the following data for averages, fits, limits, etc. • • •				

- • • We do not use the following data for averages, fits, limits, etc. • • •
- 56 + 31 ²²EVANGELIS... 97 SPEC 0.6-2.4 $\bar{p}p \rightarrow K_S^0 K_S^0$
- 135 ± 75 ^{23,24}COUPLAND 77 CNTR 0 0.7-2.4 $\bar{p}p \rightarrow \bar{p}p$
- 98 ± 8 ²⁴ALSPECTOR 73 CNTR $\bar{p}p$ S channel
- ²²Isospin 0 and 2 not separated.
- ²³From a fit to the total elastic cross section.
- ²⁴Isospins 0 and 1 not separated.

 $K\bar{K}$ MODE

VALUE (MeV)	DOCUMENT ID	TECN	COMMENT
• • • We do not use the following data for averages, fits, limits, etc. • • •			

- • • We do not use the following data for averages, fits, limits, etc. • • •
- 91 ± 62 VLADIMIRSK...06 SPEC 40 $\pi^-p \rightarrow K_S^0 K_S^0 n$
- 150 ± 30 ABLIKIM 04E BES2 $J/\psi \rightarrow \omega K^+ K^-$
- 270 ± 50 BARBERIS 99 OMEG 450 $pp \rightarrow p_S p_f K^+ K^-$

Meson Particle Listings

 $f_2(2150)$, $\rho(2150)$ $f_2(2150)$ DECAY MODES

Mode	Fraction (Γ_i/Γ)
Γ_1 $\pi\pi$	
Γ_2 $\eta\eta$	seen
Γ_3 $K\bar{K}$	seen
Γ_4 $f_2(1270)\eta$	seen
Γ_5 $a_2(1320)\pi$	seen

 $f_2(2150)$ BRANCHING RATIOS

$\Gamma(K\bar{K})/\Gamma(\eta\eta)$	Γ_3/Γ_2			
VALUE	CL%	DOCUMENT ID	TECN	COMMENT
1.28 ± 0.23		BARBERIS	00E	450 $p\bar{p} \rightarrow p_f \eta \eta P_S$

••• We do not use the following data for averages, fits, limits, etc. •••

<0.1 95 25 PROKOSHKIN 95D GAM4 300 $\pi^- N \rightarrow \pi^- N 2\eta$,
450 $p\bar{p} \rightarrow p\bar{p} 2\eta$

²⁵ Using data from ARMSTRONG 89D.

$\Gamma(\pi\pi)/\Gamma(\eta\eta)$	Γ_1/Γ_2			
VALUE	CL%	DOCUMENT ID	TECN	COMMENT
<0.33	95	26 PROKOSHKIN 95D	GAM4	300 $\pi^- N \rightarrow \pi^- N 2\eta$, 450 $p\bar{p} \rightarrow p\bar{p} 2\eta$

••• We do not use the following data for averages, fits, limits, etc. •••

<0.33 95 26 PROKOSHKIN 95D GAM4 300 $\pi^- N \rightarrow \pi^- N 2\eta$,
450 $p\bar{p} \rightarrow p\bar{p} 2\eta$

²⁶ Derived from a $\pi^0 \pi^0/\eta\eta$ limit.

$\Gamma(f_2(1270)\eta)/\Gamma(a_2(1320)\pi)$	Γ_4/Γ_5		
VALUE	DOCUMENT ID	TECN	COMMENT
0.79 ± 0.11	27	ADOMEIT	96 CBAR 1.94 $\bar{p}p \rightarrow \eta 3\pi^0$

²⁷ Using $B(a_2(1320) \rightarrow \eta\pi) = 0.145$

 $f_2(2150)$ REFERENCES

UMAN	06	PR D73 052009	I. Uman et al.	(FNAL E835)
VLADIMIRSK...	06	PAN 69 493	V.V. Vladimirov et al.	(ITEP, Moscow)
		Translated from YAF 69 515.		
ABLIKIM	04E	PL B603 138	M. Ablikim et al.	(BES Collab.)
ANISOVICH	00E	PL B477 19	A.V. Anisovich et al.	
BARBERIS	00E	PL B479 59	D. Barberis et al.	(WA 102 Collab.)
ABELE	99B	EPJ C8 67	A. Abele et al.	(Crystal Barrel Collab.)
ANISOVICH	99B	PL B449 154	A.V. Anisovich et al.	
ANISOVICH	99K	PL B468 309	A.V. Anisovich et al.	
BARBERIS	99	PL B453 305	D. Barberis et al.	(Omega Expt.)
EVANGELIS...	97	PR D56 3803	C. Evangelista et al.	(LEAR Collab.)
MARTIN	97	PR C56 1114	B.R. Martin, G.C. Oades	(LOUC, AARH)
ADOMEIT	96	ZPHY C71 227	J. Adomeit et al.	(Crystal Barrel Collab.)
KLOET	96	PR D53 6120	W.M. Kloet, F. Myhrer	(RUTG, NORO)
PROKOSHKIN	95D	SPD 40 495	Y.D. Prokoshkin	(SERP)IGJPC
		Translated from DANS 344 469.		
HASAN	94	PL B334 215	A. Hasan, D.V. Bugg	(LOQM)
OAKDEN	94	NP A574 731	M.N. Oakden, M.R. Pennington	(DURH)
SINGOVSKI	94	NC 107A 1911	A.V. Singovsky	(SERP)
ARMSTRONG	93C	PL B307 394	T.A. Armstrong et al.	(FNAL, FERR, GENO+)
ARMSTRONG	89D	PL B227 186	T.A. Armstrong, M. Benayoun	(ATHU, BARI, BIRN+)
MARTIN	80B	NP B176 355	B.R. Martin, D. Morgan	(LOUC, RHEL)JP
MARTIN	80C	NP B169 216	A.D. Martin, M.R. Pennington	(DURH)JP
CUTTS	78B	PR D17 16	D. Cutts et al.	(STON, WISC)
DULUDE	78B	PL 79B 335	R.S. Dulude et al.	(BROW, MIT, BARI)JP
COUPLAND	77	PL 71B 460	M. Coupland et al.	(LOQM, RHEL)
ALSPECTOR	73	PRL 30 511	J. Alspector et al.	(RUTG, UPNJ)

 $\rho(2150)$

$$I^G(J^{PC}) = 1^+(1^{--})$$

OMITTED FROM SUMMARY TABLE

This entry was previously called $T_1(2190)$. See our mini-review under the $\rho(1700)$.

 $\rho(2150)$ MASS

e^+e^- PRODUCED	VALUE (MeV)	DOCUMENT ID	TECN	COMMENT
2149 ± 17 OUR AVERAGE		Includes data from the datablock that follows this one.		
2150 ± 40 ± 50	AUBERT	07AU BABR	10.6	$e^+e^- \rightarrow f_1(1285)\pi^+\pi^-\gamma$
2153 ± 37	BIAGINI	91 RVUE	$e^+e^- \rightarrow \pi^+\pi^-, K^+K^-$	
2110 ± 50	¹ CLEGG	90 RVUE	$e^+e^- \rightarrow 3(\pi^+\pi^-), 2(\pi^+\pi^-\pi^0)$	

••• We do not use the following data for averages, fits, limits, etc. •••

1990 ± 80 AUBERT 07AU BABR 10.6 $e^+e^- \rightarrow \eta'\pi^+\pi^-\gamma$

$\bar{p}p \rightarrow \pi\pi$	VALUE (MeV)	DOCUMENT ID	TECN	COMMENT
~ 2191	HASAN	94 RVUE	$\bar{p}p \rightarrow \pi\pi$	
~ 2070	² OAKDEN	94 RVUE	$0.36-1.55 \bar{p}p \rightarrow \pi\pi$	
~ 2170	³ MARTIN	80B RVUE		
~ 2100	³ MARTIN	80C RVUE		

••• We do not use the following data for averages, fits, limits, etc. •••

~ 2191 4 HASAN 94 RVUE $\bar{p}p \rightarrow \pi\pi$

~ 2070 5 OAKDEN 94 RVUE $0.36-1.55 \bar{p}p \rightarrow \pi\pi$

~ 2170 6 MARTIN 80B RVUE

~ 2100 7 MARTIN 80C RVUE

S-CHANNEL $\bar{N}N$

VALUE (MeV)	DOCUMENT ID	TECN	COMMENT
2110 ± 35	⁴ ANISOVICH	02 SPEC	$0.6-1.9 \bar{p}\bar{p} \rightarrow \omega\pi^0, \omega\eta\pi^0, \pi^+\pi^-$
~ 2190	⁵ CUTTS	78B CNTR	$0.97-3 \bar{p}p \rightarrow \bar{N}N$
2155 ± 15	^{5,6} COUPLAND	77 CNTR	$0.7-2.4 \bar{p}p \rightarrow \bar{p}p$
2193 ± 2	^{5,7} ALSPECTOR	73 CNTR	$\bar{p}p$ S channel
2190 ± 10	⁸ ABRAMS	70 CNTR	S channel $\bar{p}N$

 $\pi^-p \rightarrow \omega\pi^0 n$

VALUE (MeV)	DOCUMENT ID	TECN	COMMENT
2155 ± 21 OUR AVERAGE			
2140 ± 30	ALDE	95	GAM2 38 $\pi^-p \rightarrow \omega\pi^0 n$
2170 ± 30	ALDE	92C	GAM4 100 $\pi^-p \rightarrow \omega\pi^0 n$

The data in this block is included in the average printed for a previous datablock.

¹ Includes ATKINSON 85.
² See however KLOET 96 who fit $\pi^+\pi^-$ only and find waves only up to $J = 3$ to be important but not significantly resonant.
³ $I(J^P) = 1(1^-)$ from simultaneous analysis of $\bar{p}\bar{p} \rightarrow \pi^-\pi^+$ and $\pi^0\pi^0$.
⁴ From the combined analysis of ANISOVICH 00J, ANISOVICH 01D, ANISOVICH 01E, and ANISOVICH 02.
⁵ Isospins 0 and 1 not separated.
⁶ From a fit to the total elastic cross section.
⁷ Referred to as T or T region by ALSPECTOR 73.
⁸ Seen as bump in $l = 1$ state. See also COOPER 68. PEASLEE 75 confirm $\bar{p}p$ results of ABRAMS 70, no narrow structure.

 $\rho(2150)$ WIDTH

e^+e^- PRODUCED	VALUE (MeV)	DOCUMENT ID	TECN	COMMENT
359 ± 40 OUR AVERAGE		Includes data from the datablock that follows this one.		
350 ± 40 ± 50	AUBERT	07AU BABR	10.6	$e^+e^- \rightarrow f_1(1285)\pi^+\pi^-\gamma$
389 ± 79	BIAGINI	91 RVUE	$e^+e^- \rightarrow \pi^+\pi^-, K^+K^-$	
410 ± 100	⁹ CLEGG	90 RVUE	$e^+e^- \rightarrow 3(\pi^+\pi^-), 2(\pi^+\pi^-\pi^0)$	

••• We do not use the following data for averages, fits, limits, etc. •••

310 ± 140 AUBERT 07AU BABR 10.6 $e^+e^- \rightarrow \eta'\pi^+\pi^-\gamma$

 $\bar{p}p \rightarrow \pi\pi$

VALUE (MeV)	DOCUMENT ID	TECN	COMMENT
~ 296	HASAN	94 RVUE	$\bar{p}p \rightarrow \pi\pi$
~ 40	¹⁰ OAKDEN	94 RVUE	$0.36-1.55 \bar{p}p \rightarrow \pi\pi$
~ 250	¹¹ MARTIN	80B RVUE	
~ 200	¹¹ MARTIN	80C RVUE	

S-CHANNEL $\bar{N}N$

VALUE (MeV)	DOCUMENT ID	TECN	COMMENT
230 ± 50	¹² ANISOVICH	02 SPEC	$0.6-1.9 \bar{p}\bar{p} \rightarrow \omega\pi^0, \omega\eta\pi^0, \pi^+\pi^-$
135 ± 75	^{13,14} COUPLAND	77 CNTR	$0.7-2.4 \bar{p}p \rightarrow \bar{p}p$
98 ± 8	¹⁴ ALSPECTOR	73 CNTR	$\bar{p}p$ S channel
~ 85	¹⁵ ABRAMS	70 CNTR	S channel $\bar{p}N$

 $\pi^-p \rightarrow \omega\pi^0 n$

VALUE (MeV)	DOCUMENT ID	TECN	COMMENT
320 ± 70			
ALDE	95	GAM2	38 $\pi^-p \rightarrow \omega\pi^0 n$
ALDE	92C	GAM4	100 $\pi^-p \rightarrow \omega\pi^0 n$

The data in this block is included in the average printed for a previous datablock.

••• We do not use the following data for averages, fits, limits, etc. •••

~ 300 ALDE 92C GAM4 100 $\pi^-p \rightarrow \omega\pi^0 n$

⁹ Includes ATKINSON 85.
¹⁰ See however KLOET 96 who fit $\pi^+\pi^-$ only and find waves only up to $J = 3$ to be important but not significantly resonant.
¹¹ $I(J^P) = 1(1^-)$ from simultaneous analysis of $\bar{p}\bar{p} \rightarrow \pi^-\pi^+$ and $\pi^0\pi^0$.
¹² From the combined analysis of ANISOVICH 00J, ANISOVICH 01D, ANISOVICH 01E, and ANISOVICH 02.
¹³ From a fit to the total elastic cross section.
¹⁴ Isospins 0 and 1 not separated.
¹⁵ Seen as bump in $l = 1$ state. See also COOPER 68. PEASLEE 75 confirm $\bar{p}p$ results of ABRAMS 70, no narrow structure.

 $\rho(2150)$ DECAY MODES

Mode	Fraction (Γ_i/Γ)
Γ_1 e^+e^-	
Γ_2 $\pi^+\pi^-$	seen
Γ_3 K^+K^-	seen
Γ_4 $3(\pi^+\pi^-)$	seen
Γ_5 $2(\pi^+\pi^-\pi^0)$	seen
Γ_6 $\eta'\pi^+\pi^-$	seen
Γ_7 $f_1(1285)\pi^+\pi^-$	seen
Γ_8 $\omega\pi^0$	seen
Γ_9 $\omega\pi^0\eta$	seen
Γ_{10} $\rho\bar{\rho}$	

See key on page 405

Meson Particle Listings

$\rho(2150)$, $\phi(2170)$

$\rho(2150) \Gamma(i)\Gamma(e^+e^-)/\Gamma^2(\text{total})$

$\Gamma(f_1(1285)\pi^+\pi^-)/\Gamma_{\text{total}} \times \Gamma(e^+e^-)/\Gamma_{\text{total}}$	$\Gamma_7/\Gamma \times \Gamma_1/\Gamma$			
VALUE (units 10^{-7})	DOCUMENT ID	TECN	COMMENT	
$3.1 \pm 0.6 \pm 0.5$	16	AUBERT	07AU BABR	$10.6 e^+e^- \rightarrow f_1(1285)\pi^+\pi^-\gamma$
¹⁶ Calculated by us from the reported value of cross section at the peak.				

$\Gamma(\eta'\pi^+\pi^-)/\Gamma_{\text{total}} \times \Gamma(e^+e^-)/\Gamma_{\text{total}}$	$\Gamma_6/\Gamma \times \Gamma_1/\Gamma$			
VALUE (units 10^{-8})	DOCUMENT ID	TECN	COMMENT	
4.9 ± 1.9	17	AUBERT	07AU BABR	$10.6 e^+e^- \rightarrow \eta'\pi^+\pi^-\gamma$
¹⁷ Calculated by us from the reported value of cross section at the peak.				

$\rho(2150)$ REFERENCES

AUBERT	07AU	PR D76 092005	B. Aubert et al.	(BABAR Collab.)
ANISOVICH	02	PL B542 8	A.V. Anisovich et al.	
ANISOVICH	01D	PL B508 6	A.V. Anisovich et al.	
ANISOVICH	01E	PL B513 281	A.V. Anisovich et al.	
ANISOVICH	00J	PL B491 47	A.V. Anisovich et al.	
KLOET	96	PR D53 6120	W.M. Kloet, F. Myhrer	(RUTG, NORD)
ALDE	95	ZPHY C66 379	D.M. Alde et al.	(GAMS Collab.) JP
HASAN	94	PL B334 215	A. Hasan, D.V. Bugg	(LOQM)
OAKDEN	94	NP A574 731	M.N. Oakden, M.R. Pennington	(DURH)
ALDE	92C	ZPHY C54 553	D.M. Alde et al.	(BELG, SERP, KEK, LANL+)
BIAGINI	91	NC 104A 363	M.E. Biagini et al.	(FRAS, PRAG)
CLEGG	90	ZPHY C45 677	A.B. Clegg, A. Donnachie	(LANC, MCHS)
ATKINSON	85	ZPHY C29 333	M. Atkinson et al.	(BONN, CERN, GLAS+)
MARTIN	80B	NP B176 355	B.R. Martin, D. Morgan	(LOUC, RHEL) JP
MARTIN	80C	NP B169 216	A.D. Martin, M.R. Pennington	(DURH) JP
CUTTS	78B	PR D17 16	D. Cutts et al.	(STON, WIS C)
COUPLAND	77	PL 71B 460	M. Coupland et al.	(LOQM, RHEL)
PEASLEE	75	PL 57B 189	D.C. Peaslee et al.	(CANB, BARI, BROW+)
ALSPECTOR	73	PRL 30 511	J. Alspector et al.	(RUTG, UPNJ)
ABRAMS	70	PR D1 1917	R.J. Abrams et al.	(BNL)
COOPER	68	PRL 20 1059	W.A. Cooper et al.	(ANL)

$\phi(2170)$

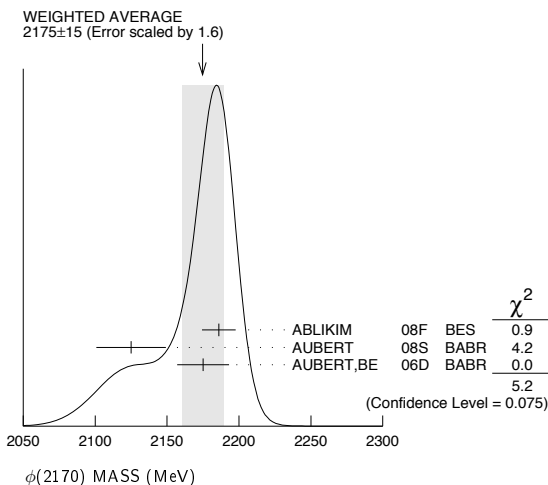
$$I^G(J^{PC}) = 0^-(1^{--})$$

Observed by AUBERT, BE 06D in the initial-state radiation process $e^+e^- \rightarrow \phi f_0(980)\gamma$.

$\phi(2170)$ MASS

VALUE (MeV)	EVTs	DOCUMENT ID	TECN	COMMENT
2175 ± 15 OUR AVERAGE	Error includes scale factor of 1.6. See the ideogram below.			
$2186 \pm 10 \pm 6$	52	ABLIKIM	08F BES	$J/\psi \rightarrow \eta\phi f_0(980)$
$2125 \pm 22 \pm 10$	483	AUBERT	08S BABR	$10.6 e^+e^- \rightarrow \phi\eta\gamma$
$2175 \pm 10 \pm 15$	201	¹ AUBERT, BE	06D BABR	$10.6 e^+e^- \rightarrow K^+K^-\pi\pi\gamma$
• • • We do not use the following data for averages, fits, limits, etc. • • •				
$2079 \pm 13 \pm 79$	4.8k	² SHEN	09 BELL	$10.6 e^+e^- \rightarrow K^+K^-\pi^+\pi^-\gamma$
2192 ± 14	116 ± 95	³ AUBERT	07AK BABR	$10.6 e^+e^- \rightarrow K^+K^-\pi^+\pi^-\gamma$
2169 ± 20	149 ± 36	³ AUBERT	07AK BABR	$10.6 e^+e^- \rightarrow K^+K^-\pi^0\pi^0\gamma$

¹ From the $\phi f_0(980)$ component.
² From a fit with two incoherent Breit-Wigners.
³ From the $K^+K^-\pi f_0(980)$ component.



$\phi(2170)$ WIDTH

VALUE (MeV)	EVTs	DOCUMENT ID	TECN	COMMENT
61 ± 18 OUR AVERAGE				
$65 \pm 23 \pm 17$	52	ABLIKIM	08F BES	$J/\psi \rightarrow \eta\phi f_0(980)$
$61 \pm 5 \pm 13$	483	AUBERT	08S BABR	$10.6 e^+e^- \rightarrow \phi\eta\gamma$
$58 \pm 16 \pm 20$	201	⁴ AUBERT, BE	06D BABR	$10.6 e^+e^- \rightarrow K^+K^-\pi\pi\gamma$

• • • We do not use the following data for averages, fits, limits, etc. • • •

$192 \pm 23 \pm 25$	4.8k	⁵ SHEN	09 BELL	$10.6 e^+e^- \rightarrow K^+K^-\pi^+\pi^-\gamma$
71 ± 21	116 ± 95	⁶ AUBERT	07AK BABR	$10.6 e^+e^- \rightarrow K^+K^-\pi^+\pi^-\gamma$
102 ± 27	149 ± 36	⁶ AUBERT	07AK BABR	$10.6 e^+e^- \rightarrow K^+K^-\pi^0\pi^0\gamma$
⁴ From the $\phi f_0(980)$ component.				
⁵ From a fit with two incoherent Breit-Wigners.				
⁶ From the $K^+K^-\pi f_0(980)$ component.				

$\phi(2170)$ DECAY MODES

Mode	Fraction (Γ_i/Γ)
$\Gamma_1 e^+e^-$	seen
$\Gamma_2 \phi\eta$	
$\Gamma_3 \phi\pi\pi$	
$\Gamma_4 \phi f_0(980)$	seen
$\Gamma_5 K^+K^-\pi^+\pi^-$	
$\Gamma_6 K^+K^-\pi^0\pi^0 \rightarrow K^+K^-\pi^+\pi^-$	seen
$\Gamma_7 K^+K^-\pi^0\pi^0$	
$\Gamma_8 K^+K^-\pi f_0(980) \rightarrow K^+K^-\pi^0\pi^0$	seen
$\Gamma_9 K^*0 K^\pm\pi^\mp$	not seen

$\phi(2170) \Gamma(i)\Gamma(e^+e^-)/\Gamma(\text{total})$

$\Gamma(\phi\eta) \times \Gamma(e^+e^-)/\Gamma_{\text{total}}$	$\Gamma_2\Gamma_1/\Gamma$			
VALUE (eV)	EVTs	DOCUMENT ID	TECN	COMMENT
$1.7 \pm 0.7 \pm 1.3$	483	AUBERT	08S BABR	$10.6 e^+e^- \rightarrow \phi\eta\gamma$

$\Gamma(\phi f_0(980)) \times \Gamma(e^+e^-)/\Gamma_{\text{total}}$	$\Gamma_4\Gamma_1/\Gamma$			
VALUE (eV)	EVTs	DOCUMENT ID	TECN	COMMENT
$2.5 \pm 0.8 \pm 0.4$	201	⁷ AUBERT, BE	06D BABR	$10.6 e^+e^- \rightarrow K^+K^-\pi\pi\gamma$
⁷ From the $\phi f_0(980)$ component.				

$\phi(2170) \Gamma(i)\Gamma(e^+e^-)/\Gamma^2(\text{total})$

$\Gamma(\phi\pi\pi)/\Gamma_{\text{total}} \times \Gamma(e^+e^-)/\Gamma_{\text{total}}$	$\Gamma_3/\Gamma \times \Gamma_1/\Gamma$			
VALUE (units 10^{-7})	EVTs	DOCUMENT ID	TECN	COMMENT
$1.65 \pm 0.15 \pm 0.18$	4.8k	⁸ SHEN	09 BELL	$10.6 e^+e^- \rightarrow K^+K^-\pi^+\pi^-\gamma$

⁸ Multiplied by 3/2 to take into account the $\phi\pi^0\pi^0$ mode. Using $B(\phi \rightarrow K^+K^-) = (49.2 \pm 0.6)\%$.

$\phi(2170)$ BRANCHING RATIOS

$\Gamma(K^+K^-\pi f_0(980) \rightarrow K^+K^-\pi^+\pi^-)/\Gamma_{\text{total}}$	Γ_6/Γ		
VALUE	DOCUMENT ID	TECN	COMMENT
seen	AUBERT	07AK BABR	$10.6 e^+e^- \rightarrow K^+K^-\pi^+\pi^-\gamma$
$\Gamma(K^+K^-\pi f_0(980) \rightarrow K^+K^-\pi^0\pi^0)/\Gamma_{\text{total}}$	Γ_8/Γ		
VALUE	DOCUMENT ID	TECN	COMMENT
seen	AUBERT	07AK BABR	$10.6 e^+e^- \rightarrow K^+K^-\pi^0\pi^0\gamma$
$\Gamma(K^*0 K^\pm\pi^\mp)/\Gamma_{\text{total}}$	Γ_9/Γ		
VALUE	DOCUMENT ID	TECN	COMMENT
not seen	AUBERT	07AK BABR	$10.6 \text{ GeV } e^+e^-$

$\phi(2170)$ REFERENCES

SHEN	09	PR D80 031101R	C.P. Shen et al.	(BELLE Collab.)
ABLIKIM	08F	PRL 100 102003	M. Ablikim et al.	(BES Collab.)
AUBERT	08S	PR D77 092002	B. Aubert et al.	(BABAR Collab.)
AUBERT	07AK	PR D76 012008	B. Aubert et al.	(BABAR Collab.)
AUBERT, BE	06D	PR D74 091103R	B. Aubert et al.	(BABAR Collab.)

Meson Particle Listings

 $f_0(2200)$, $f_j(2220)$ $f_0(2200)$

$$I^G(J^{PC}) = 0^+(0^{++})$$

OMITTED FROM SUMMARY TABLE

Seen in $K_S^0 K_S^0$ (AUGUSTIN 88), $K^+ K^-$ (ABLIKIM 05q) and $\eta\eta$ (BINON 05) system. Not seen in $T(1S)$ radiative decays (BARU 89).

 $f_0(2200)$ MASS

VALUE (MeV)	DOCUMENT ID	TECN	COMMENT
2189 ± 13 OUR AVERAGE			
2170 ± 20 ⁺¹⁰ ₋₁₅	ABLIKIM	05q	BES2 $\psi(2S) \rightarrow \gamma\pi^+\pi^-K^+K^-$
2210 ± 50	¹ BINON	05	GAMS 33 $\pi^-p \rightarrow \eta\eta n$
2197 ± 17	² AUGUSTIN	88	DM2 $J/\psi \rightarrow \gamma K_S^0 K_S^0$
• • • We do not use the following data for averages, fits, limits, etc. • • •			
~ 2122	HASAN	94	RVUE $\bar{p}p \rightarrow \pi\pi$
~ 2321	HASAN	94	RVUE $\bar{p}p \rightarrow \pi\pi$
¹ First solution, PWA is ambiguous.			
² Cannot determine spin to be 0.			

 $f_0(2200)$ WIDTH

VALUE (MeV)	DOCUMENT ID	TECN	COMMENT
238 ± 50 OUR AVERAGE			Error includes scale factor of 1.2.
220 ± 60 ⁺⁴⁰ ₋₄₅	ABLIKIM	05q	BES2 $\psi(2S) \rightarrow \gamma\pi^+\pi^-K^+K^-$
380 ± 90	³ BINON	05	GAMS 33 $\pi^-p \rightarrow \eta\eta n$
201 ± 51	⁴ AUGUSTIN	88	DM2 $J/\psi \rightarrow \gamma K_S^0 K_S^0$
• • • We do not use the following data for averages, fits, limits, etc. • • •			
~ 273	HASAN	94	RVUE $\bar{p}p \rightarrow \pi\pi$
~ 223	HASAN	94	RVUE $\bar{p}p \rightarrow \pi\pi$
³ First solution, PWA is ambiguous.			
⁴ Cannot determine spin to be 0.			

 $f_0(2200)$ REFERENCES

ABLIKIM	05q	PR D72 092002	M. Ablikim et al.	(BES Collab.)
BINON	05	PAN 68 960	F. Binon et al.	
HASAN	94	PL B334 215	A. Hasan, D.V. Bugg	(LOQM)
BARU	89	ZPHY C42 505	S.E. Baru et al.	(NOVO)
AUGUSTIN	88	PRL 60 2238	J.E. Augustin et al.	(DM2 Collab.)

 $f_j(2220)$

$$I^G(J^{PC}) = 0^+(2^{++} \text{ or } 4^{++})$$

OMITTED FROM SUMMARY TABLE

Needs confirmation. See our mini-review in the 2004 edition of this Review, PDG 04.

 $f_j(2220)$ MASS

VALUE (MeV)	EVTS	DOCUMENT ID	TECN	COMMENT
2231.1 ± 3.5 OUR AVERAGE				
2235 ± 4 ± 6	74	BAI	96B	BES $e^+e^- \rightarrow J/\psi \rightarrow \gamma\pi^+\pi^-$
2230 ± 6 ± 7	±16 46	BAI	96B	BES $e^+e^- \rightarrow J/\psi \rightarrow \gamma K^+K^-$
2232 ± 8 ± 7	±15 23	BAI	96B	BES $e^+e^- \rightarrow J/\psi \rightarrow \gamma K_S^0 K_S^0$
2235 ± 4 ± 5	32	BAI	96B	BES $e^+e^- \rightarrow J/\psi \rightarrow \gamma p\bar{p}$
2209 ± 17 ± 15	±10	ASTON	88F	LASS 11 $K^-p \rightarrow K^+K^-A$
2230 ± 20		BOLONKIN	88	SPEC 40 $\pi^-p \rightarrow K_S^0 K_S^0 n$
2220 ± 10	41	¹ ALDE	86B	GA24 38-100 $\pi p \rightarrow n\eta\eta'$
2230 ± 6 ± 14	93	BALTRUSAIT...86D	MRK3	$e^+e^- \rightarrow \gamma K^+K^-$
2232 ± 7 ± 7	23	BALTRUSAIT...86D	MRK3	$e^+e^- \rightarrow \gamma K_S^0 K_S^0$
• • • We do not use the following data for averages, fits, limits, etc. • • •				
2223.9 ± 2.5		² VLADIMIRSK...08	SPEC	40 $\pi^-p \rightarrow K_S^0 K_S^0 n + m\pi^0$
2246 ± 36		BAI	98H	BES $J/\psi \rightarrow \gamma\pi^0\pi^0$
¹ ALDE 86B uses data from both the GAMS-2000 and GAMS-4000 detectors.				
² $J^{PC} = 2^{++}$. Systematic uncertainties not evaluated				

 $f_j(2220)$ WIDTH

VALUE (MeV)	CL%	EVTS	DOCUMENT ID	TECN	COMMENT
23 ± 9 OUR AVERAGE					
19 ± 13 ± 11	±12	74	BAI	96B	BES $e^+e^- \rightarrow J/\psi \rightarrow \gamma\pi^+\pi^-$
20 ± 20 ± 15	±17	46	BAI	96B	BES $e^+e^- \rightarrow J/\psi \rightarrow \gamma K^+K^-$
20 ± 25 ± 16	±14	23	BAI	96B	BES $e^+e^- \rightarrow J/\psi \rightarrow \gamma K_S^0 K_S^0$

15 ± 12 ± 9	32	BAI	96B	BES $e^+e^- \rightarrow J/\psi \rightarrow \gamma p\bar{p}$
60 ± 107 ± 57		ASTON	88F	LASS 11 $K^-p \rightarrow K^+K^-A$
80 ± 30		BOLONKIN	88	SPEC 40 $\pi^-p \rightarrow K_S^0 K_S^0 n$
26 ± 20 ± 16 ± 17	93	BALTRUSAIT...86D	MRK3	$e^+e^- \rightarrow \gamma K^+K^-$
18 ± 23 ± 15 ± 10	23	BALTRUSAIT...86D	MRK3	$e^+e^- \rightarrow \gamma K_S^0 K_S^0$
• • • We do not use the following data for averages, fits, limits, etc. • • •				
8.6 ± 2.5		³ VLADIMIRSK...08	SPEC	40 $\pi^-p \rightarrow K_S^0 K_S^0 n + m\pi^0$
< 80	90	ALDE	87C	GAM2 38 $\pi^-p \rightarrow \eta' \eta n$
³ $J^{PC} = 2^{++}$. Systematic uncertainties not evaluated				

 $f_j(2220)$ DECAY MODES

Mode	Fraction (Γ_i/Γ)
Γ_1 $\pi\pi$	seen
Γ_2 $\pi^+\pi^-$	seen
Γ_3 $K\bar{K}$	seen
Γ_4 $p\bar{p}$	
Γ_5 $\gamma\gamma$	not seen
Γ_6 $\eta\eta'$ (958)	seen
Γ_7 $\phi\phi$	not seen
Γ_8 $\eta\eta$	not seen

 $f_j(2220)$ $\Gamma(i)\Gamma(\gamma\gamma)/\Gamma(\text{total})$

VALUE (eV)	CL%	DOCUMENT ID	TECN	COMMENT	$\Gamma_3\Gamma_5/\Gamma$
< 1.4	95	⁴ ACCIARRI	01H	L3 $\gamma\gamma \rightarrow K_S^0 K_S^0, E_{cm}^{90} = 91, 183-209$ GeV	
• • • We do not use the following data for averages, fits, limits, etc. • • •					
< 5.6	95	⁴ GODANG	97	CLE2 $\gamma\gamma \rightarrow K_S^0 K_S^0$	
< 86	95	⁴ ALBRECHT	90G	ARG $\gamma\gamma \rightarrow K^+K^-$	
< 1000	95	⁵ ALTHOFF	85B	TASS $\gamma\gamma, K\bar{K}\pi$	

 $\Gamma(\pi\pi) \times \Gamma(\gamma\gamma)/\Gamma(\text{total})$

VALUE (eV)	CL%	DOCUMENT ID	TECN	COMMENT	$\Gamma_1\Gamma_5/\Gamma$
< 2.5	95	ALAM	98c	CLE2 $\gamma\gamma \rightarrow \pi^+\pi^-$	
⁴ Assuming $J^P = 2^+$.					
⁵ True for $J^P = 0^+$ and $J^P = 2^+$.					

 $f_j(2220)$ $\Gamma(i)\Gamma(p\bar{p})/\Gamma^2(\text{total})$

VALUE (units 10 ⁻⁵)	CL%	DOCUMENT ID	TECN	COMMENT	$\Gamma_4/\Gamma \times \Gamma_1/\Gamma$
< 18	95	⁶ AMSLER	01	CBAR 1.4-1.5 $p\bar{p} \rightarrow \pi^0\pi^0$	
• • • We do not use the following data for averages, fits, limits, etc. • • •					
< (11-42)	99	⁷ HASAN	96	SPEC 1.35-1.55 $p\bar{p} \rightarrow \pi^+\pi^-$	

 $\Gamma(p\bar{p})/\Gamma(\text{total}) \times \Gamma(\phi\phi)/\Gamma(\text{total})$

VALUE (units 10 ⁻⁵)	CL%	DOCUMENT ID	TECN	COMMENT	$\Gamma_4/\Gamma \times \Gamma_7/\Gamma$
< 6	95	⁸ EVANGELIS...	98	SPEC 1.1-2.0 $p\bar{p} \rightarrow \phi\phi$	

 $\Gamma(p\bar{p})/\Gamma(\text{total}) \times \Gamma(\eta\eta)/\Gamma(\text{total})$

VALUE (units 10 ⁻⁵)	CL%	DOCUMENT ID	TECN	COMMENT	$\Gamma_4/\Gamma \times \Gamma_8/\Gamma$
< 4	95	⁶ AMSLER	01	CBAR 1.4-1.5 $p\bar{p} \rightarrow \eta\eta$	

⁶ For $J^P = 2^+$ in the mass range 2222-2240 MeV and the total width between 10 and 20 MeV.

⁷ For $J^P = 2^+$ and $J^P = 4^+$ in the mass range 2220-2245 MeV and the total width of 15 MeV.

⁸ For $J^P = 2^+$, the mass of 2235 MeV and the total width of 15 MeV.

 $f_j(2220)$ BRANCHING RATIOS

VALUE (units 10 ⁻⁴)	CL%	DOCUMENT ID	TECN	COMMENT	Γ_4/Γ
not seen		⁹ AUBERT	07AV	BABR $B \rightarrow p\bar{p}K^*$	
not seen		WANG	05A	BELL $B^+ \rightarrow \bar{p}p K^+$	
< 3.0	95	¹⁰ EVANGELIS...	97	SPEC 1.96-2.40 $p\bar{p} \rightarrow K_S^0 K_S^0$	
< 1.1	99.7	¹¹ BARNES	93	SPEC 1.3-1.57 $p\bar{p} \rightarrow K_S^0 K_S^0$	
< 2.6	99.7	¹¹ BARDIN	87	CNTR 1.3-1.5 $p\bar{p} \rightarrow K^+K^-$	
< 3.6	99.7	¹¹ SCULLI	87	CNTR 1.29-1.55 $p\bar{p} \rightarrow K^+K^-$	
⁹ Assuming $\Gamma < 30$ MeV.					
¹⁰ Assuming $\Gamma \sim 20$ MeV, $J^P = 2^+$ and $B(f_j(2220) \rightarrow K\bar{K}) = 100\%$.					
¹¹ Assuming $\Gamma = 30-35$ MeV, $J^P = 2^+$ and $B(f_j(2220) \rightarrow K\bar{K}) = 100\%$.					

See key on page 405

Meson Particle Listings

 $f_J(2220), \eta(2225), \rho_3(2250)$ $\Gamma(\pi\pi)/\Gamma(K\bar{K})$

VALUE	DOCUMENT ID	TECN	COMMENT	Γ_1/Γ_3
1.0 ± 0.5	BAI	96B	BES $e^+e^- \rightarrow J/\psi \rightarrow \gamma 2\pi, K\bar{K}$	

 $\Gamma(\rho\bar{\rho})/\Gamma(K\bar{K})$

VALUE	DOCUMENT ID	TECN	COMMENT	Γ_4/Γ_3
0.17 ± 0.09	BAI	96B	BES $e^+e^- \rightarrow J/\psi \rightarrow \gamma \rho\bar{\rho}, K\bar{K}$	

 $f_J(2220)$ REFERENCES

VLADIMIRSK...	08	PAN 71 2129	V.V. Vladimirov et al.	(ITEP)
AUBERT	07AV	PR D76 092004	B. Aubert et al.	(BABAR Collab.)
WANG	05A	PL B617 141	M.-Z. Wang et al.	(BELLE Collab.)
PDG	04	PL B592 1	S. Eidelman et al.	(PDG Collab.)
ACCIARRI	01H	PL B501 173	M. Acciarri et al.	(L3 Collab.)
AMSLER	01	PL B520 175	C. Amstler et al.	(Crystal Barrel Collab.)
ALAM	98C	PRL 81 3328	M.S. Alam et al.	(CLEO Collab.)
BAI	98H	PRL 81 1179	J.Z. Bai et al.	(BES Collab.)
EVANGELIS...	98	PR D57 5370	C. Evangelista et al.	(JETSET Collab.)
EVANGELIS...	97	PR D56 3803	C. Evangelista et al.	(LEAR Collab.)
GODANG	97	PRL 79 3829	R. Godang et al.	(CLEO Collab.)
BAI	96B	PRL 76 3502	J.Z. Bai et al.	(BES Collab.)
HASAN	96	PL B388 376	A. Hasan, D.V. Bugg	(BRUN, LOQM)
BARNES	93	PL B309 469	P.D. Barnes et al.	(PS185 Collab.)
ALBRECHT	90G	ZPHY C48 183	H. Albrecht et al.	(ARGUS Collab.)
ASTON	88F	PL B215 199	D. Aston et al.	(SLAC, NAGO, CIN, INUS, JP)
BOLONKIN	88	NP B309 426	B.V. Bolonkin et al.	(ITEP, SERP)
ALDE	87C	SJNP 45 255	D. Alde et al.	
BARDIN	87	PL B195 292	G. Bardin et al.	(SACL, FERR, CERN, PADO+)
SCULLI	87	PRL 58 1715	J. Sculli et al.	(NYU, BNL)
ALDE	86B	PL B177 120	D.M. Alde et al.	(SERP, BELG, LANL, LAPP)
BALTRUSAITIS...	86D	PRL 56 107	R.M. Baltrusaitis	(CIT, UCSC, ILL, SLAC+)
ALTHOFF	85B	ZPHY C29 189	M. Althoff et al.	(TASSO Collab.)

 $\eta(2225)$

$$I^G(J^{PC}) = 0^+(0^-)$$

OMITTED FROM SUMMARY TABLE

Seen in $J/\psi \rightarrow \gamma \phi \phi$. $\eta(2225)$ MASS

VALUE (MeV)	EVTS	DOCUMENT ID	TECN	COMMENT
2226 ± 16	OUR AVERAGE			
2240 ± 30	196 ± 19	ABLIKIM	08i	BES $J/\psi \rightarrow \gamma K^+ K^- K_S^0 K_L^0$
2230 ± 25	± 15	BAI	90b	MRK3 $J/\psi \rightarrow \gamma K^+ K^- K^+ K^-$
2214 ± 20	± 13	BAI	90b	MRK3 $J/\psi \rightarrow \gamma K^+ K^- K_S^0 K_L^0$
~ 2220		BISELLO	86b	DM2 $J/\psi \rightarrow \gamma K^+ K^- K^+ K^-$

 $\eta(2225)$ WIDTH

VALUE (MeV)	EVTS	DOCUMENT ID	TECN	COMMENT
185 ± 70	OUR AVERAGE			
190 ± 30	196 ± 19	ABLIKIM	08i	BES $J/\psi \rightarrow \gamma K^+ K^- K_S^0 K_L^0$
150 ± 300	± 60	BAI	90b	MRK3 $J/\psi \rightarrow \gamma K^+ K^- K^+ K^-$
~ 80		BISELLO	86b	DM2 $J/\psi \rightarrow \gamma K^+ K^- K^+ K^-$

 $\eta(2225)$ REFERENCES

ABLIKIM	08i	PL B662 330	M. Ablikim et al.	(BES Collab.)
BAI	90b	PRL 65 1309	Z. Bai et al.	(Mark III Collab.)
BISELLO	86b	PL B179 294	D. Bisello et al.	(DM2 Collab.)

 $\rho_3(2250)$

$$I^G(J^{PC}) = 1^+(3^-)$$

OMITTED FROM SUMMARY TABLE

Contains results mostly from formation experiments. For further production experiments see the Further States entry. See also $\rho(2150)$, $f_2(2150)$, $f_4(2300)$, $\rho_5(2350)$. $\rho_3(2250)$ MASS $\bar{p}p \rightarrow \pi\pi$ or $K\bar{K}$

VALUE (MeV)	DOCUMENT ID	TECN	CHG	COMMENT
~ 2232	HASAN	94	RVUE	$\bar{p}p \rightarrow \pi\pi$
~ 2090	1 OAKDEN	94	RVUE	$0.36-1.55 \bar{p}p \rightarrow \pi\pi$
~ 2250	2 MARTIN	80b	RVUE	
~ 2300	2 MARTIN	80c	RVUE	
~ 2140	3 CARTER	78b	CNTR	0 $0.7-2.4 \bar{p}p \rightarrow K^- K^+$
~ 2150	4 CARTER	77	CNTR	0 $0.7-2.4 \bar{p}p \rightarrow \pi\pi$

1 See however KLOET 96 who fit $\pi^+ \pi^-$ only and find waves only up to $J = 3$ to be important but not significantly resonant.

2 $I(J^P) = 1(3^-)$ from simultaneous analysis of $\bar{p}p \rightarrow \pi^- \pi^+$ and $\pi^0 \pi^0$.

3 $I = 0, 1. J^P = 3^-$ from Barrelet-zero analysis.

4 $I(J^P) = 1(3^-)$ from amplitude analysis.

S-CHANNEL $\bar{N}N$

VALUE (MeV)	DOCUMENT ID	TECN	CHG	COMMENT
2260 ± 20	5 ANISOVICH	02	SPEC	$0.6-1.9 \rho\bar{p} \rightarrow \omega \pi^0, \omega \eta \pi^0,$ $\pi^+ \pi^-$
~ 2190	6 CUTTS	78b	CNTR	$0.97-3 \bar{p}p \rightarrow \bar{N}N$
2155 ± 15	6,7 COUPLAND	77	CNTR	0 $0.7-2.4 \bar{p}p \rightarrow \bar{p}p$
2193 ± 2	6,8 ALSPECTOR	73	CNTR	$\bar{p}p$ S channel
2190 ± 10	9 ABRAMS	70	CNTR	S channel $\bar{p}N$

5 From the combined analysis of ANISOVICH 00j, ANISOVICH 01D, ANISOVICH 01E, and ANISOVICH 02.

6 Isospins 0 and 1 not separated.

7 From a fit to the total elastic cross section.

8 Referred to as T or T region by ALSPECTOR 73.

9 Seen as bump in $I = 1$ state. See also COOPER 68. PEASLEE 75 confirm $\bar{p}p$ results of ABRAMS 70, no narrow structure.

 $\pi^- p \rightarrow \eta \pi \pi$

VALUE (MeV)	DOCUMENT ID	TECN	COMMENT
$2290 \pm 20 \pm 30$	AMELIN	00	VES $37 \pi^- p \rightarrow \eta \pi^+ \pi^- n$

 $\rho_3(2250)$ WIDTH $\bar{p}p \rightarrow \pi\pi$ or $K\bar{K}$

VALUE (MeV)	DOCUMENT ID	TECN	CHG	COMMENT
~ 220	HASAN	94	RVUE	$\bar{p}p \rightarrow \pi\pi$
~ 60	10 OAKDEN	94	RVUE	$0.36-1.55 \bar{p}p \rightarrow \pi\pi$
~ 250	11 MARTIN	80b	RVUE	
~ 200	11 MARTIN	80c	RVUE	
~ 150	12 CARTER	78b	CNTR	0 $0.7-2.4 \bar{p}p \rightarrow K^- K^+$
~ 200	13 CARTER	77	CNTR	0 $0.7-2.4 \bar{p}p \rightarrow \pi\pi$

10 See however KLOET 96 who fit $\pi^+ \pi^-$ only and find waves only up to $J = 3$ to be important but not significantly resonant.

11 $I(J^P) = 1(3^-)$ from simultaneous analysis of $\bar{p}p \rightarrow \pi^- \pi^+$ and $\pi^0 \pi^0$.

12 $I = 0, 1. J^P = 3^-$ from Barrelet-zero analysis.

13 $I(J^P) = 1(3^-)$ from amplitude analysis.

S-CHANNEL $\bar{N}N$

VALUE (MeV)	DOCUMENT ID	TECN	CHG	COMMENT
160 ± 25	14 ANISOVICH	02	SPEC	$0.6-1.9 \rho\bar{p} \rightarrow \omega \pi^0, \omega \eta \pi^0,$ $\pi^+ \pi^-$
135 ± 75	15,16 COUPLAND	77	CNTR	0 $0.7-2.4 \bar{p}p \rightarrow \bar{p}p$
98 ± 8	16 ALSPECTOR	73	CNTR	$\bar{p}p$ S channel
~ 85	17 ABRAMS	70	CNTR	S channel $\bar{p}N$

14 From the combined analysis of ANISOVICH 00j, ANISOVICH 01D, ANISOVICH 01E, and ANISOVICH 02.

15 From a fit to the total elastic cross section.

16 Isospins 0 and 1 not separated.

17 Seen as bump in $I = 1$ state. See also COOPER 68. PEASLEE 75 confirm $\bar{p}p$ results of ABRAMS 70, no narrow structure.

Meson Particle Listings

$\rho_3(2250)$, $f_2(2300)$, $f_4(2300)$

$\pi^- p \rightarrow \eta \pi \pi$

VALUE (MeV)	DOCUMENT ID	TECN	COMMENT
230±50±80	AMELIN	00	VES 37 $\pi^- p \rightarrow \eta \pi^+ \pi^- n$

$\rho_3(2250)$ REFERENCES

ANISOVICH 02	PL B542 8	A.V. Anisovich et al.	
ANISOVICH 01D	PL B508 6	A.V. Anisovich et al.	
ANISOVICH 01E	PL B513 281	A.V. Anisovich et al.	
AMELIN 00	NP A668 83	D. Amelin et al.	(VES Collab.)
ANISOVICH 00J	PL B491 47	A.V. Anisovich et al.	
KLOET 96	PR D53 6120	W.M. Kloet, F. Myhrer	(RUTG, NORD)
HASAN 94	PL B334 215	A. Hasan, D.V. Bugg	(LOQM)
OAKDEN 94	NP A574 731	M.V. Oakden, M.R. Pennington	(DURH)
MARTIN 80B	NP B176 355	B.R. Martin, D. Morgan	(LOUC, RHEL) JP
MARTIN 80C	NP B169 216	A.D. Martin, M.R. Pennington	(DURH) JP
CARTER 78B	NP B141 467	A.A. Carter	(LOQM)
CUTTS 78B	PR D17 16	D. Cutts et al.	(STON, WIS C)
CARTER 77	PL 67B 117	A.A. Carter et al.	(LOQM, RHEL) JP
COUPLAND 77	PL 71B 460	M. Coupland et al.	(LOQM, RHEL)
PEASLEE 75	PL 57B 189	D.C. Peaslee et al.	(CANB, BARI, BROW+)
ALSPECTOR 73	PRL 30 511	J. Alspector et al.	(RUTG, UPNJ)
ABRAMS 70	PR D1 1917	R.J. Abrams et al.	(BNL)
COOPER 68	PRL 20 1059	W.A. Cooper et al.	(ANL)

$f_2(2300)$

$$I^G(J^{PC}) = 0^+(2^{++})$$

$f_2(2300)$ MASS

VALUE (MeV)	DOCUMENT ID	TECN	COMMENT
2297±28	¹ ETKIN 88	MPS	22 $\pi^- p \rightarrow \phi \phi n$
2270±12	VLADIMIRSK...06	SPEC	40 $\pi^- p \rightarrow K_S^0 K_S^0 n$
2327±9±6	ABE 04	BELL	10.6 $e^+ e^- \rightarrow e^+ e^- K^+ K^-$
2240±15	ANISOVICH 00J	SPEC	$p \bar{p} \rightarrow \pi^0 \pi^0 \eta$
2231±10	BOOTH 86	OMEG	85 $\pi^- Be \rightarrow 2\phi Be$
2220 ⁺⁹⁰ ₋₂₀	LINDENBAUM 84	RVUE	
2320±40	ETKIN 82	MPS	22 $\pi^- p \rightarrow 2\phi n$

¹Includes data of ETKIN 85. The percentage of the resonance going into $\phi \phi 2^+ + S_2$, D_2 , and D_0 is 6^{+15}_{-5} , 25^{+18}_{-14} , and 69^{+16}_{-27} , respectively.

$f_2(2300)$ WIDTH

VALUE (MeV)	DOCUMENT ID	TECN	COMMENT
149±41	² ETKIN 88	MPS	22 $\pi^- p \rightarrow \phi \phi n$
90±29	VLADIMIRSK...06	SPEC	40 $\pi^- p \rightarrow K_S^0 K_S^0 n$
275±36±20	ABE 04	BELL	10.6 $e^+ e^- \rightarrow e^+ e^- K^+ K^-$
241±30	ANISOVICH 00J	SPEC	$p \bar{p} \rightarrow \pi^0 \pi^0 \eta$
133±5.0	BOOTH 86	OMEG	85 $\pi^- Be \rightarrow 2\phi Be$
200±5.0	LINDENBAUM 84	RVUE	
220±7.0	ETKIN 82	MPS	22 $\pi^- p \rightarrow 2\phi n$

²Includes data of ETKIN 85.

$f_2(2300)$ DECAY MODES

Mode	Fraction (Γ_i/Γ)
Γ_1 $\phi \phi$	seen
Γ_2 $K \bar{K}$	seen
Γ_3 $\gamma \gamma$	seen

$f_2(2300)$ $\Gamma(i)\Gamma(\gamma\gamma)/\Gamma(\text{total})$

$\Gamma(K \bar{K}) \times \Gamma(\gamma\gamma)/\Gamma_{\text{total}}$	DOCUMENT ID	TECN	COMMENT	$\Gamma_2/\Gamma_3/\Gamma$
44±6±12	³ ABE 04	BELL	10.6 $e^+ e^- \rightarrow e^+ e^- K^+ K^-$	

³Assuming spin 2.

$f_2(2300)$ REFERENCES

VLADIMIRSK... 06	PAN 69 493	V.V. Vladimisky et al.	(ITEP, Moscow)
	Translated from YAF 69 515		
ABE 04	EPJ C32 323	K. Abe et al.	(BELLE Collab.)
ANISOVICH 00J	PL B491 47	A.V. Anisovich et al.	
ETKIN 88	PL B201 568	A. Etkin et al.	(BNL, CUNY)
BOOTH 86	NP B273 677	P.S.L. Booth et al.	(LIVP, GLAS, CERN)
ETKIN 85	PL 165B 217	A. Etkin et al.	(BNL, CUNY)
LINDENBAUM 84	CNPP 13 285	S.J. Lindenbaum	(CUNY)
ETKIN 82	PRL 49 1620	A. Etkin et al.	(BNL, CUNY)

$f_4(2300)$

$$I^G(J^{PC}) = 0^+(4^{++})$$

OMITTED FROM SUMMARY TABLE

This entry was previously called $U_0(2350)$. Contains results mostly from formation experiments. For further production experiments see the Further States entry. See also $\rho(2150)$, $f_2(2150)$, $\rho_3(2250)$, $\rho_5(2350)$.

$f_4(2300)$ MASS

$\bar{p} p \rightarrow \pi \pi$ or $\bar{K} K$

VALUE (MeV)	DOCUMENT ID	TECN	COMMENT
~2314	HASAN 94	RVUE	$\bar{p} p \rightarrow \pi \pi$
~2300	¹ MARTIN 80B	RVUE	
~2300	¹ MARTIN 80C	RVUE	
~2340	² CARTER 78B	CNTR	0.7-2.4 $\bar{p} p \rightarrow K^- K^+$
~2330	DULUDE 78B	OSP K	1-2 $\bar{p} p \rightarrow \pi^0 \pi^0$
~2310	³ CARTER 77	CNTR	0.7-2.4 $\bar{p} p \rightarrow \pi \pi$

¹ $I(J^P) = 0(4^+)$ from simultaneous analysis of $p \bar{p} \rightarrow \pi^- \pi^+$ and $\pi^0 \pi^0$.
² $I(J^P) = 0(4^+)$ from Barrelet-zero analysis.
³ $I(J^P) = 0(4^+)$ from amplitude analysis.

S-CHANNEL $\bar{p} p$ or $\bar{N} N$

VALUE (MeV)	DOCUMENT ID	TECN	COMMENT
2283±17	⁴ ANISOVICH 00J	SPEC	
~2380	⁵ CUTTS 78B	CNTR	0.97-3 $\bar{p} p \rightarrow \bar{N} N$
2345±15	^{5,6} COUPLAND 77	CNTR	0.7-2.4 $\bar{p} p \rightarrow \bar{p} p$
2359±2	^{5,7} ALSPECTOR 73	CNTR	$\bar{p} p$ S channel
2375±10	ABRAMS 70	CNTR	S channel $\bar{N} N$

⁴From the combined analysis of ANISOVICH 99c and ANISOVICH 99f on $\bar{p} p \rightarrow \eta \pi^0 \pi^0$, $\pi^0 \pi^0$, $\eta \eta$, $\eta \eta'$, $\pi^+ \pi^-$.
⁵Isospins 0 and 1 not separated.
⁶From a fit to the total elastic cross section.
⁷Referred to as U or U region by ALSPECTOR 73.

$\pi^- p \rightarrow \eta \pi \pi n$

VALUE (MeV)	DOCUMENT ID	TECN	COMMENT
2330±20±40	AMELIN 00	VES	37 $\pi^- p \rightarrow \eta \pi^+ \pi^- n$

$p \bar{p}$ CENTRAL PRODUCTION

VALUE (MeV)	DOCUMENT ID	COMMENT
2320±60 OUR ESTIMATE		
2332±15	BARBERIS 00F	450 $p \bar{p} \rightarrow p f \omega \omega p_S$

$f_4(2300)$ WIDTH

$\bar{p} p \rightarrow \pi \pi$ or $\bar{K} K$

VALUE (MeV)	DOCUMENT ID	TECN	COMMENT
~278	HASAN 94	RVUE	$\bar{p} p \rightarrow \pi \pi$
~200	⁸ MARTIN 80C	RVUE	
~150	⁹ CARTER 78B	CNTR	0.7-2.4 $\bar{p} p \rightarrow K^- K^+$
~210	¹⁰ CARTER 77	CNTR	0.7-2.4 $\bar{p} p \rightarrow \pi \pi$

⁸ $I(J^P) = 0(4^+)$ from simultaneous analysis of $p \bar{p} \rightarrow \pi^- \pi^+$ and $\pi^0 \pi^0$.
⁹ $I(J^P) = 0(4^+)$ from Barrelet-zero analysis.
¹⁰ $I(J^P) = 0(4^+)$ from amplitude analysis.

S-CHANNEL $\bar{p} p$ or $\bar{N} N$

VALUE (MeV)	DOCUMENT ID	TECN	COMMENT
310±25	¹¹ ANISOVICH 00J	SPEC	
135 ⁺¹⁵⁰ ₋₆₅	^{12,13} COUPLAND 77	CNTR	0.7-2.4 $\bar{p} p \rightarrow \bar{p} p$
165 ⁺¹⁸ ₋₈	¹³ ALSPECTOR 73	CNTR	$\bar{p} p$ S channel
~190	ABRAMS 70	CNTR	S channel $\bar{N} N$

¹¹From the combined analysis of ANISOVICH 99c and ANISOVICH 99f on $\bar{p} p \rightarrow \eta \pi^0 \pi^0$, $\pi^0 \pi^0$, $\eta \eta$, $\eta \eta'$, $\pi^+ \pi^-$.
¹²From a fit to the total elastic cross section.
¹³Isospins 0 and 1 not separated.

$\pi^- p \rightarrow \eta \pi \pi n$

VALUE (MeV)	DOCUMENT ID	TECN	COMMENT
235±50±40	AMELIN 00	VES	37 $\pi^- p \rightarrow \eta \pi^+ \pi^- n$

See key on page 405

Meson Particle Listings
f4(2300), f0(2330), f2(2340), rho5(2350)

pp CENTRAL PRODUCTION

Table with columns: VALUE (MeV), DOCUMENT ID, COMMENT. Row: 250±80 OUR ESTIMATE

• • • We do not use the following data for averages, fits, limits, etc. • • •
260±57 BARBERIS 00F 450 pp -> p_f omega p_S

f4(2300) DECAY MODES

Table with columns: Mode, Fraction (Gamma_i/Gamma). Rows: Gamma_1 rho rho, Gamma_2 omega omega, Gamma_3 eta pi pi, Gamma_4 pi pi, Gamma_5 K K-bar, Gamma_6 N N-bar

f4(2300) BRANCHING RATIOS

Table with columns: Gamma(rho rho)/Gamma(omega omega), Gamma_1/Gamma_2, VALUE, DOCUMENT ID, COMMENT. Row: 2.8±0.5 BARBERIS 00F 450 pp -> p_f omega p_S

f4(2300) REFERENCES

Table with columns: Author, Year, Document ID, Journal, Comment. Includes AMELIN 00 NP A668 83, ANISOVICH 00J PL B491 47, etc.

f0(2330)

J^G(J^PC) = 0^+(0^{++})

OMITTED FROM SUMMARY TABLE

f0(2330) MASS

Table with columns: VALUE (MeV), DOCUMENT ID, TECN, COMMENT. Rows: 2314±25, 2337±14, ~2321

f0(2330) WIDTH

Table with columns: VALUE (MeV), DOCUMENT ID, TECN, COMMENT. Rows: 144±20, 217±33, ~223

f0(2330) REFERENCES

Table with columns: Author, Year, Document ID, Journal, Comment. Includes BUGG 04A EPJ C36 161, ANISOVICH 00J PL B491 47, etc.

f2(2340)

J^G(J^PC) = 0^+(2^{++})

f2(2340) MASS

Table with columns: VALUE (MeV), EVTS, DOCUMENT ID, TECN, COMMENT. Rows: 2339±55, 2350±7, 2392±10, 2360±20

• • • We do not use the following data for averages, fits, limits, etc. • • •
1 Includes data of ETKIN 85. The percentage of the resonance going into phi phi 2^{++} S_2, D_2, and D_0 is 37±19, 4±12, and 59±21, respectively.
2 Statistical error only.

f2(2340) WIDTH

Table with columns: VALUE (MeV), EVTS, DOCUMENT ID, TECN, COMMENT. Rows: 319±81/69, 218±16, 198±50, 150±150

3 Includes data of ETKIN 85.
4 Statistical error only.

f2(2340) DECAY MODES

Table with columns: Mode, Fraction (Gamma_i/Gamma). Rows: Gamma_1 phi phi, Gamma_2 eta eta

f2(2340) BRANCHING RATIOS

Table with columns: Gamma(eta eta)/Gamma_total, DOCUMENT ID, TECN, COMMENT. Row: seens UMAN 06 E835 5.2 p-bar p -> eta eta pi^0

f2(2340) REFERENCES

Table with columns: Author, Year, Document ID, Journal, Comment. Includes UMAN 06 PR D73 052009, ETKIN 88 PL B201 568, etc.

rho5(2350)

J^G(J^PC) = 1^+(5^{--})

OMITTED FROM SUMMARY TABLE

This entry was previously called U_1(2400). See also rho(2150), f_2(2150), rho_3(2250), f_4(2300).

rho5(2350) MASS

Table with columns: VALUE (MeV), DOCUMENT ID, TECN, COMMENT. Row: 2330±35 ALDE 95 GAM2 38 pi^- p -> omega pi^0 n

Table with columns: VALUE (MeV), DOCUMENT ID, TECN, CHG, COMMENT. Rows: ~2303, ~2300, ~2250, ~2500, ~2480

S-CHANNEL N N-bar

Table with columns: VALUE (MeV), DOCUMENT ID, TECN, CHG, COMMENT. Rows: 2300±45, ~2380, 2345±15, 2359±2, 2350±10, 2360±25

Meson Particle Listings

$\rho_5(2350)$, $a_6(2450)$, $f_6(2510)$

$\pi^- p \rightarrow K^+ K^- n$

VALUE (MeV)	DOCUMENT ID	TECN	CHG	COMMENT
• • • We do not use the following data for averages, fits, limits, etc. • • •				
2307 ± 6	ALPER	80	CNTR	0 62 $\pi^- p \rightarrow K^+ K^- n$

- 1 $I(J^P) = 1(5^-)$ from simultaneous analysis of $p\bar{p} \rightarrow \pi^- \pi^+$ and $\pi^0 \pi^0$.
- 2 $I = 0(1)$; $J^P = 5^-$ from Barrelet-zero analysis.
- 3 $I(J^P) = 1(5^-)$ from amplitude analysis.
- 4 From the combined analysis of ANISOVICH 00J, ANISOVICH 01D, ANISOVICH 01E, and ANISOVICH 02.
- 5 Isospins 0 and 1 not separated.
- 6 From a fit to the total elastic cross section.
- 7 Referred to as U or U region by ALSPECTOR 73.
- 8 For $l = 1 \overline{N}N$.
- 9 No evidence for this bump seen in the $\bar{p}p$ data of CHAPMAN 71B. Narrow state not confirmed by OH 73 with more data.

$\rho_5(2350)$ WIDTH

$\pi^- p \rightarrow \omega \pi^0 n$

VALUE (MeV)	DOCUMENT ID	TECN	COMMENT
400 ± 100	ALDE	95	GAM2 38 $\pi^- p \rightarrow \omega \pi^0 n$

$\bar{p} p \rightarrow \pi \pi$ or $\overline{K} K$

VALUE (MeV)	DOCUMENT ID	TECN	CHG	COMMENT
• • • We do not use the following data for averages, fits, limits, etc. • • •				
~ 169	HASAN	94	RVUE	$\bar{p} p \rightarrow \pi \pi$
~ 250	10 MARTIN	80B	RVUE	
~ 300	10 MARTIN	80C	RVUE	
~ 150	11 CARTER	78B	CNTR	0 0.7-2.4 $\bar{p} p \rightarrow K^- K^+$
~ 210	12 CARTER	77	CNTR	0 0.7-2.4 $\bar{p} p \rightarrow \pi \pi$

S-CHANNEL $\overline{N} N$

VALUE (MeV)	DOCUMENT ID	TECN	CHG	COMMENT
• • • We do not use the following data for averages, fits, limits, etc. • • •				
260 ± 75	13 ANISOVICH	02	SPEC	0.6-1.9 $p\bar{p} \rightarrow \omega \pi^0, \omega \eta \pi^0, \pi^+ \pi^-$
235 ± 65 40	ANISOVICH	00J	SPEC	
135 ± 150 65	14,15 COUPLAND	77	CNTR	0 0.7-2.4 $\bar{p} p \rightarrow \bar{p} p$
165 ± 18 8	15 ALSPECTOR	73	CNTR	$\bar{p} p$ S channel
< 60	16 OH	70B	HDBC	-0 $\bar{p}(pn), K^* K 2\pi$
~ 140	ABRAMS	67C	CNTR	S channel $\bar{p} N$

$\pi^- p \rightarrow K^+ K^- n$

VALUE (MeV)	DOCUMENT ID	TECN	CHG	COMMENT
• • • We do not use the following data for averages, fits, limits, etc. • • •				
245 ± 20	ALPER	80	CNTR	0 62 $\pi^- p \rightarrow K^+ K^- n$

- 10 $I(J^P) = 1(5^-)$ from simultaneous analysis of $p\bar{p} \rightarrow \pi^- \pi^+$ and $\pi^0 \pi^0$.
- 11 $I = 0(1)$; $J^P = 5^-$ from Barrelet-zero analysis.
- 12 $I(J^P) = 1(5^-)$ from amplitude analysis.
- 13 From the combined analysis of ANISOVICH 00J, ANISOVICH 01D, ANISOVICH 01E, and ANISOVICH 02.
- 14 From a fit to the total elastic cross section.
- 15 Isospins 0 and 1 not separated.
- 16 No evidence for this bump seen in the $\bar{p}p$ data of CHAPMAN 71B. Narrow state not confirmed by OH 73 with more data.

$\rho_5(2350)$ REFERENCES

ANISOVICH 02	PL B542 8	A.V. Anisovich et al.
ANISOVICH 01D	PL B508 6	A.V. Anisovich et al.
ANISOVICH 01E	PL B513 281	A.V. Anisovich et al.
ANISOVICH 00J	PL B491 47	A.V. Anisovich et al.
ALDE 95	ZPHY C66 379	D.M. Alde et al. (GAMS Collab.) JP
HASAN 94	PL B334 215	A. Hasan, D.V. Bugg (LOQM)
ALPER 80	PL 94B 422	B. Alper et al. (AMST, CERN, CRAC, MPIM+)
MARTIN 80B	NP B176 355	B.R. Martin, D. Morgan (LOUC, RHEL) JP
MARTIN 80C	NP B169 216	A.D. Martin, M.R. Pennington (DURH) JP
CARTER 78B	NP B141 467	A.A. Carter (LOQM)
CUTTS 78B	PR D17 116	D. Cutts et al. (STON, WIS C)
CARTER 77	PL 67B 117	A.A. Carter et al. (LOQM, RHEL) JP
COUPLAND 77	PL 71B 460	M. Coupland et al. (LOQM, RHEL)
ALSPECTOR 73	PRL 30 511	J. Alspector et al. (RUTG, UPNJ)
OH 73	NP B51 57	B.Y. Oh et al. (MSU)
CHAPMAN 71B	PR D4 1275	J.W. Chapman et al. (MICH)
ABRAMS 70	PR D1 1917	R.J. Abrams et al. (BNL)
OH 70B	PRL 24 1257	B.Y. Oh et al. (MSU)
ABRAMS 67C	PRL 18 1209	R.J. Abrams et al. (BNL)

$a_6(2450)$

$$I^G(J^{PC}) = 1^-(6^{++})$$

OMITTED FROM SUMMARY TABLE
Needs confirmation.

$a_6(2450)$ MASS

VALUE (MeV)	DOCUMENT ID	TECN	CHG	COMMENT
2450 ± 130	1 CLELAND	82B	SPEC	± 50 $\pi p \rightarrow K_S^0 K^\pm p$

¹ From an amplitude analysis.

$a_6(2450)$ WIDTH

VALUE (MeV)	DOCUMENT ID	TECN	CHG	COMMENT
400 ± 250	2 CLELAND	82B	SPEC	± 50 $\pi p \rightarrow K_S^0 K^\pm p$

² From an amplitude analysis.

$a_6(2450)$ DECAY MODES

Mode	Fraction (Γ_i/Γ)
$\Gamma_1 K \overline{K}$	(6.0 ± 1.0) %

$a_6(2450)$ REFERENCES

CLELAND 82B NP B208 228 W.E. Cleland et al. (DURH, GEVA, LAUS+)

$f_6(2510)$

$$I^G(J^{PC}) = 0^+(6^{++})$$

OMITTED FROM SUMMARY TABLE
Needs confirmation.

$f_6(2510)$ MASS

VALUE (MeV)	DOCUMENT ID	TECN	COMMENT
2465 ± 50 OUR AVERAGE	Error includes scale factor of 2.1.		
2420 ± 30	ALDE	98	GAM4 100 $\pi^- p \rightarrow \pi^0 \pi^0 n$
2510 ± 30	BINON	84B	GAM2 38 $\pi^- p \rightarrow n 2\pi^0$

$f_6(2510)$ WIDTH

VALUE (MeV)	DOCUMENT ID	TECN	COMMENT
255 ± 40 OUR AVERAGE			
270 ± 60	ALDE	98	GAM4 100 $\pi^- p \rightarrow \pi^0 \pi^0 n$
240 ± 60	BINON	84B	GAM2 38 $\pi^- p \rightarrow n 2\pi^0$

$f_6(2510)$ DECAY MODES

Mode	Fraction (Γ_i/Γ)
$\Gamma_1 \pi \pi$	(6.0 ± 1.0) %

$f_6(2510)$ BRANCHING RATIOS

$\Gamma(\pi \pi)/\Gamma_{total}$	DOCUMENT ID	TECN	COMMENT	Γ_1/Γ
0.06 ± 0.01	1 BINON	83C	GAM2 38 $\pi^- p \rightarrow n 4\gamma$	

¹ Assuming one pion exchange and using data of BOLOTOV 74.

$f_6(2510)$ REFERENCES

ALDE 98	EPI A3 361	D. Alde et al. (GAM4 Collab.)
Also	PAN 62 405	D. Alde et al. (GAMS Collab.)
BINON 84B	LNC 39 41	F.G. Binon et al. (SERP, BELG, LAPP) JP
BINON 83C	SJNP 38 723	F.G. Binon et al. (SERP, BRUX+) JP
BOLOTOV 74	PL 52B 489	V.N. Bolotov et al. (SERP)

See key on page 405

Meson Particle Listings
Further States

$B(f_2\eta)/B(a_2\pi)_{L=2}$					
VALUE		DOCUMENT ID	TECN		
0.074±0.026		²⁸ ANISOVICH	00E	SPEC	
²⁸ Corrected for all decay modes.					

$f_3(2050) \quad I^G(J^{PC}) = 0^+(3^{++})$					
MASS (MeV)	WIDTH (MeV)	DOCUMENT ID	TECN	COMMENT	
2048±8	213±34	ANISOVICH	00J	SPEC	2.0 $p\bar{p} \rightarrow \eta\pi^0\pi^0$

$f_0(2060) \quad I^G(J^{PC}) = 0^+(0^{++})$					
MASS (MeV)	WIDTH (MeV)	DOCUMENT ID	TECN	COMMENT	
~2050	~120	²⁹ OAKDEN	94	RVUE	0.36-1.55 $\bar{p}p \rightarrow \pi\pi$
~2060	~50	²⁹ OAKDEN	94	RVUE	0.36-1.55 $\bar{p}p \rightarrow \pi\pi$
²⁹ See SEMENOV 99 and KLOET 96.					

$\pi(2070) \quad I^G(J^{PC}) = 1^-(0^{-+})$					
MASS (MeV)	WIDTH (MeV)	DOCUMENT ID	TECN	COMMENT	
2070±35	310 ⁺¹⁰⁰ ₋₅₀	ANISOVICH	01F	SPEC	2.0 $\bar{p}p \rightarrow 3\pi^0, \pi^0\eta, \pi^0\eta'$

$X(2075) \quad I^G(J^{PC}) = ?^?(?^{??})$					
MASS (MeV)	WIDTH (MeV)	DOCUMENT ID	TECN	COMMENT	
2075±12±5	90±35±9	³⁰ ABLIKIM	04J	BES2	$J/\psi \rightarrow K^-p\bar{\Lambda}$
³⁰ From a fit in the region $M_{p\bar{\Lambda}} - M_p - M_{\Lambda} < 150$ MeV. S-wave in the $p\bar{\Lambda}$ system preferred.					

$X(2080) \quad I^G(J^{PC}) = ?^?(?^{??})$					
MASS (MeV)	WIDTH (MeV)	DOCUMENT ID	TECN	COMMENT	
2080±10	110±20	KREYMER	80	STRC	13 $\pi^-d \rightarrow p\bar{p}n(n_S)$

$X(2080) \quad I^G(J^{PC}) = ?^?(3^{-?})$					
MASS (MeV)	WIDTH (MeV)	DOCUMENT ID	TECN	COMMENT	
2080±10	190±15	ROZANSKA	80	SPRK	18 $\pi^-p \rightarrow p\bar{p}n$

$a_1(2095) \quad I^G(J^{PC}) = 1^-(1^{++})$					
MASS (MeV)	WIDTH (MeV)	EVS	DOCUMENT ID	TECN	COMMENT
2096±17±121	451±41±81	69k	KUHN	04	B852 18 $\pi^-p \rightarrow \eta\pi^+\pi^-\pi^-p$

$B(a_1(2095) \rightarrow f_1(1285)\pi) / B(a_1(2095) \rightarrow a_1(1260))$					
VALUE	EVS	DOCUMENT ID	TECN	COMMENT	
3.18±0.64	69k	KUHN	04	B852	18 $\pi^-p \rightarrow \eta\pi^+\pi^-\pi^-p$

$\eta(2100) \quad I^G(J^{PC}) = 0^+(0^{-+})$					
MASS (MeV)	WIDTH (MeV)	EVS	DOCUMENT ID	TECN	COMMENT
2103±50	187±75	586	³¹ BISELLO	89B	DM2 $J/\psi \rightarrow 4\pi\gamma$
³¹ ASTON 81B sees no peak, has 850 events in Ajinenko+Barth bins. ARESTOV 80 sees no peak.					

$X(2100) \quad I^G(J^{PC}) = ?^?(0^{??})$					
MASS (MeV)	WIDTH (MeV)	DOCUMENT ID	TECN	COMMENT	
2100±40	250±40	ALDE	86D	GAM4	100 $\pi^-p \rightarrow 2\eta X$

$X(2110) \quad I^G(J^{PC}) = 1^+(3^{-?})$					
MASS (MeV)	WIDTH (MeV)	DOCUMENT ID	TECN	COMMENT	
2110±10	330±20	EVANGELIS...	79	OMEG	10,16 $\pi^-p \rightarrow \bar{p}pn$

$f_2(2140) \quad I^G(J^{PC}) = 0^+(2^{++})$					
MASS (MeV)	WIDTH (MeV)	EVS	DOCUMENT ID	TECN	COMMENT
2141±12	49±28	389	GREEN	86	MPSF 400 $pA \rightarrow 4KX$

$X(2150) \quad I^G(J^{PC}) = ?^?(2^{+?})$					
MASS (MeV)	WIDTH (MeV)	DOCUMENT ID	TECN	COMMENT	
2150±10	260±10	ROZANSKA	80	SPRK	18 $\pi^-p \rightarrow p\bar{p}n$

$a_2(2175) \quad I^G(J^{PC}) = 1^-(2^{++})$					
MASS (MeV)	WIDTH (MeV)	DOCUMENT ID	TECN	COMMENT	
2175±40	310 ⁺⁹⁰ ₋₄₅	ANISOVICH	01F	SPEC	2.0 $\bar{p}p \rightarrow 3\pi^0, \pi^0\eta, \pi^0\eta'$

$\eta(2190) \quad I^G(J^{PC}) = 0^+(0^{-+})$					
MASS (MeV)	WIDTH (MeV)	DOCUMENT ID	TECN	COMMENT	
2190±50	850±100	BUGG	99	BES	

$\omega_2(2195) \quad I^G(J^{PC}) = 0^-(2^{-+-})$					
MASS (MeV)	WIDTH (MeV)	DOCUMENT ID	TECN	COMMENT	
2195±30	225±40	³² ANISOVICH	02B	SPEC	0.6-1.9 $p\bar{p} \rightarrow \omega\eta, \omega\pi^0\pi^0$
³² From the combined analysis of ANISOVICH 00D, ANISOVICH 01C, and ANISOVICH 02B.					

$\omega(2205) \quad I^G(J^{PC}) = 0^-(1^{-+-})$					
MASS (MeV)	WIDTH (MeV)	DOCUMENT ID	TECN	COMMENT	
2205±30	350±90	³³ ANISOVICH	02B	SPEC	0.6-1.9 $p\bar{p} \rightarrow \omega\eta, \omega\pi^0\pi^0$
³³ From the combined analysis of ANISOVICH 00D, ANISOVICH 01C, and ANISOVICH 02B.					

$X(2210) \quad I^G(J^{PC}) = ?^?(?^{??})$					
MASS (MeV)	WIDTH (MeV)	DOCUMENT ID	TECN	COMMENT	
2210 ⁺⁷⁹ ₋₂₁	203 ⁺⁴³⁷ ₋₈₇	EVANGELIS...	79B	OMEG	10 $\pi^-p \rightarrow K^+K^-n$

$X(2210) \quad I^G(J^{PC}) = ?^?(?^{??})$					
MASS (MeV)	WIDTH (MeV)	DOCUMENT ID	TECN	COMMENT	
2207±22	130	CASO	70	HBC	11.2 π^-p

$h_1(2215) \quad I^G(J^{PC}) = 0^-(1^{+-})$					
MASS (MeV)	WIDTH (MeV)	DOCUMENT ID	TECN	COMMENT	
2215±40	325±55	³⁴ ANISOVICH	02B	SPEC	0.6-1.9 $p\bar{p} \rightarrow \omega\eta, \omega\pi^0\pi^0$
³⁴ From the combined analysis of ANISOVICH 00D, ANISOVICH 01C, and ANISOVICH 02B.					

$\rho_2(2225) \quad I^G(J^{PC}) = 1^+(2^{-+-})$					
MASS (MeV)	WIDTH (MeV)	DOCUMENT ID	TECN	COMMENT	
2225±35	335 ⁺¹⁰⁰ ₋₅₀	³⁵ ANISOVICH	02	SPEC	0.6-1.9 $p\bar{p} \rightarrow \omega\pi^0, \omega\eta\pi^0, \pi^+\pi^-$
³⁵ From the combined analysis of ANISOVICH 00J, ANISOVICH 01D, ANISOVICH 01E, and ANISOVICH 02.					

$\rho_4(2230) \quad I^G(J^{PC}) = 1^+(4^{-+-})$					
MASS (MeV)	WIDTH (MeV)	DOCUMENT ID	TECN	COMMENT	
2230±25	210±30	³⁶ ANISOVICH	02	SPEC	0.6-1.9 $p\bar{p} \rightarrow \omega\pi^0, \omega\eta\pi^0, \pi^+\pi^-$

³⁶ From the combined analysis of ANISOVICH 00J, ANISOVICH 01D, ANISOVICH 01E, and ANISOVICH 02.

$b_1(2240) \quad I^G(J^{PC}) = 1^+(1^{+-})$					
MASS (MeV)	WIDTH (MeV)	DOCUMENT ID	TECN	COMMENT	
2240±35	320±85	³⁷ ANISOVICH	02	SPEC	0.6-1.9 $p\bar{p} \rightarrow \omega\pi^0, \omega\eta\pi^0, \pi^+\pi^-$

³⁷ From the combined analysis of ANISOVICH 00J, ANISOVICH 01D, ANISOVICH 01E, and ANISOVICH 02.

$\pi_2(2245) \quad I^G(J^{PC}) = 1^-(2^{-+-})$					
MASS (MeV)	WIDTH (MeV)	DOCUMENT ID	TECN	COMMENT	
2245±60	320 ⁺¹⁰⁰ ₋₄₀	ANISOVICH	01F	SPEC	2.0 $\bar{p}p \rightarrow 3\pi^0, \pi^0\eta, \pi^0\eta'$

$b_3(2245) \quad I^G(J^{PC}) = 1^+(3^{+-})$					
MASS (MeV)	WIDTH (MeV)	DOCUMENT ID	TECN	COMMENT	
2245±50	320±70	³⁸ BUGG	04C	RVUE	

³⁸ From the combined analysis of ANISOVICH 00J, ANISOVICH 01D, ANISOVICH 01E, and ANISOVICH 02.

$\eta_2(2250) \quad I^G(J^{PC}) = 0^+(2^{-+-})$					
MASS (MeV)	WIDTH (MeV)	DOCUMENT ID	TECN	COMMENT	
2248±20	280±20	A NISOVICH	00I	SPEC	
2267±14	290±50	A NISOVICH	00J	SPEC	

$\pi_4(2250) \quad I^G(J^{PC}) = 1^-(4^{-+-})$					
MASS (MeV)	WIDTH (MeV)	DOCUMENT ID	TECN	COMMENT	
2250±15	215±25	ANISOVICH	01F	SPEC	2.0 $\bar{p}p \rightarrow 3\pi^0, \pi^0\eta, \pi^0\eta'$

$\omega_4(2250) \quad I^G(J^{PC}) = 0^-(4^{-+-})$					
MASS (MeV)	WIDTH (MeV)	DOCUMENT ID	TECN	COMMENT	
2250±30	150±50	³⁹ ANISOVICH	02B	SPEC	0.6-1.9 $p\bar{p} \rightarrow \omega\eta, \omega\pi^0\pi^0$

Meson Particle Listings

Further States

See key on page 405

X(3250) $I^G(J^{PC}) = ?^?(?^{??})$ 4-Body Decays					
MASS (MeV)	WIDTH (MeV)	DOCUMENT ID	TECN	COMMENT	
$3245 \pm 8 \pm 20$	25 ± 11	ALEEV	93 BIS2	$X(3250) \rightarrow \Lambda \bar{p} K^+ \pi^\pm$	
$3250 \pm 9 \pm 20$	50 ± 20	ALEEV	93 BIS2	$X(3250) \rightarrow \Lambda \bar{p} K^- \pi^\mp$	
$3270 \pm 8 \pm 20$	25 ± 11	ALEEV	93 BIS2	$X(3250) \rightarrow K_S^0 \rho \bar{p} K^\pm$	

X(3350) $I^G(J^{PC}) = ?^?(?^{??})$					
MASS (MeV)	WIDTH (MeV)	EVS	DOCUMENT ID	TECN	COMMENT
$3350^{+10}_{-20} \pm 20$	$70^{+40}_{-30} \pm 40$	50 ± 10	GABYSHEV	06A BELL	$B^- \rightarrow \Lambda_c^+ \bar{p} \pi^-$

REFERENCES for Further States

ABRAAMYAN	09	PR C80 034001	Kh.U. Abraamyan et al.		
VLADIMIRSK...	08	PAN 71 2129	V.V. Vladimirsky et al.	(ITEP)	
		Translated from YAF 71 2166.			
VLADIMIRSK...	07	PAN 70 1706	V. Vladimirsky et al.		
		Translated from YAF 70 1751.			
YASUI	07	PR D76 034009	S. Yasui, M. Oka		
ABLIKIM	06S	PRL 97 142002	M. Ablikim et al.	(BES Collab.)	
GABYSHEV	06A	PRL 97 242001	N. Gabyshev et al.	(BELLE Collab.)	
SCHEGELSKY	06	EPJ A27 199	V.A. Schegelsky et al.		
SCHEGELSKY	06A	EPJ A27 207	V.A. Schegelsky et al.		
UMAN	06	PR D73 052009	I. Uman et al.	(FNAL E835)	
VLADIMIRSK...	06	PAN 69 493	V.V. Vladimirsky et al.	(ITEP, Moscow)	
		Translated from YAF 69 515.			
BINON	05	PAN 68 960	F. Binon et al.		
		Translated from YAF 68 998.			
GRIGOR'EV	05	PAN 68 1271	V.K. Grigor'ev et al.	(ITEP)	
		Translated from YAF 68 1324.			
LU	05	PRL 94 032002	M. Lu et al.	(BNL E852 Collab.)	
ABLIKIM	04J	PRL 93 112002	M. Ablikim et al.	(BES Collab.)	
BUGG	04	PL B595 556 (erratum)	D.V. Bugg		
BUGG	04A	EPJ C36 161	D.V. Bugg		
BUGG	04C	PRPL 397 257	D.V. Bugg		
EVDOKIMOV	04	PRL 93 242001	A.V. Evdokimov et al.	(SELEX Collab.)	
KUHN	04	PL B595 109	J. Kuhn et al.	(BNL E852 Collab.)	
ANISOVICH	03	EPJ A16 229	V.V. Anisovich et al.		
VLADIMIRSK...	03	PAN 66 700	V.V. Vladimirsky et al.		
		Translated from YAF 66 729.			
ANISOVICH	02	PL B542 8	A.V. Anisovich et al.		
ANISOVICH	02B	PL B542 19	A.V. Anisovich et al.		
CHUNG	02	PR D65 072001	S.U. Chung et al.	(BNL E852 Collab.)	
LINK	02K	PL B545 50	J.M. Link et al.	(FNAL FOCUS Collab.)	
ANISOVICH	01C	PL B507 23	A.V. Anisovich et al.		

ANISOVICH	01D	PL B508 6	A.V. Anisovich et al.		
ANISOVICH	01E	PL B513 281	A.V. Anisovich et al.		
ANISOVICH	01F	PL B517 261	A.V. Anisovich et al.		
ANISOVICH	01G	PL B517 273	A.V. Anisovich et al.		
ANISOVICH	00D	PL B476 15	A.V. Anisovich et al.		
ANISOVICH	00E	PL B477 19	A.V. Anisovich et al.		
ANISOVICH	00I	PL B491 40	A.V. Anisovich et al.		
ANISOVICH	00J	PL B491 47	A.V. Anisovich et al.		
ANISOVICH	00M	PL B496 145	A.V. Anisovich et al.		
BARNES	00	PR C62 055203	P.D. Barnes et al.		
FILIPPI	00	PL B495 284	A. Filippi et al.	(OBELIX Experiment)	
VLADIMIRSKII	00	JETPL 72 486	V.V. Vladimirskii et al.		
		Translated from ZETFP 72 698.			
ANISOVICH	99C	PL B452 173	A.V. Anisovich et al.		
ANISOVICH	99E	PL B452 187	A.V. Anisovich et al.		
BUGG	99	PL B458 511	D.V. Bugg et al.		
FERRER	99	EPJ C10 249	A. Ferrer et al.		
SEMEVNOV	99	SFU 42 847	S.V. Semenov		
		Translated from UFN 42 937.			
KLOET	96	PR D53 6120	W.M. Kloet, F. Myhrer	(RUTG, NORD)	
PROKOSHNIK	96	SPD 41 247	Y.D. Prokoshnik, V.D. Samoilenko	(SERP)	
		Translated from DANS 348 481.			
HASAN	94	PL B334 215	A. Hasan, D.V. Bugg	(LOQM)	
OAKDEN	94	NP A574 731	M.N. Oakden, M.R. Pennington	(DURH)	
ALEEV	93	PAN 56 1358	A.N. Aleev et al.	(BIS-2 Collab.)	
		Translated from YAF 56 100.			
ARMSTRONG	93D	PL B307 399	T.A. Armstrong et al.	(FNAL, FERR, GENO+)	
ALBRECHT	91F	ZPHY C50 1	H. Albrecht et al.	(ARGUS Collab.)	
CONDO	91	PR D43 2787	G.T. Condo et al.	(SLAC Hybrid Collab.)	
BISELLO	89B	PR D39 701	G. Busetto et al.	(DM2 Collab.)	
ATKINSON	88	ZPHY C38 535	M. Atkinson et al.	(BONN, CERN, GLAS+)	
DAFTARI	87	PRL 58 859	I.K. Daftari et al.	(SYRA)	
ALDE	86D	NP B269 485	D.M. Alde et al.	(BELG, LAPP, SERP, CERN+)	
BRIDGES	86D	PL B180 313	D.L. Bridges et al.	(SYRA, BNL, CASE+)	
GREEN	86	PRL 56 1639	D.R. Green et al.	(FNAL, ARIZ, FSU+)	
ATKINSON	85	ZPHY C29 333	M. Atkinson et al.	(BONN, CERN, GLAS+)	
DENNEY	83	PR D28 2726	D.L. Denney et al.	(IOWA, MICH)	
ASTON	81B	NP B189 205	D. Aston et al.	(BONN, CERN, EPOL, GLAS+)	
ARESTOV	80	IHEP 80-165	Y.I. Arestov et al.	(SERP)	
CHLIAPNIK...	80	ZPHY C3 285	P.V. Chliapnikov et al.	(SERP, BRUX, MONS)	
KREYMER	80	PR D22 36	A.E. Kreymer et al.	(IND, PURD, SLAC+)	
ROZANSKA	80	NP B162 505	M. Rozanska et al.	(MPIM, CERN)	
EVANGELIS...	79	NP B153 253	C. Evangelista et al.	(BARI, BONN, CERN+)	
EVANGELIS...	79B	NP B154 381	C. Evangelista et al.	(BARI, BONN, CERN+)	
BALTAY	78	PR D17 52	C. Baltay et al.	(COLU, BING)	
ANTIPOV	77	NP B119 45	Y.M. Antipov et al.	(SERP, GEVA)	
BALTAY	77	PRL 39 591	C. Baltay, C.V. Cautis, M. Kateikar	(COLU)	
BALTAY	75	PRL 35 891	C. Baltay et al.	(COLU, BING)	
KALELKAR	75	Thesis Nevis 207	M.S. Kalelkar	(COLU)	
CASO	70	LCN 3 707	C. Caso et al.	(GENO, HAMB, MILA, SAEL)	

Meson Particle Listings

 K^\pm

STRANGE MESONS
($S = \pm 1, C = B = 0$)

$K^+ = u\bar{s}, K^0 = d\bar{s}, \bar{K}^0 = \bar{d}s, K^- = \bar{u}s,$ similarly for K^{*} 's

 K^\pm $I(J^P) = \frac{1}{2}(0^-)$ **THE CHARGED KAON MASS**

Revised 1994 by T.G. Trippe (LBNL).

The average of the six charged kaon mass measurements which we use in the Particle Listings is

$$m_{K^\pm} = 493.677 \pm 0.013 \text{ MeV } (S = 2.4), \quad (1)$$

where the error has been increased by the scale factor S . The large scale factor indicates a serious disagreement between different input data. The average before scaling the error is

$$m_{K^\pm} = 493.677 \pm 0.005 \text{ MeV }, \quad (2)$$

$$\chi^2 = 22.9 \text{ for } 5 \text{ D.F.}, \text{ Prob.} = 0.04\%,$$

where the high χ^2 and correspondingly low χ^2 probability further quantify the disagreement.

The main disagreement is between the two most recent and precise results,

$$m_{K^\pm} = 493.696 \pm 0.007 \text{ MeV} \quad \text{DENISOV 91}$$

$$m_{K^\pm} = 493.636 \pm 0.011 \text{ MeV } (S = 1.5) \quad \text{GALL 88}$$

$$\text{Average} = 493.679 \pm 0.006 \text{ MeV}$$

$$\chi^2 = 21.2 \text{ for } 1 \text{ D.F.}, \text{ Prob.} = 0.0004\%, \quad (3)$$

both of which are measurements of x-ray energies from kaonic atoms. Comparing the average in Eq. (3) with the overall average in Eq. (2), it is clear that DENISOV 91 and GALL 88 dominate the overall average, and that their disagreement is responsible for most of the high χ^2 .

The GALL 88 measurement was made using four different kaonic atom transitions, $K^- \text{Pb } (9 \rightarrow 8)$, $K^- \text{Pb } (11 \rightarrow 10)$, $K^- \text{W } (9 \rightarrow 8)$, and $K^- \text{W } (11 \rightarrow 10)$. The m_{K^\pm} values they obtain from each of these transitions is shown in the Particle Listings and in Fig. 1. Their $K^- \text{Pb } (9 \rightarrow 8)$ m_{K^\pm} is below and somewhat inconsistent with their other three transitions. The average of their four measurements is

$$m_{K^\pm} = 493.636 \pm 0.007, \quad (4)$$

$$\chi^2 = 7.0 \text{ for } 3 \text{ D.F.}, \text{ Prob.} = 7.2\%.$$

This is a low but acceptable χ^2 probability so, to be conservative, GALL 88 scaled up the error on their average by $S=1.5$ to obtain their published error ± 0.011 shown in Eq. (3) above and used in the Particle Listings average.

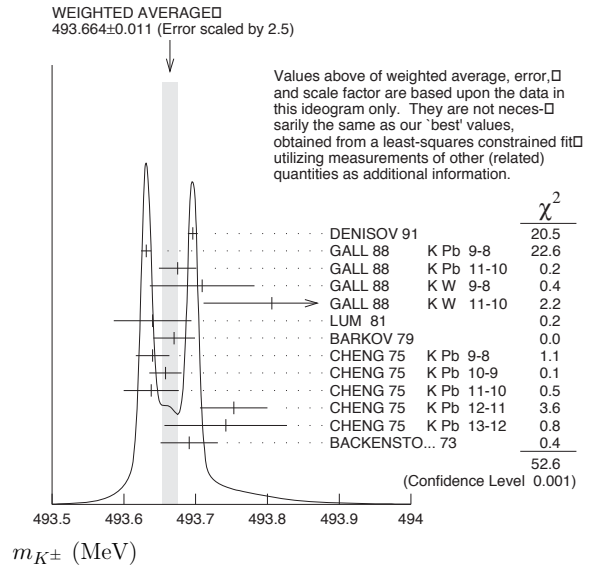


Figure 1: Ideogram of m_{K^\pm} mass measurements. GALL 88 and CHENG 75 measurements are shown separately for each transition they measured.

The ideogram in Fig. 1 shows that the DENISOV 91 measurement and the GALL 88 $K^- \text{Pb } (9 \rightarrow 8)$ measurement yield two well-separated peaks. One might suspect the GALL 88 $K^- \text{Pb } (9 \rightarrow 8)$ measurement since it is responsible both for the internal inconsistency in the GALL 88 measurements and the disagreement with DENISOV 91.

To see if the disagreement could result from a systematic problem with the $K^- \text{Pb } (9 \rightarrow 8)$ transition, we have separated the CHENG 75 data, which also used $K^- \text{Pb}$, into its separate transitions. Figure 1 shows that the CHENG 75 and GALL 88 $K^- \text{Pb } (9 \rightarrow 8)$ values are consistent, suggesting the possibility of a common effect such as contaminant nuclear γ rays near the $K^- \text{Pb } (9 \rightarrow 8)$ transition energy, although the CHENG 75 errors are too large to make a strong conclusion. The average of all 13 measurements has a χ^2 of 52.6 as shown in Fig. 1 and the first line of Table 1, yielding an unacceptable χ^2 probability of 0.00005%. The second line of Table 1 excludes both the GALL 88 and CHENG 75 measurements of the $K^- \text{Pb } (9 \rightarrow 8)$ transition and yields a χ^2 probability of 43%. The third [fourth] line of Table 1 excludes only the GALL 88 $K^- \text{Pb } (9 \rightarrow 8)$ [DENISOV 91] measurement and yields a χ^2 probability of 20% [8.6%]. Table 1 shows that removing both measurements of the $K^- \text{Pb } (9 \rightarrow 8)$ transition produces the most consistent set of data, but that excluding only the GALL 88 $K^- \text{Pb } (9 \rightarrow 8)$ transition or DENISOV 91 also produces acceptable probabilities.

See key on page 405

Table 1: m_{K^\pm} averages for some combinations of Fig. 1 data.

m_{K^\pm} (MeV)	χ^2	D.F.	Prob. (%)	Measurements used
493.664 ± 0.004	52.6	12	0.00005	all 13 measurements
493.690 ± 0.006	10.1	10	43	no K^- Pb(9→8)
493.687 ± 0.006	14.6	11	20	no GALL 88 K^- Pb(9→8)
493.642 ± 0.006	17.8	11	8.6	no DENISOV 91

Yu.M. Ivanov, representing DENISOV 91, has estimated corrections needed for the older experiments because of improved ^{192}Ir and ^{198}Au calibration γ -ray energies. He estimates that CHENG 75 and BACKENSTOSS 73 m_{K^\pm} values could be raised by about 15 keV and 22 keV, respectively. With these estimated corrections, Table 1 becomes Table 2. The last line of Table 2 shows that if such corrections are assumed, then GALL 88 K^- Pb (9 → 8) is inconsistent with the rest of the data even when DENISOV 91 is excluded. Yu.M. Ivanov warns that these are rough estimates. Accordingly, we do not use Table 2 to reject the GALL 88 K^- Pb (9 → 8) transition, but we note that a future reanalysis of the CHENG 75 data could be useful because it might provide supporting evidence for such a rejection.

Table 2: m_{K^\pm} averages for some combinations of Fig. 1 data after raising CHENG 75 and BACKENSTOSS 73 values by 0.015 and 0.022 MeV respectively.

m_{K^\pm} (MeV)	χ^2	D.F.	Prob. (%)	Measurements used
493.666 ± 0.004	53.9	12	0.00003	all 13 measurements
493.693 ± 0.006	9.0	10	53	no K^- Pb(9→8)
493.690 ± 0.006	11.5	11	40	no GALL 88 K^- Pb(9→8)
493.645 ± 0.006	23.0	11	1.8	no DENISOV 91

The GALL 88 measurement uses a Ge semiconductor spectrometer which has a resolution of about 1 keV, so they run the risk of some contaminant nuclear γ rays. Studies of γ rays following stopped π^- and Σ^- absorption in nuclei (unpublished) do not show any evidence for contaminants according to GALL 88 spokesperson, B.L. Roberts. The DENISOV 91 measurement uses a crystal diffraction spectrometer with a resolution of 6.3 eV for radiation at 22.1 keV to measure the 4f-3d transition in K^- ^{12}C . The high resolution and the light nucleus reduce the probability for overlap by contaminant γ rays, compared with the measurement of GALL 88. The DENISOV 91 measurement is supported by their high-precision measurement of the 4d-2p transition energy in π^- ^{12}C , which is good agreement with the calculated energy.

While we suspect that the GALL 88 K^- Pb (9 → 8) measurements could be the problem, we are unable to find clear grounds for rejecting it. Therefore, we retain their measurement in the average and accept the large scale factor until further information can be obtained from new measurements and/or from reanalysis of GALL 88 and CHENG 75 data.

We thank B.L. Roberts (Boston Univ.) and Yu.M. Ivanov (Petersburg Nuclear Physics Inst.) for their extensive help in understanding this problem.

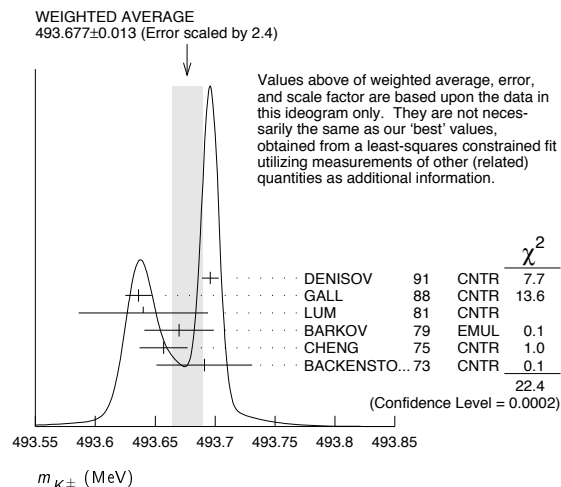
 K^\pm MASS

VALUE (MeV)	DOCUMENT ID	TECN	CHG	COMMENT
493.677 ± 0.016 OUR FIT	Error includes scale factor of 2.8.			
493.677 ± 0.013 OUR AVERAGE	Error includes scale factor of 2.4. See the ideogram below.			
493.696 ± 0.007	¹ DENISOV	91	CNTR	— Kaonic atoms
493.636 ± 0.011	² GALL	88	CNTR	— Kaonic atoms
493.640 ± 0.054	LUM	81	CNTR	— Kaonic atoms
493.670 ± 0.029	BARKOV	79	EMUL	± $e^+ e^- \rightarrow K^+ K^-$
493.657 ± 0.020	² CHENG	75	CNTR	— Kaonic atoms
493.691 ± 0.040	BACKENSTO...73	CNTR	—	Kaonic atoms
• • • We do not use the following data for averages, fits, limits, etc. • • •				
493.631 ± 0.007	GALL	88	CNTR	— K^- Pb (9 → 8)
493.675 ± 0.026	GALL	88	CNTR	— K^- Pb (11 → 10)
493.709 ± 0.073	GALL	88	CNTR	— K^- W (9 → 8)
493.806 ± 0.095	GALL	88	CNTR	— K^- W (11 → 10)
$493.640 \pm 0.022 \pm 0.008$	³ CHENG	75	CNTR	— K^- Pb (9 → 8)
$493.658 \pm 0.019 \pm 0.012$	³ CHENG	75	CNTR	— K^- Pb (10 → 9)
$493.638 \pm 0.035 \pm 0.016$	³ CHENG	75	CNTR	— K^- Pb (11 → 10)
$493.753 \pm 0.042 \pm 0.021$	³ CHENG	75	CNTR	— K^- Pb (12 → 11)
$493.742 \pm 0.081 \pm 0.027$	³ CHENG	75	CNTR	— K^- Pb (13 → 12)

¹ Error increased from 0.0059 based on the error analysis in IVANOV 92.

² This value is the authors' combination of all of the separate transitions listed for this paper.

³ The CHENG 75 values for separate transitions were calculated from their Table 7 transition energies. The first error includes a 20% systematic error in the noncircular contaminant shift. The second error is due to a ± 5 eV uncertainty in the theoretical transition energies.

 **$m_{K^+} - m_{K^-}$**

Test of CPT.

VALUE (MeV)	EVTS	DOCUMENT ID	TECN	CHG
-0.032 ± 0.090	1.5 M	⁴ FORD	72	ASPK ±

⁴ FORD 72 uses $m_{\pi^+} - m_{\pi^-} = +28 \pm 70$ keV.

 K^\pm MEAN LIFE

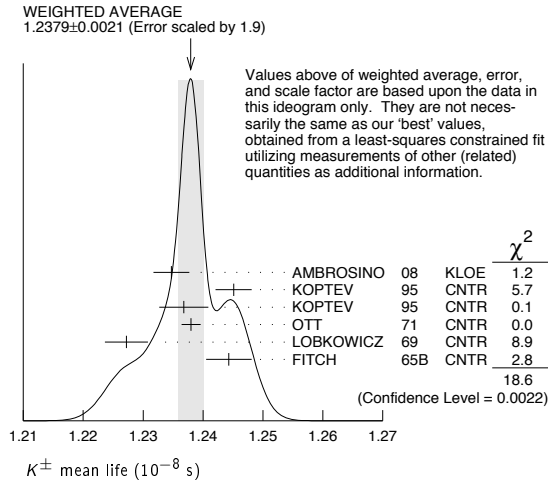
VALUE (10^{-8} s)	EVTS	DOCUMENT ID	TECN	CHG	COMMENT
1.2380 ± 0.0021 OUR FIT	Error includes scale factor of 1.9.				
1.2379 ± 0.0021 OUR AVERAGE	Error includes scale factor of 1.9. See the ideogram below.				
1.2347 ± 0.0030	15M	⁵ AMBROSINO	08	KLOE	± $\phi \rightarrow K^+ K^-$
1.2451 ± 0.0030	250k	KOPTEV	95	CNTR	K at rest, U target
1.2368 ± 0.0041	150k	KOPTEV	95	CNTR	K at rest, Cu target
1.2380 ± 0.0016	3M	OTT	71	CNTR	+ K at rest
1.2272 ± 0.0036		LOBKOWICZ	69	CNTR	+ K in flight
1.2443 ± 0.0038		FITCH	65B	CNTR	+ K at rest
• • • We do not use the following data for averages, fits, limits, etc. • • •					
1.2415 ± 0.0024	400k	⁶ KOPTEV	95	CNTR	K at rest
1.221 ± 0.011		FORD	67	CNTR	±
1.231 ± 0.011		BOYARSKI	62	CNTR	±

Meson Particle Listings

 K^\pm

⁵ Result obtained by averaging the decay length and decay time analyses taking correlations into account.

⁶ KOPTEV 95 report this weighted average of their U-target and Cu-target results, where they have weighted by $1/\sigma$ rather than $1/\sigma^2$.



$$(\tau_{K^+} - \tau_{K^-}) / \tau_{\text{average}}$$

This quantity is a measure of CPT invariance in weak interactions.

VALUE (%)	DOCUMENT ID	TECN
0.10 ± 0.09 OUR AVERAGE	Error includes scale factor of 1.2.	
-0.4 ± 0.4	AMBROSINO 08	KLOE
0.090 ± 0.078	LOBKOWICZ 69	CNTR
0.47 ± 0.30	FORD 67	CNTR

RARE KAON DECAYS

Revised November 2009 by L. Littenberg (BNL) and G. Valencia (Iowa State University).

A. Introduction: There are several useful reviews on rare kaon decays and related topics [1–14]. Activity in rare kaon decays can be divided roughly into four categories:

1. Searches for explicit violations of the Standard Model
2. Measurements of Standard Model parameters
3. Searches for CP violation
4. Studies of strong interactions at low energy.

The paradigm of Category 1 is the lepton flavor violating decay $K_L \rightarrow \mu e$. Category 2 includes processes such as $K^+ \rightarrow \pi^+ \nu \bar{\nu}$, which is sensitive to $|V_{td}|$. Much of the interest in Category 3 is focused on the decays $K_L \rightarrow \pi^0 \ell \bar{\ell}$, where $\ell \equiv e, \mu, \nu$. Category 4 includes reactions like $K^+ \rightarrow \pi^+ \ell^+ \ell^-$ which constitute a testing ground for the ideas of chiral perturbation theory. Category 4 also includes $K_L \rightarrow \pi^0 \gamma \gamma$ and $K_L \rightarrow \ell^+ \ell^- \gamma$. The former is important in understanding a CP -conserving contribution to $K_L \rightarrow \pi^0 \ell^+ \ell^-$, whereas the latter could shed light on long distance contributions to $K_L \rightarrow \mu^+ \mu^-$.

The interplay between Categories 2-4 can be illustrated in Fig. 1. The modes $K \rightarrow \pi \nu \bar{\nu}$ are the cleanest ones theoretically. They can provide accurate determinations of certain CKM parameters (shown in the figure). In combination with alternate determinations of these parameters, they also constrain new interactions. The modes $K_L \rightarrow \pi^0 e^+ e^-$ and $K_L \rightarrow \mu^+ \mu^-$ are also sensitive to CKM parameters. However, they suffer from a series of hadronic uncertainties that can be addressed, at least in part, through a systematic study of the additional modes indicated in the figure.

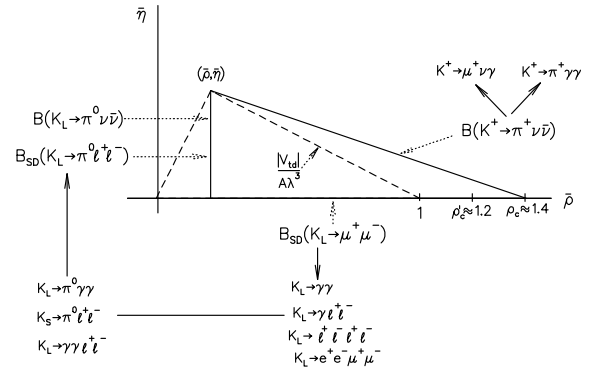


Figure 1: Role of rare kaon decays in determining the unitarity triangle. The solid arrows point to auxiliary modes needed to interpret the main results, or potential backgrounds to them.

B. Explicit violations of the Standard Model: Much activity has focussed on searches for lepton flavor violation (LFV). This is motivated by the fact that many extensions of the minimal Standard Model violate lepton flavor and by the potential to access very high energy scales. For example, the tree-level exchange of a LFV vector boson of mass M_X that couples to left-handed fermions with electroweak strength and without mixing angles yields $B(K_L \rightarrow \mu e) = 4.7 \times 10^{-12} (148 \text{ TeV}/M_X)^4$ [4]. This simple dimensional analysis may be used to read from Table 1 that the reaction $K_L \rightarrow \mu e$ is already probing scales of over 100 TeV. Table 1 summarizes the present experimental situation vis a vis LFV. The decays $K_L \rightarrow \mu^\pm e^\mp$ and $K^+ \rightarrow \pi^+ e^\mp \mu^\pm$ (or $K_L \rightarrow \pi^0 e^\mp \mu^\pm$) provide complementary information on potential family number violating interactions, since the former is sensitive to parity-odd couplings and the latter is sensitive to parity-even couplings. Limits on certain lepton-number violating kaon decays [15,16] also exist. Related searches in μ and τ processes are discussed in our section “Tests of Conservation Laws.”

Table 1: Searches for lepton flavor violation in K decay

Mode	90% CL		
	upper limit	Exp't	Yr./Ref.
$K^+ \rightarrow \pi^+ e^- \mu^+$	1.2×10^{-11}	BNL-865	2005/Ref. 17
$K^+ \rightarrow \pi^+ e^+ \mu^-$	5.2×10^{-10}	BNL-865	2000/Ref. 15
$K_L \rightarrow \mu e$	4.7×10^{-12}	BNL-871	1998/Ref. 18
$K_L \rightarrow \pi^0 e \mu$	7.6×10^{-11}	KTeV	2008/Ref. 19
$K_L \rightarrow \pi^0 \pi^0 e \mu$	1.7×10^{-10}	KTeV	2008/Ref. 19

Physics beyond the SM is also pursued through the search for $K^+ \rightarrow \pi^+ X^0$, where X^0 is a very light, long-lived particle (e.g., hyperphoton, axion, familon, etc.). The 90% CL upper limit on this process is 7.3×10^{-11} [20].

C. Measurements of Standard Model parameters:

In the SM, the decay $K^+ \rightarrow \pi^+ \nu \bar{\nu}$ is dominated by one-loop diagrams with top-quark intermediate states and long-distance contributions are known to be quite small [2,21,22]. This permits a precise calculation [23] of this rate in terms of SM parameters. Studies of this process are thus motivated by the possibility of detecting non-SM physics when comparing with the results of global fits [24,25].

BNL-787 observed two candidate events [26,27] in the clean high π^+ momentum and one event [28] in the low-momentum region. The successor experiment BNL-949 observed one more in the high-momentum region [20] and three more in the low-momentum region [29] yielding a branching ratio of $(1.73_{-1.05}^{+1.15}) \times 10^{-10}$ [30]. A new experiment, NA62, with a sensitivity goal of $\sim 10^{-12}$ /event was proposed [31] at CERN in 2005. It has been approved and is scheduled to run in 2011. In the future, this mode may provide grounds for precision tests of flavor dynamics [32]. The branching ratio can be written in terms of the very well-measured K_{e3} rate as [2]:

$$B(K^+ \rightarrow \pi^+ \nu \bar{\nu}) = \frac{\alpha^2 B(K^+ \rightarrow \pi^0 e^+ \nu)}{V_{us}^2 2\pi^2 \sin^4 \theta_W} \times \sum_{l=e,\mu,\tau} |V_{cs}^* V_{cd} X_{NL}^\ell + V_{ts}^* V_{td} X(m_t)|^2 \quad (1)$$

to eliminate the *a priori* unknown hadronic matrix element. Isospin breaking corrections to the ratio of matrix elements reduce this rate by 10% [33,23]. In Eq. (1), the Inami-Lim function $X(m_t)$ is of order 1 [34], and X_{NL}^ℓ is several hundred times smaller. This form exhibits the strong dependence of this branching ratio on $|V_{td}|$. QCD corrections, which mainly affect X_{NL}^ℓ , lead to a residual error of $< 5\%$ for the decay amplitude [11,22,35,36]. Evaluating the constants in Eq. (1), one can cast this result in terms of the CKM parameters λ , V_{cb} , $\bar{\rho}$ and $\bar{\eta}$ (see our Section on “The Cabibbo-Kobayashi-Maskawa mixing matrix”) [11]:

$$B(K^+ \rightarrow \pi^+ \nu \bar{\nu}) \approx 1.6 \times 10^{-5} |V_{cb}|^4 [\sigma \bar{\eta}^2 + (\rho_c - \bar{\rho})^2], \quad (2)$$

where $\rho_c \equiv 1 + (\frac{2}{3} X_{NL}^e + \frac{1}{3} X_{NL}^\tau) / (|V_{cb}|^2 X(m_t)) \approx 1.4$ and $\sigma \equiv 1 / (1 - \frac{1}{2} \lambda^2)^2$. Thus, $B(K^+ \rightarrow \pi^+ \nu \bar{\nu})$ determines an ellipse in the $\bar{\rho}$, $\bar{\eta}$ plane with center $(\rho_c, 0)$ and semi-axes $\approx \frac{1}{|V_{cb}|^2} \sqrt{\frac{B(K^+ \rightarrow \pi^+ \nu \bar{\nu})}{1.6 \times 10^{-5}}}$ and $\frac{1}{\sigma |V_{cb}|^2} \sqrt{\frac{B(K^+ \rightarrow \pi^+ \nu \bar{\nu})}{1.6 \times 10^{-5}}}$. Current constraints on the CKM parameters lead to a predicted branching ratio $(8.5 \pm 0.7) \times 10^{-11}$ [36], near the lower end of the measurement of BNL-787 and 949.

The decay $K_L \rightarrow \mu^+ \mu^-$ also has a short distance contribution sensitive to the CKM parameter $\bar{\rho}$, given by [11]:

$$B_{SD}(K_L \rightarrow \mu^+ \mu^-) \approx 2.7 \times 10^{-4} |V_{cb}|^4 (\rho'_c - \bar{\rho})^2 \quad (3)$$

where ρ'_c depends on the charm quark mass and is approximately 1.2. This decay, however, is dominated by a long-distance contribution from a two-photon intermediate state. The absorptive (imaginary) part of the long-distance component is determined by the measured rate for $K_L \rightarrow \gamma \gamma$ to be $B_{\text{abs}}(K_L \rightarrow \mu^+ \mu^-) =$

$(6.64 \pm 0.07) \times 10^{-9}$; and it almost completely saturates the observed rate $B(K_L \rightarrow \mu^+ \mu^-) = (6.84 \pm 0.11) \times 10^{-9}$ [37]. The difference between the observed rate and the absorptive component can be attributed to the (coherent) sum of the short-distance amplitude and the real part of the long-distance amplitude. The latter cannot be derived directly from experiment [38], but can be estimated with certain assumptions [39,40]. The decay $K_L \rightarrow e^+ e^-$ is completely dominated by long distance physics and is easier to estimate. The result, $B(K_L \rightarrow e^+ e^-) \sim 9 \times 10^{-12}$ [38,41], is in good agreement with the BNL-871 measurement, $(8.7_{-4.1}^{+5.7}) \times 10^{-12}$ [42].

D. Searches for direct CP violation: The mode $K_L \rightarrow \pi^0 \nu \bar{\nu}$ is dominantly *CP*-violating and free of hadronic uncertainties [2,43,44]. In the Standard Model, this mode is dominated by an intermediate top-quark state and does not suffer from the small uncertainty associated with the charm-quark intermediate state that affects the mode $K^+ \rightarrow \pi^+ \nu \bar{\nu}$. The branching ratio is given approximately by Ref. 11:

$$B(K_L \rightarrow \pi^0 \nu \bar{\nu}) \approx 7.6 \times 10^{-5} |V_{cb}|^4 \bar{\eta}^2. \quad (4)$$

With current constraints on the CKM parameters this leads to a predicted branching ratio $(2.6 \pm 0.3) \times 10^{-11}$ [14]. The 90% CL bound on $K^+ \rightarrow \pi^+ \nu \bar{\nu}$ provides a nearly model-independent bound $B(K_L \rightarrow \pi^0 \nu \bar{\nu}) < 1.46 \times 10^{-9}$ [45]. KEK-391a, which began data-taking in early 2004, has published a result of $B(K_L \rightarrow \pi^0 \nu \bar{\nu}) \leq 6.7 \times 10^{-8}$ [46] based on partial data. Very recently a preliminary result on the remainder of the data yielded $B(K_L \rightarrow \pi^0 \nu \bar{\nu}) \leq 6.8 \times 10^{-8}$ [47]. The KOTO experiment, whose initial goal is to reach the 10^{-11} /event level, is under construction at J-PARC [48].

There has been much theoretical work on possible contributions to rare *K* decays beyond the SM. A comprehensive discussion of these can be found in Refs. [14] and [49].

The decay $K_L \rightarrow \pi^0 e^+ e^-$ also has sensitivity to the CKM parameter η through its *CP*-violating component. There are both direct and indirect *CP*-violating amplitudes which can interfere. The direct *CP*-violating amplitude is short distance dominated and has been calculated in detail within the SM [8]. The indirect *CP*-violating amplitude can be inferred from a measurement of $K_S \rightarrow \pi^0 e^+ e^-$. The complete *CP*-violating contribution to the rate can be written as [50]:

$$B_{\text{CPV}} \approx 10^{-12} \left[15.7 |a_S|^2 \pm 1.45 \left(\frac{|V_{cb}|^2 \bar{\eta}}{10^{-4}} \right) |a_S| + 0.129 \left(\frac{|V_{cb}|^2 \bar{\eta}}{10^{-4}} \right)^2 \right] \quad (5)$$

where the three terms correspond to the indirect *CP* violation, the interference, and the direct *CP* violation respectively. The parameter a_S has been extracted by NA48 from a measurement of the decay $K_S \rightarrow \pi^0 e^+ e^-$ with the result $|a_S| = 1.06_{-0.21}^{+0.26} \pm 0.07$ [51]. With current constraints on the CKM parameters this implies that

$$B_{\text{CPV}} \approx (17.2 \pm 9.4 + 4.7) \times 10^{-12}. \quad (6)$$

Meson Particle Listings

K^\pm

The indirect CP violation is larger than the direct CP violation. While the sign of the interference is *a priori* unknown, arguments in favor of a positive sign have been put forward in Ref. 52 and Ref. 53. NA48 has also obtained the value $a_s = 1.54^{+0.40}_{-0.32} \pm 0.06$ [54] from a measurement of the $K_S \rightarrow \pi^0 \mu^+ \mu^-$ rate, in agreement with the value extracted from $K_S \rightarrow \pi^0 e^+ e^-$

$K_L \rightarrow \pi^0 \gamma \gamma$ also has a CP -conserving component dominated by a two-photon intermediate state. This component can be decomposed into an absorptive and a dispersive part. The absorptive part can be extracted from the measurement of the low $m_{\gamma\gamma}$ region of the $K_L \rightarrow \pi^0 \gamma \gamma$ spectrum. The rate and the shape of the distribution $d\Gamma/dm_{\gamma\gamma}$ in $K_L \rightarrow \pi^0 \gamma \gamma$ are well described in chiral perturbation theory in terms of three (*a priori*) unknown parameters [55,56].

Both KTeV and NA48 have studied the mode $K_L \rightarrow \pi^0 \gamma \gamma$, reporting similar results. KTeV finds $B(K_L \rightarrow \pi^0 \gamma \gamma) = (1.29 \pm 0.03_{\text{stat}} \pm 0.05_{\text{sys}}) \times 10^{-6}$ [57], while NA48 finds $B(K_L \rightarrow \pi^0 \gamma \gamma) = (1.36 \pm 0.03_{\text{stat}} \pm 0.03_{\text{sys}} \pm 0.03_{\text{norm}}) \times 10^{-6}$ [58]. Both experiments are consistent with a negligible rate in the low $m_{\gamma\gamma}$ region, suggesting a very small CP -conserving component $B_{\text{CP}}(K_L \rightarrow \pi^0 e^+ e^-) \sim \mathcal{O}(10^{-13})$ [52,56,58]. There remains some model dependence in the estimate of the dispersive part of the CP -conserving $K_L \rightarrow \pi^0 e^+ e^-$ [52].

The related process, $K_L \rightarrow \pi^0 \gamma e^+ e^-$, is potentially an additional background in some region of phase space [59]. This process has been observed with a branching ratio of $(1.62 \pm 0.14_{\text{stat}} \pm 0.09_{\text{sys}}) \times 10^{-8}$ [60].

The decay $K_L \rightarrow \gamma \gamma e^+ e^-$ constitutes the dominant background to $K_L \rightarrow \pi^0 e^+ e^-$. It was first observed by BNL-845 [61], and subsequently confirmed with a much larger sample by FNAL-799 [62]. It has been estimated that this background will enter at about the 10^{-10} level [63,64], comparable to or larger than the signal level. Because of this, the observation of $K_L \rightarrow \pi^0 e^+ e^-$ at the SM level will depend on background subtraction with good statistics. Possible alternative strategies are discussed in Ref. 52 and references cited therein.

The 90% CL upper bound for the process $K_L \rightarrow \pi^0 e^+ e^-$ is 2.8×10^{-10} [64]. For the closely related muonic process, the published upper bound is $B(K_L \rightarrow \pi^0 \mu^+ \mu^-) \leq 3.8 \times 10^{-10}$ [65], compared with the SM prediction of $(1.5 \pm 0.3) \times 10^{-11}$ [66] (assuming positive interference between the direct- and indirect- CP violating components). KTeV has additional data corresponding to about a factor 1.3 in sensitivity for the latter reaction that is under analysis.

A study of $K_L \rightarrow \pi^0 \mu^+ \mu^-$ has indicated that it might be possible to extract the direct CP -violating contribution by a joint study of the Dalitz plot variables and the components of the μ^+ polarization [67]. The latter tends to be quite substantial so that large statistics may not be necessary.

Combined information from the two $K_L \rightarrow \pi^0 \ell^+ \ell^-$ modes complements the $K \rightarrow \pi \nu \bar{\nu}$ measurements in constraining physics beyond the SM [68].

E. Other long distance dominated modes:

The decays $K^+ \rightarrow \pi^+ \ell^+ \ell^-$ ($\ell = e$ or μ) have received considerable attention. The rate and spectrum have been measured for both the electron and muon modes [69,70]. Ref. 50 has proposed a parametrization inspired by chiral perturbation theory, which provides a successful description of data but indicates the presence of large corrections beyond leading order. More work is needed to fully understand the origin of these large corrections.

The related rare hyperon decay mode $\Sigma^+ \rightarrow p \mu^+ \mu^-$, has been recently observed by the HyperCP collaboration [71]. The observed rate is in rough agreement with the standard model expectation [72] but the three events that have been observed cluster at a common $m_{\mu\mu}$ invariant mass and this can be interpreted as evidence for a new particle X^0 . The existing measurements of $K^+ \rightarrow \pi^+ \mu^+ \mu^-$ rule out a scalar X^0 and the new bounds, $B(K_L \rightarrow \pi^0 \pi^0 \mu^+ \mu^-) < 9.44 \times 10^{-11}$ [73] and $B(K_L \rightarrow \pi^0 \pi^0 \gamma \gamma) < 2.4 \times 10^{-7}$ [74] aim at closing the possibility of a pseudoscalar X^0 [75].

Much information has been recorded by KTeV and NA48 on the rates and spectrum for the Dalitz pair conversion modes $K_L \rightarrow \ell^+ \ell^- \gamma$ [76,77], and $K_L \rightarrow \ell^+ \ell^- \ell'^+ \ell'^-$ for $\ell, \ell' = e$ or μ [16,78–80]. All these results are used to test hadronic models and could further our understanding of the long distance component in $K_L \rightarrow \mu^+ \mu^-$.

References

1. D. Bryman, Int. J. Mod. Phys. **A4**, 79 (1989).
2. J. Hagelin and L. Littenberg, Prog. in Part. Nucl. Phys. **23**, 1 (1989).
3. L. Littenberg and G. Valencia, Ann. Rev. Nucl. and Part. Sci. **43**, 729 (1993).
4. J. Ritchie and S. Wojcicki, Rev. Mod. Phys. **65**, 1149 (1993).
5. B. Winstein and L. Wolfenstein, Rev. Mod. Phys. **65**, 1113 (1993).
6. G. D'Ambrosio *et al.*, *Radiative Non-Leptonic Kaon Decays*, in The DAΦNE Physics Handbook (second edition), eds. L. Maiani, G. Pancheri, and N. Paver (Frascati), Vol. I, 265 (1995).
7. A. Pich, Rept. on Prog. in Phys. **58**, 563 (1995).
8. G. Buchalla, A.J. Buras, and M.E. Lautenbacher, Rev. Mod. Phys. **68**, 1125 (1996).
9. G. D'Ambrosio and G. Isidori, Int. J. Mod. Phys. **A13**, 1 (1996).
10. P. Buchholz and B. Renk Prog. in Part. Nucl. Phys. **39**, 253 (1997).
11. A.J. Buras and R. Fleischer, TUM-HEP-275-97, hep-ph/9704376, *Heavy Flavours II*, World Scientific, eds. A.J. Buras and M. Lindner (1997), 65–238.
12. A.J. Buras, TUM-HEP-349-99, Lectures given at Lake Louise Winter Institute: Electroweak Physics, Lake Louise, Alberta, Canada, 14–20 Feb. 1999.
13. A.R. Barker and S.H. Kettell, Ann. Rev. Nucl. and Part. Sci. **50**, 249 (2000).
14. A.J. Buras, F. Schwab, and S. Uhlig, Rev. Mod. Phys. **80**, 965 (2008).
15. R. Appel *et al.*, Phys. Rev. Lett. **85**, 2877 (2000).

See key on page 405

-
16. A. Alavi-Harati *et al.*, Phys. Rev. Lett. **90**, 141801 (2003).
17. A. Sher *et al.*, Phys. Rev. **D72**, 012005 (2005).
18. D. Ambrose *et al.*, Phys. Rev. Lett. **81**, 5734 (1998).
19. E. Abouzaid *et al.*, Phys. Rev. Lett. **100**, 131803 (2008).
20. V.V. Anisimovsky *et al.*, Phys. Rev. Lett. **93**, 031801 (2004).
21. M. Lu and M.B. Wise, Phys. Lett. **B324**, 461 (1994); A.F. Falk, A. Lewandowski, and A.A. Petrov, Phys. Lett. **B505**, 107 (2001).
22. G. Isidori, F. Mescia, and C. Smith, Nucl. Phys. **B718**, 319 (2005).
23. F. Mescia and C. Smith, Phys. Rev. **D76**, 034017 (2007).
24. CKMfitter Group (J. Charles *et al.*), Eur. Phys. J. **C41**, 1 (2005), [hep-ph/0406184], updated results and plots available at: <http://ckmfitter.in2p3.fr>.
25. M. Bona *et al.*, [UTfit Collaboration] “Model-independent constraints on Delta F=2 operators and the scale of New Physics,” [arXiv:0707.0636](https://arxiv.org/abs/0707.0636) [hep-ph].
26. S. Adler *et al.*, Phys. Rev. Lett. **88**, 041803 (2002).
27. S. Adler *et al.*, Phys. Rev. Lett. **84**, 3768 (2000).
28. S. Adler *et al.*, Phys. Lett. **B537**, 237 (2002).
29. A.V. Artamonov *et al.*, Phys. Rev. Lett. **101**, 191802 (2008).
30. A.V. Artamonov *et al.*, Phys. Rev. **D79**, 092004 (2009).
31. G. Anelli *et al.*, CERN-SPSC-2005-013, 11 June 2005.
32. G. D’Ambrosio and G. Isidori, Phys. Lett. **B530**, 108 (2002).
33. W. Marciano and Z. Parsa, Phys. Rev. **D53**, 1 (1996).
34. T. Inami and C.S. Lim, Prog. Theor. Phys. **65**, 297 (1981); Erratum Prog. Theor. Phys. **65**, 172 (1981).
35. G. Buchalla and A.J. Buras, Nucl. Phys. **B548**, 309 (1999); M. Misiak and J. Urban, Phys. Lett. **B451**, 161 (1999); A.J. Buras *et al.*, Phys. Rev. Lett. **95**, 261805 (2005).
36. J. Brod and M. Gorbahn, Phys. Rev. **D78**, 034006 (2008).
37. D. Ambrose *et al.*, Phys. Rev. Lett. **84**, 1389 (2000).
38. G. Valencia, Nucl. Phys. **B517**, 339 (1998).
39. G. D’Ambrosio, G. Isidori, and J. Portoles, Phys. Lett. **B423**, 385 (1998).
40. G. Isidori and R. Unterdorfer, JHEP **0401**, 009 (2004).
41. D. Gomez-Dumm and A. Pich, Phys. Rev. Lett. **80**, 4633 (1998).
42. D. Ambrose *et al.*, Phys. Rev. Lett. **81**, 4309 (1998).
43. L. Littenberg, Phys. Rev. **D39**, 3322 (1989).
44. G. Buchalla and G. Isidori, Phys. Lett. **B440**, 170 (1998).
45. Y. Grossman and Y. Nir, Phys. Lett. **B398**, 163 (1997).
46. J.K. Ahn *et al.*, Phys. Rev. Lett. **100**, 201802 (2008).
47. H. Morii, “Search for the $K_L \rightarrow \pi^0 \nu \bar{\nu}$ at E391a Experiment,” KAON 09, 12 June 2009.
48. J. Comfort *et al.*, “Proposal for $K_L^0 \rightarrow \pi^0 \nu \bar{\nu}$ Experiment at J-Parc,” J-PARC Proposal 14 (2006).
49. D. Bryman *et al.*, Int. J. Mod. Phys. **A21**, 487 (2006).
50. G. D’Ambrosio *et al.*, JHEP **9808**, 004 (1998); C.O. Dib, I. Dunietz, and F.J. Gilman, Phys. Rev. **D39**, 2639 (1989).
51. J.R. Batley *et al.*, Phys. Lett. **B576**, 43 (2003).
52. G. Buchalla, G. D’Ambrosio, and G. Isidori, Nucl. Phys. **B672**, 387 (2003).
53. S. Friot, D. Greynat, and E. de Rafael, Phys. Lett. **B595**, 301 (2004).
54. J.R. Batley *et al.*, Phys. Lett. **B599**, 197 (2004).
55. G. Ecker, A. Pich, and E. de Rafael, Phys. Lett. **237B**, 481 (1990); L. Cappiello, G. D’Ambrosio, and M. Miragliuolo, Phys. Lett. **B298**, 423 (1993); A. Cohen, G. Ecker, and A. Pich, Phys. Lett. **B304**, 347 (1993).
56. F. Gabbiani and G. Valencia, Phys. Rev. **D66**, 074006 (2002).
57. E. Abouzaid *et al.*, Phys. Rev. **D77**, 112004 (2008).
58. A. Lai *et al.*, Phys. Lett. **B536**, 229 (2002).
59. J. Donoghue and F. Gabbiani, Phys. Rev. **D56**, 1605 (1997).
60. E. Abouzaid *et al.*, Phys. Rev. **D76**, 052001 (2007).
61. W.M. Morse *et al.*, Phys. Rev. **D45**, 36 (1992).
62. A. Alavi-Harati *et al.*, Phys. Rev. **D64**, 012003 (2001).
63. H.B. Greenlee, Phys. Rev. **D42**, 3724 (1990).
64. A. Alavi-Harati *et al.*, Phys. Rev. Lett. **93**, 021805 (2004).
65. A. Alavi-Harati *et al.*, Phys. Rev. Lett. **84**, 5279 (2000).
66. G. Isidori, C. Smith, and R. Unterdorfer, Eur. Phys. J. **C36**, 57 (2004).
67. M.V. Diwan, H. Ma, and T.L. Trueman, Phys. Rev. **D65**, 054020 (2002).
68. F. Mescia, C. Smith, and S. Trine, JHEP **0608**, 088 (2006).
69. R. Appel *et al.*, Phys. Rev. Lett. **83**, 4482 (1999); J.R. Batley *et al.*, Phys. Lett. **B677**, 246 (2009).
70. S.C. Adler *et al.*, Phys. Rev. Lett. **79**, 4756 (1997); R. Appel *et al.*, Phys. Rev. Lett. **84**, 2580 (2000); H.K. Park *et al.*, Phys. Rev. Lett. **88**, 111801 (2002).
71. H. Park *et al.*, Phys. Rev. Lett. **94**, 021801 (2005).
72. X.G. He, J. Tandean, and G. Valencia, Phys. Rev. **D72**, 074003 (2005).
73. D. Phillips “Search for the Rare Decay $K_L \rightarrow \pi^0 \pi^0 \mu^+ \mu^-$,” KAON 09, 11 June 2009.
74. Y.C. Tung *et al.*, Phys. Rev. Lett. **102**, 051802 (2009).
75. X.G. He, J. Tandean, and G. Valencia, JHEP **0806**, 002 (2008) and references therein.
76. A. Alavi-Harati *et al.*, Phys. Rev. Lett. **87**, 071801 (2001).
77. A. Abouzaid *et al.*, Phys. Rev. Lett. **99**, 051804 (2007).
78. J.R. LaDue “Understanding Dalitz Decays of the K_L in particular the decays of $K_L \rightarrow e^+ e^- \gamma$ and $K_L \rightarrow e^+ e^- e^+ e^-$ ” University of Colorado Thesis, May 2003. The preliminary result for $K_L \rightarrow e^+ e^- \gamma$ in this thesis has been superseded by the final result in [77].
79. A. Alavi-Harati *et al.*, Phys. Rev. Lett. **86**, 5425 (2001).
80. V. Fanti *et al.*, Phys. Lett. **B458**, 458 (1999).
-

Meson Particle Listings

K^\pm

K^\pm DECAY MODES

K^- modes are charge conjugates of the modes below.

Mode	Fraction (Γ_i/Γ)	Scale factor/ Confidence level
Leptonic and semileptonic modes		
Γ_1 $K^+ \rightarrow e^+ \nu_e$	$(1.584 \pm 0.020) \times 10^{-5}$	
Γ_2 $K^+ \rightarrow \mu^+ \nu_\mu$	$(63.55 \pm 0.11) \%$	S=1.2
Γ_3 $K^+ \rightarrow \pi^0 e^+ \nu_e$	$(5.07 \pm 0.04) \%$	S=2.1
Called K_{e3}^+ .		
Γ_4 $K^+ \rightarrow \pi^0 \mu^+ \nu_\mu$	$(3.353 \pm 0.034) \%$	S=1.8
Called $K_{\mu 3}^+$.		
Γ_5 $K^+ \rightarrow \pi^0 \pi^0 e^+ \nu_e$	$(2.2 \pm 0.4) \times 10^{-5}$	
Γ_6 $K^+ \rightarrow \pi^+ \pi^- e^+ \nu_e$	$(4.09 \pm 0.10) \times 10^{-5}$	
Γ_7 $K^+ \rightarrow \pi^+ \pi^- \mu^+ \nu_\mu$	$(1.4 \pm 0.9) \times 10^{-5}$	
Γ_8 $K^+ \rightarrow \pi^0 \pi^0 \pi^0 e^+ \nu_e$	$< 3.5 \times 10^{-6}$	CL=90%
Hadronic modes		
Γ_9 $K^+ \rightarrow \pi^+ \pi^0$	$(20.66 \pm 0.08) \%$	S=1.2
Γ_{10} $K^+ \rightarrow \pi^+ \pi^0 \pi^0$	$(1.761 \pm 0.022) \%$	S=1.1
Γ_{11} $K^+ \rightarrow \pi^+ \pi^+ \pi^-$	$(5.59 \pm 0.04) \%$	S=1.3
Leptonic and semileptonic modes with photons		
Γ_{12} $K^+ \rightarrow \mu^+ \nu_\mu \gamma$	[a,b] $(6.2 \pm 0.8) \times 10^{-3}$	
Γ_{13} $K^+ \rightarrow \mu^+ \nu_\mu \gamma (\text{SD}^+)$	[c,d] $(1.33 \pm 0.22) \times 10^{-5}$	
Γ_{14} $K^+ \rightarrow \mu^+ \nu_\mu \gamma (\text{SD}^+ \text{INT})$	[c,d] $< 2.7 \times 10^{-5}$	CL=90%
Γ_{15} $K^+ \rightarrow \mu^+ \nu_\mu \gamma (\text{SD}^- + \text{SD}^- \text{INT})$	[c,d] $< 2.6 \times 10^{-4}$	CL=90%
Γ_{16} $K^+ \rightarrow e^+ \nu_e \gamma$	$(9.4 \pm 0.4) \times 10^{-6}$	
Γ_{17} $K^+ \rightarrow \pi^0 e^+ \nu_e \gamma$	[a,b] $(2.56 \pm 0.16) \times 10^{-4}$	
Γ_{18} $K^+ \rightarrow \pi^0 e^+ \nu_e \gamma (\text{SD})$	[c,d] $< 5.3 \times 10^{-5}$	CL=90%
Γ_{19} $K^+ \rightarrow \pi^0 \mu^+ \nu_\mu \gamma$	[a,b] $(1.5 \pm 0.4) \times 10^{-5}$	
Γ_{20} $K^+ \rightarrow \pi^0 \pi^0 e^+ \nu_e \gamma$	$< 5 \times 10^{-6}$	CL=90%
Hadronic modes with photons or $\ell\bar{\ell}$ pairs		
Γ_{21} $K^+ \rightarrow \pi^+ \pi^0 \gamma$	[a,b] $(2.75 \pm 0.15) \times 10^{-4}$	
Γ_{22} $K^+ \rightarrow \pi^+ \pi^0 \gamma (\text{DE})$	[b,e] $(4.3 \pm 0.7) \times 10^{-6}$	
Γ_{23} $K^+ \rightarrow \pi^+ \pi^0 \pi^0 \gamma$	[a,b] $(7.6 \pm_{-3.0}^{+6.0}) \times 10^{-6}$	
Γ_{24} $K^+ \rightarrow \pi^+ \pi^+ \pi^- \gamma$	[a,b] $(1.04 \pm 0.31) \times 10^{-4}$	
Γ_{25} $K^+ \rightarrow \pi^+ \gamma \gamma$	[b] $(1.10 \pm 0.32) \times 10^{-6}$	
Γ_{26} $K^+ \rightarrow \pi^+ 3\gamma$	[b] $< 1.0 \times 10^{-4}$	CL=90%
Γ_{27} $K^\pm \rightarrow \pi^+ e^+ e^- \gamma$	$(1.19 \pm 0.13) \times 10^{-8}$	
Leptonic modes with $\ell\bar{\ell}$ pairs		
Γ_{28} $K^+ \rightarrow e^+ \nu_e \nu \bar{\nu}$	$< 6 \times 10^{-5}$	CL=90%
Γ_{29} $K^+ \rightarrow \mu^+ \nu_\mu \nu \bar{\nu}$	$< 6.0 \times 10^{-6}$	CL=90%
Γ_{30} $K^+ \rightarrow e^+ \nu_e e^+ e^-$	$(2.48 \pm 0.20) \times 10^{-8}$	
Γ_{31} $K^+ \rightarrow \mu^+ \nu_\mu e^+ e^-$	$(7.06 \pm 0.31) \times 10^{-8}$	
Γ_{32} $K^+ \rightarrow e^+ \nu_e \mu^+ \mu^-$	$(1.7 \pm 0.5) \times 10^{-8}$	
Γ_{33} $K^+ \rightarrow \mu^+ \nu_\mu \mu^+ \mu^-$	$< 4.1 \times 10^{-7}$	CL=90%
Lepton Family number (LF), Lepton number (L), $\Delta S = \Delta Q$ (SQ) violating modes, or $\Delta S = 1$ weak neutral current (SI) modes		
Γ_{34} $K^+ \rightarrow \pi^+ \pi^+ e^- \bar{\nu}_e$	SQ $< 1.2 \times 10^{-8}$	CL=90%
Γ_{35} $K^+ \rightarrow \pi^+ \pi^+ \mu^- \bar{\nu}_\mu$	SQ $< 3.0 \times 10^{-6}$	CL=95%
Γ_{36} $K^+ \rightarrow \pi^+ e^+ e^-$	SI $(3.00 \pm 0.09) \times 10^{-7}$	
Γ_{37} $K^+ \rightarrow \pi^+ \mu^+ \mu^-$	SI $(8.1 \pm 1.4) \times 10^{-8}$	S=2.7
Γ_{38} $K^+ \rightarrow \pi^+ \nu \bar{\nu}$	SI $(1.7 \pm 1.1) \times 10^{-10}$	
Γ_{39} $K^+ \rightarrow \pi^+ \pi^0 \nu \bar{\nu}$	SI $< 4.3 \times 10^{-5}$	CL=90%
Γ_{40} $K^+ \rightarrow \mu^- \nu e^+ e^+$	LF $< 2.0 \times 10^{-8}$	CL=90%
Γ_{41} $K^+ \rightarrow \mu^+ \nu_e$	LF [f] $< 4 \times 10^{-3}$	CL=90%
Γ_{42} $K^+ \rightarrow \pi^+ \mu^+ e^-$	LF $< 1.3 \times 10^{-11}$	CL=90%
Γ_{43} $K^+ \rightarrow \pi^+ \mu^- e^+$	LF $< 5.2 \times 10^{-10}$	CL=90%
Γ_{44} $K^+ \rightarrow \pi^- \mu^+ e^+$	L $< 5.0 \times 10^{-10}$	CL=90%
Γ_{45} $K^+ \rightarrow \pi^- e^+ e^+$	L $< 6.4 \times 10^{-10}$	CL=90%
Γ_{46} $K^+ \rightarrow \pi^- \mu^+ \mu^+$	L [f] $< 3.0 \times 10^{-9}$	CL=90%
Γ_{47} $K^+ \rightarrow \mu^+ \bar{\nu}_e$	L [f] $< 3.3 \times 10^{-3}$	CL=90%
Γ_{48} $K^+ \rightarrow \pi^0 e^+ \bar{\nu}_e$	L $< 3 \times 10^{-3}$	CL=90%
Γ_{49} $K^+ \rightarrow \pi^+ \gamma$	[g] $< 2.3 \times 10^{-9}$	CL=90%

- [a] Most of this radiative mode, the low-momentum γ part, is also included in the parent mode listed without γ 's.
- [b] See the Particle Listings below for the energy limits used in this measurement.

[c] See the "Note on $\pi^\pm \rightarrow \ell^\pm \nu \gamma$ and $K^\pm \rightarrow \ell^\pm \nu \gamma$ Form Factors" in the π^\pm Particle Listings for definitions and details.

[d] Structure-dependent part.

[e] Direct-emission branching fraction.

[f] Derived from an analysis of neutrino-oscillation experiments.

[g] Violates angular-momentum conservation.

CONSTRAINED FIT INFORMATION

An overall fit to the mean life, a decay rate, and 13 branching ratios uses 32 measurements and one constraint to determine 8 parameters. The overall fit has a $\chi^2 = 51.8$ for 25 degrees of freedom.

The following *off-diagonal* array elements are the correlation coefficients $\langle \delta p_i \delta p_j \rangle / (\delta p_i \delta p_j)$, in percent, from the fit to parameters p_i , including the branching fractions, $x_i \equiv \Gamma_i / \Gamma_{\text{total}}$. The fit constrains the x_i whose labels appear in this array to sum to one.

x_3	-64						
x_4	-62	90					
x_5	-3	4	3				
x_9	-65	1	-1	0			
x_{10}	-13	-6	-6	0	-6		
x_{11}	-21	-9	-9	0	-10	3	
Γ	5	2	2	0	2	-1	-24
	x_2	x_3	x_4	x_5	x_9	x_{10}	x_{11}

Mode	Rate (10^8 s^{-1})	Scale factor
Γ_2 $K^+ \rightarrow \mu^+ \nu_\mu$	0.5133 ± 0.0013	1.5
Γ_3 $K^+ \rightarrow \pi^0 e^+ \nu_e$	0.0410 ± 0.0004	2.1
Called K_{e3}^+ .		
Γ_4 $K^+ \rightarrow \pi^0 \mu^+ \nu_\mu$	0.02708 ± 0.00028	1.9
Called $K_{\mu 3}^+$.		
Γ_5 $K^+ \rightarrow \pi^0 \pi^0 e^+ \nu_e$	$(1.77 \pm_{-0.30}^{+0.35}) \times 10^{-5}$	
Γ_9 $K^+ \rightarrow \pi^+ \pi^0$	0.1669 ± 0.0007	1.3
Γ_{10} $K^+ \rightarrow \pi^+ \pi^0 \pi^0$	0.01423 ± 0.00018	1.1
Γ_{11} $K^+ \rightarrow \pi^+ \pi^+ \pi^-$	0.04518 ± 0.00029	1.2

K^\pm DECAY RATES

$\Gamma(\mu^+ \nu_\mu)$	Γ_2		
VALUE (10^6 s^{-1})	DOCUMENT ID	TECN	CHG
51.33 ± 0.13 OUR FIT	Error includes scale factor of 1.5.		
• • • We do not use the following data for averages, fits, limits, etc. • • •			
51.2 ± 0.8	FORD	67	CNTR ±

$\Gamma(\pi^+ \pi^+ \pi^-)$	Γ_{11}				
VALUE (10^6 s^{-1})	EVTS	DOCUMENT ID	TECN	CHG	
4.518 ± 0.029 OUR FIT	Error includes scale factor of 1.2.				
4.511 ± 0.024	7	FORD	70	ASPK	
• • • We do not use the following data for averages, fits, limits, etc. • • •					
4.529 ± 0.032	3.2M	7	FORD	70	ASPK
4.496 ± 0.030		7	FORD	67	CNTR ±
⁷ First FORD 70 value is second FORD 70 combined with FORD 67.					

$$(\Gamma(K^+) - \Gamma(K^-)) / \Gamma(K)$$

$K^\pm \rightarrow \mu^\pm \nu_\mu$ RATE DIFFERENCE/AVERAGE			
Test of CPT conservation.			
VALUE (%)	DOCUMENT ID	TECN	
-0.54 ± 0.41	FORD	67	CNTR

$K^\pm \rightarrow \pi^\pm \pi^+ \pi^-$ RATE DIFFERENCE/AVERAGE					
Test of CP conservation.					
VALUE (%)	EVTS	DOCUMENT ID	TECN	CHG	
0.08 ± 0.12	8	FORD	70	ASPK	
• • • We do not use the following data for averages, fits, limits, etc. • • •					
-0.02 ± 0.16	9	SMITH	73	ASPK ±	
0.10 ± 0.14	3.2M	8	FORD	70	ASPK
-0.50 ± 0.90			FLETCHER	67	OSPK
-0.04 ± 0.21	8	FORD	67	CNTR	

- ⁸ First FORD 70 value is second FORD 70 combined with FORD 67.
- ⁹ SMITH 73 value of $K^\pm \rightarrow \pi^\pm \pi^+ \pi^-$ rate difference is derived from SMITH 73 value of $K^\pm \rightarrow \pi^\pm 2\pi^0$ rate difference.

Table with columns: VALUE (%), EVTS, DOCUMENT ID, TECN, CHG. Rows: K± → π± π0 π0 RATE DIFFERENCE/AVERAGE. Includes sub-sections for CP and CPT conservation tests.

Table with columns: VALUE, EVTS, DOCUMENT ID, TECN, CHG. Row: Γ(π0 e+ νe)/[Γ(π0 μ+ νμ) + Γ(π+ π0) + Γ(π+ π0 π0)].

Table with columns: VALUE, EVTS, DOCUMENT ID, TECN, CHG, COMMENT. Row: Γ(π0 e+ νe)/Γ(π+ π0).

Table with columns: VALUE, EVTS, DOCUMENT ID, TECN, CHG. Row: Γ(π0 e+ νe)/Γ(π+ π+ π-).

Table with columns: VALUE (units 10-5), EVTS, DOCUMENT ID, TECN, CHG. Section: K+ BRANCHING RATIOS. Sub-section: Leptonic and semileptonic modes. Row: Γ(e+ νe)/Γ(μ+ νμ).

Table with columns: VALUE (units 10-2), EVTS, DOCUMENT ID, TECN, CHG, COMMENT. Row: Γ(π0 μ+ νμ)/Γtotal.

10 The ratio is defined to include internal-bremsstrahlung, ignoring direct-emission contributions. AMBROSINO 09E determined the ratio from the measurement of Γ(K → e ν(γ)), Eγ < 10 MeV / Γ(K → μ ν(γ)). 89.8% of K → e ν(γ) events had Eγ < 10 MeV.

17 Depends on K+ lifetime τ. AMBROSINO 08A uses PDG 06 value of τ = (1.2385 ± 0.0024) × 10-8 sec. The correlation between K+_{e3} and K+_{μ3} branching fraction measurements is 62.7%.

Table with columns: VALUE (units 10-2), EVTS, DOCUMENT ID, TECN, CHG, COMMENT. Row: Γ(μ+ νμ)/Γtotal.

Table with columns: VALUE, EVTS, DOCUMENT ID, TECN, CHG. Row: Γ(π0 μ+ νμ)/Γ(μ+ νμ).

Table with columns: VALUE (units 10-2), EVTS, DOCUMENT ID, TECN, CHG, COMMENT. Row: Γ(π0 e+ νe)/Γtotal.

19 GARLAND 68 changed from 0.055 ± 0.004 in agreement with μ-spectrum calculation of GAILLARD 70 appendix B. L.G.Pondrom, (private communication 73).

12 Depends on K+ lifetime τ. AMBROSINO 08A uses PDG 06 value of τ = (1.2385 ± 0.0024) × 10-8 sec. The correlation between K+_{e3} and K+_{μ3} branching fraction measurements is 62.7%.

Table with columns: VALUE, EVTS, DOCUMENT ID, TECN, CHG, COMMENT. Row: Γ(π0 μ+ νμ)/Γ(π0 e+ νe).

Table with columns: VALUE, EVTS, DOCUMENT ID, TECN, CHG. Row: Γ(π0 e+ νe)/Γ(μ+ νμ).

Table with columns: VALUE, EVTS, DOCUMENT ID, TECN, CHG, COMMENT. Row: Γ(π0 e+ νe)/Γtotal.

13 AUERBACH 67 changed from 0.0797 ± 0.0054. See comment with ratio Γ(π0 μ+ νμ)/Γ(μ+ νμ). The value 0.0785 ± 0.0025 given in AUERBACH 67 is an average of AUERBACH 67 Γ(π0 e+ νe)/Γ(μ+ νμ) and CESTER 66 Γ(π0 e+ νe)/[Γ(μ+ νμ) + Γ(π+ π0)].

21 Not used in the fit. This result enters the fit via correlation of K+_{e3} and K+_{μ3} branching fraction measurements of AMBROSINO 08A.

Table with columns: VALUE (units 10-2), EVTS, DOCUMENT ID, TECN, CHG. Row: Γ(π0 e+ νe)/[Γ(μ+ νμ) + Γ(π+ π0)].

Table with columns: VALUE (units 10-2), EVTS, DOCUMENT ID, TECN, CHG. Row: [Γ(π0 μ+ νμ) + Γ(π+ π0)]/Γtotal.

See key on page 405

 $\Gamma(\pi^+\nu\bar{\nu})/\Gamma_{\text{total}}$ Γ_{38}/Γ

Test for $\Delta S = 1$ weak neutral current. Allowed by higher-order electroweak interactions. Branching ratio values are extrapolated from the momentum or energy regions shown in the comments assuming Standard Model phase space except for those labeled "Scalar" or "Tensor" to indicate the assumed non-Standard-Model interaction.

VALUE (units 10^{-9})	CL% EVTS	DOCUMENT ID	TECN	CHG	COMMENT
$0.173^{+0.115}_{-0.105}$	7	67 ARTAMONOV 08	B949	+	$140 < P_{\pi} < 199$ MeV, $211 < P_{\pi} < 229$ MeV
••• We do not use the following data for averages, fits, limits, etc. •••					
$0.789^{+0.926}_{-0.510}$	3	68 ARTAMONOV 08	B949	+	$140 < P_{\pi} < 199$ MeV
< 2.2	90	1 69 ADLER	04 B787	+	$211 < P_{\pi} < 229$ MeV
< 2.7	90	ADLER	04 B787	+	Scalar
< 1.8	90	ADLER	04 B787	+	Tensor
$0.147^{+0.130}_{-0.089}$	3	70 ANISIMOVSK...04	B949	+	$211 < P_{\pi} < 229$ MeV
$0.157^{+0.175}_{-0.082}$	2	ADLER	02 B787	+	$P_{\pi} > 211$ MeV/c
< 4.2	90	1 ADLER	02c B787	+	$140 < P_{\pi} < 195$ MeV
< 4.7	90	71 ADLER	02c B787	+	Scalar
< 2.5	90	71 ADLER	02c B787	+	Tensor
$0.15^{+0.34}_{-0.12}$	1	ADLER	00 B787		In ADLER 02
$0.42^{+0.97}_{-0.35}$	1	ADLER	97 B787		
< 2.4	90	ADLER	96 B787		
< 7.5	90	ATIYA	93 B787	+	$T(\pi)$ 115-127 MeV
< 5.2	90	72 ATIYA	93 B787	+	
< 17	90	0 ATIYA	93B B787	+	$T(\pi)$ 60-100 MeV
< 34	90	ATIYA	90 B787	+	
< 140	90	ASANO	81B CNTR	+	$T(\pi)$ 116-127 MeV

67 Value obtained combining ANISIMOVSKY 04, ADLER 04, and the present ARTAMONOV 08 results.

68 Observed 3 events with an estimated background of $0.93 \pm 0.17^{+0.32}_{-0.24}$. Signal-to-background ratio for each of these 3 events is 0.20, 0.42, and 0.47.

69 Value obtained combining the previous result ADLER 02c with 1 event and the present result with 0 events to obtain an expected background 1.22 ± 0.24 events and 1 event observed.

70 Value obtained combining the previous E787 result ADLER 02 with 2 events and the present E949 with 1 event. The additional event has a signal-to-background ratio 0.9. Superseded by ARTAMONOV 08.

71 Sperseded by ADLER 04.

72 Combining ATIYA 93 and ATIYA 93B results. Superseded by ADLER 96.

 $\Gamma(\pi^+\pi^0\nu\bar{\nu})/\Gamma_{\text{total}}$ Γ_{39}/Γ

Test for $\Delta S = 1$ weak neutral current. Allowed by higher-order electroweak interactions.

VALUE (units 10^{-5})	CL%	DOCUMENT ID	TECN
< 4.3	90	73 ADLER 01	SPEC

73 Search region defined by $90 \text{ MeV}/c < P_{\pi^+} < 188 \text{ MeV}/c$ and $135 \text{ MeV} < E_{\pi^0} < 180 \text{ MeV}$.

 $\Gamma(\mu^-\nu e^+e^+)/\Gamma(\pi^+\pi^-e^+\nu_e)$ Γ_{40}/Γ_6

Test of lepton family number conservation.

VALUE (units 10^{-3})	CL%	EVTS	DOCUMENT ID	TECN	CHG
< 0.5	90	0	74 DIAMANT-... 76	SPEC	+

74 DIAMANT-BERGER 76 quotes this result times our 1975 $\pi^+\pi^-e\nu$ BR ratio.

 $\Gamma(\mu^+\nu_e)/\Gamma_{\text{total}}$ Γ_{41}/Γ

Forbidden by lepton family number conservation.

VALUE	CL%	EVTS	DOCUMENT ID	TECN	CHG	COMMENT
< 0.004	90	0	75 LYONS 81	HLBC	200 GeV K^+ narrow band ν beam	

••• We do not use the following data for averages, fits, limits, etc. •••

< 0.012 90 75 COOPER 82 HLBC Wideband ν beam

75 COOPER 82 and LYONS 81 limits on ν_e observation are here interpreted as limits on lepton family number violation in the absence of mixing.

 $\Gamma(\pi^+\mu^+e^-)/\Gamma_{\text{total}}$ Γ_{42}/Γ

Test of lepton family number conservation.

VALUE (units 10^{-10})	CL%	EVTS	DOCUMENT ID	TECN	CHG
< 0.13	90	0	76 SHER 05	RVUE	+

••• We do not use the following data for averages, fits, limits, etc. •••

< 0.21 90 SHER 05 B865 +

< 0.39 90 APPEL 00 B865 +

< 2.1 90 LEE 90 SPEC +

76 This result combines SHER 05 1998 data, APPEL 00 1996 data, and data from BERGMAN 97 and PISLAK 97 theses, all from BNL-E865, with LEE 90 BNL-E777 data.

 $\Gamma(\pi^+\mu^-e^+)/\Gamma_{\text{total}}$ Γ_{43}/Γ

Test of lepton family number conservation.

VALUE (units 10^{-10})	CL%	EVTS	DOCUMENT ID	TECN	CHG
< 5.2	90	0	APPEL 00B	B865	+

••• We do not use the following data for averages, fits, limits, etc. •••

< 70 90 0 77 DIAMANT-... 76 SPEC +

77 Measurement actually applies to the sum of the $\pi^+\mu^-e^+$ and $\pi^-\mu^+e^+$ modes.

 $\Gamma(\pi^-\mu^+e^+)/\Gamma_{\text{total}}$ Γ_{44}/Γ

Test of total lepton number conservation.

VALUE (units 10^{-10})	CL%	EVTS	DOCUMENT ID	TECN	CHG
< 5.0	90	0	APPEL 00B	B865	+

••• We do not use the following data for averages, fits, limits, etc. •••

< 70 90 0 78 DIAMANT-... 76 SPEC +

78 Measurement actually applies to the sum of the $\pi^+\mu^-e^+$ and $\pi^-\mu^+e^+$ modes.

 $\Gamma(\pi^-e^+e^+)/\Gamma_{\text{total}}$ Γ_{45}/Γ

Test of total lepton number conservation.

VALUE	CL%	EVTS	DOCUMENT ID	TECN	CHG
< 6.4×10^{-10}	90	0	APPEL 00B	B865	+

••• We do not use the following data for averages, fits, limits, etc. •••

< 9.2×10^{-9} 90 0 DIAMANT-... 76 SPEC +

< 1.5×10^{-5} CHANG 68 HBC -

 $\Gamma(\pi^-\mu^+\mu^+)/\Gamma_{\text{total}}$ Γ_{46}/Γ

Forbidden by total lepton number conservation.

VALUE	CL%	EVTS	DOCUMENT ID	TECN	CHG
< 3.0×10^{-9}	90	0	APPEL 00B	B865	+

••• We do not use the following data for averages, fits, limits, etc. •••

< 1.5×10^{-4} 90 79 LITTENBERG 92 HBC

79 LITTENBERG 92 is from retroactive data analysis of CHANG 68 bubble chamber data.

 $\Gamma(\mu^+\nu_e)/\Gamma_{\text{total}}$ Γ_{47}/Γ

Forbidden by total lepton number conservation.

VALUE (units 10^{-3})	CL%	EVTS	DOCUMENT ID	TECN	COMMENT
< 3.3	90	80	COOPER 82	HLBC	Wideband ν beam

80 COOPER 82 limit on $\bar{\nu}_e$ observation is here interpreted as a limit on lepton number violation in the absence of mixing.

 $\Gamma(\pi^0e^+\nu_e)/\Gamma_{\text{total}}$ Γ_{48}/Γ

Forbidden by total lepton number conservation.

VALUE	CL%	EVTS	DOCUMENT ID	TECN	COMMENT
< 0.003	90	81	COOPER 82	HLBC	Wideband ν beam

81 COOPER 82 limit on $\bar{\nu}_e$ observation is here interpreted as a limit on lepton number violation in the absence of mixing.

 $\Gamma(\pi^+\gamma)/\Gamma_{\text{total}}$ Γ_{49}/Γ

Violates angular momentum conservation and gauge invariance. Current interest in this decay is as a search for non-commutative space-time effects as discussed in ARTAMONOV 05 and for exotic physics such as a vacuum expectation value of a new vector field, non-local Superstring effects, or departures from Lorentz invariance, as discussed in ADLER 02b.

VALUE (units 10^{-3})	CL%	DOCUMENT ID	TECN	CHG
< 2.3	90	ARTAMONOV 05	B949	+

••• We do not use the following data for averages, fits, limits, etc. •••

< 360 90 ADLER 02B B787 +

< 1400 90 ASANO 82 CNTR +

< 4000 90 82 KLEMS 71 OSPK +

82 Test of model of Selli, Nuovo Cimento 60A 291 (1969).

 K^+ LONGITUDINAL POLARIZATION OF EMITTED μ^+

VALUE	CL%	DOCUMENT ID	TECN	CHG	COMMENT
< -0.990	90	83 AOKI 94	SPEC	+	

••• We do not use the following data for averages, fits, limits, etc. •••

< -0.990 90 IMAZATO 92 SPEC + Repl. by AOKI 94

-0.970 \pm 0.047 84 YAMANAKA 86 SPEC +

-1.0 \pm 0.1 84 CUTTS 69 SPRK +

-0.96 \pm 0.12 84 COOMBES 57 CNTR +

83 AOKI 94 measures $\xi P_{\mu^+} = -0.9996 \pm 0.0030 \pm 0.0048$. The above limit is obtained by summing the statistical and systematic errors in quadrature, normalizing to the physically significant region ($|\xi P_{\mu^+}| < 1$) and assuming that $\xi = 1$, its maximum value.

84 Assumes $\xi = 1$.

Meson Particle Listings

 K^\pm DALITZ PLOT PARAMETERS FOR
 $K \rightarrow 3\pi$ DECAYS

Revised 1999 by T.G. Trippe (LBNL).

The Dalitz plot distribution for $K^\pm \rightarrow \pi^\pm \pi^\pm \pi^\mp$, $K^\pm \rightarrow \pi^0 \pi^0 \pi^\pm$, and $K_L^0 \rightarrow \pi^+ \pi^- \pi^0$ can be parameterized by a series expansion such as that introduced by Weinberg [1]. We use the form

$$\begin{aligned} |M|^2 \propto & 1 + g \frac{(s_3 - s_0)}{m_{\pi^+}^2} + h \left[\frac{s_3 - s_0}{m_{\pi^+}^2} \right]^2 \\ & + j \frac{(s_2 - s_1)}{m_{\pi^+}^2} + k \left[\frac{s_2 - s_1}{m_{\pi^+}^2} \right]^2 \\ & + f \frac{(s_2 - s_1)(s_3 - s_0)}{m_{\pi^+}^2 m_{\pi^+}^2} + \dots, \end{aligned} \quad (1)$$

where $m_{\pi^+}^2$ has been introduced to make the coefficients g , h , j , and k dimensionless, and

$$\begin{aligned} s_i &= (P_K - P_i)^2 = (m_K - m_i)^2 - 2m_K T_i, \quad i = 1, 2, 3, \\ s_0 &= \frac{1}{3} \sum_i s_i = \frac{1}{3} (m_K^2 + m_1^2 + m_2^2 + m_3^2). \end{aligned}$$

Here the P_i are four-vectors, m_i and T_i are the mass and kinetic energy of the i^{th} pion, and the index 3 is used for the odd pion.

The coefficient g is a measure of the slope in the variable s_3 (or T_3) of the Dalitz plot, while h and k measure the quadratic dependence on s_3 and $(s_2 - s_1)$, respectively. The coefficient j is related to the asymmetry of the plot and must be zero if CP invariance holds. Note also that if CP is good, g , h , and k must be the same for $K^+ \rightarrow \pi^+ \pi^+ \pi^-$ as for $K^- \rightarrow \pi^- \pi^- \pi^+$.

Since different experiments use different forms for $|M|^2$, in order to compare the experiments we have converted to g , h , j , and k whatever coefficients have been measured. Where such conversions have been done, the measured coefficient a_y , a_t , a_u , or a_v is given in the comment at the right. For definitions of these coefficients, details of this conversion, and discussion of the data, see the April 1982 version of this note [2].

References

1. S. Weinberg, Phys. Rev. Lett. **4**, 87 (1960).
2. Particle Data Group, Phys. Lett. **111B**, 69 (1982).

ENERGY DEPENDENCE OF K^\pm DALITZ PLOT

$$\begin{aligned} |\text{matrix element}|^2 &= 1 + gu + hu^2 + kv^2 \\ \text{where } u &= (s_3 - s_0) / m_{\pi^+}^2 \text{ and } v = (s_2 - s_1) / m_{\pi^+}^2 \end{aligned}$$

LINEAR COEFFICIENT g FOR $K^\pm \rightarrow \pi^\pm \pi^+ \pi^-$

Some experiments use Dalitz variables x and y . In the comments we give $a_y =$ coefficient of y term. See note above on "Dalitz Plot Parameters for $K \rightarrow 3\pi$ Decays." For discussion of the conversion of a_y to g , see the earlier version of the same note in the Review published in Physics Letters **111B** 70 (1982).

VALUE	EVTS	DOCUMENT ID	TECN	CHG	COMMENT
-0.21134 ± 0.00017	471M	⁸⁵ BATLEY	07B	NA48	±
••• We do not use the following data for averages, fits, limits, etc. •••					
-0.2221 ± 0.0065	225k	DEVAUX	77	SPEC	+ $a_y = .2814 \pm .0082$
-0.199 ± 0.008	81k	⁸⁶ LUCAS	73	HBC	- $a_y = 0.252 \pm 0.011$
-0.2157 ± 0.0028	750k	FORD	72	ASPK	+ $a_y = .2734 \pm .0035$
-0.2186 ± 0.0028	750k	FORD	72	ASPK	- $a_y = .2770 \pm .0035$
-0.200 ± 0.009	39819	⁸⁷ HOFFMASTER	72	HLBC	+
-0.196 ± 0.012	17898	⁸⁸ GRAUMAN	70	HLBC	+ $a_y = 0.228 \pm 0.030$

-0.193 ± 0.010	50919	MAST	69	HBC	- $a_y = 0.244 \pm 0.013$
-0.218 ± 0.016	9994	⁸⁹ BUTLER	68	HBC	+ $a_y = 0.277 \pm 0.020$
-0.190 ± 0.023	5778	^{89,90} MOSCOSO	68	HBC	- $a_y = 0.242 \pm 0.029$
-0.22 ± 0.024	5428	^{89,90} ZINCHENKO	67	HBC	+ $a_y = 0.28 \pm 0.03$
-0.220 ± 0.035	1347	⁹¹ FERRO-LUZZI	61	HBC	- $a_y = 0.28 \pm 0.045$

⁸⁵ Final state strong interaction and radiative corrections not included in the fit.

⁸⁶ Quadratic dependence is required by K_L^0 experiments.

⁸⁷ HOFFMASTER 72 includes GRAUMAN 70 data.

⁸⁸ Emulsion data added — all events included by HOFFMASTER 72.

⁸⁹ Experiments with large errors not included in average.

⁹⁰ Also includes DBC events.

⁹¹ No radiative corrections included.

QUADRATIC COEFFICIENT h FOR $K^\pm \rightarrow \pi^\pm \pi^+ \pi^-$

VALUE (units 10^{-2})	EVTS	DOCUMENT ID	TECN	CHG	
1.848 ± 0.040	471M	⁹² BATLEY	07B	NA48	±
••• We do not use the following data for averages, fits, limits, etc. •••					
-0.06 ± 1.43	225k	DEVAUX	77	SPEC	+
1.87 ± 0.62	750k	FORD	72	ASPK	+
1.25 ± 0.62	750k	FORD	72	ASPK	-
-0.9 ± 1.4	39819	HOFFMASTER	72	HLBC	+
-0.1 ± 1.2	50919	MAST	69	HBC	-

⁹² Final state strong interaction and radiative corrections not included in the fit.

QUADRATIC COEFFICIENT k FOR $K^\pm \rightarrow \pi^\pm \pi^+ \pi^-$

VALUE (units 10^{-3})	EVTS	DOCUMENT ID	TECN	CHG	
-4.63 ± 0.14	471M	⁹³ BATLEY	07B	NA48	±
••• We do not use the following data for averages, fits, limits, etc. •••					
-20.5 ± 3.9	225k	DEVAUX	77	SPEC	+
-7.5 ± 1.9	750k	FORD	72	ASPK	+
-8.3 ± 1.9	750k	FORD	72	ASPK	-
-10.5 ± 4.5	39819	HOFFMASTER	72	HLBC	+
-14 ± 12	50919	MAST	69	HBC	-

⁹³ Final state strong interaction and radiative corrections not included in the fit.

 $(g_+ - g_-) / (g_+ + g_-)$ FOR $K^\pm \rightarrow \pi^\pm \pi^+ \pi^-$

This is a CP violating asymmetry between linear coefficients g_\pm for $K^+ \rightarrow \pi^+ \pi^+ \pi^-$ decay and g_- for $K^- \rightarrow \pi^- \pi^- \pi^+$ decay.

VALUE (units 10^{-4})	EVTS	DOCUMENT ID	TECN
-1.5 ± 1.5 ± 1.6	3.1G	⁹⁴ BATLEY	07E NA48
••• We do not use the following data for averages, fits, limits, etc. •••			
1.7 ± 2.1 ± 2.0	1.7G	⁹⁵ BATLEY	06 NA48
-70.0 ± 53	3.2M	FORD	70 ASPK

⁹⁴ BATLEY 07E includes data from BATLEY 06. Uses quadratic parametrization and value $g_+ + g_- = 2g$ from BATLEY 07B. This measurement neglects any possible charge asymmetries in higher order slope parameters h or k .

⁹⁵ This measurement neglects any possible charge asymmetries in higher order slope parameters h or k .

LINEAR COEFFICIENT g FOR $K^\pm \rightarrow \pi^\pm \pi^0 \pi^0$

Unless otherwise stated, all experiments include terms quadratic in $(s_3 - s_0) / m_{\pi^+}^2$. See note above on "Dalitz Plot Parameters for $K \rightarrow 3\pi$ Decays."

See BATUSOV 98 for a discussion of the discrepancy between their result and others, especially BOLOTOV 86. At this time we have no way to resolve the discrepancy so we depend on the large scale factor as a warning.

VALUE	EVTS	DOCUMENT ID	TECN	CHG	COMMENT
0.626 ± 0.007 OUR AVERAGE					
0.6259 ± 0.0043 ± 0.0093	493k	AKOPDZHAN.	05B	TNF	±
0.627 ± 0.004 ± 0.010	252k	^{96,97} AJINENKO	03B	ISTR	-
••• We do not use the following data for averages, fits, limits, etc. •••					
0.736 ± 0.014 ± 0.012	33k	BATUSOV	98	SPEC	+
0.582 ± 0.021	43k	BOLOTOV	86	CALO	-
0.670 ± 0.054	3263	BRAUN	76B	HLBC	+
0.630 ± 0.038	5635	SHEAFF	75	HLBC	+
0.510 ± 0.060	27k	SMITH	75	WIRE	+
0.67 ± 0.06	1365	AUBERT	72	HLBC	+
0.544 ± 0.048	4048	DAVISON	69	HLBC	+

⁹⁶ Measured using in-flight decays of the 25 GeV negative secondary beam.

⁹⁷ They form new world averages $g_- = (0.617 \pm 0.018)$ and $g_+ = (0.684 \pm 0.033)$ which give $\Delta g_{\pi^0} = 0.051 \pm 0.028$.

QUADRATIC COEFFICIENT h FOR $K^\pm \rightarrow \pi^\pm \pi^0 \pi^0$

VALUE	EVTS	DOCUMENT ID	TECN	CHG	COMMENT
0.052 ± 0.008 OUR AVERAGE					
0.0551 ± 0.0044 ± 0.0086	493k	AKOPDZHAN.	05B	TNF	±
0.046 ± 0.004 ± 0.012	252k	⁹⁸ AJINENKO	03B	ISTR	-
••• We do not use the following data for averages, fits, limits, etc. •••					
0.128 ± 0.015 ± 0.024	33k	BATUSOV	98	SPEC	+
0.037 ± 0.024	43k	BOLOTOV	86	CALO	-
0.152 ± 0.082	3263	BRAUN	76B	HLBC	+
0.041 ± 0.030	5635	SHEAFF	75	HLBC	+
0.009 ± 0.040	27k	SMITH	75	WIRE	+
-0.01 ± 0.08	1365	AUBERT	72	HLBC	+
0.026 ± 0.050	4048	DAVISON	69	HLBC	+

⁹⁸ Measured using in-flight decays of the 25 GeV negative secondary beam.

QUADRATIC COEFFICIENT k FOR $K^\pm \rightarrow \pi^\pm \pi^0 \pi^0$

VALUE	EVTS	DOCUMENT ID	TECN	CHG
0.0054 ± 0.0035	OUR AVERAGE	Error includes scale factor of 2.5.		
0.0082 ± 0.0011 ± 0.0014	493k	AKOPDZHAN.05B	TNF	±
0.001 ± 0.001 ± 0.002	252k	99 AJINENKO	03B ISTR	—
• • • We do not use the following data for averages, fits, limits, etc. • • •				
0.0197 ± 0.0045 ± 0.0029	33k	BATUSOV	98 SPEC	+

⁹⁹ Measured using in-flight decays of the 25 GeV negative secondary beam.

 $(g_+ - g_-) / (g_+ + g_-)$ FOR $K^\pm \rightarrow \pi^\pm \pi^0 \pi^0$ A nonzero value for this quantity indicates CP violation.

VALUE (units 10^{-4})	EVTS	DOCUMENT ID	TECN	CHG
1.8 ± 1.8	OUR AVERAGE			
1.8 ± 1.7 ± 0.6	91.3M	100 BATLEY	07E NA48	
2 ± 18 ± 5	619k	101 AKOPDZHAN.05	TNF	
• • • We do not use the following data for averages, fits, limits, etc. • • •				
1.8 ± 2.2 ± 1.3	47M	102 BATLEY	06A NA48	

¹⁰⁰ BATLEY 07E includes data from BATLEY 06A. Uses quadratic parametrization and PDG 06 value $g = 0.626 \pm 0.007$ to obtain $g_+ - g_- = (2.2 \pm 2.1 \pm 0.7) \times 10^{-4}$. Neglects any possible charge asymmetries in higher order slope parameters h or k .

¹⁰¹ Asymmetry obtained assuming that $g_+ + g_- = 2 \times 0.652$ (PDG 02) and that asymmetries in h and k are zero.

¹⁰² Linear and quadratic slopes from PDG 04 are used. Any possible charge asymmetries in higher order slope parameters h or k are neglected.

ALTERNATIVE PARAMETRIZATIONS OF $K^\pm \rightarrow \pi^\pm \pi^0 \pi^0$ DALITZ PLOT

The following functional form for the matrix element suggested by $\pi\pi$ rescattering in $K^+ \rightarrow \pi^+ \pi^+ \pi^- \rightarrow \pi^+ \pi^0 \pi^0$ is used for this fit (CABIBBO 04A, CABIBBO 05): Matrix element = $M_0 + M_1$ where $M_0 = 1 + (1/2)g_0 u + (1/2)h' u^2 + (1/2)k_0 v^2$ with $u = (s_3 - s_0)/(m_{\pi^+})^2$, $v = (s_2 - s_1)/(m_{\pi^+})^2$ and where M_1 takes into account the non-analytic piece due to $\pi\pi$ rescattering amplitudes a_0 and a_2 ; The parameters g_0 and h' are related to the parameters g and h of the matrix element squared given in the previous section by the approximations $g_0 \sim g^{PDG}$ and $h' \sim h^{PDG} - (g/2)^2$ and $k_0 \sim k^{PDG}$.

In addition, we also consider the effective field theory framework of COLANGELO 06A and BISSEGGGER 09 to extract g_{BB} and h'_{BB} .

LINEAR COEFFICIENT g_0 FOR $K^\pm \rightarrow \pi^\pm \pi^0 \pi^0$

VALUE	EVTS	DOCUMENT ID	TECN	CHG
0.6525 ± 0.0009 ± 0.0033	OUR AVERAGE	Error includes scale factor of 2.5.		
0.645 ± 0.004 ± 0.009	23M	104 BATLEY	06B NA48	±

• • • We do not use the following data for averages, fits, limits, etc. • • •

¹⁰³ This fit is obtained with the CABIBBO 05 matrix element in the $2\pi^0$ invariant mass squared range $0.074094 < m_{2\pi^0}^2 < 0.104244$ GeV². Electromagnetic corrections and CHPT constraints for $\pi\pi$ phase shifts (a_0 and a_2) have been used. Also measured ($a_0 - a_2$) $m_{\pi^+} = 0.2646 \pm 0.0021 \pm 0.0023$, where k_0 was kept fixed in the fit at -0.0099 .

¹⁰⁴ Superseded by BATLEY 09A. This fit is obtained with the CABIBBO 05 matrix element in the $2\pi^0$ invariant mass squared range 0.074 GeV² $< m_{2\pi^0}^2 < 0.097$ GeV², assuming $k = 0$ (no term proportional to $(s_2 - s_1)^2$) and excluding the kinematic region around the cusp ($m_{2\pi^0}^2 = (2m_{\pi^+})^2 \pm 0.000525$ GeV²). Also $\pi\pi$ phase shifts a_0 and a_2 are measured: ($a_0 - a_2$) $m_{\pi^+} = 0.268 \pm 0.010 \pm 0.004 \pm 0.013$ (external) and $a_2 m_{\pi^+} = -0.041 \pm 0.022 \pm 0.014$.

QUADRATIC COEFFICIENT h' FOR $K^\pm \rightarrow \pi^\pm \pi^0 \pi^0$

VALUE	EVTS	DOCUMENT ID	TECN	CHG
-0.0433 ± 0.0008 ± 0.0026	OUR AVERAGE	Error includes scale factor of 2.5.		
-0.047 ± 0.012 ± 0.011	23M	106 BATLEY	06B NA48	±

• • • We do not use the following data for averages, fits, limits, etc. • • •

¹⁰⁵ This fit is obtained with the CABIBBO 05 matrix element in the $2\pi^0$ invariant mass squared range $0.074094 < m_{2\pi^0}^2 < 0.104244$ GeV². Electromagnetic corrections and CHPT constraints for $\pi\pi$ phase shifts (a_0 and a_2) have been used. Also measured ($a_0 - a_2$) $m_{\pi^+} = 0.2646 \pm 0.0021 \pm 0.0023$, where k_0 was kept fixed in the fit at -0.0099 .

¹⁰⁶ Superseded by BATLEY 09A. This fit is obtained with the CABIBBO 05 matrix element in the $2\pi^0$ invariant mass squared range 0.074 GeV² $< m_{2\pi^0}^2 < 0.097$ GeV², assuming $k = 0$ (no term proportional to $(s_2 - s_1)^2$) and excluding the kinematic region around the cusp ($m_{2\pi^0}^2 = (2m_{\pi^+})^2 \pm 0.000525$ GeV²). Also $\pi\pi$ phase shifts a_0 and a_2 are measured: ($a_0 - a_2$) $m_{\pi^+} = 0.268 \pm 0.010 \pm 0.004 \pm 0.013$ (external) and $a_2 m_{\pi^+} = -0.041 \pm 0.022 \pm 0.014$.

QUADRATIC COEFFICIENT k_0 FOR $K^\pm \rightarrow \pi^\pm \pi^0 \pi^0$

VALUE	EVTS	DOCUMENT ID	TECN	CHG
0.0095 ± 0.00017 ± 0.00048	OUR AVERAGE	Error includes scale factor of 2.5.		
0.0095 ± 0.00017 ± 0.00048	60M	107 BATLEY	09A NA48	±

¹⁰⁷ Assumed $a_2 m_{\pi^+} = -0.0044$ in the fit.

LINEAR COEFFICIENT g_{BB} FOR $K^\pm \rightarrow \pi^\pm \pi^0 \pi^0$

VALUE	EVTS	DOCUMENT ID	TECN	CHG
0.6219 ± 0.0009 ± 0.0033	OUR AVERAGE	Error includes scale factor of 2.5.		
0.6219 ± 0.0009 ± 0.0033	60M	108 BATLEY	09A NA48	±

¹⁰⁸ This fit is obtained using parametrizations of COLANGELO 06A and BISSEGGGER 09 in the $2\pi^0$ invariant mass squared range $0.074094 < m_{2\pi^0}^2 < 0.104244$ GeV². Electromagnetic corrections and CHPT constraints for $\pi\pi$ phase shifts (a_0 and a_2) have been used. Also measured ($a_0 - a_2$) $m_{\pi^+} = 0.2633 \pm 0.0024 \pm 0.0024$, where k_0 was kept fixed in the fit at 0.0085.

QUADRATIC COEFFICIENT h'_{BB} FOR $K^\pm \rightarrow \pi^\pm \pi^0 \pi^0$

VALUE	EVTS	DOCUMENT ID	TECN	CHG
-0.0520 ± 0.0009 ± 0.0026	OUR AVERAGE	Error includes scale factor of 2.5.		
-0.0520 ± 0.0009 ± 0.0026	60M	109 BATLEY	09A NA48	±

¹⁰⁹ This fit is obtained using parametrizations of COLANGELO 06A and BISSEGGGER 09 in the $2\pi^0$ invariant mass squared range $0.074094 < m_{2\pi^0}^2 < 0.104244$ GeV². Electromagnetic corrections and CHPT constraints for $\pi\pi$ phase shifts (a_0 and a_2) have been used. Also measured ($a_0 - a_2$) $m_{\pi^+} = 0.2633 \pm 0.0024 \pm 0.0024$, where k_0 was kept fixed in the fit at 0.0085.

 $K_{\ell 3}^\pm$ AND $K_{\ell 3}^0$ FORM FACTORS

Updated October 2009 by T.G. Trippe (LBNL) and C.-J. Lin (LBNL).

Assuming that only the vector current contributes to $K \rightarrow \pi \ell \nu$ decays, we write the matrix element as

$$M \propto f_+(t) [(P_K + P_\pi)_\mu \bar{\ell} \gamma_\mu (1 + \gamma_5) \nu] + f_-(t) [m_\ell \bar{\ell} (1 + \gamma_5) \nu], \quad (1)$$

where P_K and P_π are the four-momenta of the K and π mesons, m_ℓ is the lepton mass, and f_+ and f_- are dimensionless form factors which can depend only on $t = (P_K - P_\pi)^2$, the square of the four-momentum transfer to the leptons. If time-reversal invariance holds, f_+ and f_- are relatively real. $K_{\mu 3}$ experiments, discussed immediately below, measure f_+ and f_- , while $K_{e 3}$ experiments, discussed further below, are sensitive only to f_+ because the small electron mass makes the f_- term negligible.

$K_{\mu 3}$ Experiments. Analyses of $K_{\mu 3}$ data frequently assume a linear dependence of f_+ and f_- on t , *i.e.*,

$$f_\pm(t) = f_\pm(0) [1 + \lambda_\pm(t/m_{\pi^+}^2)]. \quad (2)$$

Most $K_{\mu 3}$ data are adequately described by Eq. (2) for f_+ and a constant f_- (*i.e.*, $\lambda_- = 0$).

There are two equivalent parametrizations commonly used in these analyses:

(1) **λ_+ , $\xi(0)$ parametrization.** Older analyses of $K_{\mu 3}$ data often introduce the ratio of the two form factors

$$\xi(t) = f_-(t)/f_+(t). \quad (3)$$

The $K_{\mu 3}$ decay distribution is then described by the two parameters λ_+ and $\xi(0)$ (assuming time reversal invariance and $\lambda_- = 0$).

(2) **λ_+ , λ_0 parametrization.** More recent $K_{\mu 3}$ analyses have parametrized in terms of the form factors f_+ and f_0 , which are associated with vector and scalar exchange, respectively, to the lepton pair. f_0 is related to f_+ and f_- by

$$f_0(t) = f_+(t) + [t/(m_K^2 - m_\pi^2)] f_-(t). \quad (4)$$

Meson Particle Listings

K^\pm

Here $f_0(0)$ must equal $f_+(0)$ unless $f_-(t)$ diverges at $t = 0$. The earlier assumption that f_+ is linear in t and f_- is constant leads to f_0 linear in t :

$$f_0(t) = f_0(0) [1 + \lambda_0(t/m_{\pi^+}^2)] . \quad (5)$$

With the assumption that $f_0(0) = f_+(0)$, the two parametrizations, $(\lambda_+, \xi(0))$ and (λ_+, λ_0) are equivalent as long as correlation information is retained. (λ_+, λ_0) correlations tend to be less strong than $(\lambda_+, \xi(0))$ correlations.

Since the 2006 edition of the *Review* [4], we no longer quote results in the $(\lambda_+, \xi(0))$ parametrization. We have removed many older low statistics results from the Listings. See the 2004 version of this note [5] for these older results, and the 1982 version [6] for additional discussion of the $K_{\mu 3}^0$ parameters, correlations, and conversion between parametrizations.

Quadratic Parametrization. More recent high-statistics experiments have included a quadratic term in the expansion of $f_+(t)$,

$$f_+(t) = f_+(0) \left[1 + \lambda'_+(t/m_{\pi^+}^2) + \frac{\lambda''_+}{2}(t/m_{\pi^+}^2)^2 \right] . \quad (6)$$

If there is a non-vanishing quadratic term, then λ_+ of Eq. (2) represents the average slope, which is then different from λ'_+ . Our convention is to include the factor $\frac{1}{2}$ in the quadratic term, and to use m_{π^+} even for K_{e3}^+ and $K_{\mu 3}^+$ decays. We have converted other's parametrizations to match our conventions, as noted in the beginning of the “ K_{e3}^\pm and $K_{\mu 3}^0$ Form Factors” sections of the Listings.

Pole Parametrization: The pole model describes the t -dependence of $f_+(t)$ and $f_0(t)$ in terms of the exchange of the lightest vector and scalar K^* mesons with masses M_v and M_s , respectively:

$$f_+(t) = f_+(0) \left[\frac{M_v^2}{M_v^2 - t} \right] , \quad f_0(t) = f_0(0) \left[\frac{M_s^2}{M_s^2 - t} \right] . \quad (7)$$

Dispersive Parametrization [7,8]. This approach uses dispersive techniques and the known low-energy K - π phases to parametrize the vector and scalar form factors:

$$f_+(t) = f_+(0) \exp \left[\frac{t}{m_\pi^2} (\Lambda_+ + H(t)) \right] ; \quad (8)$$

$$f_0(t) = f_+(0) \exp \left[\frac{t}{(m_K^2 - m_\pi^2)} (\ln[C] - G(t)) \right] , \quad (9)$$

where Λ_+ is the slope of the vector form factor, and $\ln[C] = \ln[f_0(m_K^2 - m_\pi^2)]$ is the logarithm of the scalar form factor at the Callan-Treiman point. The functions $H(t)$ and $G(t)$ are dispersive integrals.

K_{e3} Experiments: Analysis of K_{e3} data is simpler than that of $K_{\mu 3}$ because the second term of the matrix element assuming a pure vector current [Eq. (1) above] can be neglected. Here f_+ can be assumed to be linear in t , in which case the linear coefficient λ_+ of Eq. (2) is determined, or quadratic, in which case the linear coefficient λ'_+ and quadratic coefficient λ''_+ of Eq. (6) are determined.

If we remove the assumption of a pure vector current, then the matrix element for the decay, in addition to the terms in Eq. (1), would contain

$$+2m_K f_S \bar{\ell}(1 + \gamma_5)\nu \\ + (2f_T/m_K)(P_K)_\lambda (P_\pi)_\mu \bar{\ell} \sigma_{\lambda\mu} (1 + \gamma_5)\nu , \quad (10)$$

where f_S is the scalar form factor, and f_T is the tensor form factor. In the case of the K_{e3} decays where the f_- term can be neglected, experiments have yielded limits on $|f_S/f_+|$ and $|f_T/f_+|$.

Fits for K_{e3} Form Factors. For K_{e3} data, we determine best values for the three parametrizations: linear (λ_+) , quadratic $(\lambda'_+, \lambda''_+)$ and pole (M_v) . For $K_{\mu 3}$ data, we determine best values for the three parametrizations: linear (λ_+, λ_0) , quadratic $(\lambda'_+, \lambda''_+, \lambda_0)$ and pole (M_v, M_s) . We then assume $\mu - e$ universality so that we can combine K_{e3} and $K_{\mu 3}$ data, and again determine best values for the three parametrizations: linear (λ_+, λ_0) , quadratic $(\lambda'_+, \lambda''_+, \lambda_0)$, and pole (M_v, M_s) . When there is more than one parameter, fits are done including input correlations. Simple averages suffice in the two K_{e3} cases where there is only one parameter: linear (λ_+) and pole (M_v) .

Both KTeV and KLOE see an improvement in the quality of their fits relative to linear fits when a quadratic term is introduced, as well as when the pole parametrization is used. The quadratic parametrization has the disadvantage that the quadratic parameter λ''_+ is highly correlated with the linear parameter λ'_+ , in the neighborhood of 95%, and that neither parameter is very well determined. The pole fit has the same number of parameters as the linear fit, but yields slightly better fit probabilities, so that it would be advisable for all experiments to include the pole parametrization as one of their choices [9].

The “Kaon Particle Listings” show the results with and without assuming $\mu - e$ universality. The “Meson Summary Tables” show all of the results assuming $\mu - e$ universality, but most results not assuming $\mu - e$ universality are given only in the Listings.

References

1. L.M. Chounet, J.M. Gaillard, and M.K. Gaillard, Phys. Reports **4C**, 199 (1972).
2. H.W. Fearing, E. Fischbach, and J. Smith, Phys. Rev. **D2**, 542 (1970).
3. N. Cabibbo and A. Maksymowicz, Phys. Lett. **9**, 352 (1964).
4. W.-M. Yao *et al.*, Particle Data Group, J. Phys. **G33**, 1 (2006).
5. S. Eidelman *et al.*, Particle Data Group, Phys. Lett. **B592**, 1 (2004).
6. M. Roos *et al.*, Particle Data Group, Phys. Lett. **111B**, 73 (1982).
7. V. Bernard *et al.*, Phys. Lett. **B638**, 48 (2006).
8. A. Lai *et al.*, Phys. Lett. **B647**, 341 (2007), and references therein.
9. We thank P. Franzini (Rome U. and Frascati) for useful discussions on this point.

Meson Particle Listings

 K^\pm f_T/f_+ FOR K_{S3}^\pm DECAYRatio of tensor to f_+ couplings.

VALUE (units 10^{-2})	EVTS	DOCUMENT ID	TECN	CHG	COMMENT
$-0.07 \pm 0.71 \pm 0.20$	540k	YUSHCHENKO04	ISTR	-	DP
••• We do not use the following data for averages, fits, limits, etc. •••					
$-2.1 \pm 2.8 \pm 1.4$	112k	¹³² AJINENKO	03	ISTR	- DP
2 ± 12	1585	BRAUN	75	HLBC	

¹³²The second error is the theoretical error from the uncertainty in the chiral perturbation theory prediction for λ_0 . Superseded by YUSHCHENKO 04.

 K_{A4}^\pm FORM FACTORS

Based on the parametrizations of AMOROS 99, the K_{A4}^\pm form factors can be expressed as

$$F_s = f_s + f'_s q^2 + f''_s q^4 + f'_e S_e / 4m_\pi^2$$

$$F_p = f_p + f'_p q^2$$

$$G_p = g_p + g'_p q^2$$

$$H_p = h_p + h'_p q^2$$

where $q^2 = (S_\pi / 4m_\pi^2)$, S_π is the invariant mass squared of the dipion, and S_e is the invariant mass squared of the dilepton.

 f_s FOR $K^\pm \rightarrow \pi^+ \pi^- e^\pm \nu$ DECAY

VALUE	EVTS	DOCUMENT ID	TECN	CHG
$5.75 \pm 0.02 \pm 0.08$	400k	¹³³ PISLAK	03	B865 +

¹³³Radiative corrections included. Using Roy equations and not including isospin breaking, PISLAK 03 obtains the following $\pi\pi$ scattering lengths $a_0^0 = 0.228 \pm 0.012 \pm 0.004 + 0.012$ (theor.) and $a_0^2 = -0.037 \pm 0.023 \pm 0.008 \pm 0.003$ (theor.).

 f'_s FOR $K^\pm \rightarrow \pi^+ \pi^- e^\pm \nu$ DECAY

VALUE	EVTS	DOCUMENT ID	TECN	CHG
$0.99 \pm 0.06 \pm 0.01$	670k	^{134,135} BATLEY	08A	NA48 ±
$1.06 \pm 0.10 \pm 0.40$	400k	¹³⁶ PISLAK	03	B865 +

¹³⁴BATLEY 08A reports $[f'_s] / [f_s] = (17.2 \pm 0.9 \pm 0.6) \times 10^{-2}$ which we multiply by our best value $f_s = 5.75 \pm 0.08$. Our first error is their experiment's error and our second error is the systematic error from using our best value.

¹³⁵Radiative corrections included. Using Roy equations and not including isospin breaking, BATLEY 08A obtains the following $\pi\pi$ scattering length $a_0^0 = 0.233 \pm 0.016 \pm 0.007$ $a_0^2 = -0.0471 \pm 0.011 \pm 0.004$.

¹³⁶Radiative corrections included. Using Roy equations and not including isospin breaking, PISLAK 03 obtains the following $\pi\pi$ scattering lengths $a_0^0 = 0.228 \pm 0.012 \pm 0.004 + 0.012$ (theor.) and $a_0^2 = -0.037 \pm 0.023 \pm 0.008 \pm 0.003$ (theor.).

 f''_s FOR $K^\pm \rightarrow \pi^+ \pi^- e^\pm \nu$ DECAY

VALUE	EVTS	DOCUMENT ID	TECN	CHG
$-0.52 \pm 0.07 \pm 0.01$	670k	^{137,138} BATLEY	08A	NA48 ±
$-0.59 \pm 0.12 \pm 0.40$	400k	¹³⁹ PISLAK	03	B865 +

¹³⁷BATLEY 08A reports $[f''_s] / [f_s] = (-9.0 \pm 0.9 \pm 0.7) \times 10^{-2}$ which we multiply by our best value $f_s = 5.75 \pm 0.08$. Our first error is their experiment's error and our second error is the systematic error from using our best value.

¹³⁸Radiative corrections included. Using Roy equations and not including isospin breaking, BATLEY 08A obtains the following $\pi\pi$ scattering length $a_0^0 = 0.233 \pm 0.016 \pm 0.007$ $a_0^2 = -0.0471 \pm 0.011 \pm 0.004$.

¹³⁹Radiative corrections included. Using Roy equations and not including isospin breaking, PISLAK 03 obtains the following $\pi\pi$ scattering lengths $a_0^0 = 0.228 \pm 0.012 \pm 0.004 + 0.012$ (theor.) and $a_0^2 = -0.037 \pm 0.023 \pm 0.008 \pm 0.003$ (theor.).

 f'_e FOR $K^\pm \rightarrow \pi^+ \pi^- e^\pm \nu$ DECAY

VALUE	EVTS	DOCUMENT ID	TECN	CHG
$0.47 \pm 0.07 \pm 0.01$	670k	^{140,141} BATLEY	08A	NA48 ±

¹⁴⁰BATLEY 08A reports $[f'_e] / [f_s] = (8.1 \pm 0.8 \pm 0.9) \times 10^{-2}$ which we multiply by our best value $f_s = 5.75 \pm 0.08$. Our first error is their experiment's error and our second error is the systematic error from using our best value.

¹⁴¹Radiative corrections included. Using Roy equations and not including isospin breaking, BATLEY 08A obtains the following $\pi\pi$ scattering length $a_0^0 = 0.233 \pm 0.016 \pm 0.007$ $a_0^2 = -0.0471 \pm 0.011 \pm 0.004$.

 f_p FOR $K^\pm \rightarrow \pi^+ \pi^- e^\pm \nu$ DECAY

VALUE	EVTS	DOCUMENT ID	TECN	CHG
$-0.276 \pm 0.033 \pm 0.004$	670k	^{142,143} BATLEY	08A	NA48 ±

¹⁴²BATLEY 08A reports $[f_p] / [f_s] = (-4.8 \pm 0.4 \pm 0.4) \times 10^{-2}$ which we multiply by our best value $f_s = 5.75 \pm 0.08$. Our first error is their experiment's error and our second error is the systematic error from using our best value.

¹⁴³Radiative corrections included. Using Roy equations and not including isospin breaking, BATLEY 08A obtains the following $\pi\pi$ scattering length $a_0^0 = 0.233 \pm 0.016 \pm 0.007$ $a_0^2 = -0.0471 \pm 0.011 \pm 0.004$.

 g_p FOR $K^\pm \rightarrow \pi^+ \pi^- e^\pm \nu$ DECAY

VALUE	EVTS	DOCUMENT ID	TECN	CHG
4.78 ± 0.17 OUR AVERAGE	Error includes scale factor of 2.4.			
$5.02 \pm 0.10 \pm 0.07$	670k	^{144,145} BATLEY	08A	NA48 ±
$4.66 \pm 0.05 \pm 0.07$	400k	¹⁴⁶ PISLAK	03	B865 +

¹⁴⁴BATLEY 08A reports $[g_p] / [f_s] = (87.3 \pm 1.3 \pm 1.2) \times 10^{-2}$ which we multiply by our best value $f_s = 5.75 \pm 0.08$. Our first error is their experiment's error and our second error is the systematic error from using our best value.

¹⁴⁵Radiative corrections included. Using Roy equations and not including isospin breaking, BATLEY 08A obtains the following $\pi\pi$ scattering length $a_0^0 = 0.233 \pm 0.016 \pm 0.007$ $a_0^2 = -0.0471 \pm 0.011 \pm 0.004$.

¹⁴⁶Radiative corrections included. Using Roy equations and not including isospin breaking, PISLAK 03 obtains the following $\pi\pi$ scattering lengths $a_0^0 = 0.228 \pm 0.012 \pm 0.004 + 0.012$ (theor.) and $a_0^2 = -0.037 \pm 0.023 \pm 0.008 \pm 0.003$ (theor.).

 g'_p FOR $K^\pm \rightarrow \pi^+ \pi^- e^\pm \nu$ DECAY

VALUE	EVTS	DOCUMENT ID	TECN	CHG
0.60 ± 0.10 OUR AVERAGE	Error includes scale factor of 1.1.			
$0.47 \pm 0.15 \pm 0.01$	670k	^{147,148} BATLEY	08A	NA48 ±
$0.67 \pm 0.10 \pm 0.04$	400k	¹⁴⁹ PISLAK	03	B865 +

¹⁴⁷BATLEY 08A reports $[g'_p] / [f_s] = (8.1 \pm 2.2 \pm 1.5) \times 10^{-2}$ which we multiply by our best value $f_s = 5.75 \pm 0.08$. Our first error is their experiment's error and our second error is the systematic error from using our best value.

¹⁴⁸Radiative corrections included. Using Roy equations and not including isospin breaking, BATLEY 08A obtains the following $\pi\pi$ scattering length $a_0^0 = 0.233 \pm 0.016 \pm 0.007$ $a_0^2 = -0.0471 \pm 0.011 \pm 0.004$.

¹⁴⁹Radiative corrections included. Using Roy equations and not including isospin breaking, PISLAK 03 obtains the following $\pi\pi$ scattering lengths $a_0^0 = 0.228 \pm 0.012 \pm 0.004 + 0.012$ (theor.) and $a_0^2 = -0.037 \pm 0.023 \pm 0.008 \pm 0.003$ (theor.).

 h_p FOR $K^\pm \rightarrow \pi^+ \pi^- e^\pm \nu$ DECAY

VALUE	EVTS	DOCUMENT ID	TECN	CHG
-2.46 ± 0.22 OUR AVERAGE	Error includes scale factor of 1.9.			
$-2.36 \pm 0.12 \pm 0.03$	670k	^{150,151} BATLEY	08A	NA48 ±
$-2.95 \pm 0.19 \pm 0.20$	400k	¹⁵² PISLAK	03	B865 +

¹⁵⁰BATLEY 08A reports $[h_p] / [f_s] = (-41.1 \pm 1.9 \pm 0.8) \times 10^{-2}$ which we multiply by our best value $f_s = 5.75 \pm 0.08$. Our first error is their experiment's error and our second error is the systematic error from using our best value.

¹⁵¹Radiative corrections included. Using Roy equations and not including isospin breaking, BATLEY 08A obtains the following $\pi\pi$ scattering length $a_0^0 = 0.233 \pm 0.016 \pm 0.007$ $a_0^2 = -0.0471 \pm 0.011 \pm 0.004$.

¹⁵²Radiative corrections included. Using Roy equations and not including isospin breaking, PISLAK 03 obtains the following $\pi\pi$ scattering lengths $a_0^0 = 0.228 \pm 0.012 \pm 0.004 + 0.012$ (theor.) and $a_0^2 = -0.037 \pm 0.023 \pm 0.008 \pm 0.003$ (theor.).

DECAY FORM FACTOR FOR $K^\pm \rightarrow \pi^0 \pi^0 e^\pm \nu$

Given in BOLOTOV 86b, BARMIN 88b, and SHIMIZU 04.

 $K^\pm \rightarrow \ell^\pm \nu \gamma$ FORM FACTORS

For definitions of the axial-vector F_A and vector F_V form factor, see the "Note on $\pi^\pm \rightarrow \ell^\pm \nu \gamma$ and $K^\pm \rightarrow \ell^\pm \nu \gamma$ Form Factors" in the π^\pm section. In the kaon literature, often different definitions $a_K = F_A/m_K$ and $v_K = F_V/m_K$ are used.

 $F_A + F_V$, SUM OF AXIAL-VECTOR AND VECTOR FORM FACTOR FOR $K \rightarrow e \nu \gamma$

VALUE	EVTS	DOCUMENT ID	TECN	COMMENT
0.133 ± 0.008 OUR AVERAGE	Error includes scale factor of 1.3. See the ideogram below.			
$0.125 \pm 0.007 \pm 0.001$	1.4K	¹⁵³ AMBROSINO	09E	KLOE E_γ in 10–250 MeV, $p_e > 200$ MeV/c

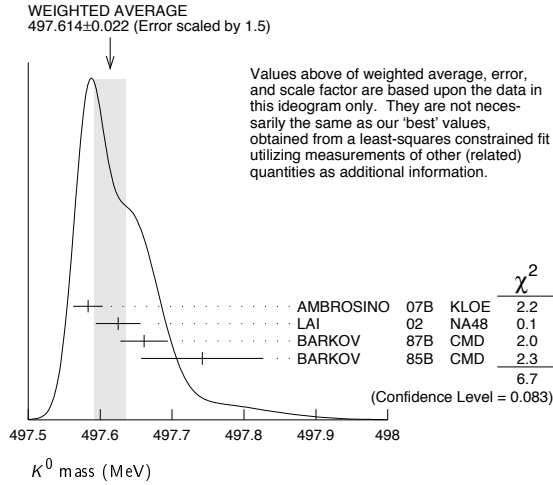
0.147 ± 0.011 51 ¹⁵⁴HEINTZE 79 SPEC

$0.150 + 0.018 - 0.023$ 56 ¹⁵⁵HEARD 75 SPEC

¹⁵³Vector form factor fitted with a linear function, $V(x) = F_V (1 + \lambda(1-x))$, $x = 2E_\gamma/m_K$. The fitted value of $\lambda = 0.38 \pm 0.20 \pm 0.02$ with a correlation of -0.93 between $(F_V + F_A)$ and λ .

¹⁵⁴HEINTZE 79 quotes absolute value of $|F_A + F_V| \sin \theta_C$. We use $\sin \theta_C = V_{us} = 0.2205$.

¹⁵⁵HEARD 75 quotes absolute value of $|F_A + F_V| \sin \theta_C$. We use $\sin \theta_C = V_{us} = 0.2205$.

 $m_{K^0} - m_{K^\pm}$

VALUE (MeV)	EVTS	DOCUMENT ID	TECN	CHG	COMMENT
3.937±0.028 OUR FIT					Error includes scale factor of 1.8.
•••					We do not use the following data for averages, fits, limits, etc. •••
3.95 ± 0.21	417	HILL	68B	DBC	+ $K^+ d \rightarrow K^0 p p$
3.90 ± 0.25	9	BURNSTEIN	65	HBC	-
3.71 ± 0.35	7	KIM	65B	HBC	- $K^- p \rightarrow n \bar{K}^0$
5.4 ± 1.1		CRAWFORD	59	HBC	+
3.9 ± 0.6		ROSENFELD	59	HBC	-

 K^0 MEAN SQUARE CHARGE RADIUS

VALUE (fm ²)	EVTS	DOCUMENT ID	TECN	COMMENT	
-0.077±0.010 OUR AVERAGE					
-0.077 ± 0.007 ± 0.011	5037	ABOUZAID	06	KTEV	$K_L^0 \rightarrow \pi^+ \pi^- e^+ e^-$
-0.090 ± 0.021		LAI	03c	NA48	$K_L^0 \rightarrow \pi^+ \pi^- e^+ e^-$
-0.054 ± 0.026		MOLZON	78		K_S regen. by electrons
•••					We do not use the following data for averages, fits, limits, etc. •••
-0.087 ± 0.046		BLATNIK	79		VMD + dispersion relations
-0.050 ± 0.130		FOETH	69B		K_S regen. by electrons

 T -VIOLATION PARAMETER IN K^0 - \bar{K}^0 MIXING

The asymmetry $A_T = \frac{\Gamma(\bar{K}^0 \rightarrow K^0) - \Gamma(K^0 \rightarrow \bar{K}^0)}{\Gamma(\bar{K}^0 \rightarrow K^0) + \Gamma(K^0 \rightarrow \bar{K}^0)}$ must vanish if T invariance holds.

ASYMMETRY A_T IN K^0 - \bar{K}^0 MIXING

VALUE (units 10^{-3})	EVTS	DOCUMENT ID	TECN
6.6±1.3±1.0	640k	1 ANGELOPOU... 98E	CPLR

¹ ANGELOPOULOS 98E measures the asymmetry $A_T = \frac{\Gamma(\bar{K}^0_{t=0} \rightarrow e^+ \pi^- \nu_{t=\tau}) - \Gamma(K^0_{t=0} \rightarrow e^- \pi^+ \bar{\nu}_{t=\tau})}{\Gamma(\bar{K}^0_{t=0} \rightarrow e^+ \pi^- \nu_{t=\tau}) + \Gamma(K^0_{t=0} \rightarrow e^- \pi^+ \bar{\nu}_{t=\tau})}$ as a function of the neutral-kaon eigentime τ . The initial strangeness of the neutral kaon is tagged by the charge of the accompanying charged kaon in the reactions $p\bar{p} \rightarrow K^- \pi^+ K^0$ and $p\bar{p} \rightarrow K^+ \pi^- \bar{K}^0$. The strangeness at the time of the decay is tagged by the lepton charge. The reported result is the average value of A_T over the interval $1\tau_S < \tau < 20\tau_S$. From this value of A_T ANGELOPOULOS 01B, assuming CPT invariance in the $e\pi\nu$ decay amplitude, determine the T -violating $\Delta S = \Delta S$ conserving parameter (for its definition, see Review below) $4\text{Re}(\epsilon) = (6.2 \pm 1.4 \pm 1.0) \times 10^{-3}$.

 CPT INVARIANCE TESTS IN NEUTRAL KAON DECAY

Updated October 2009 by M. Antonelli (LNF-INFN, Frascati) and G. D'Ambrosio (INFN Sezione di Napoli).

CPT theorem is based on three assumptions: quantum field theory, locality, and Lorentz invariance, and thus it is a fundamental probe of our basic understanding of particle physics. Strangeness oscillation in $K^0 - \bar{K}^0$ system, described by the equation

$$i \frac{d}{dt} \begin{bmatrix} K^0 \\ \bar{K}^0 \end{bmatrix} = [M - i\Gamma/2] \begin{bmatrix} K^0 \\ \bar{K}^0 \end{bmatrix},$$

where M and Γ are hermitian matrices (see PDG review [1], references [2,3], and KLOE paper [4] for notations and previous literature), allows a very accurate test of CPT symmetry; indeed since CPT requires $M_{11} = M_{22}$ and $\Gamma_{11} = \Gamma_{22}$, the mass and width eigenstates, $K_{S,L}$, have a CPT -violating piece, δ , in addition to the usual CPT -conserving parameter ϵ :

$$K_{S,L} = \frac{1}{\sqrt{2(1+|\epsilon_{S,L}|^2)}} \left[(1+\epsilon_{S,L}) K^0 + (1-\epsilon_{S,L}) \bar{K}^0 \right]$$

$$\epsilon_{S,L} = \frac{-i\Im(M_{12}) - \frac{1}{2}\Im(\Gamma_{12}) \mp \frac{1}{2} \left[M_{11} - M_{22} - \frac{i}{2}(\Gamma_{11} - \Gamma_{22}) \right]}{m_L - m_S + i(\Gamma_S - \Gamma_L)/2}$$

$$\equiv \epsilon \pm \delta.$$

Using the phase convention $\Im(\Gamma_{12}) = 0$, we determine the phase of ϵ to be $\varphi_{SW} \equiv \arctan \frac{2(m_L - m_S)}{\Gamma_S - \Gamma_L}$. Imposing unitarity to an arbitrary combination of K^0 and \bar{K}^0 wave functions, we obtain the Bell-Steinberger relation [5] connecting CP and CPT violation in the mass matrix to CP and CPT violation in the decay; in fact, neglecting $\mathcal{O}(\epsilon)$ corrections to the coefficient of the CPT -violating parameter, δ , we can write [4]

$$\left[\frac{\Gamma_S + \Gamma_L}{\Gamma_S - \Gamma_L} + i \tan \phi_{SW} \right] \left[\frac{\Re(\epsilon)}{1+|\epsilon|^2} - i\Im(\delta) \right] = \frac{1}{\Gamma_S - \Gamma_L} \sum_f A_L(f) A_S^*(f),$$

where $A_{L,S}(f) \equiv A(K_{L,S} \rightarrow f)$. We stress that this relation is phase-convention-independent. The advantage of the neutral kaon system is that only a few decay modes give significant contributions to the r.h.s. in Eq. (2); in fact, defining for the hadronic modes

$$\alpha_i \equiv \frac{1}{\Gamma_S} \langle \mathcal{A}_L(i) \mathcal{A}_S^*(i) \rangle = \eta_i \mathcal{B}(K_S \rightarrow i),$$

$$i = \pi^0 \pi^0, \pi^+ \pi^-(\gamma), 3\pi^0, \pi^0 \pi^+ \pi^-(\gamma),$$

the recent data from CPLEAR, KLOE, KTeV, and NA48 have led to the following determinations (the analysis described in Ref. 4 has been updated by using the recent measurements of K_L branching ratios from KTeV [6] and NA48 [7,8])

$$\alpha_{\pi^+ \pi^-} = ((1.112 \pm 0.013) + i(1.061 \pm 0.014)) \times 10^{-3},$$

$$\alpha_{\pi^0 \pi^0} = ((0.493 \pm 0.007) + i(0.471 \pm 0.007)) \times 10^{-3},$$

$$\alpha_{\pi^+ \pi^- \pi^0} = ((0 \pm 2) + i(0 \pm 2)) \times 10^{-6},$$

$$|\alpha_{\pi^0 \pi^0 \pi^0}| < 7 \times 10^{-6} \text{ at } 95\% \text{ CL}.$$

The semileptonic contribution to the right-handed side of Eq. (2) requires the determination of several observables: we define [2,3]

$$\mathcal{A}(K^0 \rightarrow \pi^- l^+ \nu) = \mathcal{A}_0(1 - y),$$

$$\mathcal{A}(K^0 \rightarrow \pi^+ l^- \nu) = \mathcal{A}_0^*(1 + y^*)(x_+ - x_-)^*,$$

$$\mathcal{A}(\bar{K}^0 \rightarrow \pi^+ l^- \nu) = \mathcal{A}_0^*(1 + y^*),$$

$$\mathcal{A}(\bar{K}^0 \rightarrow \pi^- l^+ \nu) = \mathcal{A}_0(1 - y)(x_+ + x_-),$$

Meson Particle Listings

 K^0

where x_+ (x_-) describes the violation of the $\Delta S = \Delta Q$ rule in CPT -conserving (violating) decay amplitudes, and y parametrizes CPT violation for $\Delta S = \Delta Q$ transitions. Taking advantage of their tagged $K^0(\bar{K}^0)$ beams, CPLEAR has measured $\Im(x_+)$, $\Re(x_-)$, $\Im(\delta)$, and $\Re(\delta)$ [10]. These determinations have been improved in Ref. 4 by including the information $A_S - A_L = 4[\Re(\delta) + \Re(x_-)]$, where $A_{L,S}$ are the K_L and K_S semileptonic charge asymmetries, respectively, from the PDG [11] and KLOE [12]. Here we are also including the T -violating asymmetry measurement from CPLEAR [13].

Table 1: Values, errors, and correlation coefficients for $\Re(\delta)$, $\Im(\delta)$, $\Re(x_-)$, $\Im(x_+)$, and $A_S + A_L$ obtained from a combined fit, including KLOE [4] and CPLEAR [13].

	value	Correlations coefficients
$\Re(\delta)$	$(3.0 \pm 2.3) \times 10^{-4}$	1
$\Im(\delta)$	$(-0.66 \pm 0.65) \times 10^{-2}$	-0.21 1
$\Re(x_-)$	$(-0.30 \pm 0.21) \times 10^{-2}$	-0.21 -0.60 1
$\Im(x_+)$	$(0.02 \pm 0.22) \times 10^{-2}$	-0.38 -0.14 0.47 1
$A_S + A_L$	$(-0.40 \pm 0.83) \times 10^{-2}$	-0.10 -0.63 0.99 0.43 1

The value $A_S + A_L$ in Table 1 can be directly included in the semileptonic contributions to the Bell Steinberger relations in Eq. (2)

$$\begin{aligned} & \sum_{\pi\ell\nu} \langle \mathcal{A}_L(\pi\ell\nu) \mathcal{A}_S^*(\pi\ell\nu) \rangle \\ &= 2\Gamma(K_L \rightarrow \pi\ell\nu) (\Re(\epsilon) - \Re(y) - i(\Im(x_+) + \Im(\delta))) \\ &= 2\Gamma(K_L \rightarrow \pi\ell\nu) ((A_S + A_L)/4 - i(\Im(x_+) + \Im(\delta))) . \end{aligned} \quad (6)$$

Defining

$$\alpha_{\pi\ell\nu} \equiv \frac{1}{\Gamma_S} \sum_{\pi\ell\nu} \langle \mathcal{A}_L(\pi\ell\nu) \mathcal{A}_S^*(\pi\ell\nu) \rangle + 2i \frac{\tau_{K_S}}{\tau_{K_L}} \mathcal{B}(K_L \rightarrow \pi\ell\nu) \Im(\delta) , \quad (7)$$

we find:

$$\alpha_{\pi\ell\nu} = ((-0.2 \pm 0.5) + i(0.1 \pm 0.5)) \times 10^{-5} .$$

Inserting the values of the α parameters into Eq. (2), we find

$$\begin{aligned} \Re(\epsilon) &= (161.2 \pm 0.6) \times 10^{-5} , \\ \Im(\delta) &= (-0.6 \pm 1.9) \times 10^{-5} . \end{aligned} \quad (8)$$

The complete information on Eq. (8) is given in Table 2.

Table 2: Summary of results: values, errors, and correlation coefficients for $\Re(\epsilon)$, $\Im(\delta)$, $\Re(\delta)$, and $\Re(x_-)$.

	value	Correlations coefficients
$\Re(\epsilon)$	$(161.2 \pm 0.6) \times 10^{-5}$	+1
$\Im(\delta)$	$(-0.6 \pm 1.9) \times 10^{-5}$	+0.26 1
$\Re(\delta)$	$(2.5 \pm 2.3) \times 10^{-4}$	+0.08 -0.09 1
$\Re(x_-)$	$(-4.2 \pm 1.7) \times 10^{-3}$	+0.13 0.17 -0.43 1

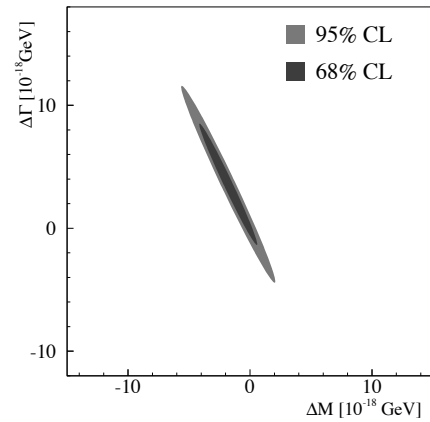
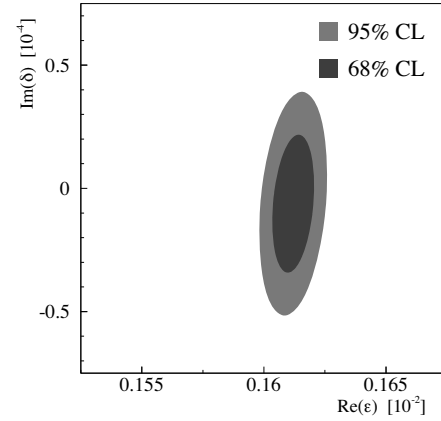


Figure 1: Top: allowed region at 68% and 95% C.L. in the $\Re(\epsilon)$, $\Im(\delta)$ plane. Bottom: allowed region at 68% and 95% C.L. in the ΔM , $\Delta\Gamma$ plane. Latest KTeV preliminary results not included in these figures.

Now the agreement with CPT conservation, $\Im(\delta) = \Re(\delta) = \Re(x_-) = 0$, is at 30% C.L.

The allowed region in the $\Re(\epsilon) - \Im(\delta)$ plane at 68% CL and 95% C.L. is shown in the top panel of Fig. 1.

The process giving the largest contribution to the size of the allowed region is $K_L \rightarrow \pi^+\pi^-$, through the uncertainty on ϕ_{+-} .

The limits on $\Im(\delta)$ and $\Re(\delta)$ can be used to constrain the $K^0 - \bar{K}^0$ mass and width difference

$$\delta = \frac{i(m_{K^0} - m_{\bar{K}^0}) + \frac{1}{2}(\Gamma_{K^0} - \Gamma_{\bar{K}^0})}{\Gamma_S - \Gamma_L} \cos \phi_{SW} e^{i\phi_{SW}} [1 + \mathcal{O}(\epsilon)].$$

The allowed region in the $\Delta M = (m_{K^0} - m_{\bar{K}^0})$, $\Delta\Gamma = (\Gamma_{K^0} - \Gamma_{\bar{K}^0})$ plane is shown in the bottom panel of Fig. 1. As a result, we improve on the previous limits (see for instance, P. Bloch in Ref. 11) and in the limit $\Gamma_{K^0} - \Gamma_{\bar{K}^0} = 0$ we obtain

$$-5.1 \times 10^{-19} \text{ GeV} < m_{K^0} - m_{\bar{K}^0} < 5.1 \times 10^{-19} \text{ GeV} \text{ at } 95 \% \text{ C.L.}$$

Adding the preliminary KTeV results on $\phi_{\pi^+\pi^-}$ and $\Delta\phi$ [14,15] we obtain: $\Re(\epsilon) = (161.2 \pm 0.6) \times 10^{-5}$, $\Im(\delta) = (-0.6 \pm 1.4) \times 10^{-5}$, leading to

$$-4.0 \times 10^{-19} \text{ GeV} < m_{K^0} - m_{\bar{K}^0} < 4.0 \times 10^{-19} \text{ GeV} \text{ at } 95 \% \text{ C.L.}$$

References

1. See the “*CP Violation in Meson Decays*,” in this *Review*.
2. L. Maiani, “*CP And CPT Violation In Neutral Kaon Decays*,” L. Maiani, G. Pancheri, and N. Paver, *The Second Daphne Physics Handbook*, Vol. 1, 2.
3. G. D’Ambrosio, G. Isidori, and A. Pugliese, “*CP and CPT measurements at DAΦNE*,” L. Maiani, G. Pancheri, and N. Paver, *The Second Daphne Physics Handbook*, Vol. 1, 2.
4. F. Ambrosino *et al.*, [KLOE Collaboration], *JHEP* **0612**, 011 (2006) [arXiv:hep-ex/0610034].
5. J. S. Bell and J. Steinberger, In Wolfenstein, L. (ed.): *CP violation*, 42-57. (In *Oxford International Symposium Conference on Elementary Particles*, September 1965, 195-208, 221-222). (See Book Index).
6. T. Alexopoulos *et al.*, [KTeV Collaboration], *Phys. Rev. D* **70**, 092006 (1998).
7. A. Lai *et al.*, [NA48 Collaboration], *Phys. Lett.* **B645**, 26 (2007);
A. Lai *et al.*, [NA48 Collaboration], *Phys. Lett.* **B602**, 41 (2004).
8. We thank G. Isidori and M. Palutan for their contribution to the original analysis [4] performed with KLOE data.
9. A. Angelopoulos *et al.*, [CPLEAR Collaboration], *Phys. Reports* **374**, 165 (2003).
10. A. Angelopoulos *et al.*, [CPLEAR Collaboration], *Phys. Lett.* **B444**, 52 (1998).
11. W. M. Yao *et al.*, [Particle Data Group], *J. Phys.* **G33**, 1 (2006).
12. F. Ambrosino *et al.*, [KLOE Collaboration], *Phys. Lett.* **B636**, 173 (2006) [arXiv:hep-ex/0601026].
13. P. Bloch, M. Fidecaro, private communication of the data in a finer binning format; A. Angelopoulos *et al.*, [CPLEAR Collaboration], *Phys. Lett.* **B444**, 43 (1998).
14. KTeV home page, <http://ktev.fnal.gov/public/>.
15. We thank M. Palutan for the collaboration in this analysis.

CP-VIOLATION PARAMETERS

Re(ϵ)

VALUE (units 10^{-3})	DOCUMENT ID	TECN
1.596 ± 0.013	² AMBROSINO 06H	KLOE
• • • We do not use the following data for averages, fits, limits, etc. • • •		
1.664 ± 0.010	³ LAI	05A NA48

- ² AMBROSINO 06H uses Bell-Steinberger relations with the following measurements: $B(K_L^0 \rightarrow \pi^+\pi^-)$ in AMBROSINO 06F, $B(K_S^0 \rightarrow \pi^0\pi^0\pi^0)$ in AMBROSINO 05B, the K_S^0 -semileptonic charge asymmetry in AMBROSINO 06E, and K^0 -semileptonic results in ANGELOPOULOS 98F.
³ LAI 05A values are obtained through unitarity (Bell-Steinberger relations), improving determination of η_{000} and combining other data from PDG 04 and APOSTOLAKIS 99B.

CPT-VIOLATION PARAMETERS

In $K^0 - \bar{K}^0$ mixing, if *CP*-violating interactions include a *T* conserving part then

$$|K_S\rangle = [|K_1\rangle + (\epsilon + \delta)|K_2\rangle] / \sqrt{1 + |\epsilon + \delta|^2}$$

$$|K_L\rangle = [|K_2\rangle + (\epsilon - \delta)|K_1\rangle] / \sqrt{1 + |\epsilon - \delta|^2}$$

where

$$|K_1\rangle = [|K^0\rangle + |\bar{K}^0\rangle] / \sqrt{2}$$

$$|K_2\rangle = [|K^0\rangle - |\bar{K}^0\rangle] / \sqrt{2}$$

and

$$|\bar{K}^0\rangle = CP|K^0\rangle.$$

The parameter δ specifies the *CPT*-violating part.

Estimates of δ are given below assuming the validity of the $\Delta S = \Delta Q$ rule. See also THOMSON 95 for a test of *CP T*-symmetry conservation in K^0 decays using the Bell-Steinberger relation.

REAL PART OF δ

A nonzero value violates *CPT* invariance.

VALUE (units 10^{-4})	EVTS	DOCUMENT ID	TECN	COMMENT
2.3 ± 2.7		⁴ AMBROSINO 06H	KLOE	
• • • We do not use the following data for averages, fits, limits, etc. • • •				
2.4 ± 2.8		⁵ APOSTOLA... 99B	RVUE	
2.9 ± 2.6 ± 0.6	1.3M	⁶ ANGELOPO... 98F	CPLR	
180 ± 200	6481	⁷ DEMIDOV 95		$K_{\ell 3}$ reanalysis

- ⁴ AMBROSINO 06H uses Bell-Steinberger relations with the following measurements: $B(K_L^0 \rightarrow \pi^+\pi^-)$ in AMBROSINO 06F, $B(K_S^0 \rightarrow \pi^0\pi^0\pi^0)$ in AMBROSINO 05B, the K_S^0 -semileptonic charge asymmetry in AMBROSINO 06E, and K^0 -semileptonic results in ANGELOPOULOS 98F.
⁵ APOSTOLAKIS 99B assumes only unitarity and combines CPLEAR and other results.
⁶ ANGELOPOULOS 98F use $\Delta S = \Delta Q$. If $\Delta S = \Delta Q$ is not assumed, they find $\text{Re}\delta = (3.0 \pm 3.3 \pm 0.6) \times 10^{-4}$.
⁷ DEMIDOV 95 reanalyzes data from HART 73 and NIEBERGALL 74.

IMAGINARY PART OF δ

A nonzero value violates *CPT* invariance.

VALUE (units 10^{-5})	EVTS	DOCUMENT ID	TECN	COMMENT
0.4 ± 2.1		⁸ AMBROSINO 06H	KLOE	
• • • We do not use the following data for averages, fits, limits, etc. • • •				
– 0.2 ± 2.0		⁹ LAI	05A NA48	
2.4 ± 5.0		¹⁰ APOSTOLA... 99B	RVUE	
– 90 ± 290 ± 100	1.3M	¹¹ ANGELOPO... 98F	CPLR	
2100 ± 3700	6481	¹² DEMIDOV 95		$K_{\ell 3}$ reanalysis

- ⁸ AMBROSINO 06H uses Bell-Steinberger relations with the following measurements: $B(K_L^0 \rightarrow \pi^+\pi^-)$ in AMBROSINO 06F, $B(K_S^0 \rightarrow \pi^0\pi^0\pi^0)$ in AMBROSINO 05B, the K_S^0 -semileptonic charge asymmetry in AMBROSINO 06E, and K^0 -semileptonic results in ANGELOPOULOS 98F.
⁹ LAI 05A values are obtained through unitarity (Bell-Steinberger relations), improving determination of η_{000} and combining other data from PDG 04 and APOSTOLAKIS 99B.
¹⁰ APOSTOLAKIS 99B assumes only unitarity and combines CPLEAR and other results.
¹¹ If $\Delta S = \Delta Q$ is not assumed, ANGELOPOULOS 98F finds $\text{Im}\delta = (-15 \pm 23 \pm 3) \times 10^{-3}$.
¹² DEMIDOV 95 reanalyzes data from HART 73 and NIEBERGALL 74.

Re(η)

A non-zero value would violate *CPT* invariance in $\Delta S = \Delta Q$ amplitude. $\text{Re}(\eta)$ is the following combination of K_{e3} decay amplitudes:

$$\text{Re}(\eta) = \text{Re} \left(\frac{A(K^0 \rightarrow e^-\pi^+\bar{\nu}_e) + A(K^0 \rightarrow e^+\pi^-\nu_e)}{A(K^0 \rightarrow e^-\pi^+\bar{\nu}_e) + A(K^0 \rightarrow e^+\pi^-\nu_e)} \right)$$

VALUE (units 10^{-3})	EVTS	DOCUMENT ID	TECN
0.4 ± 2.5	13k	¹³ AMBROSINO 06E	KLOE
• • • We do not use the following data for averages, fits, limits, etc. • • •			
0.3 ± 3.1		¹⁴ APOSTOLA... 99B	CPLR

- ¹³ They use the PDG 04 for the K_L^0 semileptonic charge asymmetry and PDG 04 (*CP* review, *CPT* NOT ASSUMED) for $\text{Re}(\epsilon)$.
¹⁴ Constrained by Bell-Steinberger (or unitarity) relation.

Meson Particle Listings

K_S^0, K_L^0

Table listing experimental data for K mesons, including authors, journals, and dates. Examples: GIBBONS 88 PRL 61 2661; BURKHARDT 87 PL B199 139; GROSSMAN 87 PRL 59 18; BARMIN 86 SJNP 44 622; etc.

OTHER RELATED PAPERS

Table listing related papers on kaon decays. Examples: LITTENBERG 93 ARNPS 43 729; BATTISTON 92 PRPL 214 293; TRILLING 65B UCRL 16473; etc.



$I(J^P) = \frac{1}{2}(0^-)$

$m_{K_L^0} - m_{K_S^0}$

For earlier measurements, beginning with GOOD 61 and FITCH 61, see our 1986 edition, Physics Letters 170B 132 (1986).

OUR FIT is described in the note on "CP violation in K_L decays" in the K_L^0 Particle Listings. The result labeled "OUR FIT Assuming CPT" ["OUR FIT Not assuming CPT"] includes all measurements except those with the comment "Not assuming CPT" ["Assuming CPT"]. Measurements with neither comment do not assume CPT and enter both fits.

Table with columns: VALUE (10^10 h s^-1), DOCUMENT ID, TECN, COMMENT. Lists various fits and measurements. Examples: 0.5292 ± 0.0009 OUR FIT; 0.5290 ± 0.0015 OUR FIT; etc.

- 1 ALAVI-HARATI 03 fit Δm and $\tau_{K_S^0}$ simultaneously. ϕ_{+-} is constrained to the Superweak value, i.e. CPT is assumed. See " K_S^0 Mean Life" section for correlation information.
2 The two ALAVI-HARATI 03 values use the same data. The first enters the "Assuming CPT " fit and the second enters the "Not assuming CPT " fit. They use 40-160 GeV K beams.
3 ALAVI-HARATI 03 fit Δm , ϕ_{+-} , and $\tau_{K_S^0}$ simultaneously. See ϕ_{+-} in the " K_L CP violation" section for correlation information.
4 Fits Δm and ϕ_{+-} simultaneously. GIBBONS 93c systematic error is from B. Winstein via private communication. 20-160 GeV K beams.
5 GIBBONS 93 value assume $\phi_{+-} = \phi_{00} = \phi_{SW} = (43.7 \pm 0.2)^\circ$, i.e. assumes CPT . 20-160 GeV K beams.
6 These two experiments have a common systematic error due to the uncertainty in the momentum scale, as pointed out in WAHL 89.
7 GJESDAL 74 uses charge asymmetry in $K_{\mu 3}^0$ decays.
8 ANGELOPOULOS 01 uses strong interactions strangeness tagging at two different times.
9 Uses K_{e3}^0 and K_{e3}^0 strangeness tagging at production and decay. Assumes CPT conservation on $\Delta S = -\Delta Q$ transitions.
10 ADLER 96c is the result of a fit which includes nearly the same data as entered into the "OUR FIT" value above.
11 ARONSON 82 find that Δm may depend on the kaon energy.
12 ARONSON 70 and CARNEGIE 71 use K_S^0 mean life = $(0.862 \pm 0.006) \times 10^{-10}$ s. We have not attempted to adjust these values for the subsequent change in the K_S^0 mean life or in η_{+-} .

K_L^0 MEAN LIFE

Table showing mean life measurements for K_L^0. Columns: VALUE (10^-8 s), EVTS, DOCUMENT ID, TECN, COMMENT. Examples: 5.116 ± 0.020 OUR FIT; 5.072 ± 0.011 ± 0.035 13M 13 AMBROSINO 06 KLOE; etc.

13 AMBROSINO 06 uses $\phi \rightarrow K_L K_S$ with K_L tagged by $K_S \rightarrow \pi^+ \pi^-$. The four major K_L BR's are measured, the small remainder ($\pi^+ \pi^-, \pi^0 \pi^0, \gamma \gamma$) is taken from PDG 04. This KLOE K_L lifetime is obtained by imposing $\sum_i B_i = 1$. The correlation matrix among the four measured K_L BR's and this K_L lifetime is

Correlation matrix table with columns $K_{e3}, K_{\mu 3}, 3\pi^0, \pi^+ \pi^-, \pi^0 \pi^0, \tau_{K_L}$. Values range from 1 to -0.43.

These correlations are taken into account in our fit. The average of this KLOE mean life measurement and the independent KLOE measurement in AMBROSINO 05c is $(5.084 \pm 0.023) \times 10^{-8}$ s.

K_L^0 DECAY MODES

Table listing decay modes for K_L^0. Columns: Mode, Fraction (Γ_i/Γ), Scale factor/Confidence level. Divided into Semileptonic modes, Hadronic modes, and Semileptonic modes with photons.

Other modes with photons or $\ell\bar{\ell}$ pairs

Table with 4 columns: Label, Mode, Value, and Comment. Rows include $\Gamma_{17} 2\gamma$, $\Gamma_{18} 3\gamma$, $\Gamma_{19} e^+e^-\gamma$, $\Gamma_{20} \mu^+\mu^-\gamma$, $\Gamma_{21} e^+e^-\gamma\gamma$, $\Gamma_{22} \mu^+\mu^-\gamma\gamma$.

Charge conjugation \times Parity (CP) or Lepton Family number (LF) violating modes, or $\Delta S = 1$ weak neutral current (SI) modes

Table with 4 columns: Label, Mode, Value, and Comment. Rows include $\Gamma_{23} \mu^+\mu^-$, $\Gamma_{24} e^+e^-$, $\Gamma_{25} \pi^+\pi^-e^+e^-$, $\Gamma_{26} \pi^0\pi^0e^+e^-$, $\Gamma_{27} \mu^+\mu^-e^+e^-$, $\Gamma_{28} e^+e^-e^+e^-$, $\Gamma_{29} \pi^0\mu^+\mu^-$, $\Gamma_{30} \pi^0e^+e^-$, $\Gamma_{31} \pi^0\nu\bar{\nu}$, $\Gamma_{32} \pi^0\pi^0\nu\bar{\nu}$, $\Gamma_{33} e^\pm\mu^\mp$, $\Gamma_{34} e^\pm e^\pm\mu^\mp\mu^\mp$, $\Gamma_{35} \pi^0\mu^\pm e^\mp$, $\Gamma_{36} \pi^0\pi^0\mu^\pm e^\mp$.

- [a] The value is for the sum of the charge states or particle/antiparticle states indicated.
[b] This mode includes gammas from inner bremsstrahlung but not the direct emission mode $K_L^0 \to \pi^+\pi^-\gamma$ (DE).
[c] Most of this radiative mode, the low-momentum γ part, is also included in the parent mode listed without γ 's.
[d] See the Particle Listings below for the energy limits used in this measurement.
[e] Allowed by higher-order electroweak interactions.
[f] Violates CP in leading order. Test of direct CP violation since the indirect CP-violating and CP-conserving contributions are expected to be suppressed.

CONSTRAINED FIT INFORMATION

An overall fit to the mean life and 15 branching ratios uses 27 measurements and one constraint to determine 11 parameters. The overall fit has a $\chi^2 = 37.3$ for 17 degrees of freedom.

The following off-diagonal array elements are the correlation coefficients $\langle \delta p_i \delta p_j \rangle / (\delta p_i \delta p_j)$, in percent, from the fit to parameters p_i , including the branching fractions, $x_i \equiv \Gamma_i / \Gamma_{total}$. The fit constrains the x_i whose labels appear in this array to sum to one.

Correlation matrix table with 11 columns and 11 rows. Rows are labeled $x_2, x_6, x_7, x_8, x_9, x_{13}, x_{14}, x_{17}, x_{19}, \Gamma$. Columns are labeled $x_1, x_2, x_6, x_7, x_8, x_9, x_{13}, x_{14}, x_{17}, x_{19}$.

Table with 3 columns: Mode, Rate ($10^8 s^{-1}$), and Scale factor. Rows include $\Gamma_1 \pi^\pm e^\mp \nu_e$, $\Gamma_2 \pi^\pm \mu^\mp \nu_\mu$, $\Gamma_6 3\pi^0$, $\Gamma_7 \pi^+\pi^-\pi^0$, $\Gamma_8 \pi^+\pi^-$, $\Gamma_9 \pi^0\pi^0$, $\Gamma_{13} \pi^+\pi^-\gamma$, $\Gamma_{14} \pi^+\pi^-\gamma$ (DE), $\Gamma_{17} 2\gamma$, $\Gamma_{19} e^+e^-\gamma$.

K_L^0 DECAY RATES

$\Gamma(\pi^+\pi^-\pi^0)$ Γ_7

VALUE ($10^6 s^{-1}$) EVTS DOCUMENT ID TECN COMMENT

Table with 6 columns: VALUE, EVTS, DOCUMENT ID, TECN, COMMENT. Rows include 2.451 ± 0.015 OUR FIT, 2.32, 2.35, 2.71, 2.5, 2.12, 2.20, 2.62, 3.26, 1.4.

$\Gamma(\pi^\pm e^\mp \nu_e)$ Γ_1

VALUE ($10^6 s^{-1}$) EVTS DOCUMENT ID TECN COMMENT

Table with 6 columns: VALUE, EVTS, DOCUMENT ID, TECN, COMMENT. Rows include 7.93 ± 0.04 OUR FIT, 7.81, 7.52.

$\Gamma(\pi^\pm e^\mp \nu_e) + \Gamma(\pi^\pm \mu^\mp \nu_\mu)$ $(\Gamma_1 + \Gamma_2)$

VALUE ($10^6 s^{-1}$) EVTS DOCUMENT ID TECN COMMENT

Table with 6 columns: VALUE, EVTS, DOCUMENT ID, TECN, COMMENT. Rows include 13.21 ± 0.06 OUR FIT, 12.4, 8.47, 13.1, 11.6, 10.3, 9.85.

K_L^0 BRANCHING RATIOS

Semileptonic modes

$\Gamma(\pi^\pm e^\mp \nu_e) / \Gamma_{total}$ Γ_1 / Γ

VALUE EVTS DOCUMENT ID TECN

Table with 4 columns: VALUE, EVTS, DOCUMENT ID, TECN. Rows include 0.4055 ± 0.0012 OUR FIT, 0.4047 ± 0.0028 OUR AVERAGE, $0.4007 \pm 0.0005 \pm 0.0015$, 0.4067 ± 0.0011 .

17 There are correlations between these five KLOE measurements: $B(K_L \to \pi e \nu)$, $B(K_L \to \pi \mu \nu)$, $B(K_L \to 3\pi^0)$, $B(K_L \to \pi^+\pi^-\pi^0)$, and τ_{K_L} measured in AMBROSINO 06. See the footnote for the τ_{K_L} measurement for the correlation matrix.

18 ALEXOPOULOS 04 constrains $\sum_i B_i = 0.9993$ for the six major K_L branching fractions. The correlations among these branching fractions are taken into account in our fit. The correlation matrix is

Correlation matrix table with 6 columns: K_{e3} , $K_{\mu 3}$, $3\pi^0$, $\pi^+\pi^-\pi^0$, $\pi^+\pi^-$, $\pi^0\pi^0$. Rows are labeled K_{e3} , $K_{\mu 3}$, $3\pi^0$, $\pi^+\pi^-\pi^0$, $\pi^+\pi^-$, $\pi^0\pi^0$.

$\Gamma(\pi^\pm \mu^\mp \nu_\mu) / \Gamma_{total}$ Γ_2 / Γ

VALUE EVTS DOCUMENT ID TECN

Table with 4 columns: VALUE, EVTS, DOCUMENT ID, TECN. Rows include 0.2704 ± 0.0007 OUR FIT, 0.2700 ± 0.0008 OUR AVERAGE, $0.2698 \pm 0.0005 \pm 0.0015$, 0.2701 ± 0.0009 .

19 There are correlations between these five KLOE measurements: $B(K_L \to \pi e \nu)$, $B(K_L \to \pi \mu \nu)$, $B(K_L \to 3\pi^0)$, $B(K_L \to \pi^+\pi^-\pi^0)$, and τ_{K_L} measured in AMBROSINO 06. See the footnote for the τ_{K_L} measurement for the correlation matrix.

20 For correlations with other ALEXOPOULOS 04 measurements, see the footnote with their $B(K_L \to \pi e \nu)$ measurement.

$[\Gamma(\pi^\pm e^\mp \nu_e) + \Gamma(\pi^\pm \mu^\mp \nu_\mu)] / \Gamma_{total}$ $(\Gamma_1 + \Gamma_2) / \Gamma$

VALUE DOCUMENT ID

Table with 2 columns: VALUE, DOCUMENT ID. Row includes 0.6759 ± 0.0013 OUR FIT.

$\Gamma(\mu^+ \mu^- e^+ e^-)/\Gamma_{\text{total}}$ Γ_{27}/Γ
 Test for $\Delta S = 1$ weak neutral current. Allowed by higher-order electroweak interaction.

VALUE (units 10^{-3})	CL%	EVTs	DOCUMENT ID	TECN	COMMENT
2.69 ± 0.27 OUR AVERAGE					
2.69 ± 0.24 ± 0.12		131	⁶⁴ ALAVI-HARATI 03B	KTEV	
2.9 ^{+6.7} _{-2.4}		1	GU	96 E799	
••• We do not use the following data for averages, fits, limits, etc. •••					
2.62 ± 0.40 ± 0.17		43	ALAVI-HARATI 01H	KTEV	Sup. by ALAVI-HARATI 03B
<4900		90	BALATS	83 SPEC	
⁶⁴ ALAVI-HARATI 03B also measures the linear slope $\alpha = -1.59 \pm 0.37$.					

$\Gamma(e^+ e^- e^+ e^-)/\Gamma_{\text{total}}$ Γ_{28}/Γ
 Test for $\Delta S = 1$ weak neutral current. Allowed by higher-order electroweak interaction.

VALUE (units 10^{-3})	EVTs	DOCUMENT ID	TECN	COMMENT
3.56 ± 0.21 OUR AVERAGE				
3.30 ± 0.24 ± 0.25	200	⁶⁵ LAI	05B NA48	
3.72 ± 0.18 ± 0.23	441	ALAVI-HARATI 01D	KTEV	
3.96 ± 0.78 ± 0.32	27	GU	94 E799	
3.07 ± 1.25 ± 0.26	6	VAGINS	93 B845	
••• We do not use the following data for averages, fits, limits, etc. •••				
6 ± 2 ± 1	18	⁶⁶ AKAGI	95 SPEC	$m_{ee} > 470$ MeV
7 ± 3 ± 2	6	⁶⁶ AKAGI	95 SPEC	$m_{ee} > 470$ MeV
10.4 ± 3.7 ± 1.1	8	⁶⁷ BARR	95 NA31	
6 ± 2 ± 1	18	AKAGI	93 CNTR	Sup. by AKAGI 95
4 ± 3	2	BARR	91 NA31	Sup. by BARR 95
⁶⁵ LAI 05B uses 1998 and 1999 data. Data are normalized to the observed events of $K_L^0 \rightarrow \pi^+ \pi^- \pi^0$ (π^0 into Dalitz pair) and PDG 04 values are used for $B(K_L^0 \rightarrow \pi^+ \pi^- \pi^0)$ and $B(\pi^0 \rightarrow e^+ e^- \gamma)$. The systematic error includes a normalization error of ± 0.10 .				
⁶⁶ Values are for the total branching fraction, acceptance-corrected for the m_{ee} cuts shown.				
⁶⁷ Distribution of angles between two $e^+ e^-$ pair planes favors $CP = -1$ for K_L^0 .				

$\Gamma(\pi^0 \mu^+ \mu^-)/\Gamma_{\text{total}}$ Γ_{29}/Γ
 Violates CP in leading order. Test for $\Delta S = 1$ weak neutral current. Allowed by higher-order electroweak interaction.

VALUE (units 10^{-3})	CL%	EVTs	DOCUMENT ID	TECN
< 0.38				
< 5.1	90	0	HARRIS	93 E799
••• We do not use the following data for averages, fits, limits, etc. •••				

$\Gamma(\pi^0 e^+ e^-)/\Gamma_{\text{total}}$ Γ_{30}/Γ
 Violates CP in leading order. Direct and indirect CP -violating contributions are expected to be comparable and to dominate the CP -conserving part. LAI 02B result suggests that CP -violation effects dominate. Test for $\Delta S = 1$ weak neutral current. Allowed by higher-order electroweak interaction.

VALUE (units 10^{-10})	CL%	EVTs	DOCUMENT ID	TECN	COMMENT
< 2.8					
< 3.5	90	0	⁶⁸ ALAVI-HARATI 04A	KTEV	combined result
0.0047 ^{+0.0022} _{-0.0018}			ALAVI-HARATI 04A	KTEV	
< 5.1	90	2	⁶⁹ LAI	02B NA48	CP -conserving part
0.01 to 0.02			ALAVI-HARATI 01	KTEV	
			ALAVI-HARATI 99B	KTEV	CP -conserving part
< 43	90	0	HARRIS	93B E799	
< 75	90	0	BARKER	90 E731	
< 55	90	0	OHL	90 B845	
< 400	90	0	BARR	88 NA31	
< 3200	90	0	JASTRZEM...	88 SPEC	

⁶⁸ Combined result of ALAVI-HARATI 04A 1999-2000 data set and ALAVI-HARATI 01 1997 data set.

⁶⁹ LAI 02B uses the absence of a signal in $K_L^0 \rightarrow \pi^0 \gamma \gamma$ with $m(\gamma\gamma) < m(\pi^0)$ and their α_V value to predict this value.

$\Gamma(\pi^0 \nu \bar{\nu})/\Gamma_{\text{total}}$ Γ_{31}/Γ
 Violates CP in leading order. Test of direct CP violation since the indirect CP -violating and CP -conserving contributions are expected to be suppressed. Test of $\Delta S = 1$ weak neutral current.

VALUE (units 10^{-7})	CL%	DOCUMENT ID	TECN
< 0.67			
< 2.1	90	⁷⁰ AHN	08 K391
< 5.9	90	⁷¹ AHN	06 K391
< 16	90	ALAVI-HARATI 100	KTEV
< 580	90	ADAMS	99 KTEV
< 2200	90	WEAVER	94 E799
	90	GRAHAM	92 CNTR

⁷⁰ Value obtained using data from February to April 2005.

⁷¹ Value obtained analyzing 10% of data of RUN 1 (performed in 2004).

$\Gamma(\pi^0 \pi^0 \nu \bar{\nu})/\Gamma_{\text{total}}$ Γ_{32}/Γ

VALUE	CL%	DOCUMENT ID	TECN
< 4.7 × 10⁻⁵			
< 4.7 × 10 ⁻⁵	90	⁷² NIX	07 K391

⁷² Observed 1 event with expected background of 0.43 ± 0.35 events. NIX 07 also measured $B(K_L^0 \rightarrow \pi^0 \pi^0 P) < 1.2 \times 10^{-6}$ at 90% CL, where P is the pseudoscalar particle and $m_P < 100$ MeV.

$\Gamma(e^\pm \mu^\mp)/\Gamma_{\text{total}}$ Γ_{33}/Γ
 Test of lepton family number conservation.

VALUE (units 10^{-11})	CL%	EVTs	DOCUMENT ID	TECN
< 0.47				
< 9.4	90	0	AMBROSE	98B B871
< 3.9	90	0	AKAGI	95 SPEC
< 3.3	90	0	⁷³ ARISAKA	93 B791
			ARISAKA	93 B791
⁷³ This is the combined result of ARISAKA 93 and MATHIAZHAGAN 89.				

$\Gamma(e^\pm e^\pm \mu^\mp \mu^\mp)/\Gamma_{\text{total}}$ Γ_{34}/Γ
 Test of lepton family number conservation.

VALUE (units 10^{-11})	CL%	EVTs	DOCUMENT ID	TECN	COMMENT
< 4.12					
< 12.3	90	0	⁷⁴ ALAVI-HARATI 01H	KTEV	Sup. by ALAVI-HARATI 03B
< 610	90	0	⁷⁴ GU	96 E799	
⁷⁴ Assuming uniform phase space distribution.					

$\Gamma(\pi^0 \mu^\pm e^\mp)/\Gamma_{\text{total}}$ Γ_{35}/Γ
 Test of lepton family number conservation.

VALUE (units 10^{-10})	CL%	DOCUMENT ID	TECN
< 0.76			
< 62	90	ABOUZAID	08c KTEV
< 62	90	ARISAKA	98 E799
••• We do not use the following data for averages, fits, limits, etc. •••			

$\Gamma(\pi^0 \pi^0 \mu^\pm e^\mp)/\Gamma_{\text{total}}$ Γ_{36}/Γ
 Test of lepton family number conservation.

VALUE (units 10^{-10})	CL%	DOCUMENT ID	TECN
< 1.7			
< 1.7	90	ABOUZAID	08c KTEV

V_{ud} , V_{us} , THE CABIBBO ANGLE, AND CKM UNITARITY

Updated November 2009 by E. Blucher (Univ. of Chicago) and W.J. Marciano (BNL)

The Cabibbo-Kobayashi-Maskawa (CKM) [1,2] three-generation quark mixing matrix written in terms of the Wolfenstein parameters (λ, A, ρ, η) [3] nicely illustrates the orthonormality constraint of unitarity and central role played by λ .

$$V_{\text{CKM}} = \begin{pmatrix} V_{ud} & V_{us} & V_{ub} \\ V_{cd} & V_{cs} & V_{cb} \\ V_{td} & V_{ts} & V_{tb} \end{pmatrix} = \begin{pmatrix} 1 - \lambda^2/2 & \lambda & A\lambda^3(\rho - i\eta) \\ -\lambda & 1 - \lambda^2/2 & A\lambda^2 \\ A\lambda^3(1 - \rho - i\eta) & -A\lambda^2 & 1 \end{pmatrix} + \mathcal{O}(\lambda^4). \quad (1)$$

That cornerstone is a carryover from the two-generation Cabibbo angle, $\lambda = \sin(\theta_{\text{Cabibbo}}) = V_{us}$. Its value is a critical ingredient in determinations of the other parameters and in tests of CKM unitarity.

Unfortunately, the precise value of λ has been somewhat controversial in the past, with kaon decays suggesting [4] $\lambda \simeq 0.220$, while hyperon decays [5] and indirect determinations via nuclear β -decays imply a somewhat larger $\lambda \simeq 0.225 - 0.230$. That discrepancy is often discussed in terms of a deviation from the unitarity requirement

$$|V_{ud}|^2 + |V_{us}|^2 + |V_{ub}|^2 = 1. \quad (2)$$

For many years, using a value of V_{us} derived from $K \rightarrow \pi e \nu$ (K_{e3}) decays, that sum was consistently 2-2.5 sigma below unity, a potential signal [6] for new physics effects. Below, we discuss the current status of V_{ud} , V_{us} , and their associated unitarity test in Eq. (2). (Since $|V_{ub}|^2 \simeq 1 \times 10^{-5}$ is negligibly small, it is ignored in this discussion.)

Meson Particle Listings

K_L^0

V_{ud}

The value of V_{ud} has been obtained from superallowed nuclear, neutron, and pion decays. Currently, the most precise determination of V_{ud} comes from superallowed nuclear beta-decays [6] ($0^+ \rightarrow 0^+$ transitions). Measuring their half-lives, t , and Q values which give the decay rate factor, f , leads to a precise determination of V_{ud} via the master formula [7–9]

$$|V_{ud}|^2 = \frac{2984.48(5) \text{ sec}}{ft(1 + \text{RC})} \quad (3)$$

where RC denotes the entire effect of electroweak radiative corrections, nuclear structure, and isospin violating nuclear effects. RC is nucleus-dependent, ranging from about +3.0% to +3.6% for the best measured superallowed decays. The most recent analysis of Hardy and Towner [10, 11] gives a weighted average (with errors combined in quadrature) of

$$V_{ud} = 0.97425(22) \text{ (superallowed)}, \quad (4)$$

which, assuming unitarity, corresponds to $\lambda = 0.2255(10)$. The new average value of V_{ud} is shifted upward compared to our 2007 value of 0.97418(27) primarily because of improvements in the experimental ft values and nuclear isospin breaking corrections employed. We note, however, that the possibility of additional nuclear coulombic corrections has been raised recently [12].

Combined measurements of the neutron lifetime, τ_n , and the ratio of axial-vector/vector couplings, $g_A \equiv G_A/G_V$, via neutron decay asymmetries can also be used to determine V_{ud} :

$$|V_{ud}|^2 = \frac{4908.7(1.9) \text{ sec}}{\tau_n(1 + 3g_A^2)}, \quad (5)$$

where the error stems from uncertainties in the electroweak radiative corrections [8] due to hadronic loop effects. Those effects have been recently updated and their error was reduced by about a factor of 2 [9], leading to a ± 0.0002 theoretical uncertainty in V_{ud} (common to all V_{ud} extractions). Using the world averages from this *Review*

$$\begin{aligned} \tau_n^{\text{ave}} &= 885.7(8) \text{ sec} \\ g_A^{\text{ave}} &= 1.2695(29) \end{aligned} \quad (6)$$

leads to

$$V_{ud} = 0.9746(4)_{\tau_n(18)g_A(2)_{\text{RC}}} \quad (7)$$

with the error dominated by g_A uncertainties (which have been expanded due to experimental inconsistencies). We note that a recent precise measurement [13] of $\tau_n = 878.5(7)(3)$ sec is also inconsistent with the world average from this *Review* and would lead to a considerably larger $V_{ud} = 0.9786(4)(18)(2)$. Alternatively, accepting the recent shorter lifetime measurement as correct, and employing it along with the value of V_{ud} in Eq. (4), leads to $g_A = 1.2763(7)$, which is outside of the range of Eq. (6) but in good accord with the most recent direct measurements of g_A [14]. Future neutron studies are expected to resolve these inconsistencies and significantly reduce the

uncertainties in g_A and τ_n , potentially making them the best way to determine V_{ud} .

The recently completed PIBETA experiment at PSI measured the very small ($\mathcal{O}(10^{-8})$) branching ratio for $\pi^+ \rightarrow \pi^0 e^+ \nu_e$ with about $\pm 1/2\%$ precision. Their result gives [15]

$$V_{ud} = 0.9749(26) \left[\frac{BR(\pi^+ \rightarrow e^+ \nu_e(\gamma))}{1.2352 \times 10^{-4}} \right]^{\frac{1}{2}} \quad (8)$$

which is normalized using the very precisely determined theoretical prediction for $BR(\pi^+ \rightarrow e^+ \nu_e(\gamma)) = 1.2352(5) \times 10^{-4}$ [7], rather than the experimental branching ratio from this *Review* of $1.230(4) \times 10^{-4}$ which would lower the value to $V_{ud} = 0.9728(30)$. Theoretical uncertainties in that determination are very small; however, much higher statistics would be required to make this approach competitive with others.

V_{us}

$|V_{us}|$ may be determined from kaon decays, hyperon decays, and tau decays. Previous determinations have most often used $K\ell 3$ decays:

$$\Gamma_{K\ell 3} = \frac{G_F^2 M_K^5}{192\pi^3} S_{EW}(1 + \delta_K^\ell + \delta_{SU2}) C^2 |V_{us}|^2 f_+^2(0) I_K^\ell. \quad (9)$$

Here, ℓ refers to either e or μ , G_F is the Fermi constant, M_K is the kaon mass, S_{EW} is the short-distance radiative correction, δ_K^ℓ is the mode-dependent long-distance radiative correction, $f_+(0)$ is the calculated form factor at zero momentum transfer for the $\ell\nu$ system, and I_K^ℓ is the phase-space integral, which depends on measured semileptonic form factors. For charged kaon decays, δ_{SU2} is the deviation from one of the ratio of $f_+(0)$ for the charged to neutral kaon decay; it is zero for the neutral kaon. C^2 is 1 (1/2) for neutral (charged) kaon decays. Most determinations of $|V_{us}|$ have been based only on $K \rightarrow \pi e \nu$ decays; $K \rightarrow \pi \mu \nu$ decays have not been used because of large uncertainties in I_K^μ . The experimental measurements are the semileptonic decay widths (based on the semileptonic branching fractions and lifetime) and form factors (allowing calculation of the phase space integrals). Theory is needed for S_{EW} , δ_K^ℓ , δ_{SU2} , and $f_+(0)$.

Many new measurements during the last few years have resulted in a significant shift in V_{us} . Most importantly, recent measurements of the $K \rightarrow \pi e \nu$ branching fractions are significantly different than earlier PDG averages, probably as a result of inadequate treatment of radiation in older experiments. This effect was first observed by BNL E865 [16] in the charged kaon system and then by KTeV [17,18] in the neutral kaon system; subsequent measurements were made by KLOE [19–22], NA48 [23–25], and ISTRA+ [26]. Current averages (*e.g.*, by the PDG [27] or Flavianet [28]) of the semileptonic branching fractions are based only on recent, high-statistics experiments where the treatment of radiation is clear. In addition to measurements of branching fractions, new measurements of lifetimes [29] and form factors [30–34], have resulted in improved precision for all of the experimental inputs

to V_{us} . Precise measurements of form factors for $K_{\mu 3}$ decay now make it possible to use both semileptonic decay modes to extract V_{us} .

Following the analysis of the Flavianet group [28], one finds the values of $|V_{us}|f_+(0)$ in Table 1. The average of these measurements gives

$$f_+(0)|V_{us}| = 0.21664(48). \quad (10)$$

Figure 1 shows a comparison of these results with the PDG evaluation from 2002 [35], as well as $f_+(0)(1 - |V_{ud}|^2 - |V_{ub}|^2)^{1/2}$, the expectation for $f_+(0)|V_{us}|$ assuming unitarity, based on $|V_{ud}| = 0.9742 \pm 0.0003$, $|V_{ub}| = (3.6 \pm 0.7) \times 10^{-3}$, and the lattice calculation of $f_+(0) = 0.9644 \pm 0.0049$ [36] (Lattice calculations of $f_+(0)$ have improved significantly in recent years, and therefore replace the classic calculation of Leutwyler and Roos [37].) Combining the result in Eq. (10) with the above value of $f_+(0)$ gives

$$|V_{us}| = \lambda = 0.2246 \pm 0.0012. \quad (11)$$

Table 1: $|V_{us}|f_+(0)$ from $K\ell 3$.

Decay Mode	$ V_{us} f_+(0)$
$K^\pm e 3$	0.2173 ± 0.0008
$K^\pm \mu 3$	0.2176 ± 0.0011
$K_L e 3$	0.2163 ± 0.0006
$K_L \mu 3$	0.2168 ± 0.0007
$K_S e 3$	0.2154 ± 0.0013
Average	0.2166 ± 0.0005

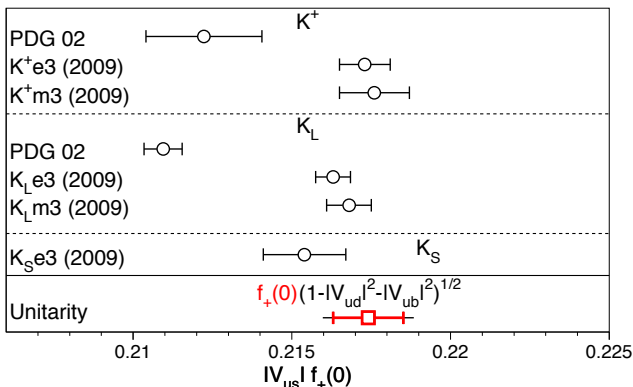


Figure 1: Comparison of determinations of $|V_{us}|f_+(0)$ from this review (labeled 2009), from the PDG 2002, and with the prediction from unitarity using $|V_{ud}|$ and the lattice calculation of $f_+(0)$ [36]. For $f_+(0)(1 - |V_{ud}|^2 - |V_{ub}|^2)^{1/2}$, the inner error bars are from the quoted uncertainty in $f_+(0)$; the total uncertainties include the $|V_{ud}|$ and $|V_{ub}|$ errors.

A value of V_{us} can also be obtained from a comparison of the radiative inclusive decay rates for $K \rightarrow \mu\nu(\gamma)$ and $\pi \rightarrow \mu\nu(\gamma)$ combined with a lattice gauge theory calculation of f_K/f_π via [42]

$$\frac{|V_{us}|f_K}{|V_{ud}|f_\pi} = 0.2387(4) \left[\frac{\Gamma(K \rightarrow \mu\nu(\gamma))}{\Gamma(\pi \rightarrow \mu\nu(\gamma))} \right]^{\frac{1}{2}} \quad (12)$$

with the small error coming from electroweak radiative corrections. Employing

$$\frac{\Gamma(K \rightarrow \mu\nu(\gamma))}{\Gamma(\pi \rightarrow \mu\nu(\gamma))} = 1.3337(46), \quad (13)$$

which averages in the KLOE result [43], $B(K \rightarrow \mu\nu(\gamma)) = 63.66(9)(15)\%$ and [44]

$$f_K/f_\pi = 1.189(7) \quad (14)$$

along with the value of V_{ud} in Eq. (4) leads to

$$|V_{us}| = 0.2259(5)(13). \quad (15)$$

It should be mentioned that hyperon decay fits suggest [5]

$$|V_{us}| = 0.2250(27) \text{ Hyperon Decays} \quad (16)$$

modulo SU(3) breaking effects that could shift that value up or down. We note that a recent representative effort [45] that incorporates SU(3) breaking found $V_{us} = 0.226(5)$. Similarly, inclusive strangeness changing tau decays give [46]

$$|V_{us}| = 0.2208(34) \text{ Tau Decays} \quad (17)$$

where the central value depends on the strange quark mass. However, a recent BaBar study [47] of $\tau \rightarrow K\nu/\tau \rightarrow \pi\nu$ using the lattice value of f_K/f_π from Eq. (14) finds $V_{us} = 0.2255(24)$, in good agreement with other determinations.

Employing the value of V_{ud} in Eq. (4) and $V_{us} = 0.2252(9)$, the average of the $K\ell 3$ (Eq. (11)) and $K\mu 2$ (Eq. (15)) determinations of V_{us} , leads to the unitarity consistency check

$$|V_{ud}|^2 + |V_{us}|^2 + |V_{ub}|^2 = 0.9999(4)(4). \quad (18)$$

where the first error is the uncertainty from $|V_{ud}|^2$ and the second error is the uncertainty from $|V_{us}|^2$.

CKM Unitarity Constraints

The current good experimental agreement with unitarity, $|V_{ud}|^2 + |V_{us}|^2 + |V_{ub}|^2 = 0.9999(6)$, provides strong confirmation of Standard Model radiative corrections (which range between 3-4% depending on the nucleus used) at better than the 50 sigma level [48]. In addition, it implies constraints on “New Physics” effects at both the tree and quantum loop levels. Those effects could be in the form of contributions to nuclear beta decays, K decays and/or muon decays, with the last of these providing normalization via the muon lifetime [49], which is used to obtain the Fermi constant, $G_\mu = 1.166371(6) \times 10^{-5} \text{ GeV}^{-2}$.

In the following sections, we illustrate the implications of CKM unitarity for (1) exotic muon decays [50] (beyond ordinary

Meson Particle Listings

 K_L^0

muon decay $\mu^+ \rightarrow e^+ \nu_e \bar{\nu}_\mu$) and (2) new heavy quark mixing V_{uD} [51]. Other examples in the literature [52,53] include Z_χ boson quantum loop effects, supersymmetry, leptoquarks, compositeness etc.

Exotic Muon Decays

If additional lepton flavor violating decays such as $\mu^+ \rightarrow e^+ \bar{\nu}_e \nu_\mu$ (wrong neutrinos) occur, they would cause confusion in searches for neutrino oscillations at, for example, muon storage rings/neutrino factories or other neutrino sources from muon decays. Calling the rate for all such decays $\Gamma(\text{exotic } \mu \text{ decays})$, they should be subtracted before the extraction of G_μ and normalization of the CKM matrix. Since that is not done and unitarity works, one has (at one-sided 95% CL)

$$|V_{ud}|^2 + |V_{us}|^2 + |V_{ub}|^2 = 1 - BR(\text{exotic } \mu \text{ decays}) \geq 0.9989 \quad (19)$$

or

$$BR(\text{exotic } \mu \text{ decays}) < 0.001 . \quad (20)$$

This bound is a factor of 10 better than the direct experimental bound on $\mu^+ \rightarrow e^+ \bar{\nu}_e \nu_\mu$.

New Heavy Quark Mixing

Heavy D quarks naturally occur in fourth quark generation models and some heavy quark “new physics” scenarios such as E_6 grand unification. Their mixing with ordinary quarks gives rise to V_{uD} which is constrained by unitarity (one sided 95% CL)

$$|V_{ud}|^2 + |V_{us}|^2 + |V_{ub}|^2 = 1 - |V_{uD}|^2 > 0.9989 \\ |V_{uD}| < 0.03 . \quad (21)$$

A similar constraint applies to heavy neutrino mixing and the couplings $V_{\mu N}$ and V_{eN} .

References

- N. Cabibbo, Phys. Rev. Lett. **10**, 531 (1963).
- M. Kobayashi and T. Maskawa, Prog. Theor. Phys. **49**, 652 (1973).
- L. Wolfenstein, Phys. Rev. Lett. **51**, 1945 (1983).
- S. Eidelman *et al.*, [Particle Data Group], Phys. Lett. **B592**, 1 (2004).
- N. Cabibbo, E.C. Swallow, and R. Winston, Phys. Rev. Lett. **92**, 251803 (2004) [hep-ph/0307214].
- J.C. Hardy and I.S. Towner, Phys. Rev. Lett. **94**, 092502 (2005) [nucl-th/0412050].
- W.J. Marciano and A. Sirlin, Phys. Rev. Lett. **71**, 3629 (1993).
- A. Czarnecki, W.J. Marciano, and A. Sirlin, Phys. Rev. **D70**, 093006 (2004) [hep-ph/0406324].
- W.J. Marciano and A. Sirlin, Phys. Rev. Lett. **96**, 032002 (2006) [hep-ph/0510099].
- J.C. Hardy and I.S. Towner, Phys. Rev. **C77**, 025501 (2008).
- J.C. Hardy and I.S. Towner, Phys. Rev. **C79**, 055502 (2009).
- G.A. Miller and A. Schwenk, Phys. Rev. **C78**, 035501 (2008); N. Auerbach, Phys. Rev. **C79**, 035502 (2009); H. Liang, N. Van Giai and J. Meng, Phys. Rev. **C79**, 064316 (2009).
- A. Serebrov *et al.*, Phys. Lett. **B605**, 72 (2005) [nucl-ex/0408009].
- H. Abele, Prog. in Part. Nucl. Phys. **60**, 1 (2008).
- D. Pocanic *et al.*, Phys. Rev. Lett. **93**, 181803 (2004) [hep-ex/0312030].
- A. Sher *et al.*, Phys. Rev. Lett. **91**, 261802 (2003).
- T. Alexopoulos *et al.*, [KTeV Collab.], Phys. Rev. Lett. **93**, 181802 (2004) [hep-ex/0406001].
- T. Alexopoulos *et al.*, [KTeV Collab.], Phys. Rev. **D70**, 092006 (2004) [hep-ex/0406002].
- F. Ambrosino *et al.*, [KLOE Collab.], Phys. Lett. **B632**, 43 (2006) [hep-ex/0508027].
- F. Ambrosino *et al.*, [KLOE Collab.], Phys. Lett. **B638**, 140 (2006) [hep-ex/0603041].
- F. Ambrosino *et al.*, [KLOE Collab.], Phys. Lett. **B636**, 173 (2006) [hep-ex/0601026].
- F. Ambrosino *et al.*, [KLOE Collab.], PoS **HEP2005**, 287 (2006) [Frascati Phys. Ser. **41**, 69 (2006)] [hep-ex/0510028].
- A. Lai *et al.*, [NA48 Collab.], Phys. Lett. **B602**, 41 (2004) [hep-ex/0410059].
- A. Lai *et al.*, [NA48 Collab.], Phys. Lett. **B645**, 26 (2007) [hep-ex/0611052].
- J.R. Batley *et al.*, [NA48/2 Collab.], Eur. Phys. J. C **50**, 329 (2007) [hep-ex/0702015].
- V.I. Romanovsky *et al.*, [hep-ex/0704.2052].
- C. Amsler *et al.*, [Particle Data Group], Phys. Lett. **B667**, 1 (2008).
- Flavianet Working Group on Precise SM Tests in K Decays, <http://www.lnf.infn.it/wg/vus>. For a recent detailed review, see M. Antonelli *et al.*, [hep-ph/0907.5386].
- F. Ambrosino *et al.*, [KLOE Collab.], Phys. Lett. **B626**, 15 (2005) [hep-ex/0507088].
- T. Alexopoulos *et al.*, [KTeV Collab.], Phys. Rev. **D70**, 092007 (2004) [hep-ex/0406003].
- E. Abouzaid *et al.*, [KTeV Collab.], Phys. Rev. **D74**, 097101 (2006) [hep-ex/0608058].
- F. Ambrosino *et al.*, [KLOE Collab.], Phys. Lett. **B636**, 166 (2006) [hep-ex/0601038].
- A. Lai *et al.*, [NA48 Collab.], Phys. Lett. **B604**, 1 (2004) [hep-ex/0410065].
- O.P. Yushchenko *et al.*, Phys. Lett. **B589**, 111 (2004) [hep-ex/0404030].
- K. Hagiwara *et al.*, [Particle Data Group], Phys. Rev. **D66**, 1 (2002).
- P.A. Boyle *et al.*, Phys. Rev. Lett. **100**, 141601 (2008).
- H. Leutwyler and M. Roos, Z. Phys. **C25**, 91 (1984).
- D. Becirevic *et al.*, Nucl. Phys. **B705**, 339 (2005) [hep-ph/0403217].
- J. Bijnens and P. Talavera, Nucl. Phys. **B669**, 341 (2003).
- V. Cirigliano *et al.*, JHEP **0504**, 006 (2005) [hep-ph/0503108].
- M. Jamin, J.A. Oller, and A. Pich, JHEP **02**, 047 (2004).
- W.J. Marciano, Phys. Rev. Lett. **93**, 231803 (2004) [hep-ph/0402299].

43. F. Ambrosino *et al.*, [KLOE Collab.], Phys. Lett. **B632**, 76 (2006) [hep-ex/0509045].
44. E. Follana *et al.*, Phys. Rev. Lett. **100**, 062002 (2008).
45. V. Mateu and A. Pich, JHEP **0510**, 041 (2005) [hep-ph/0509045].
46. E. Gamiz *et al.*, Phys. Rev. Lett. **94**, 011803 (2005) [hep-ph/0408044]; E. Gamiz *et al.*, arXiv:0709.0282 [hep-ph].
47. B. Aubert *et al.*, [BaBar Collaboration], [hep-ex/0912.0242].
48. A. Sirlin, Rev. Mod. Phys. **50**, 573 (1978).
49. D.B. Chitwood *et al.*, Phys. Rev. Lett. **99**, 032001 (2007).
50. K.S. Babu and S. Pakvasa, hep-ph/0204236.
51. W. Marciano and A. Sirlin, Phys. Rev. Lett. **56**, 22 (1986); P. Langacker and D. London, Phys. Rev. **D38**, 886 (1988).
52. W. Marciano and A. Sirlin, Phys. Rev. **D35**, 1672 (1987).
53. R. Barbieri *et al.*, Phys. Lett. **156B**, 348 (1985); K. Hagiwara *et al.*, Phys. Rev. Lett. **75**, 3605 (1995); A. Kurylov and M. Ramsey-Musolf, Phys. Rev. Lett. **88**, 071804 (2000).

ENERGY DEPENDENCE OF K_L^0 DALITZ PLOT

For discussion, see note on Dalitz plot parameters in the K^\pm section of the Particle Listings above. For definitions of a_V , a_T , a_H , and a_Y , see the earlier version of the same note in the 1982 edition of this Review published in Physics Letters **111B** 70 (1982).

$$|\text{matrix element}|^2 = 1 + gu + hu^2 + jv + kv^2 + fuv$$

where $u = (s_3 - s_0) / m_\pi^2$ and $v = (s_2 - s_1) / m_\pi^2$

LINEAR COEFFICIENT g FOR $K_L^0 \rightarrow \pi^+ \pi^- \pi^0$

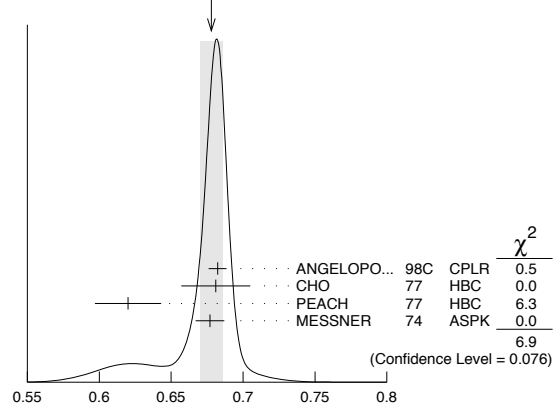
VALUE	EVTS	DOCUMENT ID	TECN	COMMENT
0.678 ± 0.008 OUR AVERAGE				Error includes scale factor of 1.5. See the ideogram below.
0.6823 ± 0.0044 ± 0.0044	500k	ANGELOPO...	98c CPLR	
0.681 ± 0.024	6499	CHO	77 HBC	
0.620 ± 0.023	4709	PEACH	77 HBC	
0.677 ± 0.010	509k	MESSNER	74 ASPK	$a_Y = -0.917 \pm 0.013$
• • • We do not use the following data for averages, fits, limits, etc. • • •				
0.69 ± 0.07	192	⁷⁵ BALDO...	75 HLBC	
0.590 ± 0.022	56k	⁷⁵ BUCHANAN	75 SPEC	$a_H = -0.277 \pm 0.010$
0.619 ± 0.027	20k	^{75,76} BISI	74 ASPK	$a_T = -0.282 \pm 0.011$
0.612 ± 0.032		⁷⁵ ALEXANDER	73B HBC	
0.73 ± 0.04	3200	⁷⁵ BRANDENB...	73 HBC	
0.608 ± 0.043	1486	⁷⁵ KRENZ	72 HLBC	$a_T = -0.277 \pm 0.018$
0.650 ± 0.012	29k	⁷⁵ ALBROW	70 ASPK	$a_Y = -0.858 \pm 0.015$
0.593 ± 0.022	36k	^{75,77} BUCHANAN	70 SPEC	$a_H = -0.278 \pm 0.010$
0.664 ± 0.056	4400	⁷⁵ SMITH	70 OSPK	$a_T = -0.306 \pm 0.024$
0.400 ± 0.045	2446	⁷⁵ BASILE	68B OSPK	$a_T = -0.188 \pm 0.020$
0.649 ± 0.044	1350	⁷⁵ HOPKINS	67 HBC	$a_T = -0.294 \pm 0.018$
0.428 ± 0.055	1198	⁷⁵ NEFKENS	67 OSPK	$a_H = -0.204 \pm 0.025$

⁷⁵ Quadratic dependence required by some experiments. (See sections on "QUADRATIC COEFFICIENT h " and "QUADRATIC COEFFICIENT k " below.) Correlations prevent us from averaging results of fits not including g , h , and k terms.

⁷⁶ BISI 74 value comes from quadratic fit with quad. term consistent with zero. g error is thus larger than if linear fit were used.

⁷⁷ BUCHANAN 70 result revised by BUCHANAN 75 to include radiative correlations and to use more reliable K_L^0 momentum spectrum of second experiment (had same beam).

WEIGHTED AVERAGE
0.678±0.008 (Error scaled by 1.5)



Linear coeff. g for $K_L^0 \rightarrow \pi^+ \pi^- \pi^0$ matrix element squared

QUADRATIC COEFFICIENT h FOR $K_L^0 \rightarrow \pi^+ \pi^- \pi^0$

VALUE	EVTS	DOCUMENT ID	TECN
0.076 ± 0.006 OUR AVERAGE			
0.061 ± 0.004 ± 0.015	500k	ANGELOPO...	98c CPLR
0.095 ± 0.032	6499	CHO	77 HBC
0.048 ± 0.036	4709	PEACH	77 HBC
0.079 ± 0.007	509k	MESSNER	74 ASPK

• • • We do not use the following data for averages, fits, limits, etc. • • •

-0.011 ± 0.018	29k	⁷⁸ ALBROW	70 ASPK
0.043 ± 0.052	4400	⁷⁸ SMITH	70 OSPK

See notes in section "LINEAR COEFFICIENT g FOR $K_L^0 \rightarrow \pi^+ \pi^- \pi^0$ | MATRIX ELEMENT²" above.

⁷⁸ Quadratic coefficients h and k required by some experiments. (See section on "QUADRATIC COEFFICIENT k " below.) Correlations prevent us from averaging results of fits not including g , h , and k terms.

QUADRATIC COEFFICIENT k FOR $K_L^0 \rightarrow \pi^+ \pi^- \pi^0$

VALUE	EVTS	DOCUMENT ID	TECN
0.0099 ± 0.0015 OUR AVERAGE			
0.0104 ± 0.0017 ± 0.0024	500k	ANGELOPO...	98c CPLR
0.024 ± 0.010	6499	CHO	77 HBC
-0.008 ± 0.012	4709	PEACH	77 HBC
0.0097 ± 0.0018	509k	MESSNER	74 ASPK

LINEAR COEFFICIENT j FOR $K_L^0 \rightarrow \pi^+ \pi^- \pi^0$ (CP-VIOLATING TERM)

Listed in CP-violation section below.

QUADRATIC COEFFICIENT f FOR $K_L^0 \rightarrow \pi^+ \pi^- \pi^0$ (CP-VIOLATING TERM)

Listed in CP-violation section below.

QUADRATIC COEFFICIENT h FOR $K_L^0 \rightarrow \pi^0 \pi^0 \pi^0$

No average is computed because not all measurements included the effect of final state rescattering.

VALUE (units 10^{-3})	EVTS	DOCUMENT ID	TECN
+0.59 ± 0.20 ± 1.16	6.8M	⁷⁹ ABOUZAID	08A KTEV
-6.1 ± 0.9 ± 0.5	14.7M	⁸⁰ LAI	01B NA48
-3.3 ± 1.1 ± 0.7	5M	^{80,81} SOMALWAR	92 E731

⁷⁹ Result obtained using Cl3pl model of CABIBBO 05 to include $\pi\pi$ rescattering effects. The systematic error includes an external error of 1.06×10^{-3} from the parametrization input of $(a_0 - a_2) m_{\pi^+} = 0.268 \pm 0.017$ from BATLEY 06B.

⁸⁰ LAI 01B and SOMALWAR 92 results do not include $\pi\pi$ final state rescattering effects.

⁸¹ SOMALWAR 92 chose m_{π^+} as normalization to make it compatible with the Particle Data Group $K_L^0 \rightarrow \pi^+ \pi^- \pi^0$ definitions.

K_L^0 FORM FACTORS

For discussion, see note on form factors in the K^\pm section of the Particle Listings above.

In the form factor comments, the following symbols are used.

f_+ and f_- are form factors for the vector matrix element.

f_S and f_T refer to the scalar and tensor term.

$$f_0(t) = f_+(t) + f_-(t) t / (m_{K^0}^2 - m_{\pi^+}^2)$$

t = momentum transfer to the π .

λ_+ and λ_0 are the linear expansion coefficients of f_+ and f_0 :

$$f_+(t) = f_+(0) (1 + \lambda_+ t / m_{\pi^+}^2)$$

For quadratic expansion

$$f_+(t) = f_+(0) (1 + \lambda'_+ t / m_{\pi^+}^2 + \frac{\lambda''_+}{2} t^2 / m_{\pi^+}^4)$$

Meson Particle Listings

K_L^0

as used by KTeV. If there is a non-vanishing quadratic term, then λ_+ represents an average slope, which is then different from λ'_+ .

NA48 (K_{e3}) and ISTRA quadratic expansion coefficients are converted with $\lambda'_+ PDG = \lambda_+ NA48$ and $\lambda''_+ PDG = 2 \lambda'_+ NA48$

$\lambda'_+ PDG = (\frac{m_{\pi^+}}{m_{\pi^0}})^2 \lambda_+ ISTRA$ and

$\lambda''_+ PDG = 2 (\frac{m_{\pi^+}}{m_{\pi^0}})^4 \lambda'_+ ISTRA$

ISTRA linear expansion coefficients are converted with $\lambda_+ PDG = (\frac{m_{\pi^+}}{m_{\pi^0}})^2 \lambda_+ ISTRA$ and $\lambda_0 PDG = (\frac{m_{\pi^+}}{m_{\pi^0}})^2 \lambda_0 ISTRA$

The pole parametrization is

$$f_+(t) = f_+(0) \left(\frac{M_V^2}{M_V^2 - t} \right)$$

$$f_0(t) = f_0(0) \left(\frac{M_S^2}{M_S^2 - t} \right)$$

where M_V and M_S are the vector and scalar pole masses.

The dispersive parametrization is

$$f_+(t) = f_+(0) \exp \left[\frac{t}{m_\pi^2} (\Lambda_+ + H(t)) \right];$$

$$f_0(t) = f_0(0) \exp \left[\frac{t}{m_K^2 - m_\pi^2} (\ln[C] - G(t)) \right],$$

where Λ_+ is the slope parameter and $\ln[C] = \ln[f_0(m_K^2 - m_\pi^2)]$ is the logarithm of the scalar form factor at the Callan-Treiman point.

$H(t)$ and $G(t)$ are dispersive integrals.

The following abbreviations are used:

DP = Dalitz plot analysis.

PI = π spectrum analysis.

MU = μ spectrum analysis.

POL = μ polarization analysis.

BR = $K_{\mu 3}^0 / K_{e 3}^0$ branching ratio analysis.

E = positron or electron spectrum analysis.

RC = radiative corrections.

λ_+ (LINEAR ENERGY DEPENDENCE OF f_+ IN K_{e3}^0 DECAY)

For radiative correction of K_{e3}^0 DP, see GINSBERG 67, BECHERRAWY 70, CIRIGLIANO 02, CIRIGLIANO 04, and ANDRE 07. Results labeled OUR FIT are discussed in the review “ K_{e3}^\pm and $K_{\mu 3}^0$ Form Factors” in the K^\pm Listings. For earlier, lower statistics results, see the 2004 edition of this review, Physics Letters **B592** 1 (2004).

VALUE (units 10^{-2})	EVTS	DOCUMENT ID	TECN	COMMENT
2.82 ± 0.04 OUR FIT	Error includes scale factor of 1.1. Assuming μ -e universality			
2.85 ± 0.04 OUR AVERAGE				

2.86 ± 0.05 ± 0.04	2M	AMBROSINO 06D	KLOE	
2.832 ± 0.037 ± 0.043	1.9M	ALEXOPOU... 04A	KTEV	PI, no $\mu = e$
2.88 ± 0.04 ± 0.11	5.6M	82 LAI 04C	NA48	DP
• • • We do not use the following data for averages, fits, limits, etc. • • •				
2.84 ± 0.07 ± 0.13	5.6M	83 LAI 04C	NA48	DP
2.45 ± 0.12 ± 0.22	366k	APOSTOLA... 00	CPLR	DP
3.06 ± 0.34	74k	BIRULEV 81	SPEC	DP
3.12 ± 0.25	500k	GJESDAL 76	SPEC	DP
2.70 ± 0.28	25k	BLUMENTHAL 75	SPEC	DP

⁸² Results from linear fit and assuming only vector and axial couplings.
⁸³ Results from linear fit with $|f_S/f_+|$ and $|f_T/f_+|$ free.

λ_+ (LINEAR ENERGY DEPENDENCE OF f_+ IN $K_{\mu 3}^0$ DECAY)

Results labeled OUR FIT are discussed in the review “ K_{e3}^\pm and $K_{\mu 3}^0$ Form Factors” in the K^\pm Listings. For earlier, lower statistics results, see the 2004 edition of this review, Physics Letters **B592** 1 (2004).

VALUE (units 10^{-2})	EVTS	DOCUMENT ID	TECN	COMMENT
2.82 ± 0.04 OUR FIT	Error includes scale factor of 1.1. Assuming μ -e universality			
2.71 ± 0.10 OUR FIT	Error includes scale factor of 1.4. Not assuming μ -e universality			
2.67 ± 0.06 ± 0.08	2.3M	84 LAI 07A	NA48	DP
2.745 ± 0.088 ± 0.063	1.5M	ALEXOPOU... 04A	KTEV	DP, no $\mu = e$
2.813 ± 0.051	3.4M	ALEXOPOU... 04A	KTEV	PI, DP, $\mu = e$
3.0 ± 0.3	1.6M	DONALDSON 74B	SPEC	DP
• • • We do not use the following data for averages, fits, limits, etc. • • •				
4.27 ± 0.44	150k	BIRULEV 81	SPEC	DP

λ_0 (LINEAR ENERGY DEPENDENCE OF f_0 IN $K_{\mu 3}^0$ DECAY)

Wherever possible, we have converted the above values of $\xi(0)$ into values of λ_0 using the associated λ_+^H and $d\xi(0)/d\lambda_+$. Results labeled OUR FIT are discussed in the review “ K_{e3}^\pm and $K_{\mu 3}^0$ Form Factors” in the K^\pm Listings. For earlier, lower statistics results, see the 2004 edition of this review, Physics Letters **B592** 1 (2004).

VALUE (units 10^{-2})	$d\lambda_0/d\lambda_+$	EVTS	DOCUMENT ID	TECN	COMMENT
1.38 ± 0.18 OUR FIT	Error includes scale factor of 2.2. Assuming μ -e universality				
1.42 ± 0.23 OUR FIT	Error includes scale factor of 2.8. Not assuming μ -e universality				
1.17 ± 0.07 ± 0.10		2.3M	85 LAI 07A	NA48	DP
1.657 ± 0.125	-0.44	1.5M	86 ALEXOPOU... 04A	KTEV	DP, no $\mu = e$

1.635 ± 0.121	-0.85	3.4M	87 ALEXOPOU... 04A	KTEV	PI, DP, $\mu = e$
+1.9 ± 0.4	-0.47	1.6M	88 DONALDSON 74B	SPEC	DP

• • • We do not use the following data for averages, fits, limits, etc. • • •
 3.41 ± 0.67 unknown 150k ⁸⁹ BIRULEV 81 SPEC DP

⁸⁵ LAI 07A gives a correlation -0.40 between their λ_0 and λ_+ measurements.

⁸⁶ ALEXOPOULOS 04A gives a correlation -0.38 between their λ_0 and λ_+ measurements.

⁸⁷ ALEXOPOULOS 04A gives a correlation -0.36 between their λ_0 and λ_+ measurements.

⁸⁸ DONALDSON 74B $d\lambda_0/d\lambda_+$ obtained from figure 18.

⁸⁹ BIRULEV 81 gives $d\lambda_0/d\lambda_+ = -1.5$, giving an unreasonably narrow error ellipse which dominates all other results. We use $d\lambda_0/d\lambda_+ = 0$.

λ'_+ (LINEAR K_{e3}^0 FORM FACTOR FROM QUADRATIC FIT)

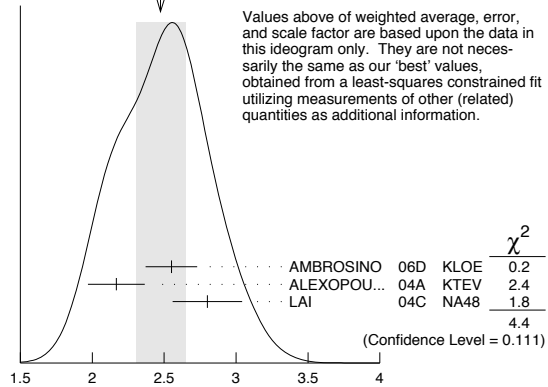
VALUE (units 10^{-2})	EVTS	DOCUMENT ID	TECN	COMMENT
2.40 ± 0.12 OUR FIT	Error includes scale factor of 1.2. Assuming μ -e universality			
2.49 ± 0.13 OUR FIT	Error includes scale factor of 1.1. Not assuming μ -e universality			
2.48 ± 0.17 OUR AVERAGE	Error includes scale factor of 1.5. See the ideogram below.			
2.55 ± 0.15 ± 0.10	2M	⁹⁰ AMBROSINO 06D	KLOE	
2.167 ± 0.137 ± 0.143	1.9M	⁹¹ ALEXOPOU... 04A	KTEV	PI, no $\mu = e$
2.80 ± 0.19 ± 0.15	5.6M	⁹² LAI 04C	NA48	DP

⁹⁰ We use AMBROSINO 06D result in the fit not assuming μ -e universality. This result enters the fit assuming μ -e universality via AMBROSINO 07C measurement of λ'_+ in $K_{\mu 3}$ decays. AMBROSINO 06D gives a correlation -0.95 between their λ'_+ and λ''_+ .

⁹¹ ALEXOPOULOS 04A gives a correlation -0.97 between their λ'_+ and λ''_+ .

⁹² For LAI 04C we calculate a correlation -0.88 between their λ'_+ and λ''_+ .

WEIGHTED AVERAGE
 2.48±0.17 (Error scaled by 1.5)



Values above of weighted average, error, and scale factor are based upon the data in this ideogram only. They are not necessarily the same as our 'best' values, obtained from a least-squares constrained fit utilizing measurements of other (related) quantities as additional information.

λ'_+ (LINEAR K_{e3}^0 FORM FACTOR FROM QUADRATIC FIT) (units 10^{-2})

λ''_+ (QUADRATIC K_{e3}^0 FORM FACTOR)

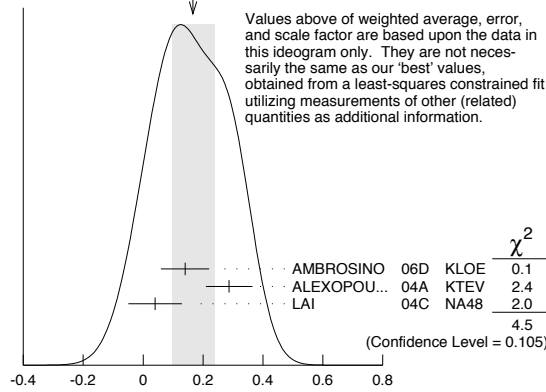
VALUE (units 10^{-2})	EVTS	DOCUMENT ID	TECN	COMMENT
0.20 ± 0.05 OUR FIT	Error includes scale factor of 1.2. Assuming μ -e universality			
0.16 ± 0.05 OUR FIT	Error includes scale factor of 1.1. Not assuming μ -e universality			
0.17 ± 0.07 OUR AVERAGE	Error includes scale factor of 1.5. See the ideogram below.			
0.14 ± 0.07 ± 0.04	2M	⁹³ AMBROSINO 06D	KLOE	
0.287 ± 0.057 ± 0.053	1.9M	⁹⁴ ALEXOPOU... 04A	KTEV	PI, no $\mu = e$
0.04 ± 0.08 ± 0.04	5.6M	^{95,96} LAI 04C	NA48	DP

⁹³ We use AMBROSINO 06D result in the fit not assuming μ -e universality. This result enters the fit assuming μ -e universality via AMBROSINO 07C measurement of λ''_+ in $K_{\mu 3}$ decays. AMBROSINO 06D gives a correlation -0.95 between their λ'_+ and λ''_+ .

⁹⁴ ALEXOPOULOS 04A gives a correlation -0.97 between their λ'_+ and λ''_+ .

⁹⁵ Values doubled to agree with PDG conventions described above.

⁹⁶ LAI 04C gives a correlation -0.88 between their λ'_+ and λ''_+ .

WEIGHTED AVERAGE
0.17±0.07 (Error scaled by 1.5) χ^2_+ (QUADRATIC K_{e3}^0 FORM FACTOR) (units 10^{-2}) χ'_+ (LINEAR $K_{\mu 3}^0$ FORM FACTOR FROM QUADRATIC FIT)

VALUE (units 10^{-2})	EVTS	DOCUMENT ID	TECN	COMMENT
2.40 ± 0.12 OUR FIT	Error	includes scale factor of 1.2.	Assuming μ -e universality	
1.89 ± 0.24 OUR FIT	Not assuming μ -e universality			
2.23 ± 0.98 ± 0.37	1.8M	97 AMBROSINO 07C	KLOE	no $\mu = e$
2.56 ± 0.15 ± 0.09	3.8M	97 AMBROSINO 07C	KLOE	$\mu = e$
2.05 ± 0.22 ± 0.24	2.3M	97 LAI 07A	NA48	DP
1.703 ± 0.319 ± 0.177	1.5M	97 ALEXOPOU... 04A	KTEV	DP, no $\mu = e$
2.064 ± 0.175	3.4M	97 ALEXOPOU... 04A	KTEV	PI, DP, $\mu = e$

⁹⁷ See section λ_0 below for correlations. χ''_+ (QUADRATIC $K_{\mu 3}^0$ FORM FACTOR)

VALUE (units 10^{-2})	EVTS	DOCUMENT ID	TECN	COMMENT
0.20 ± 0.05 OUR FIT	Error	includes scale factor of 1.2.	Assuming μ -e universality	
0.37 ± 0.12 OUR FIT	Error	includes scale factor of 1.3.	Not assuming μ -e universality	
0.48 ± 0.49 ± 0.16	1.8M	98 AMBROSINO 07C	KLOE	no $\mu = e$
0.15 ± 0.07 ± 0.04	3.8M	98 AMBROSINO 07C	KLOE	$\mu = e$
0.26 ± 0.09 ± 0.10	2.3M	98 LAI 07A	NA48	DP
0.443 ± 0.131 ± 0.072	1.5M	98 ALEXOPOU... 04A	KTEV	DP, no $\mu = e$
0.320 ± 0.069	3.4M	98 ALEXOPOU... 04A	KTEV	PI, DP, $\mu = e$

⁹⁸ See section λ_0 below for correlations. λ_0 (LINEAR f_0 $K_{\mu 3}^0$ FORM FACTOR FROM QUADRATIC FIT)

VALUE (units 10^{-2})	EVTS	DOCUMENT ID	TECN	COMMENT
1.16 ± 0.09 OUR FIT	Error	includes scale factor of 1.2.	Assuming μ -e universality	
1.07 ± 0.14 OUR FIT	Error	includes scale factor of 1.3.	Not assuming μ -e universality	
0.91 ± 0.59 ± 0.26	1.8M	99 AMBROSINO 07C	KLOE	no $\mu = e$
1.54 ± 0.18 ± 0.13	3.8M	100 AMBROSINO 07C	KLOE	$\mu = e$
0.95 ± 0.11 ± 0.08	2.3M	101 LAI 07A	NA48	DP
1.281 ± 0.136 ± 0.122	1.5M	102 ALEXOPOU... 04A	KTEV	DP, no $\mu = e$
1.372 ± 0.131	3.4M	103 ALEXOPOU... 04A	KTEV	PI, DP, $\mu = e$

⁹⁹ AMBROSINO 07C, not assuming μ -e universality, gives a correlation matrix

$$\begin{array}{cc} \chi'_+ & \chi''_+ \\ \chi''_+ & -0.97 & 1 \\ \lambda_0 & 0.81 & -0.91 \end{array}$$

¹⁰⁰ AMBROSINO 07C, assuming μ -e universality, gives a correlation matrix

$$\begin{array}{cc} \chi'_+ & \chi''_+ \\ \chi''_+ & -0.95 & 1 \\ \lambda_0 & 0.29 & -0.38 \end{array}$$

¹⁰¹ LAI 07A gives a correlation matrix

$$\begin{array}{cc} \chi'_+ & \chi''_+ \\ \chi''_+ & -0.96 & 1 \\ \lambda_0 & 0.63 & -0.73 \end{array}$$

¹⁰² ALEXOPOULOS 04A, not assuming μ -e universality, gives a correlation matrix

$$\begin{array}{ccc} \chi'_+ & & \lambda_0 \\ \chi''_+ & -0.96 & 1 \\ \lambda_0 & 0.65 & -0.75 & 1 \end{array}$$

¹⁰³ ALEXOPOULOS 04A, assuming μ -e universality, gives a correlation matrix

$$\begin{array}{ccc} \chi'_+ & & \lambda_0 \\ \chi''_+ & -0.97 & 1 \\ \lambda_0 & 0.34 & -0.44 & 1 \end{array}$$

 M_V^e (POLE MASS FOR K_{e3}^0 DECAY)

VALUE (MeV)	EVTS	DOCUMENT ID	TECN	COMMENT
878 ± 6 OUR FIT	Error	includes scale factor of 1.1.	Assuming μ -e universality	
875 ± 5 OUR AVERAGE				
870 ± 6 ± 7	2M	AMBROSINO 06D	KLOE	
881.03 ± 5.12 ± 4.94	1.9M	ALEXOPOU... 04A	KTEV	PI, no $\mu = e$
859 ± 18	5.6M	LAI 04C	NA48	

 M_V^μ (POLE MASS FOR $K_{\mu 3}^0$ DECAY)

VALUE (MeV)	EVTS	DOCUMENT ID	TECN	COMMENT
878 ± 6 OUR FIT	Error	includes scale factor of 1.1.	Assuming μ -e universality	
900 ± 21 OUR FIT	Error	includes scale factor of 1.7.	Not assuming μ -e universality	
905 ± 9 ± 17	2.3M	104 LAI 07A	NA48	DP
889.19 ± 12.81 ± 9.92	1.5M	104 ALEXOPOU... 04A	KTEV	DP, no $\mu = e$
882.32 ± 6.54	3.4M	104 ALEXOPOU... 04A	KTEV	PI, DP, $\mu = e$

¹⁰⁴ See section M_S^μ below for correlations. M_S^μ (POLE MASS FOR $K_{\mu 3}^0$ DECAY)

VALUE (MeV)	EVTS	DOCUMENT ID	TECN	COMMENT
1222 ± 80 OUR FIT	Error	includes scale factor of 2.3.	Not assuming μ -e universality	
1252 ± 90 OUR FIT	Error	includes scale factor of 2.6.	Assuming μ -e universality	
1400 ± 46 ± 53	2.3M	105 LAI 07A	NA48	DP
1167.14 ± 28.30 ± 31.04	1.5M	106 ALEXOPOU... 04A	KTEV	PI, no $\mu = e$
1173.80 ± 39.47	3.4M	107 ALEXOPOU... 04A	KTEV	PI, DP, $\mu = e$

¹⁰⁵ LAI 07A gives a correlation -0.47 between their M_S^μ and M_V^μ measurements, not assuming μ -e universality.¹⁰⁶ ALEXOPOULOS 04A gives a correlation -0.46 between their M_S^μ and M_V^μ and measurements, not assuming μ -e universality.¹⁰⁷ ALEXOPOULOS 04A gives a correlation -0.40 between their M_S^μ and M_V^μ and measurements, assuming μ -e universality. Λ_+ (DISPERSIVE VECTOR FORM FACTOR FOR $K_{\mu 3}^0$ DECAY)See the review on " K_{e3}^\pm and $K_{\mu 3}^0$ Form Factors" for details of the dispersive parametrization.

VALUE (units 10^{-1})	EVTS	DOCUMENT ID	TECN	COMMENT
0.251 ± 0.011 OUR AVERAGE	Error	includes scale factor of 2.2.		
0.257 ± 0.004 ± 0.004	3.8M	108 AMBROSINO 07C	KLOE	$\mu = e$
0.233 ± 0.005 ± 0.008	2.3M	109 LAI 07A	NA48	DP

¹⁰⁸ AMBROSINO 07C results include 2M K_{e3} events from AMBROSINO 06D. The correlation between Λ_+ and $\ln(C)$ is -0.26 .¹⁰⁹ LAI 07A gives a correlation -0.44 between their Λ_+ and $\ln(C)$ measurements. $\ln(C)$ (DISPERSIVE SCALAR FORM FACTOR FOR $K_{\mu 3}^0$ DECAY)See the review on " K_{e3}^\pm and $K_{\mu 3}^0$ Form Factors" for details of the dispersive parametrization.

VALUE (units 10^{-1})	EVTS	DOCUMENT ID	TECN	COMMENT
1.59 ± 0.26 OUR AVERAGE	Error	includes scale factor of 2.2.		
2.04 ± 0.19 ± 0.15	3.8M	110 AMBROSINO 07C	KLOE	$\mu = e$
1.438 ± 0.080 ± 0.112	2.3M	111 LAI 07A	NA48	DP

¹¹⁰ AMBROSINO 07C results include 2M K_{e3} events from AMBROSINO 06D. We convert (Λ_+, A_0) to $(\Lambda_+, \ln(C))$ parametrization using $\ln(C) = (A_0 \cdot 11.713 + 0.0398) \pm 0.0041$, where the error is due to theory parametrization of the form factor. The correlation between Λ_+ and $\ln(C)$ is -0.26 .¹¹¹ LAI 07A gives a correlation -0.44 between their Λ_+ and $\ln(C)$ measurements. $a_1(t_0, Q^2)$ FORM FACTOR PARAMETER

See HILL 06 for a definition of this parameter.

VALUE	EVTS	DOCUMENT ID	TECN
1.023 ± 0.028 ± 0.029	2M	112 ABOUZAID 06C	KTEV
$112 Q^2 = 2 \text{ GeV}^2, t_0 = 0.49 (m_K - m_\pi)^2$.			Correlation between a_1 and a_2 : $\rho_{12} = -0.064$.

 $a_2(t_0, Q^2)$ FORM FACTOR PARAMETER

See HILL 06 for a definition of this parameter.

VALUE	EVTS	DOCUMENT ID	TECN
0.75 ± 1.58 ± 1.47	2M	113 ABOUZAID 06C	KTEV
$113 Q^2 = 2 \text{ GeV}^2, t_0 = 0.49 (m_K - m_\pi)^2$.			Correlation between a_1 and a_2 : $\rho_{12} = -0.064$.

 $|f_S/f_+|$ FOR K_{e3}^0 DECAYRatio of scalar to f_+ couplings.

VALUE (units 10^{-2})	CL%	EVTS	DOCUMENT ID	TECN	COMMENT
1.5 ± 0.7 ± 1.2		5.6M	114 LAI 04C	NA48	

• • • We do not use the following data for averages, fits, limits, etc. • • •

<9.5	95	18k	HILL	78	STRC
<7.	68	48k	BIRULEV	76	SPEC
<4.	68	25k	BLUMENTHAL	75	SPEC

¹¹⁴ Results from linear fit with $|f_S/f_+|$ and $|f_T/f_+|$ free.

Meson Particle Listings

 K_L^0 $|f_T/f_+|$ FOR K_{e3}^0 DECAYRatio of tensor to f_+ couplings.

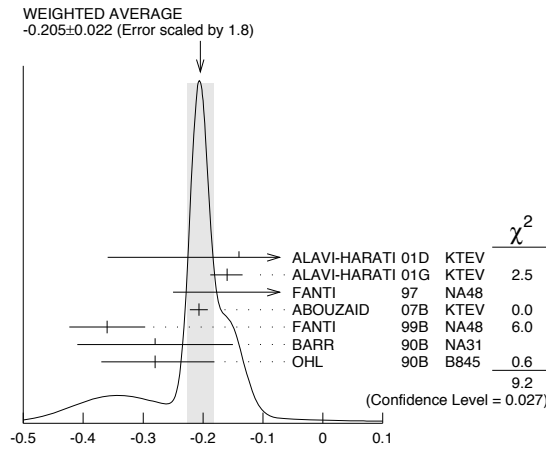
VALUE (units 10^{-2})	CL%	EVTS	DOCUMENT ID	TECN	COMMENT
5.4 ± 0.3		5.6M	115 LAI	04c	NA48
<40.	95	18k	HILL	78	STRC
<34.	68	48k	BIRULEV	76	SPEC See also BIRULEV 81
<23.	68	25k	BLUMENTHAL75	SPEC	

115 Results from linear fit with $|f_S/f_+|$ and $|f_T/f_+|$ free. $|f_T/f_+|$ FOR $K_{\mu 3}^0$ DECAYRatio of tensor to f_+ couplings.

VALUE (units 10^{-2})	DOCUMENT ID	TECN
12 ± 12	BIRULEV 81	SPEC

 α_{K^*} DECAY FORM FACTOR FOR $K_L \rightarrow \ell^+ \ell^- \gamma$, $K_L^0 \rightarrow \ell^+ \ell^- \ell'^+ \ell'^-$ Average of all α_{K^*} measurements (from each of three datablocks following this one) assuming lepton universality.

VALUE DOCUMENT ID
 -0.205 ± 0.022 OUR AVERAGE Includes data from the 3 datablocks that follow this one. Error includes scale factor of 1.8. See the ideogram below.

 α_{K^*} DECAY FORM FACTOR FOR $K_L \rightarrow \ell^+ \ell^- \gamma$, $K_L^0 \rightarrow \ell^+ \ell^- \ell'^+ \ell'^-$ α_{K^*} DECAY FORM FACTOR FOR $K_L \rightarrow e^+ e^- \gamma$

α_{K^*} is the constant in the model of BERGSTROM 83 which measures the relative strength of the vector-vector transition $K_L \rightarrow K^* \gamma$ with $K^* \rightarrow \rho, \omega, \phi \rightarrow \gamma^*$ and the pseudoscalar-pseudoscalar transition $K_L \rightarrow \pi, \eta, \eta' \rightarrow \gamma \gamma^*$.

VALUE EVTS DOCUMENT ID TECN
 The data in this block is included in the average printed for a previous datablock.

-0.217 ± 0.034 OUR AVERAGE	Error includes scale factor of 2.4.
$-0.207 \pm 0.012 \pm 0.009$	83k 116 ABOUZAID 07B KTEV
$-0.36 \pm 0.06 \pm 0.02$	6864 FANTI 99B NA48
-0.28 ± 0.13	BARR 90B NA31
-0.280 ± 0.099	OHL 90B B845

116 ABOUZAID 07B measures $C \cdot \alpha_{K^*} = -0.517 \pm 0.030 \pm 0.022$. We assume $C = 2.5$, as in all other measurements. α_{K^*} DECAY FORM FACTOR FOR $K_L \rightarrow \mu^+ \mu^- \gamma$

α_{K^*} is the constant in the model of BERGSTROM 83 described in the previous section.

VALUE EVTS DOCUMENT ID TECN
 The data in this block is included in the average printed for a previous datablock.

-0.158 ± 0.027 OUR AVERAGE	
-0.160 ± 0.026	9100 ALAVI-HARATI01G KTEV
-0.04 ± 0.24	FANTI 97 NA48

 $\alpha_{K^*}^{\text{eff}}$ DECAY FORM FACTOR FOR $K_L \rightarrow e^+ e^- e^+ e^-$

$\alpha_{K^*}^{\text{eff}}$ is the parameter describing the relative strength of an intermediate pseudoscalar decay amplitude and a vector meson decay amplitude in the model of BERGSTROM 83. It takes into account both the radiative effects and the form factor. Since there are two $e^+ e^-$ pairs here compared with one in $e^+ e^- \gamma$ decays, a factorized expression is used for the $e^+ e^- e^+ e^-$ decay form factor.

VALUE EVTS DOCUMENT ID TECN
 The data in this block is included in the average printed for a previous datablock.

$-0.14 \pm 0.16 \pm 0.15$	441 ALAVI-HARATI01D KTEV
---------------------------	--------------------------

 α_{DIP} DECAY FORM FACTOR FOR $K_L^0 \rightarrow \ell^+ \ell^- \gamma$, $K_L^0 \rightarrow \ell^+ \ell^- \ell'^+ \ell'^-$ Average of all α_{DIP} measurements (from each of three datablocks following this one) assuming lepton universality.

VALUE DOCUMENT ID
 -1.69 ± 0.08 OUR AVERAGE Includes data from the 3 datablocks that follow this one. Error includes scale factor of 1.7.

 α_{DIP} DECAY FORM FACTOR FOR $K_L^0 \rightarrow e^+ e^- \gamma$

α_{DIP} parameter in $K_L^0 \rightarrow \gamma^* \gamma^*$ form factor by DAMBROSIO 98, motivated by vector meson dominance and a proper short distance behavior.

VALUE EVTS DOCUMENT ID TECN
 The data in this block is included in the average printed for a previous datablock.

$-1.729 \pm 0.043 \pm 0.028$ 83k ABOUZAID 07B KTEV

 α_{DIP} DECAY FORM FACTOR FOR $K_L^0 \rightarrow \mu^+ \mu^- \gamma$

α_{DIP} is a constant in the model of DAMBROSIO 98 described in the previous section.

VALUE EVTS DOCUMENT ID TECN
 The data in this block is included in the average printed for a previous datablock.

-1.54 ± 0.10 9100 ALAVI-HARATI01G KTEV

 α_{DIP} DECAY FORM FACTOR FOR $K_L^0 \rightarrow e^+ e^- \mu^+ \mu^-$

α_{DIP} is a constant in the model of DAMBROSIO 98 described in the previous section.

VALUE EVTS DOCUMENT ID TECN
 The data in this block is included in the average printed for a previous datablock.

-1.59 ± 0.37 131 ALAVI-HARATI03B KTEV

 a_1/a_2 FORM FACTOR FOR M1 DIRECT EMISSION AMPLITUDEForm factor = $\tilde{g}_{M1} \left[1 + \frac{a_1/a_2}{(M_\rho^2 - M_K^2) + 2M_K E_\gamma} \right]$ as described in ALAVI-HARATI 00B.

VALUE (GeV ²)	EVTS	DOCUMENT ID	TECN	COMMENT
-0.737 ± 0.014 OUR AVERAGE				
$-0.744 \pm 0.027 \pm 0.032$	5241	117 ABOUZAID 06	KTEV	$\pi^+ \pi^- e^+ e^-$
$-0.738 \pm 0.007 \pm 0.018$	111k	118 ABOUZAID 06A	KTEV	$\pi^+ \pi^+ \gamma$
$-0.81 \pm 0.07 \pm 0.02$		119 LAI 03c	NA48	$\pi^+ \pi^- e^+ e^-$
$-0.737 \pm 0.026 \pm 0.022$		120 ALAVI-HARATI01B		$\pi^+ \pi^- \gamma$
$-0.720 \pm 0.028 \pm 0.009$	1766	121 ALAVI-HARATI00B	KTEV	$\pi^+ \pi^- e^+ e^-$

117 ABOUZAID 06 also measured $|\tilde{g}_{M1}| = 1.11 \pm 0.14$.
 118 ABOUZAID 06A also measured $|\tilde{g}_{M1}| = 1.198 \pm 0.035 \pm 0.086$.
 119 LAI 03c also measured $\tilde{g}_{M1} = 0.99 \pm 0.28$.
 120 ALAVI-HARATI 01B fit gives $\chi^2/\text{DOF} = 38.8/27$. Linear and quadratic fits give $\chi^2/\text{DOF} = 43.2/27$ and $37.6/26$ respectively.
 121 ALAVI-HARATI 00B also measured $|\tilde{g}_{M1}| = 1.35 \pm 0.20$.

 \bar{f}_S DECAY FORM FACTOR FOR $K_L^0 \rightarrow \pi^\pm \pi^0 e^\mp \nu_e$

VALUE DOCUMENT ID TECN
 0.049 ± 0.011 OUR AVERAGE Error includes scale factor of 1.7.

$0.052 \pm 0.006 \pm 0.002$	BATLEY 04	NA48
$0.010 \pm 0.016 \pm 0.017$	MAKOFF 93	E731

 \bar{f}_P DECAY FORM FACTOR FOR $K_L^0 \rightarrow \pi^\pm \pi^0 e^\mp \nu_e$

VALUE DOCUMENT ID TECN
 -0.052 ± 0.012 OUR AVERAGE

$-0.051 \pm 0.011 \pm 0.005$	BATLEY 04	NA48
$-0.079 \pm 0.049 \pm 0.022$	MAKOFF 93	E731

 λ_ρ DECAY FORM FACTOR FOR $K_L^0 \rightarrow \pi^\pm \pi^0 e^\mp \nu_e$

VALUE DOCUMENT ID TECN
 0.085 ± 0.020 OUR AVERAGE

$0.087 \pm 0.019 \pm 0.006$	BATLEY 04	NA48
$0.014 \pm 0.087 \pm 0.070$	MAKOFF 93	E731

 \bar{h} DECAY FORM FACTOR FOR $K_L^0 \rightarrow \pi^\pm \pi^0 e^\mp \nu_e$

VALUE DOCUMENT ID TECN
 -0.30 ± 0.13 OUR AVERAGE

$-0.32 \pm 0.12 \pm 0.07$	BATLEY 04	NA48
$-0.07 \pm 0.31 \pm 0.31$	MAKOFF 93	E731

 L_3 CHIRAL PERT. THEO. PARAM. FOR $K_L^0 \rightarrow \pi^\pm \pi^0 e^\mp \nu_e$

VALUE (units 10^{-3}) DOCUMENT ID TECN
 -3.96 ± 0.28 OUR AVERAGE Error includes scale factor of 1.6.

-4.1 ± 0.2	BATLEY 04	NA48
-3.4 ± 0.4	122 MAKOFF 93	E731

122 MAKOFF 93 sign has been changed to negative to agree with the sign convention used in BATLEY 04.

a_V VECTOR MESON EXCHANGE CONTRIBUTION

VALUE	EVTS	DOCUMENT ID	TECN	COMMENT
-0.43±0.06 OUR AVERAGE				Error includes scale factor of 1.5.
-0.31±0.05±0.07	1.4k	¹²³ ABOUZAID 08	KTEV	
-0.46±0.03±0.04		LAI 02B NA48	$K_L^0 \rightarrow \pi^0 2\gamma$	
-0.67±0.21±0.12		ALAVI-HARATI01E	KTEV $K_L^0 \rightarrow \pi^0 e^+ e^- \gamma$	
••• We do not use the following data for averages, fits, limits, etc. •••				
-0.72±0.05±0.06	¹²⁴	ALAVI-HARATI99B	KTEV $K_L^0 \rightarrow \pi^0 2\gamma$	

¹²³ Using KTeV dataset collected in 1996, 1997, and 1999.

¹²⁴ Superseded by ABOUZAID 08.

CP VIOLATION IN K_L DECAYS

Updated May 2010 by L. Wolfenstein (Carnegie-Mellon University), T.G. Trippe (LBNL), and C.-J. Lin (LBNL).

The symmetries C (particle-antiparticle interchange) and P (space inversion) hold for strong and electromagnetic interactions. After the discovery of large C and P violation in the weak interactions, it appeared that the product CP was a good symmetry. In 1964 CP violation was observed in K^0 decays at a level given by the parameter $\epsilon \approx 2.3 \times 10^{-3}$.

A unified treatment of CP violation in K , D , B , and B_s mesons is given in “ CP Violation in Meson Decays” by D. Kirkby and Y. Nir in this *Review*. A more detailed review including a thorough discussion of the experimental techniques used to determine CP violation parameters is given in a book by K. Kleinknecht [1]. Here we give a concise summary of the formalism needed to define the parameters of CP violation in K_L decays, and a description of our fits for the best values of these parameters.

1. Formalism for CP violation in Kaon decay:

CP violation has been observed in the semi-leptonic decays $K_L^0 \rightarrow \pi^\mp \ell^\pm \nu$, and in the nonleptonic decay $K_L^0 \rightarrow 2\pi$. The experimental numbers that have been measured are

$$A_L = \frac{\Gamma(K_L^0 \rightarrow \pi^- \ell^+ \nu) - \Gamma(K_L^0 \rightarrow \pi^+ \ell^- \nu)}{\Gamma(K_L^0 \rightarrow \pi^- \ell^+ \nu) + \Gamma(K_L^0 \rightarrow \pi^+ \ell^- \nu)} \quad (1a)$$

$$\eta_{+-} = A(K_L^0 \rightarrow \pi^+ \pi^-) / A(K_S^0 \rightarrow \pi^+ \pi^-) = |\eta_{+-}| e^{i\phi_{+-}} \quad (1b)$$

$$\eta_{00} = A(K_L^0 \rightarrow \pi^0 \pi^0) / A(K_S^0 \rightarrow \pi^0 \pi^0) = |\eta_{00}| e^{i\phi_{00}} \quad (1c)$$

CP violation can occur either in the $K^0 - \bar{K}^0$ mixing or in the decay amplitudes. Assuming CPT invariance, the mass eigenstates of the $K^0 - \bar{K}^0$ system can be written

$$|K_S\rangle = p|K^0\rangle + q|\bar{K}^0\rangle, \quad |K_L\rangle = p|K^0\rangle - q|\bar{K}^0\rangle. \quad (2)$$

If CP invariance held, we would have $q = p$ so that K_S would be CP -even and K_L CP -odd. (We define $|\bar{K}^0\rangle$ as $CP |K^0\rangle$.) CP violation in $K^0 - \bar{K}^0$ mixing is then given by the parameter $\tilde{\epsilon}$ where

$$\frac{p}{q} = \frac{(1 + \tilde{\epsilon})}{(1 - \tilde{\epsilon})}. \quad (3)$$

CP violation can also occur in the decay amplitudes

$$A(K^0 \rightarrow \pi\pi(I)) = A_I e^{i\delta_I}, \quad A(\bar{K}^0 \rightarrow \pi\pi(I)) = A_I^* e^{i\delta_I}, \quad (4)$$

where I is the isospin of $\pi\pi$, δ_I is the final-state phase shift, and A_I would be real if CP invariance held. The CP -violating

observables are usually expressed in terms of ϵ and ϵ' defined by

$$\eta_{+-} = \epsilon + \epsilon', \quad \eta_{00} = \epsilon - 2\epsilon'. \quad (5a)$$

One can then show [2]

$$\epsilon = \tilde{\epsilon} + i (\text{Im } A_0 / \text{Re } A_0), \quad (5b)$$

$$\sqrt{2}\epsilon' = i e^{i(\delta_2 - \delta_0)} (\text{Re } A_2 / \text{Re } A_0) (\text{Im } A_2 / \text{Re } A_2 - \text{Im } A_0 / \text{Re } A_0), \quad (5c)$$

$$A_L = 2\text{Re } \epsilon / (1 + |\epsilon|^2) \approx 2\text{Re } \epsilon. \quad (5d)$$

In Eqs. (5a), small corrections [3] of order $\epsilon' \times \text{Re}(A_2/A_0)$ are neglected, and Eq. (5d) assumes the $\Delta S = \Delta Q$ rule.

The quantities $\text{Im } A_0$, $\text{Im } A_2$, and $\text{Im } \tilde{\epsilon}$ depend on the choice of phase convention, since one can change the phases of K^0 and \bar{K}^0 by a transformation of the strange quark state $|s\rangle \rightarrow |s\rangle e^{i\alpha}$; of course, observables are unchanged. It is possible by a choice of phase convention to set $\text{Im } A_0$ or $\text{Im } A_2$ or $\text{Im } \tilde{\epsilon}$ to zero, but none of these is zero with the usual phase conventions in the Standard Model. The choice $\text{Im } A_0 = 0$ is called the Wu-Yang phase convention [4], in which case $\epsilon = \tilde{\epsilon}$. The value of ϵ' is independent of phase convention, and a nonzero value demonstrates CP violation in the decay amplitudes, referred to as direct CP violation. The possibility that direct CP violation is essentially zero, and that CP violation occurs only in the mixing matrix, was referred to as the superweak theory [5].

By applying CPT invariance and unitarity the phase of ϵ is given approximately by

$$\phi_\epsilon \approx \tan^{-1} \frac{2(m_{K_L} - m_{K_S})}{\Gamma_{K_S} - \Gamma_{K_L}} \approx 43.51 \pm 0.05^\circ, \quad (6a)$$

while Eq. (5c) gives the phase of ϵ' to be

$$\phi_{\epsilon'} = \delta_2 - \delta_0 + \frac{\pi}{2} \approx 42.3 \pm 1.5^\circ, \quad (6b)$$

where the numerical value is based on an analysis of $\pi - \pi$ scattering using chiral perturbation theory [6]. The approximation in Eq. (6a) depends on the assumption that direct CP violation is very small in all K^0 decays. This is expected to be good to a few tenths of a degree, as indicated by the small value of ϵ' and of η_{+-} and η_{00} , the CP -violation parameters in the decays $K_S \rightarrow \pi^+ \pi^- \pi^0$ [7], and $K_S \rightarrow \pi^0 \pi^0 \pi^0$ [8]. The relation in Eq. (6a) is exact in the superweak theory, so this is sometimes called the superweak-phase ϕ_{SW} . An important point for the analysis is that $\cos(\phi_{\epsilon'} - \phi_\epsilon) \simeq 1$. The consequence is that only two real quantities need be measured, the magnitude of ϵ and the value of (ϵ'/ϵ) , including its sign. The measured quantity $|\eta_{00}/\eta_{+-}|^2$ is very close to unity so that we can write

$$|\eta_{00}/\eta_{+-}|^2 \approx 1 - 6\text{Re}(\epsilon'/\epsilon) \approx 1 - 6\epsilon'/\epsilon, \quad (7a)$$

$$\text{Re}(\epsilon'/\epsilon) \approx \frac{1}{3}(1 - |\eta_{00}/\eta_{+-}|). \quad (7b)$$

From the experimental measurements in this edition of the *Review*, and the fits discussed in the next section, one finds

$$|\epsilon| = (2.228 \pm 0.011) \times 10^{-3}, \quad (8a)$$

Meson Particle Listings

 K_L^0

$$\phi_\epsilon = (43.5 \pm 0.7)^\circ, \quad (8b)$$

$$\text{Re}(\epsilon'/\epsilon) \approx \epsilon'/\epsilon = (1.65 \pm 0.26) \times 10^{-3}, \quad (8c)$$

$$\phi_{+-} = (43.4 \pm 0.7)^\circ, \quad (8d)$$

$$\phi_{00} - \phi_{+-} = (0.2 \pm 0.4)^\circ, \quad (8e)$$

$$A_L = (3.32 \pm 0.06) \times 10^{-3}. \quad (8f)$$

Direct CP violation, as indicated by ϵ'/ϵ , is expected in the Standard Model. However, the numerical value cannot be reliably predicted because of theoretical uncertainties [9]. The value of A_L agrees with Eq. (5d). The values of ϕ_{+-} and $\phi_{00} - \phi_{+-}$ are used to set limits on CPT violation [see “Tests of Conservation Laws”].

2. Fits for K_L^0 CP -violation parameters:

In recent years, K_L^0 CP -violation experiments have improved our knowledge of CP -violation parameters, and their consistency with the expectations of CPT invariance and unitarity. To determine the best values of the CP -violation parameters in $K_L^0 \rightarrow \pi^+\pi^-$ and $\pi^0\pi^0$ decay, we make two types of fits, one for the phases ϕ_{+-} and ϕ_{00} jointly with Δm and τ_S , and the other for the amplitudes $|\eta_{+-}|$ and $|\eta_{00}|$ jointly with the $K_L^0 \rightarrow \pi\pi$ branching fractions.

Fits to ϕ_{+-} , ϕ_{00} , $\Delta\phi$, Δm , and τ_S data: These are joint fits to the data on ϕ_{+-} , ϕ_{00} , the phase difference $\Delta\phi = \phi_{00} - \phi_{+-}$, the $K_L^0 - K_S^0$ mass difference Δm , and the K_S^0 mean life τ_S , including the effects of correlations.

Measurements of ϕ_{+-} and ϕ_{00} are highly correlated with Δm and τ_S . Some measurements of τ_S are correlated with Δm . The correlations are given in the footnotes of the ϕ_{+-} and ϕ_{00} sections of the K_L^0 Listings, and the τ_S section of the K_S^0 Listings.

In most cases, the correlations are quoted as 100%, *i.e.*, with the value and error of ϕ_{+-} or ϕ_{00} given at a fixed value of Δm and τ_S , with additional terms specifying the dependence of the value on Δm and τ_S . These cases lead to diagonal bands in Figs. [1] and [2]. The KTeV experiment [10] quotes its results as values of ϕ_{+-} , Δm , and τ_S with correlations, leading to the ellipses labeled “b.”

The data on τ_S , Δm , and ϕ_{+-} shown in Figs. [1] and [2] are combined with data on ϕ_{00} and $\phi_{00} - \phi_{+-}$ in two fits, one without assuming CPT , and the other with this assumption. The results without assuming CPT are shown as ellipses labeled “a.” These ellipses are seen to be in good agreement with the superweak phase

$$\phi_{\text{SW}} = \tan^{-1} \left(\frac{2\Delta m}{\Delta\Gamma} \right) = \tan^{-1} \left(\frac{2\Delta m \tau_S \tau_L}{\hbar(\tau_L - \tau_S)} \right). \quad (9)$$

In Figs. [1] and [2], ϕ_{SW} is shown as narrow bands labeled “j.”

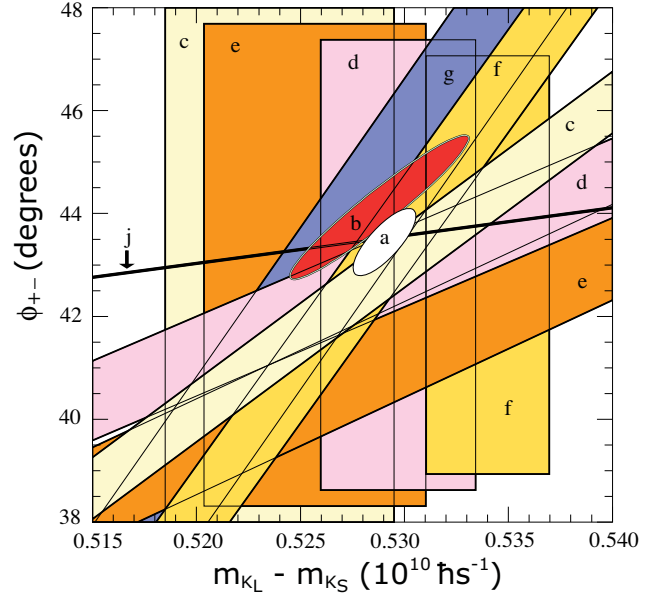


Figure 1: ϕ_{+-} vs Δm for experiments which do not assume CPT invariance. Δm measurements appear as vertical bands spanning $\Delta m \pm 1\sigma$, cut near the top and bottom to aid the eye. Most ϕ_{+-} measurements appear as diagonal bands spanning $\phi_{+-} \pm \sigma_\phi$. Data are labeled by letters: “b”–FNAL KTeV, “c”–CERN CPLEAR, “d”–FNAL E773, “e”–FNAL E731, “f”–CERN, “g”–CERN NA31, and are cited in Table 1. The narrow band “j” shows ϕ_{SW} . The ellipse “a” shows the $\chi^2 = 1$ contour of the fit result. Color version at end of book.

Table 1: References, Document ID’s, and sources corresponding to the letter labels in the figures. The data are given in the ϕ_{+-} and Δm sections of the K_L Listings, and the τ_S section of the K_S Listings.

Label	Source	PDG Document ID	Ref.
a	this Review	OUR FIT	
b	FNAL KTeV	ALAVI-HARATI 03	[10]
c	CERN CPLEAR	APOSTOLAKIS 99C	[11]
d	FNAL E773	SCHWINGENHEUER 95	[12]
e	FNAL E731	GIBBONS 93,93C	[13,14]
f	CERN	GEWENIGER 74B,74C	[15,16]
g	CERN NA31	CAROSI 90	[17]
h	CERN NA48	LAI 02C	[18]
i	CERN NA31	BERTANZA 97	[19]
j	this Review	SUPERWEAK 10	

Table 2 column 2, “Fit w/o CPT ,” gives the resulting fitted parameters, while Table 3 gives the correlation matrix for this fit. The white ellipses labeled “a” in Fig. 1 and Fig. 2 are the $\chi^2 = 1$ contours for this fit.

For experiments which have dependencies on unseen fit parameters, that is, parameters other than those shown on the

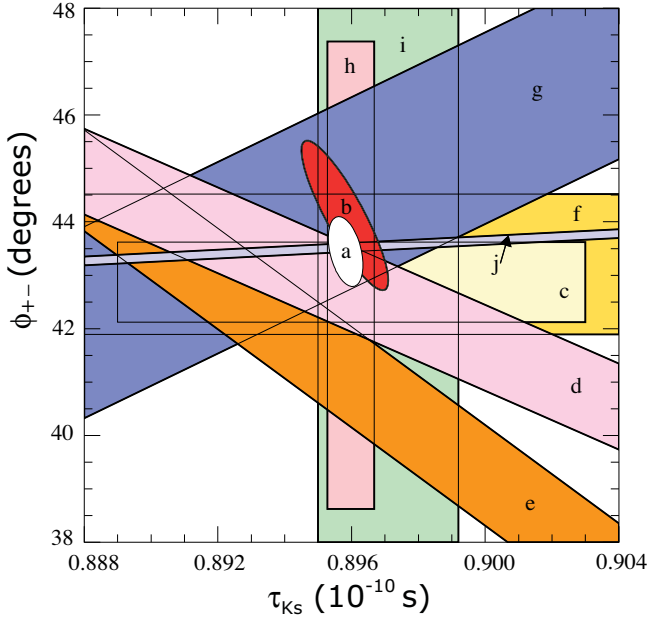


Figure 2: ϕ_{+-} vs τ_S . τ_S measurements appear as vertical bands spanning $\tau_S \pm 1\sigma$, some of which are cut near the top and bottom to aid the eye. Most ϕ_{+-} measurements appear as diagonal or horizontal bands spanning $\phi_{+-} \pm \sigma_\phi$. Data are labeled by letters: “b”–FNAL KTeV, “c”–CERN CPLEAR, “d”–FNAL E773, “e”–FNAL E731, “f”–CERN, “g”–CERN NA31, “h”–CERN NA48, “i”–CERN NA31, and are cited in Table 1. The narrow band “j” shows ϕ_{SW} . The ellipse “a” shows the fit result’s $\chi^2 = 1$ contour. Color version at end of book.

x or y axis of the figure, their band positions are evaluated using the fit results and their band widths include the fitted uncertainty in the unseen parameters. This is also true for the ϕ_{SW} bands.

If CPT invariance and unitarity are assumed, then by Eq. (6a), the phase of ϵ is constrained to be approximately equal to

$$\phi_{\text{SW}} = (43.5165 \pm 0.0002)^\circ + 54.1(\Delta m - 0.5290)^\circ + 32.0(\tau_S - 0.8958)^\circ \quad (10)$$

where we have linearized the Δm and τ_S dependence of Eq. (9). The error ± 0.0002 is due to the uncertainty in τ_L . Here Δm has units $10^{10} \hbar \text{s}^{-1}$ and τ_S has units 10^{-10}s .

If in addition we use the observation that $\text{Re}(\epsilon'/\epsilon) \ll 1$ and $\cos(\phi_{\epsilon'} - \phi_\epsilon) \simeq 1$, as well as the numerical value of $\phi_{\epsilon'}$ given in Eq. (6b), then Eqs. (5a), which are sketched in Fig. 3, lead to the constraint

$$\begin{aligned} \phi_{00} - \phi_{+-} &\approx -3 \text{Im} \left(\frac{\epsilon'}{\epsilon} \right) \\ &\approx -3 \text{Re} \left(\frac{\epsilon'}{\epsilon} \right) \tan(\phi_{\epsilon'} - \phi_\epsilon) \\ &\approx 0.006^\circ \pm 0.008^\circ, \end{aligned} \quad (11)$$

so that $\phi_{+-} \approx \phi_{00} \approx \phi_\epsilon \approx \phi_{\text{SW}}$.

Table 2: Fit results for ϕ_{+-} , Δm , τ_S , ϕ_{00} , $\Delta\phi = \phi_{00} - \phi_{+-}$, and ϕ_ϵ without and with the CPT assumption.

Quantity(units)	Fit w/o CPT	Fit w/ CPT
$\phi_{+-} (^\circ)$	43.4 ± 0.7 (S=1.3)	43.51 ± 0.05 (S=1.1)
$\Delta m (10^{10} \hbar \text{s}^{-1})$	0.5290 ± 0.0015 (S=1.1)	0.5292 ± 0.0009 (S=1.2)
$\tau_S (10^{-10} \text{s})$	0.8958 ± 0.0005	0.8953 ± 0.0005 (S=1.1)
$\phi_{00} (^\circ)$	43.7 ± 0.8 (S=1.2)	43.52 ± 0.05 (S=1.1)
$\Delta\phi (^\circ)$	0.2 ± 0.4	0.006 ± 0.014 (S=1.8)
$\phi_\epsilon (^\circ)$	43.5 ± 0.7 (S=1.3)	43.51 ± 0.05 (S=1.1)
χ^2	17.4	21.9
# Deg. Free.	13	17

In the fit assuming CPT , we constrain $\phi_\epsilon = \phi_{\text{SW}}$ using the linear expression in Eq. (10), and constrain $\phi_{00} - \phi_{+-}$ using Eq. (11). These constraints are inserted into the Listings with the Document ID of SUPERWEAK 10. Some additional data for which the authors assumed CPT are added to this fit or substitute for other less precise data for which the authors did not make this assumption. See the Listings for details.

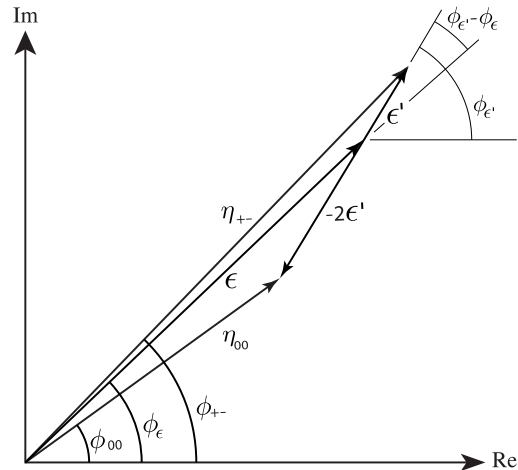


Figure 3: Sketch of Eqs. (5a). Not to scale.

The results of this fit are shown in Table 2, column 3, “Fit w/ CPT ,” and the correlation matrix is shown in Table 4. The Δm precision is improved by the CPT assumption.

Table 3: Correlation matrix for the results of the fit without the CPT assumption

	ϕ_{+-}	Δm	τ_S	ϕ_{00}	$\Delta\phi$	ϕ_ϵ
ϕ_{+-}	1.000	0.778	-0.391	0.837	-0.002	0.977
Δm	0.778	1.000	-0.424	0.665	0.024	0.766
τ_S	-0.391	-0.424	1.000	-0.327	0.001	-0.382
ϕ_{00}	0.837	0.665	-0.327	1.000	0.546	0.934
$\Delta\phi$	-0.002	0.024	0.001	0.546	1.000	0.211
ϕ_ϵ	0.977	0.766	-0.382	0.934	0.211	1.000

Meson Particle Listings

 K_L^0 **Table 4:** Correlation matrix for the results of the fit with the CPT assumption

	ϕ_{+-}	Δm	τ_S	ϕ_{00}	$\Delta\phi$	ϕ_ϵ
ϕ_{+-}	1.000	0.924	0.054	0.711	-0.283	0.964
Δm	0.924	1.000	-0.231	0.834	-0.020	0.958
τ_S	0.054	-0.231	1.000	0.056	0.009	0.059
ϕ_{00}	0.711	0.834	0.056	1.000	0.473	0.873
$\Delta\phi$	-0.283	-0.020	0.009	0.473	1.000	-0.018
ϕ_ϵ	0.964	0.958	0.059	0.873	-0.018	1.000

Fits for ϵ'/ϵ , $|\eta_{+-}|$, $|\eta_{00}|$, and $B(K_L \rightarrow \pi\pi)$

We list measurements of $|\eta_{+-}|$, $|\eta_{00}|$, $|\eta_{00}/\eta_{+-}|$, and ϵ'/ϵ . Independent information on $|\eta_{+-}|$ and $|\eta_{00}|$ can be obtained from measurements of the K_L^0 and K_S^0 lifetimes (τ_L , τ_S), and branching ratios (B) to $\pi\pi$, using the relations

$$|\eta_{+-}| = \left[\frac{B(K_L^0 \rightarrow \pi^+\pi^-)}{\tau_L} \frac{\tau_S}{B(K_S^0 \rightarrow \pi^+\pi^-)} \right]^{1/2}, \quad (12a)$$

$$|\eta_{00}| = \left[\frac{B(K_L^0 \rightarrow \pi^0\pi^0)}{\tau_L} \frac{\tau_S}{B(K_S^0 \rightarrow \pi^0\pi^0)} \right]^{1/2}. \quad (12b)$$

For historical reasons, the branching ratio fits and the CP -violation fits are done separately, but we want to include the influence of $|\eta_{+-}|$, $|\eta_{00}|$, $|\eta_{00}/\eta_{+-}|$, and ϵ'/ϵ measurements on $B(K_L^0 \rightarrow \pi^+\pi^-)$ and $B(K_L^0 \rightarrow \pi^0\pi^0)$ and vice versa. We approximate a global fit to all of these measurements by first performing two independent fits: 1) BRFIT, a fit to the K_L^0 branching ratios, rates, and mean life, and 2) ETAFIT, a fit to the $|\eta_{+-}|$, $|\eta_{00}|$, $|\eta_{+-}/\eta_{00}|$, and ϵ'/ϵ measurements. The results from fit 1, along with the K_S^0 values from this edition, are used to compute values of $|\eta_{+-}|$ and $|\eta_{00}|$, which are included as measurements in the $|\eta_{00}|$ and $|\eta_{+-}|$ sections with a document ID of BRFIT 10. Thus, the fit values of $|\eta_{+-}|$ and $|\eta_{00}|$ given in this edition include both the direct measurements and the results from the branching ratio fit.

The process is reversed in order to include the direct $|\eta|$ measurements in the branching ratio fit. The results from fit 2 above (before including BRFIT 10 values) are used along with the K_L^0 and K_S^0 mean lives and the $K_S^0 \rightarrow \pi\pi$ branching fractions to compute the K_L^0 branching ratio $\Gamma(K_L^0 \rightarrow \pi^0\pi^0)/\Gamma(K_L^0 \rightarrow \pi^+\pi^-)$. This branching ratio value is included as a measurement in the branching ratio section with a document ID of ETAFIT 10. Thus, the K_L^0 branching ratio fit values in this edition include the results of the direct measurement of $|\eta_{00}/\eta_{+-}|$ and ϵ'/ϵ . Most individual measurements of $|\eta_{+-}|$ and $|\eta_{00}|$ enter our fits directly via the corresponding measurements of $\Gamma(K_L^0 \rightarrow \pi^+\pi^-)/\Gamma(\text{total})$ and $\Gamma(K_L^0 \rightarrow \pi^0\pi^0)/\Gamma(\text{total})$, and those that do not have too large errors to have any influence on the fitted values of these branching ratios. A more detailed discussion of these fits is given in the 1990 edition of this *Review* [20].

References

1. K. Kleinknecht, "Uncovering CP violation: experimental clarification in the neutral K meson and B meson systems," *Springer Tracts in Modern Physics*, vol. 195 (Springer Verlag 2003).
2. B. Winstein and L. Wolfenstein, *Rev. Mod. Phys.* **65**, 1113 (1993).
3. M.S. Sozzi, *Eur. Phys. J.* **C36**, 37 (2004).
4. T.T. Wu and C.N. Yang, *Phys. Rev. Lett.* **13**, 380 (1964).
5. L. Wolfenstein, *Phys. Rev. Lett.* **13**, 562 (1964); L. Wolfenstein, *Comm. Nucl. Part. Phys.* **21**, 275 (1994).
6. G. Colangelo, J. Gasser, and H. Leutwyler, *Nucl. Phys.* **B603**, 125 (2001).
7. R. Adler *et al.*, (CPLEAR Collaboration), *Phys. Lett.* **B407**, 193 (1997); P. Bloch, *Proceedings of Workshop on K Physics* (Orsay 1996), ed. L. Iconomidou-Fayard, Edition Frontieres, Gif-sur-Yvette, France (1997) p. 307.
8. A. Lai *et al.*, *Phys. Lett.* **B610**, 165 (2005).
9. G. Buchalla, A.J. Buras, and M.E. Lautenbacher, *Rev. Mod. Phys.* **68**, 1125 (1996); S. Bosch *et al.*, *Nucl. Phys.* **B565**, 3 (2000); S. Bertolini, M. Fabrichesi, and J.O. Egg, *Rev. Mod. Phys.* **72**, 65 (2000).
10. A. Alavi-Harati *et al.*, *Phys. Rev.* **D67**, 012005 (2003); See also *erratum*, Alavi-Harati *et al.*, *Phys. Rev. D*, to be published, for corrections to correlation coefficients.
11. A. Apostolakis *et al.*, *Phys. Lett.* **B458**, 545 (1999).
12. B. Schwingerheuer *et al.*, *Phys. Rev. Lett.* **74**, 4376 (1995).
13. L.K. Gibbons *et al.*, *Phys. Rev. Lett.* **70**, 1199 (1993) and footnote in Ref. 12.
14. L.K. Gibbons, Thesis, RX-1487, Univ. of Chicago, 1993.
15. C. Geweniger *et al.*, *Phys. Lett.* **48B**, 487 (1974).
16. C. Geweniger *et al.*, *Phys. Lett.* **52B**, 108 (1974).
17. R. Carosi *et al.*, *Phys. Lett.* **B237**, 303 (1990).
18. A. Lai *et al.*, *Phys. Lett.* **B537**, 28 (2002).
19. L. Bertanza *et al.*, *Z. Phys.* **C73**, 629 (1997).
20. J.J. Hernandez *et al.*, Particle Data Group, *Phys. Lett.* **B239**, 1 (1990).

 CP -VIOLATION PARAMETERS IN K_L^0 DECAYS**CHARGE ASYMMETRY IN $K_{\mu 3}^0$ DECAYS**

Such asymmetry violates CP . It is related to $\text{Re}(\epsilon)$.

 $A_L =$ weighted average of $A_L(\mu)$ and $A_L(e)$

In previous editions and in the literature the symbol used for this asymmetry was δ_L or δ . We use A_L for consistency with B^0 asymmetry notation and with recent K_S^0 notation.

VALUE (%)	EVTS	DOCUMENT ID	TECN	COMMENT
0.332±0.006 OUR AVERAGE		Includes data from the 2 datablocks that follow this one.		
0.333±0.050	33M	WILLIAMS	73	ASPK $K_{\mu 3} + K_{e 3}$

 $A_L(\mu) = [\Gamma(\pi^- \mu^+ \nu_\mu) - \Gamma(\pi^+ \mu^- \bar{\nu}_\mu)]/\text{SUM}$

Only the combined value below is put into the Meson Summary Table.

VALUE (%)	EVTS	DOCUMENT ID	TECN
The data in this block is included in the average printed for a previous datablock.			

0.304±0.025 OUR AVERAGE

0.313±0.029	15M	GEWENIGER	74	ASPK
0.278±0.051	7.7M	PICCIONI	72	ASPK
••• We do not use the following data for averages, fits, limits, etc. •••				
0.60 ±0.14	4.1M	MCCARTHY	73	CNTR
0.57 ±0.17	1M	125 PACIOTTI	69	OSPK
0.403±0.134	1M	125 DORFAN	67	OSPK

¹²⁵ PACIOTTI 69 is a reanalysis of DORFAN 67 and is corrected for $\mu^+ \mu^-$ range difference in MCCARTHY 72.

$$A_L(\epsilon) = [\Gamma(\pi^- e^+ \nu_e) - \Gamma(\pi^+ e^- \bar{\nu}_e)] / \text{SUM}$$

Only the combined value below is put into the Meson Summary Table.

VALUE (%)	EVTS	DOCUMENT ID	TECN
The data in this block is included in the average printed for a previous datablock.			

0.334 ± 0.007 OUR AVERAGE

0.3322 ± 0.0058 ± 0.0047	298M	ALAVI-HARATI 02	
0.341 ± 0.018	34M	GEWENIGER 74	ASPK
0.318 ± 0.038	40M	FITCH 73	ASPK
0.346 ± 0.033	10M	MARX 70	CNTR
• • • We do not use the following data for averages, fits, limits, etc. • • •			
0.36 ± 0.18	600k	ASHFORD 72	ASPK
0.246 ± 0.059	10M	126 SAAL 69	CNTR
0.224 ± 0.036	10M	126 BENNETT 67	CNTR

126 SAAL 69 is a reanalysis of BENNETT 67.

PARAMETERS FOR $K_L^0 \rightarrow 2\pi$ DECAY

$$\eta_{+-} = A(K_L^0 \rightarrow \pi^+ \pi^-) / A(K_S^0 \rightarrow \pi^+ \pi^-)$$

$$\eta_{00} = A(K_L^0 \rightarrow \pi^0 \pi^0) / A(K_S^0 \rightarrow \pi^0 \pi^0)$$

The fitted values of $|\eta_{+-}|$ and $|\eta_{00}|$ given below are the results of a fit to $|\eta_{+-}|$, $|\eta_{00}|$, $|\eta_{00}/\eta_{+-}|$, and $\text{Re}(\epsilon'/\epsilon)$. Independent information on $|\eta_{+-}|$ and $|\eta_{00}|$ can be obtained from the fitted values of the $K_L^0 \rightarrow \pi\pi$ and $K_S^0 \rightarrow \pi\pi$ branching ratios and the K_L^0 and K_S^0 lifetimes. This information is included as data in the $|\eta_{+-}|$ and $|\eta_{00}|$ sections with a Document ID "BRFIT." See the note "CP violation in K_L decays" above for details.

$$|\eta_{00}| = |A(K_L^0 \rightarrow 2\pi^0) / A(K_S^0 \rightarrow 2\pi^0)|$$

VALUE (units 10^{-3})	DOCUMENT ID	TECN	COMMENT
2.221 ± 0.011 OUR FIT	Error includes scale factor of 1.8.		
2.243 ± 0.014	BRFIT	10	
• • • We do not use the following data for averages, fits, limits, etc. • • •			
2.47 ± 0.31 ± 0.24	ANGELOPO... 98	CPLR	
2.49 ± 0.40	127 ADLER 96B	CPLR	Sup. by ANGELOPOULOS 98
2.33 ± 0.18	CHRISTENS... 79	ASPK	
2.71 ± 0.37	128 WOLFF 71	OSPK	Cu reg., 4γ 's
2.95 ± 0.63	128 CHOLLET 70	OSPK	Cu reg., 4γ 's

127 Error is statistical only.

128 CHOLLET 70 gives $|\eta_{00}| = (1.23 \pm 0.24) \times (\text{regeneration amplitude, 2 GeV/c Cu})/10000\text{mb}$. WOLFF 71 gives $|\eta_{00}| = (1.13 \pm 0.12) \times (\text{regeneration amplitude, 2 GeV/c Cu})/10000\text{mb}$. We compute both $|\eta_{00}|$ values for (regeneration amplitude, 2 GeV/c Cu) = 24 ± 2mb. This regeneration amplitude results from averaging over FAISSNER 69, extrapolated using optical-model calculations of Bohm et al., Physics Letters **27B** 594 (1968) and the data of BALATS 71. (From H. Faissner, private communication).

$$|\eta_{+-}| = |A(K_L^0 \rightarrow \pi^+ \pi^-) / A(K_S^0 \rightarrow \pi^+ \pi^-)|$$

VALUE (units 10^{-3})	EVTS	DOCUMENT ID	TECN	COMMENT
2.232 ± 0.011 OUR FIT	Error includes scale factor of 1.8.			
2.226 ± 0.007	BRFIT	10		
• • • We do not use the following data for averages, fits, limits, etc. • • •				
2.223 ± 0.012	129 LAI	07	NA48	
2.219 ± 0.013	130 AMBROSINO 06F	KLOE		
2.228 ± 0.010	131 ALEXOPOU... 04	KTEV		
2.286 ± 0.023 ± 0.026	70M	132 APOSTOLA... 99c	CPLR	K^0 - \bar{K}^0 asymmetry
2.310 ± 0.043 ± 0.031		133 ADLER 95B	CPLR	K^0 - \bar{K}^0 asymmetry
2.32 ± 0.14 ± 0.03	10 ⁵	ADLER 92B	CPLR	K^0 - \bar{K}^0 asymmetry
2.30 ± 0.035		GEWENIGER 74B	ASPK	

129 Value obtained from the NA48 measurements of $\Gamma(K_L^0 \rightarrow \pi^+ \pi^-) / \Gamma(K_L^0 \rightarrow \pi e \nu_e)$ and $\tau_{K_S^0}$ and KLOE measurements of $B(K_S^0 \rightarrow \pi^+ \pi^-)$ and $\tau_{K_L^0}$. $\Gamma(K_L^0 \rightarrow \pi^+ \pi^-)$ is defined to include the inner bremsstrahlung component $\Gamma(K_L^0 \rightarrow \pi^+ \pi^- \gamma(\text{IB}))$ but exclude the direct emission component $B(K_S^0 \rightarrow \pi^+ \pi^- (\text{DE}))$. Their $|\eta_{+-}|$ value is not directly used in our fit, but enters the fit via their branching ratio and lifetime measurements.

130 AMBROSINO 06F uses KLOE branching ratios and τ_L together with τ_S from PDG 04. Their $|\eta_{+-}|$ value is not directly used in our fit, but enters the fit via their branching ratio and lifetime measurements.

131 ALEXOPOULOS 04 $|\eta_{+-}|$ uses their $K_L^0 \rightarrow \pi\pi$ branching fractions, $\tau_S = (0.8963 \pm 0.0005) \times 10^{-10}$ s from the average of KTeV and NA48 τ_S measurements, and assumes that $\Gamma(K_S^0 \rightarrow \pi e \nu_e) = \Gamma(K_L^0 \rightarrow \pi e \nu_e)$ giving $B(K_S^0 \rightarrow \pi e \nu_e) = 0.118\%$. Their $|\eta_{+-}|$ is not directly used in our fit, but enters our fit via their branching ratio measurements.

132 APOSTOLAKIS 99c report $(2.264 \pm 0.023 \pm 0.026 + 9.1[\tau_S - 0.8934]) \times 10^{-3}$. We evaluate for our 2006 best value $\tau_S = (0.8958 \pm 0.0005) \times 10^{-10}$ s.

133 ADLER 95B report $(2.312 \pm 0.043 \pm 0.030 - 1[\Delta m - 0.5274] + 9.1[\tau_S - 0.8926]) \times 10^{-3}$. We evaluate for our 1996 best values $\Delta m = (0.5304 \pm 0.0014) \times 10^{-10} \text{ ns}^{-1}$ and $\tau_S = (0.8927 \pm 0.0009) \times 10^{-10}$ s. Superseded by APOSTOLAKIS 99c.

$$|\epsilon| = (2|\eta_{+-}| + |\eta_{00}|) / 3$$

This expression is a very good approximation, good to about one part in 10^{-4} because of the small measured value of $\phi_{00} - \phi_{+-}$ and small theoretical ambiguities.

VALUE (units 10^{-3})	DOCUMENT ID	TECN	COMMENT
2.228 ± 0.011 OUR FIT	Error includes scale factor of 1.8.		

$$|\eta_{00}/\eta_{+-}|$$

VALUE	EVTS	DOCUMENT ID	TECN
0.9951 ± 0.0008 OUR FIT	Error includes scale factor of 1.6.		
0.9930 ± 0.0020 OUR AVERAGE			
0.9931 ± 0.0020	134,135	BARR 93D	NA31
0.9904 ± 0.0084 ± 0.0036	136	WOODS 88	E731
• • • We do not use the following data for averages, fits, limits, etc. • • •			
0.9939 ± 0.0013 ± 0.0015	1M	134 BARR 93D	NA31
0.9899 ± 0.0020 ± 0.0025	134	BURKHARDT 88	NA31

134 This is the square root of the ratio R given by BURKHARDT 88 and BARR 93D.

135 This is the combined results from BARR 93D and BURKHARDT 88, taking into account a common systematic uncertainty of 0.0014.

136 We calculate $|\eta_{00}/\eta_{+-}| = 1 - 3(\epsilon'/\epsilon)$ from WOODS 88 (ϵ'/ϵ) value.

$$\text{Re}(\epsilon'/\epsilon) = (1 - |\eta_{00}/\eta_{+-}|) / 3$$

We have neglected terms of order $\omega \cdot \text{Re}(\epsilon'/\epsilon)$, where $\omega = \text{Re}(A_2)/\text{Re}(A_0) \approx 1/22$. If included, this correction would lower $\text{Re}(\epsilon'/\epsilon)$ by about 0.04×10^{-3} . See SOZZI 04.

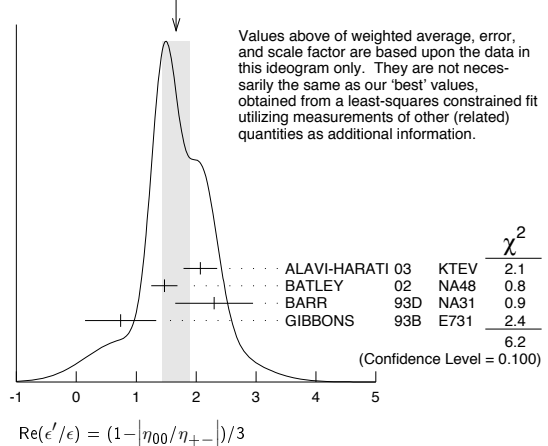
VALUE (units 10^{-3})	DOCUMENT ID	TECN	COMMENT
1.65 ± 0.26 OUR FIT	Error includes scale factor of 1.6.		
1.67 ± 0.23 OUR AVERAGE	Error includes scale factor of 1.4. See the ideogram below.		
2.07 ± 0.28	ALAVI-HARATI 03	KTEV	
1.47 ± 0.22	BATLEY 02	NA48	
2.3 ± 0.65	137,138	BARR 93D	NA31
0.74 ± 0.52 ± 0.29	GIBBONS 93B	E731	
• • • We do not use the following data for averages, fits, limits, etc. • • •			
1.53 ± 0.26	LAI	01c	NA48 Incl. in BATLEY 02
2.80 ± 0.30 ± 0.28	ALAVI-HARATI 99D	KTEV	In ALAVI-HARATI 03
1.85 ± 0.45 ± 0.58	FANTI 99c	NA48	In LAI 01c
2.0 ± 0.7	139	BARR 93D	NA31
-0.4 ± 1.4 ± 0.6	PATTERSON 90	E731	in GIBBONS 93B
3.3 ± 1.1	139	BURKHARDT 88	NA31
3.2 ± 2.8 ± 1.2	137	WOODS 88	E731

137 These values are derived from $|\eta_{00}/\eta_{+-}|$ measurements. They enter the average in this section but enter the fit via the $|\eta_{00}/\eta_{+-}|$ only.

138 This is the combined results from BARR 93D and BURKHARDT 88, taking into account their common systematic uncertainty.

139 These values are derived from $|\eta_{00}/\eta_{+-}|$ measurements.

WEIGHTED AVERAGE
1.67 ± 0.23 (Error scaled by 1.4)



ϕ_{+-} , PHASE OF η_{+-}

The dependence of the phase on Δm and τ_S is given for each experiment in the comments below, where Δm is the $K_L^0 - K_S^0$ mass difference in units 10^{10} ns^{-1} and τ_S is the K_S mean life in units 10^{-10} s. We also give the regeneration phase ϕ_r in the comments below.

OUR FIT is described in the note on "CP violation in K_L decays" in the K_L^0 Particle Listings. Most experiments in this section are included in both the "Not Assuming CPT" and "Assuming CPT" fits. In the latter fit, they have little direct influence on ϕ_{+-} because their errors are large compared to that assuming CPT, but they influence Δm and τ_S through their dependencies on these parameters, which are given in the footnotes. Only ALAVI-HARATI 03 is excluded from the "Assuming CPT" fit because we explicitly include their Δm and τ_S measurements which assume CPT.

VALUE (%)	EVTS	DOCUMENT ID	TECN	COMMENT
43.51 ± 0.05 OUR FIT	Error includes scale factor of 1.1. Assuming CPT			
43.4 ± 0.7 OUR FIT	Error includes scale factor of 1.3. Not assuming CPT			
44.12 ± 0.72 ± 1.20	140	ALAVI-HARATI 03	KTEV	Not assuming CPT
42.9 ± 0.6 ± 0.3	70M	141 APOSTOLA... 99c	CPLR	K^0 - \bar{K}^0 asymmetry
43.0 ± 0.8 ± 0.2	142,143	SCHWINGEN... 95	E773	CH_2 regenerator
41.4 ± 0.9 ± 0.3	143,144	GIBBONS 93	E731	B_4C regenerator
44.4 ± 1.6 ± 0.6	145	CAROSI 90	NA31	Vacuum regen.
43.3 ± 1.0 ± 0.5	146	GEWENIGER 74B	ASPK	Vacuum regen.

Meson Particle Listings

 K_L^0

• • • We do not use the following data for averages, fits, limits, etc. • • •

42.5 ± 0.4 ± 0.3	147,148	ADLER	96c	RVUE
43.4 ± 1.1 ± 0.3	149	ADLER	95B	CPLR $K^0\text{-}\bar{K}^0$ asymmetry
42.3 ± 4.4 ± 1.4	10 ⁵	ADLER	92B	CPLR $K^0\text{-}\bar{K}^0$ asymmetry
47.7 ± 2.0 ± 0.9	143,151	KARLSSON	90	E731
44.2 ± 2.8 ± 0.2	152	CARTHERS	75	SPEC C regenerator

140 ALAVI-HARATI 03 ϕ_{+-} is correlated with their $\Delta m = m_{K_L^0} - m_{K_S^0}$ and τ_{K_S} measurements in the K_L^0 and K_S^0 sections respectively. The correlation coefficients are

$\rho(\phi_{+-}, \Delta m) = +0.955$, $\rho(\phi_{+-}, \tau_{K_S}) = -0.871$, and $\rho(\tau_{K_S}, \Delta m) = -0.840$. *CPT* is not assumed. Uses scintillator Pb regenerator.

141 APOSTOLAKIS 99c measures $\phi_{+-} = (43.19 \pm 0.53 \pm 0.28) + 300 [\Delta m - 0.5301]$ (°). We have adjusted the measurement to use our best values of ($\Delta m = 0.5292 \pm 0.0009$) (10^{10} h s^{-1}). Our first error is their experiment's error and our second error is the systematic error from using our best values.

142 SCHWINGENHEUER 95 measures $\phi_{+-} = (43.53 \pm 0.76) + 173 [\Delta m - 0.5282] - 275 [\tau_S - 0.8926]$ (°). We have adjusted the measurement to use our best values of ($\Delta m = 0.5292 \pm 0.0009$) (10^{10} h s^{-1}), ($\tau_S = 0.8953 \pm 0.0005$) (10^{-10} s). Our first error is their experiment's error and our second error is the systematic error from using our best values.

143 These experiments measure $\phi_{+-} - \phi_f$ and calculate the regeneration phase from the power law momentum dependence of the regeneration amplitude using analyticity and dispersion relations. SCHWINGENHEUER 95 [GIBBONS 93] includes a systematic error of 0.35° [0.5°] for uncertainties in their modeling of the regeneration amplitude.

144 GIBBONS 93 measures $\phi_{+-} = (42.21 \pm 0.9) + 189 [\Delta m - 0.5257] - 460 [\tau_S - 0.8922]$ (°). We have adjusted the measurement to use our best values of ($\Delta m = 0.5292 \pm 0.0009$) (10^{10} h s^{-1}), ($\tau_S = 0.8953 \pm 0.0005$) (10^{-10} s). Our first error is their experiment's error and our second error is the systematic error from using our best values. This is actually reported in SCHWINGENHEUER 95, footnote 8. GIBBONS 93 reports ϕ_{+-} (42.2 ± 1.4)°. They measure $\phi_{+-} - \phi_f$ and calculate the regeneration phase ϕ_f from the power law momentum dependence of the regeneration amplitude using analyticity. An error of 0.6° is included for possible uncertainties in the regeneration phase.

145 CAROSI 90 measures $\phi_{+-} = (46.9 \pm 1.4 \pm 0.7) + 579 [\Delta m - 0.5351] + 303 [\tau_S - 0.8922]$ (°). We have adjusted the measurement to use our best values of ($\Delta m = 0.5292 \pm 0.0009$) (10^{10} h s^{-1}), ($\tau_S = 0.8953 \pm 0.0005$) (10^{-10} s). Our first error is their experiment's error and our second error is the systematic error from using our best values.

146 GEWENIGER 74B measures $\phi_{+-} = (49.4 \pm 1.0) + 565 [\Delta m - 0.540]$ (°). We have adjusted the measurement to use our best values of ($\Delta m = 0.5292 \pm 0.0009$) (10^{10} h s^{-1}). Our first error is their experiment's error and our second error is the systematic error from using our best values.

147 ADLER 96c measures $\phi_{+-} = (43.82 \pm 0.41) + 339 [\Delta m - 0.5307] - 252 [\tau_S - 0.8922]$ (°). We have adjusted the measurement to use our best values of ($\Delta m = 0.5292 \pm 0.0009$) (10^{10} h s^{-1}), ($\tau_S = 0.8953 \pm 0.0005$) (10^{-10} s). Our first error is their experiment's error and our second error is the systematic error from using our best values.

148 ADLER 96c is the result of a fit which includes nearly the same data as entered into the "OUR FIT" value in the 1996 edition of this Review (Physical Review D54 1 (1996)).

149 ADLER 95B measures $\phi_{+-} = (42.7 \pm 0.9 \pm 0.6) + 316 [\Delta m - 0.5274] + 30 [\tau_S - 0.8926]$ (°). We have adjusted the measurement to use our best values of ($\Delta m = 0.5292 \pm 0.0009$) (10^{10} h s^{-1}), ($\tau_S = 0.8953 \pm 0.0005$) (10^{-10} s). Our first error is their experiment's error and our second error is the systematic error from using our best values.

150 ADLER 92B quote separately two systematic errors: ± 0.4 from their experiment and ± 1.0 degrees due to the uncertainty in the value of Δm .

151 KARLSSON 90 systematic error does not include regeneration phase uncertainty.

152 CARTHERS 75 measures $\phi_{+-} = (45.5 \pm 2.8) + 224 [\Delta m - 0.5348]$ (°). We have adjusted the measurement to use our best values of ($\Delta m = 0.5292 \pm 0.0009$) (10^{10} h s^{-1}). Our first error is their experiment's error and our second error is the systematic error from using our best values. $\phi_f = -40.9 \pm 2.6^\circ$.

 ϕ_{00} , PHASE OF η_{00}

See comment in ϕ_{+-} header above for treatment of Δm and τ_S dependence, as well as for the inclusion of data in both the "Assuming *CPT*" and "Not Assuming *CPT*" fits.

OUR FIT is described in the note on "CP violation in K_L decays" in the K_L^0 Particle Listings.

VALUE (°)	DOCUMENT ID	TECN	COMMENT
43.52 ± 0.05 OUR FIT	Error includes scale factor of 1.1. Assuming <i>CPT</i>		
43.7 ± 0.8 OUR FIT	Error includes scale factor of 1.2. Not assuming <i>CPT</i>		
44.5 ± 2.3 ± 0.6	153	CAROSI	90 NA31

• • • We do not use the following data for averages, fits, limits, etc. • • •

41.6 ± 5.9 ± 0.2	154	ANGELOPOU...	98 CPLR
50.8 ± 7.1 ± 1.7	155	ADLER	96B CPLR Sup. by ANGELOPOULOS 98
47.4 ± 1.4 ± 0.9	156	KARLSSON	90 E731

153 CAROSI 90 measures $\phi_{00} = (47.1 \pm 2.1 \pm 1.0) + 579 [\Delta m - 0.5351] + 252 [\tau_S - 0.8922]$ (°). We have adjusted the measurement to use our best values of ($\Delta m = 0.5292 \pm 0.0009$) (10^{10} h s^{-1}), ($\tau_S = 0.8953 \pm 0.0005$) (10^{-10} s). Our first error is their experiment's error and our second error is the systematic error from using our best values.

154 ANGELOPOULOS 98 measures $\phi_{00} = (42.0 \pm 5.6 \pm 1.9) + 240 [\Delta m - 0.5307]$ (°). We have adjusted the measurement to use our best values of ($\Delta m = 0.5292 \pm 0.0009$) (10^{10} h s^{-1}). Our first error is their experiment's error and our second error is the systematic error from using our best values. The τ_S dependence is negligible.

155 ADLER 96B identified initial neutral kaon individually as being a K^0 or a \bar{K}^0 . The systematic uncertainty is $\pm 1.5^\circ$ combined in quadrature with $\pm 0.8^\circ$ due to Δm .

156 KARLSSON 90 systematic error does not include regeneration phase uncertainty.

$$\phi_\epsilon = (2\phi_{+-} + \phi_{00})/3$$

This expression is a very good approximation, good to about 10^{-3} degrees because of the small measured values of $\phi_{00} - \phi_{+-}$ and $\text{Re } \epsilon'/\epsilon$, and small theoretical ambiguities.

VALUE (°)	DOCUMENT ID	COMMENT
43.51 ± 0.05 OUR FIT	Error includes scale factor of 1.1. Assuming <i>CPT</i>	
43.5 ± 0.7 OUR FIT	Error includes scale factor of 1.3. Not assuming <i>CPT</i>	
43.5136 ± 0.0002 ± 0.0533	157	SUPERWEAK 10 Assuming <i>CPT</i>

157 SUPERWEAK 10 is a fake measurement used to impose the *CPT* or Superweak constraint $\phi_{+-} = \phi_{\text{SW}} = \tan^{-1}[2 \frac{\Delta m}{\hbar} (\frac{\tau_S \tau_L}{\tau_L - \tau_S})]$. This "measurement" is linearized using values near the RPP 2004 edition values of Δm , τ_S and τ_L , and then adjusted to our current values as described in the following "measurement". SUPERWEAK 10 measures $\phi_\epsilon = (43.51647 \pm 0.00020) + 54.1 [\Delta m - 0.5290] + 32.0 [\tau_S - 0.8958]$ (°). We have adjusted the measurement to use our best values of ($\Delta m = 0.5292 \pm 0.0009$) (10^{10} h s^{-1}), ($\tau_S = 0.8953 \pm 0.0005$) (10^{-10} s). Our first error is their experiment's error and our second error is the systematic error from using our best values.

DECAY-PLANE ASYMMETRY IN $\pi^+\pi^-e^+e^-$ DECAYS

This is the *CP*-violating asymmetry

$$A = \frac{N_{\sin\phi\cos\phi>0.0} - N_{\sin\phi\cos\phi<0.0}}{N_{\sin\phi\cos\phi>0.0} + N_{\sin\phi\cos\phi<0.0}}$$

where ϕ is the angle between the e^+e^- and $\pi^+\pi^-$ planes in the K_L^0 rest frame.

CP ASYMMETRY A IN $K_L^0 \rightarrow \pi^+\pi^-e^+e^-$

VALUE (%)	DOCUMENT ID	TECN
13.7 ± 1.5 OUR AVERAGE		
13.6 ± 1.4 ± 1.5	ABOUZAID 06	KTEV
14.2 ± 3.0 ± 1.9	LAI	03c NA48
13.6 ± 2.5 ± 1.2	ALAVI-HARATI00B	KTEV

PARAMETERS FOR $e^+e^-e^+e^-$ DECAYS

These are the *CP*-violating parameters in the ϕ distribution, where ϕ is the angle between the planes of the two e^+e^- pairs in the kaon rest frame:

$$d\Gamma/d\phi \propto 1 + \beta_{CP} \cos(2\phi) + \gamma_{CP} \sin(2\phi)$$

 β_{CP} from $K_L^0 \rightarrow e^+e^-e^+e^-$

VALUE	EVTS	DOCUMENT ID	TECN	COMMENT
-0.19 ± 0.07 OUR AVERAGE				
-0.13 ± 0.10 ± 0.03	200	158 LAI	05B	NA48
-0.23 ± 0.09 ± 0.02	441	ALAVI-HARATI01D	KTEV	$M_{e^+e^-} > 8 \text{ MeV}/c^2$
158 LAI 05B obtains $\beta_{CP} = -0.13 \pm 0.10$ (stat) if $\gamma_{CP} = 0$ is assumed.				

 γ_{CP} from $K_L^0 \rightarrow e^+e^-e^+e^-$

VALUE	EVTS	DOCUMENT ID	TECN	COMMENT
0.01 ± 0.11 OUR AVERAGE	Error includes scale factor of 1.6.			
+0.13 ± 0.10 ± 0.03	200	LAI	05B	NA48
-0.09 ± 0.09 ± 0.02	441	ALAVI-HARATI01D	KTEV	$M_{e^+e^-} > 8 \text{ MeV}/c^2$

CHARGE ASYMMETRY IN $\pi^+\pi^-\pi^0$ DECAYS

These are *CP*-violating charge-asymmetry parameters, defined at beginning of section "LINEAR COEFFICIENT g FOR $K_L^0 \rightarrow \pi^+\pi^-\pi^0$ above.

See also note on Dalitz plot parameters in K^\pm section and note on "CP violation in K_L decays" above.

LINEAR COEFFICIENT j FOR $K_L^0 \rightarrow \pi^+\pi^-\pi^0$

VALUE	EVTS	DOCUMENT ID	TECN
0.0012 ± 0.0008 OUR AVERAGE			
0.0010 ± 0.0024 ± 0.0030	500k	ANGELOPOU...	98c CPLR
-0.001 ± 0.011	6499	CHO	77
0.001 ± 0.003	4709	PEACH	77
0.0013 ± 0.0009	3M	SCRIBANO	70
0.0 ± 0.017	4400	SMITH	70 OSPK
0.001 ± 0.004	238k	BLANPIED	68

QUADRATIC COEFFICIENT f FOR $K_L^0 \rightarrow \pi^+\pi^-\pi^0$

VALUE	EVTS	DOCUMENT ID	TECN
0.0045 ± 0.0024 ± 0.0059	500k	ANGELOPOU...	98c CPLR

PARAMETERS for $K_L^0 \rightarrow \pi^+\pi^-\gamma$ DECAY

$$|\eta_{+-\gamma}| = |A(K_L^0 \rightarrow \pi^+\pi^-\gamma, \text{CP violating})/A(K_S^0 \rightarrow \pi^+\pi^-\gamma)|$$

VALUE (units 10^{-3})	EVTS	DOCUMENT ID	TECN
2.35 ± 0.07 OUR AVERAGE			
2.359 ± 0.062 ± 0.040	9045	MATTHEWS	95 E773
2.15 ± 0.26 ± 0.20	3671	RAMBERG	93B E731

 $\phi_{+-\gamma}$ = phase of $\eta_{+-\gamma}$

VALUE (°)	EVTS	DOCUMENT ID	TECN
44 ± 4 OUR AVERAGE			
43.8 ± 3.5 ± 1.9	9045	MATTHEWS	95 E773
72 ± 23 ± 17	3671	RAMBERG	93B E731

$|\epsilon'_{+-\gamma}|/\epsilon$ for $K_L^0 \rightarrow \pi^+\pi^-\gamma$

VALUE	CL%	EVTS	DOCUMENT ID	TECN
<0.3	90	3671	159 RAMBERG	93B E731

¹⁵⁹RAMBERG 93B limit on $|\epsilon'_{+-\gamma}|/\epsilon$ assumes that any difference between η_{+-} and $\eta_{+-\gamma}$ is due to direct CP violation.

 $|\mathcal{E}|$ for $K_L^0 \rightarrow \pi^+\pi^-\gamma$

This parameter is the amplitude of the direct emission of a CP violating E1 electric dipole photon.

VALUE	CL%	EVTS	DOCUMENT ID	TECN	COMMENT
<0.21	90	111k	ABOUZAID	06A KTEV	$E_\gamma^* > 20$ MeV

T VIOLATION TESTS IN K_L^0 DECAYS $\text{Im}(\xi)$ in $K_{\mu 3}^0$ DECAY (from transverse μ pol.)

Test of T reversal invariance.

VALUE	CL%	EVTS	DOCUMENT ID	TECN	COMMENT
-0.007 ± 0.026 OUR AVERAGE					

0.009 ± 0.030	12M	MORSE	80	CNTR	Polarization
0.35 ± 0.30	207k	160 CLARK	77	SPEC	POL, t=0
-0.085 ± 0.064	2.2M	161 SANDWEISS	73	CNTR	POL, t=0
-0.02 ± 0.08		LONGO	69	CNTR	POL, t=3.3
-0.2 ± 0.6		ABRAMS	68B	OSPK	Polarization

• • • We do not use the following data for averages, fits, limits, etc. • • •

0.012 ± 0.026 SCHMIDT 79 CNTR Repl. by MORSE 80

¹⁶⁰CLARK 77 value has additional $\xi(0)$ dependence +0.21Re $[\xi(0)]$.

¹⁶¹SANDWEISS 73 value corrected from value quoted in their paper due to new value of Re(ξ). See footnote 4 of SCHMIDT 79.

CPT-INVARIANCE TESTS IN K_L^0 DECAYSPHASE DIFFERENCE $\phi_{00} - \phi_{+-}$

Test of CPT.

OUR FIT is described in the note on "CP violation in K_L decays" in the K_L^0 Particle Listings.

VALUE (°)	DOCUMENT ID	TECN	COMMENT
-----------	-------------	------	---------

0.006 ± 0.014 OUR FIT			Error includes scale factor of 1.8. Assuming CPT
0.2 ± 0.4 OUR FIT			Not assuming CPT
0.006 ± 0.008	162 SUPERWEAK 10		Assuming CPT
0.39 ± 0.22 ± 0.45	163 ALAVI-HARATI03	KTEV	
-0.30 ± 0.88	164 SCHWINGEN...95		Combined E731, E773
• • • We do not use the following data for averages, fits, limits, etc. • • •			
0.62 ± 0.71 ± 0.75	SCHWINGEN...95	E773	
-1.6 ± 1.2	165 GIBBONS 93	E731	
0.2 ± 2.6 ± 1.2	166 CAROSI 90	NA31	
-0.3 ± 2.4 ± 1.2	KARLSSON 90	E731	

¹⁶²SUPERWEAK 10 is a fake experiment to constrain $\phi_{00} - \phi_{+-}$ to a small value as described in the note "CP violation in K_L decays."

¹⁶³ALAVI-HARATI 03 fit Re(ϵ'/ϵ), Im(ϵ'/ϵ), Δm , τ_{K_S} , and ϕ_{+-} simultaneously, not assuming CPT. Phase difference is obtained from $\phi_{00} - \phi_{+-} \approx -3\text{Im}(\epsilon'/\epsilon)$ for small $|\epsilon'/\epsilon|$.

¹⁶⁴This SCHWINGENHEUER 95 values is the combined result of SCHWINGENHEUER 95 and GIBBONS 93, accounting for correlated systematic errors.

¹⁶⁵GIBBONS 93 give detailed dependence of systematic error on lifetime (see the section on the K_S^0 mean life) and mass difference (see the section on $m_{K_L^0} - m_{K_S^0}$).

¹⁶⁶CAROSI 90 is excluded from the fit because it is not independent of ϕ_{+-} and ϕ_{00} values.

PHASE DIFFERENCE $\phi_{+-} - \phi_{SW}$

Test of CPT. The Superweak phase $\phi_{SW} \equiv \tan^{-1}(2\Delta m/\Delta\Gamma)$ where $\Delta m = m_{K_L^0} - m_{K_S^0}$ and $\Delta\Gamma = \hbar(\tau_L - \tau_S)/(\tau_L\tau_S)$.

VALUE (°)	DOCUMENT ID	TECN	COMMENT
-----------	-------------	------	---------

0.61 ± 0.62 ± 1.01	167 ALAVI-HARATI03	KTEV	
---------------------------	--------------------	------	--

¹⁶⁷ALAVI-HARATI 03 fit is the same as their ϕ_{+-} , τ_{K_S} , Δm fit, except that the parameter $\phi_{+-} - \phi_{SW}$ is used in place of ϕ .

 $\text{Re}(\frac{2}{3}\eta_{+-} + \frac{1}{3}\eta_{00}) - \frac{A_T}{2}$

Test of CPT

VALUE (units 10 ⁻⁶)	DOCUMENT ID	TECN	COMMENT
---------------------------------	-------------	------	---------

-3 ± 35	168 ALAVI-HARATI02	E799	Uses A_L from K_{e3} decays
----------------	--------------------	------	---------------------------------

¹⁶⁸ALAVI-HARATI 02 uses PDG 00 values of η_{+-} and η_{00} .

 $\Delta S = \Delta Q$ IN K^0 DECAYS

The relative amount of $\Delta S \neq \Delta Q$ component present is measured by the parameter x , defined as

$$x = A(\bar{K}^0 \rightarrow \pi^-\ell^+\nu)/A(K^0 \rightarrow \pi^-\ell^+\nu)$$

We list Re $\{x\}$ and Im $\{x\}$ for K_{e3} and $K_{\mu 3}$ combined.

$$x = A(\bar{K}^0 \rightarrow \pi^-\ell^+\nu)/A(K^0 \rightarrow \pi^-\ell^+\nu) = A(\Delta S = -\Delta Q)/A(\Delta S = \Delta Q)$$

REAL PART OF x

VALUE	EVTS	DOCUMENT ID	TECN	COMMENT
-------	------	-------------	------	---------

-0.0018 ± 0.0041 ± 0.0045		ANGELOPO...	98D CPLR	K_{e3} from K^0
----------------------------------	--	-------------	----------	---------------------

• • • We do not use the following data for averages, fits, limits, etc. • • •

0.10 +0.18 -0.19	79	SMITH	75B WIRE	$\pi^-p \rightarrow K^0\lambda$
0.04 ± 0.03	4724	NIEBERGALL	74 ASPK	$K^+p \rightarrow K^0p\pi^+$
-0.008 ± 0.044	1757	FACKLER	73 OSPK	K_{e3} from K^0
-0.03 ± 0.07	1367	HART	73 OSPK	K_{e3} from $K^0\lambda$
-0.070 ± 0.036	1079	MALLARY	73 OSPK	K_{e3} from $K^0\lambda X$
0.03 ± 0.06	410	169 BURGUN	72 HBC	$K^+p \rightarrow K^0p\pi^+$
0.04 +0.10 -0.13	100	170 GRAHAM	72 OSPK	$K_{\mu 3}$ from $K^0\lambda$
-0.05 ± 0.09	442	170 GRAHAM	72 OSPK	$\pi^-p \rightarrow K^0\lambda$
0.26 +0.10 -0.14	126	MANN	72 HBC	$K^-p \rightarrow n\bar{K}^0$
-0.13 ± 0.11	342	170 MANTSCH	72 OSPK	K_{e3} from $K^0\lambda$
0.04 +0.07 -0.08	222	169 BURGUN	71 HBC	$K^+p \rightarrow K^0p\pi^+$
0.25 +0.07 -0.09	252	WEBBER	71 HBC	$K^-p \rightarrow n\bar{K}^0$
0.12 ± 0.09	215	171 CHO	70 DBC	$K^+d \rightarrow K^0pp$
-0.020 ± 0.025		172 BENNETT	69 CNTR	Charge asym+ Cu regen.
0.09 +0.14 -0.16	686	LITTENBERG	69 OSPK	$K^+n \rightarrow K^0p$
0.03 ± 0.03		172 BENNETT	68 CNTR	
0.09 +0.07 -0.09	121	JAMES	68 HBC	$\bar{p}p$
0.17 +0.16 -0.35	116	FELDMAN	67B OSPK	$\pi^-p \rightarrow K^0\lambda$
0.17 ± 0.10	335	171 HILL	67 DBC	$K^+d \rightarrow K^0pp$
0.035 +0.11 -0.13	196	AUBERT	65 HLBC	K^+ charge exch.
0.06 +0.18 -0.44	152	173 BALDO...	65 HLBC	K^+ charge exch.
-0.08 +0.16 -0.28	109	174 FRANZINI	65 HBC	$\bar{p}p$

¹⁶⁹BURGUN 72 is a final result which includes BURGUN 71.

¹⁷⁰First GRAHAM 72 value is second GRAHAM 72 value combined with MANTSCH 72.

¹⁷¹CHO 70 is analysis of unambiguous events in new data and HILL 67.

¹⁷²BENNETT 69 is a reanalysis of BENNETT 68.

¹⁷³BALDO-CEOLIN 65 gives x and θ converted by us to Re(x) and Im(x).

¹⁷⁴FRANZINI 65 gives x and θ for Re(x) and Im(x). See SCHMIDT 67.

IMAGINARY PART OF x

Assumes $m_{K_L^0} - m_{K_S^0}$ positive. See Listings above.

VALUE	EVTS	DOCUMENT ID	TECN	COMMENT
-------	------	-------------	------	---------

0.0012 ± 0.0019 ± 0.0009	640k	ANGELOPO...	01B CPLR	K_{e3} from K^0
---------------------------------	------	-------------	----------	---------------------

• • • We do not use the following data for averages, fits, limits, etc. • • •

0.0012 ± 0.0019	640k	175 ANGELOPO...	98E CPLR	K_{e3} from K^0
-0.10 +0.16 -0.19	79	SMITH	75B WIRE	$\pi^-p \rightarrow K^0\lambda$
-0.06 ± 0.05	4724	NIEBERGALL	74 ASPK	$K^+p \rightarrow K^0p\pi^+$
-0.017 ± 0.060	1757	FACKLER	73 OSPK	K_{e3} from K^0
0.09 ± 0.07	1367	HART	73 OSPK	K_{e3} from $K^0\lambda$
0.107 +0.092 -0.074	1079	MALLARY	73 OSPK	K_{e3} from $K^0\lambda X$
0.07 +0.06 -0.07	410	176 BURGUN	72 HBC	$K^+p \rightarrow K^0p\pi^+$
0.12 +0.17 -0.16	100	177 GRAHAM	72 OSPK	$K_{\mu 3}$ from $K^0\lambda$
0.05 ± 0.13	442	177 GRAHAM	72 OSPK	$\pi^-p \rightarrow K^0\lambda$
0.21 +0.15 -0.12	126	MANN	72 HBC	$K^-p \rightarrow n\bar{K}^0$
-0.04 ± 0.16	342	177 MANTSCH	72 OSPK	K_{e3} from $K^0\lambda$
0.12 +0.08 -0.09	222	176 BURGUN	71 HBC	$K^+p \rightarrow K^0p\pi^+$
0.0 ± 0.08	252	WEBBER	71 HBC	$K^-p \rightarrow n\bar{K}^0$
-0.08 ± 0.07	215	178 CHO	70 DBC	$K^+d \rightarrow K^0pp$
-0.11 +0.10 -0.11	686	LITTENBERG	69 OSPK	$K^+n \rightarrow K^0p$
+0.22 +0.37 -0.29	121	JAMES	68 HBC	$\bar{p}p$
0.0 ± 0.25	116	FELDMAN	67B OSPK	$\pi^-p \rightarrow K^0\lambda$
-0.20 ± 0.10	335	178 HILL	67 DBC	$K^+d \rightarrow K^0pp$
-0.21 +0.11 -0.15	196	AUBERT	65 HLBC	K^+ charge exch.
-0.44 +0.32 -0.19	152	179 BALDO...	65 HLBC	K^+ charge exch.
+0.24 +0.40 -0.30	109	180 FRANZINI	65 HBC	$\bar{p}p$

¹⁷⁵Superseded by ANGELOPOULOS 01B.

¹⁷⁶BURGUN 72 is a final result which includes BURGUN 71.

¹⁷⁷First GRAHAM 72 value is second GRAHAM 72 value combined with MANTSCH 72.

¹⁷⁸Footnote 10 of HILL 67 should read +0.58, not -0.58 (private communication) CHO 70 is analysis of unambiguous events in new data and HILL 67.

¹⁷⁹BALDO-CEOLIN 65 gives x and θ converted by us to Re(x) and Im(x).

¹⁸⁰FRANZINI 65 gives x and θ for Re(x) and Im(x). See SCHMIDT 67.

See key on page 405

Meson Particle Listings

$K_L^0, K_S^{*0}(800)$

Table listing meson particles with columns for author(s), experiment, and institutional affiliation. Includes entries like Vosburgh et al. (RUTG, MASA), Firestone (YALE, BNL), and many others.

Table listing meson particles with columns for author(s), experiment, and institutional affiliation. Includes entries like Auerbach et al. (PENN), Behr et al. (EPOL, MILA, PADO), and others.

$K_0^{*}(800)$
Or K_0^{*}

$$I(J^P) = \frac{1}{2}(0^{+})$$

OMITTED FROM SUMMARY TABLE

Needs confirmation. See the mini-review on scalar mesons under $f_0(600)$ (see the index for the page number).

$K_0^{*}(800)$ MASS

Table of $K_0^{*}(800)$ mass measurements. Columns include VALUE (MeV), EVTS, DOCUMENT ID, TECN, and COMMENT. Includes entries like ABLIKIM 06c, BES2, AITALA 02, etc.

- 1 S-matrix pole. GUO 06 in a chiral unitary approach report a mass of 757 ± 33 MeV and a width of 558 ± 82 MeV.
2 A fit in the $K_0^{*}(800) + K^{*}(892) + K^{*}(1410)$ model with mass and width of the $K_0^{*}(800)$ from ABLIKIM 06c well describes the left slope of the $K_S^0 \pi^-$ invariant mass spectrum in $\tau^- \rightarrow K_S^0 \pi^- \nu_{\tau}$ decay studied by EPIFANOV 07.
3 S-matrix pole. Using Roy-Steiner equations (ROY 71) as well as unitarity, analyticity and crossing symmetry constraints.
4 Not seen by KOPP 01 using 7070 events of $D^0 \rightarrow K^- \pi^+ \pi^0$. LINK 02e and LINK 05i show clear evidence for a constant non-resonant scalar amplitude rather than $K_0^{*}(800)$ in their high statistics analysis of $D^+ \rightarrow K^- \pi^+ \mu^+ \nu_{\mu}$.
5 AUBERT 07T does not find evidence for the charged $K_0^{*}(800)$ using 11k events of $D^0 \rightarrow K^- K^+ \pi^0$.
6 S-matrix pole. Supersedes BUGG 06. Combined analysis of ASTON 88, ABLIKIM 06c, AITALA 06, and LINK 09 using an s-dependent width with couplings to $K\pi$ and $K\eta'$, and the Adler zero near thresholds.
7 T-matrix pole.
8 A Breit-Wigner mass and width.
9 S-matrix pole. Reanalysis of ASTON 88, AITALA 02, and ABLIKIM 06c using for the κ an s-dependent width with an Adler zero near threshold.
10 Breit-Wigner parameters. A significant S-wave can be also modeled as a non-resonant contribution.
11 S-matrix pole.
12 Using ASTON 88.
13 T-matrix pole. Reanalysis of data from LINGLIN 73, ESTABROOKS 78, and ASTON 88 in the unitarized ChPT model.
14 T-matrix pole. Reanalysis of ASTON 88 data.
15 Reanalysis of ASTON 88 using interfering Breit-Wigner amplitudes.

OTHER RELATED PAPERS

Table listing related papers with columns for author(s), experiment, and institutional affiliation. Includes entries like Hayakawa et al. (NAGO), Ritchie et al. (YALE), and others.

$K_0^{*}(800)$ WIDTH

Table of $K_0^{*}(800)$ width measurements. Columns include VALUE (MeV), EVTS, DOCUMENT ID, TECN, and COMMENT. Includes entries like ABLIKIM 06c, BES2, AITALA 02, etc.

Meson Particle Listings

$K_0^*(800)$, $K^*(892)$

- 16 S-matrix pole.
- 17 A fit in the $K_0^*(800) + K^*(892) + K^*(1410)$ model with mass and width of the $K_0^*(800)$ from ABLIKIM 06c well describes the left slope of the $K_S^0 \pi^-$ invariant mass spectrum in $\tau^- \rightarrow K_S^0 \pi^- \nu_\tau$ decay studied by EPIFANOV 07.
- 18 S-matrix pole. Using Roy-Steiner equations (ROY 71) as well as unitarity, analyticity and crossing symmetry constraints.
- 19 Not seen by KOPP 01 using 7070 events of $D^0 \rightarrow K^- \pi^+ \pi^0$. LINK 02e and LINK 05i show clear evidence for a constant non-resonant scalar amplitude rather than $K_0^*(800)$ in their high statistics analysis of $D^+ \rightarrow K^- \pi^+ \mu^+ \nu_\mu$.
- 20 AUBERT 07t does not find evidence for the charged $K_0^*(800)$ using 11k events of $D^0 \rightarrow K^- K^+ \pi^0$.
- 21 S-matrix pole. Supersedes BUGG 06. Combined analysis of ASTON 88, ABLIKIM 06c, AITALA 06, and LINK 09 using an s-dependent width with couplings to $K\pi$ and $K\eta'$, and the Adler zero near thresholds.
- 22 T-matrix pole.
- 23 A Breit-Wigner mass and width.
- 24 S-matrix pole. Reanalysis of ASTON 88, AITALA 02, and ABLIKIM 06c using for the π s-dependent width with an Adler zero near threshold.
- 25 Statistical error only. A fit to the Dalitz plot including the $K_0^*(800)^\pm$, $K^*(892)^\pm$, and ϕ resonances modeled as Breit-Wigners. A significant S-wave can be also modeled as a non-resonant contribution.
- 26 Using ASTON 88.
- 27 T-matrix pole. Reanalysis of data from LINGLIN 73, ESTABROOKS 78, and ASTON 88 in the unitarized ChPT model.
- 28 T-matrix pole. Reanalysis of ASTON 88 data.
- 29 Reanalysis of ASTON 88 using interfering Breit-Wigner amplitudes.

$K_0^*(800)$ REFERENCES

BUGG 10 PR D81 014002 D.V. Bugg (LOQM)	LINK 09 PL B681 14 J.M. Link et al. (FNAL FOCUS Collab.)
BONVICINI 08A PR D78 052001 G. Bonvicini et al. (CLEO Collab.)	AUBERT 07T PR D76 011102R B. Aubert et al. (BABAR Collab.)
EPIFANOV 07 PL B654 65 D. Epifanov et al. (BELLE Collab.)	LINK 07B PL B653 1 J.M. Link et al. (FNAL FOCUS Collab.)
ABLIKIM 06C PL B633 681 M. Ablikim et al. (BES Collab.)	AITALA 06 PR D73 032004 E.M. Aitala et al. (FNAL E791 Collab.)
Also PR D74 059301 (errata) E.M. Aitala et al. (FNAL E791 Collab.)	BUGG 06 PL B632 471 D.V. Bugg (LOQM)
CAWFIELD 06A PR D74 031108R C. Cawfield et al. (CLEO Collab.)	DESCOTES-G... 06 EPJ C48 553 S. Descotes-Genon, B. Moussallam
GUO 06 NP A773 78 F.K. Guo et al.	ZHOU 06 NP A775 212 Z.Y. Zhou, H.Q. Zheng
LINK 05I PL B621 72 J.M. Link et al. (FNAL FOCUS Collab.)	PELAEZ 04A MPL A19 2879 J.R. Pelaez
ZHENG 04 NP A733 235 H.Q. Zheng et al.	BUGG 03 PL B572 1 D.V. Bugg
AITALA 02 PRL 89 121801 E.M. Aitala et al. (FNAL E791 Collab.)	LINK 02E PL B535 43 J.M. Link et al. (FNAL FOCUS Collab.)
KOPP 01 PR D63 092001 S. Kopp et al. (CLEO Collab.)	ISHIDA 97B PTP 98 621 S. Ishida et al.
ASTON 88 NP B296 493 D. Aston et al. (SLAC, NAGO, CINC, INUS)	ESTABROOKS 78 NP B133 490 P.G. Estabrooks et al. (MCGI, CARL, DURH+)
LINGLIN 73 NP B85 408 D. Linglin (CERN)	ROY 71 PL 36B 353 S.M. Roy

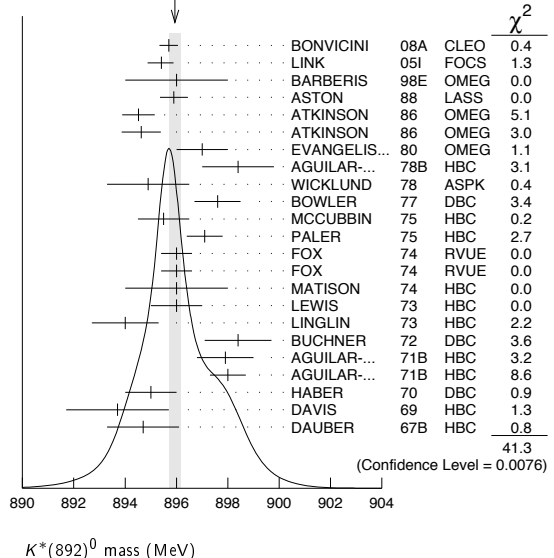
CHARGED ONLY, PRODUCED IN τ LEPTON DECAYS

VALUE (MeV)	EVTs	DOCUMENT ID	TECN	COMMENT
895.47 ± 0.20 ± 0.74	53k	6 EPIFANOV	07 BELL	$\tau^- \rightarrow K_S^0 \pi^- \nu_\tau$
892.0 ± 0.9		7,8 BOITO	09 RVUE	$\tau^- \rightarrow K_S^0 \pi^- \nu_\tau$
895.3 ± 0.2		7,9 JAMIN	08 RVUE	$\tau^- \rightarrow K_S^0 \pi^- \nu_\tau$
896.4 ± 0.9	11970	10 BONVICINI	02 CLEO	$\tau^- \rightarrow K^- \pi^0 \nu_\tau$
895 ± 2		11 BARATE	99R ALEP	$\tau^- \rightarrow K^- \pi^0 \nu_\tau$

NEUTRAL ONLY

VALUE (MeV)	EVTs	DOCUMENT ID	TECN	COMMENT
895.94 ± 0.22 OUR AVERAGE		Error includes scale factor of 1.4. See the ideogram below.		
895.7 ± 0.2 ± 0.3	141k	12 BONVICINI	08A CLEO	$D^+ \rightarrow K^- \pi^+ \pi^+$
895.41 ± 0.32 ^{+0.35} _{-0.43}	18k	13 LINK	05I FOCUS	$D^+ \rightarrow K^- \pi^+ \mu^+ \nu_\mu$
896 ± 2		BARBERIS	98E OMEG	450 $pp \rightarrow p\bar{p} p_S K^* \bar{K}^*$
895.9 ± 0.5 ± 0.2		ASTON	88 LASS	11 $K^- p \rightarrow K^- \pi^+ n$
894.52 ± 0.63	25k	1 ATKINSON	86 OMEG	20-70 γp
894.63 ± 0.76	20k	1 ATKINSON	86 OMEG	20-70 γp
897 ± 1	28k	EVANGELIS...	80 OMEG	10 $\pi^- p \rightarrow K^+ \pi^- (\Lambda, \Sigma)$
898.4 ± 1.4	1180	AGUILAR...	78B HBC	0.76 $\bar{p} p \rightarrow K^\mp K_S^0 \pi^\pm$
894.9 ± 1.6		WICKLUND	78 ASPK	3.4,6 $K^\pm N \rightarrow (K\pi)^0 N$
897.6 ± 0.9		BOWLER	77 DBC	5.4 $K^+ d \rightarrow K^+ \pi^- p p$
895.5 ± 1.0	3600	MCCUBBIN	75 HBC	3.6 $K^- p \rightarrow K^- \pi^+ n$
897.1 ± 0.7	22k	1 PALER	75 HBC	14.3 $K^- p \rightarrow (K\pi)^0 X$
896.0 ± 0.6	10k	FOX	74 RVUE	2 $K^- p \rightarrow K^- \pi^+ n$
896.0 ± 0.6		FOX	74 RVUE	2 $K^+ n \rightarrow K^+ \pi^- p$
896 ± 2		14 MATISON	74 HBC	12 $K^+ p \rightarrow K^+ \pi^- \Delta$
896 ± 1	3186	LEWIS	73 HBC	2.1-2.7 $K^+ p \rightarrow K\pi p p$
894.0 ± 1.3		14 LINGLIN	73 HBC	2-13 $K^+ p \rightarrow K^+ \pi^- \pi^+ p$
898.4 ± 1.3	1700	2 BUCHNER	72 DBC	4.6 $K^+ n \rightarrow K^+ \pi^- p$
897.9 ± 1.1	2934	2 AGUILAR...	71B HBC	3.9,4.6 $K^- p \rightarrow K^- \pi^+ n$
898.0 ± 0.7	5362	2 AGUILAR...	71B HBC	3.9,4.6 $K^- p \rightarrow (K\pi)^0 X$
895 ± 1	4300	3 HABER	70 DBC	3 $K^- N \rightarrow K^- \pi^+ X$
893.7 ± 2.0	10k	DAVIS	69 HBC	12 $K^+ p \rightarrow K^+ \pi^- \pi^+ p$
894.7 ± 1.4	1040	2 DAUBER	67B HBC	2.0 $K^- p \rightarrow K^- \pi^+ \pi^- p$
894.9 ± 0.5 ± 0.7	14.4k	15 MITCHELL	09A CLEO	$D^+ \rightarrow K^+ K^- \pi^+$
896.2 ± 0.3	20k	7 AUBERT	07AK BABR	10.6 $e^+ e^- \rightarrow K^* K^\pm \pi^\mp \gamma$
900.7 ± 1.1	5900	BARTH	83 HBC	70 $K^+ p \rightarrow K^+ \pi^- X$

WEIGHTED AVERAGE
895.94±0.22 (Error scaled by 1.4)



$K^*(892)$

$$J(P) = \frac{1}{2}(1^-)$$

$K^*(892)$ MASS

CHARGED ONLY, HADROPRODUCED

VALUE (MeV)	EVTs	DOCUMENT ID	TECN	CHG	COMMENT
891.66 ± 0.26 OUR AVERAGE					
892.6 ± 0.5	5840	BAUBILLIER 84B	HBC	-	8.25 $K^- p \rightarrow \bar{K}^0 \pi^- p$
888 ± 3		NAPIER 84	SPEC	+	200 $\pi^- p \rightarrow 2K_S^0 X$
891 ± 1		NAPIER 84	SPEC	-	200 $\pi^- p \rightarrow 2K_S^0 X$
891.7 ± 2.1	3700	BARTH 83	HBC	+	70 $K^+ p \rightarrow K^0 \pi^+ X$
891 ± 1	4100	TOAFF 81	HBC	-	6.5 $K^- p \rightarrow \bar{K}^0 \pi^- p$
892.8 ± 1.6		AJINENKO 80	HBC	+	32 $K^+ p \rightarrow K^0 \pi^+ X$
890.7 ± 0.9	1800	AGUILAR... 78B	HBC	±	0.76 $\bar{p} p \rightarrow K^\mp K_S^0 \pi^\pm$
886.6 ± 2.4	1225	BALAND 78	HBC	±	12 $\bar{p} p \rightarrow (K\pi)^\pm X$
891.7 ± 0.6	6706	COOPER 78	HBC	±	0.76 $\bar{p} p \rightarrow (K\pi)^\pm X$
891.9 ± 0.7	9000	1 PALER 75	HBC	-	14.3 $K^- p \rightarrow (K\pi)^- X$
892.2 ± 1.5	4404	AGUILAR... 71B	HBC	-	3.9,4.6 $K^- p \rightarrow (K\pi)^- p$
891 ± 2	1000	CRENNELL 69D	DBC	-	3.9 $K^- N \rightarrow K^0 \pi^- X$
890 ± 3.0	720	BARLOW 67	HBC	±	1.2 $\bar{p} p \rightarrow (K^0 \pi)^\pm K^\mp$
889 ± 3.0	600	BARLOW 67	HBC	±	1.2 $\bar{p} p \rightarrow (K^0 \pi)^\pm K\pi$
891 ± 2.3	620	2 DEBAERE 67B	HBC	+	3.5 $K^+ p \rightarrow K^0 \pi^+ p$
891.0 ± 1.2	1700	3 WOJCIKCI 64	HBC	-	1.7 $K^- p \rightarrow \bar{K}^0 \pi^- p$
893.5 ± 1.1	27k	4 ABELE 99D	CBAR	±	0.0 $\bar{p} p \rightarrow K^+ K^- \pi^0$
890.4 ± 0.2 ± 0.5	80 ± 0.8k	5 BIRD 89	LASS	-	11 $K^- p \rightarrow \bar{K}^0 \pi^- p$
890.0 ± 2.3	800	2,3 CLELAND 82	SPEC	+	30 $K^+ p \rightarrow K_S^0 \pi^+ p$
896.0 ± 1.1	3200	2,3 CLELAND 82	SPEC	+	50 $K^+ p \rightarrow K_S^0 \pi^+ p$
893 ± 1	3600	2,3 CLELAND 82	SPEC	-	50 $K^+ p \rightarrow K_S^0 \pi^- p$
896.0 ± 1.9	380	DELFOSE 81	SPEC	+	50 $K^\pm p \rightarrow K^\pm \pi^0 p$
886.0 ± 2.3	187	DELFOSE 81	SPEC	+	50 $K^\pm p \rightarrow K^\pm \pi^0 p$
894.2 ± 2.0	765	2 CLARK 73	HBC	-	3.13 $K^- p \rightarrow \bar{K}^0 \pi^- p$
894.3 ± 1.5	1150	2,3 CLARK 73	HBC	-	3.3 $K^- p \rightarrow \bar{K}^0 \pi^- p$
892.0 ± 2.6	341	2 SCHWEING...68	HBC	-	5.5 $K^- p \rightarrow \bar{K}^0 \pi^- p$

- 1 Inclusive reaction. Complicated background and phase-space effects.
- 2 Mass errors enlarged by us to Γ/\sqrt{N} . See note.
- 3 Number of events in peak reevaluated by us.
- 4 K-matrix pole.
- 5 From a partial wave amplitude analysis.
- 6 From a fit in the $K_0^*(800) + K^*(892) + K^*(1410)$ model.
- 7 Systematic uncertainties not estimated.
- 8 From the pole position of the $K\pi$ vector form factor in the complex s-plane and using EPIFANOV 07 data.
- 9 Reanalysis of EPIFANOV 07 using resonance chiral theory.
- 10 Calculated by us from the shift by 4.7 ± 0.9 MeV (statistical uncertainty only) reported in BONVICINI 02 with respect to the world average value from PDG 00.

- ¹¹ With mass and width of the $K^*(1410)$ fixed at 1412 MeV and 227 MeV, respectively.
¹² From the isobar model with a complex pole for the κ .
¹³ Fit to $K\pi$ mass spectrum includes a non-resonant scalar component.
¹⁴ From pole extrapolation.
¹⁵ This value comes from a fit with χ^2 of 178/117.

 $K^*(892)$ MASSES AND MASS DIFFERENCES

Unrealistically small errors have been reported by some experiments. We use simple “realistic” tests for the minimum errors on the determination of a mass and width from a sample of N events:

$$\delta_{\min}(m) = \frac{\Gamma}{\sqrt{N}}, \quad \delta_{\min}(\Gamma) = 4 \frac{\Gamma}{\sqrt{N}}. \quad (1)$$

We consistently increase unrealistic errors before averaging. For a detailed discussion, see the 1971 edition of this Note.

 $m_{K^*(892)^0} - m_{K^*(892)^\pm}$

VALUE (MeV)	EVTS	DOCUMENT ID	TECN	CHG	COMMENT
6.7 ± 1.2 OUR AVERAGE					
7.7 ± 1.7	2980	AGUILAR-...	78B	HBC	±0 0.76 $\bar{p}p \rightarrow K^\mp K_S^0 \pi^\pm$
5.7 ± 1.7	7338	AGUILAR-...	71B	HBC	-0 3.9,4.6 K^-p
6.3 ± 4.1	283	BARASH	67B	HBC	0.0 $\bar{p}p$

- ¹⁶ Number of events in peak reevaluated by us.

 $K^*(892)$ RANGE PARAMETER

All from partial wave amplitude analyses.

VALUE (GeV ⁻¹)	EVTS	DOCUMENT ID	TECN	CHG	COMMENT
3.96 ± 0.54 +1.31 -0.90	18k	LINK	05i	FOCS	0 $D^+ \rightarrow K^- \pi^+ \mu^+ \nu_\mu$
3.4 ± 0.7		ASTON	88	LASS	0 11 $K^-p \rightarrow K^- \pi^+ n$
12.1 ± 3.2 ± 3.0		BIRD	89	LASS	- 11 $K^-p \rightarrow \bar{K}^0 \pi^- p$

- • • We do not use the following data for averages, fits, limits, etc. • • •

- ¹⁷ Fit to $K\pi$ mass spectrum includes a non-resonant scalar component.

 $K^*(892)$ WIDTH**CHARGED ONLY, HADROPRODUCED**

VALUE (MeV)	EVTS	DOCUMENT ID	TECN	CHG	COMMENT
50.8 ± 0.9 OUR FIT					
50.8 ± 0.9 OUR AVERAGE					
49 ± 2	5840	BAUBILLIER	84B	HBC	- 8.25 $K^-p \rightarrow \bar{K}^0 \pi^- p$
56 ± 4		NAPIER	84	SPEC	- 200 $\pi^- p \rightarrow 2K_S^0 X$
51 ± 2	4100	TOAFF	81	HBC	- 6.5 $K^-p \rightarrow \bar{K}^0 \pi^- p$
50.5 ± 5.6		AJINENKO	80	HBC	+ 32 $K^+p \rightarrow K^0 \pi^+ X$
45.8 ± 3.6	1800	AGUILAR-...	78B	HBC	± 0.76 $\bar{p}p \rightarrow K^\mp K_S^0 \pi^\pm$
52.0 ± 2.5	6706	COOPER	78	HBC	± 0.76 $\bar{p}p \rightarrow (K\pi)^\pm X$
52.1 ± 2.2	9000	PALER	75	HBC	- 14.3 $K^-p \rightarrow (K\pi)^-$
46.3 ± 6.7	765	CLARK	73	HBC	- 3.13 $K^-p \rightarrow \bar{K}^0 \pi^- p$
48.2 ± 5.7	1150	CLARK	73	HBC	- 3.3 $K^-p \rightarrow \bar{K}^0 \pi^- p$
54.3 ± 3.3	4404	AGUILAR-...	71B	HBC	- 3.9,4.6 $K^-p \rightarrow (K\pi)^-$
46 ± 5	1700	WOJCICKI	64	HBC	- 1.7 $K^-p \rightarrow \bar{K}^0 \pi^- p$
54.8 ± 1.7	27k	ABELE	99d	CBAR	± 0.0 $\bar{p}p \rightarrow K^+ K^- \pi^0$
45.2 ± 1 ± 2	79.7 ± 0.8k	BIRD	89	LASS	- 11 $K^-p \rightarrow \bar{K}^0 \pi^- p$
42.8 ± 7.1	3700	BARTH	83	HBC	+ 70 $K^+p \rightarrow K^0 \pi^+ X$
64.0 ± 9.2	800	CLELAND	82	SPEC	+ 30 $K^+p \rightarrow K_S^0 \pi^+ p$
62.0 ± 4.4	3200	CLELAND	82	SPEC	+ 50 $K^+p \rightarrow K_S^0 \pi^+ p$
55 ± 4	3600	CLELAND	82	SPEC	- 50 $K^+p \rightarrow K_S^0 \pi^- p$
62.6 ± 3.8	380	DELFOSSÉ	81	SPEC	+ 50 $K^\pm p \rightarrow K^\pm \pi^0 p$
50.5 ± 3.9	187	DELFOSSÉ	81	SPEC	- 50 $K^\pm p \rightarrow K^\pm \pi^0 p$

- • • We do not use the following data for averages, fits, limits, etc. • • •

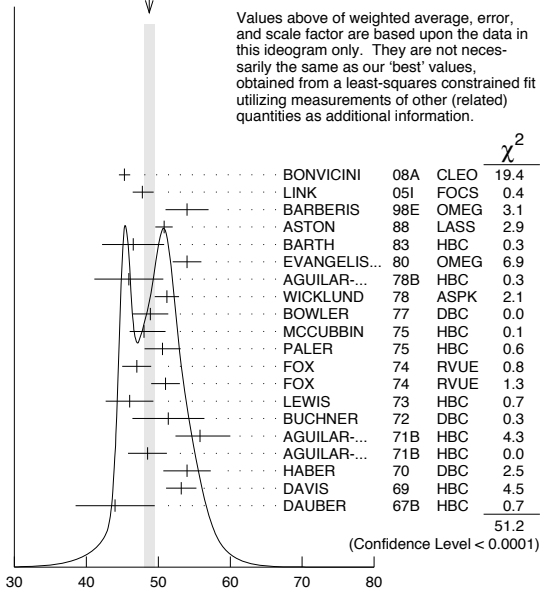
CHARGED ONLY, PRODUCED IN τ LEPTON DECAYS

VALUE (MeV)	EVTS	DOCUMENT ID	TECN	CHG	COMMENT
46.2 ± 0.6 ± 1.2	53k	EPIFANOV	07	BELL	$\tau^- \rightarrow K_S^0 \pi^- \nu_\tau$
46.2 ± 0.4		BOITO	09	RVUE	$\tau^- \rightarrow K_S^0 \pi^- \nu_\tau$
47.5 ± 0.4		JAMIN	08	RVUE	$\tau^- \rightarrow K_S^0 \pi^- \nu_\tau$
55 ± 8		BARATE	99R	ALEP	$\tau^- \rightarrow K^- \pi^0 \nu_\tau$

- • • We do not use the following data for averages, fits, limits, etc. • • •

NEUTRAL ONLY

VALUE (MeV)	EVTS	DOCUMENT ID	TECN	CHG	COMMENT
48.7 ± 0.8 OUR FIT					Error includes scale factor of 1.7.
48.7 ± 0.7 OUR AVERAGE					Error includes scale factor of 1.6. See the ideogram below.
45.3 ± 0.5 ± 0.6	141k	BONVICINI	08A	CLEO	$D^+ \rightarrow K^- \pi^+ \pi^+$
47.79 ± 0.86 ± 1.32 -1.06	18k	LINK	05i	FOCS	0 $D^+ \rightarrow K^- \pi^+ \mu^+ \nu_\mu$
54 ± 3		BARBERIS	98E	OMEG	450 $pp \rightarrow p_f p_S K^* \bar{K}^*$
50.8 ± 0.8 ± 0.9		ASTON	88	LASS	0 11 $K^-p \rightarrow K^- \pi^+ n$
46.5 ± 4.3	5900	BARTH	83	HBC	0 70 $K^+p \rightarrow K^+ \pi^- X$
54 ± 2	28k	EVANGELIS...	80	OMEG	0 10 $\pi^- p \rightarrow K^+ \pi^- (\Lambda, \Sigma)$
45.9 ± 4.8	1180	AGUILAR-...	78B	HBC	0 0.76 $\bar{p}p \rightarrow K^\mp K_S^0 \pi^\pm$
51.2 ± 1.7		WICKLUND	78	ASPK	0 3,4,6 $K^\pm N \rightarrow (K\pi)^0 N$
48.9 ± 2.5		BOWLER	77	DBC	0 5.4 $K^+ d \rightarrow K^+ \pi^- pp$
48 +3 -2	3600	MCCUBBIN	75	HBC	0 3.6 $K^-p \rightarrow K^- \pi^+ n$
50.6 ± 2.5	22k	PALER	75	HBC	0 14.3 $K^-p \rightarrow (K\pi)^0 X$
47 ± 2	10k	FOX	74	RVUE	0 2 $K^-p \rightarrow K^- \pi^+ n$
51 ± 2		FOX	74	RVUE	0 2 $K^+n \rightarrow K^+ \pi^- p$
46.0 ± 3.3	3186	LEWIS	73	HBC	0 2.1-2.7 $K^+p \rightarrow K\pi\pi p$
51.4 ± 5.0	1700	BUCHNER	72	DBC	0 4.6 $K^+n \rightarrow K^+ \pi^- p$
55.8 +4.2 -3.4	2934	AGUILAR-...	71B	HBC	0 3.9,4.6 $K^-p \rightarrow K^- \pi^+ n$
48.5 ± 2.7	5362	AGUILAR-...	71B	HBC	0 3.9,4.6 $K^-p \rightarrow K^- \pi^+ \pi^- p$
54.0 ± 3.3	4300	HABER	70	DBC	0 3 $K^-N \rightarrow K^- \pi^+ X$
53.2 ± 2.1	10k	DAVIS	69	HBC	0 1.2 $K^+p \rightarrow K^+ \pi^- \pi^+ p$
44 ± 5.5	1040	DAUBER	67B	HBC	0 2.0 $K^-p \rightarrow K^- \pi^+ \pi^- p$
• • •					We do not use the following data for averages, fits, limits, etc. • • •
45.7 ± 1.1 ± 0.5	14.4k	MITCHELL	09A	CLEO	$D_S^+ \rightarrow K^+ K^- \pi^+$
50.6 ± 0.9	20k	AUBERT	07AK	BABR	10.6 $e^+ e^- \rightarrow K^{*0} K^\pm \pi^\mp \gamma$

WEIGHTED AVERAGE
48.7 ± 0.7 (Error scaled by 1.6)**NEUTRAL ONLY (MeV)**

- ¹⁸ Width errors enlarged by us to $4 \times \Gamma/\sqrt{N}$; see note.
¹⁹ Inclusive reaction. Complicated background and phase-space effects.
²⁰ Number of events in peak reevaluated by us.
²¹ K-matrix pole.
²² From a partial wave amplitude analysis.
²³ From a fit in the $K_S^0(800) + K^*(892) + K^*(1410)$ model.
²⁴ Systematic uncertainties not estimated.
²⁵ From the pole position of the $K\pi$ vector form factor in the complex s -plane and using EPIFANOV 07 data.
²⁶ Reanalysis of EPIFANOV 07 using resonance chiral theory.
²⁷ With mass and width of the $K^*(1410)$ fixed at 1412 MeV and 227 MeV, respectively.
²⁸ From the isobar model with a complex pole for the κ .
²⁹ Fit to $K\pi$ mass spectrum includes a non-resonant scalar component.
³⁰ This value comes from a fit with χ^2 of 178/117.

Meson Particle Listings

 $K^*(892)$, $K_1(1270)$ $K^*(892)$ DECAY MODES

Mode	Fraction (Γ_i/Γ)	Confidence level
Γ_1 $K\pi$	~ 100	%
Γ_2 $(K\pi)^\pm$	(99.901 \pm 0.009) %	
Γ_3 $(K\pi)^0$	(99.761 \pm 0.021) %	
Γ_4 $K^0\gamma$	(2.39 \pm 0.21) $\times 10^{-3}$	
Γ_5 $K^\pm\gamma$	(9.9 \pm 0.9) $\times 10^{-4}$	
Γ_6 $K\pi\pi$	< 7	$\times 10^{-4}$

CONSTRAINED FIT INFORMATION

An overall fit to the total width and a partial width uses 13 measurements and one constraint to determine 3 parameters. The overall fit has a $\chi^2 = 7.8$ for 11 degrees of freedom.

The following *off-diagonal* array elements are the correlation coefficients $\langle \delta p_i \delta p_j \rangle / (\delta p_i \delta p_j)$, in percent, from the fit to parameters p_i , including the branching fractions, $x_i \equiv \Gamma_i / \Gamma_{\text{total}}$. The fit constrains the x_i whose labels appear in this array to sum to one.

x_5	-100	
Γ	19	-19
	x_2	x_5

Mode	Rate (MeV)
Γ_2 $(K\pi)^\pm$	50.7 \pm 0.9
Γ_5 $K^\pm\gamma$	0.050 \pm 0.005

CONSTRAINED FIT INFORMATION

An overall fit to the total width and a partial width uses 21 measurements and one constraint to determine 3 parameters. The overall fit has a $\chi^2 = 51.2$ for 19 degrees of freedom.

The following *off-diagonal* array elements are the correlation coefficients $\langle \delta p_i \delta p_j \rangle / (\delta p_i \delta p_j)$, in percent, from the fit to parameters p_i , including the branching fractions, $x_i \equiv \Gamma_i / \Gamma_{\text{total}}$. The fit constrains the x_i whose labels appear in this array to sum to one.

x_4	-100	
Γ	18	-18
	x_3	x_4

Mode	Rate (MeV)	Scale factor
Γ_3 $(K\pi)^0$	48.6 \pm 0.8	1.7
Γ_4 $K^0\gamma$	0.117 \pm 0.010	

 $K^*(892)$ PARTIAL WIDTHS

$\Gamma(K^0\gamma)$	Γ_4			
VALUE (keV)	DOCUMENT ID	TECN	CHG	COMMENT
117 \pm 10 OUR FIT				
116.5 \pm 9.9	584	CARLSMITH	86	SPEC 0 $K_L^0 A \rightarrow K_S^0 \pi^0 A$

$\Gamma(K^\pm\gamma)$	Γ_5			
VALUE (keV)	DOCUMENT ID	TECN	CHG	COMMENT
50 \pm 5 OUR FIT				
50 \pm 5 OUR AVERAGE				
48 \pm 11	BERG	83	SPEC	- 156 $K^- A \rightarrow \bar{K} \pi A$
51 \pm 5	CHANDLEE	83	SPEC	+ 200 $K^+ A \rightarrow K \pi A$

 $K^*(892)$ BRANCHING RATIOS

$\Gamma(K^0\gamma)/\Gamma_{\text{total}}$	Γ_4/Γ			
VALUE (units 10^{-3})	DOCUMENT ID	TECN	CHG	COMMENT
2.39 \pm 0.21 OUR FIT				
1.5 \pm 0.7	CARITHERS	75B	CNTR	0 8-16 $\bar{K}^0 A$

$\Gamma(K^\pm\gamma)/\Gamma_{\text{total}}$	Γ_5/Γ			
VALUE (units 10^{-3})	DOCUMENT ID	TECN	CHG	COMMENT
0.99 \pm 0.09 OUR FIT				
<1.6	95	BEMPORAD	73	CNTR + 10-16 $K^+ A$

 $\Gamma(K\pi\pi)/\Gamma((K\pi)^\pm)$

VALUE	CL%	DOCUMENT ID	TECN	CHG	COMMENT
$< 7 \times 10^{-4}$	95	JONGEJANS	78	HBC	4 $K^- p \rightarrow p \bar{K}^0 2\pi$
$< 20 \times 10^{-4}$		WOJCICKI	64	HBC	- 1.7 $K^- p \rightarrow \bar{K}^0 \pi^- p$

••• We do not use the following data for averages, fits, limits, etc. •••

 $K^*(892)$ REFERENCES

BOITO	09	EPJ C59	821	D.R. Boito, R. Escribano, M. Jamin	
MITCHELL	09A	PR D79	072008	R.E. Mitchell <i>et al.</i>	(CLEO Collab.)
BONVICINI	08A	PR D78	052001	G. Bonvicini <i>et al.</i>	(CLEO Collab.)
JAMIN	08	PL	B664	M. Jamin, A. Pich, J. Portoles	
AUBERT	07AK	PR D76	012008	B. Aubert <i>et al.</i>	(BABAR Collab.)
EPIFANOV	07	PL	B654	D. Epifanov <i>et al.</i>	(BELLE Collab.)
LINK	05I	PL	B621	J.M. Link <i>et al.</i>	(FNAL FOCUS Collab.)
BONVICINI	02	PRL	88	G. Bonvicini <i>et al.</i>	(CLEO Collab.)
PDG	00	EPJ	C15	D.E. Groom <i>et al.</i>	
ABELE	99D	PL	B468	A. Abele <i>et al.</i>	(Crystal Barrel Collab.)
BARATE	99R	EPJ	C11	R. Barate <i>et al.</i>	(ALEPH Collab.)
BARBERIS	98E	PL	B436	D. Barberis <i>et al.</i>	(Omega Expt.)
BIRD	89	SLAC	332	P.F. Bird	(SLAC)
ASTON	88	NP	B296	D. Aston <i>et al.</i>	(SLAC, NAGO, CINC, INUS)
ATKINSON	86	ZPHY	C30	M. Atkinson <i>et al.</i>	(BONN, CERN, GLAS+)
CARLSMITH	86	PRL	56	D. Carlsmith <i>et al.</i>	(EFI, SAFL)
BAUBILLIER	84B	ZPHY	C26	M. Baubillier <i>et al.</i>	(BIRM, CERN, GLAS+)
NAPIER	84	PL	149B	A. Napier <i>et al.</i>	(TUFTS, ARIZ, FNAL, FLOR+)
BARTH	83	NP	B223	M. Barth <i>et al.</i>	(BRUX, CERN, GENO, MONS+)
BERG	83	Thesis UMI	83-21652	D.M. Berg	(ROCH)
CHANDLEE	83	PRL	51	C. Chandlee <i>et al.</i>	(ROCH, FNAL, MINN)
CLELAND	82	NP	B208	W.E. Cleland <i>et al.</i>	(DURH, GEVA, LAUS+)
DELFOSE	81	NP	B183	A. Delfosse <i>et al.</i>	(GEVA, LAUS)
TOAFF	81	PR	D23	S. Toaff <i>et al.</i>	(ANL, KANS)
AJINENKO	80	ZPHY	C5	I.V. Ajinenko <i>et al.</i>	(SERP, BRUX, MONS+)
EVANGELIS...	80	NP	B165	C. Evangelista <i>et al.</i>	(BARI, BONN, CERN+)
AGUILAR...	78B	NP	B141	M. Aguilar-Benitez <i>et al.</i>	(MADR, TATA+)
BALAND	78	NP	B140	J.F. Baland <i>et al.</i>	(MONS, BELG, CERN+)
COOPER	78	NP	B136	A.M. Cooper <i>et al.</i>	(TATA, CERN, CDEF+)
JONGEJANS	78	NP	B139	B. Jongejans <i>et al.</i>	(ZEEM, CERN, NIJ+)
WICKLUND	78	PR	D17	A.B. Wicklund <i>et al.</i>	(ANL)
BOWLER	77	NP	B126	M.G. Bowler <i>et al.</i>	(OXF)
CARITHERS	75B	PRL	35	W.C.J. Carithers <i>et al.</i>	(ROCH, MCGI)
MCCUBBIN	75	NP	B86	N.A. McCubbin, L. Lyons	(OXF)
PALER	75	NP	B96	K. Paler <i>et al.</i>	(RHEL, SAFL, EPOL)
FOX	74	NP	B80	G.C. Fox, M.L. Griss	(CIT)
MATISON	74	PR	D3	M.J. Matison <i>et al.</i>	(LBL)
BEMPORAD	73	NP	B51	C. Bemporad <i>et al.</i>	(CERN, ETH, LOIC)
CLARK	73	NP	B54	O.G. Clark, L. Lyons, D. Radojicki	(OXF)
LEWIS	73	NP	B60	PH. Lewis <i>et al.</i>	(LOWC, LOIC, CDEF)
LINGLIN	73	NP	B55	D. Linglin	(CERN)
BUCHNER	72	NP	B45	K. Buchner <i>et al.</i>	(MPIM, CERN, BRUX)
AGUILAR...	71B	PR	D4	M. Aguilar-Benitez, R.L. Eisner, J.B. Kinson	(BNL)
HABER	70	NP	B17	B. Haber <i>et al.</i>	(REHO, SAFL, BGNA, EPOL)
CRENNELL	69D	PRL	22	D.J. Crennell <i>et al.</i>	(BNL)
DAVIS	69	PRL	23	P.J. Davis <i>et al.</i>	(LRL)
SCHWEING...	68	PR	166	F. Schweingruber <i>et al.</i>	(ANL, NWES)
BARASH	67B	PR	156	N. Barash <i>et al.</i>	(COLU)
BARLOW	67	NC	50A	J. Barlow <i>et al.</i>	(CERN, CDEF, IRAO, LYP)
DAUBER	67B	NP	153	P.M. Dauber <i>et al.</i>	(UCLA)
DEBAERE	67B	NC	51A	W. de Baere <i>et al.</i>	(BRUX, CERN)
WOJCICKI	64	PR	135	S.G. Wojcicki	(LRL)

 $K_1(1270)$

$$I(J^P) = \frac{1}{2}(1^+)$$

 $K_1(1270)$ MASS

VALUE (MeV)	DOCUMENT ID
1272 \pm 7 OUR AVERAGE	Includes data from the 2 datablocks that follow this one.

PRODUCED BY K^- , BACKWARD SCATTERING, HYPERON EXCHANGE

VALUE (MeV)	EVTS	DOCUMENT ID	TECN	CHG	COMMENT
					The data in this block is included in the average printed for a previous datablock.

1275 \pm 10	700	GAVILLET	78	HBC	+ 4.2 $K^- p \rightarrow \Xi^- (K\pi\pi)^+$
---------------------------------	-----	----------	----	-----	---

PRODUCED BY K BEAMS

VALUE (MeV)	DOCUMENT ID	TECN	CHG	COMMENT
				The data in this block is included in the average printed for a previous datablock.

1270 \pm 10	¹ DAUM	81C	CNTR	-	63 $K^- p \rightarrow K^- 2\pi p$
••• We do not use the following data for averages, fits, limits, etc. •••					
~ 1276	² TORNQVIST	82B	RVUE		
~ 1300	VERGEEST	79	HBC	-	4.2 $K^- p \rightarrow (\bar{K}\pi\pi)^- p$
1289 \pm 25	³ CARNEGIE	77	ASPK	\pm	13 $K^\pm p \rightarrow (K\pi\pi)^\pm p$
~ 1300	BRANDENB...	76	ASPK	\pm	13 $K^\pm p \rightarrow (K\pi\pi)^\pm p$
~ 1270	OTTER	76	HBC	-	10,14,16 $K^- p \rightarrow (\bar{K}\pi\pi)^- p$
1260	DAVIS	72	HBC	+	12 $K^+ p$
1234 \pm 12	FIRESTONE	72B	DBC	+	12 $K^+ d$

¹ Well described in the chiral unitary approach of GENG 07 with two poles at 1195 and 1284 MeV and widths of 246 and 146 MeV, respectively.

² From a unitarized quark-model calculation.

³ From a model-dependent fit with Gaussian background to BRANDENBURG 76 data.

PRODUCED BY BEAMS OTHER THAN K MESONS

VALUE (MeV)	EVTs	DOCUMENT ID	TECN	CHG	COMMENT
1279±10	25k	⁴ ABLIKIM	06c	BES2	$J/\psi \rightarrow \bar{K}^*(892)^0 K^+ \pi^-$
1294±10	310	RODEBACK	81	HBC	$4 \pi^- p \rightarrow \Lambda K 2\pi$
1300	40	CRENNELL	72	HBC	$4.5 \pi^- p \rightarrow \Lambda K 2\pi$
1242 ⁺⁹ ₋₁₀		⁵ ASTIER	69	HBC	$\bar{p} p$
1300	45	CRENNELL	67	HBC	$6 \pi^- p \rightarrow \Lambda K 2\pi$

⁴ Systematic errors not estimated.⁵ This was called the C meson.PRODUCED IN τ LEPTON DECAYS

VALUE (MeV)	EVTs	DOCUMENT ID	TECN	CHG	COMMENT
1254±33±34	7k	ASNER	00B	CLEO	$\tau^- \rightarrow K^- \pi^+ \pi^- \nu_\tau$

 $K_1(1270)$ WIDTH

VALUE (MeV)	DOCUMENT ID
90±20 OUR ESTIMATE	This is only an educated guess; the error given is larger than the error on the average of the published values.
87±7 OUR AVERAGE	Includes data from the 2 datablocks that follow this one.

PRODUCED BY K^- , BACKWARD SCATTERING, HYPERON EXCHANGE

VALUE (MeV)	EVTs	DOCUMENT ID	TECN	CHG	COMMENT
75±15	700	GAVILLET	78	HBC	$4.2 K^- p \rightarrow \Xi^- K \pi \pi$

PRODUCED BY K BEAMS

VALUE (MeV)	DOCUMENT ID	TECN	CHG	COMMENT
90±8	⁶ DAUM	81c	CNTR	$63 K^- p \rightarrow K^- 2\pi p$
~150	VERGEEST	79	HBC	$4.2 K^- p \rightarrow (\bar{K} \pi \pi)^- p$
150±71	⁷ CARNEGIE	77	ASPK	$13 K^\pm p \rightarrow (K \pi \pi)^\pm p$
~200	BRANDENB...	76	ASPK	$13 K^\pm p \rightarrow (K \pi \pi)^\pm p$
120	DAVIS	72	HBC	$12 K^+ p$
188±21	FIRESTONE	72B	DBC	$12 K^+ d$

⁶ Well described in the chiral unitary approach of GENG 07 with two poles at 1195 and 1284 MeV and widths of 246 and 146 MeV, respectively.⁷ From a model-dependent fit with Gaussian background to BRANDENBURG 76 data.

PRODUCED BY BEAMS OTHER THAN K MESONS

VALUE (MeV)	EVTs	DOCUMENT ID	TECN	CHG	COMMENT
131±21	25k	⁸ ABLIKIM	06c	BES2	$J/\psi \rightarrow \bar{K}^*(892)^0 K^+ \pi^-$
66±15	310	RODEBACK	81	HBC	$4 \pi^- p \rightarrow \Lambda K 2\pi$
60	40	CRENNELL	72	HBC	$4.5 \pi^- p \rightarrow \Lambda K 2\pi$
127 ⁺⁷ ₋₂₅		ASTIER	69	HBC	$\bar{p} p$
60	45	CRENNELL	67	HBC	$6 \pi^- p \rightarrow \Lambda K 2\pi$

⁸ Systematic errors not estimated.PRODUCED IN τ LEPTON DECAYS

VALUE (MeV)	EVTs	DOCUMENT ID	TECN	CHG	COMMENT
260 ⁺⁹⁰ ₋₇₀ ±80	7k	ASNER	00B	CLEO	$\tau^- \rightarrow K^- \pi^+ \pi^- \nu_\tau$

 $K_1(1270)$ DECAY MODES

Mode	Fraction (Γ_i/Γ)
Γ_1 $K \rho$	(42 ± 6) %
Γ_2 $K_0^*(1430) \pi$	(28 ± 4) %
Γ_3 $K^*(892) \pi$	(16 ± 5) %
Γ_4 $K \omega$	(11.0 ± 2.0) %
Γ_5 $K f_0(1370)$	(3.0 ± 2.0) %
Γ_6 γK^0	seen

 $K_1(1270)$ PARTIAL WIDTHS

$\Gamma(K \rho)$	Γ_1			
VALUE (MeV)	DOCUMENT ID	TECN	CHG	COMMENT
57±5	MAZZUCATO	79	HBC	$4.2 K^- p \rightarrow \Xi^- (K \pi \pi)^+$
75±6	CARNEGIE	77B	ASPK	$13 K^\pm p \rightarrow (K \pi \pi)^\pm p$
$\Gamma(K_0^*(1430) \pi)$ <td>Γ_2</td>	Γ_2			
VALUE (MeV)	DOCUMENT ID	TECN	CHG	COMMENT
26±6	CARNEGIE	77B	ASPK	$13 K^\pm p \rightarrow (K \pi \pi)^\pm p$

 $\Gamma(K^*(892) \pi)$

VALUE (MeV)	DOCUMENT ID	TECN	CHG	COMMENT	Γ_3
14±11	MAZZUCATO	79	HBC	$4.2 K^- p \rightarrow \Xi^- (K \pi \pi)^+$	
2±2	CARNEGIE	77B	ASPK	$13 K^\pm p \rightarrow (K \pi \pi)^\pm p$	

 $\Gamma(K \omega)$

VALUE (MeV)	DOCUMENT ID	TECN	CHG	COMMENT	Γ_4
4±4	MAZZUCATO	79	HBC	$4.2 K^- p \rightarrow \Xi^- (K \pi \pi)^+$	
24±3	CARNEGIE	77B	ASPK	$13 K^\pm p \rightarrow (K \pi \pi)^\pm p$	

 $\Gamma(K f_0(1370))$

VALUE (MeV)	DOCUMENT ID	TECN	CHG	COMMENT	Γ_5
22±5	CARNEGIE	77B	ASPK	$13 K^\pm p \rightarrow (K \pi \pi)^\pm p$	

 $\Gamma(\gamma K^0)$

VALUE (keV)	DOCUMENT ID	TECN	COMMENT	Γ_6
73.2±6.1±28.3	ALAVI-HARATI02B	KTEV	$K^+ A \rightarrow K^+ + A$	

 $K_1(1270)$ BRANCHING RATIOS

$\Gamma(K \rho)/\Gamma_{total}$	Γ_1/Γ			
0.42±0.06	⁹ DAUM	81c	CNTR	$63 K^- p \rightarrow K^- 2\pi p$
dominant	RODEBACK	81	HBC	$4 \pi^- p \rightarrow \Lambda K 2\pi$

 $\Gamma(K_0^*(1430) \pi)/\Gamma_{total}$

VALUE	DOCUMENT ID	TECN	COMMENT	Γ_2/Γ
0.28±0.04	⁹ DAUM	81c	CNTR	$63 K^- p \rightarrow K^- 2\pi p$

 $\Gamma(K^*(892) \pi)/\Gamma_{total}$

VALUE	DOCUMENT ID	TECN	COMMENT	Γ_3/Γ
0.16±0.05	⁹ DAUM	81c	CNTR	$63 K^- p \rightarrow K^- 2\pi p$

 $\Gamma(K \omega)/\Gamma_{total}$

VALUE	DOCUMENT ID	TECN	COMMENT	Γ_4/Γ
0.11±0.02	⁹ DAUM	81c	CNTR	$63 K^- p \rightarrow K^- 2\pi p$

 $\Gamma(K \omega)/\Gamma(K \rho)$

VALUE	CL%	DOCUMENT ID	TECN	COMMENT	Γ_4/Γ_1
<0.30	95	RODEBACK	81	HBC	$4 \pi^- p \rightarrow \Lambda K 2\pi$

 $\Gamma(K f_0(1370))/\Gamma_{total}$

VALUE	DOCUMENT ID	TECN	COMMENT	Γ_5/Γ
0.03±0.02	⁹ DAUM	81c	CNTR	$63 K^- p \rightarrow K^- 2\pi p$

D-wave/S-wave RATIO FOR $K_1(1270) \rightarrow K^*(892) \pi$

VALUE	DOCUMENT ID	TECN	COMMENT	
1.0±0.7	⁹ DAUM	81c	CNTR	$63 K^- p \rightarrow K^- 2\pi p$

⁹ Average from low and high t data. $K_1(1270)$ REFERENCES

GENG	07	PR D75 014017	L.S. Geng et al.	
ABLIKIM	06C	PL B633 681	M. Ablikim et al.	(BES Collab.)
ALAVI-HARATI	02B	PRL 89 072001	A. Alavi-Harati et al.	(FNAL KTeV Collab.)
ASNER	00B	PR D62 072006	D.M. Asner et al.	(CLEO Collab.)
TORNQVIST	82B	NP B203 268	N.A. Tornqvist	(HELS)
DAUM	81C	NP B187 1	C. Daum et al.	(AMST, CERN, CRAC, MPIM+)
RODEBACK	81	ZPHY C9 9	S. Rodeback et al.	(CERN, CDEF, MADR+)
MAZZUCATO	79	NP B156 532	M. Mazzucato et al.	(CERN, ZEEM, NIJM+)
VERGEEST	79	NP B158 265	J.S.M. Vergeest et al.	(NIJM, AMST, CERN+)
GAVILLET	78	PL 76B 517	P. Gavillet et al.	(AMST, CERN, NIJM+ JP)
CARNEGIE	77	NP B127 509	R.K. Carnegie et al.	(SLAC)
CARNEGIE	77B	PL 68B 287	R.K. Carnegie et al.	(SLAC)
BRANDENB...	76	PRL 36 703	G.W. Brandenburg et al.	(SLAC) JP
OTTER	76	NP B106 77	G. Otter et al.	(AACH3, BERL, CERN, LOIC+) JP
CRENNELL	72	PR D6 1220	D.J. Crennell et al.	(BNL)
DAVIS	72	PR D5 2688	P.J. Davis et al.	(LBL)
FIRESTONE	72B	PR D5 505	A. Firestone et al.	(LBL)
ASTIER	69	NP B10 65	A. Astier et al.	(CDEF, CERN, IPNP, LIPP) JP
CRENNELL	67	PRL 19 44	D.J. Crennell et al.	(BNL) 1

Meson Particle Listings

$K_1(1400), K^*(1410)$

$K_1(1400)$

$$I(J^P) = \frac{1}{2}(1^+)$$

$K_1(1400)$ MASS

VALUE (MeV)	EVTs	DOCUMENT ID	TECN	CHG	COMMENT
1403 ± 7 OUR AVERAGE					
1463 ± 64 ± 68	7k	ASNER	00B	CLEO	± $\tau^- \rightarrow K^- \pi^+ \pi^- \nu_\tau$
1373 ± 14 ± 18		¹ ASTON	87	LASS	0 11 $K^- p \rightarrow \bar{K}^0 \pi^+ \pi^- n$
1392 ± 18		BAUBILLIER	82B	HBC	0 8.25 $K^- p \rightarrow K_S^0 \pi^+ \pi^- n$
1410 ± 25		DAUM	81C	CNTR	- 63 $K^- p \rightarrow K^- 2\pi p$
1415 ± 15		ETKIN	80	MPS	0 6 $K^- p \rightarrow \bar{K}^0 \pi^+ \pi^- n$
1404 ± 10		² CARNEGIE	77	ASPK	± 13 $K^\pm p \rightarrow (K\pi\pi)^\pm p$
• • • We do not use the following data for averages, fits, limits, etc. • • •					
1418 ± 8	25k	³ ABLIKIM	06c	BES2	$J/\psi \rightarrow \bar{K}^*(892)^0 K^+ \pi^-$
~ 1350		⁴ TORNQVIST	82B	RVUE	
~ 1400		VERGEEST	79	HBC	- 4.2 $K^- p \rightarrow (\bar{K}\pi\pi)^- p$
~ 1400		BRANDENB...	76	ASPK	± 13 $K^\pm p \rightarrow (K\pi\pi)^\pm p$
1420		DAVIS	72	HBC	+ 12 $K^+ p$
1368 ± 18		FIRESTONE	72B	DBC	+ 12 $K^+ d$

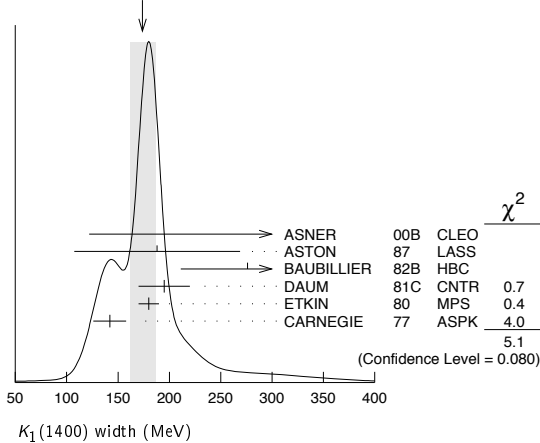
¹ From partial-wave analysis of $K^0 \pi^+ \pi^-$ system.
² From a model-dependent fit with Gaussian background to BRANDENBURG 76 data.
³ Systematic errors not estimated.
⁴ From a unitarized quark-model calculation.

$K_1(1400)$ WIDTH

VALUE (MeV)	EVTs	DOCUMENT ID	TECN	CHG	COMMENT
174 ± 13 OUR AVERAGE					Error includes scale factor of 1.6. See the ideogram below.
300 +370 -110 ± 140	7k	ASNER	00B	CLEO	± $\tau^- \rightarrow K^- \pi^+ \pi^- \nu_\tau$
188 ± 54 ± 60		⁵ ASTON	87	LASS	0 11 $K^- p \rightarrow \bar{K}^0 \pi^+ \pi^- n$
276 ± 65		BAUBILLIER	82B	HBC	0 8.25 $K^- p \rightarrow K_S^0 \pi^+ \pi^- n$
195 ± 25		DAUM	81C	CNTR	- 63 $K^- p \rightarrow K^- 2\pi p$
180 ± 10		ETKIN	80	MPS	0 6 $K^- p \rightarrow \bar{K}^0 \pi^+ \pi^- n$
142 ± 16		⁶ CARNEGIE	77	ASPK	± 13 $K^\pm p \rightarrow (K\pi\pi)^\pm p$
• • • We do not use the following data for averages, fits, limits, etc. • • •					
152 ± 16	25k	⁷ ABLIKIM	06c	BES2	$J/\psi \rightarrow \bar{K}^*(892)^0 K^+ \pi^-$
~ 200		VERGEEST	79	HBC	- 4.2 $K^- p \rightarrow (\bar{K}\pi\pi)^- p$
~ 160		BRANDENB...	76	ASPK	± 13 $K^\pm p \rightarrow (K\pi\pi)^\pm p$
80		DAVIS	72	HBC	+ 12 $K^+ p$
241 ± 30		FIRESTONE	72B	DBC	+ 12 $K^+ d$

⁵ From partial-wave analysis of $K^0 \pi^+ \pi^-$ system.
⁶ From a model-dependent fit with Gaussian background to BRANDENBURG 76 data.
⁷ Systematic errors not estimated.

WEIGHTED AVERAGE
174±13 (Error scaled by 1.6)



$K_1(1400)$ DECAY MODES

Mode	Fraction (Γ_i/Γ)
Γ_1 $K^*(892)\pi$	(94 ± 6) %
Γ_2 $K\rho$	(1.2 ± 0.6) %
Γ_3 $Kf_0(1370)$	(2.0 ± 2.0) %
Γ_4 $K\omega$	(1.0 ± 1.0) %
Γ_5 $K_0^*(1430)\pi$	not seen
Γ_6 γK^0	seen

$K_1(1400)$ PARTIAL WIDTHS

VALUE (MeV)	DOCUMENT ID	TECN	CHG	COMMENT	Γ_1
117 ± 10	CARNEGIE	77	ASPK	± 13 $K^\pm p \rightarrow (K\pi\pi)^\pm p$	
2 ± 1	CARNEGIE	77	ASPK	± 13 $K^\pm p \rightarrow (K\pi\pi)^\pm p$	Γ_2
23 ± 12	CARNEGIE	77	ASPK	± 13 $K^\pm p \rightarrow (K\pi\pi)^\pm p$	Γ_4
280.8 ± 23.2 ± 40.4	ALAVI-HARATI02B	KTEV		$K^+ A \rightarrow K^* + A$	Γ_6

$K_1(1400)$ BRANCHING RATIOS

VALUE	DOCUMENT ID	TECN	COMMENT	Γ_1/Γ
0.94 ± 0.06	⁸ DAUM	81c	CNTR 63 $K^- p \rightarrow K^- 2\pi p$	
0.03 ± 0.03	⁸ DAUM	81c	CNTR 63 $K^- p \rightarrow K^- 2\pi p$	Γ_2/Γ
0.02 ± 0.02	⁸ DAUM	81c	CNTR 63 $K^- p \rightarrow K^- 2\pi p$	Γ_3/Γ
0.01 ± 0.01	⁸ DAUM	81c	CNTR 63 $K^- p \rightarrow K^- 2\pi p$	Γ_4/Γ
not seen	⁸ DAUM	81c	CNTR 63 $K^- p \rightarrow K^- 2\pi p$	Γ_5/Γ

D-wave/S-wave RATIO FOR $K_1(1400) \rightarrow K^*(892)\pi$

VALUE	DOCUMENT ID	TECN	COMMENT
0.04 ± 0.01	⁸ DAUM	81c	CNTR 63 $K^- p \rightarrow K^- 2\pi p$

⁸ Average from low and high t data.

$K_1(1400)$ REFERENCES

ABLIKIM 06c PL B633 681 M. Ablikim et al. (BES Collab.)
 ALAVI-HARATI 02B PRL 89 072001 A. Alavi-Harati et al. (FNAL KTeV Collab.)
 ASNER 00B PR D62 072006 D.M. Asner et al. (CLEO Collab.)
 ASTON 87 NP B292 693 D. Aston et al. (SLAC, NAGO, CINC, INUS)
 BAUBILLIER 82B NP B202 21 M. Baubillier et al. (BIRM, CERN, GLAS+)
 TORNQVIST 82B NP B203 268 N.A. Tornqvist (HELS)
 DAUM 81C NP B187 1 C. Daum et al. (AMST, CERN, CRAC, MPIM+)
 ETKIN 80 PR D22 42 A. Etkin et al. (BNL, CUNY) JP
 VERGEEST 79 NP B158 265 J.S.M. Vergeest et al. (NIJM, AMST, CERN+)
 CARNEGIE 77 NP B127 509 R.K. Carnegie et al. (SLAC)
 BRANDENB... 76 PRL 36 703 G.W. Brandenburg et al. (SLAC) JP
 DAVIS 72 PR D5 2688 P.J. Davis et al. (LBL)
 FIRESTONE 72B PR D5 505 A. Firestone et al. (LBL)

$K^*(1410)$

$$I(J^P) = \frac{1}{2}(1^-)$$

$K^*(1410)$ MASS

VALUE (MeV)	DOCUMENT ID	TECN	CHG	COMMENT
1414 ± 15 OUR AVERAGE				Error includes scale factor of 1.3.
1380 ± 21 ± 19	ASTON	88	LASS	0 11 $K^- p \rightarrow K^- \pi^+ n$
1420 ± 7 ± 10	ASTON	87	LASS	0 11 $K^- p \rightarrow \bar{K}^0 \pi^+ \pi^- n$
• • • We do not use the following data for averages, fits, limits, etc. • • •				
1276 +72 -77	^{1,2} BOITO	09	RVUE	$\tau^- \rightarrow K_S^0 \pi^- \nu_\tau$
1367 ± 54	BIRD	89	LASS	- 11 $K^- p \rightarrow \bar{K}^0 \pi^- p$
1474 ± 25	BAUBILLIER	82B	HBC	0 8.25 $K^- p \rightarrow \bar{K}^0 2\pi n$
1500 ± 30	ETKIN	80	MPS	0 6 $K^- p \rightarrow \bar{K}^0 \pi^+ \pi^- n$

¹ From the pole position of the $K\pi$ vector form factor in the complex s -plane and using EPIFANOV 07 data.
² Systematic uncertainties not estimated.

$K^*(1410)$ WIDTH

VALUE (MeV)	DOCUMENT ID	TECN	CHG	COMMENT
232 ± 21 OUR AVERAGE				Error includes scale factor of 1.1.
176 ± 52 ± 22	ASTON	88	LASS	0 11 $K^- p \rightarrow K^- \pi^+ n$
240 ± 18 ± 12	ASTON	87	LASS	0 11 $K^- p \rightarrow \bar{K}^0 \pi^+ \pi^- n$

K*(1430)

CONSTRAINED FIT INFORMATION

An overall fit to the total width, a partial width, and 10 branching ratios uses 31 measurements and one constraint to determine 8 parameters. The overall fit has a chi^2 = 20.2 for 24 degrees of freedom.

The following off-diagonal array elements are the correlation coefficients <delta p_i delta p_j> / (delta p_i delta p_j), in percent, from the fit to parameters p_i, including the branching fractions, x_i = Gamma_i / Gamma_total. The fit constrains the x_i whose labels appear in this array to sum to one.

Table with correlation coefficients and branching ratios. Includes a table for Mode, Rate (MeV), and Scale factor for various decay channels like K pi, K*(892) pi, etc.

K*(1430) PARTIAL WIDTHS

Table of partial widths Gamma(K+gamma), Gamma(K0 gamma), and Gamma(K0 eta) with values, document IDs, and comments.

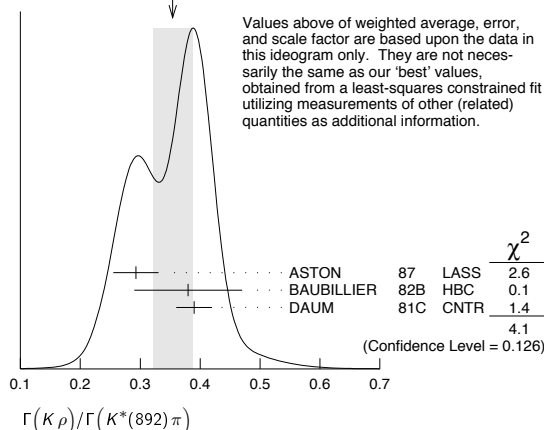
K*(1430) BRANCHING RATIOS

Table of branching ratios for various decay channels including Gamma(K pi) / Gamma_total, Gamma(K*(892) pi) / Gamma(K pi), Gamma(K omega) / Gamma(K pi), Gamma(K rho) / Gamma(K pi), and Gamma(K eta) / Gamma(K pi).

Gamma(K rho) / Gamma(K*(892) pi)

Table of Gamma(K rho) / Gamma(K*(892) pi) values from different experiments: ASTON, BAUBILLIER, DAUM.

WEIGHTED AVERAGE 0.354 +/- 0.033 (Error scaled by 1.4)



Gamma(K omega) / Gamma(K*(892) pi)

Table of Gamma(K omega) / Gamma(K*(892) pi) value from FIELD.

Gamma(K eta) / Gamma(K*(892) pi)

Table of Gamma(K eta) / Gamma(K*(892) pi) value from FIELD.

Gamma(K eta) / Gamma(K pi)

Table of Gamma(K eta) / Gamma(K pi) values from ASTON, AGUILAR..., BASSOMPIE..., BISHOP.

Gamma(K*(892) pi pi) / Gamma_total

Table of Gamma(K*(892) pi pi) / Gamma_total values from GOLDBERG.

Gamma(K*(892) pi pi) / Gamma(K pi)

Table of Gamma(K*(892) pi pi) / Gamma(K pi) values from JONGEJANS.

Gamma(K omega pi) / Gamma_total

Table of Gamma(K omega pi) / Gamma_total values from JONGEJANS with detailed comments.

K*(1430) REFERENCES

Table of references for K*(1430) from various sources like AUBERT, ALAVI-HARATI, BIRD, etc.

Meson Particle Listings

 $K_2^*(1430)$, $K(1460)$, $K_2(1580)$, $K(1630)$

ETKIN	80	PR D22 42	A. Etkin <i>et al.</i>	(BNL, CUNY) JP
ESTABROOKS	78	NP B133 490	P.G. Estabrooks <i>et al.</i>	(MCGI, CARL, DURH+)
Also		PR D17 658	P.G. Estabrooks <i>et al.</i>	(MCGI, CARL, DURH+)
JONGEJANS	78	NP B139 383	B. Jongejans <i>et al.</i>	(ZEEM, CERN, NIJM+)
MARTIN	78	NP B134 392	A.D. Martin <i>et al.</i>	(DURH, GEVA)
BOWLER	77	NP B126 31	M.G. Bowler <i>et al.</i>	(OXF)
GOLDBERG	76	LNC 17 253	J. Goldberg	(HAIF)
HENDRICK	76	NP B112 189	K. Hendrickx <i>et al.</i>	(MONS, SAFL, PARIS+)
LAUSCHER	75	NP B86 189	P. Lauscher <i>et al.</i>	(ABCLV Collab.) JP
MCCUBBIN	75	NP B86 13	N.A. McCubbin, L. Lyons	(OXF)
DEHM	74	NP B75 47	G. Dehm <i>et al.</i>	(MPIM, BRUX, MONS, CERN)
LINGLIN	73	NP B55 408	D. Linglin	(CERN)
AGUILAR...	71B	PR D4 2583	M. Aguilar-Benitez, R.L. Eisner, J.B. Kinson	(BNL)
BARNHAM	71C	NP B28 171	K.W.J. Barnham <i>et al.</i>	(BIRM, GLAS)
CORDS	71	PR D4 1974	D. Cords <i>et al.</i>	(PURD, UCD, IUPU)
BASSOMPIERRE...	69	NP B13 189	G. Bassompierre <i>et al.</i>	(CERN, BRUX) JP
BISHOP	69	NP B9 403	J.M. Bishop <i>et al.</i>	(WIS C)
CRENNELL	69D	PRL 22 487	D.J. Crennell <i>et al.</i>	(BNL)
DAVIS	69	PRL 23 1071	P.J. Davis <i>et al.</i>	(LRL)
LIND	69	NP B34 1	V.G. Lind <i>et al.</i>	(LRL) JP
SCHWEING...	68	PR 166 1317	F. Schweingruber <i>et al.</i>	(ANL, NWES)
Also		Thesis	F.L. Schweingruber	(NWES, NWES)
BASSANO	67	PRL 19 968	D. Bassano <i>et al.</i>	(BNL, SYRA)
FIELD	67	PL 24B 638	J.H. Field <i>et al.</i>	(UCSD)
BADIER	65C	PL 19 612	J. Badier <i>et al.</i>	(EPOL, SAFL, AMST)

 $K(1460)$

$$I(J^P) = \frac{1}{2}(0^-)$$

OMITTED FROM SUMMARY TABLE

Observed in $K\pi\pi$ partial-wave analysis. $K(1460)$ MASS

VALUE (MeV)	DOCUMENT ID	TECN	CHG	COMMENT
••• We do not use the following data for averages, fits, limits, etc. •••				
~ 1460	DAUM	81c CNTR	-	63 $K^-p \rightarrow K^-2\pi p$
~ 1400	¹ BRANDENB...	76B ASPK	±	13 $K^\pm p \rightarrow K^\pm 2\pi p$
¹ Coupled mainly to $K f_0(1370)$. Decay into $K^*(892)\pi$ seen.				

 $K(1460)$ WIDTH

VALUE (MeV)	DOCUMENT ID	TECN	CHG	COMMENT
••• We do not use the following data for averages, fits, limits, etc. •••				
~ 260	DAUM	81c CNTR	-	63 $K^-p \rightarrow K^-2\pi p$
~ 250	² BRANDENB...	76B ASPK	±	13 $K^\pm p \rightarrow K^\pm 2\pi p$
² Coupled mainly to $K f_0(1370)$. Decay into $K^*(892)\pi$ seen.				

 $K(1460)$ DECAY MODES

Mode	Fraction (Γ_i/Γ)
Γ_1 $K^*(892)\pi$	seen
Γ_2 $K\rho$	seen
Γ_3 $K_0^*(1430)\pi$	seen

 $K(1460)$ PARTIAL WIDTHS

$\Gamma(K^*(892)\pi)$	Γ_1		
VALUE (MeV)	DOCUMENT ID	TECN	COMMENT
••• We do not use the following data for averages, fits, limits, etc. •••			
~ 109	DAUM	81c CNTR	63 $K^-p \rightarrow K^-2\pi p$
$\Gamma(K\rho)$	Γ_2		
VALUE (MeV)	DOCUMENT ID	TECN	COMMENT
••• We do not use the following data for averages, fits, limits, etc. •••			
~ 34	DAUM	81c CNTR	63 $K^-p \rightarrow K^-2\pi p$
$\Gamma(K_0^*(1430)\pi)$	Γ_3		
VALUE (MeV)	DOCUMENT ID	TECN	COMMENT
••• We do not use the following data for averages, fits, limits, etc. •••			
~ 117	DAUM	81c CNTR	63 $K^-p \rightarrow K^-2\pi p$

 $K(1460)$ REFERENCES

DAUM	81c	NP B187 1	C. Daum <i>et al.</i>	(AMST, CERN, CRAC, MPIM+)
BRANDENB...	76B	PRL 36 1239	G.W. Brandenburg <i>et al.</i>	(SLAC) JP

 $K_2(1580)$

$$I(J^P) = \frac{1}{2}(2^-)$$

OMITTED FROM SUMMARY TABLE

Seen in partial-wave analysis of the $K^-\pi^+\pi^-$ system. Needs confirmation. $K_2(1580)$ MASS

VALUE (MeV)	DOCUMENT ID	CHG	COMMENT
••• We do not use the following data for averages, fits, limits, etc. •••			
~ 1580	OTTER	79 -	10,14,16 K^-p

 $K_2(1580)$ WIDTH

VALUE (MeV)	DOCUMENT ID	CHG	COMMENT
••• We do not use the following data for averages, fits, limits, etc. •••			
~ 110	OTTER	79 -	10,14,16 K^-p

 $K_2(1580)$ DECAY MODES

Mode	Fraction (Γ_i/Γ)
Γ_1 $K^*(892)\pi$	seen
Γ_2 $K_2^*(1430)\pi$	possibly seen

 $K_2(1580)$ BRANCHING RATIOS

$\Gamma(K^*(892)\pi)/\Gamma_{\text{total}}$	Γ_1/Γ			
VALUE	DOCUMENT ID	TECN	CHG	COMMENT
seen	OTTER	79	HBC	- 10,14,16 K^-p

$\Gamma(K_2^*(1430)\pi)/\Gamma_{\text{total}}$	Γ_2/Γ			
VALUE	DOCUMENT ID	TECN	CHG	COMMENT
possibly seen	OTTER	79	HBC	- 10,14,16 K^-p

 $K_2(1580)$ REFERENCES

OTTER	79	NP B147 1	G. Otter <i>et al.</i>	(AACH3, BERL, CERN, LOIC+) JP
-------	----	-----------	------------------------	-------------------------------

 $K(1630)$

$$I(J^P) = \frac{1}{2}(?^-)$$

OMITTED FROM SUMMARY TABLE

Seen as a narrow peak, compatible with the experimental resolution, in the invariant mass of the $K_S^0\pi^+\pi^-$ system produced in $\pi^-\pi^-$ interactions at high momentum transfers. $K(1630)$ MASS

VALUE (MeV)	EVTS	DOCUMENT ID	TECN	COMMENT
1629 ± 7	~ 75	KARNAUKHOV98	BC	16.0 $\pi^-\pi^- \rightarrow (K_S^0\pi^+\pi^-) X^+\pi^- X^0$

 $K(1630)$ WIDTH

VALUE (MeV)	EVTS	DOCUMENT ID	TECN	COMMENT
16_{-16}^{+19}	~ 75	¹ KARNAUKHOV98	BC	16.0 $\pi^-\pi^- \rightarrow (K_S^0\pi^+\pi^-) X^+\pi^- X^0$

¹ Compatible with an experimental resolution of 14 ± 1 MeV. $K(1630)$ DECAY MODES

Mode
Γ_1 $K_S^0\pi^+\pi^-$

 $K(1630)$ REFERENCES

KARNAUKHOV 98	PAN 61 203	V.M. Karnaukhov, C. Cocco, V.I. Moroz
Translated from YAF 61 252.		

See key on page 405

Meson Particle Listings

$K_1(1650)$, $K^*(1680)$, $K_2(1770)$

 $K_1(1650)$

$$I(J^P) = \frac{1}{2}(1^+)$$

OMITTED FROM SUMMARY TABLE

This entry contains various peaks in strange meson systems ($K^+\phi$, $K\pi\pi$) reported in partial-wave analysis in the 1600–1900 mass region.

 $K_1(1650)$ MASS

VALUE (MeV)	DOCUMENT ID	TECN	CHG	COMMENT
1650±50	FRAME	86	OMEG +	13 $K^+p \rightarrow \phi K^+p$
••• We do not use the following data for averages, fits, limits, etc. •••				
~1840	ARMSTRONG	83	OMEG -	18.5 $K^-p \rightarrow 3Kp$
~1800	DAUM	81c	CNTR -	63 $K^-p \rightarrow K^-2\pi p$

 $K_1(1650)$ WIDTH

VALUE (MeV)	DOCUMENT ID	TECN	CHG	COMMENT
150±50	FRAME	86	OMEG +	13 $K^+p \rightarrow \phi K^+p$
••• We do not use the following data for averages, fits, limits, etc. •••				
~250	DAUM	81c	CNTR -	63 $K^-p \rightarrow K^-2\pi p$

 $K_1(1650)$ DECAY MODES

Mode	Fraction (Γ_i/Γ)
Γ_1 $K\pi\pi$	(38.7±2.5) %
Γ_2 $K\phi$	(31.4 $^{+5.0}_{-2.1}$) %

 $K_1(1650)$ REFERENCES

FRAME	86	NP B276 667	D. Frame et al.	(GLAS)
ARMSTRONG	83	NP B221 1	T.A. Armstrong et al.	(BARI, BIRM, CERN+)
DAUM	81c	NP B187 1	C. Daum et al.	(AMST, CERN, CRAC, MPIM+)

 $K^*(1680)$

$$I(J^P) = \frac{1}{2}(1^-)$$

 $K^*(1680)$ MASS

VALUE (MeV)	DOCUMENT ID	TECN	CHG	COMMENT
1717±27 OUR AVERAGE	Error includes scale factor of 1.4.			
1677±10±32	ASTON	88	LASS 0	11 $K^-p \rightarrow K^-\pi^+n$
1735±10±20	ASTON	87	LASS 0	11 $K^-p \rightarrow \bar{K}^0\pi^+\pi^-n$
••• We do not use the following data for averages, fits, limits, etc. •••				
1678±64	BIRD	89	LASS -	11 $K^-p \rightarrow \bar{K}^0\pi^-p$
1800±70	ETKIN	80	MPS 0	6 $K^-p \rightarrow \bar{K}^0\pi^+\pi^-n$
~1650	ESTABROOKS	78	ASPK 0	13 $K^\pm p \rightarrow K^\pm\pi^\pm n$

 $K^*(1680)$ WIDTH

VALUE (MeV)	DOCUMENT ID	TECN	CHG	COMMENT
322±110 OUR AVERAGE	Error includes scale factor of 4.2.			
205±16±34	ASTON	88	LASS 0	11 $K^-p \rightarrow K^-\pi^+n$
423±18±30	ASTON	87	LASS 0	11 $K^-p \rightarrow \bar{K}^0\pi^+\pi^-n$
••• We do not use the following data for averages, fits, limits, etc. •••				
454±270	BIRD	89	LASS -	11 $K^-p \rightarrow \bar{K}^0\pi^-p$
170±30	ETKIN	80	MPS 0	6 $K^-p \rightarrow \bar{K}^0\pi^+\pi^-n$
250 to 300	ESTABROOKS	78	ASPK 0	13 $K^\pm p \rightarrow K^\pm\pi^\pm n$

 $K^*(1680)$ DECAY MODES

Mode	Fraction (Γ_i/Γ)
Γ_1 $K\pi$	(38.7±2.5) %
Γ_2 $K\rho$	(31.4 $^{+5.0}_{-2.1}$) %
Γ_3 $K^*(892)\pi$	(29.9 $^{+2.2}_{-5.0}$) %

CONSTRAINED FIT INFORMATION

An overall fit to 4 branching ratios uses 4 measurements and one constraint to determine 3 parameters. The overall fit has a $\chi^2 = 2.9$ for 2 degrees of freedom.

The following *off-diagonal* array elements are the correlation coefficients $\langle \delta x_i \delta x_j \rangle / (\delta x_i \delta x_j)$, in percent, from the fit to the branching fractions, $x_i \equiv \Gamma_i/\Gamma_{\text{total}}$. The fit constrains the x_i whose labels appear in this array to sum to one.

$$\begin{matrix} x_2 & \begin{matrix} -36 \\ -39 \end{matrix} \\ x_3 & \begin{matrix} -39 & -72 \\ x_1 & x_2 \end{matrix} \end{matrix}$$

 $K^*(1680)$ BRANCHING RATIOS

$\Gamma(K\pi)/\Gamma_{\text{total}}$	DOCUMENT ID	TECN	CHG	COMMENT	Γ_1/Γ
0.387±0.026 OUR FIT					
0.388±0.014±0.022	ASTON	88	LASS 0	11 $K^-p \rightarrow K^-\pi^+n$	

$\Gamma(K\pi)/\Gamma(K^*(892)\pi)$	DOCUMENT ID	TECN	CHG	COMMENT	Γ_1/Γ_3
1.30$^{+0.23}_{-0.14}$ OUR FIT					
2.8 ±1.1	ASTON	84	LASS 0	11 $K^-p \rightarrow \bar{K}^0 2\pi n$	

$\Gamma(K\rho)/\Gamma(K\pi)$	DOCUMENT ID	TECN	CHG	COMMENT	Γ_2/Γ_1
0.81$^{+0.14}_{-0.09}$ OUR FIT					
1.2 ±0.4	ASTON	84	LASS 0	11 $K^-p \rightarrow \bar{K}^0 2\pi n$	

$\Gamma(K\rho)/\Gamma(K^*(892)\pi)$	DOCUMENT ID	TECN	CHG	COMMENT	Γ_2/Γ_3
1.05$^{+0.27}_{-0.11}$ OUR FIT					
0.97±0.09$^{+0.30}_{-0.10}$	ASTON	87	LASS 0	11 $K^-p \rightarrow \bar{K}^0\pi^+\pi^-n$	

 $K^*(1680)$ REFERENCES

BIRD	89	SLAC-332	P.F. Bird	(SLAC)
ASTON	88	NP B296 493	D. Aston et al.	(SLAC, NAGO, CINC, INUS)
ASTON	87	NP B292 693	D. Aston et al.	(SLAC, NAGO, CINC, INUS)
ASTON	84	PL 149B 258	D. Aston et al.	(SLAC, CARL, OTTA)JP
ETKIN	80	PR D22 42	A. Etkin et al.	(BNL, CUNY)JP
ESTABROOKS	78	NP B133 490	P.G. Estabrooks et al.	(MCGI, CARL, DURH+)JP

 $K_2(1770)$

$$I(J^P) = \frac{1}{2}(2^-)$$

See our mini-review in the 2004 edition of this Review, PDG 04.

 $K_2(1770)$ MASS

VALUE (MeV)	EVTS	DOCUMENT ID	TECN	CHG	COMMENT
1773±8		¹ ASTON	93	LASS	11 $K^-p \rightarrow K^-\omega p$
••• We do not use the following data for averages, fits, limits, etc. •••					
1743±15		TIKHOMIROV	03	SPEC	40.0 $\pi^- C \rightarrow K_S^0 K_S^0 K_L^0 X$
~1730		FRAME	86	OMEG +	13 $K^+p \rightarrow \phi K^+p$
~1780		ARMSTRONG	83	OMEG -	18.5 $K^-p \rightarrow 3Kp$
1710±15	60	DAUM	81c	CNTR -	63 $K^-p \rightarrow K^-2\pi p$
1767±6		CHUNG	74	HBC -	7.3 $K^-p \rightarrow K^-\omega p$
1730±20	306	BLIEDEN	72	MMS -	11-16 K^-p
1765±40		FIRESTONE	72B	DBC +	12 K^+d
1740		COLLEY	71	HBC +	10 $K^+p \rightarrow K_2\pi N$
1745±20		DENEGRI	71	DBC -	12.6 $K^-d \rightarrow \bar{K}2\pi d$
1780±15		AGUILAR...	70c	HBC -	4.6 K^-p
1760±15		BARTSCH	70c	HBC -	10.1 K^-p
		LUDLAM	70	HBC -	12.6 K^-p

- From a partial wave analysis of the K^-p system.
- From a partial wave analysis of the $K^-2\pi$ system.
- Produced in conjunction with excited deuteron.
- Systematic errors added correspond to spread of different fits.

 $K_2(1770)$ WIDTH

VALUE (MeV)	EVTS	DOCUMENT ID	TECN	CHG	COMMENT
186±14		⁵ ASTON	93	LASS	11 $K^-p \rightarrow K^-\omega p$

Meson Particle Listings

$K_2(1770)$, $K_3^*(1780)$

• • • We do not use the following data for averages, fits, limits, etc. • • •

Table with 4 columns: Value (e.g., 147±70), Author (e.g., TIKHOMIROV), Experiment (e.g., 03), and Decay Mode (e.g., $40.0 \frac{\pi^- C \rightarrow}{K_S^0 K_S^0 K_L^0 X}$).

5 From a partial wave analysis of the $K^-\omega$ system.
6 From a partial wave analysis of the $K^-2\pi$ system.
7 Produced in conjunction with excited deuteron.
8 Systematic errors added correspond to spread of different fits.

$K_2(1770)$ REFERENCES

PDG 04 PL B592 1 S. Eidelman et al. (PDG Collab.)
TIKHOMIROV 03 PAN 66 828 G.D. Tikhomirov et al.
ASTON 93 PL B308 186 D. Aston et al. (SLAC, NAGO, CINC, INUS)
FRAME 86 NP B276 667 D. Frame et al. (GLAS)
ARMSTRONG 83 NP B221 1 T.A. Armstrong et al. (BARI, BIRM, CERN+)
DAUM 81C NP B187 1 C. Daum et al. (AMST, CERN, CRAC, MPIM+)
OTTER 81 NP B181 1 G. Otter (AACH3, BERL, LOIC, VIEN, BIRM+)
CHUNG 74 PL 51B 413 S.U. Chung et al. (BNL)
BLIEDEN 72 PL 39B 668 H.R. Blieden et al. (STON, NEAS)
FIRESTONE 72B PR D5 505 A. Firestone et al. (LBL)
COLLEY 71 NP B26 71 D.C. Colley et al. (BIRM, GLAS)
DENEGRÍ 71 NP B28 13 D. Denegri et al. (JHU JP)
AGUILAR... 70C PRL 25 54 M. Aguilar-Benitez et al. (BNL)
BARTSCH 70C PL 33B 186 J. Bartsch et al. (AACH, BERL, CERN+)
LUDLAM 70 PR D2 1234 T. Ludlam, J. Sandweiss, A.J. Slaughter (YALE)
BARBARO... 69 PRL 22 1207 A. Barbaro-Galsteri et al. (LRL)

$K_3^*(1780)$

$I(J^P) = \frac{1}{2}(3^-)$

$K_2^*(1780)$ MASS

Table with columns: VALUE (MeV), EVTS, DOCUMENT ID, TECN, CHG, COMMENT. Includes '1776±7 OUR AVERAGE' and various reference data points.

• • • We do not use the following data for averages, fits, limits, etc. • • •

$K_2(1770)$ DECAY MODES

Table with 2 columns: Mode (e.g., $K \pi \pi$) and Fraction (Γ_i/Γ).

$K_2(1770)$ BRANCHING RATIOS

$\Gamma(K_2^*(1430)\pi)/\Gamma(K\pi\pi)$ Γ_2/Γ_1

Table with columns: VALUE, DOCUMENT ID, TECN, CHG, COMMENT. Includes branching ratio data for $K_2^*(1430)\pi$ and $K_2^*(1270)\pi$.

$\Gamma(K^*(892)\pi)/\Gamma(K\pi\pi)$ Γ_3/Γ_1

Table with columns: VALUE, DOCUMENT ID, TECN, COMMENT. Includes branching ratio data for $K^*(892)\pi$.

$\Gamma(K f_2(1270))/\Gamma(K\pi\pi)$ Γ_4/Γ_1

Table with columns: VALUE, DOCUMENT ID, TECN, COMMENT. Includes branching ratio data for $K f_2(1270)$.

$\Gamma(K f_0(980))/\Gamma_{total}$ Γ_5/Γ

Table with columns: VALUE, DOCUMENT ID, TECN, COMMENT. Includes branching ratio data for $K f_0(980)$.

$\Gamma(K\phi)/\Gamma_{total}$ Γ_6/Γ

Table with columns: VALUE, DOCUMENT ID, TECN, CHG, COMMENT. Includes branching ratio data for $K\phi$.

$\Gamma(K\omega)/\Gamma_{total}$ Γ_7/Γ

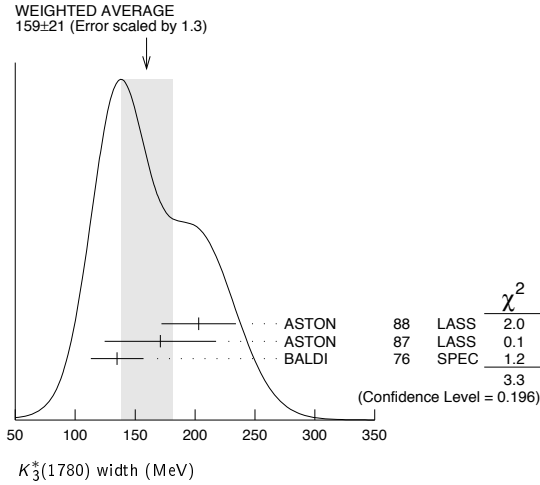
Table with columns: VALUE, DOCUMENT ID, TECN, CHG, COMMENT. Includes branching ratio data for $K\omega$.

$K_3^*(1780)$ WIDTH

Table with columns: VALUE (MeV), EVTS, DOCUMENT ID, TECN, CHG, COMMENT. Includes width data for $K_3^*(1780)$ and various reference data points.

$K_3^*(1780), K_2(1820)$

- ⁶ From energy-independent partial-wave analysis.
- ⁷ From a fit to Y_6^2 moment. $J^P = 3^-$ found.
- ⁸ From a partial wave amplitude analysis.
- ⁹ From a fit to Y_6^0 moment.
- ¹⁰ Errors enlarged by us to $4\Gamma/\sqrt{N}$; see the note with the $K^*(892)$ mass.
- ¹¹ ESTABROOKS 78 find that BRANDENBURG 76D data are consistent with 175 MeV width. Not averaged.



$K_3^*(1780)$ DECAY MODES

Mode	Fraction (Γ_i/Γ)	Confidence level
Γ_1 $K\rho$	(31 ± 9) %	
Γ_2 $K^*(892)\pi$	(20 ± 5) %	
Γ_3 $K\pi$	(18.8 ± 1.0) %	
Γ_4 $K\eta$	(30 ± 13) %	
Γ_5 $K_2^*(1430)\pi$	< 16 %	95%

CONSTRAINED FIT INFORMATION

An overall fit to 3 branching ratios uses 4 measurements and one constraint to determine 4 parameters. The overall fit has a $\chi^2 = 0.0$ for 1 degrees of freedom.

The following off-diagonal array elements are the correlation coefficients $\langle \delta x_i \delta x_j \rangle / (\delta x_i \delta x_j)$, in percent, from the fit to the branching fractions, $x_i \equiv \Gamma_i/\Gamma_{\text{total}}$. The fit constrains the x_i whose labels appear in this array to sum to one.

x_2	85		
x_3	18	21	
x_4	-98	-94	-27
	x_1	x_2	x_3

$K_3^*(1780)$ BRANCHING RATIOS

$\Gamma(K\rho)/\Gamma(K^*(892)\pi)$	Γ_1/Γ_2			
VALUE	DOCUMENT ID	TECN	CHG	COMMENT
1.52 ± 0.23 OUR FIT				
1.52 ± 0.21 ± 0.10	ASTON	87	LASS	0 11 $K^-p \rightarrow \bar{K}^0 \pi^+ \pi^- n$
$\Gamma(K^*(892)\pi)/\Gamma(K\pi)$	Γ_2/Γ_3			
VALUE	DOCUMENT ID	TECN	CHG	COMMENT
1.09 ± 0.26 OUR FIT				
1.09 ± 0.26	ASTON	84B	LASS	0 11 $K^-p \rightarrow \bar{K}^0 2\pi n$
$\Gamma(K\pi)/\Gamma_{\text{total}}$	Γ_3/Γ			
VALUE	DOCUMENT ID	TECN	CHG	COMMENT
0.188 ± 0.010 OUR FIT				
0.188 ± 0.010 OUR AVERAGE				
0.187 ± 0.008 ± 0.008	ASTON	88	LASS	0 11 $K^-p \rightarrow K^- \pi^+ n$
0.19 ± 0.02	ESTABROOKS	78	ASPK	0 13 $K^\pm p \rightarrow K\pi n$
$\Gamma(K\eta)/\Gamma(K\pi)$	Γ_4/Γ_3			
VALUE	DOCUMENT ID	TECN	CHG	COMMENT
1.6 ± 0.7 OUR FIT				
• • • We do not use the following data for averages, fits, limits, etc. • • •				
0.41 ± 0.050	¹² BIRD	89	LASS	- 11 $K^-p \rightarrow \bar{K}^0 \pi^- p$
0.50 ± 0.18	ASTON	88B	LASS	- 11 $K^-p \rightarrow K^- \eta p$

¹²This result supersedes ASTON 88B.

$\Gamma(K_2^*(1430)\pi)/\Gamma(K^*(892)\pi)$	Γ_5/Γ_2			
VALUE	DOCUMENT ID	TECN	CHG	COMMENT
< 0.78	95	ASTON	87	LASS 0 11 $K^-p \rightarrow \bar{K}^0 \pi^+ \pi^- n$

$K_3^*(1780)$ REFERENCES

BIRD	89	SLAC-332	P.F. Bird	(SLAC)
ASTON	88	NP B296 493	D. Aston et al.	(SLAC, NAGO, CINC, INUS)
ASTON	88B	PL B201 169	D. Aston et al.	(SLAC, NAGO, CINC, INUS) JP
ASTON	87	NP B292 693	D. Aston et al.	(SLAC, NAGO, CINC, INUS)
ASTON	84B	NP B247 261	D. Aston et al.	(SLAC, CARL, OTTA)
BAUBILLIER	84B	ZPHY C26 37	M. Baubillier et al.	(BIRM, CERN, GLAS+)
BAUBILLIER	82B	NP B202 21	M. Baubillier et al.	(BIRM, CERN, GLAS+)
CLELAND	82	NP B208 189	W.E. Cleland et al.	(DURH, GEVA, LAUS+)
ASTON	81D	PL 99B 502	D. Aston et al.	(SLAC, CARL, OTTA) JP
TOAFF	81	PR D23 1500	S. Toaff et al.	(ANL, KANS)
ETKIN	80	PR D22 42	A. Etkin et al.	(BNL, CUNY) JP
BEUSCH	78	PL 74B 282	W. Beusch et al.	(CERN, AACH3, ETH) JP
CHUNG	78	PRL 40 355	S.U. Chung et al.	(BNL, BRAN, CUNY+) JP
ESTABROOKS	78	NP B133 490	P.G. Estabrooks et al.	(MCGI, CARL, DURH+) JP
Also		PR D17 658	P.G. Estabrooks et al.	(MCGI, CARL, DURH+)
BALDI	76	PL 63B 344	R. Baldi et al.	(GEVA) JP
BRANDENB...	76D	PL 60B 478	G.W. Brandenburg et al.	(SLAC) JP

$K_2(1820)$

$I(J^P) = \frac{1}{2}(2^-)$

See our mini-review in the 2004 edition of this Review (PDG 04) under $K_2(1770)$.

$K_2(1820)$ MASS

VALUE (MeV)	DOCUMENT ID	TECN	COMMENT
1816 ± 13	¹ ASTON	93	LASS 11 $K^-p \rightarrow K^- \omega p$
• • • We do not use the following data for averages, fits, limits, etc. • • •			
~ 1840	² DAUM	81c	CNTR 63 $K^-p \rightarrow K^- 2\pi p$
¹ From a partial wave analysis of the $K^- \omega$ system.			
² From a partial wave analysis of the $K^- 2\pi$ system.			

$K_2(1820)$ WIDTH

VALUE (MeV)	DOCUMENT ID	TECN	COMMENT
276 ± 35	³ ASTON	93	LASS 11 $K^-p \rightarrow K^- \omega p$
• • • We do not use the following data for averages, fits, limits, etc. • • •			
~ 230	⁴ DAUM	81c	CNTR 63 $K^-p \rightarrow K^- 2\pi p$
³ From a partial wave analysis of the $K^- \omega$ system.			
⁴ From a partial wave analysis of the $K^- 2\pi$ system.			

$K_2(1820)$ DECAY MODES

Mode	Fraction (Γ_i/Γ)
Γ_1 $K\pi\pi$	
Γ_2 $K_2^*(1430)\pi$	seen
Γ_3 $K^*(892)\pi$	seen
Γ_4 $K f_2(1270)$	seen
Γ_5 $K\omega$	seen

$K_2(1820)$ BRANCHING RATIOS

$\Gamma(K_2^*(1430)\pi)/\Gamma(K\pi\pi)$	Γ_2/Γ_1		
VALUE	DOCUMENT ID	TECN	COMMENT
• • • We do not use the following data for averages, fits, limits, etc. • • •			
~ 0.77	DAUM	81c	CNTR 63 $K^-p \rightarrow \bar{K} 2\pi p$
$\Gamma(K^*(892)\pi)/\Gamma(K\pi\pi)$	Γ_3/Γ_1		
VALUE	DOCUMENT ID	TECN	COMMENT
• • • We do not use the following data for averages, fits, limits, etc. • • •			
~ 0.05	DAUM	81c	CNTR 63 $K^-p \rightarrow \bar{K} 2\pi p$
$\Gamma(K f_2(1270))/\Gamma(K\pi\pi)$	Γ_4/Γ_1		
VALUE	DOCUMENT ID	TECN	COMMENT
• • • We do not use the following data for averages, fits, limits, etc. • • •			
~ 0.18	DAUM	81c	CNTR 63 $K^-p \rightarrow \bar{K} 2\pi p$

$K_2(1820)$ REFERENCES

PDG	04	PL B592 1	S. Eitelman et al.	(PDG Collab.)
ASTON	93	PL B308 186	D. Aston et al.	(SLAC, NAGO, CINC, INUS)
DAUM	81c	NP B187 1	C. Daum et al.	(AMST, CERN, CRAC, MPIM+)

Meson Particle Listings

 $K(1830)$, $K_0^*(1950)$, $K_2^*(1980)$, $K_4^*(2045)$ $K(1830)$

$$I(J^P) = \frac{1}{2}(0^-)$$

OMITTED FROM SUMMARY TABLE

Seen in partial-wave analysis of $K^- \phi$ system. Needs confirmation. $K(1830)$ MASS

VALUE (MeV)	DOCUMENT ID	TECN	CHG	COMMENT
••• We do not use the following data for averages, fits, limits, etc. •••				
~1830	ARMSTRONG 83	OMEG	-	18.5 $K^- p \rightarrow 3Kp$

 $K(1830)$ WIDTH

VALUE (MeV)	DOCUMENT ID	TECN	CHG	COMMENT
••• We do not use the following data for averages, fits, limits, etc. •••				
~250	ARMSTRONG 83	OMEG	-	18.5 $K^- p \rightarrow 3Kp$

 $K(1830)$ DECAY MODES

Mode	Fraction (Γ_i/Γ)
Γ_1 $K \phi$	

 $K(1830)$ REFERENCESARMSTRONG 83 NP B221 1 T.A. Armstrong *et al.* (BARI, BIRM, CERN+)JP $K_0^*(1950)$

$$I(J^P) = \frac{1}{2}(0^+)$$

OMITTED FROM SUMMARY TABLE

Seen in partial-wave analysis of the $K^- \pi^+$ system. Needs confirmation. $K_0^*(1950)$ MASS

VALUE (MeV)	DOCUMENT ID	TECN	CHG	COMMENT
1945 ± 10 ± 20	¹ ASTON 88	LASS	0	11 $K^- p \rightarrow K^- \pi^+ n$
••• We do not use the following data for averages, fits, limits, etc. •••				
1917 ± 12	² ZHOU 06	RVUE		$Kp \rightarrow K^- \pi^+ n$
1820 ± 40	³ ANISOVICH 97c	RVUE		11 $K^- p \rightarrow K^- \pi^+ n$

¹ We take the central value of the two solutions and the larger error given.² S-matrix pole. Using ASTON 88 and assuming $K_0^*(800)$, $K_0^*(1430)$.³ T-matrix pole. Reanalysis of ASTON 88 data. $K_0^*(1950)$ WIDTH

VALUE (MeV)	DOCUMENT ID	TECN	CHG	COMMENT
201 ± 34 ± 79	⁴ ASTON 88	LASS	0	11 $K^- p \rightarrow K^- \pi^+ n$
••• We do not use the following data for averages, fits, limits, etc. •••				
145 ± 38	⁵ ZHOU 06	RVUE		$Kp \rightarrow K^- \pi^+ n$
250 ± 100	⁶ ANISOVICH 97c	RVUE		11 $K^- p \rightarrow K^- \pi^+ n$

⁴ We take the central value of the two solutions and the larger error given.⁵ S-matrix pole. Using ASTON 88 and assuming $K_0^*(800)$, $K_0^*(1430)$.⁶ T-matrix pole. Reanalysis of ASTON 88 data. $K_0^*(1950)$ DECAY MODES

Mode	Fraction (Γ_i/Γ)
Γ_1 $K \pi$	(52 ± 14) %

 $K_0^*(1950)$ BRANCHING RATIOS

$\Gamma(K \pi)/\Gamma_{\text{total}}$	DOCUMENT ID	TECN	CHG	COMMENT	Γ_1/Γ
0.52 ± 0.08 ± 0.12	⁷ ASTON 88	LASS	0	11 $K^- p \rightarrow K^- \pi^+ n$	
••• We do not use the following data for averages, fits, limits, etc. •••					
~0.60	⁸ ZHOU 06	RVUE		$Kp \rightarrow K^- \pi^+ n$	

⁷ We take the central value of the two solutions and the larger error given.⁸ S-matrix pole. Using ASTON 88 and assuming $K_0^*(800)$, $K_0^*(1430)$. $K_0^*(1950)$ REFERENCESZHOU 06 NP A775 212 Z.Y. Zhou, H.Q. Zheng
ANISOVICH 97c PL B413 137 A.V. Anisovich, A.V. Sarantsev
ASTON 88 NP B296 493 D. Aston *et al.* (SLAC, NAGO, CINC, INUS) $K_2^*(1980)$

$$I(J^P) = \frac{1}{2}(2^+)$$

OMITTED FROM SUMMARY TABLE

Needs confirmation.

 $K_2^*(1980)$ MASS

VALUE (MeV)	EVTS	DOCUMENT ID	TECN	CHG	COMMENT
1973 ± 8 ± 25		ASTON 87	LASS	0	11 $K^- p \rightarrow \bar{K}^0 \pi^+ \pi^- n$
••• We do not use the following data for averages, fits, limits, etc. •••					
2020 ± 20		TIKHOMIROV 03	SPEC		40.0 $\bar{K}^0 \pi^+ \pi^- n$ $K_S^0 K_S^0 K_L^0 X$
1978 ± 40	241 ± 47	BIRD 89	LASS	-	11 $K^- p \rightarrow \bar{K}^0 \pi^- p$

 $K_2^*(1980)$ WIDTH

VALUE (MeV)	EVTS	DOCUMENT ID	TECN	CHG	COMMENT
373 ± 33 ± 60		ASTON 87	LASS	0	11 $K^- p \rightarrow \bar{K}^0 \pi^+ \pi^- n$
••• We do not use the following data for averages, fits, limits, etc. •••					
180 ± 70		TIKHOMIROV 03	SPEC		40.0 $\bar{K}^0 \pi^+ \pi^- n$ $K_S^0 K_S^0 K_L^0 X$
398 ± 47	241 ± 47	BIRD 89	LASS	-	11 $K^- p \rightarrow \bar{K}^0 \pi^- p$

 $K_2^*(1980)$ DECAY MODES

Mode	Fraction (Γ_i/Γ)
Γ_1 $K^*(892) \pi$	
Γ_2 $K \rho$	
Γ_3 $K f_2(1270)$	

 $K_2^*(1980)$ BRANCHING RATIOS

$\Gamma(K \rho)/\Gamma(K^*(892) \pi)$	DOCUMENT ID	TECN	CHG	COMMENT	Γ_2/Γ_1
1.49 ± 0.24 ± 0.09	ASTON 87	LASS	0	11 $K^- p \rightarrow \bar{K}^0 \pi^+ \pi^- n$	

$\Gamma(K f_2(1270))/\Gamma_{\text{total}}$	DOCUMENT ID	TECN	COMMENT	Γ_3/Γ
---	-------------	------	---------	-------------------

••• We do not use the following data for averages, fits, limits, etc. •••

possibly seen TIKHOMIROV 03 SPEC 40.0 $\bar{K}^0 \pi^+ \pi^- n$
 $K_S^0 K_S^0 K_L^0 X$

 $K_2^*(1980)$ REFERENCESTIKHOMIROV 03 PAN 66 828 G.D. Tikhomirov *et al.*
BIRD 89 SLAC-332 Translated from YAF 66 860.
ASTON 87 NP B292 693 P.F. Bird (SLAC)
D. Aston *et al.* (SLAC, NAGO, CINC, INUS) $K_4^*(2045)$

$$I(J^P) = \frac{1}{2}(4^+)$$

 $K_4^*(2045)$ MASS

VALUE (MeV)	EVTS	DOCUMENT ID	TECN	CHG	COMMENT
2045 ± 9 OUR AVERAGE		Error includes scale factor of 1.1.			
2062 ± 14 ± 13		¹ ASTON 86	LASS	0	11 $K^- p \rightarrow K^- \pi^+ n$
2039 ± 10	400	^{2,3} CLELAND 82	SPEC	±	50 $K^- \pi^+ n$ $K_S^0 \pi^\pm p$
2070 ⁺¹⁰⁰ ₋₄₀		⁴ ASTON 81c	LASS	0	11 $K^- p \rightarrow K^- \pi^+ n$
••• We do not use the following data for averages, fits, limits, etc. •••					
2079 ± 7	431	TORRES 86	MPSF		400 $pA \rightarrow 4KX$
2088 ± 20	650	BAUBILLIER 82	HBC	-	8.25 $K^- p \rightarrow K_S^0 \pi^- p$
2115 ± 46	488	CARMONY 77	HBC	0	9 $K^+ d \rightarrow K^+ \pi^+ X$

¹ From a fit to all moments.² From a fit to 8 moments.³ Number of events evaluated by us.⁴ From energy-independent partial-wave analysis. $K_4^*(2045)$ WIDTH

VALUE (MeV)	EVTS	DOCUMENT ID	TECN	CHG	COMMENT
198 ± 30 OUR AVERAGE					
221 ± 48 ± 27		⁵ ASTON 86	LASS	0	11 $K^- p \rightarrow K^- \pi^+ n$
189 ± 35	400	^{6,7} CLELAND 82	SPEC	±	50 $K^- p \rightarrow K_S^0 \pi^\pm p$

See key on page 405

Meson Particle Listings
 $K_4^*(2045)$, $K_2(2250)$, $K_3(2320)$

••• We do not use the following data for averages, fits, limits, etc. •••

61 ± 58	431	TORRES	86	MPSF	400	$pA \rightarrow 4KX$
170^{+100}_{-50}	650	BAUBILLIER	82	HBC	—	$8.25 K^- p \rightarrow K_S^0 \pi^- p$
240^{+500}_{-100}		⁸ ASTON	81c	LASS	0	$11 K^- p \rightarrow K^- \pi^+ n$
300 ± 200		CARMONY	77	HBC	0	$9 K^+ d \rightarrow K^+ \pi^+ X$

⁵ From a fit to all moments.⁶ From a fit to 8 moments.⁷ Number of events evaluated by us.⁸ From energy-independent partial-wave analysis. $K_4^*(2045)$ DECAY MODES

Mode	Fraction (Γ_i/Γ)
$\Gamma_1 K \pi$	$(9.9 \pm 1.2) \%$
$\Gamma_2 K^*(892) \pi \pi$	$(9 \pm 5) \%$
$\Gamma_3 K^*(892) \pi \pi \pi$	$(7 \pm 5) \%$
$\Gamma_4 \rho K \pi$	$(5.7 \pm 3.2) \%$
$\Gamma_5 \omega K \pi$	$(5.0 \pm 3.0) \%$
$\Gamma_6 \phi K \pi$	$(2.8 \pm 1.4) \%$
$\Gamma_7 \phi K^*(892)$	$(1.4 \pm 0.7) \%$

 $K_4^*(2045)$ BRANCHING RATIOS

$\Gamma(K\pi)/\Gamma_{\text{total}}$	DOCUMENT ID	TECN	CHG	COMMENT	Γ_1/Γ
0.099 ± 0.012	ASTON	88	LASS	0	$11 K^- p \rightarrow K^- \pi^+ n$

$\Gamma(K^*(892)\pi\pi)/\Gamma(K\pi)$	DOCUMENT ID	TECN	CHG	COMMENT	Γ_2/Γ_1
0.89 ± 0.53	BAUBILLIER	82	HBC	—	$8.25 K^- p \rightarrow \rho K_S^0 3\pi$

$\Gamma(K^*(892)\pi\pi\pi)/\Gamma(K\pi)$	DOCUMENT ID	TECN	CHG	COMMENT	Γ_3/Γ_1
0.75 ± 0.49	BAUBILLIER	82	HBC	—	$8.25 K^- p \rightarrow \rho K_S^0 3\pi$

$\Gamma(\rho K\pi)/\Gamma(K\pi)$	DOCUMENT ID	TECN	CHG	COMMENT	Γ_4/Γ_1
0.58 ± 0.32	BAUBILLIER	82	HBC	—	$8.25 K^- p \rightarrow \rho K_S^0 3\pi$

$\Gamma(\omega K\pi)/\Gamma(K\pi)$	DOCUMENT ID	TECN	CHG	COMMENT	Γ_5/Γ_1
0.50 ± 0.30	BAUBILLIER	82	HBC	—	$8.25 K^- p \rightarrow \rho K_S^0 3\pi$

$\Gamma(\phi K\pi)/\Gamma_{\text{total}}$	DOCUMENT ID	TECN	COMMENT	Γ_6/Γ
0.028 ± 0.014	⁹ TORRES	86	MPSF	400 $pA \rightarrow 4KX$

$\Gamma(\phi K^*(892))/\Gamma_{\text{total}}$	DOCUMENT ID	TECN	COMMENT	Γ_7/Γ
0.014 ± 0.007	⁹ TORRES	86	MPSF	400 $pA \rightarrow 4KX$

⁹ Error determination is model dependent. $K_4^*(2045)$ REFERENCES

ASTON	88	NP B296 493	D. Aston et al.	(SLAC, NAGO, CINC, INUS)
ASTON	86	PL B180 308	D. Aston et al.	(SLAC, NAGO, CINC, INUS)
TORRES	86	PR D34 707	S. Torres et al.	(VPI, ARIZ, FNAL, FSU+)
BAUBILLIER	82	PL 118B 447	M. Baubillier et al.	(BIRM, CERN, GLAS+)
CLELAND	82	NP B208 189	W.E. Cleland et al.	(DURH, GEVA, LAUS+)
ASTON	81C	PL 106B 235	D. Aston et al.	(SLAC, CARL, OTTA)JP
CARMONY	77	PR D16 1251	D.D. Carmony et al.	(PURD, UCD, IUPU)

 $K_2(2250)$

$$I(J^P) = \frac{1}{2}(2^-)$$

OMITTED FROM SUMMARY TABLE

This entry contains various peaks in strange meson systems reported in the 2150–2260 MeV region, as well as enhancements seen in the antihyperon-nucleon system, either in the mass spectra or in the $J^P = 2^-$ wave.

 $K_2(2250)$ MASS

VALUE (MeV)	EVTS	DOCUMENT ID	TECN	CHG	COMMENT	
2247 ± 17 OUR AVERAGE						
2200 ± 40		¹ ARMSTRONG	83c	OMEG	—	$18 K^- p \rightarrow \Lambda \bar{p} X$
2235 ± 50		¹ BAUBILLIER	81	HBC	—	$8 K^- p \rightarrow \Lambda \bar{p} X$
2260 ± 20		¹ CLELAND	81	SPEC	±	$50 K^+ p \rightarrow \Lambda \bar{p} X$

••• We do not use the following data for averages, fits, limits, etc. •••

2280 ± 20		TIKHOMIROV	03	SPEC		$40.0 \pi^- C \rightarrow K_S^0 K_S^0 K_L^0 X$
2147 ± 4	37	CHLIAPNIK...	79	HBC	+	$32 K^+ p \rightarrow \Lambda \bar{p} X$
2240 ± 20	20	LISSAUER	70	HBC		$9 K^+ p$

¹ $J^P = 2^-$ from moments analysis.

 $K_2(2250)$ WIDTH

VALUE (MeV)	EVTS	DOCUMENT ID	TECN	CHG	COMMENT	
180 ± 30 OUR AVERAGE					Error includes scale factor of 1.4.	
150 ± 30		² ARMSTRONG	83c	OMEG	—	$18 K^- p \rightarrow \Lambda \bar{p} X$
210 ± 30		² CLELAND	81	SPEC	±	$50 K^+ p \rightarrow \Lambda \bar{p} X$

••• We do not use the following data for averages, fits, limits, etc. •••

180 ± 60		TIKHOMIROV	03	SPEC		$40.0 \pi^- C \rightarrow K_S^0 K_S^0 K_L^0 X$
~ 200		² BAUBILLIER	81	HBC	—	$8 K^- p \rightarrow \Lambda \bar{p} X$
~ 40	37	CHLIAPNIK...	79	HBC	+	$32 K^+ p \rightarrow \Lambda \bar{p} X$
80 ± 20	20	LISSAUER	70	HBC		$9 K^+ p$

² $J^P = 2^-$ from moments analysis.

 $K_2(2250)$ DECAY MODES

Mode	Fraction (Γ_i/Γ)
$\Gamma_1 K \pi \pi$	
$\Gamma_2 K f_2(1270)$	
$\Gamma_3 K^*(892) f_0(980)$	
$\Gamma_4 \rho \bar{\Lambda}$	

 $K_2(2250)$ REFERENCES

TIKHOMIROV	03	PAN 66 828	G.D. Tikhomirov et al.
		Translated from YAF 66 860.	
ARMSTRONG	83c	NP B227 365	T.A. Armstrong et al.
BAUBILLIER	81	NP B183 1	M. Baubillier et al.
CLELAND	81	NP B184 1	W.E. Cleland et al.
CHLIAPNIK...	79	NP B158 253	P.V. Chliapnikov et al.
LISSAUER	70	NP B18 491	D. Lissauer et al.

(BARI, BIRM, CERN+)
(BIRM, CERN, GLAS+JP)
(PITT, GEVA, LAUS+JP)
(CERN, BELG, MONS)
(LBL)

 $K_3(2320)$

$$I(J^P) = \frac{1}{2}(3^+)$$

OMITTED FROM SUMMARY TABLE

Seen in the $J^P = 3^+$ wave of the antihyperon-nucleon system. Needs confirmation.

 $K_3(2320)$ MASS

VALUE (MeV)	DOCUMENT ID	TECN	CHG	COMMENT	
2324 ± 24 OUR AVERAGE					
2330 ± 40	¹ ARMSTRONG	83c	OMEG	—	$18 K^- p \rightarrow \Lambda \bar{p} X$
2320 ± 30	¹ CLELAND	81	SPEC	±	$50 K^+ p \rightarrow \Lambda \bar{p} X$

¹ $J^P = 3^+$ from moments analysis.

 $K_3(2320)$ WIDTH

VALUE (MeV)	DOCUMENT ID	TECN	CHG	COMMENT	
150 ± 30	² ARMSTRONG	83c	OMEG	—	$18 K^- p \rightarrow \Lambda \bar{p} X$

••• We do not use the following data for averages, fits, limits, etc. •••

~ 250		² CLELAND	81	SPEC	±	$50 K^+ p \rightarrow \Lambda \bar{p} X$
-------	--	----------------------	----	------	---	--

² $J^P = 3^+$ from moments analysis.

 $K_3(2320)$ DECAY MODES

Mode	Fraction (Γ_i/Γ)
$\Gamma_1 \rho \bar{\Lambda}$	

 $K_3(2320)$ REFERENCES

ARMSTRONG	83c	NP B227 365	T.A. Armstrong et al.	(BARI, BIRM, CERN+)
CLELAND	81	NP B184 1	W.E. Cleland et al.	(PITT, GEVA, LAUS+)

Meson Particle Listings

 $K_5^*(2380)$, $K_4(2500)$, $K(3100)$ $K_5^*(2380)$

$$I(J^P) = \frac{1}{2}(5^-)$$

OMITTED FROM SUMMARY TABLE
Needs confirmation.

 $K_5^*(2380)$ MASS

VALUE (MeV)	DOCUMENT ID	TECN	CHG	COMMENT	
2382 ± 14 ± 19	¹ ASTON	86	LASS	0	11 $K^- p \rightarrow K^- \pi^+ n$

¹ From a fit to all the moments.

 $K_5^*(2380)$ WIDTH

VALUE (MeV)	DOCUMENT ID	TECN	CHG	COMMENT	
178 ± 37 ± 32	² ASTON	86	LASS	0	11 $K^- p \rightarrow K^- \pi^+ n$

² From a fit to all the moments.

 $K_5^*(2380)$ DECAY MODES

Mode	Fraction (Γ_i/Γ)
Γ_1 $K \pi$	(6.1 ± 1.2) %

 $K_5^*(2380)$ BRANCHING RATIOS

$\Gamma(K \pi)/\Gamma_{\text{total}}$	DOCUMENT ID	TECN	CHG	COMMENT	Γ_1/Γ
0.061 ± 0.012	ASTON	88	LASS	0	11 $K^- p \rightarrow K^- \pi^+ n$

 $K_5^*(2380)$ REFERENCES

ASTON	88	NP B296 493	D. Aston et al.	(SLAC, NAGO, CINC, INUS)
ASTON	86	PL B180 308	D. Aston et al.	(SLAC, NAGO, CINC, INUS)

 $K_4(2500)$

$$I(J^P) = \frac{1}{2}(4^-)$$

OMITTED FROM SUMMARY TABLE
Needs confirmation.

 $K_4(2500)$ MASS

VALUE (MeV)	DOCUMENT ID	TECN	CHG	COMMENT	
2490 ± 20	¹ CLELAND	81	SPEC	±	50 $K^+ p \rightarrow \Lambda \bar{p}$

¹ $J^P = 4^-$ from moments analysis.

 $K_4(2500)$ WIDTH

VALUE (MeV)	DOCUMENT ID	TECN	CHG	COMMENT	
~ 250	² CLELAND	81	SPEC	±	50 $K^+ p \rightarrow \Lambda \bar{p}$

• • • We do not use the following data for averages, fits, limits, etc. • • •

² $J^P = 4^-$ from moments analysis.

 $K_4(2500)$ DECAY MODES

Mode
Γ_1 $\rho \bar{\Lambda}$

 $K_4(2500)$ REFERENCES

CLELAND	81	NP B184 1	W.E. Cleland et al.	(PITT, GEVA, LAUS+)
---------	----	-----------	---------------------	---------------------

 $K(3100)$

$$I^G(J^PC) = ?^?(?^{??})$$

OMITTED FROM SUMMARY TABLE

Narrow peak observed in several ($\Lambda \bar{p}$ + pions) and ($\bar{\Lambda} p$ + pions) states in Σ^- Be reactions by BOURQUIN 86 and in $n p$ and $n A$ reactions by ALEEV 93. Not seen by BOEHNLEIN 91. If due to strong decays, this state has exotic quantum numbers ($B=0, Q=+1, S=-1$ for $\Lambda \bar{p} \pi^+ \pi^+$ and $I \geq 3/2$ for $\Lambda \bar{p} \pi^-$). Needs confirmation.

 $K(3100)$ MASS

VALUE (MeV)	DOCUMENT ID
≈ 3100 OUR ESTIMATE	

3-BODY DECAYS

VALUE (MeV)	DOCUMENT ID	TECN	COMMENT	
3054 ± 11 OUR AVERAGE				
3060 ± 7 ± 20	¹ ALEEV	93	BIS2	$K(3100) \rightarrow \Lambda \bar{p} \pi^+$
3056 ± 7 ± 20	¹ ALEEV	93	BIS2	$K(3100) \rightarrow \bar{\Lambda} p \pi^-$
3055 ± 8 ± 20	¹ ALEEV	93	BIS2	$K(3100) \rightarrow \Lambda \bar{p} \pi^-$
3045 ± 8 ± 20	¹ ALEEV	93	BIS2	$K(3100) \rightarrow \bar{\Lambda} p \pi^+$

4-BODY DECAYS

VALUE (MeV)	DOCUMENT ID	TECN	COMMENT	
3059 ± 11 OUR AVERAGE				
3067 ± 6 ± 20	¹ ALEEV	93	BIS2	$K(3100) \rightarrow \Lambda \bar{p} \pi^+ \pi^+$
3060 ± 8 ± 20	¹ ALEEV	93	BIS2	$K(3100) \rightarrow \Lambda \bar{p} \pi^+ \pi^-$
3055 ± 7 ± 20	¹ ALEEV	93	BIS2	$K(3100) \rightarrow \bar{\Lambda} p \pi^- \pi^-$
3052 ± 8 ± 20	¹ ALEEV	93	BIS2	$K(3100) \rightarrow \bar{\Lambda} p \pi^- \pi^+$

• • • We do not use the following data for averages, fits, limits, etc. • • •

3105 ± 30	BOURQUIN	86	SPEC	$K(3100) \rightarrow \Lambda \bar{p} \pi^+ \pi^+$
3115 ± 30	BOURQUIN	86	SPEC	$K(3100) \rightarrow \Lambda \bar{p} \pi^+ \pi^-$

5-BODY DECAYS

VALUE (MeV)	DOCUMENT ID	TECN	COMMENT	
3095 ± 30	BOURQUIN	86	SPEC	$K(3100) \rightarrow \Lambda \bar{p} \pi^+ \pi^+ \pi^-$

¹ Supersedes ALEEV 90.

 $K(3100)$ WIDTH

3-BODY DECAYS

VALUE (MeV)	DOCUMENT ID	TECN	COMMENT	
• • • We do not use the following data for averages, fits, limits, etc. • • •				
42 ± 16	² ALEEV	93	BIS2	$K(3100) \rightarrow \Lambda \bar{p} \pi^+$
36 ± 15	² ALEEV	93	BIS2	$K(3100) \rightarrow \bar{\Lambda} p \pi^-$
50 ± 18	² ALEEV	93	BIS2	$K(3100) \rightarrow \Lambda \bar{p} \pi^-$
30 ± 15	² ALEEV	93	BIS2	$K(3100) \rightarrow \bar{\Lambda} p \pi^+$

4-BODY DECAYS

VALUE (MeV)	CL%	DOCUMENT ID	TECN	COMMENT	
• • • We do not use the following data for averages, fits, limits, etc. • • •					
22 ± 8		² ALEEV	93	BIS2	$K(3100) \rightarrow \Lambda \bar{p} \pi^+ \pi^+$
28 ± 12		² ALEEV	93	BIS2	$K(3100) \rightarrow \Lambda \bar{p} \pi^+ \pi^-$
32 ± 15		² ALEEV	93	BIS2	$K(3100) \rightarrow \bar{\Lambda} p \pi^- \pi^-$
30 ± 15		² ALEEV	93	BIS2	$K(3100) \rightarrow \bar{\Lambda} p \pi^- \pi^+$
< 30	90	BOURQUIN	86	SPEC	$K(3100) \rightarrow \Lambda \bar{p} \pi^+ \pi^+$
< 80	90	BOURQUIN	86	SPEC	$K(3100) \rightarrow \Lambda \bar{p} \pi^+ \pi^-$

5-BODY DECAYS

VALUE (MeV)	CL%	DOCUMENT ID	TECN	COMMENT	
• • • We do not use the following data for averages, fits, limits, etc. • • •					
< 30	90	BOURQUIN	86	SPEC	$K(3100) \rightarrow \Lambda \bar{p} \pi^+ \pi^+ \pi^-$

² Supersedes ALEEV 90.

 $K(3100)$ DECAY MODES

Mode
Γ_1 $K(3100)^0 \rightarrow \Lambda \bar{p} \pi^+$
Γ_2 $K(3100)^{--} \rightarrow \Lambda \bar{p} \pi^-$
Γ_3 $K(3100)^- \rightarrow \Lambda \bar{p} \pi^+ \pi^-$
Γ_4 $K(3100)^+ \rightarrow \Lambda \bar{p} \pi^+ \pi^+$
Γ_5 $K(3100)^0 \rightarrow \Lambda \bar{p} \pi^+ \pi^+ \pi^-$
Γ_6 $K(3100)^0 \rightarrow \Sigma(1385)^+ \bar{p}$

 $\Gamma(\Sigma(1385)^+ \bar{p})/\Gamma(\Lambda \bar{p} \pi^+)$

VALUE	CL%	DOCUMENT ID	TECN	COMMENT	Γ_6/Γ_1
< 0.04	90	ALEEV	93	BIS2	$K(3100)^0 \rightarrow \Sigma(1385)^+ \bar{p}$

 $K(3100)$ REFERENCES

ALEEV	93	PAN 56 1358	A.N. Aliev et al.	(BIS-2 Collab.)
		Translated from YAF 56 100.		
BOEHNLEIN	91	NPBPS B21 174	A. Boehnlein et al.	(FLOR, BNL, IND+)
ALEEV	90	ZPHY C47 533	A.N. Aliev et al.	(BIS-2 Collab.)
BOURQUIN	86	PL B172 113	M.H. Bourquin et al.	(GEVA, RAL, HEIDP+)

CHARMED MESONS ($C = \pm 1$)

$D^+ = c\bar{d}, D^0 = c\bar{u}, \bar{D}^0 = \bar{c}u, D^- = \bar{c}d$, similarly for D^{*s}

D^\pm

$$I(J^P) = \frac{1}{2}(0^-)$$

D^\pm MASS

The fit includes $D^\pm, D^0, D_s^\pm, D^{*s}, D^{*0}, D_1(2420)^0, D_2^*(2460)^0$, and $D_{s1}(2536)^\pm$ mass and mass difference measurements.

VALUE (MeV)	EVTS	DOCUMENT ID	TECN	COMMENT
1869.60 ± 0.16 OUR FIT	Error includes scale factor of 1.1.			
1869.5 ± 0.4 OUR AVERAGE				
1869.53 ± 0.49 ± 0.20	110 ± 15	ANASHIN	10A	KEDR e^+e^- at $\psi(3770)$
1870.0 ± 0.5 ± 1.0	317	BARLAG	90c	ACCM π^- Cu 230 GeV
1869.4 ± 0.6		¹ TRILLING	81	RVUE e^+e^- 3.77 GeV
• • • We do not use the following data for averages, fits, limits, etc. • • •				
1875 ± 10	9	ADA MOVICH	87	EMUL Photoproduction
1860 ± 16	6	ADA MOVICH	84	EMUL Photoproduction
1863 ± 4		DERRICK	84	HRS e^+e^- 29 GeV
1868.4 ± 0.5		¹ SCHINDLER	81	MRK2 e^+e^- 3.77 GeV
1874 ± 5		GOLDHABER	77	MRK1 D^0, D^+ recoil spectra
1868.3 ± 0.9		¹ PERUZZI	77	LGW e^+e^- 3.77 GeV
1874 ± 11		PICCOLO	77	MRK1 e^+e^- 4.03, 4.41 GeV
1876 ± 15	50	PERUZZI	76	MRK1 $K^\mp \pi^\pm \pi^\pm$

¹PERUZZI 77 and SCHINDLER 81 errors do not include the 0.13% uncertainty in the absolute SPEAR energy calibration. TRILLING 81 uses the high precision $J/\psi(1S)$ and $\psi(2S)$ measurements of ZHOLENTZ 80 to determine this uncertainty and combines the PERUZZI 77 and SCHINDLER 81 results to obtain the value quoted.

D^\pm MEAN LIFE

Measurements with an error $> 100 \times 10^{-15}$ s have been omitted from the Listings.

VALUE (10^{-15} s)	EVTS	DOCUMENT ID	TECN	COMMENT
1040 ± 7 OUR AVERAGE				
1039.4 ± 4.3 ± 7.0	110k	LINK	02f	FOCS γ nucleus, ≈ 180 GeV
1033.6 ± 22.1 ^{+9.9} _{-12.7}	3777	BONVICINI	99	CLEO $e^+e^- \approx \Upsilon(4S)$
1048 ± 15 ± 11	9k	FRABETTI	94D	E687 $D^+ \rightarrow K^- \pi^+ \pi^+$
• • • We do not use the following data for averages, fits, limits, etc. • • •				
1075 ± 40 ± 18	2455	FRABETTI	91	E687 γ Be, $D^+ \rightarrow K^- \pi^+ \pi^+$
1030 ± 80 ± 60	200	ALVAREZ	90	NA14 $\gamma, D^+ \rightarrow K^- \pi^+ \pi^+$
1050 ⁺⁷⁷ ₋₇₂	317	² BARLAG	90c	ACCM π^- Cu 230 GeV
1050 ± 80 ± 70	363	ALBRECHT	88i	ARG e^+e^- 10 GeV
1050 ± 30 ± 25	2992	RAAB	88	E691 Photoproduction

²BARLAG 90c estimates the systematic error to be negligible.

D^+ DECAY MODES

Most decay modes (other than the semileptonic modes) that involve a neutral K meson are now given as K_S^0 modes, not as \bar{K}^0 modes. Nearly always it is a K_S^0 that is measured, and interference between Cabibbo-allowed and doubly Cabibbo-suppressed modes can invalidate the assumption that $2\Gamma(K_S^0) = \Gamma(\bar{K}^0)$.

Mode	Fraction (Γ_i/Γ)	Scale factor/ Confidence level
Inclusive modes		
Γ_1 e^+ semileptonic	(16.07 ± 0.30) %	
Γ_2 μ^+ anything	(17.6 ± 3.2) %	
Γ_3 K^- anything	(25.7 ± 1.4) %	
Γ_4 \bar{K}^0 anything + K^0 anything	(61 ± 5) %	
Γ_5 K^+ anything	(5.9 ± 0.8) %	
Γ_6 $K^*(892)^-$ anything	(6 ± 5) %	
Γ_7 $\bar{K}^*(892)^0$ anything	(23 ± 5) %	
Γ_8 $K^*(892)^+$ anything		
Γ_9 $K^*(892)^0$ anything	< 6.6 %	CL=90%
Γ_{10} η anything	(6.3 ± 0.7) %	
Γ_{11} η' anything	(1.04 ± 0.18) %	
Γ_{12} ϕ anything	(1.03 ± 0.12) %	

Leptonic and semileptonic modes

Γ_{13} $e^+ \nu_e$	< 8.8	$\times 10^{-6}$	CL=90%
Γ_{14} $\mu^+ \nu_\mu$	(3.82 ± 0.33)	$\times 10^{-4}$	
Γ_{15} $\tau^+ \nu_\tau$	< 1.2	$\times 10^{-3}$	CL=90%
Γ_{16} $\bar{K}^0 e^+ \nu_e$	(8.83 ± 0.22) %		
Γ_{17} $\bar{K}^0 \mu^+ \nu_\mu$	(9.4 ± 0.8) %		S=1.2
Γ_{18} $K^- \pi^+ e^+ \nu_e$	(4.1 ± 0.6) %		S=1.1
Γ_{19} $\bar{K}^*(892)^0 e^+ \nu_e$, $\bar{K}^*(892)^0 \rightarrow K^- \pi^+$	(3.68 ± 0.21) %		
Γ_{20} $K^- \pi^+ e^+ \nu_e$ nonresonant	< 7	$\times 10^{-3}$	CL=90%
Γ_{21} $K^- \pi^+ \mu^+ \nu_\mu$	(3.9 ± 0.5) %		
Γ_{22} $\bar{K}^*(892)^0 \mu^+ \nu_\mu$, $\bar{K}^*(892)^0 \rightarrow K^- \pi^+$	(3.7 ± 0.3) %		
Γ_{23} $K^- \pi^+ \mu^+ \nu_\mu$ nonresonant	(2.1 ± 0.6) $\times 10^{-3}$		
Γ_{24} $K^- \pi^+ \pi^0 \mu^+ \nu_\mu$	< 1.7	$\times 10^{-3}$	CL=90%
Γ_{25} $\pi^0 e^+ \nu_e$	(4.05 ± 0.18) $\times 10^{-3}$		
Γ_{26} $\eta e^+ \nu_e$	(1.33 ± 0.21) $\times 10^{-3}$		
Γ_{27} $\rho^0 e^+ \nu_e$	(2.2 ± 0.4) $\times 10^{-3}$		
Γ_{28} $\rho^0 \mu^+ \nu_\mu$	(2.5 ± 0.5) $\times 10^{-3}$		
Γ_{29} $\omega e^+ \nu_e$	(1.6 ^{+0.7} _{-0.6}) $\times 10^{-3}$		
Γ_{30} $\eta'(958) e^+ \nu_e$	< 3.5	$\times 10^{-4}$	CL=90%
Γ_{31} $\phi e^+ \nu_e$	< 1.6	$\times 10^{-4}$	CL=90%

Fractions of some of the following modes with resonances have already appeared above as submodes of particular charged-particle modes.

Γ_{32} $\bar{K}^*(892)^0 e^+ \nu_e$	(5.53 ± 0.32) %	S=1.2
Γ_{33} $\bar{K}^*(892)^0 \mu^+ \nu_\mu$	(5.5 ± 0.5) %	S=1.2
Γ_{34} $\bar{K}_0^*(1430)^0 \mu^+ \nu_\mu$	< 2.5	$\times 10^{-4}$
Γ_{35} $\bar{K}^*(1680)^0 \mu^+ \nu_\mu$	< 1.6	$\times 10^{-3}$

Hadronic modes with a \bar{K} or $\bar{K}\bar{K}$

Γ_{36} $K_S^0 \pi^+$	(1.49 ± 0.04) %	S=1.4
Γ_{37} $K_S^0 \pi^+$	(1.46 ± 0.05) %	
Γ_{38} $K^- 2\pi^+$	[a] (9.4 ± 0.4) %	S=2.2
Γ_{39} $(K^- \pi^+)_{S\text{-wave}} \pi^+$	(7.52 ± 0.33) %	
Γ_{40} $\bar{K}_0^*(800)^0 \pi^+, \bar{K}_0^*(800) \rightarrow$ $K^- \pi^+$		
Γ_{41} $\bar{K}_0^*(1430)^0 \pi^+$, $\bar{K}_0^*(1430)^0 \rightarrow K^- \pi^+$	[b] (1.25 ± 0.08) %	
Γ_{42} $\bar{K}^*(892)^0 \pi^+$, $\bar{K}^*(892)^0 \rightarrow K^- \pi^+$	(1.04 ± 0.12) %	
Γ_{43} $\bar{K}^*(1410)^0 \pi^+, \bar{K}^{*0} \rightarrow$	not seen	
Γ_{44} $\bar{K}_S^*(1430)^0 \pi^+$, $\bar{K}_S^*(1430)^0 \rightarrow K^- \pi^+$	[b] (2.3 ± 0.7) $\times 10^{-4}$	
Γ_{45} $\bar{K}^*(1680)^0 \pi^+$, $\bar{K}^*(1680)^0 \rightarrow K^- \pi^+$	[b] (2.2 ± 1.1) $\times 10^{-4}$	
Γ_{46} $K^- (2\pi^+)_{I=2}$	(1.45 ± 0.27) %	
Γ_{47} $K^- 2\pi^+$ nonresonant		
Γ_{48} $K_S^0 \pi^+ \pi^0$	[a] (6.90 ± 0.32) %	S=1.3
Γ_{49} $K_S^0 \rho^+$	(4.7 ± 1.0) %	
Γ_{50} $\bar{K}^*(892)^0 \pi^+$, $\bar{K}^*(892)^0 \rightarrow K_S^0 \pi^0$	(1.3 ± 0.6) %	
Γ_{51} $K_S^0 \pi^+ \pi^0$ nonresonant	(9 ± 7) $\times 10^{-3}$	
Γ_{52} $K^- 2\pi^+ \pi^0$	[c] (6.08 ± 0.29) %	S=1.6
Γ_{53} $K_S^0 2\pi^+ \pi^-$	[c] (3.10 ± 0.11) %	S=1.1
Γ_{54} $K^- 3\pi^+ \pi^-$	[a] (5.7 ± 0.6) $\times 10^{-3}$	S=1.2
Γ_{55} $\bar{K}^*(892)^0 2\pi^+ \pi^-$, $\bar{K}^*(892)^0 \rightarrow K^- \pi^+$	(1.2 ± 0.4) $\times 10^{-3}$	
Γ_{56} $\bar{K}^*(892)^0 \rho^0 \pi^+$, $\bar{K}^*(892)^0 \rightarrow K^- \pi^+$	(2.3 ± 0.4) $\times 10^{-3}$	
Γ_{57} $\bar{K}^*(892)^0 a_1(1260)^+$	[d] (9.3 ± 1.9) $\times 10^{-3}$	
Γ_{58} $\bar{K}^*(892)^0 2\pi^+ \pi^- \text{ no-}\rho$, $\bar{K}^*(892)^0 \rightarrow K^- \pi^+$		
Γ_{59} $K^- \rho^0 2\pi^+$	(1.72 ± 0.29) $\times 10^{-3}$	
Γ_{60} $K^- 3\pi^+ \pi^-$ nonresonant	(4.0 ± 3.0) $\times 10^{-4}$	
Γ_{61} $K^+ 2K_S^0$	(4.6 ± 2.1) $\times 10^{-3}$	
Γ_{62} $K^+ K^- K_S^0 \pi^+$	(2.4 ± 0.5) $\times 10^{-4}$	

Meson Particle Listings

 D^\pm $\Gamma(\tau^+ \nu_\tau)/\Gamma_{\text{total}}$ Γ_{15}/Γ

VALUE	CL%	DOCUMENT ID	TECN	COMMENT
$<1.2 \times 10^{-3}$	90	EISENSTEIN 08	CLEO	e^+e^- at $\psi(3770)$
••• We do not use the following data for averages, fits, limits, etc. •••				
$<2.1 \times 10^{-3}$	90	RUBIN 06A	CLEO	See EISENSTEIN 08

 $\Gamma(\bar{K}^0 e^+ \nu_e)/\Gamma_{\text{total}}$ Γ_{16}/Γ

VALUE (%)	EVTS	DOCUMENT ID	TECN	COMMENT
8.83 ± 0.22 OUR AVERAGE				
8.83 ± 0.10 ± 0.20	8467	18 BESSON	09 CLEO	e^+e^- at $\psi(3770)$
8.95 ± 1.59 ± 0.67	34 ± 6	19 ABLIKIM	05A BES	e^+e^- at $\psi(3770)$
••• We do not use the following data for averages, fits, limits, etc. •••				
8.53 ± 0.13 ± 0.23		20 DOBBS	08 CLEO	See BESSON 09
8.71 ± 0.38 ± 0.37	545 ± 24	HUANG	05B CLEO	See DOBBS 08

¹⁸ See the form-factor parameters near the end of this D^+ Listing.
¹⁹ The ABLIKIM 05A result together with the $D^0 \rightarrow K^- e^+ \nu_e$ branching fraction of ABLIKIM 04C and Particle Data Group lifetimes gives $\Gamma(D^0 \rightarrow K^- e^+ \nu_e) / \Gamma(D^+ \rightarrow \bar{K}^0 e^+ \nu_e) = 1.08 \pm 0.22 \pm 0.07$; isospin invariance predicts the ratio is 1.0.
²⁰ DOBBS 08 establishes $|V_{cs}^d \cdot \frac{f_+^\pi(0)}{f_+^K(0)}| = 0.188 \pm 0.008 \pm 0.002$ from the D^+ and D^0 decays to $\bar{K} e^+ \nu_e$ and $\pi e^+ \nu_e$. It also finds $\Gamma(D^0 \rightarrow K^- e^+ \nu_e) / \Gamma(D^+ \rightarrow \bar{K}^0 e^+ \nu_e) = 1.06 \pm 0.02 \pm 0.03$; isospin invariance predicts the ratio is 1.0.

 $\Gamma(\bar{K}^0 \mu^+ \nu_\mu)/\Gamma_{\text{total}}$ Γ_{17}/Γ

VALUE	EVTS	DOCUMENT ID	TECN	COMMENT
0.094 ± 0.008 OUR FIT	Error includes scale factor of 1.2.			
0.103 ± 0.023 ± 0.008	29 ± 6	ABLIKIM 07	BES2	e^+e^- at 3773 MeV

 $\Gamma(\bar{K}^0 \mu^+ \nu_\mu)/\Gamma(K^- 2\pi^+)$ Γ_{17}/Γ_{38}

VALUE	EVTS	DOCUMENT ID	TECN	COMMENT
1.01 ± 0.08 OUR FIT	Error includes scale factor of 1.1.			
1.019 ± 0.076 ± 0.065	555 ± 39	LINK 04E	FOCS	γ nucleus, $\bar{E}_\gamma \approx 180$ GeV

 $\Gamma(K^- \pi^+ e^+ \nu_e)/\Gamma_{\text{total}}$ Γ_{18}/Γ

VALUE (units 10^{-2})	EVTS	DOCUMENT ID	TECN	COMMENT
4.1 ± 0.6 OUR FIT	Error includes scale factor of 1.1.			
3.5 $\pm_{-0.6}^{+0.7}$ OUR AVERAGE				
3.50 ± 0.75 ± 0.27	29 ± 6	ABLIKIM 06o	BES2	e^+e^- at 3773 MeV
3.5 $\pm_{-0.7}^{+1.2}$ ± 0.4	14	BAI 91	MRK3	$e^+e^- \approx 3.77$ GeV

 $\Gamma(\bar{K}^*(892)^0 e^+ \nu_e)/\Gamma_{\text{total}}$ Γ_{32}/Γ

Unseen decay modes of the $\bar{K}^*(892)^0$ are included. See the end of the D^+ Listings for measurements of $D^+ \rightarrow \bar{K}^*(892)^0 \ell^+ \nu_\ell$ form-factor ratios.

VALUE (units 10^{-2})	EVTS	DOCUMENT ID	TECN	COMMENT
5.53 ± 0.32 OUR FIT	Error includes scale factor of 1.2.			
5.52 ± 0.34 OUR AVERAGE				
5.06 ± 1.21 ± 0.40	28 ± 7	ABLIKIM 06o	BES2	e^+e^- at 3773 MeV
5.56 ± 0.27 ± 0.23	422 ± 21	21 HUANG 05B	CLEO	e^+e^- at $\psi(3770)$

²¹ HUANG 05B finds $\Gamma(D^0 \rightarrow K^{*-} e^+ \nu_e) / \Gamma(D^+ \rightarrow \bar{K}^{*0} e^+ \nu_e) = 0.98 \pm 0.08 \pm 0.04$; isospin invariance predicts the ratio is 1.0.

 $\Gamma(\bar{K}^*(892)^0 e^+ \nu_e)/\Gamma(K^- \pi^+ e^+ \nu_e)$ Γ_{32}/Γ_{18}

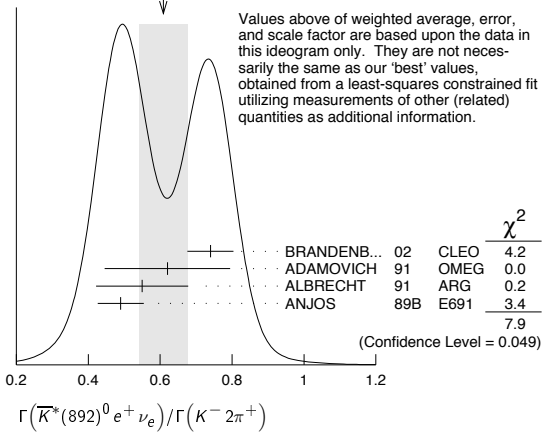
Unseen decay modes of the $\bar{K}^*(892)^0$ are included. See the end of the D^+ Listings for measurements of $D^+ \rightarrow \bar{K}^*(892)^0 \ell^+ \nu_\ell$ form-factor ratios.

VALUE	EVTS	DOCUMENT ID	TECN	COMMENT
1.36 ± 0.22 OUR FIT	Error includes scale factor of 1.2.			
1.0 ± 0.3	35	ADAMOVICH 91	OMEG	π^- 340 GeV

 $\Gamma(\bar{K}^*(892)^0 e^+ \nu_e)/\Gamma(K^- 2\pi^+)$ Γ_{32}/Γ_{38}

Unseen decay modes of the $\bar{K}^*(892)^0$ are included. See the end of the D^+ Listings for measurements of $D^+ \rightarrow \bar{K}^*(892)^0 \ell^+ \nu_\ell$ form-factor ratios.

VALUE	EVTS	DOCUMENT ID	TECN	COMMENT
0.59 ± 0.04 OUR FIT	Error includes scale factor of 1.4.			
0.61 ± 0.07 OUR AVERAGE	Error includes scale factor of 1.6. See the ideogram below.			
0.74 ± 0.04 ± 0.05		BRANDENB... 02	CLEO	$e^+e^- \approx \Upsilon(4S)$
0.62 ± 0.15 ± 0.09	35	ADAMOVICH 91	OMEG	π^- 340 GeV
0.55 ± 0.08 ± 0.10	880	ALBRECHT 91	ARG	$e^+e^- \approx 10.4$ GeV
0.49 ± 0.04 ± 0.05		ANJOS 89B	E691	Photoproduction

WEIGHTED AVERAGE
0.61 ± 0.07 (Error scaled by 1.6) $\Gamma(K^- \pi^+ e^+ \nu_e \text{ nonresonant})/\Gamma_{\text{total}}$ Γ_{20}/Γ

VALUE	CL%	DOCUMENT ID	TECN	COMMENT
<0.007	90	ANJOS 89B	E691	Photoproduction

 $\Gamma(K^- \pi^+ \mu^+ \nu_\mu)/\Gamma(\bar{K}^0 \mu^+ \nu_\mu)$ Γ_{21}/Γ_{17}

VALUE	EVTS	DOCUMENT ID	TECN	COMMENT
0.417 ± 0.030 ± 0.023	555 ± 39	LINK 04E	FOCS	γ nucleus, $\bar{E}_\gamma \approx 180$ GeV

 $\Gamma(\bar{K}^*(892)^0 \mu^+ \nu_\mu)/\Gamma(\bar{K}^0 \mu^+ \nu_\mu)$ Γ_{33}/Γ_{17}

Unseen decay modes of the $\bar{K}^*(892)^0$ are included. See the end of the D^+ Listings for measurements of $D^+ \rightarrow \bar{K}^*(892)^0 \ell^+ \nu_\ell$ form-factor ratios.

VALUE	EVTS	DOCUMENT ID	TECN	COMMENT
0.58 ± 0.05 OUR FIT	Error includes scale factor of 1.1.			
0.594 ± 0.043 ± 0.033	555 ± 39	LINK 04E	FOCS	γ nucleus, $\bar{E}_\gamma \approx 180$ GeV

 $\Gamma(\bar{K}^*(892)^0 \mu^+ \nu_\mu)/\Gamma(K^- 2\pi^+)$ Γ_{33}/Γ_{38}

Unseen decay modes of the $\bar{K}^*(892)^0$ are included. See the end of the D^+ Listings for measurements of $D^+ \rightarrow \bar{K}^*(892)^0 \ell^+ \nu_\ell$ form-factor ratios.

VALUE	EVTS	DOCUMENT ID	TECN	COMMENT
0.58 ± 0.05 OUR FIT	Error includes scale factor of 1.1.			
0.57 ± 0.06 OUR AVERAGE	Error includes scale factor of 1.2.			
0.72 ± 0.10 ± 0.05		BRANDENB... 02	CLEO	$e^+e^- \approx \Upsilon(4S)$
0.56 ± 0.04 ± 0.06	875	FRABETTI 93E	E687	γ Be $\bar{E}_\gamma \approx 200$ GeV
0.46 ± 0.07 ± 0.08	224	KODAMA 92C	E653	π^- emulsion 600 GeV
••• We do not use the following data for averages, fits, limits, etc. •••				
0.602 ± 0.010 ± 0.021	12k	22 LINK 02J	FOCS	γ nucleus, ≈ 180 GeV

²² This LINK 02J result includes the effects of an interference of a small S-wave $K^- \pi^+$ amplitude with the dominant \bar{K}^{*0} amplitude. (The interference effect is reported in LINK 02E.) This result is redundant with results of LINK 04E elsewhere in these Listings.

 $\Gamma(K^- \pi^+ \mu^+ \nu_\mu \text{ nonresonant})/\Gamma(K^- \pi^+ \mu^+ \nu_\mu)$ Γ_{23}/Γ_{21}

VALUE	EVTS	DOCUMENT ID	TECN	COMMENT
0.0530 ± 0.0074 + 0.0099 - 0.0096	14k	LINK 05i	FOCS	γ nucleus, $\bar{E}_\gamma \approx 180$ GeV

 $\Gamma(K^- \pi^+ \pi^0 \mu^+ \nu_\mu)/\Gamma(K^- \pi^+ \mu^+ \nu_\mu)$ Γ_{24}/Γ_{21}

VALUE	CL%	DOCUMENT ID	TECN	COMMENT
<0.042	90	FRABETTI 93E	E687	γ Be $\bar{E}_\gamma \approx 200$ GeV

 $\Gamma(\bar{K}_0^*(1430)^0 \mu^+ \nu_\mu)/\Gamma(K^- \pi^+ \mu^+ \nu_\mu)$ Γ_{34}/Γ_{21}

VALUE	EVTS	DOCUMENT ID	TECN	COMMENT
<0.0064	90	LINK 05i	FOCS	γ nucleus, $\bar{E}_\gamma \approx 180$ GeV

 $\Gamma(\bar{K}^*(1680)^0 \mu^+ \nu_\mu)/\Gamma(K^- \pi^+ \mu^+ \nu_\mu)$ Γ_{35}/Γ_{21}

VALUE	EVTS	DOCUMENT ID	TECN	COMMENT
<0.04	90	LINK 05i	FOCS	γ nucleus, $\bar{E}_\gamma \approx 180$ GeV

 $\Gamma(\pi^0 e^+ \nu_e)/\Gamma_{\text{total}}$ Γ_{25}/Γ

VALUE (%)	EVTS	DOCUMENT ID	TECN	COMMENT
0.405 ± 0.016 ± 0.009	838	23 BESSON 09	CLEO	e^+e^- at $\psi(3770)$
••• We do not use the following data for averages, fits, limits, etc. •••				
0.373 ± 0.022 ± 0.013		24 DOBBS 08	CLEO	See BESSON 09
0.44 ± 0.06 ± 0.03	63 ± 9	HUANG 05B	CLEO	See DOBBS 08

²³ See the form-factor parameters near the end of this D^+ Listing.

²⁴ DOBBS 08 establishes $|\frac{V_{cd}}{V_{cs}} \cdot \frac{f_+^\pi(0)}{f_+^K(0)}| = 0.188 \pm 0.008 \pm 0.002$ from the D^+ and D^0 decays to $\bar{K} e^+ \nu_e$ and $\pi e^+ \nu_e$. It finds $\Gamma(D^0 \rightarrow \pi^- e^+ \nu_e) / \Gamma(D^+ \rightarrow \pi^0 e^+ \nu_e) = 2.03 \pm 0.14 \pm 0.08$; isospin invariance predicts the ratio is 2.0.

$\Gamma(\eta e^+ \nu_e) / \Gamma_{\text{total}}$					Γ_{26} / Γ
VALUE (units 10^{-4})	EVTS	DOCUMENT ID	TECN	COMMENT	
13.3 ± 2.0 ± 0.6	46 ± 8	MITCHELL	09B	CLEO	$e^+ e^-$ at $\psi(3770)$

$\Gamma(\rho^0 e^+ \nu_e) / \Gamma_{\text{total}}$					Γ_{27} / Γ
VALUE	EVTS	DOCUMENT ID	TECN	COMMENT	
0.0022 ± 0.0004 OUR FIT					
0.0021 ± 0.0004 ± 0.0001	27 ± 6	²⁵ HUANG	05B	CLEO	$e^+ e^-$ at $\psi(3770)$
²⁵ HUANG 05B finds $\Gamma(D^0 \rightarrow \rho^- e^+ \nu_e) / 2 \Gamma(D^+ \rightarrow \rho^0 e^+ \nu_e) = 1.2^{+0.4}_{-0.3} \pm 0.1$; isospin invariance predicts the ratio is 1.0.					

$\Gamma(\rho^0 e^+ \nu_e) / \Gamma(\bar{K}^*(892)^0 e^+ \nu_e)$					$\Gamma_{27} / \Gamma_{32}$
VALUE	EVTS	DOCUMENT ID	TECN	COMMENT	
0.039 ± 0.007 OUR FIT					
0.045 ± 0.014 ± 0.009	49	²⁶ AITALA	97	E791	π^- nucleus, 500 GeV
²⁶ AITALA 97 explicitly subtracts $D^+ \rightarrow \eta' e^+ \nu_e$ and other backgrounds to get this result.					

$\Gamma(\rho^0 \mu^+ \nu_\mu) / \Gamma(\bar{K}^*(892)^0 \mu^+ \nu_\mu)$					$\Gamma_{28} / \Gamma_{33}$
VALUE	EVTS	DOCUMENT ID	TECN	COMMENT	
0.045 ± 0.007 OUR AVERAGE					Error includes scale factor of 1.1.
0.041 ± 0.006 ± 0.004	320 ± 44	LINK	06B	FOCS	$\gamma A, \bar{E}_\gamma \approx 180$ GeV
0.051 ± 0.015 ± 0.009	54	²⁷ AITALA	97	E791	π^- nucleus, 500 GeV
0.079 ± 0.019 ± 0.013	39	²⁸ FRABETTI	97	E687	γ Be, $\bar{E}_\gamma \approx 220$ GeV
²⁷ AITALA 97 explicitly subtracts $D^+ \rightarrow \eta' \mu^+ \nu_\mu$ and other backgrounds to get this result.					
²⁸ Because the reconstruction efficiency for photons is low, this FRABETTI 97 result also includes any $D^+ \rightarrow \eta' \mu^+ \nu_\mu \rightarrow \gamma \rho^0 \mu^+ \nu_\mu$ events in the numerator.					

$\Gamma(\omega e^+ \nu_e) / \Gamma_{\text{total}}$					Γ_{29} / Γ
VALUE	EVTS	DOCUMENT ID	TECN	COMMENT	
0.0016 ± 0.0007 ± 0.0001	$7.6^{+3.3}_{-2.7}$	HUANG	05B	CLEO	$e^+ e^-$ at $\psi(3770)$

$\Gamma(\eta'(958) e^+ \nu_e) / \Gamma_{\text{total}}$					Γ_{30} / Γ
VALUE	CL%	DOCUMENT ID	TECN	COMMENT	
< 3.5 × 10⁻⁴	90	MITCHELL	09B	CLEO	$e^+ e^-$ at $\psi(3770)$

$\Gamma(\phi e^+ \nu_e) / \Gamma_{\text{total}}$					Γ_{31} / Γ
VALUE	CL%	DOCUMENT ID	TECN	COMMENT	
< 1.6 × 10⁻⁴	90	MITCHELL	09B	CLEO	$e^+ e^-$ at $\psi(3770)$
• • • We do not use the following data for averages, fits, limits, etc. • • •					
< 0.0201	90	ABLIKIM	06P	BES2	$e^+ e^-$ at 3773 MeV
< 0.0209	90	BAI	91	MRK3	$e^+ e^- \approx 3.77$ GeV

Hadronic modes with a \bar{K} or $\bar{K} K \bar{K}$

$\Gamma(K_S^0 \pi^+) / \Gamma_{\text{total}}$					Γ_{36} / Γ
VALUE (units 10^{-2})	EVTS	DOCUMENT ID	TECN	COMMENT	
1.49 ± 0.04 OUR FIT					Error includes scale factor of 1.4.
1.526 ± 0.022 ± 0.038		²⁹ DOBBS	07	CLEO	$e^+ e^-$ at $\psi(3770)$
• • • We do not use the following data for averages, fits, limits, etc. • • •					
1.55 ± 0.05 ± 0.06	2230 ± 60	²⁹ HE	05	CLEO	See DOBBS 07
1.6 ± 0.3 ± 0.1	161	ADLER	88c	MRK3	$e^+ e^-$ 3.77 GeV
²⁹ DOBBS 07 and HE 05 use single- and double-tagged events in an overall fit. DOBBS 07 supersedes HE 05.					

$\Gamma(K_S^0 \pi^+) / \Gamma(K^- 2\pi^+)$					$\Gamma_{36} / \Gamma_{38}$
VALUE	EVTS	DOCUMENT ID	TECN	COMMENT	
0.159 ± 0.007 OUR FIT					Error includes scale factor of 3.3.
0.1530 ± 0.0023 ± 0.0016	10.6k	LINK	02B	FOCS	γ nucleus, $\bar{E}_\gamma \approx 180$ GeV
• • • We do not use the following data for averages, fits, limits, etc. • • •					
0.174 ± 0.012 ± 0.011	473	³⁰ BISHAI	97	CLEO	$e^+ e^- \approx \Upsilon(4S)$
0.137 ± 0.015 ± 0.016	264	ANJOS	90c	E691	Photoproduction

³⁰ See BISHAI 97 for an isospin analysis of $D^+ \rightarrow \bar{K} \pi$ amplitudes.

$\Gamma(K_L^0 \pi^+) / \Gamma_{\text{total}}$					Γ_{37} / Γ
VALUE (units 10^{-2})	EVTS	DOCUMENT ID	TECN	COMMENT	
1.460 ± 0.040 ± 0.035	2023 ± 54	³¹ HE	08	CLEO	$e^+ e^-$ at $\psi(3770)$

³¹ The difference of CLEO $D^+ \rightarrow K_S^0 \pi^+$ and $K_L^0 \pi^+$ branching fractions over the sum (DOBBS 07 and HE 08) is $+0.022 \pm 0.016 \pm 0.018$.

$\Gamma(K^- 2\pi^+) / \Gamma_{\text{total}}$					Γ_{38} / Γ
VALUE (units 10^{-2})	EVTS	DOCUMENT ID	TECN	COMMENT	
9.4 ± 0.4 OUR FIT					Error includes scale factor of 2.2.
9.14 ± 0.10 ± 0.17		³² DOBBS	07	CLEO	$e^+ e^-$ at $\psi(3770)$
• • • We do not use the following data for averages, fits, limits, etc. • • •					
9.5 ± 0.2 ± 0.3	15.1k ± 130	³² HE	05	CLEO	See DOBBS 07
9.3 ± 0.6 ± 0.8	1502	³³ BALEST	94	CLEO	$e^+ e^- \approx \Upsilon(4S)$
6.4 $^{+1.5}_{-1.4}$		³⁴ BARLAG	92c	ACCM	π^- Cu 230 GeV
9.1 ± 1.3 ± 0.4	1164	ADLER	88c	MRK3	$e^+ e^-$ 3.77 GeV
9.1 ± 1.9	239	³⁵ SCHINDLER	81	MRK2	$e^+ e^-$ 3.771 GeV
³² DOBBS 07 and HE 05 use single- and double-tagged events in an overall fit. DOBBS 07 supersedes HE 05.					
³³ BALEST 94 measures the ratio of $D^+ \rightarrow K^- \pi^+ \pi^+$ and $D^0 \rightarrow K^- \pi^+$ branching fractions to be $2.35 \pm 0.16 \pm 0.16$ and uses their absolute measurement of the $D^0 \rightarrow K^- \pi^+$ fraction (AKERIB 93).					
³⁴ BARLAG 92c computes the branching fraction by topological normalization.					
³⁵ SCHINDLER 81 (MARK-2) measures $\sigma(e^+ e^- \rightarrow \psi(3770)) \times$ branching fraction to be 0.38 ± 0.05 nb. We use the MARK-3 (ADLER 88c) value of $\sigma = 4.2 \pm 0.6 \pm 0.3$ nb.					

DALITZ PLOT ANALYSIS FORMALISM

Written January 2006 by D. Asner (Pacific Northwest National Laboratory)

Introduction: Weak nonleptonic decays of D and B mesons are expected to proceed dominantly through resonant two-body decays [1]; see Ref. [2] for a review of resonance phenomenology. The amplitudes are typically calculated with the Dalitz-plot analysis technique [3], which uses the minimum number of independent observable quantities. For three-body decays of a spin-0 particle to all pseudo-scalar final states, D or $B \rightarrow abc$, the decay rate [4] is

$$\Gamma = \frac{1}{(2\pi)^3 32 \sqrt{s^3}} |\mathcal{M}|^2 dm_{ab}^2 dm_{bc}^2, \quad (1)$$

where m_{ij} is the invariant mass of particles i and j . The coefficient of the amplitude includes all kinematic factors, and $|\mathcal{M}|^2$ contains the dynamics. The scatter plot in m_{ab}^2 versus m_{bc}^2 is the Dalitz plot. If $|\mathcal{M}|^2$ is constant, the kinematically allowed region of the plot will be populated uniformly with events. Any variation in the population over the Dalitz plot is due to dynamical rather than kinematical effects. It is straightforward to extend the formalism beyond three-body final states. For N -body final states with only spin-0 particles, phase space has dimension $3N - 7$. Other decays of interest include one vector particle or a fermion/anti-fermion pair (*e.g.*, $B \rightarrow D^* \pi \pi$, $B \rightarrow \bar{K}_c p \pi$, $B \rightarrow K \ell \ell$) in the final state. For the first case, phase space has dimension $3N - 5$, and for the latter two the dimension is $3N - 4$.

Formalism: The amplitude for the process, $R \rightarrow rc, r \rightarrow ab$ where R is a D or B , r is an intermediate resonance, and a, b, c are pseudo-scalars, is given by

$$\begin{aligned} \mathcal{M}_r(J, L, l, m_{ab}, m_{bc}) &= \sum_{\lambda} \langle ab | r_{\lambda} \rangle T_r(m_{ab}) \langle cr_{\lambda} | R_J \rangle \quad (2) \\ &= Z(J, L, l, \vec{p}, \vec{q}) B_L^R(|\vec{p}|) B_L^R(|\vec{q}|) T_r(m_{ab}). \end{aligned}$$

The sum is over the helicity states λ of r , J is the total angular momentum of R (for D and B decays, $J=0$), L is the orbital angular momentum between r and c , l is the orbital angular momentum between a and b (the spin of r), \vec{p} and \vec{q} are the momenta of c and of a in the r rest frame, Z describes the

Meson Particle Listings

D^\pm

angular distribution of the final-state particles, B_L^R and B_L' are the barrier factors for the production of rc and of ab , and T_r is the dynamical function describing the resonance r . The amplitude for modeling the Dalitz plot is a phenomenological object. Differences in the parametrizations of Z , B_L , and T_r , as well as in the set of resonances r , complicate the comparison of results from different experiments.

Usually the resonances are modeled with a Breit-Wigner form, although some more recent analyses use a K -matrix formalism [5,6,7] with the P -vector approximation [8] to describe the $\pi\pi$ S-wave.

The nonresonant (NR) contribution to $D \rightarrow abc$ is parametrized as constant (S-wave) with no variation in magnitude or phase across the Dalitz plot. The available phase space is much greater for B decays, and the nonresonant contribution to $B \rightarrow abc$ requires a more sophisticated parametrization. Theoretical models of the NR amplitude [9-12] do not reproduce the distributions observed in the data. Experimentally, several parametrizations have been used [13,14].

Barrier Factor B_L : The maximum angular momentum L in a strong decay is limited by the linear momentum q . Decay particles moving slowly with an impact parameter (meson radius) d of order 1 fm have difficulty generating sufficient angular momentum to conserve the spin of the resonance. The Blatt-Weisskopf [15,16] functions B_L , given in Table 1, weight the reaction amplitudes to account for this spin-dependent effect. These functions are normalized to give $B_L = 1$ for $z = (|q|d)^2 = 1$. Another common formulation, B_L' , also in Table 1, is normalized to give $B_L' = 1$ for $z = z_0 = (|q_0|d)^2$ where q_0 is the value of q when $m_{ab} = m_r$.

Table 1: Blatt-Weisskopf barrier factors.

L	$B_L(q)$	$B_L'(q, q_0)$
0	1	1
1	$\sqrt{\frac{2z}{1+z}}$	$\sqrt{\frac{1+z_0}{1+z}}$
2	$\sqrt{\frac{13z^2}{(z-3)^2+9z}}$	$\sqrt{\frac{(z_0-3)^2+9z_0}{(z-3)^2+9z}}$

where $z = (|q|d)^2$ and $z_0 = (|q_0|d)^2$

Angular distribution: The tensor or Zemach formalism [17,18] and the helicity formalism [19,18] yield identical descriptions of the angular distributions for the decay process $R \rightarrow rc, r \rightarrow ab$ when a, b and c all have spin-0. The angular distributions for $L = 0, 1$, and 2 are given in Table 2. For final-state particles with non-zero spin (e.g., radiative decays), the helicity formalism is required.

Table 2: Angular distributions for $L = 0, 1, 2$ where θ is the angle between particles a and c in the rest frame of resonance r , $\sqrt{1+\zeta^2} = E_r/m_{ab}$ is a relativistic correction, and $E_r = (m_R^2 + m_{ab}^2 - m_c^2)/2m_R$.

$J \rightarrow L + l$	Angular distribution
$0 \rightarrow 0+0$	uniform
$0 \rightarrow 1+1$	$(1+\zeta^2) \cos^2 \theta$
$0 \rightarrow 2+2$	$\left(\zeta^2 + \frac{3}{2}\right)^2 (\cos^2 \theta - 1/3)^2$

Dynamical Function T_r : The dynamical function T_r is derived from the S -matrix formalism. In general, the amplitude that a final state f couples to an initial state i is $S_{fi} = \langle f|S|i\rangle$, where the scattering operator S is unitary and satisfies $SS^\dagger = S^\dagger S = I$. The Lorentz-invariant transition operator \hat{T} is defined by separating the probability that $f = i$, yielding

$$S = I + 2iT = I + 2i\{\rho\}^{1/2} \hat{T} \{\rho\}^{1/2}, \quad (3)$$

where I is the identity operator, ρ is the diagonal phase-space matrix, with $\rho_{ii} = 2q_i/m$, and q_i is the momentum of a in the r rest frame for decay channel i . In the single-channel S-wave case, $S = e^{2i\delta}$ satisfies unitarity and

$$\hat{T} = \frac{1}{\rho} e^{i\delta} \sin \delta. \quad (4)$$

There are three common formulations of the dynamical function. The Breit-Wigner formalism—the first term in a Taylor expansion about a T -matrix pole—is the simplest formulation. The K -matrix formalism [5] is more general (allowing more than one T -matrix pole and coupled channels while preserving unitarity). The Flatté distribution [20] is used to parametrize resonances near threshold and is equivalent to a one-pole, two-channel K -matrix.

Breit-Wigner Formulation: The common formulation of a Breit-Wigner resonance decaying to spin-0 particles a and b is

$$T_r(m_{ab}) = \frac{1}{m_r^2 - m_{ab}^2 - im_r \Gamma_{ab}(q)}. \quad (5)$$

The “mass-dependent” width Γ is

$$\Gamma = \Gamma_r \left(\frac{q}{q_r}\right)^{2L+1} \left(\frac{m_r}{m_{ab}}\right) B_L'(q, q_0)^2, \quad (6)$$

and $B_L'(q, q_0)$ is the Blatt-Weisskopf barrier factor from Table 1. A Breit-Wigner parametrization best describes isolated, non-overlapping resonances far from the threshold of additional decay channels. For the ρ and $\rho(1450)$ a more complex parametrization suggested by Gounaris-Sakurai [21] is often used [22-26]. Unitarity can be violated when the dynamical function is parametrized as the sum of two or more overlapping Breit-Wigners. The proximity of a threshold to a resonance distorts the line shape from a simple Breit-Wigner. Here the Flatté formula provides a better description and is discussed below.

K -matrix Formalism: The T matrix can be written as

$$\hat{T} = (I - i\hat{K}\rho)^{-1}\hat{K}, \quad (7)$$

where \hat{K} is the Lorentz-invariant K -matrix describing the scattering process and ρ is the phase-space factor. Resonances appear as poles in the K -matrix:

$$\hat{K}_{ij} = \sum_{\alpha} \frac{\sqrt{m_{\alpha}\Gamma_{\alpha i}(m)m_{\alpha}\Gamma_{\alpha j}(m)}}{(m_{\alpha}^2 - m^2)\sqrt{\rho_i\rho_j}}. \quad (8)$$

The K -matrix is real by construction, and so the associated T -matrix respects unitarity.

For a single pole in a single channel, K is

$$K = \frac{m_0\Gamma(m)}{m_0^2 - m^2} \quad (9)$$

and

$$T = K(1 - iK)^{-1} = \frac{m_0\Gamma(m)}{m_0^2 - m^2 - im_0\Gamma(m)}, \quad (10)$$

which is the relativistic Breit-Wigner formula. For two poles in a single channel, K is

$$K = \frac{m_{\alpha}\Gamma_{\alpha}(m)}{m_{\alpha}^2 - m^2} + \frac{m_{\beta}\Gamma_{\beta}(m)}{m_{\beta}^2 - m^2}. \quad (11)$$

If m_{α} and m_{β} are far apart relative to the widths, the T matrix is approximately the sum of two Breit-Wigners, $T(K_{\alpha} + K_{\beta}) \approx T(K_{\alpha}) + T(K_{\beta})$, each of the form of Eq. (10). This approximation is not valid for two nearby resonances, in which case T can violate unitarity.

This formulation, which applies to S -channel production in two-body scattering, $ab \rightarrow cd$, can be generalized to describe the production of resonances in processes such as the decay of charm mesons. The key assumption here is that the two-body system described by the K -matrix does *not* interact with the rest of the final state [8]. The validity of this assumption varies with the production process and is appropriate for reactions such as $\pi^- p \rightarrow \pi^0 \pi^0 n$ and semileptonic decays such as $D \rightarrow K \pi \ell \nu$. The assumption may be of limited validity for production processes such as $p\bar{p} \rightarrow \pi\pi\pi$ or $D \rightarrow \pi\pi\pi$. In these cases, the two-body Lorentz-invariant amplitude, \hat{F} , is given by

$$\hat{F}_i = (I - i\hat{K}\rho)_{ij}^{-1}\hat{P}_j = (\hat{T}\hat{K}^{-1})_{ij}\hat{P}_j, \quad (12)$$

where P is the production vector that parametrizes the resonance production in the open channels.

For the $\pi\pi$ S-wave, a common formulation of the K -matrix [7,24,25] is

$$K_{ij}(s) = \left[\sum_{\alpha} \left(\frac{g_i^{(\alpha)} g_j^{(\alpha)}}{m_{\alpha}^2 - s} \right) + f_{ij}^{sc} \frac{1 - s_0^{sc}}{s - s_0^{sc}} \right] \left[\frac{(s - s_A m_{\pi}^2 / 2)(1 - s_{A0})}{(s - s_{A0})} \right]. \quad (13)$$

The factor $g_i^{(\alpha)}$ is the real coupling constant of the K -matrix pole m_{α} to meson channel i ; the parameters f_{ij}^{sc} and s_0^{sc} describe a smooth part of the K -matrix elements; the second factor in square brackets suppresses a false kinematical singularity near

the $\pi\pi$ threshold (the Adler zero); and the number 1 has units GeV^2 .

The production vector, with $i = 1$ denoting $\pi\pi$, is

$$P_j(s) = \left[\sum_{\alpha} \left(\frac{\beta_{\alpha} g_j^{(\alpha)}}{m_{\alpha}^2 - s} \right) + f_{1j}^{pr} \frac{1 - s_0^{pr}}{s - s_0^{pr}} \right] \left[\frac{(s - s_A m_{\pi}^2 / 2)(1 - s_{A0})}{(s - s_{A0})} \right]. \quad (14)$$

where the free parameters of the Dalitz plot fit are the complex production couplings β_{α} and the production-vector background parameters f_{1j}^{pr} and s_0^{pr} . All other parameters are fixed by scattering experiments. Ref. [6] describes the $\pi\pi$ scattering data with a 4-pole, 2-channel ($\pi\pi$, $K\bar{K}$) model, while Ref. [7] describes the scattering data with 5-pole, 5-channel ($\pi\pi$, $K\bar{K}$, $\eta\eta$, $\eta'\eta'$ and 4π) model. The former has been implemented by CLEO [27] and the latter by FOCUS [25] and BABAR [24]. In both cases, only the $\pi\pi$ channel was analyzed. A more complete coupled-channel analysis would simultaneously fit all final states accessible by rescattering.

Flatté Formalism: The Flatté formulation is used when a second channel opens close to a resonance:

$$\hat{T}(m_{ab}) = \frac{1}{m_r^2 - m_{ab}^2 - i(\rho_1 g_1^2 + \rho_2 g_2^2)}, \quad (15)$$

where $g_1^2 + g_2^2 = m_0\Gamma_r$. This situation occurs in the $\pi\pi$ S-wave where the $f_0(980)$ is near the $K\bar{K}$ threshold, and in the $\pi\eta$ channel where the $a_0(980)$ also lies near the $K\bar{K}$ threshold. For the $a_0(980)$ resonance, the relevant coupling constants are $g_1 = g_{\pi\eta}$ and $g_2 = g_{KK}$, and the phase space terms are $\rho_1 = \rho_{\pi\eta}$ and $\rho_2 = \rho_{KK}$, where

$$\rho_{ab} = \sqrt{\left(1 - \left(\frac{m_a - m_b}{m_{ab}}\right)^2\right) \left(1 - \left(\frac{m_a + m_b}{m_{ab}}\right)^2\right)}. \quad (16)$$

For the $f_0(980)$ the relevant coupling constants are $g_1 = g_{\pi\pi}$ and $g_2 = g_{KK}$, and the phase space terms are $\rho_1 = \rho_{\pi\pi}$ and $\rho_2 = \rho_{KK}$. The charged and neutral K channels are usually assumed to have the same coupling constant but different phase space factors, due to $m_{K^+} \neq m_{K^0}$; the result is

$$\rho_{KK} = \frac{1}{2} \left(\sqrt{1 - \left(\frac{2m_{K^\pm}}{m_{KK}}\right)^2} + \sqrt{1 - \left(\frac{2m_{K^0}}{m_{KK}}\right)^2} \right). \quad (17)$$

Branching Ratios from Dalitz Plot Fits: A fit to the Dalitz plot distribution using either a Breit-Wigner or a K -matrix formalism factorizes into a resonant contribution to the amplitude \mathcal{M}_j and a complex coefficient, $a_j e^{i\delta_j}$, where a_j and δ_j are real. The definition of a rate of a single process, given a set of amplitudes a_j and phases δ_j , is the square of the relevant matrix element (see Eq. (1)). The “fit fraction” is usually defined as the integral over the Dalitz plot (m_{ab} vs. m_{bc}) of a single amplitude squared divided by the integral over the Dalitz plot of the square of the coherent sum of all amplitudes, or

$$\text{fit fraction}_j = \frac{\int |a_j e^{i\delta_j} \mathcal{M}_j|^2 dm_{ab}^2 dm_{bc}^2}{\int |\sum_k a_k e^{i\delta_k} \mathcal{M}_k|^2 dm_{ab}^2 dm_{bc}^2}, \quad (18)$$

Meson Particle Listings

D^\pm

where \mathcal{M}_j is defined in Eq. (2) and described in Ref. [28]. In general, the sum of the fit fractions for all components will not be unity due to interference.

When the K -matrix of Eq. (12) is used to describe a wave (e.g., the $\pi\pi$ S-wave), then \mathcal{M}_j refers to the entire wave. In this case, it may not be straightforward to separate \mathcal{M}_j into a sum of individual resonances unless these are narrow and well separated.

Reconstruction Efficiency and Resolution: The efficiency for reconstructing an event as a function of position on the Dalitz plot is in general non-uniform. Typically, a Monte Carlo sample generated with a uniform distribution in phase space is used to determine the efficiency. The variation in efficiency across the Dalitz plot varies with experiment and decay mode. Most recent analyses utilize a full GEANT [29] detector simulation.

Finite detector resolution can usually be safely neglected as most resonances are comparatively broad. Notable exceptions where detector resolution effects must be modeled are $\phi \rightarrow K^+K^-$, $\omega \rightarrow \pi^+\pi^-$, and $a_0 \rightarrow \eta\pi^0$. One approach is to convolve the resolution function in the Dalitz-plot variables m_{ab}^2 and m_{bc}^2 with the function that parametrizes the resonant amplitudes. In high-statistics data samples, resolution effects near the phase-space boundary typically contribute to a poor goodness of fit. The momenta of the final-state particles can be recalculated with a D or B mass constraint, which forces the kinematic boundaries of the Dalitz plot to be strictly respected. If the three-body mass is not constrained, then the efficiency (and the parametrization of background) may also depend on the reconstructed mass.

Backgrounds: The contribution of background to the D and B samples varies by experiment and final state. The background naturally falls into five categories: (i) purely combinatoric background containing no resonances; (ii) combinatoric background containing intermediate resonances, such as a real K^{*-} or ρ , plus additional random particles; (iii) final states containing identical particles as in $D^0 \rightarrow K_S^0\pi^0$ background to $D^0 \rightarrow \pi^+\pi^-\pi^0$ and $B \rightarrow D\pi$ background to $B \rightarrow K\pi\pi$; (iv) mistagged decays such as a real \overline{D}^0 or \overline{B}^0 incorrectly identified as a D^0 or B^0 ; and (v) particle misidentification of the decay products such as $D^+ \rightarrow \pi^-\pi^+\pi^+$ or $D_s^+ \rightarrow K^-K^+\pi^+$ reconstructed as $D^+ \rightarrow K^-\pi^+\pi^+$.

The contribution from combinatoric background with intermediate resonances is distinct from the resonances in the signal because the former do *not* interfere with the latter since they are not from true resonances. Similarly, $D^0 \rightarrow \rho\pi$ and $D^0 \rightarrow K_S^0\pi^0$ do not interfere since strong and weak transitions proceed on different time scales. The usual identification tag of the initial particle as a D^0 or a \overline{D}^0 is the charge of the distinctive slow pion in the decay sequence $D^{*+} \rightarrow D^0\pi_s^+$ or $D^{*-} \rightarrow \overline{D}^0\pi_s^-$. Another possibility is the identification or “tagging” of one of the D mesons from $\psi(3770) \rightarrow D^0\overline{D}^0$, as is done for B mesons from $\Upsilon(4S)$. The mistagged background is subtle and may be

mistakenly enumerated in the *signal* fraction determined by a D^0 mass fit. Mistagged decays contain true \overline{D}^0 's or \overline{B}^0 's and so the resonances in the mistagged sample exhibit interference on the Dalitz plot.

References

1. M Bauer, B. Stech, and M. Wirbel, Z. Phys. C **34**, 103 (1987); P. Bedaque, A. Das, and V.S. Mathur, Phys. Rev. D **49**, 269 (1994); L.-L. Chau and H.-Y. Cheng, Phys. Rev. D **36**, 137 (1987); K. Terasaki, Int. J. Mod. Phys. A **10**, 3207 (1995); F. Buccella, M. Lusignoli, and A. Pugliese, Phys. Lett. B **379**, 249 (1996).
2. J.D. Jackson, Nuovo Cim. **34**, 1644 (1964).
3. R.H. Dalitz, *Phil. Mag.* **44**, 1068 (1953).
4. See the note on Kinematics in this *Review*.
5. S.U. Chung *et al.*, Ann. Physik. **4**, 404 (1995).
6. K.L. Au, D. Morgan, and M.R. Pennington, Phys. Rev. D **35**, 1633 (1987).
7. V.V. Anisovich and A.V. Sarantsev, Eur. Phys. J. A **16**, 229 (2003).
8. I.J.R. Aitchison, Nucl. Phys. A **189**, 417 (1972).
9. S. Fajfer, R.J. Oakes, and T.N. Pham, Phys. Rev. D **60**, 054029 (1999).
10. H.Y. Cheng and K.C. Yang, Phys. Rev. D **66**, 054015 (2002).
11. S. Fajfer, T.N. Pham, and A. Prapotnik, Phys. Rev. D **70**, 034033 (2004).
12. H.Y. Cheng, C.K. Chua, and A. Soni, Phys. Rev. **D72**, 094003 (2005).
13. A. Garmash *et al.* (Belle Collab.), Phys. Rev. D **71**, 092003 (2005).
14. B. Aubert *et al.* (BABAR Collab.), arXiv:hep-ex/0507094.
15. J. Blatt and V. Weisskopf, *Theoretical Nuclear Physics*, New York: John Wiley & Sons (1952).
16. F. von Hippel and C. Quigg, Phys. Rev. D **5**, 624, (1972).
17. C. Zemach, Phys. Rev. B **133**, 1201 (1964); C. Zemach, Phys. Rev. B **140**, 97 (1965).
18. V. Filippini, A. Fontana, and A. Rotondi, Phys. Rev. D **51**, 2247 (1995).
19. M. Jacob and G.C. Wick, Annals Phys. **7**, 404 (1959) [Annals Phys. **281**, 774 (2000)]; S.U. Chung, Phys. Rev. D **48**, 1225, (1993); J.D. Richman, CALT-68-1148.
20. S.M. Flatté, Phys. Lett. B **63**, 224 (1976).
21. G.J. Gounaris and J.J. Sakarai, Phys. Rev. Lett. **21** 244, (1968).
22. B. Aubert *et al.* (BABAR Collab.), arXiv:hep-ex/0408073.
23. K. Abe *et al.* (Belle Collab.), arXiv:hep-ex/0504013.
24. B. Aubert *et al.* (BABAR Collab.), arXiv:hep-ex/0507101.
25. J.M. Link *et al.* (FOCUS Collab.), Phys. Lett. B **585**, 200 (2004).
26. B. Aubert *et al.* (BABAR Collab.), arXiv:hep-ex/0408099.
27. D. Cronin-Hennessy *et al.* (CLEO Collab.), Phys. Rev. D **72**, 031102 (2005).
28. S. Kopp *et al.* (CLEO Collab.), Phys. Rev. D **63**, 092001 (2001).

29. R. Brun *et al.*, GEANT 3.15, CERN Report No. DD/EE/84-1 (1987); R. Brun *et al.*, GEANT 3.21, CERN Program Library Long Writeup W5013 (1993), unpublished; S. Agostinelli *et al.* (GEANT4 Collab.), Nucl. Instrum. Meth. A **506**, 250 (2003).

REVIEW OF D-MESON DALITZ PLOT ANALYSES

Revised April 2010 by D. Asner (Pacific Northwest National Laboratory)

The formalism of Dalitz-plot analysis is reviewed in the preceding note. Recent studies of multi-body decays of charm mesons probe a variety of physics, including γ/ϕ_3 , $D^0-\bar{D}^0$ mixing, searches for CP violation, doubly Cabibbo-suppressed decays, and properties of S-wave $\pi\pi$, $K\pi$, and $K\bar{K}$ resonances. In the following, we discuss: (1) $D^0 \rightarrow K_S^0\pi^+\pi^-$; (2) doubly Cabibbo-suppressed decays; and (3) CP violation. The properties of the light meson resonances determined in D-meson Dalitz-plot analyses are reported in the light unflavored meson section of this *Review*.

$D^0 \rightarrow K_S^0\pi^+\pi^-$: Several experiments have analyzed $D^0 \rightarrow K_S^0\pi^+\pi^-$ decay. A CLEO analysis [1] included ten resonances: $K_S^0\rho^0$, $K_S^0\omega$, $K_S^0f_0(980)$, $K_S^0f_2(1270)$, $K_S^0f_0(1370)$, $K^*(892)^-\pi^+$, $K_0^*(1430)^-\pi^+$, $K_2^*(1430)^-\pi^+$, $K^*(1680)^-\pi^+$, and the doubly Cabibbo-suppressed (DCS) mode $K^*(892)^+\pi^-$. The CLEO model does not provide a good description of higher-statistics BABAR and Belle data samples. An improved description is obtained in three ways: First, by adding more Breit-Wigner resonances. Second, following the methodology of FOCUS [2], by applying a K -matrix model [3–5] to the $\pi\pi$ S-wave [6,7]. Third, by adding a parameterization to the $K\pi$ S-wave motivated by the LASS experiment [8].

A BABAR analysis [7,9,10] added to the CLEO model the $K^*(1410)^-\pi^+$, $K_S^0\rho^0(1450)$, the DCS modes $K_0^*(1430)^+\pi^-$ and $K_2^*(1430)^+\pi^-$, and two Breit-Wigner $\pi\pi$ S-wave contributions. A Belle analysis [11–13] included all the components of BABAR and added two more DCS modes, $K^*(1410)^+\pi^-$ and $K^*(1680)^+\pi^-$. Recently, BABAR has modeled the $\pi\pi$ S-wave using a K -matrix model for the $\pi\pi$ and $K\pi$ S-waves [14].

The primary motivation for the analysis of the decay $D^0 \rightarrow K_S^0\pi^+\pi^-$ is to study $D^0 - \bar{D}^0$ oscillations and the CKM angles. The quasi-two-body intermediate states include both CP -even and CP -odd eigenstates as well as doubly Cabibbo-suppressed channels. Time-dependent analyses of the Dalitz plot from CLEO [15] and Belle [6] simultaneously determined the strong transition amplitudes and phases, the mixing parameters x and y without phase or sign ambiguity, and the CP -violating parameter $|q/p|$ and $\text{Arg}(q/p)$. See the note on “ $D^0 - \bar{D}^0$ Mixing” for a discussion.

The CKM angle γ/ϕ_3 [16] and the quark-mixing parameter $\cos 2\beta/\phi_1$ [17] can be determined using the decays $B^- \rightarrow D^{(*)}K^{(*)-}$ and $\bar{B}^0 \rightarrow Dh^0$, respectively, followed by the decay $D \rightarrow K_S^0\pi^+\pi^-$. The Belle and BABAR experiments measured γ/ϕ_3 (Belle [11–13] and BABAR [7,9,10,14,18]) and $\cos 2\beta/\phi_1$ (Belle [19], BABAR [20]). In these analyses, a large systematic

uncertainty in the relative phase between the D^0 and \bar{D}^0 amplitudes point by point across the Dalitz plot remains to be fully understood.

The quantum entangled production of $D^0\bar{D}^0$ pairs from $\psi(3770)$ enables a model-independent determination of the D^0/\bar{D}^0 relative phase. Studying CP -tagged Dalitz plots [21,22] provides sensitivity to the cosine of the relative phase, while studying double-tagged Dalitz plots [22] probes both the cosine and sine of the D^0/\bar{D}^0 phase difference. CLEO analyzed [23] the $D^0 \rightarrow K_S^0\pi^+\pi^-$ and $D^0 \rightarrow K_L^0\pi^+\pi^-$ samples using the CP -even tag modes K^+K^- , $\pi^+\pi^-$, $K_L^0\pi^0$ (vs. $K_S^0\pi^+\pi^-$ only), the CP -odd tag modes $K_S^0\pi^0$, $K_S^0\eta$, and the double-tag modes $(K_S^0\pi^+\pi^-)^2$ and $(K_S^0\pi^+\pi^-)(K_L^0\pi^+\pi^-)$. These measurements can reduce the model uncertainty on γ/ϕ_3 to about 3° .

Doubly Cabibbo-Suppressed Decays: There are two classes of multibody doubly Cabibbo-suppressed (DCS) decays of D mesons. The first consists of those in which the DCS and corresponding Cabibbo-favored (CF) decays populate distinct Dalitz plots; the pairs $D^0 \rightarrow K^+\pi^-\pi^0$ and $D^0 \rightarrow K^-\pi^+\pi^0$, or $D^+ \rightarrow K^+\pi^+\pi^-$ and $D^+ \rightarrow K^-\pi^+\pi^+$, are examples. Our average of three measurements of $\Gamma(D^0 \rightarrow K^+\pi^-\pi^0)/\Gamma(D^0 \rightarrow K^-\pi^+\pi^0)$ is $(2.20 \pm 0.10) \times 10^{-3}$. Our average of four measurements of $\Gamma(D^+ \rightarrow K^+\pi^-\pi^+)/\Gamma(D^+ \rightarrow K^-\pi^+\pi^+)$ is $(5.77 \pm 0.22) \times 10^{-3}$; see the Particle Listings.

The second class consists of decays in which the DCS and CF modes populate the same Dalitz plot; for example, $D^0 \rightarrow K^{*-}\pi^+$ and $D^0 \rightarrow K^{*+}\pi^-$ both contribute to $D^0 \rightarrow K_S^0\pi^+\pi^-$. In this class, the potential for interference of DCS and CF amplitudes increases the sensitivity to the DCS amplitude and allows direct measurement of the relative strong phases between amplitudes. CLEO [1] and Belle [6] have measured the relative phase between $D^0 \rightarrow K^*(892)^+\pi^-$ and $D^0 \rightarrow K^*(892)^-\pi^+$ to be $(189 \pm 10 \pm 3^{+15}_-5)^\circ$ and $(171.9 \pm 1.3)^\circ$ (statistical error only). These results are close to the 180° expected from Cabibbo factors and a small strong phase.

In addition, Belle [6] has results for both the relative phase (statistical errors only) and ratio R (central values only) of the DCS fit fraction relative to the CF fit fractions for $K^*(892)^+\pi^-$, $K_0^*(1430)^+\pi^-$, $K_2^*(1430)^+\pi^-$, $K^*(1410)^+\pi^-$, and $K^*(1680)^+\pi^-$. The systematic uncertainties on R must be evaluated. The values for R in units of $\tan^4\theta_c$ are 2.94 ± 0.12 , 22.0 ± 1.6 , 34 ± 4 , 87 ± 13 , and 500 ± 500 . For $K^+\pi^-$, the corresponding value for R_D is $(1.28 \pm 0.02) \times \tan^4\theta_c$. Similarly, BABAR [7] has reported central values for R for $K^*(892)^+\pi^-$, $K_0^*(1430)^+\pi^-$, and $K_2^*(1430)^+\pi^-$. The values for R in units of $\tan^4\theta_c$ are 3.45 ± 0.31 , 7.7 ± 3.0 , and 1.7 ± 1.7 , respectively. Recently, BABAR [14] has used a K -matrix formalism to describe the $\pi\pi$ S-wave in $K_S^0\pi^+\pi^-$. The reported values for R in units of $\tan^4\theta_c$ are 2.78 ± 0.11 , 0.5 ± 0.2 , and 1.4 ± 0.5 , respectively. The large differences in R among these final states could point to an interesting role for hadronic effects.

There are other ways, not involving DCS decays, in which D^0 and \bar{D}^0 singly Cabibbo-suppressed decays can populate the

Meson Particle Listings

 D^\pm

same Dalitz plot. Examples are D^0 and \bar{D}^0 decays to $K_S^0 K^+ \pi^-$, or to $K_S^0 K^- \pi^+$. These final states can be used to study D^0 - \bar{D}^0 mixing and the CKM angle γ/ϕ_3 .

CP Violation: In the limit of CP conservation, charge conjugate decays will have the same Dalitz-plot distribution. The $D^{*\pm}$ tag enables the discrimination between D^0 and \bar{D}^0 . The integrated CP violation across the Dalitz plot is determined in two ways. The first uses

$$\mathcal{A}_{CP} = \int \left(\frac{|\mathcal{M}|^2 - |\bar{\mathcal{M}}|^2}{|\mathcal{M}|^2 + |\bar{\mathcal{M}}|^2} \right) dm_{ab}^2 dm_{bc}^2 / \int dm_{ab}^2 dm_{bc}^2, \quad (1)$$

where \mathcal{M} and $\bar{\mathcal{M}}$ have the same normalization and represent the D^0 and \bar{D}^0 Dalitz-plot amplitudes for the three-body decay $D \rightarrow abc$, and m_{ab} (m_{bc}) is the invariant mass of ab (bc). The second uses the asymmetry in the efficiency-corrected D^0 and \bar{D}^0 yields,

$$\mathcal{A}_{CP} = \frac{N_{D^0} - N_{\bar{D}^0}}{N_{D^0} + N_{\bar{D}^0}}. \quad (2)$$

These expressions are less sensitive to CP violation than are the individual resonant submodes [24–26]. Our Particle Listings give limits on CP violation for 12 D^+ , 52 D^0 , and 13 D_S^+ decay modes. No evidence of CP violation has been observed in D -meson decays.

The possibility of interference between CP -conserving and CP -violating amplitudes provides a more sensitive probe of CP violation. The constraints on the square of the CP -violating amplitudes obtained in the resonant submodes of $D^0 \rightarrow K_S^0 \pi^+ \pi^-$ range from 3.5×10^{-4} to 28.4×10^{-4} at 95% confidence level [24]. A similar analysis has been performed by CLEO [25] searching for CP violation in $D^+ \rightarrow K^+ K^- \pi^+$. The constraints on the square of the CP -violating amplitudes in the resonant submodes range from 4×10^{-4} to 51×10^{-4} at 95%. BABAR finds no evidence for CP -violating amplitudes in the resonant submodes of $D^0 \rightarrow K^+ K^- \pi^0$ and $D^0 \rightarrow \pi^+ \pi^- \pi^0$ [26].

References

- H. Muramatsu *et al.* (CLEO Collab.), Phys. Rev. Lett. **89**, 251802 (2002).
- J.M. Link *et al.* (FOCUS Collab.), Phys. Lett. **B585**, 200 (2004).
- E. P. Wigner, Phys. Rev. **70**, 15 (1946).
- S. U. Chung *et al.*, Annalen Phys. **4**, 404 (1995).
- I. J. R. Aitchison, Nucl. Phys. **A189**, 417 (1972).
- L.M. Zhang *et al.* (Belle Collab.), Phys. Rev. Lett. **99**, 131803 (2007).
- B. Aubert *et al.* (BABAR Collab.), Phys. Rev. Lett. **95**, 121802 (2005).
- D. Aston *et al.* (LASS Collab.), Nucl. Phys. **B296**, 493 (1988).
- B. Aubert *et al.* (BABAR Collab.), hep-ex/0507101.
- B. Aubert *et al.* (BABAR Collab.), arXiv:hep-ex/0607104.
- A. Poluektov *et al.* (Belle Collab.), Phys. Rev. **D70**, 072003 (2004).
- K. Abe *et al.* (Belle Collab.), hep-ex/0411049.

- A. Poluektov *et al.* (Belle Collab.), Phys. Rev. **D73**, 112009 (2006).
- B. Aubert *et al.* (BABAR Collab.), Phys. Rev. **D78**, 034023 (2008).
- D.M. Asner *et al.* (CLEO Collab.), Phys. Rev. **D72**, 012001 (2005).
- A. Giri *et al.*, Phys. Rev. **D68**, 054018 (2003).
- A. Bondar, T. Gershon, and P. Krokovny, Phys. Lett. **B624**, 1 (2005).
- B. Aubert *et al.* (BABAR Collab.), Phys. Rev. **D79**, 072003 (2009).
- P. Krokovny *et al.* (Belle Collab.), Phys. Rev. Lett. **97**, 081801 (2006).
- B. Aubert *et al.* (BABAR Collab.), arXiv:hep-ex/0607105.
- A. Bondar and A. Poluektov, Eur. Phys. J. **C47**, 347 (2006).
- A. Bondar and A. Poluektov, arXiv:hep-ph/0703267.
- R. A. Briere *et al.* (CLEO Collab.), Phys. Rev. **D80**, 032002 (2009).
- D.M. Asner *et al.* (CLEO Collab.), Phys. Rev. **D70**, 091101R (2004).
- P. Rubin *et al.* (CLEO Collab.), Phys. Rev. **D78**, 072003 (2008).
- B. Aubert *et al.* (BABAR Collab.), Phys. Rev. **D78**, 051102 (2008).

 $\Gamma((K^- \pi^+)_{S\text{-wave}} \pi^+) / \Gamma(K^- 2\pi^+)$ Γ_{39}/Γ_{38}

This is the “fit fraction” from the Dalitz-plot analysis. The $K^- \pi^+$ S -wave includes a broad scalar κ ($\bar{K}_0^*(800)$), the $\bar{K}_0^*(1430)^0$, and non-resonant background.

VALUE	DOCUMENT ID	TECN	COMMENT
0.801 ± 0.012 OUR AVERAGE			
0.8024 ± 0.0138 ± 0.0043	³⁶ LINK	09	FOCS MIPWA fit, 53k evts
0.838 ± 0.038	³⁷ BONVICINI	08A	CLEO QMIPWA fit, 141k evts
0.786 ± 0.014 ± 0.018	AITALA	06	E791 Dalitz fit, 15.1k events
••• We do not use the following data for averages, fits, limits, etc. •••			
0.8323 ± 0.0150 ± 0.0008	³⁸ LINK	07B	FOCS See LINK 09

³⁶ This LINK 09 model-independent partial-wave analysis of the $K^- \pi^+$ S -wave slices the $K^- \pi^+$ mass range into 39 bins.

³⁷ The BONVICINI 08A QMIPWA (quasi-model-independent partial-wave analysis) of the $K^- \pi^+$ S -wave amplitude slices the $K^- \pi^+$ mass range into 26 bins but keeps the Breit-Wigner $\bar{K}_0^*(1430)^0$.

³⁸ This LINK 07B fit uses a K matrix. The $K^- \pi^+$ S -wave fit fraction given above breaks down into (207.3 ± 25.5 ± 12.4)% isospin-1/2 and (40.5 ± 9.6 ± 3.2)% isospin-3/2 — with large interference between the two. The isospin-1/2 component includes the κ (or $\bar{K}_0^*(800)^0$) and $\bar{K}_0^*(1430)^0$.

 $\Gamma(\bar{K}_0^*(800)^0 \pi^+, \bar{K}_0^*(800) \rightarrow K^- \pi^+) / \Gamma(K^- 2\pi^+)$ Γ_{40}/Γ_{38}

This is the “fit fraction” from the Dalitz-plot analysis.

VALUE	DOCUMENT ID	TECN	COMMENT
••• We do not use the following data for averages, fits, limits, etc. •••			
0.478 ± 0.121 ± 0.053	AITALA	02	E791 See AITALA 06, above

 $\Gamma(\bar{K}_0^*(1430)^0 \pi^+, \bar{K}_0^*(1430)^0 \rightarrow K^- \pi^+) / \Gamma(K^- 2\pi^+)$ Γ_{41}/Γ_{38}

This is the “fit fraction” from the Dalitz-plot analysis.

VALUE	DOCUMENT ID	TECN	COMMENT
0.1330 ± 0.0062	BONVICINI	08A	CLEO QMIPWA fit, 141k evts
••• We do not use the following data for averages, fits, limits, etc. •••			
0.125 ± 0.014 ± 0.005	AITALA	02	E791 See AITALA 06, above
0.284 ± 0.022 ± 0.059	FRABETTI	94G	E687 Dalitz fit, 8800 evts
0.248 ± 0.019 ± 0.017	ANJOS	93	E691 γ Be 90–260 GeV

 $\Gamma(\bar{K}^*(892)^0 \pi^+, \bar{K}^*(892)^0 \rightarrow K^- \pi^+) / \Gamma(K^- 2\pi^+)$ Γ_{42}/Γ_{38}

This is the “fit fraction” from the Dalitz-plot analysis.

VALUE	DOCUMENT ID	TECN	COMMENT
0.111 ± 0.012 OUR AVERAGE	Error includes scale factor of 3.7.		
0.1236 ± 0.0034 ± 0.0034	LINK	09	FOCS MIPWA fit, 53k evts
0.0988 ± 0.0046	BONVICINI	08A	CLEO QMIPWA fit, 141k evts
0.119 ± 0.002 ± 0.020	AITALA	06	E791 Dalitz fit, 15.1k events

• • • We do not use the following data for averages, fits, limits, etc. • • •

$0.1361 \pm 0.0041 \pm 0.0030$	³⁹ LINK	07b	FOCS	See LINK 09
$0.123 \pm 0.010 \pm 0.009$	AITALA	02	E791	See AITALA 06
$0.137 \pm 0.006 \pm 0.009$	FRABETTI	94c	E687	Dalitz fit, 8800 evts
$0.170 \pm 0.009 \pm 0.034$	ANJOS	93	E691	γ Be 90–260 GeV
$0.14 \pm 0.04 \pm 0.04$	ALVAREZ	91b	NA14	Photoproduction
$0.13 \pm 0.01 \pm 0.07$	ADLER	87	MRK3	e^+e^- 3.77 GeV

³⁹The statistical error on this LINK 07b value is corrected in LINK 09.

$\Gamma(\bar{K}^*(1410)^0 \pi^+, \bar{K}^{*0} \rightarrow K^- \pi^+)/\Gamma(K^- 2\pi^+)$ Γ_{43}/Γ_{38}

VALUE (units 10^{-3})	DOCUMENT ID	TECN	COMMENT
not seen	LINK	09	FOCS MIPWA fit, 53k evts
not seen	BONVICINI	08A	CLEO QMIPWA fit, 141k evts

• • • We do not use the following data for averages, fits, limits, etc. • • •

$4.8 \pm 2.1 \pm 1.7$	LINK	07b	FOCS	See LINK 09
-----------------------	------	-----	------	-------------

$\Gamma(\bar{K}_2^*(1430)^0 \pi^+, \bar{K}_2^*(1430)^0 \rightarrow K^- \pi^+)/\Gamma(K^- 2\pi^+)$ Γ_{44}/Γ_{38}

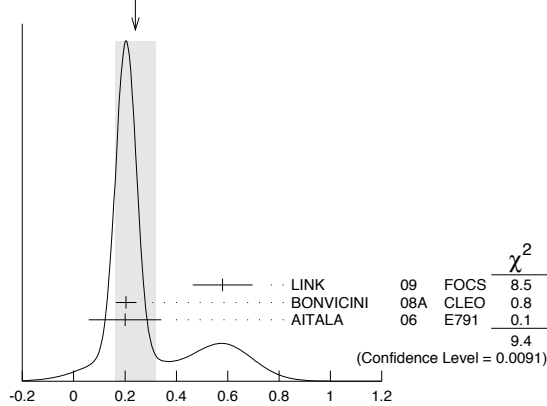
This is the “fit fraction” from the Dalitz-plot analysis.

VALUE (units 10^{-2})	DOCUMENT ID	TECN	COMMENT
0.24 ± 0.08 OUR AVERAGE	Error includes scale factor of 2.2. See the ideogram below.		
$0.58 \pm 0.10 \pm 0.06$	LINK	09	FOCS MIPWA fit, 53k evts
0.204 ± 0.040	BONVICINI	08A	CLEO QMIPWA fit, 141k evts
$0.2 \pm 0.1 \pm 0.1$	AITALA	06	E791 Dalitz fit, 15.1k events

• • • We do not use the following data for averages, fits, limits, etc. • • •

$0.39 \pm 0.09 \pm 0.05$	LINK	07b	FOCS	See LINK 09
$0.5 \pm 0.1 \pm 0.2$	AITALA	02	E791	See AITALA 06

WEIGHTED AVERAGE
 0.24 ± 0.08 (Error scaled by 2.2)



$\Gamma(\bar{K}_2^*(1430)^0 \pi^+, \bar{K}_2^*(1430)^0 \rightarrow K^- \pi^+)/\Gamma(K^- 2\pi^+)$ Γ_{44}/Γ_{38}
(units 10^{-2})

$\Gamma(\bar{K}^*(1680)^0 \pi^+, \bar{K}^*(1680)^0 \rightarrow K^- \pi^+)/\Gamma(K^- 2\pi^+)$ Γ_{45}/Γ_{38}

VALUE (units 10^{-2})	DOCUMENT ID	TECN	COMMENT
0.23 ± 0.12 OUR AVERAGE	Error includes scale factor of 1.6.		
$1.75 \pm 0.62 \pm 0.54$	LINK	09	FOCS MIPWA fit, 53k evts
0.196 ± 0.118	BONVICINI	08A	CLEO QMIPWA fit, 141k evts
$1.2 \pm 0.6 \pm 1.2$	AITALA	06	E791 Dalitz fit, 15.1k events

• • • We do not use the following data for averages, fits, limits, etc. • • •

$1.90 \pm 0.63 \pm 0.43$	LINK	07b	FOCS	See LINK 09
$2.5 \pm 0.7 \pm 0.3$	AITALA	02	E791	See AITALA 06
$4.7 \pm 0.6 \pm 0.7$	FRABETTI	94c	E687	Dalitz fit, 8800 evts
$3.0 \pm 0.4 \pm 1.3$	ANJOS	93	E691	γ Be 90–260 GeV

$\Gamma(K^- (2\pi^+)_{I=2})/\Gamma(K^- 2\pi^+)$ Γ_{46}/Γ_{38}

VALUE	DOCUMENT ID	TECN	COMMENT
0.155 ± 0.028	BONVICINI	08A	CLEO QMIPWA fit, 141k evts

$\Gamma(K^- 2\pi^+ \text{ nonresonant})/\Gamma(K^- 2\pi^+)$ Γ_{47}/Γ_{38}

This is the “fit fraction” from the Dalitz-plot analysis. Later analyses find little need for this decay mode.

VALUE	DOCUMENT ID	TECN	COMMENT
not seen	Error includes scale factor of 1.3.		
$0.130 \pm 0.058 \pm 0.044$	AITALA	02	E791 See AITALA 06
$0.998 \pm 0.037 \pm 0.072$	FRABETTI	94c	E687 Dalitz fit, 8800 evts
$0.838 \pm 0.088 \pm 0.275$	ANJOS	93	E691 γ Be 90–260 GeV
$0.79 \pm 0.07 \pm 0.15$	ADLER	87	MRK3 e^+e^- 3.77 GeV

• • • We do not use the following data for averages, fits, limits, etc. • • •

$\Gamma(K_S^0 \pi^+ \pi^0)/\Gamma_{\text{total}}$ Γ_{48}/Γ

VALUE (units 10^{-2})	EVTS	DOCUMENT ID	TECN	COMMENT
6.90 ± 0.32 OUR FIT	Error includes scale factor of 1.3.			
$6.99 \pm 0.09 \pm 0.25$	40	DOBBS	07	CLEO e^+e^- at $\psi(3770)$

• • • We do not use the following data for averages, fits, limits, etc. • • •

$7.2 \pm 0.2 \pm 0.4$	5090 ± 100	40	HE	05	CLEO	See DOBBS 07
$5.1 \pm 1.3 \pm 0.8$	159		ADLER	88c	MRK3	e^+e^- 3.77 GeV

$\Gamma(K_S^0 \rho^+)/\Gamma(K_S^0 \pi^+ \pi^0)$ Γ_{49}/Γ_{48}

VALUE	DOCUMENT ID	TECN	COMMENT
0.68 ± 0.08 ± 0.12	ADLER	87	MRK3 e^+e^- 3.77 GeV

$\Gamma(\bar{K}^*(892)^0 \pi^+, \bar{K}^*(892)^0 \rightarrow K_S^0 \pi^0)/\Gamma(K_S^0 \pi^+ \pi^0)$ Γ_{50}/Γ_{48}

VALUE	DOCUMENT ID	TECN	COMMENT
0.19 ± 0.06 ± 0.06	ADLER	87	MRK3 e^+e^- 3.77 GeV

$\Gamma(K_S^0 \pi^+ \pi^0 \text{ nonresonant})/\Gamma(K_S^0 \pi^+ \pi^0)$ Γ_{51}/Γ_{48}

VALUE	DOCUMENT ID	TECN	COMMENT
0.13 ± 0.07 ± 0.08	ADLER	87	MRK3 e^+e^- 3.77 GeV

$\Gamma(K^- 2\pi^+ \pi^0)/\Gamma_{\text{total}}$ Γ_{52}/Γ

See our 2008 Review (Physics Letters **B667** 1 (2008)) for measurements of submodes of this mode. There is nothing new since 1992, and the two papers, ANJOS 92c, with 91 ± 12 events above background, and COFFMAN 92b, with 142 ± 20 such events, could not determine submode fractions with much accuracy.

VALUE (units 10^{-2})	EVTS	DOCUMENT ID	TECN	COMMENT
6.08 ± 0.29 OUR FIT	Error includes scale factor of 1.6.			
$5.98 \pm 0.08 \pm 0.16$	41	DOBBS	07	CLEO e^+e^- at $\psi(3770)$

• • • We do not use the following data for averages, fits, limits, etc. • • •

$6.0 \pm 0.2 \pm 0.2$	4840 ± 100	41	HE	05	CLEO	See DOBBS 07
$5.8 \pm 1.2 \pm 1.2$	142		COFFMAN	92b	MRK3	e^+e^- 3.77 GeV
$6.3 \pm 1.4 \pm 1.2$	175		BALTRUSAITIS	86e	MRK3	See COFFMAN 92b

⁴¹DOBBS 07 and HE 05 use single- and double-tagged events in an overall fit. DOBBS 07 supersedes HE 05.

$\Gamma(K_S^0 2\pi^+ \pi^-)/\Gamma_{\text{total}}$ Γ_{53}/Γ

See our 2008 Review (Physics Letters **B667** 1 (2008)) for measurements of submodes of this mode. There is nothing new since 1992, and the two papers, ANJOS 92c, with 229 ± 17 events above background, and COFFMAN 92b, with 209 ± 20 such events, could not determine submode fractions with much accuracy.

VALUE (units 10^{-2})	EVTS	DOCUMENT ID	TECN	COMMENT
3.10 ± 0.11 OUR FIT	Error includes scale factor of 1.1.			
$3.122 \pm 0.046 \pm 0.096$	42	DOBBS	07	CLEO e^+e^- at $\psi(3770)$

• • • We do not use the following data for averages, fits, limits, etc. • • •

$3.2 \pm 0.1 \pm 0.2$	3210 ± 85	42	HE	05	CLEO	See DOBBS 07
$2.1 \pm 1.0 \pm 0.9$		43	BARLAG	92c	ACCM	π^- Cu 230 GeV
$3.3 \pm 0.8 \pm 0.2$	168		ADLER	88c	MRK3	e^+e^- 3.77 GeV

⁴²DOBBS 07 and HE 05 use single- and double-tagged events in an overall fit. DOBBS 07 supersedes HE 05.

⁴³BARLAG 92c computes the branching fraction by topological normalization.

$\Gamma(K^- 3\pi^+ \pi^-)/\Gamma(K^- 2\pi^+)$ Γ_{54}/Γ_{38}

VALUE	EVTS	DOCUMENT ID	TECN	COMMENT		
0.061 ± 0.005 OUR FIT	Error includes scale factor of 1.1.					
$0.058 \pm 0.002 \pm 0.006$	2923	42	DOBBS	07	CLEO	γ A, $\bar{E}_\gamma \approx 180$ GeV

• • • We do not use the following data for averages, fits, limits, etc. • • •

$0.077 \pm 0.008 \pm 0.010$	239		FRABETTI	97c	E687	γ Be, $\bar{E}_\gamma \approx 200$ GeV
$0.09 \pm 0.01 \pm 0.01$	113		ANJOS	90d	E691	Photoproduction

$\Gamma(\bar{K}^*(892)^0 2\pi^+ \pi^-, \bar{K}^*(892)^0 \rightarrow K^- \pi^+)/\Gamma(K^- 3\pi^+ \pi^-)$ Γ_{55}/Γ_{54}

VALUE	DOCUMENT ID	TECN	COMMENT
0.21 ± 0.04 ± 0.06	LINK	03d	FOCS γ A, $\bar{E}_\gamma \approx 180$ GeV

$\Gamma(\bar{K}^*(892)^0 \rho^0 \pi^+, \bar{K}^*(892)^0 \rightarrow K^- \pi^+)/\Gamma(K^- 3\pi^+ \pi^-)$ Γ_{56}/Γ_{54}

VALUE	DOCUMENT ID	TECN	COMMENT
0.40 ± 0.03 ± 0.06	LINK	03d	FOCS γ A, $\bar{E}_\gamma \approx 180$ GeV

$\Gamma(\bar{K}^*(892)^0 \rho^0 \pi^+, \bar{K}^*(892)^0 \rightarrow K^- \pi^+)/\Gamma(K^- 2\pi^+)$ Γ_{56}/Γ_{38}

VALUE	DOCUMENT ID	TECN	COMMENT
not seen	Error includes scale factor of 1.3.		
$0.016 \pm 0.007 \pm 0.004$	FRABETTI	97c	E687 γ Be, $\bar{E}_\gamma \approx 200$ GeV

$\Gamma(\bar{K}^*(892)^0 2\pi^+ \pi^- \text{ no-}\rho, \bar{K}^*(892)^0 \rightarrow K^- \pi^+)/\Gamma(K^- 2\pi^+)$ Γ_{58}/Γ_{38}

VALUE	DOCUMENT ID	TECN	COMMENT
not seen	Error includes scale factor of 1.3.		
$0.032 \pm 0.010 \pm 0.008$	FRABETTI	97c	E687 γ Be, $\bar{E}_\gamma \approx 200$ GeV

Meson Particle Listings

 D^\pm

$\Gamma(K^- \rho^0 2\pi^+)/\Gamma(K^- 3\pi^+ \pi^-)$				Γ_{59}/Γ_{54}
VALUE	DOCUMENT ID	TECN	COMMENT	
0.30 ± 0.04 ± 0.01	LINK	03D	FOCS $\gamma A, \bar{E}_\gamma \approx 180$ GeV	

$\Gamma(K^- \rho^0 2\pi^+)/\Gamma(K^- 2\pi^+)$				Γ_{59}/Γ_{38}
VALUE	DOCUMENT ID	TECN	COMMENT	
● ● ● We do not use the following data for averages, fits, limits, etc. ● ● ●				
0.034 ± 0.009 ± 0.005	FRABETTI	97c	E687 $\gamma Be, \bar{E}_\gamma \approx 200$ GeV	

$\Gamma(\bar{K}^*(892)^0 a_1(1260)^+)/\Gamma(K^- 2\pi^+)$				Γ_{57}/Γ_{38}
VALUE	DOCUMENT ID	TECN	COMMENT	
Unseen decay modes of the $\bar{K}^*(892)^0$ and $a_1(1260)^+$ are included.				
0.099 ± 0.008 ± 0.018	LINK	03D	FOCS $\gamma A, \bar{E}_\gamma \approx 180$ GeV	

$\Gamma(K^- 3\pi^+ \pi^- \text{ nonresonant})/\Gamma(K^- 3\pi^+ \pi^-)$				Γ_{60}/Γ_{54}
VALUE	CL%	DOCUMENT ID	TECN	COMMENT
0.07 ± 0.05 ± 0.01		LINK	03D	FOCS $\gamma A, \bar{E}_\gamma \approx 180$ GeV
● ● ● We do not use the following data for averages, fits, limits, etc. ● ● ●				
<0.026	90	FRABETTI	97c	E687 $\gamma Be, \bar{E}_\gamma \approx 200$ GeV

$\Gamma(K^+ 2K_S^0)/\Gamma(K^- 2\pi^+)$				Γ_{61}/Γ_{38}
VALUE	EVTS	DOCUMENT ID	TECN	COMMENT
0.049 ± 0.022 OUR AVERAGE		Error includes scale factor of 2.4.		
0.035 ± 0.010 ± 0.005	39 ± 9	ALBRECHT	94I	ARG $e^+ e^- \approx 10$ GeV
0.085 ± 0.018	70 ± 12	AMMAR	91	CLEO $e^+ e^- \approx 10.5$ GeV

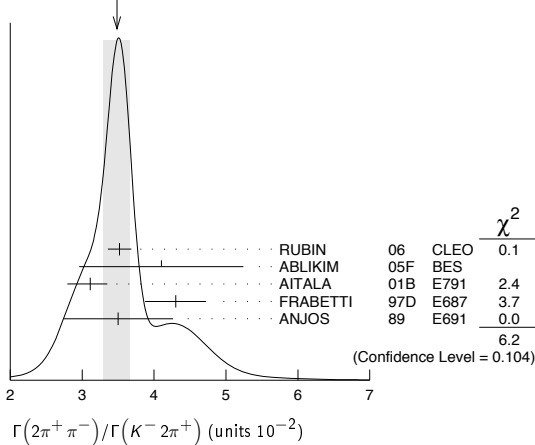
$\Gamma(K^+ K^- K_S^0 \pi^+)/\Gamma(K_S^0 2\pi^+ \pi^-)$				Γ_{62}/Γ_{53}
VALUE (units 10^{-3})	EVTS	DOCUMENT ID	TECN	COMMENT
7.7 ± 1.5 ± 0.9	35 ± 7	LINK	01c	FOCS γ nucleus, $\bar{E}_\gamma \approx 180$ GeV

Pionic modes

$\Gamma(\pi^+ \pi^0)/\Gamma(K^- 2\pi^+)$				Γ_{63}/Γ_{38}
VALUE (units 10^{-2})	EVTS	DOCUMENT ID	TECN	COMMENT
1.34 ± 0.07 OUR AVERAGE		Error includes scale factor of 1.4.		
1.33 ± 0.11 ± 0.09	1229 ± 99	AUBERT,B	06f	BABR $e^+ e^- \approx \Upsilon(4S)$
1.33 ± 0.07 ± 0.06	914 ± 46	RUBIN	06	CLEO $e^+ e^-$ at $\psi(3770)$
1.44 ± 0.19 ± 0.10	171 ± 22	ARMS	04	CLEO $e^+ e^- \approx 10$ GeV

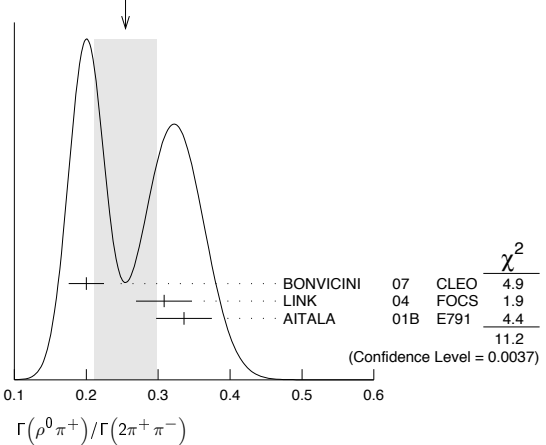
$\Gamma(2\pi^+ \pi^-)/\Gamma(K^- 2\pi^+)$				Γ_{64}/Γ_{38}
VALUE (units 10^{-2})	EVTS	DOCUMENT ID	TECN	COMMENT
3.48 ± 0.19 OUR AVERAGE		Error includes scale factor of 1.4. See the ideogram below.		
3.52 ± 0.11 ± 0.12	3303 ± 95	RUBIN	06	CLEO $e^+ e^-$ at $\psi(3770)$
4.1 ± 1.1 ± 0.3	85 ± 22	ABLIKIM	05f	BES $e^+ e^- \approx \psi(3770)$
3.11 ± 0.18 $^{+0.16}_{-0.26}$	1172	AITALA	01b	E791 π^- nucleus, 500 GeV
4.3 ± 0.3 ± 0.3	236	FRABETTI	97D	E687 $\gamma Be \approx 200$ GeV
3.5 ± 0.7 ± 0.3	83	ANJOS	89	E691 Photoproduction

WEIGHTED AVERAGE
3.48 ± 0.19 (Error scaled by 1.4)



$\Gamma(\rho^0 \pi^+)/\Gamma(2\pi^+ \pi^-)$				Γ_{65}/Γ_{64}
VALUE	DOCUMENT ID	TECN	COMMENT	
0.25 ± 0.04 OUR AVERAGE		Error includes scale factor of 2.4. See the ideogram below.		
0.200 ± 0.023 ± 0.009	BONVICINI	07	CLEO	Dalitz fit, ≈ 2240 evts
0.3082 ± 0.0314 ± 0.0230	LINK	04	FOCS	Dalitz fit, 1527 ± 51 evts
0.336 ± 0.032 ± 0.022	AITALA	01b	E791	Dalitz fit, 1172 evts

WEIGHTED AVERAGE
0.25 ± 0.04 (Error scaled by 2.4)



$\Gamma(\pi^+ (\pi^+ \pi^-)_{S\text{-wave}})/\Gamma(2\pi^+ \pi^-)$				Γ_{66}/Γ_{64}
VALUE	DOCUMENT ID	TECN	COMMENT	
0.5600 ± 0.0324 ± 0.0214	44	LINK	04	FOCS Dalitz fit, 1527 ± 51 evts

44 LINK 04 borrows a K-matrix parametrization from ANISOVICH 03 of the full $\pi-\pi$ S-wave isoscalar scattering amplitude to describe the $\pi^+ \pi^-$ S-wave component of the $\pi^+ \pi^+ \pi^-$ state. The fit fraction given above is a sum over five f_0 mesons, the $f_0(980)$, $f_0(1300)$, $f_0(1200-1600)$, $f_0(1500)$, and $f_0(1750)$. See LINK 04 for details and discussion.

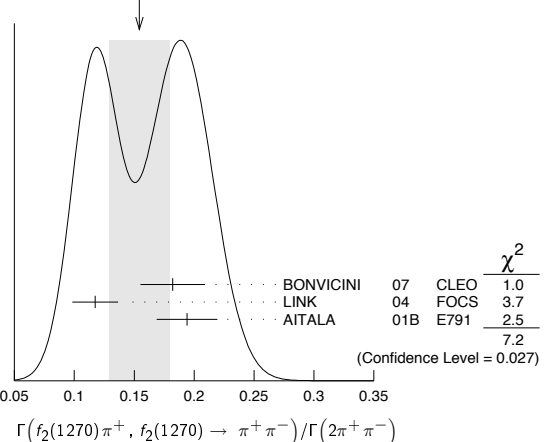
$\Gamma(\sigma \pi^+, \sigma \rightarrow \pi^+ \pi^-)/\Gamma(2\pi^+ \pi^-)$				Γ_{67}/Γ_{64}
VALUE	DOCUMENT ID	TECN	COMMENT	
0.422 ± 0.027 OUR AVERAGE		This is the "fit fraction" from the Dalitz-plot analysis.		
0.418 ± 0.014 ± 0.025	BONVICINI	07	CLEO	Dalitz fit, ≈ 2240 evts
0.463 ± 0.090 ± 0.021	AITALA	01b	E791	Dalitz fit, 1172 evts

$\Gamma(f_0(980) \pi^+, f_0(980) \rightarrow \pi^+ \pi^-)/\Gamma(2\pi^+ \pi^-)$				Γ_{68}/Γ_{64}
VALUE	DOCUMENT ID	TECN	COMMENT	
0.048 ± 0.010 OUR AVERAGE		Error includes scale factor of 1.3.		
0.041 ± 0.009 ± 0.003	BONVICINI	07	CLEO	Dalitz fit, ≈ 2240 evts
0.062 ± 0.013 ± 0.004	AITALA	01b	E791	Dalitz fit, 1172 evts

$\Gamma(f_0(1370) \pi^+, f_0(1370) \rightarrow \pi^+ \pi^-)/\Gamma(2\pi^+ \pi^-)$				Γ_{69}/Γ_{64}
VALUE	DOCUMENT ID	TECN	COMMENT	
0.024 ± 0.013 OUR AVERAGE		This is the "fit fraction" from the Dalitz-plot analysis.		
0.026 ± 0.018 ± 0.006	BONVICINI	07	CLEO	Dalitz fit, ≈ 2240 evts
0.023 ± 0.015 ± 0.008	AITALA	01b	E791	Dalitz fit, 1172 evts

$\Gamma(f_2(1270) \pi^+, f_2(1270) \rightarrow \pi^+ \pi^-)/\Gamma(2\pi^+ \pi^-)$				Γ_{70}/Γ_{64}
VALUE	DOCUMENT ID	TECN	COMMENT	
0.154 ± 0.025 OUR AVERAGE		Error includes scale factor of 1.9. See the ideogram below.		
0.182 ± 0.026 ± 0.007	BONVICINI	07	CLEO	Dalitz fit, ≈ 2240 evts
0.1174 ± 0.0190 ± 0.0029	LINK	04	FOCS	Dalitz fit, 1527 ± 51 evts
0.194 ± 0.025 ± 0.004	AITALA	01b	E791	Dalitz fit, 1172 evts

WEIGHTED AVERAGE
0.154 ± 0.025 (Error scaled by 1.9)



See key on page 405

Meson Particle Listings

 D^\pm $\Gamma(K^+ \mu^+ \mu^-)/\Gamma_{\text{total}}$ Γ_{118}/Γ

Both quarks would have to change flavor for this decay to occur.

VALUE	CL%	DOCUMENT ID	TECN	COMMENT
$<9.2 \times 10^{-6}$	90	LINK	03F	FOCS γ nucleus, $\bar{E}_\gamma \approx 180$ GeV
••• We do not use the following data for averages, fits, limits, etc. •••				
$<4.4 \times 10^{-5}$	90	AITALA	99G	E791 $\pi^- N$ 500 GeV
$<9.7 \times 10^{-5}$	90	FRABETTI	97B	E687 γ Be, $\bar{E}_\gamma \approx 220$ GeV
$<3.2 \times 10^{-4}$	90	KODAMA	95	E653 π^- emulsion 600 GeV
$<9.2 \times 10^{-3}$	90	WEIR	90B	MRK2 $e^+ e^-$ 29 GeV

 $\Gamma(\pi^+ e^\pm \mu^\mp)/\Gamma_{\text{total}}$ Γ_{119}/Γ

A test of lepton-family-number conservation.

VALUE	CL%	DOCUMENT ID	TECN	COMMENT
$<3.4 \times 10^{-5}$	90	AITALA	99G	E791 $\pi^- N$ 500 GeV

 $\Gamma(\pi^+ e^+ \mu^-)/\Gamma_{\text{total}}$ Γ_{120}/Γ

A test of lepton-family-number conservation.

VALUE	CL%	DOCUMENT ID	TECN	COMMENT
$<1.1 \times 10^{-4}$	90	FRABETTI	97B	E687 γ Be, $\bar{E}_\gamma \approx 220$ GeV
$<3.3 \times 10^{-3}$	90	WEIR	90B	MRK2 $e^+ e^-$ 29 GeV

 $\Gamma(\pi^+ e^- \mu^+)/\Gamma_{\text{total}}$ Γ_{121}/Γ

A test of lepton-family-number conservation.

VALUE	CL%	DOCUMENT ID	TECN	COMMENT
$<1.3 \times 10^{-4}$	90	FRABETTI	97B	E687 γ Be, $\bar{E}_\gamma \approx 220$ GeV
$<3.3 \times 10^{-3}$	90	WEIR	90B	MRK2 $e^+ e^-$ 29 GeV

 $\Gamma(K^+ e^\pm \mu^\mp)/\Gamma_{\text{total}}$ Γ_{122}/Γ

A test of lepton-family-number conservation.

VALUE	CL%	DOCUMENT ID	TECN	COMMENT
$<6.8 \times 10^{-5}$	90	AITALA	99G	E791 $\pi^- N$ 500 GeV

 $\Gamma(K^+ e^+ \mu^-)/\Gamma_{\text{total}}$ Γ_{123}/Γ

A test of lepton-family-number conservation.

VALUE	CL%	DOCUMENT ID	TECN	COMMENT
$<1.3 \times 10^{-4}$	90	FRABETTI	97B	E687 γ Be, $\bar{E}_\gamma \approx 220$ GeV
$<3.4 \times 10^{-3}$	90	WEIR	90B	MRK2 $e^+ e^-$ 29 GeV

 $\Gamma(K^+ e^- \mu^+)/\Gamma_{\text{total}}$ Γ_{124}/Γ

A test of lepton-family-number conservation.

VALUE	CL%	DOCUMENT ID	TECN	COMMENT
$<1.2 \times 10^{-4}$	90	FRABETTI	97B	E687 γ Be, $\bar{E}_\gamma \approx 220$ GeV
$<3.4 \times 10^{-3}$	90	WEIR	90B	MRK2 $e^+ e^-$ 29 GeV

 $\Gamma(\pi^- 2e^+)/\Gamma_{\text{total}}$ Γ_{125}/Γ

A test of lepton-number conservation.

VALUE	CL%	DOCUMENT ID	TECN	COMMENT
$<3.6 \times 10^{-6}$	90	HE	05A	CLEO $e^+ e^-$ at $\psi(3770)$
••• We do not use the following data for averages, fits, limits, etc. •••				
$<9.6 \times 10^{-5}$	90	AITALA	99G	E791 $\pi^- N$ 500 GeV
$<1.1 \times 10^{-4}$	90	FRABETTI	97B	E687 γ Be, $\bar{E}_\gamma \approx 220$ GeV
$<4.8 \times 10^{-3}$	90	WEIR	90B	MRK2 $e^+ e^-$ 29 GeV

 $\Gamma(\pi^- 2\mu^+)/\Gamma_{\text{total}}$ Γ_{126}/Γ

A test of lepton-number conservation.

VALUE	CL%	EVTS	DOCUMENT ID	TECN	COMMENT
$<4.8 \times 10^{-6}$	90		LINK	03F	FOCS γ nucleus, $\bar{E}_\gamma \approx 180$ GeV
••• We do not use the following data for averages, fits, limits, etc. •••					
$<1.7 \times 10^{-5}$	90		AITALA	99G	E791 $\pi^- N$ 500 GeV
$<8.7 \times 10^{-5}$	90		FRABETTI	97B	E687 γ Be, $\bar{E}_\gamma \approx 220$ GeV
$<2.2 \times 10^{-4}$	90	0	KODAMA	95	E653 π^- emulsion 600 GeV
$<6.8 \times 10^{-3}$	90		WEIR	90B	MRK2 $e^+ e^-$ 29 GeV

 $\Gamma(\pi^- e^+ \mu^+)/\Gamma_{\text{total}}$ Γ_{127}/Γ

A test of lepton-number conservation.

VALUE	CL%	DOCUMENT ID	TECN	COMMENT
$<5.0 \times 10^{-5}$	90	AITALA	99G	E791 $\pi^- N$ 500 GeV
••• We do not use the following data for averages, fits, limits, etc. •••				
$<1.1 \times 10^{-4}$	90	FRABETTI	97B	E687 γ Be, $\bar{E}_\gamma \approx 220$ GeV
$<3.7 \times 10^{-3}$	90	WEIR	90B	MRK2 $e^+ e^-$ 29 GeV

 $\Gamma(\rho^- 2\mu^+)/\Gamma_{\text{total}}$ Γ_{128}/Γ

A test of lepton-number conservation.

VALUE	CL%	EVTS	DOCUMENT ID	TECN	COMMENT
$<5.6 \times 10^{-4}$	90	0	KODAMA	95	E653 π^- emulsion 600 GeV

 $\Gamma(K^- 2e^+)/\Gamma_{\text{total}}$ Γ_{129}/Γ

A test of lepton-number conservation.

VALUE	CL%	DOCUMENT ID	TECN	COMMENT
$<4.5 \times 10^{-6}$	90	HE	05A	CLEO $e^+ e^-$ at $\psi(3770)$
••• We do not use the following data for averages, fits, limits, etc. •••				
$<1.2 \times 10^{-4}$	90	FRABETTI	97B	E687 γ Be, $\bar{E}_\gamma \approx 220$ GeV
$<9.1 \times 10^{-3}$	90	WEIR	90B	MRK2 $e^+ e^-$ 29 GeV

 $\Gamma(K^- 2\mu^+)/\Gamma_{\text{total}}$ Γ_{130}/Γ

A test of lepton-number conservation.

VALUE	CL%	EVTS	DOCUMENT ID	TECN	COMMENT
$<1.3 \times 10^{-5}$	90		LINK	03F	FOCS γ nucleus, $\bar{E}_\gamma \approx 180$ GeV
••• We do not use the following data for averages, fits, limits, etc. •••					
$<1.2 \times 10^{-4}$	90		FRABETTI	97B	E687 γ Be, $\bar{E}_\gamma \approx 220$ GeV
$<3.2 \times 10^{-4}$	90	0	KODAMA	95	E653 π^- emulsion 600 GeV
$<4.3 \times 10^{-3}$	90		WEIR	90B	MRK2 $e^+ e^-$ 29 GeV

 $\Gamma(K^- e^+ \mu^+)/\Gamma_{\text{total}}$ Γ_{131}/Γ

A test of lepton-number conservation.

VALUE	CL%	DOCUMENT ID	TECN	COMMENT
$<1.3 \times 10^{-4}$	90	FRABETTI	97B	E687 γ Be, $\bar{E}_\gamma \approx 220$ GeV
••• We do not use the following data for averages, fits, limits, etc. •••				
$<4.0 \times 10^{-3}$	90	WEIR	90B	MRK2 $e^+ e^-$ 29 GeV

 $\Gamma(K^*(892)^- 2\mu^+)/\Gamma_{\text{total}}$ Γ_{132}/Γ

A test of lepton-number conservation.

VALUE	CL%	EVTS	DOCUMENT ID	TECN	COMMENT
$<8.5 \times 10^{-4}$	90	0	KODAMA	95	E653 π^- emulsion 600 GeV

 D^\pm CP-VIOLATING DECAY-RATE ASYMMETRIESThis is the difference between D^+ and D^- partial widths for these modes divided by the sum of the widths. $A_{CP}(\mu^\pm \nu)$ in $D^+ \rightarrow \mu^+ \nu_\mu$, $D^- \rightarrow \mu^- \bar{\nu}_\mu$

VALUE	DOCUMENT ID	TECN	COMMENT
$+0.08 \pm 0.08$	EISENSTEIN 08	CLEO	$e^+ e^-$ at $\psi(3770)$

 $A_{CP}(K_S^0 \pi^\pm)$ in $D^\pm \rightarrow K_S^0 \pi^\pm$

VALUE	EVTS	DOCUMENT ID	TECN	COMMENT
-0.009 ± 0.009	OUR AVERAGE			
$-0.006 \pm 0.010 \pm 0.003$		DOBBS 07	CLEO	$e^+ e^-$ at $\psi(3770)$
$-0.016 \pm 0.015 \pm 0.009$	10.6k	55 LINK 02B	FOCS	γ nucleus, $\bar{E}_\gamma \approx 180$ GeV
55 LINK 02B measures $M(D^+ \rightarrow K_S^0 \pi^+)/M(D^+ \rightarrow K^- \pi^+ \pi^+)$, the ratio of numbers of events observed, and similarly for the D^- .				

 $A_{CP}(K^\mp 2\pi^\pm)$ in $D^+ \rightarrow K^- 2\pi^+$, $D^- \rightarrow K^+ 2\pi^-$

VALUE	DOCUMENT ID	TECN	COMMENT
$-0.005 \pm 0.004 \pm 0.009$	DOBBS 07	CLEO	$e^+ e^-$ at $\psi(3770)$

 $A_{CP}(K^\mp \pi^\pm \pi^\pm \pi^0)$ in $D^+ \rightarrow K^- \pi^+ \pi^+ \pi^0$, $D^- \rightarrow K^+ \pi^- \pi^- \pi^0$

VALUE	DOCUMENT ID	TECN	COMMENT
$+0.010 \pm 0.009 \pm 0.009$	DOBBS 07	CLEO	$e^+ e^-$ at $\psi(3770)$

 $A_{CP}(K_S^0 \pi^\pm \pi^0)$ in $D^+ \rightarrow K_S^0 \pi^+ \pi^0$, $D^- \rightarrow K_S^0 \pi^- \pi^0$

VALUE	DOCUMENT ID	TECN	COMMENT
$+0.003 \pm 0.009 \pm 0.003$	DOBBS 07	CLEO	$e^+ e^-$ at $\psi(3770)$

 $A_{CP}(K_S^0 \pi^\pm \pi^+ \pi^-)$ in $D^+ \rightarrow K_S^0 \pi^+ \pi^+ \pi^-$, $D^- \rightarrow K_S^0 \pi^- \pi^- \pi^+$

VALUE	DOCUMENT ID	TECN	COMMENT
$+0.001 \pm 0.011 \pm 0.006$	DOBBS 07	CLEO	$e^+ e^-$ at $\psi(3770)$

 $A_{CP}(K_S^0 K^\pm)$ in $D^\pm \rightarrow K_S^0 K^\pm$

VALUE	EVTS	DOCUMENT ID	TECN	COMMENT
$+0.071 \pm 0.061 \pm 0.012$	949	56 LINK 02B	FOCS	γ nucleus, $\bar{E}_\gamma \approx 180$ GeV
••• We do not use the following data for averages, fits, limits, etc. •••				
$+0.069 \pm 0.060 \pm 0.015$	949	57 LINK 02B	FOCS	γ nucleus, $\bar{E}_\gamma \approx 180$ GeV
56 LINK 02B measures $M(D^+ \rightarrow K_S^0 K^+)/M(D^+ \rightarrow K_S^0 \pi^+)$, the ratio of numbers of events observed, and similarly for the D^- .				
57 LINK 02B measures $M(D^+ \rightarrow K_S^0 K^+)/M(D^+ \rightarrow K^- \pi^+ \pi^+)$, the ratio of numbers of events observed, and similarly for the D^- .				

 $A_{CP}(K^+ K^- \pi^\pm)$ in $D^\pm \rightarrow K^+ K^- \pi^\pm$

VALUE (%)	EVTS	DOCUMENT ID	TECN	COMMENT
0.3 ± 0.6	OUR AVERAGE			
$-0.03 \pm 0.84 \pm 0.29$		RUBIN 08	CLEO	$e^+ e^-$, 3774 MeV
$-0.1 \pm 1.5 \pm 0.8$		DOBBS 07	CLEO	$e^+ e^-$ at $\psi(3770)$
$+1.4 \pm 1.0 \pm 0.8$	43k ± 321	58 AUBERT 05s	BABR	$e^+ e^- \approx \tau(4S)$
$+0.6 \pm 1.1 \pm 0.5$	14k	59 LINK 00B	FOCS	
-1.4 ± 2.9		59 AITALA 97B	E791	$-0.062 < A_{CP} < +0.034$ (90% CL)
-3.1 ± 6.8		59 FRABETTI 94i	E687	$-0.14 < A_{CP} < +0.081$ (90% CL)

Meson Particle Listings

 D^\pm

⁵⁸AUBERT 05s measures $N(D^+ \rightarrow K^+ K^- \pi^+)/N(D_S^+ \rightarrow K^+ K^- \pi^+)$, the ratio of the numbers of events observed, and similarly for the D^- .

⁵⁹FRABETTI 94i, AITALA 98c, and LINK 00b measure $N(D^+ \rightarrow K^- K^+ \pi^+)/N(D^+ \rightarrow K^- \pi^+ \pi^+)$, the ratio of numbers of events observed, and similarly for the D^- .

$A_{CP}(K^\pm K^*0)$ in $D^+ \rightarrow K^+ \bar{K}^{*0}, D^- \rightarrow K^- K^{*0}$

VALUE (%)	EVTS	DOCUMENT ID	TECN	COMMENT
0.1 ± 1.3 OUR AVERAGE				
-0.4 ± 2.0 ± 0.6		RUBIN 08	CLEO	Fit-fraction asymmetry
+0.9 ± 1.7 ± 0.7	11k ± 122	⁶⁰ AUBERT 05s	BABR	$e^+ e^- \approx \gamma(4S)$
-1.0 ± 5.0		⁶¹ AITALA 97b	E791	-0.092 < $A_{CP} <$ +0.072 (90% CL)
-12 ± 13		⁶¹ FRABETTI 94i	E687	-0.33 < $A_{CP} <$ +0.094 (90% CL)

⁶⁰AUBERT 05s measures $N(D^+ \rightarrow K^+ \bar{K}^{*0})/N(D_S^+ \rightarrow K^+ K^- \pi^+)$, the ratio of the numbers of events observed, and similarly for the D^- .

⁶¹FRABETTI 94i and AITALA 97b measure $N(D^+ \rightarrow K^+ \bar{K}^*(892)^0)/N(D^+ \rightarrow K^- \pi^+ \pi^+)$, the ratio of numbers of events observed, and similarly for the D^- .

$A_{CP}(\phi\pi^\pm)$ in $D^\pm \rightarrow \phi\pi^\pm$

VALUE (%)	EVTS	DOCUMENT ID	TECN	COMMENT
-0.9 ± 1.1 OUR AVERAGE				
-1.8 ± 1.6 ± 0.2		RUBIN 08	CLEO	Fit-fraction asymmetry
+0.2 ± 1.5 ± 0.6	10k ± 136	⁶² AUBERT 05s	BABR	$e^+ e^- \approx \gamma(4S)$
-2.8 ± 3.6		⁶³ AITALA 97b	E791	-0.087 < $A_{CP} <$ +0.031 (90% CL)
+6.6 ± 8.6		⁶³ FRABETTI 94i	E687	-0.075 < $A_{CP} <$ +0.21 (90% CL)

⁶²AUBERT 05s measures $N(D^+ \rightarrow \phi\pi^+)/N(D_S^+ \rightarrow K^+ K^- \pi^+)$, the ratio of the numbers of events observed, and similarly for the D^- .

⁶³FRABETTI 94i and AITALA 97b measure $N(D^+ \rightarrow \phi\pi^+)/N(D^+ \rightarrow K^- \pi^+ \pi^+)$, the ratio of numbers of events observed, and similarly for the D^- .

$A_{CP}(K^\pm K_0^*(1430)^0)$ in $D^+ \rightarrow K^+ \bar{K}_0^*(1430)^0, D^- \rightarrow K^- K_0^*(1430)^0$

VALUE (%)	DOCUMENT ID	TECN	COMMENT
+8 ± 6 ± 2	RUBIN 08	CLEO	Fit-fraction asymmetry

$A_{CP}(K^\pm K_2^*(1430)^0)$ in $D^+ \rightarrow K^+ \bar{K}_2^*(1430)^0, D^- \rightarrow K^- K_2^*(1430)^0$

VALUE (%)	DOCUMENT ID	TECN	COMMENT
+43 ± 19 ± 5	RUBIN 08	CLEO	Fit-fraction asymmetry

$A_{CP}(K^\pm K_0^*(800))$ in $D^+ \rightarrow K^+ \bar{K}_0^*(800), D^- \rightarrow K^- K_0^*(800)$

VALUE (%)	DOCUMENT ID	TECN	COMMENT
-12 ± 11 ± 6	RUBIN 08	CLEO	Fit-fraction asymmetry

$A_{CP}(a_0(1450)^0 \pi^\pm)$ in $D^\pm \rightarrow a_0(1450)^0 \pi^\pm$

VALUE (%)	DOCUMENT ID	TECN	COMMENT
-19 ± 12 ± 8	RUBIN 08	CLEO	Fit-fraction asymmetry

$A_{CP}(\phi(1680)\pi^\pm)$ in $D^\pm \rightarrow \phi(1680)\pi^\pm$

VALUE (%)	DOCUMENT ID	TECN	COMMENT
-9 ± 22 ± 14	RUBIN 08	CLEO	Fit-fraction asymmetry

$A_{CP}(\pi^+ \pi^- \pi^\pm)$ in $D^\pm \rightarrow \pi^+ \pi^- \pi^\pm$

VALUE	DOCUMENT ID	TECN	COMMENT
-0.017 ± 0.042	⁶⁴ AITALA 97b	E791	-0.086 < $A_{CP} <$ +0.052 (90% CL)

⁶⁴AITALA 97b measure $N(D^+ \rightarrow \pi^+ \pi^- \pi^+)/N(D^+ \rightarrow K^- \pi^+ \pi^+)$, the ratio of numbers of events observed, and similarly for the D^- .

$A_{CP}(K_S^0 K^\pm \pi^+ \pi^-)$ in $D^\pm \rightarrow K_S^0 K^\pm \pi^+ \pi^-$

This is the difference between D^+ and D^- partial widths for these modes divided by the sum of the widths.

VALUE	EVTS	DOCUMENT ID	TECN	COMMENT
-0.042 ± 0.064 ± 0.022	523 ± 32	LINK 05E	FOCS	$\gamma A, \bar{E}_{\gamma} \approx 180$ GeV

$D^+ D^-$ T-VIOLATING DECAY-RATE ASYMMETRIES

$A_{Tviol}(K_S^0 K^\pm \pi^+ \pi^-)$ in $D^\pm \rightarrow K_S^0 K^\pm \pi^+ \pi^-$

$C_T \equiv \bar{p}_{K^+} \cdot (\bar{p}_{\pi^+} \times \bar{p}_{\pi^-})$ is a T -odd correlation of the K^+ , π^+ , and π^- momenta for the D^+ . $\bar{C}_T \equiv \bar{p}_{K^-} \cdot (\bar{p}_{\pi^-} \times \bar{p}_{\pi^+})$ is the corresponding quantity for the D^- . $A_T \equiv [\Gamma(C_T > 0) - \Gamma(C_T < 0)] / [\Gamma(C_T > 0) + \Gamma(C_T < 0)]$ would, in the absence of strong phases, test for T violation in D^+ decays (the Γ 's are partial widths). With $\bar{A}_T \equiv [\Gamma(-\bar{C}_T > 0) - \Gamma(-\bar{C}_T < 0)] / [\Gamma(-\bar{C}_T > 0) + \Gamma(-\bar{C}_T < 0)]$, the asymmetry $A_{Tviol} \equiv \frac{1}{2}(A_T - \bar{A}_T)$ tests for T violation even with nonzero strong phases.

VALUE	EVTS	DOCUMENT ID	TECN	COMMENT
+0.023 ± 0.062 ± 0.022	523 ± 32	LINK 05E	FOCS	$\gamma A, \bar{E}_{\gamma} \approx 180$ GeV

$D^+ \rightarrow \bar{K}^0/\pi^0 \ell^+ \nu_\ell$ FORM FACTORS

$f_+(0)|V_{cs}|$ in $D^+ \rightarrow \bar{K}^0 \ell^+ \nu_\ell$

VALUE	DOCUMENT ID	TECN	COMMENT
0.707 ± 0.010 ± 0.009	BESSON 09	CLEO	$\bar{K}^0 e^+ \nu_e$ 3-parameter fit

$r_1 \equiv a_1/a_0$ in $D^+ \rightarrow \bar{K}^0 \ell^+ \nu_\ell$

VALUE	DOCUMENT ID	TECN	COMMENT
-1.66 ± 0.44 ± 0.10	BESSON 09	CLEO	$\bar{K}^0 e^+ \nu_e$ 3-parameter fit

$r_2 \equiv a_2/a_0$ in $D^+ \rightarrow \bar{K}^0 \ell^+ \nu_\ell$

VALUE	DOCUMENT ID	TECN	COMMENT
-14 ± 11 ± 1	BESSON 09	CLEO	$\bar{K}^0 e^+ \nu_e$ 3-parameter fit

$f_+(0)|V_{cd}|$ in $D^+ \rightarrow \pi^0 \ell^+ \nu_\ell$

VALUE	DOCUMENT ID	TECN	COMMENT
0.146 ± 0.007 ± 0.002	BESSON 09	CLEO	$\pi^0 e^+ \nu_e$ 3-parameter fit

$r_1 \equiv a_1/a_0$ in $D^+ \rightarrow \pi^0 \ell^+ \nu_\ell$

VALUE	DOCUMENT ID	TECN	COMMENT
-1.37 ± 0.88 ± 0.24	BESSON 09	CLEO	$\pi^0 e^+ \nu_e$ 3-parameter fit

$r_2 \equiv a_2/a_0$ in $D^+ \rightarrow \pi^0 \ell^+ \nu_\ell$

VALUE	DOCUMENT ID	TECN	COMMENT
-4 ± 5 ± 1	BESSON 09	CLEO	$\pi^0 e^+ \nu_e$ 3-parameter fit

$D^+ \rightarrow \bar{K}^*(892)^0 \ell^+ \nu_\ell$ FORM FACTORS

$r_V \equiv V(0)/A_1(0)$ in $D^+ \rightarrow \bar{K}^*(892)^0 \ell^+ \nu_\ell$

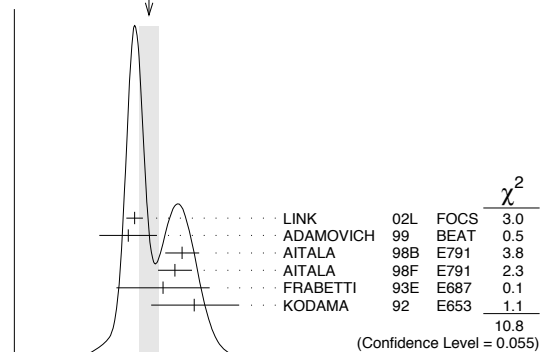
VALUE	EVTS	DOCUMENT ID	TECN	COMMENT
1.62 ± 0.08 OUR AVERAGE				
1.504 ± 0.057 ± 0.039	15k	⁶⁵ LINK 02L	FOCS	$\bar{K}^*(892)^0 \mu^+ \nu_\mu$
1.45 ± 0.23 ± 0.07	763	ADAMOVICH 99	BEAT	$\bar{K}^*(892)^0 \mu^+ \nu_\mu$
1.90 ± 0.11 ± 0.09	3000	⁶⁶ AITALA 98b	E791	$\bar{K}^*(892)^0 e^+ \nu_e$
1.84 ± 0.11 ± 0.09	3034	AITALA 98f	E791	$\bar{K}^*(892)^0 \mu^+ \nu_\mu$
1.74 ± 0.27 ± 0.28	874	FRABETTI 93e	E687	$\bar{K}^*(892)^0 \mu^+ \nu_\mu$
2.00 +0.34 -0.32 ± 0.16	305	KODAMA 92	E653	$\bar{K}^*(892)^0 \mu^+ \nu_\mu$
2.0 ± 0.6 ± 0.3	183	ANJOS 90e	E691	$\bar{K}^*(892)^0 e^+ \nu_e$

• • • We do not use the following data for averages, fits, limits, etc. • • •

⁶⁵LINK 02L includes the effects of interference with an S-wave background. This much improves the goodness of fit, but does not much shift the values of the form factors.

⁶⁶This is slightly different from the AITALA 98b value: see ref. [5] in AITALA 98f.

WEIGHTED AVERAGE
1.62 ± 0.08 (Error scaled by 1.5)



$r_V \equiv V(0)/A_1(0)$ in $D^+ \rightarrow \bar{K}^*(892)^0 \ell^+ \nu_\ell$

$r_2 \equiv A_2(0)/A_1(0)$ in $D^+ \rightarrow \bar{K}^*(892)^0 \ell^+ \nu_\ell$

VALUE	EVTS	DOCUMENT ID	TECN	COMMENT
0.83 ± 0.05 OUR AVERAGE				
0.875 ± 0.049 ± 0.064	15k	⁶⁷ LINK 02L	FOCS	$\bar{K}^*(892)^0 \mu^+ \nu_\mu$
1.00 ± 0.15 ± 0.03	763	ADAMOVICH 99	BEAT	$\bar{K}^*(892)^0 \mu^+ \nu_\mu$
0.71 ± 0.08 ± 0.09	3000	AITALA 98b	E791	$\bar{K}^*(892)^0 e^+ \nu_e$
0.75 ± 0.08 ± 0.09	3034	AITALA 98f	E791	$\bar{K}^*(892)^0 \mu^+ \nu_\mu$
0.78 ± 0.18 ± 0.10	874	FRABETTI 93e	E687	$\bar{K}^*(892)^0 \mu^+ \nu_\mu$
0.82 +0.22 -0.23 ± 0.11	305	KODAMA 92	E653	$\bar{K}^*(892)^0 \mu^+ \nu_\mu$

• • • We do not use the following data for averages, fits, limits, etc. • • •

0.0 ± 0.5 ± 0.2 183 ANJOS 90e E691 $\bar{K}^*(892)^0 e^+ \nu_e$

⁶⁷LINK 02L includes the effects of interference with an S-wave background. This much improves the goodness of fit, but does not much shift the values of the form factors.

Meson Particle Listings

D±, D0

See key on page 405

Table with 5 columns: VALUE, EVTS, DOCUMENT ID, TECN, COMMENT. Row 1: 0.04±0.33±0.29, 3034, AITALA 98F E791, K*(892)0 μ+ νμ

Table with 5 columns: VALUE, EVTS, DOCUMENT ID, TECN, COMMENT. Row 1: 1.09±0.10±0.02, 763, ADAMOVICH 99 BEAT, K*(892)0 μ+ νμ

• • • We do not use the following data for averages, fits, limits, etc. • • •

Table with 5 columns: VALUE, EVTS, DOCUMENT ID, TECN, COMMENT. Row 1: 1.8 +0.6 -0.4 ±0.3, 183, ANJOS 90E E691, K*(892)0 e+ νe

Table with 5 columns: VALUE, EVTS, DOCUMENT ID, TECN, COMMENT. Row 1: 0.22±0.06 OUR AVERAGE, Error includes scale factor of 1.6.

Table with 5 columns: VALUE, EVTS, DOCUMENT ID, TECN, COMMENT. Row 1: 0.16±0.05±0.02, 305, KODAMA 92 E653, K*(892)0 μ+ νμ

• • • We do not use the following data for averages, fits, limits, etc. • • •

Table with 5 columns: VALUE, EVTS, DOCUMENT ID, TECN, COMMENT. Row 1: 0.15 +0.07 -0.05 ±0.03, 183, ANJOS 90E E691, K*(892)0 e+ νe

D± REFERENCES

Large table of references for D± mesons, listing author names, document IDs, and collaboration names.

Large table of references for D0 mesons, listing author names, document IDs, and collaboration names.

OTHER RELATED PAPERS

Table with 3 columns: Author(s), Title/Reference, Location.



I(JP) = 1/2(0-)

D0 MASS

The fit includes D±, D0, Ds±, Ds*, D*0, Ds±, D1(2420)0, Ds±(2460)0, and Ds1(2536)± mass and mass difference measurements.

Table with 5 columns: VALUE (MeV), EVTS, DOCUMENT ID, TECN, COMMENT. Includes fit results and average values.

Meson Particle Listings

 D^0

¹PERUZZI 77 and SCHINDLER 81 errors do not include the 0.13% uncertainty in the absolute SPEAR energy calibration. TRILLING 81 uses the high precision $J/\psi(1S)$ and $\psi(2S)$ measurements of ZHOLENTZ 80 to determine this uncertainty and combines the PERUZZI 77 and SCHINDLER 81 results to obtain the value quoted. TRILLING 81 enters the fit in the D^{\pm} mass, and PERUZZI 77 and SCHINDLER 81 enter in the $m_{D^{\pm}} - m_{D^0}$, below.

²Error does not include possible systematic mass scale shift, estimated to be less than 5 MeV.

 $m_{D^{\pm}} - m_{D^0}$

The fit includes D^{\pm} , D^0 , D_s^{\pm} , $D^{*\pm}$, D^{*0} , $D_s^{*\pm}$, $D_1(2420)^0$, $D_2^*(2460)^0$, and $D_{s1}(2536)^{\pm}$ mass and mass difference measurements.

VALUE (MeV)	DOCUMENT ID	TECN	COMMENT
4.77±0.10 OUR FIT	Error includes scale factor of 1.1.		
4.74±0.28 OUR AVERAGE			
4.7 ± 0.3	³ SCHINDLER 81	MRK2	e^+e^- 3.77 GeV
5.0 ± 0.8	³ PERUZZI 77	LGW	e^+e^- 3.77 GeV

³See the footnote on TRILLING 81 in the D^0 and D^{\pm} sections on the mass.

 D^0 MEAN LIFE

Measurements with an error $> 10 \times 10^{-15}$ s have been omitted from the average.

VALUE (10^{-15} s)	EVTs	DOCUMENT ID	TECN	COMMENT
410.1± 1.5 OUR AVERAGE				
409.6± 1.1± 1.5	210k	LINK	02F FOCUS	γ nucleus, ≈ 180 GeV
407.9± 6.0± 4.3	10k	KUSHNIR...	01 SELX	$K^-\pi^+$, $K^-\pi^+\pi^+\pi^-$
413 ± 3 ± 4	35k	AITALA	99E E791	$K^-\pi^+$
408.5± 4.1± 3.5 - 3.4	25k	BONVICINI	99 CLE2	$e^+e^- \approx \Upsilon(4S)$
413 ± 4 ± 3	16k	FRABETTI	94D E687	$K^-\pi^+$, $K^-\pi^+\pi^+\pi^-$
● ● ● We do not use the following data for averages, fits, limits, etc. ● ● ●				
424 ± 11 ± 7	5118	FRABETTI	91 E687	$K^-\pi^+$, $K^-\pi^+\pi^+\pi^-$
417 ± 18 ± 15	890	ALVAREZ	90 NA14	$K^-\pi^+$, $K^-\pi^+\pi^+\pi^-$
388 $\begin{smallmatrix} +23 \\ -21 \end{smallmatrix}$	641	⁴ BARLAG	90c ACCM	π^- Cu 230 GeV
480 ± 40 ± 30	776	ALBRECHT	88i ARG	e^+e^- 10 GeV
422 ± 8 ± 10	4212	RAAB	88 E691	Photoproduction
420 ± 50	90	BARLAG	87b ACCM	K^- and π^- 200 GeV

⁴BARLAG 90c estimate systematic error to be negligible.

 $D^0-\bar{D}^0$ MIXING

Revised April 2010 by D. Asner (Pacific Northwest National Laboratory)

The detailed formalism for $D^0-\bar{D}^0$ mixing is presented in the note on “ CP Violation in Meson Decays” in this *Review*. For completeness, we present an overview here. The time evolution of the $D^0-\bar{D}^0$ system is described by the Schrödinger equation

$$i\frac{\partial}{\partial t}\begin{pmatrix} D^0(t) \\ \bar{D}^0(t) \end{pmatrix} = \left(\mathbf{M} - \frac{i}{2}\mathbf{\Gamma}\right)\begin{pmatrix} D^0(t) \\ \bar{D}^0(t) \end{pmatrix}, \quad (1)$$

where the \mathbf{M} and $\mathbf{\Gamma}$ matrices are Hermitian, and CPT invariance requires that $M_{11} = M_{22} \equiv M$ and $\Gamma_{11} = \Gamma_{22} \equiv \Gamma$. The off-diagonal elements of these matrices describe the dispersive and absorptive parts of the mixing.

Because CP violation is expected to be quite small here, it is convenient to label the mass eigenstates by the CP quantum number in the limit of CP conservation. Thus, we write

$$|D_{1,2}\rangle = p|D^0\rangle \pm q|\bar{D}^0\rangle, \quad (2)$$

where

$$\left(\frac{q}{p}\right)^2 = \frac{M_{12}^* - \frac{i}{2}\Gamma_{12}^*}{M_{12} - \frac{i}{2}\Gamma_{12}}. \quad (3)$$

The normalization condition is $|p|^2 + |q|^2 = 1$. Our phase convention is $CP|D^0\rangle = +|\bar{D}^0\rangle$, and the sign is chosen so that D_1 has CP even, or nearly so.

The corresponding eigenvalues are

$$\omega_{1,2} \equiv m_{1,2} - \frac{i}{2}\Gamma_{1,2} = \left(M - \frac{i}{2}\Gamma\right) \pm \frac{q}{p}\left(M_{12} - \frac{i}{2}\Gamma_{12}\right), \quad (4)$$

where $m_{1,2}$ and $\Gamma_{1,2}$ are the masses and widths of the $D_{1,2}$.

We define dimensionless mixing parameters x and y by

$$x \equiv (m_1 - m_2)/\Gamma = \Delta m/\Gamma \quad (5)$$

and

$$y \equiv (\Gamma_1 - \Gamma_2)/2\Gamma = \Delta\Gamma/2\Gamma, \quad (6)$$

where $\Gamma \equiv (\Gamma_1 + \Gamma_2)/2$. If CP is conserved, then M_{12} and Γ_{12} are real, $\Delta m = 2M_{12}$, $\Delta\Gamma = 2\Gamma_{12}$, and $p = q = 1/\sqrt{2}$. The signs of Δm and $\Delta\Gamma$ are to be determined experimentally.

The parameters x and y are measured in several ways. The most precise values are obtained using the time dependence of D decays. Since $D^0-\bar{D}^0$ mixing is a small effect, the identifying tag of the initial particle as a D^0 or a \bar{D}^0 must be extremely accurate. The usual tag is the charge of the distinctive slow pion in the decay sequence $D^{*+} \rightarrow D^0\pi^+$ or $D^{*-} \rightarrow \bar{D}^0\pi^-$. In current experiments, the probability of mistagging is about 0.1%. The large data samples produced at the B -factories allow the production flavor to also be determined by fully reconstructing charm on the “other side” of the event—significantly reducing the mistag rate [1]. Another tag of comparable accuracy is identification of one of the D 's produced from $\psi(3770) \rightarrow D^0\bar{D}^0$ decays. Although time-dependent analyses are not possible at symmetric charm-threshold facilities (the D^0 and \bar{D}^0 do not travel far enough), the quantum-coherent $C = -1$ $\psi(3770) \rightarrow D^0\bar{D}^0$ state provides time-integrated sensitivity [2,3].

Time-Dependent Analyses: We extend the formalism of this *Review*'s note on “ CP Violation in Meson Decays.” In addition to the “right-sign” instantaneous decay amplitudes $\bar{A}_f \equiv \langle f|H|\bar{D}^0\rangle$ and $A_{\bar{f}} \equiv \langle \bar{f}|H|D^0\rangle$ for CP conjugate final states $f = K^+\pi^-, \dots$ and $\bar{f} = K^-\pi^+, \dots$, we include “wrong-sign” amplitudes $\bar{A}_{\bar{f}} \equiv \langle \bar{f}|H|\bar{D}^0\rangle$ and $A_f \equiv \langle f|H|D^0\rangle$.

It is conventional to normalize the wrong-sign decay distributions to the integrated rate of right-sign decays and to express time in units of the precisely measured neutral D -meson mean lifetime, $\tau_{D^0} = 1/\Gamma = 2/(\Gamma_1 + \Gamma_2)$. Starting from a pure $|D^0\rangle$ or $|\bar{D}^0\rangle$ state at $t = 0$, the time-dependent rates of decay to wrong-sign final states relative to the integrated right-sign decay rates are, to leading order:

$$r(t) \equiv \frac{|\langle f|H|D^0(t)\rangle|^2}{|\bar{A}_f|^2} = \left|\frac{q}{p}\right|^2 \left|g_+(t)\lambda_f^{-1} + g_-(t)\right|^2, \quad (7)$$

and

$$\bar{r}(t) \equiv \frac{|\langle \bar{f}|H|\bar{D}^0(t)\rangle|^2}{|A_{\bar{f}}|^2} = \left|\frac{p}{q}\right|^2 \left|g_+(t)\lambda_{\bar{f}} + g_-(t)\right|^2. \quad (8)$$

where

$$\lambda_f \equiv q\bar{A}_f/pA_f, \quad \lambda_{\bar{f}} \equiv q\bar{A}_{\bar{f}}/pA_{\bar{f}}, \quad (9)$$

and

$$g_{\pm}(t) = \frac{1}{2}\left(e^{-iz_1t} \pm e^{-iz_2t}\right), \quad z_{1,2} = \frac{\omega_{1,2}}{\Gamma}. \quad (10)$$

Note that a change in the convention for the relative phase of D^0 and \bar{D}^0 would cancel between q/p and \bar{A}_f/A_f and leave λ_f unchanged. We expand $r(t)$ and $\bar{r}(t)$ to second order in x and y for modes in which the ratio of decay amplitudes, $R_D = |A_f/\bar{A}_f|^2$, is very small.

Semileptonic decays: Consider the final state $f = K^+\ell^-\bar{\nu}_\ell$, where $A_f = \bar{A}_f = 0$ in the Standard Model. The final state f is only accessible through mixing and $r(t)$ is

$$r(t) = |g_-(t)|^2 \left| \frac{q}{p} \right|^2 \approx \frac{e^{-t}}{4} (x^2 + y^2) t^2 \left| \frac{q}{p} \right|^2. \quad (11)$$

For $\bar{r}(t)$ q/p is replaced by p/q . In the Standard Model, CP violation in charm mixing is small and $|q/p| \approx 1$. In the limit of CP conservation, $r(t) = \bar{r}(t)$, and the time-integrated mixing rate relative to the time-integrated right-sign decay rate for semileptonic decays is

$$R_M = \int_0^\infty r(t) dt = \left| \frac{q}{p} \right|^2 \frac{x^2 + y^2}{2 + x^2 - y^2} = \frac{1}{2} (x^2 + y^2). \quad (12)$$

Table 1: Results for R_M in D^0 semileptonic decays.

Year	Exper.	Final state(s)	R_M ($\times 10^{-3}$)	90% C.L.
2008	Belle [4]	$K^{(*)+}e^-\bar{\nu}_e$	$0.13 \pm 0.22 \pm 0.20$	$< 0.61 \times 10^{-3}$
2007	BABAR [1]	$K^{(*)+}e^-\bar{\nu}_e$	$0.04^{+0.70}_{-0.60}$	$(-1.3, 1.2) \times 10^{-3}$
2005*	Belle [5]	$K^{(*)+}e^-\bar{\nu}_e$	$0.02 \pm 0.47 \pm 0.14$	$< 1.0 \times 10^{-3}$
2005	CLEO [6]	$K^{(*)+}e^-\bar{\nu}_e$	$1.6 \pm 2.9 \pm 2.9$	$< 7.8 \times 10^{-3}$
2004*	BABAR [7]	$K^{(*)+}e^-\bar{\nu}_e$	$2.3 \pm 1.2 \pm 0.4$	$< 4.2 \times 10^{-3}$
2002*	FOCUS [8]	$K^+\mu^-\bar{\nu}_\mu$	$-0.76^{+0.99}_{-0.93}$	$< 1.01 \times 10^{-3}$
1996	E791 [9]	$K^+\ell^-\bar{\nu}_\ell$	$(1.1^{+3.0}_{-2.7}) \times 10^{-3}$	$< 5.0 \times 10^{-3}$
HFAG [10]			0.13 ± 0.27	

*These measurements are excluded from the HFAG average. The FOCUS result is unpublished, the BABAR result has been superseded by Ref. 1, and the Belle result has been superseded by Ref. 4.

Table 1 summarizes results for R_M from semileptonic decays; the world average from the Heavy Flavor Averaging Group (HFAG) [10] is $R_M = (1.30 \pm 2.69) \times 10^{-4}$.

Wrong-sign decays to hadronic non- CP eigenstates: Consider the final state $f = K^+\pi^-$, where A_f is doubly Cabibbo-suppressed. The ratio of decay amplitudes is

$$\frac{A_f}{\bar{A}_f} = -\sqrt{R_D} e^{-i\delta_f}, \quad \left| \frac{A_f}{\bar{A}_f} \right| \sim O(\tan^2 \theta_c), \quad (13)$$

where R_D is the doubly Cabibbo-suppressed (DCS) decay rate relative to the Cabibbo-favored (CF) rate, δ_f is the strong phase difference between DCS and CF processes, and θ_c is the Cabibbo angle. The minus sign originates from the sign of V_{us} relative to V_{cd} .

We characterize the violation of CP with the real-valued parameters A_M , A_D , and ϕ . We adopt the parametrization (see Refs. 11 and 12)

$$\left| \frac{q}{p} \right|^2 = \sqrt{\frac{1+A_M}{1-A_M}}, \quad (14)$$

$$\lambda_f^{-1} \equiv \frac{pA_f}{q\bar{A}_f} = -\sqrt{R_D} \left(\frac{(1+A_D)(1-A_M)}{(1-A_D)(1+A_M)} \right)^{1/4} e^{-i(\delta_f+\phi)}, \quad (15)$$

$$\lambda_{\bar{f}} \equiv \frac{q\bar{A}_{\bar{f}}}{pA_{\bar{f}}} = -\sqrt{R_D} \left(\frac{(1-A_D)(1+A_M)}{(1+A_D)(1-A_M)} \right)^{1/4} e^{-i(\delta_f-\phi)}. \quad (16)$$

From these relations, we obtain

$$\sqrt{\frac{1+A_D}{1-A_D}} = \frac{|A_f/\bar{A}_f|}{|\bar{A}_{\bar{f}}/A_{\bar{f}}|}, \quad (17)$$

and A_D is a measure of direct CP violation, while A_M is a measure of CP violation in mixing. The angle ϕ measures CP violation in interference between mixing and decay. While A_M is independent of the decay process, A_D and ϕ , in general, depend on f .

In general, $\lambda_{\bar{f}}$ and λ_f^{-1} are independent complex numbers. More detail on CP violation in meson decays can be found in Ref. 13. To leading order, for A_D and $A_M \ll 1$,

$$r(t) = e^{-t} \left[R_D(1+A_D) + \sqrt{R_D(1+A_M)(1+A_D)} y'_- t + \frac{1}{2}(1+A_M)R_M t^2 \right] \quad (18)$$

and

$$\bar{r}(t) = e^{-t} \left[R_D(1-A_D) + \sqrt{R_D(1-A_M)(1-A_D)} y'_+ t + \frac{1}{2}(1-A_M)R_M t^2 \right] \quad (19)$$

Here

$$y'_\pm \equiv y' \cos \phi \pm x' \sin \phi = y \cos(\delta_{K\pi} \mp \phi) - x \sin(\delta_{K\pi} \mp \phi), \quad (20)$$

where

$$x' \equiv x \cos \delta_{K\pi} + y \sin \delta_{K\pi}, \quad y' \equiv y \cos \delta_{K\pi} - x \sin \delta_{K\pi}, \quad (21)$$

and $R_M = (x^2 + y^2)/2 = (x'^2 + y'^2)/2$ is the mixing rate relative to the time-integrated Cabibbo-favored rate.

The three terms in Eq. (18) and Eq. (19) probe the three fundamental types of CP violation. In the limit of CP conservation, A_M , A_D , and ϕ are all zero. Then

$$r(t) = \bar{r}(t) = e^{-t} \left(R_D + \sqrt{R_D} y' t + \frac{1}{2} R_M t^2 \right), \quad (22)$$

and the time-integrated wrong-sign rate relative to the integrated right-sign rate is

$$R = \int_0^\infty r(t) dt = R_D + \sqrt{R_D} y' + R_M. \quad (23)$$

Meson Particle Listings

D^0

The ratio R is the most readily accessible experimental quantity. In Table 2 are also reported the measurements of R_D and A_D , and their HFAG average [10] from a general fit; all allow for both mixing and CP violation. Typically, the fit parameters are R_D , x'^2 , and y' . Table 3 summarizes the results for y' and x'^2 . Allowing for CP violation, the separate contributions to R can be extracted by fitting the $D^0 \rightarrow K^+\pi^-$ and $\bar{D}^0 \rightarrow K^-\pi^+$ decay rates.

Table 2: Results for R , R_D , and A_D in $D^0 \rightarrow K^+\pi^-$.

Year	Exper.	$R(\times 10^{-3})$	$R_D(\times 10^{-3})$	$A_D(\%)$
2007	CDF [14]	4.15 ± 0.10	3.04 ± 0.55	—
2007	BABAR [15]	$3.53 \pm 0.08 \pm 0.04$	$3.03 \pm 0.16 \pm 0.10$	$-2.1 \pm 5.2 \pm 1.5$
2006	Belle [16]	$3.77 \pm 0.08 \pm 0.05$	3.64 ± 0.17	2.3 ± 4.7
2005*	FOCUS [17]	$4.29^{+0.63}_{-0.61} \pm 0.28$	$5.17^{+1.47}_{-1.58} \pm 0.76$	$13^{+33}_{-25} \pm 10$
2000*	CLEO [18]	$3.32^{+0.63}_{-0.65} \pm 0.40$	$4.8 \pm 1.2 \pm 0.4$	$-1^{+16}_{-17} \pm 1$
1998	E791 [19]	$6.8^{+3.4}_{-3.3} \pm 0.7$	—	—
Average		3.80 ± 0.05	3.37 ± 0.09 [10]	-2.2 ± 2.4 [10]

*These measurements are included in the HFAG average of R_D but are excluded from the HFAG average A_D .

Table 3: Results on the time-dependence of $r(t)$ in $D^0 \rightarrow K^+\pi^-$ and $\bar{D}^0 \rightarrow K^-\pi^+$ decays. The CDF result assumes no CP violation. The FOCUS, CLEO, and Belle results restrict x'^2 to the physical region. The confidence intervals from FOCUS, CLEO, and BABAR are obtained from the fit, whereas Belle uses a Feldman-Cousins method, and CDF uses a Bayesian method.

Year	Exper.	y' (%)	$x'^2 (\times 10^{-3})$
2007	CDF [14]	0.85 ± 0.76	-0.12 ± 0.35
2007	BABAR [15]	$0.97 \pm 0.44 \pm 0.31$	$-0.22 \pm 0.30 \pm 0.21$
2006	Belle [16]	$-2.8 < y' < 2.1$	< 0.72 (95% C.L.)
2005	FOCUS [17]	$-11.2 < y' < 6.7$	< 8.0 (95% C.L.)
2000	CLEO [18]	$-5.8 < y' < 1.0$	< 0.81 (95% C.L.)

Table 4 summarizes results for R measured in multibody final states with nonzero strangeness. Here R , defined in Eq. (23), becomes an average over the Dalitz plot.

Table 4: Results for R in $D^0 \rightarrow K^{(*)+}\pi^-(n\pi)$. The values of R need not be the same for different decay channels.

Year	Exper.	D^0 final state	$R(\%)$
2006	BABAR [24]	$K^+\pi^-\pi^0$	$0.214 \pm 0.008 \pm 0.008$
2005	Belle [25]	$K^+\pi^-\pi^+\pi^-$	$0.320 \pm 0.018^{+0.018}_{-0.013}$
2005	Belle [25]	$K^+\pi^-\pi^0$	$0.229 \pm 0.015^{+0.013}_{-0.009}$
2002	CLEO [20]	$K^{*+}\pi^-$	$0.5 \pm 0.2^{+0.6}_{-0.1}$
2001	CLEO [26]	$K^+\pi^-\pi^+\pi^-$	$0.44^{+0.13}_{-0.12} \pm 0.06$
2001	CLEO [27]	$K^+\pi^-\pi^0$	$0.43^{+0.11}_{-0.10} \pm 0.07$
1998	E791 [19]	$K^+\pi^-\pi^+\pi^-$	$0.25^{+0.36}_{-0.34} \pm 0.03$

Extraction of the mixing parameters x and y from the results in Table 3 requires knowledge of the relative strong phase $\delta_{K\pi}$. An interference effect that provides useful sensitivity to $\delta_{K\pi}$ arises in the decay chain $\psi(3770) \rightarrow D^0 \bar{D}^0 \rightarrow (f_{CP})(K^+\pi^-)$, where f_{CP} denotes a CP -even or -odd eigenstate from D^0 decay, such as K^+K^- or $K_S^0\pi^0$, respectively [28]. Here, the amplitude relation

$$\sqrt{2} A(D_{\pm} \rightarrow K^-\pi^+) = A(D^0 \rightarrow K^-\pi^+) \pm A(\bar{D}^0 \rightarrow K^-\pi^+), \quad (24)$$

where D_{\pm} denotes a CP -even or -odd eigenstate, implies that

$$\cos \delta_{K\pi} = \frac{|A(D_+ \rightarrow K^-\pi^+)|^2 - |A(D_- \rightarrow K^-\pi^+)|^2}{2\sqrt{R_D} |A(D^0 \rightarrow K^-\pi^+)|^2}. \quad (25)$$

This neglects CP violation and uses $\sqrt{R_D} \ll 1$.

For multibody final states, Eqs. (13)–(23) apply separately to each point in phase-space. Although x and y do not vary across the space, knowledge of the resonant substructure is needed to extrapolate the strong phase difference δ from point to point to determine x and y .

A time-dependent analysis of $D^0 \rightarrow K^+\pi^-\pi^0$ from BABAR [24,29] determines the *relative* strong phase variation across the Dalitz plot and reports $x'' = (2.61^{+0.57}_{-0.68} \pm 0.39)\%$, and $y'' = (-0.06^{+0.55}_{-0.64} \pm 0.34)\%$, where x'' and y'' are defined as

$$\begin{aligned} x'' &\equiv x \cos \delta_{K\pi\pi^0} + y \sin \delta_{K\pi\pi^0}, \\ y'' &\equiv y \cos \delta_{K\pi\pi^0} - x \sin \delta_{K\pi\pi^0}, \end{aligned} \quad (26)$$

in parallel to x' , y' , and $\delta_{K\pi}$ of Eq. (21). Here $\delta_{K\pi\pi^0}$ is the remaining strong phase difference between the DCS $D^0 \rightarrow K^+\rho^-$ and the CF $\bar{D}^0 \rightarrow K^+\rho^-$ amplitudes and does not vary across the Dalitz plot. Both strong phases, $\delta_{K\pi}$ and $\delta_{K\pi\pi^0}$, can be determined from time-integrated CP asymmetries in correlated $D^0 \bar{D}^0$ produced at the $\psi(3770)$ [28,30].

Both the sign and magnitude of x and y without phase or sign ambiguity may be measured using the time-dependent resonant substructure of multibody D^0 decays [31,21]. In $D^0 \rightarrow K_S^0\pi^+\pi^-$, the DCS and CF decay amplitudes populate the same Dalitz plot, which allows direct measurement of

the relative strong phases. CLEO [20] and Belle [21] have measured the relative phase between $D^0 \rightarrow K^*(892)^+\pi^-$ and $D^0 \rightarrow K^*(892)^-\pi^+$ to be $(189 \pm 10 \pm 3_{-5}^{+15})^\circ$ and $(171.9 \pm 1.3 \text{ (stat. only)})^\circ$, respectively. These results are close to the 180° expected from Cabibbo factors and a small strong phase. Table 5 summarizes the results from Belle [21] of a time-dependent Dalitz-plot analysis of $D^0 \rightarrow K_S^0\pi^+\pi^-$.

Table 5: Results from Belle time-dependent Dalitz-plot analysis of $D^0 \rightarrow K_S^0\pi^+\pi^-$ [21]. The errors are statistical, experimental systematic, and decay-model systematic, respectively.

Result	95% C.L. interval
No CP Violation	
$x = (0.80 \pm 0.29_{-0.07-0.14}^{+0.09+0.10})\%$	$(0.0, 1.6)\%$
$y = (0.33 \pm 0.24_{-0.12-0.08}^{+0.08+0.06})\%$	$(-0.34, 0.96)\%$
With CP Violation	
$x = (0.81 \pm 0.30_{-0.07-0.16}^{+0.10+0.09})\%$	$ x < 1.6\%$
$y = (0.37 \pm 0.25_{-0.13-0.08}^{+0.07+0.07})\%$	$ y < 1.04\%$
$ q/p = 0.86_{-0.29-0.03}^{+0.30+0.06} \pm 0.08$	
$\phi = (-14_{-18-3-4}^{+16+5+2})^\circ$	

In addition, Belle [21] has results for both the relative phase (statistical errors only) and ratio R (central values only) of the DCS fit fraction relative to the CF fit fractions for $K^*(892)^+\pi^-$, $K_0^*(1430)^+\pi^-$, $K_2^*(1430)^+\pi^-$, $K^*(1410)^+\pi^-$, and $K^*(1680)^+\pi^-$. The systematic uncertainties on R must be evaluated. The values for R in units of $\tan^4\theta_c$ are 2.94 ± 0.12 , 22.0 ± 1.6 , 34 ± 4 , 87 ± 13 , and 500 ± 500 . For $K^+\pi^-$, the corresponding value for R_D is $(1.28 \pm 0.02) \times \tan^4\theta_c$. Similarly, BABAR [22] has reported central values for R for $K^*(892)^+\pi^-$, $K_0^*(1430)^+\pi^-$, and $K_2^*(1430)^+\pi^-$. The values for R in units of $\tan^4\theta_c$ are 3.45 ± 0.31 , 7.7 ± 3.0 , and 1.7 ± 1.7 , respectively. Recently, BABAR [23] has used a K-matrix formalism to describe the $\pi\pi$ S-wave in $K_S^0\pi^+\pi^-$. The reported values for R in units of $\tan^4\theta_c$ are 2.78 ± 0.11 , 0.5 ± 0.2 , and 1.4 ± 0.5 , respectively. The large differences in R among these final states could point to an interesting role for hadronic effects.

Decays to CP Eigenstates: When the final state f is a CP eigenstate, there is no distinction between f and \bar{f} , and $A_f = A_{\bar{f}}$ and $\bar{A}_{\bar{f}} = \bar{A}_f$. We denote final states with CP eigenvalues ± 1 by f_\pm and write λ_\pm for λ_{f_\pm} .

The quantity y may be measured by comparing the rate for D^0 decays to non- CP eigenstates such as $K^-\pi^+$ with decays to CP eigenstates such as K^+K^- [12]. If decays to K^+K^- have a shorter effective lifetime than those to $K^-\pi^+$, y is positive.

In the limit of slow mixing ($x, y \ll 1$) and the absence of direct CP violation ($A_D = 0$), but allowing for small indirect CP violation ($|A_M|, |\phi| \ll 1$), we can write

$$\lambda_\pm = \left| \frac{q}{p} \right| e^{i\phi}. \quad (27)$$

Table 6: Results for y_{CP} from $D^0 \rightarrow K^+K^-$ and $\pi^+\pi^-$.

Year	Exper.	final state(s)	$y_{CP}(\%)$	$A_\Gamma(\times 10^{-3})$
2009	BABAR [32]	K^+K^-	$1.16 \pm 0.22 \pm 0.18$	-
2009	Belle [33]	$K_S^0K^+K^-$	$0.11 \pm 0.61 \pm 0.52$	-
2008	BABAR* [34]	$K^+K^-, \pi^+\pi^-$	$1.03 \pm 0.33 \pm 0.19$	$2.6 \pm 3.6 \pm 0.8$
2007	Belle [35]	$K^+K^-, \pi^+\pi^-$	$1.31 \pm 0.32 \pm 0.25$	$0.1 \pm 3.0 \pm 1.5$
2001	CLEO [36]	$K^+K^-, \pi^+\pi^-$	$-1.2 \pm 2.5 \pm 1.4$	—
2001	Belle [37]	K^+K^-	$-0.5 \pm 1.0_{-0.8}^{+0.7}$	—
2000	FOCUS [38]	K^+K^-	$3.42 \pm 1.39 \pm 0.74$	—
1999	E791 [39]	K^+K^-	$0.8 \pm 2.9 \pm 1.0$	—
HFAG Avg. [10]			1.11 ± 0.22	0.12 ± 0.25

*This measurement is included in the result reported by Ref. 32.

In this scenario, to a good approximation, the decay rates for states that are initially D^0 and \bar{D}^0 to a CP eigenstate have exponential time dependence:

$$r_\pm(t) \propto \exp(-t/\tau_\pm), \quad (28)$$

$$\bar{r}_\pm(t) \propto \exp(-t/\bar{\tau}_\pm), \quad (29)$$

where τ is measured in units of $1/\Gamma$.

The effective lifetimes are given by

$$1/\tau_\pm = 1 \pm \left| \frac{q}{p} \right| (y \cos \phi - x \sin \phi), \quad (30)$$

$$1/\bar{\tau}_\pm = 1 \pm \left| \frac{p}{q} \right| (y \cos \phi + x \sin \phi). \quad (31)$$

The effective decay rate to a CP eigenstate combining both D^0 and \bar{D}^0 decays is

$$r_\pm(t) + \bar{r}_\pm(t) \propto e^{-(1 \pm y_{CP})t}. \quad (32)$$

Here

$$y_{CP} = \frac{1}{2} \left(\left| \frac{q}{p} \right| + \left| \frac{p}{q} \right| \right) y \cos \phi - \frac{1}{2} \left(\left| \frac{q}{p} \right| - \left| \frac{p}{q} \right| \right) x \sin \phi \quad (33)$$

$$\approx y \cos \phi - A_M x \sin \phi. \quad (34)$$

If CP is conserved, $y_{CP} = y$.

All measurements of y_{CP} and A_Γ are relative to the $D^0 \rightarrow K^-\pi^+$ decay rate. Table 6 summarizes the current status of measurements. Belle [35] and BaBar [32,34] have reported y_{CP} and the decay-rate asymmetry for CP even final states

$$A_\Gamma = \frac{\bar{\tau}_+ - \tau_+}{\bar{\tau}_+ + \tau_+} = \frac{(1/\tau_+) - (1/\bar{\tau}_+)}{(1/\tau_+) + (1/\bar{\tau}_+)} \quad (35)$$

$$= \frac{1}{2} \left(\left| \frac{q}{p} \right| - \left| \frac{p}{q} \right| \right) y \cos \phi - \frac{1}{2} \left(\left| \frac{q}{p} \right| + \left| \frac{p}{q} \right| \right) x \sin \phi \quad (36)$$

$$\approx A_M y \cos \phi - x \sin \phi. \quad (37)$$

If CP is conserved, $A_\Gamma = 0$. Recently, Belle [33] has reported y_{CP} for the final state $K_S^0K^+K^-$ which is dominated by the CP odd final state $K_S^0\phi$.

Meson Particle Listings

D^0

Substantial work on the time-integrated CP asymmetries in decays to CP eigenstates are consistent with no CP -violation at the few-percent level [40].

Coherent $D^0\bar{D}^0$ Analyses: Measurements of R_D , $\cos\delta_{K\pi}$, x , and y can be made simultaneously in a combined fit to the single-tag (ST) and double-tag (DT) yields, or individually by a series of “targeted” analyses [28,30].

The “comprehensive” analysis simultaneously measures mixing and DCS parameters by examining various ST and DT rates. Due to quantum correlations in the $C = -1$ and $C = +1$ $D^0\bar{D}^0$ pairs produced in the reactions $e^+e^- \rightarrow D^0\bar{D}^0(\pi^0)$ and $e^+e^- \rightarrow D^0\bar{D}^0\gamma(\pi^0)$, respectively, the time-integrated $D^0\bar{D}^0$ decay rates are sensitive to interference between amplitudes for indistinguishable final states. The size of this interference is governed by the relevant amplitude ratios and can include contributions from $D^0\text{--}\bar{D}^0$ mixing.

The following categories of final states are considered:

f or \bar{f} : Hadronic states accessed from either D^0 or \bar{D}^0 decay but that are not CP eigenstates. An example is $K^-\pi^+$, which results from Cabibbo-favored D^0 transitions or DCS \bar{D}^0 transitions.

ℓ^+ or ℓ^- : Semileptonic or purely leptonic final states, which, in the absence of mixing, tag unambiguously the flavor of the parent D^0 .

f_+ or f_- : CP -even and CP -odd eigenstates, respectively.

The decay rates for $D^0\bar{D}^0$ pairs to all possible combinations of the above categories of final states are calculated in Ref. 2, for both $C = -1$ and $C = +1$, reproducing the work of Ref. 3. Such $D^0\bar{D}^0$ combinations, where both D final states are specified, are double tags. In addition, the rates for single tags, where either the D^0 or \bar{D}^0 is identified and the other neutral D decays generically are given in Ref. 2.

CLEO-c has reported results using 281 pb⁻¹ of $e^+e^- \rightarrow \psi(3770)$ data [41,42], where the quantum-coherent $D^0\bar{D}^0$ pairs are in the $C = -1$ state. The values of y , R_M , and $\cos\delta_{K\pi}$ are determined from a combined fit to the ST (hadronic only) and DT yields. The hadronic final states included are $K^-\pi^+$ (f), $K^+\pi^-$ (\bar{f}), K^-K^+ (f_+), $\pi^+\pi^-$ (f_+), $K_S^0\pi^0\pi^0$ (f_+), $K_L^0\pi^0$ (f_+), $K_S^0\pi^0$ (f_-), $K_S^0\eta$ (f_-), and $K_S^0\omega$ (f_-). The two flavored final states, $K^-\pi^+$ and $K^+\pi^-$, can be reached via CF or DCS transitions.

Semileptonic DT yields are also included, where one D is fully reconstructed in one of the hadronic modes listed above, and the other D is partially reconstructed, requiring that only an electron be found. When the electron is accompanied by a flavor tag ($D \rightarrow K^-\pi^+$ or $K^+\pi^-$), only the “right-sign” DT sample, where the electron and kaon charges are the same, is used.

The main results of the CLEO-c analysis are the determination of $\cos\delta_{K\pi} = 1.10 \pm 0.35 \pm 0.07$, and World Averages for the mixing parameters from an “extended” fit that combines the CLEO-c data with previous mixing and branching-ratio measurements [41,42]. In these fits, which allow $\cos\delta_{K\pi}$ and x^2 to be unphysical, the no-mixing result ($x = y = 0$) is excluded

at 5.0σ . Constraining $\cos\delta_{K\pi}$ and $\sin\delta_{K\pi}$ to $[-1, +1]$ —that is interpreting $\delta_{K\pi}$ as an angle—yields $\delta_{K\pi} = (22_{-12}^{+14+9})^\circ$. Note that measurements of y (Table 5 and Table 6) and y' (Table 3) contribute to the determination of $\delta_{K\pi}$.

Coherent $D^0\bar{D}^0$ production can also be used to determine the average strong phase difference, $\bar{\delta}_f$, and coherence factor, R_f , for a flavor-specific multibody final state, f , such as $K^-\pi^+\pi^0$ [43]. Determining the mixing parameters using multibody decays, without using knowledge of resonant substructure, requires both R_f and $\bar{\delta}_f$. Furthermore, the measurement of R_f improves the determination of the Unitarity Triangle angle γ [44,45]. The parameters $\bar{\delta}_f$ and R_f are defined by

$$R_f e^{-i\bar{\delta}_f} = \frac{\int \mathcal{A}_f(\mathbf{x})\mathcal{A}_{\bar{f}}(\mathbf{x})d\mathbf{x}}{A_f A_{\bar{f}}}. \quad (38)$$

Here $\mathcal{A}_f(\mathbf{x})$ ($\mathcal{A}_{\bar{f}}(\mathbf{x})$) is the amplitude for $D^0 \rightarrow f$ ($D^0 \rightarrow \bar{f}$) at a point in multibody phase space described by parameters \mathbf{x} , and $A_f^2 = \int |\mathcal{A}_f(\mathbf{x})|^2 d\mathbf{x}$. A value of R_f close to unity indicates that only a few intermediate states, with limited overlap in phase space, dominate the decay. Note that while $\bar{\delta}_{K\pi} = \delta_{K\pi}$ (defined in Eq. (13)), knowledge of the resonant substructure is required to relate $\bar{\delta}_{K\pi\pi^0}$ and $\bar{\delta}_{K3\pi}$ to $\delta_{K\pi\pi^0}$ (defined below Eq. (26)) and $\delta_{K3\pi}$, respectively.

CLEO-c has reported results for R_f and $\bar{\delta}_f$ ($f = K^-\pi^+\pi^0$, $K^-\pi^+\pi^+\pi^-$) using 818 pb⁻¹ of $e^+e^- \rightarrow \psi(3770)$ data [46]. The DT rates of f tagged by f_\pm , f , or another flavor-specific final state with a kaon of the same sign, e.g. $K^-\pi^+\pi^0$ vs. $K^-\pi^+$, provide the sensitivity to the parameters [43]. A similar analysis strategy is adopted to that reported in Refs [41,42]. Two fits to the DT rates are performed with and without external constraints on the mixing parameters x , y , and $\delta_{K\pi}$. The results of these fits are shown in Table 7. The results of Ref. 46 are not yet included in the HFAG average [10].

Table 7: Results from CLEO-c for mixing parameters from coherent $D^0\bar{D}^0$ decays.

Parameter	Mixing constrained	Mixing unconstrained
$\delta_{K\pi}(\circ)$ [41,42]	22_{-16}^{+14}	< 75 @95% C.L.
$\delta_{K\pi}(\circ)$ [46]	$28.5_{-9.5}^{+9.6}$	50_{-28}^{+38}
x (%) [46]	0.96 ± 0.25	$-0.8_{-2.5}^{+2.9}$
y (%) [46]	0.81 ± 0.16	$0.7_{-2.7}^{+2.4}$
$R_{K\pi\pi^0}$ [46]	0.84 ± 0.07	$0.78_{-0.25}^{+0.11}$
$\bar{\delta}_{K\pi\pi^0}(\circ)$ [46]	47_{-17}^{+14}	59_{-28}^{+32}
$R_{K3\pi}$ [46]	$0.33_{-0.23}^{+0.26}$	$0.36_{-0.30}^{+0.24}$
$\bar{\delta}_{K3\pi}(\circ)$ [46]	-66_{-23}^{+26}	-62_{-53}^{+62}

Summary of Experimental Results: Several recent results indicate that charm mixing is at the upper end of the range of Standard Model estimates.

For $D^0 \rightarrow K^+\pi^-$, BABAR [15] and CDF [14] find evidence for oscillations with 3.9σ ($\Delta\text{Log}\mathcal{L}$) and 3.8σ (Bayesian), respectively. The most precise measurement for mixing parameters is from Belle [16], which excludes $x^2 = y' = 0$ at 2.1σ .

For y_{CP} in $D^0 \rightarrow K^+K^-$ and $\pi^+\pi^-$, Belle [35] and BABAR [32] find 3.2σ and 4.1σ effects. The most sensitive measurement of y is in $D^0 \rightarrow K_S^0\pi^+\pi^-$ from Belle [21] and is only 1.2σ significant. In the same analysis, Belle also finds a 2.4σ result for x . The current situation would benefit from better knowledge of the strong phase difference $\delta_{K\pi}$ than provided by the current CLEO-c result [41,42]. This would allow one to unfold x and y from the $D^0 \rightarrow K^+\pi^-$ measurements of x'^2 and y' , and directly compare them to the $D^0 \rightarrow K_S^0\pi^+\pi^-$ results.

The experimental data consistently indicate that the D^0 and \bar{D}^0 do mix. The mixing is presumably dominated by long-range processes. Under the assumption that the observed mixing is due entirely to short-range processes, significant constraints on a variety of new physics models are obtained [47]. A serious limitation to the interpretation of charm oscillations in terms of New Physics is the theoretical uncertainty of the Standard Model prediction. However, recent evidence opens the window to searches for CP violation, which would provide unequivocal evidence of New Physics.

HFAG Averaging of Charm Mixing Results:

The Heavy Flavor Averaging Group (HFAG) has made a global fit to all mixing measurements to obtain values of x , y , $\delta_{K\pi}$, $\delta_{K\pi\pi^0}$, R_D , $A_D \equiv (R_D^+ - R_D^-)/(R_D^+ + R_D^-)$, $|q/p|$, and $\text{Arg}(q/p) \equiv \phi$. Correlations among observables are taken into account by using the error matrices from the experiments. The measurements of $D^0 \rightarrow K^{(*)+}\ell^-\bar{\nu}$, K^+K^- , $\pi^+\pi^-$, $K^+\pi^-$, $K^+\pi^-\pi^0$, $K^+\pi^-\pi^+\pi^-$, $K_S^0\pi^+\pi^-$, and $K_S^0K^+K^-$ decays, as well as CLEO-c results for double-tagged branching fractions measured at the $\psi(3770)$.

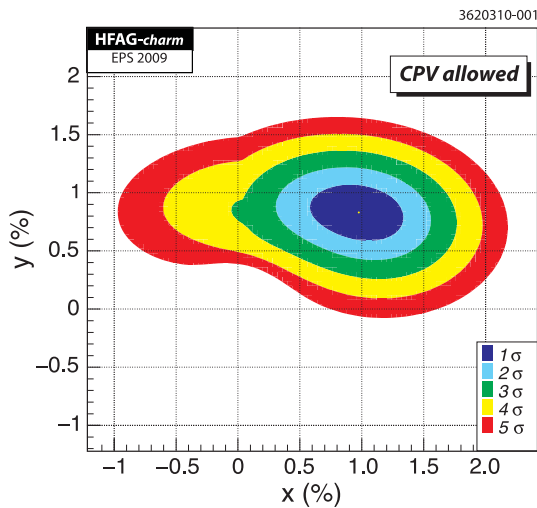


Figure 1: Two-dimensional 1σ - 5σ contours for (x, y) from measurements of $D^0 \rightarrow K^{(*)+}\ell\nu$, h^+h^- , $K^+\pi^-$, $K^+\pi^-\pi^0$, $K^+\pi^-\pi^+\pi^-$, $K_S^0\pi^+\pi^-$, and $K_S^0K^+K^-$ decays, and double-tagged branching fractions measured at the $\psi(3770)$ resonance (from HFAG [10]). Color version at end of book.

Table 8: HFAG Charm Mixing Average allowing for CP violation [10].

Parameter	HFAG average	95% C.L. interval
$x(\%)$	$0.98^{+0.24}_{-0.26}$	[0.46, 1.44]
$y(\%)$	0.83 ± 0.16	[0.51, 1.14]
$R_D(\%)$	0.337 ± 0.009	[0.320, 0.353]
$\delta_{K\pi}(\circ)$	$26.4^{+9.6}_{-9.9}$	[5.9, 45.8]
$\delta_{K\pi\pi^0}(\circ)$	$14.8^{+20.2}_{-22.1}$	[-30.3, 53.8]
$A_D(\%)$	-2.2 ± 2.4	[-6.9, 2.6]
$ q/p $	$0.86^{+0.18}_{-0.15}$	[0.60, 1.22]
$\phi(\circ)$	$-9.6^{+8.3}_{-9.5}$	[-22.1, 6.3]

For the global fit, confidence contours in the two dimensions (x, y) and $(|q/p|, \phi)$ are obtained by letting, for any point in the two-dimensional plane, all other fit parameters take their preferred values. Figures 1 and 2 show the resulting 1-to-5 σ contours. The fits exclude the no-mixing point ($x = y = 0$) at 10.2σ , whether or not CP violation is allowed. The parameters x and y differ from zero by 3.2σ and 4.8σ , respectively. One-dimensional likelihood functions for parameters are obtained by allowing, for any value of the parameter, all other fit parameters to take their preferred values. The resulting likelihood functions give central values, 68.3% C.L. intervals, and 95% C.L. intervals as listed in Table 8.

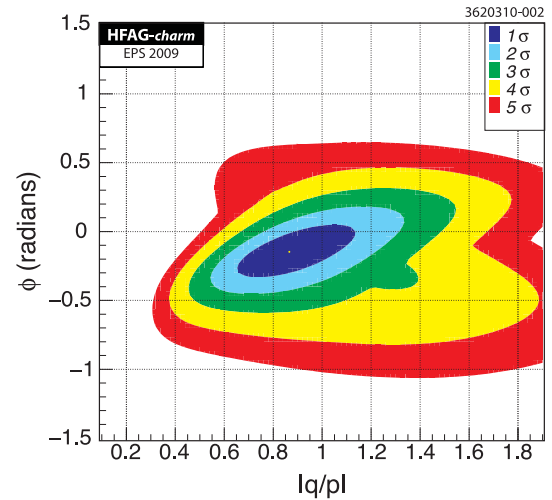


Figure 2: Two-dimensional 1σ - 5σ contours for $(|q/p|, \text{Arg}(q/p))$ from measurements of $D^0 \rightarrow K^{(*)+}\ell\nu$, h^+h^- , $K^+\pi^-$, $K^+\pi^-\pi^0$, $K^+\pi^-\pi^+\pi^-$, $K_S^0\pi^+\pi^-$, and $K_S^0K^+K^-$ decays, and double-tagged branching fractions measured at the $\psi(3770)$ resonance (from HFAG [10]). Color version at end of book.

From the results of the HFAG averaging, the following can be concluded: (1) Since CP violation is small and y_{CP} is positive, the CP -even state is shorter-lived, as in the $K^0\bar{K}^0$

Meson Particle Listings

 D^0

system. (2) However, since x appears to be positive, the CP -even state is heavier, unlike in the $K^0\bar{K}^0$ system. (3) The strong phase difference $\delta_{K\pi}$ is unlikely to be small. (4) There is no evidence yet for CP -violation in the $D^0\bar{D}^0$ system. Observing CP -violation at the current level of sensitivity would indicate new physics.

References

1. B. Aubert *et al.*, Phys. Rev. **D76**, 014018 (2007).
2. D.M. Asner and W.M. Sun, Phys. Rev. **D73**, 034024 (2006); Erratum-*ibid.*, **77**, 019901 (2008).
3. D. Atwood and A.A. Petrov, Phys. Rev. **D71**, 054032 (2005) Z.Z. Xing, Phys. Rev. **D55**, 196 (1997) M. Goldhaber and J.L. Rosner, Phys. Rev. **D15**, 1254 (1977).
4. U. Bitenc *et al.*, Phys. Rev. **D77**, 112003 (2008).
5. U. Bitenc *et al.*, Phys. Rev. **D72**, 071101R (2005).
6. C. Cawfield *et al.*, Phys. Rev. **D71**, 077101 (2005).
7. B. Aubert *et al.*, Phys. Rev. **D70**, 091102R (2004).
8. K. Stenson, presented at the April Meeting of the American Physical Society (APS 03), Philadelphia, Pennsylvania, April 5-8, 2003; M. Hosack, (FOCUS Collab.), Fermilab-Thesis-2002-25.
9. E.M. Aitala *et al.*, Phys. Rev. Lett. **77**, 2384 (1996).
10. A.J. Schwartz, for the Heavy Flavor Averaging Group, arXiv:0911.1464 [hep-ex].
11. Y. Nir, Lectures given at 27th SLAC Summer Institute on Particle Physics: CP Violation in and Beyond the Standard Model (SSI 99), Stanford, California, 7-16 Jul 1999. Published in Trieste 1999, *Particle Physics*, pp. 165-243.
12. S. Bergmann *et al.*, Phys. Lett. **B486**, 418 (2000).
13. See the Note on " CP Violation in Meson Decays" in this *Review*.
14. T. Aaltonen, Phys. Rev. Lett. **100**, 121802 (2008).
15. B. Aubert *et al.*, Phys. Rev. Lett. **98**, 211802 (2007).
16. L.M. Zhang *et al.*, Phys. Rev. Lett. **96**, 151801 (2006).
17. J.M. Link *et al.*, Phys. Lett. **B607**, 51 (2005).
18. R. Godang *et al.*, Phys. Rev. Lett. **84**, 5038 (2000).
19. E.M. Aitala *et al.*, Phys. Rev. **D57**, 13 (1998).
20. H. Muramatsu *et al.*, Phys. Rev. Lett. **89**, 251802 (2002).
21. L.M. Zhang *et al.*, Phys. Rev. Lett. **99**, 131803 (2007).
22. B. Aubert *et al.*, Phys. Rev. Lett. **95**, 121802 (2005).
23. B. Aubert *et al.*, Phys. Rev. **D78**, 034023 (2008).
24. B. Aubert *et al.*, Phys. Rev. Lett. **97**, 221803 (2006).
25. X.C. Tian *et al.*, Phys. Rev. Lett. **95**, 231801 (2005).
26. S.A. Dytman *et al.*, Phys. Rev. **D64**, 111101R (2001).
27. G. Brandenburg *et al.*, Phys. Rev. Lett. **87**, 071802 (2001).
28. R.A. Briere *et al.*, (CLEO Collab.), CLNS 01-1742, (2001).
29. B. Aubert *et al.*, Phys. Rev. Lett. **103**, 211801 (2009).
30. G. Cavoto *et al.*, Prepared for *3rd Workshop on the Unitarity Triangle: CKM 2005, San Diego, California, 15-18 Mar 2005*, hep-ph/0603019.
31. D.M. Asner *et al.*, Phys. Rev. **D72**, 012001 (2005).
32. B. Aubert *et al.*, Phys. Rev. **D80**, 071103R (2009).
33. A. Zupanc *et al.*, Phys. Rev. **D80**, 052006 (2009).
34. B. Aubert *et al.*, Phys. Rev. **D78**, 011105 (2008).
35. M. Staric *et al.*, Phys. Rev. Lett. **98**, 211803 (2007).
36. S.E. Csorna *et al.*, Phys. Rev. **D65**, 092001 (2002).
37. K. Abe *et al.*, Phys. Rev. Lett. **88**, 162001 (2002).
38. J.M. Link *et al.*, Phys. Lett. **B485**, 62 (2000).
39. E.M. Aitala *et al.*, Phys. Rev. Lett. **83**, 32 (1999).
40. See the tabulation of A_{CP} results in the D^0 and D^+ Listings in this *Review*.
41. J.L. Rosner *et al.*, Phys. Rev. Lett. **100**, 221801 (2008).
42. D.M. Asner *et al.*, Phys. Rev. **D78**, 012001 (2008).
43. D. Atwood and A. Soni, Phys. Rev. **D68**, 033003 (2003).
44. D. Atwood, I. Dunietz and A. Soni, Phys. Rev. Lett. **78**, 3257 (1997).
45. D. Atwood, I. Dunietz and A. Soni, Phys. Rev. **D63**, 036005 (2001).
46. N. Lowery *et al.*, *et al.*, Phys. Rev. **D80**, 031105 (R)(2009).
47. E. Golowich *et al.*, Phys. Rev. **D76**, 095009 (2007).

$$|m_{D_1^0} - m_{D_2^0}| = x \Gamma$$

The D_1^0 and D_2^0 are the mass eigenstates of the D^0 meson, as described in the note on " $D^0\text{-}\bar{D}^0$ Mixing," above. The experiments usually present $x \equiv \Delta m/\Gamma$. Then $\Delta m = x \Gamma = x \hbar/\tau$.

VALUE ($10^{10} \hbar s^{-1}$)	CL%	DOCUMENT ID	TECN	COMMENT
$2.39^{+0.59}_{-0.63}$		OUR EVALUATION	HFAG fit; see the note on " $D^0\text{-}\bar{D}^0$ Mixing."	
$1.98 \pm 0.73^{+0.32}_{-0.41}$		⁵ ZHANG	07B BELL	$\Delta m < 3.9$, 95% CL
••• We do not use the following data for averages, fits, limits, etc. •••				
6.4 $^{+1.4}_{-1.7} \pm 1.0$		⁶ AUBERT	09AN BABR	e^+e^- at 10.58 GeV
-2		⁷ LOWREY	09 CLEO	e^+e^- at $\psi(3770)$
< 7	95	⁸ ZHANG	06 BELL	e^+e^-
-11	to $+22$	⁵ ASNER	05 CLEO	$e^+e^- \approx 10$ GeV
< 11	90	BITENC	05 BELL	
< 30	90	CRAWFIELD	05 CLEO	
< 7	95	⁸ LI	05A BELL	See ZHANG 06
< 22	95	⁹ LINK	05H FOCS	γ nucleus
< 23	95	AUBERT	04Q BABR	
< 11	95	⁸ AUBERT	03Z BABR	e^+e^- , 10.6 GeV
< 7	95	¹⁰ GODANG	00 CLE2	e^+e^-
< 32	90	^{11,12} AITALA	98 E791	π^- nucleus, 500 GeV
< 24	90	¹³ AITALA	96c E791	π^- nucleus, 500 GeV
< 21	90	^{12,14} ANJOS	88c E691	Photoproduction

⁵The ASNER 05 and ZHANG 07B values are from the time-dependent Dalitz-plot analysis of $D^0 \rightarrow K_S^0 \pi^+ \pi^-$. Decay-time information and interference on the Dalitz plot are used to distinguish doubly Cabibbo-suppressed decays from mixing and to measure the relative phase between $D^0 \rightarrow K^{*+} \pi^-$ and $\bar{D}^0 \rightarrow K^{*+} \pi^-$. This value allows CP violation and is sensitive to the sign of Δm .

⁶The AUBERT 09AN values are inferred from the branching ratio $\Gamma(D^0 \rightarrow K^+ \pi^- \pi^0 \text{ via } \bar{D}^0)/\Gamma(D^0 \rightarrow K^- \pi^+ \pi^0)$ given near the end of this Listings. Mixing is distinguished from DCS decays using decay-time information. Interference between mixing and DCS is allowed. The phase between $D^0 \rightarrow K^+ \pi^- \pi^0$ and $\bar{D}^0 \rightarrow K^+ \pi^- \pi^0$ is assumed to be small. The width difference here is γ' , which is not the same as γ_{CP} in the note on $D^0\text{-}\bar{D}^0$ mixing.

⁷LOWREY 09 uses quantum correlations in $e^+e^- \rightarrow D^0\bar{D}^0$ at the $\psi(3770)$. See below for coherence factors and average relative strong phases for both $D^0 \rightarrow K^- \pi^+ \pi^0$ and $D^0 \rightarrow K^- \pi^- 2\pi^+$. A fit that includes external measurements of charm mixing parameters gets $\Delta m = (2.34 \pm 0.61) \times 10^{10} \hbar s^{-1}$.

⁸The AUBERT 03Z, LI 05A, and ZHANG 06 limits are inferred from the $D^0\text{-}\bar{D}^0$ mixing ratio $\Gamma(K^+ \pi^- \text{ via } \bar{D}^0)/\Gamma(K^- \pi^+)$ given near the end of this D^0 Listings. Decay-time information is used to distinguish DCS decays from $D^0\text{-}\bar{D}^0$ mixing. The limit allows interference between the DCS and mixing ratios, and also allows CP violation. AUBERT 03Z assumes the strong phase between $D^0 \rightarrow K^+ \pi^-$ and $\bar{D}^0 \rightarrow K^+ \pi^-$ amplitudes is small; if an arbitrary phase is allowed, the limit degrades by 20%. The LI 05A and ZHANG 06 limits are valid for an arbitrary strong phase.

⁹This LINK 05H limit is inferred from the $D^0\text{-}\bar{D}^0$ mixing ratio $\Gamma(K^+ \pi^- \text{ via } \bar{D}^0)/\Gamma(K^- \pi^+)$ given near the end of this D^0 Listings. Decay-time information is used to distinguish DCS decays from $D^0\text{-}\bar{D}^0$ mixing. The limit allows interference between the DCS and mixing ratios, and also allows CP violation. The strong phase between $D^0 \rightarrow K^+ \pi^-$ and $\bar{D}^0 \rightarrow K^+ \pi^-$ is assumed to be small. If an arbitrary relative strong phase is allowed, the limit degrades by 25%.

¹⁰This GODANG 00 limit is inferred from the $D^0\text{-}\bar{D}^0$ mixing ratio $\Gamma(K^+ \pi^- \text{ via } \bar{D}^0)/\Gamma(K^- \pi^+)$ given near the end of this D^0 Listings. Decay-time information is used to distinguish DCS decays from $D^0\text{-}\bar{D}^0$ mixing. The limit allows interference between the DCS and mixing ratios, and also allows CP violation. The strong phase between $D^0 \rightarrow K^+ \pi^-$ and $\bar{D}^0 \rightarrow K^+ \pi^-$ is assumed to be small. If an arbitrary relative strong phase is allowed, the limit degrades by a factor of two.

Meson Particle Listings

 D^0 $D^0 \rightarrow K^- \pi^+ \pi^0$ AVERAGE RELATIVE STRONG PHASE $\delta^{K\pi\pi^0}$

VALUE (°)	DOCUMENT ID	TECN	COMMENT
239⁺³²₋₂₈	30	LOWREY	09 CLEO $e^+e^- \rightarrow D^0\bar{D}^0$ at $\psi(3770)$

30 LOWREY 09 uses quantum correlations in $e^+e^- \rightarrow D^0\bar{D}^0$ at the $\psi(3770)$, where the decay rates of CP-tagged $K^-\pi^+\pi^0$ final states depend on $R_{K\pi\pi^0}$ and $\delta^{K\pi\pi^0}$.

A fit that includes external measurements of charm mixing parameters gets $\delta^{K\pi\pi^0} = (227^{+14}_{-17})^\circ$.

 $D^0 \rightarrow K^- \pi^- 2\pi^+$ COHERENCE FACTOR $R_{K3\pi}$

See the note on ' $D^0\bar{D}^0$ Mixing' for the definition. $R_{K3\pi}$ can have any value between 0 and 1. A value near 1 indicates the decay is dominated by a few intermediate states with limited interference.

VALUE	DOCUMENT ID	TECN	COMMENT
0.36^{+0.24}_{-0.30}	31	LOWREY	09 CLEO $e^+e^- \rightarrow D^0\bar{D}^0$ at $\psi(3770)$

31 LOWREY 09 uses quantum correlations in $e^+e^- \rightarrow D^0\bar{D}^0$ at the $\psi(3770)$, where the decay rates of CP-tagged $K^-\pi^-2\pi^+$ final states depend on $R_{K3\pi}$ and $\delta^{K3\pi}$. A fit that includes external measurements of charm mixing parameters gets $R_{K3\pi} = 0.33^{+0.26}_{-0.23}$.

 $D^0 \rightarrow K^- \pi^- 2\pi^+$ AVERAGE RELATIVE STRONG PHASE $\delta^{K3\pi}$

VALUE (°)	DOCUMENT ID	TECN	COMMENT
118⁺⁶²₋₅₃	32	LOWREY	09 CLEO $e^+e^- \rightarrow D^0\bar{D}^0$ at $\psi(3770)$

32 LOWREY 09 uses quantum correlations in $e^+e^- \rightarrow D^0\bar{D}^0$ at the $\psi(3770)$, where the decay rates of CP-tagged $K^-\pi^-2\pi^+$ final states depend on $R_{K3\pi}$ and $\delta^{K3\pi}$.

A fit that includes external measurements of charm mixing parameters gets $\delta^{K3\pi} = (114^{+26}_{-23})^\circ$.

 D^0 DECAY MODES

Most decay modes (other than the semileptonic modes) that involve a neutral K meson are now given as K_S^0 modes, not as \bar{K}^0 modes. Nearly always it is a K_S^0 that is measured, and interference between Cabibbo-allowed and doubly Cabibbo-suppressed modes can invalidate the assumption that $2\Gamma(K_S^0) = \Gamma(\bar{K}^0)$.

Mode	Fraction (Γ_i/Γ)	Scale factor/ Confidence level
------	--------------------------------	-----------------------------------

Topological modes

Γ_1 0-prongs	[a] (17 ± 6) %	
Γ_2 2-prongs	(69 ± 6) %	
Γ_3 4-prongs	[b] (14.3 ± 0.5) %	
Γ_4 6-prongs	[c] (6.4 ± 1.3) × 10 ⁻⁴	

Inclusive modes

Γ_5 e^+ anything	[d] (6.49 ± 0.11) %	
Γ_6 μ^+ anything	(6.7 ± 0.6) %	
Γ_7 K^- anything	(54.7 ± 2.8) %	S=1.3
Γ_8 \bar{K}^0 anything + K^0 anything	(47 ± 4) %	
Γ_9 K^+ anything	(3.4 ± 0.4) %	
Γ_{10} $K^*(892)^-$ anything	(15 ± 9) %	
Γ_{11} $\bar{K}^*(892)^0$ anything	(9 ± 4) %	
Γ_{12} $K^*(892)^+$ anything	< 3.6 %	CL=90%
Γ_{13} $K^*(892)^0$ anything	(2.8 ± 1.3) %	
Γ_{14} η anything	(9.5 ± 0.9) %	
Γ_{15} η' anything	(2.48 ± 0.27) %	
Γ_{16} ϕ anything	(1.05 ± 0.11) %	

Semileptonic modes

Γ_{17} $K^-\ell^+\nu_\ell$		
Γ_{18} $K^-e^+\nu_e$	(3.55 ± 0.05) %	S=1.2
Γ_{19} $K^-\mu^+\nu_\mu$	(3.31 ± 0.13) %	
Γ_{20} $K^*(892)^-e^+\nu_e$	(2.17 ± 0.16) %	
Γ_{21} $K^*(892)^-\mu^+\nu_\mu$	(1.98 ± 0.24) %	
Γ_{22} $K^-\pi^0e^+\nu_e$	(1.6 ^{+1.3} _{-0.5}) %	
Γ_{23} $\bar{K}^0\pi^-e^+\nu_e$	(2.7 ^{+0.9} _{-0.7}) %	
Γ_{24} $K^-\pi^+\pi^-\pi^0e^+\nu_e$	(2.8 ^{+1.4} _{-1.1}) × 10 ⁻⁴	
Γ_{25} $K_1(1270)^-e^+\nu_e$	(7.6 ^{+4.0} _{-3.1}) × 10 ⁻⁴	
Γ_{26} $K^-\pi^+\pi^-\mu^+\nu_\mu$	< 1.2 × 10 ⁻³	CL=90%
Γ_{27} $(\bar{K}^*(892)\pi)^-\mu^+\nu_\mu$	< 1.4 × 10 ⁻³	CL=90%
Γ_{28} $\pi^-e^+\nu_e$	(2.89 ± 0.08) × 10 ⁻³	S=1.1
Γ_{29} $\pi^-\mu^+\nu_\mu$	(2.37 ± 0.24) × 10 ⁻³	
Γ_{30} $\rho^-e^+\nu_e$	(1.9 ± 0.4) × 10 ⁻³	

Hadronic modes with one \bar{K}

Γ_{31} $K^-\pi^+$	(3.89 ± 0.05) %	S=1.2
Γ_{32} $K_S^0\pi^0$	(1.22 ± 0.05) %	
Γ_{33} $K_S^0\pi^0$	(10.0 ± 0.7) × 10 ⁻³	
Γ_{34} $K_S^0\pi^+\pi^-$	[e] (2.94 ± 0.16) %	S=1.1
Γ_{35} $K_S^0\rho^0$	(6.6 ^{+0.6} _{-0.8}) × 10 ⁻³	
Γ_{36} $K_S^0\omega, \omega \rightarrow \pi^+\pi^-$	(2.1 ± 0.6) × 10 ⁻⁴	
Γ_{37} $K_S^0(\pi^+\pi^-)_{S\text{-wave}}$	(3.5 ± 0.8) × 10 ⁻³	
Γ_{38} $K_S^0f_0(980), f_0(980) \rightarrow \pi^+\pi^-$	(1.27 ^{+0.40} _{-0.24}) × 10 ⁻³	
Γ_{39} $K_S^0f_0(1370), f_0(1370) \rightarrow \pi^+\pi^-$	(2.9 ^{+0.9} _{-1.3}) × 10 ⁻³	
Γ_{40} $K_S^0f_2(1270), f_2(1270) \rightarrow \pi^+\pi^-$	(9 ⁺¹⁰ ₋₆) × 10 ⁻⁵	
Γ_{41} $K^*(892)^-\pi^+, K^*(892)^-\pi^0 \rightarrow K_S^0\pi^-$	(1.73 ^{+0.14} _{-0.17}) %	
Γ_{42} $K_0^*(1430)^-\pi^+, K_0^*(1430)^-\pi^0 \rightarrow K_S^0\pi^-$	(2.81 ^{+0.40} _{-0.33}) × 10 ⁻³	
Γ_{43} $K_2^*(1430)^-\pi^+, K_2^*(1430)^-\pi^0 \rightarrow K_S^0\pi^-$	(3.5 ^{+2.0} _{-1.1}) × 10 ⁻⁴	
Γ_{44} $K^*(1680)^-\pi^+, K^*(1680)^-\pi^0 \rightarrow K_S^0\pi^-$	(5 ± 4) × 10 ⁻⁴	
Γ_{45} $K^*(892)^+\pi^-, K^*(892)^+\pi^0 \rightarrow K_S^0\pi^+$	[f] (1.18 ^{+0.60} _{-0.35}) × 10 ⁻⁴	
Γ_{46} $K_0^*(1430)^+\pi^-, K_0^*(1430)^+\pi^0 \rightarrow K_S^0\pi^+$	[f] < 1.5 × 10 ⁻⁵	CL=95%
Γ_{47} $K_2^*(1430)^+\pi^-, K_2^*(1430)^+\pi^0 \rightarrow K_S^0\pi^+$	[f] < 3.5 × 10 ⁻⁵	CL=95%
Γ_{48} $K_S^0\pi^+\pi^-$ nonresonant	(2.7 ^{+6.0} _{-1.7}) × 10 ⁻⁴	
Γ_{49} $K^-\pi^+\pi^0$	[e] (13.9 ± 0.5) %	S=1.7
Γ_{50} $K^-\rho^+$	(10.8 ± 0.7) %	
Γ_{51} $K^-\rho(1700)^+, \rho(1700)^+ \rightarrow \pi^+\pi^0$	(7.9 ± 1.7) × 10 ⁻³	
Γ_{52} $K^*(892)^-\pi^+, K^*(892)^-\pi^0 \rightarrow K^-\pi^0$	(2.22 ^{+0.40} _{-0.19}) %	
Γ_{53} $\bar{K}^*(892)^0\pi^0, \bar{K}^*(892)^0 \rightarrow K^-\pi^+$	(1.88 ± 0.23) %	
Γ_{54} $K_0^*(1430)^-\pi^+, K_0^*(1430)^-\pi^0 \rightarrow K^-\pi^0$	(4.6 ± 2.1) × 10 ⁻³	
Γ_{55} $\bar{K}_0^*(1430)^0\pi^0, \bar{K}_0^*(1430)^0 \rightarrow K^-\pi^+$	(5.7 ^{+5.0} _{-1.5}) × 10 ⁻³	
Γ_{56} $K^*(1680)^-\pi^+, K^*(1680)^-\pi^0 \rightarrow K^-\pi^0$	(1.8 ± 0.7) × 10 ⁻³	
Γ_{57} $K^-\pi^+\pi^0$ nonresonant	(1.11 ^{+0.50} _{-0.19}) %	
Γ_{58} $K_S^02\pi^0$	(8.3 ± 0.6) × 10 ⁻³	
Γ_{59} $\bar{K}^*(892)^0\pi^0, \bar{K}^*(892)^0 \rightarrow K_S^0\pi^0$	(6.7 ^{+1.8} _{-1.5}) × 10 ⁻³	
Γ_{60} $K_S^02\pi^0$ nonresonant	(4.5 ± 1.1) × 10 ⁻³	
Γ_{61} $K^-2\pi^+\pi^-$	[e] (8.09 ^{+0.21} _{-0.18}) %	S=1.3
Γ_{62} $K^-\pi^+\rho^0$ total	(6.76 ± 0.33) %	
Γ_{63} $K^-\pi^+\rho^0$ 3-body	(5.1 ± 2.3) × 10 ⁻³	
Γ_{64} $\bar{K}^*(892)^0\rho^0, \bar{K}^*(892)^0 \rightarrow K^-\pi^+$	(1.06 ± 0.23) %	
Γ_{65} $K^-\pi_1(1260)^+, \pi_1(1260)^+ \rightarrow 2\pi^+\pi^-$	(3.6 ± 0.6) %	
Γ_{66} $\bar{K}^*(892)^0\pi^+\pi^-$ total, $\bar{K}^*(892)^0 \rightarrow K^-\pi^+$	(1.6 ± 0.4) %	
Γ_{67} $\bar{K}^*(892)^0\pi^+\pi^-$ 3-body, $\bar{K}^*(892)^0 \rightarrow K^-\pi^+$	(9.9 ± 2.3) × 10 ⁻³	
Γ_{68} $K_1(1270)^-\pi^+, K_1(1270)^-\pi^0 \rightarrow K^-\pi^+\pi^-$	[g] (2.9 ± 0.3) × 10 ⁻³	
Γ_{69} $K^-2\pi^+\pi^-$ nonresonant	(1.88 ± 0.26) %	
Γ_{70} $K_S^0\pi^+\pi^-\pi^0$	[h] (5.4 ± 0.6) %	
Γ_{71} $K_S^0\eta, \eta \rightarrow \pi^+\pi^-\pi^0$	(9.8 ± 0.6) × 10 ⁻⁴	
Γ_{72} $K_S^0\omega, \omega \rightarrow \pi^+\pi^-\pi^0$	(9.9 ± 0.5) × 10 ⁻³	
Γ_{73} $K^-\pi^+2\pi^0$		
Γ_{74} $K^-2\pi^+\pi^-\pi^0$	(4.2 ± 0.4) %	

Meson Particle Listings

 D^0

Γ_{186}	$K^+ K^- \pi^+ \pi^-$	[j]	$(2.43 \pm 0.12) \times 10^{-3}$	
Γ_{187}	$\phi \pi^+ \pi^-$ 3-body, $\phi \rightarrow K^+ K^-$		$(2.4 \pm 2.4) \times 10^{-5}$	
Γ_{188}	$\phi \rho^0, \phi \rightarrow K^+ K^-$		$(7.1 \pm 0.6) \times 10^{-4}$	
Γ_{189}	$K^+ K^- \rho^0$ 3-body		$(5 \pm 7) \times 10^{-5}$	
Γ_{190}	$f_0(980) \pi^+ \pi^-, f_0 \rightarrow K^+ K^-$		$(3.6 \pm 0.9) \times 10^{-4}$	
Γ_{191}	$K^*(892)^0 K^\mp \pi^\pm$ 3-body,	[k]	$(2.7 \pm 0.6) \times 10^{-4}$	
	$K^{*0} \rightarrow K^\pm \pi^\mp$			
Γ_{192}	$K^*(892)^0 \bar{K}^*(892)^0, K^{*0} \rightarrow$ $K^\pm \pi^\mp$		$(7 \pm 5) \times 10^{-5}$	
Γ_{193}	$K_1(1270)^\pm K^\mp,$ $K_1(1270)^\pm \rightarrow K^\pm \pi^+ \pi^-$		$(8.0 \pm 1.8) \times 10^{-4}$	
Γ_{194}	$K_1(1400)^\pm K^\mp,$ $K_1(1400)^\pm \rightarrow K^\pm \pi^+ \pi^-$		$(5.3 \pm 1.2) \times 10^{-4}$	
Γ_{195}	$2K_S^0 \pi^+ \pi^-$		$(1.28 \pm 0.24) \times 10^{-3}$	
Γ_{196}	$K_S^0 K^- 2\pi^+ \pi^-$		$< 1.5 \times 10^{-4}$	CL=90%
Γ_{197}	$K^+ K^- \pi^+ \pi^- \pi^0$		$(3.1 \pm 2.0) \times 10^{-3}$	

Other $K\bar{K}X$ modes. They include all decay modes of the ϕ , η , and ω .

Γ_{198}	$\phi \pi^0$			
Γ_{199}	$\phi \eta$		$(1.4 \pm 0.5) \times 10^{-4}$	
Γ_{200}	$\phi \omega$		$< 2.1 \times 10^{-3}$	CL=90%

Radiative modes

Γ_{201}	$\rho^0 \gamma$		$< 2.4 \times 10^{-4}$	CL=90%
Γ_{202}	$\omega \gamma$		$< 2.4 \times 10^{-4}$	CL=90%
Γ_{203}	$\phi \gamma$		$(2.70 \pm 0.35) \times 10^{-5}$	
Γ_{204}	$\bar{K}^*(892)^0 \gamma$		$(3.28 \pm 0.34) \times 10^{-4}$	

Doubly Cabibbo suppressed (DC) modes or
 $\Delta C = 2$ forbidden via mixing (C2M) modes

Γ_{205}	$K^+ \ell^- \bar{\nu}_\ell$ via \bar{D}^0		$< 2.2 \times 10^{-5}$	CL=90%
Γ_{206}	K^+ or $K^*(892)^+$ $e^- \bar{\nu}_e$ via \bar{D}^0		$< 6 \times 10^{-5}$	CL=90%
Γ_{207}	$K^+ \pi^-$	DC	$(1.48 \pm 0.07) \times 10^{-4}$	
Γ_{208}	$K^+ \pi^-$ via DCS		$(1.31 \pm 0.08) \times 10^{-4}$	
Γ_{209}	$K^+ \pi^-$ via \bar{D}^0		$< 1.6 \times 10^{-5}$	CL=95%
Γ_{210}	$K_S^0 \pi^+ \pi^-$ in $D^0 \rightarrow \bar{D}^0$		$< 1.9 \times 10^{-4}$	CL=95%
Γ_{211}	$K^*(892)^+ \pi^-,$ $K^*(892)^+ \rightarrow K_S^0 \pi^+$	DC	$(1.18 \pm_{0.35}^{0.60}) \times 10^{-4}$	
Γ_{212}	$K_0^*(1430)^+ \pi^-,$ $K_0^*(1430)^+ \rightarrow K_S^0 \pi^+$	DC	$< 1.5 \times 10^{-5}$	
Γ_{213}	$K_2^*(1430)^+ \pi^-,$ $K_2^*(1430)^+ \rightarrow K_S^0 \pi^+$	DC	$< 3.5 \times 10^{-5}$	
Γ_{214}	$K^+ \pi^- \pi^0$	DC	$(3.05 \pm 0.17) \times 10^{-4}$	
Γ_{215}	$K^+ \pi^- \pi^0$ via \bar{D}^0		$(7.3 \pm 0.5) \times 10^{-4}$	
Γ_{216}	$K^+ \pi^+ 2\pi^-$	DC	$(2.62 \pm_{0.19}^{0.21}) \times 10^{-4}$	
Γ_{217}	$K^+ \pi^+ 2\pi^-$ via \bar{D}^0		$< 4 \times 10^{-4}$	CL=90%
Γ_{218}	$K^+ \pi^-$ or $K^+ \pi^+ 2\pi^-$ via \bar{D}^0			
Γ_{219}	μ^- anything via \bar{D}^0		$< 4 \times 10^{-4}$	CL=90%

 $\Delta C = 1$ weak neutral current (C1) modes,
Lepton Family number (LF) violating modes,
Lepton (L) or Baryon (B) number violating modes

Γ_{220}	$\gamma \gamma$	C1	$< 2.7 \times 10^{-5}$	CL=90%
Γ_{221}	$e^+ e^-$	C1	$< 1.2 \times 10^{-6}$	CL=90%
Γ_{222}	$\mu^+ \mu^-$	C1	$< 1.3 \times 10^{-6}$	CL=90%
Γ_{223}	$\pi^0 e^+ e^-$	C1	$< 4.5 \times 10^{-5}$	CL=90%
Γ_{224}	$\pi^0 \mu^+ \mu^-$	C1	$< 1.8 \times 10^{-4}$	CL=90%
Γ_{225}	$\eta e^+ e^-$	C1	$< 1.1 \times 10^{-4}$	CL=90%
Γ_{226}	$\eta \mu^+ \mu^-$	C1	$< 5.3 \times 10^{-4}$	CL=90%
Γ_{227}	$\pi^+ \pi^- e^+ e^-$	C1	$< 3.73 \times 10^{-4}$	CL=90%
Γ_{228}	$\rho^0 e^+ e^-$	C1	$< 1.0 \times 10^{-4}$	CL=90%
Γ_{229}	$\pi^+ \pi^- \mu^+ \mu^-$	C1	$< 3.0 \times 10^{-5}$	CL=90%
Γ_{230}	$\rho^0 \mu^+ \mu^-$	C1	$< 2.2 \times 10^{-5}$	CL=90%
Γ_{231}	$\omega e^+ e^-$	C1	$< 1.8 \times 10^{-4}$	CL=90%
Γ_{232}	$\omega \mu^+ \mu^-$	C1	$< 8.3 \times 10^{-4}$	CL=90%
Γ_{233}	$K^- K^+ e^+ e^-$	C1	$< 3.15 \times 10^{-4}$	CL=90%
Γ_{234}	$\phi e^+ e^-$	C1	$< 5.2 \times 10^{-5}$	CL=90%
Γ_{235}	$K^- K^+ \mu^+ \mu^-$	C1	$< 3.3 \times 10^{-5}$	CL=90%
Γ_{236}	$\phi \mu^+ \mu^-$	C1	$< 3.1 \times 10^{-5}$	CL=90%
Γ_{237}	$\bar{K}^0 e^+ e^-$	[l]	$< 1.1 \times 10^{-4}$	CL=90%
Γ_{238}	$\bar{K}^0 \mu^+ \mu^-$	[l]	$< 2.6 \times 10^{-4}$	CL=90%
Γ_{239}	$K^- \pi^+ e^+ e^-$	C1	$< 3.85 \times 10^{-4}$	CL=90%
Γ_{240}	$\bar{K}^*(892)^0 e^+ e^-$	[l]	$< 4.7 \times 10^{-5}$	CL=90%
Γ_{241}	$K^- \pi^+ \mu^+ \mu^-$	C1	$< 3.59 \times 10^{-4}$	CL=90%

Γ_{242}	$\bar{K}^*(892)^0 \mu^+ \mu^-$	[l]	$< 2.4 \times 10^{-5}$	CL=90%
Γ_{243}	$\pi^+ \pi^- \pi^0 \mu^+ \mu^-$	CI	$< 8.1 \times 10^{-4}$	CL=90%
Γ_{244}	$\mu^\pm e^\mp$	LF	[m] $< 8.1 \times 10^{-7}$	CL=90%
Γ_{245}	$\pi^0 e^\pm \mu^\mp$	LF	[m] $< 8.6 \times 10^{-5}$	CL=90%
Γ_{246}	$\eta e^\pm \mu^\mp$	LF	[m] $< 1.0 \times 10^{-4}$	CL=90%
Γ_{247}	$\pi^+ \pi^- e^\pm \mu^\mp$	LF	[m] $< 1.5 \times 10^{-5}$	CL=90%
Γ_{248}	$\rho^0 e^\pm \mu^\mp$	LF	[m] $< 4.9 \times 10^{-5}$	CL=90%
Γ_{249}	$\omega e^\pm \mu^\mp$	LF	[m] $< 1.2 \times 10^{-4}$	CL=90%
Γ_{250}	$K^- K^+ e^\pm \mu^\mp$	LF	[m] $< 1.8 \times 10^{-4}$	CL=90%
Γ_{251}	$\phi e^\pm \mu^\mp$	LF	[m] $< 3.4 \times 10^{-5}$	CL=90%
Γ_{252}	$\bar{K}^0 e^\pm \mu^\mp$	LF	[m] $< 1.0 \times 10^{-4}$	CL=90%
Γ_{253}	$K^- \pi^+ e^\pm \mu^\mp$	LF	[m] $< 5.53 \times 10^{-4}$	CL=90%
Γ_{254}	$\bar{K}^*(892)^0 e^\pm \mu^\mp$	LF	[m] $< 8.3 \times 10^{-5}$	CL=90%
Γ_{255}	$2\pi^- 2e^+ + c.c.$	L	$< 1.12 \times 10^{-4}$	CL=90%
Γ_{256}	$2\pi^- 2\mu^+ + c.c.$	L	$< 2.9 \times 10^{-5}$	CL=90%
Γ_{257}	$K^- \pi^- 2e^+ + c.c.$	L	$< 2.06 \times 10^{-4}$	CL=90%
Γ_{258}	$K^- \pi^- 2\mu^+ + c.c.$	L	$< 3.9 \times 10^{-4}$	CL=90%
Γ_{259}	$2K^- 2e^+ + c.c.$	L	$< 1.52 \times 10^{-4}$	CL=90%
Γ_{260}	$2K^- 2\mu^+ + c.c.$	L	$< 9.4 \times 10^{-5}$	CL=90%
Γ_{261}	$\pi^- \pi^- e^+ \mu^+ + c.c.$	L	$< 7.9 \times 10^{-5}$	CL=90%
Γ_{262}	$K^- \pi^- e^+ \mu^+ + c.c.$	L	$< 2.18 \times 10^{-4}$	CL=90%
Γ_{263}	$2K^- e^+ \mu^+ + c.c.$	L	$< 5.7 \times 10^{-5}$	CL=90%
Γ_{264}	$p e^-$	L,B	[n] $< 1.0 \times 10^{-5}$	CL=90%
Γ_{265}	$\bar{p} e^+$	L,B	[o] $< 1.1 \times 10^{-5}$	CL=90%

Γ_{266}	A dummy mode used by the fit.		$(39.4 \pm 1.3) \%$	S=1.1
----------------	-------------------------------	--	---------------------	-------

[a] This value is obtained by subtracting the branching fractions for 2-, 4- and 6-prongs from unity.

[b] This is the sum of our $K^- 2\pi^+ \pi^-, K^- 2\pi^+ \pi^- \pi^0, \bar{K}^0 2\pi^+ 2\pi^-, K^+ 2K^- \pi^+, 2\pi^+ 2\pi^-, 2\pi^+ 2\pi^- \pi^0, K^+ K^- \pi^+ \pi^-,$ and $K^+ K^- \pi^+ \pi^- \pi^0,$ branching fractions.

[c] This is the sum of our $K^- 3\pi^+ 2\pi^-$ and $3\pi^+ 3\pi^-$ branching fractions.

[d] The branching fractions for the $K^- e^+ \nu_e, K^*(892)^- e^+ \nu_e, \pi^- e^+ \nu_e,$ and $\rho^- e^+ \nu_e$ modes add up to $6.20 \pm 0.17 \%$.

[e] The branching fraction for this mode may differ from the sum of the submodes that contribute to it, due to interference effects. See the relevant papers.

[f] This is a doubly Cabibbo-suppressed mode.

[g] The two experiments measuring this fraction are in serious disagreement. See the Particle Listings.

[h] Submodes of the $D^0 \rightarrow K_S^0 \pi^+ \pi^- \pi^0$ mode with a K^* and/or ρ were studied by COFFMAN 92B, but with only 140 events. With nothing new for 18 years, we refer to our 2008 edition, Physics Letters B667 1 (2008), for those results.

[i] This branching fraction includes all the decay modes of the resonance in the final state.

[j] The experiments on the division of this charge mode amongst its submodes disagree, and the submode branching fractions here add up to considerably more than the charged-mode fraction.

[k] However, these upper limits are in serious disagreement with values obtained in another experiment.

[l] This mode is not a useful test for a $\Delta C=1$ weak neutral current because both quarks must change flavor in this decay.

[m] The value is for the sum of the charge states or particle/antiparticle states indicated.

[n] This limit is for either D^0 or \bar{D}^0 to $p e^-$.

[o] This limit is for either D^0 or \bar{D}^0 to $\bar{p} e^+$.

Meson Particle Listings

D⁰

⁷² See the footnote on the ALBRECHT 94F measurement of $\Gamma(K^-\pi^+)/\Gamma_{\text{total}}$ for the method used.

⁷³ SCHINDLER 81 (MARK-2) measures $\sigma(e^+e^- \rightarrow \psi(3770)) \times$ branching fraction to be 0.30 ± 0.08 nb. We use the MARK-3 (ADLER 88c) value of $\sigma = 5.8 \pm 0.5 \pm 0.6$ nb.

⁷⁴ PERUZZI 77 (MARK-1) measures $\sigma(e^+e^- \rightarrow \psi(3770)) \times$ branching fraction to be 0.46 ± 0.12 nb. We use the MARK-3 (ADLER 88c) value of $\sigma = 5.8 \pm 0.5 \pm 0.6$ nb.

$\Gamma(K_S^0 \pi^+ \pi^-) / \Gamma(K^-\pi^+) \quad \Gamma_{34} / \Gamma_{31}$

VALUE	EVTS	DOCUMENT ID	TECN	COMMENT
0.76 ± 0.04 OUR FIT	Error includes scale factor of 1.1.			
$0.81 \pm 0.05 \pm 0.08$	856 ± 35	FRABETTI 94J	E687	γ Be $E_{\gamma} = 220$ GeV
••• We do not use the following data for averages, fits, limits, etc. •••				
0.85 ± 0.40	35	AVERY 80	SPEC	γ N → D*+
1.4 ± 0.5	116	PICCOLO 77	MRK1	e ⁺ e ⁻ 4.03, 4.41 GeV

$\Gamma(K_S^0 \rho^0) / \Gamma(K_S^0 \pi^+ \pi^-) \quad \Gamma_{35} / \Gamma_{34}$

This is the "fit fraction" from the Dalitz-plot analysis.

VALUE	DOCUMENT ID	TECN	COMMENT
$0.224^{+0.017}_{-0.023}$ OUR AVERAGE	Error includes scale factor of 1.7.		
0.210 ± 0.016	⁷⁵ AUBERT	08AL BABR	Dalitz fit, ≈ 487 k evts
0.264 ± 0.009 ± $^{+0.010}_{-0.026}$	MURAMATSU 02	CLE2	Dalitz fit, 5299 evts
••• We do not use the following data for averages, fits, limits, etc. •••			
0.267 ± 0.011 ± $^{+0.009}_{-0.028}$	ASNER 04A	CLEO	See MURAMATSU 02
0.350 ± 0.028 ± 0.067	FRABETTI 94G	E687	Dalitz fit, 597 evts
0.227 ± 0.032 ± 0.009	ALBRECHT 93D	ARG	Dalitz fit, 440 evts
0.215 ± 0.051 ± 0.037	ANJOS 93	E691	γ Be 90-260 GeV
0.20 ± 0.06 ± 0.03	FRABETTI 92B	E687	γ Be, $E_{\gamma} = 221$ GeV
0.12 ± 0.01 ± 0.07	ADLER 87	MRK3	e ⁺ e ⁻ 3.77 GeV

⁷⁵ The error on this AUBERT 08AL value includes both statistical and systematic uncertainties; the latter dominates.

$\Gamma(K_S^0 \omega, \omega \rightarrow \pi^+ \pi^-) / \Gamma(K_S^0 \pi^+ \pi^-) \quad \Gamma_{36} / \Gamma_{34}$

This is the "fit fraction" from the Dalitz-plot analysis.

VALUE	DOCUMENT ID	TECN	COMMENT
0.0073 ± 0.0020 OUR AVERAGE			
0.009 ± 0.010	⁷⁶ AUBERT	08AL BABR	Dalitz fit, ≈ 487 k evts
0.0072 ± 0.0018 ± $^{+0.0010}_{-0.0009}$	MURAMATSU 02	CLE2	Dalitz fit, 5299 evts
••• We do not use the following data for averages, fits, limits, etc. •••			
0.0081 ± 0.0019 ± $^{+0.0018}_{-0.0010}$	ASNER 04A	CLEO	See MURAMATSU 02

⁷⁶ The error on this AUBERT 08AL value includes both statistical and systematic uncertainties; the latter dominates.

$\Gamma(K_S^0 (\pi^+ \pi^-)_{S\text{-wave}}) / \Gamma(K_S^0 \pi^+ \pi^-) \quad \Gamma_{37} / \Gamma_{34}$

This is the "fit fraction" from the Dalitz-plot analysis. The $(\pi^+ \pi^-)_{S\text{-wave}}$ includes what in isobar models are the $f_0(980)$ and $f_0(1370)$; see the following two data blocks.

VALUE	DOCUMENT ID	TECN	COMMENT
0.119 ± 0.026	⁷⁷ AUBERT	08AL BABR	Dalitz fit, ≈ 487 k evts

⁷⁷ The error on this AUBERT 08AL value includes both statistical and systematic uncertainties; the latter dominates.

$\Gamma(K_S^0 f_0(980), f_0(980) \rightarrow \pi^+ \pi^-) / \Gamma(K_S^0 \pi^+ \pi^-) \quad \Gamma_{38} / \Gamma_{34}$

This is the "fit fraction" from the Dalitz-plot analysis.

VALUE	DOCUMENT ID	TECN	COMMENT
$0.043 \pm 0.005 \pm ^{+0.012}_{-0.006}$	MURAMATSU 02	CLE2	Dalitz fit, 5299 evts
••• We do not use the following data for averages, fits, limits, etc. •••			
0.042 ± 0.005 ± $^{+0.011}_{-0.005}$	ASNER 04A	CLEO	See MURAMATSU 02
0.068 ± 0.016 ± 0.018	FRABETTI 94G	E687	Dalitz fit, 597 evts
0.046 ± 0.018 ± 0.006	ALBRECHT 93D	ARG	Dalitz fit, 440 evts

$\Gamma(K_S^0 f_0(1370), f_0(1370) \rightarrow \pi^+ \pi^-) / \Gamma(K_S^0 \pi^+ \pi^-) \quad \Gamma_{39} / \Gamma_{34}$

This is the "fit fraction" from the Dalitz-plot analysis.

VALUE	DOCUMENT ID	TECN	COMMENT
$0.099 \pm 0.011 \pm ^{+0.028}_{-0.044}$	MURAMATSU 02	CLE2	Dalitz fit, 5299 evts
••• We do not use the following data for averages, fits, limits, etc. •••			
0.098 ± 0.014 ± $^{+0.026}_{-0.036}$	ASNER 04A	CLEO	See MURAMATSU 02
0.077 ± 0.022 ± 0.031	FRABETTI 94G	E687	Dalitz fit, 597 evts
0.082 ± 0.028 ± 0.013	ALBRECHT 93D	ARG	Dalitz fit, 440 evts

$\Gamma(K_S^0 f_2(1270), f_2(1270) \rightarrow \pi^+ \pi^-) / \Gamma(K_S^0 \pi^+ \pi^-) \quad \Gamma_{40} / \Gamma_{34}$

This is the "fit fraction" from the Dalitz-plot analysis.

VALUE	DOCUMENT ID	TECN	COMMENT
$0.0032 \pm ^{+0.0035}_{-0.0022}$ OUR AVERAGE			
0.006 ± 0.007	⁷⁸ AUBERT	08AL BABR	Dalitz fit, ≈ 487 k evts
0.0027 ± 0.0015 ± $^{+0.0037}_{-0.0017}$	MURAMATSU 02	CLE2	Dalitz fit, 5299 evts
••• We do not use the following data for averages, fits, limits, etc. •••			
0.0036 ± 0.0022 ± $^{+0.0032}_{-0.0019}$	ASNER 04A	CLEO	See MURAMATSU 02
0.037 ± 0.014 ± 0.017	FRABETTI 94G	E687	Dalitz fit, 597 evts
0.050 ± 0.021 ± 0.008	ALBRECHT 93D	ARG	Dalitz fit, 440 evts

⁷⁸ The error on this AUBERT 08AL value includes both statistical and systematic uncertainties; the latter dominates.

$\Gamma(K^*(892)^-\pi^+, K^*(892)^-\pi^0) / \Gamma(K_S^0 \pi^+ \pi^-) \quad \Gamma_{41} / \Gamma_{34}$

This is the "fit fraction" from the Dalitz-plot analysis.

VALUE	DOCUMENT ID	TECN	COMMENT
$0.588^{+0.034}_{-0.050}$ OUR AVERAGE	Error includes scale factor of 2.0.		
0.557 ± 0.028	⁷⁹ AUBERT	08AL BABR	Dalitz fit, ≈ 487 k evts
0.657 ± 0.013 ± $^{+0.018}_{-0.040}$	MURAMATSU 02	CLE2	Dalitz fit, 5299 evts
••• We do not use the following data for averages, fits, limits, etc. •••			
0.663 ± 0.013 ± $^{+0.024}_{-0.043}$	ASNER 04A	CLEO	See MURAMATSU 02
0.625 ± 0.036 ± 0.026	FRABETTI 94G	E687	Dalitz fit, 597 evts
0.718 ± 0.042 ± 0.030	ALBRECHT 93D	ARG	Dalitz fit, 440 evts
0.480 ± 0.097	ANJOS 93	E691	γ Be 90-260 GeV
0.56 ± 0.04 ± 0.05	ADLER 87	MRK3	e ⁺ e ⁻ 3.77 GeV

⁷⁹ The error on this AUBERT 08AL value includes both statistical and systematic uncertainties; the latter dominates.

$\Gamma(K_S^*(1430)^-\pi^+, K_0^*(1430)^-\pi^0) / \Gamma(K_S^0 \pi^+ \pi^-) \quad \Gamma_{42} / \Gamma_{34}$

This is the "fit fraction" from the Dalitz-plot analysis.

VALUE	DOCUMENT ID	TECN	COMMENT
$0.095^{+0.014}_{-0.010}$ OUR AVERAGE			
0.102 ± 0.015	⁸⁰ AUBERT	08AL BABR	Dalitz fit, ≈ 487 k evts
0.073 ± 0.007 ± $^{+0.031}_{-0.011}$	MURAMATSU 02	CLE2	Dalitz fit, 5299 evts
••• We do not use the following data for averages, fits, limits, etc. •••			
0.072 ± 0.007 ± $^{+0.014}_{-0.013}$	ASNER 04A	CLEO	See MURAMATSU 02
0.109 ± 0.027 ± 0.029	FRABETTI 94G	E687	Dalitz fit, 597 evts
0.129 ± 0.034 ± 0.021	ALBRECHT 93D	ARG	Dalitz fit, 440 evts

⁸⁰ The error on this AUBERT 08AL value includes both statistical and systematic uncertainties; the latter dominates.

$\Gamma(K_S^*(1430)^-\pi^+, K_2^*(1430)^-\pi^0) / \Gamma(K_S^0 \pi^+ \pi^-) \quad \Gamma_{43} / \Gamma_{34}$

This is the "fit fraction" from the Dalitz-plot analysis.

VALUE	DOCUMENT ID	TECN	COMMENT
$0.0120^{+0.0070}_{-0.0035}$ OUR AVERAGE			
0.022 ± 0.016	⁸¹ AUBERT	08AL BABR	Dalitz fit, ≈ 487 k evts
0.011 ± 0.002 ± $^{+0.007}_{-0.003}$	MURAMATSU 02	CLE2	Dalitz fit, 5299 evts
••• We do not use the following data for averages, fits, limits, etc. •••			
0.011 ± 0.002 ± $^{+0.005}_{-0.003}$	ASNER 04A	CLEO	See MURAMATSU 02

⁸¹ The error on this AUBERT 08AL value includes both statistical and systematic uncertainties; the latter dominates.

$\Gamma(K^*(1680)^-\pi^+, K^*(1680)^-\pi^0) / \Gamma(K_S^0 \pi^+ \pi^-) \quad \Gamma_{44} / \Gamma_{34}$

This is the "fit fraction" from the Dalitz-plot analysis.

VALUE	DOCUMENT ID	TECN	COMMENT
0.016 ± 0.013 OUR AVERAGE			
0.007 ± 0.019	⁸² AUBERT	08AL BABR	Dalitz fit, ≈ 487 k evts
0.022 ± 0.004 ± $^{+0.018}_{-0.015}$	MURAMATSU 02	CLE2	Dalitz fit, 5299 evts
••• We do not use the following data for averages, fits, limits, etc. •••			
0.023 ± 0.005 ± $^{+0.007}_{-0.014}$	ASNER 04A	CLEO	See MURAMATSU 02

⁸² The error on this AUBERT 08AL value includes both statistical and systematic uncertainties; the latter dominates.

$\Gamma(K^*(892)^+\pi^-, K^*(892)^+\pi^0) / \Gamma(K_S^0 \pi^+ \pi^-) \quad \Gamma_{45} / \Gamma_{34}$

This is the "fit fraction" from the Dalitz-plot analysis. This is a doubly Cabibbo-suppressed mode.

VALUE (units 10 ⁻³)	DOCUMENT ID	TECN	COMMENT
$4.0^{+2.0}_{-1.2}$ OUR AVERAGE			
4.6 ± 2.3	⁸³ AUBERT	08AL BABR	Dalitz fit, ≈ 487 k evts
3.4 ± 1.3 ± $^{+4.1}_{-0.4}$	MURAMATSU 02	CLE2	Dalitz fit, 5299 evts
••• We do not use the following data for averages, fits, limits, etc. •••			
3.4 ± 1.3 ± $^{+3.6}_{-0.5}$	ASNER 04A	CLEO	See MURAMATSU 02

⁸³ The error on this AUBERT 08AL value includes both statistical and systematic uncertainties; the latter dominates.

$\Gamma(K_S^*(1430)^+\pi^-, K_0^*(1430)^+\pi^0) / \Gamma(K_S^0 \pi^+ \pi^-) \quad \Gamma_{46} / \Gamma_{34}$

This is the "fit fraction" from the Dalitz-plot analysis. This is a doubly Cabibbo-suppressed mode.

VALUE	CL%	DOCUMENT ID	TECN	COMMENT
$< 5 \times 10^{-4}$	95	AUBERT	08AL BABR	Dalitz fit, ≈ 487 k evts

$\Gamma(K_S^*(1430)^+\pi^-, K_2^*(1430)^+\pi^0) / \Gamma(K_S^0 \pi^+ \pi^-) \quad \Gamma_{47} / \Gamma_{34}$

This is the "fit fraction" from the Dalitz-plot analysis. This is a doubly Cabibbo-suppressed mode.

VALUE	CL%	DOCUMENT ID	TECN	COMMENT
$< 1.2 \times 10^{-3}$	95	AUBERT	08AL BABR	Dalitz fit, ≈ 487 k evts

See key on page 405

Meson Particle Listings

D⁰

$\Gamma(K_S^0 \pi^+ \pi^- \text{ nonresonant})/\Gamma(K_S^0 \pi^+ \pi^-)$ Γ_{48}/Γ_{34}

This is the "fit fraction" from the Dalitz-plot analysis. Neither FRABETTI 94G nor ALBRECHT 93D (quoted in many of the earlier submodes of $K_S^0 \pi^+ \pi^-$) sees evidence for a nonresonant component.

VALUE	DOCUMENT ID	TECN	COMMENT
0.009 ± 0.004 ± 0.020 - 0.004	MURAMATSU 02	CLE2	Dalitz fit, 5 299 evts
••• We do not use the following data for averages, fits, limits, etc. •••			
0.007 ± 0.007 ± 0.021 - 0.006	ASNER	04A CLEO	See MURAMATSU 02
0.263 ± 0.024 ± 0.041	ANJOS	93 E691	γ Be 90–260 GeV
0.26 ± 0.08 ± 0.05	FRABETTI	92B E687	γ Be, $\bar{E}_\gamma = 221$ GeV
0.33 ± 0.05 ± 0.10	ADLER	87 MRK3	e^+e^- 3.77 GeV

$\Gamma(K^- \pi^+ \pi^0)/\Gamma_{\text{total}}$ Γ_{49}/Γ

VALUE (units 10⁻²)

13.9 ± 0.5 OUR FIT Error includes scale factor of 1.7.

14.57 ± 0.12 ± 0.38

VALUE	EVTS	DOCUMENT ID	TECN	COMMENT
		⁸⁴ DOBBS	07 CLEO	e^+e^- at $\psi(3770)$
••• We do not use the following data for averages, fits, limits, etc. •••				
14.9 ± 0.3 ± 0.5	19k ± 150	⁸⁴ HE	05 CLEO	See DOBBS 07
13.3 ± 1.2 ± 1.3	931	ADLER	88c MRK3	e^+e^- ≈ 10 GeV
11.7 ± 4.3	37	⁸⁵ SCHINDLER	81 MRK2	e^+e^- 3.771 GeV

⁸⁴ DOBBS 07 and HE 05 use single- and double-tagged events in an overall fit. DOBBS 07 supersedes HE 05.

⁸⁵ SCHINDLER 81 (MARK-2) measures $\sigma(e^+e^- \rightarrow \psi(3770)) \times$ branching fraction to be 0.68 ± 0.23 nb. We use the MARK-3 (ADLER 88c) value of $\sigma = 5.8 \pm 0.5 \pm 0.6$ nb.

$\Gamma(K^- \pi^+ \pi^0)/\Gamma(K^- \pi^+)$ Γ_{49}/Γ_{31}

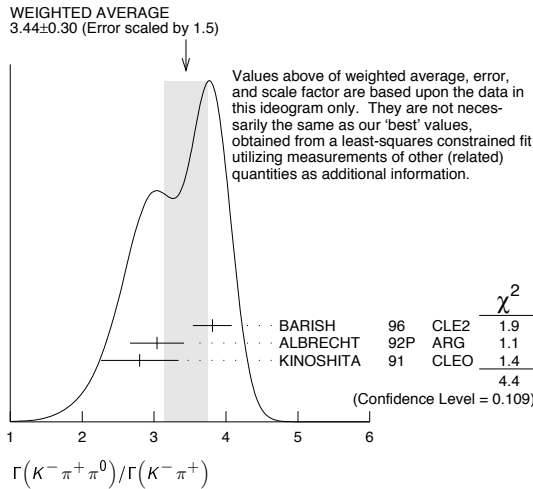
VALUE

3.57 ± 0.13 OUR FIT Error includes scale factor of 1.9.

3.44 ± 0.30 OUR AVERAGE Error includes scale factor of 1.5. See the ideogram below.

VALUE	EVTS	DOCUMENT ID	TECN	COMMENT
3.81 ± 0.07 ± 0.26	10k	BARISH	96 CLE2	$e^+e^- \approx \Upsilon(4S)$
3.04 ± 0.16 ± 0.34	931	⁸⁶ ALBRECHT	92P ARG	$e^+e^- \approx 10$ GeV
2.8 ± 0.14 ± 0.52	1050	KINOSHITA	91 CLEO	$e^+e^- \sim 10.7$ GeV

⁸⁶ This value is calculated from numbers in Table 1 of ALBRECHT 92P.



$\Gamma(K^- \rho^+) / \Gamma(K^- \pi^+ \pi^0)$ Γ_{50}/Γ_{49}

This is the "fit fraction" from the Dalitz-plot analysis.

VALUE	DOCUMENT ID	TECN	COMMENT
0.78 ± 0.04 OUR AVERAGE			
0.788 ± 0.019 ± 0.048	KOPP	01 CLE2	Dalitz fit, ≈ 7,000 evts
0.765 ± 0.041 ± 0.054	FRABETTI	94G E687	Dalitz fit, 5 30 evts
••• We do not use the following data for averages, fits, limits, etc. •••			
0.647 ± 0.039 ± 0.150	ANJOS	93 E691	γ Be 90–260 GeV
0.81 ± 0.03 ± 0.06	ADLER	87 MRK3	e^+e^- 3.77 GeV

$\Gamma(K^- \rho(1700)^+ \rho(1700)^+ \rightarrow \pi^+ \pi^0) / \Gamma(K^- \pi^+ \pi^0)$ Γ_{51}/Γ_{49}

This is the "fit fraction" from the Dalitz-plot analysis.

VALUE	DOCUMENT ID	TECN	COMMENT
0.057 ± 0.008 ± 0.009	KOPP	01 CLE2	Dalitz fit, ≈ 7,000 evts

$\Gamma(K^*(892)^- \pi^+, K^*(892)^- \rightarrow K^- \pi^0) / \Gamma(K^- \pi^+ \pi^0)$ Γ_{52}/Γ_{49}

This is the "fit fraction" from the Dalitz-plot analysis.

VALUE	DOCUMENT ID	TECN	COMMENT
0.160 ± 0.025 - 0.013 OUR AVERAGE			
0.161 ± 0.007 ± 0.027 - 0.011	KOPP	01 CLE2	Dalitz fit, ≈ 7,000 evts
0.148 ± 0.028 ± 0.049	FRABETTI	94G E687	Dalitz fit, 5 30 evts
••• We do not use the following data for averages, fits, limits, etc. •••			
0.084 ± 0.011 ± 0.012	ANJOS	93 E691	γ Be 90–260 GeV
0.12 ± 0.02 ± 0.03	ADLER	87 MRK3	e^+e^- 3.77 GeV

$\Gamma(K^*(892)^0 \pi^0, \bar{K}^*(892)^0 \rightarrow K^- \pi^+) / \Gamma(K^- \pi^+ \pi^0)$ Γ_{53}/Γ_{49}

This is the "fit fraction" from the Dalitz-plot analysis.

VALUE	DOCUMENT ID	TECN	COMMENT
0.135 ± 0.016 OUR AVERAGE			
0.127 ± 0.009 ± 0.016	KOPP	01 CLE2	Dalitz fit, ≈ 7,000 evts
0.165 ± 0.031 ± 0.015	FRABETTI	94G E687	Dalitz fit, 5 30 evts
••• We do not use the following data for averages, fits, limits, etc. •••			
0.142 ± 0.018 ± 0.024	ANJOS	93 E691	γ Be 90–260 GeV
0.13 ± 0.02 ± 0.03	ADLER	87 MRK3	e^+e^- 3.77 GeV

$\Gamma(K_0^*(1430)^- \pi^+, K_0^*(1430)^- \rightarrow K^- \pi^0) / \Gamma(K^- \pi^+ \pi^0)$ Γ_{54}/Γ_{49}

This is the "fit fraction" from the Dalitz-plot analysis.

VALUE	DOCUMENT ID	TECN	COMMENT
0.033 ± 0.006 ± 0.014	KOPP	01 CLE2	Dalitz fit, ≈ 7,000 evts

$\Gamma(\bar{K}_0^*(1430)^0 \pi^0, \bar{K}_0^*(1430)^0 \rightarrow K^- \pi^+) / \Gamma(K^- \pi^+ \pi^0)$ Γ_{55}/Γ_{49}

This is the "fit fraction" from the Dalitz-plot analysis.

VALUE	DOCUMENT ID	TECN	COMMENT
0.041 ± 0.006 ± 0.032 - 0.009	KOPP	01 CLE2	Dalitz fit, ≈ 7,000 evts

$\Gamma(K^*(1680)^- \pi^+, K^*(1680)^- \rightarrow K^- \pi^0) / \Gamma(K^- \pi^+ \pi^0)$ Γ_{56}/Γ_{49}

This is the "fit fraction" from the Dalitz-plot analysis.

VALUE	DOCUMENT ID	TECN	COMMENT
0.013 ± 0.003 ± 0.004	KOPP	01 CLE2	Dalitz fit, ≈ 7,000 evts

$\Gamma(K^- \pi^+ \pi^0 \text{ nonresonant}) / \Gamma(K^- \pi^+ \pi^0)$ Γ_{57}/Γ_{49}

This is the "fit fraction" from the Dalitz-plot analysis.

VALUE	EVTS	DOCUMENT ID	TECN	COMMENT
0.080 ± 0.040 - 0.014 OUR AVERAGE				
0.075 ± 0.009 ± 0.056 - 0.011		KOPP	01 CLE2	Dalitz fit, ≈ 7,000 evts
0.101 ± 0.033 ± 0.040		FRABETTI	94G E687	Dalitz fit, 5 30 evts
••• We do not use the following data for averages, fits, limits, etc. •••				
0.036 ± 0.004 ± 0.018		ANJOS	93 E691	γ Be 90–260 GeV
0.09 ± 0.02 ± 0.04		ADLER	87 MRK3	e^+e^- 3.77 GeV
0.51 ± 0.22	21	SUMMERS	84 E691	Photoproduction

$\Gamma(K_S^0 2\pi^0) / \Gamma_{\text{total}}$ Γ_{58}/Γ

VALUE (units 10⁻³)

8.34 ± 0.45 ± 0.42

DOCUMENT ID	TECN	COMMENT
ASNER 08	CLEO	$e^+e^- \rightarrow D^0 \bar{D}^0$, 3.77 GeV

$\Gamma(\bar{K}^*(892)^0 \pi^0, \bar{K}^*(892)^0 \rightarrow K_S^0 \pi^0) / \Gamma(K_S^0 \pi^0)$ Γ_{59}/Γ_{32}

VALUE	DOCUMENT ID	TECN	COMMENT
0.55 ± 0.13 - 0.10 ± 0.07	PROCARIO 93B	CLE2	Dalitz plot fit, 122 evts

$\Gamma(K_S^0 2\pi^0 \text{ nonresonant}) / \Gamma(K_S^0 \pi^0)$ Γ_{60}/Γ_{32}

VALUE	DOCUMENT ID	TECN	COMMENT
0.37 ± 0.08 ± 0.04	PROCARIO 93B	CLE2	Dalitz plot fit, 122 evts

$\Gamma(K^- 2\pi^+ \pi^-) / \Gamma_{\text{total}}$ Γ_{61}/Γ

VALUE (units 10⁻²)

8.09 ± 0.21 - 0.18 OUR FIT Error includes scale factor of 1.3.

8.17 ± 0.33 OUR AVERAGE Error includes scale factor of 1.7. See the ideogram below.

VALUE	EVTS	DOCUMENT ID	TECN	COMMENT
8.30 ± 0.07 ± 0.20		⁸⁷ DOBBS	07 CLEO	e^+e^- at $\psi(3770)$
7.9 ± 1.5 ± 0.9		⁸⁸ ALBRECHT	94 ARG	$e^+e^- \approx \Upsilon(4S)$
6.80 ± 0.27 ± 0.57	1430 ± 52	⁸⁹ ALBRECHT	94F ARG	$e^+e^- \approx \Upsilon(4S)$
9.1 ± 0.8 ± 0.8	992	ADLER	88c MRK3	e^+e^- 3.77 GeV
••• We do not use the following data for averages, fits, limits, etc. •••				
8.3 ± 0.2 ± 0.3	15k ± 130	⁸⁷ HE	05 CLEO	See DOBBS 07
11.7 ± 2.5	185	⁹⁰ SCHINDLER	81 MRK2	e^+e^- 3.771 GeV
6.2 ± 1.9	44	⁹¹ PERUZZI	77 LGW	e^+e^- 3.77 GeV

⁸⁷ DOBBS 07 and HE 05 use single- and double-tagged events in an overall fit. DOBBS 07 supersedes HE 05.

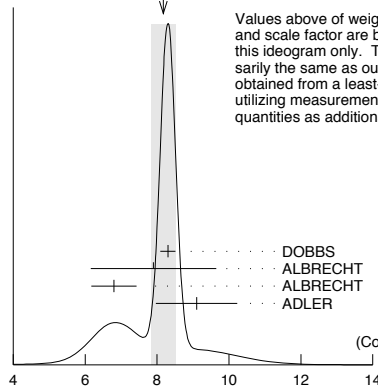
⁸⁸ ALBRECHT 94 uses D^0 mesons from $\bar{B}^0 \rightarrow D^+ \ell^- \bar{\nu}_\ell$ decays. This is a different set of events than used by ALBRECHT 94F.

⁸⁹ See the footnote on the ALBRECHT 94F measurement of $\Gamma(K^- \pi^+) / \Gamma_{\text{total}}$ for the method used.

⁹⁰ SCHINDLER 81 (MARK-2) measures $\sigma(e^+e^- \rightarrow \psi(3770)) \times$ branching fraction to be 0.68 ± 0.11 nb. We use the MARK-3 (ADLER 88c) value of $\sigma = 5.8 \pm 0.5 \pm 0.6$ nb.

⁹¹ PERUZZI 77 (MARK-1) measures $\sigma(e^+e^- \rightarrow \psi(3770)) \times$ branching fraction to be 0.36 ± 0.10 nb. We use the MARK-3 (ADLER 88c) value of $\sigma = 5.8 \pm 0.5 \pm 0.6$ nb.

Meson Particle Listings

 D^0 WEIGHTED AVERAGE
8.17±0.33 (Error scaled by 1.7)

Values above of weighted average, error, and scale factor are based upon the data in this ideogram only. They are not necessarily the same as our 'best' values, obtained from a least-squares constrained fit utilizing measurements of other (related) quantities as additional information.

DOCUMENT ID	TECN	COMMENT	χ^2
DOBBS 07	CLEO	0.4	
ALBRECHT 94	ARG		
ALBRECHT 94F	ARG	4.7	
ADLER 88C	MRK3	0.7	

(Confidence Level = 0.056)

 $\Gamma(K^-2\pi^+\pi^-)/\Gamma_{\text{total}}$ (units 10^{-2})

$\Gamma(K^-2\pi^+\pi^-)/\Gamma(K^-2\pi^+\pi^-)$		Γ_{61}/Γ_{31}			
VALUE	EVTs	DOCUMENT ID	TECN	COMMENT	
2.08 ± 0.05 OUR FIT		Error includes scale factor of 1.5.			
1.97 ± 0.09 OUR AVERAGE					
1.94 ± 0.07 ± 0.09		JUN	00	SELX	Σ^- nucleus, 600 GeV
1.7 ± 0.2 ± 0.2	1745	ANJOS	92c	E691	γ Be 90–260 GeV
1.90 ± 0.25 ± 0.20	337	ALVAREZ	91B	NA14	Photoproduction
2.12 ± 0.16 ± 0.09		BORTOLETT	O88	CLEO	e^+e^- 10.55 GeV
2.17 ± 0.28 ± 0.23		ALBRECHT	85F	ARG	e^+e^- 10 GeV
••• We do not use the following data for averages, fits, limits, etc. •••					
2.0 ± 0.9	48	BAILEY	86	ACCM	π^- Be fixed target
2.0 ± 1.0	10	BAILEY	83B	SPEC	π^- Be $\rightarrow D^0$
2.2 ± 0.8	214	PICCOLO	77	MRK1	e^+e^- 4.03, 4.41 GeV

$\Gamma(K^-2\pi^+\rho^0\text{total})/\Gamma(K^-2\pi^+\pi^-)$		Γ_{62}/Γ_{61}			
VALUE	EVTs	DOCUMENT ID	TECN	COMMENT	
0.835 ± 0.035 OUR AVERAGE					
0.80 ± 0.03 ± 0.05		ANJOS	92c	E691	1745 $K^-2\pi^+\pi^-$ evts
0.855 ± 0.032 ± 0.030		COFFMAN	92B	MRK3	1281 ± 45 $K^-2\pi^+\pi^-$ evts
••• We do not use the following data for averages, fits, limits, etc. •••					
0.98 ± 0.12 ± 0.10		ALVAREZ	91B	NA14	Photoproduction

$\Gamma(K^-2\pi^+\rho^0\text{3-body})/\Gamma(K^-2\pi^+\pi^-)$		Γ_{63}/Γ_{61}			
VALUE	EVTs	DOCUMENT ID	TECN	COMMENT	
0.063 ± 0.028 OUR AVERAGE					
0.05 ± 0.03 ± 0.02		ANJOS	92c	E691	1745 $K^-2\pi^+\pi^-$ evts
0.084 ± 0.022 ± 0.04		COFFMAN	92B	MRK3	1281 ± 45 $K^-2\pi^+\pi^-$ evts
••• We do not use the following data for averages, fits, limits, etc. •••					
0.77 ± 0.06 ± 0.06	92	ALVAREZ	91B	NA14	Photoproduction
0.85 ± 0.11 ± 0.22	180	PICCOLO	77	MRK1	e^+e^- 4.03, 4.41 GeV

⁹²This value is for $\rho^0(K^-2\pi^+)$ -nonresonant. ALVAREZ 91B cannot determine what fraction of this is $K^-a_1(1260)^+$.

$\Gamma(\bar{K}^*(892)^0\rho^0)/\Gamma(K^-2\pi^+\pi^-)$		Γ_{95}/Γ_{61}			
VALUE	EVTs	DOCUMENT ID	TECN	COMMENT	
0.195 ± 0.03 ± 0.03		ANJOS	92c	E691	1745 $K^-2\pi^+\pi^-$ evts
••• We do not use the following data for averages, fits, limits, etc. •••					
0.34 ± 0.09 ± 0.09		ALVAREZ	91B	NA14	Photoproduction
0.75 ± 0.3	5	BAILEY	83B	SPEC	π Be $\rightarrow D^0$
0.15 ± 0.16 ± 0.15	20	PICCOLO	77	MRK1	e^+e^- 4.03, 4.41 GeV

$\Gamma(\bar{K}^*(892)^0\rho^0\text{transverse})/\Gamma(K^-2\pi^+\pi^-)$		Γ_{96}/Γ_{61}			
VALUE	EVTs	DOCUMENT ID	TECN	COMMENT	
0.213 ± 0.024 ± 0.075		COFFMAN	92B	MRK3	1281 ± 45 $K^-2\pi^+\pi^-$ evts

$\Gamma(\bar{K}^*(892)^0\rho^0\text{S-wave})/\Gamma(K^-2\pi^+\pi^-)$		Γ_{97}/Γ_{61}			
VALUE	EVTs	DOCUMENT ID	TECN	COMMENT	
0.375 ± 0.045 ± 0.06		ANJOS	92c	E691	1745 $K^-2\pi^+\pi^-$ evts

$\Gamma(\bar{K}^*(892)^0\rho^0\text{S-wave long.})/\Gamma_{\text{total}}$		Γ_{98}/Γ			
VALUE	CL%	DOCUMENT ID	TECN	COMMENT	
<0.003	90	COFFMAN	92B	MRK3	1281 ± 45 $K^-2\pi^+\pi^-$ evts

$\Gamma(\bar{K}^*(892)^0\rho^0\text{P-wave})/\Gamma_{\text{total}}$		Γ_{99}/Γ			
VALUE	CL%	DOCUMENT ID	TECN	COMMENT	
<0.003	90	COFFMAN	92B	MRK3	1281 ± 45 $K^-2\pi^+\pi^-$ evts
••• We do not use the following data for averages, fits, limits, etc. •••					
<0.009	90	ANJOS	92c	E691	1745 $K^-2\pi^+\pi^-$ evts

$\Gamma(\bar{K}^*(892)^0\rho^0\text{D-wave})/\Gamma(K^-2\pi^+\pi^-)$		Γ_{100}/Γ_{61}			
VALUE	CL%	DOCUMENT ID	TECN	COMMENT	
0.255 ± 0.045 ± 0.06		ANJOS	92c	E691	1745 $K^-2\pi^+\pi^-$ evts

$\Gamma(K^-2\pi^+\rho(980))/\Gamma_{\text{total}}$		Γ_{101}/Γ			
VALUE	CL%	DOCUMENT ID	TECN	COMMENT	
<0.011	90	ANJOS	92c	E691	1745 $K^-2\pi^+\pi^-$ evts

$\Gamma(\bar{K}^*(892)^0\rho(980))/\Gamma_{\text{total}}$		Γ_{102}/Γ			
VALUE	CL%	DOCUMENT ID	TECN	COMMENT	
<0.007	90	ANJOS	92c	E691	1745 $K^-2\pi^+\pi^-$ evts

$\Gamma(K^-a_1(1260)^+)/\Gamma(K^-2\pi^+\pi^-)$		Γ_{91}/Γ_{61}			
VALUE	CL%	DOCUMENT ID	TECN	COMMENT	
0.97 ± 0.14 OUR AVERAGE					
0.94 ± 0.13 ± 0.20		ANJOS	92c	E691	1745 $K^-2\pi^+\pi^-$ evts
0.984 ± 0.048 ± 0.16		COFFMAN	92B	MRK3	1281 ± 45 $K^-2\pi^+\pi^-$ evts

$\Gamma(K^-a_2(1320)^+)/\Gamma_{\text{total}}$		Γ_{92}/Γ			
VALUE	CL%	DOCUMENT ID	TECN	COMMENT	
<0.002	90	ANJOS	92c	E691	1745 $K^-2\pi^+\pi^-$ evts
••• We do not use the following data for averages, fits, limits, etc. •••					
<0.006	90	COFFMAN	92B	MRK3	1281 ± 45 $K^-2\pi^+\pi^-$ evts

$\Gamma(K_1(1270)^-\pi^+)/\Gamma(K^-2\pi^+\pi^-)$		Γ_{103}/Γ_{61}			
VALUE	CL%	DOCUMENT ID	TECN	COMMENT	
0.194 ± 0.056 ± 0.088		COFFMAN	92B	MRK3	1281 ± 45 $K^-2\pi^+\pi^-$ evts
••• We do not use the following data for averages, fits, limits, etc. •••					
<0.013	90	ANJOS	92c	E691	1745 $K^-2\pi^+\pi^-$ evts

$\Gamma(K_1(1400)^-\pi^+)/\Gamma_{\text{total}}$		Γ_{104}/Γ			
VALUE	CL%	DOCUMENT ID	TECN	COMMENT	
<0.012	90	COFFMAN	92B	MRK3	1281 ± 45 $K^-2\pi^+\pi^-$ evts

$\Gamma(K^*(1410)^-\pi^+)/\Gamma_{\text{total}}$		Γ_{105}/Γ			
VALUE	CL%	DOCUMENT ID	TECN	COMMENT	
<0.012	90	COFFMAN	92B	MRK3	1281 ± 45 $K^-2\pi^+\pi^-$ evts

$\Gamma(\bar{K}^*(892)^0\pi^+\pi^-\text{total})/\Gamma(K^-2\pi^+\pi^-)$		Γ_{93}/Γ_{61}			
VALUE	EVTs	DOCUMENT ID	TECN	COMMENT	
0.30 ± 0.06 ± 0.03		ANJOS	92c	E691	1745 $K^-2\pi^+\pi^-$ evts

$\Gamma(\bar{K}^*(892)^0\pi^+\pi^-3\text{-body})/\Gamma(K^-2\pi^+\pi^-)$		Γ_{94}/Γ_{61}			
VALUE	EVTs	DOCUMENT ID	TECN	COMMENT	
0.18 ± 0.04 OUR AVERAGE					
0.165 ± 0.03 ± 0.045		ANJOS	92c	E691	1745 $K^-2\pi^+\pi^-$ evts
0.210 ± 0.027 ± 0.06		COFFMAN	92B	MRK3	1281 ± 45 $K^-2\pi^+\pi^-$ evts

$\Gamma(K^-2\pi^+\pi^- \text{nonresonant})/\Gamma(K^-2\pi^+\pi^-)$		Γ_{69}/Γ_{61}			
VALUE	EVTs	DOCUMENT ID	TECN	COMMENT	
0.233 ± 0.032 OUR AVERAGE					
0.23 ± 0.02 ± 0.03		ANJOS	92c	E691	1745 $K^-2\pi^+\pi^-$ evts
0.242 ± 0.025 ± 0.06		COFFMAN	92B	MRK3	1281 ± 45 $K^-2\pi^+\pi^-$ evts

$\Gamma(\rho(1450)^- \pi^+, \rho(1450)^- \rightarrow \pi^- \pi^0)/\Gamma(\pi^+ \pi^- \pi^0)$	$\Gamma_{134}/\Gamma_{128}$			
VALUE (units 10 ⁻²)	DOCUMENT ID	TECN	COMMENT	
1.79 ± 0.22 ± 0.12	AUBERT	07BJ BABR	Dalitz fit, 45k events	
$\Gamma(\rho(1700)^+ \pi^-, \rho(1700)^+ \rightarrow \pi^+ \pi^0)/\Gamma(\pi^+ \pi^- \pi^0)$	$\Gamma_{135}/\Gamma_{128}$			
VALUE (units 10 ⁻²)	DOCUMENT ID	TECN	COMMENT	
4.1 ± 0.7 ± 0.7	AUBERT	07BJ BABR	Dalitz fit, 45k events	
$\Gamma(\rho(1700)^0 \pi^0, \rho(1700)^0 \rightarrow \pi^+ \pi^-)/\Gamma(\pi^+ \pi^- \pi^0)$	$\Gamma_{136}/\Gamma_{128}$			
VALUE (units 10 ⁻²)	DOCUMENT ID	TECN	COMMENT	
5.0 ± 0.6 ± 1.0	AUBERT	07BJ BABR	Dalitz fit, 45k events	
$\Gamma(\rho(1700)^- \pi^+, \rho(1700)^- \rightarrow \pi^- \pi^0)/\Gamma(\pi^+ \pi^- \pi^0)$	$\Gamma_{137}/\Gamma_{128}$			
VALUE (units 10 ⁻²)	DOCUMENT ID	TECN	COMMENT	
3.2 ± 0.4 ± 0.6	AUBERT	07BJ BABR	Dalitz fit, 45k events	
$\Gamma(f_0(980)\pi^0, f_0(980) \rightarrow \pi^+ \pi^-)/\Gamma(\pi^+ \pi^- \pi^0)$	$\Gamma_{138}/\Gamma_{128}$			
VALUE (units 10 ⁻²)	CL%	DOCUMENT ID	TECN	COMMENT
0.25 ± 0.04 ± 0.04		AUBERT	07BJ BABR	Dalitz fit, 45k events
••• We do not use the following data for averages, fits, limits, etc. •••				
<0.026	95	107 CRONIN-HEN..05	CLEO	e ⁺ e ⁻ ≈ 10 GeV
107 The CRONIN-HENNESSY 05 fit here includes, in addition to the three ρπ charged states, only the f ₀ (980)π ⁰ mode. See also the next entries for limits obtained in the same way for the f ₀ (600)π ⁰ mode and for an S-wave π ⁺ π ⁻ parametrized using a K-matrix. Our ρπ branching ratios, given above, use the fit with the K-matrix S wave.				
$\Gamma(f_0(600)\pi^0, f_0(600) \rightarrow \pi^+ \pi^-)/\Gamma(\pi^+ \pi^- \pi^0)$	$\Gamma_{139}/\Gamma_{128}$			
The f ₀ (600) is the σ.				
VALUE (units 10 ⁻²)	CL%	DOCUMENT ID	TECN	COMMENT
0.82 ± 0.10 ± 0.10		AUBERT	07BJ BABR	Dalitz fit, 45k events
••• We do not use the following data for averages, fits, limits, etc. •••				
<0.21	95	108 CRONIN-HEN..05	CLEO	e ⁺ e ⁻ ≈ 10 GeV
108 See the note on CRONIN-HENNESSY 05 in the preceding data block.				
$\Gamma((\pi^+ \pi^-)_{S\text{-wave}} \pi^0)/\Gamma(\pi^+ \pi^- \pi^0)$	$\Gamma_{140}/\Gamma_{128}$			
VALUE	CL%	DOCUMENT ID	TECN	COMMENT
<0.019	95	109 CRONIN-HEN..05	CLEO	e ⁺ e ⁻ ≈ 10 GeV
109 See the note on CRONIN-HENNESSY 05 two data blocks up.				
$\Gamma(f_0(1370)\pi^0, f_0(1370) \rightarrow \pi^+ \pi^-)/\Gamma(\pi^+ \pi^- \pi^0)$	$\Gamma_{141}/\Gamma_{128}$			
VALUE (units 10 ⁻²)	DOCUMENT ID	TECN	COMMENT	
0.37 ± 0.11 ± 0.09	AUBERT	07BJ BABR	Dalitz fit, 45k events	
$\Gamma(f_0(1500)\pi^0, f_0(1500) \rightarrow \pi^+ \pi^-)/\Gamma(\pi^+ \pi^- \pi^0)$	$\Gamma_{142}/\Gamma_{128}$			
VALUE (units 10 ⁻²)	DOCUMENT ID	TECN	COMMENT	
0.39 ± 0.08 ± 0.07	AUBERT	07BJ BABR	Dalitz fit, 45k events	
$\Gamma(f_0(1710)\pi^0, f_0(1710) \rightarrow \pi^+ \pi^-)/\Gamma(\pi^+ \pi^- \pi^0)$	$\Gamma_{143}/\Gamma_{128}$			
VALUE (units 10 ⁻²)	DOCUMENT ID	TECN	COMMENT	
0.31 ± 0.07 ± 0.08	AUBERT	07BJ BABR	Dalitz fit, 45k events	
$\Gamma(f_2(1270)\pi^0, f_2(1270) \rightarrow \pi^+ \pi^-)/\Gamma(\pi^+ \pi^- \pi^0)$	$\Gamma_{144}/\Gamma_{128}$			
VALUE (units 10 ⁻²)	DOCUMENT ID	TECN	COMMENT	
1.32 ± 0.08 ± 0.10	AUBERT	07BJ BABR	Dalitz fit, 45k events	
$\Gamma(\pi^+ \pi^- \pi^0 \text{ nonresonant})/\Gamma(\pi^+ \pi^- \pi^0)$	$\Gamma_{145}/\Gamma_{128}$			
VALUE (units 10 ⁻²)	DOCUMENT ID	TECN	COMMENT	
0.84 ± 0.21 ± 0.12	AUBERT	07BJ BABR	Dalitz fit, 45k events	
$\Gamma(3\pi^0)/\Gamma_{\text{total}}$	Γ_{146}/Γ			
VALUE	CL%	DOCUMENT ID	TECN	COMMENT
<3.5 × 10 ⁻⁴	90	RUBIN	06	CLEO e ⁺ e ⁻ at ψ(3770)
$\Gamma(2\pi^+ 2\pi^-)/\Gamma(K^- \pi^+)$	Γ_{147}/Γ_{31}			
VALUE (units 10 ⁻²)	EVTS	DOCUMENT ID	TECN	COMMENT
19.1 ± 0.5 OUR FIT	Error includes scale factor of 1.1.			
19.1 ± 0.4 ± 0.6	7331 ± 130	RUBIN	06	CLEO e ⁺ e ⁻ at ψ(3770)
$\Gamma(2\pi^+ 2\pi^-)/\Gamma(K^- 2\pi^+ \pi^-)$	Γ_{147}/Γ_{61}			
VALUE (units 10 ⁻²)	EVTS	DOCUMENT ID	TECN	COMMENT
9.19 ± 0.23 OUR FIT	Error includes scale factor of 1.1.			
9.20 ± 0.26 OUR AVERAGE				
9.14 ± 0.18 ± 0.22	6360 ± 115	LINK	07A	FOCS γBe, E _γ ≈ 180 GeV
7.9 ± 1.8 ± 0.5	162	ABLIKIM	05F	BES e ⁺ e ⁻ ≈ ψ(3770)
9.5 ± 0.7 ± 0.2	814	FRABETTI	95c	E687 γBe, E _γ ≈ 200 GeV
10.2 ± 1.3	345	AMMAR	91	CLEO e ⁺ e ⁻ ≈ 10.5 GeV
••• We do not use the following data for averages, fits, limits, etc. •••				
11.5 ± 2.3 ± 1.6	64	ADAMOVIICH	92	OMEG π ⁻ 340 GeV
10.8 ± 2.4 ± 0.8	79	FRABETTI	92	E687 γBe
9.6 ± 1.8 ± 0.7	66	ANJOS	91	E691 γBe 80–240 GeV
$\Gamma(a_1(1260)^+ \pi^-, a_1^+ \rightarrow 2\pi^+ \pi^- \text{ total})/\Gamma(2\pi^+ 2\pi^-)$	$\Gamma_{148}/\Gamma_{147}$			
This is the fit fraction from the coherent amplitude analysis.				
VALUE (units 10 ⁻²)	DOCUMENT ID	TECN	COMMENT	
60.0 ± 3.0 ± 2.4	LINK	07A	FOCS 4-body fit, ≈ 5.7k evts	
$\Gamma(a_1(1260)^+ \pi^-, a_1^+ \rightarrow \rho^0 \pi^+ \text{ S-wave})/\Gamma(2\pi^+ 2\pi^-)$	$\Gamma_{149}/\Gamma_{147}$			
This is the fit fraction from the coherent amplitude analysis.				
VALUE (units 10 ⁻²)	DOCUMENT ID	TECN	COMMENT	
43.3 ± 2.5 ± 1.9	LINK	07A	FOCS 4-body fit, ≈ 5.7k evts	
$\Gamma(a_1(1260)^+ \pi^-, a_1^+ \rightarrow \rho^0 \pi^+ \text{ D-wave})/\Gamma(2\pi^+ 2\pi^-)$	$\Gamma_{150}/\Gamma_{147}$			
This is the fit fraction from the coherent amplitude analysis.				
VALUE (units 10 ⁻²)	DOCUMENT ID	TECN	COMMENT	
2.5 ± 0.5 ± 0.4	LINK	07A	FOCS 4-body fit, ≈ 5.7k evts	
$\Gamma(a_1(1260)^+ \pi^-, a_1^+ \rightarrow \sigma \pi^+)/\Gamma(2\pi^+ 2\pi^-)$	$\Gamma_{151}/\Gamma_{147}$			
This is the fit fraction from the coherent amplitude analysis.				
VALUE (units 10 ⁻²)	DOCUMENT ID	TECN	COMMENT	
8.3 ± 0.7 ± 0.6	LINK	07A	FOCS 4-body fit, ≈ 5.7k evts	
$\Gamma(2\rho^0 \text{ total})/\Gamma(2\pi^+ 2\pi^-)$	$\Gamma_{152}/\Gamma_{147}$			
This is the fit fraction from the coherent amplitude analysis.				
VALUE (units 10 ⁻²)	DOCUMENT ID	TECN	COMMENT	
24.5 ± 1.3 ± 1.0	LINK	07A	FOCS 4-body fit, ≈ 5.7k evts	
$\Gamma(2\rho^0, \text{ parallel helicities})/\Gamma(2\pi^+ 2\pi^-)$	$\Gamma_{153}/\Gamma_{147}$			
This is the fit fraction from the coherent amplitude analysis.				
VALUE (units 10 ⁻²)	DOCUMENT ID	TECN	COMMENT	
1.1 ± 0.3 ± 0.3	LINK	07A	FOCS 4-body fit, ≈ 5.7k evts	
$\Gamma(2\rho^0, \text{ perpendicular helicities})/\Gamma(2\pi^+ 2\pi^-)$	$\Gamma_{154}/\Gamma_{147}$			
This is the fit fraction from the coherent amplitude analysis.				
VALUE (units 10 ⁻²)	DOCUMENT ID	TECN	COMMENT	
6.4 ± 0.6 ± 0.5	LINK	07A	FOCS 4-body fit, ≈ 5.7k evts	
$\Gamma(2\rho^0, \text{ longitudinal helicities})/\Gamma(2\pi^+ 2\pi^-)$	$\Gamma_{155}/\Gamma_{147}$			
This is the fit fraction from the coherent amplitude analysis.				
VALUE (units 10 ⁻²)	DOCUMENT ID	TECN	COMMENT	
16.8 ± 1.0 ± 0.8	LINK	07A	FOCS 4-body fit, ≈ 5.7k evts	
$\Gamma(\text{Resonant } (\pi^+ \pi^-) \pi^+ \pi^- \text{ 3-body total})/\Gamma(2\pi^+ 2\pi^-)$	$\Gamma_{156}/\Gamma_{147}$			
This is the fit fraction from the coherent amplitude analysis.				
VALUE (units 10 ⁻²)	DOCUMENT ID	TECN	COMMENT	
20.0 ± 1.2 ± 1.0	LINK	07A	FOCS 4-body fit, ≈ 5.7k evts	
$\Gamma(\sigma \pi^+ \pi^-)/\Gamma(2\pi^+ 2\pi^-)$	$\Gamma_{157}/\Gamma_{147}$			
This is the fit fraction from the coherent amplitude analysis.				
VALUE (units 10 ⁻²)	DOCUMENT ID	TECN	COMMENT	
8.2 ± 0.9 ± 0.7	LINK	07A	FOCS 4-body fit, ≈ 5.7k evts	
$\Gamma(f_0(980) \pi^+ \pi^-, f_0 \rightarrow \pi^+ \pi^-)/\Gamma(2\pi^+ 2\pi^-)$	$\Gamma_{158}/\Gamma_{147}$			
This is the fit fraction from the coherent amplitude analysis.				
VALUE (units 10 ⁻²)	DOCUMENT ID	TECN	COMMENT	
2.4 ± 0.5 ± 0.4	LINK	07A	FOCS 4-body fit, ≈ 5.7k evts	
$\Gamma(f_2(1270) \pi^+ \pi^-, f_2 \rightarrow \pi^+ \pi^-)/\Gamma(2\pi^+ 2\pi^-)$	$\Gamma_{159}/\Gamma_{147}$			
This is the fit fraction from the coherent amplitude analysis.				
VALUE (units 10 ⁻²)	DOCUMENT ID	TECN	COMMENT	
4.9 ± 0.6 ± 0.5	LINK	07A	FOCS 4-body fit, ≈ 5.7k evts	
$\Gamma(\pi^+ \pi^- 2\pi^0)/\Gamma(K^- \pi^+)$	Γ_{160}/Γ_{31}			
VALUE (units 10 ⁻²)	EVTS	DOCUMENT ID	TECN	COMMENT
25.8 ± 1.5 ± 1.8	2724 ± 166	RUBIN	06	CLEO e ⁺ e ⁻ at ψ(3770)
$\Gamma(\eta \pi^0)/\Gamma_{\text{total}}$	Γ_{161}/Γ			
Unseen decay modes of the η are included.				
VALUE (units 10 ⁻⁴)	EVTS	DOCUMENT ID	TECN	COMMENT
6.4 ± 1.0 ± 0.4	156 ± 24	ARTUSO	08	CLEO e ⁺ e ⁻ at ψ(3770)
$\Gamma(\eta \pi^0)/\Gamma(K^- \pi^+)$	Γ_{161}/Γ_{31}			
Unseen decay modes of the η are included.				
VALUE (units 10 ⁻²)	EVTS	DOCUMENT ID	TECN	COMMENT
1.47 ± 0.34 ± 0.11	62 ± 14	RUBIN	06	CLEO See ARTUSO 08
$\Gamma(\omega \pi^0)/\Gamma_{\text{total}}$	Γ_{162}/Γ			
Unseen decay modes of the ω are included.				
VALUE	CL%	DOCUMENT ID	TECN	COMMENT
<2.6 × 10 ⁻⁴	90	RUBIN	06	CLEO e ⁺ e ⁻ at ψ(3770)
$\Gamma(2\pi^+ 2\pi^- \pi^0)/\Gamma(K^- \pi^+)$	Γ_{163}/Γ_{31}			
VALUE (units 10 ⁻²)	EVTS	DOCUMENT ID	TECN	COMMENT
10.7 ± 1.2 ± 0.5	1614 ± 171	RUBIN	06	CLEO e ⁺ e ⁻ at ψ(3770)

Meson Particle Listings

D^0

$\Gamma(\eta\pi^+\pi^-)/\Gamma_{\text{total}}$

Unseen decay modes of the η are included.

VALUE (units 10^{-4})	CL%	EVTS	DOCUMENT ID	TECN	COMMENT
$10.9 \pm 1.3 \pm 0.9$		257 ± 32	ARTUSO 08	CLEO	e^+e^- at $\psi(3770)$
••• We do not use the following data for averages, fits, limits, etc. •••					
<19	90		RUBIN 06	CLEO	e^+e^- at $\psi(3770)$

Γ_{164}/Γ

$\Gamma(\omega\pi^+\pi^-)/\Gamma(K^-\pi^+)$

Unseen decay modes of the ω are included.

VALUE (units 10^{-2})	EVTS	DOCUMENT ID	TECN	COMMENT
$4.1 \pm 1.2 \pm 0.4$	472 ± 132	RUBIN 06	CLEO	e^+e^- at $\psi(3770)$

Γ_{165}/Γ_{31}

$\Gamma(3\pi^+3\pi^-)/\Gamma(K^-2\pi^+\pi^-)$

VALUE (units 10^{-3})	EVTS	DOCUMENT ID	TECN	COMMENT
$5.23 \pm 0.59 \pm 1.35$	149 ± 17	LINK 04B	FOCS	$\gamma A, \bar{E}_\gamma \approx 180$ GeV

Γ_{166}/Γ_{61}

$\Gamma(3\pi^+3\pi^-)/\Gamma(K^-3\pi^+2\pi^-)$

VALUE	DOCUMENT ID	TECN	COMMENT
$1.93 \pm 0.47 \pm 0.48$	¹¹⁰ LINK 04B	FOCS	$\gamma A, \bar{E}_\gamma \approx 180$ GeV

Γ_{166}/Γ_{87}

••• We do not use the following data for averages, fits, limits, etc. •••

¹¹⁰ This LINK 04B result is not independent of other results in these Listings.

$\Gamma(\eta'(958)\pi^0)/\Gamma_{\text{total}}$

VALUE (units 10^{-4})	EVTS	DOCUMENT ID	TECN	COMMENT
$8.1 \pm 1.5 \pm 0.6$	50 ± 9	ARTUSO 08	CLEO	e^+e^- at $\psi(3770)$

Γ_{167}/Γ

$\Gamma(\eta'(958)\pi^+\pi^-)/\Gamma_{\text{total}}$

VALUE (units 10^{-4})	EVTS	DOCUMENT ID	TECN	COMMENT
$4.5 \pm 1.6 \pm 0.5$	21 ± 8	ARTUSO 08	CLEO	e^+e^- at $\psi(3770)$

Γ_{168}/Γ

$\Gamma(2\eta)/\Gamma_{\text{total}}$

VALUE (units 10^{-4})	EVTS	DOCUMENT ID	TECN	COMMENT
$16.7 \pm 1.4 \pm 1.3$	255 ± 22	ARTUSO 08	CLEO	e^+e^- at $\psi(3770)$

Γ_{169}/Γ

$\Gamma(\eta\eta'(958))/\Gamma_{\text{total}}$

VALUE (units 10^{-4})	EVTS	DOCUMENT ID	TECN	COMMENT
$12.6 \pm 2.5 \pm 1.1$	46 ± 9	ARTUSO 08	CLEO	e^+e^- at $\psi(3770)$

Γ_{170}/Γ

Hadronic modes with a $K\bar{K}$ pair

$\Gamma(K^+K^-)/\Gamma_{\text{total}}$

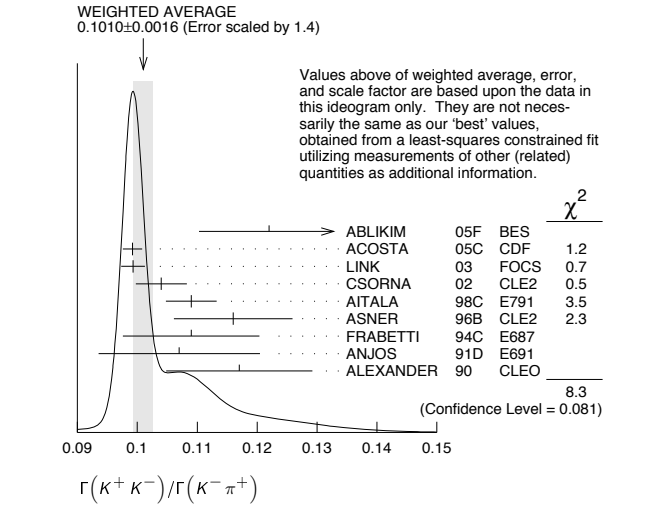
VALUE (units 10^{-3})	EVTS	DOCUMENT ID	TECN	COMMENT
3.94 ± 0.07 OUR FIT	Error includes scale factor of 1.3.			
$4.08 \pm 0.08 \pm 0.09$	4746 ± 74	BONVICINI 08	CLEO	e^+e^- at $\psi(3770)$

Γ_{171}/Γ

$\Gamma(K^+K^-)/\Gamma(K^-\pi^+)$

VALUE	EVTS	DOCUMENT ID	TECN	COMMENT
0.1015 ± 0.0015 OUR FIT	Error includes scale factor of 1.4.			
0.1010 ± 0.0016 OUR AVERAGE	Error includes scale factor of 1.4. See the ideogram below.			
$0.122 \pm 0.011 \pm 0.004$	242 ± 20	ABLIKIM 05F	BES	$e^+e^- \approx \psi(3770)$
$0.0992 \pm 0.0011 \pm 0.0012$	16k ± 200	ACOSTA 05c	CDF	$p\bar{p}, \sqrt{s}=1.96$ TeV
$0.0993 \pm 0.0014 \pm 0.0014$	11k	LINK 03	FOCS	γ nucleus, $\bar{E}_\gamma \approx 180$ GeV
$0.1040 \pm 0.0033 \pm 0.0027$	1900	CSORNA 02	CLE2	$e^+e^- \approx \Upsilon(4S)$
$0.109 \pm 0.003 \pm 0.003$	3317	AITALA 98c	E791	π^- nucleus, 500 GeV
$0.116 \pm 0.007 \pm 0.007$	1102	ASNER 96B	CLE2	$e^+e^- \approx \Upsilon(4S)$
$0.109 \pm 0.007 \pm 0.009$	581	FRABETTI 94c	E687	γ Be $\bar{E}_\gamma = 220$ GeV
$0.107 \pm 0.010 \pm 0.009$	193	ANJOS 91D	E691	Photoproduction
$0.117 \pm 0.010 \pm 0.007$	249	ALEXANDER 90	CLEO	e^+e^- 10.5–11 GeV
••• We do not use the following data for averages, fits, limits, etc. •••				
$0.107 \pm 0.029 \pm 0.015$	103	ADAMOVIH 92	OMEG	π^- 340 GeV
$0.138 \pm 0.027 \pm 0.010$	155	FRABETTI 92	E687	γ Be
0.16 ± 0.05	34	ALVAREZ 91B	NA14	Photoproduction
$0.10 \pm 0.02 \pm 0.01$	131	ALBRECHT 90c	ARG	$e^+e^- \approx 10$ GeV
$0.122 \pm 0.018 \pm 0.012$	118	BALTRUSAIT...85E	MRK3	e^+e^- 3.77 GeV
0.113 ± 0.030		ABRAMS 79D	MRK2	e^+e^- 3.77 GeV

Γ_{171}/Γ_{31}



$\Gamma(K^+K^-)/\Gamma(\pi^+\pi^-)$

$\Gamma_{171}/\Gamma_{126}$

The unused results here are redundant with $\Gamma(K^+K^-)/\Gamma(K^-\pi^+)$ and $\Gamma(\pi^+\pi^-)/\Gamma(K^-\pi^+)$ measurements by the same experiments.

VALUE	EVTS	DOCUMENT ID	TECN	COMMENT
••• We do not use the following data for averages, fits, limits, etc. •••				
$2.760 \pm 0.040 \pm 0.034$	7334	ACOSTA 05c	CDF	$p\bar{p}, \sqrt{s}=1.96$ TeV
$2.81 \pm 0.10 \pm 0.06$		LINK 03	FOCS	γ nucleus, $\bar{E}_\gamma \approx 180$ GeV
$2.96 \pm 0.16 \pm 0.15$	710	CSORNA 02	CLE2	$e^+e^- \approx \Upsilon(4S)$
$2.75 \pm 0.15 \pm 0.16$		AITALA 98c	E791	π^- nucleus, 500 GeV
$2.53 \pm 0.46 \pm 0.19$		FRABETTI 94c	E687	γ Be $\bar{E}_\gamma = 220$ GeV
$2.23 \pm 0.81 \pm 0.46$		ADAMOVIH 92	OMEG	π^- 340 GeV
$1.95 \pm 0.34 \pm 0.22$		ANJOS 91D	E691	Photoproduction
2.5 ± 0.7		ALBRECHT 90c	ARG	$e^+e^- \approx 10$ GeV
$2.35 \pm 0.37 \pm 0.28$		ALEXANDER 90	CLEO	e^+e^- 10.5–11 GeV

$\Gamma(2K_S^0)/\Gamma_{\text{total}}$

Γ_{172}/Γ

VALUE (units 10^{-4})	EVTS	DOCUMENT ID	TECN	COMMENT
1.9 ± 0.7 OUR FIT	Error includes scale factor of 2.5.			
$1.46 \pm 0.32 \pm 0.09$	68 ± 15	BONVICINI 08	CLEO	e^+e^- at $\psi(3770)$

$\Gamma(2K_S^0)/\Gamma(K_S^0\pi^+\pi^-)$

Γ_{172}/Γ_{34}

This is the same as $\Gamma(K^0\bar{K}^0)/\Gamma(\bar{K}^0\pi^+\pi^-)$ because $D^0 \rightarrow K_S^0 K_L^0$ is forbidden by CP conservation.

VALUE	EVTS	DOCUMENT ID	TECN	COMMENT
0.0065 ± 0.0025 OUR FIT	Error includes scale factor of 2.4.			
0.0120 ± 0.0022 OUR AVERAGE				
$0.0144 \pm 0.0032 \pm 0.0016$	79 ± 17	LINK 05A	FOCS	γ Be, $\bar{E}_\gamma \approx 180$ GeV
$0.0101 \pm 0.0022 \pm 0.0016$	26	ASNER 96B	CLE2	$e^+e^- \approx \Upsilon(4S)$
$0.039 \pm 0.013 \pm 0.013$	20 ± 7	FRABETTI 94J	E687	γ Be $\bar{E}_\gamma = 220$ GeV
••• We do not use the following data for averages, fits, limits, etc. •••				
$0.021 \pm 0.011 \pm 0.002$	5	ALEXANDER 90	CLEO	e^+e^- 10.5–11 GeV

$\Gamma(K_S^0 K^-\pi^+)/\Gamma(K^-\pi^+)$

Γ_{173}/Γ_{31}

VALUE	DOCUMENT ID	TECN	COMMENT
0.089 ± 0.013 OUR FIT	Error includes scale factor of 1.1.		
0.08 ± 0.03	¹¹¹ ANJOS 91	E691	γ Be 80–240 GeV

¹¹¹ The factor 100 at the top of column 2 of Table I of ANJOS 91 should be omitted.

$\Gamma(K_S^0 K^-\pi^+)/\Gamma(K_S^0\pi^+\pi^-)$

Γ_{173}/Γ_{34}

VALUE	EVTS	DOCUMENT ID	TECN	COMMENT
0.117 ± 0.017 OUR FIT	Error includes scale factor of 1.1.			
0.119 ± 0.021 OUR AVERAGE	Error includes scale factor of 1.3.			
0.108 ± 0.019	61	AMMAR 91	CLEO	$e^+e^- \approx 10.5$ GeV
$0.16 \pm 0.03 \pm 0.02$	39	ALBRECHT 90c	ARG	$e^+e^- \approx 10$ GeV

$\Gamma(\bar{K}^*(892)^0 K_S^0, \bar{K}^*(892)^0 \rightarrow K^-\pi^+)/\Gamma(K_S^0\pi^+\pi^-)$

Γ_{174}/Γ_{34}

VALUE	CL%	DOCUMENT ID	TECN	COMMENT
<0.019	90	AMMAR 91	CLEO	$e^+e^- \approx 10.5$ GeV
••• We do not use the following data for averages, fits, limits, etc. •••				
<0.02	90	ALBRECHT 90c	ARG	$e^+e^- \approx 10$ GeV

$\Gamma(K_S^0 K^+\pi^-)/\Gamma(K^-\pi^+)$

Γ_{175}/Γ_{31}

VALUE	DOCUMENT ID	TECN	COMMENT
0.068 ± 0.013 OUR FIT	Error includes scale factor of 1.1.		
0.05 ± 0.025	¹¹² ANJOS 91	E691	γ Be 80–240 GeV

¹¹² The factor 100 at the top of column 2 of Table I of ANJOS 91 should be omitted.

$\Gamma(K_S^0 K^+ \pi^-) / \Gamma(K_S^0 \pi^+ \pi^-)$					$\Gamma_{175} / \Gamma_{34}$
VALUE	EVTS	DOCUMENT ID	TECN	COMMENT	
0.089 ± 0.017 OUR FIT					
0.098 ± 0.020	55	AMMAR	91	CLEO $e^+ e^- \approx 10.5$ GeV	

$\Gamma(K^*(892)^0 K_S^0) / \Gamma(K_S^0 \pi^+ \pi^-)$					$\Gamma_{176} / \Gamma_{34}$
VALUE	CL%	DOCUMENT ID	TECN	COMMENT	
<0.010	90	AMMAR	91	CLEO $e^+ e^- \approx 10.5$ GeV	

$\Gamma(K^+ K^- \pi^0) / \Gamma(K^- \pi^+ \pi^0)$					$\Gamma_{177} / \Gamma_{49}$
VALUE (units 10 ⁻²)	EVTS	DOCUMENT ID	TECN	COMMENT	
2.37 ± 0.03 ± 0.04	11k ± 122	AUBERT,B	06X	BABR $e^+ e^- \approx \Upsilon(4S)$	
••• We do not use the following data for averages, fits, limits, etc. •••					
0.95 ± 0.26	151	ASNER	96B	CLE2 $e^+ e^- \approx \Upsilon(4S)$	

$\Gamma(K^*(892)^+ K^-) / \Gamma(K^+ K^- \pi^0)$					$\Gamma_{178} / \Gamma_{177}$
VALUE (units 10 ⁻²)	DOCUMENT ID	TECN	COMMENT		
44.4 ± 0.8 ± 0.6	AUBERT	07T	BABR	Dalitz fit II, 11k evts	
••• We do not use the following data for averages, fits, limits, etc. •••					
46.1 ± 3.1	113	CAWLFIELD	06A	CLEO Dalitz fit, 627 ± 30 evts	
113 The error on this CAWLFIELD 06A result is statistical only.					

$\Gamma(K^*(892)^- K^+) / \Gamma(K^+ K^- \pi^0)$					$\Gamma_{179} / \Gamma_{177}$
VALUE (units 10 ⁻²)	DOCUMENT ID	TECN	COMMENT		
15.9 ± 0.7 ± 0.6	AUBERT	07T	BABR	Dalitz fit II, 11k evts	
••• We do not use the following data for averages, fits, limits, etc. •••					
12.3 ± 2.2	114	CAWLFIELD	06A	CLEO Dalitz fit, 627 ± 30 evts	
114 The error on this CAWLFIELD 06A result is statistical only.					

$\Gamma((K^+ \pi^0)_{S\text{-wave}} K^-) / \Gamma(K^+ K^- \pi^0)$					$\Gamma_{180} / \Gamma_{177}$
VALUE (units 10 ⁻²)	DOCUMENT ID	TECN	COMMENT		
71.1 ± 3.7 ± 1.9	115	AUBERT	07T	BABR Dalitz fit II, 11k evts	
115 The only major difference between fits I and II in the AUBERT 07T analysis is in this mode, where the fit-I fraction is (16.3 ± 3.4 ± 2.1)%.					

$\Gamma((K^- \pi^0)_{S\text{-wave}} K^+) / \Gamma(K^+ K^- \pi^0)$					$\Gamma_{181} / \Gamma_{177}$
VALUE (units 10 ⁻²)	DOCUMENT ID	TECN	COMMENT		
3.9 ± 0.9 ± 1.0	AUBERT	07T	BABR	Dalitz fit II, 11k evts	

$\Gamma(f_0(980) \pi^0, f_0 \rightarrow K^+ K^-) / \Gamma(K^+ K^- \pi^0)$					$\Gamma_{182} / \Gamma_{177}$
VALUE (units 10 ⁻²)	DOCUMENT ID	TECN	COMMENT		
10.5 ± 1.1 ± 1.2	116	AUBERT	07T	BABR Dalitz fit II, 11k evts	
116 When AUBERT 07T replace the $f_0(980) \pi^0$ mode with $a_0(980) \pi^0$, the fit fraction is a negligibly different (11.0 ± 1.5 ± 1.2)%.					

$\Gamma(\phi \pi^0, \phi \rightarrow K^+ K^-) / \Gamma(K^+ K^- \pi^0)$					$\Gamma_{183} / \Gamma_{177}$
VALUE (units 10 ⁻²)	DOCUMENT ID	TECN	COMMENT		
19.4 ± 0.6 ± 0.5	AUBERT	07T	BABR	Dalitz fit II, 11k evts	
••• We do not use the following data for averages, fits, limits, etc. •••					
14.9 ± 1.6	117	CAWLFIELD	06A	CLEO Dalitz fit, 627 ± 30 evts	
117 The error on this CAWLFIELD 06A result is statistical only.					

$\Gamma(K^+ K^- \pi^0 \text{ nonresonant}) / \Gamma(K^+ K^- \pi^0)$					$\Gamma_{184} / \Gamma_{177}$
VALUE	DOCUMENT ID	TECN	COMMENT		
••• We do not use the following data for averages, fits, limits, etc. •••					
0.360 ± 0.037	118	CAWLFIELD	06A	CLEO Dalitz fit, 627 ± 30 evts	
118 The error is statistical only. CAWLFIELD 06A also fits the Dalitz plot replacing this flat nonresonant background with broad S-wave $\kappa^\pm \rightarrow K^\pm \pi^0$ resonances. There is no significant improvement in the fit, and $K^* K^\mp$ and $\phi \pi^0$ results are not much changed.					

$\Gamma(2K_S^0 \pi^0) / \Gamma_{\text{total}}$					Γ_{185} / Γ
VALUE	DOCUMENT ID	TECN	COMMENT		
<0.00059	ASNER	96B	CLE2	$e^+ e^- \approx \Upsilon(4S)$	

$\Gamma(\phi \pi^0) / \Gamma(K^+ K^-)$					$\Gamma_{198} / \Gamma_{171}$
NP10000 VALUE	EVTS	DOCUMENT ID	TECN	COMMENT	
••• We do not use the following data for averages, fits, limits, etc. •••					
0.194 ± 0.006 ± 0.009	1254	TAJIMA	04	BELL $e^+ e^-$ at $\Upsilon(4S)$	

$\Gamma(\phi \eta) / \Gamma(K^+ K^-)$					$\Gamma_{199} / \Gamma_{171}$
VALUE (units 10 ⁻²)	EVTS	DOCUMENT ID	TECN	COMMENT	
3.59 ± 1.14 ± 0.18	31	TAJIMA	04	BELL $e^+ e^-$ at $\Upsilon(4S)$	

$\Gamma(\phi \omega) / \Gamma_{\text{total}}$					Γ_{200} / Γ
VALUE	CL%	DOCUMENT ID	TECN	COMMENT	
<0.0021	90	ALBRECHT	94I	ARG $e^+ e^- \approx 10$ GeV	

$\Gamma(K^+ K^- \pi^+ \pi^-) / \Gamma(K^- 2\pi^+ \pi^-)$					$\Gamma_{186} / \Gamma_{61}$
VALUE (units 10 ⁻²)	EVTS	DOCUMENT ID	TECN	COMMENT	
3.00 ± 0.13 OUR AVERAGE					
2.95 ± 0.11 ± 0.08	2669 ± 101	119 LINK	05G	FOCS $\gamma\text{Be}, \bar{E}_\gamma \approx 180$ GeV	
3.13 ± 0.37 ± 0.36	136 ± 15	AITALA	98D	E791 π^- nucleus, 500 GeV	
3.5 ± 0.4 ± 0.2	244 ± 26	FRABETTI	95C	E687 $\gamma\text{Be}, \bar{E}_\gamma \approx 200$ GeV	
••• We do not use the following data for averages, fits, limits, etc. •••					
4.4 ± 1.8 ± 0.5	19 ± 8	ABLIKIM	05F	BES $e^+ e^- \approx \psi(3770)$	
4.1 ± 0.7 ± 0.5	114 ± 20	ALBRECHT	94I	ARG $e^+ e^- \approx 10$ GeV	
3.14 ± 1.0	89 ± 29	AMMAR	91	CLEO $e^+ e^- \approx 10.5$ GeV	
2.8 + _{-0.7}		ANJOS	91	E691 γBe 80–240 GeV	

119 LINK 05G uses a smaller, cleaner subset of 1279 ± 48 events for the amplitude analysis that gives the results in the next data blocks.

$\Gamma(\phi \pi^+ \pi^- \text{ 3-body}, \phi \rightarrow K^+ K^-) / \Gamma(K^+ K^- \pi^+ \pi^-)$					$\Gamma_{187} / \Gamma_{186}$
VALUE	DOCUMENT ID	TECN	COMMENT		
0.01 ± 0.01	LINK	05G	FOCS	1279 ± 48 $K^+ K^- \pi^+ \pi^-$ evts.	

$\Gamma(\phi \rho^0, \phi \rightarrow K^+ K^-) / \Gamma(K^+ K^- \pi^+ \pi^-)$					$\Gamma_{188} / \Gamma_{186}$
VALUE	DOCUMENT ID	TECN	COMMENT		
0.29 ± 0.02 ± 0.01	LINK	05G	FOCS	1279 ± 48 $K^+ K^- \pi^+ \pi^-$ evts.	

$\Gamma(K^+ K^- \rho^0 \text{ 3-body}) / \Gamma(K^+ K^- \pi^+ \pi^-)$					$\Gamma_{189} / \Gamma_{186}$
VALUE	DOCUMENT ID	TECN	COMMENT		
0.02 ± 0.02 ± 0.02	LINK	05G	FOCS	1279 ± 48 $K^+ K^- \pi^+ \pi^-$ evts.	

$\Gamma(f_0(980) \pi^+ \pi^-, f_0 \rightarrow K^+ K^-) / \Gamma(K^+ K^- \pi^+ \pi^-)$					$\Gamma_{190} / \Gamma_{186}$
VALUE	DOCUMENT ID	TECN	COMMENT		
0.15 ± 0.03 ± 0.02	LINK	05G	FOCS	1279 ± 48 $K^+ K^- \pi^+ \pi^-$ evts.	

$\Gamma(K^*(892)^0 K^\mp \pi^\pm \text{ 3-body}, K^{*0} \rightarrow K^\pm \pi^\mp) / \Gamma(K^+ K^- \pi^+ \pi^-)$					$\Gamma_{191} / \Gamma_{186}$
VALUE	DOCUMENT ID	TECN	COMMENT		
0.11 ± 0.02 ± 0.01	LINK	05G	FOCS	1279 ± 48 $K^+ K^- \pi^+ \pi^-$ evts.	

$\Gamma(K^*(892)^0 K^{*0} \pi^\pm / \Gamma(K^+ K^- \pi^+ \pi^-)$					$\Gamma_{192} / \Gamma_{186}$
VALUE	DOCUMENT ID	TECN	COMMENT		
0.03 ± 0.02 ± 0.01	LINK	05G	FOCS	1279 ± 48 $K^+ K^- \pi^+ \pi^-$ evts.	

$\Gamma(K_1(1270)^\pm K^\mp, K_1(1270)^\pm \rightarrow K^\pm \pi^\mp) / \Gamma(K^+ K^- \pi^+ \pi^-)$					$\Gamma_{193} / \Gamma_{186}$
VALUE	DOCUMENT ID	TECN	COMMENT		
0.33 ± 0.06 ± 0.04	120 LINK	05G	FOCS	1279 ± 48 $K^+ K^- \pi^+ \pi^-$ evts.	

120 This LINK 05G value includes $K_1(1270)^\pm \rightarrow \rho^0 K^\pm, \rightarrow K_0^0(1430)^\pm \pi^\pm$, and $K^*(892)^0 \pi^\pm$.

$\Gamma(K_1(1400)^\pm K^\mp, K_1(1400)^\pm \rightarrow K^\pm \pi^\mp) / \Gamma(K^+ K^- \pi^+ \pi^-)$					$\Gamma_{194} / \Gamma_{186}$
VALUE	DOCUMENT ID	TECN	COMMENT		
0.22 ± 0.03 ± 0.04	LINK	05G	FOCS	1279 ± 48 $K^+ K^- \pi^+ \pi^-$ evts.	

$\Gamma(2K_S^0 \pi^+ \pi^-) / \Gamma(K_S^0 \pi^+ \pi^-)$					$\Gamma_{195} / \Gamma_{34}$
VALUE (units 10 ⁻²)	EVTS	DOCUMENT ID	TECN	COMMENT	
4.3 ± 0.8 OUR AVERAGE					
4.16 ± 0.70 ± 0.42	113 ± 21	LINK	05A	FOCS $\gamma\text{Be}, \bar{E}_\gamma \approx 180$ GeV	
6.2 ± 2.0 ± 1.6	25	ALBRECHT	94I	ARG $e^+ e^- \approx 10$ GeV	

$\Gamma(K_S^0 K^- 2\pi^+ \pi^-) / \Gamma(K_S^0 2\pi^+ 2\pi^-)$					$\Gamma_{196} / \Gamma_{81}$
VALUE	CL%	DOCUMENT ID	TECN	COMMENT	
<0.054	90	LINK	04D	FOCS $\gamma\text{A}, \bar{E}_\gamma \approx 180$ GeV	

$\Gamma(K^+ K^- \pi^+ \pi^- \pi^0) / \Gamma_{\text{total}}$					Γ_{197} / Γ
VALUE	DOCUMENT ID	TECN	COMMENT		
0.0031 ± 0.0020	121	BARLAG	92C	ACCM π^- Cu 230 GeV	
121 BARLAG 92C computes the branching fraction using topological normalization.					

Radiative modes

$\Gamma(\rho^0 \gamma) / \Gamma_{\text{total}}$					Γ_{201} / Γ
VALUE	CL%	DOCUMENT ID	TECN	COMMENT	
<2.4 × 10⁻⁴	90	ASNER	98	CLE2	

Meson Particle Listings

D⁰

$\Gamma(\omega\gamma)/\Gamma_{\text{total}}$				Γ_{202}/Γ	
VALUE	CL%	DOCUMENT ID	TECN		
$<2.4 \times 10^{-4}$	90	ASNER	98	CLE2	

$\Gamma(\phi\gamma)/\Gamma(K^+K^-)$				$\Gamma_{203}/\Gamma_{171}$	
VALUE (units 10^{-3})	EVTS	DOCUMENT ID	TECN	COMMENT	
6.8 ± 0.9 OUR FIT					
$6.31^{+1.70+0.30}_{-1.48-0.36}$	28	TAJIMA	04	BELL	e^+e^- at $\gamma(4S)$

$\Gamma(\phi\gamma)/\Gamma(K^-\pi^+)$				Γ_{203}/Γ_{31}	
VALUE (units 10^{-4})	EVTS	DOCUMENT ID	TECN	COMMENT	
6.9 ± 0.9 OUR FIT					
$7.15 \pm 0.78 \pm 0.69$	243 ± 25	AUBERT	08AZ	BABR	$e^+e^- \approx 10.6$ GeV

$\Gamma(\bar{K}^*(892)^0\gamma)/\Gamma(K^-\pi^+)$				Γ_{204}/Γ_{31}	
VALUE (units 10^{-3})	EVTS	DOCUMENT ID	TECN	COMMENT	
8.43 ± 0.51 ± 0.70	2286 ± 113	AUBERT	08AZ	BABR	$e^+e^- \approx 10.6$ GeV

Doubly Cabibbo-suppressed / Mixing modes

$\Gamma(K^+\ell^-\nu_\ell \text{ via } \bar{D}^0)/\Gamma(K^-\ell^+\nu_\ell)$ Γ_{205}/Γ_{17}
 This is a limit on R_M without the complications of possible doubly Cabibbo-suppressed decays that occur when using hadronic modes. For the limits on $|m_1 - m_2|$ and $(\Gamma_1 - \Gamma_2)/\Gamma$ that come from the best mixing limit, see near the beginning of these D^0 Listings.

VALUE	CL%	DOCUMENT ID	TECN	COMMENT
$< 6.1 \times 10^{-4}$	90	122 BITENC	08	BELL e^+e^- , 10.58 GeV
$< 50 \times 10^{-4}$	90	123 AITALA	96C	E791 π^- nucleus, 500 GeV

122 The BITENC 08 right-sign sample includes about 15% of $D^0 \rightarrow K^-\pi^0\ell^+\nu_\ell$ and other decays.
 123 AITALA 96C uses $D^{*+} \rightarrow D^0\pi^+$ (and charge conjugate) decays to identify the charm at production and $D^0 \rightarrow K^-\ell^+\nu_\ell$ (and charge conjugate) decays to identify the charm at decay.

$\Gamma(K^+ \text{ or } K^*(892)^+ e^-\nu_e \text{ via } \bar{D}^0) / [\Gamma(K^- e^+\nu_e) + \Gamma(K^*(892)^- e^+\nu_e)]$ $\Gamma_{206}/(\Gamma_{18}+\Gamma_{20})$

This is a limit on R_M without the complications of possible doubly Cabibbo-suppressed decays that occur when using hadronic modes. The experiments use $D^{*+} \rightarrow D^0\pi^+$ (and charge conjugate) decays to identify the charm at production and the charge of the e to identify the charm at decay. These limits do not allow CP violation. For the limits on $|m_1 - m_2|$ and $(\Gamma_1 - \Gamma_2)/\Gamma$ that come from the best mixing limit, see near the beginning of these D^0 Listings.

VALUE	CL%	DOCUMENT ID	TECN	COMMENT
< 0.001	90	BITENC	05	BELL $e^+e^- \approx 10.6$ GeV
$-0.0013 < R < +0.0012$	90	AUBERT	07AB	BABR $e^+e^- \approx 10.58$ GeV
< 0.0078	90	CAWLFIELD	05	CLEO $e^+e^- \approx 10.6$ GeV
< 0.0042	90	AUBERT,B	04Q	BABR See AUBERT 07AB

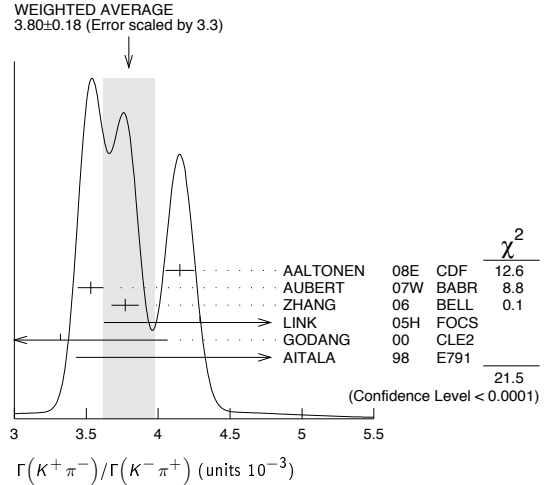
$\Gamma(K^+\pi^-)/\Gamma(K^-\pi^+)$ Γ_{207}/Γ_{31}
 This is R , the time-integrated wrong-sign rate compared to the right-sign rate. See the note on " D^0 - \bar{D}^0 Mixing," near the start of the D^0 Listings.

The experiments here use the charge of the pion in $D^*(2010)^\pm \rightarrow (D^0 \text{ or } \bar{D}^0)\pi^\pm$ decay to tell whether a D^0 or a \bar{D}^0 was born. The $D^0 \rightarrow K^+\pi^-$ decay can occur directly by doubly Cabibbo-suppressed (DCS) decay, or indirectly by $D^0 \rightarrow \bar{D}^0$ mixing followed by $\bar{D}^0 \rightarrow K^+\pi^-$ decay. Some of the experiments can use the decay-time information to disentangle the two mechanisms. Here, we list the experimental branching ratio, which if there is no mixing is the DCS ratio. See the next data block for values of the DCS ratio R_D , and the following data block for limits on the mixing ratio R_M . See the section on CP -violating asymmetries near the end of this D^0 Listing for values of A_D , and the note on " D^0 - \bar{D}^0 Mixing" for limits on x' and y' .

Some early limits have been omitted from this Listing; see our 1998 edition (The European Physical Journal **C3** 1 (1998)) and our 2006 edition (Journal of Physics, **G33** 1 (2006)).

VALUE (units 10^{-3})	EVTS	DOCUMENT ID	TECN	COMMENT
3.80 ± 0.18 OUR AVERAGE				Error includes scale factor of 3.3. See the ideogram below.
4.15 ± 0.10	$12.7 \pm 0.3k$	124 AALTONEN	08E	CDF $p\bar{p}, \sqrt{s} = 1.96$ TeV
$3.53 \pm 0.08 \pm 0.04$	4030 ± 90	125 AUBERT	07W	BABR $e^+e^- \approx 10.6$ GeV
$3.77 \pm 0.08 \pm 0.05$	4024 ± 88	124 ZHANG	06	BELL e^+e^-
$4.29^{+0.63}_{-0.61} \pm 0.27$	234	126 LINK	05H	FOCS γ nucleus
$3.32^{+0.63}_{-0.65} \pm 0.40$	45	124 GODANG	00	CLE2 e^+e^-
$6.8^{+3.4}_{-3.3} \pm 0.7$	34	125 AITALA	98	E791 π^- nucl., 500 GeV
$4.05 \pm 0.21 \pm 0.11$	$2.0 \pm 0.1k$	127 ABULENCIA	06X	CDF See AALTONEN 08E
$3.81 \pm 0.17^{+0.08}_{-0.16}$	845 ± 40	125 LI	05A	BELL See ZHANG 06
$3.57 \pm 0.22 \pm 0.27$		128 AUBERT	03Z	BABR See AUBERT 07W
$4.04 \pm 0.85 \pm 0.25$	149	129 LINK	01	FOCS γ nucleus

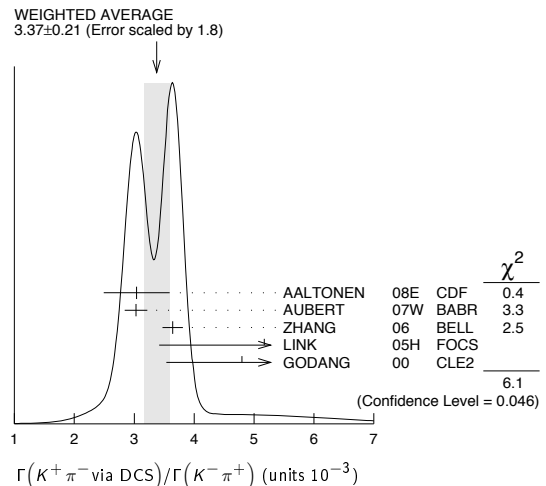
124 GODANG 00, ZHANG 06, and AALTONEN 08E allow CP violation.
 125 AITALA 98, LI 05A, and AUBERT 07W assume no CP violation.
 126 This LINK 05H result assumes no mixing but allows CP violation. If neither mixing nor CP violation is allowed, $R = (4.29 \pm 0.63 \pm 0.28) \times 10^{-3}$.
 127 This ABULENCIA 06X result assumes no mixing.
 128 This AUBERT 03Z result allows CP violation. If CP violation is not allowed, $R = 0.00359 \pm 0.00020 \pm 0.00027$.
 129 This LINK 01 result assumes no mixing or CP violation.



$\Gamma(K^+\pi^- \text{ via DCS})/\Gamma(K^-\pi^+)$ Γ_{208}/Γ_{31}
 This is R_D , the doubly Cabibbo-suppressed ratio when mixing is allowed.

VALUE (units 10^{-3})	CL%	EVTS	DOCUMENT ID	TECN	COMMENT
3.37 ± 0.21 OUR AVERAGE					Error includes scale factor of 1.8. See the ideogram below.
3.04 ± 0.55	$12.7 \pm 0.3k$		AALTONEN	08E	CDF $p\bar{p}, \sqrt{s} = 1.96$ TeV
$3.03 \pm 0.16 \pm 0.10$	4030 ± 90	130	AUBERT	07W	BABR $e^+e^- \approx 10.6$ GeV
3.64 ± 0.17	4024 ± 88	131	ZHANG	06	BELL e^+e^-
$5.17^{+1.47}_{-1.58} \pm 0.76$	234	132	LINK	05H	FOCS γ nucleus
$4.8 \pm 1.2 \pm 0.4$	45	133	GODANG	00	CLE2 e^+e^-
2.87 ± 0.37	845 ± 40		LI	05A	BELL See ZHANG 06
$2.3 < R_D < 5.2$	95		134 AUBERT	03Z	BABR See AUBERT 07W
$9.0^{+12.0}_{-10.9} \pm 4.4$	34	135	AITALA	98	E791 π^- nucl., 500 GeV

130 This AUBERT 07W result is the same whether or not CP violation is allowed.
 131 This ZHANG 06 assumes no CP violation.
 132 This LINK 05H result allows CP violation. Allowing mixing but not CP violation, $R_D = (3.81^{+1.67}_{-1.63} \pm 0.92) \times 10^{-3}$.
 133 This GODANG 00 result allows CP violation.
 134 This AUBERT 03Z result allows CP violation. If only mixing is allowed, the 95% confidence level interval is $(2.4 < R_D < 4.9) \times 10^{-3}$.
 135 This AITALA 98 result assumes no CP violation.



$\Gamma(K^+ \pi^- \text{ via } \bar{D}^0) / \Gamma(K^- \pi^+)$ $\Gamma_{209} / \Gamma_{31}$

This is R_M in the note on " D^0 - \bar{D}^0 Mixing" near the start of the D^0 Listings. The experiments here (1) use the charge of the pion in $D^*(2010)^\pm \rightarrow (D^0 \text{ or } \bar{D}^0) \pi^\pm$ decay to tell whether a D^0 or a \bar{D}^0 was born; and (2) use the decay-time distribution to disentangle doubly Cabibbo-suppressed decay and mixing. For the limits on $|m_1 - m_2|$ and $(\Gamma_1 - \Gamma_2) / \Gamma$ that come from the best mixing limit, see near the beginning of these D^0 Listings.

VALUE	CL%	EVTS	DOCUMENT ID	TECN	COMMENT
<0.00040	95		136 ZHANG	06 BELL	$e^+ e^-$
• • • We do not use the following data for averages, fits, limits, etc. • • •					
<0.00046	95	137	LI	05A BELL	See ZHANG 06
<0.0063	95	138	LINK	05H FOCs	γ nucleus
<0.0013	95	139	AUBERT	03z BABR	$e^+ e^-$, 10.6 GeV
<0.00041	95	140	GODANG	00 CLE2	$e^+ e^-$
<0.0092	95	141	BARATE	98W ALEP	$e^+ e^-$ at Z^0
<0.005	90	1 ± 4	142 ANJOS	88c E691	Photoproduction

136 This ZHANG 06 result allows CP violation, but the result does not change if CP violation is not allowed.

137 This LI 05A result allows CP violation. The limit becomes < 0.00042 (95% CL) if CP violation is not allowed.

138 LINK 05H obtains the same result whether or not CP violation is allowed.

139 This AUBERT 03z result allows CP violation and assumes that the strong phase between $D^0 \rightarrow K^+ \pi^-$ and $\bar{D}^0 \rightarrow K^+ \pi^-$ is small, and limits only $D^0 \rightarrow \bar{D}^0$ transitions via off-shell intermediate states. The limit on transitions via on-shell intermediate states is 0.0016.

140 This GODANG 00 result allows CP violation and assumes that the strong phase between $D^0 \rightarrow K^+ \pi^-$ and $\bar{D}^0 \rightarrow K^+ \pi^-$ is small, and limits only $D^0 \rightarrow \bar{D}^0$ transitions via off-shell intermediate states. The limit on transitions via on-shell intermediate states is 0.0017.

141 This BARATE 98W result assumes no interference between the DCS and mixing amplitudes ($\gamma = 0$ in the note on " D^0 - \bar{D}^0 Mixing" near the start of the D^0 Listings). When interference is allowed, the limit degrades to 0.036 (95% CL).

142 This ANJOS 88c result assumes no interference between the DCS and mixing amplitudes ($\gamma = 0$ in the note on " D^0 - \bar{D}^0 Mixing" near the start of the D^0 Listings). When interference is allowed, the limit degrades to 0.019.

 $\Gamma(K_S^0 \pi^+ \pi^- \text{ in } D^0 \rightarrow \bar{D}^0) / \Gamma(K_S^0 \pi^+ \pi^-)$ $\Gamma_{210} / \Gamma_{34}$

This is R_M in the note on " D^0 - \bar{D}^0 Mixing" near the start of the D^0 Listings. The experiments here (1) use the charge of the pion in $D^*(2010)^\pm \rightarrow (D^0 \text{ or } \bar{D}^0) \pi^\pm$ decay to tell whether a D^0 or a \bar{D}^0 was born; and (2) use the decay-time distribution to disentangle doubly Cabibbo-suppressed decay and mixing. For the limits on $|m_1 - m_2|$ and $(\Gamma_1 - \Gamma_2) / \Gamma$ that come from the best mixing limit, see near the beginning of these D^0 Listings.

VALUE	CL%	EVTS	DOCUMENT ID	TECN	COMMENT
<0.0063	95	143	ASNER	05 CLEO	$e^+ e^- \approx 10$ GeV

143 This ASNER 05 limit allows CP violation. If CP violation is not allowed, the limit is 0.0042 at 95% CL.

 $\Gamma(K^+ \pi^- \pi^0) / \Gamma(K^- \pi^+ \pi^0)$ $\Gamma_{214} / \Gamma_{49}$

The experiments here use the charge of the pion in $D^*(2010)^\pm \rightarrow (D^0 \text{ or } \bar{D}^0) \pi^\pm$ decay to tell whether a D^0 or a \bar{D}^0 was born. The $D^0 \rightarrow K^+ \pi^- \pi^0$ decay can occur directly by doubly Cabibbo-suppressed (DCS) decay, or indirectly by $D^0 \rightarrow \bar{D}^0$ mixing followed by $\bar{D}^0 \rightarrow K^+ \pi^- \pi^0$ decay.

VALUE (units 10^{-3})	CL%	EVTS	DOCUMENT ID	TECN	COMMENT
2.20 ± 0.10 OUR AVERAGE					
2.14 ± 0.08 ± 0.08	763 ± 51	144	AUBERT,B	06N BABR	$e^+ e^- \approx T(45)$
2.29 ± 0.15 ± 0.13	1978 ± 104		TIAN	05 BELL	$e^+ e^- \approx T(45)$
4.3 ± 1.1 ± 0.7	38		BRANDENB...	01 CLE2	$e^+ e^- \approx T(45)$

144 This AUBERT,B 06N result assumes no mixing.

 $\Gamma(K^+ \pi^- \pi^0 \text{ via } \bar{D}^0) / \Gamma(K^- \pi^+ \pi^0)$ $\Gamma_{215} / \Gamma_{49}$

This is R_M in the note on " D^0 - \bar{D}^0 Mixing" near the start of the D^0 Listings. The experiments here (1) use the charge of the pion in $D^*(2010)^\pm \rightarrow (D^0 \text{ or } \bar{D}^0) \pi^\pm$ decay to tell whether a D^0 or a \bar{D}^0 was born; and (2) use the decay-time distribution to disentangle doubly Cabibbo-suppressed decay and mixing. For the limits on $|m_1 - m_2|$ and $(\Gamma_1 - \Gamma_2) / \Gamma$ that come from the best mixing limit, see near the beginning of these D^0 Listings.

VALUE (units 10^{-3})	CL%	DOCUMENT ID	TECN	COMMENT
5.25 ± 0.25 ± 0.31 ± 0.12		AUBERT	09AN BABR	$e^+ e^-$ at 10.58 GeV

• • • We do not use the following data for averages, fits, limits, etc. • • •

<0.54 95 145 AUBERT,B 06N BABR $e^+ e^- \approx T(45)$

145 This AUBERT,B 06N limit assumes no CP violation. The measured value corresponding to the limit is $(2.3^{+1.8}_{-1.4} \pm 0.4) \times 10^{-4}$. If CP violation is allowed, this becomes $(1.0^{+2.2}_{-0.7} \pm 0.3) \times 10^{-4}$.

 $\Gamma(K^+ \pi^+ 2\pi^-) / \Gamma(K^- 2\pi^+ \pi^-)$ $\Gamma_{216} / \Gamma_{61}$

The experiments here use the charge of the pion in $D^*(2010)^\pm \rightarrow (D^0 \text{ or } \bar{D}^0) \pi^\pm$ decay to tell whether a D^0 or a \bar{D}^0 was born. The $D^0 \rightarrow K^+ \pi^- \pi^+ \pi^-$ decay can occur directly by doubly Cabibbo-suppressed (DCS) decay, or indirectly by $D^0 \rightarrow \bar{D}^0$ mixing followed by $\bar{D}^0 \rightarrow K^+ \pi^- \pi^+ \pi^-$ decay. Some of the experiments can use the decay-time information to disentangle the two mechanisms. Here, we list the experimental branching ratio, which if there is no mixing is the DCS ratio; in the next data block we give the limits on the mixing ratio.

Some early limits have been omitted from this Listing; see our 1998 edition (EPJ C3 1).

VALUE (units 10^{-3})	CL%	EVTS	DOCUMENT ID	TECN	COMMENT
3.24 ± 0.25 ± 0.18 ± 0.13 OUR AVERAGE					
3.20 ± 0.18 ± 0.13		1721 ± 75	146 TIAN	05 BELL	$e^+ e^- \approx T(45)$
4.4 ± 1.3 ± 1.2 ± 0.4		54	146 DYTMAN	01 CLE2	$e^+ e^- \approx T(45)$
2.5 ± 3.6 ± 3.4 ± 0.3			147 AITALA	98 E791	π^- nucl., 500 GeV

• • • We do not use the following data for averages, fits, limits, etc. • • •

<18 90 146 AMMAR 91 CLEO $e^+ e^- \approx 10.5$ GeV

<18 90 5 ± 12 148 ANJOS 88c E691 Photoproduction

146 AMMAR 91 cannot and DYTMAN 01 and TIAN 05 do not distinguish between doubly Cabibbo-suppressed decay and D^0 - \bar{D}^0 mixing.

147 This AITALA 98 result assumes no D^0 - \bar{D}^0 mixing (R_M in the note on " D^0 - \bar{D}^0 Mixing"). It becomes $-0.0020^{+0.0117}_{-0.0106} \pm 0.0035$ when mixing is allowed and decay-time information is used to distinguish doubly Cabibbo-suppressed decays from mixing.

148 ANJOS 88c uses decay-time information to distinguish doubly Cabibbo-suppressed (DCS) decays from D^0 - \bar{D}^0 mixing. However, the result assumes no interference between the DCS and mixing amplitudes ($\gamma = 0$ in the note on " D^0 - \bar{D}^0 Mixing" near the start of the D^0 Listings). When interference is allowed, the limit degrades to 0.033.

 $\Gamma(K^+ \pi^+ 2\pi^- \text{ via } \bar{D}^0) / \Gamma(K^- 2\pi^+ \pi^-)$ $\Gamma_{217} / \Gamma_{61}$

This is a D^0 - \bar{D}^0 mixing limit. The experiments here (1) use the charge of the pion in $D^*(2010)^\pm \rightarrow (D^0 \text{ or } \bar{D}^0) \pi^\pm$ decay to tell whether a D^0 or a \bar{D}^0 was born; and (2) use the decay-time distribution to disentangle doubly Cabibbo-suppressed decay and mixing. For the limits on $|m_{D_1^0} - m_{D_2^0}|$ and $(\Gamma_{D_1^0} - \Gamma_{D_2^0}) / \Gamma_{D^0}$ that come from the best mixing limit, see near the beginning of these D^0 Listings.

VALUE	CL%	EVTS	DOCUMENT ID	TECN	COMMENT
<0.005	90	0 ± 4	149 ANJOS	88c E691	Photoproduction

149 ANJOS 88c uses decay-time information to distinguish doubly Cabibbo-suppressed (DCS) decays from D^0 - \bar{D}^0 mixing. However, the result assumes no interference between the DCS and mixing amplitudes ($\gamma = 0$ in the note on " D^0 - \bar{D}^0 Mixing" near the start of the D^0 Listings). When interference is allowed, the limit degrades to 0.007.

 $\Gamma(K^+ \pi^- \text{ or } K^+ \pi^+ 2\pi^- \text{ via } \bar{D}^0) / \Gamma(K^- \pi^+ \text{ or } K^- 2\pi^+ \pi^-)$ $\Gamma_{218} / \Gamma_{60}$

This is a D^0 - \bar{D}^0 mixing limit. For the limits on $|m_{D_1^0} - m_{D_2^0}|$ and $(\Gamma_{D_1^0} - \Gamma_{D_2^0}) / \Gamma_{D^0}$ that come from the best mixing limit, see near the beginning of these D^0 Listings.

VALUE	CL%	DOCUMENT ID	TECN	COMMENT
<0.0085	90	150 AITALA	98 E791	π^- nucleus, 500 GeV
<0.0037	90	151 ANJOS	88c E691	Photoproduction

• • • We do not use the following data for averages, fits, limits, etc. • • •

<0.0085 90 150 AITALA 98 E791 π^- nucleus, 500 GeV

<0.0037 90 151 ANJOS 88c E691 Photoproduction

150 AITALA 98 uses decay-time information to distinguish doubly Cabibbo-suppressed decays from D^0 - \bar{D}^0 mixing. The fit allows interference between the two amplitudes, and also allows CP violation in this term. The central value obtained is $0.0039^{+0.0036}_{-0.0032} \pm 0.0016$. When interference is disallowed, the result becomes $0.0021 \pm 0.0009 \pm 0.0002$.

151 This combines results of ANJOS 88c on $K^+ \pi^-$ and $K^+ \pi^- \pi^+ \pi^-$ (via \bar{D}^0) reported in the data block above (see footnotes there). It assumes no interference.

 $\Gamma(\mu^- \text{ anything via } \bar{D}^0) / \Gamma(\mu^+ \text{ anything})$ $\Gamma_{219} / \Gamma_{6}$

This is a D^0 - \bar{D}^0 mixing limit. See the somewhat better limits above.

VALUE	CL%	DOCUMENT ID	TECN	COMMENT
<0.0056	90	LOUIS	86 SPEC	π^- W 225 GeV

• • • We do not use the following data for averages, fits, limits, etc. • • •

<0.012 90 BENVENUTI 85 CNTR μ C, 200 GeV

<0.044 90 BODEK 82 SPEC π^- , pFe $\rightarrow D^0$

Rare or forbidden modes

 $\Gamma(\gamma\gamma) / \Gamma(2\pi^0)$ $\Gamma_{220} / \Gamma_{127}$

$D^0 \rightarrow \gamma\gamma$ is a flavor-changing neutral-current decay, forbidden in the Standard Model at the tree level.

VALUE	CL%	DOCUMENT ID	TECN	COMMENT
<0.033	90	COAN	03 CLE2	$e^+ e^- \approx T(45)$

See key on page 405

Meson Particle Listings

$$D^*(2010)^\pm, D_0^*(2400)^0, D_0^*(2400)^\pm$$

$\Gamma(D^+\pi^0)/\Gamma_{\text{total}}$					Γ_2/Γ
VALUE	EVTs	DOCUMENT ID	TECN	COMMENT	
0.307 ± 0.005 OUR FIT					
0.3073 ± 0.0013 ± 0.0062		6,7,8 BARTELT	98 CLE2	e^+e^-	
●●● We do not use the following data for averages, fits, limits, etc. ●●●					
0.312 ± 0.011 ± 0.008	1404	ALBRECHT	95F ARG	$e^+e^- \rightarrow$ hadrons	
0.308 ± 0.004 ± 0.008	410	6 BUTLER	92 CLE2	$e^+e^- \rightarrow$ hadrons	
0.26 ± 0.02 ± 0.02		ADLER	88D MRK3	e^+e^-	
0.34 ± 0.07		COLES	82 MRK2	e^+e^-	

$\Gamma(D^+\gamma)/\Gamma_{\text{total}}$					Γ_3/Γ
VALUE	CL%	EVTs	DOCUMENT ID	TECN	COMMENT
0.016 ± 0.004 OUR FIT					
0.016 ± 0.005 OUR AVERAGE					
0.0168 ± 0.0042 ± 0.0029			6,7 BARTELT	98 CLE2	e^+e^-
0.011 ± 0.014 ± 0.016	12		6 BUTLER	92 CLE2	$e^+e^- \rightarrow$ hadrons
●●● We do not use the following data for averages, fits, limits, etc. ●●●					
<0.052	90		ALBRECHT	95F ARG	$e^+e^- \rightarrow$ hadrons
0.17 ± 0.05 ± 0.05			ADLER	88D MRK3	e^+e^-
0.22 ± 0.12			9 COLES	82 MRK2	e^+e^-

6 The branching ratios are not independent, they have been constrained by the authors to sum to 100%.
7 Systematic error includes theoretical error on the prediction of the ratio of hadronic modes.
8 Assuming that isospin is conserved in the decay.
9 Not independent of $\Gamma(D^0\pi^+)/\Gamma_{\text{total}}$ and $\Gamma(D^+\pi^0)/\Gamma_{\text{total}}$ measurement.

 $D^*(2010)^\pm$ REFERENCES

ANASTASSOV	02	PR D65 032003	A. Anastassov et al.	(CLEO Collab.)
ADINOLFI	99	NP B547 3	M. Adinolfi et al.	(Beatrice Collab.)
BREITWEG	99	EPJ C6 67	J. Breitweg et al.	(ZEUS Collab.)
BARTELT	98	PRL 80 3919	J. Bartelt et al.	(CLEO II Collab.)
ADLOFF	97B	ZPHY C72 593	C. Adloff et al.	(H1 Collab.)
BREITWEG	97	PL B401 192	J. Breitweg et al.	(ZEUS Collab.)
BREITWEG	97B	PL B407 402	J. Breitweg et al.	(ZEUS Collab.)
ALBRECHT	95F	ZPHY C66 63	H. Albrecht et al.	(ARGUS Collab.)
DERRICK	95	PL B349 225	M. Derrick et al.	(ZEUS Collab.)
BARLAG	92B	PL B278 480	S. Barlag et al.	(ACCMOR Collab.)
BORTOLETTO	92B	PRL 69 2046	D. Bortoletto et al.	(CLEO Collab.)
BUTLER	92	PRL 69 2041	F. Butler et al.	(CLEO Collab.)
ALEXANDER	91B	PL B262 341	G. Alexander et al.	(OPAL Collab.)
DECAMP	91J	PL B266 218	D. Decamp et al.	(ALEPH Collab.)
ABACHI	88B	PL B212 533	S. Abachi et al.	(ANL, IND, MICH, PURD+)
ADLER	88D	PL B208 152	J. Adler et al.	(Mark III Collab.)
ALBRECHT	85F	PL 150B 235	H. Albrecht et al.	(ARGUS Collab.)
AHLEN	83	PRL 51 1147	S.P. Ahlen et al.	(ANL, IND, LBL+)
BAILEY	83	PL 132B 230	R. Bailey et al.	(AMST, BRIS, CERN, CRAC+)
COLES	82	PR D26 2190	M.W. Coles et al.	(LBL, SLAC)
YELTON	82	PRL 49 430	J.M. Yelton et al.	(SLAC, LBL, UCB+)
FITCH	81	PRL 46 761	V.L. Fitch et al.	(PRIN, SAACL, TORI+)
AVERY	80	PRL 44 1309	P. Avery et al.	(ILL, FNAL, COLLU)
BLIETSCHAU	79	PL 86B 108	J. Bletschau et al.	(AACH3, BONN, CERN+)
FELDMAN	77B	PRL 38 1313	G.J. Feldman et al.	(Mark I Collab.)
GOLDBABER	77	PL 69B 503	G. Goldhaber et al.	(Mark I Collab.)
PERUZZI	77	PRL 39 1301	I. Peruzzi et al.	(LGW Collab.)

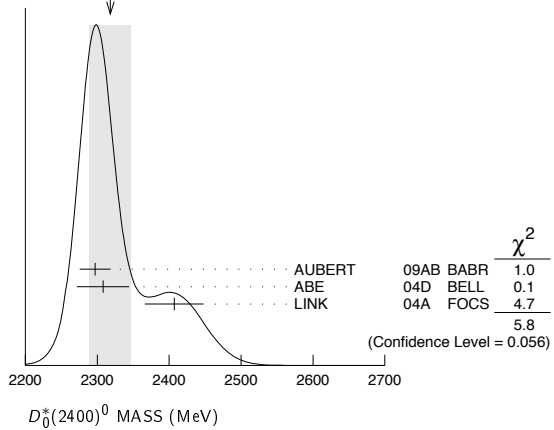
 $D_0^*(2400)^0$

$$I(J^P) = \frac{1}{2}(0^+)$$

$J = 0^+$ assignment favoured (ABE 04D).

 $D_0^*(2400)^0$ MASS

VALUE (MeV)	EVTs	DOCUMENT ID	TECN	COMMENT	
2318 ± 29 OUR AVERAGE		Error includes scale factor of 1.7. See the ideogram below.			
2297 ± 8 ± 20	3.4k	AUBERT	09AB BABR	$B^- \rightarrow D^+\pi^-\pi^-$	
2308 ± 17 ± 32		ABE	04D BELL	$B^- \rightarrow D^+\pi^-\pi^-$	
2407 ± 21 ± 35	9.8k	LINK	04A FOCS	γA	

WEIGHTED AVERAGE
2318±29 (Error scaled by 1.7) $D_0^*(2400)^0$ WIDTH

VALUE (MeV)	EVTs	DOCUMENT ID	TECN	COMMENT
267 ± 40 OUR AVERAGE				
273 ± 12 ± 48	3.4k	AUBERT	09AB BABR	$B^- \rightarrow D^+\pi^-\pi^-$
276 ± 21 ± 63		ABE	04D BELL	$B^- \rightarrow D^+\pi^-\pi^-$
240 ± 55 ± 59	9.8k	LINK	04A FOCS	γA

 $D_0^*(2400)^0$ DECAY MODES

Mode	Fraction (Γ_i/Γ)
$\Gamma_1 D^+\pi^-$	seen

 $D_0^*(2400)^0$ REFERENCES

AUBERT	09AB	PR D79 112004	B. Aubert et al.	(BABAR Collab.)
ABE	04D	PR D69 112002	K. ABE et al.	(BELLE Collab.)
LINK	04A	PL B586 11	J.M. Link et al.	(FOCUS Collab.)

 $D_0^*(2400)^\pm$

$$I(J^P) = \frac{1}{2}(0^+)$$

OMITTED FROM SUMMARY TABLE
 J, P need confirmation.

 $D_0^*(2400)^\pm$ MASS

VALUE (MeV)	EVTs	DOCUMENT ID	TECN	COMMENT
2403 ± 14 ± 35	18.8k	LINK	04A FOCS	γA

 $D_0^*(2400)^\pm$ WIDTH

VALUE (MeV)	EVTs	DOCUMENT ID	TECN	COMMENT
283 ± 24 ± 34	18.8k	LINK	04A FOCS	γA

 $D_0^*(2400)^\pm$ DECAY MODES

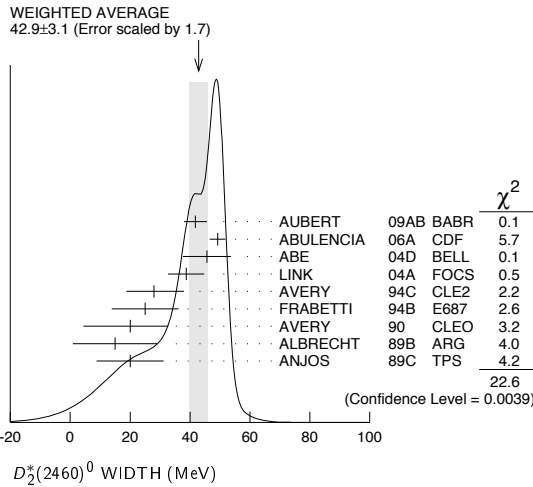
Mode	Fraction (Γ_i/Γ)
$\Gamma_1 D^0\pi^+$	seen

 $D_0^*(2400)^\pm$ REFERENCES

LINK	04A	PL B586 11	J.M. Link et al.	(FOCUS Collab.)
------	-----	------------	------------------	-----------------

Meson Particle Listings

$D_2^*(2460)^0, D_2^*(2460)^\pm$



$D_2^*(2460)^0$ WIDTH (MeV)

$D_2^*(2460)^0$ DECAY MODES

$\bar{D}_2^*(2460)^0$ modes are charge conjugates of modes below.

Mode	Fraction (Γ_i/Γ)
Γ_1 $D^+\pi^-$	seen
Γ_2 $D^*(2010)^+\pi^-$	seen
Γ_3 $D^0\pi^+\pi^-$	not seen
Γ_4 $D^{*0}\pi^+\pi^-$	not seen

$D_2^*(2460)^0$ BRANCHING RATIOS

$\Gamma(D^+\pi^-)/\Gamma_{total}$		Γ_1/Γ	
VALUE	EVTS	DOCUMENT ID	TEC/N
seen	3.4k	AUBERT	09AB BABR
seen	337	ALBRECHT	89B ARG
seen		ANJOS	89C TPS

$\Gamma(D^*(2010)^+\pi^-)/\Gamma_{total}$		Γ_2/Γ	
VALUE	TEC/N	DOCUMENT ID	COMMENT
seen		ACKERSTAFF	97W OPAL
seen		AVERY	90 CLEO
seen		ALBRECHT	89H ARG

$\Gamma(D^+\pi^-)/\Gamma(D^*(2010)^+\pi^-)$		Γ_1/Γ_2	
VALUE	EVTS	DOCUMENT ID	TEC/N

VALUE	EVTS	DOCUMENT ID	TEC/N	COMMENT
2.8±0.8±0.5	1560±230	CHEKANOV	09 ZEUS	$e^\pm p \rightarrow D^{(*)}\pi^- X$
2.2±0.7±0.6		AVERY	94C CLE2	$e^+e^- \rightarrow D^{*+}\pi^- X$
2.3±0.8		AVERY	90 CLEO	e^+e^-
3.0±1.1±1.5		ALBRECHT	89H ARG	$e^+e^- \rightarrow D^*\pi^- X$

• • • We do not use the following data for averages, fits, limits, etc. • • •

VALUE	EVTS	DOCUMENT ID	TEC/N	COMMENT
1.9±0.5		ABE	04D BELL	$B^- \rightarrow D^{(*)}\pi^- \pi^-$

VALUE	EVTS	DOCUMENT ID	TEC/N	COMMENT
0.62±0.03±0.02	8414	AUBERT	09Y BABR	$B^+ \rightarrow D_2^{*0} \ell^+ \nu_\ell$

⁵ Assuming $\Gamma(\Upsilon(4S) \rightarrow B^+ B^-) / \Gamma(\Upsilon(4S) \rightarrow B^0 \bar{B}^0) = 1.065 \pm 0.026$ and equal partial widths for charged and neutral D_2^* mesons.

$D_2^*(2460)^0$ REFERENCES

AUBERT	09AB PR D79 112004	B. Aubert et al.	(BABAR Collab.)
AUBERT	09Y PRL 103 051803	B. Aubert et al.	(BABAR Collab.)
CHEKANOV	09 EPJ C60 25	S. Chekanov et al.	(ZEUS Collab.)
ABULENCIA	06A PR D73 051104	A. Abulencia et al.	(CDF Collab.)
ABE	04D PR D69 112002	K. Abe et al.	(BELLE Collab.)
LINK	04A PL B586 11	J.M. Link et al.	(FOCUS Collab.)
ABREU	98M PL B426 231	P. Abreu et al.	(DELPHI Collab.)
ACKERSTAFF	97W ZPHY C76 425	K. Ackerstaff et al.	(OPAL Collab.)
ASRATYAN	95 ZPHY C68 43	A.E. Asratyan et al.	(BIRM, BELG, CERN+)
AVERY	94C PL B331 236	P. Avery et al.	(CLEO Collab.)
FRABETTI	94B PRL 72 324	P.L. Frabetti et al.	(FNAL E687 Collab.)
AVERY	90 PR D41 774	P. Avery, D. Besson	(CLEO Collab.)
ALBRECHT	89B PL B221 422	H. Albrecht et al.	(ARGUS Collab.) JP
ALBRECHT	89H PL B232 398	H. Albrecht et al.	(ARGUS Collab.) JP
ANJOS	89C PRL 62 1717	J.C. Anjos et al.	(FNAL E691 Collab.)

$D_2^*(2460)^\pm$

$I(J^P) = \frac{1}{2}(2^+)$

$J^P = 2^+$ assignment strongly favored (ALBRECHT 89B).

$D_2^*(2460)^\pm$ MASS

VALUE (MeV)	EVTS	DOCUMENT ID	TEC/N	COMMENT
-------------	------	-------------	-------	---------

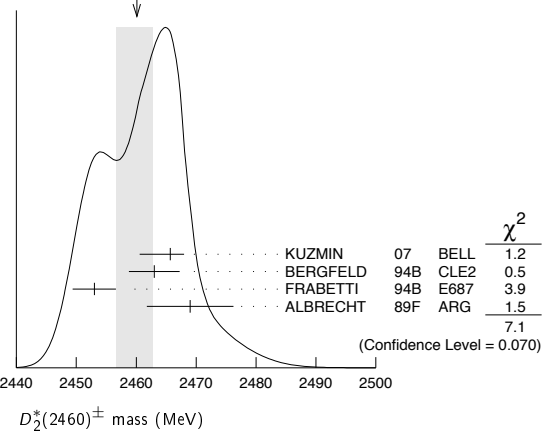
2460.1±3.5 OUR AVERAGE Error includes scale factor of 1.5. See the ideogram below.

2465.7±1.8±1.4	2909	KUZMIN	07 BELL	$e^+e^- \rightarrow$ hadrons
2463 ±3 ±3	310	BERGFELD	94B CLE2	$e^+e^- \rightarrow D^0\pi^+X$
2453 ±3 ±2	185	FRABETTI	94B E687	$\gamma Be \rightarrow D^0\pi^+X$
2469 ±4 ±6		ALBRECHT	89F ARG	$e^+e^- \rightarrow D^0\pi^+X$

• • • We do not use the following data for averages, fits, limits, etc. • • •

2467.6±1.5±0.8 3.5k LINK 04A FOCS γA
¹ Fit includes the contribution from $D_0^*(2400)^\pm$. Not independent of the corresponding mass difference measurement, $(m_{D_2^*(2460)^\pm} - m_{D_2^*(2460)^0})$.

WEIGHTED AVERAGE
2460.1±2.6-3.5 (Error scaled by 1.5)



$D_2^*(2460)^\pm$ mass (MeV)

$m_{D_2^*(2460)^\pm} - m_{D_2^*(2460)^0}$

VALUE (MeV)	EVTS	DOCUMENT ID	TEC/N	COMMENT
-------------	------	-------------	-------	---------

2.4±1.7 OUR AVERAGE

3.1±1.9±0.9		LINK	04A FOCS	γA
- 2 ±4 ±4		BERGFELD	94B CLE2	$e^+e^- \rightarrow$ hadrons
0 ±4		FRABETTI	94B E687	$\gamma Be \rightarrow D\pi X$
14 ±5 ±8		ALBRECHT	89F ARG	$e^+e^- \rightarrow D^0\pi^+X$

$D_2^*(2460)^\pm$ WIDTH

VALUE (MeV)	EVTS	DOCUMENT ID	TEC/N	COMMENT
-------------	------	-------------	-------	---------

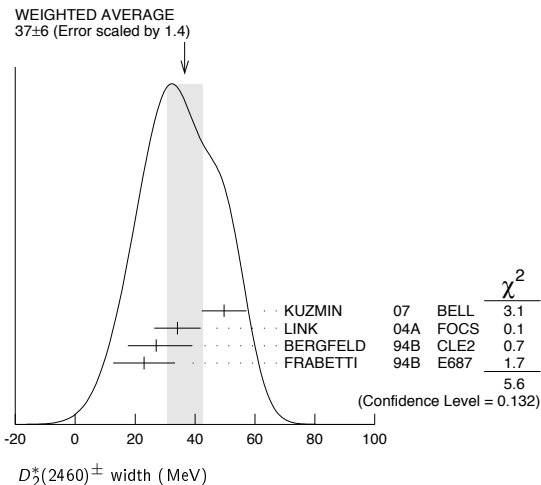
37 ± 6 OUR AVERAGE Error includes scale factor of 1.4. See the ideogram below.

49.7± 3.8±6.4	2909	KUZMIN	07 BELL	$e^+e^- \rightarrow$ hadrons
34.1± 6.5±4.2	3.5k	LINK	04A FOCS	γA
27 ±11 ±5	310	BERGFELD	94B CLE2	$e^+e^- \rightarrow D^0\pi^+X$
23 ± 9 ±5	185	FRABETTI	94B E687	$\gamma Be \rightarrow D^0\pi^+X$

² Fit includes the contribution from $D_0^*(2400)^\pm$.

See key on page 405

Meson Particle Listings

 $D_2^*(2460)^\pm, D^*(2640)^\pm$  $D_2^*(2460)^\pm$ DECAY MODES $D_2^*(2460)^\pm$ modes are charge conjugates of modes below.

Mode	Fraction (Γ_i/Γ)
Γ_1 $D^0 \pi^+$	seen
Γ_2 $D^{*0} \pi^+$	seen
Γ_3 $D^+ \pi^+ \pi^-$	not seen
Γ_4 $D^{*+} \pi^+ \pi^-$	not seen

 $D_2^*(2460)^\pm$ BRANCHING RATIOS

$\Gamma(D^0 \pi^+)/\Gamma_{\text{total}}$	Γ_1/Γ		
VALUE	DOCUMENT ID	TECN	COMMENT
seen	ALBRECHT	89F	ARG $e^+ e^- \rightarrow D^0 \pi^+ X$

$\Gamma(D^0 \pi^+)/\Gamma(D^{*0} \pi^+)$	Γ_1/Γ_2		
VALUE	DOCUMENT ID	TECN	COMMENT
$1.9 \pm 1.1 \pm 0.3$	BERGFELD	94B	CLE2 $e^+ e^- \rightarrow$ hadrons

$\Gamma(D^0 \pi^+)/[\Gamma(D^0 \pi^+) + \Gamma(D^{*0} \pi^+)]$	$\Gamma_1/(\Gamma_1 + \Gamma_2)$			
VALUE	EVTS	DOCUMENT ID	TECN	COMMENT

• • • We do not use the following data for averages, fits, limits, etc. • • •

0.62±0.03±0.02 3361 ³AUBERT 09Y BABR $\bar{B}^0 \rightarrow D_2^{*+} \ell^- \nu_\ell$ ³ Assuming $\Gamma(\Upsilon(4S) \rightarrow B^+ B^-) / \Gamma(\Upsilon(4S) \rightarrow B^0 \bar{B}^0) = 1.065 \pm 0.026$ and equal partial widths for charged and neutral D_2^* mesons. $D_2^*(2460)^\pm$ REFERENCES

AUBERT	09Y	PRL 103 051803	B. Aubert <i>et al.</i>	(BABAR Collab.)
KUZMIN	07	PR D76 012006	A. Kuzmin <i>et al.</i>	(BELLE Collab.)
LINK	04A	PL B586 11	J.M. Link <i>et al.</i>	(FOCUS Collab.)
BERGFELD	94B	PL B340 194	T. Bergfeld <i>et al.</i>	(CLEO Collab.)
FRABETTI	94B	PRL 72 324	P.L. Frabetti <i>et al.</i>	(FNAL E687 Collab.)
ALBRECHT	89B	PL B221 422	H. Albrecht <i>et al.</i>	(ARGUS Collab.)
ALBRECHT	89F	PL B231 208	H. Albrecht <i>et al.</i>	(ARGUS Collab.)

 $D^*(2640)^\pm$

$I(J^P) = \frac{1}{2}(??)$

OMITTED FROM SUMMARY TABLE

Seen in Z decays by ABREU 98M. Not seen by ABBIENDI 01N and CHEKANOV 09. Needs confirmation.

 $D^*(2640)^\pm$ MASS

VALUE (MeV)	EVTS	DOCUMENT ID	TECN	COMMENT
$2637 \pm 2 \pm 6$	66 ± 14	ABREU	98M	DLPH $e^+ e^- \rightarrow D^{*+} \pi^+ \pi^- X$

 $D^*(2640)^\pm$ WIDTH

VALUE (MeV)	CL%	DOCUMENT ID	TECN	COMMENT
<15	95	ABREU	98M	DLPH $e^+ e^- \rightarrow D^{*+} \pi^+ \pi^- X$

 $D^*(2640)^\pm$ DECAY MODES $D^*(2640)^\pm$ modes are charge conjugates of modes below.

Mode	Fraction (Γ_i/Γ)
Γ_1 $D^*(2010)^+ \pi^+ \pi^-$	seen

 $D^*(2640)^\pm$ REFERENCES

CHEKANOV	09	EPJ C60 25	S. Chekanov <i>et al.</i>	(ZEUS Collab.)
ABBIENDI	01N	EPJ C20 445	G. Abbiendi <i>et al.</i>	(OPAL Collab.)
ABREU	98M	PL B426 231	P. Abreu <i>et al.</i>	(DELPHI Collab.)

Meson Particle Listings

D_s^\pm

CHARMED, STRANGE MESONS ($C = S = \pm 1$)

$D_s^+ = c\bar{s}$, $D_s^- = \bar{c}s$, similarly for $D_s^{* \prime s}$

D_s^\pm

$$I(J^P) = 0(0^-)$$

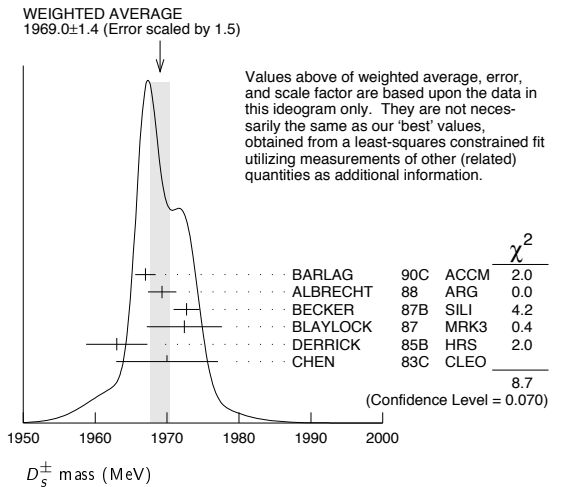
The angular distributions of the decays of the ϕ and $\bar{K}^*(892)^0$ in the $\phi\pi^+$ and $K^+\bar{K}^*(892)^0$ modes strongly indicate that the spin is zero. The parity given is that expected of a $c\bar{s}$ ground state.

D_s^\pm MASS

The fit includes D_s^\pm , D^0 , $D_s^{*\pm}$, D^{*0} , $D_s^{* \prime \pm}$, $D_1(2420)^0$, $D_2^*(2460)^0$, and $D_{s1}(2536)^\pm$ mass and mass difference measurements. Measurements of the D_s^\pm mass with an error greater than 10 MeV are omitted from the fit and average. A number of early measurements have been omitted altogether.

VALUE (MeV)	EVTS	DOCUMENT ID	TECN	COMMENT
1968.47 ± 0.33 OUR FIT	Error includes scale factor of 1.3.			
1969.0 ± 1.4 OUR AVERAGE	Error includes scale factor of 1.5. See the ideogram below.			
1967.0 ± 1.0 ± 1.0	54	BARLAG	90c ACCM	π^- Cu 230 GeV
1969.3 ± 1.4 ± 1.4		ALBRECHT	88 ARG	e^+e^- 9.4–10.6 GeV
1972.7 ± 1.5 ± 1.0	21	BECKER	87B SILI	200 GeV π, K, p
1972.4 ± 3.7 ± 3.7	27	BLAYLOCK	87 MRK3	e^+e^- 4.14 GeV
1963 ± 3 ± 3	30	DERRICK	85B HRS	e^+e^- 29 GeV
1970 ± 5 ± 5	104	CHEN	83c CLEO	e^+e^- 10.5 GeV
• • • We do not use the following data for averages, fits, limits, etc. • • •				
1968.3 ± 0.7 ± 0.7	290	¹ ANJOS	88 E691	Photoproduction
1980 ± 15	6	USHIDA	86 EMUL	ν wideband
1973.6 ± 2.6 ± 3.0	163	ALBRECHT	85D ARG	e^+e^- 10 GeV
1948 ± 28 ± 10	65	AIHARA	84D TPC	e^+e^- 29 GeV
1975 ± 9 ± 10	49	ALTHOFF	84 TASS	e^+e^- 14–25 GeV
1975 ± 4	3	BAILEY	84 ACCM	hadron $^+$ Be \rightarrow $\phi\pi^+X$

¹ ANJOS 88 enters the fit via $m_{D_s^\pm} - m_{D^\pm}$ (see below).



The fit includes D_s^\pm , D^0 , $D_s^{*\pm}$, D^{*0} , $D_s^{* \prime \pm}$, $D_1(2420)^0$, $D_2^*(2460)^0$, and $D_{s1}(2536)^\pm$ mass and mass difference measurements.

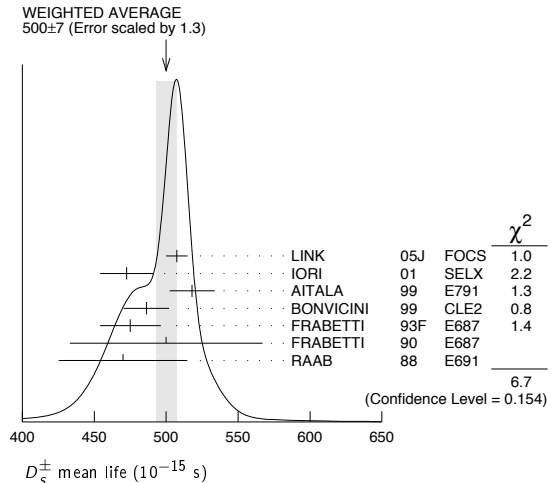
VALUE (MeV)	EVTS	DOCUMENT ID	TECN	COMMENT
98.88 ± 0.30 OUR FIT	Error includes scale factor of 1.4.			
98.85 ± 0.25 OUR AVERAGE	Error includes scale factor of 1.1.			
99.41 ± 0.38 ± 0.21		ACOSTA	03D CDF2	$\bar{p}p$, $\sqrt{s} = 1.96$ TeV
98.4 ± 0.1 ± 0.3	48k	AUBERT	02G BABR	$e^+e^- \approx \Upsilon(4S)$
99.5 ± 0.6 ± 0.3		BROWN	94 CLE2	$e^+e^- \approx \Upsilon(4S)$
98.5 ± 1.5	555	CHEN	89 CLEO	e^+e^- 10.5 GeV
99.0 ± 0.8	290	ANJOS	88 E691	Photoproduction

D_s^\pm MEAN LIFE

Measurements with an error greater than 100×10^{-15} s or with fewer than 100 events have been omitted from the Listings.

VALUE (10^{-15} s)	EVTS	DOCUMENT ID	TECN	COMMENT
500 ± 7 OUR AVERAGE	Error includes scale factor of 1.3. See the ideogram below.			
507.4 ± 5.5 ± 5.1	13.6k	LINK	05J FOCS	$\phi\pi^+$ and $\bar{K}^{*0}K^+$
472.5 ± 17.2 ± 6.6	760	IORI	01 SELX	600 GeV Σ^-, π^-, p
518 ± 14 ± 7	1662	AITALA	99 E791	π^- nucleus, 500 GeV
486.3 ± 15.0 ^{+4.9} - 5.1	2167	² BONVICINI	99 CLE2	$e^+e^- \approx \Upsilon(4S)$
475 ± 20 ± 7	900	FRABETTI	93F E687	γ Be, $\phi\pi^+$
500 ± 60 ± 30	104	FRABETTI	90 E687	γ Be, $\phi\pi^+$
470 ± 40 ± 20	228	RAAB	88 E691	Photoproduction

² BONVICINI 99 obtains 1.19 ± 0.04 for the ratio of D_s^+ to D^0 lifetimes.



D_s^\pm DECAY MODES

Unless otherwise noted, the branching fractions for modes with a resonance in the final state include all the decay modes of the resonance. D_s^- modes are charge conjugates of the modes below.

Mode	Fraction (Γ_i/Γ)	Scale factor/ Confidence level
Inclusive modes		
Γ_1 e^+ semileptonic	[a] (6.5 ± 0.4) %	
Γ_2 π^+ anything	(119.3 ± 1.4) %	
Γ_3 π^- anything	(43.2 ± 0.9) %	
Γ_4 π^0 anything	(123 ± 7) %	
Γ_5 K^- anything	(18.7 ± 0.5) %	
Γ_6 K^+ anything	(28.9 ± 0.7) %	
Γ_7 K_S^0 anything	(19.0 ± 1.1) %	
Γ_8 η anything	[b] (29.9 ± 2.8) %	
Γ_9 ω anything	(6.1 ± 1.4) %	
Γ_{10} η' anything	[c] (11.7 ± 1.8) %	
Γ_{11} $f_0(980)$ anything, $f_0 \rightarrow \pi^+\pi^-$	< 1.3	CL=90%
Γ_{12} ϕ anything	(15.7 ± 1.0) %	
Γ_{13} K^+K^- anything	(15.8 ± 0.7) %	
Γ_{14} $K_S^0K^+$ anything	(5.8 ± 0.5) %	
Γ_{15} $K_S^0K^-$ anything	(1.9 ± 0.4) %	
Γ_{16} $2K_S^0$ anything	(1.70 ± 0.32) %	
Γ_{17} $2K^+$ anything	< 2.6	$\times 10^{-3}$ CL=90%
Γ_{18} $2K^-$ anything	< 6	$\times 10^{-4}$ CL=90%
Leptonic and semileptonic modes		
Γ_{19} $e^+\nu_e$	< 1.2	$\times 10^{-4}$ CL=90%
Γ_{20} $\mu^+\nu_\mu$	(5.8 ± 0.4) $\times 10^{-3}$	
Γ_{21} $\tau^+\nu_\tau$	(5.6 ± 0.4) %	
Γ_{22} $K^+K^-e^+\nu_e$	—	
Γ_{23} $\phi e^+\nu_e$	[d] (2.49 ± 0.14) %	
Γ_{24} $\eta e^+\nu_e + \eta'(958) e^+\nu_e$	[d] (3.66 ± 0.37) %	
Γ_{25} $\eta e^+\nu_e$	[d] (2.67 ± 0.29) %	S=1.1
Γ_{26} $\eta'(958) e^+\nu_e$	[d] (9.9 ± 2.3) $\times 10^{-3}$	
Γ_{27} $K^0 e^+\nu_e$	(3.7 ± 1.0) $\times 10^{-3}$	
Γ_{28} $K^*(892)^0 e^+\nu_e$	[d] (1.8 ± 0.7) $\times 10^{-3}$	
Γ_{29} $f_0(980) e^+\nu_e, f_0 \rightarrow \pi^+\pi^-$	(2.00 ± 0.32) $\times 10^{-3}$	

Meson Particle Listings

D_s^\pm

CONSTRAINED FIT INFORMATION

An overall fit to 17 branching ratios uses 18 measurements and one constraint to determine 13 parameters. The overall fit has a $\chi^2 = 2.1$ for 6 degrees of freedom.

The following *off-diagonal* array elements are the correlation coefficients $\langle \delta x_i \delta x_j \rangle / (\delta x_i \delta x_j)$, in percent, from the fit to the branching fractions, $x_i \equiv \Gamma_i / \Gamma_{\text{total}}$. The fit constrains the x_i whose labels appear in this array to sum to one.

x_{25}	16																		
x_{26}	12	2																	
x_{30}	0	0	0																
x_{31}	0	0	0	76															
x_{41}	0	0	0	42	48														
x_{43}	0	0	0	51	59	32													
x_{54}	0	0	0	59	74	37	45												
x_{64}	0	0	0	38	43	23	29	33											
x_{65}	0	0	0	11	12	6	8	9	28										
x_{73}	0	0	0	46	53	31	37	40	27	8									
x_{83}	0	0	0	37	44	22	28	33	20	6									
x_{113}	-17	-25	-20	-69	-79	-71	-57	-62	-51	-19									

x_{83}	25																		
x_{113}	-68	-40																	

D_s^+ BRANCHING FRACTIONS

Written April 2010 by J.L. Rosner (University of Chicago) and C.G. Wohl (LBNL).

More than a dozen papers on the D_s^+ , most of them from the CLEO experiment, have been published since the 2008 Review. We now know enough to attempt an overview of the branching fractions. Figure 1 shows a partial breakdown of the fractions. The rest of this note is about how the figure was constructed. The values shown make heavy use of CLEO measurements of inclusive branching fractions [1]. For other data and references cited in the following, see the Listings.

Modes with leptons: The bottom $(20.0 \pm 0.9)\%$ of Fig. 1 shows the fractions for the exclusive modes that include leptons. Measured $e^+\nu_e$ fractions have been doubled to get the semileptonic $\ell^+\nu$ fractions. The sum of the exclusive $e^+\nu_e$ fractions is $(6.9 \pm 0.4)\%$, consistent with an inclusive semileptonic $e^+\nu_e$ measurement of $(6.5 \pm 0.4)\%$. There seems to be little missing here.

Inclusive hadronic $K\bar{K}$ fractions: The Cabibbo-favored $c \rightarrow s$ decay in D_s^+ decay produces a final state with both an s and an \bar{s} ; and thus decay modes with a $K\bar{K}$ pair or with an η , ω , η' , or ϕ predominate (see, for example, in Fig. 1 the fractions with leptons). We consider the $K\bar{K}$ modes first. A complete picture of the exclusive $K\bar{K}$ charge modes is not yet possible, because branching fractions for more than half of those modes have yet to be measured. However, CLEO has measured the inclusive K^+ , K^- , K_S^0 , K^+K^- , $K^+K_S^0$, $K^-K_S^0$, and $2K_S^0$ fractions (which include modes with leptons) [1]. And each of these inclusive fractions f with a K_S^0 is equal to the corresponding fraction with a K_L^0 : $f(K^+K_L^0) = f(K^+K_S^0)$, $f(2K_L^0) = f(2K_S^0)$, etc. Therefore, of all inclusive fractions pairing a K^+ , K_S^0 , or K_L^0 with a K^- , K_S^0 , or K_L^0 , we know all but $f(K_S^0K_L^0)$.

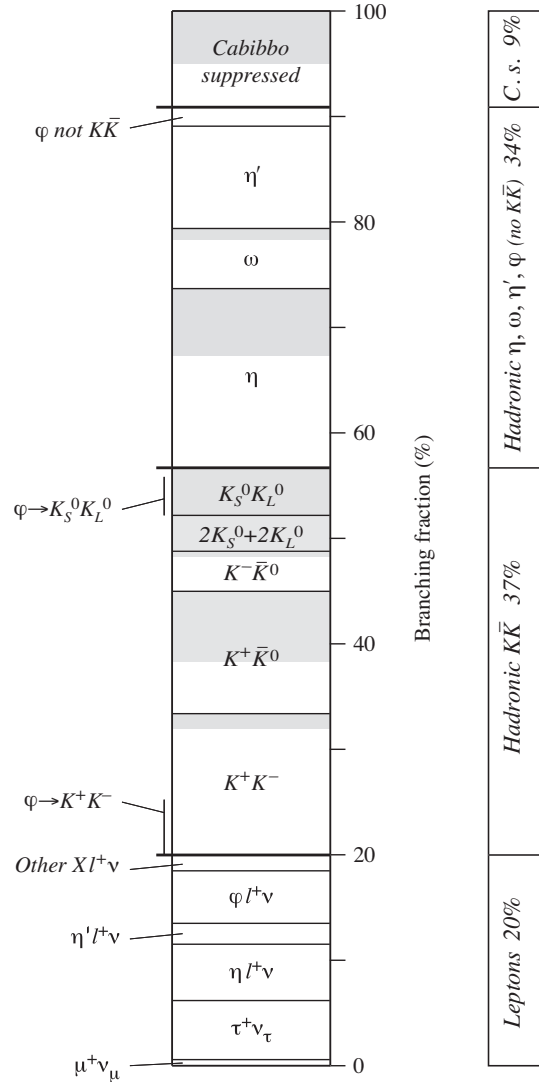


Figure : A partial breakdown of D_s^+ branching fractions. Shading indicates parts of bins allotted to as-yet unmeasured exclusive modes. The inclusive hadronic ϕ fraction is spread over three bins. See the text for further explanations.

We can get that fraction. The total K_S^0 fraction is

$$f(K_S^0) = f(K^+K_S^0) + f(K^-K_S^0) + 2f(2K_S^0) + f(K_S^0K_L^0) + f(\text{single } K_S^0),$$

where $f(\text{single } K_S^0)$ is the sum of the branching fractions for modes such as $K_S^0\pi^+2\pi^0$ with a K_S^0 and no second K . The $K_S^0\pi^+2\pi^0$ mode is in fact the only unmeasured single- K_S^0 mode (throughout, we shall assume that fractions for modes with a K or $K\bar{K}$ and more than three pions are negligible), and we shall take its fraction to be the same as for the $K_S^02\pi^+\pi^-$ mode, $(0.29 \pm 0.11)\%$. Any reasonable deviation from this value would be too small to matter much in the following. Adding the several small single- K_S^0 branching fractions, including those from semileptonic modes, we get $f(\text{single } K_S^0) = (1.67 \pm 0.26)\%$.

Using this, we have:

$$\begin{aligned} f(K_S^0 K_L^0) &= f(K_S^0) - f(K^+ K_S^0) - f(K^- K_S^0) - 2f(2K_S^0) \\ &\quad - f(\text{single } K_S^0) \\ &= (19.0 \pm 1.1) - (5.8 \pm 0.5) - (1.9 \pm 0.4) \\ &\quad - 2 \times (1.70 \pm 0.32) - (1.67 \pm 0.26) \\ &= (6.2 \pm 1.4)\% . \end{aligned}$$

Here and below we treat the errors as uncorrelated, although often they are not. However, our main aim is to get numbers for Fig. 1; errors will be secondary.

There is a check on our result: The ϕ inclusive branching fraction is $(15.7 \pm 1.0)\%$, of which 34%, or $(5.34 \pm 0.34)\%$ of D_s^+ decays, produces a $K_S^0 K_L^0$. Our $f(K_S^0 K_L^0) = (6.2 \pm 1.4)\%$ has to be at least this large—and it is.

We now make a table. The first column gives the various particle pairings; here we use $f(K^+ \bar{K}^0) = 2f(K^+ K_S^0)$, and likewise for $f(K^- K^0)$. The second column gives the inclusive branching fractions; the third column gives the fractions for $K^+ K^-$ and $K_S^0 K_L^0$ from $\phi \ell^+ \nu$ decay; the last column subtracts these off to get the purely hadronic $K\bar{K}$ inclusive fractions.

$K^+ K^-$	15.8 (0.7)%	2.44 (0.14)%	13.4 (0.7)%
$K^+ \bar{K}^0$	11.6 (1.0)		11.6 (1.0)
$K^- K^0$	3.8 (0.8)		3.8 (0.8)
$K_S^0 K_S^0 + K_L^0 K_L^0$	3.4 (0.64)		3.4 (0.64)
$K_S^0 K_L^0$	6.2 (1.4)	1.69 (0.10)	4.5 (1.4) .

The values in the last column are shown in Fig. 1. Their sum is $(36.7 \pm 2.1)\%$.

We can add more information to the figure by summing up measured branching fractions for exclusive modes within each bin:

$K^+ K^-$ modes—The sum of measured $K^+ K^- \pi^+$, $K^+ K^- \pi^+ \pi^0$, and $K^+ K^- 2\pi^+ \pi^-$ branching fractions is $(12.0 \pm 0.6)\%$. That leaves $(1.4 \pm 0.9)\%$ for the $K^+ K^- \pi^+ 2\pi^0$ mode, which is the only other $K^+ K^-$ mode with three or fewer pions. In Fig. 1, this unmeasured part of the $K^+ K^-$ bin is shaded.

$K^+ \bar{K}^0$ modes—Twice the sum of measured $K^+ K_S^0$ and $K^+ K_S^0 \pi^+ \pi^-$ branching fractions is $(4.9 \pm 0.3)\%$. This leaves $(6.7 \pm 1.0)\%$ for the unmeasured $K^+ \bar{K}^0$ modes (there are four such modes with three or fewer pions). This is shaded in the figure.

$K^- K^0$ modes—Twice the $K^- K_S^0 2\pi^+$ fraction is $(3.28 \pm 0.24)\%$, which leaves about $(0.5 \pm 0.8)\%$ for $K^- K^0 2\pi^+ \pi^0$, the only other $K^- K^0$ mode with three or fewer pions.

$K^0 \bar{K}^0$ modes—The only measurement of $K^0 \bar{K}^0$ decays is of the $2K_S^0 2\pi^+ \pi^-$ fraction, $(0.084 \pm 0.035)\%$; so nearly everything is shaded here. However, most of the $K_S^0 K_L^0$ fraction is accounted for by ϕ decays (see below).

Inclusive hadronic η , ω , η' , and ϕ fractions: These are easier. We start with the inclusive branching fractions, and then, to avoid double counting, subtract: (1) fractions for modes

with leptons; (2) η mesons that are included in the inclusive η' fraction; and (3) $K^+ K^-$ and $K_S^0 K_L^0$ from ϕ decays:

$$\begin{aligned} f(\eta \text{ hadronic}) &= f(\eta \text{ inclusive}) - 0.65 f(\eta' \text{ inclusive}) \\ &\quad - f(\eta \ell^+ \nu) = (17.0 \pm 3.1)\% \end{aligned}$$

$$\begin{aligned} f(\omega \text{ hadronic}) &= f(\omega \text{ inclusive}) - 0.03 f(\eta' \text{ inclusive}) \\ &= (5.7 \pm 1.4)\% \end{aligned}$$

$$\begin{aligned} f(\eta' \text{ hadronic}) &= f(\eta' \text{ inclusive}) - f(\eta' \ell^+ \nu) \\ &= (9.7 \pm 1.9)\% \end{aligned}$$

$$\begin{aligned} f(\phi \text{ hadronic, } \not\rightarrow K\bar{K}) &= 0.17 [f(\phi \text{ inclusive}) \\ &\quad - f(\phi \ell^+ \nu)] = (1.8 \pm 0.2)\% . \end{aligned}$$

The factors 0.65, 0.03, and 0.17 are the $\eta' \rightarrow \eta$, $\eta' \rightarrow \omega$, and $\phi \not\rightarrow K\bar{K}$ branching fractions. Figure 1 shows the results; the sum is $(34.2 \pm 3.9)\%$, which is about equal to the hadronic $K\bar{K}$ total.

Note that the bin marked ϕ near the top of Fig. 1 includes neither the $\phi \ell^+ \nu$ decays nor the 83% of other ϕ decays that produce a $K\bar{K}$ pair. Compared to the size of that ϕ bin, there is twice as much ϕ in the $K_S^0 K_L^0$ bin, and nearly three times as much in the $K^+ K^-$ bin. These contributions are indicated in those bins.

Again, we can show how much of each bin is accounted for by measured exclusive branching fractions:

η modes—The sum of $\eta \pi^+$, $\eta \rho^+$, and ηK^+ branching fractions is $(10.6 \pm 0.8)\%$, which leaves a good part of the inclusive hadronic η fraction, $(17.0 \pm 3.1)\%$, to be accounted for. This is shaded in the figure.

ω modes—The sum of $\omega \pi^+$, $\omega \pi^+ \pi^0$, and $\omega 2\pi^+ \pi^-$ fractions is $(4.6 \pm 0.9)\%$, which is nearly as large as the inclusive hadronic ω fraction, $(5.7 \pm 1.4)\%$.

η' modes—The sum of $\eta' \pi^+$, $\eta' \rho^+$, and $\eta' K^+$ fractions is $(16.5 \pm 2.2)\%$, which is much larger than the inclusive hadronic η' fraction, $(9.7 \pm 1.9)\%$. If an exclusive measurement is at fault, it almost has to be the $\eta' \rho^+$ fraction, which is $(12.5 \pm 2.2)\%$. It has been suggested that some of this signal might instead be misidentified kinematic reflections of other modes [2].

Cabibbo-suppressed modes: Remaining is $(9.1 \pm 4.5)\%$ for hadronic Cabibbo-suppressed modes having no η , ω , η' , or ϕ . The contributions are:

$K^0 + \text{pions}$ —Above, we found that $f(\text{single } K_S^0) = (1.67 \pm 0.26)\%$; subtracting leptonic contributions leaves $(1.20 \pm 0.24)\%$. The hadronic single- K^0 fraction is twice this, $(2.40 \pm 0.48)\%$.

$K^+ + \text{pions}$ —The $K^+ \pi^0$ and $K^+ \pi^+ \pi^-$ fractions sum to $(0.77 \pm 0.05)\%$. Much of the $K^+ n\pi$ modes, where $n \geq 3$, is already in the η , ω , and η' bins, and the rest is not measured. The total K^+ fraction wanted here is probably in the 1-to-2% range.

Multi-pions —The $2\pi^+ \pi^-$, $\pi^+ 2\pi^0$, and $3\pi^+ 2\pi^-$ fractions total $(2.6 \pm 0.2)\%$. Modes not measured might double this.

Meson Particle Listings

 D_s^\pm

The sum of the three contributions is certainly not inconsistent with the Cabibbo-suppressed total of $(9.1 \pm 4.5)\%$. The sum of actually measured fractions is $(4.2 \pm 0.2)\%$.

A model: With CLEO about to publish inclusive branching fractions [1], Gronau and Rosner predicted those fractions using a “statistical isospin” model [2]. Consider, say, the $D_s^+ \rightarrow K\bar{K}\pi$ charge modes: the $K^+K^-\pi^+$ branching fraction is measured, the $K^+\bar{K}^0\pi^0$ and $K^0\bar{K}^0\pi^+$ fractions are not. The statistical isospin model assumes that all the independent isospin amplitudes for $D_s^+ \rightarrow K\bar{K}\pi$ decay are equal in magnitude and incoherent in phase—in which case, the ratio of the three fractions here is 3:3:2. (Actually, use was also made of the fact that $D_s^+ \rightarrow K\bar{K}\pi$ decay is dominated by $\phi\pi^+$, $K^+\bar{K}^{*0}$, and $K^{*+}\bar{K}^0$ submodes; but the estimated charge-mode ratios were not far from 3:3:2.) A different, quark-antiquark pair-production model was used to estimate systematic uncertainties.

In this way, unmeasured exclusive fractions were calculated from measured exclusive fractions (the latter were taken from the 2008 Review, and so did not benefit from recent results). In the hadronic sector, the measured total of 59.4% of D_s^+ decays led to an estimated total of 24.2% for unmeasured modes. Weighted counts of π^+ , K_S^0 , etc., were then made to get the inclusive fractions.

Of interest here is that the sum of all the exclusive fractions—a way-stop in getting the inclusive values—was a nearly correct 103%. In the absence of complete measurements, the model is a way to, in effect, average over ignorance. It probably works better summed over a number of charge-mode sets than in detail. It is known to sometimes give incorrect results when there are sufficient measurements to test it.

References

1. S. Dobbs *et al.*, Phys. Rev. **D79**, 112008 (2009).
2. M. Gronau and J.L. Rosner, Phys. Rev. **D79**, 074022 (2009).

 D_s^\pm BRANCHING RATIOS

A number of older, now obsolete results have been omitted. They may be found in earlier editions.

Inclusive modes

$\Gamma(e^+ \text{ semileptonic})/\Gamma_{\text{total}}$		Γ_1/Γ	
This is the purely e^+ semileptonic branching fraction: the e^+ fraction from π^+ decays has been subtracted off. The sum of our (non- τ) e^+ exclusive fractions — an $e^+\nu_e$ with an η , η' , ϕ , K^0 , K^{*0} , or $f_0(980)$ — is $6.90 \pm 0.4\%$			
VALUE (units 10^{-2})	EVTS	DOCUMENT ID	TECN COMMENT
$6.52 \pm 0.39 \pm 0.15$	536 \pm 29	³ ASNER	10 CLEO e^+e^- at 3774 MeV
³ Using the D_s^+ and D^0 lifetimes, ASNER 10 finds that the ratio of the D_s^+ and D^0 semileptonic widths is $0.828 \pm 0.051 \pm 0.025$.			
$\Gamma(\pi^+ \text{ anything})/\Gamma_{\text{total}}$		Γ_2/Γ	
Events with two π^+ 's count twice, etc. But π^+ 's from $K_S^0 \rightarrow \pi^+\pi^-$ are not included.			
VALUE (units 10^{-2})	DOCUMENT ID	TECN	COMMENT
$119.3 \pm 1.2 \pm 0.7$	DOBBS	09	CLEO e^+e^- at 4170 MeV
$\Gamma(\pi^- \text{ anything})/\Gamma_{\text{total}}$		Γ_3/Γ	
Events with two π^- 's count twice, etc. But π^- 's from $K_S^0 \rightarrow \pi^+\pi^-$ are not included.			
VALUE (units 10^{-2})	DOCUMENT ID	TECN	COMMENT
$43.2 \pm 0.9 \pm 0.3$	DOBBS	09	CLEO e^+e^- at 4170 MeV

$\Gamma(\pi^0 \text{ anything})/\Gamma_{\text{total}}$		Γ_4/Γ	
Events with two π^0 's count twice, etc. But π^0 's from $K_S^0 \rightarrow 2\pi^0$ are not included.			
VALUE (units 10^{-2})	DOCUMENT ID	TECN	COMMENT
$123.4 \pm 3.8 \pm 5.3$	DOBBS	09	CLEO e^+e^- at 4170 MeV
$\Gamma(K^- \text{ anything})/\Gamma_{\text{total}}$		Γ_5/Γ	
VALUE (units 10^{-2})	DOCUMENT ID	TECN	COMMENT
$18.7 \pm 0.5 \pm 0.2$	DOBBS	09	CLEO e^+e^- at 4170 MeV
$\Gamma(K^+ \text{ anything})/\Gamma_{\text{total}}$		Γ_6/Γ	
VALUE (units 10^{-2})	DOCUMENT ID	TECN	COMMENT
$28.9 \pm 0.6 \pm 0.3$	DOBBS	09	CLEO e^+e^- at 4170 MeV
$\Gamma(K_S^0 \text{ anything})/\Gamma_{\text{total}}$		Γ_7/Γ	
VALUE (units 10^{-2})	DOCUMENT ID	TECN	COMMENT
$19.0 \pm 1.0 \pm 0.4$	DOBBS	09	CLEO e^+e^- at 4170 MeV
$\Gamma(\eta \text{ anything})/\Gamma_{\text{total}}$		Γ_8/Γ	
This ratio includes η particles from η' decays.			
VALUE (units 10^{-2})	EVTS	DOCUMENT ID	TECN COMMENT
$29.9 \pm 2.2 \pm 1.7$		DOBBS	09 CLEO e^+e^- at 4170 MeV
••• We do not use the following data for averages, fits, limits, etc. •••			
$23.5 \pm 3.1 \pm 2.0$	674 \pm 91	HUANG	06B CLEO See DOBBS 09
$\Gamma(\omega \text{ anything})/\Gamma_{\text{total}}$		Γ_9/Γ	
VALUE (units 10^{-2})	DOCUMENT ID	TECN	COMMENT
$6.1 \pm 1.4 \pm 0.3$	DOBBS	09	CLEO e^+e^- at 4170 MeV
$\Gamma(\eta' \text{ anything})/\Gamma_{\text{total}}$		Γ_{10}/Γ	
VALUE (units 10^{-2})	EVTS	DOCUMENT ID	TECN COMMENT
$11.7 \pm 1.7 \pm 0.7$		DOBBS	09 CLEO e^+e^- at 4170 MeV
••• We do not use the following data for averages, fits, limits, etc. •••			
$8.7 \pm 1.9 \pm 0.8$	68 \pm 15	HUANG	06B CLEO See DOBBS 09
$\Gamma(f_0(980) \text{ anything, } f_0 \rightarrow \pi^+\pi^-)/\Gamma_{\text{total}}$		Γ_{11}/Γ	
VALUE (units 10^{-2})	CL%	DOCUMENT ID	TECN COMMENT
<1.3	90	DOBBS	09 CLEO e^+e^- at 4170 MeV
$\Gamma(\phi \text{ anything})/\Gamma_{\text{total}}$		Γ_{12}/Γ	
VALUE (units 10^{-2})	EVTS	DOCUMENT ID	TECN COMMENT
$15.7 \pm 0.8 \pm 0.6$		DOBBS	09 CLEO e^+e^- at 4170 MeV
••• We do not use the following data for averages, fits, limits, etc. •••			
$16.1 \pm 1.2 \pm 1.1$	398 \pm 27	HUANG	06B CLEO See DOBBS 09
$\Gamma(K^+K^- \text{ anything})/\Gamma_{\text{total}}$		Γ_{13}/Γ	
VALUE (units 10^{-2})	DOCUMENT ID	TECN	COMMENT
$15.8 \pm 0.6 \pm 0.3$	DOBBS	09	CLEO e^+e^- at 4170 MeV
$\Gamma(K_S^0 K^+ \text{ anything})/\Gamma_{\text{total}}$		Γ_{14}/Γ	
VALUE (units 10^{-2})	DOCUMENT ID	TECN	COMMENT
$5.8 \pm 0.5 \pm 0.1$	DOBBS	09	CLEO e^+e^- at 4170 MeV
$\Gamma(K_S^0 K^- \text{ anything})/\Gamma_{\text{total}}$		Γ_{15}/Γ	
VALUE (units 10^{-2})	DOCUMENT ID	TECN	COMMENT
$1.9 \pm 0.4 \pm 0.1$	DOBBS	09	CLEO e^+e^- at 4170 MeV
$\Gamma(2K_S^0 \text{ anything})/\Gamma_{\text{total}}$		Γ_{16}/Γ	
VALUE (units 10^{-2})	DOCUMENT ID	TECN	COMMENT
$1.7 \pm 0.3 \pm 0.1$	DOBBS	09	CLEO e^+e^- at 4170 MeV
$\Gamma(2K^+ \text{ anything})/\Gamma_{\text{total}}$		Γ_{17}/Γ	
VALUE (units 10^{-2})	CL%	DOCUMENT ID	TECN COMMENT
<0.26	90	DOBBS	09 CLEO e^+e^- at 4170 MeV
$\Gamma(2K^- \text{ anything})/\Gamma_{\text{total}}$		Γ_{18}/Γ	
VALUE (units 10^{-2})	CL%	DOCUMENT ID	TECN COMMENT
<0.06	90	DOBBS	09 CLEO e^+e^- at 4170 MeV

Leptonic and semileptonic modes

DECAY CONSTANTS OF CHARGED PSEUDO-SCALAR MESONS

Revised April 2010 by J. Rosner (Univ. Chicago) and S. Stone (Syracuse Univ.)

Introduction. Charged mesons formed from a quark and an anti-quark can decay to a charged lepton and a neutrino when these objects annihilate via a virtual W boson [1]. Fig. 1 illustrates this process for the purely leptonic decay of a D^+ meson.

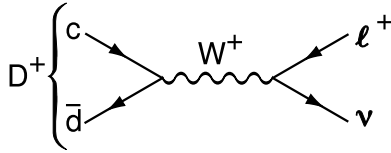


Figure 1: The annihilation process for pure D^+ leptonic decays in the Standard Model.

Similar quark-antiquark annihilations via a virtual W^+ to the $\ell^+\nu$ final states occur for the π^+ , K^+ , D_s^+ , and B^+ mesons. (Charge-conjugate particles and decays are implied.) Let P be any of these pseudoscalar mesons. To lowest order, the decay width is

$$\Gamma(P \rightarrow \ell\nu) = \frac{G_F^2}{8\pi} f_P^2 m_\ell^2 m_P \left(1 - \frac{m_\ell^2}{m_P^2}\right)^2 |V_{q_1 q_2}|^2. \quad (1)$$

Here m_P is the P mass, m_ℓ is the ℓ mass, $V_{q_1 q_2}$ is the Cabibbo-Kobayashi-Maskawa (CKM) matrix element between the constituent quarks $q_1 \bar{q}_2$ in P , and G_F is the Fermi coupling constant. The parameter f_P is the decay constant, and is related to the wave-function overlap of the quark and antiquark.

The decay P^\pm starts with a spin-0 meson, and ends up with a left-handed neutrino or right-handed antineutrino. By angular momentum conservation, the ℓ^\pm must then also be left-handed or right-handed, respectively. In the $m_\ell = 0$ limit, the decay is forbidden, and can only occur as a result of the finite ℓ mass. This helicity suppression is the origin of the m_ℓ^2 dependence of the decay width.

There is a complication in measuring purely leptonic decay rates. The process $P \rightarrow \ell\nu\gamma$ is not simply a radiative correction, although radiative corrections contribute. The P can make a transition to a virtual P^* , emitting a real photon, and the P^* decays into $\ell\nu$, avoiding helicity suppression. The importance of this amplitude depends on the decaying particle and the detection technique. The $\ell\nu\gamma$ rate for a heavy particle such as B decaying into a light particle such as a muon can be larger than the width without photon emission [2]. On the other hand, for decays into a τ^\pm , the helicity suppression is mostly broken and these effects appear to be small.

Measurements of purely leptonic decay branching fractions and lifetimes allow experimental determination of the product $|V_{q_1 q_2}| f_P$. If the CKM element is well known from other measurements, then f_P can be well measured. If, on the other hand, the CKM element is not well measured, having theoretical input on f_P can allow a determination of the CKM element. The

importance of measuring $\Gamma(P \rightarrow \ell\nu)$ depends on the particle being considered. For the B system, f_B is crucial for extracting information on the fundamental CKM parameters from measurements of $B^0\text{-}\bar{B}^0$ mixing. Knowledge of f_{B_s} is also needed, but it cannot be directly measured as the B_s is neutral, so the violation of the SU(3) relation $f_{B_s} = f_B$ must be estimated theoretically. This difficulty does not occur for D mesons as both the D^+ and D_s^+ are charged, allowing direct measurement of SU(3) breaking and a direct comparison with theory.

For B^- and D_s^+ decays, the existence of a charged Higgs boson (or any other charged object beyond the Standard Model) would modify the decay rates; however, this would not necessarily be true for the D^+ [3,4]. More generally, the ratio of $\tau\nu$ to $\mu\nu$ decays can serve as one probe of lepton universality [3,5].

As $|V_{ud}|$ has been quite accurately measured in superallowed β decays [6], with a value of 0.97425(22) [7], measurements of $\Gamma(\pi^+ \rightarrow \mu^+\nu)$ yield a value for f_π . Similarly, $|V_{us}|$ has been well measured in semileptonic kaon decays, so a value for f_K from $\Gamma(K^- \rightarrow \mu^-\bar{\nu})$ can be compared to theoretical calculations. Lattice gauge theory calculations, however, have been claimed to be very accurate in determining f_K , and these have been used to predict $|V_{us}|$ [8].

Charmed mesons. We review current measurements, starting with the charm system. The CLEO collaboration has performed the only measurement of the branching fraction for $D^+ \rightarrow \mu^+\nu$ [9]. CLEO uses e^+e^- collisions at the $\psi(3770)$ resonant energy where D^-D^+ pairs are copiously produced. They fully reconstruct one of the D mesons, find a candidate muon track of opposite sign to this tag, and then use kinematical constraints to infer the existence of a missing neutrino and hence the $\mu\nu$ decay of the other D . They find $\mathcal{B}(D^+ \rightarrow \mu^+\nu) = (3.82 \pm 0.32 \pm 0.09) \times 10^{-4}$. We use the well-measured D^+ lifetime of 1.040(7) ps, and assuming $|V_{cd}|$ equals $|V_{us}| = 0.2246(12)$ [7] minus higher order correction terms [10], we find $|V_{cd}| = 0.2245(12)$. (The errors on these quantities are included in the systematic error.) The CLEO branching fraction result then translates into a value of

$$f_{D^+} = (206.7 \pm 8.5 \pm 2.5) \text{ MeV}. \quad (2)$$

This result includes a 1% correction (reduction) of the rate due to the presence of the radiative $\mu^+\nu\gamma$ final state based on the estimate by Dobrescu and Kronfeld [11].

Before we compare this result with theoretical predictions, we discuss the D_s^+ . Measurements of $f_{D_s^+}$ have been made by several groups and are listed in Table 1 [12–16]. We exclude values [17–21] obtained by normalizing to D_s^+ decay modes (mentioned in the 2008 version of this Review) that are not well defined. Many measurements, for example, used the $\phi\pi^+$ mode. This decay is a subset of the $D_s^+ \rightarrow K^+K^-\pi^+$ channel which has interferences from other modes populating the K^+K^- mass region near the ϕ , the most prominent of which is the $f_0(980)$. Thus the extraction of effective $\phi\pi^+$ rate is sensitive to the mass resolution of the experiment and the cuts used to define the ϕ mass region [22,23].

Meson Particle Listings

 D_s^\pm

Table 1: Experimental results for $\mathcal{B}(D_s^+ \rightarrow \mu^+\nu)$, $\mathcal{B}(D_s^+ \rightarrow \tau^+\nu)$, and $f_{D_s^+}$. Numbers for $f_{D_s^+}$ have been extracted using updated values for masses and $|V_{cs}|$ (see text); radiative corrections have been included. Common systematic errors in the CLEO results have been taken into account.

Experiment	Mode	$\mathcal{B} \times 10^{-2}$	$f_{D_s^+}$ (MeV)
CLEO-c [12]	$\mu^+\nu$	$(0.565 \pm 0.045 \pm 0.017)$	$257.6 \pm 10.3 \pm 4.3$
Belle [13]	$\mu^+\nu$	$(0.638 \pm 0.076 \pm 0.057)$	$274 \pm 16 \pm 12$
Average	$\mu^+\nu$	(0.580 ± 0.043)	261.5 ± 9.7
CLEO-c [12]	$\tau^+\nu$ ($\pi^+\bar{\nu}$)	$(6.42 \pm 0.81 \pm 0.18)$	$278.0 \pm 17.5 \pm 3.8$
CLEO-c [14]	$\tau^+\nu$ ($\rho^+\bar{\nu}$)	$(5.52 \pm 0.57 \pm 0.21)$	$257.8 \pm 13.3 \pm 5.2$
CLEO-c [15]	$\tau^+\nu$ ($e^+\nu\bar{\nu}$)	$(5.30 \pm 0.47 \pm 0.22)$	$252.6 \pm 11.1 \pm 5.2$
BaBar [16]	$\tau^+\nu$ ($e^+\nu\bar{\nu}$)	$(4.54 \pm 0.53 \pm 0.40 \pm 0.28)$	$233.8 \pm 13.7 \pm 12.6$
Average	$\tau^+\nu$	(5.58 ± 0.35)	255.5 ± 7.5
Average	$\mu^+\nu + \tau^+\nu$		257.5 ± 6.1

Table 2: Theoretical predictions of $f_{D_s^+}$, f_{D^+} , and $f_{D_s^+}/f_{D^+}$. QL indicates a quenched-lattice calculation, while PQL indicates a partially-quenched lattice calculation. (Only selected results having errors are included.)

Model	$f_{D_s^+}$ (MeV)	f_{D^+} (MeV)	$f_{D_s^+}/f_{D^+}$
Experiment (our averages)	257.5 ± 6.1	206.7 ± 8.9	1.25 ± 0.06
Lattice [26]	241 ± 3	208 ± 4	1.162 ± 0.009
Lattice [27]	260 ± 10	217 ± 10	1.20 ± 0.02
PQL [28]	244 ± 8	197 ± 9	1.24 ± 0.03
QL (QCDSF) [29]	$220 \pm 6 \pm 5 \pm 11$	$206 \pm 6 \pm 3 \pm 22$	$1.07 \pm 0.02 \pm 0.02$
QL (Taiwan) [30]	$266 \pm 10 \pm 18$	$235 \pm 8 \pm 14$	$1.13 \pm 0.03 \pm 0.05$
QL (UKQCD) [31]	$236 \pm 8_{-14}^{+17}$	$210 \pm 10_{-16}^{+17}$	$1.13 \pm 0.02_{-0.02}^{+0.04}$
QL [32]	$231 \pm 12_{-1}^{+6}$	$211 \pm 14_{-12}^{+2}$	1.10 ± 0.02
QCD Sum Rules [33]	205 ± 22	177 ± 21	$1.16 \pm 0.01 \pm 0.03$
QCD Sum Rules [34]	235 ± 24	203 ± 20	1.15 ± 0.04
Field Correlators [35]	260 ± 10	210 ± 10	1.24 ± 0.03
Light Front [36]	268.3 ± 19.1	206 (fixed)	1.30 ± 0.04

The CLEO and Belle $\mu^+\nu$ results rely on fully reconstructing all the final state particles except for the neutrino and using a missing-mass technique to infer the existence of the neutrino. CLEO uses $e^+e^- \rightarrow D_s D_s^*$ collisions at 4170 MeV, while Belle uses $e^+e^- \rightarrow DKn\pi D_s^*$ collisions at energies near the $\Upsilon(4S)$.

When selecting the $\tau^+ \rightarrow \pi^+\bar{\nu}$ and $\tau^+ \rightarrow \rho^+\bar{\nu}$ decay modes, CLEO uses both calculation of the missing-mass and the fact that there should be no extra energy in the event beyond that deposited by the measured tagged D_s^- and the τ^+ decay products. The $\tau^+ \rightarrow e^+\nu\bar{\nu}$ mode, however, uses only extra energy. BaBar measures $\Gamma(D_s^+ \rightarrow \tau^+\nu)/\Gamma(D_s^+ \rightarrow \bar{K}^0 K^+)$ using the $\tau^+ \rightarrow e^+\nu\bar{\nu}$ mode. Here the D_s^- tag is formed similarly to Belle by finding events with a D a K and pions opposite a single positron and little extra energy. Then the analysis is performed selecting modes with a $\bar{K}^0 K^+$ consistent with arising from the decay of a D_s^+ . (The fourth error in Table 1 on their measurement reflects the uncertainty due to the PDG value of $\mathcal{B}(D_s^+ \rightarrow \bar{K}^0 K^+)$.)

We extract the decay constant from the measured branching ratios using the D_s^+ mass of 1.96849(34) GeV, the τ^+ mass of 1.77684(17) GeV, and a lifetime of 0.500(7) ps. We use the first order correction $|V_{cs}| = |V_{ud}| - |V_{cb}|^2/2$ [10]; taking $|V_{ud}| = 0.97425(22)$ [6], and $|V_{cb}| = 0.04$ from an average of exclusive and inclusive semileptonic B decay results as discussed in Ref. [24], we find $|V_{cs}| = 0.97345(22)$. Our experimental average,

$$f_{D_s^+} = (257.5 \pm 6.1) \text{ MeV}, \quad (3)$$

uses only those results that are included in Table 1. We have again included the radiative correction of 1% in the $\mu^+\nu$ rates listed in the table estimated by Dobrescu and Kronfeld [11] (the $\tau^+\nu$ rates need not be corrected). Other theoretical calculations show that the $\gamma\mu^+\nu$ rate is a factor of 40–100 below the $\mu^+\nu$ rate for charm [25].

Two ratios are of particular interest. The ratio of decay constants for the $\tau^+\nu : \mu^+\nu$ modes is $f_{D_s^+}(\tau^+\nu)/f_{D_s^+}(\mu^+\nu) = 0.98 \pm 0.05$, and the ratio of D_s^+ to D^+ decay constants is $f_{D_s^+}/f_{D^+} = 1.25 \pm 0.06$. Table 2 compares the experimental $f_{D_s^+}$ with theoretical calculations [26–36]. While most theories give values lower than the $f_{D_s^+}$ measurement, the errors are sufficiently large, in most cases, to declare success. An unquenched lattice calculation [26], however, differs by 2.4 standard deviations [37]. Remarkably it agrees with f_{D^+} and consequently disagrees in the ratio $f_{D_s^+}/f_{D^+}$, with less significance as the error in f_{D^+} is substantial.

The Fermilab-MILC result has been updated; the preliminary values for f_{D^+} and $f_{D_s^+}$ were raised by 10 MeV and 11 MeV, respectively [27]. These changes bring the predictions for both numbers within errors of experiment.

Akeroyd and Chen [38] pointed out that leptonic decay widths are modified in two-Higgs-doublet models (2HDM). Specifically, for the D^+ and D_s^+ , Eq. (1) is modified by a factor r_q multiplying the right-hand side [39]:

$$r_q = \left[1 + \left(\frac{1}{m_c + m_q} \right) \left(\frac{M_{D_q}}{M_{H^+}} \right)^2 \left(m_c - \frac{m_q \tan^2 \beta}{1 + \epsilon_0 \tan \beta} \right) \right]^2, \quad (4)$$

where M_{H^+} is the charged Higgs mass, M_{D_q} is the mass of the D meson (containing the light quark q), m_c is the charm quark mass, m_q is the light-quark mass, and $\tan \beta$ is the ratio of the vacuum expectation values of the two Higgs doublets. In models where the fermion mass arises from coupling to more than one vacuum expectation value ϵ_0 can be non-zero, perhaps as large as 0.01. For the D^+ , $m_d \ll m_c$, and the change due to the H^+ is very small. For the D_s^+ , however, the effect can be substantial.

A major concern is the need for the Standard Model (SM) value of $f_{D_s^+}$. We can take that from a theoretical model. Our most aggressive choice is that of the unquenched lattice calculation [26], because they claim the smallest error. Since the charged Higgs would lower the rate compared to the SM, in principle, experiment gives a lower limit on the charged Higgs mass. However, the value for the predicted decay constant using this model is 2.4 standard deviations *below* the measurement, implying that (a) either the model of Ref. 26 is not representative; (b) no value of m_{H^+} in the two-Higgs doublet model will satisfy the constraint at 99% confidence level; or (c) there is new physics, different from the 2HDM, that interferes constructively with the SM amplitude such as in the R-parity-violating model of Akeroyd and Recksiegel [40]. New physics can affect the $\mu^+\nu$ and $\tau^+\nu$ final states differently and thus these should be studied separately [39].

To sum up, the situation is not clear. To set limits on new physics we need an accurate calculation of $f_{D_s^+}$ and more precise measurements would also be useful.

The B meson. The Belle and BaBar collaborations have found evidence for $B^- \rightarrow \tau^-\bar{\nu}$ decay in $e^+e^- \rightarrow B^- B^+$ collisions at the $\Upsilon(4S)$ energy. The analysis relies on reconstructing a hadronic or semi-leptonic B decay tag, finding a τ candidate in the remaining track and or photon candidates, and examining the extra energy in the event which should be close to zero for a real τ decay opposite a B meson tag. The results are listed in Table 3.

There are large backgrounds under the signals in all cases. The systematic errors are also quite large, on the order of 20%. Thus the significances are not that large. Belle quotes 3.5σ and 3.8σ for their hadronic and semileptonic tags, respectively, while BaBar quotes 2.8σ for their combined result. We note that the four central values are remarkably close to the average considering the large errors on all the measurements. More accuracy would be useful to investigate the effects of new physics. Here the effect of a charged Higgs is different as it can either increase or decrease the expected SM branching ratio.

Meson Particle Listings

 D_s^\pm

Table 3: Experimental results for $\mathcal{B}(B^- \rightarrow \tau^- \bar{\nu})$. We have computed an average for the two Belle measurements assuming that the systematic errors are fully correlated.

Experiment	Tag	$\mathcal{B} \times 10^{-4}$
Belle [41]	Hadronic	$(1.79^{+0.56}_{-0.49} \text{ } ^{+0.46}_{-0.51})$
Belle [42]	Semileptonic	$(1.65^{+0.38}_{-0.37} \text{ } ^{+0.35}_{-0.34})$
Belle	Our Average	$(1.70^{+0.47}_{-0.46})$
BaBar [43]	Hadronic	$(1.8^{+0.9}_{-0.8} \pm 0.4)$
BaBar [44]	Semileptonic	$(1.7 \pm 0.8 \pm 0.4)$
BaBar [44]	Average	$(1.8^{+1.0}_{-0.9})$
	Our Average	$(1.72^{+0.43}_{-0.42})$

The factor r in the 2HDM that multiplies the right side of Eq. (1) is given in terms of the B meson mass, M_B , by [3,39]

$$r = \left(1 - \frac{\tan^2 \beta}{1 + \epsilon_0 \tan \beta} \frac{M_B^2}{m_{H^+}^2} \right)^2. \quad (5)$$

We can derive limits in the 2HDM $\tan\beta$ - m_{H^+} plane. Again, we need to know the SM prediction of this decay rate. We ascertain this value using Eq. (1). Here theory provides a value of $f_B = (193 \pm 11)$ MeV [45]. We also need a value for $|V_{ub}|$. Here significant differences arise between using inclusive charmless semileptonic decays and the exclusive decay $B \rightarrow \pi \ell^+ \nu$ [46]. We find that the inclusive decays give rise to a value of $|V_{ub}| = (4.21 \pm 0.25) \times 10^{-3}$, while the $\pi \ell^+ \nu$ measurements yield $|V_{ub}| = (3.50 \pm 0.35) \times 10^{-3}$. Taking an average over inclusive and exclusive determinations, and enlarging the error using the PDG prescription because the results differ, we find $|V_{ub}| = (3.97 \pm 0.55) \times 10^{-3}$, where the error is dominantly theoretical. We thus arrive at the SM prediction for the $\tau^- \bar{\nu}$ branching fraction of $(1.04 \pm 0.31) \times 10^{-4}$.

Taking the ratio of the experimental value to the predicted branching ratio at its 90% c.l. *upper* limit and using Eq. (5) with ϵ_0 set to zero, we find that we can limit $M_{H^+} / \tan\beta > 3.3$ GeV. The 90% c.l. *lower* limit also permits us to exclude the region 3.8 GeV $< M_{H^+} / \tan\beta < 18.0$ GeV [47]. Considering the large uncertainties on V_{ub} and the branching ratio measurements, this should be taken more as indication of what the data can eventually tell us when and if the situation improves.

Charged pions and kaons. We now discuss the determination of charged pion and kaon decay constants. The sum of branching fractions for $\pi^- \rightarrow \mu^- \bar{\nu}$ and $\pi^- \rightarrow \mu^- \bar{\nu} \gamma$ is 99.98770(4)%. The two modes are difficult to separate experimentally, so we use this sum, with Eq. (1) modified to include photon emission and radiative corrections [48]. The branching fraction together with the lifetime 26.033(5) ns gives

$$f_{\pi^-} = (130.41 \pm 0.03 \pm 0.20) \text{ MeV}. \quad (6)$$

The first error is due to the error on $|V_{ud}|$, 0.97425(22) [6]; the second is due to the higher-order corrections, and is much larger.

Similarly, the sum of branching fractions for $K^- \rightarrow \mu^- \bar{\nu}$ and $K^- \rightarrow \mu^- \bar{\nu} \gamma$ is 63.55(11)%, and the lifetime is 12.3840(193) ns [49]. Measurements of semileptonic kaon decays provide a value for the product $f_+(0)|V_{us}|$, where $f_+(0)$ is the form-factor at zero four-momentum transfer between the initial state kaon and the final state pion. We use a value for $f_+(0)|V_{us}|$ of 0.21664(48) [49]. The $f_+(0)$ must be determined theoretically. We follow Blucher and Marciano [7] in using the lattice calculation $f_+(0) = 0.9644 \pm 0.0049$ [50], since it appears to be more precise than the classic Leutwyler-Roos calculation $f_+(0) = 0.961 \pm 0.008$ [51]. The result is $|V_{us}| = 0.2246 \pm 0.0012$, which is consistent with the hyperon decay value of 0.2250 ± 0.0027 [52]. We derive

$$f_{K^-} = (156.1 \pm 0.2 \pm 0.8 \pm 0.2) \text{ MeV}. \quad (7)$$

The first error is due to the error on Γ ; the second is due to the CKM factor $|V_{us}|$, and the third is due to the higher-order corrections. The largest source of error in these corrections depends on the QCD part, which is based on one calculation in the large N_c framework. We have doubled the quoted error here; this would probably be unnecessary if other calculations were to come to similar conclusions. A large part of the additional uncertainty vanishes in the ratio of the K^- and π^- decay constants, which is

$$f_{K^-}/f_{\pi^-} = 1.197 \pm 0.002 \pm 0.006 \pm 0.001. \quad (8)$$

The first error is due to the measured decay rates; the second is due to the uncertainties on the CKM factors; the third is due to the uncertainties in the radiative correction ratio.

These measurements have been used in conjunction with calculations of f_K/f_π in order to find a value for $|V_{us}|/|V_{ud}|$. Two recent lattice predictions of f_K/f_π are 1.189 ± 0.007 [26] and $1.192 \pm 0.007 \pm 0.006$ [53]. Together with the precisely measured $|V_{ud}|$, this gives an independent measure of $|V_{us}|$ [8,49].

References

1. For an expanded version of this review see J. L. Rosner and S. Stone, "Leptonic Decays of Charged Pseudoscalar Mesons," arXiv:1002.1655.
2. Most predictions for the rate for $B^- \rightarrow \mu^- \bar{\nu} \gamma$ are in the range of 1 to 20 times the rate for $B^- \rightarrow \mu^- \bar{\nu}$. See G. Burdman, T. Goldman, and D. Wyler, Phys. Rev. **D51**, 111 (1995); P. Colangelo, F. De Fazio, and G. Nardulli, Phys. Lett. **B372**, 331 (1996); *ibid.*, **386**, 328 (1996); A. Khodjamirian, G. Stoll, and D. Wyler, Phys. Lett. **B358**, 129 (1995); G. Eilam, I. Halperin, and R. Mendel, Phys. Lett. **B361**, 137 (1995); D. Atwood, G. Eilam, and A. Soni, Mod. Phys. Lett. **A11**, 1061 (1996); C.Q. Geng and C.C. Lih, Phys. Rev. **D57**, 5697 (1998) and Mod. Phys. Lett. **A15**, 2087 (2000); G.P. Korchemsky, D. Pirjol, and T.M. Yang, Phys. Rev. **D61**, 114510 (2000); C.W. Hwang, Eur. Phys. J. **C46**, 379 (2006).
3. W.-S. Hou, Phys. Rev. **D48**, 2342 (1993).
4. See, for example, A.G. Akeroyd and S. Recksiegel, Phys. Lett. **B554**, 38 (2003); A.G. Akeroyd, Prog. Theor. Phys. **111**, 295 (2004).

5. J.L. Hewett, [hep-ph/9505246](#), presented at *Lafex International School on High Energy Physics (LISHEP95)*, Rio de Janeiro, Brazil, Feb. 6-22, 1995.
6. I. S. Towner and J. C. Hardy, *Phys. Rev.* **C79**, 055502 (2009); I. S. Towner and J. C. Hardy, *Phys. Rev.* **C77**, 025501 (2008).
7. E. Blucher and W. J. Marciano, “ V_{ud} , V_{us} , The Cabibbo Angle, and CKM Unitarity” in PDG 2010.
8. W.J. Marciano, *Phys. Rev. Lett.* **93**, 231803 (2004); A. Jüttner, [[arXiv:0711.1239](#)].
9. B. I. Eisenstein *et al.*, (CLEO Collab.), *Phys. Rev.* **D78**, 052003 (2008). See also M. Artuso *et al.*, (CLEO Collab.), *Phys. Rev. Lett.* **95**, 251801 (2005).
10. J. Charles *et al.*, *Eur. Phys. J.* **C41**, 1 (2005).
11. B. A. Dobrescu and A. S. Kronfeld, *Phys. Rev. Lett.* **100**, 241802 (2008).
12. J. P. Alexander *et al.*, (CLEO Collab.), *Phys. Rev.* **D79**, 052001 (2009); M. Artuso *et al.*, (CLEO Collab.), *Phys. Rev. Lett.* **99**, 071802 (2007).
13. L. Widhalm *et al.*, (Belle Collab.), *Phys. Rev. Lett.* **100**, 241801 (2008).
14. P. Naik *et al.*, (CLEO Collab.), *Phys. Rev.* **D80**, 112004 (2009).
15. P.U.E. Onyisi *et al.*, (CLEO Collab.), *Phys. Rev.* **D79**, 052002 (2009); K.M. Ecklund *et al.*, (CLEO Collab.), *Phys. Rev. Lett.* **100**, 161801 (2008).
16. J. Dingfelder, “Hot topics from Babar: Leptonic and Semileptonic B and D decays,” presented at Moriond QCD and High Energy Interactions, La Thuile, Italy March 2010; J. P. Lee *et al.* (BaBar Collab.) [arXiv:1003.3063](#).
17. M. Chadha *et al.*, (CLEO Collab.), *Phys. Rev.* **D58**, 032002 (1998).
18. Y. Alexandrov *et al.*, (BEATRICE Collab.), *Phys. Lett.* **B478**, 31 (2000).
19. A. Heister *et al.*, (ALEPH Collab.), *Phys. Lett.* **B528**, 1 (2002).
20. M. Acciarri *et al.*, (L3 Collab.), *Phys. Lett.* **B396**, 327 (1997).
21. G. Abbiendi *et al.*, (OPAL Collab.), *Phys. Lett.* **B516**, 236 (2001).
22. See J. Alexander *et al.* (CLEO Collab.), *Phys. Rev. Lett.* **100**, 161804 (2008).
23. We have not included a BaBar result: $\mathcal{B}(D_s^+ \rightarrow \mu^+\nu) = (6.67 \pm 0.83 \pm 0.26 \pm 0.66) \times 10^{-3}$ and $f_{D_s^+} = (281 \pm 17 \pm 7 \pm 14)$ MeV based on $\mathcal{B}(D_s^+ \rightarrow \phi\pi^+) = (4.71 \pm 0.46)\%$. These measurements determined the ratio of the leptonic decay to a hadronic decay, usually $\Gamma(D_s^+ \rightarrow \ell^+\nu)/\Gamma(D_s^+ \rightarrow \phi\pi^+)$. B. Aubert *et al.*, (BABAR Collab.), *Phys. Rev. Lett.* **98**, 141801 (2007).
24. M. Artuso, E. Barberio and S. Stone, *PMC Physics A*, **3:3** (2009), [arXiv:0902.3743 \[hep-ph\]](#).
25. See most papers in Ref. [2] and C. D. Lü and G. L. Song, *Phys. Lett.* **B562**, 75 (2003).
26. E. Follana *et al.*, (HPQCD and UKQCD Collaborations), *Phys. Rev. Lett.* **100**, 062002 (2008) The statistical error is given as 0.6%, with the other systematic errors added in quadrature yielding the 3 MeV total error.
27. We use the updated numbers from A. Bazavov *et al.* (Fermilab Lattice and MILC Collaborations), *PoS LATTICE 2009 249*, (2009), an update that increases both f_{D^+} and $f_{D_s^+}$ by 10 MeV and 11 MeV, respectively, from the values originally given in C. Bernard *et al.*, [[arXiv:0904.1895](#)] (2009); see also C. Aubin *et al.*, *Phys. Rev. Lett.* **95**, 122002 (2005).
28. B. Blossier *et al.*, [[arXiv:0904.0954](#)] (2009).
29. A. Ali Khan *et al.*, (QCDSF Collaboration), *Phys. Lett.* **B652**, 150 (2007).
30. T.W. Chiu *et al.*, *Phys. Lett.* **B624**, 31 (2005) [[hep-ph/0506266](#)].
31. L. Lellouch and C.-J. Lin (UKQCD Collaboration), *Phys. Rev.* **D64**, 094501 (2001).
32. D. Becirevic *et al.*, *Phys. Rev.* **D60**, 074501 (1999).
33. J. Bordes, J. Peñarrocha, and K. Schilcher, *JHEP* **0511**, 014 (2005).
34. S. Narison, [[hep-ph/0202200](#)] (2002).
35. A.M. Badalian *et al.*, *Phys. Rev.* **D75**, 116001 (2007); see also A.M. Badalian and B.L.G. Bakker, [[hep-ph/0702229](#)].
36. C.-W. Hwang, [arXiv:0910.0145 \[hep-ph\]](#) (2009).
37. The small errors quoted in Follana *et al.* [26] are still being discussed in the lattice community. See, for example, M. Della Morte [[arXiv:0711.3160](#)], page 6 (2007). See also A. S. Kronfeld [[arXiv:0912.0543](#)] (2009).
38. A.G. Akeroyd and C.H. Chen, *Phys. Rev.* **D75**, 075004 (2007) [[hep-ph/0701078](#)].
39. A.G. Akeroyd and F. Mahmoudi, *JHEP* **0904**, 121 (2009).
40. A. G. Akeroyd and S. Recksiegel, *Phys. Lett.* **B554**, 38 (2003) [[hep-ph/0210376](#)].
41. K. Ikado *et al.*, (Belle Collab.), *Phys. Rev. Lett.* **97**, 251802 (2006).
42. I. Adachi *et al.*, (Belle Collab.), [[arXiv:0809.3834](#)].
43. B. Aubert *et al.*, (BaBar Collab.), *Phys. Rev.* **D77**, 011107R (2008).
44. B. Aubert *et al.*, (BaBar Collab.) [[arXiv:0912.2453](#)].
45. C. Bernard *et al.* (Fermilab, MILC Collabs.), *PoS LATTICE 2008 278*, (2008) calculate $f_B = 195 \pm 11$ MeV, while E. Gamiz *et al.* (HPQCD Collab.) *Phys. Rev.* **D80**, 014503 (2009) find $f_B = 190 \pm 13$ MeV. We average the two results assuming the errors are fully correlated.
46. See the discussion in M. Artuso, E. Barberio and S. Stone, *PMC Physics A* **3:3** (2009) [[arXiv:0902.3743](#)].
47. In supersymmetric models there may be corrections which weaken our bound; a slightly different formula for r is given by Isidori and Paradisi, *Phys. Lett.* **B639**, 499 (2006) [[hep-ph/0605012](#)] that depends on a model dependent value of a parameter - ϵ_0 .
48. W.J. Marciano and A. Sirlin, *Phys. Rev. Lett.* **71**, 3629 (1993); V. Cirigliano and I. Rosell, *JHEP* **0710**, 005 (2007).
49. Flavianet Working Group on Precise SM Tests in K Decays, <http://www.lnf.infn.it/wg/vus>. See M. Antonelli *et al.*, *Nucl. Phys. Proc. Suppl.* **181-182**, 83 (2008). For a recent detailed review, see M. Antonelli *et al.*, [[arXiv:0907.5386](#)].
50. P. A. Boyle *et al.*, *Phys. Rev. Lett.* **100**, 141601 (2008).
51. H. Leutwyler and M. Roos, *Z. Phys.* **C25**, 91 (1984).
52. N. Cabibbo, E. C. Swallow and R. Winston, *Phys. Rev. Lett.* **92**, 251803 (2004).
53. S. Durr *et al.*, [[arXiv:1001.4692](#)] (2010).

See key on page 405

Meson Particle Listings

 $D_{s1}(2536)^{\pm}, D_{s2}(2573), D_{s1}^*(2700)^{\pm}$

$\Gamma((D^*(2010)+K^0)_{S\text{-wave}})/\Gamma(D^*(2010)+K^0)$						Γ_2/Γ_1
VALUE	EVTS	DOCUMENT ID	TECN	COMMENT		
$0.72 \pm 0.05 \pm 0.01$	5485	BALAGURA	08	BELL	$10.6 e^+ e^- \rightarrow D^* K^0 X$	
$\Gamma(D^+ \pi^- K^+)/\Gamma(D^*(2010)+K^0)$						Γ_4/Γ_1
VALUE (units 10^{-2})	EVTS	DOCUMENT ID	TECN	COMMENT		
$3.27 \pm 0.18 \pm 0.37$	1264	BALAGURA	08	BELL	$10.6 e^+ e^- \rightarrow D^+ \pi^- K^+ X$	
$\Gamma(D^+ K^0)/\Gamma(D^*(2010)+K^0)$						Γ_6/Γ_1
VALUE	CL%	DOCUMENT ID	TECN	COMMENT		
<0.40	90	ALEXANDER	93	CLEO	$e^+ e^- \rightarrow D^* K^0 X$	
<0.43	90	ALBRECHT	89E	ARG	$D_{s1}^* \rightarrow D^*(2010) K^0$	
$\Gamma(D^0 K^+)/\Gamma(D^*(2007)^0 K^+)$						Γ_7/Γ_5
VALUE	CL%	DOCUMENT ID	TECN	COMMENT		
<0.12	90	ALEXANDER	93	CLEO	$e^+ e^- \rightarrow D^{*0} K^+ X$	
$\Gamma(D_s^{*+} \gamma)/\Gamma_{\text{total}}$						Γ_8/Γ
VALUE	DOCUMENT ID	TECN	COMMENT			
possibly seen	ASRATYAN	88	HLBC	$\nu N \rightarrow D_s \gamma X$		
$\Gamma(D_s^{*+} \gamma)/\Gamma(D^*(2007)^0 K^+)$						Γ_8/Γ_5
VALUE	CL%	DOCUMENT ID	TECN	COMMENT		
<0.42	90	ALEXANDER	93	CLEO	$e^+ e^- \rightarrow D^{*0} K^+ X$	
$\Gamma(D_s^+ \pi^+ \pi^-)/\Gamma_{\text{total}}$						Γ_9/Γ
VALUE	DOCUMENT ID	TECN	COMMENT			
seen	AUBERT	06P	BABR	$10.6 e^+ e^- \rightarrow D_s^+ \pi^+ \pi^- X$		

 $D_{s1}(2536)^{\pm}$ REFERENCES

ABAZOV	09G	PRL 102 051801	V.M. Abazov et al.	(D0 Collab.)
CHEKANOV	09	EPJ C60 25	S. Chekanov et al.	(ZEUS Collab.)
AUBERT	08B	PR D77 011102R	B. Aubert et al.	(BABAR Collab.)
BALAGURA	08	PR D77 032001	V. Balagura et al.	(BELLE Collab.)
AUBERT	06P	PR D74 032007	B. Aubert et al.	(BABAR Collab.)
PDG	06	JPG 33 1	W.-M. Yao et al.	(PDG Collab.)
HEISTER	02B	PL B526 34	A. Heister et al.	(ALEPH Collab.)
ACKERSTAFF	97W	ZPHY C76 425	K. Akerstaff et al.	(OPAL Collab.)
ASRATYAN	94	ZPHY C61 563	A.E. Asratyan et al.	(BIRM, BELG, CERN+)
FRABETTI	94B	PRL 72 324	P.L. Frabetti et al.	(FNAL E807 Collab.)
ALEXANDER	93	PL B303 377	J. Alexander et al.	(CLEO Collab.)
ALBRECHT	92R	PL B297 425	H. Albrecht et al.	(ARGUS Collab.)
AVERY	90	PR D41 774	P. Avery, D. Besson	(CLEO Collab.)
ALBRECHT	89E	PL B230 162	H. Albrecht et al.	(ARGUS Collab.)
ASRATYAN	88	ZPHY C40 483	A.E. Asratyan et al.	(ITEP, SERP)

 $D_{s2}^*(2573)$

$$I(J^P) = 0(?)^?$$

 J^P is natural, width and decay modes consistent with 2^+ . $D_{s2}^*(2573)$ MASS

VALUE (MeV)	EVTS	DOCUMENT ID	TECN	CHG	COMMENT
2572.6 ± 0.9 OUR AVERAGE					
$2572.2 \pm 0.3 \pm 1.0$		AUBERT,BE	06E	BABR	$e^+ e^- \rightarrow D K X$
$2574.5 \pm 3.3 \pm 1.6$		ALBRECHT	96	ARG	$e^+ e^- \rightarrow D^0 K^+ X$
$2573.2_{-1.6}^{+1.7} \pm 0.9$	217	KUBOTA	94	CLE2	+ $e^+ e^- \sim 10.5$ GeV

••• We do not use the following data for averages, fits, limits, etc. •••

2570.0 ± 4.3 25 ¹ EVDOKIMOV 04 SELX $600 \Sigma^- A \rightarrow D^0 K^+ X$

2568.6 ± 3.2 64 ² HEISTER 02B ALEP $e^+ e^- \rightarrow D^0 K^+ X$

¹ Not independent of the mass difference below.

² Calculated using $m_{D^0} = 1864.5 \pm 0.5$ MeV and the mass difference below.

 $m_{D_{s2}^*(2573)} - m_{D^0}$

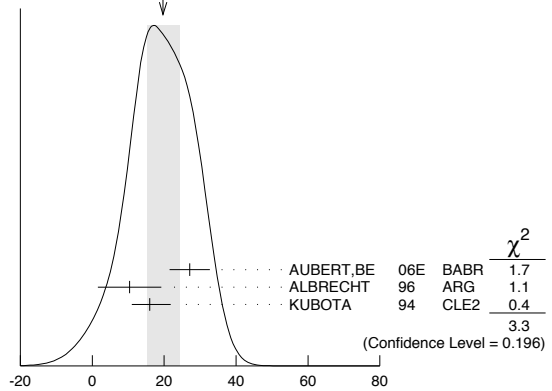
VALUE (MeV)	EVTS	DOCUMENT ID	TECN	COMMENT
$704 \pm 3 \pm 1$	64	HEISTER	02B	ALEP $e^+ e^- \rightarrow D^0 K^+ X$
••• We do not use the following data for averages, fits, limits, etc. •••				
705.4 ± 4.3	25	³ EVDOKIMOV	04	SELX $600 \Sigma^- A \rightarrow D^0 K^+ X$

³ Systematic errors not estimated.

 $D_{s2}^*(2573)$ WIDTH

VALUE (MeV)	EVTS	DOCUMENT ID	TECN	CHG	COMMENT
20 ± 5 OUR AVERAGE		Error includes scale factor of 1.3. See the ideogram below.			
$27.1 \pm 0.6 \pm 5.6$		AUBERT,BE	06E	BABR	$e^+ e^- \rightarrow D K X$
$10.4 \pm 8.3 \pm 3.0$		ALBRECHT	96	ARG	$e^+ e^- \rightarrow D^0 K^+ X$
$16_{-4}^{+5} \pm 3$	217	KUBOTA	94	CLE2	+ $e^+ e^- \sim 10.5$ GeV
••• We do not use the following data for averages, fits, limits, etc. •••					
14_{-6}^{+9}	25	⁴ EVDOKIMOV	04	SELX	$600 \Sigma^- A \rightarrow D^0 K^+ X$

⁴ Systematic errors not estimated.

WEIGHTED AVERAGE
20±5 (Error scaled by 1.3) $D_{s2}^*(2573)^+$ DECAY MODES

$D_{s2}^*(2573)^-$ modes are charge conjugates of the modes below.

Mode	Fraction (Γ_i/Γ)
$\Gamma_1 D^0 K^+$	seen
$\Gamma_2 D^*(2007)^0 K^+$	not seen

 $D_{s2}^*(2573)^+$ BRANCHING RATIOS

$\Gamma(D^0 K^+)/\Gamma_{\text{total}}$						Γ_1/Γ
VALUE	EVTS	DOCUMENT ID	TECN	CHG	COMMENT	
seen	217	KUBOTA	94	CLE2	\pm	$e^+ e^- \sim 10.5$ GeV
$\Gamma(D^*(2007)^0 K^+)/\Gamma(D^0 K^+)$						Γ_2/Γ_1
VALUE	CL%	DOCUMENT ID	TECN	CHG	COMMENT	
<0.33	90	KUBOTA	94	CLE2	+	$e^+ e^- \sim 10.5$ GeV

 $D_{s2}^*(2573)$ REFERENCES

AUBERT,BE	06E	PRL 97 222001	B. Aubert et al.	(BABAR Collab.)
EVDOKIMOV	04	PRL 93 242001	A.V. Evdokimov et al.	(SELEX Collab.)
HEISTER	02B	PL B526 34	A. Heister et al.	(ALEPH Collab.)
ALBRECHT	96	ZPHY C69 405	H. Albrecht et al.	(ARGUS Collab.)
KUBOTA	94	PRL 72 1972	Y. Kubota et al.	(CLEO Collab.)

 $D_{s1}^*(2700)^{\pm}$

$$I(J^P) = 0(1^-)$$

OMITTED FROM SUMMARY TABLE

 $D_{s1}^*(2700)^+$ MASS

VALUE (MeV)	EVTS	DOCUMENT ID	TECN	COMMENT
2709_{-6}^{+9} OUR AVERAGE				
$2710 \pm 2_{-7}^{+12}$	10.4k	¹ AUBERT	09AR	BABR $e^+ e^- \rightarrow D^{(*)} K X$
$2708 \pm 9_{-10}^{+11}$	182	BRODZICKA	08	BELL $B^+ \rightarrow D^0 \bar{D}^0 K^+$
••• We do not use the following data for averages, fits, limits, etc. •••				
$2688 \pm 4 \pm 3$		² AUBERT,BE	06E	BABR $10.6 e^+ e^- \rightarrow D K X$

¹ From simultaneous fits to the two DK mass spectra and to the total $D^* K$ mass spectrum.

² Superseded by AUBERT 09AR.

 $D_{s1}^*(2700)^+$ WIDTH

VALUE (MeV)	EVTS	DOCUMENT ID	TECN	COMMENT
125 ± 30 OUR AVERAGE				
$149 \pm 7_{-52}^{+39}$	10.4k	³ AUBERT	09AR	BABR $e^+ e^- \rightarrow D^{(*)} K X$
$108 \pm 23_{-31}^{+36}$	182	BRODZICKA	08	BELL $B^+ \rightarrow D^0 \bar{D}^0 K^+$
••• We do not use the following data for averages, fits, limits, etc. •••				
$112 \pm 7 \pm 36$		⁴ AUBERT,BE	06E	BABR $10.6 e^+ e^- \rightarrow D K X$
³ From simultaneous fits to the two DK mass spectra and to the total $D^* K$ mass spectrum.				
⁴ Superseded by AUBERT 09AR.				

Meson Particle Listings

 $D_{s1}^*(2700)^\pm, D_{sJ}^*(2860)^\pm, D_{sJ}(3040)^\pm$ $D_{s1}^*(2700)^\pm$ DECAY MODES

Mode	
Γ_1 DK	
Γ_2 $D^0 K^+$	
Γ_3 $D^+ K_S^0$	
Γ_4 $D^* K$	
Γ_5 $D^{*0} K^+$	
Γ_6 $D^{*+} K_S^0$	

 $D_{s1}^*(2700)^\pm$ BRANCHING RATIOS

$\Gamma(D^* K)/\Gamma(DK)$		Γ_4/Γ_1		
VALUE	EVTS	DOCUMENT ID	TECN	COMMENT
$0.91 \pm 0.13 \pm 0.12$	10.4k	⁵ AUBERT	09AR BABR	$e^+ e^- \rightarrow D^{(*)} KX$
⁵ From the average of the corresponding ratios with $D^{(*)0} K^+$ and $D^{(*)+} K_S^0$.				

$\Gamma(D^{*0} K^+)/\Gamma(D^0 K^+)$		Γ_5/Γ_2		
VALUE	EVTS	DOCUMENT ID	TECN	COMMENT
$0.88 \pm 0.14 \pm 0.14$	7716	⁶ AUBERT	09AR BABR	$e^+ e^- \rightarrow D^{(*)} KX$
⁶ From the $D^{*0} K^+$ and $D^0 K^+$, where $D^{*0} \rightarrow D^0 \pi^0$.				

$\Gamma(D^{*+} K_S^0)/\Gamma(D^+ K_S^0)$		Γ_6/Γ_3		
VALUE	EVTS	DOCUMENT ID	TECN	COMMENT
$1.14 \pm 0.39 \pm 0.23$	2700	⁷ AUBERT	09AR BABR	$e^+ e^- \rightarrow D^{(*)} KX$
⁷ From the $D^{*+} K_S^0$ and $D^+ K_S^0$, where $D^{*+} \rightarrow D^+ \pi^0$.				

 $D_{s1}^*(2700)^\pm$ REFERENCES

AUBERT	09AR	PR D80 092003	B. Aubert <i>et al.</i>	(BABAR Collab.)
BRODZICKA	08	PRL 100 092001	J. Brodzicka <i>et al.</i>	(BELLE Collab.)
AUBERT, BE	06E	PRL 97 222001	B. Aubert <i>et al.</i>	(BABAR Collab.)

$D_{sJ}^*(2860)^\pm$ $I(J^P) = 0(??)$

OMITTED FROM SUMMARY TABLE

Observed by AUBERT, BE 06E and AUBERT 09AR in inclusive production of DK and D^*K in e^+e^- annihilation. J^P is natural. $D_{sJ}^*(2860)^+$ MASS

VALUE (MeV)	EVTS	DOCUMENT ID	TECN	COMMENT
$2862 \pm 2 \pm \frac{5}{2}$	3122	¹ AUBERT	09AR BABR	$e^+ e^- \rightarrow D^{(*)} KX$
$\bullet \bullet \bullet$ We do not use the following data for averages, fits, limits, etc. $\bullet \bullet \bullet$				
$2856.6 \pm 1.5 \pm 5.0$		² AUBERT, BE	06E BABR	$e^+ e^- \rightarrow DKX$
¹ From simultaneous fits to the two DK mass spectra and to the total D^*K mass spectrum.				
² Superseded by AUBERT 09AR.				

 $D_{sJ}^*(2860)^+$ WIDTH

VALUE (MeV)	EVTS	DOCUMENT ID	TECN	COMMENT
$48 \pm 3 \pm 6$	3122	³ AUBERT	09AR BABR	$e^+ e^- \rightarrow D^{(*)} KX$
$\bullet \bullet \bullet$ We do not use the following data for averages, fits, limits, etc. $\bullet \bullet \bullet$				
$47 \pm 7 \pm 10$		⁴ AUBERT, BE	06E BABR	$e^+ e^- \rightarrow DKX$
³ From simultaneous fits to the two DK mass spectra and to the total D^*K mass spectrum.				
⁴ Superseded by AUBERT 09AR.				

 $D_{sJ}^*(2860)^\pm$ DECAY MODES

Mode	
Γ_1 DK	
Γ_2 $D^0 K^+$	
Γ_3 $D^+ K_S^0$	
Γ_4 $D^* K$	
Γ_5 $D^{*0} K^+$	
Γ_6 $D^{*+} K_S^0$	

 $D_{sJ}^*(2860)^\pm$ BRANCHING RATIOS

$\Gamma(D^* K)/\Gamma(DK)$		Γ_4/Γ_1		
VALUE	EVTS	DOCUMENT ID	TECN	COMMENT
$1.10 \pm 0.15 \pm 0.19$	3122	⁵ AUBERT	09AR BABR	$e^+ e^- \rightarrow D^{(*)} KX$
⁵ From the average of the corresponding ratios with $D^{(*)0} K^+$ and $D^{(*)+} K_S^0$.				

$\Gamma(D^{*0} K^+)/\Gamma(D^0 K^+)$		Γ_5/Γ_2		
VALUE	EVTS	DOCUMENT ID	TECN	COMMENT
$1.04 \pm 0.17 \pm 0.20$	2241	⁶ AUBERT	09AR BABR	$e^+ e^- \rightarrow D^{(*)} KX$
⁶ From the $D^{*0} K^+$ and $D^0 K^+$, where $D^{*0} \rightarrow D^0 \pi^0$.				

$\Gamma(D^{*+} K_S^0)/\Gamma(D^+ K_S^0)$		Γ_6/Γ_3		
VALUE	EVTS	DOCUMENT ID	TECN	COMMENT
$1.38 \pm 0.35 \pm 0.49$	881	⁷ AUBERT	09AR BABR	$e^+ e^- \rightarrow D^{(*)} KX$
⁷ From the $D^{*+} K_S^0$ and $D^+ K_S^0$, where $D^{*+} \rightarrow D^+ \pi^0$.				

 $D_{sJ}^*(2860)^\pm$ REFERENCES

AUBERT	09AR	PR D80 092003	B. Aubert <i>et al.</i>	(BABAR Collab.)
AUBERT, BE	06E	PRL 97 222001	B. Aubert <i>et al.</i>	(BABAR Collab.)

$D_{sJ}(3040)^\pm$

 $I(J^P) = 0(??)$

OMITTED FROM SUMMARY TABLE

Observed by AUBERT 09AR in inclusive production of D^*K in e^+e^- annihilation. $D_{sJ}(3040)^+$ MASS

VALUE (MeV)	DOCUMENT ID	TECN	COMMENT
$3044 \pm 8 \pm \frac{30}{5}$	AUBERT	09AR BABR	$e^+ e^- \rightarrow D^* KX$

 $D_{sJ}(3040)^+$ WIDTH

VALUE (MeV)	DOCUMENT ID	TECN	COMMENT
$239 \pm 35 \pm \frac{46}{42}$	AUBERT	09AR BABR	$e^+ e^- \rightarrow D^* KX$

 $D_{sJ}(3040)^\pm$ DECAY MODES

Mode	
Γ_1 $D^* K$	
Γ_2 $D^{*0} K^+$	
Γ_3 $D^{*+} K_S^0$	

 $D_{sJ}(3040)^\pm$ REFERENCES

AUBERT	09AR	PR D80 092003	B. Aubert <i>et al.</i>	(BABAR Collab.)
--------	------	---------------	-------------------------	-----------------

OTHER RELATED PAPERS

SUN	09	PR D80 074037	Z.-F. Sun, X. Lin
-----	----	---------------	-------------------

BOTTOM MESONS**($B = \pm 1$)** $B^+ = u\bar{d}, B^0 = d\bar{b}, \bar{B}^0 = \bar{d}b, B^- = \bar{u}b$, similarly for B^{*} 's***B*-particle organization**

Many measurements of *B* decays involve admixtures of *B* hadrons. Previously we arbitrarily included such admixtures in the B^\pm section, but because of their importance we have created two new sections: “ B^\pm/B^0 Admixture” for $\Upsilon(4S)$ results and “ $B^\pm/B^0/B_s^0/b$ -baryon Admixture” for results at higher energies. Most inclusive decay branching fractions and χ_b at high energy are found in the Admixture sections. B^0 - \bar{B}^0 mixing data are found in the B^0 section, while B_s^0 - \bar{B}_s^0 mixing data and B - \bar{B} mixing data for a B^0/B_s^0 admixture are found in the B_s^0 section. *CP*-violation data are found in the B^\pm, B^0 , and B^\pm/B^0 Admixture sections. *b*-baryons are found near the end of the Baryon section. Recently, we also created a new section: “ V_{cb} and V_{ub} CKM Matrix Elements.”

The organization of the *B* sections is now as follows, where bullets indicate particle sections and brackets indicate reviews.

[Production and Decay of *b*-flavored Hadrons]

[A Short Note on HFAG Activities]

- B^\pm
 - mass, mean life
 - branching fractions
 - polarization in B^\pm decay
 - CP* violation
- B^0
 - mass, mean life
 - branching fractions
 - [Polarization in *B* decay]
 - polarization in B^0 decay
 - [B - \bar{B} Mixing]
 - B^0 - \bar{B}^0 mixing
 - CP* violation
- B^\pm/B^0 Admixture
 - branching fractions, *CP* violation
 - CP* violation
- $B^\pm/B^0/B_s^0/b$ -baryon Admixture
 - mean life
 - production fractions
 - branching fractions
 - χ_b at high energy
 - production fractions in hadronic *Z* decay
- V_{cb} and V_{ub} CKM Matrix Elements
 - [Determination of V_{cb} and V_{ub}]

- B^*
 - mass
- $B_1(5721)^0$
 - mass
- $B_J^*(5732)$
 - mass, width
- $B_2(5747)^0$
 - mass
- B_s^0
 - mass, mean life
 - branching fractions
 - polarization in B_s^0 decay
 - B_s^0 - \bar{B}_s^0 mixing
- B_s^*
 - mass
- $B_{s,J}^*(5850)$
 - mass, width
- B_c^\pm
 - mass, mean life
 - branching fractions

At the end of Baryon Listings:

- Λ_b
 - mass, mean life
 - branching fractions
- Σ_b, Σ_b^*
 - mass
- Ξ_b^0, Ξ_b^-
 - mean life
- Ω_b^-
 - mass, mean life
 - branching fractions
- *b*-baryon Admixture
 - mean life
 - branching fractions

PRODUCTION AND DECAY OF *b*-FLAVORED HADRONS

Updated March 2010 by Y. Kwon (Yonsei U., Seoul, Korea), G. Punzi (U. and INFN, Pisa, Italy), and J.G. Smith (U. of Colorado, Boulder, CO, USA).

The *b* quark belongs to the third generation of quarks and is the weak-doublet partner of the *t* quark. The existence of the third-generation quark doublet was proposed in 1973 by Kobayashi and Maskawa [1] in their model of the quark mixing matrix (“CKM” matrix), and confirmed four years later by the first observation of a $b\bar{b}$ meson [2]. In the KM model, *CP* violation is explained within the Standard Model (SM) by an irreducible phase of the 3×3 unitary matrix. The regular pattern of the three lepton and quark families is one of the most intriguing puzzles in particle physics. The existence of families gives rise to many of the free parameters in the SM, including the fermion masses, and the elements of the CKM matrix.

Since the *b* quark is the lighter element of the third-generation quark doublet, the decays of *b*-flavored hadrons occur via generation-changing processes through this matrix. Because of this, and the fact that the CKM matrix is close to a 3×3 unit matrix, many interesting features such as loop and box diagrams, flavor oscillations, as well as large *CP* asymmetries, can be observed in the weak decays of *b*-flavored hadrons.

The CKM matrix is parameterized by three real parameters and one complex phase. This complex phase can become a source of *CP* violation in *B* meson decays. A crucial milestone was the first observation of *CP* violation in the *B* meson system in 2001, by the BaBar [3] and Belle [4] collaborations. They measured a large value for the parameter $\sin 2\beta$ ($= \sin 2\phi_1$) [5], almost four decades after the discovery of a small *CP* asymmetry in neutral kaons. A more detailed discussion of the CKM matrix and *CP* violation can be found elsewhere in this Review [6,7].

Recent developments in the physics of *b*-hadrons include the observation of direct *CP* violation, results for rare higher-order weak decays, investigations of heavier *b*-hadrons (B_s^0 , B_c , baryons, excited states), measurement of the B_s^0 -mixing frequency, increasingly accurate determinations of the CKM matrix parameters.

The structure of this mini-review is organized as follows. After a brief description of theory and terminology, we discuss *b*-quark production and current results on spectroscopy

Meson Particle Listings

b-flavored hadrons

and lifetimes of *b*-flavored hadrons. We then discuss some basic properties of *B*-meson decays, followed by summaries of hadronic, rare, and electroweak penguin decays of *B*-mesons. There are separate mini-reviews for $B\bar{B}$ mixing [8] and the extraction of the CKM matrix elements V_{cb} and V_{ub} from *B*-meson decays [9] in this *Review*.

Theory and terminology: The ground states of *b*-flavored hadrons decay via weak interactions. In most hadrons, the *b*-quark is accompanied by light-partner quarks (*d*, *u*, or *s*), and the decay modes are well described by the decay of the *b* quark (spectator model) [10]. The dominant decay mode of a *b* quark is $b \rightarrow cW^{*-}$ (referred to as a “tree” or “spectator” decay), where the virtual *W* materializes either into a pair of leptons $\ell\bar{\nu}$ (“semileptonic decay”), or into a pair of quarks which then hadronizes. The decays in which the spectator quark combines with one of the quarks from W^* to form one of the final state hadrons are suppressed by a factor $\sim (1/3)^2$, because the colors of the two quarks from different sources must match (“color-suppression”).

Many aspects of *B* decays can be understood through the Heavy Quark Effective Theory (HQET) [11]. This has been particularly successful for semileptonic decays. For further discussion of HQET, see for instance Ref. 9. For hadronic decays, one typically uses effective Hamiltonian calculations that rely on a perturbative expansion with Wilson coefficients. In addition, some form of the factorization hypothesis is commonly used, where, in analogy with semileptonic decays, two-body hadronic decays of *B* mesons are expressed as the product of two independent hadronic currents, one describing the formation of a charm meson (in case of the dominant $b \rightarrow cW^{*-}$ decays), and the other the hadronization of the remaining $\bar{u}d$ (or $\bar{c}s$) system from the virtual W^- . Qualitatively, for a *B* decay with a large energy release, the $\bar{u}d$ pair (produced as a color singlet) travels fast enough to leave the interaction region without influencing the charm meson. This is known to work well for the dominant spectator decays [12]. There are several common implementations of these ideas for hadronic *B* decays, the most common of which are QCD factorization (QCDF) [13], perturbative QCD (pQCD) [14], and soft collinear effective theory (SCET) [15].

The transition $b \rightarrow u$ is suppressed by $|V_{ub}/V_{cb}|^2 \sim (0.1)^2$ relative to $b \rightarrow c$ transitions, and gives way to rarer decay modes, *e.g.*, loop-induced $b \rightarrow s$ decays. The transition $b \rightarrow s$ is a flavor-changing neutral-current (FCNC) process, and although not allowed in the SM as a tree-process, can occur via more complex diagrams (denoted “penguin” decays). The rates for such processes are comparable or larger than CKM-suppressed $b \rightarrow u$ processes. Penguin processes involving $b \rightarrow d$ transitions are also possible, and have recently been observed [16,17]. Other decay processes discussed in this *Review* include *W*-exchange (a *W* is exchanged between initial-state quarks), penguin annihilation (the gluon from a penguin loop attaches to the spectator quark, similar to an exchange diagram), and pure-annihilation (the initial quarks annihilate to a virtual *W*, which then decays).

Production and spectroscopy: The bound states of a \bar{b} antiquark and a *u*, *d*, *s*, or *c* quark are referred to as the B_u (B^+), B_d (B^0), B_s^0 , and B_c^+ mesons, respectively. The B_c^+ is the heaviest of the ground-state *b*-flavored mesons, and the most difficult to produce: it was observed for the first time in the semileptonic mode by CDF in 1998 [18], but its mass was accurately determined only in 2006, from the fully reconstructed mode $B_c^+ \rightarrow J/\psi\pi^+$ [19].

The first excited meson is called the B^* meson, while B^{**} is the generic name for the four orbitally excited ($L = 1$) *B*-meson states that correspond to the *P*-wave mesons in the charm system, D^{**} . Excited states of the B_s^0 meson are similarly named B_s^{*0} and B_s^{**0} . Of the possible bound $\bar{b}b$ states, the Υ series (S-wave) and the χ_b (P-wave) are well studied. The pseudoscalar ground state η_b has been observed only recently by BaBar [20] (and confirmed by CLEO [21]), indirectly through the decay $\Upsilon(3S) \rightarrow \gamma\eta_b$. See Ref. 22 for classification and naming of these and other states.

Experimental studies of *b* decays have been performed in e^+e^- collisions at the $\Upsilon(4S)$ (ARGUS, CLEO, Belle, BaBar) and $\Upsilon(5S)$ (CLEO, Belle) resonances, as well as at higher energies, at the *Z* resonance (SLC, LEP) and in $p\bar{p}$ collisions (Tevatron). The $e^+e^- \rightarrow b\bar{b}$ production cross-section at the *Z*, $\Upsilon(4S)$, and $\Upsilon(5S)$ resonances are about 6.6 *nb*, 1.1 *nb*, and 0.3 *nb* respectively. High-energy hadron collisions produce *b*-flavored hadrons of all species with much larger cross-sections: $\sigma(p\bar{p} \rightarrow bX, |y| < 1) \sim 30 \mu\text{b}$ at the Tevatron ($\sqrt{s} = 1.96 \text{ TeV}$), and even higher at the energies of the LHC pp collider (up to a factor of ten at $\sqrt{s} = 14 \text{ TeV}$).

BaBar and Belle have accumulated respectively 560 fb^{-1} and 1020 fb^{-1} of data, of which 433 fb^{-1} and 710 fb^{-1} respectively at the $\Upsilon(4S)$ resonance, while CDF and D0 have currently accumulated about 7 fb^{-1} each. These numbers imply that the majority of *b*-quarks have been produced in hadron collisions, but the large backgrounds cause the hadron collider experiments to have lower efficiency. Only the few decay modes for which triggering and reconstruction are easiest have been studied so far in hadron collisions. Up to now, these have included final states with leptons, and exclusive modes with all charged particles in the final state. In contrast, detectors operating at e^+e^- colliders (“B-Factories”) have a high efficiency for most decays, and have provided large samples of a rich variety of decays of B^0 and B^+ mesons.

In hadron collisions, most production happens as $b\bar{b}$ pairs, either via *s*-channel production or gluon-splitting, with a smaller fraction of single *b*-quarks produced by flavor excitation. The total *b*-production cross section is an interesting test of our understanding of QCD processes. For many years, experimental measurements have been several times higher than predictions. With improved measurements [23], more accurate input parameters, and more advanced calculations [24], the discrepancy between theory and data is now much reduced, although the presence of inconsistencies among existing measurements makes further studies desirable.

Each quark of a $b\bar{b}$ pair produced in hadron collisions hadronizes separately and incoherently from the other, but it is still possible, although difficult, to obtain a statistical indication of the charge of a produced b/\bar{b} quark (“flavor tag” or “charge tag”) from the accompanying particles produced in the hadronization process, or from the decay products of the other quark. The momentum spectrum of produced b -quarks typically peaks near the b -quark mass, and extends to much higher momenta, dropping by about a decade for every ten GeV. This implies typical decay lengths of the order of a millimeter, that are important to resolve the fast oscillations of B_s^0 mesons.

In e^+e^- colliders, since the B mesons are very slow in the $\Upsilon(4S)$ rest frame, asymmetric beam energies are used to boost the decay products to improve the precision of time-dependent measurements that are crucial for the study of CP violation. At KEKB, the boost is $\beta\gamma = 0.43$, and the typical B -meson decay length is dilated from $\approx 20 \mu\text{m}$ to $\approx 200 \mu\text{m}$. PEP-II uses a slightly larger boost, $\beta\gamma = 0.55$. The two B mesons produced in $\Upsilon(4S)$ decay are in a coherent quantum state, which makes it easier than in hadron collision to infer the charge state of one B meson from observation of the other; however, the coherence also requires to determine the decay time of both mesons, rather than just one, in order to perform time-dependent CP -violation measurements.

For the measurement of branching fractions, the initial composition of the data sample must be known. The $\Upsilon(4S)$ resonance decays predominantly to $B^0\bar{B}^0$ and B^+B^- ; the current experimental upper limit for non- $B\bar{B}$ decays of the $\Upsilon(4S)$ is less than 4% at the 95% confidence level (CL) [25]. The only known modes of this category are decays to lower Υ states and a pion pair, recently observed with branching fractions of order 10^{-4} [26]. The ratio f_+/f_0 of the fractions of charged to neutral B productions from $\Upsilon(4S)$ decays has been measured by CLEO, BaBar, and Belle in various ways, typically based on pairs of isospin-related decays of B^+ and B^0 , such that it can be assumed that $\Gamma(B^+ \rightarrow x^+) = \Gamma(B^0 \rightarrow x^0)$. In this way, the ratio of the number of events observed in these modes is proportional to $(f_+\tau_+)/ (f_0\tau_0)$ [27–30]. BaBar has also performed an independent measurement of f_0 with a different method that does not require isospin symmetry or the value of the lifetime ratio, based on the number of events with one or two reconstructed $B^0 \rightarrow D^{*-}\ell^+\nu$ decays [31]. The combined result, from the current average of τ_+/τ_0 , is $f_+/f_0 = 1.068 \pm 0.029$ [32]. This number is currently a bit less consistent with equal production of B^+B^- and $B^0\bar{B}^0$ pairs than it used to be in the past (deviates from unity by 2.5σ), but we still assume $f_+/f_0 = 1$ in this mini-review except where explicitly stated otherwise. This assumption is also supported by the near equality of the B^+ and B^0 masses: our fit of CLEO, ARGUS, and CDF measurements yields $m(B^0) = 5279.50 \pm 0.33 \text{ MeV}/c^2$, $m(B^+) = 5279.13 \pm 0.31 \text{ MeV}/c^2$, and $m(B^0) - m(B^+) = 0.37 \pm 0.24 \text{ MeV}/c^2$.

CLEO and Belle have also collected some data at the $\Upsilon(5S)$ resonance [34,35], Belle in particular has been taking a large

fraction of its recent data at this resonance, and accumulated more than 100 fb^{-1} at the time of this writing. This resonance does not provide the simple final states of the $\Upsilon(4S)$: there are seven possible final states with a pair of non-strange B mesons and three with a pair of strange B mesons ($B_s^*\bar{B}_s^*$, $B_s^*\bar{B}_s^0$, and $B_s^0\bar{B}_s^0$). The fraction of events with a pair of B_s^0 mesons over the total number of events with a pair of b -flavored hadrons has been measured to be $f_s[\Upsilon(5S)] = 0.193 \pm 0.029$, of which 90% is made of $B_s^{*0}\bar{B}_s^{*0}$ events. A few branching fractions of the B_s^0 have been measured in this way, and if a precise knowledge of f_s can be reached, they could be made the most accurate. A few new B_s^0 modes have been observed that are difficult to reconstruct in hadron colliders, and the most precise mass measurement of the B_s^{*0} meson has been obtained [35,36]. However, the small boost of B_s^0 mesons produced in this way prevents resolution of their fast oscillations for time-dependent measurements; these are only accessible in hadron collisions or at the Z peak.

In high-energy collisions, the produced b or \bar{b} quarks can hadronize with different probabilities into the full spectrum of b -hadrons, either in their ground or excited states. Table 1 shows the measured fractions f_d , f_u , f_s , and f_{baryon} of B^0 , B^+ , B_s^0 , and b baryons, respectively, in an unbiased sample of weakly decaying b hadrons produced at the Z resonance and in $p\bar{p}$ collisions [32]. The results were obtained from a fit where the sum of the fractions were constrained to equal 1.0, neglecting production of B_c mesons. The observed yields of B_c mesons at the Tevatron [18], provide an estimate $f_c = 0.2\%$, in agreement with expectations [37], which is below the current experimental uncertainties in the other fractions.

The combined values assume identical hadronization in $p\bar{p}$ collisions and in Z decay. These could in principle differ, because of the different momentum distributions of the b -quark in these processes; the sample used in the $p\bar{p}$ measurements has momenta close to the b mass, rather than $m_Z/2$. A test of the agreement between production fractions may be given by comparison of values of the average time-integrated mixing probability parameter $\bar{\chi} = f_d\chi_d + f_s\chi_s$ [8], which is an important input in the determination of the world-averages of production fractions. The current measurements of $\bar{\chi}$ from LEP and Tevatron differ by 1.8σ [32]. This slight discrepancy causes a larger uncertainty in the combined fractions in Table 1. With the availability of increasing large samples of b -flavored mesons and baryons at $p\bar{p}$ colliders, the limited knowledge of these fractions has become an important limiting factor in the determination of their branching fractions.

Excited B -meson states have been observed by CLEO, LEP, CUSB, D0, and CDF. The current world average of the $B^{*-}B$ mass difference is $45.78 \pm 0.35 \text{ MeV}/c^2$. Evidence for B^{**} ($L=1$) production has been initially obtained at LEP [38], as a broad resonance in the mass of an inclusively reconstructed bottom hadron candidate combined with a charged pion from the primary vertex. Detailed results from exclusive modes have been recently obtained at the Tevatron, allowing separation of

Meson Particle Listings

b-flavored hadrons

Table 1: Fractions of weakly-decaying *b*-hadron species in $Z \rightarrow b\bar{b}$ decay and in $p\bar{p}$ collisions at $\sqrt{s} = 1.8$ TeV.

<i>b</i> hadron	Fraction at Z [%]	Fraction at $p\bar{p}$ [%]	Combined [%]
B^+, B^0	40.2 ± 0.9	33.2 ± 3.0	40.0 ± 1.2
B_s^0	10.5 ± 0.9	12.2 ± 1.4	11.5 ± 1.3
<i>b</i> baryons	9.1 ± 1.5	21.4 ± 6.8	8.5 ± 2.1

the narrow states B_1 and B_2^* , and at CDF also a measurement of the B_2^* width [39].

Also the narrow B_s^{**} states, first sighted by OPAL as a single broad enhancement in the B^+K mass spectrum [40], have now been clearly observed and separately measured at the Tevatron [41]: $M(B_{s1}) = 5829.4 \pm 0.7$ MeV/ c^2 (CDF) and $M(B_{s2}^*) = 5839.7 \pm 0.7$ MeV/ c^2 (CDF), $M(B_{s2}^*) = 5839.6 \pm 1.1 \pm 0.7$ MeV/ c^2 (D0).

Baryon states containing a *b* quark are labeled according to the same scheme used for non-*b* baryons, with the addition of a *b* subscript [22]. For many years, the only well-established *b* baryon was the Λ_b^0 (quark composition *udb*), with only indirect evidence for Ξ_b (*dsb*) production from LEP [42]. This situation has changed dramatically in the past few years due to the large samples being accumulated at the Tevatron. Clear signals of four strongly-decaying baryon states, $\Sigma_b^+, \Sigma_b^{*+}$ (*uub*), $\Sigma_b^-, \Sigma_b^{*-}$ (*ddb*) have been obtained by CDF in $\Lambda_b^0\pi^\pm$ final states [43]. The strange bottom baryon Ξ_b^\pm has been observed in the exclusive mode $\Xi_b^\pm \rightarrow J/\psi\Xi^\pm$ by D0 [44], and CDF [45] that also measured its lifetime individually for the first time (was previously only known from a mix). The relative production of Ξ_b and Λ_b baryons has been found to be consistent with the B_s to B_d production ratio [44]. Observation of the doubly-strange bottom baryon Ω_b^- has been published by both D0 [46] and CDF [47]. The masses measured by the two experiments show however a large discrepancy that still needs to be resolved. Apart from this discrepancy, the masses of all these new baryons have been measured to a precision of a few MeV/ c^2 , and found to be in agreement with predictions from HQET.

Lifetimes: Precise lifetimes are key in extracting the weak parameters that are important for understanding the role of the CKM matrix in *CP* violation, such as the determination of V_{cb} and $B_s^0\bar{B}_s^0$ mixing parameters. In the naive spectator model, the heavy quark can decay only via the external spectator mechanism, and thus, the lifetimes of all mesons and baryons containing *b* quarks would be equal. Non-spectator effects, such as the interference between contributing amplitudes, modify this simple picture and give rise to a lifetime hierarchy for *b*-flavored hadrons similar to the one in the charm sector. However, since the lifetime differences are expected to scale as $1/m_Q^2$, where m_Q is the mass of the heavy quark, the variations in the *b* system are expected to be significantly smaller; on the order of 10% or less [48]. We expect:

$$\tau(B^+) \geq \tau(B^0) \approx \tau(B_s^0) > \tau(\Lambda_b^0) \gg \tau(B_c^+). \quad (1)$$

In the B_c^+ , both quarks can decay weakly, resulting in a much shorter lifetime.

Measurements of the lifetimes of the different *b*-flavored hadrons thus provide a means to determine the importance of non-spectator mechanisms in the *b* sector. Over the past years, the precision of silicon vertex detectors and the increasing availability of fully-reconstructed samples yielded measurements with much-reduced statistical and systematic uncertainties, at the 1% level. The averaging of precision results from different experiments is a complex task that requires careful treatment of correlated systematic uncertainties; the world averages given in this mini-review Table 2 have been determined by the Heavy Flavor Averaging Group (HFAG) [32].

Table 2: Summary of inclusive and exclusive world-average *b*-hadron lifetime measurements. For the two B_s^0 averages, see text below.

Particle	Lifetime [ps]
B^+	1.638 ± 0.011
B^0	1.525 ± 0.009
B_s^0 (flavor-specific)	1.417 ± 0.042
B_s^0 ($1/\Gamma_s$)	$1.472^{+0.024}_{-0.026}$
B_c^+	0.453 ± 0.041
Λ_b^0	$1.391^{+0.038}_{-0.037}$
Ξ_b^-	$1.56^{+0.27}_{-0.25}$
Ω_b^-	$1.13^{+0.53}_{-0.40}$
Ξ_b mixture	$1.49^{+0.19}_{-0.18}$
<i>b</i> -baryon mixture	1.345 ± 0.032
<i>b</i> -hadron mixture	1.568 ± 0.009

The short B_c^+ lifetime is in good agreement with predictions [49]. For precision comparisons with theory, lifetime ratios are more sensitive. Experimentally we find:

$$\frac{\tau_{B^+}}{\tau_{B^0}} = 1.071 \pm 0.009, \quad \frac{\tau_{B_s^0}}{\tau_{B^0}} = 0.965 \pm 0.017,$$

$$\frac{\tau_{\Lambda_b}}{\tau_{B^0}} = 0.912 \pm 0.025,$$

while theory makes the following predictions [48,50]

$$\frac{\tau_{B^+}}{\tau_{B^0}} = 1.06 \pm 0.02, \quad \frac{\tau_{B_s^0}}{\tau_{B^0}} = 1.00 \pm 0.01, \quad \frac{\tau_{\Lambda_b}}{\tau_{B^0}} = 0.88 \pm 0.05.$$

The ratio of B^+ to B^0 is measured to better than 1%, and is significantly different from one, in agreement with predictions [48]. Conversely, the ratio of B_s^0 to B^0 lifetimes is expected to be very close to one, but exhibits a 2.5σ deviation. The Λ_b lifetime has a history of discrepancies. Predictions used to be higher than data, before the introduction of higher-order effects lowered them. The recent measurements, from CDF on the exclusive $J/\psi\Lambda$ mode [51], and from D0 [52] on both semileptonic and $J/\psi\Lambda$ mode, disagree at the 3σ level. The most recent CDF measurement [53] appears to improve the agreement with theory again.

Neutral B mesons are two-component systems similar to neutral kaons, with a light (L) and a heavy (H) mass eigenstate, and independent decay widths Γ_L and Γ_H . The SM predicts a non-zero width difference $\Delta\Gamma = \Gamma_L - \Gamma_H > 0$ for both B_s and B_d . For B_d , $\Delta\Gamma_d/\Gamma_d$ is expected to be $\sim 0.2\%$. Analysis of BaBar and DELPHI data on CP -specific modes of the B^0 yield a combined result: $\Delta\Gamma_d/\Gamma_d = 0.009 \pm 0.037$ [32]. The issue is much more interesting for the B_s , since the SM expectation for $\Delta\Gamma_s/\Gamma_s$ is of order 10%. This potentially non-negligible difference requires care when defining the B_s^0 lifetime. As indicated in Table 2, two different lifetimes are defined for the B_s^0 meson: one is defined as $1/\Gamma_s$, where Γ_s is the average width of the two mass eigenstates $(\Gamma_L + \Gamma_H)/2$; the other is obtained from “flavor-specific” decays (*e.g.*, semileptonic) and depends both on Γ_s and $\Delta\Gamma_s$. Experimentally, the quantity $\Delta\Gamma_s$ can be accessed by measuring lifetimes in decays into CP eigenstates, which are expected to be close approximations to the mass eigenstates. This has been done with the $J/\psi\phi$ mode, where the two CP eigenstates are distinguished by angular distributions, and in $B_s^0 \rightarrow K^+K^-$ which is dominated by a single CP -state. The current experimental information is dominated by CDF and D0 measurements on the $J/\psi\phi$ mode. By appropriately combining all published measurements of $J/\psi\phi$ lifetimes and flavor-specific lifetimes, the HFAG group obtains a world-average $\Delta\Gamma_s/\Gamma_s = 0.092^{+0.051}_{-0.054}$ [32]; the quoted uncertainties are, however, non-Gaussian, and a better representation of the current uncertainty is given by the 95% CL interval: $-0.020 < \Delta\Gamma_s/\Gamma_s < 0.193$ [32], which is compatible with zero; the latest theoretical predictions yield $\Delta\Gamma_s/\Gamma_s = 0.147 \pm 0.060$ [54], in agreement with the experiment within the large uncertainties on both. From the theoretical point of view, the best quantity to use is $\Delta\Gamma_s/\Delta M_s$, which is much less affected by hadronic uncertainties: $\Delta\Gamma_s/\Delta M_s = (49.7 \pm 9.4) \times 10^{-4}$ [54]. Exploiting the very accurate measurement of ΔM_s now available [58], this can be turned into a SM prediction with just 20% uncertainty: $\Delta\Gamma_s/\Gamma_s = 0.127 \pm 0.024$. This is likely to be of importance in future comparisons, as the experimental precision improves with the growth of Tevatron samples. Further improvements may come from $B_s^0 \rightarrow K^+K^-$, and alternative (model-dependent) determinations via the $B_s^0 \rightarrow D_s^{(*)+}D_s^{(*)-}$ branching fraction [57].

The width difference $\Delta\Gamma_s$ is connected to the B_s^0 mixing phase ϕ_s by $\Delta\Gamma_s = \Gamma_{12} \cos \phi_s$, where Γ_{12} is the off-diagonal term of the decay matrix [6,8,54]. Both CDF [55] and D0 [56] have produced CL contours in the $(\phi_s, \Delta\Gamma)$ plane from their measurements, and both observe a mild deviation, in the same direction, from the expectation of the Standard model of a phase ϕ_s close to zero. They have combined their measurements from samples of 2.8 fb^{-1} each to make a Tevatron average, obtaining a deviation from predictions at a level slightly above 2σ [33]. The possibility of a large value of ϕ_s has attracted significant interest, as it would be a very clean evidence for the

existence of new sources of CP violation beyond the standard model, and is currently a target of active investigation.

B meson decay properties: Semileptonic B decays $B \rightarrow X_c \ell \nu$ and $B \rightarrow X_u \ell \nu$ provide an excellent way to measure the magnitude of the CKM elements $|V_{cb}|$ and $|V_{ub}|$ respectively, because the strong interaction effects are much simplified due to the two leptons in the final state. Both exclusive and inclusive decays can be used, and the nature of uncertainties are quite complementary. For exclusive decay analysis, knowledge of the form factors for the exclusive hadronic system $X_{c(u)}$ is required. For inclusive analysis, it is usually necessary to restrict the available phase-space of the decay products to suppress backgrounds; subsequently uncertainties are introduced in the extrapolation to the full phase-space. Moreover, restriction to a small corner of the phase-space may result in breakdown of the operator-product expansion scheme, thus making theoretical calculations unreliable. A more detailed discussion of B semileptonic decays and the extraction of $|V_{cb}|$ and $|V_{ub}|$ is given elsewhere in this *Review* [9].

On the other hand, hadronic decays of B are complicated because of strong interaction effects caused by the surrounding cloud of light quarks and gluons. While this complicates the extraction of CKM matrix elements, it also provides a great opportunity to study perturbative and non-perturbative QCD, hadronization, and Final State Interaction (FSI) effects. Pure-penguin decays were first established by the observation of $B \rightarrow K^* \gamma$ [59]. Some observed decay modes such as $B^0 \rightarrow D_s^- K^+$, may be interpreted as evidence of a W -exchange process [60]. The recent evidence for the decay $B^+ \rightarrow \tau^+ \nu$ from Belle [61] and BaBar [62] is the first sign of a pure annihilation decay. There is growing evidence that penguin annihilation processes may be important in decays with two vector mesons in the final state [63].

Hadronic decays:

Most of the hadronic B decays involve $b \rightarrow c$ transition at the quark level, resulting in a charmed hadron or charmonium in the final state. Other types of hadronic decays are very rare and will be discussed separately in the next section. The experimental results on hadronic B decays have steadily improved over the past few years, and the measurements have reached sufficient precision to challenge our understanding of the dynamics of these decays. With the good neutral particle detection and hadron identification capabilities of B -factory detectors, a substantial fraction of hadronic B decay events can be fully reconstructed. Because of the kinematic constraint of $\Upsilon(4S)$, the energy sum of the final-state particles of a B meson decay is always equal to one half of the total energy in the center of mass frame. As a result, the two variables, ΔE (energy difference) and M_B (B candidate mass with a beam-energy constraint) are very effective for suppressing combinatorial background both from $\Upsilon(4S)$ and $e^+e^- \rightarrow q\bar{q}$ continuum events. In particular, the energy-constraint in M_B improves the signal resolution by almost an order of magnitude.

Meson Particle Listings

b-flavored hadrons

The kinematically clean environment of B meson decays provides an excellent opportunity to search for new states. For instance, quark-level $b \rightarrow c\bar{c}s$ decays have been used to search for new charmonium and charm-strange mesons and study their properties in detail. In 2003, BaBar discovered a new narrow charm-strange state $D_{sJ}^*(2317)$ [64], and CLEO observed a similar state $D_{sJ}(2460)$ [65]. However, the properties of these new states were not well known until Belle observed $B \rightarrow DD_{sJ}^*(2317)$ and $B \rightarrow DD_{sJ}(2460)$, which helped identify some quantum numbers of $D_{sJ}(2460)$ [66]. Further studies of $D_{sJ}^{(*)}$ meson production in B decays have been made by Belle and BaBar. In particular, BaBar has observed $B \rightarrow D_{sJ}^*(2317)^+\bar{D}^{(*)}$ ($D_{sJ}^*(2317)^+ \rightarrow D_s^+\pi^0$) and $B \rightarrow D_{sJ}(2460)^+\bar{D}^{(*)}$ ($D_{sJ}(2460)^+ \rightarrow D_s^+\pi^0$, $D_s^+\gamma$) decays. The angular analysis of $B \rightarrow D_{sJ}(2460)^+\bar{D}$ with $D_{sJ}(2460)^+ \rightarrow D_s^+\gamma$ supports the $J^P = 1^+$ assignment for $D_{sJ}(2460)$. With a sample of 449 million $B\bar{B}$ pairs, Belle has observed a new D_{sJ} meson produced in $B^+ \rightarrow \bar{D}^0 D_{sJ} \rightarrow \bar{D}^0 D^0 K^+$ [67]. The mass and width of this state are measured to be $2708 \pm 9^{+11}_{-10}$ MeV/ c^2 and $108 \pm 23^{+36}_{-31}$ MeV, respectively. An analysis of the helicity angle distribution determines its spin-parity to be 1^- .

A variety of exotic particles have been discovered in B decays. Belle found the $X(3872)$ state [68], confirmed by CDF [69] and BaBar [71]. Belle has observed a near-threshold enhancement in the $\omega J/\psi$ invariant mass for $B \rightarrow K\omega J/\psi$ decays [72]. BaBar has studied $B \rightarrow J/\psi\pi^+\pi^-K$, finding an excess of $J/\psi\pi^+\pi^-$ events with a mass just above 4.2 GeV/ c^2 ; this is consistent with the $Y(4260)$ that was observed by BaBar in ISR (Initial State Radiation) events [74]. A Belle study of $B \rightarrow K\pi^\pm\psi'$ [75] finds a state called $Z^\pm(4430)$ that decays to $\pi^\pm\psi'$. Since it is charged, it could not be a charmonium state. This state was searched for by BaBar with similar sensitivity but was not found [76]. More details about these exotic states are described in a separate mini-review [77] in this *Review*.

There have been hundreds of publications on hadronic B decays to open-charm and charmonium final states mostly from the B -factory experiments. These results are nicely summarized in a recent report by HFAG [32].

Rare B decays: All B -meson decays that do not occur through the $b \rightarrow c$ transition are usually called rare B decays. These include both semileptonic and hadronic $b \rightarrow u$ decays that are suppressed at leading order by the small CKM matrix element V_{ub} , as well as higher-order $b \rightarrow s(d)$ processes such as electroweak and gluonic penguin decays.

Charmless B meson decays into two-body hadronic final states such as $B \rightarrow \pi\pi$ and $K\pi$ are experimentally clean, and provide good opportunities to probe new physics and search for indirect and direct CP violations. Since the final state particles in these decays tend to have larger momenta than average B decay products, the event environment is cleaner than for $b \rightarrow c$ decays. Branching fractions are typically around 10^{-5} . Over the past decade, many such modes have been observed by BaBar, Belle, and CLEO. More recently,

comparable samples of the modes with all charged final particles have been reconstructed in $p\bar{p}$ collisions by CDF by triggering on the impact parameter of the charged tracks. This has also allowed observation of charmless decays of the B_s^0 , in final states $\phi\phi$ [78], K^+K^- [79], and $K^-\pi^+$ [80], and of charmless decays of the Λ_b^0 baryon [80]. Charmless B_s^0 modes are related to corresponding B^0 modes by U-spin symmetry, and are determined by similar amplitudes. Combining the observables from B_s^0 and B^0 modes is a further way of eliminating hadronic uncertainties and extracting relevant CKM information [99].

Because of relatively high-momenta for final state particles, the dominant source of background in e^+e^- collisions is $q\bar{q}$ continuum events; sophisticated background suppression techniques exploiting event shape variables are essential for these analyses. In hadron collisions, the dominant background comes from QCD or partially reconstructed heavy flavors, and is similarly suppressed by a combination of kinematic and isolation requirements. The results are in general consistent among the four experiments.

BaBar [81] and Belle [82] have observed the decays $B^+ \rightarrow \bar{K}^0 K^+$ and $B^0 \rightarrow K^0 \bar{K}^0$. The world-average branching fractions are $\mathcal{B}(B^0 \rightarrow K^0 \bar{K}^0) = (0.96^{+0.20}_{-0.18}) \times 10^{-6}$ and $\mathcal{B}(B^+ \rightarrow \bar{K}^0 K^+) = (1.36 \pm 0.27) \times 10^{-6}$. These are the first observations of hadronic $b \rightarrow d$ transitions, with significance $> 5\sigma$ for all four measurements. CP asymmetries have even been measured for these modes, though with large errors.

Most rare decay modes including $B^0 \rightarrow K^+\pi^-$ have contributions from both $b \rightarrow u$ tree and $b \rightarrow sg$ penguin processes. If the size of the two contributions are comparable, the interference between them may result in direct CP violation, seen experimentally as a charge asymmetry in the decay rate measurement. BaBar [83], Belle [84], and CDF [85] have measured the direct CP violating asymmetry in $B^0 \rightarrow K^+\pi^-$ decays. The BaBar and Belle measurements constitute observation of direct CP violation with a significance of more than 5σ . The world average for this quantity is now rather precise, -0.098 ± 0.013 . There are sum rules that relate the decay rates and decay-rate asymmetries between the four $K\pi$ charge states. The experimental measurements of the other three modes are not yet precise enough to test these sum rules.

There is now evidence for direct CP violation in three other decays: $B^+ \rightarrow \rho^0 K^+$ [86], $B^+ \rightarrow \eta K^+$ [87], and $B^0 \rightarrow \eta K^{*0}$ [88]. The significance is typically 3–4 σ , though with the most recent BaBar measurement [87], this significance for the $B^+ \rightarrow \eta K^+$ decay is now more than 4 σ . In at least the first two cases, a large direct CP violation might be expected since the penguin amplitude is suppressed so the tree and penguin amplitudes may have comparable magnitudes.

The decay $B^0 \rightarrow \pi^+\pi^-$ can be used to extract the CKM angle α . This is complicated by the presence of significant contributions from penguin diagrams. An isospin analysis [89] can be used to untangle the penguin complications. The decay $B^0 \rightarrow \pi^0\pi^0$, which is now measured by both BaBar and Belle, is crucial in this analysis. Unfortunately the amount of

penguin pollution in the $B \rightarrow \pi\pi$ system is rather large. In the past few years, measurements in the $B^0 \rightarrow \rho\rho$ system have produced more precise values of α , since penguin amplitudes are generally smaller for decays with vector mesons. An important ingredient in the analysis is the $B^0 \rightarrow \rho^0\rho^0$ branching fraction. The average of recent measurements from BaBar and Belle BaBar [90] yields a branching fraction of $(0.73 \pm 0.28) \times 10^{-6}$. This is only 3% of the $\rho^+\rho^-$ branching fraction, much smaller than the corresponding ratio in the $\pi\pi$ system.

The decay $B \rightarrow a_1\pi$ has been seen by BaBar. An analysis of the time evolution of this decay [91] together with measurements of other related decays has recently been used to measure the CKM angle α [92] in agreement with the more precise measurements from the $\rho\rho$ system.

Since $B \rightarrow \rho\rho$ has two vector mesons in the final state, the CP eigenvalue of the final state depends on the longitudinal polarization fraction f_L for the decay. Therefore, a measurement of f_L is needed to extract the CKM angle α . Both BaBar and Belle have measured the f_L for the decays $\rho^+\rho^-$ and $\rho^+\rho^0$ and in both cases the measurements show $f_L > 0.9$, making a complete angular analysis unnecessary.

By analyzing the angular distributions of the B decays to two vector mesons, we can learn a lot about both weak- and strong-interaction dynamics in B decays. Decays that are penguin-dominated surprisingly have values of f_L near 0.5. The list of such decays has now grown to include $B \rightarrow \phi K^*$, $B \rightarrow \rho K^*$, and $B \rightarrow \omega K^*$. The reasons for this ‘‘polarization puzzle’’ are not fully understood. A detailed description of the angular analysis of B decays to two vector mesons can be found in a separate mini-review [93] in this *Review*.

There has been substantial progress in measurements of many other rare- B decays. The decay $B \rightarrow \eta'K$ stood out as the largest rare- B decay for many years. The reasons for the large rate are now largely understood [13,94]. However, there are now measurements of several 3-body or quasi-3-body modes with similarly large branching fractions. States seen so far include $K\pi\pi$ (three charge states) [95], KKK (four charge states) [96], and $K^*\pi\pi$ (two charged states) [97]. Many of these analyses now include quite sophisticated Dalitz plot treatments with many intermediate resonances. There has also been an observation of the decay $B^+ \rightarrow K^+K^-\pi^+$ by BaBar [98], noteworthy because an even number of kaons is typically indicative of suppressed $b \rightarrow d$ transitions as discussed above.

Belle [61] and BaBar [62] have found evidence for $B^+ \rightarrow \tau^+\nu$ with a combined branching fraction of $(180 \pm 50) \times 10^{-6}$ in good agreement with the value expected in the SM. This is the first evidence for a pure annihilation decay. A substantial region of parameter space of charged Higgs mass vs. $\tan\beta$ is excluded by the limit on this mode.

Electroweak penguin decays:

More than a decade has passed since the CLEO experiment first observed an exclusive radiative $b \rightarrow s\gamma$ transition, $B \rightarrow K^*(892)\gamma$ [59], thus providing the first evidence for the one-loop

FCNC electromagnetic penguin decay. Using much larger data samples, both Belle and BaBar have updated this analysis [100] with an average branching fraction $\mathcal{B}(B^0 \rightarrow K^{*0}\gamma) = (43.3 \pm 1.5) \times 10^{-6}$, and have added several new decay modes such as $B \rightarrow K_1\gamma$, $K_2^*(1430)\gamma$, *etc.* [101]. With a sample of 24 fb^{-1} at $\Upsilon(5S)$, Belle observed a radiative penguin decay of B_s^0 in $\phi\gamma$ mode with a branching fraction $(57_{-19}^{+22}) \times 10^{-6}$ [102].

Compared to $b \rightarrow s\gamma$, the $b \rightarrow d\gamma$ transitions such as $B \rightarrow \rho\gamma$, are suppressed by the small CKM element V_{td} . Both Belle and BaBar have observed these decays [16,17]. The world average $\mathcal{B}(B \rightarrow (\rho, \omega)\gamma) = (1.28 \pm 0.21) \times 10^{-6}$. This can be used to calculate $|V_{td}/V_{ts}|$ [103]; the measured values are $0.233_{-0.032}^{+0.033}$ from BaBar [17] and $0.195_{-0.024}^{+0.025}$ from Belle [16].

The observed radiative penguin branching fractions can constrain a large class of SM extensions [104]. However, due to the uncertainties in the hadronization, only the inclusive $b \rightarrow s\gamma$ rate can be reliably compared with theoretical calculations. This rate can be measured from the endpoint of the inclusive photon spectrum in B decay. By combining the measurements of $B \rightarrow X_s\gamma$ from CLEO, BaBar, and Belle experiments [105,106], HFAG obtains the new average: $\mathcal{B}(B \rightarrow X_s\gamma) = (3.55 \pm 0.24 \pm 0.09) \times 10^{-4}$ [107]. Consistent results have been reported by ALEPH for inclusive b -hadrons produced at the Z . The measured branching fraction can be compared to theoretical calculations. Recent calculations of $\mathcal{B}(b \rightarrow s\gamma)$ in NNLO level predict the values of $(3.15 \pm 0.23) \times 10^{-4}$ [108] and $(2.98 \pm 0.26) \times 10^{-4}$ [109], where the latter is calculated with a cut $E_\gamma \geq 1.6 \text{ GeV}$.

The CP asymmetry in $b \rightarrow s\gamma$ is extensively studied theoretically both in the SM and beyond [110]. According to the SM, the CP asymmetry in $b \rightarrow s\gamma$ is smaller than 1%, but some non-SM models allow significantly larger CP asymmetry ($\sim 10\%$) without altering the inclusive branching fraction. The current world average is $A_{CP} = -0.012 \pm 0.028$, again dominated by BaBar and Belle [111]. In addition to the CP asymmetry, BaBar also measured the isospin asymmetry $\Delta_{0-} = 0.06 \pm 0.17$ in $b \rightarrow s\gamma$ by measuring the companion B with full reconstruction in the hadronic decay modes [112].

In addition, all three experiments have measured the inclusive photon energy spectrum for $b \rightarrow s\gamma$, and by analyzing the shape of the spectrum they obtain the first and second moments for photon energies. Belle has measured these moments covering the widest range in the photon energy ($1.7 < E_\gamma < 2.8 \text{ GeV}$) [106]. These results can be used to extract non-perturbative HQET parameters that are needed for precise determination of the CKM matrix element V_{ub} .

Additional information on FCNC processes can be obtained from $B \rightarrow X_s\ell^+\ell^-$ decays, which are mediated by electroweak penguin and W -box diagrams. Their branching fractions have been measured by Belle [113], BaBar [114], and CDF [115]. Average branching fractions over all charged and neutral modes have been determined from BaBar and Belle data for $B \rightarrow K\ell^+\ell^-$: $(0.45 \pm 0.04) \times 10^{-6}$ and for $B \rightarrow K^*(892)\ell^+\ell^-$: $(1.08 \pm 0.11) \times 10^{-6}$, consistent with the

Meson Particle Listings

b-flavored hadrons

SM expectation. Both experiments also measured the branching fractions for inclusive $B \rightarrow X_s \ell^+ \ell^-$ decays [116], with an average of $(3.66_{-0.77}^{+0.76}) \times 10^{-6}$ [117].

Finally the decays $B_{(s)}^0 \rightarrow e^+ e^-$ and $\mu^+ \mu^-$ are interesting since they only proceed at second order in weak interactions in the SM, but may have large contributions from supersymmetric loops, proportional to $(\tan \beta)^6$. CDF and D0 as well as the *B*-factory experiments have obtained results that exclude a portion of the region allowed by SUSY models. The most stringent limits in these modes are obtained by CDF. The limits in the $\mu^+ \mu^-$ mode are: $< 5.8 \times 10^{-8}$ and $< 1.8 \times 10^{-8}$, respectively, for B_s^0 and B^0 [118]. For the B_s^0 mode, the result is just one order of magnitude above SM predictions [119]. The limits for the $e^+ e^-$ modes are: $< 2.8 \times 10^{-7}$ and $< 8.3 \times 10^{-8}$, respectively, for B_s^0 and B^0 [120]. There are also limits for lepton flavor-violating channels $B_{(s)}^0 \rightarrow e^+ \mu^-$, which are around 10^{-7} [120].

Summary and Outlook: The study of *B* mesons continues to be one of the most productive fields in particle physics. With the two asymmetric *B*-factory experiments Belle and BaBar, we now have a combined data sample of well over 1 ab^{-1} . *CP* violation has been firmly established in many decays of *B* mesons. Evidence for direct *CP* violation has been observed. Many rare decays such as hadronic $b \rightarrow u$ transitions and $b \rightarrow s(d)$ penguin decays have been observed, and the emerging pattern is still full of surprises. Despite the remarkable successes of the *B*-factory experiments, many fundamental questions in the flavor sector remain unanswered.

At Fermilab, CDF and D0 each has accumulated about 7 fb^{-1} , which is the equivalent of nearly 10^{12} *b*-hadrons produced. In spite of the low trigger efficiency of hadronic experiments, a selection of modes have been reconstructed in large quantities, giving a start to a program of studies on B_s^0 and *b*-flavored baryons, in which a first major step has been the determination of the B_s^0 oscillation frequency.

In addition, the LHC will soon produce huge samples of *b*-hadrons and consequently will enable us to test the CKM paradigm with unprecedented precision. There are also proposals for higher-luminosity *B* Factories at KEK and Frascati in order to increase the samples to $\sim 50 \text{ ab}^{-1}$, which will make it possible to explore the indirect evidence of new physics beyond the SM in the heavy-flavor particles (*b*, *c*, and τ), in a way that is complementary to the LHC.

These experiments promise a rich spectrum of rare and precise measurements that have the potential to fundamentally affect our understanding of the SM and *CP*-violating phenomena.

References

1. M. Kobayashi and T. Maskawa, *Prog. Theor. Phys.* **49**, 652 (1973).
2. S. W. Herb *et al.*, *Phys. Rev. Lett.* **39**, 252 (1977).
3. B. Aubert *et al.* (BaBar Collab.), *Phys. Rev. Lett.* **87**, 091801 (2001).
4. K. Abe *et al.* (Belle Collab.), *Phys. Rev. Lett.* **87**, 091802 (2001).
5. Currently two different notations (ϕ_1, ϕ_2, ϕ_3) and (α, β, γ) are used in the literature for CKM unitarity angles. In this mini-review, we use the latter notation following the other mini-reviews in this *Review*. The two notations are related by $\phi_1 = \beta$, $\phi_2 = \alpha$ and $\phi_3 = \gamma$.
6. See the “*CP* Violation in Meson Decays” by D. Kirkby and Y. Nir in this *Review*.
7. See the “CKM Quark Mixing Matrix,” by A. Cecucci, Z. Ligeti, and Y. Sakai, in this *Review*.
8. See the “Review on B - \bar{B} Mixing,” by O. Schneider in this *Review*.
9. See the “Determination of $|V_{cb}|$ and $|V_{ub}|$,” by R. Kowalewski and T. Mannel in this *Review*.
10. The B_c is a special case, where a weak decay of the *c* quark is also possible, but the spectator model still applies.
11. B. Grinstein, *Nucl. Phys.* **B339**, 253 (1990); H. Georgi, *Phys. Lett.* **B240**, 447 (1990); A.F. Falk *et al.*, *Nucl. Phys.* **B343**, 1 (1990); E. Eichten and B. Hill, *Phys. Lett.* **B234**, 511 (1990).
12. M. Neubert, “Aspects of QCD Factorization,” [hep-ph/0110093](#), *Proceedings of HF9*, Pasadena (2001) and references therein; Z. Ligeti *et al.*, *Phys. Lett.* **B507**, 142 (2001).
13. M. Beneke *et al.*, *Phys. Rev. Lett.* **83**, 1914 (1999); *Nucl. Phys.* **B591**, 313 (2000); *Nucl. Phys.* **B606**, 245 (2001); M. Beneke and M. Neubert, *Nucl. Phys.* **B675**, 333 (2003).
14. Y.Y. Keum, H-n. Li, and A.I. Sanda, *Phys. Lett.* **B504**, 6 (2001); *Phys. Rev.* **D63**, 054008 (2001); Y.Y. Keum and H-n. Li, *Phys. Rev.* **D63**, 074006 (2001); C.D. Lü, K. Ukai, and M.Z. Yang, *Phys. Rev.* **D63**, 074009 (2001); C.D. Lü and M.Z. Yang, *Eur. Phys. J.* **C23**, 275 (2002).
15. C.W. Bauer, S. Fleming, and M.E. Luke, *Phys. Rev.* **D63**, 014006 (2001); C.W. Bauer *et al.*, *Phys. Rev.* **D63**, 114020 (2001); C.W. Bauer and I.W. Stewart, *Phys. Lett.* **B516**, 134 (2001).
16. N. Taniguchi *et al.* (Belle Collab.), *Phys. Rev. Lett.* **101**, 111801 (2008).
17. B. Aubert *et al.* (BaBar Collab.), *Phys. Rev.* **D78**, 112001 (2008).
18. F. Abe *et al.* (CDF Collab.), *Phys. Rev. Lett.* **81**, 2432 (1998); F. Abe *et al.* (CDF Collab.), *Phys. Rev.* **D58**, 112004 (1998).
19. D. Acosta *et al.* (CDF Collab.), *Phys. Rev. Lett.* **96**, 082002 (2006).
20. B. Aubert *et al.* (BABAR Collaboration), *Phys. Rev. Lett.* **101**, 071801 (2008) [Erratum-*ibid.* **102**, 029901 (2009)].
21. G. Bonvicini, *et al.* (CLEO Collaboration), *Phys. Rev.* **D81**, 031104 (2010).
22. See the note on “Naming scheme for hadrons,” by M. Roos and C.G. Wohl in this *Review*.
23. A. Abulencia *et al.* (CDF Collab.), *Phys. Rev.* **D75**, 012010 (2007), and references therein.
24. M. Cacciari *et al.*, *JHEP* **9805**, 007 (1998); S. Frixione and B. R. Webber, *JHEP* **0206**, 029 (2002); M. Cacciari

- et al.*, JHEP **0407**, 033 (2004); M. Cacciari *et al.*, JHEP **0604**, 006 (2006), and references therein.
25. B. Barish *et al.* (CLEO Collab.), Phys. Rev. Lett. **76**, 1570 (1996).
 26. B. Aubert *et al.* (BaBar Collab.), Phys. Rev. Lett. **96**, 232001 (2006); A. Sokolov *et al.* (Belle Collab.), Phys. Rev. **D75**, 071103 (R) (2007).
 27. J.P. Alexander *et al.* (CLEO Collab.), Phys. Rev. Lett. **86**, 2737 (2001).
 28. B. Aubert *et al.* (BaBar Collab.), Phys. Rev. **D65**, 032001 (2001); B. Aubert *et al.* (BaBar Collab.), Phys. Rev. **D69**, 071101 (2004).
 29. S.B. Athar *et al.* (CLEO Collab.), Phys. Rev. **D66**, 052003 (2002).
 30. N.C. Hastings *et al.* (Belle Collab.), Phys. Rev. **D67**, 052004 (2003).
 31. B. Aubert *et al.* (BaBar Collab.), Phys. Rev. Lett. **95**, 042001 (2005).
 32. E. Barberio *et al.* (Heavy Flavor Averaging Group), "Averages of b-hadron and c-hadron properties at the end of 2007," arXiv:0808.1297 [hep-ex], and online update at <http://www.slac.stanford.edu/xorg/hfag/>.
 33. "Tevatron B working group", at <http://tevbwg.fnal.gov>.
 34. G.S. Huang *et al.* (CLEO Collab.), Phys. Rev. **D75**, 012002 (2007).
 35. R. Louvot *et al.* (Belle Collab.), Phys. Rev. Lett. **102**, 021801 (2009).
 36. R. Louvot [Belle Collaboration], *Proceedings of EPS09*, Krakov, Poland (2009), arXiv:0909.2160 [hep-ex].
 37. M. Lusignoli, M. Masetti, and S. Petrarca, Phys. Lett. **B266**, 142 (1991); K. Cheung, Phys. Lett. **B472**, 408 (2000).
 38. P. Abreu *et al.* (DELPHI Collab.), Phys. Lett. **B345**, 598 (1995).
 39. T. Aaltonen *et al.* (CDF Collaboration), Phys. Rev. Lett. **102**, 102003 (2009); V.M. Abazov *et al.* (D0 Collab.), Phys. Rev. Lett. **99**, 172001 (2007).
 40. R. Akers *et al.* (OPAL Collab.), Z. Phys. **C66**, 19 (1995).
 41. T. Aaltonen *et al.* (CDF Collab.), Phys. Rev. Lett. **100**, 082001 (2008); V.M. Abazov *et al.* (D0 Collab.), Phys. Rev. Lett. **100**, 082002 (2008).
 42. D. Buskulic *et al.* (ALEPH Collab.), Phys. Lett. **B384**, 449 (1996); P. Abreu *et al.* (DELPHI Collab.), Z. Phys. **C68**, 541 (1995).
 43. T. Aaltonen *et al.* (CDF Collab.), Phys. Rev. Lett. **99**, 202001 (2007).
 44. V.M. Abazov *et al.* (Co Collab.), Phys. Rev. Lett. **99**, 052001 (2007).
 45. T. Aaltonen *et al.* (CDF Collab.), Phys. Rev. Lett. **99**, 052002 (2007).
 46. V. M. Abazov *et al.* [D0 Collaboration], Phys. Rev. Lett. **101**, 232002 (2008).
 47. T. Aaltonen *et al.* [CDF Collaboration], Phys. Rev. **D80**, 072003 (2009).
 48. C. Tarantino, Eur. Phys. J. **C33**, S895 (2004); F. Gabbiani *et al.*, Phys. Rev. **D68**, 114006 (2003); F. Gabbiani *et al.*, Phys. Rev. **D70**, 094031 (2004).
 49. C.H. Chang *et al.*, Phys. Rev. **D64**, 014003 (2001); V.V. Kiselev, A.E. Kovalsky, and A.K. Likhoded, Nucl. Phys. **B585**, 353 (2000); V.V. Kiselev, arXiv:hep-ph/0308214, and references therein.
 50. I.I. Bigi *et al.*, in *B Decays*, 2nd ed., S. Stone (ed.), World Scientific, Singapore, 1994.
 51. A. Abulencia *et al.* (CDF Collab.), Phys. Rev. Lett. **98**, 122001 (2007).
 52. V.M. Abazov *et al.* (D0 Collab.), Phys. Rev. Lett. **99**, 182001 (2007); V.M. Abazov *et al.* (D0 Collab.), Phys. Rev. Lett. **99**, 142001 (2007).
 53. T. Aaltonen *et al.* (CDF Collab.), Phys. Rev. Lett. **104**, 102002 (2010).
 54. A. Lenz and U. Nierste, JHEP **0706**, 072 (2007).
 55. T. Aaltonen *et al.* (CDF Collab.), Phys. Rev. Lett. **100**, 121803 (2008).
 56. V.M. Abazov *et al.* (D0 Collab.), Phys. Rev. **D76**, 057101 (2007).
 57. R. Barate *et al.* (ALEPH Collab.), Phys. Lett. **B486**, 286 (2000); V.M. Abazov *et al.* (D0 Collab.), Phys. Rev. Lett. **99**, 241801 (2007).
 58. A. Abulencia *et al.* (CDF Collab.), Phys. Rev. Lett. **97**, 242003 (2006).
 59. R. Ammar *et al.* (CLEO Collab.), Phys. Rev. Lett. **71**, 674 (1993).
 60. P. Krokovny *et al.* (Belle Collab.), Phys. Rev. Lett. **89**, 231804 (2002); B. Aubert *et al.* (BaBar Collab.), Phys. Rev. Lett. **98**, 081801 (2007).
 61. K. Ikado *et al.* (Belle Collab.), Phys. Rev. Lett. **97**, 251802 (2006).
 62. B. Aubert *et al.* (BaBar Collab.), Phys. Rev. **D77**, 011107 (2008); B. Aubert *et al.* (BaBar Collab.), arXiv:0912.2453 (2009).
 63. M. Beneke, J. Rohrer, and D. Yang, Nucl. Phys. **B774**, 64 (2007).
 64. B. Aubert *et al.* (BaBar Collab.), Phys. Rev. Lett. **90**, 242001 (2003).
 65. D. Besson *et al.* (CLEO Collab.), Phys. Rev. **D68**, 032002 (2003).
 66. P. Krokovny *et al.* (Belle Collab.), Phys. Rev. Lett. **91**, 262002 (2003).
 67. J. Brodzicka *et al.* (Belle Collab.), Phys. Rev. Lett. **100**, 092001 (2008).
 68. S.-K. Choi *et al.* (Belle Collab.), Phys. Rev. Lett. **91**, 262001 (2003).
 69. D. Acosta *et al.* (CDF II Collab.), Phys. Rev. Lett. **93**, 072001 (2004); BaBar Collab., B. Aubert *et al.*, Phys. Rev. **D71**, 071103 (2005).
 70. G. Gokhroo *et al.* (Belle Collab.), Phys. Rev. Lett. **97**, 162002 (2006).
 71. B. Aubert *et al.* (BaBar Collab.), Phys. Rev. **D77**, 011102 (2008); B. Aubert *et al.* (BaBar Collab.), Phys. Rev. **D71**, 031501 (2005).
 72. S.-K. Choi *et al.* (Belle Collab.), Phys. Rev. Lett. **94**, 182002 (2005).
 73. B. Aubert *et al.* (BaBar Collab.), Phys. Rev. **D73**, 011101 (2006).
 74. B. Aubert *et al.* (BaBar Collab.), Phys. Rev. Lett. **95**, 142001 (2005).
 75. S.-K. Choi *et al.* (Belle Collab.), Phys. Rev. Lett. **100**, 142001 (2008).

Meson Particle Listings

b-flavored hadrons

-
76. B. Aubert *et al.* (BaBar Collab.), Phys. Rev. **D79**, 112001 (2009).
77. See the “Non- $q\bar{q}$ mesons,” by C. Amsler in this *Review*.
78. D. Acosta *et al.* (CDF Collab.), Phys. Rev. Lett. **95**, 031801 (2005).
79. A. Abulencia *et al.* (CDF Collab.), Phys. Rev. Lett. **97**, 211802 (2006).
80. T. Aaltonen *et al.* (CDF Collab.), Phys. Rev. Lett. **103**, 031801 (2009).
81. B. Aubert *et al.* (BaBar Collab.), Phys. Rev. Lett. **97**, 171805 (2006).
82. K. Abe *et al.* (Belle Collab.), Phys. Rev. Lett. **95**, 231802 (2005).
83. B. Aubert *et al.* (BaBar Collab.), Phys. Rev. Lett. **99**, 021603 (2007).
84. Y. Chao *et al.* (Belle Collab.), Phys. Rev. Lett. **93**, 191802 (2004).
85. M. Morello (CDF Collab.), Nucl. Phys. **B170**, 39 (2007).
86. B. Aubert *et al.* (BaBar Collab.), Phys. Rev. **D72**, 072003 (2005); A. Garmash *et al.* (Belle Collab.), Phys. Rev. Lett. **96**, 251803 (2006).
87. P. Chang *et al.* (Belle Collab.), Phys. Rev. **D75**, 071104 (2007); B. Aubert *et al.* (BaBar Collab.), Phys. Rev. **D80**, 112002 (2009).
88. B. Aubert *et al.* (BaBar Collab.), Phys. Rev. Lett. **97**, 201802 (2006); C.H. Wang *et al.* (Belle Collab.), Phys. Rev. **D75**, 092005 (2007).
89. M. Gronau and D. London, Phys. Rev. Lett. **65**, 3381 (1990).
90. B. Aubert *et al.* (BaBar Collab.), Phys. Rev. Lett. **98**, 111801 (2007); C.C. Chiang *et al.* (Belle Collab.), Phys. Rev. **D78**, 111102 (2008).
91. B. Aubert *et al.* (BaBar Collab.), Phys. Rev. Lett. **98**, 181803 (2007).
92. B. Aubert *et al.* (BaBar Collab.), arXiv:0909.2171 (to appear in PRD RC).
93. See the “Polarization in *B* Decays,” by A. Gritsan and J. Smith in this *Review*.
94. A. Williamson and J. Zupan, Phys. Rev. **D74**, 014003 (2006).
95. B. Aubert *et al.* (BaBar Collab.), Phys. Rev. **D78**, 012004 (2008); A. Garmash *et al.* (Belle Collab.), Phys. Rev. Lett. **96**, 251803 (2006); P. Chang *et al.* (Belle Collab.), Phys. Lett. **B599**, 148 (2004); B. Aubert *et al.* (BaBar Collab.), Phys. Rev. **D78**, 052005 (2008); A. Garmash *et al.* (Belle Collab.), Phys. Rev. **D75**, 012006 (2007); B. Aubert *et al.* (BaBar Collab.), Phys. Rev. **D80**, 112001 (2009).
96. A. Garmash *et al.* (Belle Collab.), Phys. Rev. **D71**, 092003 (2005); B. Aubert *et al.* (BaBar Collab.), Phys. Rev. **D74**, 032003 (2006); A. Garmash *et al.* (Belle Collab.), Phys. Rev. **D69**, 012001 (2004); B. Aubert *et al.* (BaBar Collab.), Phys. Rev. Lett. **93**, 181805 (2004); B. Aubert *et al.* (BaBar Collab.), Phys. Rev. Lett. **95**, 011801 (2006).
97. B. Aubert *et al.* (BaBar Collab.), Phys. Rev. **D74**, 051104R (2006); B. Aubert *et al.* (BaBar Collab.), Phys. Rev. **D76**, 071104R (2007).
98. B. Aubert *et al.* (BaBar Collab.), Phys. Rev. Lett. **99**, 221801 (2007).
99. R. Fleischer, Phys. Lett. **B459**, 306 (1999); D. London and J. Matias, Phys. Rev. **D70**, 031502 (2004).
100. M. Nakao *et al.* (Belle Collab.), Phys. Rev. **D69**, 112001 (2004); B. Aubert *et al.* (BaBar Collab.), Phys. Rev. Lett. **103**, 211802 (2009).
101. B. Aubert *et al.* (BaBar Collab.), Phys. Rev. **D70**, 091105R (2004); H. Yang *et al.* (Belle Collab.), Phys. Rev. Lett. **94**, 111802 (2005); S. Nishida *et al.* (Belle Collab.), Phys. Lett. **B610**, 23 (2005); B. Aubert *et al.* (BaBar Collab.), Phys. Rev. **D74**, 031102R (2004).
102. J. Wicht *et al.* (Belle Collab.), Phys. Rev. Lett. **100**, 121801 (2008).
103. A. Ali *et al.*, Phys. Lett. **B595**, 323 (2004); P. Ball, G. Jones, and R. Zwicky, Phys. Rev. **D75**, 054004 (2007).
104. J.L. Hewett, Phys. Rev. Lett. **70**, 1045 (1993).
105. S. Chen *et al.* (CLEO Collab.), Phys. Rev. Lett. **87**, 251807 (2001); B. Aubert *et al.* (BaBar Collab.), Phys. Rev. Lett. **97**, 171803 (2006).
106. A. Limosani *et al.* (Belle Collab.), Phys. Rev. Lett. **103**, 241801 (2009).
107. E. Barberio *et al.* (Heavy Flavor Averaging Group), “Averages of *b*-hadron and *c*-hadron properties at the end of 2009,” In preparation, and online update at <http://www.slac.stanford.edu/xorg/hfag/>.
108. M. Misiak *et al.*, Phys. Rev. Lett. **98**, 022002 (2007).
109. T. Becher and M. Neubert, Phys. Rev. Lett. **98**, 022003 (2007).
110. L. Wolfenstein and Y.L. Wu, Phys. Rev. Lett. **73**, 2809 (1994); H.M. Asatrian and A. Ioannisian, Phys. Rev. **D54**, 5642 (1996); M. Ciuchini *et al.*, Phys. Lett. **B388**, 353 (1996); S. Baek and P. Ko, Phys. Rev. Lett. **83**, 488 (1998); A.L. Kagan and M. Neubert, Phys. Rev. **D58**, 094012 (1998); K. Kiers *et al.*, Phys. Rev. **D62**, 116004 (2000).
111. S. Nishida *et al.* (Belle Collab.), Phys. Rev. Lett. **93**, 031803 (2004); B. Aubert *et al.* (BaBar Collab.), Phys. Rev. Lett. **101**, 171804 (2008).
112. B. Aubert *et al.* (BaBar Collab.), Phys. Rev. **D77**, 051103 (2008).
113. J.-T. Wei *et al.* (Belle Collab.), Phys. Rev. Lett. **103**, 171801 (2009).
114. B. Aubert *et al.* (BaBar Collab.), Phys. Rev. Lett. **102**, 091803 (2009).
115. T. Aaltonen *et al.* (CDF Collab.), Phys. Rev. **D79**, 011104 (2009).
116. M. Iwasaki *et al.* (Belle Collab.), Phys. Rev. **D72**, 092005 (2005); B. Aubert *et al.* (BaBar Collab.), Phys. Rev. Lett. **93**, 081802 (2004).
117. The average is calculated by HFAG [32] including the recent unpublished value by Belle.
118. T. Aaltonen *et al.* (CDF Collab.), Phys. Rev. Lett. **100**, 101802 (2008).
119. G. Buchalla and A.J. Buras, Nucl. Phys. **B400**, 225 (1993); A.J. Buras, Phys. Lett. **B566**, 115 (2003).
120. T. Aaltonen *et al.* (CDF Collab.), Phys. Rev. Lett. **102**, 201801 (2009).
-

A NOTE ON HFAG ACTIVITIES

The Heavy Flavor Averaging Group (HFAG) has been formed, continuing the activities of the LEP Heavy Flavor Steering group, to provide the averages for measurements dedicated to the b -flavor related quantities. The HFAG consists of representatives and contacts from the experimental groups: BaBar, Belle, CDF, CLEO, DØ, LEP, and SLD.

In the averaging the input parameters used in the various analyses are adjusted (rescaled) to common values, and all known correlations are taken into account. The HFAG has five subgroups providing averages for b -hadron lifetimes and B -oscillation parameters, CP -violation measurements, semileptonic parameters, rare branching fractions, and b -hadron decays to charm. The averages provided by the HFAG are listed as "OUR EVALUATION" with a corresponding note.

The most up-to-date and complete listing of averages and more detailed information on the averaging procedures are available at:

<http://www.slac.stanford.edu/xorg/hfag> and also at
<http://belle.kek.jp/mirror/hfag> (KEK mirror site).



$$J(P) = \frac{1}{2}(0^-)$$

Quantum numbers not measured. Values shown are quark-model predictions.

See also the B^\pm/B^0 ADMIXTURE and $B^\pm/B^0/B_s^0/b$ -baryon ADMIXTURE sections.

 B^\pm MASS

The fit uses m_{B^\pm} , ($m_{B^0} - m_{B^\pm}$), and m_{B^0} to determine m_{B^+} , m_{B^0} , and the mass difference.

VALUE (MeV)	EVTS	DOCUMENT ID	TECN	COMMENT
5279.17 ± 0.29	OUR FIT			
5279.1 ± 0.4	OUR AVERAGE			
5279.10 ± 0.41 ± 0.36		1 ACOSTA 06	CDF	$p\bar{p}$ at 1.96 TeV
5279.1 ± 0.4 ± 0.4	526	2 CSORNA 00	CLE2	$e^+e^- \rightarrow \Upsilon(4S)$
5279.1 ± 1.7 ± 1.4	147	ABE 96B	CDF	$p\bar{p}$ at 1.8 TeV
• • • We do not use the following data for averages, fits, limits, etc. • • •				
5278.8 ± 0.54 ± 2.0	362	ALAM 94	CLE2	$e^+e^- \rightarrow \Upsilon(4S)$
5278.3 ± 0.4 ± 2.0		BORTOLETTO92	CLEO	$e^+e^- \rightarrow \Upsilon(4S)$
5280.5 ± 1.0 ± 2.0		3 ALBRECHT 90J	ARG	$e^+e^- \rightarrow \Upsilon(4S)$
5275.8 ± 1.3 ± 3.0	32	ALBRECHT 87C	ARG	$e^+e^- \rightarrow \Upsilon(4S)$
5278.2 ± 1.8 ± 3.0	12	4 ALBRECHT 87D	ARG	$e^+e^- \rightarrow \Upsilon(4S)$
5278.6 ± 0.8 ± 2.0		BEBEK 87	CLEO	$e^+e^- \rightarrow \Upsilon(4S)$

- ¹ Uses exclusively reconstructed final states containing a $J/\psi \rightarrow \mu^+\mu^-$ decays.
² CSORNA 00 uses fully reconstructed $526 B^+ \rightarrow J/\psi(\ell^+) K^+$ events and invariant masses without beam constraint.
³ ALBRECHT 90J assumes 10580 for $\Upsilon(4S)$ mass. Supersedes ALBRECHT 87C and ALBRECHT 87D.
⁴ Found using fully reconstructed decays with $J/\psi(1S)$. ALBRECHT 87D assume $m_{\Upsilon(4S)} = 10577$ MeV.

 B^\pm MEAN LIFE

See $B^\pm/B^0/B_s^0/b$ -baryon ADMIXTURE section for data on B -hadron mean life averaged over species of bottom particles.

"OUR EVALUATION" is an average using rescaled values of the data listed below. The average and rescaling were performed by the Heavy Flavor Averaging Group (HFAG) and are described at <http://www.slac.stanford.edu/xorg/hfag/>. The averaging/rescaling procedure takes into account correlations between the measurements and asymmetric lifetime errors.

VALUE (10^{-12} s)	EVTS	DOCUMENT ID	TECN	COMMENT
1.638 ± 0.011	OUR EVALUATION			
1.635 ± 0.011 ± 0.011		1 ABE 05B	BELL	$e^+e^- \rightarrow \Upsilon(4S)$
1.624 ± 0.014 ± 0.018		2 ABDALLAH 04E	DLPH	$e^+e^- \rightarrow Z$
1.636 ± 0.058 ± 0.025		3 ACOSTA 02C	CDF	$p\bar{p}$ at 1.8 TeV
1.673 ± 0.032 ± 0.023		4 AUBERT 01F	BABR	$e^+e^- \rightarrow \Upsilon(4S)$
1.648 ± 0.049 ± 0.035		5 BARATE 00R	ALEP	$e^+e^- \rightarrow Z$

1.643 ± 0.037 ± 0.025		6 ABBIENDI 99J	OPAL	$e^+e^- \rightarrow Z$
1.637 ± 0.058 ± 0.045 ± 0.043		5 ABE 98Q	CDF	$p\bar{p}$ at 1.8 TeV
1.66 ± 0.06 ± 0.03		6 ACCIARRI 98S	L3	$e^+e^- \rightarrow Z$
1.66 ± 0.06 ± 0.05		6 ABE 97J	SLD	$e^+e^- \rightarrow Z$
1.58 ± 0.21 ± 0.04 ± 0.18 ± 0.03	94	3 BUSKULIC 96J	ALEP	$e^+e^- \rightarrow Z$
1.61 ± 0.16 ± 0.12		5,7 ABREU 95Q	DLPH	$e^+e^- \rightarrow Z$
1.72 ± 0.08 ± 0.06		8 ADAM 95	DLPH	$e^+e^- \rightarrow Z$
1.52 ± 0.14 ± 0.09		5 AKERS 95T	OPAL	$e^+e^- \rightarrow Z$
• • • We do not use the following data for averages, fits, limits, etc. • • •				
1.695 ± 0.026 ± 0.015		4 ABE 02H	BELL	Repl. by ABE 05B
1.68 ± 0.07 ± 0.02		3 ABE 98B	CDF	Repl. by ACOSTA 02C
1.56 ± 0.13 ± 0.06		5 ABE 96C	CDF	Repl. by ABE 98Q
1.58 ± 0.09 ± 0.03		9 BUSKULIC 96J	ALEP	$e^+e^- \rightarrow Z$
1.58 ± 0.09 ± 0.04		5 BUSKULIC 96J	ALEP	Repl. by BARATE 00R
1.70 ± 0.09		10 ADAM 95	DLPH	$e^+e^- \rightarrow Z$
1.61 ± 0.16 ± 0.05	148	3 ABE 94D	CDF	Repl. by ABE 98B
1.30 ± 0.33 ± 0.16 ± 0.29	92	5 ABREU 93D	DLPH	Sup. by ABREU 95Q
1.56 ± 0.19 ± 0.13	134	8 ABREU 93G	DLPH	Sup. by ADAM 95
1.51 ± 0.30 ± 0.12 ± 0.28 ± 0.14	59	5 ACTON 93C	OPAL	Sup. by AKERS 95T
1.47 ± 0.22 ± 0.15 ± 0.19 ± 0.14	77	5 BUSKULIC 93D	ALEP	Sup. by BUSKULIC 96J

- ¹ Measurement performed using a combined fit of CP -violation, mixing and lifetimes.
² Measurement performed using an inclusive reconstruction and B flavor identification technique.
³ Measured mean life using fully reconstructed decays.
⁴ Events are selected in which one B meson is fully reconstructed while the second B meson is reconstructed inclusively.
⁵ Data analyzed using $D/D^* \ell X$ event vertices.
⁶ Data analyzed using charge of secondary vertex.
⁷ ABREU 95Q assumes $B(B^0 \rightarrow D^{*-} \ell^+ \nu_\ell) = 3.2 \pm 1.7\%$.
⁸ Data analyzed using vertex-charge technique to tag B charge.
⁹ Combined result of $D/D^* \ell X$ analysis and fully reconstructed B analysis.
¹⁰ Combined ABREU 95Q and ADAM 95 result.

 B^+ DECAY MODES

B^- modes are charge conjugates of the modes below. Modes which do not identify the charge state of the B are listed in the B^\pm/B^0 ADMIXTURE section.

The branching fractions listed below assume 50% $B^0\bar{B}^0$ and 50% B^+B^- production at the $\Upsilon(4S)$. We have attempted to bring older measurements up to date by rescaling their assumed $\Upsilon(4S)$ production ratio to 50:50 and their assumed D, D_s, D^* , and ψ branching ratios to current values whenever this would affect our averages and best limits significantly.

Indentation is used to indicate a subchannel of a previous reaction. All resonant subchannels have been corrected for resonance branching fractions to the final state so the sum of the subchannel branching fractions can exceed that of the final state.

For inclusive branching fractions, e.g., $B \rightarrow D^\pm$ anything, the values usually are multiplicities, not branching fractions. They can be greater than one.

Mode	Fraction (Γ_i/Γ)	Scale factor/ Confidence level
Semileptonic and leptonic modes		
Γ_1 $\ell^+ \nu_\ell$ anything	[a] (10.99 ± 0.28) %	
Γ_2 $e^+ \nu_e X_C$	(10.8 ± 0.4) %	
Γ_3 $D \ell^+ \nu_\ell$ anything	(9.8 ± 0.7) %	
Γ_4 $\bar{D}^0 \ell^+ \nu_\ell$	[a] (2.23 ± 0.11) %	
Γ_5 $\bar{D}^0 \pi^+ \nu_\tau$	(7 ± 4) × 10 ⁻³	
Γ_6 $\bar{D}^*(2007)^0 \ell^+ \nu_\ell$	[a] (5.68 ± 0.19) %	
Γ_7 $\bar{D}^*(2007)^0 \pi^+ \nu_\tau$	(2.0 ± 0.5) %	
Γ_8 $D^- \pi^+ \ell^+ \nu_\ell$	(4.2 ± 0.5) × 10 ⁻³	
Γ_9 $\bar{D}_2^0(2420)^0 \ell^+ \nu_\ell \times$ $B(\bar{D}_2^0 \rightarrow D^+ \pi^-)$	(2.5 ± 0.5) × 10 ⁻³	
Γ_{10} $\bar{D}_2^*(2460)^0 \ell^+ \nu_\ell \times$ $B(\bar{D}_2^* \rightarrow D^+ \pi^-)$	(1.67 ± 0.30) × 10 ⁻³	S=1.2
Γ_{11} $D^{(*)} n \pi \ell^+ \nu_\ell$ ($n \geq 1$)	(1.86 ± 0.26) %	
Γ_{12} $D^{*-} \pi^+ \ell^+ \nu_\ell$	(6.1 ± 0.6) × 10 ⁻³	
Γ_{13} $\bar{D}_1(2420)^0 \ell^+ \nu_\ell \times B(\bar{D}_1^0 \rightarrow$ $D^{*+} \pi^-)$	(3.03 ± 0.20) × 10 ⁻³	
Γ_{14} $\bar{D}_1'(2430)^0 \ell^+ \nu_\ell \times B(\bar{D}_1'^0 \rightarrow$ $D^{*+} \pi^-)$	(2.7 ± 0.6) × 10 ⁻³	
Γ_{15} $\bar{D}_2^*(2460)^0 \ell^+ \nu_\ell \times$ $B(\bar{D}_2^* \rightarrow D^{*+} \pi^-)$	(1.85 ± 0.27) × 10 ⁻³	S=1.3

$\Gamma_{125} \overline{D}^0 D^*(2010)^+ + \overline{D}^*(2007)^0 D^+$	< 1.30	%	CL=90%	$\Gamma_{185} X(3945)^0 K^+ \times B(X^0 \rightarrow J/\psi \gamma)$	< 1.4	$\times 10^{-5}$	CL=90%
$\Gamma_{126} \overline{D}^0 D^*(2010)^+$	(3.9 ± 0.5)	$\times 10^{-4}$		$\Gamma_{186} Z(3930)^0 K^+ \times B(Z^0 \rightarrow J/\psi \gamma)$	< 2.5	$\times 10^{-6}$	CL=90%
$\Gamma_{127} \overline{D}^0 D^+$	(3.8 ± 0.4)	$\times 10^{-4}$		$\Gamma_{187} X(3945) K^+$			
$\Gamma_{128} \overline{D}^0 D^+ K^0$	< 2.8	$\times 10^{-3}$	CL=90%	$\Gamma_{188} J/\psi(1S) K^*(892)^+$	(1.43 ± 0.08)	$\times 10^{-3}$	
$\Gamma_{129} D^+ \overline{D}^*(2007)^0$	(6.3 ± 1.7)	$\times 10^{-4}$		$\Gamma_{189} J/\psi(1S) K(1270)^+$	(1.8 ± 0.5)	$\times 10^{-3}$	
$\Gamma_{130} \overline{D}^*(2007)^0 D^+ K^0$	< 6.1	$\times 10^{-3}$	CL=90%	$\Gamma_{190} J/\psi(1S) K(1400)^+$	< 5	$\times 10^{-4}$	CL=90%
$\Gamma_{131} \overline{D}^0 \overline{D}^*(2010)^+ K^0$	(5.2 ± 1.2)	$\times 10^{-3}$		$\Gamma_{191} J/\psi(1S) \eta K^+$	(1.08 ± 0.33)	$\times 10^{-4}$	
$\Gamma_{132} \overline{D}^*(2007)^0 D^*(2010)^+ K^0$	(7.8 ± 2.6)	$\times 10^{-3}$		$\Gamma_{192} J/\psi(1S) \eta' K^+$	< 8.8	$\times 10^{-5}$	CL=90%
$\Gamma_{133} \overline{D}^0 D^0 K^+$	(2.10 ± 0.26)	$\times 10^{-3}$		$\Gamma_{193} J/\psi(1S) \phi K^+$	(5.2 ± 1.7)	$\times 10^{-5}$	S=1.2
$\Gamma_{134} \overline{D}^*(2007)^0 D^0 K^+$	< 3.8	$\times 10^{-3}$	CL=90%	$\Gamma_{194} J/\psi(1S) \omega K^+$ nonresonant	(3.5 ± 0.4)	$\times 10^{-4}$	
$\Gamma_{135} \overline{D}^0 \overline{D}^*(2007)^0 K^+$	(4.7 ± 1.0)	$\times 10^{-3}$		$\Gamma_{195} J/\psi(1S) \pi^+$	(4.9 ± 0.4)	$\times 10^{-5}$	S=1.2
$\Gamma_{136} \overline{D}^*(2007)^0 D^*(2007)^0 K^+$	(5.3 ± 1.6)	$\times 10^{-3}$		$\Gamma_{196} J/\psi(1S) \rho^+$	(5.0 ± 0.8)	$\times 10^{-5}$	
$\Gamma_{137} D^- D^+ K^+$	< 4	$\times 10^{-4}$	CL=90%	$\Gamma_{197} J/\psi(1S) \pi^+ \pi^0$ nonresonant	< 7.3	$\times 10^{-6}$	CL=90%
$\Gamma_{138} D^- D^*(2010)^+ K^+$	< 7	$\times 10^{-4}$	CL=90%	$\Gamma_{198} J/\psi(1S) a_1(1260)^+$	< 1.2	$\times 10^{-3}$	CL=90%
$\Gamma_{139} D^*(2010)^- D^+ K^+$	(1.5 ± 0.4)	$\times 10^{-3}$		$\Gamma_{199} J/\psi(1S) \rho \overline{\lambda}$	(1.18 ± 0.31)	$\times 10^{-5}$	
$\Gamma_{140} D^*(2010)^- D^*(2010)^+ K^+$	< 1.8	$\times 10^{-3}$	CL=90%	$\Gamma_{200} J/\psi(1S) \overline{\Sigma}^0 p$	< 1.1	$\times 10^{-5}$	CL=90%
$\Gamma_{141} (\overline{D}^+ \overline{D}^*) (D^+ D^*) K$	(3.5 ± 0.6)	%		$\Gamma_{201} J/\psi(1S) D^+$	< 1.2	$\times 10^{-4}$	CL=90%
$\Gamma_{142} D_s^+ \pi^0$	(1.6 ± 0.5)	$\times 10^{-5}$		$\Gamma_{202} J/\psi(1S) \overline{D}^0 \pi^+$	< 2.5	$\times 10^{-5}$	CL=90%
$\Gamma_{143} D_s^+ \pi^0$	< 2.6	$\times 10^{-4}$	CL=90%	$\Gamma_{203} \psi(2S) \pi^+$	(2.58 ± 0.29)	$\times 10^{-5}$	
$\Gamma_{144} D_s^+ \eta$	< 4	$\times 10^{-4}$	CL=90%	$\Gamma_{204} \psi(2S) K^+$	(6.46 ± 0.33)	$\times 10^{-4}$	
$\Gamma_{145} D_s^+ \eta$	< 6	$\times 10^{-4}$	CL=90%	$\Gamma_{205} \psi(2S) K^*(892)^+$	(6.2 ± 1.2)	$\times 10^{-4}$	
$\Gamma_{146} D_s^+ \rho^0$	< 3.0	$\times 10^{-4}$	CL=90%	$\Gamma_{206} \psi(2S) K^+ \pi^+ \pi^-$	(1.9 ± 1.2)	$\times 10^{-3}$	
$\Gamma_{147} D_s^+ \rho^0$	< 4	$\times 10^{-4}$	CL=90%	$\Gamma_{207} \psi(3770) K^+$	(4.9 ± 1.3)	$\times 10^{-4}$	
$\Gamma_{148} D_s^+ \omega$	< 4	$\times 10^{-4}$	CL=90%	$\Gamma_{208} \psi(3770) K^+ \times B(\psi \rightarrow D^0 \overline{D}^0)$	(1.6 ± 0.4)	$\times 10^{-4}$	S=1.1
$\Gamma_{149} D_s^+ \omega$	< 6	$\times 10^{-4}$	CL=90%	$\Gamma_{209} \psi(3770) K^+ \times B(\psi \rightarrow D^+ D^-)$	(9.4 ± 3.5)	$\times 10^{-5}$	
$\Gamma_{150} D_s^+ a_1(1260)^0$	< 1.8	$\times 10^{-3}$	CL=90%	$\Gamma_{210} \chi_{c0} \pi^+ \times B(\chi_{c0} \rightarrow \pi^+ \pi^-)$	< 1	$\times 10^{-7}$	CL=90%
$\Gamma_{151} D_s^+ a_1(1260)^0$	< 1.3	$\times 10^{-3}$	CL=90%	$\Gamma_{211} \chi_{c0}(1P) K^+$	(1.33 +0.19 / -0.16)	$\times 10^{-4}$	
$\Gamma_{152} D_s^+ \phi$	< 1.9	$\times 10^{-6}$	CL=90%	$\Gamma_{212} \chi_{c0} K^*(892)^+$	< 2.1	$\times 10^{-4}$	CL=90%
$\Gamma_{153} D_s^+ \phi$	< 1.2	$\times 10^{-5}$	CL=90%	$\Gamma_{213} \chi_{c2} \pi^+ \times B(\chi_{c2} \rightarrow \pi^+ \pi^-)$	< 1	$\times 10^{-7}$	CL=90%
$\Gamma_{154} D_s^+ \overline{K}^0$	< 8	$\times 10^{-4}$	CL=90%	$\Gamma_{214} \chi_{c2} K^+$	< 1.8	$\times 10^{-5}$	CL=90%
$\Gamma_{155} D_s^+ \overline{K}^0$	< 9	$\times 10^{-4}$	CL=90%	$\Gamma_{215} \chi_{c2} K^*(892)^+$	< 1.2	$\times 10^{-4}$	CL=90%
$\Gamma_{156} D_s^+ \overline{K}^*(892)^0$	< 4	$\times 10^{-4}$	CL=90%	$\Gamma_{216} \chi_{c1}(1P) \pi^+$	(2.0 ± 0.4)	$\times 10^{-5}$	
$\Gamma_{157} D_s^+ \overline{K}^*(892)^0$	< 3.5	$\times 10^{-4}$	CL=90%	$\Gamma_{217} \chi_{c1}(1P) K^+$	(4.6 ± 0.4)	$\times 10^{-4}$	S=1.6
$\Gamma_{158} D_s^+ \pi^+ K^+$	(1.80 ± 0.22)	$\times 10^{-4}$		$\Gamma_{218} \chi_{c1}(1P) K^*(892)^+$	(3.0 ± 0.6)	$\times 10^{-4}$	S=1.1
$\Gamma_{159} D_s^+ \pi^+ K^+$	(1.45 ± 0.24)	$\times 10^{-4}$		$\Gamma_{219} h_c(1P) K^+$	< 3.8	$\times 10^{-5}$	
$\Gamma_{160} D_s^+ \pi^+ K^*(892)^+$	< 5	$\times 10^{-3}$	CL=90%	$\Gamma_{220} K^0 \pi^+$	(2.31 ± 0.10)	$\times 10^{-5}$	
$\Gamma_{161} D_s^+ \pi^+ K^*(892)^+$	< 7	$\times 10^{-3}$	CL=90%	$\Gamma_{221} K^+ \pi^0$	(1.29 ± 0.06)	$\times 10^{-5}$	
$\Gamma_{162} D_s^+ K^+ K^+$	(1.1 ± 0.4)	$\times 10^{-5}$		$\Gamma_{222} \eta' K^+$	(7.06 ± 0.25)	$\times 10^{-5}$	
$\Gamma_{163} D_s^+ K^+ K^+$	< 1.5	$\times 10^{-5}$	CL=90%	$\Gamma_{223} \eta' K^*(892)^+$	(4.9 ± 2.0)	$\times 10^{-6}$	
Charmonium modes				$\Gamma_{224} \eta K^+$	(2.33 +0.33 / -0.29)	$\times 10^{-6}$	S=1.4
$\Gamma_{164} \eta_c K^+$	(9.1 ± 1.3)	$\times 10^{-4}$		$\Gamma_{225} \eta K^*(892)^+$	(1.93 ± 0.16)	$\times 10^{-5}$	
$\Gamma_{165} \eta_c K^*(892)^+$	(1.2 ± 0.7 / 0.6)	$\times 10^{-3}$		$\Gamma_{226} \eta K_0^*(1430)^+$	(1.8 ± 0.4)	$\times 10^{-5}$	
$\Gamma_{166} \eta_c(2S) K^+$	(3.4 ± 1.8)	$\times 10^{-4}$		$\Gamma_{227} \eta K_2^*(1430)^+$	(9.1 ± 3.0)	$\times 10^{-6}$	
$\Gamma_{167} J/\psi(1S) K^+$	(1.014 ± 0.034)	$\times 10^{-3}$		$\Gamma_{228} \eta(1295) K^+ \times B(\eta(1295) \rightarrow \eta \pi \pi)$	(2.9 +0.8 / -0.7)	$\times 10^{-6}$	
$\Gamma_{168} J/\psi(1S) K^+ \pi^+ \pi^-$	(1.07 ± 0.19)	$\times 10^{-3}$	S=1.9	$\Gamma_{229} \eta(1405) K^+ \times B(\eta(1405) \rightarrow \eta \pi \pi)$	< 1.3	$\times 10^{-6}$	CL=90%
$\Gamma_{169} h_c(1P) K^+ \times B(h_c(1P) \rightarrow J/\psi \pi^+ \pi^-)$	< 3.4	$\times 10^{-6}$	CL=90%	$\Gamma_{230} \eta(1405) K^+ \times B(\eta(1405) \rightarrow K^* K)$	< 1.2	$\times 10^{-6}$	CL=90%
$\Gamma_{170} X(3872) K^+$	< 3.2	$\times 10^{-4}$	CL=90%	$\Gamma_{231} \eta(1475) K^+ \times B(\eta(1475) \rightarrow K^* K)$	(1.38 +0.21 / -0.18)	$\times 10^{-5}$	
$\Gamma_{171} X(3872) K^+ \times B(X \rightarrow J/\psi \pi^+ \pi^-)$	(9.5 ± 1.9)	$\times 10^{-6}$	S=1.3	$\Gamma_{232} f_1(1285) K^+$	< 2.0	$\times 10^{-6}$	CL=90%
$\Gamma_{172} X(3872) K^+ \times B(X \rightarrow J/\psi \gamma)$	(2.8 ± 0.8)	$\times 10^{-6}$		$\Gamma_{233} f_1(1420) K^+ \times B(f_1(1420) \rightarrow \eta \pi \pi)$	< 2.9	$\times 10^{-6}$	CL=90%
$\Gamma_{173} X(3872) K^*(892)^+ \times B(X \rightarrow J/\psi \gamma)$	< 4.8	$\times 10^{-6}$	CL=90%	$\Gamma_{234} f_1(1420) K^+ \times B(f_1(1420) \rightarrow K^* K)$	< 4.1	$\times 10^{-6}$	CL=90%
$\Gamma_{174} X(3872) K^+ \times B(X \rightarrow \psi(2S) \gamma)$	(9.5 ± 2.8)	$\times 10^{-6}$		$\Gamma_{235} \phi(1680) K^+ \times B(\phi(1680) \rightarrow K^* K)$	< 3.4	$\times 10^{-6}$	CL=90%
$\Gamma_{175} X(3872) K^*(892)^+ \times B(X \rightarrow \psi(2S) \gamma)$	< 2.8	$\times 10^{-5}$	CL=90%	$\Gamma_{236} \omega K^+$	(6.7 ± 0.8)	$\times 10^{-6}$	S=1.8
$\Gamma_{176} X(3872) K^+ \times B(X \rightarrow D^0 \overline{D}^0)$	< 6.0	$\times 10^{-5}$	CL=90%	$\Gamma_{237} \omega K^*(892)^+$	< 7.4	$\times 10^{-6}$	CL=90%
$\Gamma_{177} X(3872) K^+ \times B(X \rightarrow D^+ D^-)$	< 4.0	$\times 10^{-5}$	CL=90%	$\Gamma_{238} \omega(K\pi)_0^{*+}$	(2.7 ± 0.4)	$\times 10^{-5}$	
$\Gamma_{178} X(3872) K^+ \times B(X \rightarrow D^0 \overline{D}^0 \pi^0)$	(1.0 ± 0.4)	$\times 10^{-4}$		$\Gamma_{239} \omega K_0^*(1430)^+$	(2.4 ± 0.5)	$\times 10^{-5}$	
$\Gamma_{179} X(3872) K^+ \times B(X \rightarrow \overline{D}^0 D^0)$	(8.5 ± 2.6)	$\times 10^{-5}$	S=1.4	$\Gamma_{240} \omega K_2^*(1430)^+$	(2.1 ± 0.4)	$\times 10^{-5}$	
$\Gamma_{180} X(3872) K^+ \times B(X(3872) \rightarrow J/\psi(1S) \eta)$	< 7.7	$\times 10^{-6}$	CL=90%	$\Gamma_{241} a_0(980)^+ K^0 \times B(a_0(980)^+ \rightarrow \eta \pi^+)$	< 3.9	$\times 10^{-6}$	CL=90%
$\Gamma_{181} X(3872)^+ K^0 \times B(X(3872)^+ \rightarrow J/\psi(1S) \pi^+ \pi^0)$	[Γ] < 2.2	$\times 10^{-5}$	CL=90%	$\Gamma_{242} a_0(980)^0 K^+ \times B(a_0(980)^0 \rightarrow \eta \pi^0)$	< 2.5	$\times 10^{-6}$	CL=90%
$\Gamma_{182} X(4430)^+ K^0 \times B(X^+ \rightarrow J/\psi \pi^+)$	< 1.5	$\times 10^{-5}$	CL=95%	$\Gamma_{243} K^*(892)^0 \pi^+$	(1.01 ± 0.09)	$\times 10^{-5}$	
$\Gamma_{183} X(4430)^+ K^0 \times B(X^+ \rightarrow \psi(2S) \pi^+)$	< 4.7	$\times 10^{-5}$	CL=95%	$\Gamma_{244} K^*(892)^+ \pi^0$	(6.9 ± 2.4)	$\times 10^{-6}$	
$\Gamma_{184} X(4260)^0 K^+ \times B(X^0 \rightarrow J/\psi \pi^+ \pi^-)$	< 2.9	$\times 10^{-5}$	CL=95%	$\Gamma_{245} K^+ \pi^- \pi^+$	(5.10 ± 0.29)	$\times 10^{-5}$	

K or K* modes

Meson Particle Listings

 B^\pm

Γ_{246}	$K^+ \pi^- \pi^+$ nonresonant	$(1.63^{+0.21}_{-0.15}) \times 10^{-5}$		Γ_{306}	$\phi K_0^*(1430)^+$	$(7.0 \pm 1.6) \times 10^{-6}$	
Γ_{247}	$\omega(782) K^+$	$(6 \pm 9) \times 10^{-6}$		Γ_{307}	$\phi K_2^*(1430)^+$	$(8.4 \pm 2.1) \times 10^{-6}$	
Γ_{248}	$K^+ f_0(980) \times B(f_0(980) \rightarrow \pi^+ \pi^-)$	$(9.4^{+1.0}_{-1.2}) \times 10^{-6}$		Γ_{308}	$\phi K_2^*(1770)^+$	< 1.50	$\times 10^{-5}$ CL=90%
Γ_{249}	$f_2(1270)^0 K^+$	$(1.07 \pm 0.27) \times 10^{-6}$		Γ_{309}	$\phi K_2^*(1820)^+$	< 1.63	$\times 10^{-5}$ CL=90%
Γ_{250}	$f_0(1370)^0 K^+ \times B(f_0(1370)^0 \rightarrow \pi^+ \pi^-)$	< 1.07	$\times 10^{-5}$ CL=90%	Γ_{310}	$K^+ \phi$	$(4.9^{+2.4}_{-2.2}) \times 10^{-6}$	S=2.9
Γ_{251}	$\rho^0(1450) K^+ \times B(\rho^0(1450) \rightarrow \pi^+ \pi^-)$	< 1.17	$\times 10^{-5}$ CL=90%	Γ_{311}	$\eta' \eta' K^+$	< 2.5	$\times 10^{-5}$ CL=90%
Γ_{252}	$K^+ f_X(1300) \times B(f_X \rightarrow \pi^+ \pi^-)$	$(7 \pm 5) \times 10^{-7}$		Γ_{312}	$\omega \phi K^+$	< 1.9	$\times 10^{-6}$ CL=90%
Γ_{253}	$f_0(1500) K^+ \times B(f_0(1500) \rightarrow \pi^+ \pi^-)$	< 4.4	$\times 10^{-6}$ CL=90%	Γ_{313}	$X(1812) K^+ \times B(X \rightarrow \omega \phi)$	< 3.2	$\times 10^{-7}$ CL=90%
Γ_{254}	$f_2'(1525) K^+ \times B(f_2'(1525) \rightarrow \pi^+ \pi^-)$	< 3.4	$\times 10^{-6}$ CL=90%	Γ_{314}	$K^*(892)^+ \gamma$	$(4.21 \pm 0.18) \times 10^{-5}$	
Γ_{255}	$K^+ \rho^0$	$(3.7 \pm 0.5) \times 10^{-6}$		Γ_{315}	$K_1^*(1270)^+ \gamma$	$(4.3 \pm 1.3) \times 10^{-5}$	
Γ_{256}	$K_0^*(1430)^0 \pi^+$	$(4.5^{+0.9}_{-0.7}) \times 10^{-5}$	S=1.5	Γ_{316}	$\eta K^+ \gamma$	$(7.9 \pm 0.9) \times 10^{-6}$	
Γ_{257}	$K_2^*(1430)^0 \pi^+$	$(5.6^{+2.2}_{-1.5}) \times 10^{-6}$		Γ_{317}	$\eta' K^+ \gamma$	< 4.2	$\times 10^{-6}$ CL=90%
Γ_{258}	$K^*(1410)^0 \pi^+$	< 4.5	$\times 10^{-5}$ CL=90%	Γ_{318}	$\phi K^+ \gamma$	$(3.5 \pm 0.6) \times 10^{-6}$	
Γ_{259}	$K^*(1680)^0 \pi^+$	< 1.2	$\times 10^{-5}$ CL=90%	Γ_{319}	$K^+ \pi^- \pi^+ \gamma$	$(2.76 \pm 0.22) \times 10^{-5}$	S=1.2
Γ_{260}	$K^- \pi^+ \pi^+$	< 9.5	$\times 10^{-7}$ CL=90%	Γ_{320}	$K^*(892)^0 \pi^+ \gamma$	$(2.0^{+0.7}_{-0.6}) \times 10^{-5}$	
Γ_{261}	$K^- \pi^+ \pi^+$ nonresonant	< 5.6	$\times 10^{-5}$ CL=90%	Γ_{321}	$K^+ \rho^0 \gamma$	< 2.0	$\times 10^{-5}$ CL=90%
Γ_{262}	$K_1(1270)^0 \pi^+$	< 4.0	$\times 10^{-5}$ CL=90%	Γ_{322}	$K^+ \pi^- \pi^+ \gamma$ nonresonant	< 9.2	$\times 10^{-6}$ CL=90%
Γ_{263}	$K_1(1400)^0 \pi^+$	< 3.9	$\times 10^{-5}$ CL=90%	Γ_{323}	$K^0 \pi^+ \pi^0 \gamma$	$(4.6 \pm 0.5) \times 10^{-5}$	
Γ_{264}	$K^0 \pi^+ \pi^0$	< 6.6	$\times 10^{-5}$ CL=90%	Γ_{324}	$K_1^*(1400)^+ \gamma$	< 1.5	$\times 10^{-5}$ CL=90%
Γ_{265}	$K^0 \rho^+$	$(8.0 \pm 1.5) \times 10^{-6}$		Γ_{325}	$K_2^*(1430)^+ \gamma$	$(1.4 \pm 0.4) \times 10^{-5}$	
Γ_{266}	$K^*(892)^+ \pi^+ \pi^-$	$(7.5 \pm 1.0) \times 10^{-5}$		Γ_{326}	$K^*(1680)^+ \gamma$	< 1.9	$\times 10^{-3}$ CL=90%
Γ_{267}	$K^*(892)^+ \rho^0$	< 6.1	$\times 10^{-6}$ CL=90%	Γ_{327}	$K_3^*(1780)^+ \gamma$	< 3.9	$\times 10^{-5}$ CL=90%
Γ_{268}	$K^*(892)^+ f_0(980)$	$(5.2 \pm 1.3) \times 10^{-6}$		Γ_{328}	$K_4^*(2045)^+ \gamma$	< 9.9	$\times 10^{-3}$ CL=90%
Γ_{269}	$a_1^+ K^0$	$(3.5 \pm 0.7) \times 10^{-5}$		Light unflavored meson modes			
Γ_{270}	$b_1^+ K^0 \times B(b_1^+ \rightarrow \omega \pi^+)$	$(9.6 \pm 1.9) \times 10^{-6}$		Γ_{329}	$\rho^+ \gamma$	$(9.8 \pm 2.5) \times 10^{-7}$	
Γ_{271}	$K^*(892)^0 \rho^+$	$(9.2 \pm 1.5) \times 10^{-6}$		Γ_{330}	$\pi^+ \pi^0$	$(5.7 \pm 0.5) \times 10^{-6}$	S=1.4
Γ_{272}	$K_1(1400)^+ \rho^0$	< 7.8	$\times 10^{-4}$ CL=90%	Γ_{331}	$\pi^+ \pi^+ \pi^-$	$(1.52 \pm 0.14) \times 10^{-5}$	
Γ_{273}	$K_2^*(1430)^+ \rho^0$	< 1.5	$\times 10^{-3}$ CL=90%	Γ_{332}	$\rho^0 \pi^+$	$(8.3 \pm 1.2) \times 10^{-6}$	
Γ_{274}	$b_1^0 K^+ \times B(b_1^0 \rightarrow \omega \pi^0)$	$(9.1 \pm 2.0) \times 10^{-6}$		Γ_{333}	$\pi^+ f_0(980) \times B(f_0(980) \rightarrow \pi^+ \pi^-)$	< 1.5	$\times 10^{-6}$ CL=90%
Γ_{275}	$b_1^+ K^* \times B(b_1^+ \rightarrow \omega \pi^+)$	< 5.9	$\times 10^{-6}$ CL=90%	Γ_{334}	$\pi^+ f_2(1270)$	$(1.6^{+0.7}_{-0.4}) \times 10^{-6}$	
Γ_{276}	$b_1^0 K^* \times B(b_1^0 \rightarrow \omega \pi^0)$	< 6.7	$\times 10^{-6}$ CL=90%	Γ_{335}	$\rho(1450)^0 \pi^+ \times B(\rho^0 \rightarrow \pi^+ \pi^-)$	$(1.4^{+0.6}_{-0.9}) \times 10^{-6}$	
Γ_{277}	$K^+ \bar{K}^0$	$(1.36 \pm 0.27) \times 10^{-6}$		Γ_{336}	$f_0(1370) \pi^+ \times B(f_0(1370) \rightarrow \pi^+ \pi^-)$	< 4.0	$\times 10^{-6}$ CL=90%
Γ_{278}	$\bar{K}^0 K^+ \pi^0$	< 2.4	$\times 10^{-5}$ CL=90%	Γ_{337}	$f_0(600) \pi^+ \times B(f_0(600) \rightarrow \pi^+ \pi^-)$	< 4.1	$\times 10^{-6}$ CL=90%
Γ_{279}	$K^+ K_S^0 K_S^0$	$(1.15 \pm 0.13) \times 10^{-5}$		Γ_{338}	$\pi^+ \pi^- \pi^+$ nonresonant	$(5.3^{+1.5}_{-1.1}) \times 10^{-6}$	
Γ_{280}	$K_S^0 K_S^0 \pi^+$	< 5.1	$\times 10^{-7}$ CL=90%	Γ_{339}	$\pi^+ \pi^0 \pi^0$	< 8.9	$\times 10^{-4}$ CL=90%
Γ_{281}	$K^+ K^- \pi^+$	$(5.0 \pm 0.7) \times 10^{-6}$		Γ_{340}	$\rho^+ \pi^0$	$(1.09 \pm 0.14) \times 10^{-5}$	
Γ_{282}	$K^+ K^- \pi^+$ nonresonant	< 7.5	$\times 10^{-5}$ CL=90%	Γ_{341}	$\pi^+ \pi^- \pi^+ \pi^0$	< 4.0	$\times 10^{-3}$ CL=90%
Γ_{283}	$K^+ \bar{K}^*(892)^0$	< 1.1	$\times 10^{-6}$ CL=90%	Γ_{342}	$\rho^+ \rho^0$	$(2.40 \pm 0.19) \times 10^{-5}$	
Γ_{284}	$K^+ \bar{K}_0^*(1430)^0$	< 2.2	$\times 10^{-6}$ CL=90%	Γ_{343}	$\rho^+ f_0(980) \times B(f_0(980) \rightarrow \pi^+ \pi^-)$	< 2.0	$\times 10^{-6}$ CL=90%
Γ_{285}	$K^+ K^+ \pi^-$	< 1.6	$\times 10^{-7}$ CL=90%	Γ_{344}	$a_1(1260)^+ \pi^0$	$(2.6 \pm 0.7) \times 10^{-5}$	
Γ_{286}	$K^+ K^+ \pi^-$ nonresonant	< 8.79	$\times 10^{-5}$ CL=90%	Γ_{345}	$a_1(1260)^0 \pi^+$	$(2.0 \pm 0.6) \times 10^{-5}$	
Γ_{287}	$K^+ f_J(2220)$	< 1.18	$\times 10^{-5}$ CL=90%	Γ_{346}	$\omega \pi^+$	$(6.9 \pm 0.5) \times 10^{-6}$	
Γ_{288}	$K^*(892)^+ K^*(892)^0$	$(1.2 \pm 0.5) \times 10^{-6}$		Γ_{347}	$\omega \rho^+$	$(1.59 \pm 0.21) \times 10^{-5}$	
Γ_{289}	$K^* K^+ \pi^-$	< 6.1	$\times 10^{-6}$ CL=90%	Γ_{348}	$\eta \pi^+$	$(4.07 \pm 0.32) \times 10^{-6}$	
Γ_{290}	$K^+ K^- K^+$	$(3.37 \pm 0.22) \times 10^{-5}$	S=1.4	Γ_{349}	$\eta \rho^+$	$(7.0 \pm 2.9) \times 10^{-6}$	S=2.8
Γ_{291}	$K^+ \phi$	$(8.3 \pm 0.7) \times 10^{-6}$		Γ_{350}	$\eta' \rho^+$	$(2.7 \pm 0.9) \times 10^{-6}$	S=1.9
Γ_{292}	$f_0(980) K^+ \times B(f_0(980) \rightarrow K^+ K^-)$	< 2.9	$\times 10^{-6}$ CL=90%	Γ_{351}	$\eta' \rho^+$	$(8.7^{+4.0}_{-3.1}) \times 10^{-6}$	
Γ_{293}	$a_2(1320) K^+ \times B(a_2(1320) \rightarrow K^+ K^-)$	< 1.1	$\times 10^{-6}$ CL=90%	Γ_{352}	$\phi \pi^+$	< 2.4	$\times 10^{-7}$ CL=90%
Γ_{294}	$f_2'(1525) K^+ \times B(f_2'(1525) \rightarrow K^+ K^-)$	< 4.9	$\times 10^{-6}$ CL=90%	Γ_{353}	$\phi \rho^+$	< 3.0	$\times 10^{-6}$ CL=90%
Γ_{295}	$X_0(1550) K^+ \times B(X_0(1550) \rightarrow K^+ K^-)$	$(4.3 \pm 0.7) \times 10^{-6}$		Γ_{354}	$a_0(980)^0 \pi^+ \times B(a_0(980)^0 \rightarrow \eta \pi^+)$	< 5.8	$\times 10^{-6}$ CL=90%
Γ_{296}	$\phi(1680) K^+ \times B(\phi(1680) \rightarrow K^+ K^-)$	< 8	$\times 10^{-7}$ CL=90%	Γ_{355}	$a_0(980)^+ \pi^0 \times B(a_0^+ \rightarrow \eta \pi^+)$	< 1.4	$\times 10^{-6}$ CL=90%
Γ_{297}	$f_0(1710) K^+ \times B(f_0(1710) \rightarrow K^+ K^-)$	$(1.7 \pm 1.0) \times 10^{-6}$		Γ_{356}	$\pi^+ \pi^+ \pi^+ \pi^-$	< 8.6	$\times 10^{-4}$ CL=90%
Γ_{298}	$K^+ K^- K^+$ nonresonant	$(2.8^{+0.9}_{-1.6}) \times 10^{-5}$	S=3.3	Γ_{357}	$\rho^0 a_1(1260)^+$	< 6.2	$\times 10^{-4}$ CL=90%
Γ_{299}	$K^*(892)^+ K^+ K^-$	$(3.6 \pm 0.5) \times 10^{-5}$		Γ_{358}	$\rho^0 a_2(1320)^+$	< 7.2	$\times 10^{-4}$ CL=90%
Γ_{300}	$K^*(892)^+ \phi$	$(10.0 \pm 2.0) \times 10^{-6}$	S=1.7	Γ_{359}	$b_1^0 \pi^+ \times B(b_1^0 \rightarrow \omega \pi^0)$	$(6.7 \pm 2.0) \times 10^{-6}$	
Γ_{301}	$\phi(K\pi)_0^{*+}$	$(8.3 \pm 1.6) \times 10^{-6}$		Γ_{360}	$b_1^+ \pi^0 \times B(b_1^+ \rightarrow \omega \pi^+)$	< 3.3	$\times 10^{-6}$ CL=90%
Γ_{302}	$\phi K_1(1270)^+$	$(6.1 \pm 1.9) \times 10^{-6}$		Γ_{361}	$\pi^+ \pi^+ \pi^+ \pi^- \pi^0$	< 6.3	$\times 10^{-3}$ CL=90%
Γ_{303}	$\phi K_1(1400)^+$	< 3.2	$\times 10^{-6}$ CL=90%	Γ_{362}	$b_1^+ \rho^0 \times B(b_1^+ \rightarrow \omega \pi^+)$	< 5.2	$\times 10^{-6}$ CL=90%
Γ_{304}	$\phi K^*(1410)^+$	< 4.3	$\times 10^{-6}$ CL=90%	Γ_{363}	$a_1(1260)^+ a_1(1260)^0$	< 1.3	$\times 10^{-6}$ CL=90%
Γ_{305}				Γ_{364}	$b_1^0 \rho^+ \times B(b_1^0 \rightarrow \omega \pi^0)$	< 3.3	$\times 10^{-6}$ CL=90%

Meson Particle Listings

B $^{\pm}$

See key on page 405

 $\Gamma(D^{*-}\pi^+\ell^+\nu_\ell)/\Gamma_{\text{total}}$ Γ_{12}/Γ

VALUE (units 10^{-3})	DOCUMENT ID	TECN	COMMENT
--------------------------	-------------	------	---------

6.1 \pm 0.6 OUR AVERAGE

5.9 \pm 0.5 \pm 0.4	1 AUBERT	08Q	BABR $e^+e^- \rightarrow \Upsilon(4S)$
6.6 \pm 1.0 \pm 0.3	1,2 LIVENTSEV	08	BELL $e^+e^- \rightarrow \Upsilon(4S)$
••• We do not use the following data for averages, fits, limits, etc. •••			
6.0 \pm 1.4 \pm 0.1	3,4 LIVENTSEV	05	BELL Repl. by LIVENTSEV 08

- 1 Uses a fully reconstructed B meson as a tag on the recoil side.
- 2 LIVENTSEV 08 reports $(6.4 \pm 0.8 \pm 0.9) \times 10^{-3}$ from a measurement of $[\Gamma(B^+ \rightarrow D^{*-}\pi^+\ell^+\nu_\ell)/\Gamma_{\text{total}}] / [B(B^+ \rightarrow \bar{D}^0\ell^+\nu_\ell)]$ assuming $B(B^+ \rightarrow \bar{D}^0\ell^+\nu_\ell) = (2.15 \pm 0.22) \times 10^{-2}$, which we rescale to our best value $B(B^+ \rightarrow \bar{D}^0\ell^+\nu_\ell) = (2.23 \pm 0.11) \times 10^{-2}$. Our first error is their experiment's error and our second error is the systematic error from using our best value.
- 3 Excludes D^{*+} contribution to $D\pi$ modes.
- 4 LIVENTSEV 05 reports $[\Gamma(B^+ \rightarrow D^{*-}\pi^+\ell^+\nu_\ell)/\Gamma_{\text{total}}] / [B(B^0 \rightarrow D^{*+}(2010)^-\ell^+\nu_\ell)] = 0.12 \pm 0.02 \pm 0.02$ which we multiply by our best value $B(B^0 \rightarrow D^{*+}(2010)^-\ell^+\nu_\ell) = (5.01 \pm 0.12) \times 10^{-2}$. Our first error is their experiment's error and our second error is the systematic error from using our best value.

 $\Gamma(\bar{D}_1(2420)^0\ell^+\nu_\ell \times B(\bar{D}_1^0 \rightarrow D^{*+}\pi^-))/\Gamma_{\text{total}}$ Γ_{13}/Γ

VALUE (units 10^{-3})	DOCUMENT ID	TECN	COMMENT
--------------------------	-------------	------	---------

3.03 \pm 0.20 OUR AVERAGE

2.97 \pm 0.17 \pm 0.17	1 AUBERT	09Y	BABR $e^+e^- \rightarrow \Upsilon(4S)$
2.9 \pm 0.3 \pm 0.3	2 AUBERT	08BL	BABR $e^+e^- \rightarrow \Upsilon(4S)$
4.2 \pm 0.7 \pm 0.7	2 LIVENTSEV	08	BELL $e^+e^- \rightarrow \Upsilon(4S)$
3.73 \pm 0.85 \pm 0.57	3 ANASTASSOV	98	CLE2 $e^+e^- \rightarrow \Upsilon(4S)$

- 1 Uses a simultaneous measurement of all B semileptonic decays without full reconstruction of events.
- 2 Uses a fully reconstructed B meson as a tag on the recoil side.
- 3 Assumes equal production of B^+ and B^0 at the $\Upsilon(4S)$.

 $\Gamma(\bar{D}_1^*(2430)^0\ell^+\nu_\ell \times B(\bar{D}_1^0 \rightarrow D^{*+}\pi^-))/\Gamma_{\text{total}}$ Γ_{14}/Γ

VALUE (units 10^{-3})	CL%	DOCUMENT ID	TECN	COMMENT
--------------------------	-----	-------------	------	---------

2.7 \pm 0.4 \pm 0.5

••• We do not use the following data for averages, fits, limits, etc. •••				
<0.7	90	1 LIVENTSEV	08	BELL $e^+e^- \rightarrow \Upsilon(4S)$

- 1 Uses a fully reconstructed B meson as a tag on the recoil side.

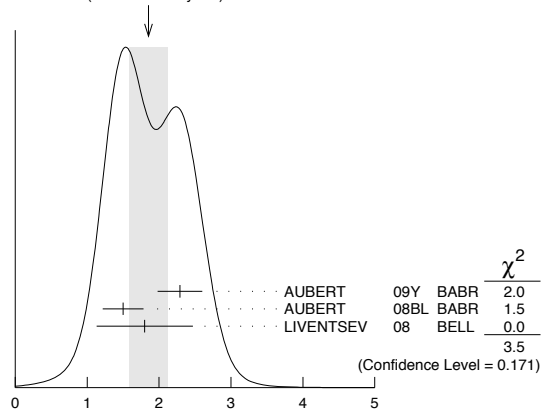
 $\Gamma(\bar{D}_2^*(2460)^0\ell^+\nu_\ell \times B(\bar{D}_2^0 \rightarrow D^{*+}\pi^-))/\Gamma_{\text{total}}$ Γ_{15}/Γ

VALUE (units 10^{-3})	CL%	DOCUMENT ID	TECN	COMMENT
--------------------------	-----	-------------	------	---------

1.85 \pm 0.27 OUR AVERAGE

2.29 \pm 0.23 \pm 0.21		1 AUBERT	09Y	BABR $e^+e^- \rightarrow \Upsilon(4S)$
1.5 \pm 0.2 \pm 0.2		2 AUBERT	08BL	BABR $e^+e^- \rightarrow \Upsilon(4S)$
1.8 \pm 0.6 \pm 0.3		2 LIVENTSEV	08	BELL $e^+e^- \rightarrow \Upsilon(4S)$
••• We do not use the following data for averages, fits, limits, etc. •••				
<1.6	90	3 ANASTASSOV	98	CLE2 $e^+e^- \rightarrow \Upsilon(4S)$

- 1 Uses a simultaneous measurement of all B semileptonic decays without full reconstruction of events.
- 2 Uses a fully reconstructed B meson as a tag on the recoil side.
- 3 Assumes equal production of B^+ and B^0 at the $\Upsilon(4S)$.

WEIGHTED AVERAGE
1.85 \pm 0.27 (Error scaled by 1.3) $\Gamma(\bar{D}_2^*(2460)^0\ell^+\nu_\ell \times B(\bar{D}_2^0 \rightarrow D^{*+}\pi^-))/\Gamma_{\text{total}}$ (units 10^{-3}) $\Gamma(\pi^0\ell^+\nu_\ell)/\Gamma_{\text{total}}$ Γ_{16}/Γ

"OUR EVALUATION" is an average using rescaled values of the data listed below. The average and rescaling were performed by the Heavy Flavor Averaging Group (HFAG) and are described at <http://www.slac.stanford.edu/xorg/hfag/>. The averaging/rescaling procedure takes into account correlations between the measurements.

VALUE (units 10^{-4})	DOCUMENT ID	TECN	COMMENT
--------------------------	-------------	------	---------

0.77 \pm 0.10 \pm 0.07 OUR EVALUATION**0.81 \pm 0.09 OUR AVERAGE**

0.82 \pm 0.09 \pm 0.05	1,2 AUBERT	08AV	BABR $e^+e^- \rightarrow \Upsilon(4S)$
0.77 \pm 0.14 \pm 0.08	3 HOKUUE	07	BELL $e^+e^- \rightarrow \Upsilon(4S)$
••• We do not use the following data for averages, fits, limits, etc. •••			
0.74 \pm 0.05 \pm 0.10	4 AUBERT,B	05O	BABR Repl. by AUBERT 08AV

- 1 Using isospin relation, B^+ and B^0 branching fractions are combined.
- 2 Assumes equal production of B^+ and B^0 at the $\Upsilon(4S)$.
- 3 The signal events are tagged by a second B meson reconstructed in the semileptonic mode $B \rightarrow D^{(*)}\ell\nu_\ell$.
- 4 B^+ and B^0 decays combined assuming isospin symmetry. Systematic errors include both experimental and form-factor uncertainties.

 $\Gamma(\pi^0e^+\nu_e)/\Gamma_{\text{total}}$ Γ_{17}/Γ

VALUE (units 10^{-4})	CL%	DOCUMENT ID	TECN	COMMENT
--------------------------	-----	-------------	------	---------

••• We do not use the following data for averages, fits, limits, etc. •••

0.9 \pm 0.2 \pm 0.2		1 ALEXANDER	96T	CLE2 $e^+e^- \rightarrow \Upsilon(4S)$
<22	90	ANTREASYAN	90B	CBAL $e^+e^- \rightarrow \Upsilon(4S)$

- 1 Derived based in the reported B^0 result by assuming isospin symmetry: $\Gamma(B^0 \rightarrow \pi^-\ell^+\nu) = 2\Gamma(B^+ \rightarrow \pi^0\ell^+\nu)$.

 $\Gamma(\eta\ell^+\nu_\ell)/\Gamma_{\text{total}}$ Γ_{18}/Γ

VALUE (units 10^{-4})	CL%	DOCUMENT ID	TECN	COMMENT
--------------------------	-----	-------------	------	---------

0.37 \pm 0.13 OUR AVERAGE

0.31 \pm 0.06 \pm 0.08		1 AUBERT	09Q	BABR $e^+e^- \rightarrow \Upsilon(4S)$
0.64 \pm 0.20 \pm 0.03		2 AUBERT	08AV	BABR $e^+e^- \rightarrow \Upsilon(4S)$
••• We do not use the following data for averages, fits, limits, etc. •••				
<1.01	90	3 ADAM	07	CLE2 $e^+e^- \rightarrow \Upsilon(4S)$
0.84 \pm 0.31 \pm 0.18		4 ATHAR	03	CLE2 Repl. by ADAM 07

- 1 Uses the neutrino reconstruction technique. Assumes $B(\Upsilon(4S) \rightarrow B^+B^-) = (51.6 \pm 0.6)\%$ and $B(\Upsilon(4S) \rightarrow B^0\bar{B}^0) = (48.4 \pm 0.6)\%$.
- 2 Assumes equal production of B^+ and B^0 at the $\Upsilon(4S)$.
- 3 The B^0 and B^+ results are combined assuming the isospin, B lifetimes, and relative charged/neutral B production at the $\Upsilon(4S)$.
- 4 ATHAR 03 reports systematic errors 0.16 ± 0.09 , which are experimental systematic and systematic due to model dependence. We combine these in quadrature.

 $\Gamma(\eta'\ell^+\nu_\ell)/\Gamma_{\text{total}}$ Γ_{19}/Γ

VALUE (units 10^{-4})	DOCUMENT ID	TECN	COMMENT
--------------------------	-------------	------	---------

0.17 \pm 0.22 OUR AVERAGE

0.04 \pm 0.22 \pm 0.05	1 AUBERT	08AV	BABR $e^+e^- \rightarrow \Upsilon(4S)$
2.66 \pm 0.80 \pm 0.56	2 ADAM	07	CLE2 $e^+e^- \rightarrow \Upsilon(4S)$

- 1 Assumes equal production of B^+ and B^0 at the $\Upsilon(4S)$.
- 2 The B^0 and B^+ results are combined assuming the isospin, B lifetimes, and relative charged/neutral B production at the $\Upsilon(4S)$. Corresponds to 90% CL interval $(1.20-4.46) \times 10^{-4}$.

 $\Gamma(\omega\ell^+\nu_\ell)/\Gamma_{\text{total}}$ Γ_{20}/Γ

VALUE (units 10^{-4})	CL%	DOCUMENT ID	TECN	COMMENT
--------------------------	-----	-------------	------	---------

1.15 \pm 0.17 OUR AVERAGE

1.14 \pm 0.16 \pm 0.08		1 AUBERT	09Q	BABR $e^+e^- \rightarrow \Upsilon(4S)$
1.3 \pm 0.4 \pm 0.4		2 SCHWANDA	04	BELL $e^+e^- \rightarrow \Upsilon(4S)$
••• We do not use the following data for averages, fits, limits, etc. •••				
<2.1	90	3 BEAN	93B	CLE2 $e^+e^- \rightarrow \Upsilon(4S)$

- 1 Uses $B(\Upsilon(4S) \rightarrow B^+B^-) = (51.6 \pm 0.6)\%$ and $B(\Upsilon(4S) \rightarrow B^0\bar{B}^0) = (48.4 \pm 0.6)\%$.
- 2 Assumes equal production of B^+ and B^0 at the $\Upsilon(4S)$.
- 3 BEAN 93B limit set using ISGW Model. Using isospin and the quark model to combine $\Gamma(\rho^0\ell^+\nu_\ell)$ and $\Gamma(\rho^-\ell^+\nu_\ell)$ with this result, they obtain a limit $<(1.6-2.7) \times 10^{-4}$ at 90% CL for $B^+ \rightarrow \omega\ell^+\nu_\ell$. The range corresponds to the ISGW, WSB, and KS models. An upper limit on $|V_{ub}/V_{cb}| < 0.8-0.13$ at 90% CL is derived as well.

 $\Gamma(\omega\mu^+\nu_\mu)/\Gamma_{\text{total}}$ Γ_{21}/Γ

VALUE	DOCUMENT ID	TECN	COMMENT
-------	-------------	------	---------

••• We do not use the following data for averages, fits, limits, etc. •••

seen 1 ALBRECHT 91C ARG

- 1 In ALBRECHT 91C, one event is fully reconstructed providing evidence for the $b \rightarrow u$ transition.

Meson Particle Listings

B[±]

Γ($\rho^0 \ell^+ \nu_\ell$)/Γ_{total} **Γ₂₂/Γ**

ℓ = e or μ, not sum over e and μ modes.

VALUE (units 10 ⁻⁴)	CL%	DOCUMENT ID	TECN	COMMENT
1.28 ± 0.18 OUR AVERAGE				
1.33 ± 0.23 ± 0.18		¹ HOKUUE 07	BELL	e ⁺ e ⁻ → T(4S)
1.16 ± 0.11 ± 0.30		² AUBERT,B 05o	BABR	e ⁺ e ⁻ → T(4S)
1.34 ± 0.15 ^{+0.28} _{-0.32}		³ BEHRENS 00	CLE2	e ⁺ e ⁻ → T(4S)

• • • We do not use the following data for averages, fits, limits, etc. • • •

1.40 ± 0.21 ^{+0.32} _{-0.33}		³ BEHRENS 00	CLE2	e ⁺ e ⁻ → T(4S)
1.2 ± 0.2 ^{+0.3} _{-0.4}		³ ALEXANDER 96T	CLE2	e ⁺ e ⁻ → T(4S)
<2.1	90	⁴ BEAN 93B	CLE2	e ⁺ e ⁻ → T(4S)

- ¹ The signal events are tagged by a second B meson reconstructed in the semileptonic mode B → D^(*)ℓνℓ.
- ² B⁺ and B⁰ decays combined assuming isospin symmetry. Systematic errors include both experimental and form-factor uncertainties.
- ³ Derived based in the reported B⁰ result by assuming isospin symmetry: Γ(B⁰ → ρ⁻ℓ⁺ν) = 2Γ(B⁺ → ρ⁰ℓ⁺ν) ≈ 2Γ(B⁺ → ωℓ⁺ν).
- ⁴ BEAN 93B limit set using ISGW Model. Using isospin and the quark model to combine Γ(ω⁰ℓ⁺ν) and Γ(ρ⁻ℓ⁺ν) with this result, they obtain a limit <(1.6-2.7) × 10⁻⁴ at 90% CL for B⁺ → ρ⁰ℓ⁺ν. The range corresponds to the ISGW, WSB, and KS models. An upper limit on |V_{ub}/V_{cb}| < 0.8-0.13 at 90% CL is derived as well.

Γ(ρ⁰e⁺ν_e)/Γ_{total} **Γ₂₃/Γ**

VALUE	CL%	DOCUMENT ID	TECN	COMMENT
<5.2 × 10⁻³	90	¹ ADAM 03B	CLE2	e ⁺ e ⁻ → T(4S)

¹ Based on phase-space model; if V-A model is used, the 90% CL upper limit becomes < 1.2 × 10⁻³.

Γ(e⁺ν_e)/Γ_{total} **Γ₂₄/Γ**

VALUE (units 10⁻⁶)

VALUE	CL%	DOCUMENT ID	TECN	COMMENT
< 1.9	90	¹ AUBERT 09V	BABR	e ⁺ e ⁻ → T(4S)

• • • We do not use the following data for averages, fits, limits, etc. • • •

< 8	90	¹ AUBERT 10E	BABR	e ⁺ e ⁻ → T(4S)
< 5.2	90	¹ AUBERT 08AD	BABR	Repl. by AUBERT 09V
< 9.8	90	¹ SATOYAMA 07	BELL	e ⁺ e ⁻ → T(4S)
<15	90	ARTUSO 95	CLE2	e ⁺ e ⁻ → T(4S)

¹ Assumes equal production of B⁺ and B⁰ at the T(4S).

Γ(μ⁺ν_μ)/Γ_{total} **Γ₂₅/Γ**

VALUE (units 10⁻⁶)

VALUE	CL%	DOCUMENT ID	TECN	COMMENT
< 1.0	90	¹ AUBERT 09V	BABR	e ⁺ e ⁻ → T(4S)

• • • We do not use the following data for averages, fits, limits, etc. • • •

<11	90	¹ AUBERT 10E	BABR	e ⁺ e ⁻ → T(4S)
< 5.6	90	¹ AUBERT 08AD	BABR	e ⁺ e ⁻ → T(4S)
< 1.7	90	¹ SATOYAMA 07	BELL	e ⁺ e ⁻ → T(4S)
< 6.6	90	AUBERT 04o	BABR	e ⁺ e ⁻ → T(4S)
<21	90	ARTUSO 95	CLE2	e ⁺ e ⁻ → T(4S)

¹ Assumes equal production of B⁺ and B⁰ at the T(4S).

Γ(τ⁺ν_τ)/Γ_{total} **Γ₂₆/Γ**

See the note on “Decay Constants of Charged Pseudoscalar Mesons” in the D_s[±] Listings.

VALUE (units 10 ⁻⁴)	CL%	DOCUMENT ID	TECN	COMMENT
1.8 ± 0.5 OUR AVERAGE				
1.7 ± 0.8 ± 0.2		^{1,2} AUBERT 10E	BABR	e ⁺ e ⁻ → T(4S)
1.8 ^{+0.9} _{-0.8} ± 0.45		^{1,3} AUBERT 08D	BABR	e ⁺ e ⁻ → T(4S)
1.79 ^{+0.56+0.46} _{-0.49-0.51}		^{1,3} IKADO 06	BELL	e ⁺ e ⁻ → T(4S)

• • • We do not use the following data for averages, fits, limits, etc. • • •

0.9 ± 0.6 ± 0.1		^{1,2} AUBERT 07AL	BABR	Repl. by AUBERT 10E
< 2.6	90	¹ AUBERT 06K	BABR	e ⁺ e ⁻ → T(4S)
< 4.2	90	¹ AUBERT,B 05B	BABR	Repl. by AUBERT 06K
< 8.3	90	⁴ BARATE 01E	ALEP	e ⁺ e ⁻ → Z
< 8.4	90	¹ BROWDER 01	CLE2	e ⁺ e ⁻ → T(4S)
< 5.7	90	⁵ ACCIARRI 97F	L3	e ⁺ e ⁻ → Z
<104	90	⁶ ALBRECHT 95D	ARG	e ⁺ e ⁻ → T(4S)
< 22	90	ARTUSO 95	CLE2	e ⁺ e ⁻ → T(4S)
< 18	90	⁷ BUSKULIC 95	ALEP	e ⁺ e ⁻ → Z

- ¹ Assumes equal production of B⁺ and B⁰ at the T(4S).
- ² Requires one reconstructed semileptonic B decay B⁻ → D⁰ℓ⁻ν_ℓX in the recoil.
- ³ The analysis is based on a sample of events with one fully reconstructed tag B in a hadronic decay mode B⁻ → D^{(*)0}X⁻.
- ⁴ The energy-flow and b-tagging algorithms were used.
- ⁵ ACCIARRI 97F uses missing-energy technique and f(b → B⁻) = (38.2 ± 2.5)%.
- ⁶ ALBRECHT 95D uses full reconstruction of one B decay as tag.
- ⁷ BUSKULIC 95 uses same missing-energy technique as in B⁻ → τ⁺ν_τX, but analysis is restricted to endpoint region of missing-energy distribution.

Γ(ℓ⁺ν_ℓγ)/Γ_{total} **Γ₂₇/Γ**

VALUE	CL%	DOCUMENT ID	TECN	COMMENT
<15.6 × 10⁻⁶	90	¹ AUBERT 09AT	BABR	e ⁺ e ⁻ → T(4S)

¹ Assumes equal production of B⁺ and B⁰ at the T(4S).

Γ(e⁺ν_eγ)/Γ_{total} **Γ₂₈/Γ**

VALUE	CL%	DOCUMENT ID	TECN	COMMENT
< 17 × 10⁻⁶	90	¹ AUBERT 09AT	BABR	e ⁺ e ⁻ → T(4S)
<200 × 10 ⁻⁶	90	² BROWDER 97	CLE2	e ⁺ e ⁻ → T(4S)

• • • We do not use the following data for averages, fits, limits, etc. • • •

- ¹ Assumes equal production of B⁺ and B⁰ at the T(4S).
- ² BROWDER 97 uses the hermiticity of the CLEOII detector to reconstruct the neutrino energy and momentum.

Γ(μ⁺ν_μγ)/Γ_{total} **Γ₂₉/Γ**

VALUE	CL%	DOCUMENT ID	TECN	COMMENT
<24 × 10⁻⁶	90	¹ AUBERT 09AT	BABR	e ⁺ e ⁻ → T(4S)
<52 × 10 ⁻⁶	90	² BROWDER 97	CLE2	e ⁺ e ⁻ → T(4S)

• • • We do not use the following data for averages, fits, limits, etc. • • •

- ¹ Assumes equal production of B⁺ and B⁰ at the T(4S).
- ² BROWDER 97 uses the hermiticity of the CLEOII detector to reconstruct the neutrino energy and momentum.

Γ(D⁰X)/Γ_{total} **Γ₃₀/Γ**

VALUE	CL%	DOCUMENT ID	TECN	COMMENT
0.086 ± 0.006 ± 0.004		¹ AUBERT 07N	BABR	e ⁺ e ⁻ → T(4S)
0.098 ± 0.009 ± 0.006		¹ AUBERT,BE 04B	BABR	Repl. by AUBERT 07N

• • • We do not use the following data for averages, fits, limits, etc. • • •

¹ Events are selected by completely reconstructing one B and searching for a reconstructed charmed particle in the rest of the event. The last error includes systematic and charm branching ratio uncertainties.

Γ(D⁰X)/Γ_{total} **Γ₃₁/Γ**

VALUE	CL%	DOCUMENT ID	TECN	COMMENT
0.786 ± 0.016^{+0.034}_{-0.033}		¹ AUBERT 07N	BABR	e ⁺ e ⁻ → T(4S)
0.793 ± 0.025 ^{+0.045} _{-0.044}		¹ AUBERT,BE 04B	BABR	Repl. by AUBERT 07N

• • • We do not use the following data for averages, fits, limits, etc. • • •

¹ Events are selected by completely reconstructing one B and searching for a reconstructed charmed particle in the rest of the event. The last error includes systematic and charm branching ratio uncertainties.

Γ(D⁰X)/[Γ(D⁰X) + Γ(D⁰X)] **Γ₃₀/(Γ₃₀+Γ₃₁)**

VALUE	CL%	DOCUMENT ID	TECN	COMMENT
0.098 ± 0.007 ± 0.001		AUBERT 07N	BABR	e ⁺ e ⁻ → T(4S)
0.110 ± 0.010 ± 0.003		AUBERT,BE 04B	BABR	Repl. by AUBERT 07N

• • • We do not use the following data for averages, fits, limits, etc. • • •

Γ(D⁺X)/Γ_{total} **Γ₃₂/Γ**

VALUE	CL%	DOCUMENT ID	TECN	COMMENT
0.025 ± 0.005 ± 0.002		¹ AUBERT 07N	BABR	e ⁺ e ⁻ → T(4S)
0.038 ± 0.009 ± 0.005		¹ AUBERT,BE 04B	BABR	Repl. by AUBERT 07N

• • • We do not use the following data for averages, fits, limits, etc. • • •

¹ Events are selected by completely reconstructing one B and searching for a reconstructed charmed particle in the rest of the event. The last error includes systematic and charm branching ratio uncertainties.

Γ(D⁻X)/Γ_{total} **Γ₃₃/Γ**

VALUE	CL%	DOCUMENT ID	TECN	COMMENT
0.099 ± 0.008 ± 0.009		¹ AUBERT 07N	BABR	e ⁺ e ⁻ → T(4S)
0.098 ± 0.012 ± 0.014		¹ AUBERT,BE 04B	BABR	Repl. by AUBERT 07N

• • • We do not use the following data for averages, fits, limits, etc. • • •

¹ Events are selected by completely reconstructing one B and searching for a reconstructed charmed particle in the rest of the event. The last error includes systematic and charm branching ratio uncertainties.

Γ(D⁺X)/[Γ(D⁺X) + Γ(D⁻X)] **Γ₃₂/(Γ₃₂+Γ₃₃)**

VALUE	CL%	DOCUMENT ID	TECN	COMMENT
0.204 ± 0.035 ± 0.001		AUBERT 07N	BABR	e ⁺ e ⁻ → T(4S)
0.278 ± 0.052 ± 0.009		AUBERT,BE 04B	BABR	Repl. by AUBERT 07N

• • • We do not use the following data for averages, fits, limits, etc. • • •

Γ(D_s⁺X)/Γ_{total} **Γ₃₄/Γ**

VALUE	CL%	DOCUMENT ID	TECN	COMMENT
0.079 ± 0.006^{+0.013}_{-0.011}		¹ AUBERT 07N	BABR	e ⁺ e ⁻ → T(4S)
0.143 ± 0.016 ^{+0.051} _{-0.034}		¹ AUBERT,BE 04B	BABR	Repl. by AUBERT 07N

• • • We do not use the following data for averages, fits, limits, etc. • • •

¹ Events are selected by completely reconstructing one B and searching for a reconstructed charmed particle in the rest of the event. The last error includes systematic and charm branching ratio uncertainties.

$\Gamma(D_s^- X)/\Gamma_{total}$					Γ_{35}/Γ
VALUE	CL%	DOCUMENT ID	TECN	COMMENT	

0.011 ± 0.004 + 0.002
-0.003 -0.001

1 AUBERT 07N BABR $e^+ e^- \rightarrow \Upsilon(4S)$

• • • We do not use the following data for averages, fits, limits, etc. • • •

<0.022 90 1 AUBERT,BE 04B BABR Repl. by AUBERT 07N

1 Events are selected by completely reconstructing one B and searching for a reconstructed charmed particle in the rest of the event. The last error includes systematic and charm branching ratio uncertainties.

$\Gamma(D_s^+ X)/[\Gamma(D_s^+ X) + \Gamma(D_s^- X)]$					$\Gamma_{34}/(\Gamma_{34} + \Gamma_{35})$
VALUE	CL%	DOCUMENT ID	TECN	COMMENT	

0.884 ± 0.038 ± 0.002

AUBERT 07N BABR $e^+ e^- \rightarrow \Upsilon(4S)$

• • • We do not use the following data for averages, fits, limits, etc. • • •

0.966 ± 0.039 ± 0.012 AUBERT,BE 04B BABR Repl. by AUBERT 07N

$\Gamma(D_s^- X)/[\Gamma(D_s^+ X) + \Gamma(D_s^- X)]$					$\Gamma_{35}/(\Gamma_{34} + \Gamma_{35})$
VALUE	CL%	DOCUMENT ID	TECN	COMMENT	

<0.126 90 AUBERT,BE 04B BABR $e^+ e^- \rightarrow \Upsilon(4S)$

$\Gamma(\Lambda_c^+ X)/\Gamma_{total}$					Γ_{36}/Γ
VALUE	CL%	DOCUMENT ID	TECN	COMMENT	

0.021 ± 0.005 + 0.008
-0.004

1 AUBERT 07N BABR $e^+ e^- \rightarrow \Upsilon(4S)$

• • • We do not use the following data for averages, fits, limits, etc. • • •

0.029 ± 0.008 + 0.011
 -0.007

1 AUBERT,BE 04B BABR Repl. by AUBERT 07N

1 Events are selected by completely reconstructing one B and searching for a reconstructed charmed particle in the rest of the event. The last error includes systematic and charm branching ratio uncertainties.

$\Gamma(\bar{\Lambda}_c^- X)/\Gamma_{total}$					Γ_{37}/Γ
VALUE	CL%	DOCUMENT ID	TECN	COMMENT	

0.028 ± 0.005 + 0.010
-0.007

1 AUBERT 07N BABR $e^+ e^- \rightarrow \Upsilon(4S)$

• • • We do not use the following data for averages, fits, limits, etc. • • •

0.035 ± 0.008 + 0.013
 -0.009

1 AUBERT,BE 04B BABR Repl. by AUBERT 07N

1 Events are selected by completely reconstructing one B and searching for a reconstructed charmed particle in the rest of the event. The last error includes systematic and charm branching ratio uncertainties.

$\Gamma(\Lambda_c^+ X)/[\Gamma(\Lambda_c^+ X) + \Gamma(\bar{\Lambda}_c^- X)]$					$\Gamma_{36}/(\Gamma_{36} + \Gamma_{37})$
VALUE	CL%	DOCUMENT ID	TECN	COMMENT	

0.427 ± 0.071 ± 0.001

AUBERT 07N BABR $e^+ e^- \rightarrow \Upsilon(4S)$

• • • We do not use the following data for averages, fits, limits, etc. • • •

0.452 ± 0.090 ± 0.003 AUBERT,BE 04B BABR Repl. by AUBERT 07N

$\Gamma(\bar{c} X)/\Gamma_{total}$					Γ_{38}/Γ
VALUE	CL%	DOCUMENT ID	TECN	COMMENT	

0.968 ± 0.019 + 0.041
-0.039

1 AUBERT 07N BABR $e^+ e^- \rightarrow \Upsilon(4S)$

• • • We do not use the following data for averages, fits, limits, etc. • • •

0.983 ± 0.030 + 0.054
 -0.051

1 AUBERT,BE 04B BABR Repl. by AUBERT 07N

1 Events are selected by completely reconstructing one B and searching for a reconstructed charmed particle in the rest of the event. The last error includes systematic and charm branching ratio uncertainties.

$\Gamma(c X)/\Gamma_{total}$					Γ_{39}/Γ
VALUE	CL%	DOCUMENT ID	TECN	COMMENT	

0.234 ± 0.012 + 0.018
-0.014

1 AUBERT 07N BABR $e^+ e^- \rightarrow \Upsilon(4S)$

• • • We do not use the following data for averages, fits, limits, etc. • • •

0.330 ± 0.022 + 0.055
 -0.037

1 AUBERT,BE 04B BABR Repl. by AUBERT 07N

1 Events are selected by completely reconstructing one B and searching for a reconstructed charmed particle in the rest of the event. The last error includes systematic and charm branching ratio uncertainties.

$\Gamma(\bar{c} c X)/\Gamma_{total}$					Γ_{40}/Γ
VALUE	CL%	DOCUMENT ID	TECN	COMMENT	

1.202 ± 0.023 + 0.053
-0.049

1 AUBERT 07N BABR $e^+ e^- \rightarrow \Upsilon(4S)$

• • • We do not use the following data for averages, fits, limits, etc. • • •

1.313 ± 0.037 + 0.088
 -0.075

1 AUBERT,BE 04B BABR Repl. by AUBERT 07N

1 Events are selected by completely reconstructing one B and searching for a reconstructed charmed particle in the rest of the event. The last error includes systematic and charm branching ratio uncertainties.

$\Gamma(\bar{D}^0 \pi^+)/\Gamma_{total}$					Γ_{41}/Γ
VALUE (units 10^{-3})	EVTS	DOCUMENT ID	TECN	COMMENT	

4.84 ± 0.15 OUR AVERAGE

4.90 ± 0.07 ± 0.22

5.3 ± 0.6 ± 0.3

4.49 ± 0.21 ± 0.23

4.97 ± 0.12 ± 0.29

5.0 ± 0.7 ± 0.6 54

5.4 +1.8 +1.2
 -1.5 -0.9 14

1 AUBERT 07H BABR $e^+ e^- \rightarrow \Upsilon(4S)$

2 ABULENCIA 06J CDF $p\bar{p}$ at 1.96 TeV

3 AUBERT,BE 06J BABR $e^+ e^- \rightarrow \Upsilon(4S)$

1,4 AHMED 02B CLE2 $e^+ e^- \rightarrow \Upsilon(4S)$

5 BORTOLETTO92 CLEO $e^+ e^- \rightarrow \Upsilon(4S)$

6 BEBEK 87 CLEO $e^+ e^- \rightarrow \Upsilon(4S)$

• • • We do not use the following data for averages, fits, limits, etc. • • •

4.75 ± 0.26 + 0.05
 -0.06 7 AUBERT,B 04P BABR Repl. by AUBERT 07H

5.5 ± 0.4 ± 0.5 304 8 ALAM 94 CLE2 Repl. by AHMED 02B

2.0 ± 0.8 ± 0.6 12 5 ALBRECHT 90J ARG $e^+ e^- \rightarrow \Upsilon(4S)$

1.9 ± 1.0 ± 0.6 7 9 ALBRECHT 88K ARG $e^+ e^- \rightarrow \Upsilon(4S)$

1 Assumes equal production of B^+ and B^0 at the $\Upsilon(4S)$.

2 ABULENCIA 06J reports $[\Gamma(B^+ \rightarrow \bar{D}^0 \pi^+)/\Gamma_{total}] / [B(B^0 \rightarrow D^- \pi^+)] = 1.97 \pm 0.10 \pm 0.21$ which we multiply by our best value $B(B^0 \rightarrow D^- \pi^+) = (2.68 \pm 0.13) \times 10^{-3}$. Our first error is their experiment's error and our second error is the systematic error from using our best value.

3 Uses a missing-mass method. Does not depend on D branching fractions or B^+/B^0 production rates.

4 AHMED 02B reports an additional uncertainty on the branching ratios to account for 4.5% uncertainty on relative production of B^0 and B^+ , which is not included here.

5 Assumes equal production of B^+ and B^0 at the $\Upsilon(4S)$ and uses the MarkIII branching fractions for the D .

6 BEBEK 87 value has been updated in BERKELMAN 91 to use same assumptions as noted for BORTOLETTO 92.

7 AUBERT,B 04P reports $[\Gamma(B^+ \rightarrow \bar{D}^0 \pi^+)/\Gamma_{total}] \times [B(D^0 \rightarrow K^- \pi^+)] = (1.846 \pm 0.032 \pm 0.097) \times 10^{-4}$ which we divide by our best value $B(D^0 \rightarrow K^- \pi^+) = (3.89 \pm 0.05) \times 10^{-2}$. Our first error is their experiment's error and our second error is the systematic error from using our best value.

8 ALAM 94 assume equal production of B^+ and B^0 at the $\Upsilon(4S)$ and use the CLEOII absolute $B(D^0 \rightarrow K^- \pi^+)$ and the PDG 1992 $B(D^0 \rightarrow K^- \pi^+ \pi^0)/B(D^0 \rightarrow K^- \pi^+)$ and $B(D^0 \rightarrow K^- 2\pi^+ \pi^-)/B(D^0 \rightarrow K^- \pi^+)$.

9 ALBRECHT 88K assumes $B^0 \bar{B}^0 : B^+ B^-$ ratio is 45:55. Superseded by ALBRECHT 90J.

$\Gamma(\bar{D}^0 \rho^+)/\Gamma_{total}$					Γ_{44}/Γ
VALUE	EVTS	DOCUMENT ID	TECN	COMMENT	

0.0134 ± 0.0018 OUR AVERAGE

0.0135 ± 0.0012 ± 0.0015 212 1 ALAM 94 CLE2 $e^+ e^- \rightarrow \Upsilon(4S)$

0.013 ± 0.004 ± 0.004 19 2 ALBRECHT 90J ARG $e^+ e^- \rightarrow \Upsilon(4S)$

• • • We do not use the following data for averages, fits, limits, etc. • • •

0.021 ± 0.008 ± 0.009 10 3 ALBRECHT 88K ARG $e^+ e^- \rightarrow \Upsilon(4S)$

1 ALAM 94 assume equal production of B^+ and B^0 at the $\Upsilon(4S)$ and use the CLEOII absolute $B(D^0 \rightarrow K^- \pi^+)$ and the PDG 1992 $B(D^0 \rightarrow K^- \pi^+ \pi^0)/B(D^0 \rightarrow K^- \pi^+)$ and $B(D^0 \rightarrow K^- 2\pi^+ \pi^-)/B(D^0 \rightarrow K^- \pi^+)$.

2 Assumes equal production of B^+ and B^0 at the $\Upsilon(4S)$ and uses the MarkIII branching fractions for the D .

3 ALBRECHT 88K assumes $B^0 \bar{B}^0 : B^+ B^-$ ratio is 45:55.

$\Gamma(\bar{D}^0 K^+)/\Gamma(\bar{D}^0 \pi^+)$					Γ_{45}/Γ_{41}
VALUE (units 10^{-2})	EVTS	DOCUMENT ID	TECN	COMMENT	

7.6 ± 0.6 OUR AVERAGE

Error includes scale factor of 2.3. See the ideogram below.

6.77 ± 0.23 ± 0.30 HORII 08 BELL $e^+ e^- \rightarrow \Upsilon(4S)$

8.31 ± 0.35 ± 0.20 AUBERT 04N BABR $e^+ e^- \rightarrow \Upsilon(4S)$

9.9 +1.4 +0.7
 -1.2 -0.6 BORNHEIM 03 CLE2 $e^+ e^- \rightarrow \Upsilon(4S)$

• • • We do not use the following data for averages, fits, limits, etc. • • •

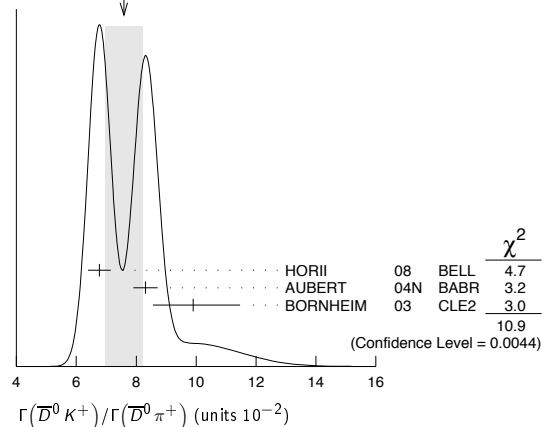
9.4 ± 0.9 ± 0.7 ABE 03D BELL Repl. by SWAIN 03

7.7 ± 0.5 ± 0.6 SWAIN 03 BELL Repl. by HORII 08

7.9 ± 0.9 ± 0.6 ABE 01I BELL Repl. by ABE 03D

5.5 ± 1.4 ± 0.5 ATHANAS 98 CLE2 Repl. by BORNHEIM 03

WEIGHTED AVERAGE
 7.6 ± 0.6 (Error scaled by 2.3)



Meson Particle Listings

B[±]

$\Gamma(D_{CP(+1)}K^+)/\Gamma(D_{CP(+1)}\pi^+)$		Γ46/Γ42	
VALUE	DOCUMENT ID	TECN	COMMENT
0.086±0.009 OUR AVERAGE			
0.086±0.008±0.007	¹ ABE	06 BELL	e ⁺ e ⁻ → $\Upsilon(4S)$
0.088±0.016±0.005	³ AUBERT	04N BABR	e ⁺ e ⁻ → $\Upsilon(4S)$
••• We do not use the following data for averages, fits, limits, etc. •••			
0.125±0.036±0.010	³ ABE	03D BELL	Repl. by SWAIN 03
0.093±0.018±0.008	³ SWAIN	03 BELL	Repl. by ABE 06

¹ Reports a double ratio of $B(B^+ \rightarrow D_{CP(+1)}K^+)/B(B^+ \rightarrow D_{CP(+1)}\pi^+)$ and $B(B^+ \rightarrow \bar{D}^0K^+)/B(B^+ \rightarrow \bar{D}^0\pi^+)$, $1.13 \pm 0.16 \pm 0.08$. We multiply by our best value of $B(B^+ \rightarrow \bar{D}^0K^+)/B(B^+ \rightarrow \bar{D}^0\pi^+) = 0.083 \pm 0.006$. Our first error is their experiment's error and the second error is systematic error from using our best value.

² ABE 06 reports $[\Gamma(B^+ \rightarrow D_{CP(+1)}K^+)/\Gamma(B^+ \rightarrow D_{CP(+1)}\pi^+)] / [\Gamma(B^+ \rightarrow \bar{D}^0K^+)/\Gamma(B^+ \rightarrow \bar{D}^0\pi^+)] = 1.13 \pm 0.06 \pm 0.08$ which we multiply by our best value $\Gamma(B^+ \rightarrow \bar{D}^0K^+)/\Gamma(B^+ \rightarrow \bar{D}^0\pi^+) = (7.6 \pm 0.6) \times 10^{-2}$. Our first error is their experiment's error and our second error is the systematic error from using our best value.

³ CP=-1 eigenstate of $D^0\bar{D}^0$ system is reconstructed via K^+K^- and $\pi^+\pi^-$.

$\Gamma(D_{CP(+1)}K^+)/\Gamma(\bar{D}^0K^+)$		Γ46/Γ45	
VALUE	DOCUMENT ID	TECN	COMMENT
0.55±0.05 OUR AVERAGE			
0.65±0.12±0.06	¹ AALTONEN	10A CDF	$p\bar{p}$ at 1.96 TeV
0.53±0.05±0.025	AUBERT	08AA BABR	e ⁺ e ⁻ → $\Upsilon(4S)$
••• We do not use the following data for averages, fits, limits, etc. •••			
0.45±0.06±0.02	AUBERT	06j BABR	Repl. by AUBERT 08AA

¹ Reports $R_{CP+} = 2 (B(B^- \rightarrow D_{CP(+1)}K^-) + B(B^- \rightarrow D_{CP(+1)}\pi^-)) / (B(B^- \rightarrow D^0K^-) + B(B^- \rightarrow \bar{D}^0\pi^-)) = 1.30 \pm 0.24 \pm 0.12$ that we have divided by 2.

$\Gamma(D_{CP(-1)}K^+)/\Gamma(D_{CP(-1)}\pi^+)$		Γ47/Γ43	
VALUE	DOCUMENT ID	TECN	COMMENT
0.097±0.016±0.007			
••• We do not use the following data for averages, fits, limits, etc. •••			
0.119±0.028±0.006	² ABE	03D BELL	Repl. by SWAIN 03
0.108±0.019±0.007	² SWAIN	03 BELL	Repl. by ABE 06

¹ Reports a double ratio of $B(B^+ \rightarrow D_{CP(-1)}K^+)/B(B^+ \rightarrow D_{CP(-1)}\pi^+)$ and $B(B^+ \rightarrow \bar{D}^0K^+)/B(B^+ \rightarrow \bar{D}^0\pi^+)$, $1.17 \pm 0.14 \pm 0.14$. We multiply by our best value of $B(B^+ \rightarrow \bar{D}^0K^+)/B(B^+ \rightarrow \bar{D}^0\pi^+) = 0.083 \pm 0.006$. Our first error is their experiment's error and the second error is systematic error from using our best value.

² CP=-1 eigenstate of $D^0\bar{D}^0$ system is reconstructed via $K_S^0\pi^0, K_S^0\omega, K_S^0\phi, K_S^0\eta$, and $K_S^0\eta'$.

$\Gamma(D_{CP(-1)}K^+)/\Gamma(\bar{D}^0K^+)$		Γ47/Γ45	
VALUE	DOCUMENT ID	TECN	COMMENT
0.515±0.05±0.025			
••• We do not use the following data for averages, fits, limits, etc. •••			
0.43 ±0.05±0.02	AUBERT	06j BABR	Repl. by AUBERT 08AA

$\Gamma([K^-\pi^+]_D K^+)/\Gamma_{total}$		Γ48/Γ	
VALUE	CL%	DOCUMENT ID	TECN COMMENT
<2.8 × 10⁻⁷	90	HORII	08 BELL e ⁺ e ⁻ → $\Upsilon(4S)$
••• We do not use the following data for averages, fits, limits, etc. •••			
<6.3 × 10 ⁻⁷	90	SAIGO	05 BELL e ⁺ e ⁻ → $\Upsilon(4S)$

$\Gamma([K^-\pi^+]_D K^+)/\Gamma([K^+\pi^-]_D K^+)$		Γ48/Γ49	
VALUE (units 10 ⁻³)	CL%	DOCUMENT ID	TECN COMMENT
7.8^{+6.2^{+2.0}}_{-5.7^{+2.8}}		HORII	08 BELL e ⁺ e ⁻ → $\Upsilon(4S)$
••• We do not use the following data for averages, fits, limits, etc. •••			
<29	90	¹ AUBERT	05G BABR e ⁺ e ⁻ → $\Upsilon(4S)$
<44	90	² SAIGO	05 BELL e ⁺ e ⁻ → $\Upsilon(4S)$
<26	90	³ AUBERT,B	04L BABR Repl. by AUBERT 05G

¹ AUBERT 05G extract a constraint on the magnitude of the ratio of amplitudes $|A(B^+ \rightarrow D^0K^+)/A(B^+ \rightarrow \bar{D}^0K^+)| < 0.23$ at 90% CL (Bayesian). Similar measurements from $B^+ \rightarrow D^*0K^+$ are also reported.

² SAIGO 05 extract a constraint on the magnitude of the ratio of amplitudes $|A(B^+ \rightarrow D^0K^+)/A(B^+ \rightarrow \bar{D}^0K^+)| < 0.27$ at 90% CL.

³ AUBERT,B 04L extract a constraint on the magnitude of the ratio of amplitudes $|A(B^+ \rightarrow D^0K^+)/A(B^+ \rightarrow \bar{D}^0K^+)| < 0.22$ at 90% CL.

$\Gamma([K^-\pi^+\pi^0]_D K^+)/\Gamma([K^+\pi^-\pi^0]_D K^+)$		Γ50/Γ51	
VALUE	CL%	DOCUMENT ID	TECN COMMENT
<0.039	95	¹ AUBERT	07BN BABR e ⁺ e ⁻ → $\Upsilon(4S)$
••• We do not use the following data for averages, fits, limits, etc. •••			
0.046±0.031±0.008		AUBERT,B	05V BABR Repl. by AUBERT 09AJ

$\Gamma([K^-\pi^+]_D K^*(892)^+)/\Gamma([K^+\pi^-]_D K^*(892)^+)$		Γ52/Γ53	
VALUE	DOCUMENT ID	TECN	COMMENT
0.066±0.031±0.010	AUBERT	09AJ BABR	e ⁺ e ⁻ → $\Upsilon(4S)$
••• We do not use the following data for averages, fits, limits, etc. •••			
0.046±0.031±0.008	AUBERT,B	05V BABR	Repl. by AUBERT 09AJ

$\Gamma([K^-\pi^+]_D \pi^+)/\Gamma_{total}$		Γ54/Γ	
VALUE (units 10 ⁻⁷)	DOCUMENT ID	TECN	COMMENT
6.29^{+1.02^{+0.37}}_{-0.98^{-0.48}}	HORII	08 BELL	e ⁺ e ⁻ → $\Upsilon(4S)$
••• We do not use the following data for averages, fits, limits, etc. •••			
6.6 ^{+1.9^{+0.5}} _{-1.7}	SAIGO	05 BELL	Repl. by HORII 08

$\Gamma([K^-\pi^+]_D \pi^+)/\Gamma([K^+\pi^-]_D \pi^+)$		Γ54/Γ55	
VALUE (units 10 ⁻³)	DOCUMENT ID	TECN	COMMENT
3.40^{+0.55^{+0.15}}_{-0.53^{-0.22}}	HORII	08 BELL	e ⁺ e ⁻ → $\Upsilon(4S)$
••• We do not use the following data for averages, fits, limits, etc. •••			
3.5 ^{+1.0^{+0.2}} _{-0.9}	SAIGO	05 BELL	Repl. by HORII 08

$\Gamma([\pi^+\pi^-\pi^0]_D K^-)/\Gamma_{total}$		Γ56/Γ	
VALUE (units 10 ⁻⁶)	DOCUMENT ID	TECN	COMMENT
4.6±0.8±0.4	¹ AUBERT	07BJ BABR	e ⁺ e ⁻ → $\Upsilon(4S)$
••• We do not use the following data for averages, fits, limits, etc. •••			
5.5±1.0±0.7	¹ AUBERT,B	05T BABR	Repl. by AUBERT 07BJ

¹ Assumes equal production of B⁺ and B⁰ at the $\Upsilon(4S)$.

$\Gamma(\bar{D}^0 K^*(892)^+)/\Gamma_{total}$		Γ57/Γ	
VALUE (units 10 ⁻⁴)	DOCUMENT ID	TECN	COMMENT
5.3 ±0.4 OUR AVERAGE			
5.29±0.30±0.34	¹ AUBERT	06z BABR	e ⁺ e ⁻ → $\Upsilon(4S)$
6.1 ±1.6 ±1.7	¹ MAHAPATRA	02 CLE2	e ⁺ e ⁻ → $\Upsilon(4S)$
••• We do not use the following data for averages, fits, limits, etc. •••			
6.3 ±0.7 ±0.5	¹ AUBERT	04Q BABR	Repl. by AUBERT 06z

¹ Assumes equal production of B⁺ and B⁰ at the $\Upsilon(4S)$.

$\Gamma(D_{CP(-1)}K^*(892)^+)/\Gamma(\bar{D}^0 K^*(892)^+)$		Γ58/Γ57	
VALUE	DOCUMENT ID	TECN	COMMENT
0.515±0.135±0.065	¹ AUBERT	09AJ BABR	e ⁺ e ⁻ → $\Upsilon(4S)$
••• We do not use the following data for averages, fits, limits, etc. •••			
0.325±0.13 ±0.04	² AUBERT,B	05U BABR	Repl. by AUBERT 09AJ

¹ The authors report $R_{CP-} = 1.03 \pm 0.27 \pm 0.13$ which is, assuming CP conservation, twice the value of the quoted above branching ratio.

² The authors report $R_{CP-} = 0.65 \pm 0.26 \pm 0.08$ which is, assuming CP conservation, twice the value of the quoted above branching ratio.

$\Gamma(D_{CP(+1)}K^*(892)^+)/\Gamma(\bar{D}^0 K^*(892)^+)$		Γ59/Γ57	
VALUE	DOCUMENT ID	TECN	COMMENT
1.085±0.175±0.045	¹ AUBERT	09AJ BABR	e ⁺ e ⁻ → $\Upsilon(4S)$
••• We do not use the following data for averages, fits, limits, etc. •••			
0.98 ±0.20 ±0.055	² AUBERT,B	05U BABR	Repl. by AUBERT 09AJ

¹ The authors report $R_{CP+} = 2.17 \pm 0.35 \pm 0.09$ which is, assuming CP conservation, twice the value of the quoted above branching ratio.

² The authors report $R_{CP+} = 1.96 \pm 0.40 \pm 0.11$ which is, assuming CP conservation, twice the value of the quoted above branching ratio.

$\Gamma(\bar{D}^0 K^+ \bar{K}^0)/\Gamma_{total}$		Γ60/Γ	
VALUE (units 10 ⁻⁴)	DOCUMENT ID	TECN	COMMENT
5.5±1.4±0.8	¹ DRUTSKOY	02 BELL	e ⁺ e ⁻ → $\Upsilon(4S)$
••• We do not use the following data for averages, fits, limits, etc. •••			
	¹ Assumes equal production of B ⁺ and B ⁰ at the $\Upsilon(4S)$.		

$\Gamma(\bar{D}^0 K^+ \bar{K}^*(892)^0)/\Gamma_{total}$		Γ61/Γ	
VALUE (units 10 ⁻⁴)	DOCUMENT ID	TECN	COMMENT
7.5±1.3±1.1	¹ DRUTSKOY	02 BELL	e ⁺ e ⁻ → $\Upsilon(4S)$
••• We do not use the following data for averages, fits, limits, etc. •••			
	¹ Assumes equal production of B ⁺ and B ⁰ at the $\Upsilon(4S)$.		

$\Gamma(\bar{D}^0 \pi^+ \pi^+ \pi^-)/\Gamma_{total}$		Γ62/Γ	
VALUE	DOCUMENT ID	TECN	COMMENT
0.0115±0.0029±0.0021	¹ BORTOLETTO	92 CLEO	e ⁺ e ⁻ → $\Upsilon(4S)$
••• We do not use the following data for averages, fits, limits, etc. •••			
	¹ BORTOLETTO 92 assumes equal production of B ⁺ and B ⁰ at the $\Upsilon(4S)$ and uses MarkIII branching fractions for the D.		

$\Gamma(\bar{D}^0 \pi^+ \pi^+ \pi^- \text{nonresonant})/\Gamma_{total}$		Γ63/Γ	
VALUE	DOCUMENT ID	TECN	COMMENT
0.0051±0.0034±0.0023	¹ BORTOLETTO	92 CLEO	e ⁺ e ⁻ → $\Upsilon(4S)$
••• We do not use the following data for averages, fits, limits, etc. •••			
	¹ BORTOLETTO 92 assumes equal production of B ⁺ and B ⁰ at the $\Upsilon(4S)$ and uses MarkIII branching fractions for the D.		

$\Gamma(\bar{D}^0 \pi^+ \rho^0)/\Gamma_{total}$		Γ64/Γ	
VALUE	DOCUMENT ID	TECN	COMMENT
0.0042±0.0023±0.0020	¹ BORTOLETTO	92 CLEO	e ⁺ e ⁻ → $\Upsilon(4S)$
••• We do not use the following data for averages, fits, limits, etc. •••			
	¹ BORTOLETTO 92 assumes equal production of B ⁺ and B ⁰ at the $\Upsilon(4S)$ and uses MarkIII branching fractions for the D.		

See key on page 405

Meson Particle Listings

 B^\pm

$\Gamma(\overline{D}^0 a_1(1260)^+)/\Gamma_{\text{total}}$		Γ_{65}/Γ	
VALUE	DOCUMENT ID	TECN	COMMENT
0.0045 ± 0.0019 ± 0.0031	¹ BORTOLETTO92	CLEO	$e^+e^- \rightarrow \Upsilon(4S)$

¹ BORTOLETTO 92 assumes equal production of B^+ and B^0 at the $\Upsilon(4S)$ and uses MarkIII branching fractions for the D .

$\Gamma(\overline{D}^0 \omega \pi^+)/\Gamma_{\text{total}}$		Γ_{66}/Γ	
VALUE	DOCUMENT ID	TECN	COMMENT
0.0041 ± 0.0007 ± 0.0006	¹ ALEXANDER 01B	CLE2	$e^+e^- \rightarrow \Upsilon(4S)$

¹ Assumes equal production of B^+ and B^0 at the $\Upsilon(4S)$. The signal is consistent with all observed $\omega\pi^+$ having proceeded through the ρ^+ resonance at mass $1349 \pm 25^{+10}_{-5}$ MeV and width $547 \pm 86^{+46}_{-45}$ MeV.

$\Gamma(D^{*}(2010)^- \pi^+ \pi^+)/\Gamma_{\text{total}}$		Γ_{67}/Γ	
VALUE (units 10^{-3})	CL% EVTS	DOCUMENT ID	TECN COMMENT
1.35 ± 0.22 OUR AVERAGE			
1.25 ± 0.08 ± 0.22		¹ ABE 04D BELL	$e^+e^- \rightarrow \Upsilon(4S)$
1.9 ± 0.7 ± 0.3	14	² ALAM 94 CLE2	$e^+e^- \rightarrow \Upsilon(4S)$
2.6 ± 1.4 ± 0.7	11	³ ALBRECHT 90J ARG	$e^+e^- \rightarrow \Upsilon(4S)$
2.4 $\begin{smallmatrix} +1.7 & +1.0 \\ -1.6 & -0.6 \end{smallmatrix}$	3	⁴ BEBEK 87 CLEO	$e^+e^- \rightarrow \Upsilon(4S)$

• • • We do not use the following data for averages, fits, limits, etc. • • •

<4. 90 ⁵ BORTOLETTO92 CLEO $e^+e^- \rightarrow \Upsilon(4S)$

5. ± 2. ± 3. 7 ⁶ ALBRECHT 87c ARG $e^+e^- \rightarrow \Upsilon(4S)$

¹ Assumes equal production of B^+ and B^0 at the $\Upsilon(4S)$.

² ALAM 94 assume equal production of B^+ and B^0 at the $\Upsilon(4S)$ and use the CLEOII $B(D^*(2010)^+ \rightarrow D^0 \pi^+)$ and absolute $B(D^0 \rightarrow K^- \pi^+)$ and the PDG 1992 $B(D^0 \rightarrow K^- \pi^+ \pi^0)/B(D^0 \rightarrow K^- \pi^+)$ and $B(D^0 \rightarrow K^- 2\pi^+ \pi^-)/B(D^0 \rightarrow K^- \pi^+)$.

³ Assumes equal production of B^+ and B^0 at the $\Upsilon(4S)$ and uses the MarkIII branching fractions for the D .

⁴ BEBEK 87 value has been updated in BERKELMAN 91 to use same assumptions as noted for BORTOLETTO 92.

⁵ BORTOLETTO 92 assumes equal production of B^+ and B^0 at the $\Upsilon(4S)$ and uses MarkIII branching fractions for the D and $D^*(2010)$. The authors also find the product branching fraction into $D^{**} \pi$ followed by $D^{**} \rightarrow D^*(2010) \pi$ to be $0.0014^{+0.0008}_{-0.0006} \pm 0.0003$ where D^{**} represents all orbitally excited D mesons.

⁶ ALBRECHT 87c use PDG 86 branching ratios for D and $D^*(2010)$ and assume $B(\Upsilon(4S) \rightarrow B^+ B^-) = 55\%$ and $B(\Upsilon(4S) \rightarrow B^0 \overline{B}^0) = 45\%$. Superseded by ALBRECHT 90.

$\Gamma(D^- \pi^+ \pi^+)/\Gamma_{\text{total}}$		Γ_{68}/Γ	
VALUE (units 10^{-3})	CL% EVTS	DOCUMENT ID	TECN COMMENT
1.07 ± 0.05 OUR AVERAGE			
1.08 ± 0.03 ± 0.05		¹ AUBERT 09AB BABR	$e^+e^- \rightarrow \Upsilon(4S)$
1.02 ± 0.04 ± 0.15		¹ ABE 04D BELL	$e^+e^- \rightarrow \Upsilon(4S)$

• • • We do not use the following data for averages, fits, limits, etc. • • •

<1.4 90 ² ALAM 94 CLE2 $e^+e^- \rightarrow \Upsilon(4S)$

<7 90 ³ BORTOLETTO92 CLEO $e^+e^- \rightarrow \Upsilon(4S)$

2.5 $\begin{smallmatrix} +4.1 & +2.4 \\ -2.3 & -0.8 \end{smallmatrix}$ 1 ⁴ BEBEK 87 CLEO $e^+e^- \rightarrow \Upsilon(4S)$

¹ Assumes equal production of B^+ and B^0 at the $\Upsilon(4S)$.

² ALAM 94 assume equal production of B^+ and B^0 at the $\Upsilon(4S)$ and use the MarkIII $B(D^+ \rightarrow K^- 2\pi^+)$.

³ BORTOLETTO 92 assumes equal production of B^+ and B^0 at the $\Upsilon(4S)$ and uses MarkIII branching fractions for the D . The product branching fraction into $D_0^*(2340) \pi$ followed by $D_0^*(2340) \rightarrow D \pi$ is < 0.005 at 90%CL and into $D_2^*(2460)$ followed by $D_2^*(2460) \rightarrow D \pi$ is < 0.004 at 90%CL.

⁴ BEBEK 87 assume the $\Upsilon(4S)$ decays 43% to $B^0 \overline{B}^0$. $B(D^- \rightarrow K^+ \pi^- \pi^-) = (9.1 \pm 1.3 \pm 0.4)\%$ is assumed.

$\Gamma(D^+ K^0)/\Gamma_{\text{total}}$		Γ_{69}/Γ	
VALUE (units 10^{-6})	CL%	DOCUMENT ID	TECN COMMENT
<5.0	90	¹ AUBERT,B 05E BABR	$e^+e^- \rightarrow \Upsilon(4S)$

¹ Assumes equal production of B^+ and B^0 at the $\Upsilon(4S)$.

$\Gamma(\overline{D}^{*0} \pi^+)/\Gamma_{\text{total}}$		Γ_{70}/Γ	
VALUE (units 10^{-3})	EVTS	DOCUMENT ID	TECN COMMENT
5.19 ± 0.26 OUR AVERAGE			
5.52 ± 0.17 ± 0.42		¹ AUBERT 07H BABR	$e^+e^- \rightarrow \Upsilon(4S)$
5.5 ± 0.4 ± 0.2		^{2,3} AUBERT,BE 06J BABR	$e^+e^- \rightarrow \Upsilon(4S)$
4.34 ± 0.47 ± 0.18		⁴ BRANDENB... 98 CLE2	$e^+e^- \rightarrow \Upsilon(4S)$
5.2 ± 0.7 ± 0.7	71	⁵ ALAM 94 CLE2	$e^+e^- \rightarrow \Upsilon(4S)$
7.2 ± 1.8 ± 1.6		⁶ BORTOLETTO92 CLEO	$e^+e^- \rightarrow \Upsilon(4S)$
4.0 ± 1.4 ± 1.2	9	⁶ ALBRECHT 90J ARG	$e^+e^- \rightarrow \Upsilon(4S)$

• • • We do not use the following data for averages, fits, limits, etc. • • •

2.7 ± 4.4 ⁷ BEBEK 87 CLEO $e^+e^- \rightarrow \Upsilon(4S)$

¹ Assumes equal production of B^+ and B^0 at the $\Upsilon(4S)$.

² AUBERT,BE 06J reports $[\Gamma(B^+ \rightarrow \overline{D}^*(2007)^0 \pi^+)/\Gamma_{\text{total}}] / [B(B^+ \rightarrow \overline{D}^0 \pi^+)] = 1.14 \pm 0.07 \pm 0.04$ which we multiply by our best value $B(B^+ \rightarrow \overline{D}^0 \pi^+) = (4.84 \pm 0.15) \times 10^{-3}$. Our first error is their experiment's error and our second error is the systematic error from using our best value.

³ Uses a missing-mass method. Does not depend on D branching fractions or B^+/B^0 production rates.

⁴ BRANDENBURG 98 assume equal production of B^+ and B^0 at $\Upsilon(4S)$ and use the D^* reconstruction technique. The first error is their experiment's error and the second error is the systematic error from the PDG 96 value of $B(D^{*0} \rightarrow D \pi)$.

⁵ ALAM 94 assume equal production of B^+ and B^0 at the $\Upsilon(4S)$ and use the CLEOII $B(D^*(2007)^0 \rightarrow D^0 \pi^0)$ and absolute $B(D^0 \rightarrow K^- \pi^+)$ and the PDG 1992 $B(D^0 \rightarrow K^- \pi^+ \pi^0)/B(D^0 \rightarrow K^- \pi^+)$ and $B(D^0 \rightarrow K^- 2\pi^+ \pi^-)/B(D^0 \rightarrow K^- \pi^+)$.

⁶ Assumes equal production of B^+ and B^0 at the $\Upsilon(4S)$ and uses MarkIII branching fractions for the D and $D^*(2010)$.

⁷ This is a derived branching ratio, using the inclusive pion spectrum and other two-body B decays. BEBEK 87 assume the $\Upsilon(4S)$ decays 43% to $B^0 \overline{B}^0$.

$\Gamma(\overline{D}^*(2007)^0 \omega \pi^+)/\Gamma_{\text{total}}$		Γ_{73}/Γ	
VALUE	DOCUMENT ID	TECN	COMMENT
0.0045 ± 0.0010 ± 0.0007	¹ ALEXANDER 01B	CLE2	$e^+e^- \rightarrow \Upsilon(4S)$

¹ Assumes equal production of B^+ and B^0 at the $\Upsilon(4S)$. The signal is consistent with all observed $\omega\pi^+$ having proceeded through the ρ^+ resonance at mass $1349 \pm 25^{+10}_{-5}$ MeV and width $547 \pm 86^{+46}_{-45}$ MeV.

$\Gamma(\overline{D}^*(2007)^0 \rho^+)/\Gamma_{\text{total}}$		Γ_{74}/Γ	
VALUE	EVTS	DOCUMENT ID	TECN COMMENT
0.0098 ± 0.0017 OUR AVERAGE			
0.0098 ± 0.0006 ± 0.0017		¹ CSORNA 03 CLE2	$e^+e^- \rightarrow \Upsilon(4S)$
0.010 ± 0.006 ± 0.004	7	² ALBRECHT 90J ARG	$e^+e^- \rightarrow \Upsilon(4S)$

• • • We do not use the following data for averages, fits, limits, etc. • • •

0.0168 ± 0.0021 ± 0.0028 86 ³ ALAM 94 CLE2 $e^+e^- \rightarrow \Upsilon(4S)$

¹ Assumes equal production of B^0 and B^+ at the $\Upsilon(4S)$ resonance. The second error combines the systematic and theoretical uncertainties in quadrature. CSORNA 03 includes data used in ALAM 94. A full angular fit to three complex helicity amplitudes is performed.

² Assumes equal production of B^+ and B^0 at the $\Upsilon(4S)$ and uses MarkIII branching fractions for the D and $D^*(2010)$.

³ ALAM 94 assume equal production of B^+ and B^0 at the $\Upsilon(4S)$ and use the CLEOII $B(D^*(2007)^0 \rightarrow D^0 \pi^0)$ and absolute $B(D^0 \rightarrow K^- \pi^+)$ and the PDG 1992 $B(D^0 \rightarrow K^- \pi^+ \pi^0)/B(D^0 \rightarrow K^- \pi^+)$ and $B(D^0 \rightarrow K^- 2\pi^+ \pi^-)/B(D^0 \rightarrow K^- \pi^+)$. The nonresonant $\pi^+ \pi^0$ contribution under the ρ^+ is negligible.

$\Gamma(\overline{D}^*(2007)^0 K^+)/\Gamma_{\text{total}}$		Γ_{75}/Γ	
VALUE (units 10^{-4})	DOCUMENT ID	TECN	COMMENT
4.21 ± 0.35 OUR AVERAGE			
4.22 $\begin{smallmatrix} +0.30 \\ -0.26 \end{smallmatrix}$ ± 0.21	¹ AUBERT 05N BABR		$e^+e^- \rightarrow \Upsilon(4S)$
4.1 ± 1.1 ± 0.2	² ABE 01I BELL		$e^+e^- \rightarrow \Upsilon(4S)$

¹ AUBERT 05N reports $[\Gamma(B^+ \rightarrow \overline{D}^*(2007)^0 K^+)/\Gamma_{\text{total}}] / [B(B^+ \rightarrow \overline{D}^*(2007)^0 \pi^+)] = 0.0813 \pm 0.0040^{+0.0042}_{-0.0031}$ which we multiply by our best value $B(B^+ \rightarrow \overline{D}^*(2007)^0 \pi^+) = (5.19 \pm 0.26) \times 10^{-3}$. Our first error is their experiment's error and our second error is the systematic error from using our best value.

² ABE 01I reports $[\Gamma(B^+ \rightarrow \overline{D}^*(2007)^0 K^+)/\Gamma_{\text{total}}] / [B(B^+ \rightarrow \overline{D}^*(2007)^0 \pi^+)] = 0.078 \pm 0.019 \pm 0.009$ which we multiply by our best value $B(B^+ \rightarrow \overline{D}^*(2007)^0 \pi^+) = (5.19 \pm 0.26) \times 10^{-3}$. Our first error is their experiment's error and our second error is the systematic error from using our best value.

$\Gamma(\overline{D}_{CP(1)}^{*0} K^+)/\Gamma_{\text{total}}$		Γ_{76}/Γ	
VALUE (units 10^{-4})	DOCUMENT ID	TECN	COMMENT
2.76 ± 0.29 $\begin{smallmatrix} +0.24 \\ -0.22 \end{smallmatrix}$	¹ AUBERT 08BF BABR		$e^+e^- \rightarrow \Upsilon(4S)$

¹ AUBERT 08BF reports $[\Gamma(B^+ \rightarrow \overline{D}_{CP(1)}^{*0} K^+)/\Gamma_{\text{total}}] / [B(B^+ \rightarrow \overline{D}^*(2007)^0 K^+)] = 0.655 \pm 0.065 \pm 0.020$ which we multiply by our best value $B(B^+ \rightarrow \overline{D}^*(2007)^0 K^+) = (4.21 \pm 0.35) \times 10^{-4}$. Our first error is their experiment's error and our second error is the systematic error from using our best value.

$\Gamma(\overline{D}_{CP(1)}^{*0} K^+)/\Gamma(\overline{D}_{CP(1)}^{*0} \pi^+)$		Γ_{76}/Γ_{71}	
VALUE	DOCUMENT ID	TECN	COMMENT
0.095 ± 0.017 OUR AVERAGE			
0.11 ± 0.02 ± 0.02	¹ ABE 06 BELL		$e^+e^- \rightarrow \Upsilon(4S)$
0.086 ± 0.021 ± 0.007	² AUBERT 05N BABR		$e^+e^- \rightarrow \Upsilon(4S)$

¹ Reports a double ratio of $B(B^+ \rightarrow D_{CP(1)}^{*0} K^+)/B(B^+ \rightarrow D_{CP(1)}^{*0} \pi^+)$ and $B(B^+ \rightarrow \overline{D}^{*0} K^+)/B(B^+ \rightarrow \overline{D}^{*0} \pi^+)$, $1.41 \pm 0.25 \pm 0.06$. We multiply by our best value of $B(B^+ \rightarrow \overline{D}^{*0} K^+)/B(B^+ \rightarrow \overline{D}^{*0} \pi^+) = 0.080 \pm 0.011$. Our first error is their experiment's error and the second error is systematic error from using our best value.

² Uses $D^{*0} \rightarrow D^0 \pi^0$ with D^0 reconstructed in the CP -even eigenstates $K^+ K^-$ and $\pi^+ \pi^-$.

Meson Particle Listings

 B^{\pm}

$\Gamma(\bar{D}_{CP(-)}^{*0} K^+)/\Gamma_{\text{total}}$ Γ_{77}/Γ

VALUE (units 10^{-4})	DOCUMENT ID	TECN	COMMENT
$2.39 \pm 0.27 \pm 0.20$ _{-0.18}	1 AUBERT	08BF	BABR $e^+ e^- \rightarrow \Upsilon(4S)$

¹AUBERT 08BF reports $[\Gamma(B^+ \rightarrow \bar{D}_{CP(-)}^{*0} K^+)/\Gamma_{\text{total}}] / [B(B^+ \rightarrow \bar{D}^*(2007)^0 K^+)] = 0.55 \pm 0.06 \pm 0.02$ which we multiply by our best value $B(B^+ \rightarrow \bar{D}^*(2007)^0 K^+) = (4.21 \pm 0.35) \times 10^{-4}$. Our first error is their experiment's error and our second error is the systematic error from using our best value.

$\Gamma(\bar{D}_{CP(-)}^{*0} K^+)/\Gamma(D_{CP(-)}^{*0} \pi^+)$ Γ_{77}/Γ_{72}

VALUE	DOCUMENT ID	TECN	COMMENT
$0.09 \pm 0.03 \pm 0.01$	1 ABE	06	BELL $e^+ e^- \rightarrow \Upsilon(4S)$

¹Reports a double ratio of $B(B^+ \rightarrow (D_{CP(-)}^{*0})^0 K^+)/B(B^+ \rightarrow (D_{CP(-)}^{*0})^0 \pi^+)$ and $B(B^+ \rightarrow \bar{D}^*(2007)^0 K^+)/B(B^+ \rightarrow \bar{D}^*(2007)^0 \pi^+)$, $1.15 \pm 0.31 \pm 0.12$. We multiply by our best value of $B(B^+ \rightarrow \bar{D}^*(2007)^0 K^+)/B(B^+ \rightarrow \bar{D}^*(2007)^0 \pi^+) = 0.080 \pm 0.011$. Our first error is their experiment's error and the second error is systematic error from using our best value.

$\Gamma(\bar{D}^*(2007)^0 K^*(892)^+)/\Gamma_{\text{total}}$ Γ_{78}/Γ

VALUE (units 10^{-4})	DOCUMENT ID	TECN	COMMENT
8.1 ± 1.4 OUR AVERAGE			
8.3 \pm 1.1 \pm 1.0	1 AUBERT	04k	BABR $e^+ e^- \rightarrow \Upsilon(4S)$
7.2 \pm 2.2 \pm 2.6	2 MAHAPATRA	02	CLE2 $e^+ e^- \rightarrow \Upsilon(4S)$

¹Assumes equal production of B^+ and B^0 at the $\Upsilon(4S)$.
²Assumes equal production of B^+ and B^0 at the $\Upsilon(4S)$ and an unpolarized final state.

$\Gamma(\bar{D}^*(2007)^0 K^+ \bar{K}^0)/\Gamma_{\text{total}}$ Γ_{79}/Γ

VALUE (units 10^{-4})	CL%	DOCUMENT ID	TECN	COMMENT
<10.6	90	1 DRUTSKOY	02	BELL $e^+ e^- \rightarrow \Upsilon(4S)$

¹Assumes equal production of B^+ and B^0 at the $\Upsilon(4S)$.

$\Gamma(\bar{D}^*(2007)^0 K^+ K^*(892)^0)/\Gamma_{\text{total}}$ Γ_{80}/Γ

VALUE (units 10^{-4})	DOCUMENT ID	TECN	COMMENT
$15.3 \pm 3.1 \pm 2.9$	1 DRUTSKOY	02	BELL $e^+ e^- \rightarrow \Upsilon(4S)$

¹Assumes equal production of B^+ and B^0 at the $\Upsilon(4S)$.

$\Gamma(\bar{D}^*(2007)^0 \pi^+ \pi^+ \pi^-)/\Gamma_{\text{total}}$ Γ_{81}/Γ

VALUE (units 10^{-2})	EVTS	DOCUMENT ID	TECN	COMMENT
1.03 ± 0.12 OUR AVERAGE				
1.055 \pm 0.047 \pm 0.129		1 MAJUMDER	04	BELL $e^+ e^- \rightarrow \Upsilon(4S)$
0.94 \pm 0.20 \pm 0.17	48	2,3 ALAM	94	CLE2 $e^+ e^- \rightarrow \Upsilon(4S)$

¹Assumes equal production of B^+ and B^0 at the $\Upsilon(4S)$.
²ALAM 94 assume equal production of B^+ and B^0 at the $\Upsilon(4S)$ and use the CLEO II $B(D^*(2007)^0 \rightarrow D^0 \pi^0)$ and absolute $B(D^0 \rightarrow K^- \pi^+)$ and the PDG 1992 $B(D^0 \rightarrow K^- \pi^+ \pi^0)/B(D^0 \rightarrow K^- \pi^+)$ and $B(D^0 \rightarrow K^- 2\pi^+ \pi^-)/B(D^0 \rightarrow K^- \pi^+)$.
³The three pion mass is required to be between 1.0 and 1.6 GeV consistent with an a_1 meson. (If this channel is dominated by a_1^+ , the branching ratio for $\bar{D}^{*0} a_1^+$ is twice that for $\bar{D}^{*0} \pi^+ \pi^+ \pi^-$.)

$\Gamma(\bar{D}^*(2007)^0 a_1(1260)^+)/\Gamma_{\text{total}}$ Γ_{82}/Γ

VALUE	DOCUMENT ID	TECN	COMMENT
$0.0188 \pm 0.0040 \pm 0.0034$	1,2 ALAM	94	CLE2 $e^+ e^- \rightarrow \Upsilon(4S)$

¹ALAM 94 value is twice their $\Gamma(\bar{D}^*(2007)^0 \pi^+ \pi^+ \pi^-)/\Gamma_{\text{total}}$ value based on their observation that the three pions are dominantly in the $a_1(1260)$ mass range 1.0 to 1.6 GeV.
²ALAM 94 assume equal production of B^+ and B^0 at the $\Upsilon(4S)$ and use the CLEO II $B(D^*(2007)^0 \rightarrow D^0 \pi^0)$ and absolute $B(D^0 \rightarrow K^- \pi^+)$ and the PDG 1992 $B(D^0 \rightarrow K^- \pi^+ \pi^0)/B(D^0 \rightarrow K^- \pi^+)$ and $B(D^0 \rightarrow K^- 2\pi^+ \pi^-)/B(D^0 \rightarrow K^- \pi^+)$.

$\Gamma(\bar{D}^*(2007)^0 \pi^- \pi^+ \pi^0)/\Gamma_{\text{total}}$ Γ_{83}/Γ

VALUE	DOCUMENT ID	TECN	COMMENT
$0.0180 \pm 0.0024 \pm 0.0027$	1 ALEXANDER	01B	CLE2 $e^+ e^- \rightarrow \Upsilon(4S)$

¹Assumes equal production of B^+ and B^0 at the $\Upsilon(4S)$. The signal is consistent with all observed $\omega \pi^+$ having proceeded through the ρ^+ resonance at mass $1349 \pm 25 \pm 10$ MeV and width $547 \pm 86 \pm 46$ MeV.

$\Gamma(\bar{D}^{*0} 3\pi^+ 2\pi^-)/\Gamma_{\text{total}}$ Γ_{84}/Γ

VALUE (units 10^{-3})	DOCUMENT ID	TECN	COMMENT
$5.67 \pm 0.91 \pm 0.85$	1 MAJUMDER	04	BELL $e^+ e^- \rightarrow \Upsilon(4S)$

¹Assumes equal production of B^+ and B^0 at the $\Upsilon(4S)$.

$\Gamma(D^*(2010)^+ \pi^0)/\Gamma_{\text{total}}$ Γ_{85}/Γ

VALUE	CL%	DOCUMENT ID	TECN	COMMENT
<3.6 \times 10 ⁻⁶		1 IWABUCHI	08	BELL $e^+ e^- \rightarrow \Upsilon(4S)$
••• We do not use the following data for averages, fits, limits, etc. •••				
<1.7 \times 10 ⁻⁴	90	2 BRANDENB...	98	CLE2 $e^+ e^- \rightarrow \Upsilon(4S)$

¹Assumes equal production of B^+ and B^0 at the $\Upsilon(4S)$.
²BRANDENBURG 98 assume equal production of B^+ and B^0 at $\Upsilon(4S)$ and use the D^* partial reconstruction technique. The first error is their experiment's error and the second error is the systematic error from the PDG 96 value of $B(D^* \rightarrow D \pi)$.

$\Gamma(D^*(2010)^+ K^0)/\Gamma_{\text{total}}$ Γ_{86}/Γ

VALUE	CL%	DOCUMENT ID	TECN	COMMENT
<9.0 \times 10 ⁻⁶	90	1 AUBERT,B	05E	BABR $e^+ e^- \rightarrow \Upsilon(4S)$
••• We do not use the following data for averages, fits, limits, etc. •••				
<9.5 \times 10 ⁻⁵	90	1 GRITSAN	01	CLE2 $e^+ e^- \rightarrow \Upsilon(4S)$

¹Assumes equal production of B^+ and B^0 at the $\Upsilon(4S)$.

$\Gamma(D^*(2010)^- \pi^+ \pi^+ \pi^0)/\Gamma_{\text{total}}$ Γ_{87}/Γ

VALUE	EVTS	DOCUMENT ID	TECN	COMMENT
$0.0152 \pm 0.0071 \pm 0.0001$	26	1 ALBRECHT	90J	ARG $e^+ e^- \rightarrow \Upsilon(4S)$
••• We do not use the following data for averages, fits, limits, etc. •••				
0.043 \pm 0.013 \pm 0.026	24	2 ALBRECHT	87c	ARG $e^+ e^- \rightarrow \Upsilon(4S)$

¹ALBRECHT 90J reports $0.018 \pm 0.007 \pm 0.005$ from a measurement of $[\Gamma(B^+ \rightarrow D^*(2010)^- \pi^+ \pi^+ \pi^0)/\Gamma_{\text{total}}] \times [B(D^*(2010)^+ \rightarrow D^0 \pi^+)]$ assuming $B(D^*(2010)^+ \rightarrow D^0 \pi^+) = 0.57 \pm 0.06$, which we rescale to our best value $B(D^*(2010)^+ \rightarrow D^0 \pi^+) = (67.7 \pm 0.5) \times 10^{-2}$. Our first error is their experiment's error and our second error is the systematic error from using our best value. Assumes equal production of B^+ and B^0 at the $\Upsilon(4S)$ and uses MarkIII branching fractions for the D .
²ALBRECHT 87c use PDG 86 branching ratios for D and $D^*(2010)$ and assume $B(\Upsilon(4S) \rightarrow B^+ B^-) = 55\%$ and $B(\Upsilon(4S) \rightarrow B^0 \bar{B}^0) = 45\%$. Superseded by ALBRECHT 90J.

$\Gamma(D^*(2010)^- \pi^+ \pi^+ \pi^+ \pi^-)/\Gamma_{\text{total}}$ Γ_{88}/Γ

VALUE (units 10^{-3})	CL%	DOCUMENT ID	TECN	COMMENT
$2.56 \pm 0.26 \pm 0.33$		1 MAJUMDER	04	BELL $e^+ e^- \rightarrow \Upsilon(4S)$
••• We do not use the following data for averages, fits, limits, etc. •••				
<10	90	2 ALBRECHT	90J	ARG $e^+ e^- \rightarrow \Upsilon(4S)$

¹Assumes equal production of B^+ and B^0 at the $\Upsilon(4S)$.
²Assumes equal production of B^+ and B^0 at the $\Upsilon(4S)$ and uses MarkIII branching fractions for the D and $D^*(2010)$.

$\Gamma(\bar{D}^{*0} \pi^+)/\Gamma_{\text{total}}$ Γ_{89}/Γ

D^{*0} represents an excited state with mass $2.2 < M < 2.8$ GeV/ c^2 .

VALUE (units 10^{-3})	DOCUMENT ID	TECN	COMMENT
$5.9 \pm 1.3 \pm 0.2$	1,2 AUBERT,BE	06J	BABR $e^+ e^- \rightarrow \Upsilon(4S)$

¹AUBERT,BE 06J reports $[\Gamma(B^+ \rightarrow \bar{D}^{*0} \pi^+)/\Gamma_{\text{total}}] / [B(B^+ \rightarrow \bar{D}^0 \pi^+)] = 1.22 \pm 0.13 \pm 0.23$ which we multiply by our best value $B(B^+ \rightarrow \bar{D}^0 \pi^+) = (4.84 \pm 0.15) \times 10^{-3}$. Our first error is their experiment's error and our second error is the systematic error from using our best value.
²Uses a missing-mass method. Does not depend on D branching fractions or B^+/B^0 production rates.

$\Gamma(\bar{D}_1^*(2420)^0 \pi^+)/\Gamma_{\text{total}}$ Γ_{90}/Γ

VALUE	EVTS	DOCUMENT ID	TECN	COMMENT
0.0015 ± 0.0006 OUR AVERAGE				Error includes scale factor of 1.3.
0.0011 \pm 0.0005 \pm 0.0002	8	1 ALAM	94	CLE2 $e^+ e^- \rightarrow \Upsilon(4S)$
0.0025 \pm 0.0007 \pm 0.0006		2 ALBRECHT	94D	ARG $e^+ e^- \rightarrow \Upsilon(4S)$

¹ALAM 94 assume equal production of B^+ and B^0 at the $\Upsilon(4S)$ and use the CLEO II $B(D^*(2010)^+ \rightarrow D^0 \pi^+)$ and absolute $B(D^0 \rightarrow K^- \pi^+)$ and the PDG 1992 $B(D^0 \rightarrow K^- \pi^+ \pi^0)/B(D^0 \rightarrow K^- \pi^+)$ and assuming $B(D_1(2420)^0 \rightarrow D^*(2010)^+ \pi^-) = 67\%$.
²ALBRECHT 94D assume equal production of B^+ and B^0 at the $\Upsilon(4S)$ and use the CLEO II $B(D^*(2010)^+ \rightarrow D^0 \pi^+)$ assuming $B(D_1(2420)^0 \rightarrow D^*(2010)^+ \pi^-) = 67\%$.

$\Gamma(\bar{D}_1(2420)^0 \pi^+ \times B(\bar{D}_1^0 \rightarrow \bar{D}^0 \pi^+ \pi^-))/\Gamma_{\text{total}}$ Γ_{91}/Γ

VALUE (units 10^{-4})	DOCUMENT ID	TECN	COMMENT
$1.85 \pm 0.29 \pm 0.35$ -0.55	1 ABE	05A	BELL $e^+ e^- \rightarrow \Upsilon(4S)$

¹Assumes equal production of B^+ and B^0 at the $\Upsilon(4S)$.

$\Gamma(\bar{D}_2^*(2462)^0 \pi^+ \times B(\bar{D}_2^0(2462)^0 \rightarrow D^- \pi^+))/\Gamma_{\text{total}}$ Γ_{92}/Γ

VALUE (units 10^{-4})	DOCUMENT ID	TECN	COMMENT
3.5 ± 0.4 OUR AVERAGE			
3.5 \pm 0.2 \pm 0.4	1 AUBERT	09AB	BABR $e^+ e^- \rightarrow \Upsilon(4S)$
3.4 \pm 0.3 \pm 0.72	1 ABE	04D	BELL $e^+ e^- \rightarrow \Upsilon(4S)$

¹Assumes equal production of B^+ and B^0 at the $\Upsilon(4S)$.

$\Gamma(\bar{D}_0^*(2400)^0 \pi^+ \times B(\bar{D}_0^0(2400)^0 \rightarrow D^- \pi^+))/\Gamma_{\text{total}}$ Γ_{93}/Γ

VALUE (units 10^{-4})	DOCUMENT ID	TECN	COMMENT
6.4 ± 1.4 OUR AVERAGE			
6.8 \pm 0.3 \pm 2.0	1 AUBERT	09AB	BABR $e^+ e^- \rightarrow \Upsilon(4S)$
6.1 \pm 0.6 \pm 1.8	1 ABE	04D	BELL $e^+ e^- \rightarrow \Upsilon(4S)$

$\Gamma(\bar{D}_1(2421)^0 \pi^+ \times B(\bar{D}_1^0(2421)^0 \rightarrow D^- \pi^+))/\Gamma_{\text{total}}$ Γ_{94}/Γ

VALUE (units 10^{-4})	DOCUMENT ID	TECN	COMMENT
$6.8 \pm 0.7 \pm 1.3$	1 ABE	04D	BELL $e^+ e^- \rightarrow \Upsilon(4S)$

¹Assumes equal production of B^+ and B^0 at the $\Upsilon(4S)$.

$\Gamma(D_s^{*-} \pi^+ K^*(892)^+)/\Gamma_{\text{total}}$ Γ_{161}/Γ

VALUE	CL%	DOCUMENT ID	TECN	COMMENT
$<7 \times 10^{-3}$	90	¹ ALBRECHT 93E	ARG	$e^+e^- \rightarrow \Upsilon(4S)$

¹ ALBRECHT 93E reports $< 1.1 \times 10^{-2}$ from a measurement of $[\Gamma(B^+ \rightarrow D_s^{*-} \pi^+ K^*(892)^+)/\Gamma_{\text{total}}] \times [B(D_s^+ \rightarrow \phi\pi^+)]$ assuming $B(D_s^+ \rightarrow \phi\pi^+) = 0.027$, which we rescale to our best value $B(D_s^+ \rightarrow \phi\pi^+) = 4.5 \times 10^{-2}$.

$\Gamma(D_s^- K^+ K^+)/\Gamma_{\text{total}}$ Γ_{162}/Γ

VALUE (units 10^{-4})	DOCUMENT ID	TECN	COMMENT
$0.11 \pm 0.04 \pm 0.02$	¹ AUBERT 08G	BABR	$e^+e^- \rightarrow \Upsilon(4S)$

¹ Assumes equal production of B^+ and B^0 at the $\Upsilon(4S)$.

$\Gamma(D_s^{*-} K^+ K^+)/\Gamma_{\text{total}}$ Γ_{163}/Γ

VALUE (units 10^{-4})	DOCUMENT ID	TECN	COMMENT
<0.15	¹ AUBERT 08G	BABR	$e^+e^- \rightarrow \Upsilon(4S)$

¹ Assumes equal production of B^+ and B^0 at the $\Upsilon(4S)$.

$\Gamma(\eta_c K^+)/\Gamma_{\text{total}}$ Γ_{164}/Γ

VALUE (units 10^{-3})	DOCUMENT ID	TECN	COMMENT
0.91 ± 0.13 OUR AVERAGE			
0.87 ± 0.15	^{1,2} AUBERT 06E	BABR	$e^+e^- \rightarrow \Upsilon(4S)$
$1.4^{+0.3}_{-0.2} \pm 0.4$	³ AUBERT,B 05L	BABR	$e^+e^- \rightarrow \Upsilon(4S)$
$1.25 \pm 0.14^{+0.39}_{-0.40}$	⁴ FANG 03	BELL	$e^+e^- \rightarrow \Upsilon(4S)$
$0.69^{+0.26}_{-0.21} \pm 0.22$	⁵ EDWARDS 01	CLE2	$e^+e^- \rightarrow \Upsilon(4S)$
$1.06 \pm 0.12 \pm 0.18$	^{2,6} AUBERT,B 04B	BABR	$e^+e^- \rightarrow \Upsilon(4S)$

- • • We do not use the following data for averages, fits, limits, etc. • • •
- ¹ Perform measurements of absolute branching fractions using a missing mass technique.
- ² The ratio of $B(B^\pm \rightarrow K^\pm \eta_c) B(\eta_c \rightarrow K\bar{K}\pi) = (7.4 \pm 0.5 \pm 0.7) \times 10^{-5}$ reported in AUBERT,B 04B and $B(B^\pm \rightarrow K^\pm \eta_c) = (8.7 \pm 1.5) \times 10^{-3}$ reported in AUBERT 06E contribute to the determination of $B(\eta_c \rightarrow K\bar{K}\pi)$, which is used by others for normalization.
- ³ AUBERT,B 05L reports $[\Gamma(B^+ \rightarrow \eta_c K^+)/\Gamma_{\text{total}}] \times [B(\eta_c(1S) \rightarrow p\bar{p})] = (1.8^{+0.3}_{-0.2} \pm 0.2) \times 10^{-6}$ which we divide by our best value $B(\eta_c(1S) \rightarrow p\bar{p}) = (1.3 \pm 0.4) \times 10^{-3}$. Our first error is their experiment's error and our second error is the systematic error from using our best value.
- ⁴ Assumes equal production of B^+ and B^0 at the $\Upsilon(4S)$.
- ⁵ EDWARDS 01 assumes equal production of B^0 and B^+ at the $\Upsilon(4S)$. The correlated uncertainties (28.3)% from $B(J/\psi(1S) \rightarrow \eta_c \gamma)$ in those modes have been accounted for.
- ⁶ AUBERT,B 04B reports $[\Gamma(B^+ \rightarrow \eta_c K^+)/\Gamma_{\text{total}}] \times [B(\eta_c(1S) \rightarrow K\bar{K}\pi)] = (0.074 \pm 0.005 \pm 0.007) \times 10^{-3}$ which we divide by our best value $B(\eta_c(1S) \rightarrow K\bar{K}\pi) = (7.0 \pm 1.2) \times 10^{-2}$. Our first error is their experiment's error and our second error is the systematic error from using our best value.

$\Gamma(B^+ \rightarrow \eta_c K^+)/\Gamma_{\text{total}} \times \Gamma(\eta_c(1S) \rightarrow \gamma\gamma)/\Gamma_{\text{total}}$ $\Gamma_{164}/\Gamma \times \Gamma_{28}^{\eta_c(1S)}/\Gamma_{\eta_c(1S)}$

VALUE (units 10^{-6})	DOCUMENT ID	TECN	COMMENT
$0.22^{+0.09+0.04}_{-0.07-0.02}$	¹ WICHT 08	BELL	$e^+e^- \rightarrow \Upsilon(4S)$

¹ Assumes equal production of B^+ and B^0 at the $\Upsilon(4S)$.

$\Gamma(\eta_c K^*(892)^+)/\Gamma_{\text{total}}$ Γ_{165}/Γ

VALUE (units 10^{-3})	DOCUMENT ID	TECN	COMMENT
$1.2^{+0.6}_{-0.4} \pm 0.4$	^{1,2} AUBERT 07AV	BABR	$e^+e^- \rightarrow \Upsilon(4S)$

- ¹ AUBERT 07AV reports $[\Gamma(B^+ \rightarrow \eta_c K^*(892)^+)/\Gamma_{\text{total}}] \times [B(\eta_c(1S) \rightarrow p\bar{p})] = (1.57^{+0.56+0.45}_{-0.46-0.36}) \times 10^{-6}$ which we divide by our best value $B(\eta_c(1S) \rightarrow p\bar{p}) = (1.3 \pm 0.4) \times 10^{-3}$. Our first error is their experiment's error and our second error is the systematic error from using our best value.
- ² Assumes equal production of B^+ and B^0 at the $\Upsilon(4S)$.

$\Gamma(\eta_c(2S) K^+)/\Gamma_{\text{total}}$ Γ_{166}/Γ

VALUE (units 10^{-4})	DOCUMENT ID	TECN	COMMENT
$3.4 \pm 1.8 \pm 0.3$	¹ AUBERT 06E	BABR	$e^+e^- \rightarrow \Upsilon(4S)$

¹ Perform measurements of absolute branching fractions using a missing mass technique.

$\Gamma(B^+ \rightarrow h_c(1P) K^+)/\Gamma_{\text{total}} \times \Gamma(h_c(1P) \rightarrow \eta_c \gamma)/\Gamma_{\text{total}}$ $\Gamma_{219}/\Gamma \times \Gamma_{4}^{h_c(1P)}/\Gamma_{h_c(1P)}$

VALUE (units 10^{-4})	DOCUMENT ID	TECN	COMMENT
<0.48	¹ AUBERT 08AB	BABR	$e^+e^- \rightarrow \Upsilon(4S)$

¹ Uses the production ratio of $(B^+ B^-)/(B^0 \bar{B}^0) = 1.026 \pm 0.032$ at $\Upsilon(4S)$.

$\Gamma(B^+ \rightarrow \eta_c(2S) K^+)/\Gamma_{\text{total}} \times \Gamma(\eta_c(2S) \rightarrow \gamma\gamma)/\Gamma_{\text{total}}$ $\Gamma_{166}/\Gamma \times \Gamma_{11}^{\eta_c(2S)}/\Gamma_{\eta_c(2S)}$

VALUE (units 10^{-6})	DOCUMENT ID	TECN	COMMENT
<0.18	¹ WICHT 08	BELL	$e^+e^- \rightarrow \Upsilon(4S)$

¹ Assumes equal production of B^+ and B^0 at the $\Upsilon(4S)$.

$\Gamma(J/\psi(1S) K^+)/\Gamma_{\text{total}}$ Γ_{167}/Γ

VALUE (units 10^{-4})	EVTS	DOCUMENT ID	TECN	COMMENT
10.14 ± 0.34 OUR FIT				
10.22 ± 0.35 OUR AVERAGE				
$8.1 \pm 1.3 \pm 0.7$		¹ AUBERT 06E	BABR	$e^+e^- \rightarrow \Upsilon(4S)$
$10.61 \pm 0.15 \pm 0.48$		² AUBERT 05J	BABR	$e^+e^- \rightarrow \Upsilon(4S)$
$10.1 \pm 1.0 \pm 0.3$		³ AUBERT,B 05L	BABR	$e^+e^- \rightarrow \Upsilon(4S)$
$10.1 \pm 0.2 \pm 0.7$		² ABE 03B	BELL	$e^+e^- \rightarrow \Upsilon(4S)$
$10.2 \pm 0.8 \pm 0.7$		² JESSOP 97	CLE2	$e^+e^- \rightarrow \Upsilon(4S)$
$9.3 \pm 3.1 \pm 0.1$		⁴ BORTOLETTO92	CLEO	$e^+e^- \rightarrow \Upsilon(4S)$
$8.1 \pm 3.5 \pm 0.1$	⁶	⁵ ALBRECHT 90J	ARG	$e^+e^- \rightarrow \Upsilon(4S)$

- • • We do not use the following data for averages, fits, limits, etc. • • •
- ¹ Perform measurements of absolute branching fractions using a missing mass technique.
- ² Assumes equal production of B^+ and B^0 at the $\Upsilon(4S)$.
- ³ AUBERT,B 05L reports $[\Gamma(B^+ \rightarrow J/\psi(1S) K^+)/\Gamma_{\text{total}}] \times [B(J/\psi(1S) \rightarrow p\bar{p})] = (2.2 \pm 0.2 \pm 0.1) \times 10^{-6}$ which we divide by our best value $B(J/\psi(1S) \rightarrow p\bar{p}) = (2.17 \pm 0.07) \times 10^{-3}$. Our first error is their experiment's error and our second error is the systematic error from using our best value.
- ⁴ BORTOLETTO 92 reports $(8 \pm 2 \pm 2) \times 10^{-4}$ from a measurement of $[\Gamma(B^+ \rightarrow J/\psi(1S) K^+)/\Gamma_{\text{total}}] \times [B(J/\psi(1S) \rightarrow e^+e^-)]$ assuming $B(J/\psi(1S) \rightarrow e^+e^-) = 0.069 \pm 0.009$, which we rescale to our best value $B(J/\psi(1S) \rightarrow e^+e^-) = (5.94 \pm 0.06) \times 10^{-2}$. Our first error is their experiment's error and our second error is the systematic error from using our best value. Assumes equal production of B^+ and B^0 at the $\Upsilon(4S)$.
- ⁵ ALBRECHT 90J reports $(7 \pm 3 \pm 1) \times 10^{-4}$ from a measurement of $[\Gamma(B^+ \rightarrow J/\psi(1S) K^+)/\Gamma_{\text{total}}] \times [B(J/\psi(1S) \rightarrow e^+e^-)]$ assuming $B(J/\psi(1S) \rightarrow e^+e^-) = 0.069 \pm 0.009$, which we rescale to our best value $B(J/\psi(1S) \rightarrow e^+e^-) = (5.94 \pm 0.06) \times 10^{-2}$. Our first error is their experiment's error and our second error is the systematic error from using our best value. Assumes equal production of B^+ and B^0 at the $\Upsilon(4S)$.
- ⁶ ALBRECHT 87D assume $B^+ B^-/B^0 \bar{B}^0$ ratio is 55/45. Superseded by ALBRECHT 90J.
- ⁷ BEBEK 87 value has been updated in BERKELMAN 91 to use same assumptions as noted for BORTOLETTO 92.
- ⁸ ALAM 86 assumes B^\pm/B^0 ratio is 60/40.

$\Gamma(\eta_c K^+)/\Gamma(J/\psi(1S) K^+)$ $\Gamma_{164}/\Gamma_{167}$

VALUE	DOCUMENT ID	TECN	COMMENT
$1.33 \pm 0.10 \pm 0.43$	¹ AUBERT,B 04B	BABR	$e^+e^- \rightarrow \Upsilon(4S)$

¹ Uses BABAR measurement of $B(B^+ \rightarrow J/\psi K^+) = (10.1 \pm 0.3 \pm 0.5) \times 10^{-4}$.

$\Gamma(B^+ \rightarrow J/\psi(1S) K^+)/\Gamma_{\text{total}} \times \Gamma(J/\psi(1S) \rightarrow \gamma\gamma)/\Gamma_{\text{total}}$ $\Gamma_{167}/\Gamma \times \Gamma_{184}^{J/\psi(1S)}/\Gamma_{J/\psi(1S)}$

VALUE (units 10^{-6})	CL%	DOCUMENT ID	TECN	COMMENT
<0.16	90	¹ WICHT 08	BELL	$e^+e^- \rightarrow \Upsilon(4S)$

¹ Assumes equal production of B^+ and B^0 at the $\Upsilon(4S)$.

$\Gamma(J/\psi(1S) K^+ \pi^+ \pi^-)/\Gamma_{\text{total}}$ Γ_{168}/Γ

VALUE (units 10^{-3})	CL%	EVTS	DOCUMENT ID	TECN	COMMENT
1.07 ± 0.19 OUR AVERAGE					Error includes scale factor of 1.9.
$1.16 \pm 0.07 \pm 0.09$			¹ AUBERT 05R	BABR	$e^+e^- \rightarrow \Upsilon(4S)$
$0.69 \pm 0.18 \pm 0.12$			² ACOSTA 02F	CDF	$p\bar{p}$ 1.8 TeV
$1.39 \pm 0.82 \pm 0.01$			³ BORTOLETTO92	CLEO	$e^+e^- \rightarrow \Upsilon(4S)$
$1.39 \pm 0.91 \pm 0.01$		⁶	⁴ ALBRECHT 87D	ARG	$e^+e^- \rightarrow \Upsilon(4S)$

- • • We do not use the following data for averages, fits, limits, etc. • • •
- ¹ Assumes equal production of B^+ and B^0 at the $\Upsilon(4S)$.
- ² ACOSTA 02F uses as reference of $B(B \rightarrow J/\psi(1S) K^+) = (10.1 \pm 0.6) \times 10^{-4}$. The second error includes the systematic error and the uncertainties of the branching ratio.
- ³ BORTOLETTO 92 reports $(1.2 \pm 0.6 \pm 0.4) \times 10^{-3}$ from a measurement of $[\Gamma(B^+ \rightarrow J/\psi(1S) K^+ \pi^+ \pi^-)/\Gamma_{\text{total}}] \times [B(J/\psi(1S) \rightarrow e^+e^-)]$ assuming $B(J/\psi(1S) \rightarrow e^+e^-) = 0.069 \pm 0.009$, which we rescale to our best value $B(J/\psi(1S) \rightarrow e^+e^-) = (5.94 \pm 0.06) \times 10^{-2}$. Our first error is their experiment's error and our second error is the systematic error from using our best value. Assumes equal production of B^+ and B^0 at the $\Upsilon(4S)$.
- ⁴ ALBRECHT 87D reports $(1.2 \pm 0.8) \times 10^{-3}$ from a measurement of $[\Gamma(B^+ \rightarrow J/\psi(1S) K^+ \pi^+ \pi^-)/\Gamma_{\text{total}}] \times [B(J/\psi(1S) \rightarrow e^+e^-)]$ assuming $B(J/\psi(1S) \rightarrow e^+e^-) = 0.069 \pm 0.009$, which we rescale to our best value $B(J/\psi(1S) \rightarrow e^+e^-) = (5.94 \pm 0.06) \times 10^{-2}$. Our first error is their experiment's error and our second error is the systematic error from using our best value. They actually report 0.0011 ± 0.0007 assuming $B^+ B^-/B^0 \bar{B}^0$ ratio is 55/45. We rescale to 50/50. Analysis explicitly removes $B^+ \rightarrow \psi(2S) K^+$.
- ⁵ ALBRECHT 90J reports $< 1.6 \times 10^{-3}$ from a measurement of $[\Gamma(B^+ \rightarrow J/\psi(1S) K^+ \pi^+ \pi^-)/\Gamma_{\text{total}}] \times [B(J/\psi(1S) \rightarrow e^+e^-)]$ assuming $B(J/\psi(1S) \rightarrow e^+e^-) = 0.069$, which we rescale to our best value $B(J/\psi(1S) \rightarrow e^+e^-) = 5.94 \times 10^{-2}$. Assumes equal production of B^+ and B^0 at the $\Upsilon(4S)$.

$\Gamma(J/\psi(1S)K^*(892)^+)/\Gamma(J/\psi(1S)K^+)$ $\Gamma_{188}/\Gamma_{167}$

VALUE	DOCUMENT ID	TECN	COMMENT
1.39 ± 0.09 OUR AVERAGE			
1.37 ± 0.05 ± 0.08	AUBERT	05J	BABR $e^+e^- \rightarrow \Upsilon(4S)$
1.45 ± 0.20 ± 0.17	¹ JESSOP	97	CLE2 $e^+e^- \rightarrow \Upsilon(4S)$
1.92 ± 0.60 ± 0.17	ABE	96Q	CDF $p\bar{p}$
• • • We do not use the following data for averages, fits, limits, etc. • • •			
1.37 ± 0.10 ± 0.08	² AUBERT	02	BABR Repl. by AUBERT 05J
¹ JESSOP 97 assumes equal production of B^+ and B^0 at the $\Upsilon(4S)$. The measurement is actually measured as an average over kaon charged and neutral states.			
² Assumes equal production of B^+ and B^0 at the $\Upsilon(4S)$.			

 $\Gamma(J/\psi(1S)K(1270)^+)/\Gamma_{total}$ Γ_{189}/Γ

VALUE (units 10^{-3})	DOCUMENT ID	TECN	COMMENT
1.80 ± 0.34 ± 0.39	¹ ABE	01L	BELL $e^+e^- \rightarrow \Upsilon(4S)$
¹ Uses the PDG value of $B(B^+ \rightarrow J/\psi(1S)K^+) = (1.00 \pm 0.10) \times 10^{-3}$.			

 $\Gamma(J/\psi(1S)K(1400)^+)/\Gamma(J/\psi(1S)K(1270)^+)$ $\Gamma_{190}/\Gamma_{189}$

VALUE	CL%	DOCUMENT ID	TECN	COMMENT
<0.30	90	ABE	01L	BELL $e^+e^- \rightarrow \Upsilon(4S)$

 $\Gamma(J/\psi(1S)\eta K^+)/\Gamma_{total}$ Γ_{191}/Γ

VALUE (units 10^{-5})	DOCUMENT ID	TECN	COMMENT
10.8 ± 2.3 ± 2.4	¹ AUBERT	04Y	BABR $e^+e^- \rightarrow \Upsilon(4S)$
¹ Assumes equal production of B^+ and B^0 at the $\Upsilon(4S)$.			

 $\Gamma(J/\psi(1S)\eta' K^+)/\Gamma_{total}$ Γ_{192}/Γ

VALUE (units 10^{-5})	CL%	DOCUMENT ID	TECN	COMMENT
<8.8	90	¹ XIE	07	BELL $e^+e^- \rightarrow \Upsilon(4S)$
¹ Assumes equal production of B^+ and B^0 at the $\Upsilon(4S)$.				

 $\Gamma(J/\psi(1S)\phi K^+)/\Gamma_{total}$ Γ_{193}/Γ

VALUE	DOCUMENT ID	TECN	COMMENT
(5.2 ± 1.7) × 10⁻⁵ OUR AVERAGE			Error includes scale factor of 1.2.
(4.4 ± 1.4 ± 0.5) × 10 ⁻⁵	¹ AUBERT	03D	BABR $e^+e^- \rightarrow \Upsilon(4S)$
(8.8 ^{+3.5} _{-3.0} ± 1.3) × 10 ⁻⁵	² ANASTASSOV	00	CLE2 $e^+e^- \rightarrow \Upsilon(4S)$
¹ Assumes equal production of B^+ and B^0 at the $\Upsilon(4S)$.			
² ANASTASSOV 00 finds 10 events on a background of 0.5 ± 0.2 . Assumes equal production of B^0 and B^+ at the $\Upsilon(4S)$, a uniform Dalitz plot distribution, isotropic $J/\psi(1S)$ and ϕ decays, and $B(B^+ \rightarrow J/\psi(1S)\phi K^+) = B(B^0 \rightarrow J/\psi(1S)\phi K^0)$.			

 $\Gamma(J/\psi(1S)\omega K^+ \text{ nonresonant})/\Gamma_{total}$ Γ_{194}/Γ

VALUE (units 10^{-4})	DOCUMENT ID	TECN	COMMENT
3.5 ± 0.2 ± 0.4	¹ AUBERT	08W	BABR $e^+e^- \rightarrow \Upsilon(4S)$
¹ Assumes equal production of B^+ and B^0 at the $\Upsilon(4S)$.			

 $\Gamma(J/\psi(1S)\pi^+)/\Gamma_{total}$ Γ_{195}/Γ

VALUE	DOCUMENT ID	TECN	COMMENT
(4.9 ± 0.4) × 10⁻⁵ OUR FIT			Error includes scale factor of 1.2.
(3.8 ± 0.6 ± 0.3) × 10⁻⁵	¹ ABE	03B	BELL $e^+e^- \rightarrow \Upsilon(4S)$
¹ Assumes equal production of B^+ and B^0 at the $\Upsilon(4S)$.			

 $\Gamma(J/\psi(1S)\pi^+)/\Gamma(J/\psi(1S)K^+)$ $\Gamma_{195}/\Gamma_{167}$

VALUE	EVTs	DOCUMENT ID	TECN	COMMENT
0.049 ± 0.004 OUR FIT				Error includes scale factor of 1.1.
0.052 ± 0.004 OUR AVERAGE				
0.0486 ± 0.0082 ± 0.0015		ABULENCIA	09	CDF $p\bar{p}$ at 1.96 TeV
0.0537 ± 0.0045 ± 0.0011		AUBERT	04P	BABR $e^+e^- \rightarrow \Upsilon(4S)$
0.050 ^{+0.019} _{-0.017} ± 0.001		ABE	96R	CDF $p\bar{p}$ 1.8 TeV
0.052 ± 0.024		BISHAI	96	CLE2 $e^+e^- \rightarrow \Upsilon(4S)$
• • • We do not use the following data for averages, fits, limits, etc. • • •				
0.0391 ± 0.0078 ± 0.0019		AUBERT	02F	BABR Repl. by AUBERT 04P
0.043 ± 0.023	5	¹ ALEXANDER	95	CLE2 Sup. by BISHAI 96
¹ Assumes equal production of B^+B^- and $B^0\bar{B}^0$ on $\Upsilon(4S)$.				

 $\Gamma(J/\psi(1S)\rho^+)/\Gamma_{total}$ Γ_{196}/Γ

VALUE (units 10^{-5})	CL%	DOCUMENT ID	TECN	COMMENT
5.0 ± 0.7 ± 0.3		¹ AUBERT	07AC	BABR $e^+e^- \rightarrow \Upsilon(4S)$
• • • We do not use the following data for averages, fits, limits, etc. • • •				
<77	90	BISHAI	96	CLE2 $e^+e^- \rightarrow \Upsilon(4S)$
¹ Assumes equal production of B^+ and B^0 at the $\Upsilon(4S)$.				

 $\Gamma(J/\psi(1S)\pi^+\pi^0 \text{ nonresonant})/\Gamma_{total}$ Γ_{197}/Γ

VALUE (units 10^{-5})	CL%	DOCUMENT ID	TECN	COMMENT
<0.73	90	¹ AUBERT	07AC	BABR $e^+e^- \rightarrow \Upsilon(4S)$
¹ Assumes equal production of B^+ and B^0 at the $\Upsilon(4S)$.				

 $\Gamma(J/\psi(1S)a_1(1260)^+)/\Gamma_{total}$ Γ_{198}/Γ

VALUE	CL%	DOCUMENT ID	TECN	COMMENT
<1.2 × 10⁻³	90	BISHAI	96	CLE2 $e^+e^- \rightarrow \Upsilon(4S)$

 $\Gamma(J/\psi(1S)\rho\bar{\Lambda})/\Gamma_{total}$ Γ_{199}/Γ

VALUE (units 10^{-6})	CL%	DOCUMENT ID	TECN	COMMENT
11.8 ± 3.1 OUR AVERAGE				
11.7 ± 2.8 ^{+1.8} _{-2.3}		¹ XIE	05	BELL $e^+e^- \rightarrow \Upsilon(4S)$
12 ⁺⁹ ₋₆		¹ AUBERT	03K	BABR $e^+e^- \rightarrow \Upsilon(4S)$
• • • We do not use the following data for averages, fits, limits, etc. • • •				
<41	90	ZANG	04	BELL $e^+e^- \rightarrow \Upsilon(4S)$
¹ Assumes equal production of B^+ and B^0 at the $\Upsilon(4S)$.				

 $\Gamma(J/\psi(1S)\Sigma^0\rho)/\Gamma_{total}$ Γ_{200}/Γ

VALUE	CL%	DOCUMENT ID	TECN	COMMENT
<1.1 × 10⁻⁵	90	¹ XIE	05	BELL $e^+e^- \rightarrow \Upsilon(4S)$
¹ Assumes equal production of B^+ and B^0 at the $\Upsilon(4S)$.				

 $\Gamma(J/\psi(1S)D^+)/\Gamma_{total}$ Γ_{201}/Γ

VALUE (units 10^{-5})	CL%	DOCUMENT ID	TECN	COMMENT
<12	90	¹ AUBERT	05U	BABR $e^+e^- \rightarrow \Upsilon(4S)$
¹ Assumes equal production of B^+ and B^0 at the $\Upsilon(4S)$.				

 $\Gamma(J/\psi(1S)D^0\pi^+)/\Gamma_{total}$ Γ_{202}/Γ

VALUE (units 10^{-5})	CL%	DOCUMENT ID	TECN	COMMENT
<2.5	90	¹ ZHANG	05B	BELL $e^+e^- \rightarrow \Upsilon(4S)$
• • • We do not use the following data for averages, fits, limits, etc. • • •				
<5.2	90	¹ AUBERT	05R	BABR $e^+e^- \rightarrow \Upsilon(4S)$
¹ Assumes equal production of B^+ and B^0 at the $\Upsilon(4S)$.				

 $\Gamma(\psi(2S)\pi^+)/\Gamma_{total}$ Γ_{203}/Γ

VALUE (units 10^{-5})	DOCUMENT ID	TECN	COMMENT
2.44 ± 0.22 ± 0.20	¹ BHARDWAJ	08	BELL $e^+e^- \rightarrow \Upsilon(4S)$
¹ Assumes equal production of B^+ and B^0 at the $\Upsilon(4S)$.			

 $\Gamma(\psi(2S)\pi^+)/\Gamma(\psi(2S)K^+)$ $\Gamma_{203}/\Gamma_{204}$

VALUE (units 10^{-2})	DOCUMENT ID	TECN	COMMENT
3.99 ± 0.36 ± 0.17	BHARDWAJ	08	BELL $e^+e^- \rightarrow \Upsilon(4S)$

 $\Gamma(\psi(2S)K^+)/\Gamma_{total}$ Γ_{204}/Γ

VALUE (units 10^{-4})	EVTs	DOCUMENT ID	TECN	COMMENT
6.46 ± 0.33 OUR FIT				
6.6 ± 0.4 OUR AVERAGE				
4.9 ± 1.6 ± 0.4		¹ AUBERT	06E	BABR $e^+e^- \rightarrow \Upsilon(4S)$
6.17 ± 0.32 ± 0.44		² AUBERT	05J	BABR $e^+e^- \rightarrow \Upsilon(4S)$
6.9 ± 0.6		² ABE	03B	BELL $e^+e^- \rightarrow \Upsilon(4S)$
7.8 ± 0.7 ± 0.9		² RICHICHI	01	CLE2 $e^+e^- \rightarrow \Upsilon(4S)$
18 ± 8 ± 4	5	² ALBRECHT	90J	ARG $e^+e^- \rightarrow \Upsilon(4S)$
• • • We do not use the following data for averages, fits, limits, etc. • • •				
6.4 ± 0.5 ± 0.8		² AUBERT	02	BABR Repl. by AUBERT 05J
6.1 ± 2.3 ± 0.9	7	² ALAM	94	CLE2 Repl. by RICHICHI 01
<5 at 90% CL		² BORTOLETTO	92	CLEO $e^+e^- \rightarrow \Upsilon(4S)$
22 ± 17	3	³ ALBRECHT	87D	ARG $e^+e^- \rightarrow \Upsilon(4S)$
¹ Perform measurements of absolute branching fractions using a missing mass technique.				
² Assumes equal production of B^+ and B^0 at the $\Upsilon(4S)$.				
³ ALBRECHT 87D assume $B^+B^-/B^0\bar{B}^0$ ratio is 55/45. Superseded by ALBRECHT 90J.				

 $\Gamma(\psi(2S)K^+)/\Gamma(J/\psi(1S)K^+)$ $\Gamma_{204}/\Gamma_{167}$

VALUE	DOCUMENT ID	TECN	COMMENT
0.64 ± 0.04 OUR FIT			
0.60 ± 0.07 OUR AVERAGE			
0.63 ± 0.05 ± 0.08	ABAZOV	09Y	D0 $p\bar{p}$ at 1.96 TeV
0.558 ± 0.082 ± 0.056	ABE	98D	CDF $p\bar{p}$ 1.8 TeV
• • • We do not use the following data for averages, fits, limits, etc. • • •			
0.64 ± 0.06 ± 0.07	¹ AUBERT	02	BABR $e^+e^- \rightarrow \Upsilon(4S)$
¹ Assumes equal production of B^+ and B^0 at the $\Upsilon(4S)$.			

 $\Gamma(\psi(2S)K^*(892)^+)/\Gamma_{total}$ Γ_{205}/Γ

VALUE (units 10^{-4})	CL%	DOCUMENT ID	TECN	COMMENT
6.7 ± 1.4 OUR AVERAGE				Error includes scale factor of 1.3.
5.92 ± 0.85 ± 0.89		¹ AUBERT	05J	BABR $e^+e^- \rightarrow \Upsilon(4S)$
9.2 ± 1.9 ± 1.2		¹ RICHICHI	01	CLE2 $e^+e^- \rightarrow \Upsilon(4S)$
• • • We do not use the following data for averages, fits, limits, etc. • • •				
<30	90	¹ ALAM	94	CLE2 Repl. by RICHICHI 01
<35	90	¹ BORTOLETTO	92	CLEO $e^+e^- \rightarrow \Upsilon(4S)$
<49	90	¹ ALBRECHT	90J	ARG $e^+e^- \rightarrow \Upsilon(4S)$
¹ Assumes equal production of B^+ and B^0 at the $\Upsilon(4S)$.				

Meson Particle Listings

 B^\pm

$\Gamma(\psi(2S)K^*(892^+))/\Gamma(\psi(2S)K^+)$				$\Gamma_{205}/\Gamma_{204}$
VALUE	DOCUMENT ID	TECN	COMMENT	
0.96 ± 0.15 ± 0.09	AUBERT	05J	BABR $e^+e^- \rightarrow \Upsilon(4S)$	

$\Gamma(\psi(2S)K^+\pi^+\pi^-)/\Gamma_{total}$				Γ_{206}/Γ
VALUE	EVTs	DOCUMENT ID	TECN	COMMENT
0.0019 ± 0.0011 ± 0.0004	3	¹ ALBRECHT	90J	ARG $e^+e^- \rightarrow \Upsilon(4S)$
¹ Assumes equal production of B^+ and B^0 at the $\Upsilon(4S)$.				

$\Gamma(\psi(3770)K^+)/\Gamma_{total}$				Γ_{207}/Γ
VALUE (units 10^{-3})	DOCUMENT ID	TECN	COMMENT	
0.49 ± 0.13 OUR AVERAGE				
3.5 ± 2.5 ± 0.3	¹ AUBERT	06E	BABR $e^+e^- \rightarrow \Upsilon(4S)$	
0.48 ± 0.11 ± 0.07	² CHISTOV	04	BELL $e^+e^- \rightarrow \Upsilon(4S)$	
¹ Perform measurements of absolute branching fractions using a missing mass technique.				
² Assumes equal production of B^+ and B^0 at the $\Upsilon(4S)$.				

$\Gamma(\psi(3770)K^+ \times B(\psi \rightarrow D^0\bar{D}^0))/\Gamma_{total}$				Γ_{208}/Γ
VALUE (units 10^{-4})	DOCUMENT ID	TECN	COMMENT	
1.6 ± 0.4 OUR AVERAGE	Error includes scale factor of 1.1.			
1.41 ± 0.30 ± 0.22	¹ AUBERT	08B	BABR $e^+e^- \rightarrow \Upsilon(4S)$	
2.2 ± 0.5 ± 0.3	¹ BRODZICKA	08	BELL $e^+e^- \rightarrow \Upsilon(4S)$	
• • • We do not use the following data for averages, fits, limits, etc. • • •				
3.4 ± 0.8 ± 0.5	¹ CHISTOV	04	BELL Repl. by BRODZICKA 08	
¹ Assumes equal production of B^+ and B^0 at the $\Upsilon(4S)$.				

$\Gamma(\psi(3770)K^+ \times B(\psi \rightarrow D^+D^-))/\Gamma_{total}$				Γ_{209}/Γ
VALUE (units 10^{-4})	DOCUMENT ID	TECN	COMMENT	
0.94 ± 0.35 OUR AVERAGE				
0.84 ± 0.32 ± 0.21	¹ AUBERT	08B	BABR $e^+e^- \rightarrow \Upsilon(4S)$	
1.4 ± 0.8 ± 0.2	¹ CHISTOV	04	BELL $e^+e^- \rightarrow \Upsilon(4S)$	
¹ Assumes equal production of B^+ and B^0 at the $\Upsilon(4S)$.				

$\Gamma(\chi_{c0}\pi^+ \times B(\chi_{c0} \rightarrow \pi^+\pi^-))/\Gamma_{total}$				Γ_{210}/Γ
VALUE (units 10^{-6})	CL%	DOCUMENT ID	TECN	COMMENT
< 0.1	90	¹ AUBERT	09L	BABR $e^+e^- \rightarrow \Upsilon(4S)$
• • • We do not use the following data for averages, fits, limits, etc. • • •				
< 0.3	90	¹ AUBERT,B	05G	BABR Repl. by AUBERT 09L
¹ Assumes equal production of B^+ and B^0 at the $\Upsilon(4S)$.				

$\Gamma(\chi_{c0}(1P)K^+)/\Gamma_{total}$				Γ_{211}/Γ
VALUE (units 10^{-4})	CL%	DOCUMENT ID	TECN	COMMENT
1.33 ± 0.19 OUR AVERAGE				
1.26 ^{+0.28} _{-0.25} ± 0.06		^{1,2} AUBERT	08A1	BABR $e^+e^- \rightarrow \Upsilon(4S)$
1.84 ± 0.32 ± 0.31		^{1,3} AUBERT	06o	BABR $e^+e^- \rightarrow \Upsilon(4S)$
5.2 ± 2.4 ± 0.4		⁴ AUBERT,BE	06M	BABR $e^+e^- \rightarrow \Upsilon(4S)$
1.12 ± 0.12 ^{+0.30} _{-0.20}		¹ GARMASH	06	BELL $e^+e^- \rightarrow \Upsilon(4S)$
• • • We do not use the following data for averages, fits, limits, etc. • • •				
< 5	90	^{1,5} WICHT	08	BELL $e^+e^- \rightarrow \Upsilon(4S)$
< 1.8	90	⁶ AUBERT	06E	BABR $e^+e^- \rightarrow \Upsilon(4S)$
< 8.9	90	¹ AUBERT	05K	BABR $e^+e^- \rightarrow \Upsilon(4S)$
1.39 ± 0.49 ± 0.11		⁷ AUBERT,B	05N	BABR Repl. by AUBERT 08A1
1.96 ± 0.35 ^{+2.00} _{-0.42}		¹ GARMASH	05	BELL Repl. by GARMASH 06
2.7 ± 0.7		⁸ AUBERT	04T	BABR Repl. by AUBERT,B 04P
3.0 ± 0.8 ± 0.3		⁹ AUBERT,B	04P	BABR Repl. by AUBERT,B 05N
6.0 ^{+2.1} _{-1.8} ± 1.1		¹⁰ ABE	02B	BELL Repl. by GARMASH 05
< 4.8	90	¹¹ EDWARDS	01B	CLE2 $e^+e^- \rightarrow \Upsilon(4S)$

- ¹ Assumes equal production of B^+ and B^0 at the $\Upsilon(4S)$.
- ² AUBERT 08A1 reports $(0.70 \pm 0.10^{+0.12}_{-0.10}) \times 10^{-6}$ for $B(B^+ \rightarrow \chi_{c0}K^+) \times B(\chi_{c0} \rightarrow \pi^+\pi^-)$. We compute $B(B^+ \rightarrow \chi_{c0}K^+)$ using the PDG value $B(\chi_{c0} \rightarrow \pi\pi) = (8.4 \pm 0.4) \times 10^{-3}$ and 2/3 for the $\pi^+\pi^-$ fraction. Our first error is their experiment's error and the second error is systematic error from using our best value.
- ³ Measured in the $B^+ \rightarrow K^+K^-K^+$ decay.
- ⁴ AUBERT,BE 06M reports $[\Gamma(B^+ \rightarrow \chi_{c0}(1P)K^+)/\Gamma_{total}] \times [B(\chi_{c0}(1P) \rightarrow \gamma J/\psi(1S))] = (6.1 \pm 2.6 \pm 1.1) \times 10^{-6}$ which we divide by our best value $B(\chi_{c0}(1P) \rightarrow \gamma J/\psi(1S)) = (1.16 \pm 0.08) \times 10^{-2}$. Our first error is their experiment's error and our second error is the systematic error from using our best value. The significance of the observed signal is 2.4 σ .
- ⁵ WICHT 08 reports $[\Gamma(B^+ \rightarrow \chi_{c0}(1P)K^+)/\Gamma_{total}] \times [B(\chi_{c0}(1P) \rightarrow \gamma\gamma)] < 0.11 \times 10^{-6}$ which we divide by our best value $B(\chi_{c0}(1P) \rightarrow \gamma\gamma) = 2.22 \times 10^{-4}$.
- ⁶ Perform measurements of absolute branching fractions using a missing mass technique.
- ⁷ AUBERT,B 05N reports $(0.66 \pm 0.22 \pm 0.08) \times 10^{-6}$ for $B(B^+ \rightarrow \chi_{c0}^0K^+) \times B(\chi_{c0}^0 \rightarrow \pi^+\pi^-)$. We compute $B(B^+ \rightarrow \chi_{c0}^0K^+)$ using the PDG value $B(\chi_{c0}^0 \rightarrow \pi^+\pi^-) = (7.1 \pm 0.6) \times 10^{-3}$ and 2/3 for the $\pi^+\pi^-$ fraction.
- ⁸ The measurement performed using decay channels $\chi_{c0}^0 \rightarrow \pi^+\pi^-$ and $\chi_{c0}^0 \rightarrow K^+K^-$. The ratio of the branching ratios for these channels is found to be consistent with world average.

⁹ AUBERT 04P reports $B(B^+ \rightarrow \chi_{c0}^0K^+) \times B(\chi_{c0}^0 \rightarrow \pi^+\pi^-) = (1.5 \pm 0.4 \pm 0.1) \times 10^{-6}$ and used PDG value of $B(\chi_{c0}^0 \rightarrow \pi\pi) = (7.4 \pm 0.8) \times 10^{-3}$ and Clebsh-Gordan coefficient to compute $B(B^+ \rightarrow \chi_{c0}^0K^+)$.

¹⁰ ABE 02b measures the ratio of $B(B^+ \rightarrow \chi_{c0}^0K^+)/B(B^+ \rightarrow J/\psi(1S)K^+) = 0.60 \pm 0.21 - 0.18 \pm 0.05 \pm 0.08$, where the third error is due to the uncertainty in the $B(\chi_{c0}^0 \rightarrow \pi^+\pi^-)$, and uses $B(B^+ \rightarrow J/\psi(1S)K^+) = (10.0 \pm 1.0) \times 10^{-4}$ to obtain the result.

¹¹ EDWARDS 01 assumes equal production of B^0 and B^+ at the $\Upsilon(4S)$. The correlated uncertainties (28.3%) from $B(J/\psi(1S) \rightarrow \gamma\eta_c)$ in those modes have been accounted for.

$\Gamma(\chi_{c0}K^*(892^+))/\Gamma_{total}$				Γ_{212}/Γ
VALUE (units 10^{-4})	CL%	DOCUMENT ID	TECN	COMMENT
< 2.1	90	¹ AUBERT	08BD	BABR $e^+e^- \rightarrow \Upsilon(4S)$
• • • We do not use the following data for averages, fits, limits, etc. • • •				
< 28.6	90	¹ AUBERT	05K	BABR Repl. by AUBERT 08BD
¹ Assumes equal production of B^+ and B^0 at the $\Upsilon(4S)$.				

$\Gamma(\chi_{c2}\pi^+ \times B(\chi_{c2} \rightarrow \pi^+\pi^-))/\Gamma_{total}$				Γ_{213}/Γ
VALUE (units 10^{-6})	CL%	DOCUMENT ID	TECN	COMMENT
< 0.1	90	¹ AUBERT	09L	BABR $e^+e^- \rightarrow \Upsilon(4S)$
¹ Assumes equal production of B^+ and B^0 at the $\Upsilon(4S)$.				

$\Gamma(\chi_{c2}K^+)/\Gamma_{total}$				Γ_{214}/Γ
VALUE	CL%	DOCUMENT ID	TECN	COMMENT
< 1.8 × 10⁻⁵	90	¹ AUBERT	09B	BABR $e^+e^- \rightarrow \Upsilon(4S)$
• • • We do not use the following data for averages, fits, limits, etc. • • •				
< 2.0 × 10 ⁻⁵	90	² AUBERT	06E	BABR $e^+e^- \rightarrow \Upsilon(4S)$
< 2.9 × 10 ⁻⁵	90	³ SONI	06	BELL $e^+e^- \rightarrow \Upsilon(4S)$
< 3.0 × 10 ⁻⁵	90	³ AUBERT	05K	BABR Repl. by AUBERT 06E
¹ Uses $\chi_{c1,2} \rightarrow J/\psi\gamma$. Assumes $B(\Upsilon(4S) \rightarrow B^+B^-) = (51.6 \pm 0.6)\%$ and $B(\Upsilon(4S) \rightarrow B^0\bar{B}^0) = (48.4 \pm 0.6)\%$.				
² Perform measurements of absolute branching fractions using a missing mass technique.				
³ Assumes equal production of B^+ and B^0 at the $\Upsilon(4S)$.				

$\Gamma(B^+ \rightarrow \chi_{c2}K^+)/\Gamma_{total} \times \Gamma(\chi_{c2}(1P) \rightarrow \gamma\gamma)/\Gamma_{total}$				$\Gamma_{214}/\Gamma \times \Gamma_{54}^{\chi_{c2}(1P)}/\Gamma_{\chi_{c2}(1P)}$
VALUE (units 10^{-6})	CL%	DOCUMENT ID	TECN	COMMENT
< 0.09	90	¹ WICHT	08	BELL $e^+e^- \rightarrow \Upsilon(4S)$
¹ Assumes equal production of B^+ and B^0 at the $\Upsilon(4S)$.				

$\Gamma(\chi_{c2}K^*(892^+))/\Gamma_{total}$				Γ_{215}/Γ
VALUE	CL%	DOCUMENT ID	TECN	COMMENT
< 12 × 10⁻⁵	90	¹ AUBERT	09B	BABR $e^+e^- \rightarrow \Upsilon(4S)$
• • • We do not use the following data for averages, fits, limits, etc. • • •				
< 12.7 × 10 ⁻⁵	90	² SONI	06	BELL $e^+e^- \rightarrow \Upsilon(4S)$
< 1.2 × 10 ⁻⁵	90	² AUBERT	05K	BABR Repl. by AUBERT 09B
¹ Uses $\chi_{c1,2} \rightarrow J/\psi\gamma$. Assumes $B(\Upsilon(4S) \rightarrow B^+B^-) = (51.6 \pm 0.6)\%$ and $B(\Upsilon(4S) \rightarrow B^0\bar{B}^0) = (48.4 \pm 0.6)\%$.				
² Assumes equal production of B^+ and B^0 at the $\Upsilon(4S)$.				

$\Gamma(\chi_{c1}(1P)\pi^+)/\Gamma_{total}$				Γ_{216}/Γ
VALUE (units 10^{-5})	CL%	DOCUMENT ID	TECN	COMMENT
2.2 ± 0.4 ± 0.3		¹ KUMAR	06	BELL $e^+e^- \rightarrow \Upsilon(4S)$
¹ Assumes equal production of B^+ and B^0 at the $\Upsilon(4S)$.				

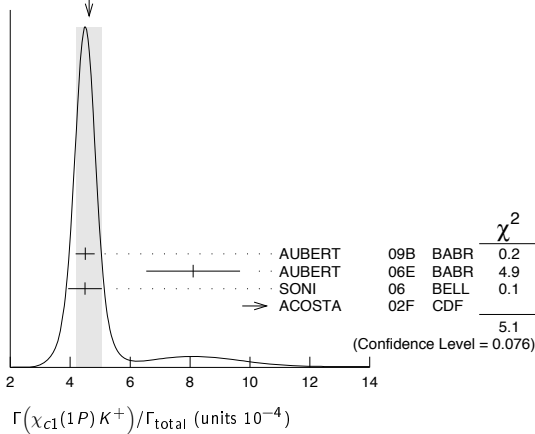
$\Gamma(\chi_{c1}(1P)K^+)/\Gamma_{total}$				Γ_{217}/Γ
VALUE (units 10^{-4})	EVTs	DOCUMENT ID	TECN	COMMENT
4.6 ± 0.4 OUR AVERAGE	Error includes scale factor of 1.6. See the ideogram below.			
4.5 ± 0.1 ± 0.3		¹ AUBERT	09B	BABR $e^+e^- \rightarrow \Upsilon(4S)$
8.1 ± 1.4 ± 0.7		² AUBERT	06E	BABR $e^+e^- \rightarrow \Upsilon(4S)$
4.49 ± 0.19 ± 0.53		³ SONI	06	BELL $e^+e^- \rightarrow \Upsilon(4S)$
15.5 ± 5.4 ± 2.0		⁴ ACOSTA	02F	CDF $p\bar{p}$ 1.8 TeV
• • • We do not use the following data for averages, fits, limits, etc. • • •				
5.1 ± 0.4 ± 0.2		⁵ AUBERT,BE	06M	BABR Repl. by AUBERT 09B
5.79 ± 0.26 ± 0.65		³ AUBERT	05J	BABR Repl. by AUBERT,BE 06M
6.0 ± 0.9 ± 0.3		⁶ AUBERT	02	BABR Repl. by AUBERT 05J
9.7 ± 4.0 ± 0.9	6	³ ALAM	94	CLE2 $e^+e^- \rightarrow \Upsilon(4S)$
19 ± 13 ± 6		⁷ ALBRECHT	92E	ARG $e^+e^- \rightarrow \Upsilon(4S)$

- ¹ Uses $\chi_{c1,2} \rightarrow J/\psi\gamma$. Assumes $B(\Upsilon(4S) \rightarrow B^+B^-) = (51.6 \pm 0.6)\%$ and $B(\Upsilon(4S) \rightarrow B^0\bar{B}^0) = (48.4 \pm 0.6)\%$.
- ² Perform measurements of absolute branching fractions using a missing mass technique.
- ³ Assumes equal production of B^+ and B^0 at the $\Upsilon(4S)$.
- ⁴ ACOSTA 02F uses as reference of $B(B \rightarrow J/\psi(1S)K^+) = (10.1 \pm 0.6) \times 10^{-4}$. The second error includes the systematic error and the uncertainties of the branching ratio.
- ⁵ AUBERT,BE 06M reports $[\Gamma(B^+ \rightarrow \chi_{c1}(1P)K^+)/\Gamma_{total}] \times [B(\chi_{c1}(1P) \rightarrow \gamma J/\psi(1S))] = (1.76 \pm 0.07 \pm 0.12) \times 10^{-4}$ which we divide by our best value $B(\chi_{c1}(1P) \rightarrow \gamma J/\psi(1S)) = (34.4 \pm 1.5) \times 10^{-2}$. Our first error is their experiment's error and our second error is the systematic error from using our best value.

⁶ AUBERT 02 reports $(7.5 \pm 0.9 \pm 0.8) \times 10^{-4}$ from a measurement of $[\Gamma(B^+ \rightarrow \chi_{c1}(1P)K^+)/\Gamma_{total}] \times [B(\chi_{c1}(1P) \rightarrow \gamma J/\psi(1S))]$ assuming $B(\chi_{c1}(1P) \rightarrow \gamma J/\psi(1S)) = 0.273 \pm 0.016$, which we rescale to our best value $B(\chi_{c1}(1P) \rightarrow \gamma J/\psi(1S)) = (34.4 \pm 1.5) \times 10^{-2}$. Our first error is their experiment's error and our second error is the systematic error from using our best value. Assumes equal production of B^+ and B^0 at the $\Upsilon(4S)$.

⁷ ALBRECHT 92E assumes no $\chi_{c2}(1P)$ production and $B(\Upsilon(4S) \rightarrow B^+B^-) = 50\%$.

WEIGHTED AVERAGE
 4.6 ± 0.4 (Error scaled by 1.6)



$\Gamma(\chi_{c1}(1P)K^+)/\Gamma(J/\psi(1S)K^+)$ $\Gamma_{217}/\Gamma_{167}$

VALUE	DOCUMENT ID	TECN	COMMENT
$0.60 \pm 0.07 \pm 0.03$	¹ AUBERT 02	BABR	$e^+e^- \rightarrow \Upsilon(4S)$

¹ AUBERT 02 reports $0.75 \pm 0.08 \pm 0.05$ from a measurement of $[\Gamma(B^+ \rightarrow \chi_{c1}(1P)K^+)/\Gamma(B^+ \rightarrow J/\psi(1S)K^+)] \times [B(\chi_{c1}(1P) \rightarrow \gamma J/\psi(1S))]$ assuming $B(\chi_{c1}(1P) \rightarrow \gamma J/\psi(1S)) = 0.273 \pm 0.016$, which we rescale to our best value $B(\chi_{c1}(1P) \rightarrow \gamma J/\psi(1S)) = (34.4 \pm 1.5) \times 10^{-2}$. Our first error is their experiment's error and our second error is the systematic error from using our best value. Assumes equal production of B^+ and B^0 at the $\Upsilon(4S)$.

$\Gamma(\chi_{c1}(1P)\pi^+)/\Gamma(\chi_{c1}(1P)K^+)$ $\Gamma_{216}/\Gamma_{217}$

VALUE	DOCUMENT ID	TECN	COMMENT
$0.043 \pm 0.008 \pm 0.003$	¹ KUMAR 06	BELL	$e^+e^- \rightarrow \Upsilon(4S)$

¹ Assumes equal production of B^+ and B^0 at the $\Upsilon(4S)$.

$\Gamma(\chi_{c1}(1P)K^*(892)^+)/\Gamma_{total}$ Γ_{218}/Γ

VALUE (units 10^{-4})	CL%	DOCUMENT ID	TECN	COMMENT
3.0 ± 0.6	OUR AVERAGE			Error includes scale factor of 1.1.
$2.6 \pm 0.5 \pm 0.4$		¹ AUBERT 09B	BABR	$e^+e^- \rightarrow \Upsilon(4S)$
$4.05 \pm 0.59 \pm 0.95$		² SONI 06	BELL	$e^+e^- \rightarrow \Upsilon(4S)$

• • • We do not use the following data for averages, fits, limits, etc. • • •

$2.94 \pm 0.95 \pm 0.98$		² AUBERT 05J	BABR	Repl. by AUBERT 09B
<21	90	² ALAM 94	CLE2	$e^+e^- \rightarrow \Upsilon(4S)$

¹ Uses $\chi_{c1,2} \rightarrow J/\psi\gamma$. Assumes $B(\Upsilon(4S) \rightarrow B^+B^-) = (51.6 \pm 0.6)\%$ and $B(\Upsilon(4S) \rightarrow B^0\bar{B}^0) = (48.4 \pm 0.6)\%$.

² Assumes equal production of B^+ and B^0 at the $\Upsilon(4S)$.

$\Gamma(\chi_{c1}(1P)K^*(892)^+)/\Gamma(\chi_{c1}(1P)K^+)$ $\Gamma_{218}/\Gamma_{217}$

VALUE	DOCUMENT ID	TECN	COMMENT
$0.51 \pm 0.17 \pm 0.16$	AUBERT 05J	BABR	$e^+e^- \rightarrow \Upsilon(4S)$

$\Gamma(h_c(1P)K^+)/\Gamma_{total}$ Γ_{219}/Γ

VALUE (units 10^{-5})	EVTS	DOCUMENT ID	TECN	COMMENT
<3.8	90	¹ FANG 06	BELL	$e^+e^- \rightarrow \Upsilon(4S)$

¹ Assumes equal production of B^+ and B^0 at the $\Upsilon(4S)$ and $B(h_c \rightarrow \eta_c\gamma) = 50\%$.

$\Gamma(K^0\pi^+)/\Gamma_{total}$ Γ_{220}/Γ

VALUE (units 10^{-6})	CL%	DOCUMENT ID	TECN	COMMENT
23.1 ± 1.0	OUR AVERAGE			
$22.8 \pm 0.8 \pm 1.3$		¹ LIN 07	BELL	$e^+e^- \rightarrow \Upsilon(4S)$
$23.9 \pm 1.1 \pm 1.0$		¹ AUBERT, BE 06C	BABR	$e^+e^- \rightarrow \Upsilon(4S)$
$18.8 \pm 3.7 \pm 2.1$		¹ BORNHEIM 03	CLE2	$e^+e^- \rightarrow \Upsilon(4S)$

• • • We do not use the following data for averages, fits, limits, etc. • • •

$26.0 \pm 1.3 \pm 1.0$		¹ AUBERT, BE 05E	BABR	Repl. by AUBERT, BE 06C
$22.3 \pm 1.7 \pm 1.1$		¹ AUBERT 04M	BABR	Repl. by AUBERT, BE 05E
$22.0 \pm 1.9 \pm 1.1$		¹ CHAO 04	BELL	Repl. by LIN 07
19.4 ± 3.1	$\pm 3.0 \pm 1.6$	¹ CASEY 02	BELL	Repl. by CHAO 04
$13.7 \pm 5.7 \pm 1.9$	$- 4.8 - 1.8$	¹ ABE 01H	BELL	Repl. by CASEY 02
18.2 ± 3.3	$\pm 3.0 \pm 2.0$	¹ AUBERT 01E	BABR	Repl. by AUBERT 04M
$18.2 \pm 4.6 \pm 1.6$	$- 4.0 - 1.6$	¹ CRONIN-HEN..00	CLE2	Repl. by BORNHEIM 03
23 ± 11	$\pm 10 \pm 3.6$	GODANG 98	CLE2	Repl. by CRONIN-HENNESSY 00
<48	90	ASNER 96	CLE2	Repl. by GODANG 98
<190	90	ALBRECHT 91B	ARG	$e^+e^- \rightarrow \Upsilon(4S)$
<100	90	² AVERY 89B	CLEO	$e^+e^- \rightarrow \Upsilon(4S)$
<680	90	AVERY 87	CLEO	$e^+e^- \rightarrow \Upsilon(4S)$

¹ Assumes equal production of B^+ and B^0 at the $\Upsilon(4S)$.

² AVERY 89B reports $<9 \times 10^{-5}$ assuming the $\Upsilon(4S)$ decays 43% to $B^0\bar{B}^0$. We rescale to 50%.

$\Gamma(K^+\pi^0)/\Gamma_{total}$ Γ_{221}/Γ

VALUE (units 10^{-6})	CL%	DOCUMENT ID	TECN	COMMENT
12.9 ± 0.6	OUR AVERAGE			
$13.6 \pm 0.6 \pm 0.7$		¹ AUBERT 07BC	BABR	$e^+e^- \rightarrow \Upsilon(4S)$
$12.4 \pm 0.5 \pm 0.6$		¹ LIN 07A	BELL	$e^+e^- \rightarrow \Upsilon(4S)$
$12.9 \pm 2.4 \pm 1.2$	$- 2.2 - 1.1$	¹ BORNHEIM 03	CLE2	$e^+e^- \rightarrow \Upsilon(4S)$

• • • We do not use the following data for averages, fits, limits, etc. • • •

$12.0 \pm 0.7 \pm 0.6$		¹ AUBERT 05L	BABR	Repl. by AUBERT 07BC
$12.0 \pm 1.3 \pm 1.3$	$- 0.9$	¹ CHAO 04	BELL	Repl. by LIN 07A
12.8 ± 1.2	± 1.0	¹ AUBERT 03L	BABR	Repl. by AUBERT 05L
13.0 ± 2.5	± 1.3	¹ CASEY 02	BELL	Repl. by CHAO 04
$16.3 \pm 3.5 \pm 1.6$	$- 3.3 - 1.8$	¹ ABE 01H	BELL	Repl. by CASEY 02
10.8 ± 2.1	± 1.0	¹ AUBERT 01E	BABR	Repl. by AUBERT 03L
$11.6 \pm 3.0 \pm 1.4$	$- 2.7 - 1.3$	¹ CRONIN-HEN..00	CLE2	Repl. by BORNHEIM 03
<16	90	GODANG 98	CLE2	Repl. by CRONIN-HENNESSY 00
<14	90	ASNER 96	CLE2	Repl. by GODANG 98

¹ Assumes equal production of B^+ and B^0 at the $\Upsilon(4S)$.

$\Gamma(K^+\pi^0)/\Gamma(K^0\pi^+)$ $\Gamma_{221}/\Gamma_{220}$

VALUE	DOCUMENT ID	TECN	COMMENT
$0.54 \pm 0.03 \pm 0.04$	LIN 07A	BELL	$e^+e^- \rightarrow \Upsilon(4S)$

• • • We do not use the following data for averages, fits, limits, etc. • • •

$2.38 \pm 0.98 \pm 0.39$	$- 1.10 - 0.26$	ABE 01H	BELL	Repl. by LIN 07A
--------------------------	-----------------	---------	------	------------------

$\Gamma(\eta'K^+)/\Gamma_{total}$ Γ_{222}/Γ

VALUE (units 10^{-6})	CL%	DOCUMENT ID	TECN	COMMENT
70.6 ± 2.5	OUR AVERAGE			
$71.5 \pm 1.3 \pm 3.2$		¹ AUBERT 09AV	BABR	$e^+e^- \rightarrow \Upsilon(4S)$
63 ± 10	$\pm 9 \pm 2$	^{1,2} WICHT 08	BELL	$e^+e^- \rightarrow \Upsilon(4S)$
$69.2 \pm 2.2 \pm 3.7$		¹ SCHUEMANN 06	BELL	$e^+e^- \rightarrow \Upsilon(4S)$
80 ± 10	$\pm 9 \pm 7$	¹ RICHICHI 00	CLE2	$e^+e^- \rightarrow \Upsilon(4S)$

• • • We do not use the following data for averages, fits, limits, etc. • • •

$70.0 \pm 1.5 \pm 2.8$		¹ AUBERT 07AE	BABR	Repl. by AUBERT 09AV
$68.9 \pm 2.0 \pm 3.2$		¹ AUBERT 05M	BABR	Repl. by AUBERT 07AE
$76.9 \pm 3.5 \pm 4.4$		¹ AUBERT 03W	BABR	Repl. by AUBERT 05M
79 ± 12	$\pm 11 \pm 9$	¹ ABE 01M	BELL	Repl. by SCHUEMANN 06
70 ± 8	± 5	¹ AUBERT 01G	BABR	Repl. by AUBERT 03W
65 ± 15	$\pm 14 \pm 9$	BEHRENS 98	CLE2	Repl. by RICHICHI 00

¹ Assumes equal production of B^+ and B^0 at the $\Upsilon(4S)$.

² WICHT 08 reports $[\Gamma(B^+ \rightarrow \eta'K^+)/\Gamma_{total}] \times [B(\eta'(958) \rightarrow \gamma\gamma)] = (1.40 \pm 0.16 \pm 0.15) \times 10^{-6}$ which we divide by our best value $B(\eta'(958) \rightarrow \gamma\gamma) = (2.22 \pm 0.08) \times 10^{-2}$. Our first error is their experiment's error and our second error is the systematic error from using our best value.

$\Gamma(\eta'K^*(892)^+)/\Gamma_{total}$ Γ_{223}/Γ

VALUE (units 10^{-6})	CL%	DOCUMENT ID	TECN	COMMENT
4.9 ± 1.9	± 0.8	¹ AUBERT 07E	BABR	$e^+e^- \rightarrow \Upsilon(4S)$

• • • We do not use the following data for averages, fits, limits, etc. • • •

<2.9	90	¹ SCHUEMANN 07	BELL	$e^+e^- \rightarrow \Upsilon(4S)$
<14	90	¹ AUBERT, B 04D	BABR	Repl. by AUBERT 07E
<35	90	¹ RICHICHI 00	CLE2	$e^+e^- \rightarrow \Upsilon(4S)$
<13	90	BEHRENS 98	CLE2	Repl. by RICHICHI 00

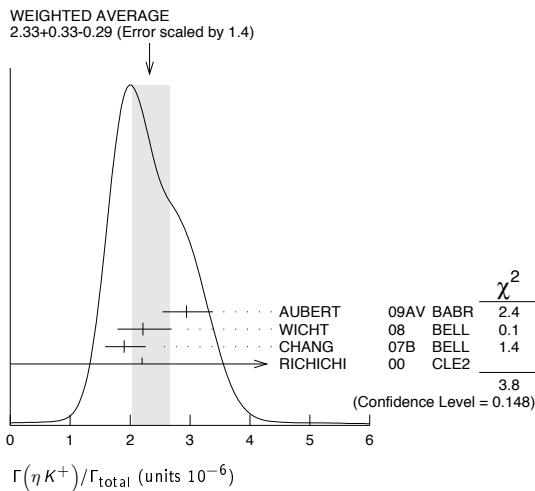
¹ Assumes equal production of B^+ and B^0 at the $\Upsilon(4S)$.

Meson Particle Listings

B^\pm

$\Gamma(\eta K^+)/\Gamma_{total}$		Γ_{224}/Γ			
VALUE (units 10^{-6})	CL%	DOCUMENT ID	TECN	COMMENT	
2.33 ± 0.33 OUR AVERAGE Error includes scale factor of 1.4. See the ideogram below.					
2.94 ± 0.39 -0.34 ± 0.21		1 AUBERT	09AV	BABR	$e^+e^- \rightarrow \Upsilon(4S)$
2.21 ± 0.48 -0.42 ± 0.01		1,2 WICHT	08	BELL	$e^+e^- \rightarrow \Upsilon(4S)$
1.9 ± 0.3 +0.2 -0.1		1 CHANG	07B	BELL	$e^+e^- \rightarrow \Upsilon(4S)$
2.2 ± 2.8 -2.2		1 RICHICHI	00	CLE2	$e^+e^- \rightarrow \Upsilon(4S)$
• • • We do not use the following data for averages, fits, limits, etc. • • •					
3.7 ± 0.4 ± 0.1		1 AUBERT	07AE	BABR	Repl. by AUBERT 09AV
3.3 ± 0.6 ± 0.3		1 AUBERT,B	05K	BABR	Repl. by AUBERT 07AE
2.1 ± 0.6 ± 0.2		1 CHANG	05A	BELL	Repl. by CHANG 07B
3.4 ± 0.8 ± 0.2		1 AUBERT	04H	BABR	Repl. by AUBERT,B 05K
<14	90	BEHRENS	98	CLE2	Repl. by RICHICHI 00

¹ Assumes equal production of B^+ and B^0 at the $\Upsilon(4S)$.
² WICHT 08 reports $[\Gamma(B^+ \rightarrow \eta K^+)/\Gamma_{total}] \times [B(\eta \rightarrow 2\gamma)] = (0.87 \pm 0.16 \pm 0.10 \pm 0.15 \pm 0.07) \times 10^{-6}$ which we divide by our best value $B(\eta \rightarrow 2\gamma) = (39.31 \pm 0.20) \times 10^{-2}$. Our first error is their experiment's error and our second error is the systematic error from using our best value.



$\Gamma(\eta K^*(892)^+)/\Gamma_{total}$		Γ_{225}/Γ			
VALUE (units 10^{-6})	CL%	DOCUMENT ID	TECN	COMMENT	
19.3 ± 1.6 OUR AVERAGE					
19.3 ± 2.0 -1.9 ± 1.5		1 WANG	07B	BELL	$e^+e^- \rightarrow \Upsilon(4S)$
18.9 ± 1.8 ± 1.3		1 AUBERT,B	06H	BABR	$e^+e^- \rightarrow \Upsilon(4S)$
26.4 ± 9.6 -8.2 ± 3.3		1 RICHICHI	00	CLE2	$e^+e^- \rightarrow \Upsilon(4S)$

• • • We do not use the following data for averages, fits, limits, etc. • • •

25.6 ± 4.0 ± 2.4		1 AUBERT,B	04D	BABR	Repl. by AUBERT,B 06H
<30	90	BEHRENS	98	CLE2	Repl. by RICHICHI 00

¹ Assumes equal production of B^+ and B^0 at the $\Upsilon(4S)$.

$\Gamma(\eta K_0^*(1430)^+)/\Gamma_{total}$		Γ_{226}/Γ			
VALUE (units 10^{-6})	CL%	DOCUMENT ID	TECN	COMMENT	
18.2 ± 2.6 ± 2.6					
		1 AUBERT,B	06H	BABR	$e^+e^- \rightarrow \Upsilon(4S)$

¹ Assumes equal production of B^+ and B^0 at the $\Upsilon(4S)$.

$\Gamma(\eta K_2^*(1430)^+)/\Gamma_{total}$		Γ_{227}/Γ			
VALUE (units 10^{-6})	CL%	DOCUMENT ID	TECN	COMMENT	
9.1 ± 2.7 ± 1.4					
		1 AUBERT,B	06H	BABR	$e^+e^- \rightarrow \Upsilon(4S)$

¹ Assumes equal production of B^+ and B^0 at the $\Upsilon(4S)$.

$\Gamma(\eta(1295) K^+ \times B(\eta(1295) \rightarrow \eta\pi\pi))/\Gamma_{total}$		Γ_{228}/Γ			
VALUE (units 10^{-6})	CL%	DOCUMENT ID	TECN	COMMENT	
2.9 ± 0.8 ± 0.7 ± 0.2					
		1 AUBERT	08X	BABR	$e^+e^- \rightarrow \Upsilon(4S)$

¹ Assumes equal production of B^+ and B^0 at the $\Upsilon(4S)$.

$\Gamma(\eta(1405) K^+ \times B(\eta(1405) \rightarrow \eta\pi\pi))/\Gamma_{total}$		Γ_{229}/Γ			
VALUE (units 10^{-6})	CL%	DOCUMENT ID	TECN	COMMENT	
<1.3					
	90	1 AUBERT	08X	BABR	$e^+e^- \rightarrow \Upsilon(4S)$

¹ Assumes equal production of B^+ and B^0 at the $\Upsilon(4S)$.

$\Gamma(\eta(1405) K^+ \times B(\eta(1405) \rightarrow K^* K))/\Gamma_{total}$		Γ_{230}/Γ			
VALUE (units 10^{-6})	CL%	DOCUMENT ID	TECN	COMMENT	
<1.2					
	90	1 AUBERT	08X	BABR	$e^+e^- \rightarrow \Upsilon(4S)$

¹ Assumes equal production of B^+ and B^0 at the $\Upsilon(4S)$.

$\Gamma(\eta(1475) K^+ \times B(\eta(1475) \rightarrow K^* K))/\Gamma_{total}$		Γ_{231}/Γ			
VALUE (units 10^{-6})	CL%	DOCUMENT ID	TECN	COMMENT	
13.8 ± 1.8 ± 1.0					
		1 AUBERT	08X	BABR	$e^+e^- \rightarrow \Upsilon(4S)$

¹ Assumes equal production of B^+ and B^0 at the $\Upsilon(4S)$.

$\Gamma(f_1(1285) K^+)/\Gamma_{total}$		Γ_{232}/Γ			
VALUE (units 10^{-6})	CL%	DOCUMENT ID	TECN	COMMENT	
<2.0					
	90	1 AUBERT	08X	BABR	$e^+e^- \rightarrow \Upsilon(4S)$

¹ Assumes equal production of B^+ and B^0 at the $\Upsilon(4S)$.

$\Gamma(f_1(1420) K^+ \times B(f_1(1420) \rightarrow \eta\pi\pi))/\Gamma_{total}$		Γ_{233}/Γ			
VALUE (units 10^{-6})	CL%	DOCUMENT ID	TECN	COMMENT	
<2.9					
	90	1 AUBERT	08X	BABR	$e^+e^- \rightarrow \Upsilon(4S)$

¹ Assumes equal production of B^+ and B^0 at the $\Upsilon(4S)$.

$\Gamma(f_1(1420) K^+ \times B(f_1(1420) \rightarrow K^* K))/\Gamma_{total}$		Γ_{234}/Γ			
VALUE (units 10^{-6})	CL%	DOCUMENT ID	TECN	COMMENT	
<4.1					
	90	1 AUBERT	08X	BABR	$e^+e^- \rightarrow \Upsilon(4S)$

¹ Assumes equal production of B^+ and B^0 at the $\Upsilon(4S)$.

$\Gamma(\phi(1680) K^+ \times B(\phi(1680) \rightarrow K^* K))/\Gamma_{total}$		Γ_{235}/Γ			
VALUE (units 10^{-6})	CL%	DOCUMENT ID	TECN	COMMENT	
<3.4					
	90	1 AUBERT	08X	BABR	$e^+e^- \rightarrow \Upsilon(4S)$

¹ Assumes equal production of B^+ and B^0 at the $\Upsilon(4S)$.

$\Gamma(\omega K^+)/\Gamma_{total}$		Γ_{236}/Γ			
VALUE (units 10^{-6})	CL%	DOCUMENT ID	TECN	COMMENT	
6.7 ± 0.8 OUR AVERAGE Error includes scale factor of 1.8.					
6.3 ± 0.5 ± 0.3		1 AUBERT	07AE	BABR	$e^+e^- \rightarrow \Upsilon(4S)$
8.1 ± 0.6 ± 0.6		1 JEN	06	BELL	$e^+e^- \rightarrow \Upsilon(4S)$
3.2 ± 2.4 ± 0.8 -1.9 ± 0.8		1 JESSOP	00	CLE2	$e^+e^- \rightarrow \Upsilon(4S)$
• • • We do not use the following data for averages, fits, limits, etc. • • •					
6.1 ± 0.6 ± 0.4		1 AUBERT,B	06E	BABR	AUBERT 07AE
4.8 ± 0.8 ± 0.4		1 AUBERT	04H	BABR	Repl. by AUBERT,B 06E
6.5 ± 1.3 -1.2 ± 0.6		1 WANG	04A	BELL	Repl. by JEN 06
9.2 ± 2.6 ± 1.0 -2.3 ± 1.0		1 LU	02	BELL	Repl. by WANG 04A
<4	90	1 AUBERT	01G	BABR	$e^+e^- \rightarrow \Upsilon(4S)$
1.5 ± 7 ± 2		1 BERGFELD	98	CLE2	Repl. by JESSOP 00

¹ Assumes equal production of B^+ and B^0 at the $\Upsilon(4S)$.

$\Gamma(\omega K^*(892)^+)/\Gamma_{total}$		Γ_{237}/Γ			
VALUE (units 10^{-6})	CL%	DOCUMENT ID	TECN	COMMENT	
< 7.4					
	90	1 AUBERT	09H	BABR	$e^+e^- \rightarrow \Upsilon(4S)$
• • • We do not use the following data for averages, fits, limits, etc. • • •					
< 3.4	90	1 AUBERT,B	06T	BABR	Repl. by AUBERT 09H
< 7.4	90	1 AUBERT	05O	BABR	Repl. by AUBERT,B 06T
< 87	90	1 BERGFELD	98	CLE2	

¹ Assumes equal production of B^+ and B^0 at the $\Upsilon(4S)$.

$\Gamma(\omega(K\pi)_0^{*+})/\Gamma_{total}$		Γ_{238}/Γ			
VALUE (units 10^{-6})	CL%	DOCUMENT ID	TECN	COMMENT	
27.5 ± 3.0 ± 2.6					
		1 AUBERT	09H	BABR	$e^+e^- \rightarrow \Upsilon(4S)$

($K\pi)_0^{*+}$ is the total S-wave composed of $K_0^*(1430)$ and nonresonant that are described using LASS shape.

¹ Assumes equal production of B^+ and B^0 at the $\Upsilon(4S)$.

$\Gamma(\omega K_0^*(1430)^+)/\Gamma_{total}$		Γ_{239}/Γ			
VALUE (units 10^{-6})	CL%	DOCUMENT ID	TECN	COMMENT	
24.0 ± 2.6 ± 4.4					
		1 AUBERT	09H	BABR	$e^+e^- \rightarrow \Upsilon(4S)$

¹ Assumes equal production of B^+ and B^0 at the $\Upsilon(4S)$.

$\Gamma(\omega K_2^*(1430)^+)/\Gamma_{total}$		Γ_{240}/Γ			
VALUE (units 10^{-6})	CL%	DOCUMENT ID	TECN	COMMENT	
21.5 ± 3.6 ± 2.4					
		1 AUBERT	09H	BABR	$e^+e^- \rightarrow \Upsilon(4S)$

¹ Assumes equal production of B^+ and B^0 at the $\Upsilon(4S)$.

Meson Particle Listings

B^\pm

$\Gamma(K^*(892)^+ K^*(892)^0)/\Gamma_{total}$ Γ_{289}/Γ

VALUE (units 10^{-6})	CL%	DOCUMENT ID	TECN	COMMENT
1.2 ± 0.5 ± 0.1		AUBERT	09F	BABR $e^+ e^- \rightarrow \Upsilon(4S)$

- • • We do not use the following data for averages, fits, limits, etc. • • •

<71	90	¹ GODANG	02	CLE2 $e^+ e^- \rightarrow \Upsilon(4S)$
-----	----	---------------------	----	---

¹ Assumes a helicity 00 configuration. For a helicity 11 configuration, the limit decreases to 4.8×10^{-5} .

$\Gamma(K^{*+} K^+ \pi^-)/\Gamma_{total}$ Γ_{290}/Γ

VALUE (units 10^{-6})	CL%	DOCUMENT ID	TECN	COMMENT
<6.1	90	¹ AUBERT,B	06u	BABR $e^+ e^- \rightarrow \Upsilon(4S)$

¹ Assumes equal production of B^+ and B^0 at the $\Upsilon(4S)$.

$\Gamma(K^+ K^- K^+)/\Gamma_{total}$ Γ_{291}/Γ

VALUE (units 10^{-6})	CL%	DOCUMENT ID	TECN	COMMENT
33.7 ± 2.2 OUR AVERAGE		Error includes scale factor of 1.4.		

35.2 ± 0.9 ± 1.6		¹ AUBERT	06o	BABR $e^+ e^- \rightarrow \Upsilon(4S)$
30.6 ± 1.2 ± 2.3		¹ GARMASH	05	BELL $e^+ e^- \rightarrow \Upsilon(4S)$
• • • We do not use the following data for averages, fits, limits, etc. • • •				
32.8 ± 1.8 ± 2.8		² GARMASH	04	BELL Repl. by GARMASH 05
29.6 ± 2.1 ± 1.6		² AUBERT	03m	BABR Repl. by AUBERT 06o
35.3 ± 3.7 ± 4.5		³ GARMASH	02	BELL Repl. by GARMASH 04
<200	90	⁴ ADAM	96d	DLPH $e^+ e^- \rightarrow Z$
<320	90	⁴ ABREU	95n	DLPH Sup. by ADAM 96d
<350	90	ALBRECHT	91E	ARG $e^+ e^- \rightarrow \Upsilon(4S)$

¹ Assumes equal production of B^+ and B^0 at the $\Upsilon(4S)$.
² Assumes equal production of B^0 and B^+ at the $\Upsilon(4S)$; charm and charmonium contributions are subtracted, otherwise no assumptions about intermediate resonances.
³ Uses a reference decay mode $B^+ \rightarrow \bar{D}^0 \pi^+$ and $\bar{D}^0 \rightarrow K^+ \pi^-$ with $B(B^+ \rightarrow \bar{D}^0 \pi^+) \cdot B(\bar{D}^0 \rightarrow K^+ \pi^-) = (20.3 \pm 2.0) \times 10^{-5}$.
⁴ Assumes B^0 and B^- production fractions of 0.39, and B_s production fraction of 0.12.

$\Gamma(K^+ \phi)/\Gamma_{total}$ Γ_{292}/Γ

VALUE (units 10^{-6})	CL%	DOCUMENT ID	TECN	COMMENT
8.3 ± 0.7 OUR AVERAGE				

8.4 ± 0.7 ± 0.7		¹ AUBERT	06o	BABR $e^+ e^- \rightarrow \Upsilon(4S)$
7.6 ± 1.3 ± 0.6		² ACOSTA	05j	CDF $p\bar{p}$ at 1.96 TeV
9.6 ± 0.92 ± 1.05 ± 0.85		¹ GARMASH	05	BELL $e^+ e^- \rightarrow \Upsilon(4S)$
5.5 ± 2.1 ± 1.8 ± 0.6		¹ BRIERE	01	CLE2 $e^+ e^- \rightarrow \Upsilon(4S)$

- • • We do not use the following data for averages, fits, limits, etc. • • •

10.0 ± 0.9 ± 0.8 ± 0.5		¹ AUBERT	04A	BABR Repl. by AUBERT 06o
9.4 ± 1.1 ± 0.7		¹ CHEN	03b	BELL Repl. by GARMASH 05
14.6 ± 3.0 ± 2.8 ± 2.0		³ GARMASH	02	BELL Repl. by CHEN 03b
7.7 ± 1.6 ± 1.4 ± 0.8		¹ AUBERT	01d	BABR $e^+ e^- \rightarrow \Upsilon(4S)$
<144	90	⁴ ABE	00c	SLD $e^+ e^- \rightarrow Z$
< 5	90	¹ BERGFELD	98	CLE2
<280	90	⁵ ADAM	96d	DLPH $e^+ e^- \rightarrow Z$
< 12	90	ASNER	96	CLE2 $e^+ e^- \rightarrow \Upsilon(4S)$
<440	90	⁶ ABREU	95n	DLPH Sup. by ADAM 96d
<180	90	ALBRECHT	91B	ARG $e^+ e^- \rightarrow \Upsilon(4S)$
< 90	90	⁷ AVERY	89b	CLEO $e^+ e^- \rightarrow \Upsilon(4S)$
<210	90	AVERY	87	CLEO $e^+ e^- \rightarrow \Upsilon(4S)$

¹ Assumes equal production of B^+ and B^0 at the $\Upsilon(4S)$.
² Uses $B(B^+ \rightarrow J/\psi K^+) = (1.00 \pm 0.04) \times 10^{-3}$ and $B(J/\psi \rightarrow \mu^+ \mu^-) = 0.0588 \pm 0.0010$.
³ Uses a reference decay mode $B^+ \rightarrow \bar{D}^0 \pi^+$ and $\bar{D}^0 \rightarrow K^+ \pi^-$ with $B(B^+ \rightarrow \bar{D}^0 \pi^+) \cdot B(\bar{D}^0 \rightarrow K^+ \pi^-) = (20.3 \pm 2.0) \times 10^{-5}$.
⁴ ABE 00c assumes $B(Z \rightarrow b\bar{b}) = (21.7 \pm 0.1)\%$ and the B fractions $f_{B^0} = f_{B^+} = (39.7 \pm 1.8) \pm 2.2) \%$ and $f_{B_s} = (10.5 \pm 1.8) \pm 2.2) \%$.
⁵ ADAM 96d assumes $f_{B^0} = f_{B^-} = 0.39$ and $f_{B_s} = 0.12$.
⁶ Assumes a B^0 , B^- production fraction of 0.39 and a B_s production fraction of 0.12.
⁷ AVERY 89b reports $< 8 \times 10^{-5}$ assuming the $\Upsilon(4S)$ decays 43% to $B^0 \bar{B}^0$. We rescale to 50%.

$\Gamma(f_0(980) K^+ \times B(f_0(980) \rightarrow K^+ K^-))/\Gamma_{total}$ Γ_{293}/Γ

VALUE (units 10^{-6})	CL%	DOCUMENT ID	TECN	COMMENT
<2.9	90	¹ GARMASH	05	BELL $e^+ e^- \rightarrow \Upsilon(4S)$

- • • We do not use the following data for averages, fits, limits, etc. • • •

6.5 ± 2.5 ± 1.6		¹ AUBERT	06o	BABR $e^+ e^- \rightarrow \Upsilon(4S)$
-----------------	--	---------------------	-----	---

¹ Assumes equal production of B^+ and B^0 at the $\Upsilon(4S)$.

$\Gamma(a_2(1320) K^+ \times B(a_2(1320) \rightarrow K^+ K^-))/\Gamma_{total}$ Γ_{294}/Γ

VALUE (units 10^{-6})	CL%	DOCUMENT ID	TECN	COMMENT
<1.1 × 10⁻⁶	90	¹ GARMASH	05	BELL $e^+ e^- \rightarrow \Upsilon(4S)$

¹ Assumes equal production of B^+ and B^0 at the $\Upsilon(4S)$.

$\Gamma(f_2'(1525) K^+ \times B(f_2'(1525) \rightarrow K^+ K^-))/\Gamma_{total}$ Γ_{295}/Γ

VALUE (units 10^{-6})	CL%	DOCUMENT ID	TECN	COMMENT
<4.9 × 10⁻⁶	90	¹ GARMASH	05	BELL $e^+ e^- \rightarrow \Upsilon(4S)$

¹ Assumes equal production of B^+ and B^0 at the $\Upsilon(4S)$.

$\Gamma(X_0(1550) K^+ \times B(X_0(1550) \rightarrow K^+ K^-))/\Gamma_{total}$ Γ_{296}/Γ

VALUE (units 10^{-6})	CL%	DOCUMENT ID	TECN	COMMENT
4.3 ± 0.6 ± 0.3		¹ AUBERT	06o	BABR $e^+ e^- \rightarrow \Upsilon(4S)$

$X_0(1550)$ is a possible spin zero state near 1.55 GeV/c² invariant mass of $K^+ K^-$.
¹ Assumes equal production of B^+ and B^0 at the $\Upsilon(4S)$.

$\Gamma(\phi(1680) K^+ \times B(\phi(1680) \rightarrow K^+ K^-))/\Gamma_{total}$ Γ_{297}/Γ

VALUE (units 10^{-6})	CL%	DOCUMENT ID	TECN	COMMENT
<0.8 × 10⁻⁶	90	¹ GARMASH	05	BELL $e^+ e^- \rightarrow \Upsilon(4S)$

¹ Assumes equal production of B^+ and B^0 at the $\Upsilon(4S)$.

$\Gamma(f_0(1710) K^+ \times B(f_0(1710) \rightarrow K^+ K^-))/\Gamma_{total}$ Γ_{298}/Γ

VALUE (units 10^{-6})	CL%	DOCUMENT ID	TECN	COMMENT
1.7 ± 1.0 ± 0.3		¹ AUBERT	06o	BABR $e^+ e^- \rightarrow \Upsilon(4S)$

¹ Assumes equal production of B^+ and B^0 at the $\Upsilon(4S)$.

$\Gamma(K^+ K^- K^+ \text{nonresonant})/\Gamma_{total}$ Γ_{299}/Γ

VALUE (units 10^{-6})	CL%	DOCUMENT ID	TECN	COMMENT
28 + 9 - 16 OUR AVERAGE		Error includes scale factor of 3.3.		

50.0 ± 6.0 ± 4.0		¹ AUBERT	06o	BABR $e^+ e^- \rightarrow \Upsilon(4S)$
24.0 ± 1.5 ± 2.6 ± 6.0		¹ GARMASH	05	BELL $e^+ e^- \rightarrow \Upsilon(4S)$

- • • We do not use the following data for averages, fits, limits, etc. • • •

<38	90	BERGFELD	96b	CLE2 $e^+ e^- \rightarrow \Upsilon(4S)$
-----	----	----------	-----	---

¹ Assumes equal production of B^+ and B^0 at the $\Upsilon(4S)$.

$\Gamma(K^*(892)^+ K^+ K^-)/\Gamma_{total}$ Γ_{300}/Γ

VALUE (units 10^{-6})	CL%	DOCUMENT ID	TECN	COMMENT
36.2 ± 3.3 ± 3.6		¹ AUBERT,B	06u	BABR $e^+ e^- \rightarrow \Upsilon(4S)$

- • • We do not use the following data for averages, fits, limits, etc. • • •

<1600	90	ALBRECHT	91E	ARG $e^+ e^- \rightarrow \Upsilon(4S)$
-------	----	----------	-----	--

¹ Assumes equal production of B^+ and B^0 at the $\Upsilon(4S)$.

$\Gamma(K^*(892)^+ \phi)/\Gamma_{total}$ Γ_{301}/Γ

VALUE (units 10^{-6})	CL%	DOCUMENT ID	TECN	COMMENT
10.0 ± 2.0 OUR AVERAGE		Error includes scale factor of 1.7.		

11.2 ± 1.0 ± 0.9		¹ AUBERT	07BA	BABR $e^+ e^- \rightarrow \Upsilon(4S)$
6.7 ± 2.1 ± 0.7 ± 1.9 ± 1.0		¹ CHEN	03B	BELL $e^+ e^- \rightarrow \Upsilon(4S)$

- • • We do not use the following data for averages, fits, limits, etc. • • •

12.7 + 2.2 - 2.0 ± 1.1		¹ AUBERT	03v	BABR Repl. by AUBERT 07BA
9.7 + 4.2 - 3.4 ± 1.7		¹ AUBERT	01d	BABR Repl. by AUBERT 03v

< 22.5	90	¹ BRIERE	01	CLE2 $e^+ e^- \rightarrow \Upsilon(4S)$
< 41	90	¹ BERGFELD	98	CLE2
< 70	90	ASNER	96	CLE2 $e^+ e^- \rightarrow \Upsilon(4S)$
<1300	90	ALBRECHT	91B	ARG $e^+ e^- \rightarrow \Upsilon(4S)$

¹ Assumes equal production of B^+ and B^0 at the $\Upsilon(4S)$.

$\Gamma(\phi(K\pi)_0^{*+})/\Gamma_{total}$ Γ_{302}/Γ

$(K\pi)_0^{*+}$ is the total S-wave composed of $K_0^*(1430)$ and nonresonant that are described using LASS shape.

VALUE (units 10^{-6})	DOCUMENT ID	TECN	COMMENT
8.3 ± 1.4 ± 0.8	¹ AUBERT	08b1	BABR $e^+ e^- \rightarrow \Upsilon(4S)$

¹ Assumes equal production of B^+ and B^0 at the $\Upsilon(4S)$.

$\Gamma(\phi K_1(1270)^+)/\Gamma_{total}$ Γ_{303}/Γ

VALUE (units 10^{-6})	DOCUMENT ID	TECN	COMMENT
6.1 ± 1.6 ± 1.1	¹ AUBERT	08b1	BABR $e^+ e^- \rightarrow \Upsilon(4S)$

¹ Assumes equal production of B^+ and B^0 at the $\Upsilon(4S)$.

$\Gamma(\phi K_1(1400)^+)/\Gamma_{total}$ Γ_{304}/Γ

VALUE (units 10^{-6})	CL%	DOCUMENT ID	TECN	COMMENT
< 3.2	90	¹ AUBERT	08b1	BABR $e^+ e^- \rightarrow \Upsilon(4S)$

- • • We do not use the following data for averages, fits, limits, etc. • • •

<1100	90	ALBRECHT	91B	ARG $e^+ e^- \rightarrow \Upsilon(4S)$
-------	----	----------	-----	--

¹ Assumes equal production of B^+ and B^0 at the $\Upsilon(4S)$.

$\Gamma(\phi K^*(1410)^+)/\Gamma_{total}$ Γ_{305}/Γ

VALUE (units 10^{-6})	CL%	DOCUMENT ID	TECN	COMMENT
<4.3	90	¹ AUBERT	08b1	BABR $e^+ e^- \rightarrow \Upsilon(4S)$

¹ Assumes equal production of B^+ and B^0 at the $\Upsilon(4S)$.

$\Gamma(\phi K_0^*(1430)^+)/\Gamma_{\text{total}}$ Γ_{306}/Γ

VALUE (units 10^{-6})	DOCUMENT ID	TECN	COMMENT
$7.0 \pm 1.3 \pm 0.9$	¹ AUBERT	08BI	BABR $e^+e^- \rightarrow \Upsilon(4S)$

¹ Assumes equal production of B^+ and B^0 at the $\Upsilon(4S)$.

 $\Gamma(\phi K_2^*(1430)^+)/\Gamma_{\text{total}}$ Γ_{307}/Γ

VALUE (units 10^{-6})	CL%	DOCUMENT ID	TECN	COMMENT
$8.4 \pm 1.8 \pm 1.0$		¹ AUBERT	08BI	BABR $e^+e^- \rightarrow \Upsilon(4S)$
< 3400	90	ALBRECHT	91B	ARG $e^+e^- \rightarrow \Upsilon(4S)$

• • • We do not use the following data for averages, fits, limits, etc. • • •
¹ Assumes equal production of B^+ and B^0 at the $\Upsilon(4S)$.

 $\Gamma(\phi K_2^*(1770)^+)/\Gamma_{\text{total}}$ Γ_{308}/Γ

VALUE (units 10^{-6})	CL%	DOCUMENT ID	TECN	COMMENT
< 15.0	90	¹ AUBERT	08BI	BABR $e^+e^- \rightarrow \Upsilon(4S)$

¹ Assumes equal production of B^+ and B^0 at the $\Upsilon(4S)$.

 $\Gamma(\phi K_2^*(1820)^+)/\Gamma_{\text{total}}$ Γ_{309}/Γ

VALUE (units 10^{-6})	CL%	DOCUMENT ID	TECN	COMMENT
< 16.3	90	¹ AUBERT	08BI	BABR $e^+e^- \rightarrow \Upsilon(4S)$

¹ Assumes equal production of B^+ and B^0 at the $\Upsilon(4S)$.

 $\Gamma(K^+ \phi \phi)/\Gamma_{\text{total}}$ Γ_{310}/Γ

VALUE (units 10^{-6})	DOCUMENT ID	TECN	COMMENT
$4.9 \pm 2.4 \pm 2.2$ OUR AVERAGE	Error includes scale factor of 2.9.		
$7.5 \pm 1.0 \pm 0.7$	¹ AUBERT, BE	06H	BABR $e^+e^- \rightarrow \Upsilon(4S)$
$2.6 \pm 1.1 \pm 0.9 \pm 0.3$	¹ HUANG	03	BELL $e^+e^- \rightarrow \Upsilon(4S)$

¹ Assumes equal production of B^0 and B^+ at the $\Upsilon(4S)$ and for a $\phi\phi$ invariant mass below 2.85 GeV/ c^2 .

 $\Gamma(\eta' \eta' K^+)/\Gamma_{\text{total}}$ Γ_{311}/Γ

VALUE (units 10^{-6})	CL%	DOCUMENT ID	TECN	COMMENT
< 25	90	¹ AUBERT, B	06P	BABR $e^+e^- \rightarrow \Upsilon(4S)$

¹ Assumes equal production of B^+ and B^0 at the $\Upsilon(4S)$.

 $\Gamma(\omega \phi K^+)/\Gamma_{\text{total}}$ Γ_{312}/Γ

VALUE (units 10^{-6})	CL%	DOCUMENT ID	TECN	COMMENT
< 1.9	90	¹ LIU	09	BELL $e^+e^- \rightarrow \Upsilon(4S)$

¹ Assumes equal production of B^+ and B^0 at the $\Upsilon(4S)$.

 $\Gamma(X(1812) K^+ \times B(X \rightarrow \omega \phi))/\Gamma_{\text{total}}$ Γ_{313}/Γ

VALUE (units 10^{-6})	CL%	DOCUMENT ID	TECN	COMMENT
< 0.32	90	¹ LIU	09	BELL $e^+e^- \rightarrow \Upsilon(4S)$

¹ Assumes equal production of B^+ and B^0 at the $\Upsilon(4S)$.

 $\Gamma(K^*(892)^+ \gamma)/\Gamma_{\text{total}}$ Γ_{314}/Γ

VALUE (units 10^{-5})	CL%	DOCUMENT ID	TECN	COMMENT
4.21 ± 0.18 OUR AVERAGE				
$4.22 \pm 0.14 \pm 0.16$		¹ AUBERT	09A0	BABR $e^+e^- \rightarrow \Upsilon(4S)$
$4.25 \pm 0.31 \pm 0.24$		² NAKAO	04	BELL $e^+e^- \rightarrow \Upsilon(4S)$
$3.76 \pm 0.89 \pm 0.83 \pm 0.28$		² COAN	00	CLE2 $e^+e^- \rightarrow \Upsilon(4S)$

• • • We do not use the following data for averages, fits, limits, etc. • • •

$3.87 \pm 0.28 \pm 0.26$		³ AUBERT, BE	04A	BABR Repl. by AUBERT 09A0
$3.83 \pm 0.62 \pm 0.22$		² AUBERT	02c	BABR Repl. by AUBERT, BE 04A
$5.7 \pm 3.1 \pm 1.1$		⁴ AMMAR	93	CLE2 Repl. by COAN 00
< 55	90	⁵ ALBRECHT	89G	ARG $e^+e^- \rightarrow \Upsilon(4S)$
< 55	90	⁵ AVERY	89B	CLEO $e^+e^- \rightarrow \Upsilon(4S)$
< 180	90	⁵ AVERY	87B	CLEO $e^+e^- \rightarrow \Upsilon(4S)$

- ¹ Uses $B(\Upsilon(4S) \rightarrow B^+ B^-) = (51.6 \pm 0.6)\%$ and $B(\Upsilon(4S) \rightarrow B^0 \bar{B}^0) = (48.4 \pm 0.6)\%$.
² Assumes equal production of B^+ and B^0 at the $\Upsilon(4S)$.
³ Uses the production ratio of charged and neutral B from $\Upsilon(4S)$ decays $R^{+0} = 1.006 \pm 0.048$.
⁴ AMMAR 93 observed 4.1 ± 2.3 events above background.
⁵ Assumes the $\Upsilon(4S)$ decays 43% to $B^0 \bar{B}^0$.

 $\Gamma(K_1(1270)^+ \gamma)/\Gamma_{\text{total}}$ Γ_{315}/Γ

VALUE (units 10^{-5})	CL%	DOCUMENT ID	TECN	COMMENT
$4.3 \pm 0.9 \pm 0.9$		¹ YANG	05	BELL $e^+e^- \rightarrow \Upsilon(4S)$

• • • We do not use the following data for averages, fits, limits, etc. • • •

< 9.9	90	¹ NISHIDA	02	BELL Repl. by YANG 05
< 730	90	² ALBRECHT	89G	ARG $e^+e^- \rightarrow \Upsilon(4S)$

- ¹ Assumes equal production of B^+ and B^0 at the $\Upsilon(4S)$.
² ALBRECHT 89G reports < 0.0066 assuming the $\Upsilon(4S)$ decays 45% to $B^0 \bar{B}^0$. We rescale to 50%.

 $\Gamma(\eta K^+ \gamma)/\Gamma_{\text{total}}$ Γ_{316}/Γ

VALUE (units 10^{-6})	DOCUMENT ID	TECN	COMMENT
7.9 ± 0.9 OUR AVERAGE			
$7.7 \pm 1.0 \pm 0.4$	^{1,2} AUBERT	09	BABR $e^+e^- \rightarrow \Upsilon(4S)$
$8.4 \pm 1.5 \pm 1.2 \pm 0.9$	^{2,3} NISHIDA	05	BELL $e^+e^- \rightarrow \Upsilon(4S)$

- • • We do not use the following data for averages, fits, limits, etc. • • •
- | | | | |
|------------------------|--------------------------|-----|-------------------------|
| $10.0 \pm 1.3 \pm 0.5$ | ^{1,2} AUBERT, B | 06M | BABR Repl. by AUBERT 09 |
|------------------------|--------------------------|-----|-------------------------|
- ¹ $m_{\eta K} < 3.25$ GeV/ c^2 .
² Assumes equal production of B^+ and B^0 at the $\Upsilon(4S)$.
³ $m_{\eta K} < 2.4$ GeV/ c^2 .

 $\Gamma(\eta' K^+ \gamma)/\Gamma_{\text{total}}$ Γ_{317}/Γ

VALUE (units 10^{-6})	CL%	DOCUMENT ID	TECN	COMMENT
< 4.2	90	^{1,2} AUBERT, B	06M	BABR $e^+e^- \rightarrow \Upsilon(4S)$

¹ $m_{\eta' K} < 3.25$ GeV/ c^2 .
² Assumes equal production of B^+ and B^0 at the $\Upsilon(4S)$.

 $\Gamma(\phi K^+ \gamma)/\Gamma_{\text{total}}$ Γ_{318}/Γ

VALUE (units 10^{-6})	DOCUMENT ID	TECN	COMMENT
3.5 ± 0.6 OUR AVERAGE			
$3.5 \pm 0.6 \pm 0.4$	¹ AUBERT	07Q	BABR $e^+e^- \rightarrow \Upsilon(4S)$
$3.4 \pm 0.9 \pm 0.4$	¹ DRUTSKOY	04	BELL $e^+e^- \rightarrow \Upsilon(4S)$

¹ Assumes equal production of B^+ and B^0 at $\Upsilon(4S)$.

 $\Gamma(K^+ \pi^- \pi^+ \pi^- \gamma)/\Gamma_{\text{total}}$ Γ_{319}/Γ

VALUE (units 10^{-5})	DOCUMENT ID	TECN	COMMENT
2.76 ± 0.22 OUR AVERAGE	Error includes scale factor of 1.2.		
$2.95 \pm 0.13 \pm 0.20$	^{1,2} AUBERT	07R	BABR $e^+e^- \rightarrow \Upsilon(4S)$
$2.50 \pm 0.18 \pm 0.22$	^{2,3} YANG	05	BELL $e^+e^- \rightarrow \Upsilon(4S)$

• • • We do not use the following data for averages, fits, limits, etc. • • •

$2.4 \pm 0.5 \pm 0.4 \pm 0.2$	^{2,4} NISHIDA	02	BELL Repl. by YANG 05
-------------------------------	------------------------	----	-----------------------

- ¹ $M_{K\pi\pi} < 1.8$ GeV/ c^2 .
² Assumes equal production of B^+ and B^0 at the $\Upsilon(4S)$.
³ $M_{K\pi\pi} < 2.0$ GeV/ c^2 .
⁴ $M_{K\pi\pi} < 2.4$ GeV/ c^2 .

 $\Gamma(K^*(892)^0 \pi^+ \gamma)/\Gamma_{\text{total}}$ Γ_{320}/Γ

VALUE	DOCUMENT ID	TECN	COMMENT
$(2.0 \pm 0.7 \pm 0.2) \times 10^{-5}$	^{1,2} NISHIDA	02	BELL $e^+e^- \rightarrow \Upsilon(4S)$

¹ Assumes equal production of B^+ and B^0 at the $\Upsilon(4S)$.
² $M_{K\pi\pi} < 2.4$ GeV/ c^2 .

 $\Gamma(K^+ \rho^0 \gamma)/\Gamma_{\text{total}}$ Γ_{321}/Γ

VALUE	CL%	DOCUMENT ID	TECN	COMMENT
$< 2.0 \times 10^{-5}$	90	^{1,2} NISHIDA	02	BELL $e^+e^- \rightarrow \Upsilon(4S)$

¹ Assumes equal production of B^+ and B^0 at the $\Upsilon(4S)$.
² $M_{K\pi\pi} < 2.4$ GeV/ c^2 .

 $\Gamma(K^+ \pi^- \pi^+ \gamma \text{ nonresonant})/\Gamma_{\text{total}}$ Γ_{322}/Γ

VALUE	CL%	DOCUMENT ID	TECN	COMMENT
$< 9.2 \times 10^{-6}$	90	^{1,2} NISHIDA	02	BELL $e^+e^- \rightarrow \Upsilon(4S)$

¹ Assumes equal production of B^+ and B^0 at the $\Upsilon(4S)$.
² $M_{K\pi\pi} < 2.4$ GeV/ c^2 .

 $\Gamma(K^0 \pi^+ \pi^0 \gamma)/\Gamma_{\text{total}}$ Γ_{323}/Γ

VALUE (units 10^{-5})	DOCUMENT ID	TECN	COMMENT
$4.56 \pm 0.42 \pm 0.31$	^{1,2} AUBERT	07R	BABR $e^+e^- \rightarrow \Upsilon(4S)$

¹ $M_{K\pi\pi} < 1.8$ GeV/ c^2 .
² Assumes equal production of B^+ and B^0 at the $\Upsilon(4S)$.

 $\Gamma(K_1(1400)^+ \gamma)/\Gamma_{\text{total}}$ Γ_{324}/Γ

VALUE (units 10^{-5})	CL%	DOCUMENT ID	TECN	COMMENT
< 1.5	90	¹ YANG	05	BELL $e^+e^- \rightarrow \Upsilon(4S)$

• • • We do not use the following data for averages, fits, limits, etc. • • •

< 5.0	90	¹ NISHIDA	02	BELL Repl. by YANG 05
< 220	90	² ALBRECHT	89G	ARG $e^+e^- \rightarrow \Upsilon(4S)$

¹ Assumes equal production of B^+ and B^0 at the $\Upsilon(4S)$.
² ALBRECHT 89G reports < 0.0020 assuming the $\Upsilon(4S)$ decays 45% to $B^0 \bar{B}^0$. We rescale to 50%.

 $\Gamma(K_2^*(1430)^+ \gamma)/\Gamma_{\text{total}}$ Γ_{325}/Γ

VALUE (units 10^{-5})	CL%	DOCUMENT ID	TECN	COMMENT
$1.45 \pm 0.40 \pm 0.15$		¹ AUBERT, B	04U	BABR $e^+e^- \rightarrow \Upsilon(4S)$

• • • We do not use the following data for averages, fits, limits, etc. • • •

< 140	90	² ALBRECHT	89G	ARG $e^+e^- \rightarrow \Upsilon(4S)$
---------	----	-----------------------	-----	---------------------------------------

- ¹ Assumes equal production of B^+ and B^0 at the $\Upsilon(4S)$.
² ALBRECHT 89G reports < 0.0013 assuming the $\Upsilon(4S)$ decays 45% to $B^0 \bar{B}^0$. We rescale to 50%.

Meson Particle Listings

B^\pm

$\Gamma(K^*(1680)^+ \gamma) / \Gamma_{\text{total}}$ Γ_{326} / Γ

VALUE	CL%	DOCUMENT ID	TECN	COMMENT
<0.0019	90	¹ ALBRECHT 89G ARG		$e^+ e^- \rightarrow \Upsilon(4S)$

¹ ALBRECHT 89G reports < 0.0017 assuming the $\Upsilon(4S)$ decays 45% to $B^0 \bar{B}^0$. We rescale to 50%.

$\Gamma(K_3^*(1780)^+ \gamma) / \Gamma_{\text{total}}$ Γ_{327} / Γ

VALUE (units 10^{-6})	CL%	DOCUMENT ID	TECN	COMMENT
< 39	90	^{1,2} NISHIDA 05 BELL		$e^+ e^- \rightarrow \Upsilon(4S)$

• • • We do not use the following data for averages, fits, limits, etc. • • •

<5500	90	³ ALBRECHT 89G ARG		$e^+ e^- \rightarrow \Upsilon(4S)$
-------	----	-------------------------------	--	------------------------------------

¹ Assumes equal production of B^+ and B^0 at the $\Upsilon(4S)$.
² Uses $B(K_3^*(1780) \rightarrow \eta K) = 0.11^{+0.05}_{-0.04}$.
³ ALBRECHT 89G reports < 0.005 assuming the $\Upsilon(4S)$ decays 45% to $B^0 \bar{B}^0$. We rescale to 50%.

$\Gamma(K_2^*(2045)^+ \gamma) / \Gamma_{\text{total}}$ Γ_{328} / Γ

VALUE	CL%	DOCUMENT ID	TECN	COMMENT
<0.0099	90	¹ ALBRECHT 89G ARG		$e^+ e^- \rightarrow \Upsilon(4S)$

¹ ALBRECHT 89G reports < 0.0090 assuming the $\Upsilon(4S)$ decays 45% to $B^0 \bar{B}^0$. We rescale to 50%.

$\Gamma(\rho^+ \gamma) / \Gamma_{\text{total}}$ Γ_{329} / Γ

VALUE (units 10^{-6})	CL%	DOCUMENT ID	TECN	COMMENT
0.98 ± 0.25 OUR AVERAGE				
$1.20^{+0.42}_{-0.37} \pm 0.20$		¹ AUBERT 08BH BABR		$e^+ e^- \rightarrow \Upsilon(4S)$
$0.87^{+0.29+0.09}_{-0.27-0.11}$		¹ TANIGUCHI 08 BELL		$e^+ e^- \rightarrow \Upsilon(4S)$

• • • We do not use the following data for averages, fits, limits, etc. • • •

$1.10^{+0.37}_{-0.33} \pm 0.09$		¹ AUBERT 07L BABR		Repl. by AUBERT 08BH
$0.55^{+0.42+0.09}_{-0.36-0.08}$		¹ MOHAPATRA 06 BELL		Repl. by TANIGUCHI 08
$0.9^{+0.6}_{-0.5} \pm 0.1$	90	¹ AUBERT 05 BABR		Repl. by AUBERT 07L
< 2.2	90	¹ MOHAPATRA 05 BELL		$e^+ e^- \rightarrow \Upsilon(4S)$
< 2.1	90	¹ AUBERT 04c BABR		$e^+ e^- \rightarrow \Upsilon(4S)$
<13	90	^{1,2} COAN 00 CLE2		$e^+ e^- \rightarrow \Upsilon(4S)$

¹ Assumes equal production of B^+ and B^0 at $\Upsilon(4S)$.
² No evidence for a nonresonant $K \pi \gamma$ contamination was seen; the central value assumes no contamination.

$\Gamma(\pi^+ \pi^0) / \Gamma_{\text{total}}$ Γ_{330} / Γ

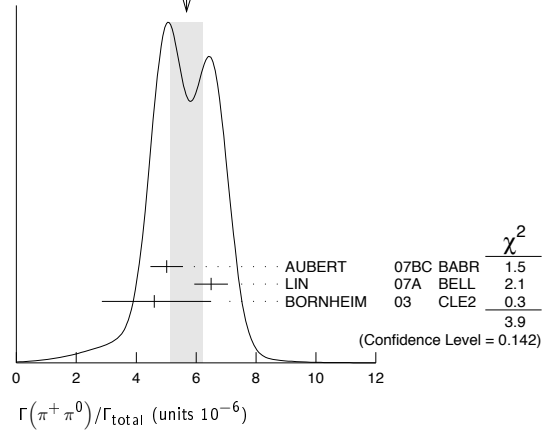
VALUE (units 10^{-6})	CL%	DOCUMENT ID	TECN	COMMENT
5.7 ± 0.5 OUR AVERAGE				Error includes scale factor of 1.4. See the ideogram below.
$5.02 \pm 0.46 \pm 0.29$		¹ AUBERT 07bC BABR		$e^+ e^- \rightarrow \Upsilon(4S)$
$6.5 \pm 0.4 \pm 0.4$		¹ LIN 07A BELL		$e^+ e^- \rightarrow \Upsilon(4S)$
$4.6^{+1.8+0.6}_{-1.6-0.7}$		¹ BORNHEIM 03 CLE2		$e^+ e^- \rightarrow \Upsilon(4S)$

• • • We do not use the following data for averages, fits, limits, etc. • • •

$5.8 \pm 0.6 \pm 0.4$		¹ AUBERT 05L BABR		Repl. by AUBERT 07bC
$5.0 \pm 1.2 \pm 0.5$		¹ CHAO 04 BELL		Repl. by LIN 07A
$5.5^{+1.0}_{-1.9} \pm 0.6$		¹ AUBERT 03L BABR		Repl. by AUBERT 05L
$7.4^{+2.3}_{-2.2} \pm 0.9$		¹ CASEY 02 BELL		Repl. by CHAO 04
< 13.4	90	¹ ABE 01H BELL		$e^+ e^- \rightarrow \Upsilon(4S)$
< 9.6	90	¹ AUBERT 01E BABR		$e^+ e^- \rightarrow \Upsilon(4S)$
< 12.7	90	¹ CRONIN-HEN.00 CLE2		$e^+ e^- \rightarrow \Upsilon(4S)$
< 20	90	GODANG 98 CLE2		Repl. by CRONIN-HENNESSY 00
< 17	90	ASNER 96 CLE2		Repl. by GODANG 98
< 240	90	¹ ALBRECHT 90B ARG		$e^+ e^- \rightarrow \Upsilon(4S)$
< 2300	90	² BEBEK 87 CLEO		$e^+ e^- \rightarrow \Upsilon(4S)$

¹ Assumes equal production of B^+ and B^0 at the $\Upsilon(4S)$.
² BEBEK 87 assume the $\Upsilon(4S)$ decays 43% to $B^0 \bar{B}^0$.

WEIGHTED AVERAGE
5.7±0.5 (Error scaled by 1.4)



$\Gamma(\pi^+ \pi^0) / \Gamma(K^0 \pi^+)$ $\Gamma_{330} / \Gamma_{220}$

VALUE	DOCUMENT ID	TECN	COMMENT
0.285 ± 0.02 ± 0.02	LIN 07A BELL		$e^+ e^- \rightarrow \Upsilon(4S)$

$\Gamma(\pi^+ \pi^+ \pi^-) / \Gamma_{\text{total}}$ Γ_{331} / Γ

VALUE (units 10^{-6})	CL%	DOCUMENT ID	TECN	COMMENT
15.2 ± 0.6 ± 1.3		¹ AUBERT 09L BABR		$e^+ e^- \rightarrow \Upsilon(4S)$

• • • We do not use the following data for averages, fits, limits, etc. • • •

$16.2 \pm 1.2 \pm 0.9$		¹ AUBERT,B 05G BABR		Repl. by AUBERT 09L
$10.9 \pm 3.3 \pm 1.6$		¹ AUBERT 03M BABR		Repl. by AUBERT 05G
<130	90	² ADAM 96D DLPH		$e^+ e^- \rightarrow Z$
<220	90	³ ABREU 95N DLPH		Sup. by ADAM 96D
<450	90	⁴ ALBRECHT 90B ARG		$e^+ e^- \rightarrow \Upsilon(4S)$
<190	90	⁵ BORTOLETTO89 CLEO		$e^+ e^- \rightarrow \Upsilon(4S)$

¹ Assumes equal production of B^0 and B^+ at the $\Upsilon(4S)$; charm and charmonium contributions are subtracted, otherwise no assumptions about intermediate resonances.
² ADAM 96D assumes $f_{B^0} = f_{B^-} = 0.39$ and $f_{B_s} = 0.12$.
³ Assumes a B^0, B^- production fraction of 0.39 and a B_s production fraction of 0.12.
⁴ ALBRECHT 90B limit assumes equal production of $B^0 \bar{B}^0$ and $B^+ B^-$ at $\Upsilon(4S)$.
⁵ BORTOLETTO 89 reports < 1.7×10^{-4} assuming the $\Upsilon(4S)$ decays 43% to $B^0 \bar{B}^0$. We rescale to 50%.

$\Gamma(\rho^0 \pi^+) / \Gamma_{\text{total}}$ Γ_{332} / Γ

VALUE (units 10^{-6})	CL%	DOCUMENT ID	TECN	COMMENT
8.3 ± 1.2 OUR AVERAGE				
$8.1 \pm 0.7^{+1.3}_{-1.6}$		¹ AUBERT 09L BABR		$e^+ e^- \rightarrow \Upsilon(4S)$
$8.0^{+2.3}_{-2.0} \pm 0.7$		¹ GORDON 02 BELL		$e^+ e^- \rightarrow \Upsilon(4S)$
$10.4^{+3.3}_{-3.4} \pm 2.1$		¹ JESSOP 00 CLE2		$e^+ e^- \rightarrow \Upsilon(4S)$

• • • We do not use the following data for averages, fits, limits, etc. • • •

$8.8 \pm 1.0^{+0.6}_{-0.9}$		¹ AUBERT,B 05G BABR		Repl. by AUBERT 09L
$9.5 \pm 1.1 \pm 0.9$		¹ AUBERT 04Z BABR		Repl. by AUBERT 05G
< 83	90	² ABE 00c SLD		$e^+ e^- \rightarrow Z$
<160	90	³ ADAM 96D DLPH		$e^+ e^- \rightarrow Z$
< 43	90	ASNER 96 CLE2		Repl. by JESSOP 00
<260	90	⁴ ABREU 95N DLPH		Sup. by ADAM 96D
<150	90	¹ ALBRECHT 90B ARG		$e^+ e^- \rightarrow \Upsilon(4S)$
<170	90	⁵ BORTOLETTO89 CLEO		$e^+ e^- \rightarrow \Upsilon(4S)$
<230	90	⁵ BEBEK 87 CLEO		$e^+ e^- \rightarrow \Upsilon(4S)$
<600	90	GILES 84 CLEO		Repl. by BEBEK 87

¹ Assumes equal production of B^+ and B^0 at the $\Upsilon(4S)$.
² ABE 00c assumes $B(Z \rightarrow b \bar{b}) = (21.7 \pm 0.1)\%$ and the B fractions $f_{B^0} = f_{B^+} = (39.7^{+1.8}_{-2.2})\%$ and $f_{B_s} = (10.5^{+1.8}_{-2.2})\%$.
³ ADAM 96D assumes $f_{B^0} = f_{B^-} = 0.39$ and $f_{B_s} = 0.12$.
⁴ Assumes a B^0, B^- production fraction of 0.39 and a B_s production fraction of 0.12.
⁵ Papers assume the $\Upsilon(4S)$ decays 43% to $B^0 \bar{B}^0$. We rescale to 50%.

$[\Gamma(K^*(892)^0 \pi^+) + \Gamma(\rho^0 \pi^+)] / \Gamma_{\text{total}}$ $(\Gamma_{243} + \Gamma_{332}) / \Gamma$

VALUE (units 10^{-6})	DOCUMENT ID	TECN	COMMENT
170 ± 120 ± 80 ± 20	¹ ADAM 96D DLPH		$e^+ e^- \rightarrow Z$

¹ ADAM 96D assumes $f_{B^0} = f_{B^-} = 0.39$ and $f_{B_s} = 0.12$.

$\Gamma(\pi^+ f_0(980) \times B(f_0(980) \rightarrow \pi^+ \pi^-))/\Gamma_{total}$ Γ_{333}/Γ

Table with columns: VALUE (units 10⁻⁶), CL%, DOCUMENT ID, TECN, COMMENT. Rows include data from AUBERT and BORTOLETTO.

1 Assumes equal production of B⁺ and B⁰ at the T(4S).
2 BORTOLETTO 89 reports < 1.2 × 10⁻⁴ assuming the T(4S) decays 43% to B⁰B⁰. We rescale to 50%.

$\Gamma(\pi^+ f_2(1270))/\Gamma_{total}$ Γ_{334}/Γ

Table with columns: VALUE (units 10⁻⁶), CL%, DOCUMENT ID, TECN, COMMENT. Rows include data from AUBERT and BORTOLETTO.

1 AUBERT 09L reports $[\Gamma(B^+ \rightarrow \pi^+ f_2(1270))/\Gamma_{total}] \times [B(f_2(1270) \rightarrow \pi^+ \pi^-)] = (0.9 \pm 0.2 \pm 0.1 + 0.3 - 0.1) \times 10^{-6}$ which we divide by our best value $B(f_2(1270) \rightarrow \pi^+ \pi^-) = (56.5 + 1.6 - 0.8) \times 10^{-2}$. Our first error is their experiment's error and our second error is the systematic error from using our best value.
2 Assumes equal production of B⁺ and B⁰ at the T(4S).
3 AUBERT,B 05G reports $[\Gamma(B^+ \rightarrow \pi^+ f_2(1270))/\Gamma_{total}] \times [B(f_2(1270) \rightarrow \pi^+ \pi^-)] = (2.3 \pm 0.6 \pm 0.4) \times 10^{-6}$ which we divide by our best value $B(f_2(1270) \rightarrow \pi^+ \pi^-) = (56.5 + 1.6 - 0.8) \times 10^{-2}$. Our first error is their experiment's error and our second error is the systematic error from using our best value.
4 BORTOLETTO 89 reports < 2.1 × 10⁻⁴ assuming the T(4S) decays 43% to B⁰B⁰. We rescale to 50%.

$\Gamma(\rho(1450)^0 \pi^+ \times B(\rho^0 \rightarrow \pi^+ \pi^-))/\Gamma_{total}$ Γ_{335}/Γ

Table with columns: VALUE (units 10⁻⁶), CL%, DOCUMENT ID, TECN, COMMENT. Rows include data from AUBERT.

1 Assumes equal production of B⁺ and B⁰ at the T(4S).

$\Gamma(f_0(1370) \pi^+ \times B(f_0(1370) \rightarrow \pi^+ \pi^-))/\Gamma_{total}$ Γ_{336}/Γ

Table with columns: VALUE (units 10⁻⁶), CL%, DOCUMENT ID, TECN, COMMENT. Rows include data from AUBERT.

1 Assumes equal production of B⁺ and B⁰ at the T(4S).

$\Gamma(f_0(600) \pi^+ \times B(f_0(600) \rightarrow \pi^+ \pi^-))/\Gamma_{total}$ Γ_{337}/Γ

Table with columns: VALUE (units 10⁻⁶), CL%, DOCUMENT ID, TECN, COMMENT. Rows include data from AUBERT.

1 Assumes equal production of B⁺ and B⁰ at the T(4S).

$\Gamma(\pi^+ \pi^- \pi^+ \text{nonresonant})/\Gamma_{total}$ Γ_{338}/Γ

Table with columns: VALUE (units 10⁻⁶), CL%, DOCUMENT ID, TECN, COMMENT. Rows include data from AUBERT, BERGFELD, and WANG.

1 Assumes equal production of B⁺ and B⁰ at the T(4S).

$\Gamma(\pi^+ \pi^0 \pi^0)/\Gamma_{total}$ Γ_{339}/Γ

Table with columns: VALUE (units 10⁻⁶), CL%, DOCUMENT ID, TECN, COMMENT. Rows include data from ALBRECHT and ZHANG.

1 ALBRECHT 90B limit assumes equal production of B⁰B⁰ and B⁺B⁻ at T(4S).

$\Gamma(\rho^+ \pi^0)/\Gamma_{total}$ Γ_{340}/Γ

Table with columns: VALUE (units 10⁻⁶), CL%, DOCUMENT ID, TECN, COMMENT. Rows include OUR AVERAGE and data from AUBERT, ZHANG, and JESSOP.

1 Assumes equal production of B⁺ and B⁰ at the T(4S).
2 Assumes no nonresonant contributions of B⁺ → π⁺π⁰π⁰.

$\Gamma(\pi^+ \pi^- \pi^+ \pi^0)/\Gamma_{total}$ Γ_{341}/Γ

Table with columns: VALUE (units 10⁻⁶), CL%, DOCUMENT ID, TECN, COMMENT. Row includes data from ALBRECHT.

1 ALBRECHT 90B limit assumes equal production of B⁰B⁰ and B⁺B⁻ at T(4S).

$\Gamma(\rho^+ \rho^0)/\Gamma_{total}$ Γ_{342}/Γ

Table with columns: VALUE (units 10⁻⁶), CL%, DOCUMENT ID, TECN, COMMENT. Rows include OUR AVERAGE and data from AUBERT, ZHANG, and BELL.

1 Assumes equal production of B⁺ and B⁰ at the T(4S).
2 The systematic error includes the error associated with the helicity-mix uncertainty.

$\Gamma(\rho^+ f_0(980) \times B(f_0(980) \rightarrow \pi^+ \pi^-))/\Gamma_{total}$ Γ_{343}/Γ

Table with columns: VALUE (units 10⁻⁶), CL%, DOCUMENT ID, TECN, COMMENT. Rows include data from AUBERT and AUBERT, BE.

1 Assumes equal production of B⁺ and B⁰ at the T(4S).

$\Gamma(a_1(1260)^+ \pi^0)/\Gamma_{total}$ Γ_{344}/Γ

Table with columns: VALUE (units 10⁻⁶), CL%, DOCUMENT ID, TECN, COMMENT. Rows include data from AUBERT and ALBRECHT.

1 Assumes equal production of B⁺ and B⁰ at the T(4S).
2 Assumes a₁⁺ decays only to 3π and B(a₁⁺ → π[±]π[∓]π[±]) = 0.5.

$\Gamma(a_1(1260)^0 \pi^+)/\Gamma_{total}$ Γ_{345}/Γ

Table with columns: VALUE (units 10⁻⁶), CL%, DOCUMENT ID, TECN, COMMENT. Rows include data from AUBERT and ALBRECHT.

1 Assumes equal production of B⁺ and B⁰ at the T(4S).
2 Assumes a₁⁰ decays only to 3π and B(a₁⁰ → π[±]π[∓]π⁰) = 1.0.

$\Gamma(\omega \pi^+)/\Gamma_{total}$ Γ_{346}/Γ

Table with columns: VALUE (units 10⁻⁶), CL%, DOCUMENT ID, TECN, COMMENT. Rows include OUR AVERAGE and data from AUBERT, JEN, and JESSOP.

1 Assumes equal production of B⁺ and B⁰ at the T(4S).

$\Gamma(\omega \rho^+)/\Gamma_{total}$ Γ_{347}/Γ

Table with columns: VALUE (units 10⁻⁶), CL%, DOCUMENT ID, TECN, COMMENT. Rows include data from AUBERT, BERGFELD, and ALBRECHT.

1 Assumes equal production of B⁺ and B⁰ at the T(4S).

$\Gamma(\omega \pi^+)/\Gamma_{total}$ Γ_{347}/Γ

Table with columns: VALUE (units 10⁻⁶), CL%, DOCUMENT ID, TECN, COMMENT. Rows include data from AUBERT, BERGFELD, and ALBRECHT.

1 Assumes equal production of B⁺ and B⁰ at the T(4S).

$\Gamma(\eta \pi^+)/\Gamma_{total}$ Γ_{348}/Γ

Table with columns: VALUE (units 10⁻⁶), CL%, DOCUMENT ID, TECN, COMMENT. Rows include OUR AVERAGE and data from AUBERT, CHANG, and RICHICHI.

1 Assumes equal production of B⁺ and B⁰ at the T(4S).

$\Gamma(\eta \pi^+)/\Gamma_{total}$ Γ_{348}/Γ

Table with columns: VALUE (units 10⁻⁶), CL%, DOCUMENT ID, TECN, COMMENT. Rows include data from AUBERT, CHANG, RICHICHI, and ALBRECHT.

1 Assumes equal production of B⁺ and B⁰ at the T(4S).

Meson Particle Listings

B^\pm

$\Gamma(K^+ e^+ e^-)/\Gamma_{total}$ Γ_{417}/Γ

Test for $\Delta B=1$ weak neutral current. Allowed by higher-order electroweak interactions.

VALUE (units 10^{-7})	CL%	DOCUMENT ID	TECN	COMMENT
5.5 ± 0.7 OUR AVERAGE				
$5.1^{+1.2}_{-1.1} \pm 0.2$		1 AUBERT	09T BABR	$e^+ e^- \rightarrow \Upsilon(4S)$
$5.7^{+0.9}_{-0.8} \pm 0.3$		1 WEI	09A BELL	$e^+ e^- \rightarrow \Upsilon(4S)$

- • • We do not use the following data for averages, fits, limits, etc. • • •

$4.2^{+1.2}_{-1.1} \pm 0.2$		1 AUBERT,B	06J BABR	Repl. by AUBERT 09T
$10.5^{+2.5}_{-2.2} \pm 0.7$		1 AUBERT	03U BABR	Repl. by AUBERT,B 06J
$6.3^{+1.9}_{-1.7} \pm 0.3$		2 ISHIKAWA	03 BELL	Repl. by WEI 09A
< 14	90	1 ABE	02 BELL	$e^+ e^- \rightarrow \Upsilon(4S)$
< 9	90	1 AUBERT	02L BABR	$e^+ e^- \rightarrow \Upsilon(4S)$
< 24	90	3 ANDERSON	01B CLE2	$e^+ e^- \rightarrow \Upsilon(4S)$
< 990	90	4 ALBRECHT	91E ARG	$e^+ e^- \rightarrow \Upsilon(4S)$
< 68000	90	5 WEIR	90B MRK2	$e^+ e^- 29$ GeV
< 600	90	6 AVERY	89B CLEO	$e^+ e^- \rightarrow \Upsilon(4S)$
< 2500	90	7 AVERY	87 CLEO	$e^+ e^- \rightarrow \Upsilon(4S)$

$\Gamma(K^+ \mu^+ \mu^-)/\Gamma_{total}$ Γ_{418}/Γ

Test for $\Delta B=1$ weak neutral current. Allowed by higher-order electroweak interactions.

VALUE (units 10^{-7})	CL%	DOCUMENT ID	TECN	COMMENT
5.2 ± 0.7 OUR AVERAGE				
$6.0 \pm 1.6 \pm 0.2$		1 AALTONEN	09B CDF	$p\bar{p}$ at 1.96 TeV
$4.1^{+1.6}_{-1.5} \pm 0.2$		2 AUBERT	09T BABR	$e^+ e^- \rightarrow \Upsilon(4S)$
$5.3^{+0.8}_{-0.7} \pm 0.3$		2 WEI	09A BELL	$e^+ e^- \rightarrow \Upsilon(4S)$

- • • We do not use the following data for averages, fits, limits, etc. • • •

$3.1^{+1.5}_{-1.2} \pm 0.3$		2 AUBERT,B	06J BABR	Repl. by AUBERT 09T
$0.7^{+1.9}_{-1.1} \pm 0.2$		2 AUBERT	03U BABR	Repl. by AUBERT,B 06J
$4.5^{+1.4}_{-1.2} \pm 0.3$		3 ISHIKAWA	03 BELL	Repl. by WEI 09A
$9.8^{+4.6}_{-3.6} \pm 1.6$		2 ABE	02 BELL	Repl. by ISHIKAWA 03
< 12	90	2 AUBERT	02L BABR	$e^+ e^- \rightarrow \Upsilon(4S)$
< 36.8	90	4 ANDERSON	01B CLE2	$e^+ e^- \rightarrow \Upsilon(4S)$
< 52	90	5 AFFOLDER	99B CDF	$p\bar{p}$ at 1.8 TeV
< 100	90	6 ABE	96L CDF	Repl. by AFFOLDER 99B
< 2400	90	7 ALBRECHT	91E ARG	$e^+ e^- \rightarrow \Upsilon(4S)$
< 64000	90	8 WEIR	90B MRK2	$e^+ e^- 29$ GeV
< 1700	90	9 AVERY	89B CLEO	$e^+ e^- \rightarrow \Upsilon(4S)$
< 3800	90	10 AVERY	87 CLEO	$e^+ e^- \rightarrow \Upsilon(4S)$

$\Gamma(K^+ \nu \nu)/\Gamma_{total}$ Γ_{419}/Γ

Test for $\Delta B=1$ weak neutral current. Allowed by higher-order electroweak interactions.

VALUE	CL%	DOCUMENT ID	TECN	COMMENT
< 1.4 × 10⁻⁵	90	1 CHEN	07D BELL	$e^+ e^- \rightarrow \Upsilon(4S)$

- • • We do not use the following data for averages, fits, limits, etc. • • •

< 5.2 × 10 ⁻⁵	90	1 AUBERT	05H BABR	$e^+ e^- \rightarrow \Upsilon(4S)$
< 2.4 × 10 ⁻⁴	90	1 BROWDER	01H CLE2	$e^+ e^- \rightarrow \Upsilon(4S)$

1 Assumes equal production of B^+ and B^0 at the $\Upsilon(4S)$.

$\Gamma(\rho^+ \nu \nu)/\Gamma_{total}$ Γ_{420}/Γ

Test for $\Delta B=1$ weak neutral current. Allowed by higher-order electroweak interaction.

VALUE	CL%	DOCUMENT ID	TECN	COMMENT
< 1.5 × 10⁻⁴	90	1 CHEN	07D BELL	$e^+ e^- \rightarrow \Upsilon(4S)$

1 Assumes equal production of B^+ and B^0 at the $\Upsilon(4S)$.

$\Gamma(K^*(892)^+ \ell^+ \ell^-)/\Gamma_{total}$ Γ_{421}/Γ

Test for $\Delta B=1$ weak neutral current. Allowed by higher-order electroweak interactions.

VALUE (units 10^{-7})	CL%	DOCUMENT ID	TECN	COMMENT
12.9 ± 2.1 OUR AVERAGE				
$14.0^{+4.0}_{-3.7} \pm 0.9$		1 AUBERT	09T BABR	$e^+ e^- \rightarrow \Upsilon(4S)$
$12.4^{+2.3}_{-2.1} \pm 1.3$		1 WEI	09A BELL	$e^+ e^- \rightarrow \Upsilon(4S)$

- • • We do not use the following data for averages, fits, limits, etc. • • •

$7.3^{+5.0}_{-4.2} \pm 2.1$		1 AUBERT,B	06J BABR	Repl. by AUBERT 09T
< 22	90	1 ISHIKAWA	03 BELL	$e^+ e^- \rightarrow \Upsilon(4S)$

1 Assumes equal production of B^+ and B^0 at the $\Upsilon(4S)$.

$\Gamma(K^*(892)^+ \nu \nu)/\Gamma_{total}$ Γ_{424}/Γ

Test for $\Delta B=1$ weak neutral current. Allowed by higher-order electroweak interaction.

VALUE	CL%	DOCUMENT ID	TECN	COMMENT
< 8 × 10⁻⁵	90	AUBERT	08Bc BABR	$e^+ e^- \rightarrow \Upsilon(4S)$

- • • We do not use the following data for averages, fits, limits, etc. • • •

< 1.4 × 10 ⁻⁴	90	1 CHEN	07D BELL	$e^+ e^- \rightarrow \Upsilon(4S)$
--------------------------	----	--------	----------	------------------------------------

1 Assumes equal production of B^+ and B^0 at the $\Upsilon(4S)$.

$\Gamma(K^*(892)^+ e^+ e^-)/\Gamma_{total}$ Γ_{422}/Γ

Test for $\Delta B=1$ weak neutral current. Allowed by higher-order electroweak interactions.

VALUE (units 10^{-7})	CL%	DOCUMENT ID	TECN	COMMENT
15.5 ± 4.0 OUR AVERAGE				
$13.8^{+4.7}_{-4.2} \pm 0.8$		1 AUBERT	09T BABR	$e^+ e^- \rightarrow \Upsilon(4S)$
$17.3^{+5.0}_{-4.2} \pm 2.0$		1 WEI	09A BELL	$e^+ e^- \rightarrow \Upsilon(4S)$

- • • We do not use the following data for averages, fits, limits, etc. • • •

$7.5^{+7.6}_{-6.5} \pm 3.8$		1 AUBERT,B	06J BABR	Repl. by AUBERT 09T
$2.0^{+13.4}_{-8.7} \pm 2.8$		1 AUBERT	03U BABR	$e^+ e^- \rightarrow \Upsilon(4S)$
< 46	90	2 ISHIKAWA	03 BELL	$e^+ e^- \rightarrow \Upsilon(4S)$
< 89	90	1 ABE	02 BELL	Repl. by ISHIKAWA 03
< 95	90	1 AUBERT	02L BABR	$e^+ e^- \rightarrow \Upsilon(4S)$
< 6900	90	3 ALBRECHT	91E ARG	$e^+ e^- \rightarrow \Upsilon(4S)$

1 Assumes equal production of B^+ and B^0 at the $\Upsilon(4S)$.

2 Assumes equal production of B^0 and B^+ at $\Upsilon(4S)$. The second error is a total of systematic uncertainties including model dependence.

3 ALBRECHT 91E reports < 6.3 × 10⁻⁴ assuming the $\Upsilon(4S)$ decays 45% to $B^0 \bar{B}^0$. We rescale to 50%.

$\Gamma(K^*(892)^+ \mu^+ \mu^-)/\Gamma_{total}$ Γ_{423}/Γ

Test for $\Delta B=1$ weak neutral current. Allowed by higher-order electroweak interactions.

VALUE (units 10^{-7})	CL%	DOCUMENT ID	TECN	COMMENT
11.6 ± 3.1 OUR AVERAGE				
$14.6^{+7.9}_{-7.5} \pm 1.2$		1 AUBERT	09T BABR	$e^+ e^- \rightarrow \Upsilon(4S)$
$11.1^{+3.2}_{-2.7} \pm 1.0$		1 WEI	09A BELL	$e^+ e^- \rightarrow \Upsilon(4S)$

- • • We do not use the following data for averages, fits, limits, etc. • • •

$9.7^{+9.4}_{-6.9} \pm 1.4$		1 AUBERT,B	06J BABR	Repl. by AUBERT 09T
$30.7^{+25.8}_{-17.8} \pm 4.2$		1 AUBERT	03U BABR	$e^+ e^- \rightarrow \Upsilon(4S)$
$6.5^{+6.9+1.5}_{-5.3-1.6}$		2 ISHIKAWA	03 BELL	Repl. by WEI 09A
< 39	90	1 ABE	02 BELL	Repl. by ISHIKAWA 03
< 170	90	1 AUBERT	02L BABR	$e^+ e^- \rightarrow \Upsilon(4S)$
< 12000	90	3 ALBRECHT	91E ARG	$e^+ e^- \rightarrow \Upsilon(4S)$

1 Assumes equal production of B^+ and B^0 at the $\Upsilon(4S)$.

2 Assumes equal production of B^0 and B^+ at $\Upsilon(4S)$. The second error is a total of systematic uncertainties including model dependence. The 90% C.L. upper limit is 2.2 × 10⁻⁶.

3 ALBRECHT 91E reports < 1.1 × 10⁻³ assuming the $\Upsilon(4S)$ decays 45% to $B^0 \bar{B}^0$. We rescale to 50%.

$\Gamma(\pi^+ e^+ \mu^-)/\Gamma_{total}$ Γ_{425}/Γ

Test of lepton family number conservation.

VALUE	CL%	DOCUMENT ID	TECN	COMMENT
< 0.0064	90	1 WEIR	90B MRK2	$e^+ e^- 29$ GeV

1 WEIR 90B assumes B^+ production cross section from LUND.

$\Gamma(\pi^+ e^- \mu^+)/\Gamma_{total}$ Γ_{426}/Γ

Test of lepton family number conservation.

VALUE	CL%	DOCUMENT ID	TECN	COMMENT
< 0.0064	90	1 WEIR	90B MRK2	$e^+ e^- 29$ GeV

1 WEIR 90B assumes B^+ production cross section from LUND.

Meson Particle Listings

 B^\pm Γ_\perp/Γ in $B^+ \rightarrow J/\psi K^{*+}$

VALUE	DOCUMENT ID	TECN	COMMENT
0.180 ± 0.014 ± 0.010	ITOH	05	BELL $e^+e^- \rightarrow \Upsilon(4S)$

 Γ_L/Γ in $B^+ \rightarrow \omega K^{*+}$

VALUE	DOCUMENT ID	TECN	COMMENT
0.41 ± 0.18 ± 0.05	AUBERT	09H	BABR $e^+e^- \rightarrow \Upsilon(4S)$

 Γ_L/Γ in $B^+ \rightarrow \omega K_2^*(1430)^+$

VALUE	DOCUMENT ID	TECN	COMMENT
0.56 ± 0.10 ± 0.04	AUBERT	09H	BABR $e^+e^- \rightarrow \Upsilon(4S)$

 Γ_L/Γ in $B^+ \rightarrow K^{*+} \bar{K}^{*0}$

VALUE	DOCUMENT ID	TECN	COMMENT
0.75^{+0.16}_{-0.26} ± 0.03	¹ AUBERT	09F	BABR $e^+e^- \rightarrow \Upsilon(4S)$

¹ Assumes equal production of B^+ and B^0 at the $\Upsilon(4S)$. Γ_L/Γ in $B^+ \rightarrow \phi K^{*+}(892)^+$

VALUE	DOCUMENT ID	TECN	COMMENT
0.50 ± 0.05 OUR AVERAGE			
0.49 ± 0.05 ± 0.03	AUBERT	07BA	BABR $e^+e^- \rightarrow \Upsilon(4S)$
0.52 ± 0.08 ± 0.03	CHEN	05A	BELL $e^+e^- \rightarrow \Upsilon(4S)$
• • • We do not use the following data for averages, fits, limits, etc. • • •			
0.46 ± 0.12 ± 0.03	AUBERT	03V	BABR Repl. by AUBERT 07BA

 Γ_\perp/Γ in $B^+ \rightarrow \phi K^{*+}$

VALUE	DOCUMENT ID	TECN	COMMENT
0.20 ± 0.05 OUR AVERAGE			
0.21 ± 0.05 ± 0.02	AUBERT	07BA	BABR $e^+e^- \rightarrow \Upsilon(4S)$
0.19 ± 0.08 ± 0.02	CHEN	05A	BELL $e^+e^- \rightarrow \Upsilon(4S)$

 ϕ_\parallel in $B^+ \rightarrow \phi K^{*+}$

VALUE (°)	DOCUMENT ID	TECN	COMMENT
2.34 ± 0.18 OUR AVERAGE			
2.47 ± 0.20 ± 0.07	AUBERT	07BA	BABR $e^+e^- \rightarrow \Upsilon(4S)$
2.10 ± 0.28 ± 0.04	CHEN	05A	BELL $e^+e^- \rightarrow \Upsilon(4S)$

 ϕ_\perp in $B^+ \rightarrow \phi K^{*+}$

VALUE (°)	DOCUMENT ID	TECN	COMMENT
2.58 ± 0.17 OUR AVERAGE			
2.69 ± 0.20 ± 0.03	AUBERT	07BA	BABR $e^+e^- \rightarrow \Upsilon(4S)$
2.31 ± 0.30 ± 0.07	CHEN	05A	BELL $e^+e^- \rightarrow \Upsilon(4S)$

 $\delta_0(B^+ \rightarrow \phi K^{*+})$

VALUE (rad)	DOCUMENT ID	TECN	COMMENT
3.07 ± 0.18 ± 0.06	AUBERT	07BA	BABR $e^+e^- \rightarrow \Upsilon(4S)$

 $A_{CP}^0(B^+ \rightarrow \phi K^{*+})$

VALUE	DOCUMENT ID	TECN	COMMENT
0.17 ± 0.11 ± 0.02	AUBERT	07BA	BABR $e^+e^- \rightarrow \Upsilon(4S)$

 $A_{CP}^1(B^+ \rightarrow \phi K^{*+})$

VALUE	DOCUMENT ID	TECN	COMMENT
0.22 ± 0.24 ± 0.08	AUBERT	07BA	BABR $e^+e^- \rightarrow \Upsilon(4S)$

 $\Delta\phi_\parallel(B^+ \rightarrow \phi K^{*+})$

VALUE (rad)	DOCUMENT ID	TECN	COMMENT
0.07 ± 0.20 ± 0.05	AUBERT	07BA	BABR $e^+e^- \rightarrow \Upsilon(4S)$

 $\Delta\phi_\perp(B^+ \rightarrow \phi K^{*+})$

VALUE (rad)	DOCUMENT ID	TECN	COMMENT
0.19 ± 0.20 ± 0.07	AUBERT	07BA	BABR $e^+e^- \rightarrow \Upsilon(4S)$

 $\Delta\delta_0(B^+ \rightarrow \phi K^{*+})$

VALUE (rad)	DOCUMENT ID	TECN	COMMENT
0.20 ± 0.18 ± 0.03	AUBERT	07BA	BABR $e^+e^- \rightarrow \Upsilon(4S)$

 Γ_L/Γ in $B^+ \rightarrow \phi K_1(1270)^+$

VALUE	DOCUMENT ID	TECN	COMMENT
0.46^{+0.12+0.06}_{-0.13-0.07}	AUBERT	08BI	BABR $e^+e^- \rightarrow \Upsilon(4S)$

 Γ_L/Γ in $B^+ \rightarrow \phi K_2^*(1430)^+$

VALUE	DOCUMENT ID	TECN	COMMENT
0.80^{+0.09}_{-0.10} ± 0.03	AUBERT	08BI	BABR $e^+e^- \rightarrow \Upsilon(4S)$

 $\delta_0(B^+ \rightarrow \phi K_2^*(1430)^+)$

VALUE (rad)	DOCUMENT ID	TECN	COMMENT
3.59 ± 0.19 ± 0.12	AUBERT	08BI	BABR $e^+e^- \rightarrow \Upsilon(4S)$

 $\Delta\delta_0(B^+ \rightarrow \phi K_2^*(1430)^+)$

VALUE (rad)	DOCUMENT ID	TECN	COMMENT
-0.05 ± 0.19 ± 0.06	AUBERT	08BI	BABR $e^+e^- \rightarrow \Upsilon(4S)$

 Γ_L/Γ in $B^+ \rightarrow \rho^0 K^{*+}(892)^+$

VALUE	DOCUMENT ID	TECN	COMMENT
• • • We do not use the following data for averages, fits, limits, etc. • • •			
0.96 ^{+0.04} _{-0.15} ± 0.04	AUBERT	03V	BABR $e^+e^- \rightarrow \Upsilon(4S)$

 $\Gamma_L/\Gamma(B^+ \rightarrow K^{*+} \rho^0)$

VALUE	DOCUMENT ID	TECN	COMMENT
0.48 ± 0.08 OUR AVERAGE			
0.52 ± 0.10 ± 0.04	AUBERT,B	06G	BABR $e^+e^- \rightarrow \Upsilon(4S)$
0.43 ± 0.11 ^{+0.05} _{-0.02}	ZHANG	05D	BELL $e^+e^- \rightarrow \Upsilon(4S)$

 Γ_L/Γ in $B^+ \rightarrow \rho^+ \rho^0$

VALUE	DOCUMENT ID	TECN	COMMENT
0.950 ± 0.016 OUR AVERAGE			
0.950 ± 0.015 ± 0.006	AUBERT	09G	BABR $e^+e^- \rightarrow \Upsilon(4S)$
0.948 ± 0.106 ± 0.021	ZHANG	03B	BELL $e^+e^- \rightarrow \Upsilon(4S)$
• • • We do not use the following data for averages, fits, limits, etc. • • •			
0.905 ± 0.042 ^{+0.023} _{-0.027}	AUBERT,BE	06G	BABR Repl. by AUBERT 09G
0.97 ± 0.03 ± 0.04	AUBERT	03V	BABR Repl. by AUBERT,BE 06G

 Γ_L/Γ in $B^+ \rightarrow \omega \rho^+$

VALUE	DOCUMENT ID	TECN	COMMENT
0.90 ± 0.05 ± 0.03	AUBERT	09H	BABR $e^+e^- \rightarrow \Upsilon(4S)$
• • • We do not use the following data for averages, fits, limits, etc. • • •			
0.82 ± 0.11 ± 0.02	AUBERT,B	06T	BABR Repl. by AUBERT 09H
0.88 ± 0.12 ± 0.03	AUBERT	05O	BABR Repl. by AUBERT,B 06T

 Γ_L/Γ in $B^+ \rightarrow \rho \bar{p} K^{*+}(892)^+$

VALUE	DOCUMENT ID	TECN	COMMENT
0.32 ± 0.17 ± 0.09	CHEN	08C	BELL $e^+e^- \rightarrow \Upsilon(4S)$

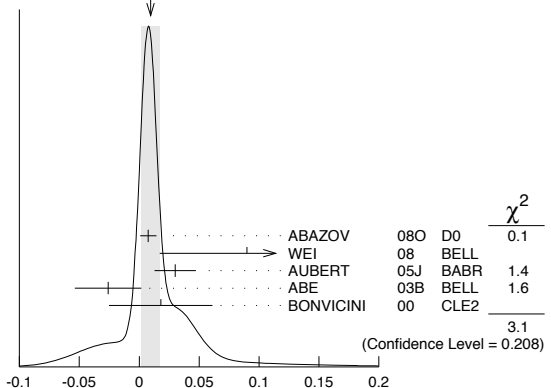
CP VIOLATION

 A_{CP} is defined as

$$\frac{B(B^- \rightarrow \bar{f}) - B(B^+ \rightarrow f)}{B(B^- \rightarrow \bar{f}) + B(B^+ \rightarrow f)}$$

the CP-violation charge asymmetry of exclusive B^- and B^+ decay. $A_{CP}(B^+ \rightarrow J/\psi(1S)K^+)$

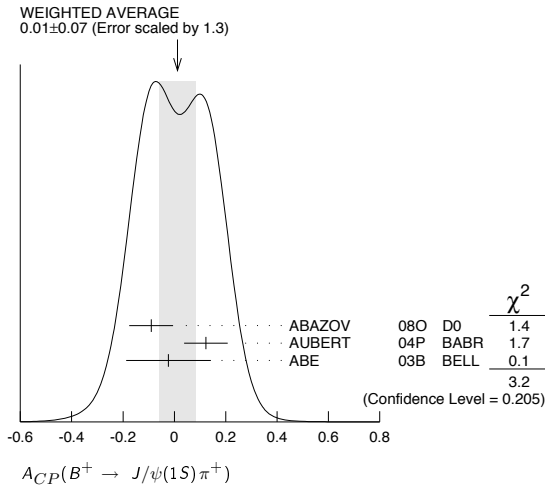
VALUE	DOCUMENT ID	TECN	COMMENT
0.009 ± 0.008 OUR AVERAGE			Error includes scale factor of 1.3. See the ideogram below.
0.0075 ± 0.0061 ± 0.0030	¹ ABAZOV	08O	D0 $p\bar{p}$ at 1.96 TeV
0.09 ± 0.07 ± 0.02	² WEI	08	BELL $e^+e^- \rightarrow \Upsilon(4S)$
0.030 ± 0.014 ± 0.010	³ AUBERT	05J	BABR $e^+e^- \rightarrow \Upsilon(4S)$
-0.026 ± 0.022 ± 0.017	ABE	03B	BELL $e^+e^- \rightarrow \Upsilon(4S)$
0.018 ± 0.043 ± 0.004	⁴ BONVICINI	00	CLE2 $e^+e^- \rightarrow \Upsilon(4S)$
• • • We do not use the following data for averages, fits, limits, etc. • • •			
0.03 ± 0.015 ± 0.006	AUBERT	04P	BABR Repl. by AUBERT 05J
0.003 ± 0.030 ± 0.004	AUBERT	02F	BABR Repl. by AUBERT 04P

¹ Uses $J/\psi \rightarrow \mu^+ \mu^-$ decay.² Uses $B^+ \rightarrow J/\psi K^+$, where $J/\psi \rightarrow p\bar{p}$.³ The result reported corresponds to $-A_{CP}$.⁴ A +0.3% correction is applied due to a slightly higher reconstruction efficiency for the positive kaons.WEIGHTED AVERAGE
0.009 ± 0.008 (Error scaled by 1.3) $A_{CP}(B^+ \rightarrow J/\psi(1S)K^+)$

$A_{CP}(B^+ \rightarrow J/\psi(1S)\pi^+)$

VALUE	DOCUMENT ID	TECN	COMMENT
0.01 ± 0.07 OUR AVERAGE	Error includes scale factor of 1.3. See the ideogram below.		
-0.09 ± 0.08 ± 0.03	¹ ABAZOV	08o D0	$p\bar{p}$ at 1.96 TeV
+0.123 ± 0.085 ± 0.004	AUBERT	04P BABR	$e^+e^- \rightarrow \Upsilon(4S)$
-0.023 ± 0.164 ± 0.015	ABE	03B BELL	$e^+e^- \rightarrow \Upsilon(4S)$
• • • We do not use the following data for averages, fits, limits, etc. • • •			
+0.01 ± 0.22 ± 0.01	AUBERT	02F BABR	Repl. by AUBERT 04P

¹ Uses $J/\psi \rightarrow \mu^+\mu^-$ decay.



$A_{CP}(B^+ \rightarrow J/\psi\rho^+)$

VALUE	DOCUMENT ID	TECN	COMMENT
-0.11 ± 0.12 ± 0.08	AUBERT	07AC BABR	$e^+e^- \rightarrow \Upsilon(4S)$

$A_{CP}(B^+ \rightarrow J/\psi K^*(892)^+)$

VALUE	DOCUMENT ID	TECN	COMMENT
-0.048 ± 0.029 ± 0.016	¹ AUBERT	05J BABR	$e^+e^- \rightarrow \Upsilon(4S)$

¹ The result reported corresponds to $-A_{CP}$.

$A_{CP}(B^+ \rightarrow \eta_c K^+)$

VALUE	DOCUMENT ID	TECN	COMMENT
-0.16 ± 0.08 ± 0.02	¹ WEI	08 BELL	$e^+e^- \rightarrow \Upsilon(4S)$

¹ Uses $B^+ \rightarrow \eta_c K^+$, where $\eta_c \rightarrow p\bar{p}$.

$A_{CP}(B^+ \rightarrow \psi(2S)\pi^+)$

VALUE	DOCUMENT ID	TECN	COMMENT
0.022 ± 0.085 ± 0.016	BHARDWAJ	08 BELL	$e^+e^- \rightarrow \Upsilon(4S)$

$A_{CP}(B^+ \rightarrow \psi(2S)K^+)$

VALUE	DOCUMENT ID	TECN	COMMENT
-0.025 ± 0.024 OUR AVERAGE			
0.052 ± 0.059 ± 0.020	AUBERT	05J BABR	$e^+e^- \rightarrow \Upsilon(4S)$
-0.042 ± 0.020 ± 0.017	ABE	03B BELL	$e^+e^- \rightarrow \Upsilon(4S)$
0.02 ± 0.091 ± 0.01	¹ BONVICINI	00 CLE2	$e^+e^- \rightarrow \Upsilon(4S)$

¹ A + 0.3% correction is applied due to a slightly higher reconstruction efficiency for the positive kaons.

$A_{CP}(B^+ \rightarrow \psi(2S)K^*(892)^+)$

VALUE	DOCUMENT ID	TECN	COMMENT
0.077 ± 0.207 ± 0.051	¹ AUBERT	05J BABR	$e^+e^- \rightarrow \Upsilon(4S)$

¹ The result reported corresponds to $-A_{CP}$.

$A_{CP}(B^+ \rightarrow \chi_{c1}(1P)\pi^+)$

VALUE	DOCUMENT ID	TECN	COMMENT
0.07 ± 0.18 ± 0.02	KUMAR	06 BELL	$e^+e^- \rightarrow \Upsilon(4S)$

$A_{CP}(B^+ \rightarrow \chi_{c0}K^+)$

VALUE	DOCUMENT ID	TECN	COMMENT
-0.11 ± 0.12 OUR AVERAGE			
-0.14 ± 0.15 ^{+0.03} _{-0.06}	AUBERT	08Ai BABR	$e^+e^- \rightarrow \Upsilon(4S)$
-0.065 ± 0.20 ^{+0.035} _{-0.024}	GARMASH	06 BELL	$e^+e^- \rightarrow \Upsilon(4S)$

$A_{CP}(B^+ \rightarrow \chi_{c1}K^+)$

VALUE	DOCUMENT ID	TECN	COMMENT
-0.009 ± 0.033 OUR AVERAGE			
-0.01 ± 0.03 ± 0.02	KUMAR	06 BELL	$e^+e^- \rightarrow \Upsilon(4S)$
-0.003 ± 0.076 ± 0.017	¹ AUBERT	05J BABR	$e^+e^- \rightarrow \Upsilon(4S)$

¹ The result reported corresponds to $-A_{CP}$.

$A_{CP}(B^+ \rightarrow \chi_{c1}K^*(892)^+)$

VALUE	DOCUMENT ID	TECN	COMMENT
0.471 ± 0.378 ± 0.268	¹ AUBERT	05J BABR	$e^+e^- \rightarrow \Upsilon(4S)$

¹ The result reported corresponds to $-A_{CP}$.

$A_{CP}(B^+ \rightarrow \bar{D}^0\pi^+)$

VALUE	DOCUMENT ID	TECN	COMMENT
-0.008 ± 0.008	ABE	06 BELL	$e^+e^- \rightarrow \Upsilon(4S)$

$A_{CP}(B^+ \rightarrow D_{CP(+)}\pi^+)$

VALUE	DOCUMENT ID	TECN	COMMENT
0.035 ± 0.024	ABE	06 BELL	$e^+e^- \rightarrow \Upsilon(4S)$

$A_{CP}(B^+ \rightarrow D_{CP(-)}\pi^+)$

VALUE	DOCUMENT ID	TECN	COMMENT
0.017 ± 0.026	ABE	06 BELL	$e^+e^- \rightarrow \Upsilon(4S)$

$A_{CP}(B^+ \rightarrow \bar{D}^0K^+)$

VALUE	DOCUMENT ID	TECN	COMMENT
0.066 ± 0.036	ABE	06 BELL	$e^+e^- \rightarrow \Upsilon(4S)$
• • • We do not use the following data for averages, fits, limits, etc. • • •			
0.003 ± 0.080 ± 0.037	¹ ABE	03D BELL	Repl. by SWAIN 03
0.04 ± 0.06 ± 0.03	² SWAIN	03 BELL	Repl. by ABE 06

¹ Corresponds to 90% confidence range $-0.15 < A_{CP} < 0.16$.
² Corresponds to 90% confidence range $-0.07 < A_{CP} < 0.15$.

$r_B(B^+ \rightarrow D^0K^+)$

$r_B^{(*)}$ and $\delta_B^{(*)}$ are the amplitude ratios and relative strong phases between the amplitudes of $A(B^+ \rightarrow D^{(*)0}K^+)$ and $A(B^+ \rightarrow \bar{D}^{(*)0}K^+)$,

VALUE	CL%	DOCUMENT ID	TECN	COMMENT
0.101 ± 0.032 OUR AVERAGE				
0.086 ± 0.032 ± 0.015		¹ AUBERT	08AL BABR	$e^+e^- \rightarrow \Upsilon(4S)$
0.159 ^{+0.054} _{-0.050} ± 0.050		² POLUEKTOV	06 BELL	$e^+e^- \rightarrow \Upsilon(4S)$
• • • We do not use the following data for averages, fits, limits, etc. • • •				
<0.19	90	HORII	08 BELL	$e^+e^- \rightarrow \Upsilon(4S)$
0.12 ± 0.08 ± 0.05		³ AUBERT,B	05Y BABR	Repl. by AUBERT 08AL

¹ Uses Dalitz plot analysis of $\bar{D}^0 \rightarrow K_S^0\pi^+\pi^-$ and $\bar{D}^0 \rightarrow K_S^0K^+K^-$ decays coming from $B^\pm \rightarrow D^{(*)}K^{(*)\pm}$ modes.
² Uses a Dalitz plot analysis of the $\bar{D}^0 \rightarrow K_S^0\pi^+\pi^-$ decays; Combines the $D K^+$, $D^* K^+$ and $D K^{*+}$ modes.
³ Uses a Dalitz analysis of neutral D decays to $K_S^0\pi^+\pi^-$ in the processes $B^\pm \rightarrow D^{(*)}K^\pm$, $D^* \rightarrow D\pi^0$, $D\gamma$.

$\delta_B(B^+ \rightarrow D^0K^+)$

VALUE (degrees)	DOCUMENT ID	TECN	COMMENT
126 ± 21 OUR AVERAGE			
109 ⁺²⁷ ₋₃₀ ± 8	¹ AUBERT	08AL BABR	$e^+e^- \rightarrow \Upsilon(4S)$
145.7 ^{+19.0} _{-19.7} ± 23.1	² POLUEKTOV	06 BELL	$e^+e^- \rightarrow \Upsilon(4S)$
• • • We do not use the following data for averages, fits, limits, etc. • • •			
104 ± 45 ⁺²³ ₋₃₂	³ AUBERT,B	05Y BABR	Repl. by AUBERT 08AL

¹ Uses Dalitz plot analysis of $\bar{D}^0 \rightarrow K_S^0\pi^+\pi^-$ and $\bar{D}^0 \rightarrow K_S^0K^+K^-$ decays coming from $B^\pm \rightarrow D^{(*)}K^{(*)\pm}$ modes.
² Uses a Dalitz plot analysis of the $\bar{D}^0 \rightarrow K_S^0\pi^+\pi^-$ decays; Combines the $D K^+$, $D^* K^+$ and $D K^{*+}$ modes.
³ Uses a Dalitz analysis of neutral D decays to $K_S^0\pi^+\pi^-$ in the processes $B^\pm \rightarrow D^{(*)}K^\pm$, $D^* \rightarrow D\pi^0$, $D\gamma$.

¹ Uses Dalitz plot analysis of $\bar{D}^0 \rightarrow K_S^0\pi^+\pi^-$ and $\bar{D}^0 \rightarrow K_S^0K^+K^-$ decays coming from $B^\pm \rightarrow D^{(*)}K^{(*)\pm}$ modes.
² Uses a Dalitz plot analysis of the $\bar{D}^0 \rightarrow K_S^0\pi^+\pi^-$ decays; Combines the $D K^+$, $D^* K^+$ and $D K^{*+}$ modes.
³ Uses a Dalitz analysis of neutral D decays to $K_S^0\pi^+\pi^-$ in the processes $B^\pm \rightarrow D^{(*)}K^\pm$, $D^* \rightarrow D\pi^0$, $D\gamma$.

$r_B(B^+ \rightarrow DK^{*+})$

r_B and δ_B are the amplitude ratios and relative strong phases between the amplitudes of $A_{CP}(B^+ \rightarrow DK^{*+})$ and $A_{CP}(B^+ \rightarrow \bar{D}K^{*+})$,

VALUE	DOCUMENT ID	TECN	COMMENT
0.34 ± 0.09 OUR AVERAGE	Error includes scale factor of 1.3.		
0.31 ± 0.07	¹ AUBERT	09AJ BABR	$e^+e^- \rightarrow \Upsilon(4S)$
0.564 ^{+0.216} _{-0.155} ± 0.093	² POLUEKTOV	06 BELL	$e^+e^- \rightarrow \Upsilon(4S)$
• • • We do not use the following data for averages, fits, limits, etc. • • •			
0.181 ^{+0.088} _{-0.108} ± 0.042	³ AUBERT	08AL BABR	Repl. by AUBERT 09AJ

¹ Obtained by combining the GLW and ADS methods. The 2-sigma range corresponds to [0.17, 0.43].
² Uses a Dalitz plot analysis of the $\bar{D}^0 \rightarrow K_S^0\pi^+\pi^-$ decays; Combines the $D K^+$, $D^* K^+$ and $D K^{*+}$ modes.
³ Uses Dalitz plot analysis of $\bar{D}^0 \rightarrow K_S^0\pi^+\pi^-$ and $\bar{D}^0 \rightarrow K_S^0K^+K^-$ decays coming from $B^\pm \rightarrow D^{(*)}K^{(*)\pm}$ modes.

Meson Particle Listings

 B^\pm $\delta_B(B^+ \rightarrow DK^{*+})$

VALUE (degrees)	DOCUMENT ID	TECN	COMMENT
157 ± 70 OUR AVERAGE	Error includes scale factor of 2.0.		
104 ⁺³⁹ ₋₃₇ ± 18	¹ AUBERT	08AL BABR	$e^+e^- \rightarrow \Upsilon(4S)$
242.6 ^{+20.2} _{-23.2} ± 49.4	² POLUEKTOV	06 BELL	$e^+e^- \rightarrow \Upsilon(4S)$
¹ Uses Dalitz plot analysis of $\bar{D}^0 \rightarrow K_S^0 \pi^+ \pi^-$ and $\bar{D}^0 \rightarrow K_S^0 K^+ K^-$ decays coming from $B^\pm \rightarrow D^{(*)} K^{(*)\pm}$ modes.			
² Uses a Dalitz plot analysis of the $\bar{D}^0 \rightarrow K_S^0 \pi^+ \pi^-$ decays; Combines the $D K^+$, $D^* K^+$ and $D K^{*+}$ modes.			

 $A_{CP}(B^+ \rightarrow [K^-\pi^+]_D K^+)$

VALUE	DOCUMENT ID	TECN	COMMENT
-0.1 ^{+0.8} _{-1.0} ± 0.4	HORII	08 BELL	$e^+e^- \rightarrow \Upsilon(4S)$
••• We do not use the following data for averages, fits, limits, etc. •••			
+0.88 ^{+0.77} _{-0.62} ± 0.06	SAIGO	05 BELL	Repl. by HORII 08

 $A_{CP}(B^+ \rightarrow [K^-\pi^+]_{\bar{D}} K^*(892)^+)$

VALUE	DOCUMENT ID	TECN	COMMENT
-0.34 ± 0.43 ± 0.16	AUBERT	09AJ BABR	$e^+e^- \rightarrow \Upsilon(4S)$
••• We do not use the following data for averages, fits, limits, etc. •••			
-0.22 ± 0.61 ± 0.17	AUBERT,B	05V BABR	Repl. by AUBERT 09AJ

 $A_{CP}(B^+ \rightarrow [K^-\pi^+]_D \pi^+)$

VALUE	DOCUMENT ID	TECN	COMMENT
-0.02 ^{+0.15} _{-0.16} ± 0.04	HORII	08 BELL	$e^+e^- \rightarrow \Upsilon(4S)$
••• We do not use the following data for averages, fits, limits, etc. •••			
+0.30 ^{+0.29} _{-0.25} ± 0.06	SAIGO	05 BELL	Repl. by HORII 08

 $A_{CP}(B^+ \rightarrow [\pi^+\pi^-\pi^0]_D K^+)$

VALUE	DOCUMENT ID	TECN	COMMENT
-0.02 ± 0.15 ± 0.03	¹ AUBERT	07BJ BABR	$e^+e^- \rightarrow \Upsilon(4S)$
••• We do not use the following data for averages, fits, limits, etc. •••			
-0.02 ± 0.16 ± 0.03	AUBERT,B	05T BABR	Repl. by AUBERT 07BJ
¹ Uses a Dalitz plot analysis of $D^0 \rightarrow \pi^+\pi^-\pi^0$. Also reports the one-sigma regions: $0.06 < r_B < 0.78$, $-30^\circ < \gamma < 76^\circ$, and $-27^\circ < \delta < 78^\circ$.			

 $A_{CP}(B^+ \rightarrow D_{CP(+1)} K^+)$

VALUE	DOCUMENT ID	TECN	COMMENT
0.24 ± 0.08 OUR AVERAGE	Error includes scale factor of 1.1.		
0.39 ± 0.17 ± 0.04	AALTONEN	10A CDF	$p\bar{p}$ at 1.96 TeV
0.27 ± 0.09 ± 0.04	AUBERT	08AA BABR	$e^+e^- \rightarrow \Upsilon(4S)$
0.06 ± 0.14 ± 0.05	ABE	06 BELL	$e^+e^- \rightarrow \Upsilon(4S)$
••• We do not use the following data for averages, fits, limits, etc. •••			
0.35 ± 0.13 ± 0.04	AUBERT	06J BABR	Repl. by AUBERT 08AA
0.07 ± 0.17 ± 0.06	AUBERT	04N BABR	Repl. by AUBERT 06J
0.29 ± 0.26 ± 0.05	¹ ABE	03D BELL	Repl. by SWAIN 03
0.06 ± 0.19 ± 0.04	² SWAIN	03 BELL	Repl. by ABE 06

- ¹ Corresponds to 90% confidence range $-0.14 < A_{CP} < 0.73$.
² Corresponds to 90% confidence range $-0.26 < A_{CP} < 0.38$.

 $A_{CP}(B^+ \rightarrow D_{CP(-1)} K^+)$

VALUE	DOCUMENT ID	TECN	COMMENT
-0.10 ± 0.08 OUR AVERAGE			
-0.09 ± 0.09 ± 0.02	AUBERT	08AA BABR	$e^+e^- \rightarrow \Upsilon(4S)$
-0.12 ± 0.14 ± 0.05	ABE	06 BELL	$e^+e^- \rightarrow \Upsilon(4S)$
••• We do not use the following data for averages, fits, limits, etc. •••			
-0.06 ± 0.13 ± 0.04	AUBERT	06J BABR	Repl. by AUBERT 08AA
-0.22 ± 0.24 ± 0.04	¹ ABE	03D BELL	Repl. by SWAIN 03
-0.19 ± 0.17 ± 0.05	² SWAIN	03 BELL	Repl. by ABE 06
¹ Corresponds to 90% confidence range $-0.62 < A_{CP} < 0.18$.			
² Corresponds to 90% confidence range $-0.47 < A_{CP} < 0.11$.			

 $A_{CP}(B^+ \rightarrow \bar{D}^{*0} \pi^+)$

VALUE	DOCUMENT ID	TECN	COMMENT
-0.014 ± 0.015	ABE	06 BELL	$e^+e^- \rightarrow \Upsilon(4S)$

 $A_{CP}(B^+ \rightarrow (D_{CP(+1)}^*)^0 \pi^+)$

VALUE	DOCUMENT ID	TECN	COMMENT
-0.021 ± 0.045	ABE	06 BELL	$e^+e^- \rightarrow \Upsilon(4S)$

 $A_{CP}(B^+ \rightarrow (D_{CP(-1)}^*)^0 \pi^+)$

VALUE	DOCUMENT ID	TECN	COMMENT
-0.090 ± 0.051	ABE	06 BELL	$e^+e^- \rightarrow \Upsilon(4S)$

 $A_{CP}(B^+ \rightarrow D^{*0} K^+)$

VALUE	DOCUMENT ID	TECN	COMMENT
-0.07 ± 0.04 OUR AVERAGE			
-0.06 ± 0.04 ± 0.01	AUBERT	08BF BABR	$e^+e^- \rightarrow \Upsilon(4S)$
-0.089 ± 0.086	ABE	06 BELL	$e^+e^- \rightarrow \Upsilon(4S)$

 $r_B^{(*)}(B^+ \rightarrow D^{*0} K^+)$

$r_B^{(*)}$ and $\delta_B^{(*)}$ are the amplitude ratios and relative strong phases between the amplitudes of $A(B^+ \rightarrow D^{(*)0} K^+)$ and $A(B^+ \rightarrow \bar{D}^{(*)0} K^+)$,

VALUE	DOCUMENT ID	TECN	COMMENT
0.14 ± 0.05 OUR AVERAGE			
0.135 ± 0.050 ± 0.012	¹ AUBERT	08AL BABR	$e^+e^- \rightarrow \Upsilon(4S)$
0.175 ^{+0.108} _{-0.099} ± 0.050	² POLUEKTOV	06 BELL	$e^+e^- \rightarrow \Upsilon(4S)$
••• We do not use the following data for averages, fits, limits, etc. •••			
0.17 ± 0.10 ± 0.04	³ AUBERT,B	05Y BABR	Repl. by AUBERT 08AL
¹ Uses Dalitz plot analysis of $\bar{D}^0 \rightarrow K_S^0 \pi^+ \pi^-$ and $\bar{D}^0 \rightarrow K_S^0 K^+ K^-$ decays coming from $B^\pm \rightarrow D^{(*)} K^{(*)\pm}$ modes.			
² Uses a Dalitz plot analysis of the $\bar{D}^0 \rightarrow K_S^0 \pi^+ \pi^-$ decays; Combines the $D K^+$, $D^* K^+$ and $D K^{*+}$ modes.			
³ Uses a Dalitz analysis of neutral D decays to $K_S^0 \pi^+ \pi^-$ in the processes $B^\pm \rightarrow D^{(*)} K^\pm, D^* \rightarrow D \pi^0, D \gamma$.			

 $\delta_B^*(B^+ \rightarrow D^{*0} K^+)$

VALUE (degrees)	DOCUMENT ID	TECN	COMMENT
299 ± 24 OUR AVERAGE			
297 ⁺²⁷ ₋₂₉ ± 6.4	¹ AUBERT	08AL BABR	$e^+e^- \rightarrow \Upsilon(4S)$
302.0 ^{+33.8} _{-35.1} ± 23.7	² POLUEKTOV	06 BELL	$e^+e^- \rightarrow \Upsilon(4S)$
••• We do not use the following data for averages, fits, limits, etc. •••			
296 ± 41 ⁺²⁰ ₋₁₉	³ AUBERT,B	05Y BABR	Repl. by AUBERT 08AL
¹ Uses Dalitz plot analysis of $\bar{D}^0 \rightarrow K_S^0 \pi^+ \pi^-$ and $\bar{D}^0 \rightarrow K_S^0 K^+ K^-$ decays coming from $B^\pm \rightarrow D^{(*)} K^{(*)\pm}$ modes.			
² Uses a Dalitz plot analysis of the $\bar{D}^0 \rightarrow K_S^0 \pi^+ \pi^-$ decays; Combines the $D K^+$, $D^* K^+$ and $D K^{*+}$ modes.			
³ Uses a Dalitz analysis of neutral D decays to $K_S^0 \pi^+ \pi^-$ in the processes $B^\pm \rightarrow D^{(*)} K^\pm, D^* \rightarrow D \pi^0, D \gamma$.			

 $A_{CP}(B^+ \rightarrow D_{CP(+1)}^{*0} K^+)$

VALUE	DOCUMENT ID	TECN	COMMENT
-0.12 ± 0.08 OUR AVERAGE			
-0.11 ± 0.09 ± 0.01	AUBERT	08BF BABR	$e^+e^- \rightarrow \Upsilon(4S)$
-0.20 ± 0.22 ± 0.04	ABE	06 BELL	$e^+e^- \rightarrow \Upsilon(4S)$
••• We do not use the following data for averages, fits, limits, etc. •••			
-0.10 ± 0.23 ^{+0.03} _{-0.04}	AUBERT	05N BABR	Repl. by AUBERT 08BF

 $A_{CP}(B^+ \rightarrow D_{CP(-1)}^{*0} K^+)$

VALUE	DOCUMENT ID	TECN	COMMENT
0.07 ± 0.10 OUR AVERAGE			
+0.06 ± 0.10 ± 0.02	AUBERT	08BF BABR	$e^+e^- \rightarrow \Upsilon(4S)$
+0.13 ± 0.30 ± 0.08	ABE	06 BELL	$e^+e^- \rightarrow \Upsilon(4S)$

 $A_{CP}(B^+ \rightarrow D_{CP(+1)} K^*(892)^+)$

VALUE	DOCUMENT ID	TECN	COMMENT
+0.09 ± 0.13 ± 0.06	AUBERT	09AJ BABR	$e^+e^- \rightarrow \Upsilon(4S)$
••• We do not use the following data for averages, fits, limits, etc. •••			
-0.08 ± 0.19 ± 0.08	AUBERT,B	05U BABR	Repl. by AUBERT 09AJ

 $A_{CP}(B^+ \rightarrow D_{CP(-1)} K^*(892)^+)$

VALUE	DOCUMENT ID	TECN	COMMENT
-0.23 ± 0.21 ± 0.07	AUBERT	09AJ BABR	$e^+e^- \rightarrow \Upsilon(4S)$
••• We do not use the following data for averages, fits, limits, etc. •••			
-0.26 ± 0.40 ± 0.12	AUBERT,B	05U BABR	Repl. by AUBERT 09AJ

 $A_{CP}(B^+ \rightarrow D^{*+} \bar{D}^{*0})$

VALUE	DOCUMENT ID	TECN	COMMENT
-0.15 ± 0.11 ± 0.02	AUBERT,B	06A BABR	$e^+e^- \rightarrow \Upsilon(4S)$

 $A_{CP}(B^+ \rightarrow D^{*+} \bar{D}^0)$

VALUE	DOCUMENT ID	TECN	COMMENT
-0.06 ± 0.13 ± 0.02	AUBERT,B	06A BABR	$e^+e^- \rightarrow \Upsilon(4S)$

 $A_{CP}(B^+ \rightarrow D^+ \bar{D}^{*0})$

VALUE	DOCUMENT ID	TECN	COMMENT
0.13 ± 0.18 ± 0.04	AUBERT,B	06A BABR	$e^+e^- \rightarrow \Upsilon(4S)$

 $A_{CP}(B^+ \rightarrow D^+ \bar{D}^0)$

VALUE	DOCUMENT ID	TECN	COMMENT
-0.03 ± 0.07 OUR AVERAGE			
0.00 ± 0.08 ± 0.02	ADACHI	08 BELL	$e^+e^- \rightarrow \Upsilon(4S)$
-0.13 ± 0.14 ± 0.02	AUBERT,B	06A BABR	$e^+e^- \rightarrow \Upsilon(4S)$

$A_{CP}(B^+ \rightarrow \rho^+ \gamma)$

VALUE	DOCUMENT ID	TECN	COMMENT
$-0.11 \pm 0.32 \pm 0.09$	TANIGUCHI	08	BELL $e^+ e^- \rightarrow \Upsilon(4S)$

 $A_{CP}(B^+ \rightarrow \pi^+ \pi^0)$

VALUE	DOCUMENT ID	TECN	COMMENT
0.06 ± 0.05 OUR AVERAGE			
$0.07 \pm 0.06 \pm 0.01$	LIN	08	BELL $e^+ e^- \rightarrow \Upsilon(4S)$
$0.03 \pm 0.08 \pm 0.01$	AUBERT	07bc	BABR $e^+ e^- \rightarrow \Upsilon(4S)$
••• We do not use the following data for averages, fits, limits, etc. •••			
$-0.01 \pm 0.10 \pm 0.02$	¹ AUBERT	05L	BABR Repl. by AUBERT 07bc
$0.00 \pm 0.10 \pm 0.02$	² CHAO	05A	BELL Repl. by CHAO 04b
$-0.02 \pm 0.10 \pm 0.01$	³ CHAO	04B	BELL Repl. by LIN 08
$-0.03 \pm 0.18 \pm 0.02$	⁴ AUBERT	03L	BABR Repl. by AUBERT 05L
$0.30 \pm 0.30 \pm 0.06$	⁵ CASEY	02	BELL Repl. by CHAO 04b

¹ Corresponds to a 90% CL interval of $-0.19 < A_{CP} < 0.21$.² Corresponds to a 90% CL interval of $-0.17 < A_{CP} < 0.16$.³ This corresponds to 90% CL interval of $-0.18 < A_{CP} < 0.14$.⁴ Corresponds to 90% confidence range $-0.32 < A_{CP} < 0.27$.⁵ Corresponds to 90% confidence range $-0.23 < A_{CP} < +0.86$. $A_{CP}(B^+ \rightarrow \pi^+ \pi^- \pi^+)$

VALUE	DOCUMENT ID	TECN	COMMENT
$0.032 \pm 0.044 \pm 0.040$ -0.037	AUBERT	09L	BABR $e^+ e^- \rightarrow \Upsilon(4S)$
••• We do not use the following data for averages, fits, limits, etc. •••			
$-0.007 \pm 0.077 \pm 0.025$	AUBERT,B	05G	BABR Repl. by AUBERT 09L
$-0.39 \pm 0.33 \pm 0.12$	AUBERT	03M	BABR Repl. by AUBERT 05G

 $A_{CP}(B^+ \rightarrow \rho^0 \pi^+)$

VALUE	DOCUMENT ID	TECN	COMMENT
$0.18 \pm 0.07 \pm 0.05$ -0.15	AUBERT	09L	BABR $e^+ e^- \rightarrow \Upsilon(4S)$
••• We do not use the following data for averages, fits, limits, etc. •••			
$-0.074 \pm 0.120 \pm 0.035$	AUBERT,B	05G	BABR Repl. by AUBERT 09L
$-0.19 \pm 0.11 \pm 0.02$	AUBERT	04Z	BABR Repl. by AUBERT,B 05G

 $A_{CP}(B^+ \rightarrow f_2(1270) \pi^+)$

VALUE	DOCUMENT ID	TECN	COMMENT
$0.41 \pm 0.25 \pm 0.18$ -0.15	AUBERT	09L	BABR $e^+ e^- \rightarrow \Upsilon(4S)$
••• We do not use the following data for averages, fits, limits, etc. •••			
$-0.004 \pm 0.247 \pm 0.028$	AUBERT,B	05G	BABR Repl. by AUBERT 09L
$-0.19 \pm 0.11 \pm 0.02$	AUBERT	04Z	BABR Repl. by AUBERT,B 05G

 $A_{CP}(B^+ \rightarrow \rho^0(1450) \pi^+)$

VALUE	DOCUMENT ID	TECN	COMMENT
$-0.06 \pm 0.28 \pm 0.23$ -0.40	AUBERT	09L	BABR $e^+ e^- \rightarrow \Upsilon(4S)$

 $A_{CP}(B^+ \rightarrow f_0(1370) \pi^+)$

VALUE	DOCUMENT ID	TECN	COMMENT
$0.72 \pm 0.15 \pm 0.16$	AUBERT	09L	BABR $e^+ e^- \rightarrow \Upsilon(4S)$

 $A_{CP}(B^+ \rightarrow \pi^+ \pi^- \pi^+ \text{ nonresonant})$

VALUE	DOCUMENT ID	TECN	COMMENT
$-0.14 \pm 0.14 \pm 0.18$ -0.08	AUBERT	09L	BABR $e^+ e^- \rightarrow \Upsilon(4S)$

 $A_{CP}(B^+ \rightarrow \rho^+ \pi^0)$

VALUE	DOCUMENT ID	TECN	COMMENT
0.02 ± 0.11 OUR AVERAGE			
$-0.01 \pm 0.13 \pm 0.02$	AUBERT	07x	BABR $e^+ e^- \rightarrow \Upsilon(4S)$
$0.06 \pm 0.17 \pm 0.04$	ZHANG	05A	BELL $e^+ e^- \rightarrow \Upsilon(4S)$
••• We do not use the following data for averages, fits, limits, etc. •••			
$0.24 \pm 0.16 \pm 0.06$	AUBERT	04Z	BABR Repl. by AUBERT 07x

 $A_{CP}(B^+ \rightarrow \rho^+ \rho^0)$

VALUE	DOCUMENT ID	TECN	COMMENT
-0.05 ± 0.05 OUR AVERAGE			
$-0.054 \pm 0.055 \pm 0.010$	AUBERT	09G	BABR $e^+ e^- \rightarrow \Upsilon(4S)$
$0.00 \pm 0.22 \pm 0.03$	ZHANG	03B	BELL $e^+ e^- \rightarrow \Upsilon(4S)$
••• We do not use the following data for averages, fits, limits, etc. •••			
$-0.12 \pm 0.13 \pm 0.10$	AUBERT,BE	06G	BABR Repl. by AUBERT 09G
$-0.19 \pm 0.23 \pm 0.03$	AUBERT	03v	BABR Repl. by AUBERT,BE 06G

 $A_{CP}(B^+ \rightarrow b_1^0 \pi^+)$

VALUE	DOCUMENT ID	TECN	COMMENT
$+0.05 \pm 0.16 \pm 0.02$	AUBERT	07B1	BABR $e^+ e^- \rightarrow \Upsilon(4S)$

 $A_{CP}(B^+ \rightarrow \omega \pi^+)$

VALUE	DOCUMENT ID	TECN	COMMENT
-0.04 ± 0.06 OUR AVERAGE			
$-0.02 \pm 0.08 \pm 0.01$	AUBERT	07AE	BABR $e^+ e^- \rightarrow \Upsilon(4S)$
$-0.02 \pm 0.09 \pm 0.01$	JEN	06	BELL $e^+ e^- \rightarrow \Upsilon(4S)$
-0.34 ± 0.25	¹ CHEN	00	CLE2 $e^+ e^- \rightarrow \Upsilon(4S)$
••• We do not use the following data for averages, fits, limits, etc. •••			
$-0.01 \pm 0.10 \pm 0.01$	AUBERT,B	06E	BABR Repl. by AUBERT 07AE
$0.03 \pm 0.16 \pm 0.01$	AUBERT	04H	BABR Repl. by AUBERT,B 06E
$0.50 \pm 0.23 \pm 0.02$	² WANG	04A	BELL Repl. by JEN 06
$-0.01 \pm 0.29 \pm 0.03$	³ AUBERT	02E	BABR Repl. by AUBERT 04H
¹ Corresponds to 90% confidence range $-0.75 < A_{CP} < 0.07$.			
² Corresponds to 90% CL interval $-0.25 < A_{CP} < 0.41$			
³ Corresponds to 90% confidence range $-0.50 < A_{CP} < 0.46$.			

 $A_{CP}(B^+ \rightarrow \omega \rho^+)$

VALUE	DOCUMENT ID	TECN	COMMENT
$-0.20 \pm 0.09 \pm 0.02$	AUBERT	09H	BABR $e^+ e^- \rightarrow \Upsilon(4S)$
••• We do not use the following data for averages, fits, limits, etc. •••			
$0.04 \pm 0.18 \pm 0.02$	AUBERT,B	06T	BABR Repl. by AUBERT 09H
$0.05 \pm 0.26 \pm 0.02$	AUBERT	05O	BABR Repl. by AUBERT,B 06T

 $A_{CP}(B^+ \rightarrow \eta \pi^+)$

VALUE	DOCUMENT ID	TECN	COMMENT
-0.13 ± 0.10 OUR AVERAGE			Error includes scale factor of 1.5.
$-0.03 \pm 0.09 \pm 0.03$	AUBERT	09AV	BABR $e^+ e^- \rightarrow \Upsilon(4S)$
$-0.23 \pm 0.09 \pm 0.02$	CHANG	07B	BELL $e^+ e^- \rightarrow \Upsilon(4S)$
••• We do not use the following data for averages, fits, limits, etc. •••			
$-0.08 \pm 0.10 \pm 0.01$	AUBERT	07AE	BABR Repl. by AUBERT 09AV
$-0.13 \pm 0.12 \pm 0.01$	AUBERT,B	05K	BABR Repl. by AUBERT 07AE
$0.07 \pm 0.15 \pm 0.03$	CHANG	05A	BELL Repl. by CHANG 07B
$-0.44 \pm 0.18 \pm 0.01$	AUBERT	04H	BABR Repl. by AUBERT,B 05K

 $A_{CP}(B^+ \rightarrow \eta' \pi^+)$

VALUE	DOCUMENT ID	TECN	COMMENT
0.06 ± 0.16 OUR AVERAGE			
$0.03 \pm 0.17 \pm 0.02$	AUBERT	09AV	BABR $e^+ e^- \rightarrow \Upsilon(4S)$
$0.20 \pm 0.37 \pm 0.04$	SCHUEMANN	06	BELL $e^+ e^- \rightarrow \Upsilon(4S)$
••• We do not use the following data for averages, fits, limits, etc. •••			
$0.21 \pm 0.17 \pm 0.01$	AUBERT	07AE	BABR Repl. by AUBERT 09AV
$0.14 \pm 0.16 \pm 0.01$	AUBERT,B	05K	BABR Repl. by AUBERT 07AE

 $A_{CP}(B^+ \rightarrow \eta \rho^+)$

VALUE	DOCUMENT ID	TECN	COMMENT
0.11 ± 0.11 OUR AVERAGE			
$0.13 \pm 0.11 \pm 0.02$	AUBERT	08AH	BABR $e^+ e^- \rightarrow \Upsilon(4S)$
$-0.04 \pm 0.34 \pm 0.01$	WANG	07B	BELL $e^+ e^- \rightarrow \Upsilon(4S)$
••• We do not use the following data for averages, fits, limits, etc. •••			
$0.02 \pm 0.18 \pm 0.02$	AUBERT,B	05K	BABR Repl. by AUBERT 08AH

 $A_{CP}(B^+ \rightarrow \eta' \rho^+)$

VALUE	DOCUMENT ID	TECN	COMMENT
$0.04 \pm 0.28 \pm 0.02$	¹ AUBERT	07E	BABR $e^+ e^- \rightarrow \Upsilon(4S)$
¹ Reports A_{CP} with the opposite sign convention.			

 $A_{CP}(B^+ \rightarrow \rho \bar{p} \pi^+)$

VALUE	DOCUMENT ID	TECN	COMMENT
0.00 ± 0.04 OUR AVERAGE			
$-0.02 \pm 0.05 \pm 0.02$	¹ WEI	08	BELL $e^+ e^- \rightarrow \Upsilon(4S)$
$+0.04 \pm 0.07 \pm 0.04$	AUBERT	07AV	BABR $e^+ e^- \rightarrow \Upsilon(4S)$
••• We do not use the following data for averages, fits, limits, etc. •••			
$-0.16 \pm 0.22 \pm 0.01$	WANG	04	BELL Repl. by WEI 08
¹ Requires $m_{p\bar{p}} < 2.85 \text{ GeV}/c^2$.			

 $A_{CP}(B^+ \rightarrow \rho \bar{p} K^+)$

VALUE	DOCUMENT ID	TECN	COMMENT
-0.16 ± 0.07 OUR AVERAGE			
$-0.17 \pm 0.10 \pm 0.02$	¹ WEI	08	BELL $e^+ e^- \rightarrow \Upsilon(4S)$
$-0.16 \pm 0.07 \pm 0.04$	¹ AUBERT,B	05L	BABR $e^+ e^- \rightarrow \Upsilon(4S)$
••• We do not use the following data for averages, fits, limits, etc. •••			
$-0.05 \pm 0.11 \pm 0.01$	WANG	04	BELL Repl. by WEI 08
¹ Requires $m_{p\bar{p}} < 2.85 \text{ GeV}/c^2$.			

 $A_{CP}(B^+ \rightarrow \rho \bar{p} K^*(892)^+)$

VALUE	DOCUMENT ID	TECN	COMMENT
0.21 ± 0.16 OUR AVERAGE			Error includes scale factor of 1.4.
$-0.01 \pm 0.19 \pm 0.02$	CHEN	08c	BELL $e^+ e^- \rightarrow \Upsilon(4S)$
$+0.32 \pm 0.13 \pm 0.05$	AUBERT	07AV	BABR $e^+ e^- \rightarrow \Upsilon(4S)$

Meson Particle Listings
B±

Table listing meson particles with columns for name, number, type, PRL reference, author(s), and classification. Includes entries like GOKHROO, IKADO, JEN, KUMAR, MOHAPATRA, etc.

¹³Data analyzed using inclusive $D/D^* \ell X$.

¹⁴Measured mean life using partially reconstructed $D^{*-} \pi^+ X$ vertices.

¹⁵ABREU 95q assumes $B(B^0 \rightarrow D^{*-} \ell^+ \nu_\ell) = 3.2 \pm 1.7\%$.

¹⁶Data analyzed using vertex-charge technique to tag B charge.

¹⁷AKERS 95T assumes $B(B^0 \rightarrow D_s^{(*)} D^0) = 5.0 \pm 0.9\%$ to find B^+/B^0 yield.

¹⁸AUBERT 03c uses a sample of approximately 14,000 exclusively reconstructed $B^0 \rightarrow D^*(2010)^- \ell \nu$ and simultaneously measures the lifetime and oscillation frequency.

¹⁹Combined result of $D/D^* \ell X$ analysis, fully reconstructed B analysis, and partially reconstructed $D^{*-} \pi^+ X$ analysis.

²⁰Combined ABREU 95q and ADAM 95 result.

²¹WAGNER 90 tagged B^0 mesons by their decays into $D^{*-} e^+ \nu$ and $D^{*-} \mu^+ \nu$ where the D^{*-} is tagged by its decay into $\pi^- \bar{D}^0$.

²²AVERRILL 89 is an estimate of the B^0 mean lifetime assuming that $B^0 \rightarrow D^{*+} X$ always.

MEAN LIFE RATIO τ_{B^+}/τ_{B^0}

τ_{B^+}/τ_{B^0} (direct measurements)

"OUR EVALUATION" is an average using rescaled values of the data listed below. The average and rescaling were performed by the Heavy Flavor Averaging Group (HFAG) and are described at <http://www.slac.stanford.edu/xorg/hfag/>. The averaging/rescaling procedure takes into account correlations between the measurements and asymmetric lifetime errors.

VALUE	EVTS	DOCUMENT ID	TECN	COMMENT
1.071 ± 0.009		OUR EVALUATION		
1.080 ± 0.016 ± 0.014		1 ABAZOV	05D D0	$p\bar{p}$ at 1.96 TeV
1.066 ± 0.008 ± 0.008		2 ABE	05B BELL	$e^+ e^- \rightarrow \Upsilon(4S)$
1.060 ± 0.021 ± 0.024		3 ABDALLAH	04E DLPH	$e^+ e^- \rightarrow Z$
1.093 ± 0.066 ± 0.028		4 ACOSTA	02C CDF	$p\bar{p}$ at 1.8 TeV
1.082 ± 0.026 ± 0.012		5 AUBERT	01F BABR	$e^+ e^- \rightarrow \Upsilon(4S)$
1.085 ± 0.059 ± 0.018		1 BARATE	00R ALEP	$e^+ e^- \rightarrow Z$
1.079 ± 0.064 ± 0.041		6 ABBIENDI	99J OPAL	$e^+ e^- \rightarrow Z$
1.110 ± 0.056 ± 0.033 -0.030		1 ABE	98Q CDF	$p\bar{p}$ at 1.8 TeV
1.09 ± 0.07 ± 0.03		6 ACCIARRI	98S L3	$e^+ e^- \rightarrow Z$
1.01 ± 0.07 ± 0.06		6 ABE	97J SLD	$e^+ e^- \rightarrow Z$
1.27 +0.23 +0.03 -0.19 -0.02		4 BUSKULIC	96J ALEP	$e^+ e^- \rightarrow Z$
1.00 +0.17 ± 0.10 -0.15		1,7 ABREU	95Q DLPH	$e^+ e^- \rightarrow Z$
1.06 +0.13 ± 0.10 -0.11		8 ADAM	95 DLPH	$e^+ e^- \rightarrow Z$
0.99 ± 0.14 +0.05 -0.04		1,9 AKERS	95T OPAL	$e^+ e^- \rightarrow Z$

••• We do not use the following data for averages, fits, limits, etc. •••

1.091 ± 0.023 ± 0.014		5 ABE	02H BELL	Repl. by ABE 05B
1.06 ± 0.07 ± 0.02		4 ABE	98B CDF	Repl. by ACOSTA 02c
1.01 ± 0.11 ± 0.02		1 ABE	96C CDF	Repl. by ABE 98Q
1.03 ± 0.08 ± 0.02		10 BUSKULIC	96J ALEP	$e^+ e^- \rightarrow Z$
0.98 ± 0.08 ± 0.03		1 BUSKULIC	96J ALEP	Repl. by BARATE 00R
1.02 ± 0.16 ± 0.05		4 ABE	94D CDF	Repl. by ABE 98B
1.11 +0.51 ± 0.11 -0.39		188 ABREU	93D DLPH	Sup. by ABREU 95q
1.01 +0.29 ± 0.12 -0.22		253 ABREU	93G DLPH	Sup. by ADAM 95
1.0 +0.33 ± 0.08 -0.25		130 ACTON	93C OPAL	Sup. by AKERS 95T
0.96 +0.19 ± 0.18 -0.15 -0.12		154 BUSKULIC	93D ALEP	Sup. by BUSKULIC 96J

¹Data analyzed using $D/D^* \mu X$ vertices.

²Measurement performed using a combined fit of CP -violation, mixing and lifetimes.

³Measurement performed using an inclusive reconstruction and B flavor identification technique.

⁴Measured using fully reconstructed decays.

⁵Events are selected in which one B meson is fully reconstructed while the second B meson is reconstructed inclusively.

⁶Data analyzed using charge of secondary vertex.

⁷ABREU 95q assumes $B(B^0 \rightarrow D^{*-} \ell^+ \nu_\ell) = 3.2 \pm 1.7\%$.

⁸Data analyzed using vertex-charge technique to tag B charge.

⁹AKERS 95T assumes $B(B^0 \rightarrow D_s^{(*)} D^0) = 5.0 \pm 0.9\%$ to find B^+/B^0 yield.

¹⁰Combined result of $D/D^* \ell X$ analysis and fully reconstructed B analysis.

τ_{B^+}/τ_{B^0} (inferred from branching fractions)

These measurements are inferred from the branching fractions for semileptonic decay or other spectator-dominated decays by assuming that the rates for such decays are equal for B^0 and B^+ . We do not use measurements which assume equal production of B^0 and B^+ because of the large uncertainty in the production ratio.

VALUE	CL%	EVTS	DOCUMENT ID	TECN	COMMENT
1.076 ± 0.034			OUR EVALUATION		
1.07 ± 0.04			OUR AVERAGE		
1.07 ± 0.04 ± 0.03			URQUIJO	07 BELL	$e^+ e^- \rightarrow \Upsilon(4S)$
1.067 ± 0.041 ± 0.033			AUBERT,B	06Y BABR	$e^+ e^- \rightarrow \Upsilon(4S)$

••• We do not use the following data for averages, fits, limits, etc. •••

0.95 +0.117 ± 0.091 -0.080		1 ARTUSO	97 CLE2	$e^+ e^- \rightarrow \Upsilon(4S)$
1.15 ± 0.17 ± 0.06		2 JESSOP	97 CLE2	$e^+ e^- \rightarrow \Upsilon(4S)$
0.93 ± 0.18 ± 0.12		3 ATHANAS	94 CLE2	Sup. by ARTUSO 97
0.91 ± 0.27 ± 0.21		4 ALBRECHT	92C ARG	$e^+ e^- \rightarrow \Upsilon(4S)$
1.0 ± 0.4		29 4,5 ALBRECHT	92G ARG	$e^+ e^- \rightarrow \Upsilon(4S)$
0.89 ± 0.19 ± 0.13		4 FULTON	91 CLEO	$e^+ e^- \rightarrow \Upsilon(4S)$
1.00 ± 0.23 ± 0.14		4 ALBRECHT	89L ARG	$e^+ e^- \rightarrow \Upsilon(4S)$
0.49 to 2.3	90	6 BEAN	87B CLEO	$e^+ e^- \rightarrow \Upsilon(4S)$

¹ARTUSO 97 uses partial reconstruction of $B \rightarrow D^* \ell \nu_\ell$ and independent of B^0 and B^+ production fraction.

²Assumes equal production of B^+ and B^0 at the $\Upsilon(4S)$.

³ATHANAS 94 uses events tagged by fully reconstructed B^- decays and partially or fully reconstructed B^0 decays.

⁴Assumes equal production of B^0 and B^+ .

⁵ALBRECHT 92G data analyzed using $B \rightarrow D_s \bar{D}, D_s \bar{D}^*, D_s^* \bar{D}, D_s^* \bar{D}^*$ events.

⁶BEAN 87B assume the fraction of $B^0 \bar{B}^0$ events at the $\Upsilon(4S)$ is 0.41.

$\text{sgn}(\text{Re}(\lambda_{CP})) \Delta \Gamma_{B_d^0} / \Gamma_{B_d^0}$

$\Gamma_{B_d^0}$ and $\Delta \Gamma_{B_d^0}$ are the decay rate average and difference between two B_d^0 CP eigenstates (light – heavy). The λ_{CP} characterizes B^0 and \bar{B}^0 decays to states of charmonium plus K_L^0 , see the review on “ CP Violation” in the reviews section.

"OUR EVALUATION" is an average using rescaled values of the data listed below. The average and rescaling were performed by the Heavy Flavor Averaging Group (HFAG) and are described at <http://www.slac.stanford.edu/xorg/hfag/>. The averaging/rescaling procedure takes into account correlations between the measurements.

VALUE	DOCUMENT ID	TECN	COMMENT
0.010 ± 0.037	OUR EVALUATION		
0.008 ± 0.037 ± 0.018	1 AUBERT,B	04C BABR	$e^+ e^- \rightarrow \Upsilon(4S)$

¹Corresponds to 90% confidence range $[-0.084, 0.068]$.

$|\Delta \Gamma_{B_d^0}| / \Gamma_{B_d^0}$

VALUE	CL%	DOCUMENT ID	TECN	COMMENT
< 0.18		95 1 ABDALLAH	03B DLPH	$e^+ e^- \rightarrow Z$

The data in this block is included in the average printed for a previous datablock.

••• We do not use the following data for averages, fits, limits, etc. •••

< 0.80	95	2,3 BEHRENS	00B CLE2	$e^+ e^- \rightarrow \Upsilon(4S)$
--------	----	-------------	----------	------------------------------------

¹Using the measured $\tau_{B^0} = 1.55 \pm 0.03$ ps.

²BEHRENS 00B uses high-momentum lepton tags and partially reconstructed $\bar{B}^0 \rightarrow D^{*+} \pi^-, \rho^-$ decays to determine the flavor of the B meson.

³Assumes $\Delta m_d = 0.478 \pm 0.018$ ps^{-1} and $\tau_{B^0} = 1.548 \pm 0.032$ ps.

B^0 DECAY MODES

\bar{B}^0 modes are charge conjugates of the modes below. Reactions indicate the weak decay vertex and do not include mixing. Modes which do not identify the charge state of the B are listed in the B^\pm/B^0 ADMIXTURE section.

The branching fractions listed below assume 50% $B^0 \bar{B}^0$ and 50% $B^+ B^-$ production at the $\Upsilon(4S)$. We have attempted to bring older measurements up to date by rescaling their assumed $\Upsilon(4S)$ production ratio to 50:50 and their assumed D, D_s, D^* , and ψ branching ratios to current values whenever this would affect our averages and best limits significantly.

Indentation is used to indicate a subchannel of a previous reaction. All resonant subchannels have been corrected for resonance branching fractions to the final state so the sum of the subchannel branching fractions can exceed that of the final state.

For inclusive branching fractions, e.g., $B \rightarrow D^\pm$ anything, the values usually are multiplicities, not branching fractions. They can be greater than one.

Mode	Fraction (Γ_i/Γ)	Scale factor/ Confidence level
Γ_1 $\ell^+ \nu_\ell$ anything	[a] (10.33 ± 0.28) %	
Γ_2 $e^+ \nu_e X_c$	(10.1 ± 0.4) %	
Γ_3 $D \ell^+ \nu_\ell$ anything	(9.3 ± 0.9) %	
Γ_4 $D^- \ell^+ \nu_\ell$	[a] (2.17 ± 0.12) %	
Γ_5 $D^- \tau^+ \nu_\tau$	(1.1 ± 0.4) %	
Γ_6 $D^*(2010)^- \ell^+ \nu_\ell$	[a] (5.01 ± 0.12) %	
Γ_7 $D^*(2010)^- \tau^+ \nu_\tau$	(1.5 ± 0.5) %	S=1.3
Γ_8 $\bar{D}^0 \pi^- \ell^+ \nu_\ell$	(4.3 ± 0.6) × 10 ⁻³	

Meson Particle Listings

 B^0

Γ_9	$D_0^*(2400)^- \ell^+ \nu_\ell \times$ $B(D_0^{*-} \rightarrow \bar{D}^0 \pi^-)$	$(3.0 \pm 1.2) \times 10^{-3}$	S=1.8	Γ_{66}	$\bar{D}_s^*(2460)^- \rho^+$	< 4.9	$\times 10^{-3}$	CL=90%
Γ_{10}	$D_2^*(2460)^- \ell^+ \nu_\ell \times$ $B(D_2^{*-} \rightarrow \bar{D}^0 \pi^-)$	$(2.2 \pm 0.6) \times 10^{-3}$		Γ_{67}	$D_0^0 \bar{D}^0$	< 4.3	$\times 10^{-5}$	CL=90%
Γ_{11}	$\bar{D}^{(*)} n \pi \ell^+ \nu_\ell (n \geq 1)$	$(2.3 \pm 0.5) \%$		Γ_{68}	$D^{*0} \bar{D}^0$	< 2.9	$\times 10^{-4}$	CL=90%
Γ_{12}	$\bar{D}^{*0} \pi^- \ell^+ \nu_\ell$	$(4.9 \pm 0.8) \times 10^{-3}$		Γ_{69}	$D^- D^+$	$(2.11 \pm 0.31) \times 10^{-4}$		S=1.2
Γ_{13}	$D_1(2420)^- \ell^+ \nu_\ell \times$ $B(D_1^- \rightarrow \bar{D}^{*0} \pi^-)$	$(2.80 \pm 0.28) \times 10^{-3}$		Γ_{70}	$D^- D_s^+$	$(7.2 \pm 0.8) \times 10^{-3}$		
Γ_{14}	$D_1'(2430)^- \ell^+ \nu_\ell \times$ $B(D_1'^- \rightarrow \bar{D}^{*0} \pi^-)$	$(3.1 \pm 0.9) \times 10^{-3}$		Γ_{71}	$D^*(2010)^- D_s^+$	$(8.0 \pm 1.1) \times 10^{-3}$		
Γ_{15}	$D_2^*(2460)^- \ell^+ \nu_\ell \times$ $B(D_2^{*-} \rightarrow \bar{D}^{*0} \pi^-)$	$(1.2 \pm 0.5) \times 10^{-3}$	S=2.7	Γ_{72}	$D^- D_s^{*+}$	$(7.4 \pm 1.6) \times 10^{-3}$		
Γ_{16}	$\rho^- \ell^+ \nu_\ell$	[a] $(2.47 \pm 0.33) \times 10^{-4}$		Γ_{73}	$D^*(2010)^- D_s^{*+}$	$(1.77 \pm 0.14) \%$		
Γ_{17}	$\pi^- \ell^+ \nu_\ell$	[a] $(1.34 \pm 0.08) \times 10^{-4}$		Γ_{74}	$D_{s0}(2317)^- K^+ \times$ $B(D_{s0}(2317)^- \rightarrow D_s^- \pi^0)$	$(4.2 \pm 1.4) \times 10^{-5}$		
Γ_{18}	$\pi^- \mu^+ \nu_\mu$			Γ_{75}	$D_{s0}(2317)^- \pi^+ \times$ $B(D_{s0}(2317)^- \rightarrow D_s^- \pi^0)$	< 2.5	$\times 10^{-5}$	CL=90%
Inclusive modes				Γ_{76}	$D_{sJ}(2457)^- K^+ \times$ $B(D_{sJ}(2457)^- \rightarrow D_s^- \pi^0)$	< 9.4	$\times 10^{-6}$	CL=90%
Γ_{19}	K^\pm anything	$(78 \pm 8) \%$		Γ_{77}	$D_{sJ}(2457)^- \pi^+ \times$ $B(D_{sJ}(2457)^- \rightarrow D_s^- \pi^0)$	< 4.0	$\times 10^{-6}$	CL=90%
Γ_{20}	$D^0 X$	$(8.1 \pm 1.5) \%$		Γ_{78}	$D_s^- D_s^+$	< 3.6	$\times 10^{-5}$	CL=90%
Γ_{21}	$\bar{D}^0 X$	$(47.4 \pm 2.8) \%$		Γ_{79}	$D_s^{*-} D_s^+$	< 1.3	$\times 10^{-4}$	CL=90%
Γ_{22}	$D^+ X$	< 3.9	CL=90%	Γ_{80}	$D_s^- D_s^{*+}$	< 2.4	$\times 10^{-4}$	CL=90%
Γ_{23}	$D^- X$	$(36.9 \pm 3.3) \%$		Γ_{81}	$D_{s0}(2317)^+ D^- \times$ $B(D_{s0}(2317)^+ \rightarrow D_s^+ \pi^0)$	(9.7 ± 4.0)	$\times 10^{-4}$	S=1.5
Γ_{24}	$D_s^+ X$	(10.3 ± 2.1)		Γ_{82}	$D_{s0}(2317)^+ D^- \times$ $B(D_{s0}(2317)^+ \rightarrow D_s^+ \gamma)$	< 9.5	$\times 10^{-4}$	CL=90%
Γ_{25}	$D_s^- X$	< 2.6	CL=90%	Γ_{83}	$D_{s0}(2317)^+ D^*(2010)^- \times$ $B(D_{s0}(2317)^+ \rightarrow D_s^+ \pi^0)$	$(1.5 \pm 0.6) \times 10^{-3}$		
Γ_{26}	$\Lambda_c^+ X$	< 3.1	CL=90%	Γ_{84}	$D_{sJ}(2457)^+ D^-$	$(3.5 \pm 1.1) \times 10^{-3}$		
Γ_{27}	$\bar{\Lambda}_c^- X$	(5.0 ± 2.1)		Γ_{85}	$D_{sJ}(2457)^+ D^- \times$ $B(D_{sJ}(2457)^+ \rightarrow D_s^+ \gamma)$	(6.5 ± 1.7)	$\times 10^{-4}$	
Γ_{28}	$\bar{c} X$	$(95 \pm 5) \%$		Γ_{86}	$D_{sJ}(2457)^+ D^- \times$ $B(D_{sJ}(2457)^+ \rightarrow D_s^+ \gamma)$	< 6.0	$\times 10^{-4}$	CL=90%
Γ_{29}	$c X$	$(24.6 \pm 3.1) \%$		Γ_{87}	$D_{sJ}(2457)^+ D^- \times$ $B(D_{sJ}(2457)^+ \rightarrow D_s^+ \pi^-)$	< 2.0	$\times 10^{-4}$	CL=90%
Γ_{30}	$\bar{c} c X$	$(119 \pm 6) \%$		Γ_{88}	$D_{sJ}(2457)^+ D^- \times$ $B(D_{sJ}(2457)^+ \rightarrow D_s^+ \pi^0)$	< 3.6	$\times 10^{-4}$	CL=90%
D, D*, or D_s modes				Γ_{89}	$D^*(2010)^- D_{sJ}(2457)^+$	$(9.3 \pm 2.2) \times 10^{-3}$		
Γ_{31}	$D^- \pi^+$	$(2.68 \pm 0.13) \times 10^{-3}$		Γ_{90}	$D_{sJ}(2457)^+ D^*(2010) \times$ $B(D_{sJ}(2457)^+ \rightarrow D_s^+ \gamma)$	(2.3 ± 0.9)	$\times 10^{-3}$	
Γ_{32}	$D^- \rho^+$	$(7.6 \pm 1.3) \times 10^{-3}$		Γ_{91}	$D^- D_{s1}(2536)^+ \times$ $B(D_{s1}(2536)^+ \rightarrow D^{*0} K^+)$	$(1.7 \pm 0.6) \times 10^{-4}$		
Γ_{33}	$D^- K^0 \pi^+$	$(4.9 \pm 0.9) \times 10^{-4}$		Γ_{92}	$D^*(2010)^- D_{s1}(2536)^+ \times$ $B(D_{s1}(2536)^+ \rightarrow D^{*0} K^+)$	$(3.3 \pm 1.1) \times 10^{-4}$		
Γ_{34}	$D^- K^*(892)^+$	$(4.5 \pm 0.7) \times 10^{-4}$		Γ_{93}	$D^- D_{s1}(2536)^+ \times$ $B(D_{s1}(2536)^+ \rightarrow D^{*+} K^0)$	$(2.6 \pm 1.1) \times 10^{-4}$		
Γ_{35}	$D^- \omega \pi^+$	$(2.8 \pm 0.6) \times 10^{-3}$		Γ_{94}	$D^{*-} D_{s1}(2536)^+ \times$ $B(D_{s1}(2536)^+ \rightarrow D^{*+} K^0)$	$(5.0 \pm 1.7) \times 10^{-4}$		
Γ_{36}	$D^- K^+$	$(2.0 \pm 0.6) \times 10^{-4}$		Γ_{95}	$D^- D_{sJ}(2573)^+ \times$ $B(D_{sJ}(2573)^+ \rightarrow D^0 K^+)$	< 1	$\times 10^{-4}$	CL=90%
Γ_{37}	$D^- K^+ \bar{K}^0$	< 3.1	CL=90%	Γ_{96}	$D^*(2010)^- D_{sJ}(2573)^+ \times$ $B(D_{sJ}(2573)^+ \rightarrow D^0 K^+)$	< 2	$\times 10^{-4}$	CL=90%
Γ_{38}	$D^- K^+ \bar{K}^*(892)^0$	$(8.8 \pm 1.9) \times 10^{-4}$		Γ_{97}	$D_s^+ \pi^-$	$(2.4 \pm 0.4) \times 10^{-5}$		
Γ_{39}	$\bar{D}^0 \pi^+ \pi^-$	$(8.4 \pm 0.9) \times 10^{-4}$		Γ_{98}	$D_s^{*+} \pi^-$	$(2.1 \pm 0.4) \times 10^{-5}$		S=1.4
Γ_{40}	$D^*(2010)^- \pi^+$	$(2.76 \pm 0.13) \times 10^{-3}$		Γ_{99}	$D_s^+ \rho^-$	< 2.4	$\times 10^{-5}$	CL=90%
Γ_{41}	$D^- \pi^+ \pi^+ \pi^-$	$(8.0 \pm 2.5) \times 10^{-3}$		Γ_{100}	$D_s^{*+} \rho^-$	$(4.1 \pm 1.3) \times 10^{-5}$		
Γ_{42}	$(D^- \pi^+ \pi^+ \pi^-)$ nonresonant	$(3.9 \pm 1.9) \times 10^{-3}$		Γ_{101}	$D_s^+ a_0^-$	< 1.9	$\times 10^{-5}$	CL=90%
Γ_{43}	$D^- \pi^+ \rho^0$	$(1.1 \pm 1.0) \times 10^{-3}$		Γ_{102}	$D_s^{*+} a_0^-$	< 3.6	$\times 10^{-5}$	CL=90%
Γ_{44}	$D^- a_1(1260)^+$	$(6.0 \pm 3.3) \times 10^{-3}$		Γ_{103}	$D_s^{*+} a_1(1260)^-$	< 2.1	$\times 10^{-3}$	CL=90%
Γ_{45}	$D^*(2010)^- \pi^+ \pi^0$	$(1.5 \pm 0.5) \%$		Γ_{104}	$D_s^{*+} a_1(1260)^-$	< 1.7	$\times 10^{-3}$	CL=90%
Γ_{46}	$D^*(2010)^- \rho^+$	$(6.8 \pm 0.9) \times 10^{-3}$		Γ_{105}	$D_s^+ a_2^-$	< 1.9	$\times 10^{-4}$	CL=90%
Γ_{47}	$D^*(2010)^- K^+$	$(2.14 \pm 0.16) \times 10^{-4}$		Γ_{106}	$D_s^{*+} a_2^-$	< 2.0	$\times 10^{-4}$	CL=90%
Γ_{48}	$D^*(2010)^- K^0 \pi^+$	$(3.0 \pm 0.8) \times 10^{-4}$		Γ_{107}	$D_s^- K^+$	$(3.0 \pm 0.4) \times 10^{-5}$		
Γ_{49}	$D^*(2010)^- K^* (892)^+$	$(3.3 \pm 0.6) \times 10^{-4}$		Γ_{108}	$D_s^{*-} K^+$	$(2.19 \pm 0.30) \times 10^{-5}$		
Γ_{50}	$D^*(2010)^- K^+ \bar{K}^0$	< 4.7	CL=90%	Γ_{109}	$D_s^- K^*(892)^+$	$(3.5 \pm 1.0) \times 10^{-5}$		
Γ_{51}	$D^*(2010)^- K^+ \bar{K}^*(892)^0$	$(1.29 \pm 0.33) \times 10^{-3}$		Γ_{110}	$D_s^{*-} K^*(892)^+$	(3.2 ± 1.5)	$\times 10^{-5}$	
Γ_{52}	$D^*(2010)^- \pi^+ \pi^+ \pi^-$	$(7.0 \pm 0.8) \times 10^{-3}$		Γ_{111}	$D_s^- \pi^+ K^0$	$(1.10 \pm 0.33) \times 10^{-4}$		
Γ_{53}	$(D^*(2010)^- \pi^+ \pi^+ \pi^-)$ non-resonant	$(0.0 \pm 2.5) \times 10^{-3}$	S=1.3	Γ_{112}	$D_s^{*-} \pi^+ K^0$	< 1.10	$\times 10^{-4}$	CL=90%
Γ_{54}	$D^*(2010)^- \pi^+ \rho^0$	$(5.7 \pm 3.2) \times 10^{-3}$		Γ_{113}	$D_s^- \pi^+ K^*(892)^0$	< 3.0	$\times 10^{-3}$	CL=90%
Γ_{55}	$D^*(2010)^- a_1(1260)^+$	$(1.30 \pm 0.27) \%$		Γ_{114}	$D_s^{*-} \pi^+ K^*(892)^0$	< 1.6	$\times 10^{-3}$	CL=90%
Γ_{56}	$D^*(2010)^- \pi^+ \pi^+ \pi^- \pi^0$	$(1.76 \pm 0.27) \%$						
Γ_{57}	$D^{*-} 3\pi^+ 2\pi^-$	$(4.7 \pm 0.9) \times 10^{-3}$						
Γ_{58}	$\bar{D}^*(2010)^- \omega \pi^+$	$(2.89 \pm 0.30) \times 10^{-3}$						
Γ_{59}	$D_1(2430)^0 \omega \times$ $B(D_1(2430)^0 \rightarrow D^{*-} \pi^+)$	$(4.1 \pm 1.6) \times 10^{-4}$						
Γ_{60}	$\bar{D}^{*-} \pi^+$	[b] $(2.1 \pm 1.0) \times 10^{-3}$						
Γ_{61}	$D_1(2420)^- \pi^+ \times B(D_1^- \rightarrow$ $D^- \pi^+ \pi^-)$	(8.9 ± 2.3)						
Γ_{62}	$D_1(2420)^- \pi^+ \times B(D_1^- \rightarrow$ $D^{*-} \pi^+ \pi^-)$	< 3.3	CL=90%					
Γ_{63}	$\bar{D}_2^*(2460)^- \pi^+ \times$ $B(D_2^*(2460)^- \rightarrow D^0 \pi^-)$	$(2.15 \pm 0.35) \times 10^{-4}$						
Γ_{64}	$\bar{D}_0^*(2400)^- \pi^+ \times$ $B(D_0^*(2400)^- \rightarrow D^0 \pi^-)$	$(6.0 \pm 3.0) \times 10^{-5}$						
Γ_{65}	$D_2^*(2460)^- \pi^+ \times B((D_2^*)^- \rightarrow$ $D^{*-} \pi^+ \pi^-)$	< 2.4	CL=90%					

Baryon modes

Γ_{366}	$\rho\bar{p}$	< 1.1	$\times 10^{-7}$	CL=90%
Γ_{367}	$\rho\bar{p}\pi^+\pi^-$	< 2.5	$\times 10^{-4}$	CL=90%
Γ_{368}	$\rho\bar{p}K^0$	(2.66 ± 0.32)	$\times 10^{-6}$	
Γ_{369}	$\Theta(1540)^+\bar{p} \times B(\Theta(1540)^+ \rightarrow [h] \rho K_S^0)$	< 5	$\times 10^{-8}$	CL=90%
Γ_{370}	$f_J(2220)K^0 \times B(f_J(2220) \rightarrow \rho\bar{p})$	< 4.5	$\times 10^{-7}$	CL=90%
Γ_{371}	$\rho\bar{p}K^*(892)^0$	(1.24 \pm $\frac{0.28}{0.25}$)	$\times 10^{-6}$	
Γ_{372}	$f_J(2220)K_0^* \times B(f_J(2220) \rightarrow \rho\bar{p})$	< 1.5	$\times 10^{-7}$	CL=90%
Γ_{373}	$\rho\bar{p}\pi^-$	(3.14 ± 0.29)	$\times 10^{-6}$	
Γ_{374}	$\rho\bar{\Sigma}^-(1385)^-$	< 2.6	$\times 10^{-7}$	CL=90%
Γ_{375}	$\Delta^0\bar{\Lambda}$	< 9.3	$\times 10^{-7}$	CL=90%
Γ_{376}	$\rho\bar{\Lambda}K^-$	< 8.2	$\times 10^{-7}$	CL=90%
Γ_{377}	$\rho\bar{\Sigma}^0\pi^-$	< 3.8	$\times 10^{-6}$	CL=90%
Γ_{378}	$\bar{\Lambda}\Lambda$	< 3.2	$\times 10^{-7}$	CL=90%
Γ_{379}	$\bar{\Lambda}\Lambda K^0$	(4.8 \pm $\frac{1.0}{0.9}$)	$\times 10^{-6}$	
Γ_{380}	$\bar{\Lambda}\Lambda K^{*0}$	(2.5 \pm $\frac{0.9}{0.8}$)	$\times 10^{-6}$	
Γ_{381}	$\bar{\Lambda}\Lambda D^0$	(1.1 \pm $\frac{0.6}{0.5}$)	$\times 10^{-5}$	
Γ_{382}	$\Delta^0\bar{\Delta}^0$	< 1.5	$\times 10^{-3}$	CL=90%
Γ_{383}	$\Delta^{++}\bar{\Delta}^{--}$	< 1.1	$\times 10^{-4}$	CL=90%
Γ_{384}	$\bar{D}^0\rho\bar{p}$	(1.14 ± 0.09)	$\times 10^{-4}$	
Γ_{385}	$D_s^-\bar{\Lambda}p$	(2.8 ± 0.9)	$\times 10^{-5}$	
Γ_{386}	$\bar{D}^*(2007)^0\rho\bar{p}$	(1.03 ± 0.13)	$\times 10^{-4}$	
Γ_{387}	$D^*(2010)^-\rho\bar{\pi}$	(1.5 ± 0.4)	$\times 10^{-3}$	
Γ_{388}	$D^-\rho\bar{p}\pi^+$	(3.38 ± 0.32)	$\times 10^{-4}$	
Γ_{389}	$D^*(2010)^-\rho\bar{p}\pi^+$	(5.0 ± 0.5)	$\times 10^{-4}$	
Γ_{390}	$\Theta_c\bar{p}\pi^+ \times B(\Theta_c \rightarrow D^-\rho)$	< 9	$\times 10^{-6}$	CL=90%
Γ_{391}	$\Theta_c\bar{p}\pi^+ \times B(\Theta_c \rightarrow D^{*-}\rho)$	< 1.4	$\times 10^{-5}$	CL=90%
Γ_{392}	$\bar{\Sigma}_c^{--}\Delta^{++}$	< 1.0	$\times 10^{-3}$	CL=90%
Γ_{393}	$\bar{\Lambda}_c^-\rho\pi^+\pi^-$	(1.3 ± 0.4)	$\times 10^{-3}$	
Γ_{394}	$\bar{\Lambda}_c^-\rho$	(2.0 ± 0.4)	$\times 10^{-5}$	
Γ_{395}	$\bar{\Lambda}_c^-\rho\pi^0$	< 5.9	$\times 10^{-4}$	CL=90%
Γ_{396}	$\bar{\Lambda}_c^-\rho\pi^+\pi^-\pi^0$	< 5.07	$\times 10^{-3}$	CL=90%
Γ_{397}	$\bar{\Lambda}_c^-\rho\pi^+\pi^-\pi^+\pi^-$	< 2.74	$\times 10^{-3}$	CL=90%
Γ_{398}	$\bar{\Lambda}_c^-\rho\pi^+\pi^-$	(1.12 ± 0.32)	$\times 10^{-3}$	
Γ_{399}	$\bar{\Lambda}_c^-\rho\pi^+\pi^-$ (nonresonant)	(6.4 ± 1.9)	$\times 10^{-4}$	
Γ_{400}	$\bar{\Sigma}_c(2520)^{--}\rho\pi^+$	(1.2 ± 0.4)	$\times 10^{-4}$	
Γ_{401}	$\bar{\Sigma}_c(2520)^0\rho\pi^-$	< 3.8	$\times 10^{-5}$	CL=90%
Γ_{402}	$\bar{\Sigma}_c(2455)^0\rho\pi^-$	(1.5 ± 0.5)	$\times 10^{-4}$	
Γ_{403}	$\bar{\Sigma}_c(2455)^0N^0 \times B(N^0 \rightarrow \rho\pi^-)$	(8.0 ± 2.9)	$\times 10^{-5}$	
Γ_{404}	$\bar{\Sigma}_c(2455)^{--}\rho\pi^+$	(2.2 ± 0.7)	$\times 10^{-4}$	
Γ_{405}	$\bar{\Lambda}_c^-pK^+\pi^-$	(4.3 ± 1.4)	$\times 10^{-5}$	
Γ_{406}	$\bar{\Sigma}_c(2455)^{--}pK^+ \times B(\bar{\Sigma}_c^{--} \rightarrow \bar{\Lambda}_c^-\pi^-)$	(1.1 ± 0.4)	$\times 10^{-5}$	
Γ_{407}	$\bar{\Lambda}_c^-pK^*(892)^0$	< 2.42	$\times 10^{-5}$	CL=90%
Γ_{408}	$\bar{\Lambda}_c^-\Lambda_c^+$	< 6.2	$\times 10^{-5}$	CL=90%
Γ_{409}	$\bar{\Lambda}_c^-(2593)^- / \bar{\Lambda}_c^-(2625)^-\rho$	< 1.1	$\times 10^{-4}$	CL=90%
Γ_{410}	$\bar{\Xi}_c^-\Lambda_c^+ \times B(\bar{\Xi}_c^- \rightarrow \bar{\Xi}^-\pi^-\pi^-)$	(2.2 ± 2.3)	$\times 10^{-5}$	S=1.9
Γ_{411}	$\Lambda_c^+\Lambda_c^-K^0$	(5.4 ± 3.2)	$\times 10^{-4}$	

Lepton Family number (LF) violating modes, or $\Delta B = 1$ weak neutral current (BI) modes

Γ_{412}	$\gamma\gamma$	B1	< 6.2	$\times 10^{-7}$	CL=90%
Γ_{413}	e^+e^-	B1	< 8.3	$\times 10^{-8}$	CL=90%
Γ_{414}	$e^+e^-\gamma$	B1	< 1.2	$\times 10^{-7}$	CL=90%
Γ_{415}	$\mu^+\mu^-$	B1	< 1.5	$\times 10^{-8}$	CL=90%
Γ_{416}	$\mu^+\mu^-\gamma$	B1	< 1.6	$\times 10^{-7}$	CL=90%
Γ_{417}	$\tau^+\tau^-$	B1	< 4.1	$\times 10^{-3}$	CL=90%
Γ_{418}	$\pi^0\ell^+\ell^-$	B1	< 1.2	$\times 10^{-7}$	CL=90%
Γ_{419}	$\pi^0e^+e^-$	B1	< 1.4	$\times 10^{-7}$	CL=90%
Γ_{420}	$\pi^0\mu^+\mu^-$	B1	< 1.8	$\times 10^{-7}$	CL=90%
Γ_{421}	$\pi^0\nu\bar{\nu}$	B1	< 2.2	$\times 10^{-4}$	CL=90%
Γ_{422}	$K^0\ell^+\ell^-$	B1	[a] (3.1 \pm $\frac{0.8}{0.7}$)	$\times 10^{-7}$	
Γ_{423}	$K^0e^+e^-$	B1	(1.6 \pm $\frac{1.0}{0.8}$)	$\times 10^{-7}$	
Γ_{424}	$K^0\mu^+\mu^-$	B1	(4.5 \pm $\frac{1.2}{1.0}$)	$\times 10^{-7}$	
Γ_{425}	$K^0\nu\bar{\nu}$	B1	< 1.6	$\times 10^{-4}$	CL=90%
Γ_{426}	$\rho^0\nu\bar{\nu}$	B1	< 4.4	$\times 10^{-4}$	CL=90%

Γ_{427}	$K^*(892)^0\ell^+\ell^-$	B1	[a] (9.9 \pm $\frac{1.2}{1.1}$)	$\times 10^{-7}$	
Γ_{428}	$K^*(892)^0e^+e^-$	B1	(1.03 \pm $\frac{0.19}{0.17}$)	$\times 10^{-6}$	
Γ_{429}	$K^*(892)^0\mu^+\mu^-$	B1	(1.05 \pm $\frac{0.16}{0.13}$)	$\times 10^{-6}$	
Γ_{430}	$K^*(892)^0\nu\bar{\nu}$	B1	< 1.2	$\times 10^{-4}$	CL=90%
Γ_{431}	$\phi\nu\bar{\nu}$	B1	< 5.8	$\times 10^{-5}$	CL=90%
Γ_{432}	$e^\pm\mu^\mp$	LF	[g] < 6.4	$\times 10^{-8}$	CL=90%
Γ_{433}	$\pi^0e^\pm\mu^\mp$	LF	< 1.4	$\times 10^{-7}$	CL=90%
Γ_{434}	$K^0e^\pm\mu^\mp$	LF	< 2.7	$\times 10^{-7}$	CL=90%
Γ_{435}	$K^*(892)^0e^+\mu^-$	LF	< 5.3	$\times 10^{-7}$	CL=90%
Γ_{436}	$K^*(892)^0e^-\mu^+$	LF	< 3.4	$\times 10^{-7}$	CL=90%
Γ_{437}	$K^*(892)^0e^\pm\mu^\mp$	LF	< 5.8	$\times 10^{-7}$	CL=90%
Γ_{438}	$e^\pm\tau^\mp$	LF	[g] < 2.8	$\times 10^{-5}$	CL=90%
Γ_{439}	$\mu^\pm\tau^\mp$	LF	[g] < 2.2	$\times 10^{-5}$	CL=90%
Γ_{440}	invisible	B1	< 2.2	$\times 10^{-4}$	CL=90%
Γ_{441}	$\nu\bar{\nu}\gamma$	B1	< 4.7	$\times 10^{-5}$	CL=90%

[a] An ℓ indicates an e or a μ mode, not a sum over these modes.

[b] \bar{D}^{**} represents an excited state with mass $2.2 < M < 2.8$ GeV/ c^2 .

[c] $X(3872)^+$ is a hypothetical charged partner of the $X(3872)$.

[d] Stands for the possible candidates of $K^*(1410)$, $K_0^*(1430)$ and $K_2^*(1430)$.

[e] B^0 and B_S^0 contributions not separated. Limit is on weighted average of the two decay rates.

[f] This decay refers to the coherent sum of resonant and nonresonant $J^P = 0^+ K\pi$ components with $1.60 < m_{K\pi} < 2.15$ GeV/ c^2 .

[g] The value is for the sum of the charge states or particle/antiparticle states indicated.

[h] $\Theta(1540)^+$ denotes a possible narrow pentaquark state.

B^0 BRANCHING RATIOS

For branching ratios in which the charge of the decaying B is not determined, see the B^\pm section.

$\Gamma(\ell^+\nu_\ell anything)/\Gamma_{total}$ Γ_1/Γ
 "OUR EVALUATION" is an average using rescaled values of the data listed below. The average and rescaling were performed by the Heavy Flavor Averaging Group (HFAG) and are described at <http://www.slac.stanford.edu/xorg/hfag/>. The averaging/rescaling procedure takes into account correlations between the measurements.

VALUE (units 10^{-2})	DOCUMENT ID	TECN	COMMENT
10.33 ± 0.28 OUR EVALUATION	Error includes scale factor of 1.1.		
10.46 ± 0.30 ± 0.23	1 URQUIJO	07 BELL	$e^+e^- \rightarrow \Upsilon(4S)$
9.64 ± 0.27 ± 0.33	2 AUBERT,B	06Y BABR	$e^+e^- \rightarrow \Upsilon(4S)$
10.78 ± 0.60 ± 0.69	3 ARTUSO	97 CLE2	$e^+e^- \rightarrow \Upsilon(4S)$
9.3 ± 1.1 ± 1.5	ALBRECHT	94 ARG	$e^+e^- \rightarrow \Upsilon(4S)$
9.9 ± 3.0 ± 0.9	HENDERSON	92 CLEO	$e^+e^- \rightarrow \Upsilon(4S)$
10.32 ± 0.36 ± 0.35	4 OKABE	05 BELL	Repl. by URQUIJO 07
10.9 ± 0.7 ± 1.1	ATHANAS	94 CLE2	Sup. by ARTUSO 97

- • • We do not use the following data for averages, fits, limits, etc. • • •
- 1 URQUIJO 07 report a measurement of $(9.80 \pm 0.29 \pm 0.21)\%$ for the partial branching fraction of $B \rightarrow e\nu_e X_c$ decay with electron energy above 0.6 GeV. We converted the result to $B \rightarrow e\nu_e X$ branching fraction.
- 2 The measurements are obtained for charged and neutral B mesons partial rates of semileptonic decay to electrons with momentum above 0.6 GeV/ c in the B rest frame. The best precision on the ratio is achieved for a momentum threshold of 1.0 GeV: $B(B^+ \rightarrow e^+\nu_e X) / B(B^0 \rightarrow e^+\nu_e X) = 1.074 \pm 0.041 \pm 0.026$.
- 3 ARTUSO 97 uses partial reconstruction of $B \rightarrow D^*\ell\nu_\ell$ and inclusive semileptonic branching ratio from BARISH 96B $(0.1049 \pm 0.0017 \pm 0.0043)$.
- 4 The measurements are obtained for charged and neutral B mesons partial rates of semileptonic decay to electrons with momentum above 0.6 GeV/ c in the B rest frame, and their ratio of $B(B^+ \rightarrow e^+\nu_e X)/B(B^0 \rightarrow e^+\nu_e X) = 1.08 \pm 0.05 \pm 0.02$.

$\Gamma(e^+\nu_e X_c)/\Gamma_{total}$ Γ_2/Γ

VALUE (units 10^{-2})	DOCUMENT ID	TECN	COMMENT
10.08 ± 0.30 ± 0.22	1 URQUIJO	07 BELL	$e^+e^- \rightarrow \Upsilon(4S)$

1 Measure the independent B^+ and B^0 partial branching fractions with electron threshold energies of 0.4 GeV.

$\Gamma(D^-\ell^+\nu_\ell)/\Gamma_{total}$ Γ_4/Γ

ℓ denotes e or μ , not the sum.

"OUR EVALUATION" is an average using rescaled values of the data listed below. The average and rescaling were performed by the Heavy Flavor Averaging Group (HFAG) and are described at <http://www.slac.stanford.edu/xorg/hfag/>. The averaging/rescaling procedure takes into account correlations between the measurements.

Meson Particle Listings

 B^0

VALUE DOCUMENT ID TECN COMMENT

0.0217 ± 0.0012 OUR EVALUATION

0.0218 ± 0.0012 OUR AVERAGE

VALUE	DOCUMENT ID	TECN	COMMENT
0.0221 ± 0.0011 ± 0.0011	¹ AUBERT	10 BABR	$e^+e^- \rightarrow \Upsilon(4S)$
0.0213 ± 0.0012 ± 0.0039	02E BELL	$e^+e^- \rightarrow \Upsilon(4S)$	
0.0209 ± 0.0013 ± 0.0018	² BARTELT	99 CLE2	$e^+e^- \rightarrow \Upsilon(4S)$
0.0235 ± 0.0020 ± 0.0044	³ BUSKULIC	97 ALEP	$e^+e^- \rightarrow Z$

• • • We do not use the following data for averages, fits, limits, etc. • • •

0.0221 ± 0.0011 ± 0.0012	¹ AUBERT	08Q BABR	Repl. by AUBERT 10
0.0187 ± 0.0015 ± 0.0032	⁴ ATHANAS	97 CLE2	Repl. by BARTELT 99
0.018 ± 0.006 ± 0.003	⁵ FULTON	91 CLEO	$e^+e^- \rightarrow \Upsilon(4S)$
0.020 ± 0.007 ± 0.006	⁶ ALBRECHT	89J ARG	$e^+e^- \rightarrow \Upsilon(4S)$

- Uses a fully reconstructed B meson as a tag on the recoil side.
- Assumes equal production of B^+ and B^0 at the $\Upsilon(4S)$.
- BUSKULIC 97 assumes fraction (B^+) = fraction (B^0) = (37.8 ± 2.2)% and PDG 96 values for B lifetime and branching ratio of D^* and D decays.
- ATHANAS 97 uses missing energy and missing momentum to reconstruct neutrino.
- FULTON 91 assumes assuming equal production of B^0 and B^+ at the $\Upsilon(4S)$ and uses Mark III D and D^* branching ratios.
- ALBRECHT 89J reports 0.018 ± 0.006 ± 0.005. We rescale using the method described in STONE 94 but with the updated PDG 94 $B(D^0 \rightarrow K^-\pi^+)$.

$\Gamma(D^-\ell^+\nu_\ell)/\Gamma(\ell^+\nu_\ell\text{anything})$ Γ_4/Γ_1

VALUE	DOCUMENT ID	TECN	COMMENT
0.230 ± 0.011 ± 0.011	¹ AUBERT	10 BABR	$e^+e^- \rightarrow \Upsilon(4S)$

- Uses a fully reconstructed B meson on the recoil side.

$\Gamma(D^-\ell^+\nu_\ell)/\Gamma(D\ell^+\nu_\ell\text{anything})$ Γ_4/Γ_3

VALUE	DOCUMENT ID	TECN	COMMENT
0.215 ± 0.016 ± 0.013	¹ AUBERT	07AN BABR	$e^+e^- \rightarrow \Upsilon(4S)$

- Uses a fully reconstructed B meson on the recoil side.

$\Gamma(D^-\tau^+\nu_\tau)/\Gamma_{\text{total}}$ Γ_5/Γ

VALUE (units 10^{-2})	DOCUMENT ID	TECN	COMMENT
• • • We do not use the following data for averages, fits, limits, etc. • • •			
1.04 ± 0.35 ± 0.18	¹ AUBERT	08N BABR	Repl. by AUBERT 09s

- Uses a fully reconstructed B meson as a tag on the recoil side.

$\Gamma(D^-\tau^+\nu_\tau)/\Gamma(D^-\ell^+\nu_\ell)$ Γ_5/Γ_4

VALUE	DOCUMENT ID	TECN	COMMENT
0.489 ± 0.165 ± 0.069	¹ AUBERT	09s BABR	$e^+e^- \rightarrow \Upsilon(4S)$

- Uses a fully reconstructed B meson as a tag on the recoil side.

$\Gamma(D^*(2010)^-\ell^+\nu_\ell)/\Gamma_{\text{total}}$ Γ_6/Γ

"OUR EVALUATION" is an average using rescaled values of the data listed below. The average and rescaling were performed by the Heavy Flavor Averaging Group (HFAG) and are described at <http://www.slac.stanford.edu/xorg/hfag/>. The averaging/rescaling procedure takes into account correlations between the measurements.

VALUE	EVS	DOCUMENT ID	TECN	COMMENT
0.0501 ± 0.0012 OUR EVALUATION				
0.0524 ± 0.0022 OUR FIT				Error includes scale factor of 1.4.
0.0523 ± 0.0022 OUR AVERAGE				Error includes scale factor of 1.4. See the ideogram below.

0.0549 ± 0.0016 ± 0.0025	¹ AUBERT	08Q BABR	$e^+e^- \rightarrow \Upsilon(4S)$
0.0469 ± 0.0004 ± 0.0034	² AUBERT	08R BABR	$e^+e^- \rightarrow \Upsilon(4S)$
0.0590 ± 0.0022 ± 0.0050	³ ABDALLAH	04D DLPH	$e^+e^- \rightarrow Z^0$
0.0609 ± 0.0019 ± 0.0040	⁴ ADAM	03 CLE2	$e^+e^- \rightarrow \Upsilon(4S)$
0.0459 ± 0.0023 ± 0.0040	⁵ ABE	02F BELL	$e^+e^- \rightarrow \Upsilon(4S)$
0.0470 ± 0.0013 ± $\frac{0.0036}{-0.0031}$	⁶ ABREU	01H DLPH	$e^+e^- \rightarrow Z$
0.0526 ± 0.0020 ± 0.0046	⁷ ABBIENDI	00Q OPAL	$e^+e^- \rightarrow Z$
0.0553 ± 0.0026 ± 0.0052	⁸ BUSKULIC	97 ALEP	$e^+e^- \rightarrow Z$

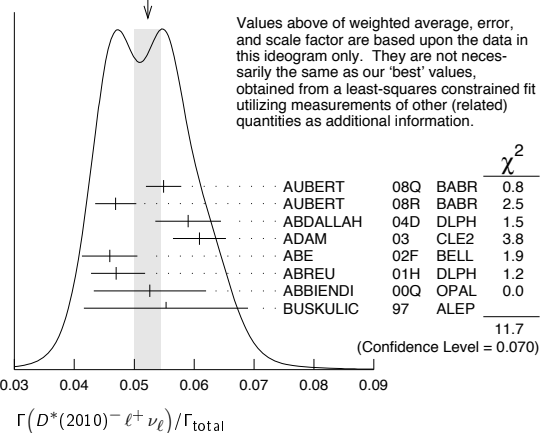
• • • We do not use the following data for averages, fits, limits, etc. • • •

0.0490 ± 0.0007 ± $\frac{0.0036}{-0.0035}$	³ AUBERT	05E BABR	Repl. by AUBERT 08r
0.0539 ± 0.0011 ± 0.0034	⁹ ABDALLAH	04D DLPH	$e^+e^- \rightarrow Z^0$
0.0609 ± 0.0019 ± 0.0040	¹⁰ BRIERE	02 CLE2	$e^+e^- \rightarrow \Upsilon(4S)$
0.0508 ± 0.0021 ± 0.0066	¹¹ ACKERSTAFF	97G OPAL	Repl. by ABBIENDI 00q

0.0552 ± 0.0017 ± 0.0068	¹² ABREU	96P DLPH	Repl. by ABREU 01H
0.0449 ± 0.0032 ± 0.0039	¹³ BARISH	95 CLE2	Repl. by ADAM 03
0.0518 ± 0.0030 ± 0.0062	¹⁴ BUSKULIC	95N ALEP	Sup. by BUSKULIC 97
0.045 ± 0.003 ± 0.004	¹⁵ ALBRECHT	94 ARG	$e^+e^- \rightarrow \Upsilon(4S)$
0.047 ± 0.005 ± 0.005	¹⁶ ALBRECHT	93 ARG	$e^+e^- \rightarrow \Upsilon(4S)$
seen	¹⁷ SANGHERA	93 CLE2	$e^+e^- \rightarrow \Upsilon(4S)$
0.070 ± 0.018 ± 0.014	¹⁸ ANTREASYAN	90B CBAL	$e^+e^- \rightarrow \Upsilon(4S)$
0.060 ± 0.010 ± 0.014	¹⁹ ALBRECHT	89C ARG	$e^+e^- \rightarrow \Upsilon(4S)$
0.040 ± 0.004 ± 0.006	²⁰ ALBRECHT	89J ARG	$e^+e^- \rightarrow \Upsilon(4S)$
0.070 ± 0.012 ± 0.019	²¹ BORTOLETTO	89B CLEO	$e^+e^- \rightarrow \Upsilon(4S)$
	²² ALBRECHT	87J ARG	$e^+e^- \rightarrow \Upsilon(4S)$

- Uses a fully reconstructed B meson as a tag on the recoil side.
- Measured using fully reconstructed D^* sample and a simultaneous fit to the Caprini-Lellouch-Neubert form factor parameters: $\rho^2 = 1.191 \pm 0.048 \pm 0.028$, $R_1(1) = 1.429 \pm 0.061 \pm 0.044$, and $R_2(1) = 0.827 \pm 0.038 \pm 0.022$.
- Measured using fully reconstructed D^* sample.
- Uses the combined fit of both $B^0 \rightarrow D^*(2010)^-\ell\nu$ and $B^+ \rightarrow \bar{D}^*(2007)^0\ell\nu$ samples.
- Assumes equal production of B^+ and B^0 at the $\Upsilon(4S)$.
- ABREU 01H measured using about 5000 partial reconstructed D^* sample.
- ABBIENDI 00Q assumes the fraction $B(b \rightarrow B^0) = (39.7 \pm 1.8) \pm 2.2\%$. This result is an average of two methods using exclusive and partial D^* reconstruction.
- BUSKULIC 97 assumes fraction (B^+) = fraction (B^0) = (37.8 ± 2.2)% and PDG 96 values for B lifetime and D^* and D branching fractions.
- Combines with previous partial reconstructed D^* measurement.
- The results are based on the same analysis and data sample reported in ADAM 03.
- ACKERSTAFF 97G assumes fraction (B^+) = fraction (B^0) = (37.8 ± 2.2)% and PDG 96 values for B lifetime and branching ratio of D^* and D decays.
- ABREU 96P result is the average of two methods using exclusive and partial D^* reconstruction.
- BARISH 95 use $B(D^0 \rightarrow K^-\pi^+) = (3.91 \pm 0.08 \pm 0.17)\%$ and $B(D^{*+} \rightarrow D^0\pi^+) = (68.1 \pm 1.0 \pm 1.3)\%$.
- BUSKULIC 95N assumes fraction (B^+) = fraction (B^0) = 38.2 ± 1.3 ± 2.2% and $\tau_{B^0} = 1.58 \pm 0.06$ ps. $\Gamma(D^{*-}\ell^+\nu_\ell)/\text{total} = [5.18 - 0.13(\text{fraction}(B^0) - 38.2) - 1.5(\tau_{B^0} - 1.58)]\%$.
- ALBRECHT 94 assumes $B(D^{*+} \rightarrow D^0\pi^+) = 68.1 \pm 1.0 \pm 1.3\%$. Uses partial reconstruction of D^{*+} and is independent of D^0 branching ratios.
- ALBRECHT 93 reports 0.052 ± 0.005 ± 0.006. We rescale using the method described in STONE 94 but with the updated PDG 94 $B(D^0 \rightarrow K^-\pi^+)$. We have taken their average e and μ value. They also obtain $\alpha = 2 * \Gamma^0 / (\Gamma^- + \Gamma^+) - 1 = 1.1 \pm 0.4 \pm 0.2$, $A_{FB} = 3/4 * (\Gamma^- - \Gamma^+) / \Gamma = 0.2 \pm 0.08 \pm 0.06$ and a value of $|V_{cb}| = 0.036 - 0.045$ depending on model assumptions.
- Combining $\bar{D}^{*0}\ell^+\nu_\ell$ and $\bar{D}^{*-}\ell^+\nu_\ell$ SANGHERA 93 test $V-A$ structure and fit the decay angular distributions to obtain $A_{FB} = 3/4 * (\Gamma^- - \Gamma^+) / \Gamma = 0.14 \pm 0.06 \pm 0.03$. Assuming a value of V_{cb} , they measure V, A_1 , and A_2 , the three form factors for the $D^*\ell\nu_\ell$ decay, where results are slightly dependent on model assumptions.
- ANTREASYAN 90B is average over B and $\bar{D}^*(2010)$ charge states.
- The measurement of ALBRECHT 89C suggests a D^* polarization γ_L/γ_T of 0.85 ± 0.45, or $\alpha = 0.7 \pm 0.9$.
- ALBRECHT 89J is ALBRECHT 87J value rescaled using $B(D^*(2010)^- \rightarrow D^0\pi^-) = 0.57 \pm 0.04 \pm 0.04$. Superseded by ALBRECHT 93.
- We have taken average of the the BORTOLETTO 89b values for electrons and muons, 0.046 ± 0.005 ± 0.007. We rescale using the method described in STONE 94 but with the updated PDG 94 $B(D^0 \rightarrow K^-\pi^+)$. The measurement suggests a D^* polarization parameter value $\alpha = 0.65 \pm 0.66 \pm 0.25$.
- ALBRECHT 87J assume $\mu-e$ universality, the $B(\Upsilon(4S) \rightarrow B^0\bar{B}^0) = 0.45$, the $B(D^0 \rightarrow K^-\pi^+) = (0.042 \pm 0.004 \pm 0.004)$, and the $B(D^*(2010)^- \rightarrow D^0\pi^-) = 0.49 \pm 0.08$. Superseded by ALBRECHT 89J.

WEIGHTED AVERAGE
0.0523 ± 0.0022 (Error scaled by 1.4)



$\Gamma(D^*(2010)^-\ell^+\nu_\ell)/\Gamma(D\ell^+\nu_\ell\text{anything})$ Γ_6/Γ_3

VALUE	DOCUMENT ID	TECN	COMMENT
0.537 ± 0.031 ± 0.036	¹ AUBERT	07AN BABR	$e^+e^- \rightarrow \Upsilon(4S)$

- Uses a fully reconstructed B meson on the recoil side.

$\Gamma(D^*(2010)^-\tau^+\nu_\tau)/\Gamma_{\text{total}}$ Γ_7/Γ

VALUE (units 10^{-2})	DOCUMENT ID	TECN	COMMENT
1.5 ± 0.5 OUR FIT			Error includes scale factor of 1.3.
2.02 ± $\frac{0.49}{-0.37}$ ± 0.37	¹ MATYJA	07 BELL	$e^+e^- \rightarrow \Upsilon(4S)$

- • • We do not use the following data for averages, fits, limits, etc. • • •
- | | | | |
|--------------------|---------------------|----------|---------------------|
| 1.11 ± 0.51 ± 0.06 | ² AUBERT | 08N BABR | Repl. by AUBERT 09s |
|--------------------|---------------------|----------|---------------------|
- Observed in the recoil of the accompanying B meson.
 - Uses a fully reconstructed B meson as a tag on the recoil side.

• • • We do not use the following data for averages, fits, limits, etc. • • •

2.86 ± 0.20 ± 0.08		1,7 AUBERT,B	04o	BABR	Repl. by AUBERT 07h
2.8 ± 0.4 ± 0.1	81	8 ALAM	94	CLE2	Repl. by AHMED 02b
3.1 ± 1.3 ± 1.0	7	5 ALBRECHT	88k	ARG	$e^+e^- \rightarrow \Upsilon(4S)$

- ¹ Assumes equal production of B^+ and B^0 at the $\Upsilon(4S)$.
² Uses a missing-mass method. Does not depend on D branching fractions or B^+/B^0 production rates.
³ AHMED 02b reports an additional uncertainty on the branching ratios to account for 4.5% uncertainty on relative production of B^0 and B^+ , which is not included here.
⁴ BORTOLETTO 92 assumes equal production of B^+ and B^0 at the $\Upsilon(4S)$ and uses Mark III branching fractions for the D .
⁵ ALBRECHT 88k assumes $B^0\bar{B}^0:B^+B^-$ production ratio is 45:55. Superseded by ALBRECHT 90j which assumes 50:50.
⁶ BEBEK 87 value has been updated in BERKELMAN 91 to use same assumptions as noted for BORTOLETTO 92.
⁷ AUBERT,B 04o reports $[\Gamma(B^0 \rightarrow D^-\pi^+)/\Gamma_{\text{total}}] \times [B(D^+ \rightarrow K_S^0\pi^+)] = (42.7 \pm 2.1 \pm 2.2) \times 10^{-6}$ which we divide by our best value $B(D^+ \rightarrow K_S^0\pi^+) = (1.49 \pm 0.04) \times 10^{-2}$. Our first error is their experiment's error and our second error is the systematic error from using our best value.
⁸ ALAM 94 reports $[\Gamma(B^0 \rightarrow D^-\pi^+)/\Gamma_{\text{total}}] \times [B(D^+ \rightarrow K^-2\pi^+)] = (0.265 \pm 0.032 \pm 0.023) \times 10^{-3}$ which we divide by our best value $B(D^+ \rightarrow K^-2\pi^+) = (9.4 \pm 0.4) \times 10^{-2}$. Our first error is their experiment's error and our second error is the systematic error from using our best value. Assumes equal production of B^+ and B^0 at the $\Upsilon(4S)$.

$\Gamma(D^- \ell^+ \nu_\ell)/\Gamma(D^- \pi^+)$ Γ_4/Γ_{31}

VALUE	DOCUMENT ID	TECN	COMMENT
9.9 ± 1.0 ± 0.9	AALTONEN	09E	CDF $p\bar{p}$ at 1.96 TeV

$\Gamma(D^- \rho^+)/\Gamma_{\text{total}}$ Γ_{32}/Γ

VALUE	EVTs	DOCUMENT ID	TECN	COMMENT
0.0076 ± 0.0013 OUR AVERAGE				
0.0075 ± 0.0013 ± 0.0003	79	1 ALAM	94	CLE2 $e^+e^- \rightarrow \Upsilon(4S)$
0.009 ± 0.005 ± 0.003	9	2 ALBRECHT	90j	ARG $e^+e^- \rightarrow \Upsilon(4S)$

- • • We do not use the following data for averages, fits, limits, etc. • • •
- | | | | | | |
|-----------------------|---|------------|-----|-----|-----------------------------------|
| 0.022 ± 0.012 ± 0.009 | 6 | 2 ALBRECHT | 88k | ARG | $e^+e^- \rightarrow \Upsilon(4S)$ |
|-----------------------|---|------------|-----|-----|-----------------------------------|
- ¹ ALAM 94 reports $[\Gamma(B^0 \rightarrow D^-\rho^+)/\Gamma_{\text{total}}] \times [B(D^+ \rightarrow K^-2\pi^+)] = 0.000704 \pm 0.000096 \pm 0.000070$ which we divide by our best value $B(D^+ \rightarrow K^-2\pi^+) = (9.4 \pm 0.4) \times 10^{-2}$. Our first error is their experiment's error and our second error is the systematic error from using our best value. Assumes equal production of B^+ and B^0 at the $\Upsilon(4S)$.
² ALBRECHT 88k assumes $B^0\bar{B}^0:B^+B^-$ production ratio is 45:55. Superseded by ALBRECHT 90j which assumes 50:50.

$\Gamma(D^- K^0\pi^+)/\Gamma_{\text{total}}$ Γ_{33}/Γ

VALUE (units 10^{-4})	DOCUMENT ID	TECN	COMMENT
4.9 ± 0.7 ± 0.5	1 AUBERT,BE	05b	BABR $e^+e^- \rightarrow \Upsilon(4S)$

- ¹ Assumes equal production of B^+ and B^0 at the $\Upsilon(4S)$.

$\Gamma(D^- K^*(892)^+)/\Gamma_{\text{total}}$ Γ_{34}/Γ

VALUE (units 10^{-4})	DOCUMENT ID	TECN	COMMENT
4.5 ± 0.7 OUR AVERAGE			
4.6 ± 0.6 ± 0.5	1 AUBERT,BE	05b	BABR $e^+e^- \rightarrow \Upsilon(4S)$
3.7 ± 1.5 ± 1.0	1 MAHAPATRA	02	CLE2 $e^+e^- \rightarrow \Upsilon(4S)$

- ¹ Assumes equal production of B^+ and B^0 at the $\Upsilon(4S)$.

$\Gamma(D^- \omega\pi^+)/\Gamma_{\text{total}}$ Γ_{35}/Γ

VALUE	DOCUMENT ID	TECN	COMMENT
0.0028 ± 0.0005 ± 0.0004	1 ALEXANDER	01b	CLE2 $e^+e^- \rightarrow \Upsilon(4S)$

- ¹ Assumes equal production of B^+ and B^0 at the $\Upsilon(4S)$. The signal is consistent with all observed $\omega\pi^+$ having proceeded through the ρ^+ resonance at mass $1349 \pm 25^{+10}_{-5}$ MeV and width $547 \pm 86^{+46}_{-45}$ MeV.

$\Gamma(D^- K^+)/\Gamma_{\text{total}}$ Γ_{36}/Γ

VALUE	DOCUMENT ID	TECN	COMMENT
(2.04 ± 0.50 ± 0.27) × 10⁻⁴	1 ABE	01i	BELL $e^+e^- \rightarrow \Upsilon(4S)$

- ¹ ABE 01i reports $B(B^0 \rightarrow D^-K^+)/B(B^0 \rightarrow D^-\pi^+) = 0.068 \pm 0.015 \pm 0.007$. We multiply by our best value $B(B^0 \rightarrow D^-\pi^+) = (3.0 \pm 0.4) \times 10^{-3}$. Our first error is their experiment's error and the second error is systematic error from using our best value.

$\Gamma(D^- K^+\bar{K}^0)/\Gamma_{\text{total}}$ Γ_{37}/Γ

VALUE (units 10^{-4})	CL%	DOCUMENT ID	TECN	COMMENT
<3.1	90	1 DRUTSKOY	02	BELL $e^+e^- \rightarrow \Upsilon(4S)$

- ¹ Assumes equal production of B^+ and B^0 at the $\Upsilon(4S)$.

$\Gamma(D^- K^+\bar{K}^*(892)^0)/\Gamma_{\text{total}}$ Γ_{38}/Γ

VALUE (units 10^{-4})	DOCUMENT ID	TECN	COMMENT
8.8 ± 1.1 ± 1.5	1 DRUTSKOY	02	BELL $e^+e^- \rightarrow \Upsilon(4S)$

- ¹ Assumes equal production of B^+ and B^0 at the $\Upsilon(4S)$.

$\Gamma(D^0\pi^+\pi^-)/\Gamma_{\text{total}}$ Γ_{39}/Γ

VALUE (units 10^{-4})	CL% EVTS	DOCUMENT ID	TECN	COMMENT
8.4 ± 0.4 ± 0.8		1 KUZMIN	07	BELL $e^+e^- \rightarrow \Upsilon(4S)$

- • • We do not use the following data for averages, fits, limits, etc. • • •
- | | | | | |
|-----------------|----|----------------|-------------|---|
| 8.0 ± 0.6 ± 1.5 | | 1,2 SATPATHY | 03 | BELL Repl. by KUZMIN 07 |
| < 16 | 90 | 1 ALAM | 94 | CLE2 $e^+e^- \rightarrow \Upsilon(4S)$ |
| < 70 | 90 | 3 BORTOLETTO92 | CLEO | $e^+e^- \rightarrow \Upsilon(4S)$ |
| < 340 | 90 | 4 BEBEK | 87 | CLEO $e^+e^- \rightarrow \Upsilon(4S)$ |
| 700 ± 500 | | 5 | 5 BEHRENDTS | 83 CLEO $e^+e^- \rightarrow \Upsilon(4S)$ |

- ¹ Assumes equal production of B^+ and B^0 at the $\Upsilon(4S)$.
² No assumption about the intermediate mechanism is made in the analysis.
³ BORTOLETTO 92 assumes equal production of B^+ and B^0 at the $\Upsilon(4S)$ and uses Mark III branching fractions for the D . The product branching fraction into $D_S^*(2340)\pi$ followed by $D_S^*(2340) \rightarrow D^0\pi$ is < 0.0001 at 90% CL and into $D_S^*(2460)$ followed by $D_S^*(2460) \rightarrow D^0\pi$ is < 0.0004 at 90% CL.
⁴ BEBEK 87 assumes the $\Upsilon(4S)$ decays 43% to $B^0\bar{B}^0$. We rescale to 50%. $B(D^0 \rightarrow K^-\pi^+) = (4.2 \pm 0.4 \pm 0.4)\%$ and $B(D^0 \rightarrow K^-\pi^+\pi^-\pi^-) = (9.1 \pm 0.8 \pm 0.8)\%$ were used.
⁵ Corrected by us using assumptions: $B(D^0 \rightarrow K^-\pi^+) = (0.042 \pm 0.006)$ and $B(\Upsilon(4S) \rightarrow B^0\bar{B}^0) = 50\%$. The product branching ratio is $B(B^0 \rightarrow \bar{D}^0\pi^+\pi^-)B(\bar{D}^0 \rightarrow K^+\pi^-) = (0.39 \pm 0.26) \times 10^{-2}$.

$\Gamma(D^*(2010)^-\pi^+)/\Gamma_{\text{total}}$ Γ_{40}/Γ

VALUE (units 10^{-3})	EVTs	DOCUMENT ID	TECN	COMMENT
2.76 ± 0.13 OUR AVERAGE				
2.79 ± 0.08 ± 0.17		1 AUBERT	07h	BABR $e^+e^- \rightarrow \Upsilon(4S)$
2.7 ± 0.4 ± 0.1		2,3 AUBERT,BE	06j	BABR $e^+e^- \rightarrow \Upsilon(4S)$
2.81 ± 0.24 ± 0.05		4 BRANDENB...	98	CLE2 $e^+e^- \rightarrow \Upsilon(4S)$
2.6 ± 0.3 ± 0.4	82	5 ALAM	94	CLE2 $e^+e^- \rightarrow \Upsilon(4S)$
3.37 ± 0.96 ± 0.02		6 BORTOLETTO92	CLEO	$e^+e^- \rightarrow \Upsilon(4S)$
2.36 ± 0.88 ± 0.02	12	7 ALBRECHT	90j	ARG $e^+e^- \rightarrow \Upsilon(4S)$
2.36 ± 1.50 ± 1.10 ± 0.02	5	8 BEBEK	87	CLEO $e^+e^- \rightarrow \Upsilon(4S)$

- • • We do not use the following data for averages, fits, limits, etc. • • •
- | | | | | |
|-----------------|----|-------------|-----|--|
| 10 ± 4 ± 1 | 8 | 9 AKERS | 94j | OPAL $e^+e^- \rightarrow Z$ |
| 2.7 ± 1.4 ± 1.0 | 5 | 10 ALBRECHT | 87c | ARG $e^+e^- \rightarrow \Upsilon(4S)$ |
| 3.5 ± 2 ± 2 | | 11 ALBRECHT | 86f | ARG $e^+e^- \rightarrow \Upsilon(4S)$ |
| 17 ± 5 ± 5 | 41 | 12 GILES | 84 | CLEO $e^+e^- \rightarrow \Upsilon(4S)$ |

- ¹ Assumes equal production of B^+ and B^0 at the $\Upsilon(4S)$.
² AUBERT,BE 06j reports $[\Gamma(B^0 \rightarrow D^*(2010)^-\pi^+)/\Gamma_{\text{total}}] / [B(B^0 \rightarrow D^-\pi^+)] = 0.99 \pm 0.11 \pm 0.08$ which we multiply by our best value $B(B^0 \rightarrow D^-\pi^+) = (2.68 \pm 0.13) \times 10^{-3}$. Our first error is their experiment's error and our second error is the systematic error from using our best value.
³ Uses a missing-mass method. Does not depend on D branching fractions or B^+/B^0 production rates.
⁴ BRANDENBURG 98 assume equal production of B^+ and B^0 at $\Upsilon(4S)$ and use the D^* reconstruction technique. The first error is their experiment's error and the second error is the systematic error from the PDG 96 value of $B(D^* \rightarrow D\pi)$.
⁵ ALAM 94 assume equal production of B^+ and B^0 at the $\Upsilon(4S)$ and use the CLEO II $B(D^*(2010)^+ \rightarrow D^0\pi^+)$ and absolute $B(D^0 \rightarrow K^-\pi^+)$ and the PDG 1992 $B(D^0 \rightarrow K^-\pi^+\pi^0)/B(D^0 \rightarrow K^-\pi^+)$ and $B(D^0 \rightarrow K^-2\pi^+\pi^-)/B(D^0 \rightarrow K^-\pi^+)$.
⁶ BORTOLETTO 92 reports $(4.0 \pm 1.0 \pm 0.7) \times 10^{-3}$ from a measurement of $[\Gamma(B^0 \rightarrow D^*(2010)^-\pi^+)/\Gamma_{\text{total}}] \times [B(D^*(2010)^+ \rightarrow D^0\pi^+)]$ assuming $B(D^*(2010)^+ \rightarrow D^0\pi^+) = 0.57 \pm 0.06$, which we rescale to our best value $B(D^*(2010)^+ \rightarrow D^0\pi^+) = (67.7 \pm 0.5) \times 10^{-2}$. Our first error is their experiment's error and our second error is the systematic error from using our best value. Assumes equal production of B^+ and B^0 at the $\Upsilon(4S)$ and uses Mark III branching fractions for the D .
⁷ ALBRECHT 90j reports $(2.8 \pm 0.9 \pm 0.6) \times 10^{-3}$ from a measurement of $[\Gamma(B^0 \rightarrow D^*(2010)^-\pi^+)/\Gamma_{\text{total}}] \times [B(D^*(2010)^+ \rightarrow D^0\pi^+)]$ assuming $B(D^*(2010)^+ \rightarrow D^0\pi^+) = 0.57 \pm 0.06$, which we rescale to our best value $B(D^*(2010)^+ \rightarrow D^0\pi^+) = (67.7 \pm 0.5) \times 10^{-2}$. Our first error is their experiment's error and our second error is the systematic error from using our best value. Assumes equal production of B^+ and B^0 at the $\Upsilon(4S)$ and uses Mark III branching fractions for the D .
⁸ BEBEK 87 reports $(2.8^{+1.5+1.0}_{-1.2-0.6}) \times 10^{-3}$ from a measurement of $[\Gamma(B^0 \rightarrow D^*(2010)^-\pi^+)/\Gamma_{\text{total}}] \times [B(D^*(2010)^+ \rightarrow D^0\pi^+)]$ assuming $B(D^*(2010)^+ \rightarrow D^0\pi^+) = 0.57 \pm 0.06$, which we rescale to our best value $B(D^*(2010)^+ \rightarrow D^0\pi^+) = (67.7 \pm 0.5) \times 10^{-2}$. Our first error is their experiment's error and our second error is the systematic error from using our best value. Updated in BERKELMAN 91 to use same assumptions as noted for BORTOLETTO 92 and ALBRECHT 90j.
⁹ Assumes $B(Z \rightarrow b\bar{b}) = 0.217$ and 38% B_d production fraction.
¹⁰ ALBRECHT 87c use PDG 86 branching ratios for D and $D^*(2010)$ and assume $B(\Upsilon(4S) \rightarrow B^+B^-) = 55\%$ and $B(\Upsilon(4S) \rightarrow B^0\bar{B}^0) = 45\%$. Superseded by ALBRECHT 90j.
¹¹ ALBRECHT 86f uses pseudomass that is independent of D^0 and D^+ branching ratios.
¹² Assumes $B(D^*(2010)^+ \rightarrow D^0\pi^+) = 0.60^{+0.08}_{-0.15}$. Assumes $B(\Upsilon(4S) \rightarrow B^0\bar{B}^0) = 0.40 \pm 0.02$ Does not depend on D branching ratios.

$\Gamma(D^*(2010)^-\ell^+\nu_\ell)/\Gamma(D^*(2010)^-\pi^+)$ Γ_6/Γ_{40}

VALUE	DOCUMENT ID	TECN	COMMENT
16.5 ± 2.3 ± 1.1	AALTONEN	09E	CDF $p\bar{p}$ at 1.96 TeV

Meson Particle Listings

 B^0

$\Gamma(D^-\pi^+\pi^-\pi^-)/\Gamma_{\text{total}}$ Γ_{41}/Γ
 VALUE DOCUMENT ID TECN COMMENT

0.0080 ± 0.0021 ± 0.0014 ¹BORTOLETTO92 CLEO $e^+e^- \rightarrow \Upsilon(4S)$
¹BORTOLETTO 92 assumes equal production of B^+ and B^0 at the $\Upsilon(4S)$ and uses MarkIII branching fractions for the D .

$\Gamma((D^-\pi^+\pi^+\pi^-) \text{ nonresonant})/\Gamma_{\text{total}}$ Γ_{42}/Γ
 VALUE DOCUMENT ID TECN COMMENT

0.0039 ± 0.0014 ± 0.0013 ¹BORTOLETTO92 CLEO $e^+e^- \rightarrow \Upsilon(4S)$
¹BORTOLETTO 92 assumes equal production of B^+ and B^0 at the $\Upsilon(4S)$ and uses MarkIII branching fractions for the D .

$\Gamma(D^-\pi^+\rho^0)/\Gamma_{\text{total}}$ Γ_{43}/Γ
 VALUE DOCUMENT ID TECN COMMENT

0.0011 ± 0.0009 ± 0.0004 ¹BORTOLETTO92 CLEO $e^+e^- \rightarrow \Upsilon(4S)$
¹BORTOLETTO 92 assumes equal production of B^+ and B^0 at the $\Upsilon(4S)$ and uses MarkIII branching fractions for the D .

$\Gamma(D^-\rho_1(1260)^+)/\Gamma_{\text{total}}$ Γ_{44}/Γ
 VALUE DOCUMENT ID TECN COMMENT

0.0060 ± 0.0022 ± 0.0024 ¹BORTOLETTO92 CLEO $e^+e^- \rightarrow \Upsilon(4S)$
¹BORTOLETTO 92 assumes equal production of B^+ and B^0 at the $\Upsilon(4S)$ and uses MarkIII branching fractions for the D .

$\Gamma(D^*(2010)^-\pi^+\pi^0)/\Gamma_{\text{total}}$ Γ_{45}/Γ
 VALUE EVTS DOCUMENT ID TECN COMMENT

0.0152 ± 0.0052 ± 0.0001 51 ¹ALBRECHT 90j ARG $e^+e^- \rightarrow \Upsilon(4S)$
 • • • We do not use the following data for averages, fits, limits, etc. • • •
 0.015 ± 0.008 ± 0.008 8 ²ALBRECHT 87c ARG $e^+e^- \rightarrow \Upsilon(4S)$

¹ALBRECHT 90j reports $0.018 \pm 0.004 \pm 0.005$ from a measurement of $[\Gamma(B^0 \rightarrow D^*(2010)^-\pi^+\pi^0)/\Gamma_{\text{total}}] \times [B(D^*(2010)^+ \rightarrow D^0\pi^+)]$ assuming $B(D^*(2010)^+ \rightarrow D^0\pi^+) = 0.57 \pm 0.06$, which we rescale to our best value $B(D^*(2010)^+ \rightarrow D^0\pi^+) = (67.7 \pm 0.5) \times 10^{-2}$. Our first error is their experiment's error and our second error is the systematic error from using our best value. Assumes equal production of B^+ and B^0 at the $\Upsilon(4S)$ and uses MarkIII branching fractions for the D .

²ALBRECHT 87c use PDG 86 branching ratios for D and $D^*(2010)$ and assume $B(\Upsilon(4S) \rightarrow B^+B^-) = 55\%$ and $B(\Upsilon(4S) \rightarrow B^0\bar{B}^0) = 45\%$. Superseded by ALBRECHT 90j.

$\Gamma(D^*(2010)^-\rho^+)/\Gamma_{\text{total}}$ Γ_{46}/Γ
 VALUE EVTS DOCUMENT ID TECN COMMENT

0.0068 ± 0.0009 OUR AVERAGE
 0.0068 ± 0.0003 ± 0.0009 ¹CSORNA 03 CLE2 $e^+e^- \rightarrow \Upsilon(4S)$
 0.0160 ± 0.0113 ± 0.0001 ²BORTOLETTO92 CLEO $e^+e^- \rightarrow \Upsilon(4S)$
 0.00589 ± 0.00352 ± 0.00004 19 ³ALBRECHT 90j ARG $e^+e^- \rightarrow \Upsilon(4S)$
 • • • We do not use the following data for averages, fits, limits, etc. • • •
 0.0074 ± 0.0010 ± 0.0014 76 ^{4,5}ALAM 94 CLE2 $e^+e^- \rightarrow \Upsilon(4S)$
 0.081 ± 0.029 ^{+0.059}_{-0.024} 19 ⁶CHEN 85 CLEO $e^+e^- \rightarrow \Upsilon(4S)$

¹Assumes equal production of B^0 and B^+ at the $\Upsilon(4S)$ resonance. The second error combines the systematic and theoretical uncertainties in quadrature. CSORNA 03 includes data used in ALAM 94. A full angular fit to three complex helicity amplitudes is performed.

²BORTOLETTO 92 reports $0.019 \pm 0.008 \pm 0.011$ from a measurement of $[\Gamma(B^0 \rightarrow D^*(2010)^-\rho^+)/\Gamma_{\text{total}}] \times [B(D^*(2010)^+ \rightarrow D^0\pi^+)]$ assuming $B(D^*(2010)^+ \rightarrow D^0\pi^+) = 0.57 \pm 0.06$, which we rescale to our best value $B(D^*(2010)^+ \rightarrow D^0\pi^+) = (67.7 \pm 0.5) \times 10^{-2}$. Our first error is their experiment's error and our second error is the systematic error from using our best value. Assumes equal production of B^+ and B^0 at the $\Upsilon(4S)$ and uses MarkIII branching fractions for the D .

³ALBRECHT 90j reports $0.007 \pm 0.003 \pm 0.003$ from a measurement of $[\Gamma(B^0 \rightarrow D^*(2010)^-\rho^+)/\Gamma_{\text{total}}] \times [B(D^*(2010)^+ \rightarrow D^0\pi^+)]$ assuming $B(D^*(2010)^+ \rightarrow D^0\pi^+) = 0.57 \pm 0.06$, which we rescale to our best value $B(D^*(2010)^+ \rightarrow D^0\pi^+) = (67.7 \pm 0.5) \times 10^{-2}$. Our first error is their experiment's error and our second error is the systematic error from using our best value. Assumes equal production of B^+ and B^0 at the $\Upsilon(4S)$ and uses MarkIII branching fractions for the D .

⁴ALAM 94 assume equal production of B^+ and B^0 at the $\Upsilon(4S)$ and use the CLEO II $B(D^*(2010)^+ \rightarrow D^0\pi^+)$ and absolute $B(D^0 \rightarrow K^-\pi^+)$ and the PDG 1992 $B(D^0 \rightarrow K^-\pi^+\pi^0)/B(D^0 \rightarrow K^-\pi^+)$ and $B(D^0 \rightarrow K^-2\pi^+\pi^-)/B(D^0 \rightarrow K^-\pi^+)$.

⁵This decay is nearly completely longitudinally polarized, $\Gamma_L/\Gamma = (93 \pm 5 \pm 5)\%$, as expected from the factorization hypothesis (ROSNER 90). The nonresonant $\pi^+\pi^0$ contribution under the ρ^+ is less than 9% at 90% CL.

⁶Uses $B(D^* \rightarrow D^0\pi^+) = 0.6 \pm 0.15$ and $B(\Upsilon(4S) \rightarrow B^0\bar{B}^0) = 0.4$. Does not depend on D branching ratios.

$\Gamma(D^*(2010)^-K^+)/\Gamma_{\text{total}}$ Γ_{47}/Γ
 VALUE (units 10^{-4}) DOCUMENT ID TECN COMMENT

2.14 ± 0.16 OUR AVERAGE
 2.14 ± 0.12 ± 0.10 ¹AUBERT 06A BABR $e^+e^- \rightarrow \Upsilon(4S)$
 2.0 ± 0.4 ± 0.1 ²ABE 01I BELL $e^+e^- \rightarrow \Upsilon(4S)$

¹AUBERT 06A reports $[\Gamma(B^0 \rightarrow D^*(2010)^-K^+)/\Gamma_{\text{total}}] / [B(B^0 \rightarrow D^*(2010)^-\pi^+)] = 0.0776 \pm 0.0034 \pm 0.0029$ which we multiply by our best value $B(B^0 \rightarrow D^*(2010)^-\pi^+) = (2.76 \pm 0.13) \times 10^{-3}$. Our first error is their experiment's error and our second error is the systematic error from using our best value.

²ABE 01i reports $[\Gamma(B^0 \rightarrow D^*(2010)^-K^+)/\Gamma_{\text{total}}] / [B(B^0 \rightarrow D^*(2010)^-\pi^+)] = 0.074 \pm 0.015 \pm 0.006$ which we multiply by our best value $B(B^0 \rightarrow D^*(2010)^-\pi^+) = (2.76 \pm 0.13) \times 10^{-3}$. Our first error is their experiment's error and our second error is the systematic error from using our best value.

$\Gamma(D^*(2010)^-K^0\pi^+)/\Gamma_{\text{total}}$ Γ_{48}/Γ
 VALUE (units 10^{-4}) DOCUMENT ID TECN COMMENT

3.0 ± 0.7 ± 0.3 ¹AUBERT, BE 05B BABR $e^+e^- \rightarrow \Upsilon(4S)$
¹Assumes equal production of B^+ and B^0 at the $\Upsilon(4S)$.

$\Gamma(D^*(2010)^-K^*(892)^+)/\Gamma_{\text{total}}$ Γ_{49}/Γ
 VALUE (units 10^{-4}) DOCUMENT ID TECN COMMENT

3.3 ± 0.6 OUR AVERAGE
 3.2 ± 0.6 ± 0.3 ¹AUBERT, BE 05B BABR $e^+e^- \rightarrow \Upsilon(4S)$
 3.8 ± 1.3 ± 0.8 ²MAHAPATRA 02 CLE2 $e^+e^- \rightarrow \Upsilon(4S)$
¹Assumes equal production of B^+ and B^0 at the $\Upsilon(4S)$.
²Assumes equal production of B^+ and B^0 at the $\Upsilon(4S)$ and an unpolarized final state.

$\Gamma(D^*(2010)^-K^+\bar{K}^0)/\Gamma_{\text{total}}$ Γ_{50}/Γ
 VALUE (units 10^{-4}) CL% DOCUMENT ID TECN COMMENT

<4.7 90 ¹DRUTSKOY 02 BELL $e^+e^- \rightarrow \Upsilon(4S)$
¹Assumes equal production of B^+ and B^0 at the $\Upsilon(4S)$.

$\Gamma(D^*(2010)^-K^+\bar{K}^*(892)^0)/\Gamma_{\text{total}}$ Γ_{51}/Γ
 VALUE (units 10^{-4}) DOCUMENT ID TECN COMMENT

12.9 ± 2.2 ± 2.5 ¹DRUTSKOY 02 BELL $e^+e^- \rightarrow \Upsilon(4S)$
¹Assumes equal production of B^+ and B^0 at the $\Upsilon(4S)$.

$\Gamma(D^*(2010)^-\pi^+\pi^+\pi^-)/\Gamma_{\text{total}}$ Γ_{52}/Γ
 VALUE CL% DOCUMENT ID TECN COMMENT

0.0070 ± 0.0008 OUR AVERAGE Error includes scale factor of 1.3. See the ideogram below.
 0.00681 ± 0.00023 ± 0.00072 ¹MAJUMDER 04 BELL $e^+e^- \rightarrow \Upsilon(4S)$
 0.0063 ± 0.0010 ± 0.0011 ^{2,3}ALAM 94 CLE2 $e^+e^- \rightarrow \Upsilon(4S)$
 0.0134 ± 0.0036 ± 0.0001 ⁴BORTOLETTO92 CLEO $e^+e^- \rightarrow \Upsilon(4S)$
 0.0101 ± 0.0041 ± 0.0001 ⁵ALBRECHT 90j ARG $e^+e^- \rightarrow \Upsilon(4S)$

• • • We do not use the following data for averages, fits, limits, etc. • • •
 0.033 ± 0.009 ± 0.016 ⁶ALBRECHT 87c ARG $e^+e^- \rightarrow \Upsilon(4S)$
 <0.042 90 ⁷BEBEK 87 CLEO $e^+e^- \rightarrow \Upsilon(4S)$

¹Assumes equal production of B^+ and B^0 at the $\Upsilon(4S)$.
²ALAM 94 assume equal production of B^+ and B^0 at the $\Upsilon(4S)$ and use the CLEO II $B(D^*(2010)^+ \rightarrow D^0\pi^+)$ and absolute $B(D^0 \rightarrow K^-\pi^+)$ and the PDG 1992 $B(D^0 \rightarrow K^-\pi^+\pi^0)/B(D^0 \rightarrow K^-\pi^+)$ and $B(D^0 \rightarrow K^-2\pi^+\pi^-)/B(D^0 \rightarrow K^-\pi^+)$.

³The three pion mass is required to be between 1.0 and 1.6 GeV consistent with an a_1 meson. (If this channel is dominated by a_1^+ , the branching ratio for $\bar{D}^*-\pi^+\pi^+\pi^-$ is twice that for $\bar{D}^*-\pi^+\pi^+\pi^-$.)

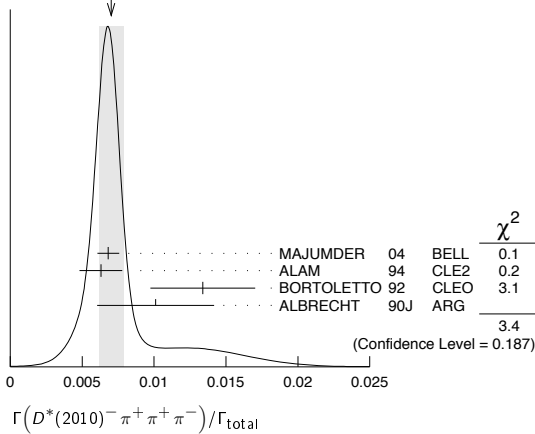
⁴BORTOLETTO 92 reports $0.0159 \pm 0.0028 \pm 0.0037$ from a measurement of $[\Gamma(B^0 \rightarrow D^*(2010)^-\pi^+\pi^+\pi^-)/\Gamma_{\text{total}}] \times [B(D^*(2010)^+ \rightarrow D^0\pi^+)]$ assuming $B(D^*(2010)^+ \rightarrow D^0\pi^+) = 0.57 \pm 0.06$, which we rescale to our best value $B(D^*(2010)^+ \rightarrow D^0\pi^+) = (67.7 \pm 0.5) \times 10^{-2}$. Our first error is their experiment's error and our second error is the systematic error from using our best value. Assumes equal production of B^+ and B^0 at the $\Upsilon(4S)$ and uses MarkIII branching fractions for the D .

⁵ALBRECHT 90j reports $0.012 \pm 0.003 \pm 0.004$ from a measurement of $[\Gamma(B^0 \rightarrow D^*(2010)^-\pi^+\pi^+\pi^-)/\Gamma_{\text{total}}] \times [B(D^*(2010)^+ \rightarrow D^0\pi^+)]$ assuming $B(D^*(2010)^+ \rightarrow D^0\pi^+) = 0.57 \pm 0.06$, which we rescale to our best value $B(D^*(2010)^+ \rightarrow D^0\pi^+) = (67.7 \pm 0.5) \times 10^{-2}$. Our first error is their experiment's error and our second error is the systematic error from using our best value. Assumes equal production of B^+ and B^0 at the $\Upsilon(4S)$ and uses MarkIII branching fractions for the D .

⁶ALBRECHT 87c use PDG 86 branching ratios for D and $D^*(2010)$ and assume $B(\Upsilon(4S) \rightarrow B^+B^-) = 55\%$ and $B(\Upsilon(4S) \rightarrow B^0\bar{B}^0) = 45\%$. Superseded by ALBRECHT 90j.

⁷BEBEK 87 value has been updated in BERKELMAN 91 to use same assumptions as noted for BORTOLETTO 92.

WEIGHTED AVERAGE
0.0070±0.0008 (Error scaled by 1.3)



$\Gamma((D^*(2010)^- \pi^+ \pi^+ \pi^-) \text{ nonresonant})/\Gamma_{\text{total}}$ Γ53/Γ

VALUE	DOCUMENT ID	TECN	COMMENT
0.0000 ± 0.0019 ± 0.0016	¹ BORTOLETTO92	CLEO	$e^+e^- \rightarrow \Upsilon(4S)$

¹ BORTOLETTO 92 assumes equal production of B^+ and B^0 at the $\Upsilon(4S)$ and uses MarkIII branching fractions for the D and $D^*(2010)$.

$\Gamma(D^*(2010)^- \pi^+ \rho^0)/\Gamma_{\text{total}}$ Γ54/Γ

VALUE	DOCUMENT ID	TECN	COMMENT
0.00573 ± 0.00317 ± 0.00004	¹ BORTOLETTO92	CLEO	$e^+e^- \rightarrow \Upsilon(4S)$

¹ BORTOLETTO 92 reports $0.0068 \pm 0.0032 \pm 0.0021$ from a measurement of $[\Gamma(B^0 \rightarrow D^*(2010)^- \pi^+ \rho^0)/\Gamma_{\text{total}}] \times [B(D^*(2010)^+ \rightarrow D^0 \pi^+)]$ assuming $B(D^*(2010)^+ \rightarrow D^0 \pi^+) = 0.57 \pm 0.06$, which we rescale to our best value $B(D^*(2010)^+ \rightarrow D^0 \pi^+) = (67.7 \pm 0.5) \times 10^{-2}$. Our first error is their experiment's error and our second error is the systematic error from using our best value. Assumes equal production of B^+ and B^0 at the $\Upsilon(4S)$ and uses MarkIII branching fractions for the D .

$\Gamma(D^*(2010)^- a_1(1260)^+)/\Gamma_{\text{total}}$ Γ55/Γ

VALUE	DOCUMENT ID	TECN	COMMENT
0.0130 ± 0.0027 OUR AVERAGE			
0.0126 ± 0.0020 ± 0.0022	^{1,2} ALAM 94	CLE2	$e^+e^- \rightarrow \Upsilon(4S)$
0.0152 ± 0.0070 ± 0.0001	³ BORTOLETTO92	CLEO	$e^+e^- \rightarrow \Upsilon(4S)$

¹ ALAM 94 value is twice their $\Gamma(D^*(2010)^- \pi^+ \pi^+ \pi^-)/\Gamma_{\text{total}}$ value based on their observation that the three pions are dominantly in the $a_1(1260)$ mass range 1.0 to 1.6 GeV.
² ALAM 94 assume equal production of B^+ and B^0 at the $\Upsilon(4S)$ and use the CLEOII $B(D^*(2010)^+ \rightarrow D^0 \pi^+)$ and absolute $B(D^0 \rightarrow K^- \pi^+)$ and the PDG 1992 $B(D^0 \rightarrow K^- \pi^+ \pi^0)/B(D^0 \rightarrow K^- \pi^+)$ and $B(D^0 \rightarrow K^- 2\pi^+ \pi^-)/B(D^0 \rightarrow K^- \pi^+)$.
³ BORTOLETTO 92 reports $0.018 \pm 0.006 \pm 0.006$ from a measurement of $[\Gamma(B^0 \rightarrow D^*(2010)^- a_1(1260)^+)/\Gamma_{\text{total}}] \times [B(D^*(2010)^+ \rightarrow D^0 \pi^+)]$ assuming $B(D^*(2010)^+ \rightarrow D^0 \pi^+) = 0.57 \pm 0.06$, which we rescale to our best value $B(D^*(2010)^+ \rightarrow D^0 \pi^+) = (67.7 \pm 0.5) \times 10^{-2}$. Our first error is their experiment's error and our second error is the systematic error from using our best value. Assumes equal production of B^+ and B^0 at the $\Upsilon(4S)$ and uses MarkIII branching fractions for the D .

$\Gamma(D^*(2010)^- \pi^+ \pi^+ \pi^- \pi^0)/\Gamma_{\text{total}}$ Γ56/Γ

VALUE	EVTs	DOCUMENT ID	TECN	COMMENT
0.0176 ± 0.0027 OUR AVERAGE				
0.0172 ± 0.0014 ± 0.0024	28	¹ ALEXANDER 01B	CLE2	$e^+e^- \rightarrow \Upsilon(4S)$
0.0345 ± 0.0181 ± 0.0003	28	² ALBRECHT 90J	ARG	$e^+e^- \rightarrow \Upsilon(4S)$

¹ Assumes equal production of B^+ and B^0 at the $\Upsilon(4S)$. The signal is consistent with all observed $\omega\pi^+$ having proceeded through the ρ^+ resonance at mass $1349 \pm 25^{+10}_{-5}$ MeV and width $547 \pm 86^{+46}_{-45}$ MeV.
² ALBRECHT 90J reports $0.041 \pm 0.015 \pm 0.016$ from a measurement of $[\Gamma(B^0 \rightarrow D^*(2010)^- \pi^+ \pi^+ \pi^- \pi^0)/\Gamma_{\text{total}}] \times [B(D^*(2010)^+ \rightarrow D^0 \pi^+)]$ assuming $B(D^*(2010)^+ \rightarrow D^0 \pi^+) = 0.57 \pm 0.06$, which we rescale to our best value $B(D^*(2010)^+ \rightarrow D^0 \pi^+) = (67.7 \pm 0.5) \times 10^{-2}$. Our first error is their experiment's error and our second error is the systematic error from using our best value. Assumes equal production of B^+ and B^0 at the $\Upsilon(4S)$ and uses MarkIII branching fractions for the D .

$\Gamma(D^{*-} 3\pi^+ 2\pi^-)/\Gamma_{\text{total}}$ Γ57/Γ

VALUE (units 10^{-3})	DOCUMENT ID	TECN	COMMENT
4.72 ± 0.59 ± 0.71	¹ MAJUMDER 04	BELL	$e^+e^- \rightarrow \Upsilon(4S)$

¹ Assumes equal production of B^+ and B^0 at the $\Upsilon(4S)$.

$\Gamma(\bar{D}^*(2010)^- \omega \pi^+)/\Gamma_{\text{total}}$ Γ58/Γ

VALUE (units 10^{-3})	DOCUMENT ID	TECN	COMMENT
2.89 ± 0.30 OUR AVERAGE			
2.88 ± 0.21 ± 0.31	¹ AUBERT 06L	BABR	$e^+e^- \rightarrow \Upsilon(4S)$
2.9 ± 0.3 ± 0.4	^{1,2} ALEXANDER 01B	CLE2	$e^+e^- \rightarrow \Upsilon(4S)$

¹ Assumes equal production of B^+ and B^0 at the $\Upsilon(4S)$.
² The signal is consistent with all observed $\omega\pi^+$ having proceeded through the ρ^+ resonance at mass $1349 \pm 25^{+10}_{-5}$ MeV and width $547 \pm 86^{+46}_{-45}$ MeV.

$\Gamma(D_1(2430)^0 \omega \times B(D_1(2430)^0 \rightarrow D^{*-} \pi^+))/\Gamma_{\text{total}}$ Γ59/Γ

VALUE (units 10^{-4})	DOCUMENT ID	TECN	COMMENT
4.1 ± 1.2 ± 1.1	¹ AUBERT 06L	BABR	$e^+e^- \rightarrow \Upsilon(4S)$

¹ Obtained by fitting the events with $\cos \theta_{D^*} < 0.5$ and scaling up the result by a factor of 4/3. No interference effects between $B^0 \rightarrow D_1^+ \omega$ and $D^* \omega \pi$ are assumed.

$\Gamma(\bar{D}^{*-} \pi^+)/\Gamma_{\text{total}}$ Γ60/Γ

D^{*-} represents an excited state with mass $2.2 < M < 2.8$ GeV/c².

VALUE (units 10^{-3})	DOCUMENT ID	TECN	COMMENT
2.1 ± 1.0 ± 0.1	^{1,2} AUBERT, BE 06J	BABR	$e^+e^- \rightarrow \Upsilon(4S)$

¹ AUBERT, BE 06J reports $[\Gamma(B^0 \rightarrow \bar{D}^{*-} \pi^+)/\Gamma_{\text{total}}] / [B(B^0 \rightarrow D^- \pi^+)] = 0.77 \pm 0.22 \pm 0.29$ which we multiply by our best value $B(B^0 \rightarrow D^- \pi^+) = (2.68 \pm 0.13) \times 10^{-3}$. Our first error is their experiment's error and our second error is the systematic error from using our best value.
² Uses a missing-mass method. Does not depend on D branching fractions or B^+ / B^0 production rates.

$\Gamma(D_1(2420)^- \pi^+ \times B(D_1^- \rightarrow D^- \pi^+ \pi^-))/\Gamma_{\text{total}}$ Γ61/Γ

VALUE (units 10^{-4})	DOCUMENT ID	TECN	COMMENT
0.89 ± 0.15 ± 0.17 - 0.32	¹ ABE 05A	BELL	$e^+e^- \rightarrow \Upsilon(4S)$

¹ Assumes equal production of B^+ and B^0 at the $\Upsilon(4S)$.

$\Gamma(D_1(2420)^- \pi^+ \times B(D_1^- \rightarrow D^{*-} \pi^+ \pi^-))/\Gamma_{\text{total}}$ Γ62/Γ

VALUE (units 10^{-4})	CL%	DOCUMENT ID	TECN	COMMENT
< 0.33	90	¹ ABE 05A	BELL	$e^+e^- \rightarrow \Upsilon(4S)$

¹ Assumes equal production of B^+ and B^0 at the $\Upsilon(4S)$.

$\Gamma(\bar{D}_2^*(2460)^- \pi^+ \times B(D_2^{*-}(2460)^- \rightarrow D^0 \pi^-))/\Gamma_{\text{total}}$ Γ63/Γ

VALUE (units 10^{-4})	CL%	DOCUMENT ID	TECN	COMMENT
2.15 ± 0.17 ± 0.31		^{1,2} KUZMIN 07	BELL	$e^+e^- \rightarrow \Upsilon(4S)$

• • • We do not use the following data for averages, fits, limits, etc. • • •
 <14.7 90 ¹ ALAM 94 CLE2 $e^+e^- \rightarrow \Upsilon(4S)$

¹ Assumes equal production of B^+ and B^0 at the $\Upsilon(4S)$.
² Our second uncertainty combines systematics and model errors quoted in the paper.

$\Gamma(\bar{D}_2^*(2400)^- \pi^+ \times B(D_2^{*0}(2400)^- \rightarrow D^0 \pi^-))/\Gamma_{\text{total}}$ Γ64/Γ

VALUE (units 10^{-4})	DOCUMENT ID	TECN	COMMENT
0.60 ± 0.13 ± 0.27	^{1,2} KUZMIN 07	BELL	$e^+e^- \rightarrow \Upsilon(4S)$

¹ Assumes equal production of B^+ and B^0 at the $\Upsilon(4S)$.
² Our second uncertainty combines systematics and model errors quoted in the paper.

$\Gamma(D_2^*(2460)^- \pi^+ \times B((D_2^{*-}(2460)^- \rightarrow D^{*-} \pi^+ \pi^-))/\Gamma_{\text{total}}$ Γ65/Γ

VALUE (units 10^{-4})	CL%	DOCUMENT ID	TECN	COMMENT
< 0.24	90	¹ ABE 05A	BELL	$e^+e^- \rightarrow \Upsilon(4S)$

¹ Assumes equal production of B^+ and B^0 at the $\Upsilon(4S)$.

$\Gamma(\bar{D}_2^*(2460)^- \rho^+)/\Gamma_{\text{total}}$ Γ66/Γ

VALUE	CL%	DOCUMENT ID	TECN	COMMENT
< 0.0049	90	¹ ALAM 94	CLE2	$e^+e^- \rightarrow \Upsilon(4S)$

¹ ALAM 94 assumes equal production of B^+ and B^0 at the $\Upsilon(4S)$ and use the CLEOII absolute $B(D^0 \rightarrow K^- \pi^+)$ and $B(D_2^*(2460)^+ \rightarrow D^0 \pi^+) = 30\%$.

$\Gamma(D^0 \bar{D}^0)/\Gamma_{\text{total}}$ Γ67/Γ

VALUE (units 10^{-4})	CL%	DOCUMENT ID	TECN	COMMENT
< 0.43	90	¹ ADACHI 08	BELL	$e^+e^- \rightarrow \Upsilon(4S)$

• • • We do not use the following data for averages, fits, limits, etc. • • •
 <0.6 90 ¹ AUBERT, B 06A BABR $e^+e^- \rightarrow \Upsilon(4S)$

¹ Assumes equal production of B^+ and B^0 at the $\Upsilon(4S)$.

$\Gamma(D^{*0} \bar{D}^0)/\Gamma_{\text{total}}$ Γ68/Γ

VALUE (units 10^{-4})	CL%	DOCUMENT ID	TECN	COMMENT
< 2.9	90	¹ AUBERT, B 06A	BABR	$e^+e^- \rightarrow \Upsilon(4S)$

¹ Assumes equal production of B^+ and B^0 at the $\Upsilon(4S)$.

Meson Particle Listings

 B^0 $\Gamma(D^- D^+)/\Gamma_{\text{total}}$ Γ_{69}/Γ

VALUE (units 10^{-4})	CL%	DOCUMENT ID	TECN	COMMENT
2.11 ± 0.31 OUR AVERAGE		Error includes scale factor of 1.2.		
1.97 ± 0.20 ± 0.20		¹ FRATINA 07	BELL	$e^+ e^- \rightarrow \Upsilon(4S)$
2.8 ± 0.4 ± 0.5		¹ AUBERT,B	06A BABR	$e^+ e^- \rightarrow \Upsilon(4S)$
• • • We do not use the following data for averages, fits, limits, etc. • • •				
1.91 ± 0.51 ± 0.30		¹ MAJUMDER 05	BELL	Repl. by FRATINA 07
< 9.4	90	¹ LIPELES 00	CLE2	$e^+ e^- \rightarrow \Upsilon(4S)$
< 59	90	BARATE 98Q	ALEP	$e^+ e^- \rightarrow Z$
< 12	90	ASNER 97	CLE2	$e^+ e^- \rightarrow \Upsilon(4S)$

¹ Assumes equal production of B^+ and B^0 at the $\Upsilon(4S)$. $\Gamma(D^- D_s^+)/\Gamma_{\text{total}}$ Γ_{70}/Γ

VALUE	EVTs	DOCUMENT ID	TECN	COMMENT
0.0072 ± 0.0008 OUR AVERAGE				
0.0073 ± 0.0004 ± 0.0007		¹ ZUPANC 07	BELL	$e^+ e^- \rightarrow \Upsilon(4S)$
0.0066 ± 0.0014 ± 0.0006		² AUBERT 06N	BABR	$e^+ e^- \rightarrow \Upsilon(4S)$
0.0068 ± 0.0024 ± 0.0006		³ GIBAUT 96	CLE2	$e^+ e^- \rightarrow \Upsilon(4S)$
0.010 ± 0.009 ± 0.001		⁴ ALBRECHT 92G	ARG	$e^+ e^- \rightarrow \Upsilon(4S)$
0.0053 ± 0.0030 ± 0.0005		⁵ BORTOLETTO92	CLEO	$e^+ e^- \rightarrow \Upsilon(4S)$
0.012 ± 0.007	3	⁶ BORTOLETTO90	CLEO	$e^+ e^- \rightarrow \Upsilon(4S)$

- ¹ ZUPANC 07 reports $(7.5 \pm 0.2 \pm 1.1) \times 10^{-3}$ from a measurement of $[\Gamma(B^0 \rightarrow D^- D_s^+)/\Gamma_{\text{total}}] \times [B(D_s^+ \rightarrow \phi\pi^+)]$ assuming $B(D_s^+ \rightarrow \phi\pi^+) = (4.4 \pm 0.6) \times 10^{-2}$, which we rescale to our best value $B(D_s^+ \rightarrow \phi\pi^+) = (4.5 \pm 0.4) \times 10^{-2}$. Our first error is their experiment's error and our second error is the systematic error from using our best value.
- ² AUBERT 06N reports $(0.64 \pm 0.13 \pm 0.10) \times 10^{-2}$ from a measurement of $[\Gamma(B^0 \rightarrow D^- D_s^+)/\Gamma_{\text{total}}] \times [B(D_s^+ \rightarrow \phi\pi^+)]$ assuming $B(D_s^+ \rightarrow \phi\pi^+) = 0.0462 \pm 0.0062$, which we rescale to our best value $B(D_s^+ \rightarrow \phi\pi^+) = (4.5 \pm 0.4) \times 10^{-2}$. Our first error is their experiment's error and our second error is the systematic error from using our best value.
- ³ GIBAUT 96 reports $0.0087 \pm 0.0024 \pm 0.0020$ from a measurement of $[\Gamma(B^0 \rightarrow D^- D_s^+)/\Gamma_{\text{total}}] \times [B(D_s^+ \rightarrow \phi\pi^+)]$ assuming $B(D_s^+ \rightarrow \phi\pi^+) = 0.035$, which we rescale to our best value $B(D_s^+ \rightarrow \phi\pi^+) = (4.5 \pm 0.4) \times 10^{-2}$. Our first error is their experiment's error and our second error is the systematic error from using our best value.
- ⁴ ALBRECHT 92G reports $0.017 \pm 0.013 \pm 0.006$ from a measurement of $[\Gamma(B^0 \rightarrow D^- D_s^+)/\Gamma_{\text{total}}] \times [B(D_s^+ \rightarrow \phi\pi^+)]$ assuming $B(D_s^+ \rightarrow \phi\pi^+) = 0.027$, which we rescale to our best value $B(D_s^+ \rightarrow \phi\pi^+) = (4.5 \pm 0.4) \times 10^{-2}$. Our first error is their experiment's error and our second error is the systematic error from using our best value. Assumes PDG 1990 D^+ branching ratios, e.g., $B(D^+ \rightarrow K^- 2\pi^+) = 7.7 \pm 1.0\%$.
- ⁵ BORTOLETTO 92 reports $0.0080 \pm 0.0045 \pm 0.0030$ from a measurement of $[\Gamma(B^0 \rightarrow D^- D_s^+)/\Gamma_{\text{total}}] \times [B(D_s^+ \rightarrow \phi\pi^+)]$ assuming $B(D_s^+ \rightarrow \phi\pi^+) = 0.030 \pm 0.011$, which we rescale to our best value $B(D_s^+ \rightarrow \phi\pi^+) = (4.5 \pm 0.4) \times 10^{-2}$. Our first error is their experiment's error and our second error is the systematic error from using our best value. Assumes equal production of B^+ and B^0 at the $\Upsilon(4S)$ and uses MarkIII branching fractions for the D .
- ⁶ BORTOLETTO 90 assume $B(D_s \rightarrow \phi\pi^+) = 2\%$. Superseded by BORTOLETTO 92.

 $\Gamma(D^*(2010)^- D_s^+)/\Gamma_{\text{total}}$ Γ_{71}/Γ

VALUE	EVTs	DOCUMENT ID	TECN	COMMENT
0.0080 ± 0.0011 OUR AVERAGE				
0.0073 ± 0.0013 ± 0.0007		¹ AUBERT 06N	BABR	$e^+ e^- \rightarrow \Upsilon(4S)$
0.0083 ± 0.0015 ± 0.0007		² AUBERT 03i	BABR	$e^+ e^- \rightarrow \Upsilon(4S)$
0.0088 ± 0.0017 ± 0.0008		³ AHMED 00b	CLE2	$e^+ e^- \rightarrow \Upsilon(4S)$
0.008 ± 0.006 ± 0.001		⁴ ALBRECHT 92G	ARG	$e^+ e^- \rightarrow \Upsilon(4S)$
0.011 ± 0.006 ± 0.001		⁵ BORTOLETTO92	CLEO	$e^+ e^- \rightarrow \Upsilon(4S)$
0.0072 ± 0.0022 ± 0.0006		⁶ GIBAUT 96	CLE2	Repl. by AHMED 00b
0.024 ± 0.014	3	⁷ BORTOLETTO90	CLEO	$e^+ e^- \rightarrow \Upsilon(4S)$

- ¹ AUBERT 06N reports $(0.71 \pm 0.13 \pm 0.09) \times 10^{-2}$ from a measurement of $[\Gamma(B^0 \rightarrow D^*(2010)^- D_s^+)/\Gamma_{\text{total}}] \times [B(D_s^+ \rightarrow \phi\pi^+)]$ assuming $B(D_s^+ \rightarrow \phi\pi^+) = 0.0462 \pm 0.0062$, which we rescale to our best value $B(D_s^+ \rightarrow \phi\pi^+) = (4.5 \pm 0.4) \times 10^{-2}$. Our first error is their experiment's error and our second error is the systematic error from using our best value.
- ² AUBERT 03i reports $0.0103 \pm 0.0014 \pm 0.0013$ from a measurement of $[\Gamma(B^0 \rightarrow D^*(2010)^- D_s^+)/\Gamma_{\text{total}}] \times [B(D_s^+ \rightarrow \phi\pi^+)]$ assuming $B(D_s^+ \rightarrow \phi\pi^+) = 0.036$, which we rescale to our best value $B(D_s^+ \rightarrow \phi\pi^+) = (4.5 \pm 0.4) \times 10^{-2}$. Our first error is their experiment's error and our second error is the systematic error from using our best value.
- ³ AHMED 00b reports $0.0110 \pm 0.0018 \pm 0.0011$ from a measurement of $[\Gamma(B^0 \rightarrow D^*(2010)^- D_s^+)/\Gamma_{\text{total}}] \times [B(D_s^+ \rightarrow \phi\pi^+)]$ assuming $B(D_s^+ \rightarrow \phi\pi^+) = 0.036$, which we rescale to our best value $B(D_s^+ \rightarrow \phi\pi^+) = (4.5 \pm 0.4) \times 10^{-2}$. Our first error is their experiment's error and our second error is the systematic error from using our best value.
- ⁴ ALBRECHT 92G reports $0.014 \pm 0.010 \pm 0.003$ from a measurement of $[\Gamma(B^0 \rightarrow D^*(2010)^- D_s^+)/\Gamma_{\text{total}}] \times [B(D_s^+ \rightarrow \phi\pi^+)]$ assuming $B(D_s^+ \rightarrow \phi\pi^+) = 0.027$, which we rescale to our best value $B(D_s^+ \rightarrow \phi\pi^+) = (4.5 \pm 0.4) \times 10^{-2}$. Our first error is their experiment's error and our second error is the systematic error from using our best value.

our best value. Assumes PDG 1990 D^+ and $D^*(2010)^+$ branching ratios, e.g., $B(D^0 \rightarrow K^- \pi^+) = 3.71 \pm 0.25\%$, $B(D^+ \rightarrow K^- 2\pi^+) = 7.1 \pm 1.0\%$, and $B(D^*(2010)^+ \rightarrow D^0 \pi^+) = 55 \pm 4\%$.

- ⁵ BORTOLETTO 92 reports $0.016 \pm 0.009 \pm 0.006$ from a measurement of $[\Gamma(B^0 \rightarrow D^*(2010)^- D_s^+)/\Gamma_{\text{total}}] \times [B(D_s^+ \rightarrow \phi\pi^+)]$ assuming $B(D_s^+ \rightarrow \phi\pi^+) = 0.030 \pm 0.011$, which we rescale to our best value $B(D_s^+ \rightarrow \phi\pi^+) = (4.5 \pm 0.4) \times 10^{-2}$. Our first error is their experiment's error and our second error is the systematic error from using our best value. Assumes equal production of B^+ and B^0 at the $\Upsilon(4S)$ and uses MarkIII branching fractions for the D and $D^*(2010)$.
- ⁶ GIBAUT 96 reports $0.0093 \pm 0.0023 \pm 0.0016$ from a measurement of $[\Gamma(B^0 \rightarrow D^*(2010)^- D_s^+)/\Gamma_{\text{total}}] \times [B(D_s^+ \rightarrow \phi\pi^+)]$ assuming $B(D_s^+ \rightarrow \phi\pi^+) = 0.035$, which we rescale to our best value $B(D_s^+ \rightarrow \phi\pi^+) = (4.5 \pm 0.4) \times 10^{-2}$. Our first error is their experiment's error and our second error is the systematic error from using our best value.
- ⁷ BORTOLETTO 90 assume $B(D_s \rightarrow \phi\pi^+) = 2\%$. Superseded by BORTOLETTO 92.

 $\Gamma(D^- D_s^{*+})/\Gamma_{\text{total}}$ Γ_{72}/Γ

VALUE	DOCUMENT ID	TECN	COMMENT
0.0074 ± 0.0016 OUR AVERAGE			
0.0071 ± 0.0016 ± 0.0006	¹ AUBERT 06N	BABR	$e^+ e^- \rightarrow \Upsilon(4S)$
0.0078 ± 0.0032 ± 0.0007	² GIBAUT 96	CLE2	$e^+ e^- \rightarrow \Upsilon(4S)$
0.016 ± 0.012 ± 0.001	³ ALBRECHT 92G	ARG	$e^+ e^- \rightarrow \Upsilon(4S)$

- ¹ AUBERT 06N reports $(0.69 \pm 0.16 \pm 0.09) \times 10^{-2}$ from a measurement of $[\Gamma(B^0 \rightarrow D^- D_s^{*+})/\Gamma_{\text{total}}] \times [B(D_s^+ \rightarrow \phi\pi^+)]$ assuming $B(D_s^+ \rightarrow \phi\pi^+) = 0.0462 \pm 0.0062$, which we rescale to our best value $B(D_s^+ \rightarrow \phi\pi^+) = (4.5 \pm 0.4) \times 10^{-2}$. Our first error is their experiment's error and our second error is the systematic error from using our best value.
- ² GIBAUT 96 reports $0.0100 \pm 0.0035 \pm 0.0022$ from a measurement of $[\Gamma(B^0 \rightarrow D^- D_s^{*+})/\Gamma_{\text{total}}] \times [B(D_s^+ \rightarrow \phi\pi^+)]$ assuming $B(D_s^+ \rightarrow \phi\pi^+) = 0.035$, which we rescale to our best value $B(D_s^+ \rightarrow \phi\pi^+) = (4.5 \pm 0.4) \times 10^{-2}$. Our first error is their experiment's error and our second error is the systematic error from using our best value.
- ³ ALBRECHT 92G reports $0.027 \pm 0.017 \pm 0.009$ from a measurement of $[\Gamma(B^0 \rightarrow D^- D_s^{*+})/\Gamma_{\text{total}}] \times [B(D_s^+ \rightarrow \phi\pi^+)]$ assuming $B(D_s^+ \rightarrow \phi\pi^+) = 0.027$, which we rescale to our best value $B(D_s^+ \rightarrow \phi\pi^+) = (4.5 \pm 0.4) \times 10^{-2}$. Our first error is their experiment's error and our second error is the systematic error from using our best value. Assumes PDG 1990 D^+ branching ratios, e.g., $B(D^+ \rightarrow K^- 2\pi^+) = 7.7 \pm 1.0\%$.

 $\Gamma(D^*(2010)^- D_s^{*+})/\Gamma_{\text{total}}$ Γ_{73}/Γ

VALUE	DOCUMENT ID	TECN	COMMENT
0.0177 ± 0.0014 OUR AVERAGE			
0.0173 ± 0.0018 ± 0.0015	¹ AUBERT 06N	BABR	$e^+ e^- \rightarrow \Upsilon(4S)$
0.0188 ± 0.0009 ± 0.0017	² AUBERT 05v	BABR	$e^+ e^- \rightarrow \Upsilon(4S)$
0.0158 ± 0.0027 ± 0.0014	³ AUBERT 03i	BABR	$e^+ e^- \rightarrow \Upsilon(4S)$
0.015 ± 0.004 ± 0.001	⁴ AHMED 00b	CLE2	$e^+ e^- \rightarrow \Upsilon(4S)$
0.016 ± 0.009 ± 0.001	⁵ ALBRECHT 92G	ARG	$e^+ e^- \rightarrow \Upsilon(4S)$
0.016 ± 0.005 ± 0.001	⁶ GIBAUT 96	CLE2	Repl. by AHMED 00b

- ¹ AUBERT 06N reports $(1.68 \pm 0.21 \pm 0.19) \times 10^{-2}$ from a measurement of $[\Gamma(B^0 \rightarrow D^*(2010)^- D_s^{*+})/\Gamma_{\text{total}}] \times [B(D_s^+ \rightarrow \phi\pi^+)]$ assuming $B(D_s^+ \rightarrow \phi\pi^+) = 0.0462 \pm 0.0062$, which we rescale to our best value $B(D_s^+ \rightarrow \phi\pi^+) = (4.5 \pm 0.4) \times 10^{-2}$. Our first error is their experiment's error and our second error is the systematic error from using our best value.
- ² A partial reconstruction technique is used and the result is independent of the particle decay rate of D_s^+ meson. It also provides a model-independent determination of $B(D_s^+ \rightarrow \phi\pi^+) = (4.81 \pm 0.52 \pm 0.38)\%$.
- ³ AUBERT 03i reports $0.0197 \pm 0.0015 \pm 0.0030$ from a measurement of $[\Gamma(B^0 \rightarrow D^*(2010)^- D_s^{*+})/\Gamma_{\text{total}}] \times [B(D_s^+ \rightarrow \phi\pi^+)]$ assuming $B(D_s^+ \rightarrow \phi\pi^+) = 0.036$, which we rescale to our best value $B(D_s^+ \rightarrow \phi\pi^+) = (4.5 \pm 0.4) \times 10^{-2}$. Our first error is their experiment's error and our second error is the systematic error from using our best value.
- ⁴ AHMED 00b reports $0.0182 \pm 0.0037 \pm 0.0025$ from a measurement of $[\Gamma(B^0 \rightarrow D^*(2010)^- D_s^{*+})/\Gamma_{\text{total}}] \times [B(D_s^+ \rightarrow \phi\pi^+)]$ assuming $B(D_s^+ \rightarrow \phi\pi^+) = 0.036$, which we rescale to our best value $B(D_s^+ \rightarrow \phi\pi^+) = (4.5 \pm 0.4) \times 10^{-2}$. Our first error is their experiment's error and our second error is the systematic error from using our best value.
- ⁵ ALBRECHT 92G reports $0.026 \pm 0.014 \pm 0.006$ from a measurement of $[\Gamma(B^0 \rightarrow D^*(2010)^- D_s^{*+})/\Gamma_{\text{total}}] \times [B(D_s^+ \rightarrow \phi\pi^+)]$ assuming $B(D_s^+ \rightarrow \phi\pi^+) = 0.027$, which we rescale to our best value $B(D_s^+ \rightarrow \phi\pi^+) = (4.5 \pm 0.4) \times 10^{-2}$. Our first error is their experiment's error and our second error is the systematic error from using our best value. Assumes PDG 1990 D^+ and $D^*(2010)^+$ branching ratios, e.g., $B(D^0 \rightarrow K^- \pi^+) = 3.71 \pm 0.25\%$, $B(D^+ \rightarrow K^- 2\pi^+) = 7.1 \pm 1.0\%$, and $B(D^*(2010)^+ \rightarrow D^0 \pi^+) = 55 \pm 4\%$.
- ⁶ GIBAUT 96 reports $0.0203 \pm 0.0050 \pm 0.0036$ from a measurement of $[\Gamma(B^0 \rightarrow D^*(2010)^- D_s^{*+})/\Gamma_{\text{total}}] \times [B(D_s^+ \rightarrow \phi\pi^+)]$ assuming $B(D_s^+ \rightarrow \phi\pi^+) = 0.035$, which we rescale to our best value $B(D_s^+ \rightarrow \phi\pi^+) = (4.5 \pm 0.4) \times 10^{-2}$. Our first error is their experiment's error and our second error is the systematic error from using our best value.

$\Gamma(D_s^{*+} a_1(1260)^-)/\Gamma_{\text{total}}$					Γ_{104}/Γ
VALUE	CL%	DOCUMENT ID	TECN	COMMENT	
$<1.7 \times 10^{-3}$	90	1 ALBRECHT 93E	ARG	$e^+e^- \rightarrow \Upsilon(4S)$	
1 ALBRECHT 93E reports $< 2.9 \times 10^{-3}$ from a measurement of $[\Gamma(B^0 \rightarrow D_s^{*+} a_1(1260)^-)/\Gamma_{\text{total}}] \times [B(D_s^+ \rightarrow \phi\pi^+)]$ assuming $B(D_s^+ \rightarrow \phi\pi^+) = 0.027$, which we rescale to our best value $B(D_s^+ \rightarrow \phi\pi^+) = 4.5 \times 10^{-2}$.					

$\Gamma(D_s^{*+} \phi_2^-)/\Gamma_{\text{total}}$					Γ_{105}/Γ
VALUE (units 10^{-5})	CL%	DOCUMENT ID	TECN	COMMENT	
<19	90	1 AUBERT 06X	BABR	$e^+e^- \rightarrow \Upsilon(4S)$	
1 Assumes equal production of B^+ and B^0 at the $\Upsilon(4S)$.					

$\Gamma(D_s^{*+} a_2^-)/\Gamma_{\text{total}}$					Γ_{106}/Γ
VALUE (units 10^{-5})	CL%	DOCUMENT ID	TECN	COMMENT	
<20	90	1 AUBERT 06X	BABR	$e^+e^- \rightarrow \Upsilon(4S)$	
1 Assumes equal production of B^+ and B^0 at the $\Upsilon(4S)$.					

$\Gamma(D_s^- K^+)/\Gamma_{\text{total}}$					Γ_{107}/Γ
VALUE (units 10^{-6})	CL%	DOCUMENT ID	TECN	COMMENT	
30 ± 4	OUR AVERAGE				
$29 \pm 4 \pm 2$		1 AUBERT 08AJ	BABR	$e^+e^- \rightarrow \Upsilon(4S)$	
$36^{+11}_{-10} \pm 3$		2 KROKOVNY 02	BELL	$e^+e^- \rightarrow \Upsilon(4S)$	
• • • We do not use the following data for averages, fits, limits, etc. • • •					
$27 \pm 5 \pm 2$		3 AUBERT 07K	BABR	Repl. by AUBERT 08AJ	
$26 \pm 10 \pm 2$		4 AUBERT 03D	BABR	Repl. by AUBERT 07K	
< 190	90	5 ALEXANDER 93B	CLE2	$e^+e^- \rightarrow \Upsilon(4S)$	
<1300	90	6 BORTOLETTO 90	CLEO	$e^+e^- \rightarrow \Upsilon(4S)$	

- 1 Assumes equal production of B^+ and B^0 at the $\Upsilon(4S)$.
- 2 KROKOVNY 02 reports $[\Gamma(B^0 \rightarrow D_s^- K^+)/\Gamma_{\text{total}}] \times [B(D_s^+ \rightarrow \phi\pi^+)] = (1.61^{+0.45}_{-0.38} \pm 0.21) \times 10^{-6}$ which we divide by our best value $B(D_s^+ \rightarrow \phi\pi^+) = (4.5 \pm 0.4) \times 10^{-2}$. Our first error is their experiment's error and our second error is the systematic error from using our best value.
- 3 AUBERT 07K reports $[\Gamma(B^0 \rightarrow D_s^- K^+)/\Gamma_{\text{total}}] \times [B(D_s^+ \rightarrow \phi\pi^+)] = (1.21 \pm 0.17 \pm 0.11) \times 10^{-6}$ which we divide by our best value $B(D_s^+ \rightarrow \phi\pi^+) = (4.5 \pm 0.4) \times 10^{-2}$. Our first error is their experiment's error and our second error is the systematic error from using our best value.
- 4 AUBERT 03D reports $[\Gamma(B^0 \rightarrow D_s^- K^+)/\Gamma_{\text{total}}] \times [B(D_s^+ \rightarrow \phi\pi^+)] = (1.16 \pm 0.36 \pm 0.24) \times 10^{-6}$ which we divide by our best value $B(D_s^+ \rightarrow \phi\pi^+) = (4.5 \pm 0.4) \times 10^{-2}$. Our first error is their experiment's error and our second error is the systematic error from using our best value.
- 5 ALEXANDER 93B reports $< 230 \times 10^{-6}$ from a measurement of $[\Gamma(B^0 \rightarrow D_s^- K^+)/\Gamma_{\text{total}}] \times [B(D_s^+ \rightarrow \phi\pi^+)]$ assuming $B(D_s^+ \rightarrow \phi\pi^+) = 0.037$, which we rescale to our best value $B(D_s^+ \rightarrow \phi\pi^+) = 4.5 \times 10^{-2}$.
- 6 BORTOLETTO 90 assume $B(D_s^+ \rightarrow \phi\pi^+) = 2\%$.

$\Gamma(D_s^{*-} K^+)/\Gamma_{\text{total}}$					Γ_{108}/Γ
VALUE (units 10^{-5})	CL%	DOCUMENT ID	TECN	COMMENT	
2.19 ± 0.30	OUR AVERAGE				
$2.02 \pm 0.33 \pm 0.22$		1 JOSHI 10	BELL	$e^+e^- \rightarrow \Upsilon(4S)$	
$2.4 \pm 0.4 \pm 0.2$		1 AUBERT 08AJ	BABR	$e^+e^- \rightarrow \Upsilon(4S)$	
• • • We do not use the following data for averages, fits, limits, etc. • • •					
$2.2 \pm 0.6 \pm 0.2$		2 AUBERT 07K	BABR	Repl. by AUBERT 08AJ	
< 2.5	90	AUBERT 03D	BABR	Repl. by AUBERT 07K	
<14	90	3 ALEXANDER 93B	CLE2	$e^+e^- \rightarrow \Upsilon(4S)$	

- 1 Assumes equal production of B^+ and B^0 at the $\Upsilon(4S)$.
- 2 AUBERT 07K reports $[\Gamma(B^0 \rightarrow D_s^{*-} K^+)/\Gamma_{\text{total}}] \times [B(D_s^+ \rightarrow \phi\pi^+)] = (0.97 \pm 0.24 \pm 0.12) \times 10^{-6}$ which we divide by our best value $B(D_s^+ \rightarrow \phi\pi^+) = (4.5 \pm 0.4) \times 10^{-2}$. Our first error is their experiment's error and our second error is the systematic error from using our best value.
- 3 ALEXANDER 93B reports $< 17 \times 10^{-5}$ from a measurement of $[\Gamma(B^0 \rightarrow D_s^{*-} K^+)/\Gamma_{\text{total}}] \times [B(D_s^+ \rightarrow \phi\pi^+)]$ assuming $B(D_s^+ \rightarrow \phi\pi^+) = 0.037$, which we rescale to our best value $B(D_s^+ \rightarrow \phi\pi^+) = 4.5 \times 10^{-2}$.

$\Gamma(D_s^- K^*(892)^+)/\Gamma_{\text{total}}$					Γ_{109}/Γ
VALUE (units 10^{-5})	CL%	DOCUMENT ID	TECN	COMMENT	
$3.5^{+1.0}_{-0.9} \pm 0.4$		1 AUBERT 08AJ	BABR	$e^+e^- \rightarrow \Upsilon(4S)$	
• • • We do not use the following data for averages, fits, limits, etc. • • •					
<280	90	2 ALBRECHT 93E	ARG	$e^+e^- \rightarrow \Upsilon(4S)$	
< 80	90	3 ALEXANDER 93B	CLE2	$e^+e^- \rightarrow \Upsilon(4S)$	

- 1 Assumes equal production of B^+ and B^0 at the $\Upsilon(4S)$.
- 2 ALBRECHT 93E reports $< 4.6 \times 10^{-3}$ from a measurement of $[\Gamma(B^0 \rightarrow D_s^- K^*(892)^+)/\Gamma_{\text{total}}] \times [B(D_s^+ \rightarrow \phi\pi^+)]$ assuming $B(D_s^+ \rightarrow \phi\pi^+) = 0.027$, which we rescale to our best value $B(D_s^+ \rightarrow \phi\pi^+) = 4.5 \times 10^{-2}$.
- 3 ALEXANDER 93B reports $< 9.7 \times 10^{-4}$ from a measurement of $[\Gamma(B^0 \rightarrow D_s^- K^*(892)^+)/\Gamma_{\text{total}}] \times [B(D_s^+ \rightarrow \phi\pi^+)]$ assuming $B(D_s^+ \rightarrow \phi\pi^+) = 0.037$, which we rescale to our best value $B(D_s^+ \rightarrow \phi\pi^+) = 4.5 \times 10^{-2}$.

$\Gamma(D_s^{*-} K^*(892)^+)/\Gamma_{\text{total}}$					Γ_{110}/Γ
VALUE (units 10^{-5})	CL%	DOCUMENT ID	TECN	COMMENT	
$3.2^{+1.4}_{-1.2} \pm 0.4$		1 AUBERT 08AJ	BABR	$e^+e^- \rightarrow \Upsilon(4S)$	
• • • We do not use the following data for averages, fits, limits, etc. • • •					
<350	90	2 ALBRECHT 93E	ARG	$e^+e^- \rightarrow \Upsilon(4S)$	
< 90	90	3 ALEXANDER 93B	CLE2	$e^+e^- \rightarrow \Upsilon(4S)$	

- 1 Assumes equal production of B^+ and B^0 at the $\Upsilon(4S)$.
- 2 ALBRECHT 93E reports $< 5.8 \times 10^{-3}$ from a measurement of $[\Gamma(B^0 \rightarrow D_s^{*-} K^*(892)^+)/\Gamma_{\text{total}}] \times [B(D_s^+ \rightarrow \phi\pi^+)]$ assuming $B(D_s^+ \rightarrow \phi\pi^+) = 0.027$, which we rescale to our best value $B(D_s^+ \rightarrow \phi\pi^+) = 4.5 \times 10^{-2}$.
- 3 ALEXANDER 93B reports $< 11.0 \times 10^{-4}$ from a measurement of $[\Gamma(B^0 \rightarrow D_s^{*-} K^*(892)^+)/\Gamma_{\text{total}}] \times [B(D_s^+ \rightarrow \phi\pi^+)]$ assuming $B(D_s^+ \rightarrow \phi\pi^+) = 0.037$, which we rescale to our best value $B(D_s^+ \rightarrow \phi\pi^+) = 4.5 \times 10^{-2}$.

$\Gamma(D_s^- \pi^+ K^0)/\Gamma_{\text{total}}$					Γ_{111}/Γ
VALUE (units 10^{-4})	CL%	DOCUMENT ID	TECN	COMMENT	
$1.10 \pm 0.26 \pm 0.20$		1 AUBERT 08G	BABR	$e^+e^- \rightarrow \Upsilon(4S)$	
• • • We do not use the following data for averages, fits, limits, etc. • • •					
<40	90	2 ALBRECHT 93E	ARG	$e^+e^- \rightarrow \Upsilon(4S)$	

- 1 Assumes equal production of B^+ and B^0 at the $\Upsilon(4S)$.
- 2 ALBRECHT 93E reports $< 7.3 \times 10^{-3}$ from a measurement of $[\Gamma(B^0 \rightarrow D_s^- \pi^+ K^0)/\Gamma_{\text{total}}] \times [B(D_s^+ \rightarrow \phi\pi^+)]$ assuming $B(D_s^+ \rightarrow \phi\pi^+) = 0.027$, which we rescale to our best value $B(D_s^+ \rightarrow \phi\pi^+) = 4.5 \times 10^{-2}$.

$\Gamma(D_s^{*-} \pi^+ K^0)/\Gamma_{\text{total}}$					Γ_{112}/Γ
VALUE (units 10^{-4})	CL%	DOCUMENT ID	TECN	COMMENT	
< 1.10	90	1 AUBERT 08G	BABR	$e^+e^- \rightarrow \Upsilon(4S)$	
• • • We do not use the following data for averages, fits, limits, etc. • • •					
<25	90	2 ALBRECHT 93E	ARG	$e^+e^- \rightarrow \Upsilon(4S)$	

- 1 Assumes equal production of B^+ and B^0 at the $\Upsilon(4S)$.
- 2 ALBRECHT 93E reports $< 4.2 \times 10^{-3}$ from a measurement of $[\Gamma(B^0 \rightarrow D_s^{*-} \pi^+ K^0)/\Gamma_{\text{total}}] \times [B(D_s^+ \rightarrow \phi\pi^+)]$ assuming $B(D_s^+ \rightarrow \phi\pi^+) = 0.027$, which we rescale to our best value $B(D_s^+ \rightarrow \phi\pi^+) = 4.5 \times 10^{-2}$.

$\Gamma(D_s^- \pi^+ K^*(892)^0)/\Gamma_{\text{total}}$					Γ_{113}/Γ
VALUE	CL%	DOCUMENT ID	TECN	COMMENT	
$<3.0 \times 10^{-3}$	90	1 ALBRECHT 93E	ARG	$e^+e^- \rightarrow \Upsilon(4S)$	
• • • We do not use the following data for averages, fits, limits, etc. • • •					
<1	90	2 ALBRECHT 93E	ARG	$e^+e^- \rightarrow \Upsilon(4S)$	

- 1 Assumes equal production of B^+ and B^0 at the $\Upsilon(4S)$.
- 2 ALBRECHT 93E reports $< 5.0 \times 10^{-3}$ from a measurement of $[\Gamma(B^0 \rightarrow D_s^- \pi^+ K^*(892)^0)/\Gamma_{\text{total}}] \times [B(D_s^+ \rightarrow \phi\pi^+)]$ assuming $B(D_s^+ \rightarrow \phi\pi^+) = 0.027$, which we rescale to our best value $B(D_s^+ \rightarrow \phi\pi^+) = 4.5 \times 10^{-2}$.

$\Gamma(D_s^{*-} \pi^+ K^*(892)^0)/\Gamma_{\text{total}}$					Γ_{114}/Γ
VALUE	CL%	DOCUMENT ID	TECN	COMMENT	
$<1.6 \times 10^{-3}$	90	1 ALBRECHT 93E	ARG	$e^+e^- \rightarrow \Upsilon(4S)$	
• • • We do not use the following data for averages, fits, limits, etc. • • •					
$< 2.7 \times 10^{-3}$		1 ALBRECHT 93E	ARG	from a measurement of $[\Gamma(B^0 \rightarrow D_s^{*-} \pi^+ K^*(892)^0)/\Gamma_{\text{total}}] \times [B(D_s^+ \rightarrow \phi\pi^+)]$ assuming $B(D_s^+ \rightarrow \phi\pi^+) = 0.027$, which we rescale to our best value $B(D_s^+ \rightarrow \phi\pi^+) = 4.5 \times 10^{-2}$.	

$\Gamma(D^0 K^0)/\Gamma_{\text{total}}$					Γ_{115}/Γ
VALUE (units 10^{-5})	CL%	DOCUMENT ID	TECN	COMMENT	
5.2 ± 0.7	OUR AVERAGE				
$5.3 \pm 0.7 \pm 0.3$		1 AUBERT,B 06L	BABR	$e^+e^- \rightarrow \Upsilon(4S)$	
$5.0^{+1.3}_{-1.2} \pm 0.6$		1 KROKOVNY 03	BELL	$e^+e^- \rightarrow \Upsilon(4S)$	
1 Assumes equal production of B^+ and B^0 at the $\Upsilon(4S)$.					

$\Gamma(D^0 K^+ \pi^-)/\Gamma_{\text{total}}$					Γ_{116}/Γ
VALUE (units 10^{-6})	CL%	DOCUMENT ID	TECN	COMMENT	
$88 \pm 15 \pm 9$		1 AUBERT 06A	BABR	$e^+e^- \rightarrow \Upsilon(4S)$	
1 Assumes equal production of B^+ and B^0 at the $\Upsilon(4S)$.					

$\Gamma(D^0 K^*(892)^0)/\Gamma_{\text{total}}$					Γ_{117}/Γ
VALUE (units 10^{-5})	CL%	DOCUMENT ID	TECN	COMMENT	
4.2 ± 0.6	OUR AVERAGE				
$4.0 \pm 0.7 \pm 0.3$		1 AUBERT,B 06L	BABR	$e^+e^- \rightarrow \Upsilon(4S)$	
$4.8^{+1.1}_{-1.0} \pm 0.5$		1 KROKOVNY 03	BELL	$e^+e^- \rightarrow \Upsilon(4S)$	
• • • We do not use the following data for averages, fits, limits, etc. • • •					
$5.7 \pm 0.9 \pm 0.6$		1 AUBERT 06A	BABR	Repl. by AUBERT,B 06L	
1 Assumes equal production of B^+ and B^0 at the $\Upsilon(4S)$.					

$\Gamma(D_2^*(2460)^- K^+ \times B(D_2^*(2460)^- \rightarrow \bar{D}^0 \pi^-))/\Gamma_{\text{total}}$					Γ_{118}/Γ
VALUE (units 10^{-6})	CL%	DOCUMENT ID	TECN	COMMENT	
$18.3 \pm 4.0 \pm 3.1$		1 AUBERT 06A	BABR	$e^+e^- \rightarrow \Upsilon(4S)$	
1 Assumes equal production of B^+ and B^0 at the $\Upsilon(4S)$.					

Meson Particle Listings

 B^0 $\Gamma(\bar{D}^0 K^+ \pi^- \text{ non-resonant})/\Gamma_{\text{total}}$ Γ_{119}/Γ

VALUE (units 10^{-6})	CL%	DOCUMENT ID	TECN	COMMENT
<37	90	¹ AUBERT	06A BABR	$e^+ e^- \rightarrow \Upsilon(4S)$

¹ Assumes equal production of B^+ and B^0 at the $\Upsilon(4S)$.

 $\Gamma(\bar{D}^0 \pi^0)/\Gamma_{\text{total}}$ Γ_{120}/Γ

VALUE (units 10^{-4})	CL%	DOCUMENT ID	TECN	COMMENT
2.61 ± 0.24 OUR AVERAGE				
2.25 ± 0.14 ± 0.35		¹ BLYTH	06 BELL	$e^+ e^- \rightarrow \Upsilon(4S)$
2.9 ± 0.2 ± 0.3		¹ AUBERT	04B BABR	$e^+ e^- \rightarrow \Upsilon(4S)$
2.74 $^{+0.36}_{-0.32}$ ± 0.55		¹ COAN	02 CLE2	$e^+ e^- \rightarrow \Upsilon(4S)$

• • • We do not use the following data for averages, fits, limits, etc. • • •

3.1 ± 0.4 ± 0.5		¹ ABE	02j BELL	Repl. by BLYTH 06
<1.2	90	² NEMAT1	98 CLE2	Repl. by COAN 02
<4.8	90	³ ALAM	94 CLE2	Repl. by NEMAT1 98

- ¹ Assumes equal production of B^+ and B^0 at the $\Upsilon(4S)$.
² NEMAT1 98 assumes equal production of B^+ and B^0 at the $\Upsilon(4S)$ and use the PDG 96 values for D^0 , D^{*0} , η , η' , and ω branching fractions.
³ ALAM 94 assume equal production of B^+ and B^0 at the $\Upsilon(4S)$ and use the CLEOII absolute $B(D^0 \rightarrow K^- \pi^+)$ and the PDG 1992 $B(D^0 \rightarrow K^- \pi^+ \pi^0)/B(D^0 \rightarrow K^- \pi^+)$ and $B(D^0 \rightarrow K^- 2\pi^+ \pi^-)/B(D^0 \rightarrow K^- \pi^+)$.

 $\Gamma(\bar{D}^0 \rho^0)/\Gamma_{\text{total}}$ Γ_{121}/Γ

VALUE (units 10^{-4})	CL%	DOCUMENT ID	TECN	COMMENT
3.19 ± 0.20 ± 0.45		^{1,2} KUZMIN	07 BELL	$e^+ e^- \rightarrow \Upsilon(4S)$
2.9 ± 1.0 ± 0.4		¹ SATPATHY	03 BELL	Repl. by KUZMIN 07
< 3.9	90	³ NEMAT1	98 CLE2	$e^+ e^- \rightarrow \Upsilon(4S)$
< 5.5	90	⁴ ALAM	94 CLE2	Repl. by NEMAT1 98
< 6.0	90	⁵ BORTOLETTO92	CLEO	$e^+ e^- \rightarrow \Upsilon(4S)$
<27.0	90	⁶ ALBRECHT	88k ARG	$e^+ e^- \rightarrow \Upsilon(4S)$

- • • We do not use the following data for averages, fits, limits, etc. • • •
- ¹ Assumes equal production of B^+ and B^0 at the $\Upsilon(4S)$.
² Our second uncertainty combines systematics and model errors quoted in the paper.
³ NEMAT1 98 assumes equal production of B^+ and B^0 at the $\Upsilon(4S)$ and use the PDG 96 values for D^0 , D^{*0} , η , η' , and ω branching fractions.
⁴ ALAM 94 assume equal production of B^+ and B^0 at the $\Upsilon(4S)$ and use the CLEOII absolute $B(D^0 \rightarrow K^- \pi^+)$ and the PDG 1992 $B(D^0 \rightarrow K^- \pi^+ \pi^0)/B(D^0 \rightarrow K^- \pi^+)$ and $B(D^0 \rightarrow K^- 2\pi^+ \pi^-)/B(D^0 \rightarrow K^- \pi^+)$.
⁵ BORTOLETTO 92 assume equal production of B^+ and B^0 at the $\Upsilon(4S)$ and use MarkIII branching fractions for the D .
⁶ ALBRECHT 88k reports < 0.003 assuming $B^0 \bar{B}^0 : B^+ B^-$ production ratio is 45:55. We rescale to 50%.

 $\Gamma(\bar{D}^0 f_2)/\Gamma_{\text{total}}$ Γ_{122}/Γ

VALUE (units 10^{-4})	CL%	DOCUMENT ID	TECN	COMMENT
1.20 ± 0.18 ± 0.38		^{1,2} KUZMIN	07 BELL	$e^+ e^- \rightarrow \Upsilon(4S)$

- ¹ Assumes equal production of B^+ and B^0 at the $\Upsilon(4S)$.
² Our second uncertainty combines systematics and model errors quoted in the paper.

 $\Gamma(\bar{D}^0 \eta)/\Gamma_{\text{total}}$ Γ_{123}/Γ

VALUE (units 10^{-4})	CL%	DOCUMENT ID	TECN	COMMENT
2.02 ± 0.35 OUR AVERAGE				Error includes scale factor of 1.6.
1.77 ± 0.16 ± 0.21		¹ BLYTH	06 BELL	$e^+ e^- \rightarrow \Upsilon(4S)$
2.5 ± 0.2 ± 0.3		¹ AUBERT	04B BABR	$e^+ e^- \rightarrow \Upsilon(4S)$
1.4 $^{+0.5}_{-0.4}$ ± 0.3		¹ ABE	02j BELL	Repl. by BLYTH 06
<1.3	90	² NEMAT1	98 CLE2	$e^+ e^- \rightarrow \Upsilon(4S)$
<6.8	90	³ ALAM	94 CLE2	Repl. by NEMAT1 98

- • • We do not use the following data for averages, fits, limits, etc. • • •
- ¹ Assumes equal production of B^+ and B^0 at the $\Upsilon(4S)$.
² NEMAT1 98 assumes equal production of B^+ and B^0 at the $\Upsilon(4S)$ and use the PDG 96 values for D^0 , D^{*0} , η , η' , and ω branching fractions.
³ ALAM 94 assume equal production of B^+ and B^0 at the $\Upsilon(4S)$ and use the CLEOII absolute $B(D^0 \rightarrow K^- \pi^+)$ and the PDG 1992 $B(D^0 \rightarrow K^- \pi^+ \pi^0)/B(D^0 \rightarrow K^- \pi^+)$ and $B(D^0 \rightarrow K^- 2\pi^+ \pi^-)/B(D^0 \rightarrow K^- \pi^+)$.

 $\Gamma(\bar{D}^0 \eta')/\Gamma_{\text{total}}$ Γ_{124}/Γ

VALUE (units 10^{-4})	CL%	DOCUMENT ID	TECN	COMMENT
1.25 ± 0.23 OUR AVERAGE				Error includes scale factor of 1.1.
1.14 ± 0.20 $^{+0.10}_{-0.13}$		¹ SCHUMANN	05 BELL	$e^+ e^- \rightarrow \Upsilon(4S)$
1.7 ± 0.4 ± 0.2		¹ AUBERT	04B BABR	$e^+ e^- \rightarrow \Upsilon(4S)$
<9.4	90	² NEMAT1	98 CLE2	$e^+ e^- \rightarrow \Upsilon(4S)$
<8.6	90	³ ALAM	94 CLE2	Repl. by NEMAT1 98

- • • We do not use the following data for averages, fits, limits, etc. • • •
- ¹ Assumes equal production of B^+ and B^0 at the $\Upsilon(4S)$.
² NEMAT1 98 assumes equal production of B^+ and B^0 at the $\Upsilon(4S)$ and use the PDG 96 values for D^0 , D^{*0} , η , η' , and ω branching fractions.
³ ALAM 94 assume equal production of B^+ and B^0 at the $\Upsilon(4S)$ and use the CLEOII absolute $B(D^0 \rightarrow K^- \pi^+)$ and the PDG 1992 $B(D^0 \rightarrow K^- \pi^+ \pi^0)/B(D^0 \rightarrow K^- \pi^+)$ and $B(D^0 \rightarrow K^- 2\pi^+ \pi^-)/B(D^0 \rightarrow K^- \pi^+)$.

 $\Gamma(\bar{D}^0 \eta')/\Gamma(\bar{D}^0 \eta)$ $\Gamma_{124}/\Gamma_{123}$

VALUE	DOCUMENT ID	TECN	COMMENT
0.7 ± 0.2 ± 0.1	AUBERT	04B BABR	$e^+ e^- \rightarrow \Upsilon(4S)$

 $\Gamma(\bar{D}^0 \omega)/\Gamma_{\text{total}}$ Γ_{125}/Γ

VALUE (units 10^{-4})	CL%	DOCUMENT ID	TECN	COMMENT
2.59 ± 0.30 OUR AVERAGE				
2.37 ± 0.23 ± 0.28		¹ BLYTH	06 BELL	$e^+ e^- \rightarrow \Upsilon(4S)$
3.0 ± 0.3 ± 0.4		¹ AUBERT	04B BABR	$e^+ e^- \rightarrow \Upsilon(4S)$
1.8 ± 0.5 $^{+0.4}_{-0.3}$		¹ ABE	02j BELL	Repl. by BLYTH 06
<5.1	90	² NEMAT1	98 CLE2	$e^+ e^- \rightarrow \Upsilon(4S)$
<6.3	90	³ ALAM	94 CLE2	Repl. by NEMAT1 98

- • • We do not use the following data for averages, fits, limits, etc. • • •
- ¹ Assumes equal production of B^+ and B^0 at the $\Upsilon(4S)$.
² NEMAT1 98 assumes equal production of B^+ and B^0 at the $\Upsilon(4S)$ and use the PDG 96 values for D^0 , D^{*0} , η , η' , and ω branching fractions.
³ ALAM 94 assume equal production of B^+ and B^0 at the $\Upsilon(4S)$ and use the CLEOII absolute $B(D^0 \rightarrow K^- \pi^+)$ and the PDG 1992 $B(D^0 \rightarrow K^- \pi^+ \pi^0)/B(D^0 \rightarrow K^- \pi^+)$ and $B(D^0 \rightarrow K^- 2\pi^+ \pi^-)/B(D^0 \rightarrow K^- \pi^+)$.

 $\Gamma(\bar{D}^0 \phi)/\Gamma_{\text{total}}$ Γ_{126}/Γ

VALUE (units 10^{-6})	CL%	DOCUMENT ID	TECN	COMMENT
<11.6	90	¹ AUBERT	07A0 BABR	$e^+ e^- \rightarrow \Upsilon(4S)$

¹ Assumes equal production of B^+ and B^0 at the $\Upsilon(4S)$.

 $\Gamma(\bar{D}^0 K^+ \pi^-)/\Gamma_{\text{total}}$ Γ_{127}/Γ

VALUE (units 10^{-6})	CL%	DOCUMENT ID	TECN	COMMENT
<19	90	¹ AUBERT	06A BABR	Repl. by AUBERT 09AE

¹ Assumes equal production of B^+ and B^0 at the $\Upsilon(4S)$.

 $\Gamma(\bar{D}^0 K^+ \pi^-)/\Gamma(\bar{D}^0 K^+ \pi^-)$ $\Gamma_{127}/\Gamma_{116}$

VALUE	DOCUMENT ID	TECN	COMMENT
0.068 ± 0.042	¹ AUBERT	09AE BABR	$e^+ e^- \rightarrow \Upsilon(4S)$

¹ Reports a signal at the level of 2.5 standard deviations after combining results from $D^0 \rightarrow K^+ \pi^-$, $K^+ \pi^- \pi^0$, and $K^+ \pi^- \pi^+ \pi^-$.

 $\Gamma(\bar{D}^0 K^*(892)^0)/\Gamma_{\text{total}}$ Γ_{128}/Γ

VALUE (units 10^{-5})	CL%	DOCUMENT ID	TECN	COMMENT
<1.1	90	¹ AUBERT,B	06L BABR	$e^+ e^- \rightarrow \Upsilon(4S)$
<1.8	90	¹ KROKOVNY	03 BELL	$e^+ e^- \rightarrow \Upsilon(4S)$

¹ Assumes equal production of B^+ and B^0 at the $\Upsilon(4S)$.

 $\Gamma(\bar{D}^{*0} \gamma)/\Gamma_{\text{total}}$ Γ_{129}/Γ

VALUE	CL%	DOCUMENT ID	TECN	COMMENT
<2.5 × 10 ⁻⁵	90	¹ AUBERT,B	05Q BABR	$e^+ e^- \rightarrow \Upsilon(4S)$
<5.0 × 10 ⁻⁵	90	¹ ARTUSO	00 CLE2	$e^+ e^- \rightarrow \Upsilon(4S)$

¹ Assumes equal production of B^+ and B^0 at the $\Upsilon(4S)$.

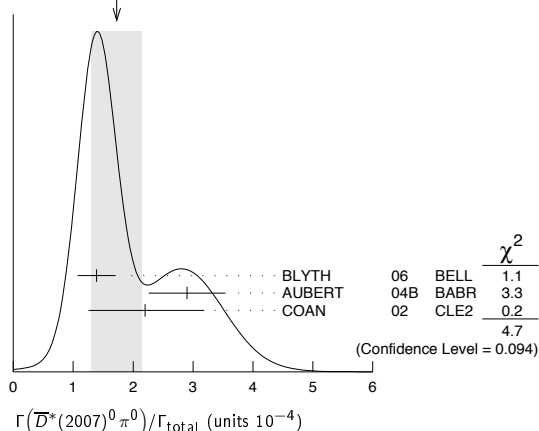
 $\Gamma(\bar{D}^{*0}(2007)^0 \pi^0)/\Gamma_{\text{total}}$ Γ_{130}/Γ

VALUE (units 10^{-4})	CL%	DOCUMENT ID	TECN	COMMENT
1.7 ± 0.4 OUR AVERAGE				Error includes scale factor of 1.5. See the ideogram below.
1.39 ± 0.18 ± 0.26		¹ BLYTH	06 BELL	$e^+ e^- \rightarrow \Upsilon(4S)$
2.9 ± 0.4 ± 0.5		¹ AUBERT	04B BABR	$e^+ e^- \rightarrow \Upsilon(4S)$
2.20 $^{+0.59}_{-0.52}$ ± 0.79		¹ COAN	02 CLE2	$e^+ e^- \rightarrow \Upsilon(4S)$

- • • We do not use the following data for averages, fits, limits, etc. • • •
- 2.7 $^{+0.8}_{-0.7}$ $^{+0.5}_{-0.6}$
- | | | | | |
|------|------------------|---------------------|-------------------|--------------------|
| | ¹ ABE | 02j BELL | Repl. by BLYTH 06 | |
| <4.4 | 90 | ² NEMAT1 | 98 CLE2 | Repl. by COAN 02 |
| <9.7 | 90 | ³ ALAM | 94 CLE2 | Repl. by NEMAT1 98 |

- ¹ Assumes equal production of B^+ and B^0 at the $\Upsilon(4S)$.
² NEMAT1 98 assumes equal production of B^+ and B^0 at the $\Upsilon(4S)$ and use the PDG 96 values for D^0 , D^{*0} , η , η' , and ω branching fractions.
³ ALAM 94 assume equal production of B^+ and B^0 at the $\Upsilon(4S)$ and use the CLEOII $B(D^{*0}(2007)^0 \rightarrow D^0 \pi^0)$ and absolute $B(D^0 \rightarrow K^- \pi^+)$ and the PDG 1992 $B(D^0 \rightarrow K^- \pi^+ \pi^0)/B(D^0 \rightarrow K^- \pi^+)$ and $B(D^0 \rightarrow K^- 2\pi^+ \pi^-)/B(D^0 \rightarrow K^- \pi^+)$.

WEIGHTED AVERAGE
1.7±0.4 (Error scaled by 1.5)



$\Gamma(\bar{D}^0 \pi^0) / \Gamma(\bar{D}^*(2007)^0 \pi^0)$		$\Gamma_{120} / \Gamma_{130}$	
VALUE	DOCUMENT ID	TECN	COMMENT
1.14±0.26 OUR AVERAGE	Error includes scale factor of 1.3.		
1.62±0.23±0.35	BLYTH 06	BELL	e ⁺ e ⁻ → T(4S)
1.0 ±0.1 ±0.2	AUBERT 04B	BABR	e ⁺ e ⁻ → T(4S)

$\Gamma(\bar{D}^*(2007)^0 \rho^0) / \Gamma_{total}$		Γ_{131} / Γ	
VALUE	CL%	DOCUMENT ID	TECN COMMENT
<5.1 × 10⁻⁴	90	1 SATPATHY 03	BELL e ⁺ e ⁻ → T(4S)
• • • We do not use the following data for averages, fits, limits, etc. • • •			
<0.00056	90	2 NEMAT1 98	CLE2 e ⁺ e ⁻ → T(4S)
<0.00117	90	3 ALAM 94	CLE2 Repl. by NEMAT1 98

¹ Assumes equal production of B⁺ and B⁰ at the T(4S).
² NEMAT1 98 assumes equal production of B⁺ and B⁰ at the T(4S) and use the PDG 96 values for D⁰, D^{*0}, η, η', and ω branching fractions.
³ ALAM 94 assume equal production of B⁺ and B⁰ at the T(4S) and use the CLEO II B(D*(2007)⁰ → D⁰π⁰) and absolute B(D⁰ → K⁻π⁺) and the PDG 1992 B(D⁰ → K⁻π⁺π⁰)/B(D⁰ → K⁻π⁺) and B(D⁰ → K⁻2π⁺π⁻)/B(D⁰ → K⁻π⁺).

$\Gamma(\bar{D}^*(2007)^0 \eta) / \Gamma_{total}$		Γ_{132} / Γ	
VALUE (units 10 ⁻⁴)	CL%	DOCUMENT ID	TECN COMMENT
1.8 ±0.6 OUR AVERAGE	Error includes scale factor of 1.8.		
1.40±0.28±0.26	1	BLYTH 06	BELL e ⁺ e ⁻ → T(4S)
2.6 ±0.4 ±0.4	1	AUBERT 04B	BABR e ⁺ e ⁻ → T(4S)
• • • We do not use the following data for averages, fits, limits, etc. • • •			
<4.6	90	1 ABE 02J	BELL e ⁺ e ⁻ → T(4S)
<2.6	90	2 NEMAT1 98	CLE2 e ⁺ e ⁻ → T(4S)
<6.9	90	3 ALAM 94	CLE2 Repl. by NEMAT1 98

¹ Assumes equal production of B⁺ and B⁰ at the T(4S).
² NEMAT1 98 assumes equal production of B⁺ and B⁰ at the T(4S) and use the PDG 96 values for D⁰, D^{*0}, η, η', and ω branching fractions.
³ ALAM 94 assume equal production of B⁺ and B⁰ at the T(4S) and use the CLEO II B(D*(2007)⁰ → D⁰π⁰) and absolute B(D⁰ → K⁻π⁺) and the PDG 1992 B(D⁰ → K⁻π⁺π⁰)/B(D⁰ → K⁻π⁺) and B(D⁰ → K⁻2π⁺π⁻)/B(D⁰ → K⁻π⁺).

$\Gamma(\bar{D}^0 \eta) / \Gamma(\bar{D}^*(2007)^0 \eta)$		$\Gamma_{123} / \Gamma_{132}$	
VALUE	DOCUMENT ID	TECN	COMMENT
0.99±0.19 OUR AVERAGE	Error includes scale factor of 1.5.		
1.27±0.29±0.25	BLYTH 06	BELL	e ⁺ e ⁻ → T(4S)
0.9 ±0.2 ±0.1	AUBERT 04B	BABR	e ⁺ e ⁻ → T(4S)

$\Gamma(\bar{D}^*(2007)^0 \eta') / \Gamma(\bar{D}^*(2007)^0 \eta)$		$\Gamma_{133} / \Gamma_{132}$	
VALUE	DOCUMENT ID	TECN	COMMENT
0.5±0.3 ±0.1	AUBERT 04B	BABR	e ⁺ e ⁻ → T(4S)

$\Gamma(\bar{D}^*(2007)^0 \eta') / \Gamma_{total}$		Γ_{133} / Γ	
VALUE (units 10 ⁻⁴)	CL%	DOCUMENT ID	TECN COMMENT
1.23±0.35 OUR AVERAGE	Error includes scale factor of 1.5.		
1.21±0.34±0.22	1	SCHUMANN 05	BELL e ⁺ e ⁻ → T(4S)
1.3 ±0.7 ±0.2	1,2	AUBERT 04B	BABR e ⁺ e ⁻ → T(4S)
• • • We do not use the following data for averages, fits, limits, etc. • • •			
<14	90	BRANDENB... 98	CLE2 e ⁺ e ⁻ → T(4S)
<19	90	3 NEMAT1 98	CLE2 e ⁺ e ⁻ → T(4S)
<27	90	4 ALAM 94	CLE2 Repl. by NEMAT1 98

¹ Assumes equal production of B⁺ and B⁰ at the T(4S).
² Reports an upper limit < 2.6 × 10⁻⁴ at 90% CL.
³ NEMAT1 98 assumes equal production of B⁺ and B⁰ at the T(4S) and use the PDG 96 values for D⁰, D^{*0}, η, η', and ω branching fractions.
⁴ ALAM 94 assume equal production of B⁺ and B⁰ at the T(4S) and use the CLEO II B(D*(2007)⁰ → D⁰π⁰) and absolute B(D⁰ → K⁻π⁺) and the PDG 1992 B(D⁰ → K⁻π⁺π⁰)/B(D⁰ → K⁻π⁺) and B(D⁰ → K⁻2π⁺π⁻)/B(D⁰ → K⁻π⁺).

$\Gamma(\bar{D}^0 \eta') / \Gamma(\bar{D}^*(2007)^0 \eta')$		$\Gamma_{124} / \Gamma_{133}$	
VALUE	DOCUMENT ID	TECN	COMMENT
1.3±0.8±0.2	AUBERT 04B	BABR	e ⁺ e ⁻ → T(4S)

$\Gamma(\bar{D}^*(2007)^0 \pi^+ \pi^-) / \Gamma_{total}$		Γ_{134} / Γ	
VALUE	DOCUMENT ID	TECN	COMMENT
(6.2±1.2±1.8) × 10⁻⁴	1,2 SATPATHY 03	BELL	e ⁺ e ⁻ → T(4S)
¹ Assumes equal production of B ⁺ and B ⁰ at the T(4S). ² No assumption about the intermediate mechanism is made in the analysis.			

$\Gamma(\bar{D}^*(2007)^0 K^0) / \Gamma_{total}$		Γ_{135} / Γ	
VALUE (units 10 ⁻⁵)	CL%	DOCUMENT ID	TECN COMMENT
3.6±1.2±0.3	1	AUBERT,B 06L	BABR e ⁺ e ⁻ → T(4S)
• • • We do not use the following data for averages, fits, limits, etc. • • •			
<6.6	90	1 KROKOVNY 03	BELL e ⁺ e ⁻ → T(4S)
¹ Assumes equal production of B ⁺ and B ⁰ at the T(4S).			

$\Gamma(\bar{D}^*(2007)^0 K^*(892)^0) / \Gamma_{total}$		Γ_{136} / Γ	
VALUE	CL%	DOCUMENT ID	TECN COMMENT
<6.9 × 10⁻⁵	90	1 KROKOVNY 03	BELL e ⁺ e ⁻ → T(4S)
¹ Assumes equal production of B ⁺ and B ⁰ at the T(4S).			

$\Gamma(D^*(2007)^0 K^*(892)^0) / \Gamma_{total}$		Γ_{137} / Γ	
VALUE	CL%	DOCUMENT ID	TECN COMMENT
<4.0 × 10⁻⁵	90	1 KROKOVNY 03	BELL e ⁺ e ⁻ → T(4S)
¹ Assumes equal production of B ⁺ and B ⁰ at the T(4S).			

$\Gamma(D^*(2007)^0 \pi^+ \pi^+ \pi^- \pi^-) / \Gamma_{total}$		Γ_{138} / Γ	
VALUE (units 10 ⁻³)	CL%	DOCUMENT ID	TECN COMMENT
2.7 ±0.5 OUR AVERAGE	Error includes scale factor of 1.5.		
2.60±0.47±0.37	1	MAJUMDER 04	BELL e ⁺ e ⁻ → T(4S)
3.0 ±0.7 ±0.6	1	EDWARDS 02	CLE2 e ⁺ e ⁻ → T(4S)
¹ Assumes equal production of B ⁺ and B ⁰ at the T(4S).			

$\Gamma(D^*(2007)^0 \pi^+ \pi^+ \pi^- \pi^-) / \Gamma(D^*(2010)^- \pi^+ \pi^+ \pi^- \pi^-)$		$\Gamma_{138} / \Gamma_{56}$	
VALUE	DOCUMENT ID	TECN	COMMENT
0.17±0.04±0.02	1	EDWARDS 02	CLE2 e ⁺ e ⁻ → T(4S)
¹ Assumes equal production of B ⁺ and B ⁰ at the T(4S).			

$\Gamma(D^*(2010)^+ D^*(2010)^-) / \Gamma_{total}$		Γ_{139} / Γ	
VALUE (units 10 ⁻⁴)	CL%	DOCUMENT ID	TECN COMMENT
8.2±0.9 OUR AVERAGE	Error includes scale factor of 1.5.		
8.1±0.6±1.0	1	AUBERT,B 06A	BABR e ⁺ e ⁻ → T(4S)
8.1±0.8±1.1	1	MIYAKE 05	BELL e ⁺ e ⁻ → T(4S)
9.9 ^{+4.2} _{-3.3} ±1.2	1	LIPELES 00	CLE2 e ⁺ e ⁻ → T(4S)
• • • We do not use the following data for averages, fits, limits, etc. • • •			
8.3±1.6±1.2	1,2	AUBERT 02M	BABR Repl. by AUBERT,B 06B
6.2 ^{+4.0} _{-2.9} ±1.0	3	ARTUSO 99	CLE2 Repl. by LIPELES 00
<61	90	4 BARATE 98Q	ALEP e ⁺ e ⁻ → Z
<22	90	5 ASNER 97	CLE2 Repl. by ARTUSO 99

¹ Assumes equal production of B⁺ and B⁰ at the T(4S).
² AUBERT 02M also assumes the measured CP-odd fraction of the final states is 0.22 ± 0.18 ± 0.03.
³ ARTUSO 99 uses B(T(4S) → B⁰ \bar{B}^0) = (48 ± 4)%.
⁴ BARATE 98Q (ALEPH) observes 2 events with an expected background of 0.10 ± 0.03 which corresponds to a branching ratio of (2.3^{+1.9}_{-1.2} ± 0.4) × 10⁻³.
⁵ ASNER 97 at CLEO observes 1 event with an expected background of 0.022 ± 0.011. This corresponds to a branching ratio of (5.3^{+7.1}_{-3.7} ± 1.0) × 10⁻⁴.

$\Gamma(\bar{D}^*(2007)^0 \omega) / \Gamma_{total}$		Γ_{140} / Γ	
VALUE (units 10 ⁻⁴)	CL%	DOCUMENT ID	TECN COMMENT
2.7 ±0.8 OUR AVERAGE	Error includes scale factor of 1.5.		
2.29±0.39±0.40	1	BLYTH 06	BELL e ⁺ e ⁻ → T(4S)
4.2 ±0.7 ±0.9	90	1 AUBERT 04B	BABR e ⁺ e ⁻ → T(4S)
• • • We do not use the following data for averages, fits, limits, etc. • • •			
< 7.9	90	1 ABE 02J	BELL e ⁺ e ⁻ → T(4S)
< 7.4	90	2 NEMAT1 98	CLE2 e ⁺ e ⁻ → T(4S)
< 21	90	3 ALAM 94	CLE2 Repl. by NEMAT1 98

¹ Assumes equal production of B⁺ and B⁰ at the T(4S).
² NEMAT1 98 assumes equal production of B⁺ and B⁰ at the T(4S) and use the PDG 96 values for D⁰, D^{*0}, η, η', and ω branching fractions.
³ ALAM 94 assume equal production of B⁺ and B⁰ at the T(4S) and use the CLEO II B(D*(2007)⁰ → D⁰π⁰) and absolute B(D⁰ → K⁻π⁺) and the PDG 1992 B(D⁰ → K⁻π⁺π⁰)/B(D⁰ → K⁻π⁺) and B(D⁰ → K⁻2π⁺π⁻)/B(D⁰ → K⁻π⁺).

$\Gamma(\bar{D}^0 \omega) / \Gamma(\bar{D}^*(2007)^0 \omega)$		$\Gamma_{125} / \Gamma_{140}$	
VALUE	DOCUMENT ID	TECN	COMMENT
0.78±0.14 OUR AVERAGE	Error includes scale factor of 1.1.		
1.04±0.20±0.17	BLYTH 06	BELL	e ⁺ e ⁻ → T(4S)
0.7 ±0.1 ±0.1	AUBERT 04B	BABR	e ⁺ e ⁻ → T(4S)

Meson Particle Listings

 B^0

$\Gamma(J/\psi(1S)\eta)/\Gamma_{\text{total}}$		Γ_{168}/Γ	
VALUE (units 10^{-6})	CL%	DOCUMENT ID	TECN COMMENT
$9.5 \pm 1.7 \pm 0.8$		¹ CHANG 07A BELL	$e^+e^- \rightarrow \Upsilon(4S)$
••• We do not use the following data for averages, fits, limits, etc. •••			
< 27	90	¹ AUBERT 03o BABR	$e^+e^- \rightarrow \Upsilon(4S)$
<1200	90	² ACCIARRI 97c L3	
¹ Assumes equal production of B^+ and B^0 at the $\Upsilon(4S)$.			
² ACCIARRI 97c assumes B^0 production fraction ($39.5 \pm 4.0\%$) and B_S ($12.0 \pm 3.0\%$).			

$\Gamma(J/\psi(1S)\pi^+\pi^-)/\Gamma_{\text{total}}$		Γ_{169}/Γ	
VALUE	CL%	DOCUMENT ID	TECN COMMENT
$(4.6 \pm 0.7 \pm 0.6) \times 10^{-5}$		¹ AUBERT 03b BABR	$e^+e^- \rightarrow \Upsilon(4S)$
¹ Assumes equal production of B^+ and B^0 at the $\Upsilon(4S)$.			

$\Gamma(J/\psi(1S)\pi^+\pi^- \text{ nonresonant})/\Gamma_{\text{total}}$		Γ_{170}/Γ	
VALUE (units 10^{-5})	CL%	DOCUMENT ID	TECN COMMENT
<1.2	90	¹ AUBERT 07Ac BABR	$e^+e^- \rightarrow \Upsilon(4S)$
¹ Assumes equal production of B^+ and B^0 at the $\Upsilon(4S)$.			

$\Gamma(J/\psi(1S)f_2)/\Gamma_{\text{total}}$		Γ_{171}/Γ	
VALUE (units 10^{-5})	CL%	DOCUMENT ID	TECN COMMENT
<0.46	90	¹ AUBERT 07Ac BABR	$e^+e^- \rightarrow \Upsilon(4S)$
¹ Assumes equal production of B^+ and B^0 at the $\Upsilon(4S)$.			

$\Gamma(J/\psi(1S)\rho^0)/\Gamma_{\text{total}}$		Γ_{172}/Γ	
VALUE (units 10^{-5})	CL%	DOCUMENT ID	TECN COMMENT
$2.7 \pm 0.3 \pm 0.2$		¹ AUBERT 07Ac BABR	$e^+e^- \rightarrow \Upsilon(4S)$
••• We do not use the following data for averages, fits, limits, etc. •••			
$1.6 \pm 0.6 \pm 0.4$		¹ AUBERT 03b BABR	Repl. by AUBERT 07Ac
<25	90	BISHAI 96 CLE2	$e^+e^- \rightarrow \Upsilon(4S)$
¹ Assumes equal production of B^+ and B^0 at the $\Upsilon(4S)$.			

$\Gamma(J/\psi(1S)\omega)/\Gamma_{\text{total}}$		Γ_{173}/Γ	
VALUE	CL%	DOCUMENT ID	TECN COMMENT
< 2.7×10^{-4}	90	BISHAI 96 CLE2	$e^+e^- \rightarrow \Upsilon(4S)$

$\Gamma(J/\psi(1S)\phi)/\Gamma_{\text{total}}$		Γ_{174}/Γ	
VALUE (units 10^{-6})	CL%	DOCUMENT ID	TECN COMMENT
<0.94	90	¹ LIU 08i BELL	$e^+e^- \rightarrow \Upsilon(4S)$
••• We do not use the following data for averages, fits, limits, etc. •••			
<9.2	90	¹ AUBERT 03o BABR	$e^+e^- \rightarrow \Upsilon(4S)$
¹ Assumes equal production of B^+ and B^0 at the $\Upsilon(4S)$.			

$\Gamma(J/\psi(1S)\eta'(958))/\Gamma_{\text{total}}$		Γ_{175}/Γ	
VALUE (units 10^{-5})	CL%	DOCUMENT ID	TECN COMMENT
<6.3	90	¹ AUBERT 03o BABR	$e^+e^- \rightarrow \Upsilon(4S)$
¹ Assumes equal production of B^+ and B^0 at the $\Upsilon(4S)$.			

$\Gamma(J/\psi(1S)K^0\pi^+\pi^-)/\Gamma_{\text{total}}$		Γ_{176}/Γ	
VALUE (units 10^{-4})	CL%	DOCUMENT ID	TECN COMMENT
$10.3 \pm 3.3 \pm 1.5$		¹ AFFOLDER 02b CDF	$p\bar{p}$ 1.8 TeV
¹ Uses $B^0 \rightarrow J/\psi(1S)K_S^0$ decay as a reference and $B(B^0 \rightarrow J/\psi(1S)K^0) = 8.3 \times 10^{-4}$.			

$\Gamma(J/\psi(1S)K^0\rho^0)/\Gamma_{\text{total}}$		Γ_{177}/Γ	
VALUE (units 10^{-4})	CL%	DOCUMENT ID	TECN COMMENT
$5.4 \pm 2.9 \pm 0.9$		¹ AFFOLDER 02b CDF	$p\bar{p}$ 1.8 TeV
¹ Uses $B^0 \rightarrow J/\psi(1S)K_S^0$ decay as a reference and $B(B^0 \rightarrow J/\psi(1S)K^0) = 8.3 \times 10^{-4}$.			

$\Gamma(J/\psi(1S)K^*(892)^+\pi^-)/\Gamma_{\text{total}}$		Γ_{178}/Γ	
VALUE (units 10^{-4})	CL%	DOCUMENT ID	TECN COMMENT
$7.7 \pm 4.1 \pm 1.3$		¹ AFFOLDER 02b CDF	$p\bar{p}$ 1.8 TeV
¹ Uses $B^0 \rightarrow J/\psi(1S)K_S^0$ decay as a reference and $B(B^0 \rightarrow J/\psi(1S)K^0) = 8.3 \times 10^{-4}$.			

$\Gamma(J/\psi(1S)K^*(892)^0\pi^+\pi^-)/\Gamma_{\text{total}}$		Γ_{179}/Γ	
VALUE (units 10^{-4})	CL%	DOCUMENT ID	TECN COMMENT
$6.6 \pm 1.9 \pm 1.1$		¹ AFFOLDER 02b CDF	$p\bar{p}$ 1.8 TeV
¹ Uses $B^0 \rightarrow J/\psi(1S)K^*(892)^0$ decay as a reference and $B(B^0 \rightarrow J/\psi(1S)K^0) = 12.4 \times 10^{-4}$.			

$\Gamma(X(3872)^-K^+)/\Gamma_{\text{total}}$		Γ_{180}/Γ	
VALUE	CL%	DOCUMENT ID	TECN COMMENT
< 5×10^{-4}	90	¹ AUBERT 06E BABR	$e^+e^- \rightarrow \Upsilon(4S)$
¹ Perform measurements of absolute branching fractions using a missing mass technique.			

$\Gamma(X(3872)^-K^+ \times B(X(3872)^- \rightarrow J/\psi(1S)\pi^-\pi^0))/\Gamma_{\text{total}}$		Γ_{181}/Γ	
VALUE (units 10^{-6})	CL%	DOCUMENT ID	TECN COMMENT
<5.4	90	¹ AUBERT 05b BABR	$e^+e^- \rightarrow \Upsilon(4S)$
¹ Assumes equal production of B^+ and B^0 at the $\Upsilon(4S)$. The isovector-X hypothesis is excluded with a likelihood test at 1×10^{-4} level.			

$\Gamma(X(3872)K^0 \times B(X \rightarrow J/\psi\pi^+\pi^-))/\Gamma_{\text{total}}$		Γ_{182}/Γ	
VALUE (units 10^{-6})	CL%	DOCUMENT ID	TECN COMMENT
< 6.0	90	¹ AUBERT 08Y BABR	$e^+e^- \rightarrow \Upsilon(4S)$
••• We do not use the following data for averages, fits, limits, etc. •••			
<10.3	90	^{1,2} AUBERT 06 BABR	Repl. by AUBERT 08Y
¹ Assumes equal production of B^+ and B^0 at the $\Upsilon(4S)$.			
² The lower limit is also given to be 1.34×10^{-6} at 90% CL.			

$\Gamma(X(3872)K^0 \times B(X \rightarrow J/\psi\gamma))/\Gamma_{\text{total}}$		Γ_{183}/Γ	
VALUE (units 10^{-6})	CL%	DOCUMENT ID	TECN COMMENT
<4.9	90	¹ AUBERT 09b BABR	$e^+e^- \rightarrow \Upsilon(4S)$
¹ Uses $B(\Upsilon(4S) \rightarrow B^+B^-) = (51.6 \pm 0.6)\%$ and $B(\Upsilon(4S) \rightarrow B^0\bar{B}^0) = (48.4 \pm 0.6)\%$.			

$\Gamma(X(3872)K^*(892)^0 \times B(X \rightarrow J/\psi\gamma))/\Gamma_{\text{total}}$		Γ_{184}/Γ	
VALUE (units 10^{-6})	CL%	DOCUMENT ID	TECN COMMENT
<2.8	90	¹ AUBERT 09b BABR	$e^+e^- \rightarrow \Upsilon(4S)$
¹ Uses $B(\Upsilon(4S) \rightarrow B^+B^-) = (51.6 \pm 0.6)\%$ and $B(\Upsilon(4S) \rightarrow B^0\bar{B}^0) = (48.4 \pm 0.6)\%$.			

$\Gamma(X(3872)K^0 \times B(X \rightarrow \psi(2S)\gamma))/\Gamma_{\text{total}}$		Γ_{185}/Γ	
VALUE (units 10^{-6})	CL%	DOCUMENT ID	TECN COMMENT
<19	90	¹ AUBERT 09b BABR	$e^+e^- \rightarrow \Upsilon(4S)$
¹ Uses $B(\Upsilon(4S) \rightarrow B^+B^-) = (51.6 \pm 0.6)\%$ and $B(\Upsilon(4S) \rightarrow B^0\bar{B}^0) = (48.4 \pm 0.6)\%$.			

$\Gamma(X(3872)K^*(892)^0 \times B(X \rightarrow \psi(2S)\gamma))/\Gamma_{\text{total}}$		Γ_{186}/Γ	
VALUE (units 10^{-6})	CL%	DOCUMENT ID	TECN COMMENT
<4.4	90	¹ AUBERT 09b BABR	$e^+e^- \rightarrow \Upsilon(4S)$
¹ Uses $B(\Upsilon(4S) \rightarrow B^+B^-) = (51.6 \pm 0.6)\%$ and $B(\Upsilon(4S) \rightarrow B^0\bar{B}^0) = (48.4 \pm 0.6)\%$.			

$\Gamma(X(3872)K^0 \times B(X \rightarrow D^0\bar{D}^0\pi^0))/\Gamma_{\text{total}}$		Γ_{187}/Γ	
VALUE (units 10^{-4})	CL%	DOCUMENT ID	TECN COMMENT
$1.66 \pm 0.70 \pm 0.32$		¹ GOKHROO 06 BELL	$e^+e^- \rightarrow \Upsilon(4S)$
¹ Measure the near-threshold enhancements in the ($D^0\bar{D}^0\pi^0$) system at a mass $3875.2 \pm 0.7 \pm 0.3 \pm 1.6 \pm 0.8$ MeV/ c^2 .			

$\Gamma(X(3872)K^0 \times B(X \rightarrow \bar{D}^{*0}D^0))/\Gamma_{\text{total}}$		Γ_{188}/Γ	
VALUE (units 10^{-4})	CL%	DOCUMENT ID	TECN COMMENT
1.2 ± 0.4		OUR AVERAGE	
$0.97 \pm 0.46 \pm 0.13$		¹ AUSHEV 10 BELL	$e^+e^- \rightarrow \Upsilon(4S)$
$2.22 \pm 1.05 \pm 0.42$		^{1,2} AUBERT 08b BABR	$e^+e^- \rightarrow \Upsilon(4S)$
¹ Assumes equal production of B^+ and B^0 at the $\Upsilon(4S)$.			
² This result is equivalent to the the 90% CL upper limit of 4.37×10^{-4}			

$\Gamma(B^0 \rightarrow X(3945)K^0)/\Gamma_{\text{total}} \times \Gamma(X(3945) \rightarrow \omega J/\psi)/\Gamma_{\text{total}}$		$\Gamma_{189}/\Gamma \times \Gamma_1^{X(3945)}/\Gamma^{X(3945)}$	
VALUE (units 10^{-5})	CL%	DOCUMENT ID	TECN COMMENT
$1.3 \pm 1.3 \pm 0.2$		^{1,2} AUBERT 08w BABR	$e^+e^- \rightarrow \Upsilon(4S)$
¹ Corresponds to upper limit of 3.9×10^{-5} at 90% CL.			
² Assumes equal production of B^+ and B^0 at the $\Upsilon(4S)$.			

$\Gamma(X(4430)^\pm K^\mp \times B(X^\pm \rightarrow \psi(2S)\pi^\pm))/\Gamma_{\text{total}}$		Γ_{190}/Γ	
VALUE (units 10^{-5})	CL%	DOCUMENT ID	TECN COMMENT
$3.2 \pm 1.8 \pm 5.3$ -0.9 ± 1.6		¹ MIZUK 09 BELL	$e^+e^- \rightarrow \Upsilon(4S)$
••• We do not use the following data for averages, fits, limits, etc. •••			
<3.1	95	¹ AUBERT 09AA BABR	$e^+e^- \rightarrow \Upsilon(4S)$
$4.1 \pm 1.0 \pm 1.4$		^{1,2} CHOI 08 BELL	Repl. by MIZUK 09
¹ Assumes equal production of B^+ and B^0 at the $\Upsilon(4S)$.			
² Establishes the $X(4430)^+$ with a significance of 6.5 sigma. Needs confirmation.			

$\Gamma(X(4430)^\pm K^\mp \times B(X^\pm \rightarrow J/\psi\pi^\pm))/\Gamma_{\text{total}}$		Γ_{191}/Γ	
VALUE (units 10^{-5})	CL%	DOCUMENT ID	TECN COMMENT
<0.4	95	¹ AUBERT 09AA BABR	$e^+e^- \rightarrow \Upsilon(4S)$
¹ Assumes equal production of B^+ and B^0 at the $\Upsilon(4S)$.			

$\Gamma(J/\psi(1S)p\bar{p})/\Gamma_{\text{total}}$		Γ_{192}/Γ	
VALUE	CL%	DOCUMENT ID	TECN COMMENT
< 8.3×10^{-7}	90	¹ XIE 05 BELL	$e^+e^- \rightarrow \Upsilon(4S)$
••• We do not use the following data for averages, fits, limits, etc. •••			
< 1.9×10^{-6}	90	¹ AUBERT 03k BABR	$e^+e^- \rightarrow \Upsilon(4S)$
¹ Assumes equal production of B^+ and B^0 at the $\Upsilon(4S)$.			

$\Gamma(J/\psi(1S)\gamma)/\Gamma_{\text{total}}$		Γ_{193}/Γ	
VALUE (units 10^{-6})	CL%	DOCUMENT ID	TECN COMMENT
<1.6	90	¹ AUBERT,B 04T BABR	$e^+e^- \rightarrow \Upsilon(4S)$
¹ Assumes equal production of B^+ and B^0 at the $\Upsilon(4S)$.			

$\Gamma(J/\psi(1S)\bar{D}^0)/\Gamma_{\text{total}}$ Γ_{194}/Γ

VALUE (units 10^{-5})	CL%	DOCUMENT ID	TECN	COMMENT
<1.3	90	¹ AUBERT 05U	BABR	$e^+e^- \rightarrow \Upsilon(4S)$
••• We do not use the following data for averages, fits, limits, etc. •••				
<2.0	90	¹ ZHANG 05B	BELL	$e^+e^- \rightarrow \Upsilon(4S)$
¹ Assumes equal production of B^+ and B^0 at the $\Upsilon(4S)$.				

 $\Gamma(\psi(2S)K^0)/\Gamma_{\text{total}}$ Γ_{195}/Γ

VALUE (units 10^{-4})	CL%	DOCUMENT ID	TECN	COMMENT
6.2 ± 0.5 OUR FIT				
6.2 ± 0.6 OUR AVERAGE				
6.46 ± 0.65 ± 0.51		¹ AUBERT 05J	BABR	$e^+e^- \rightarrow \Upsilon(4S)$
6.7 ± 1.1		¹ ABE 03B	BELL	$e^+e^- \rightarrow \Upsilon(4S)$
5.0 ± 1.1 ± 0.6		¹ RICHICHI 01	CLE2	$e^+e^- \rightarrow \Upsilon(4S)$
••• We do not use the following data for averages, fits, limits, etc. •••				
6.9 ± 1.1 ± 1.1		¹ AUBERT 02	BABR	Repl. by AUBERT 05J
< 8	90	¹ ALAM 94	CLE2	$e^+e^- \rightarrow \Upsilon(4S)$
<15	90	¹ BORTOLETTO92	CLEO	$e^+e^- \rightarrow \Upsilon(4S)$
<28	90	¹ ALBRECHT 90J	ARG	$e^+e^- \rightarrow \Upsilon(4S)$
¹ Assumes equal production of B^+ and B^0 at the $\Upsilon(4S)$.				

 $\Gamma(\psi(2S)K^0)/\Gamma(J/\psi(1S)K^0)$ $\Gamma_{195}/\Gamma_{159}$

VALUE	DOCUMENT ID	TECN	COMMENT
0.82 ± 0.13 ± 0.12	¹ AUBERT 02	BABR	$e^+e^- \rightarrow \Upsilon(4S)$
¹ Assumes equal production of B^+ and B^0 at the $\Upsilon(4S)$.			

 $\Gamma(\psi(3770)K^0 \times B(\psi \rightarrow \bar{D}^0 D^0))/\Gamma_{\text{total}}$ Γ_{196}/Γ

VALUE (units 10^{-4})	CL%	DOCUMENT ID	TECN	COMMENT
<1.23	90	¹ AUBERT 08B	BABR	$e^+e^- \rightarrow \Upsilon(4S)$
¹ Assumes equal production of B^+ and B^0 at the $\Upsilon(4S)$.				

 $\Gamma(\psi(3770)K^0 \times B(\psi \rightarrow D^- D^+))/\Gamma_{\text{total}}$ Γ_{197}/Γ

VALUE (units 10^{-4})	CL%	DOCUMENT ID	TECN	COMMENT
<1.88	90	¹ AUBERT 08B	BABR	$e^+e^- \rightarrow \Upsilon(4S)$
¹ Assumes equal production of B^+ and B^0 at the $\Upsilon(4S)$.				

 $\Gamma(\psi(2S)K^+\pi^-)/\Gamma_{\text{total}}$ Γ_{198}/Γ

VALUE (units 10^{-4})	CL%	DOCUMENT ID	TECN	COMMENT
5.68 ± 0.13 ± 0.42		¹ MIZUK 09	BELL	$e^+e^- \rightarrow \Upsilon(4S)$
••• We do not use the following data for averages, fits, limits, etc. •••				
<10	90	¹ ALBRECHT 90J	ARG	$e^+e^- \rightarrow \Upsilon(4S)$
¹ Assumes equal production of B^+ and B^0 at the $\Upsilon(4S)$.				

 $\Gamma(\psi(2S)K^*(892)^0)/\Gamma_{\text{total}}$ Γ_{199}/Γ

VALUE (units 10^{-4})	CL%	DOCUMENT ID	TECN	COMMENT
6.1 ± 0.5 OUR FIT				Error includes scale factor of 1.1.
6.1 ± 0.6 OUR AVERAGE				Error includes scale factor of 1.1.
5.52 ^{+0.35+0.53} _{-0.32-0.58}		¹ MIZUK 09	BELL	$e^+e^- \rightarrow \Upsilon(4S)$
6.49 ± 0.59 ± 0.97		¹ AUBERT 05J	BABR	$e^+e^- \rightarrow \Upsilon(4S)$
7.6 ± 1.1 ± 1.0		¹ RICHICHI 01	CLE2	$e^+e^- \rightarrow \Upsilon(4S)$
9.0 ± 2.2 ± 0.9		² ABE 98o	CDF	$p\bar{p}$ 1.8 TeV
••• We do not use the following data for averages, fits, limits, etc. •••				
<19	90	¹ ALAM 94	CLE2	Repl. by RICHICHI 01
14 ± 8 ± 4		¹ BORTOLETTO92	CLEO	$e^+e^- \rightarrow \Upsilon(4S)$
<23	90	¹ ALBRECHT 90J	ARG	$e^+e^- \rightarrow \Upsilon(4S)$

¹ Assumes equal production of B^+ and B^0 at the $\Upsilon(4S)$.
² ABE 98o reports $[B(B^0 \rightarrow \psi(2S)K^*(892)^0)]/[B(B^+ \rightarrow J/\psi(1S)K^+)] = 0.908 \pm 0.194 \pm 0.10$. We multiply by our best value $B(B^+ \rightarrow J/\psi(1S)K^+) = (9.9 \pm 1.0) \times 10^{-4}$. Our first error is their experiment's error and our second error is the systematic error from using our best value.

 $\Gamma(\psi(2S)K^*(892)^0)/\Gamma(\psi(2S)K^0)$ $\Gamma_{199}/\Gamma_{195}$

VALUE	DOCUMENT ID	TECN	COMMENT
0.99 ± 0.10 OUR FIT			
1.00 ± 0.14 ± 0.09	AUBERT 05J	BABR	$e^+e^- \rightarrow \Upsilon(4S)$

 $\Gamma(\chi_{c0}(1P)K^0)/\Gamma_{\text{total}}$ Γ_{200}/Γ

VALUE (units 10^{-6})	CL%	DOCUMENT ID	TECN	COMMENT
142⁺⁵⁵₋₄₄ ± 22		^{1,2} AUBERT 09AU	BABR	$e^+e^- \rightarrow \Upsilon(4S)$
••• We do not use the following data for averages, fits, limits, etc. •••				
< 113	90	² GARMASH 07	BELL	$e^+e^- \rightarrow \Upsilon(4S)$
<1240	90	¹ AUBERT 05K	BABR	$e^+e^- \rightarrow \Upsilon(4S)$
< 500	90	³ EDWARDS 01	CLE2	$e^+e^- \rightarrow \Upsilon(4S)$

¹ Assumes equal production of B^+ and B^0 at the $\Upsilon(4S)$.
² Uses Dalitz plot analysis of the $B^0 \rightarrow K^0\pi^+\pi^-$ final state decays.
³ EDWARDS 01 assumes equal production of B^0 and B^+ at the $\Upsilon(4S)$. The correlated uncertainties (28.3)% from $B(J/\psi(1S) \rightarrow \gamma\eta_c)$ in those modes have been accounted for.

 $\Gamma(\chi_{c0}K^*(892)^0)/\Gamma_{\text{total}}$ Γ_{201}/Γ

VALUE (units 10^{-4})	CL%	DOCUMENT ID	TECN	COMMENT
1.7 ± 0.3 ± 0.2		¹ AUBERT 08BD	BABR	$e^+e^- \rightarrow \Upsilon(4S)$
••• We do not use the following data for averages, fits, limits, etc. •••				
<7.7	90	¹ AUBERT 05K	BABR	Repl. by AUBERT 08BD
¹ Assumes equal production of B^+ and B^0 at the $\Upsilon(4S)$.				

 $\Gamma(\chi_{c2}K^0)/\Gamma_{\text{total}}$ Γ_{202}/Γ

VALUE	CL%	DOCUMENT ID	TECN	COMMENT
< 2.6 × 10⁻⁵	90	¹ SONI 06	BELL	$e^+e^- \rightarrow \Upsilon(4S)$
••• We do not use the following data for averages, fits, limits, etc. •••				
<2.8 × 10 ⁻⁵	90	² AUBERT 09B	BABR	$e^+e^- \rightarrow \Upsilon(4S)$
<4.1 × 10 ⁻⁵	90	¹ AUBERT 05K	BABR	$e^+e^- \rightarrow \Upsilon(4S)$
¹ Assumes equal production of B^+ and B^0 at the $\Upsilon(4S)$. ² Uses $\chi_{c1,2} \rightarrow J/\psi\gamma$. Assumes $B(\Upsilon(4S) \rightarrow B^+B^-) = (51.6 \pm 0.6)\%$ and $B(\Upsilon(4S) \rightarrow B^0\bar{B}^0) = (48.4 \pm 0.6)\%$.				

 $\Gamma(\chi_{c2}K^*(892)^0)/\Gamma_{\text{total}}$ Γ_{203}/Γ

VALUE (units 10^{-5})	CL%	DOCUMENT ID	TECN	COMMENT
6.6 ± 1.8 ± 0.5		¹ AUBERT 09B	BABR	$e^+e^- \rightarrow \Upsilon(4S)$
••• We do not use the following data for averages, fits, limits, etc. •••				
<7.1	90	² SONI 06	BELL	$e^+e^- \rightarrow \Upsilon(4S)$
<3.6	90	² AUBERT 05K	BABR	Repl. by AUBERT 09B
¹ Uses $\chi_{c1,2} \rightarrow J/\psi\gamma$. Assumes $B(\Upsilon(4S) \rightarrow B^+B^-) = (51.6 \pm 0.6)\%$ and $B(\Upsilon(4S) \rightarrow B^0\bar{B}^0) = (48.4 \pm 0.6)\%$. ² Assumes equal production of B^+ and B^0 at the $\Upsilon(4S)$.				

 $\Gamma(\chi_{c1}(1P)\pi^0)/\Gamma_{\text{total}}$ Γ_{204}/Γ

VALUE (units 10^{-5})	DOCUMENT ID	TECN	COMMENT
1.12 ± 0.25 ± 0.12	¹ KUMAR 08	BELL	$e^+e^- \rightarrow \Upsilon(4S)$
¹ Assumes equal production of B^+ and B^0 at the $\Upsilon(4S)$.			

 $\Gamma(\chi_{c1}(1P)K^0)/\Gamma_{\text{total}}$ Γ_{205}/Γ

VALUE (units 10^{-4})	CL%	DOCUMENT ID	TECN	COMMENT
3.90 ± 0.33 OUR AVERAGE				
4.2 ± 0.3 ± 0.3		¹ AUBERT 09B	BABR	$e^+e^- \rightarrow \Upsilon(4S)$
3.51 ± 0.33 ± 0.45		² SONI 06	BELL	$e^+e^- \rightarrow \Upsilon(4S)$
3.1 ^{+1.5} _{-1.1} ± 0.1		³ AVERY 00	CLE2	$e^+e^- \rightarrow \Upsilon(4S)$
••• We do not use the following data for averages, fits, limits, etc. •••				
4.53 ± 0.41 ± 0.51		² AUBERT 05J	BABR	Repl. by AUBERT 09B
4.3 ± 1.4 ± 0.2		⁴ AUBERT 02	BABR	Repl. by AUBERT 05J
<27	90	² ALAM 94	CLE2	$e^+e^- \rightarrow \Upsilon(4S)$
¹ Uses $\chi_{c1,2} \rightarrow J/\psi\gamma$. Assumes $B(\Upsilon(4S) \rightarrow B^+B^-) = (51.6 \pm 0.6)\%$ and $B(\Upsilon(4S) \rightarrow B^0\bar{B}^0) = (48.4 \pm 0.6)\%$. ² Assumes equal production of B^+ and B^0 at the $\Upsilon(4S)$. ³ AVERY 00 reports $(3.9+1.9-1.3 ± 0.4) \times 10^{-4}$ from a measurement of $[\Gamma(B^0 \rightarrow \chi_{c1}(1P)K^0)/\Gamma_{\text{total}}] \times [B(\chi_{c1}(1P) \rightarrow \gamma J/\psi(1S))] \times [B(\chi_{c1}(1P) \rightarrow \gamma J/\psi(1S))] = 0.273 \pm 0.016$, which we rescale to our best value $B(\chi_{c1}(1P) \rightarrow \gamma J/\psi(1S)) = (34.4 \pm 1.5) \times 10^{-2}$. Our first error is their experiment's error and our second error is the systematic error from using our best value. Assumes equal production of B^+ and B^0 at the $\Upsilon(4S)$. ⁴ AUBERT 02 reports $(5.4 \pm 1.4 \pm 1.1) \times 10^{-4}$ from a measurement of $[\Gamma(B^0 \rightarrow \chi_{c1}(1P)K^0)/\Gamma_{\text{total}}] \times [B(\chi_{c1}(1P) \rightarrow \gamma J/\psi(1S))] \times [B(\chi_{c1}(1P) \rightarrow \gamma J/\psi(1S))] = 0.273 \pm 0.016$, which we rescale to our best value $B(\chi_{c1}(1P) \rightarrow \gamma J/\psi(1S)) = (34.4 \pm 1.5) \times 10^{-2}$. Our first error is their experiment's error and our second error is the systematic error from using our best value. Assumes equal production of B^+ and B^0 at the $\Upsilon(4S)$.				

 $\Gamma(\chi_{c1}(1P)K^0)/\Gamma(J/\psi(1S)K^0)$ $\Gamma_{205}/\Gamma_{195}$

VALUE	DOCUMENT ID	TECN	COMMENT
0.52 ± 0.16 ± 0.02	¹ AUBERT 02	BABR	$e^+e^- \rightarrow \Upsilon(4S)$
¹ AUBERT 02 reports $0.66 \pm 0.11 \pm 0.17$ from a measurement of $[\Gamma(B^0 \rightarrow \chi_{c1}(1P)K^0)/\Gamma(B^0 \rightarrow J/\psi(1S)K^0)] \times [B(\chi_{c1}(1P) \rightarrow \gamma J/\psi(1S))] \times [B(\chi_{c1}(1P) \rightarrow \gamma J/\psi(1S))] = 0.273 \pm 0.016$, which we rescale to our best value $B(\chi_{c1}(1P) \rightarrow \gamma J/\psi(1S)) = (34.4 \pm 1.5) \times 10^{-2}$. Our first error is their experiment's error and our second error is the systematic error from using our best value. Assumes equal production of B^+ and B^0 at the $\Upsilon(4S)$.			

 $\Gamma(\chi_{c1}(1P)K^-\pi^+)/\Gamma_{\text{total}}$ Γ_{206}/Γ

VALUE (units 10^{-4})	DOCUMENT ID	TECN	COMMENT
3.83 ± 0.10 ± 0.39	¹ MIZUK 08	BELL	$e^+e^- \rightarrow \Upsilon(4S)$
¹ Assumes equal production of B^+ and B^0 at the $\Upsilon(4S)$.			

Meson Particle Listings

 B^0

$\Gamma(\chi_{c1}(1P)K^*(892)^0)/\Gamma_{\text{total}}$ Γ_{207}/Γ

VALUE (units 10^{-4})	CL%	DOCUMENT ID	TECN	COMMENT
2.22\pm0.40		OUR AVERAGE Error includes scale factor of 1.6.		
2.5 \pm 0.2 \pm 0.2		1 AUBERT	09B	BABR $e^+e^- \rightarrow \Upsilon(4S)$
1.73 \pm 0.15 \pm 0.34		2 MIZUK	08	BELL $e^+e^- \rightarrow \Upsilon(4S)$
3.14 \pm 0.34 \pm 0.72		2 SONI	06	BELL Repl. by MIZUK 08
3.27 \pm 0.42 \pm 0.64		2 AUBERT	05J	BABR Repl. by AUBERT 09B
3.8 \pm 1.3 \pm 0.2		3 AUBERT	02	BABR Repl. by AUBERT 05J
<21	90	4 ALAM	94	CLE2 $e^+e^- \rightarrow \Upsilon(4S)$

- ¹ Uses $\chi_{c1,2} \rightarrow J/\psi\gamma$. Assumes $B(\Upsilon(4S) \rightarrow B^+B^-) = (51.6 \pm 0.6)\%$ and $B(\Upsilon(4S) \rightarrow B^0\bar{B}^0) = (48.4 \pm 0.6)\%$.
- ² Assumes equal production of B^+ and B^0 at the $\Upsilon(4S)$.
- ³ AUBERT 02 reports $(4.8 \pm 1.4 \pm 0.9) \times 10^{-4}$ from a measurement of $[\Gamma(B^0 \rightarrow \chi_{c1}(1P)K^*(892)^0)/\Gamma_{\text{total}}] \times [B(\chi_{c1}(1P) \rightarrow \gamma J/\psi(1S))] / [\gamma J/\psi(1S)]$ assuming $B(\chi_{c1}(1P) \rightarrow \gamma J/\psi(1S)) = 0.273 \pm 0.016$, which we rescale to our best value $B(\chi_{c1}(1P) \rightarrow \gamma J/\psi(1S)) = (34.4 \pm 1.5) \times 10^{-2}$. Our first error is their experiment's error and our second error is the systematic error from using our best value. Assumes equal production of B^+ and B^0 at the $\Upsilon(4S)$.
- ⁴ BORTOLETTO 92 assumes equal production of B^+ and B^0 at the $\Upsilon(4S)$.

$\Gamma(X(4051)+K^- \times B(X^+ \rightarrow \chi_{c1}\pi^+))/\Gamma_{\text{total}}$ Γ_{208}/Γ

VALUE (units 10^{-5})	CL%	DOCUMENT ID	TECN	COMMENT
3.0\pm1.5\pm3.7		OUR AVERAGE		
-0.8 - 1.6		1 MIZUK	08	BELL $e^+e^- \rightarrow \Upsilon(4S)$

- ¹ Assumes equal production of B^+ and B^0 at the $\Upsilon(4S)$.

$\Gamma(X(4248)+K^- \times B(X^+ \rightarrow \chi_{c1}\pi^+))/\Gamma_{\text{total}}$ Γ_{209}/Γ

VALUE (units 10^{-5})	CL%	DOCUMENT ID	TECN	COMMENT
4.0\pm2.3\pm19.7		OUR AVERAGE		
0.9 - 0.5		1 MIZUK	08	BELL $e^+e^- \rightarrow \Upsilon(4S)$

- ¹ Assumes equal production of B^+ and B^0 at the $\Upsilon(4S)$.

$\Gamma(\chi_{c1}(1P)K^*(892)^0)/\Gamma(\chi_{c1}(1P)K^0)$ $\Gamma_{207}/\Gamma_{205}$

VALUE	CL%	DOCUMENT ID	TECN	COMMENT
0.72\pm0.11\pm0.12		OUR AVERAGE		
0.89 \pm 0.34 \pm 0.17		1 AUBERT	02	BABR Repl. by AUBERT 05J

- ¹ Assumes equal production of B^+ and B^0 at the $\Upsilon(4S)$.

$\Gamma(K^+\pi^-)/\Gamma_{\text{total}}$ Γ_{210}/Γ

VALUE (units 10^{-6})	CL%	DOCUMENT ID	TECN	COMMENT
19.4\pm0.6		OUR AVERAGE		
19.1 \pm 0.6 \pm 0.6		1 AUBERT	07B	BABR $e^+e^- \rightarrow \Upsilon(4S)$
19.9 \pm 0.4 \pm 0.8		1 LIN	07A	BELL $e^+e^- \rightarrow \Upsilon(4S)$
18.0 \pm 2.3 \pm 1.2		1 BORNHEIM	03	CLE2 $e^+e^- \rightarrow \Upsilon(4S)$
18.5 \pm 1.0 \pm 0.7		1 CHAO	04	BELL Repl. by LIN 07A
17.9 \pm 0.9 \pm 0.7		1 AUBERT	02Q	BABR Repl. by AUBERT 07B
22.5 \pm 1.9 \pm 1.8		1 CASEY	02	BELL Repl. by CHAO 04
19.3 \pm 3.4 \pm 1.5		1 ABE	01H	BELL Repl. by CASEY 02
16.7 \pm 1.6 \pm 1.3		1 AUBERT	01E	BABR Repl. by AUBERT 02Q
<66	90	2 ABE	00c	SLD $e^+e^- \rightarrow Z$
17.2 \pm 2.5 \pm 1.2		1 CRONIN-HEN..00	CLE2	Repl. by BORNHEIM 03
15 \pm 5. \pm 1.4		GODANG	98	CLE2 Repl. by CRONIN-HENNESSY 00
24 \pm 17. \pm 2		3 ADAM	96D	DLPH $e^+e^- \rightarrow Z$
<17	90	ASNER	96	CLE2 Sup. by ADAM 96D
<30	90	4 BUSKULIC	96V	ALEP $e^+e^- \rightarrow Z$
<90	90	5 ABREU	95N	DLPH Sup. by ADAM 96D
<81	90	6 AKERS	94L	OPAL $e^+e^- \rightarrow Z$
<26	90	7 BATTLE	93	CLE2 $e^+e^- \rightarrow \Upsilon(4S)$
<180	90	ALBRECHT	91B	ARG $e^+e^- \rightarrow \Upsilon(4S)$
<90	90	8 AVERY	89B	CLEO $e^+e^- \rightarrow \Upsilon(4S)$
<320	90	AVERY	87	CLEO $e^+e^- \rightarrow \Upsilon(4S)$

- ¹ Assumes equal production of B^+ and B^0 at the $\Upsilon(4S)$.
- ² ABE 00c assumes $B(Z \rightarrow b\bar{b}) = (21.7 \pm 0.1)\%$ and the B fractions $f_{B^0} = f_{B^+} = (39.7 \pm 1.8 \pm 2.2)\%$ and $f_{B_s} = (10.5 \pm 1.8 \pm 2.2)\%$.
- ³ ADAM 96D assumes $f_{B^0} = f_{B^-} = 0.39$ and $f_{B_s} = 0.12$. Contributions from B^0 and B_s decays cannot be separated. Limits are given for the weighted average of the decay rates for the two neutral B mesons.
- ⁴ BUSKULIC 96V assumes PDG 96 production fractions for B^0 , B^+ , B_s , b baryons.
- ⁵ Assumes a B^0 , B^- production fraction of 0.39 and a B_s production fraction of 0.12. Contributions from B^0 and B_s decays cannot be separated. Limits are given for the weighted average of the decay rates for the two neutral B mesons.
- ⁶ Assumes $B(Z \rightarrow b\bar{b}) = 0.217$ and $B_D^0(B_s^0)$ fraction 39.5% (12%).
- ⁷ BATTLE 93 assumes equal production of $B^0\bar{B}^0$ and B^+B^- at $\Upsilon(4S)$.
- ⁸ Assumes the $\Upsilon(4S)$ decays 43% to $B^0\bar{B}^0$.

$\Gamma(K^+\pi^-)/\Gamma(K^0\pi^0)$ $\Gamma_{210}/\Gamma_{211}$

VALUE	CL%	DOCUMENT ID	TECN	COMMENT
2.16\pm0.16\pm0.16		OUR AVERAGE		
1.20 \pm 0.50 \pm 0.22		1 ABE	01H	BELL Repl. by LIN 07A

- ¹ Assumes equal production of B^+ and B^0 at the $\Upsilon(4S)$.

$[\Gamma(K^+\pi^-) + \Gamma(\pi^+\pi^-)]/\Gamma_{\text{total}}$ $(\Gamma_{210} + \Gamma_{315})/\Gamma$

VALUE (units 10^{-6})	CL%	DOCUMENT ID	TECN	COMMENT
19\pm6		OUR AVERAGE		
28 \pm 15 \pm 20		1 ADAM	96D	DLPH $e^+e^- \rightarrow Z$
18 \pm 6 \pm 3		17.2	ASNER	96 CLE2 $e^+e^- \rightarrow \Upsilon(4S)$
24 \pm 8 \pm 2		2 BATTLE	93	CLE2 $e^+e^- \rightarrow \Upsilon(4S)$

- ¹ ADAM 96D assumes $f_{B^0} = f_{B^-} = 0.39$ and $f_{B_s} = 0.12$. Contributions from B^0 and B_s decays cannot be separated. Limits are given for the weighted average of the decay rates for the two neutral B mesons.
- ² BATTLE 93 assumes equal production of $B^0\bar{B}^0$ and B^+B^- at $\Upsilon(4S)$.

$\Gamma(K^0\pi^0)/\Gamma_{\text{total}}$ Γ_{211}/Γ

VALUE (units 10^{-6})	CL%	DOCUMENT ID	TECN	COMMENT
9.5\pm0.8		OUR AVERAGE		
8.7 \pm 0.5 \pm 0.6		1 FUJIKAWA	10A	BELL $e^+e^- \rightarrow \Upsilon(4S)$
10.3 \pm 0.7 \pm 0.6		1 AUBERT	08E	BABR $e^+e^- \rightarrow \Upsilon(4S)$
12.8 \pm 4.0 \pm 1.7		1 BORNHEIM	03	CLE2 $e^+e^- \rightarrow \Upsilon(4S)$

- ¹ LIN 07A BELL Repl. by FUJIKAWA 10A
- ¹ AUBERT 05Y BABR Repl. by AUBERT 08E
- ¹ AUBERT 04M BABR Repl. by AUBERT 05Y
- ¹ CHAO 04 BELL Repl. by LIN 07A
- ¹ CASEY 02 BELL Repl. by CHAO 04
- ¹ ABE 01H BELL Repl. by CASEY 02
- ¹ AUBERT 01E BABR Repl. by AUBERT 04M
- ¹ CRONIN-HEN..00 CLE2 Repl. by BORNHEIM 03
- <41 90 GODANG 98 CLE2 Repl. by CRONIN-HENNESSY 00
- <40 90 ASNER 96 CLE2 Repl. by GODANG 98
- ¹ Assumes equal production of B^+ and B^0 at the $\Upsilon(4S)$.

$\Gamma(\eta'K^0)/\Gamma_{\text{total}}$ Γ_{212}/Γ

VALUE (units 10^{-6})	CL%	DOCUMENT ID	TECN	COMMENT
66\pm4		OUR AVERAGE		
68.5 \pm 2.2 \pm 3.1		1 AUBERT	09AV	BABR $e^+e^- \rightarrow \Upsilon(4S)$
58.9 \pm 3.6 \pm 4.3		1 SCHUEMANN	06	BELL $e^+e^- \rightarrow \Upsilon(4S)$
89 \pm 18. \pm 9		1 RICHICHI	00	CLE2 $e^+e^- \rightarrow \Upsilon(4S)$

- ¹ AUBERT 07AE BABR Repl. by AUBERT 09AV
- ¹ AUBERT 05M BABR AUBERT 07AE
- ¹ AUBERT 03W BABR Repl. by AUBERT 05M
- ¹ ABE 01M BELL Repl. by SCHUEMANN 06
- ¹ AUBERT 01G BABR Repl. by AUBERT 03W
- 47 \pm 27. \pm 9

- ¹ Assumes equal production of B^+ and B^0 at the $\Upsilon(4S)$.

$\Gamma(\eta'K^*(892)^0)/\Gamma_{\text{total}}$ Γ_{213}/Γ

VALUE (units 10^{-6})	CL%	DOCUMENT ID	TECN	COMMENT
3.8\pm1.1\pm0.5		OUR AVERAGE		
<2.6	90	1 SCHUEMANN	07	BELL $e^+e^- \rightarrow \Upsilon(4S)$
<7.6	90	1 AUBERT,B	04D	BABR Repl. by AUBERT 07E
<24	90	1 RICHICHI	00	CLE2 $e^+e^- \rightarrow \Upsilon(4S)$
<39	90	BEHRENS	98	CLE2 Repl. by RICHICHI 00

- ¹ Assumes equal production of B^+ and B^0 at the $\Upsilon(4S)$.

$\Gamma(\eta K^0)/\Gamma_{\text{total}}$ Γ_{214}/Γ

VALUE (units 10^{-6})	CL%	DOCUMENT ID	TECN	COMMENT
1.15\pm0.43\pm0.09		OUR AVERAGE		
1.15 \pm 0.43 \pm 0.09		1 AUBERT	09AV	BABR $e^+e^- \rightarrow \Upsilon(4S)$

Meson Particle Listings

B^0

$\Gamma(K^+ \rho(1700)^-)/\Gamma_{total}$ Γ_{235}/Γ

VALUE (units 10^{-6})	CL%	DOCUMENT ID	TECN	COMMENT
<1.1	90	¹ AUBERT	08AQ	BABR $e^+e^- \rightarrow \Upsilon(4S)$

¹ Assumes equal production of B^+ and B^0 at the $\Upsilon(4S)$.

$\Gamma((K^+ \pi^- \pi^0) \text{ non-resonant})/\Gamma_{total}$ Γ_{236}/Γ

VALUE (units 10^{-6})	CL%	DOCUMENT ID	TECN	COMMENT
$4.4 \pm 0.9 \pm 0.5$		¹ AUBERT	08AQ	BABR $e^+e^- \rightarrow \Upsilon(4S)$

• • • We do not use the following data for averages, fits, limits, etc. • • •

<9.4	90	¹ CHANG	04	BELL $e^+e^- \rightarrow \Upsilon(4S)$
------	----	--------------------	----	--

¹ Assumes equal production of B^+ and B^0 at the $\Upsilon(4S)$.

$\Gamma((K\pi)_0^{*0} \pi^- \times B((K\pi)_0^{*0} \rightarrow K^+ \pi^-))/\Gamma_{total}$ Γ_{237}/Γ

($K\pi)_0^{*0}$ is the total S-wave composed of $K_0^*(1430)$ and nonresonant that are described using LASS shape.

VALUE (units 10^{-6})	DOCUMENT ID	TECN	COMMENT
$9.4^{+1.1+2.3}_{-1.3-2.1}$	¹ AUBERT	08AQ	BABR $e^+e^- \rightarrow \Upsilon(4S)$

¹ Assumes equal production of B^+ and B^0 at the $\Upsilon(4S)$.

$\Gamma((K\pi)_0^{*0} \pi^0 \times B((K\pi)_0^{*0} \rightarrow K^+ \pi^-))/\Gamma_{total}$ Γ_{238}/Γ

($K\pi)_0^{*0}$ is the total S-wave composed of $K_0^*(1430)$ and nonresonant that are described using LASS shape.

VALUE (units 10^{-6})	DOCUMENT ID	TECN	COMMENT
$8.7^{+1.1+2.8}_{-0.9-2.6}$	¹ AUBERT	08AQ	BABR $e^+e^- \rightarrow \Upsilon(4S)$

¹ Assumes equal production of B^+ and B^0 at the $\Upsilon(4S)$.

$\Gamma(K_2^*(1430)^0 \pi^0)/\Gamma_{total}$ Γ_{239}/Γ

VALUE (units 10^{-6})	CL%	DOCUMENT ID	TECN	COMMENT
<4.0	90	¹ AUBERT	08AQ	BABR $e^+e^- \rightarrow \Upsilon(4S)$

¹ Assumes equal production of B^+ and B^0 at the $\Upsilon(4S)$.

$\Gamma(K^*(1680)^0 \pi^0)/\Gamma_{total}$ Γ_{240}/Γ

VALUE (units 10^{-6})	CL%	DOCUMENT ID	TECN	COMMENT
<7.5	90	¹ AUBERT	08AQ	BABR $e^+e^- \rightarrow \Upsilon(4S)$

¹ Assumes equal production of B^+ and B^0 at the $\Upsilon(4S)$.

$\Gamma(K_X^{*0} \pi^0)/\Gamma_{total}$ Γ_{241}/Γ

K_X^{*0} stands for the possible candidates of $K^*(1410)$, $K_0^*(1430)$ and $K_2^*(1430)$.

VALUE (units 10^{-6})	DOCUMENT ID	TECN	COMMENT
$6.1^{+1.6+0.5}_{-1.5-0.6}$	¹ CHANG	04	BELL $e^+e^- \rightarrow \Upsilon(4S)$

¹ Assumes equal production of B^+ and B^0 at the $\Upsilon(4S)$.

$\Gamma(K^0 \pi^+ \pi^- \text{ charmless})/\Gamma_{total}$ Γ_{242}/Γ

VALUE (units 10^{-6})	CL%	DOCUMENT ID	TECN	COMMENT
49.6 ± 2.0 OUR AVERAGE				
$50.2 \pm 1.5 \pm 1.8$		¹ AUBERT	09AU	BABR $e^+e^- \rightarrow \Upsilon(4S)$
$47.5 \pm 2.4 \pm 3.7$		² GARMASH	07	BELL $e^+e^- \rightarrow \Upsilon(4S)$
$50^{+10}_{-9} \pm 7$		¹ ECKHART	02	CLE2 $e^+e^- \rightarrow \Upsilon(4S)$

• • • We do not use the following data for averages, fits, limits, etc. • • •

$43.0 \pm 2.3 \pm 2.3$		¹ AUBERT	06i	BABR Repl. by AUBERT 09AU
$43.7 \pm 3.8 \pm 3.4$		¹ AUBERT,B	04o	BABR Repl. by AUBERT 06i
$45.4 \pm 5.2 \pm 5.9$		¹ GARMASH	04	BELL Repl. by GARMASH 07
<440	90	ALBRECHT	91E	ARG $e^+e^- \rightarrow \Upsilon(4S)$

¹ Assumes equal production of B^+ and B^0 at the $\Upsilon(4S)$.
² Uses Dalitz plot analysis of the $B^0 \rightarrow K^0 \pi^+ \pi^-$ final state decays.

$\Gamma(K^0 \pi^+ \pi^- \text{ non-resonant})/\Gamma_{total}$ Γ_{243}/Γ

VALUE (units 10^{-6})	DOCUMENT ID	TECN	COMMENT
$14.7^{+4.0}_{-2.6}$ OUR AVERAGE	Error includes scale factor of 2.1.		
$11.1^{+2.5}_{-1.0} \pm 0.9$	¹ AUBERT	09AU	BABR $e^+e^- \rightarrow \Upsilon(4S)$
$19.9 \pm 2.5^{+1.7}_{-2.0}$	² GARMASH	07	BELL $e^+e^- \rightarrow \Upsilon(4S)$

¹ Assumes equal production of B^+ and B^0 at the $\Upsilon(4S)$.
² Uses Dalitz plot analysis of the $B^0 \rightarrow K^0 \pi^+ \pi^-$ final state decays.

$\Gamma(K^0 \rho^0)/\Gamma_{total}$ Γ_{244}/Γ

VALUE (units 10^{-6})	CL%	DOCUMENT ID	TECN	COMMENT
4.7 ± 0.6 OUR AVERAGE				
$4.4^{+0.7}_{-0.6} \pm 0.3$		¹ AUBERT	09AU	BABR $e^+e^- \rightarrow \Upsilon(4S)$
$6.1 \pm 1.0^{+1.1}_{-1.2}$		² GARMASH	07	BELL $e^+e^- \rightarrow \Upsilon(4S)$

• • • We do not use the following data for averages, fits, limits, etc. • • •

$4.9 \pm 0.8 \pm 0.9$		¹ AUBERT	07F	BABR Repl. by AUBERT 09AU
< 39	90	ASNER	96	CLEO $e^+e^- \rightarrow \Upsilon(4S)$
< 320	90	ALBRECHT	91B	ARG $e^+e^- \rightarrow \Upsilon(4S)$
< 500	90	³ AVERY	89B	CLEO $e^+e^- \rightarrow \Upsilon(4S)$
<64000	90	⁴ AVERY	87	CLEO $e^+e^- \rightarrow \Upsilon(4S)$

¹ Assumes equal production of B^+ and B^0 at the $\Upsilon(4S)$.
² Uses Dalitz plot analysis of the $B^0 \rightarrow K^0 \pi^+ \pi^-$ final state decays.
³ AVERY 89B reports $< 5.8 \times 10^{-4}$ assuming the $\Upsilon(4S)$ decays 43% to $B^0 \bar{B}^0$. We rescale to 50%.
⁴ AVERY 87 reports < 0.08 assuming the $\Upsilon(4S)$ decays 40% to $B^0 \bar{B}^0$. We rescale to 50%.

$\Gamma(K^*(892)^+ \pi^-)/\Gamma_{total}$ Γ_{245}/Γ

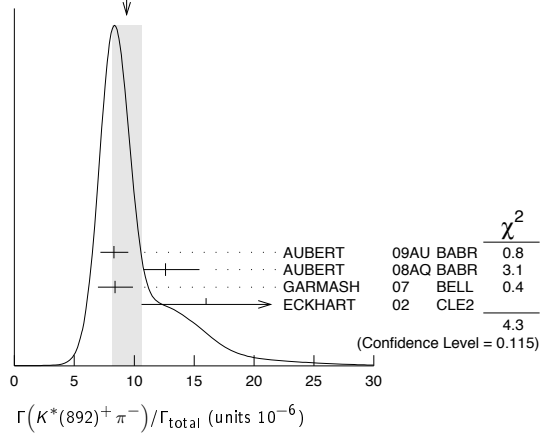
VALUE (units 10^{-6})	CL%	DOCUMENT ID	TECN	COMMENT
$9.4^{+1.3}_{-1.2}$ OUR AVERAGE		Error includes scale factor of 1.5. See the ideogram below.		
$8.3^{+0.9}_{-0.8} \pm 0.8$		^{1,2} AUBERT	09AU	BABR $e^+e^- \rightarrow \Upsilon(4S)$
$12.6^{+2.7}_{-1.6} \pm 0.9$		^{1,3} AUBERT	08AQ	BABR $e^+e^- \rightarrow \Upsilon(4S)$
$8.4 \pm 1.1^{+1.0}_{-0.9}$		² GARMASH	07	BELL $e^+e^- \rightarrow \Upsilon(4S)$
$16^{+6}_{-5} \pm 2$		¹ ECKHART	02	CLE2 $e^+e^- \rightarrow \Upsilon(4S)$

• • • We do not use the following data for averages, fits, limits, etc. • • •

$11.0 \pm 1.5 \pm 0.71$		¹ AUBERT	06i	BABR Repl. by AUBERT 09AU
$12.9 \pm 2.4 \pm 1.4$		¹ AUBERT,B	04o	BABR Repl. by AUBERT 06i
$14.8^{+4.6+2.8}_{-4.4-1.3}$		¹ CHANG	04	BELL Repl. by GARMASH 07
< 72	90	ASNER	96	CLE2 $e^+e^- \rightarrow \Upsilon(4S)$
<620	90	ALBRECHT	91B	ARG $e^+e^- \rightarrow \Upsilon(4S)$
<380	90	⁴ AVERY	89B	CLEO $e^+e^- \rightarrow \Upsilon(4S)$
<560	90	⁵ AVERY	87	CLEO $e^+e^- \rightarrow \Upsilon(4S)$

¹ Assumes equal production of B^+ and B^0 at the $\Upsilon(4S)$.
² Uses Dalitz plot analysis of the $B^0 \rightarrow K^0 \pi^+ \pi^-$ final state decays.
³ Uses Dalitz plot analysis of $B^0 \rightarrow K^+ \pi^- \pi^0$ decays.
⁴ AVERY 89B reports $< 4.4 \times 10^{-4}$ assuming the $\Upsilon(4S)$ decays 43% to $B^0 \bar{B}^0$. We rescale to 50%.
⁵ AVERY 87 reports $< 7 \times 10^{-4}$ assuming the $\Upsilon(4S)$ decays 40% to $B^0 \bar{B}^0$. We rescale to 50%.

WEIGHTED AVERAGE
 $9.4^{+1.3-1.2}$ (Error scaled by 1.5)



$\Gamma(K_0^*(1430)^+ \pi^-)/\Gamma_{total}$ Γ_{246}/Γ

VALUE (units 10^{-6})	DOCUMENT ID	TECN	COMMENT
33 ± 7 OUR AVERAGE	Error includes scale factor of 2.0.		
$29.9^{+2.3}_{-1.7} \pm 3.6$	^{1,2} AUBERT	09AU	BABR $e^+e^- \rightarrow \Upsilon(4S)$
$49.7 \pm 3.8^{+6.8}_{-8.2}$	² GARMASH	07	BELL $e^+e^- \rightarrow \Upsilon(4S)$

¹ Assumes equal production of B^+ and B^0 at the $\Upsilon(4S)$.
² Uses Dalitz plot analysis of the $B^0 \rightarrow K^0 \pi^+ \pi^-$ final state decays.

$\Gamma(K_X^{*+} \pi^-)/\Gamma_{total}$ Γ_{247}/Γ

K_X^{*+} stands for the possible candidates of $K^*(1410)$, $K_0^*(1430)$ and $K_2^*(1430)$.

VALUE (units 10^{-6})	DOCUMENT ID	TECN	COMMENT
$5.1 \pm 1.5^{+0.6}_{-0.7}$	¹ CHANG	04	BELL $e^+e^- \rightarrow \Upsilon(4S)$

¹ Assumes equal production of B^+ and B^0 at the $\Upsilon(4S)$.

See key on page 405

Meson Particle Listings

 B^0 $\Gamma(K^*(892)^0 K^+ K^-)/\Gamma_{\text{total}}$ Γ_{279}/Γ

VALUE (units 10^{-6})	CL%	DOCUMENT ID	TECN	COMMENT
$27.5 \pm 1.3 \pm 2.2$		¹ AUBERT	07As BABR	$e^+ e^- \rightarrow \Upsilon(4S)$
• • • We do not use the following data for averages, fits, limits, etc. • • •				
<610	90	ALBRECHT	91E ARG	$e^+ e^- \rightarrow \Upsilon(4S)$
¹ Assumes equal production of B^+ and B^0 at the $\Upsilon(4S)$.				

 $\Gamma(K^*(892)^0 \phi)/\Gamma_{\text{total}}$ Γ_{280}/Γ

VALUE (units 10^{-6})	CL%	DOCUMENT ID	TECN	COMMENT
9.8 ± 0.6 OUR AVERAGE				
$9.7 \pm 0.5 \pm 0.5$		¹ AUBERT	08Bg BABR	$e^+ e^- \rightarrow \Upsilon(4S)$
$10.0 \pm 1.6 \pm 0.7$ $-1.5 - 0.8$		¹ CHEN	03B BELL	$e^+ e^- \rightarrow \Upsilon(4S)$
$11.5 \pm 4.5 \pm 1.8$ $-3.7 - 1.7$		¹ BRIERE	01 CLE2	$e^+ e^- \rightarrow \Upsilon(4S)$
• • • We do not use the following data for averages, fits, limits, etc. • • •				
$9.2 \pm 0.7 \pm 0.6$		¹ AUBERT	07D BABR	Repl. by AUBERT 08Bg
$9.2 \pm 0.9 \pm 0.5$		¹ AUBERT,B	04W BABR	Repl. by AUBERT 07D
$11.2 \pm 1.3 \pm 0.8$		¹ AUBERT	03V BABR	Repl. by AUBERT,B 04W
$8.7 \pm 2.9 \pm 1.1$ -2.1		¹ AUBERT	01D BABR	Repl. by AUBERT 03V
<384	90	² ABE	00c SLD	$e^+ e^- \rightarrow Z$
<21	90	¹ BERGFELD	98 CLE2	
<43	90	ASNER	96 CLE2	$e^+ e^- \rightarrow \Upsilon(4S)$
<320	90	ALBRECHT	91B ARG	$e^+ e^- \rightarrow \Upsilon(4S)$
<380	90	³ AVERY	89B CLEO	$e^+ e^- \rightarrow \Upsilon(4S)$
<380	90	⁴ AVERY	87 CLEO	$e^+ e^- \rightarrow \Upsilon(4S)$

- ¹ Assumes equal production of B^+ and B^0 at the $\Upsilon(4S)$.
² ABE 00c assumes $B(Z \rightarrow b\bar{b}) = (21.7 \pm 0.1)\%$ and the B fractions $f_{B^0} = f_{B^+} = (39.7 \pm 2.8)\%$ and $f_{B_s} = (10.5 \pm 1.8)\%$.
³ AVERY 89B reports $< 4.4 \times 10^{-4}$ assuming the $\Upsilon(4S)$ decays 43% to $B^0 \bar{B}^0$. We rescale to 50%.
⁴ AVERY 87 reports $< 4.7 \times 10^{-4}$ assuming the $\Upsilon(4S)$ decays 40% to $B^0 \bar{B}^0$. We rescale to 50%.

 $\Gamma(K^*(892)^0 K^- \pi^+)/\Gamma_{\text{total}}$ Γ_{281}/Γ

VALUE (units 10^{-6})	CL%	DOCUMENT ID	TECN	COMMENT
$4.6 \pm 1.1 \pm 0.8$		¹ AUBERT	07As BABR	$e^+ e^- \rightarrow \Upsilon(4S)$
¹ Assumes equal production of B^+ and B^0 at the $\Upsilon(4S)$.				

 $\Gamma(K^*(892)^0 \bar{K}^*(892)^0)/\Gamma_{\text{total}}$ Γ_{282}/Γ

VALUE (units 10^{-6})	CL%	DOCUMENT ID	TECN	COMMENT
$1.28 \pm 0.35 \pm 0.11$ -0.30		¹ AUBERT	08i BABR	$e^+ e^- \rightarrow \Upsilon(4S)$
• • • We do not use the following data for averages, fits, limits, etc. • • •				
<22	90	² GODANG	02 CLE2	$e^+ e^- \rightarrow \Upsilon(4S)$
<469	90	³ ABE	00c SLD	$e^+ e^- \rightarrow Z$

- ¹ Assumes equal production of B^+ and B^0 at the $\Upsilon(4S)$.
² Assumes a helicity 00 configuration. For a helicity 11 configuration, the limit decreases to 1.9×10^{-5} .
³ ABE 00c assumes $B(Z \rightarrow b\bar{b}) = (21.7 \pm 0.1)\%$ and the B fractions $f_{B^0} = f_{B^+} = (39.7 \pm 2.8)\%$ and $f_{B_s} = (10.5 \pm 1.8)\%$.

 $\Gamma(K^*(892)^0 K^+ \pi^-)/\Gamma_{\text{total}}$ Γ_{283}/Γ

VALUE (units 10^{-6})	CL%	DOCUMENT ID	TECN	COMMENT
<2.2	90	¹ AUBERT	07As BABR	$e^+ e^- \rightarrow \Upsilon(4S)$
¹ Assumes equal production of B^+ and B^0 at the $\Upsilon(4S)$.				

 $\Gamma(K^*(892)^0 K^*(892)^0)/\Gamma_{\text{total}}$ Γ_{284}/Γ

VALUE (units 10^{-6})	CL%	DOCUMENT ID	TECN	COMMENT
<0.41	90	¹ AUBERT	08i BABR	$e^+ e^- \rightarrow \Upsilon(4S)$
• • • We do not use the following data for averages, fits, limits, etc. • • •				
<37	90	² GODANG	02 CLE2	$e^+ e^- \rightarrow \Upsilon(4S)$

- ¹ Assumes equal production of B^+ and B^0 at the $\Upsilon(4S)$.
² Assumes a helicity 00 configuration. For a helicity 11 configuration, the limit decreases to 2.9×10^{-5} .

 $\Gamma(K^*(892)^+ K^*(892)^-)/\Gamma_{\text{total}}$ Γ_{285}/Γ

VALUE (units 10^{-6})	CL%	DOCUMENT ID	TECN	COMMENT
<2.0	90	¹ AUBERT	08AP BABR	$e^+ e^- \rightarrow \Upsilon(4S)$
• • • We do not use the following data for averages, fits, limits, etc. • • •				
<141	90	² GODANG	02 CLE2	$e^+ e^- \rightarrow \Upsilon(4S)$

- ¹ Assumes equal production of B^+ and B^0 at the $\Upsilon(4S)$.
² Assumes a helicity 00 configuration. For a helicity 11 configuration, the limit decreases to 8.9×10^{-5} .

 $\Gamma(K_1(1400)^0 \phi)/\Gamma_{\text{total}}$ Γ_{286}/Γ

VALUE	CL%	DOCUMENT ID	TECN	COMMENT
< 5.0×10^{-3}	90	ALBRECHT	91B ARG	$e^+ e^- \rightarrow \Upsilon(4S)$

 $\Gamma(\phi(K\pi)_0^0)/\Gamma_{\text{total}}$ Γ_{287}/Γ

This decay refers to the coherent sum of resonant and nonresonant $J^P = 0^+ K\pi$ components with $1.13 < m_{K\pi} < 1.53 \text{ GeV}/c^2$.

VALUE (units 10^{-6})	CL%	DOCUMENT ID	TECN	COMMENT
$4.3 \pm 0.6 \pm 0.4$		¹ AUBERT	08Bg BABR	$e^+ e^- \rightarrow \Upsilon(4S)$
• • • We do not use the following data for averages, fits, limits, etc. • • •				
$5.0 \pm 0.8 \pm 0.3$		¹ AUBERT	07D BABR	Repl. by AUBERT 08Bg
¹ Assumes equal production of B^+ and B^0 at the $\Upsilon(4S)$.				

 $\Gamma(\phi(K\pi)_0^0 (1.60 < m_{K\pi} < 2.15))/\Gamma_{\text{total}}$ Γ_{288}/Γ

This decay refers to the coherent sum of resonant and nonresonant $J^P = 0^+ K\pi$ components with $1.60 < m_{K\pi} < 2.15 \text{ GeV}/c^2$.

VALUE (units 10^{-6})	CL%	DOCUMENT ID	TECN	COMMENT
<1.7	90	¹ AUBERT	07Ao BABR	$e^+ e^- \rightarrow \Upsilon(4S)$
¹ Assumes equal production of B^+ and B^0 at the $\Upsilon(4S)$.				

 $\Gamma(K_0^*(1430)^0 \phi)/\Gamma_{\text{total}}$ Γ_{289}/Γ

VALUE (units 10^{-6})	CL%	DOCUMENT ID	TECN	COMMENT
$3.9 \pm 0.5 \pm 0.6$		¹ AUBERT	08Bg BABR	$e^+ e^- \rightarrow \Upsilon(4S)$
• • • We do not use the following data for averages, fits, limits, etc. • • •				
$4.6 \pm 0.7 \pm 0.6$		¹ AUBERT	07D BABR	Repl. by AUBERT 08Bg
seen		² AUBERT,B	04W BABR	Repl. by AUBERT 07D

- ¹ Assumes equal production of B^+ and B^0 at the $\Upsilon(4S)$.
² Observed 181 ± 17 events with statistical significance greater than 10σ .

 $\Gamma(K^*(1680)^0 \phi)/\Gamma_{\text{total}}$ Γ_{290}/Γ

VALUE (units 10^{-6})	CL%	DOCUMENT ID	TECN	COMMENT
<3.5	90	¹ AUBERT	07Ao BABR	$e^+ e^- \rightarrow \Upsilon(4S)$
¹ Assumes equal production of B^+ and B^0 at the $\Upsilon(4S)$.				

 $\Gamma(K^*(1780)^0 \phi)/\Gamma_{\text{total}}$ Γ_{291}/Γ

VALUE (units 10^{-6})	CL%	DOCUMENT ID	TECN	COMMENT
<2.7	90	¹ AUBERT	07Ao BABR	$e^+ e^- \rightarrow \Upsilon(4S)$
¹ Assumes equal production of B^+ and B^0 at the $\Upsilon(4S)$.				

 $\Gamma(K^*(2045)^0 \phi)/\Gamma_{\text{total}}$ Γ_{292}/Γ

VALUE (units 10^{-6})	CL%	DOCUMENT ID	TECN	COMMENT
<15.3	90	¹ AUBERT	07Ao BABR	$e^+ e^- \rightarrow \Upsilon(4S)$
¹ Assumes equal production of B^+ and B^0 at the $\Upsilon(4S)$.				

 $\Gamma(K_2^*(1430)^0 \rho^0)/\Gamma_{\text{total}}$ Γ_{293}/Γ

VALUE (units 10^{-6})	CL%	DOCUMENT ID	TECN	COMMENT
< 1.1×10^3	90	ALBRECHT	91B ARG	$e^+ e^- \rightarrow \Upsilon(4S)$

 $\Gamma(K_2^*(1430)^0 \phi)/\Gamma_{\text{total}}$ Γ_{294}/Γ

VALUE (units 10^{-6})	CL%	DOCUMENT ID	TECN	COMMENT
$7.5 \pm 0.9 \pm 0.5$		¹ AUBERT	08Bg BABR	$e^+ e^- \rightarrow \Upsilon(4S)$
• • • We do not use the following data for averages, fits, limits, etc. • • •				
$7.8 \pm 1.1 \pm 0.6$		¹ AUBERT	07D BABR	Repl. by AUBERT 08Bg
seen		² AUBERT,B	04W BABR	Repl. by AUBERT 07D
<1400	90	ALBRECHT	91B ARG	$e^+ e^- \rightarrow \Upsilon(4S)$

- ¹ Assumes equal production of B^+ and B^0 at the $\Upsilon(4S)$.
² The angular distribution of $B \rightarrow \phi K^*(1430)$ provides evidence with statistical significance of 3.2σ .

 $\Gamma(K^0 \phi \phi)/\Gamma_{\text{total}}$ Γ_{295}/Γ

VALUE (units 10^{-6})	CL%	DOCUMENT ID	TECN	COMMENT
$4.1 \pm 1.7 \pm 0.4$ -1.4		¹ AUBERT,BE	06H BABR	$e^+ e^- \rightarrow \Upsilon(4S)$
¹ Assumes equal production of B^0 and B^+ at the $\Upsilon(4S)$ and for a $\phi\phi$ invariant mass below $2.85 \text{ GeV}/c^2$.				

 $\Gamma(\eta' \eta' K^0)/\Gamma_{\text{total}}$ Γ_{296}/Γ

VALUE (units 10^{-6})	CL%	DOCUMENT ID	TECN	COMMENT
<31	90	¹ AUBERT,B	06P BABR	$e^+ e^- \rightarrow \Upsilon(4S)$
¹ Assumes equal production of B^+ and B^0 at the $\Upsilon(4S)$.				

 $\Gamma(\eta K^0 \gamma)/\Gamma_{\text{total}}$ Γ_{297}/Γ

VALUE (units 10^{-6})	CL%	DOCUMENT ID	TECN	COMMENT
7.6 ± 1.8 OUR AVERAGE				
$7.1 \pm 2.1 \pm 0.4$ -2.0		^{1,2} AUBERT	09 BABR	$e^+ e^- \rightarrow \Upsilon(4S)$
$8.7 \pm 3.1 \pm 1.9$ $-2.7 - 1.6$		^{2,3} NISHIDA	05 BELL	$e^+ e^- \rightarrow \Upsilon(4S)$
• • • We do not use the following data for averages, fits, limits, etc. • • •				
$11.3 \pm 2.8 \pm 0.6$ -1.6		^{1,2} AUBERT,B	06M BABR	Repl. by AUBERT 09
¹ $m_{\eta K} < 3.25 \text{ GeV}/c^2$.				
² Assumes equal production of B^+ and B^0 at the $\Upsilon(4S)$.				
³ $m_{\eta K} < 2.4 \text{ GeV}/c^2$.				

Meson Particle Listings

 B^0 $\Gamma(\eta' K^0 \gamma)/\Gamma_{\text{total}}$ Γ_{298}/Γ

VALUE (units 10^{-6})	CL%	DOCUMENT ID	TECN	COMMENT
<6.6	90	1,2 AUBERT,B	06M	BABR $e^+e^- \rightarrow \Upsilon(4S)$
¹ $m_{\eta'K} < 3.25 \text{ GeV}/c^2$. ² Assumes equal production of B^+ and B^0 at the $\Upsilon(4S)$.				

 $\Gamma(K^0 \phi \gamma)/\Gamma_{\text{total}}$ Γ_{299}/Γ

VALUE (units 10^{-6})	CL%	DOCUMENT ID	TECN	COMMENT
<2.7	90	1 AUBERT	07Q	BABR $e^+e^- \rightarrow \Upsilon(4S)$
<ul style="list-style-type: none"> • • • We do not use the following data for averages, fits, limits, etc. • • • 				
<8.3	90	1 DRUTSKOY	04	BELL $e^+e^- \rightarrow \Upsilon(4S)$
¹ Assumes equal production of B^+ and B^0 at $\Upsilon(4S)$.				

 $\Gamma(K^+ \pi^- \gamma)/\Gamma_{\text{total}}$ Γ_{300}/Γ

VALUE	CL%	DOCUMENT ID	TECN	COMMENT
$(4.6 \pm 1.3 + 0.5) \times 10^{-6}$		1,2 NISHIDA	02	BELL $e^+e^- \rightarrow \Upsilon(4S)$
¹ Assumes equal production of B^+ and B^0 at the $\Upsilon(4S)$. ² $1.25 \text{ GeV}/c^2 < M_{K\pi} < 1.6 \text{ GeV}/c^2$				

 $\Gamma(K^*(892)^0 \gamma)/\Gamma_{\text{total}}$ Γ_{301}/Γ

VALUE (units 10^{-6})	CL%	DOCUMENT ID	TECN	COMMENT
43.3 ± 1.5 OUR AVERAGE				
$44.7 \pm 1.0 \pm 1.6$		1 AUBERT	09A0	BABR $e^+e^- \rightarrow \Upsilon(4S)$
$40.1 \pm 2.1 \pm 1.7$		2 NAKAO	04	BELL $e^+e^- \rightarrow \Upsilon(4S)$
$45.5 \pm 7.2 \pm 3.4$		3 COAN	00	CLE2 $e^+e^- \rightarrow \Upsilon(4S)$
<ul style="list-style-type: none"> • • • We do not use the following data for averages, fits, limits, etc. • • • 				
$39.2 \pm 2.0 \pm 2.4$		4 AUBERT,BE	04A	BABR Repl. by AUBERT 09A0
< 110	90	ACOSTA	02G	CDF $p\bar{p}$ at 1.8 TeV
$42.3 \pm 4.0 \pm 2.2$		2 AUBERT	02c	BABR Repl. by AUBERT,BE 04A
< 210	90	5 ADAM	96D	DLPH $e^+e^- \rightarrow Z$
$40 \pm 17 \pm 8$		6 AMMAR	93	CLE2 Repl. by COAN 00
< 420	90	ALBRECHT	89G	ARG $e^+e^- \rightarrow \Upsilon(4S)$
< 240	90	7 AVERY	89B	CLEO $e^+e^- \rightarrow \Upsilon(4S)$
< 2100	90	AVERY	87	CLEO $e^+e^- \rightarrow \Upsilon(4S)$

- ¹ Uses $B(\Upsilon(4S) \rightarrow B^+ B^-) = (51.6 \pm 0.6)\%$ and $B(\Upsilon(4S) \rightarrow B^0 \bar{B}^0) = (48.4 \pm 0.6)\%$.
² Assumes equal production of B^+ and B^0 at the $\Upsilon(4S)$.
³ Assumes equal production of B^+ and B^0 at the $\Upsilon(4S)$. No evidence for a nonresonant $K\pi\gamma$ contamination was seen; the central value assumes no contamination.
⁴ Uses the production ratio of charged and neutral B from $\Upsilon(4S)$ decays $R^{+0} = 1.006 \pm 0.048$.
⁵ ADAM 96D assumes $f_{B^0} = f_{B^-} = 0.39$ and $f_{B^+} = 0.12$.
⁶ AMMAR 93 observed 6.6 ± 2.8 events above background.
⁷ AVERY 89B reports $< 2.8 \times 10^{-4}$ assuming the $\Upsilon(4S)$ decays 43% to $B^0 \bar{B}^0$. We rescale to 50%.

 $\Gamma(K^*(1410)\gamma)/\Gamma_{\text{total}}$ Γ_{302}/Γ

VALUE	CL%	DOCUMENT ID	TECN	COMMENT
$<1.3 \times 10^{-4}$	90	1 NISHIDA	02	BELL $e^+e^- \rightarrow \Upsilon(4S)$
¹ Assumes equal production of B^+ and B^0 at the $\Upsilon(4S)$.				

 $\Gamma(K^+ \pi^- \gamma \text{ nonresonant})/\Gamma_{\text{total}}$ Γ_{303}/Γ

VALUE	CL%	DOCUMENT ID	TECN	COMMENT
$<2.6 \times 10^{-6}$	90	1,2 NISHIDA	02	BELL $e^+e^- \rightarrow \Upsilon(4S)$
¹ Assumes equal production of B^+ and B^0 at the $\Upsilon(4S)$. ² $1.25 \text{ GeV}/c^2 < M_{K\pi} < 1.6 \text{ GeV}/c^2$				

 $\Gamma(K^0 \pi^+ \pi^- \gamma)/\Gamma_{\text{total}}$ Γ_{304}/Γ

VALUE (units 10^{-5})	CL%	DOCUMENT ID	TECN	COMMENT
1.95 ± 0.22 OUR AVERAGE				
$1.85 \pm 0.21 \pm 0.12$		1,2 AUBERT	07R	BABR $e^+e^- \rightarrow \Upsilon(4S)$
$2.40 \pm 0.4 \pm 0.3$		2,3 YANG	05	BELL $e^+e^- \rightarrow \Upsilon(4S)$
¹ $M_{K\pi\pi} < 1.8 \text{ GeV}/c^2$. ² Assumes equal production of B^+ and B^0 at the $\Upsilon(4S)$. ³ $M_{K\pi\pi} < 2.0 \text{ GeV}/c^2$.				

 $\Gamma(K^+ \pi^- \pi^0 \gamma)/\Gamma_{\text{total}}$ Γ_{305}/Γ

VALUE (units 10^{-5})	CL%	DOCUMENT ID	TECN	COMMENT
$4.07 \pm 0.22 \pm 0.31$		1,2 AUBERT	07R	BABR $e^+e^- \rightarrow \Upsilon(4S)$
¹ $M_{K\pi\pi} < 1.8 \text{ GeV}/c^2$. ² Assumes equal production of B^+ and B^0 at the $\Upsilon(4S)$.				

 $\Gamma(K_1(1270)^0 \gamma)/\Gamma_{\text{total}}$ Γ_{306}/Γ

VALUE (units 10^{-5})	CL%	DOCUMENT ID	TECN	COMMENT
< 5.8	90	1 YANG	05	BELL $e^+e^- \rightarrow \Upsilon(4S)$
<ul style="list-style-type: none"> • • • We do not use the following data for averages, fits, limits, etc. • • • 				
< 700	90	2 ALBRECHT	89G	ARG $e^+e^- \rightarrow \Upsilon(4S)$
¹ Assumes equal production of B^+ and B^0 at the $\Upsilon(4S)$. ² ALBRECHT 89G reports < 0.0078 assuming the $\Upsilon(4S)$ decays 45% to $B^0 \bar{B}^0$. We rescale to 50%.				

 $\Gamma(K_1(1400)^0 \gamma)/\Gamma_{\text{total}}$ Γ_{307}/Γ

VALUE (units 10^{-5})	CL%	DOCUMENT ID	TECN	COMMENT
< 1.5	90	1 YANG	05	BELL $e^+e^- \rightarrow \Upsilon(4S)$
<ul style="list-style-type: none"> • • • We do not use the following data for averages, fits, limits, etc. • • • 				
< 430	90	2 ALBRECHT	89G	ARG $e^+e^- \rightarrow \Upsilon(4S)$
¹ Assumes equal production of B^+ and B^0 at the $\Upsilon(4S)$. ² ALBRECHT 89G reports < 0.0048 assuming the $\Upsilon(4S)$ decays 45% to $B^0 \bar{B}^0$. We rescale to 50%.				

 $\Gamma(K_2^*(1430)^0 \gamma)/\Gamma_{\text{total}}$ Γ_{308}/Γ

VALUE (units 10^{-5})	CL%	DOCUMENT ID	TECN	COMMENT
1.24 ± 0.24 OUR AVERAGE				
$1.22 \pm 0.25 \pm 0.10$		1 AUBERT,B	04U	BABR $e^+e^- \rightarrow \Upsilon(4S)$
$1.3 \pm 0.5 \pm 0.1$		1 NISHIDA	02	BELL $e^+e^- \rightarrow \Upsilon(4S)$
<ul style="list-style-type: none"> • • • We do not use the following data for averages, fits, limits, etc. • • • 				
< 40	90	2 ALBRECHT	89G	ARG $e^+e^- \rightarrow \Upsilon(4S)$
¹ Assumes equal production of B^+ and B^0 at the $\Upsilon(4S)$. ² ALBRECHT 89G reports $< 4.4 \times 10^{-4}$ assuming the $\Upsilon(4S)$ decays 45% to $B^0 \bar{B}^0$. We rescale to 50%.				

 $\Gamma(K^*(1680)^0 \gamma)/\Gamma_{\text{total}}$ Γ_{309}/Γ

VALUE	CL%	DOCUMENT ID	TECN	COMMENT
< 0.0020	90	1 ALBRECHT	89G	ARG $e^+e^- \rightarrow \Upsilon(4S)$
¹ ALBRECHT 89G reports < 0.0022 assuming the $\Upsilon(4S)$ decays 45% to $B^0 \bar{B}^0$. We rescale to 50%.				

 $\Gamma(K_3^*(1780)^0 \gamma)/\Gamma_{\text{total}}$ Γ_{310}/Γ

VALUE (units 10^{-6})	CL%	DOCUMENT ID	TECN	COMMENT
< 83	90	1,2 NISHIDA	05	BELL $e^+e^- \rightarrow \Upsilon(4S)$
<ul style="list-style-type: none"> • • • We do not use the following data for averages, fits, limits, etc. • • • 				
< 10000	90	3 ALBRECHT	89G	ARG $e^+e^- \rightarrow \Upsilon(4S)$
¹ Assumes equal production of B^+ and B^0 at the $\Upsilon(4S)$. ² Uses $B(K_3^*(1780) \rightarrow \eta K) = 0.11 \pm 0.05$. ³ ALBRECHT 89G reports < 0.011 assuming the $\Upsilon(4S)$ decays 45% to $B^0 \bar{B}^0$. We rescale to 50%.				

 $\Gamma(K_4^*(2045)^0 \gamma)/\Gamma_{\text{total}}$ Γ_{311}/Γ

VALUE	CL%	DOCUMENT ID	TECN	COMMENT
< 0.0043	90	1 ALBRECHT	89G	ARG $e^+e^- \rightarrow \Upsilon(4S)$
¹ ALBRECHT 89G reports < 0.0048 assuming the $\Upsilon(4S)$ decays 45% to $B^0 \bar{B}^0$. We rescale to 50%.				

 $\Gamma(\rho^0 \gamma)/\Gamma_{\text{total}}$ Γ_{312}/Γ

VALUE (units 10^{-6})	CL%	DOCUMENT ID	TECN	COMMENT
0.86 ± 0.15 OUR AVERAGE				
$0.97 \pm 0.24 \pm 0.06$		1 AUBERT	08BH	BABR $e^+e^- \rightarrow \Upsilon(4S)$
$0.78 \pm 0.17 \pm 0.09$		1 TANIGUCHI	08	BELL $e^+e^- \rightarrow \Upsilon(4S)$
<ul style="list-style-type: none"> • • • We do not use the following data for averages, fits, limits, etc. • • • 				
$0.79 \pm 0.22 \pm 0.06$		1 AUBERT	07L	BABR Repl. by AUBERT 08BH
$1.25 \pm 0.37 \pm 0.07$		1 MOHAPATRA	06	BELL Repl. by TANIGUCHI 08
$0.0 \pm 0.2 \pm 0.1$	90	1 AUBERT	05	BABR Repl. by AUBERT 07L
< 0.8	90	1 MOHAPATRA	05	BELL $e^+e^- \rightarrow \Upsilon(4S)$
< 1.2	90	1 AUBERT	04c	BABR $e^+e^- \rightarrow \Upsilon(4S)$
< 17	90	1 COAN	00	CLE2 $e^+e^- \rightarrow \Upsilon(4S)$
¹ Assumes equal production of B^+ and B^0 at the $\Upsilon(4S)$.				

 $\Gamma(\rho^0 \gamma)/\Gamma(K^*(892)^0 \gamma)$ $\Gamma_{312}/\Gamma_{301}$

VALUE (units 10^{-2})	CL%	DOCUMENT ID	TECN	COMMENT
$2.06 \pm 0.45 \pm 0.14$		TANIGUCHI	08	BELL $e^+e^- \rightarrow \Upsilon(4S)$
-0.43 ± 0.16				

 $\Gamma(\omega \gamma)/\Gamma_{\text{total}}$ Γ_{313}/Γ

VALUE (units 10^{-6})	CL%	DOCUMENT ID	TECN	COMMENT
0.44 ± 0.18 OUR AVERAGE				
$0.50 \pm 0.27 \pm 0.09$		1 AUBERT	08BH	BABR $e^+e^- \rightarrow \Upsilon(4S)$
$0.40 \pm 0.19 \pm 0.13$		1 TANIGUCHI	08	BELL $e^+e^- \rightarrow \Upsilon(4S)$
<ul style="list-style-type: none"> • • • We do not use the following data for averages, fits, limits, etc. • • • 				
$0.40 \pm 0.24 \pm 0.05$		1 AUBERT	07L	BABR Repl. by AUBERT 08BH
$0.56 \pm 0.34 \pm 0.05$		1 MOHAPATRA	06	BELL Repl. by TANIGUCHI 08
< 1.0	90	1 AUBERT	05	BABR Repl. by AUBERT 07L
< 0.8	90	1 MOHAPATRA	05	BELL Repl. by MOHAPATRA 06
< 1.0	90	1 AUBERT	04c	BABR $e^+e^- \rightarrow \Upsilon(4S)$
< 9.2	90	1 COAN	00	CLE2 $e^+e^- \rightarrow \Upsilon(4S)$
¹ Assumes equal production of B^+ and B^0 at the $\Upsilon(4S)$.				

$\Gamma(\rho^0 \pi^-)/\Gamma_{\text{total}}$					Γ_{377}/Γ
VALUE	CL%	DOCUMENT ID	TECN	COMMENT	
$<3.8 \times 10^{-6}$	90	¹ WANG 03	BELL	$e^+e^- \rightarrow \Upsilon(4S)$	
¹ Assumes equal production of B^+ and B^0 at the $\Upsilon(4S)$.					

$\Gamma(\bar{\Lambda})/\Gamma_{\text{total}}$					Γ_{378}/Γ
VALUE (units 10^{-6})	CL%	DOCUMENT ID	TECN	COMMENT	
<0.32	90	¹ TSAI 07	BELL	$e^+e^- \rightarrow \Upsilon(4S)$	
• • • We do not use the following data for averages, fits, limits, etc. • • •					
<0.69	90	¹ CHANG 05	BELL	Repl. by TSAI 2007	
<1.2	90	¹ BORNHEIM 03	CLE2	$e^+e^- \rightarrow \Upsilon(4S)$	
<1.0	90	¹ ABE 020	BELL	Repl. by CHANG 05	
<3.9	90	¹ COAN 99	CLE2	$e^+e^- \rightarrow \Upsilon(4S)$	
¹ Assumes equal production of B^+ and B^0 at the $\Upsilon(4S)$.					

$\Gamma(\bar{\Lambda}\Lambda K^0)/\Gamma_{\text{total}}$					Γ_{379}/Γ
VALUE (units 10^{-6})		DOCUMENT ID	TECN	COMMENT	
$4.76^{+0.84}_{-0.68} \pm 0.61$		^{1,2} CHANG 09	BELL	$e^+e^- \rightarrow \Upsilon(4S)$	
¹ Excluding charmonium events in $2.85 < m_{\Lambda\bar{\Lambda}} < 3.128$ GeV/ c^2 and $3.315 < m_{\Lambda\bar{\Lambda}} < 3.735$ GeV/ c^2 . Measurements in various $m_{\Lambda\bar{\Lambda}}$ bins are also reported.					
² Assumes equal production of B^+ and B^0 at the $\Upsilon(4S)$.					

$\Gamma(\bar{\Lambda}\Lambda K^{*0})/\Gamma_{\text{total}}$					Γ_{380}/Γ
VALUE (units 10^{-6})		DOCUMENT ID	TECN	COMMENT	
$2.46^{+0.87}_{-0.72} \pm 0.34$		^{1,2} CHANG 09	BELL	$e^+e^- \rightarrow \Upsilon(4S)$	
¹ Excluding charmonium events in $2.85 < m_{\Lambda\bar{\Lambda}} < 3.128$ GeV/ c^2 and $3.315 < m_{\Lambda\bar{\Lambda}} < 3.735$ GeV/ c^2 . Measurements in various $m_{\Lambda\bar{\Lambda}}$ bins are also reported.					
² Assumes equal production of B^+ and B^0 at the $\Upsilon(4S)$.					

$\Gamma(\bar{\Lambda}\Lambda D^0)/\Gamma_{\text{total}}$					Γ_{381}/Γ
VALUE (units 10^{-5})		DOCUMENT ID	TECN	COMMENT	
$1.05^{+0.57}_{-0.44} \pm 0.14$		¹ CHANG 09	BELL	$e^+e^- \rightarrow \Upsilon(4S)$	
¹ Assumes equal production of B^+ and B^0 at the $\Upsilon(4S)$.					

$\Gamma(\Delta^0 \bar{\Delta}^0)/\Gamma_{\text{total}}$					Γ_{382}/Γ
VALUE	CL%	DOCUMENT ID	TECN	COMMENT	
<0.0015	90	¹ BORTOLETTO89	CLEO	$e^+e^- \rightarrow \Upsilon(4S)$	
¹ BORTOLETTO 89 reports < 0.0018 assuming $\Upsilon(4S)$ decays 43% to $B^0\bar{B}^0$. We rescale to 50%.					

$\Gamma(\Delta^{++} \bar{\Delta}^{--})/\Gamma_{\text{total}}$					Γ_{383}/Γ
VALUE	CL%	DOCUMENT ID	TECN	COMMENT	
$<1.1 \times 10^{-4}$	90	¹ BORTOLETTO89	CLEO	$e^+e^- \rightarrow \Upsilon(4S)$	
¹ BORTOLETTO 89 reports $< 1.3 \times 10^{-4}$ assuming $\Upsilon(4S)$ decays 43% to $B^0\bar{B}^0$. We rescale to 50%.					

$\Gamma(\bar{D}^0 \rho \bar{p})/\Gamma_{\text{total}}$					Γ_{384}/Γ
VALUE (units 10^{-4})		DOCUMENT ID	TECN	COMMENT	
1.14 ± 0.09 OUR AVERAGE					
$1.13 \pm 0.06 \pm 0.08$		¹ AUBERT,B 06s	BABR	$e^+e^- \rightarrow \Upsilon(4S)$	
$1.18 \pm 0.15 \pm 0.16$		¹ ABE 02w	BELL	$e^+e^- \rightarrow \Upsilon(4S)$	
¹ Assumes equal production of B^+ and B^0 at the $\Upsilon(4S)$.					

$\Gamma(D_s^- \bar{\Lambda} p)/\Gamma_{\text{total}}$					Γ_{385}/Γ
VALUE (units 10^{-5})		DOCUMENT ID	TECN	COMMENT	
$2.8 \pm 0.8 \pm 0.3$		^{1,2} MEDVEDEVA 07	BELL	$e^+e^- \rightarrow \Upsilon(4S)$	
¹ Assumes equal production of B^+ and B^0 at the $\Upsilon(4S)$.					
² MEDVEDEVA 07 reports $(2.9 \pm 0.7 \pm 0.5 \pm 0.4) \times 10^{-5}$ from a measurement of $[\Gamma(B^0 \rightarrow D_s^- \bar{\Lambda} p)/\Gamma_{\text{total}}] \times [B(D_s^+ \rightarrow \phi \pi^+)]$ assuming $B(D_s^+ \rightarrow \phi \pi^+) = (4.4 \pm 0.6) \times 10^{-2}$, which we rescale to our best value $B(D_s^+ \rightarrow \phi \pi^+) = (4.5 \pm 0.4) \times 10^{-2}$. Our first error is their experiment's error and our second error is the systematic error from using our best value.					

$\Gamma(\bar{D}^*(2007)^0 \rho \bar{p})/\Gamma_{\text{total}}$					Γ_{386}/Γ
VALUE (units 10^{-4})		DOCUMENT ID	TECN	COMMENT	
1.03 ± 0.13 OUR AVERAGE					
$1.01 \pm 0.10 \pm 0.09$		¹ AUBERT,B 06s	BABR	$e^+e^- \rightarrow \Upsilon(4S)$	
$1.20^{+0.33}_{-0.29} \pm 0.21$		¹ ABE 02w	BELL	$e^+e^- \rightarrow \Upsilon(4S)$	
¹ Assumes equal production of B^+ and B^0 at the $\Upsilon(4S)$.					

$\Gamma(D^*(2010)^- \rho \bar{\pi})/\Gamma_{\text{total}}$					Γ_{387}/Γ
VALUE (units 10^{-4})		DOCUMENT ID	TECN	COMMENT	
$14.5^{+3.4}_{-3.0} \pm 2.7$		¹ ANDERSON 01	CLE2	$e^+e^- \rightarrow \Upsilon(4S)$	
¹ Assumes equal production of B^+ and B^0 at the $\Upsilon(4S)$.					

$\Gamma(D^- \rho \bar{p} \pi^+)/\Gamma_{\text{total}}$					Γ_{388}/Γ
VALUE (units 10^{-4})		DOCUMENT ID	TECN	COMMENT	
$3.38 \pm 0.14 \pm 0.29$		¹ AUBERT,B 06s	BABR	$e^+e^- \rightarrow \Upsilon(4S)$	
¹ Assumes equal production of B^+ and B^0 at the $\Upsilon(4S)$.					

$\Gamma(D^{*+}(2010)^- \rho \bar{p} \pi^+)/\Gamma_{\text{total}}$					Γ_{389}/Γ
VALUE (units 10^{-4})		DOCUMENT ID	TECN	COMMENT	
5.0 ± 0.5 OUR AVERAGE					
$4.81 \pm 0.22 \pm 0.44$		¹ AUBERT,B 06s	BABR	$e^+e^- \rightarrow \Upsilon(4S)$	
$6.5^{+1.3}_{-1.2} \pm 1.0$		¹ ANDERSON 01	CLE2	$e^+e^- \rightarrow \Upsilon(4S)$	
¹ Assumes equal production of B^+ and B^0 at the $\Upsilon(4S)$.					

$\Gamma(\Theta_c^- \bar{p} \pi^+ \times B(\Theta_c \rightarrow D^- \rho))/\Gamma_{\text{total}}$					Γ_{390}/Γ
VALUE (units 10^{-6})	CL%	DOCUMENT ID	TECN	COMMENT	
<9	90	¹ AUBERT,B 06s	BABR	$e^+e^- \rightarrow \Upsilon(4S)$	
¹ Assumes equal production of B^+ and B^0 at the $\Upsilon(4S)$.					

$\Gamma(\Theta_c^- \bar{p} \pi^+ \times B(\Theta_c \rightarrow D^{*-} \rho))/\Gamma_{\text{total}}$					Γ_{391}/Γ
VALUE (units 10^{-6})	CL%	DOCUMENT ID	TECN	COMMENT	
<14	90	¹ AUBERT,B 06s	BABR	$e^+e^- \rightarrow \Upsilon(4S)$	
¹ Assumes equal production of B^+ and B^0 at the $\Upsilon(4S)$.					

$\Gamma(\Sigma_c^{*-} \Delta^{++})/\Gamma_{\text{total}}$					Γ_{392}/Γ
VALUE	CL%	DOCUMENT ID	TECN	COMMENT	
$<1.0 \times 10^{-3}$	90	¹ PROCARIO 94	CLE2	$e^+e^- \rightarrow \Upsilon(4S)$	
¹ PROCARIO 94 reports < 0.0012 from a measurement of $[\Gamma(B^0 \rightarrow \Sigma_c^{*-} \Delta^{++})/\Gamma_{\text{total}}] \times [B(\Lambda_c^+ \rightarrow p K^- \pi^+)]$ assuming $B(\Lambda_c^+ \rightarrow p K^- \pi^+) = 0.043$, which we rescale to our best value $B(\Lambda_c^+ \rightarrow p K^- \pi^+) = 5.0 \times 10^{-2}$.					

$\Gamma(\bar{\Lambda}_c^- \rho \pi^+ \pi^-)/\Gamma_{\text{total}}$					Γ_{393}/Γ
VALUE (units 10^{-3})		DOCUMENT ID	TECN	COMMENT	
1.3 ± 0.4 OUR AVERAGE					
$1.7^{+0.3}_{-0.2} \pm 0.4$		¹ DYTMAN 02	CLE2	$e^+e^- \rightarrow \Upsilon(4S)$	
$1.10 \pm 0.20 \pm 0.29$		² GABYSHEV 02	BELL	$e^+e^- \rightarrow \Upsilon(4S)$	
• • • We do not use the following data for averages, fits, limits, etc. • • •					
$1.33^{+0.46}_{-0.42} \pm 0.37$		³ FU 97	CLE2	Repl. by DYTMAN 02	

¹ DYTMAN 02 reports $(1.67^{+0.27}_{-0.25}) \times 10^{-3}$ from a measurement of $[\Gamma(B^0 \rightarrow \bar{\Lambda}_c^- \rho \pi^+ \pi^-)/\Gamma_{\text{total}}] \times [B(\Lambda_c^+ \rightarrow p K^- \pi^+)]$ assuming $B(\Lambda_c^+ \rightarrow p K^- \pi^+) = 0.05$, which we rescale to our best value $B(\Lambda_c^+ \rightarrow p K^- \pi^+) = (5.0 \pm 1.3) \times 10^{-2}$. Our first error is their experiment's error and our second error is the systematic error from using our best value.					
² GABYSHEV 02 reports $(1.1 \pm 0.2) \times 10^{-3}$ from a measurement of $[\Gamma(B^0 \rightarrow \bar{\Lambda}_c^- \rho \pi^+ \pi^-)/\Gamma_{\text{total}}] \times [B(\Lambda_c^+ \rightarrow p K^- \pi^+)]$ assuming $B(\Lambda_c^+ \rightarrow p K^- \pi^+) = 0.05$, which we rescale to our best value $B(\Lambda_c^+ \rightarrow p K^- \pi^+) = (5.0 \pm 1.3) \times 10^{-2}$. Our first error is their experiment's error and our second error is the systematic error from using our best value.					
³ FU 97 uses PDG 96 values of Λ_c branching fraction.					

$\Gamma(\bar{\Lambda}_c^- \rho)/\Gamma_{\text{total}}$					Γ_{394}/Γ
VALUE (units 10^{-5})	CL%	DOCUMENT ID	TECN	COMMENT	
2.0 ± 0.4 OUR AVERAGE					
$1.9 \pm 0.2 \pm 0.5$		^{1,2} AUBERT 08BN	BABR	$e^+e^- \rightarrow \Upsilon(4S)$	
$2.19^{+0.56}_{-0.49} \pm 0.65$		^{1,3} GABYSHEV 03	BELL	$e^+e^- \rightarrow \Upsilon(4S)$	
• • • We do not use the following data for averages, fits, limits, etc. • • •					
$2.10^{+0.67+0.77}_{-0.55-0.46}$		^{1,4} AUBERT 07AV	BABR	Repl. by AUBERT 08BN	
< 9	90	^{1,5} DYTMAN 02	CLE2	$e^+e^- \rightarrow \Upsilon(4S)$	
< 3.1	90	^{1,4} GABYSHEV 02	BELL	$e^+e^- \rightarrow \Upsilon(4S)$	
< 21	90	⁶ FU 97	CLE2	$e^+e^- \rightarrow \Upsilon(4S)$	

¹ Assumes equal production of B^+ and B^0 at the $\Upsilon(4S)$.					
² AUBERT 08BN reports $(1.89 \pm 0.21 \pm 0.49) \times 10^{-5}$ from a measurement of $[\Gamma(B^0 \rightarrow \bar{\Lambda}_c^- \rho)/\Gamma_{\text{total}}] \times [B(\Lambda_c^+ \rightarrow p K^- \pi^+)]$ assuming $B(\Lambda_c^+ \rightarrow p K^- \pi^+) = (5.0 \pm 1.3) \times 10^{-2}$.					
³ The second error for GABYSHEV 03 includes the systematic and the error of $\Lambda_c \rightarrow \bar{p} K^+ \pi^-$ decay branching fraction.					
⁴ Uses the value for $\Lambda_c \rightarrow p K^- \pi^+$ branching ratio $(5.0 \pm 1.3)\%$.					
⁵ DYTMAN 02 measurement uses $B(\Lambda_c^- \rightarrow \bar{p} K^+ \pi^-) = 5.0 \pm 1.3\%$. The second error includes the systematic and the uncertainty of the branching ratio.					
⁶ FU 97 uses PDG 96 values of Λ_c branching ratio.					

$\Gamma(\bar{\Lambda}_c^- \rho \pi^0)/\Gamma_{\text{total}}$					Γ_{395}/Γ
VALUE	CL%	DOCUMENT ID	TECN	COMMENT	
$<5.9 \times 10^{-4}$	90	¹ FU 97	CLE2	$e^+e^- \rightarrow \Upsilon(4S)$	
¹ FU 97 uses PDG 96 values of Λ_c branching ratio.					

Meson Particle Listings

 B^0

$\Gamma(\bar{A}_c^- \rho \pi^+ \pi^- \pi^0)/\Gamma_{\text{total}}$					Γ_{396}/Γ
VALUE	CL%	DOCUMENT ID	TECN	COMMENT	
$<5.07 \times 10^{-3}$	90	¹ FU	97	CLE2 $e^+e^- \rightarrow \Upsilon(4S)$	

¹FU 97 uses PDG 96 values of A_c branching ratio.

$\Gamma(\bar{A}_c^- \rho \pi^+ \pi^- \pi^+ \pi^-)/\Gamma_{\text{total}}$					Γ_{397}/Γ
VALUE	CL%	DOCUMENT ID	TECN	COMMENT	
$<2.74 \times 10^{-3}$	90	¹ FU	97	CLE2 $e^+e^- \rightarrow \Upsilon(4S)$	

¹FU 97 uses PDG 96 values of A_c branching ratio.

$\Gamma(\bar{A}_c^- \rho \pi^+ \pi^-)/\Gamma_{\text{total}}$					Γ_{398}/Γ
VALUE (units 10^{-4})		DOCUMENT ID	TECN	COMMENT	
$11.2 \pm 0.5 \pm 3.2$		^{1,2} PARK	07	BELL $e^+e^- \rightarrow \Upsilon(4S)$	

¹Assumes equal production of B^+ and B^0 at the $\Upsilon(4S)$.

²PARK 07 reports $(11.2 \pm 0.5 \pm 3.2) \times 10^{-4}$ from a measurement of $[\Gamma(B^0 \rightarrow \bar{A}_c^- \rho \pi^+ \pi^-)/\Gamma_{\text{total}}] \times [B(A_c^+ \rightarrow \rho K^- \pi^+)]$ assuming $B(A_c^+ \rightarrow \rho K^- \pi^+) = (5.0 \pm 1.3) \times 10^{-2}$.

$\Gamma(\bar{A}_c^- \rho \pi^+ \pi^- (\text{nonresonant}))/\Gamma_{\text{total}}$					Γ_{399}/Γ
VALUE (units 10^{-4})		DOCUMENT ID	TECN	COMMENT	
$6.4 \pm 0.4 \pm 1.9$		^{1,2} PARK	07	BELL $e^+e^- \rightarrow \Upsilon(4S)$	

¹Assumes equal production of B^+ and B^0 at the $\Upsilon(4S)$.

²PARK 07 reports $(6.4 \pm 0.4 \pm 1.9) \times 10^{-4}$ from a measurement of $[\Gamma(B^0 \rightarrow \bar{A}_c^- \rho \pi^+ \pi^- (\text{nonresonant}))/\Gamma_{\text{total}}] \times [B(A_c^+ \rightarrow \rho K^- \pi^+)]$ assuming $B(A_c^+ \rightarrow \rho K^- \pi^+) = (5.0 \pm 1.3) \times 10^{-2}$.

$\Gamma(\bar{\Sigma}_c(2520)^- \rho \pi^+)/\Gamma_{\text{total}}$					Γ_{400}/Γ
VALUE (units 10^{-4})		DOCUMENT ID	TECN	COMMENT	
$1.2 \pm 0.1 \pm 0.4$		^{1,2} PARK	07	BELL $e^+e^- \rightarrow \Upsilon(4S)$	

• • • We do not use the following data for averages, fits, limits, etc. • • •

³GABYSHEV 02 BELL Repl. by PARK 07

¹Assumes equal production of B^+ and B^0 at the $\Upsilon(4S)$.

²PARK 07 reports $(1.2 \pm 0.1 \pm 0.4) \times 10^{-4}$ from a measurement of $[\Gamma(B^0 \rightarrow \bar{\Sigma}_c(2520)^- \rho \pi^+)/\Gamma_{\text{total}}] \times [B(A_c^+ \rightarrow \rho K^- \pi^+)]$ assuming $B(A_c^+ \rightarrow \rho K^- \pi^+) = (5.0 \pm 1.3) \times 10^{-2}$.

³GABYSHEV 02 reports $(1.63_{-0.58}^{+0.64}) \times 10^{-4}$ from a measurement of $[\Gamma(B^0 \rightarrow \bar{\Sigma}_c(2520)^- \rho \pi^+)/\Gamma_{\text{total}}] \times [B(A_c^+ \rightarrow \rho K^- \pi^+)]$ assuming $B(A_c^+ \rightarrow \rho K^- \pi^+) = 0.05$, which we rescale to our best value $B(A_c^+ \rightarrow \rho K^- \pi^+) = (5.0 \pm 1.3) \times 10^{-2}$. Our first error is their experiment's error and our second error is the systematic error from using our best value.

$\Gamma(\bar{\Sigma}_c(2520)^0 \rho \pi^-)/\Gamma_{\text{total}}$					Γ_{401}/Γ
VALUE	CL%	DOCUMENT ID	TECN	COMMENT	
$<0.38 \times 10^{-4}$	90	¹ PARK	07	BELL $e^+e^- \rightarrow \Upsilon(4S)$	

• • • We do not use the following data for averages, fits, limits, etc. • • •

^{1,2}GABYSHEV 02 BELL Repl. by PARK 07

¹Assumes equal production of B^+ and B^0 at the $\Upsilon(4S)$.

²Uses the value for $A_c \rightarrow \rho K^- \pi^+$ branching ratio $(5.0 \pm 1.3)\%$.

$\Gamma(\bar{\Sigma}_c(2455)^0 N^0 \times B(N^0 \rightarrow \rho \pi^-))/\Gamma_{\text{total}}$					Γ_{403}/Γ
VALUE (units 10^{-4})		DOCUMENT ID	TECN	COMMENT	
$0.80 \pm 0.15 \pm 0.25$		^{1,2} KIM	08	BELL $e^+e^- \rightarrow \Upsilon(4S)$	

¹Assumes equal production of B^+ and B^0 at the $\Upsilon(4S)$.

²KIM 08 reports $(0.80 \pm 0.15 \pm 0.25) \times 10^{-4}$ from a measurement of $[\Gamma(B^0 \rightarrow \bar{\Sigma}_c(2455)^0 N^0 \times B(N^0 \rightarrow \rho \pi^-))/\Gamma_{\text{total}}] \times [B(A_c^+ \rightarrow \rho K^- \pi^+)]$ assuming $B(A_c^+ \rightarrow \rho K^- \pi^+) = (5.0 \pm 1.3) \times 10^{-2}$.

$\Gamma(\bar{\Sigma}_c(2455)^0 \rho \pi^-)/\Gamma_{\text{total}}$					Γ_{402}/Γ
VALUE (units 10^{-4})	CL%	DOCUMENT ID	TECN	COMMENT	
1.5 ± 0.5	OUR AVERAGE				

^{1,2}PARK 07 BELL $e^+e^- \rightarrow \Upsilon(4S)$

³DYTMAN 02 CLE2 $e^+e^- \rightarrow \Upsilon(4S)$

• • • We do not use the following data for averages, fits, limits, etc. • • •

⁴GABYSHEV 02 BELL Repl. by PARK 07

¹Assumes equal production of B^+ and B^0 at the $\Upsilon(4S)$.

²PARK 07 reports $(1.4 \pm 0.2 \pm 0.4) \times 10^{-4}$ from a measurement of $[\Gamma(B^0 \rightarrow \bar{\Sigma}_c(2455)^0 \rho \pi^-)/\Gamma_{\text{total}}] \times [B(A_c^+ \rightarrow \rho K^- \pi^+)]$ assuming $B(A_c^+ \rightarrow \rho K^- \pi^+) = (5.0 \pm 1.3) \times 10^{-2}$.

³DYTMAN 02 reports $(2.2 \pm 0.7) \times 10^{-4}$ from a measurement of $[\Gamma(B^0 \rightarrow \bar{\Sigma}_c(2455)^0 \rho \pi^-)/\Gamma_{\text{total}}] \times [B(A_c^+ \rightarrow \rho K^- \pi^+)]$ assuming $B(A_c^+ \rightarrow \rho K^- \pi^+) = 0.05$, which we rescale to our best value $B(A_c^+ \rightarrow \rho K^- \pi^+) = (5.0 \pm 1.3) \times 10^{-2}$. Our first error is their experiment's error and our second error is the systematic error from using our best value.

⁴GABYSHEV 02 reports $(0.48_{-0.41}^{+0.46}) \times 10^{-4}$ from a measurement of $[\Gamma(B^0 \rightarrow \bar{\Sigma}_c(2455)^0 \rho \pi^-)/\Gamma_{\text{total}}] \times [B(A_c^+ \rightarrow \rho K^- \pi^+)]$ assuming $B(A_c^+ \rightarrow \rho K^- \pi^+) = 0.05$, which we rescale to our best value $B(A_c^+ \rightarrow \rho K^- \pi^+) = (5.0 \pm 1.3) \times 10^{-2}$. Our first error is their experiment's error and our second error is the systematic error from using our best value.

$\Gamma(\bar{\Sigma}_c(2455)^- \rho \pi^+)/\Gamma_{\text{total}}$					Γ_{404}/Γ
VALUE (units 10^{-4})		DOCUMENT ID	TECN	COMMENT	
2.2 ± 0.7	OUR AVERAGE				

^{1,2}PARK 07 BELL $e^+e^- \rightarrow \Upsilon(4S)$

³DYTMAN 02 CLE2 $e^+e^- \rightarrow \Upsilon(4S)$

• • • We do not use the following data for averages, fits, limits, etc. • • •

⁴GABYSHEV 02 BELL Repl. by PARK 07

¹Assumes equal production of B^+ and B^0 at the $\Upsilon(4S)$.

²PARK 07 reports $(2.1 \pm 0.2 \pm 0.6) \times 10^{-4}$ from a measurement of $[\Gamma(B^0 \rightarrow \bar{\Sigma}_c(2455)^- \rho \pi^+)/\Gamma_{\text{total}}] \times [B(A_c^+ \rightarrow \rho K^- \pi^+)]$ assuming $B(A_c^+ \rightarrow \rho K^- \pi^+) = (5.0 \pm 1.3) \times 10^{-2}$.

³DYTMAN 02 reports $(3.7 \pm 1.1) \times 10^{-4}$ from a measurement of $[\Gamma(B^0 \rightarrow \bar{\Sigma}_c(2455)^- \rho \pi^+)/\Gamma_{\text{total}}] \times [B(A_c^+ \rightarrow \rho K^- \pi^+)]$ assuming $B(A_c^+ \rightarrow \rho K^- \pi^+) = 0.05$, which we rescale to our best value $B(A_c^+ \rightarrow \rho K^- \pi^+) = (5.0 \pm 1.3) \times 10^{-2}$. Our first error is their experiment's error and our second error is the systematic error from using our best value.

⁴GABYSHEV 02 reports $(2.38_{-0.69}^{+0.75}) \times 10^{-4}$ from a measurement of $[\Gamma(B^0 \rightarrow \bar{\Sigma}_c(2455)^- \rho \pi^+)/\Gamma_{\text{total}}] \times [B(A_c^+ \rightarrow \rho K^- \pi^+)]$ assuming $B(A_c^+ \rightarrow \rho K^- \pi^+) = 0.05$, which we rescale to our best value $B(A_c^+ \rightarrow \rho K^- \pi^+) = (5.0 \pm 1.3) \times 10^{-2}$. Our first error is their experiment's error and our second error is the systematic error from using our best value.

$\Gamma(\bar{A}_c^- \rho K^+ \pi^-)/\Gamma_{\text{total}}$					Γ_{405}/Γ
VALUE (units 10^{-5})		DOCUMENT ID	TECN	COMMENT	
$4.3 \pm 0.8 \pm 1.2$		^{1,2} AUBERT	09AG BABR	$e^+e^- \rightarrow \Upsilon(4S)$	

¹AUBERT 09AG reports $(4.33 \pm 0.82 \pm 0.33 \pm 1.13) \times 10^{-5}$ from a measurement of $[\Gamma(B^0 \rightarrow \bar{A}_c^- \rho K^+ \pi^-)/\Gamma_{\text{total}}] \times [B(A_c^+ \rightarrow \rho K^- \pi^+)]$ assuming $B(A_c^+ \rightarrow \rho K^- \pi^+) = (5.0 \pm 1.3) \times 10^{-2}$.

²Assumes equal production of B^+ and B^0 at the $\Upsilon(4S)$.

$\Gamma(\bar{\Sigma}_c(2455)^- \rho K^+ \times B(\bar{\Sigma}_c^- \rightarrow \bar{A}_c^- \pi^-))/\Gamma_{\text{total}}$					Γ_{406}/Γ
VALUE (units 10^{-5})		DOCUMENT ID	TECN	COMMENT	
$1.11 \pm 0.30 \pm 0.30$		^{1,2} AUBERT	09AG BABR	$e^+e^- \rightarrow \Upsilon(4S)$	

¹AUBERT 09AG reports $(1.11 \pm 0.30 \pm 0.09 \pm 0.29) \times 10^{-5}$ from a measurement of $[\Gamma(B^0 \rightarrow \bar{\Sigma}_c(2455)^- \rho K^+ \times B(\bar{\Sigma}_c^- \rightarrow \bar{A}_c^- \pi^-))/\Gamma_{\text{total}}] \times [B(A_c^+ \rightarrow \rho K^- \pi^+)]$ assuming $B(A_c^+ \rightarrow \rho K^- \pi^+) = (5.0 \pm 1.3) \times 10^{-2}$.

²Assumes equal production of B^+ and B^0 at the $\Upsilon(4S)$.

$\Gamma(\bar{A}_c^- \rho K^*(892)^0)/\Gamma_{\text{total}}$					Γ_{407}/Γ
VALUE (units 10^{-5})	CL%	DOCUMENT ID	TECN	COMMENT	
<2.42	90	¹ AUBERT	09AG BABR	$e^+e^- \rightarrow \Upsilon(4S)$	

¹Assumes equal production of B^+ and B^0 at the $\Upsilon(4S)$.

$\Gamma(\bar{A}_c^- A_c^+)/\Gamma_{\text{total}}$					Γ_{408}/Γ
VALUE (units 10^{-5})	CL%	DOCUMENT ID	TECN	COMMENT	
<6.2	90	¹ UCHIDA	08	BELL $e^+e^- \rightarrow \Upsilon(4S)$	

¹Assumes equal production of B^+ and B^0 at the $\Upsilon(4S)$.

$\Gamma(\bar{A}_c^-(2593)^- / \bar{A}_c^-(2625)^- \rho)/\Gamma_{\text{total}}$					Γ_{409}/Γ
VALUE	CL%	DOCUMENT ID	TECN	COMMENT	
$<1.1 \times 10^{-4}$	90	^{1,2} DYTMAN	02	CLE2 $e^+e^- \rightarrow \Upsilon(4S)$	

¹Assumes equal production of B^+ and B^0 at the $\Upsilon(4S)$.

²DYTMAN 02 measurement uses $B(A_c^- \rightarrow \bar{p} K^+ \pi^-) = 5.0 \pm 1.3\%$. The second error includes the systematic and the uncertainty of the branching ratio.

$\Gamma(\bar{\Xi}_c^- A_c^+ \times B(\bar{\Xi}_c^- \rightarrow \Xi^+ \pi^- \pi^-))/\Gamma_{\text{total}}$					Γ_{410}/Γ
VALUE (units 10^{-5})		DOCUMENT ID	TECN	COMMENT	
2.2 ± 2.3	OUR AVERAGE			Error includes scale factor of 1.9.	

^{1,2}AUBERT 08H BABR $e^+e^- \rightarrow \Upsilon(4S)$

^{2,3}CHISTOV 06A BELL $e^+e^- \rightarrow \Upsilon(4S)$

¹AUBERT 08H reports $(1.5 \pm 1.07 \pm 0.44) \times 10^{-5}$ from a measurement of $[\Gamma(B^0 \rightarrow \bar{\Xi}_c^- A_c^+ \times B(\bar{\Xi}_c^- \rightarrow \Xi^+ \pi^- \pi^-))/\Gamma_{\text{total}}] \times [B(A_c^+ \rightarrow \rho K^- \pi^+)]$ assuming $B(A_c^+ \rightarrow \rho K^- \pi^+) = (5.0 \pm 1.3) \times 10^{-2}$.

²Assumes equal production of B^+ and B^0 at the $\Upsilon(4S)$.

³CHISTOV 06A reports $(9.3_{-2.8}^{+3.7} \pm 3.1) \times 10^{-5}$ from a measurement of $[\Gamma(B^0 \rightarrow \bar{\Xi}_c^- A_c^+ \times B(\bar{\Xi}_c^- \rightarrow \Xi^+ \pi^- \pi^-))/\Gamma_{\text{total}}] \times [B(A_c^+ \rightarrow \rho K^- \pi^+)]$ assuming $B(A_c^+ \rightarrow \rho K^- \pi^+) = (5.0 \pm 1.3) \times 10^{-2}$.

$\Gamma(A_c^+ A_c^- K^0)/\Gamma_{\text{total}}$					Γ_{411}/Γ
VALUE (units 10^{-4})		DOCUMENT ID	TECN	COMMENT	
5.4 ± 3.2	OUR AVERAGE				

^{1,2}AUBERT 08H BABR $e^+e^- \rightarrow \Upsilon(4S)$

^{2,3}GABYSHEV 06 BELL $e^+e^- \rightarrow \Upsilon(4S)$

Meson Particle Listings

 B^0

• • • We do not use the following data for averages, fits, limits, etc. • • •

VALUE (units 10^{-7})	CL%	DOCUMENT ID	TECN	COMMENT
$1.3^{+1.6}_{-1.1} \pm 0.2$		1 AUBERT,B	06J	BABR Repl. by AUBERT 09T
$-2.1^{+2.3}_{-1.6} \pm 0.8$		1 AUBERT	03U	BABR $e^+e^- \rightarrow \Upsilon(4S)$
< 5.4	90	2 ISHIKAWA	03	BELL $e^+e^- \rightarrow \Upsilon(4S)$
< 27	90	1 ABE	02	BELL Repl. by ISHIKAWA 03
< 38	90	1 AUBERT	02L	BABR $e^+e^- \rightarrow \Upsilon(4S)$
< 84.5	90	3 ANDERSON	01B	CLE2 $e^+e^- \rightarrow \Upsilon(4S)$
< 3000	90	ALBRECHT	91E	ARG $e^+e^- \rightarrow \Upsilon(4S)$
< 5200	90	4 AVERY	87	CLEO $e^+e^- \rightarrow \Upsilon(4S)$

¹ Assumes equal production of B^+ and B^0 at the $\Upsilon(4S)$.

² Assumes equal production of B^0 and B^+ at $\Upsilon(4S)$.

³ The result is for di-lepton masses above 0.5 GeV.

⁴ AVERY 87 reports $< 6.5 \times 10^{-4}$ assuming the $\Upsilon(4S)$ decays 40% to $B^0\bar{B}^0$. We rescale to 50%.

$\Gamma(K^0\mu^+\mu^-)/\Gamma_{\text{total}}$ Γ_{424}/Γ

Test for $\Delta B=1$ weak neutral current. Allowed by higher-order electroweak interactions.

VALUE (units 10^{-7})	CL%	DOCUMENT ID	TECN	COMMENT
$4.5^{+1.2}_{-1.0}$ OUR AVERAGE				

$4.9^{+2.9}_{-2.5} \pm 0.3$		1 AUBERT	09T	BABR $e^+e^- \rightarrow \Upsilon(4S)$
$4.4^{+1.3}_{-1.1} \pm 0.3$		1 WEI	09A	BELL $e^+e^- \rightarrow \Upsilon(4S)$

• • • We do not use the following data for averages, fits, limits, etc. • • •

$5.9^{+3.3}_{-2.6} \pm 0.7$		1 AUBERT,B	06J	BABR Repl. by AUBERT 09T
$1.63^{+0.82}_{-0.63} \pm 0.14$		1 AUBERT	03U	BABR Repl. by AUBERT,B 06J
$5.6^{+2.9}_{-2.3} \pm 0.5$		2 ISHIKAWA	03	BELL Repl. by WEI 09A
< 33	90	1 ABE	02	BELL Repl. by ISHIKAWA 03
< 36	90	AUBERT	02L	BABR $e^+e^- \rightarrow \Upsilon(4S)$
< 66.4	90	3 ANDERSON	01B	CLE2 $e^+e^- \rightarrow \Upsilon(4S)$
< 5200	90	ALBRECHT	91E	ARG $e^+e^- \rightarrow \Upsilon(4S)$
< 3600	90	4 AVERY	87	CLEO $e^+e^- \rightarrow \Upsilon(4S)$

¹ Assumes equal production of B^+ and B^0 at the $\Upsilon(4S)$.

² Assumes equal production of B^0 and B^+ at $\Upsilon(4S)$. The second error is a total of systematic uncertainties including model dependence.

³ The result is for di-lepton masses above 0.5 GeV.

⁴ AVERY 87 reports $< 4.5 \times 10^{-4}$ assuming the $\Upsilon(4S)$ decays 40% to $B^0\bar{B}^0$. We rescale to 50%.

$\Gamma(K^*(892)^0 e^+ e^-)/\Gamma_{\text{total}}$ Γ_{427}/Γ

Test for $\Delta B=1$ weak neutral current. Allowed by higher-order electroweak interactions.

VALUE (units 10^{-7})	CL%	DOCUMENT ID	TECN	COMMENT
$9.9^{+1.2}_{-1.1}$ OUR AVERAGE				

$10.3^{+2.2}_{-2.1} \pm 0.7$		1 AUBERT	09T	BABR $e^+e^- \rightarrow \Upsilon(4S)$
$9.7^{+1.3}_{-1.1} \pm 0.7$		1 WEI	09A	BELL $e^+e^- \rightarrow \Upsilon(4S)$

• • • We do not use the following data for averages, fits, limits, etc. • • •

$8.1^{+2.1}_{-1.9} \pm 0.9$		1 AUBERT,B	06J	BABR Repl. by AUBERT 09T
$11.7^{+3.0}_{-2.7} \pm 0.9$		1 ISHIKAWA	03	BELL Repl. by WEI 09A

¹ Assumes equal production of B^0 and B^+ at $\Upsilon(4S)$.

$\Gamma(K^*(892)^0 e^+ e^-)/\Gamma_{\text{total}}$ Γ_{428}/Γ

Test for $\Delta B=1$ weak neutral current. Allowed by higher-order electroweak interactions.

VALUE (units 10^{-7})	CL%	DOCUMENT ID	TECN	COMMENT
$10.3^{+1.9}_{-1.7}$ OUR AVERAGE				

$8.6^{+2.6}_{-2.4} \pm 0.5$		1 AUBERT	09T	BABR $e^+e^- \rightarrow \Upsilon(4S)$
$11.8^{+2.7}_{-2.2} \pm 0.9$		1 WEI	09A	BELL $e^+e^- \rightarrow \Upsilon(4S)$

• • • We do not use the following data for averages, fits, limits, etc. • • •

$10.4^{+3.3}_{-2.9} \pm 1.1$		1 AUBERT,B	06J	BABR Repl. by AUBERT 09T
$11.1^{+5.6}_{-4.7} \pm 1.1$		1 AUBERT	03U	BABR $e^+e^- \rightarrow \Upsilon(4S)$
< 24	90	2 ISHIKAWA	03	BELL $e^+e^- \rightarrow \Upsilon(4S)$
< 64	90	1 ABE	02	BELL Repl. by ISHIKAWA 03
< 67	90	1 AUBERT	02L	BABR $e^+e^- \rightarrow \Upsilon(4S)$
< 2900	90	ALBRECHT	91E	ARG $e^+e^- \rightarrow \Upsilon(4S)$

¹ Assumes equal production of B^+ and B^0 at the $\Upsilon(4S)$.

² Assumes equal production of B^0 and B^+ at $\Upsilon(4S)$.

$\Gamma(K^*(892)^0 \mu^+ \mu^-)/\Gamma_{\text{total}}$ Γ_{429}/Γ

Test for $\Delta B=1$ weak neutral current. Allowed by higher-order electroweak interactions.

VALUE (units 10^{-7})	CL%	DOCUMENT ID	TECN	COMMENT
$10.5^{+1.6}_{-1.3}$ OUR AVERAGE				

$8.1 \pm 3.2 \pm 0.4$		1 AALTONEN	09B	CDF $p\bar{p}$ at 1.96 TeV
$13.5^{+4.0}_{-3.7} \pm 1.0$		2 AUBERT	09T	BABR $e^+e^- \rightarrow \Upsilon(4S)$
$10.6^{+1.9}_{-1.4} \pm 0.7$		2 WEI	09A	BELL $e^+e^- \rightarrow \Upsilon(4S)$

• • • We do not use the following data for averages, fits, limits, etc. • • •

$8.7^{+3.8}_{-3.3} \pm 1.2$		2 AUBERT,B	06J	BABR Repl. by AUBERT 09T
$8.6^{+7.9}_{-5.8} \pm 1.1$		2 AUBERT	03U	BABR Repl. by AUBERT,B 06J
$13.3^{+4.2}_{-3.7} \pm 1.1$		3 ISHIKAWA	03	BELL Repl. by WEI 09A
< 42	90	2 ABE	02	BELL $e^+e^- \rightarrow \Upsilon(4S)$
< 33	90	AUBERT	02L	BABR $e^+e^- \rightarrow \Upsilon(4S)$
< 40	90	4 AFFOLDER	99B	CDF $p\bar{p}$ at 1.8 TeV
< 250	90	5 ABE	96L	CDF Repl. by AFFOLDER 99B
< 230	90	6 ALBAJAR	91C	UA1 $E_{\text{cm}}^{p\bar{p}} = 630$ GeV
< 3400	90	ALBRECHT	91E	ARG $e^+e^- \rightarrow \Upsilon(4S)$

¹ AALTONEN 09b reports $[\Gamma(B^0 \rightarrow K^*(892)^0 \mu^+ \mu^-)/\Gamma_{\text{total}}] / [B(B^0 \rightarrow J/\psi(1S) K^*(892)^0)] = (0.61 \pm 0.23 \pm 0.07) \times 10^{-3}$ which we multiply by our best value $B(B^0 \rightarrow J/\psi(1S) K^*(892)^0) = (1.33 \pm 0.06) \times 10^{-3}$. Our first error is their experiment's error and our second error is the systematic error from using our best value.

² Assumes equal production of B^+ and B^0 at the $\Upsilon(4S)$.

³ Assumes equal production of B^0 and B^+ at $\Upsilon(4S)$. The second error is a total of systematic uncertainties including model dependence.

⁴ AFFOLDER 99b measured relative to $B^0 \rightarrow J/\psi(1S) K^*(892)^0$.

⁵ ABE 96L measured relative to $B^0 \rightarrow J/\psi(1S) K^*(892)^0$ using PDG 94 branching ratios.

⁶ ALBAJAR 91c assumes 36% of \bar{b} quarks give B^0 mesons.

$\Gamma(K^*(892)^0 \nu \bar{\nu})/\Gamma_{\text{total}}$ Γ_{430}/Γ

Test for $\Delta B=1$ weak neutral current. Allowed by higher-order electroweak interactions.

VALUE	CL%	DOCUMENT ID	TECN	COMMENT
$< 1.2 \times 10^{-4}$	90	AUBERT	08Bc	BABR $e^+e^- \rightarrow \Upsilon(4S)$

• • • We do not use the following data for averages, fits, limits, etc. • • •

$< 3.4 \times 10^{-4}$	90	1 CHEN	07D	BELL $e^+e^- \rightarrow \Upsilon(4S)$
$< 1.0 \times 10^{-3}$	90	2 ADAM	96D	DLPH $e^+e^- \rightarrow Z$

¹ Assumes equal production of B^+ and B^0 at the $\Upsilon(4S)$.

² ADAM 96d assumes $f_{B^0} = f_{B^+} = 0.39$ and $f_{B_s} = 0.12$.

$\Gamma(\phi \nu \bar{\nu})/\Gamma_{\text{total}}$ Γ_{431}/Γ

Test for $\Delta B=1$ weak neutral current. Allowed by higher-order electroweak interaction.

VALUE	CL%	DOCUMENT ID	TECN	COMMENT
$< 5.8 \times 10^{-5}$	90	1 CHEN	07D	BELL $e^+e^- \rightarrow \Upsilon(4S)$

¹ Assumes equal production of B^+ and B^0 at the $\Upsilon(4S)$.

$\Gamma(e^\pm \mu^\mp)/\Gamma_{\text{total}}$ Γ_{432}/Γ

Test of lepton family number conservation. Allowed by higher-order electroweak interactions.

VALUE	CL%	DOCUMENT ID	TECN	COMMENT
$< 6.4 \times 10^{-8}$	90	AALTONEN	09P	CDF $p\bar{p}$ at 1.96 TeV

• • • We do not use the following data for averages, fits, limits, etc. • • •

$< 9.2 \times 10^{-8}$	90	1 AUBERT	08P	BABR $e^+e^- \rightarrow \Upsilon(4S)$
$< 1.8 \times 10^{-7}$	90	1 AUBERT	05W	BABR $e^+e^- \rightarrow \Upsilon(4S)$
$< 1.7 \times 10^{-7}$	90	1 CHANG	03	BELL $e^+e^- \rightarrow \Upsilon(4S)$
$< 15 \times 10^{-7}$	90	1 BERGFELD	00B	CLE2 $e^+e^- \rightarrow \Upsilon(4S)$
$< 3.5 \times 10^{-6}$	90	ABE	98V	CDF $p\bar{p}$ at 1.8 TeV
$< 1.6 \times 10^{-5}$	90	2 ACCIARRI	97B	L3 $e^+e^- \rightarrow Z$
$< 5.9 \times 10^{-6}$	90	AMMAR	94	CLE2 $e^+e^- \rightarrow \Upsilon(4S)$
$< 3.4 \times 10^{-6}$	90	3 AVERY	89B	CLEO $e^+e^- \rightarrow \Upsilon(4S)$
$< 4.5 \times 10^{-5}$	90	4 ALBRECHT	87D	ARG $e^+e^- \rightarrow \Upsilon(4S)$
$< 7.7 \times 10^{-5}$	90	5 AVERY	87	CLEO $e^+e^- \rightarrow \Upsilon(4S)$
$< 3 \times 10^{-4}$	90	GILES	84	CLEO Repl. by AVERY 87

¹ Assumes equal production of B^+ and B^0 at the $\Upsilon(4S)$.

² ACCIARRI 97b assume PDG 96 production fractions for B^+ , B^0 , B_s , and Λ_b .

³ Paper assumes the $\Upsilon(4S)$ decays 43% to $B^0\bar{B}^0$. We rescale to 50%.

⁴ ALBRECHT 87D reports $< 5 \times 10^{-5}$ assuming the $\Upsilon(4S)$ decays 45% to $B^0\bar{B}^0$. We rescale to 50%.

⁵ AVERY 87 reports $< 9 \times 10^{-5}$ assuming the $\Upsilon(4S)$ decays 40% to $B^0\bar{B}^0$. We rescale to 50%.

$\Gamma(\pi^0 e^\pm \mu^\mp)/\Gamma_{\text{total}}$ Γ_{433}/Γ

Test of lepton family number conservation.

VALUE	CL%	DOCUMENT ID	TECN	COMMENT
$< 1.4 \times 10^{-7}$	90	1 AUBERT	07Ag	BABR $e^+e^- \rightarrow \Upsilon(4S)$

¹ Assumes equal production of B^+ and B^0 at the $\Upsilon(4S)$.

$\Gamma(K^0 e^\pm \mu^\mp)/\Gamma_{\text{total}}$ Γ_{434}/Γ

Test of lepton family number conservation.

VALUE (units 10^{-7})	CL%	DOCUMENT ID	TECN	COMMENT
< 2.7	90	1 AUBERT,B	06J	BABR $e^+e^- \rightarrow \Upsilon(4S)$

• • • We do not use the following data for averages, fits, limits, etc. • • •

< 40	90	1 AUBERT	02L	BABR Repl. by AUBERT,B 06J
------	----	----------	-----	----------------------------

¹ Assumes equal production of B^+ and B^0 at the $\Upsilon(4S)$.

$\Gamma(K^*(892)^0 e^+ \mu^-)/\Gamma_{\text{total}}$ Γ_{435}/Γ

VALUE (units 10^{-7})	CL%	DOCUMENT ID	TECN	COMMENT
<5.3	90	¹ AUBERT,B 06J	BABR	$e^+ e^- \rightarrow \Upsilon(4S)$

¹ Assumes equal production of B^0 and B^+ at $\Upsilon(4S)$.

 $\Gamma(K^*(892)^0 e^- \mu^+)/\Gamma_{\text{total}}$ Γ_{436}/Γ

VALUE (units 10^{-7})	CL%	DOCUMENT ID	TECN	COMMENT
<3.4	90	¹ AUBERT,B 06J	BABR	$e^+ e^- \rightarrow \Upsilon(4S)$

¹ Assumes equal production of B^0 and B^+ at $\Upsilon(4S)$.

 $\Gamma(K^*(892)^0 e^\pm \mu^\mp)/\Gamma_{\text{total}}$ Γ_{437}/Γ

Test of lepton family number conservation.

VALUE (units 10^{-7})	CL%	DOCUMENT ID	TECN	COMMENT
< 5.8	90	¹ AUBERT,B 06J	BABR	$e^+ e^- \rightarrow \Upsilon(4S)$
•••				We do not use the following data for averages, fits, limits, etc. •••
<34	90	¹ AUBERT 02L	BABR	Repl. by AUBERT,B 06J

¹ Assumes equal production of B^+ and B^0 at the $\Upsilon(4S)$.

 $\Gamma(e^\pm \tau^\mp)/\Gamma_{\text{total}}$ Γ_{438}/Γ

Test of lepton family number conservation. Allowed by higher-order electroweak interactions.

VALUE	CL%	DOCUMENT ID	TECN	COMMENT
<2.8 $\times 10^{-5}$	90	¹ AUBERT 08AD	BABR	$e^+ e^- \rightarrow \Upsilon(4S)$
•••				We do not use the following data for averages, fits, limits, etc. •••
<1.1 $\times 10^{-4}$	90	BORNHEIM 04	CLE2	$e^+ e^- \rightarrow \Upsilon(4S)$
<5.3 $\times 10^{-4}$	90	AMMAR 94	CLE2	Repl. by BORNHEIM 04

¹ Assumes equal production of B^+ and B^0 at the $\Upsilon(4S)$.

 $\Gamma(\mu^\pm \tau^\mp)/\Gamma_{\text{total}}$ Γ_{439}/Γ

Test of lepton family number conservation. Allowed by higher-order electroweak interactions.

VALUE	CL%	DOCUMENT ID	TECN	COMMENT
<2.2 $\times 10^{-5}$	90	¹ AUBERT 08AD	BABR	$e^+ e^- \rightarrow \Upsilon(4S)$
•••				We do not use the following data for averages, fits, limits, etc. •••
<3.8 $\times 10^{-5}$	90	BORNHEIM 04	CLE2	$e^+ e^- \rightarrow \Upsilon(4S)$
<8.3 $\times 10^{-4}$	90	AMMAR 94	CLE2	Repl. by BORNHEIM 04

¹ Assumes equal production of B^+ and B^0 at the $\Upsilon(4S)$.

 $\Gamma(\text{invisible})/\Gamma_{\text{total}}$ Γ_{440}/Γ

VALUE (units 10^{-5})	CL%	DOCUMENT ID	TECN	COMMENT
<22	90	¹ AUBERT,B 04J	BABR	$e^+ e^- \rightarrow \Upsilon(4S)$

¹ Uses the fully reconstructed $B^0 \rightarrow D^{(*)} - \ell^+ \nu_\ell$ events as a tag.

 $\Gamma(\nu \bar{\nu} \gamma)/\Gamma_{\text{total}}$ Γ_{441}/Γ

VALUE (units 10^{-5})	CL%	DOCUMENT ID	TECN	COMMENT
<4.7	90	¹ AUBERT,B 04J	BABR	$e^+ e^- \rightarrow \Upsilon(4S)$

¹ Uses the fully reconstructed $B^0 \rightarrow D^{(*)} - \ell^+ \nu_\ell$ events as a tag.

POLARIZATION IN B DECAYS

Revised April 2010 by A. V. Gritsan (Johns Hopkins University) and J. G. Smith (University of Colorado at Boulder).

We review the notation used in polarization measurements in particle production and decay, with a particular emphasis on the B decays and the CP -violating observables in polarization measurements. We look at several examples of vector-vector and vector-tensor B meson decays, while more details about the theory and experimental results in B decays can be found in a separate mini-review [1] in this *Review*.

Figure 1 illustrates angular observables in an example of the sequential process $ab \rightarrow X \rightarrow P_1 P_2 \rightarrow (p_{11} p_{12})(p_{21} p_{22})$ [2]. The angular distributions are of particular interest because they are sensitive to spin correlations and reveal properties of particles and their interactions, such as quantum numbers and couplings. In the case of a spin-zero particle X , such as B meson or a Higgs boson, there are no spin correlations in the production mechanism and the decay chain is to be analyzed. The angular distribution of decay products can be expressed as a function of three helicity angles which describe the alignment

of the particles in the decay chain. The analyzer of the B -daughter polarization is normally chosen for two-body decays, as the direction of the daughters in the center-of-mass of the parent (e.g., $\rho \rightarrow 2\pi$) [3], and for three-body decays as the normal to the decay plane (e.g., $\omega \rightarrow 3\pi$) [4]. An equivalent set of transversity angles is sometimes used in polarization analyses [5]. The differential decay width depends on complex amplitudes $A_{\lambda_1 \lambda_2}$, corresponding to the X -daughter helicity states λ_i .

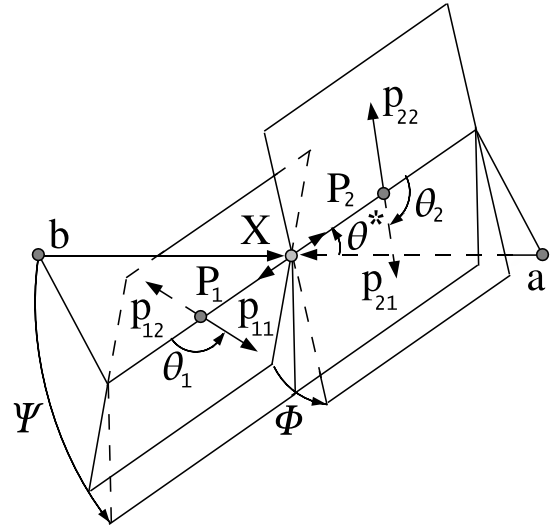


Figure 1: Definition of the production and helicity angles in the sequential process $ab \rightarrow X \rightarrow P_1 P_2 \rightarrow (p_{11} p_{12})(p_{21} p_{22})$. The three helicity angles include θ_1 and θ_2 , defined in the rest frame of the two daughters P_1 and P_2 , and Φ , defined in the X frame as the angle between the two decay planes. The two production angles θ^* and Ψ are defined in the X frame, where Ψ is the angle between the production plane and the average of the two decay planes.

In the case of a spin-zero B -meson decay, its daughter helicities are constrained to $\lambda_1 = \lambda_2 = \lambda$. Therefore we simplify amplitude notation as A_λ . Moreover, most B -decay polarization analyses are limited to the case when the spin of one of the B -meson daughters is 1. In that case, there are only three independent amplitudes corresponding to $\lambda = 0$ or ± 1 [6], where the last two can be expressed in terms of parity-even and parity-odd amplitudes $A_{\parallel, \perp} = (A_{+1} \pm A_{-1})/\sqrt{2}$. The overall decay amplitude involves three complex terms proportional to the above amplitudes and the Wigner d functions of helicity angles. The exact angular dependence would depend on the quantum numbers of the B -meson daughters and of their decay products, and can be found in the literature [6,7]. The differential decay rate would involve six real quantities α_i , including interference terms,

$$\frac{d\Gamma}{\Gamma d \cos \theta_1 d \cos \theta_2 d \Phi} = \sum_i \alpha_i f_i(\cos \theta_1, \cos \theta_2, \Phi), \quad (1)$$

Meson Particle Listings

 B^0

where each f_i ($\cos \theta_1$, $\cos \theta_2$, Φ) has unique angular dependence specific to particle quantum numbers, and the α_i parameters are defined as:

$$\alpha_1 = \frac{|A_0|^2}{\sum |A_\lambda|^2} = f_L, \quad (2)$$

$$\alpha_2 = \frac{|A_\parallel|^2 + |A_\perp|^2}{\sum |A_\lambda|^2} = (1 - f_L), \quad (3)$$

$$\alpha_3 = \frac{|A_\parallel|^2 - |A_\perp|^2}{\sum |A_\lambda|^2} = (1 - f_L - 2f_\perp), \quad (4)$$

$$\alpha_4 = \frac{\Im m(A_\perp A_\parallel^*)}{\sum |A_\lambda|^2} = \sqrt{f_\perp(1 - f_L - f_\perp)} \sin(\phi_\perp - \phi_\parallel), \quad (5)$$

$$\alpha_5 = \frac{\Re e(A_\parallel A_0^*)}{\sum |A_\lambda|^2} = \sqrt{f_L(1 - f_L - f_\perp)} \cos(\phi_\parallel), \quad (6)$$

$$\alpha_6 = \frac{\Im m(A_\perp A_0^*)}{\sum |A_\lambda|^2} = \sqrt{f_\perp f_L} \sin(\phi_\perp), \quad (7)$$

where the amplitudes have been expressed with the help of polarization parameters f_L , f_\perp , ϕ_\parallel , and ϕ_\perp defined in Table 1. Note that the terms proportional to $\Re e(A_\perp A_\parallel^*)$, $\Im m(A_\parallel A_0^*)$, and $\Re e(A_\perp A_0^*)$ are absent in Eqs. (2-7). However, these terms may appear for some three-body decays of a B -meson daughter, see Ref. 7.

Table 1: Rate, polarization, and CP -asymmetry parameters defined for the B -meson decays to mesons with non-zero spin. Numerical examples are shown for the $B^0 \rightarrow \varphi K^*(892)^0$ decay. The first six parameters are defined under the assumption of no CP violation in decay, while they are averaged between the \bar{B} and B parameters in general. The last six parameters involve differences between the \bar{B} and B meson decay parameters. The phase convention δ_0 is chosen with respect to a single A_{00} amplitude from a reference B decay mode, which is $B^0 \rightarrow \varphi K_0^*(1430)^0$ for numerical results.

parameter	definition	average
\mathcal{B}	$\Gamma/\Gamma_{\text{total}}$	$(9.8 \pm 0.6) \times 10^{-6}$
f_L	$ A_0 ^2/\sum A_\lambda ^2$	0.480 ± 0.030
f_\perp	$ A_\perp ^2/\sum A_\lambda ^2$	0.24 ± 0.05
$\phi_\parallel - \pi$	$\arg(A_\parallel/A_0) - \pi$	-0.74 ± 0.13
$\phi_\perp - \pi$	$\arg(A_\perp/A_0) - \pi$	-0.75 ± 0.13
$\delta_0 - \pi$	$\arg(A_{00}/A_0) - \pi$	-0.32 ± 0.17
A_{CP}	$(\bar{\Gamma} - \Gamma)/(\bar{\Gamma} + \Gamma)$	$+0.01 \pm 0.05$
A_{CP}^0	$(\bar{f}_L - f_L)/(\bar{f}_L + f_L)$	$+0.04 \pm 0.06$
A_{CP}^\perp	$(\bar{f}_\perp - f_\perp)/(\bar{f}_\perp + f_\perp)$	-0.11 ± 0.12
$\Delta\phi_\parallel$	$(\bar{\phi}_\parallel - \phi_\parallel)/2$	$+0.11 \pm 0.22$
$\Delta\phi_\perp$	$(\bar{\phi}_\perp - \phi_\perp - \pi)/2$	$+0.08 \pm 0.22$
$\Delta\delta_0$	$(\bar{\delta}_0 - \delta_0)/2$	$+0.27 \pm 0.16$

Overall, six real parameters describe three complex amplitudes A_0 , A_\parallel , and A_\perp . These could be chosen to be the four polarization parameters f_L , f_\perp , ϕ_\parallel , and ϕ_\perp , one overall size normalization, such as decay rate Γ , or branching fraction \mathcal{B} ,

and one overall phase δ_0 . The phase convention is arbitrary for an isolated B decay mode. However, for several B decays, the relative phase could produce meaningful and observable effects through interference with other B decays with the same final states, such as for $B \rightarrow VK_J^*$ with $J = 0, 1, 2, 3, 4, \dots$. The phase could be referenced to the single $B \rightarrow VK_0^*$ amplitude A_{00} in such a case, as shown in Table 1. Here V stands for any spin-one vector meson.

Moreover, CP violation can be tested in the angular distribution of the decay as the difference between the B and \bar{B} . Each of the six real parameters describing the three complex amplitudes would have a counterpart CP -asymmetry term, corresponding to three direct- CP asymmetries in three amplitudes, and three CP -violating phase differences, equivalent to the phase measurements from the mixing-induced CP asymmetries in the time evolution of B -decays [1]. In Table 1 and Ref. 8, these are chosen to be the direct- CP asymmetries in the overall decay rate \mathcal{A}_{CP} , in the f_L fraction \mathcal{A}_{CP}^0 , and in the f_\perp fraction \mathcal{A}_{CP}^\perp , and three weak phase differences:

$$\Delta\phi_\parallel = \frac{1}{2} \arg(\bar{A}_\parallel A_0 / A_\parallel \bar{A}_0), \quad (8)$$

$$\Delta\phi_\perp = \frac{1}{2} \arg(\bar{A}_\perp A_0 / A_\perp \bar{A}_0) - \frac{\pi}{2}, \quad (9)$$

$$\Delta\delta_0 = \frac{1}{2} \arg(\bar{A}_{00} A_0 / A_{00} \bar{A}_0). \quad (10)$$

The $\frac{\pi}{2}$ term in Eq. (9) reflects the fact that A_\perp and \bar{A}_\perp differ in phase by π if CP is conserved. The two parameters $\Delta\phi_\parallel$ and $\Delta\phi_\perp$ are equivalent to triple-product asymmetries constructed from the vectors describing the decay angular distribution [9]. The CP -violating phase difference in the reference decay mode [8] is, in the Wolfenstein CKM quark-mixing phase convention,

$$\Delta\phi_{00} = \frac{1}{2} \arg(A_{00}/\bar{A}_{00}). \quad (11)$$

This can be measured only together with the mixing-induced phase difference for some of the neutral B -meson decays similar to other mixing-induced CP asymmetry measurements [1].

It may not always be possible to have a phase-reference decay mode which would define δ_0 and $\Delta\delta_0$ parameters. In that case, it may be possible to define the phase difference directly similarly to Eq. (11):

$$\Delta\phi_0 = \frac{1}{2} \arg(A_0/\bar{A}_0). \quad (12)$$

One can measure the angles of the CKM unitarity triangle, assuming Standard Model contributions to the $\Delta\phi_0$ and B -mixing phases. Examples include measurements of $\beta = \phi_1$ with $B \rightarrow J/\psi K^*$ and $\alpha = \phi_2$ with $B \rightarrow \rho\rho$.

Most of the B decays that arise from tree-level $b \rightarrow c$ transitions have the amplitude hierarchy $|A_0| > |A_+| > |A_-|$ which is expected from analyses based on quark-helicity conservation [10]. The larger the mass of the vector-meson daughters, the weaker the inequality. The B meson decays to heavy vector particles with charm, such as $B \rightarrow J/\psi K^*$, $\psi(2S)K^*$, $\chi_{c1}K^*$,

$D^*\rho$, D^*K^* , D^*D^* , and $D^*D_s^*$, show a substantial fraction of the amplitudes corresponding to transverse polarization of the vector mesons ($A_{\pm 1}$), in agreement with the factorization prediction. The detailed amplitude analysis of the $B \rightarrow J/\psi K^*$ decays has been performed by the BABAR [11], Belle [12], CDF [13], CLEO [14], and D0 [15] collaborations. Most analyses are performed under the assumption of the absence of direct CP violation. The parameter values are given in the particle listing of this *Review*. The difference between the strong phases ϕ_{\parallel} and ϕ_{\perp} deviates significantly from zero. The recent measurements [11,12] of CP -violating terms similar to those in $B \rightarrow \varphi K^*$ [8] shown in Table 1 are consistent with zero.

In addition, the mixing-induced CP -violating asymmetry is measured in the $B^0 \rightarrow J/\psi K^{*0}$ decay [1,11,12] where angular analysis allows one to separate CP -eigenstate amplitudes. This allows one to resolve the sign ambiguity of the $\cos 2\beta$ ($\cos 2\phi_1$) term that appears in the time-dependent angular distribution due to interference of parity-even and parity-odd terms. This analysis relies on the knowledge of discrete ambiguities in the strong phases ϕ_{\parallel} and ϕ_{\perp} , as discussed below. The BABAR experiment used a method based on the dependence on the $K\pi$ invariant mass of the interference between the S - and P -waves to resolve the discrete ambiguity in the determination of the strong phases ($\phi_{\parallel}, \phi_{\perp}$) in $B \rightarrow J/\psi K^*$ decays [11]. The result is in agreement with the amplitude hierarchy expectation [10]. The CDF [13,16] and D0 [15,17] experiments have studied the $B_s^0 \rightarrow J/\psi \varphi$ decay and provided the lifetime, polarization, and phase measurements.

The amplitude hierarchy $|A_0| \gg |A_+| \gg |A_-|$ was expected in B decays to light vector particles in both penguin transitions [18,19] and tree-level transitions [10]. There is confirmation by the BABAR and BELLE experiments of predominantly longitudinal polarization in the tree-level $b \rightarrow u$ transition, such as $B^0 \rightarrow \rho^+ \rho^-$ [20], $B^+ \rightarrow \rho^0 \rho^+$ [21], and $B^+ \rightarrow \omega \rho^+$ [22]; this is consistent with the analysis of the quark helicity conservation [10]. Because the longitudinal amplitude dominates the decay, a detailed amplitude analysis is not possible with current B samples, and limits on the transverse amplitude fraction are obtained. Only limits have been set for $B^0 \rightarrow \omega \rho^0, \omega \omega$ [22]; there is some evidence for $B^0 \rightarrow \rho^0 \rho^0$ [23] decays. The small values for these branching fractions indicates that $b \rightarrow d$ penguin pollution is small in the charmless, strangeless vector-vector B decays.

The interest in the polarization and CP -asymmetry measurements in penguin transition, such as $b \rightarrow s$ decays $B \rightarrow \varphi K^*, \rho K^*, \omega K^*$, or $B_s^0 \rightarrow \varphi \varphi$, and $b \rightarrow d$ decay $B \rightarrow K^* \bar{K}^*$, is motivated by their potential sensitivity to physics beyond the Standard Model. The decay amplitudes for $B \rightarrow \varphi K^*$ have been measured by the BABAR and Belle experiments [8,24,25]. The fractions of longitudinal polarization $f_L = 0.50 \pm 0.05$ for the $B^+ \rightarrow \varphi K^{*+}$ decay, and $f_L = 0.48 \pm 0.03$ for the $B^0 \rightarrow \varphi K^{*0}$ decay, indicate significant departure from the naive expectation of predominant longitudinal polarization,

and suggest other contributions to the decay amplitude, previously neglected, either within the Standard Model, such as penguin annihilation [27] or QCD rescattering [28], or from physics beyond the Standard Model [29]. The complete set of twelve amplitude parameters measured in the $B^0 \rightarrow \varphi K^{*0}$ decay are given in Table 1. Several other parameters could be constructed from the above twelve parameters, as suggested in Ref. 30.

The discrete ambiguity in the phase ($\phi_{\parallel}, \phi_{\perp}, \Delta\phi_{\parallel}, \Delta\phi_{\perp}$) measurements has been resolved by BABAR in favor of $|A_+| \gg |A_-|$ through interference between the S - and P -waves of $K\pi$. The search for vector-tensor and vector-axialvector $B \rightarrow \varphi K_J^{(*)}$ decays with $J = 1, 2, 3, 4$ revealed a large fraction of longitudinal polarization in the decay $B \rightarrow \varphi K_2^*(1430)$ with $f_L = 0.90_{-0.07}^{+0.06}$ [8,31], but large contribution of transverse amplitude in $B \rightarrow \varphi K_1(1270)$ with $f_L = 0.46_{-0.15}^{+0.13}$ [32].

Like $B \rightarrow \varphi K^*$, the decays $B \rightarrow \rho K^*$ and $B \rightarrow \omega K^*$ may be sensitive to New Physics. Measurements of the longitudinal polarization fraction in $B^+ \rightarrow \rho^0 K^{*0}, B^+ \rightarrow \rho^+ K^{*0}$ [33] and in both vector-vector and vector-tensor final states of $B \rightarrow \omega K_J^*$ [22] reveal a large fraction of transverse polarization, indicating an anomaly similar to $B \rightarrow \varphi K^*$ except for different pattern in vector-tensor final states. At the same time, first measurement of the polarization in the $b \rightarrow d$ penguin decays $B \rightarrow K^* \bar{K}^*$ indicates a large fraction of longitudinal polarization [34]. There is also evidence for the $B_s^0 \rightarrow \varphi \varphi$ decay [35]. The polarization pattern in penguin-dominated B -meson decays is not fully understood [27,28,29].

The three-body smilpionic B -meson decays, such as $B \rightarrow V l_1 l_2$, share many features with the two-body $B \rightarrow VV$ decays. Their differential decay width can be parameterized with the two helicity angles defined in the V and $(l_1 l_2)$ frames and with the azimuthal angle, as defined in Fig. 1. However, since the $(l_1 l_2)$ pair does not come from an on-shell particle, the angular distribution is unique to each point in the dilepton mass m_{ll} spectrum. The polarization measurements as a function of m_{ll} provide complementary information on physics beyond the Standard Model, as discussed for $B \rightarrow K^* l^+ l^-$ decay in Ref. 36, though the current data in this mode [37] are not yet sufficient for precise tests.

The examples of the angular distributions and observables in $B \rightarrow K^* l^+ l^-$ are discussed in Ref. 36. With the present statistics only two angular observables have been measured in this decay when integrated over certain ranges of the dilepton mass m_{ll} [37]. One parameter is the fraction of longitudinal polarization F_L , which is determined by the K^* angular distribution and is similar to f_L defined for exclusive two-body decays. The other parameter is the forward-backward asymmetry of the lepton pair A_{FB} , which is the asymmetry of the decay rate with positive and negative values of $\cos \theta_1$.

In summary, there has been considerable recent interest in the polarization measurements of B -meson decays because they reveal both weak- and strong-interaction dynamics [27–29,38]. New measurements will further elucidate the pattern of spin

Meson Particle Listings

 B^0

alignment measurements in rare B decays, and further test the Standard Model and strong interaction dynamics, including the non-factorizable contributions to the B -decay amplitudes.

References

1. Y. Kwon, G. Punzi, and J. G. Smith, "Production and Decay of b -Flavored Hadrons," mini-review in this *Review*.
2. For a recent example and further references see Y. Y. Gao *et al.*, Phys. Rev. **D81**, 075022 (2010).
3. M. Jacob and G. C. Wick, Ann. Phys. **7**, 404 (1959).
4. S. M. Berman and M. Jacob, Phys. Rev. **139**, 1023 (1965).
5. I. Dunietz *et al.*, Phys. Rev. **D43**, 2193 (1991).
6. G. Kramer and W. F. Palmer, Phys. Rev. **D45**, 193 (1992).
7. A. Datta *et al.*, Phys. Rev. **D77**, 114025 (2008).
8. BABAR Collaboration, B. Aubert *et al.*, Phys. Rev. Lett. **93**, 231804 (2004); Phys. Rev. Lett. **98**, 051801 (2007); Phys. Rev. **D78**, 092008 (2008).
9. G. Valencia, Phys. Rev. **D39**, 3339 (1998); A. Datta and D. London, Int. J. Mod. Phys. **A19**, 2505 (2004).
10. A. Ali *et al.*, Z. Physik **C1**, 269 (1979); M. Suzuki, Phys. Rev. **D64**, 117503 (2001).
11. BABAR Collaboration, B. Aubert *et al.*, Phys. Rev. **D71**, 032005 (2005); Phys. Rev. **D76**, 031102 (2007).
12. Belle Collaboration, R. Itoh *et al.*, Phys. Rev. Lett. **95**, 091601 (2005).
13. CDF Collaboration, T. Affolder *et al.*, Phys. Rev. Lett. **85**, 4668 (2000); CDF Collaboration, D. Acosta *et al.*, Phys. Rev. Lett. **94**, 101803 (2005).
14. CLEO Collaboration, C. P. Jessop, Phys. Rev. Lett. **79**, 4533 (1997).
15. D0 Collaboration, V. M. Abazov *et al.*, Phys. Rev. Lett. **102**, 032001 (2009).
16. CDF Collaboration, T. Aaltonen *et al.*, Phys. Rev. Lett. **100**, 121803 (2008).
17. D0 Collaboration, V. M. Abazov *et al.*, Phys. Rev. Lett. **98**, 121801 (2007).
18. H. Y. Cheng and K. C. Yang, Phys. Lett. **B511**, 40 (2001); C. H. Chen, Y. Y. Keum, and H. n. Li, Phys. Rev. **D66**, 054013 (2002).
19. A. L. Kagan, Phys. Lett. **B601**, 151 (2004); Y. Grossman, Int. J. Mod. Phys. **A19**, 907 (2004).
20. Belle Collaboration, A. Somov *et al.*, Phys. Rev. Lett. **96**, 171801 (2006); BABAR Collaboration, B. Aubert *et al.*, Phys. Rev. **D76**, 052007 (2007).
21. Belle Collaboration, J. Zhang *et al.*, Phys. Rev. Lett. **91**, 221801 (2003); BABAR Collaboration, B. Aubert *et al.*, Phys. Rev. Lett. **102**, 141802 (2009).
22. BABAR Collaboration, B. Aubert *et al.*, Phys. Rev. **D74**, 051102 (2006); Phys. Rev. **D79**, 052005 (2009).
23. BABAR Collaboration, B. Aubert *et al.*, Phys. Rev. **D78**, 071104 (2008).
24. Belle Collaboration, K. F. Chen *et al.*, Phys. Rev. Lett. **94**, 221804 (2005).
25. BABAR Collaboration, B. Aubert *et al.*, Phys. Rev. Lett. **99**, 201802 (2007).

26. BABAR Collaboration, B. Aubert *et al.*, Phys. Rev. Lett. **91**, 171802 (2003); Belle Collaboration, K. F. Chen *et al.*, Phys. Rev. Lett. **91**, 201801 (2003).
27. A. L. Kagan, Phys. Lett. **B601**, 151 (2004); H. n. Li and S. Mishima, Phys. Rev. **D71**, 054025 (2005); C.-H. Chen *et al.*, Phys. Rev. **D72**, 054011 (2005); M. Beneke *et al.*, Phys. Rev. Lett. **96**, 141801 (2006); C.-H. Chen and C.-Q. Geng, Phys. Rev. **D75**, 054010 (2007); A. Datta *et al.*, Phys. Rev. **D76**, 034015 (2007); M. Beneke, J. Rohrer, and D. Yang, Nucl. Phys. **B774**, 64 (2007); H.-Y. Cheng and K.-C. Yang, Phys. Rev. **D78**, 094001 (2008).
28. C. W. Bauer *et al.*, Phys. Rev. **D70**, 054015 (2004); P. Colangelo *et al.*, Phys. Lett. **B597**, 291 (2004); M. Ladisa *et al.*, Phys. Rev. **D70**, 114025 (2004); H. Y. Cheng *et al.*, Phys. Rev. **D71**, 014030 (2005).
29. Y. Grossman, Int. J. Mod. Phys. A **19**, 907 (2004); E. Alvarez *et al.*, Phys. Rev. **D70**, 115014 (2004); P. K. Das and K. C. Yang, Phys. Rev. **D71**, 094002 (2005); C. H. Chen and C. Q. Geng, Phys. Rev. **D71**, 115004 (2005); Y. D. Yang *et al.*, Phys. Rev. **D72**, 015009 (2005); K. C. Yang, Phys. Rev. **72**, 034009 (2005); S. Baek, Phys. Rev. **D72**, 094008 (2005); C. S. Huang *et al.*, Phys. Rev. **D73**, 034026 (2006); C. H. Chen and H. Hatanaka, Phys. Rev. **D73**, 075003 (2006); A. Faessler *et al.*, Phys. Rev. **D75**, 074029 (2007).
30. D. London, N. Sinha, and R. Sinha, Phys. Rev. **D69**, 114013 (2004).
31. BABAR Collaboration, B. Aubert *et al.*, Phys. Rev. **D76**, 051103 (2007).
32. BABAR Collaboration, B. Aubert *et al.*, Phys. Rev. Lett. **101**, 161801 (2008).
33. Belle Collaboration, J. Zhang *et al.*, Phys. Rev. Lett. **95**, 141801 (2005); BABAR Collaboration, B. Aubert *et al.*, Phys. Rev. Lett. **97**, 201801 (2006).
34. BABAR Collaboration, B. Aubert *et al.*, Phys. Rev. Lett. **100**, 081801 (2008); Phys. Rev. **D79**, 051102 (2009).
35. CDF Collaboration, D. Acosta *et al.*, Phys. Rev. Lett. **95**, 031801 (2005).
36. G. Burdman, Phys. Rev. **D52**, 6400 (1995); F. Kruger and J. Matias, Phys. Rev. **D71**, 094009 (2005); E. Lunghi and J. Matias, JHEP **0704**, 058 (2007).
37. Belle Collaboration, A. Ishikawa *et al.*, Phys. Rev. Lett. **96**, 251801 (2006); BABAR Collaboration, B. Aubert *et al.*, Phys. Rev. **D73**, 092001 (2006).
38. C. H. Chen and H. n. Li, Phys. Rev. **D71**, 114008 (2005).

POLARIZATION IN B^0 DECAY

In decays involving two vector mesons, one can distinguish among the states in which meson polarizations are both longitudinal (L) or both are transverse and parallel (\parallel) or perpendicular (\perp) to each other with the parameters Γ_L/Γ , $\Gamma_{\parallel}/\Gamma$, and the relative phases ϕ_{\parallel} and ϕ_{\perp} . See the definitions in the note on "Polarization in B Decays" review in the B^0 Particle Listings.

 Γ_L/Γ in $B^0 \rightarrow J/\psi(1S)K^*(892)^0$

VALUE	EVTs	DOCUMENT ID	TECN	COMMENT
0.570 ± 0.008	OUR AVERAGE			
$0.587 \pm 0.011 \pm 0.013$		¹ ABAZOV	09E D0	$p\bar{p}$ at 1.96 TeV
$0.556 \pm 0.009 \pm 0.010$		² AUBERT	07AD BABR	$e^+e^- \rightarrow \Upsilon(4S)$
$0.562 \pm 0.026 \pm 0.018$		ACOSTA	05 CDF	$p\bar{p}$ at 1.96 TeV
$0.574 \pm 0.012 \pm 0.009$		ITOH	05 BELL	$e^+e^- \rightarrow \Upsilon(4S)$
$0.59 \pm 0.06 \pm 0.01$		³ AFFOLDER	00N CDF	$p\bar{p}$ at 1.8 TeV
$0.52 \pm 0.07 \pm 0.04$		⁴ JESSOP	97 CLE2	$e^+e^- \rightarrow \Upsilon(4S)$
$0.65 \pm 0.10 \pm 0.04$	65	ABE	95Z CDF	$p\bar{p}$ at 1.8 TeV
$0.97 \pm 0.16 \pm 0.15$	13	⁵ ALBRECHT	94G ARG	$e^+e^- \rightarrow \Upsilon(4S)$

B^0 - \bar{B}^0 MIXING

Updated April 2010 by O. Schneider (Ecole Polytechnique Fédérale de Lausanne).

There are two neutral B^0 - \bar{B}^0 meson systems, B_d^0 - \bar{B}_d^0 and B_s^0 - \bar{B}_s^0 (generically denoted B_q^0 - \bar{B}_q^0 , $q = s, d$), which exhibit particle-antiparticle mixing [1]. This mixing phenomenon is described in Ref. 2. In the following, we adopt the notation introduced in Ref. 2, and assume CPT conservation throughout. In each system, the light (L) and heavy (H) mass eigenstates,

$$|B_{L,H}\rangle = p|B_q^0\rangle \pm q|\bar{B}_q^0\rangle, \quad (1)$$

have a mass difference $\Delta m_q = m_H - m_L > 0$, and a total decay width difference $\Delta\Gamma_q = \Gamma_L - \Gamma_H$. In the absence of CP violation in the mixing, $|q/p| = 1$, these differences are given by $\Delta m_q = 2|M_{12}|$ and $|\Delta\Gamma_q| = 2|\Gamma_{12}|$, where M_{12} and Γ_{12} are the off-diagonal elements of the mass and decay matrices [2]. The evolution of a pure $|B_q^0\rangle$ or $|\bar{B}_q^0\rangle$ state at $t = 0$ is given by

$$|B_q^0(t)\rangle = g_+(t)|B_q^0\rangle + \frac{q}{p}g_-(t)|\bar{B}_q^0\rangle, \quad (2)$$

$$|\bar{B}_q^0(t)\rangle = g_+(t)|\bar{B}_q^0\rangle + \frac{p}{q}g_-(t)|B_q^0\rangle, \quad (3)$$

which means that the flavor states remain unchanged (+) or oscillate into each other (-) with time-dependent probabilities proportional to

$$|g_{\pm}(t)|^2 = \frac{e^{-\Gamma_q t}}{2} \left[\cosh\left(\frac{\Delta\Gamma_q t}{2}\right) \pm \cos(\Delta m_q t) \right], \quad (4)$$

where $\Gamma_q = (\Gamma_H + \Gamma_L)/2$. In the absence of CP violation, the time-integrated mixing probability $\int |g_-(t)|^2 dt / (\int |g_-(t)|^2 dt + \int |g_+(t)|^2 dt)$ is given by

$$\chi_q = \frac{x_q^2 + y_q^2}{2(x_q^2 + 1)}, \quad \text{where} \quad x_q = \frac{\Delta m_q}{\Gamma_q}, \quad y_q = \frac{\Delta\Gamma_q}{2\Gamma_q}. \quad (5)$$

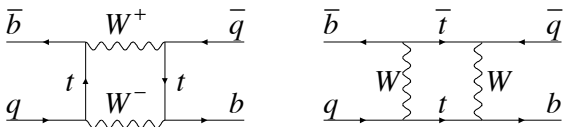


Figure 1: Dominant box diagrams for the $B_q^0 \rightarrow \bar{B}_q^0$ transitions ($q = d$ or s). Similar diagrams exist where one or both t quarks are replaced with c or u quarks.

Standard Model predictions and phenomenology

In the Standard Model, the transitions $B_q^0 \rightarrow \bar{B}_q^0$ and $\bar{B}_q^0 \rightarrow B_q^0$ are due to the weak interaction. They are described, at the lowest order, by box diagrams involving two W bosons and two up-type quarks (see Fig. 1), as is the case for K^0 - \bar{K}^0 mixing. However, the long range interactions arising from intermediate virtual states are negligible for the neutral B meson systems, because the large B mass is off the region of hadronic resonances. The calculation of the dispersive and absorptive parts of the box diagrams yields the following predictions for the off-diagonal element of the mass and decay matrices [3],

$$M_{12} = -\frac{G_F^2 m_W^2 \eta_B m_{B_q} B_{B_q} f_{B_q}^2}{12\pi^2} S_0(m_t^2/m_W^2) (V_{tq}^* V_{tb})^2, \quad (6)$$

$$\Gamma_{12} = \frac{G_F^2 m_b^2 \eta_B' m_{B_q} B_{B_q} f_{B_q}^2}{8\pi} \times \left[(V_{tq}^* V_{tb})^2 + V_{tq}^* V_{tb} V_{cq}^* V_{cb} \mathcal{O}\left(\frac{m_c^2}{m_b^2}\right) + (V_{cq}^* V_{cb})^2 \mathcal{O}\left(\frac{m_c^4}{m_b^4}\right) \right], \quad (7)$$

where G_F is the Fermi constant, m_W the W boson mass, and m_i the mass of quark i ; m_{B_q} , f_{B_q} and B_{B_q} are the B_q^0 mass, weak decay constant and bag parameter, respectively. The known function $S_0(x_t)$ can be approximated very well by $0.784 x_t^{0.76}$ [4], and V_{ij} are the elements of the CKM matrix [5]. The QCD corrections η_B and η_B' are of order unity. The only non-negligible contributions to M_{12} are from box diagrams involving two top quarks. The phases of M_{12} and Γ_{12} satisfy

$$\phi_M - \phi_\Gamma = \pi + \mathcal{O}\left(\frac{m_c^2}{m_b^2}\right), \quad (8)$$

implying that the mass eigenstates have mass and width differences of opposite signs. This means that, like in the K^0 - \bar{K}^0 system, the heavy state is expected to have a smaller decay width than that of the light state: $\Gamma_H < \Gamma_L$. Hence, $\Delta\Gamma = \Gamma_L - \Gamma_H$ is expected to be positive in the Standard Model.

Furthermore, the quantity

$$\left| \frac{\Gamma_{12}}{M_{12}} \right| \simeq \frac{3\pi m_b^2}{2 m_W^2} \frac{1}{S_0(m_t^2/m_W^2)} \sim \mathcal{O}\left(\frac{m_b^2}{m_t^2}\right) \quad (9)$$

is small, and a power expansion of $|q/p|^2$ yields

$$\left| \frac{q}{p} \right|^2 = 1 + \left| \frac{\Gamma_{12}}{M_{12}} \right| \sin(\phi_M - \phi_\Gamma) + \mathcal{O}\left(\left| \frac{\Gamma_{12}}{M_{12}} \right|^2\right). \quad (10)$$

Therefore, considering both Eqs. (8) and (9), the CP -violating parameter

$$1 - \left| \frac{q}{p} \right|^2 \simeq \text{Im}\left(\frac{\Gamma_{12}}{M_{12}}\right) \quad (11)$$

is expected to be very small: $\sim \mathcal{O}(10^{-3})$ for the B_d^0 - \bar{B}_d^0 system and $\lesssim \mathcal{O}(10^{-4})$ for the B_s^0 - \bar{B}_s^0 system [6].

In the approximation of negligible CP violation in mixing, the ratio $\Delta\Gamma_q/\Delta m_q$ is equal to the small quantity $|\Gamma_{12}/M_{12}|$ of Eq. (9); it is hence independent of CKM matrix elements, *i.e.*, the same for the B_d^0 - \bar{B}_d^0 and B_s^0 - \bar{B}_s^0 systems. Calculations [7] yield $\sim 5 \times 10^{-3}$ with a $\sim 20\%$ uncertainty. Given the current experimental knowledge on the mixing parameter x_q

$$\begin{cases} x_d = 0.774 \pm 0.008 & (B_d^0\text{-}\bar{B}_d^0 \text{ system}) \\ x_s = 26.2 \pm 0.5 & (B_s^0\text{-}\bar{B}_s^0 \text{ system}) \end{cases}, \quad (12)$$

the Standard Model thus predicts that $\Delta\Gamma_d/\Gamma_d$ is very small (below 1%), but $\Delta\Gamma_s/\Gamma_s$ considerably larger ($\sim 10\%$). These width differences are caused by the existence of final states to which both the B_q^0 and \bar{B}_q^0 mesons can decay. Such decays

Meson Particle Listings

B^0

involve $b \rightarrow c\bar{c}q$ quark-level transitions, which are Cabibbo-suppressed if $q = d$ and Cabibbo-allowed if $q = s$.

A complete set of Standard Model predictions for all mixing parameters in both the $B_d^0\text{--}\bar{B}_d^0$ and $B_s^0\text{--}\bar{B}_s^0$ systems can be found in Ref. 7.

Experimental issues and methods for oscillation analyses

Time-integrated measurements of $B^0\text{--}\bar{B}^0$ mixing were published for the first time in 1987 by UA1 [8] and ARGUS [9], and since then by many other experiments. These measurements are typically based on counting same-sign and opposite-sign lepton pairs from the semileptonic decay of the produced $b\bar{b}$ pairs. Such analyses cannot easily separate the contributions from the different b -hadron species, therefore, the clean environment of $\Upsilon(4S)$ machines (where only B_d^0 and charged B_u mesons are produced) is in principle best suited to measure χ_d .

However, better sensitivity is obtained from time-dependent analyses aiming at the direct measurement of the oscillation frequencies Δm_d and Δm_s , from the proper time distributions of B_d^0 or B_s^0 candidates identified through their decay in (mostly) flavor-specific modes, and suitably tagged as mixed or unmixed. This is particularly true for the $B_s^0\text{--}\bar{B}_s^0$ system, where the large value of x_s implies maximal mixing, *i.e.*, $\chi_s \simeq 1/2$. In such analyses, the B_d^0 or B_s^0 mesons are either fully reconstructed, partially reconstructed from a charm meson, selected from a lepton with the characteristics of a $b \rightarrow \ell^-$ decay, or selected from a reconstructed displaced vertex. At high-energy colliders (LEP, SLC, Tevatron), the proper time $t = \frac{m_B}{p}L$ is measured from the distance L between the production vertex and the B decay vertex, and from an estimate of the B momentum p . At asymmetric B factories (KEKB, PEP-II), producing $e^+e^- \rightarrow \Upsilon(4S) \rightarrow B_d^0\bar{B}_d^0$ events with a boost $\beta\gamma$ ($= 0.425, 0.55$), the proper time difference between the two B candidates is estimated as $\Delta t \simeq \frac{\Delta z}{\beta\gamma c}$, where Δz is the spatial separation between the two B decay vertices along the boost direction. In all cases, the good resolution needed on the vertex positions is obtained with silicon detectors.

The average statistical significance \mathcal{S} of a B_d^0 or B_s^0 oscillation signal can be approximated as [10]

$$\mathcal{S} \approx \sqrt{N/2} f_{\text{sig}} (1 - 2\eta) e^{-(\Delta m \sigma_t)^2/2}, \quad (13)$$

where N is the number of selected and tagged candidates, f_{sig} is the fraction of signal in that sample, η is the total mistag probability, and σ_t is the resolution on proper time (or proper time difference). The quantity \mathcal{S} decreases very quickly as Δm increases; this dependence is controlled by σ_t , which is therefore a critical parameter for Δm_s analyses. At high-energy colliders, the proper time resolution $\sigma_t \sim \frac{m_B}{\langle p \rangle} \sigma_L \oplus t \frac{\sigma_p}{p}$ includes a constant contribution due to the decay length resolution σ_L (typically 0.05–0.3 ps), and a term due to the relative momentum resolution σ_p/p (typically 10–20% for partially reconstructed decays), which increases with proper time. At B factories, the boost of the B mesons is estimated from the known beam energies,

and the term due to the spatial resolution dominates (typically 1–1.5 ps because of the much smaller B boost).

In order to tag a B candidate as mixed or unmixed, it is necessary to determine its flavor both in the initial state and in the final state. The initial and final state mistag probabilities, η_i and η_f , degrade \mathcal{S} by a total factor $(1 - 2\eta) = (1 - 2\eta_i)(1 - 2\eta_f)$. In lepton-based analyses, the final state is tagged by the charge of the lepton from $b \rightarrow \ell^-$ decays; the largest contribution to η_f is then due to $\bar{b} \rightarrow \bar{c} \rightarrow \ell^-$ decays. Alternatively, the charge of a reconstructed charm meson (D^{*-} from B_d^0 or D_s^- from B_s^0), or that of a kaon hypothesized to come from a $b \rightarrow c \rightarrow s$ decay [11], can be used. For fully-inclusive analyses based on topological vertexing, final-state tagging techniques include jet-charge [12] and charge-dipole [13,14] methods. At high-energy colliders, the methods to tag the initial state (*i.e.*, the state at production), can be divided into two groups: the ones that tag the initial charge of the \bar{b} quark contained in the B candidate itself (same-side tag), and the ones that tag the initial charge of the other b quark produced in the event (opposite-side tag). On the same side, the charge of a track from the primary vertex is correlated with the production state of the B if that track is a decay product of a B^{**} state or the first particle in the fragmentation chain [15,16]. Jet- and vertex-charge techniques work on both sides and on the opposite side, respectively. Finally, the charge of a lepton from $b \rightarrow \ell^-$ or of a kaon from $b \rightarrow c \rightarrow s$ can be used as opposite side tags, keeping in mind that their performance is degraded due to integrated mixing. At SLC, the beam polarization produced a sizeable forward-backward asymmetry in the $Z \rightarrow b\bar{b}$ decays, and provided another very interesting and effective initial state tag based on the polar angle of the B candidate [13]. Initial state tags have also been combined to reach $\eta_i \sim 26\%$ at LEP [16,17], or even 22% at SLD [13] with full efficiency. In the case $\eta_f = 0$, this corresponds to an effective tagging efficiency $Q = \epsilon D^2 = \epsilon(1 - 2\eta)^2$, where ϵ is the tagging efficiency, in the range 23 – 31%. The equivalent figure achieved by CDF during Tevatron Run I was $\sim 3.5\%$ [18], reflecting the fact that tagging is more difficult at hadron colliders. The current CDF and DØ analyses of Tevatron Run II data reach $\epsilon D^2 = (1.8 \pm 0.1)\%$ [19] and $(2.5 \pm 0.2)\%$ [20] for opposite-side tagging, while same-side kaon tagging (for B_s^0 oscillation analyses) is contributing an additional 3.7 – 4.8% at CDF [19], and pushes the combined performance to $(4.5 \pm 0.9)\%$ at DØ [21].

At B factories, the flavor of a B_d^0 meson at production cannot be determined, since the two neutral B mesons produced in a $\Upsilon(4S)$ decay evolve in a coherent P -wave state where they keep opposite flavors at any time. However, as soon as one of them decays, the other follows a time-evolution given by Eqs. (2) or (3), where t is replaced with Δt (which will take negative values half of the time). Hence, the “initial state” tag of a B can be taken as the final-state tag of the other B . Effective tagging efficiencies Q of 30% are achieved by BaBar and Belle [22], using different techniques including $b \rightarrow \ell^-$ and $b \rightarrow c \rightarrow s$ tags. It is worth noting that, in this case, mixing of

the other B (*i.e.*, the coherent mixing occurring before the first B decay) does not contribute to the mistag probability.

In the absence of experimental observation of a decay-width difference, oscillation analyses typically neglect $\Delta\Gamma$ in Eq. (4), and describe the data with the physics functions $\Gamma e^{-\Gamma t}(1 \pm \cos(\Delta m t))/2$ (high-energy colliders) or $\Gamma e^{-\Gamma|\Delta t|}(1 \pm \cos(\Delta m \Delta t))/4$ (asymmetric $\Upsilon(4S)$ machines). As can be seen from Eq. (4), a non-zero value of $\Delta\Gamma$ would effectively reduce the oscillation amplitude with a small time-dependent factor that would be very difficult to distinguish from time resolution effects. Measurements of Δm_d are usually extracted from the data using a maximum likelihood fit. To extract information useful for the interpretation of B_s^0 oscillation searches and for the combination of their results, a method [10] is followed in which a B_s^0 oscillation amplitude \mathcal{A} is measured as a function of a fixed test value of Δm_s , using a maximum likelihood fit based on the functions $\Gamma_s e^{-\Gamma_s t}(1 \pm \mathcal{A} \cos(\Delta m_s t))/2$. To a good approximation, the statistical uncertainty on \mathcal{A} is Gaussian and equal to $1/\mathcal{S}$ from Eq. (13). If Δm_s is equal to its true value, one expects $\mathcal{A} = 1$ within the total uncertainty $\sigma_{\mathcal{A}}$; in case a signal is seen, its observed (or expected) significance will be defined as $\mathcal{A}/\sigma_{\mathcal{A}}$ (or $1/\sigma_{\mathcal{A}}$). However, if Δm_s is (far) below its true value, a measurement consistent with $\mathcal{A} = 0$ is expected. A value of Δm_s can be excluded at 95% CL if $\mathcal{A} + 1.645 \sigma_{\mathcal{A}} \leq 1$ (since the integral of a normal distribution from $-\infty$ to 1.645 is equal to 0.95). Because of the proper time resolution, the quantity $\sigma_{\mathcal{A}}(\Delta m_s)$ is a steadily increasing function of Δm_s . We define the sensitivity for 95% CL exclusion of Δm_s values (or for a 3σ or 5σ observation of B_s^0 oscillations) as the value of Δm_s for which $1/\sigma_{\mathcal{A}} = 1.645$ (or $1/\sigma_{\mathcal{A}} = 3$ or 5).

B_d^0 mixing studies

Many B_d^0 - \bar{B}_d^0 oscillations analyses have been published [23] by the ALEPH [24], BaBar [25], Belle [26], CDF [15], DØ [20], DELPHI [14,27], L3 [28], and OPAL [29,30] collaborations. Although a variety of different techniques have been used, the individual Δm_d results obtained at high-energy colliders have remarkably similar precision. Their average is compatible with the recent and more precise measurements from asymmetric B factories. The systematic uncertainties are not negligible; they are often dominated by sample composition, mistag probability, or b -hadron lifetime contributions. Before being combined, the measurements are adjusted on the basis of a common set of input values, including the b -hadron lifetimes and fractions published in this *Review*. Some measurements are statistically correlated. Systematic correlations arise both from common physics sources (fragmentation fractions, lifetimes, branching ratios of b hadrons), and from purely experimental or algorithmic effects (efficiency, resolution, tagging, background description). Combining all published measurements [14,15,20,24–30] and accounting for all identified correlations yields $\Delta m_d = 0.508 \pm 0.003(\text{stat}) \pm 0.003(\text{syst}) \text{ ps}^{-1}$ [31], a result dominated by the B factories.

On the other hand, ARGUS and CLEO have published time-integrated measurements [32–34], which average to $\chi_d =$

0.182 ± 0.015 . Following Ref. 34, the width difference $\Delta\Gamma_d$ could in principle be extracted from the measured value of Γ_d and the above averages for Δm_d and χ_d (see Eq. (5)), provided that $\Delta\Gamma_d$ has a negligible impact on the Δm_d measurements. However, direct time-dependent studies published by DELPHI [14] and BaBar [35] provide stronger constraints, which can be combined to yield $\text{sign}(\text{Re}\lambda_{CP})\Delta\Gamma_d/\Gamma_d = 0.010 \pm 0.037$ [31].

Assuming $\Delta\Gamma_d = 0$ and no CP violation in mixing, and using the measured B_d^0 lifetime of $1.525 \pm 0.009 \text{ ps}$, the Δm_d and χ_d results are combined to yield the world average

$$\Delta m_d = 0.507 \pm 0.005 \text{ ps}^{-1} \quad (14)$$

or, equivalently,

$$\chi_d = 0.1873 \pm 0.0024. \quad (15)$$

Evidence for CP violation in B_d^0 mixing has been searched for, both with flavor-specific and inclusive B_d^0 decays, in samples where the initial flavor state is tagged. In the case of semileptonic (or other flavor-specific) decays, where the final-state tag is also available, the following asymmetry [2]

$$\mathcal{A}_{\text{SL}}^d = \frac{N(\bar{B}_d^0(t) \rightarrow \ell^+ \nu_\ell X) - N(B_d^0(t) \rightarrow \ell^- \bar{\nu}_\ell X)}{N(\bar{B}_d^0(t) \rightarrow \ell^+ \nu_\ell X) + N(B_d^0(t) \rightarrow \ell^- \bar{\nu}_\ell X)} \simeq 1 - |q/p|_d^2 \quad (16)$$

has been measured, either in time-integrated analyses at CLEO [34,36], CDF [37,38] and DØ [39], or in time-dependent analyses at LEP [30,40,41], BaBar [35,42,43] and Belle [44]. In the inclusive case, also investigated at LEP [40,41,45], no final-state tag is used, and the asymmetry [46]

$$\begin{aligned} & \frac{N(B_d^0(t) \rightarrow \text{all}) - N(\bar{B}_d^0(t) \rightarrow \text{all})}{N(B_d^0(t) \rightarrow \text{all}) + N(\bar{B}_d^0(t) \rightarrow \text{all})} \\ & \simeq \mathcal{A}_{\text{SL}}^d \left[\frac{x_d}{2} \sin(\Delta m_d t) - \sin^2 \left(\frac{\Delta m_d t}{2} \right) \right] \end{aligned} \quad (17)$$

must be measured as a function of the proper time to extract information on CP violation. In all cases, asymmetries compatible with zero have been found, with a precision limited by the available statistics. A simple average of all published results for the B_d^0 meson [30,34–36,39,41,42,44,45] yields $\mathcal{A}_{\text{SL}}^d = -0.0049 \pm 0.0038$, under the assumption of no CP violation in B_s^0 mixing. Published results at B factories only [34–36,42,44], where no B_s^0 is produced, average to

$$\mathcal{A}_{\text{SL}}^d = -0.0005 \pm 0.0056, \text{ or } |q/p|_d = 1.0002 \pm 0.0028, \quad (18)$$

a result which does not yet constrain the Standard Model.

The Δm_d result of Eq. (14) provides an estimate of $2|M_{12}|$, and can be used, together with Eq. (6), to extract the magnitude of the CKM matrix element V_{td} within the Standard Model [47]. The main experimental uncertainties on the resulting estimate of $|V_{td}|$ come from m_t and Δm_d ; however, the extraction is at present completely dominated by the uncertainty on the hadronic matrix element $f_{B_d} \sqrt{B_{B_d}} = 244 \pm 26 \text{ MeV}$ obtained from lattice QCD calculations [48].

Meson Particle Listings

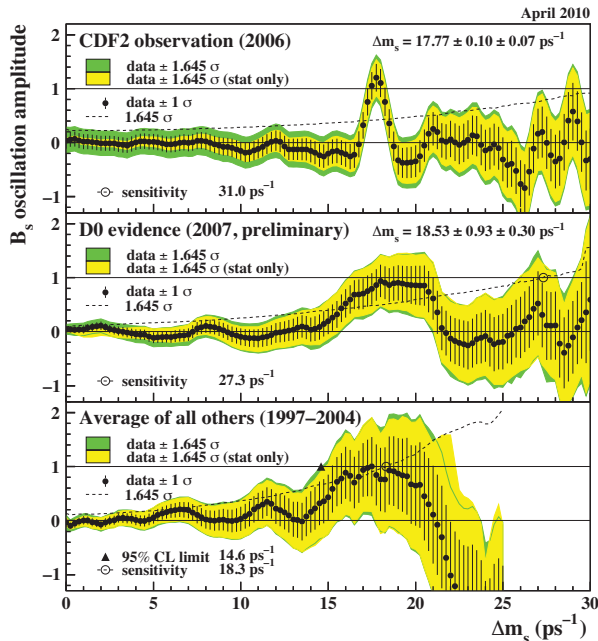
 B^0 B_s^0 mixing studies

Figure 2: Combined measurements of the B_s^0 oscillation amplitude as a function of Δm_s . Top: CDF result based on Run II data, published in 2006 [19]. Middle: Average of all preliminary $D\bar{O}$ results available at the end of 2007 [21]. Bottom: Average of all other results (mainly from LEP and SLD) published between 1997 and 2004. All measurements are dominated by statistical uncertainties. Neighboring points are statistically correlated. Color version at end of book.

Interesting Tevatron Run II results based on 1 fb^{-1} of data became available in 2006: after $D\bar{O}$ [49] reported $17 < \Delta m_s < 21 \text{ ps}^{-1}$ (90% CL) and a most probable value of 19 ps^{-1} with an observed (expected) significance of 2.5σ (0.9σ), CDF published the first direct evidence of B_s^0 oscillations shortly followed by a $> 5\sigma$ observation (shown at the top of Fig. 2). The measured value of Δm_s is [19]

$$\Delta m_s = 17.77 \pm 0.10(\text{stat}) \pm 0.07(\text{syst}) \text{ ps}^{-1}, \quad (19)$$

based on samples of flavour-tagged hadronic and semileptonic B_s^0 decays, partially or fully reconstructed in flavour-specific final states. More recently, $D\bar{O}$ [21] obtained with 2.4 fb^{-1} an independent 2.9σ preliminary evidence for B_s^0 oscillations (middle of Fig. 2) at $\Delta m_s = 18.53 \pm 0.93(\text{stat}) \pm 0.30(\text{syst}) \text{ ps}^{-1}$ [50], consistent with the CDF measurement.

In the decade before the Tevatron Run II results became available, $B_s^0\text{-}\bar{B}_s^0$ oscillations had been the subject of many studies from ALEPH [51], CDF [52], DELPHI [14,17,53], OPAL [54] and SLD [13,55,56], which only lead to lower limits on Δm_s due to the limited statistics. For comparison with the Tevatron Run II measurements, the B_s^0 oscillation amplitude obtained [31] by combining all earlier published results [13,14,17,51–55] is also shown in Fig. 2 (bottom) as a function of Δm_s . The Δm_s values between 14.6 and 21.7 ps^{-1}

could not be excluded at 95% CL, because the data was compatible with a signal in this region. However, the largest deviation from $\mathcal{A} = 0$ in this range is a 1.9σ effect only, so no signal could be claimed.

The information on $|V_{ts}|$ obtained in the framework of the Standard Model is hampered by the hadronic uncertainty, as in the B_d^0 case. However, several uncertainties cancel in the frequency ratio

$$\frac{\Delta m_s}{\Delta m_d} = \frac{m_{B_s}}{m_{B_d}} \xi^2 \left| \frac{V_{ts}}{V_{td}} \right|^2, \quad (20)$$

where $\xi = (f_{B_s} \sqrt{B_{B_s}})/(f_{B_d} \sqrt{B_{B_d}}) = 1.210_{-0.035}^{+0.047}$ is an SU(3) flavor-symmetry breaking factor obtained from lattice QCD calculations [48]. Using the measurements of Eqs. (14) and (19), one can extract

$$\left| \frac{V_{td}}{V_{ts}} \right| = 0.2061 \pm 0.0012(\text{exp})_{-0.0060}^{+0.0080}(\text{lattice}), \quad (21)$$

in good agreement with (but much more precise than) the recent results obtained by the Belle [57] and BaBar [58] collaborations based on the observation of the $b \rightarrow d\gamma$ transition. The CKM matrix can be constrained using experimental results on observables such as Δm_d , Δm_s , $|V_{ub}/V_{cb}|$, ϵ_K , and $\sin(2\beta)$ together with theoretical inputs and unitarity conditions [47,59,60]. The constraint from our knowledge on the ratio $\Delta m_s/\Delta m_d$ is presently more effective in limiting the position of the apex of the CKM unitarity triangle than the one obtained from the Δm_d measurements alone, due to the reduced hadronic uncertainty in Eq. (20). We also note that the measured value of Δm_s is consistent with the Standard Model prediction obtained from CKM fits where no experimental information on Δm_s is used, *e.g.*, $16.8 \pm 1.6 \text{ ps}^{-1}$ [59] or $17.6_{-1.8}^{+1.7} \text{ ps}^{-1}$ [60].

Information on $\Delta\Gamma_s$ can be obtained by studying the proper time distribution of untagged B_s^0 samples [61]. In the case of an inclusive B_s^0 selection [62], or a semileptonic (or flavour-specific) B_s^0 decay selection [17,63,64], both the short- and long-lived components are present, and the proper time distribution is a superposition of two exponentials with decay constants $\Gamma_{L,H} = \Gamma_s \pm \Delta\Gamma_s/2$. In principle, this provides sensitivity to both Γ_s and $(\Delta\Gamma_s/\Gamma_s)^2$. Ignoring $\Delta\Gamma_s$ and fitting for a single exponential leads to an estimate of Γ_s with a relative bias proportional to $(\Delta\Gamma_s/\Gamma_s)^2$. An alternative approach, which is directly sensitive to first order in $\Delta\Gamma_s/\Gamma_s$, is to determine the lifetime of B_s^0 candidates decaying to CP eigenstates; measurements exist for $B_s^0 \rightarrow K^+K^-$ [65], $B_s^0 \rightarrow J/\psi\phi$ [66,67], and $B_s^0 \rightarrow D_s^{(*)+}D_s^{(*)-}$ [68], which are mostly CP -even states [69]. However, in the case of $B_s^0 \rightarrow J/\psi\phi$, this technique has now been replaced by more sensitive time-dependent angular analyses that allow the simultaneous extraction of $\Delta\Gamma_s/\Gamma_s$ and the CP -even and CP -odd amplitudes [70,71]. Applying the combination procedure of Ref. 31 (including the constraint from the

flavour-specific lifetime measurements) on the published results of Refs. [17,63,66,70,71] yields

$$\Delta\Gamma_s/\Gamma_s = +0.092_{-0.054}^{+0.051} \quad \text{and} \quad 1/\Gamma_s = 1.472_{-0.026}^{+0.024} \text{ ps}, \quad (22)$$

or equivalently

$$1/\Gamma_L = 1.408_{-0.030}^{+0.033} \text{ ps} \quad \text{and} \quad 1/\Gamma_H = 1.543_{-0.060}^{+0.058} \text{ ps}, \quad (23)$$

under the assumption of no CP violation in B_s^0 mixing.

Independent estimates of $\Delta\Gamma_s/\Gamma_s$, leading to the average $\Delta\Gamma_s/\Gamma_s = +0.092 \pm 0.032$ [31], have also been obtained directly from measurements of the $B_s^0 \rightarrow D_s^{(*)+} D_s^{(*)-}$ branching ratio [68,72], under the assumption that these decays account for all CP -even final states (however, no systematic uncertainty due to this assumption is included in the above average).

Recent untagged or tagged analyses [70,73,74,71] also consider CP violation in $B_s^0 \rightarrow J/\psi\phi$ decays, and start to constrain the phase difference $-2\beta_s$ between the B_s^0 mixing diagram and the $b \rightarrow c\bar{c}s$ tree decay diagram. In the Standard Model (SM), $\beta_s = \arg(-(V_{ts}V_{tb}^*)/(V_{cs}V_{cb}^*))$ is expected to be approximately 0.02 [7,59,60]. A two-dimensional combination of the published results [70,73,71] yields $\beta_s \in [+0.14; +0.73] \cup [+0.82; +1.43]$ and $\Delta\Gamma_s \in [+0.036; +0.264] \cup [-0.264; -0.036] \text{ ps}^{-1}$ at 90% CL [31]. Another combination including preliminary results [74], treating all analyses on the same footing, and allowing the strong phases to vary freely in the fit, gives $\beta_s \in [+0.10; +1.42]$ at 95% CL [75]. The probability to obtain a result less consistent with the SM prediction if the SM is correct is estimated to be 2% (p-value).

On the other hand CP violation in B_s^0 mixing has been investigated through the asymmetry between positive and negative same-sign muon pairs from semi-leptonic decays of $b\bar{b}$ pairs [37–39], and directly through the charge asymmetry of $B_s^0 \rightarrow D_s\mu\nu X$ decays [76,77]. Combining all published results [37,39,76] with the knowledge of CP violation in B_d^0 mixing from Eq. (18) leads to

$$\mathcal{A}_{\text{SL}}^s = -0.0036 \pm 0.0094, \quad \text{or} \quad |q/p|_s = 1.0018 \pm 0.0047. \quad (24)$$

A large New Physics phase could possibly contribute to both CP violation in $B_s^0 \rightarrow J/\psi\phi$, and to the mixing phase difference of Eq. (8) on which $\mathcal{A}_{\text{SL}}^s$ depends. Combined fits [78,79] based on β_s and $\mathcal{A}_{\text{SL}}^s$ measurements already yield interesting constraints on this New Physics phase.

Average b -hadron mixing probability and b -hadron production fractions at high energy

Mixing measurements can significantly improve our knowledge on the fractions f_u , f_d , f_s , and f_{baryon} , defined as the fractions of B_u , B_d^0 , B_s^0 and b -baryon in an unbiased sample of weakly decaying b hadrons produced in high-energy collisions. Indeed, time-integrated mixing analyses performed with lepton pairs from $b\bar{b}$ events at high energy measure the quantity

$$\bar{\chi} = f'_d \chi_d + f'_s \chi_s, \quad (25)$$

where f'_d and f'_s are the fractions of B_d^0 and B_s^0 hadrons in a sample of semileptonic b -hadron decays. Assuming that all b hadrons have the same semileptonic decay width implies $f'_q = f_q/(\Gamma_q\tau_b)$ ($q = s, d$), where τ_b is the average b -hadron lifetime. Hence $\bar{\chi}$ measurements, together with the χ_d average of Eq. (15) and the very good approximation $\chi_s = 1/2$ (in fact $\chi_s = 0.49927 \pm 0.00003$ from Eqs. (5), (19) and (22)), provide constraints on the fractions f_d and f_s .

The LEP experiments have measured $f_s \times \text{BR}(B_s^0 \rightarrow D_s^- \ell^+ \nu_\ell X)$ [80], $\text{BR}(b \rightarrow \Lambda_b^0) \times \text{BR}(\Lambda_b^0 \rightarrow \Lambda_c^+ \ell^- \bar{\nu}_\ell X)$ [81], and $\text{BR}(b \rightarrow \Xi_b^-) \times \text{BR}(\Xi_b^- \rightarrow \Xi^- \ell^- \bar{\nu}_\ell X)$ [82] from partially reconstructed final states including a lepton, f_{baryon} from protons identified in b events [83], and the production rate of charged b hadrons [84]. The b -hadron fractions measured at CDF using double semileptonic $K^*\mu\mu$ and $\phi\mu\mu$ final states [85] and lepton-charm final states [86] are at slight discrepancy with the ones measured at LEP. Furthermore the averages of the $\bar{\chi}$ values measured at LEP, 0.1259 ± 0.0042 [87], and at Tevatron, 0.147 ± 0.011 [39,88], show a 1.8σ deviation with respect to each other. This is a hint that the fractions at the Tevatron might be different from the ones in Z decays, and calls for separate averages of the LEP and Tevatron results. A combination of all the available information under the constraints $f_u = f_d$ and $f_u + f_d + f_s + f_{\text{baryon}} = 1$, including the recent strange b -baryon measurements at the Tevatron [89], yields the three set of averages shown in Table 1 [31]. The third set, obtained using both LEP and Tevatron results, has larger errors than the first set, obtained using LEP results only, because scale factors have been applied as advocated by the PDG for the treatment of marginally consistent data.

Table 1: $\bar{\chi}$ and b -hadron fractions (see text).

	in Z decays	at Tevatron	combined
$\bar{\chi}$	0.1259 ± 0.0042	0.147 ± 0.011	0.1284 ± 0.0069
$f_u = f_d$	0.402 ± 0.009	0.332 ± 0.030	0.400 ± 0.012
f_s	0.105 ± 0.009	0.122 ± 0.014	0.115 ± 0.013
f_{baryon}	0.090 ± 0.015	0.214 ± 0.068	0.085 ± 0.021

Summary and prospects

B^0 - \bar{B}^0 mixing has been and still is a field of intense study. While fairly little experimental progress was achieved in the B_d^0 sector during the past few years, impressive new B_s^0 results became available from Run II of the Tevatron. B_s^0 oscillations are established and the mass difference in the B_s^0 - \bar{B}_s^0 system is measured very accurately, with a central value compatible with the Standard Model (SM) expectation and a relative precision (0.7%) matching that in the B_d^0 - \bar{B}_d^0 system (0.9%). However, the extraction of $|V_{td}/V_{ts}|$ from these measurements in the SM framework is limited by the hadronic uncertainty, which will be an important challenge to reduce in the future. New time-dependent angular analyses of $B_s^0 \rightarrow J/\psi\phi$ decays and measurements of time-integrated B_s^0 asymmetries at CDF

Meson Particle Listings

 B^0

and $D\bar{O}$ are improving our knowledge of the other B_s^0 mixing parameters: while CP violation in $B_s^0-\bar{B}_s^0$ mixing is consistent with zero, with an uncertainty still large compared to the SM prediction, the relative decay width difference $\Delta\Gamma_s/\Gamma_s$ is now determined to an absolute precision of $\sim 5\%$, smaller than the central value of the SM prediction. The data prefer $\Gamma_L > \Gamma_H$ as predicted in the SM.

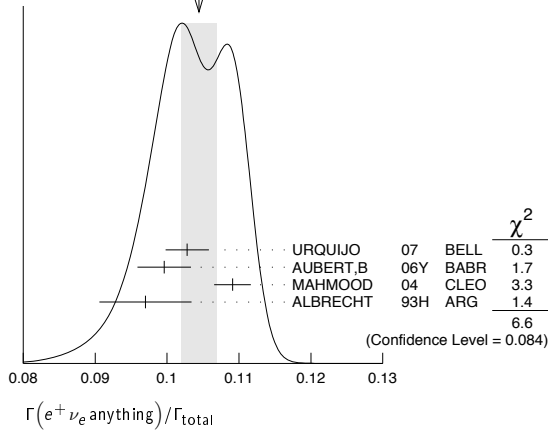
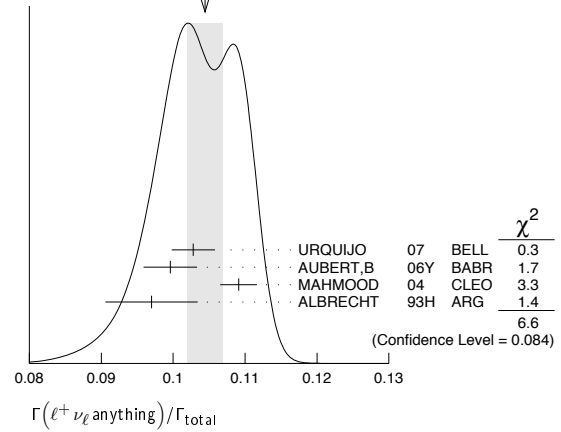
Improved B_s^0 results are still to come, with very promising short-term prospects, both for $\Delta\Gamma_s$ and CP -violating phases induced by mixing such as β_s and $\arg(-M_{12}/\Gamma_{12})$. Although first interesting experimental constraints have been published, very little is known yet about these phases, which are predicted to be very small in the SM. A full search for New Physics effects in these observables will require statistics beyond that of the Tevatron. These will eventually become available at CERN's Large Hadron Collider, which started physics operation in 2010 and where LHCb expects to be able to measure β_s down to the SM value after many years of operations [90].

B mixing may still reveal a surprize, but much effort is needed for this, both on the experimental and theoretical sides, in particular to further reduce the hadronic uncertainties of lattice QCD calculations. In the long term, a stringent check of the consistency of the B_d^0 and B_s^0 mixing amplitudes (magnitudes and phases) with all other measured flavour-physics observables will be possible within the SM, leading to very tight limits (or otherwise new interesting knowledge!) on New Physics.

References

1. T.D. Lee and C.S. Wu, *Ann. Rev. Nucl. Sci.* **16**, 511 (1966); I.I. Bigi and A.I. Sanda, “ CP violation,” Cambridge Univ. Press, 2000; G.C. Branco, L. Lavoura, and J.P. Silva, “ CP violation,” Clarendon Press Oxford, 1999.
2. See the review on CP violation in meson decays by D. Kirkby and Y. Nir in this publication.
3. A.J. Buras, W. Slominski, and H. Steger, *Nucl. Phys.* **B245**, 369 (1984).
4. T. Inami and C.S. Lim, *Prog. Theor. Phys.* **65**, 297 (1981); for the power-like approximation, see A.J. Buras and R. Fleischer, page 91 in “Heavy Flavours II,” eds. A.J. Buras and M. Lindner, Singapore World Scientific, 1998.
5. M. Kobayashi and K. Maskawa, *Prog. Theor. Phys.* **49**, 652 (1973).
6. I.I. Bigi *et al.*, in “ CP violation,” ed. C. Jarlskog, Singapore World Scientific, 1989.
7. A. Lenz and U. Nierste, *JHEP* **0607**, 072 (2007).
8. C. Albajar *et al.* (UA1 Collab.), *Phys. Lett.* **B186**, 247 (1987).
9. H. Albrecht *et al.* (ARGUS Collab.), *Phys. Lett.* **B192**, 245 (1987).
10. H.-G. Moser and A. Roussarie, *Nucl. Instrum. Methods* **384**, 491 (1997).
11. SLD Collab., SLAC-PUB-7228, SLAC-PUB-7229, and SLAC-PUB-7230, *28th Int. Conf. on High Energy Physics*, Warsaw, 1996; J. Wittlin, PhD thesis, SLAC-R-582, 2001.
12. ALEPH Collab., contrib. 596 to *Int. Europhysics Conf. on High Energy Physics*, Jerusalem, 1997.
13. K. Abe *et al.* (SLD Collab.), *Phys. Rev.* **D67**, 012006 (2003).
14. J. Abdallah *et al.* (DELPHI Collab.), *Eur. Phys. J.* **C28**, 155 (2003).
15. F. Abe *et al.* (CDF Collab.), *Phys. Rev. Lett.* **80**, 2057 (1998) and *Phys. Rev.* **D59**, 032001 (1999); *Phys. Rev.* **D60**, 051101 (1999); *Phys. Rev.* **D60**, 072003 (1999); T. Affolder *et al.* (CDF Collab.), *Phys. Rev.* **D60**, 112004 (1999).
16. R. Barate *et al.* (ALEPH Collab.), *Eur. Phys. J.* **C4**, 367 (1998); *Eur. Phys. J.* **C7**, 553 (1999).
17. P. Abreu *et al.* (DELPHI Collab.), *Eur. Phys. J.* **C16**, 555 (2000); *Eur. Phys. J.* **C18**, 229 (2000).
18. See tagging summary on page 160 of K. Anikeev *et al.*, “ B physics at the Tevatron: Run II and beyond,” FERMILAB-PUB-01/97, hep-ph/0201071, and references therein.
19. A. Abulencia *et al.* (CDF Collab.), *Phys. Rev. Lett.* **97**, 242003 (2006).
20. V.M. Abazov *et al.* (DØ Collab.), *Phys. Rev.* **D74**, 112002 (2006).
21. DØ Collab., DØ note 5474-CONF, August 2007, and DØ note 5254-CONF, October 2006.
22. B. Aubert *et al.* (BaBar Collab.), *Phys. Rev. Lett.* **94**, 161803 (2005); K.-F. Chen *et al.* (Belle Collab.), *Phys. Rev.* **D72**, 012004 (2005).
23. Throughout this paper, we omit references of results that have been superseded by new published measurements.
24. D. Buskulic *et al.* (ALEPH Collab.), *Z. Phys.* **C75**, 397 (1997).
25. B. Aubert *et al.* (BaBar Collab.), *Phys. Rev. Lett.* **88**, 221802 (2002) and *Phys. Rev.* **D66**, 032003 (2002); *Phys. Rev. Lett.* **88**, 221803 (2002); *Phys. Rev.* **D67**, 072002 (2003); *Phys. Rev.* **D73**, 012004 (2006).
26. N.C. Hastings *et al.* (Belle Collab.), *Phys. Rev.* **D67**, 052004 (2003); Y. Zheng *et al.* (Belle Collab.), *Phys. Rev.* **D67**, 092004 (2003); K. Abe *et al.* (Belle Collab.), *Phys. Rev.* **D71**, 072003 (2005).
27. P. Abreu *et al.* (DELPHI Collab.), *Z. Phys.* **C76**, 579 (1997).
28. M. Acciarri *et al.* (L3 Collab.), *Eur. Phys. J.* **C5**, 195 (1998).
29. G. Alexander *et al.* (OPAL Collab.), *Z. Phys.* **C72**, 377 (1996); K. Ackerstaff *et al.* (OPAL Collab.), *Z. Phys.* **C76**, 417 (1997); G. Abbiendi *et al.* (OPAL Collab.), *Phys. Lett.* **B493**, 266 (2000).
30. K. Ackerstaff *et al.* (OPAL Collab.), *Z. Phys.* **C76**, 401 (1997).
31. E. Barberio *et al.* (HFAG), “Averages of b -hadron and c -hadron properties at the end of 2007,” arXiv:0808.1297v3 [hep-ex], March 2009; the combined results on b -hadron fractions, lifetimes and mixing parameters published in this *Review* have been obtained by the B oscillations working group of the Heavy Flavour Averaging Group (HFAG), using the methods and procedures described in Chapter 3 of the above paper, after updating the list of inputs; for more information, see <http://www.slac.stanford.edu/xorg/hfag/osc/>.
32. H. Albrecht *et al.* (ARGUS Collab.), *Z. Phys.* **C55**, 357 (1992); *Phys. Lett.* **B324**, 249 (1994).

-
33. J. Bartelt *et al.* (CLEO Collab.), Phys. Rev. Lett. **71**, 1680 (1993).
34. B.H. Behrens *et al.* (CLEO Collab.), Phys. Lett. **B490**, 36 (2000).
35. B. Aubert *et al.* (BaBar Collab.), Phys. Rev. Lett. **92**, 181801 (2004) and Phys. Rev. **D70**, 012007 (2004).
36. D.E. Jaffe *et al.* (CLEO Collab.), Phys. Rev. Lett. **86**, 5000 (2001).
37. F. Abe *et al.* (CDF Collab.), Phys. Rev. **D55**, 2546 (1997).
38. CDF Collab., CDF note 9015, October 2007.
39. V.M. Abazov *et al.* (DØ Collab.), Phys. Rev. **D74**, 092001 (2006).
40. DELPHI Collab., contrib. 449 to *Int. Europhysics Conf. on High Energy Physics*, Jerusalem, 1997.
41. R. Barate *et al.* (ALEPH Collab.), Eur. Phys. J. **C20**, 431 (2001).
42. B. Aubert *et al.* (BaBar Collab.), Phys. Rev. Lett. **96**, 251802 (2006).
43. BaBar Collab., [arXiv:hep-ex/0607091v1](https://arxiv.org/abs/hep-ex/0607091v1), *33rd Int. Conf. on High Energy Physics*, Moscow, 2006.
44. E. Nakano *et al.* (Belle Collab.), Phys. Rev. **D73**, 112002 (2006).
45. G. Abbiendi *et al.* (OPAL Collab.), Eur. Phys. J. **C12**, 609 (2000).
46. M. Beneke, G. Buchalla, and I. Dunietz, Phys. Lett. **B393**, 132 (1997); I. Dunietz, Eur. Phys. J. **C7**, 197 (1999).
47. See the review on the CKM quark-mixing matrix by A. Ceccucci, Z. Ligeti, and Y. Sakai in this publication.
48. M. Okamoto, plenary talk at *XXIIIth Int. Symp. on Lattice Field Theory*, Dublin, July 2005, [hep-lat/0510113](https://arxiv.org/abs/hep-lat/0510113); these estimates are obtained by combining the unquenched lattice QCD calculations from A. Gray *et al.* (HPQCD Collab.), Phys. Rev. Lett. **95**, 212001 (2005) and S. Aoki *et al.* (JLQCD Collab.), Phys. Rev. Lett. **91**, 212001 (2003).
49. V.M. Abazov *et al.* (DØ Collab.), Phys. Rev. Lett. **97**, 021802 (2006).
50. DØ Collab., DØ note 5618-CONF v1.1, March 2008.
51. A. Heister *et al.* (ALEPH Collab.), Eur. Phys. J. **C29**, 143 (2003).
52. F. Abe *et al.* (CDF Collab.), Phys. Rev. Lett. **82**, 3576 (1999).
53. J. Abdallah *et al.* (DELPHI Collab.), Eur. Phys. J. **C35**, 35 (2004).
54. G. Abbiendi *et al.* (OPAL Collab.), Eur. Phys. J. **C11**, 587 (1999); Eur. Phys. J. **C19**, 241 (2001).
55. K. Abe *et al.* (SLD Collab.), Phys. Rev. **D66**, 032009 (2002).
56. SLD Collab., SLAC-PUB-8568, *30th Int. Conf. on High Energy Physics*, Osaka, 2000.
57. N. Taniguchi *et al.* (Belle Collab.), Phys. Rev. Lett. **101**, 111801 (2008), erratum *ibid.* **101**, 129904 (2008).
58. B. Aubert *et al.* (BaBar Collab.), Phys. Rev. Lett. **102**, 161803 (2009); B. Aubert *et al.* (BaBar Collab.), Phys. Rev. **D78**, 112001 (2008).
59. M. Bona *et al.* (UTfit Collab.), [arXiv:hep-ph/0606167v2](https://arxiv.org/abs/hep-ph/0606167v2); updated results at <http://www.utfit.org/>.
60. J. Charles *et al.* (CKMfitter Collab.), Eur. Phys. J. **C41**, 1 (2005); updated results at <http://ckmfitter.in2p3.fr/>.
61. K. Hartkorn and H.-G. Moser, Eur. Phys. J. **C8**, 381 (1999).
62. M. Acciarri *et al.* (L3 Collab.), Phys. Lett. **B438**, 417 (1998).
63. D. Buskulic *et al.* (ALEPH Collab.), Phys. Lett. **B377**, 205 (1996); K. Ackerstaff *et al.* (OPAL Collab.), Phys. Lett. **B426**, 161 (1998); F. Abe *et al.* (CDF Collab.), Phys. Rev. **D59**, 032004 (1999); V.M. Abazov *et al.* (DØ Collab.), Phys. Rev. Lett. **97**, 241801 (2006).
64. CDF Collab., CDF note 9203, October 2008; CDF note 7757, August 2005.
65. D. Tonelli for the CDF Collab., [arXiv:hep-ex/0605038v1](https://arxiv.org/abs/hep-ex/0605038v1), May 2006.
66. F. Abe *et al.* (CDF Collab.), Phys. Rev. **D57**, 5382 (1998).
67. V.M. Abazov *et al.* (DØ Collab.), Phys. Rev. Lett. **94**, 042001 (2005); CDF Collab., CDF note 8524, March 2007.
68. R. Barate *et al.* (ALEPH Collab.), Phys. Lett. **B486**, 286 (2000).
69. R. Aleksan *et al.*, Phys. Lett. **B316**, 567 (1993).
70. T. Aaltonen *et al.* (CDF Collab.), Phys. Rev. Lett. **100**, 121803 (2008).
71. V.M. Abazov *et al.* (DØ Collab.), Phys. Rev. Lett. **101**, 241801 (2008); this replaces both V.M. Abazov *et al.* (DØ Collab.), Phys. Rev. Lett. **98**, 121801 (2007) and V.M. Abazov *et al.* (DØ Collab.), Phys. Rev. Lett. **102**, 032001 (2009).
72. V.M. Abazov *et al.* (DØ Collab.), Phys. Rev. Lett. **102**, 091801 (2009); A. Abulencia *et al.* (CDF Collab.), Phys. Rev. Lett. **100**, 021803 (2008).
73. T. Aaltonen *et al.* (CDF Collab.), Phys. Rev. Lett. **100**, 161802 (2008).
74. CDF Collab., CDF/ANAL/BOTTOM/PUBLIC/9458, August 2008; this is a preliminary update of Ref. 73.
75. CDF and DØ combination working group on $\Delta\Gamma_s$ and β_s , CDF/PHYS/BOTTOM/CDFR/9787 and DØ note 5928-CONF, July 2009.
76. V.M. Abazov *et al.* (DØ Collab.), Phys. Rev. Lett. **98**, 151801 (2007).
77. V.M. Abazov *et al.* (DØ Collab.), [arXiv:0904.3907v1](https://arxiv.org/abs/0904.3907v1) [[hep-ex](https://arxiv.org/abs/hep-ex)], April 2009, submitted to Phys. Rev. Lett.
78. DØ Collab., DØ note 5933-CONF, May 2009; V.M. Abazov *et al.* (DØ Collab.), Phys. Rev. **D76**, 057101 (2007).
79. M. Bona *et al.* (UTfit Collab.), [arXiv:0803.0659](https://arxiv.org/abs/0803.0659) [[hep-ph](https://arxiv.org/abs/hep-ph)], March 2008.
80. P. Abreu *et al.* (DELPHI Collab.), Phys. Lett. **B289**, 199 (1992); P.D. Acton *et al.* (OPAL Collab.), Phys. Lett. **B295**, 357 (1992); D. Buskulic *et al.* (ALEPH Collab.), Phys. Lett. **B361**, 221 (1995).
81. P. Abreu *et al.* (DELPHI Collab.), Z. Phys. **C68**, 375 (1995); R. Barate *et al.* (ALEPH Collab.), Eur. Phys. J. **C2**, 197 (1998).
82. D. Buskulic *et al.* (ALEPH Collab.), Phys. Lett. **B384**, 449 (1996); J. Abdallah *et al.* (DELPHI Collab.), Eur. Phys. J. **C44**, 299 (2005).
83. R. Barate *et al.* (ALEPH Collab.), Eur. Phys. J. **C5**, 205 (1998).
84. J. Abdallah *et al.* (DELPHI Collab.), Phys. Lett. **B576**, 29 (2003).

WEIGHTED AVERAGE
0.1044±0.0025 (Error scaled by 1.5)WEIGHTED AVERAGE
0.1044±0.0025 (Error scaled by 1.5)

VALUE	CL%	DOCUMENT ID	TECN	COMMENT	Γ_2/Γ
$<5.9 \times 10^{-4}$		90	1 ADAM 03B	CLE2 $e^+e^- \rightarrow \Upsilon(4S)$	
••• We do not use the following data for averages, fits, limits, etc. •••					
<0.0016		90	ALBRECHT 90H	ARG $e^+e^- \rightarrow \Upsilon(4S)$	
¹ Based on V–A model.					

VALUE	CL%	DOCUMENT ID	TECN	COMMENT	Γ_3/Γ
0.1074 ± 0.0016		OUR EVALUATION			
••• We do not use the following data for averages, fits, limits, etc. •••					
$0.100 \pm 0.006 \pm 0.002$		1 ALBRECHT 90H	ARG	$e^+e^- \rightarrow \Upsilon(4S)$	
$0.108 \pm 0.006 \pm 0.01$		CHEN 84	CLEO	Direct μ at $\Upsilon(4S)$	
$0.112 \pm 0.009 \pm 0.01$		LEVMAN 84	CUSB	Direct μ at $\Upsilon(4S)$	
¹ ALBRECHT 90H uses the model of ALTARELLI 82 to correct over all lepton momenta. 0.097 ± 0.006 is obtained using ISGRU 89B.					

“OUR EVALUATION” is an average using rescaled values of the data listed below. The average and rescaling were performed by the Heavy Flavor Averaging Group (HFAG) and are described at <http://www.slac.stanford.edu/xorg/hfag/>. The averaging/rescaling procedure takes into account correlations between the measurements.

VALUE	CL%	DOCUMENT ID	TECN	COMMENT	Γ_4/Γ
0.1074 ± 0.0016		OUR EVALUATION			
••• We do not use the following data for averages, fits, limits, etc. •••					
$0.100 \pm 0.006 \pm 0.002$		1 ALBRECHT 90H	ARG	$e^+e^- \rightarrow \Upsilon(4S)$	
$0.108 \pm 0.006 \pm 0.01$		CHEN 84	CLEO	Direct μ at $\Upsilon(4S)$	
$0.112 \pm 0.009 \pm 0.01$		LEVMAN 84	CUSB	Direct μ at $\Upsilon(4S)$	
¹ ALBRECHT 90H uses the model of ALTARELLI 82 to correct over all lepton momenta. 0.097 ± 0.006 is obtained using ISGRU 89B.					

VALUE	CL%	DOCUMENT ID	TECN	COMMENT	Γ_5/Γ_4
0.1044 ± 0.0025		OUR AVERAGE			
••• We do not use the following data for averages, fits, limits, etc. •••					
$0.108 \pm 0.002 \pm 0.0056$		1 HENDERSON 92	CLEO	$e^+e^- \rightarrow \Upsilon(4S)$	
¹ HENDERSON 92 measurement employs e and μ . The systematic error contains 0.004 in quadrature from model dependence. The authors average a variation of the Isgru, Scora, Grinstein, and Wise model with that of the Altarelli-Cabibbo-Corbò-Maiani-Martinelli model for semileptonic decays to correct the acceptance.					

VALUE	CL%	DOCUMENT ID	TECN	COMMENT	Γ_6/Γ_4
0.1044 ± 0.0025		OUR AVERAGE			
••• We do not use the following data for averages, fits, limits, etc. •••					
$0.108 \pm 0.002 \pm 0.0056$		1 HENDERSON 92	CLEO	$e^+e^- \rightarrow \Upsilon(4S)$	
¹ HENDERSON 92 measurement employs e and μ . The systematic error contains 0.004 in quadrature from model dependence. The authors average a variation of the Isgru, Scora, Grinstein, and Wise model with that of the Altarelli-Cabibbo-Corbò-Maiani-Martinelli model for semileptonic decays to correct the acceptance.					

VALUE	CL%	DOCUMENT ID	TECN	COMMENT	Γ_5/Γ_4
$0.26 \pm 0.07 \pm 0.04$		1 FULTON 91	CLEO	$e^+e^- \rightarrow \Upsilon(4S)$	
¹ FULTON 91 uses $B(D^+ \rightarrow K^- \pi^+ \pi^+) = (9.1 \pm 1.3 \pm 0.4)\%$ as measured by MARK III.					

VALUE	CL%	DOCUMENT ID	TECN	COMMENT	Γ_6/Γ_4
$0.67 \pm 0.09 \pm 0.10$		1 FULTON 91	CLEO	$e^+e^- \rightarrow \Upsilon(4S)$	
¹ FULTON 91 uses $B(D^0 \rightarrow K^- \pi^+) = (4.2 \pm 0.4 \pm 0.4)\%$ as measured by MARK III.					

VALUE	CL%	DOCUMENT ID	TECN	COMMENT	Γ_7/Γ_4
$0.223 \pm 0.006 \pm 0.009$		1 AUBERT 10	BABR	$e^+e^- \rightarrow \Upsilon(4S)$	
¹ Uses a fully reconstructed B meson as a tag on the recoil side.					

VALUE (units 10^{-2})	CL%	DOCUMENT ID	TECN	COMMENT	Γ_8/Γ
$0.86 \pm 0.24 \pm 0.12$		1 AUBERT 08N	BABR	$e^+e^- \rightarrow \Upsilon(4S)$	
¹ Uses a fully reconstructed B meson as a tag on the recoil side.					

VALUE (units 10^{-2})	CL%	DOCUMENT ID	TECN	COMMENT	Γ_9/Γ
$0.67 \pm 0.08 \pm 0.10$		ABDALLAH 04D	DLPH	$e^+e^- \rightarrow Z^0$	
••• We do not use the following data for averages, fits, limits, etc. •••					
$0.6 \pm 0.3 \pm 0.1$		1 BARISH 95	CLE2	$e^+e^- \rightarrow \Upsilon(4S)$	
¹ BARISH 95 use $B(D^0 \rightarrow K^- \pi^+) = (3.91 \pm 0.08 \pm 0.17)\%$ and $B(D^{*+} \rightarrow D^0 \pi^+) = (68.1 \pm 1.0 \pm 1.3)\%$.					

VALUE (units 10^{-2})	CL%	DOCUMENT ID	TECN	COMMENT	Γ_{10}/Γ
$0.6 \pm 0.6 \pm 0.1$		1 BARISH 95	CLE2	$e^+e^- \rightarrow \Upsilon(4S)$	
¹ BARISH 95 use $B(D^0 \rightarrow K^- \pi^+) = (3.91 \pm 0.08 \pm 0.17)\%$, $B(D^{*+} \rightarrow D^0 \pi^+) = (68.1 \pm 1.0 \pm 1.3)\%$, $B(D^{*0} \rightarrow D^0 \pi^0) = (63.6 \pm 2.3 \pm 3.3)\%$.					

VALUE (units 10^{-2})	CL%	DOCUMENT ID	TECN	COMMENT	Γ_{11}/Γ
$1.62 \pm 0.31 \pm 0.11$		1 AUBERT 08N	BABR	$e^+e^- \rightarrow \Upsilon(4S)$	
¹ Uses a fully reconstructed B meson as a tag on the recoil side. The results are normalized to the B^+ decay rate.					

VALUE	CL%	EVTS	DOCUMENT ID	TECN	COMMENT	Γ_{12}/Γ
$0.027 \pm 0.005 \pm 0.005$		63	1 ALBRECHT 93	ARG	$e^+e^- \rightarrow \Upsilon(4S)$	
••• We do not use the following data for averages, fits, limits, etc. •••						
<0.028		95	2 BARISH 95	CLE2	$e^+e^- \rightarrow \Upsilon(4S)$	
¹ ALBRECHT 93 assumes the GISW model to correct for unseen modes. Using the BHK model, the result becomes $0.023 \pm 0.006 \pm 0.004$. Assumes $B(D^{*+} \rightarrow D^0 \pi^+) = 68.1\%$, $B(D^0 \rightarrow K^- \pi^+) = 3.65\%$, $B(D^0 \rightarrow K^- \pi^+ \pi^- \pi^+) = 7.5\%$. We have taken their average e and μ value.						
² BARISH 95 use $B(D^0 \rightarrow K^- \pi^+) = (3.91 \pm 0.08 \pm 0.17)\%$, assume all nonresonant channels are zero, and use GISW model for relative abundances of D^{**} states.						

Meson Particle Listings

B^\pm/B^0 ADMIXTURE

$\Gamma(\pi \ell \nu_\ell)/\Gamma_{\text{total}}$ Γ_{24}/Γ
 "OUR EVALUATION" is an average using rescaled values of the data listed below. The average and rescaling were performed by the Heavy Flavor Averaging Group (HFAG) and are described at <http://www.slac.stanford.edu/xorg/hfag/>. The averaging/scaling procedure takes into account correlation between the measurements.

VALUE (units 10^{-4}) DOCUMENT ID
1.35 ± 0.07 ± 0.07 OUR AVERAGE The result includes measurements of $B^0 \rightarrow \pi^- \ell^+ \ell^- \nu_\ell$ and $B^+ \rightarrow \pi^0 \ell^+ \nu_\ell$ decay rates.

$\Gamma(K^+ \ell^+ \nu_\ell \text{ anything})/\Gamma(\ell^+ \nu_\ell \text{ anything})$ Γ_{25}/Γ_4
 ℓ denotes e or μ , not the sum.
 VALUE DOCUMENT ID TECN COMMENT
0.58 ± 0.05 OUR AVERAGE
 0.594 ± 0.021 ± 0.056 ALBRECHT 94c ARG $e^+ e^- \rightarrow \Upsilon(4S)$
 0.54 ± 0.07 ± 0.06 1 ALAM 87b CLEO $e^+ e^- \rightarrow \Upsilon(4S)$

1 ALAM 87b measurement relies on lepton-kaon correlations.

$\Gamma(K^- \ell^+ \nu_\ell \text{ anything})/\Gamma(\ell^+ \nu_\ell \text{ anything})$ Γ_{26}/Γ_4
 ℓ denotes e or μ , not the sum.
 VALUE DOCUMENT ID TECN COMMENT
0.092 ± 0.035 OUR AVERAGE
 0.086 ± 0.011 ± 0.044 ALBRECHT 94c ARG $e^+ e^- \rightarrow \Upsilon(4S)$
 0.10 ± 0.05 ± 0.02 1 ALAM 87b CLEO $e^+ e^- \rightarrow \Upsilon(4S)$

1 ALAM 87b measurement relies on lepton-kaon correlations.

$\Gamma(K^0/\bar{K}^0 \ell^+ \nu_\ell \text{ anything})/\Gamma(\ell^+ \nu_\ell \text{ anything})$ Γ_{27}/Γ_4
 ℓ denotes e or μ , not the sum. Sum over K^0 and \bar{K}^0 states.
 VALUE DOCUMENT ID TECN COMMENT
0.42 ± 0.05 OUR AVERAGE
 0.452 ± 0.038 ± 0.056 1 ALBRECHT 94c ARG $e^+ e^- \rightarrow \Upsilon(4S)$
 0.39 ± 0.06 ± 0.04 2 ALAM 87b CLEO $e^+ e^- \rightarrow \Upsilon(4S)$

1 ALBRECHT 94c assume a K^0/\bar{K}^0 multiplicity twice that of K_S^0 .

2 ALAM 87b measurement relies on lepton-kaon correlations.

$\langle n_c \rangle$
 VALUE DOCUMENT ID TECN COMMENT
1.10 ± 0.05
 • • • We do not use the following data for averages, fits, limits, etc. • • •
 0.98 ± 0.16 ± 0.12 2 ALAM 87b CLEO $e^+ e^- \rightarrow \Upsilon(4S)$

1 GIBBONS 97b from charm counting using $B(D_s^+ \rightarrow \phi \pi) = 0.036 \pm 0.009$ and $B(\Lambda_c^+ \rightarrow p K^- \pi^+) = 0.044 \pm 0.006$.

2 From the difference between K^- and K^+ widths. ALAM 87b measurement relies on lepton-kaon correlations. It does not consider the possibility of $B\bar{B}$ mixing. We have thus removed it from the average.

$\Gamma(D^\pm \text{ anything})/\Gamma_{\text{total}}$ Γ_{28}/Γ
 VALUE DOCUMENT ID TECN COMMENT
0.231 ± 0.015 OUR AVERAGE
 0.230 ± 0.012 ± 0.009 1 GIBBONS 97b CLE2 $e^+ e^- \rightarrow \Upsilon(4S)$
 0.24 ± 0.04 ± 0.01 2 BORTOLETTO92 CLEO $e^+ e^- \rightarrow \Upsilon(4S)$
 0.22 ± 0.05 ± 0.01 3 ALBRECHT 91H ARG $e^+ e^- \rightarrow \Upsilon(4S)$
 • • • We do not use the following data for averages, fits, limits, etc. • • •
 0.20 ± 0.05 ± 0.01 4 BORTOLETTO87 CLEO Sup. by BORTOLETTO 92

1 GIBBONS 97b reports $[\Gamma(B \rightarrow D^\pm \text{ anything})/\Gamma_{\text{total}}] \times [B(D^+ \rightarrow K^- 2\pi^+)] = 0.0216 \pm 0.0008 \pm 0.00082$ which we divide by our best value $B(D^+ \rightarrow K^- 2\pi^+) = (9.4 \pm 0.4) \times 10^{-2}$. Our first error is their experiment's error and our second error is the systematic error from using our best value.

2 BORTOLETTO 92 reports $[\Gamma(B \rightarrow D^\pm \text{ anything})/\Gamma_{\text{total}}] \times [B(D^+ \rightarrow K^- 2\pi^+)] = 0.0226 \pm 0.0030 \pm 0.0018$ which we divide by our best value $B(D^+ \rightarrow K^- 2\pi^+) = (9.4 \pm 0.4) \times 10^{-2}$. Our first error is their experiment's error and our second error is the systematic error from using our best value.

3 ALBRECHT 91H reports $[\Gamma(B \rightarrow D^\pm \text{ anything})/\Gamma_{\text{total}}] \times [B(D^+ \rightarrow K^- 2\pi^+)] = 0.0209 \pm 0.0027 \pm 0.0040$ which we divide by our best value $B(D^+ \rightarrow K^- 2\pi^+) = (9.4 \pm 0.4) \times 10^{-2}$. Our first error is their experiment's error and our second error is the systematic error from using our best value.

4 BORTOLETTO 87 reports $[\Gamma(B \rightarrow D^\pm \text{ anything})/\Gamma_{\text{total}}] \times [B(D^+ \rightarrow K^- 2\pi^+)] = 0.019 \pm 0.004 \pm 0.002$ which we divide by our best value $B(D^+ \rightarrow K^- 2\pi^+) = (9.4 \pm 0.4) \times 10^{-2}$. Our first error is their experiment's error and our second error is the systematic error from using our best value.

$\Gamma(D^0/\bar{D}^0 \text{ anything})/\Gamma_{\text{total}}$ Γ_{29}/Γ
 VALUE DOCUMENT ID TECN COMMENT
0.625 ± 0.029 OUR AVERAGE Error includes scale factor of 1.3. See the ideogram below.
 0.646 ± 0.025 ± 0.007 EVTs 1 GIBBONS 97b CLE2 $e^+ e^- \rightarrow \Upsilon(4S)$
 0.60 ± 0.05 ± 0.01 2 BORTOLETTO92 CLEO $e^+ e^- \rightarrow \Upsilon(4S)$
 0.50 ± 0.08 ± 0.01 3 ALBRECHT 91H ARG $e^+ e^- \rightarrow \Upsilon(4S)$
 • • • We do not use the following data for averages, fits, limits, etc. • • •
 0.54 ± 0.07 ± 0.01 21k 4 BORTOLETTO87 CLEO $e^+ e^- \rightarrow \Upsilon(4S)$
 0.62 ± 0.19 ± 0.01 5 GREEN 83 CLEO Repl. by BORTOLETTO 87

1 GIBBONS 97b reports $[\Gamma(B \rightarrow D^0/\bar{D}^0 \text{ anything})/\Gamma_{\text{total}}] \times [B(D^0 \rightarrow K^- \pi^+)] = 0.0251 \pm 0.0006 \pm 0.00075$ which we divide by our best value $B(D^0 \rightarrow K^- \pi^+) = (3.89 \pm 0.05) \times 10^{-2}$. Our first error is their experiment's error and our second error is the systematic error from using our best value.

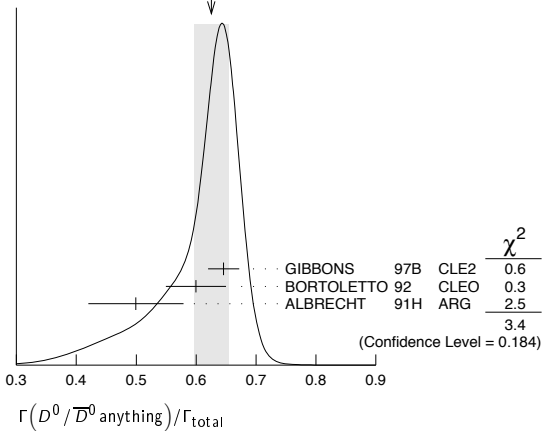
2 BORTOLETTO 92 reports $[\Gamma(B \rightarrow D^0/\bar{D}^0 \text{ anything})/\Gamma_{\text{total}}] \times [B(D^0 \rightarrow K^- \pi^+)] = 0.0233 \pm 0.0012 \pm 0.0014$ which we divide by our best value $B(D^0 \rightarrow K^- \pi^+) = (3.89 \pm 0.05) \times 10^{-2}$. Our first error is their experiment's error and our second error is the systematic error from using our best value.

3 ALBRECHT 91H reports $[\Gamma(B \rightarrow D^0/\bar{D}^0 \text{ anything})/\Gamma_{\text{total}}] \times [B(D^0 \rightarrow K^- \pi^+)] = 0.0194 \pm 0.0015 \pm 0.0025$ which we divide by our best value $B(D^0 \rightarrow K^- \pi^+) = (3.89 \pm 0.05) \times 10^{-2}$. Our first error is their experiment's error and our second error is the systematic error from using our best value.

4 BORTOLETTO 87 reports $[\Gamma(B \rightarrow D^0/\bar{D}^0 \text{ anything})/\Gamma_{\text{total}}] \times [B(D^0 \rightarrow K^- \pi^+)] = 0.0210 \pm 0.0015 \pm 0.0021$ which we divide by our best value $B(D^0 \rightarrow K^- \pi^+) = (3.89 \pm 0.05) \times 10^{-2}$. Our first error is their experiment's error and our second error is the systematic error from using our best value.

5 GREEN 83 reports $[\Gamma(B \rightarrow D^0/\bar{D}^0 \text{ anything})/\Gamma_{\text{total}}] \times [B(D^0 \rightarrow K^- \pi^+)] = 0.024 \pm 0.006 \pm 0.004$ which we divide by our best value $B(D^0 \rightarrow K^- \pi^+) = (3.89 \pm 0.05) \times 10^{-2}$. Our first error is their experiment's error and our second error is the systematic error from using our best value.

WEIGHTED AVERAGE
 0.625 ± 0.029 (Error scaled by 1.3)



$\Gamma(D^*(2010)^\pm \text{ anything})/\Gamma_{\text{total}}$ Γ_{30}/Γ
 VALUE DOCUMENT ID TECN COMMENT
0.225 ± 0.015 OUR AVERAGE
 0.247 ± 0.019 ± 0.01 1 GIBBONS 97b CLE2 $e^+ e^- \rightarrow \Upsilon(4S)$
 0.205 ± 0.019 ± 0.007 2 ALBRECHT 96D ARG $e^+ e^- \rightarrow \Upsilon(4S)$
 0.230 ± 0.028 ± 0.009 3 BORTOLETTO92 CLEO $e^+ e^- \rightarrow \Upsilon(4S)$
 • • • We do not use the following data for averages, fits, limits, etc. • • •
 0.283 ± 0.053 ± 0.002 4 ALBRECHT 91H ARG Sup. by ALBRECHT 96D
 0.22 ± 0.04 ± 0.07 EVTs 5200 5 BORTOLETTO87 CLEO $e^+ e^- \rightarrow \Upsilon(4S)$
 0.27 ± 0.06 ± 0.08 EVTs 510 6 CSORNA 85 CLEO Repl. by BORTOLETTO 87

1 GIBBONS 97b reports $B(B \rightarrow D^*(2010)^\pm \text{ anything}) = 0.239 \pm 0.015 \pm 0.014 \pm 0.009$ using CLEO measured D and D^* branching fractions. We rescale to our PDG 96 values of D and D^* branching ratios. Our first error is their experiment's error and our second error is the systematic error from using our best value.

2 ALBRECHT 96D reports $B(B \rightarrow D^*(2010)^\pm \text{ anything}) = 0.196 \pm 0.019$ using CLEO measured $B(D^*(2010)^\pm \rightarrow D^0 \pi^\pm) = 0.681 \pm 0.01 \pm 0.013$, $B(D^0 \rightarrow K^- \pi^+) = 0.0401 \pm 0.0014$, $B(D^0 \rightarrow K^- \pi^+ \pi^0) = 0.081 \pm 0.005$. We rescale to our PDG 96 values of D and D^* branching ratios. Our first error is their experiment's error and our second error is the systematic error from using our best value.

3 BORTOLETTO 92 reports $B(B \rightarrow D^*(2010)^\pm \text{ anything}) = 0.25 \pm 0.03 \pm 0.04$ using MARK II $B(D^*(2010)^\pm \rightarrow D^0 \pi^\pm) = 0.57 \pm 0.06$ and $B(D^0 \rightarrow K^- \pi^+) = 0.042 \pm 0.008$. We rescale to our PDG 96 values of D and D^* branching ratios. Our first error is their experiment's error and our second error is the systematic error from using our best value.

4 ALBRECHT 91H reports $0.348 \pm 0.060 \pm 0.035$ from a measurement of $[\Gamma(B \rightarrow D^*(2010)^\pm \text{ anything})/\Gamma_{\text{total}}] \times [B(D^*(2010)^\pm \rightarrow D^0 \pi^\pm)]$ assuming $B(D^*(2010)^\pm \rightarrow D^0 \pi^\pm) = 0.55 \pm 0.04$, which we rescale to our best value $B(D^*(2010)^\pm \rightarrow D^0 \pi^\pm) = (67.7 \pm 0.5) \times 10^{-2}$. Our first error is their experiment's error and our second error is the systematic error from using our best value. Uses the PDG 90 $B(D^0 \rightarrow K^- \pi^+) = 0.0371 \pm 0.0025$.

5 BORTOLETTO 87 uses old MARK III (BALTRUSAITIS 86E) branching ratios $B(D^0 \rightarrow K^- \pi^+) = 0.056 \pm 0.004 \pm 0.003$ and also assumes $B(D^*(2010)^\pm \rightarrow D^0 \pi^\pm) = 0.60 \pm 0.08$. The product branching ratio for $B(B \rightarrow D^*(2010)^\pm) B(D^*(2010)^\pm \rightarrow D^0 \pi^\pm) = 0.13 \pm 0.02 \pm 0.012$. Superseded by BORTOLETTO 92.

6 $V-A$ momentum spectrum used to extrapolate below $p = 1$ GeV. We correct the value assuming $B(D^0 \rightarrow K^- \pi^+) = 0.042 \pm 0.006$ and $B(D^*(2010)^\pm \rightarrow D^0 \pi^\pm) = 0.6 \pm 0.08$. The product branching fraction is $B(B \rightarrow D^*(2010)^\pm) B(D^*(2010)^\pm \rightarrow D^0 \pi^\pm) = (68 \pm 15 \pm 9) \times 10^{-4}$.

The theory underlying the determination of $|V_{qb}|$ is mature, in particular for $|V_{cb}|$. The theoretical approaches all use the fact that the mass m_b of the b quark is large compared to the scale Λ_{QCD} that determines low-energy hadronic physics. The basis for precise calculations is a systematic expansion in powers of Λ/m_b , where $\Lambda \sim 500 - 700$ MeV is a hadronic scale of the order of Λ_{QCD} , using effective-field-theory methods to separate non-perturbative from perturbative contributions. The expansion in Λ/m_b and α_s works well enough to enable a precision determination of $|V_{cb}|$ and $|V_{ub}|$ in semileptonic decays.

The large data samples available at the B factories have opened up new possibilities experimentally. Analyses where one B meson from an $\Upsilon(4S)$ decay is fully reconstructed allow a recoiling semileptonic B decay to be studied with higher purity than was previously possible. Improved knowledge of $\overline{B} \rightarrow X_c \ell \overline{\nu}_\ell$ decays allows partial rates for $\overline{B} \rightarrow X_u \ell \overline{\nu}_\ell$ transitions to be measured in regions previously considered inaccessible, increasing the acceptance for $\overline{B} \rightarrow X_u \ell \overline{\nu}_\ell$ transitions and reducing theoretical uncertainties.

Experimental measurements of the exclusive $\overline{B} \rightarrow \pi \ell \overline{\nu}_\ell$ decay are quite precise. Further improvement in the theoretical calculation of the form factor normalization is needed to fully exploit these measurements.

Throughout this review the numerical results quoted are based on the methods of the Heavy Flavor Averaging Group [2].

DETERMINATION OF $|V_{cb}|$

Summary: The determination of $|V_{cb}|$ from $\overline{B} \rightarrow D^* \ell \overline{\nu}_\ell$ decays is currently at a relative precision of about 3%. The main limitation is the knowledge of the form factor near the maximum momentum transfer to the leptons. For the $\overline{B} \rightarrow D \ell \overline{\nu}_\ell$ channel experimental measurements have recently been substantially improved, allowing this channel to provide a meaningful cross-check on $\overline{B} \rightarrow D^* \ell \overline{\nu}_\ell$.

Determinations of $|V_{cb}|$ from inclusive decays are currently below 2% relative uncertainty. The limitations arise mainly from our ignorance of higher order perturbative and non-perturbative corrections.

The values obtained from inclusive and exclusive determinations are currently only marginally consistent with each other:

$$|V_{cb}| = (41.5 \pm 0.7) \times 10^{-3} \text{ (inclusive)} \quad (1)$$

$$|V_{cb}| = (38.7 \pm 1.1) \times 10^{-3} \text{ (exclusive)}. \quad (2)$$

An average of the above gives $|V_{cb}| = (40.6 \pm 0.6) \times 10^{-3}$, with $P(\chi^2) = 0.03$. Scaling the error by $\sqrt{\chi^2/\text{ndf}} = 2.2$ we quote

$$|V_{cb}| = (40.6 \pm 1.3) \times 10^{-3}. \quad (3)$$

$|V_{cb}|$ from exclusive decays

Exclusive determinations of $|V_{cb}|$ are based on a study of semileptonic B decays into the ground state charmed mesons D and D^* . The main uncertainties in this approach stem from

our ignorance of the form factors describing the $B \rightarrow D$ and $B \rightarrow D^*$ transitions. However, in the limit of infinite bottom and charm quark masses only a single form factor appears, the Isgur-Wise function [3], which depends on the product of the four-velocities v and v' of the initial and final-state hadrons.

The extraction of $|V_{cb}|$ is based on the distribution of the variable $w \equiv v \cdot v'$, which corresponds to the energy of the final state $D^{(*)}$ meson in the rest frame of the decay. Heavy Quark Symmetry (HQS) [3,4] predicts the normalization of the rate at $w = 1$, the point of maximum momentum transfer to the leptons, and $|V_{cb}|$ is obtained from an extrapolation of the measured spectrum to $w = 1$. This extrapolation relies on a parametrization of the form factor, as explained below.

A precise determination requires corrections to the HQS prediction for the normalization as well as some information on the slope of the form factors near the point $w = 1$, since the phase space vanishes there. The corrections to the HQS prediction due to finite quark masses are given in terms of the symmetry-breaking parameter

$$\frac{1}{\mu} = \frac{1}{m_c} - \frac{1}{m_b},$$

which is essentially $1/m_c$ for realistic quark masses. HQS ensures that those matrix elements that correspond to the currents that generate the HQS are normalized at $w = 1$; as a result, some of the form factors either vanish or are normalized at $w = 1$. Due to Luke's Theorem [5] (which is an application of the Ademollo-Gatto theorem [6] to heavy quarks), the leading correction to those form factors normalized due to HQS is quadratic in $1/\mu$, while for the form factors that vanish in the infinite mass limit the corrections are in general linear in $1/m_c$ and $1/m_b$. Thus we have, using the definitions as in Eq. (2.84) of Ref. [7]

$$\begin{aligned} h_i(1) &= 1 + \mathcal{O}(1/\mu^2) & \text{for } i = +, V, A_1, A_3, \\ h_i(1) &= \mathcal{O}(1/m_c, 1/m_b) & \text{for } i = -, A_2. \end{aligned} \quad (4)$$

In addition to these corrections, there are perturbatively calculable radiative corrections from QCD and QED, which will be discussed in the relevant sections. Both - radiative corrections as well as $1/m$ corrections - are considered in the framework of Heavy Quark Effective Theory (HQET) [8], which provides for a systematic expansion.

$\overline{B} \rightarrow D^* \ell \overline{\nu}_\ell$

The decay rate for $\overline{B} \rightarrow D^* \ell \overline{\nu}_\ell$ is given by

$$\frac{d\Gamma}{dw}(\overline{B} \rightarrow D^* \ell \overline{\nu}_\ell) = \frac{G_F^2}{48\pi^3} |V_{cb}|^2 m_{D^*}^3 (w^2 - 1)^{1/2} P(w) (\mathcal{F}(w))^2 \quad (5)$$

where $P(w)$ is a phase space factor with $P(1) = 12(m_B - m_{D^*})^2$ and $\mathcal{F}(w)$ is dominated by the axial vector form factor h_{A_1} as $w \rightarrow 1$. In the infinite-mass limit, the HQS normalization gives $\mathcal{F}(1) = 1$.

Meson Particle Listings

V_{cb} and V_{ub} CKM Matrix Elements

The form factor $\mathcal{F}(w)$ must be parametrized to perform an extrapolation to the zero-recoil point. A frequently used one-parameter form motivated by analyticity and unitarity is [9,10]

$$\mathcal{F}(w) = \eta_{\text{QED}}\eta_{\text{A}} \left[1 + \delta_{1/m^2} + \dots \right] \\ \left[1 - 8\rho_{A_1}^2 z + (53\rho_{A_1}^2 - 15)z^2 - (231\rho_{A_1}^2 - 91)z^3 \right] \quad (6)$$

with $z = (\sqrt{w+1} - \sqrt{2})/(\sqrt{w+1} + \sqrt{2})$ originating from a conformal transformation. The parameter $\rho_{A_1}^2$ is the slope of the form factor at $w = 1$. The η_{QED} and η_{A} factors are the QED [11] and QCD [12] short-distance radiative corrections

$$\eta_{\text{QED}} = 1.007, \quad \eta_{\text{A}} = 0.960 \pm 0.007 \quad (7)$$

and δ_{1/m^2} comes from non-perturbative $1/m^2$ corrections.

Recently, lattice simulations which include effects from finite quark masses have been used to calculate the deviation of $\mathcal{F}(1)$ from unity. The value quoted from these calculations, multiplied by η_{QED} , is

$$\mathcal{F}(1) = 0.927 \pm 0.024 \quad (8)$$

where the errors quoted in Ref. [14] have been added in quadrature. The leading uncertainties are due to lattice statistical and dis

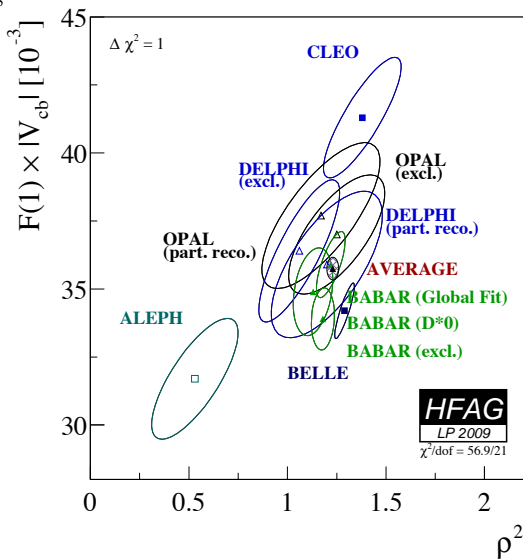


Figure 1: Measurements of $|V_{cb}|\mathcal{F}(1)$ vs. $\rho_{A_1}^2$ are shown as $\Delta\chi^2 = 1$ ellipses. Color version at end of book.

Non-lattice estimates based on sum rules for the the form factor tend to yield lower values for $\mathcal{F}(1)$ [15,16]. Omitting the contributions from excited states, the sum rules indicate that $\mathcal{F}(1) < 0.9$; including the excited states will further reduce the form factor.

Many experiments [17–25] have measured the differential rate as a function of w . Fig. 1 shows corresponding values of $|V_{cb}|\mathcal{F}(1)$ and $\rho_{A_1}^2$ (as defined in Ref. [10]) . These measurements have been updated using more precise values [23] for the form factor ratios $R_1 \propto A_2/A_1$ and $R_2 \propto V/A_1$. The

leading sources of uncertainty on $|V_{cb}|\mathcal{F}(1)$ are due to detection efficiencies and $D^{(*)}$ decay branching fractions, while for ρ^2 the uncertainties in R_1 and R_2 still dominate. Recent BABAR measurements, one using $\overline{B}^0 \rightarrow D^{*0}\ell\overline{\nu}_\ell$ decays [24] and the other using a global fit to $\overline{B} \rightarrow D\ell\overline{\nu}_\ell X$ decays [25] are completely insensitive to uncertainties related to the reconstruction of the charged pion from $D^* \rightarrow D\pi$ decays; both measurements agree with the average given below. Related measurements [26,27] of $\Gamma(\overline{B} \rightarrow D^*\ell\overline{\nu}_\ell)$ using samples at the $\Upsilon(4S)$ in which the opposite B is fully reconstructed have also been made. These use the measured missing mass squared to isolate signal decays and have very little sensitivity to the form factor slope.

The confidence level of the average based on the measurements in Fig. 1 is $\sim 0.004\%$. In light of the poor consistency we choose to rescale the errors by $\sqrt{\chi^2/\text{ndf}} = 1.65$ to find $|V_{cb}|\mathcal{F}(1) = (35.75 \pm 0.70) \times 10^{-3}$. Along with the value given above for $\mathcal{F}(1)$ this yields

$$|V_{cb}| = (38.5 \pm 0.8_{\text{exp}} \pm 1.0_{\text{theo}}) \times 10^{-3} \quad (\overline{B} \rightarrow D^*\ell\overline{\nu}_\ell). \quad (9)$$

The values of $\mathcal{F}(1)$ obtained from QCD sum rules result in larger values for $|V_{cb}|$.

$\overline{B} \rightarrow D\ell\overline{\nu}_\ell$

The differential rate for $\overline{B} \rightarrow D\ell\overline{\nu}_\ell$ is given by

$$\frac{d\Gamma}{dw}(\overline{B} \rightarrow D\ell\overline{\nu}_\ell) = \\ \frac{G_F^2}{48\pi^3} |V_{cb}|^2 (m_B + m_D)^2 m_D^3 (w^2 - 1)^{3/2} (\mathcal{G}(w))^2. \quad (10)$$

The form factor is

$$\mathcal{G}(w) = h_+(w) - \frac{m_B - m_D}{m_B + m_D} h_-(w), \quad (11)$$

where h_+ is normalized due to HQS and h_- vanishes in the heavy mass limit. Thus

$$\mathcal{G}(1) = 1 + \mathcal{O}\left(\frac{m_B - m_D}{m_B + m_D} \frac{1}{m_c}\right) \quad (12)$$

and the corrections to the HQET predictions are parametrically larger than was the case for $\overline{B} \rightarrow D^*\ell\overline{\nu}_\ell$.

In order to get a more precise prediction for the form factor $\mathcal{G}(1)$ the heavy quark limit can be supplemented by additional assumptions. It has been argued in Ref. [28] that in a limit in which the kinetic energy μ_π^2 is equal to the chromomagnetic moment μ_G^2 (these quantities are discussed below in more detail) one may obtain the value

$$\mathcal{G}(1) = 1.04 \pm 0.01_{\text{power}} \pm 0.01_{\text{pert}} \quad (13)$$

Lattice calculations including effects beyond the heavy mass limit have become available, and hence the fact that deviations from the HQET predictions are parametrically larger than in the case $\overline{B} \rightarrow D^*\ell\overline{\nu}_\ell$ is irrelevant. These unquenched calculations quote a (preliminary) value [29]

$$\mathcal{G}(1) = 1.074 \pm 0.018 \pm 0.016 \quad (14)$$

which has an error comparable to the one quoted for $\mathcal{F}(1)$, although some uncertainties have not been taken into account.

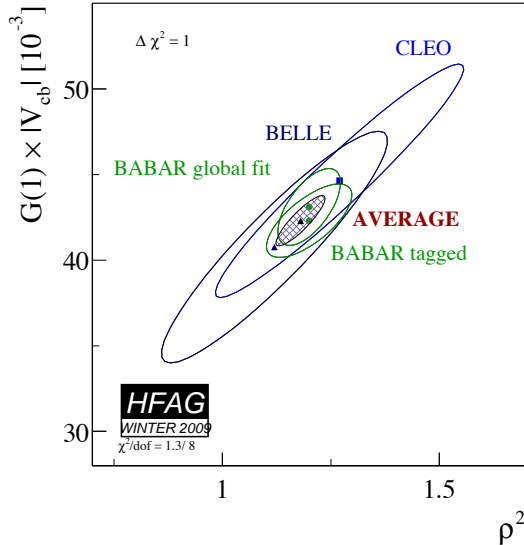


Figure 2: Measurements of $|V_{cb}|\mathcal{G}(1)$ vs. ρ^2 are shown as $\Delta\chi^2 = 1$ ellipses. Color version at end of book.

The measurements of $\bar{B} \rightarrow D\ell\bar{\nu}_\ell$ have improved substantially in the last year. The two new measurements [25,30] are consistent with previous measurements [17,31,32] but significantly more precise, as shown in Fig. 2. The average of these inputs gives $|V_{cb}|\mathcal{G}(1) = (42.3 \pm 0.7 \pm 1.3) \times 10^{-3}$. Using the value given in Eq. (14) for $\mathcal{G}(1)$, accounting for the QED correction and conservatively adding the theory uncertainties linearly results in

$$|V_{cb}| = (39.1 \pm 1.4 \pm 1.3) \times 10^{-3} \quad (\bar{B} \rightarrow D\ell\bar{\nu}_\ell) \quad (15)$$

where the first uncertainty is from experiment and the second from theory.

Using the non-lattice estimate from Eq. (13) one finds $|V_{cb}| = (40.4 \pm 1.4 \pm 0.8) \times 10^{-3}$.

Measuring the differential rate at $w = 1$ is more difficult in $\bar{B} \rightarrow D\ell\bar{\nu}_\ell$ decays than in $\bar{B} \rightarrow D^*\ell\bar{\nu}_\ell$ decays, since the rate is smaller and the background from mis-reconstructed $\bar{B} \rightarrow D^*\ell\bar{\nu}_\ell$ decays is significant; this is reflected in the larger experimental uncertainty. The B factories can address these limitations by studying decays recoiling against fully reconstructed B mesons or doing a global fit to $\bar{B} \rightarrow X_c\ell\bar{\nu}_\ell$ decays. Theoretical input on the shape of the w spectrum in $\bar{B} \rightarrow D\ell\bar{\nu}_\ell$ is valuable, as precise measurements of the total rate are easier; a recent measurement [26] of $\mathcal{B}(\bar{B} \rightarrow D\ell\bar{\nu}_\ell)$ has an uncertainty of $\sim 5\%$.

The determinations from $\bar{B} \rightarrow D^*\ell\bar{\nu}_\ell$ and $\bar{B} \rightarrow D\ell\bar{\nu}_\ell$ decays are consistent, and their uncertainties are largely uncorrelated. Averaging the two results gives

$$|V_{cb}| = (38.7 \pm 1.1) \times 10^{-3} \quad (\text{exclusive}). \quad (16)$$

Prospects for Lattice determinations of the $B \rightarrow D^{(*)}$ form factors

Lattice determinations of the $B \rightarrow D^{(*)}$ form factors have improved significantly over the last few years. The key for the

improvements [13,33] is a set of double-ratios, constructed so that all uncertainties scale with the deviation of the form factor from unity. In combination with the possibility to perform unquenched calculations, i.e. calculations with realistic sea quarks, these double ratios yield quite precise predictions for form factors.

The remaining uncertainties are due to the chiral extrapolation from the light quark masses used in the numerical lattice computation to realistic up and down quark masses, and to discretization errors. These sources of uncertainty will be reduced with larger lattice sizes and smaller lattice spacings. The total uncertainty in the lattice values of $\mathcal{F}(1)$ and $\mathcal{G}(1)$ obtained from this method will be 2-3%. However, in the light of the current $> 2\sigma$ tension between inclusive and exclusive $|V_{cb}|$ a revision of the systematic uncertainties becomes important.

In addition to the lattice calculations of form factor normalizations, first results for the w dependence of the form factors are available [34]. While these first results are still in the quenched approximation, one can expect further calculations of form factor shapes in the near future.

Decays to Excited D Meson States

Above the ground state D and D^* mesons lie four positive-parity states with one unit of orbital angular momentum, generically denoted as D^{**} . In the heavy mass limit they form two spin symmetry doublets with $j_\ell = 1/2$ and $j_\ell = 3/2$, where j_ℓ is the total angular momentum of the light degrees of freedom. The doublet with $j_\ell = 3/2$ is expected to be narrow while the states with $j_\ell = 1/2$ should be broad, consistent with experimental measurements. Furthermore, one expects that in the heavy mass limit $\Gamma(B \rightarrow D^{**}(j_\ell = 3/2)\ell\bar{\nu}) \gg \Gamma(B \rightarrow D^{**}(j_\ell = 1/2)\ell\bar{\nu})$ [35,36,37]. Recent measurements indicate that this expectation may be violated, although the experimental situation is not clear. BELLE [27] and BABAR [38] report different results for the broad states and the experiments do not have the sensitivity to identify the spin-parity of these states. If a violation is confirmed, it may indicate substantial mixing between the two spin symmetry doublets, which can occur due to terms of order $1/m_c$. However, the impact on the exclusive $|V_{cb}|$ determination is expected to be small, since the zero-recoil point is protected against corrections of order $1/m_c$ by Luke's theorem.

$|V_{cb}|$ from inclusive decays

At present the most precise determinations of $|V_{cb}|$ come from inclusive decays. The method is based on a measurement of the total semileptonic decay rate, together with the leptonic energy and the hadronic invariant mass spectra of inclusive semileptonic decays. The total decay rate can be calculated quite reliably in terms of non-perturbative parameters that can be extracted from the information contained in the spectra.

Inclusive semileptonic rate

The theoretical foundation for the calculation of the total semileptonic rate is the Operator Product Expansion (OPE) which yields the Heavy Quark Expansion (HQE), a systematic

Meson Particle Listings

V_{cb} and V_{ub} CKM Matrix Elements

expansion in inverse powers of the b -quark mass [39,40]. The validity of the OPE is proven in the deep Euclidean region for the momenta (which is satisfied, *e.g.*, in deep inelastic scattering), but its application to heavy quark decays requires a continuation to time-like momenta $p_B^2 = M_B^2$, where possible contributions which are exponentially damped in the Euclidean region could become oscillatory. The validity of the OPE for inclusive decays is equivalent to the assumption of parton-hadron duality, hereafter referred to simply as duality, and possible oscillatory contributions would be an indication of duality violation.

Duality-violating effects are hard to quantify. In practice, they would appear as unnaturally large coefficients of higher order terms in the $1/m$ expansion [41]. The description of ~ 60 measurements in terms of ~ 6 free parameters in global fits to $\bar{B} \rightarrow X_c \ell \bar{\nu}_\ell$ decays provides a non-trivial testing ground for the HQE predictions. Present fits include terms up to order $1/m_b^3$, the coefficients of which have sizes as expected a priori by theory and are in quantitative agreement with extractions from other observables. The consistency of the data with these OPE fits will be discussed later; no indication is found that terms of order $1/m_b^4$ or higher are large, and there is no evidence for duality violations in the data. Thus duality or, likewise, the validity of the OPE, is assumed in the analysis, and no further uncertainty is assigned to potential duality violations.

The OPE result for the total rate can be written schematically (the details of the expression can be found, *e.g.*, in Ref. [42]) as

$$\begin{aligned} \Gamma = & |V_{cb}|^2 \hat{\Gamma}_0 m_b^5(\mu) (1 + A_{ew}) A^{\text{pert}}(r, \mu) \times \\ & \left[z_0(r) + z_2(r) \left(\frac{\mu_\pi^2}{m_b^2}, \frac{\mu_G^2}{m_b^2} \right) + z_3(r) \left(\frac{\rho_D^3}{m_b^3}, \frac{\rho_{LS}^3}{m_b^3} \right) \right. \\ & \left. + z_4(r) \left(\frac{s_i}{m_b^4} \right) + \dots \right] \end{aligned} \quad (17)$$

where A_{ew} denotes the electroweak and $A^{\text{pert}}(r, \mu)$ the QCD radiative corrections, r is the ratio m_c/m_b and the z_i are known phase-space functions.

This expression is known up to order $1/m_b^4$, where the terms of order $1/m_b^3$ and $1/m_b^4$ have been computed only at tree level [43,44,45]. The leading term is the parton model, which is known completely to order α_s , and the terms of order $\alpha_s^2 \beta_0$ (where β_0 is the first coefficient of the QCD β function, $\beta_0 = (33 - 2n_f)/3$) have been included by the usual BLM procedure [42,46]. Furthermore, the corrections of order $\alpha_s \mu_\pi^2/m_b^2$ have been computed [47].

Starting at order $1/m_b^3$ contributions with an infrared sensitivity to the charm mass m_c appear [45,48,49]. At order $1/m_b^3$ this ‘‘intrinsic charm’’ contribution is a $\log(m_c)$ in the coefficient of the Darwin term ρ_D . At higher orders, terms such as $1/m_b^3 \times 1/m_c^2$ and $\alpha_s(m_c) 1/m_b^3 \times 1/m_c$ appear, which are comparable in size to the contributions of order $1/m_b^4$

The HQE parameters are given in terms of forward matrix elements by

$$\begin{aligned} \bar{\Lambda} &= M_B - m_b \\ \mu_\pi^2 &= -\langle B | \bar{b} (iD_\perp)^2 b | B \rangle \\ \mu_G^2 &= \langle B | \bar{b} (iD_\perp^\mu) (iD_\perp^\nu) \sigma_{\mu\nu} b | B \rangle \\ \rho_D^3 &= \langle B | \bar{b} (iD_{\perp\mu}) (ivD) (iD_\perp^\nu) b | B \rangle \\ \rho_{LS}^3 &= \langle B | \bar{b} (iD_\perp^\mu) (ivD) (iD_\perp^\nu) \sigma_{\mu\nu} b | B \rangle \end{aligned} \quad (18)$$

while the five hadronic parameters s_i of the order $1/m_b^4$ can be found in Ref. [44]; these have not yet been included in the fits. The non-perturbative matrix elements depend on the renormalization scale μ , on the chosen renormalization scheme and on the quark mass m_b . The rates and the spectra depend strongly on m_b (or equivalently on $\bar{\Lambda}$), which makes the discussion of renormalization issues mandatory.

Using the pole mass definition for the heavy quark masses, it is well known that the corresponding perturbative series of decay rates does not converge very well, making a precision determination of $|V_{cb}|$ in such a scheme impossible. The solution to this problem is to choose an appropriate ‘‘short-distance’’ mass definition. Frequently used mass definitions are the kinetic scheme [15], or the 1S scheme [50]. Both of these schemes have been applied to semi-leptonic $b \rightarrow c$ transitions, yielding comparable results and uncertainties.

The 1S scheme eliminates the b quark pole mass by relating it to the perturbative expression for the mass of the 1S state of the Υ system. The physical mass of the $\Upsilon(1S)$ contains non-perturbative contributions, which have been estimated in Ref. [52]. These non-perturbative contributions are small; nevertheless, the best determination of the b quark mass in the 1S scheme is obtained from sum rules for $e^+e^- \rightarrow b\bar{b}$ [51].

Alternatively one may use a short-distance mass definition such as the $\overline{\text{MS}}$ mass $m_b^{\overline{\text{MS}}}(m_b)$. However, it has been argued that the scale m_b is unnaturally high for B decays, while for smaller scales $\mu \sim 1 \text{ GeV}$ $m_b^{\overline{\text{MS}}}(\mu)$ is under poor control. For this reason the so-called ‘‘kinetic mass’’ $m_b^{\text{kin}}(\mu)$, has been proposed. It is the mass entering the non-relativistic expression for the kinetic energy of a heavy quark, and is defined using heavy quark sum rules [15].

The HQE parameters also depend on the renormalization scale and scheme. The matrix elements given in Eq. (18) are defined with the full QCD fields and states, which is the definition frequently used in the kinetic scheme. Sometimes slightly different parameters λ_1 and λ_2 are used, which are defined in the infinite mass limit. The relation between these parameters is

$$\begin{aligned} \bar{\Lambda}_{\text{HQET}} &= \lim_{m_b \rightarrow \infty} \bar{\Lambda}, \quad -\lambda_1 = \lim_{m_b \rightarrow \infty} \mu_\pi^2 \\ \lambda_2 &= \lim_{m_b \rightarrow \infty} \mu_G^2, \quad \rho_1 = \lim_{m_b \rightarrow \infty} \rho_D^3 \\ \rho_2 &= \lim_{m_b \rightarrow \infty} \rho_{LS}^3 \end{aligned}$$

Defining the kinetic energy and the chromomagnetic moment in the infinite-mass limit (as, *e.g.*, in the 1S scheme) requires that

$1/m_b$ corrections to the matrix elements defined in Eq. (18) be taken into account once one goes beyond order $1/m_b^2$. As a result, additional quantities $\mathcal{T}_1 \cdots \mathcal{T}_4$ appear at order $1/m_b^3$. However, these quantities are correlated such that the total number of non-perturbative parameters to order $1/m_b^3$ is the same as in the scheme where m_b is kept finite in the matrix elements which define the non-perturbative parameters. A detailed discussion of these issues can be found in Ref. [53].

In order to define the HQE parameters properly one must adopt a renormalization scheme, as was done for the heavy quark mass. Since all these parameters can again be determined by heavy quark sum rules, one may adopt a scheme similar to the kinetic scheme for the quark mass. The HQE parameters in the kinetic scheme depend on powers of the renormalization scale μ , and the above relations are valid in the limit $\mu \rightarrow 0$, leaving only logarithms of μ .

Some of these parameters also appear in the relation for the heavy hadron masses. The quantity $\bar{\Lambda}$ is determined once a definition is specified for the quark mass. The parameter μ_G^2 can be extracted from the mass splitting in the lowest spin-symmetry doublet of heavy mesons

$$\mu_G^2(\mu) = \frac{3}{4} C_G(\mu, m_b) (M_{B^*}^2 - M_B^2) \quad (19)$$

where $C_G(\mu, m_b)$ is a perturbatively-computable coefficient which depends on the scheme. In the kinetic scheme we have

$$\mu_G^2(1\text{GeV}) = 0.35_{-0.02}^{+0.03} \text{GeV}^2. \quad (20)$$

Determination of HQE Parameters and $|V_{cb}|$

Several experiments have measured moments in $\bar{B} \rightarrow X_c \ell \bar{\nu}_\ell$ decays [54–61] as a function of the minimum lepton momentum. The measurements of the moments of the electron energy spectrum (0th-3rd) and of the squared hadronic mass spectrum (0th-2nd) have statistical uncertainties that are roughly equal to their systematic uncertainties. They can be improved with more data and significant effort. The moments measured by each experiment have strong correlations; the full statistical and systematic correlation matrices are required to allow these to be used in a global fit. Measurements of photon energy moments (0th-2nd) in $B \rightarrow X_s \gamma$ decays [62–66] as a function of the minimum accepted photon energy are still primarily statistics limited.

Global fits to the full set of moments [63,67–70] have been performed in the 1S and kinetic schemes. The semileptonic moments alone determine a linear combination of m_b and m_c very accurately but leave the orthogonal combination poorly determined [71]; the addition of radiative moments allows m_b to be extracted with greater precision. The most recent global fit in the kinetic scheme gives [69]

$$|V_{cb}| = (41.54 \pm 0.44 \pm 0.58) \times 10^{-3} \quad (21)$$

$$m_b^{\text{kin}} = 4.620 \pm 0.035 \text{GeV} \quad (22)$$

$$\mu_\pi^2(\text{kin}) = 0.424 \pm 0.042 \text{GeV} \quad (23)$$

where the first error includes experimental and theoretical uncertainties and the second error on $|V_{cb}|$ is from the estimated accuracy of the HQE for the total semileptonic rate.

A fit to the same moments in the 1S scheme gives [70]

$$|V_{cb}| = (41.87 \pm 0.25 \pm 0.08) \times 10^{-3} \quad (24)$$

$$m_b^{1\text{S}} = 4.685 \pm 0.029 \text{GeV} \quad (25)$$

$$\lambda_1(1\text{S}) = -0.373 \pm 0.052 \text{GeV}^2 \quad (26)$$

where the last error on $|V_{cb}|$ is due to the uncertainties in the B meson lifetimes.

Theoretical uncertainties are estimated and included in performing the fits. The χ^2/dof is substantially below unity in all fits, suggesting that the theoretical uncertainties may be overestimated, or correlations incompletely accounted for. In any case, the low χ^2 shows no evidence for duality violations at a significant level. Similar values for the parameters are obtained when only experimental uncertainties are used in the fits. If the photon energy spectrum moments from $\bar{B} \rightarrow X_s \gamma$ are excluded from the fit input in the kinetic scheme, the results for $|V_{cb}|$ and μ_π^2 change by only small amounts, while m_b^{kin} increases to $4.68 \pm 0.05 \text{GeV}$.

The mass in the $\overline{\text{MS}}$ scheme corresponding to Eq. (22) is $m_b^{\overline{\text{MS}}} = 4.25 \pm 0.05 \text{GeV}$. This can be compared with a recent value obtained using relativistic sum rules [72], $m_b^{\overline{\text{MS}}} = 4.163 \pm 0.016 \text{GeV}$. The uncertainties on m_b are further discussed in the section on the determination of $|V_{ub}|$.

The precision of these results can be further improved. Some of the measurements, in particular of the $\bar{B} \rightarrow X_s \gamma$ photon energy spectrum, can be improved by using the full B-factory data sets. Improvements can be made in the theory by calculating higher order perturbative corrections [73] and, more importantly, by calculating perturbative corrections to the matrix elements defining the HQE parameters. The inclusion of still higher order moments may improve the sensitivity of the fits to higher order terms in the HQE.

Determination of $|V_{ub}|$

Summary: The determination of $|V_{ub}|$ is the focus of significant experimental and theoretical work. The determinations based on inclusive semileptonic decays using different calculational ansätze are consistent. The largest parametric uncertainty comes from the error on m_b . Significant progress has been made in determinations of $|V_{ub}|$ from $\bar{B} \rightarrow \pi \ell \bar{\nu}_\ell$ decays by using combined fits to theory and experimental data as a function of q^2 . Further improvements in the form factor normalization are needed to improve the precision.

The values obtained from inclusive and exclusive determinations are

$$|V_{ub}| = (4.27 \pm 0.38) \times 10^{-3} \quad (\text{inclusive}), \quad (27)$$

$$|V_{ub}| = (3.38 \pm 0.36) \times 10^{-3} \quad (\text{exclusive}). \quad (28)$$

The two determinations are independent, and the dominant uncertainties are on multiplicative factors. The inclusive and

Meson Particle Listings

V_{cb} and V_{ub} CKM Matrix Elements

exclusive values are weighted by their relative errors and the uncertainties are treated as normally distributed. The resulting average has $P(\chi^2) = 0.10$. We choose to scale the error on the average by $\sqrt{\chi^2/1} = 1.62$ to find

$$|V_{ub}| = (3.89 \pm 0.44) \times 10^{-3} \quad (29)$$

Since the dominant uncertainties come from theory, the uncertainty on the average cannot be assumed to be normally distributed.

$|V_{ub}|$ from inclusive decays

The theoretical description of inclusive $\overline{B} \rightarrow X_u \ell \overline{\nu}_\ell$ decays is based on the Heavy Quark Expansion, as for $\overline{B} \rightarrow X_c \ell \overline{\nu}_\ell$ decays, and leads to a predicted total decay rate with uncertainties below 5% [74,75]. Unfortunately, the total decay rate is hard to measure due to the large background from CKM-favored $\overline{B} \rightarrow X_c \ell \overline{\nu}_\ell$ transitions. Calculating the partial decay rate in regions of phase space where $\overline{B} \rightarrow X_c \ell \overline{\nu}_\ell$ decays are suppressed is more challenging, as the HQE convergence in these regions is spoiled, requiring the introduction of a non-perturbative distribution function, the ‘‘shape function’’ (SF) [76,77], whose form is unknown. The shape function becomes important when the light-cone momentum component $P_+ \equiv E_X - |P_X|$ is not large compared to Λ_{QCD} . This additional difficulty can be addressed in two complementary ways. The leading shape function can either be measured in the radiative decay $\overline{B} \rightarrow X_s \gamma$, or be modeled with constraints on the 0th-2nd moments, and the results applied to the calculation of the $\overline{B} \rightarrow X_u \ell \overline{\nu}_\ell$ partial decay rate [78–80]; in such an approach the largest challenges are for the theory. Alternatively, measurements of $\overline{B} \rightarrow X_u \ell \overline{\nu}_\ell$ partial decay rates can be extended further into the $\overline{B} \rightarrow X_c \ell \overline{\nu}_\ell$ -allowed region, enabling a simplified theoretical (pure HQE) treatment [81] but requiring precise experimental knowledge of the $\overline{B} \rightarrow X_c \ell \overline{\nu}_\ell$ background.

The shape function is a universal property of B mesons at leading order. It has been recognized for over a decade [76,77] that the leading SF can be measured in $\overline{B} \rightarrow X_s \gamma$ decays. However, sub-leading shape functions [82–87] arise at each order in $1/m_b$, and differ in semileptonic and radiative B decays. The form of the SFs cannot be calculated from first principles. Prescriptions that relate directly the partial rates for $\overline{B} \rightarrow X_s \gamma$ and $\overline{B} \rightarrow X_u \ell \overline{\nu}_\ell$ decays and thereby avoid any parameterization of the leading SF are available [88–91]; uncertainties due to sub-leading SF remain in these approaches. Existing measurements have tended to use parameterizations of the leading SF that respect constraints on the zeroth, first and second moments. At leading order the first and second moments are equal to $\overline{\Lambda} = M_B - m_b$ and μ_π^2 , respectively. The relations between SF moments and the non-perturbative parameters of the HQE are known to second order in α_s [92]. As a result, measurements of HQE parameters from global fits to $\overline{B} \rightarrow X_c \ell \overline{\nu}_\ell$ and $\overline{B} \rightarrow X_s \gamma$ moments can be used to constrain the SF moments, as well as provide accurate values of m_b and other parameters for use in determining $|V_{ub}|$. The

possibility of measuring these HQE parameters directly from moments in $\overline{B} \rightarrow X_u \ell \overline{\nu}_\ell$ decays has been explored [93], but the experimental precision achievable there is not competitive with other approaches.

A recent development is to use appropriate basis functions to approximate the shape function, thereby also including the known short-distance contributions as well as the renormalization properties of the SF [94], allowing finally a global fit of all inclusive B meson decay data.

The calculations that are used for the fits performed by HFAG are documented in Refs. [78] (BLNP), [95] (GGOU), [96] (DGE) and [81] (BLL).

The calculations start from the triple differential rate using the variables

$$P_l = M_B - 2E_l, \quad P_- = E_X + |\vec{P}_X|, \quad P_+ = E_X - |\vec{P}_X| \quad (30)$$

for which the differential rate becomes

$$\frac{d^3\Gamma}{dP_+ dP_- dP_l} = \frac{G_F^2 |V_{ub}|^2}{16\pi^2} (M_B - P_+) \left\{ (P_- - P_l)(M_B - P_- + P_l - P_+) \mathcal{F}_1 + (M_B - P_-)(P_- - P_+) \mathcal{F}_2 + (P_- - P_l)(P_l - P_+) \mathcal{F}_3 \right\}. \quad (31)$$

The ‘‘structure functions’’ \mathcal{F}_i can be calculated using factorization theorems that have been proven to subleading order in the $1/m_b$ expansion.

The BLNP [78] calculation uses these factorization theorems to write the \mathcal{F}_i in terms of perturbatively calculable hard coefficients H and jet functions J , which are convolved with the (soft) light-cone distribution functions S , the shape functions of the B meson.

The leading order term in the $1/m_b$ expansion of the \mathcal{F}_i contains a single non-perturbative function and is calculated to subleading order in α_s , while at subleading order in the $1/m_b$ expansion there are several independent non-perturbative functions which have been calculated only at tree level in the α_s expansion.

To extract the non-perturbative input one can study the photon energy spectrum in $B \rightarrow X_s \gamma$ [80]. This spectrum is known at a similar accuracy as the P_+ spectrum in $B \rightarrow X_u \ell \overline{\nu}_\ell$. Going to subleading order in the $1/m_b$ expansion requires the modeling of subleading SFs, a large variety of which were studied in Ref. [78].

A recent calculation (GGOU) [95] uses a hard, Wilsonian cut-off that matches the definition of the kinetic mass. The non-perturbative input is similar to what is used in BLNP, but the shape functions are defined differently. In particular, they are defined at finite m_b and depend on the light-cone component k_+ of the b quark momentum and on the momentum transfer q^2 to the leptons. These functions include sub-leading effects to all orders; as a result they are non-universal, with one shape function corresponding to each structure function in Eq. (31). Their k_+ moments can be computed in the OPE and related to observables and to the shape functions defined in Ref. [78].

Going to subleading order in α_s requires the definition of a renormalization scheme for the HQE parameters and for the SF. It has been noted that the relation between the moments of the SF and the forward matrix elements of local operators is plagued by ultraviolet problems which require additional renormalization. A possible scheme for improving this behavior has been suggested in Refs. [78,80], which introduce a particular definition of the quark mass (the so-called shape function scheme) based on the first moment of the measured spectrum. Likewise, the HQE parameters can be defined from measured moments of spectra, corresponding to moments of the SF.

One can also attempt to calculate the SF by using additional assumptions. One possible approach (DGE) is the so-called “dressed gluon exponentiation” [96], where the perturbative result is continued into the infrared regime using the renormalon structure obtained in the large β_0 limit, where β_0 has been defined following Eq. (17). Alternatively, one may assume an analytic behaviour for the strong coupling in the infrared to perform an extrapolation of perturbation theory [97].

While attempts to quantify the SF are important, the impact of uncertainties in the SF is significantly reduced in some recent measurements that cover a larger portion of the $\overline{B} \rightarrow X_u \ell \overline{\nu}_\ell$ phase space. Several measurements using a combination of cuts on the leptonic momentum transfer q^2 and the hadronic invariant mass M_X as suggested in Ref. [98] have been made. Measurements of the electron spectrum in $\overline{B} \rightarrow X_u \ell \overline{\nu}_\ell$ decays have been made down to momenta of 1.9 GeV or even lower, where SF uncertainties are not dominant. Of course, determining $\overline{B} \rightarrow X_u \ell \overline{\nu}_\ell$ partial rates in charm-dominated regions can bring in a strong dependence on the modeling of the $\overline{B} \rightarrow X_u \ell \overline{\nu}_\ell$ spectrum, which is problematic [99]. The measurements quoted below have used a variety of functional forms to parameterize the leading SF; in no case does this lead to more than a 2% uncertainty on $|V_{ub}|$.

Weak Annihilation [100,101,95] (WA) can in principle contribute significantly in the restricted region (at high q^2) accepted by measurements of $\overline{B} \rightarrow X_u \ell \overline{\nu}_\ell$ decays. An estimate [81] based on leptonic D_s decays [101,49] leads to a $\sim 3\%$ uncertainty on the total $\overline{B} \rightarrow X_u \ell \overline{\nu}_\ell$ rate from the $\Upsilon(4S)$. The differential spectrum from WA decays is not known, but they are expected to contribute predominantly at high q^2 , and may be a significant source of uncertainty for $|V_{ub}|$ measurements that only accept a small fraction, f_u , of the full $\overline{B} \rightarrow X_u \ell \overline{\nu}_\ell$ phase space. Model-dependent limits on WA were determined in Ref. [102], where the CLEO data were fitted to combinations of WA models and a spectator $\overline{B} \rightarrow X_u \ell \overline{\nu}_\ell$ component and background. More direct experimental constraints [103] on WA have recently been made by comparing the $\overline{B} \rightarrow X_u \ell \overline{\nu}_\ell$ decay rates of charged and neutral B mesons. However, these constraints are not sensitive to the isoscalar contribution to WA. The sensitivity of $|V_{ub}|$ determinations to WA can also be reduced by removing the region at high q^2 in those measurements where q^2 is determined.

Measurements

We summarize the measurements used in the determination of $|V_{ub}|$ below. Given the improved precision and more rigorous theoretical interpretation of the recent measurements, earlier determinations [104–107] will not be further considered in this review.

Inclusive electron momentum measurements [108–110] reconstruct a single charged electron to determine a partial decay rate for $\overline{B} \rightarrow X_u \ell \overline{\nu}_\ell$ near the kinematic endpoint. This results in a high $\mathcal{O}(50\%)$ selection efficiency and only modest sensitivity to the modeling of detector response. The decay rate can be cleanly extracted for $E_e > 2.3$ GeV, but this is deep in the SF region, where theoretical uncertainties are large. Measurements down to 2.0 or 1.9 GeV exist, but have low ($< 1/10$) signal-to-background (S/B) ratio, making the control of the $\overline{B} \rightarrow X_c \ell \overline{\nu}_\ell$ background a crucial point. In these analyses the inclusive electron momentum spectrum from $B\overline{B}$ events is determined by subtracting the $e^+e^- \rightarrow q\overline{q}$ continuum background using data samples collected just below $B\overline{B}$ threshold. The continuum-subtracted spectrum is fitted to a combination of a model $\overline{B} \rightarrow X_u \ell \overline{\nu}_\ell$ spectrum and several components ($D\ell\overline{\nu}_\ell$, $D^*\ell\overline{\nu}_\ell$, ...) of the $\overline{B} \rightarrow X_c \ell \overline{\nu}_\ell$ background. The resulting $|V_{ub}|$ values for various E_e cuts are given in Table 1. The leading uncertainty at the lower lepton momentum cuts comes from the $\overline{B} \rightarrow X_c \ell \overline{\nu}_\ell$ background. Prospects for reducing further the lepton momentum cut are improving in light of better knowledge of the semileptonic decays to higher mass $X_c \ell \overline{\nu}$ states [26,27]. The determination of $|V_{ub}|$ from these measurements is discussed below.

An untagged “neutrino reconstruction” measurement [111] from BABAR uses a combination [112] of a high energy electron with a measurement of the missing momentum vector. This allows a much higher S/B ~ 0.7 at the same E_e cut and a $\mathcal{O}(5\%)$ selection efficiency, but at the cost of a smaller accepted phase space for $\overline{B} \rightarrow X_u \ell \overline{\nu}_\ell$ decays and uncertainties associated with the determination of the missing momentum. A control sample of $\Upsilon(4S) \rightarrow B\overline{B}$ decays where one B is reconstructed as $\overline{B} \rightarrow D^0(X)e\overline{\nu}$ with $D^0 \rightarrow K^-\pi^+$ is used to reduce uncertainties from detector and background modeling. The corresponding values for $|V_{ub}|$ are given in Table 1.

The large samples accumulated at the B factories allow studies in which one B meson is fully reconstructed and the recoiling B decays semileptonically [113–116]. The experiments can fully reconstruct a “tag” B candidate in about 0.5% (0.3%) of B^+B^- ($B^0\overline{B}^0$) events. An electron or muon with center-of-mass momentum above 1.0 GeV is required amongst the charged tracks not assigned to the tag B and the remaining particles are assigned to the X_u system. The full set of kinematic properties (E_ℓ , M_X , q^2 , etc.) are available for studying the semileptonically decaying B , making possible selections that accept up to 70% of the full $\overline{B} \rightarrow X_u \ell \overline{\nu}_\ell$ rate. Despite requirements (e.g. on the square of the missing mass) aimed at rejecting events with

Meson Particle Listings

V_{cb} and V_{ub} CKM Matrix Elements

additional missing particles, undetected or mis-measured particles from $\overline{B} \rightarrow X_c \ell \overline{\nu}_\ell$ decay (e.g., K_L^0 and additional neutrinos) remain an important source of uncertainty.

BABAR [113] and BELLE [114,115] have measured partial rates with cuts on M_X , M_X and q^2 , and P_+ based on large samples of $B\overline{B}$ events. Correlations amongst these related partial rates are taken into account in the average given in Table 1. In each case the experimental systematics have significant contributions from the modeling of $\overline{B} \rightarrow X_u \ell \overline{\nu}_\ell$ and $\overline{B} \rightarrow X_c \ell \overline{\nu}_\ell$ decays and from the detector response to charged particles, photons and neutral hadrons.

Recoil-based analyses [115,116] of something approaching the full $\overline{B} \rightarrow X_u \ell \overline{\nu}_\ell$ rate are noteworthy for the smallness of their theoretical uncertainties, since they are in the region where the OPE is well behaved. The new Belle measurement [115] is quite precise; the leading experimental error comes from uncertainty in the modeling of $\overline{B} \rightarrow X_u \ell \overline{\nu}_\ell$ decays.

Determination of $|V_{ub}|$

The determination of $|V_{ub}|$ from the measured partial rates requires input from theory. The BLNP, GGOU and DGE calculations described previously are used to determine $|V_{ub}|$ from all measured partial $\overline{B} \rightarrow X_u \ell \overline{\nu}_\ell$ rates; the values are given in Table 1. The m_b input values used [118] are $m_b^{SF} = 4.650_{-0.037}^{+0.043}$ GeV for BLNP, $m_b^{\text{kin}} = 4.620 \pm 0.035$ GeV for GGOU, and $m_b^{MS} = 4.248 \pm 0.051$ GeV for DGE. These values come from the OPE fit to $\overline{B} \rightarrow X_c \ell \overline{\nu}_\ell$ and $\overline{B} \rightarrow X_s \gamma$ moments described above. An additional contribution for WA has been added to the DGE error budget.

As an illustration of the relative sizes of the uncertainties entering $|V_{ub}|$ we give the error breakdown for the BLNP average: statistical—2.6%; experimental—1.9%; $\overline{B} \rightarrow X_c \ell \overline{\nu}_\ell$ modeling—0.9%; $\overline{B} \rightarrow X_u \ell \overline{\nu}_\ell$ modeling—1.7%; HQE parameters—3.5%; shape function parameterization—0.4%; subleading SFs—0.7%; scale matching—3.5%; Weak Annihilation—1.2%. The uncertainty on m_b dominates the uncertainty on $|V_{ub}|$ from HQE parameters.

The correlations amongst the three BABAR recoil-based measurements are fully accounted for in the average. The statistical correlations amongst the other measurements used in the average are tiny (due to small overlaps among signal events and large differences in S/B ratios) and have been ignored. Correlated systematic and theoretical errors are taken into account, both within an experiment and between experiments.

The theoretical calculations produce very similar results for $|V_{ub}|$; the rms difference between the calculated partial rates for each measurement, averaged over the set of measurements, is 2.1%. The $|V_{ub}|$ values do not show a marked trend versus f_u , the kinematic acceptance for $\overline{B} \rightarrow X_u \ell \overline{\nu}_\ell$ decays. The P-values of the averages are all good, suggesting that the ratios of calculated partial widths in the different phase space regions are in reasonable agreement with ratios of measured widths.

A recent calculation [120] at NNLO accuracy of the leading term in the partial rate shows a surprisingly large change from the NLO calculation used in the BLNP method; these

Table 1: $|V_{ub}|$ (in units of 10^{-5}) from inclusive $\overline{B} \rightarrow X_u \ell \overline{\nu}_\ell$ measurements. The first uncertainty on $|V_{ub}|$ is experimental, while the second includes both theoretical and HQE parameter uncertainties. The values are listed in order of increasing f_u (0.19 to 0.90).

Ref.	BLNP	GGOU	DGE
[108]	$383 \pm 45 \pm 33$	$368 \pm 43 \pm 32$	$358 \pm 42 \pm 27$
[111]	$428 \pm 29 \pm 37$	not avail.	$404 \pm 27 \pm 29$
[110]	$418 \pm 24 \pm 30$	$405 \pm 23 \pm 27$	$406 \pm 27 \pm 27$
[109]	$464 \pm 43 \pm 30$	$453 \pm 42 \pm 26$	$456 \pm 42 \pm 26$
[119]	$423 \pm 45 \pm 30$	$414 \pm 44 \pm 34$	$420 \pm 44 \pm 21$
[113]	$432 \pm 28 \pm 30$	$422 \pm 28 \pm 34$	$426 \pm 28 \pm 21$
[113]	$365 \pm 24 \pm 26$	$343 \pm 22 \pm 28$	$370 \pm 24 \pm 28$
[113]	$402 \pm 19 \pm 28$	$398 \pm 19 \pm 27$	$423 \pm 20 \pm 19$
[115]	$436 \pm 26 \pm 22$	$441 \pm 26 \pm 13$	$446 \pm 26 \pm 16$
	$420 \pm 16 \pm 23$	$427 \pm 16 \pm 18$	$433 \pm 15 \pm 17$

updated calculations are not yet reflected in the values shown in Table 1. Their impact is to increase $|V_{ub}|$ by about 8%. This suggests that the uncertainties assigned to renormalization scale matching have been underestimated. While similar calculations are not yet available for the other approaches, the impact of NNLO terms may be underestimated there as well.

All calculations yield compatible $|V_{ub}|$ values and similar error estimates. We take the arithmetic mean of the values and errors to find

$$|V_{ub}| = (4.27 \pm 0.15_{\text{exp}} \pm 0.19_{\text{th}} \pm 0.30_{\text{NNLO}}) \times 10^{-3} \quad (\text{inclusive}) \quad (32)$$

where the last uncertainty (7%) has been added to account for the large shift seen at NNLO. Note that while the average $|V_{ub}|$ quoted here is not shifted, the findings in Ref. [120] imply the NNLO corrections will raise $|V_{ub}|$.

As was the case with $|V_{cb}|$, it is hard to assign an uncertainty to $|V_{ub}|$ for possible duality violations. However, theoretical arguments suggest that duality should hold even better in $b \rightarrow u \ell \overline{\nu}_\ell$ than in $b \rightarrow c \ell \overline{\nu}_\ell$ [41]. On the other hand, unless duality violations are much larger in $\overline{B} \rightarrow X_u \ell \overline{\nu}_\ell$ decays than in $\overline{B} \rightarrow X_c \ell \overline{\nu}_\ell$ decays, the precision of the $|V_{ub}|$ determination is not yet at the level where duality violations are likely to be significant.

Hadronization uncertainties also impact the $|V_{ub}|$ determination. The theoretical expressions are valid at the parton level and do not incorporate any resonant structure (e.g. $\overline{B} \rightarrow \pi \ell \overline{\nu}_\ell$); this must be added “by hand” to the simulated $\overline{B} \rightarrow X_u \ell \overline{\nu}_\ell$ event samples, since the detailed final state multiplicity and structure impacts the estimates of experimental acceptance and efficiency. The experiments have adopted procedures to input resonant structure while preserving the appropriate behavior in the kinematic variables averaged over the sample. The resulting uncertainties have been estimated to be ~ 1 -2% on $|V_{ub}|$.

A separate class of analyses follows the strategy discussed in Refs. [88–91], where integrals of differential distributions in

$\overline{B} \rightarrow X_u \ell \overline{\nu}_\ell$ decays are compared with corresponding integrals in $\overline{B} \rightarrow X_s \gamma$ decays to extract $|V_{ub}|$, thereby eliminating the need to model the leading shape function. A study [121] using the measured BABAR electron spectrum in $\overline{B} \rightarrow X_u \ell \overline{\nu}_\ell$ decays provides $|V_{ub}|$ determinations using all available “SF-free” calculations; the resulting $|V_{ub}|$ values have total uncertainties of $\sim 12\%$ and are fully compatible with the average quoted above.

The BLL [98] calculation can be used for measurements with cuts on M_X and q^2 . Using the same HQE parameter input as above yields a $|V_{ub}|$ value of $(4.87 \pm 0.24 \pm 0.38) \times 10^{-3}$, which is about 15% higher than the values given in Table 1 for these measurements.

HQE parameters and shape function input

The global fits to $\overline{B} \rightarrow X_c \ell \overline{\nu}_\ell$ and $\overline{B} \rightarrow X_s \gamma$ moments discussed earlier provide input values for the heavy quark parameters needed in calculating $\overline{B} \rightarrow X_u \ell \overline{\nu}_\ell$ partial rates. These HQE parameters are also used to constrain the first and second moments of the shape function. The determinations of m_b using $\overline{B} \rightarrow X_c \ell \overline{\nu}_\ell$ moments are on solid theoretical ground and are performed using order α_S^2 calculations. Concern has been expressed about the theoretical control of $\mathcal{O}(1/m_b)$ corrections to the $\overline{B} \rightarrow X_s \gamma$ moments. On the other hand, the $\overline{B} \rightarrow X_c \ell \overline{\nu}_\ell$ moments alone constrain only a linear combination of m_b and m_c with precision. Another way of determining precise values for m_b is to use determinations from relativistic sum rules [122,72] or Lattice QCD determinations [123], or to combine input on m_c from these sources with the global fit to $\overline{B} \rightarrow X_c \ell \overline{\nu}_\ell$ moments. Further work in this area is needed to critically assess the uncertainties quoted in the various methods. A convergence of the m_b values from these different techniques would enhance our confidence in the m_b used to extract $|V_{ub}|$ from inclusive decays. The uncertainty on m_b will continue to be a leading contribution to the uncertainty in $|V_{ub}|$.

For use in calculating inclusive $\overline{B} \rightarrow X_u \ell \overline{\nu}_\ell$ decay rates, the m_b values determined in the global fit need to be translated into the renormalization scheme used in the calculation. These translations are done at fixed-order in α_S and bring in an additional source of uncertainty. Recently, the BLNP calculation has been updated to include the full $\mathcal{O}(\alpha_S^2)$ contributions [120]. Still the dependence on the b quark mass remains a large parametric uncertainty in the $|V_{ub}|$ determination.

Status and outlook

At present, as indicated by the average given above, the uncertainty on $|V_{ub}|$ from inclusive decays is at the 9% level. A large portion of this error has been added by the authors to reflect the larger-than-expected changes seen in the BLNP calculation when including NNLO terms. Determining the impact of NNLO terms in the other partial rate calculations should be pursued with high priority. The uncertainty on m_b taken here is ~ 40 MeV, contributing an uncertainty of $\sim 4\%$ on $|V_{ub}|$. Complimentary determinations of m_b with robust error estimates can be a valuable addition to the use of B decay moments. Further progress can also be expected on some of

the other leading sources of uncertainty. The Weak Annihilation contribution is now being addressed with data; further improvement can be expected with the full B factory dataset. The uncertainties on $|V_{ub}|$ quoted in the calculations are at the few percent level, and it has been suggested that these may be underestimated. Improving our confidence in, and eventually reducing, these theory uncertainties will require improvements in the calculations. For the approaches making use of the shape function this amounts to improvements in relating the spectra from $\overline{B} \rightarrow X_u \ell \overline{\nu}_\ell$ and $\overline{B} \rightarrow X_s \gamma$ decays by calculating radiative corrections and the effects of subleading SFs, while approaches less sensitive to SFs require calculations of higher-order radiative corrections. Experimental uncertainties will be reduced through higher statistics, a better understanding of $\overline{B} \rightarrow X_c \ell \overline{\nu}_\ell$ decays and the incorporation of improved measurements on D decays. Better measurement of exclusive $\overline{B} \rightarrow X_u \ell \overline{\nu}_\ell$ decay modes will also help reduce experimental uncertainties. The two approaches stated earlier, namely determining the shape function from the $\overline{B} \rightarrow X_s \gamma$ photon spectrum and applying it to $\overline{B} \rightarrow X_u \ell \overline{\nu}_\ell$ decays and pushing the measurements into regions where shape function and duality uncertainties become negligible, are complementary and should both be pursued.

$|V_{ub}|$ from exclusive decays

Exclusive charmless semileptonic decays offer a complementary means of determining $|V_{ub}|$. For the experiments, the specification of the final state provides better background rejection, but the lower branching fraction reflects itself in lower yields compared with inclusive decays. For theory, the calculation of the form factors for $\overline{B} \rightarrow X_u \ell \overline{\nu}_\ell$ decays is challenging, but brings in a different set of uncertainties from those encountered in inclusive decays. In this review we focus on $\overline{B} \rightarrow \pi \ell \overline{\nu}_\ell$, as it is the most promising mode for both experiment and theory, and recent improvements have been made in both areas. Measurements of other exclusive states can be found in Refs. [124–129].

$\overline{B} \rightarrow \pi \ell \overline{\nu}_\ell$ form factor calculations The relevant form factors for the decay $\overline{B} \rightarrow \pi \ell \overline{\nu}_\ell$ are usually defined as

$$\langle \pi(p_\pi) | V^\mu | B(p_B) \rangle = \tag{33}$$

$$f_+(q^2) \left[p_B^\mu + p_\pi^\mu - \frac{m_B^2 - m_\pi^2}{q^2} q^\mu \right] + f_0(q^2) \frac{m_B^2 - m_\pi^2}{q^2} q^\mu$$

in terms of which the rate becomes (in the limit $m_\ell \rightarrow 0$)

$$\frac{d\Gamma}{dq^2} = \frac{G_F^2 |V_{ub}|^2}{24\pi^3} |p_\pi|^3 |f_+(q^2)|^2 \tag{34}$$

where p_π is the momentum of pion in the B meson rest frame.

Currently available non-perturbative methods for the calculation of the form factors include lattice QCD and light-cone sum rules. The two methods are complementary in phase space, since the lattice calculation is restricted to the kinematical range of high momentum transfer q^2 to the leptons, due to large discretization errors, while light-cone sum rules

Meson Particle Listings

V_{cb} and V_{ub} CKM Matrix Elements

provide information near $q^2 = 0$. Interpolations between these two regions may be constrained by unitarity and analyticity.

Unquenched simulations, for which quark loop effects in the QCD vacuum are fully incorporated, have become quite common, and the first results based on these simulations for the $\bar{B} \rightarrow \pi \ell \bar{\nu}_\ell$ form factors have been obtained recently by the Fermilab/MILC collaboration [130] and the HPQCD collaboration [131].

The two calculations differ in the way the b quark is simulated, with HPQCD using nonrelativistic QCD and Fermilab/MILC the so-called Fermilab heavy quark method; they agree within the quoted errors.

In order to obtain the partially-integrated differential rate, the BK parameterization [132]

$$f_+(q^2) = \frac{c_B(1 - \alpha_B)}{(1 - \bar{q}^2)(1 - \alpha_B \bar{q}^2)}, \quad (35)$$

$$f_0(q^2) = \frac{c_B(1 - \alpha_B)}{(1 - \bar{q}^2/\beta_B)}, \quad (36)$$

with $\bar{q}^2 \equiv q^2/m_{B^*}^2$ has been used frequently to extrapolate to small values of q^2 . It includes the leading pole contribution from B^* , and higher poles are modeled by a single pole. The heavy quark scaling is satisfied if the parameters c_B , α_B and β_B scale appropriately. However, the BK parameterization should be used with some caution, since it is not consistent with SCET [133]. More recently, analyticity and unitarity bounds have been employed to constrain the form factors. Making use of the heavy quark limit, stringent constraints on the shape of the form factor can be derived [134], and the conformal mapping of the kinematical variables onto the complex unit disc yields a rapidly converging series in this variable. The use of lattice data in combination with a data point at small q^2 from SCET or sum rules provides a stringent constraint on the shape of the form factor [135]. The most recent form factor parametrization is given in Ref. [136] and has been applied to the extraction of $|V_{ub}|$ from $B \rightarrow \pi \ell \bar{\nu}_\ell$ using lattice data in Ref. [130].

Much work remains to be done, since the current combined statistical plus systematic errors in the lattice results are still at the $\sim 10\%$ level on $|V_{ub}|$ and need to be reduced. Reduction of errors to the $5 \sim 6\%$ level for $|V_{ub}|$ may be feasible within the next few years, although that could involve carrying out a two-loop (or fully non-perturbative) matching between lattice and continuum QCD heavy-to-light current operators, and/or going to smaller lattice spacing.

Another established non-perturbative approach to obtain the form factors is through Light-Cone QCD Sum Rules (LCSR), where the heavy mass limit has been discussed from the point of view of SCET in Ref. [137]. The sum-rule approach provides an approximation for the product $f_B f_+(q^2)$, valid in the region $0 < q^2 < \sim 14 \text{ GeV}^2$. The determination of $f_+(q^2)$ itself requires knowledge of the decay constant f_B , which usually is obtained by replacing f_B by its two-point QCD (SVZ) sum rule [138] in terms of perturbative and condensate

contributions. The advantage of this procedure is the approximate cancellation of various theoretical uncertainties in the ratio $(f_B f_+)/f_B$. The LCSR for $f_B f_+$ is based on the light-cone OPE of the relevant vacuum-to-pion correlation function, calculated in full QCD at finite b -quark mass. The resulting expressions actually comprise a triple expansion: in the twist t of the operators near the light-cone, in α_s , and in the deviation of the pion distribution amplitudes from their asymptotic form, which is fixed from conformal symmetry.

There are multiple sources of uncertainties in the LCQCD calculation, which are discussed in Refs. [139,140]. The total uncertainty adds up to about 15%, resulting in the LCQCD prediction

$$f_+(0) = 0.26 \pm 0.04 \quad (37)$$

which is consistent with the values quoted in Refs. [139] and [140]. It is interesting to note that the results from the LQCD and LCSR are consistent with each other when the BK parameterization is used to relate them. This increases confidence in the theoretical predictions for the rate of $\bar{B} \rightarrow \pi \ell \bar{\nu}_\ell$.

LC-sum rules are valid in the kinematic region of small q^2 and thus can be used to obtain an estimate of the q^2 dependence in a region $q^2 \leq 14 \text{ GeV}^2$ [139]. This is complementary to the lattice results at large values of q^2 , and the results from LCQCD smoothly extrapolate the lattice data to small values of q^2 .

An alternative determination of $|V_{ub}|$ has been proposed by several authors [141,142]. It is based on a model-independent relation between rare decays such as $\bar{B} \rightarrow K^* \ell^+ \ell^-$ and $\bar{B} \rightarrow \rho \ell \bar{\nu}_\ell$, which can be obtained at large momentum transfer q to the leptons. This method is based on the HQET relations between the matrix elements of the $B \rightarrow K^*$ and the $B \rightarrow \rho$ transitions and a systematic, OPE-based expansion in powers of m_c^2/q^2 and Λ_{QCD}/q . The theoretical uncertainty is claimed to be of the order of 5% for $|V_{ub}|$; however, it requires a precise measurement of the exclusive rare decay $\bar{B} \rightarrow K^* \ell^+ \ell^-$, which is a task for future ultra-high-rate experiments.

$\bar{B} \rightarrow \pi \ell \bar{\nu}_\ell$ measurements

The $\bar{B} \rightarrow \pi \ell \bar{\nu}_\ell$ measurements fall into two broad classes: untagged, in which case the reconstruction of the missing momentum of the event serves as an estimator for the unseen neutrino, and tagged, in which the second B meson in the event is fully reconstructed in either a hadronic or semileptonic decay mode. The tagged measurements have high and uniform acceptance, S/B as high as 10, but low statistics. The untagged measurements have somewhat higher background levels (S/B ≤ 1) and make slightly more restrictive kinematic cuts, but have adequate statistics to measure the q^2 dependence of the form factor.

Table 2: Total and partial branching fractions for $\overline{B}^0 \rightarrow \pi^+ \ell^- \overline{\nu}_\ell$. The uncertainties are from statistics and systematics. Measurements of $\mathcal{B}(B^- \rightarrow \pi^0 \ell^- \overline{\nu}_\ell)$ have been multiplied by a factor $2\tau_{B^0}/\tau_{B^-}$ to obtain the values below.

	$\mathcal{B} \times 10^4$	$\mathcal{B}(q^2 > 16) \times 10^4$
CLEO π^+, π^0 [128]	$1.38 \pm 0.15 \pm 0.11$	$0.41 \pm 0.08 \pm 0.04$
BABAR π^+, π^0 [143]	$1.45 \pm 0.07 \pm 0.11$	$0.38 \pm 0.04 \pm 0.05$
BELLE SL π^+ [144]	$1.38 \pm 0.19 \pm 0.15$	$0.36 \pm 0.10 \pm 0.04$
BELLE SL π^0 [144]	$1.43 \pm 0.26 \pm 0.15$	$0.37 \pm 0.15 \pm 0.04$
BELLE had π^+ [145]	$1.12 \pm 0.18 \pm 0.05$	$0.26 \pm 0.08 \pm 0.01$
BELLE had π^0 [145]	$1.24 \pm 0.23 \pm 0.05$	$0.41 \pm 0.11 \pm 0.02$
BABAR SL π^+ [146]	$1.39 \pm 0.21 \pm 0.08$	$0.46 \pm 0.13 \pm 0.03$
BABAR SL π^0 [146]	$1.80 \pm 0.28 \pm 0.15$	$0.45 \pm 0.17 \pm 0.06$
BABAR had π^+ [147]	$1.07 \pm 0.27 \pm 0.19$	$0.65 \pm 0.20 \pm 0.13$
BABAR had π^0 [147]	$1.54 \pm 0.41 \pm 0.30$	$0.49 \pm 0.23 \pm 0.12$
Average	$1.36 \pm 0.05 \pm 0.05$	$0.37 \pm 0.03 \pm 0.02$

CLEO has analyzed $\overline{B} \rightarrow \pi \ell \overline{\nu}_\ell$ and $\overline{B} \rightarrow \rho \ell \overline{\nu}_\ell$ using an untagged analysis [128]. Similar analyses have been done by BABAR [129,143]. The leading systematic uncertainties in the untagged $\overline{B} \rightarrow \pi \ell \overline{\nu}_\ell$ analyses are associated with modeling the missing momentum reconstruction, with backgrounds from $\overline{B} \rightarrow X_c \ell \overline{\nu}_\ell$ and $\overline{B} \rightarrow X_u \ell \overline{\nu}_\ell$ decays, and with varying the form factor for the $\overline{B} \rightarrow \rho \ell \overline{\nu}_\ell$ decay. The values obtained for the full and partial branching fractions are listed in Table 2 above the horizontal line.

BABAR has measured the differential $\overline{B} \rightarrow \pi \ell \overline{\nu}_\ell$ rate versus q^2 with good accuracy [143]. A fit using the BK parameterization [132] gives $\alpha = 0.52 \pm 0.05 \pm 0.03$ with $P(\chi^2) = 65\%$. The q^2 spectrum, shown in Fig. 3, is compatible with the shapes expected from both LCSR and LQCD calculations, but is incompatible ($P(\chi^2) = 0.06\%$) with the ISGW2 [148] model.

BELLE [144] and BABAR [146] have performed analyses based on reconstructing a B in the $\overline{D}^{(*)} \ell^+ \nu_\ell$ decay mode and looking for a $\overline{B} \rightarrow \pi \ell \overline{\nu}_\ell$ or $\overline{B} \rightarrow \rho \ell \overline{\nu}_\ell$ decay amongst the remaining particles in the event. The fact that the B and \overline{B} are back-to-back in the $\Upsilon(4S)$ frame is used to construct a discriminating variable and obtain a signal-to-noise ratio above unity for all q^2 bins. A related technique was discussed in Ref. [149]. BABAR [146] and BELLE [145] have also used their samples of B mesons reconstructed in hadronic decay modes to measure exclusive charmless semileptonic decays giving very clean but low-yield samples. The resulting full and partial branching fractions are given in Table 2. The average of the tagged analyses provides an accuracy on the $\overline{B} \rightarrow \pi \ell \overline{\nu}_\ell$ branching fraction comparable to that obtained with untagged analyses.

The outlook for further improvements in these measurements with larger B-factory data samples is good. The tagged measurements in particular will improve; the current estimates of systematic uncertainties in these measurements have

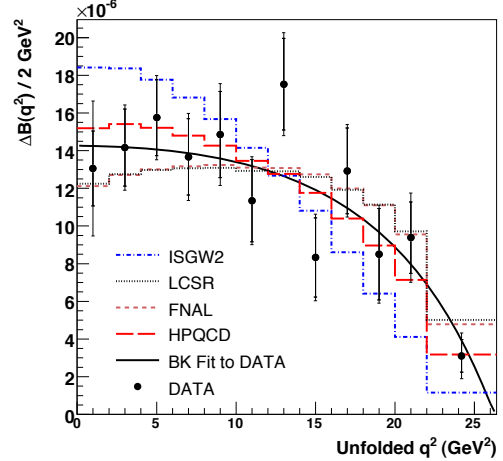


Figure 3: The differential branching fraction versus q^2 from BABAR [143] with several theoretical predictions overlaid.

a significant statistical component, so the total experimental uncertainty should fall as $1/\sqrt{N}$.

$|V_{ub}|$ can be obtained from the average $\overline{B} \rightarrow \pi \ell \overline{\nu}_\ell$ branching fraction and the measured q^2 spectrum. Fits to the measured q^2 spectrum from Ref. [143] using a theoretically motivated parameterization (e.g. from Ref. [9]) remove most of the model dependence from theoretical uncertainties in the shape of the spectrum.

Recent determinations [130,150] of $|V_{ub}|$ from $\overline{B} \rightarrow \pi \ell \overline{\nu}_\ell$ decays have used simultaneous fits to the experimental partial rate and lattice points versus q^2 , using the form factor parameterization of Ref. [9]. We quote here the value from Ref. [130],

$$|V_{ub}| = (3.38 \pm 0.36) \times 10^{-3} \quad (\text{exclusive}). \quad (38)$$

The contributions to the uncertainty from experimental, lattice statistical and lattice systematic errors are all comparable, and each can be further improved.

Conclusion

The study of semileptonic B meson decays continues to be an active area for both theory and experiment. Substantial progress has been made in the application of HQE calculations to inclusive decays, with fits to moments of $\overline{B} \rightarrow X_c \ell \overline{\nu}_\ell$ and $B \rightarrow X_s \gamma$ decays providing precise values for $|V_{cb}|$ and m_b . However, the tension between the inclusive and exclusive $|V_{cb}|$ values highlights the need for further work.

Measurements of inclusive $\overline{B} \rightarrow X_u \ell \overline{\nu}_\ell$ decays have improved, and additional theoretical treatments and improved knowledge of m_b have strengthened our determination of $|V_{ub}|$. Further progress in these areas is possible, but will require higher order radiative corrections from the theory and, in the case of $|V_{ub}|$, improved experimental knowledge of the

Meson Particle Listings

V_{cb} and V_{ub} CKM Matrix Elements

$\bar{B} \rightarrow X_c \ell \bar{\nu}_\ell$ background, and independent confirmations of the input used for m_b . While there has been impressive progress in the past few years, the quest to achieve a precision of 5% on $|V_{ub}|$ from inclusive decays remains elusive.

Progress in both $b \rightarrow u$ and $b \rightarrow c$ exclusive channels depends crucially on progress in lattice calculations. Here the prospects are good (see, *e.g.*, Ref. [151]), since unquenched lattice simulations are now possible, although the ultimate attainable precision is hard to estimate.

The measurements of $\bar{B} \rightarrow \pi \ell \bar{\nu}_\ell$ have improved significantly, including the first reasonably precise determination of the q^2 dependence. Reducing the theoretical uncertainties to a comparable level will require significant effort, but is clearly vital.

The difference between the values for $|V_{ub}|$ obtained from inclusive and exclusive decays has persisted for many years, despite significant improvements in both theory and experiment for both methods. How to reconcile these results remains an intriguing puzzle.

Both $|V_{cb}|$ and $|V_{ub}|$ are indispensable inputs into unitarity triangle fits. In particular, knowing $|V_{ub}|$ with good precision allows a test of CKM unitarity in the most direct way, by comparing the length of the $|V_{ub}|$ side of the unitarity triangle with the measurement of $\sin(2\beta)$. This comparison of a “tree” process ($b \rightarrow u$) with a “loop-induced” process ($B^0 - \bar{B}^0$ mixing) provides sensitivity to possible contributions from new physics. While the effort required to further improve our knowledge of these CKM matrix elements is large, it is well motivated.

The authors would like to acknowledge helpful discussions with M. Artuso, I. I. Bigi, A. Hoang, C. Schwanda and E. Barberio.

References

1. See R. Kowalewski and T. Mannel, Phys. Lett. **B667**, 1 (2008).
2. E. Barberio *et al.*, arXiv:0704.3575.
3. N. Isgur and M.B. Wise, Phys. Lett. **B232**, 113 (1989); *ibid.* **B237**, 527 (1990).
4. M.A. Shifman and M.B. Voloshin, Sov. J. Nucl. Phys. **47**, 511 (1988) [Yad. Fiz. **47**, 801 (1988)].
5. M.E. Luke, Phys. Lett. **B252**, 447 (1990).
6. M. Ademollo and R. Gatto, Phys. Rev. Lett. **13**, 264 (1964).
7. A.V. Manohar and M.B. Wise, Camb. Monogr. Part. Phys. Nucl. Phys. Cosmol. **10**,1(2000).
8. B. Grinstein, Nucl. Phys. **B339**, 253 (1990); H. Georgi, Phys. Lett. **B240**, 447 (1990); A.F. Falk *et al.*, Nucl. Phys. **B343**, 1 (1990); E. Eichten and B. Hill, Phys. Lett. **B234**, 511 (1990).
9. C.G. Boyd, B. Grinstein, and R.F. Lebed, Phys. Rev. **D56**, 6895 (1997); *ibid.*, Phys. Rev. Lett. **74**, 4603 (1995); C.G. Boyd and M.J. Savage, Phys. Rev. **D56**, 303 (1997).
10. I. Caprini *et al.*, Nucl. Phys. **B530**, 153 (1998).
11. A. Sirlin, Nucl. Phys. **B196**, 83 (1982).
12. A. Czarnecki and K. Melnikov, Nucl. Phys. **B505**, 65 (1997).
13. S. Hashimoto *et al.*, Phys. Rev. **D66**, 014503 (2002).
14. C. Bernard *et al.*, Phys. Rev. **D79**, 014506 (2009).
15. I.I.Y. Bigi *et al.*, Phys. Rev. **D52**, 196 (1995).
16. A. Kapustin *et al.*, Phys. Lett. B **375**, 327 (1996).
17. D. Buskulic *et al.*, (ALEPH Collab.), Phys. Lett. **B395**, 373 (1997).
18. G. Abbiendi *et al.*, (OPAL Collab.), Phys. Lett. **B482**, 15 (2000).
19. P. Abreu *et al.*, (DELPHI Collab.), Phys. Lett. **B510**, 55 (2001).
20. J. Abdallah *et al.*, (DELPHI Collab.), Eur. Phys. J. **C33**, 213 (2004).
21. N.E. Adam *et al.*, (CLEO Collab.), Phys. Rev. **D67**, 032001 (2003).
22. I. Adachi *et al.*, (BELLE Collab.), arXiv:0810.1657.
23. B. Aubert *et al.*, (BABAR Collab.), Phys. Rev. **D77**, 032002 (2008).
24. B. Aubert *et al.*, (BABAR Collab.), Phys. Rev. Lett. **100**, 231803 (2008).
25. B. Aubert *et al.*, (BABAR Collab.), Phys. Rev. **D79**, 012002 (2009).
26. B. Aubert *et al.*, (BABAR Collab.), Phys. Rev. **D76**, 051101 (2007); updated in arXiv:0708.1738.
27. D. Liventsev *et al.*, (BELLE Collab.), Phys. Rev. **D77**, 091503 (2008).
28. N. Uraltsev, Phys. Lett. **B585**, 253 (2004).
29. M. Okamoto *et al.*, Nucl. Phys. (Proc. Supp.) **B140**, 461 (2005). A. Kronfeld, talk presented at the workshop CKM05, San Diego, CA - Workshop on the Unitarity Triangle, 15-18 March 2005.
30. B. Aubert *et al.*, (BABAR Collab.), Phys. Rev. Lett. **101**, 261802 (2008).
31. J. E. Bartelt *et al.*, (CLEO Collab.), Phys. Rev. Lett. **82**, 3746 (1999).
32. K. Abe *et al.*, (BELLE Collab.), Phys. Lett. **B526**, 247 (2002).
33. S. Hashimoto *et al.*, Phys. Rev. **D61**, 014502 (2000).
34. G. M. de Divitiis, R. Petronzio, and N. Tantalo, JHEP **0710**, 062 (2007).
35. A.K. Leibovich *et al.*, Phys. Rev. D **57**, 308 (1998).
36. N. Uraltsev, arXiv:hep-ph/0409125.
37. I.I. Bigi *et al.*, Eur. Phys. J. C **52**, 975 (2007) arXiv:0708.1621 [hep-ph].
38. B. Aubert *et al.*, (BABAR Collab.), arXiv:0808.0528.
39. A.V. Manohar and M.B. Wise, Phys. Rev. **D49**, 1310 (1994).
40. I.I.Y. Bigi *et al.*, Phys. Rev. Lett. **71**, 496 (1993), Phys. Lett. **B323**, 408 (1994).
41. M.A. Shifman, hep-ph/0009131, I.I.Y. Bigi and N. Uraltsev, Int. J. Mod. Phys. **A16**, 5201 (2001).
42. D. Benson *et al.*, Nucl. Phys. **B665**, 367 (2003).
43. M. Gremm and A. Kapustin, Phys. Rev. **D55**, 6924 (1997).
44. B. M. Dassinger, T. Mannel, and S. Turczyk, JHEP **0703**, 087 (2007).
45. I. I. Bigi, N. Uraltsev, and R. Zwicky, Eur. Phys. J. **C50**, 539 (2007).
46. P. Gambino and N. Uraltsev, Eur. Phys. J. **C34**, 181 (2004).

-
47. T. Becher, H. Boos, and E. Lunghi, [arXiv:0708.0855](https://arxiv.org/abs/0708.0855).
48. C. Breidenbach *et al.*, Phys. Rev. D **78**, 014022 (2008).
49. I. Bigi *et al.*, [arXiv:0911.3322](https://arxiv.org/abs/0911.3322).
50. A.H. Hoang *et al.*, Phys. Rev. **D59**, 074017 (1999).
51. A.H. Hoang, Phys. Rev. D **61**, 034005 (2000) [[arXiv:hep-ph/9905550](https://arxiv.org/abs/hep-ph/9905550)].
52. H. Leutwyler, Phys. Lett. **B98**, 447 (1981); M.B. Voloshin, Sov. J. Nucl. Phys. **36**, 143 (1982).
53. C.W. Bauer *et al.*, Phys. Rev. **D70**, 094017 (2004).
54. S.E. Csorna *et al.*, (CLEO Collab.), Phys. Rev. **D70**, 032002 (2004).
55. A.H. Mahmood *et al.*, (CLEO Collab.), Phys. Rev. **D70**, 032003 (2004).
56. B. Aubert *et al.*, (BABAR Collab.), Phys. Rev. **D69**, 111103 (2004); updated in [arXiv:0707.2670](https://arxiv.org/abs/0707.2670).
57. B. Aubert *et al.*, (BABAR Collab.), Phys. Rev. **D69**, 111104 (2004).
58. C. Schwanda *et al.*(BELLE Collab.), Phys. Rev. **D75**, 032005 (2007).
59. P. Urquijo *et al.*(BELLE Collab.), Phys. Rev. **D75**, 032001 (2007).
60. J. Abdallah *et al.*, (DELPHI Collab.), Eur. Phys. J. **C45**, 35 (2006).
61. D. Acosta *et al.*, (CDF Collab.), Phys. Rev. **D71**, 051103 (2005).
62. A. Limosani *et al.* [BELLE Collab.], Phys. Rev. Lett. **103**, 241801 (2009).
63. C. Schwanda *et al.*, (BELLE Collab.), Phys. Rev. **D78**, 032016 (2008).
64. B. Aubert *et al.*, (BABAR Collab.), Phys. Rev. **D72**, 052004 (2005).
65. B. Aubert *et al.*, (BABAR Collab.), Phys. Rev. Lett. **97**, 171803 (2006).
66. S. Chen *et al.*, (CLEO Collab.), Phys. Rev. Lett. **87**, 251807 (2001).
67. M. Battaglia *et al.*, Phys. Lett. **B556**, 41 (2003).
68. B. Aubert *et al.*, (BABAR Collab.), Phys. Rev. Lett. **93**, 011803 (2004).
69. O. Buchmüller and H. Flächer, [hep-ph/0507253](https://arxiv.org/abs/hep-ph/0507253); updated in www.slac.stanford.edu/xorg/hfag2/semi/summer09/gbl_fits/kinetic/index.html.
70. C. W. Bauer *et al.*, Phys. Rev. **D70**, 094017 (2004) ; updated in <http://www.slac.stanford.edu/xorg/hfag2/se-mi/EndOfYear09/home.shtml>.
71. See section 5.4.2 of M. Antonelli *et al.*, [arXiv:0907.5386](https://arxiv.org/abs/0907.5386).
72. Chetyrkin *et al.*, Phys. Rev. **D80**, 074010 (2009).
73. M. Neubert, Phys. Rev. D **72**, 074025 (2005).
74. A. H. Hoang *et al.*, Phys. Rev. **D59**, 074017 (1999).
75. N. Uraltsev, Int. J. Mod. Phys. **A14**, 4641 (1999).
76. M. Neubert, Phys. Rev. **D49**, 4623 (1994); *ibid.* **D49**, 3392 (1994).
77. I. Bigi *et al.*, Int. J. Mod. Phys. **A9**, 2467 (1994).
78. B.O. Lange, M. Neubert, and G. Paz, Phys. Rev. **D72**, 073006 (2005).
79. C. W. Bauer *et al.*, Phys. Lett. **B543**, 261 (2002).
80. T. Mannel and S. Recksiegel, Phys. Rev. **D60**, 114040 (1999).
81. C. W. Bauer, Z. Ligeti, and M. E. Luke, Phys. Rev. **D64**, 113004 (2001).
82. C. W. Bauer *et al.*, Phys. Rev. **D68**, 094001 (2003).
83. S. W. Bosch *et al.*, JHEP **0411**, 073 (2004).
84. A. W. Leibovich *et al.*, Phys. Lett. **B539**, 242 (2002).
85. M. Neubert, Phys. Lett. **B543**, 269 (2002).
86. K.S.M.Lee and I.W. Stewart, Nucl. Phys. **B721**, 325 (2005).
87. M. Beneke *et al.*, JHEP **0506**, 071 (2005).
88. M. Neubert, Phys. Lett. **B513**, 88 (2001); Phys. Lett. **B543**, 269 (2002).
89. A.K. Leibovich *et al.*, Phys. Rev. **D61**, 053006 (2000); **62**, 014010 (2000); Phys. Lett. **B486**, 86 (2000); **513**, 83 (2001).
90. A.H. Hoang *et al.*, Phys. Rev. **D71**, 093007 (2005).
91. B. Lange *et al.*, JHEP **0510**, 084 (2005); B. Lange, JHEP **0601**, 104 (2006).
92. M. Neubert, Phys. Lett. **B612**, 13 (2005).
93. P. Gambino, G. Ossola, and N. Uraltsev, JHEP **0509**, 010 (2005).
94. Z. Ligeti, I. W. Stewart, and F. J. Tackmann, Phys. Rev. D **78**, 114014 (2008).
95. P. Gambino *et al.*, JHEP **0710**, 058 (2007).
96. J.R. Andersen and E. Gardi, JHEP **0601**, 097 (2006).
97. U. Aglietti *et al.*, Eur. Phys. J. **C59**, 831 (2009).
98. C. W. Bauer *et al.*, Phys. Rev. **D64**, 113004 (2001); Phys. Lett. **B479**, 395 (2000).
99. Point raised by Frank Tackmann at Vxb2009 (<https://confluence.slac.stanford.edu/display/vxb2009/>).
100. I. I. Y. Bigi and N. G. Uraltsev, Nucl. Phys. **B423**, 33 (1994).
101. M.B. Voloshin, Phys. Lett. **B515**, 74 (2001).
102. J.L. Rosner *et al.*, (CLEO Collab.), Phys. Rev. Lett. **96**, 121801 (2006).
103. B. Aubert *et al.*, (BABAR Collab.), [arXiv:0708.1753](https://arxiv.org/abs/0708.1753).
104. R. Barate *et al.*, (ALEPH Collab.), Eur. Phys. J. **C6**, 555 (1999).
105. M. Acciarri *et al.*, (L3 Collab.), Phys. Lett. **B436**, 174 (1998).
106. G. Abbiendi *et al.*, (OPAL Collab.), Eur. Phys. J. **C21**, 399 (2001).
107. P. Abreu *et al.*, (DELPHI Collab.), Phys. Lett. **B478**, 14 (2000).
108. A. Bornheim *et al.*, (CLEO Collab.), Phys. Rev. Lett. **88**, 231803 (2002).
109. A. Limosani *et al.*, (BELLE Collab.), Phys. Lett. **B621**, 28 (2005).
110. B. Aubert *et al.*, (BABAR Collab.), Phys. Rev. **D73**, 012006 (2006).
111. B. Aubert *et al.*, (BABAR Collab.), Phys. Rev. Lett. **95**, 111801 (2005), Erratum-*ibid.* **97**, 019903(E) (2006).
112. R. Kowalewski and S. Menke, Phys. Lett. **B541**, 29 (2002).
113. B. Aubert *et al.*, (BABAR Collab.), Phys. Rev. Lett. **92**, 071802 (2004); *ibid.* **100**, 171802 (2008).
114. I. Bizjak *et al.*, (BELLE Collab.), Phys. Rev. Lett. **95**, 241801 (2005).

B_S^0, B_S^*

CP VIOLATION PARAMETERS in B_S^0

$\text{Re}(\epsilon_{B_S^0}) / (1 + |\epsilon_{B_S^0}|^2)$

CP impurity in B_S^0 system.

"OUR EVALUATION" is an average using rescaled values of the data listed below. The average and rescaling were performed by the Heavy Flavor Averaging Group (HFAG) and are described at http://www.slac.stanford.edu/xorg/hfag/. The averaging/scaling procedure takes into account correlation between the measurements.

Table with columns: VALUE (units 10^-3), DOCUMENT ID, TECN, COMMENT. Row: -0.9 ± 2.6 OUR EVALUATION, 6.1 ± 4.8 ± 0.9, 138 ABAZOV, 07A D0, p-pbar at 1.96 TeV.

138 The first direct measurement of the time integrated flavor untagged charge asymmetry in semileptonic B_S^0 decays is reported as $2\chi^2_{SL}(\text{untagged}) = A_{SL}^{\pm} = (2.45 \pm 1.93 \pm 0.35) \times 10^{-2}$.

CP Violation phase β_S

$-2\beta_S$ is the weak phase difference between B_S^0 mixing amplitude and the $B_S^0 \rightarrow J/\psi\phi$ decay amplitude. The Standard Model value of β_S is $\arg(-\frac{V_{ts}V_{tb}^*}{V_{cs}V_{cb}^*})$.

"OUR EVALUATION" is an average using rescaled values of the data listed below. The average and rescaling were performed by the Heavy Flavor Averaging Group (HFAG) and are described at http://www.slac.stanford.edu/xorg/hfag/. The averaging/scaling procedure takes into account correlation between the measurements.

Table with columns: VALUE, DOCUMENT ID, TECN, COMMENT. Row: 0.47 +0.13 -0.21 or 1.09+0.21 -0.13 OUR EVALUATION, 139 AALTONEN, 08G CDF, p-pbar at 1.96 GeV.

Table with columns: VALUE, DOCUMENT ID, TECN, COMMENT. Row: 0.28 +0.12 -0.15 +0.04 -0.01, 140,141 ABAZOV, 08AM D0, p-pbar at 1.96 TeV.

• • • We do not use the following data for averages, fits, limits, etc. • • •

Table with columns: VALUE, DOCUMENT ID, TECN, COMMENT. Row: 0.395 ± 0.28 ± 0.005 -0.070, 142,143 ABAZOV, 07 D0, Repl. by ABAZOV 07N.

Table with columns: VALUE, DOCUMENT ID, TECN, COMMENT. Row: 0.35 +0.20 -0.24, 143,144 ABAZOV, 07N D0, Repl. by ABAZOV 08AM.

139 Reports $0.32 < 2\beta_S < 2.82$ at 68% C.L. and confidence regions in the two-dimensional space of $2\beta_S$ and $\Delta\Gamma$ from the first measurement of $B_S^0 \rightarrow J/\psi\phi$ decays using flavor tagging. The probability of a deviation from SM prediction as large as the level of observed data is 15%.

140 Measured using fully reconstructed $B_S \rightarrow J/\psi\phi$ decays.

141 Reports $\phi_S = -2\beta_S$ and obtains 90% CL interval $-0.03 < \beta_S < 0.60$.

142 The first direct measurement of the CP-violating mixing phase is reported from the time-dependent analysis of flavor untagged $B_S^0 \rightarrow J/\psi\phi$ decays.

143 Reports ϕ_S which equals to $-2\beta_S$.

144 Combines D0 collaboration measurements of time-dependent angular distributions in $B_S^0 \rightarrow J/\psi\phi$ and charge asymmetry in semileptonic decays. There is a 4-fold ambiguity in the solution.

B_S^0 REFERENCES

Large table of references for B_S^0. Columns: Author, Year, Journal, Comment. Includes entries like AALTONEN 09AQ PRL 103 191802, AALTONEN 09B PR D79 011104R, etc.

Large table of references for B_S^0. Columns: Author, Year, Journal, Comment. Includes entries like ABE 00C PR D62 071101R, ABREU 00Y EPJ C16 555, AFFOLDER 00N PRL 85 4668, etc.

B_S^*

$I(J^P) = 0(1^-)$

I, J, P need confirmation. Quantum numbers shown are quark-model predictions.

B_S^* MASS

From mass difference below and the B_S^0 mass.

Table with columns: VALUE (MeV), DOCUMENT ID, TECN, COMMENT. Row: 5415.4 ± 1.4 OUR FIT Error includes scale factor of 2.5, 5415.8 ± 1.5 OUR AVERAGE Error includes scale factor of 2.6.

Table with columns: VALUE, DOCUMENT ID, TECN, COMMENT. Row: 5416.4 ± 0.4 ± 0.5 LOUVOT 09 BELL e+e- -> T(5S), 5411.7 ± 1.6 ± 0.6 AQUINES 06 CLEO e+e- -> T(5S).

• • • We do not use the following data for averages, fits, limits, etc. • • •

Table with columns: VALUE, DOCUMENT ID, TECN, COMMENT. Row: 5418 ± 1 ± 3 DRUTSKOY 07A BELL Repl. by LOUVOT 09.

Table with columns: VALUE, DOCUMENT ID, TECN, COMMENT. Row: 5414 ± 1 ± 3 BONVICINI 06 CLEO e+e- -> T(5S).

1 Utilized the beam constrained invariant mass peak positions for B_S^* and B_S^* to extract the measurement.

2 Uses 14 candidates consistent with B_S decays into final states with a J/ψ and a $D_S^{(*)-}$.

$m_{B_S^*} - m_{B_S}$

Table with columns: VALUE (MeV), DOCUMENT ID, TECN, COMMENT. Row: 49.0 ± 1.5 OUR FIT Error includes scale factor of 2.0.

46.1 ± 1.5 OUR AVERAGE

Table with columns: VALUE, DOCUMENT ID, TECN, COMMENT. Row: 45.7 ± 1.7 ± 0.7 AQUINES 06 CLEO e+e- -> T(5S).

Table with columns: VALUE, DOCUMENT ID, TECN, COMMENT. Row: 47.0 ± 2.6 LEE-FRANZINI 90 CSB2 e+e- -> T(5S).

• • • We do not use the following data for averages, fits, limits, etc. • • •

Table with columns: VALUE, DOCUMENT ID, TECN, COMMENT. Row: 48 ± 1 ± 3 BONVICINI 06 CLEO Repl. by AQUINES 06.

3 Utilized the beam constrained invariant mass peak positions for B_S^* and B_S^* to extract the measurement.

4 LEE-FRANZINI 90 measure $46.7 \pm 0.4 \pm 0.2$ MeV for an admixture of $B^0, B^+,$ and B_S . They use the shape of the photon line to separate the above value for B_S .

5 Uses 14 candidates consistent with B_S decays into final states with a J/ψ and a $D_S^{(*)-}$.

$(m_{B_S^*} - m_{B_S}) - (m_{B_S^*} - m_{B_S})$

Table with columns: VALUE (MeV), CL %, DOCUMENT ID, TECN, COMMENT. Row: <6, 95, ABREU, 95R DLPH, E_cm^e_e = 88-94 GeV.

Meson Particle Listings

 B_s^* , $B_{s1}(5830)^0$, $B_{s2}^*(5840)^0$, $B_{sJ}^*(5850)$ B_s^* DECAY MODES

Mode	Fraction (Γ_i/Γ)
Γ_1 $B_s \gamma$	dominant

 B_s^* REFERENCES

LOUVOT 09	PRL 102 021801	R. Louvot <i>et al.</i>	(BELLE Collab.)
DRUTSKOY 07A	PR D76 012002	A. Drutskoy <i>et al.</i>	(BELLE Collab.)
AQUINES 06	PRL 96 152001	O. Aquines <i>et al.</i>	(CLEO Collab.)
BONVICINI 06	PRL 96 022002	G. Bonvicini <i>et al.</i>	(CLEO Collab.)
ABREU 95R	ZPHY C68 353	P. Abreu <i>et al.</i>	(DELPHI Collab.)
LEE-FRANZINI 90	PRL 65 2947	J. Lee-Franzini <i>et al.</i>	(CUSB II Collab.)

 $B_{s1}(5830)^0$ $I(J^P) = \frac{1}{2}(1^+)$ Status: ***
 I, J, P need confirmation.

Quantum numbers shown are quark-model predictions.

 $B_{s1}(5830)^0$ MASS

VALUE (MeV)	DOCUMENT ID	TECN	COMMENT
5829.4 ± 0.7	¹ AALTONEN 08k	CDF	$p\bar{p}$ at 1.96 TeV

¹ Uses two-body decays into K^- and B^+ mesons reconstructed as $B^+ \rightarrow J/\psi K^+$, $J/\psi \rightarrow \mu^+ \mu^-$ or $B^+ \rightarrow \bar{D}^0 \pi^+$, $\bar{D}^0 \rightarrow K^+ \pi^-$. $m_{B_{s1}^0} - m_{B^{*+}}$

VALUE (MeV)	DOCUMENT ID	TECN	COMMENT
504.41 ± 0.21 ± 0.14	² AALTONEN 08k	CDF	$p\bar{p}$ at 1.96 TeV

² Uses two-body decays into K^- and B^+ mesons reconstructed as $B^+ \rightarrow J/\psi K^+$, $J/\psi \rightarrow \mu^+ \mu^-$ or $B^+ \rightarrow \bar{D}^0 \pi^+$, $\bar{D}^0 \rightarrow K^+ \pi^-$. $B_{s1}(5830)^0$ DECAY MODES

Mode	Fraction (Γ_i/Γ)
Γ_1 $B^{*+} K^-$	dominant

 $B_{s1}(5830)^0$ BRANCHING RATIOS

$\Gamma(B^{*+} K^-)/\Gamma_{\text{total}}$	Γ_1/Γ
dominant	

 $B_{s1}(5830)^0$ REFERENCES

AALTONEN 08k	PRL 100 082001	T. Aaltonen <i>et al.</i>	(CDF Collab.)
--------------	----------------	---------------------------	---------------

 $B_{s2}^*(5840)^0$ $I(J^P) = \frac{1}{2}(2^+)$ Status: ***
 I, J, P need confirmation.

Quantum numbers shown are quark-model predictions.

 $B_{s2}^*(5840)^0$ MASS

VALUE (MeV)	DOCUMENT ID	TECN	COMMENT
5839.7 ± 0.6 OUR AVERAGE			
5839.7 ± 0.7	¹ AALTONEN 08k	CDF	$p\bar{p}$ at 1.96 TeV
5839.6 ± 1.1 ± 0.7	² ABAZOV 08E	D0	$p\bar{p}$ at 1.96 TeV

¹ Uses two-body decays into K^- and B^+ mesons reconstructed as $B^+ \rightarrow J/\psi K^+$, $J/\psi \rightarrow \mu^+ \mu^-$ or $B^+ \rightarrow \bar{D}^0 \pi^+$, $\bar{D}^0 \rightarrow K^+ \pi^-$.² Observed in $B_{s2}^{*0} \rightarrow B^+ K^-$. Measured production rate of B_{s2}^{*0} relative to B^+ to be $(1.15 \pm 0.23 \pm 0.13)\%$. $m_{B_{s2}^0} - m_{B_{s1}^0}$

VALUE (MeV)	DOCUMENT ID	TECN	COMMENT
10.5 ± 0.6	³ AALTONEN 08k	CDF	$p\bar{p}$ at 1.96 TeV

³ Uses two-body decays into K^- and B^+ mesons reconstructed as $B^+ \rightarrow J/\psi K^+$, $J/\psi \rightarrow \mu^+ \mu^-$ or $B^+ \rightarrow \bar{D}^0 \pi^+$, $\bar{D}^0 \rightarrow K^+ \pi^-$. $B_{s2}^*(5840)^0$ DECAY MODES

Mode	Fraction (Γ_i/Γ)
Γ_1 $B^+ K^-$	dominant

 $B_{s2}^*(5840)^0$ BRANCHING RATIOS

$\Gamma(B^+ K^-)/\Gamma_{\text{total}}$	Γ_1/Γ
dominant	

⁴ Measured production rate of B_{s2}^{*0} relative to B^+ to be $(1.15 \pm 0.23 \pm 0.13)\%$. $B_{s2}^*(5840)^0$ REFERENCES

AALTONEN 08k	PRL 100 082001	T. Aaltonen <i>et al.</i>	(CDF Collab.)
ABAZOV 08E	PRL 100 082002	V.M. Abazov <i>et al.</i>	(D0 Collab.)

 $B_{sJ}^*(5850)$ $I(J^P) = ?(??)$
 I, J, P need confirmation.

OMITTED FROM SUMMARY TABLE

Signal can be interpreted as coming from $\bar{b}s$ states. Needs confirmation. $B_{sJ}^*(5850)$ MASS

VALUE (MeV)	EVTs	DOCUMENT ID	TECN	COMMENT
5853 ± 15	141	AKERS 95E	OPAL	$E_{\text{cm}}^{\text{pe}} = 88-94$ GeV

 $B_{sJ}^*(5850)$ WIDTH

VALUE (MeV)	EVTs	DOCUMENT ID	TECN	COMMENT
47 ± 22	141	AKERS 95E	OPAL	$E_{\text{cm}}^{\text{pe}} = 88-94$ GeV

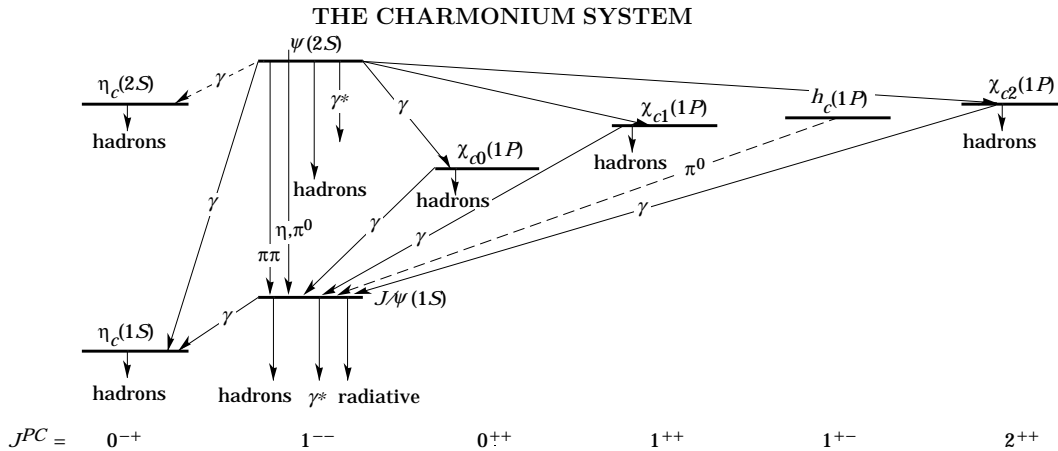
 $B_{sJ}^*(5850)$ REFERENCES

AKERS 95E	ZPHY C66 19	R. Akers <i>et al.</i>	(OPAL Collab.)
-----------	-------------	------------------------	----------------

Meson Particle Listings

Charmonium, $\eta_c(1S)$

c \bar{c} MESONS



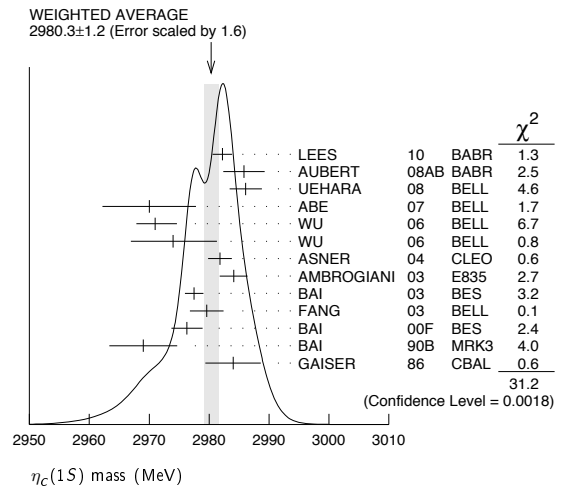
The current state of knowledge of the charmonium system and transitions, as interpreted by the charmonium model. Uncertain states and transitions are indicated by dashed lines. The notation γ^* refers to decay processes involving intermediate virtual photons, including decays to e^+e^- and $\mu^+\mu^-$.

$\eta_c(1S)$ $I^G(J^{PC}) = 0^+(0^{-+})$

$\eta_c(1S)$ MASS

VALUE (MeV)	EVTS	DOCUMENT ID	TECN	COMMENT
2980.3 ± 1.2 OUR AVERAGE		Error includes scale factor of 1.6. See the ideogram below.		
2982.2 ± 0.4 ± 1.6	14k	¹ LEES	10 BABR	10.6 $e^+e^- \rightarrow e^+e^-K_S^0K^\pm\pi^\mp$
2985.8 ± 1.5 ± 3.1	921 ± 32	AUBERT	08AB BABR	$B \rightarrow \eta_c(1S)K^{(*)} \rightarrow K\bar{K}\pi K^{(*)}$
2986.1 ± 1.0 ± 2.5	7.5k	UEHARA	08 BELL	$\gamma\gamma \rightarrow \eta_c \rightarrow \text{hadrons}$
2970 ± 5 ± 6	501	² ABE	07 BELL	$e^+e^- \rightarrow J/\psi(c\bar{c})$
2971 ± 3 ± $\frac{2}{1}$	195	WU	06 BELL	$B^+ \rightarrow \rho\bar{p}K^+$
2974 ± 7 ± $\frac{2}{1}$	20	WU	06 BELL	$B^+ \rightarrow \Lambda\bar{\Lambda}K^+$
2981.8 ± 1.3 ± 1.5	592	ASNEN	04 CLEO	$\gamma\gamma \rightarrow \eta_c \rightarrow K_S^0K^\pm\pi^\mp$
2984.1 ± 2.1 ± 1.0	190	³ AMBROGIANI	03 E835	$\bar{p}p \rightarrow \eta_c \rightarrow \gamma\gamma$
2977.5 ± 1.0 ± 1.2		^{4,5} BAI	03 BES	$J/\psi \rightarrow \gamma\eta_c$
2979.6 ± 2.3 ± 1.6	182 ± 25	FANG	03 BELL	$B \rightarrow \eta_c K$
2976.3 ± 2.3 ± 1.2		^{5,6,7} BAI	00F BES	$J/\psi \rightarrow \gamma\eta_c$ and $\psi(2S) \rightarrow \gamma\eta_c$
2969 ± 4 ± 4	80	⁵ BAI	90B MRK3	$J/\psi \rightarrow \gamma K^+K^-K^+K^-$
2984 ± 2.3 ± 4.0		⁵ GAISER	86 CBAL	$J/\psi \rightarrow \gamma X, \psi(2S) \rightarrow \gamma X$
••• We do not use the following data for averages, fits, limits, etc. •••				
2982.2 ± 0.6		⁵ MITCHELL	09 CLEO	$e^+e^- \rightarrow \gamma X$
2982 ± 5	273 ± 43	⁸ AUBERT	06E BABR	$B^\pm \rightarrow K^\pm X_{c\bar{c}}$
2982.5 ± 1.1 ± 0.9	2547 ± 90	⁹ AUBERT	04D BABR	$\gamma\gamma \rightarrow \eta_c(1S) \rightarrow K\bar{K}\pi$
2976.6 ± 2.9 ± 1.3	140	^{5,6,10} BAI	00F BES	$J/\psi \rightarrow \gamma\eta_c$
2980.4 ± 2.3 ± 0.6		¹¹ BRANDENB...	00B CLE2	$\gamma\gamma \rightarrow \eta_c \rightarrow K^\pm K_S^0\pi^\mp$
2975.8 ± 3.9 ± 1.2		^{6,10} BAI	99B BES	Sup. by BAI 00F
2999 ± 8	25	ABREU	98O DLPH	$e^+e^- \rightarrow e^+e^- + \text{hadrons}$
2988.3 ± $\frac{3.3}{3.1}$		ARMSTRONG	95F E760	$\bar{p}p \rightarrow \gamma\gamma$
2974.4 ± 1.9		^{5,10} BISELLO	91 DM2	$J/\psi \rightarrow \eta_c\gamma$
2956 ± 12 ± 12		⁵ BAI	90B MRK3	$J/\psi \rightarrow \gamma K^+K^-K_S^0K_L^0$
2982.6 ± $\frac{2.7}{2.3}$	12	BAGLIN	87B SPEC	$\bar{p}p \rightarrow \gamma\gamma$
2980.2 ± 1.6		^{5,10} BALTRUSAIT...86	MRK3	$J/\psi \rightarrow \eta_c\gamma$
2976 ± 8		^{5,12} BALTRUSAIT...84	MRK3	$J/\psi \rightarrow 2\phi\gamma$
2982 ± 8	18	¹³ HIMEL	80B MRK2	e^+e^-
2980 ± 9		¹³ PARTRIDGE	80B CBAL	e^+e^-

- ¹ Taking into account interference with the non-resonant $J^P = 0^-$ amplitude.
- ² From a fit of the J/ψ recoil mass spectrum. Supersedes ABE,K 02 and ABE 04c.
- ³ Using mass of $\psi(2S) = 3686.00$ MeV.
- ⁴ From a simultaneous fit of five decay modes of the η_c .
- ⁵ MITCHELL 09 observes a significant asymmetry in the lineshapes of $\psi(2S) \rightarrow \gamma\eta_c$ and $J/\psi \rightarrow \gamma\eta_c$ transitions. If ignored, this asymmetry could lead to significant bias whenever the mass and width are measured in $\psi(2S)$ or J/ψ radiative decays.
- ⁶ Using an η_c width of 13.2 MeV.
- ⁷ Weighted average of the $\psi(2S)$ and $J/\psi(1S)$ samples.
- ⁸ From the fit of the kaon momentum spectrum. Systematic errors not evaluated.
- ⁹ Superseded by LEES 10.
- ¹⁰ Average of several decay modes.
- ¹¹ Superseded by ASNEN 04.
- ¹² $\eta_c \rightarrow \phi\phi$.
- ¹³ Mass adjusted by us to correspond to $J/\psi(1S)$ mass = 3097 MeV.



$\eta_c(1S)$ WIDTH

VALUE (MeV)	CL%	EVTS	DOCUMENT ID	TECN	COMMENT
28.6 ± 2.2 OUR AVERAGE		Error includes scale factor of 2.0. See the ideogram below.			
31.7 ± 1.2 ± 0.8		14k	¹⁴ LEES	10 BABR	10.6 $e^+e^- \rightarrow e^+e^-K_S^0K^\pm\pi^\mp$

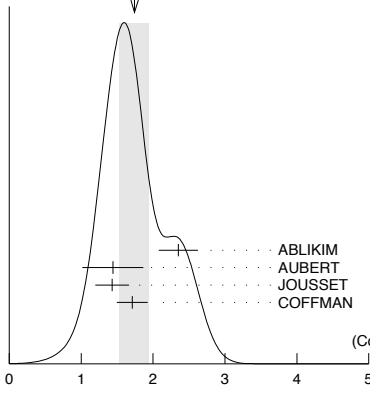
Meson Particle Listings

$J/\psi(1S)$

$\Gamma(\omega\eta)/\Gamma_{\text{total}}$				Γ_{34}/Γ	
VALUE (units 10^{-3})	EVTS	DOCUMENT ID	TECN	COMMENT	
1.74 ± 0.20	OUR AVERAGE	Error includes scale factor of 1.6. See the ideogram below.			
2.352 ± 0.273	5k	62 ABLIKIM	06F BES2	$J/\psi \rightarrow \omega\eta$	
1.44 ± 0.40 ± 0.14	13	63 AUBERT	06D BABR	$10.6 e^+e^- \rightarrow \omega\eta\gamma$	
1.43 ± 0.10 ± 0.21	378	JOUSSET	90 DM2	$J/\psi \rightarrow \text{hadrons}$	
1.71 ± 0.08 ± 0.20		COFFMAN	88 MRK3	$e^+e^- \rightarrow 3\pi\eta$	

⁶²Using $B(\eta \rightarrow 2\gamma) = (39.43 \pm 0.26)\%$, $B(\eta \rightarrow \pi^+\pi^-\pi^0) = 22.6 \pm 0.4\%$, $B(\eta \rightarrow \pi^+\pi^-\gamma) = 4.68 \pm 0.11\%$, and $B(\omega \rightarrow \pi^+\pi^-\pi^0) = (89.1 \pm 0.7)\%$.
⁶³Using $\Gamma(J/\psi \rightarrow e^+e^-) = 5.52 \pm 0.14 \pm 0.04$ keV.

WEIGHTED AVERAGE
 1.74±0.20 (Error scaled by 1.6)



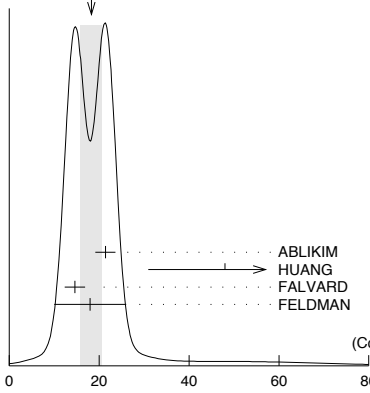
	χ^2
ABL IKIM 06F BES2	5.0
AUBERT 06D BABR	0.5
JOUSSET 90 DM2	1.8
COFFMAN 88 MRK3	0.0
	7.3

(Confidence Level = 0.062)

$\Gamma(\phi K\bar{K})/\Gamma_{\text{total}}$				Γ_{35}/Γ	
VALUE (units 10^{-4})	EVTS	DOCUMENT ID	TECN	COMMENT	
18.3 ± 2.4	OUR AVERAGE	Error includes scale factor of 1.5. See the ideogram below.			
21.4 ± 0.4 ± 2.2		ABL IKIM 05 BES2	$J/\psi \rightarrow \phi\pi^+\pi^-$		
48 ⁺²⁰ ₋₁₆ ± 6	9.0 ^{+3.7} _{-3.0}	64,65 HUANG 03 BELL	$B^+ \rightarrow (\phi K^+ K^-) K^+$		
14.6 ± 0.8 ± 2.1		⁶⁶ FALVARD 88 DM2	$J/\psi \rightarrow \text{hadrons}$		
18 ± 8	14	FELDMAN 77 MRK1	e^+e^-		

⁶⁴We have multiplied $K^+ K^-$ measurement by 2 to obtain $K\bar{K}$.
⁶⁵Using $B(B^+ \rightarrow J/\psi K^+) = (1.01 \pm 0.05) \times 10^{-3}$.
⁶⁶Addition of $\phi K^+ K^-$ and $\phi K^0 \bar{K}^0$ branching ratios.

WEIGHTED AVERAGE
 18.3±2.4 (Error scaled by 1.5)



	χ^2
ABL IKIM 05 BES2	2.0
HUANG 03 BELL	4.6
FALVARD 88 DM2	2.7
FELDMAN 77 MRK1	0.0
	4.6

(Confidence Level = 0.099)

$\Gamma(\phi f_0(1710) \rightarrow \phi K\bar{K})/\Gamma_{\text{total}}$				Γ_{36}/Γ	
VALUE (units 10^{-4})	EVTS	DOCUMENT ID	TECN	COMMENT	
3.6 ± 0.2 ± 0.6		67,68 FALVARD 88 DM2	$J/\psi \rightarrow \text{hadrons}$		

⁶⁷Including interference with $f'_2(1525)$.
⁶⁸Includes unknown branching fraction $f_0(1710) \rightarrow K\bar{K}$.

$\Gamma(\Delta(1232)^{++} \bar{\Delta}(1232)^{-})/\Gamma_{\text{total}}$				Γ_{37}/Γ	
VALUE (units 10^{-3})	EVTS	DOCUMENT ID	TECN	COMMENT	
1.10 ± 0.09 ± 0.28	233	EATON 84 MRK2	e^+e^-		

$\Gamma(\Sigma(1385)^- \bar{\Sigma}(1385)^+ \text{ (or c.c.)})/\Gamma_{\text{total}}$				Γ_{38}/Γ	
VALUE (units 10^{-3})	EVTS	DOCUMENT ID	TECN	COMMENT	
1.03 ± 0.13	OUR AVERAGE	Error includes scale factor of 2.7.			
1.00 ± 0.04 ± 0.21	631 ± 25	HENRARD 87 DM2	$e^+e^- \rightarrow \Sigma^{*-}$		
1.19 ± 0.04 ± 0.25	754 ± 27	HENRARD 87 DM2	$e^+e^- \rightarrow \Sigma^{*+}$		
0.86 ± 0.18 ± 0.22	56	EATON 84 MRK2	$e^+e^- \rightarrow \Sigma^{*-}$		
1.03 ± 0.24 ± 0.25	68	EATON 84 MRK2	$e^+e^- \rightarrow \Sigma^{*+}$		

$\Gamma(\phi f'_2(1525))/\Gamma_{\text{total}}$				Γ_{39}/Γ	
VALUE (units 10^{-4})	EVTS	DOCUMENT ID	TECN	COMMENT	
8 ± 4	OUR AVERAGE	Error includes scale factor of 2.7.			
12.3 ± 0.6 ± 2.0	69,70	FALVARD 88 DM2	$J/\psi \rightarrow \text{hadrons}$		
4.8 ± 1.8	46	⁶⁹ GIDAL 81 MRK2	$J/\psi \rightarrow K^+ K^- K^+ K^-$		

⁶⁹Re-evaluated using $B(f'_2(1525) \rightarrow K\bar{K}) = 0.713$.
⁷⁰Including interference with $f_0(1710)$.

$\Gamma(\phi\pi^+\pi^-)/\Gamma_{\text{total}}$				Γ_{40}/Γ	
VALUE (units 10^{-3})	EVTS	DOCUMENT ID	TECN	COMMENT	
0.94 ± 0.09	OUR AVERAGE	Error includes scale factor of 1.2.			
0.96 ± 0.13	103	⁷¹ AUBERT, BE 06D BABR	$10.6 e^+e^- \rightarrow K^+ K^- \pi^+ \pi^- \gamma$		
1.09 ± 0.02 ± 0.13		ABL IKIM 05 BES2	$J/\psi \rightarrow \phi\pi^+\pi^-$		
0.78 ± 0.03 ± 0.12		FALVARD 88 DM2	$J/\psi \rightarrow \text{hadrons}$		
2.1 ± 0.9	23	FELDMAN 77 MRK1	e^+e^-		

⁷¹Derived by us. AUBERT, BE 06D measures $\Gamma(J/\psi \rightarrow e^+e^-) \times B(J/\psi \rightarrow \phi\pi^+\pi^-) \times B(\phi \rightarrow K^+ K^-) = (2.61 \pm 0.30 \pm 0.18)$ eV

$\Gamma(\phi\pi^0\pi^0)/\Gamma_{\text{total}}$				Γ_{41}/Γ	
VALUE (units 10^{-3})	EVTS	DOCUMENT ID	TECN	COMMENT	
0.56 ± 0.16	23	⁷² AUBERT, BE 06D BABR	$10.6 e^+e^- \rightarrow K^+ K^- \pi^0 \pi^0 \gamma$		

⁷²Derived by us. AUBERT, BE 06D measures $\Gamma(J/\psi \rightarrow e^+e^-) \times B(J/\psi \rightarrow \phi\pi^0\pi^0) \times B(\phi \rightarrow K^+ K^-) = (1.54 \pm 0.40 \pm 0.16)$ eV

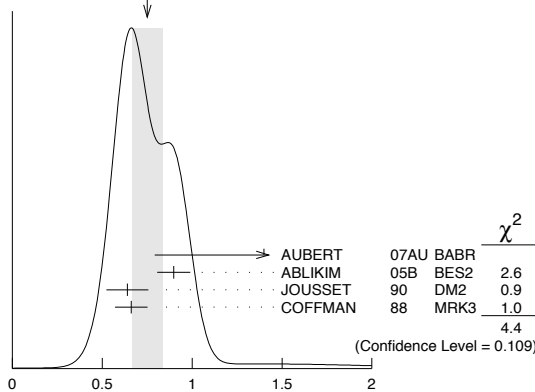
$\Gamma(\phi K^\pm K^\pm \pi^\mp)/\Gamma_{\text{total}}$				Γ_{42}/Γ	
VALUE (units 10^{-4})	EVTS	DOCUMENT ID	TECN	COMMENT	
7.2 ± 0.8	OUR AVERAGE	Error includes scale factor of 1.5.			
7.4 ± 0.6 ± 1.4	227 ± 19	ABL IKIM 08E BES2	$e^+e^- \rightarrow J/\psi$		
7.4 ± 0.9 ± 1.1		FALVARD 88 DM2	$J/\psi \rightarrow \text{hadrons}$		
7 ± 0.6 ± 1.0	163 ± 15	BECKER 87 MRK3	$e^+e^- \rightarrow \text{hadrons}$		

$\Gamma(\omega f_1(1420))/\Gamma_{\text{total}}$				Γ_{43}/Γ	
VALUE (units 10^{-4})	EVTS	DOCUMENT ID	TECN	COMMENT	
6.8 ± 1.9 ⁺³¹ ₋₂₆ ± 1.7	111	BECKER 87 MRK3	$e^+e^- \rightarrow \text{hadrons}$		

$\Gamma(\phi\eta)/\Gamma_{\text{total}}$				Γ_{44}/Γ	
VALUE (units 10^{-3})	EVTS	DOCUMENT ID	TECN	COMMENT	
0.75 ± 0.08	OUR AVERAGE	Error includes scale factor of 1.5. See the ideogram below.			
1.4 ± 0.6 ± 0.1	6	⁷³ AUBERT 07AU BABR	$10.6 e^+e^- \rightarrow \phi\eta\gamma$		
0.898 ± 0.024 ± 0.089		ABL IKIM 05B BES2	$e^+e^- \rightarrow J/\psi \rightarrow \text{hadr}$		
0.64 ± 0.04 ± 0.11	346	JOUSSET 90 DM2	$J/\psi \rightarrow \text{hadrons}$		
0.661 ± 0.045 ± 0.078		COFFMAN 88 MRK3	$e^+e^- \rightarrow K^+ K^- \eta$		

⁷³AUBERT 07AU quotes $\Gamma_{ee}^{J/\psi} \cdot B(J/\psi \rightarrow \phi\eta) \cdot B(\phi \rightarrow K^+ K^-) \cdot B(\eta \rightarrow \gamma\gamma) = 0.84 \pm 0.37 \pm 0.05$ eV.

WEIGHTED AVERAGE
 0.75±0.08 (Error scaled by 1.5)



$\Gamma(\Xi^0 \Xi^0)/\Gamma_{\text{total}}$				Γ_{45}/Γ	
VALUE (units 10^{-3})	EVTS	DOCUMENT ID	TECN	COMMENT	
1.20 ± 0.12 ± 0.21	206	ABL IKIM 08O BES2	$e^+e^- \rightarrow J/\psi$		

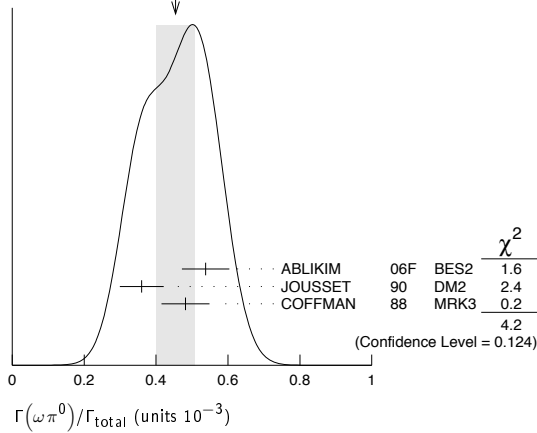
Γ(Ξ(1530) ⁻ Ξ ⁺)/Γ _{total}		Γ ₄₆ /Γ
VALUE (units 10 ⁻³)	EVTS	DOCUMENT ID
0.59 ± 0.09 ± 0.12	75 ± 11	HENRARD 87
Error includes scale factor of 1.4.		TECN COMMENT
		DM2 e ⁺ e ⁻

Γ(ρK ⁻ Σ ⁰ (1385) ⁰)/Γ _{total}		Γ ₄₇ /Γ
VALUE (units 10 ⁻³)	EVTS	DOCUMENT ID
0.51 ± 0.26 ± 0.18	89	EATON 84
Error includes scale factor of 1.4.		TECN COMMENT
		MRK2 e ⁺ e ⁻

Γ(ωπ ⁰)/Γ _{total}		Γ ₄₈ /Γ
VALUE (units 10 ⁻³)	EVTS	DOCUMENT ID
0.45 ± 0.05 OUR AVERAGE	2090	74 ABLIKIM 06F BES2
Error includes scale factor of 1.4.		TECN COMMENT
		J/ψ → ωπ ⁰
0.538 ± 0.012 ± 0.065	2090	JOUSSET 90 DM2
		J/ψ → hadrons
0.360 ± 0.028 ± 0.054	222	COFFMAN 88 MRK3
		e ⁺ e ⁻ → π ⁰ π ⁺ π ⁻ π ⁰

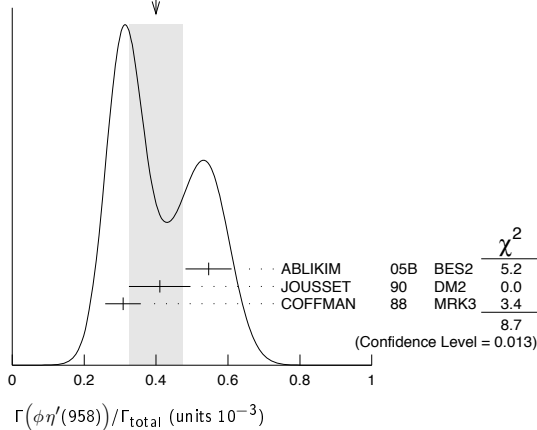
74 Using B(ω → π⁺π⁻π⁰) = (89.1 ± 0.7)%.

WEIGHTED AVERAGE
0.45±0.05 (Error scaled by 1.4)



Γ(φη'(958))/Γ _{total}		Γ ₄₉ /Γ
VALUE (units 10 ⁻³)	CL% EVTS	DOCUMENT ID
0.40 ± 0.07 OUR AVERAGE	167	ABLIKIM 05B BES2
Error includes scale factor of 2.1.		TECN COMMENT
		e ⁺ e ⁻ → J/ψ → hadr
0.546 ± 0.031 ± 0.056		JOUSSET 90 DM2
		J/ψ → hadrons
0.41 ± 0.03 ± 0.08		COFFMAN 88 MRK3
		e ⁺ e ⁻ → K ⁺ K ⁻ η'
<ul style="list-style-type: none"> • • • We do not use the following data for averages, fits, limits, etc. • • • 		
< 1.3	90	VANNUCCI 77 MRK1
		e ⁺ e ⁻

WEIGHTED AVERAGE
0.40±0.07 (Error scaled by 2.1)



Γ(φf ₀ (980))/Γ _{total}		Γ ₅₀ /Γ
VALUE (units 10 ⁻⁴)	EVTS	DOCUMENT ID
3.2 ± 0.9 OUR AVERAGE		75 FALVARD 88
Error includes scale factor of 1.9.		TECN COMMENT
		J/ψ → hadrons
4.6 ± 0.4 ± 0.8		75 GIDAL 81
		J/ψ → K ⁺ K ⁻ K ⁺ K ⁻
2.6 ± 0.6	50	MRK2

75 Assuming B(f₀(980) → ππ) = 0.78.

Γ(φf ₀ (980) → φπ ⁺ π ⁻)/Γ _{total}		Γ ₅₁ /Γ
VALUE (units 10 ⁻³)	EVTS	DOCUMENT ID
0.182 ± 0.042 ± 0.005	19.5 ± 4.5	76,77 AUBERT 07AK BABR
Error includes scale factor of 1.9.		TECN COMMENT
		10.6 e ⁺ e ⁻ → π ⁺ π ⁻ K ⁺ K ⁻ γ

76 Using B(φ → K⁺K⁻) = (49.3 ± 0.6)%.

77 AUBERT 07AK reports [Γ(J/ψ(1S) → φf₀(980) → φπ⁺π⁻)/Γ_{total}] × [Γ(J/ψ(1S) → e⁺e⁻) = (1.01 ± 0.22 ± 0.08) × 10⁻³ keV which we divide by our best value Γ(J/ψ(1S) → e⁺e⁻) = 5.55 ± 0.14 ± 0.02 keV. Our first error is their experiment's error and our second error is the systematic error from using our best value.

Γ(φf ₀ (980) → φπ ⁰ π ⁰)/Γ _{total}		Γ ₅₂ /Γ
VALUE (units 10 ⁻³)	EVTS	DOCUMENT ID
0.171 ± 0.073 ± 0.004	7.0 ± 2.8	78,79 AUBERT 07AK BABR
Error includes scale factor of 1.9.		TECN COMMENT
		10.6 e ⁺ e ⁻ → π ⁰ π ⁰ K ⁺ K ⁻ γ

78 Using B(φ → K⁺K⁻) = (49.3 ± 0.6)%.

79 AUBERT 07AK reports [Γ(J/ψ(1S) → φf₀(980) → φπ⁰π⁰)/Γ_{total}] × [Γ(J/ψ(1S) → e⁺e⁻) = (0.95 ± 0.39 ± 0.10) × 10⁻³ keV which we divide by our best value Γ(J/ψ(1S) → e⁺e⁻) = 5.55 ± 0.14 ± 0.02 keV. Our first error is their experiment's error and our second error is the systematic error from using our best value.

Γ(Ξ(1530) ⁰ Ξ ⁺)/Γ _{total}		Γ ₅₃ /Γ
VALUE (units 10 ⁻³)	EVTS	DOCUMENT ID
0.32 ± 0.12 ± 0.07	24 ± 9	HENRARD 87
Error includes scale factor of 1.4.		TECN COMMENT
		DM2 e ⁺ e ⁻

Γ(Σ(1385) ⁻ Σ ⁺ (or c.c.))/Γ _{total}		Γ ₅₄ /Γ
VALUE (units 10 ⁻³)	EVTS	DOCUMENT ID
0.31 ± 0.05 OUR AVERAGE		HENRARD 87
Error includes scale factor of 1.1.		TECN COMMENT
		DM2 e ⁺ e ⁻ → Σ ⁺ π ⁻
0.30 ± 0.03 ± 0.07	74 ± 8	HENRARD 87
		DM2 e ⁺ e ⁻ → Σ ⁺ π ⁺
0.34 ± 0.04 ± 0.07	77 ± 9	EATON 84
		MRK2 e ⁺ e ⁻ → Σ ⁺ π ⁻
0.29 ± 0.11 ± 0.10	26	EATON 84
		MRK2 e ⁺ e ⁻ → Σ ⁺ π ⁺
0.31 ± 0.11 ± 0.11	28	

Γ(φf ₁ (1285))/Γ _{total}		Γ ₅₅ /Γ
VALUE (units 10 ⁻⁴)	EVTS	DOCUMENT ID
2.6 ± 0.5 OUR AVERAGE		JOUSSET 90
Error includes scale factor of 1.1.		TECN COMMENT
		J/ψ → φ2(π ⁺ π ⁻)
3.2 ± 0.6 ± 0.4		JOUSSET 90
		DM2 J/ψ → φηπ ⁺ π ⁻
2.1 ± 0.5 ± 0.4	25	80 JOUSSET 90
		DM2 J/ψ → φηπ ⁺ π ⁻
<ul style="list-style-type: none"> • • • We do not use the following data for averages, fits, limits, etc. • • • 		
0.6 ± 0.2 ± 0.1	16 ± 6	BECKER 87
		MRK3 J/ψ → φK ⁺ K ⁻ π

80 We attribute to the f₁(1285) the signal observed in the π⁺π⁻η invariant mass distribution at 1297 MeV.

Γ(ηπ ⁺ π ⁻)/Γ _{total}		Γ ₅₆ /Γ
VALUE (units 10 ⁻³)	EVTS	DOCUMENT ID
0.40 ± 0.17 ± 0.03	9	81 AUBERT 07AU BABR
Error includes scale factor of 1.9.		TECN COMMENT
		10.6 e ⁺ e ⁻ → ηπ ⁺ π ⁻ γ

81 AUBERT 07AU quotes Γ^{J/ψ}_{ee} · B(J/ψ → ηπ⁺π⁻) · B(η → 3π) = 0.51 ± 0.22 ± 0.03 eV.

Γ(ρη)/Γ _{total}		Γ ₅₇ /Γ
VALUE (units 10 ⁻³)	EVTS	DOCUMENT ID
0.193 ± 0.023 OUR AVERAGE		JOUSSET 90
Error includes scale factor of 1.1.		TECN COMMENT
		J/ψ → hadrons
0.194 ± 0.017 ± 0.029	299	COFFMAN 88
		MRK3 e ⁺ e ⁻ → π ⁺ π ⁻ η
0.193 ± 0.013 ± 0.029		

Γ(ωη'(958))/Γ _{total}		Γ ₅₈ /Γ
VALUE (units 10 ⁻³)	EVTS	DOCUMENT ID
0.182 ± 0.021 OUR AVERAGE		ABLIKIM 06F
Error includes scale factor of 1.9.		TECN COMMENT
		BES2 J/ψ → ωη'
0.226 ± 0.043	218	82 ABLIKIM 06F
		BES2 J/ψ → ωη'
0.18 ^{+0.10} _{-0.08} ± 0.03	6	JOUSSET 90
		DM2 J/ψ → hadrons
0.166 ± 0.017 ± 0.019		COFFMAN 88
		MRK3 e ⁺ e ⁻ → 3πη'

82 Using B(η' → π⁺π⁻η) = (44.3 ± 1.5)%, B(η' → π⁺π⁻γ) = 29.5 ± 1.0%, B(η → 2γ) = 39.43 ± 0.26%, and B(ω → π⁺π⁻π⁰) = (89.1 ± 0.7)%.

Γ(ωf ₀ (980))/Γ _{total}		Γ ₅₉ /Γ
VALUE (units 10 ⁻⁴)	EVTS	DOCUMENT ID
1.41 ± 0.27 ± 0.47		83 AUGUSTIN 89
Error includes scale factor of 1.9.		TECN COMMENT
		DM2 J/ψ → 2(π ⁺ π ⁻)π ⁰

83 Assuming B(f₀(980) → ππ) = 0.78.

Γ(ρη'(958))/Γ _{total}		Γ ₆₀ /Γ
VALUE (units 10 ⁻³)	EVTS	DOCUMENT ID
0.105 ± 0.018 OUR AVERAGE		JOUSSET 90
Error includes scale factor of 1.1.		TECN COMMENT
		J/ψ → hadrons
0.083 ± 0.030 ± 0.012	19	COFFMAN 88
		MRK3 J/ψ → π ⁺ π ⁻ η'
0.114 ± 0.014 ± 0.016		

Γ(a ₂ (1320) [±] π [∓])/Γ _{total}		Γ ₆₁ /Γ
VALUE (units 10 ⁻⁴)	CL%	DOCUMENT ID
< 43	90	BRAUNSCH... 76
		DASP e ⁺ e ⁻

Meson Particle Listings

 $J/\psi(1S)$
 $\Gamma(K\bar{K}_2^*(1430) + \text{c.c.})/\Gamma_{\text{total}}$ Γ_{62}/Γ

VALUE (units 10^{-4})	CL%	DOCUMENT ID	TECN	COMMENT
<40	90	VANNUCCI 77	MRK1	$e^+e^- \rightarrow K^0\bar{K}_2^{*0}$
• • • We do not use the following data for averages, fits, limits, etc. • • •				
<66	90	BRAUNSCH... 76	DASP	$e^+e^- \rightarrow K^\pm\bar{K}_2^{*\mp}$

 $\Gamma(K_1(1270)^\pm K^\mp)/\Gamma_{\text{total}}$ Γ_{63}/Γ

VALUE (units 10^{-3})	CL%	DOCUMENT ID	TECN	COMMENT
<3.0	90	84 BAI	99c	BES e^+e^-

⁸⁴ Assuming $B(K_1(1270) \rightarrow K\rho) = 0.42 \pm 0.06$

 $\Gamma(K_2^*(1430)^0\bar{K}_2^*(1430)^0)/\Gamma_{\text{total}}$ Γ_{64}/Γ

VALUE (units 10^{-4})	CL%	DOCUMENT ID	TECN	COMMENT
<29	90	VANNUCCI 77	MRK1	$e^+e^- \rightarrow \pi^+\pi^-K^+K^-$

 $\Gamma(K^*(892)^0\bar{K}^*(892)^0)/\Gamma_{\text{total}}$ Γ_{65}/Γ

VALUE (units 10^{-4})	CL%	EPTS	DOCUMENT ID	TECN	COMMENT
2.3 ± 0.7 ± 0.1	25 ± 8	85	AUBERT 07AK	BABR	10.6 $e^+e^- \rightarrow \pi^+\pi^-K^+K^-$

• • • We do not use the following data for averages, fits, limits, etc. • • •

<5 90 VANNUCCI 77 MRK1 $e^+e^- \rightarrow \pi^+\pi^-K^+K^-$

⁸⁵ AUBERT 07AK reports [$\Gamma(J/\psi(1S) \rightarrow K^*(892)^0\bar{K}^*(892)^0)/\Gamma_{\text{total}}$] \times [$\Gamma(J/\psi(1S) \rightarrow e^+e^-)$] = $(1.28 \pm 0.40 \pm 0.11) \times 10^{-3}$ keV which we divide by our best value $\Gamma(J/\psi(1S) \rightarrow e^+e^-) = 5.55 \pm 0.14 \pm 0.02$ keV. Our first error is their experiment's error and our second error is the systematic error from using our best value.

 $\Gamma(\phi f_2(1270))/\Gamma_{\text{total}}$ Γ_{66}/Γ

VALUE (units 10^{-3})	CL%	EPTS	DOCUMENT ID	TECN	COMMENT
0.72 ± 0.13 ± 0.02	44 ± 7	86,87	AUBERT 07AK	BABR	10.6 $e^+e^- \rightarrow \pi^+\pi^-K^+K^-\gamma$

• • • We do not use the following data for averages, fits, limits, etc. • • •

< 0.45 90 FALVARD 88 DM2 $J/\psi \rightarrow \text{hadrons}$

< 0.37 90 VANNUCCI 77 MRK1 $e^+e^- \rightarrow \pi^+\pi^-K^+K^-$

⁸⁶ Using $B(f_2(1270) \rightarrow \pi\pi) = (84.8^{+2.4}_{-1.2})\%$

⁸⁷ AUBERT 07AK reports [$\Gamma(J/\psi(1S) \rightarrow \phi f_2(1270))/\Gamma_{\text{total}}$] \times [$\Gamma(J/\psi(1S) \rightarrow e^+e^-)$] = $(4.02 \pm 0.65 \pm 0.33) \times 10^{-3}$ keV which we divide by our best value $\Gamma(J/\psi(1S) \rightarrow e^+e^-) = 5.55 \pm 0.14 \pm 0.02$ keV. Our first error is their experiment's error and our second error is the systematic error from using our best value.

 $\Gamma(\phi\eta(1405) \rightarrow \phi\eta\pi\pi)/\Gamma_{\text{total}}$ Γ_{67}/Γ

VALUE (units 10^{-4})	CL%	DOCUMENT ID	TECN	COMMENT
<2.5	90	88 FALVARD 88	DM2	$J/\psi \rightarrow \text{hadrons}$

⁸⁸ Includes unknown branching fraction $\eta(1405) \rightarrow \eta\pi\pi$.

 $\Gamma(\omega f_2'(1525))/\Gamma_{\text{total}}$ Γ_{68}/Γ

VALUE (units 10^{-4})	CL%	DOCUMENT ID	TECN	COMMENT
<2.2	90	89 VANNUCCI 77	MRK1	$e^+e^- \rightarrow \pi^+\pi^-\pi^0K^+K^-$
• • • We do not use the following data for averages, fits, limits, etc. • • •				
<2.8	90	89 FALVARD 88	DM2	$J/\psi \rightarrow \text{hadrons}$

⁸⁹ Re-evaluated assuming $B(f_2'(1525) \rightarrow K\bar{K}) = 0.713$.

 $\Gamma(\Sigma(1385)^0\bar{\Lambda})/\Gamma_{\text{total}}$ Γ_{69}/Γ

VALUE (units 10^{-3})	CL%	DOCUMENT ID	TECN	COMMENT
<0.2	90	HENRRARD 87	DM2	e^+e^-

 $\Gamma(\Delta(1232)^+\bar{p})/\Gamma_{\text{total}}$ Γ_{70}/Γ

VALUE (units 10^{-3})	CL%	DOCUMENT ID	TECN	COMMENT
<0.1	90	HENRRARD 87	DM2	e^+e^-

 $\Gamma(\Theta(1540)\bar{\Theta}(1540) \rightarrow K_S^0\rho K^-\bar{p} + \text{c.c.})/\Gamma_{\text{total}}$ Γ_{71}/Γ

VALUE (units 10^{-5})	CL%	DOCUMENT ID	TECN	COMMENT
<1.1	90	BAI 04G	BES2	e^+e^-

 $\Gamma(\Theta(1540)K^-\bar{p} \rightarrow K_S^0\rho K^-\bar{p})/\Gamma_{\text{total}}$ Γ_{72}/Γ

VALUE (units 10^{-5})	CL%	DOCUMENT ID	TECN	COMMENT
<2.1	90	BAI 04G	BES2	e^+e^-

 $\Gamma(\Theta(1540)K_S^0\bar{p} \rightarrow K_S^0\rho K^+n)/\Gamma_{\text{total}}$ Γ_{73}/Γ

VALUE (units 10^{-5})	CL%	DOCUMENT ID	TECN	COMMENT
<1.6	90	BAI 04G	BES2	e^+e^-

 $\Gamma(\bar{\Theta}(1540)K^+n \rightarrow K_S^0\rho K^+n)/\Gamma_{\text{total}}$ Γ_{74}/Γ

VALUE (units 10^{-5})	CL%	DOCUMENT ID	TECN	COMMENT
<5.6	90	BAI 04G	BES2	e^+e^-

 $\Gamma(\bar{\Theta}(1540)K_S^0\rho \rightarrow K_S^0\rho K^-\bar{n})/\Gamma_{\text{total}}$ Γ_{75}/Γ

VALUE (units 10^{-5})	CL%	DOCUMENT ID	TECN	COMMENT
<1.1	90	BAI 04G	BES2	e^+e^-

 $\Gamma(\Sigma^0\bar{\Lambda})/\Gamma_{\text{total}}$ Γ_{76}/Γ

VALUE (units 10^{-4})	CL%	DOCUMENT ID	TECN	COMMENT
<0.9	90	HENRRARD 87	DM2	e^+e^-

 $\Gamma(\phi\pi^0)/\Gamma_{\text{total}}$ Γ_{77}/Γ

VALUE (units 10^{-6})	CL%	DOCUMENT ID	TECN	COMMENT
<6.4	90	ABLIKIM 05B	BES2	$e^+e^- \rightarrow J/\psi \rightarrow \phi\gamma\gamma$
• • • We do not use the following data for averages, fits, limits, etc. • • •				
<6.8	90	COFFMAN 88	MRK3	$e^+e^- \rightarrow K^+K^-\pi^0$

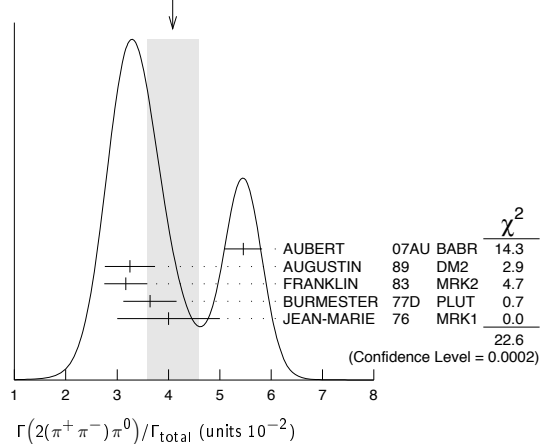
STABLE HADRONS

 $\Gamma(2(\pi^+\pi^-\pi^0))/\Gamma_{\text{total}}$ Γ_{78}/Γ

VALUE (units 10^{-2})	EPTS	DOCUMENT ID	TECN	COMMENT
4.1 ± 0.5 OUR AVERAGE		Error includes scale factor of 2.4. See the ideogram below.		
5.46 ± 0.34 ± 0.14	4990	90 AUBERT 07AU	BABR	10.6 $e^+e^- \rightarrow 2(\pi^+\pi^-\pi^0)\gamma$
3.25 ± 0.49	46055	AUGUSTIN 89	DM2	$J/\psi \rightarrow 2(\pi^+\pi^-\pi^0)$
3.17 ± 0.42	147	FRANKLIN 83	MRK2	$e^+e^- \rightarrow \text{hadrons}$
3.64 ± 0.52	1500	BURMESTER 77D	PLUT	e^+e^-
4 ± 1	675	JEAN-MARIE 76	MRK1	e^+e^-

⁹⁰ AUBERT 07AU reports [$\Gamma(J/\psi(1S) \rightarrow 2(\pi^+\pi^-\pi^0))/\Gamma_{\text{total}}$] \times [$\Gamma(J/\psi(1S) \rightarrow e^+e^-)$] = $0.303 \pm 0.005 \pm 0.018$ keV which we divide by our best value $\Gamma(J/\psi(1S) \rightarrow e^+e^-) = 5.55 \pm 0.14 \pm 0.02$ keV. Our first error is their experiment's error and our second error is the systematic error from using our best value.

WEIGHTED AVERAGE
4.1 ± 0.5 (Error scaled by 2.4)


 $\Gamma(\omega\pi^+\pi^-)/\Gamma(2(\pi^+\pi^-\pi^0))$ Γ_{12}/Γ_{78}

VALUE	DOCUMENT ID	TECN	COMMENT
0.3	91 JEAN-MARIE 76	MRK1	e^+e^-

⁹¹ Final state $(\pi^+\pi^-\pi^0)$ under the assumption that $\pi\pi$ is isospin 0.

 $\Gamma(3(\pi^+\pi^-\pi^0))/\Gamma_{\text{total}}$ Γ_{79}/Γ

VALUE	EPTS	DOCUMENT ID	TECN	COMMENT
0.029 ± 0.006 OUR AVERAGE				
0.028 ± 0.009	11	FRANKLIN 83	MRK2	$e^+e^- \rightarrow \text{hadrons}$
0.029 ± 0.007	181	JEAN-MARIE 76	MRK1	e^+e^-

 $\Gamma(\pi^+\pi^-\pi^0)/\Gamma_{\text{total}}$ Γ_{80}/Γ

VALUE (units 10^{-3})	EPTS	DOCUMENT ID	TECN	COMMENT
20.7 ± 1.2 OUR AVERAGE		Error includes scale factor of 1.6. See the ideogram below.		
23.6 ± 2.1 ± 0.5	256	92 AUBERT 07AU	BABR	10.6 $e^+e^- \rightarrow J/\psi\pi^+\pi^-\gamma$
21.8 ± 1.9		93,94 AUBERT,B	04N	BABR 10.6 $e^+e^- \rightarrow \pi^+\pi^-\pi^0\gamma$
21.84 ± 0.05 ± 2.01	220k	94,95 BAI	04H	BES e^+e^-
20.91 ± 0.21 ± 1.16		94,96 BAI	04H	BES e^+e^-
15 ± 2	168	FRANKLIN 83	MRK2	e^+e^-

⁹² AUBERT 07AU reports [$\Gamma(J/\psi(1S) \rightarrow \pi^+\pi^-\pi^0)/\Gamma_{\text{total}}$] \times [$\Gamma(\psi(2S) \rightarrow J/\psi(1S)\pi^+\pi^-) \times \Gamma(\psi(2S) \rightarrow e^+e^-)/\Gamma_{\text{total}}$] = $(18.6 \pm 1.2 \pm 1.1) \times 10^{-3}$ keV which we divide by our best value $\Gamma(\psi(2S) \rightarrow J/\psi(1S)\pi^+\pi^-) \times \Gamma(\psi(2S) \rightarrow e^+e^-)/\Gamma_{\text{total}} = 0.788 \pm 0.015$ keV. Our first error is their experiment's error and our second error is the systematic error from using our best value.

⁹³ From the ratio of $\Gamma(e^+e^-) B(\pi^+\pi^-\pi^0)$ and $\Gamma(e^+e^-) B(\mu^+\mu^-)$ (AUBERT 04).

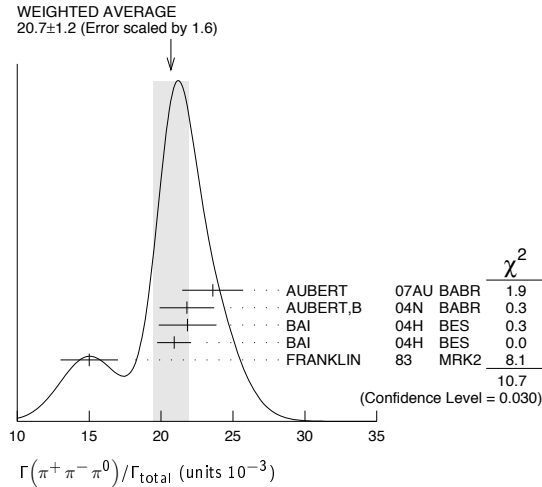
⁹⁴ Mostly $\rho\pi$, see also $\rho\pi$ subsection.

⁹⁵ From $J/\psi \rightarrow \pi^+\pi^-\pi^0$ events directly.

See key on page 405

Meson Particle Listings
 $J/\psi(1S)$

⁹⁶ Obtained comparing the rates for $\pi^+\pi^-\pi^0$ and $\mu^+\mu^-$, using J/ψ events produced via $\psi(2S) \rightarrow \pi^+\pi^- J/\psi$ and with $B(J/\psi \rightarrow \mu^+\mu^-) = 5.88 \pm 0.10\%$.



VALUE (units 10^{-2})	EVTS	DOCUMENT ID	TECN	COMMENT
1.79±0.29 OUR AVERAGE				Error includes scale factor of 2.2.
1.93±0.14±0.05	768	⁹⁷ AUBERT	07AU BABR	10.6 $e^+e^- \rightarrow K^+K^-\pi^+\pi^-\pi^0\gamma$

1.2 ± 0.3 309 VANNUCCI 77 MRK1 e^+e^-
⁹⁷AUBERT 07AU reports [$\Gamma(J/\psi(1S) \rightarrow \pi^+\pi^-\pi^0 K^+K^-)/\Gamma_{\text{total}}$] × [$\Gamma(J/\psi(1S) \rightarrow e^+e^-)$] = 0.1070 ± 0.0043 ± 0.0064 keV which we divide by our best value $\Gamma(J/\psi(1S) \rightarrow e^+e^-) = 5.55 \pm 0.14 \pm 0.02$ keV. Our first error is their experiment's error and our second error is the systematic error from using our best value.

VALUE (units 10^{-4})	EVTS	DOCUMENT ID	TECN	COMMENT
90±30	13	JEAN-MARIE	76	MRK1 e^+e^-

VALUE (units 10^{-3})	EVTS	DOCUMENT ID	TECN	COMMENT
6.6±0.5 OUR AVERAGE				
6.5±0.4±0.2	1.6k	⁹⁸ AUBERT	07AK BABR	10.6 $e^+e^- \rightarrow \pi^+\pi^-K^+K^-\gamma$
7.2±2.3	205	VANNUCCI	77	MRK1 e^+e^-

• • • We do not use the following data for averages, fits, limits, etc. • • •

6.1±0.7±0.2 233 ⁹⁹AUBERT 05D BABR 10.6 $e^+e^- \rightarrow K^+K^-\pi^+\pi^-\gamma$
⁹⁸AUBERT 07AK reports [$\Gamma(J/\psi(1S) \rightarrow \pi^+\pi^-K^+K^-)/\Gamma_{\text{total}}$] × [$\Gamma(J/\psi(1S) \rightarrow e^+e^-)$] = (36.3±1.3±2.1) × 10⁻³ keV which we divide by our best value $\Gamma(J/\psi(1S) \rightarrow e^+e^-) = 5.55 \pm 0.14 \pm 0.02$ keV. Our first error is their experiment's error and our second error is the systematic error from using our best value.

⁹⁹Superseded by AUBERT 07AK. AUBERT 05D reports [$\Gamma(J/\psi(1S) \rightarrow \pi^+\pi^-K^+K^-)/\Gamma_{\text{total}}$] × [$\Gamma(J/\psi(1S) \rightarrow e^+e^-)$] = (33.6 ± 2.7 ± 2.7) × 10⁻³ keV which we divide by our best value $\Gamma(J/\psi(1S) \rightarrow e^+e^-) = 5.55 \pm 0.14 \pm 0.02$ keV. Our first error is their experiment's error and our second error is the systematic error from using our best value.

VALUE (units 10^{-3})	EVTS	DOCUMENT ID	TECN	COMMENT
1.84±0.28±0.05	73	¹⁰⁰ AUBERT	07AU BABR	10.6 $e^+e^- \rightarrow K^+K^-\pi^+\pi^-\eta\gamma$

¹⁰⁰AUBERT 07AU reports [$\Gamma(J/\psi(1S) \rightarrow \pi^+\pi^-K^+K^-)/\Gamma_{\text{total}}$] × [$\Gamma(J/\psi(1S) \rightarrow e^+e^-)$] = (10.2±1.3±0.8) × 10⁻³ keV which we divide by our best value $\Gamma(J/\psi(1S) \rightarrow e^+e^-) = 5.55 \pm 0.14 \pm 0.02$ keV. Our first error is their experiment's error and our second error is the systematic error from using our best value.

VALUE (units 10^{-3})	EVTS	DOCUMENT ID	TECN	COMMENT
2.45±0.31±0.06	203 ± 16	¹⁰¹ AUBERT	07AK BABR	10.6 $e^+e^- \rightarrow \pi^0\pi^0 K^+K^-\gamma$

¹⁰¹AUBERT 07AK reports [$\Gamma(J/\psi(1S) \rightarrow \pi^0\pi^0 K^+K^-)/\Gamma_{\text{total}}$] × [$\Gamma(J/\psi(1S) \rightarrow e^+e^-)$] = (13.6±1.1±1.3) × 10⁻³ keV which we divide by our best value $\Gamma(J/\psi(1S) \rightarrow e^+e^-) = 5.55 \pm 0.14 \pm 0.02$ keV. Our first error is their experiment's error and our second error is the systematic error from using our best value.

VALUE (units 10^{-4})	EVTS	DOCUMENT ID	TECN	COMMENT
3.23±0.75±0.73	52	ABLIKIM	08F	BES $J/\psi \rightarrow \eta\phi f_0(980)$

VALUE (units 10^{-3})	EVTS	DOCUMENT ID	TECN	COMMENT
61 ± 10 OUR AVERAGE				
55.2±12.0	25	FRANKLIN	83	MRK2 $e^+e^- \rightarrow K^+K^-\pi^0$
78.0±21.0	126	VANNUCCI	77	MRK1 $e^+e^- \rightarrow K_S^0 K^\pm\pi^\mp$

VALUE (units 10^{-3})	EVTS	DOCUMENT ID	TECN	COMMENT
3.55±0.23 OUR AVERAGE				
3.53±0.12±0.29	1107	¹⁰² ABLIKIM	05H	BES2 $e^+e^- \rightarrow \psi(2S) \rightarrow J/\psi\pi^+\pi^-, J/\psi \rightarrow 2(\pi^+\pi^-)\gamma$

VALUE (units 10^{-3})	EVTS	DOCUMENT ID	TECN	COMMENT
3.51±0.34±0.09	270	¹⁰³ AUBERT	05D	BABR 10.6 $e^+e^- \rightarrow 2(\pi^+\pi^-)\gamma$
4.0 ± 1.0	76	JEAN-MARIE	76	MRK1 e^+e^-

¹⁰²Computed using $B(J/\psi \rightarrow \mu^+\mu^-) = 0.0588 \pm 0.0010$.

¹⁰³AUBERT 05D reports [$\Gamma(J/\psi(1S) \rightarrow 2(\pi^+\pi^-))/\Gamma_{\text{total}}$] × [$\Gamma(J/\psi(1S) \rightarrow e^+e^-)$] = (19.5 ± 1.4 ± 1.3) × 10⁻³ keV which we divide by our best value $\Gamma(J/\psi(1S) \rightarrow e^+e^-) = 5.55 \pm 0.14 \pm 0.02$ keV. Our first error is their experiment's error and our second error is the systematic error from using our best value.

VALUE (units 10^{-4})	EVTS	DOCUMENT ID	TECN	COMMENT
43 ± 4 OUR AVERAGE				
43.0± 2.9±2.8	496	¹⁰⁴ AUBERT	06D	BABR 10.6 $e^+e^- \rightarrow 3(\pi^+\pi^-)\gamma$
40 ± 20	32	JEAN-MARIE	76	MRK1 e^+e^-

¹⁰⁴Using $\Gamma(J/\psi \rightarrow e^+e^-) = 5.52 \pm 0.14 \pm 0.04$ keV.

VALUE (units 10^{-3})	EVTS	DOCUMENT ID	TECN	COMMENT
1.62±0.09±0.19	761	¹⁰⁵ AUBERT	06D	BABR 10.6 $e^+e^- \rightarrow 2(\pi^+\pi^-\pi^0)\gamma$

¹⁰⁵Using $\Gamma(J/\psi \rightarrow e^+e^-) = 5.52 \pm 0.14 \pm 0.04$ keV.

VALUE (units 10^{-3})	EVTS	DOCUMENT ID	TECN	COMMENT
2.29±0.24 OUR AVERAGE				
2.35±0.39±0.20	85	¹⁰⁶ AUBERT	07AU BABR	10.6 $e^+e^- \rightarrow 2(\pi^+\pi^-)\eta\gamma$
2.26±0.08±0.27	4839	ABLIKIM	05C	BES2 $e^+e^- \rightarrow 2(\pi^+\pi^-)\eta$

¹⁰⁶AUBERT 07AU quotes $\Gamma_{ee}^{J/\psi} \cdot B(J/\psi \rightarrow 2(\pi^+\pi^-)\eta) \cdot B(\eta \rightarrow \gamma\gamma) = 5.16 \pm 0.85 \pm 0.39$ eV.

VALUE (units 10^{-4})	EVTS	DOCUMENT ID	TECN	COMMENT
7.24±0.96±1.11	616	ABLIKIM	05C	BES2 $e^+e^- \rightarrow 3(\pi^+\pi^-)\eta$

VALUE (units 10^{-3})	EVTS	DOCUMENT ID	TECN	COMMENT
2.17±0.07 OUR AVERAGE				

VALUE (units 10^{-3})	EVTS	DOCUMENT ID	TECN	COMMENT
2.18±0.16±0.07	317	¹⁰⁷ WU	06	BELL $B^+ \rightarrow p\bar{p}K^+$
2.26±0.01±0.14	63316	BAI	04E	BES2 $e^+e^- \rightarrow J/\psi$
1.97±0.22	99	BALDINI	98	FENI e^+e^-
1.91±0.04±0.30		PALLIN	87	DM2 e^+e^-
2.16±0.07±0.15	1420	EATON	84	MRK2 e^+e^-
2.5 ± 0.4	133	BRANDELNIK	79C	DASP e^+e^-
2.0 ± 0.5		BESCH	78	BONA e^+e^-
2.2 ± 0.2	331	¹⁰⁸ PERUZZI	78	MRK1 e^+e^-

• • • We do not use the following data for averages, fits, limits, etc. • • •

2.0 ± 0.3 48 ANTONELLI 93 SPEC e^+e^-
¹⁰⁷WU 06 reports [$\Gamma(J/\psi(1S) \rightarrow p\bar{p})/\Gamma_{\text{total}}$] × [$B(B^+ \rightarrow J/\psi(1S)K^+)$] = (2.21 ± 0.13 ± 0.10) × 10⁻⁶ which we divide by our best value $B(B^+ \rightarrow J/\psi(1S)K^+) = (1.014 \pm 0.034) \times 10^{-3}$. Our first error is their experiment's error and our second error is the systematic error from using our best value.

¹⁰⁸Assuming angular distribution (1+cos²θ).

VALUE (units 10^{-3})	EVTS	DOCUMENT ID	TECN	COMMENT
1.19±0.08 OUR AVERAGE				Error includes scale factor of 1.1.

VALUE (units 10^{-3})	EVTS	DOCUMENT ID	TECN	COMMENT
1.33±0.02±0.11	11k	ABLIKIM	09B	BES2 e^+e^-
1.13±0.09±0.09	685	EATON	84	MRK2 e^+e^-
1.4 ± 0.4		BRANDELNIK	79C	DASP e^+e^-
1.00±0.15	109	PERUZZI	78	MRK1 e^+e^-

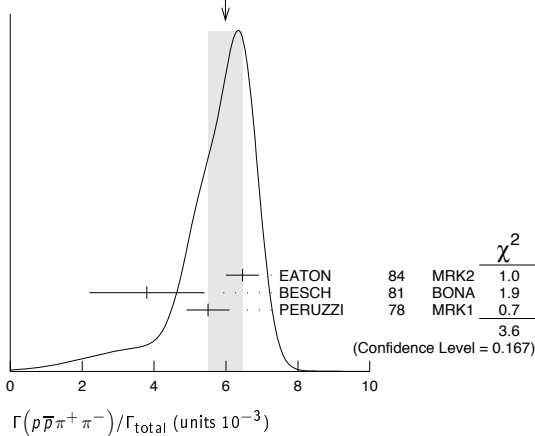
VALUE (units 10^{-3})	EVTS	DOCUMENT ID	TECN	COMMENT
6.0 ± 0.5 OUR AVERAGE				Error includes scale factor of 1.3. See the ideogram below.

VALUE (units 10^{-4})	EVTS	DOCUMENT ID	TECN	COMMENT
6.46±0.17±0.43	1435	EATON	84	MRK2 e^+e^-
3.8 ± 1.6	48	BESCH	81	BONA e^+e^-
5.5 ± 0.6	533	PERUZZI	78	MRK1 e^+e^-

Meson Particle Listings

$J/\psi(1S)$

WEIGHTED AVERAGE
6.0±0.5 (Error scaled by 1.3)



$\Gamma(p\bar{p}\pi^+\pi^-\pi^0)/\Gamma_{total}$ Γ_{96}/Γ

Including $p\bar{p}\pi^+\pi^-\gamma$ and excluding ω, η, η'
Error includes scale factor of 1.9.

VALUE (units 10^{-3})	EVTS	DOCUMENT ID	TECN	COMMENT
2.3 ± 0.9 OUR AVERAGE				
3.36 ± 0.65 ± 0.28	364	EATON 84	MRK2	e^+e^-
1.6 ± 0.6	39	PERUZZI 78	MRK1	e^+e^-

$\Gamma(p\bar{p}\eta)/\Gamma_{total}$ Γ_{97}/Γ

VALUE (units 10^{-3})	EVTS	DOCUMENT ID	TECN	COMMENT
2.00 ± 0.12 OUR AVERAGE				
1.91 ± 0.02 ± 0.17	13k	109 ABLIKIM 09	BES2	e^+e^-
2.03 ± 0.13 ± 0.15	826	EATON 84	MRK2	e^+e^-
2.5 ± 1.2		BRANDELIK 79c	DASP	e^+e^-
2.3 ± 0.4	197	PERUZZI 78	MRK1	e^+e^-

¹⁰⁹ From the combination of $p\bar{p}\eta \rightarrow p\bar{p}\gamma\gamma$ and $p\bar{p}\eta \rightarrow p\bar{p}\pi^+\pi^-\pi^0$ channels.

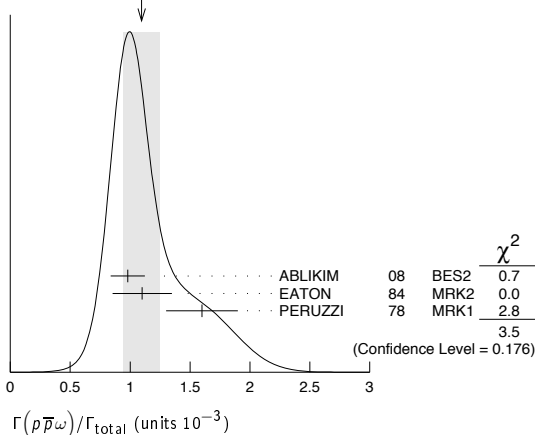
$\Gamma(p\bar{p}\rho)/\Gamma_{total}$ Γ_{98}/Γ

VALUE (units 10^{-3})	CL%	DOCUMENT ID	TECN	COMMENT
<0.31	90	EATON 84	MRK2	$e^+e^- \rightarrow \text{hadrons}\gamma$

$\Gamma(p\bar{p}\omega)/\Gamma_{total}$ Γ_{99}/Γ

VALUE (units 10^{-3})	EVTS	DOCUMENT ID	TECN	COMMENT
1.10 ± 0.15 OUR AVERAGE				Error includes scale factor of 1.3. See the ideogram below.
0.98 ± 0.03 ± 0.14	2449	ABLIKIM 08	BES2	e^+e^-
1.10 ± 0.17 ± 0.18	486	EATON 84	MRK2	e^+e^-
1.6 ± 0.3	77	PERUZZI 78	MRK1	e^+e^-

WEIGHTED AVERAGE
1.10±0.15 (Error scaled by 1.3)



$\Gamma(p\bar{p}\eta'(958))/\Gamma_{total}$ Γ_{100}/Γ

VALUE (units 10^{-3})	EVTS	DOCUMENT ID	TECN	COMMENT
0.21 ± 0.04 OUR AVERAGE				
0.200 ± 0.023 ± 0.028	265 ± 31	110 ABLIKIM 09	BES2	e^+e^-
0.68 ± 0.23 ± 0.17	19	EATON 84	MRK2	e^+e^-
1.8 ± 0.6	19	PERUZZI 78	MRK1	e^+e^-

¹¹⁰ From the combination of $p\bar{p}\eta' \rightarrow p\bar{p}\pi^+\pi^-\eta$ and $p\bar{p}\eta' \rightarrow p\bar{p}\gamma\rho^0$ channels.

$\Gamma(p\bar{p}\phi)/\Gamma_{total}$ Γ_{101}/Γ

VALUE (units 10^{-4})	DOCUMENT ID	TECN	COMMENT
0.45 ± 0.13 ± 0.07	FALVARD 88	DM2	$J/\psi \rightarrow \text{hadrons}$

$\Gamma(n\bar{n})/\Gamma_{total}$ Γ_{102}/Γ

VALUE (units 10^{-2})	EVTS	DOCUMENT ID	TECN	COMMENT
0.22 ± 0.04 OUR AVERAGE				
0.231 ± 0.049	79	BALDINI 98	FENI	e^+e^-
0.18 ± 0.09		BESCH 78	BONA	e^+e^-
• • • We do not use the following data for averages, fits, limits, etc. • • •				
0.190 ± 0.055	40	ANTONELLI 93	SPEC	e^+e^-

$\Gamma(n\bar{n}\pi^+\pi^-)/\Gamma_{total}$ Γ_{103}/Γ

VALUE (units 10^{-3})	EVTS	DOCUMENT ID	TECN	COMMENT
3.8 ± 3.6	5	BESCH 81	BONA	e^+e^-

$\Gamma(\Sigma^+\Sigma^-)/\Gamma_{total}$ Γ_{104}/Γ

VALUE (units 10^{-3})	EVTS	DOCUMENT ID	TECN	COMMENT
1.50 ± 0.10 ± 0.22	399	ABLIKIM 08o	BES2	$e^+e^- \rightarrow J/\psi$

$\Gamma(\Sigma^0\bar{\Sigma}^0)/\Gamma_{total}$ Γ_{105}/Γ

VALUE (units 10^{-3})	EVTS	DOCUMENT ID	TECN	COMMENT
1.29 ± 0.09 OUR AVERAGE				
1.15 ± 0.24 ± 0.03		111 AUBERT 07BD	BABR	10.6 $e^+e^- \rightarrow \Sigma^0\bar{\Sigma}^0\gamma$
1.33 ± 0.04 ± 0.11	1779	ABLIKIM 06	BES2	$J/\psi \rightarrow \Sigma^0\bar{\Sigma}^0$
1.06 ± 0.04 ± 0.23	884 ± 30	PALLIN 87	DM2	$e^+e^- \rightarrow \Sigma^0\bar{\Sigma}^0$
1.58 ± 0.16 ± 0.25	90	EATON 84	MRK2	$e^+e^- \rightarrow \Sigma^0\bar{\Sigma}^0$
1.3 ± 0.4	52	PERUZZI 78	MRK1	$e^+e^- \rightarrow \Sigma^0\bar{\Sigma}^0$
• • • We do not use the following data for averages, fits, limits, etc. • • •				
2.4 ± 2.6	3	BESCH 81	BONA	$e^+e^- \rightarrow \Sigma^+\Sigma^-$

¹¹¹ AUBERT 07BD reports $[\Gamma(J/\psi(1S) \rightarrow \Sigma^0\bar{\Sigma}^0)/\Gamma_{total}] \times [\Gamma(J/\psi(1S) \rightarrow e^+e^-)] = (6.4 \pm 1.2 \pm 0.6) \times 10^{-3}$ keV which we divide by our best value $\Gamma(J/\psi(1S) \rightarrow e^+e^-) = 5.55 \pm 0.14 \pm 0.02$ keV. Our first error is their experiment's error and our second error is the systematic error from using our best value.

$\Gamma(2(\pi^+\pi^-)K^+K^-)/\Gamma_{total}$ Γ_{106}/Γ

VALUE (units 10^{-4})	EVTS	DOCUMENT ID	TECN	COMMENT
47 ± 7 OUR AVERAGE				Error includes scale factor of 1.3.
49.8 ± 4.2 ± 3.4	205	112 AUBERT 06d	BABR	10.6 $e^+e^- \rightarrow \omega K^+ K^- 2(\pi^+\pi^-)\gamma$
31 ± 13	30	VANNUCCI 77	MRK1	e^+e^-
¹¹² Using $\Gamma(J/\psi \rightarrow e^+e^-) = 5.52 \pm 0.14 \pm 0.04$ keV.				

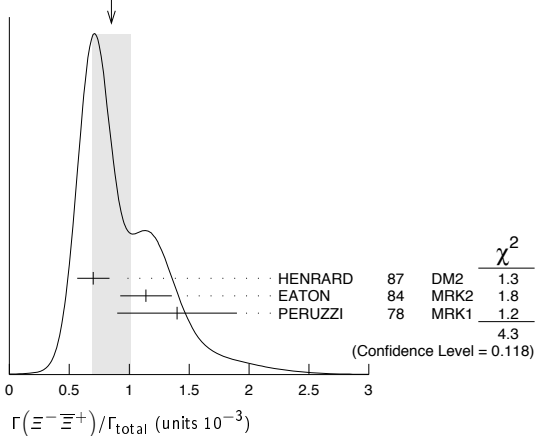
$\Gamma(p\bar{p}\pi^-)/\Gamma_{total}$ Γ_{107}/Γ

VALUE (units 10^{-3})	EVTS	DOCUMENT ID	TECN	COMMENT
2.12 ± 0.09 OUR AVERAGE				
2.36 ± 0.02 ± 0.21	59k	ABLIKIM 06k	BES2	$J/\psi \rightarrow p\pi^-\bar{n}$
2.47 ± 0.02 ± 0.24	55k	ABLIKIM 06k	BES2	$J/\psi \rightarrow \bar{p}\pi^+n$
2.02 ± 0.07 ± 0.16	1288	EATON 84	MRK2	$e^+e^- \rightarrow p\pi^-$
1.93 ± 0.07 ± 0.16	1191	EATON 84	MRK2	$e^+e^- \rightarrow \bar{p}\pi^+$
1.7 ± 0.7	32	BESCH 81	BONA	$e^+e^- \rightarrow p\pi^-$
1.6 ± 1.2	5	BESCH 81	BONA	$e^+e^- \rightarrow \bar{p}\pi^+$
2.16 ± 0.29	194	PERUZZI 78	MRK1	$e^+e^- \rightarrow p\pi^-$
2.04 ± 0.27	204	PERUZZI 78	MRK1	$e^+e^- \rightarrow \bar{p}\pi^+$

$\Gamma(\Xi^-\Xi^+)/\Gamma_{total}$ Γ_{111}/Γ

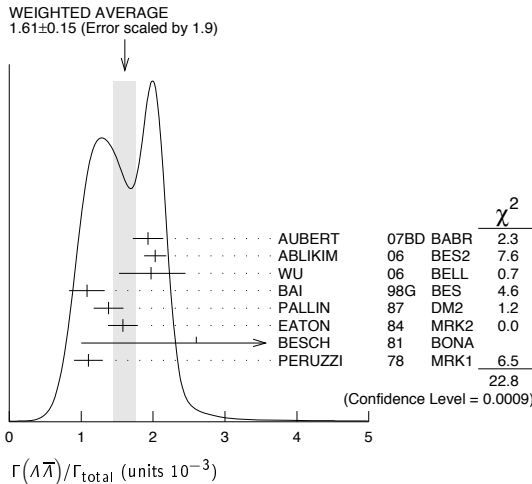
VALUE (units 10^{-3})	EVTS	DOCUMENT ID	TECN	COMMENT
0.85 ± 0.16 OUR AVERAGE				Error includes scale factor of 1.5. See the ideogram below.
0.70 ± 0.06 ± 0.12	132 ± 11	HENRARD 87	DM2	$e^+e^- \rightarrow \Xi^-\Xi^+$
1.14 ± 0.08 ± 0.20	194	EATON 84	MRK2	$e^+e^- \rightarrow \Xi^-\Xi^+$
1.4 ± 0.5	51	PERUZZI 78	MRK1	$e^+e^- \rightarrow \Xi^-\Xi^+$

WEIGHTED AVERAGE
0.85±0.16 (Error scaled by 1.5)



$\Gamma(\Lambda\bar{\Lambda})/\Gamma_{total}$				Γ_{112}/Γ
VALUE (units 10^{-3})	EVTS	DOCUMENT ID	TECN	COMMENT
1.61±0.15 OUR AVERAGE	Error includes scale factor of 1.9. See the ideogram below.			
1.93±0.21±0.05		113 AUBERT	07BD BABR	10.6 $e^+e^- \rightarrow \Lambda\bar{\Lambda}\gamma$
2.03±0.03±0.15	8887	ABLIKIM	06 BES2	$J/\psi \rightarrow \Lambda\bar{\Lambda}$
2.0 $^{+0.5}_{-0.4} \pm 0.1$	46	114 WU	06 BELL	$B^+ \rightarrow \Lambda\bar{\Lambda}K^+$
1.08±0.06±0.24	631	BAI	98G BES	e^+e^-
1.38±0.05±0.20	1847	PALLIN	87 DM2	e^+e^-
1.58±0.08±0.19	365	EATON	84 MRK2	e^+e^-
2.6±1.6	5	BESCH	81 BONA	e^+e^-
1.1±0.2	196	PERUZZI	78 MRK1	e^+e^-

- 113 AUBERT 07BD reports $[\Gamma(J/\psi(1S) \rightarrow \Lambda\bar{\Lambda})/\Gamma_{total}] \times [\Gamma(J/\psi(1S) \rightarrow e^+e^-)] = (10.7 \pm 0.9 \pm 0.7) \times 10^{-3}$ keV which we divide by our best value $\Gamma(J/\psi(1S) \rightarrow e^+e^-) = 5.55 \pm 0.14 \pm 0.02$ keV. Our first error is their experiment's error and our second error is the systematic error from using our best value.
- 114 WU 06 reports $[\Gamma(J/\psi(1S) \rightarrow \Lambda\bar{\Lambda})/\Gamma_{total}] \times [B(B^+ \rightarrow J/\psi(1S)K^+)] = (2.00^{+0.34}_{-0.29} \pm 0.34) \times 10^{-6}$ which we divide by our best value $B(B^+ \rightarrow J/\psi(1S)K^+) = (1.014 \pm 0.034) \times 10^{-3}$. Our first error is their experiment's error and our second error is the systematic error from using our best value.



$\Gamma(\Lambda\bar{\Lambda})/\Gamma(p\bar{p})$				Γ_{112}/Γ_{93}
VALUE	DOCUMENT ID	TECN	COMMENT	
0.90±0.15±0.10	115 WU	06 BELL	$B^+ \rightarrow p\bar{p}K^+, \Lambda\bar{\Lambda}K^+$	

115 Not independent of other $J/\psi \rightarrow \Lambda\bar{\Lambda}, p\bar{p}$ branching ratios reported by WU 06.

$\Gamma(\Lambda\bar{\Sigma}^- \pi^+ \text{ (or c.c.)})/\Gamma_{total}$				Γ_{113}/Γ
VALUE (units 10^{-3})	EVTS	DOCUMENT ID	TECN	COMMENT
0.83 ± 0.07 OUR AVERAGE	Error includes scale factor of 1.2.			
0.770±0.051±0.083	335	116 ABLIKIM	07H BES2	$e^+e^- \rightarrow \Lambda\bar{\Sigma}^+ \pi^-$
0.747±0.056±0.076	254	116 ABLIKIM	07H BES2	$e^+e^- \rightarrow \Lambda\bar{\Sigma}^- \pi^+$
0.90 ± 0.06 ± 0.16	225 ± 15	HENRARD	87 DM2	$e^+e^- \rightarrow \Lambda\bar{\Sigma}^+ \pi^-$
1.11 ± 0.06 ± 0.20	342 ± 18	HENRARD	87 DM2	$e^+e^- \rightarrow \Lambda\bar{\Sigma}^- \pi^+$
1.53 ± 0.17 ± 0.38	135	EATON	84 MRK2	$e^+e^- \rightarrow \Lambda\bar{\Sigma}^+ \pi^-$
1.38 ± 0.21 ± 0.35	118	EATON	84 MRK2	$e^+e^- \rightarrow \Lambda\bar{\Sigma}^- \pi^+$

$\Gamma(\rho K^- \bar{K}^-)/\Gamma_{total}$				Γ_{114}/Γ
VALUE (units 10^{-3})	EVTS	DOCUMENT ID	TECN	COMMENT
0.89±0.07±0.14	307	EATON	84 MRK2	e^+e^-

$\Gamma(2(K^+K^-))/\Gamma_{total}$				Γ_{115}/Γ
VALUE (units 10^{-3})	EVTS	DOCUMENT ID	TECN	COMMENT
0.76±0.09 OUR AVERAGE				
0.74±0.09±0.02	156 ± 15	117 AUBERT	07AK BABR	10.6 $e^+e^- \rightarrow 2(K^+K^-)\gamma$
1.4 $^{+0.5}_{-0.4} \pm 0.2$	11.0 $^{+4.3}_{-3.5}$	118 HUANG	03 BELL	$B^+ \rightarrow 2(K^+K^-)K^+$

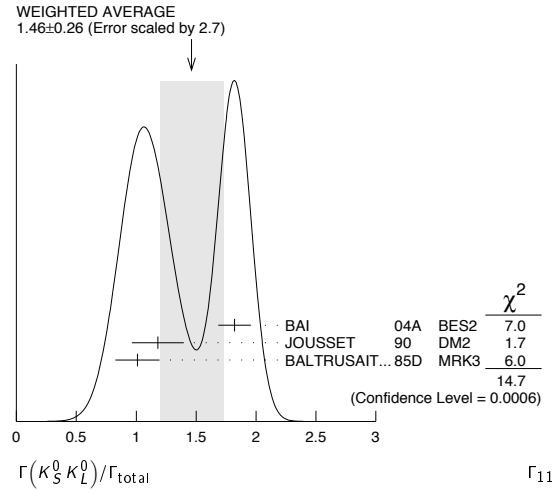
- 117 AUBERT 07AK reports $[\Gamma(J/\psi(1S) \rightarrow 2(K^+K^-))/\Gamma_{total}] \times [\Gamma(J/\psi(1S) \rightarrow e^+e^-)] = (4.11 \pm 0.39 \pm 0.30) \times 10^{-3}$ keV which we divide by our best value $\Gamma(J/\psi(1S) \rightarrow e^+e^-) = 5.55 \pm 0.14 \pm 0.02$ keV. Our first error is their experiment's error and our second error is the systematic error from using our best value.
- 118 Using $B(B^+ \rightarrow J/\psi K^+) = (1.01 \pm 0.05) \times 10^{-3}$.
- 119 Superseded by AUBERT 07AK. AUBERT 05D reports $[\Gamma(J/\psi(1S) \rightarrow 2(K^+K^-))/\Gamma_{total}] \times [\Gamma(J/\psi(1S) \rightarrow e^+e^-)] = (4.0 \pm 0.7 \pm 0.6) \times 10^{-3}$ keV which we divide by our best value $\Gamma(J/\psi(1S) \rightarrow e^+e^-) = 5.55 \pm 0.14 \pm 0.02$ keV. Our first error is their experiment's error and our second error is the systematic error from using our best value.

$\Gamma(\rho K^- \bar{K}^0)/\Gamma_{total}$				Γ_{116}/Γ
VALUE (units 10^{-3})	EVTS	DOCUMENT ID	TECN	COMMENT
0.29±0.06±0.05	90	EATON	84 MRK2	e^+e^-

$\Gamma(K^+K^-)/\Gamma_{total}$				Γ_{117}/Γ
VALUE (units 10^{-4})	EVTS	DOCUMENT ID	TECN	COMMENT
2.37±0.31 OUR AVERAGE				
2.39±0.24±0.22	107	BALTRUSAIT...85D	MRK3	e^+e^-
2.2 ± 0.9	6	BRANDELIK	79C DASP	e^+e^-

$\Gamma(K_S^0 K_L^0)/\Gamma_{total}$				Γ_{118}/Γ
VALUE (units 10^{-4})	EVTS	DOCUMENT ID	TECN	COMMENT
1.46±0.26 OUR AVERAGE	Error includes scale factor of 2.7. See the ideogram below.			
1.82±0.04±0.13	2155 ± 45	120 BAI	04A BES2	$J/\psi \rightarrow K_S^0 K_L^0 \rightarrow \pi^+\pi^-X$
1.18±0.12±0.18		JOUSSET	90 DM2	$J/\psi \rightarrow \text{hadrons}$
1.01±0.16±0.09	74	BALTRUSAIT...85D	MRK3	e^+e^-

120 Using $B(K_S^0 \rightarrow \pi^+\pi^-) = 0.6868 \pm 0.0027$.



$\Gamma(\Lambda\bar{\eta})/\Gamma_{total}$				Γ_{119}/Γ
VALUE (units 10^{-4})	EVTS	DOCUMENT ID	TECN	COMMENT
2.62±0.60±0.44	44	121 ABLIKIM	07H BES2	$e^+e^- \rightarrow \psi(2S)$

121 Using $B(\Lambda \rightarrow \pi^-p) = 63.9\%$ and $B(\eta \rightarrow \gamma\gamma) = 39.4\%$.

$\Gamma(\Lambda\bar{\Lambda} \pi^0)/\Gamma_{total}$				Γ_{120}/Γ	
VALUE (units 10^{-4})	CL%	EVTS	DOCUMENT ID	TECN	COMMENT
<0.64		90	122 ABLIKIM	07H BES2	$e^+e^- \rightarrow \psi(2S)$
••• We do not use the following data for averages, fits, limits, etc. •••					
2.3 ± 0.7 ± 0.8		11	BAI	98G BES	e^+e^-
2.2 ± 0.5 ± 0.5		19 ± 4	HENRARD	87 DM2	e^+e^-

122 Using $B(\Lambda \rightarrow \pi^-p) = 63.9\%$.

$\Gamma(\bar{\Lambda} n K_S^0 + \text{C.C.})/\Gamma_{total}$				Γ_{121}/Γ
VALUE (units 10^{-4})	EVTS	DOCUMENT ID	TECN	COMMENT
6.46±0.20±1.07	1058	123 ABLIKIM	08C BES2	$e^+e^- \rightarrow J/\psi$

123 Using $B(\bar{\Lambda} \rightarrow \bar{p}\pi^+) = 63.9\%$ and $B(K_S^0 \rightarrow \pi^+\pi^-) = 69.2\%$.

$\Gamma(\pi^+\pi^-)/\Gamma_{total}$				Γ_{122}/Γ
VALUE (units 10^{-4})	EVTS	DOCUMENT ID	TECN	COMMENT
1.47±0.23 OUR AVERAGE				
1.58±0.20±0.15	84	BALTRUSAIT...85D	MRK3	e^+e^-
1.0 ± 0.5	5	BRANDELIK	78B DASP	e^+e^-
1.6 ± 1.6	1	VANNUCCI	77 MRK1	e^+e^-

$\Gamma(\Lambda\bar{\Sigma} + \text{c.c.})/\Gamma_{total}$				Γ_{123}/Γ	
VALUE (units 10^{-3})	CL%	DOCUMENT ID	TECN	COMMENT	
<0.15		90	PERUZZI	78 MRK1	$e^+e^- \rightarrow \Lambda X$

$\Gamma(K_S^0 K_S^0)/\Gamma_{total}$				Γ_{124}/Γ	
VALUE (units 10^{-4})	CL%	DOCUMENT ID	TECN	COMMENT	
<0.01		95	124 BAI	04D BES	e^+e^-
••• We do not use the following data for averages, fits, limits, etc. •••					
<0.052		90	124 BALTRUSAIT...85C	MRK3	e^+e^-

124 Forbidden by CP.

Meson Particle Listings

J/ψ(1S)

RADIATIVE DECAYS

Γ(3γ)/Γ _{total}					Γ ₁₂₅ /Γ	
VALUE (units 10 ⁻⁶)	CL%	EVTS	DOCUMENT ID	TECN	COMMENT	
12 ± 3 ± 2		24.2 ^{+7.2} _{-6.0}	ADAMS	08	CLEO	ψ(2S) → π ⁺ π ⁻ J/ψ
<55	90		PARTRIDGE	80	CBAL	e ⁺ e ⁻

• • • We do not use the following data for averages, fits, limits, etc. • • •

Γ(4γ)/Γ _{total}					Γ ₁₂₆ /Γ	
VALUE (units 10 ⁻⁶)	CL%	EVTS	DOCUMENT ID	TECN	COMMENT	
<9	90		ADAMS	08	CLEO	ψ(2S) → π ⁺ π ⁻ J/ψ

Γ(5γ)/Γ _{total}					Γ ₁₂₇ /Γ	
VALUE (units 10 ⁻⁶)	CL%	EVTS	DOCUMENT ID	TECN	COMMENT	
<15	90		ADAMS	08	CLEO	ψ(2S) → π ⁺ π ⁻ J/ψ

Γ(γη _c (1S))/Γ _{total}					Γ ₁₂₈ /Γ	
VALUE (units 10 ⁻²)	CL%	EVTS	DOCUMENT ID	TECN	COMMENT	
1.7 ± 0.4 OUR AVERAGE						Error includes scale factor of 1.6.
2.07 ± 0.32 ± 0.03			125 MITCHELL	09	CLEO	e ⁺ e ⁻ → γX
1.27 ± 0.36			GAISER	86	CBAL	J/ψ → γX
0.79 ± 0.20		273 ± 43	126 AUBERT	06E	BABR	B [±] → K [±] X _c π
seen		16	BALTRUSAIT...84	MRK3	J/ψ	→ 2φγ

• • • We do not use the following data for averages, fits, limits, etc. • • •

125 MITCHELL 09 reports (1.98 ± 0.09 ± 0.30) × 10⁻² from a measurement of [Γ(J/ψ(1S) → γη_c(1S))/Γ_{total}] × [B(ψ(2S) → J/ψ(1S)π⁺π⁻)] assuming B(ψ(2S) → J/ψ(1S)π⁺π⁻) = (35.04 ± 0.07 ± 0.77) × 10⁻², which we rescale to our best value B(ψ(2S) → J/ψ(1S)π⁺π⁻) = (33.6 ± 0.4) × 10⁻². Our first error is their experiment's error and our second error is the systematic error from using our best value.

126 Calculated by the authors using an average of B(J/ψ → γη_c) × B(η_c → K \bar{K} π) from BALTRUSAITIS 86, BISELLO 91, BAI 04 and B(η_c → K \bar{K} π) = (8.5 ± 1.8)% from AUBERT 06E.

Γ(γη _c (1S) → 3γ)/Γ _{total}					Γ ₁₂₉ /Γ	
VALUE (units 10 ⁻⁶)	CL%	EVTS	DOCUMENT ID	TECN	COMMENT	
1.2 ± 2.7 ± 0.3		1.2 ^{+2.8} _{-1.1}	ADAMS	08	CLEO	ψ(2S) → π ⁺ π ⁻ J/ψ

Γ(γπ ⁺ π ⁻ 2π ⁰)/Γ _{total}					Γ ₁₃₀ /Γ	
VALUE (units 10 ⁻³)	CL%	EVTS	DOCUMENT ID	TECN	COMMENT	
8.3 ± 0.2 ± 3.1			127 BALTRUSAIT...86B	MRK3	J/ψ → 4πγ	
						127 4π mass less than 2.0 GeV.

Γ(γηππ)/Γ _{total}					Γ ₁₃₁ /Γ	
VALUE (units 10 ⁻³)	CL%	EVTS	DOCUMENT ID	TECN	COMMENT	
6.1 ± 1.0 OUR AVERAGE						
5.85 ± 0.3 ± 1.05			128 EDWARDS	83B	CBAL	J/ψ → ηπ ⁺ π ⁻
7.8 ± 1.2 ± 2.4			128 EDWARDS	83B	CBAL	J/ψ → η2π ⁰
						128 Broad enhancement at 1700 MeV.

Γ(γη ₂ (1870) → γηπ ⁺ π ⁻)/Γ _{total}					Γ ₁₃₂ /Γ	
VALUE (units 10 ⁻⁴)	CL%	EVTS	DOCUMENT ID	TECN	COMMENT	
6.2 ± 2.2 ± 0.9			BAI	99	BES	J/ψ → γηπ ⁺ π ⁻

Γ(γη(1405/1475) → γK \bar{K} π)/Γ _{total}					Γ ₁₃₃ /Γ	
VALUE (units 10 ⁻³)	CL%	EVTS	DOCUMENT ID	TECN	COMMENT	
2.8 ± 0.6 OUR AVERAGE						Error includes scale factor of 1.6. See the ideogram below.
1.66 ± 0.1 ± 0.58			129,130 BAI	00D	BES	J/ψ → γK [±] K ⁰ _S π [∓]
3.8 ± 0.3 ± 0.6			131 AUGUSTIN	90	DM2	J/ψ → γK \bar{K} π
4.0 ± 0.7 ± 1.0			131 EDWARDS	82E	CBAL	J/ψ → K ⁺ K ⁻ π ⁰ γ
4.3 ± 1.7			131,132 SCHARRE	80	MRK2	e ⁺ e ⁻
						• • • We do not use the following data for averages, fits, limits, etc. • • •
1.78 ± 0.21 ± 0.33			131,133,134 AUGUSTIN	92	DM2	J/ψ → γK \bar{K} π
0.83 ± 0.13 ± 0.18			131,135,136 AUGUSTIN	92	DM2	J/ψ → γK \bar{K} π
0.66 ^{+0.17+0.24} _{-0.16-0.15}			131,134,137 BAI	90C	MRK3	J/ψ → γK ⁰ _S K [±] π [∓]
1.03 ^{+0.21+0.26} _{-0.18-0.19}			131,136,138 BAI	90C	MRK3	J/ψ → γK ⁰ _S K [±] π [∓]

129 Interference with the J/ψ(1S) radiative transition to the broad K \bar{K} π pseudoscalar state around 1800 is (0.15 ± 0.01 ± 0.05) × 10⁻³.

130 Interference with J/ψ → γf₁(1420) is (-0.03 ± 0.01 ± 0.01) × 10⁻³.

131 Includes unknown branching fraction η(1405) → K \bar{K} π.

132 Corrected for spin-zero hypothesis for η(1405).

133 From fit to the a₀(980)π⁰ ⁺ partial wave.

134 a₀(980)π mode.

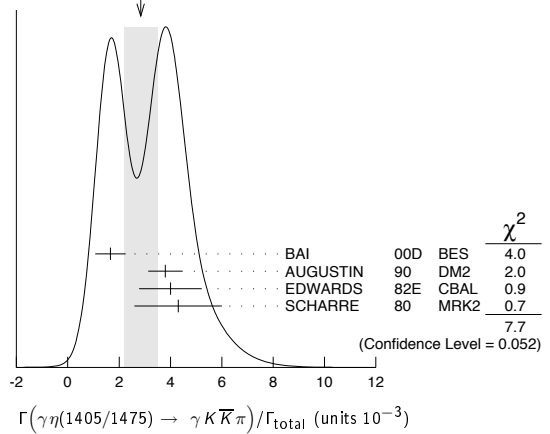
135 From fit to the K*(892)K⁰ ⁺ partial wave.

136 K* \bar{K} mode.

137 From a₀(980)π final state.

138 From K*(890)K final state.

WEIGHTED AVERAGE
2.8±0.6 (Error scaled by 1.6)



Γ(γη(1405/1475) → γγρ ⁰)/Γ _{total}					Γ ₁₃₄ /Γ	
VALUE (units 10 ⁻⁴)	CL%	EVTS	DOCUMENT ID	TECN	COMMENT	
0.78 ± 0.20 OUR AVERAGE						Error includes scale factor of 1.8.
1.07 ± 0.17 ± 0.11			139 BAI	04J	BES2	J/ψ → γγπ ⁺ π ⁻
0.64 ± 0.12 ± 0.07			139 COFFMAN	90	MRK3	J/ψ → γγπ ⁺ π ⁻
						139 Includes unknown branching fraction η(1405) → γρ ⁰ .

Γ(γη(1405/1475) → γηπ ⁺ π ⁻)/Γ _{total}					Γ ₁₃₅ /Γ	
VALUE (units 10 ⁻⁴)	CL%	EVTS	DOCUMENT ID	TECN	COMMENT	
3.0 ± 0.5 OUR AVERAGE						
2.6 ± 0.7 ± 0.4			BAI	99	BES	J/ψ → γηπ ⁺ π ⁻
3.38 ± 0.33 ± 0.64			140 BOLTON	92B	MRK3	J/ψ → γηπ ⁺ π ⁻
						• • • We do not use the following data for averages, fits, limits, etc. • • •
7.0 ± 0.6 ± 1.1		261	141 AUGUSTIN	90	DM2	J/ψ → γηπ ⁺ π ⁻
						140 Via a ₀ (980)π.
						141 Includes unknown branching fraction to ηπ ⁺ π ⁻ .

Γ(γη(1405/1475) → γγφ)/Γ _{total}					Γ ₁₃₆ /Γ	
VALUE (units 10 ⁻⁴)	CL%	EVTS	DOCUMENT ID	TECN	COMMENT	
<0.82	95		BAI	04J	BES2	J/ψ → γγK ⁺ K ⁻

Γ(γγρ)/Γ _{total}					Γ ₁₃₇ /Γ	
VALUE (units 10 ⁻³)	CL%	EVTS	DOCUMENT ID	TECN	COMMENT	
4.5 ± 0.8 OUR AVERAGE						
4.7 ± 0.3 ± 0.9			142 BALTRUSAIT...86B	MRK3	J/ψ → 4πγ	
3.75 ± 1.05 ± 1.20			143 BURKE	82	MRK2	J/ψ → 4πγ
						• • • We do not use the following data for averages, fits, limits, etc. • • •
<0.09	90		144 BISELLO	89B		J/ψ → 4πγ
						142 4π mass less than 2.0 GeV.
						143 4π mass less than 2.0 GeV. We have multiplied 2ρ ⁰ measurement by 3 to obtain 2ρ.
						144 4π mass in the range 2.0–25 GeV.

Γ(γρω)/Γ _{total}					Γ ₁₃₈ /Γ	
VALUE (units 10 ⁻⁴)	CL%	EVTS	DOCUMENT ID	TECN	COMMENT	
<5.4	90		ABLIKIM	08A	BES2	e ⁺ e ⁻ → J/ψ

Γ(γγφ)/Γ _{total}					Γ ₁₃₉ /Γ	
VALUE (units 10 ⁻⁵)	CL%	EVTS	DOCUMENT ID	TECN	COMMENT	
<8.8	90		ABLIKIM	08A	BES2	e ⁺ e ⁻ → J/ψ

Γ(η'(958))/Γ _{total}					Γ ₁₄₀ /Γ	
VALUE (units 10 ⁻³)	CL%	EVTS	DOCUMENT ID	TECN	COMMENT	
5.28 ± 0.15 OUR AVERAGE						
5.24 ± 0.12 ± 0.11			PEDLAR	09	CLE3	J/ψ → η'γ
5.55 ± 0.44		35k	ABLIKIM	06E	BES2	J/ψ → η'γ
						• • • We do not use the following data for averages, fits, limits, etc. • • •
4.50 ± 0.14 ± 0.53			BOLTON	92B	MRK3	J/ψ → γπ ⁺ π ⁻ η, η → γγ
4.30 ± 0.31 ± 0.71			BOLTON	92B	MRK3	J/ψ → γπ ⁺ π ⁻ η, η → π ⁺ π ⁻ π ⁰
4.04 ± 0.16 ± 0.85		622	AUGUSTIN	90	DM2	J/ψ → γηπ ⁺ π ⁻
4.39 ± 0.09 ± 0.66		2420	AUGUSTIN	90	DM2	J/ψ → γγπ ⁺ π ⁻
4.1 ± 0.3 ± 0.6			BLOOM	83	CBAL	e ⁺ e ⁻ → 3γ + hadrons
2.9 ± 1.1		6	BRANDELIK	79C	DASP	e ⁺ e ⁻ → 3γ
2.4 ± 0.7		57	BARTEL	76	CNTR	e ⁺ e ⁻ → 2γγ

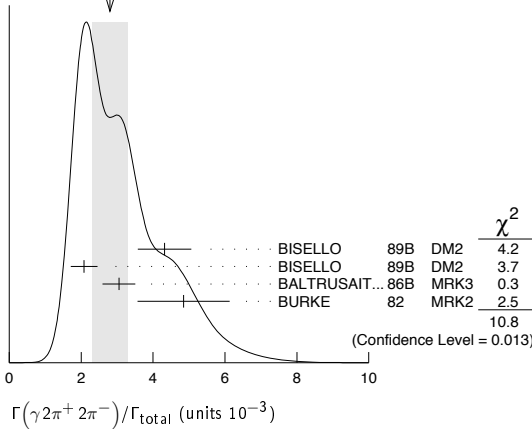
See key on page 405

Meson Particle Listings

J/ψ(1S)

Table with 4 columns: VALUE (units 10^-3), DOCUMENT ID, TECN, COMMENT. Title: Γ(γ2π+2π-)/Γtotal Γ141/Γ. Includes 'OUR AVERAGE' and error notes.

WEIGHTED AVERAGE 2.8±0.5 (Error scaled by 1.9)



- 152 ABLIKIM 06v reports [Γ(J/ψ(1S) → γf2(1270))/Γtotal] × [B(f2(1270) → ππ)] = ...
- 153 ABLIKIM 06v reports [Γ(J/ψ(1S) → γf2(1270))/Γtotal] × [B(f2(1270) → ππ)] = ...
- 154 Estimated using B(f2(1270) → ππ)=0.843 ± 0.012. The errors do not contain the uncertainty in the f2(1270) decay.
- 155 Restated by us to take account of spread of E1, M2, E3 transitions.

Table with 5 columns: VALUE (units 10^-4), CL%, DOCUMENT ID, TECN, COMMENT. Title: Γ(γf0(1710) → γK K̄)/Γtotal Γ149/Γ. Includes 'OUR AVERAGE' and error notes.

- We do not use the following data for averages, fits, limits, etc. •••
- 156 Includes unknown branching ratio to K+K- or KS0KS0.
- 157 Assuming JP = 2+ for f0(1710).
- 158 Includes unknown branching fraction to K+K- or KS0KS0. We have multiplied K+K- measurement by 2, and KS0KS0 by 4 to obtain KK̄ result.
- 159 Assuming JP = 0+ for f0(1710).
- 160 Includes unknown branching fraction to ρ0ρ0.
- 161 Includes unknown branching fraction to π+π-.
- 162 Includes unknown branching fraction to ηη.

Table with 5 columns: VALUE (units 10^-4), EVTS, DOCUMENT ID, TECN, COMMENT. Title: Γ(γf2(1270) f2(1270))/Γtotal Γ142/Γ.

Table with 4 columns: VALUE (units 10^-4), DOCUMENT ID, TECN, COMMENT. Title: Γ(γf2(1270) f2(1270) (non resonant))/Γtotal Γ143/Γ.

Table with 5 columns: VALUE (units 10^-3), EVTS, DOCUMENT ID, TECN, COMMENT. Title: Γ(γK+K-π+π-)/Γtotal Γ144/Γ.

Table with 4 columns: VALUE (units 10^-3), DOCUMENT ID, TECN, COMMENT. Title: Γ(γf4(2050))/Γtotal Γ145/Γ.

Table with 5 columns: VALUE (units 10^-3), EVTS, DOCUMENT ID, TECN, COMMENT. Title: Γ(γωω)/Γtotal Γ146/Γ.

Table with 4 columns: VALUE (units 10^-3), DOCUMENT ID, TECN, COMMENT. Title: Γ(γη(1405/1475) → γρ0ρ0)/Γtotal Γ147/Γ.

Table with 5 columns: VALUE (units 10^-3), EVTS, DOCUMENT ID, TECN, COMMENT. Title: Γ(γf2(1270))/Γtotal Γ148/Γ.

Table with 4 columns: VALUE (units 10^-4), DOCUMENT ID, TECN, COMMENT. Title: Γ(γf0(1710) → γππ)/Γtotal Γ150/Γ.

Table with 5 columns: VALUE (units 10^-3), EVTS, DOCUMENT ID, TECN, COMMENT. Title: Γ(γf0(1710) → γωω)/Γtotal Γ151/Γ.

Table with 5 columns: VALUE (units 10^-3), EVTS, DOCUMENT ID, TECN, COMMENT. Title: Γ(γη)/Γtotal Γ152/Γ.

Table with 4 columns: VALUE (units 10^-3), DOCUMENT ID, TECN, COMMENT. Title: Γ(γf1(1420) → γK K̄π)/Γtotal Γ153/Γ.

Table with 5 columns: VALUE (units 10^-3), DOCUMENT ID, TECN, COMMENT. Title: Γ(γf1(1285))/Γtotal Γ154/Γ.

See key on page 405

Meson Particle Listings

J/ψ(1S)

Table with columns: Γ(γfj(2220))/Γtotal, CL%, EVTS, DOCUMENT ID, TECN, COMMENT, Γ172/Γ. Includes data for HASAN, BAI, AUGUSTIN, BALTRUSAIT..86D.

186 Using BAI 96B.
187 Using BARNES 93.
188 Includes unknown branching fraction to K+K- or K_S^0 K_S^0.

Table with columns: Γ(γfj(2220) → γππ)/Γtotal, DOCUMENT ID, TECN, COMMENT, Γ173/Γ. Includes data for BAI 96B BES, BAI 98H BES.

Table with columns: Γ(γfj(2220) → γK K̄)/Γtotal, DOCUMENT ID, TECN, COMMENT, Γ174/Γ. Includes data for BAI 96B BES.

Table with columns: Γ(γfj(2220) → γρρ̄)/Γtotal, DOCUMENT ID, TECN, COMMENT, Γ175/Γ. Includes data for BAI 96B BES.

Table with columns: Γ(γf0(1500))/Γtotal, DOCUMENT ID, TECN, COMMENT, Γ176/Γ. Includes data for ABLIKIM 06v BES2, ABLIKIM 06v BES2, BUGG 95 MRK3.

Table with columns: Γ(γe+e-)/Γtotal, DOCUMENT ID, TECN, COMMENT, Γ177/Γ. Includes data for ARMSTRONG 96 E760.

WEAK DECAYS

Table with columns: Γ(D- e+ νe + c.c.)/Γtotal, DOCUMENT ID, TECN, COMMENT, Γ178/Γ. Includes data for ABLIKIM 06M BES2.

Table with columns: Γ(D̄0 e+ e- + c.c.)/Γtotal, DOCUMENT ID, TECN, COMMENT, Γ179/Γ. Includes data for ABLIKIM 06M BES2.

Table with columns: Γ(D_s- e+ νe + c.c.)/Γtotal, DOCUMENT ID, TECN, COMMENT, Γ180/Γ. Includes data for ABLIKIM 06M BES2.

Table with columns: Γ(D- π+ + c.c.)/Γtotal, DOCUMENT ID, TECN, COMMENT, Γ181/Γ. Includes data for ABLIKIM 08J BES2.

Table with columns: Γ(D̄0 K̄0 + c.c.)/Γtotal, DOCUMENT ID, TECN, COMMENT, Γ182/Γ. Includes data for ABLIKIM 08J BES2.

Table with columns: Γ(D_s- π+ + c.c.)/Γtotal, DOCUMENT ID, TECN, COMMENT, Γ183/Γ. Includes data for ABLIKIM 08J BES2.

Table with columns: Γ(γγ)/Γtotal, CL%, DOCUMENT ID, TECN, COMMENT, Γ184/Γ. Includes data for ADAMS 08 CLEO, WICHT 08 BELL, ABLIKIM 07J BES2, BARTEL 77 CNTR.

LEPTON FAMILY NUMBER (LF) VIOLATING MODES

Table with columns: Γ(e± μ∓)/Γtotal, CL%, DOCUMENT ID, TECN, COMMENT, Γ185/Γ. Includes data for BAI 03D BES.

Table with columns: Γ(e± τ∓)/Γtotal, CL%, DOCUMENT ID, TECN, COMMENT, Γ186/Γ. Includes data for ABLIKIM 04 BES.

Table with columns: Γ(μ± τ∓)/Γtotal, CL%, DOCUMENT ID, TECN, COMMENT, Γ187/Γ. Includes data for ABLIKIM 04 BES.

OTHER DECAYS

Table with columns: Γ(invisible)/Γ(μ+ μ-), CL%, DOCUMENT ID, TECN, COMMENT, Γ188/Γ6. Includes data for ABLIKIM 08G BES2.

J/ψ(1S) REFERENCES

List of references for J/ψ(1S) decays, including authors like Anashin, ABLIKIM, MITCHELL, PEDLAR, SHEN, AUBERT, BESSON, WICHT, ANDREOTTI, AUBERT, ABLIKIM, ADAMS, AUBERT, WU, ABLIKIM, LI, SIBIRTSSEV, AULCHENKO, HUANG, ARTAMONOV, and various collaborations like BABAR, Belle, CLEO, and BES.

Meson Particle Listings

 $J/\psi(1S)$, Branching Ratios of ψ 's and χ 's

BAI	99C	PRL 83 1918	J.Z. Bai et al.	(BES Collab.)
BAI	98D	PR D58 092006	J.Z. Bai et al.	(BES Collab.)
BAI	98G	PL B424 213	J.Z. Bai et al.	(BES Collab.)
BAI	98H	PRL 81 1179	J.Z. Bai et al.	(BES Collab.)
BALDINI	98	PL B444 111	R. Baldini et al.	(FENICE Collab.)
ARMSTRONG	96	PR D54 7067	T.A. Armstrong et al.	(E760 Collab.)
BAI	96B	PRL 76 3502	J.Z. Bai et al.	(BES Collab.)
BAI	96C	PRL 77 3959	J.Z. Bai et al.	(BES Collab.)
BAI	96D	PR D54 1221	J.Z. Bai et al.	(BES Collab.)
GRIEBUSHIN	96	PR D53 4723	A. Griebushin et al.	(E672 Collab.)
HASAN	96	PL B388 376	A. Hasan, D.V. Bugg	(BRUN, LOQM)
BAI	95B	PL B355 374	J.Z. Bai et al.	(BES Collab.)
BUGG	95	PL B353 378	D.V. Bugg et al.	(LOQM, PNPI, WASH)
ANTONELLI	93	PL B301 317	A. Antonelli et al.	(FENICE Collab.)
ARMSTRONG	93B	PR D47 772	T.A. Armstrong et al.	(FNAL E760 Collab.)
BARNES	93	PL B309 469	P.D. Barnes et al.	(PS185 Collab.)
AUGUSTIN	92	PR D46 1951	J.E. Augustin, G. Cosme	(DM2 Collab.)
BOLTON	92	PL B278 495	T. Bolton et al.	(Mark III Collab.)
BOLTON	92B	PRL 69 1328	T. Bolton et al.	(Mark III Collab.)
COFFMAN	92	PRL 68 282	D.M. Coffman et al.	(Mark III Collab.)
HSUEH	92	PR D45 R2181	S. Hsueh, S. Palestini	(FNAL, TORI)
BISELLO	91	NP B350 1	D. Bisello et al.	(DM2 Collab.)
AUGUSTIN	90	PR D42 10	J.E. Augustin et al.	(DM2 Collab.)
BAI	90B	PRL 65 1309	Z. Bai et al.	(Mark III Collab.)
BAI	90C	PRL 65 2507	Z. Bai et al.	(Mark III Collab.)
BISELLO	90	PL B241 617	D. Bisello et al.	(DM2 Collab.)
COFFMAN	90	PR D41 1410	D.M. Coffman et al.	(Mark III Collab.)
JOUSSET	90	PR D41 1389	J. Jousset et al.	(DM2 Collab.)
ALEXANDER	89	NP B320 45	J.E. Alexander et al.	(LBL, MICH, SLAC)
AUGUSTIN	89	NP B320 1	J.E. Augustin, G. Cosme	(DM2 Collab.)
BISELLO	89B	PR D39 701	G. Busetto et al.	(DM2 Collab.)
AUGUSTIN	88	PRL 60 2238	J.E. Augustin et al.	(DM2 Collab.)
COFFMAN	88	PR D38 2695	D.M. Coffman et al.	(Mark III Collab.)
FALVARD	88	PR D38 2706	A. Falvard et al.	(CLER, FRAS, LALO+)
AUGUSTIN	87	ZPHY C36 369	J.E. Augustin et al.	(LALO, CLER, FRAS+)
BAGLIN	87	NP B286 592	C. Baglin et al.	(LAPP, CERN, GENO, LYON+)
BALTRUSAITIS...	87	PR D35 2077	R.M. Baltrusaitis et al.	(Mark III Collab.)
BECKER	87	PRL 59 186	J.J. Becker et al.	(Mark III Collab.)
BISELLO	87	PL B192 239	D. Bisello et al.	(PADO, CLER, FRAS+)
COHEN	87	RMP 59 1121	E.R. Cohen, B.N. Taylor	(RIS, NBS)
HENRARD	87	NP B292 670	P. Henrard et al.	(CLER, FRAS, LALO+)
PALLIN	87	NP B292 653	D. Pallin et al.	(CLER, FRAS, LALO, PADO)
BALTRUSAITIS...	86	PR D33 629	R.M. Baltrusaitis et al.	(DM2 Collab.)
BALTRUSAITIS...	86B	PR D33 1222	R.M. Baltrusaitis et al.	(Mark III Collab.)
BALTRUSAITIS...	86D	PRL 56 107	R.M. Baltrusaitis et al.	(CIT, UCSC, ILL, SLAC+)
BISELLO	86B	PL B179 294	D. Bisello et al.	(DM2 Collab.)
GAISER	86	PR D34 711	J. Gaiser et al.	(Crystal Ball Collab.)
BALTRUSAITIS...	85C	PRL 55 1723	R.M. Baltrusaitis et al.	(CIT, UCSC+)
BALTRUSAITIS...	85D	PR D32 566	R.M. Baltrusaitis et al.	(CIT, UCSC+)
KURAEV	85	SJNP 41 466	E.A. Kurayev, V.S. Fadin	(NOVO)
BALTRUSAITIS...	84	Translated from YAF 41 733	R.M. Baltrusaitis et al.	(CIT, UCSC+)
EATON	84	PRL 52 2126	G.M. Eaton et al.	(LBL, SLAC)
BLOOM	83	ARNS 33 143	M.W. Eaton et al.	(SLAC, CIT)
EDWARDS	83B	PRL 51 859	C. Edwards et al.	(CIT, HARV, PRIN+)
FRANKLIN	83	PRL 51 963	M.E.B. Franklin et al.	(LBL, SLAC)
BURKE	82	PRL 49 632	D.L. Burke et al.	(LBL, SLAC)
EDWARDS	82B	PR D25 3065	C. Edwards et al.	(CIT, HARV, PRIN+)
EDWARDS	82D	PRL 48 458	C. Edwards et al.	(CIT, HARV, PRIN+)
Also		ARNS 33 143	E.D. Bloom, C. Peck	(SLAC, CIT)
EDWARDS	82E	PRL 49 259	C. Edwards et al.	(CIT, HARV, PRIN+)
LEMOIGNE	82	PL 113B 509	Y. Lemoigne et al.	(SACL, LOIC, SHMP+)
BESCH	81	ZPHY C9 1	H.J. Besch et al.	(BONN, DESY, MANZ)
GIDAL	81	PL 107B 153	H. Gidal et al.	(SL, LBL)
PARTRIDGE	80	PRL 44 712	R. Partridge et al.	(CIT, HARV, PRIN+)
SCHARRE	80	PL 97B 329	D.L. Scharre et al.	(SLAC, LBL)
ZHOLENTZ	80	PL 96B 214	A.A. Zholentz et al.	(NOVO)
Also		SJNP 34 814	A.A. Zholentz et al.	(NOVO)
Translated from YAF		34 1471	A.A. Zholentz et al.	
BRANDELIK	79C	ZPHY C1 233	R. Brandelik et al.	(DASP Collab.)
ALEXANDER	78	PL 72B 493	G. Alexander et al.	(DESY, HAMB, SIEG+)
BESCH	78	PL 78B 347	H.J. Besch et al.	(BONN, DESY, MANZ)
BRANDELIK	78B	PL 74B 292	R. Brandelik et al.	(DASP Collab.)
PERUZZI	78	PR D17 2901	I. Peruzzi et al.	(SLAC, LBL)
BARTEL	77	PL 66B 489	W. Bartel et al.	(DESY, HEIDP)
BURMESTER	77D	PL 72B 135	J. Burmester et al.	(DESY, HAMB, SIEG+)
FELDMAN	77	PRPL 33C 285	G.J. Feldman, M.L. Perl	(LBL, SLAC)
VANNUCCI	77	PR D15 1814	F. Vannucci et al.	(SLAC, LBL)
BARTEL	76	PL 64B 483	W. Bartel et al.	(DESY, HEIDP)
BRAUNSCH...	76	PL 63B 487	W. Braunschweig et al.	(DASP Collab.)
JEAN-MARIE	76	PRL 36 291	B. Jean-Marie et al.	(SLAC, LBL) IG
BALDINI...	75	PL 58B 471	R. Baldini-Celio et al.	(FRAS, ROMA)
BOYARSKI	75	PRL 34 1357	A.M. Boyarski et al.	(SLAC, LBL) JPC
DASP	75	PL 56B 493	W. Braunschweig et al.	(DASP Collab.)
ESPOSITO	75B	LNC 14 73	B. Esposito et al.	(FRAS, NAPL, PADO+)
FORD	75	PRL 34 604	R.L. Ford et al.	(SLAC, PENN)

BRANCHING RATIOS OF $\psi(2S)$ AND $\chi_{c0,1,2}$

Updated May 2010 by J.J. Hernández-Rey (IFIC, Valencia), S. Navas (University of Granada), and C. Patrignani (INFN, Genova).

Since 2002, the treatment of the branching ratios of the $\psi(2S)$ and $\chi_{c0,1,2}$ has undergone an important restructuring.

When measuring a branching ratio experimentally, it is not always possible to normalize the number of events observed in the corresponding decay mode to the total number of particles produced. Therefore, the experimenters sometimes report the number of observed decays with respect to another decay mode of the same or another particle in the relevant decay chain. This is actually equivalent to measuring combinations of branching fractions of several decay modes.

To extract the branching ratio of a given decay mode, the collaborations use some previously reported measurements of the required branching ratios. However, the values are frequently taken from the *Review of Particle Physics* (RPP), which in turn uses the branching ratio reported by the experiment in the following edition, giving rise either to correlations or to plain vicious circles [1,2] as discussed in more detail in earlier editions of this mini-review.

The way to avoid these dependencies and correlations is to extract the branching ratios through a fit that uses the truly measured combinations of branching fractions and partial widths. This fit, in fact, should involve decays from the four concerned particles, $\psi(2S)$, χ_{c0} , χ_{c1} , and χ_{c2} , and occasionally some combinations of branching ratios of more than one of them. This is what is done since the 2002 edition [3].

The PDG policy is to quote the results of the collaborations in a manner as close as possible to what appears in their original publications. However, in order to avoid the problems mentioned above, we had in some cases to work out the values originally measured, using the number of events and detection efficiencies given by the collaborations, or rescaling back the published results. The information was sometimes spread over several articles, and some articles referred to papers still unpublished, which in turn contained the relevant numbers in footnotes.

Even though the experimental collaborations are entitled to extract whatever branching ratios they consider appropriate by using other published results, we would like to encourage them to also quote explicitly in their articles the actual quantities measured, so that they can be used directly in averages and fits of different experimental determinations.

To inform the reader how we computed some of the values used in this edition of RPP, we use footnotes to indicate the branching ratios actually given by the experiments and the quantities they use to derive them from the true combination of branching ratios actually measured.

None of the branching ratios of the $\chi_{c0,1,2}$ are measured independently of the $\psi(2S)$ radiative decays. We tried to identify those branching ratios which can be correlated in a non-trivial way, and although we cannot preclude the existence of other cases, we are confident that the most relevant correlations have already been removed. Nevertheless, correlations in the errors of different quantities measured by the same experiment have not been taken into account.

FIT INFORMATION

This is an overall fit to 4 total widths, 1 partial width, 24 combinations of partial widths, 7 branching ratios, and 75 combinations of branching ratios. Of the latter 52 involve decays of more than one particle.

The overall fit uses 213 measurements to determine 47 parameters and has a χ^2 of 301.4 for 166 degrees of freedom.

The relatively high χ^2 of the fit, 1.8 per d.o.f., can be traced back to a few specific discrepancies in the data. No rescaling of errors has been applied.

Branching Ratios of ψ 's and χ 's, $\chi_{c0}(1P)$

In the listing we provide the correlation coefficients $\langle \delta x_i \delta x_j \rangle / (\delta x_i \cdot \delta x_j)$, in percent, from the fit to the corresponding parameter x_i .

References

1. Y.F. Gu and X.H. Li, Phys. Lett. **B449**, 361 (1999).
2. C. Patrignani, Phys. Rev. **D64**, 034017 (2001).
3. Particle Data Group, K.Hagiwara *et al.*, Phys. Rev. **D68**, 010001 (2002).

 $\chi_{c0}(1P)$

$$I^G(J^{PC}) = 0^+(0^{++})$$

 $\chi_{c0}(1P)$ MASS

VALUE (MeV)	EVTs	DOCUMENT ID	TECN	COMMENT
3414.75 ± 0.31 OUR AVERAGE				
3414.2 ± 0.5 ± 2.3	5.4k	UEHARA	08 BELL	$\gamma\gamma \rightarrow \chi_{c0} \rightarrow \text{hadrons}$
3406 ± 0.7 ± 6	230	1 ABE	07 BELL	$e^+e^- \rightarrow J/\psi(c\bar{c})$
3414.21 ± 0.39 ± 0.27		ABLIKIM	05G BES2	$\psi(2S) \rightarrow \gamma\chi_{c0}$
3414.7 ± 0.7 ± 0.2		2 ANDREOTTI	03 E835	$\bar{p}p \rightarrow \chi_{c0} \rightarrow \pi^0\pi^0$
3415.5 ± 0.4 ± 0.4	392	3 BAGNASCO	02 E835	$\bar{p}p \rightarrow \chi_{c0} \rightarrow J/\psi\gamma$
3417.4 ± 1.8 ± 0.2		2 AMBROGIANI	99B E835	$\bar{p}p \rightarrow e^+e^-\gamma$
3414.1 ± 0.6 ± 0.8		BAI	99B BES	$\psi(2S) \rightarrow \gamma X$
3417.8 ± 0.4 ± 4		2 GAISER	86 CBAL	$\psi(2S) \rightarrow \gamma X$
3416 ± 3 ± 4		4 TANENBAUM	78 MRK1	e^+e^-
• • • We do not use the following data for averages, fits, limits, etc. • • •				
3416.5 ± 3.0		EISENSTEIN	01 CLE2	$e^+e^- \rightarrow e^+e^-\chi_{c0}$
3422 ± 1.0		4 BARTEL	78B CNTR	$e^+e^- \rightarrow J/\psi 2\gamma$
3415 ± 9		4 BIDDICK	77 CNTR	$e^+e^- \rightarrow \gamma X$

¹ From a fit of the J/ψ recoil mass spectrum. Supersedes ABE,K 02 and ABE 04c.

² Using mass of $\psi(2S) = 3686.0$ MeV.

³ Recalculated by ANDREOTTI 05A, using the value of $\psi(2S)$ mass from AULCHENKO 03.

⁴ Mass value shifted by us by amount appropriate for $\psi(2S)$ mass = 3686 MeV and $J/\psi(1S)$ mass = 3097 MeV.

 $\chi_{c0}(1P)$ WIDTH

VALUE (MeV)	EVTs	DOCUMENT ID	TECN	COMMENT
10.3 ± 0.6 OUR FIT				
10.5 ± 0.8 OUR AVERAGE	Error			includes scale factor of 1.1.
10.6 ± 1.9 ± 2.6	5.4k	UEHARA	08 BELL	$\gamma\gamma \rightarrow \chi_{c0} \rightarrow \text{hadrons}$
12.6 ± 1.5 ± 0.9		ABLIKIM	05G BES2	$\psi(2S) \rightarrow \gamma\chi_{c0}$
8.6 ± 1.7 ± 0.1		ANDREOTTI	03 E835	$\bar{p}p \rightarrow \chi_{c0} \rightarrow \pi^0\pi^0$
9.7 ± 1.0	392	5 BAGNASCO	02 E835	$\bar{p}p \rightarrow \chi_{c0} \rightarrow J/\psi\gamma$
16.6 ± 5.2 ± 0.1		AMBROGIANI	99B E835	$\bar{p}p \rightarrow e^+e^-\gamma$
14.3 ± 2.0 ± 3.0		BAI	98I BES	$\psi(2S) \rightarrow \gamma\pi^+\pi^-$
13.5 ± 3.3 ± 4.2		GAISER	86 CBAL	$\psi(2S) \rightarrow \gamma X, \gamma\pi^0\pi^0$
⁵ Recalculated by ANDREOTTI 05A.				

 $\chi_{c0}(1P)$ DECAY MODES

Mode	Fraction (Γ_j/Γ)	Scale factor/ Confidence level
------	--------------------------------	-----------------------------------

Hadronic decays

Γ_1	$2(\pi^+\pi^-)$	(2.27 ± 0.19) %	
Γ_2	$\rho^0\pi^+\pi^-$	$(8.9 \pm 2.8) \times 10^{-3}$	
Γ_3	$\rho^0\rho^0$		
Γ_4	$f_0(980)f_0(980)$	$(6.8 \pm 2.2) \times 10^{-4}$	
Γ_5	$\pi^+\pi^-\pi^0\pi^0$	$(3.4 \pm 0.4) \%$	
Γ_6	$\rho^+\pi^-\pi^0 + \text{c.c.}$	$(2.9 \pm 0.4) \%$	
Γ_7	$\pi^+\pi^-K^+K^-$	$(1.80 \pm 0.15) \%$	
Γ_8	$K_0^*(1430)^0 \bar{K}_0^*(1430)^0 \rightarrow$ $\pi^+\pi^-K^+K^-$	$(1.00^{+0.40}_{-0.29}) \times 10^{-3}$	
Γ_9	$K_0^*(1430)^0 \bar{K}_2^*(1430)^0 + \text{c.c.} \rightarrow$ $\pi^+\pi^-K^+K^-$	$(8.1^{+2.0}_{-2.5}) \times 10^{-4}$	
Γ_{10}	$K_1(1270)^+K^- + \text{c.c.} \rightarrow$ $\pi^+\pi^-K^+K^-$	$(6.4 \pm 1.9) \times 10^{-3}$	
Γ_{11}	$K_1(1400)^+K^- + \text{c.c.} \rightarrow$ $\pi^+\pi^-K^+K^-$	< 2.7 $\times 10^{-3}$	CL=90%
Γ_{12}	$f_0(980)f_0(980)$	$(1.7^{+1.1}_{-0.9}) \times 10^{-4}$	
Γ_{13}	$f_0(980)f_0(2200)$	$(8.1^{+2.1}_{-2.6}) \times 10^{-4}$	

Γ_{14}	$f_0(1370)f_0(1370)$	< 2.8 $\times 10^{-4}$	CL=90%
Γ_{15}	$f_0(1370)f_0(1500)$	< 1.7 $\times 10^{-4}$	CL=90%
Γ_{16}	$f_0(1370)f_0(1710)$	$(6.8^{+4.0}_{-2.4}) \times 10^{-4}$	
Γ_{17}	$f_0(1500)f_0(1370)$	< 1.3 $\times 10^{-4}$	CL=90%
Γ_{18}	$f_0(1500)f_0(1500)$	< 5 $\times 10^{-5}$	CL=90%
Γ_{19}	$f_0(1500)f_0(1710)$	< 7 $\times 10^{-5}$	CL=90%
Γ_{20}	$K^+K^-\pi^0\pi^0$	$(5.7 \pm 0.9) \times 10^{-3}$	
Γ_{21}	$K^+\pi^-K^0\pi^0 + \text{c.c.}$	$(2.53 \pm 0.34) \%$	
Γ_{22}	$\rho^+K^-K^0 + \text{c.c.}$	$(1.23 \pm 0.22) \%$	
Γ_{23}	$K^*(892)^-K^+\pi^0 \rightarrow$ $K^+\pi^-K^0\pi^0 + \text{c.c.}$	$(4.7 \pm 1.2) \times 10^{-3}$	
Γ_{24}	$K_S^0 K_S^0 \pi^+\pi^-$	$(5.8 \pm 1.1) \times 10^{-3}$	
Γ_{25}	$K^+K^-\eta\pi^0$	$(3.1 \pm 0.7) \times 10^{-3}$	
Γ_{26}	$3(\pi^+\pi^-)$	$(1.20 \pm 0.18) \%$	
Γ_{27}	$K^+K^*(892)^0\pi^-\pi^0 + \text{c.c.}$	$(7.3 \pm 1.6) \times 10^{-3}$	
Γ_{28}	$K^*(892)^0 \bar{K}^*(892)^0$	$(1.7 \pm 0.6) \times 10^{-3}$	
Γ_{29}	$\pi\pi$	$(8.4 \pm 0.4) \times 10^{-3}$	
Γ_{30}	$\pi^0\eta$	< 1.8 $\times 10^{-4}$	
Γ_{31}	$\pi^0\eta'$	< 1.1 $\times 10^{-3}$	
Γ_{32}	$\eta\eta$	$(2.68 \pm 0.28) \times 10^{-3}$	
Γ_{33}	$\eta\eta'$	< 2.4 $\times 10^{-4}$	CL=90%
Γ_{34}	$\eta'\eta'$	$(2.03 \pm 0.22) \times 10^{-3}$	
Γ_{35}	$\omega\omega$	$(2.2 \pm 0.7) \times 10^{-3}$	
Γ_{36}	K^+K^-	$(6.10 \pm 0.35) \times 10^{-3}$	
Γ_{37}	$K_S^0 K_S^0$	$(3.16 \pm 0.18) \times 10^{-3}$	
Γ_{38}	$\pi^+\pi^-\eta$	< 2.0 $\times 10^{-4}$	CL=90%
Γ_{39}	$\pi^+\pi^-\eta'$	< 4 $\times 10^{-4}$	CL=90%
Γ_{40}	$\bar{K}^0 K^+\pi^- + \text{c.c.}$	< 1.0 $\times 10^{-4}$	CL=90%
Γ_{41}	$K^+K^-\pi^0$	< 6 $\times 10^{-5}$	CL=90%
Γ_{42}	$K^+K^-\eta$	< 2.3 $\times 10^{-4}$	CL=90%
Γ_{43}	$K^+K^-K_S^0 K_S^0$	$(1.4 \pm 0.5) \times 10^{-3}$	
Γ_{44}	$K^+K^-K^+K^-$	$(2.81 \pm 0.30) \times 10^{-3}$	
Γ_{45}	$K^+K^-\phi$	$(9.9 \pm 2.5) \times 10^{-4}$	
Γ_{46}	$\phi\phi$	$(9.2 \pm 1.9) \times 10^{-4}$	
Γ_{47}	$\rho\bar{\rho}$	$(2.28 \pm 0.13) \times 10^{-4}$	
Γ_{48}	$\rho\bar{\rho}\pi^0$	$(5.7 \pm 1.2) \times 10^{-4}$	
Γ_{49}	$\rho\bar{\rho}\eta$	$(3.7 \pm 1.1) \times 10^{-4}$	
Γ_{50}	$\pi^+\pi^-\rho\bar{\rho}$	$(2.1 \pm 0.7) \times 10^{-3}$	S=1.4
Γ_{51}	$\pi^0\pi^0\rho\bar{\rho}$	$(1.05 \pm 0.28) \times 10^{-3}$	
Γ_{52}	$K_S^0 K_S^0 \rho\bar{\rho}$	< 8.8 $\times 10^{-4}$	CL=90%
Γ_{53}	$\rho\bar{\rho}\pi^-$	$(1.14 \pm 0.31) \times 10^{-3}$	
Γ_{54}	$\Lambda\bar{\Lambda}$	$(3.3 \pm 0.4) \times 10^{-4}$	
Γ_{55}	$\Lambda\bar{\Lambda}\pi^+\pi^-$	< 4.0 $\times 10^{-3}$	CL=90%
Γ_{56}	$K^+\bar{p}\Lambda + \text{c.c.}$	$(1.03 \pm 0.20) \times 10^{-3}$	
Γ_{57}	$\Sigma^0\bar{\Sigma}^0$	$(4.2 \pm 0.7) \times 10^{-4}$	
Γ_{58}	$\Sigma^+\bar{\Sigma}^-$	$(3.1 \pm 0.7) \times 10^{-4}$	
Γ_{59}	$\Xi^0\bar{\Xi}^0$	$(3.2 \pm 0.8) \times 10^{-4}$	
Γ_{60}	$\Xi^-\bar{\Xi}^+$	$(4.9 \pm 0.7) \times 10^{-4}$	

Radiative decays

Γ_{61}	$\gamma J/\psi(1S)$	$(1.16 \pm 0.08) \%$	
Γ_{62}	$\gamma\rho^0$	< 9 $\times 10^{-6}$	CL=90%
Γ_{63}	$\gamma\omega$	< 8 $\times 10^{-6}$	CL=90%
Γ_{64}	$\gamma\phi$	< 6 $\times 10^{-6}$	CL=90%
Γ_{65}	$\gamma\gamma$	$(2.22 \pm 0.17) \times 10^{-4}$	

Meson Particle Listings

 $\chi_{c0}(1P)$

CONSTRAINED FIT INFORMATION

A multiparticle fit to $\chi_{c1}(1P)$, $\chi_{c0}(1P)$, $\chi_{c2}(1P)$, and $\psi(2S)$ with 4 total widths, a partial width, 24 combinations of partial widths obtained from integrated cross section, and 82 branching ratios uses 213 measurements to determine 47 parameters. The overall fit has a $\chi^2 = 301.4$ for 166 degrees of freedom.

The following *off-diagonal* array elements are the correlation coefficients $\langle \delta p_i \delta p_j \rangle / (\delta p_i \delta p_j)$, in percent, from the fit to parameters p_i , including the branching fractions, $x_i \equiv \Gamma_i / \Gamma_{\text{total}}$.

x_2	26										
x_7	20	5									
x_{27}	9	2	30								
x_{29}	21	5	22	8							
x_{32}	7	2	8	3	15						
x_{36}	20	5	21	8	33	13					
x_{37}	22	6	22	9	32	12	30				
x_{44}	13	3	12	5	18	7	17	17			
x_{46}	7	2	6	3	9	3	8	8	5		
x_{47}	3	1	3	1	-6	-11	4	4	2	1	
x_{54}	9	2	9	3	16	6	15	14	8	4	
x_{61}	2	0	3	0	12	9	7	6	3	1	
x_{65}	-26	-7	-19	-10	-9	-2	-11	-16	-9	-6	
Γ	-14	-4	-12	-6	-12	-4	-11	-13	-7	-4	
	x_1	x_2	x_7	x_{27}	x_{29}	x_{32}	x_{36}	x_{37}	x_{44}	x_{46}	
x_{54}	2										
x_{61}	-47	3									
x_{65}	-7	-3	11								
Γ	3	-5	-10	-57							
	x_{47}	x_{54}	x_{61}	x_{65}							

 $\chi_{c0}(1P)$ PARTIAL WIDTHS $\chi_{c0}(1P)$ $\Gamma(i)\Gamma(\gamma J/\psi(1S))/\Gamma(\text{total})$

$\Gamma(\rho\bar{\rho}) \times \Gamma(\gamma J/\psi(1S))/\Gamma_{\text{total}}$	$\Gamma_{47}\Gamma_{61}/\Gamma$
VALUE (eV)	EVTS DOCUMENT ID TECN COMMENT
27.4 ± 2.4 OUR FIT	
● ● ● We do not use the following data for averages, fits, limits, etc. ● ● ●	
26.6 ± 2.6 ± 1.4	392 ^{6,7} BAGNASCO 02 E835 $\bar{p}p \rightarrow \chi_{c0} \rightarrow J/\psi \gamma$
48.7 ^{+11.3} - 8.9 ± 2.4	^{6,7} AMBROGIANI 99B E835 $\bar{p}p \rightarrow \gamma J/\psi$

⁶ Calculated by us using $B(J/\psi(1S) \rightarrow e^+e^-) = 0.0593 \pm 0.0010$.

⁷ Values in $(\Gamma(\rho\bar{\rho}) \times \Gamma(\gamma J/\psi(1S))/\Gamma_{\text{total}})$ and $(\Gamma(\rho\bar{\rho})/\Gamma_{\text{total}}) \times \Gamma(\gamma J/\psi(1S))/\Gamma_{\text{total}}$ are not independent. The latter is used in the fit since it is less correlated to the total width.

 $\chi_{c0}(1P)$ $\Gamma(i)\Gamma(\gamma\gamma)/\Gamma(\text{total})$

$\Gamma(\pi\pi) \times \Gamma(\gamma\gamma)/\Gamma_{\text{total}}$	$\Gamma_{29}\Gamma_{65}/\Gamma$
VALUE (eV)	EVTS DOCUMENT ID TECN COMMENT
19.2 ± 1.4 OUR FIT	
23 ± 5 OUR AVERAGE	
29.7 ^{+17.4} - 12.0 ± 4.8	103 ⁺⁶⁰ - 42 ⁸ UEHARA 09 BELL 10.6 $e^+e^- \rightarrow e^+e^- \pi^0 \pi^0$
22.7 ± 3.2 ± 3.5	129 ± 18 ⁹ NAKAZAWA 05 BELL $e^+e^- \rightarrow e^+e^- \chi_{c0}$

⁸ We multiplied the measurement by 3 to convert from $\pi^0 \pi^0$ to $\pi\pi$. Interference with the continuum included.

⁹ We have multiplied $\pi^+ \pi^-$ measurement by 3/2 to obtain $\pi\pi$.

$\Gamma(K^+ K^-) \times \Gamma(\gamma\gamma)/\Gamma_{\text{total}}$	$\Gamma_{36}\Gamma_{65}/\Gamma$
VALUE (eV)	EVTS DOCUMENT ID TECN COMMENT
14.0 ± 1.1 OUR FIT	
14.3 ± 1.6 ± 2.3	153 ± 17 NAKAZAWA 05 BELL $e^+e^- \rightarrow e^+e^- \chi_{c0}$

$\Gamma(K_S^0 K_L^0) \times \Gamma(\gamma\gamma)/\Gamma_{\text{total}}$	$\Gamma_{37}\Gamma_{65}/\Gamma$
VALUE (eV)	EVTS DOCUMENT ID TECN COMMENT
7.3 ± 0.5 OUR FIT	
7.00 ± 0.65 ± 0.71	134 ± 12 CHEN 07B BELL $e^+e^- \rightarrow e^+e^- \chi_{c0}$

$\Gamma(2(\pi^+ \pi^-)) \times \Gamma(\gamma\gamma)/\Gamma_{\text{total}}$	$\Gamma_1\Gamma_{65}/\Gamma$
VALUE (eV)	EVTS DOCUMENT ID TECN COMMENT
52 ± 4 OUR FIT	
49 ± 10 OUR AVERAGE	Error includes scale factor of 1.8.
44.7 ± 3.6 ± 4.9	3.6k UEHARA 08 BELL $\gamma\gamma \rightarrow \chi_{c0} \rightarrow 2(\pi^+ \pi^-)$
75 ± 13 ± 8	EISENSTEIN 01 CLE2 $e^+e^- \rightarrow e^+e^- \chi_{c0}$

$\Gamma(\rho^0 \rho^0) \times \Gamma(\gamma\gamma)/\Gamma_{\text{total}}$	$\Gamma_3\Gamma_{65}/\Gamma$
VALUE (eV)	CL% EVTS DOCUMENT ID TECN COMMENT
● ● ● We do not use the following data for averages, fits, limits, etc. ● ● ●	
<12	90 <252 UEHARA 08 BELL $\gamma\gamma \rightarrow \chi_{c0} \rightarrow 2(\pi^+ \pi^-)$

$\Gamma(\pi^+ \pi^- K^+ K^-) \times \Gamma(\gamma\gamma)/\Gamma_{\text{total}}$	$\Gamma_7\Gamma_{65}/\Gamma$
VALUE (eV)	EVTS DOCUMENT ID TECN COMMENT
41 ± 4 OUR FIT	
38.8 ± 3.7 ± 4.7	1.7k UEHARA 08 BELL $\gamma\gamma \rightarrow \chi_{c0} \rightarrow K^+ K^- \pi^+ \pi^-$

$\Gamma(K^+ \bar{K}^*(892)^0 \pi^- + \text{c.c.}) \times \Gamma(\gamma\gamma)/\Gamma_{\text{total}}$	$\Gamma_{27}\Gamma_{65}/\Gamma$
VALUE (eV)	EVTS DOCUMENT ID TECN COMMENT
17 ± 4 OUR FIT	
16.7 ± 6.1 ± 3.0	495 ± 182 UEHARA 08 BELL $\gamma\gamma \rightarrow \chi_{c0} \rightarrow K^+ K^- \pi^+ \pi^-$

$\Gamma(K^*(892)^0 \bar{K}^*(892)^0) \times \Gamma(\gamma\gamma)/\Gamma_{\text{total}}$	$\Gamma_{28}\Gamma_{65}/\Gamma$
VALUE (eV)	CL% EVTS DOCUMENT ID TECN COMMENT
● ● ● We do not use the following data for averages, fits, limits, etc. ● ● ●	
<6	90 <148 UEHARA 08 BELL $\gamma\gamma \rightarrow \chi_{c0} \rightarrow K^+ K^- \pi^+ \pi^-$

$\Gamma(K^+ K^- K^+ K^-) \times \Gamma(\gamma\gamma)/\Gamma_{\text{total}}$	$\Gamma_{44}\Gamma_{65}/\Gamma$
VALUE (eV)	EVTS DOCUMENT ID TECN COMMENT
6.5 ± 0.7 OUR FIT	
7.9 ± 1.3 ± 1.1	215 ± 36 UEHARA 08 BELL $\gamma\gamma \rightarrow \chi_{c0} \rightarrow 2(K^+ K^-)$

$\Gamma(\phi\phi) \times \Gamma(\gamma\gamma)/\Gamma_{\text{total}}$	$\Gamma_{46}\Gamma_{65}/\Gamma$
VALUE (eV)	EVTS DOCUMENT ID TECN COMMENT
2.1 ± 0.5 OUR FIT	
2.3 ± 0.9 ± 0.4	23.6 ± 9.6 UEHARA 08 BELL $\gamma\gamma \rightarrow \chi_{c0} \rightarrow 2(K^+ K^-)$

 $\chi_{c0}(1P)$ BRANCHING RATIOS

HADRONIC DECAYS

$\Gamma(2(\pi^+ \pi^-))/\Gamma_{\text{total}}$	Γ_1/Γ
VALUE	DOCUMENT ID
0.0227 ± 0.0019 OUR FIT	

$\Gamma(\rho^0 \pi^+ \pi^-)/\Gamma(2(\pi^+ \pi^-))$	Γ_2/Γ_1
VALUE	DOCUMENT ID TECN COMMENT
0.39 ± 0.12 OUR FIT	
0.39 ± 0.12	TANENBAUM 78 MRK1 $\psi(2S) \rightarrow \gamma \chi_{c0}$

$\Gamma(\rho^0 \pi^+ \pi^-)/\Gamma_{\text{total}}$	Γ_2/Γ
VALUE	DOCUMENT ID
0.0089 ± 0.0028 OUR FIT	

$\Gamma(f_0(980) f_0(980))/\Gamma_{\text{total}}$	Γ_4/Γ
VALUE (units 10^{-4})	EVTS DOCUMENT ID TECN COMMENT
6.8 ± 2.1 ± 0.2	36 ± 9 ¹⁰ ABLIKIM 04G BES $\psi(2S) \rightarrow \gamma \pi^+ \pi^-$
¹⁰ ABLIKIM 04G reports $[\Gamma(\chi_{c0}(1P) \rightarrow f_0(980) f_0(980))/\Gamma_{\text{total}}] \times [B(\psi(2S) \rightarrow \gamma \chi_{c0}(1P))] = (6.5 \pm 1.6 \pm 1.3) \times 10^{-5}$ which we divide by our best value $B(\psi(2S) \rightarrow \gamma \chi_{c0}(1P)) = (9.62 \pm 0.31) \times 10^{-2}$. Our first error is their experiment's error and our second error is the systematic error from using our best value.	

$\Gamma(\pi^+ \pi^- \pi^0 \pi^0)/\Gamma_{\text{total}}$	Γ_5/Γ
VALUE (%)	EVTS DOCUMENT ID TECN COMMENT
3.4 ± 0.4 ± 0.1	1751.4 ¹¹ HE 08B CLEO $e^+e^- \rightarrow \gamma h^+ h^- h^0 h^0$

¹¹ HE 08B reports $3.54 \pm 0.10 \pm 0.43 \pm 0.18\%$ from a measurement of $[\Gamma(\chi_{c0}(1P) \rightarrow \pi^+ \pi^- \pi^0 \pi^0)/\Gamma_{\text{total}}] \times [B(\psi(2S) \rightarrow \gamma \chi_{c0}(1P))]$ assuming $B(\psi(2S) \rightarrow \gamma \chi_{c0}(1P)) = (9.22 \pm 0.11 \pm 0.46) \times 10^{-2}$, which we rescale to our best value $B(\psi(2S) \rightarrow \gamma \chi_{c0}(1P)) = (9.62 \pm 0.31) \times 10^{-2}$. Our first error is their experiment's error and our second error is the systematic error from using our best value.

$\Gamma(\rho^+ \pi^- \pi^0 + \text{c.c.})/\Gamma_{\text{total}}$	Γ_6/Γ
VALUE (%)	EVTS DOCUMENT ID TECN COMMENT
2.9 ± 0.4 ± 0.1	1358.5 ^{12,13} HE 08B CLEO $e^+e^- \rightarrow \gamma h^+ h^- h^0 h^0$

¹² HE 08B reports $3.04 \pm 0.18 \pm 0.42 \pm 0.16\%$ from a measurement of $[\Gamma(\chi_{c0}(1P) \rightarrow \rho^+ \pi^- \pi^0 + \text{c.c.})/\Gamma_{\text{total}}] \times [B(\psi(2S) \rightarrow \gamma \chi_{c0}(1P))]$ assuming $B(\psi(2S) \rightarrow \gamma \chi_{c0}(1P)) = (9.22 \pm 0.11 \pm 0.46) \times 10^{-2}$, which we rescale to our best value $B(\psi(2S) \rightarrow \gamma \chi_{c0}(1P)) = (9.62 \pm 0.31) \times 10^{-2}$. Our first error is their experiment's error and our second error is the systematic error from using our best value.

¹³ Calculated by us. We have added the values from HE 08B for $\rho^+ \pi^- \pi^0$ and $\rho^- \pi^+ \pi^0$ decays assuming uncorrelated statistical and fully correlated systematic uncertainties.

$\Gamma(\pi^+ \pi^- K^+ K^-)/\Gamma_{\text{total}}$	Γ_7/Γ
VALUE (units 10^{-3})	DOCUMENT ID
18.0 ± 1.5 OUR FIT	

$\Gamma(K^+ \bar{K}^*(892)^0 \pi^- + \text{c.c.})/\Gamma(\pi^+ \pi^- K^+ K^-)$	Γ_{27}/Γ_7
VALUE	DOCUMENT ID TECN COMMENT
0.41 ± 0.09 OUR FIT	
0.41 ± 0.10	TANENBAUM 78 MRK1 $\psi(2S) \rightarrow \gamma \chi_{c0}$

See key on page 405

Meson Particle Listings

 $\chi_{c0}(1P)$

- ⁴⁹ATHAR 07 reports $< 0.10 \times 10^{-3}$ from a measurement of $[\Gamma(\chi_{c0}(1P) \rightarrow \bar{K}^0 K^+ \pi^- + \text{c.c.})/\Gamma_{\text{total}}] \times [\text{B}(\psi(2S) \rightarrow \gamma \chi_{c0}(1P))]$ assuming $\text{B}(\psi(2S) \rightarrow \gamma \chi_{c0}(1P)) = (9.22 \pm 0.11 \pm 0.46) \times 10^{-2}$, which we rescale to our best value $\text{B}(\psi(2S) \rightarrow \gamma \chi_{c0}(1P)) = 9.62 \times 10^{-2}$.
- ⁵⁰ABLIKIM 06R reports $< 0.70 \times 10^{-3}$ from a measurement of $[\Gamma(\chi_{c0}(1P) \rightarrow \bar{K}^0 K^+ \pi^- + \text{c.c.})/\Gamma_{\text{total}}] \times [\text{B}(\psi(2S) \rightarrow \gamma \chi_{c0}(1P))]$ assuming $\text{B}(\psi(2S) \rightarrow \gamma \chi_{c0}(1P)) = (9.2 \pm 0.4) \times 10^{-2}$, which we rescale to our best value $\text{B}(\psi(2S) \rightarrow \gamma \chi_{c0}(1P)) = 9.62 \times 10^{-2}$.
- ⁵¹We have multiplied the $K_S^0 K^+ \pi^-$ measurement by a factor of 2 to convert to $K^0 K^+ \pi^-$.
- ⁵²Rescaled by us using $\text{B}(\psi(2S) \rightarrow \gamma \chi_{c0}) = (9.4 \pm 0.4)\%$ and $\text{B}(\psi(2S) \rightarrow J/\psi(1S) \pi^+ \pi^-) = (32.6 \pm 0.5)\%$.

$\Gamma(K^+ K^- \pi^0)/\Gamma_{\text{total}}$ Γ_{41}/Γ

VALUE (units 10^{-3})	CL%	DOCUMENT ID	TECN	COMMENT
<0.06	90	⁵³ ATHAR	07	CLEO $\psi(2S) \rightarrow \gamma h^+ h^- h^0$

- ⁵³ATHAR 07 reports $< 0.06 \times 10^{-3}$ from a measurement of $[\Gamma(\chi_{c0}(1P) \rightarrow K^+ K^- \pi^0)/\Gamma_{\text{total}}] \times [\text{B}(\psi(2S) \rightarrow \gamma \chi_{c0}(1P))]$ assuming $\text{B}(\psi(2S) \rightarrow \gamma \chi_{c0}(1P)) = (9.22 \pm 0.11 \pm 0.46) \times 10^{-2}$, which we rescale to our best value $\text{B}(\psi(2S) \rightarrow \gamma \chi_{c0}(1P)) = 9.62 \times 10^{-2}$.

$\Gamma(K^+ K^- \eta)/\Gamma_{\text{total}}$ Γ_{42}/Γ

VALUE (units 10^{-3})	CL%	DOCUMENT ID	TECN	COMMENT
<0.23	90	⁵⁴ ATHAR	07	CLEO $\psi(2S) \rightarrow \gamma h^+ h^- h^0$

- ⁵⁴ATHAR 07 reports $< 0.24 \times 10^{-3}$ from a measurement of $[\Gamma(\chi_{c0}(1P) \rightarrow K^+ K^- \eta)/\Gamma_{\text{total}}] \times [\text{B}(\psi(2S) \rightarrow \gamma \chi_{c0}(1P))]$ assuming $\text{B}(\psi(2S) \rightarrow \gamma \chi_{c0}(1P)) = (9.22 \pm 0.11 \pm 0.46) \times 10^{-2}$, which we rescale to our best value $\text{B}(\psi(2S) \rightarrow \gamma \chi_{c0}(1P)) = 9.62 \times 10^{-2}$.

$\Gamma(K^+ K^- K_S^0 \bar{K}_S^0)/\Gamma_{\text{total}}$ Γ_{43}/Γ

VALUE (units 10^{-3})	EVTS	DOCUMENT ID	TECN	COMMENT
1.43 ± 0.48 ± 0.05	16.8 ± 4.8	⁵⁵ ABLIKIM	05o	BES2 $\psi(2S) \rightarrow \gamma \chi_{c0}$

- ⁵⁵ABLIKIM 05o reports $[\Gamma(\chi_{c0}(1P) \rightarrow K^+ K^- K_S^0 \bar{K}_S^0)/\Gamma_{\text{total}}] \times [\text{B}(\psi(2S) \rightarrow \gamma \chi_{c0}(1P))]$ = $(0.138 \pm 0.039 \pm 0.025) \times 10^{-3}$ which we divide by our best value $\text{B}(\psi(2S) \rightarrow \gamma \chi_{c0}(1P)) = (9.62 \pm 0.31) \times 10^{-2}$. Our first error is their experiment's error and our second error is the systematic error from using our best value.

$\Gamma(K^+ K^- K^+ K^-)/\Gamma_{\text{total}}$ Γ_{44}/Γ

VALUE (units 10^{-3})	DOCUMENT ID
2.81 ± 0.30 OUR FIT	

$\Gamma(K^+ K^- \phi)/\Gamma_{\text{total}}$ Γ_{45}/Γ

VALUE (units 10^{-3})	EVTS	DOCUMENT ID	TECN	COMMENT
0.99 ± 0.25 ± 0.03	38	⁵⁶ ABLIKIM	06t	BES2 $\psi(2S) \rightarrow \gamma 2K^+ 2K^-$

- ⁵⁶ABLIKIM 06t reports $(1.03 \pm 0.22 \pm 0.15) \times 10^{-3}$ from a measurement of $[\Gamma(\chi_{c0}(1P) \rightarrow K^+ K^- \phi)/\Gamma_{\text{total}}] \times [\text{B}(\psi(2S) \rightarrow \gamma \chi_{c0}(1P))]$ assuming $\text{B}(\psi(2S) \rightarrow \gamma \chi_{c0}(1P)) = (9.2 \pm 0.4) \times 10^{-2}$, which we rescale to our best value $\text{B}(\psi(2S) \rightarrow \gamma \chi_{c0}(1P)) = (9.62 \pm 0.31) \times 10^{-2}$. Our first error is their experiment's error and our second error is the systematic error from using our best value.

$\Gamma(\phi\phi)/\Gamma_{\text{total}}$ Γ_{46}/Γ

VALUE (units 10^{-3})	DOCUMENT ID
0.92 ± 0.19 OUR FIT	

$\Gamma(p\bar{p})/\Gamma_{\text{total}}$ Γ_{47}/Γ

VALUE (units 10^{-4})	DOCUMENT ID
2.28 ± 0.13 OUR FIT	

$\Gamma(p\bar{p}\pi^0)/\Gamma_{\text{total}}$ Γ_{48}/Γ

VALUE (units 10^{-3})	DOCUMENT ID	TECN	COMMENT
0.57 ± 0.12 ± 0.02	⁵⁷ ATHAR	07	CLEO $\psi(2S) \rightarrow \gamma h^+ h^- h^0$

- ⁵⁷ATHAR 07 reports $(0.59 \pm 0.10 \pm 0.08) \times 10^{-3}$ from a measurement of $[\Gamma(\chi_{c0}(1P) \rightarrow p\bar{p}\pi^0)/\Gamma_{\text{total}}] \times [\text{B}(\psi(2S) \rightarrow \gamma \chi_{c0}(1P))]$ assuming $\text{B}(\psi(2S) \rightarrow \gamma \chi_{c0}(1P)) = (9.22 \pm 0.11 \pm 0.46) \times 10^{-2}$, which we rescale to our best value $\text{B}(\psi(2S) \rightarrow \gamma \chi_{c0}(1P)) = (9.62 \pm 0.31) \times 10^{-2}$. Our first error is their experiment's error and our second error is the systematic error from using our best value.

$\Gamma(p\bar{p}\eta)/\Gamma_{\text{total}}$ Γ_{49}/Γ

VALUE (units 10^{-3})	DOCUMENT ID	TECN	COMMENT
0.37 ± 0.11 ± 0.01	⁵⁸ ATHAR	07	CLEO $\psi(2S) \rightarrow \gamma h^+ h^- h^0$

- ⁵⁸ATHAR 07 reports $(0.39 \pm 0.11 \pm 0.04) \times 10^{-3}$ from a measurement of $[\Gamma(\chi_{c0}(1P) \rightarrow p\bar{p}\eta)/\Gamma_{\text{total}}] \times [\text{B}(\psi(2S) \rightarrow \gamma \chi_{c0}(1P))]$ assuming $\text{B}(\psi(2S) \rightarrow \gamma \chi_{c0}(1P)) = (9.22 \pm 0.11 \pm 0.46) \times 10^{-2}$, which we rescale to our best value $\text{B}(\psi(2S) \rightarrow \gamma \chi_{c0}(1P)) = (9.62 \pm 0.31) \times 10^{-2}$. Our first error is their experiment's error and our second error is the systematic error from using our best value.

$\Gamma(\pi^+ \pi^- \rho\bar{\rho})/\Gamma_{\text{total}}$ Γ_{50}/Γ

- | VALUE (units 10^{-3}) | DOCUMENT ID | TECN | COMMENT |
|---------------------------------|--|------|--|
| 2.1 ± 0.7 OUR EVALUATION | Error includes scale factor of 1.4. Treating systematic error as correlated. | | |
| 2.1 ± 1.0 OUR AVERAGE | Error includes scale factor of 2.0. | | |
| 1.57 ± 0.21 ± 0.53 | ⁵⁹ BAI | 99b | BES $\psi(2S) \rightarrow \gamma \chi_{c0}$ |
| 4.20 ± 1.15 ± 0.18 | ⁵⁹ TANENBAUM | 78 | MRK1 $\psi(2S) \rightarrow \gamma \chi_{c0}$ |
- ⁵⁹Rescaled by us using $\text{B}(\psi(2S) \rightarrow \gamma \chi_{c0}) = (9.4 \pm 0.4)\%$ and $\text{B}(\psi(2S) \rightarrow J/\psi(1S) \pi^+ \pi^-) = (32.6 \pm 0.5)\%$.

$\Gamma(\pi^0 \pi^0 \rho\bar{\rho})/\Gamma_{\text{total}}$ Γ_{51}/Γ

- | VALUE (%) | EVTS | DOCUMENT ID | TECN | COMMENT |
|------------------------------|------|------------------|------|---|
| 0.105 ± 0.028 ± 0.003 | 39.5 | ⁶⁰ HE | 08b | CLEO $e^+ e^- \rightarrow \gamma h^+ h^- h^0$ |
- ⁶⁰HE 08b reports $0.11 \pm 0.02 \pm 0.02 \pm 0.01$ % from a measurement of $[\Gamma(\chi_{c0}(1P) \rightarrow \pi^0 \pi^0 \rho\bar{\rho})/\Gamma_{\text{total}}] \times [\text{B}(\psi(2S) \rightarrow \gamma \chi_{c0}(1P))]$ assuming $\text{B}(\psi(2S) \rightarrow \gamma \chi_{c0}(1P)) = (9.22 \pm 0.11 \pm 0.46) \times 10^{-2}$, which we rescale to our best value $\text{B}(\psi(2S) \rightarrow \gamma \chi_{c0}(1P)) = (9.62 \pm 0.31) \times 10^{-2}$. Our first error is their experiment's error and our second error is the systematic error from using our best value.

$\Gamma(K_S^0 K_S^0 \rho\bar{\rho})/\Gamma_{\text{total}}$ Γ_{52}/Γ

- | VALUE (units 10^{-4}) | CL% | DOCUMENT ID | TECN | COMMENT |
|--------------------------|-----|-----------------------|------|--|
| <8.8 | 90 | ⁶¹ ABLIKIM | 06d | BES2 $\psi(2S) \rightarrow \chi_{c0} \gamma$ |
- ⁶¹Using $\text{B}(\psi(2S) \rightarrow \chi_{c0} \gamma) = (9.2 \pm 0.5)\%$

$\Gamma(\rho\bar{\rho}\pi^-)/\Gamma_{\text{total}}$ Γ_{53}/Γ

- | VALUE (units 10^{-4}) | DOCUMENT ID | TECN | COMMENT |
|--------------------------|-----------------------|------|--|
| 11.4 ± 3.1 ± 0.4 | ⁶² ABLIKIM | 06i | BES2 $\psi(2S) \rightarrow \gamma p \pi^- X$ |
- ⁶²ABLIKIM 06i reports $[\Gamma(\chi_{c0}(1P) \rightarrow \rho\bar{\rho}\pi^-)/\Gamma_{\text{total}}] \times [\text{B}(\psi(2S) \rightarrow \gamma \chi_{c0}(1P))]$ = $(1.10 \pm 0.24 \pm 0.18) \times 10^{-4}$ which we divide by our best value $\text{B}(\psi(2S) \rightarrow \gamma \chi_{c0}(1P)) = (9.62 \pm 0.31) \times 10^{-2}$. Our first error is their experiment's error and our second error is the systematic error from using our best value.

$\Gamma(\Lambda\bar{\Lambda})/\Gamma_{\text{total}}$ Γ_{54}/Γ

- | VALUE (units 10^{-4}) | DOCUMENT ID |
|--------------------------|-------------|
| 3.3 ± 0.4 OUR FIT | |

$\Gamma(\Lambda\bar{\Lambda}\pi^+ \pi^-)/\Gamma_{\text{total}}$ Γ_{55}/Γ

- | VALUE (units 10^{-3}) | CL% | DOCUMENT ID | TECN | COMMENT |
|--------------------------|-----|-----------------------|------|--|
| <4.0 | 90 | ⁶³ ABLIKIM | 06d | BES2 $\psi(2S) \rightarrow \chi_{c0} \gamma$ |
- ⁶³Using $\text{B}(\psi(2S) \rightarrow \chi_{c0} \gamma) = (9.2 \pm 0.5)\%$

$\Gamma(K^+ \bar{P}\Lambda + \text{c.c.})/\Gamma_{\text{total}}$ Γ_{56}/Γ

- | VALUE (units 10^{-3}) | DOCUMENT ID | TECN | COMMENT |
|---------------------------|---------------------|------|--|
| 1.03 ± 0.19 ± 0.03 | ⁶⁴ ATHAR | 07 | CLEO $\psi(2S) \rightarrow \gamma h^+ h^- h^0$ |
- ⁶⁴ATHAR 07 reports $(1.07 \pm 0.17 \pm 0.12) \times 10^{-3}$ from a measurement of $[\Gamma(\chi_{c0}(1P) \rightarrow K^+ \bar{P}\Lambda + \text{c.c.})/\Gamma_{\text{total}}] \times [\text{B}(\psi(2S) \rightarrow \gamma \chi_{c0}(1P))]$ assuming $\text{B}(\psi(2S) \rightarrow \gamma \chi_{c0}(1P)) = (9.22 \pm 0.11 \pm 0.46) \times 10^{-2}$, which we rescale to our best value $\text{B}(\psi(2S) \rightarrow \gamma \chi_{c0}(1P)) = (9.62 \pm 0.31) \times 10^{-2}$. Our first error is their experiment's error and our second error is the systematic error from using our best value.

$\Gamma(\Sigma^0 \bar{\Sigma}^0)/\Gamma_{\text{total}}$ Γ_{57}/Γ

- | VALUE (units 10^{-4}) | EVTS | DOCUMENT ID | TECN | COMMENT |
|--------------------------|---------|--------------------|------|--|
| 4.2 ± 0.7 ± 0.1 | 78 ± 10 | ⁶⁵ NAIK | 08 | CLEO $\psi(2S) \rightarrow \gamma \Sigma^0 \bar{\Sigma}^0$ |
- ⁶⁵NAIK 08 reports $(4.41 \pm 0.56 \pm 0.47) \times 10^{-4}$ from a measurement of $[\Gamma(\chi_{c0}(1P) \rightarrow \Sigma^0 \bar{\Sigma}^0)/\Gamma_{\text{total}}] \times [\text{B}(\psi(2S) \rightarrow \gamma \chi_{c0}(1P))]$ assuming $\text{B}(\psi(2S) \rightarrow \gamma \chi_{c0}(1P)) = (9.22 \pm 0.11 \pm 0.46) \times 10^{-2}$, which we rescale to our best value $\text{B}(\psi(2S) \rightarrow \gamma \chi_{c0}(1P)) = (9.62 \pm 0.31) \times 10^{-2}$. Our first error is their experiment's error and our second error is the systematic error from using our best value.

$\Gamma(\Sigma^+ \bar{\Sigma}^-)/\Gamma_{\text{total}}$ Γ_{58}/Γ

- | VALUE (units 10^{-4}) | EVTS | DOCUMENT ID | TECN | COMMENT |
|--------------------------|--------|--------------------|------|--|
| 3.1 ± 0.7 ± 0.1 | 39 ± 7 | ⁶⁶ NAIK | 08 | CLEO $\psi(2S) \rightarrow \gamma \Sigma^+ \bar{\Sigma}^-$ |
- ⁶⁶NAIK 08 reports $(3.25 \pm 0.57 \pm 0.43) \times 10^{-4}$ from a measurement of $[\Gamma(\chi_{c0}(1P) \rightarrow \Sigma^+ \bar{\Sigma}^-)/\Gamma_{\text{total}}] \times [\text{B}(\psi(2S) \rightarrow \gamma \chi_{c0}(1P))]$ assuming $\text{B}(\psi(2S) \rightarrow \gamma \chi_{c0}(1P)) = (9.22 \pm 0.11 \pm 0.46) \times 10^{-2}$, which we rescale to our best value $\text{B}(\psi(2S) \rightarrow \gamma \chi_{c0}(1P)) = (9.62 \pm 0.31) \times 10^{-2}$. Our first error is their experiment's error and our second error is the systematic error from using our best value.

$\Gamma(\Xi^0 \bar{\Xi}^0)/\Gamma_{\text{total}}$ Γ_{59}/Γ

- | VALUE (units 10^{-4}) | EVTS | DOCUMENT ID | TECN | COMMENT |
|--------------------------|------------|--------------------|------|--|
| 3.2 ± 0.8 ± 0.1 | 23.3 ± 4.9 | ⁶⁷ NAIK | 08 | CLEO $\psi(2S) \rightarrow \gamma \Xi^0 \bar{\Xi}^0$ |
- ⁶⁷NAIK 08 reports $(3.34 \pm 0.70 \pm 0.48) \times 10^{-4}$ from a measurement of $[\Gamma(\chi_{c0}(1P) \rightarrow \Xi^0 \bar{\Xi}^0)/\Gamma_{\text{total}}] \times [\text{B}(\psi(2S) \rightarrow \gamma \chi_{c0}(1P))]$ assuming $\text{B}(\psi(2S) \rightarrow \gamma \chi_{c0}(1P)) = (9.22 \pm 0.11 \pm 0.46) \times 10^{-2}$, which we rescale to our best value $\text{B}(\psi(2S) \rightarrow \gamma \chi_{c0}(1P)) = (9.62 \pm 0.31) \times 10^{-2}$. Our first error is their experiment's error and our second error is the systematic error from using our best value.

Meson Particle Listings

 $\chi_{c0}(1P)$ $\Gamma(\Xi^-\bar{\Xi}^+)/\Gamma_{total}$ Γ_{60}/Γ

VALUE (units 10^{-4})	CL%	EVTS	DOCUMENT ID	TECN	COMMENT
4.9 ± 0.7 ± 0.2		95 ± 11	68 NAIK	08 CLEO	$\psi(2S) \rightarrow \gamma \Xi^+ \Xi^-$

• • • We do not use the following data for averages, fits, limits, etc. • • •

<10.3 90 69 ABLIKIM 06D BES2 $\psi(2S) \rightarrow \chi_{c0}\gamma$

68 NAIK 08 reports $(5.14 \pm 0.60 \pm 0.47) \times 10^{-4}$ from a measurement of $[\Gamma(\chi_{c0}(1P) \rightarrow \Xi^-\bar{\Xi}^+)/\Gamma_{total}] \times [B(\psi(2S) \rightarrow \gamma\chi_{c0}(1P))]$ assuming $B(\psi(2S) \rightarrow \gamma\chi_{c0}(1P)) = (9.22 \pm 0.11 \pm 0.46) \times 10^{-2}$, which we rescale to our best value $B(\psi(2S) \rightarrow \gamma\chi_{c0}(1P)) = (9.62 \pm 0.31) \times 10^{-2}$. Our first error is their experiment's error and our second error is the systematic error from using our best value.

69 Using $B(\psi(2S) \rightarrow \chi_{c0}\gamma) = (9.2 \pm 0.5)\%$

 $\Gamma(p\bar{p})/\Gamma_{total} \times \Gamma(\pi\pi)/\Gamma_{total}$ $\Gamma_{47}/\Gamma \times \Gamma_{29}/\Gamma$

VALUE (units 10^{-7})	DOCUMENT ID	TECN	COMMENT
19.0 ± 1.4 OUR FIT			
15.3 ± 2.4 ± 0.8	70 ANDREOTTI 03	E835	$\bar{p}p \rightarrow \chi_{c0} \rightarrow \pi^0 \pi^0$

70 We have multiplied $B(p\bar{p})\text{-}B(\pi^0\pi^0)$ measurement by 3 to obtain $B(p\bar{p})\text{-}B(\pi\pi)$.

 $\Gamma(p\bar{p})/\Gamma_{total} \times \Gamma(\pi^0\eta)/\Gamma_{total}$ $\Gamma_{47}/\Gamma \times \Gamma_{30}/\Gamma$

VALUE (units 10^{-7})	DOCUMENT ID	TECN	COMMENT
<0.4	ANDREOTTI 05c	E835	$\bar{p}p \rightarrow \pi^0\eta$

 $\Gamma(p\bar{p})/\Gamma_{total} \times \Gamma(\pi^0\eta')/\Gamma_{total}$ $\Gamma_{47}/\Gamma \times \Gamma_{31}/\Gamma$

VALUE (units 10^{-7})	DOCUMENT ID	TECN	COMMENT
<2.5	ANDREOTTI 05c	E835	$\bar{p}p \rightarrow \pi^0\eta'$

 $\Gamma(p\bar{p})/\Gamma_{total} \times \Gamma(\eta\eta)/\Gamma_{total}$ $\Gamma_{47}/\Gamma \times \Gamma_{32}/\Gamma$

VALUE (units 10^{-7})	DOCUMENT ID	TECN	COMMENT
6.1 ± 0.7 OUR FIT			
4.0 ± 1.2 ± 0.5	ANDREOTTI 05c	E835	$\bar{p}p \rightarrow \eta\eta$

 $\Gamma(p\bar{p})/\Gamma_{total} \times \Gamma(\eta\eta')/\Gamma_{total}$ $\Gamma_{47}/\Gamma \times \Gamma_{33}/\Gamma$

VALUE (units 10^{-6})	DOCUMENT ID	TECN	COMMENT
2.1 ± 2.3	ANDREOTTI 05c	E835	$\bar{p}p \rightarrow \pi^0\eta$

• • • We do not use the following data for averages, fits, limits, etc. • • •

RADIATIVE DECAYS

 $\Gamma(\gamma J/\psi(1S))/\Gamma_{total}$ Γ_{61}/Γ

VALUE (units 10^{-4})	DOCUMENT ID	TECN	COMMENT
116 ± 8 OUR FIT			
200 ± 20 ± 20	71 ADAM 05A	CLEO	$e^+e^- \rightarrow \psi(2S) \rightarrow \gamma\chi_{c0}$

71 Uses $B(\psi(2S) \rightarrow \gamma\chi_{c0} \rightarrow \gamma J/\psi)$ from ADAM 05A and $B(\psi(2S) \rightarrow \gamma\chi_{c0})$ from ATHAR 04.

 $\Gamma(\gamma\rho^0)/\Gamma_{total}$ Γ_{62}/Γ

VALUE (units 10^{-6})	CL%	EVTS	DOCUMENT ID	TECN	COMMENT
<9		90 1.2 ± 4.5	72 BENNETT 08A	CLEO	$\psi(2S) \rightarrow \gamma\rho^0$

72 BENNETT 08A reports < 9.6×10^{-6} from a measurement of $[\Gamma(\chi_{c0}(1P) \rightarrow \gamma\rho^0)/\Gamma_{total}] \times [B(\psi(2S) \rightarrow \gamma\chi_{c0}(1P))]$ assuming $B(\psi(2S) \rightarrow \gamma\chi_{c0}(1P)) = (9.2 \pm 0.4) \times 10^{-2}$, which we rescale to our best value $B(\psi(2S) \rightarrow \gamma\chi_{c0}(1P)) = 9.62 \times 10^{-2}$.

 $\Gamma(\gamma\omega)/\Gamma_{total}$ Γ_{63}/Γ

VALUE (units 10^{-6})	CL%	EVTS	DOCUMENT ID	TECN	COMMENT
<8		90 0.0 ± 2.8	73 BENNETT 08A	CLEO	$\psi(2S) \rightarrow \gamma\omega$

73 BENNETT 08A reports < 8.8×10^{-6} from a measurement of $[\Gamma(\chi_{c0}(1P) \rightarrow \gamma\omega)/\Gamma_{total}] \times [B(\psi(2S) \rightarrow \gamma\chi_{c0}(1P))]$ assuming $B(\psi(2S) \rightarrow \gamma\chi_{c0}(1P)) = (9.2 \pm 0.4) \times 10^{-2}$, which we rescale to our best value $B(\psi(2S) \rightarrow \gamma\chi_{c0}(1P)) = 9.62 \times 10^{-2}$.

 $\Gamma(\gamma\phi)/\Gamma_{total}$ Γ_{64}/Γ

VALUE (units 10^{-6})	CL%	EVTS	DOCUMENT ID	TECN	COMMENT
<6		90 0.1 ± 1.6	74 BENNETT 08A	CLEO	$\psi(2S) \rightarrow \gamma\phi$

74 BENNETT 08A reports < 6.4×10^{-6} from a measurement of $[\Gamma(\chi_{c0}(1P) \rightarrow \gamma\phi)/\Gamma_{total}] \times [B(\psi(2S) \rightarrow \gamma\chi_{c0}(1P))]$ assuming $B(\psi(2S) \rightarrow \gamma\chi_{c0}(1P)) = (9.2 \pm 0.4) \times 10^{-2}$, which we rescale to our best value $B(\psi(2S) \rightarrow \gamma\chi_{c0}(1P)) = 9.62 \times 10^{-2}$.

 $\Gamma(\gamma\eta)/\Gamma_{total}$ Γ_{65}/Γ

VALUE (units 10^{-4})	CL%	DOCUMENT ID	TECN	COMMENT
2.22 ± 0.17 OUR FIT				
<8		90 75 WICHT 08	BELL	$B^\pm \rightarrow K^\pm\gamma\gamma$

75 WICHT 08 reports $[\Gamma(\chi_{c0}(1P) \rightarrow \gamma\eta)/\Gamma_{total}] \times [B(B^\pm \rightarrow \chi_{c0}(1P)K^\pm)] < 0.11 \times 10^{-6}$ which we divide by our best value $B(B^\pm \rightarrow \chi_{c0}(1P)K^\pm) = 1.33 \times 10^{-4}$.

 $\Gamma(\gamma\gamma)/\Gamma(\gamma J/\psi(1S))$ Γ_{65}/Γ_{61}

VALUE (units 10^{-2})	DOCUMENT ID	TECN	COMMENT
1.91 ± 0.19 OUR FIT			
2.0 ± 0.4 OUR AVERAGE			
2.2 ± 0.4 $^{+0.1}_{-0.2}$	76 ANDREOTTI 04	E835	$\bar{p}p \rightarrow \chi_{c0} \rightarrow \gamma\gamma$
1.45 ± 0.74	77 AMBROGIANI 00B	E835	$\bar{p}p \rightarrow \chi_{c2} \rightarrow \gamma\gamma, \gamma J/\psi$

76 The values of $B(p\bar{p})B(\gamma\gamma)$ and $B(\gamma\gamma)B(\gamma J/\psi)$ measured by ANDREOTTI 04 are not independent. The latter is used in the fit because of smaller systematics.

77 Calculated by us using $B(J/\psi(1S) \rightarrow e^+e^-) = 0.0593 \pm 0.0010$.

 $\Gamma(p\bar{p})/\Gamma_{total} \times \Gamma(\gamma J/\psi(1S))/\Gamma_{total}$ $\Gamma_{47}/\Gamma \times \Gamma_{61}/\Gamma$

VALUE (units 10^{-7})	EVTS	DOCUMENT ID	TECN	COMMENT
26.5 ± 1.8 OUR FIT				
28.2 ± 2.1 OUR AVERAGE				
28.0 ± 1.9 ± 1.3	392 78,79,80	BAGNASCO 02	E835	$\bar{p}p \rightarrow \chi_{c0} \rightarrow J/\psi\gamma$
29.3 $^{+5.7}_{-4.7}$ ± 1.5	89 78,79	AMBROGIANI 99B		$\bar{p}p \rightarrow \chi_{c0} \rightarrow J/\psi\gamma$

78 Values in $(\Gamma(p\bar{p}) \times \Gamma(\gamma J/\psi(1S))/\Gamma_{total})$ and $(\Gamma(p\bar{p})/\Gamma_{total} \times \Gamma(\gamma J/\psi(1S))/\Gamma_{total})$ are not independent. The latter is used in the fit since it is less correlated to the total width.

79 Calculated by us using $B(J/\psi(1S) \rightarrow e^+e^-) = 0.0593 \pm 0.0010$.

80 Recalculated by ANDREOTTI 05A.

 $\Gamma(p\bar{p})/\Gamma_{total} \times \Gamma(\gamma\gamma)/\Gamma_{total}$ $\Gamma_{47}/\Gamma \times \Gamma_{65}/\Gamma$

VALUE (units 10^{-8})	DOCUMENT ID	TECN	COMMENT
5.1 ± 0.5 OUR FIT			
6.52 ± 1.18 $^{+0.48}_{-0.72}$	81 ANDREOTTI 04	E835	$\bar{p}p \rightarrow \chi_{c0} \rightarrow \gamma\gamma$

81 The values of $B(p\bar{p})B(\gamma\gamma)$ and $B(\gamma\gamma)B(\gamma J/\psi)$ measured by ANDREOTTI 04 are not independent. The latter is used in the fit because of smaller systematics.

 $\chi_{c0}(1P)$ CROSS-PARTICLE BRANCHING RATIOS $\Gamma(\chi_{c0}(1P) \rightarrow p\bar{p})/\Gamma_{total} \times \Gamma(\psi(2S) \rightarrow \gamma\chi_{c0}(1P))/\Gamma_{total}$

VALUE (units 10^{-6})	EVTS	DOCUMENT ID	TECN	COMMENT
21.9 ± 1.4 OUR FIT				
23.7 ± 1.8 OUR AVERAGE				
23.7 ± 1.4 ± 1.4	383 ± 22	82 NAIK 08	CLEO	$\psi(2S) \rightarrow \gamma p\bar{p}$
23.6 $^{+3.7}_{-3.4}$ ± 3.4	89.5 $^{+14}_{-13}$	BAI	04F BES	$\psi(2S) \rightarrow \gamma\chi_{c0}(1P) \rightarrow \gamma p\bar{p}$

82 Calculated by us. NAIK 08 reports $B(\chi_{c0}^0 \rightarrow p\bar{p}) = (25.7 \pm 1.5 \pm 1.5 \pm 1.3) \times 10^{-5}$ using $B(\psi(2S) \rightarrow \gamma\chi_{c0}^0) = (9.22 \pm 0.11 \pm 0.46)\%$.

 $\Gamma(\chi_{c0}(1P) \rightarrow p\bar{p})/\Gamma_{total} \times \Gamma(\psi(2S) \rightarrow \gamma\chi_{c0}(1P))/\Gamma(\psi(2S) \rightarrow J/\psi(1S)\pi^+\pi^-)$

VALUE (units 10^{-5})	DOCUMENT ID	TECN	COMMENT
6.5 ± 0.4 OUR FIT			
4.6 ± 1.9	83 BAI	98I	BES $\psi(2S) \rightarrow \gamma\chi_{c0} \rightarrow \gamma p\bar{p}$

83 Calculated by us. The value for $B(\chi_{c0} \rightarrow p\bar{p})$ reported in BAI 98I is derived using $B(\psi(2S) \rightarrow \gamma\chi_{c0}) = (9.3 \pm 0.8)\%$ and $B(\psi(2S) \rightarrow J/\psi(1S)\pi^+\pi^-) = (32.4 \pm 2.6)\%$ [BAI 98D].

 $\Gamma(\chi_{c0}(1P) \rightarrow \Lambda\bar{\Lambda})/\Gamma_{total} \times \Gamma(\psi(2S) \rightarrow \gamma\chi_{c0}(1P))/\Gamma_{total}$

VALUE (units 10^{-6})	EVTS	DOCUMENT ID	TECN	COMMENT
32 ± 4 OUR FIT				
31.2 ± 3.3 ± 2.0	131 ± 12	84 NAIK 08	CLEO	$\psi(2S) \rightarrow \gamma\Lambda\bar{\Lambda}$

84 Calculated by us. NAIK 08 reports $B(\chi_{c0}^0 \rightarrow \Lambda\bar{\Lambda}) = (33.8 \pm 3.6 \pm 2.2 \pm 1.7) \times 10^{-5}$ using $B(\psi(2S) \rightarrow \gamma\chi_{c0}^0) = (9.22 \pm 0.11 \pm 0.46)\%$.

 $\Gamma(\chi_{c0}(1P) \rightarrow \Lambda\bar{\Lambda})/\Gamma_{total} \times \Gamma(\psi(2S) \rightarrow \gamma\chi_{c0}(1P))/\Gamma(\psi(2S) \rightarrow J/\psi(1S)\pi^+\pi^-)$

VALUE (units 10^{-5})	EVTS	DOCUMENT ID	TECN	COMMENT
9.5 ± 1.1 OUR FIT				
13.0 ± 3.6 ± 2.5	15.2 $^{+4.2}_{-4.0}$	85 BAI	03E BES	$\psi(2S) \rightarrow \gamma\Lambda\bar{\Lambda}$

85 BAI 03E reports $[B(\chi_{c0}^0 \rightarrow \Lambda\bar{\Lambda})/B(\psi(2S) \rightarrow \gamma\chi_{c0}^0)] / [B(\psi(2S) \rightarrow J/\psi\pi^+\pi^-)] \times [B^2(\Lambda \rightarrow \pi^-p) / B(J/\psi \rightarrow p\bar{p})] = (2.45 $^{+0.68}_{-0.65}$ ± 0.46)\%$. We calculate from this measurement the presented value using $B(\Lambda \rightarrow \pi^-p) = (63.9 \pm 0.5)\%$ and $B(J/\psi \rightarrow p\bar{p}) = (2.17 \pm 0.07) \times 10^{-3}$.

$$\Gamma(\chi_{c0}(1P) \rightarrow \gamma J/\psi(1S))/\Gamma_{total} \times \Gamma(\psi(2S) \rightarrow \gamma \chi_{c0}(1P))/\Gamma_{total} \\ \Gamma_{61}/\Gamma \times \Gamma_{105}^{\psi(2S)}/\Gamma_{\psi(2S)}$$

VALUE (units 10^{-2})	EVTS	DOCUMENT ID	TECN	COMMENT
0.112±0.008 OUR FIT				
0.073±0.018 OUR AVERAGE				
0.069±0.018		86 OREGLIA	82 CBAL	$\psi(2S) \rightarrow \gamma \chi_{c0}$
0.4 ±0.3		87 BRANDELIK	79B DASP	$\psi(2S) \rightarrow \gamma \chi_{c0}$
0.16 ±0.11		87 BARTEL	78B CNTR	$\psi(2S) \rightarrow \gamma \chi_{c0}$
3.3 ±1.7		88 BIDDICK	77 CNTR	$e^+ e^- \rightarrow \gamma X$
• • • We do not use the following data for averages, fits, limits, etc. • • •				
0.125±0.007±0.013	560	89 MENDEZ	08 CLEO	$\psi(2S) \rightarrow \gamma \chi_{c0}$
0.18 ±0.01 ±0.02	172	90 ADAM	05A CLEO	Repl. by MENDEZ 08
86 Recalculated by us using $B(J/\psi(1S) \rightarrow \ell^+ \ell^-) = 0.1181 \pm 0.0020$.				
87 Recalculated by us using $B(J/\psi(1S) \rightarrow \mu^+ \mu^-) = 0.0588 \pm 0.0010$.				
88 Assumes isotropic gamma distribution.				
89 Not independent from other measurements of MENDEZ 08.				
90 Not independent from other values reported by ADAM 05A.				

$$\Gamma(\chi_{c0}(1P) \rightarrow \gamma J/\psi(1S))/\Gamma_{total} \times \Gamma(\psi(2S) \rightarrow \gamma \chi_{c0}(1P))/\Gamma(\psi(2S) \rightarrow \\ J/\psi(1S) \text{ anything}) \\ \Gamma_{61}/\Gamma \times \Gamma_{105}^{\psi(2S)}/\Gamma_{\psi(2S)}$$

$$\Gamma_{61}/\Gamma \times \Gamma_{105}^{\psi(2S)}/\Gamma_{\psi(2S)} = \Gamma_{61}/\Gamma \times \Gamma_{105}^{\psi(2S)}/\Gamma_{\psi(2S)} + \Gamma_{11}^{\psi(2S)}/\Gamma_{\psi(2S)} + \Gamma_{12}^{\psi(2S)}/\Gamma_{\psi(2S)} + \Gamma_{13}^{\psi(2S)}/\Gamma_{\psi(2S)} + 0.344\Gamma_{106}^{\psi(2S)}/\Gamma_{\psi(2S)} + 0.195\Gamma_{107}^{\psi(2S)}/\Gamma_{\psi(2S)}$$

VALUE (units 10^{-2})	EVTS	DOCUMENT ID	TECN	COMMENT
0.188±0.014 OUR FIT				
0.118±0.014 OUR AVERAGE				
• • • We do not use the following data for averages, fits, limits, etc. • • •				
0.201±0.011±0.021	560	91 MENDEZ	08 CLEO	$\psi(2S) \rightarrow \gamma \chi_{c0}$
0.31 ±0.02 ±0.03	172	ADAM	05A CLEO	Repl. by MENDEZ 08
91 Not independent from other measurements of MENDEZ 08.				

$$\Gamma(\chi_{c0}(1P) \rightarrow \gamma J/\psi(1S))/\Gamma_{total} \times \Gamma(\psi(2S) \rightarrow \gamma \chi_{c0}(1P))/\Gamma(\psi(2S) \rightarrow \\ J/\psi(1S) \pi^+ \pi^-) \\ \Gamma_{61}/\Gamma \times \Gamma_{105}^{\psi(2S)}/\Gamma_{11}^{\psi(2S)}$$

VALUE (units 10^{-2})	EVTS	DOCUMENT ID	TECN	COMMENT
0.333±0.024 OUR FIT				
0.358±0.020±0.037	560	MENDEZ	08 CLEO	$\psi(2S) \rightarrow \gamma \chi_{c0}$
• • • We do not use the following data for averages, fits, limits, etc. • • •				
0.55 ±0.04 ±0.06	172	92 ADAM	05A CLEO	Repl. by MENDEZ 08
92 Not independent from other values reported by ADAM 05A.				

$$\Gamma(\chi_{c0}(1P) \rightarrow \gamma \gamma)/\Gamma_{total} \times \Gamma(\psi(2S) \rightarrow \gamma \chi_{c0}(1P))/\Gamma_{total} \\ \Gamma_{65}/\Gamma \times \Gamma_{105}^{\psi(2S)}/\Gamma_{\psi(2S)}$$

VALUE (units 10^{-5})	EVTS	DOCUMENT ID	TECN	COMMENT
2.14±0.19 OUR FIT				
2.21±0.33 OUR AVERAGE				
2.17±0.32±0.10	207 ± 31	ECKLUND	08A CLEO	$\psi(2S) \rightarrow \gamma \chi_{c0} \rightarrow 3\gamma$
3.7 ±1.8 ±1.0		LEE	85 CBAL	$\psi(2S) \rightarrow \gamma \chi_{c0}$

$$\Gamma(\chi_{c0}(1P) \rightarrow \pi \pi)/\Gamma_{total} \times \Gamma(\psi(2S) \rightarrow \gamma \chi_{c0}(1P))/\Gamma_{total} \\ \Gamma_{29}/\Gamma \times \Gamma_{105}^{\psi(2S)}/\Gamma_{\psi(2S)}$$

VALUE (units 10^{-4})	EVTS	DOCUMENT ID	TECN	COMMENT
8.03±0.32 OUR FIT				
8.7 ±0.4 OUR AVERAGE				
8.81±0.11±0.43	8.9k	93 ASNER	09 CLEO	$\psi(2S) \rightarrow \gamma \pi^+ \pi^-$
8.13±0.19±0.89	2.8k	94 ASNER	09 CLEO	$\psi(2S) \rightarrow \gamma \pi^0 \pi^0$
93 Calculated by us. ASNER 09 reports $B(\chi_{c0} \rightarrow \pi^+ \pi^-) = (6.37 \pm 0.08 \pm 0.31 \pm 0.32) \times 10^{-3}$ using $B(\psi(2S) \rightarrow \gamma \chi_{c0}) = (9.22 \pm 0.11 \pm 0.46)\%$. We have multiplied the $\pi^+ \pi^-$ measurement by 3/2 to obtain $\pi\pi$.				
94 Calculated by us. ASNER 09 reports $B(\chi_{c0} \rightarrow \pi^0 \pi^0) = (2.94 \pm 0.07 \pm 0.32 \pm 0.15) \times 10^{-3}$ using $B(\psi(2S) \rightarrow \gamma \chi_{c0}) = (9.22 \pm 0.11 \pm 0.46)\%$. We have multiplied the $\pi^0 \pi^0$ measurement by 3 to obtain $\pi\pi$.				

$$\Gamma(\chi_{c0}(1P) \rightarrow \pi \pi)/\Gamma_{total} \times \Gamma(\psi(2S) \rightarrow \gamma \chi_{c0}(1P))/\Gamma(\psi(2S) \rightarrow \\ J/\psi(1S) \pi^+ \pi^-) \\ \Gamma_{29}/\Gamma \times \Gamma_{105}^{\psi(2S)}/\Gamma_{11}^{\psi(2S)}$$

VALUE (units 10^{-4})	EVTS	DOCUMENT ID	TECN	COMMENT
23.9±1.0 OUR FIT				
20.7±1.7 OUR AVERAGE				
23.9±2.7±4.1	97 ± 11	95 BAI	03c BES	$\psi(2S) \rightarrow \gamma \chi_{c0} \rightarrow \gamma \pi^0 \pi^0$
20.2±1.1±1.5	720 ± 32	96 BAI	98B BES	$\psi(2S) \rightarrow \gamma \chi_{c0} \rightarrow \gamma \pi^+ \pi^-$
95 We have multiplied $\pi^0 \pi^0$ measurement by 3 to obtain $\pi\pi$.				
96 Calculated by us. The value for $B(\chi_{c0} \rightarrow \pi^+ \pi^-)$ reported in BAI 98B is derived using $B(\psi' \rightarrow \gamma \chi_{c0}) = (9.3 \pm 0.8)\%$ and $B(\psi' \rightarrow J/\psi \pi^+ \pi^-) = (32.4 \pm 2.6)\%$ [BAI 98D]. We have multiplied $\pi^+ \pi^-$ measurement by 3/2 to obtain $\pi\pi$.				

$$\Gamma(\chi_{c0}(1P) \rightarrow \eta \eta)/\Gamma_{total} \times \Gamma(\psi(2S) \rightarrow \gamma \chi_{c0}(1P))/\Gamma_{total} \\ \Gamma_{32}/\Gamma \times \Gamma_{105}^{\psi(2S)}/\Gamma_{\psi(2S)}$$

VALUE (units 10^{-4})	EVTS	DOCUMENT ID	TECN	COMMENT
2.57±0.26 OUR FIT				
2.93±0.12±0.29	0.9k	97 ASNER	09 CLEO	$\psi(2S) \rightarrow \gamma \eta \eta$
• • • We do not use the following data for averages, fits, limits, etc. • • •				
2.86±0.46±0.37	48	98 ADAMS	07 CLEO	$\psi(2S) \rightarrow \gamma \chi_{c0}$
97 Calculated by us. ASNER 09 reports $B(\chi_{c0} \rightarrow \eta \eta) = (3.18 \pm 0.13 \pm 0.31 \pm 0.16) \times 10^{-3}$ using $B(\psi(2S) \rightarrow \gamma \chi_{c0}) = (9.22 \pm 0.11 \pm 0.46)\%$.				
98 Superseded by ASNER 09. Calculated by us. The value of $B(\chi_{c0}(1P) \rightarrow \eta \eta)$ reported by ADAMS 07 was derived using $B(\psi(2S) \rightarrow \gamma \chi_{c0}(1P)) = (9.22 \pm 0.11 \pm 0.46)\%$ (ATHAR 04).				

$$\Gamma(\chi_{c0}(1P) \rightarrow \eta \eta)/\Gamma_{total} \times \Gamma(\psi(2S) \rightarrow \gamma \chi_{c0}(1P))/\Gamma(\psi(2S) \rightarrow \\ J/\psi(1S) \pi^+ \pi^-) \\ \Gamma_{32}/\Gamma \times \Gamma_{105}^{\psi(2S)}/\Gamma_{11}^{\psi(2S)}$$

VALUE (units 10^{-3})	DOCUMENT ID	TECN	COMMENT
0.77 ±0.08 OUR FIT			
0.578±0.241±0.158	BAI	03c BES	$\psi(2S) \rightarrow \gamma \eta \eta$

$$\Gamma(\chi_{c0}(1P) \rightarrow K^+ K^-)/\Gamma_{total} \times \Gamma(\psi(2S) \rightarrow \gamma \chi_{c0}(1P))/\Gamma_{total} \\ \Gamma_{36}/\Gamma \times \Gamma_{105}^{\psi(2S)}/\Gamma_{\psi(2S)}$$

VALUE (units 10^{-4})	EVTS	DOCUMENT ID	TECN	COMMENT
5.86±0.28 OUR FIT				
5.97±0.07±0.32	8.1k	99 ASNER	09 CLEO	$\psi(2S) \rightarrow \gamma K^+ K^-$
99 Calculated by us. ASNER 09 reports $B(\chi_{c0} \rightarrow K^+ K^-) = (6.47 \pm 0.08 \pm 0.35 \pm 0.32) \times 10^{-3}$ using $B(\psi(2S) \rightarrow \gamma \chi_{c0}) = (9.22 \pm 0.11 \pm 0.46)\%$.				

$$\Gamma(\chi_{c0}(1P) \rightarrow K^+ K^-)/\Gamma_{total} \times \Gamma(\psi(2S) \rightarrow \gamma \chi_{c0}(1P))/\Gamma(\psi(2S) \rightarrow \\ J/\psi(1S) \pi^+ \pi^-) \\ \Gamma_{36}/\Gamma \times \Gamma_{105}^{\psi(2S)}/\Gamma_{11}^{\psi(2S)}$$

VALUE (units 10^{-3})	EVTS	DOCUMENT ID	TECN	COMMENT
1.75±0.09 OUR FIT				
1.63±0.10±0.15	774 ± 38	100 BAI	98B BES	$\psi(2S) \rightarrow \gamma K^+ K^-$
100 Calculated by us. The value for $B(\chi_{c0} \rightarrow K^+ K^-)$ reported by BAI 98B is derived using $B(\psi(2S) \rightarrow \gamma \chi_{c0}) = (9.3 \pm 0.8)\%$ and $B(\psi(2S) \rightarrow J/\psi \pi^+ \pi^-) = (32.4 \pm 2.6)\%$ [BAI 98D].				

$$\Gamma(\chi_{c0}(1P) \rightarrow K_S^0 K_S^0)/\Gamma_{total} \times \Gamma(\psi(2S) \rightarrow \gamma \chi_{c0}(1P))/\Gamma_{total} \\ \Gamma_{37}/\Gamma \times \Gamma_{105}^{\psi(2S)}/\Gamma_{\psi(2S)}$$

VALUE (units 10^{-4})	EVTS	DOCUMENT ID	TECN	COMMENT
3.04±0.15 OUR FIT				
3.18±0.17 OUR AVERAGE				
3.22±0.07±0.17	2.1k	101 ASNER	09 CLEO	$\psi(2S) \rightarrow \gamma K_S^0 K_S^0$
3.02±0.19±0.33	322	ABLIKIM	05o BES2	$\psi(2S) \rightarrow \gamma K_S^0 K_S^0$
101 Calculated by us. ASNER 09 reports $B(\chi_{c0} \rightarrow K_S^0 K_S^0) = (3.49 \pm 0.08 \pm 0.18 \pm 0.17) \times 10^{-3}$ using $B(\psi(2S) \rightarrow \gamma \chi_{c0}) = (9.22 \pm 0.11 \pm 0.46)\%$.				

$$\Gamma(\chi_{c0}(1P) \rightarrow K_S^0 K_S^0)/\Gamma_{total} \times \Gamma(\psi(2S) \rightarrow \gamma \chi_{c0}(1P))/\Gamma(\psi(2S) \rightarrow \\ J/\psi(1S) \pi^+ \pi^-) \\ \Gamma_{37}/\Gamma \times \Gamma_{105}^{\psi(2S)}/\Gamma_{11}^{\psi(2S)}$$

VALUE (units 10^{-4})	DOCUMENT ID	TECN	COMMENT
9.1±0.5 OUR FIT			
5.6±0.8±1.3	102 BAI	99B BES	$\psi(2S) \rightarrow \gamma K_S^0 K_S^0$
102 Calculated by us. The value of $B(\chi_{c0} \rightarrow K_S^0 K_S^0)$ reported by BAI 99B was derived using $B(\psi(2S) \rightarrow \gamma \chi_{c0}(1P)) = (9.3 \pm 0.8)\%$ and $B(\psi(2S) \rightarrow J/\psi \pi^+ \pi^-) = (32.4 \pm 2.6)\%$ [BAI 98D].			

$$\Gamma(\chi_{c0}(1P) \rightarrow 2(\pi^+ \pi^-))/\Gamma_{total} \times \Gamma(\psi(2S) \rightarrow \gamma \chi_{c0}(1P))/\Gamma(\psi(2S) \rightarrow \\ J/\psi(1S) \pi^+ \pi^-) \\ \Gamma_{11}/\Gamma \times \Gamma_{105}^{\psi(2S)}/\Gamma_{11}^{\psi(2S)}$$

VALUE (units 10^{-3})	DOCUMENT ID	TECN	COMMENT
6.5±0.5 OUR FIT			
6.9±2.4 OUR AVERAGE			Error includes scale factor of 3.8.
4.4±0.1±0.9	103 BAI	99B BES	$\psi(2S) \rightarrow \gamma \chi_{c0}$
9.3±0.9	104 TANENBAUM	78 MRK1	$\psi(2S) \rightarrow \gamma \chi_{c0}$
103 Calculated by us. The value for $B(\chi_{c0} \rightarrow 2\pi^+ 2\pi^-)$ reported in BAI 99B is derived using $B(\psi(2S) \rightarrow \gamma \chi_{c0}) = (9.3 \pm 0.8)\%$ and $B(\psi(2S) \rightarrow J/\psi(1S) \pi^+ \pi^-) = (32.4 \pm 2.6)\%$ [BAI 98D].			
104 The value $B(\psi(1S) \rightarrow \gamma \chi_{c0}) \times B(\chi_{c0} \rightarrow 2\pi^+ 2\pi^-)$ reported in TANENBAUM 78 is derived using $B(\psi(2S) \rightarrow J/\psi(1S) \pi^+ \pi^-) \times B(J/\psi(1S) \rightarrow \ell^+ \ell^-) = (4.6 \pm 0.7)\%$. Calculated by us using $B(J/\psi(1S) \rightarrow \ell^+ \ell^-) = 0.1181 \pm 0.0020$.			

$$\Gamma(\chi_{c0}(1P) \rightarrow \pi^+ \pi^- K^+ K^-)/\Gamma_{total} \times \Gamma(\psi(2S) \rightarrow \gamma \chi_{c0}(1P))/\Gamma_{total} \\ \Gamma_{7}/\Gamma \times \Gamma_{105}^{\psi(2S)}/\Gamma_{\psi(2S)}$$

VALUE (units 10^{-3})	DOCUMENT ID	TECN	COMMENT
1.73±0.13 OUR FIT			
1.64±0.05±0.2	ABLIKIM	05q BES2	$\psi(2S) \rightarrow \gamma \chi_{c0}$

Meson Particle Listings

$\chi_{c0}(1P), \chi_{c1}(1P)$

$$\Gamma(\chi_{c0}(1P) \rightarrow \pi^+ \pi^- K^+ K^-) / \Gamma_{\text{total}} \times \Gamma(\psi(2S) \rightarrow \gamma \chi_{c0}(1P)) / \Gamma(\psi(2S) \rightarrow J/\psi(1S) \pi^+ \pi^-)$$

$$\frac{\Gamma_7 / \Gamma \times \Gamma_{105}^{\psi(2S)} / \Gamma_{11}^{\psi(2S)}}{\Gamma_{105}^{\psi(2S)} / \Gamma_{11}^{\psi(2S)}}$$

VALUE (units 10 ⁻³)	DOCUMENT ID	TECN	COMMENT
5.2 ± 0.4 OUR FIT			
5.8 ± 1.6 OUR AVERAGE			Error includes scale factor of 2.3.
4.22 ± 0.20 ± 0.97	BAI	99B BES	$\psi(2S) \rightarrow \gamma \chi_{c0}$
7.4 ± 1.0	105 TANENBAUM	78 MRK1	$\psi(2S) \rightarrow \gamma \chi_{c0}$

105 The reported value is derived using $B(\psi(2S) \rightarrow \pi^+ \pi^- J/\psi) \times B(J/\psi \rightarrow \ell^+ \ell^-) = (4.6 \pm 0.7)\%$. Calculated by us using $B(J/\psi \rightarrow \ell^+ \ell^-) = 0.1181 \pm 0.0020$.

$$\Gamma(\chi_{c0}(1P) \rightarrow K^+ K^- K^+ K^-) / \Gamma_{\text{total}} \times \Gamma(\psi(2S) \rightarrow \gamma \chi_{c0}(1P)) / \Gamma_{\text{total}}$$

$$\frac{\Gamma_{44} / \Gamma \times \Gamma_{105}^{\psi(2S)} / \Gamma_{11}^{\psi(2S)}}{\Gamma_{105}^{\psi(2S)} / \Gamma_{11}^{\psi(2S)}}$$

VALUE (units 10 ⁻⁴)	EVTS	DOCUMENT ID	TECN	COMMENT
2.70 ± 0.27 OUR FIT				
3.20 ± 0.11 ± 0.41	278	106 ABLIKIM	06T BES2	$\psi(2S) \rightarrow \gamma 2K^+ 2K^-$

106 Calculated by us. The value of $B(\chi_{c0} \rightarrow 2K^+ 2K^-)$ reported by ABLIKIM 06T was derived using $B(\psi(2S) \rightarrow \gamma \chi_{c0}(1P)) = (9.2 \pm 0.4)\%$.

$$\Gamma(\chi_{c0}(1P) \rightarrow K^+ K^- K^+ K^-) / \Gamma_{\text{total}} \times \Gamma(\psi(2S) \rightarrow \gamma \chi_{c0}(1P)) / \Gamma(\psi(2S) \rightarrow J/\psi(1S) \pi^+ \pi^-)$$

$$\frac{\Gamma_{44} / \Gamma \times \Gamma_{105}^{\psi(2S)} / \Gamma_{11}^{\psi(2S)}}{\Gamma_{105}^{\psi(2S)} / \Gamma_{11}^{\psi(2S)}}$$

VALUE (units 10 ⁻⁴)	EVTS	DOCUMENT ID	TECN	COMMENT
8.0 ± 0.8 OUR FIT				
6.1 ± 0.8 ± 0.9	107	BAI	99B BES	$\psi(2S) \rightarrow \gamma 2K^+ 2K^-$

107 Calculated by us. The value of $B(\chi_{c0} \rightarrow 2K^+ 2K^-)$ reported by BAI 99B was derived using $B(\psi(2S) \rightarrow \gamma \chi_{c0}(1P)) = (9.3 \pm 0.8)\%$ and $B(\psi(2S) \rightarrow J/\psi \pi^+ \pi^-) = (32.4 \pm 2.6)\%$ [BAI 98D].

$$\Gamma(\chi_{c0}(1P) \rightarrow \phi\phi) / \Gamma_{\text{total}} \times \Gamma(\psi(2S) \rightarrow \gamma \chi_{c0}(1P)) / \Gamma_{\text{total}}$$

$$\frac{\Gamma_{46} / \Gamma \times \Gamma_{105}^{\psi(2S)} / \Gamma_{11}^{\psi(2S)}}{\Gamma_{105}^{\psi(2S)} / \Gamma_{11}^{\psi(2S)}}$$

VALUE (units 10 ⁻⁴)	EVTS	DOCUMENT ID	TECN	COMMENT
0.88 ± 0.18 OUR FIT				
0.86 ± 0.19 ± 0.12	26	108 ABLIKIM	06T BES2	$\psi(2S) \rightarrow \gamma 2K^+ 2K^-$

108 Calculated by us. The value of $B(\chi_{c0} \rightarrow \phi\phi)$ reported by ABLIKIM 06T was derived using $B(\psi(2S) \rightarrow \gamma \chi_{c0}(1P)) = (9.2 \pm 0.4)\%$.

$$\Gamma(\chi_{c0}(1P) \rightarrow \phi\phi) / \Gamma_{\text{total}} \times \Gamma(\psi(2S) \rightarrow \gamma \chi_{c0}(1P)) / \Gamma(\psi(2S) \rightarrow J/\psi(1S) \pi^+ \pi^-)$$

$$\frac{\Gamma_{46} / \Gamma \times \Gamma_{105}^{\psi(2S)} / \Gamma_{11}^{\psi(2S)}}{\Gamma_{105}^{\psi(2S)} / \Gamma_{11}^{\psi(2S)}}$$

VALUE (units 10 ⁻⁴)	EVTS	DOCUMENT ID	TECN	COMMENT
2.6 ± 0.5 OUR FIT				
2.6 ± 1.0 ± 1.1	109	BAI	99B BES	$\psi(2S) \rightarrow \gamma 2K^+ 2K^-$

109 Calculated by us. The value of $B(\chi_{c0} \rightarrow \phi\phi)$ reported by BAI 99B was derived using $B(\psi(2S) \rightarrow \gamma \chi_{c0}(1P)) = (9.3 \pm 0.8)\%$ and $B(\psi(2S) \rightarrow J/\psi \pi^+ \pi^-) = (32.4 \pm 2.6)\%$ [BAI 98D].

$\chi_{c0}(1P)$ REFERENCES

Author	Year	Ref	TECN	Comment
ASNER	09	PR D79 072007		(CLEO Collab.)
UEHARA	09	PR D79 052009		(BELLE Collab.)
BENNETT	08A	PRL 101 151801		(CLEO Collab.)
ECKLUND	08A	PR D78 091501R		(CLEO Collab.)
HE	08B	PR D78 092004		(CLEO Collab.)
MENDEZ	08	PR D78 111102R		(CLEO Collab.)
NAIK	08	PR D78 031101R		(CLEO Collab.)
UEHARA	08	EPJ C53 1		(BELLE Collab.)
WICHT	08	PL B662 323		(BELLE Collab.)
ABE	07	PRL 98 082001		(BELLE Collab.)
ADAMS	07	PR D75 071101R		(CLEO Collab.)
ATHAR	07	PR D75 032002		(CLEO Collab.)
CHEN	07B	PL B651 15		(BELLE Collab.)
ABLIKIM	06D	PR D73 052006		(BES Collab.)
ABLIKIM	06I	PR D74 012004		(BES Collab.)
ABLIKIM	06R	PR D74 072001		(BES Collab.)
ABLIKIM	06T	PL B642 197		(BES Collab.)
ABLIKIM	05G	PR D71 092002		(BES Collab.)
ABLIKIM	05N	PL B630 7		(BES Collab.)
ABLIKIM	05O	PL B630 21		(BES Collab.)
ABLIKIM	05Q	PR D72 092002		(BES Collab.)
ADAM	05A	PRL 94 232002		(CLEO Collab.)
ANDREOTTI	05A	NP B717 34		(FNAL E835 Collab.)
ANDREOTTI	05C	PR D72 112002		(FNAL E835 Collab.)
NAKAZAWA	05	PL B615 39		(BELLE Collab.)
ABE	04G	PR D70 071102		(BELLE Collab.)
ABLIKIM	04G	PR D70 092002		(BES Collab.)
ABLIKIM	04H	PR D70 092003		(BES Collab.)
ANDREOTTI	04	PL B584 16		(E835 Collab.)
ATHAR	04	PR D70 112002		(CLEO Collab.)
BAI	04F	PR D69 092001		(BES Collab.)
ANDREOTTI	03	PRL 91 091801		(FNAL E835 Collab.)
AULCHENKO	03	PL B573 63		(KEDR Collab.)
BAI	03C	PR D67 032004		(BES Collab.)
BAI	03E	PR D67 112001		(BES Collab.)
ABE K	02	PRL 89 142001		(BELLE Collab.)
BAGNASCO	02	PL B533 237		(FNAL E835 Collab.)
EISENSTEIN	01	PRL 87 061801		(CLEO Collab.)
AMBROGIANI	00B	PR D62 052002		(FNAL E835 Collab.)
AMBROGIANI	99B	PRL 83 2902		(FNAL E835 Collab.)
BAI	99B	PR D60 072001		(BES Collab.)
BAI	98D	PR D58 092006		(BES Collab.)
BAI	98I	PRL 81 3091		(BES Collab.)
GAISER	86	PR D34 711		(Crystal Ball Collab.)
LEE	85	SLAC 282		(SLAC)
OREGLIA	82	PR D25 2259		(SLAC, CIT, HARV+)
BRANDELIK	79B	NP B160 426		(DASP Collab.)
BARTEL	78B	PL 79B 492		(DESY, HEIDP)
TANENBAUM	78	PR D17 1731		(SLAC, LBL)
Also		Private Comm.		(LBL, UCBA)
BIDDICK	77	PRL 38 1324		(UCSD, UMD, PAVI+)

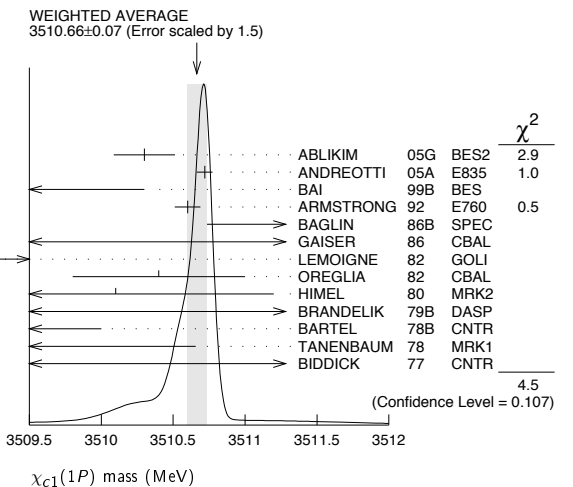
$$\chi_{c1}(1P) \quad J^G(J^PC) = 0^+(1^{++})$$

See the Review on " $\psi(2S)$ and χ_c branching ratios" before the $\chi_{c0}(1P)$ Listings.

$\chi_{c1}(1P)$ MASS

VALUE (MeV)	EVTS	DOCUMENT ID	TECN	COMMENT
3510.66 ± 0.07 OUR AVERAGE				Error includes scale factor of 1.5. See the ideogram below.
3510.30 ± 0.14 ± 0.16		ABLIKIM	05G BES2	$\psi(2S) \rightarrow \gamma \chi_{c1}$
3510.719 ± 0.051 ± 0.019		ANDREOTTI	05A E835	$p\bar{p} \rightarrow e^+ e^- \gamma$
3509.4 ± 0.9		BAI	99B BES	$\psi(2S) \rightarrow \gamma X$
3510.60 ± 0.087 ± 0.019	513	1 ARMSTRONG	92 E760	$\bar{p}p \rightarrow e^+ e^- \gamma$
3511.3 ± 0.4 ± 0.4	30	BAGLIN	86B SPEC	$\bar{p}p \rightarrow e^+ e^- X$
3512.3 ± 0.3 ± 4.0		2 GAISER	86 CBAL	$\psi(2S) \rightarrow \gamma X$
3507.4 ± 1.7	91	3 LEMOIGNE	82 GOLI	$185 \pi^- \text{Be} \rightarrow \gamma \mu^+ \mu^- A$
3510.4 ± 0.6		OREGLIA	82 CBAL	$e^+ e^- \rightarrow J/\psi 2\gamma$
3510.1 ± 1.1	254	4 HIMEL	80 MRK2	$e^+ e^- \rightarrow J/\psi 2\gamma$
3509 ± 11	21	BRANDELIK	79B DASP	$e^+ e^- \rightarrow J/\psi 2\gamma$
3507 ± 3		4 BARTEL	78B CNTR	$e^+ e^- \rightarrow J/\psi 2\gamma$
3505.0 ± 4 ± 4		4.5 TANENBAUM	78 MRK1	$e^+ e^-$
3513 ± 7	367	4 BIDDICK	77 CNTR	$\psi(2S) \rightarrow \gamma X$
3500 ± 10	40	TANENBAUM	75 MRK1	Hadrons γ

- • • We do not use the following data for averages, fits, limits, etc. • • •
- 1 Recalculated by ANDREOTTI 05A, using the value of $\psi(2S)$ mass from AULCHENKO 03.
- 2 Using mass of $\psi(2S) = 3686.0$ MeV.
- 3 $J/\psi(1S)$ mass constrained to 3097 MeV.
- 4 Mass value shifted by us by amount appropriate for $\psi(2S)$ mass = 3686 MeV and $J/\psi(1S)$ mass = 3097 MeV.
- 5 From a simultaneous fit to radiative and hadronic decay channels.



$\chi_{c1}(1P)$ WIDTH

VALUE (MeV)	CL%	EVTS	DOCUMENT ID	TECN	COMMENT
0.86 ± 0.05 OUR FIT					
0.88 ± 0.05 OUR AVERAGE					
1.39 +0.40 +0.26 -0.38 -0.77			ABLIKIM	05G BES2	$\psi(2S) \rightarrow \gamma \chi_{c1}$
0.876 ± 0.045 ± 0.026			ANDREOTTI	05A E835	$p\bar{p} \rightarrow e^+ e^- \gamma$
0.87 ± 0.11 ± 0.08		513	6 ARMSTRONG	92 E760	$\bar{p}p \rightarrow e^+ e^- \gamma$
<1.3	95		BAGLIN	86B SPEC	$\bar{p}p \rightarrow e^+ e^- X$
<3.8	90		GAISER	86 CBAL	$\psi(2S) \rightarrow \gamma X$

6 Recalculated by ANDREOTTI 05A.

$\chi_{c1}(1P)$ DECAY MODES

Mode	Fraction (Γ_i/Γ)	Scale factor/ Confidence level
Hadronic decays		
Γ_1 $3(\pi^+\pi^-)$	$(5.8 \pm 1.4) \times 10^{-3}$	S=1.2
Γ_2 $2(\pi^+\pi^-)$	$(7.6 \pm 2.6) \times 10^{-3}$	
Γ_3 $\pi^+\pi^-\pi^0\pi^0$	$(1.26 \pm 0.17) \%$	
Γ_4 $\rho^+\pi^-\pi^0 + \text{c.c.}$	$(1.53 \pm 0.26) \%$	
Γ_5 $\rho^0\pi^+\pi^-$	$(3.9 \pm 3.5) \times 10^{-3}$	
Γ_6 $\pi^+\pi^-K^+K^-$	$(4.5 \pm 1.0) \times 10^{-3}$	
Γ_7 $K^+K^-\pi^0\pi^0$	$(1.18 \pm 0.29) \times 10^{-3}$	
Γ_8 $K^+\pi^-K^0\pi^0 + \text{c.c.}$	$(9.0 \pm 1.5) \times 10^{-3}$	
Γ_9 $\rho^+K^-K^0 + \text{c.c.}$	$(5.3 \pm 1.3) \times 10^{-3}$	
Γ_{10} $K^*(892)^0K^0\pi^0 \rightarrow K^+\pi^-K^0\pi^0 + \text{c.c.}$	$(2.5 \pm 0.7) \times 10^{-3}$	
Γ_{11} $K^+K^-\eta\pi^0$	$(1.2 \pm 0.4) \times 10^{-3}$	
Γ_{12} $\pi^+\pi^-K_S^0K_S^0$	$(7.2 \pm 3.1) \times 10^{-4}$	
Γ_{13} $K^+K^-\eta$	$(3.3 \pm 1.0) \times 10^{-4}$	
Γ_{14} $K^0K^+\pi^- + \text{c.c.}$	$(7.3 \pm 0.6) \times 10^{-3}$	
Γ_{15} $K^*(892)^0\bar{K}^0 + \text{c.c.}$	$(1.0 \pm 0.4) \times 10^{-3}$	
Γ_{16} $K^*(892)^+K^- + \text{c.c.}$	$(1.5 \pm 0.7) \times 10^{-3}$	
Γ_{17} $K_J^*(1430)^0\bar{K}^0 + \text{c.c.} \rightarrow K_S^0K^+\pi^- + \text{c.c.}$	$< 8 \times 10^{-4}$	CL=90%
Γ_{18} $K_J^*(1430)^+K^- + \text{c.c.} \rightarrow K_S^0K^+\pi^- + \text{c.c.}$	$< 2.3 \times 10^{-3}$	CL=90%
Γ_{19} $K^+K^-\pi^0$	$(1.91 \pm 0.26) \times 10^{-3}$	
Γ_{20} $\eta\pi^+\pi^-$	$(5.0 \pm 0.5) \times 10^{-3}$	
Γ_{21} $a_0(980)^+\pi^- + \text{c.c.} \rightarrow \eta\pi^+\pi^-$	$(1.9 \pm 0.7) \times 10^{-3}$	
Γ_{22} $f_2(1270)\eta$	$(2.8 \pm 0.8) \times 10^{-3}$	
Γ_{23} $\pi^+\pi^-\eta'$	$(2.4 \pm 0.5) \times 10^{-3}$	
Γ_{24} $K^+\bar{K}^*(892)^0\pi^- + \text{c.c.}$	$(3.2 \pm 2.1) \times 10^{-3}$	
Γ_{25} $K^*(892)^0\bar{K}^*(892)^0$	$(1.5 \pm 0.4) \times 10^{-3}$	
Γ_{26} $K^+K^-K_S^0K_S^0$	$< 5 \times 10^{-4}$	CL=90%
Γ_{27} $K^+K^-K^+K^-$	$(5.6 \pm 1.2) \times 10^{-4}$	
Γ_{28} $K^+K^-\phi$	$(4.3 \pm 1.6) \times 10^{-4}$	
Γ_{29} $\rho\bar{\rho}$	$(7.3 \pm 0.4) \times 10^{-5}$	
Γ_{30} $\rho\bar{\rho}\pi^0$	$(1.2 \pm 0.5) \times 10^{-4}$	
Γ_{31} $\rho\bar{\rho}\eta$	$< 1.6 \times 10^{-4}$	CL=90%
Γ_{32} $\pi^+\pi^-\rho\bar{\rho}$	$(5.0 \pm 1.9) \times 10^{-4}$	
Γ_{33} $\pi^0\pi^0\rho\bar{\rho}$		
Γ_{34} $K_S^0K_S^0\rho\bar{\rho}$	$< 4.5 \times 10^{-4}$	CL=90%
Γ_{35} $\Lambda\bar{\Lambda}$	$(1.18 \pm 0.19) \times 10^{-4}$	
Γ_{36} $\Lambda\bar{\Lambda}\pi^+\pi^-$	$< 1.5 \times 10^{-3}$	CL=90%
Γ_{37} $K^+\bar{\rho}\Lambda$	$(3.2 \pm 1.0) \times 10^{-4}$	
Γ_{38} $\Sigma^0\bar{\Sigma}^0$	$< 4 \times 10^{-5}$	CL=90%
Γ_{39} $\Sigma^+\bar{\Sigma}^-$	$< 6 \times 10^{-5}$	CL=90%
Γ_{40} $=\bar{0}=\bar{0}$	$< 6 \times 10^{-5}$	CL=90%
Γ_{41} $\Xi^-\bar{\Xi}^+$	$(8.4 \pm 2.3) \times 10^{-5}$	
Γ_{42} $\pi^+\pi^- + K^+K^-$	$< 2.1 \times 10^{-3}$	
Γ_{43} $K_S^0K_S^0$	$< 6 \times 10^{-5}$	CL=90%
Radiative decays		
Γ_{44} $\gamma J/\psi(1S)$	$(34.4 \pm 1.5) \%$	
Γ_{45} $\gamma\rho^0$	$(2.29 \pm 0.27) \times 10^{-4}$	
Γ_{46} $\gamma\omega$	$(7.8 \pm 1.8) \times 10^{-5}$	
Γ_{47} $\gamma\phi$	$< 2.4 \times 10^{-5}$	CL=90%
Γ_{48} $\gamma\gamma$		

CONSTRAINED FIT INFORMATION

A multiparticle fit to $\chi_{c1}(1P)$, $\chi_{c0}(1P)$, $\chi_{c2}(1P)$, and $\psi(2S)$ with 4 total widths, a partial width, 24 combinations of partial widths obtained from integrated cross section, and 82 branching ratios uses 213 measurements to determine 47 parameters. The overall fit has a $\chi^2 = 301.4$ for 166 degrees of freedom.

The following *off-diagonal* array elements are the correlation coefficients $\langle \delta p_i \delta p_j \rangle / (\delta p_i \delta p_j)$, in percent, from the fit to parameters p_i , including the branching fractions, $x_i \equiv \Gamma_i / \Gamma_{\text{total}}$.

x_{27}	8				
x_{29}	-9	-4			
x_{35}	11	5	-5		
x_{44}	36	16	-32	20	
Γ	-13	-5	-59	-7	-30
	x_{14}	x_{27}	x_{29}	x_{35}	x_{44}

 $\chi_{c1}(1P)$ PARTIAL WIDTHS $\chi_{c1}(1P)$ $\Gamma(i)\Gamma(\gamma J/\psi(1S))/\Gamma(\text{total})$

$\Gamma(p\bar{p}) \times \Gamma(\gamma J/\psi(1S))/\Gamma_{\text{total}}$	DOCUMENT ID	TECN	COMMENT
21.7 ± 0.8 OUR FIT			
21.4 ± 0.9 OUR AVERAGE			
21.5 ± 0.5 ± 0.8	⁷ ANDREOTTI 05A	E835	$p\bar{p} \rightarrow e^+e^-\gamma$
21.4 ± 1.5 ± 2.2	^{7,8} ARMSTRONG 92	E760	$p\bar{p} \rightarrow e^+e^-\gamma$
19.9 ^{+4.4} _{-4.0}	⁷ BAGLIN 86B	SPEC	$p\bar{p} \rightarrow e^+e^-\gamma$

⁷ Calculated by us using $B(J/\psi(1S) \rightarrow e^+e^-) = 0.0593 \pm 0.0010$.

⁸ Recalculated by ANDREOTTI 05A.

 $\chi_{c1}(1P)$ BRANCHING RATIOS

HADRONIC DECAYS

$\Gamma(3(\pi^+\pi^-))/\Gamma_{\text{total}}$	DOCUMENT ID	TECN	COMMENT
5.8 ± 1.4 OUR EVALUATION			Error includes scale factor of 1.2. Treating systematic error as correlated.
5.8 ± 1.1 OUR AVERAGE			
5.4 ± 0.7 ± 0.9	⁹ BAI 99B	BES	$\psi(2S) \rightarrow \gamma\chi_{c1}$
16.0 ± 5.9 ± 0.8	⁹ TANENBAUM 78	MRK1	$\psi(2S) \rightarrow \gamma\chi_{c1}$

⁹ Rescaled by us using $B(\psi(2S) \rightarrow \gamma\chi_{c1}) = (8.8 \pm 0.4)\%$ and $B(\psi(2S) \rightarrow J/\psi(1S)\pi^+\pi^-) = (32.6 \pm 0.5)\%$.

$\Gamma(2(\pi^+\pi^-))/\Gamma_{\text{total}}$	DOCUMENT ID	TECN	COMMENT
7.6 ± 2.6 OUR EVALUATION			Treating systematic error as correlated.
8 ± 4 OUR AVERAGE			Error includes scale factor of 1.5.
4.6 ± 2.1 ± 2.6	¹⁰ BAI 99B	BES	$\psi(2S) \rightarrow \gamma\chi_{c1}$
12.5 ± 4.2 ± 0.6	¹⁰ TANENBAUM 78	MRK1	$\psi(2S) \rightarrow \gamma\chi_{c1}$

¹⁰ Rescaled by us using $B(\psi(2S) \rightarrow \gamma\chi_{c1}) = (8.8 \pm 0.4)\%$ and $B(\psi(2S) \rightarrow J/\psi(1S)\pi^+\pi^-) = (32.6 \pm 0.5)\%$.

$\Gamma(\pi^+\pi^-\pi^0\pi^0)/\Gamma_{\text{total}}$	DOCUMENT ID	TECN	COMMENT
1.26 ± 0.16 ± 0.05	604.7	11 HE 08B	CLEO $e^+e^- \rightarrow \gamma h^+ h^- h^0 h^0$

¹¹ HE 08B reports $1.28 \pm 0.06 \pm 0.15 \pm 0.08 \%$ from a measurement of $[\Gamma(\chi_{c1}(1P) \rightarrow \pi^+\pi^-\pi^0\pi^0)/\Gamma_{\text{total}}] \times [B(\psi(2S) \rightarrow \gamma\chi_{c1}(1P))]$ assuming $B(\psi(2S) \rightarrow \gamma\chi_{c1}(1P)) = (9.07 \pm 0.11 \pm 0.54) \times 10^{-2}$, which we rescale to our best value $B(\psi(2S) \rightarrow \gamma\chi_{c1}(1P)) = (9.2 \pm 0.4) \times 10^{-2}$. Our first error is their experiment's error and our second error is the systematic error from using our best value.

$\Gamma(\rho^+\pi^-\pi^0 + \text{c.c.})/\Gamma_{\text{total}}$	DOCUMENT ID	TECN	COMMENT
1.53 ± 0.25 ± 0.06	712.3	12,13 HE 08B	CLEO $e^+e^- \rightarrow \gamma h^+ h^- h^0 h^0$

¹² HE 08B reports $1.56 \pm 0.13 \pm 0.22 \pm 0.10 \%$ from a measurement of $[\Gamma(\chi_{c1}(1P) \rightarrow \rho^+\pi^-\pi^0 + \text{c.c.})/\Gamma_{\text{total}}] \times [B(\psi(2S) \rightarrow \gamma\chi_{c1}(1P))]$ assuming $B(\psi(2S) \rightarrow \gamma\chi_{c1}(1P)) = (9.07 \pm 0.11 \pm 0.54) \times 10^{-2}$, which we rescale to our best value $B(\psi(2S) \rightarrow \gamma\chi_{c1}(1P)) = (9.2 \pm 0.4) \times 10^{-2}$. Our first error is their experiment's error and our second error is the systematic error from using our best value.

¹³ Calculated by us. We have added the values from HE 08B for $\rho^+\pi^-\pi^0$ and $\rho^-\pi^+\pi^0$ decays assuming uncorrelated statistical and fully correlated systematic uncertainties.

$\Gamma(\rho^0\pi^+\pi^-)/\Gamma_{\text{total}}$	DOCUMENT ID	TECN	COMMENT
39 ± 35	14	TANENBAUM 78	MRK1 $\psi(2S) \rightarrow \gamma\chi_{c1}$

¹⁴ Estimated using $B(\psi(2S) \rightarrow \gamma\chi_{c1}(1P)) = 0.087$. The errors do not contain the uncertainty in the $\psi(2S)$ decay.

Meson Particle Listings

 $\chi_{c1}(1P)$

$\Gamma(\pi^+ \pi^- K^+ K^-)/\Gamma_{\text{total}}$	Γ_6/Γ
VALUE (units 10^{-3})	DOCUMENT ID TECN COMMENT
4.5 ± 1.0 OUR EVALUATION	Treating systematic error as correlated.
4.5 ± 0.9 OUR AVERAGE	
4.2 ± 0.4 ± 0.9	15 BAI 99B BES $\psi(2S) \rightarrow \gamma \chi_{c1}$
7.3 ± 3.0 ± 0.4	15 TANENBAUM 78 MRK1 $\psi(2S) \rightarrow \gamma \chi_{c1}$
15 Rescaled by us using $B(\psi(2S) \rightarrow \gamma \chi_{c1}) = (8.8 \pm 0.4)\%$ and $B(\psi(2S) \rightarrow J/\psi(1S) \pi^+ \pi^-) = (32.6 \pm 0.5)\%$.	

$\Gamma(K^+ K^- \pi^0 \pi^0)/\Gamma_{\text{total}}$	Γ_7/Γ
VALUE (%)	DOCUMENT ID TECN COMMENT
0.118 ± 0.029 ± 0.005	45.1 16 HE 08B CLEO $e^+ e^- \rightarrow \gamma h^+ h^- h^0 h^0$
16 HE 08B reports $0.12 \pm 0.02 \pm 0.02 \pm 0.01\%$ from a measurement of $[\Gamma(\chi_{c1}(1P) \rightarrow K^+ K^- \pi^0 \pi^0)/\Gamma_{\text{total}}] \times [B(\psi(2S) \rightarrow \gamma \chi_{c1}(1P))]$ assuming $B(\psi(2S) \rightarrow \gamma \chi_{c1}(1P)) = (9.07 \pm 0.11 \pm 0.54) \times 10^{-2}$, which we rescale to our best value $B(\psi(2S) \rightarrow \gamma \chi_{c1}(1P)) = (9.2 \pm 0.4) \times 10^{-2}$. Our first error is their experiment's error and our second error is the systematic error from using our best value.	

$\Gamma(K^+ \pi^- K^0 \pi^0 + \text{c.c.})/\Gamma_{\text{total}}$	Γ_8/Γ
VALUE (%)	DOCUMENT ID TECN COMMENT
0.90 ± 0.14 ± 0.03	141.3 17 HE 08B CLEO $e^+ e^- \rightarrow \gamma h^+ h^- h^0 h^0$
17 HE 08B reports $0.92 \pm 0.09 \pm 0.11 \pm 0.06\%$ from a measurement of $[\Gamma(\chi_{c1}(1P) \rightarrow K^+ \pi^- K^0 \pi^0 + \text{c.c.})/\Gamma_{\text{total}}] \times [B(\psi(2S) \rightarrow \gamma \chi_{c1}(1P))]$ assuming $B(\psi(2S) \rightarrow \gamma \chi_{c1}(1P)) = (9.07 \pm 0.11 \pm 0.54) \times 10^{-2}$, which we rescale to our best value $B(\psi(2S) \rightarrow \gamma \chi_{c1}(1P)) = (9.2 \pm 0.4) \times 10^{-2}$. Our first error is their experiment's error and our second error is the systematic error from using our best value.	

$\Gamma(\rho^+ K^- K^0 + \text{c.c.})/\Gamma_{\text{total}}$	Γ_9/Γ
VALUE (%)	DOCUMENT ID TECN COMMENT
0.53 ± 0.13 ± 0.02	141.3 18 HE 08B CLEO $e^+ e^- \rightarrow \gamma h^+ h^- h^0 h^0$
18 HE 08B reports $0.54 \pm 0.11 \pm 0.07 \pm 0.03\%$ from a measurement of $[\Gamma(\chi_{c1}(1P) \rightarrow \rho^+ K^- K^0 + \text{c.c.})/\Gamma_{\text{total}}] \times [B(\psi(2S) \rightarrow \gamma \chi_{c1}(1P))]$ assuming $B(\psi(2S) \rightarrow \gamma \chi_{c1}(1P)) = (9.07 \pm 0.11 \pm 0.54) \times 10^{-2}$, which we rescale to our best value $B(\psi(2S) \rightarrow \gamma \chi_{c1}(1P)) = (9.2 \pm 0.4) \times 10^{-2}$. Our first error is their experiment's error and our second error is the systematic error from using our best value.	

$\Gamma(K^*(892)^0 K^0 \pi^0 \rightarrow K^+ \pi^- K^0 \pi^0 + \text{c.c.})/\Gamma_{\text{total}}$	Γ_{10}/Γ
VALUE (%)	DOCUMENT ID TECN COMMENT
0.25 ± 0.07 ± 0.01	141.3 19 HE 08B CLEO $e^+ e^- \rightarrow \gamma h^+ h^- h^0 h^0$
19 HE 08B reports $0.25 \pm 0.06 \pm 0.03 \pm 0.02\%$ from a measurement of $[\Gamma(\chi_{c1}(1P) \rightarrow K^*(892)^0 K^0 \pi^0 \rightarrow K^+ \pi^- K^0 \pi^0 + \text{c.c.})/\Gamma_{\text{total}}] \times [B(\psi(2S) \rightarrow \gamma \chi_{c1}(1P))]$ assuming $B(\psi(2S) \rightarrow \gamma \chi_{c1}(1P)) = (9.07 \pm 0.11 \pm 0.54) \times 10^{-2}$, which we rescale to our best value $B(\psi(2S) \rightarrow \gamma \chi_{c1}(1P)) = (9.2 \pm 0.4) \times 10^{-2}$. Our first error is their experiment's error and our second error is the systematic error from using our best value.	

$\Gamma(K^+ K^- \eta \pi^0)/\Gamma_{\text{total}}$	Γ_{11}/Γ
VALUE (%)	DOCUMENT ID TECN COMMENT
0.118 ± 0.036 ± 0.005	141.3 20 HE 08B CLEO $e^+ e^- \rightarrow \gamma h^+ h^- h^0 h^0$
20 HE 08B reports $0.12 \pm 0.03 \pm 0.02 \pm 0.01\%$ from a measurement of $[\Gamma(\chi_{c1}(1P) \rightarrow K^+ K^- \eta \pi^0)/\Gamma_{\text{total}}] \times [B(\psi(2S) \rightarrow \gamma \chi_{c1}(1P))]$ assuming $B(\psi(2S) \rightarrow \gamma \chi_{c1}(1P)) = (9.07 \pm 0.11 \pm 0.54) \times 10^{-2}$, which we rescale to our best value $B(\psi(2S) \rightarrow \gamma \chi_{c1}(1P)) = (9.2 \pm 0.4) \times 10^{-2}$. Our first error is their experiment's error and our second error is the systematic error from using our best value.	

$\Gamma(\pi^+ \pi^- K_S^0 K_S^0)/\Gamma_{\text{total}}$	Γ_{12}/Γ
VALUE (units 10^{-4})	DOCUMENT ID TECN COMMENT
7.2 ± 3.1 ± 0.3	19.8 ± 7.7 21 ABLIKIM 05o BES2 $\psi(2S) \rightarrow \chi_{c1} \gamma$
21 ABLIKIM 05o reports $[\Gamma(\chi_{c1}(1P) \rightarrow \pi^+ \pi^- K_S^0 K_S^0)/\Gamma_{\text{total}}] \times [B(\psi(2S) \rightarrow \gamma \chi_{c1}(1P))] = (0.67 \pm 0.26 \pm 0.11) \times 10^{-4}$ which we divide by our best value $B(\psi(2S) \rightarrow \gamma \chi_{c1}(1P)) = (9.2 \pm 0.4) \times 10^{-2}$. Our first error is their experiment's error and our second error is the systematic error from using our best value.	

$\Gamma(K^+ K^- \eta)/\Gamma_{\text{total}}$	Γ_{13}/Γ
VALUE (units 10^{-3})	DOCUMENT ID TECN COMMENT
0.33 ± 0.10 ± 0.01	22 ATHAR 07 CLEO $\psi(2S) \rightarrow \gamma h^+ h^- h^0$
22 ATHAR 07 reports $(0.34 \pm 0.10 \pm 0.04) \times 10^{-3}$ from a measurement of $[\Gamma(\chi_{c1}(1P) \rightarrow K^+ K^- \eta)/\Gamma_{\text{total}}] \times [B(\psi(2S) \rightarrow \gamma \chi_{c1}(1P))]$ assuming $B(\psi(2S) \rightarrow \gamma \chi_{c1}(1P)) = 0.0907 \pm 0.0011 \pm 0.0054$, which we rescale to our best value $B(\psi(2S) \rightarrow \gamma \chi_{c1}(1P)) = (9.2 \pm 0.4) \times 10^{-2}$. Our first error is their experiment's error and our second error is the systematic error from using our best value.	

$\Gamma(K^0 K^+ \pi^- + \text{c.c.})/\Gamma_{\text{total}}$	Γ_{14}/Γ
VALUE (units 10^{-3})	DOCUMENT ID
7.3 ± 0.6 OUR FIT	

$\Gamma(K^*(892)^0 \bar{K}^0 + \text{c.c.})/\Gamma_{\text{total}}$	Γ_{15}/Γ
VALUE (units 10^{-3})	EVTS DOCUMENT ID TECN COMMENT
1.03 ± 0.38 ± 0.04	22 23 ABLIKIM 06R BES2 $\psi(2S) \rightarrow \gamma \chi_{c1}$
23 ABLIKIM 06R reports $(1.1 \pm 0.4 \pm 0.1) \times 10^{-3}$ from a measurement of $[\Gamma(\chi_{c1}(1P) \rightarrow K^*(892)^0 \bar{K}^0 + \text{c.c.})/\Gamma_{\text{total}}] \times [B(\psi(2S) \rightarrow \gamma \chi_{c1}(1P))]$ assuming $B(\psi(2S) \rightarrow \gamma \chi_{c1}(1P)) = (8.7 \pm 0.4) \times 10^{-2}$, which we rescale to our best value $B(\psi(2S) \rightarrow \gamma \chi_{c1}(1P)) = (9.2 \pm 0.4) \times 10^{-2}$. Our first error is their experiment's error and our second error is the systematic error from using our best value.	

$\Gamma(K^*(892)^+ K^- + \text{c.c.})/\Gamma_{\text{total}}$	Γ_{16}/Γ
VALUE (units 10^{-3})	EVTS DOCUMENT ID TECN COMMENT
1.5 ± 0.7 ± 0.1	27 24 ABLIKIM 06R BES2 $\psi(2S) \rightarrow \gamma \chi_{c1}$
24 ABLIKIM 06R reports $(1.6 \pm 0.7 \pm 0.2) \times 10^{-3}$ from a measurement of $[\Gamma(\chi_{c1}(1P) \rightarrow K^*(892)^+ K^- + \text{c.c.})/\Gamma_{\text{total}}] \times [B(\psi(2S) \rightarrow \gamma \chi_{c1}(1P))]$ assuming $B(\psi(2S) \rightarrow \gamma \chi_{c1}(1P)) = (8.7 \pm 0.4) \times 10^{-2}$, which we rescale to our best value $B(\psi(2S) \rightarrow \gamma \chi_{c1}(1P)) = (9.2 \pm 0.4) \times 10^{-2}$. Our first error is their experiment's error and our second error is the systematic error from using our best value.	

$\Gamma(K_S^*(1430)^0 \bar{K}^0 + \text{c.c.} \rightarrow K_S^0 K^+ \pi^- + \text{c.c.})/\Gamma_{\text{total}}$	Γ_{17}/Γ
VALUE (units 10^{-3})	CL% DOCUMENT ID TECN COMMENT
< 0.8	90 25 ABLIKIM 06R BES2 $\psi(2S) \rightarrow \gamma \chi_{c1}$
25 ABLIKIM 06R reports $< 0.9 \times 10^{-3}$ from a measurement of $[\Gamma(\chi_{c1}(1P) \rightarrow K_S^*(1430)^0 \bar{K}^0 + \text{c.c.} \rightarrow K_S^0 K^+ \pi^- + \text{c.c.})/\Gamma_{\text{total}}] \times [B(\psi(2S) \rightarrow \gamma \chi_{c1}(1P))]$ assuming $B(\psi(2S) \rightarrow \gamma \chi_{c1}(1P)) = (8.7 \pm 0.4) \times 10^{-2}$, which we rescale to our best value $B(\psi(2S) \rightarrow \gamma \chi_{c1}(1P)) = 9.2 \times 10^{-2}$.	

$\Gamma(K_S^*(1430)^+ K^- + \text{c.c.} \rightarrow K_S^0 K^+ \pi^- + \text{c.c.})/\Gamma_{\text{total}}$	Γ_{18}/Γ
VALUE (units 10^{-3})	CL% DOCUMENT ID TECN COMMENT
< 2.3	90 26 ABLIKIM 06R BES2 $\psi(2S) \rightarrow \gamma \chi_{c1}$
26 ABLIKIM 06R reports $< 2.4 \times 10^{-3}$ from a measurement of $[\Gamma(\chi_{c1}(1P) \rightarrow K_S^*(1430)^+ K^- + \text{c.c.} \rightarrow K_S^0 K^+ \pi^- + \text{c.c.})/\Gamma_{\text{total}}] \times [B(\psi(2S) \rightarrow \gamma \chi_{c1}(1P))]$ assuming $B(\psi(2S) \rightarrow \gamma \chi_{c1}(1P)) = (8.7 \pm 0.4) \times 10^{-2}$, which we rescale to our best value $B(\psi(2S) \rightarrow \gamma \chi_{c1}(1P)) = 9.2 \times 10^{-2}$.	

$\Gamma(K^+ K^- \pi^0)/\Gamma_{\text{total}}$	Γ_{19}/Γ
VALUE (units 10^{-3})	DOCUMENT ID TECN COMMENT
1.91 ± 0.25 ± 0.07	27 ATHAR 07 CLEO $\psi(2S) \rightarrow \gamma h^+ h^- h^0$
27 ATHAR 07 reports $(1.95 \pm 0.16 \pm 0.23) \times 10^{-3}$ from a measurement of $[\Gamma(\chi_{c1}(1P) \rightarrow K^+ K^- \pi^0)/\Gamma_{\text{total}}] \times [B(\psi(2S) \rightarrow \gamma \chi_{c1}(1P))]$ assuming $B(\psi(2S) \rightarrow \gamma \chi_{c1}(1P)) = 0.0907 \pm 0.0011 \pm 0.0054$, which we rescale to our best value $B(\psi(2S) \rightarrow \gamma \chi_{c1}(1P)) = (9.2 \pm 0.4) \times 10^{-2}$. Our first error is their experiment's error and our second error is the systematic error from using our best value.	

$\Gamma(\eta \pi^+ \pi^-)/\Gamma_{\text{total}}$	Γ_{20}/Γ
VALUE (units 10^{-3})	EVTS DOCUMENT ID TECN COMMENT
5.0 ± 0.5 OUR AVERAGE	
4.9 ± 0.5 ± 0.2	28 ATHAR 07 CLEO $\psi(2S) \rightarrow \gamma h^+ h^- h^0$
5.6 ± 1.0 ± 0.2	22 29 ABLIKIM 06R BES2 $\psi(2S) \rightarrow \gamma \chi_{c1}$
28 ATHAR 07 reports $(5.0 \pm 0.3 \pm 0.5) \times 10^{-3}$ from a measurement of $[\Gamma(\chi_{c1}(1P) \rightarrow \eta \pi^+ \pi^-)/\Gamma_{\text{total}}] \times [B(\psi(2S) \rightarrow \gamma \chi_{c1}(1P))]$ assuming $B(\psi(2S) \rightarrow \gamma \chi_{c1}(1P)) = 0.0907 \pm 0.0011 \pm 0.0054$, which we rescale to our best value $B(\psi(2S) \rightarrow \gamma \chi_{c1}(1P)) = (9.2 \pm 0.4) \times 10^{-2}$. Our first error is their experiment's error and our second error is the systematic error from using our best value.	
29 ABLIKIM 06R reports $(5.9 \pm 0.7 \pm 0.8) \times 10^{-3}$ from a measurement of $[\Gamma(\chi_{c1}(1P) \rightarrow \eta \pi^+ \pi^-)/\Gamma_{\text{total}}] \times [B(\psi(2S) \rightarrow \gamma \chi_{c1}(1P))]$ assuming $B(\psi(2S) \rightarrow \gamma \chi_{c1}(1P)) = (8.7 \pm 0.4) \times 10^{-2}$, which we rescale to our best value $B(\psi(2S) \rightarrow \gamma \chi_{c1}(1P)) = (9.2 \pm 0.4) \times 10^{-2}$. Our first error is their experiment's error and our second error is the systematic error from using our best value.	

$\Gamma(a_0(980)^+ \pi^- + \text{c.c.} \rightarrow \eta \pi^+ \pi^-)/\Gamma_{\text{total}}$	Γ_{21}/Γ
VALUE (units 10^{-3})	EVTS DOCUMENT ID TECN COMMENT
1.9 ± 0.7 ± 0.1	58 30 ABLIKIM 06R BES2 $\psi(2S) \rightarrow \gamma \chi_{c1}$
30 ABLIKIM 06R reports $(2.0 \pm 0.5 \pm 0.5) \times 10^{-3}$ from a measurement of $[\Gamma(\chi_{c1}(1P) \rightarrow a_0(980)^+ \pi^- + \text{c.c.} \rightarrow \eta \pi^+ \pi^-)/\Gamma_{\text{total}}] \times [B(\psi(2S) \rightarrow \gamma \chi_{c1}(1P))]$ assuming $B(\psi(2S) \rightarrow \gamma \chi_{c1}(1P)) = (8.7 \pm 0.4) \times 10^{-2}$, which we rescale to our best value $B(\psi(2S) \rightarrow \gamma \chi_{c1}(1P)) = (9.2 \pm 0.4) \times 10^{-2}$. Our first error is their experiment's error and our second error is the systematic error from using our best value.	

$\Gamma(f_2(1270) \eta)/\Gamma_{\text{total}}$	Γ_{22}/Γ
VALUE (units 10^{-3})	EVTS DOCUMENT ID TECN COMMENT
2.8 ± 0.8 ± 0.1	53 31 ABLIKIM 06R BES2 $\psi(2S) \rightarrow \gamma \chi_{c1}$
31 ABLIKIM 06R reports $(3.0 \pm 0.7 \pm 0.5) \times 10^{-3}$ from a measurement of $[\Gamma(\chi_{c1}(1P) \rightarrow f_2(1270) \eta)/\Gamma_{\text{total}}] \times [B(\psi(2S) \rightarrow \gamma \chi_{c1}(1P))]$ assuming $B(\psi(2S) \rightarrow \gamma \chi_{c1}(1P)) = (8.7 \pm 0.4) \times 10^{-2}$, which we rescale to our best value $B(\psi(2S) \rightarrow \gamma \chi_{c1}(1P)) = (9.2 \pm 0.4) \times 10^{-2}$. Our first error is their experiment's error and our second error is the systematic error from using our best value.	

Meson Particle Listings

$\chi_{c1}(1P)$

$\Gamma(\gamma\rho^0)/\Gamma_{total}$ Γ_{45}/Γ

VALUE (units 10^{-6})	EVTS	DOCUMENT ID	TECN	COMMENT
229 ± 25 ± 9	186 ± 15	53 BENNETT	08A CLEO	$\psi(2S) \rightarrow \gamma\gamma\rho^0$

53 BENNETT 08A reports $(243 \pm 19 \pm 22) \times 10^{-6}$ from a measurement of $[\Gamma(\chi_{c1}(1P) \rightarrow \gamma\rho^0)/\Gamma_{total}] \times [B(\psi(2S) \rightarrow \gamma\chi_{c1}(1P))]$ assuming $B(\psi(2S) \rightarrow \gamma\chi_{c1}(1P)) = (8.7 \pm 0.4) \times 10^{-2}$, which we rescale to our best value $B(\psi(2S) \rightarrow \gamma\chi_{c1}(1P)) = (9.2 \pm 0.4) \times 10^{-2}$. Our first error is their experiment's error and our second error is the systematic error from using our best value.

$\Gamma(\gamma\omega)/\Gamma_{total}$ Γ_{46}/Γ

VALUE (units 10^{-6})	EVTS	DOCUMENT ID	TECN	COMMENT
78 ± 18 ± 3	39.2 ± 7.1	54 BENNETT	08A CLEO	$\psi(2S) \rightarrow \gamma\gamma\omega$

54 BENNETT 08A reports $(83 \pm 15 \pm 12) \times 10^{-6}$ from a measurement of $[\Gamma(\chi_{c1}(1P) \rightarrow \gamma\omega)/\Gamma_{total}] \times [B(\psi(2S) \rightarrow \gamma\chi_{c1}(1P))]$ assuming $B(\psi(2S) \rightarrow \gamma\chi_{c1}(1P)) = (8.7 \pm 0.4) \times 10^{-2}$, which we rescale to our best value $B(\psi(2S) \rightarrow \gamma\chi_{c1}(1P)) = (9.2 \pm 0.4) \times 10^{-2}$. Our first error is their experiment's error and our second error is the systematic error from using our best value.

$\Gamma(\gamma\phi)/\Gamma_{total}$ Γ_{47}/Γ

VALUE (units 10^{-6})	CL%	EVTS	DOCUMENT ID	TECN	COMMENT
< 24	90	5.2 ± 3.1	55 BENNETT	08A CLEO	$\psi(2S) \rightarrow \gamma\gamma\phi$

55 BENNETT 08A reports $< 26 \times 10^{-6}$ from a measurement of $[\Gamma(\chi_{c1}(1P) \rightarrow \gamma\phi)/\Gamma_{total}] \times [B(\psi(2S) \rightarrow \gamma\chi_{c1}(1P))]$ assuming $B(\psi(2S) \rightarrow \gamma\chi_{c1}(1P)) = (8.7 \pm 0.4) \times 10^{-2}$, which we rescale to our best value $B(\psi(2S) \rightarrow \gamma\chi_{c1}(1P)) = 9.2 \times 10^{-2}$.

$\Gamma(\gamma\eta)/\Gamma_{total}$ Γ_{48}/Γ

VALUE (units 10^{-5})	CL%	DOCUMENT ID	TECN	COMMENT
• • • We do not use the following data for averages, fits, limits, etc. • • •				
< 3.5	90	ECKLUND	08A CLEO	$\psi(2S) \rightarrow \gamma\chi_{c1} \rightarrow 3\gamma$
< 15.0	90	56 YAMADA	77 DASP	$e^+e^- \rightarrow 3\gamma$

56 Estimated using $B(\psi(2S) \rightarrow \gamma\chi_{c1}(1P)) = 0.087$. The errors do not contain the uncertainty in the $\psi(2S)$ decay.

$\chi_{c1}(1P)$ CROSS-PARTICLE BRANCHING RATIOS

$\Gamma(\chi_{c1}(1P) \rightarrow \rho\bar{\rho})/\Gamma_{total} \times \Gamma(\psi(2S) \rightarrow \gamma\chi_{c1}(1P))/\Gamma(\psi(2S) \rightarrow J/\psi(1S)\pi^+\pi^-)$ $\Gamma_{29}/\Gamma \times \Gamma_{106}^{\psi(2S)}/\Gamma_{11}^{\psi(2S)}$

VALUE (units 10^{-5})	DOCUMENT ID	TECN	COMMENT
2.02 ± 0.16 OUR FIT			
1.1 ± 1.0	57 BAI	98i BES	$\psi(2S) \rightarrow \gamma\chi_{c1} \rightarrow \gamma\rho\rho$

57 Calculated by us. The value for $B(\chi_{c1} \rightarrow \rho\bar{\rho})$ reported in BAI 98i is derived using $B(\psi(2S) \rightarrow \gamma\chi_{c1}) = (8.7 \pm 0.8)\%$ and $B(\psi(2S) \rightarrow J/\psi(1S)\pi^+\pi^-) = (32.4 \pm 2.6)\%$ [BAI 98i].

$\Gamma(\chi_{c1}(1P) \rightarrow \Lambda\bar{\Lambda})/\Gamma_{total} \times \Gamma(\psi(2S) \rightarrow \gamma\chi_{c1}(1P))/\Gamma_{total}$ $\Gamma_{35}/\Gamma \times \Gamma_{106}^{\psi(2S)}/\Gamma_{11}^{\psi(2S)}$

VALUE (units 10^{-6})	EVTS	DOCUMENT ID	TECN	COMMENT
10.9 ± 1.7 OUR FIT				
10.5 ± 1.6 ± 0.6	46 ± 7	58 NAIK	08 CLEO	$\psi(2S) \rightarrow \gamma\Lambda\bar{\Lambda}$

58 Calculated by us. NAIK 08 reports $B(\chi_{c1} \rightarrow \Lambda\bar{\Lambda}) = (11.6 \pm 1.8 \pm 0.7 \pm 0.7) \times 10^{-5}$ using $B(\psi(2S) \rightarrow \gamma\chi_{c1}) = (9.07 \pm 0.11 \pm 0.54)\%$.

$\Gamma(\chi_{c1}(1P) \rightarrow \Lambda\bar{\Lambda})/\Gamma_{total} \times \Gamma(\psi(2S) \rightarrow \gamma\chi_{c1}(1P))/\Gamma(\psi(2S) \rightarrow J/\psi(1S)\pi^+\pi^-)$ $\Gamma_{35}/\Gamma \times \Gamma_{106}^{\psi(2S)}/\Gamma_{11}^{\psi(2S)}$

VALUE (units 10^{-5})	EVTS	DOCUMENT ID	TECN	COMMENT
3.3 ± 0.5 OUR FIT				
7.1 ± 2.9 ± 1.3	9.0 ± 3.5 ± 3.1	59 BAI	03E BES	$\psi(2S) \rightarrow \gamma\Lambda\bar{\Lambda}$

59 BAI 03E reports $[B(\chi_{c1} \rightarrow \Lambda\bar{\Lambda})/B(\psi(2S) \rightarrow \gamma\chi_{c1})/B(\psi(2S) \rightarrow J/\psi\pi^+\pi^-)] \times [B^2(\Lambda \rightarrow \pi^-p)/B(J/\psi \rightarrow \rho\bar{\rho})] = (1.33^{+0.52}_{-0.46} \pm 0.25)\%$. We calculate from this measurement the presented value using $B(\Lambda \rightarrow \pi^-p) = (63.9 \pm 0.5)\%$ and $B(J/\psi \rightarrow \rho\bar{\rho}) = (2.17 \pm 0.07) \times 10^{-3}$.

$\Gamma(\chi_{c1}(1P) \rightarrow \gamma J/\psi(1S))/\Gamma_{total} \times \Gamma(\psi(2S) \rightarrow \gamma\chi_{c1}(1P))/\Gamma_{total}$ $\Gamma_{44}/\Gamma \times \Gamma_{106}^{\psi(2S)}/\Gamma_{11}^{\psi(2S)}$

VALUE (units 10^{-2})	EVTS	DOCUMENT ID	TECN	COMMENT
3.18 ± 0.08 OUR FIT				
2.70 ± 0.13 OUR AVERAGE				
2.81 ± 0.05 ± 0.23	13k	BAI	04i BES2	$\psi(2S) \rightarrow J/\psi\gamma\gamma$
2.56 ± 0.12 ± 0.20		GAISER	86 CBAL	$\psi(2S) \rightarrow \gamma X$
2.78 ± 0.30		60 OREGLIA	82 CBAL	$\psi(2S) \rightarrow \gamma\chi_{c1}$
2.2 ± 0.5		61 BRANDELIK	79B DASP	$\psi(2S) \rightarrow \gamma\chi_{c1}$
2.9 ± 0.5		61 BARTEL	78B CNTR	$\psi(2S) \rightarrow \gamma\chi_{c1}$
5.0 ± 1.5		62 BIDDICK	77 CNTR	$e^+e^- \rightarrow \gamma X$
2.8 ± 0.9		60 WHITAKER	76 MRK1	e^+e^-

• • • We do not use the following data for averages, fits, limits, etc. • • •
 3.56 ± 0.03 ± 0.12 24.9k 63 MENDEZ 08 CLEO $\psi(2S) \rightarrow \gamma\chi_{c1}$
 3.44 ± 0.06 ± 0.13 3.7k 64 ADAM 05A CLEO Repl. by MENDEZ 08

60 Recalculated by us using $B(J/\psi(1S) \rightarrow \ell^+\ell^-) = 0.1181 \pm 0.0020$.
 61 Recalculated by us using $B(J/\psi(1S) \rightarrow \mu^+\mu^-) = 0.0588 \pm 0.0010$.
 62 Assumes isotropic gamma distribution.
 63 Not independent from other measurements of MENDEZ 08.
 64 Not independent from other values reported by ADAM 05A.

$\Gamma(\chi_{c1}(1P) \rightarrow \gamma J/\psi(1S))/\Gamma_{total} \times \Gamma(\psi(2S) \rightarrow \gamma\chi_{c1}(1P))/\Gamma(\psi(2S) \rightarrow J/\psi(1S)\text{anything})$ $\Gamma_{44}/\Gamma \times \Gamma_{106}^{\psi(2S)}/\Gamma_{11}^{\psi(2S)}$

VALUE (units 10^{-2})	EVTS	DOCUMENT ID	TECN	COMMENT
5.35 ± 0.12 OUR FIT				
• • • We do not use the following data for averages, fits, limits, etc. • • •				
5.70 ± 0.04 ± 0.15	24.9k	65 MENDEZ	08 CLEO	$\psi(2S) \rightarrow \gamma\chi_{c1}$
5.77 ± 0.10 ± 0.12	3.7k	ADAM	05A CLEO	Repl. by MENDEZ 08

65 Not independent from other measurements of MENDEZ 08.

$\Gamma(\chi_{c1}(1P) \rightarrow \gamma J/\psi(1S))/\Gamma_{total} \times \Gamma(\psi(2S) \rightarrow \gamma\chi_{c1}(1P))/\Gamma(\psi(2S) \rightarrow J/\psi(1S)\pi^+\pi^-)$ $\Gamma_{44}/\Gamma \times \Gamma_{106}^{\psi(2S)}/\Gamma_{11}^{\psi(2S)}$

VALUE (units 10^{-2})	EVTS	DOCUMENT ID	TECN	COMMENT
9.47 ± 0.23 OUR FIT				
10.15 ± 0.28 OUR AVERAGE				
10.17 ± 0.07 ± 0.27	24.9k	MENDEZ	08 CLEO	$\psi(2S) \rightarrow \gamma\chi_{c1}$
12.6 ± 0.3 ± 3.8	3k	66 ABLIKIM	04B BES	$\psi(2S) \rightarrow J/\psi X$
8.5 ± 2.1		67 HIMEL	80 MRK2	$\psi(2S) \rightarrow \gamma\chi_{c1}$

• • • We do not use the following data for averages, fits, limits, etc. • • •
 10.24 ± 0.17 ± 0.23 3.7k 68 ADAM 05A CLEO Repl. by MENDEZ 08

66 From a fit to the J/ψ recoil mass spectra.
 67 The value for $B(\psi(2S) \rightarrow \gamma\chi_{c1}) \times B(\chi_{c1} \rightarrow \gamma J/\psi(1S))$ quoted in HIMEL 80 is derived using $B(\psi(2S) \rightarrow J/\psi(1S)\pi^+\pi^-) = (33 \pm 3)\%$ and $B(J/\psi(1S) \rightarrow \ell^+\ell^-) = 0.138 \pm 0.018$. Calculated by us using $B(J/\psi(1S) \rightarrow \ell^+\ell^-) = 0.1181 \pm 0.0020$.
 68 Not independent from other values reported by ADAM 05A.

$\Gamma(\chi_{c1}(1P) \rightarrow K^0 K^+ \pi^- + c.c.)/\Gamma_{total} \times \Gamma(\psi(2S) \rightarrow \gamma\chi_{c1}(1P))/\Gamma_{total}$ $\Gamma_{14}/\Gamma \times \Gamma_{106}^{\psi(2S)}/\Gamma_{11}^{\psi(2S)}$

VALUE (units 10^{-4})	DOCUMENT ID	TECN	COMMENT
6.8 ± 0.5 OUR FIT			
7.2 ± 0.6 OUR AVERAGE			
7.3 ± 0.5 ± 0.5	69 ATHAR	07 CLEO	$\psi(2S) \rightarrow \gamma K_S^0 K^+ \pi^-$
7.0 ± 0.5 ± 0.9	70 ABLIKIM	06R BES2	$\psi(2S) \rightarrow \gamma\chi_{c1}$

69 Calculated by us. The value of $B(\chi_{c1} \rightarrow K^0 K^+ \pi^- + c.c.)$ reported by ATHAR 07 was derived using $B(\psi(2S) \rightarrow \gamma\chi_{c1}(1P)) = (9.07 \pm 0.11 \pm 0.54)\%$.
 70 Calculated by us. ABLIKIM 06R reports $B(\chi_{c1} \rightarrow K_S^0 K^+ \pi^-) = (4.0 \pm 0.3 \pm 0.5) \times 10^{-3}$. We use $B(\psi(2S) \rightarrow \gamma\chi_{c1}) = (8.7 \pm 0.4) \times 10^{-2}$.

$\Gamma(\chi_{c1}(1P) \rightarrow K^0 K^+ \pi^- + c.c.)/\Gamma_{total} \times \Gamma(\psi(2S) \rightarrow \gamma\chi_{c1}(1P))/\Gamma(\psi(2S) \rightarrow J/\psi(1S)\pi^+\pi^-)$ $\Gamma_{14}/\Gamma \times \Gamma_{106}^{\psi(2S)}/\Gamma_{11}^{\psi(2S)}$

VALUE (units 10^{-4})	DOCUMENT ID	TECN	COMMENT
20.2 ± 1.6 OUR FIT			
13.2 ± 2.4 ± 3.2	71 BAI	99B BES	$\psi(2S) \rightarrow \gamma K_S^0 K^+ \pi^-$

71 Calculated by us. The value of $B(\chi_{c1} \rightarrow K_S^0 K^+ \pi^-)$ reported by BAI 99B was derived using $B(\psi(2S) \rightarrow \gamma\chi_{c1}(1P)) = (8.7 \pm 0.8)\%$ and $B(\psi(2S) \rightarrow J/\psi\pi^+\pi^-) = (32.4 \pm 2.6)\%$ [BAI 98d].

$\Gamma(\chi_{c1}(1P) \rightarrow K^+ K^- K^+ K^-)/\Gamma_{total} \times \Gamma(\psi(2S) \rightarrow \gamma\chi_{c1}(1P))/\Gamma_{total}$ $\Gamma_{27}/\Gamma \times \Gamma_{106}^{\psi(2S)}/\Gamma_{11}^{\psi(2S)}$

VALUE (units 10^{-4})	EVTS	DOCUMENT ID	TECN	COMMENT
0.52 ± 0.11 OUR FIT				
0.61 ± 0.11 ± 0.08	54	72 ABLIKIM	06T BES2	$\psi(2S) \rightarrow \gamma K^+ K^+ K^- K^-$

72 Calculated by us. The value of $B(\chi_{c1} \rightarrow 2K^+ 2K^-)$ reported by ABLIKIM 06T was derived using $B(\psi(2S) \rightarrow \gamma\chi_{c1}(1P)) = (8.7 \pm 0.8)\%$.

$\Gamma(\chi_{c1}(1P) \rightarrow K^+ K^- K^+ K^-)/\Gamma_{total} \times \Gamma(\psi(2S) \rightarrow \gamma\chi_{c1}(1P))/\Gamma(\psi(2S) \rightarrow J/\psi(1S)\pi^+\pi^-)$ $\Gamma_{27}/\Gamma \times \Gamma_{106}^{\psi(2S)}/\Gamma_{11}^{\psi(2S)}$

VALUE (units 10^{-4})	DOCUMENT ID	TECN	COMMENT
1.54 ± 0.31 OUR FIT			
1.13 ± 0.40 ± 0.29	73 BAI	99B BES	$\psi(2S) \rightarrow \gamma K^+ K^+ K^- K^-$

73 Calculated by us. The value of $B(\chi_{c1} \rightarrow 2K^+ 2K^-)$ reported by BAI 99B was derived using $B(\psi(2S) \rightarrow \gamma\chi_{c1}(1P)) = (8.7 \pm 0.8)\%$ and $B(\psi(2S) \rightarrow J/\psi\pi^+\pi^-) = (32.4 \pm 2.6)\%$ [BAI 98d].

See key on page 405

Meson Particle Listings

$\chi_{c1}(1P), h_c(1P)$

$$\Gamma(\chi_{c1}(1P) \rightarrow p\bar{p})/\Gamma_{\text{total}} \times \Gamma(\psi(2S) \rightarrow \gamma\chi_{c1}(1P))/\Gamma_{\text{total}}$$

$$\Gamma_{29}/\Gamma \times \Gamma_{\psi(2S)}^{\psi(2S)}/\Gamma_{\psi(2S)}$$

VALUE (units 10^{-6})	EVTS	DOCUMENT ID	TECN	COMMENT
6.8 ± 0.5	OUR FIT			
7.5 ± 1.4	OUR AVERAGE Error includes scale factor of 2.0.			
$8.2 \pm 0.7 \pm 0.4$	141 ± 13	⁷⁴ NAIK 08	CLEO	$\psi(2S) \rightarrow \gamma p\bar{p}$
$4.8 \pm 1.4 \pm 0.6$	18.2 ± 5.5 -1.3 ± 4.9	BAI 04F	BES	$\psi(2S) \rightarrow \gamma\chi_{c1}(1P) \rightarrow \gamma p\bar{p}$

⁷⁴ Calculated by us. NAIK 08 reports $B(\chi_{c1} \rightarrow p\bar{p}) = (9.0 \pm 0.8 \pm 0.4 \pm 0.5) \times 10^{-5}$ using $B(\psi(2S) \rightarrow \gamma\chi_{c1}) = (9.07 \pm 0.11 \pm 0.54)\%$.

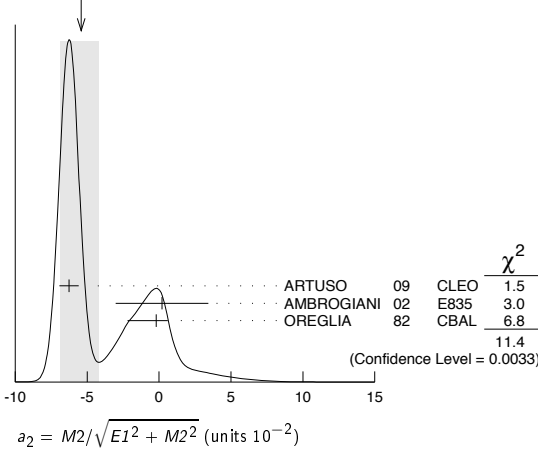
MULTIPOLE AMPLITUDES IN $\chi_{c1}(1P) \rightarrow \gamma J/\psi(1S)$

$$a_2 = M_2/\sqrt{E_1^2 + M_2^2}$$

Magnetic quadrupole fractional transition amplitude

VALUE (units 10^{-2})	EVTS	DOCUMENT ID	TECN	COMMENT
-5.4 ± 1.2	OUR AVERAGE Error includes scale factor of 2.4. See the ideogram below.			
$-6.26 \pm 0.63 \pm 0.24$	39k	ARTUSO 09	CLEO	$\psi(2S) \rightarrow \gamma\gamma\ell^+\ell^-$
$0.2 \pm 3.2 \pm 0.4$	2090	AMBROGIANI 02	E835	$p\bar{p} \rightarrow \chi_{c1} \rightarrow J/\psi\gamma$
-0.2 ± 0.8 -2.0	921	OREGLIA 82	CBAL	$\psi(2S) \rightarrow \chi_{c1}\gamma \rightarrow J/\psi\gamma\gamma$

WEIGHTED AVERAGE
-5.4±1.2-1.5 (Error scaled by 2.4)



MULTIPOLE AMPLITUDES IN $\psi(2S) \rightarrow \gamma\chi_{c1}(1S)$ RADIATIVE DECAY

$$b_2 = M_2/\sqrt{E_1^2 + M_2^2}$$

Magnetic quadrupole fractional transition amplitude

VALUE (units 10^{-2})	EVTS	DOCUMENT ID	TECN	COMMENT
2.9 ± 0.8	OUR AVERAGE			
$2.76 \pm 0.73 \pm 0.23$	39k	ARTUSO 09	CLEO	$\psi(2S) \rightarrow \gamma\gamma\ell^+\ell^-$
7.7 ± 5.0 -4.5	921	OREGLIA 82	CBAL	$\psi(2S) \rightarrow \gamma\gamma\ell^+\ell^-$

MULTIPOLE AMPLITUDE RATIOS IN RADIATIVE DECAYS $\psi(2S) \rightarrow \gamma\chi_{c1}(1S)$ and $\chi_{c1} \rightarrow \gamma J/\psi(1S)$

$$a_2/b_2$$

Magnetic quadrupole transition amplitude ratio

VALUE	EVTS	DOCUMENT ID	TECN	COMMENT
-2.27 ± 0.57 -0.99	39k	⁷⁵ ARTUSO 09	CLEO	$\psi(2S) \rightarrow \gamma\gamma\ell^+\ell^-$

⁷⁵ Statistical and systematic errors combined. Not independent of $a_2(\chi_{c1})$ and $b_2(\chi_{c1})$ values from ARTUSO 09.

$\chi_{c1}(1P)$ REFERENCES

ARTUSO 09 PR D80 112003	M. Artuso <i>et al.</i>	(CLEO Collab.)
BENNETT 08A PRL 101 151801	J.V. Bennett <i>et al.</i>	(CLEO Collab.)
ECKLUND 08A PR D78 091501R	K.M. Ecklund <i>et al.</i>	(CLEO Collab.)
HE 08B PR D78 092004	Q. He <i>et al.</i>	(CLEO Collab.)
MENDEZ 08 PR D78 011102R	H. Mendez <i>et al.</i>	(CLEO Collab.)
NAIK 08 PR D78 031101R	P. Naik <i>et al.</i>	(CLEO Collab.)
ATHAR 07 PR D75 032002	S.B. Athar <i>et al.</i>	(CLEO Collab.)
ABLIKIM 06D PR D73 052006	M. Ablikim <i>et al.</i>	(BES Collab.)
ABLIKIM 06R PR D74 072001	M. Ablikim <i>et al.</i>	(BES Collab.)
ABLIKIM 06T PL B642 197	M. Ablikim <i>et al.</i>	(BES Collab.)
ABLIKIM 05G PR D71 092002	M. Ablikim <i>et al.</i>	(BES Collab.)
ABLIKIM 05O PL B630 21	M. Ablikim <i>et al.</i>	(BES Collab.)
ADAM 05A PRL 94 232002	N.E. Adam <i>et al.</i>	(CLEO Collab.)
ANDREOTTI 05A NP B717 34	M. Andreotti <i>et al.</i>	(FNAL E835 Collab.)
ABLIKIM 04B PR D70 012003	M. Ablikim <i>et al.</i>	(BES Collab.)
ABLIKIM 04H PR D70 092003	M. Ablikim <i>et al.</i>	(BES Collab.)
ATHAR 04 PR D70 112002	S.B. Athar <i>et al.</i>	(CLEO Collab.)
BAI 04F PR D69 092001	J.Z. Bai <i>et al.</i>	(BES Collab.)
BAI 04I PR D70 012006	J.Z. Bai <i>et al.</i>	(BES Collab.)
AULCHENKO 03 PL B573 63	V.M. Aulchenko <i>et al.</i>	(KEDR Collab.)
BAI 03E PR D67 112001	J.Z. Bai <i>et al.</i>	(BES Collab.)

AMBROGIANI 02 PR D65 052002	M. Ambrogiani <i>et al.</i>	(FNAL E835 Collab.)
BAI 99B PR D60 072001	J.Z. Bai <i>et al.</i>	(BES Collab.)
BAI 98D PR D58 092006	J.Z. Bai <i>et al.</i>	(BES Collab.)
BAI 98I PRL 81 3091	J.Z. Bai <i>et al.</i>	(BES Collab.)
ARMSTRONG 92 NP B373 35	T.A. Armstrong <i>et al.</i>	(FNAL FERR, GENO+)
Also PRL 68 1468	T.A. Armstrong <i>et al.</i>	(FNAL FERR, GENO+)
BAGLIN 86B PL B172 455	C. Baglin (LAPP, CERN, GENO, LYON, OSLO+)	
GAISER 86 PR D34 711	J. Gaiser <i>et al.</i>	(Crystal Ball Collab.)
LEMOIGNE 82 PL 113B 509	Y. Lemoigne <i>et al.</i>	(SACL, LOIC, SHMP+)
OREGLIA 82 PR D25 2259	M.J. Oreglia <i>et al.</i>	(SLAC, CIT, HARV+)
Also Private Comm.	M.J. Oreglia	(EFI)
HIMEL 80 PRL 44 920	T. Himel <i>et al.</i>	(LBL, SLAC)
Also Private Comm.	G. Trilling	(LBL, UCB)
BRANDELIK 79B NP B160 426	R. Brandelik <i>et al.</i>	(DASP Collab.)
BARTEL 78B PL 79B 492	W. Bartel <i>et al.</i>	(DESY, HEIDP)
TANENBAUM 78 PR D17 1731	W.M. Tanenbaum <i>et al.</i>	(SLAC, LBL)
Also Private Comm.	G. Trilling	(LBL, UCB)
BIDDICK 77 PRL 38 1324	C.J. Biddick <i>et al.</i>	(UCSD, UMD, PAV+)
FELDMAN 77 PRPL 33C 285	G.J. Feldman, M.L. Perl	(LBL, SLAC)
YAMADA 77 Hamburg Conf. 69	S. Yamada	(DASP Collab.)
WHITAKER 76 PRL 37 1536	J.S. Whitaker <i>et al.</i>	(SLAC, LBL)
TANENBAUM 75 PRL 35 1323	W.M. Tanenbaum <i>et al.</i>	(LBL, SLAC)

$h_c(1P)$

$$J^P(C) = ?(1^{+-})$$

Quantum numbers are quark model prediction, C = - established by $\eta_c\gamma$ decay.

$h_c(1P)$ MASS

VALUE (MeV)	EVTS	DOCUMENT ID	TECN	COMMENT
3525.42 ± 0.29	OUR AVERAGE Error includes scale factor of 1.7.			
$3525.20 \pm 0.18 \pm 0.12$	1282	¹ DOBBS 08A	CLEO	$\psi(2S) \rightarrow \pi^0\eta_c\gamma$
$3525.8 \pm 0.2 \pm 0.2$	13	ANDREOTTI 05B	E835	$\bar{p}p \rightarrow \eta_c\gamma$
• • • We do not use the following data for averages, fits, limits, etc. • • •				
3525.6 ± 0.5	92 ± 23 -22	ADAMS 09	CLEO	$\psi(2S) \rightarrow 2(\pi^+\pi^-\pi^0)$
$3524.4 \pm 0.6 \pm 0.4$	168 ± 40	² ROSNER 05	CLEO	$\psi(2S) \rightarrow \pi^0\eta_c\gamma$
3527 ± 8	42	ANTONIAZZI 94	E705	$300 \pi^\pm, pLi \rightarrow J/\psi\pi^0 X$
$3526.28 \pm 0.18 \pm 0.19$	59	³ ARMSTRONG 92D	E760	$\bar{p}p \rightarrow J/\psi\pi^0$
$3525.4 \pm 0.8 \pm 0.4$	5	BAGLIN 86	SPEC	$\bar{p}p \rightarrow J/\psi X$

¹ Combination of exclusive and inclusive analyses for the reaction $\psi(2S) \rightarrow \pi^0\eta_c \rightarrow \pi^0\eta_c\gamma$. This result is the average of DOBBS 08A and ROSNER 05.

² Superseded by DOBBS 08A.

³ Mass central value and systematic error recalculated by us according to Eq. (16) in ARMSTRONG 93B, using the value for the $\psi(2S)$ mass from AULCHENKO 03.

$h_c(1P)$ WIDTH

VALUE (MeV)	CL%	EVTS	DOCUMENT ID	TECN	COMMENT
<1		13	ANDREOTTI 05B	E835	$\bar{p}p \rightarrow \eta_c\gamma$
• • • We do not use the following data for averages, fits, limits, etc. • • •					
<1.1	90	59	ARMSTRONG 92D	E760	$\bar{p}p \rightarrow J/\psi\pi^0$

$h_c(1P)$ DECAY MODES

Mode	Fraction (Γ_i/Γ)
Γ_1 $J/\psi(1S)\pi^0$	
Γ_2 $J/\psi(1S)\pi\pi$	not seen
Γ_3 $p\bar{p}$	
Γ_4 $\eta_c\gamma$	seen
Γ_5 $\pi^+\pi^-\pi^0$	not seen
Γ_6 $2\pi^+2\pi^-\pi^0$	seen
Γ_7 $3\pi^+3\pi^-\pi^0$	not seen

$h_c(1P)$ PARTIAL WIDTHS

$$h_c(1P) \Gamma(i)\Gamma(\bar{p}p)/\Gamma(\text{total})$$

$\Gamma(\eta_c\gamma) \times \Gamma(\bar{p}p)/\Gamma_{\text{total}}$	$\Gamma_4\Gamma_3/\Gamma$			
VALUE (eV)	EVTS	DOCUMENT ID	TECN	COMMENT
• • • We do not use the following data for averages, fits, limits, etc. • • •				
12.0 ± 4.5	13	⁴ ANDREOTTI 05B	E835	$\bar{p}p \rightarrow \eta_c\gamma$

⁴ Assuming $\Gamma = 1$ MeV.

$h_c(1P)$ BRANCHING RATIOS

$\Gamma(J/\psi(1S)\pi\pi)/\Gamma(J/\psi(1S)\pi^0)$	Γ_2/Γ_1			
VALUE	CL%	DOCUMENT ID	TECN	COMMENT
<0.18	90	ARMSTRONG 92D	E760	$\bar{p}p \rightarrow J/\psi\pi^0$

Meson Particle Listings

 $h_c(1P), \chi_{c2}(1P)$

$\Gamma(\eta_c\gamma)/\Gamma_{\text{total}}$	VALUE	EVTs	DOCUMENT ID	TECN	COMMENT	Γ_4/Γ
seen	1282		⁵ DOBBS	08A	CLEO $\psi(2S) \rightarrow \pi^0 \eta_c \gamma$	
seen	168 ± 40		⁶ ROSNER	05	CLEO $\psi(2S) \rightarrow \pi^0 \eta_c \gamma$	

⁵ DOBBS 08A measures the product $B(\psi(2S) \rightarrow \pi^0 h_c) \times B(h_c \rightarrow \eta_c \gamma)$ to be $(4.19 \pm 0.32 \pm 0.45) \times 10^{-4}$ from the combination of exclusive and inclusive analyses.
⁶ ROSNER 05 measures the product $B(\psi(2S) \rightarrow \pi^0 h_c) \times B(h_c \rightarrow \eta_c \gamma)$ to be $(4.0 \pm 0.8 \pm 0.7) \times 10^{-4}$.

$\Gamma(\pi^+ \pi^- \pi^0)/\Gamma_{\text{total}}$	VALUE	DOCUMENT ID	TECN	COMMENT	Γ_5/Γ
not seen		⁷ ADAMS	09	CLEO $\psi(2S) \rightarrow \pi^+ \pi^- 2\pi^0$	

⁷ ADAMS 09 measures the branching fractions product $B(h_c(1P) \rightarrow \pi^+ \pi^- \pi^0) \times B(\psi(2S) \rightarrow \pi^0 h_c(1P)) < 0.19 \times 10^{-5}$.

$\Gamma(2\pi^+ 2\pi^- \pi^0)/\Gamma_{\text{total}}$	VALUE	EVTs	DOCUMENT ID	TECN	COMMENT	Γ_6/Γ
seen	$92 \pm_{-22}^{+23}$		⁸ ADAMS	09	CLEO $\psi(2S) \rightarrow 2\pi^+ 2\pi^- \pi^0$	

⁸ ADAMS 09 measures the branching fractions product $B(h_c(1P) \rightarrow 2\pi^+ 2\pi^- \pi^0) \times B(\psi(2S) \rightarrow \pi^0 h_c(1P)) = (1.88 \pm_{-0.45}^{+0.48} \pm_{-0.30}^{+0.47}) \times 10^{-5}$.

$\Gamma(3\pi^+ 3\pi^- \pi^0)/\Gamma_{\text{total}}$	VALUE	DOCUMENT ID	TECN	COMMENT	Γ_7/Γ
not seen		⁹ ADAMS	09	CLEO $\psi(2S) \rightarrow 3\pi^+ 3\pi^- \pi^0$	

⁹ ADAMS 09 measures the branching fractions product $B(h_c(1P) \rightarrow 3\pi^+ 3\pi^- \pi^0) \times B(\psi(2S) \rightarrow \pi^0 h_c(1P)) < 2.5 \times 10^{-5}$.

 $h_c(1P)$ REFERENCES

ADAMS 09	PR D80 051106	G.S. Adams et al.	(CLEO Collab.)
DOBBS 08A	PRL 101 182003	S. Dobbs et al.	(CLEO Collab.)
ANDREOTTI 05B	PR D72 032001	M. Andreotti et al.	(FNAL E835 Collab.)
ROSNER 05	PRL 95 102003	J.L. Rosner et al.	(CLEO Collab.)
AULCHENKO 03	PL B573 63	V.M. Aulchenko et al.	(KEDR Collab.)
ANTONIAZZI 94	PR D50 4258	L. Antoniazzi et al.	(E705 Collab.)
ARMSTRONG 93B	PR D47 772	T.A. Armstrong et al.	(FNAL E760 Collab.)
ARMSTRONG 92D	PRL 69 2337	T.A. Armstrong et al.	(FNAL, FERR, GENO+)
BAGLIN 86	PL B171 135	C. Baglin et al.	(LAPP, CERN, TORI, STRB+)

 $\chi_{c2}(1P)$

$$J^{PC} = 0^+(2^{++})$$

See the Review on " $\psi(2S)$ and χ_c branching ratios" before the $\chi_{c0}(1P)$ Listings.

 $\chi_{c2}(1P)$ MASS

VALUE (MeV)	EVTs	DOCUMENT ID	TECN	COMMENT
3556.20 ± 0.09	OUR AVERAGE			
$3555.3 \pm 0.6 \pm 2.2$	2.5k	UEHARA	08	BELL $\gamma\gamma \rightarrow \text{hadrons}$
$3555.70 \pm 0.59 \pm 0.39$		ABLIKIM	05G	BES2 $\psi(2S) \rightarrow \gamma \chi_{c2}$
$3556.173 \pm 0.123 \pm 0.020$		ANDREOTTI	05A	E835 $p\bar{p} \rightarrow e^+ e^- \gamma$
3559.9 ± 2.9		EISENSTEIN	01	CLE2 $e^+ e^- \rightarrow \chi_{c2}$
3556.4 ± 0.7		BAI	99B	BES $\psi(2S) \rightarrow \gamma X$
$3556.22 \pm 0.131 \pm 0.020$	585	¹ ARMSTRONG	92	E760 $\bar{p}p \rightarrow e^+ e^- \gamma$
$3556.9 \pm 0.4 \pm 0.5$	50	BAGLIN	86B	SPEC $\bar{p}p \rightarrow e^+ e^- X$
$3557.8 \pm 0.2 \pm 4$		² GAISER	86	CBAL $\psi(2S) \rightarrow \gamma X$
3553.4 ± 2.2	66	³ LEMOIGNE	82	GOLI $185 \pi^- \text{Be} \rightarrow \gamma \mu^+ \mu^- \text{A}$
3555.9 ± 0.7		⁴ OREGLIA	82	CBAL $e^+ e^- \rightarrow J/\psi 2\gamma$
3557 ± 1.5	69	⁵ HIMEL	80	MRK2 $e^+ e^- \rightarrow J/\psi 2\gamma$
3551 ± 11	15	BRANDELIC	79B	DASP $e^+ e^- \rightarrow J/\psi 2\gamma$
3553 ± 4		⁵ BARTEL	78B	CNTR $e^+ e^- \rightarrow J/\psi 2\gamma$
$3553 \pm 4 \pm 4$		^{5,6} TANENBAUM	78	MRK1 $e^+ e^-$
3563 ± 7	360	⁵ BIDDICK	77	CNTR $e^+ e^- \rightarrow \gamma X$
3543 ± 10	4	WHITAKER	76	MRK1 $e^+ e^- \rightarrow J/\psi 2\gamma$

¹ Recalculated by ANDREOTTI 05A, using the value of $\psi(2S)$ mass from AULCHENKO 03.
² Using mass of $\psi(2S) = 3686.0$ MeV.
³ $J/\psi(1S)$ mass constrained to 3097 MeV.
⁴ Assuming $\psi(2S)$ mass = 3686 MeV and $J/\psi(1S)$ mass = 3097 MeV.
⁵ Mass value shifted by us by amount appropriate for $\psi(2S)$ mass = 3686 MeV and $J/\psi(1S)$ mass = 3097 MeV.
⁶ From a simultaneous fit to radiative and hadronic decay channels.

 $\chi_{c2}(1P)$ WIDTH

VALUE (MeV)	EVTs	DOCUMENT ID	TECN	COMMENT
1.97 ± 0.11	OUR FIT			
1.95 ± 0.13	OUR AVERAGE			
$1.915 \pm 0.188 \pm 0.013$		ANDREOTTI	05A	E835 $p\bar{p} \rightarrow e^+ e^- \gamma$
$1.96 \pm 0.17 \pm 0.07$	585	⁷ ARMSTRONG	92	E760 $\bar{p}p \rightarrow e^+ e^- \gamma$
$2.6 \pm_{-1.0}^{+1.4}$	50	BAGLIN	86B	SPEC $\bar{p}p \rightarrow e^+ e^- X$
$2.8 \pm_{-2.0}^{+2.1}$		⁸ GAISER	86	CBAL $\psi(2S) \rightarrow \gamma X$

⁷ Recalculated by ANDREOTTI 05A.

⁸ Errors correspond to 90% confidence level; authors give only width range.

 $\chi_{c2}(1P)$ DECAY MODES

Mode	Fraction (Γ_i/Γ)	Confidence level
Hadronic decays		
Γ_1 $2(\pi^+ \pi^-)$	$(1.11 \pm 0.11) \%$	
Γ_2 $\rho\rho$		
Γ_3 $\pi^+ \pi^- \pi^0 \pi^0$	$(2.00 \pm 0.26) \%$	
Γ_4 $\rho^+ \pi^- \pi^0 + \text{C.C.}$	$(2.4 \pm 0.4) \%$	
Γ_5 $K^+ K^- \pi^0 \pi^0$	$(2.2 \pm 0.4) \times 10^{-3}$	
Γ_6 $K^+ \pi^- K^0 \pi^0 + \text{C.C.}$	$(1.50 \pm 0.22) \%$	
Γ_7 $\rho^+ K^- K^0 + \text{C.C.}$	$(4.5 \pm 1.4) \times 10^{-3}$	
Γ_8 $K^*(892)^0 K^+ \pi^- \rightarrow K^+ \pi^- K^0 \pi^0 + \text{C.C.}$	$(3.2 \pm 0.9) \times 10^{-3}$	
Γ_9 $K^*(892)^0 K^0 \pi^0 \rightarrow K^+ \pi^- K^0 \pi^0 + \text{C.C.}$	$(4.2 \pm 0.9) \times 10^{-3}$	
Γ_{10} $K^*(892)^- K^+ \pi^0 \rightarrow K^+ \pi^- K^0 \pi^0 + \text{C.C.}$	$(4.1 \pm 0.9) \times 10^{-3}$	
Γ_{11} $K^*(892)^+ K^0 \pi^- \rightarrow K^+ \pi^- K^0 \pi^0 + \text{C.C.}$	$(3.2 \pm 0.9) \times 10^{-3}$	
Γ_{12} $K^+ K^- \eta \pi^0$	$(1.4 \pm 0.5) \times 10^{-3}$	
Γ_{13} $\pi^+ \pi^- K^+ K^-$	$(9.2 \pm 1.1) \times 10^{-3}$	
Γ_{14} $K^+ \bar{K}^*(892)^0 \pi^- + \text{C.C.}$	$(2.3 \pm 1.2) \times 10^{-3}$	
Γ_{15} $K^*(892)^0 \bar{K}^*(892)^0$	$(2.5 \pm 0.5) \times 10^{-3}$	
Γ_{16} $3(\pi^+ \pi^-)$	$(8.6 \pm 1.8) \times 10^{-3}$	
Γ_{17} $\phi\phi$	$(1.48 \pm 0.28) \times 10^{-3}$	
Γ_{18} $\omega\omega$	$(1.9 \pm 0.6) \times 10^{-3}$	
Γ_{19} $\pi\pi$	$(2.39 \pm 0.14) \times 10^{-3}$	
Γ_{20} $\rho^0 \pi^+ \pi^-$	$(4.0 \pm 1.7) \times 10^{-3}$	
Γ_{21} $\pi^+ \pi^- \eta$	$(5.2 \pm 1.4) \times 10^{-4}$	
Γ_{22} $\pi^+ \pi^- \eta'$	$(5.4 \pm 2.0) \times 10^{-4}$	
Γ_{23} $\eta\eta$	$(5.4 \pm 0.8) \times 10^{-4}$	
Γ_{24} $K^+ K^-$	$(1.09 \pm 0.08) \times 10^{-3}$	
Γ_{25} $K_S^0 K_S^0$	$(5.8 \pm 0.5) \times 10^{-4}$	
Γ_{26} $\bar{K}^0 K^+ \pi^- + \text{C.C.}$	$(1.32 \pm 0.20) \times 10^{-3}$	
Γ_{27} $K^+ K^- \pi^0$	$(3.3 \pm 0.8) \times 10^{-4}$	
Γ_{28} $K^+ K^- \eta$	$< 3.5 \times 10^{-4}$	90%
Γ_{29} $\eta\eta'$	$< 6 \times 10^{-5}$	90%
Γ_{30} $\eta'\eta'$	$< 1.1 \times 10^{-4}$	90%
Γ_{31} $\pi^+ \pi^- K_S^0 K_S^0$	$(2.4 \pm 0.6) \times 10^{-3}$	
Γ_{32} $K^+ K^- K_S^0 K_S^0$	$< 4 \times 10^{-4}$	90%
Γ_{33} $K^+ K^- K^+ K^-$	$(1.78 \pm 0.22) \times 10^{-3}$	
Γ_{34} $K^+ K^- \phi$	$(1.55 \pm 0.32) \times 10^{-3}$	
Γ_{35} $K_S^0 K_S^0 \rho\bar{\rho}$	$< 7.9 \times 10^{-4}$	90%
Γ_{36} $\rho\bar{\rho}$	$(7.2 \pm 0.4) \times 10^{-5}$	
Γ_{37} $\rho\bar{\rho}\pi^0$	$(4.7 \pm 1.0) \times 10^{-4}$	
Γ_{38} $\rho\bar{\rho}\eta$	$(2.0 \pm 0.8) \times 10^{-4}$	
Γ_{39} $\pi^+ \pi^- \rho\bar{\rho}$	$(1.32 \pm 0.34) \times 10^{-3}$	
Γ_{40} $\pi^0 \pi^0 \rho\bar{\rho}$	$(8.5 \pm 2.6) \times 10^{-4}$	
Γ_{41} $\rho\bar{\rho}\pi^-$	$(1.1 \pm 0.4) \times 10^{-3}$	
Γ_{42} $\Lambda\bar{\Lambda}$	$(1.86 \pm 0.27) \times 10^{-4}$	
Γ_{43} $\Lambda\bar{\Lambda}\pi^+\pi^-$	$< 3.5 \times 10^{-3}$	90%
Γ_{44} $K^+ \bar{p} \Lambda + \text{C.C.}$	$(9.1 \pm 1.8) \times 10^{-4}$	
Γ_{45} $\Sigma^0 \bar{\Sigma}^0$	$< 8 \times 10^{-5}$	90%
Γ_{46} $\Sigma^+ \bar{\Sigma}^-$	$< 7 \times 10^{-5}$	90%
Γ_{47} $\Xi^0 \bar{\Xi}^0$	$< 1.1 \times 10^{-4}$	90%
Γ_{48} $\Xi^- \bar{\Xi}^+$	$(1.55 \pm 0.35) \times 10^{-4}$	
Γ_{49} $J/\psi(1S) \pi^+ \pi^- \pi^0$	$< 1.5 \%$	90%
Radiative decays		
Γ_{50} $\gamma J/\psi(1S)$	$(19.5 \pm 0.8) \%$	
Γ_{51} $\gamma\rho^0$	$< 5 \times 10^{-5}$	90%
Γ_{52} $\gamma\omega$	$< 6 \times 10^{-6}$	90%
Γ_{53} $\gamma\phi$	$< 1.2 \times 10^{-5}$	90%
Γ_{54} $\gamma\gamma$	$(2.56 \pm 0.16) \times 10^{-4}$	

Meson Particle Listings

 $\chi_{c2}(1P)$

$\Gamma(K^+ K^- \pi^0 \pi^0)/\Gamma_{\text{total}}$		Γ_5/Γ	
VALUE (%)	EVTS	DOCUMENT ID	TECN COMMENT

0.22±0.04±0.01 76.9 22 HE 08B CLEO $e^+e^- \rightarrow \gamma h^+ h^- h^0 h^0$
 22 HE 08B reports $0.21 \pm 0.03 \pm 0.03 \pm 0.01$ % from a measurement of $[\Gamma(\chi_{c2}(1P) \rightarrow K^+ K^- \pi^0 \pi^0)/\Gamma_{\text{total}}] \times [B(\psi(2S) \rightarrow \gamma \chi_{c2}(1P))]$ assuming $B(\psi(2S) \rightarrow \gamma \chi_{c2}(1P)) = (9.33 \pm 0.14 \pm 0.61) \times 10^{-2}$, which we rescale to our best value $B(\psi(2S) \rightarrow \gamma \chi_{c2}(1P)) = (8.74 \pm 0.35) \times 10^{-2}$. Our first error is their experiment's error and our second error is the systematic error from using our best value.

$\Gamma(K^+ \pi^- K^0 \pi^0 + \text{c.c.})/\Gamma_{\text{total}}$		Γ_6/Γ	
VALUE (%)	EVTS	DOCUMENT ID	TECN COMMENT

1.50±0.21±0.06 211.6 23 HE 08B CLEO $e^+e^- \rightarrow \gamma h^+ h^- h^0 h^0$
 23 HE 08B reports $1.41 \pm 0.11 \pm 0.16 \pm 0.10$ % from a measurement of $[\Gamma(\chi_{c2}(1P) \rightarrow K^+ \pi^- K^0 \pi^0 + \text{c.c.})/\Gamma_{\text{total}}] \times [B(\psi(2S) \rightarrow \gamma \chi_{c2}(1P))]$ assuming $B(\psi(2S) \rightarrow \gamma \chi_{c2}(1P)) = (9.33 \pm 0.14 \pm 0.61) \times 10^{-2}$, which we rescale to our best value $B(\psi(2S) \rightarrow \gamma \chi_{c2}(1P)) = (8.74 \pm 0.35) \times 10^{-2}$. Our first error is their experiment's error and our second error is the systematic error from using our best value.

$\Gamma(\rho^+ K^- K^0 + \text{c.c.})/\Gamma_{\text{total}}$		Γ_7/Γ	
VALUE (%)	EVTS	DOCUMENT ID	TECN COMMENT

0.45±0.13±0.02 62.9 24 HE 08B CLEO $e^+e^- \rightarrow \gamma h^+ h^- h^0 h^0$
 24 HE 08B reports $0.42 \pm 0.11 \pm 0.06 \pm 0.03$ % from a measurement of $[\Gamma(\chi_{c2}(1P) \rightarrow \rho^+ K^- K^0 + \text{c.c.})/\Gamma_{\text{total}}] \times [B(\psi(2S) \rightarrow \gamma \chi_{c2}(1P))]$ assuming $B(\psi(2S) \rightarrow \gamma \chi_{c2}(1P)) = (9.33 \pm 0.14 \pm 0.61) \times 10^{-2}$, which we rescale to our best value $B(\psi(2S) \rightarrow \gamma \chi_{c2}(1P)) = (8.74 \pm 0.35) \times 10^{-2}$. Our first error is their experiment's error and our second error is the systematic error from using our best value.

$\Gamma(K^*(892)^0 K^+ \pi^- \rightarrow K^+ \pi^- K^0 \pi^0 + \text{c.c.})/\Gamma_{\text{total}}$		Γ_8/Γ	
VALUE (%)	EVTS	DOCUMENT ID	TECN COMMENT

0.32±0.09±0.01 38.7 25 HE 08B CLEO $e^+e^- \rightarrow \gamma h^+ h^- h^0 h^0$
 25 HE 08B reports $0.30 \pm 0.07 \pm 0.04 \pm 0.02$ % from a measurement of $[\Gamma(\chi_{c2}(1P) \rightarrow K^*(892)^0 K^+ \pi^- \rightarrow K^+ \pi^- K^0 \pi^0 + \text{c.c.})/\Gamma_{\text{total}}] \times [B(\psi(2S) \rightarrow \gamma \chi_{c2}(1P))]$ assuming $B(\psi(2S) \rightarrow \gamma \chi_{c2}(1P)) = (9.33 \pm 0.14 \pm 0.61) \times 10^{-2}$, which we rescale to our best value $B(\psi(2S) \rightarrow \gamma \chi_{c2}(1P)) = (8.74 \pm 0.35) \times 10^{-2}$. Our first error is their experiment's error and our second error is the systematic error from using our best value.

$\Gamma(K^*(892)^0 K^0 \pi^0 \rightarrow K^+ \pi^- K^0 \pi^0 + \text{c.c.})/\Gamma_{\text{total}}$		Γ_9/Γ	
VALUE (%)	EVTS	DOCUMENT ID	TECN COMMENT

0.42±0.09±0.02 63.0 26 HE 08B CLEO $e^+e^- \rightarrow \gamma h^+ h^- h^0 h^0$
 26 HE 08B reports $0.39 \pm 0.07 \pm 0.05 \pm 0.03$ % from a measurement of $[\Gamma(\chi_{c2}(1P) \rightarrow K^*(892)^0 K^0 \pi^0 \rightarrow K^+ \pi^- K^0 \pi^0 + \text{c.c.})/\Gamma_{\text{total}}] \times [B(\psi(2S) \rightarrow \gamma \chi_{c2}(1P))]$ assuming $B(\psi(2S) \rightarrow \gamma \chi_{c2}(1P)) = (9.33 \pm 0.14 \pm 0.61) \times 10^{-2}$, which we rescale to our best value $B(\psi(2S) \rightarrow \gamma \chi_{c2}(1P)) = (8.74 \pm 0.35) \times 10^{-2}$. Our first error is their experiment's error and our second error is the systematic error from using our best value.

$\Gamma(K^*(892)^- K^+ \pi^0 \rightarrow K^+ \pi^- K^0 \pi^0 + \text{c.c.})/\Gamma_{\text{total}}$		Γ_{10}/Γ	
VALUE (%)	EVTS	DOCUMENT ID	TECN COMMENT

0.41±0.09±0.02 51.1 27 HE 08B CLEO $e^+e^- \rightarrow \gamma h^+ h^- h^0 h^0$
 27 HE 08B reports $0.38 \pm 0.07 \pm 0.04 \pm 0.03$ % from a measurement of $[\Gamma(\chi_{c2}(1P) \rightarrow K^*(892)^- K^+ \pi^0 \rightarrow K^+ \pi^- K^0 \pi^0 + \text{c.c.})/\Gamma_{\text{total}}] \times [B(\psi(2S) \rightarrow \gamma \chi_{c2}(1P))]$ assuming $B(\psi(2S) \rightarrow \gamma \chi_{c2}(1P)) = (9.33 \pm 0.14 \pm 0.61) \times 10^{-2}$, which we rescale to our best value $B(\psi(2S) \rightarrow \gamma \chi_{c2}(1P)) = (8.74 \pm 0.35) \times 10^{-2}$. Our first error is their experiment's error and our second error is the systematic error from using our best value.

$\Gamma(K^*(892)^+ K^0 \pi^- \rightarrow K^+ \pi^- K^0 \pi^0 + \text{c.c.})/\Gamma_{\text{total}}$		Γ_{11}/Γ	
VALUE (%)	EVTS	DOCUMENT ID	TECN COMMENT

0.32±0.09±0.01 39.3 28 HE 08B CLEO $e^+e^- \rightarrow \gamma h^+ h^- h^0 h^0$
 28 HE 08B reports $0.30 \pm 0.07 \pm 0.04 \pm 0.02$ % from a measurement of $[\Gamma(\chi_{c2}(1P) \rightarrow K^*(892)^+ K^0 \pi^- \rightarrow K^+ \pi^- K^0 \pi^0 + \text{c.c.})/\Gamma_{\text{total}}] \times [B(\psi(2S) \rightarrow \gamma \chi_{c2}(1P))]$ assuming $B(\psi(2S) \rightarrow \gamma \chi_{c2}(1P)) = (9.33 \pm 0.14 \pm 0.61) \times 10^{-2}$, which we rescale to our best value $B(\psi(2S) \rightarrow \gamma \chi_{c2}(1P)) = (8.74 \pm 0.35) \times 10^{-2}$. Our first error is their experiment's error and our second error is the systematic error from using our best value.

$\Gamma(K^+ K^- \eta \pi^0)/\Gamma_{\text{total}}$		Γ_{12}/Γ	
VALUE (%)	EVTS	DOCUMENT ID	TECN COMMENT

0.14±0.05±0.01 22.9 29 HE 08B CLEO $e^+e^- \rightarrow \gamma h^+ h^- h^0 h^0$
 29 HE 08B reports $0.13 \pm 0.04 \pm 0.02 \pm 0.01$ % from a measurement of $[\Gamma(\chi_{c2}(1P) \rightarrow K^+ K^- \eta \pi^0)/\Gamma_{\text{total}}] \times [B(\psi(2S) \rightarrow \gamma \chi_{c2}(1P))]$ assuming $B(\psi(2S) \rightarrow \gamma \chi_{c2}(1P)) = (9.33 \pm 0.14 \pm 0.61) \times 10^{-2}$, which we rescale to our best value $B(\psi(2S) \rightarrow \gamma \chi_{c2}(1P)) = (8.74 \pm 0.35) \times 10^{-2}$. Our first error is their experiment's error and our second error is the systematic error from using our best value.

$\Gamma(\pi^+ \pi^- K^+ K^-)/\Gamma_{\text{total}}$		Γ_{13}/Γ	
VALUE (units 10^{-3})	DOCUMENT ID	TECN COMMENT	

9.2±1.1 OUR FIT

$\Gamma(K^+ \bar{K}^*(892)^0 \pi^- + \text{c.c.})/\Gamma(\pi^+ \pi^- K^+ K^-)$		Γ_{14}/Γ_{13}	
VALUE	DOCUMENT ID	TECN COMMENT	

0.25±0.13 OUR FIT

0.25±0.13 TANENBAUM 78 MRK1 $\psi(2S) \rightarrow \gamma \chi_{c2}$

$\Gamma(K^+ \bar{K}^*(892)^0 \pi^- + \text{c.c.})/\Gamma_{\text{total}}$		Γ_{14}/Γ	
VALUE (units 10^{-4})	DOCUMENT ID	TECN COMMENT	

23±12 OUR FIT

$\Gamma(K^*(892)^0 \bar{K}^*(892)^0)/\Gamma_{\text{total}}$		Γ_{15}/Γ	
VALUE (units 10^{-3})	DOCUMENT ID	TECN COMMENT	

2.5±0.5 OUR FIT

$\Gamma(3(\pi^+ \pi^-))/\Gamma_{\text{total}}$		Γ_{16}/Γ	
VALUE (units 10^{-3})	DOCUMENT ID	TECN COMMENT	

8.6±1.8 OUR EVALUATION Treating systematic error as correlated.

8.6±1.8 OUR AVERAGE

$8.6 \pm 0.9 \pm 1.6$

$8.7 \pm 5.9 \pm 0.4$

30 BAI 99B BES $\psi(2S) \rightarrow \gamma \chi_{c2}$
 30 TANENBAUM 78 MRK1 $\psi(2S) \rightarrow \gamma \chi_{c2}$
 30 Rescaled by us using $B(\psi(2S) \rightarrow \gamma \chi_{c2}) = (8.3 \pm 0.4)\%$ and $B(\psi(2S) \rightarrow J/\psi(1S) \pi^+ \pi^-) = (32.6 \pm 0.5)\%$. Multiplied by a factor of 2 to convert from $K_S^0 K^+ \pi^-$ to $K^0 K^+ \pi^-$ decay.

$\Gamma(\phi\phi)/\Gamma_{\text{total}}$		Γ_{17}/Γ	
VALUE (units 10^{-3})	DOCUMENT ID	TECN COMMENT	

1.48±0.28 OUR FIT

$\Gamma(\omega\omega)/\Gamma_{\text{total}}$		Γ_{18}/Γ	
VALUE (units 10^{-3})	EVTS	DOCUMENT ID	TECN COMMENT

1.9±0.6±0.1 27.7±7.4 31 ABLIKIM 05N BES2 $\psi(2S) \rightarrow \gamma \chi_{c2} \rightarrow \gamma \pi \pi$

31 ABLIKIM 05N reports $[\Gamma(\chi_{c2}(1P) \rightarrow \omega\omega)/\Gamma_{\text{total}}] \times [B(\psi(2S) \rightarrow \gamma \chi_{c2}(1P))]$ = $(0.165 \pm 0.044 \pm 0.032) \times 10^{-3}$ which we divide by our best value $B(\psi(2S) \rightarrow \gamma \chi_{c2}(1P)) = (8.74 \pm 0.35) \times 10^{-2}$. Our first error is their experiment's error and our second error is the systematic error from using our best value.

$\Gamma(\pi\pi)/\Gamma_{\text{total}}$		Γ_{19}/Γ	
VALUE (units 10^{-3})	DOCUMENT ID	TECN COMMENT	

2.39±0.14 OUR FIT

$\Gamma(\rho^0 \pi^+ \pi^-)/\Gamma_{\text{total}}$		Γ_{20}/Γ	
VALUE (units 10^{-4})	DOCUMENT ID	TECN COMMENT	

40±17 OUR FIT

$\Gamma(\pi^+ \pi^- \eta)/\Gamma_{\text{total}}$		Γ_{21}/Γ	
VALUE (units 10^{-3})	CL%	DOCUMENT ID	TECN COMMENT

0.52±0.14±0.02

32 ATHAR 07 CLEO $\psi(2S) \rightarrow \gamma h^+ h^- h^0$

••• We do not use the following data for averages, fits, limits, etc. •••

<1.6 90 33 ABLIKIM 06R BES2 $\psi(2S) \rightarrow \gamma \chi_{c2}$

32 ATHAR 07 reports $(0.49 \pm 0.12 \pm 0.06) \times 10^{-3}$ from a measurement of $[\Gamma(\chi_{c2}(1P) \rightarrow \pi^+ \pi^- \eta)/\Gamma_{\text{total}}] \times [B(\psi(2S) \rightarrow \gamma \chi_{c2}(1P))]$ assuming $B(\psi(2S) \rightarrow \gamma \chi_{c2}(1P)) = (9.33 \pm 0.14 \pm 0.61) \times 10^{-2}$, which we rescale to our best value $B(\psi(2S) \rightarrow \gamma \chi_{c2}(1P)) = (8.74 \pm 0.35) \times 10^{-2}$. Our first error is their experiment's error and our second error is the systematic error from using our best value.

33 ABLIKIM 06R reports $< 1.7 \times 10^{-3}$ from a measurement of $[\Gamma(\chi_{c2}(1P) \rightarrow \pi^+ \pi^- \eta)/\Gamma_{\text{total}}] \times [B(\psi(2S) \rightarrow \gamma \chi_{c2}(1P))]$ assuming $B(\psi(2S) \rightarrow \gamma \chi_{c2}(1P)) = (8.1 \pm 0.4) \times 10^{-2}$, which we rescale to our best value $B(\psi(2S) \rightarrow \gamma \chi_{c2}(1P)) = 8.74 \times 10^{-2}$.

$\Gamma(\pi^+ \pi^- \eta')/\Gamma_{\text{total}}$		Γ_{22}/Γ	
VALUE (units 10^{-3})	DOCUMENT ID	TECN COMMENT	

0.54±0.20±0.02

34 ATHAR 07 CLEO $\psi(2S) \rightarrow \gamma h^+ h^- h^0$

34 ATHAR 07 reports $(0.51 \pm 0.18 \pm 0.06) \times 10^{-3}$ from a measurement of $[\Gamma(\chi_{c2}(1P) \rightarrow \pi^+ \pi^- \eta')/\Gamma_{\text{total}}] \times [B(\psi(2S) \rightarrow \gamma \chi_{c2}(1P))]$ assuming $B(\psi(2S) \rightarrow \gamma \chi_{c2}(1P)) = (9.33 \pm 0.14 \pm 0.61) \times 10^{-2}$, which we rescale to our best value $B(\psi(2S) \rightarrow \gamma \chi_{c2}(1P)) = (8.74 \pm 0.35) \times 10^{-2}$. Our first error is their experiment's error and our second error is the systematic error from using our best value.

$\Gamma(\eta\eta)/\Gamma_{\text{total}}$		Γ_{23}/Γ		
VALUE (units 10^{-4})	CL%	EVTS	DOCUMENT ID	TECN COMMENT

5.4±0.7±0.2 156±14 35 ASNER 09 CLEO $\psi(2S) \rightarrow \gamma \eta \eta$

••• We do not use the following data for averages, fits, limits, etc. •••

< 5 90 36 ADAMS 07 CLEO $\psi(2S) \rightarrow \gamma \chi_{c2}$

<12 90 37 BAI 03c BES $\psi(2S) \rightarrow \gamma \eta \eta \rightarrow 5 \gamma$

7.9±4.1±2.4 38 LEE 85 CBAL $\psi' \rightarrow \text{photons}$

35 ASNER 09 reports $(5.1 \pm 0.5 \pm 0.6) \times 10^{-4}$ from a measurement of $[\Gamma(\chi_{c2}(1P) \rightarrow \eta\eta)/\Gamma_{\text{total}}] \times [B(\psi(2S) \rightarrow \gamma \chi_{c2}(1P))]$ assuming $B(\psi(2S) \rightarrow \gamma \chi_{c2}(1P)) = (9.33 \pm 0.14 \pm 0.61) \times 10^{-2}$, which we rescale to our best value $B(\psi(2S) \rightarrow \gamma \chi_{c2}(1P)) = (8.74 \pm 0.35) \times 10^{-2}$. Our first error is their experiment's error and our second error is the systematic error from using our best value.

36 Superseded by ASNER 09. ADAMS 07 reports $< 4.7 \times 10^{-4}$ from a measurement of $[\Gamma(\chi_{c2}(1P) \rightarrow \eta\eta)/\Gamma_{\text{total}}] \times [B(\psi(2S) \rightarrow \gamma \chi_{c2}(1P))]$ assuming $B(\psi(2S) \rightarrow \gamma \chi_{c2}(1P)) = 0.0933 \pm 0.0014 \pm 0.0061$, which we rescale to our best value $B(\psi(2S) \rightarrow \gamma \chi_{c2}(1P)) = 8.74 \times 10^{-2}$.

37 Rescaled by us using $B(\psi(2S) \rightarrow \gamma \chi_{c2}) = (8.3 \pm 0.4)\%$ and $B(\psi(2S) \rightarrow J/\psi(1S) \pi^+ \pi^-) = (32.6 \pm 0.5)\%$. Multiplied by a factor of 2 to convert from $K_S^0 K^+ \pi^-$ to $K^0 K^+ \pi^-$ decay.

38 Calculated using $B(\psi(2S) \rightarrow \gamma \chi_{c2}(1P)) = 0.078 \pm 0.008$.

See key on page 405

Meson Particle Listings

 $\chi_{c2}(1P)$

$\Gamma(K^+ K^-)/\Gamma_{\text{total}}$	Γ_{24}/Γ
<u>VALUE (units 10^{-3})</u>	<u>DOCUMENT ID</u>
1.09 ± 0.08 OUR FIT	

$\Gamma(K_S^0 \bar{K}_S^0)/\Gamma_{\text{total}}$	Γ_{25}/Γ
<u>VALUE (units 10^{-3})</u>	<u>DOCUMENT ID</u>
0.58 ± 0.05 OUR FIT	

$\Gamma(K_S^0 \bar{K}_S^0)/\Gamma(\pi\pi)$	Γ_{25}/Γ_{19}
<u>VALUE</u>	<u>DOCUMENT ID</u> <u>TECN</u> <u>COMMENT</u>
0.242 ± 0.020 OUR FIT	

• • • We do not use the following data for averages, fits, limits, etc. • • •

0.27 ± 0.07 ± 0.04 ^{39,40} CHEN 07B BELL $e^+ e^- \rightarrow e^+ e^- \chi_{c2}$

³⁹ Using $\Gamma(\pi\pi) \times \Gamma(\gamma\gamma)/\Gamma_{\text{total}}$ from the $\pi^+ \pi^-$ measurement of NAKAZAWA 05 rescaled by 3/2 to convert to $\pi\pi$.

⁴⁰ Not independent from other measurements.

$\Gamma(K_S^0 \bar{K}_S^0)/\Gamma(K^+ K^-)$	Γ_{25}/Γ_{24}
<u>VALUE</u>	<u>DOCUMENT ID</u> <u>TECN</u> <u>COMMENT</u>
0.53 ± 0.05 OUR FIT	

• • • We do not use the following data for averages, fits, limits, etc. • • •

0.70 ± 0.21 ± 0.12 ^{41,42} CHEN 07B BELL $e^+ e^- \rightarrow e^+ e^- \chi_{c2}$

⁴¹ Using $\Gamma(K^+ K^-) \times \Gamma(\gamma\gamma)/\Gamma_{\text{total}}$ from NAKAZAWA 05.

⁴² Not independent from other measurements.

$\Gamma(\bar{K}^0 K^+ \pi^- + \text{c.c.})/\Gamma_{\text{total}}$	Γ_{26}/Γ
<u>VALUE (units 10^{-3})</u> <u>CL%</u> <u>EVTS</u>	<u>DOCUMENT ID</u> <u>TECN</u> <u>COMMENT</u>
1.32 ± 0.20 OUR AVERAGE	

1.39 ± 0.22 ± 0.05 ⁴³ ATHAR 07 CLEO $\psi(2S) \rightarrow \gamma h^+ h^- h^0$

1.11 ± 0.41 ± 0.04 28 ⁴⁴ ABLIKIM 06R BES2 $\psi(2S) \rightarrow \gamma \chi_{c2}$

• • • We do not use the following data for averages, fits, limits, etc. • • •

<2.0 90 ⁴⁵ BAI 99B BES $\psi(2S) \rightarrow \gamma \chi_{c2}$

⁴³ ATHAR 07 reports $(1.3 \pm 0.2 \pm 0.1) \times 10^{-3}$ from a measurement of $[\Gamma(\chi_{c2}(1P) \rightarrow \bar{K}^0 K^+ \pi^- + \text{c.c.})/\Gamma_{\text{total}}] \times [B(\psi(2S) \rightarrow \gamma \chi_{c2}(1P))]$ assuming $B(\psi(2S) \rightarrow \gamma \chi_{c2}(1P)) = (9.33 \pm 0.14 \pm 0.61) \times 10^{-2}$, which we rescale to our best value $B(\psi(2S) \rightarrow \gamma \chi_{c2}(1P)) = (8.74 \pm 0.35) \times 10^{-2}$. Our first error is their experiment's error and our second error is the systematic error from using our best value.

⁴⁴ We have multiplied the $K_S^0 K^+ \pi^-$ measurement by a factor of 2 to convert to $K^0 K^+ \pi^-$. ABLIKIM 06R reports $(1.2 \pm 0.4 \pm 0.2) \times 10^{-3}$ from a measurement of $[\Gamma(\chi_{c2}(1P) \rightarrow \bar{K}^0 K^+ \pi^- + \text{c.c.})/\Gamma_{\text{total}}] \times [B(\psi(2S) \rightarrow \gamma \chi_{c2}(1P))]$ assuming $B(\psi(2S) \rightarrow \gamma \chi_{c2}(1P)) = (8.1 \pm 0.6) \times 10^{-2}$, which we rescale to our best value $B(\psi(2S) \rightarrow \gamma \chi_{c2}(1P)) = (8.74 \pm 0.35) \times 10^{-2}$. Our first error is their experiment's error and our second error is the systematic error from using our best value.

⁴⁵ Rescaled by us using $B(\psi(2S) \rightarrow \gamma \chi_{c2}) = (8.3 \pm 0.4)\%$ and $B(\psi(2S) \rightarrow J/\psi(1S) \pi^+ \pi^-) = (32.6 \pm 0.5)\%$. Multiplied by a factor of 2 to convert from $K_S^0 K^+ \pi^-$ to $K^0 K^+ \pi^-$ decay.

$\Gamma(K^+ K^- \pi^0)/\Gamma_{\text{total}}$	Γ_{27}/Γ
<u>VALUE (units 10^{-3})</u>	<u>DOCUMENT ID</u> <u>TECN</u> <u>COMMENT</u>
0.33 ± 0.08 ± 0.01	

⁴⁶ ATHAR 07 reports $(0.31 \pm 0.07 \pm 0.04) \times 10^{-3}$ from a measurement of $[\Gamma(\chi_{c2}(1P) \rightarrow K^+ K^- \pi^0)/\Gamma_{\text{total}}] \times [B(\psi(2S) \rightarrow \gamma \chi_{c2}(1P))]$ assuming $B(\psi(2S) \rightarrow \gamma \chi_{c2}(1P)) = (9.33 \pm 0.14 \pm 0.61) \times 10^{-2}$, which we rescale to our best value $B(\psi(2S) \rightarrow \gamma \chi_{c2}(1P)) = (8.74 \pm 0.35) \times 10^{-2}$. Our first error is their experiment's error and our second error is the systematic error from using our best value.

$\Gamma(K^+ K^- \eta)/\Gamma_{\text{total}}$	Γ_{28}/Γ
<u>VALUE (units 10^{-3})</u> <u>CL%</u>	<u>DOCUMENT ID</u> <u>TECN</u> <u>COMMENT</u>
<0.35	

⁴⁷ ATHAR 07 reports $< 0.33 \times 10^{-3}$ from a measurement of $[\Gamma(\chi_{c2}(1P) \rightarrow K^+ K^- \eta)/\Gamma_{\text{total}}] \times [B(\psi(2S) \rightarrow \gamma \chi_{c2}(1P))]$ assuming $B(\psi(2S) \rightarrow \gamma \chi_{c2}(1P)) = (9.33 \pm 0.14 \pm 0.61) \times 10^{-2}$, which we rescale to our best value $B(\psi(2S) \rightarrow \gamma \chi_{c2}(1P)) = 8.74 \times 10^{-2}$.

$\Gamma(\eta\eta')/\Gamma_{\text{total}}$	Γ_{29}/Γ
<u>VALUE (units 10^{-4})</u> <u>CL%</u> <u>EVTS</u>	<u>DOCUMENT ID</u> <u>TECN</u> <u>COMMENT</u>
<0.6	

• • • We do not use the following data for averages, fits, limits, etc. • • •

<2.5 90 ⁴⁹ ADAMS 07 CLEO $\psi(2S) \rightarrow \gamma \chi_{c2}$

⁴⁸ ASNER 09 reports $< 0.6 \times 10^{-4}$ from a measurement of $[\Gamma(\chi_{c2}(1P) \rightarrow \eta\eta')/\Gamma_{\text{total}}] \times [B(\psi(2S) \rightarrow \gamma \chi_{c2}(1P))]$ assuming $B(\psi(2S) \rightarrow \gamma \chi_{c2}(1P)) = (9.33 \pm 0.14 \pm 0.61) \times 10^{-2}$, which we rescale to our best value $B(\psi(2S) \rightarrow \gamma \chi_{c2}(1P)) = 8.74 \times 10^{-2}$.

⁴⁹ Superseded by ASNER 09. ADAMS 07 reports $< 2.3 \times 10^{-4}$ from a measurement of $[\Gamma(\chi_{c2}(1P) \rightarrow \eta\eta')/\Gamma_{\text{total}}] \times [B(\psi(2S) \rightarrow \gamma \chi_{c2}(1P))]$ assuming $B(\psi(2S) \rightarrow \gamma \chi_{c2}(1P)) = 0.0933 \pm 0.0014 \pm 0.0061$, which we rescale to our best value $B(\psi(2S) \rightarrow \gamma \chi_{c2}(1P)) = 8.74 \times 10^{-2}$.

$\Gamma(\eta'\eta')/\Gamma_{\text{total}}$	Γ_{30}/Γ
<u>VALUE (units 10^{-4})</u> <u>CL%</u> <u>EVTS</u>	<u>DOCUMENT ID</u> <u>TECN</u> <u>COMMENT</u>
<1.1	

• • • We do not use the following data for averages, fits, limits, etc. • • •

<3.3 90 ⁵¹ ADAMS 07 CLEO $\psi(2S) \rightarrow \gamma \chi_{c2}$

⁵⁰ ASNER 09 reports $< 1.0 \times 10^{-4}$ from a measurement of $[\Gamma(\chi_{c2}(1P) \rightarrow \eta'\eta')/\Gamma_{\text{total}}] \times [B(\psi(2S) \rightarrow \gamma \chi_{c2}(1P))]$ assuming $B(\psi(2S) \rightarrow \gamma \chi_{c2}(1P)) = (9.33 \pm 0.14 \pm 0.61) \times 10^{-2}$, which we rescale to our best value $B(\psi(2S) \rightarrow \gamma \chi_{c2}(1P)) = 8.74 \times 10^{-2}$.

⁵¹ Superseded by ASNER 09. ADAMS 07 reports $< 3.1 \times 10^{-4}$ from a measurement of $[\Gamma(\chi_{c2}(1P) \rightarrow \eta'\eta')/\Gamma_{\text{total}}] \times [B(\psi(2S) \rightarrow \gamma \chi_{c2}(1P))]$ assuming $B(\psi(2S) \rightarrow \gamma \chi_{c2}(1P)) = 0.0933 \pm 0.0014 \pm 0.0061$, which we rescale to our best value $B(\psi(2S) \rightarrow \gamma \chi_{c2}(1P)) = 8.74 \times 10^{-2}$.

$\Gamma(\pi^+ \pi^- K_S^0 \bar{K}_S^0)/\Gamma_{\text{total}}$	Γ_{31}/Γ
<u>VALUE (units 10^{-3})</u> <u>CL%</u> <u>EVTS</u>	<u>DOCUMENT ID</u> <u>TECN</u> <u>COMMENT</u>
2.4 ± 0.6 ± 0.1	

⁵² ABLIKIM 05o reports $[\Gamma(\chi_{c2}(1P) \rightarrow \pi^+ \pi^- K_S^0 \bar{K}_S^0)/\Gamma_{\text{total}}] \times [B(\psi(2S) \rightarrow \gamma \chi_{c2}(1P))]$ = $(0.207 \pm 0.039 \pm 0.033) \times 10^{-3}$ which we divide by our best value $B(\psi(2S) \rightarrow \gamma \chi_{c2}(1P)) = (8.74 \pm 0.35) \times 10^{-2}$. Our first error is their experiment's error and our second error is the systematic error from using our best value.

$\Gamma(K^+ K^- K_S^0 \bar{K}_S^0)/\Gamma_{\text{total}}$	Γ_{32}/Γ
<u>VALUE (units 10^{-4})</u> <u>CL%</u> <u>EVTS</u>	<u>DOCUMENT ID</u> <u>TECN</u> <u>COMMENT</u>
<4	

⁵³ ABLIKIM 05o reports $[\Gamma(\chi_{c2}(1P) \rightarrow K^+ K^- K_S^0 \bar{K}_S^0)/\Gamma_{\text{total}}] \times [B(\psi(2S) \rightarrow \gamma \chi_{c2}(1P))]$ < 3.5×10^{-5} which we divide by our best value $B(\psi(2S) \rightarrow \gamma \chi_{c2}(1P)) = 8.74 \times 10^{-2}$.

$\Gamma(K^+ K^- K^+ K^-)/\Gamma_{\text{total}}$	Γ_{33}/Γ
<u>VALUE (units 10^{-3})</u>	<u>DOCUMENT ID</u>
1.78 ± 0.22 OUR FIT	

$\Gamma(K^+ K^- \phi)/\Gamma_{\text{total}}$	Γ_{34}/Γ
<u>VALUE (units 10^{-3})</u> <u>EVTS</u>	<u>DOCUMENT ID</u> <u>TECN</u> <u>COMMENT</u>
1.55 ± 0.32 ± 0.06	

⁵⁴ ABLIKIM 06T reports $(1.67 \pm 0.26 \pm 0.24) \times 10^{-3}$ from a measurement of $[\Gamma(\chi_{c2}(1P) \rightarrow K^+ K^- \phi)/\Gamma_{\text{total}}] \times [B(\psi(2S) \rightarrow \gamma \chi_{c2}(1P))]$ assuming $B(\psi(2S) \rightarrow \gamma \chi_{c2}(1P)) = (8.1 \pm 0.4) \times 10^{-2}$, which we rescale to our best value $B(\psi(2S) \rightarrow \gamma \chi_{c2}(1P)) = (8.74 \pm 0.35) \times 10^{-2}$. Our first error is their experiment's error and our second error is the systematic error from using our best value.

$\Gamma(K_S^0 \bar{K}_S^0 \rho \bar{\rho})/\Gamma_{\text{total}}$	Γ_{35}/Γ
<u>VALUE (units 10^{-4})</u> <u>CL%</u>	<u>DOCUMENT ID</u> <u>TECN</u> <u>COMMENT</u>
<7.9	

⁵⁵ Using $B(\psi(2S) \rightarrow \chi_{c2} \gamma) = (9.3 \pm 0.6)\%$.

$\Gamma(\rho \bar{\rho})/\Gamma_{\text{total}}$	Γ_{36}/Γ
<u>VALUE (units 10^{-4})</u>	<u>DOCUMENT ID</u>
0.72 ± 0.04 OUR FIT	

$\Gamma(\rho \bar{\rho} \pi^0)/\Gamma_{\text{total}}$	Γ_{37}/Γ
<u>VALUE (units 10^{-3})</u>	<u>DOCUMENT ID</u> <u>TECN</u> <u>COMMENT</u>
0.47 ± 0.10 ± 0.02	

⁵⁶ ATHAR 07 reports $(0.44 \pm 0.08 \pm 0.05) \times 10^{-3}$ from a measurement of $[\Gamma(\chi_{c2}(1P) \rightarrow \rho \bar{\rho} \pi^0)/\Gamma_{\text{total}}] \times [B(\psi(2S) \rightarrow \gamma \chi_{c2}(1P))]$ assuming $B(\psi(2S) \rightarrow \gamma \chi_{c2}(1P)) = (9.33 \pm 0.14 \pm 0.61) \times 10^{-2}$, which we rescale to our best value $B(\psi(2S) \rightarrow \gamma \chi_{c2}(1P)) = (8.74 \pm 0.35) \times 10^{-2}$. Our first error is their experiment's error and our second error is the systematic error from using our best value.

$\Gamma(\rho \bar{\rho} \eta)/\Gamma_{\text{total}}$	Γ_{38}/Γ
<u>VALUE (units 10^{-3})</u>	<u>DOCUMENT ID</u> <u>TECN</u> <u>COMMENT</u>
0.20 ± 0.08 ± 0.01	

⁵⁷ ATHAR 07 reports $(0.19 \pm 0.07 \pm 0.02) \times 10^{-3}$ from a measurement of $[\Gamma(\chi_{c2}(1P) \rightarrow \rho \bar{\rho} \eta)/\Gamma_{\text{total}}] \times [B(\psi(2S) \rightarrow \gamma \chi_{c2}(1P))]$ assuming $B(\psi(2S) \rightarrow \gamma \chi_{c2}(1P)) = (9.33 \pm 0.14 \pm 0.61) \times 10^{-2}$, which we rescale to our best value $B(\psi(2S) \rightarrow \gamma \chi_{c2}(1P)) = (8.74 \pm 0.35) \times 10^{-2}$. Our first error is their experiment's error and our second error is the systematic error from using our best value.

$\Gamma(\pi^+ \pi^- \rho \bar{\rho})/\Gamma_{\text{total}}$	Γ_{39}/Γ
<u>VALUE (units 10^{-3})</u>	<u>DOCUMENT ID</u> <u>TECN</u> <u>COMMENT</u>
1.32 ± 0.34 OUR EVALUATION	Treating systematic error as correlated.

1.3 ± 0.4 OUR AVERAGE Error includes scale factor of 1.3.

1.17 ± 0.19 ± 0.30 ⁵⁸ BAI 99B BES $\psi(2S) \rightarrow \gamma \chi_{c2}$

2.64 ± 1.03 ± 0.14 ⁵⁸ TANENBAUM 78 MRK1 $\psi(2S) \rightarrow \gamma \chi_{c2}$

⁵⁸ Rescaled by us using $B(\psi(2S) \rightarrow \gamma \chi_{c2}) = (8.3 \pm 0.4)\%$ and $B(\psi(2S) \rightarrow J/\psi(1S) \pi^+ \pi^-) = (32.6 \pm 0.5)\%$. Multiplied by a factor of 2 to convert from $K_S^0 K^+ \pi^-$ to $K^0 K^+ \pi^-$ decay.

See key on page 405

Meson Particle Listings

$\chi_{c2}(1P)$

$$\Gamma(\chi_{c2}(1P) \rightarrow \Lambda\bar{\Lambda})/\Gamma_{\text{total}} \times \Gamma(\psi(2S) \rightarrow \gamma\chi_{c2}(1P))/\Gamma_{\text{total}}$$

VALUE (units 10^{-6})	EVTS	DOCUMENT ID	TECN	COMMENT
16.3 ± 2.3 OUR FIT				
15.9 ± 2.1 ± 1.0	71 ± 9	76 NAIK	08	CLEO $\psi(2S) \rightarrow \gamma\Lambda\bar{\Lambda}$
⁷⁶ Calculated by us. NAIK 08 reports $B(\chi_{c2} \rightarrow \Lambda\bar{\Lambda}) = (17.0 \pm 2.2 \pm 1.1 \pm 1.1) \times 10^{-5}$ using $B(\psi(2S) \rightarrow \gamma\chi_{c2}) = (9.33 \pm 0.14 \pm 0.61)\%$.				

$$\Gamma(\chi_{c2}(1P) \rightarrow \Lambda\bar{\Lambda})/\Gamma_{\text{total}} \times \Gamma(\psi(2S) \rightarrow \gamma\chi_{c2}(1P))/\Gamma(\psi(2S) \rightarrow J/\psi(1S)\pi^+\pi^-)$$

VALUE (units 10^{-9})	EVTS	DOCUMENT ID	TECN	COMMENT
4.8 ± 0.7 OUR FIT				
7.1 ± 3.1 ± 1.3	8.3 ± 3.7	77 BAI	03E	BES $\psi(2S) \rightarrow \gamma\Lambda\bar{\Lambda}$

⁷⁷ BAI 03E reports $[B(\chi_{c2} \rightarrow \Lambda\bar{\Lambda}) B(\psi(2S) \rightarrow \gamma\chi_{c2}) / B(\psi(2S) \rightarrow J/\psi\pi^+\pi^-)] \times [B^2(\Lambda \rightarrow \pi^-p) / B(J/\psi \rightarrow p\bar{p})] = (1.33^{+0.59}_{-0.55} \pm 0.25)\%$. We calculate from this measurement the presented value using $B(\Lambda \rightarrow \pi^-p) = (63.9 \pm 0.5)\%$ and $B(J/\psi \rightarrow p\bar{p}) = (2.17 \pm 0.07) \times 10^{-3}$.

$$\Gamma(\chi_{c2}(1P) \rightarrow \pi\pi)/\Gamma_{\text{total}} \times \Gamma(\psi(2S) \rightarrow \gamma\chi_{c2}(1P))/\Gamma_{\text{total}}$$

VALUE (units 10^{-4})	EVTS	DOCUMENT ID	TECN	COMMENT
2.09 ± 0.09 OUR FIT				
2.16 ± 0.14 OUR AVERAGE				Error includes scale factor of 1.3.
2.23 ± 0.06 ± 0.10	2.5k	78 ASNER	09	CLEO $\psi(2S) \rightarrow \gamma\pi^+\pi^-$
1.90 ± 0.08 ± 0.20	0.8k	79 ASNER	09	CLEO $\psi(2S) \rightarrow \gamma\pi^0\pi^0$

⁷⁸ Calculated by us. ASNER 09 reports $B(\chi_{c2} \rightarrow \pi^+\pi^-) = (1.59 \pm 0.04 \pm 0.07 \pm 0.10) \times 10^{-3}$ using $B(\psi(2S) \rightarrow \gamma\chi_{c2}) = (9.33 \pm 0.14 \pm 0.61)\%$. We have multiplied the $\pi^+\pi^-$ measurement by 3/2 to obtain $\pi\pi$.
⁷⁹ Calculated by us. ASNER 09 reports $B(\chi_{c2} \rightarrow \pi^0\pi^0) = (0.68 \pm 0.03 \pm 0.07 \pm 0.04) \times 10^{-3}$ using $B(\psi(2S) \rightarrow \gamma\chi_{c2}) = (9.33 \pm 0.14 \pm 0.61)\%$. We have multiplied the $\pi^0\pi^0$ measurement by 3 to obtain $\pi\pi$.

$$\Gamma(\chi_{c2}(1P) \rightarrow \pi\pi)/\Gamma_{\text{total}} \times \Gamma(\psi(2S) \rightarrow \gamma\chi_{c2}(1P))/\Gamma(\psi(2S) \rightarrow J/\psi(1S)\pi^+\pi^-)$$

VALUE (units 10^{-3})	EVTS	DOCUMENT ID	TECN	COMMENT
0.623 ± 0.028 OUR FIT				
0.54 ± 0.06 OUR AVERAGE				
0.66 ± 0.18 ± 0.37	21 ± 6	80 BAI	03c	BES $\psi(2S) \rightarrow \gamma\pi^0\pi^0$
0.54 ± 0.05 ± 0.04	185 ± 16	81 BAI	98i	BES $\psi(2S) \rightarrow \gamma\pi^+\pi^-$

⁸⁰ We have multiplied $\pi^0\pi^0$ measurement by 3 to obtain $\pi\pi$.
⁸¹ Calculated by us. The value for $B(\chi_{c2} \rightarrow \pi^+\pi^-)$ reported by BAI 98i is derived using $B(\psi(2S) \rightarrow \gamma\chi_{c2}) = (7.8 \pm 0.8)\%$ and $B(\psi(2S) \rightarrow J/\psi\pi^+\pi^-) = (32.4 \pm 2.6)\%$ [BAI 98d]. We have multiplied $\pi^+\pi^-$ measurement by 3/2 to obtain $\pi\pi$.

$$\Gamma(\chi_{c2}(1P) \rightarrow K^+K^-)/\Gamma_{\text{total}} \times \Gamma(\psi(2S) \rightarrow \gamma\chi_{c2}(1P))/\Gamma_{\text{total}}$$

VALUE (units 10^{-5})	EVTS	DOCUMENT ID	TECN	COMMENT
9.5 ± 0.6 OUR FIT				
10.5 ± 0.3 ± 0.6	1.6k	82 ASNER	09	CLEO $\psi(2S) \rightarrow \gamma K^+K^-$
⁸² Calculated by us. ASNER 09 reports $B(\chi_{c2} \rightarrow K^+K^-) = (1.13 \pm 0.03 \pm 0.06 \pm 0.07) \times 10^{-3}$ using $B(\psi(2S) \rightarrow \gamma\chi_{c2}) = (9.33 \pm 0.14 \pm 0.61)\%$.				

$$\Gamma(\chi_{c2}(1P) \rightarrow K^+K^-)/\Gamma_{\text{total}} \times \Gamma(\psi(2S) \rightarrow \gamma\chi_{c2}(1P))/\Gamma(\psi(2S) \rightarrow J/\psi(1S)\pi^+\pi^-)$$

VALUE (units 10^{-3})	EVTS	DOCUMENT ID	TECN	COMMENT
0.283 ± 0.017 OUR FIT				
0.190 ± 0.034 ± 0.019	115 ± 13	83 BAI	98i	BES $\psi(2S) \rightarrow \gamma K^+K^-$
⁸³ Calculated by us. The value for $B(\chi_{c2} \rightarrow K^+K^-)$ reported by BAI 98i is derived using $B(\psi(2S) \rightarrow \gamma\chi_{c2}) = (7.8 \pm 0.8)\%$ and $B(\psi(2S) \rightarrow J/\psi\pi^+\pi^-) = (32.4 \pm 2.6)\%$ [BAI 98d].				

$$\Gamma(\chi_{c2}(1P) \rightarrow K_S^0 K_S^0)/\Gamma_{\text{total}} \times \Gamma(\psi(2S) \rightarrow \gamma\chi_{c2}(1P))/\Gamma_{\text{total}}$$

VALUE (units 10^{-5})	EVTS	DOCUMENT ID	TECN	COMMENT
5.1 ± 0.4 OUR FIT				
5.0 ± 0.4 OUR AVERAGE				
4.9 ± 0.3 ± 0.3	373 ± 20	84 ASNER	09	CLEO $\psi(2S) \rightarrow \gamma K_S^0 K_S^0$
5.72 ± 0.76 ± 0.63	65	ABLIIKIM	05o	BES2 $\psi(2S) \rightarrow \gamma K_S^0 K_S^0$

⁸⁴ Calculated by us. ASNER 09 reports $B(\chi_{c2} \rightarrow K_S^0 K_S^0) = (0.53 \pm 0.03 \pm 0.03 \pm 0.03) \times 10^{-3}$ using $B(\psi(2S) \rightarrow \gamma\chi_{c2}) = (9.33 \pm 0.14 \pm 0.61)\%$.

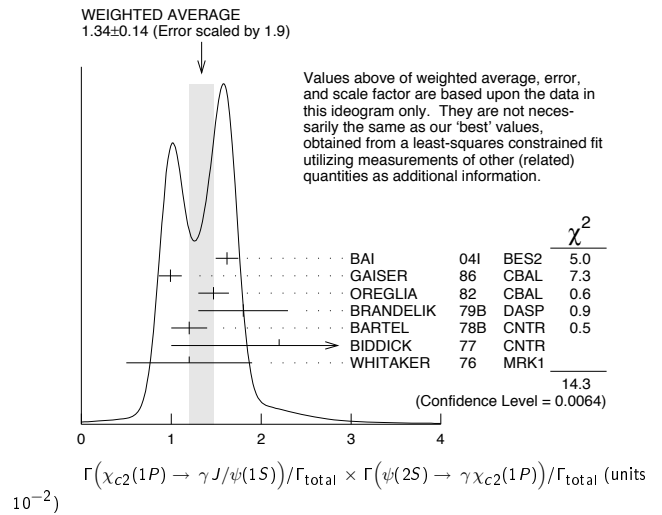
$$\Gamma(\chi_{c2}(1P) \rightarrow K_S^0 K_S^0)/\Gamma_{\text{total}} \times \Gamma(\psi(2S) \rightarrow \gamma\chi_{c2}(1P))/\Gamma(\psi(2S) \rightarrow J/\psi(1S)\pi^+\pi^-)$$

VALUE (units 10^{-5})	DOCUMENT ID	TECN	COMMENT
15.1 ± 1.1 OUR FIT			
14.7 ± 4.1 ± 3.3	85 BAI	99B	BES $\psi(2S) \rightarrow \gamma K_S^0 K_S^0$
⁸⁵ Calculated by us. The value of $B(\chi_{c2} \rightarrow K_S^0 K_S^0)$ reported by BAI 99B was derived using $B(\psi(2S) \rightarrow \gamma\chi_{c2}(1P)) = (7.8 \pm 0.8)\%$ and $B(\psi(2S) \rightarrow J/\psi\pi^+\pi^-) = (32.4 \pm 2.6)\%$ [BAI 98d].			

$$\Gamma(\chi_{c2}(1P) \rightarrow \gamma J/\psi(1S))/\Gamma_{\text{total}} \times \Gamma(\psi(2S) \rightarrow \gamma\chi_{c2}(1P))/\Gamma_{\text{total}}$$

VALUE (units 10^{-2})	EVTS	DOCUMENT ID	TECN	COMMENT
1.70 ± 0.04 OUR FIT				
1.34 ± 0.14 OUR AVERAGE				Error includes scale factor of 1.9. See the ideogram below.
1.62 ± 0.04 ± 0.12	5.8k	BAI	04i	BES2 $\psi(2S) \rightarrow J/\psi\gamma\gamma$
0.99 ± 0.10 ± 0.08		GAISER	86	CBAL $\psi(2S) \rightarrow \gamma X$
1.47 ± 0.17		86 OREGLIA	82	CBAL $\psi(2S) \rightarrow \gamma\chi_{c2}$
1.8 ± 0.5		87 BRANDELIK	79B	DASP $\psi(2S) \rightarrow \gamma\chi_{c2}$
1.2 ± 0.2		87 BARTEL	78B	CNTR $\psi(2S) \rightarrow \gamma\chi_{c2}$
2.2 ± 1.2		88 BIDDICK	77	CNTR $e^+e^- \rightarrow \gamma X$
1.2 ± 0.7		86 WHITAKER	76	MRK1 e^+e^-
● ● ● We do not use the following data for averages, fits, limits, etc. ● ● ●				
1.95 ± 0.02 ± 0.07	12.4k	89 MENDEZ	08	CLEO $\psi(2S) \rightarrow \gamma\chi_{c2}$
1.85 ± 0.04 ± 0.07	1.9k	90 ADAM	05A	CLEO Repl. by MENDEZ 08

⁸⁶ Recalculated by us using $B(J/\psi(1S) \rightarrow \ell^+\ell^-) = 0.1181 \pm 0.0020$.
⁸⁷ Recalculated by us using $B(J/\psi(1S) \rightarrow \mu^+\mu^-) = 0.0588 \pm 0.0010$.
⁸⁸ Assumes isotropic gamma distribution.
⁸⁹ Not independent from other measurements of MENDEZ 08.
⁹⁰ Not independent from other values reported by ADAM 05A.



$$\Gamma(\chi_{c2}(1P) \rightarrow \gamma J/\psi(1S))/\Gamma_{\text{total}} \times \Gamma(\psi(2S) \rightarrow \gamma\chi_{c2}(1P))/\Gamma(\psi(2S) \rightarrow J/\psi(1S)\text{anything})$$

VALUE (units 10^{-2})	EVTS	DOCUMENT ID	TECN	COMMENT
2.86 ± 0.07 OUR FIT				
● ● ● We do not use the following data for averages, fits, limits, etc. ● ● ●				
3.12 ± 0.03 ± 0.09	12.4k	91 MENDEZ	08	CLEO $\psi(2S) \rightarrow \gamma\chi_{c2}$
3.11 ± 0.07 ± 0.07	1.9k	ADAM	05A	CLEO Repl. by MENDEZ 08
⁹¹ Not independent from other measurements of MENDEZ 08.				

$$\Gamma(\chi_{c2}(1P) \rightarrow \gamma J/\psi(1S))/\Gamma_{\text{total}} \times \Gamma(\psi(2S) \rightarrow \gamma\chi_{c2}(1P))/\Gamma(\psi(2S) \rightarrow J/\psi(1S)\pi^+\pi^-)$$

VALUE (units 10^{-2})	EVTS	DOCUMENT ID	TECN	COMMENT
5.07 ± 0.13 OUR FIT				
5.53 ± 0.17 OUR AVERAGE				
5.56 ± 0.05 ± 0.16	12.4k	MENDEZ	08	CLEO $\psi(2S) \rightarrow \gamma\chi_{c2}$
6.0 ± 2.8	1.3k	92 ABLIIKIM	04B	BES $\psi(2S) \rightarrow J/\psi X$
3.9 ± 1.2		93 HIMEL	80	MRK2 $\psi(2S) \rightarrow \gamma\chi_{c2}$
● ● ● We do not use the following data for averages, fits, limits, etc. ● ● ●				
5.52 ± 0.13 ± 0.13	1.9k	94 ADAM	05A	CLEO Repl. by MENDEZ 08

⁹² From a fit to the J/ψ recoil mass spectra.
⁹³ The value for $B(\psi(2S) \rightarrow \gamma\chi_{c2}) \times B(\chi_{c2} \rightarrow \gamma J/\psi(1S))$ reported in HIMEL 80 is derived using $B(\psi(2S) \rightarrow J/\psi(1S)\pi^+\pi^-) = (33 \pm 3)\%$ and $B(J/\psi(1S) \rightarrow \ell^+\ell^-) = 0.138 \pm 0.018$. Calculated by us using $B(J/\psi(1S) \rightarrow \ell^+\ell^-) = (0.1181 \pm 0.0020)$.
⁹⁴ Not independent from other values reported by ADAM 05A.

BAGLIN	86B	PL B172 455	C. Baglin	(LAPP, CERN, GENO, LYON, OSLO+)
GAISER	86	PR D34 711	J. Gaiser et al.	(Crystal Ball Collab.)
LEE	85	SLAC 282	R.A. Lee	(SLAC)
LEMOIGNE	82	PL 113B 509	Y. Lemoigne et al.	(SACL, LOIC, SHMP+)
OREGLIA	82	PR D25 2259	M.J. Oreglia et al.	(SLAC, CIT, HARV+)
Also		Private Comm.	M.J. Oreglia	(EFI)
BARATE	81	PR D24 2994	R. Barate et al.	(SACL, LOIC, SHMP, CERN+)
HIMEL	80	PRL 44 920	T. Himel et al.	(LBL, SLAC)
Also		Private Comm.	G. Trilling	(LBL, UCB)
BRANDELIK	79B	NP B160 426	R. Brandelik et al.	(DASP Collab.)
BARTEL	78B	PL 79B 492	W. Bartel et al.	(DESY, HEIDP)
TANENBAUM	78	PR D17 1731	W.M. Tanenbaum et al.	(SLAC, LBL)
Also		Private Comm.	G. Trilling	(LBL, UCB)
BIDDICK	77	PRL 38 1324	C.J. Biddick et al.	(UCSD, UMD, PAWI+)
WHITAKER	76	PRL 37 1596	J.S. Whitaker et al.	(SLAC, LBL)

$\eta_c(2S)$ DECAY MODES

Mode	Fraction (Γ_i/Γ)	Confidence level
Γ_1 hadrons	not seen	
Γ_2 $K\bar{K}\pi$	(1.9 ± 1.2) %	
Γ_3 $2\pi^+2\pi^-$	not seen	
Γ_4 $3\pi^+3\pi^-$	not seen	
Γ_5 $K^+K^-\pi^+\pi^-$	not seen	
Γ_6 $K^+K^-\pi^+\pi^-\pi^0$	not seen	
Γ_7 $K^+K^-2\pi^+2\pi^-$	not seen	
Γ_8 $K_S^0 K^-2\pi^+\pi^- + c.c.$	not seen	
Γ_9 $2K^+2K^-$	not seen	
Γ_{10} $p\bar{p}$	not seen	
Γ_{11} $\gamma\gamma$	< 5 $\times 10^{-4}$	90%
Γ_{12} $\pi^+\pi^-\eta$	not seen	
Γ_{13} $\pi^+\pi^-\eta'$	not seen	
Γ_{14} $K^+K^-\eta$	not seen	
Γ_{15} $\pi^+\pi^-\eta_c(1S)$	not seen	

$\eta_c(2S)$

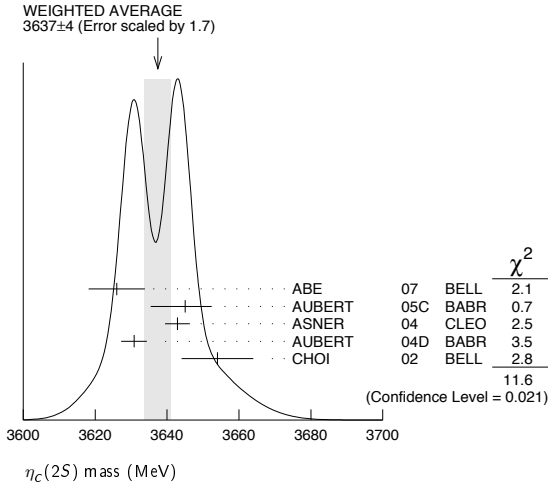
$$I^G(J^{PC}) = 0^+(0^{-+})$$

Quantum numbers are quark model predictions.

$\eta_c(2S)$ MASS

VALUE (MeV)	EVTs	DOCUMENT ID	TECN	COMMENT
3637 ± 4 OUR AVERAGE		Error includes scale factor of 1.7. See the ideogram below.		
3626 $\pm 5 \pm 6$	311	¹ ABE	07 BELL	$e^+e^- \rightarrow J/\psi(c\bar{c})$
3645.0 $\pm 5.5^{+4.9}_{-7.8}$	121 ± 27	AUBERT	05c BABR	$e^+e^- \rightarrow J/\psi c\bar{c}$
3642.9 $\pm 3.1 \pm 1.5$	61	ASNER	04 CLEO	$\gamma\gamma \rightarrow \eta_c \rightarrow K_S^0 K^\pm \pi^\mp$
3630.8 $\pm 3.4 \pm 1.0$	112 ± 24	AUBERT	04d BABR	$\gamma\gamma \rightarrow \eta_c(2S) \rightarrow K\bar{K}\pi$
3654 $\pm 6 \pm 8$	39 ± 11	CHOI	02 BELL	$B \rightarrow K K_S K^- \pi^+$
• • • We do not use the following data for averages, fits, limits, etc. • • •				
3639 ± 7	98 ± 52	² AUBERT	06e BABR	$B^\pm \rightarrow K^\pm X_{c2}^-$
3594 ± 5		³ EDWARDS	82c CBAL	$e^+e^- \rightarrow \gamma X$

¹ From a fit of the J/ψ recoil mass spectrum. Supersedes ABE, K 02 and ABE 04g.
² From the fit of the kaon momentum spectrum. Systematic errors not evaluated.
³ Assuming mass of $\psi(2S) = 3686$ MeV.



$\eta_c(2S)$ WIDTH

VALUE (MeV)	CL%	EVTs	DOCUMENT ID	TECN	COMMENT
14 ± 7 OUR AVERAGE					
6.3 $\pm 12.4 \pm 4.0$		61	ASNER	04 CLEO	$\gamma\gamma \rightarrow \eta_c \rightarrow K_S^0 K^\pm \pi^\mp$
17.0 $\pm 8.3 \pm 2.5$		112 ± 24	AUBERT	04d BABR	$\gamma\gamma \rightarrow \eta_c(2S) \rightarrow K\bar{K}\pi$
• • • We do not use the following data for averages, fits, limits, etc. • • •					
<23	90	98 ± 52	⁴ AUBERT	06e BABR	$B^\pm \rightarrow K^\pm X_{c2}^-$
22 ± 14		121 ± 27	AUBERT	05c BABR	$e^+e^- \rightarrow J/\psi c\bar{c}$
<55	90	39 ± 11	⁵ CHOI	02 BELL	$B \rightarrow K K_S K^- \pi^+$
<8.0	95		⁶ EDWARDS	82c CBAL	$e^+e^- \rightarrow \gamma X$

⁴ From the fit of the kaon momentum spectrum. Systematic errors not evaluated.
⁵ For a mass value of 3654 ± 6 MeV
⁶ For a mass value of 3594 ± 5 MeV

$\eta_c(2S)$ PARTIAL WIDTHS

$\Gamma(\gamma\gamma)$	DOCUMENT ID	TECN	COMMENT	Γ_{11}
VALUE (keV)				
• • • We do not use the following data for averages, fits, limits, etc. • • •				
1.3 ± 0.6	⁷ ASNER	04 CLEO	$\gamma\gamma \rightarrow \eta_c \rightarrow K_S^0 K^\pm \pi^\mp$	
⁷ They measure $\Gamma(\eta_c(2S)\gamma\gamma) B(\eta_c(2S) \rightarrow K\bar{K}\pi) = (0.18 \pm 0.05 \pm 0.02) \Gamma(\eta_c(1S)\gamma\gamma) B(\eta_c(1S) \rightarrow K\bar{K}\pi)$. The value for $\Gamma(\eta_c(2S) \rightarrow \gamma\gamma)$ is derived assuming that the branching fractions for $\eta_c(2S)$ and $\eta_c(1S)$ decays to $K_S K \pi$ are equal and using $\Gamma(\eta_c(1S) \rightarrow \gamma\gamma) = 7.4 \pm 0.4 \pm 2.3$ keV.				

$\eta_c(2S)$ $\Gamma(i)\Gamma(\gamma\gamma)/\Gamma(\text{total})$

$\Gamma(2\pi^+2\pi^-) \times \Gamma(\gamma\gamma)/\Gamma_{\text{total}}$	$\Gamma_3 \Gamma_{11}/\Gamma$
VALUE (eV) CL%	DOCUMENT ID TECN COMMENT
<6.5 90	UEHARA 08 BELL $\gamma\gamma \rightarrow \eta_c(2S) \rightarrow 2(\pi^+\pi^-)$
$\Gamma(K^+K^-\pi^+\pi^-) \times \Gamma(\gamma\gamma)/\Gamma_{\text{total}}$	$\Gamma_5 \Gamma_{11}/\Gamma$
VALUE (eV) CL%	DOCUMENT ID TECN COMMENT
<5.0 90	UEHARA 08 BELL $\gamma\gamma \rightarrow \eta_c(2S) \rightarrow K^+K^-\pi^+\pi^-$
$\Gamma(2K^+2K^-) \times \Gamma(\gamma\gamma)/\Gamma_{\text{total}}$	$\Gamma_9 \Gamma_{11}/\Gamma$
VALUE (eV) CL%	DOCUMENT ID TECN COMMENT
<2.9 90	UEHARA 08 BELL $\gamma\gamma \rightarrow \eta_c(2S) \rightarrow 2(K^+K^-)$

$\eta_c(2S)$ $\Gamma(i)\Gamma(\gamma\gamma)/\Gamma^2(\text{total})$

$\Gamma(p\bar{p})/\Gamma_{\text{total}} \times \Gamma(\gamma\gamma)/\Gamma_{\text{total}}$	$\Gamma_{10}/\Gamma \times \Gamma_{11}/\Gamma$
VALUE (units 10^{-8}) CL%	DOCUMENT ID TECN COMMENT
< 5.6 90	^{8,9,10} AMBROGIANI 01 E835 $p\bar{p} \rightarrow \gamma\gamma$
• • • We do not use the following data for averages, fits, limits, etc. • • •	
< 8.0 90	^{8,9,11} AMBROGIANI 01 E835 $p\bar{p} \rightarrow \gamma\gamma$
<12.0 90	^{9,11} AMBROGIANI 01 E835 $p\bar{p} \rightarrow \gamma\gamma$
⁸ Including the measurements of of ARMSTRONG 95f in the AMBROGIANI 01 analysis.	
⁹ For a total width $\Gamma=5$ MeV.	
¹⁰ For the resonance mass region 3589–3599 MeV/ c^2 .	
¹¹ For the resonance mass region 3575–3660 MeV/ c^2 .	

$\eta_c(2S)$ BRANCHING RATIOS

$\Gamma(\text{hadrons})/\Gamma_{\text{total}}$	Γ_1/Γ
VALUE	DOCUMENT ID TECN COMMENT
not seen	ABREU 98o DLPH $e^+e^- \rightarrow e^+e^- + \text{hadrons}$
• • • We do not use the following data for averages, fits, limits, etc. • • •	
seen	¹² EDWARDS 82c CBAL $e^+e^- \rightarrow \gamma X$
¹² For a mass value of 3594 ± 5 MeV	

$\Gamma(K\bar{K}\pi)/\Gamma_{\text{total}}$	Γ_2/Γ
VALUE (units 10^{-2}) EVT	DOCUMENT ID TECN COMMENT
$1.9 \pm 0.4 \pm 1.1$	59 ± 12 ¹³ AUBERT 08AB BABR $B \rightarrow \eta_c(2S) K \rightarrow K\bar{K}\pi K$
• • • We do not use the following data for averages, fits, limits, etc. • • •	
seen	39 ± 11 ¹⁴ CHOI 02 BELL $B \rightarrow K K_S K^- \pi^+$
¹³ Derived from a measurement of $[B(B^+ \rightarrow \eta_c(2S)K^+) \times B(\eta_c(2S) \rightarrow K\bar{K}\pi)] / [B(B^+ \rightarrow \eta_c K^+) \times B(\eta_c \rightarrow K\bar{K}\pi)] = (9.6^{+2.0}_{-1.9} \pm 2.5)\%$ and using $B(B^+ \rightarrow \eta_c(2S)K^+) = (3.4 \pm 1.8) \times 10^{-4}$, and $[B(B^+ \rightarrow \eta_c K^+) \times B(\eta_c \rightarrow K\bar{K}\pi)] = (6.88 \pm 0.77^{+0.55}_{-0.66}) \times 10^{-5}$.	
¹⁴ For a mass value of 3654 ± 6 MeV	

Meson Particle Listings

$\eta_c(2S), \psi(2S)$

$\Gamma(2\pi^+2\pi^-)/\Gamma_{\text{total}}$	DOCUMENT ID	TECN	COMMENT	Γ_3/Γ
VALUE not seen	UEHARA	08	BELL $\gamma\gamma \rightarrow \eta_c(2S)$	

$\Gamma(K^+K^-\pi^+\pi^-)/\Gamma_{\text{total}}$	DOCUMENT ID	TECN	COMMENT	Γ_5/Γ
VALUE not seen	UEHARA	08	BELL $\gamma\gamma \rightarrow \eta_c(2S)$	

$\Gamma(2K^+2K^-)/\Gamma_{\text{total}}$	DOCUMENT ID	TECN	COMMENT	Γ_9/Γ
VALUE not seen	UEHARA	08	BELL $\gamma\gamma \rightarrow \eta_c(2S)$	

	DOCUMENT ID	TECN	COMMENT	Γ_{11}/Γ
VALUE not seen	AMBROGIANI	01	E835 $\bar{p}p \rightarrow \gamma\gamma$	

$\Gamma(\gamma\gamma)/\Gamma_{\text{total}}$	CL%	DOCUMENT ID	TECN	COMMENT	Γ_{11}/Γ
$<5 \times 10^{-4}$	90	15 WICHT	08	BELL $B^\pm \rightarrow K^\pm \gamma\gamma$	
• • • We do not use the following data for averages, fits, limits, etc. • • •					
<0.01	90	LEE	85	CBAL $\psi' \rightarrow \text{photons}$	
15 WICHT 08 reports $[\Gamma(\eta_c(2S) \rightarrow \gamma\gamma)/\Gamma_{\text{total}}] \times [B(B^+ \rightarrow \eta_c(2S) K^+)] < 0.18 \times 10^{-6}$ which we divide by our best value $B(B^+ \rightarrow \eta_c(2S) K^+) = 3.4 \times 10^{-4}$.					

$\eta_c(2S)$ CROSS-PARTICLE BRANCHING RATIOS

$\Gamma(\eta_c(2S) \rightarrow 2\pi^+2\pi^-)/\Gamma_{\text{total}} \times \Gamma(\psi(2S) \rightarrow \gamma\eta_c(2S))/\Gamma_{\text{total}}$	DOCUMENT ID	TECN	COMMENT	$\Gamma_3/\Gamma \times \Gamma_{110}^{\psi(2S)}/\Gamma_{\psi(2S)}$	
VALUE $<14.6 \times 10^{-6}$	CL% 90	DOCUMENT ID 16 CRONIN-HEN..10	TECN CLEO	COMMENT $\psi(2S) \rightarrow \gamma 2\pi^+ 2\pi^-$	

16 Assuming $\Gamma(\eta_c(2S)) = 14$ MeV. CRONIN-HENNESSY 10 gives the analytic dependence of limits on width.

$\Gamma(\eta_c(2S) \rightarrow 3\pi^+3\pi^-)/\Gamma_{\text{total}} \times \Gamma(\psi(2S) \rightarrow \gamma\eta_c(2S))/\Gamma_{\text{total}}$	DOCUMENT ID	TECN	COMMENT	$\Gamma_4/\Gamma \times \Gamma_{110}^{\psi(2S)}/\Gamma_{\psi(2S)}$	
VALUE $<13.2 \times 10^{-6}$	CL% 90	DOCUMENT ID 17 CRONIN-HEN..10	TECN CLEO	COMMENT $\psi(2S) \rightarrow \gamma 3\pi^+ 3\pi^-$	

17 Assuming $\Gamma(\eta_c(2S)) = 14$ MeV. CRONIN-HENNESSY 10 gives the analytic dependence of limits on width.

$\Gamma(\eta_c(2S) \rightarrow K^+K^-\pi^+\pi^-)/\Gamma_{\text{total}} \times \Gamma(\psi(2S) \rightarrow \gamma\eta_c(2S))/\Gamma_{\text{total}}$	DOCUMENT ID	TECN	COMMENT	$\Gamma_5/\Gamma \times \Gamma_{110}^{\psi(2S)}/\Gamma_{\psi(2S)}$	
VALUE $<9.6 \times 10^{-6}$	CL% 90	DOCUMENT ID 18 CRONIN-HEN..10	TECN CLEO	COMMENT $\psi(2S) \rightarrow \gamma K^+ K^- \pi^+ \pi^-$	

18 Assuming $\Gamma(\eta_c(2S)) = 14$ MeV. CRONIN-HENNESSY 10 gives the analytic dependence of limits on width.

$\Gamma(\eta_c(2S) \rightarrow K^+K^-\pi^+\pi^0)/\Gamma_{\text{total}} \times \Gamma(\psi(2S) \rightarrow \gamma\eta_c(2S))/\Gamma_{\text{total}}$	DOCUMENT ID	TECN	COMMENT	$\Gamma_6/\Gamma \times \Gamma_{110}^{\psi(2S)}/\Gamma_{\psi(2S)}$	
VALUE $<43.0 \times 10^{-6}$	CL% 90	DOCUMENT ID 19 CRONIN-HEN..10	TECN CLEO	COMMENT $\psi(2S) \rightarrow \gamma K^+ K^- \pi^+ \pi^0$	

19 Assuming $\Gamma(\eta_c(2S)) = 14$ MeV. CRONIN-HENNESSY 10 gives the analytic dependence of limits on width.

$\Gamma(\eta_c(2S) \rightarrow K^+K^-2\pi^+2\pi^-)/\Gamma_{\text{total}} \times \Gamma(\psi(2S) \rightarrow \gamma\eta_c(2S))/\Gamma_{\text{total}}$	DOCUMENT ID	TECN	COMMENT	$\Gamma_7/\Gamma \times \Gamma_{110}^{\psi(2S)}/\Gamma_{\psi(2S)}$	
VALUE $<9.7 \times 10^{-6}$	CL% 90	DOCUMENT ID 20 CRONIN-HEN..10	TECN CLEO	COMMENT $\psi(2S) \rightarrow \gamma K^+ K^- 2\pi^+ 2\pi^-$	

20 Assuming $\Gamma(\eta_c(2S)) = 14$ MeV. CRONIN-HENNESSY 10 gives the analytic dependence of limits on width.

$\Gamma(\eta_c(2S) \rightarrow K_S^0 K^- 2\pi^+ \pi^- + \text{c.c.})/\Gamma_{\text{total}} \times \Gamma(\psi(2S) \rightarrow \gamma\eta_c(2S))/\Gamma_{\text{total}}$	DOCUMENT ID	TECN	COMMENT	$\Gamma_8/\Gamma \times \Gamma_{110}^{\psi(2S)}/\Gamma_{\psi(2S)}$	
VALUE $<15.2 \times 10^{-6}$	CL% 90	DOCUMENT ID 21 CRONIN-HEN..10	TECN CLEO	COMMENT $\psi(2S) \rightarrow \gamma K_S^0 K^- 2\pi^+ \pi^- + \text{c.c.}$	

21 Assuming $\Gamma(\eta_c(2S)) = 14$ MeV. CRONIN-HENNESSY 10 gives the analytic dependence of limits on width.

$\Gamma(\eta_c(2S) \rightarrow \pi^+\pi^-\eta)/\Gamma_{\text{total}} \times \Gamma(\psi(2S) \rightarrow \gamma\eta_c(2S))/\Gamma_{\text{total}}$	DOCUMENT ID	TECN	COMMENT	$\Gamma_{12}/\Gamma \times \Gamma_{110}^{\psi(2S)}/\Gamma_{\psi(2S)}$	
VALUE $<4.3 \times 10^{-6}$	CL% 90	DOCUMENT ID 22 CRONIN-HEN..10	TECN CLEO	COMMENT $\psi(2S) \rightarrow \gamma \pi^+ \pi^- \eta$	

22 Assuming $\Gamma(\eta_c(2S)) = 14$ MeV. CRONIN-HENNESSY 10 gives the analytic dependence of limits on width.

$\Gamma(\eta_c(2S) \rightarrow \pi^+\pi^-\eta')/\Gamma_{\text{total}} \times \Gamma(\psi(2S) \rightarrow \gamma\eta_c(2S))/\Gamma_{\text{total}}$	DOCUMENT ID	TECN	COMMENT	$\Gamma_{13}/\Gamma \times \Gamma_{110}^{\psi(2S)}/\Gamma_{\psi(2S)}$	
VALUE $<14.2 \times 10^{-6}$	CL% 90	DOCUMENT ID 23 CRONIN-HEN..10	TECN CLEO	COMMENT $\psi(2S) \rightarrow \gamma \pi^+ \pi^- \eta'$	

23 Assuming $\Gamma(\eta_c(2S)) = 14$ MeV. CRONIN-HENNESSY 10 gives the analytic dependence of limits on width.

$\Gamma(\eta_c(2S) \rightarrow K^+K^-\eta)/\Gamma_{\text{total}} \times \Gamma(\psi(2S) \rightarrow \gamma\eta_c(2S))/\Gamma_{\text{total}}$	DOCUMENT ID	TECN	COMMENT	$\Gamma_{14}/\Gamma \times \Gamma_{110}^{\psi(2S)}/\Gamma_{\psi(2S)}$	
VALUE $<5.9 \times 10^{-6}$	CL% 90	DOCUMENT ID 24 CRONIN-HEN..10	TECN CLEO	COMMENT $\psi(2S) \rightarrow \gamma K^+ K^- \eta$	

24 Assuming $\Gamma(\eta_c(2S)) = 14$ MeV. CRONIN-HENNESSY 10 gives the analytic dependence of limits on width.

$\Gamma(\eta_c(2S) \rightarrow \pi^+\pi^-\eta_c(1S))/\Gamma_{\text{total}} \times \Gamma(\psi(2S) \rightarrow \gamma\eta_c(2S))/\Gamma_{\text{total}}$	DOCUMENT ID	TECN	COMMENT	$\Gamma_{15}/\Gamma \times \Gamma_{110}^{\psi(2S)}/\Gamma_{\psi(2S)}$	
VALUE $<1.7 \times 10^{-4}$	CL% 90	DOCUMENT ID 25 CRONIN-HEN..10	TECN CLEO	COMMENT $\psi(2S) \rightarrow \gamma \pi^+ \pi^- \eta_c(1S)$	

25 Assuming $\Gamma(\eta_c(2S)) = 14$ MeV. CRONIN-HENNESSY 10 gives the analytic dependence of limits on width.

$\eta_c(2S)$ REFERENCES

CRONIN-HEN..10	PR D81 052002	D. Cronin-Hennessey et al.	(CLEO Collab.)
AUBERT	08AB PR D78 012006	B. Aubert et al.	(BABAR Collab.)
UEHARA	08 EPJ C33 1	S. Uehara et al.	(BELLE Collab.)
WICHT	08 PL B662 323	J. Wicht et al.	(BELLE Collab.)
ABE	07 PRL 98 082001	K. ABE et al.	(BELLE Collab.)
AUBERT	06E PRL 96 052002	B. Aubert et al.	(BABAR Collab.)
AUBERT	05C PR D72 031101R	B. Aubert et al.	(BABAR Collab.)
ABE	04G PR D70 071102	K. ABE et al.	(BELLE Collab.)
ASNER	04 PRL 92 142001	D.M. Asner et al.	(CLEO Collab.)
AUBERT	04D PRL 92 142002	B. Aubert et al.	(BABAR Collab.)
ABE,K	02 PRL 89 142001	K. ABE et al.	(BELLE Collab.)
CHOI	02 PRL 89 102001	S.-K. Choi et al.	(BELLE Collab.)
AMBROGIANI	01 PR D64 052003	M. Ambrogiani et al.	(FNAL E835 Collab.)
ABREU	98O PL B441 479	P. Abreu et al.	(DELPHI Collab.)
ARMSTRONG	95F PR D52 4839	T.A. Armstrong et al.	(FNAL, FERR, GENO+)
LEE	85 SLAC 282	R.A. Lee	(SLAC)
EDWARDS	82C PRL 48 70	C. Edwards et al.	(CIT, HARV, PRIN+)

$\psi(2S)$

$$J^{PC} = 0^-(1^{--})$$

See the Review on " $\psi(2S)$ and χ_c branching ratios" before the $\chi_{c0}(1P)$ Listings.

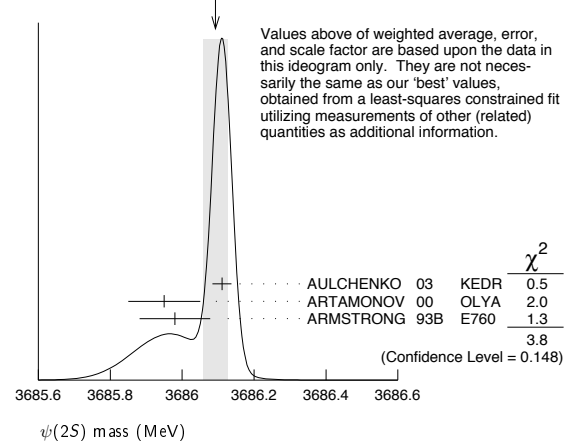
$\psi(2S)$ MASS

OUR FIT includes measurements of $m_{\psi(2S)}$, $m_{\psi(3770)}$, and $m_{\psi(3770)} - m_{\psi(2S)}$.

VALUE (MeV)	EVTS	DOCUMENT ID	TECN	COMMENT
3686.09 ± 0.04	OUR FIT			Error includes scale factor of 1.6.
3686.093 ± 0.034	OUR AVERAGE			Error includes scale factor of 1.4. See the ideogram below.
3686.111 ± 0.025 ± 0.009		AULCHENKO 03	KEDR	$e^+e^- \rightarrow \text{hadrons}$
3685.95 ± 0.10	413	1 ARTAMONOV 00	OLYA	$e^+e^- \rightarrow \text{hadrons}$
3685.98 ± 0.09 ± 0.04		2 ARMSTRONG 93B	E760	$\bar{p}p \rightarrow e^+e^-$
• • • We do not use the following data for averages, fits, limits, etc. • • •				
3686.00 ± 0.10	413	3 ZHOLENTZ 80	OLYA	e^+e^-

- 1 Reanalysis of ZHOLENTZ 80 using new electron mass (COHEN 87) and radiative corrections (KURAEV 85).
- 2 Mass central value and systematic error recalculated by us according to Eq. (16) in ARMSTRONG 93B, using the value for the $J/\psi(1S)$ mass from AULCHENKO 03.
- 3 Superseded by ARTAMONOV 00.

WEIGHTED AVERAGE
3686.093 ± 0.034 (Error scaled by 1.4)



$m_{\psi(2S)} - m_{J/\psi(1S)}$

VALUE (MeV)	DOCUMENT ID	TECN	COMMENT
589.188 ± 0.028 OUR AVERAGE			
589.194 ± 0.027 ± 0.011	⁴ AULCHENKO 03	KEDR	$e^+e^- \rightarrow$ hadrons
589.7 ± 1.2	LEMOIGNE 82	GOLI	$185\pi^- Be \rightarrow \gamma\mu^+\mu^- A$
589.07 ± 0.13	⁴ ZHOLENTZ 80	OLYA	e^+e^-
588.7 ± 0.8	LUTH 75	MRK1	
• • • We do not use the following data for averages, fits, limits, etc. • • •			
588 ± 1	⁵ BAI 98E	BES	e^+e^-
⁴ Redundant with data in mass above. ⁵ Systematic errors not evaluated.			

$\psi(2S)$ WIDTH

VALUE (keV)	EVTS	DOCUMENT ID	TECN	COMMENT
304 ± 9 OUR FIT				
286 ± 16 OUR AVERAGE				
358 ± 88 ± 4		ABLIKIM 08B	BES2	$e^+e^- \rightarrow$ hadrons
290 ± 25 ± 4	2.7k	ANDREOTTI 07	E835	$p\bar{p} \rightarrow e^+e^-, J/\psi X$
331 ± 58 ± 2		ABLIKIM 06L	BES2	$e^+e^- \rightarrow$ hadrons
264 ± 27		⁶ BAI 02B	BES2	e^+e^-
287 ± 37 ± 16		⁷ ARMSTRONG 93B	E760	$p\bar{p} \rightarrow e^+e^-$
⁶ From a simultaneous fit to the hadronic and $\mu^+\mu^-$ cross section, assuming $\Gamma = \Gamma_h + \Gamma_e + \Gamma_\mu + \Gamma_\tau$ and lepton universality. Does not include vacuum polarization correction. ⁷ The initial-state radiation correction reevaluated by ANDREOTTI 07 in its Ref. [4].				

$\psi(2S)$ DECAY MODES

Mode	Fraction (Γ_i/Γ)	Scale factor/ Confidence level
Γ_1 hadrons	(97.85 ± 0.13) %	
Γ_2 virtual $\gamma \rightarrow$ hadrons	(1.73 ± 0.14) %	S=1.5
Γ_3 ggg	(10.6 ± 1.6) %	
Γ_4 γgg	(1.02 ± 0.29) %	
Γ_5 light hadrons	(15.4 ± 1.5) %	
Γ_6 e^+e^-	(7.72 ± 0.17) × 10 ⁻³	
Γ_7 $\mu^+\mu^-$	(7.7 ± 0.8) × 10 ⁻³	
Γ_8 $\tau^+\tau^-$	(3.0 ± 0.4) × 10 ⁻³	
Decays into $J/\psi(1S)$ and anything		
Γ_9 $J/\psi(1S)$ anything	(59.5 ± 0.8) %	
Γ_{10} $J/\psi(1S)$ neutrals	(24.5 ± 0.4) %	
Γ_{11} $J/\psi(1S)\pi^+\pi^-$	(33.6 ± 0.4) %	
Γ_{12} $J/\psi(1S)\pi^0\pi^0$	(17.73 ± 0.34) %	
Γ_{13} $J/\psi(1S)\eta$	(3.28 ± 0.07) %	
Γ_{14} $J/\psi(1S)\pi^0$	(1.30 ± 0.10) × 10 ⁻³	S=1.4
Hadronic decays		
Γ_{15} $\pi^0 h_c(1P)$	seen	
Γ_{16} $3(\pi^+\pi^-)\pi^0$	(3.5 ± 1.6) × 10 ⁻³	
Γ_{17} $2(\pi^+\pi^-)\pi^0$	(2.9 ± 1.0) × 10 ⁻³	S=4.6
Γ_{18} $\rho\partial_2(1320)$	(2.6 ± 0.9) × 10 ⁻⁴	
Γ_{19} $\rho\bar{p}$	(2.76 ± 0.12) × 10 ⁻⁴	
Γ_{20} $\Delta^{++}\bar{\Delta}^{--}$	(1.28 ± 0.35) × 10 ⁻⁴	
Γ_{21} $\Lambda\bar{\Lambda}\pi^0$	< 1.2 × 10 ⁻⁴	CL=90%
Γ_{22} $\Lambda\bar{\Lambda}\eta$	< 4.9 × 10 ⁻⁵	CL=90%
Γ_{23} $\Lambda\bar{p}K^+$	(1.00 ± 0.14) × 10 ⁻⁴	
Γ_{24} $\Lambda\bar{p}K^+\pi^+\pi^-$	(1.8 ± 0.4) × 10 ⁻⁴	
Γ_{25} $\Lambda\bar{\Lambda}\pi^+\pi^-$	(2.8 ± 0.6) × 10 ⁻⁴	
Γ_{26} $\Lambda\bar{\Lambda}$	(2.8 ± 0.5) × 10 ⁻⁴	S=2.6
Γ_{27} $\Sigma^+\bar{\Sigma}^-$	(2.6 ± 0.8) × 10 ⁻⁴	
Γ_{28} $\Sigma^0\bar{\Sigma}^0$	(2.2 ± 0.4) × 10 ⁻⁴	S=1.5
Γ_{29} $\Sigma(1385)^+\bar{\Sigma}(1385)^-$	(1.1 ± 0.4) × 10 ⁻⁴	
Γ_{30} $\Xi^-\bar{\Xi}^+$	(1.8 ± 0.6) × 10 ⁻⁴	S=2.8
Γ_{31} $\Xi^0\bar{\Xi}^0$	(2.8 ± 0.9) × 10 ⁻⁴	
Γ_{32} $\Xi(1530)^0\bar{\Xi}(1530)^0$	< 8.1 × 10 ⁻⁵	CL=90%
Γ_{33} $\Omega^-\bar{\Omega}^+$	< 7.3 × 10 ⁻⁵	CL=90%
Γ_{34} $\pi^0\rho\bar{p}$	(1.33 ± 0.17) × 10 ⁻⁴	
Γ_{35} $\eta\rho\bar{p}$	(6.0 ± 1.2) × 10 ⁻⁵	
Γ_{36} $\omega\rho\bar{p}$	(6.9 ± 2.1) × 10 ⁻⁵	
Γ_{37} $\phi\rho\bar{p}$	< 2.4 × 10 ⁻⁵	CL=90%
Γ_{38} $\pi^+\pi^-\rho\bar{p}$	(6.0 ± 0.4) × 10 ⁻⁴	
Γ_{39} $p\bar{p}\pi^-$ or c.c.	(2.48 ± 0.17) × 10 ⁻⁴	
Γ_{40} $p\bar{p}\pi^-\pi^0$	(3.2 ± 0.7) × 10 ⁻⁴	
Γ_{41} $2(\pi^+\pi^-\pi^0)$	(4.8 ± 1.5) × 10 ⁻³	
Γ_{42} $\eta\pi^+\pi^-$	< 1.6 × 10 ⁻⁴	CL=90%
Γ_{43} $\eta\pi^+\pi^-\pi^0$	(9.5 ± 1.7) × 10 ⁻⁴	
Γ_{44} $2(\pi^+\pi^-\eta)$	(1.2 ± 0.6) × 10 ⁻³	

Γ_{45} $\eta'\pi^+\pi^-\pi^0$	(4.5 ± 2.1) × 10 ⁻⁴	
Γ_{46} $\omega\pi^+\pi^-$	(7.3 ± 1.2) × 10 ⁻⁴	S=2.1
Γ_{47} $b_1^{\pm}\pi^{\mp}$	(4.0 ± 0.6) × 10 ⁻⁴	S=1.1
Γ_{48} $b_1^0\pi^0$	(2.4 ± 0.6) × 10 ⁻⁴	
Γ_{49} $\omega f_2(1270)$	(2.2 ± 0.4) × 10 ⁻⁴	
Γ_{50} $\pi^+\pi^-K^+K^-$	(7.5 ± 0.9) × 10 ⁻⁴	S=1.9
Γ_{51} $\rho^0K^+K^-$	(2.2 ± 0.4) × 10 ⁻⁴	
Γ_{52} $K^*(892)^0\bar{K}_2^*(1430)^0$	(1.9 ± 0.5) × 10 ⁻⁴	
Γ_{53} $K^+K^-\pi^+\pi^-\eta$	(1.3 ± 0.7) × 10 ⁻³	
Γ_{54} $K^+K^-2(\pi^+\pi^-)\pi^0$	(1.00 ± 0.31) × 10 ⁻³	
Γ_{55} $K^+K^-2(\pi^+\pi^-)$	(1.9 ± 0.9) × 10 ⁻³	
Γ_{56} $K_1^*(1270)^{\pm}K^{\mp}$	(1.00 ± 0.28) × 10 ⁻³	
Γ_{57} $K_S^0 K_S^0 \pi^+ \pi^-$	(2.2 ± 0.4) × 10 ⁻⁴	
Γ_{58} $\rho^0 p\bar{p}$	(5.0 ± 2.2) × 10 ⁻⁵	
Γ_{59} $K^+K^*(892)^0\pi^- + c.c.$	(6.7 ± 2.5) × 10 ⁻⁴	
Γ_{60} $2(\pi^+\pi^-)$	(2.4 ± 0.6) × 10 ⁻⁴	S=2.2
Γ_{61} $\rho^0\pi^+\pi^-$	(2.2 ± 0.6) × 10 ⁻⁴	S=1.4
Γ_{62} $K^+K^-\pi^+\pi^-\pi^0$	(1.26 ± 0.09) × 10 ⁻³	
Γ_{63} $\omega f_0(1710) \rightarrow \omega K^+K^-$	(5.9 ± 2.2) × 10 ⁻⁵	
Γ_{64} $K^*(892)^0 K^-\pi^+\pi^0 + c.c.$	(8.6 ± 2.2) × 10 ⁻⁴	
Γ_{65} $K^*(892)^+ K^-\pi^+\pi^- + c.c.$	(9.6 ± 2.8) × 10 ⁻⁴	
Γ_{66} $K^*(892)^+ K^-\rho^0 + c.c.$	(7.3 ± 2.6) × 10 ⁻⁴	
Γ_{67} $K^*(892)^0 K^-\rho^+ + c.c.$	(6.1 ± 1.8) × 10 ⁻⁴	
Γ_{68} ηK^+K^-	< 1.3 × 10 ⁻⁴	CL=90%
Γ_{69} ωK^+K^-	(1.85 ± 0.25) × 10 ⁻⁴	S=1.1
Γ_{70} $3(\pi^+\pi^-)$	(3.5 ± 2.0) × 10 ⁻⁴	S=2.8
Γ_{71} $p\bar{p}\pi^+\pi^-\pi^0$	(7.3 ± 0.7) × 10 ⁻⁴	
Γ_{72} K^+K^-	(6.3 ± 0.7) × 10 ⁻⁵	
Γ_{73} $K_S^0 K_L^0$	(5.4 ± 0.5) × 10 ⁻⁵	
Γ_{74} $\pi^+\pi^-\pi^0$	(1.68 ± 0.26) × 10 ⁻⁴	S=1.4
Γ_{75} $\rho(2150)\pi \rightarrow \pi^+\pi^-\pi^0$	(1.9 $\begin{smallmatrix} +1.2 \\ -0.4 \end{smallmatrix}$) × 10 ⁻⁴	
Γ_{76} $\rho(770)\pi \rightarrow \pi^+\pi^-\pi^0$	(3.2 ± 1.2) × 10 ⁻⁵	S=1.8
Γ_{77} $\pi^+\pi^-$	(8 ± 5) × 10 ⁻⁵	
Γ_{78} $K_1^*(1400)^{\pm}K^{\mp}$	< 3.1 × 10 ⁻⁴	CL=90%
Γ_{79} $K^+K^-\pi^0$	< 2.96 × 10 ⁻⁵	CL=90%
Γ_{80} $K^+\bar{K}^*(892)^- + c.c.$	(1.7 $\begin{smallmatrix} +0.8 \\ -0.7 \end{smallmatrix}$) × 10 ⁻⁵	
Γ_{81} $K^*(892)^0\bar{K}^0 + c.c.$	(1.09 ± 0.20) × 10 ⁻⁴	
Γ_{82} $\phi\pi^+\pi^-$	(1.17 ± 0.29) × 10 ⁻⁴	S=1.7
Γ_{83} $\phi f_0(980) \rightarrow \pi^+\pi^-$	(6.8 ± 2.4) × 10 ⁻⁵	S=1.1
Γ_{84} $2(K^+K^-)$	(6.0 ± 1.4) × 10 ⁻⁵	
Γ_{85} ϕK^+K^-	(7.0 ± 1.6) × 10 ⁻⁵	
Γ_{86} $2(K^+K^+)\pi^0$	(1.10 ± 0.28) × 10 ⁻⁴	
Γ_{87} $\phi\eta$	(2.8 $\begin{smallmatrix} +1.0 \\ -0.8 \end{smallmatrix}$) × 10 ⁻⁵	
Γ_{88} $\phi\eta'$	(3.1 ± 1.6) × 10 ⁻⁵	
Γ_{89} $\omega\eta'$	(3.2 $\begin{smallmatrix} +2.5 \\ -2.1 \end{smallmatrix}$) × 10 ⁻⁵	
Γ_{90} $\omega\pi^0$	(2.1 ± 0.6) × 10 ⁻⁵	
Γ_{91} $\rho\eta'$	(1.9 $\begin{smallmatrix} +1.7 \\ -1.2 \end{smallmatrix}$) × 10 ⁻⁵	
Γ_{92} $\rho\eta$	(2.2 ± 0.6) × 10 ⁻⁵	S=1.1
Γ_{93} $\omega\eta$	< 1.1 × 10 ⁻⁵	CL=90%
Γ_{94} $\phi\pi^0$	< 4 × 10 ⁻⁶	CL=90%
Γ_{95} $\eta_c\pi^+\pi^-\pi^0$	< 1.0 × 10 ⁻³	CL=90%
Γ_{96} $p\bar{p}K^+K^-$	(2.7 ± 0.7) × 10 ⁻⁵	
Γ_{97} $\bar{\Lambda}n K_S^0 + c.c.$	(8.1 ± 1.8) × 10 ⁻⁵	
Γ_{98} $\phi f_2'(1525)$	(4.4 ± 1.6) × 10 ⁻⁵	
Γ_{99} $\Theta(1540)\bar{\Theta}(1540) \rightarrow K_S^0 p K^- \bar{n} + c.c.$	< 8.8 × 10 ⁻⁶	CL=90%
Γ_{100} $\Theta(1540)K^-\bar{n} \rightarrow K_S^0 p K^- \bar{n}$	< 1.0 × 10 ⁻⁵	CL=90%
Γ_{101} $\Theta(1540)K_S^0\bar{p} \rightarrow K_S^0\bar{p}K^+n$	< 7.0 × 10 ⁻⁶	CL=90%
Γ_{102} $\bar{\Theta}(1540)K^+n \rightarrow K_S^0\bar{p}K^+n$	< 2.6 × 10 ⁻⁵	CL=90%
Γ_{103} $\bar{\Theta}(1540)K_S^0p \rightarrow K_S^0pK^-\bar{n}$	< 6.0 × 10 ⁻⁶	CL=90%
Γ_{104} $K_S^0 K_S^0$	< 4.6 × 10 ⁻⁶	
Radiative decays		
Γ_{105} $\gamma X_{c0}(1P)$	(9.62 ± 0.31) %	
Γ_{106} $\gamma X_{c1}(1P)$	(9.2 ± 0.4) %	
Γ_{107} $\gamma X_{c2}(1P)$	(8.74 ± 0.35) %	
Γ_{108} $\pi^0 h_c \rightarrow \gamma\eta_c(1S)\pi^0$	(4.2 ± 0.5) × 10 ⁻⁴	
Γ_{109} $\gamma\eta_c(1S)$	(3.4 ± 0.5) × 10 ⁻³	S=1.3
Γ_{110} $\gamma\eta_c(2S)$	< 8 × 10 ⁻⁴	CL=90%
Γ_{111} $\gamma\pi^0$	< 5 × 10 ⁻⁶	CL=90%
Γ_{112} $\gamma\eta'(958)$	(1.21 ± 0.08) × 10 ⁻⁴	
Γ_{113} $\gamma f_2(1270)$	(2.1 ± 0.4) × 10 ⁻⁴	

Meson Particle Listings

$\psi(2S)$

Γ	Decay	Value	CL
Γ_{114}	$\gamma f_0(1710)$		
Γ_{115}	$\gamma f_0(1710) \rightarrow \gamma \pi \pi$	$(3.0 \pm 1.3) \times 10^{-5}$	
Γ_{116}	$\gamma f_0(1710) \rightarrow \gamma K \bar{K}$	$(6.0 \pm 1.6) \times 10^{-5}$	
Γ_{117}	$\gamma \gamma$	$< 1.4 \times 10^{-4}$	CL=90%
Γ_{118}	$\gamma \eta$	$< 2 \times 10^{-6}$	CL=90%
Γ_{119}	$\gamma \eta \pi^+ \pi^-$	$(8.7 \pm 2.1) \times 10^{-4}$	
Γ_{120}	$\gamma \eta(1405)$		
Γ_{121}	$\gamma \eta(1405) \rightarrow \gamma K \bar{K} \pi$	$< 9 \times 10^{-5}$	CL=90%
Γ_{122}	$\gamma \eta(1405) \rightarrow \eta \pi^+ \pi^-$	$(3.6 \pm 2.5) \times 10^{-5}$	
Γ_{123}	$\gamma \eta(1475)$		
Γ_{124}	$\gamma \eta(1475) \rightarrow K \bar{K} \pi$	$< 1.4 \times 10^{-4}$	CL=90%
Γ_{125}	$\gamma \eta(1475) \rightarrow \eta \pi^+ \pi^-$	$< 8.8 \times 10^{-5}$	CL=90%
Γ_{126}	$\gamma 2(\pi^+ \pi^-)$	$(4.0 \pm 0.6) \times 10^{-4}$	
Γ_{127}	$\gamma K^{*0} K^+ \pi^- + c.c.$	$(3.7 \pm 0.9) \times 10^{-4}$	
Γ_{128}	$\gamma K^{*0} \bar{K}^{*0}$	$(2.4 \pm 0.7) \times 10^{-4}$	
Γ_{129}	$\gamma K_S^0 K^+ \pi^- + c.c.$	$(2.6 \pm 0.5) \times 10^{-4}$	
Γ_{130}	$\gamma K^+ K^- \pi^+ \pi^-$	$(1.9 \pm 0.5) \times 10^{-4}$	
Γ_{131}	$\gamma \rho \bar{\rho}$	$(2.9 \pm 0.6) \times 10^{-5}$	
Γ_{132}	$\gamma \pi^+ \pi^- \rho \bar{\rho}$	$(2.8 \pm 1.4) \times 10^{-5}$	
Γ_{133}	$\gamma 2(\pi^+ \pi^-) K^+ K^-$	$< 2.2 \times 10^{-4}$	CL=90%
Γ_{134}	$\gamma 3(\pi^+ \pi^-)$	$< 1.7 \times 10^{-4}$	CL=90%
Γ_{135}	$\gamma K^+ K^- K^+ K^-$	$< 4 \times 10^{-5}$	CL=90%

CONSTRAINED FIT INFORMATION

A multiparticle fit to $\chi_{c1}(1P)$, $\chi_{c0}(1P)$, $\chi_{c2}(1P)$, and $\psi(2S)$ with 4 total widths, a partial width, 24 combinations of partial widths obtained from integrated cross section, and 82 branching ratios uses 213 measurements to determine 47 parameters. The overall fit has a $\chi^2 = 301.4$ for 166 degrees of freedom.

The following off-diagonal array elements are the correlation coefficients $\langle \delta p_i \delta p_j \rangle / (\delta p_i \delta p_j)$, in percent, from the fit to parameters p_i , including the branching fractions, $x_i \equiv \Gamma_i / \Gamma_{\text{total}}$.

x_7	5										
x_8	1	0									
x_{11}	44	12	3								
x_{12}	40	8	2	64							
x_{13}	28	7	2	58	35						
x_{19}	2	1	0	7	5	4					
x_{105}	2	1	0	5	3	3	0				
x_{106}	2	1	0	5	2	3	0	0			
x_{107}	3	1	0	6	4	4	0	0	0		
Γ	-79	-6	-2	-52	-46	-32	-10	-2	-3	-4	
		x_6	x_7	x_8	x_{11}	x_{12}	x_{13}	x_{19}	x_{105}	x_{106}	x_{107}

$\psi(2S)$ PARTIAL WIDTHS

$\Gamma(\text{hadrons})$	DOCUMENT ID	TECN	COMMENT	Γ_1
VALUE (keV)				
• • • We do not use the following data for averages, fits, limits, etc. • • •				
258 ± 26	BAI	02B	BES2 $e^+ e^-$	
224 ± 56	LUTH	75	MRK1 $e^+ e^-$	

$\Gamma(e^+ e^-)$	DOCUMENT ID	TECN	COMMENT	Γ_6
VALUE (keV)				
2.35 ± 0.04 OUR FIT				
2.33 ± 0.07 OUR AVERAGE				
2.338 ± 0.037 ± 0.096	ABLIKIM	08B	BES2 $e^+ e^- \rightarrow \text{hadrons}$	
2.330 ± 0.036 ± 0.110	ABLIKIM	06L	BES2 $e^+ e^- \rightarrow \text{hadrons}$	
2.44 ± 0.21	⁸ BAI	02B	BES2 $e^+ e^-$	
2.14 ± 0.21	ALEXANDER	89	RVUE See Υ mini-review	
• • • We do not use the following data for averages, fits, limits, etc. • • •				
2.0 ± 0.3	BRANDELIK	79C	DASP $e^+ e^-$	
2.1 ± 0.3	⁹ LUTH	75	MRK1 $e^+ e^-$	

⁸From a simultaneous fit to $e^+ e^-$, $\mu^+ \mu^-$, and hadronic channel, assuming $\Gamma_e = \Gamma_\mu = \Gamma_\tau / 0.38847$.

⁹From a simultaneous fit to $e^+ e^-$, $\mu^+ \mu^-$, and hadronic channels assuming $\Gamma(e^+ e^-) = \Gamma(\mu^+ \mu^-)$.

$\Gamma(\gamma \gamma)$	DOCUMENT ID	TECN	COMMENT	Γ_{117}
VALUE (eV)				
CL%				
<43	BRANDELIK	79C	DASP $e^+ e^-$	

$\psi(2S) \Gamma(i) \Gamma(e^+ e^-) / \Gamma(\text{total})$

This combination of a partial width with the partial width into $e^+ e^-$ and with the total width is obtained from the integrated cross section into channel(i) in the $e^+ e^-$ annihilation. We list only data that have not been used to determine the partial width $\Gamma(i)$ or the branching ratio $\Gamma(i) / \text{total}$.

$\Gamma(\text{hadrons}) \times \Gamma(e^+ e^-) / \Gamma_{\text{total}}$	DOCUMENT ID	TECN	COMMENT	$\Gamma_1 \Gamma_6 / \Gamma$
VALUE (keV)				
• • • We do not use the following data for averages, fits, limits, etc. • • •				
2.2 ± 0.4	ABRAMS	75	MRK1 $e^+ e^-$	

$\Gamma(\tau^+ \tau^-) \times \Gamma(e^+ e^-) / \Gamma_{\text{total}}$	DOCUMENT ID	TECN	COMMENT	$\Gamma_8 \Gamma_6 / \Gamma$
VALUE (eV)				
• • • We do not use the following data for averages, fits, limits, etc. • • •				
9.0 ± 2.6	79	¹⁰ ANASHIN	07 KEDR $e^+ e^- \rightarrow \psi(2S) \rightarrow \tau^+ \tau^-$	
¹⁰ Using $\psi(2S)$ total width of 337 ± 13 keV. Systematic errors not evaluated.				

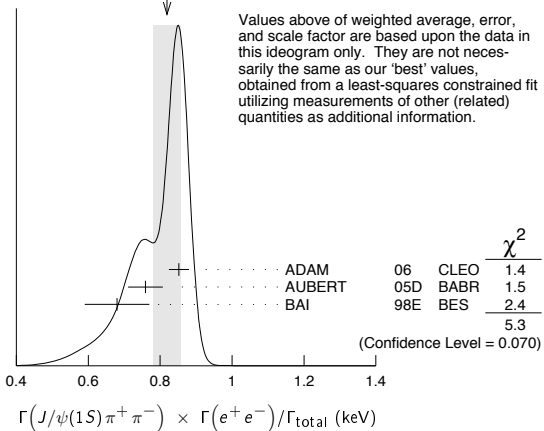
$\Gamma(J/\psi(1S) \pi^+ \pi^-) \times \Gamma(e^+ e^-) / \Gamma_{\text{total}}$	DOCUMENT ID	TECN	COMMENT	$\Gamma_{11} \Gamma_6 / \Gamma$
VALUE (keV)				
0.788 ± 0.015 OUR FIT				
0.82 ± 0.04 OUR AVERAGE Error includes scale factor of 1.6. See the ideogram below.				
0.852 ± 0.010 ± 0.026	19.5k ± 243	ADAM	06 CLEO 3.773 $e^+ e^- \rightarrow \gamma \psi(2S)$	
0.76 ± 0.05 ± 0.01	544	¹¹ AUBERT	05D BABR 10.6 $e^+ e^- \rightarrow \pi^+ \pi^- \mu^+ \mu^- \gamma$	
0.68 ± 0.09	12	BAI	98E BES $e^+ e^-$	
• • • We do not use the following data for averages, fits, limits, etc. • • •				
0.90 ± 0.08 ± 0.05	256	¹³ AUBERT	07AU BABR 10.6 $e^+ e^- \rightarrow J/\psi \pi^+ \pi^- \gamma$	

¹¹AUBERT 05D reports $[\Gamma(\psi(2S) \rightarrow J/\psi(1S) \pi^+ \pi^-) \times \Gamma(\psi(2S) \rightarrow e^+ e^-) / \Gamma_{\text{total}}] \times [B(J/\psi(1S) \rightarrow \mu^+ \mu^-)] = 0.0450 \pm 0.0018 \pm 0.0022$ keV which we divide by our best value $B(J/\psi(1S) \rightarrow \mu^+ \mu^-) = (5.93 \pm 0.06) \times 10^{-2}$. Our first error is their experiment's error and our second error is the systematic error from using our best value.

¹²The value of $\Gamma(e^+ e^-)$ quoted in BAI 98E is derived using $B(\psi(2S) \rightarrow J/\psi(1S) \pi^+ \pi^-) = (32.4 \pm 2.6) \times 10^{-2}$ and $B(J/\psi(1S) \rightarrow \ell^+ \ell^-) = 0.1203 \pm 0.0038$. Recalculated by us using $B(J/\psi(1S) \rightarrow \ell^+ \ell^-) = 0.1181 \pm 0.0020$.

¹³AUBERT 07AU reports $[\Gamma(\psi(2S) \rightarrow J/\psi(1S) \pi^+ \pi^-) \times \Gamma(\psi(2S) \rightarrow e^+ e^-) / \Gamma_{\text{total}}] \times [B(J/\psi(1S) \rightarrow \pi^+ \pi^- \pi^0)] = 0.0186 \pm 0.0012 \pm 0.0011$ keV which we divide by our best value $B(J/\psi(1S) \rightarrow \pi^+ \pi^- \pi^0) = (2.07 \pm 0.12) \times 10^{-2}$. Our first error is their experiment's error and our second error is the systematic error from using our best value.

WEIGHTED AVERAGE
0.82 ± 0.04 (Error scaled by 1.6)



Values above of weighted average, error, and scale factor are based upon the data in this ideogram only. They are not necessarily the same as our 'best' values, obtained from a least-squares constrained fit utilizing measurements of other (related) quantities as additional information.

$\Gamma(J/\psi(1S) \pi^0 \pi^0) \times \Gamma(e^+ e^-) / \Gamma_{\text{total}}$	DOCUMENT ID	TECN	COMMENT	$\Gamma_{12} \Gamma_6 / \Gamma$
VALUE (keV)				
0.416 ± 0.010 OUR FIT				
0.411 ± 0.008 ± 0.018 3.6k ± 96 ADAM 06 CLEO 3.773 $e^+ e^- \rightarrow \gamma \psi(2S)$				

$\Gamma(J/\psi(1S) \eta) \times \Gamma(e^+ e^-) / \Gamma_{\text{total}}$	DOCUMENT ID	TECN	COMMENT	$\Gamma_{13} \Gamma_6 / \Gamma$
VALUE (eV)				
77.0 ± 1.9 OUR FIT				
87 ± 9 OUR AVERAGE				
83 ± 25 ± 5	14	¹⁴ AUBERT	07AU BABR 10.6 $e^+ e^- \rightarrow J/\psi \pi^+ \pi^- \pi^0 \gamma$	
88 ± 6 ± 7	291 ± 24	ADAM	06 CLEO 3.773 $e^+ e^- \rightarrow \gamma \psi(2S)$	
¹⁴ AUBERT 07AU quotes $\Gamma_{ee}^{\psi(2S)} \cdot B(\psi(2S) \rightarrow J/\psi \eta) \cdot B(J/\psi \rightarrow \mu^+ \mu^-) \cdot B(\eta \rightarrow \pi^+ \pi^- \pi^0) = 1.11 \pm 0.33 \pm 0.07$ eV.				

$\Gamma(J/\psi(1S) \pi^0) \times \Gamma(e^+ e^-) / \Gamma_{\text{total}}$	DOCUMENT ID	TECN	COMMENT	$\Gamma_{14} \Gamma_6 / \Gamma$
VALUE (eV)				
CL%				
<8	90	<37	ADAM 06 CLEO 3.773 $e^+ e^- \rightarrow \gamma \psi(2S)$	

$$\Gamma(p\bar{p}) \times \Gamma(e^+e^-)/\Gamma_{total} \quad \Gamma_{19}\Gamma_6/\Gamma$$

VALUE (eV)	EVTS	DOCUMENT ID	TECN	COMMENT
0.647±0.028 OUR FIT				
0.59 ±0.05 OUR AVERAGE				
0.579±0.038±0.036	2.7k	ANDREOTTI 07	E835	$p\bar{p} \rightarrow e^+e^-, J/\psi X$
0.70 ±0.17 ±0.03	22	AUBERT 06B		$e^+e^- \rightarrow p\bar{p}\gamma$

$$\Gamma(\Lambda\bar{\Lambda}) \times \Gamma(e^+e^-)/\Gamma_{total} \quad \Gamma_{26}\Gamma_6/\Gamma$$

VALUE (eV)	DOCUMENT ID	TECN	COMMENT
1.5±0.4±0.1	AUBERT 07BD	BABR	10.6 $e^+e^- \rightarrow \Lambda\bar{\Lambda}\gamma$

$$\Gamma(2(\pi^+\pi^-\pi^0)) \times \Gamma(e^+e^-)/\Gamma_{total} \quad \Gamma_{41}\Gamma_6/\Gamma$$

VALUE (eV)	EVTS	DOCUMENT ID	TECN	COMMENT
11.2±3.3±1.3	43	AUBERT 06D	BABR	10.6 $e^+e^- \rightarrow 2(\pi^+\pi^-\pi^0)\gamma$

$$\Gamma(K^+K^-2(\pi^+\pi^-)) \times \Gamma(e^+e^-)/\Gamma_{total} \quad \Gamma_{55}\Gamma_6/\Gamma$$

VALUE (eV)	EVTS	DOCUMENT ID	TECN	COMMENT
4.4±2.1±0.3	26	AUBERT 06D	BABR	10.6 $e^+e^- \rightarrow K^+K^-2(\pi^+\pi^-)\gamma$

$$\Gamma(\pi^+\pi^-K^+K^-) \times \Gamma(e^+e^-)/\Gamma_{total} \quad \Gamma_{50}\Gamma_6/\Gamma$$

VALUE (eV)	EVTS	DOCUMENT ID	TECN	COMMENT
2.56±0.42±0.16	85	AUBERT 07AK	BABR	10.6 $e^+e^- \rightarrow \pi^+\pi^-K^+K^-\gamma$

$$\Gamma(\phi_0(980) \rightarrow \pi^+\pi^-) \times \Gamma(e^+e^-)/\Gamma_{total} \quad \Gamma_{83}\Gamma_6/\Gamma$$

VALUE (eV)	EVTS	DOCUMENT ID	TECN	COMMENT
0.347±0.169±0.003	6 ± 3	15 AUBERT	07AK BABR	10.6 $e^+e^- \rightarrow \pi^+\pi^-K^+K^-\gamma$

¹⁵ AUBERT 07AK reports $[\Gamma(\psi(2S) \rightarrow \phi_0(980) \rightarrow \pi^+\pi^-) \times \Gamma(\psi(2S) \rightarrow e^+e^-)/\Gamma_{total}] \times [B(\phi(1020) \rightarrow K^+K^-)] = 0.17 \pm 0.08 \pm 0.02$ eV which we divide by our best value $B(\phi(1020) \rightarrow K^+K^-) = (48.9 \pm 0.5) \times 10^{-2}$. Our first error is their experiment's error and our second error is the systematic error from using our best value.

$$\Gamma(\phi\pi^+\pi^-) \times \Gamma(e^+e^-)/\Gamma_{total} \quad \Gamma_{82}\Gamma_6/\Gamma$$

VALUE (eV)	EVTS	DOCUMENT ID	TECN	COMMENT
0.57±0.23±0.01	10	16 AUBERT, BE	06D BABR	10.6 $e^+e^- \rightarrow K^+K^-\pi^+\pi^-\gamma$

¹⁶ AUBERT, BE 06D reports $[\Gamma(\psi(2S) \rightarrow \phi\pi^+\pi^-) \times \Gamma(\psi(2S) \rightarrow e^+e^-)/\Gamma_{total}] \times [B(\phi(1020) \rightarrow K^+K^-)] = 0.28 \pm 0.11 \pm 0.02$ eV which we divide by our best value $B(\phi(1020) \rightarrow K^+K^-) = (48.9 \pm 0.5) \times 10^{-2}$. Our first error is their experiment's error and our second error is the systematic error from using our best value.

$$\Gamma(2(\pi^+\pi^-\pi^0)) \times \Gamma(e^+e^-)/\Gamma_{total} \quad \Gamma_{17}\Gamma_6/\Gamma$$

VALUE (eV)	EVTS	DOCUMENT ID	TECN	COMMENT
29.7±2.2±1.8	410	AUBERT 07AU	BABR	10.6 $e^+e^- \rightarrow 2(\pi^+\pi^-\pi^0)\gamma$

$$\Gamma(\omega\pi^+\pi^-) \times \Gamma(e^+e^-)/\Gamma_{total} \quad \Gamma_{46}\Gamma_6/\Gamma$$

VALUE (eV)	EVTS	DOCUMENT ID	TECN	COMMENT
3.01±0.84±0.02	37	17 AUBERT	07AU BABR	10.6 $e^+e^- \rightarrow \omega\pi^+\pi^-\gamma$

¹⁷ AUBERT 07AU reports $[\Gamma(\psi(2S) \rightarrow \omega\pi^+\pi^-) \times \Gamma(\psi(2S) \rightarrow e^+e^-)/\Gamma_{total}] \times [B(\omega(782) \rightarrow \pi^+\pi^-\pi^0)] = 2.69 \pm 0.73 \pm 0.16$ eV which we divide by our best value $B(\omega(782) \rightarrow \pi^+\pi^-\pi^0) = (89.2 \pm 0.7) \times 10^{-2}$. Our first error is their experiment's error and our second error is the systematic error from using our best value.

$$\Gamma(2(\pi^+\pi^-\eta)) \times \Gamma(e^+e^-)/\Gamma_{total} \quad \Gamma_{44}\Gamma_6/\Gamma$$

VALUE (eV)	EVTS	DOCUMENT ID	TECN	COMMENT
2.87±1.41±0.01	16	18 AUBERT	07AU BABR	10.6 $e^+e^- \rightarrow 2(\pi^+\pi^-\eta)\gamma$

¹⁸ AUBERT 07AU reports $[\Gamma(\psi(2S) \rightarrow 2(\pi^+\pi^-\eta)) \times \Gamma(\psi(2S) \rightarrow e^+e^-)/\Gamma_{total}] \times [B(\eta \rightarrow 2\gamma)] = 1.13 \pm 0.55 \pm 0.08$ eV which we divide by our best value $B(\eta \rightarrow 2\gamma) = (39.31 \pm 0.20) \times 10^{-2}$. Our first error is their experiment's error and our second error is the systematic error from using our best value.

$$\Gamma(K^+K^-\pi^+\pi^-\pi^0) \times \Gamma(e^+e^-)/\Gamma_{total} \quad \Gamma_{62}\Gamma_6/\Gamma$$

VALUE (eV)	EVTS	DOCUMENT ID	TECN	COMMENT
4.4±1.3±0.3	32	AUBERT 07AU	BABR	10.6 $e^+e^- \rightarrow K^+K^-\pi^+\pi^-\pi^0\gamma$

$$\Gamma(K^+K^-\pi^+\pi^-\eta) \times \Gamma(e^+e^-)/\Gamma_{total} \quad \Gamma_{53}\Gamma_6/\Gamma$$

VALUE (eV)	EVTS	DOCUMENT ID	TECN	COMMENT
3.05±1.80±0.02	7	19 AUBERT	07AU BABR	10.6 $e^+e^- \rightarrow K^+K^-\pi^+\pi^-\eta\gamma$

¹⁹ AUBERT 07AU reports $[\Gamma(\psi(2S) \rightarrow K^+K^-\pi^+\pi^-\eta) \times \Gamma(\psi(2S) \rightarrow e^+e^-)/\Gamma_{total}] \times [B(\eta \rightarrow 2\gamma)] = 1.2 \pm 0.7 \pm 0.1$ eV which we divide by our best value $B(\eta \rightarrow 2\gamma) = (39.31 \pm 0.20) \times 10^{-2}$. Our first error is their experiment's error and our second error is the systematic error from using our best value.

$\psi(2S)$ BRANCHING RATIOS

$$\Gamma(\text{hadrons})/\Gamma_{total} \quad \Gamma_1/\Gamma$$

VALUE	DOCUMENT ID	TECN	COMMENT
0.9785±0.0013 OUR AVERAGE			
0.9779±0.0015	20 BAI	02B	BES2 e^+e^-
0.981 ±0.003	20 LUTH	75	MRK1 e^+e^-

²⁰ Includes cascade decay into $J/\psi(1S)$.

$$\Gamma(\text{virtual } \gamma \rightarrow \text{hadrons})/\Gamma_{total} \quad \Gamma_2/\Gamma$$

VALUE	DOCUMENT ID	TECN	COMMENT
0.0173±0.0014 OUR AVERAGE			Error includes scale factor of 1.5.
0.0166±0.0010	21,22 SETH	04	RVUE e^+e^-
0.0199±0.0019	21 BAI	02B	BES2 e^+e^-

• • • We do not use the following data for averages, fits, limits, etc. • • •
0.029 ±0.004 ²¹ LUTH 75 MRK1 e^+e^-

²¹ Included in $\Gamma(\text{hadrons})/\Gamma_{total}$.
²² Using $B(\psi(2S) \rightarrow \ell^+\ell^-) = (0.73 \pm 0.04)\%$ from RPP-2002 and $R = 2.28 \pm 0.04$ determined by a fit to data from BAI 00 and BAI 02c.

$$\Gamma(g\bar{g})/\Gamma_{total} \quad \Gamma_3/\Gamma$$

VALUE (units 10^{-2})	EVTS	DOCUMENT ID	TECN	COMMENT
10.58±1.62	2.9 M	23 LIBBY	09	CLEO $\psi(2S) \rightarrow \text{hadrons}$

²³ Calculated using $\Gamma(\gamma g\bar{g})/\Gamma(g\bar{g}) = 0.097 \pm 0.026 \pm 0.016$ from LIBBY 09, $B(\psi(2S) \rightarrow X J/\psi)$ relative and absolute branching fractions from MENDEZ 08, $B(\psi(2S) \rightarrow \gamma\eta_c)$ from MITCHELL 09, and $B(\psi(2S) \rightarrow \text{virtual } \gamma \rightarrow \text{hadrons})$, $B(\psi(2S) \rightarrow \gamma\chi_{cJ})$, and $B(\psi(2S) \rightarrow \ell^+\ell^-)$ from PDG 08. The statistical error is negligible and the systematic error is largely uncorrelated with that of $\Gamma(\gamma g\bar{g})/\Gamma_{total}$ LIBBY 09 measurement.

$$\Gamma(\gamma g\bar{g})/\Gamma_{total} \quad \Gamma_4/\Gamma$$

VALUE (units 10^{-2})	EVTS	DOCUMENT ID	TECN	COMMENT
1.025±0.288	200 k	24 LIBBY	09	CLEO $\psi(2S) \rightarrow \gamma + \text{hadrons}$

²⁴ Calculated using $\Gamma(\gamma g\bar{g})/\Gamma(g\bar{g}) = 0.097 \pm 0.026 \pm 0.016$ from LIBBY 09. The statistical error is negligible and the systematic error is largely uncorrelated with that of $\Gamma(g\bar{g})/\Gamma_{total}$ LIBBY 09 measurement.

$$\Gamma(\gamma g\bar{g})/\Gamma(g\bar{g}) \quad \Gamma_4/\Gamma_3$$

VALUE (units 10^{-2})	EVTS	DOCUMENT ID	TECN	COMMENT
9.7±2.6±1.6	2.9 M	LIBBY 09	CLEO	$\psi(2S) \rightarrow (\gamma +) \text{hadrons}$

$$\Gamma(\text{light hadrons})/\Gamma_{total} \quad \Gamma_5/\Gamma$$

VALUE	DOCUMENT ID	TECN	COMMENT
0.154±0.015	25 MENDEZ 08	CLEO	$e^+e^- \rightarrow \psi(2S)$

• • • We do not use the following data for averages, fits, limits, etc. • • •
0.169±0.026 ²⁶ ADAM 05A CLEO $e^+e^- \rightarrow \psi(2S)$

²⁵ Uses $B(\psi(2S) \rightarrow J/\psi X)$ from MENDEZ 08 and other branching fractions from PDG 07.
²⁶ Uses $B(J/\psi X)$ from ADAM 05A, $B(\chi_{cJ})$, $B(\eta_c\gamma)$ from ATHAR 04 and $B(\ell^+\ell^-)$ from PDG 04. Superseded by MENDEZ 08.

$$\Gamma(e^+e^-)/\Gamma_{total} \quad \Gamma_6/\Gamma$$

VALUE (units 10^{-4})	DOCUMENT ID	TECN	COMMENT
77.2± 1.7 OUR FIT			
88 ±13	27 FELDMAN 77	RVUE	e^+e^-

• • • We do not use the following data for averages, fits, limits, etc. • • •
²⁷ From an overall fit assuming equal partial widths for e^+e^- and $\mu^+\mu^-$. For a measurement of the ratio see the entry $\Gamma(\mu^+\mu^-)/\Gamma(e^+e^-)$ below. Includes LUTH 75, HILGER 75, BURMESTER 77.

$$\Gamma(\mu^+\mu^-)/\Gamma_{total} \quad \Gamma_7/\Gamma$$

VALUE (units 10^{-4})	DOCUMENT ID
77±8 OUR FIT	

$$\Gamma(\mu^+\mu^-)/\Gamma(e^+e^-) \quad \Gamma_7/\Gamma_6$$

VALUE	DOCUMENT ID	TECN	COMMENT
1.00±0.11 OUR FIT			
0.89±0.16	BOYARSKI 75c	MRK1	e^+e^-

• • • We do not use the following data for averages, fits, limits, etc. • • •

$$\Gamma(\tau^+\tau^-)/\Gamma_{total} \quad \Gamma_8/\Gamma$$

VALUE (units 10^{-4})	DOCUMENT ID	TECN	COMMENT
30 ±4 OUR FIT			
30.8±2.1±3.8	28 ABLIKIM 06w	BES	$e^+e^- \rightarrow \psi(2S)$

²⁸ Computed using PDG 02 value of $B(\psi(2S) \rightarrow \text{hadrons}) = 0.9810 \pm 0.0030$ to estimate the total number of $\psi(2S)$ events.

DECAYS INTO $J/\psi(1S)$ AND ANYTHING

$$\Gamma(J/\psi(1S) \text{ anything})/\Gamma_{total} \quad \Gamma_9/\Gamma$$

VALUE	EVTS	DOCUMENT ID	TECN	COMMENT
0.595 ±0.008 OUR FIT				
0.55 ±0.07 OUR AVERAGE				

0.51 ±0.12		BRANDELIK 79c	DASP	$e^+e^- \rightarrow \mu^+\mu^-X$
0.57 ±0.08		ABRAMS 75b	MRK1	$e^+e^- \rightarrow \mu^+\mu^-X$

• • • We do not use the following data for averages, fits, limits, etc. • • •
0.6254±0.0016±0.0155 1.1M ²⁹ MENDEZ 08 CLEO $\psi(2S) \rightarrow \ell^+\ell^-X$
0.5950±0.0015±0.0190 151k ADAM 05A CLEO Repl. by MENDEZ 08

²⁹ Not independent from other measurements of MENDEZ 08.

Meson Particle Listings

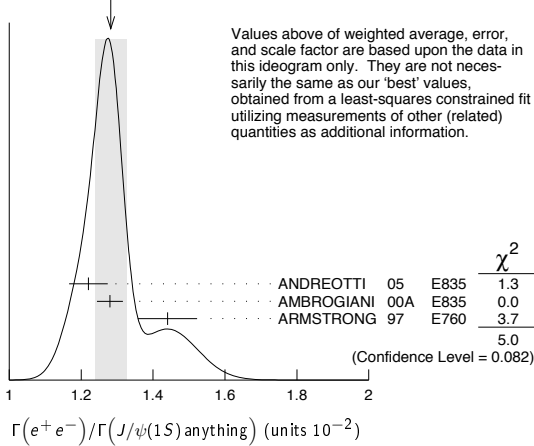
$\psi(2S)$

$\Gamma(e^+e^-)/\Gamma(J/\psi(1S)\text{ anything})$
 $\Gamma_6/\Gamma_9 = \Gamma_6/(\Gamma_{11} + \Gamma_{12} + \Gamma_{13} + 0.344\Gamma_{106} + 0.195\Gamma_{107})$

VALUE (units 10^{-2})	EVTS	DOCUMENT ID	TECN	COMMENT
1.299 ± 0.026 OUR FIT				
1.28 ± 0.04 OUR AVERAGE				Error includes scale factor of 1.6. See the ideogram below.
$1.22 \pm 0.02 \pm 0.05$	5097 ± 73	30 ANDREOTTI 05	E835	$p\bar{p} \rightarrow \psi(2S) \rightarrow e^+e^-$
$1.28 \pm 0.03 \pm 0.02$		30 AMBROGIANI 00A	E835	$p\bar{p} \rightarrow \psi(2S)$
$1.44 \pm 0.08 \pm 0.02$		30 ARMSTRONG 97	E760	$p\bar{p} \rightarrow \psi(2S)$

³⁰ Using $B(J/\psi(1S) \rightarrow e^+e^-) = 0.0593 \pm 0.0010$.

WEIGHTED AVERAGE
 1.28 ± 0.04 (Error scaled by 1.6)



$\Gamma(\mu^+\mu^-)/\Gamma(J/\psi(1S)\text{ anything})$
 $\Gamma_7/\Gamma_9 = \Gamma_7/(\Gamma_{11} + \Gamma_{12} + \Gamma_{13} + 0.344\Gamma_{106} + 0.195\Gamma_{107})$

VALUE	DOCUMENT ID	TECN	COMMENT
0.0130 ± 0.0014 OUR FIT			
0.014 ± 0.003	HILGER 75	SPEC	e^+e^-

$\Gamma(J/\psi(1S)\text{ neutrals})/\Gamma_{total}$ Γ_{10}/Γ

VALUE	DOCUMENT ID
0.245 ± 0.004 OUR FIT	

$\Gamma(J/\psi(1S)\pi^+\pi^-)/\Gamma_{total}$ Γ_{11}/Γ

VALUE	EVTS	DOCUMENT ID	TECN	COMMENT
0.336 ± 0.004 OUR FIT				
0.343 ± 0.011 OUR AVERAGE				Error includes scale factor of 1.7.
$0.3504 \pm 0.0007 \pm 0.0077$	$565k$	MENDEZ 08	CLEO	$\psi(2S) \rightarrow \ell^+\ell^-\pi^+\pi^-$
0.323 ± 0.014		BAI 02B	BES2	e^+e^-
0.32 ± 0.04		ABRAMS 75B	MRK1	$e^+e^- \rightarrow J/\psi\pi^+\pi^-$

••• We do not use the following data for averages, fits, limits, etc. •••

$0.3354 \pm 0.0014 \pm 0.0110$	$60k$	31 ADAM 05A	CLEO	Repl. by MENDEZ 08
--------------------------------	-------	-------------	------	--------------------

³¹ Not independent from other values reported by ADAM 05A.

$\Gamma(e^+e^-)/\Gamma(J/\psi(1S)\pi^+\pi^-)$ Γ_6/Γ_{11}

VALUE	DOCUMENT ID	TECN	COMMENT
0.0230 ± 0.0005 OUR FIT			
$0.0252 \pm 0.0028 \pm 0.0011$	32 AUBERT 02B	BABR	e^+e^-

³² Using $B(J/\psi(1S) \rightarrow e^+e^-) = 0.0593 \pm 0.0010$.

$\Gamma(\mu^+\mu^-)/\Gamma(J/\psi(1S)\pi^+\pi^-)$ Γ_7/Γ_{11}

VALUE	DOCUMENT ID	TECN	COMMENT
0.0229 ± 0.0025 OUR FIT			
0.0224 ± 0.0029 OUR AVERAGE			
$0.0216 \pm 0.0026 \pm 0.0014$	33 AUBERT 02B	BABR	e^+e^-
$0.0327 \pm 0.0077 \pm 0.0072$	33 GRIBUSHIN 96	FMP5	$515\pi^-\text{Be} \rightarrow 2\mu X$

³³ Using $B(J/\psi(1S) \rightarrow \mu^+\mu^-) = 0.0588 \pm 0.0010$.

$\Gamma(\tau^+\tau^-)/\Gamma(J/\psi(1S)\pi^+\pi^-)$ Γ_8/Γ_{11}

VALUE (units 10^{-3})	DOCUMENT ID	TECN	COMMENT
9.1 ± 1.1 OUR FIT			
$8.73 \pm 1.39 \pm 1.57$	BAI 02	BES	e^+e^-

$\Gamma(J/\psi(1S)\pi^+\pi^-)/\Gamma(J/\psi(1S)\text{ anything})$ Γ_{11}/Γ_9

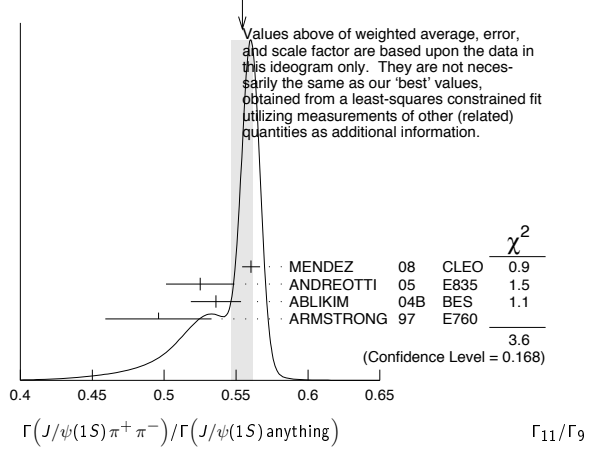
VALUE	EVTS	DOCUMENT ID	TECN	COMMENT
0.5646 ± 0.0026 OUR FIT				
0.554 ± 0.008 OUR AVERAGE				Error includes scale factor of 1.3. See the ideogram below.
$0.5604 \pm 0.0009 \pm 0.0062$	$565k$	MENDEZ 08	CLEO	$\psi(2S) \rightarrow \ell^+\ell^-\pi^+\pi^-$
$0.525 \pm 0.009 \pm 0.022$	$4k$	ANDREOTTI 05	E835	$\psi(2S) \rightarrow J/\psi X$
$0.536 \pm 0.007 \pm 0.016$	$20k$	34,35 ABLIKIM 04B	BES	$\psi(2S) \rightarrow J/\psi X$
0.496 ± 0.037		ARMSTRONG 97	E760	$p\bar{p} \rightarrow \psi(2S)$

••• We do not use the following data for averages, fits, limits, etc. •••

$0.5637 \pm 0.0027 \pm 0.0046$	$60k$	ADAM 05A	CLEO	Repl. by MENDEZ 08
--------------------------------	-------	----------	------	--------------------

³⁴ From a fit to the J/ψ recoil mass spectra.
³⁵ ABLIKIM 04B quotes $B(\psi(2S) \rightarrow J/\psi X) / B(\psi(2S) \rightarrow J/\psi\pi^+\pi^-)$.

WEIGHTED AVERAGE
 0.554 ± 0.008 (Error scaled by 1.3)



$\Gamma(J/\psi(1S)\text{ neutrals})/\Gamma(J/\psi(1S)\pi^+\pi^-)$
 $\Gamma_{10}/\Gamma_{11} = (0.9761\Gamma_{12} + 0.719\Gamma_{13} + 0.344\Gamma_{106} + 0.195\Gamma_{107})/\Gamma_{11}$

VALUE	DOCUMENT ID	TECN	COMMENT
0.731 ± 0.008 OUR FIT			
0.73 ± 0.09	TANENBAUM 76	MRK1	e^+e^-

$\Gamma(J/\psi(1S)\pi^0\pi^0)/\Gamma_{total}$ Γ_{12}/Γ

VALUE	EVTS	DOCUMENT ID	TECN	COMMENT
0.1773 ± 0.0034 OUR FIT				
••• We do not use the following data for averages, fits, limits, etc. •••				
$0.1769 \pm 0.0008 \pm 0.0053$	$61k$	36 MENDEZ 08	CLEO	$\psi(2S) \rightarrow \ell^+\ell^-\pi^0$
$0.1652 \pm 0.0014 \pm 0.0058$	$13.4k$	37 ADAM 05A	CLEO	Repl. by MENDEZ 08

³⁶ Not independent from other measurements of MENDEZ 08.
³⁷ Not independent from other values reported by ADAM 05A.

$\Gamma(J/\psi(1S)\pi^0\pi^0)/\Gamma(J/\psi(1S)\text{ anything})$ Γ_{12}/Γ_9

VALUE	EVTS	DOCUMENT ID	TECN	COMMENT
0.2982 ± 0.0032 OUR FIT				
0.320 ± 0.012 OUR AVERAGE				
$0.300 \pm 0.008 \pm 0.022$	1655 ± 44	ANDREOTTI 05	E835	$\psi(2S) \rightarrow J/\psi X$
$0.328 \pm 0.013 \pm 0.008$		AMBROGIANI 00A	E835	$p\bar{p} \rightarrow \psi(2S)$
0.323 ± 0.033		ARMSTRONG 97	E760	$p\bar{p} \rightarrow \psi(2S)$

••• We do not use the following data for averages, fits, limits, etc. •••

$0.2829 \pm 0.0012 \pm 0.0056$	$61k$	MENDEZ 08	CLEO	$\psi(2S) \rightarrow \ell^+\ell^-\pi^0$
$0.2776 \pm 0.0025 \pm 0.0043$	$13.4k$	ADAM 05A	CLEO	Repl. by MENDEZ 08

$\Gamma(J/\psi(1S)\pi^0\pi^0)/\Gamma(J/\psi(1S)\pi^+\pi^-)$ Γ_{12}/Γ_{11}

VALUE	EVTS	DOCUMENT ID	TECN	COMMENT
0.528 ± 0.008 OUR FIT				
0.513 ± 0.022 OUR AVERAGE				Error includes scale factor of 2.2.
$0.5047 \pm 0.0022 \pm 0.0102$	$61k$	MENDEZ 08	CLEO	$\psi(2S) \rightarrow \ell^+\ell^-\pi^0$
$0.570 \pm 0.009 \pm 0.026$	$14k$	38 ABLIKIM 04B	BES	$\psi(2S) \rightarrow J/\psi X$

••• We do not use the following data for averages, fits, limits, etc. •••

$0.4924 \pm 0.0047 \pm 0.0086$	$73k$	39,40 ADAM 05A	CLEO	Repl. by MENDEZ 08
$0.571 \pm 0.018 \pm 0.044$		41 ANDREOTTI 05	E835	$\psi(2S) \rightarrow J/\psi X$
0.53 ± 0.06		TANENBAUM 76	MRK1	e^+e^-
0.64 ± 0.15		42 HILGER 75	SPEC	e^+e^-

³⁸ From a fit to the J/ψ recoil mass spectra.

³⁹ Not independent from other values reported by ADAM 05A.

⁴⁰ Using 13,217 $J/\psi\pi^0\pi^0$ and 60,010 $J/\psi\pi^+\pi^-$ events.

⁴¹ Not independent from other values reported by ANDREOTTI 05.

⁴² Ignoring the $J/\psi(1S)\eta$ and $J/\psi(1S)\gamma\gamma$ decays.

$\Gamma(J/\psi(1S)\eta)/\Gamma_{total}$ Γ_{13}/Γ

VALUE	EVTS	DOCUMENT ID	TECN	COMMENT
0.0328 ± 0.0007 OUR FIT				
0.0296 ± 0.0031 OUR AVERAGE				Error includes scale factor of 1.8. See the ideogram below.
$0.0298 \pm 0.0009 \pm 0.0023$	$5.7k$	BAI 04I	BES2	$\psi(2S) \rightarrow J/\psi\gamma\gamma$
0.0255 ± 0.0029	386	43 OREGLIA 80	CBAL	$e^+e^- \rightarrow J/\psi 2\gamma$
0.045 ± 0.012	17	44 BRANDELIK 79B	DASP	$e^+e^- \rightarrow J/\psi 2\gamma$
0.042 ± 0.006	164	44 BARTEL 78B	CNTR	e^+e^-

••• We do not use the following data for averages, fits, limits, etc. •••

$0.0343 \pm 0.0004 \pm 0.0009$	$18.4k$	45 MENDEZ 08	CLEO	$\psi(2S) \rightarrow \ell^+\ell^-\eta$
$0.0325 \pm 0.0006 \pm 0.0011$	$2.8k$	46 ADAM 05A	CLEO	Repl. by MENDEZ 08
0.043 ± 0.008	44	TANENBAUM 76	MRK1	e^+e^-

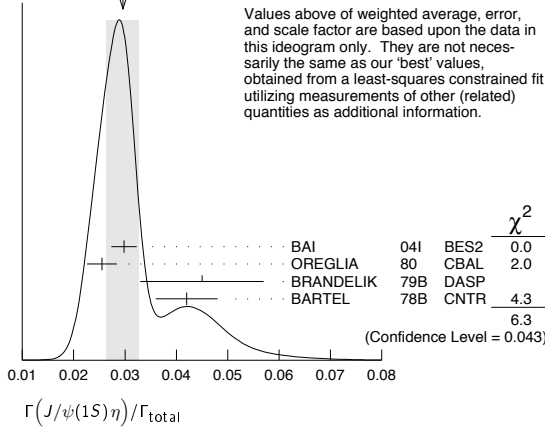
See key on page 405

Meson Particle Listings

$\psi(2S)$

- 43 Recalculated by us using $B(J/\psi(1S) \rightarrow \ell^+ \ell^-) = 0.1181 \pm 0.0020$.
- 44 Recalculated by us using $B(J/\psi(1S) \rightarrow \mu^+ \mu^-) = 0.0588 \pm 0.0010$.
- 45 Not independent from other measurements of MENDEZ 08.
- 46 Not independent from other values reported by ADAM 05A.

WEIGHTED AVERAGE
0.0296±0.0031 (Error scaled by 1.8)

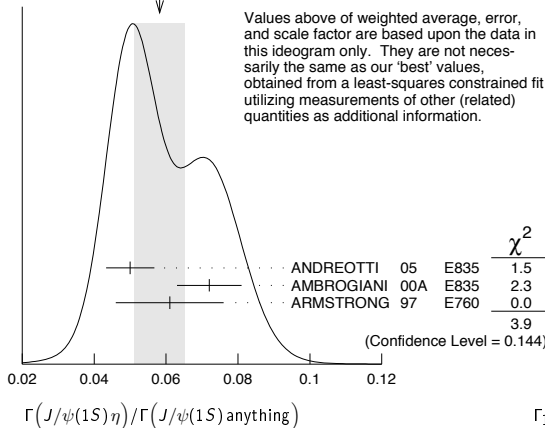


$\Gamma(J/\psi(1S)\eta)/\Gamma(J/\psi(1S)\text{anything})$ Γ_{13}/Γ_9

VALUE	EVTS	DOCUMENT ID	TECN	COMMENT
0.0551 ± 0.0009 OUR FIT				
0.058 ± 0.007 OUR AVERAGE				Error includes scale factor of 1.4. See the ideogram below.
0.050 ± 0.006 ± 0.003	298 ± 20	ANDREOTTI 05	E835	$\psi(2S) \rightarrow J/\psi X$
0.072 ± 0.009		AMBROGIANI 00A	E835	$p\bar{p} \rightarrow \psi(2S)$
0.061 ± 0.015		ARMSTRONG 97	E760	$\bar{p}p \rightarrow \psi(2S)$
• • • We do not use the following data for averages, fits, limits, etc. • • •				
0.0549 ± 0.0006 ± 0.0009	18.4k	47 MENDEZ 08	CLEO	$\psi(2S) \rightarrow \ell^+ \ell^- \eta$
0.0546 ± 0.0010 ± 0.0007	2.8k	ADAM 05A	CLEO	Repl. by MENDEZ 08

- 47 Not independent from other measurements of MENDEZ 08.

WEIGHTED AVERAGE
0.058±0.007 (Error scaled by 1.4)



$\Gamma(J/\psi(1S)\eta)/\Gamma(J/\psi(1S)\pi^+\pi^-)$ Γ_{13}/Γ_{11}

VALUE	EVTS	DOCUMENT ID	TECN	COMMENT
0.0976 ± 0.0016 OUR FIT				
0.0979 ± 0.0018 OUR AVERAGE				
0.0979 ± 0.0010 ± 0.0015	18.4k	MENDEZ 08	CLEO	$\psi(2S) \rightarrow \ell^+ \ell^- \eta$
0.098 ± 0.005 ± 0.010	2k	48 ABLIKIM 04b	BES	$\psi(2S) \rightarrow J/\psi X$
0.091 ± 0.021		49 HIMEL 80	MRK2	$e^+ e^- \rightarrow \psi(2S) X$
• • • We do not use the following data for averages, fits, limits, etc. • • •				
0.0968 ± 0.0019 ± 0.0013	2.8k	50 ADAM 05A	CLEO	Repl. by MENDEZ 08
0.095 ± 0.007 ± 0.007		51 ANDREOTTI 05	E835	$\psi(2S) \rightarrow J/\psi X$

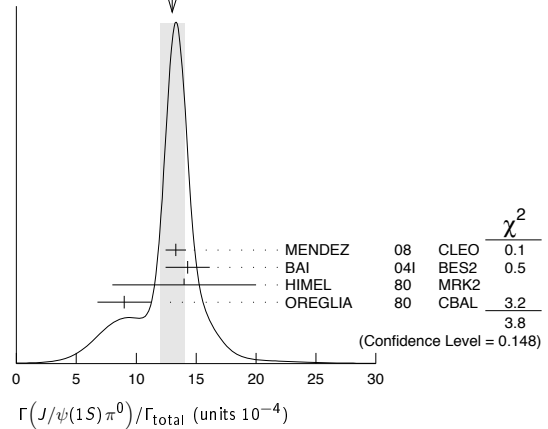
- 48 From a fit to the J/ψ recoil mass spectra.
- 49 The value for $B(\psi(2S) \rightarrow J/\psi(1S)\eta)$ reported in HIMEL 80 is derived using $B(\psi(2S) \rightarrow J/\psi(1S)\pi^+\pi^-) = (33 \pm 3)\%$ and $B(J/\psi(1S) \rightarrow \ell^+ \ell^-) = 0.138 \pm 0.018$. Calculated by us using $B(J/\psi(1S) \rightarrow \ell^+ \ell^-) = (0.1181 \pm 0.0020)$.
- 50 Not independent from other values reported by ADAM 05A.
- 51 Not independent from other values reported by ANDREOTTI 05.

$\Gamma(J/\psi(1S)\pi^0)/\Gamma_{total}$ Γ_{14}/Γ

VALUE (units 10^{-4})	EVTS	DOCUMENT ID	TECN	COMMENT
13.0 ± 1.0 OUR AVERAGE				Error includes scale factor of 1.4. See the ideogram below.
13.3 ± 0.8 ± 0.3	530	MENDEZ 08	CLEO	$\psi(2S) \rightarrow \ell^+ \ell^- 2\gamma$
14.3 ± 1.4 ± 1.2	280	BAI 041	BES2	$\psi(2S) \rightarrow J/\psi \gamma \gamma$
14 ± 6	7	HIMEL 80	MRK2	$e^+ e^-$
9 ± 2 ± 1	23	52 OREGLIA 80	CBAL	$\psi(2S) \rightarrow J/\psi 2\gamma$
• • • We do not use the following data for averages, fits, limits, etc. • • •				
13 ± 1 ± 1	88	ADAM 05A	CLEO	Repl. by MENDEZ 08

- 52 Recalculated by us using $B(J/\psi(1S) \rightarrow \ell^+ \ell^-) = 0.1181 \pm 0.0020$.

WEIGHTED AVERAGE
13.0±1.0 (Error scaled by 1.4)



$\Gamma(J/\psi(1S)\pi^0)/\Gamma(J/\psi(1S)\text{anything})$ $\Gamma_{14}/\Gamma_9 = \Gamma_{14}/(\Gamma_{11} + \Gamma_{12} + \Gamma_{13} + 0.344\Gamma_{106} + 0.195\Gamma_{107})$

VALUE (units 10^{-2})	EVTS	DOCUMENT ID	TECN	COMMENT
0.213 ± 0.012 ± 0.003	527	53 MENDEZ 08	CLEO	$e^+ e^- \rightarrow J/\psi \gamma \gamma$
0.22 ± 0.02 ± 0.01		54 ADAM 05A	CLEO	$e^+ e^- \rightarrow \psi(2S) \rightarrow J/\psi \gamma \gamma$

- 53 Not independent from other values reported by MENDEZ 08. Supersedes ADAM 05A.
- 54 Not independent from other values reported by ADAM 05A.

$\Gamma(J/\psi(1S)\pi^0)/\Gamma(J/\psi(1S)\pi^+\pi^-)$ Γ_{14}/Γ_{11}

VALUE (units 10^{-2})	EVTS	DOCUMENT ID	TECN	COMMENT
0.380 ± 0.022 ± 0.005	527	55 MENDEZ 08	CLEO	$e^+ e^- \rightarrow J/\psi \gamma \gamma$
0.39 ± 0.04 ± 0.01		56 ADAM 05A	CLEO	$e^+ e^- \rightarrow \psi(2S) \rightarrow J/\psi \gamma \gamma$

- 55 Not independent from other values reported by MENDEZ 08. Supersedes ADAM 05A.
- 56 Not independent from other values reported by ADAM 05A.

HADRONIC DECAYS

$\Gamma(\pi^0 h_C(1P))/\Gamma_{total}$ Γ_{15}/Γ

VALUE	EVTS	DOCUMENT ID	TECN	COMMENT
seen	92 $^{+23}_{-22}$	ADAMS 09	CLEO	$\psi(2S) \rightarrow 2\pi^+ 2\pi^- 2\pi^0$
seen	1282	DOBBS 08A	CLEO	$\psi(2S) \rightarrow \pi^0 \eta_C \gamma$
• • • We do not use the following data for averages, fits, limits, etc. • • •				
seen	168 ± 40	ROSNER 05	CLEO	$\psi(2S) \rightarrow \pi^0 \eta_C \gamma$

$\Gamma(3(\pi^+\pi^-)\pi^0)/\Gamma_{total}$ Γ_{16}/Γ

VALUE (units 10^{-4})	EVTS	DOCUMENT ID	TECN	COMMENT
35 ± 16	6	FRANKLIN 83	MRK2	$e^+ e^- \rightarrow \text{hadrons}$

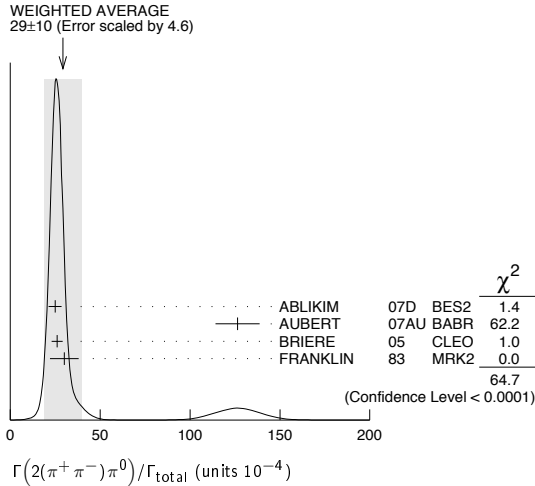
$\Gamma(2(\pi^+\pi^-)\pi^0)/\Gamma_{total}$ Γ_{17}/Γ

VALUE (units 10^{-4})	EVTS	DOCUMENT ID	TECN	COMMENT
29 ± 10 OUR AVERAGE				Error includes scale factor of 4.6. See the ideogram below.
24.9 ± 0.7 ± 3.6	2173	ABLIKIM 07b	BES2	$e^+ e^- \rightarrow \psi(2S)$
126 ± 12 ± 2	410	57 AUBERT 07a	BABR	10.6 $e^+ e^- \rightarrow 2(\pi^+\pi^-)\pi^0 \gamma$
26.1 ± 0.7 ± 3.0	1703	BRIERE 05	CLEO	$e^+ e^- \rightarrow \psi(2S) \rightarrow 2(\pi^+\pi^-)\pi^0$
30 ± 8	42	FRANKLIN 83	MRK2	$e^+ e^-$

Meson Particle Listings

$\psi(2S)$

⁵⁷ AUBERT 07AU reports $[\Gamma(\psi(2S) \rightarrow 2\pi^+\pi^-\pi^0)/\Gamma_{total}] \times [\Gamma(\psi(2S) \rightarrow e^+e^-)] = (297 \pm 22 \pm 18) \times 10^{-4}$ keV which we divide by our best value $\Gamma(\psi(2S) \rightarrow e^+e^-) = 2.35 \pm 0.04$ keV. Our first error is their experiment's error and our second error is the systematic error from using our best value.



$\Gamma(\rho_2(1320))/\Gamma_{total}$ Γ₁₈/Γ

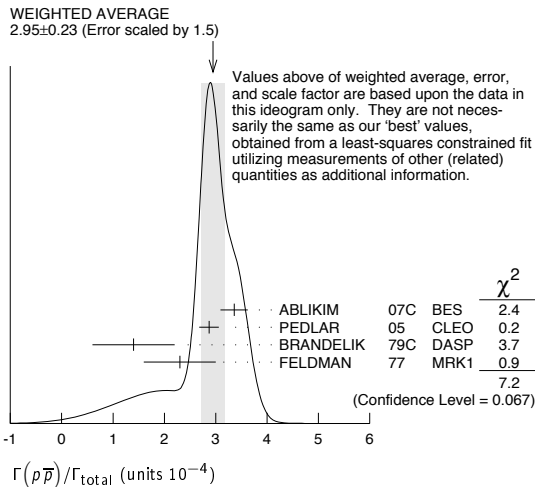
VALUE (units 10^{-4})	CL%	EVTS	DOCUMENT ID	TECN	COMMENT
2.55±0.73±0.47		112 ± 31	BAI	04c BES2	$\psi(2S) \rightarrow 2(\pi^+\pi^-\pi^0)$

• • • We do not use the following data for averages, fits, limits, etc. • • •

<2.3	90	BAI	98J	BES	e^+e^-
------	----	-----	-----	-----	----------

$\Gamma(p\bar{p})/\Gamma_{total}$ Γ₁₉/Γ

VALUE (units 10^{-4})	EVTS	DOCUMENT ID	TECN	COMMENT
2.76±0.12 OUR FIT				
2.95±0.23 OUR AVERAGE		Error includes scale factor of 1.5. See the ideogram below.		
3.36±0.09±0.25	1618	ABLIKIM	07c BES	$e^+e^- \rightarrow \psi(2S) \rightarrow p\bar{p}$
2.87±0.12±0.15	557	PEDLAR	05 CLEO	$e^+e^- \rightarrow \psi(2S) \rightarrow p\bar{p}$
1.4 ± 0.8	4	BRANDELIK	79c DASP	$e^+e^- \rightarrow \psi(2S) \rightarrow p\bar{p}$
2.3 ± 0.7		FELDMAN	77 MRK1	$e^+e^- \rightarrow \psi(2S) \rightarrow p\bar{p}$



$\Gamma(p\bar{p})/\Gamma(J/\psi(1S)\pi^+\pi^-)$ Γ₁₉/Γ₁₁

VALUE (units 10^{-4})	DOCUMENT ID	TECN	COMMENT
8.2 ± 0.4 OUR FIT			
6.98±0.49±0.97	BAI	01	BES $e^+e^- \rightarrow \psi(2S) \rightarrow p\bar{p}$

$\Gamma(\Delta^{++}\bar{\Delta}^{--})/\Gamma_{total}$ Γ₂₀/Γ

VALUE (units 10^{-5})	EVTS	DOCUMENT ID	TECN	COMMENT
12.8±1.0±3.4	157	58 BAI	01	BES $e^+e^- \rightarrow \psi(2S) \rightarrow$ hadrons

⁵⁸ Estimated using $B(\psi(2S) \rightarrow J/\psi\pi^+\pi^-) = 0.310 \pm 0.028$.

$\Gamma(\Lambda\bar{\Lambda}\pi^0)/\Gamma_{total}$ Γ₂₁/Γ

VALUE (units 10^{-4})	CL%	DOCUMENT ID	TECN	COMMENT
<1.2	90	59 ABLIKIM	07H BES2	$e^+e^- \rightarrow \psi(2S)$

⁵⁹ Using $B(\Lambda \rightarrow \pi^-p) = 63.9\%$ and $B(\eta \rightarrow \gamma\gamma) = 39.4\%$.

$\Gamma(\Lambda\bar{\Lambda}\eta)/\Gamma_{total}$ Γ₂₂/Γ

VALUE (units 10^{-4})	CL%	DOCUMENT ID	TECN	COMMENT
<0.49	90	60 ABLIKIM	07H BES2	$e^+e^- \rightarrow \psi(2S)$

⁶⁰ Using $B(\Lambda \rightarrow \pi^-p) = 63.9\%$.

$\Gamma(\Lambda\bar{p}K^+)/\Gamma_{total}$ Γ₂₃/Γ

VALUE (units 10^{-4})	EVTS	DOCUMENT ID	TECN	COMMENT
1.0±0.1 ±0.1	74.0	BRIERE	05 CLEO	$e^+e^- \rightarrow \psi(2S) \rightarrow$ $p\bar{p}K^+\pi^-$

$\Gamma(\Lambda\bar{p}K^+\pi^+\pi^-)/\Gamma_{total}$ Γ₂₄/Γ

VALUE (units 10^{-4})	EVTS	DOCUMENT ID	TECN	COMMENT
1.8±0.3±0.3	45.8	BRIERE	05 CLEO	$e^+e^- \rightarrow \psi(2S) \rightarrow$ $p\bar{p}K^+\pi^+\pi^-$

$\Gamma(\Lambda\bar{\Lambda}\pi^+\pi^-)/\Gamma_{total}$ Γ₂₅/Γ

VALUE (units 10^{-4})	EVTS	DOCUMENT ID	TECN	COMMENT
2.8±0.4±0.5	73.4	BRIERE	05 CLEO	$e^+e^- \rightarrow \psi(2S) \rightarrow$ $p\bar{p}2(\pi^+\pi^-)$

$\Gamma(\Lambda\bar{\Lambda})/\Gamma_{total}$ Γ₂₆/Γ

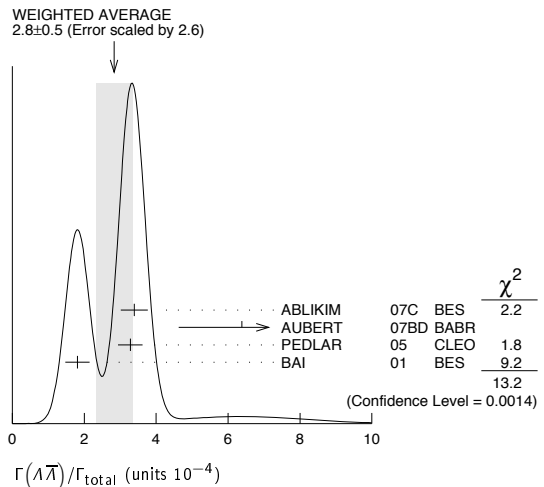
VALUE (units 10^{-4})	CL%	EVTS	DOCUMENT ID	TECN	COMMENT
2.8 ± 0.5 OUR AVERAGE			Error includes scale factor of 2.6. See the ideogram below.		
3.39±0.20±0.32		337	ABLIKIM	07c BES	$e^+e^- \rightarrow \psi(2S) \rightarrow$ hadrons
6.4 ± 1.8 ± 0.1			61 AUBERT	07BD BABR	10.6 $e^+e^- \rightarrow \Lambda\bar{\Lambda}\gamma$
3.28±0.23±0.25		208	PEDLAR	05 CLEO	$e^+e^- \rightarrow \psi(2S) \rightarrow$ hadrons
1.81±0.20±0.27		80	62 BAI	01 BES	$e^+e^- \rightarrow \psi(2S) \rightarrow$ hadrons

• • • We do not use the following data for averages, fits, limits, etc. • • •

< 4	90	FELDMAN	77	MRK1	$e^+e^- \rightarrow \psi(2S) \rightarrow$ hadrons
-----	----	---------	----	------	---

⁶¹ AUBERT 07BD reports $[\Gamma(\psi(2S) \rightarrow \Lambda\bar{\Lambda})/\Gamma_{total}] \times [\Gamma(\psi(2S) \rightarrow e^+e^-)] = (15 \pm 4 \pm 1) \times 10^{-4}$ keV which we divide by our best value $\Gamma(\psi(2S) \rightarrow e^+e^-) = 2.35 \pm 0.04$ keV. Our first error is their experiment's error and our second error is the systematic error from using our best value.

⁶² Estimated using $B(\psi(2S) \rightarrow J/\psi\pi^+\pi^-) = 0.310 \pm 0.028$.



$\Gamma(\Sigma^+\Sigma^-)/\Gamma_{total}$ Γ₂₇/Γ

VALUE (units 10^{-5})	EVTS	DOCUMENT ID	TECN	COMMENT
25.7±4.4±6.8	35	PEDLAR	05 CLEO	$e^+e^- \rightarrow \psi(2S) \rightarrow$ hadrons

$\Gamma(\Sigma^0\Sigma^0)/\Gamma_{total}$ Γ₂₈/Γ

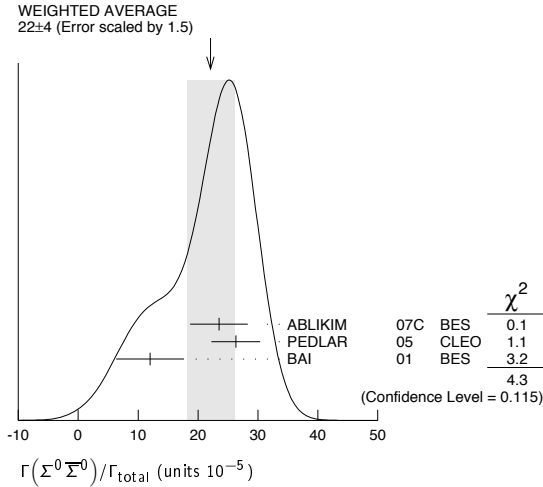
VALUE (units 10^{-5})	EVTS	DOCUMENT ID	TECN	COMMENT
22 ± 4 OUR AVERAGE		Error includes scale factor of 1.5. See the ideogram below.		
23.5±3.6±3.2	59	ABLIKIM	07c BES	$e^+e^- \rightarrow \psi(2S) \rightarrow$ hadrons
26.3±3.5±2.1	58	PEDLAR	05 CLEO	$e^+e^- \rightarrow \psi(2S) \rightarrow$ hadrons
12 ± 4 ± 4	8	63 BAI	01 BES	$e^+e^- \rightarrow \psi(2S) \rightarrow$ hadrons

⁶³ Estimated using $B(\psi(2S) \rightarrow J/\psi\pi^+\pi^-) = 0.310 \pm 0.028$.

See key on page 405

Meson Particle Listings

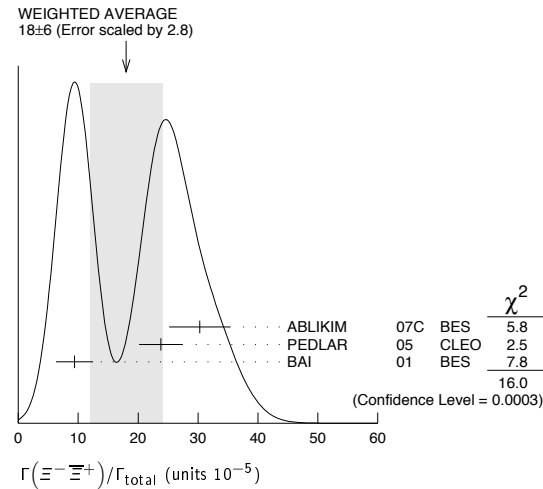
$\psi(2S)$



$\Gamma(\Sigma(1385)^+\Sigma(1385)^-)/\Gamma_{total}$ Γ₂₉/Γ				
VALUE (units 10 ⁻⁵)	EVTS	DOCUMENT ID	TECN	COMMENT
11±3±3	14	64 BAI	01 BES	$e^+e^- \rightarrow \psi(2S) \rightarrow$ hadrons

⁶⁴ Estimated using $B(\psi(2S) \rightarrow J/\psi\pi^+\pi^-) = 0.310 \pm 0.028$.

$\Gamma(\Xi^-\Xi^+)/\Gamma_{total}$ Γ₃₀/Γ					
VALUE (units 10 ⁻⁵)	CL%	EVTS	DOCUMENT ID	TECN	COMMENT
18 ± 6 OUR AVERAGE					Error includes scale factor of 2.8. See the ideogram below.
30.3±4.0±3.2		67	ABLIKIM	07c BES	$e^+e^- \rightarrow \psi(2S) \rightarrow$ hadrons
23.8±3.0±2.1		63	PEDLAR	05 CLEO	$e^+e^- \rightarrow \psi(2S) \rightarrow$ hadrons
9.4±2.7±1.5		12	65 BAI	01 BES	$e^+e^- \rightarrow \psi(2S) \rightarrow$ hadrons
• • • We do not use the following data for averages, fits, limits, etc. • • •					
<20		90	FELDMAN	77 MRK1	$e^+e^- \rightarrow \psi(2S) \rightarrow$ hadrons
⁶⁵ Estimated using $B(\psi(2S) \rightarrow J/\psi\pi^+\pi^-) = 0.310 \pm 0.028$.					



$\Gamma(\Xi^0\Xi^0)/\Gamma_{total}$ Γ₃₁/Γ				
VALUE (units 10 ⁻⁵)	EVTS	DOCUMENT ID	TECN	COMMENT
27.5±6.4±6.1	19	PEDLAR	05 CLEO	$e^+e^- \rightarrow \psi(2S) \rightarrow$ hadrons

$\Gamma(\Xi(1530)^0\Xi(1530)^0)/\Gamma_{total}$ Γ₃₂/Γ				
VALUE (units 10 ⁻⁵)	CL%	DOCUMENT ID	TECN	COMMENT
< 8.1	90	66 BAI	01 BES	$e^+e^- \rightarrow \psi(2S) \rightarrow$ hadrons
• • • We do not use the following data for averages, fits, limits, etc. • • •				
<32		90	PEDLAR	05 CLEO $e^+e^- \rightarrow \psi(2S) \rightarrow$ hadrons
⁶⁶ Estimated using $B(\psi(2S) \rightarrow J/\psi\pi^+\pi^-) = 0.310 \pm 0.028$.				

$\Gamma(\Omega^-\bar{\Omega}^+)/\Gamma_{total}$ Γ₃₃/Γ				
VALUE (units 10 ⁻⁵)	CL%	DOCUMENT ID	TECN	COMMENT
< 7.3	90	67 BAI	01 BES	$e^+e^- \rightarrow \psi(2S) \rightarrow$ hadrons
• • • We do not use the following data for averages, fits, limits, etc. • • •				
<16		90	PEDLAR	05 CLEO $e^+e^- \rightarrow \psi(2S) \rightarrow$ hadrons
⁶⁷ Estimated using $B(\psi(2S) \rightarrow J/\psi\pi^+\pi^-) = 0.310 \pm 0.028$.				

$\Gamma(\pi^0\rho\bar{\rho})/\Gamma_{total}$ Γ₃₄/Γ				
VALUE (units 10 ⁻⁴)	EVTS	DOCUMENT ID	TECN	COMMENT
1.33±0.17 OUR AVERAGE				
1.32±0.10±0.15	256 ± 18	68 ABLIKIM	05E BES2	$e^+e^- \rightarrow \psi(2S) \rightarrow$ $\rho\bar{\rho}\gamma\gamma$
1.4 ± 0.5	9	FRANKLIN	83 MRK2	$e^+e^- \rightarrow \rho\bar{\rho}\gamma\gamma$
⁶⁸ Computed using $B(\pi^0 \rightarrow \gamma\gamma) = (98.80 \pm 0.03)\%$.				

$\Gamma(\eta\rho\bar{\rho})/\Gamma_{total}$ Γ₃₅/Γ				
VALUE (units 10 ⁻⁴)	EVTS	DOCUMENT ID	TECN	COMMENT
0.60±0.12 OUR AVERAGE				
0.58±0.11±0.07	44.8 ± 8.5	69 ABLIKIM	05E BES2	$e^+e^- \rightarrow \psi(2S) \rightarrow$ $\rho\bar{\rho}\gamma\gamma$
0.8 ± 0.3 ± 0.3	9.8	BRIERE	05 CLEO	$e^+e^- \rightarrow \psi(2S) \rightarrow$ $\rho\bar{\rho}\pi^+\pi^-\pi^0$
⁶⁹ Computed using $B(\eta \rightarrow \gamma\gamma) = (39.43 \pm 0.26)\%$.				

$\Gamma(\omega\rho\bar{\rho})/\Gamma_{total}$ Γ₃₆/Γ				
VALUE (units 10 ⁻⁴)	EVTS	DOCUMENT ID	TECN	COMMENT
0.69±0.21 OUR AVERAGE				
0.6 ± 0.2 ± 0.2	21.2	BRIERE	05 CLEO	$e^+e^- \rightarrow \psi(2S) \rightarrow$ $\rho\bar{\rho}\pi^+\pi^-\pi^0$
0.8 ± 0.3 ± 0.1	14.9 ± 0.1	70 BAI	03B BES	$\psi(2S) \rightarrow \rho\bar{\rho}\pi^+\pi^-\pi^0$
⁷⁰ Normalized to $B(\psi(2S) \rightarrow J/\psi\pi^+\pi^-) = 0.305 \pm 0.016$.				

$\Gamma(\phi\rho\bar{\rho})/\Gamma_{total}$ Γ₃₇/Γ				
VALUE (units 10 ⁻⁴)	CL%	DOCUMENT ID	TECN	COMMENT
<0.24	90	BRIERE	05 CLEO	$e^+e^- \rightarrow \psi(2S) \rightarrow$ $\rho\bar{\rho}K^+K^-$
• • • We do not use the following data for averages, fits, limits, etc. • • •				
<0.26		90	71 BAI	03B BES $\psi(2S) \rightarrow K^+K^-\rho\bar{\rho}$
⁷¹ Normalized to $B(\psi(2S) \rightarrow J/\psi\pi^+\pi^-) = 0.305 \pm 0.016$.				

$\Gamma(\pi^+\pi^-\rho\bar{\rho})/\Gamma_{total}$ Γ₃₈/Γ				
VALUE (units 10 ⁻⁴)	EVTS	DOCUMENT ID	TECN	COMMENT
6.0±0.4 OUR AVERAGE				
5.9±0.2±0.4	904.5	BRIERE	05 CLEO	$e^+e^- \rightarrow \psi(2S) \rightarrow$ $\rho\bar{\rho}\pi^+\pi^-$
8 ± 2		72 TANENBAUM	78 MRK1	e^+e^-
⁷² Assuming entirely strong decay.				

$\Gamma(\rho\bar{\rho}\pi^- \text{ or c.c.})/\Gamma_{total}$ Γ₃₉/Γ				
VALUE (units 10 ⁻⁴)	EVTS	DOCUMENT ID	TECN	COMMENT
2.48±0.17 OUR AVERAGE				
2.45±0.11±0.21	851	ABLIKIM	06i BES2	$e^+e^- \rightarrow p\pi^-X$
2.52±0.12±0.22	849	ABLIKIM	06i BES2	$e^+e^- \rightarrow \bar{p}\pi^+X$

$\Gamma(\rho\bar{\rho}\pi^-\pi^0)/\Gamma_{total}$ Γ₄₀/Γ				
VALUE (units 10 ⁻⁴)	EVTS	DOCUMENT ID	TECN	COMMENT
3.18±0.50±0.50	135 ± 21	ABLIKIM	06i BES2	$e^+e^- \rightarrow p\pi^-\pi^0X$

$\Gamma(\eta\pi^+\pi^-)/\Gamma_{total}$ Γ₄₂/Γ				
VALUE (units 10 ⁻⁴)	CL%	DOCUMENT ID	TECN	COMMENT
<1.6	90	BRIERE	05 CLEO	$e^+e^- \rightarrow \psi(2S) \rightarrow$ $2(\pi^+\pi^-\pi^0)$

$\Gamma(\eta\pi^+\pi^-\pi^0)/\Gamma_{total}$ Γ₄₃/Γ				
VALUE (units 10 ⁻⁴)	EVTS	DOCUMENT ID	TECN	COMMENT
9.5±0.7±1.5		73 BRIERE	05 CLEO	$e^+e^- \rightarrow \psi(2S) \rightarrow$ hadr
• • • We do not use the following data for averages, fits, limits, etc. • • •				
10.3±0.8±1.4	201.7	74 BRIERE	05 CLEO	$e^+e^- \rightarrow \psi(2S) \rightarrow$ $\eta 3\pi(\eta \rightarrow \gamma\gamma)$
8.1±1.4±1.6	50.0	74 BRIERE	05 CLEO	$e^+e^- \rightarrow \psi(2S) \rightarrow$ $\eta 3\pi(\eta \rightarrow 3\pi)$
⁷³ Average of $\eta \rightarrow \gamma\gamma$ and $\eta \rightarrow 3\pi$.				
⁷⁴ Not independent from other values reported by BRIERE 05.				

$\Gamma(2(\pi^+\pi^-\eta))/\Gamma_{total}$ Γ₄₄/Γ				
VALUE (units 10 ⁻³)	EVTS	DOCUMENT ID	TECN	COMMENT
1.2±0.6±0.1	16	75 AUBERT	07AU BABR	10.6 $e^+e^- \rightarrow 2(\pi^+\pi^-\eta)\gamma$
⁷⁵ AUBERT 07AU quotes $\Gamma_{ee}^{\psi(2S)} \cdot B(\psi(2S) \rightarrow 2(\pi^+\pi^-\eta)) \cdot B(\eta \rightarrow \gamma\gamma) = 1.2 \pm 0.7 \pm 0.1 \text{ eV}$.				

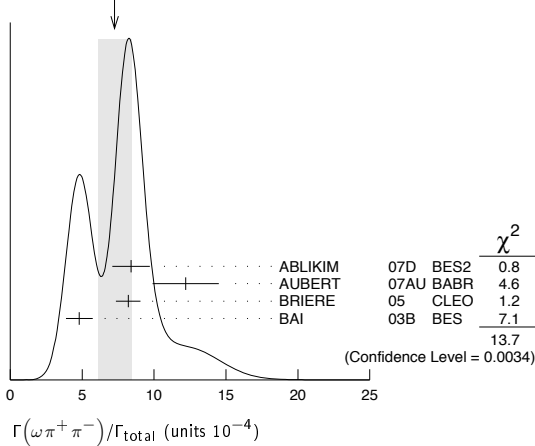
$\Gamma(\eta^+\pi^-\pi^-\pi^0)/\Gamma_{total}$ Γ₄₅/Γ				
VALUE (units 10 ⁻⁴)	EVTS	DOCUMENT ID	TECN	COMMENT
4.5±1.6±1.3	12.8	BRIERE	05 CLEO	$e^+e^- \rightarrow \psi(2S) \rightarrow$ hadr

Meson Particle Listings

 $\psi(2S)$

$\Gamma(\omega\pi^+\pi^-)/\Gamma_{\text{total}}$	Γ_{46}/Γ
7.3±1.2 OUR AVERAGE	Error includes scale factor of 2.1. See the ideogram below.
8.4±0.5±1.2 386	ABLIKIM 07D BES2 $e^+e^- \rightarrow \psi(2S)$
12.2±2.2±0.7 37	76 AUBERT 07AU BABR 10.6 $e^+e^- \rightarrow \omega\pi^+\pi^-\gamma$
8.2±0.5±0.7 391	BRIERE 05 CLEO $e^+e^- \rightarrow \psi(2S) \rightarrow 2(\pi^+\pi^-)\pi^0$
4.8±0.6±0.7 100±22	77 BAI 03B BES $\psi(2S) \rightarrow 2(\pi^+\pi^-)\pi^0$
76 AUBERT 07AU quotes $\Gamma_{ee}^{\psi(2S)} \cdot B(\psi(2S) \rightarrow \omega\pi^+\pi^-) \cdot B(\omega \rightarrow 3\pi) = 2.69 \pm 0.73 \pm 0.16$ eV.	
77 Normalized to $B(\psi(2S) \rightarrow J/\psi\pi^+\pi^-) = 0.305 \pm 0.016$.	

WEIGHTED AVERAGE
7.3±1.2 (Error scaled by 2.1)



$\Gamma(b_1^+\pi^\mp)/\Gamma_{\text{total}}$	Γ_{47}/Γ
4.0 ± 0.6 OUR AVERAGE	Error includes scale factor of 1.1.
5.1 ± 0.6 ± 0.8 202	ABLIKIM 07D BES2 $e^+e^- \rightarrow \psi(2S)$
4.18 ^{+0.43} _{-0.42} ± 0.92 170	ADAM 05 CLEO $e^+e^- \rightarrow \psi(2S)$
3.2 ± 0.6 ± 0.5 61 ± 11	78,79 BAI 03B BES $\psi(2S) \rightarrow 2(\pi^+\pi^-)\pi^0$
• • • We do not use the following data for averages, fits, limits, etc. • • •	
5.2 ± 0.8 ± 1.0	78 BAI 99c BES Repl. by BAI 03B
78 Assuming $B(b_1 \rightarrow \omega\pi) = 1$.	
79 Normalized to $B(\psi(2S) \rightarrow J/\psi\pi^+\pi^-) = 0.305 \pm 0.016$.	

$\Gamma(b_1^0\pi^0)/\Gamma_{\text{total}}$	Γ_{48}/Γ
2.35^{+0.47}_{-0.42} ± 0.40	
45	ADAM 05 CLEO $e^+e^- \rightarrow \psi(2S)$

$\Gamma(\omega f_2(1270))/\Gamma_{\text{total}}$	Γ_{49}/Γ
2.2 ± 0.4 OUR AVERAGE	
2.3 ± 0.5 ± 0.4 57	ABLIKIM 07D BES2 $e^+e^- \rightarrow \psi(2S)$
2.05 ± 0.41 ± 0.38 62 ± 12	BAI 04c BES2 $\psi(2S) \rightarrow 2(\pi^+\pi^-)\pi^0$
• • • We do not use the following data for averages, fits, limits, etc. • • •	
<1.5 90	80 BAI 03B BES $\psi(2S) \rightarrow 2(\pi^+\pi^-)\pi^0$
<1.7 90	BAI 98J BES Repl. by BAI 03B
80 Normalized to $B(\psi(2S) \rightarrow J/\psi\pi^+\pi^-) = 0.305 \pm 0.016$.	

$\Gamma(\pi^+\pi^-K^+K^-)/\Gamma_{\text{total}}$	Γ_{50}/Γ
7.5 ± 0.9 OUR AVERAGE	Error includes scale factor of 1.9.
10.9 ± 1.9 ± 0.2 85	81 AUBERT 07AK BABR 10.6 $e^+e^- \rightarrow \pi^+\pi^-K^+K^-\gamma$
7.1 ± 0.3 ± 0.4 817.2	BRIERE 05 CLEO $e^+e^- \rightarrow \psi(2S) \rightarrow K^+K^-\pi^+\pi^-$
16 ± 4	82 TANENBAUM 78 MRK1 e^+e^-
81 AUBERT 07AK reports $[\Gamma(\psi(2S) \rightarrow \pi^+\pi^-K^+K^-)/\Gamma_{\text{total}}] \times [\Gamma(\psi(2S) \rightarrow e^+e^-)] = (2.56 \pm 0.42 \pm 0.16) \times 10^{-3}$ keV which we divide by our best value $\Gamma(\psi(2S) \rightarrow e^+e^-) = 2.35 \pm 0.04$ keV. Our first error is their experiment's error and our second error is the systematic error from using our best value.	
82 Assuming entirely strong decay.	

$\Gamma(\rho^0 K^+ K^-)/\Gamma_{\text{total}}$	Γ_{51}/Γ
2.2 ± 0.2 ± 0.4	
223.8	BRIERE 05 CLEO $e^+e^- \rightarrow \psi(2S) \rightarrow K^+K^-\pi^+\pi^-$

$\Gamma(K^*(892)^0 \bar{K}_2^0(1430)^0)/\Gamma_{\text{total}}$	Γ_{52}/Γ
1.86 ± 0.32 ± 0.43	
93 ± 16	BAI 04c $\psi(2S) \rightarrow K^+K^-\pi^+\pi^-$
• • • We do not use the following data for averages, fits, limits, etc. • • •	
<1.2 90	BAI 98J BES e^+e^-

$\Gamma(K^+K^-\pi^+\pi^-)/\Gamma_{\text{total}}$	Γ_{53}/Γ
1.3 ± 0.7 ± 0.1	
7	83 AUBERT 07AU BABR 10.6 $e^+e^- \rightarrow K^+K^-\pi^+\pi^-\eta\gamma$
83 AUBERT 07AU quotes $\Gamma_{ee}^{\psi(2S)} \cdot B(\psi(2S) \rightarrow 2(\pi^+\pi^-)\eta) \cdot B(\eta \rightarrow \gamma\gamma) = 1.2 \pm 0.7 \pm 0.1$ eV.	

$\Gamma(K^+K^-2(\pi^+\pi^-)\pi^0)/\Gamma_{\text{total}}$	Γ_{54}/Γ
10.0 ± 2.5 ± 1.8	
65	ABLIKIM 07D BES2 $e^+e^- \rightarrow \psi(2S)$

$\Gamma(K_1(1270)^\pm K^\mp)/\Gamma_{\text{total}}$	Γ_{56}/Γ
10.0 ± 1.8 ± 2.1	
84 BAI 99c BES e^+e^-	
84 Assuming $B(K_1(1270) \rightarrow K\rho) = 0.42 \pm 0.06$	

$\Gamma(K_S^0 K_S^0 \pi^+\pi^-)/\Gamma_{\text{total}}$	Γ_{57}/Γ
2.20 ± 0.25 ± 0.37	
83 ± 9	ABLIKIM 05b BES2 $e^+e^- \rightarrow \psi(2S)$

$\Gamma(\rho^0 \rho^0)/\Gamma_{\text{total}}$	Γ_{58}/Γ
0.5 ± 0.1 ± 0.2	
61.1	BRIERE 05 CLEO $e^+e^- \rightarrow \psi(2S) \rightarrow \rho^0\pi^+\pi^-$

$\Gamma(K^+\bar{K}^*(892)^0\pi^- + \text{c.c.})/\Gamma_{\text{total}}$	Γ_{59}/Γ
6.7 ± 2.5	
	TANENBAUM 78 MRK1 e^+e^-

$\Gamma(2(\pi^+\pi^-))/\Gamma_{\text{total}}$	Γ_{60}/Γ
2.4 ± 0.6 OUR AVERAGE	Error includes scale factor of 2.2.
2.2 ± 0.2 ± 0.2 308	BRIERE 05 CLEO $e^+e^- \rightarrow \psi(2S) \rightarrow 2(\pi^+\pi^-)$
4.5 ± 1.0	TANENBAUM 78 MRK1 e^+e^-

$\Gamma(\rho^0\pi^+\pi^-)/\Gamma_{\text{total}}$	Γ_{61}/Γ
2.2 ± 0.6 OUR AVERAGE	Error includes scale factor of 1.4.
2.0 ± 0.2 ± 0.4 285.5	BRIERE 05 CLEO $e^+e^- \rightarrow \psi(2S) \rightarrow 2(\pi^+\pi^-)$
4.2 ± 1.5	TANENBAUM 78 MRK1 e^+e^-

$\Gamma(K^+K^-\pi^+\pi^-)/\Gamma_{\text{total}}$	Γ_{62}/Γ
12.6 ± 0.9 OUR AVERAGE	
18.7 ± 5.7 ± 0.3 32	85 AUBERT 07AU BABR 10.6 $e^+e^- \rightarrow K^+K^-\pi^+\pi^-\pi^0\gamma$
11.7 ± 1.0 ± 1.5 597	ABLIKIM 06G BES2 $\psi(2S) \rightarrow K^+K^-\pi^+\pi^-\pi^0$
12.7 ± 0.5 ± 1.0 711.6	BRIERE 05 CLEO $e^+e^- \rightarrow \psi(2S) \rightarrow K^+K^-\pi^+\pi^-\pi^0$
85 AUBERT 07AU reports $[\Gamma(\psi(2S) \rightarrow K^+K^-\pi^+\pi^-\pi^0)/\Gamma_{\text{total}}] \times [\Gamma(\psi(2S) \rightarrow e^+e^-)] = (44 \pm 13 \pm 3) \times 10^{-4}$ keV which we divide by our best value $\Gamma(\psi(2S) \rightarrow e^+e^-) = 2.35 \pm 0.04$ keV. Our first error is their experiment's error and our second error is the systematic error from using our best value.	

$\Gamma(\omega f_0(1710) \rightarrow \omega K^+ K^-)/\Gamma_{\text{total}}$	Γ_{63}/Γ
5.9 ± 2.0 ± 0.9	
19	ABLIKIM 06G BES2 $\psi(2S) \rightarrow K^+K^-\pi^+\pi^-\pi^0$

$\Gamma(K^*(892)^0 K^-\pi^+\pi^0 + \text{c.c.})/\Gamma_{\text{total}}$	Γ_{64}/Γ
8.6 ± 1.3 ± 1.8	
238	ABLIKIM 06G BES2 $\psi(2S) \rightarrow K^+K^-\pi^+\pi^-\pi^0$

$\Gamma(K^*(892)^+ K^-\pi^+\pi^- + \text{c.c.})/\Gamma_{\text{total}}$	Γ_{65}/Γ
9.6 ± 2.2 ± 1.7	
133	ABLIKIM 06G BES2 $\psi(2S) \rightarrow K^+K^-\pi^+\pi^-\pi^0$

$\Gamma(K^*(892)^+ K^-\rho^0 + \text{c.c.})/\Gamma_{\text{total}}$	Γ_{66}/Γ
7.3 ± 2.2 ± 1.4	
78	ABLIKIM 06G BES2 $\psi(2S) \rightarrow K^+K^-\pi^+\pi^-\pi^0$

See key on page 405

Meson Particle Listings

$\psi(2S)$

$\Gamma(K^*(892)^0 K^- \rho^+ + \text{c.c.})/\Gamma_{\text{total}}$					Γ_{67}/Γ
VALUE (units 10^{-4})	EVTS	DOCUMENT ID	TECN	COMMENT	
6.1 ± 1.3 ± 1.2	125	ABLIKIM	06G BES2	$\psi(2S) \rightarrow K^+ K^- \pi^+ \pi^- \pi^0$	

$\Gamma(\eta K^+ K^-)/\Gamma_{\text{total}}$					Γ_{68}/Γ
VALUE (units 10^{-4})	CL%	DOCUMENT ID	TECN	COMMENT	
<1.3	90	BRIERE	05 CLEO	$e^+ e^- \rightarrow \psi(2S) \rightarrow K^+ K^- \pi^+ \pi^- \pi^0$	

$\Gamma(\omega K^+ K^-)/\Gamma_{\text{total}}$					Γ_{69}/Γ
VALUE (units 10^{-4})	EVTS	DOCUMENT ID	TECN	COMMENT	
1.85 ± 0.25 OUR AVERAGE	Error includes scale factor of 1.1.				
2.38 ± 0.37 ± 0.29	78	ABLIKIM	06G BES2	$\psi(2S) \rightarrow K^+ K^- \pi^+ \pi^- \pi^0$	
1.9 ± 0.3 ± 0.3	76.8	BRIERE	05 CLEO	$e^+ e^- \rightarrow \psi(2S) \rightarrow K^+ K^- \pi^+ \pi^- \pi^0$	
1.5 ± 0.3 ± 0.2	23.0 ± 5.2	⁸⁶ BAI	03B BES	$\psi(2S) \rightarrow K^+ K^- \pi^+ \pi^- \pi^0$	

⁸⁶ Normalized to $B(\psi(2S) \rightarrow J/\psi \pi^+ \pi^-) = 0.305 \pm 0.016$.

$\Gamma(3(\pi^+ \pi^-))/\Gamma_{\text{total}}$					Γ_{70}/Γ
VALUE (units 10^{-4})	EVTS	DOCUMENT ID	TECN	COMMENT	
3.5 ± 2.0 OUR AVERAGE	Error includes scale factor of 2.8.				
5.45 ± 0.42 ± 0.87	671	ABLIKIM	05H BES2	$e^+ e^- \rightarrow \psi(2S) \rightarrow 3(\pi^+ \pi^-)$	
1.5 ± 1.0		⁸⁷ TANENBAUM	78 MRK1	$e^+ e^-$	

⁸⁷ Assuming entirely strong decay.

$\Gamma(p\bar{p} \pi^+ \pi^- \pi^0)/\Gamma_{\text{total}}$					Γ_{71}/Γ
VALUE (units 10^{-4})	EVTS	DOCUMENT ID	TECN	COMMENT	
7.3 ± 0.4 ± 0.6	434.9	BRIERE	05 CLEO	$e^+ e^- \rightarrow \psi(2S) \rightarrow p\bar{p} \pi^+ \pi^- \pi^0$	

$\Gamma(K^+ K^-)/\Gamma_{\text{total}}$					Γ_{72}/Γ
VALUE (units 10^{-5})	CL%	DOCUMENT ID	TECN	COMMENT	
6.3 ± 0.7 OUR AVERAGE					
6.3 ± 0.6 ± 0.3		DOBBS	06A CLEO	$e^+ e^-$	
10 ± 7		BRANDELIK	79C DASP	$e^+ e^-$	

••• We do not use the following data for averages, fits, limits, etc. •••

< 5	90	FELDMAN	77 MRK1	$e^+ e^-$	
-----	----	---------	---------	-----------	--

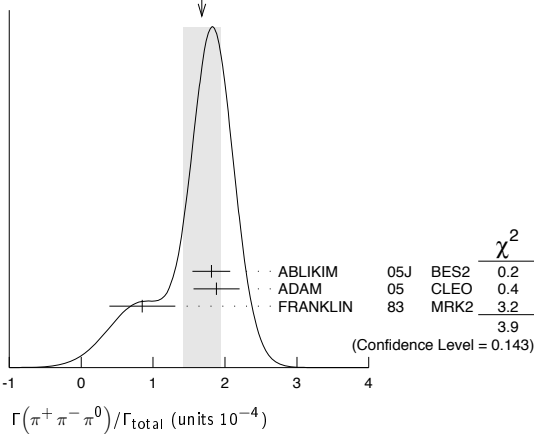
$\Gamma(K_S^0 K_L^0)/\Gamma_{\text{total}}$					Γ_{73}/Γ
VALUE (units 10^{-5})	EVTS	DOCUMENT ID	TECN	COMMENT	
5.4 ± 0.5 OUR AVERAGE					
5.8 ± 0.8 ± 0.4		DOBBS	06A CLEO	$e^+ e^-$	
5.24 ± 0.47 ± 0.48	156 ± 14	⁸⁸ BAI	04B BES2	$\psi(2S) \rightarrow K_S^0 K_L^0 \rightarrow \pi^+ \pi^- X$	

⁸⁸ Using $B(K_S^0 \rightarrow \pi^+ \pi^-) = 0.6860 \pm 0.0027$.

$\Gamma(\pi^+ \pi^- \pi^0)/\Gamma_{\text{total}}$					Γ_{74}/Γ
VALUE (units 10^{-4})	EVTS	DOCUMENT ID	TECN	COMMENT	
1.68 ± 0.26 OUR AVERAGE	Error includes scale factor of 1.4. See the ideogram below.				
1.81 ± 0.18 ± 0.19	260 ± 19	⁸⁹ ABLIKIM	05J BES2	$e^+ e^- \rightarrow \psi(2S)$	
1.88 ± 0.16 ± 0.28	194	ADAM	05 CLEO	$e^+ e^- \rightarrow \psi(2S)$	
0.85 ± 0.46	4	FRANKLIN	83 MRK2	$e^+ e^- \rightarrow \text{hadrons}$	

⁸⁹ From a PW analysis of $\psi(2S) \rightarrow \pi^+ \pi^- \pi^0$.

WEIGHTED AVERAGE
1.68 ± 0.26 (Error scaled by 1.4)



$\Gamma(\rho(2150) \pi \rightarrow \pi^+ \pi^- \pi^0)/\Gamma_{\text{total}}$					Γ_{75}/Γ
VALUE (units 10^{-4})	DOCUMENT ID	TECN	COMMENT		
1.94 ± 0.25 ± 1.15 - 0.34	⁹⁰ ABLIKIM	05J BES2	$\psi(2S) \rightarrow \rho(2150) \pi \rightarrow \pi^+ \pi^- \pi^0$		

⁹⁰ From a PW analysis of $\psi(2S) \rightarrow \pi^+ \pi^- \pi^0$.

$\Gamma(\rho(770) \pi \rightarrow \pi^+ \pi^- \pi^0)/\Gamma_{\text{total}}$					Γ_{76}/Γ
VALUE (units 10^{-4})	CL%	EVTS	DOCUMENT ID	TECN	COMMENT
0.32 ± 0.12 OUR AVERAGE	Error includes scale factor of 1.8.				
0.51 ± 0.07 ± 0.11			⁹¹ ABLIKIM	05J BES2	$\psi(2S) \rightarrow \rho(770) \pi \rightarrow \pi^+ \pi^- \pi^0$
0.24 + 0.08 - 0.07 ± 0.02		22	ADAM	05 CLEO	$e^+ e^- \rightarrow \psi(2S)$

••• We do not use the following data for averages, fits, limits, etc. •••

< 0.83	90	1	FRANKLIN	83 MRK2	$e^+ e^-$
< 10	90		BARTEL	76 CNTR	$e^+ e^-$
< 10	90		⁹² ABRAMS	75 MRK1	$e^+ e^-$

⁹¹ From a PW analysis of $\psi(2S) \rightarrow \pi^+ \pi^- \pi^0$.
⁹² Final state $\rho^0 \pi^0$.

$\Gamma(\pi^+ \pi^-)/\Gamma_{\text{total}}$					Γ_{77}/Γ
VALUE (units 10^{-5})	CL%	DOCUMENT ID	TECN	COMMENT	
8 ± 5		BRANDELIK	79C DASP	$e^+ e^-$	

••• We do not use the following data for averages, fits, limits, etc. •••

< 2.1	90	DOBBS	06A CLEO	$e^+ e^- \rightarrow \psi(2S)$
< 5	90	FELDMAN	77 MRK1	$e^+ e^-$

$\Gamma(K_1(1400)^\pm K^\mp)/\Gamma_{\text{total}}$					Γ_{78}/Γ
VALUE (units 10^{-4})	CL%	DOCUMENT ID	TECN	COMMENT	
< 3.1	90	⁹³ BAI	99C BES	$e^+ e^-$	

⁹³ Assuming $B(K_1(1400) \rightarrow K^* \pi) = 0.94 \pm 0.06$.

$\Gamma(K^+ K^- \pi^0)/\Gamma_{\text{total}}$					Γ_{79}/Γ
VALUE (units 10^{-5})	CL%	EVTS	DOCUMENT ID	TECN	COMMENT
< 2.96	90	1	FRANKLIN	83 MRK2	$e^+ e^- \rightarrow \text{hadrons}$

$\Gamma(K^+ \bar{K}^*(892)^- + \text{c.c.})/\Gamma_{\text{total}}$					Γ_{80}/Γ
VALUE (units 10^{-5})	CL%	EVTS	DOCUMENT ID	TECN	COMMENT
1.7 + 0.8 - 0.7 OUR AVERAGE					
2.9 + 1.3 - 1.7 ± 0.4	9.6 ± 4.2		ABLIKIM	05I BES2	$e^+ e^- \rightarrow \psi(2S)$
1.3 + 1.0 - 0.7 ± 0.3	7		ADAM	05 CLEO	$e^+ e^- \rightarrow \psi(2S)$

••• We do not use the following data for averages, fits, limits, etc. •••

< 5.4	90		FRANKLIN	83 MRK2	$e^+ e^- \rightarrow \text{hadrons}$
-------	----	--	----------	---------	--------------------------------------

$\Gamma(K^*(892)^0 \bar{K}^0 + \text{c.c.})/\Gamma_{\text{total}}$					Γ_{81}/Γ
VALUE (units 10^{-5})	EVTS	DOCUMENT ID	TECN	COMMENT	
10.9 ± 2.0 OUR AVERAGE					
13.3 + 2.4 - 2.8 ± 1.7	65.6 ± 9.0		ABLIKIM	05I BES2	$e^+ e^- \rightarrow \psi(2S)$
9.2 + 2.7 - 2.2 ± 0.9	25		ADAM	05 CLEO	$e^+ e^- \rightarrow \psi(2S)$

$\Gamma(K^+ \bar{K}^*(892)^- + \text{c.c.})/\Gamma(K^*(892)^0 \bar{K}^0 + \text{c.c.})$					Γ_{80}/Γ_{81}
VALUE	DOCUMENT ID	TECN	COMMENT		
0.16 ± 0.06 OUR AVERAGE					
0.22 + 0.10 - 0.14	ABLIKIM	05I BES2	$e^+ e^- \rightarrow \psi(2S)$		
0.14 + 0.08 - 0.06	ADAM	05 CLEO	$e^+ e^- \rightarrow \psi(2S)$		

$\Gamma(\phi \pi^+ \pi^-)/\Gamma_{\text{total}}$					Γ_{82}/Γ
VALUE (units 10^{-4})	EVTS	DOCUMENT ID	TECN	COMMENT	
1.17 ± 0.29 OUR AVERAGE	Error includes scale factor of 1.7.				
2.43 ± 0.95 ± 0.04	10 ± 4	^{94,95} AUBERT	07AK BABR	$10.6 e^+ e^- \rightarrow \pi^+ \pi^- K^+ K^- \gamma$	
0.9 ± 0.2 ± 0.1	47.6	BRIERE	05 CLEO	$e^+ e^- \rightarrow \psi(2S) \rightarrow K^+ K^- \pi^+ \pi^-$	
1.5 ± 0.2 ± 0.2	51.5 ± 8.3	⁹⁶ BAI	03B BES	$\psi(2S) \rightarrow K^+ K^- \pi^+ \pi^-$	

⁹⁴ AUBERT 07AK reports $[\Gamma(\psi(2S) \rightarrow \phi \pi^+ \pi^-)/\Gamma_{\text{total}}] \times [\Gamma(\psi(2S) \rightarrow e^+ e^-)] = (0.57 \pm 0.22 \pm 0.04) \times 10^{-3}$ keV which we divide by our best value $\Gamma(\psi(2S) \rightarrow e^+ e^-) = 2.35 \pm 0.04$ keV. Our first error is their experiment's error and our second error is the systematic error from using our best value.
⁹⁵ Using $B(\phi \rightarrow K^+ K^-) = (49.3 \pm 0.6)\%$.
⁹⁶ Normalized to $B(\psi(2S) \rightarrow J/\psi \pi^+ \pi^-) = 0.305 \pm 0.016$.

$$[\Gamma(\gamma\chi_{c0}(1P)) + \Gamma(\gamma\chi_{c1}(1P)) + \Gamma(\gamma\chi_{c2}(1P))]/\Gamma_{\text{total}} \quad (\Gamma_{105} + \Gamma_{106} + \Gamma_{107})/\Gamma$$

VALUE	DOCUMENT ID	TECN	COMMENT
$27.6 \pm 0.3 \pm 2.0$	110 ATHAR	04	CLEO $e^+e^- \rightarrow \gamma X$
110 Not independent from ATHAR 04 measurements of $B(\gamma\chi_{cJ})$.			

$$\Gamma(\gamma\chi_{c0}(1P))/\Gamma(\gamma\chi_{c1}(1P)) \quad \Gamma_{105}/\Gamma_{106}$$

VALUE	DOCUMENT ID	TECN	COMMENT
$1.02 \pm 0.01 \pm 0.07$	111 ATHAR	04	CLEO $e^+e^- \rightarrow \gamma X$
111 Not independent from ATHAR 04 measurements of $B(\gamma\chi_{cJ})$.			

$$\Gamma(\gamma\chi_{c2}(1P))/\Gamma(\gamma\chi_{c1}(1P)) \quad \Gamma_{107}/\Gamma_{106}$$

VALUE	DOCUMENT ID	TECN	COMMENT
$1.03 \pm 0.02 \pm 0.03$	112 ATHAR	04	CLEO $e^+e^- \rightarrow \gamma X$
112 Not independent from ATHAR 04 measurements of $B(\gamma\chi_{cJ})$.			

$$\Gamma(\gamma\chi_{c0}(1P))/\Gamma(\gamma\chi_{c2}(1P)) \quad \Gamma_{105}/\Gamma_{107}$$

VALUE	DOCUMENT ID	TECN	COMMENT
$0.99 \pm 0.02 \pm 0.08$	113 ATHAR	04	CLEO $e^+e^- \rightarrow \gamma X$
113 Not independent from ATHAR 04 measurements of $B(\gamma\chi_{cJ})$.			

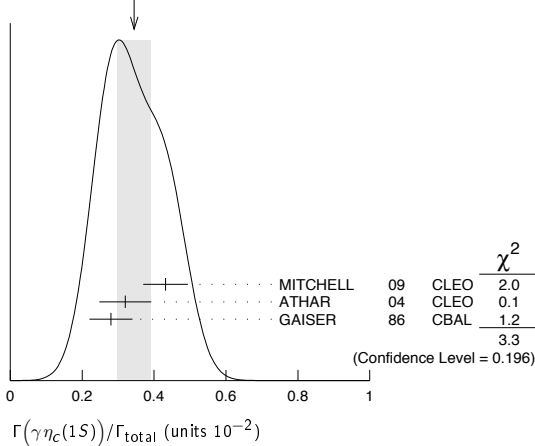
$$\Gamma(\pi^0 h_c \rightarrow \gamma \eta_c(1S) \pi^0)/\Gamma_{\text{total}} \quad \Gamma_{108}/\Gamma$$

VALUE (units 10^{-4})	EVTS	DOCUMENT ID	TECN	COMMENT
$4.16 \pm 0.30 \pm 0.37$	1282	114 DOBBS	08A	CLEO $\psi(2S) \rightarrow \pi^0 \eta_c \gamma$
114 Combination of exclusive and inclusive analyses for the reaction $\psi(2S) \rightarrow \pi^0 h_c \rightarrow \pi^0 \eta_c \gamma$. This result is the average of DOBBS 08A and ROSNER 05.				

$$\Gamma(\gamma \eta_c(1S))/\Gamma_{\text{total}} \quad \Gamma_{109}/\Gamma$$

VALUE (units 10^{-2})	EVTS	DOCUMENT ID	TECN	COMMENT
0.34 ± 0.05 OUR AVERAGE		Error includes scale factor of 1.3.		See the ideogram below.
$0.432 \pm 0.016 \pm 0.060$		MITCHELL	09	CLEO $e^+e^- \rightarrow \gamma X$
$0.32 \pm 0.04 \pm 0.06$	2560	115 ATHAR	04	CLEO $e^+e^- \rightarrow \gamma X$
0.28 ± 0.06		116 GAISER	86	CBAL $e^+e^- \rightarrow \gamma X$
115 ATHAR 04 used $\Gamma_{\eta_c(1S)} = 24.8 \pm 4.9$ MeV to obtain this result.				
116 GAISER 86 used $\Gamma_{\eta_c(1S)} = 11.5 \pm 4.5$ MeV to obtain this result.				

WEIGHTED AVERAGE
 0.34 ± 0.05 (Error scaled by 1.3)



$$\Gamma(\gamma \eta_c(2S))/\Gamma_{\text{total}} \quad \Gamma_{110}/\Gamma$$

VALUE	CL%	DOCUMENT ID	TECN	COMMENT
$< 8 \times 10^{-4}$	90	117 CRONIN-HEN.10	CLEO	$\psi(2S) \rightarrow \gamma K \bar{K} \pi$
••• We do not use the following data for averages, fits, limits, etc. •••				
$< 2 \times 10^{-3}$	90	ATHAR	04	CLEO $e^+e^- \rightarrow \gamma X$
$0.2-1.3 \times 10^{-2}$	95	EDWARDS	82C	CBAL $e^+e^- \rightarrow \gamma X$
117 CRONIN-HENNESSY 10 reports $[\Gamma(\psi(2S) \rightarrow \gamma \eta_c(2S))/\Gamma_{\text{total}}] \times [B(\eta_c(2S) \rightarrow K \bar{K} \pi)] < 14.5 \times 10^{-6}$ which we divide by our best value $B(\eta_c(2S) \rightarrow K \bar{K} \pi) = 1.9 \times 10^{-2}$. This measurement assumes $\Gamma(\eta_c(2S)) = 14$ MeV. CRONIN-HENNESSY 10 gives the analytic dependence of limits on width.				

$$\Gamma(\gamma \pi^0)/\Gamma_{\text{total}} \quad \Gamma_{111}/\Gamma$$

VALUE (units 10^{-4})	CL%	DOCUMENT ID	TECN	COMMENT
< 0.05	90	PEDLAR	09	CLE3 $\psi(2S) \rightarrow \gamma X$
••• We do not use the following data for averages, fits, limits, etc. •••				
< 54	95	118 LIBERMAN	75	SPEC e^+e^-
< 100	90	WIK	75	DASP e^+e^-
118 Restated by us using $B(\psi(2S) \rightarrow \mu^+ \mu^-) = 0.0077$.				

$$\Gamma(\gamma \eta'(958))/\Gamma_{\text{total}} \quad \Gamma_{112}/\Gamma$$

VALUE (units 10^{-4})	CL%	EVTS	DOCUMENT ID	TECN	COMMENT
1.21 ± 0.08 OUR AVERAGE					
$1.19 \pm 0.08 \pm 0.03$			PEDLAR	09	CLE3 $\psi(2S) \rightarrow \gamma X$
$1.24 \pm 0.27 \pm 0.15$	23		ABLIKIM	06R	BES2 $e^+e^- \rightarrow \psi(2S)$
$1.54 \pm 0.31 \pm 0.20$	~ 43		BAI	98F	BES $\psi(2S) \rightarrow \pi^+ \pi^- 2\gamma$, $\pi^+ \pi^- 3\gamma$
••• We do not use the following data for averages, fits, limits, etc. •••					
< 60	90		119 BRAUNSCH...	77	DASP e^+e^-
< 11	90		120 BARTEL	76	CNTR e^+e^-
119 Restated by us using total decay width 228 keV.					
120 The value is normalized to the branching ratio for $\Gamma(J/\psi(1S) \eta)/\Gamma_{\text{total}}$.					

$$\Gamma(\gamma f_2(1270))/\Gamma_{\text{total}} \quad \Gamma_{113}/\Gamma$$

VALUE (units 10^{-4})	EVTS	DOCUMENT ID	TECN	COMMENT
$2.12 \pm 0.19 \pm 0.32$	121,122	BAI	03c	BES $\psi(2S) \rightarrow \gamma \pi \pi$
••• We do not use the following data for averages, fits, limits, etc. •••				
$2.08 \pm 0.19 \pm 0.33$	200.6 ± 18.8	121 BAI	03c	BES $\psi(2S) \rightarrow \gamma \pi^+ \pi^-$
$2.90 \pm 1.08 \pm 1.07$	29.9 ± 11.1	121 BAI	03c	BES $\psi(2S) \rightarrow \gamma \pi^0 \pi^0$
121 Normalized to $B(\psi(2S) \rightarrow J/\psi \pi^+ \pi^-) = 0.305 \pm 0.016$.				
122 Combining the results from $\pi^+ \pi^-$ and $\pi^0 \pi^0$ decay modes.				

$$\Gamma(\gamma f_0(1710) \rightarrow \gamma \pi \pi)/\Gamma_{\text{total}} \quad \Gamma_{115}/\Gamma$$

VALUE (units 10^{-4})	EVTS	DOCUMENT ID	TECN	COMMENT
$0.301 \pm 0.041 \pm 0.124$	35.6 ± 4.8	123 BAI	03c	BES $\psi(2S) \rightarrow \gamma \pi^+ \pi^-$
123 Normalized to $B(\psi(2S) \rightarrow J/\psi \pi^+ \pi^-) = 0.305 \pm 0.016$.				

$$\Gamma(\gamma f_0(1710) \rightarrow \gamma K \bar{K})/\Gamma_{\text{total}} \quad \Gamma_{116}/\Gamma$$

VALUE (units 10^{-4})	CL%	EVTS	DOCUMENT ID	TECN	COMMENT
$0.604 \pm 0.090 \pm 0.132$	39.6 ± 5.9 ^{24,125}	BAI	03c	BES $\psi(2S) \rightarrow \gamma K^+ K^-$	
••• We do not use the following data for averages, fits, limits, etc. •••					
< 1.56	90	6.8 ± 3.1 ^{24,125}	BAI	03c	BES $\psi(2S) \rightarrow \gamma K_S^0 K_S^0$
124 Includes unknown branching fractions to $K^+ K^-$ or $K_S^0 K_S^0$. We have multiplied the $K^+ K^-$ result by a factor of 2 and the $K_S^0 K_S^0$ result by a factor of 4 to obtain the $K \bar{K}$ result.					
125 Normalized to $B(\psi(2S) \rightarrow J/\psi \pi^+ \pi^-) = 0.305 \pm 0.016$.					

$$\Gamma(\gamma \eta)/\Gamma_{\text{total}} \quad \Gamma_{118}/\Gamma$$

VALUE (units 10^{-4})	CL%	DOCUMENT ID	TECN	COMMENT
< 0.02	90	PEDLAR	09	CLE3 $\psi(2S) \rightarrow \gamma X$
••• We do not use the following data for averages, fits, limits, etc. •••				
< 0.9	90	BAI	98F	BES $\psi(2S) \rightarrow \pi^+ \pi^- 3\gamma$
< 2	90	YAMADA	77	DASP $e^+e^- \rightarrow 3\gamma$

$$\Gamma(\gamma \eta \pi^+ \pi^-)/\Gamma_{\text{total}} \quad \Gamma_{119}/\Gamma$$

VALUE (units 10^{-4})	EVTS	DOCUMENT ID	TECN	COMMENT
$8.71 \pm 1.25 \pm 1.64$	418	ABLIKIM	06R	BES2 $\psi(2S) \rightarrow \gamma \eta \pi^+ \pi^-$

$$\Gamma(\gamma \eta(1405) \rightarrow \gamma K \bar{K} \pi)/\Gamma_{\text{total}} \quad \Gamma_{121}/\Gamma$$

VALUE (units 10^{-4})	CL%	DOCUMENT ID	TECN	COMMENT
< 0.9	90	ABLIKIM	06R	BES2 $\psi(2S) \rightarrow \gamma K_S^0 K^+ \pi^- + \text{c.c.}$
••• We do not use the following data for averages, fits, limits, etc. •••				
< 1.3	90	ABLIKIM	06R	BES2 $\psi(2S) \rightarrow \gamma K^+ K^- \pi^0$
< 1.2	90	126 SCHARRE	80	MRK1 e^+e^-
126 Includes unknown branching fraction $\eta(1405) \rightarrow K \bar{K} \pi$.				

$$\Gamma(\gamma \eta(1405) \rightarrow \eta \pi^+ \pi^-)/\Gamma_{\text{total}} \quad \Gamma_{122}/\Gamma$$

VALUE (units 10^{-4})	EVTS	DOCUMENT ID	TECN	COMMENT
$0.36 \pm 0.25 \pm 0.05$	10	ABLIKIM	06R	BES2 $\psi(2S) \rightarrow \gamma \eta \pi^+ \pi^-$

$$\Gamma(\gamma \eta(1475) \rightarrow K \bar{K} \pi)/\Gamma_{\text{total}} \quad \Gamma_{124}/\Gamma$$

VALUE (units 10^{-4})	CL%	DOCUMENT ID	TECN	COMMENT
< 1.4	90	ABLIKIM	06R	BES2 $\psi(2S) \rightarrow \gamma K^+ K^- \pi^0$
••• We do not use the following data for averages, fits, limits, etc. •••				
< 1.5	90	ABLIKIM	06R	BES2 $\psi(2S) \rightarrow \gamma K_S^0 K^+ \pi^- + \text{c.c.}$

$$\Gamma(\gamma \eta(1475) \rightarrow \eta \pi^+ \pi^-)/\Gamma_{\text{total}} \quad \Gamma_{125}/\Gamma$$

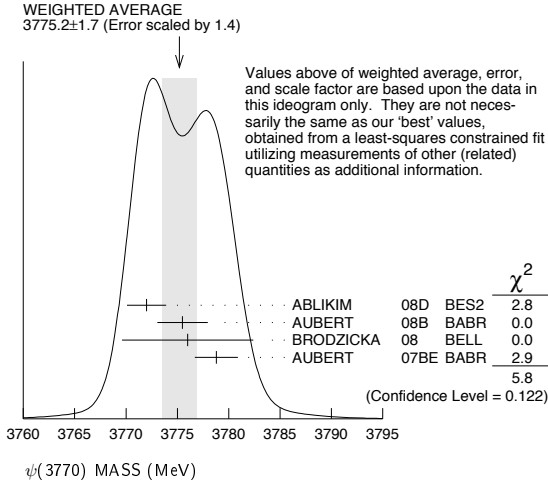
VALUE (units 10^{-4})	CL%	DOCUMENT ID	TECN	COMMENT
< 0.88	90	ABLIKIM	06R	BES2 $\psi(2S) \rightarrow \gamma \eta \pi^+ \pi^-$

See key on page 405

Meson Particle Listings

$\psi(3770)$

¹ Reanalysis of data presented in BAI 02c. From a global fit over the center-of-mass energy region 3.7–5.0 GeV covering the $\psi(3770)$, $\psi(4040)$, $\psi(4160)$, and $\psi(4415)$ resonances. Phase angle fixed in the fit to $\delta = 0^\circ$.

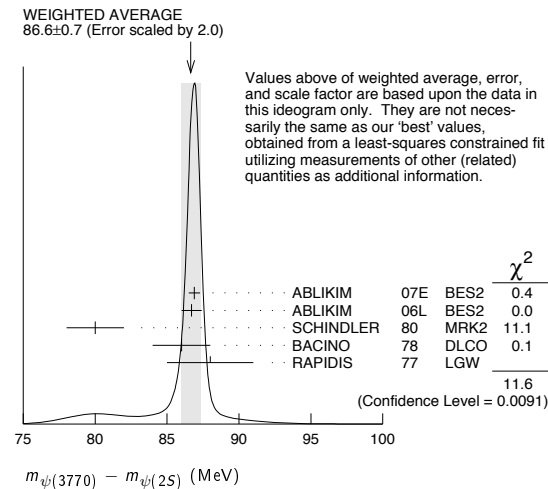


$m_{\psi(3770)} - m_{\psi(2S)}$

OUR FIT includes measurements of $m_{\psi(2S)}$, $m_{\psi(3770)}$, and $m_{\psi(3770)} - m_{\psi(2S)}$.

VALUE (MeV)	DOCUMENT ID	TECN	COMMENT
86.83 ± 0.35 OUR FIT	Error includes scale factor of 1.1.		
86.6 ± 0.7 OUR AVERAGE	Error includes scale factor of 2.0. See the ideogram below.		
86.9 ± 0.4	2 ABLIKIM 07E	BES2	$e^+e^- \rightarrow$ hadrons
86.7 ± 0.7	ABLIKIM 06L	BES2	$e^+e^- \rightarrow$ hadrons
80 ± 2	SCHINDLER 80	MRK2	e^+e^-
86 ± 2	3 BACINO 78	DLCO	e^+e^-
88 ± 3	RAPIDIS 77	LGW	e^+e^-

² BES-II $\psi(2S)$ mass subtracted (see ABLIKIM 06L).
³ SPEAR $\psi(2S)$ mass subtracted (see SCHINDLER 80).



$\psi(3770)$ WIDTH

VALUE (MeV)	EVTS	DOCUMENT ID	TECN	COMMENT
27.3 ± 1.0 OUR FIT				
27.6 ± 1.0 OUR AVERAGE				
30.4 ± 8.5		4 ABLIKIM 08D	BES2	$e^+e^- \rightarrow$ hadrons
27 ± 10 ± 5	68	BRODZICKA 08	BELL	$B^+ \rightarrow D^0 \bar{D}^0 K^+$
28.5 ± 1.2 ± 0.2		ABLIKIM 07E	BES2	$e^+e^- \rightarrow$ hadrons
23.5 ± 3.7 ± 0.9		AUBERT 07BE	BABR	$e^+e^- \rightarrow D \bar{D} \gamma$
26.9 ± 2.4 ± 0.3		ABLIKIM 06L	BES2	$e^+e^- \rightarrow$ hadrons
24 ± 5		SCHINDLER 80	MRK2	e^+e^-
24 ± 5		BACINO 78	DLCO	e^+e^-
28 ± 5		RAPIDIS 77	LGW	e^+e^-

⁴ Reanalysis of data presented in BAI 02c. From a global fit over the center-of-mass energy region 3.7–5.0 GeV covering the $\psi(3770)$, $\psi(4040)$, $\psi(4160)$, and $\psi(4415)$ resonances. Phase angle fixed in the fit to $\delta = 0^\circ$.

$\psi(3770)$ DECAY MODES

In addition to the dominant decay mode to $D\bar{D}$, $\psi(3770)$ was found to decay into the final states containing the J/ψ (BAI 05, ADAM 06). ADAMS 06 and HUANG 06A searched for various decay modes with light hadrons and found a statistically significant signal for the decay to $\phi\eta$ only (ADAMS 06).

Mode	Fraction (Γ_i/Γ)	Scale factor / Confidence level
$\Gamma_1 D\bar{D}$	(93 $^{+8}_{-9}$) %	S=2.0
$\Gamma_2 D^0 \bar{D}^0$	(52 ± 5) %	S=2.0
$\Gamma_3 D^+ D^-$	(41 ± 4) %	S=2.0
$\Gamma_4 J/\psi \pi^+ \pi^-$	(1.93 ± 0.28) × 10 ⁻³	
$\Gamma_5 J/\psi \pi^0 \pi^0$	(8.0 ± 3.0) × 10 ⁻⁴	
$\Gamma_6 J/\psi \eta$	(9 ± 4) × 10 ⁻⁴	
$\Gamma_7 J/\psi \pi^0$	< 2.8 × 10 ⁻⁴	CL=90%
$\Gamma_8 \gamma \chi_{c0}$	(7.3 ± 0.9) × 10 ⁻³	
$\Gamma_9 \gamma \chi_{c1}$	(2.9 ± 0.6) × 10 ⁻³	
$\Gamma_{10} \gamma \chi_{c2}$	< 9 × 10 ⁻⁴	CL=90%
$\Gamma_{11} e^+ e^-$	(9.7 ± 0.7) × 10 ⁻⁶	S=1.2
$\Gamma_{12} K_S^0 K_L^0$	< 1.2 × 10 ⁻⁵	CL=90%
$\Gamma_{13} 2(\pi^+ \pi^-)$	< 1.12 × 10 ⁻³	CL=90%
$\Gamma_{14} 2(\pi^+ \pi^-) \pi^0$	< 1.06 × 10 ⁻³	CL=90%
$\Gamma_{15} 2(\pi^+ \pi^- \pi^0)$	< 5.85 %	CL=90%
$\Gamma_{16} \omega \pi^+ \pi^-$	< 6.0 × 10 ⁻⁴	CL=90%
$\Gamma_{17} 3(\pi^+ \pi^-)$	< 9.1 × 10 ⁻³	
$\Gamma_{18} 3(\pi^+ \pi^-) \pi^0$	< 1.37 %	
$\Gamma_{19} 3(\pi^+ \pi^-) 2\pi^0$	< 11.74 %	CL=90%
$\Gamma_{20} \eta \pi^+ \pi^-$	< 1.24 × 10 ⁻³	CL=90%
$\Gamma_{21} \pi^+ \pi^- 2\pi^0$	< 8.9 × 10 ⁻³	CL=90%
$\Gamma_{22} \rho^0 \pi^+ \pi^-$	< 6.9 × 10 ⁻³	CL=90%
$\Gamma_{23} \eta 3\pi$	< 1.34 × 10 ⁻³	CL=90%
$\Gamma_{24} \eta 2(\pi^+ \pi^-)$	< 2.43 %	
$\Gamma_{25} \eta' 3\pi$	< 2.44 × 10 ⁻³	CL=90%
$\Gamma_{26} K^+ K^- \pi^+ \pi^-$	< 9.0 × 10 ⁻⁴	CL=90%
$\Gamma_{27} \phi \pi^+ \pi^-$	< 4.1 × 10 ⁻⁴	CL=90%
$\Gamma_{28} K^+ K^- 2\pi^0$	< 4.2 × 10 ⁻³	CL=90%
$\Gamma_{29} \phi \pi^0$	not seen	
$\Gamma_{30} \phi \eta$	(3.1 ± 0.7) × 10 ⁻⁴	
$\Gamma_{31} 4(\pi^+ \pi^-)$	< 1.67 %	CL=90%
$\Gamma_{32} 4(\pi^+ \pi^-) \pi^0$	< 3.06 %	CL=90%
$\Gamma_{33} \phi f_0(980)$	< 4.5 × 10 ⁻⁴	CL=90%
$\Gamma_{34} K^+ K^- \pi^+ \pi^- \pi^0$	< 2.36 × 10 ⁻³	CL=90%
$\Gamma_{35} K^+ K^- \rho^0 \pi^0$	< 8 × 10 ⁻⁴	CL=90%
$\Gamma_{36} K^+ K^- \rho^+ \pi^-$	< 1.46 %	CL=90%
$\Gamma_{37} \omega K^+ K^-$	< 3.4 × 10 ⁻⁴	CL=90%
$\Gamma_{38} \phi \pi^+ \pi^- \pi^0$	< 3.8 × 10 ⁻³	CL=90%
$\Gamma_{39} K^{*0} K^- \pi^+ \pi^0 + c.c.$	< 1.62 %	CL=90%
$\Gamma_{40} K^{*+} K^- \pi^+ \pi^- + c.c.$	< 3.23 %	CL=90%
$\Gamma_{41} K^+ K^- \pi^+ \pi^- 2\pi^0$	< 2.67 %	CL=90%
$\Gamma_{42} K^+ K^- 2(\pi^+ \pi^-)$	< 1.03 %	CL=90%
$\Gamma_{43} K^+ K^- 2(\pi^+ \pi^-) \pi^0$	< 3.60 %	CL=90%
$\Gamma_{44} \eta K^+ K^-$	< 4.1 × 10 ⁻⁴	CL=90%
$\Gamma_{45} \rho^0 K^+ K^-$	< 5.0 × 10 ⁻³	CL=90%
$\Gamma_{46} 2(K^+ K^-)$	< 6.0 × 10 ⁻⁴	CL=90%
$\Gamma_{47} \phi K^+ K^-$	< 7.5 × 10 ⁻⁴	CL=90%
$\Gamma_{48} 2(K^+ K^-) \pi^0$	< 2.9 × 10 ⁻⁴	CL=90%
$\Gamma_{49} 2(K^+ K^-) \pi^+ \pi^-$	< 3.2 × 10 ⁻³	CL=90%
$\Gamma_{50} K_S^0 K^- \pi^+$	< 3.2 × 10 ⁻³	CL=90%
$\Gamma_{51} K_S^0 K^- \pi^+ \pi^0$	< 1.33 %	CL=90%
$\Gamma_{52} K_S^0 K^- \rho^+$	< 6.6 × 10 ⁻³	CL=90%
$\Gamma_{53} K_S^0 K^- 2\pi^+ \pi^-$	< 8.7 × 10 ⁻³	CL=90%
$\Gamma_{54} K_S^0 K^- \pi^+ \rho^0$	< 1.6 %	CL=90%
$\Gamma_{55} K_S^0 K^- \pi^+ \eta$	< 1.3 %	CL=90%
$\Gamma_{56} K_S^0 K^- 2\pi^+ \pi^- \pi^0$	< 4.18 %	CL=90%
$\Gamma_{57} K_S^0 K^- 2\pi^+ \pi^- \eta$	< 4.8 %	CL=90%
$\Gamma_{58} K_S^0 K^- \pi^+ 2(\pi^+ \pi^-)$	< 1.22 %	CL=90%
$\Gamma_{59} K_S^0 K^- \pi^+ 2\pi^0$	< 2.65 %	CL=90%
$\Gamma_{60} K_S^0 K^- K^+ K^- \pi^+$	< 4.9 × 10 ⁻³	CL=90%
$\Gamma_{61} K_S^0 K^- K^+ K^- \pi^+ \pi^0$	< 3.0 %	CL=90%
$\Gamma_{62} K_S^0 K^- K^+ K^- \pi^+ \eta$	< 2.2 %	CL=90%
$\Gamma_{63} K^{*0} K^- \pi^+ + c.c.$	< 9.7 × 10 ⁻³	CL=90%
$\Gamma_{64} p \bar{p} \pi^0$	< 1.2 × 10 ⁻³	CL=90%
$\Gamma_{65} p \bar{p} \pi^+ \pi^-$	< 5.8 × 10 ⁻⁴	CL=90%

Meson Particle Listings

 $\psi(3770)$

Γ_{66}	$\Lambda\bar{\Lambda}$	< 1.2	$\times 10^{-4}$	CL=90%
Γ_{67}	$\rho\bar{\rho}\pi^+\pi^-\pi^0$	< 1.85	$\times 10^{-3}$	CL=90%
Γ_{68}	$\omega\rho\bar{\rho}$	< 2.9	$\times 10^{-4}$	CL=90%
Γ_{69}	$\Lambda\bar{\Lambda}\pi^0$	< 1.2	$\times 10^{-3}$	CL=90%
Γ_{70}	$\rho\bar{\rho}2(\pi^+\pi^-)$	< 2.6	$\times 10^{-3}$	CL=90%
Γ_{71}	$\eta\rho\bar{\rho}$	< 5.4	$\times 10^{-4}$	CL=90%
Γ_{72}	$\rho^0\rho\bar{\rho}$	< 1.7	$\times 10^{-3}$	CL=90%
Γ_{73}	$\rho\bar{\rho}K^+K^-$	< 3.2	$\times 10^{-4}$	CL=90%
Γ_{74}	$\phi\rho\bar{\rho}$	< 1.3	$\times 10^{-4}$	CL=90%
Γ_{75}	$\Lambda\bar{\Lambda}\pi^+\pi^-$	< 2.5	$\times 10^{-4}$	CL=90%
Γ_{76}	$\Lambda\bar{\rho}K^+$	< 2.8	$\times 10^{-4}$	CL=90%
Γ_{77}	$\Lambda\bar{\rho}K^+\pi^+\pi^-$	< 6.3	$\times 10^{-4}$	CL=90%
Γ_{78}	$\pi^+\pi^-\pi^0$	not seen		
Γ_{79}	$\rho\pi$	not seen		
Γ_{80}	$\omega\pi^0$	not seen		
Γ_{81}	$\rho\eta$	not seen		
Γ_{82}	$\omega\eta$	not seen		
Γ_{83}	$\rho\eta'$	not seen		
Γ_{84}	$\omega\eta'$	not seen		
Γ_{85}	$\phi\eta'$	not seen		
Γ_{86}	$K^{*0}\bar{K}^0$	not seen		
Γ_{87}	$K^{*+}K^-$	not seen		
Γ_{88}	$b_1\pi$	not seen		

Radiative decays

Γ_{89}	$\gamma\pi^0$	< 2	$\times 10^{-4}$	CL=90%
Γ_{90}	$\gamma\eta$	< 1.5	$\times 10^{-4}$	CL=90%
Γ_{91}	$\gamma\eta'$	< 1.8	$\times 10^{-4}$	CL=90%

CONSTRAINED FIT INFORMATION

An overall fit to the total width, a partial width, and 3 branching ratios uses 21 measurements and one constraint to determine 5 parameters. The overall fit has a $\chi^2 = 17.9$ for 17 degrees of freedom.

The following *off-diagonal* array elements are the correlation coefficients $\langle\delta p_i\delta p_j\rangle/(\delta p_i\delta p_j)$, in percent, from the fit to parameters p_i , including the branching fractions, $x_i \equiv \Gamma_i/\Gamma_{\text{total}}$. The fit constrains the x_i whose labels appear in this array to sum to one.

x_3	98		
x_{11}	0	0	
Γ	0	0	-46
	x_2	x_3	x_{11}

Mode	Rate (MeV)	Scale factor	
Γ_2	$D^0\bar{D}^0$	14.1 \pm 1.4	1.7
Γ_3	D^+D^-	11.2 \pm 1.1	1.7
Γ_{11}	e^+e^-	(2.65 \pm 0.18) $\times 10^{-4}$	1.3

 $\psi(3770)$ PARTIAL WIDTHS

$\Gamma(e^+e^-)$	VALUE (keV)	EVTS	DOCUMENT ID	TECN	COMMENT	Γ_{11}
0.265 \pm 0.018 OUR FIT					Error includes scale factor of 1.3.	
0.259 \pm 0.016 OUR AVERAGE					Error includes scale factor of 1.2.	
0.22 \pm 0.05			⁵ ABLIKIM	08D BES2	$e^+e^- \rightarrow$ hadrons	
0.277 \pm 0.011 \pm 0.013			ABLIKIM	07E BES2	$e^+e^- \rightarrow$ hadrons	
0.203 \pm 0.003 \pm $\frac{0.041}{0.027}$	1.427M		⁶ BESSON	06 CLEO	$e^+e^- \rightarrow$ hadrons	
0.276 \pm 0.050			SCHINDLER	80 MRK2	e^+e^-	
0.18 \pm 0.06			BACINO	78 DLCO	e^+e^-	
0.37 \pm 0.09			⁷ RAPIDIS	77 LGW	e^+e^-	

⁵ Reanalysis of data presented in BAI 02c. From a global fit over the center-of-mass energy region 3.7–5.0 GeV covering the $\psi(3770)$, $\psi(4040)$, $\psi(4160)$, and $\psi(4415)$ resonances. Phase angle fixed in the fit to $\delta = 0^\circ$.

⁶ BESSON 06 (as corrected in BESSON 10) measure $\sigma(e^+e^- \rightarrow \psi(3770) \rightarrow \text{hadrons}) = 6.36 \pm 0.08 \pm \frac{0.41}{-0.30}$ nb at $\sqrt{s} = 3773 \pm 1$ MeV, and obtain $\Gamma_{e^+e^-}$ from the Born-level cross section calculated using $\psi(3770)$ mass and width from our 2004 edition, PDG 04.

⁷ See also $\Gamma(e^+e^-)/\Gamma_{\text{total}}$ below.

 $\psi(3770)$ BRANCHING RATIOS

$\Gamma(D\bar{D})/\Gamma_{\text{total}}$	VALUE	EVTS	DOCUMENT ID	TECN	COMMENT	$\Gamma_1/\Gamma = (\Gamma_2+\Gamma_3)/\Gamma$
0.93 \pm $\frac{0.08}{-0.09}$ OUR FIT					Error includes scale factor of 2.0.	
0.93 \pm $\frac{0.08}{-0.09}$ OUR AVERAGE					Error includes scale factor of 2.1.	
0.849 \pm 0.056 \pm 0.018			⁸ ABLIKIM	08B BES2	$e^+e^- \rightarrow$ non- $D\bar{D}$	
1.033 \pm 0.014 \pm $\frac{0.048}{-0.066}$	1.427M		⁹ BESSON	06 CLEO	$e^+e^- \rightarrow$ hadrons	
••• We do not use the following data for averages, fits, limits, etc. •••						
0.866 \pm 0.050 \pm 0.036			^{10,11} ABLIKIM	07K BES2	$e^+e^- \rightarrow$ non- $D\bar{D}$	
0.836 \pm 0.073 \pm 0.042			¹¹ ABLIKIM	06L BES2	$e^+e^- \rightarrow D\bar{D}$	
0.855 \pm 0.017 \pm 0.058			^{11,12} ABLIKIM	06N BES2	$e^+e^- \rightarrow D\bar{D}$	

$\Gamma(D^0\bar{D}^0)/\Gamma_{\text{total}}$	VALUE	EVTS	DOCUMENT ID	TECN	COMMENT	Γ_2/Γ
0.52 \pm 0.05 OUR FIT					Error includes scale factor of 2.0.	
••• We do not use the following data for averages, fits, limits, etc. •••						
0.467 \pm 0.047 \pm 0.023			ABLIKIM	06L BES2	$e^+e^- \rightarrow D^0\bar{D}^0$	
0.499 \pm 0.013 \pm 0.038			¹² ABLIKIM	06N BES2	$e^+e^- \rightarrow D^0\bar{D}^0$	

$\Gamma(D^+D^-)/\Gamma_{\text{total}}$	VALUE	EVTS	DOCUMENT ID	TECN	COMMENT	Γ_3/Γ
0.41 \pm 0.04 OUR FIT					Error includes scale factor of 2.0.	
••• We do not use the following data for averages, fits, limits, etc. •••						
0.369 \pm 0.037 \pm 0.028			ABLIKIM	06L BES2	$e^+e^- \rightarrow D^+D^-$	
0.357 \pm 0.011 \pm 0.034			¹² ABLIKIM	06N BES2	$e^+e^- \rightarrow D^+D^-$	

$\Gamma(D^0\bar{D}^0)/\Gamma(D^+D^-)$	VALUE	EVTS	DOCUMENT ID	TECN	COMMENT	Γ_2/Γ_3
1.260 \pm 0.021 OUR FIT						
1.260 \pm 0.021 OUR AVERAGE						
1.39 \pm 0.31 \pm 0.12			PAKHOLOVA	08 BELL	10.6 $e^+e^- \rightarrow D\bar{D}\gamma$	
1.78 \pm 0.33 \pm 0.24			AUBERT	07BE BABR	$e^+e^- \rightarrow D\bar{D}\gamma$	
1.258 \pm 0.016 \pm 0.014			DOBBS	07 CLEO	$e^+e^- \rightarrow D\bar{D}$	
1.27 \pm 0.12 \pm 0.08			ABLIKIM	06L BES2	$e^+e^- \rightarrow D\bar{D}$	
2.43 \pm 1.50 \pm 0.43	34		¹³ CHISTOV	04 BELL	$B^+ \rightarrow \psi(3770) K^+$	

$\Gamma(J/\psi\pi^+\pi^-)/\Gamma_{\text{total}}$	VALUE (units 10^{-3})	EVTS	DOCUMENT ID	TECN	COMMENT	Γ_4/Γ
1.93 \pm 0.28 OUR AVERAGE						
1.89 \pm 0.20 \pm 0.20		231 \pm 33	ADAM	06 CLEO	$e^+e^- \rightarrow \psi(3770)$	
3.4 \pm 1.4 \pm 0.9		17.8 \pm 4.8	BAI	05 BES2	$e^+e^- \rightarrow \psi(3770)$	

$\Gamma(J/\psi\pi^0\pi^0)/\Gamma_{\text{total}}$	VALUE (units 10^{-2})	EVTS	DOCUMENT ID	TECN	COMMENT	Γ_5/Γ
0.080 \pm 0.025 \pm 0.016		39 \pm 14	ADAM	06 CLEO	$e^+e^- \rightarrow \psi(3770)$	

$\Gamma(J/\psi\eta)/\Gamma_{\text{total}}$	VALUE (units 10^{-5})	EVTS	DOCUMENT ID	TECN	COMMENT	Γ_6/Γ
87 \pm 33 \pm 22		22 \pm 10	ADAM	06 CLEO	$e^+e^- \rightarrow \psi(3770)$	

$\Gamma(J/\psi\pi^0)/\Gamma_{\text{total}}$	VALUE (units 10^{-5})	CL%	EVTS	DOCUMENT ID	TECN	COMMENT	Γ_7/Γ
< 28		90	< 10	ADAM	06 CLEO	$e^+e^- \rightarrow \psi(3770)$	

$\Gamma(\gamma\chi_{c0})/\Gamma_{\text{total}}$	VALUE (units 10^{-3})	CL%	EVTS	DOCUMENT ID	TECN	COMMENT	Γ_8/Γ
7.3 \pm 0.7 \pm 0.6			274 \pm 27	¹⁴ BRIERE	06 CLEO	$e^+e^- \rightarrow \psi(3770) \rightarrow \gamma + \text{hadrons}$	
••• We do not use the following data for averages, fits, limits, etc. •••							
< 44			90	¹⁵ COAN	06A CLEO	$e^+e^- \rightarrow \psi(3770) \rightarrow \gamma\gamma J/\psi$	

$\Gamma(\gamma\chi_{c1})/\Gamma_{\text{total}}$	VALUE (units 10^{-3})	EVTS	DOCUMENT ID	TECN	COMMENT	Γ_9/Γ	
2.9 \pm 0.5 \pm 0.4				¹⁶ BRIERE	06 CLEO	$e^+e^- \rightarrow \psi(3770) \rightarrow \gamma + \text{hadrons}, \gamma\gamma J/\psi$	
••• We do not use the following data for averages, fits, limits, etc. •••							
3.9 \pm 1.4 \pm 0.6		54 \pm 17	¹⁷ BRIERE	06 CLEO	$e^+e^- \rightarrow \psi(3770) \rightarrow \gamma + \text{hadrons}$		
2.8 \pm 0.5 \pm 0.4		53 \pm 10	¹⁵ COAN	06A CLEO	$e^+e^- \rightarrow \psi(3770) \rightarrow \gamma\gamma J/\psi$		

$\Gamma(\gamma\chi_{c1})/\Gamma(J/\psi\pi^+\pi^-)$	VALUE	EVTS	DOCUMENT ID	TECN	COMMENT	Γ_9/Γ_4
1.49 \pm 0.31 \pm 0.26		53 \pm 10	¹⁸ COAN	06A CLEO	$e^+e^- \rightarrow \psi(3770) \rightarrow \gamma\gamma J/\psi$	

$\Gamma(\gamma\chi_{c0})/\Gamma(\gamma\chi_{c1})$	VALUE	DOCUMENT ID	TECN	COMMENT	Γ_8/Γ_9
••• We do not use the following data for averages, fits, limits, etc. •••					
2.5 \pm 0.6		¹⁹ BRIERE	06 CLEO	$e^+e^- \rightarrow \psi(3770)$	

Meson Particle Listings

 $\psi(3770)$

$\Gamma(K^+K^-2(\pi^+\pi^-))/\Gamma_{\text{total}}$					Γ_{42}/Γ	$\Gamma(K_S^0K^-K^+K^-\pi^+)/\Gamma_{\text{total}}$					Γ_{60}/Γ	
VALUE (units 10^{-3})	CL%	DOCUMENT ID	TECN	COMMENT		VALUE (units 10^{-3})	CL%	DOCUMENT ID	TECN	COMMENT		
<10.3	90	24,25 ABLIKIM	07F	BES2	$e^+e^- \rightarrow \psi(3770)$	<4.9	90	ABLIKIM	09c	BES2	$e^+e^- \rightarrow \psi(3770)$	
$\Gamma(K^+K^-2(\pi^+\pi^-)\pi^0)/\Gamma_{\text{total}}$					Γ_{43}/Γ	$\Gamma(K_S^0K^-K^+K^-\pi^0)/\Gamma_{\text{total}}$					Γ_{61}/Γ	
<36.0	90	24,25 ABLIKIM	07F	BES2	$e^+e^- \rightarrow \psi(3770)$	<3.0	90	ABLIKIM	09c	BES2	$e^+e^- \rightarrow \psi(3770)$	
$\Gamma(\eta K^+K^-)/\Gamma_{\text{total}}$					Γ_{44}/Γ	$\Gamma(K_S^0K^-K^+K^-\pi^+\eta)/\Gamma_{\text{total}}$					Γ_{62}/Γ	
<4.1	90	23 HUANG	06A	CLEO	$e^+e^- \rightarrow \psi(3770)$	<2.2	90	ABLIKIM	09c	BES2	$e^+e^- \rightarrow \psi(3770)$	
$\Gamma(\rho^0K^+K^-)/\Gamma_{\text{total}}$					Γ_{45}/Γ	$\Gamma(K^{*0}K^-\pi^++\text{c.c.})/\Gamma_{\text{total}}$					Γ_{63}/Γ	
<5.0	90	24,25 ABLIKIM	07F	BES2	$e^+e^- \rightarrow \psi(3770)$	<9.7	90	24,25 ABLIKIM	07F	BES2	$e^+e^- \rightarrow \psi(3770)$	
$\Gamma(2(K^+K^-))/\Gamma_{\text{total}}$					Γ_{46}/Γ	$\Gamma(\rho\bar{\rho}\pi^0)/\Gamma_{\text{total}}$					Γ_{64}/Γ	
< 6.0	90	23 HUANG	06A	CLEO	$e^+e^- \rightarrow \psi(3770)$	<12	24,25	ABLIKIM	07B	BES2	$e^+e^- \rightarrow \psi(3770)$	
••• We do not use the following data for averages, fits, limits, etc. •••												
<17		24,25 ABLIKIM	07B	BES2	$e^+e^- \rightarrow \psi(3770)$							
$\Gamma(\phi K^+K^-)/\Gamma_{\text{total}}$					Γ_{47}/Γ	$\Gamma(\rho\bar{\rho}\pi^+\pi^-)/\Gamma_{\text{total}}$					Γ_{65}/Γ	
< 7.5	90	23 HUANG	06A	CLEO	$e^+e^- \rightarrow \psi(3770)$	< 5.8	90	23 HUANG	06A	CLEO	$e^+e^- \rightarrow \psi(3770)$	
••• We do not use the following data for averages, fits, limits, etc. •••						••• We do not use the following data for averages, fits, limits, etc. •••						
<24		24,25 ABLIKIM	07B	BES2	$e^+e^- \rightarrow \psi(3770)$	<16		24,25 ABLIKIM	07B	BES2	$e^+e^- \rightarrow \psi(3770)$	
$\Gamma(2(K^+K^-)\pi^0)/\Gamma_{\text{total}}$					Γ_{48}/Γ	$\Gamma(\Lambda\bar{\Lambda})/\Gamma_{\text{total}}$					Γ_{66}/Γ	
< 2.9	90	23 HUANG	06A	CLEO	$e^+e^- \rightarrow \psi(3770)$	<1.2	90	23 HUANG	06A	CLEO	$e^+e^- \rightarrow \psi(3770)$	
••• We do not use the following data for averages, fits, limits, etc. •••						••• We do not use the following data for averages, fits, limits, etc. •••						
<46		24,25 ABLIKIM	07B	BES2	$e^+e^- \rightarrow \psi(3770)$	<4		24,25 ABLIKIM	07F	BES2	$e^+e^- \rightarrow \psi(3770)$	
$\Gamma(2(K^+K^-)\pi^+\pi^-)/\Gamma_{\text{total}}$					Γ_{49}/Γ	$\Gamma(\rho\bar{\rho}\pi^+\pi^-)/\Gamma_{\text{total}}$					Γ_{67}/Γ	
<3.2	90	24,25 ABLIKIM	07F	BES2	$e^+e^- \rightarrow \psi(3770)$	<18.5	90	23 HUANG	06A	CLEO	$e^+e^- \rightarrow \psi(3770)$	
						••• We do not use the following data for averages, fits, limits, etc. •••						
						<73		24,25 ABLIKIM	07B	BES2	$e^+e^- \rightarrow \psi(3770)$	
$\Gamma(K_S^0K^-\pi^+)/\Gamma_{\text{total}}$					Γ_{50}/Γ	$\Gamma(\omega\rho\bar{\rho})/\Gamma_{\text{total}}$					Γ_{68}/Γ	
<3.2	90	18 ABLIKIM	08M	BES2	$e^+e^- \rightarrow \psi(3770)$	< 2.9	90	23 HUANG	06A	CLEO	$e^+e^- \rightarrow \psi(3770)$	
						••• We do not use the following data for averages, fits, limits, etc. •••						
						<30		90	26 ABLIKIM	07I	BES2	$3.77 e^+e^-$
$\Gamma(K_S^0K^-\pi^0)/\Gamma_{\text{total}}$					Γ_{51}/Γ	$\Gamma(\Lambda\bar{\Lambda}\pi^0)/\Gamma_{\text{total}}$					Γ_{69}/Γ	
<13.3	90	40 ABLIKIM	08M	BES2	$e^+e^- \rightarrow \psi(3770)$	<12	90	26 ABLIKIM	07I	BES2	$3.77 e^+e^-$	
$\Gamma(K_S^0K^-\rho^+)/\Gamma_{\text{total}}$					Γ_{52}/Γ	$\Gamma(\rho\bar{\rho}2(\pi^+\pi^-))/\Gamma_{\text{total}}$					Γ_{70}/Γ	
<6.6	90	ABLIKIM	09c	BES2	$e^+e^- \rightarrow \psi(3770)$	<2.6	90	24,25 ABLIKIM	07F	BES2	$e^+e^- \rightarrow \psi(3770)$	
$\Gamma(K_S^0K^-2\pi^+\pi^-)/\Gamma_{\text{total}}$					Γ_{53}/Γ	$\Gamma(\eta\rho\bar{\rho})/\Gamma_{\text{total}}$					Γ_{71}/Γ	
<8.7	90	39 ABLIKIM	08M	BES2	$e^+e^- \rightarrow \psi(3770)$	<5.4	90	23 HUANG	06A	CLEO	$e^+e^- \rightarrow \psi(3770)$	
$\Gamma(K_S^0K^-\pi^+\rho^0)/\Gamma_{\text{total}}$					Γ_{54}/Γ	$\Gamma(\rho^0\rho\bar{\rho})/\Gamma_{\text{total}}$					Γ_{72}/Γ	
<1.6	90	ABLIKIM	09c	BES2	$e^+e^- \rightarrow \psi(3770)$	<1.7	90	24,25 ABLIKIM	07F	BES2	$e^+e^- \rightarrow \psi(3770)$	
$\Gamma(K_S^0K^-\pi^+\eta)/\Gamma_{\text{total}}$					Γ_{55}/Γ	$\Gamma(\rho\bar{\rho}K^+K^-)/\Gamma_{\text{total}}$					Γ_{73}/Γ	
<1.3	90	ABLIKIM	09c	BES2	$e^+e^- \rightarrow \psi(3770)$	< 3.2	90	23 HUANG	06A	CLEO	$e^+e^- \rightarrow \psi(3770)$	
						••• We do not use the following data for averages, fits, limits, etc. •••						
						<11		24,25 ABLIKIM	07B	BES2	$e^+e^- \rightarrow \psi(3770)$	
$\Gamma(K_S^0K^-2\pi^+\pi^-)/\Gamma_{\text{total}}$					Γ_{56}/Γ	$\Gamma(\phi\rho\bar{\rho})/\Gamma_{\text{total}}$					Γ_{74}/Γ	
<41.8	90	23 ABLIKIM	08M	BES2	$e^+e^- \rightarrow \psi(3770)$	<1.3	90	23 HUANG	06A	CLEO	$e^+e^- \rightarrow \psi(3770)$	
						••• We do not use the following data for averages, fits, limits, etc. •••						
						<9		24,25 ABLIKIM	07B	BES2	$e^+e^- \rightarrow \psi(3770)$	
$\Gamma(K_S^0K^-\pi^+2(\pi^+\pi^-))/\Gamma_{\text{total}}$					Γ_{58}/Γ	$\Gamma(\Lambda\bar{\Lambda}\pi^+\pi^-)/\Gamma_{\text{total}}$					Γ_{75}/Γ	
<12.2	90	4 ABLIKIM	08M	BES2	$e^+e^- \rightarrow \psi(3770)$	< 2.5	90	23 HUANG	06A	CLEO	$e^+e^- \rightarrow \psi(3770)$	
						••• We do not use the following data for averages, fits, limits, etc. •••						
						<39		24,25 ABLIKIM	07F	BES2	$e^+e^- \rightarrow \psi(3770)$	
$\Gamma(K_S^0K^-\pi^+2\pi^0)/\Gamma_{\text{total}}$					Γ_{59}/Γ							
<26.5	90	17 ABLIKIM	08M	BES2	$e^+e^- \rightarrow \psi(3770)$							

$\Gamma(\Lambda\bar{P}K^+)/\Gamma_{total}$					Γ_{76}/Γ
VALUE (units 10^{-4})	CL%	DOCUMENT ID	TECN	COMMENT	
<2.8	90	23 HUANG	06A CLEO	$e^+e^- \rightarrow \psi(3770)$	

$\Gamma(\Lambda\bar{P}K^+\pi^+\pi^-)/\Gamma_{total}$					Γ_{77}/Γ
VALUE (units 10^{-4})	CL%	DOCUMENT ID	TECN	COMMENT	
<6.3	90	23 HUANG	06A CLEO	$e^+e^- \rightarrow \psi(3770)$	

- ⁸ Neglecting interference.
⁹ Obtained by comparing a measurement of the total cross section (corrected in BESSON 10) with that of $D\bar{D}$ reported by CLEO in DOBBS 07.
¹⁰ Using $\sigma_{obs} = 7.07 \pm 0.58$ nb and neglecting interference.
¹¹ Not independent of ABLIKIM 08B.
¹² From a measurement of $\sigma(e^+e^- \rightarrow D\bar{D})$ at $\sqrt{s} = 3773$ MeV, using the $\psi(3770)$ resonance parameters measured by ABLIKIM 06L.
¹³ See ADLER 88c for older measurements of this quantity.
¹⁴ Uses $B(\psi(2S) \rightarrow \gamma\chi_{c0}) = 9.33 \pm 0.14 \pm 0.61\%$ from ATHAR 04, $\psi(2S)$ mass and width from PDG 04, and $\Gamma_{ee}(\psi(2S)) = 2.54 \pm 0.03 \pm 0.11$ keV from ADAM 06.
¹⁵ Using $\Gamma_{ee}(\psi(2S)) = (2.54 \pm 0.03 \pm 0.11)$ keV from ADAM 06 and taking $\sigma(e^+e^- \rightarrow D\bar{D})$ from HE 05 for $\sigma(e^+e^- \rightarrow \psi(3770))$.
¹⁶ Averages the two measurements from COAN 06A and BRIERE 06.
¹⁷ Uses $B(\psi(2S) \rightarrow \gamma\chi_{c1}) = 9.07 \pm 0.11 \pm 0.54\%$ from ATHAR 04, $\psi(2S)$ mass and width from PDG 04, and $\Gamma_{ee}(\psi(2S)) = 2.54 \pm 0.03 \pm 0.11$ keV from ADAM 06.
¹⁸ Using $B(\psi(3770) \rightarrow J/\psi\pi^+\pi^-) = (1.89 \pm 0.20 \pm 0.20) \times 10^{-3}$ from ADAM 06.
¹⁹ Not independent of other results in BRIERE 06.
²⁰ Uses $B(\psi(2S) \rightarrow \gamma\chi_{c2}) = 9.22 \pm 0.11 \pm 0.46\%$ from ATHAR 04, $\psi(2S)$ mass and width from PDG 04, and $\Gamma_{ee}(\psi(2S)) = 2.54 \pm 0.03 \pm 0.11$ keV from ADAM 06.
²¹ Using $\sigma(e^+e^- \rightarrow \psi(3770) \rightarrow \text{hadrons}) = (6.38 \pm 0.08^{+0.41}_{-0.30})$ nb from BESSON 06 and $B(K_S^0 \rightarrow \pi^+\pi^-) = 0.6895 \pm 0.0014$.
²² Using $B(K_S^0 \rightarrow \pi^+\pi^-) = 0.6860 \pm 0.0027$.
²³ Using $\sigma_{tot}(e^+e^- \rightarrow \psi(3770)) = 7.9 \pm 0.6$ nb at the resonance.
²⁴ Assuming that interference effects between resonance and continuum can be neglected.
²⁵ Using $\sigma_{obs}(e^+e^- \rightarrow \psi(3770)) = 7.15 \pm 0.38$ nb.
²⁶ Using $\sigma_{obs} = 7.15 \pm 0.27 \pm 0.27$ nb and neglecting interference.
²⁷ Comparing $\sigma(e^+e^- \rightarrow \phi\eta)$ at $\sqrt{s} = 3.773$ GeV and $\sqrt{s} = 3.671$ GeV, and using $\sigma(\psi(3770) \rightarrow D\bar{D}) = 6.39 \pm 0.20$ nb.

RADIATIVE DECAYS

$\Gamma(\gamma\pi^0)/\Gamma_{total}$					Γ_{89}/Γ
VALUE (units 10^{-4})	CL%	DOCUMENT ID	TECN	COMMENT	
<2	90	PEDLAR	09 CLE3	$\psi(2S) \rightarrow \gamma X$	

$\Gamma(\gamma\eta)/\Gamma_{total}$					Γ_{90}/Γ
VALUE (units 10^{-4})	CL%	DOCUMENT ID	TECN	COMMENT	
<1.5	90	28 PEDLAR	09 CLE3	$\psi(2S) \rightarrow \gamma X$	

$\Gamma(\gamma\eta')/\Gamma_{total}$					Γ_{91}/Γ
VALUE (units 10^{-4})	CL%	DOCUMENT ID	TECN	COMMENT	
<1.8	90	28 PEDLAR	09 CLE3	$\psi(2S) \rightarrow \gamma X$	

²⁸ Assuming maximal destructive interference between $\psi(3770)$ and continuum sources.

$\psi(3770)$ REFERENCES

BESSON	10	PRL 104 159901 (err.)	D. Besson <i>et al.</i>	(CLEO Collab.)
ABLIKIM	09C	EPJ C64 243	M. Ablikim <i>et al.</i>	(BES Collab.)
PEDLAR	09	PR D79 111101	T.K. Pedlar <i>et al.</i>	(CLEO Collab.)
ABLIKIM	08B	PL B659 74	M. Ablikim <i>et al.</i>	(BES Collab.)
ABLIKIM	05D	PL B660 315	M. Ablikim <i>et al.</i>	(BES Collab.)
ABLIKIM	05M	PL B670 179	M. Ablikim <i>et al.</i>	(BES Collab.)
ABLIKIM	05N	PL B670 184	M. Ablikim <i>et al.</i>	(BES Collab.)
AUBERT	08B	PR D77 011102R	B. Aubert <i>et al.</i>	(BABAR Collab.)
BRODZICKA	08	PRL 100 092001	J. Brodzicka <i>et al.</i>	(BELLE Collab.)
PAKHOLOVA	08	PR D77 011103R	G. Pakhlova <i>et al.</i>	(BELLE Collab.)
ABLIKIM	07B	PL B650 111	M. Ablikim <i>et al.</i>	(BES Collab.)
ABLIKIM	07E	PL B652 238	M. Ablikim <i>et al.</i>	(BES Collab.)
ABLIKIM	07F	PL B656 30	M. Ablikim <i>et al.</i>	(BES Collab.)
ABLIKIM	07I	EPJ C52 805	M. Ablikim <i>et al.</i>	(BES Collab.)
ABLIKIM	07K	PR D76 122002	M. Ablikim <i>et al.</i>	(BES Collab.)
AUBERT	07BE	PR D76 111105R	B. Aubert <i>et al.</i>	(BABAR Collab.)
DOBBS	07	PR D76 112001	S. Dobbs <i>et al.</i>	(CLEO Collab.)
ABLIKIM	06L	PRL 97 121801	M. Ablikim <i>et al.</i>	(BES Collab.)
ABLIKIM	06N	PL B641 145	M. Ablikim <i>et al.</i>	(BES Collab.)
ADAM	06	PRL 96 082004	N.E. Adam <i>et al.</i>	(CLEO Collab.)
ADAMS	06	PR D73 012002	G.S. Adams <i>et al.</i>	(CLEO Collab.)
BESSON	06	PRL 96 092002	D. Besson <i>et al.</i>	(CLEO Collab.)
Also		PRL 104 159901 (err.)	D. Besson <i>et al.</i>	(CLEO Collab.)
BRIERE	06	PR D74 031106R	R.A. Briere <i>et al.</i>	(CLEO Collab.)
COAN	06A	PRL 96 102002	T.E. Coan <i>et al.</i>	(CLEO Collab.)
CRONIN-HEN...	06	PR D74 012005	D. Cronin-Hennessy <i>et al.</i>	(CLEO Collab.)
HUANG	06A	PRL 96 032003	G.S. Huang <i>et al.</i>	(CLEO Collab.)
BAI	05	PL B605 63	J.Z. Bai <i>et al.</i>	(BES Collab.)
HE	05	PRL 95 121801	Q. He <i>et al.</i>	(CLEO Collab.)
Also		PRL 96 199903 (err.)	Q. He <i>et al.</i>	(CLEO Collab.)
ABLIKIM	04F	PR D70 077101	M. Ablikim <i>et al.</i>	(BES Collab.)
ATHAR	04	PR D70 112002	S.B. Athar <i>et al.</i>	(CLEO Collab.)
CHISTOV	04	PRL 93 051803	R. Chistov <i>et al.</i>	(BELLE Collab.)
PDG	04	PL B592 1	S. Eidelman <i>et al.</i>	(PDG Collab.)
BAI	02C	PRL 88 101802	J.Z. Bai <i>et al.</i>	(BES Collab.)
ADLER	88C	PR 80 89	J. Adler <i>et al.</i>	(Mark II Collab.)
SCHINDLER	80	PR D21 2716	R.H. Schindler <i>et al.</i>	(Mark II Collab.)
BACINO	78	PRL 40 671	W.J. Bacino <i>et al.</i>	(SLAC, UCLA, UCI)
RAPIDIS	77	PRL 39 526	P.A. Rapidis <i>et al.</i>	(LGW Collab.)

$X(3872)$

$I^G(J^{PC}) = 0^?(?^{?+})$

Seen by CHOI 03 in $B \rightarrow K\pi^+\pi^- J/\psi(1S)$ decays as a narrow peak in the invariant mass distribution of the $\pi^+\pi^- J/\psi(1S)$ final state, but not seen in the $\gamma\chi_{c1}$ final state of these decays. Possibly absent in the invariant mass spectrum of the final state $\pi^+\pi^- J/\psi(1S)$ in e^+e^- collisions. Interpretation as a 1^{--} charmonium state not favored. Isovector hypothesis excluded by AUBERT 05B. A helicity amplitude analysis of the $X(3872) \rightarrow J/\psi\pi^+\pi^-$ decay gives two possible J^{PC} assignments: $J^{PC} = 1^{++}$ and 2^{--} (ABULENCIA 07E).

See our note "New charmonium-like states" in the 2008 edition of this Review (PDG 08) and the extensive chapter on Spectroscopy in N. Brambilla *et al.* (Quarkonium Working Group), to be published in the Eur. Phys. J. in 2010.

$X(3872)$ MASS FROM $J/\psi\pi\pi$ MODE

VALUE (MeV)	EVTS	DOCUMENT ID	TECN	COMMENT
3871.56 ± 0.22 OUR AVERAGE				
3871.61 ± 0.16 ± 0.19	6k	1,2 AALTONEN	09AU CDF2	$p\bar{p} \rightarrow J/\psi\pi^+\pi^- X$
3871.4 ± 0.6 ± 0.1	93.4	AUBERT	08Y BABR	$B^+ \rightarrow K^+ J/\psi\pi^+\pi^-$
3868.7 ± 1.5 ± 0.4	9.4	AUBERT	08Y BABR	$B^0 \rightarrow K_S^0 J/\psi\pi^+\pi^-$
3871.8 ± 3.1 ± 3.0	522	2,3 ABAZOV	04F D0	$p\bar{p} \rightarrow J/\psi\pi^+\pi^- X$
3872.0 ± 0.6 ± 0.5	36	CHOI	03 BELL	$B \rightarrow K\pi^+\pi^- J/\psi$
• • • We do not use the following data for averages, fits, limits, etc. • • •				
3868.6 ± 1.2 ± 0.2	8	4 AUBERT	06 BABR	$B^0 \rightarrow K_S^0 J/\psi\pi^+\pi^-$
3871.3 ± 0.6 ± 0.1	61	4 AUBERT	06 BABR	$B^- \rightarrow K^- J/\psi\pi^+\pi^-$
3873.4 ± 1.4	25	5 AUBERT	05R BABR	$B^+ \rightarrow K^+ J/\psi\pi^+\pi^-$
3871.3 ± 0.7 ± 0.4	730	2,6 ACOSTA	04 CDF2	$p\bar{p} \rightarrow J/\psi\pi^+\pi^- X$
3836 ± 13	58	2,7 ANTONIAZZI	94 E705	$300\pi^\pm Li \rightarrow J/\psi\pi^+\pi^- X$

- ¹ A possible equal mixture of two states with a mass difference greater than 3.6 MeV/ c^2 is excluded at 95% CL.
² Width consistent with detector resolution.
³ Calculated from the corresponding $m_{X(3872)} - m_{J/\psi}$ using $m_{J/\psi} = 3096.916$ MeV.
⁴ Calculated from the corresponding $m_{X(3872)} - m_{\psi(2S)}$ using $m_{\psi(2S)} = 3686.093$ MeV. Superseded by AUBERT 08Y.
⁵ Calculated from the corresponding $m_{X(3872)} - m_{\psi(2S)}$ using $m_{\psi(2S)} = 3685.96$ MeV. Superseded by AUBERT 06.
⁶ Superseded by AALTONEN 09AU.
⁷ A lower mass value can be due to an incorrect momentum scale for soft pions.

$X(3872)$ MASS FROM $D^{*0}D^0$ MODE

VALUE (MeV)	EVTS	DOCUMENT ID	TECN	COMMENT
• • • We do not use the following data for averages, fits, limits, etc. • • •				
3872.9 ^{+0.6+0.4} _{-0.4-0.5}	50	8,9 AUSHEV	10 BELL	$B \rightarrow \bar{D}^{*0}D^0 K$
3875.1 ^{+0.7+0.5} _{-0.5-0.5}	33 ± 6	9 AUBERT	08B BABR	$B \rightarrow \bar{D}^{*0}D^0 K$
3875.2 ± 0.7 ^{+0.9} _{-1.8}	24 ± 6	9,10 GOKHROO	06 BELL	$B \rightarrow D^0\bar{D}^0\pi^0 K$

- ⁸ Calculated from the measured $m_{X(3872)} - m_{D^{*0}} - m_{D^0} = 1.1^{+0.6+0.1}_{-0.4-0.3}$ MeV.
⁹ Experiments report $D^{*0}D^0$ invariant mass above $D^{*0}D^0$ threshold because D^{*0} decay products are kinematically constrained to the D^{*0} mass, even though the D^{*0} may decay off-shell.
¹⁰ Superseded by AUSHEV 10.

$m_{X(3872)} - m_{J/\psi}$

VALUE (MeV)	EVTS	DOCUMENT ID	TECN	COMMENT
774.9 ± 3.1 ± 3.0	522	ABAZOV	04F D0	$p\bar{p} \rightarrow J/\psi\pi^+\pi^- X$

$m_{X(3872)} - m_{\psi(2S)}$

VALUE (MeV)	EVTS	DOCUMENT ID	TECN	COMMENT
• • • We do not use the following data for averages, fits, limits, etc. • • •				
187.4 ± 1.4	25	11 AUBERT	05R BABR	$B^+ \rightarrow K^+ J/\psi\pi^+\pi^-$

¹¹ Superseded by AUBERT 06.

$X(3872)$ WIDTH

VALUE (MeV)	CL%	EVTS	DOCUMENT ID	TECN	COMMENT
<2.3	90	36	CHOI	03 BELL	$B \rightarrow K\pi^+\pi^- J/\psi$
• • • We do not use the following data for averages, fits, limits, etc. • • •					
<3.3	90		AUBERT	08Y BABR	$B^+ \rightarrow K^+ J/\psi\pi^+\pi^-$
<4.1	90	69	AUBERT	06 BABR	$B \rightarrow K\pi^+\pi^- J/\psi$

Meson Particle Listings

 $X(3872)$ $X(3872)$ WIDTH FROM $\bar{D}^{*0} D^0$ MODE

VALUE (MeV)	EVTS	DOCUMENT ID	TECN	COMMENT
•••				We do not use the following data for averages, fits, limits, etc. •••
$3.9^{+2.8+0.2}_{-1.4-1.1}$	50	12 AUSHEV	10 BELL	$B \rightarrow \bar{D}^{*0} D^0 K$
$3.0^{+1.9}_{-1.4} \pm 0.9$	33 ± 6	AUBERT	08B BABR	$B \rightarrow \bar{D}^{*0} D^0 K$
¹² With a measured value of $B(B \rightarrow X(3872) K) \times B(X(3872) \rightarrow D^{*0} \bar{D}^0) = (0.80 \pm 0.20 \pm 0.10) \times 10^{-4}$, assumed to be equal for both charged and neutral modes.				

 $X(3872)$ DECAY MODES

Mode	Fraction (Γ_i/Γ)
Γ_1 $e^+ e^-$	
Γ_2 $\pi^+ \pi^- J/\psi(1S)$	$> 2.6\%$
Γ_3 $\rho^0 J/\psi(1S)$	
Γ_4 $D^0 \bar{D}^0 \pi^0$	$> 3.2 \times 10^{-3}$
Γ_5 $\bar{D}^{*0} D^0$	$> 5 \times 10^{-3}$
Γ_6 $\gamma\gamma$	
Γ_7 $D^0 \bar{D}^0$	
Γ_8 $D^+ D^-$	
Γ_9 $\gamma\chi_{c1}$	
Γ_{10} $\eta J/\psi$	
Γ_{11} $\gamma J/\psi$	$> 9 \times 10^{-3}$
Γ_{12} $\gamma\psi(2S)$	$> 3.0\%$

 $X(3872)$ PARTIAL WIDTHS

$\Gamma(e^+ e^-)$ Γ_1				
VALUE (keV)	CL%	DOCUMENT ID	TECN	COMMENT
•••				We do not use the following data for averages, fits, limits, etc. •••
< 0.28	90	13 YUAN	04 RVUE	$e^+ e^- \rightarrow \pi^+ \pi^- J/\psi$
¹³ Using BABAR 98E data on $e^+ e^- \rightarrow \pi^+ \pi^- \ell^+ \ell^-$. Assuming that $\Gamma(\pi^+ \pi^- J/\psi)$ of $X(3872)$ is the same as that of $\psi(2S)$ (85.4 keV).				

 $X(3872)$ $\Gamma(i)\Gamma(e^+ e^-)/\Gamma(\text{total})$

$\Gamma(\pi^+ \pi^- J/\psi(1S)) \times \Gamma(e^+ e^-)/\Gamma(\text{total})$ $\Gamma_2 \Gamma_1/\Gamma$				
VALUE (eV)	CL%	DOCUMENT ID	TECN	COMMENT
< 6.2	90	14,15 AUBERT	05D BABR	$10.6 e^+ e^- \rightarrow K^+ K^- \pi^+ \pi^- \gamma$
•••				We do not use the following data for averages, fits, limits, etc. •••
< 8.3	90	15 DOBBS	05 CLE3	$e^+ e^- \rightarrow \pi^+ \pi^- J/\psi$
< 10	90	16 YUAN	04 RVUE	$e^+ e^- \rightarrow \pi^+ \pi^- J/\psi$
¹⁴ Using $B(X(3872) \rightarrow J/\psi \pi^+ \pi^-) \cdot B(J/\psi \rightarrow \mu^+ \mu^-) \cdot \Gamma(X(3872) \rightarrow e^+ e^-) < 0.37$ eV from AUBERT 05D and $B(J/\psi \rightarrow \mu^+ \mu^-) = 0.0588 \pm 0.0010$ from the PDG 04.				
¹⁵ Assuming $X(3872)$ has $J^{PC} = 1^{--}$.				
¹⁶ Using BABAR 98E data on $e^+ e^- \rightarrow \pi^+ \pi^- \ell^+ \ell^-$. From theoretical calculation of the production cross section and using $B(J/\psi \rightarrow \mu^+ \mu^-) = (5.88 \pm 0.10)\%$.				

 $X(3872)$ $\Gamma(i)\Gamma(\gamma\gamma)/\Gamma(\text{total})$

$\Gamma(\gamma\gamma) \times \Gamma(\pi^+ \pi^- J/\psi(1S))/\Gamma(\text{total})$ $\Gamma_6 \Gamma_2/\Gamma$				
VALUE (eV)	CL%	DOCUMENT ID	TECN	COMMENT
•••				We do not use the following data for averages, fits, limits, etc. •••
< 12.9	90	17 DOBBS	05 CLE3	$e^+ e^- \rightarrow \pi^+ \pi^- J/\psi\gamma$
¹⁷ Assuming $X(3872)$ has positive C parity and spin 0.				

 $X(3872)$ BRANCHING RATIOS

$\Gamma(\pi^+ \pi^- J/\psi(1S))/\Gamma(\text{total})$ Γ_2/Γ				
VALUE	EVTS	DOCUMENT ID	TECN	COMMENT
> 0.026	93 ± 17	18 AUBERT	08Y BABR	$B \rightarrow X(3872) K$
•••				We do not use the following data for averages, fits, limits, etc. •••
> 0.04	30	19 AUBERT	05R BABR	$B^+ \rightarrow K^+ J/\psi \pi^+ \pi^-$
> 0.04	36 ± 7	20 CHOI	03 BABR	$B^+ \rightarrow K^+ J/\psi \pi^+ \pi^-$
¹⁸ AUBERT 08Y reports $[\Gamma(X(3872) \rightarrow \pi^+ \pi^- J/\psi(1S))/\Gamma(\text{total})] \times [B(B^+ \rightarrow X(3872) K^+)] = (8.4 \pm 1.5 \pm 0.7) \times 10^{-6}$ which we divide by our best value $B(B^+ \rightarrow X(3872) K^+) < 3.2 \times 10^{-4}$.				
¹⁹ Superseded by AUBERT 08Y. AUBERT 05R reports $[\Gamma(X(3872) \rightarrow \pi^+ \pi^- J/\psi(1S))/\Gamma(\text{total})] \times [B(B^+ \rightarrow X(3872) K^+)] = (1.28 \pm 0.41) \times 10^{-5}$ which we divide by our best value $B(B^+ \rightarrow X(3872) K^+) < 3.2 \times 10^{-4}$.				
²⁰ CHOI 03 reports $[\Gamma(X(3872) \rightarrow \pi^+ \pi^- J/\psi(1S))/\Gamma(\text{total})] \times [B(B^+ \rightarrow X(3872) K^+)] / [B(B^+ \rightarrow \psi(2S) K^+)] / [B(\psi(2S) \rightarrow J/\psi(1S) \pi^+ \pi^-)] = 0.063 \pm 0.012 \pm 0.007$ which we multiply or divide by our best values $B(B^+ \rightarrow X(3872) K^+) < 3.2 \times 10^{-4}$, $B(B^+ \rightarrow \psi(2S) K^+) = (6.46 \pm 0.33) \times 10^{-4}$, $B(\psi(2S) \rightarrow J/\psi(1S) \pi^+ \pi^-) = (33.6 \pm 0.4) \times 10^{-2}$.				

 $\Gamma(D^0 \bar{D}^0 \pi^0)/\Gamma(\text{total})$ Γ_4/Γ

VALUE	EVTS	DOCUMENT ID	TECN	COMMENT
$> 3.2 \times 10^{-3}$	17 ± 5	21 GOKHROO	06 BELL	$B^+ \rightarrow D^0 \bar{D}^0 \pi^0 K^+$
²¹ GOKHROO 06 reports $[\Gamma(X(3872) \rightarrow D^0 \bar{D}^0 \pi^0)/\Gamma(\text{total})] \times [B(B^+ \rightarrow X(3872) K^+)] = (1.02 \pm 0.31^{+0.21}_{-0.29}) \times 10^{-6}$ which we divide by our best value $B(B^+ \rightarrow X(3872) K^+) < 3.2 \times 10^{-4}$.				

 $\Gamma(\bar{D}^{*0} D^0)/\Gamma(\text{total})$ Γ_5/Γ

VALUE	EVTS	DOCUMENT ID	TECN	COMMENT
$> 5 \times 10^{-3}$	27 ± 6	22 AUBERT	08B BABR	$B^+ \rightarrow \bar{D}^{*0} D^0 K^+$
²² AUBERT 08B reports $[\Gamma(X(3872) \rightarrow \bar{D}^{*0} D^0)/\Gamma(\text{total})] \times [B(B^+ \rightarrow X(3872) K^+)] = (1.67 \pm 0.36 \pm 0.47) \times 10^{-6}$ which we divide by our best value $B(B^+ \rightarrow X(3872) K^+) < 3.2 \times 10^{-4}$.				

 $\Gamma(D^0 \bar{D}^0 \pi^0)/\Gamma(\pi^+ \pi^- J/\psi(1S))$ Γ_4/Γ_2

VALUE	DOCUMENT ID	TECN	COMMENT
seen	23 GOKHROO	06 BELL	$B \rightarrow D^0 \bar{D}^0 \pi^0 K$
•••			We do not use the following data for averages, fits, limits, etc. •••
seen	AUSHEV	10 BELL	$B \rightarrow D^0 \bar{D}^0 \pi^0 K$
²³ May not necessarily be the same state as that observed in the $J/\psi \pi^+ \pi^-$ mode. Supersedes CHISTOV 04.			

 $\Gamma(D^0 \bar{D}^0)/\Gamma(\pi^+ \pi^- J/\psi(1S))$ Γ_7/Γ_2

VALUE	DOCUMENT ID	TECN	COMMENT
•••			We do not use the following data for averages, fits, limits, etc. •••
not seen	CHISTOV	04 BELL	$B \rightarrow K D^0 \bar{D}^0$

 $\Gamma(D^+ D^-)/\Gamma(\pi^+ \pi^- J/\psi(1S))$ Γ_8/Γ_2

VALUE	DOCUMENT ID	TECN	COMMENT
•••			We do not use the following data for averages, fits, limits, etc. •••
not seen	CHISTOV	04 BELL	$B \rightarrow K D^+ D^-$

 $\Gamma(\gamma\chi_{c1})/\Gamma(\pi^+ \pi^- J/\psi(1S))$ Γ_9/Γ_2

VALUE	CL%	DOCUMENT ID	TECN	COMMENT
< 0.89	90	CHOI	03 BELL	$B \rightarrow K \pi^+ \pi^- J/\psi$

 $\Gamma(\eta J/\psi)/\Gamma(\pi^+ \pi^- J/\psi(1S))$ Γ_{10}/Γ_2

VALUE	CL%	DOCUMENT ID	TECN	COMMENT
•••				We do not use the following data for averages, fits, limits, etc. •••
< 0.6	90	AUBERT	04Y BABR	$B \rightarrow K \eta J/\psi$

 $\Gamma(\gamma J/\psi)/\Gamma(\text{total})$ Γ_{11}/Γ

VALUE	EVTS	DOCUMENT ID	TECN	COMMENT
$> 9 \times 10^{-3}$	23 ± 6	24 AUBERT	09B BABR	$B^+ \rightarrow \gamma J/\psi K^+$
•••				We do not use the following data for averages, fits, limits, etc. •••
> 0.010	19	25 AUBERT, BE	06M BABR	$B^+ \rightarrow \gamma J/\psi K^+$
²⁴ AUBERT 09B reports $[\Gamma(X(3872) \rightarrow \gamma J/\psi)/\Gamma(\text{total})] \times [B(B^+ \rightarrow X(3872) K^+)] = (2.8 \pm 0.8 \pm 0.1) \times 10^{-6}$ which we divide by our best value $B(B^+ \rightarrow X(3872) K^+) < 3.2 \times 10^{-4}$.				
²⁵ Superseded by AUBERT 09B. AUBERT, BE 06M reports $[\Gamma(X(3872) \rightarrow \gamma J/\psi)/\Gamma(\text{total})] \times [B(B^+ \rightarrow X(3872) K^+)] = (3.3 \pm 1.0 \pm 0.3) \times 10^{-6}$ which we divide by our best value $B(B^+ \rightarrow X(3872) K^+) < 3.2 \times 10^{-4}$.				

 $\Gamma(\gamma\psi(2S))/\Gamma(\text{total})$ Γ_{12}/Γ

VALUE	EVTS	DOCUMENT ID	TECN	COMMENT
> 0.030	25 ± 7	26 AUBERT	09B BABR	$B^+ \rightarrow \gamma\psi(2S) K^+$
²⁶ AUBERT 09B reports $[\Gamma(X(3872) \rightarrow \gamma\psi(2S))/\Gamma(\text{total})] \times [B(B^+ \rightarrow X(3872) K^+)] = (9.5 \pm 2.7 \pm 0.6) \times 10^{-6}$ which we divide by our best value $B(B^+ \rightarrow X(3872) K^+) < 3.2 \times 10^{-4}$.				

 $\Gamma(\gamma\psi(2S))/\Gamma(\gamma J/\psi)$ Γ_{12}/Γ_{11}

VALUE	DOCUMENT ID	TECN	COMMENT
3.4 ± 1.4	AUBERT	09B BABR	$B^+ \rightarrow \gamma c \bar{c} K^+$

 $X(3872)$ REFERENCES

AUSHEV	10	PR D81 031103	T. Aushev et al.	(BELLE Collab.)
AALTONEN	09AU	PRL 103 152001	T. Aaltonen et al.	(CDF Collab.)
AUBERT	09B	PRL 102 132001	B. Aubert et al.	(BABAR Collab.)
AUBERT	08B	PR D77 011102R	B. Aubert et al.	(BABAR Collab.)
AUBERT	08Y	PR D77 111101R	B. Aubert et al.	(BABAR Collab.)
PDG	08	PL B667 1	C. Amsler et al.	(PDG Collab.)
ABUENENCIA	07E	PRL 98 132002	A. Abuencia et al.	(CDF Collab.)
AUBERT	06	PR D73 011101R	B. Aubert et al.	(BABAR Collab.)
AUBERT, BE	06M	PR D74 071101R	B. Aubert et al.	(BABAR Collab.)
GOKHROO	06	PRL 97 162002	G. Gokhroo et al.	(BELLE Collab.)
AUBERT	05B	PR D71 031501R	B. Aubert et al.	(BABAR Collab.)
AUBERT	05D	PR D71 052001	B. Aubert et al.	(BABAR Collab.)
AUBERT	05R	PR D71 071103R	B. Aubert et al.	(BABAR Collab.)
DOBBS	05	PRL 94 032004	S. Dobbs et al.	(CLEO Collab.)
ABAZOV	04F	PRL 93 162002	V.M. Abazov et al.	(DO Collab.)
ACOSTA	04	PRL 93 072001	D. Acosta et al.	(CDF Collab.)
AUBERT	04Y	PRL 93 041801	B. Aubert et al.	(BABAR Collab.)
CHISTOV	04	PRL 93 051803	R. Chistov et al.	(BELLE Collab.)
PDG	04	PL B592 1	S. Eidelman et al.	(PDG Collab.)
YUAN	04	PL B579 74	S.-K. Choi et al.	(PDG Collab.)
CHOI	03	PRL 91 262001	S.-K. Choi et al.	(BELLE Collab.)
BAI	98E	PR D57 3854	J.Z. Bai et al.	(BES Collab.)
ANTONIAZZI	94	PR D50 4258	L. Antoniazzi et al.	(E705 Collab.)

See key on page 405

Meson Particle Listings

$\chi_{c2}(2P)$, X(3940), X(3945)

$\chi_{c2}(2P)$

$I^G(J^{PC}) = 0^+(2^{++})$

OMITTED FROM SUMMARY TABLE

$\chi_{c2}(2P)$ MASS

VALUE (MeV)	EVTS	DOCUMENT ID	TECN	COMMENT
3929 ± 5 ± 2	64	UEHARA	06	BELL $10.6 e^+ e^- \rightarrow e^+ e^- D\bar{D}$

$\chi_{c2}(2P)$ WIDTH

VALUE (MeV)	CL%	EVTS	DOCUMENT ID	TECN	COMMENT
29 ± 10 ± 2		64	UEHARA	06	BELL $10.6 e^+ e^- \rightarrow e^+ e^- D\bar{D}$

$\chi_{c2}(2P)$ DECAY MODES

Mode	Fraction (Γ_i/Γ)
Γ_1 $\gamma\gamma$	
Γ_2 $D\bar{D}$	
Γ_3 $D^+ D^-$	
Γ_4 $D^0 \bar{D}^0$	

$\chi_{c2}(2P)$ PARTIAL WIDTHS

$\chi_{c2}(2P) \Gamma(\gamma\gamma)\Gamma(i)/\Gamma(\text{total})$

VALUE (keV)	CL%	EVTS	DOCUMENT ID	TECN	COMMENT
0.18 ± 0.05 ± 0.03		64	¹ UEHARA	06	BELL $10.6 e^+ e^- \rightarrow e^+ e^- D\bar{D}$

¹ Assuming $B(D^+ D^-) = 0.89 B(D^0 \bar{D}^0)$.

$\chi_{c2}(2P)$ BRANCHING RATIOS

VALUE	CL%	EVTS	DOCUMENT ID	TECN	COMMENT
0.74 ± 0.43 ± 0.16		64	UEHARA	06	BELL $10.6 e^+ e^- \rightarrow e^+ e^- D\bar{D}$

$\chi_{c2}(2P)$ REFERENCES

UEHARA 06 PRL 96 082003 S. Uehara et al. (BELLE Collab.)

X(3940)

$I^G(J^{PC}) = ?^?(?^{??})$

OMITTED FROM SUMMARY TABLE

Reported by ABE 07, observed in $e^+ e^- \rightarrow J/\psi X$.

X(3940) MASS

VALUE (MeV)	CL%	EVTS	DOCUMENT ID	TECN	COMMENT
3942⁺⁷₋₆ ± 6		52	PAKHLOV	08	BELL $e^+ e^- \rightarrow J/\psi X$

••• We do not use the following data for averages, fits, limits, etc. •••

3943 ± 6 ± 6 25 ¹ABE 07 BELL $e^+ e^- \rightarrow J/\psi X$

3936 ± 14 266 ²ABE 07 BELL $e^+ e^- \rightarrow J/\psi(c\bar{c})$

¹ From a fit to $D^{*+} D^-$ and $D^{*0} \bar{D}^0$ events.
² From the inclusive fit. Not independent of the exclusive measurement by ABE 07.

X(3940) WIDTH

VALUE (MeV)	CL%	EVTS	DOCUMENT ID	TECN	COMMENT
37⁺²⁶₋₁₅ ± 8		52	PAKHLOV	08	BELL $e^+ e^- \rightarrow J/\psi X$
<52	90	25	ABE	07	BELL $e^+ e^- \rightarrow J/\psi X$

X(3940) DECAY MODES

Mode	Fraction (Γ_i/Γ)
Γ_1 $D\bar{D}^* + \text{c.c.}$	seen
Γ_2 $D\bar{D}$	not seen
Γ_3 $J/\psi\omega$	not seen

X(3940) BRANCHING RATIOS

VALUE	CL%	EVTS	DOCUMENT ID	TECN	COMMENT
>0.45	90	25	^{3,4} ABE	07	BELL $e^+ e^- \rightarrow J/\psi X$

••• We do not use the following data for averages, fits, limits, etc. •••

³ For X(3940) decaying to final states with more than two tracks.
⁴ PAKHLOV 08 finds that the inclusive peak near 3940 MeV/c² may consist of several states.

VALUE	CL%	EVTS	DOCUMENT ID	TECN	COMMENT
<0.41	90	5,6	ABE	07	BELL $e^+ e^- \rightarrow J/\psi X$

••• We do not use the following data for averages, fits, limits, etc. •••

⁵ For X(3940) decaying to final states with more than two tracks.
⁶ PAKHLOV 08 finds that the inclusive peak near 3940 MeV/c² may consist of several states.

VALUE	CL%	EVTS	DOCUMENT ID	TECN	COMMENT
<0.26	90	7,8	ABE	07	BELL $e^+ e^- \rightarrow J/\psi X$

••• We do not use the following data for averages, fits, limits, etc. •••

⁷ For X(3940) decaying to final states with more than two tracks.
⁸ PAKHLOV 08 finds that the inclusive peak near 3940 MeV/c² may consist of several states.

X(3940) REFERENCES

PAKHLOV 08 PRL 100 202001 P. Pakhlov et al. (BELLE Collab.)
 ABE 07 PRL 98 082001 K. Abe et al. (BELLE Collab.)

X(3945)

$I^G(J^{PC}) = 0^+(?^{?+})$

OMITTED FROM SUMMARY TABLE

Observed in $\omega J/\psi$, thus C = +. May be the same state as $\chi_{c2}(2P)$.

X(3945) MASS

VALUE (MeV)	CL%	EVTS	DOCUMENT ID	TECN	COMMENT
3915.5 ± 2.7 OUR AVERAGE		49 ± 15			

3915 ± 3 ± 2 49 ± 15 ¹UEHARA 10 BELL $10.6 e^+ e^- \rightarrow e^+ e^- \omega J/\psi$
 3914.6^{+3.8}_{-3.4} ± 2.0 ²AUBERT 08w BABR $B \rightarrow \omega J/\psi K$
 3943 ± 11 ± 13 58 ± 11 ²CHOI 05 BELL $B \rightarrow \omega J/\psi K$

¹ May be $\chi_{c2}(2P)$.
² $\omega J/\psi$ threshold enhancement fitted as an S-wave Breit-Wigner resonance.

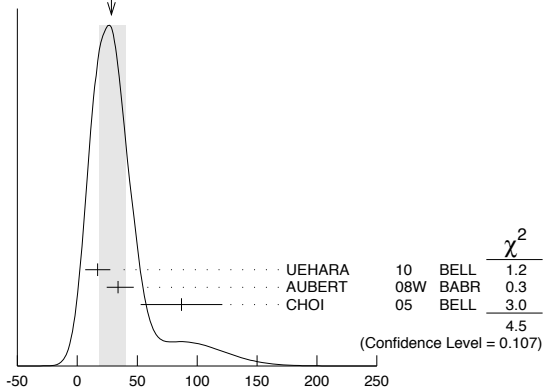
X(3945) WIDTH

VALUE (MeV)	CL%	EVTS	DOCUMENT ID	TECN	COMMENT
28⁺¹²₋₁₀ OUR AVERAGE		49 ± 15			

Error includes scale factor of 1.5. See the ideogram below.
 17 ± 10 ± 3 49 ± 15 ³UEHARA 10 BELL $10.6 e^+ e^- \rightarrow e^+ e^- \omega J/\psi$
 34⁺¹²₋₈ ± 5 ⁴AUBERT 08w BABR $B \rightarrow \omega J/\psi K$
 87 ± 22 ± 26 58 ± 11 ⁴CHOI 05 BELL $B \rightarrow \omega J/\psi K$

³ May be $\chi_{c2}(2P)$.
⁴ $\omega J/\psi$ threshold enhancement fitted as an S-wave Breit-Wigner resonance.

WEIGHTED AVERAGE
 28+12-10 (Error scaled by 1.5)



X(3945) WIDTH (MeV)

Meson Particle Listings

 $X(3945)$, $\psi(4040)$ $X(3945)$ DECAY MODES

Mode	Fraction (Γ_i/Γ)
Γ_1 $\omega J/\psi$	seen
Γ_2 $\overline{D}^{*0} D^0$	
Γ_3 $\gamma\gamma$	seen

 $X(3945)$ $\Gamma(i)\Gamma(\gamma\gamma)/\Gamma(\text{total})$

$\Gamma(\omega J/\psi) \times \Gamma(\gamma\gamma)/\Gamma_{\text{total}}$		$\Gamma_1\Gamma_3/\Gamma$	
VALUE (eV)	EVTs	DOCUMENT ID	TECN COMMENT
$18 \pm 5 \pm 2$	49 ± 15	5,6 UEHARA	10 BELL $10.6 e^+ e^- \rightarrow e^+ e^- \omega J/\psi$
••• We do not use the following data for averages, fits, limits, etc. •••			
$61 \pm 17 \pm 8$	49 ± 15	5,7 UEHARA	10 BELL $10.6 e^+ e^- \rightarrow e^+ e^- \omega J/\psi$
5 May be $\chi_{c2}(2P)$.			
6 For $J^P = 2^+$, helicity-2.			
7 For $J^P = 0^+$.			

 $X(3945)$ BRANCHING RATIOS

$\Gamma(\gamma\gamma)/\Gamma_{\text{total}}$		Γ_3/Γ	
VALUE	DOCUMENT ID	TECN	COMMENT
seen	8 UEHARA	10 BELL	$10.6 e^+ e^- \rightarrow e^+ e^- \omega J/\psi$
8 May be $\chi_{c2}(2P)$.			
$\Gamma(\omega J/\psi)/\Gamma(\overline{D}^{*0} D^0)$		Γ_1/Γ_2	
VALUE	CL%	DOCUMENT ID	TECN COMMENT
>0.71	90	9 AUSHEV	10 BELL $B \rightarrow \overline{D}^{*0} D^0 K$
9 By combining the upper limit $B(B \rightarrow X(3945) K) \times B(X(3945) \rightarrow D^{*0} \overline{D}^0) < 0.67 \times 10^{-4}$ from AUSHEV 10 with the average of CHOI 05 and AUBERT 08w measurements $B(B \rightarrow X(3945) K) \times B(X(3945) \rightarrow \omega J/\psi) = (0.51 \pm 0.11) \times 10^{-4}$.			

 $X(3945)$ REFERENCES

AUSHEV	10	PR D81 031103	T. Aushet et al.	(BELLE Collab.)
UEHARA	10	PRL 104 092001	S. Uehara et al.	(BELLE Collab.)
AUBERT	08w	PRL 101 082001	B. Aubert et al.	(BABAR Collab.)
CHOI	05	PRL 94 182002	S.-K. Choi et al.	(BELLE Collab.)

 $\psi(4040)$

$$J^{PC} = 0^-(1^{--})$$

 $\psi(4040)$ MASS

VALUE (MeV)	DOCUMENT ID	TECN	COMMENT
4039 ± 1	OUR ESTIMATE		
4039.6 ± 4.3	1 ABLIKIM	08d BES2	$e^+ e^- \rightarrow \text{hadrons}$
••• We do not use the following data for averages, fits, limits, etc. •••			
4037 ± 2	2 SETH	05A RVUE	$e^+ e^- \rightarrow \text{hadrons}$
4040 ± 1	3 SETH	05A RVUE	$e^+ e^- \rightarrow \text{hadrons}$
4040 ± 10	BRANDELIK	78c DASP	$e^+ e^-$
1 Reanalysis of data presented in BAI 02c. From a global fit over the center-of-mass energy region 3.7–5.0 GeV covering the $\psi(3770)$, $\psi(4040)$, $\psi(4160)$, and $\psi(4415)$ resonances. Phase angle fixed in the fit to $\delta = (130 \pm 46)^\circ$.			
2 From a fit to Crystal Ball (OSTERHELD 86) data.			
3 From a fit to BES (BAI 02c) data.			

 $\psi(4040)$ WIDTH

VALUE (MeV)	DOCUMENT ID	TECN	COMMENT
80 ± 10	OUR ESTIMATE		
84.5 ± 12.3	4 ABLIKIM	08d BES2	$e^+ e^- \rightarrow \text{hadrons}$
••• We do not use the following data for averages, fits, limits, etc. •••			
85 ± 10	5 SETH	05A RVUE	$e^+ e^- \rightarrow \text{hadrons}$
89 ± 6	6 SETH	05A RVUE	$e^+ e^- \rightarrow \text{hadrons}$
52 ± 10	BRANDELIK	78c DASP	$e^+ e^-$
4 Reanalysis of data presented in BAI 02c. From a global fit over the center-of-mass energy region 3.7–5.0 GeV covering the $\psi(3770)$, $\psi(4040)$, $\psi(4160)$, and $\psi(4415)$ resonances. Phase angle fixed in the fit to $\delta = (130 \pm 46)^\circ$.			
5 From a fit to Crystal Ball (OSTERHELD 86) data.			
6 From a fit to BES (BAI 02c) data.			

 $\psi(4040)$ DECAY MODES

Mode	Fraction (Γ_i/Γ)	Confidence level
Γ_1 $e^+ e^-$	$(1.07 \pm 0.16) \times 10^{-5}$	
Γ_2 $D\overline{D}$	seen	
Γ_3 $D^0 \overline{D}^0$	seen	
Γ_4 $D^+ D^-$	seen	
Γ_5 $D^* \overline{D} + \text{c.c.}$	seen	
Γ_6 $D^*(2007)^0 \overline{D}^0 + \text{c.c.}$	seen	
Γ_7 $D^*(2010)^+ D^- + \text{c.c.}$	seen	
Γ_8 $D^* \overline{D}^*$	not seen	
Γ_9 $D^*(2007)^0 \overline{D}^*(2007)^0$	not seen	
Γ_{10} $D^*(2010)^+ D^*(2010)^-$	not seen	
Γ_{11} $J/\psi(1S)$ hadrons		
Γ_{12} $J/\psi \pi^+ \pi^-$	< 4	$\times 10^{-3}$ 90%
Γ_{13} $J/\psi \pi^0 \pi^0$	< 2	$\times 10^{-3}$ 90%
Γ_{14} $J/\psi \eta$	< 7	$\times 10^{-3}$ 90%
Γ_{15} $J/\psi \pi^0$	< 2	$\times 10^{-3}$ 90%
Γ_{16} $J/\psi \pi^+ \pi^- \pi^0$	< 2	$\times 10^{-3}$ 90%
Γ_{17} $\chi_{c1} \gamma$	< 1.1	% 90%
Γ_{18} $\chi_{c2} \gamma$	< 1.7	% 90%
Γ_{19} $\chi_{c1} \pi^+ \pi^- \pi^0$	< 1.1	% 90%
Γ_{20} $\chi_{c2} \pi^+ \pi^- \pi^0$	< 3.2	% 90%
Γ_{21} $\phi \pi^+ \pi^-$	< 3	$\times 10^{-3}$ 90%
Γ_{22} $\mu^+ \mu^-$		

 $\psi(4040)$ PARTIAL WIDTHS

$\Gamma(e^+ e^-)$		Γ_1	
VALUE (keV)	DOCUMENT ID	TECN	COMMENT
0.86 ± 0.07	OUR ESTIMATE		
0.83 ± 0.20	7 ABLIKIM	08d BES2	$e^+ e^- \rightarrow \text{hadrons}$
••• We do not use the following data for averages, fits, limits, etc. •••			
0.88 ± 0.11	8 SETH	05A RVUE	$e^+ e^- \rightarrow \text{hadrons}$
0.91 ± 0.13	9 SETH	05A RVUE	$e^+ e^- \rightarrow \text{hadrons}$
0.75 ± 0.15	BRANDELIK	78c DASP	$e^+ e^-$
7 Reanalysis of data presented in BAI 02c. From a global fit over the center-of-mass energy region 3.7–5.0 GeV covering the $\psi(3770)$, $\psi(4040)$, $\psi(4160)$, and $\psi(4415)$ resonances. Phase angle fixed in the fit to $\delta = (130 \pm 46)^\circ$.			
8 From a fit to Crystal Ball (OSTERHELD 86) data.			
9 From a fit to BES (BAI 02c) data.			

 $\psi(4040)$ BRANCHING RATIOS

$\Gamma(e^+ e^-)/\Gamma_{\text{total}}$		Γ_1/Γ	
VALUE (units 10^{-5})	DOCUMENT ID	TECN	COMMENT
~ 1.0	FELDMAN	77 MRK1	$e^+ e^-$
••• We do not use the following data for averages, fits, limits, etc. •••			
$\Gamma(D\overline{D})/\Gamma(D^* \overline{D} + \text{c.c.})$		Γ_2/Γ_5	
VALUE	DOCUMENT ID	TECN	COMMENT
$0.24 \pm 0.05 \pm 0.12$	AUBERT	09m BABR	$e^+ e^- \rightarrow \gamma D^{(*)} \overline{D}$
$\Gamma(D^0 \overline{D}^0)/\Gamma(D^*(2007)^0 \overline{D}^0 + \text{c.c.})$		Γ_3/Γ_6	
VALUE	DOCUMENT ID	TECN	COMMENT
0.05 ± 0.03	10 GOLDHABER	77 MRK1	$e^+ e^-$
$\Gamma(D^*(2010)^+ D^- + \text{c.c.})/\Gamma(D^*(2007)^0 \overline{D}^0 + \text{c.c.})$		Γ_7/Γ_6	
VALUE	DOCUMENT ID	TECN	COMMENT
$0.95 \pm 0.09 \pm 0.10$	AUBERT	09m BABR	$e^+ e^- \rightarrow \gamma D^* \overline{D}$
$\Gamma(D^* \overline{D}^*)/\Gamma(D^* \overline{D} + \text{c.c.})$		Γ_8/Γ_5	
VALUE	DOCUMENT ID	TECN	COMMENT
$0.18 \pm 0.14 \pm 0.03$	AUBERT	09m BABR	$e^+ e^- \rightarrow \gamma D^{(*)} \overline{D}^{(*)}$
$\Gamma(D^*(2007)^0 \overline{D}^*(2007)^0)/\Gamma(D^*(2007)^0 \overline{D}^0 + \text{c.c.})$		Γ_9/Γ_6	
VALUE	DOCUMENT ID	TECN	COMMENT
32.0 ± 12.0	10 GOLDHABER	77 MRK1	$e^+ e^-$
$\Gamma(J/\psi \pi^+ \pi^-)/\Gamma_{\text{total}}$		Γ_{12}/Γ	
VALUE (units 10^{-3})	CL%	DOCUMENT ID	TECN COMMENT
< 4	90	COAN	06 CLEO $3.97\text{--}4.06 e^+ e^- \rightarrow \text{hadrons}$
$\Gamma(J/\psi \pi^0 \pi^0)/\Gamma_{\text{total}}$		Γ_{13}/Γ	
VALUE (units 10^{-3})	CL%	DOCUMENT ID	TECN COMMENT
< 2	90	COAN	06 CLEO $3.97\text{--}4.06 e^+ e^- \rightarrow \text{hadrons}$
$\Gamma(J/\psi \eta)/\Gamma_{\text{total}}$		Γ_{14}/Γ	
VALUE (units 10^{-3})	CL%	DOCUMENT ID	TECN COMMENT
< 7	90	COAN	06 CLEO $3.97\text{--}4.06 e^+ e^- \rightarrow \text{hadrons}$

See key on page 405

Meson Particle Listings

$\psi(4040)$, $X(4050)^\pm$, $X(4140)$, $\psi(4160)$

$\Gamma(J/\psi\pi^0)/\Gamma_{total}$				Γ_{15}/Γ
VALUE (units 10^{-3})	CL%	DOCUMENT ID	TECN COMMENT	
<2	90	COAN 06	CLEO 3.97-4.06 $e^+e^- \rightarrow$ hadrons	
$\Gamma(J/\psi\pi^+\pi^-\pi^0)/\Gamma_{total}$				Γ_{16}/Γ
VALUE (units 10^{-3})	CL%	DOCUMENT ID	TECN COMMENT	
<2	90	COAN 06	CLEO 3.97-4.06 $e^+e^- \rightarrow$ hadrons	
$\Gamma(\chi_{c1}\gamma)/\Gamma_{total}$				Γ_{17}/Γ
VALUE (units 10^{-3})	CL%	DOCUMENT ID	TECN COMMENT	
<11	90	COAN 06	CLEO 3.97-4.06 $e^+e^- \rightarrow$ hadrons	
$\Gamma(\chi_{c2}\gamma)/\Gamma_{total}$				Γ_{18}/Γ
VALUE (units 10^{-3})	CL%	DOCUMENT ID	TECN COMMENT	
<17	90	COAN 06	CLEO 3.97-4.06 $e^+e^- \rightarrow$ hadrons	
$\Gamma(\chi_{c1}\pi^+\pi^-\pi^0)/\Gamma_{total}$				Γ_{19}/Γ
VALUE (units 10^{-3})	CL%	DOCUMENT ID	TECN COMMENT	
<11	90	COAN 06	CLEO 3.97-4.06 $e^+e^- \rightarrow$ hadrons	
$\Gamma(\chi_{c2}\pi^+\pi^-\pi^0)/\Gamma_{total}$				Γ_{20}/Γ
VALUE (units 10^{-3})	CL%	DOCUMENT ID	TECN COMMENT	
<32	90	COAN 06	CLEO 3.97-4.06 $e^+e^- \rightarrow$ hadrons	
$\Gamma(\phi\pi^+\pi^-)/\Gamma_{total}$				Γ_{21}/Γ
VALUE (units 10^{-3})	CL%	DOCUMENT ID	TECN COMMENT	
<3	90	COAN 06	CLEO 3.97-4.06 $e^+e^- \rightarrow$ hadrons	

¹⁰Phase-space factor (p^3) explicitly removed.

$\psi(4040)$ REFERENCES

AUBERT 09M	PR D79 092001	B. Aubert et al.	(BABAR Collab.)
ABLIKIM 08D	PL B660 315	M. Ablikim et al.	(BES Collab.)
COAN 06	PRL 96 162003	T.E. Coan et al.	(CLEO Collab.)
SETH 05A	PR D72 017501	K.K. Seth	
BAI 02C	PRL 88 101802	J.Z. Bai et al.	(BES Collab.)
OSTERHELD 86	SLAC-PUB-4160	A. Osterheld et al.	(SLAC Crystal Ball Collab.)
BRANDELIK 78C	PL 76B 361	R. Brandelik et al.	(DASP Collab.)
	ZPHY C1 233	R. Brandelik et al.	(DASP Collab.)
FELDMAN 77	PRPL 33C 285	G.J. Feldman, M.L. Perl	(LBL, SLAC)
GOLDBABER 77	PL 69B 503	G. Goldhaber et al.	(Mark I Collab.)

$X(4050)^\pm$

$I(J^P) = ?(??)$

OMITTED FROM SUMMARY TABLE
Observed by MIZUK 08 in the $\pi^+\chi_{c1}(1P)$ invariant mass distribution in $\bar{B}^0 \rightarrow K^-\pi^+\chi_{c1}(1P)$ decays.

$X(4050)^\pm$ MASS

VALUE (MeV)	DOCUMENT ID	TECN	COMMENT
$4051 \pm 14 \pm 20$ -41	¹ MIZUK 08	BELL	$\bar{B}^0 \rightarrow K^-\pi^+\chi_{c1}(1P)$

¹ From a Dalitz plot analysis with two Breit-Wigner amplitudes.

$X(4050)^\pm$ WIDTH

VALUE (MeV)	DOCUMENT ID	TECN	COMMENT
$82 \pm 21 \pm 47$ $-17 - 22$	² MIZUK 08	BELL	$\bar{B}^0 \rightarrow K^-\pi^+\chi_{c1}(1P)$

² From a Dalitz plot analysis with two Breit-Wigner amplitudes.

$X(4050)^\pm$ DECAY MODES

Mode	Fraction (Γ_i/Γ)
$\Gamma_1 \pi^+\chi_{c1}(1P)$	seen

$X(4050)$ BRANCHING RATIOS

$\Gamma(\pi^+\chi_{c1}(1P))/\Gamma_{total}$				Γ_1/Γ
VALUE	DOCUMENT ID	TECN	COMMENT	
seen	³ MIZUK 08	BELL	$\bar{B}^0 \rightarrow K^-\pi^+\chi_{c1}(1P)$	

³With a product branching fraction measurement of $B(\bar{B}^0 \rightarrow K^-X(4050)^+) \times B(X(4050)^+ \rightarrow \pi^+\chi_{c1}(1P)) = (3.0^{+1.5+3.7}_{-0.8-1.6}) \times 10^{-5}$.

$X(4050)^\pm$ REFERENCES

MIZUK 08	PR D78 072004	R. Mizuk et al.	(BELLE Collab.)
----------	---------------	-----------------	-----------------

$X(4140)$

$I^G(J^{PC}) = 0^+(?^?+)$

OMITTED FROM SUMMARY TABLE
Needs confirmation.
Seen by AALTONEN 09AH in the $B^+ \rightarrow XK^+, X \rightarrow J/\psi\phi$. Not seen by SHEN 10 in $\gamma\gamma \rightarrow J/\psi\phi$.

$X(4140)$ MASS

VALUE (MeV)	EVTS	DOCUMENT ID	TECN	COMMENT
$4143.0 \pm 2.9 \pm 1.2$	14 ± 5	¹ AALTONEN 09AH	CDF	$B^+ \rightarrow J/\psi\phi K^+$

¹ Statistical significance of 3.8 σ .

$X(4140)$ WIDTH

VALUE (MeV)	EVTS	DOCUMENT ID	TECN	COMMENT
11.7 ± 8.3 -5.0 ± 3.7	14 ± 5	² AALTONEN 09AH	CDF	$B^+ \rightarrow J/\psi\phi K^+$

² Statistical significance of 3.8 σ .

$X(4140)$ DECAY MODES

Mode	Fraction (Γ_i/Γ)
$\Gamma_1 J/\psi\phi$	seen
$\Gamma_2 \gamma\gamma$	not seen

$X(4140)$ $\Gamma(i)\Gamma(\gamma\gamma)/\Gamma_{total}$

$\Gamma(\gamma\gamma) \times \Gamma(J/\psi\phi)/\Gamma_{total}$				$\Gamma_2\Gamma_1/\Gamma$
VALUE (eV)	CL%	DOCUMENT ID	TECN COMMENT	
<41	90	³ SHEN 10	BELL	$10.6 e^+e^- \rightarrow e^+e^- J/\psi\phi$
< 6	90	⁴ SHEN 10	BELL	$10.6 e^+e^- \rightarrow e^+e^- J/\psi\phi$

••• We do not use the following data for averages, fits, limits, etc. •••
³ For $J^P = 0^+$.
⁴ For $J^P = 2^+$.

$X(4140)$ BRANCHING RATIOS

$\Gamma(J/\psi\phi)/\Gamma_{total}$				Γ_1/Γ
VALUE	EVTS	DOCUMENT ID	TECN COMMENT	
seen	14 ± 5	⁵ AALTONEN 09AH	CDF	$B^+ \rightarrow J/\psi\phi K^+$

⁵ Statistical significance of 3.8 σ .

$\Gamma(\gamma\gamma)/\Gamma_{total}$				Γ_2/Γ
VALUE	DOCUMENT ID	TECN	COMMENT	
not seen	SHEN 10	BELL	$10.6 e^+e^- \rightarrow e^+e^- J/\psi\phi$	

$X(4140)$ REFERENCES

SHEN 10	PRL 104 112004	C.P. Shen et al.	(BELLE Collab.)
AALTONEN 09AH	PRL 102 242002	T. Aaltonen et al.	(CDF Collab.)

$\psi(4160)$

$I^G(J^{PC}) = 0^-(1^{--})$

$\psi(4160)$ MASS

VALUE (MeV)	DOCUMENT ID	TECN	COMMENT
4153 ± 3 OUR ESTIMATE			
4191.7 ± 6.5	¹ ABLIKIM 08D	BES2	$e^+e^- \rightarrow$ hadrons
4151 ± 4	² SETH 05A	RVUE	$e^+e^- \rightarrow$ hadrons
4155 ± 5	³ SETH 05A	RVUE	$e^+e^- \rightarrow$ hadrons
4159 ± 20	BRANDELIK 78C	DASP	e^+e^-

••• We do not use the following data for averages, fits, limits, etc. •••

¹ Reanalysis of data presented in BAI 02c. From a global fit over the center-of-mass energy region 3.7-5.0 GeV covering the $\psi(3770)$, $\psi(4040)$, $\psi(4160)$, and $\psi(4415)$ resonances. Phase angle fixed in the fit to $\delta = (293 \pm 57)^\circ$.
² From a fit to Crystal Ball (OSTERHELD 86) data.
³ From a fit to BES (BAI 02c) data.

$\psi(4160)$ WIDTH

VALUE (MeV)	DOCUMENT ID	TECN	COMMENT
103 ± 8 OUR ESTIMATE			
71.8 ± 12.3	⁴ ABLIKIM 08D	BES2	$e^+e^- \rightarrow$ hadrons

Meson Particle Listings

$\psi(4160)$, $X(4160)$

• • • We do not use the following data for averages, fits, limits, etc. • • •

107 ± 10	⁵ SETH	05A	RVUE	$e^+e^- \rightarrow$	hadrons
107 ± 16	⁶ SETH	05A	RVUE	$e^+e^- \rightarrow$	hadrons
78 ± 20	BRANDELIK	78C	DASP	e^+e^-	

⁴ Reanalysis of data presented in BAI 02c. From a global fit over the center-of-mass energy region 3.7–5.0 GeV covering the $\psi(3770)$, $\psi(4040)$, $\psi(4160)$, and $\psi(4415)$ resonances. Phase angle fixed in the fit to $\delta = (293 \pm 57)^\circ$.

⁵ From a fit to Crystal Ball (OSTERHELD 86) data.

⁶ From a fit to BES (BAI 02c) data.

$\psi(4160)$ DECAY MODES

Mode	Fraction (Γ_i/Γ)	Confidence level
Γ_1 e^+e^-	$(8.1 \pm 0.9) \times 10^{-6}$	
Γ_2 $D\bar{D}$	not seen	
Γ_3 $D^0\bar{D}^0$	not seen	
Γ_4 D^+D^-	not seen	
Γ_5 $D^*\bar{D} + c.c.$	not seen	
Γ_6 $D^*(2007)^0\bar{D}^0 + c.c.$	not seen	
Γ_7 $D^*(2010)^+D^- + c.c.$	not seen	
Γ_8 $D^*\bar{D}^*$	seen	
Γ_9 $D^*(2007)^0\bar{D}^*(2007)^0$	seen	
Γ_{10} $D^*(2010)^+D^*(2010)^-$	seen	
Γ_{11} $J/\psi\pi^+\pi^-$	$< 3 \times 10^{-3}$	90%
Γ_{12} $J/\psi\pi^0\pi^0$	$< 3 \times 10^{-3}$	90%
Γ_{13} $J/\psi K^+K^-$	$< 2 \times 10^{-3}$	90%
Γ_{14} $J/\psi\eta$	$< 8 \times 10^{-3}$	90%
Γ_{15} $J/\psi\pi^0$	$< 1 \times 10^{-3}$	90%
Γ_{16} $J/\psi\eta'$	$< 5 \times 10^{-3}$	90%
Γ_{17} $J/\psi\pi^+\pi^-\pi^0$	$< 1 \times 10^{-3}$	90%
Γ_{18} $\psi(2S)\pi^+\pi^-$	$< 4 \times 10^{-3}$	90%
Γ_{19} $\chi_{c1}\gamma$	$< 7 \times 10^{-3}$	90%
Γ_{20} $\chi_{c2}\gamma$	$< 1.3\%$	90%
Γ_{21} $\chi_{c1}\pi^+\pi^-\pi^0$	$< 2 \times 10^{-3}$	90%
Γ_{22} $\chi_{c2}\pi^+\pi^-\pi^0$	$< 8 \times 10^{-3}$	90%
Γ_{23} $\phi\pi^+\pi^-$	$< 2 \times 10^{-3}$	90%

$\psi(4160)$ PARTIAL WIDTHS

$\Gamma(e^+e^-)$	DOCUMENT ID	TECN	COMMENT	Γ_1
0.83 ± 0.07 OUR ESTIMATE				
0.49 ± 0.22	⁷ ABLIKIM	08D	BES2 $e^+e^- \rightarrow$ hadrons	
0.83 ± 0.08	⁸ SETH	05A	RVUE $e^+e^- \rightarrow$ hadrons	
0.84 ± 0.13	⁹ SETH	05A	RVUE $e^+e^- \rightarrow$ hadrons	
0.77 ± 0.23	BRANDELIK	78C	DASP e^+e^-	

⁷ Reanalysis of data presented in BAI 02c. From a global fit over the center-of-mass energy region 3.7–5.0 GeV covering the $\psi(3770)$, $\psi(4040)$, $\psi(4160)$, and $\psi(4415)$ resonances. Phase angle fixed in the fit to $\delta = (293 \pm 57)^\circ$.

⁸ From a fit to Crystal Ball (OSTERHELD 86) data.

⁹ From a fit to BES (BAI 02c) data.

$\psi(4160)$ BRANCHING RATIOS

$\Gamma(D\bar{D})/\Gamma(D^*\bar{D}^*)$	Γ_2/Γ_8		
VALUE	DOCUMENT ID	TECN	COMMENT
$0.02 \pm 0.03 \pm 0.02$	AUBERT	09M	BABR $e^+e^- \rightarrow \gamma D^{(*)}\bar{D}^{(*)}$
$\Gamma(D^*\bar{D} + c.c.)/\Gamma(D^*\bar{D}^*)$	Γ_5/Γ_8		
VALUE	DOCUMENT ID	TECN	COMMENT
$0.34 \pm 0.14 \pm 0.05$	AUBERT	09M	BABR $e^+e^- \rightarrow \gamma D^{(*)}\bar{D}^{(*)}$
$\Gamma(J/\psi\pi^+\pi^-)/\Gamma_{\text{total}}$	Γ_{11}/Γ		
VALUE (units 10^{-3})	DOCUMENT ID	TECN	COMMENT
< 3	COAN	06	CLEO 4.12–4.2 $e^+e^- \rightarrow$ hadrons
$\Gamma(J/\psi\pi^0\pi^0)/\Gamma_{\text{total}}$	Γ_{12}/Γ		
VALUE (units 10^{-3})	DOCUMENT ID	TECN	COMMENT
< 3	COAN	06	CLEO 4.12–4.2 $e^+e^- \rightarrow$ hadrons
$\Gamma(J/\psi K^+K^-)/\Gamma_{\text{total}}$	Γ_{13}/Γ		
VALUE (units 10^{-3})	DOCUMENT ID	TECN	COMMENT
< 2	COAN	06	CLEO 4.12–4.2 $e^+e^- \rightarrow$ hadrons
$\Gamma(J/\psi\eta)/\Gamma_{\text{total}}$	Γ_{14}/Γ		
VALUE (units 10^{-3})	DOCUMENT ID	TECN	COMMENT
< 8	COAN	06	CLEO 4.12–4.2 $e^+e^- \rightarrow$ hadrons

$\Gamma(J/\psi\pi^0)/\Gamma_{\text{total}}$	Γ_{15}/Γ		
VALUE (units 10^{-3})	DOCUMENT ID	TECN	COMMENT
< 1	90	COAN	06 CLEO 4.12–4.2 $e^+e^- \rightarrow$ hadrons

$\Gamma(J/\psi\eta')/\Gamma_{\text{total}}$	Γ_{16}/Γ		
VALUE (units 10^{-3})	DOCUMENT ID	TECN	COMMENT
< 5	90	COAN	06 CLEO 4.12–4.2 $e^+e^- \rightarrow$ hadrons

$\Gamma(J/\psi\pi^+\pi^-\pi^0)/\Gamma_{\text{total}}$	Γ_{17}/Γ		
VALUE (units 10^{-3})	DOCUMENT ID	TECN	COMMENT
< 1	90	COAN	06 CLEO 4.12–4.2 $e^+e^- \rightarrow$ hadrons

$\Gamma(\psi(2S)\pi^+\pi^-)/\Gamma_{\text{total}}$	Γ_{18}/Γ		
VALUE (units 10^{-3})	DOCUMENT ID	TECN	COMMENT
< 4	90	COAN	06 CLEO 4.12–4.2 $e^+e^- \rightarrow$ hadrons

$\Gamma(\chi_{c1}\gamma)/\Gamma_{\text{total}}$	Γ_{19}/Γ		
VALUE (units 10^{-3})	DOCUMENT ID	TECN	COMMENT
< 7	90	COAN	06 CLEO 4.12–4.2 $e^+e^- \rightarrow$ hadrons

$\Gamma(\chi_{c2}\gamma)/\Gamma_{\text{total}}$	Γ_{20}/Γ		
VALUE (units 10^{-3})	DOCUMENT ID	TECN	COMMENT
< 13	90	COAN	06 CLEO 4.12–4.2 $e^+e^- \rightarrow$ hadrons

$\Gamma(\chi_{c1}\pi^+\pi^-\pi^0)/\Gamma_{\text{total}}$	Γ_{21}/Γ		
VALUE (units 10^{-3})	DOCUMENT ID	TECN	COMMENT
< 2	90	COAN	06 CLEO 4.12–4.2 $e^+e^- \rightarrow$ hadrons

$\Gamma(\chi_{c2}\pi^+\pi^-\pi^0)/\Gamma_{\text{total}}$	Γ_{22}/Γ		
VALUE (units 10^{-3})	DOCUMENT ID	TECN	COMMENT
< 8	90	COAN	06 CLEO 4.12–4.2 $e^+e^- \rightarrow$ hadrons

$\Gamma(\phi\pi^+\pi^-)/\Gamma_{\text{total}}$	Γ_{23}/Γ		
VALUE (units 10^{-3})	DOCUMENT ID	TECN	COMMENT
< 2	90	COAN	06 CLEO 4.12–4.2 $e^+e^- \rightarrow$ hadrons

$\psi(4160)$ REFERENCES

AUBERT	09M	PR D79 092001	B. Aubert <i>et al.</i>	(BABAR Collab.)
ABLIKIM	08D	PL B660 315	M. Ablikim <i>et al.</i>	(BES Collab.)
COAN	06	PRL 96 162003	T.E. Coan <i>et al.</i>	(CLEO Collab.)
SETH	05A	PR D72 017501	K.K. Seth	
BAI	02C	PRL 88 101802	J.Z. Bai <i>et al.</i>	(BES Collab.)
OSTERHELD	86	SLAC-PUB-4160	A. Osterheld <i>et al.</i>	(SLAC Crystal Ball Collab.)
BRANDELIK	78C	PL 76B 361	R. Brandelik <i>et al.</i>	(DASP Collab.)

$X(4160)$

$$I^G(J^{PC}) = ?(???)$$

OMITTED FROM SUMMARY TABLE
Seen by PAKHLOV 08 in $e^+e^- \rightarrow J/\psi X$, $X \rightarrow D^*\bar{D}^*$

$X(4160)$ MASS

VALUE (MeV)	EVTS	DOCUMENT ID	TECN	COMMENT
$4156^{+25}_{-20} \pm 15$	24	PAKHLOV	08	BELL $e^+e^- \rightarrow J/\psi X$

$X(4160)$ WIDTH

VALUE (MeV)	EVTS	DOCUMENT ID	TECN	COMMENT
$139^{+111}_{-61} \pm 21$	24	PAKHLOV	08	BELL $e^+e^- \rightarrow J/\psi X$

$X(4160)$ DECAY MODES

Mode	Fraction (Γ_i/Γ)
Γ_1 $D\bar{D}$	not seen
Γ_2 $D^*\bar{D} + c.c.$	not seen
Γ_3 $D^*\bar{D}^*$	seen

$X(4160)$ BRANCHING RATIOS

$\Gamma(D\bar{D})/\Gamma(D^*\bar{D}^*)$	Γ_1/Γ_3		
VALUE	DOCUMENT ID	TECN	COMMENT
< 0.09	90	PAKHLOV	08 BELL $e^+e^- \rightarrow J/\psi X$

$\Gamma(D^*\bar{D} + c.c.)/\Gamma(D^*\bar{D}^*)$	Γ_2/Γ_3		
VALUE	DOCUMENT ID	TECN	COMMENT
< 0.22	90	PAKHLOV	08 BELL $e^+e^- \rightarrow J/\psi X$

$X(4160)$ REFERENCES

PAKHLOV	08	PRL 100 202001	P. Pakhlov <i>et al.</i>	(BELLE Collab.)
---------	----	----------------	--------------------------	-----------------

See key on page 405

Meson Particle Listings

X(4250)[±], X(4260)

X(4250)[±] $I(J^P) = ?(?^?)$
 OMITTED FROM SUMMARY TABLE
 Observed by MIZUK 08 in the $\pi^+\chi_{c1}(1P)$ invariant mass distribution in $\bar{B}^0 \rightarrow K^-\pi^+\chi_{c1}(1P)$ decays.

X(4250)[±] MASS

VALUE (MeV)	DOCUMENT ID	TECN	COMMENT
$4248^{+44}_{-29} +^{180}_{-35}$	¹ MIZUK	08	BELL $\bar{B}^0 \rightarrow K^-\pi^+\chi_{c1}(1P)$

¹ From a Dalitz plot analysis with two Breit-Wigner amplitudes.

X(4250)[±] WIDTH

VALUE (MeV)	DOCUMENT ID	TECN	COMMENT
$177^{+54}_{-39} +^{316}_{-61}$	² MIZUK	08	BELL $\bar{B}^0 \rightarrow K^-\pi^+\chi_{c1}(1P)$

² From a Dalitz plot analysis with two Breit-Wigner amplitudes.

X(4250)[±] DECAY MODES

Mode	Fraction (Γ_i/Γ)
$\Gamma_1 \pi^+\chi_{c1}(1P)$	seen

X(4250)[±] BRANCHING RATIOS

$\Gamma(\pi^+\chi_{c1}(1P))/\Gamma_{total}$	VALUE	DOCUMENT ID	TECN	COMMENT	Γ_1/Γ
seen	$4.0^{+2.3}_{-0.9} +^{19.7}_{-0.5} \times 10^{-5}$	³ MIZUK	08	BELL $\bar{B}^0 \rightarrow K^-\pi^+\chi_{c1}(1P)$	

³ With a product branching fraction measurement of $B(\bar{B}^0 \rightarrow K^-X(4250)^+) \times B(X(4250)^+ \rightarrow \pi^+\chi_{c1}(1P)) = (4.0^{+2.3}_{-0.9} +^{19.7}_{-0.5}) \times 10^{-5}$.

X(4250)[±] REFERENCES
 MIZUK 08 PR D78 072004 R. Mizuk et al. (BELLE Collab.)

X(4260) $I^G(J^{PC}) = ?^?(1^{--})$
 Seen in radiative return from e^+e^- collisions at $\sqrt{s} = 9.54\text{--}10.58$ GeV by AUBERT,B 05i, HE 06B, and YUAN 07, and in e^+e^- collisions at $\sqrt{s} \approx 4.26$ GeV by COAN 06. Possibly seen by AUBERT 06 in $B^- \rightarrow K^-\pi^+\pi^-J/\psi$. See also the mini-review under the X(3872). (See the index for the page number.)

X(4260) MASS

VALUE (MeV)	EVTs	DOCUMENT ID	TECN	COMMENT
4263^{+8}_{-9} OUR AVERAGE				Error includes scale factor of 1.1.
$4247 \pm 12^{+17}_{-32}$		¹ YUAN	07	BELL 10.58 $e^+e^- \rightarrow \gamma\pi^+\pi^-J/\psi$
$4284^{+17}_{-16} \pm 4$	13.6	HE	06B	CLEO 9.4–10.6 $e^+e^- \rightarrow \gamma\pi^+\pi^-J/\psi$
$4259 \pm 8^{+2}_{-6}$	125	² AUBERT,B	05i	BABR 10.58 $e^+e^- \rightarrow \gamma\pi^+\pi^-J/\psi$

¹ From a two-resonance fit.
² From a single-resonance fit. Two interfering resonances are not excluded.

X(4260) WIDTH

VALUE (MeV)	EVTs	DOCUMENT ID	TECN	COMMENT
95 ± 14 OUR AVERAGE				
$108 \pm 19 \pm 10$		³ YUAN	07	BELL 10.58 $e^+e^- \rightarrow \gamma\pi^+\pi^-J/\psi$
$73^{+39}_{-25} \pm 5$	13.6	HE	06B	CLEO 9.4–10.6 $e^+e^- \rightarrow \gamma\pi^+\pi^-J/\psi$
$88 \pm 23^{+6}_{-4}$	125	⁴ AUBERT,B	05i	BABR 10.58 $e^+e^- \rightarrow \gamma\pi^+\pi^-J/\psi$

³ From a two-resonance fit.
⁴ From a single-resonance fit. Two interfering resonances are not excluded.

X(4260) DECAY MODES

Mode	Fraction (Γ_i/Γ)
$\Gamma_1 e^+e^-$	
$\Gamma_2 J/\psi\pi^+\pi^-$	seen
$\Gamma_3 J/\psi\pi^0\pi^0$	[a] seen
$\Gamma_4 J/\psi K^+K^-$	[a] seen
$\Gamma_5 J/\psi\eta$	[a] not seen
$\Gamma_6 J/\psi\pi^0$	[a] not seen
$\Gamma_7 J/\psi\eta'$	[a] not seen
$\Gamma_8 J/\psi\pi^+\pi^-\pi^0$	[a] not seen
$\Gamma_9 J/\psi\eta\eta$	[a] not seen
$\Gamma_{10} \psi(2S)\pi^+\pi^-$	[a] not seen
$\Gamma_{11} \psi(2S)\eta$	[a] not seen
$\Gamma_{12} \chi_{c0}\omega$	[a] not seen
$\Gamma_{13} \chi_{c1}\gamma$	[a] not seen
$\Gamma_{14} \chi_{c2}\gamma$	[a] not seen
$\Gamma_{15} \chi_{c1}\pi^+\pi^-\pi^0$	[a] not seen
$\Gamma_{16} \chi_{c2}\pi^+\pi^-\pi^0$	[a] not seen
$\Gamma_{17} \phi\pi^+\pi^-$	[a] not seen
$\Gamma_{18} \phi f_0(980) \rightarrow \phi\pi^+\pi^-$	not seen
$\Gamma_{19} D\bar{D}$	not seen
$\Gamma_{20} D^0 D^{*-}\pi^+$	not seen
$\Gamma_{21} D^* \bar{D}$	not seen
$\Gamma_{22} D^* \bar{D}^*$	not seen
$\Gamma_{23} D^* \bar{D}\pi$	not seen
$\Gamma_{24} D^* \bar{D}^*\pi$	not seen
$\Gamma_{25} D_s^+ D_s^-$	not seen
$\Gamma_{26} D_s^{*+} D_s^-$	not seen
$\Gamma_{27} D_s^{*+} D_s^{*-}$	not seen
$\Gamma_{28} p\bar{p}$	not seen
$\Gamma_{29} K_S^0 K^\pm\pi^\mp$	not seen
$\Gamma_{30} K^+ K^-\pi^0$	not seen

[a] See COAN 06 for details.

X(4260) $\Gamma(i)\Gamma(e^+e^-)/\Gamma(total)$

$\Gamma(J/\psi\pi^+\pi^-) \times \Gamma(e^+e^-)/\Gamma_{total}$	VALUE (eV)	EVTs	DOCUMENT ID	TECN	COMMENT	$\Gamma_2\Gamma_1/\Gamma$
$5.9^{+1.2}_{-0.9}$ OUR AVERAGE						
$6.0 \pm 1.2^{+4.7}_{-0.5}$			⁵ YUAN	07	BELL 10.58 $e^+e^- \rightarrow \gamma\pi^+\pi^-J/\psi$	
$8.9^{+3.9}_{-3.1} \pm 1.8$	8.1		HE	06B	CLEO 9.4–10.6 $e^+e^- \rightarrow \gamma\pi^+\pi^-J/\psi$	
$5.5 \pm 1.0^{+0.8}_{-0.7}$	125		⁶ AUBERT,B	05i	BABR 10.58 $e^+e^- \rightarrow \gamma\pi^+\pi^-J/\psi$	
$20.6 \pm 2.3^{+9.1}_{-1.7}$			⁷ YUAN	07	BELL 10.58 $e^+e^- \rightarrow \gamma\pi^+\pi^-J/\psi$	

••• We do not use the following data for averages, fits, limits, etc. •••
⁵ Solution I of two equivalent solutions in a fit using two interfering resonances.
⁶ From a single-resonance fit. Two interfering resonances are not excluded.
⁷ Solution II of two equivalent solutions in a fit using two interfering resonances.

$\Gamma(J/\psi K^+K^-) \times \Gamma(e^+e^-)/\Gamma_{total}$ $\Gamma_4\Gamma_1/\Gamma$

VALUE (eV)	CL%	DOCUMENT ID	TECN	COMMENT
<1.2	90	⁸ YUAN	08	BELL $e^+e^- \rightarrow \gamma K^+K^-J/\psi$

⁸ From a fit of the broad K^+K^-J/ψ enhancement including a coherent X(4260) amplitude with mass and width from YUAN 07.

$\Gamma(\psi(2S)\pi^+\pi^-) \times \Gamma(e^+e^-)/\Gamma_{total}$ $\Gamma_{10}\Gamma_1/\Gamma$

VALUE (eV)	CL%	DOCUMENT ID	TECN	COMMENT
<4.3	90	⁹ LIU	08H	RVUE 10.58 $e^+e^- \rightarrow \psi(2S)\pi^+\pi^-\gamma$
$7.4^{+2.1}_{-1.7}$		¹⁰ LIU	08H	RVUE 10.58 $e^+e^- \rightarrow \psi(2S)\pi^+\pi^-\gamma$

⁹ For constructive interference with the X(4360) in a combined fit of AUBERT 07s and WANG 07d data with three resonances.
¹⁰ For destructive interference with the X(4360) in a combined fit of AUBERT 07s and WANG 07d data with three resonances.

$\Gamma(\phi\pi^+\pi^-) \times \Gamma(e^+e^-)/\Gamma_{total}$ $\Gamma_{17}\Gamma_1/\Gamma$

VALUE (eV)	CL%	DOCUMENT ID	TECN	COMMENT
<0.4	90	AUBERT,BE	06D	BABR 10.6 $e^+e^- \rightarrow K^+K^-\pi^+\pi^-\gamma$

Meson Particle Listings

X(4260), X(4350)

 $\Gamma(\phi f_0(980) \rightarrow \phi \pi^+ \pi^-) \times \Gamma(e^+ e^-) / \Gamma_{\text{total}}$ $\Gamma_{18} \Gamma_1 / \Gamma$

VALUE (eV)	CL%	DOCUMENT ID	TECN	COMMENT
<0.29	90	11 AUBERT	07AK BABR	10.6 $e^+ e^- \rightarrow \pi^+ \pi^- K^+ K^- \gamma$

¹¹AUBERT 07AK reports $[\Gamma(X(4260) \rightarrow \phi f_0(980) \rightarrow \phi \pi^+ \pi^-) \times \Gamma(X(4260) \rightarrow e^+ e^-) / \Gamma_{\text{total}}] \times [B(\phi(1020) \rightarrow K^+ K^-)] < 0.14$ eV which we divide by our best value $B(\phi(1020) \rightarrow K^+ K^-) = 48.9 \times 10^{-2}$.

 $\Gamma(K_S^0 K^\pm \pi^\mp) \times \Gamma(e^+ e^-) / \Gamma_{\text{total}}$ $\Gamma_{29} \Gamma_1 / \Gamma$

VALUE (eV)	CL%	DOCUMENT ID	TECN	COMMENT
<0.5	90	AUBERT	08s BABR	10.6 $e^+ e^- \rightarrow K_S^0 K^\pm \pi^\mp \gamma$

• • • We do not use the following data for averages, fits, limits, etc. • • •

 $\Gamma(K^+ K^- \pi^0) \times \Gamma(e^+ e^-) / \Gamma_{\text{total}}$ $\Gamma_{30} \Gamma_1 / \Gamma$

VALUE (eV)	CL%	DOCUMENT ID	TECN	COMMENT
<0.6	90	AUBERT	08s BABR	10.6 $e^+ e^- \rightarrow K^+ K^- \pi^0 \gamma$

• • • We do not use the following data for averages, fits, limits, etc. • • •

X(4260) BRANCHING RATIOS

 $\Gamma(D\bar{D}) / \Gamma(J/\psi \pi^+ \pi^-)$ Γ_{19} / Γ_2

VALUE	CL%	DOCUMENT ID	TECN	COMMENT
<1.0	90	12 AUBERT	07BE BABR	$e^+ e^- \rightarrow D\bar{D} \gamma$

• • • We do not use the following data for averages, fits, limits, etc. • • •

<4.0 90 CRONIN-HEN..09 CLEO $e^+ e^-$

¹²Using 4259 ± 10 MeV for the mass and 88 ± 24 MeV for the width of X(4260).

 $\Gamma(D^0 D^{*-} \pi^+) / \Gamma(J/\psi \pi^+ \pi^-)$ Γ_{20} / Γ_2

VALUE	CL%	DOCUMENT ID	TECN	COMMENT
<9	90	PAKHLOVA	09 BELL	$e^+ e^- \rightarrow X(4260) \rightarrow D^0 D^{*-} \pi^+$

 $\Gamma(D^0 D^{*-} \pi^+) / \Gamma_{\text{total}} \times \Gamma(e^+ e^-) / \Gamma_{\text{total}}$ $\Gamma_{20} / \Gamma \times \Gamma_1 / \Gamma$

VALUE	CL%	DOCUMENT ID	TECN	COMMENT
<0.42 × 10 ⁻⁶	90	13 PAKHLOVA	09 BELL	$e^+ e^- \rightarrow X(4260) \rightarrow D^0 D^{*-} \pi^+$

¹³Using 4263⁺⁸/₋₉ MeV for the mass of X(4260).

 $\Gamma(D^* \bar{D}) / \Gamma(J/\psi \pi^+ \pi^-)$ Γ_{21} / Γ_2

VALUE	CL%	DOCUMENT ID	TECN	COMMENT
<34	90	AUBERT	09M BABR	$e^+ e^- \rightarrow \gamma D^* \bar{D}$

• • • We do not use the following data for averages, fits, limits, etc. • • •

<45 90 CRONIN-HEN..09 CLEO $e^+ e^-$

 $\Gamma(D^* \bar{D}^*) / \Gamma(J/\psi \pi^+ \pi^-)$ Γ_{22} / Γ_2

VALUE	CL%	DOCUMENT ID	TECN	COMMENT
<11	90	CRONIN-HEN..09	CLEO	$e^+ e^-$

• • • We do not use the following data for averages, fits, limits, etc. • • •

<40 90 AUBERT 09M BABR $e^+ e^- \rightarrow \gamma D^* \bar{D}^*$

 $\Gamma(D^* \bar{D} \pi) / \Gamma(J/\psi \pi^+ \pi^-)$ Γ_{23} / Γ_2

VALUE	CL%	DOCUMENT ID	TECN	COMMENT
<15	90	CRONIN-HEN..09	CLEO	$e^+ e^-$

 $\Gamma(D^* \bar{D}^* \pi) / \Gamma(J/\psi \pi^+ \pi^-)$ Γ_{24} / Γ_2

VALUE	CL%	DOCUMENT ID	TECN	COMMENT
<8.2	90	CRONIN-HEN..09	CLEO	$e^+ e^-$

 $\Gamma(D_s^+ D_s^-) / \Gamma(J/\psi \pi^+ \pi^-)$ Γ_{25} / Γ_2

VALUE	CL%	DOCUMENT ID	TECN	COMMENT
<1.3	90	CRONIN-HEN..09	CLEO	$e^+ e^-$

 $\Gamma(D_s^{*+} D_s^-) / \Gamma(J/\psi \pi^+ \pi^-)$ Γ_{26} / Γ_2

VALUE	CL%	DOCUMENT ID	TECN	COMMENT
<0.8	90	CRONIN-HEN..09	CLEO	$e^+ e^-$

 $\Gamma(D_s^{*+} D_s^{*-}) / \Gamma(J/\psi \pi^+ \pi^-)$ Γ_{27} / Γ_2

VALUE	CL%	DOCUMENT ID	TECN	COMMENT
<9.5	90	CRONIN-HEN..09	CLEO	$e^+ e^-$

 $\Gamma(p\bar{p}) / \Gamma(J/\psi \pi^+ \pi^-)$ Γ_{28} / Γ_2

VALUE	CL%	DOCUMENT ID	COMMENT
<0.13	90	14 AUBERT	06B $e^+ e^- \rightarrow p\bar{p} \gamma$

¹⁴Using 4259 ± 10 MeV for the mass and 88 ± 24 MeV for the width of X(4260).

X(4260) REFERENCES

AUBERT	09M	PR D79 092001	B. Aubert <i>et al.</i>	(BABAR Collab.)
CRONIN-HEN..	09	PR D80 072001	D. Cronin-Hennessy <i>et al.</i>	(CLEO Collab.)
PAKHLOVA	09	PR D80 091101R	G. Pakhlova <i>et al.</i>	(BELLE Collab.)
AUBERT	08S	PR D77 092002	B. Aubert <i>et al.</i>	(BABAR Collab.)
LIU	08H	PR D78 014032	Z.Q. Liu, X.S. Qin, C.Z. Yuan	
YUAN	08	PR D77 011105R	C.Z. Yuan <i>et al.</i>	(BELLE Collab.)
AUBERT	07AK	PR D76 012008	B. Aubert <i>et al.</i>	(BABAR Collab.)
AUBERT	07BE	PR D76 111105R	B. Aubert <i>et al.</i>	(BABAR Collab.)
AUBERT	07S	PRL 98 212001	B. Aubert <i>et al.</i>	(BABAR Collab.)
WANG	07D	PRL 99 142002	X.L. Wang <i>et al.</i>	(BELLE Collab.)
YUAN	07	PRL 99 182004	C.Z. Yuan <i>et al.</i>	(BELLE Collab.)
AUBERT	06	PR D73 011101R	B. Aubert <i>et al.</i>	(BABAR Collab.)
AUBERT	06B	PR D73 012005	B. Aubert <i>et al.</i>	(BABAR Collab.)
AUBERT,BE	06D	PR D74 091103R	B. Aubert <i>et al.</i>	(BABAR Collab.)
COAN	06	PRL 96 162003	T.E. Coan <i>et al.</i>	(CLEO Collab.)
HE	06B	PR D74 091104R	Q. He <i>et al.</i>	(CLEO Collab.)
AUBERT,B	05I	PRL 95 142001	B. Aubert <i>et al.</i>	(BABAR Collab.)

X(4350)

$$J^G(J^{PC}) = 0^+(?^?+)$$

OMITTED FROM SUMMARY TABLE

Seen by SHEN 10 in the $\gamma\gamma \rightarrow J/\psi\phi$. Needs confirmation.

X(4350) MASS

VALUE (MeV)	EVTS	DOCUMENT ID	TECN	COMMENT
4350.6 ^{+4.6} / _{-5.1} ± 0.7	8.8 ^{+4.2} / _{-3.2}	¹ SHEN	10 BELL	10.6 $e^+ e^- \rightarrow e^+ e^- J/\psi\phi$

¹ Statistical significance of 3.2 σ .

X(4350) WIDTH

VALUE (MeV)	EVTS	DOCUMENT ID	TECN	COMMENT
13 ⁻¹⁸ / ₉ ± 4	8.8 ^{+4.2} / _{-3.2}	² SHEN	10 BELL	10.6 $e^+ e^- \rightarrow e^+ e^- J/\psi\phi$

² Statistical significance of 3.2 σ .

X(4350) DECAY MODES

Mode	Fraction (Γ_i / Γ)
Γ_1 $J/\psi\phi$	seen
Γ_2 $\gamma\gamma$	seen

X(4350) $\Gamma(i) \Gamma(\gamma\gamma) / \Gamma(\text{total})$ $\Gamma(\gamma\gamma) \times \Gamma(J/\psi\phi) / \Gamma_{\text{total}}$ $\Gamma_2 \Gamma_1 / \Gamma$

VALUE (eV)	EVTS	DOCUMENT ID	TECN	COMMENT
6.7 ^{+3.2} / _{-2.4} ± 1.1	8.8 ^{+4.2} / _{-3.2}	³ SHEN	10 BELL	10.6 $e^+ e^- \rightarrow e^+ e^- J/\psi\phi$

• • • We do not use the following data for averages, fits, limits, etc. • • •

1.5^{+0.7}/_{-0.6} ± 0.3 8.8^{+4.2}/_{-3.2} ⁴ SHEN 10 BELL 10.6 $e^+ e^- \rightarrow e^+ e^- J/\psi\phi$

³ For $J^P = 0^+$. Statistical significance of 3.2 σ .

⁴ For $J^P = 2^+$. Statistical significance of 3.2 σ .

X(4350) BRANCHING RATIOS

 $\Gamma(J/\psi\phi) / \Gamma_{\text{total}}$ Γ_1 / Γ

VALUE	DOCUMENT ID	TECN	COMMENT
seen	⁵ SHEN	10 BELL	10.6 $e^+ e^- \rightarrow e^+ e^- J/\psi\phi$

⁵ Statistical significance of 3.2 σ .

 $\Gamma(\gamma\gamma) / \Gamma_{\text{total}}$ Γ_2 / Γ

VALUE	DOCUMENT ID	TECN	COMMENT
seen	⁶ SHEN	10 BELL	10.6 $e^+ e^- \rightarrow e^+ e^- J/\psi\phi$

⁶ Statistical significance of 3.2 σ .

X(4350) REFERENCES

SHEN	10	PRL 104 112004	C.P. Shen <i>et al.</i>	(BELLE Collab.)
------	----	----------------	-------------------------	-----------------

X(4360)

$$I^G(J^{PC}) = ?^?(1^{--})$$

OMITTED FROM SUMMARY TABLE

Seen in radiative return from e^+e^- collisions at $\sqrt{s} = 9.54\text{--}10.58$ GeV by AUBERT 07S and WANG 07D. See also the review under the X(3872) particle listings. (See the index for the page number.)

X(4360) MASS

VALUE (MeV)	DOCUMENT ID	TECN	COMMENT
4361 ± 9 ± 9	¹ WANG	07D	BELL 10.58 $e^+e^- \rightarrow \gamma\pi^+\pi^-\psi(2S)$
4355 ⁺⁹ ₋₁₀ ± 9	² LIU	08H	RVUE 10.58 $e^+e^- \rightarrow \psi(2S)\pi^+\pi^-\gamma$
4324 ± 24	³ AUBERT	07s	BABR 10.58 $e^+e^- \rightarrow \gamma\pi^+\pi^-\psi(2S)$

• • • We do not use the following data for averages, fits, limits, etc. • • •

¹ From a two-resonance fit.
² From a combined fit of AUBERT 07s and WANG 07D data with two resonances.
³ From a single-resonance fit. Systematic errors not estimated.

X(4360) WIDTH

VALUE (MeV)	DOCUMENT ID	TECN	COMMENT
74 ± 15 ± 10	⁴ WANG	07D	BELL 10.58 $e^+e^- \rightarrow \gamma\pi^+\pi^-\psi(2S)$
103 ⁺¹⁷ ₋₁₅ ± 11	⁵ LIU	08H	RVUE 10.58 $e^+e^- \rightarrow \psi(2S)\pi^+\pi^-\gamma$
172 ± 33	⁶ AUBERT	07s	BABR 10.58 $e^+e^- \rightarrow \gamma\pi^+\pi^-\psi(2S)$

• • • We do not use the following data for averages, fits, limits, etc. • • •

⁴ From a two-resonance fit.
⁵ From a combined fit of AUBERT 07s and WANG 07D data with two resonances.
⁶ From a single-resonance fit. Systematic errors not estimated.

X(4360) DECAY MODES

Mode	Fraction (Γ_i/Γ)
Γ_1 e^+e^-	
Γ_2 $\psi(2S)\pi^+\pi^-$	seen
Γ_3 $D^0D^{*-}\pi^+$	

X(4360) $\Gamma(i)\Gamma(e^+e^-)/\Gamma(\text{total})$

VALUE (eV)	DOCUMENT ID	TECN	COMMENT	$\Gamma_2\Gamma_1/\Gamma$
11.1^{+1.3}_{-1.2}	⁷ LIU	08H	RVUE 10.58 $e^+e^- \rightarrow \psi(2S)\pi^+\pi^-\gamma$	
12.3 ± 1.2	⁸ LIU	08H	RVUE 10.58 $e^+e^- \rightarrow \psi(2S)\pi^+\pi^-\gamma$	
10.4 ± 1.7 ± 1.5	⁹ WANG	07D	BELL 10.58 $e^+e^- \rightarrow \gamma\pi^+\pi^-\psi(2S)$	
11.8 ± 1.8 ± 1.4	¹⁰ WANG	07D	BELL 10.58 $e^+e^- \rightarrow \gamma\pi^+\pi^-\psi(2S)$	

• • • We do not use the following data for averages, fits, limits, etc. • • •

⁷ Solution I in a combined fit of AUBERT 07s and WANG 07D data with two resonances.
⁸ Solution II in a combined fit of AUBERT 07s and WANG 07D data with two resonances.
⁹ Solution I of two equivalent solutions in a fit using two interfering resonances.
¹⁰ Solution II of two equivalent solutions in a fit using two interfering resonances.

X(4360) BRANCHING RATIOS

VALUE	CL%	DOCUMENT ID	TECN	COMMENT	Γ_3/Γ_2
< 8	90	PAKHLOVA	09	BELL $e^+e^- \rightarrow X(4360) \rightarrow D^0D^{*-}\pi^+$	

VALUE	CL%	DOCUMENT ID	TECN	COMMENT	$\Gamma_3/\Gamma \times \Gamma_1/\Gamma$
< 0.72 × 10⁻⁶	90	PAKHLOVA	09	BELL $e^+e^- \rightarrow X(4360) \rightarrow D^0D^{*-}\pi^+$	

¹¹ Using 4355⁺⁹₋₁₀ ± 9 MeV for the mass of X(4360).

X(4360) REFERENCES

PAKHLOVA	09	PR D80 091101R	G. Pakhlova et al.	(BELLE Collab.)
LIU	08H	PR D78 014032	Z.Q. Liu, X.S. Qin, C.Z. Yuan	
AUBERT	07S	PRL 98 212001	B. Aubert et al.	(BABAR Collab.)
WANG	07D	PRL 99 142002	X.L. Wang et al.	(BELLE Collab.)

 $\psi(4415)$

$$I^G(J^{PC}) = 0^-(1^{--})$$

 $\psi(4415)$ MASS

VALUE (MeV)	DOCUMENT ID	TECN	COMMENT
4421 ± 4	OUR ESTIMATE		
4415.1 ± 7.9	¹ ABLIKIM	08D	BES2 $e^+e^- \rightarrow$ hadrons
4411 ± 7	² PAKHLOVA	08A	BELL 10.6 $e^+e^- \rightarrow D^0D^-\pi^+\gamma$
4425 ± 6	³ SETH	05A	RVUE $e^+e^- \rightarrow$ hadrons
4429 ± 9	⁴ SETH	05A	RVUE $e^+e^- \rightarrow$ hadrons
4417 ± 10	BRANDELIK	78c	DASP e^+e^-
4414 ± 7	SIEGRIST	76	MRK1 e^+e^-

• • • We do not use the following data for averages, fits, limits, etc. • • •

¹ Reanalysis of data presented in BAI 02c. From a global fit over the center-of-mass energy region 3.7–5.0 GeV covering the $\psi(3770)$, $\psi(4040)$, $\psi(4160)$, and $\psi(4415)$ resonances. Phase angle fixed in the fit to $\delta = (234 \pm 88)^\circ$.
² Systematic uncertainties not estimated.
³ From a fit to Crystal Ball (OSTERHELD 86) data.
⁴ From a fit to BES (BAI 02c) data.

 $\psi(4415)$ WIDTH

VALUE (MeV)	DOCUMENT ID	TECN	COMMENT
62 ± 20	OUR ESTIMATE		
71.5 ± 19.0	⁵ ABLIKIM	08D	BES2 $e^+e^- \rightarrow$ hadrons
77 ± 20	⁶ PAKHLOVA	08A	BELL 10.6 $e^+e^- \rightarrow D^0D^-\pi^+\gamma$
119 ± 16	⁷ SETH	05A	RVUE $e^+e^- \rightarrow$ hadrons
118 ± 35	⁸ SETH	05A	RVUE $e^+e^- \rightarrow$ hadrons
66 ± 15	BRANDELIK	78c	DASP e^+e^-
33 ± 10	SIEGRIST	76	MRK1 e^+e^-

• • • We do not use the following data for averages, fits, limits, etc. • • •

⁵ Reanalysis of data presented in BAI 02c. From a global fit over the center-of-mass energy region 3.7–5.0 GeV covering the $\psi(3770)$, $\psi(4040)$, $\psi(4160)$, and $\psi(4415)$ resonances. Phase angle fixed in the fit to $\delta = (234 \pm 88)^\circ$.
⁶ Systematic uncertainties not estimated.
⁷ From a fit to Crystal Ball (OSTERHELD 86) data.
⁸ From a fit to BES (BAI 02c) data.

 $\psi(4415)$ DECAY MODES

Mode	Fraction (Γ_i/Γ)	Confidence level
Γ_1 hadrons	dominant	
Γ_2 $D\bar{D}$	not seen	
Γ_3 $D^0\bar{D}^0$	not seen	
Γ_4 D^+D^-	not seen	
Γ_5 $D^*D^+ + c.c.$	not seen	
Γ_6 $D^*(2007)^0\bar{D}^0 + c.c.$	not seen	
Γ_7 $D^*(2010)^+D^- + c.c.$	not seen	
Γ_8 D^*D^*	not seen	
Γ_9 $D^*(2007)^0D^*(2007)^0 + c.c.$	not seen	
Γ_{10} $D^*(2010)^+D^*(2010)^- + c.c.$	not seen	
Γ_{11} $D^0D^-\pi^+$		
Γ_{12} $(D^0D^-\pi^+)_{non-res}$	< 2.3 %	90%
Γ_{13} $D\bar{D}_2^*(2460) \rightarrow D^0D^-\pi^+$	(10 ± 4) %	
Γ_{14} $D^0D^{*-}\pi^+$	< 11 %	90%
Γ_{15} e^+e^-	(9.4 ± 3.2) × 10 ⁻⁶	

 $\psi(4415)$ PARTIAL WIDTHS

VALUE (keV)	DOCUMENT ID	TECN	COMMENT	Γ_{15}
0.58 ± 0.07	OUR ESTIMATE			
0.35 ± 0.12	⁹ ABLIKIM	08D	BES2 $e^+e^- \rightarrow$ hadrons	
0.72 ± 0.11	¹⁰ SETH	05A	RVUE $e^+e^- \rightarrow$ hadrons	
0.64 ± 0.23	¹¹ SETH	05A	RVUE $e^+e^- \rightarrow$ hadrons	
0.49 ± 0.13	BRANDELIK	78c	DASP e^+e^-	
0.44 ± 0.14	SIEGRIST	76	MRK1 e^+e^-	

• • • We do not use the following data for averages, fits, limits, etc. • • •

⁹ Reanalysis of data presented in BAI 02c. From a global fit over the center-of-mass energy region 3.7–5.0 GeV covering the $\psi(3770)$, $\psi(4040)$, $\psi(4160)$, and $\psi(4415)$ resonances. Phase angle fixed in the fit to $\delta = (234 \pm 88)^\circ$.
¹⁰ From a fit to Crystal Ball (OSTERHELD 86) data.
¹¹ From a fit to BES (BAI 02c) data.

 $\psi(4415)$ BRANCHING RATIOS

VALUE	DOCUMENT ID	TECN	COMMENT	Γ_1/Γ
dominant	SIEGRIST	76	MRK1 e^+e^-	

Meson Particle Listings

$\psi(4415)$, $X(4430)^\pm$, $X(4660)$

$\Gamma(D\bar{D})/\Gamma(D^*\bar{D}^*)$	DOCUMENT ID	TECN	COMMENT	Γ_2/Γ_8
VALUE 0.14 ± 0.12 ± 0.03	AUBERT	09M	BABR $e^+e^- \rightarrow \gamma D^*(*)\bar{D}^*(*)$	

$\Gamma(D^*\bar{D} + c.c.)/\Gamma(D^*\bar{D}^*)$	DOCUMENT ID	TECN	COMMENT	Γ_5/Γ_8
VALUE 0.17 ± 0.25 ± 0.03	AUBERT	09M	BABR $e^+e^- \rightarrow \gamma D^*(*)\bar{D}^*(*)$	

$\Gamma(D\bar{D}_2^*(2460) \rightarrow D^0 D^- \pi^+)/\Gamma_{total}$	DOCUMENT ID	TECN	COMMENT	Γ_{13}/Γ
VALUE (units 10^{-2}) 10.5 ± 2.4 ± 3.8	12 PAKHLOVA	08A	BELL $10.6 e^+e^- \rightarrow D^0 D^- \pi^+ \gamma$	
¹² Using 4421 ± 4 MeV for the mass and 62 ± 20 MeV for the width of $\psi(4415)$.				

$\Gamma((D^0 D^- \pi^+)_{non-res})/\Gamma(D\bar{D}_2^*(2460) \rightarrow D^0 D^- \pi^+)$	DOCUMENT ID	TECN	COMMENT	Γ_{12}/Γ_{13}
VALUE <0.22	90 13 PAKHLOVA	08A	BELL $10.6 e^+e^- \rightarrow D^0 D^- \pi^+ \gamma$	
¹³ Using 4421 ± 4 MeV for the mass and 62 ± 20 MeV for the width of $\psi(4415)$.				

$\Gamma(D^0 D^{*-} \pi^+)/\Gamma_{total} \times \Gamma(e^+e^-)/\Gamma_{total}$	DOCUMENT ID	TECN	COMMENT	$\Gamma_{14}/\Gamma \times \Gamma_{15}/\Gamma$
VALUE <0.99 × 10⁻⁶	90 14 PAKHLOVA	09	BELL $e^+e^- \rightarrow \psi(4415) \rightarrow D^0 D^{*-} \pi^+$	
¹⁴ Using 4421 ± 4 MeV for the mass of $\psi(4415)$.				

$\psi(4415)$ REFERENCES

AUBERT	09M	PR D79 092001	B. Aubert <i>et al.</i>	(BABAR Collab.)
PAKHOVA	09	PR D80 091101R	G. Pakhlova <i>et al.</i>	(BELLE Collab.)
ABELIKIM	08D	PL B660 315	M. Ablikim <i>et al.</i>	(BES Collab.)
PAKHOVA	08A	PRL 100 062001	G. Pakhlova <i>et al.</i>	(BELLE Collab.)
SETH	05A	PR D72 017501	K.K. Seth	
BAI	02C	PRL 88 101802	J.Z. Bai <i>et al.</i>	(BES Collab.)
OSTERHELD	86	SLAC-PUB-4160	A. Osterheld <i>et al.</i>	(SLAC Crystal Ball Collab.)
BRANDELIC	78C	PL 76B 361	R. Brandelik <i>et al.</i>	(DASP Collab.)
SIEGRIST	76	PRL 36 700	J.L. Siegrist <i>et al.</i>	(LBL, SLAC)

$X(4430)^\pm$

$$I(J^P) = ?(??)$$

OMITTED FROM SUMMARY TABLE

Seen by CHOI 08 in $B \rightarrow K\pi^+\psi(2S)$ decays and confirmed by reanalysis of the same data sample in MIZUK 09. Not seen by AUBERT 09AA.

$X(4430)^\pm$ MASS

VALUE (MeV)	DOCUMENT ID	TECN	COMMENT
4443⁺¹⁵⁺¹⁹₋₁₂₋₁₃	1 MIZUK	09	BELL $B \rightarrow K\pi^+\psi(2S)$
••• We do not use the following data for averages, fits, limits, etc. •••			
4433 ± 4 ± 2	2 CHOI	08	BELL $B \rightarrow K\pi^+\psi(2S)$

¹From a Dalitz plot analysis.
²Superseded by MIZUK 09.

$X(4430)^\pm$ WIDTH

VALUE (MeV)	DOCUMENT ID	TECN	COMMENT
107⁺⁸⁶⁺⁷⁴₋₄₃₋₅₆	3 MIZUK	09	BELL $B \rightarrow K\pi^+\psi(2S)$
••• We do not use the following data for averages, fits, limits, etc. •••			
45 ⁺¹⁸⁺³⁰ ₋₁₃₋₁₃	4 CHOI	08	BELL $B \rightarrow K\pi^+\psi(2S)$

³From a Dalitz plot analysis.
⁴Superseded by MIZUK 09.

$X(4430)^\pm$ DECAY MODES

Mode	Fraction (Γ_i/Γ)
Γ_1 $\pi^+\psi(2S)$	seen
Γ_2 π^+J/ψ	not seen

$X(4430)^\pm$ BRANCHING RATIOS

$\Gamma(\pi^+\psi(2S))/\Gamma_{total}$	DOCUMENT ID	TECN	COMMENT	Γ_1/Γ
seen	5 MIZUK	09	BELL $B \rightarrow K\pi^+\psi(2S)$	
••• We do not use the following data for averages, fits, limits, etc. •••				
not seen	6 AUBERT	09AA	BABR $K \rightarrow K\pi^+\psi(2S)$	

⁵Measured a product of branching fractions $B(\bar{B}^0 \rightarrow K^- X(4430)^+) \times B(X(4430)^+ \rightarrow \pi^+\psi(2S)) = (3.2_{-0.9-1.6}^{+1.8+5.3}) \times 10^{-5}$.

⁶AUBERT 09AA quotes $B(B^+ \rightarrow \bar{K}^0 X(4430)^+) \times B(X(4430)^+ \rightarrow \pi^+\psi(2S)) < 4.7 \times 10^{-5}$ and $B(\bar{B}^0 \rightarrow K^- X(4430)^+) \times B(X(4430)^+ \rightarrow \pi^+\psi(2S)) < 3.1 \times 10^{-5}$ at 95% CL.

$\Gamma(\pi^+J/\psi)/\Gamma_{total}$	DOCUMENT ID	TECN	COMMENT	Γ_2/Γ
not seen	7 AUBERT	09AA	BABR $K \rightarrow K\pi^+J/\psi$	

⁷AUBERT 09AA quotes $B(B^+ \rightarrow \bar{K}^0 X(4430)^+) \times B(X(4430)^+ \rightarrow \pi^+J/\psi) < 1.5 \times 10^{-5}$ and $B(\bar{B}^0 \rightarrow K^- X(4430)^+) \times B(X(4430)^+ \rightarrow \pi^+J/\psi) < 0.4 \times 10^{-5}$ at 95% CL.

$X(4430)^\pm$ REFERENCES

AUBERT	09AA	PR D79 112001	B. Aubert <i>et al.</i>	(BABAR Collab.)
MIZUK	09	PR D80 031104R	R. Mizuk <i>et al.</i>	(BELLE Collab.)
CHOI	08	PRL 100 142001	S.-K. Choi <i>et al.</i>	(BELLE Collab.)

$X(4660)$

$$I(J^{PC}) = ?^2(1^{--})$$

OMITTED FROM SUMMARY TABLE

Seen in radiative return from e^+e^- collisions at $\sqrt{s} = 9.54\text{--}10.58$ GeV by WANG 07D. Also obtained in a combined fit of WANG 07D and AUBERT 07S. See also the review under the $X(3872)$ particle listings. (See the index for the page number.)

$X(4660)$ MASS

VALUE (MeV)	DOCUMENT ID	TECN	COMMENT
4664 ± 11 ± 5	WANG	07D	BELL $10.58 e^+e^- \rightarrow \psi(2S)\pi^+\pi^-\gamma$
••• We do not use the following data for averages, fits, limits, etc. •••			
4661 ⁺⁹ ₋₈ ± 6	1 LIU	08H	RVUE $10.58 e^+e^- \rightarrow \psi(2S)\pi^+\pi^-\gamma$

¹From a combined fit of AUBERT 07S and WANG 07D data with two resonances.

$X(4660)$ WIDTH

VALUE (MeV)	DOCUMENT ID	TECN	COMMENT
48 ± 15 ± 3	WANG	07D	BELL $10.58 e^+e^- \rightarrow \psi(2S)\pi^+\pi^-\gamma$
••• We do not use the following data for averages, fits, limits, etc. •••			
42 ⁺¹⁷ ₋₁₂ ± 6	2 LIU	08H	RVUE $10.58 e^+e^- \rightarrow \psi(2S)\pi^+\pi^-\gamma$

²From a combined fit of AUBERT 07S and WANG 07D data with two resonances.

$X(4660)$ DECAY MODES

Mode	Fraction (Γ_i/Γ)
Γ_1 e^+e^-	
Γ_2 $\psi(2S)\pi^+\pi^-$	seen
Γ_3 $D^0 D^{*-} \pi^+$	

$X(4660)$ $\Gamma(i)\Gamma(e^+e^-)/\Gamma_{total}$

$\Gamma(\psi(2S)\pi^+\pi^-) \times \Gamma(e^+e^-)/\Gamma_{total}$	DOCUMENT ID	TECN	COMMENT	$\Gamma_2\Gamma_1/\Gamma$
••• We do not use the following data for averages, fits, limits, etc. •••				
2.2 ^{+0.7} _{-0.6}	3 LIU	08H	RVUE $10.58 e^+e^- \rightarrow \psi(2S)\pi^+\pi^-\gamma$	
5.9 ± 1.6	4 LIU	08H	RVUE $10.58 e^+e^- \rightarrow \psi(2S)\pi^+\pi^-\gamma$	
3.0 ± 0.9 ± 0.3	5 WANG	07D	BELL $10.58 e^+e^- \rightarrow \psi(2S)\pi^+\pi^-\gamma$	
7.6 ± 1.8 ± 0.8	6 WANG	07D	BELL $10.58 e^+e^- \rightarrow \psi(2S)\pi^+\pi^-\gamma$	

³Solution I in a combined fit of AUBERT 07S and WANG 07D data with two resonances.
⁴Solution II in a combined fit of AUBERT 07S and WANG 07D data with two resonances.
⁵Solution I of two equivalent solutions in a fit using two interfering resonances.
⁶Solution II of two equivalent solutions in a fit using two interfering resonances.

$X(4660)$ BRANCHING RATIOS

$\Gamma(D^0 D^{*-} \pi^+)/\Gamma(\psi(2S)\pi^+\pi^-)$	DOCUMENT ID	TECN	COMMENT	Γ_3/Γ_2
<10	90	PAKHOVA	09	BELL $e^+e^- \rightarrow X(4660) \rightarrow D^0 D^{*-} \pi^+$

$\Gamma(D^0 D^{*-} \pi^+)/\Gamma_{total} \times \Gamma(e^+e^-)/\Gamma_{total}$	DOCUMENT ID	TECN	COMMENT	$\Gamma_3/\Gamma \times \Gamma_1/\Gamma$
<0.37 × 10 ⁻⁶	90	7 PAKHOVA	09	BELL $e^+e^- \rightarrow X(4660) \rightarrow D^0 D^{*-} \pi^+$

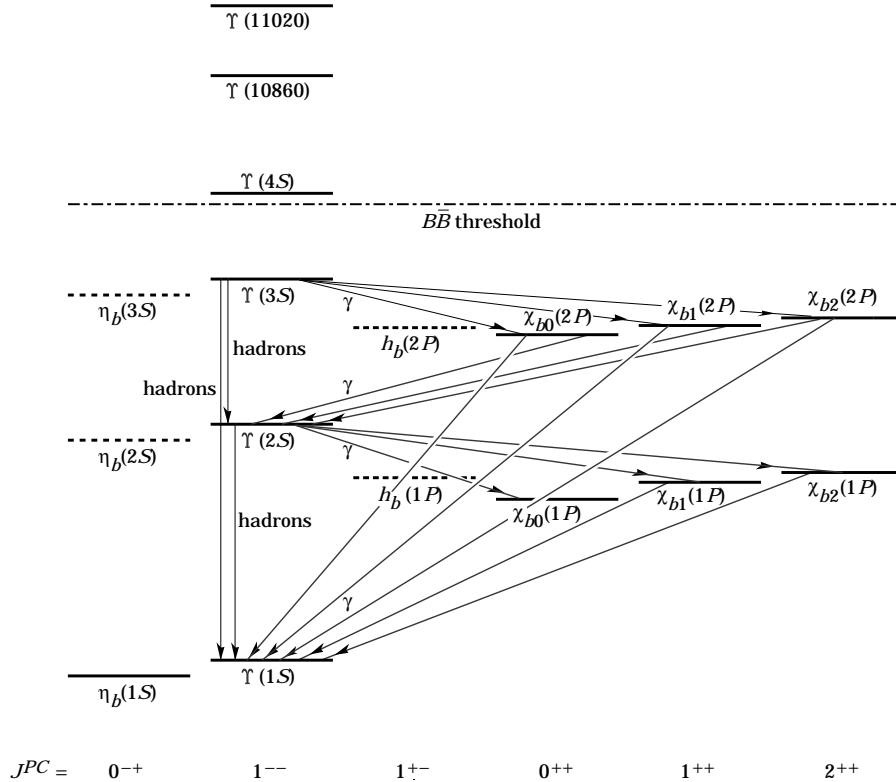
⁷Using 4664 ± 11 ± 5 MeV for the mass of $X(4660)$.

$X(4660)$ REFERENCES

PAKHOVA	09	PR D80 091101R	G. Pakhlova <i>et al.</i>	(BELLE Collab.)
LIU	08H	PR D78 014032	Z.Q. Liu, X.S. Qin, C.Z. Yuan	
AUBERT	07S	PRL 98 212001	B. Aubert <i>et al.</i>	(BABAR Collab.)
WANG	07D	PRL 99 142002	X.L. Wang <i>et al.</i>	(BELLE Collab.)

$b\bar{b}$ MESONS

THE BOTTOMONIUM SYSTEM



The level scheme of the $b\bar{b}$ states showing experimentally established states with solid lines. Singlet states are called η_b and h_b , triplet states Υ and χ_{bJ} . In parentheses it is sufficient to give the radial quantum number and the orbital angular momentum to specify the states with all their quantum numbers. *E.g.*, $h_b(2P)$ means 2^1P_1 with $n = 2, L = 1, S = 0, J = 1, PC = +- -$. If found, *D*-wave states would be called $\eta_b(nD)$ and $\Upsilon_J(nD)$, with $J = 1, 2, 3$ and $n = 1, 2, 3, 4, \dots$. For the χ_b states, the spins of only the $\chi_{b2}(1P)$ and $\chi_{b1}(1P)$ have been experimentally established. The spins of the other χ_b are given as the preferred values, based on the quarkonium models. The figure also shows the observed hadronic and radiative transitions.

WIDTH DETERMINATIONS OF THE Υ STATES

As is the case for the $J/\psi(1S)$ and $\psi(2S)$, the full widths of the $b\bar{b}$ states $\Upsilon(1S)$, $\Upsilon(2S)$, and $\Upsilon(3S)$ are not directly measurable, since they are much narrower than the energy resolution of the e^+e^- storage rings where these states are produced. The common indirect method to determine Γ starts from

$$\Gamma = \Gamma_{\ell\ell} / B_{\ell\ell} , \tag{1}$$

where $\Gamma_{\ell\ell}$ is one leptonic partial width and $B_{\ell\ell}$ is the corresponding branching fraction ($\ell = e, \mu, \text{ or } \tau$). One then assumes $e\text{-}\mu\text{-}\tau$ universality and uses

$$\begin{aligned} \Gamma_{\ell\ell} &= \Gamma_{ee} \\ B_{\ell\ell} &= \text{average of } B_{ee}, B_{\mu\mu}, \text{ and } B_{\tau\tau} . \end{aligned} \tag{2}$$

The electronic partial width Γ_{ee} is also not directly measurable at e^+e^- storage rings, only in the combination $\Gamma_{ee}\Gamma_{\text{had}}/\Gamma$, where Γ_{had} is the hadronic partial width and

$$\Gamma_{\text{had}} + 3\Gamma_{ee} = \Gamma . \tag{3}$$

This combination is obtained experimentally from the energy-integrated hadronic cross section

$$\begin{aligned} &\int_{\text{resonance}} \sigma(e^+e^- \rightarrow \Upsilon \rightarrow \text{hadrons}) dE \\ &= \frac{6\pi^2 \Gamma_{ee} \Gamma_{\text{had}}}{M^2 \Gamma} C_r = \frac{6\pi^2 \Gamma_{ee}^{(0)} \Gamma_{\text{had}}}{M^2 \Gamma} C_r^{(0)} , \end{aligned} \tag{4}$$

where M is the Υ mass, and C_r and $C_r^{(0)}$ are radiative correction factors. C_r is used for obtaining Γ_{ee} as defined in Eq. (1), and contains corrections from all orders of QED for describing $(b\bar{b}) \rightarrow e^+e^-$. The lowest order QED value $\Gamma_{ee}^{(0)}$, relevant for comparison with potential-model calculations, is defined by the

Meson Particle Listings

Bottomonium, $\eta_b(1S)$, $\Upsilon(1S)$

lowest order QED graph (Born term) alone, and is about 7% lower than Γ_{ee} .

The Listings give experimental results on B_{ee} , $B_{\mu\mu}$, $B_{\tau\tau}$, and $\Gamma_{ee}\Gamma_{had}/\Gamma$. The entries of the last quantity have been re-evaluated consistently using the correction procedure of KU-RAEV 85. The partial width Γ_{ee} is obtained from the average values for $\Gamma_{ee}\Gamma_{had}/\Gamma$ and $B_{\ell\ell}$ using

$$\Gamma_{ee} = \frac{\Gamma_{ee}\Gamma_{had}}{\Gamma(1-3B_{\ell\ell})}. \quad (5)$$

The total width Γ is then obtained from Eq. (1). We do not list Γ_{ee} and Γ values of individual experiments. The Γ_{ee} values in the Meson Summary Table are also those defined in Eq. (1).

 $\eta_b(1S)$

$$I^G(J^{PC}) = 0^+(0^{-+})$$

OMITTED FROM SUMMARY TABLE

Quantum numbers shown are quark-model predictions. Observed in radiative decay of the $\Upsilon(3S)$, therefore $C = +$.

 $\eta_b(1S)$ MASS

VALUE (MeV)	EVTS	DOCUMENT ID	TECN	COMMENT
9390.9 ± 2.8 OUR AVERAGE				
9391.8 ± 6.6 ± 2.0	2.3 ± 0.5k	¹ BONVICINI	10 CLEO	$\Upsilon(3S) \rightarrow \gamma X$
9394 ± 4.8 ± 2.0	13 ± 5k	¹ AUBERT	09Aq BABR	$\Upsilon(2S) \rightarrow \gamma X$
9388.9 ± 3.1 ± 2.7	19 ± 3k	¹ AUBERT	08v BABR	$\Upsilon(3S) \rightarrow \gamma X$
• • • We do not use the following data for averages, fits, limits, etc. • • •				
9300 ± 20 ± 20		HEISTER	02d ALEP	181–209 e^+e^-

¹ Assuming $\Gamma_{\eta_b(1S)} = 10$ MeV. Not independent of the corresponding γ energy or mass difference measurements.

 $m\Upsilon(1S) - m\eta_b$

VALUE (MeV)	EVTS	DOCUMENT ID	TECN	COMMENT
69.3 ± 2.8 OUR AVERAGE				
68.5 ± 6.6 ± 2.0	2.3 ± 0.5k	² BONVICINI	10 CLEO	$\Upsilon(3S) \rightarrow \gamma X$
66.1 ± 4.8 ± 2.0	13 ± 5k	² AUBERT	09Aq BABR	$\Upsilon(2S) \rightarrow \gamma X$
71.4 ± 2.3 ± 2.7	19 ± 3k	² AUBERT	08v BABR	$\Upsilon(3S) \rightarrow \gamma X$
² Assuming $\Gamma_{\eta_b(1S)} = 10$ MeV. Not independent of the corresponding γ energy or mass measurements.				

 γ ENERGY IN $\Upsilon(3S)$ DECAY

VALUE (MeV)	EVTS	DOCUMENT ID	TECN	COMMENT
920.6 ± 2.8 OUR AVERAGE				
918.6 ± 6.0 ± 1.9	2.3 ± 0.5k	³ BONVICINI	10 CLEO	$\Upsilon(3S) \rightarrow \gamma X$
921.2 ± 2.1 ± 2.4	19 ± 3k	³ AUBERT	08v BABR	$\Upsilon(3S) \rightarrow \gamma X$
³ Assuming $\Gamma_{\eta_b(1S)} = 10$ MeV. Not independent of the corresponding mass or mass difference measurements.				

 γ ENERGY IN $\Upsilon(2S)$ DECAY

VALUE (MeV)	EVTS	DOCUMENT ID	TECN	COMMENT
609.3 ± 4.6 ± 1.9	13 ± 5k	⁴ AUBERT	09Aq BABR	$\Upsilon(2S) \rightarrow \gamma X$
⁴ Assuming $\Gamma_{\eta_b(1S)} = 10$ MeV. Not independent of the corresponding mass or mass difference measurements.				

 $\eta_b(1S)$ DECAY MODES

Mode	Fraction (Γ_i/Γ)	Confidence level
Γ_1 $3h^+3h^-$	not seen	
Γ_2 $2h^+2h^-$	not seen	
Γ_3 $4h^+4h^-$		
Γ_4 $\gamma\gamma$	not seen	
Γ_5 $\mu^+\mu^-$	$<9 \times 10^{-3}$	90%
Γ_6 $\tau^+\tau^-$	$<8\%$	90%

 $\eta_b(1S)$ $\Gamma(i)\Gamma(\gamma\gamma)/\Gamma(\text{total})$

VALUE (eV)	CL%	DOCUMENT ID	TECN	COMMENT	$\Gamma_1\Gamma_4/\Gamma$
• • • We do not use the following data for averages, fits, limits, etc. • • •					
<470	95	ABDALLAH	06 DLPH	161–209 e^+e^-	
<132	95	HEISTER	02d ALEP	181–209 e^+e^-	
• • • We do not use the following data for averages, fits, limits, etc. • • •					
<190	95	ABDALLAH	06 DLPH	161–209 e^+e^-	
<48	95	HEISTER	02d ALEP	181–209 e^+e^-	
• • • We do not use the following data for averages, fits, limits, etc. • • •					
<660	95	ABDALLAH	06 DLPH	161–209 e^+e^-	

 $\eta_b(1S)$ BRANCHING RATIOS

VALUE	CL%	DOCUMENT ID	TECN	COMMENT	Γ_5/Γ
$<9 \times 10^{-3}$	90	⁵ AUBERT	09z BABR	$e^+e^- \rightarrow \Upsilon(2S, 3S) \rightarrow \gamma\eta_b$	
⁵ Obtained using $B(\Upsilon(2S) \rightarrow \gamma\eta_b) = (4.2^{+1.1}_{-1.0} \pm 0.9) \times 10^{-4}$ and $B(\Upsilon(3S) \rightarrow \gamma\eta_b) = (4.8 \pm 0.5 \pm 0.6) \times 10^{-4}$. This limit is equivalent to $B(\eta_b \rightarrow \mu^+\mu^-) = (-0.25 \pm 0.51 \pm 0.33)\%$ measurement.					

VALUE	CL%	DOCUMENT ID	TECN	COMMENT	Γ_6/Γ
$<8 \times 10^{-2}$	90	AUBERT	09p BABR	$e^+e^- \rightarrow \gamma\tau^+\tau^-$	

 $\eta_b(1S)$ REFERENCES

BONVICINI	10	PR D81 031104R	G. Bonvicini et al.	(CLEO Collab.)
AUBERT	09Aq	PRL 103 161801	B. Aubert et al.	(BABAR Collab.)
AUBERT	09p	PRL 103 181801	B. Aubert et al.	(BABAR Collab.)
AUBERT	09z	PRL 103 081803	B. Aubert et al.	(BABAR Collab.)
AUBERT	08v	PRL 101 071801	B. Aubert et al.	(BABAR Collab.)
ABDALLAH	06	PL B634 340	J.M. Abdallah et al.	(DELPHI Collab.)
HEISTER	02d	PL B530 56	A. Heister et al.	(ALEPH Collab.)

 $\Upsilon(1S)$

$$I^G(J^{PC}) = 0^-(1^{--})$$

 $\Upsilon(1S)$ MASS

VALUE (MeV)	DOCUMENT ID	TECN	COMMENT
9460.30 ± 0.26 OUR AVERAGE	Error includes scale factor of 3.3.		
9460.51 ± 0.09 ± 0.05	¹ ARTAMONOV	00 MD1	$e^+e^- \rightarrow$ hadrons
9459.97 ± 0.11 ± 0.07	MACKAY	84 REDE	$e^+e^- \rightarrow$ hadrons
• • • We do not use the following data for averages, fits, limits, etc. • • •			
9460.60 ± 0.09 ± 0.05	^{2,3} BARU	92b REDE	$e^+e^- \rightarrow$ hadrons
9460.59 ± 0.12	BARU	86 REDE	$e^+e^- \rightarrow$ hadrons
9460.6 ± 0.4	^{3,4} ARTAMONOV	84 REDE	$e^+e^- \rightarrow$ hadrons
¹ Reanalysis of BARU 92b and ARTAMONOV 84 using new electron mass (COHEN 87).			
² Superseding BARU 86.			
³ Superseded by ARTAMONOV 00.			
⁴ Value includes data of ARTAMONOV 82.			

 $\Upsilon(1S)$ WIDTH

VALUE (keV)	DOCUMENT ID
54.02 ± 1.25 OUR EVALUATION	See the Note on "Width Determinations of the Υ States"

 $\Upsilon(1S)$ DECAY MODES

Mode	Fraction (Γ_i/Γ)	Confidence level
Γ_1 $\tau^+\tau^-$	(2.60 ± 0.10) %	
Γ_2 e^+e^-	(2.48 ± 0.07) %	
Γ_3 $\mu^+\mu^-$	(2.48 ± 0.05) %	

Hadronic decays

Γ_4	ggg	$(81.7 \pm 0.7) \%$	
Γ_5	γgg	$(2.21 \pm 0.22) \%$	
Γ_6	$\eta'(958)$ anything	$(2.94 \pm 0.24) \%$	
Γ_7	$J/\psi(1S)$ anything	$(6.5 \pm 0.7) \times 10^{-4}$	
Γ_8	χ_{c0} anything	$< 5 \times 10^{-3}$	90%
Γ_9	χ_{c1} anything	$(2.3 \pm 0.7) \times 10^{-4}$	
Γ_{10}	χ_{c2} anything	$(3.4 \pm 1.0) \times 10^{-4}$	
Γ_{11}	$\psi(2S)$ anything	$(2.7 \pm 0.9) \times 10^{-4}$	
Γ_{12}	$\rho\pi$	$< 2 \times 10^{-4}$	90%
Γ_{13}	$\pi^+\pi^-$	$< 5 \times 10^{-4}$	90%
Γ_{14}	K^+K^-	$< 5 \times 10^{-4}$	90%
Γ_{15}	$p\bar{p}$	$< 5 \times 10^{-4}$	90%
Γ_{16}	$\pi^0\pi^+\pi^-$	$< 1.84 \times 10^{-5}$	90%
Γ_{17}	$D^*(2010)^\pm$ anything	$(2.52 \pm 0.20) \%$	
Γ_{18}	\bar{d} anything	$(2.86 \pm 0.28) \times 10^{-5}$	

Radiative decays

Γ_{19}	$\gamma\pi^+\pi^-$	$(6.3 \pm 1.8) \times 10^{-5}$	
Γ_{20}	$\gamma\pi^0\pi^0$	$(1.7 \pm 0.7) \times 10^{-5}$	
Γ_{21}	$\gamma\pi^0\eta$	$< 2.4 \times 10^{-6}$	90%
Γ_{22}	γK^+K^-	[a] $(1.14 \pm 0.13) \times 10^{-5}$	
Γ_{23}	$\gamma p\bar{p}$	[b] $< 6 \times 10^{-6}$	90%
Γ_{24}	$\gamma 2h^+2h^-$	$(7.0 \pm 1.5) \times 10^{-4}$	
Γ_{25}	$\gamma 3h^+3h^-$	$(5.4 \pm 2.0) \times 10^{-4}$	
Γ_{26}	$\gamma 4h^+4h^-$	$(7.4 \pm 3.5) \times 10^{-4}$	
Γ_{27}	$\gamma\pi^+\pi^-K^+K^-$	$(2.9 \pm 0.9) \times 10^{-4}$	
Γ_{28}	$\gamma 2\pi^+2\pi^-$	$(2.5 \pm 0.9) \times 10^{-4}$	
Γ_{29}	$\gamma 3\pi^+3\pi^-$	$(2.5 \pm 1.2) \times 10^{-4}$	
Γ_{30}	$\gamma 2\pi^+2\pi^-K^+K^-$	$(2.4 \pm 1.2) \times 10^{-4}$	
Γ_{31}	$\gamma\pi^+\pi^-p\bar{p}$	$(1.5 \pm 0.6) \times 10^{-4}$	
Γ_{32}	$\gamma 2\pi^+2\pi^-p\bar{p}$	$(4 \pm 6) \times 10^{-5}$	
Γ_{33}	$\gamma 2K^+2K^-$	$(2.0 \pm 2.0) \times 10^{-5}$	
Γ_{34}	$\gamma\eta'(958)$	$< 1.9 \times 10^{-6}$	90%
Γ_{35}	$\gamma\eta$	$< 1.0 \times 10^{-6}$	90%
Γ_{36}	$\gamma f_0(980)$	$< 3 \times 10^{-5}$	90%
Γ_{37}	$\gamma f_2'(1525)$	$(3.7 \pm 1.2 \pm 1.1) \times 10^{-5}$	
Γ_{38}	$\gamma f_2(1270)$	$(1.01 \pm 0.09) \times 10^{-4}$	
Γ_{39}	$\gamma\eta(1405)$	$< 8.2 \times 10^{-5}$	90%
Γ_{40}	$\gamma f_0(1500)$	$< 1.5 \times 10^{-5}$	90%
Γ_{41}	$\gamma f_0(1710)$	$< 2.6 \times 10^{-4}$	90%
Γ_{42}	$\gamma f_0(1710) \rightarrow \gamma K^+K^-$	$< 7 \times 10^{-6}$	90%
Γ_{43}	$\gamma f_0(1710) \rightarrow \gamma\pi^0\pi^0$	$< 1.4 \times 10^{-6}$	90%
Γ_{44}	$\gamma f_0(1710) \rightarrow \gamma\eta\eta$	$< 1.8 \times 10^{-6}$	90%
Γ_{45}	$\gamma f_4(2050)$	$< 5.3 \times 10^{-5}$	90%
Γ_{46}	$\gamma f_0(2200) \rightarrow \gamma K^+K^-$	$< 2 \times 10^{-4}$	90%
Γ_{47}	$\gamma f_J(2220) \rightarrow \gamma K^+K^-$	$< 8 \times 10^{-7}$	90%
Γ_{48}	$\gamma f_J(2220) \rightarrow \gamma\pi^+\pi^-$	$< 6 \times 10^{-7}$	90%
Γ_{49}	$\gamma f_J(2220) \rightarrow \gamma p\bar{p}$	$< 1.1 \times 10^{-6}$	90%
Γ_{50}	$\gamma\eta(2225) \rightarrow \gamma\phi\phi$	$< 3 \times 10^{-3}$	90%
Γ_{51}	γX	[c] $< 3 \times 10^{-5}$	90%
Γ_{52}	$\gamma X\bar{X}$	[d] $< 1 \times 10^{-3}$	90%
Γ_{53}	$\gamma X \rightarrow \gamma + \geq 4$ prongs	[e] $< 1.78 \times 10^{-4}$	95%
Γ_{54}	$\gamma a_1^0 \rightarrow \gamma\mu^+\mu^-$	[f] $< 9 \times 10^{-6}$	90%
Γ_{55}	$\gamma a_1^0 \rightarrow \gamma\tau^+\tau^-$	[a] $< 5.0 \times 10^{-5}$	90%

Lepton Flavor (LF) violating or Invisible decays

Γ_{56}	$\mu^\pm\tau^\mp$	LF	$< 6.0 \times 10^{-6}$	95%
Γ_{57}	invisible		$< 3.0 \times 10^{-4}$	90%

[a] $2m_\tau < M(\tau^+\tau^-) < 7500$ MeV.

[b] $2 < m_{K^+K^-} < 3$ GeV.

[c] X = pseudoscalar with $m < 7.2$ GeV

[d] $X\bar{X}$ = vectors with $m < 3.1$ GeV

[e] 1.5 GeV $< m_X < 5.0$ GeV

[f] $201 < M(\mu^+\mu^-) < 3565$ MeV.

$\Upsilon(1S)$ $\Gamma(\eta)(\Upsilon(e^+e^-))/\Gamma(\text{total})$

$\Gamma(e^+e^-) \times \Gamma(\mu^+\mu^-)/\Gamma(\text{total})$	DOCUMENT ID	TECN	COMMENT	Γ_2/Γ
31.2±1.6±1.7	KOBEL	92	CBAL $e^+e^- \rightarrow \mu^+\mu^-$	

$\Gamma(\text{hadrons}) \times \Gamma(e^+e^-)/\Gamma(\text{total})$

VALUE (keV)	DOCUMENT ID	TECN	COMMENT	Γ_0/Γ
1.240±0.016 OUR AVERAGE				
1.252±0.004±0.019	5 ROSNER	06	CLEO $9.5 e^+e^- \rightarrow \text{hadrons}$	
1.187±0.023±0.031	5 BARU	92B	MD1 $e^+e^- \rightarrow \text{hadrons}$	
1.23 ±0.02 ±0.05	5 JA KUBOWSKI	88	CBAL $e^+e^- \rightarrow \text{hadrons}$	
1.37 ±0.06 ±0.09	6 GILES	84B	CLEO $e^+e^- \rightarrow \text{hadrons}$	
1.23 ±0.08 ±0.04	6 ALBRECHT	82	DASP $e^+e^- \rightarrow \text{hadrons}$	
1.13 ±0.07 ±0.11	6 NICZYPORUK	82	LENA $e^+e^- \rightarrow \text{hadrons}$	
1.09 ±0.25	6 BOCK	80	CNTR $e^+e^- \rightarrow \text{hadrons}$	
1.35 ±0.14	7 BERGER	79	PLUT $e^+e^- \rightarrow \text{hadrons}$	

⁵ Radiative corrections evaluated following KURAEV 85.

⁶ Radiative corrections reevaluated by BUCHMUELLER 88 following KURAEV 85.

⁷ Radiative corrections reevaluated by ALEXANDER 89 using $B(\mu\mu) = 0.026$.

$\Upsilon(1S)$ PARTIAL WIDTHS

$\Gamma(e^+e^-)$	DOCUMENT ID	Γ_2
VALUE (keV)		
1.340±0.018 OUR EVALUATION		

$\Upsilon(1S)$ BRANCHING RATIOS

$\Gamma(\tau^+\tau^-)/\Gamma(\text{total})$	DOCUMENT ID	TECN	COMMENT	Γ_1/Γ
VALUE (units 10^{-2})	EVTS			
2.60±0.10 OUR AVERAGE				
2.53±0.13±0.05	60k	⁸ BESSON	07 CLEO $e^+e^- \rightarrow \Upsilon(1S) \rightarrow \tau^+\tau^-$	
2.61±0.12 ^{+0.09} _{-0.13}	25k	CINABRO	94B CLE2 $e^+e^- \rightarrow \tau^+\tau^-$	
2.7 ±0.4 ±0.2		⁹ ALBRECHT	85c ARG $\Upsilon(2S) \rightarrow \pi^+\pi^-\tau^+\tau^-$	
3.4 ±0.4 ±0.4		GILES	83 CLEO $e^+e^- \rightarrow \tau^+\tau^-$	

⁸ BESSON 07 reports $[\Gamma(\Upsilon(1S) \rightarrow \tau^+\tau^-)/\Gamma(\text{total})] / [B(\Upsilon(1S) \rightarrow \mu^+\mu^-)] = 1.02 \pm 0.02 \pm 0.05$ which we multiply by our best value $B(\Upsilon(1S) \rightarrow \mu^+\mu^-) = (2.48 \pm 0.05) \times 10^{-2}$. Our first error is their experiment's error and our second error is the systematic error from using our best value.

⁹ Using $B(\Upsilon(1S) \rightarrow ee) = B(\Upsilon(1S) \rightarrow \mu\mu) = 0.0256$; not used for width evaluations.

$\Gamma(e^+e^-)/\Gamma(\text{total})$	DOCUMENT ID	TECN	COMMENT	Γ_2/Γ
VALUE (units 10^{-2})	EVTS			
2.38±0.11 OUR AVERAGE				
2.29±0.08±0.11		ALEXANDER	98 CLE2 $\Upsilon(2S) \rightarrow \pi^+\pi^-e^+e^-$	
2.42±0.14±0.14	307	ALBRECHT	87 ARG $\Upsilon(2S) \rightarrow \pi^+\pi^-e^+e^-$	
2.8 ±0.3 ±0.2	826	BESSON	84 CLEO $\Upsilon(2S) \rightarrow \pi^+\pi^-e^+e^-$	
5.1 ±3.0		BERGER	80c PLUT $e^+e^- \rightarrow e^+e^-$	

$\Gamma(\mu^+\mu^-)/\Gamma(\text{total})$	DOCUMENT ID	TECN	COMMENT	Γ_3/Γ
VALUE	EVTS			
0.0248±0.0005 OUR AVERAGE				
0.0249±0.0002±0.0007	345k	ADAMS	05 CLEO $e^+e^- \rightarrow \mu^+\mu^-$	
0.0249±0.0008±0.0013		ALEXANDER	98 CLE2 $\Upsilon(2S) \rightarrow \mu^+\mu^-$	

0.0212±0.0020±0.0010		¹⁰ BARU	92 MD1 $e^+e^- \rightarrow \mu^+\mu^-$	
0.0231±0.0012±0.0010		¹⁰ KOBEL	92 CBAL $e^+e^- \rightarrow \mu^+\mu^-$	
0.0252±0.0007±0.0007		CHEN	89B CLEO $e^+e^- \rightarrow \mu^+\mu^-$	
0.0261±0.0009±0.0011		KAARSBERG	89 CSB2 $e^+e^- \rightarrow \mu^+\mu^-$	
0.0230±0.0025±0.0013	86	ALBRECHT	87 ARG $\Upsilon(2S) \rightarrow \mu^+\mu^-$	
0.029 ±0.003 ±0.002	864	BESSON	84 CLEO $\Upsilon(2S) \rightarrow \mu^+\mu^-$	
0.027 ±0.003 ±0.003		ANDREWS	83 CLEO $e^+e^- \rightarrow \mu^+\mu^-$	
0.032 ±0.013 ±0.003		ALBRECHT	82 DASP $e^+e^- \rightarrow \mu^+\mu^-$	
0.038 ±0.015 ±0.002		NICZYPORUK	82 LENA $e^+e^- \rightarrow \mu^+\mu^-$	
0.014 ^{+0.034} _{-0.014}		BOCK	80 CNTR $e^+e^- \rightarrow \mu^+\mu^-$	
0.022 ±0.020		BERGER	79 PLUT $e^+e^- \rightarrow \mu^+\mu^-$	

¹⁰ Taking into account interference between the resonance and continuum.

$\Gamma(\tau^+\tau^-)/\Gamma(\mu^+\mu^-)$	DOCUMENT ID	TECN	COMMENT	Γ_1/Γ_3
VALUE	EVTS			
1.02±0.02±0.05	60k	BESSON	07 CLEO $e^+e^- \rightarrow \Upsilon(1S)$	

$\Gamma(ggg)/\Gamma(\text{total})$	DOCUMENT ID	TECN	COMMENT	Γ_4/Γ
VALUE (units 10^{-2})	EVTS			
81.7±0.7	20M	¹¹ BESSON	06A CLEO $\Upsilon(1S) \rightarrow \text{hadrons}$	

¹¹ Calculated using the value $\Gamma(\gamma gg)/\Gamma(ggg) = (2.70 \pm 0.01 \pm 0.13 \pm 0.24) \%$ from BESSON 06A and PDG 08 values of $B(\mu^+\mu^-) = (2.48 \pm 0.05) \%$ and $R_{\text{hadrons}} = 3.51$. The statistical error is negligible and the systematic error is partially correlated with that of $\Gamma(\gamma gg)/\Gamma(\text{total})$ measurement of BESSON 06A.

$\Gamma(ggg)/\Gamma(\text{total})$	DOCUMENT ID	TECN	COMMENT	Γ_5/Γ
VALUE (units 10^{-2})	EVTS			
2.20±0.60	400k	¹² BESSON	06A CLEO $\Upsilon(1S) \rightarrow \gamma + \text{hadrons}$	

¹² Calculated using BESSON 06A values of $\Gamma(\gamma gg)/\Gamma(ggg) = (2.70 \pm 0.01 \pm 0.13 \pm 0.24) \%$ and $\Gamma(ggg)/\Gamma(\text{total})$. The statistical error is negligible and the systematic error is partially correlated with that of $\Gamma(ggg)/\Gamma(\text{total})$ measurement of BESSON 06A.

Meson Particle Listings

 $\Upsilon(1S)$

$\Gamma(\gamma g g)/\Gamma(g g g)$		Γ_5/Γ_4			$\Gamma(\gamma\pi^+\pi^-)/\Gamma_{total}$			Γ_{19}/Γ						
VALUE (units 10^{-2})	EVTS	DOCUMENT ID	TECN	COMMENT	VALUE (units 10^{-5})	DOCUMENT ID	TECN	COMMENT	VALUE (units 10^{-5})	DOCUMENT ID	TECN	COMMENT		
$2.70 \pm 0.01 \pm 0.27$	20M	BESSON	06A	CLEO $\Upsilon(1S) \rightarrow (\gamma^+) \text{ hadrons}$	$6.3 \pm 1.2 \pm 1.3$	17	ANASTASSOV	99 CLE2	$e^+ e^- \rightarrow \text{hadrons}$					
$\Gamma(\eta'(958) \text{ anything})/\Gamma_{total}$		Γ_6/Γ			$\Gamma(\gamma\pi^0\pi^0)/\Gamma_{total}$			Γ_{20}/Γ						
VALUE	EVTS	DOCUMENT ID	TECN	COMMENT	VALUE (units 10^{-5})	DOCUMENT ID	TECN	COMMENT	VALUE (units 10^{-5})	DOCUMENT ID	TECN	COMMENT		
0.0294 ± 0.0024 OUR AVERAGE					$1.7 \pm 0.6 \pm 0.3$	18	ANASTASSOV	99 CLE2	$e^+ e^- \rightarrow \text{hadrons}$					
$0.030 \pm 0.002 \pm 0.002$		AQUINES	06A	CLE3 $\Upsilon(1S) \rightarrow \eta' \text{ anything}$										
$0.028 \pm 0.004 \pm 0.002$		ARTUSO	03	CLE2 $\Upsilon(1S) \rightarrow \eta' \text{ anything}$	17 For $m_{\pi\pi} > 1$ GeV.			18 For $m_{\pi\pi} > 1$ GeV.						
$\Gamma(J/\psi(1S) \text{ anything})/\Gamma_{total}$		Γ_7/Γ			$\Gamma(\gamma\pi^0\eta)/\Gamma_{total}$			Γ_{21}/Γ						
VALUE (units 10^{-3})	CL% EVTS	DOCUMENT ID	TECN	COMMENT	VALUE (units 10^{-6})	CL%	DOCUMENT ID	TECN	COMMENT	VALUE (units 10^{-6})	CL%	DOCUMENT ID	TECN	COMMENT
$0.64 \pm 0.04 \pm 0.06$	730 ± 40	BRIERE	04	CLEO $e^+ e^- \rightarrow J/\psi X$	< 2.4		19	BESSON	07A CLEO	$e^+ e^- \rightarrow \Upsilon(1S)$				
$1.1 \pm 0.4 \pm 0.2$		13 FULTON	89	CLEO $e^+ e^- \rightarrow \mu^+ \mu^- X$										
< 0.68	90	ALBRECHT	92J	ARG $e^+ e^- \rightarrow e^+ e^- X, \mu^+ \mu^- X$	19 BESSON 07A obtained this limit for $0.7 < m_{\pi^0\eta} < 3$ GeV.									
< 1.7	90	MASCHMANN	90	CBAL $e^+ e^- \rightarrow \text{hadrons}$	$\Gamma(\gamma K^+ K^-)/\Gamma_{total}$			Γ_{22}/Γ						
< 20	90	NICZYPORUK	83	LENA $e^+ e^- \rightarrow \text{hadrons}$	(2 < $m_{K^+ K^-} < 3$ GeV)			2 < $m_{\rho\bar{\rho}} < 3$ GeV)			Γ_{23}/Γ			
13 Using $B(J/\psi \rightarrow \mu^+ \mu^-) = (6.9 \pm 0.9)\%$.					VALUE (units 10^{-5})	CL%	DOCUMENT ID	TECN	COMMENT	VALUE (units 10^{-5})	CL%	DOCUMENT ID	TECN	COMMENT
$\Gamma(\chi_{c0} \text{ anything})/\Gamma(J/\psi(1S) \text{ anything})$		Γ_8/Γ_7			$\Gamma(\gamma\rho\bar{\rho})/\Gamma_{total}$			Γ_{24}/Γ						
VALUE	CL%	DOCUMENT ID	TECN	COMMENT	VALUE (units 10^{-4})	EVTS	DOCUMENT ID	TECN	COMMENT	VALUE (units 10^{-4})	EVTS	DOCUMENT ID	TECN	COMMENT
< 7.4	90	BRIERE	04	CLEO $e^+ e^- \rightarrow J/\psi X$	$1.14 \pm 0.08 \pm 0.10$	90	ATHAR	06 CLE3	$\Upsilon(1S) \rightarrow \gamma K^+ K^-$	< 0.6	90	ATHAR	06 CLE3	$\Upsilon(1S) \rightarrow \gamma\rho\bar{\rho}$
$\Gamma(\chi_{c1} \text{ anything})/\Gamma(J/\psi(1S) \text{ anything})$		Γ_9/Γ_7			$\Gamma(\gamma 2h^+ 2h^-)/\Gamma_{total}$			Γ_{25}/Γ						
VALUE	EVTS	DOCUMENT ID	TECN	COMMENT	VALUE (units 10^{-4})	EVTS	DOCUMENT ID	TECN	COMMENT	VALUE (units 10^{-4})	EVTS	DOCUMENT ID	TECN	COMMENT
$0.35 \pm 0.08 \pm 0.06$	52 ± 12	BRIERE	04	CLEO $e^+ e^- \rightarrow J/\psi X$	$7.0 \pm 1.1 \pm 1.0$	80 ± 12	FULTON	90B CLEO	$e^+ e^- \rightarrow \text{hadrons}$	$5.4 \pm 1.5 \pm 1.3$	39 ± 11	FULTON	90B CLEO	$e^+ e^- \rightarrow \text{hadrons}$
$\Gamma(\chi_{c2} \text{ anything})/\Gamma(J/\psi(1S) \text{ anything})$		Γ_{10}/Γ_7			$\Gamma(\gamma 3h^+ 3h^-)/\Gamma_{total}$			Γ_{26}/Γ						
VALUE	EVTS	DOCUMENT ID	TECN	COMMENT	VALUE (units 10^{-4})	EVTS	DOCUMENT ID	TECN	COMMENT	VALUE (units 10^{-4})	EVTS	DOCUMENT ID	TECN	COMMENT
$0.52 \pm 0.12 \pm 0.09$	47 ± 11	BRIERE	04	CLEO $e^+ e^- \rightarrow J/\psi X$	$7.4 \pm 2.5 \pm 2.5$	36 ± 12	FULTON	90B CLEO	$e^+ e^- \rightarrow \text{hadrons}$	$5.4 \pm 1.5 \pm 1.3$	39 ± 11	FULTON	90B CLEO	$e^+ e^- \rightarrow \text{hadrons}$
$\Gamma(\psi(2S) \text{ anything})/\Gamma(J/\psi(1S) \text{ anything})$		Γ_{11}/Γ_7			$\Gamma(\gamma 4h^+ 4h^-)/\Gamma_{total}$			Γ_{27}/Γ						
VALUE	EVTS	DOCUMENT ID	TECN	COMMENT	VALUE (units 10^{-4})	EVTS	DOCUMENT ID	TECN	COMMENT	VALUE (units 10^{-4})	EVTS	DOCUMENT ID	TECN	COMMENT
$0.41 \pm 0.11 \pm 0.08$	42 ± 11	BRIERE	04	CLEO $e^+ e^- \rightarrow J/\psi\pi^+\pi^- X$	$2.9 \pm 0.7 \pm 0.6$	29 ± 8	FULTON	90B CLEO	$e^+ e^- \rightarrow \text{hadrons}$	$2.9 \pm 0.7 \pm 0.6$	29 ± 8	FULTON	90B CLEO	$e^+ e^- \rightarrow \text{hadrons}$
$\Gamma(\rho\pi)/\Gamma_{total}$		Γ_{12}/Γ			$\Gamma(\gamma\pi^+\pi^- K^+ K^-)/\Gamma_{total}$			Γ_{28}/Γ						
VALUE (units 10^{-4})	CL%	DOCUMENT ID	TECN	COMMENT	VALUE (units 10^{-4})	EVTS	DOCUMENT ID	TECN	COMMENT	VALUE (units 10^{-4})	EVTS	DOCUMENT ID	TECN	COMMENT
< 2	90	FULTON	90B	$\Upsilon(1S) \rightarrow \rho^0 \pi^0$	$2.5 \pm 0.7 \pm 0.5$	26 ± 7	FULTON	90B CLEO	$e^+ e^- \rightarrow \text{hadrons}$	$7.4 \pm 2.5 \pm 2.5$	36 ± 12	FULTON	90B CLEO	$e^+ e^- \rightarrow \text{hadrons}$
••• We do not use the following data for averages, fits, limits, etc. •••					$2.9 \pm 0.7 \pm 0.6$	29 ± 8	FULTON	90B CLEO	$e^+ e^- \rightarrow \text{hadrons}$	$2.9 \pm 0.7 \pm 0.6$	29 ± 8	FULTON	90B CLEO	$e^+ e^- \rightarrow \text{hadrons}$
< 10	90	BLINOV	90	MD1 $\Upsilon(1S) \rightarrow \rho^0 \pi^0$	$\Gamma(\gamma 2\pi^+ 2\pi^-)/\Gamma_{total}$			Γ_{29}/Γ						
< 21	90	NICZYPORUK	83	LENA $\Upsilon(1S) \rightarrow \rho^0 \pi^0$	VALUE (units 10^{-4})	EVTS	DOCUMENT ID	TECN	COMMENT	VALUE (units 10^{-4})	EVTS	DOCUMENT ID	TECN	COMMENT
$\Gamma(\pi^+ \pi^-)/\Gamma_{total}$		Γ_{13}/Γ			$\Gamma(\gamma 3\pi^+ 3\pi^-)/\Gamma_{total}$			Γ_{30}/Γ						
VALUE (units 10^{-4})	CL%	DOCUMENT ID	TECN	COMMENT	VALUE (units 10^{-4})	EVTS	DOCUMENT ID	TECN	COMMENT	VALUE (units 10^{-4})	EVTS	DOCUMENT ID	TECN	COMMENT
< 5	90	BARU	92	MD1 $\Upsilon(1S) \rightarrow \pi^+ \pi^-$	$2.5 \pm 0.9 \pm 0.8$	17 ± 5	FULTON	90B CLEO	$e^+ e^- \rightarrow \text{hadrons}$	$2.4 \pm 0.9 \pm 0.8$	18 ± 7	FULTON	90B CLEO	$e^+ e^- \rightarrow \text{hadrons}$
$\Gamma(K^+ K^-)/\Gamma_{total}$		Γ_{14}/Γ			$\Gamma(\gamma 2\pi^+ 2\pi^- K^+ K^-)/\Gamma_{total}$			Γ_{31}/Γ						
VALUE (units 10^{-4})	CL%	DOCUMENT ID	TECN	COMMENT	VALUE (units 10^{-4})	EVTS	DOCUMENT ID	TECN	COMMENT	VALUE (units 10^{-4})	EVTS	DOCUMENT ID	TECN	COMMENT
< 5	90	BARU	92	MD1 $\Upsilon(1S) \rightarrow K^+ K^-$	$1.5 \pm 0.5 \pm 0.3$	22 ± 6	FULTON	90B CLEO	$e^+ e^- \rightarrow \text{hadrons}$	$1.5 \pm 0.5 \pm 0.3$	22 ± 6	FULTON	90B CLEO	$e^+ e^- \rightarrow \text{hadrons}$
$\Gamma(\rho\bar{\rho})/\Gamma_{total}$		Γ_{15}/Γ			$\Gamma(\gamma\pi^+ \pi^- \rho\bar{\rho})/\Gamma_{total}$			Γ_{32}/Γ						
VALUE (units 10^{-4})	CL%	DOCUMENT ID	TECN	COMMENT	VALUE (units 10^{-4})	EVTS	DOCUMENT ID	TECN	COMMENT	VALUE (units 10^{-4})	EVTS	DOCUMENT ID	TECN	COMMENT
< 5	90	14 BARU	96	MD1 $\Upsilon(1S) \rightarrow \rho\bar{\rho}$	$0.4 \pm 0.4 \pm 0.4$	7 ± 6	FULTON	90B CLEO	$e^+ e^- \rightarrow \text{hadrons}$	$0.4 \pm 0.4 \pm 0.4$	7 ± 6	FULTON	90B CLEO	$e^+ e^- \rightarrow \text{hadrons}$
14 Supersedes BARU 92 in this node.					$\Gamma(\gamma 2K^+ 2K^-)/\Gamma_{total}$			Γ_{33}/Γ						
$\Gamma(\pi^0 \pi^+ \pi^-)/\Gamma_{total}$		Γ_{16}/Γ			$\Gamma(\gamma\eta'(958))/\Gamma_{total}$			Γ_{34}/Γ						
VALUE (units 10^{-5})	CL%	DOCUMENT ID	TECN	COMMENT	VALUE (units 10^{-6})	CL%	DOCUMENT ID	TECN	COMMENT	VALUE (units 10^{-6})	CL%	DOCUMENT ID	TECN	COMMENT
< 1.84	90	ANASTASSOV	99	CLE2 $e^+ e^- \rightarrow \text{hadrons}$	< 1.9	90	ATHAR	07A CLEO	$\Upsilon(1S) \rightarrow \gamma\eta' \rightarrow \gamma\pi^+\pi^-\eta, \gamma\rho$					
$\Gamma(D^*(2010)^\pm \text{ anything})/\Gamma_{total}$		Γ_{17}/Γ			••• We do not use the following data for averages, fits, limits, etc. •••			••• We do not use the following data for averages, fits, limits, etc. •••						
VALUE (units 10^{-3})	CL% EVTS	DOCUMENT ID	TECN	COMMENT	< 16	90	RICHICHI	01B CLE2	$\Upsilon(1S) \rightarrow \gamma\eta' \rightarrow \gamma\eta\pi^+\pi^-$					
$25.2 \pm 1.3 \pm 1.5$	$\approx 2k$	15 AUBERT	10c	BABR $\Upsilon(2S) \rightarrow \pi^+\pi^-\Upsilon(1S)$	$\Gamma(\gamma\eta)/\Gamma_{total}$			Γ_{35}/Γ						
••• We do not use the following data for averages, fits, limits, etc. •••					VALUE (units 10^{-5})	CL%	DOCUMENT ID	TECN	COMMENT	VALUE (units 10^{-5})	CL%	DOCUMENT ID	TECN	COMMENT
< 19	90	16 ALBRECHT	92J	ARG $e^+ e^- \rightarrow D^0 \pi^\pm X$	< 1.0	90	ATHAR	07A CLEO	$\Upsilon(1S) \rightarrow \gamma\eta \rightarrow \gamma\gamma\gamma, \gamma\pi^+\pi^-\pi^0, \gamma 3\pi^0$					
15 For $x_p > 0.1$.					$\Gamma(\bar{d} \text{ anything})/\Gamma_{total}$			Γ_{18}/Γ						
16 For $x_p > 0.2$.					VALUE (units 10^{-5})	EVTS	DOCUMENT ID	TECN	COMMENT	VALUE (units 10^{-5})	EVTS	DOCUMENT ID	TECN	COMMENT
$\Gamma(\bar{d} \text{ anything})/\Gamma_{total}$		Γ_{18}/Γ			$\Gamma(ggg, g\bar{g}\gamma \rightarrow \bar{d} \text{ anything})/\Gamma(ggg, g\bar{g}\gamma \rightarrow \text{anything})$									
VALUE (units 10^{-5})	EVTS	DOCUMENT ID	TECN	COMMENT	VALUE (units 10^{-5})	EVTS	DOCUMENT ID	TECN	COMMENT	VALUE (units 10^{-5})	EVTS	DOCUMENT ID	TECN	COMMENT
$2.86 \pm 0.19 \pm 0.21$	455	ASNER	07	CLEO $e^+ e^- \rightarrow \bar{d} X$	$3.36 \pm 0.23 \pm 0.25$	455	ASNER	07	CLEO $e^+ e^- \rightarrow \bar{d} X$					
$\Gamma(ggg, g\bar{g}\gamma \rightarrow \bar{d} \text{ anything})/\Gamma(ggg, g\bar{g}\gamma \rightarrow \text{anything})$					••• We do not use the following data for averages, fits, limits, etc. •••									
VALUE (units 10^{-5})	EVTS	DOCUMENT ID	TECN	COMMENT	< 21	90	MASEK	02	CLEO $\Upsilon(1S) \rightarrow \gamma\eta$					
$3.36 \pm 0.23 \pm 0.25$	455	ASNER	07	CLEO $e^+ e^- \rightarrow \bar{d} X$	••• We do not use the following data for averages, fits, limits, etc. •••									

Meson Particle Listings
 $\Upsilon(1S)$

$\Gamma(\gamma f_0(980))/\Gamma_{total}$ Γ_{36}/Γ

VALUE (units 10^{-5})	CL%	DOCUMENT ID	TECN	COMMENT
<3	90	20 ATHAR	06 CLE3	$\Upsilon(1S) \rightarrow \gamma \pi^+ \pi^-$

²⁰ Assuming $B(f_0(980) \rightarrow \pi\pi) = 1$.

$\Gamma(\gamma f_2'(1525))/\Gamma_{total}$ Γ_{37}/Γ

VALUE (units 10^{-5})	CL%	DOCUMENT ID	TECN	COMMENT
$3.7 \pm 0.9 \pm 0.8$		ATHAR	06 CLE3	$\Upsilon(1S) \rightarrow \gamma K^+ K^-$

• • • We do not use the following data for averages, fits, limits, etc. • • •

<14	90	21 FULTON	90B CLEO	$\Upsilon(1S) \rightarrow \gamma K^+ K^-$
<19.4	90	21 ALBRECHT	89 ARG	$\Upsilon(1S) \rightarrow \gamma K^+ K^-$

²¹ Assuming $B(f_2'(1525) \rightarrow K\bar{K}) = 0.71$.

$\Gamma(\gamma f_2(1270))/\Gamma_{total}$ Γ_{38}/Γ

VALUE (units 10^{-5})	CL%	DOCUMENT ID	TECN	COMMENT
10.1 ± 0.9 OUR AVERAGE				
$10.5 \pm 1.6 \pm 1.9$		22 BESSON	07A CLE3	$\Upsilon(1S) \rightarrow \gamma \pi^0 \pi^0$
$10.2 \pm 0.8 \pm 0.7$		ATHAR	06 CLE3	$\Upsilon(1S) \rightarrow \gamma \pi^+ \pi^-$
$8.1 \pm 2.3 \pm 2.9$ -0.12		23 ANASTASSOV	99 CLE2	$e^+ e^- \rightarrow$ hadrons

• • • We do not use the following data for averages, fits, limits, etc. • • •

<21	90	23 FULTON	90B CLEO	$\Upsilon(1S) \rightarrow \gamma \pi^+ \pi^-$
<13	90	23 ALBRECHT	89 ARG	$\Upsilon(1S) \rightarrow \gamma \pi^+ \pi^-$
<81	90	SCHMITT	88 CBAL	$\Upsilon(1S) \rightarrow \gamma X$

²² Using $B(f_2(1270) \rightarrow \pi^0 \pi^0) = B(f_2(1270) \rightarrow \pi\pi)/3$ and $B(f_2(1270) \rightarrow \pi\pi) = (0.845 \pm 0.025 - 0.012)\%$.

²³ Using $B(f_2(1270) \rightarrow \pi\pi) = 0.84$.

$\Gamma(\gamma \eta(1405))/\Gamma_{total}$ Γ_{39}/Γ

VALUE (units 10^{-5})	CL%	DOCUMENT ID	TECN	COMMENT
<8.2	90	24 FULTON	90B CLEO	$\Upsilon(1S) \rightarrow \gamma K^\pm \pi^\mp K_S^0$

²⁴ Includes unknown branching ratio of $\eta(1405) \rightarrow K^\pm \pi^\mp K_S^0$.

$\Gamma(\gamma f_0(1500))/\Gamma_{total}$ Γ_{40}/Γ

VALUE (units 10^{-5})	CL%	DOCUMENT ID	TECN	COMMENT
<1.5	90	25 BESSON	07A CLEO	$e^+ e^- \rightarrow \Upsilon(1S) \rightarrow \gamma \pi^0 \pi^0$

• • • We do not use the following data for averages, fits, limits, etc. • • •

<6.1	90	26 BESSON	07A CLEO	$e^+ e^- \rightarrow \Upsilon(1S) \rightarrow \gamma \eta \eta$
------	----	-----------	----------	---

²⁵ Using $B(f_0(1500) \rightarrow \pi^0 \pi^0) = B(f_0(1500) \rightarrow \pi\pi)/3$ and $B(f_0(1500) \rightarrow \pi\pi) = (0.349 \pm 0.023)\%$.

²⁶ Calculated by us using $B(f_0(1500) \rightarrow \eta\eta) = (5.1 \pm 0.9)\%$.

$\Gamma(\gamma f_0(1710))/\Gamma_{total}$ Γ_{41}/Γ

VALUE (units 10^{-4})	CL%	DOCUMENT ID	TECN	COMMENT
< 2.6	90	27 ALBRECHT	89 ARG	$\Upsilon(1S) \rightarrow \gamma K^+ K^-$

• • • We do not use the following data for averages, fits, limits, etc. • • •

< 6.3	90	27 FULTON	90B CLEO	$\Upsilon(1S) \rightarrow \gamma K^+ K^-$
<19	90	27 FULTON	90B CLEO	$\Upsilon(1S) \rightarrow \gamma K_S^0 K_S^0$
< 8	90	28 ALBRECHT	89 ARG	$\Upsilon(1S) \rightarrow \gamma \pi^+ \pi^-$
<24	90	29 SCHMITT	88 CBAL	$\Upsilon(1S) \rightarrow \gamma X$

²⁷ Assuming $B(f_0(1710) \rightarrow K\bar{K}) = 0.38$.

²⁸ Assuming $B(f_0(1710) \rightarrow \pi\pi) = 0.04$.

²⁹ Assuming $B(f_0(1710) \rightarrow \eta\eta) = 0.18$.

$\Gamma(\gamma f_0(1710) \rightarrow \gamma K^+ K^-)/\Gamma_{total}$ Γ_{42}/Γ

VALUE (units 10^{-5})	CL%	DOCUMENT ID	TECN	COMMENT
<0.7	90	ATHAR	06 CLEO	$e^+ e^- \rightarrow \Upsilon(1S) \rightarrow \gamma K^+ K^-$

$\Gamma(\gamma f_0(1710) \rightarrow \gamma \pi^0 \pi^0)/\Gamma_{total}$ Γ_{43}/Γ

VALUE (units 10^{-6})	CL%	DOCUMENT ID	TECN	COMMENT
<1.4	90	BESSON	07A CLEO	$e^+ e^- \rightarrow \Upsilon(1S) \rightarrow \gamma \pi^0 \pi^0$

$\Gamma(\gamma f_0(1710) \rightarrow \gamma \eta \eta)/\Gamma_{total}$ Γ_{44}/Γ

VALUE (units 10^{-6})	CL%	DOCUMENT ID	TECN	COMMENT
<1.8	90	BESSON	07A CLEO	$e^+ e^- \rightarrow \Upsilon(1S) \rightarrow \gamma \eta \eta$

$\Gamma(\gamma f_4(2050))/\Gamma_{total}$ Γ_{45}/Γ

VALUE (units 10^{-5})	CL%	DOCUMENT ID	TECN	COMMENT
<5.3	90	30 ATHAR	06 CLE3	$\Upsilon(1S) \rightarrow \gamma \pi^+ \pi^-$

³⁰ Assuming $B(f_4(2050) \rightarrow \pi\pi) = 0.17$.

$\Gamma(\gamma f_0(2200) \rightarrow \gamma K^+ K^-)/\Gamma_{total}$ Γ_{46}/Γ

VALUE	CL%	DOCUMENT ID	TECN	COMMENT
<0.0002	90	BARU	89 MD1	$\Upsilon(1S) \rightarrow \gamma K^+ K^-$

$\Gamma(\gamma f_J(2220) \rightarrow \gamma K^+ K^-)/\Gamma_{total}$ Γ_{47}/Γ

VALUE (units 10^{-7})	CL%	DOCUMENT ID	TECN	COMMENT
< 8	90	ATHAR	06 CLE3	$\Upsilon(1S) \rightarrow \gamma K^+ K^-$

• • • We do not use the following data for averages, fits, limits, etc. • • •

< 160	90	MASEK	02 CLEO	$\Upsilon(1S) \rightarrow \gamma K^+ K^-$
< 150	90	FULTON	90B CLEO	$\Upsilon(1S) \rightarrow \gamma K^+ K^-$
< 290	90	ALBRECHT	89 ARG	$\Upsilon(1S) \rightarrow \gamma K^+ K^-$
<2000	90	BARU	89 MD1	$\Upsilon(1S) \rightarrow \gamma K^+ K^-$

$\Gamma(\gamma f_J(2220) \rightarrow \gamma \pi^+ \pi^-)/\Gamma_{total}$ Γ_{48}/Γ

VALUE (units 10^{-7})	CL%	DOCUMENT ID	TECN	COMMENT
< 6	90	ATHAR	06 CLE3	$\Upsilon(1S) \rightarrow \gamma \pi^+ \pi^-$

• • • We do not use the following data for averages, fits, limits, etc. • • •

<120	90	MASEK	02 CLEO	$\Upsilon(1S) \rightarrow \gamma \pi^+ \pi^-$
------	----	-------	---------	---

$\Gamma(\gamma f_J(2220) \rightarrow \gamma \rho \bar{\rho})/\Gamma_{total}$ Γ_{49}/Γ

VALUE (units 10^{-7})	CL%	DOCUMENT ID	TECN	COMMENT
< 11	90	ATHAR	06 CLE3	$\Upsilon(1S) \rightarrow \gamma \rho \bar{\rho}$

• • • We do not use the following data for averages, fits, limits, etc. • • •

<160	90	MASEK	02 CLEO	$\Upsilon(1S) \rightarrow \gamma \rho \bar{\rho}$
------	----	-------	---------	---

$\Gamma(\gamma \eta(2225) \rightarrow \gamma \phi \phi)/\Gamma_{total}$ Γ_{50}/Γ

VALUE	CL%	DOCUMENT ID	TECN	COMMENT
<0.003	90	BARU	89 MD1	$\Upsilon(1S) \rightarrow \gamma K^+ K^- K^+ K^-$

$\Gamma(\gamma X)/\Gamma_{total}$ Γ_{51}/Γ
 (X = pseudoscalar with $m < 7.2$ GeV)

VALUE (units 10^{-5})	CL%	DOCUMENT ID	TECN	COMMENT
<3	90	31 BALEST	95 CLEO	$e^+ e^- \rightarrow \gamma + X$

³¹ For a noninteracting pseudoscalar X with mass < 7.2 GeV.

$\Gamma(\gamma X \bar{X})/\Gamma_{total}$ Γ_{52}/Γ
 (X = vectors with $m < 3.1$ GeV)

VALUE (units 10^{-3})	CL%	DOCUMENT ID	TECN	COMMENT
<1	90	32 BALEST	95 CLEO	$e^+ e^- \rightarrow \gamma + X \bar{X}$

³² For a noninteracting vector X with mass < 3.1 GeV.

$\Gamma(\gamma X \rightarrow \gamma + \geq 4 \text{ prongs})/\Gamma_{total}$ Γ_{53}/Γ
 (1.5 GeV $< m_X < 5.0$ GeV)

VALUE (units 10^{-4})	CL%	DOCUMENT ID	TECN	COMMENT
<1.78	95	ROSNER	07A CLEO	$e^+ e^- \rightarrow \gamma X$

$\Gamma(\gamma a_1^0 \rightarrow \gamma \mu^+ \mu^-)/\Gamma_{total}$ Γ_{54}/Γ
 (201 $< M(\mu^+ \mu^-) < 3565$ MeV)

VALUE (units 10^{-6})	CL%	DOCUMENT ID	TECN	COMMENT
<9	90	33 LOVE	08 CLEO	$e^+ e^- \rightarrow \gamma a_1^0 \rightarrow \gamma \mu^+ \mu^-$

³³ For a narrow scalar or pseudoscalar a_1^0 with 201 $< M(\mu^+ \mu^-) < 3565$ MeV, excluding J/ψ . Measured 90% CL limits as a function of $M(\mu^+ \mu^-)$ range from $1-9 \times 10^{-6}$.

$\Gamma(\gamma a_1^0 \rightarrow \gamma \tau^+ \tau^-)/\Gamma_{total}$ Γ_{55}/Γ
 ($2m_\tau < M(\tau^+ \tau^-) < 7500$ MeV)

VALUE (units 10^{-6})	CL%	DOCUMENT ID	TECN	COMMENT
<50	90	34 LOVE	08 CLEO	$e^+ e^- \rightarrow \gamma a_1^0 \rightarrow \gamma \tau^+ \tau^-$

³⁴ For a narrow scalar or pseudoscalar a_1^0 with $2m_\tau < M(\tau^+ \tau^-) < 7500$ MeV. Measured 90% CL limits as a function of $M(\tau^+ \tau^-)$ range from $1-5 \times 10^{-5}$.

$\Gamma(\mu^\pm \tau^\mp)/\Gamma_{total}$ Γ_{56}/Γ

VALUE (units 10^{-6})	CL%	DOCUMENT ID	TECN	COMMENT
<6.0	95	LOVE	08A CLEO	$e^+ e^- \rightarrow \mu^\pm \tau^\mp$

$\Gamma(\text{invisible})/\Gamma_{total}$ Γ_{57}/Γ

VALUE (units 10^{-4})	CL%	DOCUMENT ID	TECN	COMMENT
< 3.0	90	AUBERT	09AX BABR	$\Upsilon(3S) \rightarrow \pi^+ \pi^- \Upsilon(1S)$

• • • We do not use the following data for averages, fits, limits, etc. • • •

<39	90	RUBIN	07 CLEO	$\Upsilon(2S) \rightarrow \pi^+ \pi^- \Upsilon(1S)$
<25	90	TAJIMA	07 BELL	$\Upsilon(3S) \rightarrow \pi^+ \pi^- \Upsilon(1S)$

$\Upsilon(1S)$ REFERENCES

AUBERT	10C	PR D81 011102	B. Aubert <i>et al.</i>	(BABAR Collab.)
AUBERT	09AX	PRL 103 251801	B. Aubert <i>et al.</i>	(BABAR Collab.)
LOVE	08	PRL 101 151802	W. Love <i>et al.</i>	(CLEO Collab.)
LOVE	08A	PRL 101 201601	W. Love <i>et al.</i>	(CLEO Collab.)
PDG	08	PL B667 1	C. Amsler <i>et al.</i>	(PDG Collab.)
ASNER	07	PR D75 012009	D.M. Asner <i>et al.</i>	(CLEO Collab.)
ATHAR	07A	PR D76 072003	S.B. Athar <i>et al.</i>	(CLEO Collab.)
BESSON	07	PRL 98 052002	D. Besson <i>et al.</i>	(CLEO Collab.)
BESSON	07A	PR D75 072001	D. Besson <i>et al.</i>	(CLEO Collab.)
ROSNER	07A	PR D76 117102	J.L. Rosner <i>et al.</i>	(CLEO Collab.)
RUBIN	07	PR D75 031104	P. Rubin <i>et al.</i>	(CLEO Collab.)
TAJIMA	07	PRL 98 132001	O. Tajima <i>et al.</i>	(BELLE Collab.)
AQUINES	06A	PR D74 092006	O. Aquines <i>et al.</i>	(CLEO Collab.)
ATHAR	06	PR D73 032001	S.B. Athar <i>et al.</i>	(CLEO Collab.)
BESSON	06A	PR D74 012003	D. Besson <i>et al.</i>	(CLEO Collab.)

$\Gamma(3\pi^+3\pi^-2\pi^0)/\Gamma_{total}$					Γ_{12}/Γ
VALUE (units 10^{-4})	CL%	DOCUMENT ID	TECN	COMMENT	

<6 90 12 ASNER 08A CLEO $\Upsilon(2S) \rightarrow \gamma 3\pi^+3\pi^-2\pi^0$
 12 ASNER 08A reports $[\Gamma(\chi_{b0}(1P) \rightarrow 3\pi^+3\pi^-2\pi^0)/\Gamma_{total}] \times [B(\Upsilon(2S) \rightarrow \gamma\chi_{b0}(1P))]$
 $< 22 \times 10^{-6}$ which we divide by our best value $B(\Upsilon(2S) \rightarrow \gamma\chi_{b0}(1P)) = 3.8 \times 10^{-2}$.

$\Gamma(3\pi^+3\pi^-K^+K^-)/\Gamma_{total}$					Γ_{13}/Γ
VALUE (units 10^{-4})	EVTS	DOCUMENT ID	TECN	COMMENT	

2.4 ± 1.2 ± 0.2 9 13 ASNER 08A CLEO $\Upsilon(2S) \rightarrow \gamma 3\pi^+3\pi^-K^+K^-$
 13 ASNER 08A reports $[\Gamma(\chi_{b0}(1P) \rightarrow 3\pi^+3\pi^-K^+K^-)/\Gamma_{total}] \times [B(\Upsilon(2S) \rightarrow \gamma\chi_{b0}(1P))]$
 $= (9 \pm 4 \pm 2) \times 10^{-6}$ which we divide by our best value $B(\Upsilon(2S) \rightarrow \gamma\chi_{b0}(1P)) = (3.8 \pm 0.4) \times 10^{-2}$. Our first error is their experiment's error and our second error is the systematic error from using our best value.

$\Gamma(3\pi^+3\pi^-K^+K^-\pi^0)/\Gamma_{total}$					Γ_{14}/Γ
VALUE (units 10^{-4})	CL%	DOCUMENT ID	TECN	COMMENT	

<10 90 14 ASNER 08A CLEO $\Upsilon(2S) \rightarrow \gamma 3\pi^+3\pi^-K^+K^-\pi^0$
 14 ASNER 08A reports $[\Gamma(\chi_{b0}(1P) \rightarrow 3\pi^+3\pi^-K^+K^-\pi^0)/\Gamma_{total}] \times [B(\Upsilon(2S) \rightarrow \gamma\chi_{b0}(1P))]$
 $< 37 \times 10^{-6}$ which we divide by our best value $B(\Upsilon(2S) \rightarrow \gamma\chi_{b0}(1P)) = 3.8 \times 10^{-2}$.

$\Gamma(4\pi^+4\pi^-)/\Gamma_{total}$					Γ_{15}/Γ
VALUE (units 10^{-4})	CL%	DOCUMENT ID	TECN	COMMENT	

<0.8 90 15 ASNER 08A CLEO $\Upsilon(2S) \rightarrow \gamma 4\pi^+4\pi^-$
 15 ASNER 08A reports $[\Gamma(\chi_{b0}(1P) \rightarrow 4\pi^+4\pi^-)/\Gamma_{total}] \times [B(\Upsilon(2S) \rightarrow \gamma\chi_{b0}(1P))]$
 $< 3 \times 10^{-6}$ which we divide by our best value $B(\Upsilon(2S) \rightarrow \gamma\chi_{b0}(1P)) = 3.8 \times 10^{-2}$.

$\Gamma(4\pi^+4\pi^-2\pi^0)/\Gamma_{total}$					Γ_{16}/Γ
VALUE (units 10^{-4})	CL%	DOCUMENT ID	TECN	COMMENT	

<21 90 16 ASNER 08A CLEO $\Upsilon(2S) \rightarrow \gamma 4\pi^+4\pi^-2\pi^0$
 16 ASNER 08A reports $[\Gamma(\chi_{b0}(1P) \rightarrow 4\pi^+4\pi^-2\pi^0)/\Gamma_{total}] \times [B(\Upsilon(2S) \rightarrow \gamma\chi_{b0}(1P))]$
 $< 77 \times 10^{-6}$ which we divide by our best value $B(\Upsilon(2S) \rightarrow \gamma\chi_{b0}(1P)) = 3.8 \times 10^{-2}$.

$\chi_{b0}(1P)$ REFERENCES

ASNER 08A PR D78 091103 D. M. Asner et al. (CLEO Collab.)
BRIERE 08 PR D78 092007 R. A. Briere et al. (CLEO Collab.)
ARTUSO 05 PRL 94 032001 M. Artuso et al. (CLEO Collab.)
EDWARDS 99 PR D59 032003 K. W. Edwards et al. (CLEO Collab.)
WALK 86 PR D34 2611 W. S. Walk et al. (Crystal Ball Collab.)
ALBRECHT 85E PL 160B 331 H. Albrecht et al. (ARGUS Collab.)
NERNST 85 PRL 54 2195 R. Nernst et al. (Crystal Ball Collab.)
HAAS 84 PRL 52 799 J. Haas et al. (CLEO Collab.)
KLOPFEN... 83 PRL 51 160 C. Klopffenstein et al. (CUSB Collab.)
PAUSS 83 PL 130B 439 F. Pauss et al. (MPIM, COLU, CORN, LSU+)

$\chi_{b1}(1P)$

$J^G(J^{PC}) = 0^+(1^{++})$
 J needs confirmation.

Observed in radiative decay of the $\Upsilon(2S)$, therefore $C = +$. Branching ratio requires E1 transition, M1 is strongly disfavored, therefore $P = +$. $J = 1$ from SKWARNICKI 87.

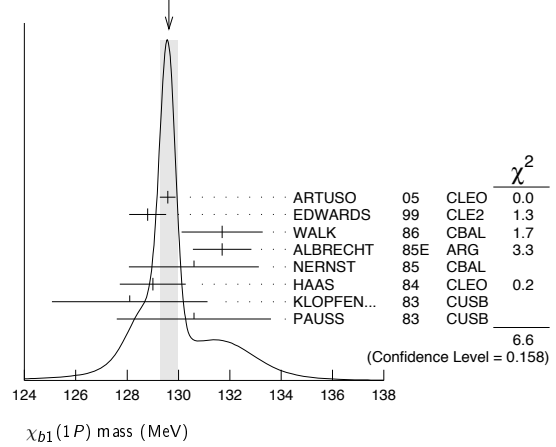
$\chi_{b1}(1P)$ MASS

VALUE (MeV) DOCUMENT ID
9892.78 ± 0.26 ± 0.31 OUR AVERAGE From average γ energy below, using $\Upsilon(2S)$ mass = 10023.26 ± 0.31 MeV

γ ENERGY IN $\Upsilon(2S)$ DECAY

VALUE (MeV)	DOCUMENT ID	TECN	COMMENT
129.63 ± 0.33 OUR AVERAGE	Error includes scale factor of 1.3. See the ideogram below.		
129.58 ± 0.09 ± 0.29	ARTUSO 05 CLEO	$\Upsilon(2S) \rightarrow \gamma X$	
128.8 ± 0.4 ± 0.6	EDWARDS 99 CLE2	$\Upsilon(2S) \rightarrow \gamma\chi(1P)$	
131.7 ± 0.9 ± 1.3	WALK 86 CBAL	$\Upsilon(2S) \rightarrow \gamma\gamma\ell^+\ell^-$	
131.7 ± 0.3 ± 1.1	ALBRECHT 85E ARG	$\Upsilon(2S) \rightarrow \text{conv.}\gamma X$	
130.6 ± 0.8 ± 2.4	NERNST 85 CBAL	$\Upsilon(2S) \rightarrow \gamma X$	
129 ± 0.8 ± 1	HAAS 84 CLEO	$\Upsilon(2S) \rightarrow \text{conv.}\gamma X$	
128.1 ± 0.4 ± 3.0	KLOPFEN... 83 CUSB	$\Upsilon(2S) \rightarrow \gamma X$	
130.6 ± 3.0	PAUSS 83 CUSB	$\Upsilon(2S) \rightarrow \gamma\gamma\ell^+\ell^-$	

WEIGHTED AVERAGE
 129.63±0.33 (Error scaled by 1.3)



$\chi_{b1}(1P)$ DECAY MODES

Mode	Fraction (Γ_i/Γ)	Confidence level
$\Gamma_1 \gamma \Upsilon(1S)$	(35 ± 8) %	
$\Gamma_2 D^0 X$	(12.6 ± 2.2) %	
$\Gamma_3 \pi^+\pi^-K^+K^-\pi^0$	(2.0 ± 0.6) × 10 ⁻⁴	
$\Gamma_4 2\pi^+\pi^-K^-K_S^0$	(1.3 ± 0.5) × 10 ⁻⁴	
$\Gamma_5 2\pi^+\pi^-K^-K_S^0 2\pi^0$	< 6 × 10 ⁻⁴	90%
$\Gamma_6 2\pi^+2\pi^-2\pi^0$	(8.0 ± 2.5) × 10 ⁻⁴	
$\Gamma_7 2\pi^+2\pi^-K^+K^-$	(1.5 ± 0.5) × 10 ⁻⁴	
$\Gamma_8 2\pi^+2\pi^-K^+K^-\pi^0$	(3.5 ± 1.2) × 10 ⁻⁴	
$\Gamma_9 2\pi^+2\pi^-K^+K^-2\pi^0$	(8.6 ± 3.2) × 10 ⁻⁴	
$\Gamma_{10} 3\pi^+2\pi^-K^-K_S^0\pi^0$	(9.3 ± 3.3) × 10 ⁻⁴	
$\Gamma_{11} 3\pi^+3\pi^-$	(1.9 ± 0.6) × 10 ⁻⁴	
$\Gamma_{12} 3\pi^+3\pi^-2\pi^0$	(1.7 ± 0.5) × 10 ⁻³	
$\Gamma_{13} 3\pi^+3\pi^-K^+K^-$	(2.6 ± 0.8) × 10 ⁻⁴	
$\Gamma_{14} 3\pi^+3\pi^-K^+K^-\pi^0$	(7.5 ± 2.6) × 10 ⁻⁴	
$\Gamma_{15} 4\pi^+4\pi^-$	(2.6 ± 0.9) × 10 ⁻⁴	
$\Gamma_{16} 4\pi^+4\pi^-2\pi^0$	(1.4 ± 0.6) × 10 ⁻³	

$\chi_{b1}(1P)$ BRANCHING RATIOS

$\Gamma(\gamma \Upsilon(1S))/\Gamma_{total}$	Γ_1/Γ
VALUE	DOCUMENT ID TECN COMMENT
0.35 ± 0.08 OUR AVERAGE	
0.32 ± 0.06 ± 0.07	WALK 86 CBAL $\Upsilon(2S) \rightarrow \gamma\gamma\ell^+\ell^-$
0.47 ± 0.18	KLOPFEN... 83 CUSB $\Upsilon(2S) \rightarrow \gamma\gamma\ell^+\ell^-$

$\Gamma(D^0 X)/\Gamma_{total}$	Γ_2/Γ
VALUE (units 10^{-2})	EVTS DOCUMENT ID TECN COMMENT
12.6 ± 1.9 ± 1.1	2310 1 BRIERE 08 CLEO $\Upsilon(2S) \rightarrow \gamma D^0 X$

¹ For $p_{D^0} > 2.5$ GeV/c.

$\Gamma(\pi^+\pi^-K^+K^-\pi^0)/\Gamma_{total}$	Γ_3/Γ
VALUE (units 10^{-4})	EVTS DOCUMENT ID TECN COMMENT
2.0 ± 0.6 ± 0.1	18 2 ASNER 08A CLEO $\Upsilon(2S) \rightarrow \gamma\pi^+\pi^-K^+K^-\pi^0$

² ASNER 08A reports $[\Gamma(\chi_{b1}(1P) \rightarrow \pi^+\pi^-K^+K^-\pi^0)/\Gamma_{total}] \times [B(\Upsilon(2S) \rightarrow \gamma\chi_{b1}(1P))]$ = (14 ± 3 ± 3) × 10⁻⁶ which we divide by our best value $B(\Upsilon(2S) \rightarrow \gamma\chi_{b1}(1P)) = (6.9 \pm 0.4) \times 10^{-2}$. Our first error is their experiment's error and our second error is the systematic error from using our best value.

$\Gamma(2\pi^+\pi^-K^-K_S^0)/\Gamma_{total}$	Γ_4/Γ
VALUE (units 10^{-4})	EVTS DOCUMENT ID TECN COMMENT
1.3 ± 0.5 ± 0.1	11 3 ASNER 08A CLEO $\Upsilon(2S) \rightarrow \gamma 2\pi^+\pi^-K^-K_S^0$

³ ASNER 08A reports $[\Gamma(\chi_{b1}(1P) \rightarrow 2\pi^+\pi^-K^-K_S^0)/\Gamma_{total}] \times [B(\Upsilon(2S) \rightarrow \gamma\chi_{b1}(1P))]$ = (9 ± 3 ± 2) × 10⁻⁶ which we divide by our best value $B(\Upsilon(2S) \rightarrow \gamma\chi_{b1}(1P)) = (6.9 \pm 0.4) \times 10^{-2}$. Our first error is their experiment's error and our second error is the systematic error from using our best value.

$\Gamma(2\pi^+\pi^-K^-K_S^0 2\pi^0)/\Gamma_{total}$	Γ_5/Γ
VALUE (units 10^{-4})	CL% DOCUMENT ID TECN COMMENT
<6	90 4 ASNER 08A CLEO $\Upsilon(2S) \rightarrow \gamma 2\pi^+\pi^-K^-2\pi^0$

⁴ ASNER 08A reports $[\Gamma(\chi_{b1}(1P) \rightarrow 2\pi^+\pi^-K^-K_S^0 2\pi^0)/\Gamma_{total}] \times [B(\Upsilon(2S) \rightarrow \gamma\chi_{b1}(1P))]$ < 42 × 10⁻⁶ which we divide by our best value $B(\Upsilon(2S) \rightarrow \gamma\chi_{b1}(1P)) = 6.9 \times 10^{-2}$.

$\Gamma(D^0 X)/\Gamma_{\text{total}}$		Γ_2/Γ	
VALUE	CL%	DOCUMENT ID	TECN COMMENT
$<7.9 \times 10^{-2}$	90	1,2 BRIERE	08 CLEO $\Upsilon(2S) \rightarrow \gamma D^0 X$

¹ For $p_{D^0} > 2.5$ GeV/c.

² The authors also present their result as $(5.4 \pm 1.9 \pm 0.5) \times 10^{-2}$.

$\Gamma(\pi^+ \pi^- K^+ K^- \pi^0)/\Gamma_{\text{total}}$		Γ_3/Γ	
VALUE (units 10^{-4})	EVTS	DOCUMENT ID	TECN COMMENT
$0.84 \pm 0.50 \pm 0.04$	8	³ ASNER	08A CLEO $\Upsilon(2S) \rightarrow \gamma \pi^+ \pi^- K^+ K^- \pi^0$

³ ASNER 08A reports $[\Gamma(\chi_{b2}(1P) \rightarrow \pi^+ \pi^- K^+ K^- \pi^0)/\Gamma_{\text{total}}] \times [B(\Upsilon(2S) \rightarrow \gamma \chi_{b2}(1P))] = (6 \pm 3 \pm 2) \times 10^{-6}$ which we divide by our best value $B(\Upsilon(2S) \rightarrow \gamma \chi_{b2}(1P)) = (7.15 \pm 0.35) \times 10^{-2}$. Our first error is their experiment's error and our second error is the systematic error from using our best value.

$\Gamma(2\pi^+ \pi^- K^- K_S^0)/\Gamma_{\text{total}}$		Γ_4/Γ	
VALUE (units 10^{-4})	CL%	DOCUMENT ID	TECN COMMENT
<1.0	90	⁴ ASNER	08A CLEO $\Upsilon(2S) \rightarrow \gamma 2\pi^+ \pi^- K^- K_S^0$

⁴ ASNER 08A reports $[\Gamma(\chi_{b2}(1P) \rightarrow 2\pi^+ \pi^- K^- K_S^0)/\Gamma_{\text{total}}] \times [B(\Upsilon(2S) \rightarrow \gamma \chi_{b2}(1P))] < 7 \times 10^{-6}$ which we divide by our best value $B(\Upsilon(2S) \rightarrow \gamma \chi_{b2}(1P)) = 7.15 \times 10^{-2}$.

$\Gamma(2\pi^+ \pi^- K^- K_S^0 2\pi^0)/\Gamma_{\text{total}}$		Γ_5/Γ	
VALUE (units 10^{-4})	EVTS	DOCUMENT ID	TECN COMMENT
$5.3 \pm 2.4 \pm 0.3$	11	⁵ ASNER	08A CLEO $\Upsilon(2S) \rightarrow \gamma 2\pi^+ \pi^- K^- 2\pi^0$

⁵ ASNER 08A reports $[\Gamma(\chi_{b2}(1P) \rightarrow 2\pi^+ \pi^- K^- K_S^0 2\pi^0)/\Gamma_{\text{total}}] \times [B(\Upsilon(2S) \rightarrow \gamma \chi_{b2}(1P))] = (38 \pm 14 \pm 10) \times 10^{-6}$ which we divide by our best value $B(\Upsilon(2S) \rightarrow \gamma \chi_{b2}(1P)) = (7.15 \pm 0.35) \times 10^{-2}$. Our first error is their experiment's error and our second error is the systematic error from using our best value.

$\Gamma(2\pi^+ 2\pi^- 2\pi^0)/\Gamma_{\text{total}}$		Γ_6/Γ	
VALUE (units 10^{-4})	EVTS	DOCUMENT ID	TECN COMMENT
$3.5 \pm 1.4 \pm 0.2$	19	⁶ ASNER	08A CLEO $\Upsilon(2S) \rightarrow \gamma 2\pi^+ 2\pi^- 2\pi^0$

⁶ ASNER 08A reports $[\Gamma(\chi_{b2}(1P) \rightarrow 2\pi^+ 2\pi^- 2\pi^0)/\Gamma_{\text{total}}] \times [B(\Upsilon(2S) \rightarrow \gamma \chi_{b2}(1P))] = (25 \pm 8 \pm 6) \times 10^{-6}$ which we divide by our best value $B(\Upsilon(2S) \rightarrow \gamma \chi_{b2}(1P)) = (7.15 \pm 0.35) \times 10^{-2}$. Our first error is their experiment's error and our second error is the systematic error from using our best value.

$\Gamma(2\pi^+ 2\pi^- K^+ K^-)/\Gamma_{\text{total}}$		Γ_7/Γ	
VALUE (units 10^{-4})	EVTS	DOCUMENT ID	TECN COMMENT
$1.1 \pm 0.4 \pm 0.1$	14	⁷ ASNER	08A CLEO $\Upsilon(2S) \rightarrow \gamma 2\pi^+ 2\pi^- K^+ K^-$

⁷ ASNER 08A reports $[\Gamma(\chi_{b2}(1P) \rightarrow 2\pi^+ 2\pi^- K^+ K^-)/\Gamma_{\text{total}}] \times [B(\Upsilon(2S) \rightarrow \gamma \chi_{b2}(1P))] = (8 \pm 2 \pm 2) \times 10^{-6}$ which we divide by our best value $B(\Upsilon(2S) \rightarrow \gamma \chi_{b2}(1P)) = (7.15 \pm 0.35) \times 10^{-2}$. Our first error is their experiment's error and our second error is the systematic error from using our best value.

$\Gamma(2\pi^+ 2\pi^- K^+ K^- \pi^0)/\Gamma_{\text{total}}$		Γ_8/Γ	
VALUE (units 10^{-4})	EVTS	DOCUMENT ID	TECN COMMENT
$2.1 \pm 0.9 \pm 0.1$	13	⁸ ASNER	08A CLEO $\Upsilon(2S) \rightarrow \gamma 2\pi^+ 2\pi^- K^+ K^- \pi^0$

⁸ ASNER 08A reports $[\Gamma(\chi_{b2}(1P) \rightarrow 2\pi^+ 2\pi^- K^+ K^- \pi^0)/\Gamma_{\text{total}}] \times [B(\Upsilon(2S) \rightarrow \gamma \chi_{b2}(1P))] = (15 \pm 5 \pm 4) \times 10^{-6}$ which we divide by our best value $B(\Upsilon(2S) \rightarrow \gamma \chi_{b2}(1P)) = (7.15 \pm 0.35) \times 10^{-2}$. Our first error is their experiment's error and our second error is the systematic error from using our best value.

$\Gamma(2\pi^+ 2\pi^- K^+ K^- 2\pi^0)/\Gamma_{\text{total}}$		Γ_9/Γ	
VALUE (units 10^{-4})	EVTS	DOCUMENT ID	TECN COMMENT
$3.9 \pm 1.8 \pm 0.2$	11	⁹ ASNER	08A CLEO $\Upsilon(2S) \rightarrow \gamma 2\pi^+ 2\pi^- K^+ K^- 2\pi^0$

⁹ ASNER 08A reports $[\Gamma(\chi_{b2}(1P) \rightarrow 2\pi^+ 2\pi^- K^+ K^- 2\pi^0)/\Gamma_{\text{total}}] \times [B(\Upsilon(2S) \rightarrow \gamma \chi_{b2}(1P))] = (28 \pm 11 \pm 7) \times 10^{-6}$ which we divide by our best value $B(\Upsilon(2S) \rightarrow \gamma \chi_{b2}(1P)) = (7.15 \pm 0.35) \times 10^{-2}$. Our first error is their experiment's error and our second error is the systematic error from using our best value.

$\Gamma(3\pi^+ 2\pi^- K^- K_S^0 \pi^0)/\Gamma_{\text{total}}$		Γ_{10}/Γ	
VALUE (units 10^{-4})	CL%	DOCUMENT ID	TECN COMMENT
<5	90	¹⁰ ASNER	08A CLEO $\Upsilon(2S) \rightarrow \gamma 3\pi^+ 2\pi^- K^- K_S^0 \pi^0$

¹⁰ ASNER 08A reports $[\Gamma(\chi_{b2}(1P) \rightarrow 3\pi^+ 2\pi^- K^- K_S^0 \pi^0)/\Gamma_{\text{total}}] \times [B(\Upsilon(2S) \rightarrow \gamma \chi_{b2}(1P))] < 36 \times 10^{-6}$ which we divide by our best value $B(\Upsilon(2S) \rightarrow \gamma \chi_{b2}(1P)) = 7.15 \times 10^{-2}$.

$\Gamma(3\pi^+ 3\pi^-)/\Gamma_{\text{total}}$		Γ_{11}/Γ	
VALUE (units 10^{-4})	EVTS	DOCUMENT ID	TECN COMMENT
$0.70 \pm 0.31 \pm 0.03$	9	¹¹ ASNER	08A CLEO $\Upsilon(2S) \rightarrow \gamma 3\pi^+ 3\pi^-$

¹¹ ASNER 08A reports $[\Gamma(\chi_{b2}(1P) \rightarrow 3\pi^+ 3\pi^-)/\Gamma_{\text{total}}] \times [B(\Upsilon(2S) \rightarrow \gamma \chi_{b2}(1P))] = (5 \pm 2 \pm 1) \times 10^{-6}$ which we divide by our best value $B(\Upsilon(2S) \rightarrow \gamma \chi_{b2}(1P)) = (7.15 \pm 0.35) \times 10^{-2}$. Our first error is their experiment's error and our second error is the systematic error from using our best value.

$\Gamma(3\pi^+ 3\pi^- 2\pi^0)/\Gamma_{\text{total}}$		Γ_{12}/Γ	
VALUE (units 10^{-4})	EVTS	DOCUMENT ID	TECN COMMENT
$10.2 \pm 3.6 \pm 0.5$	34	¹² ASNER	08A CLEO $\Upsilon(2S) \rightarrow \gamma 3\pi^+ 3\pi^- 2\pi^0$

¹² ASNER 08A reports $[\Gamma(\chi_{b2}(1P) \rightarrow 3\pi^+ 3\pi^- 2\pi^0)/\Gamma_{\text{total}}] \times [B(\Upsilon(2S) \rightarrow \gamma \chi_{b2}(1P))] = (73 \pm 16 \pm 20) \times 10^{-6}$ which we divide by our best value $B(\Upsilon(2S) \rightarrow \gamma \chi_{b2}(1P)) = (7.15 \pm 0.35) \times 10^{-2}$. Our first error is their experiment's error and our second error is the systematic error from using our best value.

$\Gamma(3\pi^+ 3\pi^- K^+ K^-)/\Gamma_{\text{total}}$		Γ_{13}/Γ	
VALUE (units 10^{-4})	CL%	DOCUMENT ID	TECN COMMENT
<0.8	90	¹³ ASNER	08A CLEO $\Upsilon(2S) \rightarrow \gamma 3\pi^+ 3\pi^- K^+ K^-$

¹³ ASNER 08A reports $[\Gamma(\chi_{b2}(1P) \rightarrow 3\pi^+ 3\pi^- K^+ K^-)/\Gamma_{\text{total}}] \times [B(\Upsilon(2S) \rightarrow \gamma \chi_{b2}(1P))] < 6 \times 10^{-6}$ which we divide by our best value $B(\Upsilon(2S) \rightarrow \gamma \chi_{b2}(1P)) = 7.15 \times 10^{-2}$.

$\Gamma(3\pi^+ 3\pi^- K^+ K^- \pi^0)/\Gamma_{\text{total}}$		Γ_{14}/Γ	
VALUE (units 10^{-4})	EVTS	DOCUMENT ID	TECN COMMENT
$3.6 \pm 1.5 \pm 0.2$	14	¹⁴ ASNER	08A CLEO $\Upsilon(2S) \rightarrow \gamma 3\pi^+ 3\pi^- K^+ K^- \pi^0$

¹⁴ ASNER 08A reports $[\Gamma(\chi_{b2}(1P) \rightarrow 3\pi^+ 3\pi^- K^+ K^- \pi^0)/\Gamma_{\text{total}}] \times [B(\Upsilon(2S) \rightarrow \gamma \chi_{b2}(1P))] = (26 \pm 8 \pm 7) \times 10^{-6}$ which we divide by our best value $B(\Upsilon(2S) \rightarrow \gamma \chi_{b2}(1P)) = (7.15 \pm 0.35) \times 10^{-2}$. Our first error is their experiment's error and our second error is the systematic error from using our best value.

$\Gamma(4\pi^+ 4\pi^-)/\Gamma_{\text{total}}$		Γ_{15}/Γ	
VALUE (units 10^{-4})	EVTS	DOCUMENT ID	TECN COMMENT
$0.84 \pm 0.40 \pm 0.04$	7	¹⁵ ASNER	08A CLEO $\Upsilon(2S) \rightarrow \gamma 4\pi^+ 4\pi^-$

¹⁵ ASNER 08A reports $[\Gamma(\chi_{b2}(1P) \rightarrow 4\pi^+ 4\pi^-)/\Gamma_{\text{total}}] \times [B(\Upsilon(2S) \rightarrow \gamma \chi_{b2}(1P))] = (6 \pm 2 \pm 2) \times 10^{-6}$ which we divide by our best value $B(\Upsilon(2S) \rightarrow \gamma \chi_{b2}(1P)) = (7.15 \pm 0.35) \times 10^{-2}$. Our first error is their experiment's error and our second error is the systematic error from using our best value.

$\Gamma(4\pi^+ 4\pi^- 2\pi^0)/\Gamma_{\text{total}}$		Γ_{16}/Γ	
VALUE (units 10^{-4})	EVTS	DOCUMENT ID	TECN COMMENT
$18 \pm 7 \pm 1$	29	¹⁶ ASNER	08A CLEO $\Upsilon(2S) \rightarrow \gamma 4\pi^+ 4\pi^- 2\pi^0$

¹⁶ ASNER 08A reports $[\Gamma(\chi_{b2}(1P) \rightarrow 4\pi^+ 4\pi^- 2\pi^0)/\Gamma_{\text{total}}] \times [B(\Upsilon(2S) \rightarrow \gamma \chi_{b2}(1P))] = (132 \pm 31 \pm 40) \times 10^{-6}$ which we divide by our best value $B(\Upsilon(2S) \rightarrow \gamma \chi_{b2}(1P)) = (7.15 \pm 0.35) \times 10^{-2}$. Our first error is their experiment's error and our second error is the systematic error from using our best value.

 $\chi_{b2}(1P)$ REFERENCES

ASNER	08A	PR D78 091103	D.M. Asner et al.	(CLEO Collab.)
BRIERE	08	PR D78 092007	R.A. Briere et al.	(CLEO Collab.)
ARTUSO	05	PRL 94 032001	M. Artuso et al.	(CLEO Collab.)
EDWARDS	99	PR D59 032003	K.W. Edwards et al.	(CLEO Collab.)
SKWARNICKI	87	PRL 58 972	T. Skwarnicki et al.	(Crystal Ball Collab.)
WALK	86	PR D34 2611	W.S. Walk et al.	(Crystal Ball Collab.)
ALBRECHT	85E	PL 160B 331	H. Albrecht et al.	(ARGUS Collab.)
NERNST	85	PRL 54 2195	R. Nernst et al.	(Crystal Ball Collab.)
HAAS	84	PRL 52 799	J. Haas et al.	(CLEO Collab.)
KLOPFEN...	83	PRL 51 160	C. Klopffenstein et al.	(CUSB Collab.)
PAUSS	83	PL 130B 439	F. Pauss et al.	(MPIM, COLU, CORN, LSU)

 $\Upsilon(2S)$

$$I^G(J^{PC}) = 0^-(1^--)$$

 $\Upsilon(2S)$ MASS

VALUE (GeV)	DOCUMENT ID	TECN	COMMENT
10.02326 ± 0.00031 OUR AVERAGE			
10.0235 ± 0.0005	¹ ARTAMONOV 00	MD1	$e^+ e^- \rightarrow$ hadrons
10.0231 ± 0.0004	BARBER 84	REDE	$e^+ e^- \rightarrow$ hadrons
••• We do not use the following data for averages, fits, limits, etc. •••			
10.0236 ± 0.0005	^{2,3} BARU	86B	$e^+ e^- \rightarrow$ hadrons

¹ Reanalysis of BARU 86B using new electron mass (COHEN 87).

² Reanalysis of ARTAMONOV 84.

³ Superseded by ARTAMONOV 00.

 $\Upsilon(2S)$ WIDTH

VALUE (keV)	DOCUMENT ID
31.98 ± 2.63 OUR EVALUATION	See the Note on "Width Determinations of the Υ States"

Meson Particle Listings

$\Upsilon(2S)$

$\Upsilon(2S)$ DECAY MODES

Mode	Fraction (Γ_i/Γ)	Scale factor/ Confidence level
Γ_1 $\Upsilon(1S)\pi^+\pi^-$	$(18.1 \pm 0.4) \%$	
Γ_2 $\Upsilon(1S)\pi^0\pi^0$	$(8.6 \pm 0.4) \%$	
Γ_3 $\tau^+\tau^-$	$(2.00 \pm 0.21) \%$	
Γ_4 $\mu^+\mu^-$	$(1.93 \pm 0.17) \%$	S=2.2
Γ_5 e^+e^-	$(1.91 \pm 0.16) \%$	
Γ_6 $\Upsilon(1S)\pi^0$	$< 1.8 \times 10^{-4}$	CL=90%
Γ_7 $\Upsilon(1S)\eta$	$(2.1 \pm 0.8) \times 10^{-4}$	
Γ_8 $J/\psi(1S)$ anything	$< 6 \times 10^{-3}$	CL=90%
Γ_9 \bar{d} anything	$(3.4 \pm 0.6) \times 10^{-5}$	
Γ_{10} hadrons	$(94 \pm 11) \%$	
Γ_{11} ggg	$(58.8 \pm 1.2) \%$	
Γ_{12} γgg	$(1.87 \pm 0.28) \%$	

Radiative decays

Γ_{13} $\gamma\chi_{b1}(1P)$	$(6.9 \pm 0.4) \%$	
Γ_{14} $\gamma\chi_{b2}(1P)$	$(7.15 \pm 0.35) \%$	
Γ_{15} $\gamma\chi_{b0}(1P)$	$(3.8 \pm 0.4) \%$	
Γ_{16} $\gamma f_0(1710)$	$< 5.9 \times 10^{-4}$	CL=90%
Γ_{17} $\gamma f_2'(1525)$	$< 5.3 \times 10^{-4}$	CL=90%
Γ_{18} $\gamma f_2(1270)$	$< 2.41 \times 10^{-4}$	CL=90%
Γ_{19} $\gamma f_J(2220)$		
Γ_{20} $\gamma\eta_b(1S)$	$(3.9 \pm 1.5) \times 10^{-4}$	
Γ_{21} $\gamma X \rightarrow \gamma + \geq 4$ prongs	$[a] < 1.95 \times 10^{-4}$	CL=95%

Lepton Flavor (LF) violating decays

Γ_{22} $\mu^\pm\tau^\mp$	LF $< 1.44 \times 10^{-5}$	CL=95%
---------------------------------	----------------------------	--------

[a] $1.5 \text{ GeV} < m_X < 5.0 \text{ GeV}$

$\Upsilon(2S)$ $\Gamma(i)\Gamma(e^+e^-)/\Gamma(\text{total})$

$\Gamma(\mu^+\mu^-) \times \Gamma(e^+e^-)/\Gamma_{\text{total}}$	DOCUMENT ID	TECN	COMMENT	$\Gamma_4\Gamma_5/\Gamma$
6.5 ± 1.5 ± 1.0	KOBEL	92	CBAL $e^+e^- \rightarrow \mu^+\mu^-$	

$\Gamma(\Upsilon(1S)\pi^+\pi^-) \times \Gamma(e^+e^-)/\Gamma_{\text{total}}$	DOCUMENT ID	TECN	COMMENT	$\Gamma_1\Gamma_5/\Gamma$
105.4 ± 1.0 ± 4.2	11.8K 4 AUBERT	08BP BABR	10.58 $e^+e^- \rightarrow \gamma\pi^+\pi^-\ell^+\ell^-$	

⁴Using $B(\Upsilon(1S) \rightarrow e^+e^-) = (2.38 \pm 0.11)\%$ and $B(\Upsilon(1S) \rightarrow \mu^+\mu^-) = (2.48 \pm 0.05)\%$.

$\Gamma(\text{hadrons}) \times \Gamma(e^+e^-)/\Gamma_{\text{total}}$	DOCUMENT ID	TECN	COMMENT	$\Gamma_{10}\Gamma_5/\Gamma$
0.577 ± 0.009 OUR AVERAGE				

0.581 ± 0.004 ± 0.009	5 ROSNER	06 CLEO	10.0 $e^+e^- \rightarrow \text{hadrons}$
0.552 ± 0.031 ± 0.017	5 BARU	96 MD1	$e^+e^- \rightarrow \text{hadrons}$
0.54 ± 0.04 ± 0.02	5 JAKUBOWSKI	88 CBAL	$e^+e^- \rightarrow \text{hadrons}$
0.58 ± 0.03 ± 0.04	6 GILES	84B CLEO	$e^+e^- \rightarrow \text{hadrons}$
0.60 ± 0.12 ± 0.07	6 ALBRECHT	82 DASP	$e^+e^- \rightarrow \text{hadrons}$
0.54 ± 0.07 ^{+0.09} / _{-0.05}	6 NICZYPORUK	81c LENA	$e^+e^- \rightarrow \text{hadrons}$
0.41 ± 0.18	6 BOCK	80 CNTR	$e^+e^- \rightarrow \text{hadrons}$

⁵Radiative corrections evaluated following KURAEV 85.

⁶Radiative corrections reevaluated by BUCHMUELLER 88 following KURAEV 85.

$\Upsilon(2S)$ PARTIAL WIDTHS

$\Gamma(e^+e^-)$	DOCUMENT ID	COMMENT	Γ_5
0.612 ± 0.011 OUR EVALUATION			

$\Upsilon(2S)$ BRANCHING RATIOS

$\Gamma(\Upsilon(1S)\pi^+\pi^-)/\Gamma_{\text{total}}$	DOCUMENT ID	TECN	COMMENT	Γ_1/Γ
18.1 ± 0.4 OUR AVERAGE				

18.02 ± 0.02 ± 0.61	851k	7 BHARI	09 CLEO $e^+e^- \rightarrow \pi^+\pi^-$ MM
17.22 ± 0.17 ± 0.75	11.8K	8,9 AUBERT	08BP BABR $e^+e^- \rightarrow \gamma\pi^+\pi^-\ell^+\ell^-$
19.2 ± 0.2 ± 1.0	52.6k	10 ALEXANDER	98 CLE2 $\pi^+\pi^-\ell^+\ell^-$, $\pi^+\pi^-$ MM
18.1 ± 0.5 ± 1.0	11.6k	ALBRECHT	87 ARG $e^+e^- \rightarrow \pi^+\pi^-$ MM
16.9 ± 4.0		GELPHMAN	85 CBAL $e^+e^- \rightarrow e^+e^-\pi^+\pi^-$
19.1 ± 1.2 ± 0.6		BESSION	84 CLEO $\pi^+\pi^-$ MM
18.9 ± 2.6		FONSECA	84 CUSB $e^+e^- \rightarrow \ell^+\ell^-\pi^+\pi^-$
21 ± 7	7	NICZYPORUK	81B LENA $e^+e^- \rightarrow \ell^+\ell^-\pi^+\pi^-$

Abbreviation MM in the COMMENT field below stands for missing mass.

⁷A weighted average of the inclusive and exclusive results.

⁸Using $B(\Upsilon(2S) \rightarrow e^+e^-) = (1.91 \pm 0.16)\%$ and $B(\Upsilon(2S) \rightarrow \mu^+\mu^-) = (1.93 \pm 0.17)\%$.

⁹Using $\Gamma_{ee}(\Upsilon(2S)) = 0.612 \pm 0.011 \text{ keV}$.

¹⁰Using $B(\Upsilon(1S) \rightarrow e^+e^-) = (2.52 \pm 0.17)\%$ and $B(\Upsilon(1S) \rightarrow \mu^+\mu^-) = (2.48 \pm 0.07)\%$.

$\Gamma(\Upsilon(1S)\pi^0\pi^0)/\Gamma_{\text{total}}$ Γ_2/Γ

VALUE (units 10^{-2})	EVTS	DOCUMENT ID	TECN	COMMENT
8.6 ± 0.4 OUR AVERAGE				
8.43 ± 0.16 ± 0.42	38k	11 BHARI	09 CLEO	$e^+e^- \rightarrow \pi^0\pi^0\ell^+\ell^-$
9.2 ± 0.6 ± 0.8	275	12 ALEXANDER	98 CLE2	$e^+e^- \rightarrow \pi^0\pi^0\ell^+\ell^-$
9.5 ± 1.9 ± 1.9	25	ALBRECHT	87 ARG	$e^+e^- \rightarrow \pi^0\pi^0\ell^+\ell^-$
8.0 ± 1.5		GELPHMAN	85 CBAL	$e^+e^- \rightarrow \pi^0\pi^0\ell^+\ell^-$
10.3 ± 2.3		FONSECA	84 CUSB	$e^+e^- \rightarrow \pi^0\pi^0\ell^+\ell^-$

¹¹Authors assume $B(\Upsilon(1S) \rightarrow e^+e^-) + B(\Upsilon(1S) \rightarrow \mu^+\mu^-) = 4.96\%$.

¹²Using $B(\Upsilon(1S) \rightarrow e^+e^-) = (2.52 \pm 0.17)\%$ and $B(\Upsilon(1S) \rightarrow \mu^+\mu^-) = (2.48 \pm 0.07)\%$.

$\Gamma(\Upsilon(1S)\pi^0\pi^0)/\Gamma(\Upsilon(1S)\pi^+\pi^-)$ Γ_2/Γ_1

VALUE	DOCUMENT ID	TECN	COMMENT
0.462 ± 0.037	13 BHARI	09 CLEO	$e^+e^- \rightarrow \Upsilon(2S)$

¹³Not independent of other values reported by BHARI 09.

$\Gamma(\tau^+\tau^-)/\Gamma_{\text{total}}$ Γ_3/Γ

VALUE (units 10^{-2})	EVTS	DOCUMENT ID	TECN	COMMENT
2.00 ± 0.21 OUR AVERAGE				
2.00 ± 0.12 ± 0.18	22k	14 BESSION	07 CLEO	$e^+e^- \rightarrow \Upsilon(2S) \rightarrow \tau^+\tau^-$
1.7 ± 1.5 ± 0.6		HAAS	84B CLEO	$e^+e^- \rightarrow \tau^+\tau^-$

¹⁴BESSION 07 reports $[\Gamma(\Upsilon(2S) \rightarrow \tau^+\tau^-)/\Gamma_{\text{total}}] / [B(\Upsilon(2S) \rightarrow \mu^+\mu^-)] = 1.04 \pm 0.04 \pm 0.05$ which we multiply by our best value $B(\Upsilon(2S) \rightarrow \mu^+\mu^-) = (1.93 \pm 0.17) \times 10^{-2}$. Our first error is their experiment's error and our second error is the systematic error from using our best value.

$\Gamma(\mu^+\mu^-)/\Gamma_{\text{total}}$ Γ_4/Γ

0.0193 ± 0.0017 OUR AVERAGE Error includes scale factor of 2.2. See the ideogram below.

0.0203 ± 0.0003 ± 0.0008	120k	ADAMS	05 CLEO	$e^+e^- \rightarrow \mu^+\mu^-$
0.0122 ± 0.0028 ± 0.0019		15 KOBEL	92 CBAL	$e^+e^- \rightarrow \mu^+\mu^-$
0.0138 ± 0.0025 ± 0.0015		KAARSBERG	89 CSB2	$e^+e^- \rightarrow \mu^+\mu^-$
0.009 ± 0.006 ± 0.006		16 ALBRECHT	85 ARG	$e^+e^- \rightarrow \mu^+\mu^-$
0.018 ± 0.008 ± 0.005		HAAS	84B CLEO	$e^+e^- \rightarrow \mu^+\mu^-$

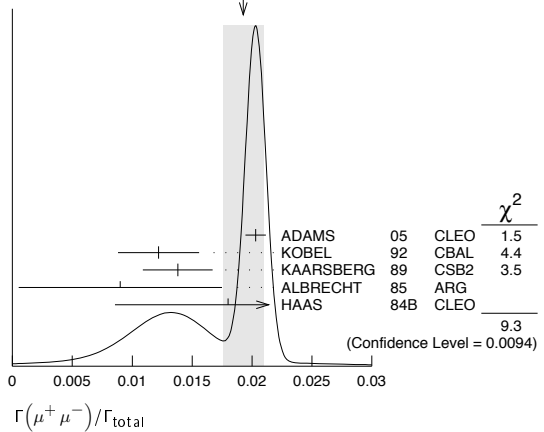
¹⁵We do not use the following data for averages, fits, limits, etc. ● ● ●

<0.038 90 NICZYPORUK 81c LENA $e^+e^- \rightarrow \mu^+\mu^-$

¹⁶Taking into account interference between the resonance and continuum.

¹⁷Re-evaluated using $B(\Upsilon(1S) \rightarrow \mu^+\mu^-) = 0.026$.

WEIGHTED AVERAGE
0.0193 ± 0.0017 (Error scaled by 2.2)



$\Gamma(\tau^+\tau^-)/\Gamma(\mu^+\mu^-)$ Γ_3/Γ_4

VALUE	EVTS	DOCUMENT ID	TECN	COMMENT
1.04 ± 0.04 ± 0.05	22k	BESSION	07 CLEO	$e^+e^- \rightarrow \Upsilon(2S)$

$\Gamma(\Upsilon(1S)\pi^0)/\Gamma_{\text{total}}$ Γ_6/Γ

VALUE (units 10^{-3})	CL%	DOCUMENT ID	TECN	COMMENT
<0.18		17 HE	90 08A CLEO	$e^+e^- \rightarrow \ell^+\ell^-\gamma\gamma$
<1.1	90	ALEXANDER	98 CLE2	$e^+e^- \rightarrow \ell^+\ell^-\gamma\gamma$
<8	90	LURZ	87 CBAL	$e^+e^- \rightarrow \ell^+\ell^-\gamma\gamma$

¹⁷Authors assume $B(\Upsilon(1S) \rightarrow e^+e^-) + B(\Upsilon(1S) \rightarrow \mu^+\mu^-) = 4.96\%$.

T(1S)eta / Gamma_total, T7/T

Table with columns: VALUE (units 10^-3), CL%, EVTS, DOCUMENT ID, TECN, COMMENT. Rows include HE 08A CLEO, AUBERT 08BP BABR, ALEXANDER 98 CLE2, ALBRECHT 87 ARG, LURZ 87 CBAL, BESSON 84 CLEO, FONSECA 84 CUSB.

18 Authors assume B(T(1S) -> e+e-) + B(T(1S) -> mu+mu-) = 4.96%.
19 Using B(T(1S) -> e+e-) = (2.38 +/- 0.11)% and B(T(1S) -> mu+mu-) = (2.48 +/- 0.05)%.
20 Using Gamma_ee(T(2S)) = 0.612 +/- 0.011 keV.

T(1S)eta / Gamma(T(1S)pi+pi-) , T7/T1

Table with columns: VALUE (units 10^-2), CL%, DOCUMENT ID, TECN, COMMENT. Rows include AUBERT 08BP BABR.

J/psi(1S) anything / Gamma_total, T8/T

Table with columns: VALUE, CL%, DOCUMENT ID, TECN, COMMENT. Rows include MASCHMANN 90.

d anything / Gamma_total, T9/T

Table with columns: VALUE (units 10^-5), EVTS, DOCUMENT ID, TECN, COMMENT. Rows include ASNER 07.

ggg / Gamma_total, T11/T

Table with columns: VALUE (units 10^-2), EVTS, DOCUMENT ID, TECN, COMMENT. Rows include BESSON 06A.

gamma g g / Gamma_total, T12/T

Table with columns: VALUE (units 10^-2), EVTS, DOCUMENT ID, TECN, COMMENT. Rows include BESSON 06A.

gamma g g / Gamma(T(2S)), T12/T11

Table with columns: VALUE (units 10^-2), EVTS, DOCUMENT ID, TECN, COMMENT. Rows include BESSON 06A.

gamma chi_b1(1P) / Gamma_total, T13/T

Table with columns: VALUE, EVTS, DOCUMENT ID, TECN, COMMENT. Rows include ARTUSO 05, EDWARDS 99, ALBRECHT 85E, NERNST 85, HAAS 84, KLOPFEN... 83.

gamma chi_b0(1P) / Gamma_total, T15/T

Table with columns: VALUE, EVTS, DOCUMENT ID, TECN, COMMENT. Rows include ARTUSO 05, EDWARDS 99, ALBRECHT 85E, NERNST 85, HAAS 84, KLOPFEN... 83.

T(70(1710)) / Gamma_total, T16/T

Table with columns: VALUE (units 10^-9), CL%, DOCUMENT ID, TECN, COMMENT. Rows include ALBRECHT 89 ARG, ALBRECHT 89 ARG.

T(f2'(1525)) / Gamma_total, T17/T

Table with columns: VALUE (units 10^-9), CL%, DOCUMENT ID, TECN, COMMENT. Rows include ALBRECHT 89 ARG.

T(f2(1270)) / Gamma_total, T18/T

Table with columns: VALUE (units 10^-5), CL%, DOCUMENT ID, TECN, COMMENT. Rows include ALBRECHT 89 ARG.

T(fJ(2220)) / Gamma_total, T19/T

Table with columns: VALUE (units 10^-3), CL%, DOCUMENT ID, TECN, COMMENT. Rows include ALBRECHT 89 ARG.

T(eta_b(1S)) / Gamma_total, T20/T

Table with columns: VALUE (units 10^-4), CL%, EVTS, DOCUMENT ID, TECN, COMMENT. Rows include AUBERT 09A, BONVICINI 10, ARTUSO 05.

T(gamma -> gamma + 2 prongs) / Gamma_total, T21/T

Table with columns: VALUE (units 10^-4), CL%, DOCUMENT ID, TECN, COMMENT. Rows include ROSNER 07A, ROSNER 06.

T(mu+/- tau+/-) / Gamma_total, T22/T

Table with columns: VALUE (units 10^-6), CL%, DOCUMENT ID, TECN, COMMENT. Rows include LOVE 08A.

T(2S) REFERENCES

List of references for T(2S) meson, including authors like BONVICINI, AUBERT, BHARI, ALBRECHT, EDWARDS, etc., and journals like PR, PL, PRL, ZPHY, etc.

Meson Particle Listings

$\Upsilon(1D)$, $\chi_{b0}(2P)$

$\Upsilon(1D)$

$$I^G(J^{PC}) = 0^-(2^{--})$$

OMITTED FROM SUMMARY TABLE
J needs confirmation.

$\Upsilon(1D)$ MASS

VALUE (MeV)	EVTS	DOCUMENT ID	TECN	COMMENT
10161.1 ± 0.6 ± 1.6	38	BONVICINI	04	CLE3 $\Upsilon(3S) \rightarrow \gamma X$

$\Upsilon(1D)$ DECAY MODES

Mode	Fraction (Γ_i/Γ)
Γ_1 $\gamma\gamma \Upsilon(1S)$	seen
Γ_2 $\gamma\chi_{bJ}(1P)$	
Γ_3 $\eta \Upsilon(1S)$	
Γ_4 $\pi^+\pi^- \Upsilon(1S)$	

$\Upsilon(1D)$ BRANCHING RATIOS

$\Gamma(\eta \Upsilon(1S))/\Gamma(\gamma\gamma \Upsilon(1S))$					Γ_3/Γ_1
VALUE	CL%	DOCUMENT ID	TECN	COMMENT	
<0.25	90	BONVICINI	04	CLE3 $\Upsilon(3S) \rightarrow \gamma X$	

$\Gamma(\pi^+\pi^- \Upsilon(1S))/\Gamma(\gamma\gamma \Upsilon(1S))$					Γ_4/Γ_1
VALUE	CL%	DOCUMENT ID	TECN	COMMENT	
<1.2	90	¹ BONVICINI	04	CLE3 $\Upsilon(3S) \rightarrow \gamma X$	

¹ Assuming $J = 2$.

$\Upsilon(1D)$ REFERENCES

BONVICINI 04 PR D70 032001 G. Bonvicini et al. (CLEO Collab.)

$\chi_{b0}(2P)$

$$I^G(J^{PC}) = 0^+(0^{++})$$

J needs confirmation.

Observed in radiative decay of the $\Upsilon(3S)$, therefore $C = +$. Branching ratio requires E1 transition, M1 is strongly disfavored, therefore $P = +$.

$\chi_{b0}(2P)$ MASS

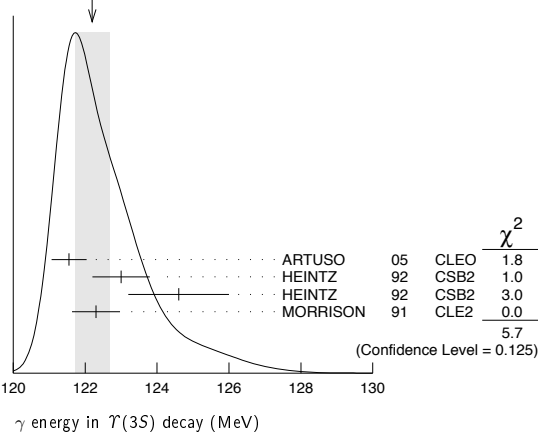
VALUE (GeV)	DOCUMENT ID
10.2325 ± 0.0004 ± 0.0005 OUR EVALUATION	From γ energy below, using $\Upsilon(3S)$ mass = 10355.2 ± 0.5 MeV

γ ENERGY IN $\Upsilon(3S)$ DECAY

VALUE (MeV)	EVTS	DOCUMENT ID	TECN	COMMENT
121.9 ± 0.4 OUR EVALUATION				Treating systematic errors as correlated
122.2 ± 0.5 OUR AVERAGE				Error includes scale factor of 1.4. See the ideogram below.
121.55 ± 0.16 ± 0.46		ARTUSO 05	CLEO	$\Upsilon(3S) \rightarrow \gamma X$
123.0 ± 0.8	4959	¹ HEINTZ 92	CSB2	$e^+e^- \rightarrow \gamma X$
124.6 ± 1.4	17	² HEINTZ 92	CSB2	$e^+e^- \rightarrow \ell^+\ell^-\gamma\gamma$
122.3 ± 0.3 ± 0.6	9903	MORRISON 91	CLE2	$e^+e^- \rightarrow \gamma X$

¹ A systematic uncertainty on the energy scale of 0.9% not included. Supersedes NARAIN 91.
² A systematic uncertainty on the energy scale of 0.9% not included. Supersedes HEINTZ 91.

WEIGHTED AVERAGE
122.2 ± 0.5 (Error scaled by 1.4)



$\chi_{b0}(2P)$ DECAY MODES

Mode	Fraction (Γ_i/Γ)	Confidence level
Γ_1 $\gamma \Upsilon(2S)$	(4.6 ± 2.1) %	
Γ_2 $\gamma \Upsilon(1S)$	(9 ± 6) × 10 ⁻³	
Γ_3 $D^0 X$	< 8.2 %	90%
Γ_4 $\pi^+\pi^- K^+ K^- \pi^0$	< 3.4 × 10 ⁻⁵	90%
Γ_5 $2\pi^+\pi^- K^- K_S^0$	< 5 × 10 ⁻⁵	90%
Γ_6 $2\pi^+\pi^- K^- K_S^0 2\pi^0$	< 2.2 × 10 ⁻⁴	90%
Γ_7 $2\pi^+ 2\pi^- 2\pi^0$	< 2.4 × 10 ⁻⁴	90%
Γ_8 $2\pi^+ 2\pi^- K^+ K^-$	< 1.5 × 10 ⁻⁴	90%
Γ_9 $2\pi^+ 2\pi^- K^+ K^- \pi^0$	< 2.2 × 10 ⁻⁴	90%
Γ_{10} $2\pi^+ 2\pi^- K^+ K^- 2\pi^0$	< 1.1 × 10 ⁻³	90%
Γ_{11} $3\pi^+ 2\pi^- K^- K_S^0 \pi^0$	< 7 × 10 ⁻⁴	90%
Γ_{12} $3\pi^+ 3\pi^-$	< 7 × 10 ⁻⁵	90%
Γ_{13} $3\pi^+ 3\pi^- 2\pi^0$	< 1.2 × 10 ⁻³	90%
Γ_{14} $3\pi^+ 3\pi^- K^+ K^-$	< 1.5 × 10 ⁻⁴	90%
Γ_{15} $3\pi^+ 3\pi^- K^+ K^- \pi^0$	< 7 × 10 ⁻⁴	90%
Γ_{16} $4\pi^+ 4\pi^-$	< 1.7 × 10 ⁻⁴	90%
Γ_{17} $4\pi^+ 4\pi^- 2\pi^0$	< 6 × 10 ⁻⁴	90%

$\chi_{b0}(2P)$ BRANCHING RATIOS

$\Gamma(\gamma \Upsilon(2S))/\Gamma_{total}$					Γ_1/Γ
VALUE	CL%	DOCUMENT ID	TECN	COMMENT	
0.046 ± 0.020 ± 0.007		³ HEINTZ 92	CSB2	$e^+e^- \rightarrow \ell^+\ell^-\gamma\gamma$	

• • • We do not use the following data for averages, fits, limits, etc. • • •

<0.089 90 ⁴CRAWFORD 92B CLE2 $e^+e^- \rightarrow \ell^+\ell^-\gamma\gamma$

³ Using $B(\Upsilon(2S) \rightarrow \mu^+\mu^-) = (1.44 \pm 0.10)\%$, $B(\Upsilon(3S) \rightarrow \gamma\chi_{b0}(2P)) = (6.0 \pm 0.4 \pm 0.6)\%$ and assuming $e\mu$ universality. Supersedes HEINTZ 91.

⁴ Using $B(\Upsilon(2S) \rightarrow \mu^+\mu^-) = (1.37 \pm 0.26)\%$, $B(\Upsilon(3S) \rightarrow \gamma\gamma \Upsilon(2S)) \times 2 B(\Upsilon(2S) \rightarrow \mu^+\mu^-) < 1.19 \times 10^{-4}$, and $B(\Upsilon(3S) \rightarrow \chi_{b0}(2P)\gamma) = 0.049$.

$\Gamma(\gamma \Upsilon(1S))/\Gamma_{total}$					Γ_2/Γ
VALUE	CL%	DOCUMENT ID	TECN	COMMENT	
0.009 ± 0.006 ± 0.001		⁵ HEINTZ 92	CSB2	$e^+e^- \rightarrow \ell^+\ell^-\gamma\gamma$	

• • • We do not use the following data for averages, fits, limits, etc. • • •

<0.025 90 ⁶CRAWFORD 92B CLE2 $e^+e^- \rightarrow \ell^+\ell^-\gamma\gamma$

⁵ Using $B(\Upsilon(1S) \rightarrow \mu^+\mu^-) = (2.57 \pm 0.07)\%$, $B(\Upsilon(3S) \rightarrow \gamma\chi_{b0}(2P)) = (6.0 \pm 0.4 \pm 0.6)\%$ and assuming $e\mu$ universality. Supersedes HEINTZ 91.

⁶ Using $B(\Upsilon(1S) \rightarrow \mu^+\mu^-) = (2.57 \pm 0.07)\%$, $B(\Upsilon(3S) \rightarrow \gamma\gamma \Upsilon(1S)) \times 2 B(\Upsilon(1S) \rightarrow \mu^+\mu^-) < 0.63 \times 10^{-4}$, and $B(\Upsilon(3S) \rightarrow \chi_{b0}(2P)\gamma) = 0.049$.

$\Gamma(D^0 X)/\Gamma_{total}$					Γ_3/Γ
VALUE	CL%	DOCUMENT ID	TECN	COMMENT	
<8.2 × 10⁻²	90	^{7,8} BRIERE 08	CLEO	$\Upsilon(3S) \rightarrow \gamma D^0 X$	

⁷ For $p_{D^0} > 2.5$ GeV/c.

⁸ The authors also present their result as $(4.1 \pm 3.0 \pm 0.4) \times 10^{-2}$.

$\Gamma(\pi^+\pi^- K^+ K^- \pi^0)/\Gamma_{total}$					Γ_4/Γ
VALUE (units 10 ⁻⁴)	CL%	DOCUMENT ID	TECN	COMMENT	
<0.34	90	⁹ ASNER 08A	CLEO	$\Upsilon(3S) \rightarrow \gamma\pi^+\pi^- K^+ K^- \pi^0$	

⁹ ASNER 08A reports $[\Gamma(\chi_{b0}(2P) \rightarrow \pi^+\pi^- K^+ K^- \pi^0)/\Gamma_{total}] \times [B(\Upsilon(3S) \rightarrow \gamma\chi_{b0}(2P))] < 2 \times 10^{-6}$ which we divide by our best value $B(\Upsilon(3S) \rightarrow \gamma\chi_{b0}(2P)) = 5.9 \times 10^{-2}$.

$\Gamma(2\pi^+\pi^- K^- K_S^0)/\Gamma_{total}$					Γ_5/Γ
VALUE (units 10 ⁻⁴)	CL%	DOCUMENT ID	TECN	COMMENT	
<0.5	90	¹⁰ ASNER 08A	CLEO	$\Upsilon(3S) \rightarrow \gamma 2\pi^+\pi^- K^- K_S^0$	

¹⁰ ASNER 08A reports $[\Gamma(\chi_{b0}(2P) \rightarrow 2\pi^+\pi^- K^- K_S^0)/\Gamma_{total}] \times [B(\Upsilon(3S) \rightarrow \gamma\chi_{b0}(2P))] < 3 \times 10^{-6}$ which we divide by our best value $B(\Upsilon(3S) \rightarrow \gamma\chi_{b0}(2P)) = 5.9 \times 10^{-2}$.

$\Gamma(2\pi^+\pi^- K^- K_S^0 2\pi^0)/\Gamma_{total}$					Γ_6/Γ
VALUE (units 10 ⁻⁴)	CL%	DOCUMENT ID	TECN	COMMENT	
<2.2	90	¹¹ ASNER 08A	CLEO	$\Upsilon(3S) \rightarrow \gamma 2\pi^+\pi^- K^- 2\pi^0$	

¹¹ ASNER 08A reports $[\Gamma(\chi_{b0}(2P) \rightarrow 2\pi^+\pi^- K^- K_S^0 2\pi^0)/\Gamma_{total}] \times [B(\Upsilon(3S) \rightarrow \gamma\chi_{b0}(2P))] < 13 \times 10^{-6}$ which we divide by our best value $B(\Upsilon(3S) \rightarrow \gamma\chi_{b0}(2P)) = 5.9 \times 10^{-2}$.

$\Gamma(2\pi^+ 2\pi^- 2\pi^0)/\Gamma_{total}$					Γ_7/Γ
VALUE (units 10 ⁻⁴)	CL%	DOCUMENT ID	TECN	COMMENT	
<2.4	90	¹² ASNER 08A	CLEO	$\Upsilon(3S) \rightarrow \gamma 2\pi^+ 2\pi^- 2\pi^0$	

¹² ASNER 08A reports $[\Gamma(\chi_{b0}(2P) \rightarrow 2\pi^+ 2\pi^- 2\pi^0)/\Gamma_{total}] \times [B(\Upsilon(3S) \rightarrow \gamma\chi_{b0}(2P))] < 14 \times 10^{-6}$ which we divide by our best value $B(\Upsilon(3S) \rightarrow \gamma\chi_{b0}(2P)) = 5.9 \times 10^{-2}$.

$\Gamma(2\pi^+2\pi^-K^+K^-)/\Gamma_{\text{total}}$ Γ_8/Γ

VALUE (units 10^{-4})	CL%	DOCUMENT ID	TECN	COMMENT
<1.5	90	13 ASNER	08A CLEO	$\Upsilon(3S) \rightarrow \gamma 2\pi^+ 2\pi^- K^+ K^-$
13 ASNER 08A reports $[\Gamma(\chi_{b0}(2P) \rightarrow 2\pi^+ 2\pi^- K^+ K^-)/\Gamma_{\text{total}}] \times [B(\Upsilon(3S) \rightarrow \gamma \chi_{b0}(2P))] < 9 \times 10^{-6}$ which we divide by our best value $B(\Upsilon(3S) \rightarrow \gamma \chi_{b0}(2P)) = 5.9 \times 10^{-2}$.				

 $\Gamma(2\pi^+2\pi^-K^+K^-\pi^0)/\Gamma_{\text{total}}$ Γ_9/Γ

VALUE (units 10^{-4})	CL%	DOCUMENT ID	TECN	COMMENT
<2.2	90	14 ASNER	08A CLEO	$\Upsilon(3S) \rightarrow \gamma 2\pi^+ 2\pi^- K^+ K^-\pi^0$
14 ASNER 08A reports $[\Gamma(\chi_{b0}(2P) \rightarrow 2\pi^+ 2\pi^- K^+ K^-\pi^0)/\Gamma_{\text{total}}] \times [B(\Upsilon(3S) \rightarrow \gamma \chi_{b0}(2P))] < 13 \times 10^{-6}$ which we divide by our best value $B(\Upsilon(3S) \rightarrow \gamma \chi_{b0}(2P)) = 5.9 \times 10^{-2}$.				

 $\Gamma(2\pi^+2\pi^-K^+K^-2\pi^0)/\Gamma_{\text{total}}$ Γ_{10}/Γ

VALUE (units 10^{-4})	CL%	DOCUMENT ID	TECN	COMMENT
<11	90	15 ASNER	08A CLEO	$\Upsilon(3S) \rightarrow \gamma 2\pi^+ 2\pi^- K^+ K^- 2\pi^0$
15 ASNER 08A reports $[\Gamma(\chi_{b0}(2P) \rightarrow 2\pi^+ 2\pi^- K^+ K^- 2\pi^0)/\Gamma_{\text{total}}] \times [B(\Upsilon(3S) \rightarrow \gamma \chi_{b0}(2P))] < 63 \times 10^{-6}$ which we divide by our best value $B(\Upsilon(3S) \rightarrow \gamma \chi_{b0}(2P)) = 5.9 \times 10^{-2}$.				

 $\Gamma(3\pi^+2\pi^-K^-K_S^0\pi^0)/\Gamma_{\text{total}}$ Γ_{11}/Γ

VALUE (units 10^{-4})	CL%	DOCUMENT ID	TECN	COMMENT
<7	90	16 ASNER	08A CLEO	$\Upsilon(3S) \rightarrow \gamma 3\pi^+ 2\pi^- K^- K_S^0\pi^0$
16 ASNER 08A reports $[\Gamma(\chi_{b0}(2P) \rightarrow 3\pi^+ 2\pi^- K^- K_S^0\pi^0)/\Gamma_{\text{total}}] \times [B(\Upsilon(3S) \rightarrow \gamma \chi_{b0}(2P))] < 39 \times 10^{-6}$ which we divide by our best value $B(\Upsilon(3S) \rightarrow \gamma \chi_{b0}(2P)) = 5.9 \times 10^{-2}$.				

 $\Gamma(3\pi^+3\pi^-)/\Gamma_{\text{total}}$ Γ_{12}/Γ

VALUE (units 10^{-4})	CL%	DOCUMENT ID	TECN	COMMENT
<0.7	90	17 ASNER	08A CLEO	$\Upsilon(3S) \rightarrow \gamma 3\pi^+ 3\pi^-$
17 ASNER 08A reports $[\Gamma(\chi_{b0}(2P) \rightarrow 3\pi^+ 3\pi^-)/\Gamma_{\text{total}}] \times [B(\Upsilon(3S) \rightarrow \gamma \chi_{b0}(2P))] < 4 \times 10^{-6}$ which we divide by our best value $B(\Upsilon(3S) \rightarrow \gamma \chi_{b0}(2P)) = 5.9 \times 10^{-2}$.				

 $\Gamma(3\pi^+3\pi^-2\pi^0)/\Gamma_{\text{total}}$ Γ_{13}/Γ

VALUE (units 10^{-4})	CL%	DOCUMENT ID	TECN	COMMENT
<12	90	18 ASNER	08A CLEO	$\Upsilon(3S) \rightarrow \gamma 3\pi^+ 3\pi^- 2\pi^0$
18 ASNER 08A reports $[\Gamma(\chi_{b0}(2P) \rightarrow 3\pi^+ 3\pi^- 2\pi^0)/\Gamma_{\text{total}}] \times [B(\Upsilon(3S) \rightarrow \gamma \chi_{b0}(2P))] < 72 \times 10^{-6}$ which we divide by our best value $B(\Upsilon(3S) \rightarrow \gamma \chi_{b0}(2P)) = 5.9 \times 10^{-2}$.				

 $\Gamma(3\pi^+3\pi^-K^+K^-)/\Gamma_{\text{total}}$ Γ_{14}/Γ

VALUE (units 10^{-4})	CL%	DOCUMENT ID	TECN	COMMENT
<1.5	90	19 ASNER	08A CLEO	$\Upsilon(3S) \rightarrow \gamma 3\pi^+ 3\pi^- K^+ K^-$
19 ASNER 08A reports $[\Gamma(\chi_{b0}(2P) \rightarrow 3\pi^+ 3\pi^- K^+ K^-)/\Gamma_{\text{total}}] \times [B(\Upsilon(3S) \rightarrow \gamma \chi_{b0}(2P))] < 9 \times 10^{-6}$ which we divide by our best value $B(\Upsilon(3S) \rightarrow \gamma \chi_{b0}(2P)) = 5.9 \times 10^{-2}$.				

 $\Gamma(3\pi^+3\pi^-K^+K^-\pi^0)/\Gamma_{\text{total}}$ Γ_{15}/Γ

VALUE (units 10^{-4})	CL%	DOCUMENT ID	TECN	COMMENT
<7	90	20 ASNER	08A CLEO	$\Upsilon(3S) \rightarrow \gamma 3\pi^+ 3\pi^- K^+ K^-\pi^0$
20 ASNER 08A reports $[\Gamma(\chi_{b0}(2P) \rightarrow 3\pi^+ 3\pi^- K^+ K^-\pi^0)/\Gamma_{\text{total}}] \times [B(\Upsilon(3S) \rightarrow \gamma \chi_{b0}(2P))] < 43 \times 10^{-6}$ which we divide by our best value $B(\Upsilon(3S) \rightarrow \gamma \chi_{b0}(2P)) = 5.9 \times 10^{-2}$.				

 $\Gamma(4\pi^+4\pi^-)/\Gamma_{\text{total}}$ Γ_{16}/Γ

VALUE (units 10^{-4})	CL%	DOCUMENT ID	TECN	COMMENT
<1.7	90	21 ASNER	08A CLEO	$\Upsilon(3S) \rightarrow \gamma 4\pi^+ 4\pi^-$
21 ASNER 08A reports $[\Gamma(\chi_{b0}(2P) \rightarrow 4\pi^+ 4\pi^-)/\Gamma_{\text{total}}] \times [B(\Upsilon(3S) \rightarrow \gamma \chi_{b0}(2P))] < 10 \times 10^{-6}$ which we divide by our best value $B(\Upsilon(3S) \rightarrow \gamma \chi_{b0}(2P)) = 5.9 \times 10^{-2}$.				

 $\Gamma(4\pi^+4\pi^-2\pi^0)/\Gamma_{\text{total}}$ Γ_{17}/Γ

VALUE (units 10^{-4})	CL%	DOCUMENT ID	TECN	COMMENT
<6	90	22 ASNER	08A CLEO	$\Upsilon(3S) \rightarrow \gamma 4\pi^+ 4\pi^- 2\pi^0$
22 ASNER 08A reports $[\Gamma(\chi_{b0}(2P) \rightarrow 4\pi^+ 4\pi^- 2\pi^0)/\Gamma_{\text{total}}] \times [B(\Upsilon(3S) \rightarrow \gamma \chi_{b0}(2P))] < 38 \times 10^{-6}$ which we divide by our best value $B(\Upsilon(3S) \rightarrow \gamma \chi_{b0}(2P)) = 5.9 \times 10^{-2}$.				

 $\chi_{b0}(2P)$ REFERENCES

ASNER	08A	PR D78 091103	D.M. Asner et al.	(CLEO Collab.)
BRIERE	08	PR D78 092007	R.A. Briere et al.	(CLEO Collab.)
ARTUSO	05	PRL 94 032001	M. Artuso et al.	(CLEO Collab.)
CRAWFORD	92B	PL B294 139	G. Crawford, R. Fullton	(CLEO Collab.)
HEINTZ	92	PR D46 1928	U. Heintz et al.	(CUSP II Collab.)
HEINTZ	91	PRL 66 1563	U. Heintz et al.	(CUSB Collab.)
MORRISON	91	PRL 67 1696	R.J. Morrison et al.	(CLEO Collab.)
NARAIN	91	PRL 66 3113	M. Narain et al.	(CUSB Collab.)

 $\chi_{b1}(2P)$

$$J^{G(JPC)} = 0^+(1^{++})$$

J needs confirmation.

Observed in radiative decay of the $\Upsilon(3S)$, therefore $C = +$. Branching ratio requires E1 transition, M1 is strongly disfavored, therefore $P = +$.

 $\chi_{b1}(2P)$ MASS

VALUE (GeV)	DOCUMENT ID
10.25546 ± 0.00022 ± 0.00050 OUR EVALUATION	From γ energy below, using $\Upsilon(3S)$ mass = 10355.2 ± 0.5 MeV

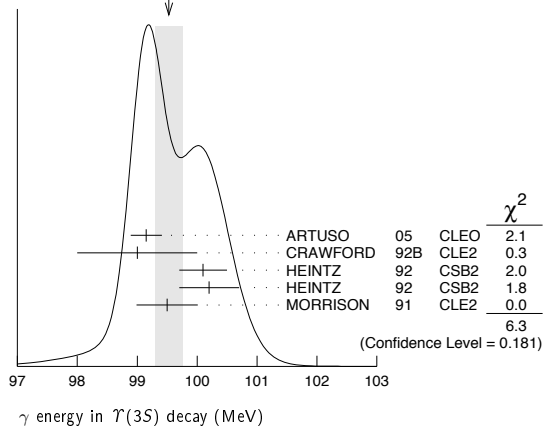
 $m_{\chi_{b1}(2P)} - m_{\chi_{b0}(2P)}$

VALUE (MeV)	DOCUMENT ID	TECN	COMMENT
23.5 ± 0.7 ± 0.7	¹ HEINTZ 92 CSB2		$e^+e^- \rightarrow \gamma X, \ell^+\ell^-\gamma\gamma$
¹ From the average photon energy for inclusive and exclusive events. Supersedes NARAIN 91.			

 γ ENERGY IN $\Upsilon(3S)$ DECAY

VALUE (MeV)	EVTs	DOCUMENT ID	TECN	COMMENT
99.26 ± 0.22 OUR EVALUATION		Treating systematic errors as correlated		
99.53 ± 0.23 OUR AVERAGE		Error includes scale factor of 1.3. See the ideogram below.		
99.15 ± 0.07 ± 0.25		ARTUSO 05 CLEO		$\Upsilon(3S) \rightarrow \gamma X$
99 ± 1	169	CRAWFORD 92B CLE2		$e^+e^- \rightarrow \ell^+\ell^-\gamma\gamma$
100.1 ± 0.4	11147	² HEINTZ 92 CSB2		$e^+e^- \rightarrow \gamma X$
100.2 ± 0.5	223	³ HEINTZ 92 CSB2		$e^+e^- \rightarrow \ell^+\ell^-\gamma\gamma$
99.5 ± 0.1 ± 0.5	25759	MORRISON 91 CLE2		$e^+e^- \rightarrow \gamma X$
² A systematic uncertainty on the energy scale of 0.9% not included. Supersedes NARAIN 91.				
³ A systematic uncertainty on the energy scale of 0.9% not included. Supersedes HEINTZ 91.				

WEIGHTED AVERAGE
99.53 ± 0.23 (Error scaled by 1.3)

 $\chi_{b1}(2P)$ DECAY MODES

Mode	Fraction (Γ_i/Γ)	Scale factor
Γ_1 $\omega \Upsilon(1S)$	(1.63 ± 0.40) %	
Γ_2 $\gamma \Upsilon(2S)$	(21 ± 4) %	1.5
Γ_3 $\gamma \Upsilon(1S)$	(8.5 ± 1.3) %	1.3
Γ_4 $\pi\pi\chi_{b1}(1P)$	(8.6 ± 3.1) × 10 ⁻³	
Γ_5 $D^0 X$	(8.8 ± 1.7) %	
Γ_6 $\pi^+\pi^-K^+K^-\pi^0$	(3.1 ± 1.0) × 10 ⁻⁴	
Γ_7 $2\pi^+\pi^-K^-K_S^0\pi^0$	(1.1 ± 0.5) × 10 ⁻⁴	
Γ_8 $2\pi^+\pi^-K^-K_S^0 2\pi^0$	(7.7 ± 3.2) × 10 ⁻⁴	
Γ_9 $2\pi^+2\pi^-2\pi^0$	(5.9 ± 2.0) × 10 ⁻⁴	
Γ_{10} $2\pi^+2\pi^-K^+K^-$	(10 ± 4) × 10 ⁻⁵	
Γ_{11} $2\pi^+2\pi^-K^+K^-\pi^0$	(5.5 ± 1.8) × 10 ⁻⁴	
Γ_{12} $2\pi^+2\pi^-K^+K^-2\pi^0$	(10 ± 4) × 10 ⁻⁴	
Γ_{13} $3\pi^+2\pi^-K^-K_S^0\pi^0$	(6.7 ± 2.6) × 10 ⁻⁴	
Γ_{14} $3\pi^+3\pi^-$	(1.2 ± 0.4) × 10 ⁻⁴	
Γ_{15} $3\pi^+3\pi^-2\pi^0$	(1.2 ± 0.4) × 10 ⁻³	
Γ_{16} $3\pi^+3\pi^-K^+K^-$	(2.0 ± 0.8) × 10 ⁻⁴	
Γ_{17} $3\pi^+3\pi^-K^+K^-\pi^0$	(6.1 ± 2.2) × 10 ⁻⁴	
Γ_{18} $4\pi^+4\pi^-$	(1.7 ± 0.6) × 10 ⁻⁴	
Γ_{19} $4\pi^+4\pi^-2\pi^0$	(1.9 ± 0.7) × 10 ⁻³	

See key on page 405

Meson Particle Listings

$$\chi_{b1}(2P), \chi_{b2}(2P)$$

B($\chi_{b0}(2P) \rightarrow pX + \bar{p}X$)/B($\chi_{b1}(2P) \rightarrow pX + \bar{p}X$)			
VALUE	DOCUMENT ID	TECN	COMMENT
1.082 ± 0.025 ± 0.060	BRIERE	07	CLEO $\Upsilon(3S) \rightarrow \gamma\chi_{bJ}(2P)$

$\chi_{b1}(2P)$ REFERENCES

ASNER	08A	PR D78 091103	D.M. Asner et al.	(CLEO Collab.)
BRIERE	08	PR D78 092007	R.A. Briere et al.	(CLEO Collab.)
BRIERE	07	PR D76 012005	R.A. Briere et al.	(CLEO Collab.)
CAWLFIELD	06	PR D73 012003	C. Crawford et al.	(CLEO Collab.)
ARTUSO	05	PRL 94 032001	M. Artuso et al.	(CLEO Collab.)
CRONIN-HEN..	04	PRL 92 222002	D. Cronin-Hennessy et al.	(CLEO3 Collab.)
CRAWFORD	92B	PL B294 139	G. Crawford, R. Fulton	(CLEO Collab.)
HEINTZ	92	PR D46 1928	U. Heintz et al.	(CUSB II Collab.)
HEINTZ	91	PR L66 1563	U. Heintz et al.	(CUSB Collab.)
MORRISON	91	PRL 67 1696	R.J. Morrison et al.	(CLEO Collab.)
NARAIN	91	PRL 66 3113	M. Narain et al.	(CUSB Collab.)

$\chi_{b2}(2P)$

$$J^G(JPC) = 0^+(2^{++})$$

J needs confirmation.

Observed in radiative decay of the $\Upsilon(3S)$, therefore $C = +$. Branching ratio requires E1 transition, M1 is strongly disfavored, therefore $P = +$.

$\chi_{b2}(2P)$ MASS

VALUE (GeV)	DOCUMENT ID	TECN	COMMENT
10.26865 ± 0.00022 ± 0.00050 OUR EVALUATION			From γ energy below, using $\Upsilon(3S)$ mass = 10355.2 ± 0.5 MeV

$m_{\chi_{b2}(2P)} - m_{\chi_{b1}(2P)}$

VALUE (MeV)	DOCUMENT ID	TECN	COMMENT
13.5 ± 0.4 ± 0.5	¹ HEINTZ	92	CSB2 $e^+e^- \rightarrow \gamma\chi, \ell^+\ell^-\gamma\gamma$
			¹ From the average photon energy for inclusive and exclusive events. Supersedes NARAIN 91.

γ ENERGY IN $\Upsilon(3S)$ DECAY

VALUE (MeV)	EVTS	DOCUMENT ID	TECN	COMMENT
86.19 ± 0.22 OUR EVALUATION	Treating systematic errors as correlated			
86.40 ± 0.18 OUR AVERAGE				
86.04 ± 0.06 ± 0.27		ARTUSO	05	CLEO $\Upsilon(3S) \rightarrow \gamma\chi$
86 ± 1	101	CRAWFORD	92B	CLE2 $e^+e^- \rightarrow \ell^+\ell^-\gamma\gamma$
86.7 ± 0.4	10319	² HEINTZ	92	CSB2 $e^+e^- \rightarrow \gamma\chi$
86.9 ± 0.4	157	³ HEINTZ	92	CSB2 $e^+e^- \rightarrow \ell^+\ell^-\gamma\gamma$
86.4 ± 0.1 ± 0.4	30741	MORRISON	91	CLE2 $e^+e^- \rightarrow \gamma\chi$
				² A systematic uncertainty on the energy scale of 0.9% not included. Supersedes NARAIN 91.
				³ A systematic uncertainty on the energy scale of 0.9% not included. Supersedes HEINTZ 91.

$\chi_{b2}(2P)$ DECAY MODES

Mode	Fraction (Γ_i/Γ)	Confidence level
Γ_1 $\omega \Upsilon(1S)$	(1.10 ± 0.34) %	
Γ_2 $\gamma \Upsilon(2S)$	(16.2 ± 2.4) %	
Γ_3 $\gamma \Upsilon(1S)$	(7.1 ± 1.0) %	
Γ_4 $\pi\pi\chi_{b2}(1P)$	(6.0 ± 2.1) × 10 ⁻³	
Γ_5 $D^0 X$	< 2.4 %	90%
Γ_6 $\pi^+\pi^-K^+K^-\pi^0$	< 1.1 %	90%
Γ_7 $2\pi^+\pi^-K^-K_S^0$	< 9 %	90%
Γ_8 $2\pi^+\pi^-K^-K_S^0 2\pi^0$	< 7 %	90%
Γ_9 $2\pi^+2\pi^-2\pi^0$	(3.9 ± 1.6) × 10 ⁻⁴	
Γ_{10} $2\pi^+2\pi^-K^+K^-$	(9 ± 4) × 10 ⁻⁵	
Γ_{11} $2\pi^+2\pi^-K^+K^-\pi^0$	(2.4 ± 1.1) × 10 ⁻⁴	
Γ_{12} $2\pi^+2\pi^-K^+K^-2\pi^0$	(4.7 ± 2.3) × 10 ⁻⁴	
Γ_{13} $3\pi^+2\pi^-K^-K_S^0\pi^0$	< 4 %	90%
Γ_{14} $3\pi^+3\pi^-$	(9 ± 4) × 10 ⁻⁵	
Γ_{15} $3\pi^+3\pi^-2\pi^0$	(1.2 ± 0.4) × 10 ⁻³	
Γ_{16} $3\pi^+3\pi^-K^+K^-$	(1.4 ± 0.7) × 10 ⁻⁴	
Γ_{17} $3\pi^+3\pi^-K^+K^-\pi^0$	(4.2 ± 1.7) × 10 ⁻⁴	
Γ_{18} $4\pi^+4\pi^-$	(9 ± 5) × 10 ⁻⁵	
Γ_{19} $4\pi^+4\pi^-2\pi^0$	(1.3 ± 0.5) × 10 ⁻³	

$\chi_{b2}(2P)$ BRANCHING RATIOS

$\Gamma(\omega \Upsilon(1S))/\Gamma_{total}$				Γ_1/Γ
VALUE (units 10 ⁻²)	EVTS	DOCUMENT ID	TECN	COMMENT
1.10^{+0.32} ± 0.28^{-0.10}	20.1 ^{+5.8} _{-5.1}	⁴ CRONIN-HEN..04	CLE3	$\Upsilon(3S) \rightarrow \gamma\omega \Upsilon(1S)$

⁴ Using B($\Upsilon(3S) \rightarrow \gamma\chi_{b2}(2P)$) = (11.4 ± 0.8)% and B($\Upsilon(1S) \rightarrow \ell^+\ell^-$) = 2 B($\Upsilon(1S) \rightarrow \mu^+\mu^-$) = 2 (2.48 ± 0.06)%.

$\Gamma(\gamma \Upsilon(2S))/\Gamma_{total}$				Γ_2/Γ
VALUE	DOCUMENT ID	TECN	COMMENT	
0.162 ± 0.024 OUR AVERAGE				
0.135 ± 0.025 ± 0.035	⁵ CRAWFORD 92B	CLE2	$e^+e^- \rightarrow \ell^+\ell^-\gamma\gamma$	
0.173 ± 0.021 ± 0.019	⁶ HEINTZ 92	CSB2	$e^+e^- \rightarrow \ell^+\ell^-\gamma\gamma$	

⁵ Using B($\Upsilon(2S) \rightarrow \mu^+\mu^-$) = (1.37 ± 0.26)%, B($\Upsilon(3S) \rightarrow \gamma\gamma \Upsilon(2S)$) × 2 B($\Upsilon(2S) \rightarrow \mu^+\mu^-$) = (4.98 ± 0.94 ± 0.62) × 10⁻⁴, and B($\Upsilon(3S) \rightarrow \gamma\chi_{b2}(2P)$) = 0.135 ± 0.003 ± 0.017.

⁶ Using B($\Upsilon(2S) \rightarrow \mu^+\mu^-$) = (1.44 ± 0.10)%, B($\Upsilon(3S) \rightarrow \gamma\chi_{b2}(2P)$) = (11.1 ± 0.5 ± 0.4)% and assuming $e\mu$ universality. Supersedes HEINTZ 91.

$\Gamma(\gamma \Upsilon(1S))/\Gamma_{total}$				Γ_3/Γ
VALUE	DOCUMENT ID	TECN	COMMENT	
0.071 ± 0.010 OUR AVERAGE				
0.072 ± 0.014 ± 0.013	⁷ CRAWFORD 92B	CLE2	$e^+e^- \rightarrow \ell^+\ell^-\gamma\gamma$	
0.070 ± 0.010 ± 0.006	⁸ HEINTZ 92	CSB2	$e^+e^- \rightarrow \ell^+\ell^-\gamma\gamma$	

⁷ Using B($\Upsilon(1S) \rightarrow \mu^+\mu^-$) = (2.57 ± 0.07)%, B($\Upsilon(3S) \rightarrow \gamma\gamma \Upsilon(2S)$) × 2 B($\Upsilon(1S) \rightarrow \mu^+\mu^-$) = (5.03 ± 0.94 ± 0.63) × 10⁻⁴, and B($\Upsilon(3S) \rightarrow \gamma\chi_{b2}(2P)$) = 0.135 ± 0.003 ± 0.017.

⁸ Using B($\Upsilon(1S) \rightarrow \mu^+\mu^-$) = (2.57 ± 0.07)%, B($\Upsilon(3S) \rightarrow \gamma\chi_{b2}(2P)$) = (11.1 ± 0.5 ± 0.4)% and assuming $e\mu$ universality. Supersedes HEINTZ 91.

$\Gamma(\pi\pi\chi_{b2}(1P))/\Gamma_{total}$				Γ_4/Γ
VALUE (units 10 ⁻³)	DOCUMENT ID	TECN	COMMENT	
6.0 ± 1.6 ± 1.4	⁹ CAWLFIELD 06	CLE3	$\Upsilon(3S) \rightarrow 2(\gamma\pi\ell)$	
			⁹ CAWLFIELD 06 quote $\Gamma(\chi_{b2}(2P) \rightarrow \pi\pi\chi_b(1P)) = 0.83 \pm 0.22 \pm 0.08 \pm 0.19$ keV assuming l-spin conservation, no D-wave contribution, $\Gamma(\chi_{b1}(2P)) = 96 \pm 16$ keV, and $\Gamma(\chi_{b2}(2P)) = 138 \pm 19$ keV.	

$\Gamma(D^0 X)/\Gamma_{total}$				Γ_5/Γ
VALUE	CL%	DOCUMENT ID	TECN	COMMENT
< 2.4 × 10 ⁻²	90,11	BRIERE	08	CLEO $\Upsilon(3S) \rightarrow \gamma D^0 X$
				¹⁰ For $p_{D^0} > 2.5$ GeV/c.
				¹¹ The authors also present their result as (0.2 ± 1.4 ± 0.1) × 10 ⁻² .

$\Gamma(\pi^+\pi^-K^+K^-\pi^0)/\Gamma_{total}$				Γ_6/Γ
VALUE (units 10 ⁻⁴)	CL%	DOCUMENT ID	TECN	COMMENT
< 1.1	90	¹² ASNER	08A	CLEO $\Upsilon(3S) \rightarrow \gamma\pi^+\pi^-K^+K^-\pi^0$
				¹² ASNER 08A reports $[\Gamma(\chi_{b2}(2P) \rightarrow \pi^+\pi^-K^+K^-\pi^0)/\Gamma_{total}] \times [B(\Upsilon(3S) \rightarrow \gamma\chi_{b2}(2P))]$ < 14 × 10 ⁻⁶ which we divide by our best value B($\Upsilon(3S) \rightarrow \gamma\chi_{b2}(2P)$) = 13.1 × 10 ⁻² .

$\Gamma(2\pi^+\pi^-K^-K_S^0)/\Gamma_{total}$				Γ_7/Γ
VALUE (units 10 ⁻⁴)	CL%	DOCUMENT ID	TECN	COMMENT
< 0.9	90	¹³ ASNER	08A	CLEO $\Upsilon(3S) \rightarrow \gamma 2\pi^+\pi^-K^-K_S^0$
				¹³ ASNER 08A reports $[\Gamma(\chi_{b2}(2P) \rightarrow 2\pi^+\pi^-K^-K_S^0)/\Gamma_{total}] \times [B(\Upsilon(3S) \rightarrow \gamma\chi_{b2}(2P))]$ < 12 × 10 ⁻⁶ which we divide by our best value B($\Upsilon(3S) \rightarrow \gamma\chi_{b2}(2P)$) = 13.1 × 10 ⁻² .

$\Gamma(2\pi^+\pi^-K^-K_S^0 2\pi^0)/\Gamma_{total}$				Γ_8/Γ
VALUE (units 10 ⁻⁴)	CL%	DOCUMENT ID	TECN	COMMENT
< 7	90	¹⁴ ASNER	08A	CLEO $\Upsilon(3S) \rightarrow \gamma 2\pi^+\pi^-K^-K_S^0 2\pi^0$
				¹⁴ ASNER 08A reports $[\Gamma(\chi_{b2}(2P) \rightarrow 2\pi^+\pi^-K^-K_S^0 2\pi^0)/\Gamma_{total}] \times [B(\Upsilon(3S) \rightarrow \gamma\chi_{b2}(2P))]$ < 87 × 10 ⁻⁶ which we divide by our best value B($\Upsilon(3S) \rightarrow \gamma\chi_{b2}(2P)$) = 13.1 × 10 ⁻² .

$\Gamma(2\pi^+2\pi^-2\pi^0)/\Gamma_{total}$				Γ_9/Γ
VALUE (units 10 ⁻⁴)	EVTS	DOCUMENT ID	TECN	COMMENT
3.9 ± 1.6 ± 0.5	23	¹⁵ ASNER	08A	CLEO $\Upsilon(3S) \rightarrow \gamma 2\pi^+2\pi^-2\pi^0$
				¹⁵ ASNER 08A reports $[\Gamma(\chi_{b2}(2P) \rightarrow 2\pi^+2\pi^-2\pi^0)/\Gamma_{total}] \times [B(\Upsilon(3S) \rightarrow \gamma\chi_{b2}(2P))]$ = (51 ± 16 ± 13) × 10 ⁻⁶ which we divide by our best value B($\Upsilon(3S) \rightarrow \gamma\chi_{b2}(2P)$) = (13.1 ± 1.6) × 10 ⁻² . Our first error is their experiment's error and our second error is the systematic error from using our best value.

$\Gamma(2\pi^+2\pi^-K^+K^-)/\Gamma_{total}$				Γ_{10}/Γ
VALUE (units 10 ⁻⁴)	EVTS	DOCUMENT ID	TECN	COMMENT
0.9 ± 0.4 ± 0.1	11	¹⁶ ASNER	08A	CLEO $\Upsilon(3S) \rightarrow \gamma 2\pi^+2\pi^-K^+K^-$
				¹⁶ ASNER 08A reports $[\Gamma(\chi_{b2}(2P) \rightarrow 2\pi^+2\pi^-K^+K^-)/\Gamma_{total}] \times [B(\Upsilon(3S) \rightarrow \gamma\chi_{b2}(2P))]$ = (12 ± 4 ± 3) × 10 ⁻⁶ which we divide by our best value B($\Upsilon(3S) \rightarrow \gamma\chi_{b2}(2P)$) = (13.1 ± 1.6) × 10 ⁻² . Our first error is their experiment's error and our second error is the systematic error from using our best value.

Meson Particle Listings

 $\chi_{b2}(2P), \Upsilon(3S)$ $\Gamma(2\pi^+2\pi^-K^+K^-\pi^0)/\Gamma_{\text{total}}$ Γ_{11}/Γ

VALUE (units 10^{-4})	EVTS	DOCUMENT ID	TECN	COMMENT
$2.4 \pm 1.0 \pm 0.3$	16	17 ASNER	08A CLEO	$\Upsilon(3S) \rightarrow \gamma 2\pi^+ 2\pi^- K^+ K^-\pi^0$
17 ASNER 08A reports $[\Gamma(\chi_{b2}(2P) \rightarrow 2\pi^+ 2\pi^- K^+ K^-\pi^0)/\Gamma_{\text{total}}] \times [B(\Upsilon(3S) \rightarrow \gamma \chi_{b2}(2P))]$ = $(32 \pm 11 \pm 8) \times 10^{-6}$ which we divide by our best value $B(\Upsilon(3S) \rightarrow \gamma \chi_{b2}(2P))$ = $(13.1 \pm 1.6) \times 10^{-2}$. Our first error is their experiment's error and our second error is the systematic error from using our best value.				

 $\Gamma(2\pi^+2\pi^-K^+K^-\pi^0)/\Gamma_{\text{total}}$ Γ_{12}/Γ

VALUE (units 10^{-4})	EVTS	DOCUMENT ID	TECN	COMMENT
$4.7 \pm 2.2 \pm 0.6$	14	18 ASNER	08A CLEO	$\Upsilon(3S) \rightarrow \gamma 2\pi^+ 2\pi^- K^+ K^-\pi^0$
18 ASNER 08A reports $[\Gamma(\chi_{b2}(2P) \rightarrow 2\pi^+ 2\pi^- K^+ K^-\pi^0)/\Gamma_{\text{total}}] \times [B(\Upsilon(3S) \rightarrow \gamma \chi_{b2}(2P))]$ = $(62 \pm 23 \pm 17) \times 10^{-6}$ which we divide by our best value $B(\Upsilon(3S) \rightarrow \gamma \chi_{b2}(2P))$ = $(13.1 \pm 1.6) \times 10^{-2}$. Our first error is their experiment's error and our second error is the systematic error from using our best value.				

 $\Gamma(3\pi^+2\pi^-K^0K_S^0\pi^0)/\Gamma_{\text{total}}$ Γ_{13}/Γ

VALUE (units 10^{-4})	CL%	DOCUMENT ID	TECN	COMMENT
<4	90	19 ASNER	08A CLEO	$\Upsilon(3S) \rightarrow \gamma 3\pi^+ 2\pi^- K^0 K_S^0 \pi^0$
19 ASNER 08A reports $[\Gamma(\chi_{b2}(2P) \rightarrow 3\pi^+ 2\pi^- K^0 K_S^0 \pi^0)/\Gamma_{\text{total}}] \times [B(\Upsilon(3S) \rightarrow \gamma \chi_{b2}(2P))]$ < 58×10^{-6} which we divide by our best value $B(\Upsilon(3S) \rightarrow \gamma \chi_{b2}(2P))$ = 13.1×10^{-2} .				

 $\Gamma(3\pi^+3\pi^-)/\Gamma_{\text{total}}$ Γ_{14}/Γ

VALUE (units 10^{-4})	EVTS	DOCUMENT ID	TECN	COMMENT
$0.9 \pm 0.4 \pm 0.1$	14	20 ASNER	08A CLEO	$\Upsilon(3S) \rightarrow \gamma 3\pi^+ 3\pi^-$
20 ASNER 08A reports $[\Gamma(\chi_{b2}(2P) \rightarrow 3\pi^+ 3\pi^-)/\Gamma_{\text{total}}] \times [B(\Upsilon(3S) \rightarrow \gamma \chi_{b2}(2P))]$ = $(12 \pm 4 \pm 3) \times 10^{-6}$ which we divide by our best value $B(\Upsilon(3S) \rightarrow \gamma \chi_{b2}(2P))$ = $(13.1 \pm 1.6) \times 10^{-2}$. Our first error is their experiment's error and our second error is the systematic error from using our best value.				

 $\Gamma(3\pi^+3\pi^-2\pi^0)/\Gamma_{\text{total}}$ Γ_{15}/Γ

VALUE (units 10^{-4})	EVTS	DOCUMENT ID	TECN	COMMENT
$12 \pm 4 \pm 1$	45	21 ASNER	08A CLEO	$\Upsilon(3S) \rightarrow \gamma 3\pi^+ 3\pi^- 2\pi^0$
21 ASNER 08A reports $[\Gamma(\chi_{b2}(2P) \rightarrow 3\pi^+ 3\pi^- 2\pi^0)/\Gamma_{\text{total}}] \times [B(\Upsilon(3S) \rightarrow \gamma \chi_{b2}(2P))]$ = $(159 \pm 33 \pm 43) \times 10^{-6}$ which we divide by our best value $B(\Upsilon(3S) \rightarrow \gamma \chi_{b2}(2P))$ = $(13.1 \pm 1.6) \times 10^{-2}$. Our first error is their experiment's error and our second error is the systematic error from using our best value.				

 $\Gamma(3\pi^+3\pi^-K^+K^-)/\Gamma_{\text{total}}$ Γ_{16}/Γ

VALUE (units 10^{-4})	EVTS	DOCUMENT ID	TECN	COMMENT
$1.4 \pm 0.7 \pm 0.2$	12	22 ASNER	08A CLEO	$\Upsilon(3S) \rightarrow \gamma 3\pi^+ 3\pi^- K^+ K^-$
22 ASNER 08A reports $[\Gamma(\chi_{b2}(2P) \rightarrow 3\pi^+ 3\pi^- K^+ K^-)/\Gamma_{\text{total}}] \times [B(\Upsilon(3S) \rightarrow \gamma \chi_{b2}(2P))]$ = $(19 \pm 7 \pm 5) \times 10^{-6}$ which we divide by our best value $B(\Upsilon(3S) \rightarrow \gamma \chi_{b2}(2P))$ = $(13.1 \pm 1.6) \times 10^{-2}$. Our first error is their experiment's error and our second error is the systematic error from using our best value.				

 $\Gamma(3\pi^+3\pi^-K^+K^-\pi^0)/\Gamma_{\text{total}}$ Γ_{17}/Γ

VALUE (units 10^{-4})	EVTS	DOCUMENT ID	TECN	COMMENT
$4.2 \pm 1.7 \pm 0.5$	16	23 ASNER	08A CLEO	$\Upsilon(3S) \rightarrow \gamma 3\pi^+ 3\pi^- K^+ K^-\pi^0$
23 ASNER 08A reports $[\Gamma(\chi_{b2}(2P) \rightarrow 3\pi^+ 3\pi^- K^+ K^-\pi^0)/\Gamma_{\text{total}}] \times [B(\Upsilon(3S) \rightarrow \gamma \chi_{b2}(2P))]$ = $(55 \pm 16 \pm 15) \times 10^{-6}$ which we divide by our best value $B(\Upsilon(3S) \rightarrow \gamma \chi_{b2}(2P))$ = $(13.1 \pm 1.6) \times 10^{-2}$. Our first error is their experiment's error and our second error is the systematic error from using our best value.				

 $\Gamma(4\pi^+4\pi^-)/\Gamma_{\text{total}}$ Γ_{18}/Γ

VALUE (units 10^{-4})	EVTS	DOCUMENT ID	TECN	COMMENT
$0.9 \pm 0.4 \pm 0.1$	9	24 ASNER	08A CLEO	$\Upsilon(3S) \rightarrow \gamma 4\pi^+ 4\pi^-$
24 ASNER 08A reports $[\Gamma(\chi_{b2}(2P) \rightarrow 4\pi^+ 4\pi^-)/\Gamma_{\text{total}}] \times [B(\Upsilon(3S) \rightarrow \gamma \chi_{b2}(2P))]$ = $(12 \pm 5 \pm 3) \times 10^{-6}$ which we divide by our best value $B(\Upsilon(3S) \rightarrow \gamma \chi_{b2}(2P))$ = $(13.1 \pm 1.6) \times 10^{-2}$. Our first error is their experiment's error and our second error is the systematic error from using our best value.				

 $\Gamma(4\pi^+4\pi^-2\pi^0)/\Gamma_{\text{total}}$ Γ_{19}/Γ

VALUE (units 10^{-4})	EVTS	DOCUMENT ID	TECN	COMMENT
$13 \pm 5 \pm 2$	27	25 ASNER	08A CLEO	$\Upsilon(3S) \rightarrow \gamma 4\pi^+ 4\pi^- 2\pi^0$
25 ASNER 08A reports $[\Gamma(\chi_{b2}(2P) \rightarrow 4\pi^+ 4\pi^- 2\pi^0)/\Gamma_{\text{total}}] \times [B(\Upsilon(3S) \rightarrow \gamma \chi_{b2}(2P))]$ = $(165 \pm 46 \pm 50) \times 10^{-6}$ which we divide by our best value $B(\Upsilon(3S) \rightarrow \gamma \chi_{b2}(2P))$ = $(13.1 \pm 1.6) \times 10^{-2}$. Our first error is their experiment's error and our second error is the systematic error from using our best value.				

 $\chi_{b2}(2P)$ REFERENCES

ASNER	08A	PR D78 091103	D.M. Asner <i>et al.</i>	(CLEO Collab.)
BRIERE	08	PR D78 092007	R.A. Briere <i>et al.</i>	(CLEO Collab.)
CRAWFIELD	06	PR D73 012003	C. Crawford <i>et al.</i>	(CLEO Collab.)
ARTUSO	05	PRL 94 032001	M. Artuso <i>et al.</i>	(CLEO Collab.)
CRONIN-HENNESSY	04	PRL 92 222002	D. Cronin-Hennessy <i>et al.</i>	(CLEO3 Collab.)
CRAWFORD	92B	PL B294 139	G. Crawford, R. Fulton	(CLEO Collab.)
HEINTZ	92	PR D46 1928	U. Heintz <i>et al.</i>	(CUSB II Collab.)
HEINTZ	91	PRL 66 1563	U. Heintz <i>et al.</i>	(CUSB Collab.)
MORRISON	91	PRL 67 1696	R.J. Morrison <i>et al.</i>	(CLEO Collab.)
NARAIN	91	PRL 66 3113	M. Narain <i>et al.</i>	(CUSB Collab.)

 $\Upsilon(3S)$

$$J^{PC} = 0^-(1^--)$$

 $\Upsilon(3S)$ MASS

VALUE (GeV)	DOCUMENT ID	TECN	COMMENT
10.3552 ± 0.0005	1 ARTAMONOV 00	MD1	$e^+e^- \rightarrow$ hadrons
••• We do not use the following data for averages, fits, limits, etc. •••			
10.3553 ± 0.0005	2,3 BARU	86B REDE	$e^+e^- \rightarrow$ hadrons
1 Reanalysis of BARU 86B using new electron mass (COHEN 87).			
2 Reanalysis of ARTAMONOV 84.			
3 Superseded by ARTAMONOV 00.			

 $\Upsilon(3S)$ WIDTH

VALUE (keV)	DOCUMENT ID
20.32 ± 1.85 OUR EVALUATION	See the Note on "Width Determinations of the Υ States"

 $\Upsilon(3S)$ DECAY MODES

Mode	Fraction (Γ_i/Γ)	Scale factor/ Confidence level
Γ_1 $\Upsilon(2S)$ anything	(10.6 ± 0.8) %	
Γ_2 $\Upsilon(2S)\pi^+\pi^-$	(2.45 ± 0.23) %	S=1.1
Γ_3 $\Upsilon(2S)\pi^0\pi^0$	(1.85 ± 0.14) %	
Γ_4 $\Upsilon(2S)\gamma\gamma$	(5.0 ± 0.7) %	
Γ_5 $\Upsilon(2S)\pi^0$	< 5.1	CL=90%
Γ_6 $\Upsilon(1S)\pi^+\pi^-$	(4.40 ± 0.10) %	
Γ_7 $\Upsilon(1S)\pi^0\pi^0$	(2.20 ± 0.13) %	
Γ_8 $\Upsilon(1S)\eta$	< 1.8	CL=90%
Γ_9 $\Upsilon(1S)\pi^0$	< 7	CL=90%
Γ_{10} $\tau^+\tau^-$	(2.29 ± 0.30) %	
Γ_{11} $\mu^+\mu^-$	(2.18 ± 0.21) %	S=2.1
Γ_{12} e^+e^-	seen	
Γ_{13} ggg	(35.7 ± 2.6) %	
Γ_{14} γgg	$(9.7 \pm 1.8) \times 10^{-3}$	

Radiative decays

Γ_{15} hadrons		
Γ_{16} $\gamma \chi_{b2}(2P)$	(13.1 ± 1.6) %	S=3.4
Γ_{17} $\gamma \chi_{b1}(2P)$	(12.6 ± 1.2) %	S=2.4
Γ_{18} $\gamma \chi_{b0}(2P)$	(5.9 ± 0.6) %	S=1.4
Γ_{19} $\gamma \chi_{b2}(1P)$	< 1.9	CL=90%
Γ_{20} $\gamma \chi_{b1}(1P)$	< 1.7	CL=90%
Γ_{21} $\gamma \chi_{b0}(1P)$	$(3.0 \pm 1.1) \times 10^{-3}$	
Γ_{22} $\gamma \eta_b(2S)$	< 6.2	CL=90%
Γ_{23} $\gamma \eta_b(1S)$	$(5.1 \pm 0.7) \times 10^{-4}$	
Γ_{24} $\gamma X \rightarrow \gamma + \geq 4$ prongs	[a] < 2.2	CL=95%
Γ_{25} $\gamma a_1^0 \rightarrow \gamma \tau^+ \tau^-$	[b] < 1.6	CL=90%

Lepton Flavor (LF) violating decays

Γ_{26} $\mu^\pm \tau^\mp$	LF	< 2.03	$\times 10^{-5}$	CL=95%
----------------------------------	----	--------	------------------	--------

[a] 1.5 GeV < m_X < 5.0 GeV[b] For $m_{\tau^+\tau^-}$ in the ranges 4.03–9.52 and 9.61–10.10 GeV. $\Upsilon(3S)$ $\Gamma(i)\Gamma(e^+e^-)/\Gamma(\text{total})$

VALUE (keV)	DOCUMENT ID	TECN	COMMENT	$\Gamma_{15}\Gamma_{12}/\Gamma$
0.414 ± 0.007 OUR AVERAGE				
$0.413 \pm 0.004 \pm 0.006$	ROSNER 06	CLEO	$10.4 e^+e^- \rightarrow$ hadrons	
$0.45 \pm 0.03 \pm 0.03$	4 GILES 84B	CLEO	$e^+e^- \rightarrow$ hadrons	

4 Radiative corrections reevaluated by BUCHMUELLER 88 following KURAEV 85.

$\Gamma(\Upsilon(1S)\pi^+\pi^-) \times \Gamma(e^+e^-)/\Gamma_{\text{total}}$		Γ_{612}/Γ	
VALUE (eV)	EVTS	DOCUMENT ID	TECN COMMENT
18.46 ± 0.27 ± 0.77	6.4K	5 AUBERT	08BP BABR $e^+e^- \rightarrow \gamma\pi^+\pi^-\ell^+\ell^-$

⁵ Using $B(\Upsilon(1S) \rightarrow e^+e^-) = (2.38 \pm 0.11)\%$ and $B(\Upsilon(1S) \rightarrow \mu^+\mu^-) = (2.48 \pm 0.05)\%$.

 $\Upsilon(3S)$ PARTIAL WIDTHS

$\Gamma(e^+e^-)$		Γ_{12}
VALUE (keV)	DOCUMENT ID	
0.443 ± 0.008 OUR EVALUATION		

 $\Upsilon(3S)$ BRANCHING RATIOS

$\Gamma(\Upsilon(2S)\text{anything})/\Gamma_{\text{total}}$		Γ_1/Γ
VALUE	EVTS	DOCUMENT ID
0.106 ± 0.008 OUR AVERAGE		
0.1023 ± 0.0105	4625	6,7,8 BUTLER
0.111 ± 0.012	4891	7,8,9 BROCK

⁶ Using $B(\Upsilon(2S) \rightarrow \Upsilon(1S)\gamma\gamma) = (0.038 \pm 0.007)\%$, and $B(\Upsilon(2S) \rightarrow \Upsilon(1S)\pi^0\pi^0) = (1/2)B(\Upsilon(2S) \rightarrow \Upsilon(1S)\pi^+\pi^-)$.

⁷ Using $B(\Upsilon(1S) \rightarrow \mu^+\mu^-) = (2.48 \pm 0.06)\%$. With the assumption of $e\mu$ universality.

⁸ Using $B(\Upsilon(2S) \rightarrow \Upsilon(1S)\pi^+\pi^-) = (18.5 \pm 0.8)\%$.

⁹ Using $B(\Upsilon(2S) \rightarrow \mu^+\mu^-) = (1.31 \pm 0.21)\%$, $B(\Upsilon(2S) \rightarrow \Upsilon(1S)\gamma\gamma) \times 2B(\Upsilon(1S) \rightarrow \mu^+\mu^-) = (0.188 \pm 0.035)\%$, and $B(\Upsilon(2S) \rightarrow \Upsilon(1S)\pi^0\pi^0) \times 2B(\Upsilon(1S) \rightarrow \mu^+\mu^-) = (0.436 \pm 0.056)\%$. With the assumption of $e\mu$ universality.

$\Gamma(\Upsilon(2S)\pi^+\pi^-)/\Gamma_{\text{total}}$		Γ_{21}/Γ
VALUE (units 10^{-2})	EVTS	DOCUMENT ID
2.45 ± 0.23 OUR AVERAGE		
2.40 ± 0.10 ± 0.26	800	10 AUBERT
3.12 ± 0.49	980	11,12 BUTLER
2.13 ± 0.38	974	13 BROCK

Error includes scale factor of 1.1.

$e^+e^- \rightarrow \gamma\pi^+\pi^-\ell^+\ell^-$

$e^+e^- \rightarrow \pi^+\pi^-\ell^+\ell^-$

$e^+e^- \rightarrow \pi^+\pi^-\ell^+\ell^- X$

- • • We do not use the following data for averages, fits, limits, etc. • • •

4.82 ± 0.65 ± 0.53 138 13 WU 93 CUSB $\Upsilon(3S) \rightarrow \pi^+\pi^-\ell^+\ell^-$

3.1 ± 2.0 5 5 MAGERAS 82 CUSB $\Upsilon(3S) \rightarrow \pi^+\pi^-\ell^+\ell^-$

¹⁰ Using $B(\Upsilon(1S) \rightarrow e^+e^-) = (2.38 \pm 0.11)\%$, $B(\Upsilon(1S) \rightarrow \mu^+\mu^-) = (2.48 \pm 0.05)\%$, and $\Gamma_{ee}(\Upsilon(3S)) = 0.443 \pm 0.008$ keV.

¹¹ From the exclusive mode.

¹² Using $B(\Upsilon(2S) \rightarrow \Upsilon(1S)\gamma\gamma) = (0.038 \pm 0.007)\%$, and $B(\Upsilon(2S) \rightarrow \Upsilon(1S)\pi^0\pi^0) = (1/2)B(\Upsilon(2S) \rightarrow \Upsilon(1S)\pi^+\pi^-)$.

¹³ Using $B(\Upsilon(2S) \rightarrow \mu^+\mu^-) = (1.31 \pm 0.21)\%$, $B(\Upsilon(2S) \rightarrow \Upsilon(1S)\gamma\gamma) \times 2B(\Upsilon(1S) \rightarrow \mu^+\mu^-) = (0.188 \pm 0.035)\%$, and $B(\Upsilon(2S) \rightarrow \Upsilon(1S)\pi^0\pi^0) \times 2B(\Upsilon(1S) \rightarrow \mu^+\mu^-) = (0.436 \pm 0.056)\%$. With the assumption of $e\mu$ universality.

$\Gamma(\Upsilon(2S)\pi^0\pi^0)/\Gamma_{\text{total}}$		Γ_{31}/Γ
VALUE (units 10^{-2})	EVTS	DOCUMENT ID
1.85 ± 0.14 OUR AVERAGE		
1.82 ± 0.09 ± 0.12	4391	14 BHARI
2.16 ± 0.39	15,16	BUTLER
1.7 ± 0.5 ± 0.2	10	17 HEINTZ

$e^+e^- \rightarrow \pi^0\pi^0\ell^+\ell^-$

$e^+e^- \rightarrow \pi^0\pi^0\ell^+\ell^-$

$e^+e^- \rightarrow \pi^0\pi^0\ell^+\ell^-$

¹⁴ Authors assume $B(\Upsilon(1S) \rightarrow e^+e^-) + B(\Upsilon(1S) \rightarrow \mu^+\mu^-) = 4.06\%$.

¹⁵ $B(\Upsilon(2S) \rightarrow \mu^+\mu^-) = (1.31 \pm 0.21)\%$ and assuming $e\mu$ universality.

¹⁶ From the exclusive mode.

¹⁷ $B(\Upsilon(2S) \rightarrow \mu^+\mu^-) = (1.44 \pm 0.10)\%$ and assuming $e\mu$ universality. Supersedes HEINTZ 91.

$\Gamma(\Upsilon(2S)\gamma\gamma)/\Gamma_{\text{total}}$		Γ_{41}/Γ
VALUE	DOCUMENT ID	TECN COMMENT
0.0502 ± 0.0069	18 BUTLER	94B CLE2 $e^+e^- \rightarrow \ell^+\ell^-\gamma\gamma$

¹⁸ From the exclusive mode.

$\Gamma(\Upsilon(2S)\pi^0)/\Gamma_{\text{total}}$		Γ_{51}/Γ
VALUE (units 10^{-3})	CL%	DOCUMENT ID
<0.51	90	19 HE 08A CLEO $e^+e^- \rightarrow \ell^+\ell^-\gamma\gamma$

¹⁹ Authors assume $B(\Upsilon(2S) \rightarrow e^+e^-) + B(\Upsilon(1S) \rightarrow \mu^+\mu^-) = 4.06\%$.

$\Gamma(\Upsilon(1S)\pi^+\pi^-)/\Gamma_{\text{total}}$		Γ_{61}/Γ
VALUE (units 10^{-2})	EVTS	DOCUMENT ID
4.40 ± 0.10 OUR AVERAGE		
4.46 ± 0.01 ± 0.13	190k	20 BHARI
4.17 ± 0.06 ± 0.19	6.4K	21 AUBERT
4.52 ± 0.35	11830	22 BUTLER
4.46 ± 0.34 ± 0.50	451	22 WU
4.46 ± 0.30	11221	22 BROCK

Abbreviation MM in the COMMENT field below stands for missing mass.

$e^+e^- \rightarrow \pi^+\pi^- MM$

10.58 $e^+e^- \rightarrow \gamma\pi^+\pi^-\ell^+\ell^-$

$e^+e^- \rightarrow \pi^+\pi^-\ell^+\ell^-$

$e^+e^- \rightarrow \pi^+\pi^-\ell^+\ell^- X$

$\pi^+\pi^-\ell^+\ell^-$

$\Upsilon(3S) \rightarrow \pi^+\pi^-\ell^+\ell^-$

$e^+e^- \rightarrow \pi^+\pi^-\ell^+\ell^- X$

$\pi^+\pi^-\ell^+\ell^-$

- • • We do not use the following data for averages, fits, limits, etc. • • •

4.9 ± 1.0 22 GREEN 82 CLEO $\Upsilon(3S) \rightarrow \pi^+\pi^-\ell^+\ell^-$

3.9 ± 1.3 26 MAGERAS 82 CUSB $\Upsilon(3S) \rightarrow \pi^+\pi^-\ell^+\ell^-$

²⁰ A weighted average of the inclusive and exclusive results.

²¹ Using $B(\Upsilon(2S) \rightarrow e^+e^-) = (1.91 \pm 0.16)\%$, $B(\Upsilon(2S) \rightarrow \mu^+\mu^-) = (1.93 \pm 0.17)\%$, and $\Gamma_{ee}(\Upsilon(3S)) = 0.443 \pm 0.008$ keV.

²² Using $B(\Upsilon(1S) \rightarrow \mu^+\mu^-) = (2.48 \pm 0.06)\%$. With the assumption of $e\mu$ universality.

$\Gamma(\Upsilon(2S)\pi^+\pi^-)/\Gamma(\Upsilon(1S)\pi^+\pi^-)$		Γ_{21}/Γ_6
VALUE	EVTS	DOCUMENT ID
• • • We do not use the following data for averages, fits, limits, etc. • • •		
0.577 ± 0.026 ± 0.060	800	23 AUBERT

$e^+e^- \rightarrow \gamma\pi^+\pi^-\ell^+\ell^-$

²³ Using $B(\Upsilon(1S) \rightarrow e^+e^-) = (2.38 \pm 0.11)\%$, $B(\Upsilon(1S) \rightarrow \mu^+\mu^-) = (2.48 \pm 0.05)\%$, $B(\Upsilon(2S) \rightarrow e^+e^-) = (1.91 \pm 0.16)\%$, and $B(\Upsilon(2S) \rightarrow \mu^+\mu^-) = (1.93 \pm 0.17)\%$. Not independent of other values reported by AUBERT 08BP.

$\Gamma(\Upsilon(1S)\pi^0\pi^0)/\Gamma_{\text{total}}$		Γ_{71}/Γ
VALUE (units 10^{-2})	EVTS	DOCUMENT ID
2.20 ± 0.13 OUR AVERAGE		
2.24 ± 0.09 ± 0.11	6584	24 BHARI
1.99 ± 0.34	56	25 BUTLER
2.2 ± 0.4 ± 0.3	33	26 HEINTZ

$e^+e^- \rightarrow \pi^0\pi^0\ell^+\ell^-$

$e^+e^- \rightarrow \pi^0\pi^0\ell^+\ell^-$

$e^+e^- \rightarrow \pi^0\pi^0\ell^+\ell^-$

²⁴ Authors assume $B(\Upsilon(1S) \rightarrow e^+e^-) + B(\Upsilon(1S) \rightarrow \mu^+\mu^-) = 4.96\%$.

²⁵ Using $B(\Upsilon(1S) \rightarrow \mu^+\mu^-) = (2.48 \pm 0.06)\%$ and assuming $e\mu$ universality.

²⁶ Using $B(\Upsilon(1S) \rightarrow \mu^+\mu^-) = (2.57 \pm 0.07)\%$ and assuming $e\mu$ universality. Supersedes HEINTZ 91.

$\Gamma(\Upsilon(1S)\pi^0\pi^0)/\Gamma(\Upsilon(1S)\pi^+\pi^-)$		Γ_{71}/Γ_6
VALUE	DOCUMENT ID	TECN COMMENT
• • • We do not use the following data for averages, fits, limits, etc. • • •		
0.501 ± 0.043	27 BHARI	09 CLEO $e^+e^- \rightarrow \Upsilon(3S)$

²⁷ Not independent of other values reported by BHARI 09.

$\Gamma(\Upsilon(1S)\eta)/\Gamma_{\text{total}}$		Γ_{81}/Γ
VALUE (units 10^{-3})	CL%	DOCUMENT ID
<0.18	90	28 HE 08A CLEO $e^+e^- \rightarrow \ell^+\ell^-\eta$
• • • We do not use the following data for averages, fits, limits, etc. • • •		
<0.8	90	29 AUBERT
<2.2	90	BROCK

$e^+e^- \rightarrow \gamma\pi^+\pi^-\pi^0\ell^+\ell^-$

$e^+e^- \rightarrow \ell^+\ell^-\eta$

²⁸ Authors assume $B(\Upsilon(1S) \rightarrow e^+e^-) + B(\Upsilon(1S) \rightarrow \mu^+\mu^-) = 4.96\%$.

²⁹ Using $B(\Upsilon(1S) \rightarrow e^+e^-) = (2.38 \pm 0.11)\%$, $B(\Upsilon(1S) \rightarrow \mu^+\mu^-) = (2.48 \pm 0.05)\%$, and $\Gamma_{ee}(\Upsilon(3S)) = 0.443 \pm 0.008$ keV.

$\Gamma(\Upsilon(1S)\eta)/\Gamma(\Upsilon(1S)\pi^+\pi^-)$		Γ_{81}/Γ_6
VALUE (units 10^{-2})	CL%	DOCUMENT ID
• • • We do not use the following data for averages, fits, limits, etc. • • •		
<1.9	90	30 AUBERT

Not independent of other values reported by AUBERT 08BP.

$\Gamma(\Upsilon(1S)\pi^0)/\Gamma_{\text{total}}$		Γ_{91}/Γ
VALUE (units 10^{-3})	CL%	DOCUMENT ID
<0.07	90	31 HE 08A CLEO $e^+e^- \rightarrow \ell^+\ell^-\gamma\gamma$

³¹ Authors assume $B(\Upsilon(1S) \rightarrow e^+e^-) + B(\Upsilon(1S) \rightarrow \mu^+\mu^-) = 4.96\%$.

$\Gamma(\tau^+\tau^-)/\Gamma_{\text{total}}$		Γ_{10}/Γ
VALUE (units 10^{-2})	EVTS	DOCUMENT ID
2.29 ± 0.21 ± 0.22	15k	32 BESSON

07 CLEO $e^+e^- \rightarrow \Upsilon(3S) \rightarrow \tau^+\tau^-$

³² BESSON 07 reports $[\Gamma(\Upsilon(3S) \rightarrow \tau^+\tau^-)/\Gamma_{\text{total}}] / [B(\Upsilon(3S) \rightarrow \mu^+\mu^-)] = 1.05 \pm 0.08 \pm 0.05$ which we multiply by our best value $B(\Upsilon(3S) \rightarrow \mu^+\mu^-) = (2.18 \pm 0.21) \times 10^{-2}$. Our first error is their experiment's error and our second error is the systematic error from using our best value.

$\Gamma(\tau^+\tau^-)/\Gamma(\mu^+\mu^-)$		Γ_{10}/Γ_{11}
VALUE	EVTS	DOCUMENT ID
1.05 ± 0.08 ± 0.05	15k	BESSON

07 CLEO $e^+e^- \rightarrow \Upsilon(3S)$

$\Gamma(\mu^+\mu^-)/\Gamma_{\text{total}}$		Γ_{11}/Γ
VALUE	EVTS	DOCUMENT ID
0.0218 ± 0.0021 OUR AVERAGE		
0.0239 ± 0.0007 ± 0.0010	81k	ADAMS
0.0202 ± 0.0019 ± 0.0033		CHEN
0.0173 ± 0.0015 ± 0.0011		KAARSBERG
0.033 ± 0.013 ± 0.007	1096	ANDREWS

05 CLEO $e^+e^- \rightarrow \mu^+\mu^-$

89B CLEO $e^+e^- \rightarrow \mu^+\mu^-$

89 CLEO $e^+e^- \rightarrow \mu^+\mu^-$

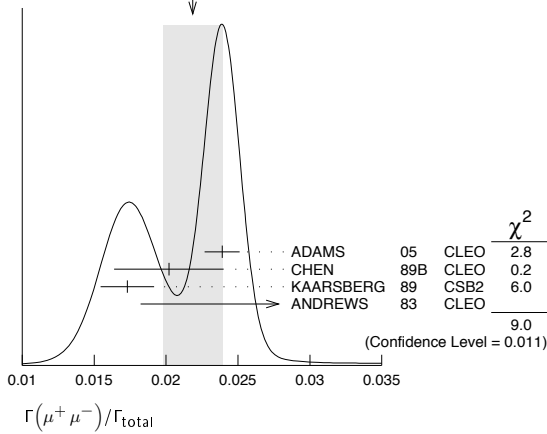
83 CLEO $e^+e^- \rightarrow \mu^+\mu^-$

Error includes scale factor of 2.1. See the ideogram below.

Meson Particle Listings

$\Upsilon(3S)$

WEIGHTED AVERAGE
0.0218±0.0021 (Error scaled by 2.1)



$\Gamma(gg)/\Gamma_{total}$ Γ_{13}/Γ

VALUE (units 10^{-2})	EVTS	DOCUMENT ID	TECN	COMMENT
35.7±2.6	3M	³³ BESSON 06A	CLEO	$\Upsilon(3S) \rightarrow \text{hadrons}$

³³ Calculated using BESSON 06A value of $\Gamma(\gamma gg)/\Gamma(gg) = (2.72 \pm 0.06 \pm 0.32 \pm 0.37)\%$ and the PDG 08 values of $B(\Upsilon(2S) + \text{anything}) = (10.6 \pm 0.8)\%$, $B(\pi^+ \pi^- \Upsilon(1S)) = (4.40 \pm 0.10)\%$, $B(\pi^0 \pi^0 \Upsilon(1S)) = (2.20 \pm 0.13)\%$, $B(\gamma \chi_{b2}(2P)) = (13.1 \pm 1.6)\%$, $B(\gamma \chi_{b1}(2P)) = (12.6 \pm 1.2)\%$, $B(\gamma \chi_{b0}(2P)) = (5.9 \pm 0.6)\%$, $B(\gamma \chi_{b0}(1P)) = (0.30 \pm 0.11)\%$, $B(\mu^+ \mu^-) = (2.18 \pm 0.21)\%$, and $R_{\text{hadrons}} = 3.51$. The statistical error is negligible and the systematic error is partially correlated with $\Gamma(\gamma gg)/\Gamma_{total}$ BESSON 06A value.

$\Gamma(\gamma gg)/\Gamma_{total}$ Γ_{14}/Γ

VALUE (units 10^{-2})	EVTS	DOCUMENT ID	TECN	COMMENT
0.97±0.18	60k	³⁴ BESSON 06A	CLEO	$\Upsilon(3S) \rightarrow \gamma + \text{hadrons}$

³⁴ Calculated using BESSON 06A values of $\Gamma(\gamma gg)/\Gamma(gg) = (2.72 \pm 0.06 \pm 0.32 \pm 0.37)\%$ and $\Gamma(gg)/\Gamma_{total}$. The statistical error is negligible and the systematic error is partially correlated with $\Gamma(gg)/\Gamma_{total}$ BESSON 06A value.

$\Gamma(\gamma gg)/\Gamma(gg)$ Γ_{14}/Γ_{13}

VALUE (units 10^{-2})	EVTS	DOCUMENT ID	TECN	COMMENT
2.72±0.06±0.49	3M	BESSON 06A	CLEO	$\Upsilon(3S) \rightarrow (\gamma +) \text{hadrons}$

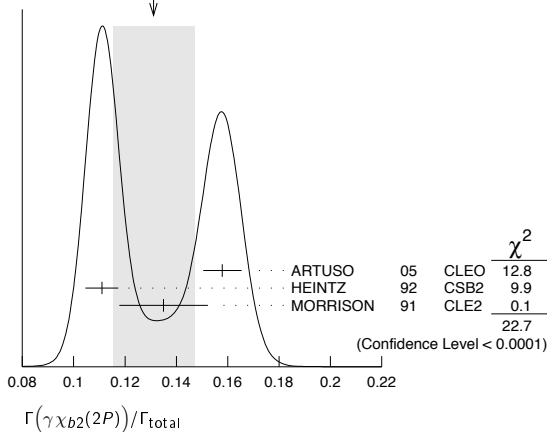
$\Gamma(\gamma \chi_{b2}(2P))/\Gamma_{total}$ Γ_{16}/Γ

VALUE	EVTS	DOCUMENT ID	TECN	COMMENT
0.131 ± 0.016 OUR AVERAGE				Error includes scale factor of 3.4. See the ideogram below.

0.1579±0.0017±0.0073	568k	ARTUSO	05 CLEO	$e^+ e^- \rightarrow \gamma X$
0.111 ± 0.005 ± 0.004	10319	³⁵ HEINTZ	92 CSB2	$e^+ e^- \rightarrow \gamma X$
0.135 ± 0.003 ± 0.017	30741	MORRISON	91 CLE2	$e^+ e^- \rightarrow \gamma X$

³⁵ Supersedes NARAIN 91.

WEIGHTED AVERAGE
0.131±0.016 (Error scaled by 3.4)



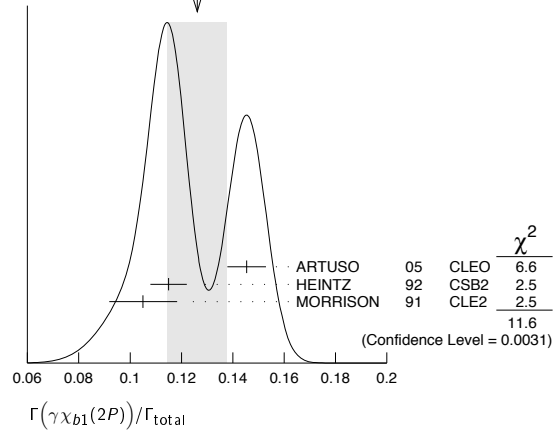
$\Gamma(\gamma \chi_{b1}(2P))/\Gamma_{total}$ Γ_{17}/Γ

VALUE	EVTS	DOCUMENT ID	TECN	COMMENT
0.126 ± 0.012 OUR AVERAGE				Error includes scale factor of 2.4. See the ideogram below.

0.1454±0.0018±0.0073	537k	ARTUSO	05 CLEO	$e^+ e^- \rightarrow \gamma X$
0.115 ± 0.005 ± 0.005	11147	³⁶ HEINTZ	92 CSB2	$e^+ e^- \rightarrow \gamma X$
0.105 +0.003 -0.002 ± 0.013	25759	MORRISON	91 CLE2	$e^+ e^- \rightarrow \gamma X$

³⁶ Supersedes NARAIN 91.

WEIGHTED AVERAGE
0.126±0.012 (Error scaled by 2.4)



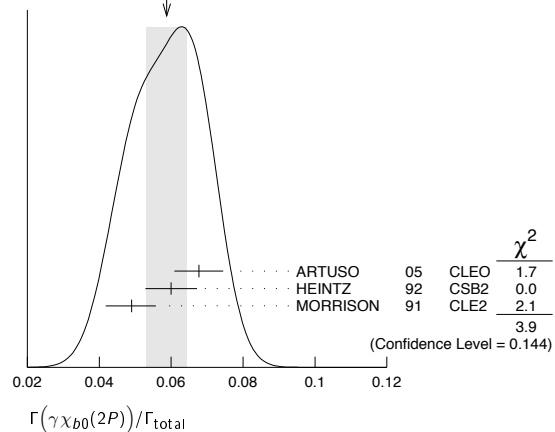
$\Gamma(\gamma \chi_{b0}(2P))/\Gamma_{total}$ Γ_{18}/Γ

VALUE	EVTS	DOCUMENT ID	TECN	COMMENT
0.059 ± 0.006 OUR AVERAGE				Error includes scale factor of 1.4. See the ideogram below.

0.0677±0.0020±0.0065	225k	ARTUSO	05 CLEO	$e^+ e^- \rightarrow \gamma X$
0.060 ± 0.004 ± 0.006	4959	³⁷ HEINTZ	92 CSB2	$e^+ e^- \rightarrow \gamma X$
0.049 +0.003 -0.004 ± 0.006	9903	MORRISON	91 CLE2	$e^+ e^- \rightarrow \gamma X$

³⁷ Supersedes NARAIN 91.

WEIGHTED AVERAGE
0.059±0.006 (Error scaled by 1.4)



$\Gamma(\gamma \chi_{b2}(1P))/\Gamma_{total}$ Γ_{19}/Γ

VALUE (units 10^{-4})	CL%	DOCUMENT ID	TECN	COMMENT
<190	90	³⁸ ASNER 08A	CLEO	$\Upsilon(3S) \rightarrow \gamma + \text{hadrons}$

³⁸ ASNER 08A reports $[\Gamma(\Upsilon(3S) \rightarrow \gamma \chi_{b2}(1P))/\Gamma_{total}] / [B(\Upsilon(2S) \rightarrow \gamma \chi_{b2}(1P))]$ < 27.1×10^{-2} which we multiply by our best value $B(\Upsilon(2S) \rightarrow \gamma \chi_{b2}(1P)) = 7.15 \times 10^{-2}$.

$\Gamma(\gamma \chi_{b1}(1P))/\Gamma_{total}$ Γ_{20}/Γ

VALUE (units 10^{-4})	CL%	DOCUMENT ID	TECN	COMMENT
<17	90	³⁹ ASNER 08A	CLEO	$\Upsilon(3S) \rightarrow \gamma + \text{hadrons}$

³⁹ ASNER 08A reports $[\Gamma(\Upsilon(3S) \rightarrow \gamma \chi_{b1}(1P))/\Gamma_{total}] / [B(\Upsilon(2S) \rightarrow \gamma \chi_{b1}(1P))]$ < 2.5×10^{-2} which we multiply by our best value $B(\Upsilon(2S) \rightarrow \gamma \chi_{b1}(1P)) = 6.9 \times 10^{-2}$.

See key on page 405

Meson Particle Listings

$\Upsilon(3S), \Upsilon(4S)$

$\Gamma(\gamma\chi_{b0}(1P))/\Gamma_{total}$ Γ_{21}/Γ

VALUE (units 10^{-2})	CL%	EVTS	DOCUMENT ID	TECN	COMMENT
0.30±0.04±0.10		8.7k	ARTUSO	05	CLEO $e^+e^- \rightarrow \gamma X$
••• We do not use the following data for averages, fits, limits, etc. •••					
<0.8	90	40	ASNER	08A	CLEO $\Upsilon(3S) \rightarrow \gamma + \text{hadrons}$
⁴⁰ ASNER 08A reports $[\Gamma(\Upsilon(3S) \rightarrow \gamma\chi_{b0}(1P))/\Gamma_{total}] / [B(\Upsilon(2S) \rightarrow \gamma\chi_{b0}(1P))]$ < 21.9×10^{-2} which we multiply by our best value $B(\Upsilon(2S) \rightarrow \gamma\chi_{b0}(1P)) = 3.8 \times 10^{-2}$.					

$\Gamma(\gamma\eta_b(2S))/\Gamma_{total}$ Γ_{22}/Γ

VALUE (units 10^{-4})	CL%	DOCUMENT ID	TECN	COMMENT
<6.2	90	ARTUSO	05	CLEO $e^+e^- \rightarrow \gamma X$

$\Gamma(\gamma\eta_b(1S))/\Gamma_{total}$ Γ_{23}/Γ

VALUE (units 10^{-4})	CL%	EVTS	DOCUMENT ID	TECN	COMMENT
5.1±0.7 OUR AVERAGE					
7.1±1.8±1.3	2.3±0.5k	41	BONVICINI	10	CLEO $\Upsilon(3S) \rightarrow \gamma X$
4.8±0.5±0.6	19±3k	41	AUBERT	09AQ	BABR $\Upsilon(3S) \rightarrow \gamma X$
••• We do not use the following data for averages, fits, limits, etc. •••					
4.8±0.5±1.2	19±3k	41,42	AUBERT	08V	BABR $\Upsilon(3S) \rightarrow \gamma X$
<4.3	90	43	ARTUSO	05	CLEO $e^+e^- \rightarrow \gamma X$
⁴¹ Assuming $\Gamma_{\eta_b(1S)} = 10$ MeV.					
⁴² Systematic error re-evaluated by AUBERT 09AQ.					
⁴³ Superseded by BONVICINI 10.					

$\Gamma(\gamma X \rightarrow \gamma + \geq 4 \text{ prongs})/\Gamma_{total}$ Γ_{24}/Γ

(1.5 GeV < m_X < 5.0 GeV)

VALUE (units 10^{-4})	CL%	DOCUMENT ID	TECN	COMMENT
<2.2	95	ROSNER	07A	CLEO $e^+e^- \rightarrow \gamma X$

$\Gamma(\gamma a_1^0 \rightarrow \gamma\tau^+\tau^-)/\Gamma_{total}$ Γ_{25}/Γ

VALUE	CL%	DOCUMENT ID	TECN	COMMENT	
<1.6 × 10⁻⁴	90	44	AUBERT	09P	BABR $e^+e^- \rightarrow \gamma a_1^0 \rightarrow \gamma\tau^+\tau^-$
⁴⁴ For a narrow scalar or pseudoscalar a_1^0 with $M(\tau^+\tau^-)$ in the ranges 4.03–9.52 and 9.61–10.10 GeV. Measured 90% CL limits as a function of $M(\tau^+\tau^-)$ range from 1.5–16 × 10 ⁻⁵ .					

$\Gamma(\mu^\pm\tau^\mp)/\Gamma_{total}$ Γ_{26}/Γ

VALUE (units 10^{-6})	CL%	DOCUMENT ID	TECN	COMMENT
<20.3	95	LOVE	08A	CLEO $e^+e^- \rightarrow \mu^\pm\tau^\mp$

$\Upsilon(3S)$ REFERENCES

BONVICINI 10	PR D81 031104R	G. Bonvicini <i>et al.</i>	(CLEO Collab.)
AUBERT 09AQ	PRL 103 161801	B. Aubert <i>et al.</i>	(BABAR Collab.)
AUBERT 09P	PRL 103 181801	B. Aubert <i>et al.</i>	(BABAR Collab.)
BHARI 09	PR D79 011103	S.R. Bhari <i>et al.</i>	(CLEO Collab.)
ASNER 08A	PR D78 091103	D.M. Asner <i>et al.</i>	(CLEO Collab.)
AUBERT 08BP	PR D78 112002	B. Aubert <i>et al.</i>	(BABAR Collab.)
AUBERT 08V	PRL 101 071801	B. Aubert <i>et al.</i>	(BABAR Collab.)
HE 08A	PRL 101 192001	Q. He <i>et al.</i>	(CLEO Collab.)
LOVE 08A	PRL 101 201601	W. Love <i>et al.</i>	(CLEO Collab.)
PDG 08	PL B667 1	C. Amsler <i>et al.</i>	(PDG Collab.)
BESSION 07	PRL 98 052002	D. Besson <i>et al.</i>	(CLEO Collab.)
ROSNER 07A	PR D76 117102	J.L. Rosner <i>et al.</i>	(CLEO Collab.)
BESSION 06A	PR D74 012003	D. Besson <i>et al.</i>	(CLEO Collab.)
ROSNER 06	PRL 96 092003	J.L. Rosner <i>et al.</i>	(CLEO Collab.)
ADAMS 05	PRL 94 012001	G.S. Adams <i>et al.</i>	(CLEO Collab.)
ARTUSO 05	PRL 94 032001	M. Artuso <i>et al.</i>	(CLEO Collab.)
ARTAMONOV 00	PL B474 427	A.S. Artamonov <i>et al.</i>	(CLEO Collab.)
BUTLER 94B	PR D49 40	F. Butler <i>et al.</i>	(CLEO Collab.)
WU 93	PL B301 307	Q.W. Wu <i>et al.</i>	(CUSB Collab.)
HEINTZ 92	PR D46 1928	U. Heintz <i>et al.</i>	(CUSB II Collab.)
BROCK 91	PR D43 1448	I.C. Brock <i>et al.</i>	(CLEO Collab.)
HEINTZ 91	PRL 66 1563	U. Heintz <i>et al.</i>	(CLEO Collab.)
MORRISON 91	PRL 67 1696	R.J. Morrison <i>et al.</i>	(CLEO Collab.)
NARAIN 91	PRL 66 3113	M. Narain <i>et al.</i>	(CUSB Collab.)
CHEN 89B	PR D39 3528	W.Y. Chen <i>et al.</i>	(CLEO Collab.)
KAARSBERG 89	PRL 62 2077	T.M. Kaarsberg <i>et al.</i>	(CUSB Collab.)
BUCHMUELLER... 88	HE e^+e^- Physics 412	W. Buchmuller, S. Cooper	(HANN, DESY, MIT)
Editors: A. Ali and P. Soeding, World Scientific, Singapore.			
COHEN 87	RMP 59 1121	E.R. Cohen, B.N. Taylor	(RIS C, NBS)
BARU 86B	ZPHY C32 622 (erratum)	S.E. Baru <i>et al.</i>	(NOVO)
KURAEV 85	SJNP 41 466	E.A. Kuraev, V.S. Fadin	(NOVO)
Translated from YAF 41 733.			
ARTAMONOV 84	PL 137B 272	A.S. Artamonov <i>et al.</i>	(NOVO)
GILES 84B	PR D29 1285	B. Giles <i>et al.</i>	(CLEO Collab.)
ANDREWS 83	PRL 50 807	D.E. Andrews <i>et al.</i>	(CLEO Collab.)
GREEN 82	PRL 49 617	J. Green <i>et al.</i>	(CLEO Collab.)
MAGERAS 82	PL 118B 453	G. Mageras <i>et al.</i>	(COLU, CORN, LSU+)

$\Upsilon(4S)$ or $\Upsilon(10580)$

$$J^G(J^{PC}) = 0^-(1^{--})$$

$\Upsilon(4S)$ MASS

VALUE (GeV)	DOCUMENT ID	TECN	COMMENT
10.5794±0.0012 OUR AVERAGE			
10.5793±0.0004±0.0012	AUBERT	05Q	BABR $e^+e^- \rightarrow \text{hadrons}$
10.5800±0.0035	¹ BEBEK	87	CLEO $e^+e^- \rightarrow \text{hadrons}$
••• We do not use the following data for averages, fits, limits, etc. •••			
10.5774±0.0010	² LOVELOCK	85	CUSB $e^+e^- \rightarrow \text{hadrons}$
¹ Reanalysis of BESSON 85.			
² No systematic error given.			

$\Upsilon(4S)$ WIDTH

VALUE (MeV)	DOCUMENT ID	TECN	COMMENT
20.5±2.5 OUR AVERAGE			
20.7±1.6±2.5	AUBERT	05Q	BABR $e^+e^- \rightarrow \text{hadrons}$
20 ±2 ±4	BESSION	85	CLEO $e^+e^- \rightarrow \text{hadrons}$
••• We do not use the following data for averages, fits, limits, etc. •••			
25 ±2.5	LOVELOCK	85	CUSB $e^+e^- \rightarrow \text{hadrons}$

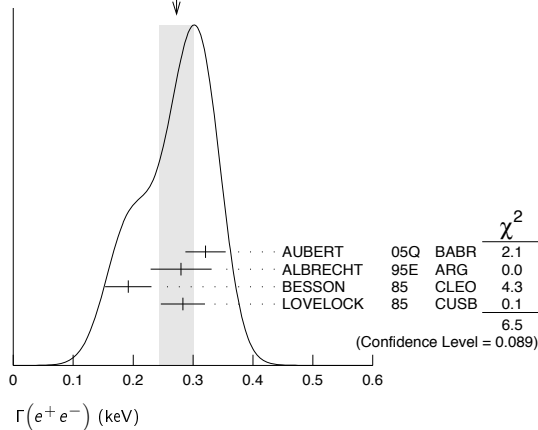
$\Upsilon(4S)$ DECAY MODES

Mode	Fraction (Γ_i/Γ)	Confidence level
Γ_1 $B\bar{B}$	> 96 %	95%
Γ_2 B^+B^-	(51.6 ±0.6) %	
Γ_3 D^+ anything + c.c.	(17.8 ±2.6) %	
Γ_4 $B^0\bar{B}^0$	(48.4 ±0.6) %	
Γ_5 $J/\psi K_S^0(J/\psi, \eta_c) K_S^0$	< 4 × 10 ⁻⁷	90%
Γ_6 non- $B\bar{B}$	< 4 %	95%
Γ_7 e^+e^-	(1.57±0.08) × 10 ⁻⁵	
Γ_8 $\rho^+\rho^-$	< 5.7 × 10 ⁻⁶	90%
Γ_9 $J/\psi(1S)$ anything	< 1.9 × 10 ⁻⁴	95%
Γ_{10} D^{*+} anything + c.c.	< 7.4 %	90%
Γ_{11} ϕ anything	(7.1 ±0.6) %	
Γ_{12} $\phi\eta$	< 1.8 × 10 ⁻⁶	90%
Γ_{13} $\phi\eta'$	< 4.3 × 10 ⁻⁶	90%
Γ_{14} $\rho\eta$	< 1.3 × 10 ⁻⁶	90%
Γ_{15} $\rho\eta'$	< 2.5 × 10 ⁻⁶	90%
Γ_{16} $\Upsilon(1S)$ anything	< 4 × 10 ⁻³	90%
Γ_{17} $\Upsilon(1S)\pi^+\pi^-$	(8.1 ±0.6) × 10 ⁻⁵	
Γ_{18} $\Upsilon(1S)\eta$	(1.96±0.11) × 10 ⁻⁴	
Γ_{19} $\Upsilon(2S)\pi^+\pi^-$	(8.6 ±1.3) × 10 ⁻⁵	
Γ_{20} \bar{d} anything	< 1.3 × 10 ⁻⁵	90%

$\Upsilon(4S)$ PARTIAL WIDTHS

$\Gamma(e^+e^-)$	DOCUMENT ID	TECN	COMMENT
0.272±0.029 OUR AVERAGE			Error includes scale factor of 1.5. See the ideogram below.
0.321±0.017±0.029	AUBERT	05Q	BABR $e^+e^- \rightarrow \text{hadrons}$
0.28 ±0.05 ±0.01	³ ALBRECHT	95E	ARG $e^+e^- \rightarrow \text{hadrons}$
0.192±0.007±0.038	BESSION	85	CLEO $e^+e^- \rightarrow \text{hadrons}$
0.283±0.037	LOVELOCK	85	CUSB $e^+e^- \rightarrow \text{hadrons}$
³ Using LEYAOUAN 77 parametrization of $\Gamma(s)$.			

Meson Particle Listings

 $\Upsilon(4S)$ WEIGHTED AVERAGE
0.272±0.029 (Error scaled by 1.5) $\Upsilon(4S)$ BRANCHING RATIOS $B\bar{B}$ DECAYS

The ratio of branching fraction to charged and neutral B mesons is often derived assuming isospin invariance in the decays, and relies on the knowledge of the B^+/B^0 lifetime ratio. "OUR EVALUATION" is obtained based on averages of rescaled data listed below. The average and rescaling were performed by the Heavy Flavor Averaging Group (HFAG) and are described at <http://www.slac.stanford.edu/xoig/hfag/>. The averaging/rescaling procedure takes into account the common dependence of the measurement on the value of the lifetime ratio.

 $\Gamma(B^+B^-)/\Gamma_{\text{total}}$ Γ_2/Γ

VALUE	DOCUMENT ID	TECN	COMMENT
0.516±0.006 OUR EVALUATION	Assuming $B(\Upsilon(4S) \rightarrow B\bar{B}) = 1$		

 $\Gamma(D_s^+ \text{ anything} + \text{c.c.})/\Gamma_{\text{total}}$ Γ_3/Γ

VALUE	DOCUMENT ID	TECN	COMMENT
0.178±0.021±0.016	4 ARTUSO	05B	CLE3 $e^+e^- \rightarrow D_s X$

4 ARTUSO 05B reports $[\Gamma(\Upsilon(4S) \rightarrow D_s^+ \text{ anything} + \text{c.c.})/\Gamma_{\text{total}}] \times [B(D_s^+ \rightarrow \phi\pi^+)] = (8.0 \pm 0.2 \pm 0.9) \times 10^{-3}$ which we divide by our best value $B(D_s^+ \rightarrow \phi\pi^+) = (4.5 \pm 0.4) \times 10^{-2}$. Our first error is their experiment's error and our second error is the systematic error from using our best value.

 $\Gamma(B^0\bar{B}^0)/\Gamma_{\text{total}}$ Γ_4/Γ

VALUE	DOCUMENT ID	TECN	COMMENT
0.484±0.006 OUR EVALUATION	Assuming $B(\Upsilon(4S) \rightarrow B\bar{B}) = 1$		

••• We do not use the following data for averages, fits, limits, etc. •••
0.487±0.010±0.008 5 AUBERT,B 05H BABR $\Upsilon(4S) \rightarrow B\bar{B} \rightarrow D^* \ell \nu \ell$

5 Direct measurement. This value is averaged with the value extracted from the $\Gamma(B^+B^-)/\Gamma(B^0\bar{B}^0)$ measurements.

 $\Gamma(B^+B^-)/\Gamma(B^0\bar{B}^0)$ Γ_2/Γ_4

VALUE	DOCUMENT ID	TECN	COMMENT
1.065±0.026 OUR EVALUATION			

1.006±0.036±0.031	6 AUBERT	04F	BABR $\Upsilon(4S) \rightarrow B\bar{B} \rightarrow J/\psi K$
1.01 ± 0.03 ± 0.09	6 HASTINGS	03	BELL $\Upsilon(4S) \rightarrow B\bar{B} \rightarrow \text{dileptons}$
1.058±0.084±0.136	7 ATHAR	02	CLEO $\Upsilon(4S) \rightarrow B\bar{B} \rightarrow D^* \ell \nu$
1.10 ± 0.06 ± 0.05	8 AUBERT	02	BABR $\Upsilon(4S) \rightarrow B\bar{B} \rightarrow (c\bar{c})K^*$
1.04 ± 0.07 ± 0.04	9 ALEXANDER	01	CLEO $\Upsilon(4S) \rightarrow B\bar{B} \rightarrow J/\psi K^*$

6 HASTINGS 03 and AUBERT 04F assume $\tau(B^+)/\tau(B^0) = 1.083 \pm 0.017$.

7 ATHAR 02 assumes $\tau(B^+)/\tau(B^0) = 1.074 \pm 0.028$. Supersedes BARISH 95.

8 AUBERT 02 assumes $\tau(B^+)/\tau(B^0) = 1.062 \pm 0.029$.

9 ALEXANDER 01 assumes $\tau(B^+)/\tau(B^0) = 1.066 \pm 0.024$.

 $\Gamma(J/\psi K_S^0/J/\psi, \eta_c) K_S^0/\Gamma_{\text{total}}$ Γ_5/Γ

Forbidden by CP invariance.

VALUE (units 10^{-7})	CL%	DOCUMENT ID	TECN	COMMENT
<4	90	10 TAJIMA	07A	BELL $\Upsilon(4S) \rightarrow B^0\bar{B}^0$

10 $\Upsilon(4S)$ with CP = +1 decays to the final state with CP = -1.

non- $B\bar{B}$ DECAYS $\Gamma(\text{non-}B\bar{B})/\Gamma_{\text{total}}$ Γ_6/Γ

VALUE	CL%	DOCUMENT ID	TECN	COMMENT
<0.04	95	BARISH	96B	CLEO e^+e^-

 $\Gamma(e^+e^-)/\Gamma_{\text{total}}$ Γ_7/Γ

VALUE (units 10^{-9})	DOCUMENT ID	TECN	COMMENT
1.57±0.08 OUR AVERAGE			

1.55±0.04±0.07	AUBERT	05Q	BABR $e^+e^- \rightarrow \text{hadrons}$
2.77±0.50±0.49	11 ALBRECHT	95E	ARG $e^+e^- \rightarrow \text{hadrons}$

11 Using LEYAOUANC 77 parametrization of $\Gamma(s)$.

 $\Gamma(\rho^+\rho^-)/\Gamma_{\text{total}}$ Γ_8/Γ

VALUE	CL%	DOCUMENT ID	TECN	COMMENT
<5.7 × 10⁻⁶	90	AUBERT	08B0	BABR $e^+e^- \rightarrow \pi^+\pi^-2\pi^0$

 $\Gamma(J/\psi(1S) \text{ anything})/\Gamma_{\text{total}}$ Γ_9/Γ

VALUE (units 10^{-4})	CL%	DOCUMENT ID	TECN	COMMENT
<1.9	95	12 ABE	02D	BELL $e^+e^- \rightarrow J/\psi X \rightarrow \ell^+\ell^-X$

••• We do not use the following data for averages, fits, limits, etc. •••

<4.7	90	12 AUBERT	01c	BABR $e^+e^- \rightarrow J/\psi X \rightarrow \ell^+\ell^-X$
------	----	-----------	-----	--

12 Uses $B(J/\psi \rightarrow e^+e^-) = 0.0593 \pm 0.0010$ and $B(J/\psi \rightarrow \mu^+\mu^-) = 0.0588 \pm 0.0010$.

 $\Gamma(D^{*+} \text{ anything} + \text{c.c.})/\Gamma_{\text{total}}$ Γ_{10}/Γ

VALUE	CL%	DOCUMENT ID	TECN	COMMENT
<0.074	90	13 ALEXANDER	90c	CLEO e^+e^-

13 For $x > 0.473$.

 $\Gamma(\phi \text{ anything})/\Gamma_{\text{total}}$ Γ_{11}/Γ

VALUE (units 10^{-2})	CL%	DOCUMENT ID	TECN	COMMENT
7.1 ± 0.1 ± 0.6		HUANG	07	CLEO $\Upsilon(4S) \rightarrow \phi X$

••• We do not use the following data for averages, fits, limits, etc. •••

<0.23	90	14 ALEXANDER	90c	CLEO e^+e^-
-------	----	--------------	-----	---------------

14 For $x > 0.52$.

 $\Gamma(\phi\eta)/\Gamma_{\text{total}}$ Γ_{12}/Γ

VALUE (units 10^{-6})	CL%	DOCUMENT ID	TECN	COMMENT
<1.8	90	15 BELOUS	09	BELL $e^+e^- \rightarrow \phi\eta$

••• We do not use the following data for averages, fits, limits, etc. •••

<2.5	90	AUBERT,BE	06F	BABR $e^+e^- \rightarrow \phi\eta$
------	----	-----------	-----	------------------------------------

15 Using all intermediate branching fraction values from PDG 08.

 $\Gamma(\phi\eta')/\Gamma_{\text{total}}$ Γ_{13}/Γ

VALUE (units 10^{-6})	CL%	DOCUMENT ID	TECN	COMMENT
<4.3	90	16 BELOUS	09	BELL $e^+e^- \rightarrow \phi\eta'$

16 Using all intermediate branching fraction values from PDG 08.

 $\Gamma(\rho\eta)/\Gamma_{\text{total}}$ Γ_{14}/Γ

VALUE (units 10^{-6})	CL%	DOCUMENT ID	TECN	COMMENT
<1.3	90	17 BELOUS	09	BELL $e^+e^- \rightarrow \rho\eta$

17 Using all intermediate branching fraction values from PDG 08.

 $\Gamma(\rho\eta')/\Gamma_{\text{total}}$ Γ_{15}/Γ

VALUE (units 10^{-6})	CL%	DOCUMENT ID	TECN	COMMENT
<2.5	90	18 BELOUS	09	BELL $e^+e^- \rightarrow \rho\eta'$

18 Using all intermediate branching fraction values from PDG 08.

 $\Gamma(\Upsilon(1S) \text{ anything})/\Gamma_{\text{total}}$ Γ_{16}/Γ

VALUE	CL%	DOCUMENT ID	TECN	COMMENT
<0.004	90	ALEXANDER	90c	CLEO e^+e^-

 $\Gamma(\Upsilon(1S)\pi^+\pi^-)/\Gamma_{\text{total}}$ Γ_{17}/Γ

VALUE (units 10^{-5})	CL%	EVS	DOCUMENT ID	TECN	COMMENT
8.1 ± 0.6 OUR AVERAGE					

8.5 ± 1.3 ± 0.2	113 ± 16	19	SOKOLOV	09	BELL $e^+e^- \rightarrow \pi^+\pi^-\mu^+\mu^-$
8.00±0.64±0.27	430	20	AUBERT	08BP	BABR $\Upsilon(4S) \rightarrow \pi^+\pi^-\ell^+\ell^-$

••• We do not use the following data for averages, fits, limits, etc. •••

17.8 ± 4.0 ± 0.3		21,22	SOKOLOV	07	BELL $e^+e^- \rightarrow \pi^+\pi^-\mu^+\mu^-$
9.0 ± 1.5 ± 0.2	167 ± 19	23	AUBERT	06R	BABR $e^+e^- \rightarrow \pi^+\pi^-\mu^+\mu^-$

<12 90 GLENN 99 CLE2 e^+e^-

19 SOKOLOV 09 reports $[\Gamma(\Upsilon(4S) \rightarrow \Upsilon(1S)\pi^+\pi^-)/\Gamma_{\text{total}}] \times [B(\Upsilon(1S) \rightarrow \mu^+\mu^-)] = (0.211 \pm 0.030 \pm 0.014) \times 10^{-5}$ which we divide by our best value $B(\Upsilon(1S) \rightarrow \mu^+\mu^-) = (2.48 \pm 0.05) \times 10^{-2}$. Our first error is their experiment's error and our second error is the systematic error from using our best value.

20 Using $B(\Upsilon(1S) \rightarrow e^+e^-) = (2.38 \pm 0.11)\%$ and $B(\Upsilon(1S) \rightarrow \mu^+\mu^-) = (2.48 \pm 0.05)\%$.

21 SOKOLOV 07 reports $[\Gamma(\Upsilon(4S) \rightarrow \Upsilon(1S)\pi^+\pi^-)/\Gamma_{\text{total}}] \times [B(\Upsilon(1S) \rightarrow \mu^+\mu^-)] = (4.42 \pm 0.81 \pm 0.56) \times 10^{-6}$ which we divide by our best value $B(\Upsilon(1S) \rightarrow \mu^+\mu^-) = (2.48 \pm 0.05) \times 10^{-2}$. Our first error is their experiment's error and our second error is the systematic error from using our best value.

22 According to the authors, systematic errors were underestimated.

23 Superseded by AUBERT 08BP. AUBERT 06R reports $[\Gamma(\Upsilon(4S) \rightarrow \Upsilon(1S)\pi^+\pi^-)/\Gamma_{\text{total}}] \times [B(\Upsilon(1S) \rightarrow \mu^+\mu^-)] = (2.23 \pm 0.25 \pm 0.27) \times 10^{-6}$ which we divide by our best value $B(\Upsilon(1S) \rightarrow \mu^+\mu^-) = (2.48 \pm 0.05) \times 10^{-2}$. Our first error is their experiment's error and our second error is the systematic error from using our best value.

Meson Particle Listings

$\Upsilon(4S), \Upsilon(10860)$

$\Gamma(\Upsilon(1S)\eta)/\Gamma_{\text{total}}$ Γ_{18}/Γ

VALUE (units 10^{-4})	EVTS	DOCUMENT ID	TECN	COMMENT
1.96 ± 0.06 ± 0.09	56	²⁴ AUBERT	08BP BABR	$\Upsilon(4S) \rightarrow \pi^+ \pi^- \pi^0 \ell^+ \ell^-$

²⁴ Using $B(\Upsilon(1S) \rightarrow e^+ e^-) = (2.38 \pm 0.11)\%$ and $B(\Upsilon(1S) \rightarrow \mu^+ \mu^-) = (2.48 \pm 0.05)\%$.

$\Gamma(\Upsilon(1S)\eta)/\Gamma(\Upsilon(1S)\pi^+ \pi^-)$ Γ_{18}/Γ_{17}

VALUE	EVTS	DOCUMENT ID	TECN	COMMENT
2.41 ± 0.40 ± 0.12	56	²⁵ AUBERT	08BP BABR	$\Upsilon(4S) \rightarrow \pi^+ \pi^- (\pi^0) \ell^+ \ell^-$

²⁵ Not independent of other values reported by AUBERT 08BP.

$\Gamma(\Upsilon(2S)\pi^+ \pi^-)/\Gamma_{\text{total}}$ Γ_{19}/Γ

VALUE (units 10^{-4})	CL%	EVTS	DOCUMENT ID	TECN	COMMENT
0.86 ± 0.11 ± 0.07		220	²⁶ AUBERT	08BP BABR	$\Upsilon(4S) \rightarrow \pi^+ \pi^- \ell^+ \ell^-$

• • • We do not use the following data for averages, fits, limits, etc. • • •

VALUE	EVTS	DOCUMENT ID	TECN	COMMENT
0.88 ± 0.17 ± 0.08	97 ± 15	²⁷ AUBERT	06R BABR	$e^+ e^- \rightarrow \pi^+ \pi^- \mu^+ \mu^-$
< 3.9	90	GLENN	99 CLE2	$e^+ e^-$

²⁶ Using $B(\Upsilon(2S) \rightarrow e^+ e^-) = (1.91 \pm 0.16)\%$ and $B(\Upsilon(2S) \rightarrow \mu^+ \mu^-) = (1.93 \pm 0.17)\%$.

²⁷ Superseded by AUBERT 08BP. AUBERT 06R reports $[\Gamma(\Upsilon(4S) \rightarrow \Upsilon(2S)\pi^+ \pi^-)/\Gamma_{\text{total}}] \times [B(\Upsilon(2S) \rightarrow \mu^+ \mu^-)] = (1.69 \pm 0.26 \pm 0.20) \times 10^{-6}$ which we divide by our best value $B(\Upsilon(2S) \rightarrow \mu^+ \mu^-) = (1.93 \pm 0.17) \times 10^{-2}$. Our first error is their experiment's error and our second error is the systematic error from using our best value.

$\Gamma(\Upsilon(2S)\pi^+ \pi^-)/\Gamma(\Upsilon(1S)\pi^+ \pi^-)$ Γ_{19}/Γ_{17}

VALUE	EVTS	DOCUMENT ID	TECN	COMMENT
1.16 ± 0.16 ± 0.14	220	²⁸ AUBERT	08BP BABR	$\Upsilon(4S) \rightarrow \pi^+ \pi^- \ell^+ \ell^-$

²⁸ Using $B(\Upsilon(1S) \rightarrow e^+ e^-) = (2.38 \pm 0.11)\%$, $B(\Upsilon(1S) \rightarrow \mu^+ \mu^-) = (2.48 \pm 0.05)\%$, $B(\Upsilon(2S) \rightarrow e^+ e^-) = (1.91 \pm 0.16)\%$, and $B(\Upsilon(2S) \rightarrow \mu^+ \mu^-) = (1.93 \pm 0.17)\%$. Not independent of other values reported by AUBERT 08BP.

$\Gamma(\bar{d} \text{ anything})/\Gamma_{\text{total}}$ Γ_{20}/Γ

VALUE (units 10^{-3})	CL%	DOCUMENT ID	TECN	COMMENT
< 1.3	90	ASNER	07 CLEO	$e^+ e^- \rightarrow \bar{d} X$

$\Upsilon(4S)$ REFERENCES

BELOUS	09	PL B681 400	K. Belous et al.	(BELLE Collab.)
SOKOLOV	09	PR D79 051103R	A. Sokolov et al.	(BELLE Collab.)
AUBERT	08BO	PR D78 071103	B. Aubert et al.	(BABAR Collab.)
AUBERT	08BP	PR D78 112002	B. Aubert et al.	(BABAR Collab.)
PDG	08	PL B667 1	C. Amser et al.	(PDG Collab.)
ASNER	07	PR D75 012009	D.M. Asner et al.	(CLEO Collab.)
HUANG	07	PR D75 012002	G.S. Huang et al.	(CLEO Collab.)
SOKOLOV	07	PR D75 071103R	A. Sokolov et al.	(BELLE Collab.)
TAJIMA	07A	PRL 99 211601	O. Tajima et al.	(BELLE Collab.)
AUBERT	06R	PRL 96 232001	B. Aubert et al.	(BABAR Collab.)
AUBERT,BE	06F	PR D74 111103R	B. Aubert et al.	(BABAR Collab.)
ARTUSO	05B	PRL 95 261801	M. Artuso et al.	(CLEO Collab.)
AUBERT	05Q	PR D72 032005	B. Aubert et al.	(BABAR Collab.)
AUBERT,B	05H	PRL 95 042001	B. Aubert et al.	(BABAR Collab.)
AUBERT	04F	PR D69 071101	B. Aubert et al.	(BABAR Collab.)
HASTINGS	03	PR D67 052004	N.C. Hastings et al.	(BELLE Collab.)
ABE	02D	PRL 88 052001	K. Abe et al.	(BELLE Collab.)
ATHAR	02	PR D66 052003	S.B. Athar et al.	(CLEO Collab.)
AUBERT	02	PR D65 032001	B. Aubert et al.	(BaBar Collab.)
ALEXANDER	01	PRL 86 2737	J.P. Alexander et al.	(CLEO Collab.)
AUBERT	01C	PRL 87 162002	B. Aubert et al.	(BaBar Collab.)
GLENN	99	PR D59 052003	S. Glenn et al.	(CLEO Collab.)
BARISH	96B	PRL 76 1570	B.C. Barish et al.	(ARGUS Collab.)
ALBRECHT	95E	ZPHY C65 619	H. Albrecht et al.	(ARGUS Collab.)
BARISH	95	PR D51 1014	B.C. Barish et al.	(CLEO Collab.)
ALEXANDER	90C	PRL 64 2226	J. Alexander et al.	(CLEO Collab.)
BEBEK	87	PR D36 1289	C. Bebek et al.	(CLEO Collab.)
BESSON	85	PRL 54 381	D. Besson et al.	(CLEO Collab.)
LOVELOCK	85	PRL 54 377	D.M.J. Lovelock et al.	(CUSB Collab.)
LEYAOUANC	77	PL B71 397	A. Le Yaouanc et al.	(ORSAY)

$\Upsilon(10860)$

$$J^{G(J^{PC})} = 0^-(1^{--})$$

$\Upsilon(10860)$ MASS

VALUE (GeV)	DOCUMENT ID	TECN	COMMENT
10.865 ± 0.008 OUR AVERAGE	Error includes scale factor of 1.1.		
10.868 ± 0.006 ± 0.005	BESSON	85 CLEO	$e^+ e^- \rightarrow \text{hadrons}$
10.845 ± 0.020	LOVELOCK	85 CUSB	$e^+ e^- \rightarrow \text{hadrons}$

• • • We do not use the following data for averages, fits, limits, etc. • • •

10.876 ± 0.002	¹ AUBERT	09E BABR	$e^+ e^- \rightarrow \text{hadrons}$
10.869 ± 0.002	² AUBERT	09E BABR	$e^+ e^- \rightarrow \text{hadrons}$

¹ In a model where a flat non-resonant $b\bar{b}$ -continuum is incoherently added to a second flat component interfering with two Breit-Wigner resonances. Systematic uncertainties not estimated.

² In a model where a non-resonant $b\bar{b}$ -continuum represented by a threshold function at $\sqrt{s}=2m_B$ is incoherently added to a flat component interfering with two Breit-Wigner resonances. Not independent of other AUBERT 09E results. Systematic uncertainties not estimated.

$\Upsilon(10860)$ WIDTH

VALUE (MeV)	DOCUMENT ID	TECN	COMMENT
110 ± 13 OUR AVERAGE			
112 ± 17 ± 23	BESSON	85 CLEO	$e^+ e^- \rightarrow \text{hadrons}$
110 ± 15	LOVELOCK	85 CUSB	$e^+ e^- \rightarrow \text{hadrons}$

• • • We do not use the following data for averages, fits, limits, etc. • • •

43 ± 4	³ AUBERT	09E BABR	$e^+ e^- \rightarrow \text{hadrons}$
74 ± 4	⁴ AUBERT	09E BABR	$e^+ e^- \rightarrow \text{hadrons}$

³ In a model where a flat non-resonant $b\bar{b}$ -continuum is incoherently added to a second flat component interfering with two Breit-Wigner resonances. Systematic uncertainties not estimated.

⁴ In a model where a non-resonant $b\bar{b}$ -continuum represented by a threshold function at $\sqrt{s}=2m_B$ is incoherently added to a flat component interfering with two Breit-Wigner resonances. Not independent of other AUBERT 09E results. Systematic uncertainties not estimated.

$\Upsilon(10860)$ DECAY MODES

Mode	Fraction (Γ_i/Γ)	Confidence level
Γ_1 $e^+ e^-$	(2.8 ± 0.7) × 10 ⁻⁶	
Γ_2 $B\bar{B}X$	(59 ± 14) %	90%
Γ_3 $B\bar{B}$	< 13.8 %	
Γ_4 $B\bar{B}^* + \text{c.c.}$	(14 ± 6) %	
Γ_5 $B^* \bar{B}^*$	(44 ± 11) %	
Γ_6 $B\bar{B}^*(*)\pi$	< 19.7 %	90%
Γ_7 $B\bar{B}\pi\pi$	< 8.9 %	
Γ_8 $B_s^*(*)\bar{B}_s^*(*)$	(19.3 ± 2.9) %	90%
Γ_9 $B_s \bar{B}_s$	(5 ± 5) × 10 ⁻³	
Γ_{10} $B_s \bar{B}_s^* + \text{c.c.}$	(1.4 ± 0.6) %	
Γ_{11} $B_s^* \bar{B}_s^*$	(17.4 ± 2.7) %	
Γ_{12} $\Upsilon(1S)\pi^+ \pi^-$	(5.3 ± 0.6) × 10 ⁻³	
Γ_{13} $\Upsilon(2S)\pi^+ \pi^-$	(7.8 ± 1.3) × 10 ⁻³	
Γ_{14} $\Upsilon(3S)\pi^+ \pi^-$	(4.8 ± 1.9) × 10 ⁻³	
Γ_{15} $\Upsilon(1S)K^+ K^-$	(6.1 ± 1.8) × 10 ⁻⁴	

Inclusive Decays.

These decay modes are submodes of one or more of the decay modes above.

Γ_{16} ϕ anything	(13.8 ± 2.4) %
Γ_{17} D^0 anything + c.c.	(108 ± 8) %
Γ_{18} D_s anything + c.c.	(46 ± 6) %
Γ_{19} J/ψ anything	(2.06 ± 0.21) %

$\Upsilon(10860)$ PARTIAL WIDTHS

$\Gamma(e^+ e^-)$	VALUE (keV)	DOCUMENT ID	TECN	COMMENT	Γ_1
0.31 ± 0.07 OUR AVERAGE	Error includes scale factor of 1.3.				
0.22 ± 0.05 ± 0.07	BESSON	85 CLEO		$e^+ e^- \rightarrow \text{hadrons}$	
0.365 ± 0.070	LOVELOCK	85 CUSB		$e^+ e^- \rightarrow \text{hadrons}$	

$\Upsilon(10860)$ BRANCHING RATIOS

$\Gamma(B\bar{B}X)/\Gamma_{\text{total}}$	DOCUMENT ID	TECN	COMMENT	Γ_2/Γ
0.589 ± 0.100 ± 0.092	⁵ HUANG	07 CLEO	$\Upsilon(5S) \rightarrow \text{hadrons}$	

$\Gamma(B\bar{B})/\Gamma_{\text{total}}$	DOCUMENT ID	TECN	COMMENT	Γ_3/Γ
< 0.138	⁵ HUANG	07 CLEO	$\Upsilon(5S) \rightarrow \text{hadrons}$	

$\Gamma(B\bar{B})/\Gamma(B\bar{B}X)$	DOCUMENT ID	TECN	COMMENT	Γ_3/Γ_2
< 0.22	AQUINES	06 CLE3	$\Upsilon(5S) \rightarrow \text{hadrons}$	

$\Gamma(B\bar{B}^* + \text{c.c.})/\Gamma_{\text{total}}$	DOCUMENT ID	TECN	COMMENT	Γ_4/Γ
0.143 ± 0.053 ± 0.027	⁵ HUANG	07 CLEO	$\Upsilon(5S) \rightarrow \text{hadrons}$	

$\Gamma(B\bar{B}^* + \text{c.c.})/\Gamma(B\bar{B}X)$	DOCUMENT ID	TECN	COMMENT	Γ_4/Γ_2
0.24 ± 0.09 ± 0.03	AQUINES	06 CLE3	$\Upsilon(5S) \rightarrow \text{hadrons}$	

Meson Particle Listings

 $\Upsilon(10860)$, $\Upsilon(11020)$

$\Gamma(B^*\bar{B}^*)/\Gamma_{\text{total}}$	DOCUMENT ID	TECN	COMMENT	Γ_5/Γ
VALUE $0.436 \pm 0.083 \pm 0.072$	5 HUANG	07	CLEO $\Upsilon(5S) \rightarrow$ hadrons	

$\Gamma(B^*\bar{B}^*)/\Gamma(B\bar{B}X)$	DOCUMENT ID	TECN	COMMENT	Γ_5/Γ_2
VALUE $0.74 \pm 0.15 \pm 0.08$	EVTS 31	AQUINES	06 CLE3 $\Upsilon(5S) \rightarrow$ hadrons	

$\Gamma(B\bar{B}^*\pi)/\Gamma_{\text{total}}$	DOCUMENT ID	TECN	COMMENT	Γ_6/Γ
VALUE <0.197	CL% 90	5 HUANG	07 CLEO $\Upsilon(5S) \rightarrow$ hadrons	

$\Gamma(B\bar{B}^*\pi)/\Gamma(B\bar{B}X)$	DOCUMENT ID	TECN	COMMENT	Γ_6/Γ_2
VALUE <0.32	CL% 90	AQUINES	06 CLE3 $\Upsilon(5S) \rightarrow$ hadrons	

$\Gamma(B\bar{B}\pi\pi)/\Gamma_{\text{total}}$	DOCUMENT ID	TECN	COMMENT	Γ_7/Γ
VALUE <0.089	CL% 90	5 HUANG	07 CLEO $\Upsilon(5S) \rightarrow$ hadrons	

$\Gamma(B\bar{B}\pi\pi)/\Gamma(B\bar{B}X)$	DOCUMENT ID	TECN	COMMENT	Γ_7/Γ_2
VALUE <0.14	CL% 90	AQUINES	06 CLE3 $\Upsilon(5S) \rightarrow$ hadrons	

$\Gamma(B_s^{(*)}\bar{B}_s^{(*)})/\Gamma_{\text{total}}$	DOCUMENT ID	TECN	COMMENT	$\Gamma_8/\Gamma = (\Gamma_9 + \Gamma_{10} + \Gamma_{11})/\Gamma$
VALUE 0.193 ± 0.029 OUR EVALUATION	Taking into account common systematics.			
0.195 ± 0.030 OUR AVERAGE				

$0.180 \pm 0.013 \pm 0.032$	6 DRUTSKOY	07	BELL $\Upsilon(5S) \rightarrow D^0 X, D_s X$	
0.21 ± 0.06 -0.03	7 HUANG	07	CLEO $\Upsilon(5S) \rightarrow D_s X$	
• • • We do not use the following data for averages, fits, limits, etc. • • •				
$0.160 \pm 0.026 \pm 0.058$	8 ARTUSO	05B	CLEO $e^+e^- \rightarrow D_X X$	

$\Gamma(B_s^{(*)}\bar{B}_s^{(*)})/\Gamma(B_s^{(*)}\bar{B}_s^{(*)})$	DOCUMENT ID	TECN	COMMENT	$\Gamma_{11}/\Gamma_8 = \Gamma_{11}/(\Gamma_9 + \Gamma_{10} + \Gamma_{11})$
VALUE (units 10^{-2}) 90.1 ± 3.8 4.0 ± 0.2	9 LOUVOT	09	BELL $10.86 e^+e^- \rightarrow B_s^{(*)}\bar{B}_s^{(*)}$	
• • • We do not use the following data for averages, fits, limits, etc. • • •				
93 ± 7 -9 ± 1	9 DRUTSKOY	07A	BELL Superseded by LOUVOT 09	

$\Gamma(B_s\bar{B}_s)/\Gamma(B_s^{(*)}\bar{B}_s^{(*)})$	DOCUMENT ID	TECN	COMMENT	$\Gamma_9/\Gamma_8 = \Gamma_9/(\Gamma_9 + \Gamma_{10} + \Gamma_{11})$
VALUE (units 10^{-2}) 2.6 ± 2.6 -2.5	LOUVOT	09	BELL $10.86 e^+e^- \rightarrow B_s^{(*)}\bar{B}_s^{(*)}$	

$\Gamma(B_s\bar{B}_s)/\Gamma(B_s^{(*)}\bar{B}_s^{(*)})$	DOCUMENT ID	TECN	COMMENT	Γ_9/Γ_{11}
VALUE <0.16	CL% 90	BONVICINI	06 CLE3 e^+e^-	

$\Gamma(B_s\bar{B}_s + \text{c.c.})/\Gamma(B_s^{(*)}\bar{B}_s^{(*)})$	DOCUMENT ID	TECN	COMMENT	$\Gamma_{10}/\Gamma_8 = \Gamma_{10}/(\Gamma_9 + \Gamma_{10} + \Gamma_{11})$
VALUE (units 10^{-2}) 7.3 ± 3.3 -3.0 ± 0.1	LOUVOT	09	BELL $10.86 e^+e^- \rightarrow B_s^{(*)}\bar{B}_s^{(*)}$	

$\Gamma(B_s\bar{B}_s + \text{c.c.})/\Gamma(B_s^{(*)}\bar{B}_s^{(*)})$	DOCUMENT ID	TECN	COMMENT	Γ_{10}/Γ_{11}
VALUE <0.16	CL% 90	BONVICINI	06 CLE3 e^+e^-	

$\Gamma(\Upsilon(1S)\pi^+\pi^-)/\Gamma_{\text{total}}$	DOCUMENT ID	TECN	COMMENT	Γ_{12}/Γ
VALUE (units 10^{-3}) $5.3 \pm 0.3 \pm 0.5$	EVTS 325	10 CHEN	08 BELL $10.87 e^+e^- \rightarrow \Upsilon(1S)\pi^+\pi^-$	

$\Gamma(\Upsilon(2S)\pi^+\pi^-)/\Gamma_{\text{total}}$	DOCUMENT ID	TECN	COMMENT	Γ_{13}/Γ
VALUE (units 10^{-3}) $7.8 \pm 0.6 \pm 1.1$	EVTS 186	10 CHEN	08 BELL $10.87 e^+e^- \rightarrow \Upsilon(2S)\pi^+\pi^-$	

$\Gamma(\Upsilon(3S)\pi^+\pi^-)/\Gamma_{\text{total}}$	DOCUMENT ID	TECN	COMMENT	Γ_{14}/Γ
VALUE (units 10^{-3}) 4.8 ± 1.9 -1.5 ± 0.7	EVTS 10	10 CHEN	08 BELL $10.87 e^+e^- \rightarrow \Upsilon(3S)\pi^+\pi^-$	

$\Gamma(\Upsilon(1S)K^+K^-)/\Gamma_{\text{total}}$	DOCUMENT ID	TECN	COMMENT	Γ_{15}/Γ
VALUE (units 10^{-4}) 6.1 ± 1.6 -1.4 ± 1.0	EVTS 20	10 CHEN	08 BELL $10.87 e^+e^- \rightarrow \Upsilon(1S)K^+K^-$	

$\Gamma(\phi \text{ anything})/\Gamma_{\text{total}}$	DOCUMENT ID	TECN	COMMENT	Γ_{16}/Γ
VALUE $0.138 \pm 0.007 \pm 0.023$ -0.015	HUANG	07	CLEO $\Upsilon(5S) \rightarrow \phi X$	

$\Gamma(D^0 \text{ anything} + \text{c.c.})/\Gamma_{\text{total}}$	DOCUMENT ID	TECN	COMMENT	Γ_{17}/Γ
VALUE $1.076 \pm 0.040 \pm 0.068$	DRUTSKOY	07	BELL $\Upsilon(5S) \rightarrow D^0 X$	

$\Gamma(D_s \text{ anything} + \text{c.c.})/\Gamma_{\text{total}}$	DOCUMENT ID	TECN	COMMENT	Γ_{18}/Γ
VALUE 0.46 ± 0.06 OUR AVERAGE				
$0.472 \pm 0.024 \pm 0.072$	6 DRUTSKOY	07	BELL $\Upsilon(5S) \rightarrow D_s X$	
$0.44 \pm 0.09 \pm 0.04$	11 ARTUSO	05B	CLE3 $e^+e^- \rightarrow D_X X$	

$\Gamma(J/\psi \text{ anything})/\Gamma_{\text{total}}$	DOCUMENT ID	TECN	COMMENT	Γ_{19}/Γ
VALUE (units 10^{-2}) $2.060 \pm 0.160 \pm 0.134$	DRUTSKOY	07	BELL $\Upsilon(5S) \rightarrow J/\psi X$	

⁵ Using measurements or limits from AQUINES 06.
⁶ Using $B(D_s^+ \rightarrow \phi\pi^+) = (4.4 \pm 0.6)\%$ from PDG 06.
⁷ Supersedes ARTUSO 05B. Combining inclusive ϕ , D_s , and B measurements. Using $B(D_s^+ \rightarrow \phi\pi^+) = 4.4 \pm 0.6\%$ from PDG 06.
⁸ Uses a model-dependent estimate $B(B_s \rightarrow D_s X) = (92 \pm 11)\%$.
⁹ From a measurement of $\sigma(e^+e^- \rightarrow B_s^*\bar{B}_s^*) / \sigma(e^+e^- \rightarrow B_s^{(*)}\bar{B}_s^{(*)})$ at $\sqrt{s} = 10.86$ GeV.
¹⁰ Assuming that the observed events are solely due to the $\Upsilon(5S)$ resonance.
¹¹ ARTUSO 05B reports $[\Gamma(\Upsilon(10860) \rightarrow D_s \text{ anything} + \text{c.c.})/\Gamma_{\text{total}}] \times [B(D_s^+ \rightarrow \phi\pi^+)] = 0.0198 \pm 0.0019 \pm 0.0038$ which we divide by our best value $B(D_s^+ \rightarrow \phi\pi^+) = (4.5 \pm 0.4) \times 10^{-2}$. Our first error is their experiment's error and our second error is the systematic error from using our best value.

 $\Upsilon(10860)$ REFERENCES

AUBERT	09E	PRL 102 012001	B. Aubert <i>et al.</i>	(BABAR Collab.)
LOUVOT	09	PRL 102 021801	R. Louvot <i>et al.</i>	(BELLE Collab.)
CHEN	08	PRL 100 112001	K.-F. Chen <i>et al.</i>	(BELLE Collab.)
DRUTSKOY	07	PRL 98 052001	A. Drutskoy <i>et al.</i>	(BELLE Collab.)
DRUTSKOY	07A	PR D76 012002	A. Drutskoy <i>et al.</i>	(BELLE Collab.)
HUANG	07	PR D75 012002	G.S. Huang <i>et al.</i>	(CLEO Collab.)
AQUINES	06	PRL 96 152001	O. Aquines <i>et al.</i>	(CLEO Collab.)
BONVICINI	06	PRL 96 022002	G. Bonvicini <i>et al.</i>	(CLEO Collab.)
PDG	06	JPG 33 1	W.-M. Yao <i>et al.</i>	(PDG Collab.)
ARTUSO	05B	PRL 95 261801	M. Artuso <i>et al.</i>	(CLEO Collab.)
BESSON	85	PRL 54 381	D. Besson <i>et al.</i>	(CLEO Collab.)
LOVELOCK	85	PRL 54 377	D.M.J. Lovelock <i>et al.</i>	(CUSB Collab.)

 $\Upsilon(11020)$

$$I^G(J^{PC}) = 0^-(1^--)$$

 $\Upsilon(11020)$ MASS

VALUE (GeV)	DOCUMENT ID	TECN	COMMENT
11.019 ± 0.008 OUR AVERAGE			
$11.019 \pm 0.005 \pm 0.007$	BESSON	85	CLEO $e^+e^- \rightarrow$ hadrons
11.020 ± 0.030	LOVELOCK	85	CUSB $e^+e^- \rightarrow$ hadrons
• • • We do not use the following data for averages, fits, limits, etc. • • •			
10.996 ± 0.002	1 AUBERT	09E	BABR $e^+e^- \rightarrow$ hadrons

¹ In a model where a flat non-resonant $b\bar{b}$ -continuum is incoherently added to a second flat component interfering with two Breit-Wigner resonances. Systematic uncertainties not estimated.

 $\Upsilon(11020)$ WIDTH

VALUE (MeV)	DOCUMENT ID	TECN	COMMENT
79 ± 16 OUR AVERAGE			
$61 \pm 13 \pm 22$	BESSON	85	CLEO $e^+e^- \rightarrow$ hadrons
90 ± 20	LOVELOCK	85	CUSB $e^+e^- \rightarrow$ hadrons
• • • We do not use the following data for averages, fits, limits, etc. • • •			
37 ± 3	2 AUBERT	09E	BABR $e^+e^- \rightarrow$ hadrons

² In a model where a flat non-resonant $b\bar{b}$ -continuum is incoherently added to a second flat component interfering with two Breit-Wigner resonances. Systematic uncertainties not estimated.

 $\Upsilon(11020)$ DECAY MODES

Mode	Fraction (Γ_i/Γ)
$\Gamma_1 e^+e^-$	$(1.6 \pm 0.5) \times 10^{-6}$

 $\Upsilon(11020)$ PARTIAL WIDTHS

$\Gamma(e^+e^-)$	DOCUMENT ID	TECN	COMMENT	Γ_1
VALUE (keV) 0.130 ± 0.030 OUR AVERAGE				
$0.095 \pm 0.03 \pm 0.035$	BESSON	85	CLEO $e^+e^- \rightarrow$ hadrons	
0.156 ± 0.040	LOVELOCK	85	CUSB $e^+e^- \rightarrow$ hadrons	

 $\Upsilon(11020)$ REFERENCES

AUBERT	09E	PRL 102 012001	B. Aubert <i>et al.</i>	(BABAR Collab.)
BESSON	85	PRL 54 381	D. Besson <i>et al.</i>	(CLEO Collab.)
LOVELOCK	85	PRL 54 377	D.M.J. Lovelock <i>et al.</i>	(CUSB Collab.)

NON- $q\bar{q}$ CANDIDATES

We include here reference lists on gluonium and other non- $q\bar{q}$ candidates. For a review see PDG 06, Journal of Physics, G 33 1 (2006). See also the "Note on scalar mesons" in the $f_0(600)$ Particle Listings, our note "New charmonium-like states" in PDG 08, Physics Letters B667 1 (2008), and the extensive chapter on Spectroscopy in N. Brambilla et al. (Quarkonium Working Group), to be published in the Eur. Phys. J. in 2010.

Non- $q\bar{q}$ Candidates

OMITTED FROM SUMMARY TABLE

NON- $q\bar{q}$ CANDIDATES REFERENCES

CHOI 08 PRL 100 142001 S.-K. Choi et al. (BELLE Collab.)
LEE 08 PL B661 28 S.H. Lee et al.
LI 08 PR D77 054001 Y. Li, C.-D. Lu, W. Wang
LIU 08A PR D75 034003 X. Liu et al.
AMBROSINO 07A PL B648 267 F. Ambrosino et al. (KLOE Collab.)
BUISSERET 07 PR C76 025206 F. Buissere et al.
CHEN 07E PR D76 094025 H.-X. Chen, A. Hosaka, S.L. Zhu
CHIU 07 PL B646 95 T.-W. Chiu, T.-H. Hsieh
DING 07A PL B657 49 G.-J. Ding, M.-L. Yan
FAESSLER 07B PR D76 114008 A. Faessler et al.
GENERAL 07 EPJ C51 347 I.J. General, S.R. Contanch, F.J. Llanes-Estrada
GENERAL 07A PL B653 216 L.J. General et al.
GLOZMAN 07 PRPL 444 1 L.Ya. Glzman
GUO 07 PL B647 133 F.-K. Guo et al.
HANHART 07 PR D75 074015 C. Hanhart et al.
LEMMER 07 PL B650 152 R.H. Lemmer
MAIANI 07 EPJ C50 609 L. Maiani et al.
MATHEUS 07 PR D75 014005 R. Matheus et al.
MATHUR 07 PR D76 114505 N. Mathur
ROSNER 07 PR D76 114002 J. Rosner
SANTOPINTO 07 PR C75 045206 E. Santopinto, G. Galata
YANG 07 PR D76 094001 K.-C. Yang
ABD-EL-HADY 06 PR D73 073010 A. Abd-El-Hady (L3 Collab.)
ACHARD 06A PL B638 128 P. Achard et al. (WAYN)
ALFIKY 06 PL B640 238 M. Alfiky, F. Gabbiani, A.A. Petrov
ANSOVICH 06A PAN 620 520 V.V. Anisovich et al. (BABAR Collab.)
AUBERT 06 PR D73 011101R B. Aubert et al.
BRAATEN 06 PR D73 011501 E. Braaten (UMH)
BUISSERET 06 EPJ A29 343 F. Buissere, V. Mathieu
BURNS 06 PR D74 034003 T.J. Burns, F.E. Close
CHEN 06 PR D73 014516 Y. Chen, A. Alexandru, S.J. Dong
CHENG 06 PR D73 014017 H.-Y. Cheng, C.-K. Chua, K.-C. Yang
CHENG 06A PR D74 094005 H.-Y. Cheng, C.-K. Chua, K.-F. Liu
CHIU 06 PR D73 094510 T.-W. Chiu, T.-H. Hsieh
COOK 06 PR D74 094501 M.S. Cook, H.R. Fiebig
CUI 06 PR D73 014018 Y. Cui et al. (CST)
DING 06 PL B643 33 G.-J. Ding, M.-L. Yan
DMITRASINOVIC 06 MPL A21 533 V. Dmitrasinovic
DUBYNYSKIY 06 PR D74 094017 S. Dubynskiy, M. Voloshin
FARIBORZ 06 PR D74 054030 A.H. Fariborz
GIACOSA 06 PR D74 014028 F. Giacosa
GUO 06A PR D74 097503 F.-K. Guo, P.-N. Shen
HE 06 PR D73 051502R X.-G. He, X.-Q. Li, X.-Q. Zeng
HOGAASEN 06 PR D73 054013 H. Hogaasen et al.
KARLINER 06 PL B638 221 M. Karliner, H.J. Lipkin
KOCHOLEV 06 PL B633 283 N. Kochelev, D.-P. Min (SEOUL, JINR)
LEE 06A EPJ A30 423 H.-J. Lee
LI 06 PR D74 034019 B.A. Li
LI 06A PR D74 054017 B.A. Li
LI 06B MPL A21 743 D.M. Li et al.
LOAN 06 UMP A21 2905 M. Loan et al.
NAVARRA 06 PL B639 272 F.S. Navarra, M. Nielsen
NIELSEN 06 PL B634 35 M. Nielsen
PELAEZ 06 PRL 97 242002 J.R. Pelaez, G. Rios
QIAO 06 PL B639 263 C. Qiao
SWANSON 06 PRPL 429 243 E.S. Swanson (PITT)
UEHARA 06 PRL 96 082003 S. Uehara et al. (BELLE Collab.)
VENTO 06 PR D73 054006 V. Vento
VIJANDE 06 PR D73 034002 F. Vijande, F. Fernandez, A. Valcarce
VOLOSHIN 06 UMP A21 1239 M. Voloshin
WANG 06 PR D73 094020 Z.-G. Wang, S.-L. Wu
YUAN 06 PL B634 399 C.Z. Yuan, P. Wang, X.H. Mo
ZHAO 06 PR D74 114025 Q. Zhao, B.S. Zhou
ABLIKIM 05 PL B607 243 M. Ablikim et al. (BES Collab.)
ABLIKIM 05R PRL 95 262001 M. Ablikim et al. (BES Collab.)
ACHARD 05B PL B615 19 P. Achard et al. (L3 Collab.)
ANIKIN 05 PL B626 86 I.V. Anikin, B. Pire, O.V. Teryaev
ANISOVICH 05 JETPL 80 715 V.V. Anisovich
ANISOVICH 05A Translated from ZETFP 80 845, JETPL 81 417, Anisovich, A.V. Sarantsev
ANISOVICH 05C UMP A20 6327 V.V. Anisovich, M.A. Matveev, A.V. Sarantsev
AUBERT 05B PR D71 031501R B. Aubert et al. (BABAR Collab.)
AUBERT 05R PR D71 071103R B. Aubert et al. (BABAR Collab.)
AUBERT.B 05I PRL 95 142001 B. Aubert et al. (BABAR Collab.)
BICUDO 05 NP A748 537 P. Bicudo
BIGI 05 PR D72 114016 I. Bigi et al.
BRAATEN 05 PR D72 014012 E. Braaten, M. Kusunoki
BRAATEN 05A PR D72 054022 E. Braaten, M. Kusunoki
BRAATEN 05B PR D71 074005 E. Braaten, M. Kusunoki
BRACCO 05 PL B624 217 M.E. Bracco, A. Lozae, R.D. Matheus
BRITO 05 PL B608 69 T.V. Brito et al.
CHANG 05B PL B623 218 C.-H. Chang, C.S. Kim, G. Wang
CHANOWITZ 05 PRL 95 172001 M. Chanowitz
CHOI 05 PRL 94 182002 S.-K. Choi et al. (BELLE Collab.)
CLOSE 05 PR D71 094022 F.E. Close, Q. Zhao
CLOSE 05A PL B628 215 F.E. Close, P.R. Page
DING 05 PR C72 015208 G.-J. Ding, M.-L. Yan (CST)
GIACOSA 05 PR C71 025207 F. Giacosa et al.
GIACOSA 05A PL B622 277 F. Giacosa et al.
GUO 05 NP A764 269 F.-K. Guo et al.
HEDDITCH 05 PR D72 114507 J.N. Hedditch et al.
HUANG 05A PR D71 114015 M.Q. Huang, D.W. Wang
IWASAKI 05A PR D72 094016 M. Iwasaki, T. Fukutome

JAFFE 05 PRPL 409 1 R.L. Jaffe
KALASHNIK... 05 EPJ A24 437 Yu.S. Kalashnikova, A.E. Kudryavtsev, A.V. Nefediev
KANADA-EN... 05 PR D71 094005 Y. Kanada-Enyo, O. Morimatsu, T. Nishikawa
KIM 05 PR D71 034025 T. Kim, P. Ko
KIM 05A PR D72 074012 H. Kim, Y. Oh
KOU 05 PL B631 164 E. Kou
LI 05 PL B605 306 B.A. Li
LI 05E MPL A20 2497 D.-M. Li et al.
LIU 05 PR D72 054023 X. Liu, X.Q. Zeng, X.Q. Li
LOISEAU 05 PR C72 011001 B. Loiseau, S. Wycech (CURCP, WINR)
LU 05 PRL 94 032002 M. Lu et al. (BNL E852 Collab.)
MAIANI 05 PR D71 014028 L. Maiani et al.
MAIANI 05A PR D72 031502R L. Maiani et al.
POPLAWSKI 05 PR D71 056003 N.J. Poplawski, A.P. Szczepaniak, J.T. Londergan
SETH 05 PL B612 1 K.K. Seth
SUZUKI 05 PR D72 114013 M. Suzuki
VIJANDE 05 PR D72 034025 J. Vijande, A. Valcarce, F. Fernandez
VOLOSHIN 05 PR D71 114003 M.B. Voloshin
WANG 05A PL B617 341 M.-Z. Wang et al. (BELLE Collab.)
WANG 05C EPJ C42 89 Z.-G. Wang, W.-M. Yang
ZHANG 05 PR D71 011502R Z.F. Zhang, H.Y. Jin
ZHAO 05 PR D72 074001 Q. Zhao
ZHAO 05A PL B631 22 Q. Zhao, B.-S. Zou, Z.-B. Ma
ZHU 05 PL B625 212 S.-L. Zhu
ABAZOV 04F PRL 93 162002 V.M. Abazov et al. (D0 Collab.)
ABE 04 EPJ C32 323 K. Abe et al. (BELLE Collab.)
ABLIKIM 04E PL B603 138 M. Ablikim et al. (BES Collab.)
ACOSTA 04 PRPL 93 072001 D. Acosta et al. (CDF Collab.)
AMSLER 04 PRPL 389 61 C. Amshler, N.A. Tornqvist
AMSLER 04A NP A740 130 C. Amshler et al.
BARNES 04 PR D69 054008 T. Barnes, S. Godfrey
BARNES 04A PL B600 223 T. Barnes et al.
BARU 04 PL B586 53 V. Baru et al.
BRAATEN 04 PR D69 074005 E. Braaten et al.
BRAATEN 04B PRL 93 162001 E. Braaten, M. Kusunoki, S. Nussinov
BUGG 04 PRPL 397 257 D.V. Bugg
CHAO 04A PL B599 43 K.-T. Chao
CHEN 04 PR D69 076003 J.-X. Chen, J.-C. Su
CHEN 04A PR D69 054002 C.-H. Chen
CHEN 04C PRL 93 232001 Y.-Q. Chen, X.-Q. Li
CLOSE 04A PR D70 094015 F.E. Close, J.J. Dudek (BELLE Collab.)
CLOSE 04B PR D69 034010 F.E. Close, J.J. Dudek
COHEN 04 PL B578 359 T.D. Cohen et al.
DAI 04 JHEP 0411 043 Y.-B. Dai et al.
DMITRASINOVIC 04 PR D70 096011 V. Dmitrasinovic
EICHTEEN 04 PR D69 094019 E. Eichten, K. Lane, C. Quigg
FADDEEV 04 PR D70 114033 L. Faddeev et al.
FARIBORZ 04 UMP A19 2095 A.H. Fariborz
GLOZMAN 04 PL B587 69 L.Ya. Glzman
KREWALD 04 PR D69 016003 S. Krewald, R.H. Lemmer, F.P. Sassen
KUHN 04 PL B595 109 J. Kuhn et al. (BNL E852 Collab.)
LIPKIN 04 PL B580 50 H.J. Lipkin
LIU 04A PR D70 094009 Y.-R. Liu
LONGACRE 04 PR D70 094041 R.S. Longacre, S.J. Lindenbaum
MAIANI 04 PR D70 054009 L. Maiani et al.
NAPSUCIALE 04A PR D70 094043 N.N. Napsuciale, S. Rodriguez
PELAEZ 04 PRL 92 102001 J.R. Pelaez
PELAEZ 04A MPL A19 2879 J.R. Pelaez
SWANSON 04 PL B582 167 E. Swanson
SWANSON 04A PL B588 189 E. Swanson
SWANSON 04B PL B598 197 E. Swanson
TESHIMA 04 JPG 30 663 T. Teshima et al.
TORNVIST 04 PL B590 209 N. Tornqvist
VANBEVEREN 04 MPL A19 1949 E. van Beveren, G. Rupp
VOLOSHIN 04A PL B604 69 M.B. Voloshin
WONG 04 PR C69 052002 C. Wong
ZOU 04 PR D69 034004 B.S. Zou, H.C. Chiang
AUBERT 03G PRL 90 242001 B. Aubert et al. (BaBar Collab.)
BARNES 03 PR D68 054006 T. Barnes et al.
BESSON 03 PR D68 032002 D. Besson et al. (CLEO Collab.)
CHENG 03B PR D67 054021 H.Y. Cheng
CHENG 03C PL B566 193 H.-Y. Cheng, W.-S. Hou
CHOI 03 PRL 91 262001 S.-K. Choi et al. (BELLE Collab.)
TERASAKI 03 PR D68 011501 K. Terasaki
ABE 02K PRL 88 181803 K. Abe et al. (BELLE Collab.)
ALOISIO 02C PL B536 209 A. Aloisio et al. (KLOE Collab.)
ALOISIO 02D PL B537 21 A. Aloisio et al.
AMSLER 02 EPJ C23 29 C. Amshler et al.
AMSLER 02B PL B541 22 C. Amshler
CHUNG 02C EPJ A15 539 S.U. Chung, E. Klempt, J.G. Korener
CLOSE 02B JPG 28 R249 F.E. Close, N. Tornqvist
ABELE 01 EPJ C19 667 A. Abele et al. (Crystal Barrel Collab.)
ABELE 01B EPJ C21 261 A. Abele et al. (Crystal Barrel Collab.)
ACCIARRI 01H PL B501 173 M. Acciarri et al. (L3 Collab.)
AITALA 01A PRL 86 765 E.M. Aitala et al. (FNAL E791 Collab.)
AMSLER 01 PL B575 175 C. Amshler et al.
CLOSE 01 EPJ C21 531 F.E. Close, A. Kirk
IDDIR 01 PL B507 183 F. Ididir, A.S. Satir
IVANOV 01 PRL 86 3977 E.I. Ivanov et al. (BNL E852 Collab.)
ACHASOV 00F PL B479 53 M.N. Achasov et al. (Novosibirsk SND Collab.)
ALFORD 00 NP B578 367 M. Alford, R.L. Jaffe
BARATE 00E PL B472 189 R. Barate et al. (ALEPH Collab.)
BARBERIS 00C PL B471 440 D. Barberis et al. (WA 102 Collab.)
KIRK 00 PL B489 29 A. Kirk
LEE 00 PR D61 014015 W. Lee, D. Weingarten
ABELE 99 PL B446 349 A. Abele et al. (Crystal Barrel Collab.)
AKHMETSHIN 99B PL B462 371 R.R. Akhmetshin et al. (Novosibirsk CMD-2 Collab.)
BAKER 99 PR D57 3810 C.A. Baker et al.
BARBERIS 99D PL B462 462 D. Barberis et al. (Omega Expt.)
CHUNG 99 PR D60 092001 S.U. Chung et al. (BNL E852 Collab.)
DELBORGGO 99 PR B446 332 R. Delbourgo, D. Liu, M. Scadron
DONNACHIE 99 PR D60 114011 A. Donnachie, Yu.S. Kalashnikova
DUENNEWEBER 99 NP A 663 + 664, 592C W. Duennebeber Proc. XV Particles and Nuclei Int. Conf., Uppsala
MINKOWSKI 99 EPJ C9 283 P. Minkowski, W. Ochs
MORNINGSTAR 99 PR D60 034509 C.J. Morningstar, M. Peardon
PAGE 99 PR D59 034016 P.R. Page, E.S. Swanson, A.P. Szczepaniak
ABELE 98 PR D57 3810 A. Abele et al. (Crystal Barrel Collab.)
ABELE 98B PL B423 175 A. Abele et al. (Crystal Barrel Collab.)
ADAMS 98B PRL 81 5760 G.S. Adams et al. (BNL E852 Collab.)
AMSLER 98 RMP 70 1293 C. Amshler
BARBERIS 98 PL B432 436 D. Barberis et al. (Omega Expt.)
BERTIN 98 PR D57 55 A. Bertin et al. (OBELIX Collab.)
CLOSE 98B PL B419 387 F.E. Close
DONNACHIE 98 PR D58 114012 A. Donnachie et al.
EVANGELISTA 98 PR D57 5370 C. Evangelista et al. (JETSET Collab.)
LOCHER 98 EPJ C4 317 M.P. Locher et al. (PSI)
ANISOVICH 97B PL B395 123 A.V. Anisovich, A.V. Sarantsev (PNPI)
BARBERIS 97B PL B413 217 D. Barberis et al. (WA 102 Collab.)
BARNES 97 PR D55 4157 T. Barnes et al. (ORNL, RAL, MCHS)
BERNARD 97 PR D56 7039 C. Bernard et al. (MILC Collab.)
BOGLIONE 97 PRL 79 1998 M. Boglione et al.

Meson Particle Listings

CLOSE	97	PL B397 333	F. Close <i>et al.</i>	(RAL, BIRM)	LEE	94	PL B323 227	J.H. Lee <i>et al.</i>	(BNL, IND, KYUN, MASD+)
FRABETTI	97	PL B391 235	P.L. Frabetti <i>et al.</i>	(FNAL E687 Collab.)	BALI	93	PL B309 378	G.S. Bali <i>et al.</i>	(LIVP)
LACOCK	97	PL B401 308	P. Lacock <i>et al.</i>	(EDIN, LIVP)	BELADIDZE	93	PL B313 276	G.M. Beladidze <i>et al.</i>	(VES Collab.)
MICHAEL	97	Hadron 97 Conf.	C. Michael		ADAMO	92	PL B287 368	A. Adamo <i>et al.</i>	(OBELIX Collab.)
AIP Conf.	Proc.	432 657			GOUZ	92	Dallas HEP 92, p. 572	Yu.P. Gouz <i>et al.</i>	(VES Collab.)
OLLER	97B	Hadron 97 Conf.	J.A. Oller, E. Oset		Proceedings XXVI Int. Conf. on High Energy Physics				
AIP Conf.	Proc.	432 413			KARCH	92	ZPHY C54 33	K. Karch <i>et al.</i>	(Crystal Ball Collab.)
THOMPSON	97	PRL 79 1630	D.R. Thompson <i>et al.</i>	(BNL E852 Collab.)	ALDE	90	PL B241 600	D.M. Alde <i>et al.</i>	(SERP, BELG, LANL, LAPP+)
WEINGARTEN	97	NPPS 53 232	D. Weingarten		MAY	90	ZPHY C46 203	B. May <i>et al.</i>	(ASTERIX Collab.)
ABELE	96B	PL B385 425	A. Abele <i>et al.</i>	(Crystal Barrel Collab.)	WEINSTEIN	90	PR D41 2236	J. Weinstein, N. Isgur	(TNTO)
ADOMEIT	96	ZPHY C71 227	J. Adomeit <i>et al.</i>	(Crystal Barrel Collab.)	ALDE	88B	PL B205 397	D.M. Alde <i>et al.</i>	(SERP, BELG, LANL, LAPP)
AMSLER	96	PR D53 295	C. Amstler, F.E. Close	(ZURI, RAL)	ASTON	88D	NP B301 525	D. Aston <i>et al.</i>	(SLAC, NAGO, CINC, INUS)
BAI	96B	PRL 76 3502	J.Z. Bai <i>et al.</i>	(BES Collab.)	ETKIN	88	PL B201 568	A. Etkin <i>et al.</i>	(BNL, CUNY)
TORNQVIST	96	PRL 76 1575	N.A. Tornqvist, M. Roos	(HELS)	CLOSE	87B	PL B196 245	F.E. Close, H.J. Lipkin	
AMELIN	95B	PL B356 595	D.V. Amelin <i>et al.</i>	(SERP, TBIL)	BOOTH	86	NP B273 677	P.S.L. Booth <i>et al.</i>	(LIVP, GLAS, CERN)
CLOSE	95	NP B443 233	F.E. Close, P.R. Page	(RAL)	BARNES	85	PL B165 434	T. Barnes	
PROKOSHKIN	95B	PAN 58 606	Y.D. Prokoshkin, S.A. Sadovsky	(SERP)	ISGUR	85	PRL 54 869	N. Isgur, R. Kokoski, J. Paton	(TNTO)
		Translated from YAF 58 662			JAFFE	77	PR D15 267,281	R. Jaffe	(MIT)
PROKOSHKIN	95C	PAN 58 853	Y.D. Prokoshkin, S.A. Sadovsky	(SERP)					
		Translated from YAF 58 921							
SEXTON	95	PRL 75 4563	J. Sexton <i>et al.</i>	(IBM)					

<i>N</i> BARYONS (<i>S</i> = 0, <i>I</i> = 1/2)	
<i>p</i>	1135
<i>n</i>	1143
<i>N</i> resonances	1150

Δ BARYONS (<i>S</i> = 0, <i>I</i> = 3/2)	
Δ resonances	1178

EXOTIC BARYONS	
Pentaquarks	1199

Λ BARYONS (<i>S</i> = -1, <i>I</i> = 0)	
Λ	1201
Λ resonances	1205

Σ BARYONS (<i>S</i> = -1, <i>I</i> = 1)	
Σ^+	1217
Σ^0	1219
Σ^-	1220
Σ resonances	1222

Ξ BARYONS (<i>S</i> = -2, <i>I</i> = 1/2)	
Ξ^0	1241
Ξ^-	1243
Ξ resonances	1246

Ω BARYONS (<i>S</i> = -3, <i>I</i> = 0)	
Ω^-	1254
Ω resonances	1255

CHARMED BARYONS (<i>C</i> = +1)	
Λ_c^+	1259
$\Lambda_c(2595)^+$	1265
$\Lambda_c(2625)^+$	1266
$\Lambda_c(2765)^+$	1267
$\Lambda_c(2880)^+$	1267
$\Lambda_c(2940)^+$	1267
$\Sigma_c(2455)$	1268
$\Sigma_c(2520)$	1268
$\Sigma_c(2800)$	1269
Ξ_c^+	1270
Ξ_c^0	1271
$\Xi_c^{'+}$	1272
$\Xi_c^{'0}$	1272
$\Xi_c(2645)$	1273
$\Xi_c(2790)$	1273
$\Xi_c(2815)$	1273
$\Xi_c(2930)$	1274
$\Xi_c(2980)$	1274
$\Xi_c(3055)$	1275
$\Xi_c(3080)$	1275
$\Xi_c(3123)$	1275
Ω_c^0	1275
$\Omega_c(2770)^0$	1276

DOUBLY-CHARMED BARYONS (<i>C</i> = +2)	
Ξ_{cc}^+	1277

BOTTOM (BEAUTY) BARYONS (<i>B</i> = -1)	
Λ_b^0	1278
Σ_b	1280
Σ_b^*	1280
Ξ_b^0, Ξ_b^-	1280
<i>b</i> -baryon ADMIXTURE ($\Lambda_b, \Xi_b, \Sigma_b, \Omega_b$)	1281

Notes in the Baryon Listings

Baryon Decay Parameters	1146
<i>N</i> and Δ Resonances	1149
Pentaquarks	1199
Baryon Magnetic Moments	1201
Λ and Σ Resonances	1203
The $\Sigma(1670)$ Region	1227
Radiative Hyperon Decays	1242
Ξ Resonances	1246
Charmed Baryons (rev.)	1257
Λ_c^+ Branching Fractions	1260



N BARYONS (S = 0, I = 1/2)

$$p, N^+ = uud; \quad n, N^0 = udd$$

p

$$I(J^P) = \frac{1}{2}(\frac{1}{2}^+) \text{ Status: } ***$$

p MASS (atomic mass units u)

The mass is known much more precisely in u (atomic mass units) than in MeV. See the next data block.

VALUE (u)	DOCUMENT ID	TECN	COMMENT
1.00727646677 ± 0.00000000010	MOHR 08	RVUE	2006 CODATA value
• • • We do not use the following data for averages, fits, limits, etc. • • •			
1.00727646688 ± 0.00000000013	MOHR 05	RVUE	2002 CODATA value
1.00727646688 ± 0.00000000013	MOHR 99	RVUE	1998 CODATA value
1.007276470 ± 0.000000012	COHEN 87	RVUE	1986 CODATA value

p MASS (MeV)

The mass is known much more precisely in u (atomic mass units) than in MeV. The conversion from u to MeV, $1 \text{ u} = 931.494028 \pm 0.000023 \text{ MeV}/c^2$ (MOHR 08, the 2006 CODATA value), involves the relatively poorly known electronic charge.

VALUE (MeV)	DOCUMENT ID	TECN	COMMENT
938.272013 ± 0.000023	MOHR 08	RVUE	2006 CODATA value
• • • We do not use the following data for averages, fits, limits, etc. • • •			
938.272029 ± 0.000080	MOHR 05	RVUE	2002 CODATA value
938.271998 ± 0.000038	MOHR 99	RVUE	1998 CODATA value
938.27231 ± 0.00028	COHEN 87	RVUE	1986 CODATA value
938.2796 ± 0.0027	COHEN 73	RVUE	1973 CODATA value

$|m_p - m_{\bar{p}}|/m_p$

A test of CPT invariance. Note that the comparison of the \bar{p} and p charge-to-mass ratio, given in the next data block, is much better determined.

VALUE	CL%	DOCUMENT ID	TECN	COMMENT
< 2 × 10⁻⁹	90	¹ HORI 06	SPEC	$\bar{p}e^-$ He atom
• • • We do not use the following data for averages, fits, limits, etc. • • •				
< 1.0 × 10 ⁻⁸	90	¹ HORI 03	SPEC	$\bar{p}e^-^4\text{He}, \bar{p}e^-^3\text{He}$
< 6 × 10 ⁻⁸	90	¹ HORI 01	SPEC	$\bar{p}e^-$ He atom
< 5 × 10 ⁻⁷		² TORII 99	SPEC	$\bar{p}e^-$ He atom

¹ HORI 01, HORI 03, and HORI 06 use the more-precisely-known constraint on the \bar{p} charge-to-mass ratio of GABRIELSE 99 (see below) to get their results. Their results are not independent of the HORI 01, HORI 03, and HORI 06 values for $|q_p + q_{\bar{p}}|/e$, below.

² TORII 99 uses the more-precisely-known constraint on the \bar{p} charge-to-mass ratio of GABRIELSE 95 (see below) to get this result. This is not independent of the TORII 99 value for $|q_p + q_{\bar{p}}|/e$, below.

\bar{p}/p CHARGE-TO-MASS RATIO, $|q_{\bar{p}}/m_{\bar{p}}|/(q_p/m_p)$

A test of CPT invariance. Listed here are measurements involving the inertial masses. For a discussion of what may be inferred about the ratio of \bar{p} and p gravitational masses, see ERICSON 90; they obtain an upper bound of 10^{-6} – 10^{-7} for violation of the equivalence principle for \bar{p} 's.

VALUE	DOCUMENT ID	TECN	COMMENT
0.99999999991 ± 0.00000000009	GABRIELSE 99	TRAP	Penning trap
• • • We do not use the following data for averages, fits, limits, etc. • • •			
1.0000000015 ± 0.0000000011	³ GABRIELSE 95	TRAP	Penning trap
1.0000000023 ± 0.0000000042	⁴ GABRIELSE 90	TRAP	Penning trap

³ Equation (2) of GABRIELSE 95 should read $M(\bar{p})/M(p) = 0.999\,999\,9985(11)$ (G. Gabrielse, private communication).

⁴ GABRIELSE 90 also measures $m_{\bar{p}}/m_{e^-} = 1836.152660 \pm 0.000083$ and $m_p/m_{e^-} = 1836.152680 \pm 0.000088$. Both are completely consistent with the 1986 CODATA (COHEN 87) value for m_p/m_{e^-} of 1836.152701 ± 0.000037 .

$$\left(\frac{q_{\bar{p}}}{m_{\bar{p}}} - \frac{q_p}{m_p} \right) / \frac{q_p}{m_p}$$

A test of CPT invariance. Taken from the \bar{p}/p charge-to-mass ratio, above.

VALUE	DOCUMENT ID
(-9 ± 9) × 10⁻¹¹ OUR EVALUATION	

$|q_p + q_{\bar{p}}|/e$

A test of CPT invariance. Note that the comparison of the \bar{p} and p charge-to-mass ratios given above is much better determined. See also a similar test involving the electron.

VALUE	CL%	DOCUMENT ID	TECN	COMMENT
< 2 × 10⁻⁹	90	⁵ HORI 06	SPEC	$\bar{p}e^-$ He atom
• • • We do not use the following data for averages, fits, limits, etc. • • •				
< 1.0 × 10 ⁻⁸	90	⁵ HORI 03	SPEC	$\bar{p}e^-^4\text{He}, \bar{p}e^-^3\text{He}$
< 6 × 10 ⁻⁸	90	⁵ HORI 01	SPEC	$\bar{p}e^-$ He atom
< 5 × 10 ⁻⁷		⁶ TORII 99	SPEC	$\bar{p}e^-$ He atom
< 2 × 10 ⁻⁵		⁷ HUGHES 92	RVUE	

⁵ HORI 01, HORI 03, and HORI 06 use the more-precisely-known constraint on the \bar{p} charge-to-mass ratio of GABRIELSE 99 (see above) to get their results. Their results are not independent of the HORI 01, HORI 03, and HORI 06 values for $|m_p - m_{\bar{p}}|/m_p$, above.

⁶ TORII 99 uses the more-precisely-known constraint on the \bar{p} charge-to-mass ratio of GABRIELSE 95 (see above) to get this result. This is not independent of the TORII 99 value for $|m_p - m_{\bar{p}}|/m_p$, above.

⁷ HUGHES 92 uses recent measurements of Rydberg-energy and cyclotron-frequency ratios.

$|q_p + q_e|/e$

See DYLLA 73 for a summary of experiments on the neutrality of matter. See also "n CHARGE" in the neutron Listings.

VALUE	DOCUMENT ID	COMMENT
< 1.0 × 10⁻²¹	⁸ DYLLA 73	Neutrality of SF ₆
• • • We do not use the following data for averages, fits, limits, etc. • • •		
< 3.2 × 10 ⁻²⁰	⁹ SENGUPTA 00	binary pulsar
< 0.8 × 10 ⁻²¹	MARINELLI 84	Magnetic levitation

⁸ Assumes that $q_n = q_p + q_e$.

⁹ SENGUPTA 00 uses the difference between the observed rate of rotational energy loss by the binary pulsar PSR B1913+16 and the rate predicted by general relativity to set this limit. See the paper for assumptions.

p MAGNETIC MOMENT

See the "Note on Baryon Magnetic Moments" in the A Listings.

VALUE (μ_N)	DOCUMENT ID	TECN	COMMENT
2.792847356 ± 0.000000023	MOHR 08	RVUE	2006 CODATA value
• • • We do not use the following data for averages, fits, limits, etc. • • •			
2.792847351 ± 0.000000028	MOHR 05	RVUE	2002 CODATA value
2.792847337 ± 0.000000029	MOHR 99	RVUE	1998 CODATA value
2.792847386 ± 0.000000063	COHEN 87	RVUE	1986 CODATA value
2.7928456 ± 0.0000011	COHEN 73	RVUE	1973 CODATA value

\bar{p} MAGNETIC MOMENT

A few early results have been omitted.

VALUE (μ_N)	DOCUMENT ID	TECN	COMMENT
-2.793 ± 0.006 OUR AVERAGE			
-2.7862 ± 0.0083	PASK 09	CNTR	\bar{p} He ⁺ hyperfine structure
-2.8005 ± 0.0090	KREISSL 88	CNTR	$\bar{p}^{208}\text{Pb } 11 \rightarrow 10 \text{ X-ray}$
-2.817 ± 0.048	ROBERTS 78	CNTR	
-2.791 ± 0.021	HU 75	CNTR	Exotic atoms

$(\mu_p + \mu_{\bar{p}}) / \mu_p$

A test of CPT invariance. Calculated from the p and \bar{p} magnetic moments, above.

VALUE	DOCUMENT ID
(-0.1 ± 2.1) × 10⁻³ OUR EVALUATION	

p ELECTRIC DIPOLE MOMENT

A nonzero value is forbidden by both T invariance and P invariance.

VALUE (10 ⁻²³ ecm)	EVTS	DOCUMENT ID	TECN	COMMENT
< 0.54	¹⁰	DMITRIEV 03		Uses ¹⁹⁹ Hg atom EDM
• • • We do not use the following data for averages, fits, limits, etc. • • •				
- 3.7 ± 6.3		CHO 89	NMR	TI F molecules
< 400		DZUBA 85	THEO	Uses ¹²⁹ Xe moment
130 ± 200		¹¹ WILKENING 84		
900 ± 1400		¹² WILKENING 84		
700 ± 900	1G	HARRISON 69	MBR	Molecular beam

Baryon Particle Listings

ρ

¹⁰DMITRIEV 03 calculates this limit from the limit on the electric dipole moment of the ¹⁹⁹Hg atom.

¹¹This WILKENING 84 value includes a finite-size effect and a magnetic effect.

¹²This WILKENING 84 value is more cautious than the other and excludes the finite-size effect, which relies on uncertain nuclear integrals.

ρ ELECTRIC POLARIZABILITY α_p

For a very complete review of the "polarizability of the nucleon and Compton scattering," see SCHUMACHER 05. His recommended values for the proton are $\alpha_p = (12.0 \pm 0.6) \times 10^{-4} \text{ fm}^3$ and $\beta_p = (1.9 \pm 0.6) \times 10^{-4} \text{ fm}^3$, almost exactly our averages.

VALUE (10^{-4} fm^3)	DOCUMENT ID	TECN	COMMENT
12.0 ± 0.6 OUR AVERAGE			
12.1 ± 1.1 ± 0.5	¹³ BEANE 03		EFT + γp
11.82 ± 0.98 +0.52 / -0.98	¹⁴ BLANPIED 01	LEGS	$p(\vec{\gamma}, \gamma), p(\vec{\gamma}, \pi^0), p(\vec{\gamma}, \pi^+)$
11.9 ± 0.5 ± 1.3	¹⁵ OLMOSDEL... 01	CNTR	γp Compton scattering
12.1 ± 0.8 ± 0.5	¹⁶ MACGIBBON 95	RVUE	global average
● ● ● We do not use the following data for averages, fits, limits, etc. ● ● ●			
11.7 ± 0.8 ± 0.7	¹⁷ BARANOV 01	RVUE	Global average
12.5 ± 0.6 ± 0.9	MACGIBBON 95	CNTR	γp Compton scattering
9.8 ± 0.4 ± 1.1	HALLIN 93	CNTR	γp Compton scattering
10.62 +1.25 +1.07 / -1.19 -1.03	ZIEGER 92	CNTR	γp Compton scattering
10.9 ± 2.2 ± 1.3	¹⁸ FEDERSPIEL 91	CNTR	γp Compton scattering

¹³BEANE 03 uses effective field theory and low-energy γp and γd Compton-scattering data. It also gets for the isoscalar polarizabilities (see the erratum) $\alpha_N = (13.0 \pm 1.9 +3.9) \times 10^{-4} \text{ fm}^3$ and $\beta_N = (-1.8 \pm 1.9 +2.1) \times 10^{-4} \text{ fm}^3$.

¹⁴BLANPIED 01 gives $\alpha_p + \beta_p$ and $\alpha_p - \beta_p$. The separate α_p and β_p are provided to us by A. Sandorfi. The first error above is statistics plus systematics; the second is from the model.

¹⁵This OLMOSDELEON 01 result uses the TAPS data alone, and does not use the (re-evaluated) sum-rule constraint that $\alpha + \beta = (13.8 \pm 0.4) \times 10^{-4} \text{ fm}^3$. See the paper for a discussion.

¹⁶MACGIBBON 95 combine the results of ZIEGER 92, FEDERSPIEL 91, and their own experiment to get a "global average" in which model errors and systematic errors are treated in a consistent way. See MACGIBBON 95 for a discussion.

¹⁷BARANOV 01 combines the results of 10 experiments from 1958 through 1995 to get a global average that takes into account both systematic and model errors and does not use the theoretical constraint on the sum $\alpha_p + \beta_p$.

¹⁸FEDERSPIEL 91 obtains for the (static) electric polarizability α_p , defined in terms of the induced electric dipole moment by $\mathbf{D} = 4\pi\epsilon_0\alpha_p\mathbf{E}$, the value $(7.0 \pm 2.2 \pm 1.3) \times 10^{-4} \text{ fm}^3$.

ρ MAGNETIC POLARIZABILITY β_p

The electric and magnetic polarizabilities are subject to a dispersion sum-rule constraint $\overline{\alpha} + \overline{\beta} = (14.2 \pm 0.5) \times 10^{-4} \text{ fm}^3$. Errors here are anticorrelated with those on $\overline{\alpha}_p$ due to this constraint.

VALUE (10^{-4} fm^3)	DOCUMENT ID	TECN	COMMENT
1.9 ± 0.5 OUR AVERAGE			
3.4 ± 1.1 ± 0.1	¹⁹ BEANE 03		EFT + γp
1.43 ± 0.98 +0.52 / -0.98	²⁰ BLANPIED 01	LEGS	$p(\vec{\gamma}, \gamma), p(\vec{\gamma}, \pi^0), p(\vec{\gamma}, \pi^+)$
1.2 ± 0.7 ± 0.5	²¹ OLMOSDEL... 01	CNTR	γp Compton scattering
2.1 ± 0.8 ± 0.5	²² MACGIBBON 95	RVUE	global average
● ● ● We do not use the following data for averages, fits, limits, etc. ● ● ●			
2.3 ± 0.9 ± 0.7	²³ BARANOV 01	RVUE	Global average
1.7 ± 0.6 ± 0.9	MACGIBBON 95	CNTR	γp Compton scattering
4.4 ± 0.4 ± 1.1	HALLIN 93	CNTR	γp Compton scattering
3.58 +1.19 +1.03 / -1.25 -1.07	ZIEGER 92	CNTR	γp Compton scattering
3.3 ± 2.2 ± 1.3	FEDERSPIEL 91	CNTR	γp Compton scattering

¹⁹BEANE 03 uses effective field theory and low-energy γp and γd Compton-scattering data. It also gets for the isoscalar polarizabilities (see the erratum) $\alpha_N = (13.0 \pm 1.9 +3.9) \times 10^{-4} \text{ fm}^3$ and $\beta_N = (-1.8 \pm 1.9 +2.1) \times 10^{-4} \text{ fm}^3$.

²⁰BLANPIED 01 gives $\alpha_p + \beta_p$ and $\alpha_p - \beta_p$. The separate α_p and β_p are provided to us by A. Sandorfi. The first error above is statistics plus systematics; the second is from the model.

²¹This OLMOSDELEON 01 result uses the TAPS data alone, and does not use the (re-evaluated) sum-rule constraint that $\alpha + \beta = (13.8 \pm 0.4) \times 10^{-4} \text{ fm}^3$. See the paper for a discussion.

²²MACGIBBON 95 combine the results of ZIEGER 92, FEDERSPIEL 91, and their own experiment to get a "global average" in which model errors and systematic errors are treated in a consistent way. See MACGIBBON 95 for a discussion.

²³BARANOV 01 combines the results of 10 experiments from 1958 through 1995 to get a global average that takes into account both systematic and model errors and does not use the theoretical constraint on the sum $\alpha_p + \beta_p$.

ρ CHARGE RADIUS

This is the rms charge radius, $\sqrt{\langle r^2 \rangle}$.

VALUE (fm)	DOCUMENT ID	TECN	COMMENT
0.8768 ± 0.0069			
● ● ● We do not use the following data for averages, fits, limits, etc. ● ● ●			
0.897 ± 0.018	BLUNDEN 05		SICK 03 + 2γ correction
0.8750 ± 0.0068	MOHR 05	RVUE	2002 CODATA value
0.895 ± 0.010 ± 0.013	SICK 03		$ep \rightarrow ep$ reanalysis
0.830 ± 0.040 ± 0.040	²⁴ ESCHRICH 01		$ep \rightarrow ep$
0.883 ± 0.014	MELNIKOV 00		1S Lamb Shift in H
0.880 ± 0.015	ROSENFELDR.00		$ep + \text{Coul. corrections}$
0.847 ± 0.008	MERGELL 96		$ep + \text{disp. relations}$
0.877 ± 0.024	WONG 94		reanalysis of Mainz ep data
0.865 ± 0.020	MCCORD 91		$ep \rightarrow ep$
0.862 ± 0.012	SIMON 80		$ep \rightarrow ep$
0.880 ± 0.030	BORKOWSKI 74		$ep \rightarrow ep$
0.810 ± 0.020	AKIMOV 72		$ep \rightarrow ep$
0.800 ± 0.025	FREREJACQ... 66		$ep \rightarrow ep$ (CH_2 tgt.)
0.805 ± 0.011	HAND 63		$ep \rightarrow ep$
²⁴ ESCHRICH 01 actually gives $\langle r^2 \rangle = (0.69 \pm 0.06 \pm 0.06) \text{ fm}^2$.			

ρ MEAN LIFE

A test of baryon conservation. See the "p Partial Mean Lives" section below for limits for identified final states. The limits here are to "anything" or are for "disappearance" modes of a bound proton (p) or (n). See also the 3ν modes in the "Partial Mean Lives" section. Table 1 of BACK 03 is a nice summary.

LIMIT (years)	PARTICLE	CL%	DOCUMENT ID	TECN	COMMENT
>5.8 × 10²⁹	n	90	²⁵ ARAKI 06	06	KLND $n \rightarrow$ invisible
>2.1 × 10²⁹	p	90	²⁶ AHMED 04	04	SNO $p \rightarrow$ invisible
● ● ● We do not use the following data for averages, fits, limits, etc. ● ● ●					
>1.9 × 10 ²⁹	n	90	²⁶ AHMED 04	SNO	$n \rightarrow$ invisible
>1.8 × 10 ²⁵	n	90	²⁷ BACK 03	BORX	
>1.1 × 10 ²⁶	p	90	²⁷ BACK 03	BORX	
>3.5 × 10 ²⁸	p	90	²⁸ ZDESENKO 03		$p \rightarrow$ invisible
>1 × 10 ²⁸	p	90	²⁹ AHMAD 02	SNO	$p \rightarrow$ invisible
>4 × 10 ²³	p	95	TRETYAK 01		$d \rightarrow n + ?$
>1.9 × 10 ²⁴	p	90	³⁰ BERNABEI 00B	DAMA	
>1.6 × 10 ²⁵	p, n	31,32	EVANS 77		
>3 × 10 ²³	p	32	DIX 70	CNTR	
>3 × 10 ²³	p, n	32,33	FLEROV 58		

²⁵ARAKI 06 looks for signs of de-excitation of the residual nucleus after disappearance of a neutron from the s shell of ¹²C.

²⁶AHMED 04 looks for γ rays from the de-excitation of a residual ¹⁵O* or ¹⁵N* following the disappearance of a neutron or proton in ¹⁶O.

²⁷BACK 03 looks for decays of unstable nuclides left after N decays of parent ¹²C, ¹³C, ¹⁶O nuclei. These are "invisible channel" limits.

²⁸ZDESENKO 03 gets this limit on proton disappearance in deuterium by analyzing SNO data in AHMAD 02.

²⁹AHMAD 02 (see its footnote 7) looks for neutrons left behind after the disappearance of the proton in deuterons.

³⁰BERNABEI 00b looks for the decay of a ¹²⁸₅₃ nucleus following the disappearance of a proton in the otherwise-stable ¹²⁹Xe nucleus.

³¹EVANS 77 looks for the daughter nuclide ¹²⁹Xe from possible ¹³⁰Te decays in ancient Te ore samples.

³²This mean-life limit has been obtained from a half-life limit by dividing the latter by $\ln(2) = 0.693$.

³³FLEROV 58 looks for the spontaneous fission of a ²³²Th nucleus after the disappearance of one of its nucleons.

\bar{p} MEAN LIFE

Of the two astrophysical limits here, that of GEER 00b involves considerably more refinements in its modeling. The other limits come from direct observations of stored antiprotons. See also "p Partial Mean Lives" after "p Partial Mean Lives," below, for exclusive-mode limits. The best (lifetime/branching fraction) limit there is 7×10^5 years, for $\bar{p} \rightarrow e^- \gamma$. We advance only the exclusive-mode limits to our Summary Tables.

LIMIT (years)	CL%	EVTS	DOCUMENT ID	TECN	COMMENT
● ● ● We do not use the following data for averages, fits, limits, etc. ● ● ●					
>8 × 10 ⁵	90		³⁴ GEER 00b		\bar{p}/p ratio, cosmic rays
>0.28			GABRIELSE 90	TRAP	Penning trap
>0.08			BELL 79	CNTR	Storage ring
>1 × 10 ⁷	90	1	GOLDEN 79	SPEC	\bar{p}/p ratio, cosmic rays
>3.7 × 10 ⁻³			BREGMAN 78	CNTR	Storage ring

³⁴GEER 00b uses agreement between a model of galactic \bar{p} production and propagation and the observed \bar{p}/p cosmic-ray spectrum to set this limit.

p DECAY MODES

See the "Note on Nucleon Decay" in our 1994 edition (Phys. Rev. D50, 1173) for a short review.

The "partial mean life" limits tabulated here are the limits on τ/B_i , where τ is the total mean life and B_i is the branching fraction for the mode in question. For N decays, p and n indicate proton and neutron partial lifetimes.

Mode	Partial mean life (10 ³⁰ years)	Confidence level
Antilepton + meson		
$\tau_1 N \rightarrow e^+ \pi$	> 158 (n), > 1600 (p)	90%
$\tau_2 N \rightarrow \mu^+ \pi$	> 100 (n), > 473 (p)	90%
$\tau_3 N \rightarrow \nu \pi$	> 112 (n), > 25 (p)	90%
$\tau_4 p \rightarrow e^+ \eta$	> 313	90%
$\tau_5 p \rightarrow \mu^+ \eta$	> 126	90%
$\tau_6 n \rightarrow \nu \eta$	> 158	90%
$\tau_7 N \rightarrow e^+ \rho$	> 217 (n), > 75 (p)	90%
$\tau_8 N \rightarrow \mu^+ \rho$	> 228 (n), > 110 (p)	90%
$\tau_9 N \rightarrow \nu \rho$	> 19 (n), > 162 (p)	90%
$\tau_{10} p \rightarrow e^+ \omega$	> 107	90%
$\tau_{11} p \rightarrow \mu^+ \omega$	> 117	90%
$\tau_{12} n \rightarrow \nu \omega$	> 108	90%
$\tau_{13} N \rightarrow e^+ K$	> 17 (n), > 150 (p)	90%
$\tau_{14} p \rightarrow e^+ K_S^0$	> 120	90%
$\tau_{15} p \rightarrow e^+ K_L^0$	> 51	90%
$\tau_{16} N \rightarrow \mu^+ K$	> 26 (n), > 120 (p)	90%
$\tau_{17} p \rightarrow \mu^+ K_S^0$	> 150	90%
$\tau_{18} p \rightarrow \mu^+ K_L^0$	> 83	90%
$\tau_{19} N \rightarrow \nu K$	> 86 (n), > 670 (p)	90%
$\tau_{20} n \rightarrow \nu K_S^0$	> 51	90%
$\tau_{21} p \rightarrow e^+ K^*(892)^0$	> 84	90%
$\tau_{22} N \rightarrow \nu K^*(892)$	> 78 (n), > 51 (p)	90%
Antilepton + mesons		
$\tau_{23} p \rightarrow e^+ \pi^+ \pi^-$	> 82	90%
$\tau_{24} p \rightarrow e^+ \pi^0 \pi^0$	> 147	90%
$\tau_{25} n \rightarrow e^+ \pi^- \pi^0$	> 52	90%
$\tau_{26} p \rightarrow \mu^+ \pi^+ \pi^-$	> 133	90%
$\tau_{27} p \rightarrow \mu^+ \pi^0 \pi^0$	> 101	90%
$\tau_{28} n \rightarrow \mu^+ \pi^- \pi^0$	> 74	90%
$\tau_{29} n \rightarrow e^+ K^0 \pi^-$	> 18	90%
Lepton + meson		
$\tau_{30} n \rightarrow e^- \pi^+$	> 65	90%
$\tau_{31} n \rightarrow \mu^- \pi^+$	> 49	90%
$\tau_{32} n \rightarrow e^- \rho^+$	> 62	90%
$\tau_{33} n \rightarrow \mu^- \rho^+$	> 7	90%
$\tau_{34} n \rightarrow e^- K^+$	> 32	90%
$\tau_{35} n \rightarrow \mu^- K^+$	> 57	90%
Lepton + mesons		
$\tau_{36} p \rightarrow e^- \pi^+ \pi^+$	> 30	90%
$\tau_{37} n \rightarrow e^- \pi^+ \pi^0$	> 29	90%
$\tau_{38} p \rightarrow \mu^- \pi^+ \pi^+$	> 17	90%
$\tau_{39} n \rightarrow \mu^- \pi^+ \pi^0$	> 34	90%
$\tau_{40} p \rightarrow e^- \pi^+ K^+$	> 75	90%
$\tau_{41} p \rightarrow \mu^- \pi^+ K^+$	> 245	90%
Antilepton + photon(s)		
$\tau_{42} p \rightarrow e^+ \gamma$	> 670	90%
$\tau_{43} p \rightarrow \mu^+ \gamma$	> 478	90%
$\tau_{44} n \rightarrow \nu \gamma$	> 28	90%
$\tau_{45} p \rightarrow e^+ \gamma \gamma$	> 100	90%
$\tau_{46} n \rightarrow \nu \gamma \gamma$	> 219	90%
Three (or more) leptons		
$\tau_{47} p \rightarrow e^+ e^+ e^-$	> 793	90%
$\tau_{48} p \rightarrow e^+ \mu^+ \mu^-$	> 359	90%
$\tau_{49} p \rightarrow e^+ \nu \nu$	> 17	90%
$\tau_{50} n \rightarrow e^+ e^- \nu$	> 257	90%
$\tau_{51} n \rightarrow \mu^+ e^- \nu$	> 83	90%
$\tau_{52} n \rightarrow \mu^+ \mu^- \nu$	> 79	90%
$\tau_{53} p \rightarrow \mu^+ e^+ e^-$	> 529	90%

$\tau_{54} p \rightarrow \mu^+ \mu^+ \mu^-$	> 675	90%
$\tau_{55} p \rightarrow \mu^+ \nu \nu$	> 21	90%
$\tau_{56} p \rightarrow e^- \mu^+ \mu^+$	> 6	90%
$\tau_{57} n \rightarrow 3 \nu$	> 0.0005	90%
$\tau_{58} n \rightarrow 5 \nu$		

Inclusive modes

$\tau_{59} N \rightarrow e^+$ anything	> 0.6 (n, p)	90%
$\tau_{60} N \rightarrow \mu^+$ anything	> 12 (n, p)	90%
$\tau_{61} N \rightarrow \nu$ anything		
$\tau_{62} N \rightarrow e^+ \pi^0$ anything	> 0.6 (n, p)	90%
$\tau_{63} N \rightarrow 2$ bodies, ν -free		

$\Delta B = 2$ dinucleon modes

The following are lifetime limits per iron nucleus.

$\tau_{64} p p \rightarrow \pi^+ \pi^+$	> 0.7	90%
$\tau_{65} p n \rightarrow \pi^+ \pi^0$	> 2	90%
$\tau_{66} n n \rightarrow \pi^+ \pi^-$	> 0.7	90%
$\tau_{67} n n \rightarrow \pi^0 \pi^0$	> 3.4	90%
$\tau_{68} p p \rightarrow e^+ e^+$	> 5.8	90%
$\tau_{69} p p \rightarrow e^+ \mu^+$	> 3.6	90%
$\tau_{70} p p \rightarrow \mu^+ \mu^+$	> 1.7	90%
$\tau_{71} p n \rightarrow e^+ \bar{\nu}$	> 2.8	90%
$\tau_{72} p n \rightarrow \mu^+ \bar{\nu}$	> 1.6	90%
$\tau_{73} n n \rightarrow \nu_e \bar{\nu}_e$	> 0.000049	90%
$\tau_{74} n n \rightarrow \nu_\mu \bar{\nu}_\mu$		
$\tau_{75} p n \rightarrow$ invisible	> 2.1×10^{-5}	90%
$\tau_{76} p p \rightarrow$ invisible	> 0.00005	90%

\bar{p} DECAY MODES

Mode	Partial mean life (years)	Confidence level
$\tau_{77} \bar{p} \rightarrow e^- \gamma$	> 7×10^5	90%
$\tau_{78} \bar{p} \rightarrow \mu^- \gamma$	> 5×10^4	90%
$\tau_{79} \bar{p} \rightarrow e^- \pi^0$	> 4×10^5	90%
$\tau_{80} \bar{p} \rightarrow \mu^- \pi^0$	> 5×10^4	90%
$\tau_{81} \bar{p} \rightarrow e^- \eta$	> 2×10^4	90%
$\tau_{82} \bar{p} \rightarrow \mu^- \eta$	> 8×10^3	90%
$\tau_{83} \bar{p} \rightarrow e^- K_S^0$	> 900	90%
$\tau_{84} \bar{p} \rightarrow \mu^- K_S^0$	> 4×10^3	90%
$\tau_{85} \bar{p} \rightarrow e^- K_L^0$	> 9×10^3	90%
$\tau_{86} \bar{p} \rightarrow \mu^- K_L^0$	> 7×10^3	90%
$\tau_{87} \bar{p} \rightarrow e^- \gamma \gamma$	> 2×10^4	90%
$\tau_{88} \bar{p} \rightarrow \mu^- \gamma \gamma$	> 2×10^4	90%
$\tau_{89} \bar{p} \rightarrow e^- \rho$		
$\tau_{90} \bar{p} \rightarrow e^- \omega$	> 200	90%
$\tau_{91} \bar{p} \rightarrow e^- K^*(892)^0$		

p PARTIAL MEAN LIVES

The "partial mean life" limits tabulated here are the limits on τ/B_i , where τ is the total mean life for the proton and B_i is the branching fraction for the mode in question.

Decaying particle: p = proton, n = bound neutron. The same event may appear under more than one partial decay mode. Background estimates may be accurate to a factor of two.

Antilepton + meson

$\tau(N \rightarrow e^+ \pi)$	τ_1					
LIMIT (10 ³⁰ years)	PARTICLE	CL%	EVTS	BKGD EST	DOCUMENT ID	TECN
> 8200	p	90	0	0.3	NISHINO 09	SKAM
> 158	n	90	3	5	MCGREW 99	IMB3
● ● ● We do not use the following data for averages, fits, limits, etc. ● ● ●						
> 540	p	90	0	0.2	MCGREW 99	IMB3
> 1600	p	90	0	0.1	SHIOZAWA 98	SKAM
> 70	p	90	0	0.5	BERGER 91	FREJ
> 70	n	90	0	≤ 0.1	BERGER 91	FREJ
> 550	p	90	0	0.7	35 BECKER-SZ... 90	IMB3
> 260	p	90	0	< 0.04	HIRATA 89c	KAMI
> 130	n	90	0	< 0.2	HIRATA 89c	KAMI
> 310	p	90	0	0.6	SEIDEL 88	IMB
> 100	n	90	0	1.6	SEIDEL 88	IMB
> 1.3	n	90	0		BARTELT 87	SOUND
> 1.3	p	90	0		BARTELT 87	SOUND
> 250	p	90	0	0.3	HAINES 86	IMB

Baryon Particle Listings

ρ

> 31	n	90	8	9	HAINES	86	IMB
> 64	p	90	0	<0.4	ARISAKA	85	KAMI
> 26	n	90	0	<0.7	ARISAKA	85	KAMI
> 82	p (free)	90	0	0.2	BLEWITT	85	IMB
> 250	p	90	0	0.2	BLEWITT	85	IMB
> 25	n	90	4	4	PARK	85	IMB
> 15	p, n	90	0		BATTISTONI	84	NUSX
> 0.5	p	90	1	0.3	³⁶ BARTELT	83	SOUD
> 0.5	n	90	1	0.3	³⁶ BARTELT	83	SOUD
> 5.8	p	90	2		³⁷ KRISHNA...	82	KOLR
> 5.8	n	90	2		³⁷ KRISHNA...	82	KOLR
> 0.1	n	90			³⁸ GURR	67	CNTR

³⁵ This BECKER-SZENDY 90 result includes data from SEIDEL 88.
³⁶ Limit based on zero events.
³⁷ We have calculated 90% CL limit from 1 confined event.
³⁸ We have converted half-life to 90% CL mean life.

$\tau(N \rightarrow \mu^+ \pi)$ 72

LIMIT	PARTICLE	CL%	EVTs	BKGD EST	DOCUMENT ID	TECN
(10 ³⁰ years)						
>6600	p	90	0	0.3	NISHINO	09 SKA M
>100	n	90	0	<0.2	HIRATA	89c KAMI
••• We do not use the following data for averages, fits, limits, etc. •••						
> 473	p	90	0	0.6	MCGREW	99 IMB3
> 90	n	90	1	1.9	MCGREW	99 IMB3
> 81	p	90	0	0.2	BERGER	91 FREJ
> 35	n	90	1	1.0	BERGER	91 FREJ
> 230	p	90	0	<0.07	HIRATA	89c KAMI
> 270	p	90	0	0.5	SEIDEL	88 IMB
> 63	n	90	0	0.5	SEIDEL	88 IMB
> 76	p	90	2	1	HAINES	86 IMB
> 23	n	90	8	7	HAINES	86 IMB
> 46	p	90	0	<0.7	ARISAKA	85 KAMI
> 20	n	90	0	<0.4	ARISAKA	85 KAMI
> 59	p (free)	90	0	0.2	BLEWITT	85 IMB
> 100	p	90	1	0.4	BLEWITT	85 IMB
> 38	n	90	1	4	PARK	85 IMB
> 10	p, n	90	0		BATTISTONI	84 NUSX
> 1.3	p, n	90	0		ALEKSEEV	81 BAKS

$\tau(N \rightarrow \nu \pi)$ 73

LIMIT	PARTICLE	CL%	EVTs	BKGD EST	DOCUMENT ID	TECN
(10 ³⁰ years)						
> 16	p	90	6	6.7	WALL	00b SOU2
>112	n	90	6	6.6	MCGREW	99 IMB3
••• We do not use the following data for averages, fits, limits, etc. •••						
> 39	n	90	4	3.8	WALL	00b SOU2
> 10	p	90	15	20.3	MCGREW	99 IMB3
> 13	n	90	1	1.2	BERGER	89 FREJ
> 10	p	90	11	14	BERGER	89 FREJ
> 25	p	90	32	32.8	³⁹ HIRATA	89c KAMI
>100	n	90	1	3	HIRATA	89c KAMI
> 6	n	90	73	60	HAINES	86 IMB
> 2	p	90	16	13	KAJITA	86 KAMI
> 40	n	90	0	1	KAJITA	86 KAMI
> 7	n	90	28	19	PARK	85 IMB
> 7	n	90	0		BATTISTONI	84 NUSX
> 2	p	90	≤ 3		BATTISTONI	84 NUSX
> 5.8	p	90	1		⁴⁰ KRISHNA...	82 KOLR
> 0.3	p	90	2		⁴¹ CHERRY	81 HOME
> 0.1	p	90			⁴² GURR	67 CNTR

³⁹ In estimating the background, this HIRATA 89c limit (as opposed to the later limits of WALL 00b and MCGREW 99) does not take into account present understanding that the flux of ν_μ originating in the upper atmosphere is depleted. Doing so would reduce the background and thus also would reduce the limit here.

⁴⁰ We have calculated 90% CL limit from 1 confined event.
⁴¹ We have converted 2 possible events to 90% CL limit.
⁴² We have converted half-life to 90% CL mean life.

$\tau(\rho \rightarrow e^+ \eta)$ 74

LIMIT	PARTICLE	CL%	EVTs	BKGD EST	DOCUMENT ID	TECN
(10 ³⁰ years)						
>313	p	90	0	0.2	MCGREW	99 IMB3
••• We do not use the following data for averages, fits, limits, etc. •••						
> 81	p	90	1	1.7	WALL	00b SOU2
> 44	p	90	0	0.1	BERGER	91 FREJ
>140	p	90	0	<0.04	HIRATA	89c KAMI
>100	p	90	0	0.6	SEIDEL	88 IMB
>200	p	90	5	3.3	HAINES	86 IMB
> 64	p	90	0	<0.8	ARISAKA	85 KAMI
> 64	p (free)	90	5	6.5	BLEWITT	85 IMB
>200	p	90	5	4.7	BLEWITT	85 IMB
> 1.2	p	90	2		⁴³ CHERRY	81 HOME

⁴³ We have converted 2 possible events to 90% CL limit.

$\tau(\rho \rightarrow \mu^+ \eta)$ 75

LIMIT	PARTICLE	CL%	EVTs	BKGD EST	DOCUMENT ID	TECN
(10 ³⁰ years)						
>126	p	90	3	2.8	MCGREW	99 IMB3
••• We do not use the following data for averages, fits, limits, etc. •••						
> 89	p	90	0	1.6	WALL	00b SOU2
> 26	p	90	1	0.8	BERGER	91 FREJ
> 69	p	90	1	<0.08	HIRATA	89c KAMI
> 1.3	p	90	0	0.7	PHILLIPS	89 HPW
> 34	p	90	1	1.5	SEIDEL	88 IMB
> 46	p	90	7	6	HAINES	86 IMB
> 26	p	90	1	<0.8	ARISAKA	85 KAMI
> 17	p (free)	90	6	6	BLEWITT	85 IMB
> 46	p	90	7	8	BLEWITT	85 IMB

$\tau(N \rightarrow \nu \eta)$ 76

LIMIT	PARTICLE	CL%	EVTs	BKGD EST	DOCUMENT ID	TECN
(10 ³⁰ years)						
>158	n	90	0	1.2	MCGREW	99 IMB3
••• We do not use the following data for averages, fits, limits, etc. •••						
> 71	n	90	2	3.7	WALL	00b SOU2
> 29	n	90	0	0.9	BERGER	89 FREJ
> 54	n	90	2	0.9	HIRATA	89c KAMI
> 16	n	90	3	2.1	SEIDEL	88 IMB
> 25	n	90	7	6	HAINES	86 IMB
> 30	n	90	0	0.4	KAJITA	86 KAMI
> 18	n	90	4	3	PARK	85 IMB
> 0.6	n	90	2		⁴⁴ CHERRY	81 HOME

⁴⁴ We have converted 2 possible events to 90% CL limit.

$\tau(N \rightarrow e^+ \rho)$ 77

LIMIT	PARTICLE	CL%	EVTs	BKGD EST	DOCUMENT ID	TECN
(10 ³⁰ years)						
>217	p	90	4	4.8	MCGREW	99 IMB3
> 75	p	90	2	2.7	HIRATA	89c KAMI
••• We do not use the following data for averages, fits, limits, etc. •••						
> 29	p	90	0	2.2	BERGER	91 FREJ
> 41	n	90	0	1.4	BERGER	91 FREJ
> 58	n	90	0	1.9	HIRATA	89c KAMI
> 38	n	90	2	4.1	SEIDEL	88 IMB
> 1.2	p	90	0		BARTELT	87 SOUD
> 1.5	n	90	0		BARTELT	87 SOUD
> 17	p	90	7	7	HAINES	86 IMB
> 14	n	90	9	4	HAINES	86 IMB
> 12	p	90	0	<1.2	ARISAKA	85 KAMI
> 6	n	90	2	<1	ARISAKA	85 KAMI
> 6.7	p (free)	90	6	6	BLEWITT	85 IMB
> 17	p	90	7	7	BLEWITT	85 IMB
> 12	n	90	4	2	PARK	85 IMB
> 0.6	n	90	1	0.3	⁴⁵ BARTELT	83 SOUD
> 0.5	p	90	1	0.3	⁴⁵ BARTELT	83 SOUD
> 9.8	p	90	1		⁴⁶ KRISHNA...	82 KOLR
> 0.8	p	90	2		⁴⁷ CHERRY	81 HOME

⁴⁵ Limit based on zero events.
⁴⁶ We have calculated 90% CL limit from 0 confined events.
⁴⁷ We have converted 2 possible events to 90% CL limit.

$\tau(N \rightarrow \mu^+ \rho)$ 78

LIMIT	PARTICLE	CL%	EVTs	BKGD EST	DOCUMENT ID	TECN
(10 ³⁰ years)						
>228	n	90	3	9.5	MCGREW	99 IMB3
>110	p	90	0	1.7	HIRATA	89c KAMI
••• We do not use the following data for averages, fits, limits, etc. •••						
> 12	p	90	0	0.5	BERGER	91 FREJ
> 22	n	90	0	1.1	BERGER	91 FREJ
> 23	n	90	1	1.8	HIRATA	89c KAMI
> 4.3	p	90	0	0.7	PHILLIPS	89 HPW
> 30	p	90	0	0.5	SEIDEL	88 IMB
> 11	n	90	1	1.1	SEIDEL	88 IMB
> 16	p	90	4	4.5	HAINES	86 IMB
> 7	n	90	6	5	HAINES	86 IMB
> 12	p	90	0	<0.7	ARISAKA	85 KAMI
> 5	n	90	1	<1.2	ARISAKA	85 KAMI
> 5.5	p (free)	90	4	5	BLEWITT	85 IMB
> 16	p	90	4	5	BLEWITT	85 IMB
> 9	n	90	1	2	PARK	85 IMB

$\tau(N \rightarrow \nu \rho)$ 79

LIMIT	PARTICLE	CL%	EVTs	BKGD EST	DOCUMENT ID	TECN
(10 ³⁰ years)						
>162	p	90	18	21.7	MCGREW	99 IMB3
> 19	n	90	0	0.5	SEIDEL	88 IMB

••• We do not use the following data for averages, fits, limits, etc. •••

Table with columns: > (value), n/p, 90, CL%, EVTS, BKGD EST, DOCUMENT ID, TECN. Rows include BERGER, HIRATA, SEIDEL, HAINES, KAJITA, BLEWITT, PARK, CHERRY.

48 We have converted 2 possible events to 90% CL limit.

τ(p → e+ ω) τ10

Table with columns: LIMIT (10^30 years), PARTICLE, CL%, EVTS, BKGD EST, DOCUMENT ID, TECN. Row: >107 p 90 7 10.8 MCGREW 99 IMB3

••• We do not use the following data for averages, fits, limits, etc. •••

Table with columns: > (value), p, 90, CL%, EVTS, BKGD EST, DOCUMENT ID, TECN. Rows include BERGER, HIRATA, SEIDEL, BARTELT, HAINES, ARISAKA, BLEWITT, BARTELT, KRISHNA, CHERRY.

49 Limit based on zero events.

50 We have calculated 90% CL limit from 0 confined events.

51 We have converted 2 possible events to 90% CL limit.

τ(p → μ+ ω) τ11

Table with columns: LIMIT (10^30 years), PARTICLE, CL%, EVTS, BKGD EST, DOCUMENT ID, TECN. Row: >117 p 90 11 12.1 MCGREW 99 IMB3

••• We do not use the following data for averages, fits, limits, etc. •••

Table with columns: > (value), p, 90, CL%, EVTS, BKGD EST, DOCUMENT ID, TECN. Rows include BERGER, HIRATA, PHILLIPS, SEIDEL, HAINES, BLEWITT.

τ(n → ν ω) τ12

Table with columns: LIMIT (10^30 years), PARTICLE, CL%, EVTS, BKGD EST, DOCUMENT ID, TECN. Row: >108 n 90 12 22.5 MCGREW 99 IMB3

••• We do not use the following data for averages, fits, limits, etc. •••

Table with columns: > (value), n, 90, CL%, EVTS, BKGD EST, DOCUMENT ID, TECN. Rows include BERGER, HIRATA, SEIDEL, HAINES, KAJITA, PARK, CHERRY.

52 We have converted 2 possible events to 90% CL limit.

τ(N → e+ K) τ13

Table with columns: LIMIT (10^30 years), PARTICLE, CL%, EVTS, BKGD EST, DOCUMENT ID, TECN. Rows: >17 n 90 35 29.4 MCGREW 99 IMB3; >150 p 90 0 <0.27 HIRATA 89c KAMI

••• We do not use the following data for averages, fits, limits, etc. •••

Table with columns: > (value), p/n, 90, CL%, EVTS, BKGD EST, DOCUMENT ID, TECN. Rows include WALL, MCGREW, BERGER, SEIDEL, HAINES, ARISAKA, BLEWITT, ALEKSEEV.

τ(p → e+ K_S^0) τ14

Table with columns: LIMIT (10^30 years), PARTICLE, CL%, EVTS, BKGD EST, DOCUMENT ID, TECN. Row: >2000 p 90 6 4.7 53 KOBAYASHI 05 SKAM

••• We do not use the following data for averages, fits, limits, etc. •••

Table with columns: > (value), p, 90, CL%, EVTS, BKGD EST, DOCUMENT ID, TECN. Rows: >120 p 90 1 1.3 WALL 00 SOU2; >76 p 90 0 0.5 BERGER 91 FREJ

53 We have doubled the p → e+ K^0 limit given in KOBAYASHI 05 to obtain this p → e+ K_S^0 limit.

τ(p → e+ K_L^0) τ15

Table with columns: LIMIT (10^30 years), PARTICLE, CL%, EVTS, BKGD EST, DOCUMENT ID, TECN. Row: >51 p 90 2 3.5 WALL 00 SOU2

••• We do not use the following data for averages, fits, limits, etc. •••

Table with columns: > (value), p, 90, CL%, EVTS, BKGD EST, DOCUMENT ID, TECN. Row: >44 p 90 0 ≤0.1 BERGER 91 FREJ

τ(N → μ+ K) τ16

Table with columns: LIMIT (10^30 years), PARTICLE, CL%, EVTS, BKGD EST, DOCUMENT ID, TECN. Rows: >120 p 90 0 <1.2 WALL 00 SOU2; >120 p 90 4 7.2 MCGREW 99 IMB3; >26 n 90 20 28.4 MCGREW 99 IMB3; >120 p 90 1 0.4 HIRATA 89c KAMI

••• We do not use the following data for averages, fits, limits, etc. •••

Table with columns: > (value), p/n, 90, CL%, EVTS, BKGD EST, DOCUMENT ID, TECN. Rows include BERGER, PHILLIPS, SEIDEL, BARTELT, HAINES, ARISAKA, BLEWITT, BARTELT, KRISHNA, CHERRY, GURR.

54 BARTELT 87 limit applies to p → μ+ K_S^0.

55 Limit based on zero events.

56 We have calculated 90% CL limit from 1 confined event.

57 We have converted half-life to 90% CL mean life.

τ(p → μ+ K_S^0) τ17

Table with columns: LIMIT (10^30 years), PARTICLE, CL%, EVTS, BKGD EST, DOCUMENT ID, TECN. Row: >2600 p 90 3 3.9 58 KOBAYASHI 05 SKAM

••• We do not use the following data for averages, fits, limits, etc. •••

Table with columns: > (value), p, 90, CL%, EVTS, BKGD EST, DOCUMENT ID, TECN. Rows: >150 p 90 0 <0.8 WALL 00 SOU2; >64 p 90 0 1.2 BERGER 91 FREJ

58 We have doubled the p → μ+ K^0 limit given in KOBAYASHI 05 to obtain this p → μ+ K_S^0 limit.

τ(p → μ+ K_L^0) τ18

Table with columns: LIMIT (10^30 years), PARTICLE, CL%, EVTS, BKGD EST, DOCUMENT ID, TECN. Row: >83 p 90 0 0.4 WALL 00 SOU2

••• We do not use the following data for averages, fits, limits, etc. •••

Table with columns: > (value), p, 90, CL%, EVTS, BKGD EST, DOCUMENT ID, TECN. Row: >44 p 90 0 ≤0.1 BERGER 91 FREJ

τ(N → ν K) τ19

Table with columns: LIMIT (10^30 years), PARTICLE, CL%, EVTS, BKGD EST, DOCUMENT ID, TECN. Rows: >2300 p 90 0 1.3 KOBAYASHI 05 SKAM; >86 n 90 0 2.4 HIRATA 89c KAMI

••• We do not use the following data for averages, fits, limits, etc. •••

Table with columns: > (value), n/p, 90, CL%, EVTS, BKGD EST, DOCUMENT ID, TECN. Rows include WALL, HAYATO, MCGREW, BERGER, ARISAKA, BLEWITT, PHILLIPS, BARTELT, HAINES, ALEKSEEV.

Baryon Particle Listings

ρ

>	32	<i>n</i>	90	0	1.4	KAJITA	86	KAMI
>	1.8	<i>p</i> (free)	90	6	11	BLEWITT	85	IMB
>	9.6	<i>p</i>	90	6	5	BLEWITT	85	IMB
>	10	<i>n</i>	90	2	2	PARK	85	IMB
>	5	<i>n</i>	90	0		BATTISTONI	84	NUSX
>	2	<i>p</i>	90	0		BATTISTONI	84	NUSX
>	0.3	<i>n</i>	90	0		61 BARTELT	83	Soud
>	0.1	<i>p</i>	90	0		61 BARTELT	83	Soud
>	5.8	<i>p</i>	90	1		62 KRISHNA...	82	KOLR
>	0.3	<i>n</i>	90	2		63 CHERRY	81	HOME

⁵⁹This ALLISON 98 limit is with no background subtraction; with subtraction the limit becomes > 46 × 10³⁰ years.

⁶⁰BARTELT 87 limit applies to $n \rightarrow \nu K_S^0$.

⁶¹Limit based on zero events.

⁶²We have calculated 90% CL limit from 1 confined event.

⁶³We have converted 2 possible events to 90% CL limit.

$\tau(n \rightarrow \nu K_S^0)$ 720

LIMIT (10 ³⁰ years)	PARTICLE	CL%	EVTs	BKGD EST	DOCUMENT ID	TECN
>260	<i>n</i>	90	34	30	64 KOBAYASHI 05	SKAM
... We do not use the following data for averages, fits, limits, etc. ...						
>51	<i>n</i>	90	16	9.1	WALL 00	SOU2

⁶⁴We have doubled the $n \rightarrow \nu K^0$ limit given in KOBAYASHI 05 to obtain this $n \rightarrow \nu K_S^0$ limit.

$\tau(\rho \rightarrow e^+ K^*(892)^0)$ 721

LIMIT (10 ³⁰ years)	PARTICLE	CL%	EVTs	BKGD EST	DOCUMENT ID	TECN
>84	ρ	90	38	52.0	MCGREW 99	IMB3
... We do not use the following data for averages, fits, limits, etc. ...						
>10	<i>p</i>	90	0	0.8	BERGER 91	FREJ
>52	<i>p</i>	90	2	1.55	HIRATA 89c	KAMI
>10	<i>p</i>	90	1	<1	ARISAKA 85	KAMI

$\tau(N \rightarrow \nu K^*(892))$ 722

LIMIT (10 ³⁰ years)	PARTICLE	CL%	EVTs	BKGD EST	DOCUMENT ID	TECN
>51	ρ	90	7	9.1	MCGREW 99	IMB3
>78	<i>n</i>	90	40	50	MCGREW 99	IMB3
... We do not use the following data for averages, fits, limits, etc. ...						
>22	<i>n</i>	90	0	2.1	BERGER 89	FREJ
>17	<i>p</i>	90	0	2.4	BERGER 89	FREJ
>20	<i>p</i>	90	5	2.1	HIRATA 89c	KAMI
>21	<i>n</i>	90	4	2.4	HIRATA 89c	KAMI
>10	<i>p</i>	90	7	6	HAINES 86	IMB
>5	<i>n</i>	90	8	7	HAINES 86	IMB
>8	<i>p</i>	90	3	2	KAJITA 86	KAMI
>6	<i>n</i>	90	2	1.6	KAJITA 86	KAMI
>5.8	<i>p</i> (free)	90	10	16	BLEWITT 85	IMB
>9.6	<i>p</i>	90	7	6	BLEWITT 85	IMB
>7	<i>n</i>	90	1	4	PARK 85	IMB
>2.1	<i>p</i>	90	1		65 BATTISTONI 82	NUSX

⁶⁵We have converted 1 possible event to 90% CL limit.

Antilepton + mesons

$\tau(\rho \rightarrow e^+ \pi^+ \pi^-)$ 723

LIMIT (10 ³⁰ years)	PARTICLE	CL%	EVTs	BKGD EST	DOCUMENT ID	TECN
>82	ρ	90	16	23.1	MCGREW 99	IMB3
... We do not use the following data for averages, fits, limits, etc. ...						
>21	<i>p</i>	90	0	2.2	BERGER 91	FREJ

$\tau(\rho \rightarrow e^+ \pi^0 \pi^0)$ 724

LIMIT (10 ³⁰ years)	PARTICLE	CL%	EVTs	BKGD EST	DOCUMENT ID	TECN
>147	ρ	90	2	0.8	MCGREW 99	IMB3
... We do not use the following data for averages, fits, limits, etc. ...						
>38	<i>p</i>	90	1	0.5	BERGER 91	FREJ

$\tau(n \rightarrow e^+ \pi^- \pi^0)$ 725

LIMIT (10 ³⁰ years)	PARTICLE	CL%	EVTs	BKGD EST	DOCUMENT ID	TECN
>52	<i>n</i>	90	38	34.2	MCGREW 99	IMB3
... We do not use the following data for averages, fits, limits, etc. ...						
>32	<i>n</i>	90	1	0.8	BERGER 91	FREJ

$\tau(\rho \rightarrow \mu^+ \pi^+ \pi^-)$ 726

LIMIT (10 ³⁰ years)	PARTICLE	CL%	EVTs	BKGD EST	DOCUMENT ID	TECN
>133	ρ	90	25	38.0	MCGREW 99	IMB3
... We do not use the following data for averages, fits, limits, etc. ...						
>17	<i>p</i>	90	1	2.6	BERGER 91	FREJ
>3.3	<i>p</i>	90	0	0.7	PHILLIPS 89	HPW

$\tau(\rho \rightarrow \mu^+ \pi^0 \pi^0)$ 727

LIMIT (10 ³⁰ years)	PARTICLE	CL%	EVTs	BKGD EST	DOCUMENT ID	TECN
>101	ρ	90	3	1.6	MCGREW 99	IMB3
... We do not use the following data for averages, fits, limits, etc. ...						
>33	<i>p</i>	90	1	0.9	BERGER 91	FREJ

$\tau(n \rightarrow \mu^+ \pi^- \pi^0)$ 728

LIMIT (10 ³⁰ years)	PARTICLE	CL%	EVTs	BKGD EST	DOCUMENT ID	TECN
>74	<i>n</i>	90	17	20.8	MCGREW 99	IMB3
... We do not use the following data for averages, fits, limits, etc. ...						
>33	<i>n</i>	90	0	1.1	BERGER 91	FREJ

$\tau(n \rightarrow e^+ K^0 \pi^-)$ 729

LIMIT (10 ³⁰ years)	PARTICLE	CL%	EVTs	BKGD EST	DOCUMENT ID	TECN
>18	<i>n</i>	90	1	0.2	BERGER 91	FREJ

Lepton + meson

$\tau(n \rightarrow e^- \pi^+)$ 730

LIMIT (10 ³⁰ years)	PARTICLE	CL%	EVTs	BKGD EST	DOCUMENT ID	TECN
>65	<i>n</i>	90	0	1.6	SEIDEL 88	IMB
... We do not use the following data for averages, fits, limits, etc. ...						
>55	<i>n</i>	90	0	1.09	BERGER 91B	FREJ
>16	<i>n</i>	90	9	7	HAINES 86	IMB
>25	<i>n</i>	90	2	4	PARK 85	IMB

$\tau(n \rightarrow \mu^- \pi^+)$ 731

LIMIT (10 ³⁰ years)	PARTICLE	CL%	EVTs	BKGD EST	DOCUMENT ID	TECN
>49	<i>n</i>	90	0	0.5	SEIDEL 88	IMB
... We do not use the following data for averages, fits, limits, etc. ...						
>33	<i>n</i>	90	0	1.40	BERGER 91B	FREJ
>2.7	<i>n</i>	90	0	0.7	PHILLIPS 89	HPW
>85	<i>n</i>	90	7	6	HAINES 86	IMB
>27	<i>n</i>	90	2	3	PARK 85	IMB

$\tau(n \rightarrow e^- \rho^+)$ 732

LIMIT (10 ³⁰ years)	PARTICLE	CL%	EVTs	BKGD EST	DOCUMENT ID	TECN
>62	<i>n</i>	90	2	4.1	SEIDEL 88	IMB
... We do not use the following data for averages, fits, limits, etc. ...						
>12	<i>n</i>	90	13	6	HAINES 86	IMB
>12	<i>n</i>	90	5	3	PARK 85	IMB

$\tau(n \rightarrow \mu^- \rho^+)$ 733

LIMIT (10 ³⁰ years)	PARTICLE	CL%	EVTs	BKGD EST	DOCUMENT ID	TECN
>7	<i>n</i>	90	1	1.1	SEIDEL 88	IMB
... We do not use the following data for averages, fits, limits, etc. ...						
>2.6	<i>n</i>	90	0	0.7	PHILLIPS 89	HPW
>9	<i>n</i>	90	7	5	HAINES 86	IMB
>9	<i>n</i>	90	2	2	PARK 85	IMB

$\tau(n \rightarrow e^- K^+)$ 734

LIMIT (10 ³⁰ years)	PARTICLE	CL%	EVTs	BKGD EST	DOCUMENT ID	TECN
>32	<i>n</i>	90	3	2.96	BERGER 91B	FREJ
... We do not use the following data for averages, fits, limits, etc. ...						
>0.23	<i>n</i>	90	0	0.7	PHILLIPS 89	HPW

$\tau(n \rightarrow \mu^- K^+)$ 735

LIMIT (10 ³⁰ years)	PARTICLE	CL%	EVTs	BKGD EST	DOCUMENT ID	TECN
>57	<i>n</i>	90	0	2.18	BERGER 91B	FREJ
... We do not use the following data for averages, fits, limits, etc. ...						
>4.7	<i>n</i>	90	0	0.7	PHILLIPS 89	HPW

Lepton + mesons

$\tau(\rho \rightarrow e^- \pi^+ \pi^+)$ 736

LIMIT (10 ³⁰ years)	PARTICLE	CL%	EVTs	BKGD EST	DOCUMENT ID	TECN
>30	ρ	90	1	2.50	BERGER 91B	FREJ
... We do not use the following data for averages, fits, limits, etc. ...						
>2.0	<i>p</i>	90	0	0.7	PHILLIPS 89	HPW

$\tau(n \rightarrow e^- \pi^+ \pi^0)$ 737

LIMIT (10 ³⁰ years)	PARTICLE	CL%	EVTs	BKGD EST	DOCUMENT ID	TECN
>29	<i>n</i>	90	1	0.78	BERGER 91B	FREJ

$\tau(p \rightarrow \mu^- \pi^+ \pi^+)$ 738

LIMIT (10 ³⁰ years)	PARTICLE	CL%	EVTs	BKGD EST	DOCUMENT ID	TECN
>17	p	90	1	1.72	BERGER 91B	FREJ

... We do not use the following data for averages, fits, limits, etc. ...

> 7.8	p	90	0	0.7	PHILLIPS 89	HPW
-------	---	----	---	-----	-------------	-----

$\tau(n \rightarrow \mu^- \pi^+ \pi^0)$ 739

LIMIT (10 ³⁰ years)	PARTICLE	CL%	EVTs	BKGD EST	DOCUMENT ID	TECN
>34	n	90	0	0.78	BERGER 91B	FREJ

$\tau(p \rightarrow e^- \pi^+ K^+)$ 740

LIMIT (10 ³⁰ years)	PARTICLE	CL%	EVTs	BKGD EST	DOCUMENT ID	TECN
>75	p	90	81	127.2	MCGREW 99	IMB3

... We do not use the following data for averages, fits, limits, etc. ...

>20	p	90	3	2.50	BERGER 91B	FREJ
-----	---	----	---	------	------------	------

$\tau(p \rightarrow \mu^- \pi^+ K^+)$ 741

LIMIT (10 ³⁰ years)	PARTICLE	CL%	EVTs	BKGD EST	DOCUMENT ID	TECN
>245	p	90	3	4.0	MCGREW 99	IMB3

... We do not use the following data for averages, fits, limits, etc. ...

> 5	p	90	2	0.78	BERGER 91B	FREJ
-----	---	----	---	------	------------	------

Antilepton + photon(s)

$\tau(p \rightarrow e^+ \gamma)$ 742

LIMIT (10 ³⁰ years)	PARTICLE	CL%	EVTs	BKGD EST	DOCUMENT ID	TECN
>670	p	90	0	0.1	MCGREW 99	IMB3

... We do not use the following data for averages, fits, limits, etc. ...

>133	p	90	0	0.3	BERGER 91	FREJ
>460	p	90	0	0.6	SEIDEL 88	IMB
>360	p	90	0	0.3	HAINES 86	IMB
> 87	p (free)	90	0	0.2	BLEWITT 85	IMB
>360	p	90	0	0.2	BLEWITT 85	IMB
> 0.1	p	90			66 GURR 67	CNTR

⁶⁶We have converted half-life to 90% CL mean life.

$\tau(p \rightarrow \mu^+ \gamma)$ 743

LIMIT (10 ³⁰ years)	PARTICLE	CL%	EVTs	BKGD EST	DOCUMENT ID	TECN
>478	p	90	0	0.1	MCGREW 99	IMB3

... We do not use the following data for averages, fits, limits, etc. ...

>155	p	90	0	0.1	BERGER 91	FREJ
>380	p	90	0	0.5	SEIDEL 88	IMB
> 97	p	90	3	2	HAINES 86	IMB
> 61	p (free)	90	0	0.2	BLEWITT 85	IMB
>280	p	90	0	0.6	BLEWITT 85	IMB
> 0.3	p	90			67 GURR 67	CNTR

⁶⁷We have converted half-life to 90% CL mean life.

$\tau(n \rightarrow \nu \gamma)$ 744

LIMIT (10 ³⁰ years)	PARTICLE	CL%	EVTs	BKGD EST	DOCUMENT ID	TECN
>28	n	90	163	144.7	MCGREW 99	IMB3

... We do not use the following data for averages, fits, limits, etc. ...

>24	n	90	10	6.86	BERGER 91B	FREJ
> 9	n	90	73	60	HAINES 86	IMB
>11	n	90	28	19	PARK 85	IMB

$\tau(p \rightarrow e^+ \gamma \gamma)$ 745

LIMIT (10 ³⁰ years)	PARTICLE	CL%	EVTs	BKGD EST	DOCUMENT ID	TECN
>100	p	90	1	0.8	BERGER 91	FREJ

$\tau(n \rightarrow \nu \gamma \gamma)$ 746

LIMIT (10 ³⁰ years)	PARTICLE	CL%	EVTs	BKGD EST	DOCUMENT ID	TECN
>219	n	90	5	7.5	MCGREW 99	IMB3

Three (or more) leptons

$\tau(p \rightarrow e^+ e^+ e^-)$ 747

LIMIT (10 ³⁰ years)	PARTICLE	CL%	EVTs	BKGD EST	DOCUMENT ID	TECN
>793	p	90	0	0.5	MCGREW 99	IMB3

... We do not use the following data for averages, fits, limits, etc. ...

>147	p	90	0	0.1	BERGER 91	FREJ
>510	p	90	0	0.3	HAINES 86	IMB
> 89	p (free)	90	0	0.5	BLEWITT 85	IMB
>510	p	90	0	0.7	BLEWITT 85	IMB

$\tau(p \rightarrow e^+ \mu^+ \mu^-)$ 748

LIMIT (10 ³⁰ years)	PARTICLE	CL%	EVTs	BKGD EST	DOCUMENT ID	TECN
>359	p	90	1	0.9	MCGREW 99	IMB3

... We do not use the following data for averages, fits, limits, etc. ...

> 81	p	90	0	0.16	BERGER 91	FREJ
> 5.0	p	90	0	0.7	PHILLIPS 89	HPW

$\tau(p \rightarrow e^+ \nu \nu)$ 749

LIMIT (10 ³⁰ years)	PARTICLE	CL%	EVTs	BKGD EST	DOCUMENT ID	TECN
>17	p	90	152	153.7	MCGREW 99	IMB3

... We do not use the following data for averages, fits, limits, etc. ...

>11	p	90	11	6.08	BERGER 91B	FREJ
-----	---	----	----	------	------------	------

$\tau(n \rightarrow e^+ e^- \nu)$ 750

LIMIT (10 ³⁰ years)	PARTICLE	CL%	EVTs	BKGD EST	DOCUMENT ID	TECN
>257	n	90	5	7.5	MCGREW 99	IMB3

... We do not use the following data for averages, fits, limits, etc. ...

> 74	n	90	0	< 0.1	BERGER 91B	FREJ
> 45	n	90	5	5	HAINES 86	IMB
> 26	n	90	4	3	PARK 85	IMB

$\tau(n \rightarrow \mu^+ e^- \nu)$ 751

LIMIT (10 ³⁰ years)	PARTICLE	CL%	EVTs	BKGD EST	DOCUMENT ID	TECN
>83	n	90	25	29.4	MCGREW 99	IMB3

... We do not use the following data for averages, fits, limits, etc. ...

>47	n	90	0	< 0.1	BERGER 91B	FREJ
-----	---	----	---	-------	------------	------

$\tau(n \rightarrow \mu^+ \mu^- \nu)$ 752

LIMIT (10 ³⁰ years)	PARTICLE	CL%	EVTs	BKGD EST	DOCUMENT ID	TECN
>79	n	90	100	145	MCGREW 99	IMB3

... We do not use the following data for averages, fits, limits, etc. ...

>42	n	90	0	1.4	BERGER 91B	FREJ
> 5.1	n	90	0	0.7	PHILLIPS 89	HPW
>16	n	90	14	7	HAINES 86	IMB
>19	n	90	4	7	PARK 85	IMB

$\tau(p \rightarrow \mu^+ e^+ e^-)$ 753

LIMIT (10 ³⁰ years)	PARTICLE	CL%	EVTs	BKGD EST	DOCUMENT ID	TECN
>529	p	90	0	1.0	MCGREW 99	IMB3

... We do not use the following data for averages, fits, limits, etc. ...

> 91	p	90	0	≤ 0.1	BERGER 91	FREJ
------	---	----	---	-------	-----------	------

$\tau(p \rightarrow \mu^+ \mu^+ \mu^-)$ 754

LIMIT (10 ³⁰ years)	PARTICLE	CL%	EVTs	BKGD EST	DOCUMENT ID	TECN
>675	p	90	0	0.3	MCGREW 99	IMB3

... We do not use the following data for averages, fits, limits, etc. ...

>119	p	90	0	0.2	BERGER 91	FREJ
> 10.5	p	90	0	0.7	PHILLIPS 89	HPW
>190	p	90	1	0.1	HAINES 86	IMB
> 44	p (free)	90	1	0.7	BLEWITT 85	IMB
>190	p	90	1	0.9	BLEWITT 85	IMB
> 2.1	p	90	1		68 BATTISTONI 82	NUSX

⁶⁸We have converted 1 possible event to 90% CL limit.

$\tau(p \rightarrow \mu^+ \nu \nu)$ 755

LIMIT (10 ³⁰ years)	PARTICLE	CL%	EVTs	BKGD EST	DOCUMENT ID	TECN
>21	p	90	7	11.23	BERGER 91B	FREJ

$\tau(p \rightarrow e^- \mu^+ \mu^+)$ 756

LIMIT (10 ³⁰ years)	PARTICLE	CL%	EVTs	BKGD EST	DOCUMENT ID	TECN
>6.0	p	90	0	0.7	PHILLIPS 89	HPW

$\tau(n \rightarrow 3\nu)$ 757

See also the "to anything" and "disappearance" limits for bound nucleons in the "p Mean Life" data block just in front of the list of possible p decay modes. Such modes could of course be three (or five) neutrinos, and the limits are stronger, but we do not repeat them here.

LIMIT (10 ³⁰ years)	PARTICLE	CL%	EVTs	BKGD EST	DOCUMENT ID	TECN
>0.00049	n	90	2	2	69 SUZUKI 93B	KAMI

... We do not use the following data for averages, fits, limits, etc. ...

>0.0023	n	90			70 GLICENSTEIN 97	KAMI
>0.00003	n	90	11	6.1	71 BERGER 91B	FREJ
>0.00012	n	90	7	11.2	71 BERGER 91B	FREJ
>0.0005	n	90	0		LEARNED 79	RVUE

⁶⁹The SUZUKI 93B limit applies to any of $\nu_e \nu_e \bar{\nu}_e$, $\nu_\mu \nu_\mu \bar{\nu}_\mu$, or $\nu_\tau \nu_\tau \bar{\nu}_\tau$.

⁷⁰GLICENSTEIN 97 uses Kamioka data and the idea that the disappearance of the neutron's magnetic moment should produce radiation.

⁷¹The first BERGER 91B limit is for $n \rightarrow \nu_e \nu_e \bar{\nu}_e$, the second is for $n \rightarrow \nu_\mu \nu_\mu \bar{\nu}_\mu$.

Baryon Particle Listings

p

$\tau(n \rightarrow 5\nu)$ 758

See the note on $\tau(n \rightarrow 3\nu)$ on the previous data block.

LIMIT (10^{30} years)	PARTICLE	CL%	EVTs	BKGD EST	DOCUMENT ID	TECN	COMMENT
>0.0017	n	90			72 GLICENSTEIN 97	KAMI	

72 GLICENSTEIN 97 uses Kamioka data and the idea that the disappearance of the neutron's magnetic moment should produce radiation.

Inclusive modes

$\tau(N \rightarrow e^+$ anything) 759

LIMIT (10^{30} years)	PARTICLE	CL%	EVTs	BKGD EST	DOCUMENT ID	TECN	COMMENT
>0.6	p, n	90			73 LEARNED 79	RVUE	

73 The electron may be primary or secondary.

$\tau(N \rightarrow \mu^+$ anything) 760

LIMIT (10^{30} years)	PARTICLE	CL%	EVTs	BKGD EST	DOCUMENT ID	TECN	COMMENT
>12	p, n	90	2		74,75 CHERRY 81	HOME	
> 1.8	p, n	90			75 COWSIK 80	CNTR	
> 6	p, n	90			75 LEARNED 79	RVUE	

74 We have converted 2 possible events to 90% CL limit.

75 The muon may be primary or secondary.

$\tau(N \rightarrow \nu$ anything) 761

Anything = π, ρ, K , etc.

LIMIT (10^{30} years)	PARTICLE	CL%	EVTs	BKGD EST	DOCUMENT ID	TECN	COMMENT
>0.0002	p, n	90	0		LEARNED 79	RVUE	

$\tau(N \rightarrow e^+ \pi^0$ anything) 762

LIMIT (10^{30} years)	PARTICLE	CL%	EVTs	BKGD EST	DOCUMENT ID	TECN	COMMENT
>0.6	p, n	90	0		LEARNED 79	RVUE	

$\tau(N \rightarrow 2$ bodies, ν -free) 763

LIMIT (10^{30} years)	PARTICLE	CL%	EVTs	BKGD EST	DOCUMENT ID	TECN	COMMENT
>1.3	p, n	90	0		ALEKSEEV 81	BAKS	

$\Delta B = 2$ dinucleon modes

$\tau(pp \rightarrow \pi^+ \pi^+)$ 764

LIMIT (10^{30} years)	CL%	EVTs	BKGD EST	DOCUMENT ID	TECN	COMMENT
>0.7	90	4	2.34	BERGER 91b	FREJ	τ per iron nucleus

$\tau(pp \rightarrow \pi^+ \pi^0)$ 765

LIMIT (10^{30} years)	CL%	EVTs	BKGD EST	DOCUMENT ID	TECN	COMMENT
>2.0	90	0	0.31	BERGER 91b	FREJ	τ per iron nucleus

$\tau(nn \rightarrow \pi^+ \pi^-)$ 766

LIMIT (10^{30} years)	CL%	EVTs	BKGD EST	DOCUMENT ID	TECN	COMMENT
>0.7	90	4	2.18	BERGER 91b	FREJ	τ per iron nucleus

$\tau(nn \rightarrow \pi^0 \pi^0)$ 767

LIMIT (10^{30} years)	CL%	EVTs	BKGD EST	DOCUMENT ID	TECN	COMMENT
>3.4	90	0	0.78	BERGER 91b	FREJ	τ per iron nucleus

$\tau(pp \rightarrow e^+ e^+)$ 768

LIMIT (10^{30} years)	CL%	EVTs	BKGD EST	DOCUMENT ID	TECN	COMMENT
>5.8	90	0	<0.1	BERGER 91b	FREJ	τ per iron nucleus

$\tau(pp \rightarrow e^+ \mu^+)$ 769

LIMIT (10^{30} years)	CL%	EVTs	BKGD EST	DOCUMENT ID	TECN	COMMENT
>3.6	90	0	<0.1	BERGER 91b	FREJ	τ per iron nucleus

$\tau(pp \rightarrow \mu^+ \mu^+)$ 770

LIMIT (10^{30} years)	CL%	EVTs	BKGD EST	DOCUMENT ID	TECN	COMMENT
>1.7	90	0	0.62	BERGER 91b	FREJ	τ per iron nucleus

$\tau(pn \rightarrow e^+ \bar{\nu})$ 771

LIMIT (10^{30} years)	CL%	EVTs	BKGD EST	DOCUMENT ID	TECN	COMMENT
>2.8	90	5	9.67	BERGER 91b	FREJ	τ per iron nucleus

$\tau(pn \rightarrow \mu^+ \bar{\nu})$ 772

LIMIT (10^{30} years)	CL%	EVTs	BKGD EST	DOCUMENT ID	TECN	COMMENT
>1.6	90	4	4.37	BERGER 91b	FREJ	τ per iron nucleus

$\tau(nn \rightarrow \nu_e \bar{\nu}_e)$ 773

We include "invisible" modes here.

LIMIT (10^{30} years)	CL%	EVTs	BKGD EST	DOCUMENT ID	TECN	COMMENT
>1.4	90			76 ARAKI 06	KLND	$nn \rightarrow$ invisible
>0.00042	90			77 TRETAK 04	CNTR	
>0.00049	90			78 BACK 03	BORX	
>0.00012	90			79 BERNABEI 00b	DAMA	
>0.00012	90	5	9.7	BERGER 91b	FREJ	τ per iron nucleus

76 ARAKI 06 looks for signs of de-excitation of the residual nucleus after disappearance of two neutrons from the s shell of ^{12}C .

77 TRETAK 04 uses data from an old Homestake-mine radiochemical experiment on limits for invisible decays of ^{39}K to ^{37}Ar .

78 BACK 03 looks for decays of unstable nuclides left after NN decays of parent ^{12}C , ^{13}C , ^{16}O nuclei. These are "invisible channel" limits.

79 BERNABEI 00b looks for the decay of a $^{129}_{54}\text{Xe}$ nucleus following the disappearance of an nn pair in the otherwise-stable $^{129}_{54}\text{Xe}$ nucleus. The limit here applies as well to $nn \rightarrow \nu_\mu \bar{\nu}_\mu, nn \rightarrow \nu_\tau \bar{\nu}_\tau$, or any "disappearance" mode.

$\tau(nn \rightarrow \nu_\mu \bar{\nu}_\mu)$ 774

LIMIT (10^{30} years)	CL%	EVTs	BKGD EST	DOCUMENT ID	TECN	COMMENT
>0.00006	90	4	4.4	BERGER 91b	FREJ	τ per iron nucleus

$\tau(pn \rightarrow \text{invisible})$ 775

This violates charge conservation as well as baryon number conservation.

VALUE (10^{30} years)	CL%	DOCUMENT ID	TECN
>0.00021	90	80 TRETAK 04	CNTR

80 TRETAK 04 uses data from an old Homestake-mine radiochemical experiment on limits for invisible decays of ^{39}K to ^{37}Ar .

$\tau(pp \rightarrow \text{invisible})$ 776

This violates charge conservation as well as baryon number conservation.

LIMIT (10^{30} years)	CL%	EVTs	BKGD EST	CL%	DOCUMENT ID	TECN
>0.00005	90				81 BACK 03	BORX
>0.0000055	90				82 BERNABEI 00b	DAMA

81 BACK 03 looks for decays of unstable nuclides left after NN decays of parent ^{12}C , ^{13}C , ^{16}O nuclei. These are "invisible channel" limits.

82 BERNABEI 00b looks for the decay of a $^{129}_{54}\text{Xe}$ nucleus following the disappearance of a pp pair in the otherwise-stable $^{129}_{54}\text{Xe}$ nucleus.

\bar{p} PARTIAL MEAN LIVES

The "partial mean life" limits tabulated here are the limits on $\bar{\tau}/B_i$, where $\bar{\tau}$ is the total mean life for the antiproton and B_i is the branching fraction for the mode in question.

$\tau(\bar{p} \rightarrow e^- \gamma)$ 777

VALUE (years)	CL%	DOCUMENT ID	TECN	COMMENT
> 7×10^5	90	GEER 00	APEX	8.9 GeV/c \bar{p} beam
>1848	95	GEER 94	CALO	8.9 GeV/c \bar{p} beam

$\tau(\bar{p} \rightarrow \mu^- \gamma)$ 778

VALUE (years)	CL%	DOCUMENT ID	TECN	COMMENT
> 5×10^4	90	GEER 00	APEX	8.9 GeV/c \bar{p} beam
> 5.0×10^4	90	HU 98b	APEX	8.9 GeV/c \bar{p} beam

$\tau(\bar{p} \rightarrow e^- \pi^0)$ 779

VALUE (years)	CL%	DOCUMENT ID	TECN	COMMENT
> 4×10^5	90	GEER 00	APEX	8.9 GeV/c \bar{p} beam
>554	95	GEER 94	CALO	8.9 GeV/c \bar{p} beam

$\tau(\bar{p} \rightarrow \mu^- \pi^0)$ 780

VALUE (years)	CL%	DOCUMENT ID	TECN	COMMENT
> 5×10^4	90	GEER 00	APEX	8.9 GeV/c \bar{p} beam
> 4.8×10^4	90	HU 98b	APEX	8.9 GeV/c \bar{p} beam

$\tau(\bar{p} \rightarrow e^- \eta)$ 781

Table with columns: VALUE (years), CL%, DOCUMENT ID, TECN, COMMENT. Includes data for GEER 00 APEX 8.9 GeV/c p beam and a note: 'We do not use the following data for averages, fits, limits, etc.'

$\tau(\bar{p} \rightarrow \mu^- \eta)$ 782

Table with columns: VALUE (years), CL%, DOCUMENT ID, TECN, COMMENT. Includes data for GEER 00 APEX 8.9 GeV/c p beam and a note: 'We do not use the following data for averages, fits, limits, etc.'

$\tau(\bar{p} \rightarrow e^- K_S^0)$ 783

Table with columns: VALUE (years), CL%, DOCUMENT ID, TECN, COMMENT. Includes data for GEER 00 APEX 8.9 GeV/c p beam and GEER 94 CALO 8.9 GeV/c p beam, and a note: 'We do not use the following data for averages, fits, limits, etc.'

$\tau(\bar{p} \rightarrow \mu^- K_S^0)$ 784

Table with columns: VALUE (years), CL%, DOCUMENT ID, TECN, COMMENT. Includes data for GEER 00 APEX 8.9 GeV/c p beam and HU 98B APEX 8.9 GeV/c p beam, and a note: 'We do not use the following data for averages, fits, limits, etc.'

$\tau(\bar{p} \rightarrow e^- K_L^0)$ 785

Table with columns: VALUE (years), CL%, DOCUMENT ID, TECN, COMMENT. Includes data for GEER 00 APEX 8.9 GeV/c p beam and GEER 94 CALO 8.9 GeV/c p beam, and a note: 'We do not use the following data for averages, fits, limits, etc.'

$\tau(\bar{p} \rightarrow \mu^- K_L^0)$ 786

Table with columns: VALUE (years), CL%, DOCUMENT ID, TECN, COMMENT. Includes data for GEER 00 APEX 8.9 GeV/c p beam and HU 98B APEX 8.9 GeV/c p beam, and a note: 'We do not use the following data for averages, fits, limits, etc.'

$\tau(\bar{p} \rightarrow e^- \gamma \gamma)$ 787

Table with columns: VALUE (years), CL%, DOCUMENT ID, TECN, COMMENT. Includes data for GEER 00 APEX 8.9 GeV/c p beam.

$\tau(\bar{p} \rightarrow \mu^- \gamma \gamma)$ 788

Table with columns: VALUE (years), CL%, DOCUMENT ID, TECN, COMMENT. Includes data for GEER 00 APEX 8.9 GeV/c p beam and HU 98B APEX 8.9 GeV/c p beam, and a note: 'We do not use the following data for averages, fits, limits, etc.'

$\tau(\bar{p} \rightarrow e^- \rho)$ 789

Table with columns: VALUE (years), CL%, DOCUMENT ID, TECN, COMMENT. Includes data for GEER 00 APEX 8.9 GeV/c p beam. Note: 'This GEER 00 measurement has been withdrawn; see GEER 00c.'

$\tau(\bar{p} \rightarrow e^- \omega)$ 790

Table with columns: VALUE (years), CL%, DOCUMENT ID, TECN, COMMENT. Includes data for GEER 00 APEX 8.9 GeV/c p beam.

$\tau(\bar{p} \rightarrow e^- K^*(892)^0)$ 791

Table with columns: VALUE (years), CL%, DOCUMENT ID, TECN, COMMENT. Includes data for GEER 00 APEX 8.9 GeV/c p beam. Note: 'This GEER 00 measurement has been withdrawn; see GEER 00c.'

Main table of references with columns: NAME, ORG, YEAR, TECH, COMMENT. Lists various experiments and publications like BLANPIED, ESCHRICH, HORI, etc., with their respective technical details and affiliations.

REFERENCES

Table of references with columns: NAME, ORG, YEAR, TECN, COMMENT. Lists references such as NISHINO 09 PRL 102 141801, PASK 09 PL B678 55, MOHR 08 RMP 80 633, etc.

n

$I(J^P) = \frac{1}{2}(1^+)$ Status: * * * *

We have omitted some results that have been superseded by later experiments. See our earlier editions.

n MASS (atomic mass units u)

The mass is known much more precisely in u (atomic mass units) than in MeV. See the next data block.

Table with columns: VALUE (u), DOCUMENT ID, TECN, COMMENT. Lists mass values for n from MOHR 08 RVUE 2006 CODATA value to COHEN 87 RVUE 1986 CODATA value.

Baryon Particle Listings

*n****n* MASS (MeV)**

The mass is known much more precisely in *u* (atomic mass units) than in MeV. The conversion from *u* to MeV, $1 \text{ u} = 931.494028 \pm 0.000023 \text{ MeV}/c^2$ (MOHR 08, the 2006 CODATA value), involves the relatively poorly known electronic charge.

VALUE (MeV)	DOCUMENT ID	TECN	COMMENT
939.565346 ± 0.000023	MOHR	08	RVUE 2006 CODATA value
• • • We do not use the following data for averages, fits, limits, etc. • • •			
939.565360 ± 0.000081	MOHR	05	RVUE 2002 CODATA value
939.565331 ± 0.000037	¹ KESSLER	99	SPEC $np \rightarrow d\gamma$
939.565330 ± 0.000038	MOHR	99	RVUE 1998 CODATA value
939.56565 ± 0.00028	^{2,3} DIFILIPPO	94	TRAP Penning trap
939.56563 ± 0.00028	COHEN	87	RVUE 1986 CODATA value
939.56564 ± 0.00028	^{3,4} GREENE	86	SPEC $np \rightarrow d\gamma$
939.5731 ± 0.0027	³ COHEN	73	RVUE 1973 CODATA value

¹ We use the 1998 CODATA *u*-to-MeV conversion factor (see the heading above) to get this mass in MeV from the much more precisely measured KESSLER 99 value of $1.00866491637 \pm 0.0000000082 \text{ u}$.

² The mass is known much more precisely in *u*: $m = 1.0086649235 \pm 0.0000000023 \text{ u}$. We use the 1986 CODATA conversion factor to get the mass in MeV.

³ These determinations are not independent of the $m_n - m_p$ measurements below.

⁴ The mass is known much more precisely in *u*: $m = 1.008664919 \pm 0.000000014 \text{ u}$.

 \bar{n} MASS

VALUE (MeV)	EVTS	DOCUMENT ID	TECN	COMMENT
939.485 ± 0.051	59	⁵ CRESTI	86	HBC $\bar{p}p \rightarrow \bar{n}n$

⁵ This is a corrected result (see the erratum). The error is statistical. The maximum systematic error is 0.029 MeV.

 $(m_n - m_{\bar{n}}) / m_n$

A test of *CPT* invariance. Calculated from the *n* and \bar{n} masses, above.

VALUE	DOCUMENT ID
$(9 \pm 6) \times 10^{-5}$ OUR EVALUATION	

 $m_n - m_p$

VALUE (MeV)	DOCUMENT ID	TECN	COMMENT
1.29333214 ± 0.00000043	⁶ MOHR	08	RVUE 2006 CODATA value
• • • We do not use the following data for averages, fits, limits, etc. • • •			
1.2933317 ± 0.00000005	⁷ MOHR	05	RVUE 2002 CODATA value
1.2933318 ± 0.00000005	⁸ MOHR	99	RVUE 1998 CODATA value
1.293318 ± 0.0000009	⁹ COHEN	87	RVUE 1986 CODATA value
1.293328 ± 0.0000072	GREENE	86	SPEC $np \rightarrow d\gamma$
1.293429 ± 0.000036	COHEN	73	RVUE 1973 CODATA value

⁶ Calculated by us from the MOHR 08 ratio $m_n/m_p = 1.00137841918(46)$. In *u*, $m_n - m_p = 1.38844920(46) \times 10^{-3} \text{ u}$.

⁷ Calculated by us from the MOHR 05 ratio $m_n/m_p = 1.00137841870 \pm 0.00000000058$. In *u*, $m_n - m_p = (1.3884487 \pm 0.00000006) \times 10^{-3} \text{ u}$.

⁸ Calculated by us from the MOHR 99 ratio $m_n/m_p = 1.00137841887 \pm 0.00000000058$. In *u*, $m_n - m_p = (1.3884489 \pm 0.00000006) \times 10^{-3} \text{ u}$.

⁹ Calculated by us from the COHEN 87 ratio $m_n/m_p = 1.001378404 \pm 0.000000009$. In *u*, $m_n - m_p = 0.001388434 \pm 0.000000009 \text{ u}$.

***n* MEAN LIFE**

We now compile only direct measurements of the lifetime, not those inferred from decay correlation measurements. For the average, we only use measurements with an error less than 10 s.

The most recent result, that of SEREBROV 05 (for a more detailed account, see SEREBROV 08A), is so far from other results that it makes no sense to include it in the average. It is up to workers in this field to resolve this issue. Until this major disagreement is understood our present average of $885.7 \pm 0.8 \text{ s}$ must be suspect.

For recent reviews of neutron physics, see NICO 05A, SEVERIJNS 06, ABELE 08, and NICO 09.

Limits on lifetimes for *bound* neutrons are given in the section "*p* PARTIAL MEAN LIVES."

VALUE (s)	DOCUMENT ID	TECN	COMMENT
885.7 ± 0.8 OUR AVERAGE			
886.3 ± 1.2 ± 3.2	NICO	05	CNTR In-beam <i>n</i> , trapped <i>p</i>
885.4 ± 0.9 ± 0.4	ARZUMANOV	00	CNTR UCN double bottle
889.2 ± 3.0 ± 3.8	BYRNE	96	CNTR Penning trap
882.6 ± 2.7	¹⁰ MAMPE	93	CNTR Gravitational trap
888.4 ± 3.1 ± 1.1	NESVIZHEV...	92	CNTR Gravitational trap
887.6 ± 3.0	MAMPE	89	CNTR Gravitational trap
891 ± 9	SPIVAK	88	CNTR Beam

• • • We do not use the following data for averages, fits, limits, etc. • • •

878.5 ± 0.7 ± 0.3	¹¹ SEREBROV	05	CNTR Gravitational trap
886.8 ± 1.2 ± 3.2	DEWEY	03	CNTR See NICO 05
888.4 ± 2.9	ALFIMENKOV	90	CNTR See NESVIZHEVSKII 92
893.6 ± 3.8 ± 3.7	BYRNE	90	CNTR See BYRNE 96
878 ± 27 ± 14	KOSSAKOW...	89	TPC Pulsed beam
877 ± 10	PAUL	89	CNTR Storage ring
876 ± 10 ± 19	LAST	88	SPEC Pulsed beam
903 ± 13	KOSVINTSEV	86	CNTR Gravitational trap
937 ± 18	¹² BYRNE	80	CNTR
875 ± 95	KOSVINTSEV	80	CNTR
881 ± 8	BONDAREN...	78	CNTR See SPIVAK 88
918 ± 14	CHRISTENSEN72		CNTR

¹⁰ IGNATOVICH 95 calls into question some of the corrections and averaging procedures used by MAMPE 93. The response, BONDARENKO 96, denies the validity of the criticisms.

¹¹ This SEREBROV 05 result is 6.5 standard deviations from our average of previous results and 5.6 standard deviations from the previous most precise result (that of ARZUMANOV 00).

¹² This measurement has been withdrawn (J. Byrne, private communication, 1990).

***n* MAGNETIC MOMENT**

See the "Note on Baryon Magnetic Moments" in the *A* Listings.

VALUE (μ_N)	DOCUMENT ID	TECN	COMMENT
-1.91304273 ± 0.00000045	MOHR	08	RVUE 2006 CODATA value
• • • We do not use the following data for averages, fits, limits, etc. • • •			
-1.91304273 ± 0.00000045	MOHR	05	RVUE 2002 CODATA value
-1.91304272 ± 0.00000045	MOHR	99	RVUE 1998 CODATA value
-1.91304275 ± 0.00000045	COHEN	87	RVUE 1986 CODATA value
-1.91304277 ± 0.00000048	¹³ GREENE	82	MRS

¹³ GREENE 82 measures the moment to be $(1.04187564 \pm 0.00000026) \times 10^{-3}$ Bohr magnetons. The value above is obtained by multiplying this by $m_p/m_e = 1836.152701 \pm 0.0000037$ (the 1986 CODATA value from COHEN 87).

***n* ELECTRIC DIPOLE MOMENT**

A nonzero value is forbidden by both *T* invariance and *P* invariance. A number of early results have been omitted. See RAMSEY 90, GOLUB 94, and LAMOREAUX 09 for reviews.

VALUE (10^{-25} ecm)	CL%	DOCUMENT ID	TECN	COMMENT
< 0.29	90	¹⁴ BAKER	06	MRS UCN's, $h\nu = 2\mu_n B \pm 2d_n E$
• • • We do not use the following data for averages, fits, limits, etc. • • •				
< 0.63	90	¹⁵ HARRIS	99	MRS $d = (-0.1 \pm 0.36) \times 10^{-25}$
< 0.97	90	ALTAREV	96	MRS $(+0.26 \pm 0.40 \pm 0.16) \times 10^{-25}$
< 1.1	95	ALTAREV	92	MRS See ALTAREV 96
< 1.2	95	SMITH	90	MRS See HARRIS 99
< 2.6	95	ALTAREV	86	MRS $d = (-1.4 \pm 0.6) \times 10^{-25}$
0.3 ± 4.8	90	PENDLEBURY	84	MRS Ultracold neutrons
< 6	90	ALTAREV	81	MRS $d = (2.1 \pm 2.4) \times 10^{-25}$
< 16	90	ALTAREV	79	MRS $d = (4.0 \pm 7.5) \times 10^{-25}$

¹⁴ LAMOREAUX 07 faults BAKER 06 for not including in the estimate of systematic error an effect due to the Earth's rotation. BAKER 07 replies (1) that the effect was included implicitly in the analysis and (2) that further analysis confirms that the BAKER 06 limit is correct as is. See also SILENKO 07.

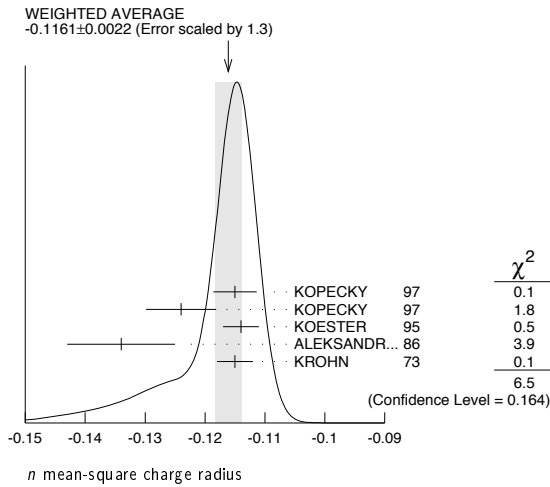
¹⁵ This HARRIS 99 result includes the result of SMITH 90. However, the averaging of the results of these two experiments has been criticized by LAMOREAUX 00.

***n* MEAN-SQUARE CHARGE RADIUS**

The mean-square charge radius of the neutron, $\langle r_n^2 \rangle$, is related to the neutron-electron scattering length b_{ne} by $\langle r_n^2 \rangle = 3(m_e a_0 / m_n) b_{ne}$, where m_e and m_n are the masses of the electron and neutron, and a_0 is the Bohr radius. Numerically, $\langle r_n^2 \rangle = 86.34 b_{ne}$, if we use a_0 for a nucleus with infinite mass.

VALUE (fm^2)	DOCUMENT ID	COMMENT
-0.1161 ± 0.0022 OUR AVERAGE		Error includes scale factor of 1.3. See the ideogram below.
-0.115 ± 0.002 ± 0.003	KOPECKY	97 <i>ne</i> scattering (Pb)
-0.124 ± 0.003 ± 0.005	KOPECKY	97 <i>ne</i> scattering (Bi)
-0.114 ± 0.003	KOESTER	95 <i>ne</i> scattering (Pb, Bi)
-0.134 ± 0.009	ALEKSANDR...	86 <i>ne</i> scattering (Bi)
-0.115 ± 0.003	¹⁶ KROHN	73 <i>ne</i> scattering (Ne, Ar, Kr, Xe)
• • • We do not use the following data for averages, fits, limits, etc. • • •		
-0.113 ± 0.003 ± 0.004	KOPECKY	95 <i>ne</i> scattering (Pb)
-0.114 ± 0.003	KOESTER	86 <i>ne</i> scattering (Pb, Bi)
-0.118 ± 0.002	KOESTER	76 <i>ne</i> scattering (Pb)
-0.120 ± 0.002	KOESTER	76 <i>ne</i> scattering (Bi)
-0.116 ± 0.003	KROHN	66 <i>ne</i> scattering (Ne, Ar, Kr, Xe)

¹⁶This value is as corrected by KOESTER 76.



n ELECTRIC POLARIZABILITY α_n

Following is the electric polarizability α_n defined in terms of the induced electric dipole moment by $\mathbf{D} = 4\pi\epsilon_0\alpha_n\mathbf{E}$. For a review, see SCHMIEDMAYER 89.

For a very complete review of the "polarizability of the nucleon and Compton scattering," see SCHUMACHER 05. His recommended values for the neutron are $\alpha_n = (12.5 \pm 1.7) \times 10^{-4} \text{ fm}^3$ and $\beta_n = (2.7 \mp 1.8) \times 10^{-4} \text{ fm}^3$, which agree with our averages within errors.

VALUE (10^{-4} fm^3)	DOCUMENT ID	TECN	COMMENT
11.6± 1.5 OUR AVERAGE			
12.5± 1.8+1.6 -1.3	17 KOSSERT 03	CNTR	$\gamma d \rightarrow \gamma pn$
8.8± 2.4±3.0	18 LUNDIN 03	CNTR	$\gamma d \rightarrow \gamma d$
12.0± 1.5±2.0	SCHMIEDM... 91	CNTR	n Pb transmission
10.7+ 3.3 -10.7	ROSE 90B	CNTR	$\gamma d \rightarrow \gamma pn$
• • • We do not use the following data for averages, fits, limits, etc. • • •			
13.6	19 KOLB 00	CNTR	$\gamma d \rightarrow \gamma pn$
0.0± 5.0	20 KOESTER 95	CNTR	n Pb, n Bi transmission
11.7+ 4.3 -11.7	ROSE 90	CNTR	See ROSE 90B
8 ±10	KOESTER 88	CNTR	n Pb, n Bi transmission
12 ±10	SCHMIEDM... 88	CNTR	n Pb, n C transmission

¹⁷KOSSERT 03 gets $\alpha_n - \beta_n = (9.8 \pm 3.6_{-1.1}^{+2.1} \pm 2.2) \times 10^{-4} \text{ fm}^3$, and uses $\alpha_n + \beta_n = (15.2 \pm 0.5) \times 10^{-4} \text{ fm}^3$ from LEVCHUK 00. Thus the errors on α_n and β_n are anti-correlated.

¹⁸LUNDIN 03 measures $\alpha_N - \beta_N = (6.4 \pm 2.4) \times 10^{-4} \text{ fm}^3$ and uses accurate values for α_p and β_p and a precise sum-rule result for $\alpha_n + \beta_n$. The second error is a model uncertainty, and errors on α_n and β_n are anticorrelated.

¹⁹KOLB 00 obtains this value with a lower limit of $7.6 \times 10^{-4} \text{ fm}^3$ but no upper limit from this experiment alone. Combined with results of ROSE 90, the $1\text{-}\sigma$ range is $(7.6\text{--}14.0) \times 10^{-4} \text{ fm}^3$.

²⁰KOESTER 95 uses natural Pb and the isotopes 208, 207, and 206. See this paper for a discussion of methods used by various groups to extract α_n from data.

n MAGNETIC POLARIZABILITY β_n

VALUE (10^{-4} fm^3)	DOCUMENT ID	TECN	COMMENT
3.7±2.0 OUR AVERAGE			
2.7±1.8+1.3 -1.6	21 KOSSERT 03	CNTR	$\gamma d \rightarrow \gamma pn$
6.5±2.4±3.0	22 LUNDIN 03	CNTR	$\gamma d \rightarrow \gamma d$
• • • We do not use the following data for averages, fits, limits, etc. • • •			
1.6	23 KOLB 00	CNTR	$\gamma d \rightarrow \gamma pn$

²¹KOSSERT 03 gets $\alpha_n - \beta_n = (9.8 \pm 3.6_{-1.1}^{+2.1} \pm 2.2) \times 10^{-4} \text{ fm}^3$, and uses $\alpha_n + \beta_n = (15.2 \pm 0.5) \times 10^{-4} \text{ fm}^3$ from LEVCHUK 00. Thus the errors on α_n and β_n are anti-correlated.

²²LUNDIN 03 measures $\alpha_N - \beta_N = (6.4 \pm 2.4) \times 10^{-4} \text{ fm}^3$ and uses accurate values for α_p and β_p and a precise sum-rule result for $\alpha_n + \beta_n$. The second error is a model uncertainty, and errors on α_n and β_n are anticorrelated.

²³KOLB 00 obtains this value with an upper limit of $7.6 \times 10^{-4} \text{ fm}^3$ but no lower limit from this experiment alone. Combined with results of ROSE 90, the $1\text{-}\sigma$ range is $(1.2\text{--}7.6) \times 10^{-4} \text{ fm}^3$.

n CHARGE

See also " $|q_p + q_e|/e$ " in the proton Listings.

VALUE ($10^{-21} e$)	DOCUMENT ID	TECN	COMMENT
- 0.4± 1.1	24 BAUMANN 88	88	Cold n deflection
• • • We do not use the following data for averages, fits, limits, etc. • • •			
-15 ± 22	25 GAEHLER 82	CNTR	Cold n deflection
²⁴ The BAUMANN 88 error ± 1.1 gives the 68% CL limits about the value -0.4 .			
²⁵ The GAEHLER 82 error ± 22 gives the 90% CL limits about the the value -15 .			

LIMIT ON nπ OSCILLATIONS

Mean Time for nπ Transition in Vacuum

A test of $\Delta B=2$ baryon number nonconservation. MOHAPATRA 80 and MOHAPATRA 89 discuss the theoretical motivations for looking for $n\pi$ oscillations. DOVER 83 and DOVER 85 give phenomenological analyses. The best limits come from looking for the decay of neutrons bound in nuclei. However, these analyses require model-dependent corrections for nuclear effects. See KABIR 83, DOVER 89, ALBERICO 91, and GAL 00 for discussions. Direct searches for $n \rightarrow \pi$ transitions using reactor neutrons are cleaner but give somewhat poorer limits. We include limits for both free and bound neutrons in the Summary Table. See MOHAPATRA 09 for a recent review.

VALUE (s)	CL%	DOCUMENT ID	TECN	COMMENT
>1.3 × 10⁸	90	CHUNG 02B	SOU2	n bound in iron
>8.6 × 10⁷	90	BALDO-...	94	CNTR Reactor (free) neutrons
• • • We do not use the following data for averages, fits, limits, etc. • • •				
>1 × 10 ⁷	90	BALDO-...	90	CNTR See BALDO-CEOLIN 94
>1.2 × 10 ⁸	90	BERGER 90	FREJ	n bound in iron
>4.9 × 10 ⁵	90	BRESSI 90	CNTR	Reactor neutrons
>4.7 × 10 ⁵	90	BRESSI 89	CNTR	See BRESSI 90
>1.2 × 10 ⁸	90	TAKITA 86	CNTR	n bound in oxygen
>1 × 10 ⁶	90	FIDECARO 85	CNTR	Reactor neutrons
>8.8 × 10 ⁷	90	PARK 85B	CNTR	
>3 × 10 ⁷		BATTISTONI 84	NUSX	
> 2.7 × 10 ⁷ -1.1 × 10 ⁸		JONES 84	CNTR	
>2 × 10 ⁷		CHERRY 83	CNTR	

LIMIT ON nn' OSCILLATIONS

Lee and Yang (LEE 56) proposed the existence of mirror world in an attempt to restore global parity symmetry. See BEREZHIANI 06 for a recent discussion.

VALUE (s)	CL%	DOCUMENT ID	TECN	COMMENT
>414	90	SEREBROV 08	CNTR	UCN, B field on & off
• • • We do not use the following data for averages, fits, limits, etc. • • •				
> 12	95	²⁶ ALTAREV 09A	CNTR	UCN, scan $0 \leq B \leq 12.5 \mu\text{T}$
>103	95	BAN 07	CNTR	UCN, B field on & off
²⁶ Losses of neutrons due to oscillations to mirror neutrons would be maximal when the magnetic fields B and B' in the two worlds were equal. Hence the scan over B by ALTAREV 09A: the limit applies for any B' over the given range. At $B' = 0$, the limit is 141 s (95% CL).				

n DECAY MODES

Mode	Fraction (Γ_i/Γ)	Confidence level
Γ_1 $p e^- \bar{\nu}_e$	100	%
Γ_2 hydrogen-atom $\bar{\nu}_e$		
Γ_3 $p e^- \bar{\nu}_e \gamma$	[a] $(3.13 \pm 0.35) \times 10^{-3}$	

Charge conservation (Q) violating mode

Γ_4 $p \nu_e \bar{\nu}_e$	Q	< 8	$\times 10^{-27}$	68%
----------------------------------	---	-----	-------------------	-----

[a] This limit is for γ energies between 15 and 340 keV.

n BRANCHING RATIOS

$\Gamma(\text{hydrogen-atom } \bar{\nu}_e)/\Gamma_{\text{total}}$ Γ_2/Γ

VALUE	CL%	DOCUMENT ID	TECN	COMMENT
• • • We do not use the following data for averages, fits, limits, etc. • • •				
<3 × 10 ⁻²	95	²⁷ GREEN 90	RVUE	
²⁷ GREEN 90 infers that $\tau(\text{hydrogen-atom } \bar{\nu}_e) > 3 \times 10^4 \text{ s}$ by comparing neutron lifetime measurements made in storage experiments with those made in β -decay experiments. However, the result depends sensitively on the lifetime measurements, and does not of course take into account more recent measurements of same.				

$\Gamma(p e^- \bar{\nu}_e \gamma)/\Gamma_{\text{total}}$ Γ_3/Γ

VALUE (units 10^{-3})	CL%	DOCUMENT ID	TECN	COMMENT
3.13±0.11±0.33		²⁸ NICO 06	CNTR	γ, p, e^- coincidence
• • • We do not use the following data for averages, fits, limits, etc. • • •				
<6.9	90	²⁹ BECK 02	CNTR	γ, p, e^- coincidence

²⁸This NICO 06 result is for γ energies between 15 and 340 keV.

²⁹This BECK 02 limit is for γ energies between 35 and 100 keV.

Baryon Particle Listings

 n

$\Gamma(\nu_e \bar{\nu}_e)/\Gamma_{\text{total}}$				Γ_4/Γ	
Forbidden by charge conservation.					
VALUE	CL%	DOCUMENT ID	TECN	COMMENT	
$< 8 \times 10^{-27}$	68	30 NORMAN	96	RVUE	${}^{71}\text{Ga} \rightarrow {}^{71}\text{Ge}$ neutrals
••• We do not use the following data for averages, fits, limits, etc. •••					
$< 9.7 \times 10^{-18}$	90	ROY	83	CNTR	${}^{113}\text{Cd} \rightarrow {}^{113m}\text{In}$ neut.
$< 7.9 \times 10^{-21}$		VAIDYA	83	CNTR	${}^{87}\text{Rb} \rightarrow {}^{87m}\text{Sr}$ neut.
$< 9 \times 10^{-24}$	90	BARABANOV	80	CNTR	${}^{71}\text{Ga} \rightarrow {}^{71}\text{GeX}$
$< 3 \times 10^{-19}$		NORMAN	79	CNTR	${}^{87}\text{Rb} \rightarrow {}^{87m}\text{Sr}$ neut.
³⁰ NORMAN 96 gets this limit by attributing SAGE and GALLEX counting rates to the charge-nonconserving transition ${}^{71}\text{Ga} \rightarrow {}^{71}\text{Ge} + \text{neutrals}$ rather than to solar-neutrino reactions.					

BARYON DECAY PARAMETERS

Written 1996 by E.D. Commins (University of California, Berkeley).

Baryon semileptonic decays

The typical spin-1/2 baryon semileptonic decay is described by a matrix element, the hadronic part of which may be written as:

$$\bar{B}_f [f_1(q^2)\gamma_\lambda + i f_2(q^2)\sigma_{\lambda\mu}q^\mu + g_1(q^2)\gamma_\lambda\gamma_5 + g_3(q^2)\gamma_5q_\lambda] B_i. \quad (1)$$

Here B_i and \bar{B}_f are spinors describing the initial and final baryons, and $q = p_i - p_f$, while the terms in f_1 , f_2 , g_1 , and g_3 account for vector, induced tensor (“weak magnetism”), axial vector, and induced pseudoscalar contributions [1]. Second-class current contributions are ignored here. In the limit of zero momentum transfer, f_1 reduces to the vector coupling constant g_V , and g_1 reduces to the axial-vector coupling constant g_A . The latter coefficients are related by Cabibbo’s theory [2], generalized to six quarks (and three mixing angles) by Kobayashi and Maskawa [3]. The g_3 term is negligible for transitions in which an e^\pm is emitted, and gives a very small correction, which can be estimated by PCAC [4], for μ^\pm modes. Recoil effects include weak magnetism, and are taken into account adequately by considering terms of first order in

$$\delta = \frac{m_i - m_f}{m_i + m_f}, \quad (2)$$

where m_i and m_f are the masses of the initial and final baryons.

The experimental quantities of interest are the total decay rate, the lepton-neutrino angular correlation, the asymmetry coefficients in the decay of a polarized initial baryon, and the polarization of the decay baryon in its own rest frame for an unpolarized initial baryon. Formulae for these quantities are derived by standard means [5] and are analogous to formulae for nuclear beta decay [6]. We use the notation of Ref. 6 in the Listings for neutron beta decay. For comparison with experiments at higher q^2 , it is necessary to modify the form factors at $q^2 = 0$ by a “dipole” q^2 dependence, and for high-precision comparisons to apply appropriate radiative corrections [7].

The ratio g_A/g_V may be written as

$$g_A/g_V = |g_A/g_V| e^{i\phi_{AV}}. \quad (3)$$

The presence of a “triple correlation” term in the transition probability, proportional to $\text{Im}(g_A/g_V)$ and of the form

$$\sigma_i \cdot (\mathbf{p}_\ell \times \mathbf{p}_\nu) \quad (4)$$

for initial baryon polarization or

$$\sigma_f \cdot (\mathbf{p}_\ell \times \mathbf{p}_\nu) \quad (5)$$

for final baryon polarization, would indicate failure of time-reversal invariance. The phase angle ϕ has been measured precisely only in neutron decay (and in ${}^{19}\text{Ne}$ nuclear beta decay), and the results are consistent with T invariance.

Hyperon nonleptonic decays

The amplitude for a spin-1/2 hyperon decaying into a spin-1/2 baryon and a spin-0 meson may be written in the form

$$M = G_F m_\pi^2 \cdot \bar{B}_f (A - B\gamma_5) B_i, \quad (6)$$

where A and B are constants [1]. The transition rate is proportional to

$$R = 1 + \gamma \hat{\omega}_f \cdot \hat{\omega}_i + (1 - \gamma)(\hat{\omega}_f \cdot \hat{\mathbf{n}})(\hat{\omega}_i \cdot \hat{\mathbf{n}}) + \alpha(\hat{\omega}_f \cdot \hat{\mathbf{n}} + \hat{\omega}_i \cdot \hat{\mathbf{n}}) + \beta \hat{\mathbf{n}} \cdot (\hat{\omega}_f \times \hat{\omega}_i), \quad (7)$$

where $\hat{\mathbf{n}}$ is a unit vector in the direction of the final baryon momentum, and $\hat{\omega}_i$ and $\hat{\omega}_f$ are unit vectors in the directions of the initial and final baryon spins. (The sign of the last term in the above equation was incorrect in our 1988 and 1990 editions.) The parameters α , β , and γ are defined as

$$\begin{aligned} \alpha &= 2 \text{Re}(s^*p)/(|s|^2 + |p|^2), \\ \beta &= 2 \text{Im}(s^*p)/(|s|^2 + |p|^2), \\ \gamma &= (|s|^2 - |p|^2)/(|s|^2 + |p|^2), \end{aligned} \quad (8)$$

where $s = A$ and $p = |\mathbf{p}_f| B/(E_f + m_f)$; here E_f and \mathbf{p}_f are the energy and momentum of the final baryon. The parameters α , β , and γ satisfy

$$\alpha^2 + \beta^2 + \gamma^2 = 1. \quad (9)$$

If the hyperon polarization is \mathbf{P}_Y , the polarization \mathbf{P}_B of the decay baryons is

$$\mathbf{P}_B = \frac{(\alpha + \mathbf{P}_Y \cdot \hat{\mathbf{n}})\hat{\mathbf{n}} + \beta(\mathbf{P}_Y \times \hat{\mathbf{n}}) + \gamma\hat{\mathbf{n}} \times (\mathbf{P}_Y \times \hat{\mathbf{n}})}{1 + \alpha\mathbf{P}_Y \cdot \hat{\mathbf{n}}}. \quad (10)$$

Here \mathbf{P}_B is defined in the rest system of the baryon, obtained by a Lorentz transformation along $\hat{\mathbf{n}}$ from the hyperon rest frame, in which $\hat{\mathbf{n}}$ and \mathbf{P}_Y are defined.

An additional useful parameter ϕ is defined by

$$\beta = (1 - \alpha^2)^{1/2} \sin \phi. \quad (11)$$

In the Listings, we compile α and ϕ for each decay, since these quantities are most closely related to experiment and are essentially uncorrelated. When necessary, we have changed the signs of reported values to agree with our sign conventions. In the Baryon Summary Table, we give α , ϕ , and Δ (defined below) with errors, and also give the value of γ without error.

Time-reversal invariance requires, in the absence of final-state interactions, that s and p be relatively real, and therefore

that $\beta = 0$. However, for the decays discussed here, the final-state interaction is strong. Thus

$$s = |s| e^{i\delta_s} \text{ and } p = |p| e^{i\delta_p}, \quad (12)$$

where δ_s and δ_p are the pion-baryon *s*- and *p*-wave strong interaction phase shifts. We then have

$$\beta = \frac{-2|s||p|}{|s|^2 + |p|^2} \sin(\delta_s - \delta_p). \quad (13)$$

One also defines $\Delta = -\tan^{-1}(\beta/\alpha)$. If *T* invariance holds, $\Delta = \delta_s - \delta_p$. For $\Lambda \rightarrow p\pi^-$ decay, the value of Δ may be compared with the *s*- and *p*-wave phase shifts in low-energy π^-p scattering, and the results are consistent with *T* invariance.

See also the note on "Radiative Hyperon Decays" in the Ξ^0 Listings in this *Review*.

References

1. E.D. Commins and P.H. Bucksbaum, *Weak Interactions of Leptons and Quarks* (Cambridge University Press, Cambridge, England, 1983).
2. N. Cabibbo, Phys. Rev. Lett. **10**, 531 (1963).
3. M. Kobayashi and T. Maskawa, Prog. Theor. Phys. **49**, 652 (1973).
4. M.L. Goldberger and S.B. Treiman, Phys. Rev. **111**, 354 (1958).
5. P.H. Frampton and W.K. Tung, Phys. Rev. **D3**, 1114 (1971).
6. J.D. Jackson, S.B. Treiman, and H.W. Wyld, Jr., Phys. Rev. **106**, 517 (1957), and Nucl. Phys. **4**, 206 (1957).
7. Y. Yokoo, S. Suzuki, and M. Morita, Prog. Theor. Phys. **50**, 1894 (1973).

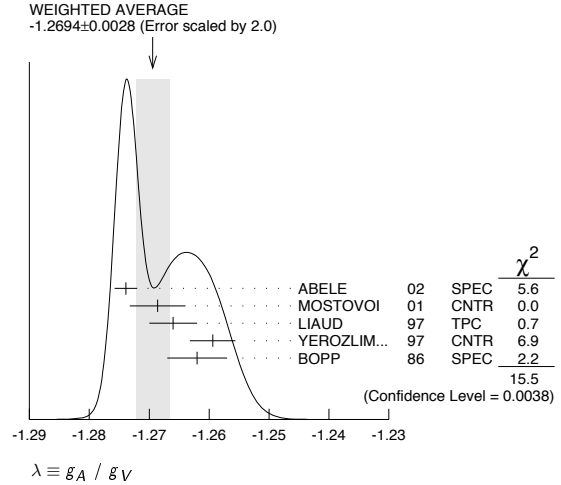
$n \rightarrow p e^- \bar{\nu}_e$ DECAY PARAMETERS

See the above "Note on Baryon Decay Parameters." For discussions of recent results, see the references cited at the beginning of the section on the neutron mean life. For discussions of the values of the weak coupling constants g_A and g_V obtained using the neutron lifetime and asymmetry parameter *A*, comparisons with other methods of obtaining these constants, and implications for particle physics and for astrophysics, see DUBBERS 91 and WOOLCOCK 91. For tests of the *V*-*A* theory of neutron decay, see EROZOLIMSKII 91B, MOSTOVOI 96, NICO 05, SEVERIJNS 06, and ABELE 08.

$\lambda \equiv g_A / g_V$

VALUE	DOCUMENT ID	TECN	COMMENT
-1.2694 ± 0.0028 OUR AVERAGE	Error includes scale factor of 2.0. See the ideogram below.		
-1.2739 ± 0.0019	31 ABELE	02 SPEC	Cold <i>n</i> , polarized, <i>A</i>
-1.2686 ± 0.0046 ± 0.0007	32 MOSTOVOI	01 CNTR	<i>A</i> and <i>B</i> × polarizations
-1.266 ± 0.004	LIAUD	97 TPC	Cold <i>n</i> , polarized, <i>A</i>
-1.2594 ± 0.0038	33 YEROZLIM...	97 CNTR	Cold <i>n</i> , polarized, <i>A</i>
-1.262 ± 0.005	BOPP	86 SPEC	Cold <i>n</i> , polarized, <i>A</i>
● ● ● We do not use the following data for averages, fits, limits, etc. ● ● ●			
-1.275 ± 0.006 ± 0.015	SCHUMANN	08 CNTR	Cold <i>n</i> , polarized
-1.274 ± 0.003	ABELE	97D SPEC	Cold <i>n</i> , polarized, <i>A</i>
-1.266 ± 0.004	SCHRECK...	95 TPC	See LIAUD 97
-1.2544 ± 0.0036	EROZOLIM...	91 CNTR	See YEROZOLIMSKY 97
-1.226 ± 0.042	MOSTOVOY	83 RVUE	
-1.261 ± 0.012	EROZOLIM...	79 CNTR	Cold <i>n</i> , polarized, <i>A</i>
-1.259 ± 0.017	34 STRATOWA	78 CNTR	<i>p</i> recoil spectrum, <i>a</i>
-1.263 ± 0.015	EROZOLIM...	77 CNTR	See EROZOLIMSKII 79
-1.250 ± 0.036	34 DOBROZE...	75 CNTR	See STRATOWA 78
-1.258 ± 0.015	35 KROHN	75 CNTR	Cold <i>n</i> , polarized, <i>A</i>
-1.263 ± 0.016	36 KROPF	74 RVUE	<i>n</i> decay alone
-1.250 ± 0.009	36 KROPF	74 RVUE	<i>n</i> decay + nuclear ft

- 31 This is the combined result of ABELE 02 and ABELE 97D.
- 32 MOSTOVOI 01 measures the two *P*-odd correlations *A* and *B*, or rather *SA* and *SB*, where *S* is the *n* polarization, in free neutron decay.
- 33 YEROZOLIMSKY 97 makes a correction to the EROZOLIMSKII 91 value.
- 34 These experiments measure the absolute value of g_A/g_V only.
- 35 KROHN 75 includes events of CHRISTENSEN 70.
- 36 KROPF 74 reviews all data through 1972.

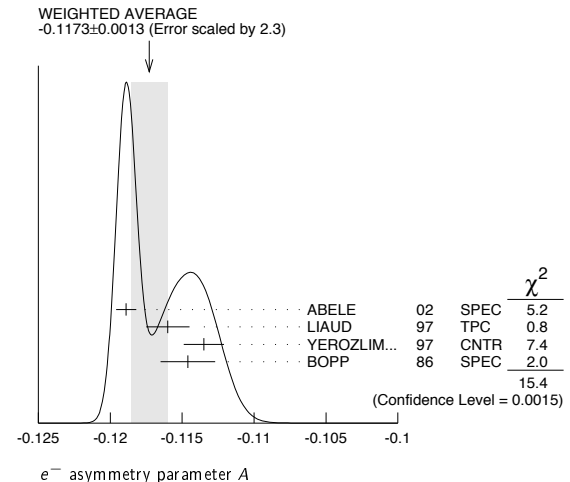


e^- ASYMMETRY PARAMETER *A*

This is the neutron-spin electron-momentum correlation coefficient. Unless otherwise noted, the values are corrected for radiative effects and weak magnetism. In the Standard Model, *A* is related to $\lambda \equiv g_A/g_V$ by $A = -2\lambda(\lambda + 1) / (1 + 3\lambda^2)$; this assumes that g_A and g_V are real.

VALUE	DOCUMENT ID	TECN	COMMENT
-0.1173 ± 0.0013 OUR AVERAGE	Error includes scale factor of 2.3. See the ideogram below.		
-0.1189 ± 0.0007	37 ABELE	02 SPEC	Cold <i>n</i> , polarized
-0.1160 ± 0.0009 ± 0.0012	LIAUD	97 TPC	Cold <i>n</i> , polarized
-0.1135 ± 0.0014	38 YEROZLIM...	97 CNTR	Cold <i>n</i> , polarized
-0.1146 ± 0.0019	BOPP	86 SPEC	Cold <i>n</i> , polarized
● ● ● We do not use the following data for averages, fits, limits, etc. ● ● ●			
-0.1138 ± 0.0046 ± 0.0021	PATTIE	09 SPEC	Ultracold <i>n</i> , polarized
-0.1168 ± 0.0017	39 MOSTOVOI	01 CNTR	Inferred
-0.1189 ± 0.0012	ABELE	97D SPEC	Cold <i>n</i> , polarized
-0.1160 ± 0.0009 ± 0.0011	SCHRECK...	95 TPC	See LIAUD 97
-0.1116 ± 0.0014	EROZOLIM...	91 CNTR	See YEROZOLIMSKY 97
-0.114 ± 0.005	40 EROZOLIM...	79 CNTR	Cold <i>n</i> , polarized
-0.113 ± 0.006	40 KROHN	75 CNTR	Cold <i>n</i> , polarized

- 37 This is the combined result of ABELE 02 and ABELE 97D.
- 38 YEROZOLIMSKY 97 makes a correction to the EROZOLIMSKII 91 value.
- 39 MOSTOVOI 01 calculates this from its measurement of $\lambda = g_A/g_V$ above.
- 40 These results are not corrected for radiative effects and weak magnetism, but the corrections are small compared to the errors.



See key on page 405

Baryon Particle Listings

n, *N*'s and Δ 's

ALTAREV	86	JETPL 44 460 Translated from ZETFP 44 360.	I.S. Altarev et al.	(PNPI)
BOPP	86	PRL 56 919 ZPHY C37 179	P. Bopp et al. E. Klempf et al.	(HEIDP, ANL, ILLG) (HEIDP, ANL, ILLG)
CRESTI	86	PL B177 206 Also PRL B200 587 (erratum)	M. Cresti et al. M. Cresti et al.	(PADO) (PADO)
GREENE	86	PRL 56 819	G.L. Greene et al.	(NBS, ILLG)
KOESTER	86	Physica B137 282	L. Koester et al.	(NBS, ILLG)
KOSVINTSEV	86	JETPL 44 571 Translated from ZETFP 44 444.	Y.Y. Kosvintsev, V.I. Morozov, G.I. Terekhov	(KIAE)
TAKITA	86	PR D34 902	M. Takita et al.	(KEK, TOKY+)
DOVER	85	PR C31 1423	C.B. Dover, A. Gal, J.M. Richard	(BNL)
FIDECARO	85	PL 156B 122	G. Fidecaro et al.	(CERN, ILLG, PADO+)
PARK	85B	NP B252 261	H.S. Park et al.	(IMB Collab.)
BATTISTONI	84	PL 133B 454	G. Battistoni et al.	(NUSEX Collab.)
JONES	84	PRL 52 720	T.W. Jones et al.	(IMB Collab.)
PENDBLEBURY	84	PL 136B 327	J.M. Pendlebury et al.	(SUSS, HARV, RAL+)
CHERRY	83	PRL 50 1354	M.L. Cherry et al.	(PENN, BNL)
DOVER	83	PR D27 1090	C.B. Dover, A. Gal, J.M. Richard	(BNL)
KABIR	83	PRL 51 231	P.K. Kabir	(HARV)
MOSTOVOY	83	JETPL 37 196 Translated from ZETFP 37 162.	Y.A. Mostovoy	(KIAE)
ROY	83	PR D28 1770	A. Roy et al.	(TATA)
VAIDYA	83	PR D27 486	S.C. Vaidya et al.	(TATA)
GAEHLER	82	PR D25 2887	R. Gähler, J. Kalus, W. Mampe	(BAYR, ILLG)
GREENE	82	Metrologia 18 93	G.L. Greene et al.	(YALE, HARV, ILLG+)
ALTAREV	81	PL 102B 13	I.S. Altarev et al.	(PNPI)
BARABANOV	80	JETPL 32 359 Translated from ZETFP 32 384.	I.R. Barabanov et al.	(PNPI)
BYRNE	80	PL 92B 274	J. Byrne et al.	(SUSS, RL)
KOSVINTSEV	80	JETPL 31 236	Y.Y. Kosvintsev et al.	(JINR)
MOHAPATRA	80	PRL 44 1316	R.N. Mohapatra, R.E. Marshak	(CUNY, VPI)
ALTAREV	79	JETPL 29 730 Translated from ZETFP 29 794.	I.S. Altarev et al.	(PNPI)
EROZOLIM...	79	SJNP 30 356 Translated from YAF 30 692.	B.G. Erozolimsky et al.	(KIAE)
NORMAN	79	PRL 43 1226	E.B. Norman, A.G. Seamster	(WASH)
BONDAREN...	78	JETPL 28 303 Translated from ZETFP 28 326.	L.N. Bondarenko et al.	(KIAE)
Also		Smolence Conf.	P.G. Bondarenko	(KIAE)
EROZOLIM...	78	SJNP 28 48 Translated from YAF 28 98.	B.G. Erozolimsky et al.	(KIAE)
STRATOWA	78	PR D18 3970	C. Stratowa, R. Dobrozemsky, P. Weinzierl	(SEIB)
EROZOLIM...	77	JETPL 23 663 Translated from ZETFP 23 720.	B.G. Erozolimsky et al.	(KIAE)
KOESTER	76	PRL 36 1021	Koester et al.	(YALE, ISNG)
STEINBERG	76	PR D13 2469	R. Steinberg et al.	(SEIB)
DOBROZE...	75	PR D11 510	R. Dobrozemsky et al.	(ANL)
KROHN	75	PL 55B 175	V.E. Krohn, G.R. Ringo	(ANL)
EROZOLIM...	74	JETPL 20 345 Translated from ZETFP 20 745.	B.G. Erozolimsky et al.	(KIAE)
KROPF	74	ZPHY 267 129 Also NP A154 160	H. Kropf, E. Paul	(LINZ) (VIEN)
STEINBERG	74	PRL 33 41	R.L. Steinberg et al.	(YALE, ISNG)
COHEN	73	JPCRD 2 664	E.F. Cohen, B.N. Taylor	(RSC, NBS)
KROHN	73	PR D8 1305	V.E. Krohn, G.R. Ringo	(RISO)
CHRISTENSEN	72	PR D5 1628	C.J. Christensen et al.	(ANL)
CHRISTENSEN	70C	PR C1 1693	C.J. Christensen, V.E. Krohn, G.R. Ringo	(KIAE)
EROZOLIM...	70C	PL 33B 351	B.G. Erozolimsky et al.	(KIAE)
GRIGOREV	68	SJNP 6 239 Translated from YAF 6 329.	V.K. Grigoriev et al.	(ITEP)
KROHN	66	PR 148 1303	V.E. Krohn, G.R. Ringo	(COLU, BNL)
LEE	56	PR 104 254	T.D. Lee, C.N. Yang	(COLU, BNL)

N AND Δ RESONANCES

I. Introduction

The excited states of the nucleon have been studied in a large number of formation and production experiments. The conventional (*i.e.*, Breit-Wigner) masses, pole positions, widths, and elasticities of the *N* and Δ resonances in the Baryon Summary Table come largely from partial-wave analyses of πN total, elastic, and charge-exchange scattering data. Partial-wave analyses have also been performed on much smaller data sets to get $N\eta$, ΔK , and ΣK branching fractions. Other branching fractions come from isobar-model analyses of $\pi N \rightarrow N\pi\pi$ data. Finally, many $N\gamma$ branching fractions have been determined from photoproduction experiments (see Sec. III).

Table 1 lists all the *N* and Δ entries in the Baryon Listings and gives our evaluation of the status of each, both overall and channel by channel. Only the ‘‘established’’ resonances (overall status 3 or 4 stars) appear in the Baryon Summary Table. We generally consider a resonance to be established only if it has been seen in at least two independent analyses of elastic scattering and if the relevant partial-wave amplitudes do not behave erratically or have large errors.

We have, in this 2006 *Review*, made slight adjustments to our estimates of *N* and Δ masses, widths, and elasticities.

II. Using the *N* and Δ listings

Written 2002 by G. Höhler (University of Karlsruhe) and R.L. Workman, (George Washington University).

In the inelastic region, a resonance is associated with a cluster of poles on different Riemann sheets. If one of these poles is located near the real axis and far enough from branch points, it will be strongly dominant. If one of the final-state particles itself has a strong decay, it is also necessary to consider branch points in the lower half plane that belong to thresholds for two-particle final states; see for example Refs. 3 and 4.

Table 1. The status of the *N* and Δ resonances. Only those with an overall status of *** or **** are included in the main Baryon Summary Table.

Particle	$L_{2I,2J}$	Overall status	Status as seen in —						
			$N\pi$	$N\eta$	ΔK	ΣK	$\Delta\pi$	$N\rho$	$N\gamma$
$N(939)$	P_{11}	****							
$N(1440)$	P_{11}	****	****	*			***	*	***
$N(1520)$	D_{13}	****	****	***			****	****	****
$N(1535)$	S_{11}	****	****	****			*	**	***
$N(1650)$	S_{11}	****	****	*	***	**	***	**	***
$N(1675)$	D_{15}	****	****	*	*		****	*	****
$N(1680)$	F_{15}	****	****	*			****	****	****
$N(1700)$	D_{13}	***	***	*	**	*	**	*	**
$N(1710)$	P_{11}	***	***	**	**	*	**	*	***
$N(1720)$	P_{13}	****	****	*	**	*	*	**	**
$N(1900)$	P_{13}	**	**					*	
$N(1990)$	F_{17}	**	**	*	*	*	*	*	*
$N(2000)$	F_{15}	**	**	*	*	*	*	**	*
$N(2080)$	D_{13}	**	**	*	*				*
$N(2090)$	S_{11}	*	*						
$N(2100)$	P_{11}	*	*	*					
$N(2190)$	G_{17}	****	****	*	*	*	*	*	*
$N(2200)$	D_{15}	**	**	*	*				
$N(2220)$	H_{19}	****	****	*					
$N(2250)$	G_{19}	****	****	*					
$N(2600)$	I_{11}	***	***						
$N(2700)$	K_{113}	**	**						
$\Delta(1232)$	P_{33}	****	****	F					****
$\Delta(1600)$	P_{33}	***	***	o				***	*
$\Delta(1620)$	S_{31}	****	****	r				****	****
$\Delta(1700)$	D_{33}	****	****	b		*		***	**
$\Delta(1750)$	P_{31}	*	*	i					
$\Delta(1900)$	S_{31}	**	**	d		*	*	**	*
$\Delta(1905)$	F_{35}	****	****	d		*	*	**	***
$\Delta(1910)$	P_{31}	****	****	e		*	*	*	*
$\Delta(1920)$	P_{33}	***	***	n		*	**	*	*
$\Delta(1930)$	D_{35}	***	***			*			**
$\Delta(1940)$	D_{33}	*	*	F					
$\Delta(1950)$	F_{37}	****	****	o		*		****	****
$\Delta(2000)$	F_{35}	**	**	r				**	
$\Delta(2150)$	S_{31}	*	*	b					
$\Delta(2200)$	G_{37}	*	*	i					
$\Delta(2300)$	H_{39}	**	**	d					
$\Delta(2350)$	D_{35}	*	*	d					
$\Delta(2390)$	F_{37}	*	*	e					
$\Delta(2400)$	G_{39}	**	**	n					
$\Delta(2420)$	H_{31}	****	****						*
$\Delta(2750)$	J_{313}	**	**						
$\Delta(2950)$	K_{315}	**	**						

**** Existence is certain, and properties are at least fairly well explored.
 *** Existence ranges from very likely to certain, but further confirmation is desirable and/or quantum numbers, branching fractions, etc. are not well determined.
 ** Evidence of existence is only fair.
 * Evidence of existence is poor.

Baryon Particle Listings

N 's and Δ 's, $N(1440)$

Our Particle Listings and Summary Tables include pole parameters for the N and Δ resonances. However, the Breit-Wigner parameters are most often quoted and are used in model-based studies of the baryons and associated reaction dynamics. Problems associated with this choice were discussed in our 2000 edition [5]. Here we just point out that the use of Breit-Wigner parameters for complicated structures, such as the $N(1440)$, should be avoided. In this case, the method used in Ref. 4 is suitable for the analysis.

In the search for “missing” quark-model states, indications of new structures occasionally are found. Often these are associated (if possible) with the one- and two-star states listed in Table 1. We caution against this: The status of the one- and two-star states found in the Karlsruhe-Helsinki (KH80) [2] and Carnegie-Mellon/Berkeley (CMB80) [6] fits is now doubtful. Predictions for π^+p spin-rotation parameters from those fits are in significant disagreement with recent ITEP/PNPI measurements [7], whereas the predictions of Ref. 8 are good. This discrepancy has been associated in Ref. 7 with the behavior of a zero trajectory at a “critical point” (see Sec. 2.1.1 of Ref. 2) near a pion lab momentum of 0.8 GeV/c. According to Ref. 7, the effect on the 4-star resonances $\Delta(1905)$ and $\Delta(1950)$ is small, but the effect on the 3-star resonances $\Delta(1920)$ and $\Delta(1930)$ is large. For a study of the approximation made in Ref. 7 and of problems with some higher resonances, the detailed treatment of zero trajectories in Ref. 9 is relevant. This problem should also be considered in any multi-channel analysis that uses the KH80 and CMB80 amplitudes as input.

III. Electromagnetic interactions

Revised 2003 by R.L. Workman (George Washington University).

Nearly all the entries in the Listings concerning electromagnetic properties of the N and Δ resonances are $N\gamma$ couplings. These couplings, the helicity amplitudes $A_{1/2}$ and $A_{3/2}$, have been obtained in partial-wave analyses of single-pion photoproduction, η photoproduction, and Compton scattering. Most photoproduction analyses have taken the existence, masses, and widths of the resonances from the $\pi N \rightarrow \pi N$ analyses, and have only determined the $N\gamma$ couplings. This approach is only applicable to resonances with a significant $N\pi$ coupling. A brief description of the various methods of analysis of photoproduction data may be found in our 1992 edition [10].

Our Listings omit a number of analyses that are now obsolete. Most of the older results may be found in our 1982 edition [11]. The errors quoted for the couplings in the Listings are calculated in different ways in different analyses and therefore should be used with care. In general, the systematic differences between the analyses caused by using different parameterization schemes are probably more indicative of the true uncertainties than are the quoted errors.

Probably the most reliable analyses, for most resonances, are ARAI 80, CRAWFORD 80, AWAJI 81, FUJII 81, CRAWFORD 83, and ARNDT 96. There is an update to the Crawford

analysis [1]. The errors we give on $N\gamma$ couplings are a combination of the stated statistical errors on the analyses and the systematic differences between them. The analyses are given equal weight, except ARNDT 96 is weighted, rather arbitrarily, by a factor of two because its data set is at least 50% larger than those of the other analyses and contains many new high-quality measurements. The $\Delta(1232)$ and $N(1535)$ are special cases and are discussed in the 2002 *Review* [12].

The Baryon Summary Table gives $N\gamma$ branching fractions for those resonances whose couplings are considered to be reasonably well established. The $N\gamma$ partial width Γ_γ is given in terms of the helicity amplitudes $A_{1/2}$ and $A_{3/2}$ by

$$\Gamma_\gamma = \frac{k^2}{\pi} \frac{2M_N}{(2J+1)M_R} [|A_{1/2}|^2 + |A_{3/2}|^2] .$$

Here M_N and M_R are the nucleon and resonance masses, J is the resonance spin, and k is the photon c.m. decay momentum.

See our 2002 *Review* [12] for some further discussion.

References

1. Proceedings of the Workshop on the Physics of Excited Nucleons (NSTAR2001), eds. D. Drechsel and L. Tiator (World Scientific, Singapore, 2001).
2. G. Höhler, Pion-Nucleon Scattering, Landolt-Börnstein Vol. I/9b2 (1983), ed. H. Schopper, Springer Verlag.
3. W.R. Frazier and A.W. Hendry, Phys. Rev. **134**, B1307 (1964).
4. R.E. Cutkosky and S. Wang, Phys. Rev. **D42**, 235 (1990).
5. D.E. Groom *et al.*, Eur. Phys. J. **C15**, 1 (2000).
6. R.E. Cutkosky *et al.*, Baryon 1980, *IV International Conference on Baryon Resonances*, Toronto, ed. N. Isgur, p. 19.
7. I.G. Alekseev *et al.*, Phys. Rev. **C55**, 2049 (1997); Phys. Lett. **B485**, 32 (2000); Eur. Phys. J. **A12**, 117 (2001).
8. R.A. Arndt *et al.*, Phys. Rev. **C52**, 2120 (1995).
9. I. Sabba-Stefanescu, Progress of Physics **35**, 573 (1987).
10. K. Hikasa *et al.*, Phys. Rev. **D45**, S1 (1992).
11. M. Roos *et al.*, Phys. Lett. **B111**, 1 (1982).
12. K. Hagiwara *et al.*, Phys. Rev. **D66**, 010001 (2002).

$N(1440) P_{11}$

$I(J^P) = \frac{1}{2}(\frac{1}{2}^+)$ Status: * * * *

Most of the results published before 1975 were last included in our 1982 edition, Physics Letters **111B** 1 (1982). Some further obsolete results published before 1984 were last included in our 2006 edition, Journal of Physics, G **33** 1 (2006).

$N(1440)$ BREIT-WIGNER MASS

VALUE (MeV)	DOCUMENT ID	TECN	COMMENT
1420 to 1470 (≈ 1440) OUR ESTIMATE			
1485.0 \pm 1.2	ARNDT	06	DPWA $\pi N \rightarrow \pi N, \eta N$
1462 \pm 10	MANLEY	92	IPWA $\pi N \rightarrow \pi N \& N\pi\pi$
1440 \pm 30	CUTKOSKY	80	IPWA $\pi N \rightarrow \pi N$
1410 \pm 12	HOEHLER	79	IPWA $\pi N \rightarrow \pi N$

• • • We do not use the following data for averages, fits, limits, etc. • • •

1436 ± 15	SARANTSEV	08	DPWA	Multichannel
1468.0 ± 4.5	ARNDT	04	DPWA	$\pi N \rightarrow \pi N, \eta N$
1518 ± 5	PENNER	02c	DPWA	Multichannel
1479 ± 80	VRANA	00	DPWA	Multichannel
1463 ± 7	ARNDT	96	IPWA	$\gamma N \rightarrow \pi N$
1467	ARNDT	95	DPWA	$\pi N \rightarrow N\pi$
1421 ± 18	BATINIC	95	DPWA	$\pi N \rightarrow N\pi, N\eta$
1465	LI	93	IPWA	$\gamma N \rightarrow \pi N$
1471	CUTKOSKY	90	IPWA	$\pi N \rightarrow \pi N$
1380	¹ LONGACRE	77	IPWA	$\pi N \rightarrow N\pi\pi$
1390	² LONGACRE	75	IPWA	$\pi N \rightarrow N\pi\pi$

N(1440) BREIT-WIGNER WIDTH

VALUE (MeV)	DOCUMENT ID	TECN	COMMENT
200 to 450 (≈ 300) OUR ESTIMATE			
284 ± 18	ARNDT	06	DPWA $\pi N \rightarrow \pi N, \eta N$
391 ± 34	MANLEY	92	IPWA $\pi N \rightarrow \pi N \& N\pi\pi$
340 ± 70	CUTKOSKY	80	IPWA $\pi N \rightarrow \pi N$
135 ± 10	HOEHLER	79	IPWA $\pi N \rightarrow \pi N$
• • • We do not use the following data for averages, fits, limits, etc. • • •			
335 ± 40	SARANTSEV	08	DPWA Multichannel
360 ± 26	ARNDT	04	DPWA $\pi N \rightarrow \pi N, \eta N$
668 ± 41	PENNER	02c	DPWA Multichannel
490 ± 120	VRANA	00	DPWA Multichannel
360 ± 20	ARNDT	96	IPWA $\gamma N \rightarrow \pi N$
440	ARNDT	95	DPWA $\pi N \rightarrow N\pi$
250 ± 63	BATINIC	95	DPWA $\pi N \rightarrow N\pi, N\eta$
315	LI	93	IPWA $\gamma N \rightarrow \pi N$
545 ± 170	CUTKOSKY	90	IPWA $\pi N \rightarrow \pi N$
200	¹ LONGACRE	77	IPWA $\pi N \rightarrow N\pi\pi$
200	² LONGACRE	75	IPWA $\pi N \rightarrow N\pi\pi$

N(1440) POLE POSITION

REAL PART

VALUE (MeV)	DOCUMENT ID	TECN	COMMENT
1350 to 1380 (≈ 1365) OUR ESTIMATE			
1359	³ ARNDT	06	DPWA $\pi N \rightarrow \pi N, \eta N$
1385	⁴ HOEHLER	93	SPED $\pi N \rightarrow \pi N$
1375 ± 30	CUTKOSKY	80	IPWA $\pi N \rightarrow \pi N$
• • • We do not use the following data for averages, fits, limits, etc. • • •			
1371 ± 7	SARANTSEV	08	DPWA Multichannel
1357	⁵ ARNDT	04	DPWA $\pi N \rightarrow \pi N, \eta N$
1383	VRANA	00	DPWA Multichannel
1346	⁶ ARNDT	95	DPWA $\pi N \rightarrow N\pi$
1360	⁷ ARNDT	91	DPWA $\pi N \rightarrow \pi N$ Soln SM90
1370	CUTKOSKY	90	IPWA $\pi N \rightarrow \pi N$
1381 or 1379	⁸ LONGACRE	78	IPWA $\pi N \rightarrow N\pi\pi$
1360 or 1333	¹ LONGACRE	77	IPWA $\pi N \rightarrow N\pi\pi$

−2×IMAGINARY PART

VALUE (MeV)	DOCUMENT ID	TECN	COMMENT
160 to 220 (≈ 190) OUR ESTIMATE			
162	³ ARNDT	06	DPWA $\pi N \rightarrow \pi N, \eta N$
164	⁴ HOEHLER	93	SPED $\pi N \rightarrow \pi N$
180 ± 40	CUTKOSKY	80	IPWA $\pi N \rightarrow \pi N$
• • • We do not use the following data for averages, fits, limits, etc. • • •			
192 ± 20	SARANTSEV	08	DPWA Multichannel
160	⁵ ARNDT	04	DPWA $\pi N \rightarrow \pi N, \eta N$
316	VRANA	00	DPWA Multichannel
176	⁶ ARNDT	95	DPWA $\pi N \rightarrow N\pi$
252	⁷ ARNDT	91	DPWA $\pi N \rightarrow \pi N$ Soln SM90
228	CUTKOSKY	90	IPWA $\pi N \rightarrow \pi N$
209 or 210	⁸ LONGACRE	78	IPWA $\pi N \rightarrow N\pi\pi$
167 or 234	¹ LONGACRE	77	IPWA $\pi N \rightarrow N\pi\pi$

N(1440) ELASTIC POLE RESIDUE

MODULUS |r|

VALUE (MeV)	DOCUMENT ID	TECN	COMMENT
38	³ ARNDT	06	DPWA $\pi N \rightarrow \pi N, \eta N$
40	HOEHLER	93	SPED $\pi N \rightarrow \pi N$
52 ± 5	CUTKOSKY	80	IPWA $\pi N \rightarrow \pi N$
• • • We do not use the following data for averages, fits, limits, etc. • • •			
36	⁵ ARNDT	04	DPWA $\pi N \rightarrow \pi N, \eta N$
42	⁶ ARNDT	95	DPWA $\pi N \rightarrow N\pi$
109	⁷ ARNDT	91	DPWA $\pi N \rightarrow \pi N$ Soln SM90
74	CUTKOSKY	90	IPWA $\pi N \rightarrow \pi N$

PHASE θ

VALUE (°)	DOCUMENT ID	TECN	COMMENT
−98	³ ARNDT	06	DPWA $\pi N \rightarrow \pi N, \eta N$
−100 ± 35	CUTKOSKY	80	IPWA $\pi N \rightarrow \pi N$
• • • We do not use the following data for averages, fits, limits, etc. • • •			
−102	⁵ ARNDT	04	DPWA $\pi N \rightarrow \pi N, \eta N$
−101	⁶ ARNDT	95	DPWA $\pi N \rightarrow N\pi$
−93	⁷ ARNDT	91	DPWA $\pi N \rightarrow \pi N$ Soln SM90
−84	CUTKOSKY	90	IPWA $\pi N \rightarrow \pi N$

N(1440) DECAY MODES

The following branching fractions are our estimates, not fits or averages.

Mode	Fraction (Γ_i/Γ)
Γ_1 $N\pi$	0.55 to 0.75
Γ_2 $N\eta$	
Γ_3 $N\pi\pi$	30–40 %
Γ_4 $\Delta\pi$	20–30 %
Γ_5 $\Delta(1232)\pi$, P-wave	
Γ_6 $N\rho$	<8 %
Γ_7 $N\rho$, S=1/2, P-wave	
Γ_8 $N\rho$, S=3/2, P-wave	
Γ_9 $N(\pi\pi)_{S\text{-wave}}^{I=0}$	5–10 %
Γ_{10} $p\gamma$	0.035–0.048 %
Γ_{11} $p\gamma$, helicity=1/2	0.035–0.048 %
Γ_{12} $n\gamma$	0.009–0.032 %
Γ_{13} $n\gamma$, helicity=1/2	0.009–0.032 %

N(1440) BRANCHING RATIOS

$\Gamma(N\pi)/\Gamma_{\text{total}}$	DOCUMENT ID	TECN	COMMENT	Γ_1/Γ
0.55 to 0.75 OUR ESTIMATE				
0.787 ± 0.016	ARNDT	06	DPWA $\pi N \rightarrow \pi N, \eta N$	
0.69 ± 0.03	MANLEY	92	IPWA $\pi N \rightarrow \pi N \& N\pi\pi$	
0.68 ± 0.04	CUTKOSKY	80	IPWA $\pi N \rightarrow \pi N$	
0.51 ± 0.05	HOEHLER	79	IPWA $\pi N \rightarrow \pi N$	
• • • We do not use the following data for averages, fits, limits, etc. • • •				
0.750 ± 0.024	ARNDT	04	DPWA $\pi N \rightarrow \pi N, \eta N$	
0.57 ± 0.01	PENNER	02c	DPWA Multichannel	
0.72 ± 0.05	VRANA	00	DPWA Multichannel	
0.68	ARNDT	95	DPWA $\pi N \rightarrow N\pi$	
0.56 ± 0.08	BATINIC	95	DPWA $\pi N \rightarrow N\pi, N\eta$	
$\Gamma(N\eta)/\Gamma_{\text{total}}$				
VALUE	DOCUMENT ID	TECN	COMMENT	Γ_2/Γ
0.00 ± 0.01	VRANA	00	DPWA Multichannel	

Note: Signs of couplings from $\pi N \rightarrow N\pi\pi$ analyses were changed in the 1986 edition to agree with the baryon-first convention; the overall phase ambiguity is resolved by choosing a negative sign for the $\Delta(1620) S_{31}$ coupling to $\Delta(1232)\pi$.

$(\Gamma_i\Gamma_j)^{1/2}/\Gamma_{\text{total}}$ in $N\pi \rightarrow N(1440) \rightarrow \Delta(1232)\pi$, P-wave	$(\Gamma_1\Gamma_5)^{1/2}/\Gamma$			
+0.37 to +0.41 OUR ESTIMATE				
+0.39 ± 0.02	MANLEY 92 IPWA $\pi N \rightarrow \pi N \& N\pi\pi$			
+0.41	^{1,9} LONGACRE 77 IPWA $\pi N \rightarrow N\pi\pi$			
+0.37	² LONGACRE 75 IPWA $\pi N \rightarrow N\pi\pi$			
$\Gamma(\Delta(1232)\pi, \text{P-wave})/\Gamma_{\text{total}}$				
VALUE	DOCUMENT ID	TECN	COMMENT	Γ_5/Γ
0.16 ± 0.01	VRANA	00	DPWA Multichannel	
$(\Gamma_i\Gamma_j)^{1/2}/\Gamma_{\text{total}}$ in $N\pi \rightarrow N(1440) \rightarrow N\rho$, S=1/2, P-wave				
$(\Gamma_1\Gamma_7)^{1/2}/\Gamma$				
VALUE	DOCUMENT ID	TECN	COMMENT	Γ_7/Γ
−0.11	^{1,9} LONGACRE	77	IPWA $\pi N \rightarrow N\pi\pi$	
+0.23	² LONGACRE	75	IPWA $\pi N \rightarrow N\pi\pi$	
$\Gamma(N\rho, \text{S=1/2, P-wave})/\Gamma_{\text{total}}$				
VALUE	DOCUMENT ID	TECN	COMMENT	Γ_7/Γ
0.00 ± 0.01	VRANA	00	DPWA Multichannel	
$(\Gamma_i\Gamma_j)^{1/2}/\Gamma_{\text{total}}$ in $N\pi \rightarrow N(1440) \rightarrow N\rho$, S=3/2, P-wave				
$(\Gamma_1\Gamma_8)^{1/2}/\Gamma$				
VALUE	DOCUMENT ID	TECN	COMMENT	Γ_8/Γ
+0.18	^{1,9} LONGACRE	77	IPWA $\pi N \rightarrow N\pi\pi$	

Baryon Particle Listings

N(1440), N(1520)

$(\Gamma_1\Gamma_2)^{1/2}/\Gamma_{total}$ in $N\pi \rightarrow N(1440) \rightarrow N(\pi\pi)_{S=0}^J=0$ $(\Gamma_1\Gamma_2)^{1/2}/\Gamma$
 VALUE DOCUMENT ID TECN COMMENT

± 0.17 to ± 0.25 OUR ESTIMATE

+0.24 ± 0.03	MANLEY	92	IPWA	$\pi N \rightarrow \pi N & N\pi\pi$
-0.18	1,9 LONGACRE	77	IPWA	$\pi N \rightarrow N\pi\pi$
-0.23	2 LONGACRE	75	IPWA	$\pi N \rightarrow N\pi\pi$

$\Gamma(N(\pi\pi)_{S=0}^J=0)/\Gamma_{total}$ Γ_9/Γ
 VALUE DOCUMENT ID TECN COMMENT

0.12 ± 0.01	VRANA	00	DPWA	Multichannel
-------------	-------	----	------	--------------

N(1440) PHOTON DECAY AMPLITUDES

Papers on γN amplitudes predating 1981 may be found in our 2006 edition, Journal of Physics, G 33 1 (2006).

N(1440) → pγ, helicity-1/2 amplitude A_{1/2}

VALUE (GeV^{-1/2}) DOCUMENT ID TECN COMMENT

-0.065 ± 0.004 OUR ESTIMATE

-0.051 ± 0.002	DUGGER	07	DPWA	$\gamma N \rightarrow \pi N$
-0.063 ± 0.005	ARNDT	96	IPWA	$\gamma N \rightarrow \pi N$
-0.069 ± 0.018	CRAWFORD	83	IPWA	$\gamma N \rightarrow \pi N$
-0.063 ± 0.008	AWAJI	81	DPWA	$\gamma N \rightarrow \pi N$

• • • We do not use the following data for averages, fits, limits, etc. • • •

-0.061	DRECHSEL	07	DPWA	$\gamma N \rightarrow \pi N$
-0.087	PENNER	02D	DPWA	Multichannel
-0.085 ± 0.003	LI	93	IPWA	$\gamma N \rightarrow \pi N$
-0.129	10 WADA	84	DPWA	Compton scattering

N(1440) → nγ, helicity-1/2 amplitude A_{1/2}

VALUE (GeV^{-1/2}) DOCUMENT ID TECN COMMENT

+0.040 ± 0.010 OUR ESTIMATE

0.045 ± 0.015	ARNDT	96	IPWA	$\gamma N \rightarrow \pi N$
0.037 ± 0.010	AWAJI	81	DPWA	$\gamma N \rightarrow \pi N$
0.030 ± 0.003	FUJII	81	DPWA	$\gamma N \rightarrow \pi N$

• • • We do not use the following data for averages, fits, limits, etc. • • •

0.054	DRECHSEL	07	DPWA	$\gamma N \rightarrow \pi N$
0.121	PENNER	02D	DPWA	Multichannel
0.085 ± 0.006	LI	93	IPWA	$\gamma N \rightarrow \pi N$

N(1440) FOOTNOTES

- LONGACRE 77 pole positions are from a search for poles in the unitarized T-matrix; the first (second) value uses, in addition to $\pi N \rightarrow N\pi\pi$ data, elastic amplitudes from a Saclay (CERN) partial-wave analysis. The other LONGACRE 77 values are from eyeball fits with Breit-Wigner circles to the T-matrix amplitudes.
- From method II of LONGACRE 75: eyeball fits with Breit-Wigner circles to the T-matrix amplitudes.
- ARNDT 06 also finds a second-sheet pole with real part = 1388 MeV, $-2 \times$ imaginary part = 165 MeV, and residue with modulus 86 MeV and phase = -46 degrees.
- See HOEHLER 93 for a detailed discussion of the evidence for and the pole parameters of N and Δ resonances as determined from Argand diagrams of πN elastic partial-wave amplitudes and from plots of the speeds with which the amplitudes traverse the diagrams.
- ARNDT 04 also finds a second-sheet pole with real part = 1385 MeV, $-2 \times$ imaginary part = 166 MeV, and residue with modulus 82 MeV and phase = -51° .
- ARNDT 95 also finds a second-sheet pole with real part = 1383 MeV, $-2 \times$ imaginary part = 210 MeV, and residue with modulus 92 MeV and phase = -54° .
- ARNDT 91 (Soln SM90) also finds a second-sheet pole with real part = 1413 MeV, $-2 \times$ imaginary part = 256 MeV, and residue = $(78-153i)$ MeV.
- LONGACRE 78 values are from a search for poles in the unitarized T-matrix. The first (second) value uses, in addition to $\pi N \rightarrow N\pi\pi$ data, elastic amplitudes from a Saclay (CERN) partial-wave analysis.
- LONGACRE 77 considers this coupling to be well determined.
- WADA 84 is inconsistent with other analyses; see the Note on N and Δ Resonances.

N(1440) REFERENCES

For early references, see Physics Letters 111B 1 (1982).

SARANTSEV	08	PL B659 94	A.V. Sarantsev et al.	(CB-ELSA/A2-TAPS Collab.)
DRECHSEL	07	EPJ A34 69	D. Drechsel, S.S. Kamalov, L. Tiator	(MAIN Z, JINR)
DUGGER	07	PR C76 025211	M. Dugger et al.	(Jefferson Lab CLAS Collab.)
ARNDT	06	PR C74 045205	R.A. Arndt et al.	(GWU)
PDG	06	JPG 33 1	W.-M. Yao et al.	(PDG Collab.)
ARNDT	04	PR C69 035213	R.A. Arndt et al.	(GWU, TRIU)
PENNER	02C	PR C66 055211	G. Penner, U. Mosel	(GIES)
PENNER	02D	PR C66 055212	G. Penner, U. Mosel	(GIES)
VRANA	00	PRPL 328 181	T.P. Vrana, S.A. Dytman,, T.-S.H. Lee	(PITT+)
ARNDT	96	PR C53 430	R.A. Arndt, I.I. Strakovsky, R.L. Workman	(VPI)
ARNDT	95	PR C52 2120	R.A. Arndt et al.	(VPI, BRCO)
BATINIC	95	PR C51 2310	M. Batinic et al.	(BOSK, UCLA)
Also		PR C57 1004 (erratum)	M. Batinic et al.	
HOEHLER	93	πN Newsletter 9 1	G. Hoehler	(KARL)
LI	93	PR C47 2759	Z.J. Li et al.	(VPI)
MANLEY	92	PR D45 4002	D.M. Manley, E.M. Saleski	(KENT) IJP
Also		PR D30 904	D.M. Manley et al.	(VPI)
ARNDT	91	PR D43 2131	R.A. Arndt et al.	(VPI, TELE) IJP
CUTKOSKY	90	PR D42 235	R.E. Cutkosky, S. Wang	(CMU)
WADA	84	NP B247 313	Y. Wada et al.	(INUS)

CRAWFORD	83	NP B211 1	R.L. Crawford, W.T. Morton	(GLAS)
PDG	82	PL 111B 1	M. Roos et al.	(HELS, CIT, CERN)
AWAJI	81	Bonn Conf. 352	N. Awaji, R. Kajikawa	(NAGO)
Also		NP B197 365	K. Fujii et al.	(NAGO)
FUJII	81	NP B187 53	K. Fujii et al.	(NAGO, OSAK)
CUTKOSKY	80	Toronto Conf. 19	R.E. Cutkosky et al.	(CMU, LBL) IJP
Also		PR D20 2839	R.E. Cutkosky et al.	(CMU, LBL) IJP
HOEHLER	79	PDAT 12-1	G. Hoehler et al.	(KARL) IJP
Also		Toronto Conf. 3	R. Koch	(KARL) IJP
LONGACRE	78	PR D17 1795	R.S. Longacre et al.	(LBL, SLAC)
LONGACRE	77	NP B122 493	R.S. Longacre, J. Dolbeau	(SACL) IJP
Also		NP B108 365	J. Dolbeau et al.	(SACL) IJP
LONGACRE	75	PL 55B 415	R.S. Longacre et al.	(LBL, SLAC) IJP

N(1520) D₁₃

$I(J^P) = \frac{1}{2}(\frac{3}{2}^-)$ Status: * * * *

Most of the results published before 1975 were last included in our 1982 edition, Physics Letters 111B 1 (1982). Some further obsolete results published before 1984 were last included in our 2006 edition, Journal of Physics, G 33 1 (2006).

N(1520) BREIT-WIGNER MASS

VALUE (MeV) DOCUMENT ID TECN COMMENT

1515 to 1525 (≈ 1520) OUR ESTIMATE

1514.5 ± 0.2	ARNDT	06	DPWA	$\pi N \rightarrow \pi N, \eta N$
1524 ± 4	MANLEY	92	IPWA	$\pi N \rightarrow \pi N & N\pi\pi$
1525 ± 10	CUTKOSKY	80	IPWA	$\pi N \rightarrow \pi N$
1519 ± 4	HOEHLER	79	IPWA	$\pi N \rightarrow \pi N$

• • • We do not use the following data for averages, fits, limits, etc. • • •

1520 ± 10	THOMA	08	DPWA	Multichannel
1516.3 ± 0.8	ARNDT	04	DPWA	$\pi N \rightarrow \pi N, \eta N$
1509 ± 1	PENNER	02C	DPWA	Multichannel
1518 ± 3	VRANA	00	DPWA	Multichannel
1516 ± 10	ARNDT	96	IPWA	$\gamma N \rightarrow \pi N$
1515	ARNDT	95	DPWA	$\pi N \rightarrow \pi N$
1526 ± 18	BATINIC	95	DPWA	$\pi N \rightarrow N\pi, N\eta$
1510	LI	93	IPWA	$\gamma N \rightarrow \pi N$
1510	1 LONGACRE	77	IPWA	$\pi N \rightarrow N\pi\pi$
1520	2 LONGACRE	75	IPWA	$\pi N \rightarrow N\pi\pi$

N(1520) BREIT-WIGNER WIDTH

VALUE (MeV) DOCUMENT ID TECN COMMENT

100 to 125 (≈ 115) OUR ESTIMATE

103.6 ± 0.4	ARNDT	06	DPWA	$\pi N \rightarrow \pi N, \eta N$
124 ± 8	MANLEY	92	IPWA	$\pi N \rightarrow \pi N & N\pi\pi$
120 ± 15	CUTKOSKY	80	IPWA	$\pi N \rightarrow \pi N$
114 ± 7	HOEHLER	79	IPWA	$\pi N \rightarrow \pi N$

• • • We do not use the following data for averages, fits, limits, etc. • • •

125 ± 15	THOMA	08	DPWA	Multichannel
98.6 ± 2.6	ARNDT	04	DPWA	$\pi N \rightarrow \pi N, \eta N$
100 ± 2	PENNER	02C	DPWA	Multichannel
124 ± 4	VRANA	00	DPWA	Multichannel
106 ± 4	ARNDT	96	IPWA	$\gamma N \rightarrow \pi N$
106	ARNDT	95	DPWA	$\pi N \rightarrow \pi N$
143 ± 32	BATINIC	95	DPWA	$\pi N \rightarrow N\pi, N\eta$
120	LI	93	IPWA	$\gamma N \rightarrow \pi N$
110	1 LONGACRE	77	IPWA	$\pi N \rightarrow N\pi\pi$
150	2 LONGACRE	75	IPWA	$\pi N \rightarrow N\pi\pi$

N(1520) POLE POSITION

REAL PART
 VALUE (MeV) DOCUMENT ID TECN COMMENT

1505 to 1515 (≈ 1510) OUR ESTIMATE

1515	ARNDT	06	DPWA	$\pi N \rightarrow \pi N, \eta N$
1510	3 HOEHLER	93	ARGD	$\pi N \rightarrow \pi N$
1510 ± 5	CUTKOSKY	80	IPWA	$\pi N \rightarrow \pi N$

• • • We do not use the following data for averages, fits, limits, etc. • • •

1509 ± 7	THOMA	08	DPWA	Multichannel
1514	ARNDT	04	DPWA	$\pi N \rightarrow \pi N, \eta N$
1504	VRANA	00	DPWA	Multichannel
1515	ARNDT	95	DPWA	$\pi N \rightarrow \pi N$
1511	ARNDT	91	DPWA	$\pi N \rightarrow \pi N$ Soln SM90
1514 or 1511	4 LONGACRE	78	IPWA	$\pi N \rightarrow N\pi\pi$
1508 or 1505	1 LONGACRE	77	IPWA	$\pi N \rightarrow N\pi\pi$

-2xIMAGINARY PART
 VALUE (MeV) DOCUMENT ID TECN COMMENT

105 to 120 (≈ 110) OUR ESTIMATE

113	ARNDT	06	DPWA	$\pi N \rightarrow \pi N, \eta N$
120	3 HOEHLER	93	ARGD	$\pi N \rightarrow \pi N$
114 ± 10	CUTKOSKY	80	IPWA	$\pi N \rightarrow \pi N$

• • • We do not use the following data for averages, fits, limits, etc. • • •

113±12	THOMA	08	DPWA	Multichannel
102	ARNDT	04	DPWA	$\pi N \rightarrow \pi N, \eta N$
112	VRANA	00	DPWA	Multichannel
110	ARNDT	95	DPWA	$\pi N \rightarrow N\pi$
108	ARNDT	91	DPWA	$\pi N \rightarrow \pi N$ Soln SM90
146 or 137	⁴ LONGACRE	78	IPWA	$\pi N \rightarrow N\pi\pi$
109 or 107	¹ LONGACRE	77	IPWA	$\pi N \rightarrow N\pi\pi$

• • • We do not use the following data for averages, fits, limits, etc. • • •

0.002 ± 0.001	THOMA	08	DPWA	Multichannel
0.0008 to 0.0012	ARNDT	05	DPWA	Multichannel
0.0008 ± 0.0001	TIATOR	99	DPWA	$\gamma p \rightarrow p\eta$
0.001 ± 0.002	BATINIC	95	DPWA	$\pi N \rightarrow N\pi, N\eta$

Note: Signs of couplings from $\pi N \rightarrow N\pi\pi$ analyses were changed in the 1986 edition to agree with the baryon-first convention; the overall phase ambiguity is resolved by choosing a negative sign for the $\Delta(1620) S_{31}$ coupling to $\Delta(1232)\pi$.

N(1520) ELASTIC POLE RESIDUE

MODULUS |r|

VALUE (MeV)	DOCUMENT ID	TECN	COMMENT
38	ARNDT	06	DPWA $\pi N \rightarrow \pi N, \eta N$
32	HOEHLER	93	ARGD $\pi N \rightarrow \pi N$
35 ± 2	CUTKOSKY	80	IPWA $\pi N \rightarrow \pi N$
• • • We do not use the following data for averages, fits, limits, etc. • • •			
35	ARNDT	04	DPWA $\pi N \rightarrow \pi N, \eta N$
34	ARNDT	95	DPWA $\pi N \rightarrow N\pi$
33	ARNDT	91	DPWA $\pi N \rightarrow \pi N$ Soln SM90

PHASE θ

VALUE (°)	DOCUMENT ID	TECN	COMMENT
- 5	ARNDT	06	DPWA $\pi N \rightarrow \pi N, \eta N$
- 8	HOEHLER	93	ARGD $\pi N \rightarrow \pi N$
-12 ± 5	CUTKOSKY	80	IPWA $\pi N \rightarrow \pi N$
• • • We do not use the following data for averages, fits, limits, etc. • • •			
- 6	ARNDT	04	DPWA $\pi N \rightarrow \pi N, \eta N$
- 7	ARNDT	95	DPWA $\pi N \rightarrow N\pi$
-10	ARNDT	91	DPWA $\pi N \rightarrow \pi N$ Soln SM90

N(1520) DECAY MODES

The following branching fractions are our estimates, not fits or averages.

Mode	Fraction (Γ_i/Γ)
$\Gamma_1 N\pi$	0.55 to 0.65
$\Gamma_2 N\eta$	(2.3 ± 0.4) × 10 ⁻³
$\Gamma_3 N\pi\pi$	40-50 %
$\Gamma_4 \Delta\pi$	15-25 %
$\Gamma_5 \Delta(1232)\pi, S\text{-wave}$	5-12 %
$\Gamma_6 \Delta(1232)\pi, D\text{-wave}$	10-14 %
$\Gamma_7 N\rho$	15-25 %
$\Gamma_8 N\rho, S=1/2, D\text{-wave}$	
$\Gamma_9 N\rho, S=3/2, S\text{-wave}$	
$\Gamma_{10} N\rho, S=3/2, D\text{-wave}$	
$\Gamma_{11} N(\pi\pi)_{S\text{-wave}}^{I=0}$	<8 %
$\Gamma_{12} p\gamma$	0.46-0.56 %
$\Gamma_{13} p\gamma, \text{helicity}=1/2$	0.001-0.034 %
$\Gamma_{14} p\gamma, \text{helicity}=3/2$	0.44-0.53 %
$\Gamma_{15} n\gamma$	0.30-0.53 %
$\Gamma_{16} n\gamma, \text{helicity}=1/2$	0.04-0.10 %
$\Gamma_{17} n\gamma, \text{helicity}=3/2$	0.25-0.45 %

N(1520) BRANCHING RATIOS

$\Gamma(N\pi)/\Gamma_{\text{total}}$

VALUE	DOCUMENT ID	TECN	COMMENT
0.55 to 0.65 OUR ESTIMATE			
0.632 ± 0.001	ARNDT	06	DPWA $\pi N \rightarrow \pi N, \eta N$
0.59 ± 0.03	MANLEY	92	IPWA $\pi N \rightarrow \pi N \& N\pi\pi$
0.58 ± 0.03	CUTKOSKY	80	IPWA $\pi N \rightarrow \pi N$
0.54 ± 0.03	HOEHLER	79	IPWA $\pi N \rightarrow \pi N$
• • • We do not use the following data for averages, fits, limits, etc. • • •			
0.58 ± 0.08	THOMA	08	DPWA Multichannel
0.640 ± 0.005	ARNDT	04	DPWA $\pi N \rightarrow \pi N, \eta N$
0.56 ± 0.01	PENNER	02c	DPWA Multichannel
0.63 ± 0.02	VRANA	00	DPWA Multichannel
0.61	ARNDT	95	DPWA $\pi N \rightarrow N\pi$
0.46 ± 0.06	BATINIC	95	DPWA $\pi N \rightarrow N\pi, N\eta$

$\Gamma(N\eta)/\Gamma_{\text{total}}$

VALUE	DOCUMENT ID	TECN	COMMENT
0.0023 ± 0.0004 OUR AVERAGE			
0.0023 ± 0.0004	PENNER	02c	DPWA Multichannel
0.00 ± 0.01	VRANA	00	DPWA Multichannel

$(\Gamma_i \Gamma_j)^{1/2}/\Gamma_{\text{total}}$ in $N\pi \rightarrow N(1520) \rightarrow \Delta(1232)\pi, S\text{-wave}$

VALUE	DOCUMENT ID	TECN	COMMENT
- 0.26 to - 0.20 OUR ESTIMATE			
- 0.18 ± 0.05	MANLEY	92	IPWA $\pi N \rightarrow \pi N \& N\pi\pi$
- 0.26	^{1,5} LONGACRE	77	IPWA $\pi N \rightarrow N\pi\pi$
- 0.24	² LONGACRE	75	IPWA $\pi N \rightarrow N\pi\pi$

$\Gamma(\Delta(1232)\pi, S\text{-wave})/\Gamma_{\text{total}}$

VALUE	DOCUMENT ID	TECN	COMMENT
0.15 ± 0.02	VRANA	00	DPWA Multichannel
• • • We do not use the following data for averages, fits, limits, etc. • • •			
0.12 ± 0.04	THOMA	08	DPWA Multichannel

$(\Gamma_i \Gamma_j)^{1/2}/\Gamma_{\text{total}}$ in $N\pi \rightarrow N(1520) \rightarrow \Delta(1232)\pi, D\text{-wave}$

VALUE	DOCUMENT ID	TECN	COMMENT
- 0.28 to - 0.24 OUR ESTIMATE			
- 0.29 ± 0.03	MANLEY	92	IPWA $\pi N \rightarrow \pi N \& N\pi\pi$
- 0.21	^{1,5} LONGACRE	77	IPWA $\pi N \rightarrow N\pi\pi$
- 0.30	² LONGACRE	75	IPWA $\pi N \rightarrow N\pi\pi$

$\Gamma(\Delta(1232)\pi, D\text{-wave})/\Gamma_{\text{total}}$

VALUE	DOCUMENT ID	TECN	COMMENT
0.11 ± 0.02	VRANA	00	DPWA Multichannel
• • • We do not use the following data for averages, fits, limits, etc. • • •			
0.14 ± 0.05	THOMA	08	DPWA Multichannel

$(\Gamma_i \Gamma_j)^{1/2}/\Gamma_{\text{total}}$ in $N\pi \rightarrow N(1520) \rightarrow N\rho, S=3/2, S\text{-wave}$

VALUE	DOCUMENT ID	TECN	COMMENT
- 0.35 to - 0.31 OUR ESTIMATE			
- 0.35 ± 0.03	MANLEY	92	IPWA $\pi N \rightarrow \pi N \& N\pi\pi$
- 0.35	^{1,5} LONGACRE	77	IPWA $\pi N \rightarrow N\pi\pi$
- 0.24	² LONGACRE	75	IPWA $\pi N \rightarrow N\pi\pi$

$\Gamma(N\rho, S=3/2, S\text{-wave})/\Gamma_{\text{total}}$

VALUE	DOCUMENT ID	TECN	COMMENT
0.09 ± 0.01	VRANA	00	DPWA Multichannel

$(\Gamma_i \Gamma_j)^{1/2}/\Gamma_{\text{total}}$ in $N\pi \rightarrow N(1520) \rightarrow N(\pi\pi)_{S\text{-wave}}^{I=0}$

VALUE	DOCUMENT ID	TECN	COMMENT
- 0.22 to - 0.06 OUR ESTIMATE			
- 0.13	^{1,5} LONGACRE	77	IPWA $\pi N \rightarrow N\pi\pi$
- 0.17	² LONGACRE	75	IPWA $\pi N \rightarrow N\pi\pi$

$\Gamma(N(\pi\pi)_{S\text{-wave}}^{I=0})/\Gamma_{\text{total}}$

VALUE	DOCUMENT ID	TECN	COMMENT
0.01 ± 0.01	VRANA	00	DPWA Multichannel
• • • We do not use the following data for averages, fits, limits, etc. • • •			
<0.04	THOMA	08	DPWA Multichannel

N(1520) PHOTON DECAY AMPLITUDES

Papers on γN amplitudes predating 1981 may be found in our 2006 edition, Journal of Physics, G **33** 1 (2006).

N(1520) → pγ, helicity-1/2 amplitude A_{1/2}

VALUE (GeV ^{-1/2})	DOCUMENT ID	TECN	COMMENT
- 0.024 ± 0.009 OUR ESTIMATE			
- 0.028 ± 0.002	DUGGER	07	DPWA $\gamma N \rightarrow \pi N$
- 0.038 ± 0.003	AHRENS	02	DPWA $\gamma N \rightarrow \pi N$
- 0.020 ± 0.007	ARNDT	96	IPWA $\gamma N \rightarrow \pi N$
- 0.028 ± 0.014	CRAWFORD	83	IPWA $\gamma N \rightarrow \pi N$
- 0.007 ± 0.004	AWAJI	81	DPWA $\gamma N \rightarrow \pi N$
• • • We do not use the following data for averages, fits, limits, etc. • • •			
- 0.027	DRECHSEL	07	DPWA $\gamma N \rightarrow \pi N$
- 0.003	PENNER	02d	DPWA Multichannel
- 0.052 ± 0.010 ± 0.007	⁶ MUKHOPAD...	98	$\gamma p \rightarrow \eta p$
- 0.020 ± 0.002	LI	93	IPWA $\gamma N \rightarrow \pi N$
- 0.012	WADA	84	DPWA Compton scattering

Baryon Particle Listings

N(1535), N(1650)

••• We do not use the following data for averages, fits, limits, etc. •••

0.066	DRECHSEL	07	DPWA	$\gamma N \rightarrow \pi N$
0.090	PENNER	02D	DPWA	Multichannel
0.110 to 0.140	KRUSCHE	95	DPWA	$\gamma p \rightarrow p \eta$
0.125 ± 0.025	KRUSCHE	95c	IPWA	$\gamma d \rightarrow \eta N(N)$
0.061 ± 0.003	LI	93	IPWA	$\gamma N \rightarrow \pi N$
0.055	WADA	84	DPWA	Compton scattering

N(1535) → nγ, helicity-1/2 amplitude A_{1/2}

VALUE (GeV ^{-1/2})	DOCUMENT ID	TECN	COMMENT
-0.046 ± 0.027 OUR ESTIMATE			
-0.080 ± 0.020	¹¹ ANISOVICH	09A	DPWA $\gamma d \rightarrow \eta N(N)$
-0.020 to 0.035	ARNDT	96	IPWA $\gamma N \rightarrow \pi N$
0.035 ± 0.014	AWAJI	81	DPWA $\gamma N \rightarrow \pi N$
-0.062 ± 0.003	FUJII	81	DPWA $\gamma N \rightarrow \pi N$

••• We do not use the following data for averages, fits, limits, etc. •••

-0.051	DRECHSEL	07	DPWA	$\gamma N \rightarrow \pi N$
-0.024	PENNER	02D	DPWA	Multichannel
-0.100 ± 0.030	KRUSCHE	95c	IPWA	$\gamma d \rightarrow \eta N(N)$
-0.046 ± 0.005	LI	93	IPWA	$\gamma N \rightarrow \pi N$

N(1535) → Nγ, ratio A_{1/2}ⁿ/A_{1/2}^p

VALUE (GeV ^{-1/2})	DOCUMENT ID	TECN
-0.84 ± 0.15		
	MUKHOPAD... 95B	IPWA

N(1535) FOOTNOTES

- LONGACRE 77 pole positions are from a search for poles in the unitarized T-matrix; the first (second) value uses, in addition to $\pi N \rightarrow N\pi$ data, elastic amplitudes from a Saclay (CERN) partial-wave analysis. The other LONGACRE 77 values are from eyeball fits with Breit-Wigner circles to the T-matrix amplitudes.
- From method II of LONGACRE 75: eyeball fits with Breit-Wigner circles to the T-matrix amplitudes.
- KRUSCHE 97 fits with the mass fixed at 1544 MeV.
- See HOEHLER 93 for a detailed discussion of the evidence for and the pole parameters of N and Δ resonances as determined from Argand diagrams of πN elastic partial-wave amplitudes and from plots of the speeds with which the amplitudes traverse the diagrams.
- ARNDT 98 also lists pole residues, which display more model dependence than do the associated pole positions.
- LONGACRE 78 values are from a search for poles in the unitarized T-matrix. The first (second) value uses, in addition to $\pi N \rightarrow N\pi$ data, elastic amplitudes from a Saclay (CERN) partial-wave analysis.
- The best value ARMSTRONG 99B obtains is ≈ 0.55 ; this assumes S_{11} dominance in the reaction $p(e, e'p) \eta$ at $Q^2 = 4$ (GeV/c)².
- This STAROSTIN 03 value is an estimate made using simplest assumptions.
- This ANISOVICH 09A amplitude is evaluated at the pole position; the phase is (20 ± 15)°.
- BENMERROUCHE 91 uses an effective Lagrangian approach to analyze η photoproduction data.
- This ANISOVICH 09A amplitude is evaluated at the pole position; the phase is (20 ± 20)°.

N(1535) REFERENCES

For early references, see Physics Letters **111B** 1 (1982).

ANISOVICH 09A	EPJ A41 13	A.V. Anisovich et al.	(BONN, PNPI, BASL)
AZNAURYAN 09	PR C80 055203	I.G. Aznauryan et al.	(JLAB CLAS Collab.)
THOMA 08	PL B659 87	U. Thoma et al.	(CB-ELSA Collab.)
DRECHSEL 07	EPJ A34 69	D. Drechsel, S.S. Kamalov, L. Tiator	(MAINZ, JINR)
DUGGER 07	PR C76 025211	M. Dugger et al.	(Jefferson Lab CLAS Collab.)
ARNDT 06	PR C74 045205	R.A. Arndt et al.	(GWU)
PDG 06	JPG 33 1	W.-M. Yao et al.	(PDG Collab.)
ARNDT 04	PR C69 035213	R.A. Arndt et al.	(GWU, TRIU)
STAROSTIN 03	PR C67 068201	A. Starostin et al.	(BNL Crystal Ball Collab.)
PENNER 02C	PR C66 055211	G. Penner, U. Mosel	(GIES)
PENNER 02D	PR C66 055212	G. Penner, U. Mosel	(GIES)
BAI 01B	PL B510 75	J.Z. Bai et al.	(BES Collab.)
THOMPSON 01	PR L6 1702	R. Thompson et al.	(Jefferson CLAS Collab.)
VRANA 00	PRPL 328 181	T.P. Vrana, S.A. Dytman, T.-S.H. Lee	(PITT+)
ARMSTRONG 99B	PR D60 052004	C.S. Armstrong et al.	
ARNDT 98	PR C58 3636	R.A. Arndt et al.	
GREEN 97	PR C55 R2167	A.M. Green, S. Wycech	(HEL5, WINR)
KRUSCHE 97	PL B397 171	B. Krusche et al.	(GIES, RPI, SASK)
ABAEV 96	PR C53 385	V.V. Abaev, B.M.K. Nefkens	(UCLA)
ARNDT 96	PR C53 430	R.A. Arndt, I.I. Strakovsky, R.L. Workman	(VPI)
ARNDT 95	PR C52 2120	R.A. Arndt et al.	(VPI, BRCC)
BATINIC 95	PR C51 2310	M. Batinic et al.	(BOSK, UCLA)
Also	PR C57 1004 (erratum)	M. Batinic et al.	
BATINIC 95B	PR C52 2188	M. Batinic, I. Slauas, A. Svarc	(BOSK)
BENMERROU... 95	PR D51 3237	M. Benmerrouche, N.C. Mukhopadhyay, J.F. Zhang	
KRUSCHE 95	PR L74 3736	B. Krusche et al.	(GIES, MANZ, GLAS+)
KRUSCHE 95C	PL B358 40	B. Krusche et al.	(GIES, MANZ, GLAS+)
MUKHOPAD... 95B	PL B364 1	N.C. Mukhopadhyay, J.F. Zhang, M. Benmerrouche	
HOEHLER 93	π N Newsletter 9 1	G. Hohler	(KARL)
LI 93	PR C47 2759	Z.J. Li et al.	(VPI)
MANLEY 92	PR D45 4002	D.M. Manley, E.M. Saleski	(KENT) IJP
Also	PR D30 904	D.M. Manley et al.	(VPI)
ARNDT 91	PR D43 2131	R.A. Arndt et al.	(VPI, TELE) IJP
BENMERROU... 91	PR L67 1070	M. Benmerrouche, N.C. Mukhopadhyay	(RPI)
WADA 84	NP B247 313	Y. Wada et al.	(INUS)
CRAWFORD 83	NP B211 1	R.L. Crawford, W.T. Morton	(GLAS)
PDG 82	PL 11B 1	M. Roos et al.	(HEL5, CIT, CERN)
AWAJI 81	Bonn Conf. 352	N. Awaji, R. Kajikawa	(NAGO)
Also	NP B197 365	K. Fujii et al.	(NAGO)
FUJII 81	NP B187 53	K. Fujii et al.	(NAGO, OSAK)
CUTKOSKY 80	Toronto Conf. 19	R.E. Cutkosky et al.	(CMU, LBL) IJP
Also	PR D20 2839	R.E. Cutkosky et al.	(CMU, LBL) IJP

HOEHLER 79	PDAT 12-1	G. Hohler et al.	(KARLT) IJP
Also	Toronto Conf. 3	R. Koch	(KARLT) IJP
LONGACRE 78	PR D17 1795	R.S. Longacre et al.	(LBL, SLAC)
LONGACRE 77	NP B122 493	R.S. Longacre, J. Dolbeau	(SACL) IJP
Also	NP B108 365	J. Dolbeau et al.	(SACL) IJP
LONGACRE 75	PL 55B 415	R.S. Longacre et al.	(LBL, SLAC) IJP

N(1650) S₁₁

$$I(J^P) = \frac{1}{2}(\frac{1}{2}^-) \text{ Status: } ***$$

Most of the results published before 1975 were last included in our 1982 edition, Physics Letters **111B** 1 (1982). Some further obsolete results published before 1984 were last included in our 2006 edition, Journal of Physics, **G 33** 1 (2006).

N(1650) BREIT-WIGNER MASS

VALUE (MeV)	DOCUMENT ID	TECN	COMMENT
1645 to 1670 (≈ 1655) OUR ESTIMATE			
1634.7 ± 1.1	ARNDT	06	DPWA $\pi N \rightarrow \pi N, \eta N$
1659 ± 9	MANLEY	92	IPWA $\pi N \rightarrow \pi N$ & $N\pi\pi$
1650 ± 30	CUTKOSKY	80	IPWA $\pi N \rightarrow \pi N$
1670 ± 8	HOEHLER	79	IPWA $\pi N \rightarrow \pi N$
••• We do not use the following data for averages, fits, limits, etc. •••			
1655 ± 15	THOMA	08	DPWA Multichannel
1651.2 ± 4.7	ARNDT	04	DPWA $\pi N \rightarrow \pi N, \eta N$
1665 ± 2	PENNER	02C	DPWA Multichannel
1647 ± 20	BAI	01B	BES $J/\psi \rightarrow p\bar{p}\eta$
1689 ± 12	VRANA	00	DPWA Multichannel
1677 ± 8	ARNDT	96	IPWA $\gamma N \rightarrow \pi N$
1667	ARNDT	95	DPWA $\pi N \rightarrow N\pi$
1712	¹ ARNDT	95	DPWA $\pi N \rightarrow N\pi$
1669 ± 17	BATINIC	95	DPWA $\pi N \rightarrow N\pi, N\eta$
1713 ± 27	² BATINIC	95	DPWA $\pi N \rightarrow N\pi, N\eta$
1674	LI	93	IPWA $\gamma N \rightarrow \pi N$
1672	MUSETTE	80	IPWA $\pi^- p \rightarrow \Lambda K^0$
1680	SAXON	80	DPWA $\pi^- p \rightarrow \Lambda K^0$
1700	³ LONGACRE	77	IPWA $\pi N \rightarrow N\pi\pi$
1660	⁴ LONGACRE	75	IPWA $\pi N \rightarrow N\pi\pi$

N(1650) BREIT-WIGNER WIDTH

VALUE (MeV)	DOCUMENT ID	TECN	COMMENT
145 to 185 (≈ 165) OUR ESTIMATE			
115.4 ± 2.8	ARNDT	06	DPWA $\pi N \rightarrow \pi N, \eta N$
167.9 ± 9.4	GREEN	97	DPWA $\pi N \rightarrow \pi N, \eta N$
173 ± 12	MANLEY	92	IPWA $\pi N \rightarrow \pi N$ & $N\pi\pi$
150 ± 40	CUTKOSKY	80	IPWA $\pi N \rightarrow \pi N$
180 ± 20	HOEHLER	79	IPWA $\pi N \rightarrow \pi N$
••• We do not use the following data for averages, fits, limits, etc. •••			
180 ± 20	THOMA	08	DPWA Multichannel
130.6 ± 7.0	ARNDT	04	DPWA $\pi N \rightarrow \pi N, \eta N$
138 ± 7	PENNER	02C	DPWA Multichannel
145 +8 -45	BAI	01B	BES $J/\psi \rightarrow p\bar{p}\eta$
202 ± 40	VRANA	00	DPWA Multichannel
160 ± 12	ARNDT	96	IPWA $\gamma N \rightarrow \pi N$
90	ARNDT	95	DPWA $\pi N \rightarrow N\pi$
184	¹ ARNDT	95	DPWA $\pi N \rightarrow N\pi$
215 ± 32	BATINIC	95	DPWA $\pi N \rightarrow N\pi, N\eta$
279 ± 54	² BATINIC	95	DPWA $\pi N \rightarrow N\pi, N\eta$
225	LI	93	IPWA $\gamma N \rightarrow \pi N$
179	MUSETTE	80	IPWA $\pi^- p \rightarrow \Lambda K^0$
120	SAXON	80	DPWA $\pi^- p \rightarrow \Lambda K^0$
170	³ LONGACRE	77	IPWA $\pi N \rightarrow N\pi\pi$
130	⁴ LONGACRE	75	IPWA $\pi N \rightarrow N\pi\pi$

N(1650) POLE POSITION

VALUE (MeV)	DOCUMENT ID	TECN	COMMENT
1640 to 1670 (≈ 1655) OUR ESTIMATE			
1648	ARNDT	06	DPWA $\pi N \rightarrow \pi N, \eta N$
1670	⁵ HOEHLER	93	ARGD $\pi N \rightarrow \pi N$
1640 ± 20	CUTKOSKY	80	IPWA $\pi N \rightarrow \pi N$
••• We do not use the following data for averages, fits, limits, etc. •••			
1645 ± 15	THOMA	08	DPWA Multichannel
1653	ARNDT	04	DPWA $\pi N \rightarrow \pi N, \eta N$
1663	VRANA	00	DPWA Multichannel
1660 ± 10	⁶ ARNDT	98	DPWA $\pi N \rightarrow \pi N, \eta N$
1673	ARNDT	95	DPWA $\pi N \rightarrow N\pi$
1689	¹ ARNDT	95	DPWA $\pi N \rightarrow N\pi$
1657	ARNDT	91	DPWA $\pi N \rightarrow \pi N$ Soln SM90
1648 or 1651	⁷ LONGACRE	78	IPWA $\pi N \rightarrow N\pi\pi$
1699 or 1698	³ LONGACRE	77	IPWA $\pi N \rightarrow N\pi\pi$

-2xIMAGINARY PART

VALUE (MeV)	DOCUMENT ID	TECN	COMMENT
150 to 180 (≈ 165) OUR ESTIMATE			
80	ARNDT 06	DPWA	$\pi N \rightarrow \pi N, \eta N$
163	⁵ HOEHLER 93	ARGD	$\pi N \rightarrow \pi N$
150 ± 30	CUTKOSKY 80	IPWA	$\pi N \rightarrow \pi N$
● ● ● We do not use the following data for averages, fits, limits, etc. ● ● ●			
187 ± 20	THOMA 08	DPWA	Multichannel
182	ARNDT 04	DPWA	$\pi N \rightarrow \pi N, \eta N$
240	VRANA 00	DPWA	Multichannel
140 ± 20	⁶ ARNDT 98	DPWA	$\pi N \rightarrow \pi N, \eta N$
82	ARNDT 95	DPWA	$\pi N \rightarrow N\pi$
192	¹ ARNDT 95	DPWA	$\pi N \rightarrow N\pi$
160	ARNDT 91	DPWA	$\pi N \rightarrow \pi N$ Soln SM90
117 or 119	⁷ LONGACRE 78	IPWA	$\pi N \rightarrow N\pi\pi$
174 or 173	³ LONGACRE 77	IPWA	$\pi N \rightarrow N\pi\pi$

N(1650) ELASTIC POLE RESIDUE**MODULUS |r|**

VALUE (MeV)	DOCUMENT ID	TECN	COMMENT
14	ARNDT 06	DPWA	$\pi N \rightarrow \pi N, \eta N$
39	HOEHLER 93	ARGD	$\pi N \rightarrow \pi N$
60 ± 10	CUTKOSKY 80	IPWA	$\pi N \rightarrow \pi N$
● ● ● We do not use the following data for averages, fits, limits, etc. ● ● ●			
69	ARNDT 04	DPWA	$\pi N \rightarrow \pi N, \eta N$
22	ARNDT 95	DPWA	$\pi N \rightarrow N\pi$
72	¹ ARNDT 95	DPWA	$\pi N \rightarrow N\pi$
54	ARNDT 91	DPWA	$\pi N \rightarrow \pi N$ Soln SM90

PHASE θ

VALUE (°)	DOCUMENT ID	TECN	COMMENT
-69	ARNDT 06	DPWA	$\pi N \rightarrow \pi N, \eta N$
-37	HOEHLER 93	ARGD	$\pi N \rightarrow \pi N$
-75 ± 25	CUTKOSKY 80	IPWA	$\pi N \rightarrow \pi N$
● ● ● We do not use the following data for averages, fits, limits, etc. ● ● ●			
-55	ARNDT 04	DPWA	$\pi N \rightarrow \pi N, \eta N$
29	ARNDT 95	DPWA	$\pi N \rightarrow N\pi$
-85	¹ ARNDT 95	DPWA	$\pi N \rightarrow N\pi$
-38	ARNDT 91	DPWA	$\pi N \rightarrow \pi N$ Soln SM90

N(1650) DECAY MODES

The following branching fractions are our estimates, not fits or averages.

Mode	Fraction (Γ_i/Γ)
Γ_1 $N\pi$	0.60 to 0.95
Γ_2 $N\eta$	3-10 %
Γ_3 ΛK	3-11 %
Γ_4 ΣK	
Γ_5 $N\pi\pi$	10-20 %
Γ_6 $\Delta\pi$	1-7 %
Γ_7 $\Delta(1232)\pi, D\text{-wave}$	
Γ_8 $N\rho$	4-12 %
Γ_9 $N\rho, S=1/2, S\text{-wave}$	
Γ_{10} $N\rho, S=3/2, D\text{-wave}$	
Γ_{11} $N(\pi\pi)_{S=0}^{I=0}$	<4 %
Γ_{12} $N(1440)\pi$	<5 %
Γ_{13} $p\gamma$	0.04-0.18 %
Γ_{14} $p\gamma, \text{ helicity}=1/2$	0.04-0.18 %
Γ_{15} $n\gamma$	0.003-0.17 %
Γ_{16} $n\gamma, \text{ helicity}=1/2$	0.003-0.17 %

N(1650) BRANCHING RATIOS

$\Gamma(N\pi)/\Gamma_{\text{total}}$	DOCUMENT ID	TECN	COMMENT	Γ_1/Γ
0.60 to 0.95 OUR ESTIMATE				
1.0	ARNDT 06	DPWA	$\pi N \rightarrow \pi N, \eta N$	
0.735 ± 0.011	GREEN 97	DPWA	$\pi N \rightarrow \pi N, \eta N$	
0.89 ± 0.07	MANLEY 92	IPWA	$\pi N \rightarrow \pi N \& N\pi\pi$	
0.65 ± 0.10	CUTKOSKY 80	IPWA	$\pi N \rightarrow \pi N$	
0.61 ± 0.04	HOEHLER 79	IPWA	$\pi N \rightarrow \pi N$	
● ● ● We do not use the following data for averages, fits, limits, etc. ● ● ●				
0.70 ± 0.15	THOMA 08	DPWA	Multichannel	
1.000	ARNDT 04	DPWA	$\pi N \rightarrow \pi N, \eta N$	
0.65 ± 0.04	PENNER 02c	DPWA	Multichannel	
0.74 ± 0.02	VRANA 00	DPWA	Multichannel	
0.99	ARNDT 95	DPWA	$\pi N \rightarrow N\pi$	
0.27	¹ ARNDT 95	DPWA	$\pi N \rightarrow N\pi$	
0.94 ± 0.07	BATINIC 95	DPWA	$\pi N \rightarrow N\pi, N\eta$	
0.49 ± 0.21	² BATINIC 95	DPWA	$\pi N \rightarrow N\pi, N\eta$	

 $\Gamma(N\eta)/\Gamma_{\text{total}}$

VALUE	DOCUMENT ID	TECN	COMMENT	Γ_2/Γ
0.023 ± 0.022 OUR AVERAGE Error includes scale factor of 4.3.				
0.010 ± 0.006	PENNER 02c	DPWA	Multichannel	
0.06 ± 0.01	VRANA 00	DPWA	Multichannel	
● ● ● We do not use the following data for averages, fits, limits, etc. ● ● ●				
0.15 ± 0.06	THOMA 08	DPWA	Multichannel	
0.06 ± 0.05	BATINIC 95	DPWA	$\pi N \rightarrow N\pi, N\eta$	
0.02 ± 0.03	² BATINIC 95	DPWA	$\pi N \rightarrow N\pi, N\eta$	

 $\Gamma(\Lambda K)/\Gamma_{\text{total}}$

VALUE	DOCUMENT ID	TECN	COMMENT	Γ_3/Γ
0.029 ± 0.004 OUR AVERAGE Error includes scale factor of 1.2.				
0.04 ± 0.01	SHKLYAR 05	DPWA	Multichannel	
0.027 ± 0.004	PENNER 02c	DPWA	Multichannel	

 $(\Gamma_i \Gamma_f)^{1/2}/\Gamma_{\text{total}}$ in $N\pi \rightarrow N(1650) \rightarrow \Lambda K$

VALUE	DOCUMENT ID	TECN	COMMENT	$(\Gamma_1 \Gamma_3)^{1/2}/\Gamma$
-0.27 to -0.17 OUR ESTIMATE				
-0.22	BELL 83	DPWA	$\pi^- p \rightarrow \Lambda K^0$	
-0.22	SAXON 80	DPWA	$\pi^- p \rightarrow \Lambda K^0$	

 $(\Gamma_i \Gamma_f)^{1/2}/\Gamma_{\text{total}}$ in $N\pi \rightarrow N(1650) \rightarrow \Sigma K$

VALUE	DOCUMENT ID	TECN	COMMENT	$(\Gamma_1 \Gamma_4)^{1/2}/\Gamma$
● ● ● We do not use the following data for averages, fits, limits, etc. ● ● ●				
-0.254	LIVANOS 80	DPWA	$\pi p \rightarrow \Sigma K$	

Note: Signs of couplings from $\pi N \rightarrow N\pi\pi$ analyses were changed in the 1986 edition to agree with the baryon-first convention; the overall phase ambiguity is resolved by choosing a negative sign for the $\Delta(1620) S_{31}$ coupling to $\Delta(1232)\pi$. $(\Gamma_i \Gamma_f)^{1/2}/\Gamma_{\text{total}}$ in $N\pi \rightarrow N(1650) \rightarrow \Delta(1232)\pi, D\text{-wave}$

VALUE	DOCUMENT ID	TECN	COMMENT	$(\Gamma_1 \Gamma_7)^{1/2}/\Gamma$
+0.15 to 0.23 OUR ESTIMATE				
+0.12 ± 0.04	MANLEY 92	IPWA	$\pi N \rightarrow \pi N \& N\pi\pi$	
+0.29	^{3,8} LONGACRE 77	IPWA	$\pi N \rightarrow N\pi\pi$	
+0.15	⁴ LONGACRE 75	IPWA	$\pi N \rightarrow N\pi\pi$	
● ● ● We do not use the following data for averages, fits, limits, etc. ● ● ●				
+0.26 ± 0.14	THOMA 08	DPWA	Multichannel	

 $\Gamma(\Delta(1232)\pi, D\text{-wave})/\Gamma_{\text{total}}$

VALUE	DOCUMENT ID	TECN	COMMENT	Γ_7/Γ
0.02 ± 0.01	VRANA 00	DPWA	Multichannel	
● ● ● We do not use the following data for averages, fits, limits, etc. ● ● ●				
0.10 ± 0.05	THOMA 08	DPWA	Multichannel	

 $(\Gamma_i \Gamma_f)^{1/2}/\Gamma_{\text{total}}$ in $N\pi \rightarrow N(1650) \rightarrow N\rho, S=1/2, S\text{-wave}$

VALUE	DOCUMENT ID	TECN	COMMENT	$(\Gamma_1 \Gamma_9)^{1/2}/\Gamma$
±0.03 to ±0.19 OUR ESTIMATE				
-0.01 ± 0.09	MANLEY 92	IPWA	$\pi N \rightarrow \pi N \& N\pi\pi$	
+0.17	^{3,8} LONGACRE 77	IPWA	$\pi N \rightarrow N\pi\pi$	
-0.16	⁴ LONGACRE 75	IPWA	$\pi N \rightarrow N\pi\pi$	

 $\Gamma(N\rho, S=1/2, S\text{-wave})/\Gamma_{\text{total}}$

VALUE	DOCUMENT ID	TECN	COMMENT	Γ_9/Γ
0.01 ± 0.01	VRANA 00	DPWA	Multichannel	

 $(\Gamma_i \Gamma_f)^{1/2}/\Gamma_{\text{total}}$ in $N\pi \rightarrow N(1650) \rightarrow N\rho, S=3/2, D\text{-wave}$

VALUE	DOCUMENT ID	TECN	COMMENT	$(\Gamma_1 \Gamma_{10})^{1/2}/\Gamma$
+0.17 to +0.29 OUR ESTIMATE				
+0.16 ± 0.06	MANLEY 92	IPWA	$\pi N \rightarrow \pi N \& N\pi\pi$	
+0.29	^{3,8} LONGACRE 77	IPWA	$\pi N \rightarrow N\pi\pi$	

 $\Gamma(N\rho, S=3/2, D\text{-wave})/\Gamma_{\text{total}}$

VALUE	DOCUMENT ID	TECN	COMMENT	Γ_{10}/Γ
0.13 ± 0.03	VRANA 00	DPWA	Multichannel	

 $(\Gamma_i \Gamma_f)^{1/2}/\Gamma_{\text{total}}$ in $N\pi \rightarrow N(1650) \rightarrow N(\pi\pi)_{S=0}^{I=0}$

VALUE	DOCUMENT ID	TECN	COMMENT	$(\Gamma_1 \Gamma_{11})^{1/2}/\Gamma$
+0.04 to +0.18 OUR ESTIMATE				
+0.12 ± 0.08	MANLEY 92	IPWA	$\pi N \rightarrow \pi N \& N\pi\pi$	
0.00	^{3,8} LONGACRE 77	IPWA	$\pi N \rightarrow N\pi\pi$	
+0.25	⁴ LONGACRE 75	IPWA	$\pi N \rightarrow N\pi\pi$	

 $\Gamma(N(\pi\pi)_{S=0}^{I=0})/\Gamma_{\text{total}}$

VALUE	DOCUMENT ID	TECN	COMMENT	Γ_{11}/Γ
0.01 ± 0.01	VRANA 00	DPWA	Multichannel	

 $(\Gamma_i \Gamma_f)^{1/2}/\Gamma_{\text{total}}$ in $N\pi \rightarrow N(1650) \rightarrow N(1440)\pi$

VALUE	DOCUMENT ID	TECN	COMMENT	$(\Gamma_1 \Gamma_{12})^{1/2}/\Gamma$
+0.11 ± 0.06	MANLEY 92	IPWA	$\pi N \rightarrow \pi N \& N\pi\pi$	

−2×IMAGINARY PART

VALUE (MeV)	DOCUMENT ID	TECN	COMMENT
125 to 150 (≈ 135) OUR ESTIMATE			
139	ARNDT 06	DPWA	$\pi N \rightarrow \pi N, \eta N$
126	³ HOEHLER 93	ARGD	$\pi N \rightarrow \pi N$
140±10	CUTKOSKY 80	IPWA	$\pi N \rightarrow \pi N$
••• We do not use the following data for averages, fits, limits, etc. •••			
180±20	THOMA 08	DPWA	Multichannel
146	ARNDT 04	DPWA	$\pi N \rightarrow \pi N, \eta N$
120	VRANA 00	DPWA	Multichannel
152	ARNDT 95	DPWA	$\pi N \rightarrow N\pi$
124	ARNDT 91	DPWA	$\pi N \rightarrow \pi N$ Soln SM90
146 or 171	⁴ LONGACRE 78	IPWA	$\pi N \rightarrow N\pi\pi$
127 or 127	¹ LONGACRE 77	IPWA	$\pi N \rightarrow N\pi\pi$

N(1675) ELASTIC POLE RESIDUE

MODULUS |r|

VALUE (MeV)	DOCUMENT ID	TECN	COMMENT
27	ARNDT 06	DPWA	$\pi N \rightarrow \pi N, \eta N$
23	HOEHLER 93	ARGD	$\pi N \rightarrow \pi N$
31±5	CUTKOSKY 80	IPWA	$\pi N \rightarrow \pi N$
••• We do not use the following data for averages, fits, limits, etc. •••			
29	ARNDT 04	DPWA	$\pi N \rightarrow \pi N, \eta N$
29	ARNDT 95	DPWA	$\pi N \rightarrow N\pi$
28	ARNDT 91	DPWA	$\pi N \rightarrow \pi N$ Soln SM90

PHASE θ

VALUE (°)	DOCUMENT ID	TECN	COMMENT
−21	ARNDT 06	DPWA	$\pi N \rightarrow \pi N, \eta N$
−22	HOEHLER 93	ARGD	$\pi N \rightarrow \pi N$
−30±10	CUTKOSKY 80	IPWA	$\pi N \rightarrow \pi N$
••• We do not use the following data for averages, fits, limits, etc. •••			
−22	ARNDT 04	DPWA	$\pi N \rightarrow \pi N, \eta N$
−6	ARNDT 95	DPWA	$\pi N \rightarrow N\pi$
−17	ARNDT 91	DPWA	$\pi N \rightarrow \pi N$ Soln SM90

N(1675) DECAY MODES

The following branching fractions are our estimates, not fits or averages.

Mode	Fraction (Γ_i/Γ)
Γ_1 $N\pi$	0.35 to 0.45
Γ_2 $N\eta$	(0.0 ±1.0) %
Γ_3 ΛK	<1 %
Γ_4 ΣK	
Γ_5 $N\pi\pi$	50–60 %
Γ_6 $\Delta\pi$	50–60 %
Γ_7 $\Delta(1232)\pi$, D-wave	
Γ_8 $\Delta(1232)\pi$, G-wave	
Γ_9 $N\rho$	<1–3 %
Γ_{10} $N\rho$, S=1/2, D-wave	
Γ_{11} $N\rho$, S=3/2, D-wave	
Γ_{12} $N\rho$, S=3/2, G-wave	
Γ_{13} $N(\pi\pi)_{S=0}^0$	
Γ_{14} $p\gamma$	0.004–0.023 %
Γ_{15} $p\gamma$, helicity=1/2	0.0–0.015 %
Γ_{16} $p\gamma$, helicity=3/2	0.0–0.011 %
Γ_{17} $n\gamma$	0.02–0.12 %
Γ_{18} $n\gamma$, helicity=1/2	0.006–0.046 %
Γ_{19} $n\gamma$, helicity=3/2	0.01–0.08 %

N(1675) BRANCHING RATIOS

$\Gamma(N\pi)/\Gamma_{\text{total}}$	DOCUMENT ID	TECN	COMMENT
0.35 to 0.45 OUR ESTIMATE			
0.393±0.001	ARNDT 06	DPWA	$\pi N \rightarrow \pi N, \eta N$
0.47 ±0.02	MANLEY 92	IPWA	$\pi N \rightarrow \pi N \& N\pi\pi$
0.38 ±0.05	CUTKOSKY 80	IPWA	$\pi N \rightarrow \pi N$
0.38 ±0.03	HOEHLER 79	IPWA	$\pi N \rightarrow \pi N$
••• We do not use the following data for averages, fits, limits, etc. •••			
0.30 ±0.08	THOMA 08	DPWA	Multichannel
0.400±0.002	ARNDT 04	DPWA	$\pi N \rightarrow \pi N, \eta N$
0.35 ±0.01	VRANA 00	DPWA	Multichannel
0.38	ARNDT 95	DPWA	$\pi N \rightarrow N\pi$
0.31 ±0.06	BATINIC 95	DPWA	$\pi N \rightarrow N\pi, N\eta$

$\Gamma(N\eta)/\Gamma_{\text{total}}$

VALUE	DOCUMENT ID	TECN	COMMENT
0.00 ±0.01			
••• We do not use the following data for averages, fits, limits, etc. •••			
0.03 ±0.03	THOMA 08	DPWA	Multichannel
0.001±0.001	BATINIC 95	DPWA	$\pi N \rightarrow N\pi, N\eta$

$(\Gamma_1\Gamma_f)^{1/2}/\Gamma_{\text{total}}$ in $N\pi \rightarrow N(1675) \rightarrow \Lambda K$

VALUE	DOCUMENT ID	TECN	COMMENT
±0.04 to ±0.08 OUR ESTIMATE			
−0.01	BELL 83	DPWA	$\pi^- p \rightarrow \Lambda K^0$
+0.036	⁵ SAXON 80	DPWA	$\pi^- p \rightarrow \Lambda K^0$

Note: Signs of couplings from $\pi N \rightarrow N\pi\pi$ analyses were changed in the 1986 edition to agree with the baryon-first convention; the overall phase ambiguity is resolved by choosing a negative sign for the $\Delta(1620) S_{31}$ coupling to $\Delta(1232)\pi$.

$(\Gamma_1\Gamma_f)^{1/2}/\Gamma_{\text{total}}$ in $N\pi \rightarrow N(1675) \rightarrow \Delta(1232)\pi$, D-wave

VALUE	DOCUMENT ID	TECN	COMMENT
+0.46 to +0.50 OUR ESTIMATE			
+0.496±0.003	MANLEY 92	IPWA	$\pi N \rightarrow \pi N \& N\pi\pi$
+0.46	^{1,6} LONGACRE 77	IPWA	$\pi N \rightarrow N\pi\pi$
+0.50	² LONGACRE 75	IPWA	$\pi N \rightarrow N\pi\pi$

$\Gamma(\Delta(1232)\pi, \text{D-wave})/\Gamma_{\text{total}}$

VALUE	DOCUMENT ID	TECN	COMMENT
0.63±0.02	VRANA 00	DPWA	Multichannel
••• We do not use the following data for averages, fits, limits, etc. •••			
0.24±0.08	THOMA 08	DPWA	Multichannel

$(\Gamma_1\Gamma_f)^{1/2}/\Gamma_{\text{total}}$ in $N\pi \rightarrow N(1675) \rightarrow N\rho, S=1/2, \text{D-wave}$

VALUE	DOCUMENT ID	TECN	COMMENT
+0.04±0.02	MANLEY 92	IPWA	$\pi N \rightarrow \pi N \& N\pi\pi$

$\Gamma(N\rho, S=1/2, \text{D-wave})/\Gamma_{\text{total}}$

VALUE	DOCUMENT ID	TECN	COMMENT
0.00±0.01	VRANA 00	DPWA	Multichannel

$(\Gamma_1\Gamma_f)^{1/2}/\Gamma_{\text{total}}$ in $N\pi \rightarrow N(1675) \rightarrow N\rho, S=3/2, \text{D-wave}$

VALUE	DOCUMENT ID	TECN	COMMENT
−0.12 to −0.06 OUR ESTIMATE			
−0.03±0.02	MANLEY 92	IPWA	$\pi N \rightarrow \pi N \& N\pi\pi$
−0.15	^{1,6} LONGACRE 77	IPWA	$\pi N \rightarrow N\pi\pi$

$\Gamma(N\rho, S=3/2, \text{D-wave})/\Gamma_{\text{total}}$

VALUE	DOCUMENT ID	TECN	COMMENT
0.01±0.01	VRANA 00	DPWA	Multichannel

$(\Gamma_1\Gamma_f)^{1/2}/\Gamma_{\text{total}}$ in $N\pi \rightarrow N(1675) \rightarrow N(\pi\pi)_{S=0}^0$

VALUE	DOCUMENT ID	TECN	COMMENT
+0.03	^{1,6} LONGACRE 77	IPWA	$\pi N \rightarrow N\pi\pi$

N(1675) PHOTON DECAY AMPLITUDES

Papers on γN amplitudes predating 1981 may be found in our 2006 edition, Journal of Physics, G **33** 1 (2006).

N(1675) → $p\gamma$, helicity-1/2 amplitude $A_{1/2}$

VALUE ($\text{GeV}^{-1/2}$)	DOCUMENT ID	TECN	COMMENT
+0.019±0.008 OUR ESTIMATE			
0.018±0.002	DUGGER 07	DPWA	$\gamma N \rightarrow \pi N$
0.015±0.010	ARNDT 96	IPWA	$\gamma N \rightarrow \pi N$
0.021±0.011	CRAWFORD 83	IPWA	$\gamma N \rightarrow \pi N$
0.034±0.005	AWAJI 81	DPWA	$\gamma N \rightarrow \pi N$
••• We do not use the following data for averages, fits, limits, etc. •••			
0.015	DRECHSEL 07	DPWA	$\gamma N \rightarrow \pi N$
0.012±0.002	LI 93	IPWA	$\gamma N \rightarrow \pi N$

N(1675) → $p\gamma$, helicity-3/2 amplitude $A_{3/2}$

VALUE ($\text{GeV}^{-1/2}$)	DOCUMENT ID	TECN	COMMENT
+0.015±0.009 OUR ESTIMATE			
0.021±0.001	DUGGER 07	DPWA	$\gamma N \rightarrow \pi N$
0.010±0.007	ARNDT 96	IPWA	$\gamma N \rightarrow \pi N$
0.015±0.009	CRAWFORD 83	IPWA	$\gamma N \rightarrow \pi N$
0.024±0.008	AWAJI 81	DPWA	$\gamma N \rightarrow \pi N$
••• We do not use the following data for averages, fits, limits, etc. •••			
0.022	DRECHSEL 07	DPWA	$\gamma N \rightarrow \pi N$
0.021±0.002	LI 93	IPWA	$\gamma N \rightarrow \pi N$

Baryon Particle Listings

N(1675), N(1680)

N(1675) -> n-gamma, helicity-1/2 amplitude A1/2

Table with columns: VALUE (GeV^-1/2), DOCUMENT ID, TECN, COMMENT. Includes our estimate and data points from ARNDT, AWAJI, FUJII, DRECHSEL, LI.

N(1675) -> n-gamma, helicity-3/2 amplitude A3/2

Table with columns: VALUE (GeV^-1/2), DOCUMENT ID, TECN, COMMENT. Includes our estimate and data points from ARNDT, AWAJI, FUJII, DRECHSEL, LI.

N(1675) FOOTNOTES

- 1 LONGACRE 77 pole positions are from a search for poles in the unitarized T-matrix; the first (second) value uses, in addition to pi N -> N pi pi data, elastic amplitudes from a Saclay (CERN) partial-wave analysis. The other LONGACRE 77 values are from eyeball fits with Breit-Wigner circles to the T-matrix amplitudes.
2 From method II of LONGACRE 75: eyeball fits with Breit-Wigner circles to the T-matrix amplitudes.
3 See HOEHLER 93 for a detailed discussion of the evidence for and the pole parameters of N and Delta resonances as determined from Argand diagrams of pi N elastic partial-wave amplitudes and from plots of the speeds with which the amplitudes traverse the diagrams.
4 LONGACRE 78 values are from a search for poles in the unitarized T-matrix. The first (second) value uses, in addition to pi N -> N pi pi data, elastic amplitudes from a Saclay (CERN) partial-wave analysis.
5 SAXON 80 finds the coupling phase is near 90 degrees.
6 LONGACRE 77 considers this coupling to be well determined.

N(1675) REFERENCES

For early references, see Physics Letters 111B 1 (1982).

Table of references for N(1675) with columns: AUTHOR, YEAR, DOCUMENT ID, TECN, COMMENT. Lists various physics papers and conference proceedings.

Boxed section for N(1680) F15. Includes the equation J^P = 1/2(5/2+) Status: *** and text describing the results published before 1975 were last included in our 1982 edition, Physics Letters 111B 1 (1982).

N(1680) BREIT-WIGNER MASS

Table with columns: VALUE (MeV), DOCUMENT ID, TECN, COMMENT. Includes our estimate for N(1680) mass and data points from ARNDT, MANLEY, CUTKOSKY, HOEHLER.

... We do not use the following data for averages, fits, limits, etc. ...

Table with columns: VALUE, DOCUMENT ID, TECN, COMMENT. Lists data points for N(1680) mass from THOMA, ARNDT, VRANA, ARNDT, BATINIC, LONGACRE.

N(1680) BREIT-WIGNER WIDTH

Table with columns: VALUE (MeV), DOCUMENT ID, TECN, COMMENT. Includes our estimate for N(1680) width and data points from ARNDT, MANLEY, CUTKOSKY, HOEHLER, THOMA, ARNDT, VRANA, ARNDT, BATINIC, LONGACRE.

N(1680) POLE POSITION

REAL PART

Table with columns: VALUE (MeV), DOCUMENT ID, TECN, COMMENT. Includes our estimate for the real part of the N(1680) pole position and data points from ARNDT, HOEHLER, CUTKOSKY, THOMA, ARNDT, VRANA, ARNDT, ARNDT, LONGACRE, LONGACRE.

-2xIMAGINARY PART

Table with columns: VALUE (MeV), DOCUMENT ID, TECN, COMMENT. Includes our estimate for the imaginary part of the N(1680) pole position and data points from ARNDT, HOEHLER, CUTKOSKY, THOMA, ARNDT, VRANA, ARNDT, ARNDT, LONGACRE, LONGACRE.

N(1680) ELASTIC POLE RESIDUE

MODULUS |r|

Table with columns: VALUE (MeV), DOCUMENT ID, TECN, COMMENT. Lists data points for the elastic pole residue from ARNDT, HOEHLER, CUTKOSKY, ARNDT, ARNDT, ARNDT.

PHASE theta

Table with columns: VALUE (degrees), DOCUMENT ID, TECN, COMMENT. Lists data points for the phase of the elastic pole residue from ARNDT, HOEHLER, CUTKOSKY, ARNDT, ARNDT, ARNDT.

See key on page 405

Baryon Particle Listings
N(1680)

N(1680) DECAY MODES

The following branching fractions are our estimates, not fits or averages.

Mode	Fraction (Γ_i/Γ)
Γ_1 $N\pi$	0.65 to 0.70
Γ_2 $N\eta$	(0.0 \pm 1.0) %
Γ_3 ΛK	
Γ_4 ΣK	
Γ_5 $N\pi\pi$	30–40 %
Γ_6 $\Delta\pi$	5–15 %
Γ_7 $\Delta(1232)\pi, P\text{-wave}$	6–14 %
Γ_8 $\Delta(1232)\pi, F\text{-wave}$	<2 %
Γ_9 $N\rho$	3–15 %
Γ_{10} $N\rho, S=1/2, F\text{-wave}$	
Γ_{11} $N\rho, S=3/2, P\text{-wave}$	<12 %
Γ_{12} $N\rho, S=3/2, F\text{-wave}$	1–5 %
Γ_{13} $N(\pi\pi)_{S\text{-wave}}^{J=0}$	5–20 %
Γ_{14} $p\gamma$	0.21–0.32 %
Γ_{15} $p\gamma, \text{helicity}=1/2$	0.001–0.011 %
Γ_{16} $p\gamma, \text{helicity}=3/2$	0.20–0.32 %
Γ_{17} $n\gamma$	0.021–0.046 %
Γ_{18} $n\gamma, \text{helicity}=1/2$	0.004–0.029 %
Γ_{19} $n\gamma, \text{helicity}=3/2$	0.01–0.024 %

N(1680) BRANCHING RATIOS

$\Gamma(N\pi)/\Gamma_{\text{total}}$				Γ_1/Γ
VALUE	DOCUMENT ID	TECN	COMMENT	
0.65 to 0.70 OUR ESTIMATE				
0.701 \pm 0.001	ARNDT	06	DPWA $\pi N \rightarrow \pi N, \eta N$	
0.70 \pm 0.03	MANLEY	92	IPWA $\pi N \rightarrow \pi N \& N\pi\pi$	
0.62 \pm 0.05	CUTKOSKY	80	IPWA $\pi N \rightarrow \pi N$	
0.65 \pm 0.02	HOEHLER	79	IPWA $\pi N \rightarrow \pi N$	
●●● We do not use the following data for averages, fits, limits, etc. ●●●				
0.72 \pm 0.15	THOMA	08	DPWA Multichannel	
0.670 \pm 0.004	ARNDT	04	DPWA $\pi N \rightarrow \pi N, \eta N$	
0.69 \pm 0.02	VRANA	00	DPWA Multichannel	
0.68	ARNDT	95	DPWA $\pi N \rightarrow N\pi$	
0.69 \pm 0.04	BATINIC	95	DPWA $\pi N \rightarrow N\pi, N\eta$	

$(\Gamma_i\Gamma_f)^{1/2}/\Gamma_{\text{total}}$ in $N\pi \rightarrow N(1680) \rightarrow N\eta$				$(\Gamma_1\Gamma_2)^{1/2}/\Gamma$
VALUE	DOCUMENT ID	TECN	COMMENT	
●●● We do not use the following data for averages, fits, limits, etc. ●●●				
not seen	BAKER	79	DPWA $\pi^- \rho \rightarrow n\eta$	

$\Gamma(N\eta)/\Gamma_{\text{total}}$				Γ_2/Γ
VALUE	DOCUMENT ID	TECN	COMMENT	
0.00 \pm 0.01				
	VRANA	00	DPWA Multichannel	
●●● We do not use the following data for averages, fits, limits, etc. ●●●				
<0.01	THOMA	08	DPWA Multichannel	
0.0015 \pm 0.0035 -0.0010	TIATOR	99	DPWA $\gamma\rho \rightarrow p\eta$	
0.01 \pm 0.004	BATINIC	95	DPWA $\pi N \rightarrow N\pi, N\eta$	

$(\Gamma_i\Gamma_f)^{1/2}/\Gamma_{\text{total}}$ in $N\pi \rightarrow N(1680) \rightarrow \Lambda K$				$(\Gamma_1\Gamma_3)^{1/2}/\Gamma$
VALUE	DOCUMENT ID	TECN	COMMENT	
Coupling to ΛK not required in the analyses of SAXON 80 or BELL 83.				

Note: Signs of couplings from $\pi N \rightarrow N\pi\pi$ analyses were changed in the 1986 edition to agree with the baryon-first convention; the overall phase ambiguity is resolved by choosing a negative sign for the $\Delta(1620) S_{31}$ coupling to $\Delta(1232)\pi$.

$(\Gamma_i\Gamma_f)^{1/2}/\Gamma_{\text{total}}$ in $N\pi \rightarrow N(1680) \rightarrow \Delta(1232)\pi, P\text{-wave}$				$(\Gamma_1\Gamma_7)^{1/2}/\Gamma$
VALUE	DOCUMENT ID	TECN	COMMENT	
-0.31 to -0.21 OUR ESTIMATE				
-0.26 \pm 0.04	MANLEY	92	IPWA $\pi N \rightarrow \pi N \& N\pi\pi$	
-0.27	1.5 LONGACRE	77	IPWA $\pi N \rightarrow N\pi\pi$	
-0.25	2 LONGACRE	75	IPWA $\pi N \rightarrow N\pi\pi$	

$\Gamma(\Delta(1232)\pi, P\text{-wave})/\Gamma_{\text{total}}$				Γ_7/Γ
VALUE	DOCUMENT ID	TECN	COMMENT	
0.14 \pm 0.03	VRANA	00	DPWA Multichannel	
●●● We do not use the following data for averages, fits, limits, etc. ●●●				
0.08 \pm 0.03	THOMA	08	DPWA Multichannel	

$(\Gamma_i\Gamma_f)^{1/2}/\Gamma_{\text{total}}$ in $N\pi \rightarrow N(1680) \rightarrow \Delta(1232)\pi, F\text{-wave}$				$(\Gamma_1\Gamma_8)^{1/2}/\Gamma$
VALUE	DOCUMENT ID	TECN	COMMENT	
+0.03 to +0.11 OUR ESTIMATE				
+0.07 \pm 0.03	MANLEY	92	IPWA $\pi N \rightarrow \pi N \& N\pi\pi$	
+0.07	1.5 LONGACRE	77	IPWA $\pi N \rightarrow N\pi\pi$	
+0.08	2 LONGACRE	75	IPWA $\pi N \rightarrow N\pi\pi$	

$\Gamma(\Delta(1232)\pi, F\text{-wave})/\Gamma_{\text{total}}$				Γ_8/Γ
VALUE	DOCUMENT ID	TECN	COMMENT	
0.01 \pm 0.01	VRANA	00	DPWA Multichannel	
●●● We do not use the following data for averages, fits, limits, etc. ●●●				
0.04 \pm 0.03	THOMA	08	DPWA Multichannel	

$(\Gamma_i\Gamma_f)^{1/2}/\Gamma_{\text{total}}$ in $N\pi \rightarrow N(1680) \rightarrow N\rho, S=3/2, P\text{-wave}$				$(\Gamma_1\Gamma_{11})^{1/2}/\Gamma$
VALUE	DOCUMENT ID	TECN	COMMENT	
-0.30 to -0.10 OUR ESTIMATE				
-0.20 \pm 0.05	MANLEY	92	IPWA $\pi N \rightarrow \pi N \& N\pi\pi$	
-0.23	1.5 LONGACRE	77	IPWA $\pi N \rightarrow N\pi\pi$	
-0.30	2 LONGACRE	75	IPWA $\pi N \rightarrow N\pi\pi$	

$\Gamma(N\rho, S=3/2, P\text{-wave})/\Gamma_{\text{total}}$				Γ_{11}/Γ
VALUE	DOCUMENT ID	TECN	COMMENT	
0.05 \pm 0.01	VRANA	00	DPWA Multichannel	

$(\Gamma_i\Gamma_f)^{1/2}/\Gamma_{\text{total}}$ in $N\pi \rightarrow N(1680) \rightarrow N\rho, S=3/2, F\text{-wave}$				$(\Gamma_1\Gamma_{12})^{1/2}/\Gamma$
VALUE	DOCUMENT ID	TECN	COMMENT	
-0.18 to -0.10 OUR ESTIMATE				
-0.13 \pm 0.03	MANLEY	92	IPWA $\pi N \rightarrow \pi N \& N\pi\pi$	
-0.15	1.5 LONGACRE	77	IPWA $\pi N \rightarrow N\pi\pi$	

$\Gamma(N\rho, S=3/2, F\text{-wave})/\Gamma_{\text{total}}$				Γ_{12}/Γ
VALUE	DOCUMENT ID	TECN	COMMENT	
0.03 \pm 0.01	VRANA	00	DPWA Multichannel	

$(\Gamma_i\Gamma_f)^{1/2}/\Gamma_{\text{total}}$ in $N\pi \rightarrow N(1680) \rightarrow N(\pi\pi)_{S\text{-wave}}^{J=0}$				$(\Gamma_1\Gamma_{13})^{1/2}/\Gamma$
VALUE	DOCUMENT ID	TECN	COMMENT	
+0.25 to +0.35 OUR ESTIMATE				
+0.29 \pm 0.04	MANLEY	92	IPWA $\pi N \rightarrow \pi N \& N\pi\pi$	
+0.31	1.5 LONGACRE	77	IPWA $\pi N \rightarrow N\pi\pi$	
+0.30	2 LONGACRE	75	IPWA $\pi N \rightarrow N\pi\pi$	

$\Gamma(N(\pi\pi)_{S\text{-wave}}^{J=0})/\Gamma_{\text{total}}$				Γ_{13}/Γ
VALUE	DOCUMENT ID	TECN	COMMENT	
0.09 \pm 0.01	VRANA	00	DPWA Multichannel	
●●● We do not use the following data for averages, fits, limits, etc. ●●●				
0.11 \pm 0.05	THOMA	08	DPWA Multichannel	

N(1680) PHOTON DECAY AMPLITUDES

Papers on γN amplitudes predating 1981 may be found in our 2006 edition, Journal of Physics, G **33** 1 (2006).

N(1680) $\rightarrow p\gamma, \text{helicity-1/2}$ amplitude $A_{1/2}$

VALUE (GeV $^{-1/2}$)	DOCUMENT ID	TECN	COMMENT
-0.015 \pm 0.006 OUR ESTIMATE			
-0.017 \pm 0.001	DUGGER	07	DPWA $\gamma N \rightarrow \pi N$
-0.010 \pm 0.004	ARNDT	96	IPWA $\gamma N \rightarrow \pi N$
-0.017 \pm 0.018	CRAWFORD	83	IPWA $\gamma N \rightarrow \pi N$
-0.009 \pm 0.006	AWAJI	81	DPWA $\gamma N \rightarrow \pi N$
●●● We do not use the following data for averages, fits, limits, etc. ●●●			
-0.025	DRECHSEL	07	DPWA $\gamma N \rightarrow \pi N$
-0.006 \pm 0.002	LI	93	IPWA $\gamma N \rightarrow \pi N$

N(1680) $\rightarrow p\gamma, \text{helicity-3/2}$ amplitude $A_{3/2}$

VALUE (GeV $^{-1/2}$)	DOCUMENT ID	TECN	COMMENT
+0.133 \pm 0.012 OUR ESTIMATE			
0.134 \pm 0.002	DUGGER	07	DPWA $\gamma N \rightarrow \pi N$
0.145 \pm 0.005	ARNDT	96	IPWA $\gamma N \rightarrow \pi N$
0.132 \pm 0.010	CRAWFORD	83	IPWA $\gamma N \rightarrow \pi N$
0.115 \pm 0.008	AWAJI	81	DPWA $\gamma N \rightarrow \pi N$
●●● We do not use the following data for averages, fits, limits, etc. ●●●			
0.134	DRECHSEL	07	DPWA $\gamma N \rightarrow \pi N$
0.154 \pm 0.002	LI	93	IPWA $\gamma N \rightarrow \pi N$

N(1680) $\rightarrow n\gamma, \text{helicity-1/2}$ amplitude $A_{1/2}$

VALUE (GeV $^{-1/2}$)	DOCUMENT ID	TECN	COMMENT
+0.029 \pm 0.010 OUR ESTIMATE			
0.030 \pm 0.005	ARNDT	96	IPWA $\gamma N \rightarrow \pi N$
0.017 \pm 0.014	AWAJI	81	DPWA $\gamma N \rightarrow \pi N$
0.032 \pm 0.003	FUJII	81	DPWA $\gamma N \rightarrow \pi N$
●●● We do not use the following data for averages, fits, limits, etc. ●●●			
0.028	DRECHSEL	07	DPWA $\gamma N \rightarrow \pi N$
0.022 \pm 0.002	LI	93	IPWA $\gamma N \rightarrow \pi N$

Baryon Particle Listings

N(1680), N(1700)

N(1680) → nγ, helicity-3/2 amplitude A_{3/2}

VALUE (GeV ^{-1/2})	DOCUMENT ID	TECN	COMMENT
-0.033 ± 0.009 OUR ESTIMATE			
-0.040 ± 0.015	ARNDT 96	IPWA	γ N → π N
-0.033 ± 0.013	AWAJI 81	DPWA	γ N → π N
-0.023 ± 0.005	FUJII 81	DPWA	γ N → π N
• • • We do not use the following data for averages, fits, limits, etc. • • •			
-0.038	DRECHSEL 07	DPWA	γ N → π N
-0.048 ± 0.002	LI 93	IPWA	γ N → π N

N(1680) FOOTNOTES

- LONGACRE 77 pole positions are from a search for poles in the unitarized T-matrix; the first (second) value uses, in addition to π N → N π π data, elastic amplitudes from a Saclay (CERN) partial-wave analysis. The other LONGACRE 77 values are from eyeball fits with Breit-Wigner circles to the T-matrix amplitudes.
- From method II of LONGACRE 75: eyeball fits with Breit-Wigner circles to the T-matrix amplitudes.
- See HOEHLER 93 for a detailed discussion of the evidence for and the pole parameters of N and Δ resonances as determined from Argand diagrams of π N elastic partial-wave amplitudes and from plots of the speeds with which the amplitudes traverse the diagrams.
- LONGACRE 78 values are from a search for poles in the unitarized T-matrix. The first (second) value uses, in addition to π N → N π π data, elastic amplitudes from a Saclay (CERN) partial-wave analysis.
- LONGACRE 77 considers this coupling to be well determined.

N(1680) REFERENCES

For early references, see Physics Letters **111B** 1 (1982). For very early references, see Reviews of Modern Physics **37** 633 (1965).

THOMA 08	PL B659 87	U. Thoma et al.	(CB-ELSA Collab.)
DRECHSEL 07	EPJ A34 69	D. Drechsel, S.S. Kamalov, L. Tiator	(MAINZ, JINR)
DUGGER 07	PR C76 025211	M. Dugger et al.	(Jefferson Lab CLAS Collab.)
ARNDT 06	PR C74 045205	R.A. Arndt et al.	(GWU)
PDG 06	JPG 33 1	W.-M. Yao et al.	(PDG Collab.)
ARNDT 04	PR C69 035213	R.A. Arndt et al.	(GWU, TRIU)
VRANA 00	PRPL 328 181	T.P. Vrana, S.A. Dytman, T.-S.H. Lee	(PITT+)
TIATOR 99	PR C60 035210	L. Tiator et al.	
ARNDT 96	PR C53 430	R.A. Arndt, I.I. Strakovsky, R.L. Workman	(VPI)
ARNDT 95	PR C52 2120	R.A. Arndt et al.	(VPI, BRCO)
BATINIC 95	PR C51 2310	M. Batinic et al.	(BOSK, UCLA)
Also	PR C57 1004 (erratum)	M. Batinic et al.	
HOEHLER 93	π N Newsletter 9 1	G. Hoehler	(KARL)
LI 93	PR C47 2759	Z.J. Li et al.	(VPI)
MANLEY 92	PR D45 4002	D.M. Manley, E.M. Saleski	(KENT) IJP
Also	PR D30 904	D.M. Manley et al.	(VPI)
ARNDT 91	PR D43 2131	R.A. Arndt et al.	(VPI, TELE) IJP
BELL 83	NP B222 389	K.W. Bell et al.	(RL) IJP
CRAWFORD 83	NP B211 1	R.L. Crawford, W.T. Morton	(GLAS)
PDG 82	PL 111B 1	M. Roos et al.	(HELS, CIT, CERN)
AWAJI 81	Bonn Conf. 352	N. Awaji, R. Kajikawa	(NAGO)
Also	NP B197 365	K. Fujii et al.	(NAGO)
FUJII 81	NP B187 53	K. Fujii et al.	(NAGO, OSAK)
CUTKOSKY 80	Toronto Conf. 19	R.E. Cutkosky et al.	(CMU, LBL) IJP
Also	PR D20 2839	R.E. Cutkosky et al.	(CMU, LBL) IJP
SAXON 80	NP B162 522	D.H. Saxon et al.	(RHEL, BRIS) IJP
BAKER 79	NP B156 93	R.D. Baker et al.	(RHEL) IJP
HOEHLER 79	PDAT 12-1	G. Hoehler et al.	(KARLT) IJP
Also	Toronto Conf. 3	R. Koch	(KARLT) IJP
LONGACRE 78	PR D17 1795	R.S. Longacre et al.	(LBL, SLAC)
LONGACRE 77	NP B122 493	R.S. Longacre, J. Dolbeau	(SACL) IJP
Also	NP B108 365	J. Dolbeau et al.	(SACL) IJP
LONGACRE 75	PL 55B 415	R.S. Longacre et al.	(LBL, SLAC) IJP

N(1700) D₁₃

$$I(J^P) = \frac{1}{2}(\frac{3}{2}^-) \text{ Status: } ***$$

Most of the results published before 1975 are now obsolete and have been omitted. They may be found in our 1982 edition, Physics Letters **111B** 1 (1982). Some further obsolete results published before 1984 were last included in our 2006 edition, Journal of Physics, G **33** 1 (2006).

The various partial-wave analyses do not agree very well.

The latest GWU analysis (ARNDT 06) finds no evidence for this resonance.

N(1700) BREIT-WIGNER MASS

VALUE (MeV)	DOCUMENT ID	TECN	COMMENT
1650 to 1750 (≈ 1700) OUR ESTIMATE			
1737 ± 44	MANLEY 92	IPWA	π N → π N & N π π
1675 ± 25	CUTKOSKY 80	IPWA	π N → π N
1731 ± 15	HOEHLER 79	IPWA	π N → π N
• • • We do not use the following data for averages, fits, limits, etc. • • •			
1740 ± 20	THOMA 08	DPWA	Multichannel
1736 ± 33	VRANA 00	DPWA	Multichannel
1791 ± 46	BATINIC 95	DPWA	π N → N π, N η
1650	SAXON 80	DPWA	π ⁻ p → Λ K ⁰
1690 to 1710	BAKER 78	DPWA	π ⁻ p → Λ K ⁰
1719	BARBOUR 78	DPWA	γ N → π N
1670 ± 10	¹ BAKER 77	IPWA	π ⁻ p → Λ K ⁰
1690	¹ BAKER 77	DPWA	π ⁻ p → Λ K ⁰
1660	² LONGACRE 77	IPWA	π N → N π π
1710	³ LONGACRE 75	IPWA	π N → N π π

N(1700) BREIT-WIGNER WIDTH

VALUE (MeV)	DOCUMENT ID	TECN	COMMENT
50 to 150 (≈ 100) OUR ESTIMATE			
250 ± 220	MANLEY 92	IPWA	π N → π N & N π π
90 ± 40	CUTKOSKY 80	IPWA	π N → π N
110 ± 30	HOEHLER 79	IPWA	π N → π N
• • • We do not use the following data for averages, fits, limits, etc. • • •			
180 ± 30	THOMA 08	DPWA	Multichannel
175 ± 133	VRANA 00	DPWA	Multichannel
215 ± 60	BATINIC 95	DPWA	π N → N π, N η
70	SAXON 80	DPWA	π ⁻ p → Λ K ⁰
70 to 100	BAKER 78	DPWA	π ⁻ p → Λ K ⁰
126	BARBOUR 78	DPWA	γ N → π N
90 ± 25	¹ BAKER 77	IPWA	π ⁻ p → Λ K ⁰
100	¹ BAKER 77	DPWA	π ⁻ p → Λ K ⁰
600	² LONGACRE 77	IPWA	π N → N π π
300	³ LONGACRE 75	IPWA	π N → N π π

N(1700) POLE POSITION

REAL PART

VALUE (MeV)	DOCUMENT ID	TECN	COMMENT
1630 to 1730 (≈ 1680) OUR ESTIMATE			
1700	⁴ HOEHLER 93	SPED	π N → π N
1660 ± 30	CUTKOSKY 80	IPWA	π N → π N
• • • We do not use the following data for averages, fits, limits, etc. • • •			
1710 ± 15	THOMA 08	DPWA	Multichannel
1704	VRANA 00	DPWA	Multichannel
not seen	ARNDT 91	DPWA	π N → π N Soln SM90
1710 or 1678	⁵ LONGACRE 78	IPWA	π N → N π π
1616 or 1613	² LONGACRE 77	IPWA	π N → N π π

−2×IMAGINARY PART

VALUE (MeV)	DOCUMENT ID	TECN	COMMENT
50 to 150 (≈ 100) OUR ESTIMATE			
120	⁴ HOEHLER 93	SPED	π N → π N
90 ± 40	CUTKOSKY 80	IPWA	π N → π N
• • • We do not use the following data for averages, fits, limits, etc. • • •			
155 ± 25	THOMA 08	DPWA	Multichannel
156	VRANA 00	DPWA	Multichannel
not seen	ARNDT 91	DPWA	π N → π N Soln SM90
607 or 567	⁵ LONGACRE 78	IPWA	π N → N π π
577 or 575	² LONGACRE 77	IPWA	π N → N π π

N(1700) ELASTIC POLE RESIDUE

MODULUS |r|

VALUE (MeV)	DOCUMENT ID	TECN	COMMENT
5	HOEHLER 93	SPED	π N → π N
6 ± 3	CUTKOSKY 80	IPWA	π N → π N

PHASE θ

VALUE (°)	DOCUMENT ID	TECN	COMMENT
0 ± 50	CUTKOSKY 80	IPWA	π N → π N

N(1700) DECAY MODES

The following branching fractions are our estimates, not fits or averages.

Mode	Fraction (Γ _i /Γ)
Γ ₁ N π	5–15 %
Γ ₂ N η	(0.0 ± 1.0) %
Γ ₃ Λ K	< 3 %
Γ ₄ Σ K	
Γ ₅ N π π	85–95 %
Γ ₆ Δ π	
Γ ₇ Δ(1232) π, S-wave	
Γ ₈ Δ(1232) π, D-wave	
Γ ₉ N ρ	< 35 %
Γ ₁₀ N ρ, S=1/2, D-wave	
Γ ₁₁ N ρ, S=3/2, S-wave	
Γ ₁₂ N ρ, S=3/2, D-wave	
Γ ₁₃ N(π π) _{S-wave} ^{L=0}	
Γ ₁₄ p γ	0.01–0.05 %
Γ ₁₅ p γ, helicity=1/2	0.0–0.024 %
Γ ₁₆ p γ, helicity=3/2	0.002–0.026 %
Γ ₁₇ n γ	0.01–0.13 %
Γ ₁₈ n γ, helicity=1/2	0.0–0.09 %
Γ ₁₉ n γ, helicity=3/2	0.01–0.05 %

See key on page 405

Baryon Particle Listings

N(1700)

N(1700) BRANCHING RATIOS

$\Gamma(N\pi)/\Gamma_{\text{total}}$				Γ_1/Γ
VALUE	DOCUMENT ID	TECN	COMMENT	
0.05 to 0.15 OUR ESTIMATE				
0.01 ± 0.02	MANLEY	92	IPWA	$\pi N \rightarrow \pi N \text{ \& } N\pi\pi$
0.11 ± 0.05	CUTKOSKY	80	IPWA	$\pi N \rightarrow \pi N$
0.08 ± 0.03	HOEHLER	79	IPWA	$\pi N \rightarrow \pi N$
• • • We do not use the following data for averages, fits, limits, etc. • • •				
0.08 ^{+0.08} / _{-0.04}	THOMA	08	DPWA	Multichannel
0.04 ± 0.02	VRANA	00	DPWA	Multichannel
0.04 ± 0.05	BATINIC	95	DPWA	$\pi N \rightarrow N\pi, N\eta$

$\Gamma(N\eta)/\Gamma_{\text{total}}$				Γ_2/Γ
VALUE	DOCUMENT ID	TECN	COMMENT	
0.00 ± 0.01				
• • • We do not use the following data for averages, fits, limits, etc. • • •				
0.10 ± 0.05	THOMA	08	DPWA	Multichannel
0.10 ± 0.06	BATINIC	95	DPWA	$\pi N \rightarrow N\pi, N\eta$

$(\Gamma_1\Gamma_7)^{1/2}/\Gamma_{\text{total}}$ in $N\pi \rightarrow N(1700) \rightarrow \Lambda K$				$(\Gamma_1\Gamma_3)^{1/2}/\Gamma$
VALUE	DOCUMENT ID	TECN	COMMENT	
-0.06 to +0.04 OUR ESTIMATE				
-0.012	BELL	83	DPWA	$\pi^- p \rightarrow \Lambda K^0$
-0.012	SAXON	80	DPWA	$\pi^- p \rightarrow \Lambda K^0$
• • • We do not use the following data for averages, fits, limits, etc. • • •				
-0.04	⁶ BAKER	78	DPWA	See SAXON 80
-0.03 ± 0.004	¹ BAKER	77	IPWA	$\pi^- p \rightarrow \Lambda K^0$
-0.03	¹ BAKER	77	DPWA	$\pi^- p \rightarrow \Lambda K^0$
+0.026 ± 0.019	DEVENISH	748		Fixed- <i>t</i> dispersion rel.

$(\Gamma_1\Gamma_7)^{1/2}/\Gamma_{\text{total}}$ in $N\pi \rightarrow N(1700) \rightarrow \Sigma K$				$(\Gamma_1\Gamma_4)^{1/2}/\Gamma$
VALUE	DOCUMENT ID	TECN	COMMENT	
• • • We do not use the following data for averages, fits, limits, etc. • • •				
not seen	LIVANOS	80	DPWA	$\pi p \rightarrow \Sigma K$
<0.017	⁷ DEANS	75	DPWA	$\pi N \rightarrow \Sigma K$

Note: Signs of couplings from $\pi N \rightarrow N\pi\pi$ analyses were changed in the 1986 edition to agree with the baryon-first convention; the overall phase ambiguity is resolved by choosing a negative sign for the $\Delta(1620) S_{31}$ coupling to $\Delta(1232)\pi$.

$(\Gamma_1\Gamma_7)^{1/2}/\Gamma_{\text{total}}$ in $N\pi \rightarrow N(1700) \rightarrow \Delta(1232)\pi, S\text{-wave}$				$(\Gamma_1\Gamma_7)^{1/2}/\Gamma$
VALUE	DOCUMENT ID	TECN	COMMENT	
0.00 to ±0.08 OUR ESTIMATE				
+0.02 ± 0.03	MANLEY	92	IPWA	$\pi N \rightarrow \pi N \text{ \& } N\pi\pi$
0.00	² LONGACRE	77	IPWA	$\pi N \rightarrow N\pi\pi$
-0.16	³ LONGACRE	75	IPWA	$\pi N \rightarrow N\pi\pi$

$\Gamma(\Delta(1232)\pi, S\text{-wave})/\Gamma_{\text{total}}$				Γ_7/Γ
VALUE	DOCUMENT ID	TECN	COMMENT	
0.11 ± 0.01	VRANA	00	DPWA	Multichannel
• • • We do not use the following data for averages, fits, limits, etc. • • •				
0.10 ± 0.05	THOMA	08	DPWA	Multichannel

$(\Gamma_1\Gamma_7)^{1/2}/\Gamma_{\text{total}}$ in $N\pi \rightarrow N(1700) \rightarrow \Delta(1232)\pi, D\text{-wave}$				$(\Gamma_1\Gamma_8)^{1/2}/\Gamma$
VALUE	DOCUMENT ID	TECN	COMMENT	
±0.04 to ±0.20 OUR ESTIMATE				
+0.10 ± 0.09	MANLEY	92	IPWA	$\pi N \rightarrow \pi N \text{ \& } N\pi\pi$
-0.12	² LONGACRE	77	IPWA	$\pi N \rightarrow N\pi\pi$
+0.14	³ LONGACRE	75	IPWA	$\pi N \rightarrow N\pi\pi$

$\Gamma(\Delta(1232)\pi, D\text{-wave})/\Gamma_{\text{total}}$				Γ_8/Γ
VALUE	DOCUMENT ID	TECN	COMMENT	
0.79 ± 0.56	VRANA	00	DPWA	Multichannel
• • • We do not use the following data for averages, fits, limits, etc. • • •				
0.20 ± 0.11	THOMA	08	DPWA	Multichannel

$(\Gamma_1\Gamma_7)^{1/2}/\Gamma_{\text{total}}$ in $N\pi \rightarrow N(1700) \rightarrow N\rho, S=3/2, S\text{-wave}$				$(\Gamma_1\Gamma_{11})^{1/2}/\Gamma$
VALUE	DOCUMENT ID	TECN	COMMENT	
±0.01 to ±0.13 OUR ESTIMATE				
-0.04 ± 0.06	MANLEY	92	IPWA	$\pi N \rightarrow \pi N \text{ \& } N\pi\pi$
-0.07	² LONGACRE	77	IPWA	$\pi N \rightarrow N\pi\pi$
+0.07	³ LONGACRE	75	IPWA	$\pi N \rightarrow N\pi\pi$

$\Gamma(N\rho, S=3/2, S\text{-wave})/\Gamma_{\text{total}}$				Γ_{11}/Γ
VALUE	DOCUMENT ID	TECN	COMMENT	
0.07 ± 0.01	VRANA	00	DPWA	Multichannel

$(\Gamma_1\Gamma_7)^{1/2}/\Gamma_{\text{total}}$ in $N\pi \rightarrow N(1700) \rightarrow N(\pi\pi)_{S=0}^{J=0}$				$(\Gamma_1\Gamma_{13})^{1/2}/\Gamma$
VALUE	DOCUMENT ID	TECN	COMMENT	
±0.02 to ±0.28 OUR ESTIMATE				
+0.02 ± 0.02	MANLEY	92	IPWA	$\pi N \rightarrow \pi N \text{ \& } N\pi\pi$
0.00	² LONGACRE	77	IPWA	$\pi N \rightarrow N\pi\pi$
+0.2	³ LONGACRE	75	IPWA	$\pi N \rightarrow N\pi\pi$

$\Gamma(N(\pi\pi)_{S=0}^{J=0})/\Gamma_{\text{total}}$				Γ_{13}/Γ
VALUE	DOCUMENT ID	TECN	COMMENT	
0.00 ± 0.01	VRANA	00	DPWA	Multichannel
• • • We do not use the following data for averages, fits, limits, etc. • • •				
0.18 ± 0.12	THOMA	08	DPWA	Multichannel

N(1700) PHOTON DECAY AMPLITUDES

Papers on γN amplitudes predating 1981 may be found in our 2006 edition, Journal of Physics, G **33** 1 (2006).

$N(1700) \rightarrow p\gamma, \text{ helicity-1/2 amplitude } A_{1/2}$				
VALUE (GeV ^{-1/2})	DOCUMENT ID	TECN	COMMENT	
-0.018 ± 0.013 OUR ESTIMATE				
-0.016 ± 0.014	CRAWFORD	83	IPWA	$\gamma N \rightarrow \pi N$
-0.002 ± 0.013	AWAJI	81	DPWA	$\gamma N \rightarrow \pi N$
• • • We do not use the following data for averages, fits, limits, etc. • • •				
-0.033 ± 0.021	BARBOUR	78	DPWA	$\gamma N \rightarrow \pi N$

$N(1700) \rightarrow p\gamma, \text{ helicity-3/2 amplitude } A_{3/2}$				
VALUE (GeV ^{-1/2})	DOCUMENT ID	TECN	COMMENT	
-0.002 ± 0.024 OUR ESTIMATE				
-0.009 ± 0.012	CRAWFORD	83	IPWA	$\gamma N \rightarrow \pi N$
0.029 ± 0.014	AWAJI	81	DPWA	$\gamma N \rightarrow \pi N$
• • • We do not use the following data for averages, fits, limits, etc. • • •				
-0.014 ± 0.025	BARBOUR	78	DPWA	$\gamma N \rightarrow \pi N$

$N(1700) \rightarrow n\gamma, \text{ helicity-1/2 amplitude } A_{1/2}$				
VALUE (GeV ^{-1/2})	DOCUMENT ID	TECN	COMMENT	
0.000 ± 0.050 OUR ESTIMATE				
0.006 ± 0.024	AWAJI	81	DPWA	$\gamma N \rightarrow \pi N$
-0.002 ± 0.013	FUJII	81	DPWA	$\gamma N \rightarrow \pi N$
• • • We do not use the following data for averages, fits, limits, etc. • • •				
+0.050 ± 0.042	BARBOUR	78	DPWA	$\gamma N \rightarrow \pi N$

$N(1700) \rightarrow n\gamma, \text{ helicity-3/2 amplitude } A_{3/2}$				
VALUE (GeV ^{-1/2})	DOCUMENT ID	TECN	COMMENT	
-0.003 ± 0.044 OUR ESTIMATE				
-0.033 ± 0.017	AWAJI	81	DPWA	$\gamma N \rightarrow \pi N$
0.018 ± 0.018	FUJII	81	DPWA	$\gamma N \rightarrow \pi N$
• • • We do not use the following data for averages, fits, limits, etc. • • •				
+0.035 ± 0.030	BARBOUR	78	DPWA	$\gamma N \rightarrow \pi N$

N(1700) $\gamma p \rightarrow \Lambda K^+$ AMPLITUDES

$(\Gamma_1\Gamma_7)^{1/2}/\Gamma_{\text{total}}$ in $p\gamma \rightarrow N(1700) \rightarrow \Lambda K^+$				$(E_{2-} \text{ amplitude})$
VALUE (units 10 ⁻³)	DOCUMENT ID	TECN	COMMENT	
• • • We do not use the following data for averages, fits, limits, etc. • • •				
4.09	TANABE	89	DPWA	

$(\Gamma_1\Gamma_7)^{1/2}/\Gamma_{\text{total}}$ in $p\gamma \rightarrow N(1700) \rightarrow \Lambda K^+$				$(M_{2-} \text{ amplitude})$
VALUE (units 10 ⁻³)	DOCUMENT ID	TECN	COMMENT	
• • • We do not use the following data for averages, fits, limits, etc. • • •				
-7.09	TANABE	89	DPWA	

$p\gamma \rightarrow N(1700) \rightarrow \Lambda K^+ \text{ phase angle } \theta$				$(E_{2-} \text{ amplitude})$
VALUE (degrees)	DOCUMENT ID	TECN	COMMENT	
• • • We do not use the following data for averages, fits, limits, etc. • • •				
-35.9	TANABE	89	DPWA	

N(1700) FOOTNOTES

- ¹ The two BAKER 77 entries are from an IPWA using the Barrelet-zero method and from a conventional energy-dependent analysis.
- ² LONGACRE 77 pole positions are from a search for poles in the unitarized T-matrix; the first (second) value uses, in addition to $\pi N \rightarrow N\pi\pi$ data, elastic amplitudes from a Saclay (CERN) partial-wave analysis. The other LONGACRE 77 values are from eyeball fits with Breit-Wigner circles to the T-matrix amplitudes.
- ³ From method II of LONGACRE 75: eyeball fits with Breit-Wigner circles to the T-matrix amplitudes.
- ⁴ See HOEHLER 93 for a detailed discussion of the evidence for and the pole parameters of N and Δ resonances as determined from Argand diagrams of πN elastic partial-wave amplitudes and from plots of the speeds with which the amplitudes traverse the diagrams.
- ⁵ LONGACRE 78 values are from a search for poles in the unitarized T-matrix. The first (second) value uses, in addition to $\pi N \rightarrow N\pi\pi$ data, elastic amplitudes from a Saclay (CERN) partial-wave analysis.
- ⁶ The overall phase of BAKER 78 couplings has been changed to agree with previous conventions.
- ⁷ The range given is from the four best solutions.

Baryon Particle Listings

$N(1710)$

$\Gamma(N\omega)/\Gamma_{\text{total}}$	DOCUMENT ID	TECN	COMMENT	Γ_3/Γ
0.13±0.02	PENNER	02c	DPWA Multichannel	

$(\Gamma_i\Gamma_f)^{1/2}/\Gamma_{\text{total}}$ in $N\pi \rightarrow N(1710) \rightarrow \Lambda K$	DOCUMENT ID	TECN	COMMENT	$(\Gamma_1\Gamma_4)^{1/2}/\Gamma$
+0.12 to +0.18 OUR ESTIMATE				
+0.16	BELL	83	DPWA $\pi^- p \rightarrow \Lambda K^0$	
+0.14	SAXON	80	DPWA $\pi^- p \rightarrow \Lambda K^0$	

$\Gamma(\Lambda K)/\Gamma_{\text{total}}$	DOCUMENT ID	TECN	COMMENT	Γ_4/Γ
0.05±0.03	SHKLYAR	05	DPWA Multichannel	
0.05±0.02	PENNER	02c	DPWA Multichannel	
0.1±0.1	VRANA	00	DPWA Multichannel	

$\Gamma(\Sigma K)/\Gamma_{\text{total}}$	DOCUMENT ID	TECN	COMMENT	Γ_5/Γ
••• We do not use the following data for averages, fits, limits, etc. •••				
0.07±0.07	PENNER	02c	DPWA Multichannel	

$(\Gamma_i\Gamma_f)^{1/2}/\Gamma_{\text{total}}$ in $N\pi \rightarrow N(1710) \rightarrow \Sigma K$	DOCUMENT ID	TECN	COMMENT	$(\Gamma_1\Gamma_5)^{1/2}/\Gamma$
••• We do not use the following data for averages, fits, limits, etc. •••				
-0.034	LIVANOS	80	DPWA $\pi p \rightarrow \Sigma K$	

Note: Signs of couplings from $\pi N \rightarrow N\pi\pi$ analyses were changed in the 1986 edition to agree with the baryon-first convention; the overall phase ambiguity is resolved by choosing a negative sign for the $\Delta(1620) S_{31}$ coupling to $\Delta(1232)\pi$.

$(\Gamma_i\Gamma_f)^{1/2}/\Gamma_{\text{total}}$ in $N\pi \rightarrow N(1710) \rightarrow \Delta(1232)\pi$, P -wave	DOCUMENT ID	TECN	COMMENT	$(\Gamma_1\Gamma_8)^{1/2}/\Gamma$
±0.16 to ±0.22 OUR ESTIMATE				
-0.21±0.04	MANLEY	92	IPWA $\pi N \rightarrow \pi N$ & $N\pi\pi$	
-0.17	2 LONGACRE	77	IPWA $\pi N \rightarrow N\pi\pi$	
+0.20	3 LONGACRE	75	IPWA $\pi N \rightarrow N\pi\pi$	

$\Gamma(\Delta(1232)\pi, P\text{-wave})/\Gamma_{\text{total}}$	DOCUMENT ID	TECN	COMMENT	Γ_8/Γ
0.39±0.08	VRANA	00	DPWA Multichannel	

$(\Gamma_i\Gamma_f)^{1/2}/\Gamma_{\text{total}}$ in $N\pi \rightarrow N(1710) \rightarrow N\rho, S=1/2, P$ -wave	DOCUMENT ID	TECN	COMMENT	$(\Gamma_1\Gamma_{10})^{1/2}/\Gamma$
±0.09 to ±0.19 OUR ESTIMATE				
+0.05±0.06	MANLEY	92	IPWA $\pi N \rightarrow \pi N$ & $N\pi\pi$	
+0.19	2 LONGACRE	77	IPWA $\pi N \rightarrow N\pi\pi$	
-0.20	3 LONGACRE	75	IPWA $\pi N \rightarrow N\pi\pi$	

$\Gamma(N\rho, S=1/2, P\text{-wave})/\Gamma_{\text{total}}$	DOCUMENT ID	TECN	COMMENT	Γ_{10}/Γ
0.17±0.01	VRANA	00	DPWA Multichannel	

$(\Gamma_i\Gamma_f)^{1/2}/\Gamma_{\text{total}}$ in $N\pi \rightarrow N(1710) \rightarrow N\rho, S=3/2, P$ -wave	DOCUMENT ID	TECN	COMMENT	$(\Gamma_1\Gamma_{11})^{1/2}/\Gamma$
+0.31	2 LONGACRE	77	IPWA $\pi N \rightarrow N\pi\pi$	

$(\Gamma_i\Gamma_f)^{1/2}/\Gamma_{\text{total}}$ in $N\pi \rightarrow N(1710) \rightarrow N(\pi\pi)_{S=0}^{J=0}$	DOCUMENT ID	TECN	COMMENT	$(\Gamma_1\Gamma_{12})^{1/2}/\Gamma$
±0.14 to ±0.22 OUR ESTIMATE				
+0.04±0.05	MANLEY	92	IPWA $\pi N \rightarrow \pi N$ & $N\pi\pi$	
-0.26	2 LONGACRE	77	IPWA $\pi N \rightarrow N\pi\pi$	
-0.28	3 LONGACRE	75	IPWA $\pi N \rightarrow N\pi\pi$	

$\Gamma(N(\pi\pi)_{S=0}^{J=0})/\Gamma_{\text{total}}$	DOCUMENT ID	TECN	COMMENT	Γ_{12}/Γ
0.01±0.01	VRANA	00	DPWA Multichannel	

$N(1710)$ PHOTON DECAY AMPLITUDES

Papers on γN amplitudes predating 1981 may be found in our 2006 edition, *Journal of Physics*, G **33** 1 (2006).

$N(1710) \rightarrow \rho\gamma$, helicity-1/2 amplitude $A_{1/2}$	DOCUMENT ID	TECN	COMMENT
+0.009±0.022 OUR ESTIMATE			
0.007±0.015	ARNDT	96	IPWA $\gamma N \rightarrow \pi N$
0.006±0.018	CRAWFORD	83	IPWA $\gamma N \rightarrow \pi N$
0.028±0.009	AWAJI	81	DPWA $\gamma N \rightarrow \pi N$
••• We do not use the following data for averages, fits, limits, etc. •••			
0.044	PENNER	02d	DPWA Multichannel
-0.037±0.002	LI	93	IPWA $\gamma N \rightarrow \pi N$

$N(1710) \rightarrow n\gamma$, helicity-1/2 amplitude $A_{1/2}$	DOCUMENT ID	TECN	COMMENT
-0.002±0.014 OUR ESTIMATE			
-0.002±0.015	ARNDT	96	IPWA $\gamma N \rightarrow \pi N$
0.000±0.018	AWAJI	81	DPWA $\gamma N \rightarrow \pi N$
-0.001±0.003	FUJII	81	DPWA $\gamma N \rightarrow \pi N$
••• We do not use the following data for averages, fits, limits, etc. •••			
-0.024	PENNER	02d	DPWA Multichannel
0.052±0.003	LI	93	IPWA $\gamma N \rightarrow \pi N$

$N(1710) \gamma\rho \rightarrow \Lambda K^+$ AMPLITUDES

$(\Gamma_i\Gamma_f)^{1/2}/\Gamma_{\text{total}}$ in $p\gamma \rightarrow N(1710) \rightarrow \Lambda K^+$	DOCUMENT ID	TECN	$(M_{1-}$ amplitude)
••• We do not use the following data for averages, fits, limits, etc. •••			
-10.6±0.4	WORKMAN	90	DPWA
-7.21	TANABE	89	DPWA

$p\gamma \rightarrow N(1710) \rightarrow \Lambda K^+$ phase angle θ	DOCUMENT ID	TECN	$(M_{1-}$ amplitude)
••• We do not use the following data for averages, fits, limits, etc. •••			
215±3	WORKMAN	90	DPWA
176.3	TANABE	89	DPWA

$N(1710)$ FOOTNOTES

- BATINIC 95 finds a second state with a 6 MeV mass difference.
- LONGACRE 77 pole positions are from a search for poles in the unitarized T-matrix; the first (second) value uses, in addition to $\pi N \rightarrow N\pi\pi$ data, elastic amplitudes from a Saclay (CERN) partial-wave analysis. The other LONGACRE 77 values are from eyeball fits with Breit-Wigner circles to the T-matrix amplitudes.
- From method II of LONGACRE 75: eyeball fits with Breit-Wigner circles to the T-matrix amplitudes.
- See HOEHLER 93 for a detailed discussion of the evidence for and the pole parameters of N and Δ resonances as determined from Argand diagrams of πN elastic partial-wave amplitudes and from plots of the speeds with which the amplitudes traverse the diagrams.
- LONGACRE 78 values are from a search for poles in the unitarized T-matrix. The first (second) value uses, in addition to $\pi N \rightarrow N\pi\pi$ data, elastic amplitudes from a Saclay (CERN) partial-wave analysis.

$N(1710)$ REFERENCES

For early references, see *Physics Letters* **111B** 1 (1982).

ARNDT 06	PR C74 045205	R.A. Arndt <i>et al.</i>	(GWU)
PDG 06	JPG 33 1	W.-M. Yao <i>et al.</i>	(PDG Collab.)
SHKLYAR 05	PR C72 015210	V. Shklyar, H. Lenske, U. Mosel	(GIES)
PENNER 02c	PR C66 055211	G. Penner, U. Mosel	(GIES)
PENNER 02d	PR C66 055212	G. Penner, U. Mosel	(GIES)
VRANA 00	PRPL 328 181	T.P. Vrana, S.A. Dytman, T.-S.H. Lee	(PITT+)
ARNDT 96	PR C53 430	R.A. Arndt, I.I. Strakovsky, R.L. Workman	(VPI)
ARNDT 95	PR C52 2120	R.A. Arndt <i>et al.</i>	(VPI, BRCO)
BATINIC 95	PR C51 2310	M. Batinic <i>et al.</i>	(BOSK, UCLA)
Also	PR C57 1004 (erratum)	M. Batinic <i>et al.</i>	
HOEHLER 93	πN Newsletter 9 1	G. Hohlner	(KARL)
LI 93	PR C47 2759	Z.J. Li <i>et al.</i>	(VPI)
MANLEY 92	PR D45 4002	D.M. Manley, E.M. Saleski	(KENT) IJP
Also	PR D30 904	D.M. Manley <i>et al.</i>	(VPI)
ARNDT 91	PR D43 2131	R.A. Arndt <i>et al.</i>	(VPI, TELE) IJP
CUTKOSKY 90	PR D42 235	R.E. Cutkosky, S. Wang	(CMU)
WORKMAN 90	PR C42 781	R.L. Workman	(VPI)
TANABE 89	PR C39 741	H. Tanabe, M. Kohno, C. Bennhold	(MANZ)
Also	NC 102A 193	M. Kohno, H. Tanabe, C. Bennhold	(MANZ)
BELL 83	NP B222 389	K.W. Bell <i>et al.</i>	(RL) IJP
CRAWFORD 83	NP B211 1	R.L. Crawford, W.T. Morton	(GLAS)
PDG 82	PL 111B 1	M. Roos <i>et al.</i>	(HELS, CIT, CERN)
AWAJI 81	Bonn Conf. 352	N. Awaji, R. Kajikawa	(NAGO)
Also	NP B197 365	K. Fujii <i>et al.</i>	(NAGO)
FUJII 81	NP B187 53	K. Fujii <i>et al.</i>	(NAGO, OSAK)
CUTKOSKY 80	Toronto Conf. 19	R.E. Cutkosky <i>et al.</i>	(CMU, LBL) IJP
Also	PR D20 2839	R.E. Cutkosky <i>et al.</i>	(CMU, LBL) IJP
LIVANOS 80	Toronto Conf. 35	P. Livanos <i>et al.</i>	(SACL) IJP
SAXON 80	NP B162 522	D.H. Saxon <i>et al.</i>	(RHEL, BRIS) IJP
HOEHLER 79	PDAT 12-1	G. Hohlner <i>et al.</i>	(KARL) IJP
Also	Toronto Conf. 3	R. Koch	(KARL) IJP
LONGACRE 78	PR D17 1795	R.S. Longacre <i>et al.</i>	(LBL, SLAC)
LONGACRE 77	NP B122 493	R.S. Longacre, J. Dolbeau	(SACL) IJP
Also	NP B108 365	J. Dolbeau <i>et al.</i>	(SACL) IJP
LONGACRE 75	PL 55B 415	R.S. Longacre <i>et al.</i>	(LBL, SLAC) IJP

Baryon Particle Listings

 $N(1720)$ $N(1720) P_{13}$

$$I(J^P) = \frac{1}{2}(\frac{3}{2}^+) \text{ Status: } ****$$

Most of the results published before 1975 were last included in our 1982 edition, Physics Letters **111B** 1 (1982). Some further obsolete results published before 1984 were last included in our 2006 edition, Journal of Physics, G **33** 1 (2006).

 $N(1720)$ BREIT-WIGNER MASS

VALUE (MeV)	DOCUMENT ID	TECN	COMMENT
1700 to 1750 (≈ 1720) OUR ESTIMATE			
1763.8 \pm 4.6	ARNDT 06	DPWA	$\pi N \rightarrow \pi N, \eta N$
1717 \pm 31	MANLEY 92	IPWA	$\pi N \rightarrow \pi N \& N\pi\pi$
1700 \pm 50	CUTKOSKY 80	IPWA	$\pi N \rightarrow \pi N$
1710 \pm 20	HOEHLER 79	IPWA	$\pi N \rightarrow \pi N$
••• We do not use the following data for averages, fits, limits, etc. •••			
1790 \pm 100	THOMA 08	DPWA	Multichannel
1749.6 \pm 4.5	ARNDT 04	DPWA	$\pi N \rightarrow \pi N, \eta N$
1705 \pm 10	PENNER 02c	DPWA	Multichannel
1716 \pm 112	VRANA 00	DPWA	Multichannel
1713 \pm 10	ARNDT 96	IPWA	$\gamma N \rightarrow \pi N$
1820	ARNDT 95	DPWA	$\pi N \rightarrow N\pi$
1711 \pm 26	BATINIC 95	DPWA	$\pi N \rightarrow N\pi, N\eta$
1720	LI 93	IPWA	$\gamma N \rightarrow \pi N$
1690	SAXON 80	DPWA	$\pi^- \rho \rightarrow \Lambda K^0$
1750	¹ LONGACRE 77	IPWA	$\pi N \rightarrow N\pi\pi$
1720	² LONGACRE 75	IPWA	$\pi N \rightarrow N\pi\pi$

 $N(1720)$ BREIT-WIGNER WIDTH

VALUE (MeV)	DOCUMENT ID	TECN	COMMENT
150 to 300 (≈ 200) OUR ESTIMATE			
210 \pm 22	ARNDT 06	DPWA	$\pi N \rightarrow \pi N, \eta N$
380 \pm 180	MANLEY 92	IPWA	$\pi N \rightarrow \pi N \& N\pi\pi$
125 \pm 70	CUTKOSKY 80	IPWA	$\pi N \rightarrow \pi N$
190 \pm 30	HOEHLER 79	IPWA	$\pi N \rightarrow \pi N$
••• We do not use the following data for averages, fits, limits, etc. •••			
690 \pm 100	THOMA 08	DPWA	Multichannel
256 \pm 22	ARNDT 04	DPWA	$\pi N \rightarrow \pi N, \eta N$
237 \pm 73	PENNER 02c	DPWA	Multichannel
121 \pm 39	VRANA 00	DPWA	Multichannel
153 \pm 15	ARNDT 96	IPWA	$\gamma N \rightarrow \pi N$
354	ARNDT 95	DPWA	$\pi N \rightarrow N\pi$
235 \pm 51	BATINIC 95	DPWA	$\pi N \rightarrow N\pi, N\eta$
200	LI 93	IPWA	$\gamma N \rightarrow \pi N$
120	SAXON 80	DPWA	$\pi^- \rho \rightarrow \Lambda K^0$
130	¹ LONGACRE 77	IPWA	$\pi N \rightarrow N\pi\pi$
150	² LONGACRE 75	IPWA	$\pi N \rightarrow N\pi\pi$

 $N(1720)$ POLE POSITION

REAL PART

VALUE (MeV)	DOCUMENT ID	TECN	COMMENT
1660 to 1690 (≈ 1675) OUR ESTIMATE			
1666	ARNDT 06	DPWA	$\pi N \rightarrow \pi N, \eta N$
1686	³ HOEHLER 93	SPED	$\pi N \rightarrow \pi N$
1680 \pm 30	CUTKOSKY 80	IPWA	$\pi N \rightarrow \pi N$
••• We do not use the following data for averages, fits, limits, etc. •••			
1630 \pm 90	THOMA 08	DPWA	Multichannel
1655	ARNDT 04	DPWA	$\pi N \rightarrow \pi N, \eta N$
1692	VRANA 00	DPWA	Multichannel
1717	ARNDT 95	DPWA	$\pi N \rightarrow N\pi$
1675	ARNDT 91	DPWA	$\pi N \rightarrow \pi N$ Soln SM90
1716 or 1716	⁴ LONGACRE 78	IPWA	$\pi N \rightarrow N\pi\pi$
1745 or 1748	¹ LONGACRE 77	IPWA	$\pi N \rightarrow N\pi\pi$

-2 \times IMAGINARY PART

VALUE (MeV)	DOCUMENT ID	TECN	COMMENT
115 to 275 OUR ESTIMATE			
355	ARNDT 06	DPWA	$\pi N \rightarrow \pi N, \eta N$
187	³ HOEHLER 93	SPED	$\pi N \rightarrow \pi N$
120 \pm 40	CUTKOSKY 80	IPWA	$\pi N \rightarrow \pi N$
••• We do not use the following data for averages, fits, limits, etc. •••			
460 \pm 80	THOMA 08	DPWA	Multichannel
278	ARNDT 04	DPWA	$\pi N \rightarrow \pi N, \eta N$
94	VRANA 00	DPWA	Multichannel
388	ARNDT 95	DPWA	$\pi N \rightarrow N\pi$
114	ARNDT 91	DPWA	$\pi N \rightarrow \pi N$ Soln SM90
124 or 126	⁴ LONGACRE 78	IPWA	$\pi N \rightarrow N\pi\pi$
135 or 123	¹ LONGACRE 77	IPWA	$\pi N \rightarrow N\pi\pi$

 $N(1720)$ ELASTIC POLE RESIDUEMODULUS $|r|$

VALUE (MeV)	DOCUMENT ID	TECN	COMMENT
25	ARNDT 06	DPWA	$\pi N \rightarrow \pi N, \eta N$
15	HOEHLER 93	SPED	$\pi N \rightarrow \pi N$
8 \pm 2	CUTKOSKY 80	IPWA	$\pi N \rightarrow \pi N$
••• We do not use the following data for averages, fits, limits, etc. •••			
20	ARNDT 04	DPWA	$\pi N \rightarrow \pi N, \eta N$
39	ARNDT 95	DPWA	$\pi N \rightarrow N\pi$
11	ARNDT 91	DPWA	$\pi N \rightarrow \pi N$ Soln SM90

PHASE θ

VALUE ($^\circ$)	DOCUMENT ID	TECN	COMMENT
-94	ARNDT 06	DPWA	$\pi N \rightarrow \pi N, \eta N$
-160 \pm 30	CUTKOSKY 80	IPWA	$\pi N \rightarrow \pi N$
••• We do not use the following data for averages, fits, limits, etc. •••			
-88	ARNDT 04	DPWA	$\pi N \rightarrow \pi N, \eta N$
-70	ARNDT 95	DPWA	$\pi N \rightarrow N\pi$
-130	ARNDT 91	DPWA	$\pi N \rightarrow \pi N$ Soln SM90

 $N(1720)$ DECAY MODES

The following branching fractions are our estimates, not fits or averages.

Mode	Fraction (Γ_i/Γ)
Γ_1 $N\pi$	10-20 %
Γ_2 $N\eta$	(4.0 \pm 1.0) %
Γ_3 ΛK	1-15 %
Γ_4 ΣK	
Γ_5 $N\pi\pi$	>70 %
Γ_6 $\Delta\pi$	
Γ_7 $\Delta(1232)\pi, P\text{-wave}$	
Γ_8 $N\rho$	70-85 %
Γ_9 $N\rho, S=1/2, P\text{-wave}$	
Γ_{10} $N\rho, S=3/2, P\text{-wave}$	
Γ_{11} $N(\pi\pi)_{S\text{-wave}}^{j=0}$	
Γ_{12} $p\gamma$	0.003-0.10 %
Γ_{13} $p\gamma, \text{helicity}=1/2$	0.003-0.08 %
Γ_{14} $p\gamma, \text{helicity}=3/2$	0.001-0.03 %
Γ_{15} $n\gamma$	0.002-0.39 %
Γ_{16} $n\gamma, \text{helicity}=1/2$	0.0-0.002 %
Γ_{17} $n\gamma, \text{helicity}=3/2$	0.001-0.39 %

 $N(1720)$ BRANCHING RATIOS $\Gamma(N\pi)/\Gamma_{\text{total}}$

VALUE	DOCUMENT ID	TECN	COMMENT	Γ_1/Γ
0.10 to 0.20 OUR ESTIMATE				
0.094 \pm 0.005	ARNDT 06	DPWA	$\pi N \rightarrow \pi N, \eta N$	
0.13 \pm 0.05	MANLEY 92	IPWA	$\pi N \rightarrow \pi N \& N\pi\pi$	
0.10 \pm 0.04	CUTKOSKY 80	IPWA	$\pi N \rightarrow \pi N$	
0.14 \pm 0.03	HOEHLER 79	IPWA	$\pi N \rightarrow \pi N$	
••• We do not use the following data for averages, fits, limits, etc. •••				
0.09 \pm 0.06	THOMA 08	DPWA	Multichannel	
0.190 \pm 0.004	ARNDT 04	DPWA	$\pi N \rightarrow \pi N, \eta N$	
0.17 \pm 0.02	PENNER 02c	DPWA	Multichannel	
0.05 \pm 0.05	VRANA 00	DPWA	Multichannel	
0.16	ARNDT 95	DPWA	$\pi N \rightarrow N\pi$	
0.18 \pm 0.04	BATINIC 95	DPWA	$\pi N \rightarrow N\pi, N\eta$	

 $\Gamma(N\eta)/\Gamma_{\text{total}}$

VALUE	DOCUMENT ID	TECN	COMMENT	Γ_2/Γ
0.04 \pm 0.01				
0.10 \pm 0.07	THOMA 08	DPWA	Multichannel	
0.002 \pm 0.002	PENNER 02c	DPWA	Multichannel	
0.002 \pm 0.01	BATINIC 95	DPWA	$\pi N \rightarrow N\pi, N\eta$	

 $\Gamma(\Lambda K)/\Gamma_{\text{total}}$

VALUE	DOCUMENT ID	TECN	COMMENT	Γ_3/Γ
0.044 \pm 0.004 OUR AVERAGE				
0.043 \pm 0.004	SHKLYAR 05	DPWA	Multichannel	
0.09 \pm 0.03	PENNER 02c	DPWA	Multichannel	
••• We do not use the following data for averages, fits, limits, etc. •••				
0.12 \pm 0.09	THOMA 08	DPWA	Multichannel	

$(\Gamma_1 \Gamma_f)^{1/2} / \Gamma_{\text{total}}$ in $N\pi \rightarrow N(1720) \rightarrow \Lambda K$ ($\Gamma_1 \Gamma_3)^{1/2} / \Gamma$

VALUE	DOCUMENT ID	TECN	COMMENT
-0.14 to -0.06 OUR ESTIMATE			
-0.09	BELL 83	DPWA	$\pi^- p \rightarrow \Lambda K^0$
-0.11	SAXON 80	DPWA	$\pi^- p \rightarrow \Lambda K^0$

Note: Signs of couplings from $\pi N \rightarrow N\pi\pi$ analyses were changed in the 1986 edition to agree with the baryon-first convention; the overall phase ambiguity is resolved by choosing a negative sign for the $\Delta(1620)$ S_{31} coupling to $\Delta(1232)\pi$.

$(\Gamma_1 \Gamma_f)^{1/2} / \Gamma_{\text{total}}$ in $N\pi \rightarrow N(1720) \rightarrow \Delta(1232)\pi$, P-wave ($\Gamma_1 \Gamma_7)^{1/2} / \Gamma$

VALUE	DOCUMENT ID	TECN	COMMENT
± 0.27 to ± 0.37 OUR ESTIMATE			
-0.17	¹ LONGACRE 77	IPWA	$\pi N \rightarrow N\pi\pi$

$(\Gamma_1 \Gamma_f)^{1/2} / \Gamma_{\text{total}}$ in $N\pi \rightarrow N(1720) \rightarrow N\rho$, $S=1/2$, P-wave ($\Gamma_1 \Gamma_9)^{1/2} / \Gamma$

VALUE	DOCUMENT ID	TECN	COMMENT
+0.34 \pm 0.05	MANLEY 92	IPWA	$\pi N \rightarrow \pi N$ & $N\pi\pi$
-0.26	¹ LONGACRE 77	IPWA	$\pi N \rightarrow N\pi\pi$
+0.40	² LONGACRE 75	IPWA	$\pi N \rightarrow N\pi\pi$

$\Gamma(N\rho, S=1/2, \text{P-wave}) / \Gamma_{\text{total}}$ (Γ_9 / Γ)

VALUE	DOCUMENT ID	TECN	COMMENT
0.91 \pm 0.01	VRANA 00	DPWA	Multichannel

$(\Gamma_1 \Gamma_f)^{1/2} / \Gamma_{\text{total}}$ in $N\pi \rightarrow N(1720) \rightarrow N\rho$, $S=3/2$, P-wave ($\Gamma_1 \Gamma_{10})^{1/2} / \Gamma$

VALUE	DOCUMENT ID	TECN	COMMENT
+0.15	¹ LONGACRE 77	IPWA	$\pi N \rightarrow N\pi\pi$

$(\Gamma_1 \Gamma_f)^{1/2} / \Gamma_{\text{total}}$ in $N\pi \rightarrow N(1720) \rightarrow N(\pi\pi)_{S=0}^{I=0}$ ($\Gamma_1 \Gamma_{11})^{1/2} / \Gamma$

VALUE	DOCUMENT ID	TECN	COMMENT
-0.19	¹ LONGACRE 77	IPWA	$\pi N \rightarrow N\pi\pi$

$N(1720)$ PHOTON DECAY AMPLITUDES

Papers on γN amplitudes predating 1981 may be found in our 2006 edition, Journal of Physics, G 33 1 (2006).

$N(1720) \rightarrow \rho\gamma$, helicity-1/2 amplitude $A_{1/2}$

VALUE (GeV ^{-1/2})	DOCUMENT ID	TECN	COMMENT
$\pm 0.018 \pm 0.030$ OUR ESTIMATE			
0.097 \pm 0.003	DUGGER 07	DPWA	$\gamma N \rightarrow \pi N$
-0.015 \pm 0.015	ARNDT 96	IPWA	$\gamma N \rightarrow \pi N$
0.044 \pm 0.066	CRAWFORD 83	IPWA	$\gamma N \rightarrow \pi N$
-0.004 \pm 0.007	AWAJI 81	DPWA	$\gamma N \rightarrow \pi N$
• • • We do not use the following data for averages, fits, limits, etc. • • •			
0.073	DRECHSEL 07	DPWA	$\gamma N \rightarrow \pi N$
-0.053	PENNER 02D	DPWA	Multichannel
0.012 \pm 0.003	LI 93	IPWA	$\gamma N \rightarrow \pi N$

$N(1720) \rightarrow \rho\gamma$, helicity-3/2 amplitude $A_{3/2}$

VALUE (GeV ^{-1/2})	DOCUMENT ID	TECN	COMMENT
$\pm 0.019 \pm 0.020$ OUR ESTIMATE			
-0.039 \pm 0.003	DUGGER 07	DPWA	$\gamma N \rightarrow \pi N$
0.007 \pm 0.010	ARNDT 96	IPWA	$\gamma N \rightarrow \pi N$
-0.024 \pm 0.006	CRAWFORD 83	IPWA	$\gamma N \rightarrow \pi N$
-0.040 \pm 0.016	AWAJI 81	DPWA	$\gamma N \rightarrow \pi N$
• • • We do not use the following data for averages, fits, limits, etc. • • •			
-0.011	DRECHSEL 07	DPWA	$\gamma N \rightarrow \pi N$
0.027	PENNER 02D	DPWA	Multichannel
-0.022 \pm 0.003	LI 93	IPWA	$\gamma N \rightarrow \pi N$

$N(1720) \rightarrow n\gamma$, helicity-1/2 amplitude $A_{1/2}$

VALUE (GeV ^{-1/2})	DOCUMENT ID	TECN	COMMENT
$\pm 0.001 \pm 0.015$ OUR ESTIMATE			
0.007 \pm 0.015	ARNDT 96	IPWA	$\gamma N \rightarrow \pi N$
0.002 \pm 0.005	AWAJI 81	DPWA	$\gamma N \rightarrow \pi N$
• • • We do not use the following data for averages, fits, limits, etc. • • •			
-0.003	DRECHSEL 07	DPWA	$\gamma N \rightarrow \pi N$
-0.004	PENNER 02D	DPWA	Multichannel
0.050 \pm 0.004	LI 93	IPWA	$\gamma N \rightarrow \pi N$

$N(1720) \rightarrow n\gamma$, helicity-3/2 amplitude $A_{3/2}$

VALUE (GeV ^{-1/2})	DOCUMENT ID	TECN	COMMENT
$\pm 0.029 \pm 0.061$ OUR ESTIMATE			
-0.005 \pm 0.025	ARNDT 96	IPWA	$\gamma N \rightarrow \pi N$
-0.015 \pm 0.019	AWAJI 81	DPWA	$\gamma N \rightarrow \pi N$
• • • We do not use the following data for averages, fits, limits, etc. • • •			
-0.031	DRECHSEL 07	DPWA	$\gamma N \rightarrow \pi N$
0.003	PENNER 02D	DPWA	Multichannel
-0.017 \pm 0.004	LI 93	IPWA	$\gamma N \rightarrow \pi N$

$N(1720) \gamma p \rightarrow \Lambda K^+$ AMPLITUDES

$(\Gamma_1 \Gamma_f)^{1/2} / \Gamma_{\text{total}}$ in $p\gamma \rightarrow N(1720) \rightarrow \Lambda K^+$ (E_{1+} amplitude)

VALUE (units 10^{-3})	DOCUMENT ID	TECN	
• • • We do not use the following data for averages, fits, limits, etc. • • •			
10.2 \pm 0.2	WORKMAN 90	DPWA	
9.52	TANABE 89	DPWA	

$p\gamma \rightarrow N(1720) \rightarrow \Lambda K^+$ phase angle θ (E_{1+} amplitude)

VALUE (degrees)	DOCUMENT ID	TECN	
• • • We do not use the following data for averages, fits, limits, etc. • • •			
-124 \pm 2	WORKMAN 90	DPWA	
-103.4	TANABE 89	DPWA	

$(\Gamma_1 \Gamma_f)^{1/2} / \Gamma_{\text{total}}$ in $p\gamma \rightarrow N(1720) \rightarrow \Lambda K^+$ (M_{1+} amplitude)

VALUE (units 10^{-3})	DOCUMENT ID	TECN	
• • • We do not use the following data for averages, fits, limits, etc. • • •			
-4.5 \pm 0.2	WORKMAN 90	DPWA	
3.18	TANABE 89	DPWA	

$N(1720)$ FOOTNOTES

- ¹ LONGACRE 77 pole positions are from a search for poles in the unitarized T-matrix; the first (second) value uses, in addition to $\pi N \rightarrow N\pi\pi$ data, elastic amplitudes from a Saclay (CERN) partial-wave analysis. The other LONGACRE 77 values are from eyeball fits with Breit-Wigner circles to the T-matrix amplitudes.
- ² From method II of LONGACRE 75: eyeball fits with Breit-Wigner circles to the T-matrix amplitudes.
- ³ See HOEHLER 93 for a detailed discussion of the evidence for and the pole parameters of N and Δ resonances as determined from Argand diagrams of πN elastic partial-wave amplitudes and from plots of the speeds with which the amplitudes traverse the diagrams.
- ⁴ LONGACRE 78 values are from a search for poles in the unitarized T-matrix. The first (second) value uses, in addition to $\pi N \rightarrow N\pi\pi$ data, elastic amplitudes from a Saclay (CERN) partial-wave analysis.

$N(1720)$ REFERENCES

For early references, see Physics Letters 111B 1 (1982).

THOMA 08	PL B659 87	U. Thoma et al.	(CB-ELSA Collab.)
DRECHSEL 07	EPJ A34 69	D. Drechsel, S.S. Kamalov, L. Tiator	(MAINZ, JINR)
DUGGER 07	PR C76 025211	M. Dugger et al.	(Jefferson Lab CLAS Collab.)
ARNDT 06	PR C74 045205	R.A. Arndt et al.	(GWU)
PDG 06	JPG 33 1	W.-M. Yao et al.	(PDG Collab.)
SHKLYAR 05	PR C72 015210	V. Shklyar, H. Lenske, U. Mosel	(GIES)
ARNDT 04	PR C69 035213	R.A. Arndt et al.	(GWU, TRIU)
PENNER 02C	PR C66 055211	G. Penner, U. Mosel	(GIES)
PENNER 02D	PR C66 055212	G. Penner, U. Mosel	(GIES)
VRANA 00	PR L 328 181	T.P. Vrana, S.A. Dytman, T.-S.H. Lee	(PIT+
ARNDT 96	PR C53 4030	R.A. Arndt, I.I. Strakovsky, R.L. Workman	(VPI)
ARNDT 95	PR C52 2120	R.A. Arndt et al.	(VPI, BRCC)
BATINIC 95	PR C51 2310	M. Batinic et al.	(BOSK, UCLA)
Also	PR C57 1004 (erratum)	G. Hohler et al.	
HOEHLER 93	πN Newsletter 9 1	G. Hohler	(KARL)
LI 93	PR C47 2759	Z.J. Li et al.	(VPI)
MANLEY 92	PR D45 4002	D.M. Manley, E.M. Saleski	(KENT) IJP
Also	PR D30 904	D.M. Manley et al.	(VPI)
ARNDT 91	PR D43 2131	R.A. Arndt et al.	(VPI, TELE) IJP
WORKMAN 90	PR C42 781	R.L. Workman	(VPI)
TANABE 89	PR C39 741	H. Tanabe, M. Kohno, C. Bennhold	(MANZ)
Also	NC 102A 193	M. Kohno, H. Tanabe, C. Bennhold	(MANZ)
BELL 83	NP B222 389	K.W. Bell et al.	(RL) IJP
CRAWFORD 83	NP B211 1	R.L. Crawford, W.T. Morton	(GLAS)
PDG 82	PL 111B 1	M. Roos et al.	(HEL, CIT, CERN)
AWAJI 81	Bonn Conf. 352	N. Awaji, R. Kajikawa	(NAGO)
Also	NP B197 365	K. Fujii et al.	(NAGO)
CUTKOSKY 80	Toronto Conf. 19	R.E. Cutkosky et al.	(CMU, LBL) IJP
Also	PR D20 2839	R.E. Cutkosky et al.	(CMU, LBL) IJP
SAXON 80	NP B162 522	D.H. Saxon et al.	(RHEL, BRIS) IJP
HOEHLER 79	PDAT 12-1	G. Hohler et al.	(KARL) IJP
Also	Toronto Conf. 3	R. Koch	(KARL) IJP
LONGACRE 78	PR D17 1795	R.S. Longacre et al.	(LBL, SLAC)
LONGACRE 77	NP B122 493	R.S. Longacre, J. Dolbeau	(SACL) IJP
Also	NP B108 365	J. Dolbeau et al.	(SACL) IJP
LONGACRE 75	PL 55B 415	R.S. Longacre et al.	(LBL, SLAC) IJP

$N(1900) P_{13}$

$$I(J^P) = \frac{1}{2}(\frac{3}{2}^+) \text{ Status: } **$$

OMITTED FROM SUMMARY TABLE

The latest GWU analysis (ARNDT 06) finds no evidence for this resonance.

$N(1900)$ BREIT-WIGNER MASS

VALUE (MeV)	DOCUMENT ID	TECN	COMMENT
≈ 1900 OUR ESTIMATE			
1915 \pm 60	NIKONOV 08	DPWA	Multichannel
1879 \pm 17	MANLEY 92	IPWA	$\pi N \rightarrow \pi N$ & $N\pi\pi$
• • • We do not use the following data for averages, fits, limits, etc. • • •			
1951 \pm 53	PENNER 02C	DPWA	Multichannel

Baryon Particle Listings

N(1900), N(1990)

N(1900) BREIT-WIGNER WIDTH

VALUE (MeV)	DOCUMENT ID	TECN	COMMENT
180±40	NIKONOV 08	DPWA	Multichannel
498±78	MANLEY 92	IPWA	$\pi N \rightarrow \pi N$ & $N\pi\pi$
• • • We do not use the following data for averages, fits, limits, etc. • • •			
622±42	PENNER 02c	DPWA	Multichannel

N(1900) DECAY MODES

Mode	Fraction (Γ_i/Γ)
Γ_1 $N\pi$	
Γ_2 $N\pi\pi$	
Γ_3 $N\rho, S=1/2, P$ -wave	
Γ_4 $N\eta$	(14 ±5) %
Γ_5 $N\omega$	(39 ±9) %
Γ_6 ΛK	(2.40±0.30) %
Γ_7 ΣK	

N(1900) BRANCHING RATIOS

$\Gamma(N\pi)/\Gamma_{total}$	DOCUMENT ID	TECN	COMMENT	Γ_1/Γ
0.26±0.06	MANLEY 92	IPWA	$\pi N \rightarrow \pi N$ & $N\pi\pi$	
• • • We do not use the following data for averages, fits, limits, etc. • • •				
0.02 - 0.09	NIKONOV 08	DPWA	Multichannel	
0.16±0.02	PENNER 02c	DPWA	Multichannel	

$\Gamma(N\eta)/\Gamma_{total}$	DOCUMENT ID	TECN	COMMENT	Γ_4/Γ
0.14±0.05	PENNER 02c	DPWA	Multichannel	

$\Gamma(N\omega)/\Gamma_{total}$	DOCUMENT ID	TECN	COMMENT	Γ_5/Γ
0.39±0.09	PENNER 02c	DPWA	Multichannel	

$(\Gamma_1\Gamma_3)^{1/2}/\Gamma_{total}$ in $N\pi \rightarrow N(1900) \rightarrow N\rho, S=1/2, P$ -wave	DOCUMENT ID	TECN	COMMENT	$(\Gamma_1\Gamma_3)^{1/2}/\Gamma$
-0.34 ± 0.03	MANLEY 92	IPWA	$\pi N \rightarrow \pi N$ & $N\pi\pi$	

$\Gamma(\Lambda K)/\Gamma_{total}$	DOCUMENT ID	TECN	COMMENT	Γ_6/Γ
0.024±0.003	SHKLYAR 05	DPWA	Multichannel	
• • • We do not use the following data for averages, fits, limits, etc. • • •				
0.05 - 0.15	NIKONOV 08	DPWA	Multichannel	
0.001±0.001	PENNER 02c	DPWA	Multichannel	

$\Gamma(\Sigma K)/\Gamma_{total}$	DOCUMENT ID	TECN	COMMENT	Γ_7/Γ
0.01±0.01	PENNER 02c	DPWA	Multichannel	

N(1900) PHOTON DECAY AMPLITUDES

Papers on γN amplitudes predating 1981 may be found in our 2006 edition, Journal of Physics, G **33** 1 (2006).

N(1900) → pγ, helicity-1/2 amplitude A_{1/2}

VALUE (GeV ^{-1/2})	DOCUMENT ID	TECN	COMMENT
-0.017	PENNER 02D	DPWA	Multichannel

N(1900) → pγ, helicity-3/2 amplitude A_{3/2}

VALUE (GeV ^{-1/2})	DOCUMENT ID	TECN	COMMENT
0.031	PENNER 02D	DPWA	Multichannel

N(1900) → nγ, helicity-1/2 amplitude A_{1/2}

VALUE (GeV ^{-1/2})	DOCUMENT ID	TECN	COMMENT
-0.016	PENNER 02D	DPWA	Multichannel

N(1900) → nγ, helicity-3/2 amplitude A_{3/2}

VALUE (GeV ^{-1/2})	DOCUMENT ID	TECN	COMMENT
-0.002	PENNER 02D	DPWA	Multichannel

N(1900) REFERENCES

NIKONOV 08	PL B662 245	V.A. Nikonov <i>et al.</i>	(Bonn, Gatchina)
ARNDT 06	PR C74 045205	R.A. Arndt <i>et al.</i>	(GWU)
PDG 06	JPG 33 1	W.-M. Yao <i>et al.</i>	(PDG Collab.)
SHKLYAR 05	PR C72 015210	V. Shklyar, H. Lenske, U. Mosel	(GIES)
PENNER 02C	PR C66 055211	G. Penner, U. Mosel	(GIES)
PENNER 02D	PR C66 055212	G. Penner, U. Mosel	(GIES)
MANLEY 92	PR D45 4002	D.M. Manley, E.M. Saleski	(KENT)
Also	PR D30 904	D.M. Manley <i>et al.</i>	(VPI)

N(1990) F₁₇

$$I(J^P) = \frac{1}{2}(\frac{7}{2}^+) \text{ Status: } **$$

OMITTED FROM SUMMARY TABLE

Most of the results published before 1975 are now obsolete and have been omitted. They may be found in our 1982 edition, Physics Letters **111B** 1 (1982). Some further obsolete results published before 1984 were last included in our 2006 edition, Journal of Physics, G **33** 1 (2006).

The various analyses do not agree very well with one another.

The latest GWU analysis (ARNDT 06) finds no evidence for this resonance.

N(1990) BREIT-WIGNER MASS

VALUE (MeV)	DOCUMENT ID	TECN	COMMENT
≈ 1990 OUR ESTIMATE			
2086±28	MANLEY 92	IPWA	$\pi N \rightarrow \pi N$ & $N\pi\pi$
1970±50	CUTKOSKY 80	IPWA	$\pi N \rightarrow \pi N$
2005±150	HOEHLER 79	IPWA	$\pi N \rightarrow \pi N$
1999	BARBOUR 78	DPWA	$\gamma N \rightarrow \pi N$
• • • We do not use the following data for averages, fits, limits, etc. • • •			
2311±16	VRANA 00	DPWA	Multichannel

N(1990) BREIT-WIGNER WIDTH

VALUE (MeV)	DOCUMENT ID	TECN	COMMENT
535±120	MANLEY 92	IPWA	$\pi N \rightarrow \pi N$ & $N\pi\pi$
350±120	CUTKOSKY 80	IPWA	$\pi N \rightarrow \pi N$
350±100	HOEHLER 79	IPWA	$\pi N \rightarrow \pi N$
216	BARBOUR 78	DPWA	$\gamma N \rightarrow \pi N$
• • • We do not use the following data for averages, fits, limits, etc. • • •			
205±72	VRANA 00	DPWA	Multichannel

N(1990) POLE POSITION

REAL PART

VALUE (MeV)	DOCUMENT ID	TECN	COMMENT
1900±30	CUTKOSKY 80	IPWA	$\pi N \rightarrow \pi N$
• • • We do not use the following data for averages, fits, limits, etc. • • •			
2301	VRANA 00	DPWA	Multichannel
not seen	ARNDT 91	DPWA	$\pi N \rightarrow \pi N$ Soln SM90

-2xIMAGINARY PART

VALUE (MeV)	DOCUMENT ID	TECN	COMMENT
260±60	CUTKOSKY 80	IPWA	$\pi N \rightarrow \pi N$
• • • We do not use the following data for averages, fits, limits, etc. • • •			
202	VRANA 00	DPWA	Multichannel
not seen	ARNDT 91	DPWA	$\pi N \rightarrow \pi N$ Soln SM90

N(1990) ELASTIC POLE RESIDUE

MODULUS |r|

VALUE (MeV)	DOCUMENT ID	TECN	COMMENT
9±3	CUTKOSKY 80	IPWA	$\pi N \rightarrow \pi N$

PHASE θ

VALUE (°)	DOCUMENT ID	TECN	COMMENT
-60±30	CUTKOSKY 80	IPWA	$\pi N \rightarrow \pi N$

N(1990) DECAY MODES

Mode	
Γ_1 $N\pi$	
Γ_2 $N\eta$	
Γ_3 ΛK	
Γ_4 ΣK	
Γ_5 $N\pi\pi$	
Γ_6 $p\gamma, \text{ helicity}=1/2$	
Γ_7 $p\gamma, \text{ helicity}=3/2$	
Γ_8 $n\gamma, \text{ helicity}=1/2$	
Γ_9 $n\gamma, \text{ helicity}=3/2$	

N(1990) BRANCHING RATIOS

$\Gamma(N\pi)/\Gamma_{\text{total}}$	DOCUMENT ID	TECN	COMMENT	Γ_1/Γ
0.06±0.02	MANLEY 92	IPWA	$\pi N \rightarrow \pi N \text{ \& } N\pi\pi$	
0.06±0.02	CUTKOSKY 80	IPWA	$\pi N \rightarrow \pi N$	
0.04±0.02	HOEHLER 79	IPWA	$\pi N \rightarrow \pi N$	
••• We do not use the following data for averages, fits, limits, etc. •••				
0.22±0.11	VRANA 00	DPWA	Multichannel	

$(\Gamma_1\Gamma_f)^{1/2}/\Gamma_{\text{total}}$ in $N\pi \rightarrow N(1990) \rightarrow N\eta$	DOCUMENT ID	TECN	COMMENT	$(\Gamma_1\Gamma_2)^{1/2}/\Gamma$
−0.043	BAKER 79	DPWA	$\pi^- p \rightarrow n\eta$	

$\Gamma(N\eta)/\Gamma_{\text{total}}$	DOCUMENT ID	TECN	COMMENT	Γ_2/Γ
0.00±0.01	VRANA 00	DPWA	Multichannel	

$(\Gamma_1\Gamma_f)^{1/2}/\Gamma_{\text{total}}$ in $N\pi \rightarrow N(1990) \rightarrow \Lambda K$	DOCUMENT ID	TECN	COMMENT	$(\Gamma_1\Gamma_3)^{1/2}/\Gamma$
+0.01	BELL 83	DPWA	$\pi^- p \rightarrow \Lambda K^0$	
not seen	SAXON 80	DPWA	$\pi^- p \rightarrow \Lambda K^0$	
−0.021±0.033	DEVENISH 74B		Fixed- t dispersion rel.	

$(\Gamma_1\Gamma_f)^{1/2}/\Gamma_{\text{total}}$ in $N\pi \rightarrow N(1990) \rightarrow \Sigma K$	DOCUMENT ID	TECN	COMMENT	$(\Gamma_1\Gamma_4)^{1/2}/\Gamma$
0.010 to 0.023	¹ DEANS 75	DPWA	$\pi N \rightarrow \Sigma K$	
0.06	LANGBEIN 73	IPWA	$\pi N \rightarrow \Sigma K$ (sol. 1)	

$(\Gamma_1\Gamma_f)^{1/2}/\Gamma_{\text{total}}$ in $N\pi \rightarrow N(1990) \rightarrow N\pi\pi$	DOCUMENT ID	TECN	COMMENT	$(\Gamma_1\Gamma_5)^{1/2}/\Gamma$
not seen	LONGACRE 75	IPWA	$\pi N \rightarrow N\pi\pi$	

N(1990) PHOTON DECAY AMPLITUDES

Papers on γN amplitudes predating 1981 may be found in our 2006 edition, Journal of Physics, G 33 1 (2006).

$N(1990) \rightarrow p\gamma$, helicity-1/2 amplitude $A_{1/2}$	DOCUMENT ID	TECN	COMMENT
0.030±0.029	AWAJI 81	DPWA	$\gamma N \rightarrow \pi N$
••• We do not use the following data for averages, fits, limits, etc. •••			
0.040	BARBOUR 78	DPWA	$\gamma N \rightarrow \pi N$

$N(1990) \rightarrow p\gamma$, helicity-3/2 amplitude $A_{3/2}$	DOCUMENT ID	TECN	COMMENT
0.086±0.060	AWAJI 81	DPWA	$\gamma N \rightarrow \pi N$
••• We do not use the following data for averages, fits, limits, etc. •••			
+0.004	BARBOUR 78	DPWA	$\gamma N \rightarrow \pi N$

$N(1990) \rightarrow n\gamma$, helicity-1/2 amplitude $A_{1/2}$	DOCUMENT ID	TECN	COMMENT
−0.001	AWAJI 81	DPWA	$\gamma N \rightarrow \pi N$
••• We do not use the following data for averages, fits, limits, etc. •••			
−0.069	BARBOUR 78	DPWA	$\gamma N \rightarrow \pi N$

$N(1990) \rightarrow n\gamma$, helicity-3/2 amplitude $A_{3/2}$	DOCUMENT ID	TECN	COMMENT
−0.178	AWAJI 81	DPWA	$\gamma N \rightarrow \pi N$
••• We do not use the following data for averages, fits, limits, etc. •••			
−0.072	BARBOUR 78	DPWA	$\gamma N \rightarrow \pi N$

N(1990) FOOTNOTES

¹ The range given for DEANS 75 is from the four best solutions.

N(1990) REFERENCES

For early references, see Physics Letters 111B 1 (1982).

ARNDT 06	PR C74 045205	R.A. Arndt <i>et al.</i>	(GWU)
PDG 06	JPG 33 1	W.-M. Yao <i>et al.</i>	(PDG Collab.)
VRANA 00	PRPL 328 181	T.P. Vrana, S.A. Dytman, T.-S.H. Lee	(PITT+)
MANLEY 92	PR D45 4002	D.M. Manley, E.M. Saleski	(KENT) IJP
Also	PR D30 904	D.M. Manley <i>et al.</i>	(VPI)
ARNDT 91	PR D43 2131	R.A. Arndt <i>et al.</i>	(VPI, TELE) IJP
BELL 83	NP B222 389	K.V. Bell <i>et al.</i>	(RL) IJP
PDG 82	PL 111B 1	M. Roos <i>et al.</i>	(HELS, CIT, CERN)
AWAJI 81	Bonn Conf. 352	N. Awaji, R. Kajikawa	(NAGO)
Also	NP B197 365	K. Fujii <i>et al.</i>	(NAGO)
CUTKOSKY 80	Toronto Conf. 19	R.E. Cutkosky <i>et al.</i>	(CMU, LBL) IJP
Also	PR D20 2839	R.E. Cutkosky <i>et al.</i>	(CMU, LBL) IJP
SAXON 80	NP B162 522	D.H. Saxon <i>et al.</i>	(RHEL, BRIS) IJP
BAKER 79	NP B156 93	R.D. Baker <i>et al.</i>	(RHEL) IJP
HOEHLER 79	PDAT 12-1	G. Hohlner <i>et al.</i>	(KARLT) IJP
Also	Toronto Conf. 3	R. Koch	(KARLT) IJP
BARBOUR 78	NP B141 253	I.M. Barbour, R.L. Crawford, N.H. Parsons	(GLAS)
DEANS 75	NP B96 90	S.R. Deans <i>et al.</i>	(SFLA, ALAH) IJP
LONGACRE 75	PL 55B 415	R.S. Longacre <i>et al.</i>	(LBL, SLAC) IJP
DEVENISH 74B	NP B81 330	R.C.E. Devenish, C.D. Froggatt, B.R. Martin	(DESY+) IJP
LANGBEIN 73	NP B53 251	W. Langbein, F. Wagner	(MUNI) IJP

N(2000) F₁₅

$$I(J^P) = \frac{1}{2}(\frac{5}{2}^+) \text{ Status: } **$$

OMITTED FROM SUMMARY TABLE

Older results have been retained simply because there is little information at all about this possible state.

N(2000) BREIT-WIGNER MASS

VALUE (MeV)	DOCUMENT ID	TECN	COMMENT
≈ 2000 OUR ESTIMATE			
1817.7	ARNDT 06	DPWA	$\pi N \rightarrow \pi N, \eta N$
1903 ± 87	MANLEY 92	IPWA	$\pi N \rightarrow \pi N \text{ \& } N\pi\pi$
1882 ± 10	HOEHLER 79	IPWA	$\pi N \rightarrow \pi N$
2025	AYED 76	IPWA	$\pi N \rightarrow \pi N$
1970	¹ LANGBEIN 73	IPWA	$\pi N \rightarrow \Sigma K$ (sol. 2)
2175	ALMEHED 72	IPWA	$\pi N \rightarrow \pi N$
1930	DEANS 72	MPWA	$\gamma p \rightarrow \Lambda K$ (sol. D)
••• We do not use the following data for averages, fits, limits, etc. •••			
1814	ARNDT 95	DPWA	$\pi N \rightarrow N\pi$

N(2000) BREIT-WIGNER WIDTH

VALUE (MeV)	DOCUMENT ID	TECN	COMMENT
117.6	ARNDT 06	DPWA	$\pi N \rightarrow \pi N, \eta N$
490 ± 310	MANLEY 92	IPWA	$\pi N \rightarrow \pi N \text{ \& } N\pi\pi$
95 ± 20	HOEHLER 79	IPWA	$\pi N \rightarrow \pi N$
157	AYED 76	IPWA	$\pi N \rightarrow \pi N$
170	¹ LANGBEIN 73	IPWA	$\pi N \rightarrow \Sigma K$ (sol. 2)
150	ALMEHED 72	IPWA	$\pi N \rightarrow \pi N$
112	DEANS 72	MPWA	$\gamma p \rightarrow \Lambda K$ (sol. D)
••• We do not use the following data for averages, fits, limits, etc. •••			
176	ARNDT 95	DPWA	$\pi N \rightarrow N\pi$

N(2000) POLE POSITION

REAL PART

VALUE (MeV)	DOCUMENT ID	TECN	COMMENT
1807	ARNDT 06	DPWA	$\pi N \rightarrow \pi N, \eta N$
••• We do not use the following data for averages, fits, limits, etc. •••			
1779	ARNDT 04	DPWA	$\pi N \rightarrow \pi N, \eta N$

−2×IMAGINARY PART

VALUE (MeV)	DOCUMENT ID	TECN	COMMENT
109	ARNDT 06	DPWA	$\pi N \rightarrow \pi N, \eta N$
••• We do not use the following data for averages, fits, limits, etc. •••			
248	ARNDT 04	DPWA	$\pi N \rightarrow \pi N, \eta N$

N(2000) ELASTIC POLE RESIDUE

MODULUS |r|

VALUE (MeV)	DOCUMENT ID	TECN	COMMENT
60	ARNDT 06	DPWA	$\pi N \rightarrow \pi N, \eta N$
••• We do not use the following data for averages, fits, limits, etc. •••			
47	ARNDT 04	DPWA	$\pi N \rightarrow \pi N, \eta N$

PHASE θ

VALUE (°)	DOCUMENT ID	TECN	COMMENT
−67	ARNDT 06	DPWA	$\pi N \rightarrow \pi N, \eta N$
••• We do not use the following data for averages, fits, limits, etc. •••			
−61	ARNDT 04	DPWA	$\pi N \rightarrow \pi N, \eta N$

N(2000) DECAY MODES

Mode
Γ_1 $N\pi$
Γ_2 $N\eta$
Γ_3 ΛK
Γ_4 ΣK
Γ_5 $N\pi\pi$
Γ_6 $\Delta(1232)\pi$, P-wave
Γ_7 $N\rho$, $S=3/2$, P-wave
Γ_8 $N\rho$, $S=3/2$, F-wave
Γ_9 $p\gamma$

$\Gamma(N\eta)/\Gamma_{\text{total}}$	DOCUMENT ID	TECN	COMMENT
0.035 ± 0.035 OUR AVERAGE	Error includes scale factor of 2.5.		
0.07 ± 0.02	PENNER	02c	DPWA Multichannel
0.00 ± 0.02	VRANA	00	DPWA Multichannel
• • • We do not use the following data for averages, fits, limits, etc. • • •			
0.07 ± 0.04	BATINIC	95	DPWA $\pi N \rightarrow N\pi, N\eta$

$(\Gamma_1\Gamma_2)^{1/2}/\Gamma_{\text{total}}$ in $N\pi \rightarrow N(2080) \rightarrow N\eta$	DOCUMENT ID	TECN	COMMENT
0.065	BAKER	79	DPWA $\pi^- p \rightarrow N\eta$

$\Gamma(N\omega)/\Gamma_{\text{total}}$	DOCUMENT ID	TECN	COMMENT
0.21 ± 0.07	PENNER	02c	DPWA Multichannel

$\Gamma(\Lambda K)/\Gamma_{\text{total}}$	DOCUMENT ID	TECN	COMMENT
• • • We do not use the following data for averages, fits, limits, etc. • • •			
0.002 ± 0.002	PENNER	02c	DPWA Multichannel

$(\Gamma_1\Gamma_2)^{1/2}/\Gamma_{\text{total}}$ in $N\pi \rightarrow N(2080) \rightarrow \Lambda K$	DOCUMENT ID	TECN	COMMENT
+0.04	BELL	83	DPWA $\pi^- p \rightarrow \Lambda K^0$
+0.03	SAXON	80	DPWA $\pi^- p \rightarrow \Lambda K^0$

$\Gamma(\Sigma K)/\Gamma_{\text{total}}$	DOCUMENT ID	TECN	COMMENT
0.007 ± 0.004	PENNER	02c	DPWA Multichannel

$(\Gamma_1\Gamma_2)^{1/2}/\Gamma_{\text{total}}$ in $N\pi \rightarrow N(2080) \rightarrow \Sigma K$	DOCUMENT ID	TECN	COMMENT
0.014 ± 0.037	2 DEANS	75	DPWA $\pi N \rightarrow \Sigma K$

$(\Gamma_1\Gamma_2)^{1/2}/\Gamma_{\text{total}}$ in $N\pi \rightarrow N(2080) \rightarrow \Delta(1232)\pi, S\text{-wave}$	DOCUMENT ID	TECN	COMMENT
-0.09 ± 0.09	MANLEY	92	IPWA $\pi N \rightarrow \pi N \& N\pi\pi$

$\Gamma(\Delta(1232)\pi, S\text{-wave})/\Gamma_{\text{total}}$	DOCUMENT ID	TECN	COMMENT
0.40 ± 0.10	VRANA	00	DPWA Multichannel

$(\Gamma_1\Gamma_2)^{1/2}/\Gamma_{\text{total}}$ in $N\pi \rightarrow N(2080) \rightarrow \Delta(1232)\pi, D\text{-wave}$	DOCUMENT ID	TECN	COMMENT
+0.22 ± 0.07	MANLEY	92	IPWA $\pi N \rightarrow \pi N \& N\pi\pi$

$\Gamma(\Delta(1232)\pi, D\text{-wave})/\Gamma_{\text{total}}$	DOCUMENT ID	TECN	COMMENT
0.17 ± 0.10	VRANA	00	DPWA Multichannel

$(\Gamma_1\Gamma_2)^{1/2}/\Gamma_{\text{total}}$ in $N\pi \rightarrow N(2080) \rightarrow N\rho, S=3/2, S\text{-wave}$	DOCUMENT ID	TECN	COMMENT
-0.24 ± 0.06	MANLEY	92	IPWA $\pi N \rightarrow \pi N \& N\pi\pi$

$\Gamma(N\rho, S=3/2, S\text{-wave})/\Gamma_{\text{total}}$	DOCUMENT ID	TECN	COMMENT
0.06 ± 0.06	VRANA	00	DPWA Multichannel

$(\Gamma_1\Gamma_2)^{1/2}/\Gamma_{\text{total}}$ in $N\pi \rightarrow N(2080) \rightarrow N(\pi\pi)_{S\text{-wave}}^{J=0}$	DOCUMENT ID	TECN	COMMENT
+0.25 ± 0.06	MANLEY	92	IPWA $\pi N \rightarrow \pi N \& N\pi\pi$

$\Gamma(N(\pi\pi)_{S\text{-wave}}^{J=0})/\Gamma_{\text{total}}$	DOCUMENT ID	TECN	COMMENT
0.24 ± 0.24	VRANA	00	DPWA Multichannel

$(\Gamma_1\Gamma_2)^{1/2}/\Gamma_{\text{total}}$ in $p\gamma \rightarrow N(2080) \rightarrow N\eta$	DOCUMENT ID	TECN	COMMENT
0.0037	HICKS	73	MPWA $\gamma p \rightarrow p\eta$

N(2080) PHOTON DECAY AMPLITUDES

Papers on γN amplitudes predating 1981 may be found in our 2006 edition, Journal of Physics, G 33 1 (2006).

N(2080) $\rightarrow p\gamma$, helicity-1/2 amplitude $A_{1/2}$

VALUE (GeV ^{-1/2})	DOCUMENT ID	TECN	COMMENT
-0.020 ± 0.008	AWAJI	81	DPWA $\gamma N \rightarrow \pi N$
• • • We do not use the following data for averages, fits, limits, etc. • • •			
0.012	PENNER	02D	DPWA Multichannel
0.026 ± 0.052	DEVENISH	74	DPWA $\gamma N \rightarrow \pi N$

N(2080) $\rightarrow p\gamma$, helicity-3/2 amplitude $A_{3/2}$

VALUE (GeV ^{-1/2})	DOCUMENT ID	TECN	COMMENT
0.017 ± 0.011	AWAJI	81	DPWA $\gamma N \rightarrow \pi N$
• • • We do not use the following data for averages, fits, limits, etc. • • •			
-0.010	PENNER	02D	DPWA Multichannel
0.128 ± 0.057	DEVENISH	74	DPWA $\gamma N \rightarrow \pi N$

N(2080) $\rightarrow n\gamma$, helicity-1/2 amplitude $A_{1/2}$

VALUE (GeV ^{-1/2})	DOCUMENT ID	TECN	COMMENT
0.007 ± 0.013	AWAJI	81	DPWA $\gamma N \rightarrow \pi N$
• • • We do not use the following data for averages, fits, limits, etc. • • •			
0.023	PENNER	02D	DPWA Multichannel
0.053 ± 0.083	DEVENISH	74	DPWA $\gamma N \rightarrow \pi N$

N(2080) $\rightarrow n\gamma$, helicity-3/2 amplitude $A_{3/2}$

VALUE (GeV ^{-1/2})	DOCUMENT ID	TECN	COMMENT
-0.053 ± 0.034	AWAJI	81	DPWA $\gamma N \rightarrow \pi N$
• • • We do not use the following data for averages, fits, limits, etc. • • •			
-0.009	PENNER	02D	DPWA Multichannel
0.100 ± 0.141	DEVENISH	74	DPWA $\gamma N \rightarrow \pi N$

N(2080) $\gamma p \rightarrow \Lambda K^+$ AMPLITUDES

$(\Gamma_1\Gamma_2)^{1/2}/\Gamma_{\text{total}}$ in $p\gamma \rightarrow N(2080) \rightarrow \Lambda K^+$	DOCUMENT ID	TECN	COMMENT
• • • We do not use the following data for averages, fits, limits, etc. • • •			
2.29 ^{+0.7} _{-0.2}	MART	00	DPWA $\gamma p \rightarrow \Lambda K^+$
5.5 ± 0.3	WORKMAN	90	DPWA
4.09	TANABE	89	DPWA

 $p\gamma \rightarrow N(2080) \rightarrow \Lambda K^+$ phase angle θ

VALUE (degrees)	DOCUMENT ID	TECN	COMMENT
• • • We do not use the following data for averages, fits, limits, etc. • • •			
-48 ± 5	WORKMAN	90	DPWA
-35.9	TANABE	89	DPWA

 $(\Gamma_1\Gamma_2)^{1/2}/\Gamma_{\text{total}}$ in $p\gamma \rightarrow N(2080) \rightarrow \Lambda K^+$

VALUE (units 10 ⁻³)	DOCUMENT ID	TECN	COMMENT
• • • We do not use the following data for averages, fits, limits, etc. • • •			
-6.7 ± 0.2	WORKMAN	90	DPWA
-4.09	TANABE	89	DPWA

N(2080) FOOTNOTES

- CUTKOSKY 80 finds a lower mass D_{13} resonance, as well as one in this region. Both are listed here.
- The range given for DEANS 75 is from the four best solutions. Disagrees with $\pi^+ p \rightarrow \Sigma^+ K^+$ data of WINNIK 77 around 1920 MeV.

N(2080) REFERENCES

For early references, see Physics Letters 111B 1 (1982).

ARNDT	06	PR C74 045205	R.A. Arndt <i>et al.</i>	(GWU)
PDG	06	JPG 33 1	W.-M. Yao <i>et al.</i>	(PDG Collab.)
PENNER	02C	PR C66 055211	G. Penner, U. Mosel	(GIES)
PENNER	02D	PR C66 055212	G. Penner, U. Mosel	(GIES)
MART	00	PR C61 012201	T. Mart, C. Bennhold	
VRANA	00	PRPL 328 181	T.P. Vrana, S.A. Dytman., T.-S.H. Lee	(PITT+)
BATINIC	95	PR C51 2310	M. Batinic <i>et al.</i>	(BOSK, UCLA)
Also		PR C57 1004 (erratum)	M. Batinic <i>et al.</i>	
MANLEY	92	PR D45 4002	D.M. Manley, E.M. Saleski	(KENT) IJP
Also		PR D30 904	D.M. Manley <i>et al.</i>	(VPI)
ARNDT	91	PR D43 2131	R.A. Arndt <i>et al.</i>	(VPI, TELE) IJP
WORKMAN	90	PR C42 781	R.L. Workman	(VPI)
TANABE	89	PR C39 741	H. Tanabe, M. Kohno, C. Bennhold	(MANZ)
Also		NC 102A 193	M. Kohno, H. Tanabe, C. Bennhold	(MANZ)
BELL	83	NP B222 389	K.W. Bell <i>et al.</i>	(RL) IJP
PDG	82	PL 111B 1	M. Roos <i>et al.</i>	(HELS, CIT, CERN)
AWAJI	81	Bonn Conf. 352	N. Awaji, R. Kajikawa	(NAGO)
Also		NP B197 365	K. Fujii <i>et al.</i>	(NAGO)
CUTKOSKY	80	Toronto Conf. 19	R.E. Cutkosky <i>et al.</i>	(CMU, LBL) IJP
Also		PR D20 2839	R.E. Cutkosky <i>et al.</i>	(CMU, LBL) IJP
SAXON	80	NP B162 522	D.H. Saxon <i>et al.</i>	(RHEL, BRIS) IJP
BAKER	79	NP B156 93	R.D. Baker <i>et al.</i>	(RHEL) IJP
HOEHLER	79	PDAT 12-1	G. Hoehler <i>et al.</i>	(KARLT) IJP
Also		Toronto Conf. 3	R. Koch	(KARLT) IJP
WINNIK	77	NP B128 66	M. Winnik <i>et al.</i>	(HAIF) I
DEANS	75	NP B96 90	S.R. Deans <i>et al.</i>	(SFLA, ALAH) IJP
DEVENISH	74	PL B28 227	R.C.E. Devenish, D.H. Lyth, W.A. Rankin	(DESY+) IJP
HICKS	73	PR D7 2614	H.R. Hicks <i>et al.</i>	(CMU, ORNL, SFLA) IJP

Baryon Particle Listings

 $N(2090)$, $N(2100)$ $N(2090) S_{11}$

$$I(J^P) = \frac{1}{2}(\frac{1}{2}^-) \text{ Status: } *$$

OMITTED FROM SUMMARY TABLE

Any structure in the S_{11} wave above 1800 MeV is listed here. A few early results that are now obsolete have been omitted.

The latest GWU analysis (ARNDT 06) finds no evidence for this resonance.

 $N(2090)$ BREIT-WIGNER MASS

VALUE (MeV)	DOCUMENT ID	TECN	COMMENT
≈ 2090 OUR ESTIMATE			
1928±59	MANLEY 92	IPWA	$\pi N \rightarrow \pi N$ & $N\pi\pi$
2180±80	CUTKOSKY 80	IPWA	$\pi N \rightarrow \pi N$
1880±20	HOEHLER 79	IPWA	$\pi N \rightarrow \pi N$
••• We do not use the following data for averages, fits, limits, etc. •••			
1822±43	VRANA 00	DPWA	Multichannel
1897±50 $^{+30}_{-2}$	PLOETZKE 98	SPEC	$\gamma p \rightarrow p\eta'$ (958)

 $N(2090)$ BREIT-WIGNER WIDTH

VALUE (MeV)	DOCUMENT ID	TECN	COMMENT
414±157	MANLEY 92	IPWA	$\pi N \rightarrow \pi N$ & $N\pi\pi$
350±100	CUTKOSKY 80	IPWA	$\pi N \rightarrow \pi N$
95±30	HOEHLER 79	IPWA	$\pi N \rightarrow \pi N$
••• We do not use the following data for averages, fits, limits, etc. •••			
248±185	VRANA 00	DPWA	Multichannel
396±155 $^{+35}_{-45}$	PLOETZKE 98	SPEC	$\gamma p \rightarrow p\eta'$ (958)

 $N(2090)$ POLE POSITION

REAL PART

VALUE (MeV)	DOCUMENT ID	TECN	COMMENT
2150±70	CUTKOSKY 80	IPWA	$\pi N \rightarrow \pi N$
1937 or 1949	¹ LONGACRE 78	IPWA	$\pi N \rightarrow N\pi\pi$
••• We do not use the following data for averages, fits, limits, etc. •••			
1795	VRANA 00	DPWA	Multichannel

-2*x*IMAGINARY PART

VALUE (MeV)	DOCUMENT ID	TECN	COMMENT
350±100	CUTKOSKY 80	IPWA	$\pi N \rightarrow \pi N$
139 or 131	¹ LONGACRE 78	IPWA	$\pi N \rightarrow N\pi\pi$
••• We do not use the following data for averages, fits, limits, etc. •••			
220	VRANA 00	DPWA	Multichannel

 $N(2090)$ ELASTIC POLE RESIDUEMODULUS $|r|$

VALUE (MeV)	DOCUMENT ID	TECN	COMMENT
40±20	CUTKOSKY 80	IPWA	$\pi N \rightarrow \pi N$

PHASE θ

VALUE (°)	DOCUMENT ID	TECN	COMMENT
0±90	CUTKOSKY 80	IPWA	$\pi N \rightarrow \pi N$

 $N(2090)$ DECAY MODES

Mode
Γ_1 $N\pi$
Γ_2 $N\eta$
Γ_3 ΛK
Γ_4 $N\pi\pi$
Γ_5 $\Delta\pi$
Γ_6 $\Delta(1232)\pi$, D-wave
Γ_7 $N\rho$
Γ_8 $N\rho$, $S=1/2$, S-wave
Γ_9 $N\rho$, $S=3/2$, D-wave
Γ_{10} $N(\pi\pi)_{S=0}^{I=0}$
Γ_{11} $N(1440)\pi$

 $N(2090)$ BRANCHING RATIOS

$\Gamma(N\pi)/\Gamma_{\text{total}}$	DOCUMENT ID	TECN	COMMENT	Γ_1/Γ
0.10±0.10	MANLEY 92	IPWA	$\pi N \rightarrow \pi N$ & $N\pi\pi$	
0.18±0.08	CUTKOSKY 80	IPWA	$\pi N \rightarrow \pi N$	
0.09±0.05	HOEHLER 79	IPWA	$\pi N \rightarrow \pi N$	
••• We do not use the following data for averages, fits, limits, etc. •••				
0.17±0.03	VRANA 00	DPWA	Multichannel	

$\Gamma(N\eta)/\Gamma_{\text{total}}$	DOCUMENT ID	TECN	COMMENT	Γ_2/Γ
0.41±0.04	VRANA 00	DPWA	Multichannel	

$(\Gamma_1\Gamma_2)^{1/2}/\Gamma_{\text{total}}$ in $N\pi \rightarrow N(2090) \rightarrow \Lambda K$	DOCUMENT ID	TECN	COMMENT	$(\Gamma_1\Gamma_3)^{1/2}/\Gamma$
not seen	SAXON 80	DPWA	$\pi^- p \rightarrow \Lambda K^0$	

$\Gamma(\Delta(1232)\pi, D\text{-wave})/\Gamma_{\text{total}}$	DOCUMENT ID	TECN	COMMENT	Γ_6/Γ
0.01±0.01	VRANA 00	DPWA	Multichannel	

$\Gamma(N\rho, S=1/2, S\text{-wave})/\Gamma_{\text{total}}$	DOCUMENT ID	TECN	COMMENT	Γ_8/Γ
0.36±0.01	VRANA 00	DPWA	Multichannel	

$\Gamma(N\rho, S=3/2, D\text{-wave})/\Gamma_{\text{total}}$	DOCUMENT ID	TECN	COMMENT	Γ_9/Γ
0.01±0.01	VRANA 00	DPWA	Multichannel	

$\Gamma(N(\pi\pi)_{S=0}^{I=0})/\Gamma_{\text{total}}$	DOCUMENT ID	TECN	COMMENT	Γ_{10}/Γ
0.02±0.01	VRANA 00	DPWA	Multichannel	

$\Gamma(N(1440)\pi)/\Gamma_{\text{total}}$	DOCUMENT ID	TECN	COMMENT	Γ_{11}/Γ
0.02±0.01	VRANA 00	DPWA	Multichannel	

 $N(2090)$ FOOTNOTES

¹ LONGACRE 78 values are from a search for poles in the unitarized T-matrix. The first (second) value uses, in addition to $\pi N \rightarrow N\pi\pi$ data, elastic amplitudes from a Saclay (CERN) partial-wave analysis.

 $N(2090)$ REFERENCES

ARNDT 06	PR C74 045205	R.A. Arndt <i>et al.</i>	(GWU)
VRANA 00	PRPL 328 181	T.P. Vrana, S.A. Dytman., T.-S.H. Lee	(PITT+)
PLOETZKE 98	PL B444 555	R. Ploetzke <i>et al.</i>	(Bonn SAPHIR Collab.)
MANLEY 92	PR D45 4002	D.M. Manley, E.M. Saleski	(KENT) IJP
Also	PR D30 904	D.M. Manley <i>et al.</i>	(VPI)
CUTKOSKY 80	Toronto Conf. 19	R.E. Cutkosky <i>et al.</i>	(CMU, LBL) IJP
Also	PR D20 2839	R.E. Cutkosky <i>et al.</i>	(CMU, LBL)
SAXON 80	NP B162 522	D.H. Saxon <i>et al.</i>	(RHEL, BRIS) IJP
HOEHLER 79	PDAT 12-1	G. Hoehler <i>et al.</i>	(KARLT) IJP
Also	Toronto Conf. 3	R. Koch	(KARLT) IJP
LONGACRE 78	PR D17 1795	R.S. Longacre <i>et al.</i>	(LBL, SLAC)

 $N(2100) P_{11}$

$$I(J^P) = \frac{1}{2}(\frac{1}{2}^+) \text{ Status: } *$$

OMITTED FROM SUMMARY TABLE

The latest GWU analysis (ARNDT 06) finds no evidence for this resonance.

 $N(2100)$ BREIT-WIGNER MASS

VALUE (MeV)	DOCUMENT ID	TECN	COMMENT
≈ 2100 OUR ESTIMATE			
1885±30	MANLEY 92	IPWA	$\pi N \rightarrow \pi N$ & $N\pi\pi$
2125±75	CUTKOSKY 80	IPWA	$\pi N \rightarrow \pi N$
2050±20	HOEHLER 79	IPWA	$\pi N \rightarrow \pi N$
••• We do not use the following data for averages, fits, limits, etc. •••			
2068±3 $^{+15}_{-40}$	ABLIKIM 06k	BES	$J/\psi \rightarrow (p\pi^-)\pi$
2084±93	VRANA 00	DPWA	Multichannel
1986±26 $^{+10}_{-30}$	PLOETZKE 98	SPEC	$\gamma p \rightarrow p\eta'$ (958)
2203±70	BATINIC 95	DPWA	$\pi N \rightarrow N\pi$, $N\eta$

 $N(2100)$ BREIT-WIGNER WIDTH

VALUE (MeV)	DOCUMENT ID	TECN	COMMENT
113±44	MANLEY 92	IPWA	$\pi N \rightarrow \pi N$ & $N\pi\pi$
260±100	CUTKOSKY 80	IPWA	$\pi N \rightarrow \pi N$
200±30	HOEHLER 79	IPWA	$\pi N \rightarrow \pi N$
••• We do not use the following data for averages, fits, limits, etc. •••			
165±14±40	ABLIKIM 06k	BES	$J/\psi \rightarrow (p\pi^-)\pi$
1077±643	VRANA 00	DPWA	Multichannel
296±100 $^{+60}_{-10}$	PLOETZKE 98	SPEC	$\gamma p \rightarrow p\eta'$ (958)
418±171	BATINIC 95	DPWA	$\pi N \rightarrow N\pi$, $N\eta$

See key on page 405

Baryon Particle Listings
N(2100), N(2190)

N(2100) POLE POSITION

REAL PART

Table with columns: VALUE (MeV), DOCUMENT ID, TECN, COMMENT. Rows include data for 2120 ± 40, 1810, and not seen.

-2xIMAGINARY PART

Table with columns: VALUE (MeV), DOCUMENT ID, TECN, COMMENT. Rows include data for 240 ± 80, 622, and not seen.

N(2100) ELASTIC POLE RESIDUE

MODULUS |r|

Table with columns: VALUE (MeV), DOCUMENT ID, TECN, COMMENT. Row includes data for 14 ± 7.

PHASE θ

Table with columns: VALUE (°), DOCUMENT ID, TECN, COMMENT. Row includes data for 35 ± 25.

N(2100) DECAY MODES

Table with columns: Mode, Fraction (Γj/Γ). Rows include Nπ, Nη, ΔK, Nππ, Δ(1232)π, P-wave, Nρ, S=1/2, P-wave, and N(ππ)S=0.

N(2100) BRANCHING RATIOS

Table with columns: Γ(Nπ)/Γtotal, VALUE, DOCUMENT ID, TECN, COMMENT, Γ1/Γ. Rows include 0.15 ± 0.06, 0.12 ± 0.03, 0.10 ± 0.04, 0.02 ± 0.05, and 0.11 ± 0.07.

Table with columns: Γ(Nη)/Γtotal, VALUE, DOCUMENT ID, TECN, COMMENT, Γ2/Γ. Rows include 0.61 ± 0.61 and 0.86 ± 0.07.

Table with columns: Γ(ΔK)/Γtotal, VALUE, DOCUMENT ID, TECN, COMMENT, Γ3/Γ. Row includes 0.21 ± 0.20.

Table with columns: (Γ1Γ2)1/2/Γtotal in Nπ → N(2100) → Δ(1232)π, P-wave, VALUE, DOCUMENT ID, TECN, COMMENT, (Γ1Γ5)1/2/Γ. Row includes -0.19 ± 0.08.

Table with columns: Γ(Δ(1232)π, P-wave)/Γtotal, VALUE, DOCUMENT ID, TECN, COMMENT, Γ5/Γ. Row includes 0.02 ± 0.01.

Table with columns: Γ(Nρ, S=1/2, P-wave)/Γtotal, VALUE, DOCUMENT ID, TECN, COMMENT, Γ6/Γ. Row includes 0.04 ± 0.01.

Table with columns: Γ(N(ππ)S=0)/Γtotal, VALUE, DOCUMENT ID, TECN, COMMENT, Γ7/Γ. Row includes 0.10 ± 0.01.

N(2100) REFERENCES

List of references for N(2100) including authors like Ablikim, Arndt, Vrana, Ploetzke, Batinic, Manley, ARNDT, CUTKOSKY, HOEHLER and their respective publications.

N(2190) G17

I(J^P) = 1/2(1/2^-) Status: ***

Most of the results published before 1975 were last included in our 1982 edition, Physics Letters 111B 1 (1982). Some further obsolete results published before 1984 were last included in our 2006 edition, Journal of Physics, G 33 1 (2006).

N(2190) BREIT-WIGNER MASS

Table with columns: VALUE (MeV), DOCUMENT ID, TECN, COMMENT. Rows include data for 2152.4 ± 1.4, 2127 ± 9, 2200 ± 70, 2140 ± 12, 2140 ± 40, 2192.1 ± 8.7, 2168 ± 18, 2131, 2198 ± 68, and 2180.

N(2190) BREIT-WIGNER WIDTH

Table with columns: VALUE (MeV), DOCUMENT ID, TECN, COMMENT. Rows include data for 484 ± 13, 550 ± 50, 500 ± 150, 390 ± 30, 270 ± 50, 726 ± 62, 453 ± 101, 476, 805 ± 140, and 80.

N(2190) POLE POSITION

REAL PART

Table with columns: VALUE (MeV), DOCUMENT ID, TECN, COMMENT. Rows include data for 2070, 2042, 2100 ± 50, 2076, 2107, 2030, and 2060.

-2xIMAGINARY PART

Table with columns: VALUE (MeV), DOCUMENT ID, TECN, COMMENT. Rows include data for 400 ± 160, 502, 380, 460, and 464.

N(2190) ELASTIC POLE RESIDUE

MODULUS |r|

Table with columns: VALUE (MeV), DOCUMENT ID, TECN, COMMENT. Rows include data for 72, 45, 25 ± 10, 68, 46, and 54.

PHASE θ

Table with columns: VALUE (°), DOCUMENT ID, TECN, COMMENT. Rows include data for -32, -30 ± 50, -32, -23, and -44.

Baryon Particle Listings

$N(2190)$, $N(2200)$

$N(2190)$ DECAY MODES

The following branching fractions are our estimates, not fits or averages.

Mode	Fraction (Γ_i/Γ)
Γ_1 $N\pi$	10–20 %
Γ_2 $N\eta$	(0.0 ± 1.0) %
Γ_3 $N\omega$	seen
Γ_4 ΛK	seen
Γ_5 ΣK	
Γ_6 $N\pi\pi$	seen
Γ_7 $N\rho$	seen
Γ_8 $N\rho$, $S=3/2$, D -wave	
Γ_9 $\rho\gamma$, helicity=1/2	
Γ_{10} $\rho\gamma$, helicity=3/2	
Γ_{11} $n\gamma$, helicity=1/2	
Γ_{12} $n\gamma$, helicity=3/2	

$N(2190)$ BRANCHING RATIOS

$\Gamma(N\pi)/\Gamma_{total}$	DOCUMENT ID	TECN	COMMENT	Γ_1/Γ
0.1 to 0.2 OUR ESTIMATE				
0.238 ± 0.001	ARNDT 06	DPWA	$\pi N \rightarrow \pi N, \eta N$	
0.22 ± 0.01	MANLEY 92	IPWA	$\pi N \rightarrow \pi N & N\pi\pi$	
0.12 ± 0.06	CUTKOSKY 80	IPWA	$\pi N \rightarrow \pi N$	
0.14 ± 0.02	HOEHLER 79	IPWA	$\pi N \rightarrow \pi N$	
0.16 ± 0.04	HENDRY 78	MPWA	$\pi N \rightarrow \pi N$	
• • • We do not use the following data for averages, fits, limits, etc. • • •				
0.230 ± 0.002	ARNDT 04	DPWA	$\pi N \rightarrow \pi N, \eta N$	
0.20 ± 0.04	VRANA 00	DPWA	Multichannel	
0.23	ARNDT 95	DPWA	$\pi N \rightarrow N\pi$	
0.19 ± 0.05	BATINIC 95	DPWA	$\pi N \rightarrow N\pi, N\eta$	

$\Gamma(N\eta)/\Gamma_{total}$	DOCUMENT ID	TECN	COMMENT	Γ_2/Γ
0.00 ± 0.01	VRANA 00	DPWA	Multichannel	
• • • We do not use the following data for averages, fits, limits, etc. • • •				
0.001 ± 0.003	BATINIC 95	DPWA	$\pi N \rightarrow N\pi, N\eta$	

$\Gamma(N\omega)/\Gamma_{total}$	DOCUMENT ID	TECN	COMMENT	Γ_3/Γ
seen	WILLIAMS 09	IPWA	$\gamma\rho \rightarrow \rho\omega$	

$(\Gamma_i\Gamma_f)^{1/2}/\Gamma_{total}$ in $N\pi \rightarrow N(2190) \rightarrow \Lambda K$	DOCUMENT ID	TECN	COMMENT	$(\Gamma_1\Gamma_4)^{1/2}/\Gamma$
–0.02	BELL 83	DPWA	$\pi^- \rho \rightarrow \Lambda K^0$	
–0.02	SAXON 80	DPWA	$\pi^- \rho \rightarrow \Lambda K^0$	

$(\Gamma_i\Gamma_f)^{1/2}/\Gamma_{total}$ in $N\pi \rightarrow N(2190) \rightarrow N\rho$, $S=3/2$, D -wave	DOCUMENT ID	TECN	COMMENT	$(\Gamma_1\Gamma_8)^{1/2}/\Gamma$
–0.25 ± 0.03	MANLEY 92	IPWA	$\pi N \rightarrow \pi N & N\pi\pi$	

$\Gamma(N\rho, S=3/2, D\text{-wave})/\Gamma_{total}$	DOCUMENT ID	TECN	COMMENT	Γ_8/Γ
0.29 ± 0.28	VRANA 00	DPWA	Multichannel	

$N(2190)$ PHOTON DECAY AMPLITUDES

Papers on γN amplitudes predating 1981 may be found in our 2006 edition, Journal of Physics, G **33** 1 (2006).

$N(2190) \rightarrow \rho\gamma$, ratio of helicity amplitudes $A_{3/2}/A_{1/2}$	DOCUMENT ID	TECN	COMMENT
• • • We do not use the following data for averages, fits, limits, etc. • • •			
–0.17 ± 0.15	WILLIAMS 09	IPWA	$\gamma\rho \rightarrow \rho\omega$

$N(2190)$ $\gamma\rho \rightarrow \Lambda K^+$ AMPLITUDES

$(\Gamma_i\Gamma_f)^{1/2}/\Gamma_{total}$ in $\rho\gamma \rightarrow N(2190) \rightarrow \Lambda K^+$ (E_4- amplitude)	DOCUMENT ID	TECN	COMMENT
• • • We do not use the following data for averages, fits, limits, etc. • • •			
2.5 ± 1.0	WORKMAN 90	DPWA	
2.04	TANABE 89	DPWA	

$\rho\gamma \rightarrow N(2190) \rightarrow \Lambda K^+$ phase angle θ (E_4- amplitude)	DOCUMENT ID	TECN	COMMENT
• • • We do not use the following data for averages, fits, limits, etc. • • •			
–4 ± 9	WORKMAN 90	DPWA	
–27.5	TANABE 89	DPWA	

$(\Gamma_i\Gamma_f)^{1/2}/\Gamma_{total}$ in $\rho\gamma \rightarrow N(2190) \rightarrow \Lambda K^+$ (M_{4-} amplitude)

VALUE (units 10^{-3})	DOCUMENT ID	TECN	COMMENT
• • • We do not use the following data for averages, fits, limits, etc. • • •			
–7.0 ± 0.7	WORKMAN 90	DPWA	
–5.78	TANABE 89	DPWA	

$N(2190)$ FOOTNOTES

¹ See HOEHLER 93 for a detailed discussion of the evidence for and the pole parameters of N and Δ resonances as determined from Argand diagrams of πN elastic partial-wave amplitudes and from plots of the speeds with which the amplitudes traverse the diagrams.

$N(2190)$ REFERENCES

For early references, see Physics Letters **111B** 1 (1982).

WILLIAMS 09	PR C80 065209	M. Williams <i>et al.</i>	(CEBAF CLAS Collab.)
ARNDT 06	PR C74 045205	R.A. Arndt <i>et al.</i>	(GWU)
PDG 06	JPG 33 1	W.-M. Yao <i>et al.</i>	(PDG Collab.)
ARNDT 04	PR C69 035213	R.A. Arndt <i>et al.</i>	(GWU, TRIU)
VRANA 00	PRPL 320 181	T.P. Vrana, S.A. Dytman, T.-S.H. Lee	(PITT+)
ARNDT 95	PR C52 2120	R.A. Arndt <i>et al.</i>	(VPI, BRCO)
BATINIC 95	PR C51 2310	M. Batinic <i>et al.</i>	(BOSK, UCLA)
Also	PR C57 1004 (erratum)	M. Batinic <i>et al.</i>	
HOEHLER 93	πN Newsletter 9 1	G. Hohler	(KARL)
MANLEY 92	PR D45 4002	D.M. Manley, E.M. Saleski	(KENT) IJP
Also	PR D30 904	D.M. Manley <i>et al.</i>	(VPI)
ARNDT 91	PR D43 2131	R.A. Arndt <i>et al.</i>	(VPI, TELE) IJP
WORKMAN 90	PR C42 781	R.L. Workman	(VPI)
TANABE 89	PR C39 741	H. Tanabe, M. Kohno, C. Bennhold	(MANZ)
Also	NC 102A 193	M. Kohno, H. Tanabe, C. Bennhold	(MANZ)
BELL 83	NP B222 389	K.W. Bell <i>et al.</i>	(RL) IJP
PDG 82	PL 111B 1	M. Roos <i>et al.</i>	(CEBN)
CUTKOSKY 80	Toronto Conf. 19	R.E. Cutkosky <i>et al.</i>	(HELS, CIT, CERN)
Also	PR D20 2839	R.E. Cutkosky <i>et al.</i>	(CMU, LBL) IJP
SAXON 80	NP B162 522	D.H. Saxon <i>et al.</i>	(RHEL, BRIS) IJP
HOEHLER 79	PDAT 12-1	G. Hohler <i>et al.</i>	(KARL) IJP
Also	Toronto Conf. 3	R. Koch	(KARL) IJP
HENDRY 78	PRL 41 222	A.W. Hendry	(IND, LBL) IJP
Also	ANP 136 1	A.W. Hendry	(IND)

$N(2200) D_{15}$

$$I(J^P) = \frac{1}{2}(\frac{5}{2}^-) \text{ Status: } * *$$

OMITTED FROM SUMMARY TABLE

The mass is not well determined. A few early results have been omitted.

The latest GWU analysis (ARNDT 06) finds no evidence for this resonance.

$N(2200)$ BREIT-WIGNER MASS

VALUE (MeV)	DOCUMENT ID	TECN	COMMENT
≈ 2200 OUR ESTIMATE			
1900	BELL 83	DPWA	$\pi^- \rho \rightarrow \Lambda K^0$
2180 ± 80	CUTKOSKY 80	IPWA	$\pi N \rightarrow \pi N$
1920	SAXON 80	DPWA	$\pi^- \rho \rightarrow \Lambda K^0$
2228 ± 30	HOEHLER 79	IPWA	$\pi N \rightarrow \pi N$
• • • We do not use the following data for averages, fits, limits, etc. • • •			
2240 ± 65	BATINIC 95	DPWA	$\pi N \rightarrow N\pi, N\eta$

$N(2200)$ BREIT-WIGNER WIDTH

VALUE (MeV)	DOCUMENT ID	TECN	COMMENT
130	BELL 83	DPWA	$\pi^- \rho \rightarrow \Lambda K^0$
400 ± 100	CUTKOSKY 80	IPWA	$\pi N \rightarrow \pi N$
220	SAXON 80	DPWA	$\pi^- \rho \rightarrow \Lambda K^0$
310 ± 50	HOEHLER 79	IPWA	$\pi N \rightarrow \pi N$
• • • We do not use the following data for averages, fits, limits, etc. • • •			
761 ± 139	BATINIC 95	DPWA	$\pi N \rightarrow N\pi, N\eta$

$N(2200)$ POLE POSITION

REAL PART	DOCUMENT ID	TECN	COMMENT
VALUE (MeV)			
2100 ± 60	CUTKOSKY 80	IPWA	$\pi N \rightarrow \pi N$

–2×IMAGINARY PART

VALUE (MeV)	DOCUMENT ID	TECN	COMMENT
360 ± 80	CUTKOSKY 80	IPWA	$\pi N \rightarrow \pi N$

$N(2200)$ ELASTIC POLE RESIDUE

MODULUS $ r $	DOCUMENT ID	TECN	COMMENT
VALUE (MeV)			
20 ± 10	CUTKOSKY 80	IPWA	$\pi N \rightarrow \pi N$

PHASE θ	DOCUMENT ID	TECN	COMMENT
VALUE (°)			
–90 ± 50	CUTKOSKY 80	IPWA	$\pi N \rightarrow \pi N$

See key on page 405

Baryon Particle Listings

 $N(2200)$, $N(2220)$ $N(2200)$ DECAY MODES

Mode	
Γ_1	$N\pi$
Γ_2	$N\eta$
Γ_3	ΛK

 $N(2200)$ BRANCHING RATIOS

$\Gamma(N\pi)/\Gamma_{\text{total}}$	VALUE	DOCUMENT ID	TECN	COMMENT	Γ_1/Γ
0.10 ± 0.03		CUTKOSKY	80	IPWA $\pi N \rightarrow \pi N$	
0.07 ± 0.02		HOEHLER	79	IPWA $\pi N \rightarrow \pi N$	
• • • We do not use the following data for averages, fits, limits, etc. • • •					
0.08 ± 0.04		BATINIC	95	DPWA $\pi N \rightarrow N\pi, N\eta$	

$\Gamma(N\eta)/\Gamma_{\text{total}}$	VALUE	DOCUMENT ID	TECN	COMMENT	Γ_2/Γ
• • • We do not use the following data for averages, fits, limits, etc. • • •					
0.001 ± 0.01		BATINIC	95	DPWA $\pi N \rightarrow N\pi, N\eta$	

$(\Gamma_1\Gamma_2)^{1/2}/\Gamma_{\text{total}}$ in $N\pi \rightarrow N(2200) \rightarrow N\eta$	VALUE	DOCUMENT ID	TECN	COMMENT	$(\Gamma_1\Gamma_2)^{1/2}/\Gamma$
0.066		BAKER	79	DPWA $\pi^- p \rightarrow n\eta$	

$(\Gamma_1\Gamma_3)^{1/2}/\Gamma_{\text{total}}$ in $N\pi \rightarrow N(2200) \rightarrow \Lambda K$	VALUE	DOCUMENT ID	TECN	COMMENT	$(\Gamma_1\Gamma_3)^{1/2}/\Gamma$
-0.03		BELL	83	DPWA $\pi^- p \rightarrow \Lambda K^0$	
-0.05		SAXON	80	DPWA $\pi^- p \rightarrow \Lambda K^0$	

 $N(2200)$ REFERENCES

ARNDT	06	PR C74 045205	R.A. Arndt <i>et al.</i>	(GWU)
BATINIC	95	PR C51 2310	M. Batinic <i>et al.</i>	(BOSK, UCLA)
Also		PR C57 1004 (erratum)	M. Batinic <i>et al.</i>	
BELL	83	NP B222 389	K.W. Bell <i>et al.</i>	(RL) IJP
CUTKOSKY	80	Toronto Conf. 19	R.E. Cutkosky <i>et al.</i>	(CMU, LBL) IJP
Also		PR D20 2839	R.E. Cutkosky <i>et al.</i>	(CMU, LBL)
SAXON	80	NP B162 522	D.H. Saxon <i>et al.</i>	(RHEL, BRIS) IJP
BAKER	79	NP B156 93	R.D. Baker <i>et al.</i>	(RHEL) IJP
HOEHLER	79	PDAT 12-1	G. Hohler <i>et al.</i>	(KARLT) IJP
Also		Toronto Conf. 3	R. Koch	(KARLT) IJP

 $N(2220) H_{19}$

$$I(J^P) = \frac{1}{2}(\frac{3}{2}^+) \text{ Status: } ****$$

Most of the results published before 1975 were last included in our 1982 edition, Physics Letters **111B** 1 (1982). Some further obsolete results published before 1980 were last included in our 2006 edition, Journal of Physics, G **33** 1 (2006).

 $N(2220)$ BREIT-WIGNER MASS

VALUE (MeV)	DOCUMENT ID	TECN	COMMENT
2200 to 2300 (\approx 2250) OUR ESTIMATE			
2316.3 ± 2.9	ARNDT	06	DPWA $\pi N \rightarrow \pi N, \eta N$
2230 ± 80	CUTKOSKY	80	IPWA $\pi N \rightarrow \pi N$
2205 ± 10	HOEHLER	79	IPWA $\pi N \rightarrow \pi N$
2300 ± 100	HENDRY	78	MPWA $\pi N \rightarrow \pi N$
• • • We do not use the following data for averages, fits, limits, etc. • • •			
2270 ± 11	ARNDT	04	DPWA $\pi N \rightarrow \pi N, \eta N$
2258	ARNDT	95	DPWA $\pi N \rightarrow N\pi$

 $N(2220)$ BREIT-WIGNER WIDTH

VALUE (MeV)	DOCUMENT ID	TECN	COMMENT
350 to 500 (\approx 400) OUR ESTIMATE			
633 ± 17	ARNDT	06	DPWA $\pi N \rightarrow \pi N, \eta N$
500 ± 150	CUTKOSKY	80	IPWA $\pi N \rightarrow \pi N$
365 ± 30	HOEHLER	79	IPWA $\pi N \rightarrow \pi N$
450 ± 150	HENDRY	78	MPWA $\pi N \rightarrow \pi N$
• • • We do not use the following data for averages, fits, limits, etc. • • •			
366 ± 42	ARNDT	04	DPWA $\pi N \rightarrow \pi N, \eta N$
334	ARNDT	95	DPWA $\pi N \rightarrow N\pi$

 $N(2220)$ POLE POSITION

REAL PART	VALUE (MeV)	DOCUMENT ID	TECN	COMMENT
2130 to 2200 (\approx 2170) OUR ESTIMATE				
2199		ARNDT	06	DPWA $\pi N \rightarrow \pi N, \eta N$
2135		1 HOEHLER	93	ARGD $\pi N \rightarrow \pi N$
2160 ± 80		CUTKOSKY	80	IPWA $\pi N \rightarrow \pi N$
• • • We do not use the following data for averages, fits, limits, etc. • • •				
2209		ARNDT	04	DPWA $\pi N \rightarrow \pi N, \eta N$
2203		ARNDT	95	DPWA $\pi N \rightarrow N\pi$
2253		ARNDT	91	DPWA $\pi N \rightarrow \pi N$ Soln SM90

 $-2 \times$ IMAGINARY PART

VALUE (MeV)	DOCUMENT ID	TECN	COMMENT	
400 to 560 (\approx 480) OUR ESTIMATE				
372		ARNDT	06	DPWA $\pi N \rightarrow \pi N, \eta N$
400		2 HOEHLER	93	ARGD $\pi N \rightarrow \pi N$
480 ± 100		CUTKOSKY	80	IPWA $\pi N \rightarrow \pi N$
• • • We do not use the following data for averages, fits, limits, etc. • • •				
564		ARNDT	04	DPWA $\pi N \rightarrow \pi N, \eta N$
536		ARNDT	95	DPWA $\pi N \rightarrow N\pi$
640		ARNDT	91	DPWA $\pi N \rightarrow \pi N$ Soln SM90

 $N(2220)$ ELASTIC POLE RESIDUEMODULUS $|r|$

VALUE (MeV)	DOCUMENT ID	TECN	COMMENT	
33		ARNDT	06	DPWA $\pi N \rightarrow \pi N, \eta N$
40		HOEHLER	93	ARGD $\pi N \rightarrow \pi N$
45 ± 20		CUTKOSKY	80	IPWA $\pi N \rightarrow \pi N$
• • • We do not use the following data for averages, fits, limits, etc. • • •				
96		ARNDT	04	DPWA $\pi N \rightarrow \pi N, \eta N$
68		ARNDT	95	DPWA $\pi N \rightarrow N\pi$
85		ARNDT	91	DPWA $\pi N \rightarrow \pi N$ Soln SM90

PHASE θ

VALUE ($^\circ$)	DOCUMENT ID	TECN	COMMENT	
-33		ARNDT	06	DPWA $\pi N \rightarrow \pi N, \eta N$
-50		HOEHLER	93	ARGD $\pi N \rightarrow \pi N$
-45 ± 25		CUTKOSKY	80	IPWA $\pi N \rightarrow \pi N$
• • • We do not use the following data for averages, fits, limits, etc. • • •				
-71		ARNDT	04	DPWA $\pi N \rightarrow \pi N, \eta N$
-43		ARNDT	95	DPWA $\pi N \rightarrow N\pi$
-62		ARNDT	91	DPWA $\pi N \rightarrow \pi N$ Soln SM90

 $N(2220)$ DECAY MODES

The following branching fractions are our estimates, not fits or averages.

Mode	Fraction (Γ_i/Γ)	
Γ_1	$N\pi$	10–20 %
Γ_2	$N\eta$	
Γ_3	ΛK	

 $N(2220)$ BRANCHING RATIOS

$\Gamma(N\pi)/\Gamma_{\text{total}}$	VALUE	DOCUMENT ID	TECN	COMMENT	Γ_1/Γ
0.1 to 0.2 OUR ESTIMATE					
0.246 ± 0.001		ARNDT	06	DPWA $\pi N \rightarrow \pi N, \eta N$	
0.15 ± 0.03		CUTKOSKY	80	IPWA $\pi N \rightarrow \pi N$	
0.18 ± 0.015		HOEHLER	79	IPWA $\pi N \rightarrow \pi N$	
0.12 ± 0.04		HENDRY	78	MPWA $\pi N \rightarrow \pi N$	
• • • We do not use the following data for averages, fits, limits, etc. • • •					
0.200 ± 0.006		ARNDT	04	DPWA $\pi N \rightarrow \pi N, \eta N$	
0.26		ARNDT	95	DPWA $\pi N \rightarrow N\pi$	

$(\Gamma_1\Gamma_3)^{1/2}/\Gamma_{\text{total}}$ in $N\pi \rightarrow N(2220) \rightarrow \Lambda K$	VALUE	DOCUMENT ID	TECN	COMMENT	$(\Gamma_1\Gamma_3)^{1/2}/\Gamma$
not required		BELL	83	DPWA $\pi^- p \rightarrow \Lambda K^0$	
not seen		SAXON	80	DPWA $\pi^- p \rightarrow \Lambda K^0$	

 $N(2220)$ FOOTNOTES

- See HOEHLER 93 for a detailed discussion of the evidence for and the pole parameters of N and Δ resonances as determined from Argand diagrams of πN elastic partial-wave amplitudes and from plots of the speeds with which the amplitudes traverse the diagrams.
- See HOEHLER 93 for a detailed discussion of the evidence for and the pole parameters of N and Δ resonances as determined from Argand diagrams of πN elastic partial-wave amplitudes and from plots of the speeds with which the amplitudes traverse the diagrams.

 $N(2220)$ REFERENCES

For early references, see Physics Letters **111B** 1 (1982).

ARNDT	06	PR C74 045205	R.A. Arndt <i>et al.</i>	(GWU)
PDG	06	JPG 33 1	W.-M. Yao <i>et al.</i>	(PDG Collab.)
ARNDT	04	PR C69 035213	R.A. Arndt <i>et al.</i>	(GWU, TRIU)
ARNDT	95	PR C52 2120	R.A. Arndt <i>et al.</i>	(VPI, BRCO)
HOEHLER	93	πN Newsletter 9 1	G. Hohler	(KARL)
ARNDT	91	PR D43 2131	R.A. Arndt <i>et al.</i>	(VPI, TELE) IJP
BELL	83	NP B222 389	K.W. Bell <i>et al.</i>	(RL) IJP
PDG	82	PL 111B 1	M. Roos <i>et al.</i>	(HELS, CIT, CERN)
CUTKOSKY	80	Toronto Conf. 19	R.E. Cutkosky <i>et al.</i>	(CMU, LBL) IJP
Also		PR D20 2839	R.E. Cutkosky <i>et al.</i>	(CMU, LBL) IJP

Baryon Particle Listings

$N(2220)$, $N(2250)$, $N(2600)$

SAXON	80	NP B162 522	D.H. Saxon <i>et al.</i>	(RHEL, BRIS) IJP
HOEHLER	79	PDAT 12-1	G. H\"ohler <i>et al.</i>	(KARLT) IJP
Also		Toronto Conf. 3	R. Koch	(KARLT) IJP
HENDRY	78	PRL 41 222	A.W. Hendry	(IND, LBL) IJP
Also		ANP 136 1	A.W. Hendry	(IND)

$N(2250) G_{19}$ $I(J^P) = \frac{1}{2}(\frac{9}{2}^-)$ Status: * * * *

Some obsolete results published before 1980 were last included in our 2006 edition, *Journal of Physics*, G **33** 1 (2006).

$N(2250)$ BREIT-WIGNER MASS

VALUE (MeV)	DOCUMENT ID	TECN	COMMENT
2200 to 2350 (≈ 2275) OUR ESTIMATE			
2302 \pm 6	ARNDT 06	DPWA	$\pi N \rightarrow \pi N, \eta N$
2250 \pm 80	CUTKOSKY 80	IPWA	$\pi N \rightarrow \pi N$
2268 \pm 15	HOEHLER 79	IPWA	$\pi N \rightarrow \pi N$
2200 \pm 100	HENDRY 78	MPWA	$\pi N \rightarrow \pi N$
• • • We do not use the following data for averages, fits, limits, etc. • • •			
2376 \pm 43	ARNDT 04	DPWA	$\pi N \rightarrow \pi N, \eta N$
2291	ARNDT 95	DPWA	$\pi N \rightarrow N\pi$

$N(2250)$ BREIT-WIGNER WIDTH

VALUE (MeV)	DOCUMENT ID	TECN	COMMENT
230 to 800 (≈ 500) OUR ESTIMATE			
628 \pm 28	ARNDT 06	DPWA	$\pi N \rightarrow \pi N, \eta N$
480 \pm 120	CUTKOSKY 80	IPWA	$\pi N \rightarrow \pi N$
300 \pm 40	HOEHLER 79	IPWA	$\pi N \rightarrow \pi N$
350 \pm 100	HENDRY 78	MPWA	$\pi N \rightarrow \pi N$
• • • We do not use the following data for averages, fits, limits, etc. • • •			
924 \pm 178	ARNDT 04	DPWA	$\pi N \rightarrow \pi N, \eta N$
772	ARNDT 95	DPWA	$\pi N \rightarrow N\pi$

$N(2250)$ POLE POSITION

REAL PART

VALUE (MeV)	DOCUMENT ID	TECN	COMMENT
2150 to 2250 (≈ 2200) OUR ESTIMATE			
2217	ARNDT 06	DPWA	$\pi N \rightarrow \pi N, \eta N$
2187	¹ HOEHLER 93	SPED	$\pi N \rightarrow \pi N$
2150 \pm 50	CUTKOSKY 80	IPWA	$\pi N \rightarrow \pi N$
• • • We do not use the following data for averages, fits, limits, etc. • • •			
2238	ARNDT 04	DPWA	$\pi N \rightarrow \pi N, \eta N$
2087	ARNDT 95	DPWA	$\pi N \rightarrow N\pi$
2243	ARNDT 91	DPWA	$\pi N \rightarrow \pi N$ Soln SM90

-2xIMAGINARY PART

VALUE (MeV)	DOCUMENT ID	TECN	COMMENT
350 to 550 (≈ 450) OUR ESTIMATE			
431	ARNDT 06	DPWA	$\pi N \rightarrow \pi N, \eta N$
388	¹ HOEHLER 93	SPED	$\pi N \rightarrow \pi N$
360 \pm 100	CUTKOSKY 80	IPWA	$\pi N \rightarrow \pi N$
• • • We do not use the following data for averages, fits, limits, etc. • • •			
536	ARNDT 04	DPWA	$\pi N \rightarrow \pi N, \eta N$
680	ARNDT 95	DPWA	$\pi N \rightarrow N\pi$
650	ARNDT 91	DPWA	$\pi N \rightarrow \pi N$ Soln SM90

$N(2250)$ ELASTIC POLE RESIDUE

MODULUS $|r|$

VALUE (MeV)	DOCUMENT ID	TECN	COMMENT
21	ARNDT 06	DPWA	$\pi N \rightarrow \pi N, \eta N$
21	HOEHLER 93	SPED	$\pi N \rightarrow \pi N$
20 \pm 6	CUTKOSKY 80	IPWA	$\pi N \rightarrow \pi N$
• • • We do not use the following data for averages, fits, limits, etc. • • •			
33	ARNDT 04	DPWA	$\pi N \rightarrow \pi N, \eta N$
24	ARNDT 95	DPWA	$\pi N \rightarrow N\pi$
47	ARNDT 91	DPWA	$\pi N \rightarrow \pi N$ Soln SM90

PHASE θ

VALUE ($^\circ$)	DOCUMENT ID	TECN	COMMENT
-20	ARNDT 06	DPWA	$\pi N \rightarrow \pi N, \eta N$
-50 \pm 20	CUTKOSKY 80	IPWA	$\pi N \rightarrow \pi N$
• • • We do not use the following data for averages, fits, limits, etc. • • •			
-25	ARNDT 04	DPWA	$\pi N \rightarrow \pi N, \eta N$
-44	ARNDT 95	DPWA	$\pi N \rightarrow N\pi$
-37	ARNDT 91	DPWA	$\pi N \rightarrow \pi N$ Soln SM90

$N(2250)$ DECAY MODES

The following branching fractions are our estimates, not fits or averages.

Mode	Fraction (Γ_i/Γ)
Γ_1 $N\pi$	5-15 %
Γ_2 $N\eta$	
Γ_3 ΛK	

$N(2250)$ BRANCHING RATIOS

$\Gamma(N\pi)/\Gamma_{total}$	DOCUMENT ID	TECN	COMMENT	Γ_1/Γ
0.05 to 0.15 OUR ESTIMATE				
0.089 \pm 0.001	ARNDT 06	DPWA	$\pi N \rightarrow \pi N, \eta N$	
0.10 \pm 0.02	CUTKOSKY 80	IPWA	$\pi N \rightarrow \pi N$	
0.10 \pm 0.02	HOEHLER 79	IPWA	$\pi N \rightarrow \pi N$	
0.09 \pm 0.02	HENDRY 78	MPWA	$\pi N \rightarrow \pi N$	
• • • We do not use the following data for averages, fits, limits, etc. • • •				
0.110 \pm 0.004	ARNDT 04	DPWA	$\pi N \rightarrow \pi N, \eta N$	
0.10	ARNDT 95	DPWA	$\pi N \rightarrow N\pi$	

$(\Gamma_1\Gamma_2)^{1/2}/\Gamma_{total}$ in $N\pi \rightarrow N(2250) \rightarrow \Lambda K$ $(\Gamma_1\Gamma_3)^{1/2}/\Gamma$

VALUE	DOCUMENT ID	TECN	COMMENT
-0.02	BELL 83	DPWA	$\pi^- p \rightarrow \Lambda K^0$
not seen	SAXON 80	DPWA	$\pi^- p \rightarrow \Lambda K^0$

$N(2250)$ FOOTNOTES

¹ See HOEHLER 93 for a detailed discussion of the evidence for and the pole parameters of N and Δ resonances as determined from Argand diagrams of πN elastic partial-wave amplitudes and from plots of the speeds with which the amplitudes traverse the diagrams.

$N(2250)$ REFERENCES

ARNDT 06	PR C74 045205	R.A. Arndt <i>et al.</i>	(GWU)
PDG 06	JPG 33 1	W.-M. Yao <i>et al.</i>	(PDG Collab.)
ARNDT 04	PR C69 035213	R.A. Arndt <i>et al.</i>	(GWU, TRIU)
ARNDT 95	PR C52 2120	R.A. Arndt <i>et al.</i>	(VPI, BRCO)
HOEHLER 93	πN Newsletter 9 1	G. H\"ohler	(KARL)
ARNDT 91	PR D43 2131	R.A. Arndt <i>et al.</i>	(VPI, TELE) IJP
BELL 83	NP B222 389	K.V. Bell <i>et al.</i>	(RL) IJP
CUTKOSKY 80	Toronto Conf. 19	R.E. Cutkosky <i>et al.</i>	(CMU, LBL) IJP
Also	PR D20 2839	R.E. Cutkosky <i>et al.</i>	(CMU, LBL) IJP
SAXON 80	NP B162 522	D.H. Saxon <i>et al.</i>	(RHEL, BRIS) IJP
HOEHLER 79	PDAT 12-1	G. H\"ohler <i>et al.</i>	(KARLT) IJP
Also	Toronto Conf. 3	R. Koch	(KARLT) IJP
HENDRY 78	PRL 41 222	A.W. Hendry	(IND, LBL) IJP
Also	ANP 136 1	A.W. Hendry	(IND)

$N(2600) I_{1,11}$

$I(J^P) = \frac{1}{2}(\frac{11}{2}^-)$ Status: * * *

$N(2600)$ BREIT-WIGNER MASS

VALUE (MeV)	DOCUMENT ID	TECN	COMMENT
2550 to 2750 (≈ 2600) OUR ESTIMATE			
2623 \pm 197	ARNDT 06	DPWA	$\pi N \rightarrow \pi N, \eta N$
2577 \pm 50	HOEHLER 79	IPWA	$\pi N \rightarrow \pi N$
2700 \pm 100	HENDRY 78	MPWA	$\pi N \rightarrow \pi N$

$N(2600)$ BREIT-WIGNER WIDTH

VALUE (MeV)	DOCUMENT ID	TECN	COMMENT
500 to 800 (≈ 650) OUR ESTIMATE			
1311 \pm 996	ARNDT 06	DPWA	$\pi N \rightarrow \pi N, \eta N$
400 \pm 100	HOEHLER 79	IPWA	$\pi N \rightarrow \pi N$
900 \pm 100	HENDRY 78	MPWA	$\pi N \rightarrow \pi N$

$N(2600)$ DECAY MODES

Mode	Fraction (Γ_i/Γ)
Γ_1 $N\pi$	5-10 %

$N(2600)$ BRANCHING RATIOS

$\Gamma(N\pi)/\Gamma_{total}$	DOCUMENT ID	TECN	COMMENT	Γ_1/Γ
0.05 to 0.1 OUR ESTIMATE				
0.050 \pm 0.018	ARNDT 06	DPWA	$\pi N \rightarrow \pi N, \eta N$	
0.05 \pm 0.01	HOEHLER 79	IPWA	$\pi N \rightarrow \pi N$	
0.08 \pm 0.02	HENDRY 78	MPWA	$\pi N \rightarrow \pi N$	

See key on page 405

Baryon Particle Listings
 $N(2600)$, $N(2700)$, $N(\sim 3000)$

$N(2600)$ REFERENCES

ARNDT	06	PR C74 045205	R.A. Arndt <i>et al.</i>	(GWU)
HOEHLER	79	PDAT 12-1	G. Hohlner <i>et al.</i>	(KARLT) IJP
Also		Toronto Conf. 3	R. Koch	(KARLT) IJP
HENDRY	78	PRL 41 222	A.W. Hendry	(IND, LBL) IJP
Also		ANP 136 1	A.W. Hendry	(IND)

$N(2700) K_{1,13}$

$I(J^P) = \frac{1}{2}(1\frac{3}{2}^+)$ Status: **

OMITTED FROM SUMMARY TABLE

The latest GWU analysis (ARNDT 06) finds no evidence for this resonance.

$N(2700)$ BREIT-WIGNER MASS

VALUE (MeV)	DOCUMENT ID	TECN	COMMENT
≈ 2700 OUR ESTIMATE			
2612 ± 45	HOEHLER 79	IPWA	$\pi N \rightarrow \pi N$
3000 ± 100	HENDRY 78	MPWA	$\pi N \rightarrow \pi N$

$N(2700)$ BREIT-WIGNER WIDTH

VALUE (MeV)	DOCUMENT ID	TECN	COMMENT
350 ± 50	HOEHLER 79	IPWA	$\pi N \rightarrow \pi N$
900 ± 150	HENDRY 78	MPWA	$\pi N \rightarrow \pi N$

$N(2700)$ DECAY MODES

Mode	Γ_1	$N \pi$
	Γ_1	$N \pi$

$N(2700)$ BRANCHING RATIOS

$\Gamma(N\pi)/\Gamma_{total}$	DOCUMENT ID	TECN	COMMENT	Γ_1/Γ
0.04 ± 0.01	HOEHLER 79	IPWA	$\pi N \rightarrow \pi N$	
0.07 ± 0.02	HENDRY 78	MPWA	$\pi N \rightarrow \pi N$	

$N(2700)$ REFERENCES

ARNDT	06	PR C74 045205	R.A. Arndt <i>et al.</i>	(GWU)
HOEHLER	79	PDAT 12-1	G. Hohlner <i>et al.</i>	(KARLT) IJP
Also		Toronto Conf. 3	R. Koch	(KARLT) IJP
HENDRY	78	PRL 41 222	A.W. Hendry	(IND, LBL) IJP
Also		ANP 136 1	A.W. Hendry	(IND)

**$N(\sim 3000)$ Region
 Partial-Wave Analyses**

OMITTED FROM SUMMARY TABLE

We list here miscellaneous high-mass candidates for isospin-1/2 resonances found in partial-wave analyses.

Our 1982 edition had an $N(3245)$, an $N(3690)$, and an $N(3755)$, each a narrow peak seen in a production experiment. Since nothing has been heard from them since the 1960's, we declare them to be dead. There was also an $N(3030)$, deduced from total cross-section and 180° elastic cross-section measurements; it is the KOCH 80 $L_{1,15}$ state below.

$N(\sim 3000)$ BREIT-WIGNER MASS

VALUE (MeV)	DOCUMENT ID	TECN	COMMENT
≈ 3000 OUR ESTIMATE			
2600	KOCH 80	IPWA	$\pi N \rightarrow \pi N D_{13}$
3100	KOCH 80	IPWA	$\pi N \rightarrow \pi N L_{1,15}$ wave
3500	KOCH 80	IPWA	$\pi N \rightarrow \pi N M_{1,17}$ wave
3500 to 4000	KOCH 80	IPWA	$\pi N \rightarrow \pi N N_{1,19}$ wave
3500 ± 200	HENDRY 78	MPWA	$\pi N \rightarrow \pi N L_{1,15}$ wave
3800 ± 200	HENDRY 78	MPWA	$\pi N \rightarrow \pi N M_{1,17}$ wave
4100 ± 200	HENDRY 78	MPWA	$\pi N \rightarrow \pi N N_{1,19}$ wave

$N(\sim 3000)$ BREIT-WIGNER WIDTH

VALUE (MeV)	DOCUMENT ID	TECN	COMMENT
1300 ± 200	HENDRY 78	MPWA	$\pi N \rightarrow \pi N L_{1,15}$ wave
1600 ± 200	HENDRY 78	MPWA	$\pi N \rightarrow \pi N M_{1,17}$ wave
1900 ± 300	HENDRY 78	MPWA	$\pi N \rightarrow \pi N N_{1,19}$ wave

$N(\sim 3000)$ DECAY MODES

Mode	Γ_1	$N \pi$
	Γ_1	$N \pi$

$N(\sim 3000)$ BRANCHING RATIOS

$\Gamma(N\pi)/\Gamma_{total}$	DOCUMENT ID	TECN	COMMENT	Γ_1/Γ
0.055 ± 0.02	HENDRY 78	MPWA	$\pi N \rightarrow \pi N L_{1,15}$ wave	
0.040 ± 0.015	HENDRY 78	MPWA	$\pi N \rightarrow \pi N M_{1,17}$ wave	
0.030 ± 0.015	HENDRY 78	MPWA	$\pi N \rightarrow \pi N N_{1,19}$ wave	

$N(\sim 3000)$ REFERENCES

KOCH	80	Toronto Conf. 3	R. Koch	(KARLT) IJP
HENDRY	78	PRL 41 222	A.W. Hendry	(IND, LBL) IJP
Also		ANP 136 1	A.W. Hendry	(IND) IJP

Baryon Particle Listings

$\Delta(1232)$

Δ BARYONS

($S = 0, I = 3/2$)

$\Delta^{++} = uuu, \Delta^+ = uud, \Delta^0 = udd, \Delta^- = ddd$

$\Delta(1232) P_{33} \quad I(J^P) = \frac{3}{2}(\frac{3}{2}^+)$ Status: * * * *

Most of the results published before 1975 were last included in our 1982 edition, Physics Letters **111B** 1 (1982). Some further obsolete results published before 1984 were last included in our 2006 edition, Journal of Physics, G **33** 1 (2006).

$\Delta(1232)$ BREIT-WIGNER MASSES

MIXED CHARGES

VALUE (MeV)	DOCUMENT ID	TECN	COMMENT
1231 to 1233 (≈ 1232) OUR ESTIMATE			
1233.4 \pm 0.4	ARNDT 06	DPWA	$\pi N \rightarrow \pi N, \eta N$
1231 \pm 1	MANLEY 92	IPWA	$\pi N \rightarrow \pi N \& N\pi\pi$
1232 \pm 3	CUTKOSKY 80	IPWA	$\pi N \rightarrow \pi N$
1233 \pm 2	HOEHLER 79	IPWA	$\pi N \rightarrow \pi N$
• • • We do not use the following data for averages, fits, limits, etc. • • •			
1232.9 \pm 1.2	ARNDT 04	DPWA	$\pi N \rightarrow \pi N, \eta N$
1228 \pm 1	PENNER 02c	DPWA	Multichannel
1234 \pm 5	VRANA 00	DPWA	Multichannel
1233	ARNDT 95	DPWA	$\pi N \rightarrow N\pi$

$\Delta(1232)^{++}$ MASS

VALUE (MeV)	DOCUMENT ID	TECN	COMMENT
• • • We do not use the following data for averages, fits, limits, etc. • • •			
1230.55 \pm 0.20	GRIDNEV 06	DPWA	$\pi N \rightarrow \pi N$
1231.88 \pm 0.29	BERNICHIA 96		Fit to PEDRONI 78
1230.5 \pm 0.2	ABAEV 95	IPWA	$\pi N \rightarrow \pi N$
1230.9 \pm 0.3	KOCH 80b	IPWA	$\pi N \rightarrow \pi N$
1231.1 \pm 0.2	PEDRONI 78		$\pi N \rightarrow \pi N$ 70-370 MeV

$\Delta(1232)^+$ MASS

VALUE (MeV)	DOCUMENT ID	COMMENT
• • • We do not use the following data for averages, fits, limits, etc. • • •		
1234.9 \pm 1.4	MIROSHNIC... 79	Fit photoproduction

$\Delta(1232)^0$ MASS

VALUE (MeV)	DOCUMENT ID	TECN	COMMENT
• • • We do not use the following data for averages, fits, limits, etc. • • •			
1231.3 \pm 0.6	BREITSCHOP..06	CNTR	Using new CHEX data
1233.40 \pm 0.22	GRIDNEV 06	DPWA	$\pi N \rightarrow \pi N$
1234.35 \pm 0.75	BERNICHIA 96		Fit to PEDRONI 78
1233.1 \pm 0.3	ABAEV 95	IPWA	$\pi N \rightarrow \pi N$
1233.6 \pm 0.5	KOCH 80b	IPWA	$\pi N \rightarrow \pi N$
1233.8 \pm 0.2	PEDRONI 78		$\pi N \rightarrow \pi N$ 70-370 MeV

$m_{\Delta^0} - m_{\Delta^{++}}$

VALUE (MeV)	DOCUMENT ID	TECN	COMMENT
• • • We do not use the following data for averages, fits, limits, etc. • • •			
2.86 \pm 0.30	GRIDNEV 06	DPWA	$\pi N \rightarrow \pi N$
2.25 \pm 0.68	BERNICHIA 96		Fit to PEDRONI 78
2.6 \pm 0.4	ABAEV 95	IPWA	$\pi N \rightarrow \pi N$
2.7 \pm 0.3	¹ PEDRONI 78		See the masses
¹ Using $\pi^{\pm}d$ as well, PEDRONI 78 determine $(M^- - M^{++}) + (M^0 - M^+)/3 = 4.6 \pm 0.2$ MeV.			

$\Delta(1232)$ BREIT-WIGNER WIDTHS

MIXED CHARGES

VALUE (MeV)	DOCUMENT ID	TECN	COMMENT
116 to 120 (≈ 118) OUR ESTIMATE			
118.7 \pm 0.6	ARNDT 06	DPWA	$\pi N \rightarrow \pi N, \eta N$
118 \pm 4	MANLEY 92	IPWA	$\pi N \rightarrow \pi N \& N\pi\pi$
120 \pm 5	CUTKOSKY 80	IPWA	$\pi N \rightarrow \pi N$
116 \pm 5	HOEHLER 79	IPWA	$\pi N \rightarrow \pi N$
• • • We do not use the following data for averages, fits, limits, etc. • • •			
118.0 \pm 2.2	ARNDT 04	DPWA	$\pi N \rightarrow \pi N, \eta N$
106 \pm 1	PENNER 02c	DPWA	Multichannel
112 \pm 18	VRANA 00	DPWA	Multichannel
114	ARNDT 95	DPWA	$\pi N \rightarrow N\pi$

$\Delta(1232)^{++}$ WIDTH

VALUE (MeV)	DOCUMENT ID	TECN	COMMENT
• • • We do not use the following data for averages, fits, limits, etc. • • •			
112.2 \pm 0.7	GRIDNEV 06	DPWA	$\pi N \rightarrow \pi N$
109.07 \pm 0.48	BERNICHIA 96		Fit to PEDRONI 78
111.0 \pm 1.0	KOCH 80b	IPWA	$\pi N \rightarrow \pi N$
111.3 \pm 0.5	PEDRONI 78		$\pi N \rightarrow \pi N$ 70-370 MeV

$\Delta(1232)^+$ WIDTH

VALUE (MeV)	DOCUMENT ID	COMMENT
• • • We do not use the following data for averages, fits, limits, etc. • • •		
131.1 \pm 2.4	MIROSHNIC... 79	Fit photoproduction

$\Delta(1232)^0$ WIDTH

VALUE (MeV)	DOCUMENT ID	TECN	COMMENT
• • • We do not use the following data for averages, fits, limits, etc. • • •			
112.5 \pm 1.9	BREITSCHOP..06	CNTR	Using new CHEX data
116.9 \pm 0.7	GRIDNEV 06	DPWA	$\pi N \rightarrow \pi N$
117.58 \pm 1.16	BERNICHIA 96		Fit to PEDRONI 78
113.0 \pm 1.5	KOCH 80b	IPWA	$\pi N \rightarrow \pi N$
117.9 \pm 0.9	PEDRONI 78		$\pi N \rightarrow \pi N$ 70-370 MeV

$\Delta^0 - \Delta^{++}$ WIDTH DIFFERENCE

VALUE (MeV)	DOCUMENT ID	TECN	COMMENT
• • • We do not use the following data for averages, fits, limits, etc. • • •			
4.66 \pm 1.0	GRIDNEV 06	DPWA	$\pi N \rightarrow \pi N$
8.45 \pm 1.11	BERNICHIA 96		Fit to PEDRONI 78
5.1 \pm 1.0	ABAEV 95	IPWA	$\pi N \rightarrow \pi N$
6.6 \pm 1.0	PEDRONI 78		See the widths

$\Delta(1232)$ POLE POSITIONS

REAL PART, MIXED CHARGES

VALUE (MeV)	DOCUMENT ID	TECN	COMMENT
1209 to 1211 (≈ 1210) OUR ESTIMATE			
1211	ARNDT 06	DPWA	$\pi N \rightarrow \pi N, \eta N$
1209	² HOEHLER 93	ARGD	$\pi N \rightarrow \pi N$
1210 \pm 1	CUTKOSKY 80	IPWA	$\pi N \rightarrow \pi N$
• • • We do not use the following data for averages, fits, limits, etc. • • •			
1210	ARNDT 04	DPWA	$\pi N \rightarrow \pi N, \eta N$
1217	VRANA 00	DPWA	Multichannel
1211	ARNDT 95	DPWA	$\pi N \rightarrow N\pi$
1210	ARNDT 91	DPWA	$\pi N \rightarrow \pi N$ Soln SM90

-2xIMAGINARY PART, MIXED CHARGES

VALUE (MeV)	DOCUMENT ID	TECN	COMMENT
98 to 102 (≈ 100) OUR ESTIMATE			
99	ARNDT 06	DPWA	$\pi N \rightarrow \pi N, \eta N$
100	² HOEHLER 93	ARGD	$\pi N \rightarrow \pi N$
100 \pm 2	CUTKOSKY 80	IPWA	$\pi N \rightarrow \pi N$
• • • We do not use the following data for averages, fits, limits, etc. • • •			
100	ARNDT 04	DPWA	$\pi N \rightarrow \pi N, \eta N$
96	VRANA 00	DPWA	Multichannel
100	ARNDT 95	DPWA	$\pi N \rightarrow N\pi$
100	ARNDT 91	DPWA	$\pi N \rightarrow \pi N$ Soln SM90

REAL PART, $\Delta(1232)^{++}$

VALUE (MeV)	DOCUMENT ID	COMMENT
• • • We do not use the following data for averages, fits, limits, etc. • • •		
1212.50 \pm 0.24	BERNICHIA 96	Fit to PEDRONI 78

-2xIMAGINARY PART, $\Delta(1232)^{++}$

VALUE (MeV)	DOCUMENT ID	COMMENT
• • • We do not use the following data for averages, fits, limits, etc. • • •		
97.37 \pm 0.42	BERNICHIA 96	Fit to PEDRONI 78

REAL PART, $\Delta(1232)^+$

VALUE (MeV)	DOCUMENT ID	TECN	COMMENT
• • • We do not use the following data for averages, fits, limits, etc. • • •			
1211 \pm 1 to 1212 \pm 1	HANSTEIN 96	DPWA	$\gamma N \rightarrow \pi N$
1206.9 \pm 0.9 to 1210.5 \pm 1.8	MIROSHNIC... 79		Fit photoproduction

-2xIMAGINARY PART, $\Delta(1232)^+$

VALUE (MeV)	DOCUMENT ID	TECN	COMMENT
• • • We do not use the following data for averages, fits, limits, etc. • • •			
102 \pm 2 to 99 \pm 2	³ HANSTEIN 96	DPWA	$\gamma N \rightarrow \pi N$
111.2 \pm 2.0 to 116.6 \pm 2.2	MIROSHNIC... 79		Fit photoproduction

REAL PART, $\Delta(1232)^0$

VALUE (MeV)	DOCUMENT ID	COMMENT
• • • We do not use the following data for averages, fits, limits, etc. • • •		
1213.20 \pm 0.66	BERNICHIA 96	Fit to PEDRONI 78

Baryon Particle Listings
Δ(1232)

-2xIMAGINARY PART, Δ(1232)0

Table with columns: VALUE (MeV), DOCUMENT ID, COMMENT. Includes data for BERNICHA 96 and a footnote about HOEHLER 93.

Δ(1232) ELASTIC POLE RESIDUES

ABSOLUTE VALUE, MIXED CHARGES

Table with columns: VALUE (MeV), DOCUMENT ID, TECN, COMMENT. Lists data for ARNDT, HOEHLER, CUTKOSKY, and ARNDT.

PHASE, MIXED CHARGES

Table with columns: VALUE (°), DOCUMENT ID, TECN, COMMENT. Lists phase values for ARNDT, HOEHLER, CUTKOSKY, and ARNDT.

Footnote: This ARNDT 95 value is in error, as pointed out by HOHLER 01. The corrected value is in line with the ARNDT 91 value (R.A. Arndt, private communication).

Δ(1232) DECAY MODES

The following branching fractions are our estimates, not fits or averages.

Table with columns: Mode, Fraction (Γj/Γ). Lists decay modes like Nπ, Nγ, and their branching fractions.

Δ(1232) BRANCHING RATIOS

Table with columns: Γ(Nπ)/Γtotal, DOCUMENT ID, TECN, COMMENT, Γ1/Γ. Lists branching ratios for ARNDT, MANLEY, CUTKOSKY, HOEHLER, ARNDT, PENNER, VRANA, and ARNDT.

Δ(1232) PHOTON DECAY AMPLITUDES

Papers on γN amplitudes predating 1981 may be found in our 2006 edition, Journal of Physics, G 33 1 (2006).

Δ(1232) → Nγ, helicity-1/2 amplitude A1/2

Table with columns: VALUE (GeV-1/2), DOCUMENT ID, TECN, COMMENT. Lists A1/2 values for DUGGER, AHRENS, ARNDT, BLANPIED, BECK, KAMALOV, HANSTEIN, ARNDT, DAVIDSON, ARNDT, DAVIDSON, CRAWFORD, AWAJI, DRECHSEL, PENNER, HANSTEIN, LI, DAVIDSON.

Δ(1232) → Nγ, helicity-3/2 amplitude A3/2

Table with columns: VALUE (GeV-1/2), DOCUMENT ID, TECN, COMMENT. Lists A3/2 values for DUGGER, AHRENS, ARNDT, BLANPIED, BECK, KAMALOV, HANSTEIN, ARNDT, DAVIDSON, ARNDT, DAVIDSON, CRAWFORD, AWAJI, DRECHSEL, PENNER, HANSTEIN, LI, DAVIDSON.

Δ(1232) → Nγ, E2/M1 ratio

Table with columns: VALUE, DOCUMENT ID, TECN, COMMENT. Lists E2/M1 ratios for AHRENS, ARNDT, BLANPIED, GALLER, BECK, HANSTEIN, ARNDT, DAVIDSON, DRECHSEL, PENNER, HANSTEIN, BECK, BLANPIED, KHANDAKER, WORKMAN, DAVIDSON, DAVIDSON, DAVIDSON, TANABE.

Δ(1232) → Nγ, absolute value of E2/M1 ratio at pole

Table with columns: VALUE, DOCUMENT ID, TECN, COMMENT. Lists absolute values for ARNDT and HANSTEIN.

Δ(1232) → Nγ, phase of E2/M1 ratio at pole

Table with columns: VALUE, DOCUMENT ID, TECN, COMMENT. Lists phase values for ARNDT and HANSTEIN.

Footnote: This ARNDT 97 value is very sensitive to the database being fitted. The result is from a fit to the full pion photoproduction database, apart from the BLANPIED 97 cross-section measurements.

Δ(1232) MAGNETIC MOMENTS

Δ(1232)++ MAGNETIC MOMENT

The values are extracted from UCLA and SIN data on π+p bremsstrahlung using a variety of different theoretical approximations and methods. Our estimate is only a rough guess of the range we expect the moment to lie within.

Table with columns: VALUE (μN), DOCUMENT ID, TECN, COMMENT. Lists magnetic moments for LOPEZCAST...01, BOSSHARD, LIN, LIN, WITTMAN, HELLER, NEFKENS.

Δ(1232)+ MAGNETIC MOMENT

Table with columns: VALUE (μN), DOCUMENT ID, COMMENT. Lists magnetic moments for KOTULLA and a footnote about systematic errors.

$\Delta(1600)$ BRANCHING RATIOS

$\Gamma(N\pi)/\Gamma_{total}$				Γ_1/Γ
VALUE	DOCUMENT ID	TECN	COMMENT	
0.10 to 0.25 OUR ESTIMATE				
0.12±0.02	MANLEY	92	IPWA	$\pi N \rightarrow \pi N$ & $N\pi\pi$
0.18±0.04	CUTKOSKY	80	IPWA	$\pi N \rightarrow \pi N$
0.21±0.06	HOEHLER	79	IPWA	$\pi N \rightarrow \pi N$
●●● We do not use the following data for averages, fits, limits, etc. ●●●				
0.10±0.03	HORN	08A	DPWA	Multichannel
0.13±0.01	PENNER	02C	DPWA	Multichannel
0.28±0.05	VRANA	00	DPWA	Multichannel

$(\Gamma_1\Gamma_f)^{1/2}/\Gamma_{total}$ in $N\pi \rightarrow \Delta(1600) \rightarrow \Sigma K$				$(\Gamma_1\Gamma_2)^{1/2}/\Gamma$
VALUE	DOCUMENT ID	TECN	COMMENT	
-0.36 to -0.28 OUR ESTIMATE				
●●● We do not use the following data for averages, fits, limits, etc. ●●●				
0.006 to 0.042	5 DEANS	75	DPWA	$\pi N \rightarrow \Sigma K$

Note: Signs of couplings from $\pi N \rightarrow N\pi\pi$ analyses were changed in the 1986 edition to agree with the baryon-first convention; the overall phase ambiguity is resolved by choosing a negative sign for the $\Delta(1620) S_{31}$ coupling to $\Delta(1232)\pi$.

$(\Gamma_1\Gamma_f)^{1/2}/\Gamma_{total}$ in $N\pi \rightarrow \Delta(1600) \rightarrow \Delta(1232)\pi, P\text{-wave}$				$(\Gamma_1\Gamma_5)^{1/2}/\Gamma$
VALUE	DOCUMENT ID	TECN	COMMENT	
+0.27 to +0.33 OUR ESTIMATE				
+0.29±0.02	MANLEY	92	IPWA	$\pi N \rightarrow \pi N$ & $N\pi\pi$
+0.24±0.05	BARNHAM	80	IPWA	$\pi N \rightarrow N\pi\pi$
+0.34	1,6 LONGACRE	77	IPWA	$\pi N \rightarrow N\pi\pi$
+0.30	2 LONGACRE	75	IPWA	$\pi N \rightarrow N\pi\pi$

$\Gamma(\Delta(1232)\pi, P\text{-wave})/\Gamma_{total}$				Γ_5/Γ
VALUE	DOCUMENT ID	TECN	COMMENT	
0.59±0.10	VRANA	00	DPWA	Multichannel

$(\Gamma_1\Gamma_f)^{1/2}/\Gamma_{total}$ in $N\pi \rightarrow \Delta(1600) \rightarrow \Delta(1232)\pi, F\text{-wave}$				$(\Gamma_1\Gamma_6)^{1/2}/\Gamma$
VALUE	DOCUMENT ID	TECN	COMMENT	
-0.15 to -0.03 OUR ESTIMATE				
-0.07	1,6 LONGACRE	77	IPWA	$\pi N \rightarrow N\pi\pi$

$(\Gamma_1\Gamma_f)^{1/2}/\Gamma_{total}$ in $N\pi \rightarrow \Delta(1600) \rightarrow N\rho, S=1/2, P\text{-wave}$				$(\Gamma_1\Gamma_8)^{1/2}/\Gamma$
VALUE	DOCUMENT ID	TECN	COMMENT	
+0.10				
+0.10	1,6 LONGACRE	77	IPWA	$\pi N \rightarrow N\pi\pi$

$(\Gamma_1\Gamma_f)^{1/2}/\Gamma_{total}$ in $N\pi \rightarrow \Delta(1600) \rightarrow N\rho, S=3/2, P\text{-wave}$				$(\Gamma_1\Gamma_9)^{1/2}/\Gamma$
VALUE	DOCUMENT ID	TECN	COMMENT	
+0.10				
+0.10	1,6 LONGACRE	77	IPWA	$\pi N \rightarrow N\pi\pi$

$(\Gamma_1\Gamma_f)^{1/2}/\Gamma_{total}$ in $N\pi \rightarrow \Delta(1600) \rightarrow N(1440)\pi, P\text{-wave}$				$(\Gamma_1\Gamma_{12})^{1/2}/\Gamma$
VALUE	DOCUMENT ID	TECN	COMMENT	
+0.15 to +0.23 OUR ESTIMATE				
+0.16±0.02	MANLEY	92	IPWA	$\pi N \rightarrow \pi N$ & $N\pi\pi$
+0.23±0.04	BARNHAM	80	IPWA	$\pi N \rightarrow N\pi\pi$

$\Gamma(N(1440)\pi)/\Gamma_{total}$				Γ_{11}/Γ
VALUE	DOCUMENT ID	TECN	COMMENT	
0.13±0.04	VRANA	00	DPWA	Multichannel

$\Delta(1600)$ PHOTON DECAY AMPLITUDES

Papers on γN amplitudes predating 1981 may be found in our 2006 edition, Journal of Physics, G **33** 1 (2006).

$\Delta(1600) \rightarrow N\gamma, \text{helicity-1/2 amplitude } A_{1/2}$

VALUE (GeV ^{-1/2})	DOCUMENT ID	TECN	COMMENT
-0.023±0.020 OUR ESTIMATE			
-0.018±0.015	ARNDT	96	IPWA $\gamma N \rightarrow \pi N$
-0.039±0.030	CRAWFORD	83	IPWA $\gamma N \rightarrow \pi N$
-0.046±0.013	AWAJI	81	DPWA $\gamma N \rightarrow \pi N$
●●● We do not use the following data for averages, fits, limits, etc. ●●●			
0.0	PENNER	02D	DPWA Multichannel
-0.026±0.002	LI	93	IPWA $\gamma N \rightarrow \pi N$
-0.200	7 WADA	84	DPWA Compton scattering
0.000±0.030	BARBOUR	78	DPWA $\gamma N \rightarrow \pi N$

$\Delta(1600) \rightarrow N\gamma, \text{helicity-3/2 amplitude } A_{3/2}$

VALUE (GeV ^{-1/2})	DOCUMENT ID	TECN	COMMENT
-0.009±0.021 OUR ESTIMATE			
-0.025±0.015	ARNDT	96	IPWA $\gamma N \rightarrow \pi N$
-0.013±0.014	CRAWFORD	83	IPWA $\gamma N \rightarrow \pi N$
0.025±0.031	AWAJI	81	DPWA $\gamma N \rightarrow \pi N$
●●● We do not use the following data for averages, fits, limits, etc. ●●●			
-0.024	PENNER	02D	DPWA Multichannel
-0.016±0.002	LI	93	IPWA $\gamma N \rightarrow \pi N$
0.023	WADA	84	DPWA Compton scattering
0.000±0.045	BARBOUR	78	DPWA $\gamma N \rightarrow \pi N$

$\Delta(1600)$ FOOTNOTES

- LONGACRE 77 pole positions are from a search for poles in the unitarized T-matrix; the first (second) value uses, in addition to $\pi N \rightarrow N\pi\pi$ data, elastic amplitudes from a Saclay (CERN) partial-wave analysis. The other LONGACRE 77 values are from eyeball fits with Breit-Wigner circles to the T-matrix amplitudes.
- From method II of LONGACRE 75: eyeball fits with Breit-Wigner circles to the T-matrix amplitudes.
- See HOEHLER 93 for a detailed discussion of the evidence for and the pole parameters of N and Δ resonances as determined from Argand diagrams of πN elastic partial-wave amplitudes and from plots of the speeds with which the amplitudes traverse the diagrams.
- LONGACRE 78 values are from a search for poles in the unitarized T-matrix. The first (second) value uses, in addition to $\pi N \rightarrow N\pi\pi$ data, elastic amplitudes from a Saclay (CERN) partial-wave analysis.
- The range given is from the four best solutions. DEANS 75 disagrees with $\pi^+ p \rightarrow \Sigma^+ K^+ K^+$ data of WINNIK 77 around 1920 MeV.
- LONGACRE 77 considers this coupling to be well determined.
- WADA 84 is inconsistent with other analyses — see the Note on N and Δ Resonances.

$\Delta(1600)$ REFERENCES

For early references, see Physics Letters **111B** 1 (1982).

HORN 08A	EPJ A38 173	I. Horn <i>et al.</i>	(CB-ELSA Collab.)
Also	PRL 101 202002	I. Horn <i>et al.</i>	(CB-ELSA Collab.)
ARNDT 06	PR C74 045205	R.A. Arndt <i>et al.</i>	(GWU)
PDG 06	JPG 33 1	W.-M. Yao <i>et al.</i>	(PDG Collab.)
PENNER 02C	PR C66 055211	G. Penner, U. Mosel	(GIES)
PENNER 02D	PR C66 055212	G. Penner, U. Mosel	(GIES)
VRANA 00	PRPL 328 181	T.P. Vrana, S.A. Dytman, T.-S.H. Lee	(PITT+)
ARNDT 96	PR C53 430	R.A. Arndt, I.I. Strakovsky, R.L. Workman	(VPI)
ARNDT 95	PR C52 2120	R.A. Arndt <i>et al.</i>	(VPI, BRCC)
HOEHLER 93	πN Newsletter 9 1	G. Hohlner	(KARL)
LI 93	PR C47 2759	Z.J. Li <i>et al.</i>	(VPI)
MANLEY 92	PR D45 4002	D.M. Manley, E.M. Saleski	(KEAT) IJP
Also	PR D30 904	D.M. Manley <i>et al.</i>	(VPI)
ARNDT 91	PR D43 2131	R.A. Arndt <i>et al.</i>	(VPI, TELE) IJP
WADA 84	NP B247 313	Y. Wada <i>et al.</i>	(INUS)
CRAWFORD 83	NP B211 1	R.L. Crawford, W.T. Morton	(GLAS)
PDG 82	PL 111B 1	M. Roos <i>et al.</i>	(HELS, CIT, CERN)
AWAJI 81	Bonn Conf. 352	N. Awaji, R. Kajikawa	(NAGO)
Also	NP B197 365	K. Fujii <i>et al.</i>	(NAGO)
BARNHAM 80	NP B168 243	K.W.J. Barnham <i>et al.</i>	(LOIC)
CUTKOSKY 80	Toronto Conf. 19	R.E. Cutkosky <i>et al.</i>	(CMU, LBL) IJP
Also	PR D20 2839	R.E. Cutkosky <i>et al.</i>	(CMU, LBL) IJP
HOEHLER 79	PDAT 12-1	G. Hohlner <i>et al.</i>	(KARL) IJP
Also	Toronto Conf. 3	R. Koch	(KARL) IJP
BARBOUR 78	NP B141 253	I.M. Barbour, R.L. Crawford, N.H. Parsons	(GLAS)
LONGACRE 78	PR D17 1795	R.S. Longacre <i>et al.</i>	(LBL, SLAC)
LONGACRE 77	NP B122 493	R.S. Longacre, J. Dolbeau	(SACL) IJP
Also	NP B108 365	J. Dolbeau <i>et al.</i>	(SACL) IJP
WINNIK 77	NP B128 66	M. Winnik <i>et al.</i>	(HAIF) I
DEANS 75	NP B96 90	S.R. Deans <i>et al.</i>	(SFLA, LAH) IJP
LONGACRE 75	PL 55B 415	R.S. Longacre <i>et al.</i>	(LBL, SLAC) IJP

$\Delta(1620) S_{31}$

$i(J^P) = \frac{3}{2}(\frac{1}{2}^-)$ Status: * * * *

Most of the results published before 1975 were last included in our 1982 edition, Physics Letters **111B** 1 (1982). Some further obsolete results published before 1984 were last included in our 2006 edition, Journal of Physics, G **33** 1 (2006).

$\Delta(1620)$ BREIT-WIGNER MASS

VALUE (MeV)	DOCUMENT ID	TECN	COMMENT
1600 to 1660 (\approx 1630) OUR ESTIMATE			
1615.2± 0.4	ARNDT	06	DPWA $\pi N \rightarrow \pi N, \eta N$
1672 ± 7	MANLEY	92	IPWA $\pi N \rightarrow \pi N$ & $N\pi\pi$
1620 ± 20	CUTKOSKY	80	IPWA $\pi N \rightarrow \pi N$
1610 ± 7	HOEHLER	79	IPWA $\pi N \rightarrow \pi N$
●●● We do not use the following data for averages, fits, limits, etc. ●●●			
1650 ± 25	THOMA	08	DPWA Multichannel
1614.1 ± 1.1	ARNDT	04	DPWA $\pi N \rightarrow \pi N, \eta N$
1612 ± 2	PENNER	02C	DPWA Multichannel
1617 ± 15	VRANA	00	DPWA Multichannel
1672 ± 5	ARNDT	96	IPWA $\gamma N \rightarrow \pi N$
1617	ARNDT	95	DPWA $\pi N \rightarrow N\pi$
1669	LI	93	IPWA $\gamma N \rightarrow \pi N$
1620	BARNHAM	80	IPWA $\pi N \rightarrow N\pi\pi$
1712.8± 6.0	1 CHEW	80	BPWA $\pi^+ p \rightarrow \pi^+ p$
1786.7± 2.0	1 CHEW	80	BPWA $\pi^+ p \rightarrow \pi^+ p$
1580	2 LONGACRE	77	IPWA $\pi N \rightarrow N\pi\pi$
1600	3 LONGACRE	75	IPWA $\pi N \rightarrow N\pi\pi$

Baryon Particle Listings

 $\Delta(1620)$ $\Delta(1620)$ BREIT-WIGNER WIDTH

VALUE (MeV)	DOCUMENT ID	TECN	COMMENT
135 to 150 (≈ 145) OUR ESTIMATE			
146.9 ± 1.9	ARNDT 06	DPWA	$\pi N \rightarrow \pi N, \eta N$
154 ± 37	MANLEY 92	IPWA	$\pi N \rightarrow \pi N \& N\pi\pi$
140 ± 20	CUTKOSKY 80	IPWA	$\pi N \rightarrow \pi N$
139 ± 18	HOEHLER 79	IPWA	$\pi N \rightarrow \pi N$
••• We do not use the following data for averages, fits, limits, etc. •••			
250 ± 60	THOMA 08	DPWA	Multichannel
141.0 ± 6.0	ARNDT 04	DPWA	$\pi N \rightarrow \pi N, \eta N$
202 ± 7	PENNER 02c	DPWA	Multichannel
143 ± 4.2	VRANA 00	DPWA	Multichannel
147 ± 8	ARNDT 96	IPWA	$\gamma N \rightarrow \pi N$
108	ARNDT 95	DPWA	$\pi N \rightarrow N\pi$
184	LI 93	IPWA	$\gamma N \rightarrow \pi N$
120	BARNHAM 80	IPWA	$\pi N \rightarrow N\pi\pi$
228.3 ± 18.0	¹ CHEW 80	BPWA	$\pi^+ p \rightarrow \pi^+ p$ (lower mass)
30.0 ± 6.4	¹ CHEW 80	BPWA	$\pi^+ p \rightarrow \pi^+ p$ (higher mass)
120	² LONGACRE 77	IPWA	$\pi N \rightarrow N\pi\pi$
150	³ LONGACRE 75	IPWA	$\pi N \rightarrow N\pi\pi$

 $\Delta(1620)$ POLE POSITION

REAL PART

VALUE (MeV)	DOCUMENT ID	TECN	COMMENT
1590 to 1610 (≈ 1600) OUR ESTIMATE			
1595	ARNDT 06	DPWA	$\pi N \rightarrow \pi N, \eta N$
1608	⁴ HOEHLER 93	SPED	$\pi N \rightarrow \pi N$
1600 ± 15	CUTKOSKY 80	IPWA	$\pi N \rightarrow \pi N$
••• We do not use the following data for averages, fits, limits, etc. •••			
1615 ± 25	THOMA 08	DPWA	Multichannel
1594	ARNDT 04	DPWA	$\pi N \rightarrow \pi N, \eta N$
1607	VRANA 00	DPWA	Multichannel
1585	ARNDT 95	DPWA	$\pi N \rightarrow N\pi$
1587	ARNDT 91	DPWA	$\pi N \rightarrow \pi N$ Soln SM90
1583 or 1583	⁵ LONGACRE 78	IPWA	$\pi N \rightarrow N\pi\pi$
1575 or 1572	² LONGACRE 77	IPWA	$\pi N \rightarrow N\pi\pi$

-2xIMAGINARY PART

VALUE (MeV)	DOCUMENT ID	TECN	COMMENT
115 to 120 (≈ 118) OUR ESTIMATE			
135	ARNDT 06	DPWA	$\pi N \rightarrow \pi N, \eta N$
116	⁴ HOEHLER 93	SPED	$\pi N \rightarrow \pi N$
120 ± 20	CUTKOSKY 80	IPWA	$\pi N \rightarrow \pi N$
••• We do not use the following data for averages, fits, limits, etc. •••			
180 ± 35	THOMA 08	DPWA	Multichannel
118	ARNDT 04	DPWA	$\pi N \rightarrow \pi N, \eta N$
148	VRANA 00	DPWA	Multichannel
104	ARNDT 95	DPWA	$\pi N \rightarrow N\pi$
120	ARNDT 91	DPWA	$\pi N \rightarrow \pi N$ Soln SM90
143 or 149	⁵ LONGACRE 78	IPWA	$\pi N \rightarrow N\pi\pi$
119 or 128	² LONGACRE 77	IPWA	$\pi N \rightarrow N\pi\pi$

 $\Delta(1620)$ ELASTIC POLE RESIDUEMODULUS $|r|$

VALUE (MeV)	DOCUMENT ID	TECN	COMMENT
15	ARNDT 06	DPWA	$\pi N \rightarrow \pi N, \eta N$
19	HOEHLER 93	SPED	$\pi N \rightarrow \pi N$
15 ± 2	CUTKOSKY 80	IPWA	$\pi N \rightarrow \pi N$
••• We do not use the following data for averages, fits, limits, etc. •••			
17	ARNDT 04	DPWA	$\pi N \rightarrow \pi N, \eta N$
14	ARNDT 95	DPWA	$\pi N \rightarrow N\pi$
15	ARNDT 91	DPWA	$\pi N \rightarrow \pi N$ Soln SM90

PHASE θ

VALUE ($^\circ$)	DOCUMENT ID	TECN	COMMENT
-92	ARNDT 06	DPWA	$\pi N \rightarrow \pi N, \eta N$
-95	HOEHLER 93	SPED	$\pi N \rightarrow \pi N$
-110 ± 20	CUTKOSKY 80	IPWA	$\pi N \rightarrow \pi N$
••• We do not use the following data for averages, fits, limits, etc. •••			
-104	ARNDT 04	DPWA	$\pi N \rightarrow \pi N, \eta N$
-121	ARNDT 95	DPWA	$\pi N \rightarrow N\pi$
-125	ARNDT 91	DPWA	$\pi N \rightarrow \pi N$ Soln SM90

 $\Delta(1620)$ DECAY MODES

The following branching fractions are our estimates, not fits or averages.

Mode	Fraction (Γ_i/Γ)
Γ_1 $N\pi$	20-30 %
Γ_2 $N\pi\pi$	70-80 %
Γ_3 $\Delta\pi$	30-60 %
Γ_4 $\Delta(1232)\pi, D\text{-wave}$	
Γ_5 $N\rho$	7-25 %
Γ_6 $N\rho, S=1/2, S\text{-wave}$	
Γ_7 $N\rho, S=3/2, D\text{-wave}$	
Γ_8 $N(1440)\pi$	
Γ_9 $N\gamma$	0.004-0.044 %
Γ_{10} $N\gamma, \text{helicity}=1/2$	0.004-0.044 %

 $\Delta(1620)$ BRANCHING RATIOS

$\Gamma(N\pi)/\Gamma_{\text{total}}$	DOCUMENT ID	TECN	COMMENT	Γ_1/Γ
0.2 to 0.3 OUR ESTIMATE				
0.315 ± 0.001	ARNDT 06	DPWA	$\pi N \rightarrow \pi N, \eta N$	
0.09 ± 0.02	MANLEY 92	IPWA	$\pi N \rightarrow \pi N \& N\pi\pi$	
0.25 ± 0.03	CUTKOSKY 80	IPWA	$\pi N \rightarrow \pi N$	
0.35 ± 0.06	HOEHLER 79	IPWA	$\pi N \rightarrow \pi N$	
••• We do not use the following data for averages, fits, limits, etc. •••				
0.22 ± 0.12	THOMA 08	DPWA	Multichannel	
0.310 ± 0.004	ARNDT 04	DPWA	$\pi N \rightarrow \pi N, \eta N$	
0.34 ± 0.01	PENNER 02c	DPWA	Multichannel	
0.45 ± 0.05	VRANA 00	DPWA	Multichannel	
0.29	ARNDT 95	DPWA	$\pi N \rightarrow N\pi$	
0.60	¹ CHEW 80	BPWA	$\pi^+ p \rightarrow \pi^+ p$ (lower mass)	
0.36	¹ CHEW 80	BPWA	$\pi^+ p \rightarrow \pi^+ p$ (higher mass)	

Note: Signs of couplings from $\pi N \rightarrow N\pi\pi$ analyses were changed in the 1986 edition to agree with the baryon-first convention; the overall phase ambiguity is resolved by choosing a negative sign for the $\Delta(1620) S_{31}$ coupling to $\Delta(1232)\pi$.

$(\Gamma_1\Gamma_7)^{1/2}/\Gamma_{\text{total}}$ in $N\pi \rightarrow \Delta(1620) \rightarrow \Delta(1232)\pi, D\text{-wave}$	DOCUMENT ID	TECN	COMMENT	$(\Gamma_1\Gamma_4)^{1/2}/\Gamma$
0.36 to -0.28 OUR ESTIMATE				
-0.24 ± 0.03	MANLEY 92	IPWA	$\pi N \rightarrow \pi N \& N\pi\pi$	
-0.33 ± 0.06	BARNHAM 80	IPWA	$\pi N \rightarrow N\pi\pi$	
-0.39	^{2,6} LONGACRE 77	IPWA	$\pi N \rightarrow N\pi\pi$	
-0.40	³ LONGACRE 75	IPWA	$\pi N \rightarrow N\pi\pi$	

$\Gamma(\Delta(1232)\pi, D\text{-wave})/\Gamma_{\text{total}}$	DOCUMENT ID	TECN	COMMENT	Γ_4/Γ
0.39 ± 0.02				
0.39 ± 0.02	VRANA 00	DPWA	Multichannel	
••• We do not use the following data for averages, fits, limits, etc. •••				
0.48 ± 0.25	THOMA 08	DPWA	Multichannel	

$(\Gamma_1\Gamma_7)^{1/2}/\Gamma_{\text{total}}$ in $N\pi \rightarrow \Delta(1620) \rightarrow N\rho, S=1/2, S\text{-wave}$	DOCUMENT ID	TECN	COMMENT	$(\Gamma_1\Gamma_6)^{1/2}/\Gamma$
+0.12 to +0.22 OUR ESTIMATE				
+0.15 ± 0.02	MANLEY 92	IPWA	$\pi N \rightarrow \pi N \& N\pi\pi$	
+0.40 ± 0.10	BARNHAM 80	IPWA	$\pi N \rightarrow N\pi\pi$	
+0.08	^{2,6} LONGACRE 77	IPWA	$\pi N \rightarrow N\pi\pi$	
+0.28	³ LONGACRE 75	IPWA	$\pi N \rightarrow N\pi\pi$	

$\Gamma(N\rho, S=1/2, S\text{-wave})/\Gamma_{\text{total}}$	DOCUMENT ID	TECN	COMMENT	Γ_6/Γ
0.14 ± 0.03				
0.14 ± 0.03	VRANA 00	DPWA	Multichannel	

$(\Gamma_1\Gamma_7)^{1/2}/\Gamma_{\text{total}}$ in $N\pi \rightarrow \Delta(1620) \rightarrow N\rho, S=3/2, D\text{-wave}$	DOCUMENT ID	TECN	COMMENT	$(\Gamma_1\Gamma_7)^{1/2}/\Gamma$
-0.15 to -0.03 OUR ESTIMATE				
-0.06 ± 0.02	MANLEY 92	IPWA	$\pi N \rightarrow \pi N \& N\pi\pi$	
-0.13	^{2,6} LONGACRE 77	IPWA	$\pi N \rightarrow N\pi\pi$	

$\Gamma(N\rho, S=3/2, D\text{-wave})/\Gamma_{\text{total}}$	DOCUMENT ID	TECN	COMMENT	Γ_7/Γ
0.02 ± 0.01				
0.02 ± 0.01	VRANA 00	DPWA	Multichannel	

$(\Gamma_1\Gamma_8)^{1/2}/\Gamma_{\text{total}}$ in $N\pi \rightarrow \Delta(1620) \rightarrow N(1440)\pi$	DOCUMENT ID	TECN	COMMENT	$(\Gamma_1\Gamma_8)^{1/2}/\Gamma$
0.11 ± 0.05				
0.11 ± 0.05	BARNHAM 80	IPWA	$\pi N \rightarrow N\pi\pi$	

See key on page 405

Baryon Particle Listings

$\Delta(1620)$, $\Delta(1700)$

$\Gamma(N(1440)\pi)/\Gamma_{\text{total}}$	DOCUMENT ID	TECN	COMMENT	Γ_B/Γ
0.00±0.01	VRANA	00	DPWA Multichannel	
0.19±0.12	THOMA	08	DPWA Multichannel	

$\Delta(1620)$ PHOTON DECAY AMPLITUDES

Papers on γN amplitudes predating 1981 may be found in our 2006 edition, Journal of Physics, G **33** 1 (2006).

$\Delta(1620) \rightarrow N\gamma$, helicity-1/2 amplitude $A_{1/2}$	DOCUMENT ID	TECN	COMMENT
+0.027±0.011 OUR ESTIMATE			
0.050±0.002	DUGGER	07	DPWA $\gamma N \rightarrow \pi N$
0.035±0.020	ARNDT	96	IPWA $\gamma N \rightarrow \pi N$
0.035±0.010	CRAWFORD	83	IPWA $\gamma N \rightarrow \pi N$
0.010±0.015	AWAJI	81	DPWA $\gamma N \rightarrow \pi N$
••• We do not use the following data for averages, fits, limits, etc. •••			
0.066	DRECHSEL	07	DPWA $\gamma N \rightarrow \pi N$
-0.050	PENNER	02D	DPWA Multichannel
0.042±0.003	LI	93	IPWA $\gamma N \rightarrow \pi N$
0.066	WADA	84	DPWA Compton scattering

$\Delta(1620)$ FOOTNOTES

- ¹ CHEW 80 reports two S_{31} resonances at somewhat higher masses than other analyses. Problems with this analysis are discussed in section 2.1.11 of HOEHLER 83.
- ² LONGACRE 77 pole positions are from a search for poles in the unitarized T-matrix; the first (second) value uses, in addition to $\pi N \rightarrow N\pi\pi$ data, elastic amplitudes from a Saclay (CERN) partial-wave analysis. The other LONGACRE 77 values are from eyeball fits with Breit-Wigner circles to the T-matrix amplitudes.
- ³ From method II of LONGACRE 75: eyeball fits with Breit-Wigner circles to the T-matrix amplitudes.
- ⁴ See HOEHLER 93 for a detailed discussion of the evidence for and the pole parameters of N and Δ resonances as determined from Argand diagrams of πN elastic partial-wave amplitudes and from plots of the speeds with which the amplitudes traverse the diagrams.
- ⁵ LONGACRE 78 values are from a search for poles in the unitarized T-matrix. The first (second) value uses, in addition to $\pi N \rightarrow N\pi\pi$ data, elastic amplitudes from a Saclay (CERN) partial-wave analysis.
- ⁶ LONGACRE 77 considers this coupling to be well determined.

$\Delta(1620)$ REFERENCES

For early references, see Physics Letters **111B** 1 (1982).

THOMA	08	PL B659 87	U. Thoma <i>et al.</i>	(CB-ELSA Collab.)
DRECHSEL	07	EPJ A34 69	D. Drechsel, S.S. Kamalov, L. Tiator	(MAINZ, JINR)
DUGGER	07	PR C76 025211	M. Dugger <i>et al.</i>	(Jefferson Lab CLAS Collab.)
ARNDT	06	PR C74 045205	R.A. Arndt <i>et al.</i>	(GWU)
PDG	06	JPG 33 1	W.-M. Yao <i>et al.</i>	(PDG Collab.)
ARNDT	04	PR C69 035213	R.A. Arndt <i>et al.</i>	(GWU, TRIU)
PENNER	02C	PR C66 055211	G. Penner, U. Mosel	(GIES)
PENNER	02D	PR C66 055212	G. Penner, U. Mosel	(GIES)
VRANA	00	PR PL 326 181	T.P. Vrana, S.A. Dytman, T.-S.H. Lee	(PITT+)
ARNDT	96	PR C53 4930	R.A. Arndt, I.I. Strakovsky, R.L. Workman	(VPI)
ARNDT	95	PR C52 2120	R.A. Arndt <i>et al.</i>	(VPI, BRCC)
HOEHLER	93	πN Newsletter 9 1	G. Hohler	(KARL)
LI	93	PR C47 2759	Z.J. Li <i>et al.</i>	(VPI)
MANLEY	92	PR D45 4002	D.M. Manley, E.M. Saleski	(KENT) IJP
Also		PR D30 904	D.M. Manley <i>et al.</i>	(VPI)
ARNDT	91	PR D43 2131	R.A. Arndt <i>et al.</i>	(VPI, TELE) IJP
WADA	84	NP B247 313	Y. Wada <i>et al.</i>	(INUS)
CRAWFORD	83	NP B211 1	R.L. Crawford, W.T. Morton	(GLAS)
HOEHLER	83	Landoth-Boernstein 1/982	G. Hohler	(KARLT)
PDG	82	PL 111B 1	M. Roos <i>et al.</i>	(HELS, CIT, CERN)
AWAJI	81	Bonn Conf. 352	N. Awaji, R. Kajikawa	(NAGO)
Also		NP B197 365	K. Fujii <i>et al.</i>	(NAGO)
BARNHAM	80	NP B168 243	K.W.J. Barnham <i>et al.</i>	(LOIC)
CHEW	80	Toronto Conf. 123	D.M. Chew	(LBL) IJP
CUTKOSKY	80	Toronto Conf. 19	R.E. Cutkosky <i>et al.</i>	(CMU, LBL) IJP
Also		PR D20 2839	R.E. Cutkosky <i>et al.</i>	(CMU, LBL) IJP
HOEHLER	79	PDAT 12-1	G. Hohler <i>et al.</i>	(KARLT) IJP
Also		Toronto Conf. 3	R. Koch	(KARLT) IJP
LONGACRE	78	PR D17 1795	R.S. Longacre <i>et al.</i>	(LBL, SLAC)
LONGACRE	77	NP B122 493	R.S. Longacre, J. Dolbeau	(SACL) IJP
Also		NP B108 365	J. Dolbeau <i>et al.</i>	(SACL) IJP
LONGACRE	75	PL 55B 415	R.S. Longacre <i>et al.</i>	(LBL, SLAC) IJP

$\Delta(1700) D_{33}$

 $I(J^P) = \frac{3}{2}(\frac{3}{2}^-)$ Status: * * * *

Most of the results published before 1975 were last included in our 1982 edition, Physics Letters **111B** 1 (1982). Some further obsolete results published before 1984 were last included in our 2006 edition, Journal of Physics, G **33** 1 (2006).

$\Delta(1700)$ BREIT-WIGNER MASS

VALUE (MeV)	DOCUMENT ID	TECN	COMMENT
1670 to 1750 (≈ 1700) OUR ESTIMATE			
1695.0±1.3	ARNDT	06	DPWA $\pi N \rightarrow \pi N, \eta N$
1762 ±44	MANLEY	92	IPWA $\pi N \rightarrow \pi N \& N\pi\pi$
1710 ±30	CUTKOSKY	80	IPWA $\pi N \rightarrow \pi N$
1680 ±70	HOEHLER	79	IPWA $\pi N \rightarrow \pi N$

••• We do not use the following data for averages, fits, limits, etc. •••

1790 ±30	HORN	08A	DPWA Multichannel
1770 ±40	THOMA	08	DPWA Multichannel
1687.9±2.5	ARNDT	04	DPWA $\pi N \rightarrow \pi N, \eta N$
1678 ±1	PENNER	02C	DPWA Multichannel
1732 ±23	VRANA	00	DPWA Multichannel
1690 ±15	ARNDT	96	IPWA $\gamma N \rightarrow \pi N$
1680	ARNDT	95	DPWA $\pi N \rightarrow N\pi$
1655	LI	93	IPWA $\gamma N \rightarrow \pi N$
1650	BARNHAM	80	IPWA $\pi N \rightarrow N\pi\pi$
1718.4 $^{+13.1}_{-13.0}$	¹ CHEW	80	BPWA $\pi^+ p \rightarrow \pi^+ p$
1600	² LONGACRE	77	IPWA $\pi N \rightarrow N\pi\pi$
1680	³ LONGACRE	75	IPWA $\pi N \rightarrow N\pi\pi$

$\Delta(1700)$ BREIT-WIGNER WIDTH

VALUE (MeV)	DOCUMENT ID	TECN	COMMENT
200 to 400 (≈ 300) OUR ESTIMATE			
375.5±7.0	ARNDT	06	DPWA $\pi N \rightarrow \pi N, \eta N$
600 ±250	MANLEY	92	IPWA $\pi N \rightarrow \pi N \& N\pi\pi$
280 ±80	CUTKOSKY	80	IPWA $\pi N \rightarrow \pi N$
230 ±80	HOEHLER	79	IPWA $\pi N \rightarrow \pi N$
••• We do not use the following data for averages, fits, limits, etc. •••			
580 ±60	HORN	08A	DPWA Multichannel
630 ±150	THOMA	08	DPWA Multichannel
364.8±16.6	ARNDT	04	DPWA $\pi N \rightarrow \pi N, \eta N$
606 ±15	PENNER	02C	DPWA Multichannel
119 ±70	VRANA	00	DPWA Multichannel
285 ±20	ARNDT	96	IPWA $\gamma N \rightarrow \pi N$
272	ARNDT	95	DPWA $\pi N \rightarrow N\pi$
348	LI	93	IPWA $\gamma N \rightarrow \pi N$
160	BARNHAM	80	IPWA $\pi N \rightarrow N\pi\pi$
193.3±26.0	¹ CHEW	80	BPWA $\pi^+ p \rightarrow \pi^+ p$
200	² LONGACRE	77	IPWA $\pi N \rightarrow N\pi\pi$
240	³ LONGACRE	75	IPWA $\pi N \rightarrow N\pi\pi$

$\Delta(1700)$ POLE POSITION

VALUE (MeV)	DOCUMENT ID	TECN	COMMENT
1620 to 1680 (≈ 1650) OUR ESTIMATE			
1632	ARNDT	06	DPWA $\pi N \rightarrow \pi N, \eta N$
1651	⁴ HOEHLER	93	SPED $\pi N \rightarrow \pi N$
1675±25	CUTKOSKY	80	IPWA $\pi N \rightarrow \pi N$
••• We do not use the following data for averages, fits, limits, etc. •••			
1640±25	HORN	08A	DPWA Multichannel
1610±35	THOMA	08	DPWA Multichannel
1617	ARNDT	04	DPWA $\pi N \rightarrow \pi N, \eta N$
1726	VRANA	00	DPWA Multichannel
1655	ARNDT	95	DPWA $\pi N \rightarrow N\pi$
1646	ARNDT	91	DPWA $\pi N \rightarrow \pi N$ Soln SM90
1681 or 1672	⁵ LONGACRE	78	IPWA $\pi N \rightarrow N\pi\pi$
1600 or 1594	² LONGACRE	77	IPWA $\pi N \rightarrow N\pi\pi$

-2xIMAGINARY PART

VALUE (MeV)	DOCUMENT ID	TECN	COMMENT
160 to 240 (≈ 200) OUR ESTIMATE			
253	ARNDT	06	DPWA $\pi N \rightarrow \pi N, \eta N$
159	⁴ HOEHLER	93	SPED $\pi N \rightarrow \pi N$
220±40	CUTKOSKY	80	IPWA $\pi N \rightarrow \pi N$
••• We do not use the following data for averages, fits, limits, etc. •••			
325±35	HORN	08A	DPWA Multichannel
320±60	THOMA	08	DPWA Multichannel
226	ARNDT	04	DPWA $\pi N \rightarrow \pi N, \eta N$
118	VRANA	00	DPWA Multichannel
242	ARNDT	95	DPWA $\pi N \rightarrow N\pi$
208	ARNDT	91	DPWA $\pi N \rightarrow \pi N$ Soln SM90
245 or 241	⁵ LONGACRE	78	IPWA $\pi N \rightarrow N\pi\pi$
208 or 201	² LONGACRE	77	IPWA $\pi N \rightarrow N\pi\pi$

$\Delta(1700)$ ELASTIC POLE RESIDUE

VALUE (MeV)	DOCUMENT ID	TECN	COMMENT
18	ARNDT	06	DPWA $\pi N \rightarrow \pi N, \eta N$
10	HOEHLER	93	SPED $\pi N \rightarrow \pi N$
13±3	CUTKOSKY	80	IPWA $\pi N \rightarrow \pi N$
••• We do not use the following data for averages, fits, limits, etc. •••			
16	ARNDT	04	DPWA $\pi N \rightarrow \pi N, \eta N$
16	ARNDT	95	DPWA $\pi N \rightarrow N\pi$
13	ARNDT	91	DPWA $\pi N \rightarrow \pi N$ Soln SM90

Baryon Particle Listings

 $\Delta(1700)$ PHASE θ

VALUE ($^\circ$)	DOCUMENT ID	TECN	COMMENT
-40	ARNDT 06	DPWA	$\pi N \rightarrow \pi N, \eta N$
-20 \pm 25	CUTKOSKY 80	IPWA	$\pi N \rightarrow \pi N$
• • • We do not use the following data for averages, fits, limits, etc. • • •			
-47	ARNDT 04	DPWA	$\pi N \rightarrow \pi N, \eta N$
-12	ARNDT 95	DPWA	$\pi N \rightarrow N\pi$
-22	ARNDT 91	DPWA	$\pi N \rightarrow \pi N$ Soln SM90

 $\Delta(1700)$ DECAY MODES

The following branching fractions are our estimates, not fits or averages.

Mode	Fraction (Γ_i/Γ)
Γ_1 $N\pi$	10–20 %
Γ_2 ΣK	
Γ_3 $N\pi\pi$	80–90 %
Γ_4 $\Delta\pi$	30–60 %
Γ_5 $\Delta(1232)\pi, S$ -wave	25–50 %
Γ_6 $\Delta(1232)\pi, D$ -wave	1–7 %
Γ_7 $N\rho$	30–55 %
Γ_8 $N\rho, S=1/2, D$ -wave	
Γ_9 $N\rho, S=3/2, S$ -wave	5–20 %
Γ_{10} $N\rho, S=3/2, D$ -wave	
Γ_{11} $N(1535)\pi$	
Γ_{12} $\Delta(1232)\eta$	
Γ_{13} $N\gamma$	0.12–0.26 %
Γ_{14} $N\gamma, \text{helicity}=1/2$	0.08–0.16 %
Γ_{15} $N\gamma, \text{helicity}=3/2$	0.025–0.12 %

 $\Delta(1700)$ BRANCHING RATIOS

$\Gamma(N\pi)/\Gamma_{\text{total}}$	DOCUMENT ID	TECN	COMMENT	Γ_1/Γ
0.10 to 0.20 OUR ESTIMATE				
0.156 \pm 0.001	ARNDT 06	DPWA	$\pi N \rightarrow \pi N, \eta N$	
0.14 \pm 0.06	MANLEY 92	IPWA	$\pi N \rightarrow \pi N$ & $N\pi\pi$	
0.12 \pm 0.03	CUTKOSKY 80	IPWA	$\pi N \rightarrow \pi N$	
0.20 \pm 0.03	HOEHLER 79	IPWA	$\pi N \rightarrow \pi N$	
• • • We do not use the following data for averages, fits, limits, etc. • • •				
0.20 \pm 0.07	HORN 08A	DPWA	Multichannel	
0.15 \pm 0.08	THOMA 08	DPWA	Multichannel	
0.150 \pm 0.001	ARNDT 04	DPWA	$\pi N \rightarrow \pi N, \eta N$	
0.14 \pm 0.01	PENNER 02C	DPWA	Multichannel	
0.05 \pm 0.01	VRANA 00	DPWA	Multichannel	
0.16	ARNDT 95	DPWA	$\pi N \rightarrow N\pi$	
0.16	¹ CHEW 80	BPWA	$\pi^+ p \rightarrow \pi^+ p$	

Note: Signs of couplings from $\pi N \rightarrow N\pi\pi$ analyses were changed in the 1986 edition to agree with the baryon-first convention; the overall phase ambiguity is resolved by choosing a negative sign for the $\Delta(1620) S_{31}$ coupling to $\Delta(1232)\pi$.

$(\Gamma_i\Gamma_f)^{1/2}/\Gamma_{\text{total}}$ in $N\pi \rightarrow \Delta(1700) \rightarrow \Delta(1232)\pi, S$ -wave	DOCUMENT ID	TECN	COMMENT	$(\Gamma_1\Gamma_5)^{1/2}/\Gamma$
+0.21 to +0.29 OUR ESTIMATE				
+0.32 \pm 0.06	MANLEY 92	IPWA	$\pi N \rightarrow \pi N$ & $N\pi\pi$	
+0.18 \pm 0.04	BARNHAM 80	IPWA	$\pi N \rightarrow N\pi\pi$	
+0.30	^{2,6} LONGACRE 77	IPWA	$\pi N \rightarrow N\pi\pi$	
+0.24	³ LONGACRE 75	IPWA	$\pi N \rightarrow N\pi\pi$	

$\Gamma(\Delta(1232)\pi, S\text{-wave})/\Gamma_{\text{total}}$	DOCUMENT ID	TECN	COMMENT	Γ_5/Γ
0.90 \pm 0.02	VRANA 00	DPWA	Multichannel	

$(\Gamma_i\Gamma_f)^{1/2}/\Gamma_{\text{total}}$ in $N\pi \rightarrow \Delta(1700) \rightarrow \Delta(1232)\pi, D$ -wave	DOCUMENT ID	TECN	COMMENT	$(\Gamma_1\Gamma_6)^{1/2}/\Gamma$
+0.05 to +0.11 OUR ESTIMATE				
+0.08 \pm 0.03	MANLEY 92	IPWA	$\pi N \rightarrow \pi N$ & $N\pi\pi$	
0.14 \pm 0.04	BARNHAM 80	IPWA	$\pi N \rightarrow N\pi\pi$	
+0.05	^{2,6} LONGACRE 77	IPWA	$\pi N \rightarrow N\pi\pi$	
+0.10	³ LONGACRE 75	IPWA	$\pi N \rightarrow N\pi\pi$	

$\Gamma(\Delta(1232)\pi, D\text{-wave})/\Gamma_{\text{total}}$	DOCUMENT ID	TECN	COMMENT	Γ_6/Γ
0.04 \pm 0.01	VRANA 00	DPWA	Multichannel	

$(\Gamma_i\Gamma_f)^{1/2}/\Gamma_{\text{total}}$ in $N\pi \rightarrow \Delta(1700) \rightarrow N\rho, S=1/2, D$ -wave	DOCUMENT ID	TECN	COMMENT	$(\Gamma_1\Gamma_8)^{1/2}/\Gamma$
+0.17 \pm 0.05	BARNHAM 80	IPWA	$\pi N \rightarrow N\pi\pi$	

$(\Gamma_i\Gamma_f)^{1/2}/\Gamma_{\text{total}}$ in $N\pi \rightarrow \Delta(1700) \rightarrow N\rho, S=3/2, S$ -wave	DOCUMENT ID	TECN	COMMENT	$(\Gamma_1\Gamma_9)^{1/2}/\Gamma$
± 0.11 to ± 0.19 OUR ESTIMATE				
+0.10 \pm 0.03	MANLEY 92	IPWA	$\pi N \rightarrow \pi N$ & $N\pi\pi$	
+0.04	^{2,6} LONGACRE 77	IPWA	$\pi N \rightarrow N\pi\pi$	
-0.30	³ LONGACRE 75	IPWA	$\pi N \rightarrow N\pi\pi$	

$\Gamma(N\rho, S=3/2, S\text{-wave})/\Gamma_{\text{total}}$	DOCUMENT ID	TECN	COMMENT	Γ_9/Γ
0.01 \pm 0.01	VRANA 00	DPWA	Multichannel	

$(\Gamma_i\Gamma_f)^{1/2}/\Gamma_{\text{total}}$ in $N\pi \rightarrow \Delta(1700) \rightarrow N\rho, S=3/2, D$ -wave	DOCUMENT ID	TECN	COMMENT	$(\Gamma_1\Gamma_{10})^{1/2}/\Gamma$
0.18 \pm 0.07	BARNHAM 80	IPWA	$\pi N \rightarrow N\pi\pi$	

$\Gamma(N(1535)\pi)/\Gamma_{\text{total}}$	DOCUMENT ID	TECN	COMMENT	Γ_{11}/Γ
0.04 \pm 0.02	HORN 08A	DPWA	Multichannel	
• • • We do not use the following data for averages, fits, limits, etc. • • •				

$\Gamma(\Delta(1232)\eta)/\Gamma_{\text{total}}$	DOCUMENT ID	TECN	COMMENT	Γ_{12}/Γ
0.02 \pm 0.01	HORN 08A	DPWA	Multichannel	
• • • We do not use the following data for averages, fits, limits, etc. • • •				

$\Gamma(N(1535)\pi)/\Gamma(\Delta(1232)\eta)$	DOCUMENT ID	TECN	COMMENT	Γ_{11}/Γ_{12}
0.67	KASHEVAROV 09	CBAL	$\gamma p \rightarrow p\pi^0\eta$	
• • • We do not use the following data for averages, fits, limits, etc. • • •				

 $\Delta(1700)$ PHOTON DECAY AMPLITUDES

Papers on γN amplitudes predating 1981 may be found in our 2006 edition, Journal of Physics, G 33 1 (2006).

 $\Delta(1700) \rightarrow N\gamma, \text{helicity}=1/2$ amplitude $A_{1/2}$

VALUE ($\text{GeV}^{-1/2}$)	DOCUMENT ID	TECN	COMMENT
+0.104 \pm 0.015 OUR ESTIMATE			
0.125 \pm 0.003	DUGGER 07	DPWA	$\gamma N \rightarrow \pi N$
0.090 \pm 0.025	ARNDT 96	IPWA	$\gamma N \rightarrow \pi N$
0.111 \pm 0.017	CRAWFORD 83	IPWA	$\gamma N \rightarrow \pi N$
0.089 \pm 0.033	AWAJI 81	DPWA	$\gamma N \rightarrow \pi N$
• • • We do not use the following data for averages, fits, limits, etc. • • •			
0.160 \pm 0.040	HORN 08A	DPWA	Multichannel
0.226	DRECHSEL 07	DPWA	$\gamma N \rightarrow \pi N$
0.096	PENNER 02D	DPWA	Multichannel
0.121 \pm 0.004	LI 93	IPWA	$\gamma N \rightarrow \pi N$

 $\Delta(1700) \rightarrow N\gamma, \text{helicity}=3/2$ amplitude $A_{3/2}$

VALUE ($\text{GeV}^{-1/2}$)	DOCUMENT ID	TECN	COMMENT
+0.085 \pm 0.022 OUR ESTIMATE			
0.105 \pm 0.003	DUGGER 07	DPWA	$\gamma N \rightarrow \pi N$
0.097 \pm 0.020	ARNDT 96	IPWA	$\gamma N \rightarrow \pi N$
0.107 \pm 0.015	CRAWFORD 83	IPWA	$\gamma N \rightarrow \pi N$
0.060 \pm 0.015	AWAJI 81	DPWA	$\gamma N \rightarrow \pi N$
• • • We do not use the following data for averages, fits, limits, etc. • • •			
0.150 \pm 0.030	HORN 08A	DPWA	Multichannel
0.210	DRECHSEL 07	DPWA	$\gamma N \rightarrow \pi N$
0.154	PENNER 02D	DPWA	Multichannel
0.115 \pm 0.004	LI 93	IPWA	$\gamma N \rightarrow \pi N$

 $\Delta(1700)$ FOOTNOTES

- Problems with CHEW 80 are discussed in section 2.1.11 of HOEHLER 83.
- LONGACRE 77 pole positions are from a search for poles in the unitarized T-matrix; the first (second) value uses, in addition to $\pi N \rightarrow N\pi\pi$ data, elastic amplitudes from a Saclay (CERN) partial-wave analysis. The other LONGACRE 77 values are from eyeball fits with Breit-Wigner circles to the T-matrix amplitudes.
- From method II of LONGACRE 75: eyeball fits with Breit-Wigner circles to the T-matrix amplitudes.
- See HOEHLER 93 for a detailed discussion of the evidence for and the pole parameters of N and Δ resonances as determined from Argand diagrams of πN elastic partial-wave amplitudes and from plots of the speeds with which the amplitudes traverse the diagrams.
- LONGACRE 78 values are from a search for poles in the unitarized T-matrix. The first (second) value uses, in addition to $\pi N \rightarrow N\pi\pi$ data, elastic amplitudes from a Saclay (CERN) partial-wave analysis.
- LONGACRE 77 considers this coupling to be well determined.

See key on page 405

Baryon Particle Listings

$\Delta(1700)$, $\Delta(1750)$, $\Delta(1900)$

$\Delta(1700)$ REFERENCES

For early references, see Physics Letters **111B** 1 (1982).

KASHEVAROV 09	EPJ A42 141	V.L. Kashevarov et al.	(MAMI Crystal Ball/TAPS)
HORN 08A	EPJ A38 173	I. Horn et al.	(CB-ELSA Collab.)
Also	PRL 101 202002	I. Horn et al.	(CB-ELSA Collab.)
THOMA 08	PL B659 67	U. Thoma et al.	(CB-ELSA Collab.)
DRECHSEL 07	EPJ A34 69	D. Drechsel, S.S. Kamalov, L. Tiator	(MAIN Z. JINR)
DUGGER 07	PR C76 025211	M. Dugger et al.	(Jefferson Lab CLAS Collab.)
ARNDT 06	PR C74 045205	R.A. Arndt et al.	(GWU)
PDG 06	JPG 33 1	W.-M. Yao et al.	(PDG Collab.)
ARNDT 04	PR C69 035213	R.A. Arndt et al.	(GWU, TRIU)
PENNER 02C	PR C66 055211	G. Penner, U. Mosel	(GIES)
PENNER 02D	PR C66 055212	G. Penner, U. Mosel	(GIES)
VRANA 00	PRPL 328 181	T.P. Vrana, S.A. Dytman, T.-S.H. Lee	(PITT+)
ARNDT 96	PR C53 430	R.A. Arndt et al.	(VPI)
ARNDT 95	PR C52 2120	R.A. Arndt et al.	(VPI, BRCO)
HOEHLER 93	πN Newsletter 9 1	G. Hohler	(KARL)
LI 93	PR C47 2759	Z.J. Li et al.	(VPI)
MANLEY 92	PR D45 4002	D.M. Manley, E.M. Saleski	(KENT IJUP)
Also	PR D30 904	D.M. Manley et al.	(VPI)
ARNDT 91	PR D43 2131	R.A. Arndt et al.	(VPI, TELE) IJUP
CRAWFORD 83	NP B211 1	R.L. Crawford, W.T. Morton	(GLAS)
HOEHLER 83	Landolt-Boernstein 1/9B2	G. Hohler	(KARLT)
PDG 82	PL 111B 1	M. Roos et al.	(HELS, CIT, CERN)
AWAJI 81	Bonn Conf. 352	N. Awaji, R. Kajikawa	(NAGO)
Also	NP B197 365	K. Fuji et al.	(NAGO)
BARNHAM 80	NP B168 243	K.W.J. Barnham et al.	(LOIC)
CHEW 80	Toronto Conf. 123	D.M. Chew	(LBL) IJUP
CUTKOSKY 80	Toronto Conf. 19	R.E. Cutkosky et al.	(CMU, LBL) IJUP
Also	PR D20 2839	R.E. Cutkosky et al.	(CMU, LBL) IJUP
HOEHLER 79	PDAT 12-1	G. Hohler et al.	(KARLT) IJUP
Also	Toronto Conf. 3	R. Koch	(KARLT) IJUP
LONGACRE 78	PR D17 1795	R.S. Longacre et al.	(LBL, SLAC)
LONGACRE 77	NP B122 493	R.S. Longacre, J. Dolbeau	(SACL) IJUP
Also	NP B108 365	J. Dolbeau et al.	(SACL) IJUP
LONGACRE 75	PL 55B 415	R.S. Longacre et al.	(LBL, SLAC) IJUP

$\Delta(1750) P_{31}$

$$J(P) = \frac{3}{2}(\frac{1}{2}^+) \text{ Status: } *$$

OMITTED FROM SUMMARY TABLE

The latest GWU analysis (ARNDT 06) finds no evidence for this resonance.

$\Delta(1750)$ BREIT-WIGNER MASS

VALUE (MeV)	DOCUMENT ID	TECN	COMMENT
≈ 1750 OUR ESTIMATE			
1744 \pm 36	MANLEY 92	IPWA	$\pi N \rightarrow \pi N \& N\pi\pi$
••• We do not use the following data for averages, fits, limits, etc. •••			
1712 \pm 1	PENNER 02c	DPWA	Multichannel
1721 \pm 61	VRANA 00	DPWA	Multichannel
1715.2 \pm 21.0	¹ CHEW 80	BPWA	$\pi^+ p \rightarrow \pi^+ p$
1778.4 \pm 9.0	¹ CHEW 80	BPWA	$\pi^+ p \rightarrow \pi^+ p$

$\Delta(1750)$ BREIT-WIGNER WIDTH

VALUE (MeV)	DOCUMENT ID	TECN	COMMENT
300 \pm 120	MANLEY 92	IPWA	$\pi N \rightarrow \pi N \& N\pi\pi$
••• We do not use the following data for averages, fits, limits, etc. •••			
643 \pm 17	PENNER 02c	DPWA	Multichannel
70 \pm 50	VRANA 00	DPWA	Multichannel
93.3 \pm 55.0	¹ CHEW 80	BPWA	$\pi^+ p \rightarrow \pi^+ p$
23.0 \pm 29.0	¹ CHEW 80	BPWA	$\pi^+ p \rightarrow \pi^+ p$

$\Delta(1750)$ POLE POSITION

REAL PART VALUE (MeV)	DOCUMENT ID	TECN	COMMENT
1748	² ARNDT 04	DPWA	$\pi N \rightarrow \pi N, \eta N$
••• We do not use the following data for averages, fits, limits, etc. •••			
1714	VRANA 00	DPWA	Multichannel

-2xIMAGINARY PART VALUE (MeV)	DOCUMENT ID	TECN	COMMENT
524	² ARNDT 04	DPWA	$\pi N \rightarrow \pi N, \eta N$
••• We do not use the following data for averages, fits, limits, etc. •••			
68	VRANA 00	DPWA	Multichannel

$\Delta(1750)$ ELASTIC POLE RESIDUE

MODULUS r VALUE (MeV)	DOCUMENT ID	TECN	COMMENT
48	² ARNDT 04	DPWA	$\pi N \rightarrow \pi N, \eta N$

PHASE θ VALUE ($^\circ$)	DOCUMENT ID	TECN	COMMENT
158	² ARNDT 04	DPWA	$\pi N \rightarrow \pi N, \eta N$

$\Delta(1750)$ DECAY MODES

Mode	
Γ_1	$N\pi$
Γ_2	$N\pi\pi$
Γ_3	$N(1440)\pi$
Γ_4	ΣK

$\Delta(1750)$ BRANCHING RATIOS

$\Gamma(N\pi)/\Gamma_{total}$	DOCUMENT ID	TECN	COMMENT	Γ_1/Γ
0.08 \pm 0.03	MANLEY 92	IPWA	$\pi N \rightarrow \pi N \& N\pi\pi$	
••• We do not use the following data for averages, fits, limits, etc. •••				
0.01 \pm 0.01	PENNER 02c	DPWA	Multichannel	
0.06 \pm 0.09	VRANA 00	DPWA	Multichannel	
0.18	¹ CHEW 80	BPWA	$\pi^+ p \rightarrow \pi^+ p$	
0.20	¹ CHEW 80	BPWA	$\pi^+ p \rightarrow \pi^+ p$	

$(\Gamma_1 \Gamma_2)^{1/2} / \Gamma_{total}$ in $N\pi \rightarrow \Delta(1700) \rightarrow N(1440)\pi$	DOCUMENT ID	TECN	COMMENT	$(\Gamma_1 \Gamma_3)^{1/2} / \Gamma$
+0.15 \pm 0.03	MANLEY 92	IPWA	$\pi N \rightarrow \pi N \& N\pi\pi$	

$\Gamma(N(1440)\pi)/\Gamma_{total}$	DOCUMENT ID	TECN	COMMENT	Γ_3/Γ
0.83 \pm 0.01	VRANA 00	DPWA	Multichannel	

$\Gamma(\Sigma K)/\Gamma_{total}$	DOCUMENT ID	TECN	COMMENT	Γ_4/Γ
0.001 \pm 0.001	PENNER 02c	DPWA	Multichannel	

$\Delta(1750)$ PHOTON DECAY AMPLITUDES

Papers on γN amplitudes predating 1981 may be found in our 2006 edition, Journal of Physics, G **33** 1 (2006).

$\Delta(1750) \rightarrow N\gamma$, helicity-1/2 amplitude $A_{1/2}$

VALUE (GeV $^{-1/2}$)	DOCUMENT ID	TECN	COMMENT
0.053	PENNER 02d	DPWA	Multichannel

$\Delta(1750)$ FOOTNOTES

- ¹ CHEW 80 reports four resonances in the P_{31} wave — see also the $\Delta(1910)$. Problems with this analysis are discussed in section 2.1.11 of HOEHLER 83.
- ² ARNDT 04 gives no corresponding Breit-Wigner parameters for this state, because the mass so obtained is about 500 MeV higher than that suggested by the position of the pole.

$\Delta(1750)$ REFERENCES

ARNDT 06	PR C74 045205	R.A. Arndt et al.	(GWU)
PDG 06	JPG 33 1	W.-M. Yao et al.	(PDG Collab.)
ARNDT 04	PR C69 035213	R.A. Arndt et al.	(GWU, TRIU)
PENNER 02C	PR C66 055211	G. Penner, U. Mosel	(GIES)
PENNER 02D	PR C66 055212	G. Penner, U. Mosel	(GIES)
VRANA 00	PRPL 328 181	T.P. Vrana, S.A. Dytman, T.-S.H. Lee	(PITT+)
MANLEY 92	PR D45 4002	D.M. Manley, E.M. Saleski	(KENT)
Also	PR D30 904	D.M. Manley et al.	(VPI)
HOEHLER 83	Landolt-Boernstein 1/9B2	G. Hohler	(KARLT)
CHEW 80	Toronto Conf. 123	D.M. Chew	(LBL)

$\Delta(1900) S_{31}$

$$J(P) = \frac{3}{2}(\frac{1}{2}^-) \text{ Status: } **$$

OMITTED FROM SUMMARY TABLE

Some obsolete results published before 1980 were last included in our 2006 edition, Journal of Physics, G **33** 1 (2006). Some further obsolete results published before 1984 were last included in our 2006 edition, Journal of Physics, G **33** 1 (2006).

The latest GWU analysis (ARNDT 06) finds no evidence for this resonance.

$\Delta(1900)$ BREIT-WIGNER MASS

VALUE (MeV)	DOCUMENT ID	TECN	COMMENT
1850 to 1950 (\approx 1900) OUR ESTIMATE			
1920 \pm 24	MANLEY 92	IPWA	$\pi N \rightarrow \pi N \& N\pi\pi$
1890 \pm 50	CUTKOSKY 80	IPWA	$\pi N \rightarrow \pi N$
1908 \pm 30	HOEHLER 79	IPWA	$\pi N \rightarrow \pi N$
••• We do not use the following data for averages, fits, limits, etc. •••			
1802 \pm 87	VRANA 00	DPWA	Multichannel
1918.5 \pm 23.0	CHEW 80	BPWA	$\pi^+ p \rightarrow \pi^+ p$

Baryon Particle Listings

$\Delta(1900), \Delta(1905)$

$\Delta(1900)$ BREIT-WIGNER WIDTH

VALUE (MeV)	DOCUMENT ID	TECN	COMMENT
140 to 240 (≈ 200) OUR ESTIMATE			
263 \pm 39	MANLEY 92	IPWA	$\pi N \rightarrow \pi N$ & $N\pi\pi$
170 \pm 5.0	CUTKOSKY 80	IPWA	$\pi N \rightarrow \pi N$
140 \pm 4.0	HOEHLER 79	IPWA	$\pi N \rightarrow \pi N$
• • • We do not use the following data for averages, fits, limits, etc. • • •			
48 \pm 4.5	VRANA 00	DPWA	Multichannel
93.5 \pm 54.0	CHEW 80	BPWA	$\pi^+ p \rightarrow \pi^+ p$

$\Delta(1900)$ POLE POSITION

REAL PART

VALUE (MeV)	DOCUMENT ID	TECN	COMMENT
1780	¹ HOEHLER 93	SPED	$\pi N \rightarrow \pi N$
1870 \pm 40	CUTKOSKY 80	IPWA	$\pi N \rightarrow \pi N$
• • • We do not use the following data for averages, fits, limits, etc. • • •			
1795	VRANA 00	DPWA	Multichannel
not seen	ARNDT 91	DPWA	$\pi N \rightarrow \pi N$ Soln SM90
2029 or 2025	² LONGACRE 78	IPWA	$\pi N \rightarrow N\pi\pi$

-2xIMAGINARY PART

VALUE (MeV)	DOCUMENT ID	TECN	COMMENT
180 \pm 5.0	CUTKOSKY 80	IPWA	$\pi N \rightarrow \pi N$
• • • We do not use the following data for averages, fits, limits, etc. • • •			
58	VRANA 00	DPWA	Multichannel
not seen	ARNDT 91	DPWA	$\pi N \rightarrow \pi N$ Soln SM90
164 or 163	² LONGACRE 78	IPWA	$\pi N \rightarrow N\pi\pi$

$\Delta(1900)$ ELASTIC POLE RESIDUE

MODULUS $|r|$

VALUE (MeV)	DOCUMENT ID	TECN	COMMENT
10 \pm 3	CUTKOSKY 80	IPWA	$\pi N \rightarrow \pi N$

PHASE θ

VALUE ($^\circ$)	DOCUMENT ID	TECN	COMMENT
+20 \pm 40	CUTKOSKY 80	IPWA	$\pi N \rightarrow \pi N$

$\Delta(1900)$ DECAY MODES

The following branching fractions are our estimates, not fits or averages.

Mode	Fraction (Γ_i/Γ)
Γ_1 $N\pi$	10-30 %
Γ_2 ΣK	
Γ_3 $N\pi\pi$	
Γ_4 $\Delta\pi$	
Γ_5 $\Delta(1232)\pi, D$ -wave	
Γ_6 $N\rho$	
Γ_7 $N\rho, S=1/2, S$ -wave	
Γ_8 $N\rho, S=3/2, D$ -wave	
Γ_9 $N(1440)\pi, S$ -wave	
Γ_{10} $N\gamma, \text{ helicity}=1/2$	

$\Delta(1900)$ BRANCHING RATIOS

$\Gamma(N\pi)/\Gamma_{\text{total}}$	DOCUMENT ID	TECN	COMMENT	Γ_1/Γ
0.1 to 0.3 OUR ESTIMATE				
0.41 \pm 0.04	MANLEY 92	IPWA	$\pi N \rightarrow \pi N$ & $N\pi\pi$	
0.10 \pm 0.03	CUTKOSKY 80	IPWA	$\pi N \rightarrow \pi N$	
0.08 \pm 0.04	HOEHLER 79	IPWA	$\pi N \rightarrow \pi N$	
• • • We do not use the following data for averages, fits, limits, etc. • • •				
0.33 \pm 0.10	VRANA 00	DPWA	Multichannel	
0.28	CHEW 80	BPWA	$\pi^+ p \rightarrow \pi^+ p$	
$(\Gamma_1\Gamma_7)^{1/2}/\Gamma_{\text{total}}$ in $N\pi \rightarrow \Delta(1900) \rightarrow \Sigma K$ $(\Gamma_1\Gamma_2)^{1/2}/\Gamma$				
VALUE	DOCUMENT ID	TECN	COMMENT	
<0.03	CANDLIN 84	DPWA	$\pi^+ p \rightarrow \Sigma^+ K^+$	
$(\Gamma_1\Gamma_7)^{1/2}/\Gamma_{\text{total}}$ in $N\pi \rightarrow \Delta(1900) \rightarrow \Delta(1232)\pi, D$-wave $(\Gamma_1\Gamma_5)^{1/2}/\Gamma$				
VALUE	DOCUMENT ID	TECN	COMMENT	
+0.25 \pm 0.07	MANLEY 92	IPWA	$\pi N \rightarrow \pi N$ & $N\pi\pi$	
$\Gamma(\Delta(1232)\pi, D\text{-wave})/\Gamma_{\text{total}}$ Γ_5/Γ				
VALUE	DOCUMENT ID	TECN	COMMENT	
0.28 \pm 0.01	VRANA 00	DPWA	Multichannel	
$(\Gamma_1\Gamma_7)^{1/2}/\Gamma_{\text{total}}$ in $N\pi \rightarrow \Delta(1900) \rightarrow N\rho, S=1/2, S$-wave $(\Gamma_1\Gamma_7)^{1/2}/\Gamma$				
VALUE	DOCUMENT ID	TECN	COMMENT	
-0.14 \pm 0.11	MANLEY 92	IPWA	$\pi N \rightarrow \pi N$ & $N\pi\pi$	

$\Gamma(N\rho, S=1/2, S\text{-wave})/\Gamma_{\text{total}}$

VALUE	DOCUMENT ID	TECN	COMMENT	Γ_7/Γ
0.30 \pm 0.02	VRANA 00	DPWA	Multichannel	

$(\Gamma_1\Gamma_7)^{1/2}/\Gamma_{\text{total}}$ in $N\pi \rightarrow \Delta(1900) \rightarrow N\rho, S=3/2, D$ -wave $(\Gamma_1\Gamma_8)^{1/2}/\Gamma$

VALUE	DOCUMENT ID	TECN	COMMENT
-0.37 \pm 0.07	MANLEY 92	IPWA	$\pi N \rightarrow \pi N$ & $N\pi\pi$

$\Gamma(N\rho, S=3/2, D\text{-wave})/\Gamma_{\text{total}}$

VALUE	DOCUMENT ID	TECN	COMMENT	Γ_8/Γ
0.05 \pm 0.01	VRANA 00	DPWA	Multichannel	

$(\Gamma_1\Gamma_7)^{1/2}/\Gamma_{\text{total}}$ in $N\pi \rightarrow \Delta(1900) \rightarrow N(1440)\pi, S$ -wave $(\Gamma_1\Gamma_9)^{1/2}/\Gamma$

VALUE	DOCUMENT ID	TECN	COMMENT
-0.16 \pm 0.11	MANLEY 92	IPWA	$\pi N \rightarrow \pi N$ & $N\pi\pi$

$\Gamma(N(1440)\pi, S\text{-wave})/\Gamma_{\text{total}}$

VALUE	DOCUMENT ID	TECN	COMMENT	Γ_9/Γ
0.04 \pm 0.01	VRANA 00	DPWA	Multichannel	

$\Delta(1900)$ PHOTON DECAY AMPLITUDES

Papers on γN amplitudes predating 1981 may be found in our 2006 edition, Journal of Physics, G **33** 1 (2006).

$\Delta(1900) \rightarrow N\gamma, \text{ helicity}=1/2$ amplitude $A_{1/2}$

VALUE (GeV $^{-1/2}$)	DOCUMENT ID	TECN	COMMENT
-0.004 \pm 0.016	CRAWFORD 83	IPWA	$\gamma N \rightarrow \pi N$
0.029 \pm 0.008	AWAJI 81	DPWA	$\gamma N \rightarrow \pi N$

$\Delta(1900)$ FOOTNOTES

- See HOEHLER 93 for a detailed discussion of the evidence for and the pole parameters of N and Δ resonances as determined from Argand diagrams of πN elastic partial-wave amplitudes and from plots of the speeds with which the amplitudes traverse the diagrams.
- LONGACRE 78 values are from a search for poles in the unitarized T-matrix. The first (second) value uses, in addition to $\pi N \rightarrow N\pi\pi$ data, elastic amplitudes from a Saclay (CERN) partial-wave analysis.

$\Delta(1900)$ REFERENCES

For early references, see Physics Letters **111B** 1 (1982).

ARNDT 06	PR C74 045205	R.A. Arndt <i>et al.</i>	(GWU)
PDG 06	JPG 33 1	W.-M. Yao <i>et al.</i>	(PDG Collab.)
VRANA 00	PRPL 328 181	T.P. Vrana, S.A. Dytman, T.-S.H. Lee	(PITT+)
HOEHLER 93	πN Newsletter 9 1	G. Hohlner	(KARL)
MANLEY 92	PR D45 4002	D.M. Manley, E.M. Saleski	(KENT) IJP
	Also	D.M. Manley <i>et al.</i>	(VPI)
ARNDT 91	PR D30 904	R.A. Arndt <i>et al.</i>	(VPI, TELE) IJP
CANDLIN 84	NP B238 477	D.J. Candlin <i>et al.</i>	(EDIN, RAL, LOWC)
CRAWFORD 83	NP B211 1	R.L. Crawford, W.T. Morton	(GLAS)
AWAJI 81	Bonn Conf. 352	N. Awaji, R. Kajikawa	(NAGO)
	Also	K. Fujii <i>et al.</i>	(NAGO)
CHEW 80	Toronto Conf. 123	D.M. Chew	(LBL) IJP
CUTKOSKY 80	Toronto Conf. 19	R.E. Cutkosky <i>et al.</i>	(CMU, LBL) IJP
	Also	R.E. Cutkosky <i>et al.</i>	(CMU, LBL) IJP
HOEHLER 79	PDAT 12-1	G. Hohlner <i>et al.</i>	(KARLT) IJP
	Also	R. Koch	(KARLT) IJP
LONGACRE 78	Toronto Conf. 3	R.S. Longacre <i>et al.</i>	(LBL, SLAC)
	Also	R.S. Longacre <i>et al.</i>	(LBL, SLAC)

$\Delta(1905) F_{35}$

$$I(J^P) = \frac{3}{2}(\frac{5}{2}^+) \text{ Status: } ***$$

Most of the results published before 1975 were last included in our 1982 edition, Physics Letters **111B** 1 (1982). Some further obsolete results published before 1984 were last included in our 2006 edition, Journal of Physics, G **33** 1 (2006).

$\Delta(1905)$ BREIT-WIGNER MASS

VALUE (MeV)	DOCUMENT ID	TECN	COMMENT
1865 to 1915 (≈ 1890) OUR ESTIMATE			
1857.8 \pm 1.6	ARNDT 06	DPWA	$\pi N \rightarrow \pi N, \eta N$
1881 \pm 18	MANLEY 92	IPWA	$\pi N \rightarrow \pi N$ & $N\pi\pi$
1910 \pm 30	CUTKOSKY 80	IPWA	$\pi N \rightarrow \pi N$
1905 \pm 20	HOEHLER 79	IPWA	$\pi N \rightarrow \pi N$
• • • We do not use the following data for averages, fits, limits, etc. • • •			
1855.7 \pm 4.2	ARNDT 04	DPWA	$\pi N \rightarrow \pi N, \eta N$
1873 \pm 77	VRANA 00	DPWA	Multichannel
1895 \pm 8	ARNDT 96	IPWA	$\gamma N \rightarrow \pi N$
1850	ARNDT 95	DPWA	$\pi N \rightarrow N\pi$
1960 \pm 40	CANDLIN 84	DPWA	$\pi^+ p \rightarrow \Sigma^+ K^+$
1787.0 $^{+6.0}_{-5.7}$	CHEW 80	BPWA	$\pi^+ p \rightarrow \Sigma^+ p$
1830	¹ LONGACRE 75	IPWA	$\pi N \rightarrow N\pi\pi$

See key on page 405

Baryon Particle Listings
 $\Delta(1905)$ $\Delta(1905)$ BREIT-WIGNER WIDTH

VALUE (MeV)	DOCUMENT ID	TECN	COMMENT
270 to 400 (≈ 330) OUR ESTIMATE			
320.6 \pm 8.6	ARNDT 06	DPWA	$\pi N \rightarrow \pi N, \eta N$
327 \pm 51	MANLEY 92	IPWA	$\pi N \rightarrow \pi N \& N\pi\pi$
400 \pm 100	CUTKOSKY 80	IPWA	$\pi N \rightarrow \pi N$
260 \pm 20	HOEHLER 79	IPWA	$\pi N \rightarrow \pi N$
••• We do not use the following data for averages, fits, limits, etc. •••			
334 \pm 22	ARNDT 04	DPWA	$\pi N \rightarrow \pi N, \eta N$
461 \pm 111	VRANA 00	DPWA	Multichannel
354 \pm 10	ARNDT 96	IPWA	$\gamma N \rightarrow \pi N$
294	ARNDT 95	DPWA	$\pi N \rightarrow N\pi$
270 \pm 40	CANDLIN 84	DPWA	$\pi^+ p \rightarrow \Sigma^+ K^+$
66.0 ⁺ 24.0 - 16.0	CHEW 80	BPWA	$\pi^+ p \rightarrow \pi^+ p$
220	¹ LONGACRE 75	IPWA	$\pi N \rightarrow N\pi\pi$

 $\Delta(1905)$ POLE POSITION

VALUE (MeV)	DOCUMENT ID	TECN	COMMENT
1825 to 1835 (≈ 1830) OUR ESTIMATE			
1819	ARNDT 06	DPWA	$\pi N \rightarrow \pi N, \eta N$
1829	² HOEHLER 93	SPED	$\pi N \rightarrow \pi N$
1830 \pm 40	CUTKOSKY 80	IPWA	$\pi N \rightarrow \pi N$
••• We do not use the following data for averages, fits, limits, etc. •••			
1825	ARNDT 04	DPWA	$\pi N \rightarrow \pi N, \eta N$
1793	VRANA 00	DPWA	Multichannel
1832	ARNDT 95	DPWA	$\pi N \rightarrow N\pi$
1794	ARNDT 91	DPWA	$\pi N \rightarrow \pi N$ Soln SM90
1813 or 1808	³ LONGACRE 78	IPWA	$\pi N \rightarrow N\pi\pi$

 $-2\times$ IMAGINARY PART

VALUE (MeV)	DOCUMENT ID	TECN	COMMENT
265 to 300 (≈ 280) OUR ESTIMATE			
247	ARNDT 06	DPWA	$\pi N \rightarrow \pi N, \eta N$
303	² HOEHLER 93	SPED	$\pi N \rightarrow \pi N$
280 \pm 60	CUTKOSKY 80	IPWA	$\pi N \rightarrow \pi N$
••• We do not use the following data for averages, fits, limits, etc. •••			
270	ARNDT 04	DPWA	$\pi N \rightarrow \pi N, \eta N$
302	VRANA 00	DPWA	Multichannel
254	ARNDT 95	DPWA	$\pi N \rightarrow N\pi$
230	ARNDT 91	DPWA	$\pi N \rightarrow \pi N$ Soln SM90
193 or 187	³ LONGACRE 78	IPWA	$\pi N \rightarrow N\pi\pi$

 $\Delta(1905)$ ELASTIC POLE RESIDUEMODULUS $|r|$

VALUE (MeV)	DOCUMENT ID	TECN	COMMENT
15	ARNDT 06	DPWA	$\pi N \rightarrow \pi N, \eta N$
25	HOEHLER 93	SPED	$\pi N \rightarrow \pi N$
25 \pm 8	CUTKOSKY 80	IPWA	$\pi N \rightarrow \pi N$
••• We do not use the following data for averages, fits, limits, etc. •••			
16	ARNDT 04	DPWA	$\pi N \rightarrow \pi N, \eta N$
12	ARNDT 95	DPWA	$\pi N \rightarrow N\pi$
14	ARNDT 91	DPWA	$\pi N \rightarrow \pi N$ Soln SM90

PHASE θ

VALUE ($^\circ$)	DOCUMENT ID	TECN	COMMENT
-30	ARNDT 06	DPWA	$\pi N \rightarrow \pi N, \eta N$
-50 \pm 20	CUTKOSKY 80	IPWA	$\pi N \rightarrow \pi N$
••• We do not use the following data for averages, fits, limits, etc. •••			
-25	ARNDT 04	DPWA	$\pi N \rightarrow \pi N, \eta N$
-4	ARNDT 95	DPWA	$\pi N \rightarrow N\pi$
-40	ARNDT 91	DPWA	$\pi N \rightarrow \pi N$ Soln SM90

 $\Delta(1905)$ DECAY MODES

The following branching fractions are our estimates, not fits or averages.

Mode	Fraction (Γ_i/Γ)
Γ_1 $N\pi$	0.09 to 0.15
Γ_2 ΣK	
Γ_3 $N\pi\pi$	85-95 %
Γ_4 $\Delta\pi$	<25 %
Γ_5 $\Delta(1232)\pi, P$ -wave	
Γ_6 $\Delta(1232)\pi, F$ -wave	
Γ_7 $N\rho$	>60 %
Γ_8 $N\rho, S=3/2, P$ -wave	
Γ_9 $N\rho, S=3/2, F$ -wave	
Γ_{10} $N\rho, S=1/2, F$ -wave	
Γ_{11} $N\gamma$	0.01-0.03 %
Γ_{12} $N\gamma, \text{helicity}=1/2$	0.0-0.1 %
Γ_{13} $N\gamma, \text{helicity}=3/2$	0.004-0.03 %

 $\Delta(1905)$ BRANCHING RATIOS

$\Gamma(N\pi)/\Gamma_{\text{total}}$	DOCUMENT ID	TECN	COMMENT	Γ_1/Γ
0.09 to 0.15 OUR ESTIMATE				
0.122 \pm 0.001	ARNDT 06	DPWA	$\pi N \rightarrow \pi N, \eta N$	
0.12 \pm 0.03	MANLEY 92	IPWA	$\pi N \rightarrow \pi N \& N\pi\pi$	
0.08 \pm 0.03	CUTKOSKY 80	IPWA	$\pi N \rightarrow \pi N$	
0.15 \pm 0.02	HOEHLER 79	IPWA	$\pi N \rightarrow \pi N$	
••• We do not use the following data for averages, fits, limits, etc. •••				
0.120 \pm 0.002	ARNDT 04	DPWA	$\pi N \rightarrow \pi N, \eta N$	
0.09 \pm 0.01	VRANA 00	DPWA	Multichannel	
0.12	ARNDT 95	DPWA	$\pi N \rightarrow N\pi$	
0.11	CHEW 80	BPWA	$\pi^+ p \rightarrow \pi^+ p$	
$(\Gamma_i\Gamma_f)^{1/2}/\Gamma_{\text{total}}$ in $N\pi \rightarrow \Delta(1905) \rightarrow \Sigma K$				$(\Gamma_1\Gamma_2)^{1/2}/\Gamma$
VALUE	DOCUMENT ID	TECN	COMMENT	
-0.015 \pm 0.003	CANDLIN 84	DPWA	$\pi^+ p \rightarrow \Sigma^+ K^+$	

Note: Signs of couplings from $\pi N \rightarrow N\pi\pi$ analyses were changed in the 1986 edition to agree with the baryon-first convention; the overall phase ambiguity is resolved by choosing a negative sign for the $\Delta(1620) S_{31}$ coupling to $\Delta(1232)\pi$.

$(\Gamma_i\Gamma_f)^{1/2}/\Gamma_{\text{total}}$ in $N\pi \rightarrow \Delta(1905) \rightarrow \Delta(1232)\pi, P$ -wave	DOCUMENT ID	TECN	COMMENT	$(\Gamma_1\Gamma_5)^{1/2}/\Gamma$
VALUE				
-0.04 \pm 0.05	MANLEY 92	IPWA	$\pi N \rightarrow \pi N \& N\pi\pi$	

$\Gamma(\Delta(1232)\pi, P$ -wave)/ Γ_{total}	DOCUMENT ID	TECN	COMMENT	Γ_5/Γ
VALUE				
0.23 \pm 0.01	VRANA 00	DPWA	Multichannel	

$(\Gamma_i\Gamma_f)^{1/2}/\Gamma_{\text{total}}$ in $N\pi \rightarrow \Delta(1905) \rightarrow \Delta(1232)\pi, F$ -wave	DOCUMENT ID	TECN	COMMENT	$(\Gamma_1\Gamma_6)^{1/2}/\Gamma$
VALUE				
+0.02 \pm 0.03	MANLEY 92	IPWA	$\pi N \rightarrow \pi N \& N\pi\pi$	
+0.20	¹ LONGACRE 75	IPWA	$\pi N \rightarrow N\pi\pi$	

$\Gamma(\Delta(1232)\pi, F$ -wave)/ Γ_{total}	DOCUMENT ID	TECN	COMMENT	Γ_6/Γ
VALUE				
0.44 \pm 0.01	VRANA 00	DPWA	Multichannel	

$(\Gamma_i\Gamma_f)^{1/2}/\Gamma_{\text{total}}$ in $N\pi \rightarrow \Delta(1905) \rightarrow N\rho, S=3/2, P$ -wave	DOCUMENT ID	TECN	COMMENT	$(\Gamma_1\Gamma_8)^{1/2}/\Gamma$
VALUE				
+0.030 to +0.36 OUR ESTIMATE				
+0.33 \pm 0.03	MANLEY 92	IPWA	$\pi N \rightarrow \pi N \& N\pi\pi$	
+0.33	¹ LONGACRE 75	IPWA	$\pi N \rightarrow N\pi\pi$	

$\Gamma(N\rho, S=3/2, P$ -wave)/ Γ_{total}	DOCUMENT ID	TECN	COMMENT	Γ_8/Γ
VALUE				
0.24 \pm 0.01	VRANA 00	DPWA	Multichannel	

 $\Delta(1905)$ PHOTON DECAY AMPLITUDESPapers on γN amplitudes predating 1981 may be found in our 2006 edition, Journal of Physics, G 33 1 (2006). $\Delta(1905) \rightarrow N\gamma, \text{helicity}=1/2$ amplitude $A_{1/2}$

VALUE ($\text{GeV}^{-1/2}$)	DOCUMENT ID	TECN	COMMENT
+0.026 \pm 0.011 OUR ESTIMATE			
0.021 \pm 0.004	DUGGER 07	DPWA	$\gamma N \rightarrow \pi N$
0.022 \pm 0.005	ARNDT 96	IPWA	$\gamma N \rightarrow \pi N$
0.021 \pm 0.010	CRAWFORD 83	IPWA	$\gamma N \rightarrow \pi N$
0.043 \pm 0.020	AWAJI 81	DPWA	$\gamma N \rightarrow \pi N$
••• We do not use the following data for averages, fits, limits, etc. •••			
0.018	DRECHSEL 07	DPWA	$\gamma N \rightarrow \pi N$
0.055 \pm 0.004	LI 93	IPWA	$\gamma N \rightarrow \pi N$

 $\Delta(1905) \rightarrow N\gamma, \text{helicity}=3/2$ amplitude $A_{3/2}$

VALUE ($\text{GeV}^{-1/2}$)	DOCUMENT ID	TECN	COMMENT
-0.045 \pm 0.020 OUR ESTIMATE			
-0.046 \pm 0.005	DUGGER 07	DPWA	$\gamma N \rightarrow \pi N$
-0.045 \pm 0.005	ARNDT 96	IPWA	$\gamma N \rightarrow \pi N$
-0.056 \pm 0.028	CRAWFORD 83	IPWA	$\gamma N \rightarrow \pi N$
-0.025 \pm 0.023	AWAJI 81	DPWA	$\gamma N \rightarrow \pi N$
••• We do not use the following data for averages, fits, limits, etc. •••			
-0.028	DRECHSEL 07	DPWA	$\gamma N \rightarrow \pi N$
0.002 \pm 0.003	LI 93	IPWA	$\gamma N \rightarrow \pi N$

Baryon Particle Listings

$\Delta(1905)$, $\Delta(1910)$

$\Delta(1905)$ FOOTNOTES

- 1 From method II of LONGACRE 75: eyeball fits with Breit-Wigner circles to the T-matrix amplitudes.
- 2 See HOEHLER 93 for a detailed discussion of the evidence for and the pole parameters of N and Δ resonances as determined from Argand diagrams of πN elastic partial-wave amplitudes and from plots of the speeds with which the amplitudes traverse the diagrams.
- 3 LONGACRE 78 values are from a search for poles in the unitarized T-matrix. The first (second) value uses, in addition to $\pi N \rightarrow N\pi\pi$ data, elastic amplitudes from a Saclay (CERN) partial-wave analysis.

$\Delta(1905)$ REFERENCES

For early references, see Physics Letters **111B** 1 (1982).

Author	Year	Document ID	TECN	COMMENT
DRECHSEL	07	EPJ A34 69		D. Drechsel, S.S. Kamalov, L. Tiator (MAIN Z, JINR)
DUGGER	07	PR C76 025211		M. Dugger et al. (Jefferson Lab CLAS Collab.)
ARNDT	06	PR C74 045205		R.A. Arndt et al. (GWU)
PDG	06	JPG 33 1		W.-M. Yao et al. (PDG Collab.)
ARNDT	04	PR C69 035213		R.A. Arndt et al. (GWU, TRIU)
VRANA	00	PRPL 328 181		T.P. Vrana, S.A. Dytman, T.-S.H. Lee (PITT+)
ARNDT	96	PR C53 430		R.A. Arndt, I.I. Strakovsky, R.L. Workman (VPI)
ARNDT	95	PR C52 2120		R.A. Arndt et al. (VPI, BRCO)
HOEHLER	93	πN Newsletter 9 1		G. Hohler (KARL)
LI	93	PR C47 2759		Z.J. Li et al. (VPI)
MANLEY	92	PR D45 4002		D.M. Manley, E.M. Saleski (KENT) IJP
Also		PR D30 904		D.M. Manley et al. (VPI)
ARNDT	91	PR D43 2131		R.A. Arndt et al. (VPI, TELE) IJP
CANDLIN	84	NP B238 477		D.J. Candlin et al. (EDIN, RAL, LOWC)
CRAWFORD	83	NP B211 1		R.L. Crawford, W.T. Morton (GLAS)
PDG	82	PL 111B 1		M. Roos et al. (HELS, CIT, CERN)
AWAJI	81	Bonn Conf. 352		N. Awaji, R. Kajikawa (NAGO)
Also		NP B197 365		K. Fujii et al. (NAGO)
CHEW	80	Toronto Conf. 123		D.M. Chew (LBL) IJP
CUTKOSKY	80	Toronto Conf. 19		R.E. Cutkosky et al. (CMU, LBL) IJP
Also		PR D20 2839		R.E. Cutkosky et al. (CMU, LBL) IJP
HOEHLER	79	PDAT 12-1		G. Hohler et al. (KARLT) IJP
Also		Toronto Conf. 3		R. Koch (KARLT) IJP
LONGACRE	78	PR D17 1795		R.S. Longacre et al. (LBL, SLAC) IJP
LONGACRE	75	PL 55B 415		R.S. Longacre et al. (LBL, SLAC) IJP

$\Delta(1910) P_{31}$

$$I(J^P) = \frac{3}{2}(\frac{1}{2}^+) \text{ Status: } ****$$

Most of the results published before 1975 were last included in our 1982 edition, Physics Letters **111B** 1 (1982). Some further obsolete results published before 1984 were last included in our 2006 edition, Journal of Physics, G **33** 1 (2006).

$\Delta(1910)$ BREIT-WIGNER MASS

VALUE (MeV)	DOCUMENT ID	TECN	COMMENT
1870 to 1920 (≈ 1910) OUR ESTIMATE			
2067.9 \pm 1.7	ARNDT 06	DPWA	$\pi N \rightarrow \pi N, \eta N$
1882 \pm 10	MANLEY 92	IPWA	$\pi N \rightarrow \pi N \& N\pi\pi$
1910 \pm 40	CUTKOSKY 80	IPWA	$\pi N \rightarrow \pi N$
1888 \pm 20	HOEHLER 79	IPWA	$\pi N \rightarrow \pi N$
••• We do not use the following data for averages, fits, limits, etc. •••			
1995 \pm 12	VRANA 00	DPWA	Multichannel
2152	ARNDT 95	DPWA	$\pi N \rightarrow N\pi$
1960.1 \pm 21.0	1 CHEW 80	BPWA	$\pi^+ p \rightarrow \pi^+ p$
2121.4 \pm 13.0	1 CHEW 80	BPWA	$\pi^+ p \rightarrow \pi^+ p$
-14.3	2 LONGACRE 77	IPWA	$\pi N \rightarrow N\pi\pi$
1790			

$\Delta(1910)$ BREIT-WIGNER WIDTH

VALUE (MeV)	DOCUMENT ID	TECN	COMMENT
190 to 270 (≈ 250) OUR ESTIMATE			
543 \pm 10	ARNDT 06	DPWA	$\pi N \rightarrow \pi N, \eta N$
239 \pm 25	MANLEY 92	IPWA	$\pi N \rightarrow \pi N \& N\pi\pi$
225 \pm 50	CUTKOSKY 80	IPWA	$\pi N \rightarrow \pi N$
280 \pm 50	HOEHLER 79	IPWA	$\pi N \rightarrow \pi N$
••• We do not use the following data for averages, fits, limits, etc. •••			
713 \pm 465	VRANA 00	DPWA	Multichannel
760	ARNDT 95	DPWA	$\pi N \rightarrow N\pi$
152.9 \pm 60.0	1 CHEW 80	BPWA	$\pi^+ p \rightarrow \pi^+ p$
172.2 \pm 37.0	1 CHEW 80	BPWA	$\pi^+ p \rightarrow \pi^+ p$
170	2 LONGACRE 77	IPWA	$\pi N \rightarrow N\pi\pi$

$\Delta(1910)$ POLE POSITION

REAL PART	DOCUMENT ID	TECN	COMMENT
1830 to 1880 (≈ 1855) OUR ESTIMATE			
1771	ARNDT 06	DPWA	$\pi N \rightarrow \pi N, \eta N$
1874	3 HOEHLER 93	SPED	$\pi N \rightarrow \pi N$
1880 \pm 30	CUTKOSKY 80	IPWA	$\pi N \rightarrow \pi N$
••• We do not use the following data for averages, fits, limits, etc. •••			
1880	VRANA 00	DPWA	Multichannel
1810	ARNDT 95	DPWA	$\pi N \rightarrow N\pi$
1950	ARNDT 91	DPWA	$\pi N \rightarrow \pi N$ Soln SM90
1792 or 1801	2 LONGACRE 77	IPWA	$\pi N \rightarrow N\pi\pi$

$-2\times$ IMAGINARY PART

VALUE (MeV)	DOCUMENT ID	TECN	COMMENT
200 to 500 (≈ 350) OUR ESTIMATE			
479	ARNDT 06	DPWA	$\pi N \rightarrow \pi N, \eta N$
283	3 HOEHLER 93	SPED	$\pi N \rightarrow \pi N$
200 \pm 40	CUTKOSKY 80	IPWA	$\pi N \rightarrow \pi N$
••• We do not use the following data for averages, fits, limits, etc. •••			
496	VRANA 00	DPWA	Multichannel
494	ARNDT 95	DPWA	$\pi N \rightarrow N\pi$
398	ARNDT 91	DPWA	$\pi N \rightarrow \pi N$ Soln SM90
172 or 165	2 LONGACRE 77	IPWA	$\pi N \rightarrow N\pi\pi$

$\Delta(1910)$ ELASTIC POLE RESIDUE

MODULUS $ r $	DOCUMENT ID	TECN	COMMENT
VALUE (MeV)			
45	ARNDT 06	DPWA	$\pi N \rightarrow \pi N, \eta N$
38	HOEHLER 93	SPED	$\pi N \rightarrow \pi N$
20 \pm 4	CUTKOSKY 80	IPWA	$\pi N \rightarrow \pi N$
••• We do not use the following data for averages, fits, limits, etc. •••			
53	ARNDT 95	DPWA	$\pi N \rightarrow N\pi$
37	ARNDT 91	DPWA	$\pi N \rightarrow \pi N$ Soln SM90
PHASE θ			
VALUE ($^\circ$)			
+172	ARNDT 06	DPWA	$\pi N \rightarrow \pi N, \eta N$
-90 \pm 30	CUTKOSKY 80	IPWA	$\pi N \rightarrow \pi N$
••• We do not use the following data for averages, fits, limits, etc. •••			
-176	ARNDT 95	DPWA	$\pi N \rightarrow N\pi$
-91	ARNDT 91	DPWA	$\pi N \rightarrow \pi N$ Soln SM90

$\Delta(1910)$ DECAY MODES

The following branching fractions are our estimates, not fits or averages.

Mode	Fraction (Γ_i/Γ)
Γ_1 $N\pi$	15-30 %
Γ_2 ΣK	
Γ_3 $N\pi\pi$	
Γ_4 $\Delta\pi$	
Γ_5 $\Delta(1232)\pi, P\text{-wave}$	
Γ_6 $N\rho$	
Γ_7 $N\rho, S=3/2, P\text{-wave}$	
Γ_8 $N(1440)\pi$	
Γ_9 $N(1440)\pi, P\text{-wave}$	
Γ_{10} $N\gamma$	0.0-0.2 %
Γ_{11} $N\gamma, \text{helicity}=1/2$	0.0-0.2 %

$\Delta(1910)$ BRANCHING RATIOS

$\Gamma(N\pi)/\Gamma_{\text{total}}$	DOCUMENT ID	TECN	COMMENT	Γ_1/Γ
0.15 to 0.3 OUR ESTIMATE				
0.239 \pm 0.001	ARNDT 06	DPWA	$\pi N \rightarrow \pi N, \eta N$	
0.23 \pm 0.08	MANLEY 92	IPWA	$\pi N \rightarrow \pi N \& N\pi\pi$	
0.19 \pm 0.03	CUTKOSKY 80	IPWA	$\pi N \rightarrow \pi N$	
0.24 \pm 0.06	HOEHLER 79	IPWA	$\pi N \rightarrow \pi N$	
••• We do not use the following data for averages, fits, limits, etc. •••				
0.29 \pm 0.21	VRANA 00	DPWA	Multichannel	
0.26	ARNDT 95	DPWA	$\pi N \rightarrow N\pi$	
0.17	1 CHEW 80	BPWA	$\pi^+ p \rightarrow \pi^+ p$	
0.40	1 CHEW 80	BPWA	$\pi^+ p \rightarrow \pi^+ p$	
$(\Gamma_1\Gamma_f)^{1/2}/\Gamma_{\text{total}}$ in $N\pi \rightarrow \Delta(1910) \rightarrow \Sigma K$				
VALUE				
< 0.03	CANDLIN 84	DPWA	$\pi^+ p \rightarrow \Sigma^+ K^+$	$(\Gamma_1\Gamma_2)^{1/2}/\Gamma$
••• We do not use the following data for averages, fits, limits, etc. •••				
-0.019	LIVANOS 80	DPWA	$\pi p \rightarrow \Sigma K$	

Note: Signs of couplings from $\pi N \rightarrow N\pi\pi$ analyses were changed in the 1986 edition to agree with the baryon-first convention; the overall phase ambiguity is resolved by choosing a negative sign for the $\Delta(1620) S_{31}$ coupling to $\Delta(1232)\pi$.

$(\Gamma_1\Gamma_f)^{1/2}/\Gamma_{\text{total}}$ in $N\pi \rightarrow \Delta(1910) \rightarrow \Delta(1232)\pi, P\text{-wave}$	DOCUMENT ID	TECN	COMMENT	$(\Gamma_1\Gamma_5)^{1/2}/\Gamma$
VALUE				
+0.06	2 LONGACRE 77	IPWA	$\pi N \rightarrow N\pi\pi$	
$(\Gamma_1\Gamma_f)^{1/2}/\Gamma_{\text{total}}$ in $N\pi \rightarrow \Delta(1910) \rightarrow N\rho, S=3/2, P\text{-wave}$				
VALUE				
+0.29	2 LONGACRE 77	IPWA	$\pi N \rightarrow N\pi\pi$	

See key on page 405

Baryon Particle Listings

$\Delta(1910), \Delta(1920)$

$(\Gamma_1 \Gamma_2)^{1/2} / \Gamma_{\text{total}}$ in $N\pi \rightarrow \Delta(1910) \rightarrow N(1440)\pi, P\text{-wave}$				$(\Gamma_1 \Gamma_2)^{1/2} / \Gamma$
VALUE	DOCUMENT ID	TECN	COMMENT	
-0.39 ± 0.04	MANLEY	92	IPWA	$\pi N \rightarrow \pi N \& N\pi\pi$

$\Gamma(N(1440)\pi) / \Gamma_{\text{total}}$				Γ_8 / Γ
VALUE	DOCUMENT ID	TECN	COMMENT	
0.56 ± 0.07	VRANA	00	DPWA	Multichannel

$\Delta(1910)$ PHOTON DECAY AMPLITUDES

Papers on γN amplitudes predating 1981 may be found in our 2006 edition, Journal of Physics, G **33** 1 (2006).

$\Delta(1910) \rightarrow N\gamma, \text{ helicity-1/2 amplitude } A_{1/2}$

VALUE (GeV ^{-1/2})	DOCUMENT ID	TECN	COMMENT
+0.003 ± 0.014 OUR ESTIMATE			
-0.002 ± 0.008	ARNDT	96	IPWA $\gamma N \rightarrow \pi N$
0.014 ± 0.030	CRAWFORD	83	IPWA $\gamma N \rightarrow \pi N$
0.025 ± 0.011	AWAJI	81	DPWA $\gamma N \rightarrow \pi N$
• • • We do not use the following data for averages, fits, limits, etc. • • •			
0.032 ± 0.003	LI	93	IPWA $\gamma N \rightarrow \pi N$

$\Delta(1910)$ FOOTNOTES

- 1 CHEW 80 reports four resonances in the P_{31} wave — see also the $\Delta(1750)$. Problems with this analysis are discussed in section 2.1.11 of HOEHLER 83.
- 2 LONGACRE 77 pole positions are from a search for poles in the unitarized T-matrix; the first (second) value uses, in addition to $\pi N \rightarrow N\pi\pi$ data, elastic amplitudes from a Saclay (CERN) partial-wave analysis. The other LONGACRE 77 values are from eyeball fits with Breit-Wigner circles to the T-matrix amplitudes.
- 3 See HOEHLER 93 for a detailed discussion of the evidence for and the pole parameters of N and Δ resonances as determined from Argand diagrams of πN elastic partial-wave amplitudes and from plots of the speeds with which the amplitudes traverse the diagrams.

$\Delta(1910)$ REFERENCES

For early references, see Physics Letters **111B** 1 (1982).

ARNDT 06 PR C74 045205	R.A. Arndt et al.	(GWU)
PDG 06 JPC 33 1	W.-M. Yao et al.	(PDG Collab.)
VRANA 00 PRPL 323 181	T.P. Vrana, S.A. Dytman, T.-S.H. Lee	(PITT+)
ARNDT 96 PR C53 430	R.A. Arndt, I.I. Strakovsky, R.L. Workman	(VPI)
ARNDT 95 PR C52 2120	R.A. Arndt et al.	(VPI, BRCO)
HOEHLER 93 πN Newsletter 9 1	G. Hohler	(KARL)
LI 93 PR C47 2759	Z.J. Li et al.	(VPI)
MANLEY 92 PR D45 4002	D.M. Manley, E.M. Saleski	(KENT) IJP
Also PR D30 904	D.M. Manley et al.	(VPI)
ARNDT 91 PR D43 2131	R.A. Arndt et al.	(VPI, TELE) IJP
CANDLIN 84 NP B238 477	D.J. Candlin et al.	(EDIN, RAL, LOWC)
CRAWFORD 83 NP B211 1	R.L. Crawford, W.T. Morton	(GLAS)
HOEHLER 83 Landolt-Boernstein 1/9B2	G. Hohler	(KARL)
PDG 82 PL 111B 1	M. Roos et al.	(HEL5, CIT, CERN)
AWAJI 81 Bonn Conf. 352	N. Awaji, R. Kajikawa	(NAGO)
Also NP B197 365	K. Fujii et al.	(NAGO)
CHEW 80 Toronto Conf. 123	D.M. Chew	(LBL) IJP
CUTKOSKY 80 Toronto Conf. 19	R.E. Cutkosky et al.	(CMU, LBL) IJP
Also PR D20 2839	R.E. Cutkosky et al.	(CMU, LBL) IJP
LIVANOS 80 Toronto Conf. 35	P. Livanos et al.	(SACL) IJP
HOEHLER 79 PDAT 12-1	G. Hohler et al.	(KARL) IJP
Also Toronto Conf. 3	R. Koch	(KARL) IJP
LONGACRE 77 NP B122 493	R.S. Longacre, J. Dolbeau	(SACL) IJP
Also NP B108 365	J. Dolbeau et al.	(SACL) IJP

$\Delta(1920) P_{33}$

$$J(P) = \frac{3}{2}(\frac{3}{2}^+) \text{ Status: } ***$$

Most of the results published before 1975 were last included in our 1982 edition, Physics Letters **111B** 1 (1982). Some further obsolete results published before 1984 were last included in our 2006 edition, Journal of Physics, G **33** 1 (2006).

The latest GWU analysis (ARNDT 06) finds no evidence for this resonance.

$\Delta(1920)$ BREIT-WIGNER MASS

VALUE (MeV)	DOCUMENT ID	TECN	COMMENT
1900 to 1970 (≈ 1920) OUR ESTIMATE			
1914 ± 16	MANLEY	92	IPWA $\pi N \rightarrow \pi N \& N\pi\pi$
1920 ± 80	CUTKOSKY	80	IPWA $\pi N \rightarrow \pi N$
1868 ± 10	HOEHLER	79	IPWA $\pi N \rightarrow \pi N$
• • • We do not use the following data for averages, fits, limits, etc. • • •			
1990 ± 35	HORN	08A	DPWA Multichannel
2057 ± 1	PENNER	02C	DPWA Multichannel
1889 ± 100	VRANA	00	DPWA Multichannel
1840 ± 40	CANDLIN	84	DPWA $\pi^+ p \rightarrow \Sigma^+ K^+$
1955.0 ± 13.0	¹ CHEW	80	BPWA $\pi^+ p \rightarrow \pi^+ p$
2065.0 ± 13.6	¹ CHEW	80	BPWA $\pi^+ p \rightarrow \pi^+ p$
12.9			

$\Delta(1920)$ BREIT-WIGNER WIDTH

VALUE (MeV)	DOCUMENT ID	TECN	COMMENT
150 to 300 (≈ 200) OUR ESTIMATE			
152 ± 55	MANLEY	92	IPWA $\pi N \rightarrow \pi N \& N\pi\pi$
300 ± 100	CUTKOSKY	80	IPWA $\pi N \rightarrow \pi N$
220 ± 80	HOEHLER	79	IPWA $\pi N \rightarrow \pi N$
• • • We do not use the following data for averages, fits, limits, etc. • • •			
330 ± 60	HORN	08A	DPWA Multichannel
525 ± 32	PENNER	02C	DPWA Multichannel
123 ± 53	VRANA	00	DPWA Multichannel
200 ± 40	CANDLIN	84	DPWA $\pi^+ p \rightarrow \Sigma^+ K^+$
88.3 ± 35.0	¹ CHEW	80	BPWA $\pi^+ p \rightarrow \pi^+ p$
62.0 ± 44.0	¹ CHEW	80	BPWA $\pi^+ p \rightarrow \pi^+ p$

$\Delta(1920)$ POLE POSITION

REAL PART	DOCUMENT ID	TECN	COMMENT
VALUE (MeV)			
1850 to 1950 (≈ 1900) OUR ESTIMATE			
1900	² HOEHLER	93	SPED $\pi N \rightarrow \pi N$
1900 ± 80	CUTKOSKY	80	IPWA $\pi N \rightarrow \pi N$
• • • We do not use the following data for averages, fits, limits, etc. • • •			
1980 ± 25	HORN	08A	DPWA Multichannel
45			
1880	VRANA	00	DPWA Multichannel
not seen	ARNDT	91	DPWA $\pi N \rightarrow \pi N$ Soln SM90

IMAGINARY PART	DOCUMENT ID	TECN	COMMENT
VALUE (MeV)			
200 to 400 (≈ 300) OUR ESTIMATE			
300 ± 100	CUTKOSKY	80	IPWA $\pi N \rightarrow \pi N$
• • • We do not use the following data for averages, fits, limits, etc. • • •			
310 ± 40	HORN	08A	DPWA Multichannel
60			
120	VRANA	00	DPWA Multichannel
not seen	ARNDT	91	DPWA $\pi N \rightarrow \pi N$ Soln SM90

$\Delta(1920)$ ELASTIC POLE RESIDUE

MODULUS $ r $	DOCUMENT ID	TECN	COMMENT
VALUE (MeV)			
24 ± 4	CUTKOSKY	80	IPWA $\pi N \rightarrow \pi N$

PHASE θ	DOCUMENT ID	TECN	COMMENT
VALUE ($^\circ$)			
-15.0 ± 3.0	CUTKOSKY	80	IPWA $\pi N \rightarrow \pi N$

$\Delta(1920)$ DECAY MODES

The following branching fractions are our estimates, not fits or averages.

Mode	Fraction (Γ_i / Γ)
$\Gamma_1 N\pi$	5–20 %
$\Gamma_2 \Sigma K$	(2.10 ± 0.30) %
$\Gamma_3 N\pi\pi$	
$\Gamma_4 \Delta(1232)\pi, P\text{-wave}$	
$\Gamma_5 N(1440)\pi, P\text{-wave}$	
$\Gamma_6 N(1535)\pi$	
$\Gamma_7 N_{a_0}(980)$	
$\Gamma_8 \Delta(1232)\eta$	
$\Gamma_9 N\gamma, \text{ helicity}=1/2$	
$\Gamma_{10} N\gamma, \text{ helicity}=3/2$	

$\Delta(1920)$ BRANCHING RATIOS

$\Gamma(N\pi) / \Gamma_{\text{total}}$	DOCUMENT ID	TECN	COMMENT	Γ_1 / Γ
VALUE				
0.05 to 0.2 OUR ESTIMATE				
0.02 ± 0.02	MANLEY	92	IPWA $\pi N \rightarrow \pi N \& N\pi\pi$	
0.20 ± 0.05	CUTKOSKY	80	IPWA $\pi N \rightarrow \pi N$	
0.14 ± 0.04	HOEHLER	79	IPWA $\pi N \rightarrow \pi N$	
• • • We do not use the following data for averages, fits, limits, etc. • • •				
0.15 ± 0.08	HORN	08A	DPWA Multichannel	
0.15 ± 0.01	PENNER	02C	DPWA Multichannel	
0.05 ± 0.04	VRANA	00	DPWA Multichannel	
0.24	¹ CHEW	80	BPWA $\pi^+ p \rightarrow \pi^+ p$	
0.18	¹ CHEW	80	BPWA $\pi^+ p \rightarrow \pi^+ p$	

$(\Gamma_1 \Gamma_2)^{1/2} / \Gamma_{\text{total}}$ in $N\pi \rightarrow \Delta(1920) \rightarrow \Sigma K$	DOCUMENT ID	TECN	COMMENT	$(\Gamma_1 \Gamma_2)^{1/2} / \Gamma$
VALUE				
-0.052 ± 0.015	CANDLIN	84	DPWA $\pi^+ p \rightarrow \Sigma^+ K^+$	
• • • We do not use the following data for averages, fits, limits, etc. • • •				
-0.049	LIVANOS	80	DPWA $\pi p \rightarrow \Sigma K$	

Baryon Particle Listings

$\Delta(1920)$, $\Delta(1930)$

$\Gamma(\Sigma K)/\Gamma_{total}$	DOCUMENT ID	TECN	COMMENT	Γ_2/Γ
VALUE 0.021 ± 0.003	PENNER	02C	DPWA	Multichannel

$(\Gamma_1 \Gamma_7)^{1/2}/\Gamma_{total}$ in $N\pi \rightarrow \Delta(1920) \rightarrow \Delta(1232)\pi$, P -wave	DOCUMENT ID	TECN	COMMENT	$(\Gamma_1 \Gamma_4)^{1/2}/\Gamma$
VALUE -0.13 ± 0.04	MANLEY	92	IPWA	$\pi N \rightarrow \pi N$ & $N\pi\pi$

$\Gamma(\Delta(1232)\pi, P\text{-wave})/\Gamma_{total}$	DOCUMENT ID	TECN	COMMENT	Γ_4/Γ
VALUE 0.41 ± 0.03	VRANA	00	DPWA	Multichannel

$(\Gamma_1 \Gamma_7)^{1/2}/\Gamma_{total}$ in $N\pi \rightarrow \Delta(1920) \rightarrow N(1440)\pi$, P -wave	DOCUMENT ID	TECN	COMMENT	$(\Gamma_1 \Gamma_5)^{1/2}/\Gamma$
VALUE +0.06 ± 0.07	MANLEY	92	IPWA	$\pi N \rightarrow \pi N$ & $N\pi\pi$

$\Gamma(N(1440)\pi, P\text{-wave})/\Gamma_{total}$	DOCUMENT ID	TECN	COMMENT	Γ_5/Γ
VALUE 0.53 ± 0.08	VRANA	00	DPWA	Multichannel

$\Gamma(N(1535)\pi)/\Gamma_{total}$	DOCUMENT ID	TECN	COMMENT	Γ_6/Γ
VALUE 0.06 ± 0.04	HORN	08A	DPWA	Multichannel

$\Gamma(Na_0(980))/\Gamma_{total}$	DOCUMENT ID	TECN	COMMENT	Γ_7/Γ
VALUE 0.04 ± 0.02	HORN	08A	DPWA	Multichannel

$\Gamma(\Delta(1232)\eta)/\Gamma_{total}$	DOCUMENT ID	TECN	COMMENT	Γ_8/Γ
VALUE 0.10 ± 0.05	HORN	08A	DPWA	Multichannel

$\Delta(1920)$ PHOTON DECAY AMPLITUDES

Papers on γN amplitudes predating 1981 may be found in our 2006 edition, Journal of Physics, G **33** 1 (2006).

$\Delta(1920) \rightarrow N\gamma$, helicity-1/2 amplitude $A_{1/2}$	DOCUMENT ID	TECN	COMMENT
VALUE (GeV ^{-1/2}) 0.040 ± 0.014	AWAJI	81	DPWA $\gamma N \rightarrow \pi N$
• • • We do not use the following data for averages, fits, limits, etc. • • •			
0.022 ± 0.008	HORN	08A	DPWA Multichannel
-0.007	PENNER	02D	DPWA Multichannel

$\Delta(1920) \rightarrow N\gamma$, helicity-3/2 amplitude $A_{3/2}$	DOCUMENT ID	TECN	COMMENT
VALUE (GeV ^{-1/2}) 0.023 ± 0.017	AWAJI	81	DPWA $\gamma N \rightarrow \pi N$
• • • We do not use the following data for averages, fits, limits, etc. • • •			
0.042 ± 0.012	HORN	08A	DPWA Multichannel
-0.001	PENNER	02D	DPWA Multichannel

$\Delta(1920)$ FOOTNOTES

- ¹ CHEW 80 reports two P_{33} resonances in this mass region. Problems with this analysis are discussed in section 2.1.11 of HOEHLER 83.
- ² See HOEHLER 93 for a detailed discussion of the evidence for and the pole parameters of N and Δ resonances as determined from Argand diagrams of πN elastic partial-wave amplitudes and from plots of the speeds with which the amplitudes traverse the diagrams.

$\Delta(1920)$ REFERENCES

For early references, see Physics Letters **111B** 1 (1982).

HORN	08A	EPJ A38 173	I. Horn et al.	(CB-ELSA Collab.)
Also		PRL 101 202002	I. Horn et al.	(CB-ELSA Collab.)
ARNDT	06	PR C74 045205	R.A. Arndt et al.	(GWU)
PDG	06	JPG 33 1	W.-M. Yao et al.	(PDG Collab.)
PENNER	02C	PR C66 055211	G. Penner, U. Mosel	(GIES)
PENNER	02D	PR C66 055212	G. Penner, U. Mosel	(GIES)
VRANA	00	PRPL 326 181	T.P. Vrana, S.A. Dytman, T.-S.H. Lee	(PITT+)
HOEHLER	93	πN Newsletter 9 1	G. Hohler	(KARL)
MANLEY	92	PR D45 4002	D.M. Manley, E.M. Saleski	(KENT) IJP
Also		PR D30 904	D.M. Manley et al.	(VPI)
ARNDT	91	PR D43 2131	R.A. Arndt et al.	(VPI, TELE) IJP
CANDLIN	84	NP B238 477	D.J. Candlin et al.	(EDIN, RAL, LOWC)
HOEHLER	83	Landolt-Boernstein 1/9B2	G. Hohler	(KARLT)
PDG	82	PL 111B 1	M. Roos et al.	(HELZ, CIT, CERN)
AWAJI	81	Bonn Conf. 352	N. Awaji, R. Kajikawa	(NAGO)
Also		NP B197 365	K. Fujii et al.	(NAGO)
CHEW	80	Toronto Conf. 123	D.M. Chew	(LBL) IJP
CUTKOSKY	80	Toronto Conf. 19	R.E. Cutkosky et al.	(CMU, LBL) IJP
Also		PR D20 2839	R.E. Cutkosky et al.	(CMU, LBL) IJP
LIVANOS	80	Toronto Conf. 35	P. Livanos et al.	(SACL) IJP
HOEHLER	79	PDAT 12-1	G. Hohler et al.	(KARLT) IJP
Also		Toronto Conf. 3	R. Koch	(KARLT) IJP

$\Delta(1930) D_{35}$

$$I(J^P) = \frac{3}{2}(\frac{5}{2}^-) \text{ Status: } ***$$

Most of the results published before 1975 were last included in our 1982 edition, Physics Letters **111B** 1 (1982). Some further obsolete results published before 1984 were last included in our 2006 edition, Journal of Physics, G **33** 1 (2006).

$\Delta(1930)$ BREIT-WIGNER MASS

VALUE (MeV)	DOCUMENT ID	TECN	COMMENT
1900 to 2020 (\approx 1960) OUR ESTIMATE			
2233 ± 53	ARNDT	06	DPWA $\pi N \rightarrow \pi N, \eta N$
1956 ± 22	MANLEY	92	IPWA $\pi N \rightarrow \pi N$ & $N\pi\pi$
1940 ± 30	CUTKOSKY	80	IPWA $\pi N \rightarrow \pi N$
1901 ± 15	HOEHLER	79	IPWA $\pi N \rightarrow \pi N$
• • • We do not use the following data for averages, fits, limits, etc. • • •			
2046 ± 45	ARNDT	04	DPWA $\pi N \rightarrow \pi N, \eta N$
1932 ± 100	VRANA	00	DPWA Multichannel
1955 ± 15	ARNDT	96	IPWA $\gamma N \rightarrow \pi N$
2056	ARNDT	95	DPWA $\pi N \rightarrow N\pi$
1963	LI	93	IPWA $\gamma N \rightarrow \pi N$
1910.0 ⁺ 15.0 - 17.2	CHEW	80	BPWA $\pi^+ p \rightarrow \pi^+ p$

$\Delta(1930)$ BREIT-WIGNER WIDTH

VALUE (MeV)	DOCUMENT ID	TECN	COMMENT
220 to 500 (\approx 360) OUR ESTIMATE			
773 ± 187	ARNDT	06	DPWA $\pi N \rightarrow \pi N, \eta N$
530 ± 140	MANLEY	92	IPWA $\pi N \rightarrow \pi N$ & $N\pi\pi$
320 ± 60	CUTKOSKY	80	IPWA $\pi N \rightarrow \pi N$
195 ± 60	HOEHLER	79	IPWA $\pi N \rightarrow \pi N$
• • • We do not use the following data for averages, fits, limits, etc. • • •			
402 ± 198	ARNDT	04	DPWA $\pi N \rightarrow \pi N, \eta N$
316 ± 237	VRANA	00	DPWA Multichannel
350 ± 20	ARNDT	96	IPWA $\gamma N \rightarrow \pi N$
590	ARNDT	95	DPWA $\pi N \rightarrow N\pi$
260	LI	93	IPWA $\gamma N \rightarrow \pi N$
74.8 ⁺ 17.0 - 16.0	CHEW	80	BPWA $\pi^+ p \rightarrow \pi^+ p$

$\Delta(1930)$ POLE POSITION

REAL PART	DOCUMENT ID	TECN	COMMENT
VALUE (MeV)			
1840 to 1960 (\approx 1900) OUR ESTIMATE			
2001	ARNDT	06	DPWA $\pi N \rightarrow \pi N, \eta N$
1850	¹ HOEHLER	93	SPED $\pi N \rightarrow \pi N$
1890 ± 50	CUTKOSKY	80	IPWA $\pi N \rightarrow \pi N$
• • • We do not use the following data for averages, fits, limits, etc. • • •			
1966	ARNDT	04	DPWA $\pi N \rightarrow \pi N, \eta N$
1883	VRANA	00	DPWA Multichannel
1913	ARNDT	95	DPWA $\pi N \rightarrow N\pi$
2018	ARNDT	91	DPWA $\pi N \rightarrow \pi N$ Soln SM90

-2xIMAGINARY PART

VALUE (MeV)	DOCUMENT ID	TECN	COMMENT
175 to 360 (\approx 270) OUR ESTIMATE			
387	ARNDT	06	DPWA $\pi N \rightarrow \pi N, \eta N$
180	¹ HOEHLER	93	SPED $\pi N \rightarrow \pi N$
260 ± 60	CUTKOSKY	80	IPWA $\pi N \rightarrow \pi N$
• • • We do not use the following data for averages, fits, limits, etc. • • •			
364	ARNDT	04	DPWA $\pi N \rightarrow \pi N, \eta N$
250	VRANA	00	DPWA Multichannel
246	ARNDT	95	DPWA $\pi N \rightarrow N\pi$
398	ARNDT	91	DPWA $\pi N \rightarrow \pi N$ Soln SM90

$\Delta(1930)$ ELASTIC POLE RESIDUE

MODULUS $ r $	DOCUMENT ID	TECN	COMMENT
VALUE (MeV)			
7	ARNDT	06	DPWA $\pi N \rightarrow \pi N, \eta N$
20	HOEHLER	93	SPED $\pi N \rightarrow \pi N$
18 ± 6	CUTKOSKY	80	IPWA $\pi N \rightarrow \pi N$
• • • We do not use the following data for averages, fits, limits, etc. • • •			
16	ARNDT	04	DPWA $\pi N \rightarrow \pi N, \eta N$
8	ARNDT	95	DPWA $\pi N \rightarrow N\pi$
15	ARNDT	91	DPWA $\pi N \rightarrow \pi N$ Soln SM90

Baryon Particle Listings
Δ(1930), Δ(1940)

PHASE θ

Table with columns: VALUE (°), DOCUMENT ID, TECN, COMMENT. Rows include ARNDT 06 DPWA πN → πN, ηN and CUTKOSKY 80 IPWA πN → πN.

• • • We do not use the following data for averages, fits, limits, etc. • • •

Δ(1930) DECAY MODES

The following branching fractions are our estimates, not fits or averages.

Table with columns: Mode, Fraction (Γ_i/Γ). Rows include Nπ, ΣK, Nππ, Nγ, Nγ, helicity=1/2, Nγ, helicity=3/2.

Δ(1930) BRANCHING RATIOS

Table with columns: Γ(Nπ)/Γ_{total}, DOCUMENT ID, TECN, COMMENT, Γ₁/Γ. Includes OUR ESTIMATE values and document references.

Table with columns: (Γ₁Γ₂)^{1/2}/Γ_{total} in Nπ → Δ(1930) → ΣK, DOCUMENT ID, TECN, COMMENT. Includes values < 0.015 and -0.031.

Table with columns: (Γ₁Γ₂)^{1/2}/Γ_{total} in Nπ → Δ(1930) → Nππ, DOCUMENT ID, TECN, COMMENT. Includes value not seen.

Δ(1930) PHOTON DECAY AMPLITUDES

Papers on γN amplitudes predating 1981 may be found in our 2006 edition, Journal of Physics, G 33 1 (2006).

Δ(1930) → Nγ, helicity-1/2 amplitude A_{1/2}

Table with columns: VALUE (GeV^{-1/2}), DOCUMENT ID, TECN, COMMENT. Includes OUR ESTIMATE values and document references.

Δ(1930) → Nγ, helicity-3/2 amplitude A_{3/2}

Table with columns: VALUE (GeV^{-1/2}), DOCUMENT ID, TECN, COMMENT. Includes OUR ESTIMATE values and document references.

Δ(1930) FOOTNOTES

¹ See HOEHLER 93 for a detailed discussion of the evidence for and the pole parameters of N and Δ resonances as determined from Argand diagrams of πN elastic partial-wave amplitudes and from plots of the speeds with which the amplitudes traverse the diagrams.

Δ(1930) REFERENCES

For early references, see Physics Letters 111B 1 (1982).

Reference list for Δ(1930) with columns: DOCUMENT ID, TECN, COMMENT. Includes entries like ARNDT 06 PR C74 045205 and PDG Collab.

Δ(1940) D₃₃

I(J^P) = 3/2(3/2⁻) Status: *

OMITTED FROM SUMMARY TABLE

The latest GWU analysis (ARNDT 06) finds no evidence for this resonance.

Δ(1940) BREIT-WIGNER MASS

Table with columns: VALUE (MeV), DOCUMENT ID, TECN, COMMENT. Includes OUR ESTIMATE values and document references.

Δ(1940) BREIT-WIGNER WIDTH

Table with columns: VALUE (MeV), DOCUMENT ID, TECN, COMMENT. Includes values like 460 ± 320 and 1985 ± 30.

Δ(1940) POLE POSITION

REAL PART

Table with columns: VALUE (MeV), DOCUMENT ID, TECN, COMMENT. Includes values like 1900 ± 100 and 1985 ± 30.

-2xIMAGINARY PART

Table with columns: VALUE (MeV), DOCUMENT ID, TECN, COMMENT. Includes values like 200 ± 60 and 390 ± 50.

Δ(1940) ELASTIC POLE RESIDUE

MODULUS |r|

Table with columns: VALUE (MeV), DOCUMENT ID, TECN, COMMENT. Includes value 8 ± 3.

PHASE θ

Table with columns: VALUE (°), DOCUMENT ID, TECN, COMMENT. Includes value 135 ± 45.

Baryon Particle Listings

$\Delta(1940), \Delta(1950)$

$\Delta(1940)$ DECAY MODES

Mode	
Γ_1	$N\pi$
Γ_2	ΣK
Γ_3	$N\pi\pi$
Γ_4	$\Delta(1232)\pi, S\text{-wave}$
Γ_5	$\Delta(1232)\pi, D\text{-wave}$
Γ_6	$N\rho, S=3/2, S\text{-wave}$
Γ_7	$N(1535)\pi$
Γ_8	$N a_0(980)$
Γ_9	$\Delta(1232)\eta$
Γ_{10}	$N\gamma, \text{helicity}=1/2$
Γ_{11}	$N\gamma, \text{helicity}=3/2$

$\Delta(1940)$ BRANCHING RATIOS

$\Gamma(N\pi)/\Gamma_{\text{total}}$	DOCUMENT ID	TECN	COMMENT	Γ_1/Γ
0.18±0.12	MANLEY 92	IPWA	$\pi N \rightarrow \pi N \& N\pi\pi$	
0.18	CHEW 80	BPWA	$\pi^+ p \rightarrow \pi^+ p$	
0.05±0.02	CUTKOSKY 80	IPWA	$\pi N \rightarrow \pi N$	
••• We do not use the following data for averages, fits, limits, etc. •••				
0.09±0.04	HORN 08A	DPWA	Multichannel	

$(\Gamma_1\Gamma_7)^{1/2}/\Gamma_{\text{total}}$ in $N\pi \rightarrow \Delta(1940) \rightarrow \Sigma K$	DOCUMENT ID	TECN	COMMENT	$(\Gamma_1\Gamma_2)^{1/2}/\Gamma$
<0.015	CANDLIN 84	DPWA	$\pi^+ p \rightarrow \Sigma^+ K^+$	

$(\Gamma_1\Gamma_7)^{1/2}/\Gamma_{\text{total}}$ in $N\pi \rightarrow \Delta(1940) \rightarrow \Delta(1232)\pi, S\text{-wave}$	DOCUMENT ID	TECN	COMMENT	$(\Gamma_1\Gamma_4)^{1/2}/\Gamma$
+0.11±0.10	MANLEY 92	IPWA	$\pi N \rightarrow \pi N \& N\pi\pi$	

$(\Gamma_1\Gamma_7)^{1/2}/\Gamma_{\text{total}}$ in $N\pi \rightarrow \Delta(1940) \rightarrow \Delta(1232)\pi, D\text{-wave}$	DOCUMENT ID	TECN	COMMENT	$(\Gamma_1\Gamma_5)^{1/2}/\Gamma$
+0.27±0.16	MANLEY 92	IPWA	$\pi N \rightarrow \pi N \& N\pi\pi$	

$(\Gamma_1\Gamma_7)^{1/2}/\Gamma_{\text{total}}$ in $N\pi \rightarrow \Delta(1940) \rightarrow N\rho, S=3/2, S\text{-wave}$	DOCUMENT ID	TECN	COMMENT	$(\Gamma_1\Gamma_6)^{1/2}/\Gamma$
+0.25±0.10	MANLEY 92	IPWA	$\pi N \rightarrow \pi N \& N\pi\pi$	

$\Gamma(N(1535)\pi)/\Gamma_{\text{total}}$	DOCUMENT ID	TECN	COMMENT	Γ_7/Γ
0.02±0.01	HORN 08A	DPWA	Multichannel	

$\Gamma(N a_0(980))/\Gamma_{\text{total}}$	DOCUMENT ID	TECN	COMMENT	Γ_8/Γ
0.02±0.01	HORN 08A	DPWA	Multichannel	

$\Gamma(\Delta(1232)\eta)/\Gamma_{\text{total}}$	DOCUMENT ID	TECN	COMMENT	Γ_9/Γ
0.04±0.02	HORN 08A	DPWA	Multichannel	

$\Delta(1940)$ PHOTON DECAY AMPLITUDES

Papers on γN amplitudes predating 1981 may be found in our 2006 edition, Journal of Physics, G **33** 1 (2006).

$\Delta(1940) \rightarrow N\gamma, \text{helicity-1/2}$ amplitude $A_{1/2}$

VALUE (GeV ^{-1/2})	DOCUMENT ID	TECN	COMMENT
-0.036±0.058	AWAJI 81	DPWA	$\gamma N \rightarrow \pi N$
••• We do not use the following data for averages, fits, limits, etc. •••			
0.160±0.040	HORN 08A	DPWA	Multichannel

$\Delta(1940) \rightarrow N\gamma, \text{helicity-3/2}$ amplitude $A_{3/2}$

VALUE (GeV ^{-1/2})	DOCUMENT ID	TECN	COMMENT
-0.031±0.012	AWAJI 81	DPWA	$\gamma N \rightarrow \pi N$
••• We do not use the following data for averages, fits, limits, etc. •••			
0.110±0.030	HORN 08A	DPWA	Multichannel

$\Delta(1940)$ FOOTNOTES

¹ LONGACRE 78 values are from a search for poles in the unitarized T-matrix. The first (second) value uses, in addition to $\pi N \rightarrow N\pi\pi$ data, elastic amplitudes from a Saclay (CERN) partial-wave analysis.

$\Delta(1940)$ REFERENCES

HORN 08A	EPI A38 173	I. Horn <i>et al.</i>	(CB-ELSA Collab.)
Also	PRL 101 202002	I. Horn <i>et al.</i>	(CB-ELSA Collab.)
ARNDT 06	PR C74 045205	R.A. Arndt <i>et al.</i>	(GWU)
PDG 06	JPG 33 1	W.-M. Yao <i>et al.</i>	(PDG Collab.)
MANLEY 92	PR D45 4002	D.M. Manley, E.M. Saleski	(KENT) IJP
Also	PR D30 904	D.M. Manley <i>et al.</i>	(VPI)
CANDLIN 84	NP B238 477	D.J. Candlin <i>et al.</i>	(EDIN, RAL, LOWC)
AWAJI 81	Bonn Conf. 352	N. Awaji, R. Kajikawa	(NAGO)
Also	NP B197 365	K. Fujii <i>et al.</i>	(NAGO)
CHEW 80	Toronto Conf. 123	D.M. Chew	(LBL) IJP
CUTKOSKY 80	Toronto Conf. 19	R.E. Cutkosky <i>et al.</i>	(CMU, LBL) IJP
Also	PR D20 2839	R.E. Cutkosky <i>et al.</i>	(CMU, LBL)
LONGACRE 78	PR D17 1795	R.S. Longacre <i>et al.</i>	(LBL, SLAC)

$\Delta(1950) F_{37}$

$$I(J^P) = \frac{3}{2}(\frac{7}{2}^+) \text{ Status: } ***$$

Most of the results published before 1975 were last included in our 1982 edition, Physics Letters **111B** 1 (1982). Some further obsolete results published before 1984 were last included in our 2006 edition, Journal of Physics, G **33** 1 (2006).

$\Delta(1950)$ BREIT-WIGNER MASS

VALUE (MeV)	DOCUMENT ID	TECN	COMMENT
1915 to 1950 (\approx 1930) OUR ESTIMATE			
1921.3± 0.2	ARNDT 06	DPWA	$\pi N \rightarrow \pi N, \eta N$
1945 ± 2	MANLEY 92	IPWA	$\pi N \rightarrow \pi N \& N\pi\pi$
1950 ± 15	CUTKOSKY 80	IPWA	$\pi N \rightarrow \pi N$
1913 ± 8	HOEHLER 79	IPWA	$\pi N \rightarrow \pi N$
••• We do not use the following data for averages, fits, limits, etc. •••			
1923.3± 0.5	ARNDT 04	DPWA	$\pi N \rightarrow \pi N, \eta N$
1936 ± 5	VRANA 00	DPWA	Multichannel
1947 ± 9	ARNDT 96	IPWA	$\gamma N \rightarrow \pi N$
1921	ARNDT 95	DPWA	$\pi N \rightarrow N\pi$
1940	LI 93	IPWA	$\gamma N \rightarrow \pi N$
1925 ± 20	CANDLIN 84	DPWA	$\pi^+ p \rightarrow \Sigma^+ K^+$
1855.0 ^{+11.0} _{-10.0}	CHEW 80	BPWA	$\pi^+ p \rightarrow \pi^+ p$
1925	¹ LONGACRE 75	IPWA	$\pi N \rightarrow N\pi\pi$

$\Delta(1950)$ BREIT-WIGNER WIDTH

VALUE (MeV)	DOCUMENT ID	TECN	COMMENT
235 to 335 (\approx 285) OUR ESTIMATE			
271.1± 1.1	ARNDT 06	DPWA	$\pi N \rightarrow \pi N, \eta N$
300 ± 7	MANLEY 92	IPWA	$\pi N \rightarrow \pi N \& N\pi\pi$
340 ± 50	CUTKOSKY 80	IPWA	$\pi N \rightarrow \pi N$
224 ± 10	HOEHLER 79	IPWA	$\pi N \rightarrow \pi N$
••• We do not use the following data for averages, fits, limits, etc. •••			
278.2± 3.0	ARNDT 04	DPWA	$\pi N \rightarrow \pi N, \eta N$
245 ± 12	VRANA 00	DPWA	Multichannel
302 ± 9	ARNDT 96	IPWA	$\gamma N \rightarrow \pi N$
232	ARNDT 95	DPWA	$\pi N \rightarrow N\pi$
306	LI 93	IPWA	$\gamma N \rightarrow \pi N$
330 ± 40	CANDLIN 84	DPWA	$\pi^+ p \rightarrow \Sigma^+ K^+$
157.2 ^{+22.0} _{-19.0}	CHEW 80	BPWA	$\pi^+ p \rightarrow \pi^+ p$
240	¹ LONGACRE 75	IPWA	$\pi N \rightarrow N\pi\pi$

$\Delta(1950)$ POLE POSITION

REAL PART

VALUE (MeV)	DOCUMENT ID	TECN	COMMENT
1870 to 1890 (\approx 1880) OUR ESTIMATE			
1876	ARNDT 06	DPWA	$\pi N \rightarrow \pi N, \eta N$
1878	² HOEHLER 93	ARGD	$\pi N \rightarrow \pi N$
1890±15	CUTKOSKY 80	IPWA	$\pi N \rightarrow \pi N$
••• We do not use the following data for averages, fits, limits, etc. •••			
1874	ARNDT 04	DPWA	$\pi N \rightarrow \pi N, \eta N$
1910	VRANA 00	DPWA	Multichannel
1880	ARNDT 95	DPWA	$\pi N \rightarrow N\pi$
1884	ARNDT 91	DPWA	$\pi N \rightarrow \pi N$ Soln SM90
1924 or 1924	³ LONGACRE 78	IPWA	$\pi N \rightarrow N\pi\pi$

-2xIMAGINARY PART

VALUE (MeV)	DOCUMENT ID	TECN	COMMENT
220 to 260 (\approx 240) OUR ESTIMATE			
227	ARNDT 06	DPWA	$\pi N \rightarrow \pi N, \eta N$
230	² HOEHLER 93	ARGD	$\pi N \rightarrow \pi N$
260±40	CUTKOSKY 80	IPWA	$\pi N \rightarrow \pi N$
••• We do not use the following data for averages, fits, limits, etc. •••			
236	ARNDT 04	DPWA	$\pi N \rightarrow \pi N, \eta N$
230	VRANA 00	DPWA	Multichannel
236	ARNDT 95	DPWA	$\pi N \rightarrow N\pi$
238	ARNDT 91	DPWA	$\pi N \rightarrow \pi N$ Soln SM90
258 or 258	³ LONGACRE 78	IPWA	$\pi N \rightarrow N\pi\pi$

$\Delta(1950)$ ELASTIC POLE RESIDUE

MODULUS $|r|$

VALUE (MeV)	DOCUMENT ID	TECN	COMMENT
53	ARNDT 06	DPWA	$\pi N \rightarrow \pi N, \eta N$
47	HOEHLER 93	ARGD	$\pi N \rightarrow \pi N$
50±7	CUTKOSKY 80	IPWA	$\pi N \rightarrow \pi N$
••• We do not use the following data for averages, fits, limits, etc. •••			
57	ARNDT 04	DPWA	$\pi N \rightarrow \pi N, \eta N$
54	ARNDT 95	DPWA	$\pi N \rightarrow N\pi$
61	ARNDT 91	DPWA	$\pi N \rightarrow \pi N$ Soln SM90

PHASE θ

VALUE (°)	DOCUMENT ID	TECN	COMMENT
-31	ARNDT 06	DPWA	$\pi N \rightarrow \pi N, \eta N$
-32	HOEHLER 93	ARGD	$\pi N \rightarrow \pi N$
-33±8	CUTKOSKY 80	IPWA	$\pi N \rightarrow \pi N$
••• We do not use the following data for averages, fits, limits, etc. •••			
-34	ARNDT 04	DPWA	$\pi N \rightarrow \pi N, \eta N$
-17	ARNDT 95	DPWA	$\pi N \rightarrow N\pi$
-23	ARNDT 91	DPWA	$\pi N \rightarrow \pi N$ Soln SM90

$\Delta(1950)$ DECAY MODES

The following branching fractions are our estimates, not fits or averages.

Mode	Fraction (Γ_i/Γ)
Γ_1 $N\pi$	0.35 to 0.45
Γ_2 ΣK	
Γ_3 $N\pi\pi$	
Γ_4 $\Delta\pi$	20-30 %
Γ_5 $\Delta(1232)\pi, F\text{-wave}$	
Γ_6 $\Delta(1232)\pi, H\text{-wave}$	
Γ_7 $N\rho$	<10 %
Γ_8 $N\rho, S=1/2, F\text{-wave}$	
Γ_9 $N\rho, S=3/2, F\text{-wave}$	
Γ_{10} $N\gamma$	0.08-0.13 %
Γ_{11} $N\gamma, \text{helicity}=1/2$	0.03-0.055 %
Γ_{12} $N\gamma, \text{helicity}=3/2$	0.05-0.075 %

$\Delta(1950)$ BRANCHING RATIOS

$\Gamma(N\pi)/\Gamma_{\text{total}}$	DOCUMENT ID	TECN	COMMENT	Γ_1/Γ
0.35 to 0.45 OUR ESTIMATE				
0.471±0.001	ARNDT 06	DPWA	$\pi N \rightarrow \pi N, \eta N$	
0.38±0.01	MANLEY 92	IPWA	$\pi N \rightarrow \pi N \& N\pi\pi$	
0.39±0.04	CUTKOSKY 80	IPWA	$\pi N \rightarrow \pi N$	
0.38±0.02	HOEHLER 79	IPWA	$\pi N \rightarrow \pi N$	
••• We do not use the following data for averages, fits, limits, etc. •••				
0.480±0.002	ARNDT 04	DPWA	$\pi N \rightarrow \pi N, \eta N$	
0.44±0.01	VRANA 00	DPWA	Multichannel	
0.49	ARNDT 95	DPWA	$\pi N \rightarrow N\pi$	
0.44	CHEW 80	BPWA	$\pi^+\rho \rightarrow \pi^+\rho$	

$(\Gamma_1\Gamma_f)^{1/2}/\Gamma_{\text{total}}$ in $N\pi \rightarrow \Delta(1950) \rightarrow \Sigma K$	DOCUMENT ID	TECN	COMMENT	$(\Gamma_1\Gamma_2)^{1/2}/\Gamma$
-0.053±0.005	CANDLIN 84	DPWA	$\pi^+\rho \rightarrow \Sigma^+ K^+$	

Note: Signs of couplings from $\pi N \rightarrow N\pi\pi$ analyses were changed in the 1986 edition to agree with the baryon-first convention; the overall phase ambiguity is resolved by choosing a negative sign for the $\Delta(1620) S_{31}$ coupling to $\Delta(1232)\pi$.

$(\Gamma_1\Gamma_f)^{1/2}/\Gamma_{\text{total}}$ in $N\pi \rightarrow \Delta(1950) \rightarrow \Delta(1232)\pi, F\text{-wave}$	DOCUMENT ID	TECN	COMMENT	$(\Gamma_1\Gamma_5)^{1/2}/\Gamma$
+0.28 to +0.32 OUR ESTIMATE				
+0.27±0.02	MANLEY 92	IPWA	$\pi N \rightarrow \pi N \& N\pi\pi$	
+0.32	¹ LONGACRE 75	IPWA	$\pi N \rightarrow N\pi\pi$	

$\Gamma(\Delta(1232)\pi, F\text{-wave})/\Gamma_{\text{total}}$	DOCUMENT ID	TECN	COMMENT	Γ_5/Γ
0.36±0.01	VRANA 00	DPWA	Multichannel	

$(\Gamma_1\Gamma_f)^{1/2}/\Gamma_{\text{total}}$ in $N\pi \rightarrow \Delta(1950) \rightarrow N\rho, S=3/2, F\text{-wave}$	DOCUMENT ID	TECN	COMMENT	$(\Gamma_1\Gamma_9)^{1/2}/\Gamma$
+0.24	¹ LONGACRE 75	IPWA	$\pi N \rightarrow N\pi\pi$	

$\Delta(1950)$ PHOTON DECAY AMPLITUDES

Papers on γN amplitudes predating 1981 may be found in our 2006 edition, Journal of Physics, G **33** 1 (2006).

$\Delta(1950) \rightarrow N\gamma, \text{helicity-1/2}$ amplitude $A_{1/2}$

VALUE (GeV ^{-1/2})	DOCUMENT ID	TECN	COMMENT
-0.076±0.012 OUR ESTIMATE			
-0.079±0.006	ARNDT 96	IPWA	$\gamma N \rightarrow \pi N$
-0.068±0.007	AWAJI 81	DPWA	$\gamma N \rightarrow \pi N$
••• We do not use the following data for averages, fits, limits, etc. •••			
-0.094	DRECHSEL 07	DPWA	$\gamma N \rightarrow \pi N$
-0.102±0.003	LI 93	IPWA	$\gamma N \rightarrow \pi N$

$\Delta(1950) \rightarrow N\gamma, \text{helicity-3/2}$ amplitude $A_{3/2}$

VALUE (GeV ^{-1/2})	DOCUMENT ID	TECN	COMMENT
-0.097±0.010 OUR ESTIMATE			
-0.103±0.006	ARNDT 96	IPWA	$\gamma N \rightarrow \pi N$
-0.094±0.016	AWAJI 81	DPWA	$\gamma N \rightarrow \pi N$
••• We do not use the following data for averages, fits, limits, etc. •••			
-0.121	DRECHSEL 07	DPWA	$\gamma N \rightarrow \pi N$
-0.115±0.003	LI 93	IPWA	$\gamma N \rightarrow \pi N$

$\Delta(1950)$ FOOTNOTES

- From method II of LONGACRE 75: eyeball fits with Breit-Wigner circles to the T-matrix amplitudes.
- See HOEHLER 93 for a detailed discussion of the evidence for and the pole parameters of N and Δ resonances as determined from Argand diagrams of πN elastic partial-wave amplitudes and from plots of the speeds with which the amplitudes traverse the diagrams.
- LONGACRE 78 values are from a search for poles in the unitarized T-matrix. The first (second) value uses, in addition to $\pi N \rightarrow N\pi\pi$ data, elastic amplitudes from a Saclay (CERN) partial-wave analysis.

$\Delta(1950)$ REFERENCES

DRECHSEL 07	EPJ A34 69	D. Drechsel, S.S. Kamalov, L. Tiator	(MAINZ, JINR)
ARNDT 06	PR C74 045205	R.A. Arndt et al.	(GWU)
PDG 06	JPG 33 1	W.-M. Yao et al.	(PDG Collab.)
ARNDT 04	PR C69 035213	R.A. Arndt et al.	(GWU, TRIU)
VRANA 00	PRPL 328 181	T.P. Vrana, S.A. Dytman., T.-S.H. Lee	(PITT+)
ARNDT 96	PR C53 430	R.A. Arndt, I.I. Strakovsky, R.L. Workman	(VPI)
ARNDT 95	PR C52 2120	R.A. Arndt et al.	(VPI, BRGO)
HOEHLER 93	πN Newsletter 9 1	G. Hohlner	(KARL)
LI 93	PR C47 2759	Z.J. Li et al.	(VPI)
MANLEY 92	PR D45 4002	D.M. Manley, E.M. Saleski	(KENT) IUP
Also	PR D30 904	D.M. Manley et al.	(VPI)
ARNDT 91	PR D43 2131	R.A. Arndt et al.	(VPI, TELE) IUP
CANDLIN 84	NP B238 477	D.J. Candlin et al.	(EDIN, RAL, LOWC)
PDG 82	PL 111B 1	M. Roos et al.	(HEL5, CIT, CERN)
AWAJI 81	Bonn Conf. 352	N. Awaji, R. Kajikawa	(NAGO)
Also	NP B197 365	K. Fujii et al.	(NAGO)
CHEW 80	Toronto Conf. 123	D.M. Chew	(LBL) IUP
CUTKOSKY 80	Toronto Conf. 19	R.E. Cutkosky et al.	(CMU, LBL) IUP
Also	PR D20 2839	R.E. Cutkosky et al.	(CMU, LBL) IUP
HOEHLER 79	PDAT 12-1	G. Hohlner et al.	(KARLT) IUP
Also	Toronto Conf. 3	R. Koch	(KARLT) IUP
LONGACRE 78	PR D17 1795	R.S. Longacre et al.	(LBL, SLAC)
LONGACRE 75	PL 55B 415	R.S. Longacre et al.	(LBL, SLAC) IUP

$\Delta(2000) F_{35}$

$I(J^P) = \frac{3}{2}(\frac{5}{2}^+)$ Status: **

OMITTED FROM SUMMARY TABLE

The latest GWU analysis (ARNDT 06) finds no evidence for this resonance.

$\Delta(2000)$ BREIT-WIGNER MASS

VALUE (MeV)	DOCUMENT ID	TECN	COMMENT
≈ 2000 OUR ESTIMATE			
1724±61	VRANA 00	DPWA	Multichannel
1752±32	MANLEY 92	IPWA	$\pi N \rightarrow \pi N \& N\pi\pi$
2200±125	CUTKOSKY 80	IPWA	$\pi N \rightarrow \pi N$

$\Delta(2000)$ BREIT-WIGNER WIDTH

VALUE (MeV)	DOCUMENT ID	TECN	COMMENT
138±68	VRANA 00	DPWA	Multichannel
251±93	MANLEY 92	IPWA	$\pi N \rightarrow \pi N \& N\pi\pi$
400±125	CUTKOSKY 80	IPWA	$\pi N \rightarrow \pi N$

$\Delta(2000)$ POLE POSITION

REAL PART			
VALUE (MeV)	DOCUMENT ID	TECN	COMMENT
1697	VRANA 00	DPWA	Multichannel
2150±100	CUTKOSKY 80	IPWA	$\pi N \rightarrow \pi N$
-2×IMAGINARY PART			
VALUE (MeV)	DOCUMENT ID	TECN	COMMENT
112	VRANA 00	DPWA	Multichannel
350±100	CUTKOSKY 80	IPWA	$\pi N \rightarrow \pi N$

Baryon Particle Listings

 $\Delta(2000)$, $\Delta(2150)$, $\Delta(2200)$ $\Delta(2000)$ ELASTIC POLE RESIDUEMODULUS $|r|$

VALUE (MeV)	DOCUMENT ID	TECN	COMMENT
16±5	CUTKOSKY 80	IPWA	$\pi N \rightarrow \pi N$

PHASE θ

VALUE (°)	DOCUMENT ID	TECN	COMMENT
150±90	CUTKOSKY 80	IPWA	$\pi N \rightarrow \pi N$

 $\Delta(2000)$ DECAY MODES

Mode	
Γ_1	$N\pi$
Γ_2	$N\pi\pi$
Γ_3	$\Delta(1232)\pi$, P-wave
Γ_4	$\Delta(1232)\pi$, F-wave
Γ_5	$N\rho$, S=3/2, P-wave

 $\Delta(2000)$ BRANCHING RATIOS

$\Gamma(N\pi)/\Gamma_{\text{total}}$	DOCUMENT ID	TECN	COMMENT	Γ_1/Γ
0.00±0.01	VRANA 00	DPWA	Multichannel	
0.02±0.01	MANLEY 92	IPWA	$\pi N \rightarrow \pi N$ & $N\pi\pi$	
0.07±0.04	CUTKOSKY 80	IPWA	$\pi N \rightarrow \pi N$	

$(\Gamma_1\Gamma_2)^{1/2}/\Gamma_{\text{total}}$ in $N\pi \rightarrow \Delta(2000) \rightarrow \Delta(1232)\pi$, P-wave	DOCUMENT ID	TECN	COMMENT	$(\Gamma_1\Gamma_3)^{1/2}/\Gamma$
+0.07±0.03	MANLEY 92	IPWA	$\pi N \rightarrow \pi N$ & $N\pi\pi$	

$\Gamma(\Delta(1232)\pi, \text{P-wave})/\Gamma_{\text{total}}$	DOCUMENT ID	TECN	COMMENT	Γ_3/Γ
0.00±0.01	VRANA 00	DPWA	Multichannel	

$(\Gamma_1\Gamma_2)^{1/2}/\Gamma_{\text{total}}$ in $N\pi \rightarrow \Delta(2000) \rightarrow \Delta(1232)\pi$, F-wave	DOCUMENT ID	TECN	COMMENT	$(\Gamma_1\Gamma_4)^{1/2}/\Gamma$
+0.09±0.04	MANLEY 92	IPWA	$\pi N \rightarrow \pi N$ & $N\pi\pi$	

$\Gamma(\Delta(1232)\pi, \text{F-wave})/\Gamma_{\text{total}}$	DOCUMENT ID	TECN	COMMENT	Γ_4/Γ
0.40±0.01	VRANA 00	DPWA	Multichannel	

$(\Gamma_1\Gamma_2)^{1/2}/\Gamma_{\text{total}}$ in $N\pi \rightarrow \Delta(2000) \rightarrow N\rho$, S=3/2, P-wave	DOCUMENT ID	TECN	COMMENT	$(\Gamma_1\Gamma_5)^{1/2}/\Gamma$
-0.06±0.01	MANLEY 92	IPWA	$\pi N \rightarrow \pi N$ & $N\pi\pi$	

$\Gamma(N\rho, \text{S=3/2, P-wave})/\Gamma_{\text{total}}$	DOCUMENT ID	TECN	COMMENT	Γ_5/Γ
0.60±0.60	VRANA 00	DPWA	Multichannel	

 $\Delta(2000)$ REFERENCES

ARNDT 06	PR C74 045205	R.A. Arndt et al.	(GWU)
VRANA 00	PRPL 328 181	T.P. Vrana, S.A. Dytman., T.-S.H. Lee	(PITT+)
MANLEY 92	PR D45 4002	D.M. Manley, E.M. Saleski	(KENT) IUP
Also	PR D30 904	D.M. Manley et al.	(VPI)
CUTKOSKY 80	Toronto Conf. 19	R.E. Cutkosky et al.	(CMU, LBL) IUP
Also	PR D20 2839	R.E. Cutkosky et al.	(CMU, LBL)

 $\Delta(2150) S_{31}$

$$I(J^P) = \frac{3}{2}(\frac{1}{2}^-) \text{ Status: } *$$

OMITTED FROM SUMMARY TABLE

The latest GWU analysis (ARNDT 06) finds no evidence for this resonance.

 $\Delta(2150)$ BREIT-WIGNER MASS

VALUE (MeV)	DOCUMENT ID	TECN	COMMENT
≈ 2150 OUR ESTIMATE			
2047.4±27.0	¹ CHEW 80	BPWA	$\pi^+ p \rightarrow \pi^+ p$
2203.2±8.4	¹ CHEW 80	BPWA	$\pi^+ p \rightarrow \pi^+ p$
2150 ±100	CUTKOSKY 80	IPWA	$\pi N \rightarrow \pi N$

 $\Delta(2150)$ BREIT-WIGNER WIDTH

VALUE (MeV)	DOCUMENT ID	TECN	COMMENT
121.6±62.0	¹ CHEW 80	BPWA	$\pi^+ p \rightarrow \pi^+ p$
120.5±45.0	¹ CHEW 80	BPWA	$\pi^+ p \rightarrow \pi^+ p$
200 ±100	CUTKOSKY 80	IPWA	$\pi N \rightarrow \pi N$

 $\Delta(2150)$ POLE POSITION

REAL PART

VALUE (MeV)	DOCUMENT ID	TECN	COMMENT
2140±80	CUTKOSKY 80	IPWA	$\pi N \rightarrow \pi N$

-2xIMAGINARY PART

VALUE (MeV)	DOCUMENT ID	TECN	COMMENT
200±80	CUTKOSKY 80	IPWA	$\pi N \rightarrow \pi N$

 $\Delta(2150)$ ELASTIC POLE RESIDUEMODULUS $|r|$

VALUE (MeV)	DOCUMENT ID	TECN	COMMENT
7±2	CUTKOSKY 80	IPWA	$\pi N \rightarrow \pi N$

PHASE θ

VALUE (°)	DOCUMENT ID	TECN	COMMENT
-60±90	CUTKOSKY 80	IPWA	$\pi N \rightarrow \pi N$

 $\Delta(2150)$ DECAY MODES

Mode	
Γ_1	$N\pi$
Γ_2	ΣK

 $\Delta(2150)$ BRANCHING RATIOS

$\Gamma(N\pi)/\Gamma_{\text{total}}$	DOCUMENT ID	TECN	COMMENT	Γ_1/Γ
0.41	¹ CHEW 80	BPWA	$\pi^+ p \rightarrow \pi^+ p$	
0.37	¹ CHEW 80	BPWA	$\pi^+ p \rightarrow \pi^+ p$	
0.08±0.02	CUTKOSKY 80	IPWA	$\pi N \rightarrow \pi N$	

$(\Gamma_1\Gamma_2)^{1/2}/\Gamma_{\text{total}}$ in $N\pi \rightarrow \Delta(2150) \rightarrow \Sigma K$	DOCUMENT ID	TECN	COMMENT	$(\Gamma_1\Gamma_2)^{1/2}/\Gamma$
<0.03	CANDLIN 84	DPWA	$\pi^+ p \rightarrow \Sigma^+ K^+$	

 $\Delta(2150)$ FOOTNOTES

¹ CHEW 80 reports two S_{31} resonances in this mass region. Problems with this analysis are discussed in section 2.1.11 of HOEHLER 83.

 $\Delta(2150)$ REFERENCES

ARNDT 06	PR C74 045205	R.A. Arndt et al.	(GWU)
CANDLIN 84	NP B238 477	D.J. Candlin et al.	(EDIN, RAL, LOWC)
HOEHLER 83	Landolt-Boernstein 1/9B2	G. Hoehler	(KARLT)
CHEW 80	Toronto Conf. 123	D.M. Chew	(LBL) IUP
CUTKOSKY 80	Toronto Conf. 19	R.E. Cutkosky et al.	(CMU, LBL) IUP
Also	PR D20 2839	R.E. Cutkosky et al.	(CMU, LBL)

 $\Delta(2200) G_{37}$

$$I(J^P) = \frac{3}{2}(\frac{1}{2}^-) \text{ Status: } *$$

OMITTED FROM SUMMARY TABLE

The various analyses are not in good agreement.

The latest GWU analysis (ARNDT 06) finds no evidence for this resonance.

 $\Delta(2200)$ BREIT-WIGNER MASS

VALUE (MeV)	DOCUMENT ID	TECN	COMMENT
≈ 2200 OUR ESTIMATE			
2200±80	CUTKOSKY 80	IPWA	$\pi N \rightarrow \pi N$
2215±60	HOEHLER 79	IPWA	$\pi N \rightarrow \pi N$
2280±80	HENDRY 78	MPWA	$\pi N \rightarrow \pi N$
••• We do not use the following data for averages, fits, limits, etc. •••			
2280±40	CANDLIN 84	DPWA	$\pi^+ p \rightarrow \Sigma^+ K^+$

 $\Delta(2200)$ BREIT-WIGNER WIDTH

VALUE (MeV)	DOCUMENT ID	TECN	COMMENT
450±100	CUTKOSKY 80	IPWA	$\pi N \rightarrow \pi N$
400±100	HOEHLER 79	IPWA	$\pi N \rightarrow \pi N$
400±150	HENDRY 78	MPWA	$\pi N \rightarrow \pi N$
••• We do not use the following data for averages, fits, limits, etc. •••			
400±50	CANDLIN 84	DPWA	$\pi^+ p \rightarrow \Sigma^+ K^+$

 $\Delta(2200)$ POLE POSITION

REAL PART

VALUE (MeV)	DOCUMENT ID	TECN	COMMENT
2100±50	CUTKOSKY 80	IPWA	$\pi N \rightarrow \pi N$

See key on page 405

Baryon Particle Listings

$\Delta(2200)$, $\Delta(2300)$, $\Delta(2350)$

-2xIMAGINARY PART

VALUE (MeV)	DOCUMENT ID	TECN	COMMENT
340 ± 80	CUTKOSKY 80	IPWA	$\pi N \rightarrow \pi N$

$\Delta(2200)$ ELASTIC POLE RESIDUE

MODULUS |r|

VALUE (MeV)	DOCUMENT ID	TECN	COMMENT
8 ± 3	CUTKOSKY 80	IPWA	$\pi N \rightarrow \pi N$

PHASE θ

VALUE (°)	DOCUMENT ID	TECN	COMMENT
-70 ± 40	CUTKOSKY 80	IPWA	$\pi N \rightarrow \pi N$

$\Delta(2200)$ DECAY MODES

Mode	Γ_1	Γ_2
$N\pi$	$N\pi$	
ΣK		ΣK

$\Delta(2200)$ BRANCHING RATIOS

$\Gamma(N\pi)/\Gamma_{total}$	DOCUMENT ID	TECN	COMMENT	Γ_1/Γ
0.06 ± 0.02	CUTKOSKY 80	IPWA	$\pi N \rightarrow \pi N$	
0.05 ± 0.02	HOEHLER 79	IPWA	$\pi N \rightarrow \pi N$	
0.09 ± 0.02	HENDRY 78	MPWA	$\pi N \rightarrow \pi N$	

$(\Gamma_1\Gamma_2)^{1/2}/\Gamma_{total}$ in $N\pi \rightarrow \Delta(2200) \rightarrow \Sigma K$	DOCUMENT ID	TECN	COMMENT	$(\Gamma_1\Gamma_2)^{1/2}/\Gamma$
-0.014 ± 0.005	CANDLIN 84	DPWA	$\pi^+ p \rightarrow \Sigma^+ K^+$	

$\Delta(2200)$ REFERENCES

ARNDT 06	PR C74 045205	R.A. Arndt et al.	(GWU)
CANDLIN 84	NP B238 477	D.J. Candlin et al.	(EDIN, RAL, LOWC)
CUTKOSKY 80	Toronto Conf. 19	R.E. Cutkosky et al.	(CMU, LBL) IJP
Also	PR D20 2839	R.E. Cutkosky et al.	(CMU, LBL)
HOEHLER 79	PDAT 12-1	G. Hoehler et al.	(KARLT) IJP
Also	Toronto Conf. 3	R. Koch	(KARLT) IJP
HENDRY 78	PRL 41 222	A.W. Hendry	(IND, LBL) IJP
Also	ANP 136 1	A.W. Hendry	(IND)

$\Delta(2300) H_{39}$

$I(J^P) = \frac{3}{2}(\frac{9}{2}^+)$ Status: **

OMITTED FROM SUMMARY TABLE

The latest GWU analysis (ARNDT 06) finds no evidence for this resonance.

$\Delta(2300)$ BREIT-WIGNER MASS

VALUE (MeV)	DOCUMENT ID	TECN	COMMENT
≈ 2300 OUR ESTIMATE			
2204.5 ± 3.4	CHEW 80	BPWA	$\pi^+ p \rightarrow \pi^+ p$
2400 ± 125	CUTKOSKY 80	IPWA	$\pi N \rightarrow \pi N$
2217 ± 80	HOEHLER 79	IPWA	$\pi N \rightarrow \pi N$
2450 ± 100	HENDRY 78	MPWA	$\pi N \rightarrow \pi N$
••• We do not use the following data for averages, fits, limits, etc. •••			
2400	CANDLIN 84	DPWA	$\pi^+ p \rightarrow \Sigma^+ K^+$

$\Delta(2300)$ BREIT-WIGNER WIDTH

VALUE (MeV)	DOCUMENT ID	TECN	COMMENT
32.3 ± 1.0	CHEW 80	BPWA	$\pi^+ p \rightarrow \pi^+ p$
425 ± 150	CUTKOSKY 80	IPWA	$\pi N \rightarrow \pi N$
300 ± 100	HOEHLER 79	IPWA	$\pi N \rightarrow \pi N$
500 ± 200	HENDRY 78	MPWA	$\pi N \rightarrow \pi N$
••• We do not use the following data for averages, fits, limits, etc. •••			
200	CANDLIN 84	DPWA	$\pi^+ p \rightarrow \Sigma^+ K^+$

$\Delta(2300)$ POLE POSITION

REAL PART	DOCUMENT ID	TECN	COMMENT
2370 ± 80	CUTKOSKY 80	IPWA	$\pi N \rightarrow \pi N$

-2xIMAGINARY PART	DOCUMENT ID	TECN	COMMENT
420 ± 160	CUTKOSKY 80	IPWA	$\pi N \rightarrow \pi N$

$\Delta(2300)$ ELASTIC POLE RESIDUE

MODULUS |r|

VALUE (MeV)	DOCUMENT ID	TECN	COMMENT
10 ± 4	CUTKOSKY 80	IPWA	$\pi N \rightarrow \pi N$

PHASE θ

VALUE (°)	DOCUMENT ID	TECN	COMMENT
-20 ± 30	CUTKOSKY 80	IPWA	$\pi N \rightarrow \pi N$

$\Delta(2300)$ DECAY MODES

Mode	Γ_1	Γ_2
$N\pi$	$N\pi$	
ΣK		ΣK

$\Delta(2300)$ BRANCHING RATIOS

$\Gamma(N\pi)/\Gamma_{total}$	DOCUMENT ID	TECN	COMMENT	Γ_1/Γ
0.05	CHEW 80	BPWA	$\pi^+ p \rightarrow \pi^+ p$	
0.06 ± 0.02	CUTKOSKY 80	IPWA	$\pi N \rightarrow \pi N$	
0.03 ± 0.02	HOEHLER 79	IPWA	$\pi N \rightarrow \pi N$	
0.08 ± 0.02	HENDRY 78	MPWA	$\pi N \rightarrow \pi N$	

$(\Gamma_1\Gamma_2)^{1/2}/\Gamma_{total}$ in $N\pi \rightarrow \Delta(2300) \rightarrow \Sigma K$	DOCUMENT ID	TECN	COMMENT	$(\Gamma_1\Gamma_2)^{1/2}/\Gamma$
-0.017	CANDLIN 84	DPWA	$\pi^+ p \rightarrow \Sigma^+ K^+$	

$\Delta(2300)$ REFERENCES

ARNDT 06	PR C74 045205	R.A. Arndt et al.	(GWU)
CANDLIN 84	NP B238 477	D.J. Candlin et al.	(EDIN, RAL, LOWC)
CHEW 80	Toronto Conf. 123	D.M. Chew	(LBL) IJP
CUTKOSKY 80	Toronto Conf. 19	R.E. Cutkosky et al.	(CMU, LBL) IJP
Also	PR D20 2839	R.E. Cutkosky et al.	(CMU, LBL)
HOEHLER 79	PDAT 12-1	G. Hoehler et al.	(KARLT) IJP
Also	Toronto Conf. 3	R. Koch	(KARLT) IJP
HENDRY 78	PRL 41 222	A.W. Hendry	(IND, LBL) IJP
Also	ANP 136 1	A.W. Hendry	(IND)

$\Delta(2350) D_{35}$

$I(J^P) = \frac{3}{2}(\frac{5}{2}^-)$ Status: *

OMITTED FROM SUMMARY TABLE

The latest GWU analysis (ARNDT 06) finds no evidence for this resonance.

$\Delta(2350)$ BREIT-WIGNER MASS

VALUE (MeV)	DOCUMENT ID	TECN	COMMENT
≈ 2350 OUR ESTIMATE			
2171 ± 18	MANLEY 92	IPWA	$\pi N \rightarrow \pi N$ & $N\pi\pi$
2400 ± 125	CUTKOSKY 80	IPWA	$\pi N \rightarrow \pi N$
2305 ± 26	HOEHLER 79	IPWA	$\pi N \rightarrow \pi N$
••• We do not use the following data for averages, fits, limits, etc. •••			
2459 ± 100	VRANA 00	DPWA	Multichannel

$\Delta(2350)$ BREIT-WIGNER WIDTH

VALUE (MeV)	DOCUMENT ID	TECN	COMMENT
264 ± 51	MANLEY 92	IPWA	$\pi N \rightarrow \pi N$ & $N\pi\pi$
400 ± 150	CUTKOSKY 80	IPWA	$\pi N \rightarrow \pi N$
300 ± 70	HOEHLER 79	IPWA	$\pi N \rightarrow \pi N$
••• We do not use the following data for averages, fits, limits, etc. •••			
480 ± 360	VRANA 00	DPWA	Multichannel

$\Delta(2350)$ POLE POSITION

REAL PART	DOCUMENT ID	TECN	COMMENT
2400 ± 125	CUTKOSKY 80	IPWA	$\pi N \rightarrow \pi N$
••• We do not use the following data for averages, fits, limits, etc. •••			
2427	VRANA 00	DPWA	Multichannel

-2xIMAGINARY PART	DOCUMENT ID	TECN	COMMENT
400 ± 150	CUTKOSKY 80	IPWA	$\pi N \rightarrow \pi N$
••• We do not use the following data for averages, fits, limits, etc. •••			
458	VRANA 00	DPWA	Multichannel

Baryon Particle Listings

 $\Delta(2350)$, $\Delta(2390)$, $\Delta(2400)$ $\Delta(2350)$ ELASTIC POLE RESIDUEMODULUS $|r|$

VALUE (MeV)	DOCUMENT ID	TECN	COMMENT
15 ± 8	CUTKOSKY 80	IPWA	$\pi N \rightarrow \pi N$

PHASE θ

VALUE ($^\circ$)	DOCUMENT ID	TECN	COMMENT
-70 ± 70	CUTKOSKY 80	IPWA	$\pi N \rightarrow \pi N$

 $\Delta(2350)$ DECAY MODES

Mode
Γ_1 $N\pi$
Γ_2 ΣK

 $\Delta(2350)$ BRANCHING RATIOS

$\Gamma(N\pi)/\Gamma_{\text{total}}$	VALUE	DOCUMENT ID	TECN	COMMENT	Γ_1/Γ
	0.020 ± 0.003	MANLEY 92	IPWA	$\pi N \rightarrow \pi N$ & $N\pi\pi$	
	0.20 ± 0.10	CUTKOSKY 80	IPWA	$\pi N \rightarrow \pi N$	
	0.04 ± 0.02	HOEHLER 79	IPWA	$\pi N \rightarrow \pi N$	
	0.07 ± 0.14	VRANA 00	DPWA	Multichannel	

• • • We do not use the following data for averages, fits, limits, etc. • • •

$(\Gamma_1\Gamma_2)^{1/2}/\Gamma_{\text{total}}$ in $N\pi \rightarrow \Delta(2350) \rightarrow \Sigma K$	VALUE	DOCUMENT ID	TECN	COMMENT	$(\Gamma_1\Gamma_2)^{1/2}/\Gamma$
	< 0.015	CANDLIN 84	DPWA	$\pi^+ p \rightarrow \Sigma^+ K^+$	

 $\Delta(2350)$ REFERENCES

ARNDT 06	PR C74 045205	R.A. Arndt et al.	(GWU)
VRANA 00	PRPL 328 181	T.P. Vrana, S.A. Dytman., T.-S.H. Lee	(PITT+)
MANLEY 92	PR D45 4002	D.M. Manley, E.M. Saleski	(KENT) IJP
Also	PR D30 904	D.M. Manley et al.	(VPI)
CANDLIN 84	NP B238 477	D.J. Candlin et al.	(EDIN, RAL, LOWC)
CUTKOSKY 80	Toronto Conf. 19	R.E. Cutkosky et al.	(CMU, LBL) IJP
Also	PR D20 2839	R.E. Cutkosky et al.	(CMU, LBL)
HOEHLER 79	PDAT 12-1	G. Hohlner et al.	(KARLT) IJP
Also	Toronto Conf. 3	R. Koch	(KARLT) IJP

$$\Delta(2390) F_{37} \quad I(J^P) = \frac{3}{2}(\frac{7}{2}^+) \text{ Status: } *$$

OMITTED FROM SUMMARY TABLE

The latest GWU analysis (ARNDT 06) finds no evidence for this resonance.

 $\Delta(2390)$ BREIT-WIGNER MASS

VALUE (MeV)	DOCUMENT ID	TECN	COMMENT
≈ 2390 OUR ESTIMATE			
2350 ± 100	CUTKOSKY 80	IPWA	$\pi N \rightarrow \pi N$
2425 ± 60	HOEHLER 79	IPWA	$\pi N \rightarrow \pi N$

 $\Delta(2390)$ BREIT-WIGNER WIDTH

VALUE (MeV)	DOCUMENT ID	TECN	COMMENT
300 ± 100	CUTKOSKY 80	IPWA	$\pi N \rightarrow \pi N$
300 ± 80	HOEHLER 79	IPWA	$\pi N \rightarrow \pi N$

 $\Delta(2390)$ POLE POSITION

REAL PART	VALUE (MeV)	DOCUMENT ID	TECN	COMMENT
	2350 ± 100	CUTKOSKY 80	IPWA	$\pi N \rightarrow \pi N$

-2xIMAGINARY PART	VALUE (MeV)	DOCUMENT ID	TECN	COMMENT
	260 ± 100	CUTKOSKY 80	IPWA	$\pi N \rightarrow \pi N$

 $\Delta(2390)$ ELASTIC POLE RESIDUE

MODULUS $ r $	VALUE (MeV)	DOCUMENT ID	TECN	COMMENT
	12 ± 6	CUTKOSKY 80	IPWA	$\pi N \rightarrow \pi N$

PHASE θ	VALUE ($^\circ$)	DOCUMENT ID	TECN	COMMENT
	-90 ± 60	CUTKOSKY 80	IPWA	$\pi N \rightarrow \pi N$

 $\Delta(2390)$ DECAY MODES

Mode
Γ_1 $N\pi$
Γ_2 ΣK

 $\Delta(2390)$ BRANCHING RATIOS

$\Gamma(N\pi)/\Gamma_{\text{total}}$	VALUE	DOCUMENT ID	TECN	COMMENT	Γ_1/Γ
	0.08 ± 0.04	CUTKOSKY 80	IPWA	$\pi N \rightarrow \pi N$	
	0.07 ± 0.04	HOEHLER 79	IPWA	$\pi N \rightarrow \pi N$	

$(\Gamma_1\Gamma_2)^{1/2}/\Gamma_{\text{total}}$ in $N\pi \rightarrow \Delta(2390) \rightarrow \Sigma K$	VALUE	DOCUMENT ID	TECN	COMMENT	$(\Gamma_1\Gamma_2)^{1/2}/\Gamma$
	< 0.015	CANDLIN 84	DPWA	$\pi^+ p \rightarrow \Sigma^+ K^+$	

 $\Delta(2390)$ REFERENCES

ARNDT 06	PR C74 045205	R.A. Arndt et al.	(GWU)
CANDLIN 84	NP B238 477	D.J. Candlin et al.	(EDIN, RAL, LOWC)
CUTKOSKY 80	Toronto Conf. 19	R.E. Cutkosky et al.	(CMU, LBL) IJP
Also	PR D20 2839	R.E. Cutkosky et al.	(CMU, LBL)
HOEHLER 79	PDAT 12-1	G. Hohlner et al.	(KARLT) IJP
Also	Toronto Conf. 3	R. Koch	(KARLT) IJP

 $\Delta(2400) G_{39}$

$$I(J^P) = \frac{3}{2}(\frac{9}{2}^-) \text{ Status: } **$$

OMITTED FROM SUMMARY TABLE

 $\Delta(2400)$ BREIT-WIGNER MASS

VALUE (MeV)	DOCUMENT ID	TECN	COMMENT
≈ 2400 OUR ESTIMATE			
2643 ± 141	ARNDT 06	DPWA	$\pi N \rightarrow \pi N, \eta N$
2300 ± 100	CUTKOSKY 80	IPWA	$\pi N \rightarrow \pi N$
2468 ± 50	HOEHLER 79	IPWA	$\pi N \rightarrow \pi N$
2200 ± 100	HENDRY 78	MPWA	$\pi N \rightarrow \pi N$

 $\Delta(2400)$ BREIT-WIGNER WIDTH

VALUE (MeV)	DOCUMENT ID	TECN	COMMENT
895 ± 432	ARNDT 06	DPWA	$\pi N \rightarrow \pi N, \eta N$
330 ± 100	CUTKOSKY 80	IPWA	$\pi N \rightarrow \pi N$
480 ± 100	HOEHLER 79	IPWA	$\pi N \rightarrow \pi N$
450 ± 200	HENDRY 78	MPWA	$\pi N \rightarrow \pi N$

 $\Delta(2400)$ POLE POSITION

REAL PART	VALUE (MeV)	DOCUMENT ID	TECN	COMMENT
	1983	ARNDT 06	DPWA	$\pi N \rightarrow \pi N, \eta N$
	2260 ± 60	CUTKOSKY 80	IPWA	$\pi N \rightarrow \pi N$

-2xIMAGINARY PART	VALUE (MeV)	DOCUMENT ID	TECN	COMMENT
	878	ARNDT 06	DPWA	$\pi N \rightarrow \pi N, \eta N$
	320 ± 160	CUTKOSKY 80	IPWA	$\pi N \rightarrow \pi N$

 $\Delta(2400)$ ELASTIC POLE RESIDUE

MODULUS $ r $	VALUE (MeV)	DOCUMENT ID	TECN	COMMENT
	24	ARNDT 06	DPWA	$\pi N \rightarrow \pi N, \eta N$
	8 ± 4	CUTKOSKY 80	IPWA	$\pi N \rightarrow \pi N$

PHASE θ	VALUE ($^\circ$)	DOCUMENT ID	TECN	COMMENT
	-139	ARNDT 06	DPWA	$\pi N \rightarrow \pi N, \eta N$
	-25 ± 15	CUTKOSKY 80	IPWA	$\pi N \rightarrow \pi N$

 $\Delta(2400)$ DECAY MODES

Mode
Γ_1 $N\pi$
Γ_2 ΣK

 $\Delta(2400)$ BRANCHING RATIOS

$\Gamma(N\pi)/\Gamma_{\text{total}}$	VALUE	DOCUMENT ID	TECN	COMMENT	Γ_1/Γ
	0.064 ± 0.022	ARNDT 06	DPWA	$\pi N \rightarrow \pi N, \eta N$	
	0.05 ± 0.02	CUTKOSKY 80	IPWA	$\pi N \rightarrow \pi N$	
	0.06 ± 0.03	HOEHLER 79	IPWA	$\pi N \rightarrow \pi N$	
	0.10 ± 0.03	HENDRY 78	MPWA	$\pi N \rightarrow \pi N$	

See key on page 405

Baryon Particle Listings
 $\Delta(2400)$, $\Delta(2420)$, $\Delta(2750)$, $\Delta(2950)$

$(\Gamma_i \Gamma_f)^{1/2} / \Gamma_{\text{total}}$ in $N\pi \rightarrow \Delta(2400) \rightarrow \Sigma K$	DOCUMENT ID	TECN	COMMENT	$(\Gamma_1 \Gamma_2)^{1/2} / \Gamma$
<0.015	CANDLIN	84	DPWA $\pi^+ p \rightarrow \Sigma^+ K^+$	

$\Delta(2400)$ REFERENCES

ARNDT	06	PR C74 045205	R.A. Arndt et al.	(GWU)
CANDLIN	84	NP B238 477	D.J. Candlin et al.	(EDIN, RAL, LOWC)
CUTKOSKY	80	Toronto Conf. 19	R.E. Cutkosky et al.	(CMU, LBL) IJP
		Also PR D20 2839	R.E. Cutkosky et al.	(CMU, LBL)
HOEHLER	79	PDAT 12-1	G. Hohler et al.	(KARLT) IJP
		Also Toronto Conf. 3	R. Koch	(KARLT) IJP
HENDRY	78	PRL 41 222	A.W. Hendry	(IND, LBL) IJP
		Also ANP 136 1	A.W. Hendry	(IND)

$\Delta(2420) H_{3,11} \quad I(J^P) = \frac{3}{2}(\frac{1}{2}^+)$ Status: ***

Most of the results published before 1975 are now obsolete and have been omitted. They may be found in our 1982 edition, Physics Letters **111B** 1 (1982).

$\Delta(2420)$ BREIT-WIGNER MASS

VALUE (MeV)	DOCUMENT ID	TECN	COMMENT
2300 to 2500 (≈ 2420) OUR ESTIMATE			
2633 \pm 29	ARNDT	06	DPWA $\pi N \rightarrow \pi N, \eta N$
2400 \pm 125	CUTKOSKY	80	IPWA $\pi N \rightarrow \pi N$
2416 \pm 17	HOEHLER	79	IPWA $\pi N \rightarrow \pi N$
2400 \pm 60	HENDRY	78	MPWA $\pi N \rightarrow \pi N$
••• We do not use the following data for averages, fits, limits, etc. •••			
2400	CANDLIN	84	DPWA $\pi^+ p \rightarrow \Sigma^+ K^+$
2358.0 \pm 9.0	CHEW	80	BPWA $\pi^+ p \rightarrow \pi^+ p$

$\Delta(2420)$ BREIT-WIGNER WIDTH

VALUE (MeV)	DOCUMENT ID	TECN	COMMENT
300 to 500 (≈ 400) OUR ESTIMATE			
692 \pm 47	ARNDT	06	DPWA $\pi N \rightarrow \pi N, \eta N$
450 \pm 150	CUTKOSKY	80	IPWA $\pi N \rightarrow \pi N$
340 \pm 28	HOEHLER	79	IPWA $\pi N \rightarrow \pi N$
460 \pm 100	HENDRY	78	MPWA $\pi N \rightarrow \pi N$
••• We do not use the following data for averages, fits, limits, etc. •••			
400	CANDLIN	84	DPWA $\pi^+ p \rightarrow \Sigma^+ K^+$
202.2 \pm 45.0	CHEW	80	BPWA $\pi^+ p \rightarrow \pi^+ p$

$\Delta(2420)$ POLE POSITION

REAL PART

VALUE (MeV)	DOCUMENT ID	TECN	COMMENT
2260 to 2400 (≈ 2330) OUR ESTIMATE			
2529	ARNDT	06	DPWA $\pi N \rightarrow \pi N, \eta N$
2300	¹ HOEHLER	93	ARGD $\pi N \rightarrow \pi N$
2360 \pm 100	CUTKOSKY	80	IPWA $\pi N \rightarrow \pi N$

-2xIMAGINARY PART

VALUE (MeV)	DOCUMENT ID	TECN	COMMENT
350 to 750 (≈ 550) OUR ESTIMATE			
621	ARNDT	06	DPWA $\pi N \rightarrow \pi N, \eta N$
620	¹ HOEHLER	93	ARGD $\pi N \rightarrow \pi N$
420 \pm 100	CUTKOSKY	80	IPWA $\pi N \rightarrow \pi N$

$\Delta(2420)$ ELASTIC POLE RESIDUE

MODULUS $|r|$

VALUE (MeV)	DOCUMENT ID	TECN	COMMENT
33	ARNDT	06	DPWA $\pi N \rightarrow \pi N, \eta N$
39	HOEHLER	93	ARGD $\pi N \rightarrow \pi N$
18 \pm 6	CUTKOSKY	80	IPWA $\pi N \rightarrow \pi N$

PHASE θ

VALUE ($^\circ$)	DOCUMENT ID	TECN	COMMENT
-45	ARNDT	06	DPWA $\pi N \rightarrow \pi N, \eta N$
-60	HOEHLER	93	ARGD $\pi N \rightarrow \pi N$
-30 \pm 40	CUTKOSKY	80	IPWA $\pi N \rightarrow \pi N$

$\Delta(2420)$ DECAY MODES

The following branching fractions are our estimates, not fits or averages.

Mode	Fraction (Γ_i / Γ)
$\Gamma_1 \quad N\pi$	5-15 %
$\Gamma_2 \quad \Sigma K$	

$\Delta(2420)$ BRANCHING RATIOS

$\Gamma(N\pi) / \Gamma_{\text{total}}$	DOCUMENT ID	TECN	COMMENT	Γ_1 / Γ
0.05 to 0.15 OUR ESTIMATE				
0.085 \pm 0.008	ARNDT	06	DPWA $\pi N \rightarrow \pi N, \eta N$	
0.08 \pm 0.03	CUTKOSKY	80	IPWA $\pi N \rightarrow \pi N$	
0.08 \pm 0.015	HOEHLER	79	IPWA $\pi N \rightarrow \pi N$	
0.11 \pm 0.02	HENDRY	78	MPWA $\pi N \rightarrow \pi N$	
••• We do not use the following data for averages, fits, limits, etc. •••				
0.22	CHEW	80	BPWA $\pi^+ p \rightarrow \pi^+ p$	

$(\Gamma_i \Gamma_f)^{1/2} / \Gamma_{\text{total}}$ in $N\pi \rightarrow \Delta(2420) \rightarrow \Sigma K$	DOCUMENT ID	TECN	COMMENT	$(\Gamma_1 \Gamma_2)^{1/2} / \Gamma$
-0.016	CANDLIN	84	DPWA $\pi^+ p \rightarrow \Sigma^+ K^+$	

$\Delta(2420)$ FOOTNOTES

¹ See HOEHLER 93 for a detailed discussion of the evidence for and the pole parameters of N and Δ resonances as determined from Argand diagrams of πN elastic partial-wave amplitudes and from plots of the speeds with which the amplitudes traverse the diagrams.

$\Delta(2420)$ REFERENCES

ARNDT	06	PR C74 045205	R.A. Arndt et al.	(GWU)
HOEHLER	93	πN Newsletter 9 1	G. Hohler	(KARL)
CANDLIN	84	NP B238 477	D.J. Candlin et al.	(EDIN, RAL, LOWC)
PDC	82	PL 111B 1	M. Roos et al.	(HELS, CIT, CERN)
CHEW	80	Toronto Conf. 123	D.M. Chew	(LBL) IJP
CUTKOSKY	80	Toronto Conf. 19	R.E. Cutkosky et al.	(CMU, LBL) IJP
		Also PR D20 2839	R.E. Cutkosky et al.	(CMU, LBL)
HOEHLER	79	PDAT 12-1	G. Hohler et al.	(KARLT) IJP
		Also Toronto Conf. 3	R. Koch	(KARLT) IJP
HENDRY	78	PRL 41 222	A.W. Hendry	(IND, LBL) IJP
		Also ANP 136 1	A.W. Hendry	(IND)

$\Delta(2750) I_{3,13} \quad I(J^P) = \frac{3}{2}(\frac{1}{2}^-)$ Status: **

OMITTED FROM SUMMARY TABLE

The latest GWU analysis (ARNDT 06) finds no evidence for this resonance.

$\Delta(2750)$ BREIT-WIGNER MASS

VALUE (MeV)	DOCUMENT ID	TECN	COMMENT
≈ 2750 OUR ESTIMATE			
2794 \pm 80	HOEHLER	79	IPWA $\pi N \rightarrow \pi N$
2650 \pm 100	HENDRY	78	MPWA $\pi N \rightarrow \pi N$

$\Delta(2750)$ BREIT-WIGNER WIDTH

VALUE (MeV)	DOCUMENT ID	TECN	COMMENT
350 \pm 100	HOEHLER	79	IPWA $\pi N \rightarrow \pi N$
500 \pm 100	HENDRY	78	MPWA $\pi N \rightarrow \pi N$

$\Delta(2750)$ DECAY MODES

Mode	Γ_1	$N\pi$

$\Delta(2750)$ BRANCHING RATIOS

$\Gamma(N\pi) / \Gamma_{\text{total}}$	DOCUMENT ID	TECN	COMMENT	Γ_1 / Γ
0.04 \pm 0.015	HOEHLER	79	IPWA $\pi N \rightarrow \pi N$	
0.05 \pm 0.01	HENDRY	78	MPWA $\pi N \rightarrow \pi N$	

$\Delta(2750)$ REFERENCES

ARNDT	06	PR C74 045205	R.A. Arndt et al.	(GWU)
HOEHLER	79	PDAT 12-1	G. Hohler et al.	(KARLT) IJP
		Also Toronto Conf. 3	R. Koch	(KARLT) IJP
HENDRY	78	PRL 41 222	A.W. Hendry	(IND, LBL) IJP
		Also ANP 136 1	A.W. Hendry	(IND)

$\Delta(2950) K_{3,15} \quad I(J^P) = \frac{3}{2}(\frac{1}{2}^+)$ Status: **

OMITTED FROM SUMMARY TABLE

$\Delta(2950)$ BREIT-WIGNER MASS

VALUE (MeV)	DOCUMENT ID	TECN	COMMENT
≈ 2950 OUR ESTIMATE			
2990 \pm 100	HOEHLER	79	IPWA $\pi N \rightarrow \pi N$
2850 \pm 100	HENDRY	78	MPWA $\pi N \rightarrow \pi N$

Baryon Particle Listings

 $\Delta(2950)$, $\Delta(\sim 3000)$ $\Delta(2950)$ BREIT-WIGNER WIDTH

VALUE (MeV)	DOCUMENT ID	TECN	COMMENT
330 ± 100	HOEHLER 79	IPWA	$\pi N \rightarrow \pi N$
700 ± 200	HENDRY 78	MPWA	$\pi N \rightarrow \pi N$

 $\Delta(2950)$ DECAY MODES

Mode
$\Gamma_1 \quad N\pi$

 $\Delta(2950)$ BRANCHING RATIOS

$\Gamma(N\pi)/\Gamma_{\text{total}}$	DOCUMENT ID	TECN	COMMENT	Γ_1/Γ
0.04 ± 0.02	HOEHLER 79	IPWA	$\pi N \rightarrow \pi N$	
0.03 ± 0.01	HENDRY 78	MPWA	$\pi N \rightarrow \pi N$	

 $\Delta(2950)$ REFERENCES

HOEHLER 79	PDAT 12-1	G. Hohler et al.	(KARLT) IJP
Also	Toronto Conf. 3	R. Koch	(KARLT) IJP
HENDRY 78	PRL 41 222	A.W. Hendry	(IND, LBL) IJP
Also	ANP 136 1	A.W. Hendry	(IND)

$\Delta(\sim 3000)$ Region
Partial-Wave Analyses

OMITTED FROM SUMMARY TABLE

We list here miscellaneous high-mass candidates for isospin-3/2 resonances found in partial-wave analyses.

Our 1982 edition also had a $\Delta(2850)$ and a $\Delta(3230)$. The evidence for them was deduced from total cross-section and 180° elastic cross-section measurements. The $\Delta(2850)$ has been resolved into the $\Delta(2750) \quad l_{3,13}$ and $\Delta(2950) \quad K_{3,15}$. The $\Delta(3230)$ is perhaps related to the $K_{3,13}$ of HENDRY 78 and to the $L_{3,17}$ of KOCH 80.

 $\Delta(\sim 3000)$ BREIT-WIGNER MASS

VALUE (MeV)	DOCUMENT ID	TECN	COMMENT
≈ 3000 OUR ESTIMATE			
3300	¹ KOCH 80	IPWA	$\pi N \rightarrow \pi N \quad L_{3,17}$ wave
3500	¹ KOCH 80	IPWA	$\pi N \rightarrow \pi N \quad M_{3,19}$ wave
2850 ± 150	HENDRY 78	MPWA	$\pi N \rightarrow \pi N \quad l_{3,11}$ wave
3200 ± 200	HENDRY 78	MPWA	$\pi N \rightarrow \pi N \quad K_{3,13}$ wave
3300 ± 200	HENDRY 78	MPWA	$\pi N \rightarrow \pi N \quad L_{3,17}$ wave
3700 ± 200	HENDRY 78	MPWA	$\pi N \rightarrow \pi N \quad M_{3,19}$ wave
4100 ± 300	HENDRY 78	MPWA	$\pi N \rightarrow \pi N \quad N_{3,21}$ wave

 $\Delta(\sim 3000)$ BREIT-WIGNER WIDTH

VALUE (MeV)	DOCUMENT ID	TECN	COMMENT
700 ± 200	HENDRY 78	MPWA	$\pi N \rightarrow \pi N \quad l_{3,11}$ wave
1000 ± 300	HENDRY 78	MPWA	$\pi N \rightarrow \pi N \quad K_{3,13}$ wave
1100 ± 300	HENDRY 78	MPWA	$\pi N \rightarrow \pi N \quad L_{3,17}$ wave
1300 ± 400	HENDRY 78	MPWA	$\pi N \rightarrow \pi N \quad M_{3,19}$ wave
1600 ± 500	HENDRY 78	MPWA	$\pi N \rightarrow \pi N \quad N_{3,21}$ wave

 $\Delta(\sim 3000)$ DECAY MODES

Mode
$\Gamma_1 \quad N\pi$

 $\Delta(\sim 3000)$ BRANCHING RATIOS

$\Gamma(N\pi)/\Gamma_{\text{total}}$	DOCUMENT ID	TECN	COMMENT	Γ_1/Γ
0.06 ± 0.02	HENDRY 78	MPWA	$\pi N \rightarrow \pi N \quad l_{3,11}$ wave	
0.045 ± 0.02	HENDRY 78	MPWA	$\pi N \rightarrow \pi N \quad K_{3,13}$ wave	
0.03 ± 0.01	HENDRY 78	MPWA	$\pi N \rightarrow \pi N \quad L_{3,17}$ wave	
0.025 ± 0.01	HENDRY 78	MPWA	$\pi N \rightarrow \pi N \quad M_{3,19}$ wave	
0.018 ± 0.01	HENDRY 78	MPWA	$\pi N \rightarrow \pi N \quad N_{3,21}$ wave	

 $\Delta(\sim 3000)$ FOOTNOTES

¹In addition, KOCH 80 reports some evidence for an $S_{31} \quad \Delta(2700)$ and a $P_{33} \quad \Delta(2800)$.

 $\Delta(\sim 3000)$ REFERENCES

KOCH 80	Toronto Conf. 3	R. Koch	(KARLT) IJP
HENDRY 78	PRL 41 222	A.W. Hendry	(IND, LBL) IJP
Also	ANP 136 1	A.W. Hendry	(IND)

EXOTIC BARYONS

PENTAQUARKS

Written May 2008 by C.G. Wohl (LBNL).

See pp. 1019–1022 of the 2006 *Review* [1] for the evidence for the $\Theta(1540)$, $\Phi(1860)$, and $\Theta_c(3100)$, and for the early unsuccessful attempts to confirm them. The table below lists papers published since then giving results of further unsuccessful searches. There are experiments at high energies and low; in new reactions and old; there are experiments—some by the same groups that claimed the original discoveries—with orders-of-magnitude greater statistics than before; there are experiments that find 100,000 $\Lambda(1520)$ s in $\bar{K}N$, but no hint of a $\Theta(1540)$ in KN . Many of the experiments search over large ranges of mass. The limits on production of a pentaquark given in the

last column of the table are at 90 or 95% confidence level; the cross-section limits are in some cases now fractions of a nanobarn. The limits often involve assumptions about the width of the pentaquark, its production angular distribution, or other matters. There is not room (or reason) to give here all the details—for which, see the papers.

There are two or three recent experiments that find weak evidence for signals near the nominal masses, but there is simply no point in tabulating them in view of the overwhelming evidence that the claimed pentaquarks do not exist. The only advance in particle physics thought worthy of mention in the American Institute of Physics “Physics News in 2003” was a false alarm. The whole story—the discoveries themselves, the tidal wave of papers by theorists and phenomenologists that followed, and the eventual “undiscovery”—is a curious episode in the history of science.

Table 1: Unsuccessful searches for pentaquarks. There are ten more unsuccessful searches for the $\Theta(1540)$, nine for the $\Phi(1860)$, and three for the $\Theta_c(3100)$ listed in our 2006 edition [1].

Experiment	Reaction	Energy, etc.	Limits, etc.
<u>Searches for the $\Theta(1540)^+$</u>			
BABAR [2]	$B^0 \rightarrow (pK_S^0)\bar{p}$	\sqrt{s} 10.58 GeV	$< 2 \times 10^{-7}$ per B^0
CLAS [3]	$\gamma p \rightarrow (nK^+/pK_S^0)K^0$	E_γ 1.6–3.8 GeV	$\sigma < 0.7$ nb, 100k $\Lambda(1520)$
CLAS [4]	$\gamma d \rightarrow (nK^+)pK^-$	E_γ 0.8–3.6 GeV	$\sigma < 0.3$ nb
CLAS [5]	$\gamma d \rightarrow (nK^+)\Lambda$	E_γ 0.8–3.6 GeV	$\sigma < 5$ –25 nb
COSY-ANKE [6]	$pp \rightarrow (pK_S^0)\Lambda\pi^+$	p_p 3.65 GeV/c	$\sigma < 58$ nb
COSY-TOF [7]	$pp \rightarrow (pK_S^0)\Sigma^+$	p_p 3.059 GeV/c	$\sigma < 150$ nb
DELPHI [8]	$Z \rightarrow (pK_S^0)X$	\sqrt{s} 91.2 GeV	$< 5.1 \times 10^{-4}$ per Z
FOCUS [9]	$\gamma A \rightarrow (pK_S^0)X$	\bar{E}_γ 180 GeV	400k $\Sigma(1385)^+$
HERA-H1 [10]	$ep \rightarrow (p/\bar{p}K_S^0)eX$	$5 < Q^2 < 100$ GeV ²	$\sigma < 30$ –90 pb
KEK-E522 [11]	$\pi^- p \rightarrow K^-(X)$	p_π 1.9 GeV/c	$\sigma < 3.9$ nb
L3 [12]	$\gamma^*\gamma^* \rightarrow (p/\bar{p}K_S^0)X$	$E_{\gamma\gamma} > 5$ GeV	$\sigma < 1.8$ nb
NOMAD [13]	$\nu_\mu N \rightarrow (pK_S^0)X$		$< 2.13 \times 10^{-3}$ per evt
<u>Searches for a pK^+ state</u>			
CLAS [14]	$\gamma p \rightarrow (pK^+)K^-$	E_γ 1.8–3.8 GeV	$\sigma < 0.15$ nb
DELPHI [8]	$Z \rightarrow (pK^+)X$	\sqrt{s} 91.2 GeV	$< 1.6 \times 10^{-3}$ per Z
JLAB-HALL-A [15]	$ep \rightarrow eK^-(X)$	E_e 5 GeV	$< 5\%$ of $\Lambda(1520)$
<u>Searches for the $\Phi(1860)$</u>			
CDF [16]	$\bar{p}p \rightarrow (\Xi^-\pi^\pm)X$	\sqrt{s} 1.96 TeV	1.9k $\Xi(1530)^0$
DELPHI [8]	$Z \rightarrow (\Xi^-\pi^-)X$	\sqrt{s} 91.2 GeV	$< 2.9 \times 10^{-4}$ per Z
FOCUS [17]	$\gamma N \rightarrow (\Xi^-\pi^-)X$	\bar{E}_γ 180 GeV	65k $\Xi(1530)^0$
HERA-H1 [18]	$ep \rightarrow (\Xi^-\pi^\pm)eX$	$2 < Q^2 < 100$ GeV ²	163 $\Xi(1530)^0$
SERP-EXCHARM [19]	$nC \rightarrow (\Xi^-\pi^\pm)X$	\bar{E}_n 51 GeV	1.5k $\Xi(1530)^0$
<u>Searches for the $\Theta_c(3100)$</u>			
BABAR [20]	$e^+e^- \rightarrow (pD^{*-})X$	\sqrt{s} 10.58 GeV	125k evts
CHORUS [21]	$\bar{\nu}_\mu A \rightarrow \mu^+X$	\bar{E}_ν 18 GeV	2262 evts
DELPHI [8]	$Z \rightarrow (pD^{*-})X$	\sqrt{s} 91.2 GeV	$< 8.8 \times 10^{-4}$ per Z

References

1. W.-M Yao *et al.*, J. Phys. **G33**, 1 (2006).
 2. B. Aubert *et al.*, Phys. Rev. **D76**, 092004 (2007).
 3. R. De Vita *et al.*, Phys. Rev. **D74**, 032001 (2006).
 4. B. McKinnon *et al.*, Phys. Rev. Lett. **96**, 212001 (2006).
 5. S. Niccolai *et al.*, Phys. Rev. Lett. **97**, 032001 (2006).
 6. M. Nekipelov *et al.*, J. Phys. **G34**, 627 (2007).
 7. M. Abdel-Bary *et al.*, Phys. Lett. **B649**, 252 (2007).
 8. J. Abdallah *et al.*, Phys. Lett. **B653**, 151 (2007).
 9. J.M. Link *et al.*, Phys. Lett. **B639**, 604 (2006).
 10. A. Aktas *et al.*, Phys. Lett. **B639**, 202 (2006).
 11. K. Miwa *et al.*, Phys. Lett. **B635**, 72 (2006).
 12. P. Achard *et al.*, Eur. Phys. J. **C49**, 395 (2007).
 13. O. Samoylov *et al.*, Eur. Phys. J. **C49**, 499 (2007).
 14. V. Kubarovsky *et al.*, Phys. Rev. Lett. **97**, 102001 (2006).
 15. Y. Qiang *et al.*, Phys. Rev. **C75**, 055208 (2007).
 16. A. Abulencia *et al.*, Phys. Rev. **D75**, 032003 (2007).
 17. J.M. Link *et al.*, Phys. Lett. **B661**, 14 (2008).
 18. A. Aktas *et al.*, Eur. Phys. J. **C52**, 507 (2007).
 19. A.N. Aleev *et al.*, Sov. J. Nucl. Phys. **70**, 1527 (2007).
 20. B. Aubert *et al.*, Phys. Rev. **D73**, 091101 (2006).
 21. G. De Lellis *et al.*, Nucl. Phys. **B763**, 268 (2007).
-

Λ BARYONS

$(S = -1, I = 0)$

$\Lambda^0 = uds$

Λ $I(J^P) = 0(\frac{1}{2}^+)$ Status: ****

We have omitted some results that have been superseded by later experiments. See our earlier editions.

Λ MASS

The fit uses Λ, Σ⁺, Σ⁰, Σ⁻ mass and mass-difference measurements.

VALUE (MeV)	EVTS	DOCUMENT ID	TECN	COMMENT
1115.683 ± 0.006 OUR FIT				
1115.683 ± 0.006 OUR AVERAGE				
1115.678 ± 0.006 ± 0.006	20k	HARTOUNI	94	SPEC <i>pp</i> 27.5 GeV/ <i>c</i>
1115.690 ± 0.008 ± 0.006	18k	¹ HARTOUNI	94	SPEC <i>pp</i> 27.5 GeV/ <i>c</i>
• • • We do not use the following data for averages, fits, limits, etc. • • •				
1115.59 ± 0.08	935	HYMAN	72	HEBC
1115.39 ± 0.12	195	MAYEUR	67	EMUL
1115.6 ± 0.4		LONDON	66	HBC
1115.65 ± 0.07	488	² SCHMIDT	65	HBC
1115.44 ± 0.12		³ BHOWMIK	63	RVUE

¹We assume *CPT* invariance: this is the $\bar{\Lambda}$ mass as measured by HARTOUNI 94. See below for the fractional mass difference, testing *CPT*.
²The SCHMIDT 65 masses have been reevaluated using our April 1973 proton and K^\pm and π^\pm masses. P. Schmidt, private communication (1974).
³The mass has been raised 35 keV to take into account a 46 keV increase in the proton mass and an 11 keV decrease in the π^\pm mass (note added Reviews of Modern Physics **39** 1 (1967)).

$$(m_\Lambda - m_{\bar{\Lambda}}) / m_\Lambda$$

A test of *CPT* invariance.

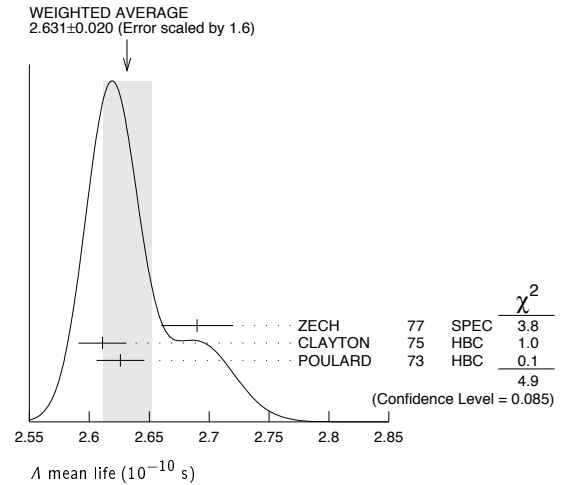
VALUE (units 10 ⁻⁵)	EVTS	DOCUMENT ID	TECN	COMMENT
- 0.1 ± 1.1 OUR AVERAGE				
+ 1.3 ± 1.2	31k	⁴ RYBICKI	96	NA32 π^- Cu, 230 GeV
- 1.08 ± 0.90		HARTOUNI	94	SPEC <i>pp</i> 27.5 GeV/ <i>c</i>
4.5 ± 5.4		CHIEN	66	HBC 6.9 GeV/ <i>c</i> $\bar{p}p$
• • • We do not use the following data for averages, fits, limits, etc. • • •				
-26 ± 13		BADIER	67	HBC 2.4 GeV/ <i>c</i> $\bar{p}p$

⁴RYBICKI 96 is an analysis of old ACCMOR (NA32) data.

Λ MEAN LIFE

Measurements with an error $\geq 0.1 \times 10^{-10}$ s have been omitted altogether, and only the latest high-statistics measurements are used for the average.

VALUE (10 ⁻¹⁰ s)	EVTS	DOCUMENT ID	TECN	COMMENT
2.631 ± 0.020 OUR AVERAGE				
2.69 ± 0.03	53k	ZECH	77	SPEC Neutral hyperon beam
2.611 ± 0.020	34k	CLAYTON	75	HBC 0.96-1.4 GeV/ <i>c</i> $K^- p$
2.626 ± 0.020	36k	POULARD	73	HBC 0.4-2.3 GeV/ <i>c</i> $K^- p$
• • • We do not use the following data for averages, fits, limits, etc. • • •				
2.69 ± 0.05	6582	ALTHOFF	73B	OSPK $\pi^+ n \rightarrow \Lambda K^+$
2.54 ± 0.04	4572	BALTAY	71B	HBC $K^- p$ at rest
2.535 ± 0.035	8342	GRIMM	68	HBC
2.47 ± 0.08	2600	HEPP	68	HBC
2.35 ± 0.09	916	BURAN	66	HLBC
2.452 ^{+0.056} _{-0.054}	2213	ENGELMANN	66	HBC
2.59 ± 0.09	794	HUBBARD	64	HBC
2.59 ± 0.07	1378	SCHWARTZ	64	HBC
2.36 ± 0.06	2239	BLOCK	63	HEBC



$$(\tau_\Lambda - \tau_{\bar{\Lambda}}) / \tau_\Lambda$$

A test of *CPT* invariance.

VALUE	DOCUMENT ID	TECN	COMMENT
- 0.001 ± 0.009 OUR AVERAGE			
- 0.0018 ± 0.0066 ± 0.0056	BARNES	96	CNTR LEAR $\bar{p}p \rightarrow \bar{\Lambda}\Lambda$
0.044 ± 0.085	BADIER	67	HBC 2.4 GeV/ <i>c</i> $\bar{p}p$

BARYON MAGNETIC MOMENTS

Written 1994 by C.G. Wohl (LBNL).

The figure below shows the measured magnetic moments of the stable baryons. It also shows the predictions of the simplest quark model, using the measured *p*, *n*, and Λ moments as input. In this model, the moments are [1]

$$\begin{aligned} \mu_p &= (4\mu_u - \mu_d)/3 & \mu_n &= (4\mu_d - \mu_u)/3 \\ \mu_{\Sigma^+} &= (4\mu_u - \mu_s)/3 & \mu_{\Sigma^-} &= (4\mu_d - \mu_s)/3 \\ \mu_{\Sigma^0} &= (4\mu_s - \mu_u)/3 & \mu_{\Xi^-} &= (4\mu_s - \mu_d)/3 \\ \mu_\Lambda &= \mu_s & \mu_{\Sigma^0} &= (2\mu_u + 2\mu_d - \mu_s)/3 \\ \mu_{\Omega^-} &= 3\mu_s \end{aligned}$$

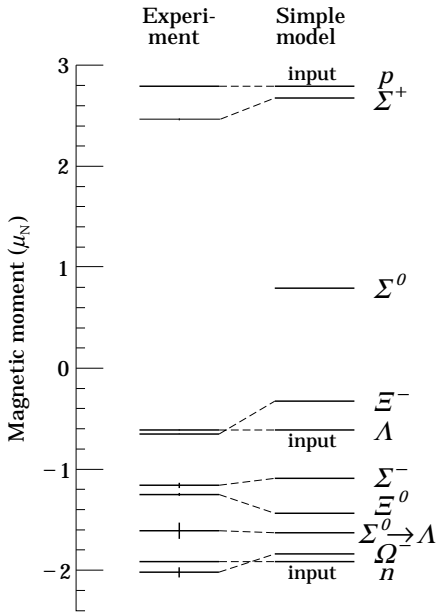
and the $\Sigma^0 \rightarrow \Lambda$ transition moment is

$$\mu_{\Sigma^0\Lambda} = (\mu_d - \mu_u)/\sqrt{3}.$$

The quark moments that result from this model are $\mu_u = +1.852 \mu_N$, $\mu_d = -0.972 \mu_N$, and $\mu_s = -0.613 \mu_N$. The corresponding effective quark masses, taking the quarks to be Dirac point particles, where $\mu = q\hbar/2m$, are 338, 322, and 510 MeV. As the figure shows, the model gives a good first approximation to the experimental moments. For efforts to make a better model, we refer to the literature [2].

Baryon Particle Listings

Λ



Λ DECAY MODES

Mode	Fraction (Γ_i/Γ)
Γ_1 $p\pi^-$	$(63.9 \pm 0.5) \%$
Γ_2 $n\pi^0$	$(35.8 \pm 0.5) \%$
Γ_3 $n\gamma$	$(1.75 \pm 0.15) \times 10^{-3}$
Γ_4 $p\pi^-\gamma$	[a] $(8.4 \pm 1.4) \times 10^{-4}$
Γ_5 $p e^- \bar{\nu}_e$	$(8.32 \pm 0.14) \times 10^{-4}$
Γ_6 $p\mu^- \bar{\nu}_\mu$	$(1.57 \pm 0.35) \times 10^{-4}$

[a] See the Listings below for the pion momentum range used in this measurement.

CONSTRAINED FIT INFORMATION

An overall fit to 5 branching ratios uses 20 measurements and one constraint to determine 5 parameters. The overall fit has a $\chi^2 = 10.5$ for 16 degrees of freedom.

The following *off-diagonal* array elements are the correlation coefficients $\langle \delta x_i \delta x_j \rangle / (\delta x_i \delta x_j)$, in percent, from the fit to the branching fractions, $x_i \equiv \Gamma_i/\Gamma_{\text{total}}$. The fit constrains the x_i whose labels appear in this array to sum to one.

x_2	-100			
x_3	-2	-1		
x_5	46	-46	-1	
x_6	0	0	0	0
	x_1	x_2	x_3	x_5

Λ BRANCHING RATIOS

$\Gamma(p\pi^-)/\Gamma(N\pi)$				$\Gamma_1/(\Gamma_1+\Gamma_2)$
VALUE	EVTS	DOCUMENT ID	TECN	COMMENT
0.641 ± 0.005 OUR FIT				
0.640 ± 0.005 OUR AVERAGE				
0.646 ± 0.008	4572	BALTAY	71B	HBC $K^- p$ at rest
0.635 ± 0.007	6736	DOYLE	69	HBC $\pi^- p \rightarrow \Lambda K^0$
0.643 ± 0.016	903	HUMPHREY	62	HBC
0.624 ± 0.030		CRAWFORD	59B	HBC $\pi^- p \rightarrow \Lambda K^0$

$\Gamma(n\pi^0)/\Gamma(N\pi)$				$\Gamma_2/(\Gamma_1+\Gamma_2)$
VALUE	EVTS	DOCUMENT ID	TECN	COMMENT
0.359 ± 0.005 OUR FIT				
0.310 ± 0.028 OUR AVERAGE				
0.35 ± 0.05		BROWN	63	HLBC
0.291 ± 0.034	75	CHRETIEN	63	HLBC

$\Gamma(n\gamma)/\Gamma_{\text{total}}$				Γ_3/Γ
VALUE (units 10^{-3})	EVTS	DOCUMENT ID	TECN	COMMENT
1.75 ± 0.15 OUR FIT				
1.75 ± 0.15	1816	LARSON	93	SPEC $K^- p$ at rest
••• We do not use the following data for averages, fits, limits, etc. •••				
$1.78 \pm 0.24^{+0.14}_{-0.16}$	287	NOBLE	92	SPEC See LARSON 93

$\Gamma(n\gamma)/\Gamma(n\pi^0)$				Γ_3/Γ_2
VALUE (units 10^{-3})	EVTS	DOCUMENT ID	TECN	COMMENT
••• We do not use the following data for averages, fits, limits, etc. •••				
$2.86 \pm 0.74 \pm 0.57$	24	BIAGI	86	SPEC SPS hyperon beam

$\Gamma(p\pi^-\gamma)/\Gamma(p\pi^-)$				Γ_4/Γ_1
VALUE (units 10^{-3})	EVTS	DOCUMENT ID	TECN	COMMENT
1.32 ± 0.22	72	BAGGETT	72C	HBC $\pi^- < 95$ MeV/c

$\Gamma(p e^- \bar{\nu}_e)/\Gamma(p\pi^-)$				Γ_5/Γ_1
VALUE (units 10^{-3})	EVTS	DOCUMENT ID	TECN	COMMENT
1.301 ± 0.019 OUR FIT				
1.301 ± 0.019 OUR AVERAGE				
1.335 ± 0.056	7111	BOURQUIN	83	SPEC SPS hyperon beam
1.313 ± 0.024	10k	WISE	80	SPEC
1.23 ± 0.11	544	LINDQUIST	77	SPEC $\pi^- p \rightarrow K^0 \Lambda$
1.27 ± 0.07	1089	KATZ	73	HBC
1.31 ± 0.06	1078	ALTHOFF	71	OSPK
1.17 ± 0.13	86	CANTER	71	HBC $K^- p$ at rest
1.20 ± 0.12	143	MALONEY	69	HBC
1.17 ± 0.18	120	BAGLIN	64	FBC K^- freon 1.45 GeV/c
1.23 ± 0.20	150	ELY	63	FBC
••• We do not use the following data for averages, fits, limits, etc. •••				
1.32 ± 0.15	218	LINDQUIST	71	OSPK See LINDQUIST 77

⁷ Changed by us from $\Gamma(p e^- \bar{\nu}_e)/\Gamma(N\pi)$ assuming the authors used $\Gamma(p\pi^-)/\Gamma_{\text{total}} = 2/3$.

⁸ Changed by us from $\Gamma(p e^- \bar{\nu}_e)/\Gamma(N\pi)$ because $\Gamma(p e^- \nu)/\Gamma(p\pi^-)$ is the directly measured quantity.

References

- See, for example, D.H. Perkins, *Introduction to High Energy Physics* (Addison-Wesley, Reading, MA, 1987), or D. Griffiths, *Introduction to Elementary Particles* (Harper & Row, New York, 1987).
- See, for example, J. Franklin, Phys. Rev. **D29**, 2648 (1984); H.J. Lipkin, Nucl. Phys. **B241**, 477 (1984); K. Suzuki, H. Kumagai, and Y. Tanaka, Europhys. Lett. **2**, 109 (1986); S.K. Gupta and S.B. Khadkikar, Phys. Rev. **D36**, 307 (1987); M.I. Krivoruchenko, Sov. J. Nucl. Phys. **45**, 109 (1987); L. Brekke and J.L. Rosner, Comm. Nucl. Part. Phys. **18**, 83 (1988); K.-T. Chao, Phys. Rev. **D41**, 920 (1990) and references cited therein Also, see references cited in discussions of results in the experimental papers..

Λ MAGNETIC MOMENT

See the "Note on Baryon Magnetic Moments" above. Measurements with an error $\geq 0.15 \mu_N$ have been omitted.

VALUE (μ_N)	EVTS	DOCUMENT ID	TECN	COMMENT
-0.613 ± 0.004 OUR AVERAGE				
-0.606 ± 0.015	200k	COX	81	SPEC
-0.6138 ± 0.0047	3M	SCHACHIN...	78	SPEC
-0.59 ± 0.07	350k	HELLER	77	SPEC
-0.57 ± 0.05	1.2M	BUNCE	76	SPEC
-0.66 ± 0.07	1300	DAHL-JENSEN71	EMUL	200 kG field

Λ ELECTRIC DIPOLE MOMENT

A nonzero value is forbidden by both T invariance and P invariance.

VALUE ($10^{-16} e\text{-cm}$)	CL%	DOCUMENT ID	TECN	COMMENT
< 1.5	95	⁵ PONDROM	81	SPEC
••• We do not use the following data for averages, fits, limits, etc. •••				
< 100	95	⁶ BARONI	71	EMUL
< 500	95	GIBSON	66	EMUL

⁵ PONDROM 81 measures $(-3.0 \pm 7.4) \times 10^{-17} e\text{-cm}$.

⁶ BARONI 71 measures $(-5.9 \pm 2.9) \times 10^{-15} e\text{-cm}$.

$\Gamma(\rho\mu^- \nu_\mu)/\Gamma(N\pi)$		$\Gamma_6/(\Gamma_1+\Gamma_2)$		
VALUE (units 10^{-4})	EVTS	DOCUMENT ID	TECN	COMMENT
1.57 ± 0.35 OUR FIT				
1.57 ± 0.35 OUR AVERAGE				
1.4 ± 0.5	14	BAGGETT	72B	HBC $K^- p$ at rest
2.4 ± 0.8	9	CANTER	71B	HBC $K^- p$ at rest
1.3 ± 0.7	3	LIND	64	RVUE
1.5 ± 1.2	2	RONNE	64	FBC

Λ DECAY PARAMETERS

See the "Note on Baryon Decay Parameters" in the neutron Listings. Some early results have been omitted.

α_- FOR $\Lambda \rightarrow p\pi^-$

VALUE	EVTS	DOCUMENT ID	TECN	COMMENT
0.642 ± 0.013 OUR AVERAGE				
0.584 ± 0.046	8500	ASTBURY	75	SPEC
0.649 ± 0.023	10325	CLELAND	72	OSPK
0.67 ± 0.06	3520	DAUBER	69	HBC From Ξ decay
0.645 ± 0.017	10130	OVERSETH	67	OSPK Λ from $\pi^- p$
0.62 ± 0.07	1156	CRONIN	63	CNTR Λ from $\pi^- p$

α_+ FOR $\Lambda \rightarrow \bar{p}\pi^+$

VALUE	EVTS	DOCUMENT ID	TECN	COMMENT
-0.71 ± 0.08 OUR AVERAGE				
-0.755 ± 0.083 ± 0.063	≈ 8.7k	ABLIKIM	10	BES $J/\psi \rightarrow \Lambda \bar{\Lambda}$
-0.63 ± 0.13	770	TIXIER	88	DM2 $J/\psi \rightarrow \Lambda \bar{\Lambda}$

ϕ ANGLE FOR $\Lambda \rightarrow p\pi^-$

($\tan\phi = \beta / \gamma$)

VALUE (°)	EVTS	DOCUMENT ID	TECN	COMMENT
-6.5 ± 3.5 OUR AVERAGE				
-7.0 ± 4.5	10325	CLELAND	72	OSPK Λ from $\pi^- p$
-8.0 ± 6.0	10130	OVERSETH	67	OSPK Λ from $\pi^- p$
13.0 ± 17.0	1156	CRONIN	63	OSPK Λ from $\pi^- p$

$\alpha_0 / \alpha_- = \alpha(\Lambda \rightarrow n\pi^0) / \alpha(\Lambda \rightarrow p\pi^-)$

VALUE	EVTS	DOCUMENT ID	TECN	COMMENT
1.01 ± 0.07 OUR AVERAGE				
1.000 ± 0.068	4760	⁹ OLSEN	70	OSPK $\pi^+ n \rightarrow \Lambda K^+$
1.10 ± 0.27		CORK	60	CNTR

⁹OLSEN 70 compares proton and neutron distributions from Λ decay.

$(\alpha + \bar{\alpha}) / (\alpha - \bar{\alpha})$ in $\Lambda \rightarrow p\pi^-, \bar{\Lambda} \rightarrow \bar{p}\pi^+$

Zero if CP is conserved; α_- and α_+ are the asymmetry parameters for $\Lambda \rightarrow p\pi^-$ and $\bar{\Lambda} \rightarrow \bar{p}\pi^+$ decay. See also the Ξ^- for a similar test involving the decay chain $\Xi^- \rightarrow \Lambda\pi^-, \Lambda \rightarrow p\pi^-$ and the corresponding antiparticle chain.

VALUE	EVTS	DOCUMENT ID	TECN	COMMENT
0.006 ± 0.021 OUR AVERAGE				
-0.081 ± 0.055 ± 0.059	≈ 8.7k	ABLIKIM	10	BES $J/\psi \rightarrow \Lambda \bar{\Lambda}$
+0.013 ± 0.022	96k	BARNES	96	CNTR LEAR $\bar{p}p \rightarrow \bar{\Lambda}\Lambda$
+0.01 ± 0.10	770	TIXIER	88	DM2 $J/\psi \rightarrow \Lambda \bar{\Lambda}$
-0.02 ± 0.14	10k	¹⁰ CHAUVAT	85	CNTR $pp, \bar{p}p$ ISR

••• We do not use the following data for averages, fits, limits, etc. •••
 -0.07 ± 0.09 4063 BARNES 87 CNTR See BARNES 96

¹⁰CHAUVAT 85 actually gives $\alpha_+(\bar{\Lambda})/\alpha_-(\Lambda) = -1.04 \pm 0.29$. Assumes polarization is same in $\bar{p}p \rightarrow \bar{\Lambda}X$ and $pp \rightarrow \Lambda X$. Tests of this assumption, based on C-invariance and fragmentation, are satisfied by the data.

g_A / g_V FOR $\Lambda \rightarrow pe^- \nu_e$

Measurements with fewer than 500 events have been omitted. Where necessary, signs have been changed to agree with our conventions, which are given in the "Note on Baryon Decay Parameters" in the neutron Listings. The measurements all assume that the form factor $g_2 = 0$. See also the footnote on DWORKIN 90.

VALUE	EVTS	DOCUMENT ID	TECN	COMMENT
-0.718 ± 0.015 OUR AVERAGE				
-0.719 ± 0.016 ± 0.012	37k	¹¹ DWORKIN	90	SPEC $e\nu$ angular corr.
-0.70 ± 0.03	7111	BOURQUIN	83	SPEC $\Xi \rightarrow \Lambda\pi^-$
-0.734 ± 0.031	10k	¹² WISE	81	SPEC $e\nu$ angular correl.
-0.63 ± 0.06	817	ALTHOFF	73	OSPK Polarized Λ

¹¹The tabulated result assumes the weak-magnetism coupling $w \equiv g_W(0)/g_V(0)$ to be 0.97, as given by the CVC hypothesis and as assumed by the other listed measurements. However, DWORKIN 90 measures w to be 0.15 ± 0.30 , and then $g_A/g_V = -0.731 \pm 0.016$.

¹²This experiment measures only the absolute value of g_A/g_V .

Λ REFERENCES

We have omitted some papers that have been superseded by later experiments. See our earlier editions.

ABLIKIM	10	PR D81 012003	M. Ablikim <i>et al.</i>	(BES Collab.)
BARNES	96	PR C54 1877	P.D. Barnes <i>et al.</i>	(CERN PS-185 Collab.)
RYBICKI	96	APP B27 2155	K. Rybicki	
HARTOUNI	94	PRL 72 1322	E.P. Hartouni <i>et al.</i>	(BNL E766 Collab.)
Also		PRL 72 2821 (erratum)	E.P. Hartouni <i>et al.</i>	(BNL E766 Collab.)
LARSON	93	PR D47 799	K.D. Larson <i>et al.</i>	(BNL-811 Collab.)
NOBLE	92	PRL 69 414	A.J. Noble <i>et al.</i>	(BIRM, BOST, BRCO+)
DWORKIN	90	PR D41 780	J. Dworkin <i>et al.</i>	(BRIS, GEVA, HEIDP+)
TIXIER	88	PL B212 523	M.H. Tixier <i>et al.</i>	(DM2 Collab.)
BARNES	87	PL B199 147	P.D. Barnes <i>et al.</i>	(CMU, SAFL, LANL+)
BIAGI	86	ZPHY C30 201	S.F. Biagi <i>et al.</i>	(BRIS, CERN, GEVA+)
CHAUVAT	85	PL 163B 273	P. Chauvat <i>et al.</i>	(CERN, CLER, UCLA+)
BOURQUIN	83	ZPHY C21 1	M.H. Bourquin <i>et al.</i>	(BRIS, GEVA, HEIDP+)
COX	81	PRL 46 877	P.T. Cox <i>et al.</i>	(MICH, WISC, RUTG, MINN+)
PONDROM	81	PR D23 814	L. Pondrom <i>et al.</i>	(WISC, MICH, RUTG+)
WISE	81	PL 98B 123	J.E. Wise <i>et al.</i>	(MASA, BNL)
WISE	80	PL 91B 165	J.E. Wise <i>et al.</i>	(MASA, BNL)
SCHACHIN...	78	PRL 41 1348	L. Schachinger <i>et al.</i>	(MICH, RUTG, WISC)
HELLER	77	PL 68B 480	K. Heller <i>et al.</i>	(MICH, WISC, HEID)
LINDQUIST	77	PR D16 2104	J. Lindquist <i>et al.</i>	(EFI, OSU, ANL)
Also		JPG 2 L211	J. Lindquist <i>et al.</i>	(EFI, WUSL, OSU+)
ZECH	77	NP B124 413	G. Zech <i>et al.</i>	(SIEG, CERN, DORT, HEID)
BUNCE	76	PRL 36 1113	G.R.M. Bunce <i>et al.</i>	(WISC, MICH, RUTG)
ASTBURY	75	NP B99 30	P. Astbury <i>et al.</i>	(LOIC, CERN, ET+)
CLAYTON	75	NP B95 130	E.F. Clayton <i>et al.</i>	(LOIC, RHEL)
ALTHOFF	73	PL 43B 237	K.H. Althoff <i>et al.</i>	(CERN, HEID)
ALTHOFF	73B	NP B66 29	K.H. Althoff <i>et al.</i>	(CERN, HEID)
KATZ	73	Thesis MDDP-TR-74-044	C.N. Katz	(UMD)
POULARD	73	PL 46B 135	G. Poulard, A. Givernaud, A.C. Borg	(SAFL)
BAGGETT	72B	ZPHY 252 362	M.J. Baggett <i>et al.</i>	(HEID)
BAGGETT	72C	PL 42B 379	M.J. Baggett <i>et al.</i>	(HEID)
CLELAND	72	NP B40 221	W.E. Cleland <i>et al.</i>	(CERN, GEVA, LUND)
HYMAN	72	PR D5 1063	L.G. Hyman <i>et al.</i>	(ANL, CMU)
ALTHOFF	71	PL 37B 531	K.H. Althoff <i>et al.</i>	(CERN, HEID)
BALTAY	71B	PR D4 670	C. Baltay <i>et al.</i>	(COLU, BING)
BARONI	71	LNC 2 1256	G. Baroni, S. Petrer, G. Romano	(ROMA)
CANTER	71	PRL 26 868	J. Canter <i>et al.</i>	(STON, COLU)
CANTER	71B	PR 27 59	J. Canter <i>et al.</i>	(STON, COLU)
DAHL-JENSEN	71	NC 3A 1	E. Dahl-Jensen <i>et al.</i>	(CERN, ANKA, LAUS+)
LINDQUIST	71	PRL 27 612	J. Lindquist <i>et al.</i>	(EFI, WUSL, OSU+)
OLSEN	70	PRL 24 843	S.L. Olsen <i>et al.</i>	(WISC, MICH)
DAUBER	69	PR 179 1262	P.M. Dauber <i>et al.</i>	(LRL)
DOYLE	69	Thesis UCLR 18139	J.C. Doyle	(LRL)
MALONEY	69	PRL 23 425	J.E. Maloney, B. Sechi-Zorn	(UMD)
GRIMM	68	NC 54A 187	H.J. Grimm	(HEID)
HEPP	68	ZPHY 214 71	V. Hepp, H. Schleich	(HEID)
BADIER	67	PL 25B 152	J. Badier <i>et al.</i>	(EPOL)
MAYEUR	67	U Libr.Brux.Bul. 32	C. Mayeur, E. Tompa, J.H. Wickens	(BELG, LOUC)
OVERSETH	67	PRL 19 391	O.E. Overseth, R.F. Roth	(MICH, PRIN)
PDG	67	RMP 39 1	A.H. Rosenfeld <i>et al.</i>	(LRL, CERN, YALE)
BURAN	66	PL 20 318	T. Buran <i>et al.</i>	(OSLO)
CHIEN	66	PR 152 1171	C.Y. Chien <i>et al.</i>	(YALE, BNL)
ENGELMANN	66	NC 45A 1038	R. Engelmann <i>et al.</i>	(HEID, REHO)
GIBSON	66	NC 45A 882	W.M. Gibson, K. Green	(BRIS)
LONDON	66	PR 143 1034	G.W. London <i>et al.</i>	(BNL, SYRA)
SCHMIDT	65	PR 140B 1328	P. Schmidt	(COLU)
BAGLIN	64	NC 35 977	C. Baglin <i>et al.</i>	(EPOL, CERN, LOUC, RHEL+)
HUBBARD	64	PR 135 B183	J.R. Hubbard <i>et al.</i>	(LRL)
LIND	64	PR 135 B1483	W.G. Lind <i>et al.</i>	(WISC)
RONNE	64	PL 11 357	B.E. Ronne <i>et al.</i>	(CERN, EPOL, LOUC+)
SCHWARTZ	64	Thesis UCLR 11360	J.A. Schwartz	(LRL)
BHOWMIK	63	NC 28 1494	B. Bhowmik, D.P. Goyal	(DELH)
BLOCK	63	PR 130 766	M.M. Block <i>et al.</i>	(NWES, BGNA, SYRA+)
BROWN	63	PR 130 769	J.L. Brown <i>et al.</i>	(LRL, MICH)
CHRETIEN	63	PR 131 2208	M. Chretien <i>et al.</i>	(BRAN, BROW, HARV+)
CRONIN	63	PR 129 1795	J.W. Cronin, O.E. Overseth	(PRIN)
ELY	63	PR 131 868	R.P. Ely <i>et al.</i>	(LRL)
HUMPHREY	62	PR 127 1305	W.E. Humphrey, R.R. Ross	(LRL)
CORK	60	PR 120 1000	B. Cork <i>et al.</i>	(LRL, PRIN, BNL)
CRAWFORD	59B	PRL 2 266	F.S. Crawford <i>et al.</i>	(LRL)

Baryon Particle Listings

 Λ 's and Σ 's Λ AND Σ RESONANCES

Introduction: The only new data entries in this 2006 Review are two measurements of the $\Lambda(1520) \rightarrow \Lambda\gamma$ branching fraction and measurements of the $\Sigma(1385) \rightarrow \Lambda\gamma$ and $\Sigma^- \gamma$ branching fractions. The field remains at a standstill. What follows is a much abbreviated version of the note on Λ and Σ Resonances from our 1990 edition [1]. In particular, see that edition for some representative Argand plots from partial-wave analyses.

Table 1 is an attempt to evaluate the status, both overall and channel by channel, of each Λ and Σ resonance in the Particle Listings. The evaluations are of course partly subjective. A blank indicates there is no evidence at all: either the relevant couplings are small or the resonance does not really exist. The main Baryon Summary Table includes only the established resonances (overall status 3 or 4 stars). A number of the 1- and 2-star entries may eventually disappear, but there are certainly many resonances yet to be discovered underlying the established ones.

Sign conventions for resonance couplings: In terms of the isospin-0 and -1 elastic scattering amplitudes A_0 and A_1 , the amplitude for $K^- p \rightarrow \bar{K}^0 n$ scattering is $\pm(A_1 - A_0)/2$, where the sign depends on conventions used in conjunction with the Clebsch-Gordan coefficients (such as, is the baryon or the meson the “first” particle). If this reaction is partial-wave analyzed and if the overall phase is chosen so that, say, the $\Sigma(1775)D_{15}$ amplitude at resonance points along the positive imaginary axis (points “up”), then any Σ at resonance will point “up” and any Λ at resonance will point “down” (along the negative imaginary axis). Thus the phase at resonance determines the isospin. The above ignores background amplitudes in the resonating partial waves.

That is the basic idea. In a similar but somewhat more complicated way, the phases of the $\bar{K}N \rightarrow \Lambda\pi$ and $\bar{K}N \rightarrow \Sigma\pi$ amplitudes for a resonating wave help determine the SU(3) multiplet to which the resonance belongs. Again, a convention has to be adopted for some overall arbitrary phases: which way is “up”? Our convention is that of Levi-Setti [2] and is shown in Fig. 1, which also compares experimental results with theoretical predictions for the signs of several resonances. In the Listings, a + or - sign in front of a measurement of an inelastic resonance coupling indicates the sign (the *absence* of a sign means that the sign is not determined, *not* that it is positive). For more details, see Appendix II of our 1982 edition [3].

Errors on masses and widths: The errors quoted on resonance parameters from partial-wave analyses are often only statistical, and the parameters can change by more than these errors when a different parametrization of the waves is used. Furthermore, the different analyses use more or less the same data, so it is not really appropriate to treat the different determinations of the resonance parameters as independent or to average them together. In any case, the spread of the masses, widths, and branching fractions from the different analyses is certainly a better indication of the uncertainties than are the quoted errors. In the Baryon Summary Table, we usually give a range reflecting the spread of the values rather than a particular value with error.

For three states, the $\Lambda(1520)$, the $\Lambda(1820)$, and the $\Sigma(1775)$, there is enough information to make an overall fit to the various branching fractions. It is then necessary to use the quoted errors, but the errors obtained from the fit should not be taken seriously.

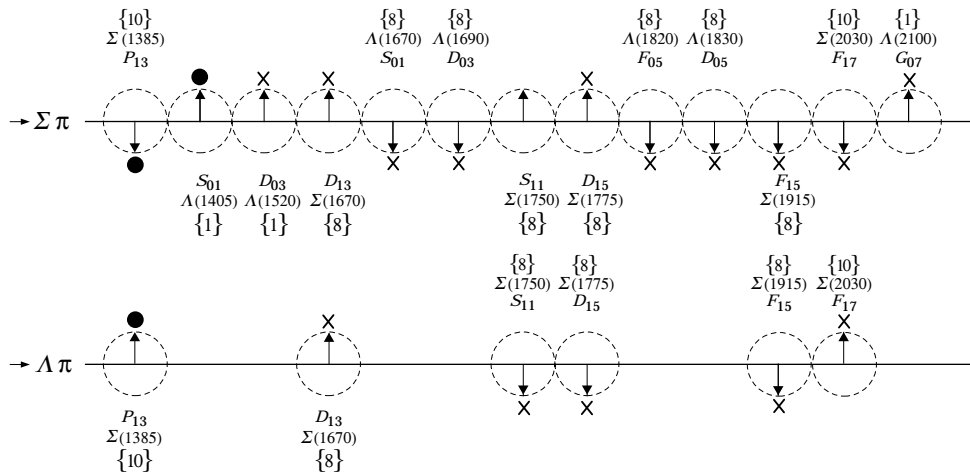


Figure 1. The signs of the imaginary parts of resonating amplitudes in the $\bar{K}N \rightarrow \Lambda\pi$ and $\Sigma\pi$ channels. The signs of the $\Sigma(1385)$ and $\Lambda(1405)$, marked with a \bullet , are set by convention, and then the others are determined relative to them. The signs required by the SU(3) assignments of the resonances are shown with an arrow, and the experimentally determined signs are shown with an \times .

Table 1. The status of the Λ and Σ resonances. Only those with an overall status of *** or **** are included in the main Baryon Summary Table.

Particle	$L_{I,2J}$	Overall status	Status as seen in —			
			$N\bar{K}$	$\Lambda\pi$	$\Sigma\pi$	Other channels
Λ(1116)	P_{01}	****		F		$N\pi$ (weakly)
Λ(1405)	S_{01}	****	****	o	****	
Λ(1520)	D_{03}	****	****	r	****	$\Lambda\pi\pi, \Lambda\gamma$
Λ(1600)	P_{01}	***	***	b	**	
Λ(1670)	S_{01}	****	****	i	****	$\Lambda\eta$
Λ(1690)	D_{03}	****	****	d	****	$\Lambda\pi\pi, \Sigma\pi\pi$
Λ(1800)	S_{01}	***	***	d	**	$N\bar{K}^*, \Sigma(1385)\pi$
Λ(1810)	P_{01}	***	***	e	**	$N\bar{K}^*$
Λ(1820)	F_{05}	****	****	n	****	$\Sigma(1385)\pi$
Λ(1830)	D_{05}	****	***	F	****	$\Sigma(1385)\pi$
Λ(1890)	P_{03}	****	****	o	**	$N\bar{K}^*, \Sigma(1385)\pi$
Λ(2000)	*	*	*	r	*	$\Lambda\omega, N\bar{K}^*$
Λ(2020)	F_{07}	*	*	b	*	
Λ(2100)	G_{07}	****	****	i	***	$\Lambda\omega, N\bar{K}^*$
Λ(2110)	F_{05}	***	**	d	*	$\Lambda\omega, N\bar{K}^*$
Λ(2325)	D_{03}	*	*	d	*	$\Lambda\omega$
Λ(2350)	***	***	*	e	*	
Λ(2585)	**	**	*	n	*	
Σ(1193)	P_{11}	****				$N\pi$ (weakly)
Σ(1385)	P_{13}	****		****	****	
Σ(1480)	*	*	*	*	*	
Σ(1560)	**	**	**	**	**	
Σ(1580)	D_{13}	*	*	*	*	
Σ(1620)	S_{11}	**	**	*	*	
Σ(1660)	P_{11}	***	***	*	**	
Σ(1670)	D_{13}	****	****	****	****	several others
Σ(1690)	**	*	**	*	*	$\Lambda\pi\pi$
Σ(1750)	S_{11}	***	***	**	*	$\Sigma\eta$
Σ(1770)	P_{11}	*	*	*	*	
Σ(1775)	D_{15}	****	****	****	***	several others
Σ(1840)	P_{13}	*	*	**	*	
Σ(1880)	P_{11}	**	**	**	*	$N\bar{K}^*$
Σ(1915)	F_{15}	****	***	****	***	$\Sigma(1385)\pi$
Σ(1940)	D_{13}	***	*	***	**	quasi-2-body
Σ(2000)	S_{11}	*	*	*	*	$N\bar{K}^*, \Lambda(1520)\pi$
Σ(2030)	F_{17}	****	****	****	**	several others
Σ(2070)	F_{15}	*	*	*	*	
Σ(2080)	P_{13}	**	**	*	*	
Σ(2100)	G_{17}	*	*	*	*	
Σ(2250)	***	***	*	*	*	
Σ(2455)	**	*	*	*	*	
Σ(2620)	**	*	*	*	*	
Σ(3000)	*	*	*	*	*	
Σ(3170)	*	*	*	*	*	multi-body

**** Existence is certain, and properties are at least fairly well explored.
 *** Existence ranges from very likely to certain, but further confirmation is desirable and/or quantum numbers, branching fractions, etc. are not well determined.
 ** Evidence of existence is only fair.
 * Evidence of existence is poor.

Production experiments: Partial-wave analyses of course separate partial waves, whereas a peak in a cross section or an invariant mass distribution usually cannot be disentangled from background and analyzed for its quantum numbers; and more than one resonance may be contributing to the peak. Results from partial-wave analyses and from production experiments are generally kept separate in the Listings, and in the Baryon Summary Table results from production experiments are used only for the low-mass states. The Σ(1385) and Λ(1405) of course lie below the $\bar{K}N$ threshold and nearly everything about them is learned from production experiments; and production and formation experiments agree quite well in the case

of Λ(1520) and results have been combined. There is some disagreement between production and formation experiments in the 1600–1700 MeV region: see the note on the Σ(1670).

References

1. Particle Data Group, Phys. Lett. **B239**, VIII.64 (1990).
2. R. Levi-Setti, in *Proceedings of the Lund International Conference on Elementary Particles* (Lund, 1969), p. 339.
3. Particle Data Group, Phys. Lett. **111B** (1982).

Λ(1405) S_{01}
 $I(J^P) = 0(\frac{1}{2}^-)$ Status: ****

It seems to be the universal opinion of the chiral-unitary community that there are two poles in the 1400-MeV region. For discussions and earlier references, see for example MAGAS 05 and JIDO 03. ZYCHOR 08 presents experimental evidence against the two-pole model, but this is disputed by GENG 07A. See also REVAI 09, which finds little basis for choosing between one- and two-pole models.

See also the “Note on the Λ(1405)” in our 2000 edition, *The European Physical Journal* **C15** 1 (2000).

A single, ordinary three-quark Λ(1405) fits nicely into a $J^P = 1/2^-$ SU(4) $\bar{4}$ multiplet, whose other members are the $\Lambda_c(2595)^+$, $\Xi_c(2790)^+$, and $\Xi_c(2790)^0$; see Fig. 1 of our note on “Charmed Baryons.”

Λ(1405) MASS

PRODUCTION EXPERIMENTS

VALUE (MeV)	EVTS	DOCUMENT ID	TECN	COMMENT
1406.5 ± 4.0		¹ DALITZ	91	M-matrix fit
• • • We do not use the following data for averages, fits, limits, etc. • • •				
1391 ± 1	700	¹ HEMINGWAY	85	HBC K^-p 4.2 GeV/c
~ 1405	400	² THOMAS	73	HBC π^-p 1.69 GeV/c
1405	120	BARBARO...	68B	DBC K^-d 2.1–2.7 GeV/c
1400 ± 5	67	BIRMINGHAM	66	HBC K^-p 3.5 GeV/c
1382 ± 8		ENGLER	65	HDHC π^-p, π^+d 1.68 GeV/c
1400 ± 24		MUSGRAVE	65	HBC $\bar{p}p$ 3–4 GeV/c
1410		ALEXANDER	62	HBC π^-p 2.1 GeV/c
1405		ALSTON	62	HBC K^-p 1.2–0.5 GeV/c
1405		ALSTON	61B	HBC K^-p 1.15 GeV/c

EXTRAPOLATIONS BELOW $N\bar{K}$ THRESHOLD

VALUE (MeV)	DOCUMENT ID	TECN	COMMENT
• • • We do not use the following data for averages, fits, limits, etc. • • •			
1407.56 or 1407.50	³ KIMURA	00	potential model
1411	⁴ MARTIN	81	K-matrix fit
1406	⁵ CHAO	73	DPWA 0-range fit (sol. B)
1421	MARTIN	70	RVUE Constant K-matrix
1416 ± 4	MARTIN	69	HBC Constant K-matrix
1403 ± 3	KIM	67	HBC K-matrix fit
1407.5 ± 1.2	⁶ KITTEL	66	HBC 0-effective-range fit
1410.7 ± 1.0	KIM	65	HBC 0-effective-range fit
1409.6 ± 1.7	⁶ SAKITT	65	HBC 0-effective-range fit

Λ(1405) WIDTH

PRODUCTION EXPERIMENTS

VALUE (MeV)	EVTS	DOCUMENT ID	TECN	COMMENT
50 ± 2		¹ DALITZ	91	M-matrix fit
• • • We do not use the following data for averages, fits, limits, etc. • • •				
32 ± 1	700	¹ HEMINGWAY	85	HBC K^-p 4.2 GeV/c
45 to 55	400	² THOMAS	73	HBC π^-p 1.69 GeV/c
35	120	BARBARO...	68B	DBC K^-d 2.1–2.7 GeV/c
50 ± 10	67	BIRMINGHAM	66	HBC K^-p 3.5 GeV/c
89 ± 20		ENGLER	65	HDHC
60 ± 20		MUSGRAVE	65	HBC
35 ± 5		ALEXANDER	62	HBC
50		ALSTON	62	HBC
20		ALSTON	61B	HBC

Baryon Particle Listings

$\Lambda(1405)$, $\Lambda(1520)$

EXTRAPOLATIONS BELOW $N\bar{K}$ THRESHOLD

VALUE (MeV)	DOCUMENT ID	TECN	COMMENT
••• We do not use the following data for averages, fits, limits, etc. •••			
50.24 or 50.26	3 KIMURA 00		potential model
30	4 MARTIN 81		K-matrix fit
55	5,7 CHAO 73	DPWA	0-range fit (sol. B)
20	MARTIN 70	RVUE	Constant K-matrix
29 ± 6	MARTIN 69	HBC	Constant K-matrix
50 ± 5	KIM 67	HBC	K-matrix fit
34.1 ± 4.1	6 KITTEL 66	HBC	
37.0 ± 3.2	KIM 65	HBC	
28.2 ± 4.1	6 SAKITT 65	HBC	

$\Lambda(1405)$ DECAY MODES

Mode	Fraction (Γ_i/Γ)
Γ_1 $\Sigma \pi$	100 %
Γ_2 $\Lambda \gamma$	
Γ_3 $\Sigma^0 \gamma$	
Γ_4 $N\bar{K}$	

$\Lambda(1405)$ PARTIAL WIDTHS

$\Gamma(\Lambda_i)$	DOCUMENT ID	COMMENT	Γ_2
••• We do not use the following data for averages, fits, limits, etc. •••			
27 ± 8	BURKHARDT 91	Isobar model fit	

$\Gamma(\Sigma^0 \gamma)$	DOCUMENT ID	COMMENT	Γ_3
••• We do not use the following data for averages, fits, limits, etc. •••			
10 ± 4 or 23 ± 7	BURKHARDT 91	Isobar model fit	

$\Lambda(1405)$ BRANCHING RATIOS

$\Gamma(N\bar{K})/\Gamma(\Sigma \pi)$	CL%	DOCUMENT ID	TECN	COMMENT	Γ_4/Γ_1
••• We do not use the following data for averages, fits, limits, etc. •••					
<3	95	HEMINGWAY 85	HBC	$K^- p$ 4.2 GeV/c	

$\Lambda(1405)$ FOOTNOTES

- ¹ DALITZ 91 fits the HEMINGWAY 85 data.
- ² THOMAS 73 data is fit by CHAO 73 (see next section).
- ³ The KIMURA 00 values are from fits A and B from a coupled-channel potential model using low-energy $\bar{K}N$ and $\Sigma \pi$ data, kaonic-hydrogen x-ray measurements, and our $\Lambda(1405)$ mass and width. The results bear mainly on the nature of the $\Lambda(1405)$: three-quark state or $\bar{K}N$ bound state.
- ⁴ The MARTIN 81 fit includes the $K^\pm p$ forward scattering amplitudes and the dispersion relations they must satisfy.
- ⁵ See also the accompanying paper of THOMAS 73.
- ⁶ Data of SAKITT 65 are used in the fit by KITTEL 66.
- ⁷ An asymmetric shape, with $\Gamma/2 = 41$ MeV below resonance, 14 MeV above.

$\Lambda(1405)$ REFERENCES

REVAI 09	PR C79 035202	J. Revai, N.V. Shevchenko (BUDA, NPI-Czech Rep.)
ZYCHOR 08	PL B660 167	I. Zychor et al. (COSY ANKE Collab.)
GENG 07A	EPJ A34 405	L.S. Geng, E. Oset (VALE)
MAGAS 05	PRL 95 052301	V.K. Magas, E. Oset, A. Ramos (BARC, VALE)
JIDO 03	NP A725 181	D. Jido et al. (OSAC, MURC, VALE, BARC+)
KIMURA 00	PR C62 015206	M. Kimura et al.
PDG 00	EPJ C15 1	D.E. Groom et al.
BURKHARDT 91	PR C44 607	H. Burkhardt, J. Lowe (NOTT, UNM, BIRM)
DALITZ 91	JPG 17 289	R.H. Dalitz, A. Deloff (OXFTP, WINR)
HEMINGWAY 85	NP B253 742	R.J. Hemingway (CERN) J
MARTIN 81	NP B179 33	A.D. Martin (DURH)
CHAO 73	NP B56 46	Y.A. Chao et al. (RHEL, CMU, LOUC)
THOMAS 73	NP B56 15	D.W. Thomas et al. (CMU) J
MARTIN 70	NP B16 479	A.D. Martin, G.G. Ross (DURH)
MARTIN 69	PR 183 1352	B.R. Martin, M. Saktitt (LOUC, BNL)
Also	PR 183 1345	B.R. Martin, M. Saktitt (LOUC, BNL)
BARBARO-... 68B	PRL 21 573	A. Barbaro-Galtieri et al. (LRL, SLAC)
KIM 67	PRL 19 1074	J.K. Kim (YALE)
BIRMINGHAM 66	PR 152 1148	M. Haque et al. (BIRM, GLAS, LOIC, OXF+)
KITTEL 66	PL 21 349	W. Kittel, G. Otter, I. Wacek (VIEN)
ENGLER 65	PRL 15 224	A. Engler et al. (CMU, BNL) JJ
KIM 65	PRL 14 29	J.K. Kim (COLU)
MUSGRAVE 65	NC 35 735	B. Musgrave et al. (BIRM, CERN, EPOL+)
SAKITT 65	PR 139 8719	M. Saktitt et al. (UMD, LRL)
ALEXANDER 62	PRL 8 447	G. Alexander et al. (LRL) I
ALSTON 62	CERN Conf. 311	M.H. Alston et al. (LRL) I
ALSTON 61B	PRL 6 698	M.H. Alston et al. (LRL) I

OTHER RELATED PAPERS

IWASAKI 97	PRL 78 3067	M. Iwasaki et al. (KEK 228 Collab.)
FINK 90	PR C41 2720	P.J.Jr. Fink et al. (IBMV, ORST, ANSM)
LEINWEBER 90	ANP 198 203	D.B. Leinweber (MCMS)
MUELLER-GR... 90	NP A513 557	A. Mueller-Groeling, K. Holinde, J. Speth (JULI)
BARRETT 89	NC 102A 179	R.C. Barrett (SURR)
BATTY 89	NC 102A 255	C.J. Batty, A. Gal (RAL, HEBR)
CAPSTICK 89	Excited Baryons 88, p.32	S. Capstick (GUEL)
LOWE 89	NC 102A 167	J. Lowe (BIRM)
WHITEHOUSE 89	PRL 63 1352	D.A. Whitehouse et al. (BIRM, BOST, BRCO+)
SIEGEL 88	PR C38 2221	P.B. Siegel, W. Weise (REGE)
WORKMAN 88	PR D37 3117	R.L. Workman, H.W. Fearing (TRIU)
SCHNICK 87	PRL 58 1719	J. Schnick, R.H. Landau (ORST)
CAPSTICK 86	PR D34 2809	S. Capstick, N. Isgur (TNTO)
JENNINGS 86	PL B176 229	B.K. Jennings (TRIU)
MALTMAN 86	PR D34 1372	K. Maltman, N. Isgur (LANL, TNTO)
ZHONG 86	PL B171 471	Y.S. Zhong et al. (ADLD, TRIU, SURR)
BURKHARDT 85	NP A440 653	H. Burkhardt, J. Lowe, A.S. Rosenthal (NOTT+)
DAREWYCH 85	PR D32 1765	J.W. Darewych, R. Koniuk, N. Isgur (YORKC, TNTO)
VEIT 85	PR D31 1033	E.A. Veit et al. (TRIU, ADLD, SURR)
KIANG 84	PR C30 1638	D. Kiang et al. (DALH, MCMS)
MILLER 84	Conference paper	D.J. Miller (LOUC)
Conf. Intersections between Particle and Nuclear Physics, p. 783		
VANDIJK 84	PR D30 937	W. van Dijk (MCMS)
VEIT 84	PL 137B 415	E.A. Veit et al. (TRIU, SURR, CERN)
DALITZ 82	Heid. Conf.	R.H. Dalitz et al. (OXFTP)
Heidelberg Conf., p. 201		
DALITZ 81	Kaon Conf.	R.H. Dalitz, J.G. McGinley (OXFTP)
Low and Intermediate Energy Kaon-Nucleon Physics, p.381		
MARTIN 81B	Kaon Conf.	A.D. Martin (DURH)
Low and Intermediate Energy Kaon-Nucleon Physics, p. 97		
OADES 77	NC 42A 462	G.C. Oades, G. Rasche (AARH, ZURI)
SHAW 73	Purdue Conf. 417	G.L. Shaw (UCI)
BARBARO-... 72	LBL-555	A. Barbaro-Galtieri (LBL)
DOBS ON 72	PR D6 3256	P.N. Dobson, R. McElhaneay (HAWA)
RAJASEKAR... 72	PR D5 610	G. Rajasekaran (TATA)
Earlier papers also cited in RAJASEKARAN 72		
CLINE 71	PRL 26 1194	D. Cline, R. Laumann, J. Mapp (WISC)
MARTIN 71	PL 35B 62	A.D. Martin, A.D. Martin, G.G. Ross (DURH, LOUC+)
DALITZ 67	PR 153 1617	R.H. Dalitz, T.C. Wong, G. Rajasekaran (OXFTP+)
DONALD 66	PL 22 711	R.A. Donald et al. (LVP)
KADYK 66	PRL 17 599	J.A. Kadyk et al. (LRL)
ABRAMS 65	PR 139 B454	G.S. Abrams, B. Sechi-Zorn (UMD)

$\Lambda(1520) D_{03}$

$$I(J^P) = 0(\frac{3}{2}^-) \text{ Status: } ***$$

Discovered by FERRO-LUZZI 62; the elaboration in WATSON 63 is the classic paper on the Breit-Wigner analysis of a multichannel resonance.

The measurements of the mass, width, and elasticity published before 1975 are now obsolete and have been omitted. They were last listed in our 1982 edition Physics Letters **111B** 1 (1982).

Production and formation experiments agree quite well, so they are listed together here.

$\Lambda(1520)$ MASS

VALUE (MeV)	EVTS	DOCUMENT ID	TECN	COMMENT
1519.5 ± 1.0 OUR ESTIMATE				
1519.50 ± 0.18 OUR AVERAGE				
1517.3 ± 1.5	300	BARBER 80D	SPEC	$\gamma p \rightarrow \Lambda(1520) K^+$
1519 ± 1		GOPAL 80	DPWA	$\bar{K} N \rightarrow \bar{K} N$
1517.8 ± 1.2	5k	BARLAG 79	HBC	$K^- p$ 4.2 GeV/c
1520.0 ± 0.5		ALSTON-... 78	DPWA	$\bar{K} N \rightarrow \bar{K} N$
1519.7 ± 0.3	4k	CAMERON 77	HBC	$K^- p$ 0.96-1.36 GeV/c
1519 ± 1		GOPAL 77	DPWA	$\bar{K} N$ multichannel
1519.4 ± 0.3	2000	CORDEN 75	DBC	$K^- d$ 1.4-1.8 GeV/c

$\Lambda(1520)$ WIDTH

VALUE (MeV)	EVTS	DOCUMENT ID	TECN	COMMENT
15.6 ± 1.0 OUR ESTIMATE				
15.59 ± 0.27 OUR AVERAGE				
16.3 ± 3.3	300	BARBER 80D	SPEC	$\gamma p \rightarrow \Lambda(1520) K^+$
16 ± 1		GOPAL 80	DPWA	$\bar{K} N \rightarrow \bar{K} N$
14 ± 3	677	1 BARLAG 79	HBC	$K^- p$ 4.2 GeV/c
15.4 ± 0.5		ALSTON-... 78	DPWA	$\bar{K} N \rightarrow \bar{K} N$
16.3 ± 0.5	4k	CAMERON 77	HBC	$K^- p$ 0.96-1.36 GeV/c
15.0 ± 0.5		GOPAL 77	DPWA	$\bar{K} N$ multichannel
15.5 ± 1.6	2000	CORDEN 75	DBC	$K^- d$ 1.4-1.8 GeV/c

$\Lambda(1520)$ DECAY MODES

Mode	Fraction (Γ_i/Γ)
Γ_1 $N\bar{K}$	45 ± 1%
Γ_2 $\Sigma \pi$	42 ± 1%
Γ_3 $\Lambda \pi \pi$	10 ± 1%
Γ_4 $\Sigma(1385) \pi$	
Γ_5 $\Sigma(1385) \pi (\rightarrow \Lambda \pi \pi)$	
Γ_6 $\Lambda(\pi \pi) s$ -wave	
Γ_7 $\Sigma \pi \pi$	0.9 ± 0.1%
Γ_8 $\Lambda \gamma$	0.85 ± 0.15%
Γ_9 $\Sigma^0 \gamma$	

CONSTRAINED FIT INFORMATION

An overall fit to 9 branching ratios uses 26 measurements and one constraint to determine 6 parameters. The overall fit has a $\chi^2 = 17.6$ for 21 degrees of freedom.

The following *off-diagonal* array elements are the correlation coefficients $\langle \delta x_i \delta x_j \rangle / (\delta x_i \delta x_j)$, in percent, from the fit to the branching fractions, $x_i \equiv \Gamma_i / \Gamma_{\text{total}}$. The fit constrains the x_i whose labels appear in this array to sum to one.

x_2	-64				
x_3	-32	-34			
x_7	-4	-3	-1		
x_8	-8	-7	-3	0	
x_9	-24	-21	-10	-1	-1
	x_1	x_2	x_3	x_7	x_8

$\Lambda(1520)$ BRANCHING RATIOS

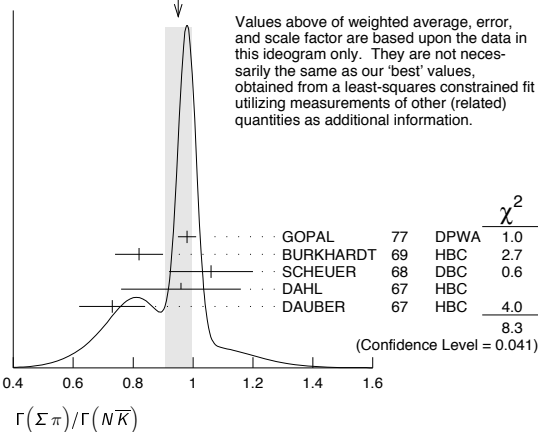
See "Sign conventions for resonance couplings" in the Note on Λ and Σ Resonances.

$\Gamma(N\bar{K})/\Gamma_{\text{total}}$	DOCUMENT ID	TECN	COMMENT	Γ_1/Γ
0.45 ± 0.01 OUR ESTIMATE				
0.447 ± 0.007 OUR FIT			Error includes scale factor of 1.2.	
0.455 ± 0.011 OUR AVERAGE				
0.47 ± 0.02	GOPAL	80	DPWA $\bar{K}N \rightarrow \bar{K}N$	
0.45 ± 0.03	ALSTON-...	78	DPWA $\bar{K}N \rightarrow \bar{K}N$	
0.448 ± 0.014	CORDEN	75	DBC $K^- d$ 1.4-1.8 GeV/c	
• • • We do not use the following data for averages, fits, limits, etc. • • •				
0.47 ± 0.01	GOPAL	77	DPWA See GOPAL 80	
0.42	MAST	76	HBC $K^- p \rightarrow \bar{K}^0 n$	

$\Gamma(\Sigma\pi)/\Gamma_{\text{total}}$	DOCUMENT ID	TECN	COMMENT	Γ_2/Γ
0.42 ± 0.01 OUR ESTIMATE				
0.420 ± 0.007 OUR FIT			Error includes scale factor of 1.2.	
0.423 ± 0.011 OUR AVERAGE				
0.426 ± 0.014	CORDEN	75	DBC $K^- d$ 1.4-1.8 GeV/c	
0.418 ± 0.017	BARBARO-...	69B	HBC $K^- p$ 0.28-0.45 GeV/c	
• • • We do not use the following data for averages, fits, limits, etc. • • •				
0.46	KIM	71	DPWA K-matrix analysis	

$\Gamma(\Sigma\pi)/\Gamma(N\bar{K})$	DOCUMENT ID	TECN	COMMENT	Γ_2/Γ_1
0.940 ± 0.026 OUR FIT			Error includes scale factor of 1.3.	
0.95 ± 0.04 OUR AVERAGE			Error includes scale factor of 1.7. See the ideogram below.	
0.98 ± 0.03	² GOPAL	77	DPWA $\bar{K}N$ multichannel	
0.82 ± 0.08	BURKHARDT	69	HBC $K^- p$ 0.8-1.2 GeV/c	
1.06 ± 0.14	SCHEUER	68	DBC $K^- N$ 3 GeV/c	
0.96 ± 0.20	DAHL	67	HBC $\pi^- p$ 1.6-4 GeV/c	
0.73 ± 0.11	DAUBER	67	HBC $K^- p$ 2 GeV/c	
• • • We do not use the following data for averages, fits, limits, etc. • • •				
1.06 ± 0.12	BERTHON	74	HBC Quasi-2-body σ	
1.72 ± 0.78	MUSGRAVE	65	HBC	

WEIGHTED AVERAGE
 0.95 ± 0.04 (Error scaled by 1.7)



$\Gamma(\Lambda\pi\pi)/\Gamma_{\text{total}}$	DOCUMENT ID	TECN	COMMENT	Γ_3/Γ
0.10 ± 0.01 OUR ESTIMATE				
0.095 ± 0.005 OUR FIT			Error includes scale factor of 1.2.	
0.096 ± 0.008 OUR AVERAGE			Error includes scale factor of 1.6.	
0.091 ± 0.006	CORDEN	75	DBC $K^- d$ 1.4-1.8 GeV/c	
0.11 ± 0.01	³ MAST	73B	IPWA $K^- p \rightarrow \Lambda\pi\pi$	

$\Gamma(\Lambda\pi\pi)/\Gamma(N\bar{K})$	DOCUMENT ID	TECN	COMMENT	Γ_3/Γ_1
0.213 ± 0.012 OUR FIT			Error includes scale factor of 1.2.	
0.202 ± 0.021 OUR AVERAGE				
0.22 ± 0.03	BURKHARDT	69	HBC $K^- p$ 0.8-1.2 GeV/c	
0.19 ± 0.04	SCHEUER	68	DBC $K^- N$ 3 GeV/c	
0.17 ± 0.05	DAHL	67	HBC $\pi^- p$ 1.6-4 GeV/c	
0.21 ± 0.18	DAUBER	67	HBC $K^- p$ 2 GeV/c	
• • • We do not use the following data for averages, fits, limits, etc. • • •				
0.27 ± 0.13	BERTHON	74	HBC Quasi-2-body σ	
0.2	KIM	71	DPWA K-matrix analysis	

$\Gamma(\Sigma\pi)/\Gamma(\Lambda\pi\pi)$	DOCUMENT ID	TECN	COMMENT	Γ_2/Γ_3
4.42 ± 0.25 OUR FIT			Error includes scale factor of 1.2.	
3.9 ± 0.6 OUR AVERAGE				
3.9 ± 1.0	UHLIG	67	HBC $K^- p$ 0.9-1.0 GeV/c	
3.3 ± 1.1	BIRMINGHAM	66	HBC $K^- p$ 3.5 GeV/c	
4.5 ± 1.0	ARMENTEROS65c		HBC	

$\Gamma(\Sigma(1385)\pi)/\Gamma_{\text{total}}$	DOCUMENT ID	TECN	COMMENT	Γ_4/Γ
0.041 ± 0.005				
	CHAN	72	HBC $K^- p \rightarrow \Lambda\pi\pi$	

$\Gamma(\Sigma(1385)\pi(\rightarrow\Lambda\pi\pi))/\Gamma(\Lambda\pi\pi)$	DOCUMENT ID	TECN	COMMENT	Γ_5/Γ_3
The $\Lambda\pi\pi$ mode is largely due to $\Sigma(1385)\pi$. Only the values of $(\Sigma(1385)\pi) / (\Lambda\pi\pi)$ given by MAST 73B and CORDEN 75 are based on real 3-body partial-wave analyses. The discrepancy between the two results is essentially due to the different hypotheses made concerning the shape of the $(\pi\pi)_{S\text{-wave}}$ state.				
0.58 ± 0.22	CORDEN	75	DBC $K^- d$ 1.4-1.8 GeV/c	
0.82 ± 0.10	⁴ MAST	73B	IPWA $K^- p \rightarrow \Lambda\pi\pi$	
• • • We do not use the following data for averages, fits, limits, etc. • • •				
0.39 ± 0.10	⁵ BURKHARDT	71	HBC $K^- p \rightarrow (\Lambda\pi\pi)\pi$	

$\Gamma(\Lambda(\pi\pi)_{S\text{-wave}})/\Gamma(\Lambda\pi\pi)$	DOCUMENT ID	TECN	COMMENT	Γ_6/Γ_3
0.20 ± 0.08				
	CORDEN	75	DBC $K^- d$ 1.4-1.8 GeV/c	

$\Gamma(\Sigma\pi\pi)/\Gamma_{\text{total}}$	DOCUMENT ID	TECN	COMMENT	Γ_7/Γ
0.009 ± 0.001 OUR ESTIMATE				
0.0086 ± 0.0005 OUR FIT				
0.0086 ± 0.0005 OUR AVERAGE				
0.007 ± 0.002	⁶ CORDEN	75	DBC $K^- d$ 1.4-1.8 GeV/c	
0.0085 ± 0.0006	⁷ MAST	73	MPWA $K^- p \rightarrow \Sigma\pi\pi$	
0.010 ± 0.0015	BARBARO-...	69B	HBC $K^- p$ 0.28-0.45 GeV/c	

$\Gamma(\Lambda\gamma)/\Gamma_{\text{total}}$	DOCUMENT ID	TECN	COMMENT	Γ_8/Γ
8.5 ± 1.5 OUR ESTIMATE				
8.8 ± 1.1 OUR FIT				
8.8 ± 1.1 OUR AVERAGE				
10.7 ± 2.9 ^{+1.5} _{-0.4}	TAYLOR	05	CLAS $\gamma p \rightarrow K^+ \Lambda\gamma$	
10.2 ± 2.1 ± 1.5	ANTIPOV	04A	SPNX $pN(C) \rightarrow \Lambda(1520) K^+ N(C)$	
8.0 ± 1.4	MAST	68B	HBC Using $\Gamma(N\bar{K})/\Gamma_{\text{total}} = 0.45$	

$\Gamma(\Sigma^0\gamma)/\Gamma_{\text{total}}$	DOCUMENT ID	TECN	COMMENT	Γ_9/Γ
0.0195 ± 0.0034 OUR FIT				
0.02 ± 0.0035	⁸ MAST	68B	HBC Not measured; see note	

$\Lambda(1520)$ FOOTNOTES

- From the best-resolution sample of $\Lambda\pi\pi$ events only.
- The $\bar{K}N \rightarrow \Sigma\pi$ amplitude at resonance is $+0.46 \pm 0.01$.
- Assumes $\Gamma(N\bar{K})/\Gamma_{\text{total}} = 0.46 \pm 0.02$.
- Both $\Sigma(1385)\pi$ DS_{03} and $\Sigma(\pi\pi)$ DP_{03} contribute.
- The central bin (1514-1524 MeV) gives 0.74 ± 0.10 ; other bins are lower by 2-to-5 standard deviations.
- Much of the $\Sigma\pi\pi$ decay proceeds via $\Sigma(1385)\pi$.
- Assumes $\Gamma(N\bar{K})/\Gamma_{\text{total}} = 0.46$.
- Calculated from $\Gamma(\Lambda\gamma)/\Gamma_{\text{total}}$, assuming SU(3). Needed to constrain the sum of all the branching ratios to be unity.

Baryon Particle Listings

 $\Lambda(1520)$, $\Lambda(1600)$, $\Lambda(1670)$ $\Lambda(1520)$ REFERENCES

Author	Year	Document ID	TECN	COMMENT
TAYLOR	05	PR C71 054609		S. Taylor et al. (JLab CLAS Collab.)
Also		PR C72 039902 (errat.)		S. Taylor et al. (JLab CLAS Collab.)
ANTIPOV	04A	PL B604 22		Yu.M. Antipov et al. (IHEP SPHINX Collab.)
PDG	82	PL 111B 1		M. Roos et al. (HEL5, CIT, CERN)
BARBER	80D	ZPHY C7 17		D.P. Barber et al. (DARE, LANC, SHEF)
GOPAL	80	Toronto Conf. 159		G.P. Gopal (RHEL) IJP
BARLAG	79	NP B149 220		S.J.M. Barlag et al. (AMST, CERN, NIJM+)
ALSTON-...	78	PR D18 182		M. Alston-Garnjost et al. (LBL, MTHO+) IJP
Also		PRL 38 1007		M. Alston-Garnjost et al. (LBL, MTHO+) IJP
CAMERON	77	NP B131 399		W. Cameron et al. (RHEL, LOIC) IJP
GOPAL	77	NP B119 362		G.P. Gopal et al. (LOIC, RHEL) IJP
MAST	76	PR D14 13		T.S. Mast et al. (LBL)
CORDEN	75	NP B84 306		M.J. Corden et al. (BIRM)
BERTHON	74	NC 21A 146		A. Berthon et al. (CDEF, RHEL, SACL+)
MAST	73	PR D7 3212		T.S. Mast et al. (LBL) IJP
MAST	73B	PR D7 5		T.S. Mast et al. (LBL) IJP
CHAN	72	PRL 28 256		S.B. Chan et al. (MASA, YALE)
BURKHARDT	71	NP B27 64		E. Burkhardt et al. (HEID, CERN, SACL)
KIM	71	PRL 27 356		J.K. Kim (HARV) IJP
Also		Duke Conf. 161		J.K. Kim (HARV) IJP
Hyperon Resonances, 1970				
BARBARO-...	69B	Lund Conf. 352		A. Barbaro-Galiteri et al. (LRL)
Also		Duke Conf. 95		R.D. Tripp (LRL)
Hyperon Resonances 1970				
BURKHARDT	69	NP B14 106		E. Burkhardt et al. (HEID, EFI, CERN+)
MAST	68B	PRL 21 1715		T.S. Mast et al. (LRL)
SCHUEER	68	NP B8 503		J.C. Schueer et al. (SABRE Collab.)
DAHL	67	PR 163 1377		O.I. Dahl et al. (LRL)
DAUBER	67	PL 24B 525		P.M. Dauber et al. (UCLA)
UHLIG	67	PR 155 1448		R.P. Uhlig et al. (UMD, NRL)
BIRMINGHAM	66	PR 152 1148		M. Haque et al. (BIRM, GLAS, LOIC, OXF+)
ARMENTEROS	65C	PL 19 338		R. Armenteros et al. (CERN, HEID, SACL)
MUSGRAVE	65	NC 35 735		B. Musgrave et al. (BIRM, CERN, EPOL+)
WATSON	63	PR 131 2248		M.B. Watson, M. Ferro-Luzzi, R.D. Tripp (LRL) IJP
FERRO-LUZZI	62	PRL 8 28		M. Ferro-Luzzi, R.D. Tripp, M.B. Watson (LRL) IJP

 $\Lambda(1600) P_{01}$

$$I(J^P) = 0(\frac{1}{2}^+) \text{ Status: } ***$$

See also the $\Lambda(1810) P_{01}$. There are quite possibly two P_{01} states in this region.

 $\Lambda(1600)$ MASS

VALUE (MeV)	DOCUMENT ID	TECN	COMMENT
1560 to 1700 (≈ 1600) OUR ESTIMATE			
1568 \pm 20	GOPAL 80	DPWA	$\bar{K}N \rightarrow \bar{K}N$
1703 \pm 100	ALSTON-... 78	DPWA	$\bar{K}N \rightarrow \bar{K}N$
1573 \pm 25	GOPAL 77	DPWA	$\bar{K}N$ multichannel
1596 \pm 6	KANE 74	DPWA	$K^- p \rightarrow \Sigma\pi$
1620 \pm 10	LANGBEIN 72	IPWA	$\bar{K}N$ multichannel
••• We do not use the following data for averages, fits, limits, etc. •••			
1572 or 1617	¹ MARTIN 77	DPWA	$\bar{K}N$ multichannel
1646 \pm 7	² CARROLL 76	DPWA	Isospin-0 total σ
1570	KIM 71	DPWA	K-matrix analysis

 $\Lambda(1600)$ WIDTH

VALUE (MeV)	DOCUMENT ID	TECN	COMMENT
50 to 250 (≈ 150) OUR ESTIMATE			
116 \pm 20	GOPAL 80	DPWA	$\bar{K}N \rightarrow \bar{K}N$
593 \pm 200	ALSTON-... 78	DPWA	$\bar{K}N \rightarrow \bar{K}N$
147 \pm 50	GOPAL 77	DPWA	$\bar{K}N$ multichannel
175 \pm 20	KANE 74	DPWA	$K^- p \rightarrow \Sigma\pi$
60 \pm 10	LANGBEIN 72	IPWA	$\bar{K}N$ multichannel
••• We do not use the following data for averages, fits, limits, etc. •••			
247 or 271	¹ MARTIN 77	DPWA	$\bar{K}N$ multichannel
20	² CARROLL 76	DPWA	Isospin-0 total σ
50	KIM 71	DPWA	K-matrix analysis

 $\Lambda(1600)$ DECAY MODES

Mode	Fraction (Γ_i/Γ)
Γ_1 $N\bar{K}$	15–30 %
Γ_2 $\Sigma\pi$	10–60 %

The above branching fractions are our estimates, not fits or averages.

 $\Lambda(1600)$ BRANCHING RATIOS

See "Sign conventions for resonance couplings" in the Note on Λ and Σ Resonances.

$\Gamma(N\bar{K})/\Gamma_{\text{total}}$	DOCUMENT ID	TECN	COMMENT	Γ_1/Γ
0.15 to 0.30 OUR ESTIMATE				
0.23 \pm 0.04	GOPAL 80	DPWA	$\bar{K}N \rightarrow \bar{K}N$	
0.14 \pm 0.05	ALSTON-... 78	DPWA	$\bar{K}N \rightarrow \bar{K}N$	
0.25 \pm 0.15	LANGBEIN 72	IPWA	$\bar{K}N$ multichannel	
••• We do not use the following data for averages, fits, limits, etc. •••				
0.24 \pm 0.04	GOPAL 77	DPWA	See GOPAL 80	
0.30 or 0.29	¹ MARTIN 77	DPWA	$\bar{K}N$ multichannel	

 $(\Gamma_1\Gamma_2)^{1/2}/\Gamma_{\text{total}}$ in $N\bar{K} \rightarrow \Lambda(1600) \rightarrow \Sigma\pi$ $(\Gamma_1\Gamma_2)^{1/2}/\Gamma$

VALUE	DOCUMENT ID	TECN	COMMENT
-0.16 \pm 0.04	GOPAL 77	DPWA	$\bar{K}N$ multichannel
-0.33 \pm 0.11	KANE 74	DPWA	$K^- p \rightarrow \Sigma\pi$
0.28 \pm 0.09	LANGBEIN 72	IPWA	$\bar{K}N$ multichannel
••• We do not use the following data for averages, fits, limits, etc. •••			
-0.39 or -0.39	¹ MARTIN 77	DPWA	$\bar{K}N$ multichannel
not seen	HEPP 76B	DPWA	$K^- N \rightarrow \Sigma\pi$

 $\Lambda(1600)$ FOOTNOTES

- ¹ The two MARTIN 77 values are from a T-matrix pole and from a Breit-Wigner fit.
² A total cross-section bump with $(J+1/2)\Gamma_{\text{el}}/\Gamma_{\text{total}} = 0.04$.

 $\Lambda(1600)$ REFERENCES

Author	Year	Document ID	TECN	COMMENT
GOPAL	80	Toronto Conf. 159		G.P. Gopal (RHEL) IJP
ALSTON-...	78	PR D18 182		M. Alston-Garnjost et al. (LBL, MTHO+) IJP
Also		PRL 38 1007		M. Alston-Garnjost et al. (LBL, MTHO+) IJP
GOPAL	77	NP B119 362		G.P. Gopal et al. (LOIC, RHEL) IJP
MARTIN	77	NP B127 349		B.R. Martin, M.K. Pidcock, R.G. Moorhouse (LOUC+) IJP
Also		NP B126 266		B.R. Martin, M.K. Pidcock (LOUC) IJP
Also		NP B126 285		B.R. Martin, M.K. Pidcock (LOUC) IJP
CARROLL	76	PRL 37 806		A.S. Carroll et al. (BNL) I
HEPP	76B	PL 65B 487		V. Hepp et al. (CERN, HEIDH, MPIM) IJP
KANE	74	LBL-2452		D.F. Kane (LBL) IJP
LANGBEIN	72	NP B47 477		W. Langbein, F. Wagner (MPIM) IJP
KIM	71	PRL 27 356		J.K. Kim (HARV) IJP

 $\Lambda(1670) S_{01}$

$$I(J^P) = 0(\frac{1}{2}^-) \text{ Status: } ***$$

The measurements of the mass, width, and elasticity published before 1974 are now obsolete and have been omitted. They were last listed in our 1982 edition Physics Letters **111B** 1 (1982).

 $\Lambda(1670)$ MASS

VALUE (MeV)	DOCUMENT ID	TECN	COMMENT
1660 to 1680 (≈ 1670) OUR ESTIMATE			
1677.5 \pm 0.8	¹ GARCIA-REC... 03	DPWA	$\bar{K}N$ multichannel
1673 \pm 2	MANLEY 02	DPWA	$\bar{K}N$ multichannel
1670.8 \pm 1.7	KOISO 85	DPWA	$K^- p \rightarrow \Sigma\pi$
1667 \pm 5	GOPAL 80	DPWA	$\bar{K}N \rightarrow \bar{K}N$
1671 \pm 3	ALSTON-... 78	DPWA	$\bar{K}N \rightarrow \bar{K}N$
1670 \pm 5	GOPAL 77	DPWA	$\bar{K}N$ multichannel
1675 \pm 2	HEPP 76B	DPWA	$K^- N \rightarrow \Sigma\pi$
1679 \pm 1	KANE 74	DPWA	$K^- p \rightarrow \Sigma\pi$
1665 \pm 5	PREVOST 74	DPWA	$K^- N \rightarrow \Sigma(1385)\pi$
••• We do not use the following data for averages, fits, limits, etc. •••			
1668.9 \pm 2.0	ABAEV 96	DPWA	$K^- p \rightarrow \Lambda\eta$
1664	² MARTIN 77	DPWA	$\bar{K}N$ multichannel

 $\Lambda(1670)$ WIDTH

VALUE (MeV)	DOCUMENT ID	TECN	COMMENT
25 to 50 (≈ 35) OUR ESTIMATE			
29.2 \pm 1.4	¹ GARCIA-REC... 03	DPWA	$\bar{K}N$ multichannel
23 \pm 6	MANLEY 02	DPWA	$\bar{K}N$ multichannel
34.1 \pm 3.7	KOISO 85	DPWA	$K^- p \rightarrow \Sigma\pi$
29 \pm 5	GOPAL 80	DPWA	$\bar{K}N \rightarrow \bar{K}N$
29 \pm 5	ALSTON-... 78	DPWA	$\bar{K}N \rightarrow \bar{K}N$
45 \pm 10	GOPAL 77	DPWA	$\bar{K}N$ multichannel
46 \pm 5	HEPP 76B	DPWA	$K^- N \rightarrow \Sigma\pi$
40 \pm 3	KANE 74	DPWA	$K^- p \rightarrow \Sigma\pi$
19 \pm 5	PREVOST 74	DPWA	$K^- N \rightarrow \Sigma(1385)\pi$
••• We do not use the following data for averages, fits, limits, etc. •••			
21.1 \pm 3.6	ABAEV 96	DPWA	$K^- p \rightarrow \Lambda\eta$
12	² MARTIN 77	DPWA	$\bar{K}N$ multichannel

 $\Lambda(1670)$ DECAY MODES

Mode	Fraction (Γ_i/Γ)
Γ_1 $N\bar{K}$	20–30 %
Γ_2 $\Sigma\pi$	25–55 %
Γ_3 $\Lambda\eta$	10–25 %
Γ_4 $\Sigma(1385)\pi$	

The above branching fractions are our estimates, not fits or averages.

See key on page 405

Baryon Particle Listings
 $\Lambda(1670), \Lambda(1690)$ $\Lambda(1670)$ BRANCHING RATIOSSee "Sign conventions for resonance couplings" in the Note on Λ and Σ Resonances.

$\Gamma(N\bar{K})/\Gamma_{\text{total}}$	DOCUMENT ID	TECN	COMMENT	Γ_1/Γ
0.20 to 0.30 OUR ESTIMATE				
0.37±0.07	MANLEY 02	DPWA	$\bar{K}N$ multichannel	
0.18±0.03	GOPAL 80	DPWA	$\bar{K}N \rightarrow \bar{K}N$	
0.17±0.03	ALSTON... 78	DPWA	$\bar{K}N \rightarrow \bar{K}N$	
••• We do not use the following data for averages, fits, limits, etc. •••				
0.20±0.03	GOPAL 77	DPWA	See GOPAL 80	
0.15	² MARTIN 77	DPWA	$\bar{K}N$ multichannel	

$\Gamma(\Lambda\eta)/\Gamma_{\text{total}}$	DOCUMENT ID	TECN	COMMENT	Γ_3/Γ
0.30±0.08	ABAEV 96	DPWA	$K^-p \rightarrow \Lambda\eta$	
••• We do not use the following data for averages, fits, limits, etc. •••				

$(\Gamma_1\Gamma_2)^{1/2}/\Gamma_{\text{total}}$ in $N\bar{K} \rightarrow \Lambda(1670) \rightarrow \Sigma\pi$	DOCUMENT ID	TECN	COMMENT	$(\Gamma_1\Gamma_2)^{1/2}/\Gamma$
VALUE				
-0.38±0.03	MANLEY 02	DPWA	$\bar{K}N$ multichannel	
-0.26±0.02	KOISO 85	DPWA	$K^-p \rightarrow \Sigma\pi$	
-0.31±0.03	GOPAL 77	DPWA	$\bar{K}N$ multichannel	
-0.29±0.03	HEPP 76B	DPWA	$K^-N \rightarrow \Sigma\pi$	
-0.23±0.03	LONDON 75	HLBC	$K^-p \rightarrow \Sigma^0\pi^0$	
-0.27±0.02	KANE 74	DPWA	$K^-p \rightarrow \Sigma\pi$	
••• We do not use the following data for averages, fits, limits, etc. •••				
-0.13	² MARTIN 77	DPWA	$\bar{K}N$ multichannel	

$(\Gamma_1\Gamma_3)^{1/2}/\Gamma_{\text{total}}$ in $N\bar{K} \rightarrow \Lambda(1670) \rightarrow \Lambda\eta$	DOCUMENT ID	TECN	COMMENT	$(\Gamma_1\Gamma_3)^{1/2}/\Gamma$
VALUE				
+0.24±0.04	MANLEY 02	DPWA	$\bar{K}N$ multichannel	
+0.20±0.05	BAXTER 73	DPWA	$K^-p \rightarrow$ neutrals	
••• We do not use the following data for averages, fits, limits, etc. •••				
0.24	KIM 71	DPWA	K-matrix analysis	
0.26	ARMENTEROS69C	HBC		
0.20 or 0.23	BERLEY 65	HBC		

$(\Gamma_1\Gamma_4)^{1/2}/\Gamma_{\text{total}}$ in $N\bar{K} \rightarrow \Lambda(1670) \rightarrow \Sigma(1385)\pi$	DOCUMENT ID	TECN	COMMENT	$(\Gamma_1\Gamma_4)^{1/2}/\Gamma$
VALUE				
-0.17±0.06	MANLEY 02	DPWA	$\bar{K}N$ multichannel	
-0.18±0.05	PREVOST 74	DPWA	$K^-N \rightarrow \Sigma(1385)\pi$	

 $\Lambda(1670)$ FOOTNOTES

- ¹ GARCIA-RECIO 03 gives pole, not Breit-Wigner, parameters, but the narrow width of the $\Lambda(1670)$ means there will be little difference.
² MARTIN 77 obtains identical resonance parameters from a T-matrix pole and from a Breit-Wigner fit.

 $\Lambda(1670)$ REFERENCES

GARCIA-RECIO 03	PR D67 076009	C. Garcia-Recio et al.	(GRAN, VALE)
MANLEY 02	PRL 88 012002	D.M. Manley et al.	(BNL Crystal Ball Collab.)
ABAEV 96	PR C53 385	V.V. Aboev, B.M.K. Nefkens	(UCLA)
KOISO 85	NP A433 619	H. Koiso et al.	(TOKY, MASA)
PDG 82	PL 111B 1	M. Roos et al.	(HEL5, CIT, CERN)
GOPAL 80	Toronto Conf. 159	G.P. Gopal	(RHEL) IJP
ALSTON... 78	PR D18 182	M. Alston-Garnjost et al.	(LBL, MTHO+) IJP
Also	PRL 38 1007	M. Alston-Garnjost et al.	(LBL, MTHO+) IJP
GOPAL 77	NP B119 362	G.P. Gopal et al.	(LOIC, RHEL) IJP
MARTIN 77	NP B127 349	B.R. Martin, M.K. Piddcock, R.G. Moorhouse	(LOUC+) IJP
Also	NP B126 266	B.R. Martin, M.K. Piddcock	(LOUC) IJP
Also	NP B126 285	B.R. Martin, M.K. Piddcock	(LOUC) IJP
HEPP 76B	PL 65B 487	V. Hepp et al.	(CERN, HEID, MPIM) IJP
LONDON 75	NP B95 289	G.W. London et al.	(BNL, CERN, EPOL+) IJP
KANE 74	LBL-2452	D.F. Kane	(LBL) IJP
PREVOST 74	NP B69 246	J. Prevost et al.	(SACL, CERN, HEID)
BAXTER 73	NP B67 125	D.F. Baxter et al.	(OXF) IJP
KIM 71	PRL 27 356	J.K. Kim	(HARV) IJP
Also	Duke Conf. 161	J.K. Kim	(HARV) IJP
ARMENTEROS 69C	Lund Paper 229	R. Armenteros et al.	(CERN, HEID, SACL) IJP
Values are quoted in LEVI-SETTI 69.			
BERLEY 65	PRL 15 641	D. Berley et al.	(BNL) IJP

 $\Lambda(1690) D_{03}$

$$I(J^P) = 0(\frac{3}{2}^-) \text{ Status: } ***$$

The measurements of the mass, width, and elasticity published before 1974 are now obsolete and have been omitted. They were last listed in our 1982 edition Physics Letters **111B** 1 (1982). $\Lambda(1690)$ MASS

VALUE (MeV)	DOCUMENT ID	TECN	COMMENT
1685 to 1695 (≈ 1690) OUR ESTIMATE			
1695.7±2.6	KOISO 85	DPWA	$K^-p \rightarrow \Sigma\pi$
1690 ±5	GOPAL 80	DPWA	$\bar{K}N \rightarrow \bar{K}N$
1692 ±5	ALSTON... 78	DPWA	$\bar{K}N \rightarrow \bar{K}N$
1690 ±5	GOPAL 77	DPWA	$\bar{K}N$ multichannel
1690 ±3	HEPP 76B	DPWA	$K^-N \rightarrow \Sigma\pi$
1689 ±1	KANE 74	DPWA	$K^-p \rightarrow \Sigma\pi$
••• We do not use the following data for averages, fits, limits, etc. •••			
1687 or 1689	¹ MARTIN 77	DPWA	$\bar{K}N$ multichannel
1692 ±4	CARROLL 76	DPWA	Isospin-0 total σ

 $\Lambda(1690)$ WIDTH

VALUE (MeV)	DOCUMENT ID	TECN	COMMENT
50 to 70 (≈ 60) OUR ESTIMATE			
67.2±5.6	KOISO 85	DPWA	$K^-p \rightarrow \Sigma\pi$
61 ±5	GOPAL 80	DPWA	$\bar{K}N \rightarrow \bar{K}N$
64 ±10	ALSTON... 78	DPWA	$\bar{K}N \rightarrow \bar{K}N$
60 ±5	GOPAL 77	DPWA	$\bar{K}N$ multichannel
82 ±8	HEPP 76B	DPWA	$K^-N \rightarrow \Sigma\pi$
60 ±4	KANE 74	DPWA	$K^-p \rightarrow \Sigma\pi$
••• We do not use the following data for averages, fits, limits, etc. •••			
62 or 62	¹ MARTIN 77	DPWA	$\bar{K}N$ multichannel
38	CARROLL 76	DPWA	Isospin-0 total σ

 $\Lambda(1690)$ DECAY MODES

Mode	Fraction (Γ_i/Γ)
Γ_1 $N\bar{K}$	20-30 %
Γ_2 $\Sigma\pi$	20-40 %
Γ_3 $\Lambda\pi\pi$	~ 25 %
Γ_4 $\Sigma\pi\pi$	~ 20 %
Γ_5 $\Lambda\eta$	
Γ_6 $\Sigma(1385)\pi, S$ -wave	

The above branching fractions are our estimates, not fits or averages.

 $\Lambda(1690)$ BRANCHING RATIOSThe sum of all the quoted branching ratios is more than 1.0. The two-body ratios are from partial-wave analyses, and thus probably are more reliable than the three-body ratios, which are determined from bumps in cross sections. Of the latter, the $\Sigma\pi\pi$ bump looks more significant. (The error given for the $\Lambda\pi\pi$ ratio looks unreasonably small.) Hardly any of the $\Sigma\pi\pi$ decay can be via $\Sigma(1385)$, for then seven times as much $\Lambda\pi\pi$ decay would be required. See "Sign conventions for resonance couplings" in the Note on Λ and Σ Resonances.

$\Gamma(N\bar{K})/\Gamma_{\text{total}}$	DOCUMENT ID	TECN	COMMENT	Γ_1/Γ
0.2 to 0.3 OUR ESTIMATE				
0.23±0.03	GOPAL 80	DPWA	$\bar{K}N \rightarrow \bar{K}N$	
0.22±0.03	ALSTON... 78	DPWA	$\bar{K}N \rightarrow \bar{K}N$	
••• We do not use the following data for averages, fits, limits, etc. •••				
0.24±0.03	GOPAL 77	DPWA	See GOPAL 80	
0.28 or 0.26	¹ MARTIN 77	DPWA	$\bar{K}N$ multichannel	

$(\Gamma_1\Gamma_2)^{1/2}/\Gamma_{\text{total}}$ in $N\bar{K} \rightarrow \Lambda(1690) \rightarrow \Sigma\pi$	DOCUMENT ID	TECN	COMMENT	$(\Gamma_1\Gamma_2)^{1/2}/\Gamma$
VALUE				
-0.34±0.02	KOISO 85	DPWA	$K^-p \rightarrow \Sigma\pi$	
-0.25±0.03	GOPAL 77	DPWA	$\bar{K}N$ multichannel	
-0.29±0.03	HEPP 76B	DPWA	$K^-N \rightarrow \Sigma\pi$	
-0.28±0.03	LONDON 75	HLBC	$K^-p \rightarrow \Sigma^0\pi^0$	
-0.28±0.02	KANE 74	DPWA	$K^-p \rightarrow \Sigma\pi$	
••• We do not use the following data for averages, fits, limits, etc. •••				
-0.30 or -0.28	¹ MARTIN 77	DPWA	$\bar{K}N$ multichannel	

$(\Gamma_1\Gamma_3)^{1/2}/\Gamma_{\text{total}}$ in $N\bar{K} \rightarrow \Lambda(1690) \rightarrow \Lambda\eta$	DOCUMENT ID	TECN	COMMENT	$(\Gamma_1\Gamma_3)^{1/2}/\Gamma$
VALUE				
0.00±0.03	BAXTER 73	DPWA	$K^-p \rightarrow$ neutrals	

Baryon Particle Listings

 $\Lambda(1690)$, $\Lambda(1800)$, $\Lambda(1810)$

$(\Gamma_1 \Gamma_7)_{1/2} / \Gamma_{\text{total}}$ in $N\bar{K} \rightarrow \Lambda(1690) \rightarrow \Lambda \pi \pi$ $(\Gamma_1 \Gamma_3)_{1/2} / \Gamma$
 VALUE DOCUMENT ID TECN COMMENT

••• We do not use the following data for averages, fits, limits, etc. •••
 0.25 ± 0.02 ² BARTLEY 68 HDBC $K^- p \rightarrow \Lambda \pi \pi$

$(\Gamma_1 \Gamma_7)_{1/2} / \Gamma_{\text{total}}$ in $N\bar{K} \rightarrow \Lambda(1690) \rightarrow \Sigma \pi \pi$ $(\Gamma_1 \Gamma_4)_{1/2} / \Gamma$
 VALUE DOCUMENT ID TECN COMMENT

0.21 ARMENTEROS68C HDBC $K^- N \rightarrow \Sigma \pi \pi$

$(\Gamma_1 \Gamma_7)_{1/2} / \Gamma_{\text{total}}$ in $N\bar{K} \rightarrow \Lambda(1690) \rightarrow \Sigma(1385) \pi$, S-wave $(\Gamma_1 \Gamma_6)_{1/2} / \Gamma$
 VALUE DOCUMENT ID TECN COMMENT

+0.27 ± 0.04 PREVOST 74 DPWA $K^- N \rightarrow \Sigma(1385) \pi$

 $\Lambda(1690)$ FOOTNOTES

- ¹ The two MARTIN 77 values are from a T-matrix pole and from a Breit-Wigner fit. Another D_{03} Λ at 1966 MeV is also suggested by MARTIN 77, but is very uncertain.
² BARTLEY 68 uses only cross-section data. The enhancement is not seen by PREVOST 71.

 $\Lambda(1690)$ REFERENCES

KOISO 85	NP A433 619	H. Koiso <i>et al.</i>	(TOKY, MASA)
PDG 82	PL 111B 1	M. Roos <i>et al.</i>	(HEL5, CIT, CERN)
GOPAL 80	Toronto Conf. 159	G.P. Gopal	(RHEL) IJP
ALSTON-... 78	PR D18 182	M. Alston-Garnjost <i>et al.</i>	(LBL, MTHO+) IJP
Also	PRL 38 1007	M. Alston-Garnjost <i>et al.</i>	(LBL, MTHO+) IJP
GOPAL 77	NP B119 362	G.P. Gopal <i>et al.</i>	(LOIC, RHEL) IJP
MARTIN 77	NP B127 349	B.R. Martin, M.K. Pidcock, R.G. Moorhouse	(LOUC+) IJP
Also	NP B126 266	B.R. Martin, M.K. Pidcock	(LOUC) IJP
Also	NP B126 285	B.R. Martin, M.K. Pidcock	(LOUC) IJP
CARROLL 76	PRL 37 806	A.S. Carroll <i>et al.</i>	(BNL) I
HEPP 76B	PL 65B 487	V. Hepp <i>et al.</i>	(CERN, HEIDH, MPIM) IJP
LONDON 75	NP B85 289	G.W. London <i>et al.</i>	(BNL, CERN, EPOL+) I
KANE 74	LBL-2452	D.F. Kane	(LBL) IJP
PREVOST 74	NP B69 246	J. Prevost <i>et al.</i>	(SACL, CERN, HEID) I
BAXTER 73	NP B67 125	D.F. Baxter <i>et al.</i>	(OXF) IJP
PREVOST 71	Amsterdam Conf.	J. Prevost	(CERN, HEID, SACL) I
ARMENTEROS 68C	NP B8 216	R. Armenteros <i>et al.</i>	(CERN, HEID, SACL) I
BARTLEY 68	PRL 21 1111	J.H. Bartley <i>et al.</i>	(TUFTS, FSU, BRAN) I

$\Lambda(1800) S_{01}$ $I(J^P) = 0(\frac{1}{2}^-)$ Status: ***

This is the second resonance in the S_{01} wave, the first being the $\Lambda(1670)$.

 $\Lambda(1800)$ MASS

VALUE (MeV)	DOCUMENT ID	TECN	COMMENT
1720 to 1850 (≈ 1800) OUR ESTIMATE			
1845 ± 10	MANLEY 02	DPWA	$\bar{K} N$ multichannel
1841 ± 10	GOPAL 80	DPWA	$\bar{K} N \rightarrow \bar{K} N$
1725 ± 20	ALSTON-... 78	DPWA	$\bar{K} N \rightarrow \bar{K} N$
1825 ± 20	GOPAL 77	DPWA	$\bar{K} N$ multichannel
1830 ± 20	LANGBEIN 72	IPWA	$\bar{K} N$ multichannel
••• We do not use the following data for averages, fits, limits, etc. •••			
1767 or 1842	¹ MARTIN 77	DPWA	$\bar{K} N$ multichannel
1780	KIM 71	DPWA	K-matrix analysis
1872 ± 10	BRICMAN 70B	DPWA	$\bar{K} N \rightarrow \bar{K} N$

 $\Lambda(1800)$ WIDTH

VALUE (MeV)	DOCUMENT ID	TECN	COMMENT
200 to 400 (≈ 300) OUR ESTIMATE			
518 ± 84	MANLEY 02	DPWA	$\bar{K} N$ multichannel
228 ± 20	GOPAL 80	DPWA	$\bar{K} N \rightarrow \bar{K} N$
185 ± 20	ALSTON-... 78	DPWA	$\bar{K} N \rightarrow \bar{K} N$
230 ± 20	GOPAL 77	DPWA	$\bar{K} N$ multichannel
70 ± 15	LANGBEIN 72	IPWA	$\bar{K} N$ multichannel
••• We do not use the following data for averages, fits, limits, etc. •••			
435 or 473	¹ MARTIN 77	DPWA	$\bar{K} N$ multichannel
40	KIM 71	DPWA	K-matrix analysis
100 ± 20	BRICMAN 70B	DPWA	$\bar{K} N \rightarrow \bar{K} N$

 $\Lambda(1800)$ DECAY MODES

Mode	Fraction (Γ_i / Γ)
Γ_1 $N\bar{K}$	25–40 %
Γ_2 $\Sigma \pi$	seen
Γ_3 $\Sigma(1385) \pi$	seen
Γ_4 $N\bar{K}^*(892)$	seen
Γ_5 $N\bar{K}^*(892)$, S=1/2, S-wave	
Γ_6 $N\bar{K}^*(892)$, S=3/2, D-wave	

The above branching fractions are our estimates, not fits or averages.

 $\Lambda(1800)$ BRANCHING RATIOS

See "Sign conventions for resonance couplings" in the Note on Λ and Σ Resonances.

$\Gamma(N\bar{K}) / \Gamma_{\text{total}}$	DOCUMENT ID	TECN	COMMENT	Γ_1 / Γ
0.25 to 0.40 OUR ESTIMATE				
0.24 ± 0.10	MANLEY 02	DPWA	$\bar{K} N$ multichannel	
0.36 ± 0.04	GOPAL 80	DPWA	$\bar{K} N \rightarrow \bar{K} N$	
0.28 ± 0.05	ALSTON-... 78	DPWA	$\bar{K} N \rightarrow \bar{K} N$	
0.35 ± 0.15	LANGBEIN 72	IPWA	$\bar{K} N$ multichannel	
••• We do not use the following data for averages, fits, limits, etc. •••				
0.37 ± 0.05	GOPAL 77	DPWA	See GOPAL 80	
1.21 or 0.70	¹ MARTIN 77	DPWA	$\bar{K} N$ multichannel	
0.80	KIM 71	DPWA	K-matrix analysis	
0.18 ± 0.02	BRICMAN 70B	DPWA	$\bar{K} N \rightarrow \bar{K} N$	

$(\Gamma_1 \Gamma_7)_{1/2} / \Gamma_{\text{total}}$ in $N\bar{K} \rightarrow \Lambda(1800) \rightarrow \Sigma \pi$	DOCUMENT ID	TECN	COMMENT	$(\Gamma_1 \Gamma_2)_{1/2} / \Gamma$
−0.08 ± 0.05	GOPAL 77	DPWA	$\bar{K} N$ multichannel	
••• We do not use the following data for averages, fits, limits, etc. •••				
−0.74 or −0.43	¹ MARTIN 77	DPWA	$\bar{K} N$ multichannel	
0.24	KIM 71	DPWA	K-matrix analysis	

$(\Gamma_1 \Gamma_7)_{1/2} / \Gamma_{\text{total}}$ in $N\bar{K} \rightarrow \Lambda(1800) \rightarrow \Sigma(1385) \pi$	DOCUMENT ID	TECN	COMMENT	$(\Gamma_1 \Gamma_3)_{1/2} / \Gamma$
+0.056 ± 0.028	² CAMERON 78	DPWA	$K^- p \rightarrow \Sigma(1385) \pi$	

$(\Gamma_1 \Gamma_7)_{1/2} / \Gamma_{\text{total}}$ in $N\bar{K} \rightarrow \Lambda(1800) \rightarrow N\bar{K}^*(892)$, S=1/2, S-wave	DOCUMENT ID	TECN	COMMENT	$(\Gamma_1 \Gamma_5)_{1/2} / \Gamma$
−0.17 ± 0.03	² CAMERON 78B	DPWA	$K^- p \rightarrow N\bar{K}^*$	

$(\Gamma_1 \Gamma_7)_{1/2} / \Gamma_{\text{total}}$ in $N\bar{K} \rightarrow \Lambda(1800) \rightarrow N\bar{K}^*(892)$, S=3/2, D-wave	DOCUMENT ID	TECN	COMMENT	$(\Gamma_1 \Gamma_6)_{1/2} / \Gamma$
−0.13 ± 0.04	CAMERON 78B	DPWA	$K^- p \rightarrow N\bar{K}^*$	

 $\Lambda(1800)$ FOOTNOTES

- ¹ The two MARTIN 77 values are from a T-matrix pole and from a Breit-Wigner fit.
² The published sign has been changed to be in accord with the baryon-first convention.

 $\Lambda(1800)$ REFERENCES

MANLEY 02	PRL 88 012002	D.M. Manley <i>et al.</i>	(BNL Crystal Ball Collab.)
GOPAL 80	Toronto Conf. 159	G.P. Gopal	(RHEL) IJP
ALSTON-... 78	PR D18 182	M. Alston-Garnjost <i>et al.</i>	(LBL, MTHO+) IJP
Also	PRL 38 1007	M. Alston-Garnjost <i>et al.</i>	(LBL, MTHO+) IJP
CAMERON 78	NP B143 189	W. Cameron <i>et al.</i>	(RHEL, LOIC) IJP
CAMERON 78B	NP B146 327	W. Cameron <i>et al.</i>	(RHEL, LOIC) IJP
GOPAL 77	NP B119 362	G.P. Gopal <i>et al.</i>	(LOIC, RHEL) IJP
MARTIN 77	NP B127 349	B.R. Martin, M.K. Pidcock, R.G. Moorhouse	(LOUC+) IJP
Also	NP B126 266	B.R. Martin, M.K. Pidcock	(LOUC) IJP
Also	NP B126 285	B.R. Martin, M.K. Pidcock	(LOUC) IJP
LANGBEIN 72	NP B47 477	W. Langbein, F. Wagner	(MPIM) IJP
KIM 71	PRL 27 356	J.K. Kim	(HARV) IJP
Also	Duke Conf. 161	J.K. Kim	(HARV) IJP
BRICMAN 70B	PL 33B 511	C. Bricman, M. Ferro-Luzzi, J.P. Lagnaux	(CERN) IJP

$\Lambda(1810) P_{01}$ $I(J^P) = 0(\frac{1}{2}^+)$ Status: ***

Almost all the recent analyses contain a P_{01} state, and sometimes two of them, but the masses, widths, and branching ratios vary greatly. See also the $\Lambda(1600) P_{01}$.

 $\Lambda(1810)$ MASS

VALUE (MeV)	DOCUMENT ID	TECN	COMMENT
1750 to 1850 (≈ 1810) OUR ESTIMATE			
1841 ± 20	GOPAL 80	DPWA	$\bar{K} N \rightarrow \bar{K} N$
1853 ± 20	GOPAL 77	DPWA	$\bar{K} N$ multichannel
1735 ± 5	CARROLL 76	DPWA	Isospin-0 total σ
1746 ± 10	PREVOST 74	DPWA	$K^- N \rightarrow \Sigma(1385) \pi$
1780 ± 20	LANGBEIN 72	IPWA	$\bar{K} N$ multichannel
••• We do not use the following data for averages, fits, limits, etc. •••			
1861 or 1953	¹ MARTIN 77	DPWA	$\bar{K} N$ multichannel
1755	KIM 71	DPWA	K-matrix analysis
1800	ARMENTEROS70	HBC	$\bar{K} N \rightarrow \bar{K} N$
1750	ARMENTEROS70	HBC	$\bar{K} N \rightarrow \Sigma \pi$
1690 ± 10	BARBARO-... 70	HBC	$\bar{K} N \rightarrow \Sigma \pi$
1740	BAILEY 69	DPWA	$\bar{K} N \rightarrow \bar{K} N$
1745	ARMENTEROS68B	HBC	$\bar{K} N \rightarrow \bar{K} N$

Baryon Particle Listings

$\Lambda(1810), \Lambda(1820)$

$\Lambda(1810)$ WIDTH

VALUE (MeV)	DOCUMENT ID	TECN	COMMENT
50 to 250 (≈ 150) OUR ESTIMATE			
164 \pm 20	GOPAL 80	DPWA	$\bar{K}N \rightarrow \bar{K}N$
90 \pm 20	CAMERON 78B	DPWA	$K^-p \rightarrow N\bar{K}^*$
166 \pm 20	GOPAL 77	DPWA	$\bar{K}N$ multichannel
46 \pm 20	PREVOST 74	DPWA	$K^-N \rightarrow \Sigma(1385)\pi$
120 \pm 10	LANGBEIN 72	IPWA	$\bar{K}N$ multichannel
••• We do not use the following data for averages, fits, limits, etc. •••			
535 or 585	¹ MARTIN 77	DPWA	$\bar{K}N$ multichannel
28	CARROLL 76	DPWA	Isospin-0 total σ
35	KIM 71	DPWA	K-matrix analysis
30	ARMENTEROS70	HBC	$\bar{K}N \rightarrow \bar{K}N$
70	ARMENTEROS70	HBC	$\bar{K}N \rightarrow \Sigma\pi$
22	BARBARO... 70	HBC	$\bar{K}N \rightarrow \Sigma\pi$
300	BAILEY 69	DPWA	$\bar{K}N \rightarrow \bar{K}N$
147	ARMENTEROS68B	HBC	

$\Lambda(1810)$ DECAY MODES

Mode	Fraction (Γ_i/Γ)
Γ_1 $N\bar{K}$	20-50 %
Γ_2 $\Sigma\pi$	10-40 %
Γ_3 $\Sigma(1385)\pi$	seen
Γ_4 $N\bar{K}^*(892)$	30-60 %
Γ_5 $N\bar{K}^*(892), S=1/2, P$ -wave	
Γ_6 $N\bar{K}^*(892), S=3/2, P$ -wave	

The above branching fractions are our estimates, not fits or averages.

$\Lambda(1810)$ BRANCHING RATIOS

See "Sign conventions for resonance couplings" in the Note on Λ and Σ Resonances.

$\Gamma(N\bar{K})/\Gamma_{\text{total}}$	DOCUMENT ID	TECN	COMMENT	Γ_1/Γ
0.2 to 0.5 OUR ESTIMATE				
0.24 \pm 0.04	GOPAL 80	DPWA	$\bar{K}N \rightarrow \bar{K}N$	
0.36 \pm 0.05	LANGBEIN 72	IPWA	$\bar{K}N$ multichannel	
••• We do not use the following data for averages, fits, limits, etc. •••				
0.21 \pm 0.04	GOPAL 77	DPWA	See GOPAL 80	
0.52 or 0.49	¹ MARTIN 77	DPWA	$\bar{K}N$ multichannel	
0.30	KIM 71	DPWA	K-matrix analysis	
0.15	ARMENTEROS70	DPWA	$\bar{K}N \rightarrow \bar{K}N$	
0.55	BAILEY 69	DPWA	$\bar{K}N \rightarrow \bar{K}N$	
0.4	ARMENTEROS68B	DPWA	$\bar{K}N \rightarrow \bar{K}N$	

$(\Gamma_1\Gamma_f)^{1/2}/\Gamma_{\text{total}}$ in $N\bar{K} \rightarrow \Lambda(1810) \rightarrow \Sigma\pi$	DOCUMENT ID	TECN	COMMENT	$(\Gamma_1\Gamma_2)^{1/2}/\Gamma$
VALUE				
-0.24 \pm 0.04	GOPAL 77	DPWA	$\bar{K}N$ multichannel	
••• We do not use the following data for averages, fits, limits, etc. •••				
+0.25 or +0.23	¹ MARTIN 77	DPWA	$\bar{K}N$ multichannel	
< 0.01	LANGBEIN 72	IPWA	$\bar{K}N$ multichannel	
0.17	KIM 71	DPWA	K-matrix analysis	
+0.20	² ARMENTEROS70	DPWA	$\bar{K}N \rightarrow \Sigma\pi$	
-0.13 \pm 0.03	BARBARO... 70	DPWA	$\bar{K}N \rightarrow \Sigma\pi$	

$(\Gamma_1\Gamma_f)^{1/2}/\Gamma_{\text{total}}$ in $N\bar{K} \rightarrow \Lambda(1810) \rightarrow \Sigma(1385)\pi$	DOCUMENT ID	TECN	COMMENT	$(\Gamma_1\Gamma_3)^{1/2}/\Gamma$
VALUE				
+0.18 \pm 0.10	PREVOST 74	DPWA	$K^-N \rightarrow \Sigma(1385)\pi$	

$(\Gamma_1\Gamma_f)^{1/2}/\Gamma_{\text{total}}$ in $N\bar{K} \rightarrow \Lambda(1810) \rightarrow N\bar{K}^*(892), S=1/2, P$ -wave	DOCUMENT ID	TECN	COMMENT	$(\Gamma_1\Gamma_5)^{1/2}/\Gamma$
VALUE				
-0.14 \pm 0.03	² CAMERON 78B	DPWA	$K^-p \rightarrow N\bar{K}^*$	

$(\Gamma_1\Gamma_f)^{1/2}/\Gamma_{\text{total}}$ in $N\bar{K} \rightarrow \Lambda(1810) \rightarrow N\bar{K}^*(892), S=3/2, P$ -wave	DOCUMENT ID	TECN	COMMENT	$(\Gamma_1\Gamma_6)^{1/2}/\Gamma$
VALUE				
+0.35 \pm 0.06	CAMERON 78B	DPWA	$K^-p \rightarrow N\bar{K}^*$	

$\Lambda(1810)$ FOOTNOTES

- The two MARTIN 77 values are from a T-matrix pole and from a Breit-Wigner fit.
- The published sign has been changed to be in accord with the baryon-first convention.

$\Lambda(1810)$ REFERENCES

GOPAL 80	Toronto Conf. 159	G.P. Gopal	(RHEL) IJP
CAMERON 78B	NP B146 327	W. Cameron et al.	(RHEL, LOIC) IJP
GOPAL 77	NP B119 362	G.P. Gopal et al.	(LOIC, RHEL) IJP
MARTIN 77	NP B127 349	B.R. Martin, M.K. Pidcock, R.G. Moorhouse	(LOUC+) IJP
	Also NP B126 266	B.R. Martin, M.K. Pidcock	(LOUC) IJP
	Also NP B126 285	B.R. Martin, M.K. Pidcock	(LOUC) IJP
CARROLL 76	PRL 37 806	A.S. Carroll et al.	(BNL) I
PREVOST 74	NP B69 246	J. Prevost et al.	(SACL, CERN, HEID) IJP
LANGBEIN 72	NP B47 477	W. Langbein, F. Wagner	(MPIM) IJP
KIM 71	PRL 27 356	J.K. Kim	(HARV) IJP
	Also Duke Conf. 161	J.K. Kim	(HARV) IJP
	Hyperon Resonances, 1970		
ARMENTEROS 70	Duke Conf. 123	R. Armenteros et al.	(CERN, HEID, SACL) IJP
	Hyperon Resonances, 1970		
BARBARO... 70	Duke Conf. 173	A. Barbaro-Galtieri	(LRL) IJP
	Hyperon Resonances, 1970		
BAILEY 69	Thesis UCL 50617	J.M. Bailey	(LLL) IJP
ARMENTEROS 68B	NP B8 195	R. Armenteros et al.	(CERN, HEID, SACL) IJP

$\Lambda(1820) F_{05}$

$$I(J^P) = 0(\frac{5}{2}^+) \text{ Status: } ***$$

This resonance is the cornerstone for all partial-wave analyses in this region. Most of the results published before 1973 are now obsolete and have been omitted. They may be found in our 1982 edition Physics Letters **111B** 1 (1982).

Most of the quoted errors are statistical only; the systematic errors due to the particular parametrizations used in the partial-wave analyses are not included. For this reason we do not calculate weighted averages for the mass and width.

$\Lambda(1820)$ MASS

VALUE (MeV)	DOCUMENT ID	TECN	COMMENT
1815 to 1825 (≈ 1820) OUR ESTIMATE			
1823 \pm 3	GOPAL 80	DPWA	$\bar{K}N \rightarrow \bar{K}N$
1819 \pm 2	ALSTON... 78	DPWA	$\bar{K}N \rightarrow \bar{K}N$
1822 \pm 2	GOPAL 77	DPWA	$\bar{K}N$ multichannel
1821 \pm 2	KANE 74	DPWA	$K^-p \rightarrow \Sigma\pi$
••• We do not use the following data for averages, fits, limits, etc. •••			
1830	DECLAIS 77	DPWA	$\bar{K}N \rightarrow \bar{K}N$
1817 or 1819	¹ MARTIN 77	DPWA	$\bar{K}N$ multichannel

$\Lambda(1820)$ WIDTH

VALUE (MeV)	DOCUMENT ID	TECN	COMMENT
70 to 90 (≈ 80) OUR ESTIMATE			
77 \pm 5	GOPAL 80	DPWA	$\bar{K}N \rightarrow \bar{K}N$
72 \pm 5	ALSTON... 78	DPWA	$\bar{K}N \rightarrow \bar{K}N$
81 \pm 5	GOPAL 77	DPWA	$\bar{K}N$ multichannel
87 \pm 3	KANE 74	DPWA	$K^-p \rightarrow \Sigma\pi$
••• We do not use the following data for averages, fits, limits, etc. •••			
82	DECLAIS 77	DPWA	$\bar{K}N \rightarrow \bar{K}N$
76 or 76	¹ MARTIN 77	DPWA	$\bar{K}N$ multichannel

$\Lambda(1820)$ DECAY MODES

Mode	Fraction (Γ_i/Γ)
Γ_1 $N\bar{K}$	55-65 %
Γ_2 $\Sigma\pi$	8-14 %
Γ_3 $\Sigma(1385)\pi$	5-10 %
Γ_4 $\Sigma(1385)\pi, P$ -wave	
Γ_5 $\Sigma(1385)\pi, F$ -wave	
Γ_6 $\Lambda\eta$	
Γ_7 $\Sigma\pi\pi$	

The above branching fractions are our estimates, not fits or averages.

$\Lambda(1820)$ BRANCHING RATIOS

Errors quoted do not include uncertainties in the parametrizations used in the partial-wave analyses and are thus too small. See also "Sign conventions for resonance couplings" in the Note on Λ and Σ Resonances.

$\Gamma(N\bar{K})/\Gamma_{\text{total}}$	DOCUMENT ID	TECN	COMMENT	Γ_1/Γ
0.55 to 0.65 OUR ESTIMATE				
0.58 \pm 0.02	GOPAL 80	DPWA	$\bar{K}N \rightarrow \bar{K}N$	
0.60 \pm 0.03	ALSTON... 78	DPWA	$\bar{K}N \rightarrow \bar{K}N$	
••• We do not use the following data for averages, fits, limits, etc. •••				
0.51	DECLAIS 77	DPWA	$\bar{K}N \rightarrow \bar{K}N$	
0.57 \pm 0.02	GOPAL 77	DPWA	See GOPAL 80	
0.59 or 0.58	¹ MARTIN 77	DPWA	$\bar{K}N$ multichannel	

Baryon Particle Listings

$\Lambda(1820)$, $\Lambda(1830)$, $\Lambda(1890)$

$(\Gamma_1 \Gamma_2)^{1/2} / \Gamma_{\text{total}}$ in $N\bar{K} \rightarrow \Lambda(1820) \rightarrow \Sigma \pi$	DOCUMENT ID	TECN	COMMENT	$(\Gamma_1 \Gamma_2)^{1/2} / \Gamma$
VALUE				
-0.28 ± 0.03	GOPAL	77	DPWA $\bar{K}N$ multichannel	
-0.28 ± 0.01	KANE	74	DPWA $K^- p \rightarrow \Sigma \pi$	
••• We do not use the following data for averages, fits, limits, etc. •••				
-0.25 or -0.25	¹ MARTIN	77	DPWA $\bar{K}N$ multichannel	

$(\Gamma_1 \Gamma_2)^{1/2} / \Gamma_{\text{total}}$ in $N\bar{K} \rightarrow \Lambda(1820) \rightarrow \Lambda \eta$	DOCUMENT ID	TECN	COMMENT	$(\Gamma_1 \Gamma_2)^{1/2} / \Gamma$
VALUE				
$-0.096^{+0.040}_{-0.020}$	RADER	73	MPWA	

$\Gamma(\Sigma \pi \pi) / \Gamma_{\text{total}}$	DOCUMENT ID	TECN	COMMENT	Γ_7 / Γ
VALUE				
no clear signal	² ARMENTEROS68c	HDBC	$K^- N \rightarrow \Sigma \pi \pi$	

$(\Gamma_1 \Gamma_2)^{1/2} / \Gamma_{\text{total}}$ in $N\bar{K} \rightarrow \Lambda(1820) \rightarrow \Sigma(1385)\pi$, P-wave	DOCUMENT ID	TECN	COMMENT	$(\Gamma_1 \Gamma_2)^{1/2} / \Gamma$
VALUE				
-0.167 ± 0.054	³ CAMERON	78	DPWA $K^- p \rightarrow \Sigma(1385)\pi$	
$+0.27 \pm 0.03$	PREVOST	74	DPWA $K^- N \rightarrow \Sigma(1385)\pi$	

$(\Gamma_1 \Gamma_2)^{1/2} / \Gamma_{\text{total}}$ in $N\bar{K} \rightarrow \Lambda(1820) \rightarrow \Sigma(1385)\pi$, F-wave	DOCUMENT ID	TECN	COMMENT	$(\Gamma_1 \Gamma_2)^{1/2} / \Gamma$
VALUE				
$+0.065 \pm 0.029$	³ CAMERON	78	DPWA $K^- p \rightarrow \Sigma(1385)\pi$	

$\Lambda(1820)$ FOOTNOTES

- The two MARTIN 77 values are from a T-matrix pole and from a Breit-Wigner fit.
- There is a suggestion of a bump, enough to be consistent with what is expected from $\Sigma(1385) \rightarrow \Sigma \pi$ decay.
- The published sign has been changed to be in accord with the baryon-first convention.

$\Lambda(1820)$ REFERENCES

PDG	82	PL 111B 1	M. Roos <i>et al.</i>	(HEL5, CIT, CERN)
GOPAL	80	Toronto Conf. 159	G.P. Gopal	(RHEL) IJP
ALSTON-...	78	PR D18 182	M. Alston-Garnjost <i>et al.</i>	(LBL, MTHO+) IJP
Also		PRL 38 1007	M. Alston-Garnjost <i>et al.</i>	(LBL, MTHO+) IJP
CAMERON	78	NP B143 189	W. Cameron <i>et al.</i>	(RHEL, LOIC) IJP
DECLAIS	77	CERN 77-16	Y. Declais <i>et al.</i>	(CAEN, CERN) IJP
GOPAL	77	NP B119 362	G.P. Gopal <i>et al.</i>	(LOIC, RHEL) IJP
MARTIN	77	NP B127 349	B.R. Martin, M.K. Pidcock, R.G. Moorhouse	(LOUC+) IJP
Also		NP B126 266	B.R. Martin, M.K. Pidcock	(LOUC) IJP
Also		NP B126 285	B.R. Martin, M.K. Pidcock	(LOUC) IJP
KANE	74	LBL-2452	D.F. Kane	(LBL) IJP
PREVOST	74	NP B69 246	J. Prevost <i>et al.</i>	(SACL, CERN, HEID)
RADER	73	NC 16A 178	R.K. Rader <i>et al.</i>	(SACL, HEID, CERN+)
ARMENTEROS 68c		NP B8 216	R. Armenteros <i>et al.</i>	(CERN, HEID, SACL) I

$\Lambda(1830) D_{05}$

$I(J^P) = 0(\frac{5}{2}^-)$ Status: * * * *

For results published before 1973 (they are now obsolete), see our 1982 edition Physics Letters **111B** 1 (1982).

The best evidence for this resonance is in the $\Sigma \pi$ channel.

$\Lambda(1830)$ MASS

VALUE (MeV)	DOCUMENT ID	TECN	COMMENT
1810 to 1830 (≈ 1830) OUR ESTIMATE			
1831 ± 10	GOPAL	80	DPWA $\bar{K}N \rightarrow \bar{K}N$
1825 ± 10	GOPAL	77	DPWA $\bar{K}N$ multichannel
1825 ± 1	KANE	74	DPWA $K^- p \rightarrow \Sigma \pi$
••• We do not use the following data for averages, fits, limits, etc. •••			
1817 or 1818	¹ MARTIN	77	DPWA $\bar{K}N$ multichannel

$\Lambda(1830)$ WIDTH

VALUE (MeV)	DOCUMENT ID	TECN	COMMENT
60 to 110 (≈ 95) OUR ESTIMATE			
100 ± 10	GOPAL	80	DPWA $\bar{K}N \rightarrow \bar{K}N$
94 ± 10	GOPAL	77	DPWA $\bar{K}N$ multichannel
119 ± 3	KANE	74	DPWA $K^- p \rightarrow \Sigma \pi$
••• We do not use the following data for averages, fits, limits, etc. •••			
56 or 56	¹ MARTIN	77	DPWA $\bar{K}N$ multichannel

$\Lambda(1830)$ DECAY MODES

Mode	Fraction (Γ_i / Γ)
Γ_1 $N\bar{K}$	3–10 %
Γ_2 $\Sigma \pi$	35–75 %
Γ_3 $\Sigma(1385)\pi$	>15 %
Γ_4 $\Sigma(1385)\pi$, D-wave	
Γ_5 $\Lambda \eta$	

The above branching fractions are our estimates, not fits or averages.

$\Lambda(1830)$ BRANCHING RATIOS

See "Sign conventions for resonance couplings" in the Note on Λ and Σ Resonances.

$\Gamma(N\bar{K}) / \Gamma_{\text{total}}$	DOCUMENT ID	TECN	COMMENT	Γ_1 / Γ
VALUE				
0.03 to 0.10 OUR ESTIMATE				
0.08 ± 0.03	GOPAL	80	DPWA $\bar{K}N \rightarrow \bar{K}N$	
0.02 ± 0.02	ALSTON-...	78	DPWA $\bar{K}N \rightarrow \bar{K}N$	
••• We do not use the following data for averages, fits, limits, etc. •••				
0.04 ± 0.03	GOPAL	77	DPWA See GOPAL 80	
0.04 or 0.04	¹ MARTIN	77	DPWA $\bar{K}N$ multichannel	

$(\Gamma_1 \Gamma_2)^{1/2} / \Gamma_{\text{total}}$ in $N\bar{K} \rightarrow \Lambda(1830) \rightarrow \Sigma \pi$	DOCUMENT ID	TECN	COMMENT	$(\Gamma_1 \Gamma_2)^{1/2} / \Gamma$
VALUE				
-0.17 ± 0.03	GOPAL	77	DPWA $\bar{K}N$ multichannel	
-0.15 ± 0.01	KANE	74	DPWA $K^- p \rightarrow \Sigma \pi$	
••• We do not use the following data for averages, fits, limits, etc. •••				
-0.17 or -0.17	¹ MARTIN	77	DPWA $\bar{K}N$ multichannel	

$(\Gamma_1 \Gamma_2)^{1/2} / \Gamma_{\text{total}}$ in $N\bar{K} \rightarrow \Lambda(1830) \rightarrow \Lambda \eta$	DOCUMENT ID	TECN	COMMENT	$(\Gamma_1 \Gamma_2)^{1/2} / \Gamma$
VALUE				
-0.044 ± 0.020	RADER	73	MPWA	

$(\Gamma_1 \Gamma_2)^{1/2} / \Gamma_{\text{total}}$ in $N\bar{K} \rightarrow \Lambda(1830) \rightarrow \Sigma(1385)\pi$	DOCUMENT ID	TECN	COMMENT	$(\Gamma_1 \Gamma_2)^{1/2} / \Gamma$
VALUE				
$+0.141 \pm 0.014$	² CAMERON	78	DPWA $K^- p \rightarrow \Sigma(1385)\pi$	
$+0.13 \pm 0.03$	PREVOST	74	DPWA $K^- N \rightarrow \Sigma(1385)\pi$	

$\Lambda(1830)$ FOOTNOTES

- The two MARTIN 77 values are from a T-matrix pole and from a Breit-Wigner fit.
- The CAMERON 78 upper limit on G-wave decay is 0.03. The published sign has been changed to be in accord with the baryon-first convention.

$\Lambda(1830)$ REFERENCES

PDG	82	PL 111B 1	M. Roos <i>et al.</i>	(HEL5, CIT, CERN)
GOPAL	80	Toronto Conf. 159	G.P. Gopal	(RHEL) IJP
ALSTON-...	78	PR D18 182	M. Alston-Garnjost <i>et al.</i>	(LBL, MTHO+) IJP
Also		PRL 38 1007	M. Alston-Garnjost <i>et al.</i>	(LBL, MTHO+) IJP
CAMERON	78	NP B143 189	W. Cameron <i>et al.</i>	(RHEL, LOIC) IJP
GOPAL	77	NP B119 362	G.P. Gopal <i>et al.</i>	(LOIC, RHEL) IJP
MARTIN	77	NP B127 349	B.R. Martin, M.K. Pidcock, R.G. Moorhouse	(LOUC+) IJP
Also		NP B126 266	B.R. Martin, M.K. Pidcock	(LOUC) IJP
Also		NP B126 285	B.R. Martin, M.K. Pidcock	(LOUC) IJP
KANE	74	LBL-2452	D.F. Kane	(LBL) IJP
PREVOST	74	NP B69 246	J. Prevost <i>et al.</i>	(SACL, CERN, HEID)
RADER	73	NC 16A 178	R.K. Rader <i>et al.</i>	(SACL, HEID, CERN+)

$\Lambda(1890) P_{03}$

$I(J^P) = 0(\frac{3}{2}^+)$ Status: * * * *

For results published before 1974 (they are now obsolete), see our 1982 edition Physics Letters **111B** 1 (1982).

The $J^P = 3/2^+$ assignment is consistent with all available data (including polarization) and recent partial-wave analyses. The dominant inelastic modes remain unknown.

$\Lambda(1890)$ MASS

VALUE (MeV)	DOCUMENT ID	TECN	COMMENT
1850 to 1910 (≈ 1890) OUR ESTIMATE			
1897 ± 5	GOPAL	80	DPWA $\bar{K}N \rightarrow \bar{K}N$
1908 ± 10	ALSTON-...	78	DPWA $\bar{K}N \rightarrow \bar{K}N$
1900 ± 10	GOPAL	77	DPWA $\bar{K}N$ multichannel
1894 ± 10	HEMINGWAY	75	DPWA $K^- p \rightarrow \bar{K}N$
••• We do not use the following data for averages, fits, limits, etc. •••			
1856 or 1868	¹ MARTIN	77	DPWA $\bar{K}N$ multichannel
1900	² NAKKASYAN	75	DPWA $K^- p \rightarrow \Lambda \omega$

$\Lambda(1890)$ WIDTH

VALUE (MeV)	DOCUMENT ID	TECN	COMMENT
60 to 200 (≈ 100) OUR ESTIMATE			
74 ± 10	GOPAL	80	DPWA $\bar{K}N \rightarrow \bar{K}N$
119 ± 20	ALSTON-...	78	DPWA $\bar{K}N \rightarrow \bar{K}N$
72 ± 10	GOPAL	77	DPWA $\bar{K}N$ multichannel
107 ± 10	HEMINGWAY	75	DPWA $K^- p \rightarrow \bar{K}N$
••• We do not use the following data for averages, fits, limits, etc. •••			
191 or 193	¹ MARTIN	77	DPWA $\bar{K}N$ multichannel
100	² NAKKASYAN	75	DPWA $K^- p \rightarrow \Lambda \omega$

$\Lambda(1890)$ DECAY MODES

Mode	Fraction (Γ_i/Γ)
Γ_1 $N\bar{K}$	20–35 %
Γ_2 $\Sigma\pi$	3–10 %
Γ_3 $\Sigma(1385)\pi$	seen
Γ_4 $\Sigma(1385)\pi$, P -wave	
Γ_5 $\Sigma(1385)\pi$, F -wave	
Γ_6 $N\bar{K}^*(892)$	seen
Γ_7 $N\bar{K}^*(892)$, $S=1/2$, P -wave	
Γ_8 $\Lambda\omega$	

The above branching fractions are our estimates, not fits or averages.

 $\Lambda(1890)$ BRANCHING RATIOS

See "Sign conventions for resonance couplings" in the Note on Λ and Σ Resonances.

$\Gamma(N\bar{K})/\Gamma_{\text{total}}$	DOCUMENT ID	TECN	COMMENT	Γ_1/Γ
0.20 to 0.35 OUR ESTIMATE				
0.20±0.02	GOPAL	80	DPWA $\bar{K}N \rightarrow \bar{K}N$	
0.34±0.05	ALSTON-...	78	DPWA $\bar{K}N \rightarrow \bar{K}N$	
0.24±0.04	HEMINGWAY	75	DPWA $K^-p \rightarrow \bar{K}N$	
••• We do not use the following data for averages, fits, limits, etc. •••				
0.18±0.02	GOPAL	77	DPWA See GOPAL 80	
0.36 or 0.34	¹ MARTIN	77	DPWA $\bar{K}N$ multichannel	

$(\Gamma_i\Gamma_f)^{1/2}/\Gamma_{\text{total}}$ in $N\bar{K} \rightarrow \Lambda(1890) \rightarrow \Sigma\pi$	DOCUMENT ID	TECN	COMMENT	$(\Gamma_1\Gamma_2)^{1/2}/\Gamma$
0.20 to 0.35 OUR ESTIMATE				
−0.09±0.03	GOPAL	77	DPWA $\bar{K}N$ multichannel	
••• We do not use the following data for averages, fits, limits, etc. •••				
+0.15 or +0.14	¹ MARTIN	77	DPWA $\bar{K}N$ multichannel	

$(\Gamma_i\Gamma_f)^{1/2}/\Gamma_{\text{total}}$ in $N\bar{K} \rightarrow \Lambda(1890) \rightarrow \Lambda\omega$	DOCUMENT ID	TECN	COMMENT	$(\Gamma_1\Gamma_8)^{1/2}/\Gamma$
seen	BACCARI	77	IPWA $K^-p \rightarrow \Lambda\omega$	
0.032	² NAKKASYAN	75	DPWA $K^-p \rightarrow \Lambda\omega$	

$(\Gamma_i\Gamma_f)^{1/2}/\Gamma_{\text{total}}$ in $N\bar{K} \rightarrow \Lambda(1890) \rightarrow \Sigma(1385)\pi$, P -wave	DOCUMENT ID	TECN	COMMENT	$(\Gamma_1\Gamma_4)^{1/2}/\Gamma$
<0.03	CAMERON	78	DPWA $K^-p \rightarrow \Sigma(1385)\pi$	

$(\Gamma_i\Gamma_f)^{1/2}/\Gamma_{\text{total}}$ in $N\bar{K} \rightarrow \Lambda(1890) \rightarrow \Sigma(1385)\pi$, F -wave	DOCUMENT ID	TECN	COMMENT	$(\Gamma_1\Gamma_5)^{1/2}/\Gamma$
−0.126±0.055	³ CAMERON	78	DPWA $K^-p \rightarrow \Sigma(1385)\pi$	

$(\Gamma_i\Gamma_f)^{1/2}/\Gamma_{\text{total}}$ in $N\bar{K} \rightarrow \Lambda(1890) \rightarrow N\bar{K}^*(892)$	DOCUMENT ID	TECN	COMMENT	$(\Gamma_1\Gamma_6)^{1/2}/\Gamma$
−0.07±0.03	^{3,4} CAMERON	78B	DPWA $K^-p \rightarrow N\bar{K}^*$	

 $\Lambda(1890)$ FOOTNOTES

- The two MARTIN 77 values are from a T-matrix pole and from a Breit-Wigner fit.
- Found in one of two best solutions.
- The published sign has been changed to be in accord with the baryon-first convention.
- Upper limits on the P_3 and F_3 waves are each 0.03.

 $\Lambda(1890)$ REFERENCES

PDG	82	PL 111B 1	M. Roos <i>et al.</i>	(HEL5, CIT, CERN)
GOPAL	80	Toronto Conf. 159	G.P. Gopal	(RHEL) IJP
ALSTON-...	78	PR D18 182	M. Alston-Garnjost <i>et al.</i>	(LBL, MTHO+) IJP
Also		PRL 38 1007	M. Alston-Garnjost <i>et al.</i>	(LBL, MTHO+) IJP
CAMERON	78	NP B143 189	W. Cameron <i>et al.</i>	(RHEL, LOIC) IJP
CAMERON	78B	NP B146 327	W. Cameron <i>et al.</i>	(RHEL, LOIC) IJP
BACCARI	77	NC 41A 96	B. Baccari <i>et al.</i>	(SACL, CDEF) IJP
GOPAL	77	NP B119 362	G.P. Gopal <i>et al.</i>	(LOIC, RHEL) IJP
MARTIN	77	NP B127 349	B.R. Martin, M.K. Pidcock, R.G. Moorhouse	(LOIC+) IJP
Also		NP B126 266	B.R. Martin, M.K. Pidcock	(LOIC) IJP
Also		NP B126 285	B.R. Martin, M.K. Pidcock	(LOIC) IJP
HEMINGWAY	75	NP B91 12	R.J. Hemingway <i>et al.</i>	(CERN, HEIDH, MPIM) IJP
NAKKASYAN	75	NP B93 85	A. Nakkasyan	(CERN) IJP

 $\Lambda(2000)$

$$I(J^P) = 0(?)^? \quad \text{Status: } *$$

OMITTED FROM SUMMARY TABLE

We list here all the ambiguous resonance possibilities with a mass around 2 GeV. The proposed quantum numbers are D_3 (BARBARO-GALTIERI 70 in $\Sigma\pi$), D_3+F_5 , P_3+D_5 , or P_1+D_3 (BRANDSTETTER 72 in $\Lambda\omega$), and S_1 (CAMERON 78B in $N\bar{K}^*$). The first two of the above analyses should now be considered obsolete. See also NAKKASYAN 75.

 $\Lambda(2000)$ MASS

VALUE (MeV)	DOCUMENT ID	TECN	COMMENT
≈ 2000 OUR ESTIMATE			
2030±30	CAMERON	78B	DPWA $K^-p \rightarrow N\bar{K}^*$
1935 to 1971	¹ BRANDSTET...72		DPWA $K^-p \rightarrow \Lambda\omega$
1951 to 2034	¹ BRANDSTET...72		DPWA $K^-p \rightarrow \Lambda\omega$
2010±30	BARBARO-...	70	DPWA $K^-p \rightarrow \Sigma\pi$

 $\Lambda(2000)$ WIDTH

VALUE (MeV)	DOCUMENT ID	TECN	COMMENT
125±25	CAMERON	78B	DPWA $K^-p \rightarrow N\bar{K}^*$
180 to 240	¹ BRANDSTET...72		DPWA (lower mass)
73 to 154	¹ BRANDSTET...72		DPWA (higher mass)
130±50	BARBARO-...	70	DPWA $K^-p \rightarrow \Sigma\pi$

 $\Lambda(2000)$ DECAY MODES

Mode
Γ_1 $N\bar{K}$
Γ_2 $\Sigma\pi$
Γ_3 $\Lambda\omega$
Γ_4 $N\bar{K}^*(892)$, $S=1/2$, S -wave
Γ_5 $N\bar{K}^*(892)$, $S=3/2$, D -wave

 $\Lambda(2000)$ BRANCHING RATIOS

See "Sign conventions for resonance couplings" in the Note on Λ and Σ Resonances.

$(\Gamma_i\Gamma_f)^{1/2}/\Gamma_{\text{total}}$ in $N\bar{K} \rightarrow \Lambda(2000) \rightarrow \Sigma\pi$	DOCUMENT ID	TECN	COMMENT	$(\Gamma_1\Gamma_2)^{1/2}/\Gamma$
−0.20±0.04	BARBARO-...	70	DPWA $K^-p \rightarrow \Sigma\pi$	

$(\Gamma_i\Gamma_f)^{1/2}/\Gamma_{\text{total}}$ in $N\bar{K} \rightarrow \Lambda(2000) \rightarrow \Lambda\omega$	DOCUMENT ID	TECN	COMMENT	$(\Gamma_1\Gamma_3)^{1/2}/\Gamma$
0.17 to 0.25	¹ BRANDSTET...72		DPWA (lower mass)	
0.04 to 0.15	¹ BRANDSTET...72		DPWA (higher mass)	

$(\Gamma_i\Gamma_f)^{1/2}/\Gamma_{\text{total}}$ in $N\bar{K} \rightarrow \Lambda(2000) \rightarrow N\bar{K}^*(892)$, $S=1/2$, S -wave	DOCUMENT ID	TECN	COMMENT	$(\Gamma_1\Gamma_4)^{1/2}/\Gamma$
−0.12±0.03	² CAMERON	78B	DPWA $K^-p \rightarrow N\bar{K}^*$	

$(\Gamma_i\Gamma_f)^{1/2}/\Gamma_{\text{total}}$ in $N\bar{K} \rightarrow \Lambda(2000) \rightarrow N\bar{K}^*(892)$, $S=3/2$, D -wave	DOCUMENT ID	TECN	COMMENT	$(\Gamma_1\Gamma_5)^{1/2}/\Gamma$
+0.09±0.03	CAMERON	78B	DPWA $K^-p \rightarrow N\bar{K}^*$	

 $\Lambda(2000)$ FOOTNOTES

- The parameters quoted here are ranges from the three best fits; the lower state probably has $J \leq 3/2$, and the higher one probably has $J \leq 5/2$.
- The published sign has been changed to be in accord with the baryon-first convention.

 $\Lambda(2000)$ REFERENCES

CAMERON	78B	NP B146 327	W. Cameron <i>et al.</i>	(RHEL, LOIC) IJP
NAKKASYAN	75	NP B93 85	A. Nakkasyan	(CERN) IJP
BRANDSTET...72	NP B39 13	A.A. Brandstetter <i>et al.</i>		(RHEL, CDEF+) IJP
BARBARO-...	70	Duke Conf. 173	A. Barbaro-Galtieri	(LRL) IJP

Hyperon Resonances, 1970

Baryon Particle Listings

 $\Lambda(2020)$, $\Lambda(2100)$ $\Lambda(2020) F_{07}$

$$I(J^P) = 0(\frac{7}{2}^+) \text{ Status: } *$$

OMITTED FROM SUMMARY TABLE

In LITCHFIELD 71, need for the state rests solely on a possibly inconsistent polarization measurement at 1.784 GeV/c. HEMINGWAY 75 does not require this state. GOPAL 77 does not need it in either $N\bar{K}$ or $\Sigma\pi$. With new K^-n angular distributions included, DECLAIS 77 sees it. However, this and other new data are included in GOPAL 80 and the state is not required. BACCARI 77 weakly supports it.

 $\Lambda(2020)$ MASS

VALUE (MeV)	DOCUMENT ID	TECN	COMMENT
≈ 2020 OUR ESTIMATE			
2140	BACCARI 77	DPWA	$K^-p \rightarrow \Lambda\omega$
2117	DECLAIS 77	DPWA	$\bar{K}N \rightarrow \bar{K}N$
2100 \pm 30	LITCHFIELD 71	DPWA	$K^-p \rightarrow \bar{K}N$
2020 \pm 20	BARBARO-... 70	DPWA	$K^-p \rightarrow \Sigma\pi$

 $\Lambda(2020)$ WIDTH

VALUE (MeV)	DOCUMENT ID	TECN	COMMENT
128	BACCARI 77	DPWA	$K^-p \rightarrow \Lambda\omega$
167	DECLAIS 77	DPWA	$\bar{K}N \rightarrow \bar{K}N$
120 \pm 30	LITCHFIELD 71	DPWA	$K^-p \rightarrow \bar{K}N$
160 \pm 30	BARBARO-... 70	DPWA	$K^-p \rightarrow \Sigma\pi$

 $\Lambda(2020)$ DECAY MODES

Mode	Fraction (Γ_i/Γ)
Γ_1 $N\bar{K}$	25–35 %
Γ_2 $\Sigma\pi$	\sim 5 %
Γ_3 $\Lambda\eta$	< 3 %
Γ_4 ΞK	< 3 %
Γ_5 $\Lambda\omega$	< 8 %
Γ_6 $N\bar{K}^*(892)$	10–20 %
Γ_7 $N\bar{K}^*(892)$, $S=1/2$, G-wave	
Γ_8 $N\bar{K}^*(892)$, $S=3/2$, D-wave	

••• We do not use the following data for averages, fits, limits, etc. •••

2094	BACCARI 77	DPWA	$K^-p \rightarrow \Lambda\omega$
2094	DECLAIS 77	DPWA	$\bar{K}N \rightarrow \bar{K}N$
2110 or 2089	¹ NAKKASYAN 75	DPWA	$K^-p \rightarrow \Lambda\omega$

 $\Lambda(2100)$ WIDTH

VALUE (MeV)	DOCUMENT ID	TECN	COMMENT
100 to 250 (≈ 200) OUR ESTIMATE			
157 \pm 40	DEBELLEFON 78	DPWA	$\bar{K}N \rightarrow \bar{K}N$
250 \pm 30	GOPAL 77	DPWA	$\bar{K}N$ multichannel
241 \pm 30	HEMINGWAY 75	DPWA	$K^-p \rightarrow \bar{K}N$
152 \pm 15	KANE 74	DPWA	$K^-p \rightarrow \Sigma\pi$
••• We do not use the following data for averages, fits, limits, etc. •••			
98	BACCARI 77	DPWA	$K^-p \rightarrow \Lambda\omega$
250	DECLAIS 77	DPWA	$\bar{K}N \rightarrow \bar{K}N$
244 or 302	¹ NAKKASYAN 75	DPWA	$K^-p \rightarrow \Lambda\omega$

 $\Lambda(2100)$ DECAY MODES

Mode	Fraction (Γ_i/Γ)
Γ_1 $N\bar{K}$	25–35 %
Γ_2 $\Sigma\pi$	\sim 5 %
Γ_3 $\Lambda\eta$	< 3 %
Γ_4 ΞK	< 3 %
Γ_5 $\Lambda\omega$	< 8 %
Γ_6 $N\bar{K}^*(892)$	10–20 %
Γ_7 $N\bar{K}^*(892)$, $S=1/2$, G-wave	
Γ_8 $N\bar{K}^*(892)$, $S=3/2$, D-wave	

The above branching fractions are our estimates, not fits or averages.

 $\Lambda(2100)$ BRANCHING RATIOSSee "Sign conventions for resonance couplings" in the Note on Λ and Σ Resonances. $\Lambda(2020)$ BRANCHING RATIOSSee "Sign conventions for resonance couplings" in the Note on Λ and Σ Resonances.

$\Gamma(N\bar{K})/\Gamma_{\text{total}}$	DOCUMENT ID	TECN	COMMENT	Γ_1/Γ
0.25 to 0.35 OUR ESTIMATE				
0.34 \pm 0.03	GOPAL 80	DPWA	$\bar{K}N \rightarrow \bar{K}N$	
0.24 \pm 0.06	DEBELLEFON 78	DPWA	$\bar{K}N \rightarrow \bar{K}N$	
0.31 \pm 0.03	HEMINGWAY 75	DPWA	$K^-p \rightarrow \bar{K}N$	

$(\Gamma_1\Gamma_2)^{1/2}/\Gamma_{\text{total}}$ in $N\bar{K} \rightarrow \Lambda(2020) \rightarrow \Sigma\pi$	DOCUMENT ID	TECN	COMMENT	$(\Gamma_1\Gamma_2)^{1/2}/\Gamma$
0.29	DECLAIS 77	DPWA	$\bar{K}N \rightarrow \bar{K}N$	
0.30 \pm 0.03	GOPAL 77	DPWA	See GOPAL 80	

$(\Gamma_1\Gamma_2)^{1/2}/\Gamma_{\text{total}}$ in $N\bar{K} \rightarrow \Lambda(2020) \rightarrow \Lambda\omega$	DOCUMENT ID	TECN	COMMENT	$(\Gamma_1\Gamma_3)^{1/2}/\Gamma$
–0.15 \pm 0.02	BARBARO-... 70	DPWA	$K^-p \rightarrow \Sigma\pi$	
< 0.05	BACCARI 77	DPWA	$K^-p \rightarrow \Lambda\omega$	

 $\Lambda(2020)$ REFERENCES

GOPAL 80	Toronto Conf. 159	G.P. Gopal	(RHEL)
BACCARI 77	NC 41A 96	B. Baccari et al.	(SACL, CDEF) IJP
DECLAIS 77	CERN 77-16	Y. Declais et al.	(CAEN, CERN) IJP
GOPAL 77	NP B119 362	G.P. Gopal et al.	(LOIC, RHEL)
HEMINGWAY 75	NP B91 12	R.J. Hemingway et al.	(CERN, HEIDH, MPIM) IJP
LITCHFIELD 71	NP B30 125	P.J. Litchfield et al.	(RHEL, CDEF, SACL) IJP
BARBARO-... 70	Duke Conf. 173	A. Barbaro-Galtri	(LRL) IJP
Hyperon Resonances, 1970			

 $\Lambda(2100) G_{07}$

$$I(J^P) = 0(\frac{7}{2}^-) \text{ Status: } ***$$

Discovered by COOL 66 and by WOHL 66. Most of the results published before 1973 are now obsolete and have been omitted. They may be found in our 1982 edition Physics Letters **111B** 1 (1982).

This entry only includes results from partial-wave analyses. Parameters of peaks seen in cross sections and in invariant-mass distributions around 2100 MeV used to be listed in a separate entry immediately following. It may be found in our 1986 edition Physics Letters **170B** 1 (1986).

 $\Lambda(2100)$ MASS

VALUE (MeV)	DOCUMENT ID	TECN	COMMENT
2090 to 2110 (≈ 2100) OUR ESTIMATE			
2104 \pm 10	GOPAL 80	DPWA	$\bar{K}N \rightarrow \bar{K}N$
2106 \pm 30	DEBELLEFON 78	DPWA	$\bar{K}N \rightarrow \bar{K}N$
2110 \pm 10	GOPAL 77	DPWA	$\bar{K}N$ multichannel
2105 \pm 10	HEMINGWAY 75	DPWA	$K^-p \rightarrow \bar{K}N$
2115 \pm 10	KANE 74	DPWA	$K^-p \rightarrow \Sigma\pi$

$\Gamma(N\bar{K})/\Gamma_{\text{total}}$	DOCUMENT ID	TECN	COMMENT	Γ_1/Γ
0.25 to 0.35 OUR ESTIMATE				
0.34 \pm 0.03	GOPAL 80	DPWA	$\bar{K}N \rightarrow \bar{K}N$	
0.24 \pm 0.06	DEBELLEFON 78	DPWA	$\bar{K}N \rightarrow \bar{K}N$	
0.31 \pm 0.03	HEMINGWAY 75	DPWA	$K^-p \rightarrow \bar{K}N$	

$(\Gamma_1\Gamma_2)^{1/2}/\Gamma_{\text{total}}$ in $N\bar{K} \rightarrow \Lambda(2100) \rightarrow \Sigma\pi$	DOCUMENT ID	TECN	COMMENT	$(\Gamma_1\Gamma_2)^{1/2}/\Gamma$
0.29	DECLAIS 77	DPWA	$\bar{K}N \rightarrow \bar{K}N$	
0.30 \pm 0.03	GOPAL 77	DPWA	See GOPAL 80	

$(\Gamma_1\Gamma_2)^{1/2}/\Gamma_{\text{total}}$ in $N\bar{K} \rightarrow \Lambda(2100) \rightarrow \Xi K$	DOCUMENT ID	TECN	COMMENT	$(\Gamma_1\Gamma_4)^{1/2}/\Gamma$
+0.12 \pm 0.04	GOPAL 77	DPWA	$\bar{K}N$ multichannel	
+0.11 \pm 0.01	KANE 74	DPWA	$K^-p \rightarrow \Sigma\pi$	

$(\Gamma_1\Gamma_2)^{1/2}/\Gamma_{\text{total}}$ in $N\bar{K} \rightarrow \Lambda(2100) \rightarrow \Lambda\eta$	DOCUMENT ID	TECN	COMMENT	$(\Gamma_1\Gamma_3)^{1/2}/\Gamma$
–0.05 \pm 0.020	RADER 73	MPWA	$K^-p \rightarrow \Lambda\eta$	

$(\Gamma_1\Gamma_2)^{1/2}/\Gamma_{\text{total}}$ in $N\bar{K} \rightarrow \Lambda(2100) \rightarrow \Xi K$	DOCUMENT ID	TECN	COMMENT	$(\Gamma_1\Gamma_4)^{1/2}/\Gamma$
0.035 \pm 0.018	LITCHFIELD 71	DPWA	$K^-p \rightarrow \Xi K$	

••• We do not use the following data for averages, fits, limits, etc. •••

0.003	MULLER 69B	DPWA	$K^-p \rightarrow \Xi K$
0.05	TRIPP 67	RVUE	$K^-p \rightarrow \Xi K$

$(\Gamma_1\Gamma_2)^{1/2}/\Gamma_{\text{total}}$ in $N\bar{K} \rightarrow \Lambda(2100) \rightarrow \Lambda\omega$	DOCUMENT ID	TECN	COMMENT	$(\Gamma_1\Gamma_5)^{1/2}/\Gamma$
–0.070	² BACCARI 77	DPWA	GD_{37} wave	
+0.011	² BACCARI 77	DPWA	GG_{17} wave	
+0.008	² BACCARI 77	DPWA	GG_{37} wave	
0.122 or 0.154	¹ NAKKASYAN 75	DPWA	$K^-p \rightarrow \Lambda\omega$	

$(\Gamma_1\Gamma_2)^{1/2}/\Gamma_{\text{total}}$ in $N\bar{K} \rightarrow \Lambda(2100) \rightarrow N\bar{K}^*(892)$, $S=3/2$, D-wave	DOCUMENT ID	TECN	COMMENT	$(\Gamma_1\Gamma_6)^{1/2}/\Gamma$
+0.21 \pm 0.04	CAMERON 78B	DPWA	$K^-p \rightarrow N\bar{K}^*$	

$(\Gamma_1\Gamma_2)^{1/2}/\Gamma_{\text{total}}$ in $N\bar{K} \rightarrow \Lambda(2100) \rightarrow N\bar{K}^*(892)$, $S=1/2$, G-wave	DOCUMENT ID	TECN	COMMENT	$(\Gamma_1\Gamma_7)^{1/2}/\Gamma$
–0.04 \pm 0.03	³ CAMERON 78B	DPWA	$K^-p \rightarrow N\bar{K}^*$	

See key on page 405

Baryon Particle Listings

$\Lambda(2100)$, $\Lambda(2110)$, $\Lambda(2325)$

$\Lambda(2100)$ FOOTNOTES

- The NAKKASYAN 75 values are from the two best solutions found. Each has the $\Lambda(2100)$ and one additional resonance (P_3 or F_5).
- Note that the three for BACCARI 77 entries are for three different waves.
- The published sign has been changed to be in accord with the baryon-first convention. The upper limit on the G_3 wave is 0.03.

$\Lambda(2100)$ REFERENCES

PDG				
PDG	86	PL 170B 1	M. Aguilar-Benitez et al.	(CERN, CIT+)
PDG	82	PL 111B 1	M. Roos et al.	(HELS, CIT, CERN)
GOPAL	80	Toronto Conf. 159	G.P. Gopal	(RHEL) IJP
CAMERON	78B	NP B146 327	W. Cameron et al.	(RHEL, LOIC) IJP
DEBELLEFON	78	NC 42A 403	A. de Bellefon et al.	(CDEF, SAACL) IJP
BACCARI	77	NC 41A 96	B. Baccari et al.	(SAACL, CDEF) IJP
DECLAIS	77	CERN 77-16	Y. Declais et al.	(CAEN, CERN) IJP
GOPAL	77	NP B119 362	G.P. Gopal et al.	(LOIC, RHEL) IJP
HEMINGWAY	75	NP B91 12	R.J. Hemingway et al.	(CERN, HEIDH, MPIM) IJP
NAKKASYAN	75	NP B93 85	A. Nakkasyan	(CERN) IJP
KANE	74	LBL-2452	D.F. Kane	(LBL) IJP
RADER	73	NC 16A 178	R.K. Rader et al.	(SAACL, HEID, CERN+) IJP
LITCHEFIELD	71	NP B30 125	P.J. Litchefield et al.	(RHEL, CDEF, SAACL) IJP
MULLER	69B	Thesis UCRL 19372	R.A. Muller	(LRL)
TRIPP	67	NP B3 10	R.D. Tripp et al.	(LRL, SLAC, CERN+) IJP
COOL	66	PRL 16 1228	R.L. Cool et al.	(BNL)
WOHL	66	PRL 17 107	C.G. Wohl, F.T. Solmitz, M.L. Stevenson	(LRL) IJP

$\Lambda(2110)$ F_{05}

$$I(J^P) = 0(\frac{5}{2}^+) \text{ Status: } ***$$

For results published before 1974 (they are now obsolete), see our 1982 edition Physics Letters **111B 1** (1982). All the references have been retained.

This resonance is in the Baryon Summary Table, but the evidence for it could be better.

$\Lambda(2110)$ MASS

VALUE (MeV)	DOCUMENT ID	TECN	COMMENT
2090 to 2140 (≈ 2110) OUR ESTIMATE			
2092 \pm 25	GOPAL 80	DPWA	$\bar{K}N \rightarrow \bar{K}N$
2125 \pm 25	CAMERON 78B	DPWA	$K^-p \rightarrow N\bar{K}^*$
2106 \pm 50	DEBELLEFON 78	DPWA	$\bar{K}N \rightarrow \bar{K}N$
2140 \pm 20	DEBELLEFON 77	DPWA	$K^-p \rightarrow \Sigma\pi$
2100 \pm 50	GOPAL 77	DPWA	$\bar{K}N$ multichannel
2112 \pm 7	KANE 74	DPWA	$K^-p \rightarrow \Sigma\pi$
••• We do not use the following data for averages, fits, limits, etc. •••			
2137	BACCARI 77	DPWA	$K^-p \rightarrow \Lambda\omega$
2103	¹ NAKKASYAN 75	DPWA	$K^-p \rightarrow \Lambda\omega$

$\Lambda(2110)$ WIDTH

VALUE (MeV)	DOCUMENT ID	TECN	COMMENT
150 to 250 (≈ 200) OUR ESTIMATE			
245 \pm 25	GOPAL 80	DPWA	$\bar{K}N \rightarrow \bar{K}N$
160 \pm 30	CAMERON 78B	DPWA	$K^-p \rightarrow N\bar{K}^*$
251 \pm 50	DEBELLEFON 78	DPWA	$\bar{K}N \rightarrow \bar{K}N$
140 \pm 20	DEBELLEFON 77	DPWA	$K^-p \rightarrow \Sigma\pi$
200 \pm 50	GOPAL 77	DPWA	$\bar{K}N$ multichannel
190 \pm 30	KANE 74	DPWA	$K^-p \rightarrow \Sigma\pi$
••• We do not use the following data for averages, fits, limits, etc. •••			
132	BACCARI 77	DPWA	$K^-p \rightarrow \Lambda\omega$
391	¹ NAKKASYAN 75	DPWA	$K^-p \rightarrow \Lambda\omega$

$\Lambda(2110)$ DECAY MODES

Mode	Fraction (Γ_i/Γ)
Γ_1 $N\bar{K}$	5–25 %
Γ_2 $\Sigma\pi$	10–40 %
Γ_3 $\Lambda\omega$	seen
Γ_4 $\Sigma(1385)\pi$	seen
Γ_5 $\Sigma(1385)\pi, P$ -wave	
Γ_6 $N\bar{K}^*(892)$	10–60 %
Γ_7 $N\bar{K}^*(892), S=1/2, F$ -wave	

The above branching fractions are our estimates, not fits or averages.

$\Lambda(2110)$ BRANCHING RATIOS

See "Sign conventions for resonance couplings" in the Note on Λ and Σ Resonances.

$\Gamma(N\bar{K})/\Gamma_{\text{total}}$	DOCUMENT ID	TECN	COMMENT	Γ_1/Γ
0.05 to 0.25 OUR ESTIMATE				
0.07 \pm 0.03	GOPAL 80	DPWA	$\bar{K}N \rightarrow \bar{K}N$	
0.27 \pm 0.06	² DEBELLEFON 78	DPWA	$\bar{K}N \rightarrow \bar{K}N$	
••• We do not use the following data for averages, fits, limits, etc. •••				
0.07 \pm 0.03	GOPAL 77	DPWA	See GOPAL 80	

$(\Gamma_1\Gamma_2)^{1/2}/\Gamma_{\text{total}}$ in $N\bar{K} \rightarrow \Lambda(2110) \rightarrow \Sigma\pi$

VALUE	DOCUMENT ID	TECN	COMMENT	$(\Gamma_1\Gamma_2)^{1/2}/\Gamma$
+0.14 \pm 0.01	DEBELLEFON 77	DPWA	$K^-p \rightarrow \Sigma\pi$	
+0.20 \pm 0.03	KANE 74	DPWA	$K^-p \rightarrow \Sigma\pi$	
••• We do not use the following data for averages, fits, limits, etc. •••				
+0.10 \pm 0.03	GOPAL 77	DPWA	$\bar{K}N$ multichannel	

$(\Gamma_1\Gamma_3)^{1/2}/\Gamma_{\text{total}}$ in $N\bar{K} \rightarrow \Lambda(2110) \rightarrow \Lambda\omega$

VALUE	DOCUMENT ID	TECN	COMMENT	$(\Gamma_1\Gamma_3)^{1/2}/\Gamma$
<0.05	BACCARI 77	DPWA	$K^-p \rightarrow \Lambda\omega$	
0.112	¹ NAKKASYAN 75	DPWA	$K^-p \rightarrow \Lambda\omega$	

$(\Gamma_1\Gamma_4)^{1/2}/\Gamma_{\text{total}}$ in $N\bar{K} \rightarrow \Lambda(2110) \rightarrow \Sigma(1385)\pi$

VALUE	DOCUMENT ID	TECN	COMMENT	$(\Gamma_1\Gamma_4)^{1/2}/\Gamma$
+0.071 \pm 0.025	³ CAMERON 78	DPWA	$K^-p \rightarrow \Sigma(1385)\pi$	

$(\Gamma_1\Gamma_6)^{1/2}/\Gamma_{\text{total}}$ in $N\bar{K} \rightarrow \Lambda(2110) \rightarrow N\bar{K}^*(892)$

VALUE	DOCUMENT ID	TECN	COMMENT	$(\Gamma_1\Gamma_6)^{1/2}/\Gamma$
-0.17 \pm 0.04	⁴ CAMERON 78B	DPWA	$K^-p \rightarrow N\bar{K}^*$	

$\Lambda(2110)$ FOOTNOTES

- Found in one of two best solutions.
- The published error of 0.6 was a misprint.
- The CAMERON 78 upper limit on F -wave decay is 0.03. The sign here has been changed to be in accord with the baryon-first convention.
- The published sign has been changed to be in accord with the baryon-first convention. The CAMERON 78B upper limits on the P_3 and F_3 waves are each 0.03.

$\Lambda(2110)$ REFERENCES

PDG				
PDG	82	PL 111B 1	M. Roos et al.	(HELS, CIT, CERN)
GOPAL	80	Toronto Conf. 159	G.P. Gopal	(RHEL) IJP
CAMERON	78	NP B143 189	W. Cameron et al.	(RHEL, LOIC) IJP
CAMERON	78B	NP B146 327	W. Cameron et al.	(RHEL, LOIC) IJP
DEBELLEFON	78	NC 42A 403	A. de Bellefon et al.	(CDEF, SAACL) IJP
BACCARI	77	NC 41A 96	B. Baccari et al.	(SAACL, CDEF) IJP
DEBELLEFON	77	NC 37A 175	A. de Bellefon et al.	(CDEF, SAACL) IJP
GOPAL	77	NP B119 362	G.P. Gopal et al.	(LOIC, RHEL) IJP
NAKKASYAN	75	NP B93 85	A. Nakkasyan	(CERN) IJP
KANE	74	LBL-2452	D.F. Kane	(LBL) IJP

$\Lambda(2325)$ D_{03}

$$I(J^P) = 0(\frac{3}{2}^-) \text{ Status: } *$$

OMITTED FROM SUMMARY TABLE

BACCARI 77 finds this state with either $J^P = 3/2^-$ or $3/2^+$ in a energy-dependent partial-wave analyses of $K^-p \rightarrow \Lambda\omega$ from 2070 to 2436 MeV. A subsequent semi-energy-independent analysis from threshold to 2436 MeV selects $3/2^-$. DEBELLEFON 78 (same group) also sees this state in an energy-dependent partial-wave analysis of $K^-p \rightarrow \bar{K}N$ data, and finds $J^P = 3/2^-$ or $3/2^+$. They again prefer $J^P = 3/2^-$, but only on the basis of model-dependent considerations.

$\Lambda(2325)$ MASS

VALUE (MeV)	DOCUMENT ID	TECN	COMMENT
≈ 2325 OUR ESTIMATE			
2342 \pm 30	DEBELLEFON 78	DPWA	$\bar{K}N \rightarrow \bar{K}N$
2327 \pm 20	BACCARI 77	DPWA	$K^-p \rightarrow \Lambda\omega$

$\Lambda(2325)$ WIDTH

VALUE (MeV)	DOCUMENT ID	TECN	COMMENT
177 \pm 40	DEBELLEFON 78	DPWA	$\bar{K}N \rightarrow \bar{K}N$
160 \pm 40	BACCARI 77	IPWA	$K^-p \rightarrow \Lambda\omega$

$\Lambda(2325)$ DECAY MODES

Mode	Fraction (Γ_i/Γ)
Γ_1 $N\bar{K}$	
Γ_2 $\Lambda\omega$	

$\Lambda(2325)$ BRANCHING RATIOS

$\Gamma(N\bar{K})/\Gamma_{\text{total}}$	DOCUMENT ID	TECN	COMMENT	Γ_1/Γ
0.19 \pm 0.06	DEBELLEFON 78	DPWA	$\bar{K}N \rightarrow \bar{K}N$	

Baryon Particle Listings

 $\Lambda(2325)$, $\Lambda(2350)$, $\Lambda(2585)$ Bumps

$(\Gamma_1 \Gamma_f)^{1/2} / \Gamma_{\text{total}}$ in $N\bar{K} \rightarrow \Lambda(2325) \rightarrow \Lambda\omega$	DOCUMENT ID	TECN	COMMENT	$(\Gamma_1 \Gamma_2)^{1/2} / \Gamma$
0.06 ± 0.02	¹ BACCARI 77	IPWA	DS_{33} wave	
0.05 ± 0.02	¹ BACCARI 77	DPWA	DD_{13} wave	
0.08 ± 0.03	¹ BACCARI 77	DPWA	DD_{33} wave	

 $\Lambda(2325)$ FOOTNOTES

¹ Note that the three BACCARI 77 entries are for three different waves.

 $\Lambda(2325)$ REFERENCES

DEBELLEFON 78	NC 42A 403	A. de Bellefón et al.	(CDEF, SACL) IJP
BACCARI 77	NC 41A 96	B. Baccari et al.	(SACL, CDEF) IJP

 $\Lambda(2350) H_{09}$

$$I(J^P) = 0(\frac{9}{2}^+) \text{ Status: } ***$$

DAUM 68 favors $J^P = 7/2^-$ or $9/2^+$. BRICMAN 70 favors $9/2^+$. LASINSKI 71 suggests three states in this region using a Pomeron + resonances model. There are now also three formation experiments from the College de France-Saclay group, DEBELLEFON 77, BACCARI 77, and DEBELLEFON 78, which find $9/2^+$ in energy-dependent partial-wave analyses of $\bar{K}N \rightarrow \Sigma\pi, \Lambda\omega$, and $N\bar{K}$.

 $\Lambda(2350)$ MASS

VALUE (MeV)	DOCUMENT ID	TECN	COMMENT
2340 to 2370 (≈ 2350) OUR ESTIMATE			
2370 ± 50	DEBELLEFON 78	DPWA	$\bar{K}N \rightarrow \bar{K}N$
2365 ± 20	DEBELLEFON 77	DPWA	$K^-p \rightarrow \Sigma\pi$
2358 ± 6	BRICMAN 70	CNTR	Total, charge exchange
• • • We do not use the following data for averages, fits, limits, etc. • • •			
2372	BACCARI 77	DPWA	$K^-p \rightarrow \Lambda\omega$
2344 ± 15	COOL 70	CNTR	K^-p, K^-d total
2360 ± 20	LU 70	CNTR	$\gamma p \rightarrow K^+Y^*$
2340 ± 7	BUGG 68	CNTR	K^-p, K^-d total

 $\Lambda(2350)$ WIDTH

VALUE (MeV)	DOCUMENT ID	TECN	COMMENT
100 to 250 (≈ 150) OUR ESTIMATE			
204 ± 50	DEBELLEFON 78	DPWA	$\bar{K}N \rightarrow \bar{K}N$
110 ± 20	DEBELLEFON 77	DPWA	$K^-p \rightarrow \Sigma\pi$
324 ± 30	BRICMAN 70	CNTR	Total, charge exchange
• • • We do not use the following data for averages, fits, limits, etc. • • •			
257	BACCARI 77	DPWA	$K^-p \rightarrow \Lambda\omega$
190	COOL 70	CNTR	K^-p, K^-d total
55	LU 70	CNTR	$\gamma p \rightarrow K^+Y^*$
140 ± 20	BUGG 68	CNTR	K^-p, K^-d total

 $\Lambda(2350)$ DECAY MODES

Mode	Fraction (Γ_i/Γ)
Γ_1 $N\bar{K}$	~ 12 %
Γ_2 $\Sigma\pi$	~ 10 %
Γ_3 $\Lambda\omega$	

The above branching fractions are our estimates, not fits or averages.

 $\Lambda(2350)$ BRANCHING RATIOS

See "Sign conventions for resonance couplings" in the Note on Λ and Σ Resonances.

$\Gamma(N\bar{K})/\Gamma_{\text{total}}$	DOCUMENT ID	TECN	COMMENT	Γ_1/Γ
≈ 0.12 OUR ESTIMATE				
0.12 ± 0.04	DEBELLEFON 78	DPWA	$\bar{K}N \rightarrow \bar{K}N$	

$(\Gamma_1 \Gamma_f)^{1/2} / \Gamma_{\text{total}}$ in $N\bar{K} \rightarrow \Lambda(2350) \rightarrow \Sigma\pi$	DOCUMENT ID	TECN	COMMENT	$(\Gamma_1 \Gamma_2)^{1/2} / \Gamma$
-0.11 ± 0.02	DEBELLEFON 77	DPWA	$K^-p \rightarrow \Sigma\pi$	

$(\Gamma_1 \Gamma_f)^{1/2} / \Gamma_{\text{total}}$ in $N\bar{K} \rightarrow \Lambda(2350) \rightarrow \Lambda\omega$	DOCUMENT ID	TECN	COMMENT	$(\Gamma_1 \Gamma_3)^{1/2} / \Gamma$
<0.05	BACCARI 77	DPWA	$K^-p \rightarrow \Lambda\omega$	

 $\Lambda(2350)$ REFERENCES

DEBELLEFON 78	NC 42A 403	A. de Bellefón et al.	(CDEF, SACL) IJP
BACCARI 77	NC 41A 96	B. Baccari et al.	(SACL, CDEF) IJP
DEBELLEFON 77	NC 37A 175	A. de Bellefón et al.	(CDEF, SACL) IJP
LASINSKI 71	NP B29 125	T.A. Lasinski	(EF) IJP
BRICMAN 70	PL 31B 152	C. Bricman et al.	(CERN, CAEN, SACL)
COOL 70	PR D1 1887	R.L. Cool et al.	(BNL) I
Also	PRL 16 1228	R.L. Cool et al.	(BNL) I
LU 70	PR D2 1846	D.C. Lu et al.	(YALE)
BUGG 68	PR 168 1466	D.V. Bugg et al.	(RHEL, BIRM, CAVE) I
DAUM 68	NP B7 19	C. Daum et al.	(CERN) JP

 $\Lambda(2585)$ Bumps

$$I(J^P) = 0(?^?) \text{ Status: } **$$

OMITTED FROM SUMMARY TABLE

 $\Lambda(2585)$ MASS (BUMPS)

VALUE (MeV)	DOCUMENT ID	TECN	COMMENT
≈ 2585 OUR ESTIMATE			
2585 ± 45	ABRAMS 70	CNTR	K^-p, K^-d total
2530 ± 25	LU 70	CNTR	$\gamma p \rightarrow K^+Y^*$

 $\Lambda(2585)$ WIDTH (BUMPS)

VALUE (MeV)	DOCUMENT ID	TECN	COMMENT
300	ABRAMS 70	CNTR	K^-p, K^-d total
150	LU 70	CNTR	$\gamma p \rightarrow K^+Y^*$

 $\Lambda(2585)$ DECAY MODES (BUMPS)

Mode	Γ_1
$N\bar{K}$	

 $\Lambda(2585)$ BRANCHING RATIOS (BUMPS)

$$(J+\frac{1}{2}) \times \Gamma(N\bar{K}) / \Gamma_{\text{total}} \quad \Gamma_1/\Gamma$$

J is not known, so only $(J+\frac{1}{2}) \times \Gamma(N\bar{K}) / \Gamma_{\text{total}}$ can be given.

VALUE	DOCUMENT ID	TECN	COMMENT
1	ABRAMS 70	CNTR	K^-p, K^-d total
0.12 ± 0.12	¹ BRICMAN 70	CNTR	Total, charge exchange

 $\Lambda(2585)$ FOOTNOTES (BUMPS)

¹ The resonance is at the end of the region analyzed — no clear signal.

 $\Lambda(2585)$ REFERENCES (BUMPS)

ABRAMS 70	PR D1 1917	R.J. Abrams et al.	(BNL) I
Also	PRL 16 1228	R.L. Cool et al.	(BNL) I
BRICMAN 70	PL 31B 152	C. Bricman et al.	(CERN, CAEN, SACL)
LU 70	PR D2 1846	D.C. Lu et al.	(YALE)

Σ BARYONS

($S = -1, I = 1$)

$\Sigma^+ = uus, \Sigma^0 = uds, \Sigma^- = dds$

Σ^+

$$I(J^P) = 1(\frac{1}{2}^+)$$
 Status: ****

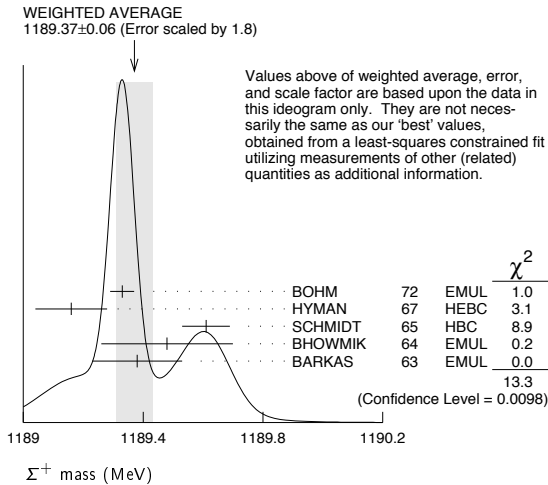
We have omitted some results that have been superseded by later experiments. See our earlier editions.

Σ^+ MASS

The fit uses $\Sigma^+, \Sigma^0, \Sigma^-$, and Λ mass and mass-difference measurements.

VALUE (MeV)	EVTS	DOCUMENT ID	TECN	COMMENT
1189.37 ± 0.07 OUR FIT				Error includes scale factor of 2.2.
1189.37 ± 0.06 OUR AVERAGE				Error includes scale factor of 1.8. See the ideogram below.
1189.33 ± 0.04	607	¹ BOHM	72	EMUL
1189.16 ± 0.12		HYMAN	67	HEBC
1189.61 ± 0.08	4205	SCHMIDT	65	HBC See note with Λ mass
1189.48 ± 0.22	58	² BHOWMIK	64	EMUL
1189.38 ± 0.15	144	² BARKAS	63	EMUL

¹ BOHM 72 is updated with our 1973 $K^-, \pi^-,$ and π^0 masses (Reviews of Modern Physics **45** S1 (1973)).
² These masses have been raised 30 keV to take into account a 46 keV increase in the proton mass and a 21 keV decrease in the π^0 mass (note added 1967 edition, Reviews of Modern Physics **39** 1 (1967)).



Σ^+ MEAN LIFE

Measurements with fewer than 1000 events have been omitted.

VALUE (10^{-10} s)	EVTS	DOCUMENT ID	TECN	COMMENT
0.8018 ± 0.0026 OUR AVERAGE				
0.8038 ± 0.0040 ± 0.0014		BARBOSA	00	E761 hyperons, 375 GeV
0.8043 ± 0.0080 ± 0.0014		³ BARBOSA	00	E761 hyperons, 375 GeV
0.798 ± 0.005	30k	MARRAFFINO	80	HBC $K^-\rho$ 0.42-0.5 GeV/c
0.807 ± 0.013	5719	CONFORTO	76	HBC $K^-\rho$ 1-1.4 GeV/c
0.795 ± 0.010	20k	EISELE	70	HBC $K^-\rho$ at rest
0.803 ± 0.008	10664	BARLOUTAUD	69	HBC $K^-\rho$ 0.4-1.2 GeV/c
0.83 ± 0.032	1300	⁴ CHANG	66	HBC

³ This is a measurement of the Σ^- lifetime. Here we assume CPT invariance; see below for the fractional $\Sigma^+ - \Sigma^-$ lifetime difference obtained by BARBOSA 00.
⁴ We have increased the CHANG 66 error of 0.018; see our 1970 edition, Reviews of Modern Physics **42** 87 (1970).

$$(\tau_{\Sigma^+} - \tau_{\Sigma^-}) / \tau_{\Sigma^+}$$

A test of CPT invariance.

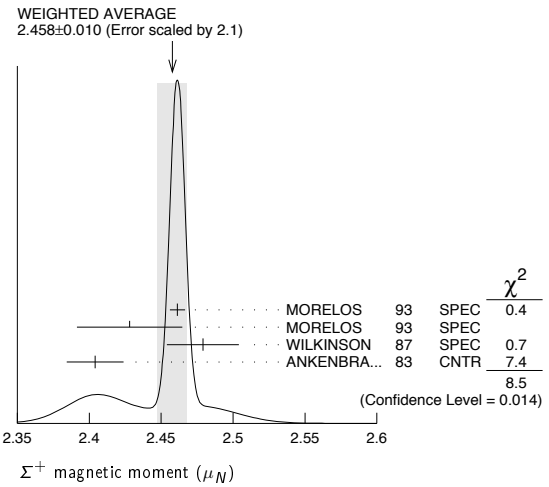
VALUE	DOCUMENT ID	TECN	COMMENT
(-6 ± 12) × 10⁻⁴	BARBOSA	00	E761 hyperons, 375 GeV

Σ^+ MAGNETIC MOMENT

See the "Note on Baryon Magnetic Moments" in the Λ Listings. Measurements with an error $\geq 0.1 \mu_N$ have been omitted.

VALUE (μ_N)	EVTS	DOCUMENT ID	TECN	COMMENT
2.458 ± 0.010 OUR AVERAGE				Error includes scale factor of 2.1. See the ideogram below.
2.4613 ± 0.0034 ± 0.0040	250k	MORELOS	93	SPEC p Cu 800 GeV
2.428 ± 0.036 ± 0.007	12k	⁵ MORELOS	93	SPEC p Cu 800 GeV
2.479 ± 0.012 ± 0.022	137k	WILKINSON	87	SPEC p Be 400 GeV
2.4040 ± 0.0198	44k	⁶ ANKENBRA...	83	CNTR p Cu 400 GeV

⁵ We assume CPT invariance: this is (minus) the Σ^- magnetic moment as measured by MORELOS 93. See below for the moment difference testing CPT .
⁶ ANKENBRANDT 83 gives the value $2.38 \pm 0.02 \mu_N$. MORELOS 93 uses the same hyperon magnet and channel and claims to determine the field integral better, leading to the revised value given here.



$$(\mu_{\Sigma^+} + \mu_{\Sigma^-}) / \mu_{\Sigma^+}$$

A test of CPT invariance.

VALUE	DOCUMENT ID	TECN	COMMENT
0.014 ± 0.015	⁷ MORELOS	93	SPEC p Cu 800 GeV

⁷ This is our calculation from the MORELOS 93 measurements of the Σ^+ and Σ^- magnetic moments given above. The statistical error on μ_{Σ^-} dominates the error here.

Σ^+ DECAY MODES

Mode	Fraction (Γ_i / Γ)	Confidence level
Γ_1 $p \pi^0$	(51.57 ± 0.30) %	
Γ_2 $n \pi^+$	(48.31 ± 0.30) %	
Γ_3 $p \gamma$	(1.23 ± 0.05) × 10 ⁻³	
Γ_4 $n \pi^+ \gamma$	[a] (4.5 ± 0.5) × 10 ⁻⁴	
Γ_5 $\Lambda e^+ \nu_e$	(2.0 ± 0.5) × 10 ⁻⁵	

$\Delta S = \Delta Q$ (SQ) violating modes or $\Delta S = 1$ weak neutral current ($S1$) modes

Mode	Fraction	Confidence level
Γ_6 $n e^+ \nu_e$	$SQ < 5 \times 10^{-6}$	90%
Γ_7 $n \mu^+ \nu_\mu$	$SQ < 3.0 \times 10^{-5}$	90%
Γ_8 $p e^+ e^-$	$S1 < 7 \times 10^{-6}$	
Γ_9 $p \mu^+ \mu^-$	$S1 (9 \begin{smallmatrix} +9 \\ -8 \end{smallmatrix}) \times 10^{-8}$	

[a] See the Listings below for the pion momentum range used in this measurement.

CONSTRAINED FIT INFORMATION

An overall fit to 2 branching ratios uses 14 measurements and one constraint to determine 3 parameters. The overall fit has a $\chi^2 = 7.7$ for 12 degrees of freedom.

The following *off-diagonal* array elements are the correlation coefficients $\langle \delta x_i \delta x_j \rangle / (\delta x_i \delta x_j)$, in percent, from the fit to the branching fractions, $x_i \equiv \Gamma_i / \Gamma_{\text{total}}$. The fit constrains the x_i whose labels appear in this array to sum to one.

x_2	-100
x_3	12 -14
	x_1 x_2

Baryon Particle Listings

 Σ^+ Σ^+ BRANCHING RATIOS $\Gamma(n\pi^+)/\Gamma(N\pi)$

VALUE	EVTS	DOCUMENT ID	TECN	COMMENT	$\Gamma_2/(\Gamma_1+\Gamma_2)$
0.4836 ± 0.0030 OUR FIT					
0.4836 ± 0.0030 OUR AVERAGE					
0.4828 ± 0.0036	10k	⁸ MARRAFFINO 80	HBC	$K^- p$ 0.42–0.5 GeV/c	
0.488 ± 0.008	1861	NOWAK 78	HBC		
0.484 ± 0.015	537	TOVEE 71	EMUL		
0.488 ± 0.010	1331	BARLOUTAUD 69	HBC	$K^- p$ 0.4–1.2 GeV/c	
0.46 ± 0.02	534	CHANG 66	HBC		
0.490 ± 0.024	308	HUMPHREY 62	HBC		

⁸ MARRAFFINO 80 actually gives $\Gamma(p\pi^0)/\Gamma(\text{total}) = 0.5172 \pm 0.0036$. $\Gamma(p\gamma)/\Gamma(p\pi^0)$

VALUE (units 10^{-3})	EVTS	DOCUMENT ID	TECN	COMMENT	Γ_3/Γ_1
2.38 ± 0.10 OUR FIT					
2.38 ± 0.10 OUR AVERAGE					
2.32 ± 0.11 ± 0.10	32k	TIMM 95	E761	Σ^+ 375 GeV	
2.81 ± 0.39 +0.21 -0.43	408	HESSEY 89	CNTR	$K^- p \rightarrow \Sigma^+ \pi^-$ at rest	
2.52 ± 0.28	190	⁹ KOBAYASHI 87	CNTR	$\pi^+ p \rightarrow \Sigma^+ K^+$	
2.46 +0.30 -0.35	155	BIAGI 85	CNTR	CERN hyperon beam	
2.11 ± 0.38	46	MANZ 80	HBC	$K^- p \rightarrow \Sigma^+ \pi^-$	
2.1 ± 0.3	45	ANG 69B	HBC	$K^- p$ at rest	
2.76 ± 0.51	31	GERSHWIN 69B	HBC	$K^- p \rightarrow \Sigma^+ \pi^-$	
3.7 ± 0.8	24	BAZIN 65	HBC	$K^- p$ at rest	

⁹ KOBAYASHI 87 actually gives $\Gamma(p\gamma)/\Gamma(\text{total}) = (1.30 \pm 0.15) \times 10^{-3}$. $\Gamma(n\pi^+\gamma)/\Gamma(n\pi^+)$

VALUE (units 10^{-3})	EVTS	DOCUMENT ID	TECN	COMMENT	Γ_4/Γ_2
0.93 ± 0.10	180	EBENHOH 73	HBC	$\pi^+ < 150$ MeV/c	
0.27 ± 0.05	29	ANG 69B	HBC	$\pi^+ < 110$ MeV/c	
~ 1.8		BAZIN 65B	HBC	$\pi^+ < 116$ MeV/c	

The π^+ momentum cuts differ, so we do not average the results but simply use the latest value in the Summary Table. $\Gamma(\Lambda e^+ \nu_e)/\Gamma_{\text{total}}$

VALUE (units 10^{-5})	EVTS	DOCUMENT ID	TECN	COMMENT	Γ_5/Γ
2.0 ± 0.5 OUR AVERAGE					
1.6 ± 0.7	5	BALTAY 69	HBC	$K^- p$ at rest	
2.9 ± 1.0	10	EISELE 69	HBC	$K^- p$ at rest	
2.0 ± 0.8	6	BARASH 67	HBC	$K^- p$ at rest	

 $\Gamma(n e^+ \nu_e)/\Gamma(n\pi^+)$

EFFECTIVE DENOM.	EVTS	DOCUMENT ID	TECN	COMMENT	Γ_6/Γ_2
< 1.1 × 10⁻⁵ OUR LIMIT				Our 90% CL limit = (2.3 events)/(effective denominator sum). [Number of events increased to 2.3 for a 90% confidence level.]	
111000	0	¹⁰ EBENHOH 74	HBC	$K^- p$ at rest	
105000	0	¹⁰ SECHI-ZORN 73	HBC	$K^- p$ at rest	

¹⁰ Effective denominator calculated by us. $\Gamma(n\mu^+ \nu_\mu)/\Gamma(n\pi^+)$

EFFECTIVE DENOM.	EVTS	DOCUMENT ID	TECN	COMMENT	Γ_7/Γ_2
< 6.2 × 10⁻⁵ OUR LIMIT				Our 90% CL limit = (6.7 events)/(effective denominator sum). [Number of events increased to 6.7 for a 90% confidence level.]	
33800	0	BAGGETT 69B	HBC		
62000	2	¹¹ EISELE 69B	HBC		
10150	0	¹² COURANT 64	HBC		
1710	0	¹² NAUENBERG 64	HBC		
120	1	GALTIERI 62	EMUL		

¹¹ Effective denominator calculated by us.¹² Effective denominator taken from EISELE 67. $\Gamma(p e^+ e^-)/\Gamma_{\text{total}}$

VALUE (units 10^{-6})	DOCUMENT ID	TECN	COMMENT	Γ_8/Γ
< 7	¹³ ANG 69B	HBC	$K^- p$ at rest	

¹³ ANG 69B found three $p e^+ e^-$ events in agreement with $\gamma \rightarrow e^+ e^-$ conversion from $\Sigma^+ \rightarrow p\gamma$. The limit given here is for neutral currents. $\Gamma(p\mu^+ \mu^-)/\Gamma_{\text{total}}$

VALUE (units 10^{-8})	EVTS	DOCUMENT ID	TECN	COMMENT	Γ_9/Γ
8.6 +6.6 -5.4 ± 5.5	3	¹⁴ PARK 05	HYCP	p Cu, 800 GeV	

¹⁴ The masses of the three dimuons of PARK 05 are within 1 MeV of one another, perhaps indicating the existence of a new state P^0 with mass 214.3 ± 0.5 MeV. In that case, the decay is $\Sigma^+ \rightarrow p P^0$, $P^0 \rightarrow \mu^+ \mu^-$, with a branching fraction of $(3.1^{+2.4}_{-1.9} \pm 1.5) \times 10^{-8}$. $\Gamma(\Sigma^+ \rightarrow n e^+ \nu_e)/\Gamma(\Sigma^- \rightarrow n e^- \bar{\nu}_e)$

VALUE	CL%	EVTS	DOCUMENT ID	TECN	COMMENT	$\Gamma_6/\Gamma_3^{\Sigma^-}$
< 0.009 OUR LIMIT					Our 90% CL limit, using $\Gamma(n e^+ \nu_e)/\Gamma(n\pi^+)$ above.	
• • •					We do not use the following data for averages, fits, limits, etc. • • •	
< 0.019	90	0	EBENHOH 74	HBC	$K^- p$ at rest	
< 0.018	90	0	SECHI-ZORN 73	HBC	$K^- p$ at rest	
< 0.12	95	0	COLE 71	HBC	$K^- p$ at rest	
< 0.03	90	0	EISELE 69B	HBC	See EBENHOH 74	

 $\Gamma(\Sigma^+ \rightarrow n\mu^+ \nu_\mu)/\Gamma(\Sigma^- \rightarrow n\mu^- \bar{\nu}_\mu)$

VALUE	EVTS	DOCUMENT ID	TECN	COMMENT	$\Gamma_7/\Gamma_4^{\Sigma^-}$	
< 0.12 OUR LIMIT					Our 90% CL limit, using $\Gamma(n\mu^+ \nu_\mu)/\Gamma(n\pi^+)$ above.	
• • •					We do not use the following data for averages, fits, limits, etc. • • •	
0.06 +0.045 -0.03	2	EISELE 69B	HBC	$K^- p$ at rest		

 $\Gamma(\Sigma^+ \rightarrow n\ell^+ \nu)/\Gamma(\Sigma^- \rightarrow n\ell^- \bar{\nu})$

VALUE	EVTS	DOCUMENT ID	TECN	COMMENT	$(\Gamma_6 + \Gamma_7)/(\Gamma_3^{\Sigma^-} + \Gamma_4^{\Sigma^-})$	
< 0.043 OUR LIMIT					Our 90% CL limit, using $[\Gamma(n e^+ \nu_e) + \Gamma(n\mu^+ \nu_\mu)]/\Gamma(n\pi^+)$.	
• • •					We do not use the following data for averages, fits, limits, etc. • • •	
< 0.08	1	NORTON 69	HBC			
< 0.034	0	BAGGETT 67	HBC			

 Σ^+ DECAY PARAMETERS

See the "Note on Baryon Decay Parameters" in the neutron Listings. A few early results have been omitted.

 α_0 FOR $\Sigma^+ \rightarrow p\pi^0$

VALUE	EVTS	DOCUMENT ID	TECN	COMMENT
-0.980 ± 0.017 -0.015 OUR FIT				
-0.980 ± 0.017 -0.013 OUR AVERAGE				
-0.945 +0.055 -0.042	1259	¹⁵ LIPMAN 73	OSPK	$\pi^+ p \rightarrow \Sigma^+$
-0.940 ± 0.045	16k	BELLA MY 72	ASPK	$\pi^+ p \rightarrow \Sigma^+ K^+$
-0.98 +0.05 -0.02	1335	¹⁶ HARRIS 70	OSPK	$\pi^+ p \rightarrow \Sigma^+ K^+$
-0.999 ± 0.022	32k	BANGERTER 69	HBC	$K^- p$ 0.4 GeV/c

¹⁵ Decay protons scattered off aluminum.¹⁶ Decay protons scattered off carbon. ϕ_0 ANGLE FOR $\Sigma^+ \rightarrow p\pi^0$

VALUE (°)	EVTS	DOCUMENT ID	TECN	COMMENT	($\tan \phi_0 = \beta/\gamma$)
36 ± 34 OUR AVERAGE					
38.1 +35.7 -37.1	1259	¹⁷ LIPMAN 73	OSPK	$\pi^+ p \rightarrow \Sigma^+ K^+$	
22 ± 90		¹⁸ HARRIS 70	OSPK	$\pi^+ p \rightarrow \Sigma^+ K^+$	

¹⁷ Decay proton scattered off aluminum.¹⁸ Decay protons scattered off carbon. α_+ / α_0

VALUE	EVTS	DOCUMENT ID	TECN	COMMENT
-0.069 ± 0.013 OUR FIT				
-0.073 ± 0.021	23k	MARRAFFINO 80	HBC	$K^- p$ 0.42–0.5 GeV/c

 α_+ FOR $\Sigma^+ \rightarrow n\pi^+$

VALUE	EVTS	DOCUMENT ID	TECN	COMMENT
0.068 ± 0.013 OUR FIT				
0.066 ± 0.016 OUR AVERAGE				
0.037 ± 0.049	4101	BERLEY 70B	HBC	
0.069 ± 0.017	35k	BANGERTER 69	HBC	$K^- p$ 0.4 GeV/c

 ϕ_+ ANGLE FOR $\Sigma^+ \rightarrow n\pi^+$

VALUE (°)	EVTS	DOCUMENT ID	TECN	COMMENT	($\tan \phi_+ = \beta/\gamma$)
167 ± 20 OUR AVERAGE				Error includes scale factor of 1.1.	
184 ± 24	1054	¹⁹ BERLEY 70B	HBC		
143 ± 29	560	BANGERTER 69B	HBC	$K^- p$ 0.4 GeV/c	

¹⁹ Changed from 176 to 184° to agree with our sign convention. α_γ FOR $\Sigma^+ \rightarrow p\gamma$

VALUE	EVTS	DOCUMENT ID	TECN	COMMENT
-0.76 ± 0.08 OUR AVERAGE				
-0.720 ± 0.086 ± 0.045	35k	²⁰ FOUCHER 92	SPEC	Σ^+ 375 GeV
-0.86 ± 0.13 ± 0.04	190	KOBAYASHI 87	CNTR	$\pi^+ p \rightarrow \Sigma^+ K^+$
-0.53 +0.38 -0.36	46	MANZ 80	HBC	$K^- p \rightarrow \Sigma^+ \pi^-$
-1.03 +0.52 -0.42	61	GERSHWIN 69B	HBC	$K^- p \rightarrow \Sigma^+ \pi^-$

²⁰ See TIMM 95 for a detailed description of the analysis.

Σ^+ REFERENCES

We have omitted some papers that have been superseded by later experiments. See our earlier editions.

PARK	05	PRL 94 021801	H.K. Park <i>et al.</i>	(FNAL HyperCP Collab.)
BARBOSA	00	PR D61 031101R	R.F. Barbosa <i>et al.</i>	(FNAL E761 Collab.)
TIMM	95	PR D51 4638	S. Timm <i>et al.</i>	(FNAL E761 Collab.)
MORELOS	93	PRL 71 3417	A. Morelos <i>et al.</i>	(FNAL E761 Collab.)
FOUCHER	92	PRL 68 3004	M. Foucher <i>et al.</i>	(FNAL E761 Collab.)
HESSEY	89	ZPHY C42 175	N.P. Hessey <i>et al.</i>	(BNL-811 Collab.)
KOBAYASHI	87	PRL 59 868	M. Kobayashi <i>et al.</i>	(KYOT)
WILKINSON	87	PRL 58 855	C.A. Wilkinson <i>et al.</i>	(WISC, MICH, RUTG+)
BIAGI	85	ZPHY C28 495	S.F. Biagi <i>et al.</i>	(CERN WA62 Collab.)
ANKENBRA...	83	PRL 51 863	C.M. Ankenbrandt <i>et al.</i>	(FNAL, IOWA, ISU+)
MANZ	80	PL 96B 217	A. Manz <i>et al.</i>	(MPIM, VAND)
MARRAFFINO	80	PR D21 2501	J. Marraffino <i>et al.</i>	(VAND, MPIM)
NOWAK	78	NP B139 61	R.J. Nowak <i>et al.</i>	(LOUC, BELG, DURH+)
CONFORTO	76	NP B105 189	B. Conforto <i>et al.</i>	(RHEL, LOUC)
EBENHOH	74	ZPHY 264 367	H. Ebenhoh <i>et al.</i>	(HEIDT)
EBENHOH	73	ZPHY 264 413	W. Ebenhoh <i>et al.</i>	(HEIDT)
LIPMAN	73	PL 43B 89	N.H. Lipman <i>et al.</i>	(RHEL, SUSS, LOWC)
PDG	73	RMP 45 51	T.A. Lasinski <i>et al.</i>	(LBL, BRAN, CERN+)
SECHI-ZORN	73	PR D8 12	B. Sechi-Zorn, G.A. Snow	(UMD)
BELLAMY	72	PL 39B 299	E.H. Bellamy <i>et al.</i>	(LOWC, RHEL, SUSS)
BOHM	72	NP B48 1	G. Bohm <i>et al.</i>	(BERL, KIDR, BRUX, IASD+)
Also		IIHE-73.2 Nov	G. Bohm	(BERL, KIDR, BRUX, IASD+)
COLE	71	PR D4 631	J. Cole <i>et al.</i>	(STON, COLU)
TOWEE	71	NP B33 493	D.W. Towe <i>et al.</i>	(LOUC, KIDR, BERL+)
BERLEY	70B	PR D1 2015	D. Berley <i>et al.</i>	(BNL, MASA, YALE)
EISELE	70	ZPHY 238 372	F. Eisele <i>et al.</i>	(HEID)
HARRIS	70	PRL 24 165	F. Harris <i>et al.</i>	(MICH, WISC)
PDG	70	RMP 42 87	A. Barbaro-Gatti <i>et al.</i>	(LRL, BRAN+)
ANG	69B	ZPHY 228 151	G. Ang <i>et al.</i>	(HEID)
BAGGETT	69B	Thesis MDDP-TR-973	N.V. Baggett	(UMD)
BALTAY	69	PRL 22 615	C. Baltay <i>et al.</i>	(COLU, STON)
BANGERTER	69	Thesis UCRL 19244	R.O. Bangenter	(LRL)
BANGERTER	69B	PR 187 1821	R.O. Bangenter <i>et al.</i>	(LRL)
BARLOUTAUD	69	NP B14 153	R. Barloutaud <i>et al.</i>	(SACL, CERN, HEID)
EISELE	69	ZPHY 221 1	F. Eisele <i>et al.</i>	(HEID)
Also		PRL 13 291	W. Willis <i>et al.</i>	(BNL, CERN, HEID, UMD)
EISELE	69B	ZPHY 221 401	F. Eisele <i>et al.</i>	(HEID)
GERSHWIN	69B	PR 188 2077	L.K. Gershwin <i>et al.</i>	(LRL)
Also		Thesis UCRL 19246	L.K. Gershwin	(LRL)
NORTON	69	Thesis Nevis 175	H. Norton	(COLU)
BAGGETT	67	PRL 19 1458	N. Baggett <i>et al.</i>	(UMD)
Also		Vienna Abs. 374	N.V. Baggett, B. Kehoe	(UMD)
Also		Private Comm.	N.V. Baggett	(UMD)
BARASH	67	PRL 19 181	N. Barash <i>et al.</i>	(UMD)
EISELE	67	ZPHY 205 409	F. Eisele <i>et al.</i>	(HEID)
HYMAN	67	PL 25B 376	L.G. Hyman <i>et al.</i>	(ANL, CMU, IWES)
PDG	67	RMP 39 1	A.H. Rosenthal <i>et al.</i>	(LRL, CERN, YALE)
CHANG	66	PR 151 1081	C.Y. Chang	(COLU)
Also		Thesis Nevis 145	C.Y. Chang	(COLU)
BAZIN	65	PRL 14 154	M. Bazin <i>et al.</i>	(PRIN, COLU)
BAZIN	65B	PR 140B 1358	M. Bazin <i>et al.</i>	(PRIN, RUTG, COLU)
SCHMIDT	65	PR 140B 1328	P. Schmidt	(COLU)
BHOWMIK	64	NP 53 22	B. Bhowmik <i>et al.</i>	(DELH)
COURANT	64	PR 136 B1791	H. Courant <i>et al.</i>	(CERN, HEID, UMD+)
NAUENBERG	64	PRL 12 679	U. Nauenberg <i>et al.</i>	(COLU, RUTG, PRIN)
BARKAS	63	PRL 11 26	W.H. Barkas, J.N. Dyer, H.H. Heckman	(LRL)
Also		Thesis UCRL 9450	J.N. Dyer	(LRL)
GALTIERI	62	PRL 9 24	A. Barbaro-Gatti <i>et al.</i>	(LRL)
HUMPHREY	62	PR 127 1305	W.E. Humphrey, R.R. Ross	(LRL)

Σ^0

$I(J^P) = 1(\frac{1}{2}^+)$ Status: ***

COURANT 63 and ALFF-STEINBERGER 65, using $\Sigma^0 \rightarrow \Lambda e^+ e^-$ decays (Dalitz decays), determined the Σ^0 parity to be positive, given that $J = 1/2$ and that certain very reasonable assumptions about form factors are true. The results of experiments involving the Primakoff effect, from which the Σ^0 mean life and $\Sigma^0 \rightarrow \Lambda$ transition magnetic moment come (see below), strongly support $J = 1/2$.

Σ^0 MASS

The fit uses $\Sigma^+, \Sigma^0, \Sigma^-,$ and Λ mass and mass-difference measurements.

VALUE (MeV)	EVTS	DOCUMENT ID	TECN	COMMENT
1192.642 ± 0.024 OUR FIT				

••• We do not use the following data for averages, fits, limits, etc. •••
 1192.65 ± 0.020 ± 0.014 3327 ¹ WANG 97 SPEC $\Sigma^0 \rightarrow \Lambda \gamma \rightarrow (p\pi^-)(e^+e^-)$

¹ This WANG 97 result is redundant with the Σ^0 - Λ mass-difference measurement below.

$m_{\Sigma^-} - m_{\Sigma^0}$

VALUE (MeV)	EVTS	DOCUMENT ID	TECN	COMMENT
4.807 ± 0.035 OUR FIT	Error			includes scale factor of 1.1.
4.86 ± 0.08 OUR AVERAGE	Error			includes scale factor of 1.2.
4.87 ± 0.12	37	DOSCH 65	HBC	
5.01 ± 0.12	12	SCHMIDT 65	HBC	See note with Λ mass
4.75 ± 0.1	18	BURNSTEIN 64	HBC	

$m_{\Sigma^0} - m_{\Lambda}$

VALUE (MeV)	EVTS	DOCUMENT ID	TECN	COMMENT
76.959 ± 0.023 OUR FIT				
76.966 ± 0.020 ± 0.013	3327	WANG 97	SPEC	$\Sigma^0 \rightarrow \Lambda \gamma \rightarrow (p\pi^-)(e^+e^-)$

••• We do not use the following data for averages, fits, limits, etc. •••

76.23 ± 0.55	109	COLAS	75	HLBC	$\Sigma^0 \rightarrow \Lambda \gamma$
76.63 ± 0.28	208	SCHMIDT	65	HBC	See note with Λ mass

Σ^0 MEAN LIFE

These lifetimes are deduced from measurements of the cross sections for the Primakoff process $\Lambda \rightarrow \Sigma^0$ in nuclear Coulomb fields. An alternative expression of the same information is the Σ^0 - Λ transition magnetic moment given in the following section. The relation is $(\mu_{\Sigma\Lambda}/\mu_N)^2 \tau = 1.92951 \times 10^{-19}$ s (see DEVLIN 86).

VALUE (10^{-20} s)	DOCUMENT ID	TECN	COMMENT
7.4 ± 0.7 OUR EVALUATION	Using $\mu_{\Sigma\Lambda}$ (see the above note).		
6.5 ^{+1.7} _{-1.1}	² DEVLIN	86	SPEC Primakoff effect
7.6 ± 0.5 ± 0.7	³ PETERSEN	86	SPEC Primakoff effect
••• We do not use the following data for averages, fits, limits, etc. •••			
5.8 ± 1.3	² DYDAK	77	SPEC See DEVLIN 86
² DEVLIN 86 is a recalculation of the results of DYDAK 77 removing a numerical approximation made in that work.			
³ An additional uncertainty of the Primakoff formalism is estimated to be < 5%.			

$|\mu(\Sigma^0 \rightarrow \Lambda)|$ TRANSITION MAGNETIC MOMENT

See the note in the Σ^0 mean-life section above. Also, see the "Note on Baryon Magnetic Moments" in the Λ Listings.

VALUE (μ_N)	DOCUMENT ID	TECN	COMMENT
1.61 ± 0.08 OUR AVERAGE			
1.72 ^{+0.17} _{-0.19}	⁴ DEVLIN	86	SPEC Primakoff effect
1.59 ± 0.05 ± 0.07	⁵ PETERSEN	86	SPEC Primakoff effect
••• We do not use the following data for averages, fits, limits, etc. •••			
1.82 ^{+0.25} _{-0.18}	⁴ DYDAK	77	SPEC See DEVLIN 86
⁴ DEVLIN 86 is a recalculation of the results of DYDAK 77 removing a numerical approximation made in that work.			
⁵ An additional uncertainty of the Primakoff formalism is estimated to be < 2.5%.			

Σ^0 DECAY MODES

Mode	Fraction (Γ_i/Γ)	Confidence level
$\Gamma_1 \Lambda \gamma$	100 %	
$\Gamma_2 \Lambda \gamma \gamma$	< 3 %	90%
$\Gamma_3 \Lambda e^+ e^-$	[a] 5 × 10 ⁻³	

[a] A theoretical value using QED.

Σ^0 BRANCHING RATIOS

$\Gamma(\Lambda \gamma \gamma)/\Gamma_{total}$	Γ_2/Γ		
VALUE	CL%	DOCUMENT ID	TECN
< 0.03	90	COLAS	75 HLBC
$\Gamma(\Lambda e^+ e^-)/\Gamma_{total}$	Γ_3/Γ		
See COURANT 63 and ALFF-STEINBERGER 65 for measurements of the invariant-mass spectrum of the Dalitz pairs.			
VALUE	DOCUMENT ID	COMMENT	
0.00545	FEINBERG 58	Theoretical QED calculation	

Σ^0 REFERENCES

WANG	97	PR D56 2544	M.H.L.S. Wang <i>et al.</i>	(BNL-E766 Collab.)
DEVLIN	86	PR D34 1626	T. Devlin, P.C. Petersen, A. Beretvas	(RUTG)
PETERSEN	86	PRL 57 949	P.C. Petersen <i>et al.</i>	(RUTG, WISC, MICH+)
DYDAK	77	NP B118 1	F. Dydak <i>et al.</i>	(CERN, DORT, HEID)
COLAS	75	NP B91 253	J. Colas <i>et al.</i>	(ORSAY)
ALFF-...	65	PR 137 B1105	C. Alff-Steinberger <i>et al.</i>	(COLU, RUTG+)
DOSCH	65	PL 14 239	H.C. Dorsch <i>et al.</i>	(HEID)
SCHMIDT	65	PR 140B 1328	P. Schmidt	(COLU)
BURNSTEIN	64	PRL 13 66	R.A. Burnstein <i>et al.</i>	(UMD)
COURANT	63	PRL 10 409	H. Courant <i>et al.</i>	(CERN, UMD)
FEINBERG	58	PR 109 1019	G. Feinberg	(BNL)

Baryon Particle Listings

Σ^-



$I(J^P) = 1(\frac{1}{2}^+)$ Status: * * * *

We have omitted some results that have been superseded by later experiments. See our earlier editions.

Σ^- MASS

The fit uses Σ^+ , Σ^0 , Σ^- , and Λ mass and mass-difference measurements.

VALUE (MeV)	EVTS	DOCUMENT ID	TECN	COMMENT
1197.449 ± 0.030 OUR FIT				Error includes scale factor of 1.2.
1197.45 ± 0.04 OUR AVERAGE				Error includes scale factor of 1.2.
1197.417 ± 0.040		GUREV 93	SPEC	Σ^- C atom, crystal diff.
1197.532 ± 0.057		GALL 88	CNTR	Σ^- Pb, Σ^- W atoms
1197.43 ± 0.08	3000	SCHMIDT 65	HBC	See note with Λ mass
• • • We do not use the following data for averages, fits, limits, etc. • • •				
1197.24 ± 0.15	1	DUGAN 75	CNTR	Exotic atoms
¹ GALL 88 concludes that the DUGAN 75 mass needs to be reevaluated.				

$m_{\Sigma^-} - m_{\Sigma^+}$

VALUE (MeV)	EVTS	DOCUMENT ID	TECN	COMMENT
8.08 ± 0.08 OUR FIT				Error includes scale factor of 1.9.
8.09 ± 0.16 OUR AVERAGE				
7.91 ± 0.23	86	BOHM 72	EMUL	
8.25 ± 0.25	2500	DOSCH 65	HBC	
8.25 ± 0.40	87	BARKAS 63	EMUL	

$m_{\Sigma^-} - m_{\Lambda}$

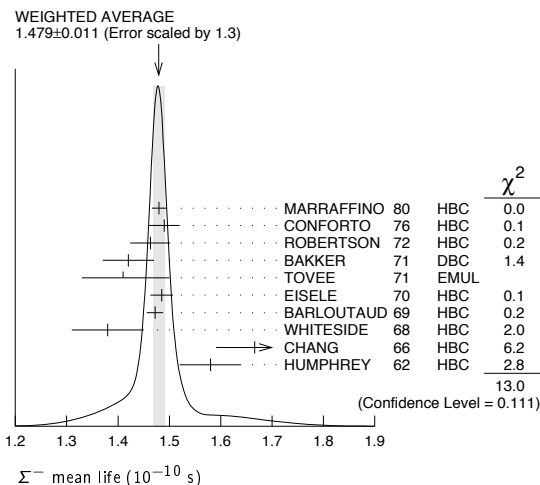
VALUE (MeV)	EVTS	DOCUMENT ID	TECN	COMMENT
81.766 ± 0.030 OUR FIT				Error includes scale factor of 1.2.
81.69 ± 0.07 OUR AVERAGE				
81.64 ± 0.09	2279	HEPP 68	HBC	
81.80 ± 0.13	85	SCHMIDT 65	HBC	See note with Λ mass
81.70 ± 0.19		BURNSTEIN 64	HBC	

Σ^- MEAN LIFE

Measurements with an error $\geq 0.2 \times 10^{-10}$ s have been omitted.

VALUE (10^{-10} s)	EVTS	DOCUMENT ID	TECN	COMMENT
1.479 ± 0.011 OUR AVERAGE				Error includes scale factor of 1.3. See the ideogram below.
1.480 ± 0.014	16k	MARRAFFINO 80	HBC	$K^- p$ 0.42–0.5 GeV/c
1.49 ± 0.03	8437	CONFORTO 76	HBC	$K^- p$ 1–1.4 GeV/c
1.463 ± 0.039	2400	ROBERTSON 72	HBC	$K^- p$ 0.25 GeV/c
1.42 ± 0.05	1383	BAKKER 71	DBC	$K^- N \rightarrow \Sigma^- \pi \pi$
1.41 ^{+0.09} / _{-0.08}		TOVEE 71	EMUL	
1.485 ± 0.022	100k	EISELE 70	HBC	$K^- p$ at rest
1.472 ± 0.016	10k	BARLOUTAUD 69	HBC	$K^- p$ 0.4–1.2 GeV/c
1.38 ± 0.07	506	WHITESIDE 68	HBC	$K^- p$ at rest
1.666 ± 0.075	3267	² CHANG 66	HBC	$K^- p$ at rest
1.58 ± 0.06	1208	HUMPHREY 62	HBC	$K^- p$ at rest

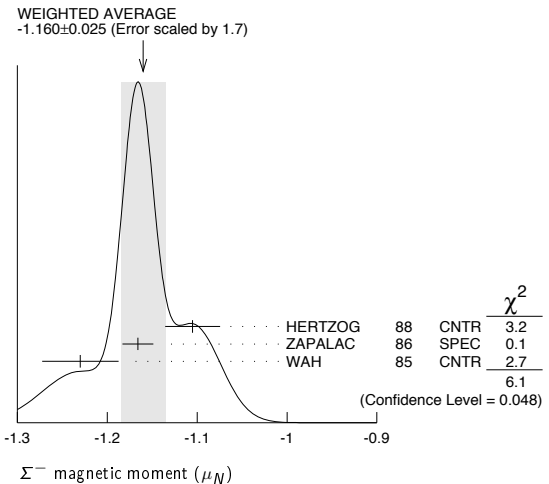
²We have increased the CHANG 66 error of 0.026; see our 1970 edition, Reviews of Modern Physics **42** 87 (1970).



Σ^- MAGNETIC MOMENT

See the "Note on Baryon Magnetic Moments" in the Λ Listings. Measurements with an error $\geq 0.3 \mu_N$ have been omitted.

VALUE (μ_N)	EVTS	DOCUMENT ID	TECN	COMMENT
-1.160 ± 0.025 OUR AVERAGE				Error includes scale factor of 1.7. See the ideogram below.
-1.105 ± 0.029 ± 0.010		HERTZOG 88	CNTR	Σ^- Pb, Σ^- W atoms
-1.166 ± 0.014 ± 0.010	671k	ZAPALAC 86	SPEC	$n e^- \nu, n \pi^-$ decays
-1.23 ± 0.03 ± 0.03		WAH 85	CNTR	ρ Cu $\rightarrow \Sigma^- X$
• • • We do not use the following data for averages, fits, limits, etc. • • •				
-0.89 ± 0.14	516k	DECK 83	SPEC	ρ Be $\rightarrow \Sigma^- X$



Σ^- CHARGE RADIUS

VALUE (fm)	DOCUMENT ID	TECN	COMMENT
0.780 ± 0.080 ± 0.060	³ ESCHRICH 01	SELX	$\Sigma^- e \rightarrow \Sigma^- e$
³ ESCHRICH 01 actually gives $\langle r^2 \rangle = (0.61 \pm 0.12 \pm 0.09) \text{ fm}^2$.			

Σ^- DECAY MODES

Mode	Fraction (Γ_i/Γ)
Γ_1 $n \pi^-$	(99.848 ± 0.005) %
Γ_2 $n \pi^- \gamma$	[a] (4.6 ± 0.6) × 10 ⁻⁴
Γ_3 $n e^- \bar{\nu}_e$	(1.017 ± 0.034) × 10 ⁻³
Γ_4 $n \mu^- \bar{\nu}_\mu$	(4.5 ± 0.4) × 10 ⁻⁴
Γ_5 $\Lambda e^- \bar{\nu}_e$	(5.73 ± 0.27) × 10 ⁻⁵

[a] See the Listings below for the pion momentum range used in this measurement.

CONSTRAINED FIT INFORMATION

An overall fit to 3 branching ratios uses 16 measurements and one constraint to determine 4 parameters. The overall fit has a $\chi^2 = 8.7$ for 13 degrees of freedom.

The following *off-diagonal* array elements are the correlation coefficients $\langle \delta x_i \delta x_j \rangle / (\delta x_i \delta x_j)$, in percent, from the fit to the branching fractions, $x_i \equiv \Gamma_i / \Gamma_{\text{total}}$. The fit constrains the x_i whose labels appear in this array to sum to one.

x_3	-64		
x_4	-77	0	
x_5	-5	0	0
	x_1	x_3	x_4

Σ^- BRANCHING RATIOS

$\Gamma(n \pi^- \gamma) / \Gamma(n \pi^-)$ Γ_2 / Γ_1
 The π^+ momentum cuts differ, so we do not average the results but simply use the latest value for the Summary Table.

VALUE (units 10^{-3})	EVTS	DOCUMENT ID	TECN	COMMENT
0.46 ± 0.06	292	EBENHOH 73	HBC	$\pi^+ < 150 \text{ MeV}/c$
• • • We do not use the following data for averages, fits, limits, etc. • • •				
0.10 ± 0.02	23	ANG 69B	HBC	$\pi^+ < 110 \text{ MeV}/c$
~ 1.1		BAZIN 65B	HBC	$\pi^+ < 166 \text{ MeV}/c$

See key on page 405

Baryon Particle Listings

Σ^-

$\Gamma(n e^- \bar{\nu}_e) / \Gamma(n \pi^-)$ Γ_3 / Γ_1

Measurements with an error $\geq 0.2 \times 10^{-3}$ have been omitted.

VALUE (units 10^{-3})	EVTS	DOCUMENT ID	TECN	COMMENT
1.019 ± 0.035 OUR FIT				
1.019 ± 0.031 OUR AVERAGE				
0.96 ± 0.05	2847	BOURQUIN	83c	SPEC SPS hyperon beam
$1.09 \begin{matrix} +0.06 \\ -0.08 \end{matrix}$	601	⁴ EBENHOH	74	HBC $K^- p$ at rest
$1.05 \begin{matrix} +0.07 \\ -0.13 \end{matrix}$	455	⁴ SECHI-ZORN	73	HBC $K^- p$ at rest
0.97 ± 0.15	57	COLE	71	HBC $K^- p$ at rest
1.11 ± 0.09	180	BIERMAN	68	HBC

⁴ An additional negative systematic error is included for internal radiative corrections and latest form factors; see BOURQUIN 83c.

$\Gamma(n \mu^- \bar{\nu}_\mu) / \Gamma(n \pi^-)$ Γ_4 / Γ_1

VALUE (units 10^{-3})	EVTS	DOCUMENT ID	TECN	COMMENT
0.45 ± 0.04 OUR FIT				
0.45 ± 0.04 OUR AVERAGE				
0.38 ± 0.11	13	COLE	71	HBC $K^- p$ at rest
0.43 ± 0.06	72	ANG	69	HBC $K^- p$ at rest
0.43 ± 0.09	56	BAGGETT	69	HBC $K^- p$ at rest
0.56 ± 0.20	11	BAZIN	65B	HBC $K^- p$ at rest
0.66 ± 0.15	22	COURANT	64	HBC

$\Gamma(\Lambda e^- \bar{\nu}_e) / \Gamma(n \pi^-)$ Γ_5 / Γ_1

VALUE (units 10^{-4})	EVTS	DOCUMENT ID	TECN	COMMENT
0.574 ± 0.027 OUR FIT				
0.574 ± 0.027 OUR AVERAGE				
0.561 ± 0.031	1620	⁵ BOURQUIN	82	SPEC SPS hyperon beam
0.63 ± 0.11	114	THOMPSON	80	ASPK Hyperon beam
0.52 ± 0.09	31	BALTAY	69	HBC $K^- p$ at rest
0.69 ± 0.12	31	EISELE	69	HBC $K^- p$ at rest
0.64 ± 0.12	35	BARASH	67	HBC $K^- p$ at rest
0.75 ± 0.28	11	COURANT	64	HBC $K^- p$ at rest

⁵ The value is from BOURQUIN 83b, and includes radiation corrections and new acceptance.

Σ^- DECAY PARAMETERS

See the "Note on Baryon Decay Parameters" in the neutron Listings. Older, outdated results have been omitted.

α_- FOR $\Sigma^- \rightarrow n \pi^-$

VALUE	EVTS	DOCUMENT ID	TECN	COMMENT
-0.068 ± 0.008 OUR AVERAGE				
-0.062 ± 0.024	28k	HANSL	78	HBC $K^- p \rightarrow \Sigma^- \pi^+$
-0.067 ± 0.011	60k	BOGERT	70	HBC $K^- p$ 0.4 GeV/c
-0.071 ± 0.012	51k	BANGERTER	69	HBC $K^- p$ 0.4 GeV/c

ϕ ANGLE FOR $\Sigma^- \rightarrow n \pi^-$ ($\tan \phi = \beta / \gamma$)

VALUE ($^\circ$)	EVTS	DOCUMENT ID	TECN	COMMENT
10 ± 15 OUR AVERAGE				
$+5 \pm 23$	1092	⁶ BERLEY	70B	HBC n rescattering
14 ± 19	1385	BANGERTER	69B	HBC $K^- p$ 0.4 GeV/c

⁶ BERLEY 70b changed from -5 to $+5^\circ$ to agree with our sign convention.

g_A/g_V FOR $\Sigma^- \rightarrow n e^- \bar{\nu}_e$

Measurements with fewer than 500 events have been omitted. Where necessary, signs have been changed to agree with our conventions, which are given in the "Note on Baryon Decay Parameters" in the neutron Listings. What is actually listed is $|g_1/f_1 - 0.237g_2/f_1|$. This reduces to $g_A/g_V \equiv g_1(0)/f_1(0)$ on making the usual assumption that $g_2 = 0$. See also the note on HSUEH 88.

VALUE	EVTS	DOCUMENT ID	TECN	COMMENT
0.340 ± 0.017 OUR AVERAGE				
$+0.327 \pm 0.007 \pm 0.019$	50k	⁷ HSUEH	88	SPEC Σ^- 250 GeV
$+0.34 \pm 0.05$	4456	⁸ BOURQUIN	83c	SPEC SPS hyperon beam
0.385 ± 0.037	3507	⁹ TANENBAUM	74	ASPK

• • • We do not use the following data for averages, fits, limits, etc. • • •

0.29 ± 0.07	25k	HSUEH	85	SPEC See HSUEH 88
$0.17 \begin{matrix} +0.07 \\ -0.09 \end{matrix}$	519	DECAMP	77	ELEC Hyperon beam

⁷ The sign is, with our conventions, unambiguously positive. The value assumes, as usual, that $g_2 = 0$. If g_2 is included in the fit, than (with our sign convention) $g_2 = -0.56 \pm 0.37$, with a corresponding reduction of g_A/g_V to $+0.20 \pm 0.08$.

⁸ BOURQUIN 83c favors the positive sign by at least 2.6 standard deviations.

⁹ TANENBAUM 74 gives 0.435 ± 0.035 , assuming no q^2 dependence in g_A and g_V . The listed result allows q^2 dependence, and is taken from HSUEH 88.

$f_2(0)/f_1(0)$ FOR $\Sigma^- \rightarrow n e^- \bar{\nu}_e$

The signs have been changed to be in accord with our conventions, given in the "Note on Baryon Decay Parameters" in the neutron Listings.

VALUE	EVTS	DOCUMENT ID	TECN	COMMENT
0.97 ± 0.14 OUR AVERAGE				
$+0.96 \pm 0.07 \pm 0.13$	50k	HSUEH	88	SPEC Σ^- 250 GeV
$+1.02 \pm 0.34$	4456	BOURQUIN	83c	SPEC SPS hyperon beam

TRIPLE CORRELATION COEFFICIENT D FOR $\Sigma^- \rightarrow n e^- \bar{\nu}_e$

The coefficient D of the term $D \mathbf{P}(\hat{p}_e \times \hat{p}_\nu)$ in the $\Sigma^- \rightarrow n e^- \bar{\nu}$ decay angular distribution. A nonzero value would indicate a violation of time-reversal invariance.

VALUE	EVTS	DOCUMENT ID	TECN	COMMENT
0.11 ± 0.10	50k	HSUEH	88	SPEC Σ^- 250 GeV

g_V/g_A FOR $\Sigma^- \rightarrow \Lambda e^- \bar{\nu}_e$

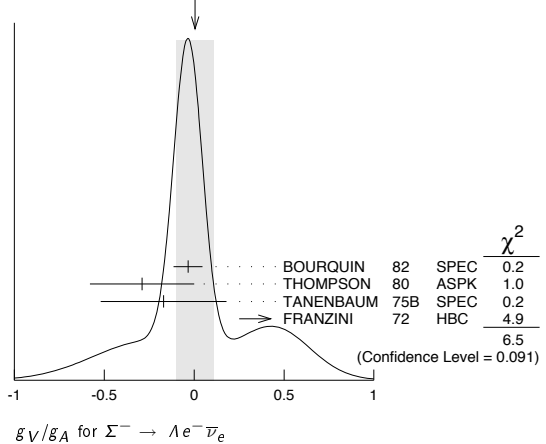
For the sign convention, see the "Note on Baryon Decay Parameters" in the neutron Listings. The value is predicted to be zero by conserved vector current theory. The values averaged assume CVC-SU(3) weak magnetism term.

VALUE	EVTS	DOCUMENT ID	TECN	COMMENT
0.01 ± 0.10 OUR AVERAGE				Error includes scale factor of 1.5. See the ideogram below.
-0.034 ± 0.080	1620	¹⁰ BOURQUIN	82	SPEC SPS hyperon beam
-0.29 ± 0.29	114	THOMPSON	80	ASPK BNL hyperon beam
-0.17 ± 0.35	55	TANENBAUM	75B	SPEC BNL hyperon beam
$+0.45 \pm 0.20$	186	^{10,11} FRANZINI	72	HBC

¹⁰ The sign has been changed to agree with our convention.

¹¹ The FRANZINI 72 value includes the events of earlier papers.

WEIGHTED AVERAGE
 0.01 ± 0.10 (Error scaled by 1.5)



g_{WM}/g_A FOR $\Sigma^- \rightarrow \Lambda e^- \bar{\nu}_e$

The values quoted assume the CVC prediction $g_V = 0$.

VALUE	EVTS	DOCUMENT ID	TECN	COMMENT
2.4 ± 1.7 OUR AVERAGE				
1.75 ± 3.5	114	THOMPSON	80	ASPK BNL hyperon beam
3.5 ± 4.5	55	TANENBAUM	75B	SPEC BNL hyperon beam
2.4 ± 2.1	186	FRANZINI	72	HBC

Σ^- REFERENCES

We have omitted some papers that have been superseded by later experiments. See our earlier editions.

ESCHRICH	01	PL B522 233	I. Eschrich et al.	(FNAL SELEX Collab.)
GUREV	93	JETPL 57 400	M.P. Gurev et al.	(PNPI)
		Translated from ZETFP 57 383.		
GALL	88	PRL 60 186	K.P. Gall et al.	(BOST, MIT, WILL, CIT+)
HERTZOG	88	PR D37 1142	D.W. Hertzog et al.	(WILL, BOST, MIT+)
HSUEH	88	PR D38 2056	S.Y. Hsueh et al.	(CHIC, ELMT, FNAL+)
ZAPALAC	86	PRL 57 1526	G. Zapalac et al.	(EFI, ELMT, FNAL+)
HSUEH	85	PRL 54 2399	S.Y. Hsueh et al.	(CHIC, ELMT, FNAL+)
WAH	85	PRL 55 2551	Y.W. Wah et al.	(FNAL, IOWA, ISU)
BOURQUIN	83B	ZPHY C21 27	M.H. Bourquin et al.	(BRIS, GEVA, HEIDP+)
BOURQUIN	83C	ZPHY C21 17	M.H. Bourquin et al.	(BRIS, GEVA, HEIDP+)
DECK	83	PR D28 1	L. Deck et al.	(RUTG, WBS C, MICH, MINN)
BOURQUIN	82	ZPHY C12 307	M.H. Bourquin et al.	(BRIS, GEVA, HEIDP+)
MARRAFFINO	80	PR D21 2501	J. Marraffino et al.	(VAND, MFRIM)
THOMPSON	80	PR D21 25	J.A. Thompson et al.	(PITT, BNL)
HANSL	78	NP B132 45	T. Hansl et al.	(MPIM, VAND)
DECAMP	77	PL 66B 295	D. Decamp et al.	(LALO, EPOL)
CONFORTO	76	NP B105 189	B. Conforto et al.	(RHEL, LOIC)
DUGAN	75	NP A254 396	G. Dugan et al.	(COLU, YALE)
TANENBAUM	75B	PR D12 1871	W. Tanenbaum et al.	(YALE, FNAL, BNL)
EBENHOH	74	ZPHY 266 367	H. Ebenhoeh et al.	(HEIDT)
TANENBAUM	74	PRL 33 175	W. Tanenbaum et al.	(YALE, FNAL, BNL)
EBENHOH	73	ZPHY 264 413	W. Ebenhoeh et al.	(HEIDT)
SECHI-ZORN	73	PR D8 12	B. Sechi-Zorn, G.A. Snow	(UMD)
BOHM	72	NP B48 1	G. Bohm et al.	(BERL, KIDR, BRUX, IASD+)
FRANZINI	72	PR D6 2417	P. Franzini et al.	(COLU, HEID, UMD+)
ROBERTSON	72	Thesis UMI 78-00877	R.M. Robertson	(IIT)
BAKKER	71	LCN 1 37	A.M. Bakker et al.	(SABRE Collab.)
COLE	71	PR D4 631	J. Cole et al.	(STON, COLU)
		Also Thesis Nevis 175	H. Norton	(COLU)
TOVEE	71	NP B33 493	D.N. Tovee et al.	(LOUC, KIDR, BERL+)
BERLEY	70B	PR D1 2015	D. Berley et al.	(BNL, MASA, YALE)
BOGERT	70	PR D2 6	D.V. Bogert et al.	(BNL, MASA, YALE)
EISELE	70	ZPHY 238 372	F. Eisele et al.	(HEID)
PDG	70	RMP 42 87	A. Barbaro-Gatti et al.	(LRL, BRAN+)
ANG	69	ZPHY 223 103	G. Ang et al.	(HEID)
ANG	69B	ZPHY 228 151	G. Ang et al.	(HEID)

Baryon Particle Listings

$\Sigma^-, \Sigma(1385)$

BAGGETT 69	PRL 23 249	N.V. Baggett, B. Kehoe, G.A. Snow	(UMD)
BALTY 69	PRL 22 615	C. Balty <i>et al.</i>	(COLU, STON)
BANGERTER 69	Thesis UCRL 19244	R.O. Bangener	(LRL)
BANGERTER 69B	PR 187 1821	R.O. Bangener <i>et al.</i>	(LRL)
BARLOUTAUD 69	NP B14 153	R. Barloutaud <i>et al.</i>	(SACL, CERN, HEID)
EISELE 69	ZPHY 221 1	F. Eisele <i>et al.</i>	(HEID)
BIERMAN 68	PRL 20 1459	E. Bierman <i>et al.</i>	(PRIN)
HEPP 68	ZPHY 214 71	V. Hepp, H. Schleich	(HEID)
WHITESIDE 68	NC 54A 537	H. Whiteside, J. Gollub	(OBER)
BARASH 67	PRL 19 181	N. Barash <i>et al.</i>	(UMD)
CHANG 66	PR 151 1081	C.Y. Chang	(COLU)
BAZIN 65B	PR 140B 1358	M. Bazin <i>et al.</i>	(PRIN, RUTG, COLU)
DOSCH 65	PL 14 239	H.C. Dosch <i>et al.</i>	(HEID)
Also	PR 151 1081	C.Y. Chang	(COLU)
SCHMIDT 65	PR 140B 1328	P. Schmidt	(COLU)
BURNSTEIN 64	PRL 13 66	R.A. Burnstein <i>et al.</i>	(UMD)
COURANT 64	PR 136 B1791	H. Courant <i>et al.</i>	(CERN, HEID, UMD+)
BARKAS 63	PRL 11 26	W.H. Barkas, J.N. Dyer, H.H. Heckman	(LRL)
HUMPHREY 62	PR 127 1305	W.E. Humphrey, R.R. Ross	(LRL)

$\Sigma(1385) P_{13}$

$$I(J^P) = 1(\frac{3}{2}^+) \text{ Status: } ****$$

Discovered by ALSTON 60. Early measurements of the mass and width for combined charge states have been omitted. They may be found in our 1984 edition Reviews of Modern Physics **56** S1 (1984).

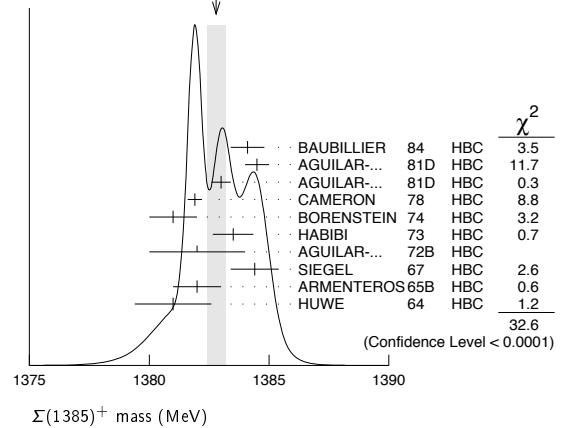
We average only the most significant determinations. We do not average results from inclusive experiments with large backgrounds or results which are not accompanied by some discussion of experimental resolution. Nevertheless systematic differences between experiments remain. (See the ideograms in the Listings below.) These differences could arise from interference effects that change with production mechanism and/or beam momentum. They can also be accounted for in part by differences in the parametrizations employed. (See BORENSTEIN 74 for a discussion on this point.) Thus BORENSTEIN 74 uses a Breit-Wigner with energy-independent width, since a P -wave was found to give unsatisfactory fits. CAMERON 78 uses the same form. On the other hand HOLMGREN 77 obtains a good fit to their $\Lambda\pi$ spectrum with a P -wave Breit-Wigner, but includes the partial width for the $\Sigma\pi$ decay mode in the parametrization. AGUILAR-BENITEZ 81D gives masses and widths for five different Breit-Wigner shapes. The results vary considerably. Only the best-fit S -wave results are given here.

$\Sigma(1385)$ MASSES

$\Sigma(1385)^+$ MASS

VALUE (MeV)	EVTS	DOCUMENT ID	TECN	COMMENT
1382.8 ± 0.4 OUR AVERAGE				Error includes scale factor of 2.0. See the ideogram below.
1384.1 ± 0.7	1897	BAUBILLIER 84	HBC	K^-p 8.25 GeV/c
1384.5 ± 0.5	5256	AGUILAR-... 81D	HBC	$K^-p \rightarrow \Lambda\pi\pi$ 4.2 GeV/c
1383.0 ± 0.4	9361	AGUILAR-... 81D	HBC	$K^-p \rightarrow \Lambda 3\pi$ 4.2 GeV/c
1381.9 ± 0.3	6900	CAMERON 78	HBC	K^-p 0.96-1.36 GeV/c
1381 ± 1	6846	BORENSTEIN 74	HBC	K^-p 2.18 GeV/c
1383.5 ± 0.85	2300	HABIBI 73	HBC	$K^-p \rightarrow \Lambda\pi\pi$
1382 ± 2	400	AGUILAR-... 72B	HBC	$K^-p \rightarrow \Lambda\pi$'s
1384.4 ± 1.0	1260	SIEGEL 67	HBC	K^-p 2.1 GeV/c
1382 ± 1	750	ARMENTEROS65B	HBC	K^-p 0.9-1.2 GeV/c
1381.0 ± 1.6	859	HUWE 64	HBC	K^-p 1.22 GeV/c
••• We do not use the following data for averages, fits, limits, etc. •••				
1385.1 ± 1.2	600	BAKER 80	HYBR	π^+p 7 GeV/c
1383.2 ± 1.0	750	BAKER 80	HYBR	K^-p 7 GeV/c
1381 ± 2	7k	¹ BAUBILLIER 79B	HBC	K^-p 8.25 GeV/c
1391 ± 2	2k	CAUTIS 79	HYBR	π^+p/K^-p 11.5 GeV
1390 ± 2	100	¹ SUGAHARA 79B	HBC	π^-p 6 GeV/c
1385 ± 3	22k	^{1,2} BARREIRO 77B	HBC	K^-p 4.2 GeV/c
1385 ± 1	2594	HOLMGREN 77	HBC	See AGUILAR-BENITEZ 81D
1380 ± 2		¹ BARDADIN-... 75	HBC	K^-p 14.3 GeV/c
1382 ± 1	3740	³ BERTHON 74	HBC	K^-p 1263-1843 MeV/c
1390 ± 6	46	AGUILAR-... 70B	HBC	$K^-p \rightarrow \Sigma\pi$'s 4 GeV/c
1383 ± 8	62	⁴ BIRMINGHAM 66	HBC	K^-p 3.5 GeV/c
1378 ± 5	135	LONDON 66	HBC	K^-p 2.24 GeV/c
1384.3 ± 1.9	250	⁴ SMITH 65	HBC	K^-p 1.8 GeV/c
1382.6 ± 2.1	250	⁴ SMITH 65	HBC	K^-p 1.95 GeV/c
1375.0 ± 3.9	170	COOPER 64	HBC	K^-p 1.45 GeV/c
1376.0 ± 3.9	154	⁴ ELY 61	HLBC	K^-p 1.11 GeV/c

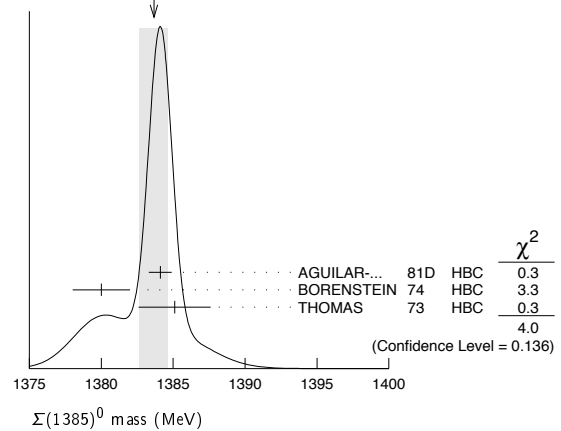
WEIGHTED AVERAGE
1382.8 ± 0.4 (Error scaled by 2.0)



$\Sigma(1385)^0$ MASS

VALUE (MeV)	EVTS	DOCUMENT ID	TECN	COMMENT
1383.7 ± 1.0 OUR AVERAGE				Error includes scale factor of 1.4. See the ideogram below.
1384.1 ± 0.8	5722	AGUILAR-... 81D	HBC	$K^-p \rightarrow \Lambda 3\pi$ 4.2 GeV/c
1380 ± 2	3100	⁵ BORENSTEIN 74	HBC	$K^-p \rightarrow \Lambda 3\pi$ 2.18 GeV/c
1385.1 ± 2.5	240	⁴ THOMAS 73	HBC	$\pi^-p \rightarrow \Lambda\pi^0 K^0$
••• We do not use the following data for averages, fits, limits, etc. •••				
1389 ± 3	500	⁶ BAUBILLIER 79B	HBC	K^-p 8.25 GeV/c

WEIGHTED AVERAGE
1383.7 ± 1.0 (Error scaled by 1.4)



$\Sigma(1385)^-$ MASS

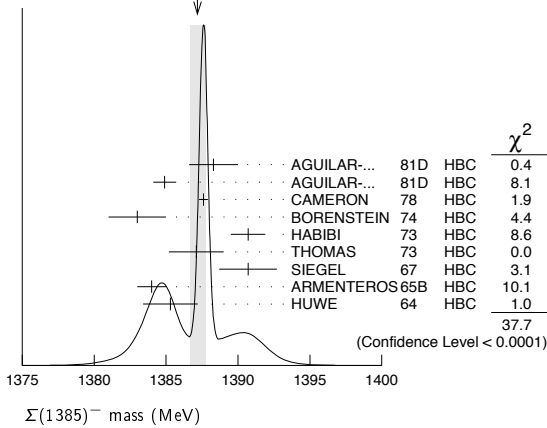
VALUE (MeV)	EVTS	DOCUMENT ID	TECN	COMMENT
1387.2 ± 0.5 OUR AVERAGE				Error includes scale factor of 2.2. See the ideogram below.
1388.3 ± 1.7	620	AGUILAR-... 81D	HBC	$K^-p \rightarrow \Lambda\pi\pi$ 4.2 GeV/c
1384.9 ± 0.8	3346	AGUILAR-... 81D	HBC	$K^-p \rightarrow \Lambda 3\pi$ 4.2 GeV/c
1387.6 ± 0.3	9720	CAMERON 78	HBC	K^-p 0.96-1.36 GeV/c
1383 ± 2	2303	BORENSTEIN 74	HBC	K^-p 2.18 GeV/c
1390.7 ± 1.2	1900	HABIBI 73	HBC	$K^-p \rightarrow \Lambda\pi\pi$
1387.1 ± 1.9	630	⁴ THOMAS 73	HBC	$\pi^-p \rightarrow \Lambda\pi^- K^+$
1390.7 ± 2.0	370	SIEGEL 67	HBC	K^-p 2.1 GeV/c
1384 ± 1	1380	ARMENTEROS65B	HBC	K^-p 0.9-1.2 GeV/c
1385.3 ± 1.9	1086	⁴ HUWE 64	HBC	K^-p 1.15-1.30 GeV/c
••• We do not use the following data for averages, fits, limits, etc. •••				
1383 ± 1	4.5k	¹ BAUBILLIER 79B	HBC	K^-p 8.25 GeV/c
1380 ± 6	150	¹ SUGAHARA 79B	HBC	π^-p 6 GeV/c
1387 ± 3	12k	^{1,2} BARREIRO 77B	HBC	K^-p 4.2 GeV/c
1391 ± 3	193	HOLMGREN 77	HBC	See AGUILAR-BENITEZ 81D
1383 ± 2		¹ BARDADIN-... 75	HBC	K^-p 14.3 GeV/c
1389 ± 1	3060	³ BERTHON 74	HBC	K^-p 1263-1843 MeV/c
1389 ± 9	15	LONDON 66	HBC	K^-p 2.24 GeV/c
1391.5 ± 2.6	120	⁴ SMITH 65	HBC	K^-p 1.8 GeV/c
1399.8 ± 2.2	58	⁴ SMITH 65	HBC	K^-p 1.95 GeV/c
1392.0 ± 6.2	200	COOPER 64	HBC	K^-p 1.45 GeV/c
1382 ± 3	93	DAHL 61	DBC	K^-d 0.45 GeV/c
1376.0 ± 4.4	224	⁴ ELY 61	HLBC	K^-p 1.11 GeV/c

See key on page 405

Baryon Particle Listings

$\Sigma(1385)$

WEIGHTED AVERAGE
1387.2±0.5 (Error scaled by 2.2)



$m_{\Sigma(1385)^-} - m_{\Sigma(1385)^+}$

VALUE (MeV)	CL%	DOCUMENT ID	TECN	COMMENT
••• We do not use the following data for averages, fits, limits, etc. •••				
- 2 to +6	95	7 BORENSTEIN 74	HBC	$K^- p$ 2.18 GeV/c
7.2±1.4		7 HABIBI 73	HBC	$K^- p \rightarrow \Lambda \pi \pi$
6.3±2.0		7 SIEGEL 67	HBC	$K^- p$ 2.1 GeV/c
11 ± 9		7 LONDON 66	HBC	$K^- p$ 2.24 GeV/c
9 ± 6		7 LONDON 66	HBC	Λ 3 π events
2.0±1.5		7 ARMENTEROS65B	HBC	$K^- p$ 0.9-1.2 GeV/c
7.2±2.1		7 SMITH 65	HBC	$K^- p$ 1.8 GeV/c
17.2±2.0		7 SMITH 65	HBC	$K^- p$ 1.95 GeV/c
17 ± 7		7 COOPER 64	HBC	$K^- p$ 1.45 GeV/c
4.3±2.2		7 HUWE 64	HBC	$K^- p$ 1.22 GeV/c
0.0±4.2		7 ELY 61	HLBC	$K^- p$ 1.11 GeV/c

$m_{\Sigma(1385)^0} - m_{\Sigma(1385)^+}$

VALUE (MeV)	CL%	DOCUMENT ID	TECN	COMMENT
••• We do not use the following data for averages, fits, limits, etc. •••				
-4 to +4	95	7 BORENSTEIN 74	HBC	$K^- p$ 2.18 GeV/c

$m_{\Sigma(1385)^-} - m_{\Sigma(1385)^0}$

VALUE (MeV)	DOCUMENT ID	TECN	COMMENT
••• We do not use the following data for averages, fits, limits, etc. •••			
2.0±2.4	7 THOMAS 73	HBC	$\pi^- p \rightarrow \Lambda \pi^- K^+$

$\Sigma(1385)$ WIDTHS

$\Sigma(1385)^+$ WIDTH

VALUE (MeV)	EVTS	DOCUMENT ID	TECN	COMMENT
35.8± 0.8 OUR AVERAGE				
37.2± 2.0	1897	BAUBILLIER 84	HBC	$K^- p$ 8.25 GeV/c
35.1± 1.7	5256	AGUILAR-... 81D	HBC	$K^- p \rightarrow \Lambda \pi \pi$ 4.2 GeV/c
37.5± 2.0	9361	AGUILAR-... 81D	HBC	$K^- p \rightarrow \Lambda$ 3 π 4.2 GeV/c
35.5± 1.9	6900	CAMERON 78	HBC	$K^- p$ 0.96-1.36 GeV/c
34.0± 1.6	6846	8 BORENSTEIN 74	HBC	$K^- p$ 2.18 GeV/c
38.3± 3.2	2300	9 HABIBI 73	HBC	$K^- p \rightarrow \Lambda \pi \pi$
32.5± 6.0	400	AGUILAR-... 72B	HBC	$K^- p \rightarrow \pi$'s
36 ± 4	1260	9 SIEGEL 67	HBC	$K^- p$ 2.1 GeV/c
32.0± 4.7	750	9 ARMENTEROS65B	HBC	$K^- p$ 0.95-1.20 GeV/c
46.5± 6.4	859	9 HUWE 64	HBC	$K^- p$ 1.15-1.30 GeV/c
••• We do not use the following data for averages, fits, limits, etc. •••				
40 ± 3	600	BAKER 80	HYBR	$\pi^+ p$ 7 GeV/c
37 ± 2	750	BAKER 80	HYBR	$K^- p$ 7 GeV/c
37 ± 2	7k	1 BAUBILLIER 79B	HBC	$K^- p$ 8.25 GeV/c
30 ± 4	2k	CAUTIS 79	HYBR	$\pi^+ p/K^- p$ 11.5 GeV
30 ± 6	100	1 SUGAHARA 79B	HBC	$\pi^- p$ 6 GeV/c
43 ± 5	22k	1,2 BARREIRO 77B	HBC	$K^- p$ 4.2 GeV/c
34 ± 2	2594	HOLMGREN 77	HBC	See AGUILAR-BENITEZ 81D
40.0± 3.2		1 BARDADIN-... 75	HBC	$K^- p$ 14.3 GeV/c
48 ± 3	3740	3 BERTHON 74	HBC	$K^- p$ 1263-1843 MeV/c
33 ± 20	46	9 AGUILAR-... 70B	HBC	$K^- p \rightarrow \Sigma \pi$'s 4 GeV/c
25 ± 32	62	9 BIRMINGHAM 66	HBC	$K^- p$ 3.5 GeV/c
30.3± 7.5	250	9 SMITH 65	HBC	$K^- p$ 1.8 GeV/c
33.1± 8.3	250	9 SMITH 65	HBC	$K^- p$ 1.95 GeV/c
51 ± 16	170	9 COOPER 64	HBC	$K^- p$ 1.45 GeV/c
48 ± 16	154	9 ELY 61	HLBC	$K^- p$ 1.11 GeV/c

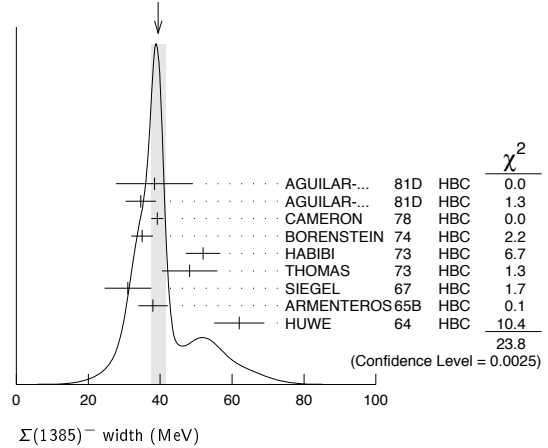
$\Sigma(1385)^0$ WIDTH

VALUE (MeV)	EVTS	DOCUMENT ID	TECN	COMMENT
36 ± 5 OUR AVERAGE				
34.8± 5.6	5722	AGUILAR-... 81D	HBC	$K^- p \rightarrow \Lambda$ 3 π 4.2 GeV/c
39.3± 10.2	240	9 THOMAS 73	HBC	$\pi^- p \rightarrow \Lambda \pi^0 K^0$
••• We do not use the following data for averages, fits, limits, etc. •••				
53 ± 8	3100	10 BORENSTEIN 74	HBC	$K^- p \rightarrow \Lambda$ 3 π 2.18 GeV/c
30 ± 9	106	CURTIS 63	OSPK	$\pi^- p$ 1.5 GeV/c

$\Sigma(1385)^-$ WIDTH

VALUE (MeV)	EVTS	DOCUMENT ID	TECN	COMMENT
39.4± 2.1 OUR AVERAGE				
Error includes scale factor of 1.7. See the ideogram below.				
38.4± 10.7	620	AGUILAR-... 81D	HBC	$K^- p \rightarrow \Lambda \pi \pi$ 4.2 GeV/c
34.6± 4.2	3346	AGUILAR-... 81D	HBC	$K^- p \rightarrow \Lambda$ 3 π 4.2 GeV/c
39.2± 1.7	9720	CAMERON 78	HBC	$K^- p$ 0.96-1.36 GeV/c
35 ± 3	2303	8 BORENSTEIN 74	HBC	$K^- p$ 2.18 GeV/c
51.9± 4.8	1900	9 HABIBI 73	HBC	$K^- p \rightarrow \Lambda \pi \pi$
48.2± 7.7	630	9 THOMAS 73	HBC	$\pi^- p \rightarrow \Lambda \pi^- K^0$
31.0± 6.5	370	9 SIEGEL 67	HBC	$K^- p$ 2.1 GeV/c
38.0± 4.1	1382	9 ARMENTEROS65B	HBC	$K^- p$ 0.95-1.20 GeV/c
62 ± 7	1086	HUWE 64	HBC	$K^- p$ 1.15-1.30 GeV/c
••• We do not use the following data for averages, fits, limits, etc. •••				
44 ± 4	4.5k	1 BAUBILLIER 79B	HBC	$K^- p$ 8.25 GeV/c
58 ± 4	150	1 SUGAHARA 79B	HBC	$\pi^- p$ 6 GeV/c
45 ± 5	12k	1,2 BARREIRO 77B	HBC	$K^- p$ 4.2 GeV/c
35 ± 10	193	HOLMGREN 77	HBC	See AGUILAR-BENITEZ 81D
47 ± 6		1 BARDADIN-... 75	HBC	$K^- p$ 14.3 GeV/c
40 ± 3	3060	3 BERTHON 74	HBC	$K^- p$ 1263-1843 MeV/c
29.2± 10.6	120	9 SMITH 65	HBC	$K^- p$ 1.80 GeV/c
17.1± 8.9	58	9 SMITH 65	HBC	$K^- p$ 1.95 GeV/c
88 ± 24	200	9 COOPER 64	HBC	$K^- p$ 1.45 GeV/c
40		DAHL 61	DBC	$K^- d$ 0.45 GeV/c
66 ± 18	224	9 ELY 61	HLBC	$K^- p$ 1.11 GeV/c

WEIGHTED AVERAGE
39.4±2.1 (Error scaled by 1.7)



$\Sigma(1385)$ POLE POSITIONS

$\Sigma(1385)^+$ REAL PART

VALUE	DOCUMENT ID	COMMENT
1379±1	LICHTENBERG74	Extrapolates HABIBI 73

$\Sigma(1385)^+$ -IMAGINARY PART

VALUE	DOCUMENT ID	COMMENT
17.5±1.5	LICHTENBERG74	Extrapolates HABIBI 73

$\Sigma(1385)^-$ REAL PART

VALUE	DOCUMENT ID	COMMENT
1383±1	LICHTENBERG74	Extrapolates HABIBI 73

$\Sigma(1385)^-$ -IMAGINARY PART

VALUE	DOCUMENT ID	COMMENT
22.5±1.5	LICHTENBERG74	Extrapolates HABIBI 73

Baryon Particle Listings

$\Sigma(1385)$, $\Sigma(1480)$ Bumps

$\Sigma(1385)$ DECAY MODES

Mode	Fraction (Γ_i/Γ)	Confidence level
$\Gamma_1 \Lambda\pi$	$(87.0 \pm 1.5)\%$	
$\Gamma_2 \Sigma\pi$	$(11.7 \pm 1.5)\%$	
$\Gamma_3 \Lambda\gamma$	$(1.3 \pm 0.4)\%$	
$\Gamma_4 \Sigma^-\gamma$	$< 2.4 \times 10^{-4}$	90%
$\Gamma_5 N\bar{K}$		

The above branching fractions are our estimates, not fits or averages.

$\Sigma(1385)$ BRANCHING RATIOS

$\Gamma(\Sigma\pi)/\Gamma(\Lambda\pi)$	Γ_2/Γ_1			
VALUE	DOCUMENT ID	TECN	CHG	COMMENT
0.135 ± 0.011 OUR AVERAGE				
0.20 ± 0.06	DIONISI	78B	HBC	\pm $K^-p \rightarrow Y^* K\bar{K}$
0.16 ± 0.03	BERTHON	74	HBC	$+$ K^-p 1.26–1.84 GeV/c
0.11 ± 0.02	BERTHON	74	HBC	$-$ K^-p 1.26–1.84 GeV/c
0.21 ± 0.05	BORENSTEIN	74	HBC	$+$ $K^-p \rightarrow \Lambda\pi^+\pi^-$, $\Sigma^0\pi^+\pi^-$
0.18 ± 0.04	MAST	73	MPWA	\pm $K^-p \rightarrow \Lambda\pi^+\pi^-$, $\Sigma^0\pi^+\pi^-$
0.10 ± 0.05	THOMAS	73	HBC	$-$ $\pi^-p \rightarrow \Lambda K\pi, \Sigma K\pi$
0.16 ± 0.07	AGUILAR...	72B	HBC	$+$ K^-p 3.9, 4.6 GeV/c
0.13 ± 0.04	COLLEY	71B	DBC	-0 K^-N 1.5 GeV/c
0.13 ± 0.04	PAN	69	HBC	$+$ $\pi^+p \rightarrow \Lambda K\pi, \Sigma K\pi$
0.08 ± 0.06	LONDON	66	HBC	$+$ K^-p 2.24 GeV/c
0.163 ± 0.041	ARMENTEROS65B	HBC	\pm	K^-p 0.95–1.20 GeV/c
0.09 ± 0.04	HUWE	64	HBC	\pm K^-p 1.2–1.7 GeV
• • • We do not use the following data for averages, fits, limits, etc. • • •				
<0.04	ALSTON	62	HBC	± 0 K^-p 1.15 GeV/c
0.04 ± 0.04	BASTIEN	61	HBC	\pm

$\Gamma(\Lambda\gamma)/\Gamma(\Lambda\pi)$	Γ_3/Γ_1				
VALUE (units 10^{-2})	CL%	EVTS	DOCUMENT ID	TECN	COMMENT
1.53 ± 0.39 ^{+0.15}/_{-0.24}		61	TAYLOR	05	CLAS $\gamma p \rightarrow K^+\Lambda\gamma$
• • • We do not use the following data for averages, fits, limits, etc. • • •					
<6	90		COLAS	75	HLBC K^-p , 575–970 MeV

$\Gamma(\Sigma^-\gamma)/\Gamma_{total}$	Γ_4/Γ				
VALUE	CL%	DOCUMENT ID	TECN	CHG	COMMENT
<2.4 × 10⁻⁴	90	11	MOLCHANOV	04	SELX $-$ $\Sigma^-p \rightarrow \Sigma(1385)^- p$, 600 GeV
• • • We do not use the following data for averages, fits, limits, etc. • • •					
<6.1 × 10 ⁻⁴	90	12	ARIK	77	SPEC $-$ $\Sigma^-p \rightarrow \Sigma(1385)^- p$, 23 GeV

$(\Gamma_i\Gamma_f)^{1/2}/\Gamma_{total}$ in $N\bar{K} \rightarrow \Sigma(1385) \rightarrow \Lambda\pi$	$(\Gamma_5\Gamma_1)^{1/2}/\Gamma$		
VALUE	DOCUMENT ID	CHG	COMMENT
+0.586 ± 0.319	13	DEVENISH	74B 0 Fixed-t dispersion rel.

$\Sigma(1385)$ FOOTNOTES

- 1 From fit to inclusive $\Lambda\pi$ spectrum.
- 2 Includes data of HOLMGREN 77.
- 3 The errors are statistical only. The resolution is not unfolded.
- 4 The error is enlarged to Γ/\sqrt{N} . See the note on the $K^*(892)$ mass in the 1984 edition.
- 5 From a fit to $\Lambda\pi^0$ with the width fixed at 34 MeV.
- 6 From fit to inclusive $\Lambda\pi^0$ spectrum with the width fixed at 40 MeV.
- 7 Redundant with data in the mass Listings.
- 8 Results from $\Lambda\pi^+\pi^-$ and $\Lambda\pi^+\pi^-\pi^0$ combined by us.
- 9 The error is enlarged to $4\Gamma/\sqrt{N}$. See the note on the $K^*(892)$ mass in the 1984 edition.
- 10 Consistent with +, 0, and – widths equal.
- 11 We calculate this from the MOLCHANOV 04 upper limit of 9.5 keV on the $\Sigma^-\gamma$ width.
- 12 We calculate this from the ARIK 77 upper limit of 24 keV on the $\Sigma^-\gamma$ width.
- 13 An extrapolation of the parameterized amplitude below threshold.

$\Sigma(1385)$ REFERENCES

TAYLOR 05	PR C71 054609	S. Taylor et al.	(JLab CLAS Collab.)
Also	PR C72 039902 (errata.)	S. Taylor et al.	(JLab CLAS Collab.)
MOLCHANOV 04	PL B590 161	V.V. Molchanov et al.	(FNAL SELEX Collab.)
BAUBILLIER 84	ZPHY C23 213	M. Baubillier et al.	(BIRM, CERN, GLAS+)
PDG 84	RMP 56 51	C.G. Wohl et al.	(LBL, CIT, CERN)
AGUILAR... 81D	AFIS A77 144	M. Aguilar-Benitez, J. Salicio	(MADR)
BAKER 80	NP B166 207	P.A. Baker et al.	(LOIC)
BAUBILLIER 79B	NP B148 18	M. Baubillier et al.	(BIRM, CERN, GLAS+)
CAUTIS 75	NP B156 507	C.V. Cautis et al.	(SLAC)
SUGAHARA 79B	NP B156 237	R. Sugahara et al.	(KEK, OSKC, KIBK)
CAMERON 78	NP B143 189	W. Cameron et al.	(RHEL, LOIC)
DIONISI 78B	PL 78B 154	C. Dionisi, R. Armenteros, J. Diaz	(CERN, AMST+)
ARIK 77	PRL 38 1000	E. Arik et al.	(PITT, BNL, MASA)
BARREIRO 77B	NP B126 319	F. Barreiro et al.	(CERN, AMST, NIUM)
HOLMGREN 77	NP B119 261	S.O. Holmgren et al.	(CERN, AMST, NIUM)
BARDADIN... 75	NP B98 418	M. Bardadin-Otwinowska et al.	(SACL, EPOL+)
COLAS 75	NP B91 253	J. Colas et al.	(ORSAY)
BERTHON 74	NC 21A 146	A. Berthon et al.	(CDEF, RHEL, SACL+)
BORENSTEIN 74	PR D9 3006	S.R. Borenstein et al.	(BNL, MICH)
DEVENISH 74B	NP B81 330	R.C.E. Devenish, C.D. Froggatt, B.R. Martin	(DESY+)

LICHTENBERG 74	PR D10 3865	D.B. Lichtenberg	(IND)
Also	Private Comm.	D.B. Lichtenberg	(IND)
HABIBI 73	Thesis Nevis 199	M. Habibi	(COLU)
Also	Purdue Conf. 387	C. Baltay et al.	(COLU, BING)
MAST 73	PR D7 3212	T.S. Mast et al.	(LBL)JJP
Also	PR D7 5	T.S. Mast et al.	(LBL)JJP
THOMAS 73	NP B56 15	D.W. Thomas et al.	(CMU)JP
AGUILAR... 72B	PR D6 29	M. Aguilar-Benitez et al.	(BNL)
COLLEY 71B	NP B51 61	D.C. Colley et al.	(BIRM, EDIN, GLAS+)
AGUILAR... 70B	PRL 25 58	M. Aguilar-Benitez et al.	(BNL, SYRA)
PAN 69	PRL 23 808	Y.L. Pan, F.L. Forman	(PENNI)
SIEGEL 67	Thesis UCRL 18041	D.M. Siegel	(LRL)
BIRMINGHAM 66	PR 152 1148	M. Haque et al.	(BIRM, GLAS, LOIC, OXF+)
LONDON 66	PR 143 1034	G.W. London et al.	(BNL, SYRA)J
ARMENTEROS 65B	PL 19 75	R. Armenteros et al.	(CERN, HEID, SACL)
SMITH 65	Thesis UCLA	L.T. Smith	(UCLA)
COOPER 64	PL 8 365	W.A. Cooper et al.	(CERN, AMST)
HUWE 64	Thesis UCRL 11291	D.O. Huwe	(LRL)JP
Also	PR 181 1824	D.O. Huwe	(LRL)JP
CURTIS 63	PR 132 1771	L.J. Curtis et al.	(MICH)J
ALSTON 62	CERN Conf. 311	M.H. Alston et al.	(LRL)
BASTIEN 61	PRL 6 702	P.L. Bastien, M. Ferro-Luzzi, A.H. Rosenfeld	(LRL)
DAHL 61	PRL 6 142	O.I. Dahl et al.	(LRL)
ELY 61	PRL 7 461	R.P. Ely et al.	(LRL)J
ALSTON 60	PRL 5 520	M.H. Alston et al.	(LRL)J

$\Sigma(1480)$ Bumps

$$I(J^P) = 1(?^?) \text{ Status: } *$$

OMITTED FROM SUMMARY TABLE

These are peaks seen in $\Lambda\pi$ and $\Sigma\pi$ spectra in the reaction $\pi^+p \rightarrow (Y\pi)K^+$ at 1.7 GeV/c. Also, the Y polarization oscillates in the same region.

MILLER 70 suggests a possible alternate explanation in terms of a reflection of $N(1675) \rightarrow \Lambda K$ decay. However, such an explanation for the $(\Sigma^+\pi^0)K^+$ channel in terms of $\Delta(1650) \rightarrow \Sigma K$ decay seems unlikely (see PAN 70). In addition such reflections would also have to account for the oscillation of the Y polarization in the 1480 MeV region.

HANSON 71, with less data than PAN 70, can neither confirm nor deny the existence of this state. MAST 75 sees no structure in this region in $K^-p \rightarrow \Lambda\pi^0$.

ENGELEN 80 performs a multichannel analysis of $K^-p \rightarrow p\bar{K}^0\pi^-$ at 4.2 GeV/c. They observe a 3.5 standard-deviation signal at 1480 MeV in $p\bar{K}^0$ which cannot be explained as a reflection of any competing channel.

PRAKHOV 04 sees no evidence for this or other light Σ resonances, aside from the $\Sigma(1385)$, in $K^-p \rightarrow \Lambda\pi^0\pi^0$.

ZYCHOR 06 finds peaks in $pp \rightarrow pK^+(\pi^\pm X^\mp)$ at $p_{beam} = 3.65$ GeV/c.

$\Sigma(1480)$ MASS (PRODUCTION EXPERIMENTS)

VALUE (MeV)	EVTS	DOCUMENT ID	TECN	COMMENT
≈ 1480 OUR ESTIMATE				
1480 ± 15	365 ± 60	ZYCHOR	06	SPEC $pp \rightarrow pK^+(\pi^\pm X^\mp)$
1480	120	ENGELEN	80	HBC $K^-p \rightarrow (p\bar{K}^0)\pi^-$
1485 ± 10		CLINE	73	MPWA $K^-d \rightarrow (\Lambda\pi^-)p$
1479 ± 10		PAN	70	HBC $\pi^+p \rightarrow (\Lambda\pi^+)K^+$
1465 ± 15		PAN	70	HBC $\pi^+p \rightarrow (\Sigma\pi)K^+$

$\Sigma(1480)$ WIDTH (PRODUCTION EXPERIMENTS)

VALUE (MeV)	EVTS	DOCUMENT ID	TECN	COMMENT
60 ± 15	365 ± 60	ZYCHOR	06	SPEC $pp \rightarrow pK^+(\pi^\pm X^\mp)$
80 ± 20	120	ENGELEN	80	HBC $K^-p \rightarrow (p\bar{K}^0)\pi^-$
40 ± 20		CLINE	73	MPWA $K^-d \rightarrow (\Lambda\pi^-)p$
31 ± 15		PAN	70	HBC $\pi^+p \rightarrow (\Lambda\pi^+)K^+$
30 ± 20		PAN	70	HBC $\pi^+p \rightarrow (\Sigma\pi)K^+$

$\Sigma(1480)$ DECAY MODES (PRODUCTION EXPERIMENTS)

Mode	Γ_3/Γ_2
$\Gamma_1 N\bar{K}$	
$\Gamma_2 \Lambda\pi$	
$\Gamma_3 \Sigma\pi$	

$\Sigma(1480)$ BRANCHING RATIOS (PRODUCTION EXPERIMENTS)

$\Gamma(\Sigma\pi)/\Gamma(\Lambda\pi)$	Γ_3/Γ_2		
VALUE	DOCUMENT ID	TECN	CHG
0.82 ± 0.51	PAN	70	HBC +

See key on page 405

Baryon Particle Listings

$\Sigma(1480)$ Bumps, $\Sigma(1560)$ Bumps, $\Sigma(1580)$

$\Gamma(N\bar{K})/\Gamma(\Lambda\pi)$	Γ_1/Γ_2			
VALUE	DOCUMENT ID	TECN	CHG	
0.72±0.50	PAN	70	HBC	+

$\Gamma(N\bar{K})/\Gamma_{\text{total}}$	Γ_1/Γ			
VALUE	DOCUMENT ID	TECN	COMMENT	
small	CLINE	73	MPVA	$K^-d \rightarrow (\Lambda\pi^-)p$

$\Sigma(1480)$ REFERENCES (PRODUCTION EXPERIMENTS)

ZYCHOR	06	PRL 96 012002	I. Zychor <i>et al.</i>	(ANKE Collab.)
PRAKHOV	04	PR C69 042202R	S. Prakhov <i>et al.</i>	(BNL Crystal Ball Collab.)
ENGELN	80	NP B167 61	J.J. Engelen <i>et al.</i>	(NIJM, AMST, CERN+)
MAST	75	PR D11 3078	T.S. Mast <i>et al.</i>	(LBL)
CLINE	73	LNC 6 205	D. Cline, R. Laumann, J. Mapp	(WISC) IJP
HANSON	71	PR D4 1296	P. Hanson, G.E. Kalmus, J. Louie	(LBL) I
MILLER	70	Duke Conf. 229	D.H. Miller	(PURD)
PAN	70	PR D2 449	Y.L. Pan <i>et al.</i>	(PENN)
Also		PRL 23 808	Y.L. Pan, F.L. Forman	(PENN) I
Also		PRL 23 806	Y.L. Pan, F.L. Forman	(PENN) I

$\Sigma(1560)$ Bumps $I(J^P) = 1(?)^?$ Status: **

OMITTED FROM SUMMARY TABLE

This entry lists peaks reported in mass spectra around 1560 MeV without implying that they are necessarily related.

DIONISI 78B observes a 6 standard-deviation enhancement at 1553 MeV in the charged $\Lambda/\Sigma\pi$ mass spectra from $K^-p \rightarrow (\Lambda/\Sigma)\pi K\bar{K}$ at 4.2 GeV/c. In a CERN ISR experiment, LOCKMAN 78 reports a narrow 6 standard-deviation enhancement at 1572 MeV in $\Lambda\pi^\pm$ from the reaction $pp \rightarrow \Lambda\pi^+\pi^-X$. These enhancements are unlikely to be associated with the $\Sigma(1580)$ (which has not been confirmed by several recent experiments – see the next entry in the Listings).

CARROLL 76 observes a bump at 1550 MeV (as well as one at 1580 MeV) in the isospin-1 $\bar{K}N$ total cross section, but uncertainties in cross section measurements outside the mass range of the experiment preclude estimating its significance.

See also MEADOWS 80 for a review of this state.

$\Sigma(1560)$ MASS (PRODUCTION EXPERIMENTS)

VALUE (MeV)	EVTS	DOCUMENT ID	TECN	CHG	COMMENT
≈ 1560 OUR ESTIMATE					
1553±7	121	DIONISI	78B	HBC	$K^-p \rightarrow (Y\pi)K\bar{K}$
1572±4	40	LOCKMAN	78	SPEC	$pp \rightarrow \Lambda\pi^+\pi^-X$

$\Sigma(1560)$ WIDTH (PRODUCTION EXPERIMENTS)

VALUE (MeV)	EVTS	DOCUMENT ID	TECN	CHG	COMMENT
79±30	121	DIONISI	78B	HBC	$K^-p \rightarrow (Y\pi)K\bar{K}$
15±6	40	¹ LOCKMAN	78	SPEC	$pp \rightarrow \Lambda\pi^+\pi^-X$

$\Sigma(1560)$ DECAY MODES (PRODUCTION EXPERIMENTS)

Mode	Fraction (Γ_i/Γ)
Γ_1 $\Lambda\pi$	seen
Γ_2 $\Sigma\pi$	

$\Sigma(1560)$ BRANCHING RATIOS (PRODUCTION EXPERIMENTS)

$\Gamma(\Sigma\pi)/[\Gamma(\Lambda\pi) + \Gamma(\Sigma\pi)]$	$\Gamma_2/(\Gamma_1+\Gamma_2)$			
VALUE	DOCUMENT ID	TECN	CHG	COMMENT
0.35±0.12	DIONISI	78B	HBC	$K^-p \rightarrow (Y\pi)K\bar{K}$

$\Gamma(\Lambda\pi)/\Gamma_{\text{total}}$	Γ_1/Γ			
VALUE	DOCUMENT ID	TECN	CHG	COMMENT
seen	LOCKMAN	78	SPEC	$pp \rightarrow \Lambda\pi^+\pi^-X$

$\Sigma(1560)$ FOOTNOTES (PRODUCTION EXPERIMENTS)

¹The width observed by LOCKMAN 78 is consistent with experimental resolution.

$\Sigma(1560)$ REFERENCES (PRODUCTION EXPERIMENTS)

MEADOWS	80	Toronto Conf. 283	B.T. Meadows	(CINC)
DIONISI	78B	PL 78B 154	C. Dionisi, R. Armenteros, J. Diaz	(CERN, AMST+)
LOCKMAN	78	Saclay DHPPE 78-01	W. Lockman <i>et al.</i>	(UCLA, SACL)
CARROLL	76	PRL 37 806	A.S. Carroll <i>et al.</i>	(BNL) I

$\Sigma(1580) D_{13}$

$$I(J^P) = 1(\frac{3}{2}^-) \text{ Status: } *$$

OMITTED FROM SUMMARY TABLE

Seen in the isospin-1 $\bar{K}N$ cross section at BNL (LI 73, CARROLL 76) and in a partial-wave analysis of $K^-p \rightarrow \Lambda\pi^0$ for c.m. energies 1560–1600 MeV by LITCHFIELD 74. LITCHFIELD 74 finds $J^P = 3/2^-$. Not seen by ENGLER 78 or by CAMERON 78C (with larger statistics in $K_L^0 p \rightarrow \Lambda\pi^+$ and $\Sigma^0\pi^+$).

Neither OLMSTED 04 (in $K^-p \rightarrow \Lambda\pi^0$) nor PRAKHOV 04 (in $K^-p \rightarrow \Lambda\pi^0\pi^0$) see any evidence for this state.

$\Sigma(1580)$ MASS

VALUE (MeV)	DOCUMENT ID	TECN	COMMENT
≈ 1580 OUR ESTIMATE			
1583±4	¹ CARROLL	76	DPWA Isospin-1 total σ
1582±4	² LITCHFIELD	74	DPWA $K^-p \rightarrow \Lambda\pi^0$

$\Sigma(1580)$ WIDTH

VALUE (MeV)	DOCUMENT ID	TECN	COMMENT
15	¹ CARROLL	76	DPWA Isospin-1 total σ
11±4	² LITCHFIELD	74	DPWA $K^-p \rightarrow \Lambda\pi^0$

$\Sigma(1580)$ DECAY MODES

Mode
Γ_1 $N\bar{K}$
Γ_2 $\Lambda\pi$
Γ_3 $\Sigma\pi$

$\Sigma(1580)$ BRANCHING RATIOS

See "Sign conventions for resonance couplings" in the Note on Λ and Σ Resonances.

$\Gamma(N\bar{K})/\Gamma_{\text{total}}$	Γ_1/Γ			
VALUE	DOCUMENT ID	TECN	COMMENT	
+0.03±0.01	² LITCHFIELD	74	DPWA	$\bar{K}N$ multichannel

$(\Gamma_1\Gamma_f)^{1/2}/\Gamma_{\text{total}}$ in $N\bar{K} \rightarrow \Sigma(1580) \rightarrow \Lambda\pi$	$(\Gamma_1\Gamma_2)^{1/2}/\Gamma$			
VALUE	DOCUMENT ID	TECN	COMMENT	
not seen	CAMERON	78C	HBC	$K_L^0 p \rightarrow \Lambda\pi^+$
not seen	ENGLER	78	HBC	$K_L^0 p \rightarrow \Lambda\pi^+$
+0.10±0.02	² LITCHFIELD	74	DPWA	$K^-p \rightarrow \Lambda\pi^0$

$(\Gamma_1\Gamma_f)^{1/2}/\Gamma_{\text{total}}$ in $N\bar{K} \rightarrow \Sigma(1580) \rightarrow \Sigma\pi$	$(\Gamma_1\Gamma_3)^{1/2}/\Gamma$			
VALUE	DOCUMENT ID	TECN	COMMENT	
not seen	CAMERON	78C	HBC	$K_L^0 p \rightarrow \Sigma^0\pi^+$
not seen	ENGLER	78	HBC	$K_L^0 p \rightarrow \Sigma^0\pi^+$
+0.03±0.04	² LITCHFIELD	74	DPWA	$\bar{K}N$ multichannel

$\Sigma(1580)$ FOOTNOTES

¹CARROLL 76 sees a total-cross-section bump with $(J+1/2)\Gamma_{\text{el}}/\Gamma_{\text{total}} = 0.06$.

²The main effect observed by LITCHFIELD 74 is in the $\Lambda\pi$ final state; the $\bar{K}N$ and $\Sigma\pi$ couplings are estimated from a multichannel fit including total-cross-section data of LI 73.

$\Sigma(1580)$ REFERENCES

OLMSTED	04	PL B588 29	J. Olmsted <i>et al.</i>	(BNL Crystal Ball Collab.)
PRAKHOV	04	PR C69 042202R	S. Prakhov <i>et al.</i>	(BNL Crystal Ball Collab.)
CAMERON	78C	NP B132 189	W. Cameron <i>et al.</i>	(BGNA, EDIN, GLAS+)
ENGLER	78	PR D18 3061	A. Engler <i>et al.</i>	(CMU, ANL)
CARROLL	76	PRL 37 806	A.S. Carroll <i>et al.</i>	(BNL) I
LITCHFIELD	74	PL 51B 509	P.J. Litchfield	(CERN) IJP
LI	73	Purdue Conf. 283	K.K. Li	(BNL) I

Baryon Particle Listings

 $\Sigma(1620)$, $\Sigma(1620)$ Production Experiments $\Sigma(1620) S_{11}$

$$I(J^P) = 1(\frac{1}{2}^-) \text{ Status: } **$$

OMITTED FROM SUMMARY TABLE

The S_{11} state at 1697 MeV reported by VANHORN 75 is tentatively listed under the $\Sigma(1750)$. CARROLL 76 sees two bumps in the isospin-1 total cross section near this mass.

Production experiments are listed separately in the next entry.

 $\Sigma(1620)$ MASS

VALUE (MeV)	DOCUMENT ID	TECN	COMMENT
≈ 1620 OUR ESTIMATE			
1600 \pm 6	1 MORRIS	78	DPWA $K^- n \rightarrow \Lambda \pi^-$
1608 \pm 5	2 CARROLL	76	DPWA isospin-1 total σ
1633 \pm 10	3 CARROLL	76	DPWA isospin-1 total σ
1630 \pm 10	LANGBEIN	72	IPWA $\bar{K} N$ multichannel
1620	KIM	71	DPWA K-matrix analysis

 $\Sigma(1620)$ WIDTH

VALUE (MeV)	DOCUMENT ID	TECN	COMMENT
87 \pm 19	1 MORRIS	78	DPWA $K^- n \rightarrow \Lambda \pi^-$
15	2 CARROLL	76	DPWA isospin-1 total σ
10	3 CARROLL	76	DPWA isospin-1 total σ
65 \pm 20	LANGBEIN	72	IPWA $\bar{K} N$ multichannel
40	KIM	71	DPWA K-matrix analysis

 $\Sigma(1620)$ DECAY MODES

Mode	Γ
Γ_1 $N\bar{K}$	
Γ_2 $\Lambda\pi$	
Γ_3 $\Sigma\pi$	

 $\Sigma(1620)$ BRANCHING RATIOS

$\Gamma(N\bar{K})/\Gamma_{\text{total}}$	DOCUMENT ID	TECN	COMMENT	Γ_1/Γ
0.22 \pm 0.02	LANGBEIN	72	IPWA $\bar{K} N$ multichannel	
0.05	KIM	71	DPWA K-matrix analysis	

$(\Gamma_1\Gamma_2)^{1/2}/\Gamma_{\text{total}}$ in $N\bar{K} \rightarrow \Sigma(1620) \rightarrow \Lambda\pi$	DOCUMENT ID	TECN	COMMENT	$(\Gamma_1\Gamma_2)^{1/2}/\Gamma$
0.12 \pm 0.02	1 MORRIS	78	DPWA $K^- n \rightarrow \Lambda \pi^-$	
not seen	BAILLON	75	IPWA $\bar{K} N \rightarrow \Lambda \pi$	
0.15	KIM	71	DPWA K-matrix analysis	

$(\Gamma_1\Gamma_3)^{1/2}/\Gamma_{\text{total}}$ in $N\bar{K} \rightarrow \Sigma(1620) \rightarrow \Sigma\pi$	DOCUMENT ID	TECN	COMMENT	$(\Gamma_1\Gamma_3)^{1/2}/\Gamma$
not seen	HEPP	76B	DPWA $K^- N \rightarrow \Sigma\pi$	
0.40 \pm 0.06	LANGBEIN	72	IPWA $\bar{K} N$ multichannel	
0.08	KIM	71	DPWA K-matrix analysis	

 $\Sigma(1620)$ FOOTNOTES

- ¹ MORRIS 78 obtains an equally good fit without including this resonance.
² Total cross-section bump with $(J+1/2)$ $\Gamma_{\text{el}}/\Gamma_{\text{total}}$ is 0.06 seen by CARROLL 76.
³ Total cross-section bump with $(J+1/2)$ $\Gamma_{\text{el}}/\Gamma_{\text{total}}$ is 0.04 seen by CARROLL 76.

 $\Sigma(1620)$ REFERENCES

MORRIS	78	PR D17 55	W.A. Morris et al.	(FSU) IJP
CARROLL	76	PRL 37 806	A.S. Carroll et al.	(BNL) I
HEPP	76B	PL 65B 487	V. Hepp et al.	(CERN, HEIDH, MPIM) IJP
BAILLON	75	NP B94 39	P.H. Baillon, P.J. Litchfield	(CERN, RHEL) IJP
VANHORN	75	NP B87 145	A.J. van Horn	(LBL) IJP
Also		NP B87 157	A.J. van Horn	(LBL) IJP
LANGBEIN	72	NP B47 477	W. Langbein, F. Wagner	(MPIM) IJP
KIM	71	PRL 27 356	J.K. Kim	(HARV) IJP
Also		Duke Conf. 161	J.K. Kim	(HARV) IJP
		Hyperon Resonances, 1970		

 $\Sigma(1620)$ Production Experiments

$$I(J^P) = 1(?^?)$$

OMITTED FROM SUMMARY TABLE

Formation experiments are listed separately in the previous entry.

The results of CRENNELL 69B at 3.9 GeV/c are not confirmed by SABRE 70 at 3.0 GeV/c. However, at 4.5 GeV/c, AMMANN 70 sees a peak at 1642 MeV which on the basis of branching ratios they do not associate with the $\Sigma(1670)$. See MILLER 70 for a review of these conflicts.

 $\Sigma(1620)$ MASS (PRODUCTION EXPERIMENTS)

VALUE (MeV)	EVTS	DOCUMENT ID	TECN	CHG	COMMENT
≈ 1620 OUR ESTIMATE					
1642 \pm 12		AMMANN	70	DBC	$K^- N$ 4.5 GeV/c
1618 \pm 3	20	BLUMENFELD	69	HBC +	$K_L^0 p$
1619 \pm 8		CRENNELL	69B	DBC \pm	$K^- N \rightarrow \Lambda \pi \pi$
					••• We do not use the following data for averages, fits, limits, etc. •••
1616 \pm 8		CRENNELL	68	DBC \pm	See CRENNELL 69B

 $\Sigma(1620)$ WIDTH (PRODUCTION EXPERIMENTS)

VALUE (MeV)	EVTS	DOCUMENT ID	TECN	CHG	COMMENT
55 \pm 24		AMMANN	70	DBC	$K^- N$ 4.5 GeV/c
30 \pm 10	20	BLUMENFELD	69	HBC +	
72 \pm $\frac{22}{15}$		CRENNELL	69B	DBC \pm	
					••• We do not use the following data for averages, fits, limits, etc. •••
66 \pm 16		CRENNELL	68	DBC \pm	See CRENNELL 69B

 $\Sigma(1620)$ DECAY MODES (PRODUCTION EXPERIMENTS)

Mode	Γ
Γ_1 $N\bar{K}$	
Γ_2 $\Lambda\pi$	
Γ_3 $\Sigma\pi$	
Γ_4 $\Lambda\pi\pi$	
Γ_5 $\Sigma(1385)\pi$	
Γ_6 $\Lambda(1405)\pi$	

 $\Sigma(1620)$ BRANCHING RATIOS (PRODUCTION EXPERIMENTS)

$\Gamma(\Lambda\pi\pi)/\Gamma(\Lambda\pi)$	DOCUMENT ID	TECN	CHG	Γ_4/Γ_2
~ 2.5	BLUMENFELD	69	HBC +	

$\Gamma(N\bar{K})/\Gamma(\Lambda\pi)$	DOCUMENT ID	TECN	CHG	COMMENT	Γ_1/Γ_2
0.4 \pm 0.4	AMMANN	70	DBC	$K^- p$ 4.5 GeV/c	
0.0 \pm 0.1	CRENNELL	68	DBC +	See CRENNELL 69B	

$\Gamma(\Lambda\pi)/\Gamma_{\text{total}}$	DOCUMENT ID	TECN	CHG	Γ_2/Γ
large	CRENNELL	68	DBC \pm	

$\Gamma(\Sigma(1385)\pi)/\Gamma(\Lambda\pi)$	DOCUMENT ID	TECN	CHG	COMMENT	Γ_5/Γ_2
< 0.3	AMMANN	70	DBC	$K^- p$ 4.5 GeV/c	
0.2 \pm 0.1	CRENNELL	68	DBC \pm		

$\Gamma(\Sigma\pi)/\Gamma(\Lambda\pi)$	DOCUMENT ID	TECN	COMMENT	Γ_3/Γ_2
< 1.1	AMMANN	70	DBC	$K^- N$ 4.5 GeV/c

$\Gamma(\Lambda(1405)\pi)/\Gamma(\Lambda\pi)$	DOCUMENT ID	TECN	COMMENT	Γ_6/Γ_2
0.7 \pm 0.4	AMMANN	70	DBC	$K^- p$ 4.5 GeV/c

$\Sigma(1620)$ Production Experiments, $\Sigma(1660)$, $\Sigma(1670)$

$\Sigma(1620)$ REFERENCES
(PRODUCTION EXPERIMENTS)

AMMANN 70 PRL 24 327	A.C. Ammann <i>et al.</i>	(PURD, IND)
Also PR D7 1345	A.C. Ammann <i>et al.</i>	(PURD, IUPU)
MILLER 70 Duke Conf. 229	D.H. Miller	(PURD)
Hyperon Resonances, 1970		
SABRE 70 NP B16 201	R. Barloutaud <i>et al.</i>	(SABRE Collab.)
BLUMENFELD 69 PL 29B 58	B.J. Blumenfeld, G.R. Kalbfleisch	(BNL)1
CRENNELL 69B Lund Paper 183	D.J. Crennell <i>et al.</i>	(BNL, CUNY)1
Results are quoted in LEVI-SETTI 69C.		
Also Lund Conf.	R. Levi-Setti	(EFI)
CRENNELL 68 PRL 21 648	D.J. Crennell <i>et al.</i>	(BNL, CUNY)1

$\Sigma(1660) P_{11}$ $I(J^P) = 1(\frac{1}{2}^+)$ Status: ***

For results published before 1974 (they are now obsolete), see our 1982 edition Physics Letters **111B** 1 (1982).

$\Sigma(1660)$ MASS

VALUE (MeV)	DOCUMENT ID	TECN	COMMENT
1630 to 1690 (≈ 1660) OUR ESTIMATE			
1665.1 \pm 11.2	1 KOISO	85	DPWA $K^-p \rightarrow \Sigma\pi$
1670 \pm 10	GOPAL	80	DPWA $\bar{K}N \rightarrow \bar{K}N$
1679 \pm 10	ALSTON-...	78	DPWA $\bar{K}N \rightarrow \bar{K}N$
1676 \pm 15	GOPAL	77	DPWA $\bar{K}N$ multichannel
1668 \pm 25	VANHORN	75	DPWA $K^-p \rightarrow \Lambda\pi^0$
1670 \pm 20	KANE	74	DPWA $K^-p \rightarrow \Sigma\pi$
••• We do not use the following data for averages, fits, limits, etc. •••			
1565 or 1597	2 MARTIN	77	DPWA $\bar{K}N$ multichannel
1660 \pm 30	3 BAILLON	75	IPWA $\bar{K}N \rightarrow \Lambda\pi$
1671 \pm 2	4 PONTE	75	DPWA $K^-p \rightarrow \Lambda\pi^0$

$\Sigma(1660)$ WIDTH

VALUE (MeV)	DOCUMENT ID	TECN	COMMENT
40 to 200 (≈ 100) OUR ESTIMATE			
81.5 \pm 22.2	1 KOISO	85	DPWA $K^-p \rightarrow \Sigma\pi$
152 \pm 20	GOPAL	80	DPWA $\bar{K}N \rightarrow \bar{K}N$
38 \pm 10	ALSTON-...	78	DPWA $\bar{K}N \rightarrow \bar{K}N$
120 \pm 20	GOPAL	77	DPWA $\bar{K}N$ multichannel
230 $+165$ -60	VANHORN	75	DPWA $K^-p \rightarrow \Lambda\pi^0$
250 \pm 110	KANE	74	DPWA $K^-p \rightarrow \Sigma\pi$
••• We do not use the following data for averages, fits, limits, etc. •••			
202 or 217	2 MARTIN	77	DPWA $\bar{K}N$ multichannel
80 \pm 40	3 BAILLON	75	IPWA $\bar{K}N \rightarrow \Lambda\pi$
81 \pm 10	4 PONTE	75	DPWA $K^-p \rightarrow \Lambda\pi^0$

$\Sigma(1660)$ DECAY MODES

Mode	Fraction (Γ_i/Γ)
Γ_1 $N\bar{K}$	10–30 %
Γ_2 $\Lambda\pi$	seen
Γ_3 $\Sigma\pi$	seen

$\Sigma(1660)$ BRANCHING RATIOS

See "Sign conventions for resonance couplings" in the Note on Λ and Σ Resonances.

$\Gamma(N\bar{K})/\Gamma_{total}$	DOCUMENT ID	TECN	COMMENT	Γ_1/Γ
0.1 to 0.3 OUR ESTIMATE				
0.12 \pm 0.03	GOPAL	80	DPWA $\bar{K}N \rightarrow \bar{K}N$	
0.10 \pm 0.05	ALSTON-...	78	DPWA $\bar{K}N \rightarrow \bar{K}N$	
••• We do not use the following data for averages, fits, limits, etc. •••				
<0.04	GOPAL	77	DPWA See GOPAL 80	
0.27 or 0.29	2 MARTIN	77	DPWA $\bar{K}N$ multichannel	

$(\Gamma_1\Gamma_2)^{1/2}/\Gamma_{total}$ in $N\bar{K} \rightarrow \Sigma(1660) \rightarrow \Lambda\pi$	DOCUMENT ID	TECN	COMMENT	$(\Gamma_1\Gamma_2)^{1/2}/\Gamma$
0.1 to 0.3 OUR ESTIMATE				
< 0.04	GOPAL	77	DPWA $\bar{K}N$ multichannel	
0.12 $+0.12$ -0.04	VANHORN	75	DPWA $K^-p \rightarrow \Lambda\pi^0$	
••• We do not use the following data for averages, fits, limits, etc. •••				
–0.10 or –0.11	2 MARTIN	77	DPWA $\bar{K}N$ multichannel	
–0.04 \pm 0.02	3 BAILLON	75	IPWA $\bar{K}N \rightarrow \Lambda\pi$	
+0.16 \pm 0.01	4 PONTE	75	DPWA $K^-p \rightarrow \Lambda\pi^0$	

$(\Gamma_1\Gamma_2)^{1/2}/\Gamma_{total}$ in $N\bar{K} \rightarrow \Sigma(1660) \rightarrow \Sigma\pi$	DOCUMENT ID	TECN	COMMENT	$(\Gamma_1\Gamma_3)^{1/2}/\Gamma$
–0.13 \pm 0.04	1 KOISO	85	DPWA $K^-p \rightarrow \Sigma\pi$	
–0.16 \pm 0.03	GOPAL	77	DPWA $\bar{K}N$ multichannel	
–0.11 \pm 0.01	KANE	74	DPWA $K^-p \rightarrow \Sigma\pi$	
••• We do not use the following data for averages, fits, limits, etc. •••				
–0.34 or –0.37	2 MARTIN	77	DPWA $\bar{K}N$ multichannel	
not seen	HEPP	76B	DPWA $K^-N \rightarrow \Sigma\pi$	

$\Sigma(1660)$ FOOTNOTES

- The evidence of KOISO 85 is weak.
- The two MARTIN 77 values are from a T-matrix pole and from a Breit-Wigner fit.
- From solution 1 of BAILLON 75; not present in solution 2.
- From solution 2 of PONTE 75; not present in solution 1.

$\Sigma(1660)$ REFERENCES

KOISO 85 NP A433 619	H. Koiso <i>et al.</i>	(TOKY, MASA)
PDG 82 PL 111B 1	M. Roos <i>et al.</i>	(HELS, CIT, CERN)
GOPAL 80 Toronto Conf. 159	G.P. Gopal	(RHEL) IJP
ALSTON-... 78 PR D18 182	M. Alston-Garnjost <i>et al.</i>	(LBL, MTHO+) IJP
Also PRL 38 1007	M. Alston-Garnjost <i>et al.</i>	(LBL, MTHO+) IJP
GOPAL 77 NP B19 302	G.P. Gopal <i>et al.</i>	(LOIC, RHEL) IJP
MARTIN 77 NP B127 349	B.R. Martin, M.K. Pidcock, R.G. Moorhouse	(LOUC+) IJP
Also NP B126 266	B.R. Martin, M.K. Pidcock	(LOUC) IJP
Also NP B126 285	B.R. Martin, M.K. Pidcock	(LOUC) IJP
HEPP 76B PL 65B 487	V. Hepp <i>et al.</i>	(CERN, HEIDH, MPIM) IJP
BAILLON 75 NP B94 39	P.H. Baillon, P.J. Lichfield	(CERN, RHEL) IJP
PONTE 75 NP D12 2597	R.A. Ponte <i>et al.</i>	(MASA, TENN, UCR) IJP
VANHORN 75 NP B87 145	A.J. van Horn	(LBL) IJP
Also NP B87 157	A.J. van Horn	(LBL) IJP
KANE 74 LBL-2452	D.F. Kane	(LBL) IJP

THE $\Sigma(1670)$ REGION

Production experiments: The measured $\Sigma\pi/\Sigma\pi\pi$ branching ratio for the $\Sigma(1670)$ produced in the reaction $K^-p \rightarrow \pi^-\Sigma(1670)^+$ is strongly dependent on momentum transfer. This was first discovered by EBERHARD 69, who suggested that there exist two Σ resonances with the same mass and quantum numbers: one with a large $\Sigma\pi\pi$ (mainly $\Lambda(1405)\pi$) branching fraction produced peripherally, and the other with a large $\Sigma\pi$ branching fraction produced at larger angles. The experimental results have been confirmed by AGUILAR-BENITEZ 70, ASPELL 74, ESTES 74, and TIMMERMANS 76. If, in fact, there are two resonances, the most likely quantum numbers for both the $\Sigma\pi$ and the $\Lambda(1405)\pi$ states are D_{13} . There is also possibly a third Σ in this region, the $\Sigma(1690)$ in the Listings, the main evidence for which is a large $\Lambda\pi/\Sigma\pi$ branching ratio. These topics have been reviewed by EBERHARD 73 and by MILLER 70.

Formation experiments: Two states are also observed near this mass in formation experiments. One of these, the $\Sigma(1670)D_{13}$, has the same quantum numbers as those observed in production and has a large $\Sigma\pi/\Sigma\pi\pi$ branching ratio; it may well be the $\Sigma(1670)$ produced at larger angles (see TIMMERMANS 76). The other state, the $\Sigma(1660)P_{11}$, has different quantum numbers, its $\Sigma\pi/\Sigma\pi\pi$ branching ratio is unknown, and its relation to the produced $\Sigma(1670)$ states is obscure.

Baryon Particle Listings

 $\Sigma(1670)$ $\Sigma(1670) D_{13}$

$$I(J^P) = 1(\frac{3}{2}^-) \text{ Status: } ****$$

For most results published before 1974 (they are now obsolete), see our 1982 edition Physics Letters **111B** 1 (1982).

Results from production experiments are listed separately in the next entry.

 $\Sigma(1670)$ MASS

VALUE (MeV)	DOCUMENT ID	TECN	COMMENT
1665 to 1685 (≈ 1670) OUR ESTIMATE			
1665.1 ± 4.1	KOISO	85	DPWA $K^- p \rightarrow \Sigma \pi$
1682 ± 5	GOPAL	80	DPWA $\bar{K} N \rightarrow \bar{K} N$
1679 ± 10	ALSTON-...	78	DPWA $\bar{K} N \rightarrow \bar{K} N$
1670 ± 5	GOPAL	77	DPWA $\bar{K} N$ multichannel
1670 ± 6	HEPP	76B	DPWA $K^- N \rightarrow \Sigma \pi$
1685 ± 20	BAILLON	75	IPWA $\bar{K} N \rightarrow \Lambda \pi$
$1659 \pm \frac{12}{5}$	VANHORN	75	DPWA $K^- p \rightarrow \Lambda \pi^0$
1670 ± 2	KANE	74	DPWA $K^- p \rightarrow \Sigma \pi$
●●● We do not use the following data for averages, fits, limits, etc. ●●●			
1667 or 1668	¹ MARTIN	77	DPWA $\bar{K} N$ multichannel
1650	DEBELLEFON	76	IPWA $K^- p \rightarrow \Lambda \pi^0$
1671 ± 3	PONTE	75	DPWA $K^- p \rightarrow \Lambda \pi^0$ (sol. 1)
1655 ± 2	PONTE	75	DPWA $K^- p \rightarrow \Lambda \pi^0$ (sol. 2)

 $\Sigma(1670)$ WIDTH

VALUE (MeV)	DOCUMENT ID	TECN	COMMENT
40 to 80 (≈ 60) OUR ESTIMATE			
65.0 ± 7.3	KOISO	85	DPWA $K^- p \rightarrow \Sigma \pi$
79 ± 10	GOPAL	80	DPWA $\bar{K} N \rightarrow \bar{K} N$
56 ± 20	ALSTON-...	78	DPWA $\bar{K} N \rightarrow \bar{K} N$
50 ± 5	GOPAL	77	DPWA $\bar{K} N$ multichannel
56 ± 3	HEPP	76B	DPWA $K^- N \rightarrow \Sigma \pi$
85 ± 25	BAILLON	75	IPWA $\bar{K} N \rightarrow \Lambda \pi$
32 ± 11	VANHORN	75	DPWA $K^- p \rightarrow \Lambda \pi^0$
79 ± 6	KANE	74	DPWA $K^- p \rightarrow \Sigma \pi$
●●● We do not use the following data for averages, fits, limits, etc. ●●●			
46 or 46	¹ MARTIN	77	DPWA $\bar{K} N$ multichannel
80	DEBELLEFON	76	IPWA $K^- p \rightarrow \Lambda \pi^0$
44 ± 11	PONTE	75	DPWA $K^- p \rightarrow \Lambda \pi^0$ (sol. 1)
76 ± 5	PONTE	75	DPWA $K^- p \rightarrow \Lambda \pi^0$ (sol. 2)

 $\Sigma(1670)$ DECAY MODES

Mode	Fraction (Γ_i/Γ)
Γ_1 $N\bar{K}$	7–13 %
Γ_2 $\Lambda\pi$	5–15 %
Γ_3 $\Sigma\pi$	30–60 %
Γ_4 $\Lambda\pi\pi$	
Γ_5 $\Sigma\pi\pi$	
Γ_6 $\Sigma(1385)\pi$	
Γ_7 $\Sigma(1385)\pi, S$ -wave	
Γ_8 $\Lambda(1405)\pi$	
Γ_9 $\Lambda(1520)\pi$	

The above branching fractions are our estimates, not fits or averages.

 $\Sigma(1670)$ BRANCHING RATIOS

See "Sign conventions for resonance couplings" in the Note on Λ and Σ Resonances.

$\Gamma(N\bar{K})/\Gamma_{\text{total}}$	DOCUMENT ID	TECN	COMMENT	Γ_1/Γ
0.07 to 0.13 OUR ESTIMATE				
0.10 ± 0.03	GOPAL	80	DPWA $\bar{K} N \rightarrow \bar{K} N$	
0.11 ± 0.03	ALSTON-...	78	DPWA $\bar{K} N \rightarrow \bar{K} N$	
●●● We do not use the following data for averages, fits, limits, etc. ●●●				
0.08 ± 0.03	GOPAL	77	DPWA See GOPAL 80	
0.07 or 0.07	¹ MARTIN	77	DPWA $\bar{K} N$ multichannel	
$(\Gamma_i\Gamma_f)^{1/2}/\Gamma_{\text{total}}$ in $N\bar{K} \rightarrow \Sigma(1670) \rightarrow \Lambda\pi$	DOCUMENT ID	TECN	COMMENT	$(\Gamma_1\Gamma_2)^{1/2}/\Gamma$
0.17 ± 0.03	² MORRIS	78	DPWA $K^- n \rightarrow \Lambda \pi^-$	
0.13 ± 0.02	² MORRIS	78	DPWA $K^- n \rightarrow \Lambda \pi^-$	
$+0.10 \pm 0.02$	GOPAL	77	DPWA $\bar{K} N$ multichannel	
$+0.06 \pm 0.02$	BAILLON	75	IPWA $\bar{K} N \rightarrow \Lambda \pi$	
$+0.09 \pm 0.02$	VANHORN	75	DPWA $K^- p \rightarrow \Lambda \pi^0$	
$+0.018 \pm 0.060$	DEVENISH	74B	Fixed- t dispersion rel.	

●●● We do not use the following data for averages, fits, limits, etc. ●●●

$+0.08$ or $+0.08$	¹ MARTIN	77	DPWA $\bar{K} N$ multichannel
$+0.05$	DEBELLEFON	76	IPWA $K^- p \rightarrow \Lambda \pi^0$
0.08 ± 0.01	PONTE	75	DPWA $K^- p \rightarrow \Lambda \pi^0$ (sol. 1)
0.17 ± 0.01	PONTE	75	DPWA $K^- p \rightarrow \Lambda \pi^0$ (sol. 2)

$$(\Gamma_i\Gamma_f)^{1/2}/\Gamma_{\text{total}}$$

VALUE	DOCUMENT ID	TECN	COMMENT	$(\Gamma_1\Gamma_3)^{1/2}/\Gamma$
$+0.20 \pm 0.02$	KOISO	85	DPWA $K^- p \rightarrow \Sigma \pi$	
$+0.21 \pm 0.02$	GOPAL	77	DPWA $\bar{K} N$ multichannel	
$+0.20 \pm 0.01$	HEPP	76B	DPWA $K^- N \rightarrow \Sigma \pi$	
$+0.21 \pm 0.03$	KANE	74	DPWA $K^- p \rightarrow \Sigma \pi$	
●●● We do not use the following data for averages, fits, limits, etc. ●●●				
$+0.18$ or $+0.17$	¹ MARTIN	77	DPWA $\bar{K} N$ multichannel	

$$\Gamma(\Lambda\pi\pi)/\Gamma_{\text{total}}$$

VALUE	DOCUMENT ID	TECN	COMMENT	Γ_4/Γ
<0.11	ARMENTEROS68E	HBC	$K^- p$ ($\Gamma_1=0.09$)	

$$(\Gamma_i\Gamma_f)^{1/2}/\Gamma_{\text{total}}$$

VALUE	DOCUMENT ID	TECN	COMMENT	$(\Gamma_1\Gamma_7)^{1/2}/\Gamma$
$+0.11 \pm 0.03$	PREVOST	74	DPWA $K^- N \rightarrow \Sigma(1385)\pi$	
●●● We do not use the following data for averages, fits, limits, etc. ●●●				
0.17 ± 0.02	³ SIMS	68	DBC $K^- N \rightarrow \Lambda\pi\pi$	

$$\Gamma(\Sigma\pi\pi)/\Gamma_{\text{total}}$$

VALUE	DOCUMENT ID	TECN	COMMENT	Γ_5/Γ
<0.14	⁴ ARMENTEROS68E	HBC	$K^- p, K^- d$ ($\Gamma_1=0.09$)	

$$\Gamma(\Lambda(1405)\pi)/\Gamma_{\text{total}}$$

VALUE	DOCUMENT ID	TECN	COMMENT	Γ_8/Γ
<0.06	ARMENTEROS68E	HBC	$K^- p, K^- d$ ($\Gamma_1=0.09$)	

$$\Gamma_i\Gamma_f/\Gamma_{\text{total}}^2$$

VALUE	DOCUMENT ID	TECN	COMMENT	$\Gamma_1\Gamma_8/\Gamma^2$
0.007 ± 0.002	⁵ BRUCKER	70	DBC $K^- N \rightarrow \Sigma\pi\pi$	
●●● We do not use the following data for averages, fits, limits, etc. ●●●				
<0.03	BERLEY	69	HBC $K^- p$ 0.6–0.82 GeV/c	

$$\Gamma(\Lambda(1405)\pi)/\Gamma(\Sigma(1385)\pi)$$

VALUE	DOCUMENT ID	TECN	COMMENT	Γ_8/Γ_6
0.23 ± 0.08	BRUCKER	70	DBC $K^- N \rightarrow \Sigma\pi\pi$	

$$(\Gamma_i\Gamma_f)^{1/2}/\Gamma_{\text{total}}$$

VALUE	DOCUMENT ID	TECN	COMMENT	$(\Gamma_1\Gamma_9)^{1/2}/\Gamma$
0.081 ± 0.016	⁶ CAMERON	77	DPWA P -wave decay	

 $\Sigma(1670)$ FOOTNOTES

- The two MARTIN 77 values are from a T-matrix pole and from a Breit-Wigner fit.
- Results are with and without an S_{11} $\Sigma(1620)$ in the fit.
- SIMS 68 uses only cross-section data. Result used as upper limit only.
- Ratio only for $\Sigma\pi\pi$ system in $l=1$, which cannot be $\Sigma(1385)$.
- Assuming the $\Lambda(1405)\pi$ cross-section bump is due only to $3/2^-$ resonance.
- The CAMERON 77 upper limit on F -wave decay is 0.03.

 $\Sigma(1670)$ REFERENCES

KOISO	85	NP A433 619	H. Koiso et al.	(TOKY, MASA)
PDG	82	PL 111B 1	M. Roos et al.	(HELS, CIT, CERN)
GOPAL	80	Toronto Conf. 159	G.P. Gopal	(RHEL) IJP
ALSTON-...	78	PR D18 182	M. Alston-Garnjost et al.	(LBL, MTHO+) IJP
		Also	M. Alston-Garnjost et al.	(LBL, MTHO+) IJP
MORRIS	78	PR D17 55	W.A. Morris et al.	(FSU) IJP
CAMERON	77	NP B131 399	W. Cameron et al.	(RHEL, LOIC) IJP
GOPAL	77	NP B119 362	G.P. Gopal et al.	(LOIC, RHEL) IJP
MARTIN	77	NP B127 349	B.R. Martin, M.K. Pidcock, R.G. Moorhouse	(LOUC+) IJP
		Also	B.R. Martin, M.K. Pidcock	(LOUC) IJP
		Also	B.R. Martin, M.K. Pidcock	(LOUC) IJP
DEBELLEFON	76	NP B109 129	A. de Bellefon, A. Berthon	(CDFE) IJP
HEPP	76B	PL 65B 487	V. Hepp et al.	(CERN, HEID, MFIM) IJP
BAILLON	75	NP B94 39	P.H. Baillon, P.J. Lichfield	(CERN, RHEL) IJP
PONTE	75	PR D12 2597	R.A. Ponte et al.	(MASA, TENN, UCR) IJP
VANHORN	75	NP B87 145	A.J. van Horn	(LBL) IJP
		Also	A.J. van Horn	(LBL) IJP
DEVENISH	74B	NP B81 330	R.C.E. Devenish, C.D. Froggatt, B.R. Martin	(DESY+) IJP
KANE	74	LBL-2452	D.F. Kane	(LBL) IJP
PREVOST	74	NP B69 246	J. Prevost et al.	(SACL, CERN, HEID)
BRUCKER	70	Duke Conf. 155	E.B. Brucker et al.	(FSU) I
		Hyperon Resonances, 1970		
		Also	D. Berley et al.	(BNL)
ARMENTEROS 68E	68E	PL 28B 521	R. Armenteros et al.	(CERN, HEID, SACL) I
SIMS	68	PRL 21 1413	W.H. Sims et al.	(FSU, TUFTS, BRAN)

Σ(1670) Bumps

$$I(J^P) = 1(?)^2$$

OMITTED FROM SUMMARY TABLE

Formation experiments are listed separately in the preceding entry.

Probably there are two states at the same mass with the same quantum numbers, one decaying to Σπ and Λπ, the other to Λ(1405)π. See the note in front of the preceding entry.

**Σ(1670) MASS
(PRODUCTION EXPERIMENTS)**

VALUE (MeV)	EVTs	DOCUMENT ID	TECN	CHG	COMMENT
≈ 1670 OUR ESTIMATE					
1670 ± 4		¹ CARROLL 76	DPWA		Isospin-1 total σ
1675 ± 10		² HEPP 76	DBC	-	K ⁻ N 1.6-1.75 GeV/c
1665 ± 1		APSELL 74	HBC		K ⁻ p 2.87 GeV/c
1688 ± 2 or 1683 ± 5	1.2k	BERTHON 74	HBC	0	Quasi-2-body σ
1670 ± 6		AGUILAR-... 70B	HBC		K ⁻ p → Σππ 4 GeV
1668 ± 10		AGUILAR-... 70B	HBC		K ⁻ p → Σ3π 4 GeV
1660 ± 10		ALVAREZ 63	HBC	+	K ⁻ p 1.51 GeV/c
• • • We do not use the following data for averages, fits, limits, etc. • • •					
1668 ± 10	150	³ FERRERSORIA 81	OMEG	-	π ⁻ p 9,12 GeV/c
1655 to 1677		TIMMERMANS76	HBC	+	K ⁻ p 4.2 GeV/c
1665 ± 5		BUGG 68	CNTR		K ⁻ p, d total σ
1661 ± 9	70	PRIMER 68	HBC	+	See BARNES 69E
1685		ALEXANDER 62C	HBC	-0	π ⁻ p 2-2.2 GeV/c

**Σ(1670) WIDTH
(PRODUCTION EXPERIMENTS)**

VALUE (MeV)	EVTs	DOCUMENT ID	TECN	CHG	COMMENT
67.0 ± 2.4		APSELL 74	HBC		K ⁻ p 2.87 GeV/c
110 ± 12		AGUILAR-... 70B	HBC		K ⁻ p → Σππ 4 GeV
135 ⁺⁴⁰ / ₋₃₀		AGUILAR-... 70B	HBC		K ⁻ p → Σ3π 4 GeV
40 ± 10		ALVAREZ 63	HBC	+	
• • • We do not use the following data for averages, fits, limits, etc. • • •					
90 ± 20	150	³ FERRERSORIA 81	OMEG	-	π ⁻ p 9,12 GeV/c
52		¹ CARROLL 76	DPWA		Isospin-1 total σ
48 to 63		TIMMERMANS76	HBC	+	K ⁻ p 4.2 GeV/c
30 ± 15		BUGG 68	CNTR		
60 ± 20	70	PRIMER 68	HBC	+	See BARNES 69E
45		ALEXANDER 62C	HBC	-0	

**Σ(1670) DECAY MODES
(PRODUCTION EXPERIMENTS)**

Mode	
Γ ₁	N \bar{K}
Γ ₂	Λπ
Γ ₃	Σπ
Γ ₄	Λππ
Γ ₅	Σππ
Γ ₆	Σ(1385)π
Γ ₇	Λ(1405)π

**Σ(1670) BRANCHING RATIOS
(PRODUCTION EXPERIMENTS)**

Γ(N \bar{K})/Γ(Σπ)	Γ ₁ /Γ ₃				
VALUE	EVTs	DOCUMENT ID	TECN	CHG	COMMENT
<0.03		TIMMERMANS76	HBC	+	K ⁻ p 4.2 GeV/c
<0.10		BERTHON 74	HBC	0	Quasi-2-body σ
<0.2		AGUILAR-... 70B	HBC		
<0.26		BARNES 69E	HBC	+	K ⁻ p 3.9-5 GeV/c
0.025		BUGG 68	CNTR	0	Assuming J = 3/2
<0.24	0	PRIMER 68	HBC	+	K ⁻ p 4.6-5 GeV/c
<0.6		LONDON 66	HBC	+	K ⁻ p 2.25 GeV/c
<0.19	0	ALVAREZ 63	HBC	+	K ⁻ p 1.15 GeV/c
≥ 0.5 ± 0.25		SMITH 63	HBC	-0	

Γ(Λπ)/Γ(Σπ)

VALUE	EVTs	DOCUMENT ID	TECN	CHG	COMMENT	Γ ₂ /Γ ₃
0.76 ± 0.09		ESTES 74	HBC	0	K ⁻ p 2.1,2.6 GeV/c	
0.45 ± 0.15		BARNES 69E	HBC	+	K ⁻ p 3.9-5 GeV/c	
0.15 ± 0.07		HUWE 69	HBC	+		
0.11 ± 0.06	33	BUTTON-...	68	HBC	+	K ⁻ p 1.7 GeV/c
• • • We do not use the following data for averages, fits, limits, etc. • • •						
≤ 0.45 ± 0.07		TIMMERMANS76	HBC	+	K ⁻ p 4.2 GeV/c	
0.55 ± 0.11		BERTHON 74	HBC	0	Quasi-2-body σ	
0	0	PRIMER 68	HBC	+	See BARNES 69E	
<0.6		LONDON 66	HBC	+	K ⁻ p 2.25 GeV/c	
1.2	130	ALVAREZ 63	HBC	+	K ⁻ p 1.15 GeV/c	
1.2		SMITH 63	HBC	-0		

Γ(Λππ)/Γ(Σπ)

VALUE	EVTs	DOCUMENT ID	TECN	CHG	COMMENT	Γ ₄ /Γ ₃
<0.6		LONDON 66	HBC	+	K ⁻ p 2.25 GeV/c	
0.56	90	ALVAREZ 63	HBC	+	K ⁻ p 1.15 GeV/c	
0.17		SMITH 63	HBC	-0		

Γ(Σππ)/Γ(Σπ)

VALUE	EVTs	DOCUMENT ID	TECN	CHG	COMMENT	Γ ₅ /Γ ₃
largest at small angles		ESTES 74	HBC	0	K ⁻ p 2.1,2.6 GeV/c	
• • • We do not use the following data for averages, fits, limits, etc. • • •						
<0.2	²	HEPP 76	DBC	-	K ⁻ N 1.6-1.75 GeV/c	
0.56	180	ALVAREZ 63	HBC	+	K ⁻ p 1.15 GeV/c	

Γ(Λ(1405)π)/Γ(Σπ)

VALUE	EVTs	DOCUMENT ID	TECN	CHG	COMMENT	Γ ₇ /Γ ₃
1.8 ± 0.3 to 0.02 ± 0.07		^{3,4} TIMMERMANS76	HBC	+	K ⁻ p 4.2 GeV/c	
largest at small angles		ESTES 74	HBC	±	K ⁻ p 2.1,2.6 GeV/c	
3.0 ± 1.6	50	LONDON 66	HBC	+	K ⁻ p 2.25 GeV/c	
• • • We do not use the following data for averages, fits, limits, etc. • • •						
0.58 ± 0.20	17	PRIMER 68	HBC	+	See BARNES 69E	

Γ(Σπ)/Γ(Σππ)

VALUE	DOCUMENT ID	TECN	CHG	COMMENT	Γ ₃ /Γ ₅
varies with prod. angle	⁵ APSELL 74	HBC	+	K ⁻ p 2.87 GeV/c	
1.39 ± 0.16	BERTHON 74	HBC	0	Quasi-2-body σ	
2.5 to 0.24	⁴ EBERHARD 69	HBC		K ⁻ p 2.6 GeV/c	
<0.4	BIRMINGHAM 66	HBC	+	K ⁻ p 3.5 GeV/c	
0.30 ± 0.15	LONDON 66	HBC	+	K ⁻ p 2.25 GeV/c	

Γ(Λ(1405)π)/Γ(Σππ)

VALUE	DOCUMENT ID	TECN	CHG	COMMENT	Γ ₇ /Γ ₅
0.97 ± 0.08	TIMMERMANS76	HBC		K ⁻ p 4.2 GeV/c	
1.00 ± 0.02	APSELL 74	HBC		K ⁻ p 2.87 GeV/c	
0.90 ^{+0.10} / _{-0.16}	EBERHARD 65	HBC	+	K ⁻ p 2.45 GeV/c	

Γ(Λ(1405)π)/Γ(Σ(1385)π)

VALUE	DOCUMENT ID	TECN	CHG	COMMENT	Γ ₇ /Γ ₆
<0.8	EBERHARD 65	HBC	+	K ⁻ p 2.45 GeV/c	

Γ(Λππ)/Γ(Σππ)

VALUE	DOCUMENT ID	TECN	CHG	COMMENT	Γ ₄ /Γ ₅
0.35 ± 0.2	BIRMINGHAM 66	HBC	+	K ⁻ p 3.5 GeV/c	

Γ(Λπ)/Γ(Σππ)

VALUE	DOCUMENT ID	TECN	CHG	COMMENT	Γ ₂ /Γ ₅
<0.2	BIRMINGHAM 66	HBC	+	K ⁻ p 3.5 GeV/c	

Γ(Λπ)/[Γ(Λπ) + Γ(Σπ)]

VALUE	DOCUMENT ID	TECN	CHG	COMMENT	Γ ₂ /[Γ ₂ +Γ ₃]
<0.6	AGUILAR-... 70B	HBC			

Baryon Particle Listings

 $\Sigma(1670)$ Bumps, $\Sigma(1690)$ Bumps, $\Sigma(1750)$ $\Gamma(\Sigma(1385)\pi)/\Gamma(\Sigma\pi)$

VALUE	DOCUMENT ID	TECN	COMMENT	Γ_6/Γ_3
$\leq 0.21 \pm 0.05$	TIMMERMANS76	HBC	$K^- p$ 4.2 GeV/c	

 $\Sigma(1670)$ QUANTUM NUMBERS
(PRODUCTION EXPERIMENTS)

VALUE	EVTS	DOCUMENT ID	TECN	CHG	COMMENT
$J^P = 3/2^-$	400	BUTTON-...	68	HBC	\pm $\Sigma^0 \pi$
$J^P = 3/2^-$		EBERHARD	67	HBC	$+$ $\Lambda(1405) \pi$
$J^P = 3/2^+$		LEVEQUE	65	HBC	$\Lambda(1405) \pi$

 $\Sigma(1670)$ FOOTNOTES

- Total cross-section bump with $(J+1/2) \Gamma_{el} / \Gamma_{total} = 0.23$.
- Enhancements in $\Sigma \pi$ and $\Sigma \pi \pi$ cross sections.
- Backward production in the $\Lambda \pi^- K^+$ final state.
- Depending on production angle.
- APSELL 74, ESTES 74, and TIMMERMANS 76 find strong branching ratio dependence on production angle, as in earlier production experiments.

 $\Sigma(1670)$ REFERENCES
(PRODUCTION EXPERIMENTS)

FERRERSORIA 81	NP B178 373	A. Ferrer Soria et al.	(CERN, CDEF, EPOL+)
CARROLL 76	PRL 37 806	A.S. Carroll et al.	(BNL) I
HEPP 76	NP B115 82	V. Hepp et al.	(CERN, HEID, MPIM) I
TIMMERMANS 76	NP B112 77	J.J.M. Timmermans et al.	(NIJM, CERN+) JP
APSELL 74	PR D10 1419	S.P. Apsell et al.	(BRAN, UMD, SYRA+) I
BERTHON 74	NC 21A 146	A. Berthon et al.	(CDEF, RHEL, SACL+) I
ESTES 74	Thesis LBL-3827	R.D. Estes	(LBL)
AGUILAR-... 70B	PRL 25 58	M. Aguilar-Benitez et al.	(BNL, SYRA)
BARNES 69E	BNL 13823	V.E. Barnes et al.	(BNL, SYRA)
EBERHARD 69	PRL 22 200	P.H. Eberhard et al.	(LRL)
HUVE 69	PR 181 1824	D.O. Huve	(LRL)
BUGG 68	PR 168 1466	D.V. Bugg et al.	(RHEL, BIRM, CAVE) I
BUTTON-... 68	PRL 21 1123	J. Button-Shafer	(MASA, LRL) JP
PRIMER 68	PRL 20 610	M. Primer et al.	(SYRA, BNL)
EBERHARD 67	PR 163 1446	P. Eberhard et al.	(LRL, ILL) IJP
BIRMINGHAM 66	PR 152 1148	M. Haque et al.	(BIRM, GLAS, LOIC, OXF+) I
LONDON 66	PR 143 1034	G.W. London et al.	(BNL, SYRA) IJ
EBERHARD 65	PRL 14 466	P.H. Eberhard et al.	(LRL, ILL) I
LEVEQUE 65	PL 18 69	A. Leveque et al.	(SACL, EPOL, GLAS+) JP
ALVAREZ 63	PRL 10 184	L.W. Alvarez et al.	(LRL) I
SMITH 63	Athens Conf. 67	G.A. Smith	(LRL)
ALEXANDER 62C	CERN Conf. 320	G. Alexander et al.	(LRL) I

 $\Sigma(1690)$ Bumps

$$I(J^P) = 1(?)^? \quad \text{Status: **}$$

OMITTED FROM SUMMARY TABLE

See the note preceding the $\Sigma(1670)$ Listings. Seen in production experiments only, mainly in $\Lambda \pi$. $\Sigma(1690)$ MASS
(PRODUCTION EXPERIMENTS)

VALUE (MeV)	EVTS	DOCUMENT ID	TECN	CHG	COMMENT
≈ 1690 OUR ESTIMATE					
1698 ± 20	70	¹ GODDARD	79	HBC	$+$ $\pi^+ p$ 10.3 GeV/c
1707 ± 20	40	² GODDARD	79	HBC	$+$ $\pi^+ p$ 10.3 GeV/c
1698 ± 20	15	ADERHOLZ	69	HBC	$+$ $\pi^+ p$ 8 GeV/c
1682 ± 2	46	BLUMENFELD	69	HBC	$+$ $K_L^0 p$
1700 ± 20		MOTT	69	HBC	$+$ $K^- p$ 5.5 GeV/c
1694 ± 24	60	³ PRIMER	68	HBC	$+$ $K^- p$ 4.6-5 GeV/c
1700 ± 6		⁴ SIMS	68	HBC	$-$ $K^- N \rightarrow \Lambda \pi \pi$
1715 ± 12	30	COLLEY	67	HBC	$+$ $K^- p$ 6 GeV/c

 $\Sigma(1690)$ WIDTH
(PRODUCTION EXPERIMENTS)

VALUE (MeV)	EVTS	DOCUMENT ID	TECN	CHG	COMMENT
240 ± 60	70	¹ GODDARD	79	HBC	$+$ $\pi^+ p$ 10.3 GeV/c
$130^+_{-100} \pm 60$	40	² GODDARD	79	HBC	$+$ $\pi^+ p$ 10.3 GeV/c
142 ± 40	15	ADERHOLZ	69	HBC	$+$ $\pi^+ p$ 8 GeV/c
25 ± 10	46	BLUMENFELD	69	HBC	$+$ $K_L^0 p$
130 ± 25		MOTT	69	HBC	$+$ $K^- p$ 5.5 GeV/c
105 ± 35	60	³ PRIMER	68	HBC	$+$ $K^- p$ 4.6-5 GeV/c
62 ± 14		⁴ SIMS	68	HBC	$-$ $K^- N \rightarrow \Lambda \pi \pi$
100 ± 35	30	COLLEY	67	HBC	$+$ $K^- p$ 6 GeV/c

 $\Sigma(1690)$ DECAY MODES
(PRODUCTION EXPERIMENTS)

Mode	Γ_1/Γ_2
Γ_1 $N \bar{K}$	
Γ_2 $\Lambda \pi$	
Γ_3 $\Sigma \pi$	
Γ_4 $\Sigma(1385) \pi$	
Γ_5 $\Lambda \pi \pi$ (including $\Sigma(1385) \pi$)	

 $\Sigma(1690)$ BRANCHING RATIOS
(PRODUCTION EXPERIMENTS)

$\Gamma(N \bar{K})/\Gamma(\Lambda \pi)$	VALUE	EVTS	DOCUMENT ID	TECN	CHG	COMMENT	Γ_1/Γ_2
	small		GODDARD	79	HBC	$+$ $\pi^+ p$ 10.2 GeV/c	
	< 0.2		MOTT	69	HBC	$+$ $K^- p$ 5.5 GeV/c	
	0.4 ± 0.25	18	COLLEY	67	HBC	$+$ 6/30 events	

$\Gamma(\Sigma \pi)/\Gamma(\Lambda \pi)$	VALUE	CL%	DOCUMENT ID	TECN	CHG	COMMENT	Γ_3/Γ_2
	small		GODDARD	79	HBC	$+$ $\pi^+ p$ 10.2 GeV/c	
	< 0.4	90	MOTT	69	HBC	$+$ $K^- p$ 5.5 GeV/c	
	0.3 ± 0.3		COLLEY	67	HBC	$+$ 4/30 events	

$\Gamma(\Sigma(1385) \pi)/\Gamma(\Lambda \pi)$	VALUE	DOCUMENT ID	TECN	CHG	COMMENT	Γ_4/Γ_2
	< 0.5	MOTT	69	HBC	$+$ $K^- p$ 5.5 GeV/c	

$\Gamma(\Lambda \pi \pi \text{ (including } \Sigma(1385) \pi))/\Gamma(\Lambda \pi)$	VALUE	DOCUMENT ID	TECN	CHG	COMMENT	Γ_5/Γ_2
	2.0 ± 0.6	BLUMENFELD	69	HBC	$+$ 31/15 events	
	0.5 ± 0.25	COLLEY	67	HBC	$+$ 15/30 events	

$\Gamma(\Sigma(1385) \pi)/\Gamma(\Lambda \pi \pi \text{ (including } \Sigma(1385) \pi))$	VALUE	DOCUMENT ID	TECN	CHG	COMMENT	Γ_4/Γ_5
	large	SIMS	68	HBC	$-$ $K^- N \rightarrow \Lambda \pi \pi$	
	small	COLLEY	67	HBC	$+$ $K^- p$ 6 GeV/c	

 $\Sigma(1690)$ FOOTNOTES
(PRODUCTION EXPERIMENTS)

- From $\pi^+ p \rightarrow (\Lambda \pi^+) K^+$, $J > 1/2$ is not required by the data.
- From $\pi^+ p \rightarrow (\Lambda \pi^+) (K \pi)^+$, $J > 1/2$ is indicated, but large background precludes a definite conclusion.
- See the $\Sigma(1670)$ Listings. AGUILAR-BENITEZ 70B with three times the data of PRIMER 68 find no evidence for the $\Sigma(1690)$.
- This analysis, which is difficult and requires several assumptions and shows no unambiguous $\Sigma(1690)$ signal, suggests $J^P = 5/2^+$. Such a state would lead all previously known Y^* trajectories.

 $\Sigma(1690)$ REFERENCES
(PRODUCTION EXPERIMENTS)

GODDARD 79	PR D19 1350	M.C. Goddard et al.	(TNT0, BNL) IJ
AGUILAR-... 70B	PRL 25 58	M. Aguilar-Benitez et al.	(BNL, SYRA)
ADERHOLZ 69	NP B11 259	M. Aderholz et al.	(AACH3, BERL, CERN+) I
BLUMENFELD 69	PL 29B 58	B.J. Blumenfeld, G.R. Kabfleisch	(BNL) I
MOTT 69	PR 177 1966	J. Mott et al.	(NWES, ANL) I
Also	PRL 18 266	M. Derrick et al.	(ANL, NWES) I
PRIMER 68	PRL 20 610	M. Primer et al.	(SYRA, BNL) I
SIMS 68	PRL 21 1413	W.H. Sims et al.	(FSU, TUFTS, BRAN) I
COLLEY 67	PL 24B 489	D.C. Colley	(BIRM, GLAS, LOIC, MUNI, OXF+) I

 $\Sigma(1750) S_{11}$

$$I(J^P) = 1(\frac{1}{2}^-) \quad \text{Status: ***}$$

For most results published before 1974 (they are now obsolete), see our 1982 edition Physics Letters **111B** 1 (1982).There is evidence for this state in many partial-wave analyses, but with wide variations in the mass, width, and couplings. The latest analyses indicated significant couplings to $N \bar{K}$ and $\Lambda \pi$, as well as to $\Sigma \eta$ whose threshold is at 1746 MeV (JONES 74). $\Sigma(1750)$ MASS

VALUE (MeV)	DOCUMENT ID	TECN	COMMENT
1730 ± 1800 (≈ 1750) OUR ESTIMATE			
1756 ± 10	GOPAL 80	DPWA	$\bar{K} N \rightarrow \bar{K} N$
1770 ± 10	ALSTON-... 78	DPWA	$\bar{K} N \rightarrow \bar{K} N$
1770 ± 15	GOPAL 77	DPWA	$\bar{K} N$ multichannel

See key on page 405

Baryon Particle Listings
 $\Sigma(1750)$, $\Sigma(1770)$

• • • We do not use the following data for averages, fits, limits, etc. • • •

1800 or 1813	1	MARTIN	77	DPWA	$\bar{K}N$ multichannel
1715 ± 10	2	CARROLL	76	DPWA	Isospin-1 total σ
1730		DEBELLEFON	76	IPWA	$K^- p \rightarrow \Lambda \pi^0$
1780 ± 30		BAILLON	75	IPWA	$\bar{K}N \rightarrow \Lambda \pi$ (sol. 1)
1700 ± 30		BAILLON	75	IPWA	$\bar{K}N \rightarrow \Lambda \pi$ (sol. 2)
1697 ⁺²⁰ ₋₁₀		VANHORN	75	DPWA	$K^- p \rightarrow \Lambda \pi^0$
1785 ± 12		CHU	74	DBC	Fits $\sigma(K^- n \rightarrow \Sigma^- \eta)$
1760 ± 5	3	JONES	74	HBC	Fits $\sigma(K^- p \rightarrow \Sigma^0 \eta)$
1739 ± 10		PREVOST	74	DPWA	$K^- N \rightarrow \Sigma(1385) \pi$

 $\Sigma(1750)$ WIDTH

VALUE (MeV)	DOCUMENT ID	TECN	COMMENT		
60 to 160 (≈ 90) OUR ESTIMATE					
64 ± 10	GOPAL	80	DPWA $\bar{K}N \rightarrow \bar{K}N$		
161 ± 20	ALSTON-...	78	DPWA $\bar{K}N \rightarrow \bar{K}N$		
60 ± 10	GOPAL	77	DPWA $\bar{K}N$ multichannel		
• • • We do not use the following data for averages, fits, limits, etc. • • •					
117 or 119	1	MARTIN	77	DPWA	$\bar{K}N$ multichannel
10	2	CARROLL	76	DPWA	Isospin-1 total σ
110		DEBELLEFON	76	IPWA	$K^- p \rightarrow \Lambda \pi^0$
140 ± 30		BAILLON	75	IPWA	$\bar{K}N \rightarrow \Lambda \pi$ (sol. 1)
160 ± 5.0		BAILLON	75	IPWA	$\bar{K}N \rightarrow \Lambda \pi$ (sol. 2)
66 ⁺¹⁴ ₋₁₂		VANHORN	75	DPWA	$K^- p \rightarrow \Lambda \pi^0$
89 ± 33		CHU	74	DBC	Fits $\sigma(K^- n \rightarrow \Sigma^- \eta)$
92 ± 7	3	JONES	74	HBC	Fits $\sigma(K^- p \rightarrow \Sigma^0 \eta)$
108 ± 20		PREVOST	74	DPWA	$K^- N \rightarrow \Sigma(1385) \pi$

 $\Sigma(1750)$ DECAY MODES

Mode	Fraction (Γ_i/Γ)
Γ_1 $N\bar{K}$	10–40 %
Γ_2 $\Lambda\pi$	seen
Γ_3 $\Sigma\pi$	< 8 %
Γ_4 $\Sigma\eta$	15–55 %
Γ_5 $\Sigma(1385)\pi$	
Γ_6 $\Lambda(1520)\pi$	

The above branching fractions are our estimates, not fits or averages.

 $\Sigma(1750)$ BRANCHING RATIOSSee "Sign conventions for resonance couplings" in the Note on Λ and Σ Resonances. $\Gamma(N\bar{K})/\Gamma_{\text{total}}$ Γ_1/Γ

VALUE	DOCUMENT ID	TECN	COMMENT		
0.1 to 0.4 OUR ESTIMATE					
0.14 ± 0.03	GOPAL	80	DPWA $\bar{K}N \rightarrow \bar{K}N$		
0.33 ± 0.05	ALSTON-...	78	DPWA $\bar{K}N \rightarrow \bar{K}N$		
• • • We do not use the following data for averages, fits, limits, etc. • • •					
0.15 ± 0.03	GOPAL	77	DPWA See GOPAL 80		
0.06 or 0.05	1	MARTIN	77	DPWA	$\bar{K}N$ multichannel

 $(\Gamma_1\Gamma_2)^{1/2}/\Gamma_{\text{total}}$ in $N\bar{K} \rightarrow \Sigma(1750) \rightarrow \Lambda\pi$ $(\Gamma_1\Gamma_2)^{1/2}/\Gamma$

VALUE	DOCUMENT ID	TECN	COMMENT		
0.04 ± 0.03	GOPAL	77	DPWA $\bar{K}N$ multichannel		
• • • We do not use the following data for averages, fits, limits, etc. • • •					
−0.10 or −0.09	1	MARTIN	77	DPWA	$\bar{K}N$ multichannel
−0.12		DEBELLEFON	76	IPWA	$K^- p \rightarrow \Lambda \pi^0$
−0.12 ± 0.02		BAILLON	75	IPWA	$\bar{K}N \rightarrow \Lambda \pi$ (sol. 1)
−0.13 ± 0.03		BAILLON	75	IPWA	$\bar{K}N \rightarrow \Lambda \pi$ (sol. 2)
−0.13 ± 0.04		VANHORN	75	DPWA	$K^- p \rightarrow \Lambda \pi^0$
−0.120 ± 0.077		DEVENISH	74B		Fixed- t dispersion rel.

 $(\Gamma_1\Gamma_2)^{1/2}/\Gamma_{\text{total}}$ in $N\bar{K} \rightarrow \Sigma(1750) \rightarrow \Sigma\pi$ $(\Gamma_1\Gamma_3)^{1/2}/\Gamma$

VALUE	DOCUMENT ID	TECN	COMMENT		
−0.09 ± 0.05	GOPAL	77	DPWA $\bar{K}N$ multichannel		
• • • We do not use the following data for averages, fits, limits, etc. • • •					
+0.06 or +0.06	1	MARTIN	77	DPWA	$\bar{K}N$ multichannel
0.13 ± 0.02		LANGBEIN	72	IPWA	$\bar{K}N$ multichannel

 $(\Gamma_1\Gamma_2)^{1/2}/\Gamma_{\text{total}}$ in $N\bar{K} \rightarrow \Sigma(1750) \rightarrow \Sigma\eta$ $(\Gamma_1\Gamma_4)^{1/2}/\Gamma$

VALUE	DOCUMENT ID	TECN	COMMENT		
0.23 ± 0.01	3	JONES	74	HBC	Fits $\sigma(K^- p \rightarrow \Sigma^0 \eta)$
• • • We do not use the following data for averages, fits, limits, etc. • • •					
seen		CLINE	69	DBC	Threshold bump

 $(\Gamma_1\Gamma_2)^{1/2}/\Gamma_{\text{total}}$ in $N\bar{K} \rightarrow \Sigma(1750) \rightarrow \Sigma(1385)\pi$ $(\Gamma_1\Gamma_5)^{1/2}/\Gamma$

VALUE	DOCUMENT ID	TECN	COMMENT		
+0.18 ± 0.15		PREVOST	74	DPWA	$K^- N \rightarrow \Sigma(1385) \pi$

 $(\Gamma_1\Gamma_2)^{1/2}/\Gamma_{\text{total}}$ in $N\bar{K} \rightarrow \Sigma(1750) \rightarrow \Lambda(1520)\pi$ $(\Gamma_1\Gamma_6)^{1/2}/\Gamma$

VALUE	DOCUMENT ID	TECN	COMMENT		
0.032 ± 0.021		CAMERON	77	DPWA	P -wave decay

 $\Sigma(1750)$ FOOTNOTES

1 The two MARTIN 77 values are from a T-matrix pole and from a Breit-Wigner fit.

2 A total cross-section bump with $(J+1/2) \Gamma_{\text{el}} / \Gamma_{\text{total}} = 0.30$.

3 An S-wave Breit-Wigner fit to the threshold cross section with no background and errors statistical only.

 $\Sigma(1750)$ REFERENCES

PDG	82	PL 111B 1	M. Roos et al.	(HELS, CIT, CERN)
GOPAL	80	Toronto Conf. 159	G.P. Gopal	(RHEL) IJP
ALSTON-...	78	PR D18 182	M. Alston-Garnjost et al.	(LBL, MTHO+) IJP
Also		PRL 38 1007	M. Alston-Garnjost et al.	(LBL, MTHO+) IJP
CAMERON	77	NP B131 399	W. Cameron et al.	(RHEL, LOIC) IJP
GOPAL	77	NP B119 362	G.P. Gopal et al.	(LOIC, RHEL) IJP
MARTIN	77	NP B127 349	B.R. Martin, M.K. Pidcock, R.G. Moorhouse	(LOUC+) IJP
Also		NP B126 266	B.R. Martin, M.K. Pidcock	(LOUC) IJP
Also		NP B126 285	B.R. Martin, M.K. Pidcock	(LOUC) IJP
CARROLL	76	PRL 37 806	A.S. Carroll et al.	(BNL) I
DEBELLEFON	76	NP B109 129	A. de Bellefon, A. Berthon	(CDEF) IJP
BAILLON	75	NP B94 39	P.H. Baillon, P.J. Litchfield	(CERN, RHEL) IJP
VANHORN	75	NP B87 145	A.J. van Horn	(LBL) IJP
Also		NP B87 157	A.J. van Horn	(LBL) IJP
CHU	74B	NC 20A 35	R.Y.L. Chu et al.	(PLAT, TUFTS, BRAN) IJP
DEVENISH	74B	NP B81 330	R.C.E. Devenish, C.D. Froggatt, B.R. Martin	(DESY+) IJP
JONES	74	NP B73 141	M.D. Jones	(CHIC) IJP
PREVOST	74	NP B69 246	J. Prevost et al.	(SACL, CERN, HEID) IJP
LANGBEIN	72	NP B47 477	W. Langbein, F. Wagner	(MFIM) IJP
CLINE	69	LCN 2 407	D. Cline, R. Laumann, J. Mapp	(WISC) IJP

 $\Sigma(1770) P_{11}$ $I(J^P) = 1(\frac{1}{2}^+)$ Status: *

OMITTED FROM SUMMARY TABLE

Evidence for this state now rests solely on solution 1 of BAILLON 75, (see the footnotes) but the $\Lambda\pi$ partial-wave amplitudes of this solution are in disagreement with amplitudes from most other $\Lambda\pi$ analyses. $\Sigma(1770)$ MASS

VALUE (MeV)	DOCUMENT ID	TECN	COMMENT		
≈ 1770 OUR ESTIMATE					
1738 ± 10	1	GOPAL	77	DPWA	$\bar{K}N$ multichannel
1770 ± 20	2	BAILLON	75	IPWA	$\bar{K}N \rightarrow \Lambda\pi$
1772	3	KANE	72	DPWA	$K^- p \rightarrow \Sigma\pi$

 $\Sigma(1770)$ WIDTH

VALUE (MeV)	DOCUMENT ID	TECN	COMMENT		
72 ± 10	1	GOPAL	77	DPWA	$\bar{K}N$ multichannel
80 ± 30	2	BAILLON	75	IPWA	$\bar{K}N \rightarrow \Lambda\pi$
80	3	KANE	72	DPWA	$K^- p \rightarrow \Sigma\pi$

 $\Sigma(1770)$ DECAY MODES

Mode
Γ_1 $N\bar{K}$
Γ_2 $\Lambda\pi$
Γ_3 $\Sigma\pi$

 $\Sigma(1770)$ BRANCHING RATIOSSee "Sign conventions for resonance couplings" in the Note on Λ and Σ Resonances. $\Gamma(N\bar{K})/\Gamma_{\text{total}}$ Γ_1/Γ

VALUE	DOCUMENT ID	TECN	COMMENT		
0.14 ± 0.04	1	GOPAL	77	DPWA	$\bar{K}N$ multichannel

 $(\Gamma_1\Gamma_2)^{1/2}/\Gamma_{\text{total}}$ in $N\bar{K} \rightarrow \Sigma(1770) \rightarrow \Lambda\pi$ $(\Gamma_1\Gamma_2)^{1/2}/\Gamma$

VALUE	DOCUMENT ID	TECN	COMMENT		
< 0.04		GOPAL	77	DPWA	$\bar{K}N$ multichannel
−0.08 ± 0.02	2	BAILLON	75	IPWA	$\bar{K}N \rightarrow \Lambda\pi$

 $(\Gamma_1\Gamma_2)^{1/2}/\Gamma_{\text{total}}$ in $N\bar{K} \rightarrow \Sigma(1770) \rightarrow \Sigma\pi$ $(\Gamma_1\Gamma_3)^{1/2}/\Gamma$

VALUE	DOCUMENT ID	TECN	COMMENT		
< 0.04		GOPAL	77	DPWA	$\bar{K}N$ multichannel
−0.108	3	KANE	72	DPWA	$K^- p \rightarrow \Sigma\pi$

Baryon Particle Listings

 $\Sigma(1770)$, $\Sigma(1775)$ $\Sigma(1770)$ FOOTNOTES

- ¹ Required to fit the isospin-1 total cross section of CARROLL 76 in the $\bar{K}N$ channel. The addition of new K^-p polarization and K^-n differential cross-section data in GOPAL 80 find it to be more consistent with the $\Sigma(1660) P_{11}$.
- ² From solution 1 of BAILLON 75; not present in solution 2.
- ³ Not required in KANE 74, which supersedes KANE 72.

 $\Sigma(1770)$ REFERENCES

Author	Year	Conference	Document ID	TECN	COMMENT
GOPAL	80	Toronto Conf.	159		(RHEL)
GOPAL	77	NP B119	362		(LOIC, RHEL) IJP
CARROLL	76	PRL	37 806		A.S. Carroll et al. (BNL) I
BAILLON	75	NP B94	39		P.H. Baillon, P.J. Litchfield (CERN, RHEL) IJP
KANE	74	LBL-2452			D.F. Kane (LBL) IJP
KANE	72	PR D5	1583		D.F.J. Kane (LBL)

 $\Sigma(1775) D_{15}$

$$J(J^P) = 1(\frac{5}{2}^-) \text{ Status: } ****$$

Discovered by GALTIERI 63, this resonance plays the same role as cornerstone for isospin-1 analyses in this region as the $\Lambda(1820)F_{05}$ does in the isospin-0 channel.

For most results published before 1974 (they are now obsolete), see our 1982 edition Physics Letters **111B** 1 (1982).

 $\Sigma(1775)$ MASS

VALUE (MeV)	DOCUMENT ID	TECN	COMMENT
1770 to 1780 (≈ 1775) OUR ESTIMATE			
1778 \pm 5	GOPAL 80	DPWA	$\bar{K}N \rightarrow \bar{K}N$
1777 \pm 5	ALSTON-... 78	DPWA	$\bar{K}N \rightarrow \bar{K}N$
1774 \pm 5	GOPAL 77	DPWA	$\bar{K}N$ multichannel
1775 \pm 10	BAILLON 75	IPWA	$\bar{K}N \rightarrow \Lambda\pi$
1774 \pm 10	VANHORN 75	DPWA	$K^-p \rightarrow \Lambda\pi^0$
1772 \pm 6	KANE 74	DPWA	$K^-p \rightarrow \Sigma\pi$
••• We do not use the following data for averages, fits, limits, etc. •••			
1772 or 1777	¹ MARTIN 77	DPWA	$\bar{K}N$ multichannel
1765	DEBELLEFON 76	IPWA	$K^-p \rightarrow \Lambda\pi^0$

 $\Sigma(1775)$ WIDTH

VALUE (MeV)	DOCUMENT ID	TECN	COMMENT
105 to 135 (≈ 120) OUR ESTIMATE			
137 \pm 10	GOPAL 80	DPWA	$\bar{K}N \rightarrow \bar{K}N$
116 \pm 10	ALSTON-... 78	DPWA	$\bar{K}N \rightarrow \bar{K}N$
130 \pm 10	GOPAL 77	DPWA	$\bar{K}N$ multichannel
125 \pm 15	BAILLON 75	IPWA	$\bar{K}N \rightarrow \Lambda\pi$
146 \pm 18	VANHORN 75	DPWA	$K^-p \rightarrow \Lambda\pi^0$
154 \pm 10	KANE 74	DPWA	$K^-p \rightarrow \Sigma\pi$
••• We do not use the following data for averages, fits, limits, etc. •••			
102 or 103	¹ MARTIN 77	DPWA	$\bar{K}N$ multichannel
120	DEBELLEFON 76	IPWA	$K^-p \rightarrow \Lambda\pi^0$

 $\Sigma(1775)$ DECAY MODES

Mode	Fraction (Γ_i/Γ)
Γ_1 $N\bar{K}$	37-43%
Γ_2 $\Lambda\pi$	14-20%
Γ_3 $\Sigma\pi$	2-5%
Γ_4 $\Sigma(1385)\pi$	8-12%
Γ_5 $\Sigma(1385)\pi, D\text{-wave}$	
Γ_6 $\Lambda(1520)\pi$	17-23%
Γ_7 $\Sigma\pi\pi$	

The above branching fractions are our estimates, not fits or averages.

CONSTRAINED FIT INFORMATION

An overall fit to 8 branching ratios uses 16 measurements and one constraint to determine 5 parameters. The overall fit has a $\chi^2 = 63.9$ for 12 degrees of freedom.

The following *off-diagonal* array elements are the correlation coefficients $\langle \delta x_i \delta x_j \rangle / (\delta x_i \delta x_j)$, in percent, from the fit to the branching fractions, $x_i \equiv \Gamma_i/\Gamma_{\text{total}}$. The fit constrains the x_i whose labels appear in this array to sum to one.

x_2	-30			
x_3	-17	-21		
x_4	-37	-49	-14	
x_6	-81	6	8	16
	x_1	x_2	x_3	x_4

 $\Sigma(1775)$ BRANCHING RATIOS

See "Sign conventions for resonance couplings" in the Note on Λ and Σ Resonances. Also, the errors quoted do not include uncertainties due to the parametrization used in the partial-wave analyses and are thus too small.

$\Gamma(N\bar{K})/\Gamma_{\text{total}}$	DOCUMENT ID	TECN	COMMENT
0.37 to 0.43 OUR ESTIMATE			
0.45 \pm 0.04 OUR FIT			Error includes scale factor of 3.1.
0.391 \pm 0.017 OUR AVERAGE			

VALUE	DOCUMENT ID	TECN	COMMENT
0.40 \pm 0.02	GOPAL 80	DPWA	$\bar{K}N \rightarrow \bar{K}N$
0.37 \pm 0.03	ALSTON-... 78	DPWA	$\bar{K}N \rightarrow \bar{K}N$
••• We do not use the following data for averages, fits, limits, etc. •••			
0.41 \pm 0.03	GOPAL 77	DPWA	See GOPAL 80
0.37 or 0.36	¹ MARTIN 77	DPWA	$\bar{K}N$ multichannel

$(\Gamma_i\Gamma_f)^{1/2}/\Gamma_{\text{total}}$ in $N\bar{K} \rightarrow \Sigma(1775) \rightarrow \Lambda\pi$	DOCUMENT ID	TECN	COMMENT
0.305 \pm 0.018 OUR FIT			Error includes scale factor of 2.4.
-0.262 \pm 0.015 OUR AVERAGE			

VALUE	DOCUMENT ID	TECN	COMMENT
-0.28 \pm 0.03	GOPAL 77	DPWA	$\bar{K}N$ multichannel
-0.25 \pm 0.02	BAILLON 75	IPWA	$\bar{K}N \rightarrow \Lambda\pi$
-0.28 \pm 0.04	VANHORN 75	DPWA	$K^-p \rightarrow \Lambda\pi^0$
-0.259 \pm 0.048	DEVENISH 74B		Fixed- t dispersion rel.
••• We do not use the following data for averages, fits, limits, etc. •••			
-0.29 or -0.28	¹ MARTIN 77	DPWA	$\bar{K}N$ multichannel
-0.30	DEBELLEFON 76	IPWA	$K^-p \rightarrow \Lambda\pi^0$

$(\Gamma_i\Gamma_f)^{1/2}/\Gamma_{\text{total}}$ in $N\bar{K} \rightarrow \Sigma(1775) \rightarrow \Sigma\pi$	DOCUMENT ID	TECN	COMMENT
0.105 \pm 0.025 OUR FIT			Error includes scale factor of 3.1.
0.098 \pm 0.016 OUR AVERAGE			Error includes scale factor of 1.8.

VALUE	DOCUMENT ID	TECN	COMMENT
+0.13 \pm 0.02	GOPAL 77	DPWA	$\bar{K}N$ multichannel
0.09 \pm 0.01	KANE 74	DPWA	$K^-p \rightarrow \Sigma\pi$
••• We do not use the following data for averages, fits, limits, etc. •••			
+0.08 or +0.08	¹ MARTIN 77	DPWA	$\bar{K}N$ multichannel

$(\Gamma_i\Gamma_f)^{1/2}/\Gamma_{\text{total}}$ in $N\bar{K} \rightarrow \Sigma(1775) \rightarrow \Lambda(1520)\pi$	DOCUMENT ID	TECN	COMMENT
0.315 \pm 0.010 OUR FIT			Error includes scale factor of 1.5.
0.303 \pm 0.009 OUR AVERAGE			Signs on measurements were ignored.

VALUE	DOCUMENT ID	TECN	COMMENT
-0.305 \pm 0.010	² CAMERON 77	DPWA	$K^-p \rightarrow \Lambda(1520)\pi^0$
0.31 \pm 0.02	BARLETTA 72	DPWA	$K^-p \rightarrow \Lambda(1520)\pi^0$
0.27 \pm 0.03	ARMENTEROS65c	HBC	$K^-p \rightarrow \Lambda(1520)\pi^0$

$(\Gamma_i\Gamma_f)^{1/2}/\Gamma_{\text{total}}$ in $N\bar{K} \rightarrow \Sigma(1775) \rightarrow \Sigma(1385)\pi$	DOCUMENT ID	TECN	COMMENT
0.211 \pm 0.022 OUR FIT			Error includes scale factor of 2.8.
0.188 \pm 0.010 OUR AVERAGE			Signs on measurements were ignored.

VALUE	DOCUMENT ID	TECN	COMMENT
-0.184 \pm 0.011	³ CAMERON 78	DPWA	$K^-p \rightarrow \Sigma(1385)\pi$
+0.20 \pm 0.02	PREVOST 74	DPWA	$K^-n \rightarrow \Sigma(1385)\pi$
••• We do not use the following data for averages, fits, limits, etc. •••			
0.32 \pm 0.06	SIMS 68	DBC	$K^-n \rightarrow \Lambda\pi\pi$
0.24 \pm 0.03	ARMENTEROS67c	HBC	$K^-p \rightarrow \Lambda\pi\pi$

$\Gamma(\Lambda\pi)/\Gamma(N\bar{K})$	DOCUMENT ID	TECN	COMMENT
0.46 \pm 0.09 OUR FIT			Error includes scale factor of 2.9.
0.33 \pm 0.05	UHLIG 67	HBC	K^-p 0.9 GeV/c

$\Gamma(\Sigma\pi\pi)/\Gamma_{\text{total}}$	DOCUMENT ID	TECN	COMMENT
0.12	⁴ ARMENTEROS68c	HDBC	$K^-n \rightarrow \Sigma\pi\pi$

$\Gamma(\Sigma(1385)\pi)/\Gamma(N\bar{K})$	DOCUMENT ID	TECN	COMMENT
0.22 \pm 0.07 OUR FIT			Error includes scale factor of 3.6.
0.25 \pm 0.09	UHLIG 67	HBC	K^-p 0.9 GeV/c

$\Gamma(\Lambda(1520)\pi)/\Gamma(N\bar{K})$	DOCUMENT ID	TECN	COMMENT
0.49 \pm 0.11 OUR FIT			Error includes scale factor of 3.5.
0.28 \pm 0.05	UHLIG 67	HBC	K^-p 0.9 GeV/c

 $\Sigma(1775)$ FOOTNOTES

- ¹ The two MARTIN 77 values are from a T-matrix pole and from a Breit-Wigner fit.
- ² This rate combines P -wave- and F -wave decays. The CAMERON 77 results for the separate P -wave- and F -wave decays are -0.303 ± 0.010 and -0.037 ± 0.014 . The published signs have been changed here to be in accord with the baryon-first convention.
- ³ The CAMERON 78 upper limit on G -wave decay is 0.03.
- ⁴ For about 3/4 of this, the $\Sigma\pi$ system has $l = 0$ and is almost entirely $\Lambda(1520)$. For the rest, the $\Sigma\pi$ has $l = 1$, which is about what is expected from the known $\Sigma(1775) \rightarrow \Sigma(1385)\pi$ rate, as seen in $\Lambda\pi\pi$.

See key on page 405

Baryon Particle Listings

$\Sigma(1775)$, $\Sigma(1840)$, $\Sigma(1880)$

 $\Sigma(1775)$ REFERENCES

PDG	82	PL 111B 1	M. Roos <i>et al.</i>	(HEL5, CIT, CERN)
GOPAL	80	Toronto Conf. 159	G.P. Gopal	(RHEL) IJP
ALSTON...	78	PR D18 182	M. Alston-Garnjost <i>et al.</i>	(LBL, MTHO+) IJP
Also		PRL 38 1007	M. Alston-Garnjost <i>et al.</i>	(LBL, MTHO+) IJP
CAMERON	78	NP B143 189	W. Cameron <i>et al.</i>	(RHEL, LOIC) IJP
CAMERON	77	NP B131 399	W. Cameron <i>et al.</i>	(RHEL, LOIC) IJP
GOPAL	77	NP B119 362	G.P. Gopal <i>et al.</i>	(LOIC, RHEL) IJP
MARTIN	77	NP B127 349	B.R. Martin, M.K. Pidcock, R.G. Moorhouse	(LOUC+) IJP
Also		NP B126 266	B.R. Martin, M.K. Pidcock	(LOUC) IJP
Also		NP B126 285	B.R. Martin, M.K. Pidcock	(LOUC) IJP
DEBELLEFON	76	NP B109 129	A. de Bellefon, A. Berthon	(CDEF) IJP
BAILLON	75	NP B94 39	P.H. Baillon, P.J. Litchfield	(CERN, RHEL) IJP
VANHORN	75	NP B87 145	A.J. van Horn	(LBL) IJP
Also		NP B87 157	A.J. van Horn	(LBL) IJP
DEVENISH	74B	NP B81 330	R.C.E. Devenish, C.D. Froggatt, B.R. Martin	(DESY+) IJP
KANE	74	LBL-2452	D.F. Kane	(LBL) IJP
PREVOST	74	NP B69 246	J. Prevost <i>et al.</i>	(SACL, CERN, HEID) IJP
BARLETTA	72	NP B40 45	W.A. Barletta	(EFI) IJP
Also		PRL 17 841	S. Fenster <i>et al.</i>	(CHIC, ANL, CERN) IJP
ARMENTEROS	68C	NP B8 216	R. Armenteros <i>et al.</i>	(CERN, HEID, SACL) I
SIMS	68	PRL 21 1413	W.H. Sims <i>et al.</i>	(FSU, TUFTS, BRAN)
ARMENTEROS	67C	ZPHY 202 486	R. Armenteros <i>et al.</i>	(CERN, HEID, SACL)
UHLIG	67	PR 155 1448	R.P. Uhlig <i>et al.</i>	(UMD, NRL)
ARMENTEROS	65C	PL 19 338	R. Armenteros <i>et al.</i>	(CERN, HEID, SACL) IJP
GALTIERI	63	PL 6 296	A. Galtieri, A. Hussain, R. Tripp	(LRL) IJ

 $\Sigma(1840)$ REFERENCES

MARTIN	77	NP B127 349	B.R. Martin, M.K. Pidcock, R.G. Moorhouse	(LOUC+) IJP
Also		NP B126 266	B.R. Martin, M.K. Pidcock	(LOUC) IJP
Also		NP B126 285	B.R. Martin, M.K. Pidcock	(LOUC) IJP
BAILLON	75	NP B94 39	P.H. Baillon, P.J. Litchfield	(CERN, RHEL) IJP
VANHORN	75	NP B87 145	A.J. van Horn	(LBL) IJP
Also		NP B87 157	A.J. van Horn	(LBL) IJP
DEVENISH	74B	NP B81 330	R.C.E. Devenish, C.D. Froggatt, B.R. Martin	(DESY+) IJP
LANGBEIN	72	NP B47 477	W. Langbein, F. Wagner	(MFM) IJP

 $\Sigma(1880) P_{11}$

$$I(J^P) = 1(\frac{1}{2}^+) \text{ Status: } **$$

OMITTED FROM SUMMARY TABLE

A P_{11} resonance is suggested by several partial-wave analyses, but with wide variations in the mass and other parameters. We list here all claims which lie well above the $P_{11} \Sigma(1770)$.

 $\Sigma(1880)$ MASS

VALUE (MeV)	DOCUMENT ID	TECN	COMMENT
≈ 1880 OUR ESTIMATE			
1826 ± 20	GOPAL 80	DPWA	$\bar{K}N \rightarrow \bar{K}N$
1870 ± 10	CAMERON 78B	DPWA	$K^- p \rightarrow N\bar{K}^*$
$1847 \text{ or } 1863$	1 MARTIN 77	DPWA	$\bar{K}N$ multichannel
1960 ± 30	2 BAILLON 75	IPWA	$\bar{K}N \rightarrow \Lambda\pi$
1985 ± 50	VANHORN 75	DPWA	$K^- p \rightarrow \Lambda\pi^0$
1898	3 LEA 73	DPWA	Multichannel K-matrix
~ 1850	ARMENTEROS70	IPWA	$\bar{K}N \rightarrow \bar{K}N$
1950 ± 50	BARBARO... 70	DPWA	$K^- N \rightarrow \Lambda\pi$
1920 ± 30	LITCHFIELD 70	DPWA	$K^- N \rightarrow \Lambda\pi$
1850	BAILEY 69	DPWA	$\bar{K}N \rightarrow \bar{K}N$
1882 ± 40	SMART 68	DPWA	$K^- N \rightarrow \Lambda\pi$

 $\Sigma(1880)$ WIDTH

VALUE (MeV)	DOCUMENT ID	TECN	COMMENT
86 ± 15	GOPAL 80	DPWA	$\bar{K}N \rightarrow \bar{K}N$
80 ± 10	CAMERON 78B	DPWA	$K^- p \rightarrow N\bar{K}^*$
$216 \text{ or } 220$	1 MARTIN 77	DPWA	$\bar{K}N$ multichannel
260 ± 40	2 BAILLON 75	IPWA	$\bar{K}N \rightarrow \Lambda\pi$
220 ± 140	VANHORN 75	DPWA	$K^- p \rightarrow \Lambda\pi^0$
222	3 LEA 73	DPWA	Multichannel K-matrix
~ 30	ARMENTEROS70	IPWA	$\bar{K}N \rightarrow \bar{K}N$
200 ± 50	BARBARO... 70	DPWA	$K^- N \rightarrow \Lambda\pi$
170 ± 40	LITCHFIELD 70	DPWA	$K^- N \rightarrow \Lambda\pi$
200	BAILEY 69	DPWA	$\bar{K}N \rightarrow \bar{K}N$
222 ± 150	SMART 68	DPWA	$K^- N \rightarrow \Lambda\pi$

 $\Sigma(1880)$ DECAY MODES

Mode
Γ_1 $N\bar{K}$
Γ_2 $\Lambda\pi$
Γ_3 $\Sigma\pi$
Γ_4 $N\bar{K}^*(892)$, $S=1/2$, P -wave
Γ_5 $N\bar{K}^*(892)$, $S=3/2$, P -wave

 $\Sigma(1880)$ BRANCHING RATIOS

See "Sign conventions for resonance couplings" in the Note on Λ and Σ Resonances.

$\Gamma(N\bar{K})/\Gamma_{\text{total}}$	DOCUMENT ID	TECN	COMMENT	Γ_1/Γ
0.06 ± 0.02	GOPAL 80	DPWA	$\bar{K}N \rightarrow \bar{K}N$	
$0.27 \text{ or } 0.27$	1 MARTIN 77	DPWA	$\bar{K}N$ multichannel	
0.31	3 LEA 73	DPWA	Multichannel K-matrix	
0.20	ARMENTEROS70	IPWA	$\bar{K}N \rightarrow \bar{K}N$	
0.22	BAILEY 69	DPWA	$\bar{K}N \rightarrow \bar{K}N$	

$(\Gamma_1\Gamma_2)^{1/2}/\Gamma_{\text{total}}$ in $N\bar{K} \rightarrow \Sigma(1880) \rightarrow \Lambda\pi$	DOCUMENT ID	TECN	COMMENT	$(\Gamma_1\Gamma_2)^{1/2}/\Gamma$
-0.24 or -0.24	1 MARTIN 77	DPWA	$\bar{K}N$ multichannel	
-0.12 ± 0.02	2 BAILLON 75	IPWA	$\bar{K}N \rightarrow \Lambda\pi$	
$+0.05$ or $+0.07$ -0.02	VANHORN 75	DPWA	$K^- p \rightarrow \Lambda\pi^0$	
-0.169 ± 0.119	DEVENISH 74B		Fixed- t dispersion rel.	
-0.30	3 LEA 73	DPWA	Multichannel K-matrix	
-0.09 ± 0.04	BARBARO... 70	DPWA	$K^- N \rightarrow \Lambda\pi$	
-0.14 ± 0.03	LITCHFIELD 70	DPWA	$K^- N \rightarrow \Lambda\pi$	
-0.11 ± 0.03	SMART 68	DPWA	$K^- N \rightarrow \Lambda\pi$	

 $\Sigma(1840)$ MASS

VALUE (MeV)	DOCUMENT ID	TECN	COMMENT
≈ 1840 OUR ESTIMATE			
$1798 \text{ or } 1802$	1 MARTIN 77	DPWA	$\bar{K}N$ multichannel
1720 ± 30	2 BAILLON 75	IPWA	$\bar{K}N \rightarrow \Lambda\pi$
1925 ± 200	VANHORN 75	DPWA	$K^- p \rightarrow \Lambda\pi^0$
1840 ± 10	LANGBEIN 72	IPWA	$\bar{K}N$ multichannel

 $\Sigma(1840)$ WIDTH

VALUE (MeV)	DOCUMENT ID	TECN	COMMENT
$93 \text{ or } 93$	1 MARTIN 77	DPWA	$\bar{K}N$ multichannel
120 ± 30	2 BAILLON 75	IPWA	$\bar{K}N \rightarrow \Lambda\pi$
65 or $+50$ -20	VANHORN 75	DPWA	$K^- p \rightarrow \Lambda\pi^0$
120 ± 10	LANGBEIN 72	IPWA	$\bar{K}N$ multichannel

 $\Sigma(1840)$ DECAY MODES

Mode
Γ_1 $N\bar{K}$
Γ_2 $\Lambda\pi$
Γ_3 $\Sigma\pi$

 $\Sigma(1840)$ BRANCHING RATIOS

See "Sign conventions for resonance couplings" in the Note on Λ and Σ Resonances.

$\Gamma(N\bar{K})/\Gamma_{\text{total}}$	DOCUMENT ID	TECN	COMMENT	Γ_1/Γ
0 or 0	1 MARTIN 77	DPWA	$\bar{K}N$ multichannel	
0.37 ± 0.13	LANGBEIN 72	IPWA	$\bar{K}N$ multichannel	

$(\Gamma_1\Gamma_2)^{1/2}/\Gamma_{\text{total}}$ in $N\bar{K} \rightarrow \Sigma(1840) \rightarrow \Lambda\pi$	DOCUMENT ID	TECN	COMMENT	$(\Gamma_1\Gamma_2)^{1/2}/\Gamma$
$+0.03$ or $+0.03$	1 MARTIN 77	DPWA	$\bar{K}N$ multichannel	
$+0.11 \pm 0.02$	2 BAILLON 75	IPWA	$\bar{K}N \rightarrow \Lambda\pi$	
$+0.06 \pm 0.04$	VANHORN 75	DPWA	$K^- p \rightarrow \Lambda\pi^0$	
$+0.122 \pm 0.078$	DEVENISH 74B		Fixed- t dispersion rel.	
0.20 ± 0.04	LANGBEIN 72	IPWA	$\bar{K}N$ multichannel	

$(\Gamma_1\Gamma_3)^{1/2}/\Gamma_{\text{total}}$ in $N\bar{K} \rightarrow \Sigma(1840) \rightarrow \Sigma\pi$	DOCUMENT ID	TECN	COMMENT	$(\Gamma_1\Gamma_3)^{1/2}/\Gamma$
-0.04 or -0.04	1 MARTIN 77	DPWA	$\bar{K}N$ multichannel	
0.15 ± 0.04	LANGBEIN 72	IPWA	$\bar{K}N$ multichannel	

 $\Sigma(1840)$ FOOTNOTES

- 1 The two MARTIN 77 values are from a T-matrix pole and from a Breit-Wigner fit.
2 From solution 1 of BAILLON 75; not present in solution 2.

Baryon Particle Listings

$\Sigma(1880), \Sigma(1915)$

$(\Gamma_i \Gamma_f)^{1/2} / \Gamma_{\text{total}}$ in $N\bar{K} \rightarrow \Sigma(1880) \rightarrow \Sigma \pi$ $(\Gamma_1 \Gamma_3)^{1/2} / \Gamma$

VALUE	DOCUMENT ID	TECN	COMMENT
+0.30 or +0.29 not seen	1 MARTIN 77 3 LEA 73	DPWA	$\bar{K}N$ multichannel Multichannel K-matrix

$(\Gamma_i \Gamma_f)^{1/2} / \Gamma_{\text{total}}$ in $N\bar{K} \rightarrow \Sigma(1880) \rightarrow N\bar{K}^*(892), S=1/2, P\text{-wave}$ $(\Gamma_1 \Gamma_4)^{1/2} / \Gamma$

VALUE	DOCUMENT ID	TECN	COMMENT
-0.05 ± 0.03	4 CAMERON 78B	DPWA	$K^- \rho \rightarrow N\bar{K}^*$

$(\Gamma_i \Gamma_f)^{1/2} / \Gamma_{\text{total}}$ in $N\bar{K} \rightarrow \Sigma(1880) \rightarrow N\bar{K}^*(892), S=3/2, P\text{-wave}$ $(\Gamma_1 \Gamma_5)^{1/2} / \Gamma$

VALUE	DOCUMENT ID	TECN	COMMENT
+0.11 ± 0.03	CAMERON 78B	DPWA	$K^- \rho \rightarrow N\bar{K}^*$

$\Sigma(1880)$ FOOTNOTES

- The two MARTIN 77 values are from a T-matrix pole and from a Breit-Wigner fit.
- From solution 1 of BAILLON 75; not present in solution 2.
- Only unconstrained states from table 1 of LEA 73 are listed.
- The published sign has been changed to be in accord with the baryon-first convention.

$\Sigma(1880)$ REFERENCES

GOPAL 80	Toronto Conf. 159	G.P. Gopal	(RHEL) IJP
CAMERON 78B	NP B146 327	W. Cameron et al.	(RHEL, LOIC) IJP
MARTIN 77	NP B127 349	B.R. Martin, M.K. Pidcock, R.G. Moorhouse	(LOUC+) IJP
Also	NP B126 266	B.R. Martin, M.K. Pidcock	(LOUC) IJP
Also	NP B126 285	B.R. Martin, M.K. Pidcock	(LOUC) IJP
BAILLON 75	NP B94 39	P.H. Baillon, P.J. Litchfield	(CERN, RHEL) IJP
VANHORN 75	NP B87 145	A.J. van Horn	(LBL) IJP
Also	NP B87 157	A.J. van Horn	(LBL) IJP
DEVENISH 74B	NP B81 330	R.C.E. Devenish, C.D. Froggatt, B.R. Martin	(DESY+) IJP
LEA 73	NP B56 77	A.T. Lea et al.	(RHEL, LOUC, GLAS, AARH) IJP
ARMENTEROS 70	Duke Conf. 123	R. Armenteros et al.	(CERN, HEID, SACL) IJP
Hyperon Resonances, 1970			
BARBARO... 70	Duke Conf. 173	A. Barbaro-Galiteri	(LRL) IJP
Hyperon Resonances, 1970			
LITCHFIELD 70	NP B22 269	P.J. Litchfield	(RHEL) IJP
BAILEY 69	Thesis UCLR 50617	J.M. Bailey	(LLL) IJP
SMART 68	PR 169 1330	W.M. Smart	(LRL) IJP

$\Sigma(1915) F_{15}$

$$I(J^P) = 1(\frac{5}{2}^+) \text{ Status: } ****$$

Discovered by COOL 66. For results published before 1974 (they are now obsolete), see our 1982 edition Physics Letters **111B** 1 (1982).

This entry only includes results from partial-wave analyses. Parameters of peaks seen in cross sections and invariant-mass distributions in this region used to be listed in a separate entry immediately following. They may be found in our 1986 edition Physics Letters **170B** 1 (1986).

$\Sigma(1915)$ MASS

VALUE (MeV)	DOCUMENT ID	TECN	COMMENT
1900 to 1935 (≈ 1915) OUR ESTIMATE			
1937 ± 20	ALSTON-...	DPWA	$\bar{K}N \rightarrow \bar{K}N$
1894 ± 5	1 CORDEN 77C		$K^- n \rightarrow \Sigma \pi$
1909 ± 5	1 CORDEN 77C		$K^- n \rightarrow \Sigma \pi$
1920 ± 10	GOPAL 77	DPWA	$\bar{K}N$ multichannel
1900 ± 4	2 CORDEN 76	DPWA	$K^- n \rightarrow \Lambda \pi^-$
1920 ± 30	BAILLON 75	IPWA	$\bar{K}N \rightarrow \Lambda \pi$
1914 ± 10	HEMINGWAY 75	DPWA	$K^- \rho \rightarrow \bar{K}N$
1920 ± 15	VANHORN 75	DPWA	$K^- \rho \rightarrow \Lambda \pi^0$
1920 ± 5	KANE 74	DPWA	$K^- \rho \rightarrow \Sigma \pi$
••• We do not use the following data for averages, fits, limits, etc. •••			
not seen	DECLAIS 77	DPWA	$\bar{K}N \rightarrow \bar{K}N$
1925 or 1933	3 MARTIN 77	DPWA	$\bar{K}N$ multichannel
1915	DEBELLEFON 76	IPWA	$K^- \rho \rightarrow \Lambda \pi^0$

$\Sigma(1915)$ WIDTH

VALUE (MeV)	DOCUMENT ID	TECN	COMMENT
80 to 160 (≈ 120) OUR ESTIMATE			
161 ± 20	ALSTON-...	DPWA	$\bar{K}N \rightarrow \bar{K}N$
107 ± 14	1 CORDEN 77C		$K^- n \rightarrow \Sigma \pi$
85 ± 13	1 CORDEN 77C		$K^- n \rightarrow \Sigma \pi$
130 ± 10	GOPAL 77	DPWA	$\bar{K}N$ multichannel
75 ± 14	2 CORDEN 76	DPWA	$K^- n \rightarrow \Lambda \pi^-$
70 ± 20	BAILLON 75	IPWA	$\bar{K}N \rightarrow \Lambda \pi$
85 ± 15	HEMINGWAY 75	DPWA	$K^- \rho \rightarrow \bar{K}N$
102 ± 18	VANHORN 75	DPWA	$K^- \rho \rightarrow \Lambda \pi^0$
162 ± 25	KANE 74	DPWA	$K^- \rho \rightarrow \Sigma \pi$
••• We do not use the following data for averages, fits, limits, etc. •••			
171 or 173	3 MARTIN 77	DPWA	$\bar{K}N$ multichannel
60	DEBELLEFON 76	IPWA	$K^- \rho \rightarrow \Lambda \pi^0$

$\Sigma(1915)$ DECAY MODES

Mode	Fraction (Γ_i/Γ)
Γ_1 $N\bar{K}$	5–15 %
Γ_2 $\Lambda \pi$	seen
Γ_3 $\Sigma \pi$	seen
Γ_4 $\Sigma(1385)\pi$	< 5 %
Γ_5 $\Sigma(1385)\pi, P\text{-wave}$	
Γ_6 $\Sigma(1385)\pi, F\text{-wave}$	

The above branching fractions are our estimates, not fits or averages.

$\Sigma(1915)$ BRANCHING RATIOS

See "Sign conventions for resonance couplings" in the Note on Λ and Σ Resonances.

$\Gamma(N\bar{K})/\Gamma_{\text{total}}$ Γ_1/Γ

VALUE	DOCUMENT ID	TECN	COMMENT
0.05 to 0.15 OUR ESTIMATE			
0.03 ± 0.02	4 GOPAL 80	DPWA	$\bar{K}N \rightarrow \bar{K}N$
0.14 ± 0.05	ALSTON-... 78	DPWA	$\bar{K}N \rightarrow \bar{K}N$
0.11 ± 0.04	HEMINGWAY 75	DPWA	$K^- \rho \rightarrow \bar{K}N$
••• We do not use the following data for averages, fits, limits, etc. •••			
0.05 ± 0.03	GOPAL 77	DPWA	See GOPAL 80
0.08 or 0.08	3 MARTIN 77	DPWA	$\bar{K}N$ multichannel

$(\Gamma_i \Gamma_f)^{1/2} / \Gamma_{\text{total}}$ in $N\bar{K} \rightarrow \Sigma(1915) \rightarrow \Lambda \pi$ $(\Gamma_1 \Gamma_2)^{1/2} / \Gamma$

VALUE	DOCUMENT ID	TECN	COMMENT
-0.09 ± 0.03	GOPAL 77	DPWA	$\bar{K}N$ multichannel
-0.10 ± 0.01	2 CORDEN 76	DPWA	$K^- n \rightarrow \Lambda \pi^-$
-0.06 ± 0.02	BAILLON 75	IPWA	$\bar{K}N \rightarrow \Lambda \pi$
-0.09 ± 0.02	VANHORN 75	DPWA	$K^- \rho \rightarrow \Lambda \pi^0$
-0.087 ± 0.056	DEVENISH 74B		Fixed-t dispersion rel.
••• We do not use the following data for averages, fits, limits, etc. •••			
-0.09 or -0.09	3 MARTIN 77	DPWA	$\bar{K}N$ multichannel
-0.10	DEBELLEFON 76	IPWA	$K^- \rho \rightarrow \Lambda \pi^0$

$(\Gamma_i \Gamma_f)^{1/2} / \Gamma_{\text{total}}$ in $N\bar{K} \rightarrow \Sigma(1915) \rightarrow \Sigma \pi$ $(\Gamma_1 \Gamma_3)^{1/2} / \Gamma$

VALUE	DOCUMENT ID	TECN	COMMENT
-0.17 ± 0.01	1 CORDEN 77C		$K^- n \rightarrow \Sigma \pi$
-0.15 ± 0.02	1 CORDEN 77C		$K^- n \rightarrow \Sigma \pi$
-0.19 ± 0.03	GOPAL 77	DPWA	$\bar{K}N$ multichannel
-0.16 ± 0.03	KANE 74	DPWA	$K^- \rho \rightarrow \Sigma \pi$
••• We do not use the following data for averages, fits, limits, etc. •••			
-0.05 or -0.05	3 MARTIN 77	DPWA	$\bar{K}N$ multichannel

$(\Gamma_i \Gamma_f)^{1/2} / \Gamma_{\text{total}}$ in $N\bar{K} \rightarrow \Sigma(1915) \rightarrow \Sigma(1385)\pi, P\text{-wave}$ $(\Gamma_1 \Gamma_5)^{1/2} / \Gamma$

VALUE	DOCUMENT ID	TECN	COMMENT
< 0.01	CAMERON 78	DPWA	$K^- \rho \rightarrow \Sigma(1385)\pi$

$(\Gamma_i \Gamma_f)^{1/2} / \Gamma_{\text{total}}$ in $N\bar{K} \rightarrow \Sigma(1915) \rightarrow \Sigma(1385)\pi, F\text{-wave}$ $(\Gamma_1 \Gamma_6)^{1/2} / \Gamma$

VALUE	DOCUMENT ID	TECN	COMMENT
+0.039 ± 0.009	5 CAMERON 78	DPWA	$K^- \rho \rightarrow \Sigma(1385)\pi$

$\Sigma(1915)$ FOOTNOTES

- The two entries for CORDEN 77C are from two different acceptable solutions.
- Preferred solution 3; see CORDEN 76 for other possibilities.
- The two MARTIN 77 values are from a T-matrix pole and from a Breit-Wigner fit.
- The mass and width are fixed to the GOPAL 77 values due to the low elasticity.
- The published sign has been changed to be in accord with the baryon-first convention.

$\Sigma(1915)$ REFERENCES

PDG 86	PL 170B 1	M. Aguilar-Benitez et al.	(CERN, CIT+)
PDG 82	PL 111B 1	M. Roos et al.	(HELS, CIT, CERN)
GOPAL 80	Toronto Conf. 159	G.P. Gopal	(RHEL) IJP
ALSTON-... 78	PR D18 182	M. Alston-Garnjost et al.	(LBL, MTHO+) IJP
Also	PRL 38 1007	M. Alston-Garnjost et al.	(LBL, MTHO+) IJP
CAMERON 78	NP B143 189	W. Cameron et al.	(RHEL, LOIC) IJP
CORDEN 77C	NP B125 61	M.J. Corden et al.	(BIRM) IJP
DECLAIS 77	CERN 77-16	Y. Declais et al.	(CAEN, CERN) IJP
GOPAL 77	NP B119 362	G.P. Gopal et al.	(LOIC, CERN) IJP
MARTIN 77	NP B127 349	B.R. Martin, M.K. Pidcock, R.G. Moorhouse	(LOUC+) IJP
Also	NP B126 266	B.R. Martin, M.K. Pidcock	(LOUC) IJP
Also	NP B126 285	B.R. Martin, M.K. Pidcock	(LOUC) IJP
CORDEN 76	NP B104 382	M.J. Corden et al.	(BIRM) IJP
DEBELLEFON 76	NP B109 129	A. de Bellefon, A. Berthon	(CERN, RHEL) IJP
BAILLON 75	NP B94 39	P.H. Baillon, P.J. Litchfield	(CERN, RHEL) IJP
HEMINGWAY 75	NP B91 12	R.J. Hemingway et al.	(CERN, HEIDH, MPIM) IJP
VANHORN 75	NP B87 145	A.J. van Horn	(LBL) IJP
Also	NP B87 157	A.J. van Horn	(LBL) IJP
DEVENISH 74B	NP B81 330	R.C.E. Devenish, C.D. Froggatt, B.R. Martin	(DESY+) IJP
KANE 74	LBL-2452	D.F. Kane	(LBL) IJP
COOL 66	PRL 16 1228	R.L. Cool et al.	(BNL)

See key on page 405

Baryon Particle Listings

$\Sigma(1940), \Sigma(2000)$

$\Sigma(1940) D_{13}$ $I(J^P) = 1(\frac{3}{2}^-)$ Status: ***

For results published before 1974 (they are now obsolete), see our 1982 edition Physics Letters **111B** 1 (1982).

Not all analyses require this state. It is not required by the GOYAL 77 analysis of $K^- n \rightarrow (\Sigma\pi)^-$ nor by the GOPAL 80 analysis of $K^- n \rightarrow K^- n$. See also HEMINGWAY 75.

$\Sigma(1940)$ MASS

VALUE (MeV)	DOCUMENT ID	TECN	COMMENT
1900 to 1950 (≈ 1940) OUR ESTIMATE			
1920 \pm 50	GOPAL 77	DPWA	$\bar{K}N$ multichannel
1950 \pm 30	BAILLON 75	IPWA	$\bar{K}N \rightarrow \Lambda\pi$
1949 $^{+40}_{-60}$	VANHORN 75	DPWA	$K^- p \rightarrow \Lambda\pi^0$
1935 \pm 80	KANE 74	DPWA	$K^- p \rightarrow \Sigma\pi$
1940 \pm 20	LITCHFIELD 74B	DPWA	$K^- p \rightarrow \Lambda(1520)\pi^0$
1950 \pm 20	LITCHFIELD 74C	DPWA	$K^- p \rightarrow \Delta(1232)\bar{K}$
••• We do not use the following data for averages, fits, limits, etc. •••			
1886 or 1893	¹ MARTIN 77	DPWA	$\bar{K}N$ multichannel
1940	DEBELLEFON 76	IPWA	$K^- p \rightarrow \Lambda\pi^0, F_{17}$ wave

$\Sigma(1940)$ WIDTH

VALUE (MeV)	DOCUMENT ID	TECN	COMMENT
150 to 300 (≈ 220) OUR ESTIMATE			
170 \pm 25	CAMERON 78B	DPWA	$K^- p \rightarrow N\bar{K}^*$
300 \pm 80	GOPAL 77	DPWA	$\bar{K}N$ multichannel
150 \pm 75	BAILLON 75	IPWA	$\bar{K}N \rightarrow \Lambda\pi$
160 $^{+70}_{-40}$	VANHORN 75	DPWA	$K^- p \rightarrow \Lambda\pi^0$
330 \pm 80	KANE 74	DPWA	$K^- p \rightarrow \Sigma\pi$
60 \pm 20	LITCHFIELD 74B	DPWA	$K^- p \rightarrow \Lambda(1520)\pi^0$
70 $^{+30}_{-20}$	LITCHFIELD 74C	DPWA	$K^- p \rightarrow \Delta(1232)\bar{K}$
••• We do not use the following data for averages, fits, limits, etc. •••			
157 or 159	¹ MARTIN 77	DPWA	$\bar{K}N$ multichannel

$\Sigma(1940)$ DECAY MODES

Mode	Fraction (Γ_i/Γ)
Γ_1 $N\bar{K}$	<20 %
Γ_2 $\Lambda\pi$	seen
Γ_3 $\Sigma\pi$	seen
Γ_4 $\Sigma(1385)\pi$	seen
Γ_5 $\Sigma(1385)\pi, S$ -wave	
Γ_6 $\Lambda(1520)\pi$	seen
Γ_7 $\Lambda(1520)\pi, P$ -wave	
Γ_8 $\Lambda(1520)\pi, F$ -wave	
Γ_9 $\Delta(1232)\bar{K}$	seen
Γ_{10} $\Delta(1232)\bar{K}, S$ -wave	
Γ_{11} $\Delta(1232)\bar{K}, D$ -wave	
Γ_{12} $N\bar{K}^*(892)$	seen
Γ_{13} $N\bar{K}^*(892), S=3/2, S$ -wave	

$\Sigma(1940)$ BRANCHING RATIOS

See "Sign conventions for resonance couplings" in the Note on Λ and Σ Resonances.

$\Gamma(N\bar{K})/\Gamma_{total}$	Γ_1/Γ
OUR ESTIMATE	
<0.04	
0.14 or 0.13	
$(\Gamma_i/\Gamma)^{1/2}/\Gamma_{total}$ in $N\bar{K} \rightarrow \Sigma(1940) \rightarrow \Lambda\pi$	
OUR ESTIMATE	
-0.06 \pm 0.03	
-0.04 \pm 0.02	
-0.05 $^{+0.03}_{-0.02}$	
-0.153 \pm 0.070	
••• We do not use the following data for averages, fits, limits, etc. •••	
-0.15 or -0.14	

$(\Gamma_i/\Gamma)^{1/2}/\Gamma_{total}$ in $N\bar{K} \rightarrow \Sigma(1940) \rightarrow \Sigma\pi$	$(\Gamma_1/\Gamma_3)^{1/2}/\Gamma$
OUR ESTIMATE	
-0.08 \pm 0.04	
-0.14 \pm 0.04	
••• We do not use the following data for averages, fits, limits, etc. •••	
+0.16 or +0.16	

$(\Gamma_i/\Gamma)^{1/2}/\Gamma_{total}$ in $N\bar{K} \rightarrow \Sigma(1940) \rightarrow \Lambda(1520)\pi, P$ -wave	$(\Gamma_1/\Gamma_7)^{1/2}/\Gamma$
OUR ESTIMATE	
< 0.03	
-0.11 \pm 0.04	

$(\Gamma_i/\Gamma)^{1/2}/\Gamma_{total}$ in $N\bar{K} \rightarrow \Sigma(1940) \rightarrow \Lambda(1520)\pi, F$ -wave	$(\Gamma_1/\Gamma_8)^{1/2}/\Gamma$
OUR ESTIMATE	
0.062 \pm 0.021	
-0.08 \pm 0.04	

$(\Gamma_i/\Gamma)^{1/2}/\Gamma_{total}$ in $N\bar{K} \rightarrow \Sigma(1940) \rightarrow \Delta(1232)\bar{K}, S$ -wave	$(\Gamma_1/\Gamma_{10})^{1/2}/\Gamma$
OUR ESTIMATE	
-0.16 \pm 0.05	

$(\Gamma_i/\Gamma)^{1/2}/\Gamma_{total}$ in $N\bar{K} \rightarrow \Sigma(1940) \rightarrow \Delta(1232)\bar{K}, D$ -wave	$(\Gamma_1/\Gamma_{11})^{1/2}/\Gamma$
OUR ESTIMATE	
-0.14 \pm 0.05	

$(\Gamma_i/\Gamma)^{1/2}/\Gamma_{total}$ in $N\bar{K} \rightarrow \Sigma(1940) \rightarrow \Sigma(1385)\pi$	$(\Gamma_1/\Gamma_4)^{1/2}/\Gamma$
OUR ESTIMATE	
+0.066 \pm 0.025	

$(\Gamma_i/\Gamma)^{1/2}/\Gamma_{total}$ in $N\bar{K} \rightarrow \Sigma(1940) \rightarrow N\bar{K}^*(892)$	$(\Gamma_1/\Gamma_{12})^{1/2}/\Gamma$
OUR ESTIMATE	
-0.09 \pm 0.02	

$\Sigma(1940)$ FOOTNOTES

- ¹ The two MARTIN 77 values are from a T-matrix pole and from a Breit-Wigner fit.
- ² The published sign has been changed to be in accord with the baryon-first convention.
- ³ Upper limits on the D_1 and D_3 waves are each 0.03.

$\Sigma(1940)$ REFERENCES

PDG 82	PL 111B 1	M. Roos et al.	(HELS, CIT, CERN)
GOPAL 80	Toronto Conf. 159	G.P. Gopal	(RHEL)
CAMERON 78	NP B143 189	W. Cameron et al.	(RHEL, LOIC) IJP
CAMERON 78B	NP B146 327	W. Cameron et al.	(RHEL, LOIC) IJP
CAMERON 77	NP B131 399	W. Cameron et al.	(RHEL, LOIC) IJP
GOPAL 77	NP B119 362	G.P. Gopal et al.	(LOIC, RHEL) IJP
GOYAL 77	PR D16 2746	D.P. Goyal, A.V. Sodhi	(DELH)
MARTIN 77	NP B127 349	B.R. Martin, M.K. Pidcock, R.G. Moorhouse	(LOUC+) IJP
Also	NP B126 266	B.R. Martin, M.K. Pidcock	(LOUC)
Also	NP B126 285	B.R. Martin, M.K. Pidcock	(LOUC) IJP
DEBELLEFON 76	NP B109 129	A. de Bellefon, A. Berthon	(CDEF) IJP
BAILLON 75	NP B94 39	P.H. Baillon, P.J. Litchfield	(CERN, RHEL) IJP
HEMINGWAY 75	NP B91 12	R.J. Hemingway et al.	(CERN, HEIDH, MPIM) IJP
VANHORN 75	NP B87 145	A.J. van Horn	(LBL) IJP
Also	NP B87 157	A.J. van Horn	(LBL) IJP
DEVENISH 74B	NP B81 330	R.C.E. Devenish, C.D. Froggatt, B.R. Martin	(DESY+) IJP
KANE 74	LBL-2452	D.F. Kane	(LBL) IJP
LITCHFIELD 74B	NP B74 19	P.J. Litchfield et al.	(CERN, HEIDH) IJP
LITCHFIELD 74C	NP B74 39	P.J. Litchfield et al.	(CERN, HEIDH) IJP

$\Sigma(2000) S_{11}$ $I(J^P) = 1(\frac{1}{2}^-)$ Status: *

OMITTED FROM SUMMARY TABLE

We list here all reported S_{11} states lying above the $\Sigma(1750) S_{11}$.

$\Sigma(2000)$ MASS

VALUE (MeV)	DOCUMENT ID	TECN	COMMENT
≈ 2000 OUR ESTIMATE			
1944 \pm 15	GOPAL 80	DPWA	$\bar{K}N \rightarrow \bar{K}N$
1955 \pm 15	GOPAL 77	DPWA	$\bar{K}N$ multichannel
1755 or 1834	¹ MARTIN 77	DPWA	$\bar{K}N$ multichannel
2004 \pm 40	VANHORN 75	DPWA	$K^- p \rightarrow \Lambda\pi^0$

$\Sigma(2000)$ WIDTH

VALUE (MeV)	DOCUMENT ID	TECN	COMMENT
215 \pm 25	GOPAL 80	DPWA	$\bar{K}N \rightarrow \bar{K}N$
170 \pm 40	GOPAL 77	DPWA	$\bar{K}N$ multichannel
413 or 450	¹ MARTIN 77	DPWA	$\bar{K}N$ multichannel
116 \pm 40	VANHORN 75	DPWA	$K^- p \rightarrow \Lambda\pi^0$

Baryon Particle Listings

 $\Sigma(2000)$, $\Sigma(2030)$ $\Sigma(2000)$ DECAY MODES

Mode	
Γ_1	$N\bar{K}$
Γ_2	$\Lambda\pi$
Γ_3	$\Sigma\pi$
Γ_4	$\Lambda(1520)\pi$
Γ_5	$N\bar{K}^*(892)$, $S=1/2$, S -wave
Γ_6	$N\bar{K}^*(892)$, $S=3/2$, D -wave

 $\Sigma(2000)$ BRANCHING RATIOS

See "Sign conventions for resonance couplings" in the Note on Λ and Σ Resonances.

$\Gamma(N\bar{K})/\Gamma_{\text{total}}$	DOCUMENT ID	TECN	COMMENT	Γ_1/Γ
0.51 ± 0.05	GOPAL	80	DPWA $\bar{K}N \rightarrow \bar{K}N$	
0.44 ± 0.05	GOPAL	77	DPWA See GOPAL 80	
0.62 or 0.57	¹ MARTIN	77	DPWA $\bar{K}N$ multichannel	

$(\Gamma_1\Gamma_2)^{1/2}/\Gamma_{\text{total}}$ in $N\bar{K} \rightarrow \Sigma(2000) \rightarrow \Lambda\pi$	DOCUMENT ID	TECN	COMMENT	$(\Gamma_1\Gamma_2)^{1/2}/\Gamma$
0.08 ± 0.03	GOPAL	77	DPWA $\bar{K}N$ multichannel	
-0.19 or -0.18	¹ MARTIN	77	DPWA $\bar{K}N$ multichannel	
not seen	BAILLON	75	IPWA $\bar{K}N \rightarrow \Lambda\pi$	
+0.07 ± 0.02 -0.01	VANHORN	75	DPWA $K^-p \rightarrow \Lambda\pi^0$	

$(\Gamma_1\Gamma_2)^{1/2}/\Gamma_{\text{total}}$ in $N\bar{K} \rightarrow \Sigma(2000) \rightarrow \Sigma\pi$	DOCUMENT ID	TECN	COMMENT	$(\Gamma_1\Gamma_2)^{1/2}/\Gamma$
+0.20 ± 0.04	GOPAL	77	DPWA $\bar{K}N$ multichannel	
+0.26 or +0.24	¹ MARTIN	77	DPWA $\bar{K}N$ multichannel	

$(\Gamma_1\Gamma_2)^{1/2}/\Gamma_{\text{total}}$ in $N\bar{K} \rightarrow \Sigma(2000) \rightarrow \Lambda(1520)\pi$	DOCUMENT ID	TECN	COMMENT	$(\Gamma_1\Gamma_2)^{1/2}/\Gamma$
+0.081 ± 0.021	² CAMERON	77	DPWA P -wave decay	

$(\Gamma_1\Gamma_2)^{1/2}/\Gamma_{\text{total}}$ in $N\bar{K} \rightarrow \Sigma(2000) \rightarrow N\bar{K}^*(892)$, $S=1/2$, S -wave	DOCUMENT ID	TECN	COMMENT	$(\Gamma_1\Gamma_2)^{1/2}/\Gamma$
+0.10 ± 0.02	² CAMERON	78B	DPWA $K^-p \rightarrow N\bar{K}^*$	

$(\Gamma_1\Gamma_2)^{1/2}/\Gamma_{\text{total}}$ in $N\bar{K} \rightarrow \Sigma(2000) \rightarrow N\bar{K}^*(892)$, $S=3/2$, D -wave	DOCUMENT ID	TECN	COMMENT	$(\Gamma_1\Gamma_2)^{1/2}/\Gamma$
-0.07 ± 0.03	CAMERON	78B	DPWA $K^-p \rightarrow N\bar{K}^*$	

 $\Sigma(2000)$ FOOTNOTES

- ¹The two MARTIN 77 values are from a T-matrix pole and from a Breit-Wigner fit.
²The published sign has been changed to be in accord with the baryon-first convention.

 $\Sigma(2000)$ REFERENCES

GOPAL	80	Toronto Conf.	159	G.P. Gopal	(RHEL)IJP
CAMERON	78B	NP B146	327	W. Cameron et al.	(RHEL, LOIC)IJP
CAMERON	77	NP B131	399	W. Cameron et al.	(RHEL, LOIC)IJP
GOPAL	77	NP B119	362	G.P. Gopal et al.	(LOIC, RHEL)IJP
MARTIN	77	NP B127	349	B.R. Martin, M.K. Pldcock, R.G. Moorhouse	(LOUC+)IJP
Also		NP B126	266	B.R. Martin, M.K. Pldcock	(LOUC)IJP
Also		NP B126	285	B.R. Martin, M.K. Pldcock	(LOUC)IJP
BAILLON	75	NP B94	39	P.H. Bailion, P.J. Litchfield	(CERN, RHEL)IJP
VANHORN	75	NP B87	145	A.J. van Horn	(LBL)IJP
Also		NP B87	157	A.J. van Horn	(LBL)IJP

 $\Sigma(2030) F_{17}$

$$I(J^P) = 1(\frac{7}{2}^+) \text{ Status: } ***$$

Discovered by COOL 66 and by WOHL 66. For most results published before 1974 (they are now obsolete), see our 1982 edition Physics Letters **111B** 1 (1982).

This entry only includes results from partial-wave analyses. Parameters of peaks seen in cross sections and invariant-mass distributions around 2030 MeV may be found in our 1984 edition, Reviews of Modern Physics **56** S1 (1984).

 $\Sigma(2030)$ MASS

VALUE (MeV)	DOCUMENT ID	TECN	COMMENT
2025 to 2040 (≈ 2030) OUR ESTIMATE			
2036 ± 5	GOPAL	80	DPWA $\bar{K}N \rightarrow \bar{K}N$
2038 ± 10	CORDEN	77B	$K^-N \rightarrow N\bar{K}^*$
2040 ± 5	GOPAL	77	DPWA $\bar{K}N$ multichannel
2030 ± 3	¹ CORDEN	76	DPWA $K^-n \rightarrow \Lambda\pi^-$
2035 ± 15	BAILLON	75	IPWA $\bar{K}N \rightarrow \Lambda\pi$

2038 ± 10	HEMINGWAY	75	DPWA $K^-p \rightarrow \bar{K}N$
2042 ± 11	VANHORN	75	DPWA $K^-p \rightarrow \Lambda\pi^0$
2020 ± 6	KANE	74	DPWA $K^-p \rightarrow \Sigma\pi$
2035 ± 10	LITCHFIELD	74B	DPWA $K^-p \rightarrow \Lambda(1520)\pi^0$
2020 ± 30	LITCHFIELD	74C	DPWA $K^-p \rightarrow \Delta(1232)\bar{K}$
2025 ± 10	LITCHFIELD	74D	DPWA $K^-p \rightarrow \Lambda(1820)\pi^0$
• • • We do not use the following data for averages, fits, limits, etc. • • •			
2027 to 2057	GOYAL	77	DPWA $K^-N \rightarrow \Sigma\pi$
2030	DEBELLEFON	76	IPWA $K^-p \rightarrow \Lambda\pi^0$

 $\Sigma(2030)$ WIDTH

VALUE (MeV)	DOCUMENT ID	TECN	COMMENT
150 to 200 (≈ 180) OUR ESTIMATE			
172 ± 10	GOPAL	80	DPWA $\bar{K}N \rightarrow \bar{K}N$
137 ± 40	CORDEN	77B	$K^-N \rightarrow N\bar{K}^*$
190 ± 10	GOPAL	77	DPWA $\bar{K}N$ multichannel
201 ± 9	¹ CORDEN	76	DPWA $K^-n \rightarrow \Lambda\pi^-$
180 ± 20	BAILLON	75	IPWA $\bar{K}N \rightarrow \Lambda\pi$
172 ± 15	HEMINGWAY	75	DPWA $K^-p \rightarrow \bar{K}N$
178 ± 13	VANHORN	75	DPWA $K^-p \rightarrow \Lambda\pi^0$
111 ± 5	KANE	74	DPWA $K^-p \rightarrow \Sigma\pi$
160 ± 20	LITCHFIELD	74B	DPWA $K^-p \rightarrow \Lambda(1520)\pi^0$
200 ± 30	LITCHFIELD	74C	DPWA $K^-p \rightarrow \Delta(1232)\bar{K}$
• • • We do not use the following data for averages, fits, limits, etc. • • •			
260	DECLAIS	77	DPWA $\bar{K}N \rightarrow \bar{K}N$
126 to 195	GOYAL	77	DPWA $K^-N \rightarrow \Sigma\pi$
160	DEBELLEFON	76	IPWA $K^-p \rightarrow \Lambda\pi^0$
70 to 125	LITCHFIELD	74D	DPWA $K^-p \rightarrow \Lambda(1820)\pi^0$

 $\Sigma(2030)$ DECAY MODES

Mode	Fraction (Γ_i/Γ)	
Γ_1	$N\bar{K}$	17–23 %
Γ_2	$\Lambda\pi$	17–23 %
Γ_3	$\Sigma\pi$	5–10 %
Γ_4	ΞK	<2 %
Γ_5	$\Sigma(1385)\pi$	5–15 %
Γ_6	$\Sigma(1385)\pi$, F -wave	
Γ_7	$\Lambda(1520)\pi$	10–20 %
Γ_8	$\Lambda(1520)\pi$, D -wave	
Γ_9	$\Lambda(1520)\pi$, G -wave	
Γ_{10}	$\Delta(1232)\bar{K}$	10–20 %
Γ_{11}	$\Delta(1232)\bar{K}$, F -wave	
Γ_{12}	$\Delta(1232)\bar{K}$, H -wave	
Γ_{13}	$N\bar{K}^*(892)$	<5 %
Γ_{14}	$N\bar{K}^*(892)$, $S=1/2$, F -wave	
Γ_{15}	$N\bar{K}^*(892)$, $S=3/2$, F -wave	
Γ_{16}	$\Lambda(1820)\pi$, P -wave	

The above branching fractions are our estimates, not fits or averages.

 $\Sigma(2030)$ BRANCHING RATIOS

See "Sign conventions for resonance couplings" in the Note on Λ and Σ Resonances.

$\Gamma(N\bar{K})/\Gamma_{\text{total}}$	DOCUMENT ID	TECN	COMMENT	Γ_1/Γ
0.17 to 0.23 OUR ESTIMATE				
0.19 ± 0.03	GOPAL	80	DPWA $\bar{K}N \rightarrow \bar{K}N$	
0.18 ± 0.03	HEMINGWAY	75	DPWA $K^-p \rightarrow \bar{K}N$	
• • • We do not use the following data for averages, fits, limits, etc. • • •				
0.15	DECLAIS	77	DPWA $\bar{K}N \rightarrow \bar{K}N$	
0.24 ± 0.02	GOPAL	77	DPWA See GOPAL 80	

$(\Gamma_1\Gamma_2)^{1/2}/\Gamma_{\text{total}}$ in $N\bar{K} \rightarrow \Sigma(2030) \rightarrow \Lambda\pi$	DOCUMENT ID	TECN	COMMENT	$(\Gamma_1\Gamma_2)^{1/2}/\Gamma$
+0.18 ± 0.02	GOPAL	77	DPWA $\bar{K}N$ multichannel	
+0.20 ± 0.01	¹ CORDEN	76	DPWA $K^-n \rightarrow \Lambda\pi^-$	
+0.18 ± 0.02	BAILLON	75	IPWA $\bar{K}N \rightarrow \Lambda\pi$	
+0.20 ± 0.01	VANHORN	75	DPWA $K^-p \rightarrow \Lambda\pi^0$	
+0.195 ± 0.053	DEVENISH	74B	Fixed- t dispersion rel.	
• • • We do not use the following data for averages, fits, limits, etc. • • •				
0.20	DEBELLEFON	76	IPWA $K^-p \rightarrow \Lambda\pi^0$	

See key on page 405

Baryon Particle Listings

$\Sigma(2030)$, $\Sigma(2070)$, $\Sigma(2080)$

$(\Gamma_1 \Gamma_2) \frac{1}{2} / \Gamma_{\text{total}}$ in $N\bar{K} \rightarrow \Sigma(2030) \rightarrow \Sigma\pi$ $(\Gamma_1 \Gamma_3) \frac{1}{2} / \Gamma$

VALUE	DOCUMENT ID	TECN	COMMENT
-0.09 ± 0.01	2 CORDEN 77C		$K^- n \rightarrow \Sigma\pi$
-0.06 ± 0.01	2 CORDEN 77C		$K^- n \rightarrow \Sigma\pi$
-0.15 ± 0.03	GOPAL 77	DPWA	$\bar{K}N$ multichannel
-0.10 ± 0.01	KANE 74	DPWA	$K^- p \rightarrow \Sigma\pi$
• • • We do not use the following data for averages, fits, limits, etc. • • •			
-0.085 ± 0.02	3 GOYAL 77	DPWA	$K^- N \rightarrow \Sigma\pi$

$(\Gamma_1 \Gamma_2) \frac{1}{2} / \Gamma_{\text{total}}$ in $N\bar{K} \rightarrow \Sigma(2030) \rightarrow \Xi K$ $(\Gamma_1 \Gamma_4) \frac{1}{2} / \Gamma$

VALUE	DOCUMENT ID	TECN	COMMENT
0.023	MULLER 69B	DPWA	$K^- p \rightarrow \Xi K$
<0.05	BURGUN 68	DPWA	$K^- p \rightarrow \Xi K$
<0.05	TRIPP 67	RVUE	$K^- p \rightarrow \Xi K$

$(\Gamma_1 \Gamma_2) \frac{1}{2} / \Gamma_{\text{total}}$ in $N\bar{K} \rightarrow \Sigma(2030) \rightarrow \Lambda(1820)\pi$, P-wave $(\Gamma_1 \Gamma_5) \frac{1}{2} / \Gamma$

VALUE	DOCUMENT ID	TECN	COMMENT
0.14 ± 0.02	CORDEN 75B	DBC	$K^- n \rightarrow N\bar{K}\pi^-$
0.18 ± 0.04	LITCHFIELD 74D	DPWA	$K^- p \rightarrow \Lambda(1820)\pi^0$

$(\Gamma_1 \Gamma_2) \frac{1}{2} / \Gamma_{\text{total}}$ in $N\bar{K} \rightarrow \Sigma(2030) \rightarrow \Lambda(1520)\pi$, D-wave $(\Gamma_1 \Gamma_6) \frac{1}{2} / \Gamma$

VALUE	DOCUMENT ID	TECN	COMMENT
+0.114 ± 0.010	4 CAMERON 77	DPWA	$K^- p \rightarrow \Lambda(1520)\pi^0$
0.14 ± 0.03	LITCHFIELD 74B	DPWA	$K^- p \rightarrow \Lambda(1520)\pi^0$
• • • We do not use the following data for averages, fits, limits, etc. • • •			
0.10 ± 0.03	5 CORDEN 75B	DBC	$K^- n \rightarrow N\bar{K}\pi^-$

$(\Gamma_1 \Gamma_2) \frac{1}{2} / \Gamma_{\text{total}}$ in $N\bar{K} \rightarrow \Sigma(2030) \rightarrow \Lambda(1520)\pi$, G-wave $(\Gamma_1 \Gamma_7) \frac{1}{2} / \Gamma$

VALUE	DOCUMENT ID	TECN	COMMENT
+0.146 ± 0.010	4 CAMERON 77	DPWA	$K^- p \rightarrow \Lambda(1520)\pi^0$
0.02 ± 0.02	LITCHFIELD 74B	DPWA	$K^- p \rightarrow \Lambda(1520)\pi^0$

$(\Gamma_1 \Gamma_2) \frac{1}{2} / \Gamma_{\text{total}}$ in $N\bar{K} \rightarrow \Sigma(2030) \rightarrow \Delta(1232)\bar{K}$, F-wave $(\Gamma_1 \Gamma_{11}) \frac{1}{2} / \Gamma$

VALUE	DOCUMENT ID	TECN	COMMENT
0.16 ± 0.03	LITCHFIELD 74C	DPWA	$K^- p \rightarrow \Delta(1232)\bar{K}$
• • • We do not use the following data for averages, fits, limits, etc. • • •			
0.17 ± 0.03	5 CORDEN 75B	DBC	$K^- n \rightarrow N\bar{K}\pi^-$

$(\Gamma_1 \Gamma_2) \frac{1}{2} / \Gamma_{\text{total}}$ in $N\bar{K} \rightarrow \Sigma(2030) \rightarrow \Delta(1232)\bar{K}$, H-wave $(\Gamma_1 \Gamma_{12}) \frac{1}{2} / \Gamma$

VALUE	DOCUMENT ID	TECN	COMMENT
0.00 ± 0.02	LITCHFIELD 74C	DPWA	$K^- p \rightarrow \Delta(1232)\bar{K}$

$(\Gamma_1 \Gamma_2) \frac{1}{2} / \Gamma_{\text{total}}$ in $N\bar{K} \rightarrow \Sigma(2030) \rightarrow \Sigma(1385)\pi$ $(\Gamma_1 \Gamma_5) \frac{1}{2} / \Gamma$

VALUE	DOCUMENT ID	TECN	COMMENT
+0.153 ± 0.026	4 CAMERON 78	DPWA	$K^- p \rightarrow \Sigma(1385)\pi$

$(\Gamma_1 \Gamma_2) \frac{1}{2} / \Gamma_{\text{total}}$ in $N\bar{K} \rightarrow \Sigma(2030) \rightarrow N\bar{K}^*(892)$, S=1/2, F-wave $(\Gamma_1 \Gamma_{14}) \frac{1}{2} / \Gamma$

VALUE	DOCUMENT ID	TECN	COMMENT
+0.06 ± 0.03	4 CAMERON 78B	DPWA	$K^- p \rightarrow N\bar{K}^*$
-0.02 ± 0.01	CORDEN 77B		$K^- d \rightarrow NN\bar{K}^*$

$(\Gamma_1 \Gamma_2) \frac{1}{2} / \Gamma_{\text{total}}$ in $N\bar{K} \rightarrow \Sigma(2030) \rightarrow N\bar{K}^*(892)$, S=3/2, F-wave $(\Gamma_1 \Gamma_{15}) \frac{1}{2} / \Gamma$

VALUE	DOCUMENT ID	TECN	COMMENT
+0.04 ± 0.03	6 CAMERON 78B	DPWA	$K^- p \rightarrow N\bar{K}^*$
-0.12 ± 0.02	CORDEN 77B		$K^- d \rightarrow NN\bar{K}^*$

$\Sigma(2030)$ FOOTNOTES

- 1 Preferred solution 3; see CORDEN 76 for other possibilities.
- 2 The two entries for CORDEN 77C are from two different acceptable solutions.
- 3 This coupling is extracted from unnormalized data.
- 4 The published sign has been changed to be in accord with the baryon-first convention.
- 5 An upper limit.
- 6 The upper limit on the G_3 wave is 0.03.

$\Sigma(2030)$ REFERENCES

PDG 84	RMP 56 51	C.G. Wohl et al.	(LBL, CIT, CERN)
PDG 82	PL 111B 1	M. Roos et al.	(HELS, CIT, CERN)
GOPAL 80	Toronto Conf. 159	G.P. Gopal	(RHEL) IJP
CAMERON 78	NP B143 189	W. Cameron et al.	(RHEL, LOIC) IJP
CAMERON 78B	NP B146 327	W. Cameron et al.	(RHEL, LOIC) IJP
CAMERON 77	NP B131 399	W. Cameron et al.	(RHEL, LOIC) IJP
CORDEN 77B	NP B121 365	M.J. Corden et al.	(BIRM) IJP
CORDEN 77C	NP B125 61	M.J. Corden et al.	(BIRM) IJP
DECLAIS 77	CERN 77-16	Y. Declais et al.	(CAEN, CERN) IJP
GOPAL 77	NP B119 362	G.P. Gopal et al.	(LOIC, RHEL) IJP
GOYAL 77	PR D16 2746	D.P. Goyal, A.V. Sodhi	(DELH) IJP
CORDEN 76	NP B104 382	M.J. Corden et al.	(BIRM) IJP
DEBELLEFON 76	NP B109 129	A. de Bellefon, A. Berthon	(CDFE) IJP
BAILLON 75	NP B94 39	P.H. Baillon, P.J. Litchfield	(CERN, RHEL) IJP

CORDEN 75B	NP B92 365	M.J. Corden et al.	(BIRM) IJP
HEMINGWAY 75	NP B91 12	R.J. Hemingway et al.	(CERN, HEIDH, MPIM) IJP
VANHORN 75	NP B87 145	A.J. van Horn	(LBL) IJP
Also	NP B87 157	A.J. van Horn	(LBL) IJP
DEVENISH 74B	NP B81 330	R.C.E. Devenish, C.D. Froggatt, B.R. Martin	(DESY+) IJP
KANE 74	LBL-2452	D.F. Kane	(LBL) IJP
LITCHFIELD 74B	NP B74 19	P.J. Litchfield et al.	(CERN, HEIDH) IJP
LITCHFIELD 74C	NP B74 39	P.J. Litchfield et al.	(CERN, HEIDH) IJP
LITCHFIELD 74D	NP B74 12	P.J. Litchfield et al.	(CERN, HEIDH) IJP
MULLER 69B	Thesis UCRL 19372	R.A. Muller	(LRL) IJP
BURGUN 68	NP B8 447	G. Burgun et al.	(SACL, CDEF, RHEL)
TRIPP 67	NP B3 10	R.D. Tripp et al.	(LRL, SLAC, CERN+)
COOL 66	PRL 16 1228	R.L. Cool et al.	(BNL) IJP
WOHL 66	PRL 17 107	C.G. Wohl, F.T. Solmitz, M.L. Stevenson	(LRL) IJP

$\Sigma(2070) F_{15}$

$I(J^P) = 1(\frac{5}{2}^+)$ Status: *

OMITTED FROM SUMMARY TABLE

This state suggested by BERTHON 70B finds support in GOPAL 80 with new $K^- p$ polarization and $K^- n$ angular distributions. The very broad state seen in KANE 72 is not required in the later (KANE 74) analysis of $\bar{K}N \rightarrow \Sigma\pi$.

$\Sigma(2070)$ MASS

VALUE (MeV)	DOCUMENT ID	TECN	COMMENT
≈ 2070 OUR ESTIMATE			
2051 ± 25	GOPAL 80	DPWA	$\bar{K}N \rightarrow \bar{K}N$
2057	KANE 72	DPWA	$K^- p \rightarrow \Sigma\pi$
2070 ± 10	BERTHON 70B	DPWA	$K^- p \rightarrow \Sigma\pi$

$\Sigma(2070)$ WIDTH

VALUE (MeV)	DOCUMENT ID	TECN	COMMENT
300 ± 30	GOPAL 80	DPWA	$\bar{K}N \rightarrow \bar{K}N$
906	KANE 72	DPWA	$K^- p \rightarrow \Sigma\pi$
140 ± 20	BERTHON 70B	DPWA	$K^- p \rightarrow \Sigma\pi$

$\Sigma(2070)$ DECAY MODES

Mode
$\Gamma_1 N\bar{K}$
$\Gamma_2 \Sigma\pi$

$\Sigma(2070)$ BRANCHING RATIOS

See "Sign conventions for resonance couplings" in the Note on Λ and Σ Resonances.

$\Gamma(N\bar{K}) / \Gamma_{\text{total}}$ Γ_1 / Γ

VALUE	DOCUMENT ID	TECN	COMMENT
0.08 ± 0.03	GOPAL 80	DPWA	$\bar{K}N \rightarrow \bar{K}N$

$(\Gamma_1 \Gamma_2) \frac{1}{2} / \Gamma_{\text{total}}$ in $N\bar{K} \rightarrow \Sigma(2070) \rightarrow \Sigma\pi$ $(\Gamma_1 \Gamma_2) \frac{1}{2} / \Gamma$

VALUE	DOCUMENT ID	TECN	COMMENT
+0.104	KANE 72	DPWA	$K^- p \rightarrow \Sigma\pi$
+0.12 ± 0.02	BERTHON 70B	DPWA	$K^- p \rightarrow \Sigma\pi$

$\Sigma(2070)$ REFERENCES

GOPAL 80	Toronto Conf. 159	G.P. Gopal	(RHEL) IJP
KANE 74	LBL-2452	D.F. Kane	(LBL) IJP
KANE 72	PR D5 1583	D.F.J. Kane	(LBL) IJP
BERTHON 70B	NP B24 417	A. Berthon et al.	(CDFE, RHEL, SACL) IJP

$\Sigma(2080) P_{13}$

$I(J^P) = 1(\frac{3}{2}^+)$ Status: **

OMITTED FROM SUMMARY TABLE

Suggested by some but not all partial-wave analyses across this region.

$\Sigma(2080)$ MASS

VALUE (MeV)	DOCUMENT ID	TECN	COMMENT
≈ 2080 OUR ESTIMATE			
2091 ± 7	1 CORDEN 76	DPWA	$K^- n \rightarrow \Lambda\pi^-$
2070 to 2120	DEBELLEFON 76	IPWA	$K^- p \rightarrow \Lambda\pi^0$
2120 ± 40	BAILLON 75	IPWA	$\bar{K}N \rightarrow \Lambda\pi$ (sol. 1)
2140 ± 40	BAILLON 75	IPWA	$\bar{K}N \rightarrow \Lambda\pi$ (sol. 2)
2082 ± 4	COX 70	DPWA	See CORDEN 76
2070 ± 30	LITCHFIELD 70	DPWA	$K^- N \rightarrow \Lambda\pi$

Baryon Particle Listings

 $\Sigma(2080)$, $\Sigma(2100)$, $\Sigma(2250)$ $\Sigma(2080)$ WIDTH

VALUE (MeV)	DOCUMENT ID	TECN	COMMENT
186 ± 48	¹ CORDEN 76	DPWA	$K^- n \rightarrow \Lambda \pi^-$
100	DEBELLEFON 76	IPWA	$K^- p \rightarrow \Lambda \pi^0$
240 ± 5.0	BAILLON 75	IPWA	$\bar{K} N \rightarrow \Lambda \pi$ (sol. 1)
200 ± 5.0	BAILLON 75	IPWA	$\bar{K} N \rightarrow \Lambda \pi$ (sol. 2)
87 ± 2.0	COX 70	DPWA	See CORDEN 76
250 ± 4.0	LITCHFIELD 70	DPWA	$K^- N \rightarrow \Lambda \pi$

 $\Sigma(2080)$ DECAY MODES

Mode	
Γ_1	$N\bar{K}$
Γ_2	$\Lambda\pi$

 $\Sigma(2080)$ BRANCHING RATIOS

See "Sign conventions for resonance couplings" in the Note on Λ and Σ Resonances.

$(\Gamma_1 \Gamma_2)^{1/2} / \Gamma_{\text{total}}$ in $N\bar{K} \rightarrow \Sigma(2080) \rightarrow \Lambda\pi$	DOCUMENT ID	TECN	COMMENT	$(\Gamma_1 \Gamma_2)^{1/2} / \Gamma$
-0.10 ± 0.03	¹ CORDEN 76	DPWA	$K^- n \rightarrow \Lambda \pi^-$	
-0.10	DEBELLEFON 76	IPWA	$K^- p \rightarrow \Lambda \pi^0$	
-0.13 ± 0.04	BAILLON 75	IPWA	$\bar{K} N \rightarrow \Lambda \pi$ (sol. 1 and 2)	
-0.16 ± 0.03	COX 70	DPWA	See CORDEN 76	
-0.09 ± 0.03	LITCHFIELD 70	DPWA	$K^- N \rightarrow \Lambda \pi$	

 $\Sigma(2080)$ FOOTNOTES

¹ Preferred solution 3; see CORDEN 76 for other possibilities, including a D_{15} at this mass.

 $\Sigma(2080)$ REFERENCES

CORDEN 76	NP B104 282	M.J. Cordón et al.	(BIRM) IJF
DEBELLEFON 76	NP B109 129	A. de Bellefont, A. Berthon	(CDEF) IJF
	Also NP B90 1	A. de Bellefont et al.	(CDEF, SACL) IJF
BAILLON 75	NP B94 39	P.H. Baillon, P.J. Litchfield	(CERN, RHEL) IJF
COX 70	NP B19 61	G.F. Cox et al.	(BIRM, EDIN, GLAS, LOIC) IJF
LITCHFIELD 70	NP B22 269	P.J. Litchfield	(RHEL) IJF

 $\Sigma(2100)$ G_{17}

$$I(J^P) = 1(\frac{7}{2}^-) \text{ Status: } *$$

OMITTED FROM SUMMARY TABLE

 $\Sigma(2100)$ MASS

VALUE (MeV)	DOCUMENT ID	TECN	COMMENT
≈ 2100 OUR ESTIMATE			
2060 ± 20	BARBARO-... 70	DPWA	$K^- p \rightarrow \Lambda \pi^0$
2120 ± 30	BARBARO-... 70	DPWA	$K^- p \rightarrow \Sigma \pi$

 $\Sigma(2100)$ WIDTH

VALUE (MeV)	DOCUMENT ID	TECN	COMMENT
70 ± 30	BARBARO-... 70	DPWA	$K^- p \rightarrow \Lambda \pi^0$
135 ± 30	BARBARO-... 70	DPWA	$K^- p \rightarrow \Sigma \pi$

 $\Sigma(2100)$ DECAY MODES

Mode	
Γ_1	$N\bar{K}$
Γ_2	$\Lambda\pi$
Γ_3	$\Sigma\pi$

 $\Sigma(2100)$ BRANCHING RATIOS

See "Sign conventions for resonance couplings" in the Note on Λ and Σ Resonances.

$(\Gamma_1 \Gamma_2)^{1/2} / \Gamma_{\text{total}}$ in $N\bar{K} \rightarrow \Sigma(2100) \rightarrow \Lambda\pi$	DOCUMENT ID	TECN	COMMENT	$(\Gamma_1 \Gamma_2)^{1/2} / \Gamma$
-0.07 ± 0.02	BARBARO-... 70	DPWA	$K^- p \rightarrow \Lambda \pi^0$	

$(\Gamma_1 \Gamma_3)^{1/2} / \Gamma_{\text{total}}$ in $N\bar{K} \rightarrow \Sigma(2100) \rightarrow \Sigma\pi$	DOCUMENT ID	TECN	COMMENT	$(\Gamma_1 \Gamma_3)^{1/2} / \Gamma$
+0.13 ± 0.02	BARBARO-... 70	DPWA	$K^- p \rightarrow \Sigma \pi$	

 $\Sigma(2100)$ REFERENCES

BARBARO-... 70	Duke Conf. 173	A. Barbaro-Galileri	(LRL) IJF
	Hyperon Resonances, 1970		

 $\Sigma(2250)$

$$I(J^P) = 1(?^?) \text{ Status: } ***$$

Results from partial-wave analyses are too weak to warrant separating them from the production and cross-section experiments. LASINSKI 71 in $\bar{K}N$ using a Pomeron + resonances model, and DEBELLEFON 76, DEBELLEFON 77, and DEBELLEFON 78 in energy-dependent partial-wave analyses of $\bar{K}N \rightarrow \Lambda\pi$, $\Sigma\pi$, and $N\bar{K}$, respectively, suggest two resonances around this mass.

 $\Sigma(2250)$ MASS

VALUE (MeV)	DOCUMENT ID	TECN	COMMENT
2210 to 2280 (≈ 2250) OUR ESTIMATE			
2270 ± 5.0	DEBELLEFON 78	DPWA	D_5 wave
2210 ± 30	DEBELLEFON 78	DPWA	G_9 wave
2275 ± 20	DEBELLEFON 77	DPWA	D_5 wave
2215 ± 20	DEBELLEFON 77	DPWA	G_9 wave
2300 ± 30	¹ DEBELLEFON 75B	HBC	$K^- p \rightarrow \Xi^*0 K^0$
2251 $^{+30}_{-20}$	VANHORN 75	DPWA	$K^- p \rightarrow \Lambda \pi^0, F_5$ wave
2280 ± 14	AGUILAR-... 70B	HBC	$K^- p$ 3.9, 4.6 GeV/c
2237 ± 11	BRICMAN 70	CNTR	Total, charge exchange
2255 ± 10	COOL 70	CNTR	$K^- p, K^- d$ total
2250 ± 7	BUGG 68	CNTR	$K^- p, K^- d$ total
••• We do not use the following data for averages, fits, limits, etc. •••			
2260	DEBELLEFON 76	IPWA	D_5 wave
2215	DEBELLEFON 76	IPWA	G_9 wave
2250 ± 20	LU 70	CNTR	$\gamma p \rightarrow K^+ Y^*$
2245	BLANPIED 65	CNTR	$\gamma p \rightarrow K^+ Y^*$
2299 ± 6	BOCK 65	HBC	$\bar{p} p$ 5.7 GeV/c

 $\Sigma(2250)$ WIDTH

VALUE (MeV)	DOCUMENT ID	TECN	COMMENT
60 to 150 (≈ 100) OUR ESTIMATE			
120 ± 4.0	DEBELLEFON 78	DPWA	D_5 wave
80 ± 2.0	DEBELLEFON 78	DPWA	G_9 wave
70 ± 2.0	DEBELLEFON 77	DPWA	D_5 wave
60 ± 2.0	DEBELLEFON 77	DPWA	G_9 wave
130 ± 20	¹ DEBELLEFON 75B	HBC	$K^- p \rightarrow \Xi^*0 K^0$
192 ± 30	VANHORN 75	DPWA	$K^- p \rightarrow \Lambda \pi^0, F_5$ wave
100 ± 20	AGUILAR-... 70B	HBC	$K^- p$ 3.9, 4.6 GeV/c
164 ± 5.0	BRICMAN 70	CNTR	Total, charge exchange
230 ± 20	BUGG 68	CNTR	$K^- p, K^- d$ total
••• We do not use the following data for averages, fits, limits, etc. •••			
100	DEBELLEFON 76	IPWA	D_5 wave
140	DEBELLEFON 76	IPWA	G_9 wave
170	COOL 70	CNTR	$K^- p, K^- d$ total
125	LU 70	CNTR	$\gamma p \rightarrow K^+ Y^*$
150	BLANPIED 65	CNTR	$\gamma p \rightarrow K^+ Y^*$
21 $^{+17}_{-21}$	BOCK 65	HBC	$\bar{p} p$ 5.7 GeV/c

 $\Sigma(2250)$ DECAY MODES

Mode	Fraction (Γ_i / Γ)
Γ_1	$N\bar{K}$
Γ_2	$\Lambda\pi$
Γ_3	$\Sigma\pi$
Γ_4	$N\bar{K}\pi$
Γ_5	$\Xi(1530)K$

The above branching fractions are our estimates, not fits or averages.

 $\Sigma(2250)$ BRANCHING RATIOS

See "Sign conventions for resonance couplings" in the Note on Λ and Σ Resonances.

$\Gamma(N\bar{K}) / \Gamma_{\text{total}}$	DOCUMENT ID	TECN	COMMENT	Γ_1 / Γ
<0.1 OUR ESTIMATE				
0.08 ± 0.02	DEBELLEFON 78	DPWA	D_5 wave	
0.02 ± 0.01	DEBELLEFON 78	DPWA	G_9 wave	

$(J+\frac{1}{2}) \times \Gamma(N\bar{K}) / \Gamma_{\text{total}}$	DOCUMENT ID	TECN	COMMENT	Γ_1 / Γ
0.16 ± 0.12	BRICMAN 70	CNTR	Total, charge exchange	
0.42	COOL 70	CNTR	$K^- p, K^- d$ total	
0.47	BUGG 68	CNTR		

••• We do not use the following data for averages, fits, limits, etc. •••

See key on page 405

Baryon Particle Listings

$\Sigma(2250)$, $\Sigma(2455)$ Bumps, $\Sigma(2620)$ Bumps, $\Sigma(3000)$ Bumps

$(\Gamma_1 \Gamma_f)^{1/2} / \Gamma_{\text{total}}$ in $N\bar{K} \rightarrow \Sigma(2250) \rightarrow \Lambda\pi$ $(\Gamma_1 \Gamma_2)^{1/2} / \Gamma$

VALUE	DOCUMENT ID	TECN	COMMENT
-0.16 ± 0.03	VANHORN 75	DPWA	$K^- p \rightarrow \Lambda\pi^0, F_5$ wave
••• We do not use the following data for averages, fits, limits, etc. •••			
+0.11	DEBELLEFON 76	IPWA	D_5 wave
-0.10	DEBELLEFON 76	IPWA	G_9 wave
-0.18	BARBARO... 70	DPWA	$K^- p \rightarrow \Lambda\pi^0, G_9$ wave

$(\Gamma_1 \Gamma_f)^{1/2} / \Gamma_{\text{total}}$ in $N\bar{K} \rightarrow \Sigma(2250) \rightarrow \Sigma\pi$ $(\Gamma_1 \Gamma_3)^{1/2} / \Gamma$

VALUE	DOCUMENT ID	TECN	COMMENT
+0.06 ± 0.02	DEBELLEFON 77	DPWA	D_5 wave
-0.03 ± 0.02	DEBELLEFON 77	DPWA	G_9 wave
+0.07	BARBARO... 70	DPWA	$K^- p \rightarrow \Sigma\pi, G_9$ wave

$\Gamma(N\bar{K}) / \Gamma(\Sigma\pi)$ Γ_1 / Γ_3

VALUE	DOCUMENT ID	TECN	COMMENT
<0.18	BARNES 69	HBC	1 standard dev. limit

$\Gamma(\Lambda\pi) / \Gamma(\Sigma\pi)$ Γ_2 / Γ_3

VALUE	DOCUMENT ID	TECN	COMMENT
<0.18	BARNES 69	HBC	1 standard dev. limit

$(\Gamma_1 \Gamma_f)^{1/2} / \Gamma_{\text{total}}$ in $N\bar{K} \rightarrow \Sigma(2250) \rightarrow \Xi(1530)K$ $(\Gamma_1 \Gamma_5)^{1/2} / \Gamma$

VALUE	DOCUMENT ID	TECN	COMMENT
0.18 ± 0.04	1 DEBELLEFON 75B	HBC	$K^- p \rightarrow \Xi^* K^0$

$\Sigma(2250)$ FOOTNOTES

¹ Seen in the (initial and final state) D_5 wave. Isospin not determined.

$\Sigma(2250)$ REFERENCES

DEBELLEFON 78	NC 42A 403	A. de Bellefon et al.	(CDEF, SACL) IJP
DEBELLEFON 77	NC 37A 175	A. de Bellefon et al.	(CDEF, SACL) IJP
DEBELLEFON 76	NP B109 129	A. de Bellefon, A. Berthon	(CDEF) IJP
Also	NP B90 1	A. de Bellefon et al.	(CDEF, SACL) IJP
DEBELLEFON 75B	NC 28A 289	A. de Bellefon et al.	(CDEF, SACL) IJP
VANHORN 75	NP B87 145	A.J. van Horn	(LBL) IJP
Also	NP B87 157	A.J. van Horn	(LBL) IJP
LASINSKI 71	NP B29 125	T.A. Lasinski	(EFI) IJP
AGUILAR... 70B	PRL 25 58	M. Aguilar-Benitez et al.	(BNL, SYRA)
BARBARO... 70	Duke Conf. 173	A. Barbaro-Galieri	(LRL) IJP
BRICMAN 70	PL 31B 152	C. Bricman et al.	(CERN, CAEN, SACL)
COOL 70	PR D1 1887	R.L. Cool et al.	(BNL) I
Also	PRL 16 1228	R.L. Cool et al.	(BNL) I
LU 70	PR D2 1846	D.C. Lu et al.	(YALE)
BARNES 69	PR 22 479	V.E. Barnes et al.	(BNL, SYRA)
BUGG 68	PR 168 1466	D.V. Bugg et al.	(RHEL, BIRM, CAVE) I
BLANPIED 65	PRL 14 741	W.A. Blanpied et al.	(YALE, CEA)
BOCK 65	PL 17 166	R.K. Bock et al.	(CERN, SACL)

$\Sigma(2455)$ Bumps

$I(J^P) = 1(?)^?$ Status: **

OMITTED FROM SUMMARY TABLE

There is also some slight evidence for Y^* states in this mass region from the reaction $\gamma p \rightarrow K^+ X$ — see GREENBERG 68.

$\Sigma(2455)$ MASS

VALUE (MeV)	DOCUMENT ID	TECN	COMMENT
≈ 2455 OUR ESTIMATE			
2455 ± 10	ABRAMS 70	CNTR	$K^- p, K^- d$ total
2455 ± 7	BUGG 68	CNTR	$K^- p, K^- d$ total

$\Sigma(2455)$ WIDTH

VALUE (MeV)	DOCUMENT ID	TECN	COMMENT
140	ABRAMS 70	CNTR	$K^- p, K^- d$ total
100 ± 20	BUGG 68	CNTR	

$\Sigma(2455)$ DECAY MODES

Mode	Γ_1
$N\bar{K}$	

$\Sigma(2455)$ BRANCHING RATIOS

$(J+\frac{1}{2}) \times \Gamma(N\bar{K}) / \Gamma_{\text{total}}$ Γ_1 / Γ

VALUE	DOCUMENT ID	TECN	COMMENT
0.39	ABRAMS 70	CNTR	$K^- p, K^- d$ total
0.05 ± 0.05	¹ BRICMAN 70	CNTR	Total, charge exchange
0.3	BUGG 68	CNTR	

$\Sigma(2455)$ FOOTNOTES

¹ Fit of total cross section given by BRICMAN 70 is poor in this region.

$\Sigma(2455)$ REFERENCES

ABRAMS 70	PR D1 1917	R.J. Abrams et al.	(BNL) I
Also	PRL 19 678	R.J. Abrams et al.	(BNL)
BRICMAN 70	PL 31B 152	C. Bricman et al.	(CERN, CAEN, SACL)
BUGG 68	PR 168 1466	D.V. Bugg et al.	(RHEL, BIRM, CAVE) I
GREENBERG 68	PRL 20 221	J.S. Greenberg et al.	(YALE)

$\Sigma(2620)$ Bumps

$I(J^P) = 1(?)^?$ Status: **

OMITTED FROM SUMMARY TABLE

$\Sigma(2620)$ MASS

VALUE (MeV)	DOCUMENT ID	TECN	COMMENT
≈ 2620 OUR ESTIMATE			
2542 ± 22	DIBIANCA 75	DBC	$K^- N \rightarrow \Xi K\pi$
2620 ± 15	ABRAMS 70	CNTR	$K^- p, K^- d$ total

$\Sigma(2620)$ WIDTH

VALUE (MeV)	DOCUMENT ID	TECN	COMMENT
221 ± 81	DIBIANCA 75	DBC	$K^- N \rightarrow \Xi K\pi$
175	ABRAMS 70	CNTR	$K^- p, K^- d$ total

$\Sigma(2620)$ DECAY MODES

Mode	Γ_1
$N\bar{K}$	

$\Sigma(2620)$ BRANCHING RATIOS

$(J+\frac{1}{2}) \times \Gamma(N\bar{K}) / \Gamma_{\text{total}}$ Γ_1 / Γ

VALUE	DOCUMENT ID	TECN	COMMENT
0.32	ABRAMS 70	CNTR	$K^- p, K^- d$ total
0.36 ± 0.12	BRICMAN 70	CNTR	Total, charge exchange

$\Sigma(2620)$ REFERENCES

DIBIANCA 75	NP B98 137	F.A. Dibianca, R.J. Endorf	(CMU)
ABRAMS 70	PR D1 1917	R.J. Abrams et al.	(BNL) I
Also	PRL 19 678	R.J. Abrams et al.	(BNL)
BRICMAN 70	PL 31B 152	C. Bricman et al.	(CERN, CAEN, SACL)

$\Sigma(3000)$ Bumps

$I(J^P) = 1(?)^?$ Status: *

OMITTED FROM SUMMARY TABLE

Seen as an enhancement in $\Lambda\pi$ and $\bar{K}N$ invariant mass spectra and in the missing mass of neutrals recoiling against a K^0 .

$\Sigma(3000)$ MASS

VALUE (MeV)	DOCUMENT ID	TECN	CHG	COMMENT
≈ 3000 OUR ESTIMATE				
3000	EHRlich 66	HBC	0	$\pi^- p$ 7.91 GeV/c

$\Sigma(3000)$ DECAY MODES

Mode	Γ_1	Γ_2
$N\bar{K}$		
$\Lambda\pi$		

$\Sigma(3000)$ REFERENCES

EHRlich 66	PR 152 1194	R. Ehrlich, W. Selove, H. Yuta	(PENN) I
------------	-------------	--------------------------------	----------

Baryon Particle Listings

 $\Sigma(3170)$ Bumps **$\Sigma(3170)$ Bumps** $I(J^P) = 1(?^?)$ Status: *

OMITTED FROM SUMMARY TABLE

Seen by AMIRZADEH 79 as a narrow 6.5-standard-deviation enhancement in the reaction $K^- p \rightarrow Y^{*+} \pi^-$ using data from independent high statistics bubble chamber experiments at 8.25 and 6.5 GeV/c. The dominant decay modes are multibody, multistrange final states and the production is via isospin-3/2 baryon exchange. Isospin 1 is favored.

Not seen in a $K^- p$ experiment in LASS at 11 GeV/c (ASTON 85B).

 **$\Sigma(3170)$ MASS
(PRODUCTION EXPERIMENTS)**

VALUE (MeV)	EVTS	DOCUMENT ID	TECN	COMMENT
≈ 3170 OUR ESTIMATE				
3170 ± 5	35	AMIRZADEH 79	HBC	$K^- p \rightarrow Y^{*+} \pi^-$

 **$\Sigma(3170)$ WIDTH
(PRODUCTION EXPERIMENTS)**

VALUE (MeV)	EVTS	DOCUMENT ID	TECN	COMMENT
<20	35	¹ AMIRZADEH 79	HBC	$K^- p \rightarrow Y^{*+} \pi^-$

 **$\Sigma(3170)$ DECAY MODES
(PRODUCTION EXPERIMENTS)**

Mode	Fraction (Γ_i/Γ)
Γ_1 $\Lambda K \bar{K} \pi$'s	seen
Γ_2 $\Sigma K \bar{K} \pi$'s	seen
Γ_3 $\Xi K \pi$'s	seen

 **$\Sigma(3170)$ BRANCHING RATIOS
(PRODUCTION EXPERIMENTS)**

$\Gamma(\Lambda K \bar{K} \pi \text{'s})/\Gamma_{\text{total}}$	Γ_1/Γ		
VALUE	DOCUMENT ID	TECN	COMMENT
seen	AMIRZADEH 79	HBC	$K^- p \rightarrow Y^{*+} \pi^-$
$\Gamma(\Sigma K \bar{K} \pi \text{'s})/\Gamma_{\text{total}}$	Γ_2/Γ		
VALUE	DOCUMENT ID	TECN	COMMENT
seen	AMIRZADEH 79	HBC	$K^- p \rightarrow Y^{*+} \pi^-$
$\Gamma(\Xi K \pi \text{'s})/\Gamma_{\text{total}}$	Γ_3/Γ		
VALUE	DOCUMENT ID	TECN	COMMENT
seen	AMIRZADEH 79	HBC	$K^- p \rightarrow Y^{*+} \pi^-$

 **$\Sigma(3170)$ FOOTNOTES
(PRODUCTION EXPERIMENTS)**

¹ Observed width consistent with experimental resolution.

 **$\Sigma(3170)$ REFERENCES
(PRODUCTION EXPERIMENTS)**

ASTON 85B	PR D32 2270	D. Aston <i>et al.</i>	(SLAC, CARL, CNRC, CINC)
AMIRZADEH 79	PL 89B 125	J. Amirzadeh <i>et al.</i>	(BIRM, CERN, GLAS+) ¹
Also	Toronto Conf. 263	J.B. Kinson <i>et al.</i>	(BIRM, CERN, GLAS+) ¹

Ξ BARYONS

$(S = -2, I = 1/2)$

$\Xi^0 = uss, \Xi^- = dss$

Ξ^0 $I(J^P) = \frac{1}{2}(\frac{1}{2}^+)$ Status: * * * *

The parity has not actually been measured, but + is of course expected.

Ξ^0 MASS

The fit uses the $\Xi^0, \Xi^-,$ and Ξ^+ masses and the $\Xi^- - \Xi^0$ mass difference. It assumes that the Ξ^- and Ξ^+ masses are the same.

VALUE (MeV)	EVTS	DOCUMENT ID	TECN	COMMENT
1314.86 ± 0.20 OUR FIT				
1314.82 ± 0.06 ± 0.20	3120	FANTI	00 NA48	p Be, 450 GeV
• • • We do not use the following data for averages, fits, limits, etc. • • •				
1315.2 ± 0.92	49	WILQUET	72 HLBC	
1313.4 ± 1.8	1	PALMER	68 HBC	

$m_{\Xi^-} - m_{\Xi^0}$

The fit uses the $\Xi^0, \Xi^-,$ and Ξ^+ masses and the $\Xi^- - \Xi^0$ mass difference. It assumes that the Ξ^- and Ξ^+ masses are the same.

VALUE (MeV)	EVTS	DOCUMENT ID	TECN	COMMENT
6.85 ± 0.21 OUR FIT				
6.3 ± 0.7 OUR AVERAGE				
6.9 ± 2.2	29	LONDON	66 HBC	
6.1 ± 0.9	88	PJERROU	65B HBC	
6.8 ± 1.6	23	JAUNEAU	63 FBC	
• • • We do not use the following data for averages, fits, limits, etc. • • •				
6.1 ± 1.6	45	CARMONY	64B HBC	See PJERROU 65B

Ξ^0 MEAN LIFE

VALUE (10^{-10} s)	EVTS	DOCUMENT ID	TECN	COMMENT
2.90 ± 0.09 OUR AVERAGE				
2.83 ± 0.16	6300	1 ZECH	77 SPEC	Neutral hyperon beam
2.88 ^{+0.21} _{-0.19}	652	BALTAY	74 HBC	1.75 GeV/c $K^- p$
2.90 ^{+0.32} _{-0.27}	157	2 MAYEUR	72 HLBC	2.1 GeV/c K^-
3.07 ^{+0.22} _{-0.20}	340	DAUBER	69 HBC	
3.0 ± 0.5	80	PJERROU	65B HBC	
2.5 ^{+0.4} _{-0.3}	101	HUBBARD	64 HBC	
3.9 ^{+1.4} _{-0.8}	24	JAUNEAU	63 FBC	
• • • We do not use the following data for averages, fits, limits, etc. • • •				
3.5 ^{+1.0} _{-0.8}	45	CARMONY	64B HBC	See PJERROU 65B

¹ The ZECH 77 result is $\tau_{\Xi^0} = [2.77 - (\tau_A - 2.69)] \times 10^{-10}$ s, in which we use $\tau_A = 2.63 \times 10^{-10}$ s.

² The MAYEUR 72 value is modified by the erratum.

Ξ^0 MAGNETIC MOMENT

See the "Note on Baryon Magnetic Moments" in the Λ Listings.

VALUE (μ_N)	EVTS	DOCUMENT ID	TECN	COMMENT
-1.250 ± 0.014 OUR AVERAGE				
-1.253 ± 0.014	270k	COX	81 SPEC	
-1.20 ± 0.06	42k	BUNCE	79 SPEC	

Ξ^0 DECAY MODES

Mode	Fraction (Γ_i/Γ)	Confidence level
$\Gamma_1 \Lambda\pi^0$	(99.525 ± 0.012) %	
$\Gamma_2 \Lambda\gamma$	(1.17 ± 0.07) × 10 ⁻³	
$\Gamma_3 \Lambda e^+ e^-$	(7.6 ± 0.6) × 10 ⁻⁶	
$\Gamma_4 \Sigma^0 \gamma$	(3.33 ± 0.10) × 10 ⁻³	
$\Gamma_5 \Sigma^+ e^- \bar{\nu}_e$	(2.53 ± 0.08) × 10 ⁻⁴	
$\Gamma_6 \Sigma^+ \mu^- \bar{\nu}_\mu$	(4.6 ^{+1.8} _{-1.4}) × 10 ⁻⁶	

$\Delta S = \Delta Q$ (SQ) violating modes or $\Delta S = 2$ forbidden (S2) modes

$\Gamma_7 \Sigma^- e^+ \nu_e$	SQ < 9	× 10 ⁻⁴	90%
$\Gamma_8 \Sigma^- \mu^+ \nu_\mu$	SQ < 9	× 10 ⁻⁴	90%
$\Gamma_9 \rho \pi^-$	S2 < 8	× 10 ⁻⁶	90%
$\Gamma_{10} \rho e^- \bar{\nu}_e$	S2 < 1.3	× 10 ⁻³	
$\Gamma_{11} \rho \mu^- \bar{\nu}_\mu$	S2 < 1.3	× 10 ⁻³	

CONSTRAINED FIT INFORMATION

An overall fit to 3 branching ratios uses 9 measurements and one constraint to determine 4 parameters. The overall fit has a $\chi^2 = 4.6$ for 6 degrees of freedom.

The following *off-diagonal* array elements are the correlation coefficients $\langle \delta x_i \delta x_j \rangle / (\delta x_i \delta x_j)$, in percent, from the fit to the branching fractions, $x_i \equiv \Gamma_i / \Gamma_{\text{total}}$. The fit constrains the x_i whose labels appear in this array to sum to one.

x_2	-57		
x_4	-82	0	
x_5	-7	0	0
	x_1	x_2	x_4

Ξ^0 BRANCHING RATIOS

$\Gamma(\Lambda\gamma)/\Gamma(\Lambda\pi^0)$ Γ_2/Γ_1

VALUE (units 10 ⁻³)	EVTS	DOCUMENT ID	TECN	COMMENT
1.17 ± 0.07 OUR FIT				
1.17 ± 0.07 OUR AVERAGE				
1.17 ± 0.05 ± 0.06	672	³ LAI	04A NA48	p Be, 450 GeV
1.91 ± 0.34 ± 0.19	31	⁴ FANTI	00 NA48	p Be, 450 GeV
1.06 ± 0.12 ± 0.11	116	JAMES	90 SPEC	FNAL hyperons

³ LAI 04A used our 2002 value of 99.5% for the $\Xi^0 \rightarrow \Lambda\pi^0$ branching fraction to get $\Gamma(\Xi^0 \rightarrow \Lambda\gamma)/\Gamma_{\text{total}} = (1.16 \pm 0.05 \pm 0.06) \times 10^{-3}$. We adjust slightly to go back to what was directly measured.

⁴ FANTI 00 used our 1998 value of 99.5% for the $\Xi^0 \rightarrow \Lambda\pi^0$ branching fraction to get $\Gamma(\Xi^0 \rightarrow \Lambda\gamma)/\Gamma_{\text{total}} = (1.90 \pm 0.34 \pm 0.19) \times 10^{-3}$. We adjust slightly to go back to what was directly measured.

$\Gamma(\Lambda e^+ e^-)/\Gamma_{\text{total}}$ Γ_3/Γ

VALUE (units 10 ⁻⁶)	EVTS	DOCUMENT ID	TECN	COMMENT
7.6 ± 0.4 ± 0.5	397 ± 21	⁵ BATLEY	07C NA48	p Be, 400 GeV

⁵ This BATLEY 07C result is consistent with internal bremsstrahlung.

$\Gamma(\Sigma^0 \gamma)/\Gamma(\Lambda\pi^0)$ Γ_4/Γ_1

VALUE (units 10 ⁻³)	EVTS	DOCUMENT ID	TECN	COMMENT
3.35 ± 0.10 OUR FIT				
3.35 ± 0.10 OUR AVERAGE				
3.34 ± 0.05 ± 0.09	4045	ALAVI-HARATI	01C KTEV	p nucleus, 800 GeV
3.16 ± 0.76 ± 0.32	17	⁶ FANTI	00 NA48	p Be, 450 GeV
3.56 ± 0.42 ± 0.10	85	TEIGE	89 SPEC	FNAL hyperons

⁶ FANTI 00 used our 1998 value of 99.5% for the $\Xi^0 \rightarrow \Lambda\pi^0$ branching fraction to get $\Gamma(\Xi^0 \rightarrow \Sigma^0 \gamma)/\Gamma_{\text{total}} = (3.14 \pm 0.76 \pm 0.32) \times 10^{-3}$. We adjust slightly to go back to what was directly measured.

$\Gamma(\Sigma^+ e^- \bar{\nu}_e)/\Gamma_{\text{total}}$ Γ_5/Γ

VALUE (units 10 ⁻⁴)	EVTS	DOCUMENT ID	TECN	COMMENT
2.53 ± 0.08 OUR FIT				
2.53 ± 0.08 OUR AVERAGE				
2.51 ± 0.03 ± 0.09	6101	BATLEY	07 NA48	p Be, 400 GeV
2.55 ± 0.14 ± 0.10	419	⁷ BATLEY	07 NA48	p Be, 400 GeV
2.71 ± 0.22 ± 0.31	176	AFFOLDER	99 KTEV	p nucleus, 800 GeV

⁷ This BATLEY 07 result is for $\Xi^0 \rightarrow \Sigma^- e^+ \nu_e$ events.

$\Gamma(\Sigma^+ \mu^- \bar{\nu}_\mu)/\Gamma(\Sigma^+ e^- \bar{\nu}_e)$ Γ_6/Γ_5

VALUE	EVTS	DOCUMENT ID	TECN	COMMENT
0.018 ± 0.007 ± 0.005 ± 0.002	9	ABOUZAID	05 KTEV	p nucleus 800 GeV

$\Gamma(\Sigma^+ \mu^- \bar{\nu}_\mu)/\Gamma(\Lambda\pi^0)$ Γ_6/Γ_1

VALUE (units 10 ⁻³)	CL%	EVTS	DOCUMENT ID	TECN	COMMENT
• • • We do not use the following data for averages, fits, limits, etc. • • •					
<1.1	90	0	YEH	74 HBC	Effective denom.=2100
<1.5			DAUBER	69 HBC	
<7			HUBBARD	66 HBC	

$\Gamma(\Sigma^- e^+ \nu_e)/\Gamma(\Lambda\pi^0)$ Γ_7/Γ_1

VALUE (units 10 ⁻³)	CL%	EVTS	DOCUMENT ID	TECN	COMMENT
<0.9	90	0	YEH	74 HBC	Effective denom.=2500
• • • We do not use the following data for averages, fits, limits, etc. • • •					
<1.5			DAUBER	69 HBC	
<6			HUBBARD	66 HBC	

Baryon Particle Listings

 Ξ^0 $\Gamma(\Sigma^- \mu^+ \nu_\mu)/\Gamma(\Lambda\pi^0)$ Γ_8/Γ_1 Test of $\Delta S = \Delta Q$ rule.

VALUE (units 10^{-3})	CL%	EVTS	DOCUMENT ID	TECN	COMMENT
<0.9	90	0	YEH	74	HBC Effective denom.=2500
••• We do not use the following data for averages, fits, limits, etc. •••					
<1.5			DAUBER	69	HBC
<6			HUBBARD	66	HBC

 $\Gamma(p\pi^-)/\Gamma(\Lambda\pi^0)$ Γ_9/Γ_1 $\Delta S=2$. Forbidden in first-order weak interaction.

VALUE (units 10^{-6})	CL%	EVTS	DOCUMENT ID	TECN	COMMENT
< 8.2	90		WHITE	05	HYCP p Cu, 800 GeV
••• We do not use the following data for averages, fits, limits, etc. •••					
< 36	90		GEWENIGER	75	SPEC
<1800	90	0	YEH	74	HBC Effective denom.=1300
< 900			DAUBER	69	HBC
<5000			HUBBARD	66	HBC

 $\Gamma(p e^- \bar{\nu}_e)/\Gamma(\Lambda\pi^0)$ Γ_{10}/Γ_1 $\Delta S=2$. Forbidden in first-order weak interaction.

VALUE (units 10^{-3})	CL%	EVTS	DOCUMENT ID	TECN	COMMENT
<1.3			DAUBER	69	HBC
••• We do not use the following data for averages, fits, limits, etc. •••					
<3.4	90	0	YEH	74	HBC Effective denom.=670
<6			HUBBARD	66	HBC

 $\Gamma(p\mu^- \bar{\nu}_\mu)/\Gamma(\Lambda\pi^0)$ Γ_{11}/Γ_1 $\Delta S=2$. Forbidden in first-order weak interaction.

VALUE (units 10^{-3})	CL%	EVTS	DOCUMENT ID	TECN	COMMENT
<1.3			DAUBER	69	HBC
••• We do not use the following data for averages, fits, limits, etc. •••					
<3.5	90	0	YEH	74	HBC Effective denom.=664
<6			HUBBARD	66	HBC

 Ξ^0 DECAY PARAMETERS

See the "Note on Baryon Decay Parameters" in the neutron Listings.

 $\alpha(\Xi^0) \alpha_-(\Lambda)$

VALUE	EVTS	DOCUMENT ID	TECN	COMMENT
-0.264 ± 0.013 OUR AVERAGE				Error includes scale factor of 2.1.
-0.260 ± 0.004 ± 0.005	300k	HANDLER	82	SPEC FNAL hyperons
-0.317 ± 0.027	6075	BUNCE	78	SPEC FNAL hyperons
-0.35 ± 0.06	505	BALTAY	74	HBC $K^- p$ 1.75 GeV/c
-0.28 ± 0.06	739	DAUBER	69	HBC $K^- p$ 1.7-2.6 GeV/c

 α FOR $\Xi^0 \rightarrow \Lambda\pi^0$

The above average, $\alpha(\Xi^0)\alpha_-(\Lambda) = -0.264 \pm 0.013$, where the error includes a scale factor of 2.1, divided by our current average $\alpha_-(\Lambda) = 0.642 \pm 0.013$, gives the following value for $\alpha(\Xi^0)$.

VALUE	DOCUMENT ID
-0.411 ± 0.022 OUR EVALUATION	Error includes scale factor of 2.1.

 ϕ ANGLE FOR $\Xi^0 \rightarrow \Lambda\pi^0$ ($\tan\phi = \beta/\gamma$)

VALUE (°)	EVTS	DOCUMENT ID	TECN	COMMENT
21 ± 12 OUR AVERAGE				
16 ± 17	652	BALTAY	74	HBC 1.75 GeV/c $K^- p$
38 ± 19	739	⁸ DAUBER	69	HBC
- 8 ± 30	146	⁹ BERGE	66	HBC

⁸ DAUBER 69 uses $\alpha_\Lambda = 0.647 \pm 0.020$.⁹ The errors have been multiplied by 1.2 due to approximations used for the Ξ polarization; see DAUBER 69 for a discussion.

RADIATIVE HYPERON DECAYS

Written September 2003 by J.D. Jackson (LBNL).

The weak radiative decays of spin-1/2 hyperons, $B_i \rightarrow B_f \gamma$, yield information about matrix elements (form factors) similar to that gained from weak hadronic decays. For a polarized spin-1/2 hyperon decaying radiatively via a $\Delta Q = 0$, $\Delta S = 1$ transition, the angular distribution of the direction \hat{p} of the final spin-1/2 baryon in the hyperon rest frame is

$$\frac{dN}{d\Omega} = \frac{N}{4\pi} (1 + \alpha_\gamma \mathbf{P}_i \cdot \hat{p}). \quad (1)$$

Here \mathbf{P}_i is the polarization of the decaying hyperon, and α_γ is the asymmetry parameter. In terms of the form factors $F_1(q^2)$,

$F_2(q^2)$, and $G(q^2)$ of the effective hadronic weak electromagnetic vertex,

$$F_1(q^2)\gamma_\lambda + iF_2(q^2)\sigma_{\lambda\mu}q^\mu + G(q^2)\gamma_\lambda\gamma_5,$$

 α_γ is

$$\alpha_\gamma = \frac{2\text{Re}[G(0)F_M^*(0)]}{|G(0)|^2 + |F_M(0)|^2}, \quad (2)$$

where $F_M = (m_i - m_f)[F_2 - F_1/(m_i + m_f)]$. If the decaying hyperon is unpolarized, the decay baryon has a longitudinal polarization given by $P_f = -\alpha_\gamma$ [1].

The angular distribution for the weak hadronic decay, $B_i \rightarrow B_f \pi$, has the same form as Eq. (1), but of course with a different asymmetry parameter, α_π . Now, however, if the decaying hyperon is unpolarized, the decay baryon has a longitudinal polarization given by $P_f = +\alpha_\pi$ [2,3]. The difference of sign is because the spins of the pion and photon are different.

$\Xi^0 \rightarrow \Lambda\gamma$ decay—The radiative decay $\Xi^0 \rightarrow \Lambda\gamma$ of an unpolarized Ξ^0 uses the hadronic decay $\Lambda \rightarrow p\pi^-$ as the analyzer. As noted above, the longitudinal polarization of the Λ will be $P_\Lambda = -\alpha_{\Xi\Lambda\gamma}$. Let α_- be the $\Lambda \rightarrow p\pi^-$ asymmetry parameter and $\theta_{\Lambda p}$ be the angle, as seen in the Λ rest frame, between the Λ line of flight and the proton momentum. Then the hadronic version of Eq. (1) applied to the $\Lambda \rightarrow p\pi^-$ decay gives

$$\frac{dN}{d\cos\theta_{\Lambda p}} = \frac{N}{2} (1 - \alpha_{\Xi\Lambda\gamma} \alpha_- \cos\theta_{\Lambda p}) \quad (3)$$

for the angular distribution of the proton in the Λ frame. The only published measurement of $\alpha_{\Xi\Lambda\gamma}$ [4] got the sign wrong, as explained in an erratum 12 years later [5]. The corrected result is $\alpha_{\Xi\Lambda\gamma} = -0.43 \pm 0.44$.

$\Xi^0 \rightarrow \Sigma^0\gamma$ decay—The asymmetry parameter here, $\alpha_{\Xi\Sigma\gamma}$, is measured by following the decay chain $\Xi^0 \rightarrow \Sigma^0\gamma$, $\Sigma^0 \rightarrow \Lambda\gamma$, $\Lambda \rightarrow p\pi^-$. Again, for an unpolarized Ξ^0 , the longitudinal polarization of the Σ^0 will be $P_\Sigma = -\alpha_{\Xi\Sigma\gamma}$. In the $\Sigma^0 \rightarrow \Lambda\gamma$ decay, a parity-conserving magnetic-dipole transition, the polarization of the Σ^0 is transferred to the Λ , as may be seen as follows. Let $\theta_{\Sigma\Lambda}$ be the angle seen in the Σ^0 rest frame between the Σ^0 line of flight and the Λ momentum. For Σ^0 helicity +1/2, the probability amplitudes for positive and negative spin states of the Σ^0 along the Λ momentum are $\cos(\theta_{\Sigma\Lambda}/2)$ and $\sin(\theta_{\Sigma\Lambda}/2)$. Then the amplitude for a negative helicity photon and a negative helicity Λ is $\cos(\theta_{\Sigma\Lambda}/2)$, while the amplitude for positive helicities for the photon and Λ is $\sin(\theta_{\Sigma\Lambda}/2)$. For Σ^0 helicity -1/2, the amplitudes are interchanged. If the Σ^0 has longitudinal polarization P_Σ , the probabilities for Λ helicities $\pm 1/2$ are therefore

$$p(\pm 1/2) = \frac{1}{2}(1 \mp P_\Sigma) \cos^2(\theta_{\Sigma\Lambda}/2) + \frac{1}{2}(1 \pm P_\Sigma) \sin^2(\theta_{\Sigma\Lambda}/2), \quad (4)$$

and the longitudinal polarization of the Λ is

$$P_\Lambda = -P_\Sigma \cos\theta_{\Sigma\Lambda} = +\alpha_{\Xi\Sigma\gamma} \cos\theta_{\Sigma\Lambda}. \quad (5)$$

Using Eq. (1) for the $\Lambda \rightarrow p\pi^-$ decay again, we get for the joint angular distribution of the $\Sigma^0 \rightarrow \Lambda\gamma$, $\Lambda \rightarrow p\pi^-$ chain,

$$\frac{d^2N}{d\cos\theta_{\Sigma\Lambda}d\cos\theta_{\Lambda p}} = \frac{N}{4} (1 + \alpha_{\Xi\Sigma\gamma} \cos\theta_{\Sigma\Lambda} \alpha_- \cos\theta_{\Lambda p}). \quad (6)$$

The KTeV collaboration recently measured $\alpha_{\Xi\Sigma\gamma}$ to be -0.63 ± 0.09 [6]. The only other measurement has been withdrawn [7].

References

1. R.E. Behrends, Phys. Rev. **111**, 1691 (1958); see Eq. (7) or (8).
2. In ancient times, the signs of the asymmetry term in the angular distributions of radiative and hadronic decays of polarized hyperons were sometimes opposite. For roughly 40 years, however, the overwhelming convention has been to make them the same. The aim, not always achieved, is to remove ambiguities.
3. For the definition of α_{π} , see the note on “Baryon Decay Parameters,” in the Neutron Listings in this Review..
4. C. James *et al.*, Phys. Rev. Lett. **64**, 843 (1990).
5. C. James *et al.*, Phys. Rev. Lett. **89**, 169901 (2002) (erratum). The various sign conventions spelled out here are discussed.
6. A. Alavi-Harati *et al.*, Phys. Rev. Lett. **86**, 3239 (2001).
7. S. Teige *et al.*, Phys. Rev. Lett. **63**, 2717 (1989); erratum, Phys. Rev. Lett. **89**, 169902 (2002).

α FOR $\Xi^0 \rightarrow \Lambda\gamma$

See the note above on “Radiative Hyperon Decays.”

VALUE	EVTS	DOCUMENT ID	TECN	COMMENT
-0.73 ± 0.17 OUR AVERAGE				
$-0.78 \pm 0.18 \pm 0.06$	672	LAI	04A NA48	p Be, 450 GeV
-0.43 ± 0.44	87	¹⁰ JAMES	90 SPEC	FNAL hyperons

¹⁰The sign has been changed; see the erratum, JAMES 02.

α FOR $\Xi^0 \rightarrow \Lambda e^+ e^-$

VALUE	EVTS	DOCUMENT ID	TECN	COMMENT
-0.8 ± 0.2	397 ± 21	¹¹ BATLEY	07c NA48	p Be, 400 GeV

¹¹This BATLEY 07c result is consistent with the asymmetry α for $\Xi^0 \rightarrow \Lambda\gamma$, as expected if the mechanism is internal bremsstrahlung.

α FOR $\Xi^0 \rightarrow \Sigma^0\gamma$

See the note above on “Radiative Hyperon Decays.”

VALUE	EVTS	DOCUMENT ID	TECN	COMMENT
$-0.63 \pm 0.08 \pm 0.05$	4045	ALAVI-HARATI01c	KTEV	p nucleus, 800 GeV
$+0.20 \pm 0.32 \pm 0.05$	85	¹² TEIGE	89 SPEC	FNAL hyperons

¹²This result has been withdrawn, due to an error. See the erratum, TEIGE 02.

$g_1(0)/f_1(0)$ FOR $\Xi^0 \rightarrow \Sigma^+ e^- \bar{\nu}_e$

VALUE	EVTS	DOCUMENT ID	TECN	COMMENT
1.21 ± 0.05 OUR AVERAGE				
$+1.20 \pm 0.04 \pm 0.03$	6520	¹³ BATLEY	07 NA48	p Be, 400 GeV
$+1.32 \pm 0.21 \pm 0.05$	487	¹⁴ ALAVI-HARATI01i	KTEV	p nucleus, 800 GeV

¹³This BATLEY 07 result uses our 2006 value of V_{us} from semileptonic kaon decays as input.

¹⁴ALAVI-HARATI 01i assumes here that the second-class current is zero and that the weak-magnetism term takes its exact SU(3) value.

$g_2(0)/f_1(0)$ FOR $\Xi^0 \rightarrow \Sigma^+ e^- \bar{\nu}_e$

VALUE	EVTS	DOCUMENT ID	TECN	COMMENT
$-1.7 \pm 2.1 \pm 2.0 \pm 0.5$	487	¹⁵ ALAVI-HARATI01i	KTEV	p nucleus, 800 GeV

¹⁵ALAVI-HARATI 01i thus assumes that $g_2 = 0$ in calculating g_2/f_1 , above.

$f_2(0)/f_1(0)$ FOR $\Xi^0 \rightarrow \Sigma^+ e^- \bar{\nu}_e$

VALUE	EVTS	DOCUMENT ID	TECN	COMMENT
$2.0 \pm 1.2 \pm 0.5$	487	ALAVI-HARATI01i	KTEV	p nucleus, 800 GeV

≡⁰ REFERENCES

BATLEY	07	PL B645 36	J.R. Batley <i>et al.</i>	(CERN NA48/1 Collab.)
BATLEY	07C	PL B650 1	J.R. Batley <i>et al.</i>	(CERN NA48 Collab.)
ABOUZAID	05	PRL 95 081801	E. Abouzaid <i>et al.</i>	(FNAL KTeV Collab.)
WHITE	05	PRL 94 101804	C.G. White <i>et al.</i>	(FNAL HyperCP Collab.)
LAI	04A	PL B584 251	A. Lai <i>et al.</i>	(CERN NA48 Collab.)
JAMES	02	PRL 89 169901 (erratum)	C. James <i>et al.</i>	(MINN, MICH, WIS C, RUTG)
TEIGE	02	PRL 89 169902 (erratum)	S. Teige <i>et al.</i>	(RUTG, MICH, MINN)
ALAVI-HARATI	01C	PRL 86 3239	A. Alavi-Harati <i>et al.</i>	(FNAL KTeV Collab.)
ALAVI-HARATI	01i	PRL 87 132001	A. Alavi-Harati <i>et al.</i>	(FNAL KTeV Collab.)
FANTI	00	EPJ C12 69	V. Fanti <i>et al.</i>	(CERN NA48 Collab.)
AFFOLDER	99	PRL 82 3751	A. Affolder <i>et al.</i>	(FNAL KTeV Collab.)
JAMES	90	PRL 64 843	C. James <i>et al.</i>	(MINN, MICH, WIS C, RUTG)
TEIGE	89	PRL 63 2717	S. Teige <i>et al.</i>	(RUTG, MICH, MINN)
HANDLER	82	PR D25 639	R. Handler <i>et al.</i>	(WISC, MICH, MINN+)
COX	81	PRL 46 877	P.T. Cox <i>et al.</i>	(MICH, WISC, RUTG, MINN+)
BUNCE	79	PL 86B 386	G.R.M. Bunce <i>et al.</i>	(BNL, MICH, RUTG+)
BUNCE	78	PR D18 633	G.R.M. Bunce <i>et al.</i>	(WISC, MICH, RUTG)
ZECH	77	NP B124 413	G. Zech <i>et al.</i>	(SIEG, CERN, DORT, HEIDH)
GEWENIGER	75	PL 57B 193	C. Geweniger <i>et al.</i>	(CERN, HEIDH)
BALTAY	74	PR D9 49	C. Baltay <i>et al.</i>	(COLU, BING, J)
YEH	74	PR D10 3545	N. Yeh <i>et al.</i>	(BING, COLU)
MAYEUR	72	NP B47 333	C. Mayeur <i>et al.</i>	(BRUX, CERN, TUFTS, LOUC)
Also		NP B53 268 (erratum)	C. Mayeur	
WILQUET	72	PL 42B 372	G. Wilquet <i>et al.</i>	(BRUX, CERN, TUFTS+)
DAUBER	69	PR 179 1262	P.M. Dauber <i>et al.</i>	(LRL)
PALMER	68	PL 26B 323	R.B. Palmer <i>et al.</i>	(BNL, SYRA)
BERGE	66	PR 147 945	J.P. Berge <i>et al.</i>	(LRL)
HUBBARD	66	Thesis UCRL 11510	J.R. Hubbard	(LRL)
LONDON	66	PR 143 1034	G.V. London <i>et al.</i>	(BNL, SYRA)
PJERROU	65B	PRL 14 275	G.M. Pjerrou <i>et al.</i>	(UCLA)
Also		Thesis	G.M. Pjerrou	(UCLA)
CARMONY	64B	PRL 12 482	D.D. Carmony <i>et al.</i>	(UCLA)
HUBBARD	64	PR 135 B183	J.R. Hubbard <i>et al.</i>	(LRL)
JAUNEAU	63	PL 4 49	L. Jauneau <i>et al.</i>	(EPOL, CERN, LOUC+)
Also		Siena Conf. 1 1	L. Jauneau <i>et al.</i>	(EPOL, CERN, LOUC+)



$$I(J^P) = \frac{1}{2}(1^+)$$
 Status: * * * *

The parity has not actually been measured, but + is of course expected.

We have omitted some results that have been superseded by later experiments. See our earlier editions.

≡⁻ MASS

The fit uses the Ξ^- , Ξ^+ , and Ξ^0 masses and the $\Xi^- - \Xi^+$ mass difference. It assumes that the Ξ^- and Ξ^+ masses are the same.

VALUE (MeV)	EVTS	DOCUMENT ID	TECN	COMMENT
1321.71 ± 0.07 OUR FIT				
$1321.70 \pm 0.08 \pm 0.05$	2478 ± 68	ABDALLAH	06E DLPH	from Z decays
• • • We do not use the following data for averages, fits, limits, etc. • • •				
1321.46 ± 0.34	632	DIBIANCA	75 DBC	4.9 GeV/c $K^- n$
1321.12 ± 0.41	268	WILQUET	72 HLBC	
1321.87 ± 0.51	195	¹ GOLDWASSER 70	HBC	5.5 GeV/c $K^- p$
1321.67 ± 0.52	6	CHIEN	66 HBC	6.9 GeV/c $\bar{p} p$
1321.4 ± 1.1	299	LONDON	66 HBC	
1321.3 ± 0.4	149	PJERROU	65B HBC	
1321.1 ± 0.3	241	² BADIER	64 HBC	
1321.4 ± 0.4	517	² JAUNEAU	63D FBC	
1321.1 ± 0.65	62	² SCHNEIDER	63 HBC	

¹ GOLDWASSER 70 uses $m_\Lambda = 1115.58$ MeV.

² These masses have been increased 0.09 MeV because the Λ mass increased.

≡⁺ MASS

The fit uses the Ξ^- , Ξ^+ , and Ξ^0 masses and the $\Xi^- - \Xi^+$ mass difference. It assumes that the Ξ^- and Ξ^+ masses are the same.

VALUE (MeV)	EVTS	DOCUMENT ID	TECN	COMMENT
1321.71 ± 0.07 OUR FIT				
$1321.73 \pm 0.08 \pm 0.05$	2256 ± 63	ABDALLAH	06E DLPH	from Z decays
• • • We do not use the following data for averages, fits, limits, etc. • • •				
1321.6 ± 0.8	35	VOTRUBA	72 HBC	10 GeV/c $K^+ p$
1321.2 ± 0.4	34	STONE	70 HBC	
1320.69 ± 0.93	5	CHIEN	66 HBC	6.9 GeV/c $\bar{p} p$

$$(m_{\Xi^-} - m_{\Xi^+}) / m_{\Xi^-}$$

A test of CPT invariance.

VALUE	DOCUMENT ID	TECN	COMMENT
$(-2.5 \pm 8.7) \times 10^{-5}$	ABDALLAH	06E DLPH	from Z decays

≡⁻ MEAN LIFE

Baryon Particle Listings



Measurements with an error $> 0.2 \times 10^{-10}$ s or with systematic errors not included have been omitted.

VALUE (10^{-10} s)	EVTS	DOCUMENT ID	TECN	COMMENT
1.639±0.015 OUR AVERAGE				
1.65 ± 0.07 ± 0.12	2478 ± 68	ABDALLAH	06E	DLPH from Z decays
1.652±0.051	32k	BOURQUIN	84	SPEC Hyperon beam
1.665±0.065	41k	BOURQUIN	79	SPEC Hyperon beam
1.609±0.028	4286	HEMINGWAY	78	HBC 4.2 GeV/c $K^- p$
1.67 ± 0.08		DIBIANCA	75	DBC 4.9 GeV/c $K^- d$
1.63 ± 0.03	4303	BALTAY	74	HBC 1.75 GeV/c $K^- p$
1.73 $\begin{smallmatrix} +0.08 \\ -0.07 \end{smallmatrix}$	680	MAYEUR	72	HLBC 2.1 GeV/c K^-
1.61 ± 0.04	2610	DAUBER	69	HBC
1.80 ± 0.16	299	LONDON	66	HBC
1.70 ± 0.12	246	PJERROU	65B	HBC
1.69 ± 0.07	794	HUBBARD	64	HBC
1.86 $\begin{smallmatrix} +0.15 \\ -0.14 \end{smallmatrix}$	517	JAUNEAU	63D	FBC

Ξ⁺ MEAN LIFE

VALUE (10^{-10} s)	EVTS	DOCUMENT ID	TECN	COMMENT
1.70±0.08±0.12	2256 ± 63	ABDALLAH	06E	DLPH from Z decays
••• We do not use the following data for averages, fits, limits, etc. •••				
1.55 $\begin{smallmatrix} +0.35 \\ -0.20 \end{smallmatrix}$	35	³ VOTRUBA	72	HBC 10 GeV/c $K^+ p$
1.6 ± 0.3	34	STONE	70	HBC
1.9 $\begin{smallmatrix} +0.7 \\ -0.5 \end{smallmatrix}$	12	³ SHEN	67	HBC
1.51±0.55	5	³ CHIEN	66	HBC 6.9 GeV/c $\bar{p} p$

³The error is statistical only.

$$(\tau_{\Xi^-} - \tau_{\Xi^+}) / \tau_{\Xi^-}$$

A test of CPT invariance.

VALUE	DOCUMENT ID	TECN	COMMENT
-0.01±0.07	ABDALLAH	06E	DLPH from Z decays

Ξ⁻ MAGNETIC MOMENT

See the "Note on Baryon Magnetic Moments" in the Λ Listings.

VALUE (μ_N)	EVTS	DOCUMENT ID	TECN	COMMENT
-0.6507±0.0025 OUR AVERAGE				
-0.6505±0.0025	4.36M	DURYEA	92	SPEC 800 GeV p Be
-0.661 ± 0.036 ± 0.036	44k	TROST	89	SPEC $\Xi^- \sim 250$ GeV
-0.69 ± 0.04	218k	RAMEIKA	84	SPEC 400 GeV p Be
••• We do not use the following data for averages, fits, limits, etc. •••				
-0.674 ± 0.021 ± 0.020	122k	HO	90	SPEC See DURYEA 92
-2.1 ± 0.8	2436	COOL	74	OSPK 1.8 GeV/c $K^- p$
-0.1 ± 2.1	2724	BINGHAM	70B	OSPK 1.8 GeV/c $K^- p$

Ξ⁺ MAGNETIC MOMENT

See the "Note on Baryon Magnetic Moments" in the Λ Listings.

VALUE (μ_N)	EVTS	DOCUMENT ID	TECN	COMMENT
+0.657±0.028±0.020	70k	HO	90	SPEC 800 GeV p Be

$$(\mu_{\Xi^-} + \mu_{\Xi^+}) / |\mu_{\Xi^-}|$$

A test of CPT invariance. We calculate this from the Ξ^- and Ξ^+ magnetic moments above.

VALUE	DOCUMENT ID
+0.01±0.05 OUR EVALUATION	

Ξ⁻ DECAY MODES

Mode	Fraction (Γ_i/Γ)	Confidence level
Γ_1 $\Lambda \pi^-$	(99.887±0.035) %	
Γ_2 $\Sigma^- \gamma$	(1.27 ± 0.23) × 10 ⁻⁴	
Γ_3 $\Lambda e^- \bar{\nu}_e$	(5.63 ± 0.31) × 10 ⁻⁴	
Γ_4 $\Lambda \mu^- \bar{\nu}_\mu$	(3.5 $\begin{smallmatrix} +3.5 \\ -2.2 \end{smallmatrix}$) × 10 ⁻⁴	
Γ_5 $\Sigma^0 e^- \bar{\nu}_e$	(8.7 ± 1.7) × 10 ⁻⁵	
Γ_6 $\Sigma^0 \mu^- \bar{\nu}_\mu$	< 8 × 10 ⁻⁴	90%
Γ_7 $\Xi^0 e^- \bar{\nu}_e$	< 2.3 × 10 ⁻³	90%

ΔS = 2 forbidden (S2) modes

Γ_8 $n \pi^-$	S2 < 1.9	× 10 ⁻⁵	90%
Γ_9 $n e^- \bar{\nu}_e$	S2 < 3.2	× 10 ⁻³	90%
Γ_{10} $n \mu^- \bar{\nu}_\mu$	S2 < 1.5	%	90%
Γ_{11} $\rho \pi^- \pi^-$	S2 < 4	× 10 ⁻⁴	90%
Γ_{12} $\rho \pi^- e^- \bar{\nu}_e$	S2 < 4	× 10 ⁻⁴	90%
Γ_{13} $\rho \pi^- \mu^- \bar{\nu}_\mu$	S2 < 4	× 10 ⁻⁴	90%
Γ_{14} $\rho \mu^- \mu^-$	L < 4	× 10 ⁻⁸	90%

CONSTRAINED FIT INFORMATION

An overall fit to 4 branching ratios uses 5 measurements and one constraint to determine 5 parameters. The overall fit has a $\chi^2 = 1.0$ for 1 degrees of freedom.

The following *off-diagonal* array elements are the correlation coefficients $\langle \delta x_i \delta x_j \rangle / (\delta x_i \delta x_j)$, in percent, from the fit to the branching fractions, $x_i \equiv \Gamma_i/\Gamma_{\text{total}}$. The fit constrains the x_i whose labels appear in this array to sum to one.

x_2	-6			
x_3	-8	0		
x_4	-99	0	-1	
x_5	-5	0	0	0
	x_1	x_2	x_3	x_4

Ξ⁻ BRANCHING RATIOS

A number of early results have been omitted.

$$\Gamma(\Sigma^- \gamma) / \Gamma(\Lambda \pi^-) \quad \Gamma_2/\Gamma_1$$

VALUE (units 10 ⁻⁴)	EVTS	DOCUMENT ID	TECN	COMMENT
1.27±0.24 OUR FIT				
1.27±0.23 OUR AVERAGE				
1.22±0.23±0.06	211	⁴ DUBBS	94	E761 Ξ^- 375 GeV
2.27±1.02	9	BIAGI	87B	SPEC SPS hyperon beam

⁴DUBBS 94 also finds weak evidence that the asymmetry parameter α_γ is positive ($\alpha_\gamma = 1.0 \pm 1.3$).

$$\Gamma(\Lambda e^- \bar{\nu}_e) / \Gamma(\Lambda \pi^-) \quad \Gamma_3/\Gamma_1$$

VALUE (units 10 ⁻³)	EVTS	DOCUMENT ID	TECN	COMMENT
0.564±0.031 OUR FIT				
0.564±0.031	2857	BOURQUIN	83	SPEC SPS hyperon beam
••• We do not use the following data for averages, fits, limits, etc. •••				
0.30 ± 0.13	11	THOMPSON	80	ASPK Hyperon beam

$$\Gamma(\Lambda \mu^- \bar{\nu}_\mu) / \Gamma(\Lambda \pi^-) \quad \Gamma_4/\Gamma_1$$

VALUE (units 10 ⁻³)	CL%	EVTS	DOCUMENT ID	TECN	COMMENT
0.35 $\begin{smallmatrix} +0.35 \\ -0.22 \end{smallmatrix}$ OUR FIT					
0.35±0.35	1	YEH	74	HBC	Effective denom.=2859
••• We do not use the following data for averages, fits, limits, etc. •••					
< 2.3	90	0	THOMPSON	80	ASPK Effective denom.=1017
< 1.3			DAUBER	69	HBC
< 12			BERGE	66	HBC

$$\Gamma(\Sigma^0 e^- \bar{\nu}_e) / \Gamma(\Lambda \pi^-) \quad \Gamma_5/\Gamma_1$$

VALUE (units 10 ⁻³)	EVTS	DOCUMENT ID	TECN	COMMENT
0.087±0.017 OUR FIT				
0.087±0.017	154	BOURQUIN	83	SPEC SPS hyperon beam

$$[\Gamma(\Lambda e^- \bar{\nu}_e) + \Gamma(\Sigma^0 e^- \bar{\nu}_e)] / \Gamma(\Lambda \pi^-) \quad (\Gamma_3 + \Gamma_5) / \Gamma_1$$

VALUE (units 10 ⁻³)	EVTS	DOCUMENT ID	TECN	COMMENT
••• We do not use the following data for averages, fits, limits, etc. •••				
0.651 ± 0.031	3011	⁵ BOURQUIN	83	SPEC SPS hyperon beam
0.68 ± 0.22	17	⁶ DUCLOS	71	OSPK

⁵ See the separate BOURQUIN 83 values for $\Gamma(\Lambda e^- \bar{\nu}_e) / \Gamma(\Lambda \pi^-)$ and $\Gamma(\Sigma^0 e^- \bar{\nu}_e) / \Gamma(\Lambda \pi^-)$ above.

⁶ DUCLOS 71 cannot distinguish Σ^0 s from Λ 's. The Cabibbo theory predicts the Σ^0 rate is about a factor 6 smaller than the Λ rate.

$$\Gamma(\Sigma^0 \mu^- \bar{\nu}_\mu) / \Gamma(\Lambda \pi^-) \quad \Gamma_6/\Gamma_1$$

VALUE (units 10 ⁻³)	CL%	EVTS	DOCUMENT ID	TECN	COMMENT
<0.76	90	0	YEH	74	HBC Effective denom.=3026
••• We do not use the following data for averages, fits, limits, etc. •••					
<5			BERGE	66	HBC

$$\Gamma(\Xi^0 e^- \bar{\nu}_e) / \Gamma(\Lambda \pi^-) \quad \Gamma_7/\Gamma_1$$

VALUE (units 10 ⁻³)	CL%	EVTS	DOCUMENT ID	TECN	COMMENT
<2.3	90	0	YEH	74	HBC Effective denom.=1000

See key on page 405

Baryon Particle Listings



$\Gamma(n\pi^-)/\Gamma(\Lambda\pi^-)$ **Γ_8/Γ_1**
 $\Delta S=2$. Forbidden in first-order weak interaction.

VALUE (units 10^{-3})	CL%	EVTS	DOCUMENT ID	TECN	COMMENT
<0.019	90		BIAGI 82B	SPEC	SPS hyperon beam
•••	We do not use the following data for averages, fits, limits, etc. •••				
<3.0	90	0	YEH 74	HBC	Effective denom.=760
<1.1			DAUBER 69	HBC	
<5.0			FERRO-LUZZI 63	HBC	

$\Gamma(ne^-\bar{\nu}_e)/\Gamma(\Lambda\pi^-)$ **Γ_9/Γ_1**
 $\Delta S=2$. Forbidden in first-order weak interaction.

VALUE (units 10^{-3})	CL%	EVTS	DOCUMENT ID	TECN	COMMENT
< 3.2	90	0	YEH 74	HBC	Effective denom.=715
•••	We do not use the following data for averages, fits, limits, etc. •••				
<10	90		BINGHAM 65	RVUE	

$\Gamma(n\mu^-\bar{\nu}_\mu)/\Gamma(\Lambda\pi^-)$ **Γ_{10}/Γ_1**
 $\Delta S=2$. Forbidden in first-order weak interaction.

VALUE (units 10^{-3})	CL%	EVTS	DOCUMENT ID	TECN	COMMENT
<15.3	90	0	YEH 74	HBC	Effective denom.=150

$\Gamma(p\pi^-\pi^-)/\Gamma(\Lambda\pi^-)$ **Γ_{11}/Γ_1**
 $\Delta S=2$. Forbidden in first-order weak interaction.

VALUE (units 10^{-4})	CL%	EVTS	DOCUMENT ID	TECN	COMMENT
<3.7	90	0	YEH 74	HBC	Effective denom.=6200

$\Gamma(p\pi^-e^-\bar{\nu}_e)/\Gamma(\Lambda\pi^-)$ **Γ_{12}/Γ_1**
 $\Delta S=2$. Forbidden in first-order weak interaction.

VALUE (units 10^{-4})	CL%	EVTS	DOCUMENT ID	TECN	COMMENT
<3.7	90	0	YEH 74	HBC	Effective denom.=6200

$\Gamma(p\pi^-\mu^-\bar{\nu}_\mu)/\Gamma(\Lambda\pi^-)$ **Γ_{13}/Γ_1**
 $\Delta S=2$. Forbidden in first-order weak interaction.

VALUE (units 10^{-4})	CL%	EVTS	DOCUMENT ID	TECN	COMMENT
<3.7	90	0	YEH 74	HBC	Effective denom.=6200

$\Gamma(p\mu^-\mu^-)/\Gamma(\Lambda\pi^-)$ **Γ_{14}/Γ_1**
 $\Delta L=2$ decay, forbidden by total lepton number conservation.

VALUE (units 10^{-8})	CL%	DOCUMENT ID	TECN	COMMENT
<4.0	90	RAJARAM 05	HYCP	p Cu, 800 GeV
•••	We do not use the following data for averages, fits, limits, etc. •••			
<3.7 $\times 10^4$	90	7 LITTENBERG 92B	HBC	Uses YEH 74 data

⁷This LITTENBERG 92B limit and the identical YEH 74 limits for the preceding three modes all result from nonobservance of any 3-prong decays of the Ξ^- . One could as well apply the limit to the *sum* of the four modes.

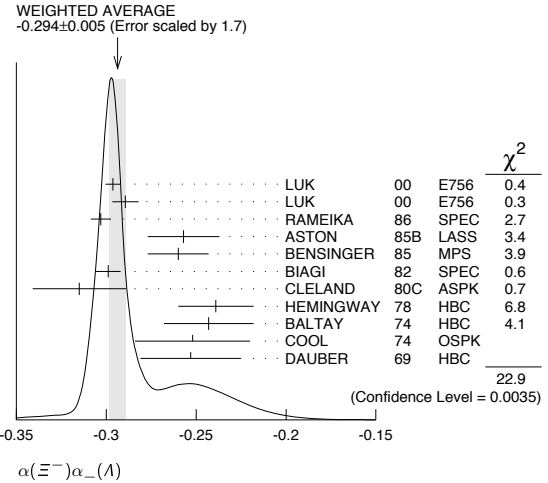
Ξ^- DECAY PARAMETERS

See the "Note on Baryon Decay Parameters" in the neutron Listings.

$\alpha(\Xi^-)\alpha_-(\Lambda)$

VALUE	EVTS	DOCUMENT ID	TECN	COMMENT
-0.294 ± 0.005 OUR AVERAGE				Error includes scale factor of 1.7. See the ideogram below.
-0.2963 ± 0.0042	189k	LUK	00 E756	p Be, 800 GeV
-0.2894 ± 0.0073	63k	⁸ LUK	00 E756	p Be, 800 GeV
-0.303 ± 0.004 ± 0.004	192k	RAMEIKA	86 SPEC	400 GeV pBe
-0.257 ± 0.020	11k	ASTON	85B LASS	11 GeV/c K^-p
-0.260 ± 0.017	21k	BENSINGER	85 MPS	5 GeV/c K^-p
-0.299 ± 0.007	150k	BIAGI	82 SPEC	SPS hyperon beam
-0.315 ± 0.026	9046	CLELAND	80c ASPK	BNL hyperon beam
-0.239 ± 0.021	6599	HEMINGWAY	78 HBC	4.2 GeV/c K^-p
-0.243 ± 0.025	4303	BALTAY	74 HBC	1.75 GeV/c K^-p
-0.252 ± 0.032	2436	COOL	74 OSPK	1.8 GeV/c K^-p
-0.253 ± 0.028	2781	DAUBER	69 HBC	

⁸This LUK 00 value is for $\alpha(\Xi^+)\alpha_+(\bar{\Lambda})$. We assume CP conservation here by including it in the average for $\alpha(\Xi^-)\alpha_-(\Lambda)$. But see the second data block below for the CP test.



α FOR $\Xi^- \rightarrow \Lambda\pi^-$
The above average, $\alpha(\Xi^-)\alpha_-(\Lambda) = -0.294 \pm 0.005$, where the error includes a scale factor of 1.7, divided by our current average $\alpha_-(\Lambda) = 0.642 \pm 0.013$, gives the following value for $\alpha(\Xi^-)$.

VALUE	DOCUMENT ID
-0.458 ± 0.012 OUR EVALUATION	Error includes scale factor of 1.8.

$\frac{[\alpha(\Xi^-)\alpha_-(\Lambda) - \alpha(\Xi^+)\alpha_+(\bar{\Lambda})]}{[\alpha(\Xi^-)\alpha_-(\Lambda) + \alpha(\Xi^+)\alpha_+(\bar{\Lambda})]}$
This is zero if CP is conserved. The α 's are the decay-asymmetry parameters for $\Xi^- \rightarrow \Lambda\pi^-$ and $\Lambda \rightarrow p\pi^-$ and for $\Xi^+ \rightarrow \bar{\Lambda}\pi^+$ and $\bar{\Lambda} \rightarrow \bar{p}\pi^+$.

VALUE (units 10^{-4})	EVTS	DOCUMENT ID	TECN	COMMENT
0.0 ± 5.1 ± 4.4	158M	HOLMSTROM 04	HYCP	p Cu, 800 GeV
•••	We do not use the following data for averages, fits, limits, etc. •••			
+120 ± 140	252k	LUK	00 E756	p Be, 800 GeV

ϕ ANGLE FOR $\Xi^- \rightarrow \Lambda\pi^-$ ($\tan\phi = \beta/\gamma$)

VALUE (°)	EVTS	DOCUMENT ID	TECN	COMMENT
-2.1 ± 0.8 OUR AVERAGE				
-2.39 ± 0.64 ± 0.64	144M	⁹ HUANG	04 HYCP	p Cu, 800 GeV
-1.61 ± 2.66 ± 0.37	1.35M	¹⁰ CHAKRAVO...	03 E756	p Be, 800 GeV
5 ± 10	11k	ASTON	85B LASS	K^-p
14.7 ± 16.0	21k	¹¹ BENSINGER	85 MPS	5 GeV/c K^-p
11 ± 9	4303	BALTAY	74 HBC	1.75 GeV/c K^-p
5 ± 16	2436	COOL	74 OSPK	1.8 GeV/c K^-p
-14 ± 11	2781	DAUBER	69 HBC	Uses $\alpha_\Lambda = 0.647 \pm 0.020$
0 ± 12	1004	¹² BERGE	66 HBC	
•••	We do not use the following data for averages, fits, limits, etc. •••			
-26 ± 30	2724	BINGHAM	70B OSPK	
0 ± 20.4	364	¹² LONDON	66 HBC	Using $\alpha_\Lambda = 0.62$
54 ± 30	356	¹² CARMONY	64B HBC	

⁹From this result and α_Ξ , HUANG 04 gets $\beta_\Xi = -0.037 \pm 0.011 \pm 0.010$ and $\gamma_\Xi = 0.888 \pm 0.0004 \pm 0.006$. And the strong p-s phase difference for $\Lambda\pi^-$ scattering is $(4.6 \pm 1.4 \pm 1.2)^\circ$.
¹⁰From this result and α_Ξ , CHAKRAVORTY 03 obtains $\beta_\Xi = -0.025 \pm 0.042 \pm 0.006$ and $\gamma_\Xi = 0.889 \pm 0.001 \pm 0.007$. And the strong p-s phase difference for $\Lambda\pi^-$ scattering is $(3.17 \pm 5.28 \pm 0.73)^\circ$.
¹¹BENSINGER 85 used $\alpha_\Lambda = 0.642 \pm 0.013$.
¹²The errors have been multiplied by 1.2 due to approximations used for the Ξ polarization; see DAUBER 69 for a discussion.

g_A/g_V FOR $\Xi^- \rightarrow \Lambda e^-\bar{\nu}_e$

VALUE	EVTS	DOCUMENT ID	TECN	COMMENT
-0.25 ± 0.05	1992	¹³ BOURQUIN	83 SPEC	SPS hyperon beam

¹³BOURQUIN 83 assumes that $g_2 = 0$. Also, the sign has been changed to agree with our conventions, given in the "Note on Baryon Decay Parameters" in the neutron Listings.

Ξ^- REFERENCES

We have omitted some papers that have been superseded by later experiments. See our earlier editions.

ABDALLAH 06E	PL B639 179	J. Abdallah et al.	(DELPHI Collab.)
RAJARAM 05	PRL 94 181801	D. Rajaram et al.	(FNAL HyperCP Collab.)
HOLMSTROM 04	PRL 93 262001	T. Holmstrom et al.	(FNAL HyperCP Collab.)
HUANG 04	PRL 93 011802	M. Huang et al.	(FNAL HyperCP Collab.)
CHAKRAVO... 03	PRL 91 031601	A. Chakravorty et al.	(FNAL E756 Collab.)
LUK 00	PRL 85 4860	K.B. Luk et al.	(FNAL E756 Collab.)
DUBBS 94	PRL 72 808	T. Dubbs et al.	(FNAL E761 Collab.)
DURYEA 92	PRL 68 768	J. Duryea et al.	(MINN, FNAL, MICH, RUTG)
LITTENBERG 92B	PR D46 R892	L.S. Littenberg, R.E. Shrock	(BNL, STON)
HO 90	PRL 65 1713	P.M. Ho et al.	(MICH, FNAL, MINN, RUTG)
Also	PR D44 3402	P.M. Ho et al.	(MICH, FNAL, MINN, RUTG)
TROST 89	PR D40 1703	L.H. Trost et al.	(FNAL-715 Collab.)
BIAGI 87B	ZPHY C35 143	S.F. Biagi et al.	(BRIS, CERN, GEVA+)
RAMEIKA 86	PR D33 3172	R. Rameika et al.	(RUTG, MICH, WISC+)

Baryon Particle Listings

$\Xi^-, \Xi^0, \Xi(1530)$

ASTON	85B	PR D32 2270	D. Aston <i>et al.</i>	(SLAC, CARL, CNRC, CINC)
BENSINGER	85	NP B252 561	J.R. Bensingier <i>et al.</i>	(CHIC, ELMT, FNAL+)
BOURQUIN	84	NP B241 1	M.H. Bourquin <i>et al.</i>	(BRIS, GEVA, HEIDP+)
RAMEIKA	84	PL 52 581	R. Rameika <i>et al.</i>	(RUTG, MICH, WISC+)
BOURQUIN	83	ZPHY C21 1	M.H. Bourquin <i>et al.</i>	(BRIS, GEVA, HEIDP+)
BIAGI	82	PL 112B 265	S.F. Biagi <i>et al.</i>	(BRIS, CAVE, GEVA+)
BIAGI	82B	PL 112B 277	S.F. Biagi <i>et al.</i>	(LOQM, GEVA, RL+)
CLELAND	80C	PR D21 12	W.E. Cleland <i>et al.</i>	(PITT, BNL)
THOMPSON	80	PR D21 25	J.A. Thompson <i>et al.</i>	(PITT, BNL)
BOURQUIN	79	PL 87B 297	M.H. Bourquin <i>et al.</i>	(BRIS, GEVA, HEIDP+)
HEMINGWAY	78	NP B142 205	R.J. Hemingway <i>et al.</i>	(CERN, ZEEM, NIJH+)
DIBIANCA	75	NP B98 137	F.A. Dibiaccia, R.J. Endorf	(CMU)
BALTAY	74	PR D9 49	C. Baltay <i>et al.</i>	(COLU, BING, J)
COOL	74	PR D10 792	R.L. Cool <i>et al.</i>	(BNL)
Also		PRL 29 1630	R.L. Cool <i>et al.</i>	(BNL)
YEH	74	PR D10 3545	N. Yeh <i>et al.</i>	(BING, COLU)
MAYEUR	72	NP B47 333	C. Mayeur <i>et al.</i>	(BRUX, CERN, TUFTS, LOUC)
VOTRUBA	72	NP B45 77	M.F. Votruba, A. Saffler, T.M. Ratcliffe	(BIRM+)
WILQUET	72	PL 42B 372	G. Wilquet <i>et al.</i>	(BRUX, CERN, TUFTS+)
DUCLOS	71	NP B32 493	J. Duclos <i>et al.</i>	(CERN)
BINGHAM	70B	PR D1 3010	G.M. Bingham <i>et al.</i>	(UCSD, WASH)
GOLDWASSER	70	PR D1 1960	E.L. Goldwasser, P.F. Schultz	(ILL)
STONE	70	PL 32B 515	S.L. Stone <i>et al.</i>	(ROCH)
DAUBER	69	PR 179 1262	P.M. Dauber <i>et al.</i>	(LRL, J)
SHEN	67	PL 25B 443	B.C. Shen, A. Firestone, G. Goldhaber	(UCB+)
BERGE	66	PR 147 945	J.P. Berge <i>et al.</i>	(LRL)
CHIEN	66	PR 152 1171	C.Y. Chien <i>et al.</i>	(YALE, BNL)
LONDON	66	PR 143 1034	G.W. London <i>et al.</i>	(BNL, SYRA)
BINGHAM	65	PRSL 285 202	H.H. Bingham	(CERN)
PJERROU	65B	PRL 14 275	G.M. Pjerrou <i>et al.</i>	(UCLA)
Also		Thesis	G.M. Pjerrou	(UCLA)
BADIER	64	Dubna Conf. 1 593	J. Badier <i>et al.</i>	(EPOL, SACL, ZEEM)
CARMONY	64B	PRL 12 482	D.D. Carmony <i>et al.</i>	(UCLA, J)
HUBBARD	64	PR 135 B183	J.R. Hubbard <i>et al.</i>	(LRL)
FERRI-LUZZI	63	PR 130 1568	M. Ferro-Luzzi <i>et al.</i>	(LRL)
JAUNEAU	63D	Siena Conf. 4	L. Jauneau <i>et al.</i>	(EPOL, CERN, LOUC+)
Also		PL 5 261	L. Jauneau <i>et al.</i>	(EPOL, CERN, LOUC+)
SCHNEIDER	63	PL 4 360	J. Schneider	(CERN)

Ξ RESONANCES

The accompanying table gives our evaluation of the present status of the Ξ resonances. Not much is known about Ξ resonances. This is because (1) they can only be produced as a part of a final state, and so the analysis is more complicated than if direct formation were possible, (2) the production cross sections are small (typically a few μb), and (3) the final states are topologically complicated and difficult to study with electronic techniques. Thus early information about Ξ resonances came entirely from bubble chamber experiments, where the numbers of events are small, and only in the 1980's did electronic experiments make any significant contributions. However, nothing of significance on Ξ resonances has been added since our 1988 edition.

For a detailed earlier review, see Meadows [1].

Table 1. The status of the Ξ resonances. Only those with an overall status of *** or **** are included in the Baryon Summary Table.

Particle	$L_{2I,2J}$	Overall status	Status as seen in —				
			$\Xi\pi$	ΛK	ΣK	$\Xi(1530)\pi$	Other channels
$\Xi(1318)$	P_{11}	****					Decays weakly
$\Xi(1530)$	P_{13}	****	****				
$\Xi(1620)$		*	*				
$\Xi(1690)$		***		***	**		
$\Xi(1820)$	D_{13}	***	**	***	**	**	
$\Xi(1950)$		***	**	**		*	
$\Xi(2030)$	1	***		**	***		
$\Xi(2120)$		*		*			
$\Xi(2250)$		**					3-body decays
$\Xi(2370)$	1	**					3-body decays
$\Xi(2500)$		*		*			3-body decays

**** Existence is certain, and properties are at least fairly well explored.
 *** Existence ranges from very likely to certain, but further confirmation is desirable and/or quantum numbers, branching fractions, etc. are not well determined.
 ** Evidence of existence is only fair.
 * Evidence of existence is poor.

Reference

- B.T. Meadows, in *Proceedings of the IVth International Conference on Baryon Resonances* (Toronto, 1980), ed. N. Isgur, p. 283.

$\Xi(1530) P_{13}$

$$I(J^P) = \frac{1}{2}(\frac{3}{2}^+) \text{ Status: } ***$$

This is the only Ξ resonance whose properties are all reasonably well known. Assuming that the Λ_c^+ has $J^P = 1/2^+$, AUBERT 08AK, in a study of $\Lambda_c^+ \rightarrow \Xi^- \pi^+ K^+$, finds conclusively that the spin of the $\Xi(1530)^0$ is 3/2. In conjunction with SCHLEIN 63B and BUTTON-SHAFFER 66, this proves also that the parity is +.

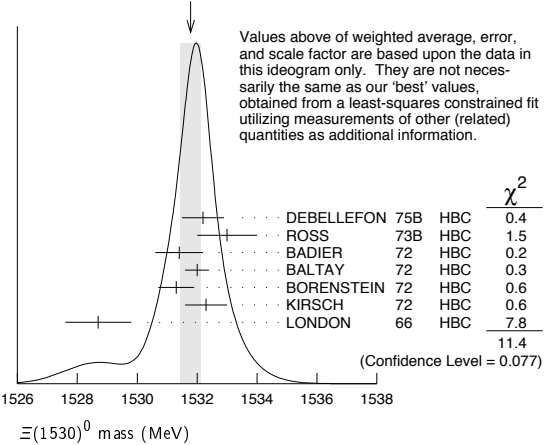
We use only those determinations of the mass and width that are accompanied by some discussion of systematics and resolution.

$\Xi(1530)$ MASSES

$\Xi(1530)^0$ MASS

VALUE (MeV)	EVTS	DOCUMENT ID	TECN	COMMENT
1531.80 ± 0.32 OUR FIT				Error includes scale factor of 1.3.
1531.78 ± 0.34 OUR AVERAGE				Error includes scale factor of 1.4. See the ideogram below.
1532.2 ± 0.7		DEBELLEFON 75B	HBC	$K^- p \rightarrow \Xi^- \bar{K} \pi$
1533 ± 1		ROSS 73B	HBC	$K^- p \rightarrow \Xi \bar{K} \pi(\pi)$
1531.4 ± 0.8	59	BADIER 72	HBC	$K^- p$ 3.95 GeV/c
1532.0 ± 0.4	1262	BALTAY 72	HBC	$K^- p$ 1.75 GeV/c
1531.3 ± 0.6	324	BORENSTEIN 72	HBC	$K^- p$ 2.2 GeV/c
1532.3 ± 0.7	286	KIRSCH 72	HBC	$K^- p$ 2.87 GeV/c
1528.7 ± 1.1	76	LONDON 66	HBC	$K^- p$ 2.24 GeV/c
••• We do not use the following data for averages, fits, limits, etc. •••				
1532.1 ± 0.4	1244	ASTON 85B	LASS	$K^- p$ 11 GeV/c
1532.1 ± 0.6	2700	¹ BAUBILLIER 81B	HBC	$K^- p$ 8.25 GeV/c
1530 ± 1	450	BIAGI 81	SPEC	SPS hyperon beam
1527 ± 0.6	80	SIXEL 79	HBC	$K^- p$ 10 GeV/c
1535 ± 0.4	100	SIXEL 79	HBC	$K^- p$ 16 GeV/c
1533.6 ± 1.4	97	BERTHON 74	HBC	Quasi-2-body σ

WEIGHTED AVERAGE
1531.78±0.34 (Error scaled by 1.4)



Values above of weighted average, error, and scale factor are based upon the data in this ideogram only. They are not necessarily the same as our 'best' values, obtained from a least-squares constrained fit utilizing measurements of other (related) quantities as additional information.

$\Xi(1530)^-$ MASS

VALUE (MeV)	EVTS	DOCUMENT ID	TECN	COMMENT
1535.0 ± 0.6 OUR FIT				
1535.2 ± 0.8 OUR AVERAGE				
1534.5 ± 1.2		DEBELLEFON 75B	HBC	$K^- p \rightarrow \Xi^- \bar{K} \pi$
1535.3 ± 2.0		ROSS 73B	HBC	$K^- p \rightarrow \Xi \bar{K} \pi(\pi)$
1536.2 ± 1.6	185	KIRSCH 72	HBC	$K^- p$ 2.87 GeV/c
1535.7 ± 3.2	38	LONDON 66	HBC	$K^- p$ 2.24 GeV/c
••• We do not use the following data for averages, fits, limits, etc. •••				
1540 ± 3	48	BERTHON 74	HBC	Quasi-2-body σ
1534.7 ± 1.1	334	BALTAY 72	HBC	$K^- p$ 1.75 GeV/c

$m_{\Xi(1530)^-} - m_{\Xi(1530)}$

VALUE (MeV)	DOCUMENT ID	TECN	COMMENT
3.2 ± 0.6 OUR FIT			
2.9 ± 0.9 OUR AVERAGE			
2.7 ± 1.0	BALTAY 72	HBC	$K^- p$ 1.75 GeV/c
2.0 ± 3.2	MERRILL 66	HBC	$K^- p$ 1.7-2.7 GeV/c
5.7 ± 3.0	PJERROU 65B	HBC	$K^- p$ 1.8-1.95 GeV/c
••• We do not use the following data for averages, fits, limits, etc. •••			

See key on page 405

Baryon Particle Listings
 $\Xi(1530)$, $\Xi(1620)$, $\Xi(1690)$

3.9±1.8	2	KIRSCH	72	HBC	$K^- p$ 2.87 GeV/c
7 ±4	2	LONDON	66	HBC	$K^- p$ 2.24 GeV/c

$\Xi(1530)$ WIDTHS

$\Xi(1530)^0$ WIDTH

VALUE (MeV)	EVTS	DOCUMENT ID	TECN	COMMENT
9.1±0.5 OUR AVERAGE				
9.5±1.2		DEBELLEFON	75B	HBC $K^- p \rightarrow \Xi^- \bar{K} \pi$
9.1±2.4		ROSS	73B	HBC $K^- p \rightarrow \Xi^- \bar{K} \pi(\pi)$
11 ±2		BADIER	72	HBC $K^- p$ 3.95 GeV/c
9.0±0.7		BALTAY	72	HBC $K^- p$ 1.75 GeV/c
8.4±1.4		BORENSTEIN	72	HBC $\Xi^- \pi^+$
11.0±1.8		KIRSCH	72	HBC $\Xi^- \pi^+$
7 ±7		BERGE	66	HBC $K^- p$ 1.5-1.7 GeV/c
8.5±3.5		LONDON	66	HBC $K^- p$ 2.24 GeV/c
7 ±2		SCHLEIN	63B	HBC $K^- p$ 1.8, 1.95 GeV/c
• • • We do not use the following data for averages, fits, limits, etc. • • •				
12.8±1.0	2700	1 BAUBILLIER	81B	HBC $K^- p$ 8.25 GeV/c
19 ±6	80	3 SIXEL	79	HBC $K^- p$ 10 GeV/c
14 ±5	100	3 SIXEL	79	HBC $K^- p$ 16 GeV/c

$\Xi(1530)^-$ WIDTH

VALUE (MeV)	DOCUMENT ID	TECN	COMMENT
9.9±1.7 OUR AVERAGE			
9.6±2.8	DEBELLEFON 75B	HBC	$K^- p \rightarrow \Xi^- \bar{K} \pi$
8.3±3.6	ROSS 73B	HBC	$K^- p \rightarrow \Xi^- \bar{K} \pi(\pi)$
7.8±3.5	BALTAY 72	HBC	$K^- p$ 1.75 GeV/c
16.2±4.6	KIRSCH 72	HBC	$\Xi^- \pi^0, \Xi^0 \pi^-$

$\Xi(1530)$ POLE POSITIONS

$\Xi(1530)^0$ REAL PART

VALUE	DOCUMENT ID	COMMENT
1531.6±0.4	LICHTENBERG74	Using HABIBI 73

$\Xi(1530)^0$ IMAGINARY PART

VALUE	DOCUMENT ID	COMMENT
4.45±0.35	LICHTENBERG74	Using HABIBI 73

$\Xi(1530)^-$ REAL PART

VALUE	DOCUMENT ID	COMMENT
1534.4±1.1	LICHTENBERG74	Using HABIBI 73

$\Xi(1530)^-$ IMAGINARY PART

VALUE	DOCUMENT ID	COMMENT
3.9 +1.75 - 3.9	LICHTENBERG74	Using HABIBI 73

$\Xi(1530)$ DECAY MODES

Mode	Fraction (Γ_i/Γ)	Confidence level
$\Gamma_1 \Xi \pi$	100 %	
$\Gamma_2 \Xi \gamma$	<4 %	90%

$\Xi(1530)$ BRANCHING RATIOS

$\Gamma(\Xi \gamma)/\Gamma_{total}$	CL%	DOCUMENT ID	TECN	COMMENT	Γ_2/Γ
<0.04	90	KALBFLEISCH 75	HBC	$K^- p$ 2.18 GeV/c	

$\Xi(1530)$ FOOTNOTES

- 1 BAUBILLIER 81B is a fit to the inclusive spectrum. The resolution (5 MeV) is not unfolded.
- 2 Redundant with data in the mass Listings.
- 3 SIXEL 79 doesn't unfold the experimental resolution of 15 MeV.

$\Xi(1530)$ REFERENCES

AUBERT	08AK	PR D78 034008	B. Aubert et al.	(BABAR Collab.)
ASTON	85B	PR D32 2270	D. Aston et al.	(SLAC, CARL, CNRC, CINC)
BAUBILLIER	81B	NP B192 1	M. Baubillier et al.	(BIRM, CERN, GLAS+)
BIAGI	81	ZPHY C9 305	S.F. Biagi et al.	(BRIS, CAVE, GEVA+)
SIXEL	79	NP B159 125	P. Sixel et al.	(AACH3, BERL, CERN, LOIC+)
DEBELLEFON	75B	NC 28A 289	A. de Bellefon et al.	(CDEF, SACL)
KALBFLEISCH	75	PR D11 987	G.R. Kalbfleisch, R.C. Strand, J.W. Chapman	(BNL+)
BERTHON	74	NC 21A 146	A. Berthon et al.	(CDEF, RHEL, SACL+)
LICHTENBERG	74	PR D10 3865	D.B. Lichtenberg	(IND)
		Also Private Comm.	D.B. Lichtenberg	(IND)
HABIBI	73	Thesis Nevis 199	M. Habibi	(COLU)
ROSS	73B	Purdue Conf. 355	R.T. Ross, J.L. Lloyd, D. Radojicic	(OXF)
BADIER	72	NP B37 429	J. Badier et al.	(EPOL)
BALTAY	72	PL 42B 129	C. Baltay et al.	(COLU, BING)
BORENSTEIN	72	PR D5 1559	S.R. Borenstein et al.	(BNL, MICH)1
KIRSCH	72	NP B40 349	L.E. Kirsch et al.	(BRAN, UMD, SYRA+)1
BERGE	66	PR 147 945	J.P. Berge et al.	(LRL)1
BUTTON...	66	PR 142 883	J. Button-Shafer et al.	(LRL)JP
LONDON	66	PR 143 1034	G.W. London et al.	(BNL, SYRA)1J
MERRILL	66	Thesis UCRL 16455	D.W. Merrill	(LRL)JP
PJERROU	65B	PRL 14 275	G.M. Pjerrou et al.	(UCLA)
SCHLEIN	63B	PRL 11 167	P.E. Schlein et al.	(UCLA)1JP

OTHER RELATED PAPERS

MAZZUCATO	81	NP B178 1	M. Mazzucato et al.	(AMST, CERN, NIIM+)
BRIEFEL	77	PR D16 2706	E. Briefel et al.	(BRAN, UMD, SYRA+)
BRIEFEL	75	PR D12 1859	E. Briefel et al.	(BRAN, UMD, SYRA+)
HUNGERBU...	74	PR D10 2051	V. Hungerbuhler et al.	(YALE, FNAL, BNL+)
BUTTON...	66	PR 142 883	J. Button-Shafer et al.	(LRL)JP

$\Xi(1620)$

$I(J^P) = \frac{1}{2}(?)^?$ Status: *
 J, P need confirmation.

OMITTED FROM SUMMARY TABLE

What little evidence there is consists of weak signals in the $\Xi \pi$ channel. A number of other experiments (e.g., BORENSTEIN 72 and HASSALL 81) have looked for but not seen any effect.

$\Xi(1620)$ MASS

VALUE (MeV)	EVTS	DOCUMENT ID	TECN	COMMENT
≈ 1620 OUR ESTIMATE				
1624±3	31	BRIEFEL 77	HBC	$K^- p$ 2.87 GeV/c
1633±12	34	DEBELLEFON 75B	HBC	$K^- p \rightarrow \Xi^- \bar{K} \pi$
1606±6	29	ROSS 72	HBC	$K^- p$ 3.1-3.7 GeV/c

$\Xi(1620)$ WIDTH

VALUE (MeV)	EVTS	DOCUMENT ID	TECN	COMMENT
22.5	31	1 BRIEFEL 77	HBC	$K^- p$ 2.87 GeV/c
40 ±15	34	DEBELLEFON 75B	HBC	$K^- p \rightarrow \Xi^- \bar{K} \pi$
21 ±7	29	ROSS 72	HBC	$K^- p \rightarrow \Xi^- \pi^+ K^*0(892)$

$\Xi(1620)$ DECAY MODES

Mode
$\Gamma_1 \Xi \pi$

$\Xi(1620)$ FOOTNOTES

- 1 The fit is insensitive to values between 15 and 30 MeV.

$\Xi(1620)$ REFERENCES

HASSALL	81	NP B189 397	J.K. Hassall et al.	(CAVE, MSU)
BRIEFEL	77	PR D16 2706	E. Briefel et al.	(BRAN, UMD, SYRA+)
		Also Duke Conf. 317	E. Briefel et al.	(BRAN, UMD, SYRA+)
		Hyperon Resonances, 1970		
		Also PR D12 1859	E. Briefel et al.	(BRAN, UMD, SYRA+)
DEBELLEFON	75B	NC 28A 289	A. de Bellefon et al.	(CDEF, SACL)
BORENSTEIN	72	PR D5 1559	S.R. Borenstein et al.	(BNL, MICH)1
ROSS	72	PL 38B 177	R.T. Ross et al.	(OXF)1

OTHER RELATED PAPERS

HUNGERBU...	74	PR D10 2051	V. Hungerbuhler et al.	(YALE, FNAL, BNL+)
SCHMIDT	73	Purdue Conf. 363	P.E. Schmidt	(BRAN)
KALBFLEISCH	70	Duke Conf. 331	G.R. Kalbfleisch	(BNL)1
		Hyperon Resonances 1970		
APSELL	69	PRL 23 884	S.P. Apseil et al.	(BRAN, UMD, SYRA+)
BARTSCH	69	PL 28B 439	J. Bartsch et al.	(AACH, BERL, CERN+)

$\Xi(1690)$

$I(J^P) = \frac{1}{2}(?)^?$ Status: ***

AUBERT 08AK, in a study of $\Lambda_c^+ \rightarrow \Xi^- \pi^+ K^+$, finds some evidence that the $\Xi(1690)$ has $J^P = 1/2^-$.

DIONISI 78 sees a threshold enhancement in both the neutral and negatively charged $\Sigma \bar{K}$ mass spectra in $K^- p \rightarrow (\Sigma \bar{K}) K \pi$ at 4.2 GeV/c. The data from the $\Sigma \bar{K}$ channels alone cannot distinguish between a resonance and a large scattering length. Weaker evidence at the same mass is seen in the corresponding $\Lambda \bar{K}$ channels, and a coupled-channel analysis yields results consistent with a new Ξ .

BIAGI 81 sees an enhancement at 1700 MeV in the diffractively produced ΛK^- system. A peak is also observed in the $\Lambda \bar{K}^0$ mass spectrum at 1660 MeV that is consistent with a 1720 MeV resonance decaying to $\Sigma^0 \bar{K}^0$, with the γ from the Σ^0 decay not detected.

BIAGI 87 provides further confirmation of this state in diffractive dissociation of Ξ^- into ΛK^- . The significance claimed is 6.7 standard deviations.

ADAMOVIICH 98 sees a peak of 1400 ± 300 events in the $\Xi^- \pi^+$ spectrum produced by 345 GeV/c Σ^- -nucleus interactions.

Baryon Particle Listings

 $\Xi(1690), \Xi(1820)$ $\Xi(1690)$ MASSES

MIXED CHARGES

VALUE (MeV) DOCUMENT ID
1690 ± 10 OUR ESTIMATE This is only an educated guess; the error given is larger than the error on the average of the published values.

 $\Xi(1690)^0$ MASS

VALUE (MeV)	EVTS	DOCUMENT ID	TECN	CHG	COMMENT
1686 ± 4	1400	ADAMOVICH	98	WA89	Σ^- nucleus, 345 GeV/c
1699 ± 5	175	¹ DIONISI	78	HBC	$K^- p$ 4.2 GeV/c
1684 ± 5	183	² DIONISI	78	HBC	$K^- p$ 4.2 GeV/c

 $\Xi(1690)^-$ MASS

VALUE (MeV)	EVTS	DOCUMENT ID	TECN	CHG	COMMENT
1691.1 ± 1.9 ± 2.0	104	BIAGI	87	SPEC	Ξ^- Be 116 GeV
1700 ± 10	150	³ BIAGI	81	SPEC	Ξ^- H 100, 135 GeV
1694 ± 6	45	⁴ DIONISI	78	HBC	$K^- p$ 4.2 GeV/c

 $\Xi(1690)$ WIDTHS

MIXED CHARGES

VALUE (MeV) DOCUMENT ID
<30 OUR ESTIMATE

 $\Xi(1690)^0$ WIDTH

VALUE (MeV)	EVTS	DOCUMENT ID	TECN	CHG	COMMENT
10 ± 6	1400	ADAMOVICH	98	WA89	Σ^- nucleus, 345 GeV/c
44 ± 23	175	¹ DIONISI	78	HBC	$K^- p$ 4.2 GeV/c
20 ± 4	183	² DIONISI	78	HBC	$K^- p$ 4.2 GeV/c

 $\Xi(1690)^-$ WIDTH

VALUE (MeV)	CL%	EVTS	DOCUMENT ID	TECN	CHG	COMMENT
< 8	90	104	BIAGI	87	SPEC	Ξ^- Be 116 GeV
47 ± 14		150	³ BIAGI	81	SPEC	Ξ^- H 100, 135 GeV
26 ± 6		45	⁴ DIONISI	78	HBC	$K^- p$ 4.2 GeV/c

 $\Xi(1690)$ DECAY MODES

Mode	Fraction (Γ_i/Γ)
Γ_1 $\Lambda \bar{K}$	seen
Γ_2 $\Sigma \bar{K}$	seen
Γ_3 $\Xi \pi$	seen
Γ_4 $\Xi^- \pi^+ \pi^0$	
Γ_5 $\Xi^- \pi^+ \pi^-$	possibly seen
Γ_6 $\Xi(1530) \pi$	

 $\Xi(1690)$ BRANCHING RATIOS

$\Gamma(\Lambda \bar{K})/\Gamma_{\text{total}}$	Γ_1/Γ
VALUE EVTS DOCUMENT ID TECN CHG COMMENT	
seen 104 BIAGI 87 SPEC - Ξ^- Be 116 GeV	

$\Gamma(\Sigma \bar{K})/\Gamma(\Lambda \bar{K})$	Γ_2/Γ_1
VALUE EVTS DOCUMENT ID TECN CHG COMMENT	
0.75 ± 0.39 75 ABE 02c BELL $e^+ e^- \approx \gamma(4S)$	
2.7 ± 0.9 DIONISI 78 HBC 0 $K^- p$ 4.2 GeV/c	
3.1 ± 1.4 DIONISI 78 HBC - $K^- p$ 4.2 GeV/c	

$\Gamma(\Xi \pi)/\Gamma(\Sigma \bar{K})$	Γ_3/Γ_2
VALUE DOCUMENT ID TECN CHG COMMENT	
<0.09 DIONISI 78 HBC 0 $K^- p$ 4.2 GeV/c	

$\Gamma(\Xi \pi)/\Gamma_{\text{total}}$	Γ_3/Γ
VALUE DOCUMENT ID TECN COMMENT	
seen ADAMOVICH 98 WA89 Σ^- nucleus, 345 GeV/c	

$\Gamma(\Xi^- \pi^+ \pi^0)/\Gamma(\Sigma \bar{K})$	Γ_4/Γ_2
VALUE DOCUMENT ID TECN CHG COMMENT	
<0.04 DIONISI 78 HBC 0 $K^- p$ 4.2 GeV/c	

$\Gamma(\Xi^- \pi^+ \pi^-)/\Gamma_{\text{total}}$	Γ_5/Γ
VALUE EVTS DOCUMENT ID TECN CHG COMMENT	
possibly seen 4 BIAGI 87 SPEC - Ξ^- Be 116 GeV	

$\Gamma(\Xi^- \pi^+ \pi^-)/\Gamma(\Sigma \bar{K})$	Γ_5/Γ_2
VALUE DOCUMENT ID TECN CHG COMMENT	
<0.03 DIONISI 78 HBC - $K^- p$ 4.2 GeV/c	

 $\Gamma(\Xi(1530)\pi)/\Gamma(\Sigma \bar{K})$

VALUE	DOCUMENT ID	TECN	CHG	COMMENT
<0.06	DIONISI	78	HBC	- $K^- p$ 4.2 GeV/c

 Γ_6/Γ_2 $\Xi(1690)$ FOOTNOTES

- From a fit to the $\Sigma^+ K^-$ spectrum.
- From a coupled-channel analysis of the $\Sigma^+ K^-$ and $\Lambda \bar{K}^0$ spectra.
- A fit to the inclusive spectrum from $\Xi^- N \rightarrow \Lambda K^- X$.
- From a coupled-channel analysis of the $\Sigma^0 K^-$ and ΛK^- spectra.

 $\Xi(1690)$ REFERENCES

AUBERT	08AK	PR D78	034008	B. Aubert <i>et al.</i>	(BABAR Collab.)
ABE	02C	PL B524	33	K. Abe <i>et al.</i>	(KEK BELLE Collab.)
ADAMOVICH	98	EPJ C5	621	M.I. Adamovich <i>et al.</i>	(CERN WA89 Collab.)
BIAGI	87	ZPHY C34	15	S.F. Biagi <i>et al.</i>	(BRIS, CERN, GEVA+)
BIAGI	81	ZPHY C9	305	S.F. Biagi <i>et al.</i>	(BRIS, CAVE, GEVA+)
DIONISI	78	PL B0B	145	C. Dionisi <i>et al.</i>	(CERN, AMST, NIJM+)

 $\Xi(1820) D_{13}$

$$J(P) = \frac{1}{2}(\frac{3}{2}^-) \text{ Status: } ***$$

The clearest evidence is an 8-standard-deviation peak in ΛK^- seen by GAY 76C. TEODORO 78 favors $J=3/2$, but cannot make a parity discrimination. BIAGI 87C is consistent with $J=3/2$ and favors negative parity for this J value.

 $\Xi(1820)$ MASS

We only average the measurements that appear to us to be most significant and best determined.

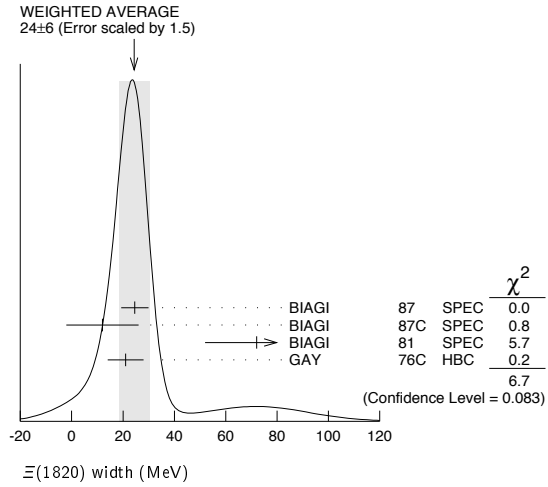
VALUE (MeV)	EVTS	DOCUMENT ID	TECN	CHG	COMMENT
1823 ± 5 OUR ESTIMATE					
1823.4 ± 1.4 OUR AVERAGE					
1819.4 ± 3.1 ± 2.0	280	¹ BIAGI	87	SPEC	0 Ξ^- Be \rightarrow (ΛK^-) X
1826 ± 3 ± 1	54	BIAGI	87c	SPEC	0 Ξ^- Be \rightarrow ($\Lambda \bar{K}^0$) X
1822 ± 6		JENKINS	83	MPS	- $K^- p \rightarrow K^+$ (MM)
1830 ± 6	300	BIAGI	81	SPEC	- SPS hyperon beam
1823 ± 2	130	GAY	76c	HBC	- $K^- p$ 4.2 GeV/c
••• We do not use the following data for averages, fits, limits, etc. •••					
1817 ± 3		ADAMOVICH	99b	WA89	Σ^- nucleus, 345 GeV
1797 ± 19	74	BRIEFEL	77	HBC	0 $K^- p$ 2.87 GeV/c
1829 ± 9	68	BRIEFEL	77	HBC	-0 $\Xi(1530) \pi$
1860 ± 14	39	BRIEFEL	77	HBC	- $\Sigma^- \bar{K}^0$
1870 ± 9	44	BRIEFEL	77	HBC	0 $\Lambda \bar{K}^0$
1813 ± 4	57	BRIEFEL	77	HBC	- ΛK^-
1807 ± 27		DIBIANCA	75	DBC	-0 $\Xi \pi \pi, \Xi^* \pi$
1762 ± 8	28	² BADIER	72	HBC	-0 $\Xi \pi, \Xi \pi \pi, Y K$
1838 ± 5	38	² BADIER	72	HBC	-0 $\Xi \pi, \Xi \pi \pi, Y K$
1830 ± 10	25	³ CRENNELL	70b	DBC	-0 3.6, 3.9 GeV/c
1826 ± 12		⁴ CRENNELL	70b	DBC	-0 3.6, 3.9 GeV/c
1830 ± 10	40	ALITTI	69	HBC	- $\Lambda, \Sigma \bar{K}$
1814 ± 4	30	BADIER	65	HBC	0 $\Lambda \bar{K}^0$
1817 ± 7	29	SMITH	65c	HBC	-0 $\Lambda \bar{K}^0, \Lambda K^-$
1770		HALSTEINSLID63	FBC	-0	K^- freon 3.5 GeV/c

 $\Xi(1820)$ WIDTH

VALUE (MeV)	EVTS	DOCUMENT ID	TECN	CHG	COMMENT
24 +15 -10 OUR ESTIMATE					
24 ± 6 OUR AVERAGE					Error includes scale factor of 1.5. See the ideogram below.
24.6 ± 5.3	280	¹ BIAGI	87	SPEC	0 Ξ^- Be \rightarrow (ΛK^-) X
12 ± 14 ± 1.7	54	BIAGI	87c	SPEC	0 Ξ^- Be \rightarrow ($\Lambda \bar{K}^0$) X
72 ± 20	300	BIAGI	81	SPEC	- SPS hyperon beam
21 ± 7	130	GAY	76c	HBC	- $K^- p$ 4.2 GeV/c
••• We do not use the following data for averages, fits, limits, etc. •••					
23 ± 13		ADAMOVICH	99b	WA89	Σ^- nucleus, 345 GeV
99 ± 57	74	BRIEFEL	77	HBC	0 $K^- p$ 2.87 GeV/c
52 ± 34	68	BRIEFEL	77	HBC	-0 $\Xi(1530) \pi$
72 ± 17	39	BRIEFEL	77	HBC	- $\Sigma^- \bar{K}^0$
44 ± 11	44	BRIEFEL	77	HBC	0 $\Lambda \bar{K}^0$
26 ± 11	57	BRIEFEL	77	HBC	- ΛK^-
85 ± 58		DIBIANCA	75	DBC	-0 $\Xi \pi \pi, \Xi^* \pi$
51 ± 13		² BADIER	72	HBC	-0 Lower mass

$\Xi(1820)$

58 ± 13	2	BADIER	72	HBC	-0	Higher mass
103 ⁺³⁸ ₋₂₄	3	CRENNELL	70B	DBC	-0	3.6, 3.9 GeV/c
48 ⁺³⁶ ₋₁₉	4	CRENNELL	70B	DBC	-0	3.6, 3.9 GeV/c
55 ⁺⁴⁰ ₋₂₀		ALITTI	69	HBC	-	$\Lambda, \Sigma \bar{K}$
12 ± 4		BADIER	65	HBC	0	$\Lambda \bar{K}^0$
30 ± 7		SMITH	65B	HBC	-0	$\Lambda \bar{K}$
< 80		HALSTEINSLID63	FBC	-0	-	K^- from 3.5 GeV/c



$\Xi(1820)$ DECAY MODES

Mode	Fraction (Γ_i/Γ)
Γ_1 $\Lambda \bar{K}$	large
Γ_2 $\Sigma \bar{K}$	small
Γ_3 $\Xi \pi$	small
Γ_4 $\Xi(1530) \pi$	small
Γ_5 $\Xi \pi \pi$ (not $\Xi(1530) \pi$)	

$\Xi(1820)$ BRANCHING RATIOS

The dominant modes seem to be $\Lambda \bar{K}$ and (perhaps) $\Xi(1530) \pi$, but the branching fractions are very poorly determined.

$\Gamma(\Lambda \bar{K})/\Gamma_{total}$	VALUE	DOCUMENT ID	TECN	CHG	COMMENT	Γ_1/Γ
0.30 ± 0.15		ALITTI	69	HBC	-	$K^- p$ 3.9-5 GeV/c

$\Gamma(\Xi \pi)/\Gamma_{total}$	VALUE	DOCUMENT ID	TECN	CHG	COMMENT	Γ_3/Γ
0.10 ± 0.10		ALITTI	69	HBC	-	$K^- p$ 3.9-5 GeV/c

$\Gamma(\Xi \pi)/\Gamma(\Lambda \bar{K})$	VALUE	CL%	DOCUMENT ID	TECN	CHG	COMMENT	Γ_3/Γ_1
< 0.36		95	GAY	76c	HBC	-	$K^- p$ 4.2 GeV/c
0.20 ± 0.20			BADIER	65	HBC	0	$K^- p$ 3 GeV/c

$\Gamma(\Xi \pi)/\Gamma(\Xi(1530) \pi)$	VALUE	DOCUMENT ID	TECN	CHG	COMMENT	Γ_3/Γ_4
1.5 ± 0.6 -0.4		APSELL	70	HBC	0	$K^- p$ 2.87 GeV/c

$\Gamma(\Sigma \bar{K})/\Gamma_{total}$	VALUE	DOCUMENT ID	TECN	CHG	COMMENT	Γ_2/Γ
0.30 ± 0.15		ALITTI	69	HBC	-	$K^- p$ 3.9-5 GeV/c

• • • We do not use the following data for averages, fits, limits, etc. • • •
<0.02 TRIPP 67 RVUE Use SMITH 65c

$\Gamma(\Sigma \bar{K})/\Gamma(\Lambda \bar{K})$	VALUE	DOCUMENT ID	TECN	CHG	COMMENT	Γ_2/Γ_1
0.24 ± 0.10		GAY	76c	HBC	-	$K^- p$ 4.2 GeV/c

$\Gamma(\Xi(1530) \pi)/\Gamma_{total}$	VALUE	DOCUMENT ID	TECN	CHG	COMMENT	Γ_4/Γ
0.30 ± 0.15		ALITTI	69	HBC	-	$K^- p$ 3.9-5 GeV/c

• • • We do not use the following data for averages, fits, limits, etc. • • •
seen ASTON 85B LASS $K^- p$ 11 GeV/c
not seen 5 HASSALL 81 HBC $K^- p$ 6.5 GeV/c
<0.25 6 DAUBER 69 HBC $K^- p$ 2.7 GeV/c

$\Gamma(\Xi(1530) \pi)/\Gamma(\Lambda \bar{K})$	VALUE	DOCUMENT ID	TECN	CHG	COMMENT	Γ_4/Γ_1
0.38 ± 0.27 OUR AVERAGE		Error includes scale factor of 2.3.				
1.0 ± 0.3		GAY	76c	HBC	-	$K^- p$ 4.2 GeV/c
0.26 ± 0.13		SMITH	65c	HBC	-0	$K^- p$ 2.45-2.7 GeV/c

$\Gamma(\Xi \pi \pi \text{ (not } \Xi(1530) \pi))/\Gamma(\Lambda \bar{K})$	VALUE	DOCUMENT ID	TECN	CHG	COMMENT	Γ_5/Γ_1
0.30 ± 0.20		BIAGI	87	SPEC	-	Ξ^- Be 116 GeV
<0.14		7 BADIER	65	HBC	0	1 st. dev. limit
>0.1		SMITH	65c	HBC	-0	$K^- p$ 2.45-2.7 GeV/c

$\Gamma(\Xi \pi \pi \text{ (not } \Xi(1530) \pi))/\Gamma(\Xi(1530) \pi)$	VALUE	DOCUMENT ID	TECN	CHG	COMMENT	Γ_5/Γ_4
consistent with zero		GAY	76c	HBC	-	$K^- p$ 4.2 GeV/c
0.3 ± 0.5		8 APSELL	70	HBC	0	$K^- p$ 2.87 GeV/c

$\Xi(1820)$ FOOTNOTES

- BIAGI 87 also sees weak signals in the in the $\Xi^- \pi^+ \pi^-$ channel at 1782.6 ± 1.4 MeV ($\Gamma = 6.0 \pm 1.5$ MeV) and 1831.9 ± 2.8 MeV ($\Gamma = 9.6 \pm 9.9$ MeV).
- BADIER 72 adds all channels and divides the peak into lower and higher mass regions. The data can also be fitted with a single Breit-Wigner of mass 1800 MeV and width 150 MeV.
- From a fit to inclusive $\Xi \pi, \Xi \pi \pi$, and ΛK^- spectra.
- From a fit to inclusive $\Xi \pi$ and $\Xi \pi \pi$ spectra only.
- Including $\Xi \pi \pi$.
- DAUBER 69 uses in part the same data as SMITH 65c.
- For the decay mode $\Xi^- \pi^+ \pi^0$ only. This limit includes $\Xi(1530) \pi$.
- Or less. Upper limit for the 3-body decay.

$\Xi(1820)$ REFERENCES

ADAMOVICH 99B	EPJ C11 271	M.I. Adamovich et al.	(CERN WA89 Collab.)
BIAGI 87	ZPHY C34 15	S.F. Biagi et al.	(BRIS, CERN, GEVA+)
BIAGI 87C	ZPHY C34 175	S.F. Biagi et al.	(BRIS, CERN, GEVA+)
ASTON 85B	PR D32 2270	D. Aston et al.	(SLAC, CARL, CNRC, CINC)
JENKINS 83	PRL 51 951	C.M. Jenkins et al.	(FSU, BRAN, LBL+)
BIAGI 81	ZPHY C9 305	S.F. Biagi et al.	(BRIS, CAVE, GEVA+)
HASSALL 81	NP B189 397	J.K. Hassall et al.	(CAVE, MSU)
TEODORO 78	PL 77B 451	D. Teodoro et al.	(AMST, CERN, NIJM+)
BRIEFEL 77	PR D16 2706	E. Briefel et al.	(BRAN, UMD, SYRA+)
Also	PRL 23 884	S.P. Apseil et al.	(BRAN, UMD, SYRA+)
GAY 76C	PL 62B 477	J.B. Gay et al.	(AMST, CERN, NIJM+)
DIBIANCA 75	NP B98 137	F.A. Dibianca, R.J. Endorf	(CNU)
BADIER 72	NP B37 429	J. Badier et al.	(EPOL)
APSELL 70	PRL 24 777	S.P. Apseil et al.	(BRAN, UMD, SYRA+)
CRENNELL 70B	PR D1 847	D.J. Crennell et al.	(BNL)
ALITTI 69	PRL 22 79	J. Alitti et al.	(BNL, SYRA+)
DAUBER 69	PR 179 1262	P.M. Dauber et al.	(LRL)
TRIPP 67	NP B3 10	R.D. Tripp et al.	(LRL, SLAC, CERN+)
BADIER 65	PL 16 171	J. Badier et al.	(EPOL, SACL, AMST+)
SMITH 65B	Athens Conf. 251	G.A. Smith, J.S. Lindsey	(LRL)
SMITH 65C	PRL 14 25	G.A. Smith et al.	(LRL) IJP
HALSTEINSLID 63	Siena Conf. 1 73	A. Halsteinslid et al.	(BERG, CERN, EPOL+)

OTHER RELATED PAPERS

TEODORO 78	PL 77B 451	D. Teodoro et al.	(AMST, CERN, NIJM+)
BRIEFEL 75	PR D12 1859	E. Briefel et al.	(BRAN, UMD, SYRA+)
SCHMIDT 73	Purdue Conf. 363	P.E. Schmidt	(BRAN)
MERRILL 68	PR 167 1202	D.W. Merrill, J. Button-Shafer	(LRL)
SMITH 64	PRL 13 61	G.A. Smith et al.	(LRL) IJP

Baryon Particle Listings

$\Xi(1950), \Xi(2030)$

$\Xi(1950)$

$$I(J^P) = \frac{1}{2}(?)^? \text{ Status: } ***$$

We list here everything reported between 1875 and 2000 MeV. The accumulated evidence for a Ξ near 1950 MeV seems strong enough to include a $\Xi(1950)$ in the main Baryon Table, but not much can be said about its properties. In fact, there may be more than one Ξ near this mass.

$\Xi(1950)$ MASS

VALUE (MeV)	EVTS	DOCUMENT ID	TECN	COMMENT
1950 ± 15 OUR ESTIMATE				
1955 ± 6		ADAMOVICH 99b	WA89	Σ^- nucleus, 345 GeV
1944 ± 9	129	BIAGI 87	SPEC	$\Xi^- \text{Be} \rightarrow (\Xi^- \pi^+) \pi^- X$
1963 ± 5 ± 2	63	BIAGI 87c	SPEC	$\Xi^- \text{Be} \rightarrow (\Lambda \bar{K}^0) X$
1937 ± 7	150	BIAGI 81	SPEC	SPS hyperon beam
1961 ± 18	139	BRIEFEL 77	HBC	$2.87 K^- p \rightarrow \Xi^- \pi^+ X$
1936 ± 22	44	BRIEFEL 77	HBC	$2.87 K^- p \rightarrow \Xi^0 \pi^- X$
1964 ± 10	56	BRIEFEL 77	HBC	$\Xi(1530) \pi$
1900 ± 12		DIBIANCA 75	DBC	$\Xi \pi$
1952 ± 11	25	ROSS 73c		$(\Xi \pi)^-$
1956 ± 6	29	BADIER 72	HBC	$\Xi \pi, \Xi \pi \pi, \gamma K$
1955 ± 14	21	GOLDWASSER 70	HBC	$\Xi \pi$
1894 ± 18	66	DAUBER 69	HBC	$\Xi \pi$
1930 ± 20	27	ALITTI 68	HBC	$\Xi^- \pi^+$
1933 ± 16	35	BADIER 65	HBC	$\Xi^- \pi^+$

$\Xi(1950)$ WIDTH

VALUE (MeV)	EVTS	DOCUMENT ID	TECN	COMMENT
60 ± 20 OUR ESTIMATE				
68 ± 22		ADAMOVICH 99b	WA89	Σ^- nucleus, 345 GeV
100 ± 31	129	BIAGI 87	SPEC	$\Xi^- \text{Be} \rightarrow (\Xi^- \pi^+) \pi^- X$
25 ± 15 ± 1.2	63	BIAGI 87c	SPEC	$\Xi^- \text{Be} \rightarrow (\Lambda \bar{K}^0) X$
60 ± 8	150	BIAGI 81	SPEC	SPS hyperon beam
159 ± 5.7	139	BRIEFEL 77	HBC	$2.87 K^- p \rightarrow \Xi^- \pi^+ X$
87 ± 26	44	BRIEFEL 77	HBC	$2.87 K^- p \rightarrow \Xi^0 \pi^- X$
60 ± 39	56	BRIEFEL 77	HBC	$\Xi(1530) \pi$
63 ± 7.8		DIBIANCA 75	DBC	$\Xi \pi$
38 ± 10		ROSS 73c		$(\Xi \pi)^-$
35 ± 11	29	BADIER 72	HBC	$\Xi \pi, \Xi \pi \pi, \gamma K$
56 ± 26	21	GOLDWASSER 70	HBC	$\Xi \pi$
98 ± 23	66	DAUBER 69	HBC	$\Xi \pi$
80 ± 4.0	27	ALITTI 68	HBC	$\Xi^- \pi^+$
140 ± 35	35	BADIER 65	HBC	$\Xi^- \pi^+$

$\Xi(1950)$ DECAY MODES

Mode	Fraction (Γ_i/Γ)
$\Gamma_1 \Lambda \bar{K}$	seen
$\Gamma_2 \Sigma \bar{K}$	possibly seen
$\Gamma_3 \Xi \pi$	seen
$\Gamma_4 \Xi(1530) \pi$	
$\Gamma_5 \Xi \pi \pi$ (not $\Xi(1530) \pi$)	

$\Xi(1950)$ BRANCHING RATIOS

$\Gamma(\Sigma \bar{K})/\Gamma(\Lambda \bar{K})$					Γ_2/Γ_1
VALUE	CL%	EVTS	DOCUMENT ID	TECN	COMMENT
<2.3	90	0	BIAGI 87c	SPEC	$\Xi^- \text{Be} 116 \text{ GeV}$
$\Gamma(\Sigma \bar{K})/\Gamma_{\text{total}}$					Γ_2/Γ
VALUE	CL%	EVTS	DOCUMENT ID	TECN	COMMENT
possibly seen		17	HASSALL 81	HBC	$K^- p 6.5 \text{ GeV/c}$
$\Gamma(\Xi \pi)/\Gamma(\Xi(1530) \pi)$					Γ_3/Γ_4
VALUE	CL%	EVTS	DOCUMENT ID	TECN	COMMENT
$2.8^{+0.7}_{-0.6}$			APSELL 70	HBC	
$\Gamma(\Xi \pi \pi \text{ (not } \Xi(1530) \pi))/\Gamma(\Xi(1530) \pi)$					Γ_5/Γ_4
VALUE	CL%	EVTS	DOCUMENT ID	TECN	COMMENT
0.0 ± 0.3			APSELL 70	HBC	

$\Xi(1950)$ REFERENCES

ADAMOVICH 99b	EPJ C11 271	M.I. Adamovich et al.	(CERN WA89 Collab.)
BIAGI 87	ZPHY C34 15	S.F. Biagi et al.	(BRIS, CERN, GEVA+)
BIAGI 87c	ZPHY C34 175	S.F. Biagi et al.	(BRIS, CERN, GEVA+)
BIAGI 81	ZPHY C9 305	S.F. Biagi et al.	(BRIS, CAVE, GEVA+)
HASSALL 81	NP B189 397	J.K. Hassall et al.	(CAVE, MSU)
BRIEFEL 77	PR D16 2706	E. Briefel et al.	(BRAN, UMD, SYRA+)
Also	Duke Conf. 317	E. Briefel et al.	(BRAN, UMD, SYRA+)
Hyperon Resonances, 1970			
DIBIANCA 75	NP B98 137	F.A. Dibianna, R.J. Endorf	(CMU)
ROSS 73c	Purdue Conf. 345	R.T. Ross, J.L. Lloyd, D. Radojick	(OXF)
BADIER 72	NP B37 429	J. Badier et al.	(EPOL)
APSELL 70	PRL 24 777	S.P. Apse et al.	(BRAN, UMD, SYRA+)
GOLDWASSER 70	PR D1 1960	E.L. Goldwasser, P.F. Schultz	(ILL)
DAUBER 69	PR 179 1262	P.M. Dauber et al.	(LRL)
ALITTI 68	PRL 21 1119	J. Alitti et al.	(BNL, SYRA)
BADIER 65	PL 16 171	J. Badier et al.	(EPOL, SACL, AMST)

$\Xi(2030)$

$$I(J^P) = \frac{1}{2}(\geq \frac{5}{2})^? \text{ Status: } ***$$

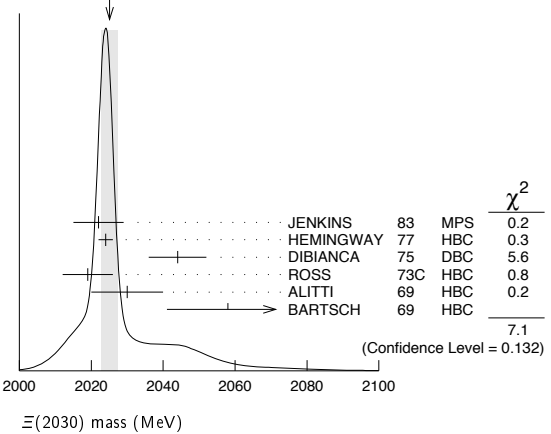
The evidence for this state has been much improved by HEMINGWAY 77, who see an eight standard deviation enhancement in $\Sigma \bar{K}$ and a weaker coupling to $\Lambda \bar{K}$. ALITTI 68 and HEMINGWAY 77 observe no signals in the $\Xi \pi \pi$ (or $\Xi(1530) \pi$) channel, in contrast to DIBIANCA 75. The decay $(\Lambda/\Sigma) \bar{K} \pi$ reported by BARTSCH 69 is also not confirmed by HEMINGWAY 77.

A moments analysis of the HEMINGWAY 77 data indicates at a level of three standard deviations that $J \geq 5/2$.

$\Xi(2030)$ MASS

VALUE (MeV)	EVTS	DOCUMENT ID	TECN	CHG	COMMENT
2025 ± 5 OUR ESTIMATE					
2025.1 ± 2.4 OUR AVERAGE Error includes scale factor of 1.3. See the ideogram below.					
2022 ± 7		JENKINS 83	MPS	-	$K^- p \rightarrow K^+$
2024 ± 2	200	HEMINGWAY 77	HBC	-	$K^- p 4.2 \text{ GeV/c}$
2044 ± 8		DIBIANCA 75	DBC	-0	$\Xi \pi \pi, \Xi^* \pi$
2019 ± 7	15	ROSS 73c	HBC	-0	$\Sigma \bar{K}$
2030 ± 10	42	ALITTI 69	HBC	-	$K^- p 3.9-5 \text{ GeV/c}$
2058 ± 17	40	BARTSCH 69	HBC	-0	$K^- p 10 \text{ GeV/c}$

WEIGHTED AVERAGE
2025.1 ± 2.4 (Error scaled by 1.3)

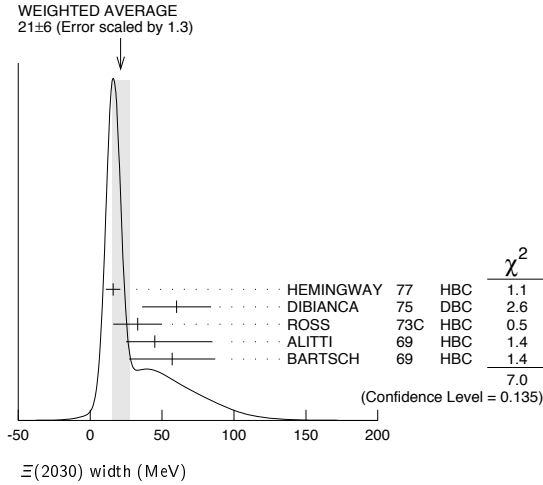


$\Xi(2030)$ WIDTH

VALUE (MeV)	EVTS	DOCUMENT ID	TECN	CHG	COMMENT
20 ± 15 OUR ESTIMATE					
21 ± 6 OUR AVERAGE Error includes scale factor of 1.3. See the ideogram below.					
16 ± 5	200	HEMINGWAY 77	HBC	-	$K^- p 4.2 \text{ GeV/c}$
60 ± 24		DIBIANCA 75	DBC	-0	$\Xi \pi \pi, \Xi^* \pi$
33 ± 17	15	ROSS 73c	HBC	-0	$\Sigma \bar{K}$
$45^{+4.0}_{-2.0}$		ALITTI 69	HBC	-	$K^- p 3.9-5 \text{ GeV/c}$
57 ± 30		BARTSCH 69	HBC	-0	$K^- p 10 \text{ GeV/c}$

See key on page 405

Baryon Particle Listings
 $\Xi(2030), \Xi(2120)$



$\Xi(2030)$ DECAY MODES

Mode	Fraction (Γ_i/Γ)
$\Gamma_1 \Lambda\bar{K}$	~ 20 %
$\Gamma_2 \Sigma\bar{K}$	~ 80 %
$\Gamma_3 \Xi\pi$	small
$\Gamma_4 \Xi(1530)\pi$	small
$\Gamma_5 \Xi\pi\pi$ (not $\Xi(1530)\pi$)	small
$\Gamma_6 \Lambda\bar{K}\pi$	small
$\Gamma_7 \Sigma\bar{K}\pi$	small

$\Xi(2030)$ BRANCHING RATIOS

$\Gamma(\Xi\pi)/[\Gamma(\Lambda\bar{K}) + \Gamma(\Sigma\bar{K}) + \Gamma(\Xi\pi) + \Gamma(\Xi(1530)\pi)]$	$\Gamma_3/(\Gamma_1+\Gamma_2+\Gamma_3+\Gamma_4)$			
VALUE	DOCUMENT ID	TECN	CHG	COMMENT
<0.30	ALITTI	69	HBC	— 1 standard dev. limit

$\Gamma(\Xi\pi)/\Gamma(\Sigma\bar{K})$	Γ_3/Γ_2				
VALUE	CL%	DOCUMENT ID	TECN	CHG	COMMENT
<0.19	95	HEMINGWAY	77	HBC	— K^-p 4.2 GeV/c

$\Gamma(\Lambda\bar{K})/[\Gamma(\Lambda\bar{K}) + \Gamma(\Sigma\bar{K}) + \Gamma(\Xi\pi) + \Gamma(\Xi(1530)\pi)]$	$\Gamma_1/(\Gamma_1+\Gamma_2+\Gamma_3+\Gamma_4)$			
VALUE	DOCUMENT ID	TECN	CHG	COMMENT
0.25 ± 0.15	ALITTI	69	HBC	— K^-p 3.9-5 GeV/c

$\Gamma(\Lambda\bar{K})/\Gamma(\Sigma\bar{K})$	Γ_1/Γ_2			
VALUE	DOCUMENT ID	TECN	CHG	COMMENT
0.22 ± 0.09	HEMINGWAY	77	HBC	— K^-p 4.2 GeV/c

$\Gamma(\Sigma\bar{K})/[\Gamma(\Lambda\bar{K}) + \Gamma(\Sigma\bar{K}) + \Gamma(\Xi\pi) + \Gamma(\Xi(1530)\pi)]$	$\Gamma_2/(\Gamma_1+\Gamma_2+\Gamma_3+\Gamma_4)$			
VALUE	DOCUMENT ID	TECN	CHG	COMMENT
0.75 ± 0.20	ALITTI	69	HBC	— K^-p 3.9-5 GeV/c

$\Gamma(\Xi(1530)\pi)/[\Gamma(\Lambda\bar{K}) + \Gamma(\Sigma\bar{K}) + \Gamma(\Xi\pi) + \Gamma(\Xi(1530)\pi)]$	$\Gamma_4/(\Gamma_1+\Gamma_2+\Gamma_3+\Gamma_4)$			
VALUE	DOCUMENT ID	TECN	CHG	COMMENT
<0.15	ALITTI	69	HBC	— 1 standard dev. limit

$[\Gamma(\Xi(1530)\pi) + \Gamma(\Xi\pi\pi(\text{not } \Xi(1530)\pi))]/\Gamma(\Sigma\bar{K})$	$(\Gamma_4+\Gamma_5)/\Gamma_2$				
VALUE	CL%	DOCUMENT ID	TECN	CHG	COMMENT
<0.11	95	¹ HEMINGWAY	77	HBC	— K^-p 4.2 GeV/c

$\Gamma(\Lambda\bar{K}\pi)/\Gamma_{\text{total}}$	Γ_6/Γ		
VALUE	DOCUMENT ID	TECN	COMMENT
seen	BARTSCH	69	HBC K^-p 10 GeV

$\Gamma(\Lambda\bar{K}\pi)/\Gamma(\Sigma\bar{K})$	Γ_6/Γ_2				
VALUE	CL%	DOCUMENT ID	TECN	CHG	COMMENT
<0.32	95	HEMINGWAY	77	HBC	— K^-p 4.2 GeV/c

$\Gamma(\Sigma\bar{K}\pi)/\Gamma_{\text{total}}$	Γ_7/Γ		
VALUE	DOCUMENT ID	TECN	COMMENT
••• We do not use the following data for averages, fits, limits, etc. •••			
seen	BARTSCH	69	HBC K^-p 10 GeV

$\Gamma(\Sigma\bar{K}\pi)/\Gamma(\Sigma\bar{K})$	Γ_7/Γ_2				
VALUE	CL%	DOCUMENT ID	TECN	CHG	COMMENT
<0.04	95	² HEMINGWAY	77	HBC	— K^-p 4.2 GeV/c

$\Xi(2030)$ FOOTNOTES

- ¹ For the decay mode $\Xi^- \pi^+ \pi^-$ only.
- ² For the decay mode $\Sigma^\pm K^- \pi^\mp$ only.

$\Xi(2030)$ REFERENCES

JENKINS 83	PRL 51 951	C.M. Jenkins et al.	(FSU, BRAN, LBL+)
HEMINGWAY 77	PL 68B 197	R.J. Hemingway et al.	(AMST, CERN, NIJM+)U
Also	PL 62B 477	J.B. Gay et al.	(AMST, CERN, NIJM)
DIBIANCA 75	NP B98 137	F.A. Dibianca, R.J. Endorf	(CMU)
ROSS 73C	Purdue Conf. 345	R.T. Ross, J.L. Lloyd, D. Radojicic	(OXF)
ALITTI 69	PRL 22 79	J. Alitti et al.	(BNL, SYRA)I
BARTSCH 69	PL 28B 439	J. Bartsch et al.	(AACH, BERL, CERN+)
ALITTI 68	PRL 21 1119	J. Alitti et al.	(BNL, SYRA)

$\Xi(2120)$

$I(J^P) = \frac{1}{2}(?)^?$ Status: *
 J, P need confirmation.

OMITTED FROM SUMMARY TABLE

$\Xi(2120)$ MASS

VALUE (MeV)	EVTS	DOCUMENT ID	TECN	COMMENT
≈ 2120 OUR ESTIMATE				
2137 ± 4	18	¹ CHLIAPNIK...	79 HBC	K^+p 32 GeV/c
2123 ± 7		² GAY	76c HBC	K^-p 4.2 GeV/c

$\Xi(2120)$ WIDTH

VALUE (MeV)	EVTS	DOCUMENT ID	TECN	COMMENT
<20	18	¹ CHLIAPNIK...	79 HBC	K^+p 32 GeV/c
25 ± 12		² GAY	76c HBC	K^-p 4.2 GeV/c

$\Xi(2120)$ DECAY MODES

Mode	Fraction (Γ_i/Γ)
$\Gamma_1 \Lambda\bar{K}$	seen

$\Xi(2120)$ BRANCHING RATIOS

$\Gamma(\Lambda\bar{K})/\Gamma_{\text{total}}$	Γ_1/Γ		
VALUE	DOCUMENT ID	TECN	COMMENT
seen	¹ CHLIAPNIK...	79 HBC	$K^+p \rightarrow (\bar{\Lambda} K^+) X$
seen	² GAY	76c HBC	K^-p 4.2 GeV/c

$\Xi(2120)$ FOOTNOTES

- ¹ CHLIAPNIKOV 79 does not uniquely identify the K^+ in the $(\bar{\Lambda} K^+) X$ final state. It also reports bumps with fewer events at 2240, 2540, and 2830 MeV.
- ² GAY 76c sees a 4-standard deviation signal. However, HEMINGWAY 77, with more events from the same experiment points out that the signal is greatly reduced if a cut is made on the 4-momentum u . This suggests an anomalous production mechanism if the $\Xi(2120)$ is real.

$\Xi(2120)$ REFERENCES

CHLIAPNIK... 79	NP B158 253	P.V. Chliapnikov et al.	(CERN, BELG, MONS)
HEMINGWAY 77	PL 68B 197	R.J. Hemingway et al.	(AMST, CERN, NIJM+)
GAY 76c	PL 62B 477	J.B. Gay et al.	(AMST, CERN, NIJM)

Baryon Particle Listings

 $\Xi(2250)$, $\Xi(2370)$, $\Xi(2500)$ $\Xi(2250)$
 $I(J^P) = \frac{1}{2}(?)$ Status: **
 J, P need confirmation.

OMITTED FROM SUMMARY TABLE

The evidence for this state is mixed. BARTSCH 69 sees a bump of not much statistical significance in $\Lambda\bar{K}\pi$, $\Sigma\bar{K}\pi$, and $\Xi\pi\pi$ mass spectra. GOLDWASSER 70 sees a narrower bump in $\Xi\pi\pi$ at a higher mass. Not seen by HASSALL 81 with 45 events/ μb at 6.5 GeV/c. Seen by JENKINS 83. Perhaps seen by BIAGI 87.

 $\Xi(2250)$ MASS

VALUE (MeV)	EVTS	DOCUMENT ID	TECN	CHG	COMMENT
≈ 2250 OUR ESTIMATE					
2189 ± 7	66	BIAGI	87	SPEC	$\Xi^- \text{Be} \rightarrow (\Xi^- \pi^+ \pi^-)$ X
2214 ± 5		JENKINS	83	MPS	$K^- p \rightarrow K^+$ MM
2295 ± 15	18	GOLDWASSER 70	HBC	-	$K^- p$ 5.5 GeV/c
2244 ± 52	35	BARTSCH 69	HBC	-	$K^- p$ 10 GeV/c

 $\Xi(2250)$ WIDTH

VALUE (MeV)	EVTS	DOCUMENT ID	TECN	CHG	COMMENT
46 ± 27	66	BIAGI	87	SPEC	$\Xi^- \text{Be} \rightarrow (\Xi^- \pi^+ \pi^-)$ X
< 30		GOLDWASSER 70	HBC	-	$K^- p$ 5.5 GeV/c
130 ± 80		BARTSCH 69	HBC	-	

 $\Xi(2250)$ DECAY MODES

Mode	Fraction (Γ_i/Γ)
Γ_1 $\Xi\pi\pi$	
Γ_2 $\Lambda\bar{K}\pi$	
Γ_3 $\Sigma\bar{K}\pi$	

 $\Xi(2250)$ REFERENCES

BIAGI 87	ZPHY C34 15	S.F. Biagi <i>et al.</i>	(BRIS, CERN, GEVA+)
JENKINS 83	PRL 51 951	C.M. Jenkins <i>et al.</i>	(FSU, BRAN, LBL+)
HASSALL 81	NP B189 397	J.K. Hassall <i>et al.</i>	(CAVE, MSU)
GOLDWASSER 70	PR D1 1960	E.L. Goldwasser, P.F. Schultz	(ILL)
BARTSCH 69	PL 28B 439	J. Bartsch <i>et al.</i>	(AACH, BERL, CERN+)

 $\Xi(2370)$
 $I(J^P) = \frac{1}{2}(?)$ Status: **
 J, P need confirmation.

OMITTED FROM SUMMARY TABLE

 $\Xi(2370)$ MASS

VALUE (MeV)	EVTS	DOCUMENT ID	TECN	CHG	COMMENT
≈ 2370 OUR ESTIMATE					
2356 ± 10		JENKINS	83	MPS	$K^- p \rightarrow K^+$ MM
2370	50	HASSALL	81	HBC	$K^- p$ 6.5 GeV/c
2373 ± 8	94	AMIRZADEH	80	HBC	$K^- p$ 8.25 GeV/c
2392 ± 27		DIBIANCA	75	DBC	$\Xi 2\pi$

 $\Xi(2370)$ WIDTH

VALUE (MeV)	EVTS	DOCUMENT ID	TECN	CHG	COMMENT
80	50	HASSALL	81	HBC	$K^- p$ 6.5 GeV/c
80 ± 25	94	AMIRZADEH	80	HBC	$K^- p$ 8.25 GeV/c
75 ± 69		DIBIANCA	75	DBC	$\Xi 2\pi$

 $\Xi(2370)$ DECAY MODES

Mode	Fraction (Γ_i/Γ)
Γ_1 $\Lambda\bar{K}\pi$ Includes $\Gamma_4 + \Gamma_6$.	seen
Γ_2 $\Sigma\bar{K}\pi$ Includes $\Gamma_5 + \Gamma_6$.	seen
Γ_3 $\Omega^- K$	
Γ_4 $\Lambda\bar{K}^*(892)$	
Γ_5 $\Sigma\bar{K}^*(892)$	
Γ_6 $\Sigma(1385)\bar{K}$	

 $\Xi(2370)$ BRANCHING RATIOS

$\Gamma(\Lambda\bar{K}\pi)/\Gamma_{\text{total}}$	DOCUMENT ID	TECN	CHG	COMMENT	Γ_1/Γ
VALUE					
seen	AMIRZADEH 80	HBC	-0	$K^- p$ 8.25 GeV/c	

$\Gamma(\Sigma\bar{K}\pi)/\Gamma_{\text{total}}$	DOCUMENT ID	TECN	CHG	COMMENT	Γ_2/Γ
VALUE					
seen	AMIRZADEH 80	HBC	-0	$K^- p$ 8.25 GeV/c	

$[\Gamma(\Lambda\bar{K}\pi) + \Gamma(\Sigma\bar{K}\pi)]/\Gamma_{\text{total}}$	DOCUMENT ID	TECN	CHG	COMMENT	$(\Gamma_1 + \Gamma_2)/\Gamma$
VALUE					
seen	HASSALL 81	HBC	-0	$K^- p$ 6.5 GeV/c	

$\Gamma(\Omega^- K)/\Gamma_{\text{total}}$	DOCUMENT ID	TECN	CHG	COMMENT	Γ_3/Γ
VALUE					
0.09 ± 0.04	¹ KINSON 80	HBC	-	$K^- p$ 8.25 GeV/c	

$[\Gamma(\Lambda\bar{K}^*(892)) + \Gamma(\Sigma\bar{K}^*(892))]/\Gamma_{\text{total}}$	DOCUMENT ID	TECN	CHG	COMMENT	$(\Gamma_4 + \Gamma_5)/\Gamma$
VALUE					
0.22 ± 0.13	¹ KINSON 80	HBC	-	$K^- p$ 8.25 GeV/c	

$\Gamma(\Sigma(1385)\bar{K})/\Gamma_{\text{total}}$	DOCUMENT ID	TECN	CHG	COMMENT	Γ_6/Γ
VALUE					
0.12 ± 0.08	¹ KINSON 80	HBC	-	$K^- p$ 8.25 GeV/c	

 $\Xi(2370)$ FOOTNOTES¹ KINSON 80 is a reanalysis of AMIRZADEH 80 with 50% more events. $\Xi(2370)$ REFERENCES

JENKINS 83	PRL 51 951	C.M. Jenkins <i>et al.</i>	(FSU, BRAN, LBL+)
HASSALL 81	NP B189 397	J.K. Hassall <i>et al.</i>	(CAVE, MSU)
AMIRZADEH 80	PL 90B 324	J. Amirzadeh <i>et al.</i>	(BIRM, CERN, GLAS+) ¹
KINSON 80	Toronto Conf. 263	J.B. Kinson <i>et al.</i>	(BIRM, CERN, GLAS+) ¹
DIBIANCA 75	NP B98 137	F.A. Dibiaanca, R.J. Endorf	(CMU)

 $\Xi(2500)$
 $I(J^P) = \frac{1}{2}(?)$ Status: *
 J, P need confirmation.

OMITTED FROM SUMMARY TABLE

The ALITTI 69 peak might be instead the $\Xi(2370)$ or might be neither the $\Xi(2370)$ nor the $\Xi(2500)$.

 $\Xi(2500)$ MASS

VALUE (MeV)	EVTS	DOCUMENT ID	TECN	CHG	COMMENT
≈ 2500 OUR ESTIMATE					
2505 ± 10		JENKINS	83	MPS	$K^- p \rightarrow K^+$ MM
2430 ± 20	30	ALITTI 69	HBC	-	$K^- p$ 4.6-5 GeV/c
2500 ± 10	45	BARTSCH 69	HBC	-0	$K^- p$ 10 GeV/c

 $\Xi(2500)$ WIDTH

VALUE (MeV)	DOCUMENT ID	TECN	CHG
150 ± 60 -40	ALITTI 69	HBC	-
59 ± 27	BARTSCH 69	HBC	-0

 $\Xi(2500)$ DECAY MODES

Mode	Fraction (Γ_i/Γ)
Γ_1 $\Xi\pi\pi$	
Γ_2 $\Lambda\bar{K}$	
Γ_3 $\Sigma\bar{K}$	
Γ_4 $\Xi\pi\pi$	seen
Γ_5 $\Xi(1530)\pi$	
Γ_6 $\Lambda\bar{K}\pi + \Sigma\bar{K}\pi$	seen

See key on page 405

Baryon Particle Listings

 $\Xi(2500)$ $\Xi(2500)$ BRANCHING RATIOS

$\frac{\Gamma(\Xi\pi)}{[\Gamma(\Xi\pi) + \Gamma(\Lambda\bar{K}) + \Gamma(\Sigma\bar{K}) + \Gamma(\Xi(1530)\pi)]}$	$\frac{\Gamma_1}{(\Gamma_1 + \Gamma_2 + \Gamma_3 + \Gamma_5)}$
VALUE	DOCUMENT ID TECN COMMENT
<0.5	ALITTI 69 HBC 1 standard dev. limit
$\frac{\Gamma(\Lambda\bar{K})}{[\Gamma(\Xi\pi) + \Gamma(\Lambda\bar{K}) + \Gamma(\Sigma\bar{K}) + \Gamma(\Xi(1530)\pi)]}$	$\frac{\Gamma_2}{(\Gamma_1 + \Gamma_2 + \Gamma_3 + \Gamma_5)}$
VALUE	DOCUMENT ID TECN CHG
0.5 ± 0.2	ALITTI 69 HBC -
$\frac{\Gamma(\Sigma\bar{K})}{[\Gamma(\Xi\pi) + \Gamma(\Lambda\bar{K}) + \Gamma(\Sigma\bar{K}) + \Gamma(\Xi(1530)\pi)]}$	$\frac{\Gamma_3}{(\Gamma_1 + \Gamma_2 + \Gamma_3 + \Gamma_5)}$
VALUE	DOCUMENT ID TECN CHG
0.5 ± 0.2	ALITTI 69 HBC -
$\frac{\Gamma(\Xi(1530)\pi)}{[\Gamma(\Xi\pi) + \Gamma(\Lambda\bar{K}) + \Gamma(\Sigma\bar{K}) + \Gamma(\Xi(1530)\pi)]}$	$\frac{\Gamma_5}{(\Gamma_1 + \Gamma_2 + \Gamma_3 + \Gamma_5)}$
VALUE	DOCUMENT ID TECN COMMENT
<0.2	ALITTI 69 HBC 1 standard dev. limit

 $\frac{\Gamma(\Xi\pi)}{\Gamma_{\text{total}}}$

VALUE	DOCUMENT ID	TECN	CHG
seen	BARTSCH	69	HBC -0

 Γ_4/Γ $\frac{[\Gamma(\Lambda\bar{K}\pi) + \Gamma(\Sigma\bar{K}\pi)]}{\Gamma_{\text{total}}}$

VALUE	DOCUMENT ID	TECN	CHG
seen	BARTSCH	69	HBC -0

 Γ_6/Γ $\Xi(2500)$ REFERENCES

JENKINS	83	PRL 51 951	C.M. Jenkins <i>et al.</i>	(FSU, BRAN, LBL+)
ALITTI	69	PRL 22 79	J. Alitti <i>et al.</i>	(BNL, SYRA)1
BARTSCH	69	PL 28B 439	J. Bartsch <i>et al.</i>	(AACH, BERL, CERN+)

Baryon Particle Listings

 Ω^- **Ω^- BARYONS**
($S = -3, I = 0$)

$$\Omega^- = sss$$

 Ω^-

$$I(J^P) = 0(\frac{3}{2}^+) \text{ Status: } ****$$

The unambiguous discovery in both production and decay was by BARNES 64. The quantum numbers follow from the assignment of the particle to the baryon decuplet. DEUTSCHMANN 78 and BAUBILLIER 78 rule out $J = 1/2$ and find consistency with $J = 3/2$. AUBERT, BE 06 finds from the decay angular distributions of $\Xi_c^0 \rightarrow \Omega^- K^+$ and $\Omega_c^0 \rightarrow \Omega^- K^+$ that $J = 3/2$; this depends on the spins of the Ξ_c^0 and Ω_c^0 being $J = 1/2$, their supposed values.

We have omitted some results that have been superseded by later experiments. See our earlier editions.

 Ω^- MASS

The fit assumes the Ω^- and $\overline{\Omega}^+$ masses are the same, and averages them together.

VALUE (MeV)	EVTS	DOCUMENT ID	TECN	COMMENT
1672.45 ± 0.29 OUR FIT				
1672.43 ± 0.32 OUR AVERAGE				
1673 ± 1	100	HARTOUNI 85	SPEC	80–280 GeV $K_L^0 C$
1673.0 ± 0.8	41	BAUBILLIER 78	HBC	8.25 GeV/c $K^- p$
1671.7 ± 0.6	27	HEMINGWAY 78	HBC	4.2 GeV/c $K^- p$
1673.4 ± 1.7	4	¹ DIBIANCA 75	DBC	4.9 GeV/c $K^- d$
1673.3 ± 1.0	3	PALMER 68	HBC	$K^- p$ 4.6, 5 GeV/c
1671.8 ± 0.8	3	SCHULTZ 68	HBC	$K^- p$ 5.5 GeV/c
1674.2 ± 1.6	5	SCOTTER 68	HBC	$K^- p$ 6 GeV/c
1672.1 ± 1.0	1	² FRY 55	EMUL	
• • • We do not use the following data for averages, fits, limits, etc. • • •				
1671.43 ± 0.78	13	³ DEUTSCH... 73	HBC	$K^- p$ 10 GeV/c
1671.9 ± 1.2	6	³ SPETH 69	HBC	See DEUTSCHMANN 73
1673.0 ± 8.0	1	ABRAMS 64	HBC	$\rightarrow \Xi^- \pi^0$
1670.6 ± 1.0	1	² FRY 55B	EMUL	
1615	1	⁴ EISENBERG 54	EMUL	

¹DIBIANCA 75 gives a mass for each event. We quote the average.

²The FRY 55 and FRY 55B events were identified as Ω^- by ALVAREZ 73. The masses assume decay to ΛK^- at rest. For FRY 55B, decay from an atomic orbit could Doppler shift the K^- energy and the resulting Ω^- mass by several MeV. This shift is negligible for FRY 55 because the Ω decay is approximately perpendicular to its orbital velocity, as is known because the Λ strikes the nucleus (L.Alvarez, private communication 1973). We have calculated the error assuming that the orbital n is 4 or larger.

³Excluded from the average; the Ω^- lifetimes measured by the experiments differ significantly from other measurements.

⁴The EISENBERG 54 mass was calculated for decay in flight. ALVAREZ 73 has shown that the Ω interacted with an Ag nucleus to give $K^- \Xi Ag$.

 $\overline{\Omega}^+$ MASS

The fit assumes the Ω^- and $\overline{\Omega}^+$ masses are the same, and averages them together.

VALUE (MeV)	EVTS	DOCUMENT ID	TECN	COMMENT
1672.45 ± 0.29 OUR FIT				
1672.5 ± 0.7 OUR AVERAGE				
1672 ± 1	72	HARTOUNI 85	SPEC	80–280 GeV $K_L^0 C$
1673.1 ± 1.0	1	FIRESTONE 71B	HBC	12 GeV/c $K^+ d$

$$(m_{\Omega^-} - m_{\overline{\Omega}^+}) / m_{\Omega^-}$$

A test of CPT invariance.

VALUE	DOCUMENT ID	TECN	COMMENT
(-1.44 ± 7.98) × 10⁻⁵	CHAN 98	E756	p Be, 800 GeV

 Ω^- MEAN LIFE

Measurements with an error $> 0.1 \times 10^{-10}$ s have been omitted. The fit assumes the Ω^- and $\overline{\Omega}^+$ mean lives are the same, and averages them together.

VALUE (10 ⁻¹⁰ s)	EVTS	DOCUMENT ID	TECN	COMMENT
0.821 ± 0.011 OUR FIT				
0.821 ± 0.011 OUR AVERAGE				
0.817 ± 0.013 ± 0.018	6934	CHAN 98	E756	p Be, 800 GeV
0.811 ± 0.037	1096	LUK 88	SPEC	p Be 400 GeV
0.823 ± 0.013	12k	BOURQUIN 84	SPEC	SPS hyperon beam
• • • We do not use the following data for averages, fits, limits, etc. • • •				

0.822 ± 0.028 2437 BOURQUIN 79B SPEC See BOURQUIN 84

 $\overline{\Omega}^+$ MEAN LIFE

The fit assumes the Ω^- and $\overline{\Omega}^+$ mean lives are the same, and averages them together.

VALUE (10 ⁻¹⁰ s)	EVTS	DOCUMENT ID	TECN	COMMENT
0.821 ± 0.011 OUR FIT				
0.823 ± 0.031 ± 0.022	1801	CHAN 98	E756	p Be, 800 GeV

$$(\tau_{\Omega^-} - \tau_{\overline{\Omega}^+}) / \tau_{\Omega^-}$$

A test of CPT invariance. Our calculation, from the averages in the preceding two data blocks.

VALUE	DOCUMENT ID
0.00 ± 0.05 OUR ESTIMATE	

 Ω^- MAGNETIC MOMENT

VALUE (μ_N)	EVTS	DOCUMENT ID	TECN	COMMENT
-2.02 ± 0.05 OUR AVERAGE				
-2.024 ± 0.056	235k	WALLACE 95	SPEC	Ω^- 300–550 GeV
-1.94 ± 0.17 ± 0.14	25k	DIEHL 91	SPEC	Spin-transfer production

 Ω^- DECAY MODES

Mode	Fraction (Γ_i/Γ)	Confidence level
$\Gamma_1 \Lambda K^-$	(67.8 ± 0.7) %	
$\Gamma_2 \Xi^0 \pi^-$	(23.6 ± 0.7) %	
$\Gamma_3 \Xi^- \pi^0$	(8.6 ± 0.4) %	
$\Gamma_4 \Xi^- \pi^+ \pi^-$	(4.3 ^{+3.4} _{-1.3}) × 10 ⁻⁴	
$\Gamma_5 \Xi(1530)^0 \pi^-$	(6.4 ^{+5.0} _{-2.0}) × 10 ⁻⁴	
$\Gamma_6 \Xi^0 e^- \overline{\nu}_e$	(5.6 ± 2.8) × 10 ⁻³	
$\Gamma_7 \Xi^- \gamma$	< 4.6 × 10 ⁻⁴	90%
$\Delta S = 2$ forbidden (S_2) modes		
$\Gamma_8 \Lambda \pi^-$	$S_2 < 2.9$ × 10 ⁻⁶	90%

 Ω^- BRANCHING RATIOS

The BOURQUIN 84 values (which include results of BOURQUIN 79B, a separate experiment) are much more accurate than any other results, and so the other results have been omitted.

$\Gamma(\Lambda K^-)/\Gamma_{\text{total}}$	VALUE	EVTS	DOCUMENT ID	TECN	COMMENT	Γ_1/Γ
	0.678 ± 0.007	14k	BOURQUIN 84	SPEC	SPS hyperon beam	
• • • We do not use the following data for averages, fits, limits, etc. • • •						
	0.686 ± 0.013	1920	BOURQUIN 79B	SPEC	See BOURQUIN 84	

$\Gamma(\Xi^0 \pi^-)/\Gamma_{\text{total}}$	VALUE	EVTS	DOCUMENT ID	TECN	COMMENT	Γ_2/Γ
	0.236 ± 0.007	1947	BOURQUIN 84	SPEC	SPS hyperon beam	
• • • We do not use the following data for averages, fits, limits, etc. • • •						
	0.234 ± 0.013	317	BOURQUIN 79B	SPEC	See BOURQUIN 84	

$\Gamma(\Xi^- \pi^0)/\Gamma_{\text{total}}$	VALUE	EVTS	DOCUMENT ID	TECN	COMMENT	Γ_3/Γ
	0.086 ± 0.004	759	BOURQUIN 84	SPEC	SPS hyperon beam	
• • • We do not use the following data for averages, fits, limits, etc. • • •						
	0.080 ± 0.008	145	BOURQUIN 79B	SPEC	See BOURQUIN 84	

$\Gamma(\Xi^- \pi^+ \pi^-)/\Gamma_{\text{total}}$	VALUE (units 10 ⁻⁴)	EVTS	DOCUMENT ID	TECN	COMMENT	Γ_4/Γ
	4.3^{+3.4}_{-1.3}	4	BOURQUIN 84	SPEC	SPS hyperon beam	

$\Gamma(\Xi(1530)^0 \pi^-)/\Gamma_{\text{total}}$	VALUE (units 10 ⁻⁴)	EVTS	DOCUMENT ID	TECN	COMMENT	Γ_5/Γ
	6.4^{+5.1}_{-2.0}	4	⁵ BOURQUIN 84	SPEC	SPS hyperon beam	
• • • We do not use the following data for averages, fits, limits, etc. • • •						
~ 20	1	1	BOURQUIN 79B	SPEC	See BOURQUIN 84	

⁵The same 4 events as in the previous mode, with the isospin factor to take into account $\Xi(1530)^0 \rightarrow \Xi^0 \pi^0$ decays included.

See key on page 405

Baryon Particle Listings

$\Omega^-, \Omega(2250)^-, \Omega(2380)^-$

$\Gamma(\Xi^0 e^- \bar{\nu}_e)/\Gamma_{total}$ Γ_6/Γ

VALUE (units 10^{-3})	EVTS	DOCUMENT ID	TECN	COMMENT
5.6 ± 2.8	14	BOURQUIN 84	SPEC	SPS hyperon beam
••• We do not use the following data for averages, fits, limits, etc. •••				
~ 10	3	BOURQUIN 79B	SPEC	See BOURQUIN 84

$\Gamma(\Xi^- \gamma)/\Gamma_{total}$ Γ_7/Γ

VALUE (units 10^{-4})	CL%	EVTS	DOCUMENT ID	TECN	COMMENT
< 4.6	90	0	ALBUQUERQ..94	E761	Ω^- 375 GeV
••• We do not use the following data for averages, fits, limits, etc. •••					
<22	90	9	BOURQUIN 84	SPEC	SPS hyperon beam
<31	90	0	BOURQUIN 79B	SPEC	See BOURQUIN 84

$\Gamma(\Lambda \pi^-)/\Gamma_{total}$ Γ_8/Γ

$\Delta S=2$. Forbidden in first-order weak interaction.

VALUE (units 10^{-6})	CL%	DOCUMENT ID	TECN	COMMENT
< 2.9	90	WHITE 05	HYCP	p Cu, 800 GeV
••• We do not use the following data for averages, fits, limits, etc. •••				
< 190	90	BOURQUIN 84	SPEC	SPS hyperon beam
<1300	90	BOURQUIN 79B	SPEC	See BOURQUIN 84

Ω^- DECAY PARAMETERS

α FOR $\Omega^- \rightarrow \Lambda K^-$

Some early results have been omitted.

VALUE	EVTS	DOCUMENT ID	TECN	COMMENT
0.0180 ± 0.0024 OUR AVERAGE				
$+0.0207 \pm 0.0051 \pm 0.0081$	960k	⁶ CHEN 05	HYCP	p Cu, 800 GeV
$+0.0178 \pm 0.0019 \pm 0.0016$	4.5M	⁶ LU 05A	HYCP	p Cu, 800 GeV
••• We do not use the following data for averages, fits, limits, etc. •••				
-0.028 ± 0.047	6953	CHAN 98	E756	p Be, 800 GeV
-0.034 ± 0.079	1743	LUK 88	SPEC	p Be 400 GeV
-0.025 ± 0.028	12k	BOURQUIN 84	SPEC	SPS hyperon beam

⁶The results of CHEN 05 and LU 05A are from different experimental runs.

$\bar{\alpha}$ FOR $\bar{\Omega}^+ \rightarrow \bar{\Lambda} K^+$

VALUE	EVTS	DOCUMENT ID	TECN	COMMENT
$-0.0181 \pm 0.0028 \pm 0.0026$	1.89M	LU 06	HYCP	p Cu, 800 GeV
••• We do not use the following data for averages, fits, limits, etc. •••				
$+0.017 \pm 0.077$	1823	CHAN 98	E756	p Be, 800 GeV

$(\alpha + \bar{\alpha})/(\alpha - \bar{\alpha})$ in $\Omega^- \rightarrow \Lambda K^-, \bar{\Omega}^+ \rightarrow \bar{\Lambda} K^+$

Zero if CP is conserved.

VALUE	DOCUMENT ID	TECN	COMMENT
$-0.016 \pm 0.092 \pm 0.089$	⁷ LU 06	HYCP	p Cu, 800 GeV

⁷This value uses the results of CHEN 05, LU 05A, and LU 06.

α FOR $\Omega^- \rightarrow \Xi^0 \pi^-$

VALUE	EVTS	DOCUMENT ID	TECN	COMMENT
$+0.09 \pm 0.14$	1630	BOURQUIN 84	SPEC	SPS hyperon beam

α FOR $\Omega^- \rightarrow \Xi^- \pi^0$

VALUE	EVTS	DOCUMENT ID	TECN	COMMENT
$+0.05 \pm 0.21$	614	BOURQUIN 84	SPEC	SPS hyperon beam

Ω^- REFERENCES

We have omitted some papers that have been superseded by later experiments. See our earlier editions.

AUBERT,BE 06	PRL 97 112001	B. Aubert et al.	(BABAR Collab.)
LU 06	PRL 96 242001	L.C. Lu et al.	(FNAL HyperCP Collab.)
CHEN 05	PR D71 051102R	Y.C. Chen et al.	(FNAL HyperCP Collab.)
LU 05A	PL B617 11	L.C. Lu et al.	(FNAL HyperCP Collab.)
WHITE 05	PRL 94 101804	C.G. White et al.	(FNAL HyperCP Collab.)
CHAN 98	PR D58 072002	A.W. Chan et al.	(FNAL E756 Collab.)
WALLACE 95	PRL 74 3732	N.B. Wallace et al.	(MINN, ARIZ, MICH+)
ALBUQUERQ.. 94	PR D50 R18	I.F. Albuquerque et al.	(FNAL E761 Collab.)
DIEHL 91	PRL 67 804	H.T. Diehl et al.	(RUTG, FNAL, MICH+)
LUK 88	PR D38 19	K.B. Luk et al.	(RUTG, WIS C, MICH, MINN)
HARTOUNI 85	PRL 54 628	E.P. Hartouni et al.	(COLU, ILL, FNAL)
BOURQUIN 84	NP B241 1	M.H. Bourquin et al.	(BRIS, GEVA, HEIDP+)
Also	PL 87B 297	M.H. Bourquin et al.	(BRIS, GEVA, HEIDP+)
BOURQUIN 79B	PL 88B 192	M.H. Bourquin et al.	(BRIS, GEVA, HEIDP+)
BAUBILLIER 78	PL 78B 342	M. Baubillier et al.	(BIRM, CERN, GLAS+)
DEUTSCH... 78	PL 73B 96	M. Deuschmann et al.	(AACH3, BERL, CERN+)
HEMINGWAY 78	NP B142 205	R.J. Hemingway et al.	(CERN, ZEEM, NIJM+)
DIBIANCA 75	NP B98 137	F.A. Dibianca, R.J. Endorf	(CMU)
ALVAREZ 73	PR D8 702	L.W. Alvarez	(LBL)
DEUTSCH... 73	NP B61 102	M. Deuschmann et al.	(ABCLV Collab.)
FIRESTONE 71B	PRL 26 410	I. Firestone et al.	(LRL)
SPEITH 69	PL 29B 252	R. Speith et al.	(AACH, BERL, CERN, LOIC+)
PALMER 68	PL 26B 323	R.B. Palmer et al.	(BNL, SYRA)
SCHULTZ 68	PR 168 1509	P.F. Schultz et al.	(ILL, ANL, NNWS+)
SCOTTER 68	PL 26B 474	D. Scotter et al.	(BIRM, GLAS, LOIC+)
ABRAMS 64	PRL 13 670	G.S. Abrams et al.	(UMD, NRL)
BARNES 64	PRL 12 204	V.E. Barnes et al.	(BNL)
FRY 55	PR 97 1189	W.F. Fry, J. Schneps, M.S. Swami	(WIS C)
FRY 55B	NC 2 346	W.F. Fry, J. Schneps, M.S. Swami	(WIS C)
EISENBERG 54	PR 96 541	Y. Eisenberg	(CORN)

$\Omega(2250)^-$

$I(J^P) = 0(?)^?$ Status: ***

$\Omega(2250)^-$ MASS

VALUE (MeV)	EVTS	DOCUMENT ID	TECN	COMMENT
2252 ± 9 OUR AVERAGE				
2253 ± 13	44	ASTON 87B	LASS	$K^- p$ 11 GeV/c
$2251 \pm 9 \pm 8$	78	BIAGI 86B	SPEC	SPS Ξ^- beam

$\Omega(2250)^-$ WIDTH

VALUE (MeV)	EVTS	DOCUMENT ID	TECN	COMMENT
55 ± 18 OUR AVERAGE				
81 ± 38	44	ASTON 87B	LASS	$K^- p$ 11 GeV/c
48 ± 20	78	BIAGI 86B	SPEC	SPS Ξ^- beam

$\Omega(2250)^-$ DECAY MODES

Mode	Fraction (Γ_i/Γ)
$\Gamma_1 \Xi^- \pi^+ K^-$	seen
$\Gamma_2 \Xi(1530)^0 K^-$	seen

$\Omega(2250)^-$ BRANCHING RATIOS

$\Gamma(\Xi(1530)^0 K^-)/\Gamma(\Xi^- \pi^+ K^-)$	Γ_2/Γ_1			
~ 1.0	44	ASTON 87B	LASS	$K^- p$ 11 GeV/c
0.70 ± 0.20	49	BIAGI 86B	SPEC	Ξ^- Be 116 GeV/c

$\Omega(2250)^-$ REFERENCES

ASTON 87B	PL B194 579	D. Aston et al.	(SLAC, NAGO, CINC, INUS)
BIAGI 86B	ZPHY C31 33	S.F. Biagi et al.	(LOQM, GEVA, RAL+)

$\Omega(2380)^-$

Status: **

OMITTED FROM SUMMARY TABLE

$\Omega(2380)^-$ MASS

VALUE (MeV)	EVTS	DOCUMENT ID	TECN	COMMENT
≈ 2380 OUR ESTIMATE				
$2384 \pm 9 \pm 8$	45	BIAGI 86B	SPEC	SPS Ξ^- beam

$\Omega(2380)^-$ WIDTH

VALUE (MeV)	EVTS	DOCUMENT ID	TECN	COMMENT
26 ± 23	45	BIAGI 86B	SPEC	SPS Ξ^- beam

$\Omega(2380)^-$ DECAY MODES

Mode	Fraction (Γ_i/Γ)
$\Gamma_1 \Xi^- \pi^+ K^-$	
$\Gamma_2 \Xi(1530)^0 K^-$	seen
$\Gamma_3 \Xi^- \bar{K}^*(892)^0$	

$\Omega(2380)^-$ BRANCHING RATIOS

$\Gamma(\Xi(1530)^0 K^-)/\Gamma(\Xi^- \pi^+ K^-)$	Γ_2/Γ_1				
< 0.44	90	9	BIAGI 86B	SPEC	Ξ^- Be 116 GeV/c

$\Gamma(\Xi^- \bar{K}^*(892)^0)/\Gamma(\Xi^- \pi^+ K^-)$	Γ_3/Γ_1			
0.5 ± 0.3	21	BIAGI 86B	SPEC	Ξ^- Be 116 GeV/c

$\Omega(2380)^-$ REFERENCES

BIAGI 86B	ZPHY C31 33	S.F. Biagi et al.	(LOQM, GEVA, RAL+)
-----------	-------------	-------------------	--------------------

Baryon Particle Listings

 $\Omega(2470)^-$ $\Omega(2470)^-$

Status: **

OMITTED FROM SUMMARY TABLE

A peak in the $\Omega^- \pi^+ \pi^-$ mass spectrum with a signal significance claimed to be at least 5.5 standard deviations. There is no reason to seriously doubt the existence of this state, but unless the evidence is overwhelming we usually wait for confirmation from a second experiment before elevating peaks to the Summary Table.

 $\Omega(2470)^-$ MASS

VALUE (MeV)	EVTS	DOCUMENT ID	TECN	COMMENT
2474 ± 12	59	ASTON	88G LASS	$K^- p$ 11 GeV/c

 $\Omega(2470)^-$ WIDTH

VALUE (MeV)	EVTS	DOCUMENT ID	TECN	COMMENT
72 ± 33	59	ASTON	88G LASS	$K^- p$ 11 GeV/c

 $\Omega(2470)^-$ DECAY MODES

Mode
$\Gamma_1 \quad \Omega^- \pi^+ \pi^-$

 $\Omega(2470)^-$ REFERENCES

ASTON	88G	PL B215 799	D. Aston <i>et al.</i>	(SLAC, NAGO, CINC, INUS)
-------	-----	-------------	------------------------	--------------------------

CHARMED BARYONS

(C = +1)

$\Lambda_c^+ = udc, \Sigma_c^{++} = uuc, \Sigma_c^+ = udc, \Sigma_c^0 = ddc,$

$\Xi_c^+ = usc, \Xi_c^0 = dsc, \Omega_c^0 = ssc$

CHARMED BARYONS

Revised January 2010 by C.G. Wohl (LBNL).

There are 17 known charmed baryons, and four other candidates not well enough established to be promoted to the Summary Tables.* Fig. 1(a) shows the mass spectrum, and for comparison Fig. 1(b) shows the spectrum of the lightest strange baryons. The Λ_c and Σ_c spectra ought to look much like the Λ and Σ spectra, since a Λ_c or a Σ_c differs from a Λ or a Σ only by the replacement of the s quark with a c quark. However, a Ξ or an Ω has more than one s quark, only *one* of which is changed to a c quark to make a Ξ_c or an Ω_c . Thus the Ξ_c and Ω_c spectra ought to be richer than the Ξ and Ω spectra.**

Before discussing the observed spectra, we review the theory of SU(4) multiplets, which tells what charmed baryons to expect; this is essential, because few of the spin-parity values given in Fig. 1(a) have been measured. Rather, they have been assigned in accord with expectations of the theory. However, they are all very likely as shown (see below).

SU(4) multiplets—Baryons made from $u, d, s,$ and c quarks belong to SU(4) multiplets. The multiplet numerology, analogous to $3 \times 3 \times 3 = 10 + 8_1 + 8_2 + 1$ for the subset of baryons made from just $u, d,$ and s quarks, is $4 \times 4 \times 4 = 20 + 20'_1 + 20'_2 + \bar{4}$. Figure 2(a) shows the 20-plet whose bottom level is an SU(3) decuplet, such as the decuplet that includes the $\Delta(1232)$. Figure 2(b) shows the 20'-plet whose bottom level is an SU(3) octet, such as the octet that includes the nucleon. Figure 2(c) shows the $\bar{4}$ multiplet, an inverted tetrahedron. One level up from the bottom level of each multiplet are the baryons with one c quark. All the baryons in a given multiplet have the same spin and parity. Each N or Δ or SU(3)-singlet- Λ resonance calls for another 20'- or 20- or $\bar{4}$ -plet, respectively.

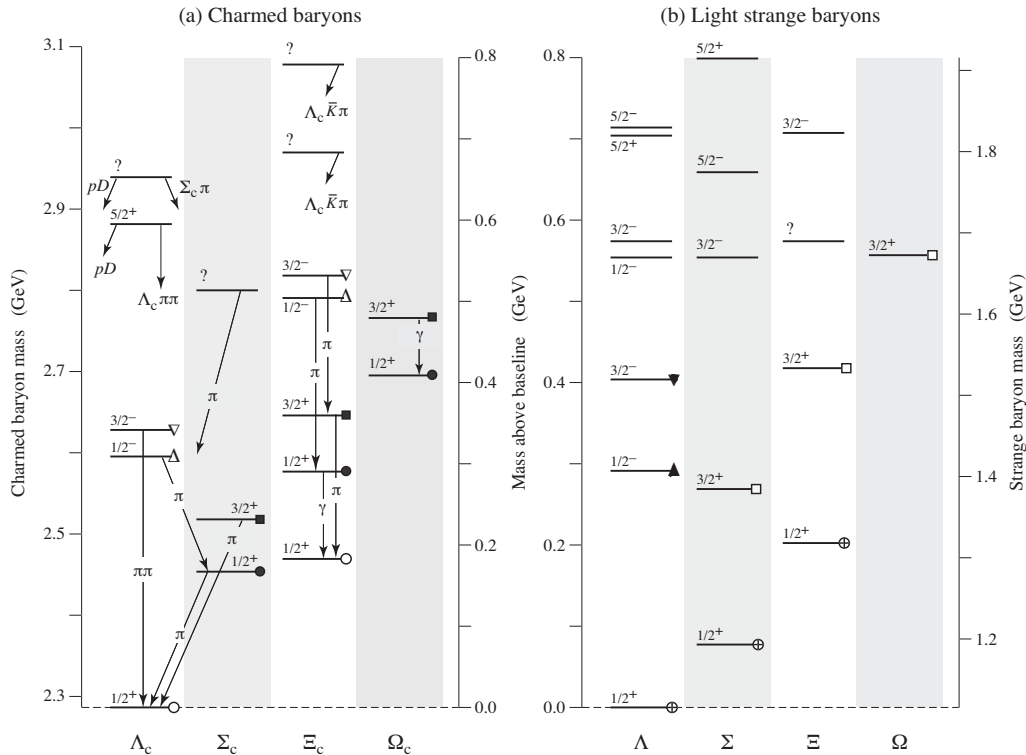


Fig. 1. (a) The known charmed baryons, and (b) the lightest “4-star” strange baryons. Note that there are two $J^P = 1/2^+$ Ξ_c states, and that the lightest Ω_c does not have $J = 3/2$. The $J^P = 1/2^+$ states, all tabbed with a circle, belong to the SU(4) multiplet that includes the nucleon; states with a circle with the same fill belong to the same SU(3) multiplet within that SU(4) multiplet. Similar remarks apply to the other states: same shape of tab, same SU(4) multiplet; same fill of that shape, same SU(3) multiplet. The $J^P = 1/2^-$ and $3/2^-$ states tabbed with triangles complete two SU(4) $\bar{4}$ multiplets.

Baryon Particle Listings

Charmed Baryons

The flavor symmetries shown in Fig. 2 are of course badly broken, but the figure is the simplest way to see what charmed baryons should exist. For example, from Fig. 2(b), we expect to find, in the same $J^P = 1/2^+$ 20'-plet as the nucleon, a Λ_c , a Σ_c , two Ξ_c 's, and an Ω_c . Note that this Ω_c has $J^P = 1/2^+$ and is not in the same SU(4) multiplet as the famous $J^P = 3/2^+$ Ω^- .

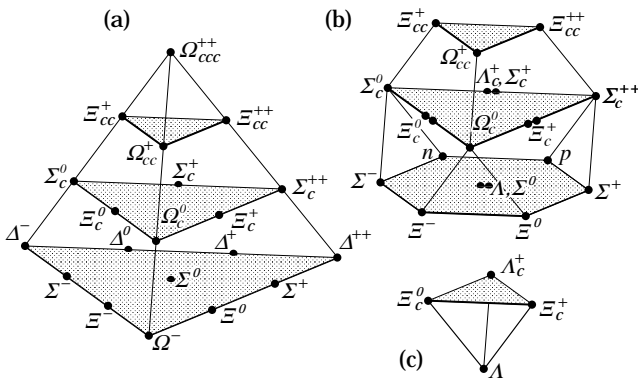


Figure 2: SU(4) multiplets of baryons made of $u, d, s,$ and c quarks. (a) The 20-plet with an SU(3) decuplet on the lowest level. (b) The 20'-plet with an SU(3) octet on the lowest level. (c) The $\bar{4}$ -plet. Note that here and in Fig. 3, but not in Fig. 1, each charge state is shown separately.

Figure 3 shows in more detail the middle level of the 20'-plet of Fig. 2(b); it splits apart into two SU(3) multiplets, a $\bar{3}$ and a 6. The states of the $\bar{3}$ are antisymmetric under the interchange of the two light quarks (the $u, d,$ and s quarks), whereas the states of the 6 are symmetric under this interchange. We use a prime to distinguish the Ξ_c in the 6 from the one in the $\bar{3}$.

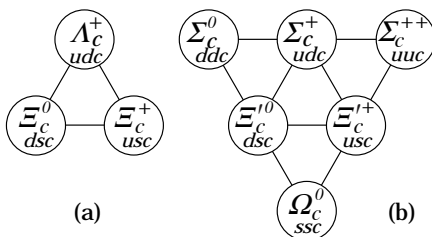


Figure 3: The SU(3) multiplets on the second level of the SU(4) multiplet of Fig. 2(b). The Λ_c and Ξ_c tabbed with open circles in Fig. 1(a) complete a $J^P = 1/2^+$ SU(3) $\bar{3}$ -plet, as in (a) here. The $\Sigma_c, \Xi_c,$ and Ω_c tabbed with closed circles in Fig. 1(a) complete a $J^P = 1/2^+$ SU(3) 6-plet, as in (b) here. Together the nine particles complete the charm = +1 level of a $J^P = 1/2^+$ SU(4) 20'-plet, as in Fig. 2(b).

The observed spectra—(1) The parity of the lightest Λ_c is defined to be positive (as are the parities of the $p, n,$ and Λ); the limited evidence about its spin is consistent with $J = 1/2$. However, few of the J^P quantum numbers given in Fig. 1(a) have been measured. Models using spin-spin and spin-orbit interactions between the quarks, with parameters determined using a few of the masses as input, lead to the J^P assignments shown.[†] There are no surprises: the $J^P = 1/2^+$ states come first, then the $J^P = 3/2^+$ states . . .

(2) There is, however, evidence that many of the J^P assignments in Fig. 1(a) must be correct. As is well known, the successive mass differences between the $J^P = 3/2^+$ particles, the $\Delta(1232)^-, \Sigma(1385)^-, \Xi(1535)^-,$ and Ω^- , which lie along the lower left edge of the 20-plet in Fig. 2(a), should according to SU(3) be about equal; and indeed experimentally they nearly are. In the same way, the mass differences between the $J^P = 1/2^+$ $\Sigma_c(2455)^0, \Xi_c^0,$ and Ω_c^0 ,[‡] the particles along the left edge of Fig. 3(b), should be about equal—assuming, of course, that they *do* all have the same J^P . The measured differences are 124.1 ± 2.9 MeV and 117.3 ± 3.4 MeV—not perfect, but close. Similarly, the mass differences between the presumed $J^P = 3/2^+$ $\Sigma_c(2520)^0, \Xi_c(2645)^0,$ and $\Omega_c(2770)^0$ are 127.9 ± 0.8 MeV and 122.4 ± 3.1 MeV. In Fig. 1(a), these two sets of charm particles are tabbed with solid circles and solid squares.

(3) Other evidence comes from the decay of the $\Lambda_c(2593)$. The only allowed strong decay is $\Lambda_c(2593)^+ \rightarrow \Lambda_c^+ \pi \pi$, and this appears to be dominated by the submode $\Sigma_c(2455)\pi$, despite little available phase space for the latter (the “ Q ” is about 2 MeV, the c.m. decay momentum about 20 MeV/c). Thus the decay is almost certainly s -wave, which, assuming that the $\Sigma_c(2455)$ does indeed have $J^P = 1/2^+$, makes $J^P = 1/2^-$ for the $\Lambda_c(2593)$.

(4) The heavier charmed baryons, such as the $J^P = 1/2^-$ and $3/2^-$ Λ_c 's, have much narrower widths than do their strange counterparts, such as the $\Lambda(1405)$ and $\Lambda(1520)$. The clean Λ_c spectrum has in fact been taken to settle the decades-long discussion about the nature of the $\Lambda(1405)$ —true 3-quark state or mere $\bar{K}N$ threshold effect?—unambiguously in favor of the first interpretation (which is not to say that the proximity of the $\bar{K}N$ threshold has no effect on the $\Lambda(1405)$). In fact, models of baryon-resonance spectroscopy should now *start* with the narrow charmed baryons, and work back to those broad old resonances.

Footnotes:

* The unpromoted states are a $\Lambda_c(2765)^+,$ a $\Xi_c(2930),$ a $\Xi_c(3055),$ and a $\Xi_c(3123)$. There is also weak evidence for a baryon with *two* c quarks, a Ξ_{cc}^+ at 3519 MeV. See the Particle Listings.

** For example, there are three Ω_c^0 states (properly symmetrized states of $ssc, scs,$ and css) corresponding to each Ω^- (sss) state.

† This is not the place to discuss the details of the models, nor to attempt a guide to the literature. See the discovery

papers of the various charmed baryons for references to the models that lead to the quantum-number assignments.

‡ A reminder about the Particle Data Group naming scheme: A particle has its mass as part of its name if and only if it decays strongly. Thus $\Sigma(1385)$ and $\Sigma_c(2455)$ but Ω^- and Ξ_c' .

Λ_c^+

$I(J^P) = 0(\frac{1}{2}^+)$ Status: * * * *

The parity of the Λ_c^+ is defined to be positive (as are the parities of the proton, neutron, and Λ). The quark content is udc . The spin J has not actually been measured. Results of an analysis of $pK^-\pi^+$ decays (JEZABEK 92) are consistent with the expected $J = 1/2$.

We have omitted some results that have been superseded by later experiments. The omitted results may be found in earlier editions.

Λ_c^+ MASS

Our value in 2004, 2284.9 ± 0.6 MeV, was the average of the measurements now filed below as "not used." The BABAR measurement is so much better that we use it alone. Note that it is about 2.6 (old) standard deviations above the 2004 value.

The fit also includes $\Sigma_c-\Lambda_c^+$ and $\Lambda_c^{*+}-\Lambda_c^+$ mass-difference measurements, but this doesn't affect the Λ_c^+ mass. The new (in 2006) Λ_c^+ mass simply pushes all those other masses higher.

VALUE (MeV)	EVTS	DOCUMENT ID	TECN	COMMENT
2286.46 ± 0.14 OUR FIT				
2286.46 ± 0.14	4891	¹ AUBERT,B	05s BABR	$\Lambda_c^0 K^+$ and $\Sigma^0 K_S^0 K^+$
• • • We do not use the following data for averages, fits, limits, etc. • • •				
2284.7 ± 0.6 ± 0.7	1134	AVERY	91 CLEO	Six modes
2281.7 ± 2.7 ± 2.6	29	ALVAREZ	90b NA14	$pK^-\pi^+$
2285.8 ± 0.6 ± 1.2	101	BARLAG	89 NA32	$pK^-\pi^+$
2284.7 ± 2.3 ± 0.5	5	AGUILAR-...	88b LEBC	$pK^-\pi^+$
2283.1 ± 1.7 ± 2.0	628	ALBRECHT	88c ARG	$pK^-\pi^+$, $p\bar{K}^0$, $\Lambda 3\pi$
2286.2 ± 1.7 ± 0.7	97	ANJOS	88b E691	$pK^-\pi^+$
2281 ± 3	2	JONES	87 HBC	$pK^-\pi^+$
2283 ± 3	3	BOSETTI	82 HBC	$pK^-\pi^+$
2290 ± 3	1	CALICCHIO	80 HYBR	$pK^-\pi^+$

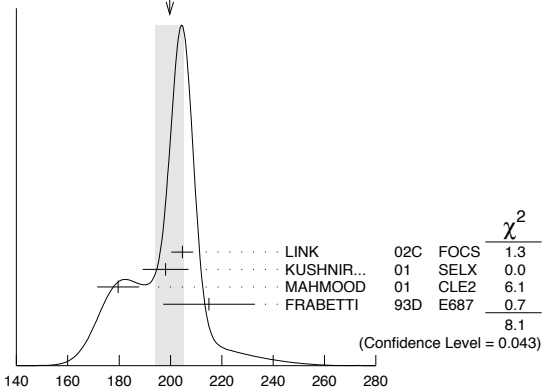
¹AUBERT,B 05s uses low-Q $\Lambda_c^0 K^+$ and $\Sigma^0 K_S^0 K^+$ decays to minimize systematic errors. The error above includes systematic as well as statistical errors. Many cross checks and adjustments to properties of the BABAR detector, as well as the large number of clean events, make this by far the best measurement of the Λ_c^+ mass.

Λ_c^+ MEAN LIFE

Measurements with an error $\geq 100 \times 10^{-15}$ s or with fewer than 20 events have been omitted from the Listings.

VALUE (10^{-15} s)	EVTS	DOCUMENT ID	TECN	COMMENT
200 ± 6 OUR AVERAGE				Error includes scale factor of 1.6. See the ideogram below.
204.6 ± 3.4 ± 2.5	8034	LINK	02c FOCS	$pK^-\pi^+$
198.1 ± 7.0 ± 5.6	1630	KUSHNIR...	01 SELX	$\Lambda_c^+ \rightarrow pK^-\pi^+$
179.6 ± 6.9 ± 4.4	4749	MAHMOOD	01 CLE2	$e^+e^- \approx \Upsilon(4S)$
215 ± 16 ± 8	1340	FRABETTI	93D E687	$\gamma Be, \Lambda_c^+ \rightarrow pK^-\pi^+$
• • • We do not use the following data for averages, fits, limits, etc. • • •				
180 ± 30 ± 30	29	ALVAREZ	90 NA14	$\gamma, \Lambda_c^+ \rightarrow pK^-\pi^+$
200 ± 30 ± 30	90	FRABETTI	90 E687	$\gamma Be, \Lambda_c^+ \rightarrow pK^-\pi^+$
196 ⁺²³ ₋₂₀	101	BARLAG	89 NA32	$pK^-\pi^+$ + c.c.
220 ± 30 ± 20	97	ANJOS	88b E691	$pK^-\pi^+$ + c.c.

WEIGHTED AVERAGE 200±6 (Error scaled by 1.6)



Λ_c^+ DECAY MODES

Nearly all branching fractions of the Λ_c^+ are measured relative to the $pK^-\pi^+$ mode, but there are no model-independent measurements of this branching fraction. We explain how we arrive at our value of $B(\Lambda_c^+ \rightarrow pK^-\pi^+)$ in a Note at the beginning of the branching-ratio measurements, below. When this branching fraction is eventually well determined, all the other branching fractions will slide up or down proportionally as the true value differs from the value we use here.

Mode	Fraction (Γ_i/Γ)	Scale factor/ Confidence level
Hadronic modes with a p: S = -1 final states		
Γ_1 $p\bar{K}^0$	(2.3 ± 0.6) %	
Γ_2 $pK^-\pi^+$	[a] (5.0 ± 1.3) %	
Γ_3 $p\bar{K}^*(892)^0$	[b] (1.6 ± 0.5) %	
Γ_4 $\Delta(1232)^{++}K^-$	(8.6 ± 3.0) $\times 10^{-3}$	
Γ_5 $\Lambda(1520)\pi^+$	[b] (1.8 ± 0.6) %	
Γ_6 $pK^-\pi^+$ nonresonant	(2.8 ± 0.8) %	
Γ_7 $p\bar{K}^0\pi^0$	(3.3 ± 1.0) %	
Γ_8 $p\bar{K}^0\eta$	(1.2 ± 0.4) %	
Γ_9 $p\bar{K}^0\pi^+\pi^-$	(2.6 ± 0.7) %	
Γ_{10} $pK^-\pi^+\pi^0$	(3.4 ± 1.0) %	
Γ_{11} $pK^*(892)^-\pi^+$	[b] (1.1 ± 0.5) %	
Γ_{12} $p(K^-\pi^+)_{\text{nonresonant}}\pi^0$	(3.6 ± 1.2) %	
Γ_{13} $\Delta(1232)\bar{K}^*(892)$	seen	
Γ_{14} $pK^-\pi^+\pi^+\pi^-$	(1.1 ± 0.8) $\times 10^{-3}$	
Γ_{15} $pK^-\pi^+\pi^0\pi^0$	(8 ± 4) $\times 10^{-3}$	
Γ_{16} $pK^-\pi^+3\pi^0$		
Hadronic modes with a p: S = 0 final states		
Γ_{17} $p\pi^+\pi^-$	(3.5 ± 2.0) $\times 10^{-3}$	
Γ_{18} $p f_0(980)$	[b] (2.8 ± 1.9) $\times 10^{-3}$	
Γ_{19} $p\pi^+\pi^+\pi^-\pi^-$	(1.8 ± 1.2) $\times 10^{-3}$	
Γ_{20} pK^+K^-	(7.7 ± 3.5) $\times 10^{-4}$	
Γ_{21} $p\phi$	[b] (8.2 ± 2.7) $\times 10^{-4}$	
Γ_{22} $pK^+K^-\text{non-}\phi$	(3.5 ± 1.7) $\times 10^{-4}$	
Hadronic modes with a hyperon: S = -1 final states		
Γ_{23} $\Lambda\pi^+$	(1.07 ± 0.28) %	
Γ_{24} $\Lambda\pi^+\pi^0$	(3.6 ± 1.3) %	
Γ_{25} $\Lambda\rho^+$	< 5 %	CL=95%
Γ_{26} $\Lambda\pi^+\pi^+\pi^-$	(2.6 ± 0.7) %	
Γ_{27} $\Sigma(1385)^+\pi^+\pi^-, \Sigma^{*+} \rightarrow \Lambda\pi^+$	(7 ± 4) $\times 10^{-3}$	
Γ_{28} $\Sigma(1385)^-\pi^+\pi^+, \Sigma^{*-} \rightarrow \Lambda\pi^+$	(5.5 ± 1.7) $\times 10^{-3}$	
Γ_{29} $\Lambda\pi^+\rho^0$	(1.1 ± 0.5) %	
Γ_{30} $\Sigma(1385)^+\rho^0, \Sigma^{*+} \rightarrow \Lambda\pi^+$	(3.7 ± 3.1) $\times 10^{-3}$	
Γ_{31} $\Lambda\pi^+\pi^+\pi^-\text{nonresonant}$	< 8 $\times 10^{-3}$	CL=90%
Γ_{32} $\Lambda\pi^+\pi^+\pi^-\pi^0\text{total}$	(1.8 ± 0.8) %	
Γ_{33} $\Lambda\pi^+\eta$	[b] (1.8 ± 0.6) %	
Γ_{34} $\Sigma(1385)^+\eta$	[b] (8.5 ± 3.3) $\times 10^{-3}$	
Γ_{35} $\Lambda\pi^+\omega$	[b] (1.2 ± 0.5) %	
Γ_{36} $\Lambda\pi^+\pi^+\pi^-\pi^0, \text{no } \eta \text{ or } \omega$	< 7 $\times 10^{-3}$	CL=90%
Γ_{37} $\Lambda K^+\bar{K}^0$	(4.7 ± 1.5) $\times 10^{-3}$	S=1.2

Baryon Particle Listings

 Λ_c^+

Γ_{38}	$\Xi(1690)^0 K^+, \Xi^{*0} \rightarrow \Lambda \bar{K}^0$	$(1.3 \pm 0.5) \times 10^{-3}$	
Γ_{39}	$\Sigma^0 \pi^+$	$(1.05 \pm 0.28) \%$	
Γ_{40}	$\Sigma^+ \pi^0$	$(1.00 \pm 0.34) \%$	
Γ_{41}	$\Sigma^+ \eta$	$(5.5 \pm 2.3) \times 10^{-3}$	
Γ_{42}	$\Sigma^+ \pi^+ \pi^-$	$(3.6 \pm 1.0) \%$	
Γ_{43}	$\Sigma^+ \rho^0$	< 1.4	CL=95%
Γ_{44}	$\Sigma^- \pi^+ \pi^+$	$(1.7 \pm 0.5) \%$	
Γ_{45}	$\Sigma^0 \pi^+ \pi^0$	$(1.8 \pm 0.8) \%$	
Γ_{46}	$\Sigma^0 \pi^+ \pi^+ \pi^-$	$(8.3 \pm 3.1) \times 10^{-3}$	
Γ_{47}	$\Sigma^+ \pi^+ \pi^- \pi^0$	—	
Γ_{48}	$\Sigma^+ \omega$	[b] $(2.7 \pm 1.0) \%$	
Γ_{49}	$\Sigma^+ K^+ K^-$	$(2.8 \pm 0.8) \times 10^{-3}$	
Γ_{50}	$\Sigma^+ \phi$	[b] $(3.1 \pm 0.9) \times 10^{-3}$	
Γ_{51}	$\Xi(1690)^0 K^+, \Xi^{*0} \rightarrow$	$(8.1 \pm 3.0) \times 10^{-4}$	
Γ_{52}	$\Sigma^+ K^+ K^-$ nonresonant	< 6	CL=90%
Γ_{53}	$\Xi^0 K^+$	$(3.9 \pm 1.4) \times 10^{-3}$	
Γ_{54}	$\Xi^- K^+ \pi^+$	$(5.1 \pm 1.4) \times 10^{-3}$	
Γ_{55}	$\Xi(1530)^0 K^+$	[b] $(2.6 \pm 1.0) \times 10^{-3}$	

Hadronic modes with a hyperon: S = 0 final states

Γ_{56}	ΛK^+	$(5.0 \pm 1.6) \times 10^{-4}$	
Γ_{57}	$\Lambda K^+ \pi^+ \pi^-$	< 4	CL=90%
Γ_{58}	$\Sigma^0 K^+$	$(4.2 \pm 1.3) \times 10^{-4}$	
Γ_{59}	$\Sigma^0 K^+ \pi^+ \pi^-$	< 2.1	CL=90%
Γ_{60}	$\Sigma^+ K^+ \pi^-$	$(1.7 \pm 0.7) \times 10^{-3}$	
Γ_{61}	$\Sigma^+ K^*(892)^0$	[b] $(2.8 \pm 1.1) \times 10^{-3}$	
Γ_{62}	$\Sigma^- K^+ \pi^+$	< 1.0	CL=90%

Doubly Cabibbo-suppressed modes

Γ_{63}	$p K^+ \pi^-$	< 2.3	CL=90%
---------------	---------------	---------	--------

Semileptonic modes

Γ_{64}	$\Lambda \ell^+ \nu_\ell$	[c] $(2.0 \pm 0.6) \%$	
Γ_{65}	$\Lambda e^+ \nu_e$	$(2.1 \pm 0.6) \%$	
Γ_{66}	$\Lambda \mu^+ \nu_\mu$	$(2.0 \pm 0.7) \%$	

Inclusive modes

Γ_{67}	e^+ anything	$(4.5 \pm 1.7) \%$	
Γ_{68}	$p e^+$ anything	$(1.8 \pm 0.9) \%$	
Γ_{69}	Λe^+ anything		
Γ_{70}	p anything	$(50 \pm 16) \%$	
Γ_{71}	p anything (no Λ)	$(12 \pm 19) \%$	
Γ_{72}	p hadrons		
Γ_{73}	n anything	$(50 \pm 16) \%$	
Γ_{74}	n anything (no Λ)	$(29 \pm 17) \%$	
Γ_{75}	Λ anything	$(35 \pm 11) \%$	S=1.4
Γ_{76}	Σ^\pm anything	[d] $(10 \pm 5) \%$	
Γ_{77}	3prongs	$(24 \pm 8) \%$	

 $\Delta C = 1$ weak neutral current (C1) modes, or Lepton number (L) violating modes

Γ_{78}	$p \mu^+ \mu^-$	C1 < 3.4	$\times 10^{-4}$	CL=90%
Γ_{79}	$\Sigma^- \mu^+ \mu^+$	L < 7.0	$\times 10^{-4}$	CL=90%

[a] See the note on " Λ_c^+ Branching Fractions" below.

[b] This branching fraction includes all the decay modes of the final-state resonance.

[c] An ℓ indicates an e or a μ mode, not a sum over these modes.

[d] The value is for the sum of the charge states or particle/antiparticle states indicated.

CONSTRAINED FIT INFORMATION

An overall fit to 18 branching ratios uses 33 measurements and one constraint to determine 12 parameters. The overall fit has a $\chi^2 = 15.5$ for 22 degrees of freedom.

The following *off-diagonal* array elements are the correlation coefficients $\langle \delta x_i \delta x_j \rangle / (\delta x_i \delta x_j)$, in percent, from the fit to the branching fractions, $x_i \equiv \Gamma_i / \Gamma_{\text{total}}$. The fit constrains the x_i whose labels appear in this array to sum to one.

x_{23}	96																				
x_{26}	97	93																			
x_{37}	82	83	80																		
x_{39}	95	98	92	82																	
x_{42}	93	90	91	77	88																
x_{44}	82	79	80	68	78	80															
x_{46}	69	66	70	57	66	65	57														
x_{49}	88	85	86	72	84	93	75	61													
x_{50}	85	82	83	70	81	90	72	59	84												
x_{54}	93	96	90	80	94	87	77	64	82	79											
	x_2	x_{23}	x_{26}	x_{37}	x_{39}	x_{42}	x_{44}	x_{46}	x_{49}	x_{50}											

 Λ_c^+ BRANCHING FRACTIONS

Revised 2002 by P.R. Burchat (Stanford University).

Most Λ_c^+ branching fractions are measured relative to the decay mode $\Lambda_c^+ \rightarrow p K^- \pi^+$. However, there are no completely model-independent measurements of the absolute branching fraction for $\Lambda_c^+ \rightarrow p K^- \pi^+$. Here we describe the measurements that have been used to extract $B(\Lambda_c^+ \rightarrow p K^- \pi^+)$, the model-dependence of the results, and the method we have used to average the results.

ARGUS (ALBRECHT 88C) and CLEO (CRAWFORD 92) measure $B(\bar{B} \rightarrow \Lambda_c^+ X) \cdot B(\Lambda_c^+ \rightarrow p K^- \pi^+)$ to be $(0.30 \pm 0.12 \pm 0.06) \%$ and $(0.273 \pm 0.051 \pm 0.039) \%$. Under the assumptions that decays of \bar{B} mesons to baryons are dominated by $\bar{B} \rightarrow \Lambda_c^+ X$ and that $\Lambda_c^+ X$ final states other than $\Lambda_c^+ \bar{N} X$ can be neglected, they also measure $B(\bar{B} \rightarrow \Lambda_c^+ X)$ to be $(6.8 \pm 0.5 \pm 0.3) \%$ (ALBRECHT 92O) and $(6.4 \pm 0.8 \pm 0.8) \%$ (CRAWFORD 92). Combining these results, we get $B(\Lambda_c^+ \rightarrow p K^- \pi^+) = (4.14 \pm 0.91) \%$. However, the assumption that \bar{B} decay modes to baryons other than $\Lambda_c^+ \bar{N} X$ are negligible is not on solid ground experimentally or theoretically [2]. Therefore, the branching fraction for $\Lambda_c^+ \rightarrow p K^- \pi^+$ given above may be low by some undetermined amount.

A second type of model-dependent determination of $B(\Lambda_c^+ \rightarrow p K^- \pi^+)$ is based on measurements by ARGUS (ALBRECHT 91G) and CLEO (BERGFELD 94) of $\sigma(e^+ e^- \rightarrow \Lambda_c^+ X) \cdot B(\Lambda_c^+ \rightarrow \Lambda \ell^+ \nu_\ell) = (4.15 \pm 1.03 \pm 1.18)$ pb and $(4.77 \pm 0.25 \pm 0.66)$ pb. ARGUS (ALBRECHT 96E) and CLEO (AVERY 91) have also measured $\sigma(e^+ e^- \rightarrow \Lambda_c^+ X) \cdot B(\Lambda_c^+ \rightarrow p K^- \pi^+)$. The weighted average is (11.2 ± 1.3) pb.

From these measurements, we extract $R \equiv B(\Lambda_c^+ \rightarrow p K^- \pi^+) / B(\Lambda_c^+ \rightarrow \Lambda \ell^+ \nu_\ell) = 2.40 \pm 0.43$. We estimate the $\Lambda_c^+ \rightarrow p K^- \pi^+$ branching fraction from the equation

$$B(\Lambda_c^+ \rightarrow p K^- \pi^+) = R f F \frac{\Gamma(D \rightarrow X \ell^+ \nu_\ell)}{1 + |V_{cd}/V_{cs}|^2} \cdot \tau(\Lambda_c^+), \quad (1)$$

where $f = B(\Lambda_c^+ \rightarrow \Lambda \ell^+ \nu_\ell) / B(\Lambda_c^+ \rightarrow X_s \ell^+ \nu_\ell)$ and $F = \Gamma(\Lambda_c^+ \rightarrow X_s \ell^+ \nu_\ell) / \Gamma(D^0 \rightarrow X_s \ell^+ \nu_\ell)$. When we use

Λ_c^+

$1+|V_{cd}/V_{cs}|^2 = 1.05$ and the world averages $\Gamma(D \rightarrow X\ell^+\nu_\ell) = (0.166 \pm 0.006) \times 10^{12} \text{ s}^{-1}$ and $\tau(\Lambda_c^+) = (0.192 \pm 0.005) \times 10^{-12} \text{ s}$, we calculate $B(\Lambda_c^+ \rightarrow pK^-\pi^+) = (7.3 \pm 1.4)\% \cdot fF$. Theoretical estimates for f and F are near 1.0 with significant uncertainties.

So, we have two results with significant model-dependence: $B(\Lambda_c^+ \rightarrow pK^-\pi^+) = (4.14 \pm 0.91)\%$ from \overline{B} decays, and $B(\Lambda_c^+ \rightarrow pK^-\pi^+) = (7.3 \pm 1.4)\% \cdot fF$ from semileptonic Λ_c^+ decays. If we set $fF = 1.0$ in the second result, and assign an uncertainty of 30% to each result to account for the unknown model-dependence, we get the consistent results $B(\Lambda_c^+ \rightarrow pK^-\pi^+) = (4.14 \pm 0.91 \pm 1.24)\%$ and $B(\Lambda_c^+ \rightarrow pK^-\pi^+) = (7.3 \pm 1.4 \pm 2.2)\%$. The weighted average of these two results is $B(\Lambda_c^+ \rightarrow pK^-\pi^+) = (5.0 \pm 1.3)\%$, where the uncertainty contains both the experimental uncertainty and the 30% estimate of model dependence in each result. We assigned the value $(5.0 \pm 1.3)\%$ to the $\Lambda_c^+ \rightarrow pK^-\pi^+$ branching fraction in our 2000 *Review* [1].

A third type of measurement of $B(\Lambda_c^+ \rightarrow pK^-\pi^+)$ has been published by CLEO (JAFPE 00). Under the assumption that a \overline{D} meson and an antiproton in opposite hemispheres is evidence for a Λ_c^+ in the hemisphere of the \overline{p} , the fraction of such $\overline{D}\overline{p}$ events with a $\Lambda_c^+ \rightarrow pK^-\pi^+$ decay can be used to determine the $\Lambda_c^+ \rightarrow pK^-\pi^+$ branching fraction. CLEO measures $B(\Lambda_c^+ \rightarrow pK^-\pi^+) = (5.0 \pm 1.3)\%$, which is coincidentally exactly the same value as our PDG 00 average given above. The quoted uncertainty includes significant contributions from model-dependent effects (*e.g.*, differences between the \overline{p} momentum spectrum in events with a Λ_c^+ and \overline{p} in the same hemisphere, and with a \overline{D} and \overline{p} in opposite hemispheres; extrapolation of the Λ_c^+ and \overline{D} momentum spectrum below the minimum value used for rejecting B decay products; and our limited understanding of backgrounds such as $D\overline{D}N\overline{p}$ events).

We have chosen to continue to assign the value $(5.0 \pm 1.3)\%$ to the $\Lambda_c^+ \rightarrow pK^-\pi^+$ branching fraction (given as PDG 02 below). As was noted earlier, most of the other Λ_c^+ decay modes are measured relative to this mode.

New methods for measuring the Λ_c^+ absolute branching fractions have been proposed [2,3].

References

1. D.E. Groom *et al.* (Particle Data Group), *Review of Particle Physics*, Eur. Phys. J. **C15**, 1 (2000).
2. I. Dunietz, Phys. Rev. **D58**, 094010 (1998).
3. P. Miglioni *et al.*, Phys. Lett. **B462**, 217 (1999).

Λ_c^+ BRANCHING RATIOS

Hadronic modes with a p : $S = -1$ final states

$\Gamma(p\overline{K}^0)/\Gamma(pK^-\pi^+)$		Γ_1/Γ_2		
VALUE	EVTS	DOCUMENT ID	TECN	COMMENT
0.47±0.04 OUR AVERAGE				
0.46±0.02±0.04	1025	ALAM	98 CLE2	$e^+e^- \approx \Upsilon(4S)$
0.44±0.07±0.05	133	AVERY	91 CLEO	$e^+e^- 10.5 \text{ GeV}$
0.55±0.17±0.14	45	ANJOS	90 E691	$\gamma\text{Be } 70\text{--}260 \text{ GeV}$
0.62±0.15±0.03	73	ALBRECHT	88c ARG	$e^+e^- 10 \text{ GeV}$

$\Gamma(pK^-\pi^+)/\Gamma_{\text{total}}$

See the note on " Λ_c^+ Branching Fractions" above.

VALUE	EVTS	DOCUMENT ID	TECN	COMMENT
0.050±0.013 OUR FIT				
0.050±0.013		PDG	02	See note at top of ratios
••• We do not use the following data for averages, fits, limits, etc. •••				
0.050±0.005±0.012	1205	² JAFFE	00 CLE2	$e^+e^- 10.52\text{--}10.58 \text{ GeV}$
0.041±0.010		^{3,4} ALBRECHT	92o ARG	$e^+e^- \approx \Upsilon(4S)$
0.044±0.012		^{3,5} CRAWFORD	92 CLEO	$e^+e^- 10.5 \text{ GeV}$
² JAFFE 00 assumes that a \overline{D} meson and an antiproton in opposite hemispheres tags for a Λ_c^+ in the hemisphere of the \overline{p} . The fraction of such $\overline{D}\overline{p}$ events with a $\Lambda_c^+ \rightarrow pK^-\pi^+$ decay then gives the $pK^-\pi^+$ branching fraction. See the paper for assumptions, caveats, etc.				
³ To extract $\Gamma(pK^-\pi^+)/\Gamma_{\text{total}}$, we use $B(\overline{B} \rightarrow \Lambda_c^+ X) \cdot B(\Lambda_c^+ \rightarrow pK^-\pi^+) = (0.28 \pm 0.06)\%$, which is the average of measurements from ARGUS (ALBRECHT 88c) and CLEO (CRAWFORD 92).				
⁴ ALBRECHT 92o measures $B(\overline{B} \rightarrow \Lambda_c^+ X) = (6.8 \pm 0.5 \pm 0.3)\%$.				
⁵ CRAWFORD 92 measures $B(\overline{B} \rightarrow \Lambda_c^+ X) = (6.4 \pm 0.8 \pm 0.8)\%$.				

$\Gamma(p\overline{K}^*(892)^0)/\Gamma(pK^-\pi^+)$

Unseen decay modes of the $\overline{K}^*(892)^0$ are included.

VALUE	EVTS	DOCUMENT ID	TECN	COMMENT
0.31±0.04 OUR AVERAGE				
0.29±0.04±0.03		⁶ AITALA	00 E791	$\pi^- N, 500 \text{ GeV}$
0.35 $^{+0.06}_{-0.07}$ ±0.03	39	BOZEK	93 NA32	$\pi^- \text{Cu } 230 \text{ GeV}$
0.42±0.24	12	BASILE	81B CNTR	$p\overline{p} \rightarrow \Lambda_c^+ e^- X$
••• We do not use the following data for averages, fits, limits, etc. •••				
0.35±0.11		BARLAG	90D NA32	See BOZEK 93
⁶ AITALA 00 makes a coherent 5-dimensional amplitude analysis of $946 \pm 38 \Lambda_c^+ \rightarrow pK^-\pi^+$ decays.				

$\Gamma(\Delta(1232)^{++}K^-)/\Gamma(pK^-\pi^+)$

VALUE	EVTS	DOCUMENT ID	TECN	COMMENT
0.17±0.04 OUR AVERAGE				Error includes scale factor of 1.1.
0.18±0.03±0.03		⁷ AITALA	00 E791	$\pi^- N, 500 \text{ GeV}$
0.12 $^{+0.04}_{-0.05}$ ±0.05	14	BOZEK	93 NA32	$\pi^- \text{Cu } 230 \text{ GeV}$
0.40±0.17	17	BASILE	81B CNTR	$p\overline{p} \rightarrow \Lambda_c^+ e^- X$
⁷ AITALA 00 makes a coherent 5-dimensional amplitude analysis of $946 \pm 38 \Lambda_c^+ \rightarrow pK^-\pi^+$ decays.				

$\Gamma(\Lambda(1520)\pi^+)/\Gamma(pK^-\pi^+)$

Unseen decay modes of the $\Lambda(1520)$ are included.

VALUE	EVTS	DOCUMENT ID	TECN	COMMENT
0.35±0.08 OUR AVERAGE				
0.34±0.08±0.05		⁸ AITALA	00 E791	$\pi^- N, 500 \text{ GeV}$
0.40 $^{+0.18}_{-0.13}$ ±0.09	12	BOZEK	93 NA32	$\pi^- \text{Cu } 230 \text{ GeV}$
⁸ AITALA 00 makes a coherent 5-dimensional amplitude analysis of $946 \pm 38 \Lambda_c^+ \rightarrow pK^-\pi^+$ decays.				

$\Gamma(pK^-\pi^+ \text{ nonresonant})/\Gamma(pK^-\pi^+)$

VALUE	EVTS	DOCUMENT ID	TECN	COMMENT
0.55±0.06 OUR AVERAGE				
0.55±0.06±0.04		⁹ AITALA	00 E791	$\pi^- N, 500 \text{ GeV}$
0.56 $^{+0.07}_{-0.09}$ ±0.05	71	BOZEK	93 NA32	$\pi^- \text{Cu } 230 \text{ GeV}$
⁹ AITALA 00 makes a coherent 5-dimensional amplitude analysis of $946 \pm 38 \Lambda_c^+ \rightarrow pK^-\pi^+$ decays.				

$\Gamma(p\overline{K}^0\pi^0)/\Gamma(pK^-\pi^+)$

VALUE	EVTS	DOCUMENT ID	TECN	COMMENT
0.66±0.05±0.07	774	ALAM	98 CLE2	$e^+e^- \approx \Upsilon(4S)$

$\Gamma(p\overline{K}^0\eta)/\Gamma(pK^-\pi^+)$

Unseen decay modes of the η are included.

VALUE	EVTS	DOCUMENT ID	TECN	COMMENT
0.25±0.04±0.04	57	AMMAR	95 CLE2	$e^+e^- \approx \Upsilon(4S)$

$\Gamma(p\overline{K}^0\pi^+\pi^-)/\Gamma(pK^-\pi^+)$

VALUE	EVTS	DOCUMENT ID	TECN	COMMENT
0.51±0.06 OUR AVERAGE				
0.52±0.04±0.05	985	ALAM	98 CLE2	$e^+e^- \approx \Upsilon(4S)$
0.43±0.12±0.04	83	AVERY	91 CLEO	$e^+e^- 10.5 \text{ GeV}$
0.98±0.36±0.08	12	BARLAG	90D NA32	$\pi^- 230 \text{ GeV}$

$\Gamma(pK^-\pi^+\pi^0)/\Gamma(pK^-\pi^+)$

VALUE	EVTS	DOCUMENT ID	TECN	COMMENT
0.67±0.04±0.11	2606	ALAM	98 CLE2	$e^+e^- \approx \Upsilon(4S)$

Baryon Particle Listings

 Λ_C^+ $\Gamma(\rho K^*(892)^-\pi^+)/\Gamma(\rho\bar{K}^0\pi^+\pi^-)$ Γ_{11}/Γ_9

Unseen decay modes of the $K^*(892)^-$ are included.

VALUE	EVTS	DOCUMENT ID	TECN	COMMENT
0.44±0.14	17	ALEEV	94	BIS2 nN 20–70 GeV

 $\Gamma(\rho(K^-\pi^+)_{\text{nonresonant}}\pi^0)/\Gamma(\rho K^-\pi^+)$ Γ_{12}/Γ_2

VALUE	EVTS	DOCUMENT ID	TECN	COMMENT
0.73±0.12±0.05	67	BOZEK	93	NA32 π^- Cu 230 GeV

 $\Gamma(\Delta(1232)\bar{K}^*(892))/\Gamma_{\text{total}}$ Γ_{13}/Γ

VALUE	EVTS	DOCUMENT ID	TECN	COMMENT
seen	35	AMENDOLIA	87	SPEC γ Ge-Si

 $\Gamma(\rho K^-\pi^+\pi^-\pi^-)/\Gamma(\rho K^-\pi^+)$ Γ_{14}/Γ_2

VALUE	DOCUMENT ID	TECN	COMMENT
0.022±0.015	BARLAG 90D	NA32	π^- 230 GeV

 $\Gamma(\rho K^-\pi^+\pi^0\pi^0)/\Gamma(\rho K^-\pi^+)$ Γ_{15}/Γ_2

VALUE	EVTS	DOCUMENT ID	TECN	COMMENT
0.16±0.07±0.03	15	BOZEK	93	NA32 π^- Cu 230 GeV

 $\Gamma(\rho K^-\pi^+3\pi^0)/\Gamma(\rho K^-\pi^+)$ Γ_{16}/Γ_2

VALUE	EVTS	DOCUMENT ID	TECN	COMMENT
•••				We do not use the following data for averages, fits, limits, etc. •••
0.10±0.06±0.02	8	BOZEK	93	NA32 π^- Cu 230 GeV

Hadronic modes with a ρ : $S = 0$ final states $\Gamma(\rho\pi^+\pi^-)/\Gamma(\rho K^-\pi^+)$ Γ_{17}/Γ_2

VALUE	DOCUMENT ID	TECN	COMMENT
0.069±0.036	BARLAG 90D	NA32	π^- 230 GeV

 $\Gamma(\rho f_0(980))/\Gamma(\rho K^-\pi^+)$ Γ_{18}/Γ_2

Unseen decay modes of the $f_0(980)$ are included.

VALUE	DOCUMENT ID	TECN	COMMENT
0.055±0.036	BARLAG 90D	NA32	π^- 230 GeV

 $\Gamma(\rho\pi^+\pi^-\pi^-\pi^-)/\Gamma(\rho K^-\pi^+)$ Γ_{19}/Γ_2

VALUE	DOCUMENT ID	TECN	COMMENT
0.036±0.023	BARLAG 90D	NA32	π^- 230 GeV

 $\Gamma(\rho K^+K^-)/\Gamma(\rho K^-\pi^+)$ Γ_{20}/Γ_2

VALUE	EVTS	DOCUMENT ID	TECN	COMMENT
0.015±0.006 OUR AVERAGE				Error includes scale factor of 2.1.
0.014±0.002±0.002	676	ABE	02c	BELL $e^+e^- \approx \Upsilon(4S)$
0.039±0.009±0.007	214	ALEXANDER	96c	CLE2 $e^+e^- \approx \Upsilon(4S)$
•••				We do not use the following data for averages, fits, limits, etc. •••
0.096±0.029±0.010	30	FRABETTI	93H	E687 γ Be, \bar{E}_γ 220 GeV
0.048±0.027		BARLAG	90D	NA32 π^- 230 GeV

 $\Gamma(\rho\phi)/\Gamma(\rho K^-\pi^+)$ Γ_{21}/Γ_2

Unseen decay modes of the ϕ are included.

VALUE	EVTS	DOCUMENT ID	TECN	COMMENT
0.0164±0.0032 OUR AVERAGE				Error includes scale factor of 1.2.
0.015±0.002±0.002	345	ABE	02c	BELL $e^+e^- \approx \Upsilon(4S)$
0.024±0.006±0.003	54	ALEXANDER	96c	CLE2 $e^+e^- \approx \Upsilon(4S)$
•••				We do not use the following data for averages, fits, limits, etc. •••
0.040±0.027		BARLAG	90D	NA32 π^- 230 GeV

 $\Gamma(\rho K^+K^-\text{non-}\phi)/\Gamma(\rho K^-\pi^+)$ Γ_{22}/Γ_2

VALUE	EVTS	DOCUMENT ID	TECN	COMMENT
0.007±0.002±0.002	344	ABE	02c	BELL $e^+e^- \approx \Upsilon(4S)$

Hadronic modes with a hyperon: $S = -1$ final states $\Gamma(\Lambda\pi^+)/\Gamma(\rho K^-\pi^+)$ Γ_{23}/Γ_2

VALUE	CL%	EVTS	DOCUMENT ID	TECN	COMMENT
0.214±0.016 OUR FIT					Error includes scale factor of 1.1.
0.204±0.019 OUR AVERAGE					
0.217±0.013±0.020		750	LINK	05F	FOCS γ nucleus, $\bar{E}_\gamma \approx 180$ GeV
0.18±0.03±0.04			ALBRECHT	92	ARG $e^+e^- \approx 10.4$ GeV
0.18±0.03±0.03		87	AVERY	91	CLEO $e^+e^- \approx 10.5$ GeV
•••					We do not use the following data for averages, fits, limits, etc. •••
<0.33		90	ANJOS	90	E691 γ Be 70–260 GeV
<0.16		90	ALBRECHT	88c	ARG e^+e^- 10 GeV

 $\Gamma(\Lambda\pi^+\pi^0)/\Gamma(\rho K^-\pi^+)$ Γ_{24}/Γ_2

VALUE	EVTS	DOCUMENT ID	TECN	COMMENT
0.73±0.09±0.16	464	AVERY	94	CLE2 $e^+e^- \approx \Upsilon(3S), \Upsilon(4S)$

 $\Gamma(\Lambda\rho^+)/\Gamma(\rho K^-\pi^+)$ Γ_{25}/Γ_2

VALUE	CL%	DOCUMENT ID	TECN	COMMENT	
<0.95		95	AVERY	94	CLE2 $e^+e^- \approx \Upsilon(3S), \Upsilon(4S)$

 $\Gamma(\Lambda\pi^+\pi^-\pi^-)/\Gamma(\rho K^-\pi^+)$ Γ_{26}/Γ_2

VALUE	EVTS	DOCUMENT ID	TECN	COMMENT
0.525±0.032 OUR FIT				
0.522±0.032 OUR AVERAGE				
0.508±0.024±0.024	1356	LINK	05F	FOCS γ nucleus, $\bar{E}_\gamma \approx 180$ GeV
0.65±0.11±0.12	289	AVERY	91	CLEO e^+e^- 10.5 GeV
0.82±0.29±0.27	44	ANJOS	90	E691 γ Be 70–260 GeV
0.94±0.41±0.13	10	BARLAG	90D	NA32 π^- 230 GeV
0.61±0.16±0.04	105	ALBRECHT	88c	ARG e^+e^- 10 GeV

 $\Gamma(\Sigma(1385)^+\pi^+\pi^-, \Sigma^{*+} \rightarrow \Lambda\pi^+)/\Gamma(\Lambda\pi^+\pi^-\pi^-)$ Γ_{27}/Γ_{26}

VALUE	DOCUMENT ID	TECN	COMMENT
0.28±0.10±0.08	LINK	05F	FOCS γ nucleus, $\bar{E}_\gamma \approx 180$ GeV

 $\Gamma(\Sigma(1385)^-\pi^+\pi^+, \Sigma^{*-} \rightarrow \Lambda\pi^-)/\Gamma(\Lambda\pi^+\pi^-\pi^-)$ Γ_{28}/Γ_{26}

VALUE	DOCUMENT ID	TECN	COMMENT
0.21±0.03±0.02	LINK	05F	FOCS γ nucleus, $\bar{E}_\gamma \approx 180$ GeV

 $\Gamma(\Lambda\pi^+\rho^0)/\Gamma(\Lambda\pi^+\pi^-\pi^-)$ Γ_{29}/Γ_{26}

VALUE	DOCUMENT ID	TECN	COMMENT
0.40±0.12±0.12	LINK	05F	FOCS γ nucleus, $\bar{E}_\gamma \approx 180$ GeV

 $\Gamma(\Sigma(1385)^+\rho^0, \Sigma^{*+} \rightarrow \Lambda\pi^+)/\Gamma(\Lambda\pi^+\pi^-\pi^-)$ Γ_{30}/Γ_{26}

VALUE	DOCUMENT ID	TECN	COMMENT
0.14±0.09±0.07	LINK	05F	FOCS γ nucleus, $\bar{E}_\gamma \approx 180$ GeV

 $\Gamma(\Lambda\pi^+\pi^-\pi^- \text{nonresonant})/\Gamma(\Lambda\pi^+\pi^-\pi^-)$ Γ_{31}/Γ_{26}

VALUE	CL%	DOCUMENT ID	TECN	COMMENT	
<0.3		90	LINK	05F	FOCS γ nucleus, $\bar{E}_\gamma \approx 180$ GeV

 $\Gamma(\rho\bar{K}^0\pi^+\pi^-)/\Gamma(\Lambda\pi^+\pi^-\pi^-)$ Γ_9/Γ_{26}

VALUE	EVTS	DOCUMENT ID	TECN	COMMENT
•••				We do not use the following data for averages, fits, limits, etc. •••
2.6±1.2		ALEEV	96	SPEC n nucleus, 50 GeV/c
4.3±1.2	130	ALEEV	84	BIS2 n C 40–70 GeV

 $\Gamma(\Lambda\pi^+\pi^-\pi^0 \text{total})/\Gamma(\rho K^-\pi^+)$ Γ_{32}/Γ_2

VALUE	EVTS	DOCUMENT ID	TECN	COMMENT
0.36±0.09±0.09	50	10	CRONIN-HEN..03	CLE3 $e^+e^- \approx \Upsilon(4S)$
				¹⁰ CRONIN-HENNESSY 03 finds this channel to be dominantly $\Lambda\eta\pi^+$ and $\Lambda\omega\pi^+$; see below.

 $\Gamma(\Lambda\pi^+\eta)/\Gamma(\rho K^-\pi^+)$ Γ_{33}/Γ_2

Unseen decay modes of the η are included.

VALUE	EVTS	DOCUMENT ID	TECN	COMMENT
0.36±0.07 OUR AVERAGE				
0.41±0.17±0.10	11	CRONIN-HEN..03	CLE3	$e^+e^- \approx \Upsilon(4S)$
0.35±0.05±0.06	116	AMMAR	95	CLE2 $e^+e^- \approx \Upsilon(4S)$

 $\Gamma(\Sigma(1385)^+\eta)/\Gamma(\rho K^-\pi^+)$ Γ_{34}/Γ_2

Unseen decay modes of the $\Sigma(1385)^+$ and η are included.

VALUE	EVTS	DOCUMENT ID	TECN	COMMENT
0.17±0.04±0.03	54	AMMAR	95	CLE2 $e^+e^- \approx \Upsilon(4S)$

 $\Gamma(\Lambda\pi^+\omega)/\Gamma(\rho K^-\pi^+)$ Γ_{35}/Γ_2

Unseen decay modes of the ω are included.

VALUE	EVTS	DOCUMENT ID	TECN	COMMENT
0.24±0.06±0.06	32	CRONIN-HEN..03	CLE3	$e^+e^- \approx \Upsilon(4S)$

 $\Gamma(\Lambda\pi^+\pi^-\pi^0, \text{no } \eta \text{ or } \omega)/\Gamma(\rho K^-\pi^+)$ Γ_{36}/Γ_2

VALUE	CL%	DOCUMENT ID	TECN	COMMENT
<0.13		90	CRONIN-HEN..03	CLE3 $e^+e^- \approx \Upsilon(4S)$

 $\Gamma(\Lambda K^+\bar{K}^0)/\Gamma(\rho K^-\pi^+)$ Γ_{37}/Γ_2

VALUE	EVTS	DOCUMENT ID	TECN	COMMENT
0.093±0.018 OUR FIT				Error includes scale factor of 1.7.
0.131±0.020 OUR AVERAGE				
0.142±0.018±0.022	251	LINK	05F	FOCS γ nucleus, $\bar{E}_\gamma \approx 180$ GeV
0.12±0.02±0.02	59	AMMAR	95	CLE2 $e^+e^- \approx \Upsilon(4S)$

 $\Gamma(\Xi(1690)^0 K^+, \Xi^{*0} \rightarrow \Lambda\bar{K}^0)/\Gamma(\Lambda K^+\bar{K}^0)$ Γ_{38}/Γ_{37}

VALUE	EVTS	DOCUMENT ID	TECN	COMMENT
0.28±0.07 OUR AVERAGE				
0.32±0.10±0.04	84±24	LINK	05F	FOCS γ nucleus, $\bar{E}_\gamma \approx 180$ GeV
0.26±0.08±0.03	93	ABE	02c	BELL $e^+e^- \approx \Upsilon(4S)$

 $\Gamma(\Lambda K^+\bar{K}^0)/\Gamma(\Lambda\pi^+)$ Γ_{37}/Γ_{23}

VALUE	EVTS	DOCUMENT ID	TECN	COMMENT
0.43±0.08 OUR FIT				Error includes scale factor of 2.0.
0.395±0.026±0.036	460±30	AUBERT	07U	BABR $e^+e^- \approx \Upsilon(4S)$

$\Gamma(\Sigma^0 \pi^+)/\Gamma(\rho K^- \pi^+)$ Γ_{39}/Γ_2

VALUE	EVTS	DOCUMENT ID	TECN	COMMENT
0.210±0.018 OUR FIT				
0.20 ±0.04 OUR AVERAGE				
0.21 ±0.02 ±0.04	196	AVERY	94	CLE2 $e^+ e^- \approx \Upsilon(3S), \Upsilon(4S)$
0.17 ±0.06 ±0.04		ALBRECHT	92	ARG $e^+ e^- \approx 10.4$ GeV

$\Gamma(\Sigma^0 \pi^+)/\Gamma(\Lambda \pi^+)$ Γ_{39}/Γ_{23}

VALUE	EVTS	DOCUMENT ID	TECN	COMMENT
0.98 ±0.05 OUR FIT				
0.98 ±0.05 OUR AVERAGE				
0.977±0.015±0.051	33k	AUBERT	07u	BABR $e^+ e^- \approx \Upsilon(4S)$
1.09 ±0.11 ±0.19	750	LINK	05F	FOCS γ nucleus, $\bar{E}_\gamma \approx 180$ GeV

$\Gamma(\Sigma^+ \pi^0)/\Gamma(\rho K^- \pi^+)$ Γ_{40}/Γ_2

VALUE	EVTS	DOCUMENT ID	TECN	COMMENT
0.20±0.03±0.03	93	KUBOTA	93	CLE2 $e^+ e^- \approx \Upsilon(4S)$

$\Gamma(\Sigma^+ \eta)/\Gamma(\rho K^- \pi^+)$ Γ_{41}/Γ_2

Unseen decay modes of the η are included.

VALUE	EVTS	DOCUMENT ID	TECN	COMMENT
0.11±0.03±0.02	26	AMMAR	95	CLE2 $e^+ e^- \approx \Upsilon(4S)$

$\Gamma(\Sigma^+ \pi^+ \pi^-)/\Gamma(\rho K^- \pi^+)$ Γ_{42}/Γ_2

VALUE	EVTS	DOCUMENT ID	TECN	COMMENT
0.72±0.07 OUR FIT				
0.69±0.08 OUR AVERAGE				
0.72±0.14	47 ± 9	VAZQUEZ-JA...	08	SELX Σ^- nucleus, 600 GeV
0.74±0.07±0.09	487	KUBOTA	93	CLE2 $e^+ e^- \approx \Upsilon(4S)$
0.54 ^{+0.18} _{-0.15}	11	BARLAG	92	NA32 π^- Cu 230 GeV

$\Gamma(\Sigma^+ \rho^0)/\Gamma(\rho K^- \pi^+)$ Γ_{43}/Γ_2

VALUE	CL%	DOCUMENT ID	TECN	COMMENT
<0.27	95	KUBOTA	93	CLE2 $e^+ e^- \approx \Upsilon(4S)$

$\Gamma(\Sigma^- \pi^+ \pi^+)/\Gamma(\rho K^- \pi^+)$ Γ_{44}/Γ_2

VALUE	EVTS	DOCUMENT ID	TECN	COMMENT
0.33 ±0.06 OUR FIT				
0.314±0.067	30 ± 6	VAZQUEZ-JA...	08	SELX Σ^- nucleus, 600 GeV

$\Gamma(\Sigma^- \pi^+ \pi^+)/\Gamma(\Sigma^+ \pi^+ \pi^-)$ Γ_{44}/Γ_{42}

VALUE	EVTS	DOCUMENT ID	TECN	COMMENT
0.46±0.09 OUR FIT				
0.53±0.15±0.07	56	FRABETTI	94E	E687 γ Be, \bar{E}_γ 220 GeV

$\Gamma(\Sigma^0 \pi^+ \pi^0)/\Gamma(\rho K^- \pi^+)$ Γ_{45}/Γ_2

VALUE	EVTS	DOCUMENT ID	TECN	COMMENT
0.36±0.09±0.10	117	AVERY	94	CLE2 $e^+ e^- \approx \Upsilon(3S), \Upsilon(4S)$

$\Gamma(\Sigma^0 \pi^+ \pi^+ \pi^-)/\Gamma(\rho K^- \pi^+)$ Γ_{46}/Γ_2

VALUE	EVTS	DOCUMENT ID	TECN	COMMENT
0.17±0.04 OUR FIT				
0.21±0.05±0.05	90	AVERY	94	CLE2 $e^+ e^- \approx \Upsilon(3S), \Upsilon(4S)$

$\Gamma(\Sigma^0 \pi^+ \pi^+ \pi^-)/\Gamma(\Lambda \pi^+ \pi^+ \pi^-)$ Γ_{46}/Γ_{26}

VALUE	EVTS	DOCUMENT ID	TECN	COMMENT
0.31±0.08 OUR FIT				
0.26±0.06±0.09	480	LINK	05F	FOCS γ nucleus, $\bar{E}_\gamma \approx 180$ GeV

$\Gamma(\Sigma^+ \omega)/\Gamma(\rho K^- \pi^+)$ Γ_{48}/Γ_2

Unseen decay modes of the ω are included.

VALUE	EVTS	DOCUMENT ID	TECN	COMMENT
0.54±0.13±0.06	107	KUBOTA	93	CLE2 $e^+ e^- \approx \Upsilon(4S)$

$\Gamma(\Sigma^+ K^+ K^-)/\Gamma(\rho K^- \pi^+)$ Γ_{49}/Γ_2

VALUE	EVTS	DOCUMENT ID	TECN	COMMENT
0.056±0.008 OUR FIT				
0.070±0.011±0.011	59	AVERY	93	CLE2 $e^+ e^- \approx 10.5$ GeV

$\Gamma(\Sigma^+ K^+ K^-)/\Gamma(\Sigma^+ \pi^+ \pi^-)$ Γ_{49}/Γ_{42}

VALUE	EVTS	DOCUMENT ID	TECN	COMMENT
0.078±0.009 OUR FIT				
0.074±0.009 OUR AVERAGE				
0.076±0.007±0.009	246	ABE	02c	BELL $e^+ e^- \approx \Upsilon(4S)$
0.071±0.011±0.011	103	LINK	02g	FOCS γ nucleus, ≈ 180 GeV

$\Gamma(\Sigma^+ \phi)/\Gamma(\rho K^- \pi^+)$ Γ_{50}/Γ_2

Unseen decay modes of the ϕ are included.

VALUE	EVTS	DOCUMENT ID	TECN	COMMENT
0.062±0.010 OUR FIT				
0.069±0.023±0.016	26	AVERY	93	CLE2 $e^+ e^- \approx 10.5$ GeV

$\Gamma(\Sigma^+ \phi)/\Gamma(\Sigma^+ \pi^+ \pi^-)$ Γ_{50}/Γ_{42}

Unseen decay modes of the ϕ are included.

VALUE	EVTS	DOCUMENT ID	TECN	COMMENT
0.087±0.012 OUR FIT				
0.086±0.012 OUR AVERAGE				
0.085±0.012±0.012	129	ABE	02c	BELL $e^+ e^- \approx \Upsilon(4S)$
0.087±0.016±0.006	57	LINK	02g	FOCS γ nucleus, ≈ 180 GeV

$\Gamma(\Xi(1690)^0 K^+, \Xi^{*0} \rightarrow \Sigma^+ K^-)/\Gamma(\Sigma^+ \pi^+ \pi^-)$ Γ_{51}/Γ_{42}

VALUE	EVTS	DOCUMENT ID	TECN	COMMENT
0.023±0.005 OUR AVERAGE				
0.023±0.005±0.005	75	ABE	02c	BELL $e^+ e^- \approx \Upsilon(4S)$
0.022±0.006±0.006	34	LINK	02g	FOCS γ nucleus, ≈ 180 GeV

$\Gamma(\Sigma^+ K^+ K^- \text{ nonresonant})/\Gamma(\Sigma^+ \pi^+ \pi^-)$ Γ_{52}/Γ_{42}

VALUE	CL%	DOCUMENT ID	TECN	COMMENT
<0.018	90	ABE	02c	BELL $e^+ e^- \approx \Upsilon(4S)$
••• We do not use the following data for averages, fits, limits, etc. •••				
<0.028	90	LINK	02g	FOCS γ nucleus, ≈ 180 GeV

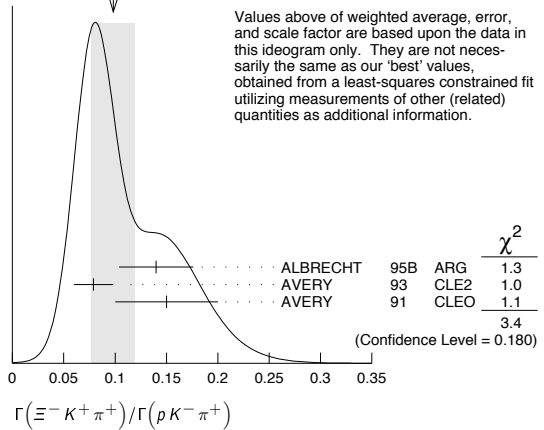
$\Gamma(\Xi^0 K^+)/\Gamma(\rho K^- \pi^+)$ Γ_{53}/Γ_2

VALUE	EVTS	DOCUMENT ID	TECN	COMMENT
0.078±0.013±0.013	56	AVERY	93	CLE2 $e^+ e^- \approx 10.5$ GeV

$\Gamma(\Xi^- K^+ \pi^+)/\Gamma(\rho K^- \pi^+)$ Γ_{54}/Γ_2

VALUE	EVTS	DOCUMENT ID	TECN	COMMENT
0.102±0.010 OUR FIT				Error includes scale factor of 1.1.
0.098±0.021 OUR AVERAGE				Error includes scale factor of 1.3. See the ideogram below.
0.14 ±0.03 ±0.02	34	ALBRECHT	95b	ARG $e^+ e^- \approx 10.4$ GeV
0.079±0.013±0.014	60	AVERY	93	CLE2 $e^+ e^- \approx 10.5$ GeV
0.15 ±0.04 ±0.03	30	AVERY	91	CLEO $e^+ e^- 10.5$ GeV

WEIGHTED AVERAGE
0.098±0.021 (Error scaled by 1.3)



$\Gamma(\Xi(1530)^0 K^+)/\Gamma(\rho K^- \pi^+)$ Γ_{55}/Γ_2

Unseen decay modes of the $\Xi(1530)^0$ are included.

VALUE	EVTS	DOCUMENT ID	TECN	COMMENT
0.052±0.014 OUR AVERAGE				
0.05 ±0.02 ±0.01	11	ALBRECHT	95b	ARG $e^+ e^- \approx 10.4$ GeV
0.053±0.016±0.010	24	AVERY	93	CLE2 $e^+ e^- \approx 10.5$ GeV

$\Gamma(\Xi^- K^+ \pi^+)/\Gamma(\Lambda \pi^+)$ Γ_{54}/Γ_{23}

VALUE	EVTS	DOCUMENT ID	TECN	COMMENT
0.47 ±0.04 OUR FIT				
0.480±0.016±0.039	2665 ± 84	AUBERT	07u	BABR $e^+ e^- \approx \Upsilon(4S)$

Hadronic modes with a hyperon: S = 0 final states

$\Gamma(\Lambda K^+)/\Gamma(\Lambda \pi^+)$ Γ_{56}/Γ_{23}

VALUE	EVTS	DOCUMENT ID	TECN	COMMENT
0.047±0.009 OUR AVERAGE				Error includes scale factor of 1.8.
0.044±0.004±0.003	1162 ± 101	AUBERT	07u	BABR $e^+ e^- \approx \Upsilon(4S)$
0.074±0.010±0.012	265	ABE	02c	BELL $e^+ e^- \approx \Upsilon(4S)$

$\Gamma(\Lambda K^+ \pi^+ \pi^-)/\Gamma(\Lambda \pi^+)$ Γ_{57}/Γ_{23}

VALUE	CL%	DOCUMENT ID	TECN	COMMENT
<4.1 × 10⁻²	90	AUBERT	07u	BABR $e^+ e^- \approx \Upsilon(4S)$

$\Gamma(\Sigma^0 K^+)/\Gamma(\Sigma^0 \pi^+)$ Γ_{58}/Γ_{39}

VALUE	EVTS	DOCUMENT ID	TECN	COMMENT
0.040±0.006 OUR AVERAGE				
0.038±0.005±0.003	366 ± 52	AUBERT	07u	BABR $e^+ e^- \approx \Upsilon(4S)$
0.056±0.014±0.008	75	ABE	02c	BELL $e^+ e^- \approx \Upsilon(4S)$

Baryon Particle Listings

 Λ_c^+

$\Gamma(\Sigma^0 K^+ \pi^+ \pi^-)/\Gamma(\Sigma^0 \pi^+)$		Γ_{59}/Γ_{39}	
VALUE	CL%	DOCUMENT ID	TECN COMMENT
$<2.0 \times 10^{-2}$	90	AUBERT	07u BABR $e^+ e^- \approx \Upsilon(4S)$

$\Gamma(\Sigma^+ K^+ \pi^-)/\Gamma(\Sigma^+ \pi^+ \pi^-)$		Γ_{60}/Γ_{42}	
VALUE	EVTS	DOCUMENT ID	TECN COMMENT
$0.047 \pm 0.011 \pm 0.008$	105	ABE	02c BELL $e^+ e^- \approx \Upsilon(4S)$

$\Gamma(\Sigma^+ K^*(892)^0)/\Gamma(\Sigma^+ \pi^+ \pi^-)$		Γ_{61}/Γ_{42}	
VALUE	EVTS	DOCUMENT ID	TECN COMMENT
$0.078 \pm 0.018 \pm 0.013$	49	LINK	02g FOCS γ nucleus, ≈ 180 GeV

Unseen decay modes of the $K^*(892)^0$ are included.

$\Gamma(\Sigma^- K^+ \pi^+)/\Gamma(\Sigma^+ K^*(892)^0)$		Γ_{62}/Γ_{61}	
VALUE	CL%	DOCUMENT ID	TECN COMMENT
<0.35	90	LINK	02g FOCS γ nucleus, ≈ 180 GeV

Doubly Cabibbo-suppressed modes

$\Gamma(p K^+ \pi^-)/\Gamma(p K^- \pi^+)$		Γ_{63}/Γ_{2}	
VALUE	CL%	DOCUMENT ID	TECN COMMENT
<0.0046	90	LINK	05k FOCS $R = (0.05 \pm 0.26 \pm 0.02)\%$

Semileptonic modes

$\Gamma(\Lambda e^+ \nu_e)/\Gamma(p K^- \pi^+)$		Γ_{64}/Γ_2	
VALUE	EVTS	DOCUMENT ID	COMMENT
0.41 ± 0.05 OUR AVERAGE			
0.42 ± 0.07		PDG	02 Our $\Gamma(\Lambda e^+ \nu_e)/\Gamma(p K^- \pi^+)$
0.39 ± 0.08		PDG	02 Our $\Gamma(\Lambda \mu^+ \nu_\mu)/\Gamma(p K^- \pi^+)$

We average here the averages of the next two data blocks.

$\Gamma(\Lambda e^+ \nu_e)/\Gamma(p K^- \pi^+)$		Γ_{65}/Γ_2	
VALUE	EVTS	DOCUMENT ID	TECN COMMENT
0.42 ± 0.07 OUR AVERAGE			
0.43 ± 0.08	11,12	BERGFELD	94 CLE2 $e^+ e^- \approx \Upsilon(4S)$
0.38 ± 0.14	12,13	ALBRECHT	91g ARG $e^+ e^- \approx 10.4$ GeV

¹¹ BERGFELD 94 measures $\sigma(e^+ e^- \rightarrow \Lambda_c^+ X) \cdot B(\Lambda_c^+ \rightarrow \Lambda e^+ \nu_e) = (4.87 \pm 0.28 \pm 0.69)$ pb.

¹² To extract $\Gamma(\Lambda_c^+ \rightarrow \Lambda e^+ \nu_e)/\Gamma(\Lambda_c^+ \rightarrow p K^- \pi^+)$, we use $\sigma(e^+ e^- \rightarrow \Lambda_c^+ X) \cdot B(\Lambda_c^+ \rightarrow p K^- \pi^+) = (11.2 \pm 1.3)$ pb, which is the weighted average of measurements from ARGUS (ALBRECHT 96e) and CLEO (AVERY 91).

¹³ ALBRECHT 91g measures $\sigma(e^+ e^- \rightarrow \Lambda_c^+ X) \cdot B(\Lambda_c^+ \rightarrow \Lambda e^+ \nu_e) = (4.20 \pm 1.28 \pm 0.71)$ pb.

$\Gamma(\Lambda \mu^+ \nu_\mu)/\Gamma(p K^- \pi^+)$		Γ_{66}/Γ_2	
VALUE	EVTS	DOCUMENT ID	TECN COMMENT
0.39 ± 0.08 OUR AVERAGE			
0.40 ± 0.09	14,15	BERGFELD	94 CLE2 $e^+ e^- \approx \Upsilon(4S)$
0.35 ± 0.20	15,16	ALBRECHT	91g ARG $e^+ e^- \approx 10.4$ GeV

¹⁴ BERGFELD 94 measures $\sigma(e^+ e^- \rightarrow \Lambda_c^+ X) \cdot B(\Lambda_c^+ \rightarrow \Lambda \mu^+ \nu_\mu) = (4.43 \pm 0.51 \pm 0.64)$ pb.

¹⁵ To extract $\Gamma(\Lambda_c^+ \rightarrow \Lambda \mu^+ \nu_\mu)/\Gamma(\Lambda_c^+ \rightarrow p K^- \pi^+)$, we use $\sigma(e^+ e^- \rightarrow \Lambda_c^+ X) \cdot B(\Lambda_c^+ \rightarrow p K^- \pi^+) = (11.2 \pm 1.3)$ pb, which is the weighted average of measurements from ARGUS (ALBRECHT 96e) and CLEO (AVERY 91).

¹⁶ ALBRECHT 91g measures $\sigma(e^+ e^- \rightarrow \Lambda_c^+ X) \cdot B(\Lambda_c^+ \rightarrow \Lambda \mu^+ \nu_\mu) = (3.91 \pm 2.02 \pm 0.90)$ pb.

Inclusive modes

$\Gamma(e^+ \text{ anything})/\Gamma_{\text{total}}$		Γ_{67}/Γ	
VALUE	CL%	DOCUMENT ID	TECN COMMENT
0.045 ± 0.017		VELLA	82 MRK2 $e^+ e^-$ 4.5–6.8 GeV

$\Gamma(p e^+ \text{ anything})/\Gamma_{\text{total}}$		Γ_{68}/Γ	
VALUE	CL%	DOCUMENT ID	TECN COMMENT
0.018 ± 0.009		17 VELLA	82 MRK2 $e^+ e^-$ 4.5–6.8 GeV

¹⁷ VELLA 82 includes protons from Λ decay.

$\Gamma(\Lambda e^+ \text{ anything})/\Gamma_{\text{total}}$		Γ_{69}/Γ	
VALUE	CL%	DOCUMENT ID	TECN COMMENT
0.011 ± 0.008		18 VELLA	82 MRK2 $e^+ e^-$ 4.5–6.8 GeV

¹⁸ VELLA 82 includes Λ 's from Σ^0 decay.

$\Gamma(p \text{ anything})/\Gamma_{\text{total}}$		Γ_{70}/Γ	
VALUE	CL%	DOCUMENT ID	TECN COMMENT
$0.50 \pm 0.08 \pm 0.14$		19 CRAWFORD	92 CLEO $e^+ e^-$ 10.5 GeV

¹⁹ This CRAWFORD 92 value includes protons from Λ decay. The value is model dependent, but account is taken of this in the systematic error.

$\Gamma(p \text{ anything (no } \Lambda))/\Gamma_{\text{total}}$		Γ_{71}/Γ	
VALUE	CL%	DOCUMENT ID	TECN COMMENT
$0.12 \pm 0.10 \pm 0.16$		CRAWFORD	92 CLEO $e^+ e^-$ 10.5 GeV

$\Gamma(n \text{ anything})/\Gamma_{\text{total}}$		Γ_{73}/Γ	
VALUE	CL%	DOCUMENT ID	TECN COMMENT
$0.50 \pm 0.08 \pm 0.14$		20 CRAWFORD	92 CLEO $e^+ e^-$ 10.5 GeV

²⁰ This CRAWFORD 92 value includes neutrons from Λ decay. The value is model dependent, but account is taken of this in the systematic error.

$\Gamma(n \text{ anything (no } \Lambda))/\Gamma_{\text{total}}$		Γ_{74}/Γ	
VALUE	CL%	DOCUMENT ID	TECN COMMENT
$0.29 \pm 0.09 \pm 0.15$		CRAWFORD	92 CLEO $e^+ e^-$ 10.5 GeV

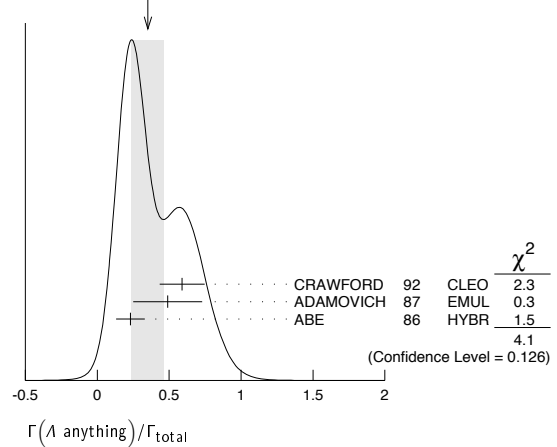
$\Gamma(p \text{ hadrons})/\Gamma_{\text{total}}$		Γ_{72}/Γ	
VALUE	CL%	DOCUMENT ID	TECN COMMENT
0.41 ± 0.24		ADAMOVICH	87 EMUL γ A 20–70 GeV/c

••• We do not use the following data for averages, fits, limits, etc. •••

$\Gamma(\Lambda \text{ anything})/\Gamma_{\text{total}}$		Γ_{75}/Γ	
VALUE	EVTS	DOCUMENT ID	TECN COMMENT
0.35 ± 0.11 OUR AVERAGE			Error includes scale factor of 1.4. See the ideogram below.
$0.59 \pm 0.10 \pm 0.12$		CRAWFORD	92 CLEO $e^+ e^-$ 10.5 GeV
0.49 ± 0.24		ADAMOVICH	87 EMUL γ A 20–70 GeV/c
0.23 ± 0.10	8	21 ABE	86 HYBR 20 GeV γ p

²¹ ABE 86 includes Λ 's from Σ^0 decay.

WEIGHTED AVERAGE
0.35±0.11 (Error scaled by 1.4)



$\Gamma(\Sigma^\pm \text{ anything})/\Gamma_{\text{total}}$		Γ_{76}/Γ	
VALUE	EVTS	DOCUMENT ID	TECN COMMENT
0.1 ± 0.05	5	ABE	86 HYBR 20 GeV γ p

$\Gamma(3\text{prongs})/\Gamma_{\text{total}}$		Γ_{77}/Γ	
VALUE	EVTS	DOCUMENT ID	TECN COMMENT
$0.24 \pm 0.07 \pm 0.04$		KAYIS-TOPAK.03	CHRS ν_μ emulsion, $\bar{E}=27$ GeV

Rare or forbidden modes

$\Gamma(p \mu^+ \mu^-)/\Gamma_{\text{total}}$		Γ_{78}/Γ	
VALUE	CL%	DOCUMENT ID	TECN COMMENT
$<3.4 \times 10^{-4}$	90	0	KODA MA 95 E653 π^- emulsion 600 GeV

A test for the $\Delta C=1$ weak neutral current. Allowed by higher-order electroweak interactions.

$\Gamma(\Sigma^- \mu^+ \mu^-)/\Gamma_{\text{total}}$		Γ_{79}/Γ	
VALUE	CL%	DOCUMENT ID	TECN COMMENT
$<7.0 \times 10^{-4}$	90	0	KODA MA 95 E653 π^- emulsion 600 GeV

A test of lepton-number conservation.

 Λ_c^+ DECAY PARAMETERS

See the note on "Baryon Decay Parameters" in the neutron Listings.

α FOR $\Lambda_c^+ \rightarrow \Lambda \pi^+$			
VALUE	EVTS	DOCUMENT ID	TECN COMMENT
-0.91 ± 0.15 OUR AVERAGE			
$-0.78 \pm 0.16 \pm 0.19$		LINK	06A FOCS γ A, $\bar{E}_\gamma \approx 180$ GeV
$-0.94 \pm 0.21 \pm 0.12$	414	22 BISHAI	95 CLE2 $e^+ e^- \approx \Upsilon(4S)$
-0.96 ± 0.42		ALBRECHT	92 ARG $e^+ e^- \approx 10.4$ GeV
-1.1 ± 0.4	86	AVERY	90b CLEO $e^+ e^- \approx 10.6$ GeV

²² BISHAI 95 actually gives $\alpha = -0.94 \pm 0.21 \pm 0.12$ limit -1.0 . However, for $\alpha \approx -1.0$, some experiments should get unphysical values ($\alpha < -1.0$), and for averaging with other measurements such values (or errors that extend below -1.0) should not be chopped.

α FOR $\Lambda_c^+ \rightarrow \Sigma^+ \pi^0$

VALUE	EVTS	DOCUMENT ID	TECN	COMMENT
$-0.45 \pm 0.31 \pm 0.06$	89	BISHAI	95	CLE2 $e^+e^- \approx \gamma(4S)$

 α FOR $\Lambda_c^+ \rightarrow \Lambda e^+ \nu_e$

The experiments don't cover the complete (or same incomplete) $M(\Lambda e^+)$ range, but we average them together anyway.

VALUE	EVTS	DOCUMENT ID	TECN	COMMENT
-0.86 ± 0.04 OUR AVERAGE				
$-0.86 \pm 0.03 \pm 0.02$	3201	23 HINSON	05	CLEO $e^+e^- \approx \gamma(4S)$
$-0.91 \pm 0.42 \pm 0.25$		24 ALBRECHT	94B	ARG $e^+e^- \approx 10$ GeV
$-0.82 \pm 0.09 \pm 0.06$ $-0.06 - 0.03$	700	25 CRAWFORD	95	CLE2 See HINSON 05
$-0.89 \pm 0.17 \pm 0.09$ $-0.11 - 0.05$	350	26 BERGFELD	94	CLE2 See CRAWFORD 95

- • • We do not use the following data for averages, fits, limits, etc. • • •
- 23 HINSON 05 measures the form-factor ratio $R \equiv f_2/f_1$ for $\Lambda_c^+ \rightarrow \Lambda e^+ \nu_e$ events to be $-0.31 \pm 0.05 \pm 0.04$ and the pole mass to be $2.21 \pm 0.08 \pm 0.14$ GeV/c², and from these calculates α , averaged over q^2 , where $\langle q^2 \rangle = 0.67$ (GeV/c)².
- 24 ALBRECHT 94B uses Λe^+ and $\Lambda \mu^+$ events in the mass range $1.85 < M(\Lambda e^+) < 2.20$ GeV.
- 25 CRAWFORD 95 measures the form-factor ratio $R \equiv f_2/f_1$ for $\Lambda_c^+ \rightarrow \Lambda e^+ \nu_e$ events to be $-0.25 \pm 0.14 \pm 0.08$ and from this calculates α , averaged over q^2 , to be the above.
- 26 BERGFELD 94 uses Λe^+ events.

 $\Lambda_c^+, \bar{\Lambda}_c^-$ CP-VIOLATING DECAY ASYMMETRIES $(\alpha + \bar{\alpha})/(\alpha - \bar{\alpha})$ in $\Lambda_c^+ \rightarrow \Lambda \pi^+, \bar{\Lambda}_c^- \rightarrow \bar{\Lambda} \pi^-$

This is zero if CP is conserved.

VALUE	DOCUMENT ID	TECN	COMMENT
$-0.07 \pm 0.19 \pm 0.24$	LINK	06A	FOCS $\gamma A, \bar{E}_\gamma \approx 180$ GeV

 $(\alpha + \bar{\alpha})/(\alpha - \bar{\alpha})$ in $\Lambda_c^+ \rightarrow \Lambda e^+ \nu_e, \bar{\Lambda}_c^- \rightarrow \bar{\Lambda} e^- \bar{\nu}_e$

This is zero if CP is conserved.

VALUE	DOCUMENT ID	TECN	COMMENT
$0.00 \pm 0.03 \pm 0.02$	HINSON	05	CLEO $e^+e^- \approx \gamma(4S)$

 Λ_c^+ REFERENCES

We have omitted some papers that have been superseded by later experiments. The omitted papers may be found in our 1992 edition (Physical Review D45, 1 June, Part II) or in earlier editions.

VÁZQUEZ-JA...	08	PL B666 299	E. Vázquez-Jauregui et al.	(SLEX Collab.)
AUBERT	07U	PL D75 052002	B. Aubert et al.	(BABAR Collab.)
LINK	06A	PL B634 165	J.M. Link et al.	(FNAL FOCUS Collab.)
AUBERT,B	05S	PL D72 052006	B. Aubert et al.	(BABAR Collab.)
HINSON	05	PRL 94 191801	J.W. Hinson et al.	(CLEO Collab.)
LINK	05F	PL B624 22	J.M. Link et al.	(FNAL FOCUS Collab.)
LINK	05K	PL B624 166	J.M. Link et al.	(FNAL FOCUS Collab.)
CRONIN-HE...	03	PR D67 012001	D. Cronin-Hennessy et al.	(CLEO Collab.)
KAYIS-TOPAK...	03	PL B555 156	A. Kayis-Topaksu et al.	(CERN CHORUS Collab.)
ABE	02C	PL B524 33	K. Abe et al.	(KEK BELLE Collab.)
LINK	02C	PRL 89 161801	J.M. Link et al.	(FNAL FOCUS Collab.)
LINK	02G	PL B540 25	J.M. Link et al.	(FNAL FOCUS Collab.)
PDG	02	PR D66 010001	K. Hagiwara et al.	(FNAL FOCUS Collab.)
KUSHNIR...	01	PRL 86 5243	A. Kushnirenko et al.	(FNAL SLEX Collab.)
MAHMOOD	01	PRL 86 2232	A.H. Mahmood et al.	(CLEO Collab.)
AITALA	00	PL B471 449	E.M. Aitala et al.	(FNAL E791 Collab.)
JAFFE	00	PR D62 072005	D.E. Jaffe et al.	(CLEO Collab.)
ALAM	98	PR D57 4467	M.S. Alam et al.	(CLEO Collab.)
ALBRECHT	96E	PRPL 276 223	H. Albrecht et al.	(ARGUS Collab.)
ALEEV	96	JINRRC 3-77 31	A.N. Aleev et al.	(Serpukhov EXCHARM Collab.)
ALEXANDER	96C	PR D53 R1013	J.P. Alexander et al.	(CLEO Collab.)
ALBRECHT	95B	PL B342 397	H. Albrecht et al.	(ARGUS Collab.)
AMMAR	95	PRL 74 3634	R. Ammar et al.	(CLEO Collab.)
BISHAI	95	PL B350 256	M. Bishai et al.	(CLEO Collab.)
CRAWFORD	95	PRL 75 624	G. Crawford et al.	(CLEO Collab.)
KODAMA	95	PL B345 85	K. Kodama et al.	(FNAL E653 Collab.)
ALBRECHT	94B	PL B326 320	H. Albrecht et al.	(ARGUS Collab.)
ALEEV	94	PAN 57 1370	A.N. Aleev et al.	(Serpukhov BIS-2 Collab.)
AVERY	94	PL B325 257	P. Avery et al.	(CLEO Collab.)
BERGFELD	94	PL B323 219	T. Bergfeld et al.	(CLEO Collab.)
FRABETTI	94E	PL B328 193	P. Frabetti et al.	(FNAL E687 Collab.)
AVERY	93	PRL 71 2391	P. Avery et al.	(CLEO Collab.)
BOZEK	93	PL B312 247	A. Bozek et al.	(CERN NA32 Collab.)
FRABETTI	93D	PRL 70 1755	P.L. Frabetti et al.	(FNAL E687 Collab.)
FRABETTI	93H	PL B314 477	P.L. Frabetti et al.	(FNAL E687 Collab.)
KUBOTA	93	PRL 71 3255	Y. Kubota et al.	(CLEO Collab.)
ALBRECHT	92	PL B274 239	H. Albrecht et al.	(ARGUS Collab.)
ALBRECHT	92O	ZPHY C56 1	H. Albrecht et al.	(ARGUS Collab.)
BARLAG	92	PL B283 465	S. Barlag et al.	(ACCMOR Collab.)
CRAWFORD	92	PR D45 752	G. Crawford et al.	(CLEO Collab.)
JEZABEK	92	PL B286 175	M. Jezabek, K. Rybicki, R. Rylko	(CRAC Collab.)
ALBRECHT	91G	PL B269 234	H. Albrecht et al.	(ARGUS Collab.)
AVERY	91	PR D43 3539	P. Avery et al.	(CLEO Collab.)
ALVAREZ	90	ZPHY C47 539	M.P. Alvarez et al.	(CERN NA14/2 Collab.)
ALVAREZ	90B	PL B246 256	M.P. Alvarez et al.	(CERN NA14/2 Collab.)
ANJOS	90	PR D41 801	J.C. Anjos et al.	(FNAL E691 Collab.)
AVERY	90B	PRL 65 2842	P. Avery et al.	(CLEO Collab.)
BARLAG	90D	ZPHY C48 29	S. Barlag et al.	(ACCMOR Collab.)
FRABETTI	90	PL B251 639	P.L. Frabetti et al.	(FNAL E687 Collab.)
BARLAG	89	PL B218 374	S. Barlag et al.	(ACCMOR Collab.)
AGUILAR...	88B	ZPHY C40 321	M. Aguilar-Benitez et al.	(LEBC-EHS Collab.)
Also		PL B189 254	M. Aguilar-Benitez et al.	(LEBC-EHS Collab.)
Also		PL B199 462	M. Aguilar-Benitez et al.	(LEBC-EHS Collab.)
Also		SJNP 48 833	M. Begalli et al.	(LEBC-EHS Collab.)
		Translated from YAF 48 1310.		
ALBRECHT	88C	PL B207 109	H. Albrecht et al.	(ARGUS Collab.)
ANJOS	88B	PRL 60 1379	J.C. Anjos et al.	(FNAL E691 Collab.)
ADAMOVIČ	87	EPL 4 887	M.I. Adamovič et al.	(Photon Emulsion Collab.)
Also		SJNP 46 447	F. Viaggi et al.	(Photon Emulsion Collab.)
		Translated from YAF 46 799.		

AMENDOLIA	87	ZPHY C36 513	S.R. Amendolia et al.	(CERN NA1 Collab.)
JONES	87	ZPHY C36 593	G.T. Jones et al.	(CERN WA21 Collab.)
ABE	86	PR D33 1	K. Abe et al.	
ALEEV	84	ZPHY C23 333	A.N. Aleev et al.	(BIS-2 Collab.)
BOSETTI	82	PL 109B 234	P.C. Bosetti et al.	(AACH3, BONN, CERN +)
VELLA	82	PRL 48 1515	E. Vella et al.	(SLAC, LBL, UCB)
BASILE	81B	NC 62A 14	M. Basile et al.	(CERN, BGNA, PGIA, FRAS)
CALICCHIO	80	PL 93B 521	M. Calicchio et al.	(BARI, BIRM, BRUX +)

OTHER RELATED PAPERS

MIGLIOZZI	99	PL B462 217	P. Migliozi et al.
DUNIETZ	98	PR D58 094010	I. Dunietz

 $\Lambda_c(2595)^+$

$$J(P) = 0(\frac{1}{2}^-) \text{ Status: } ***$$

Seen in $\Lambda_c^+ \pi^+ \pi^-$ but not in $\Lambda_c^+ \pi^0$, so this is indeed an excited Λ_c^+ rather than a Σ_c^+ . The $\Lambda_c^+ \pi^+ \pi^-$ mode is largely, and perhaps entirely, $\Sigma_c \pi$, which is just at threshold; thus (assuming, as has not yet been proven, that the Σ_c has $J^P = 1/2^+$) the J^P here is almost certainly $1/2^-$. This result is in accord with the theoretical expectation that this is the charm counterpart of the strange $\Lambda(1405)$.

 $\Lambda_c(2595)^+$ MASS

The mass is obtained from the $\Lambda_c(2595)^+ - \Lambda_c^+$ mass-difference measurements below. But the mass may be 2 or 3 MeV lower: see the footnote to BLECHMAN 03 in the next data block.

VALUE (MeV)	DOCUMENT ID
2595.4 ± 0.6 OUR FIT	Error includes scale factor of 1.1.

 $\Lambda_c(2595)^+ - \Lambda_c^+$ MASS DIFFERENCE

VALUE (MeV)	EVTS	DOCUMENT ID	TECN	COMMENT
308.9 ± 0.6 OUR FIT				Error includes scale factor of 1.1.
308.9 ± 0.6 OUR AVERAGE				Error includes scale factor of 1.1.
$309.7 \pm 0.9 \pm 0.4$	19	ALBRECHT	97	ARG $e^+e^- \approx 10$ GeV
$309.2 \pm 0.7 \pm 0.3$	14 ± 4.5	FRABETTI	96	E687 $\gamma \text{Be}, \bar{E}_\gamma \approx 220$ GeV
$307.5 \pm 0.4 \pm 1.0$	112 ± 17	EDWARDS	95	CLE2 $e^+e^- \approx 10.5$ GeV
305.6 ± 0.3		1 BLECHMAN	03	Threshold shift

1 BLECHMAN 03 finds that a more sophisticated treatment than a simple Breit-Wigner for the proximity of the threshold of the dominant decay, $\Sigma_c(2455)\pi$, lowers the $\Lambda_c(2595)^+ - \Lambda_c^+$ mass difference by 2 or 3 MeV.

 $\Lambda_c(2595)^+$ WIDTH

VALUE (MeV)	EVTS	DOCUMENT ID	TECN	COMMENT
3.6 ± 2.0 -1.3 OUR AVERAGE				
$2.9 \pm 2.9 \pm 1.8$ $-2.1 - 1.4$	19	ALBRECHT	97	ARG $e^+e^- \approx 10$ GeV
$3.9 \pm 1.4 \pm 2.0$ $-1.2 - 1.0$	112 ± 17	EDWARDS	95	CLE2 $e^+e^- \approx 10.5$ GeV

 $\Lambda_c(2595)^+$ DECAY MODES

$\Lambda_c^+ \pi \pi$ and its submode $\Sigma_c(2455)\pi$ — the latter just barely — are the only strong decays allowed to an excited Λ_c^+ having this mass; and the submode seems to dominate.

Mode	Fraction (Γ_i/Γ)
$\Gamma_1 \Lambda_c^+ \pi^+ \pi^-$	[a] $\approx 67\%$
$\Gamma_2 \Sigma_c(2455)^{++} \pi^-$	$24 \pm 7\%$
$\Gamma_3 \Sigma_c(2455)^0 \pi^+$	$24 \pm 7\%$
$\Gamma_4 \Lambda_c^+ \pi^+ \pi^-$ 3-body	$18 \pm 10\%$
$\Gamma_5 \Lambda_c^+ \pi^0$	[b] not seen
$\Gamma_6 \Lambda_c^+ \gamma$	not seen

[a] Assuming isospin conservation, so that the other third is $\Lambda_c^+ \pi^0 \pi^0$.

[b] A test that the isospin is indeed 0, so that the particle is indeed a Λ_c^+ .

 $\Lambda_c(2595)^+$ BRANCHING RATIOS

VALUE	DOCUMENT ID	TECN	COMMENT
$\Gamma(\Sigma_c(2455)^{++} \pi^-)/\Gamma(\Lambda_c^+ \pi^+ \pi^-)$			Γ_2/Γ_1
0.36 ± 0.10 OUR AVERAGE			
$0.37 \pm 0.12 \pm 0.13$	ALBRECHT	97	ARG $e^+e^- \approx 10$ GeV
$0.36 \pm 0.09 \pm 0.09$	EDWARDS	95	CLE2 $e^+e^- \approx 10.5$ GeV

Baryon Particle Listings

$\Lambda_c(2595)^+$, $\Lambda_c(2625)^+$

$\Gamma(\Sigma_c(2455)^0 \pi^+) / \Gamma(\Lambda_c^+ \pi^+ \pi^-)$ Γ_3/Γ_1

VALUE	DOCUMENT ID	TECN	COMMENT
0.37 ± 0.10 OUR AVERAGE			
0.29 ± 0.10 ± 0.11	ALBRECHT 97	ARG	$e^+ e^- \approx 10$ GeV
0.42 ± 0.09 ± 0.09	EDWARDS 95	CLE2	$e^+ e^- \approx 10.5$ GeV

$[\Gamma(\Sigma_c(2455)^{++} \pi^-) + \Gamma(\Sigma_c(2455)^0 \pi^+)] / \Gamma(\Lambda_c^+ \pi^+ \pi^-)$ $(\Gamma_2 + \Gamma_3) / \Gamma_1$

VALUE	CL%	DOCUMENT ID	TECN	COMMENT
0.66 ^{+0.13} _{-0.16} ± 0.07		ALBRECHT 97	ARG	$e^+ e^- \approx 10$ GeV
> 0.51	90	2 FRABETTI 96	E687	γ Be, $\bar{E}_\gamma \approx 220$ GeV

• • • We do not use the following data for averages, fits, limits, etc. • • •
 2 The results of FRABETTI 96 are consistent with this ratio being 100%.

$\Gamma(\Lambda_c^+ \pi^0) / \Gamma(\Lambda_c^+ \pi^+ \pi^-)$ Γ_5/Γ_1

$\Lambda_c^+ \pi^0$ decay is forbidden by isospin conservation if this state is in fact a Λ_c .

VALUE	CL%	DOCUMENT ID	TECN	COMMENT
< 3.53	90	EDWARDS 95	CLE2	$e^+ e^- \approx 10.5$ GeV

$\Gamma(\Lambda_c^+ \gamma) / \Gamma(\Lambda_c^+ \pi^+ \pi^-)$ Γ_6/Γ_1

VALUE	CL%	DOCUMENT ID	TECN	COMMENT
< 0.98	90	EDWARDS 95	CLE2	$e^+ e^- \approx 10.5$ GeV

$\Lambda_c(2595)^+$ REFERENCES

BLECHMAN 03	PR D67 074033	A.E. Blechman et al.	(JHU, FLOR)
ALBRECHT 97	PL B402 207	H. Albrecht et al.	(ARGUS Collab.)
FRABETTI 96	PL B365 461	P.L. Frabetti et al.	(FNAL E687 Collab.)
EDWARDS 95	PRL 74 3331	K.W. Edwards et al.	(CLEO Collab.)

$\Lambda_c(2625)^+$

$$I(J^P) = 0(\frac{3}{2}^-) \text{ Status: } ***$$

Seen in $\Lambda_c^+ \pi^+ \pi^-$ but not in $\Lambda_c^+ \pi^0$ so this is indeed an excited Λ_c^+ rather than a Σ_c^+ . The spin-parity has not been measured but is expected to be $3/2^-$: this is presumably the charm counterpart of the strange $\Lambda(1520)$.

$\Lambda_c(2625)^+$ MASS

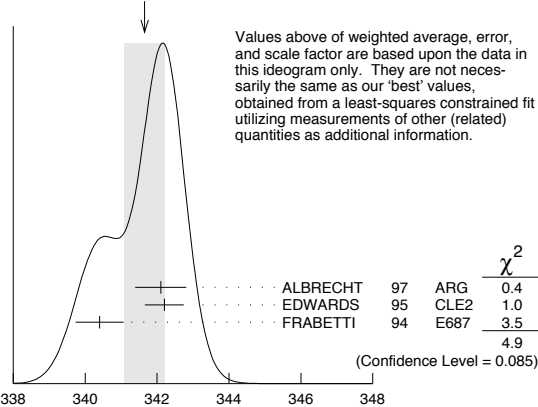
The mass is obtained from the $\Lambda_c(2625)^+ - \Lambda_c^+$ mass-difference measurements below.

VALUE (MeV)	EVTs	DOCUMENT ID	TECN	COMMENT
2628.1 ± 0.6 OUR FIT				Error includes scale factor of 1.5.
2626.6 ± 0.5 ± 1.5	42 ± 9	ALBRECHT 93F	ARG	See ALBRECHT 97

$\Lambda_c(2625)^+ - \Lambda_c^+$ MASS DIFFERENCE

VALUE (MeV)	EVTs	DOCUMENT ID	TECN	COMMENT
341.7 ± 0.6 OUR FIT				Error includes scale factor of 1.6.
341.7 ± 0.6 OUR AVERAGE				Error includes scale factor of 1.6. See the ideogram below.
342.1 ± 0.5 ± 0.5	51	ALBRECHT 97	ARG	$e^+ e^- \approx 10$ GeV
342.2 ± 0.2 ± 0.5	245 ± 19	EDWARDS 95	CLE2	$e^+ e^- \approx 10.5$ GeV
340.4 ± 0.6 ± 0.3	40 ± 9	FRABETTI 94	E687	γ Be, $\bar{E}_\gamma = 220$ GeV

WEIGHTED AVERAGE
 341.7 ± 0.6 (Error scaled by 1.6)



$\Lambda_c(2625)^+$ WIDTH

VALUE (MeV)	CL%	EVTs	DOCUMENT ID	TECN	COMMENT
< 1.9	90	245 ± 19	EDWARDS 95	CLE2	$e^+ e^- \approx 10.5$ GeV
• • • We do not use the following data for averages, fits, limits, etc. • • •					
< 3.2	90		ALBRECHT 93F	ARG	$e^+ e^- \approx \Upsilon(4S)$

$\Lambda_c(2625)^+$ DECAY MODES

$\Lambda_c^+ \pi \pi$ and its submode $\Sigma(2455) \pi$ are the only strong decays allowed to an excited Λ_c^+ having this mass.

Mode	Fraction (Γ_i/Γ)	Confidence level
Γ_1 $\Lambda_c^+ \pi^+ \pi^-$	[a] $\approx 67\%$	
Γ_2 $\Sigma_c(2455)^{++} \pi^-$	< 5	90%
Γ_3 $\Sigma_c(2455)^0 \pi^+$	< 5	90%
Γ_4 $\Lambda_c^+ \pi^+ \pi^-$ 3-body	large	
Γ_5 $\Lambda_c^+ \pi^0$	[b] not seen	
Γ_6 $\Lambda_c^+ \gamma$	not seen	

[a] Assuming isospin conservation, so that the other third is $\Lambda_c^+ \pi^0 \pi^0$.

[b] A test that the isospin is indeed 0, so that the particle is indeed a Λ_c^+ .

$\Lambda_c(2625)^+$ BRANCHING RATIOS

$\Gamma(\Sigma_c(2455)^{++} \pi^-) / \Gamma(\Lambda_c^+ \pi^+ \pi^-)$	Γ_2/Γ_1
VALUE CL% DOCUMENT ID TECN COMMENT	
< 0.08 90 EDWARDS 95 CLE2 $e^+ e^- \approx 10.5$ GeV	

$\Gamma(\Sigma_c(2455)^0 \pi^+) / \Gamma(\Lambda_c^+ \pi^+ \pi^-)$	Γ_3/Γ_1
VALUE CL% DOCUMENT ID TECN COMMENT	
< 0.07 90 EDWARDS 95 CLE2 $e^+ e^- \approx 10.5$ GeV	

$[\Gamma(\Sigma_c(2455)^{++} \pi^-) + \Gamma(\Sigma_c(2455)^0 \pi^+)] / \Gamma(\Lambda_c^+ \pi^+ \pi^-)$	$(\Gamma_2 + \Gamma_3) / \Gamma_1$
VALUE CL% EVTS DOCUMENT ID TECN COMMENT	
• • • We do not use the following data for averages, fits, limits, etc. • • •	
< 0.36 90 FRABETTI 94 E687 γ Be, $\bar{E}_\gamma = 220$ GeV	
0.46 ± 0.14 21 ALBRECHT 93F ARG $e^+ e^- \approx \Upsilon(4S)$	

$\Gamma(\Lambda_c^+ \pi^+ \pi^- \text{ 3-body}) / \Gamma(\Lambda_c^+ \pi^+ \pi^-)$	Γ_4/Γ_1
VALUE EVTS DOCUMENT ID TECN COMMENT	
• • • We do not use the following data for averages, fits, limits, etc. • • •	
0.54 ± 0.14 16 ALBRECHT 93F ARG $e^+ e^- \approx \Upsilon(4S)$	

$\Gamma(\Lambda_c^+ \pi^0) / \Gamma(\Lambda_c^+ \pi^+ \pi^-)$	Γ_5/Γ_1
VALUE CL% DOCUMENT ID TECN COMMENT	
< 0.91 90 EDWARDS 95 CLE2 $e^+ e^- \approx 10.5$ GeV	

$\Gamma(\Lambda_c^+ \gamma) / \Gamma(\Lambda_c^+ \pi^+ \pi^-)$	Γ_6/Γ_1
VALUE CL% DOCUMENT ID TECN COMMENT	
< 0.52 90 EDWARDS 95 CLE2 $e^+ e^- \approx 10.5$ GeV	

$\Lambda_c(2625)^+$ REFERENCES

ALBRECHT 97	PL B402 207	H. Albrecht et al.	(ARGUS Collab.)
EDWARDS 95	PRL 74 3331	K.W. Edwards et al.	(CLEO Collab.)
FRABETTI 94	PRL 72 951	P.L. Frabetti et al.	(FNAL E687 Collab.)
ALBRECHT 93F	PL B317 227	H. Albrecht et al.	(ARGUS Collab.)

See key on page 405

Baryon Particle Listings

$\Lambda_c(2765)^+$, $\Lambda_c(2880)^+$, $\Lambda_c(2940)^+$

$\Lambda_c(2765)^+$ or $\Sigma_c(2765)$ $I(J^P) = ?(??)$ Status: *

OMITTED FROM SUMMARY TABLE

A broad, statistically significant peak (997^{+141}_{-129} events) seen in $\Lambda_c^+ \pi^+ \pi^-$. However, nothing at all is known about its quantum numbers, including whether it is a Λ_c^+ or a Σ_c , or whether the width might be due to overlapping states.

 $\Lambda_c(2765)^+$ MASS

The mass is obtained from the $\Lambda_c(2765)^+ - \Lambda_c^+$ mass-difference measurement below.

VALUE (MeV)	DOCUMENT ID
2766.6 ± 2.4 OUR FIT	

 $\Lambda_c(2765)^+ - \Lambda_c^+$ MASS DIFFERENCE

VALUE (MeV)	EVTS	DOCUMENT ID	TECN	COMMENT
480.1 ± 2.4 OUR FIT				
480.1 ± 2.4	997^{+141}_{-129}	ARTUSO	01 CLE2	$e^+ e^- \approx \Upsilon(4S)$

 $\Lambda_c(2765)^+$ WIDTH

VALUE (MeV)	DOCUMENT ID	TECN	COMMENT
50	ARTUSO	01 CLE2	$e^+ e^- \approx \Upsilon(4S)$

 $\Lambda_c(2765)^+$ DECAY MODES

Mode	Fraction (Γ_i/Γ)
$\Gamma_1 \Lambda_c^+ \pi^+ \pi^-$	seen

 $\Lambda_c(2765)^+$ REFERENCES

ARTUSO	01	PRL 86 4479	M. Artuso et al.	(CLEO Collab.)
--------	----	-------------	------------------	----------------

$\Lambda_c(2880)^+$ $I(J^P) = 0(\frac{5}{2}^+)$ Status: ***

A narrow peak seen in $\Lambda_c^+ \pi^+ \pi^-$ and in pD^0 . It is not seen in pD^+ , and therefore it is probably a Λ_c^+ and not a Σ_c . The evidence for spin $5/2$ comes from the $\Sigma_c(2455)\pi$ decay angular distribution, and the evidence for parity $+$ comes from agreement of the $\Sigma_c(2520)/\Sigma_c(2455)$ branching ratio with a prediction of heavy quark symmetry (see MIZUK 07).

 $\Lambda_c(2880)^+$ MASS

VALUE (MeV)	EVTS	DOCUMENT ID	TECN	COMMENT
2881.53 ± 0.35 OUR FIT				
2881.50 ± 0.35 OUR AVERAGE				
$2881.9 \pm 0.1 \pm 0.5$	$2.8k \pm 190$	AUBERT	07 BABR	in pD^0
$2881.2 \pm 0.2 \pm 0.4$	690 ± 50	MIZUK	07 BELL	in $\Sigma_c(2455)^0, ++ \pi^\pm$

 $\Lambda_c(2880)^+ - \Lambda_c^+$ MASS DIFFERENCE

VALUE (MeV)	EVTS	DOCUMENT ID	TECN	COMMENT
595.1 ± 0.4 OUR FIT				
596 ± 1 ± 2	350^{+57}_{-55}	ARTUSO	01 CLE2	in $\Lambda_c^+ \pi^+ \pi^-$

 $\Lambda_c(2880)^+$ WIDTH

VALUE (MeV)	CL%	EVTS	DOCUMENT ID	TECN	COMMENT
5.8 ± 1.1 OUR AVERAGE					
$5.8 \pm 1.5 \pm 1.1$	$2.8k \pm 190$	AUBERT	07 BABR	in pD^0	
$5.8 \pm 0.7 \pm 1.1$	690 ± 50	MIZUK	07 BELL	in $\Sigma_c(2455)^0, ++ \pi^\pm$	
• • • We do not use the following data for averages, fits, limits, etc. • • •					
<8	90	ARTUSO	01 CLEO	in $\Lambda_c^+ \pi^+ \pi^-$	

 $\Lambda_c(2880)^+$ DECAY MODES

Mode	Fraction (Γ_i/Γ)
$\Gamma_1 \Lambda_c^+ \pi^+ \pi^-$	seen
$\Gamma_2 \Sigma_c(2455)^0, ++ \pi^\pm$	seen
$\Gamma_3 \Sigma_c(2520)^0, ++ \pi^\pm$	seen
$\Gamma_4 pD^0$	seen

 $\Lambda_c(2880)^+$ BRANCHING RATIOS

$\Gamma(\Sigma_c(2455)^0, ++ \pi^\pm)/\Gamma(\Lambda_c^+ \pi^+ \pi^-)$ Γ_2/Γ_1

VALUE	EVTS	DOCUMENT ID	TECN	COMMENT
0.392 ± 0.031 OUR AVERAGE				Error includes scale factor of 1.3.
$0.404 \pm 0.021 \pm 0.014$		MIZUK	07 BELL	in $\Sigma_c(2455)^0, ++ \pi^\pm$
$0.31 \pm 0.06 \pm 0.03$	96	ARTUSO	01 CLE2	$e^+ e^- \approx \Upsilon(4S)$

$\Gamma(\Sigma_c(2520)^0, ++ \pi^\pm)/\Gamma(\Lambda_c^+ \pi^+ \pi^-)$ Γ_3/Γ_1

VALUE	CL%	DOCUMENT ID	TECN	COMMENT
0.091 ± 0.025 ± 0.010				
$0.091 \pm 0.025 \pm 0.010$		MIZUK	07 BELL	in $\Sigma_c(2455)^0, ++ \pi^\pm$
• • • We do not use the following data for averages, fits, limits, etc. • • •				
<0.11	90	ARTUSO	01 CLE2	$e^+ e^- \approx \Upsilon(4S)$

$\Gamma(\Sigma_c(2520)^0, ++ \pi^\pm)/\Gamma(\Sigma_c(2455)^0, ++ \pi^\pm)$ Γ_3/Γ_2

VALUE	DOCUMENT ID	TECN	COMMENT
0.225 ± 0.062 ± 0.025			
$0.225 \pm 0.062 \pm 0.025$	¹ MIZUK	07 BELL	in $\Sigma_c(2455)^0, ++ \pi^\pm$
¹ This MIZUK 07 ratio is redundant with MIZUK 07 ratios given above.			

 $\Lambda_c(2880)^+$ REFERENCES

AUBERT	07	PRL 98 012001	B. Aubert et al.	(BABAR Collab.)
MIZUK	07	PRL 98 262001	R. Mizuk et al.	(BELLE Collab.)
ARTUSO	01	PRL 86 4479	M. Artuso et al.	(CLEO Collab.)

$\Lambda_c(2940)^+$ $I(J^P) = 0(??)$ Status: ***

A fairly narrow peak of good statistical significance first seen in the pD^0 mass spectrum. It is not seen in pD^+ , and thus it is probably a Λ_c^+ and not a Σ_c . It is also seen in $\Sigma_c(2455)^0, ++ \pi^\pm$.

 $\Lambda_c(2940)^+$ MASS

VALUE (MeV)	EVTS	DOCUMENT ID	TECN	COMMENT
2939.3 ± 1.4 OUR AVERAGE				
$2939.8 \pm 1.3 \pm 1.0$	2280 ± 310	AUBERT	07 BABR	in pD^0
$2938.0 \pm 1.3^{+2.0}_{-4.0}$	220^{+80}_{-60}	MIZUK	07 BELL	in $\Sigma_c(2455)^0, ++ \pi^\pm$

 $\Lambda_c(2940)^+$ WIDTH

VALUE (MeV)	EVTS	DOCUMENT ID	TECN	COMMENT
17 $\frac{+8}{-6}$ OUR AVERAGE				
$17.5 \pm 5.2 \pm 5.9$	2280 ± 310	AUBERT	07 BABR	in pD^0
$13 \frac{+8}{-5} \frac{+27}{-7}$	220^{+80}_{-60}	MIZUK	07 BELL	in $\Sigma_c(2455)^0, ++ \pi^\pm$

 $\Lambda_c(2940)^+$ DECAY MODES

Mode	Fraction (Γ_i/Γ)
$\Gamma_1 pD^0$	seen
$\Gamma_2 \Sigma_c(2455)^0, ++ \pi^\pm$	seen

 $\Lambda_c(2940)^+$ REFERENCES

AUBERT	07	PRL 98 012001	B. Aubert et al.	(BABAR Collab.)
MIZUK	07	PRL 98 262001	R. Mizuk et al.	(BELLE Collab.)

Baryon Particle Listings

 $\Sigma_c(2455), \Sigma_c(2520)$ $\Sigma_c(2455)$

$$I(J^P) = 1(\frac{1}{2}^+) \text{ Status: } ****$$

Neither J nor P has been measured; $1/2^+$ is the quark model prediction.

 $\Sigma_c(2455)$ MASSES

The masses are obtained from the mass-difference measurements that follow.

 $\Sigma_c(2455)^{++}$ MASS

VALUE (MeV) DOCUMENT ID
2454.02 ± 0.18 OUR FIT

 $\Sigma_c(2455)^+$ MASS

VALUE (MeV) DOCUMENT ID
2452.9 ± 0.4 OUR FIT

 $\Sigma_c(2455)^0$ MASS

VALUE (MeV) DOCUMENT ID
2453.76 ± 0.18 OUR FIT

 $\Sigma_c(2455) - \Lambda_c^+$ MASS DIFFERENCES $m_{\Sigma_c^{++}} - m_{\Lambda_c^+}$

VALUE (MeV)	EVTS	DOCUMENT ID	TECN	COMMENT
167.56 ± 0.11 OUR FIT				
167.57 ± 0.13 OUR AVERAGE				
167.4 ± 0.1 ± 0.2	2k	ARTUSO 02	CLE2	$e^+e^- \approx \Upsilon(4S)$
167.35 ± 0.19 ± 0.12	461	LINK 00C	FOCS	γ nucleus, \bar{E}_γ 180 GeV
167.76 ± 0.29 ± 0.15	122	AITALA 96B	E791	$\pi^- N$, 500 GeV
167.6 ± 0.6 ± 0.6	56	FRABETTI 96	E687	γ Be, $\bar{E}_\gamma \approx 220$ GeV
168.2 ± 0.3 ± 0.2	126	CRAWFORD 93	CLE2	$e^+e^- \approx \Upsilon(4S)$
167.8 ± 0.4 ± 0.3	54	BOWCOCK 89	CLEO	e^+e^- 10 GeV
168.2 ± 0.5 ± 1.6	92	ALBRECHT 88D	ARG	e^+e^- 10 GeV
167.4 ± 0.5 ± 2.0	46	DIESBURG 87	SPEC	$nA \sim 600$ GeV
••• We do not use the following data for averages, fits, limits, etc. •••				
167 ± 1	2	JONES 87	HBC	νp in BEBC
166 ± 1	1	BOSETTI 82	HBC	See JONES 87
168 ± 3	6	BALTAY 79	HLBC	ν Ne-H in 15-ft
166 ± 15	1	CAZZOLI 75	HBC	νp in BNL 7-ft

 $m_{\Sigma_c^+} - m_{\Lambda_c^+}$

VALUE (MeV)	EVTS	DOCUMENT ID	TECN	COMMENT
166.4 ± 0.4 OUR FIT				
166.4 ± 0.2 ± 0.3	661	AMMAR 01	CLE2	$e^+e^- \approx \Upsilon(4S)$
••• We do not use the following data for averages, fits, limits, etc. •••				
168.5 ± 0.4 ± 0.2	111	CRAWFORD 93	CLE2	See AMMAR 01
168 ± 3	1	CALICCHIO 80	HBC	νp in BEBC-TST

 $m_{\Sigma_c^0} - m_{\Lambda_c^+}$

VALUE (MeV)	EVTS	DOCUMENT ID	TECN	COMMENT
167.30 ± 0.11 OUR FIT				
167.29 ± 0.13 OUR AVERAGE				
167.2 ± 0.1 ± 0.2	2k	ARTUSO 02	CLE2	$e^+e^- \approx \Upsilon(4S)$
167.38 ± 0.21 ± 0.13	362	LINK 00C	FOCS	γ nucleus, \bar{E}_γ 180 GeV
167.38 ± 0.29 ± 0.15	143	AITALA 96B	E791	$\pi^- N$, 500 GeV
167.8 ± 0.6 ± 0.2		AILEEV 96	SPEC	n nucleus, 50 GeV/c
166.6 ± 0.5 ± 0.6	69	FRABETTI 96	E687	γ Be, $\bar{E}_\gamma \approx 220$ GeV
167.1 ± 0.3 ± 0.2	124	CRAWFORD 93	CLE2	$e^+e^- \approx \Upsilon(4S)$
168.4 ± 1.0 ± 0.3	14	ANJOS 89D	E691	γ Be 90-260 GeV
••• We do not use the following data for averages, fits, limits, etc. •••				
167.9 ± 0.5 ± 0.3	48	¹ BOWCOCK 89	CLEO	e^+e^- 10 GeV
167.0 ± 0.5 ± 1.6	70	¹ ALBRECHT 88D	ARG	e^+e^- 10 GeV
178.2 ± 0.4 ± 2.0	85	² DIESBURG 87	SPEC	$nA \sim 600$ GeV
163 ± 2	1	AMMAR 86	EMUL	νA

¹ This result enters the fit through $m_{\Sigma_c^{++}} - m_{\Sigma_c^0}$ given below.

² See the note on DIESBURG 87 in the $m_{\Sigma_c^{++}} - m_{\Sigma_c^0}$ section below.

 $\Sigma_c(2455)$ MASS DIFFERENCES $m_{\Sigma_c^{++}} - m_{\Sigma_c^0}$

VALUE (MeV)	DOCUMENT ID	TECN	COMMENT
0.27 ± 0.11 OUR FIT			Error includes scale factor of 1.1.
0.26 ± 0.14 OUR AVERAGE			Error includes scale factor of 1.2.
+ 0.2 ± 0.1 ± 0.1	ARTUSO 02	CLE2	$e^+e^- \approx \Upsilon(4S)$
- 0.03 ± 0.28 ± 0.11	LINK 00C	FOCS	γ nucleus, \bar{E}_γ 180 GeV
+ 0.38 ± 0.40 ± 0.15	AITALA 96B	E791	$\pi^- N$, 500 GeV
+ 1.1 ± 0.4 ± 0.1	CRAWFORD 93	CLE2	$e^+e^- \approx \Upsilon(4S)$
- 0.1 ± 0.6 ± 0.1	BOWCOCK 89	CLEO	e^+e^- 10 GeV
+ 1.2 ± 0.7 ± 0.3	ALBRECHT 88D	ARG	$e^+e^- \sim 10$ GeV
••• We do not use the following data for averages, fits, limits, etc. •••			
- 10.8 ± 2.9	³ DIESBURG 87	SPEC	$nA \sim 600$ GeV

³DIESBURG 87 is completely incompatible with the other experiments, which is surprising since it agrees with them about $m_{\Sigma_c(2455)^{++}} - m_{\Lambda_c^+}$. We go with the majority here.

 $m_{\Sigma_c^{++}} - m_{\Sigma_c^0}$

VALUE (MeV) DOCUMENT ID TECN COMMENT

-0.9 ± 0.4 OUR FIT

••• We do not use the following data for averages, fits, limits, etc. •••

1.4 ± 0.5 ± 0.3 CRAWFORD 93 CLE2 See AMMAR 01

 $\Sigma_c(2455)$ WIDTHS $\Sigma_c(2455)^{++}$ WIDTH

VALUE (MeV)	EVTS	DOCUMENT ID	TECN	COMMENT
2.23 ± 0.30 OUR AVERAGE				
2.3 ± 0.2 ± 0.3	2k	ARTUSO 02	CLE2	$e^+e^- \approx \Upsilon(4S)$
2.05 ± 0.41 ± 0.38	1110	LINK 02	FOCS	γ nucleus, $\bar{E}_\gamma \approx 180$ GeV

 $\Sigma_c(2455)^+$ WIDTH

VALUE (MeV)	CL%	EVTS	DOCUMENT ID	TECN	COMMENT
<4.6	90	661	AMMAR 01	CLE2	$e^+e^- \approx \Upsilon(4S)$

 $\Sigma_c(2455)^0$ WIDTH

VALUE (MeV)	EVTS	DOCUMENT ID	TECN	COMMENT
2.2 ± 0.4 OUR AVERAGE				Error includes scale factor of 1.4.
2.5 ± 0.2 ± 0.3	2k	ARTUSO 02	CLE2	$e^+e^- \approx \Upsilon(4S)$
1.55 ± 0.41 ± 0.38	913	LINK 02	FOCS	γ nucleus, $\bar{E}_\gamma \approx 180$ GeV

 $\Sigma_c(2455)$ DECAY MODES

$\Lambda_c^+ \pi$ is the only strong decay allowed to a Σ_c having this mass.

Mode	Fraction (Γ_i/Γ)
$\Gamma_1 \Lambda_c^+ \pi$	$\approx 100\%$

 $\Sigma_c(2455)$ REFERENCES

ARTUSO 02	PR D65 071101R	M. Artuso <i>et al.</i>	(CLEO Collab.)
LINK 02	PL B525 205	J.M. Link <i>et al.</i>	(FNAL FOCUS Collab.)
AMMAR 01	PRL 86 1167	R. Ammar <i>et al.</i>	(CLEO Collab.)
LINK 00C	PL B488 218	J.M. Link <i>et al.</i>	(FNAL FOCUS Collab.)
AITALA 96B	PL B379 292	E.M. Aitala <i>et al.</i>	(FNAL E791 Collab.)
AILEEV 96	JINRRC 3-77 31	A.N. Aileev <i>et al.</i>	(Serpuukhov EXCHARM Collab.)
FRABETTI 96	PL B365 461	P.L. Frabetti <i>et al.</i>	(FNAL E687 Collab.)
CRAWFORD 93	PRL 71 3259	G. Crawford <i>et al.</i>	(CLEO Collab.)
ANJOS 89D	PRL 62 1721	J.C. Anjos <i>et al.</i>	(FNAL E691 Collab.)
BOWCOCK 89	PRL 62 1240	T.J.V. Bowcock <i>et al.</i>	(CLEO Collab.)
ALBRECHT 88D	PL B211 489	H. Albrecht <i>et al.</i>	(ARGUS Collab.)
DIESBURG 87	PRL 59 2711	M. Diesburg <i>et al.</i>	(FNAL E400 Collab.)
JONES 87	ZPHY C36 593	G.T. Jones <i>et al.</i>	(CERN WA21 Collab.)
AMMAR 86	JETPL 43 515	R. Ammar <i>et al.</i>	(ITEP)
	Translated from ZETFP 43 401.		
BOSETTI 82	PL 109B 234	P.C. Bosetti <i>et al.</i>	(AACH3, BONN, CERN+)
CALICCHIO 80	PL 93B 521	M. Calicchio <i>et al.</i>	(BARI, BIRM, BRUX+)
BALTAY 79	PRL 42 1721	C. Baltay <i>et al.</i>	(COLU, BNL)
CAZZOLI 75	PRL 34 1125	E.G. Cazzoli <i>et al.</i>	(BNL)

 $\Sigma_c(2520)$

$$I(J^P) = 1(\frac{3}{2}^+) \text{ Status: } ***$$

Seen in the $\Lambda_c^+ \pi^+$ mass spectrum. The natural assignment is that this is the $J^P = 3/2^+$ excitation of the $\Sigma_c(2455)$, the charm counterpart of the $\Sigma(1385)$, but neither J nor P has been measured.

 $\Sigma_c(2520)$ MASSES

The masses are obtained from the mass-difference measurements that follow.

 $\Sigma_c(2520)^{++}$ MASS

VALUE (MeV) EVTS DOCUMENT ID TECN COMMENT
2518.4 ± 0.6 OUR FIT Error includes scale factor of 1.4.

••• We do not use the following data for averages, fits, limits, etc. •••

2530 ± 5 ± 5 6 ¹AMMOSOV 93 HLBC $\nu p \rightarrow \mu^- \Sigma_c(2530)^{++}$

¹ AMMOSOV 93 sees a cluster of 6 events and estimates the background to be 1 event.

 $\Sigma_c(2520)^+$ MASS

VALUE (MeV) DOCUMENT ID
2517.5 ± 2.3 OUR FIT

 $\Sigma_c(2520)^0$ MASS

VALUE (MeV) DOCUMENT ID
2518.0 ± 0.5 OUR FIT

$\Sigma_c(2520)$ MASS DIFFERENCES

$$m_{\Sigma_c(2520)^{++}} - m_{\Lambda_c^+}$$

VALUE (MeV)	EVTs	DOCUMENT ID	TECN	COMMENT
231.9 ± 0.6 OUR FIT				Error includes scale factor of 1.5.
231.9 ± 1.0 OUR AVERAGE				Error includes scale factor of 2.1.
231.5 ± 0.4 ± 0.3	1330 ± 110	ATHAR 05	CLEO	e^+e^- , 9.4–11.5 GeV
234.5 ± 1.1 ± 0.8	677	BRANDENB... 97	CLE2	$e^+e^- \approx \Upsilon(4S)$

$$m_{\Sigma_c(2520)^+} - m_{\Lambda_c^+}$$

VALUE (MeV)	EVTs	DOCUMENT ID	TECN	COMMENT
231.0 ± 2.3 OUR FIT				
231.0 ± 1.1 ± 2.0	327	AMMAR 01	CLE2	$e^+e^- \approx \Upsilon(4S)$

$$m_{\Sigma_c(2520)^0} - m_{\Lambda_c^+}$$

VALUE (MeV)	EVTs	DOCUMENT ID	TECN	COMMENT
231.6 ± 0.5 OUR FIT				Error includes scale factor of 1.1.
231.6 ± 0.5 OUR AVERAGE				
231.4 ± 0.5 ± 0.3	1350 ± 120	ATHAR 05	CLEO	e^+e^- , 9.4–11.5 GeV
232.6 ± 1.0 ± 0.8	504	BRANDENB... 97	CLE2	$e^+e^- \approx \Upsilon(4S)$

$$m_{\Sigma_c(2520)^{++}} - m_{\Sigma_c(2520)^0}$$

VALUE (MeV)	DOCUMENT ID	TECN	COMMENT
0.3 ± 0.6 OUR FIT			Error includes scale factor of 1.2.
0.5 ± 0.8 OUR AVERAGE			
+0.1 ± 0.8 ± 0.3	2 ATHAR 05	CLEO	e^+e^- , 9.4–11.5 GeV
1.9 ± 1.4 ± 1.0	3 BRANDENB... 97	CLE2	$e^+e^- \approx \Upsilon(4S)$
2 This ATHAR 05 result is redundant with measurements in earlier entries.			
3 This BRANDENBURG 97 result is redundant with measurements in earlier entries.			

 $\Sigma_c(2520)$ WIDTHS $\Sigma_c(2520)^{++}$ WIDTH

VALUE (MeV)	EVTs	DOCUMENT ID	TECN	COMMENT
14.9 ± 1.9 OUR AVERAGE				
14.4 $^{+1.6}_{-1.5}$ ± 1.4	1330 ± 110	ATHAR 05	CLEO	e^+e^- , 9.4–11.5 GeV
17.9 $^{+3.8}_{-3.2}$ ± 4.0	677	BRANDENB... 97	CLE2	$e^+e^- \approx \Upsilon(4S)$

 $\Sigma_c(2520)^+$ WIDTH

VALUE (MeV)	CL%	EVTs	DOCUMENT ID	TECN	COMMENT
<17	90	327	AMMAR 01	CLE2	$e^+e^- \approx \Upsilon(4S)$

 $\Sigma_c(2520)^0$ WIDTH

VALUE (MeV)	EVTs	DOCUMENT ID	TECN	COMMENT
16.1 ± 2.1 OUR AVERAGE				
16.6 $^{+1.9}_{-1.7}$ ± 1.4	1350 ± 120	ATHAR 05	CLEO	e^+e^- , 9.4–11.5 GeV
13.0 $^{+3.7}_{-3.0}$ ± 4.0	504	BRANDENB... 97	CLE2	$e^+e^- \approx \Upsilon(4S)$

 $\Sigma_c(2520)$ DECAY MODES

$\Lambda_c^+ \pi$ is the only strong decay allowed to a Σ_c having this mass.

Mode	Fraction (Γ_j/Γ)
$\Gamma_1 \Lambda_c^+ \pi$	$\approx 100\%$

 $\Sigma_c(2520)$ REFERENCES

ATHAR 05	PR D71 051101R	S.B. Athar <i>et al.</i>	(CLEO Collab.)
AMMAR 01	PRL 86 1167	R. Ammar <i>et al.</i>	(CLEO Collab.)
BRANDENB... 97	PRL 78 2304	G. Brandenburg <i>et al.</i>	(CLEO Collab.)
AMMOSOV 93	JETPL 58 247	V.V. Ammosov <i>et al.</i>	(SERP)
Translated from ZETFP 58 241.			

 $\Sigma_c(2800)$

$$I(J^P) = 1(?)^? \quad \text{Status: } ***$$

Seen in the $\Lambda_c^+ \pi^+$, $\Lambda_c^+ \pi^0$, and $\Lambda_c^+ \pi^-$ mass spectra.

 $\Sigma_c(2800)$ MASSES

The masses are obtained from the mass-difference measurements that follow.

 $\Sigma_c(2800)^{++}$ MASS

VALUE (MeV)	DOCUMENT ID
2801 $^{+4}_{-6}$ OUR FIT	

 $\Sigma_c(2800)^+$ MASS

VALUE (MeV)	DOCUMENT ID
2792 $^{+14}_{-5}$ OUR FIT	

 $\Sigma_c(2800)^0$ MASS

VALUE (MeV)	DOCUMENT ID
2802 $^{+4}_{-7}$ OUR FIT	

 $\Sigma_c(2800)$ MASS DIFFERENCES

$$m_{\Sigma_c(2800)^{++}} - m_{\Lambda_c^+}$$

VALUE (MeV)	EVTs	DOCUMENT ID	TECN	COMMENT
514 $^{+4}_{-6}$ OUR FIT				
514.5 $^{+3.4}_{-3.1}$ $^{+2.8}_{-4.9}$	2810 $^{+1090}_{-775}$	MIZUK 05	BELL	$e^+e^- \approx \Upsilon(4S)$

$$m_{\Sigma_c(2800)^+} - m_{\Lambda_c^+}$$

VALUE (MeV)	EVTs	DOCUMENT ID	TECN	COMMENT
505 $^{+14}_{-5}$ OUR FIT				
505.4 $^{+5.8}_{-4.6}$ $^{+12.4}_{-2.0}$	1540 $^{+1750}_{-1050}$	MIZUK 05	BELL	$e^+e^- \approx \Upsilon(4S)$

$$m_{\Sigma_c(2800)^0} - m_{\Lambda_c^+}$$

VALUE (MeV)	EVTs	DOCUMENT ID	TECN	COMMENT
515 $^{+4}_{-7}$ OUR FIT				
515.4 $^{+3.2}_{-3.1}$ $^{+2.1}_{-6.0}$	2240 $^{+1300}_{-740}$	MIZUK 05	BELL	$e^+e^- \approx \Upsilon(4S)$

 $\Sigma_c(2800)$ WIDTHS $\Sigma_c(2800)^{++}$ WIDTH

VALUE (MeV)	EVTs	DOCUMENT ID	TECN	COMMENT
75 $^{+18}_{-13}$ $^{+12}_{-11}$	2810 $^{+1090}_{-775}$	MIZUK 05	BELL	$e^+e^- \approx \Upsilon(4S)$

 $\Sigma_c(2800)^+$ WIDTH

VALUE (MeV)	EVTs	DOCUMENT ID	TECN	COMMENT
62 $^{+37}_{-23}$ $^{+52}_{-38}$	1540 $^{+1750}_{-1050}$	MIZUK 05	BELL	$e^+e^- \approx \Upsilon(4S)$

 $\Sigma_c(2800)^0$ WIDTH

VALUE (MeV)	EVTs	DOCUMENT ID	TECN	COMMENT
61 $^{+18}_{-13}$ $^{+22}_{-13}$	2240 $^{+1300}_{-740}$	MIZUK 05	BELL	$e^+e^- \approx \Upsilon(4S)$

 $\Sigma_c(2800)$ DECAY MODES

Mode	Fraction (Γ_j/Γ)
$\Gamma_1 \Lambda_c^+ \pi$	seen

 $\Sigma_c(2800)$ REFERENCES

MIZUK 05	PRL 94 122002	R. Mizuk <i>et al.</i>	(BELLE Collab.)
----------	---------------	------------------------	-----------------

Baryon Particle Listings



$$I(J^P) = \frac{1}{2}(\frac{1}{2}^+) \text{ Status: } ***$$

According to the quark model, the Ξ_c^+ (quark content usc) and Ξ_c^0 form an isospin doublet, and the spin-parity ought to be $J^P = 1/2^+$. None of $I, J,$ or P has actually been measured.

Ξ_c^+ MASS

The fit uses the Ξ_c^+ and Ξ_c^0 mass and mass-difference measurements.

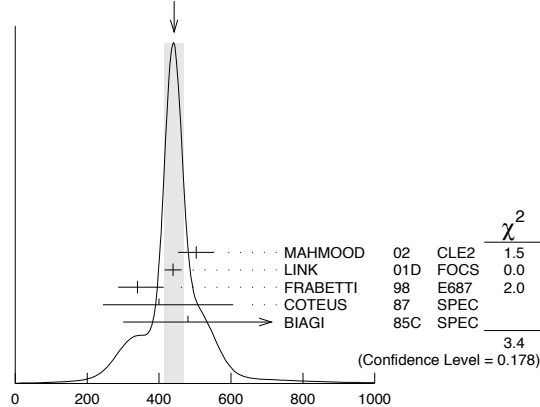
VALUE (MeV)	EVTs	DOCUMENT ID	TECN	COMMENT
2467.8^{+0.4}_{-0.6} OUR FIT				
2467.6^{+0.4}_{-1.0} OUR AVERAGE				
2468.1 ± 0.4 ^{+0.2} _{-1.4}	4950 ± 286	¹ LESIAK	05 BELL	e ⁺ e ⁻ , $\Upsilon(4S)$
2465.8 ± 1.9 ± 2.5	90	FRABETTI	98 E687	γ Be, $\bar{E}_\gamma \approx 220$ GeV
2467.0 ± 1.6 ± 2.0	147	EDWARDS	96 CLE2	e ⁺ e ⁻ $\approx \Upsilon(4S)$
2465.1 ± 3.6 ± 1.9	30	ALBRECHT	90F ARG	e ⁺ e ⁻ at $\Upsilon(4S)$
2467 ± 3 ± 4	23	ALAM	89 CLEO	e ⁺ e ⁻ 10.6 GeV
2466.5 ± 2.7 ± 1.2	5	BARLAG	89c ACCM	π^- Cu 230 GeV
• • • We do not use the following data for averages, fits, limits, etc. • • •				
2464.4 ± 2.0 ± 1.4	30	FRABETTI	93B E687	See FRABETTI 98
2459 ± 5 ± 30	56	² COTEUS	87 SPEC	nA ≈ 600 GeV
2460 ± 25	82	BIAGI	83 SPEC	Σ^- Be 135 GeV

¹ The systematic error was (wrongly) given the other way round in LESIAK 05; see the erratum.
² Although COTEUS 87 claims to agree well with BIAGI 83 on the mass and width, there appears to be a discrepancy between the two experiments. BIAGI 83 sees a single peak (stated significance about 6 standard deviations) in the $\Lambda K^- \pi^+ \pi^+$ mass spectrum. COTEUS 87 sees two peaks in the same spectrum, one at the Ξ_c^+ mass, the other 75 MeV lower. The latter is attributed to $\Xi_c^+ \rightarrow \Sigma^0 K^- \pi^+ \pi^+ \rightarrow (\Lambda \gamma) K^- \pi^+ \pi^+$, with the γ unseen. The combined significance of the double peak is stated to be 5.5 standard deviations. But the absence of any trace of a lower peak in BIAGI 83 seems to us to throw into question the interpretation of the lower peak of COTEUS 87.

Ξ_c^+ MEAN LIFE

VALUE (10 ⁻¹⁵ s)	EVTs	DOCUMENT ID	TECN	COMMENT
442 ± 26 OUR AVERAGE				Error includes scale factor of 1.3. See the ideogram below.
503 ± 47 ± 18	250	MAHMOOD	02 CLE2	e ⁺ e ⁻ $\approx \Upsilon(4S)$
439 ± 22 ± 9	532	LINK	01D FOCS	γ nucleus, $\bar{E}_\gamma \approx 180$ GeV
340 ⁺⁷⁰ ₋₅₀ ± 20	56	FRABETTI	98 E687	γ Be, $\bar{E}_\gamma \approx 220$ GeV
400 ⁺¹⁸⁰ ₋₁₂₀ ± 100	102	COTEUS	87 SPEC	nA ≈ 600 GeV
480 ⁺²¹⁰ ₋₁₅₀ ± 200	53	BIAGI	85c SPEC	Σ^- Be 135 GeV
• • • We do not use the following data for averages, fits, limits, etc. • • •				
410 ⁺¹¹⁰ ₋₈₀ ± 20	30	FRABETTI	93B E687	See FRABETTI 98
200 ⁺¹¹⁰ ₋₆₀	6	BARLAG	89c ACCM	π^- (K ⁻) Cu 230 GeV

WEIGHTED AVERAGE
442±26 (Error scaled by 1.3)



Ξ_c^+ mean life

Ξ_c^+ DECAY MODES

Mode	Fraction (Γ_i/Γ)	Confidence level
------	--------------------------------	------------------

No absolute branching fractions have been measured. The following are branching ratios relative to $\Xi^- 2\pi^+$.

Cabibbo-favored ($S = -2$) decays

Γ_i	Decay Mode	Value	Comment
Γ_1	$p 2K_S^0$	[a] 0.087 ± 0.022	
Γ_2	$\Lambda \bar{K}^0 \pi^+$	—	
Γ_3	$\Sigma(1385)^+ \bar{K}^0$	[a,b] 1.0 ± 0.5	
Γ_4	$\Lambda K^- 2\pi^+$	[a] 0.323 ± 0.033	
Γ_5	$\Lambda \bar{K}^*(892)^0 \pi^+$	[a,b] < 0.2	90%
Γ_6	$\Sigma(1385)^+ K^- \pi^+$	[a,b] < 0.3	90%
Γ_7	$\Sigma^+ K^- \pi^+$	[a] 0.94 ± 0.11	
Γ_8	$\Sigma^+ \bar{K}^*(892)^0$	[a,b] 0.81 ± 0.15	
Γ_9	$\Sigma^0 K^- 2\pi^+$	[a] 0.29 ± 0.16	
Γ_{10}	$\Xi^0 \pi^+$	[a] 0.55 ± 0.16	
Γ_{11}	$\Xi^- 2\pi^+$	[a] DEFINED AS 1	
Γ_{12}	$\Xi(1530)^0 \pi^+$	[a,b] < 0.1	90%
Γ_{13}	$\Xi^0 \pi^+ \pi^0$	[a] 2.34 ± 0.68	
Γ_{14}	$\Xi^0 \pi^- 2\pi^+$	[a] 1.74 ± 0.50	
Γ_{15}	$\Xi^0 e^+ \nu_e$	[a] 2.3 ^{+0.7} _{-0.9}	
Γ_{16}	$\Omega^- K^+ \pi^+$	[a] 0.07 ± 0.04	

Cabibbo-suppressed decays

Γ_i	Decay Mode	Value	Comment
Γ_{17}	$p K^- \pi^+$	[a] 0.21 ± 0.03	
Γ_{18}	$p \bar{K}^*(892)^0$	[a,b] 0.12 ± 0.02	
Γ_{19}	$\Sigma^+ \pi^+ \pi^-$	[a] 0.48 ± 0.20	
Γ_{20}	$\Sigma^- 2\pi^+$	[a] 0.18 ± 0.09	
Γ_{21}	$\Sigma^+ K^+ K^-$	[a] 0.15 ± 0.07	
Γ_{22}	$\Sigma^+ \phi$	[a,b] < 0.11	90%
Γ_{23}	$\Xi(1690)^0 K^+, \Xi(1690)^0 \rightarrow \Sigma^+ K^-$	[a] < 0.05	90%

[a] No absolute branching fractions have been measured. The value here is the branching ratio relative to $\Xi^- 2\pi^+$.

[b] This branching fraction includes all the decay modes of the final-state resonance.

Ξ_c^+ BRANCHING RATIOS

Cabibbo-favored ($S = -2$) decays

$\Gamma(p 2K_S^0)/\Gamma(\Xi^- 2\pi^+)$	Γ_1/Γ_{11}			
VALUE	EVTs	DOCUMENT ID	TECN	COMMENT
0.087 ± 0.016 ± 0.014	168 ± 27	LESIAK	05 BELL	e ⁺ e ⁻ , $\Upsilon(4S)$
$\Gamma(\Sigma(1385)^+ \bar{K}^0)/\Gamma(\Xi^- 2\pi^+)$	Γ_3/Γ_{11}			
Unseen decay modes of the $\Sigma(1385)^+$ are included.				
VALUE	EVTs	DOCUMENT ID	TECN	COMMENT
1.00 ± 0.49 ± 0.24	20	LINK	03E FOCS	< 1.72, 90% CL
$\Gamma(\Lambda K^- 2\pi^+)/\Gamma(\Xi^- 2\pi^+)$	Γ_4/Γ_{11}			
VALUE	EVTs	DOCUMENT ID	TECN	COMMENT
0.323 ± 0.033 OUR AVERAGE				
0.32 ± 0.03 ± 0.02	1177 ± 55	LESIAK	05 BELL	e ⁺ e ⁻ , $\Upsilon(4S)$
0.28 ± 0.06 ± 0.06	58	LINK	03E FOCS	γ nucleus, $\bar{E}_\gamma \approx 180$ GeV
0.58 ± 0.16 ± 0.07	61	BERGFELD	96 CLE2	e ⁺ e ⁻ $\approx \Upsilon(4S)$
$\Gamma(\Lambda \bar{K}^*(892)^0 \pi^+)/\Gamma(\Lambda K^- 2\pi^+)$	Γ_5/Γ_4			
Unseen decay modes of the $\bar{K}^*(892)^0$ are included.				
VALUE	CL%	DOCUMENT ID	TECN	COMMENT
< 0.5	90	BERGFELD	96 CLE2	e ⁺ e ⁻ $\approx \Upsilon(4S)$
$\Gamma(\Sigma(1385)^+ K^- \pi^+)/\Gamma(\Lambda K^- 2\pi^+)$	Γ_6/Γ_4			
Unseen decay modes of the $\Sigma(1385)^+$ are included.				
VALUE	CL%	DOCUMENT ID	TECN	COMMENT
< 0.7	90	BERGFELD	96 CLE2	e ⁺ e ⁻ $\approx \Upsilon(4S)$
$\Gamma(\Sigma^+ K^- \pi^+)/\Gamma(\Xi^- 2\pi^+)$	Γ_7/Γ_{11}			
VALUE	EVTs	DOCUMENT ID	TECN	COMMENT
0.94 ± 0.10 OUR AVERAGE				
0.91 ± 0.11 ± 0.04	251	LINK	03E FOCS	γ nucleus, $\bar{E}_\gamma \approx 180$ GeV
0.92 ± 0.20 ± 0.07		³ JUN	00 SELX	Σ^- nucleus, 600 GeV
1.18 ± 0.26 ± 0.17	119	BERGFELD	96 CLE2	e ⁺ e ⁻ $\approx \Upsilon(4S)$
³ This JUN 00 result is redundant with other results given below.				
$\Gamma(\Sigma^+ \bar{K}^*(892)^0)/\Gamma(\Xi^- 2\pi^+)$	Γ_8/Γ_{11}			
Unseen decay modes of the $\bar{K}^*(892)^0$ are included.				
VALUE	EVTs	DOCUMENT ID	TECN	COMMENT
0.81 ± 0.15 OUR AVERAGE				
0.78 ± 0.16 ± 0.06	119	LINK	03E FOCS	γ nucleus, $\bar{E}_\gamma \approx 180$ GeV
0.92 ± 0.27 ± 0.14	61	BERGFELD	96 CLE2	e ⁺ e ⁻ $\approx \Upsilon(4S)$

See key on page 405

Baryon Particle Listings

$$\Xi_c^+, \Xi_c^0$$

$\Gamma(\Sigma^0 K^- 2\pi^+)/\Gamma(\Lambda K^- 2\pi^+)$ Γ_9/Γ_4

VALUE	EVTs	DOCUMENT ID	TECN	COMMENT
0.84 ± 0.36	47	4 COTEUS	87	SPEC $nA \approx 600$ GeV

⁴ See, however, the note on the COTEUS 87 Ξ_c^+ mass measurement.

$\Gamma(\Xi^0 \pi^+)/\Gamma(\Xi^- 2\pi^+)$ Γ_{10}/Γ_{11}

VALUE	EVTs	DOCUMENT ID	TECN	COMMENT
0.55 ± 0.13 ± 0.09	39	EDWARDS	96	CLE2 $e^+ e^- \approx \gamma(4S)$

$\Gamma(\Xi^- 2\pi^+)/\Gamma_{total}$ Γ_{11}/Γ

VALUE	EVTs	DOCUMENT ID	TECN	COMMENT
• • • We do not use the following data for averages, fits, limits, etc. • • •				
seen	131	BERGFELD	96	CLE2 $e^+ e^- \approx \gamma(4S)$
seen	160	VERY	95	CLE2 $e^+ e^- \approx \gamma(4S)$
seen	30	FRABETTI	93B	E687 $\gamma Be, \bar{E}_\gamma = 220$ GeV
seen	30	ALBRECHT	90F	ARG $e^+ e^-$ at $\gamma(4S)$
seen	23	ALAM	89	CLEO $e^+ e^- 10.6$ GeV

$\Gamma(\Xi(1530)^0 \pi^+)/\Gamma(\Xi^- 2\pi^+)$ Γ_{12}/Γ_{11}

Unseen decay modes of the $\Xi(1530)^0$ are included.

VALUE	CL%	DOCUMENT ID	TECN	COMMENT
<0.1	90	LINK	03E	FOCS γ nucleus, $\bar{E}_\gamma \approx 180$ GeV

• • • We do not use the following data for averages, fits, limits, etc. • • •

<0.2 90 BERGFELD 96 CLE2 $e^+ e^- \approx \gamma(4S)$

$\Gamma(\Xi^0 \pi^+ \pi^0)/\Gamma(\Xi^- 2\pi^+)$ Γ_{13}/Γ_{11}

VALUE	EVTs	DOCUMENT ID	TECN	COMMENT
2.34 ± 0.57 ± 0.37	81	EDWARDS	96	CLE2 $e^+ e^- \approx \gamma(4S)$

$\Gamma(\Xi(1530)^0 \pi^+)/\Gamma(\Xi^0 \pi^+ \pi^0)$ Γ_{12}/Γ_{13}

VALUE	CL%	DOCUMENT ID	TECN	COMMENT
<0.3	90	EDWARDS	96	CLE2 $e^+ e^- \approx \gamma(4S)$

$\Gamma(\Xi^0 \pi^- 2\pi^+)/\Gamma(\Xi^- 2\pi^+)$ Γ_{14}/Γ_{11}

VALUE	EVTs	DOCUMENT ID	TECN	COMMENT
1.74 ± 0.42 ± 0.27	57	EDWARDS	96	CLE2 $e^+ e^- \approx \gamma(4S)$

$\Gamma(\Xi^0 e^+ \nu_e)/\Gamma(\Xi^- 2\pi^+)$ Γ_{15}/Γ_{11}

VALUE	EVTs	DOCUMENT ID	TECN	COMMENT
2.3 ± 0.6^{+0.3}_{-0.6}	41	ALEXANDER	95B	CLE2 $e^+ e^- \approx \gamma(4S)$

$\Gamma(\Omega^- K^+ \pi^+)/\Gamma(\Xi^- 2\pi^+)$ Γ_{16}/Γ_{11}

VALUE	EVTs	DOCUMENT ID	TECN	COMMENT
0.07 ± 0.03 ± 0.03	14	LINK	03E	FOCS < 0.12, 90% CL

Cabibbo-suppressed decays

$\Gamma(p K^- \pi^+)/\Gamma(\Xi^- 2\pi^+)$ Γ_{17}/Γ_{11}

VALUE	EVTs	DOCUMENT ID	TECN	COMMENT
0.21 ± 0.04 OUR AVERAGE				
0.194 ± 0.054	47 ± 11	VAZQUEZ-JA...08	SELX	Σ^- nucleus, 600 GeV
0.234 ± 0.047 ± 0.022	202	LINK	01B	FOCS γ nucleus

• • • We do not use the following data for averages, fits, limits, etc. • • •

0.20 ± 0.04 ± 0.02	76	JUN	00	SELX See VAZQUEZ-JAUREGUI 08
--------------------	----	-----	----	------------------------------

$\Gamma(p \bar{K}^*(892)^0)/\Gamma(p K^- \pi^+)$ Γ_{18}/Γ_{17}

Unseen decay modes of the $\bar{K}^*(892)^0$ are included.

VALUE	DOCUMENT ID	TECN	COMMENT
0.54 ± 0.09 ± 0.05	LINK	01B	FOCS γ nucleus

$\Gamma(\Sigma^+ \pi^+ \pi^-)/\Gamma(\Xi^- 2\pi^+)$ Γ_{19}/Γ_{11}

VALUE	EVTs	DOCUMENT ID	TECN	COMMENT
0.40 ± 0.20	21 ± 8	VAZQUEZ-JA...08	SELX	Σ^- nucleus, 600 GeV

$\Gamma(\Sigma^- 2\pi^+)/\Gamma(\Xi^- 2\pi^+)$ Γ_{20}/Γ_{11}

VALUE	EVTs	DOCUMENT ID	TECN	COMMENT
0.18 ± 0.09	10 ± 4	VAZQUEZ-JA...08	SELX	Σ^- nucleus, 600 GeV

$\Gamma(\Sigma^+ K^+ K^-)/\Gamma(\Sigma^+ K^- \pi^+)$ Γ_{21}/Γ_7

VALUE	EVTs	DOCUMENT ID	TECN	COMMENT
0.16 ± 0.06 ± 0.01	17	LINK	03E	FOCS γ nucleus, $\bar{E}_\gamma \approx 180$ GeV

$\Gamma(\Sigma^+ \phi)/\Gamma(\Sigma^+ K^- \pi^+)$ Γ_{22}/Γ_7

Unseen decay modes of the ϕ are included.

VALUE	CL%	DOCUMENT ID	TECN	COMMENT
<0.12	90	LINK	03E	FOCS γ nucleus, $\bar{E}_\gamma \approx 180$ GeV

$\Gamma(\Xi(1690)^0 K^+ \times B(\Xi(1690)^0 \rightarrow \Sigma^+ K^-))/\Gamma(\Sigma^+ K^- \pi^+)$ Γ_{23}/Γ_7

VALUE	CL%	DOCUMENT ID	TECN	COMMENT
<0.05	90	LINK	03E	FOCS γ nucleus, $\bar{E}_\gamma \approx 180$ GeV

Ξ_c^+ REFERENCES

Author	Year	PL	Page	Erratum	Collab.
VAZQUEZ-JA...	08	PL	B666 299		(SELEX Collab.)
LESIAK	05	PL	B605 237		(BELLE Collab.)
Also			PL B617 198	(erratum)	(BELLE Collab.)
LINK	03E	PL	B571 139		(FNAL FOCUS Collab.)
MAHMOOD	02	PR	D55 031102		(CLEO Collab.)
LINK	01B	PL	B512 277		(FNAL FOCUS Collab.)
LINK	01D	PL	B523 53		(FNAL FOCUS Collab.)
JUN	00	PRL	84 1857		(FNAL SELEX Collab.)
FRABETTI	98	PL	B427 211		(FNAL E687 Collab.)
BERGFELD	96	PL	B365 431		(CLEO Collab.)
EDWARDS	96	PL	B373 261		(CLEO Collab.)
ALEXANDER	95B	PRL	74 3113		(CLEO Collab.)
Also			PRL 75 4155	(erratum)	(CLEO Collab.)
VERY	95	PRL	75 4364		(CLEO Collab.)
FRABETTI	93B	PRL	70 1381		(FNAL E687 Collab.)
ALBRECHT	90F	PL	B247 121		(ARGUS Collab.)
ALAM	89	PL	B226 401		(CLEO Collab.)
BARLAG	89C	PL	B233 522		(ACCMO Collab.)
COTEUS	87	PRL	59 1530		(FNAL E400 Collab.)
BIAGI	85C	PL	150B 230		(CERN WA62 Collab.)
BIAGI	83	PL	122B 455		(CERN WA62 Collab.)

$$\Xi_c^0$$

$$I(J^P) = \frac{1}{2}(\frac{1}{2}^+) \text{ Status: } ***$$

According to the quark model, the Ξ_c^0 (quark content dsc) and Ξ_c^+ form an isospin doublet, and the spin-parity ought to be $J^P = 1/2^+$. None of $I, J, \text{ or } P$ has actually been measured.

Ξ_c^0 MASS

The fit uses the Ξ_c^0 and Ξ_c^+ mass and mass-difference measurements.

VALUE (MeV)	EVTs	DOCUMENT ID	TECN	COMMENT
-------------	------	-------------	------	---------

2470.88^{+0.34}_{-0.80} OUR FIT Error includes scale factor of 1.1.

2471.09^{+0.35}_{-1.00} OUR AVERAGE

2471.0 ± 0.3 ^{+0.2} _{-1.4}	8620 ± 355	¹ LESIAK	05	BELL $e^+ e^-$, $\gamma(4S)$
2470.0 ± 2.8 ± 2.6	85	FRABETTI	98B	E687 $\gamma Be, \bar{E}_\gamma = 220$ GeV
2469 ± 2 ± 3	9	HENDERSON	92B	CLEO $\Omega^- K^+$
2472.1 ± 2.7 ± 1.6	54	ALBRECHT	90F	ARG $e^+ e^-$ at $\gamma(4S)$
2473.3 ± 1.9 ± 1.2	4	BARLAG	90	ACCM $\pi^- (K^-)$ Cu 230
2472 ± 3 ± 4	19	ALAM	89	CLEO $e^+ e^- 10.6$ GeV
• • • We do not use the following data for averages, fits, limits, etc. • • •				
2462.1 ± 3.1 ± 1.4	42	² FRABETTI	93C	E687 See FRABETTI 98B
2471 ± 3 ± 4	14	VERY	89	CLEO See ALAM 89

¹ The systematic error was (wrongly) given the other way round in LESIAK 05.

² The FRABETTI 93C mass is well below the other measurements.

$\Xi_c^0 - \Xi_c^+$ MASS DIFFERENCE

VALUE (MeV)	DOCUMENT ID	TECN	COMMENT
-------------	-------------	------	---------

3.1^{+0.4}_{-0.5} OUR FIT

3.1 ± 0.5 OUR AVERAGE

+2.9 ± 0.5	LESIAK	05	BELL $e^+ e^-$, $\gamma(4S)$
+7.0 ± 4.5 ± 2.2	ALBRECHT	90F	ARG $e^+ e^-$ at $\gamma(4S)$
+6.8 ± 3.3 ± 0.5	BARLAG	90	ACCM $\pi^- (K^-)$ Cu 230 GeV
+5 ± 4 ± 1	ALAM	89	CLEO $\Xi_c^0 \rightarrow \Xi^- \pi^+, \Xi_c^+ \rightarrow \Xi^- \pi^+ \pi^+$

Ξ_c^0 MEAN LIFE

VALUE (10 ⁻¹⁵ s)	EVTs	DOCUMENT ID	TECN	COMMENT
-----------------------------	------	-------------	------	---------

112⁺¹³₋₁₀ OUR AVERAGE

118 ⁺¹⁴ ₋₁₂ ± 5	110	LINK	02H	FOCS γ nucleus, ≈ 180 GeV
101 ⁺²⁵ ₋₁₇ ± 5	42	FRABETTI	93C	E687 $\gamma Be, \bar{E}_\gamma = 220$ GeV
82 ⁺⁵⁹ ₋₃₀	4	BARLAG	90	ACCM $\pi^- (K^-)$ Cu 230 GeV

Ξ_c^0 DECAY MODES

No absolute branching fractions have been measured. Several measurements of ratios of fractions may be found in the Listings that follow.

Mode	Fraction (Γ_i/Γ)
Γ_1 $p K^- K^- \pi^+$	seen
Γ_2 $p K^- \bar{K}^*(892)^0$	seen
Γ_3 $p K^- K^- \pi^+$ no $\bar{K}^*(892)^0$	seen
Γ_4 ΛK_S^0	seen
Γ_5 $\Lambda K^- \pi^+$	

Baryon Particle Listings

$$\Xi_c^0, \Xi_c^{'+}, \Xi_c^{'0}$$

Γ_6	$\Lambda \bar{K}^0 \pi^+ \pi^-$	seen
Γ_7	$\Lambda K^- \pi^+ \pi^+ \pi^-$	seen
Γ_8	$\Xi^- \pi^+$	seen
Γ_9	$\Xi^- \pi^+ \pi^+ \pi^-$	seen
Γ_{10}	$\Omega^- K^+$	seen
Γ_{11}	$\Xi^- e^+ \nu_e$	seen
Γ_{12}	$\Xi^- \ell^+$ anything	seen

Ξ_c^0 BRANCHING RATIOS

$\Gamma(\rho K^- K^- \pi^+)/\Gamma(\Xi^- \pi^+)$		Γ_1/Γ_8	
VALUE	EVTS	DOCUMENT ID	TECN COMMENT
0.34 ± 0.04 OUR AVERAGE			
0.33 ± 0.03 ± 0.03	1908 ± 62	LESLIAK 05	BELL $e^+ e^-$, $\Upsilon(4S)$
0.35 ± 0.06 ± 0.03	148 ± 18	DANKO 04	CLEO $e^+ e^-$

$\Gamma(\rho K^- \bar{K}^*(892)^0)/\Gamma(\Xi^- \pi^+)$		Γ_2/Γ_8	
VALUE	EVTS	DOCUMENT ID	TECN COMMENT
0.210 ± 0.045 ± 0.015			
Unseen decay modes of the $\bar{K}^*(892)^0$ are included.			
• • • We do not use the following data for averages, fits, limits, etc. • • •			
seen		BARLAG 90	ACCM $\pi^- (K^-)$ Cu 230 GeV

$\Gamma(\rho K^- K^- \pi^+ \text{ no } \bar{K}^*(892)^0)/\Gamma(\Xi^- \pi^+)$		Γ_3/Γ_8	
VALUE	EVTS	DOCUMENT ID	TECN COMMENT
0.21 ± 0.04 ± 0.02			
		DANKO 04	CLEO $e^+ e^-$

$\Gamma(\Lambda K_S^0)/\Gamma(\Xi^- \pi^+)$		Γ_4/Γ_8	
VALUE	EVTS	DOCUMENT ID	TECN COMMENT
0.21 ± 0.02 ± 0.02			
465 ± 37			
LESLIAK 05 BELL $e^+ e^-$, $\Upsilon(4S)$			
• • • We do not use the following data for averages, fits, limits, etc. • • •			
seen	7	ALBRECHT 95B	ARG $e^+ e^- \approx 10.4$ GeV

$\Gamma(\Lambda K^- \pi^+)/\Gamma(\Xi^- \pi^+)$		Γ_5/Γ_8	
VALUE	EVTS	DOCUMENT ID	TECN COMMENT
1.07 ± 0.12 ± 0.07			
	2979 ± 211	LESLIAK 05	BELL $e^+ e^-$, $\Upsilon(4S)$

$\Gamma(\Lambda \bar{K}^0 \pi^+ \pi^-)/\Gamma_{\text{total}}$		Γ_6/Γ	
VALUE	EVTS	DOCUMENT ID	TECN COMMENT
seen			
		FRABETTI 98B	E687 γ Be, $\bar{E}_\gamma = 220$ GeV

$\Gamma(\Lambda K^- \pi^+ \pi^+ \pi^-)/\Gamma_{\text{total}}$		Γ_7/Γ	
VALUE	EVTS	DOCUMENT ID	TECN COMMENT
seen			
		FRABETTI 98B	E687 γ Be, $\bar{E}_\gamma = 220$ GeV

$\Gamma(\Xi^- \pi^+)/\Gamma(\Xi^- \pi^+ \pi^+ \pi^-)$		Γ_8/Γ_9	
VALUE	EVTS	DOCUMENT ID	TECN COMMENT
0.30 ± 0.12 ± 0.05			
		ALBRECHT 90F	ARG $e^+ e^-$ at $\Upsilon(4S)$

$\Gamma(\Omega^- K^+)/\Gamma(\Xi^- \pi^+)$		Γ_{10}/Γ_8	
VALUE	EVTS	DOCUMENT ID	TECN COMMENT
0.297 ± 0.024 OUR AVERAGE			
0.294 ± 0.018 ± 0.016	65 0	AUBERT,B 05M	BABR $e^+ e^- \approx \Upsilon(4S)$
0.50 ± 0.21 ± 0.05	9	HENDERSON 92B	CLEO $e^+ e^- \approx 10.6$ GeV

$\Gamma(\Xi^- e^+ \nu_e)/\Gamma(\Xi^- \pi^+)$		Γ_{11}/Γ_8	
VALUE	EVTS	DOCUMENT ID	TECN COMMENT
3.1 ± 1.0^{+0.3}_{-0.5}			
	54	ALEXANDER 95B	CLE2 $e^+ e^- \approx \Upsilon(4S)$

$\Gamma(\Xi^- \ell^+ \text{ anything})/\Gamma(\Xi^- \pi^+)$		Γ_{12}/Γ_8	
VALUE	EVTS	DOCUMENT ID	TECN COMMENT
The ratio is for the average (not the sum) of the $\Xi^- e^+$ anything and $\Xi^- \mu^+$ anything modes.			
0.96 ± 0.43 ± 0.18			
	18	ALBRECHT 93B	ARG $e^+ e^- \approx 10.4$ GeV

$\Gamma(\Xi^- \ell^+ \text{ anything})/\Gamma(\Xi^- \pi^+ \pi^+ \pi^-)$		Γ_{12}/Γ_9	
VALUE	EVTS	DOCUMENT ID	TECN COMMENT
The ratio is for the average (not the sum) of the $\Xi^- e^+$ anything and $\Xi^- \mu^+$ anything modes.			
0.29 ± 0.12 ± 0.04			
	18	ALBRECHT 93B	ARG $e^+ e^- \approx 10.4$ GeV

Ξ_c^0 DECAY PARAMETERS

See the note on "Baryon Decay Parameters" in the neutron Listings.

α FOR $\Xi_c^0 \rightarrow \Xi^- \pi^+$	
VALUE	EVTS
-0.56 ± 0.39^{+0.10}_{-0.09}	
	138
CHAN 01	CLE2 $e^+ e^- \approx \Upsilon(4S)$

Ξ_c^0 REFERENCES

AUBERT,B 05M	PRL 95 142003	B. Aubert <i>et al.</i>	(BABAR Collab.)
LESLIAK 05	PL B605 237	T. Lesiak <i>et al.</i>	(BELLE Collab.)
Also	PL B617 198 (erratum)	T. Lesiak <i>et al.</i>	(BELLE Collab.)
DANKO 04	PR D59 052004	I. Danko <i>et al.</i>	(CLEO Collab.)
LINK 02H	PL B541 211	J.M. Link <i>et al.</i>	(FNAL FOCUS Collab.)
CHAN 01	PR D63 111102R	S. Chan <i>et al.</i>	(CLEO Collab.)
FRABETTI 98B	PL B426 403	P.L. Frabetti <i>et al.</i>	(FNAL E687 Collab.)
ALBRECHT 95B	PL B342 397	H. Albrecht <i>et al.</i>	(ARGUS Collab.)
ALEXANDER 95B	PRL 74 3113	J. Alexander <i>et al.</i>	(CLEO Collab.)
Also	PRL 75 4155 (erratum)	J. Alexander <i>et al.</i>	(CLEO Collab.)
ALBRECHT 93B	PL B303 368	H. Albrecht <i>et al.</i>	(ARGUS Collab.)
FRABETTI 93C	PRL 70 2058	P.L. Frabetti <i>et al.</i>	(FNAL E687 Collab.)
HENDERSON 92B	PL B283 161	S. Henderson <i>et al.</i>	(CLEO Collab.)
ALBRECHT 90F	PL B247 121	H. Albrecht <i>et al.</i>	(ARGUS Collab.)
BARLAG 90	PL B236 495	S. Barlag <i>et al.</i>	(ACCMOR Collab.)
ALAM 89	PL B226 401	M.S. Alam <i>et al.</i>	(CLEO Collab.)
AVERY 89	PRL 62 863	P. Avery <i>et al.</i>	(CLEO Collab.)

$$\Xi_c^{'+}$$

$$I(J^P) = \frac{1}{2}(\frac{1}{2}^+) \text{ Status: } ***$$

The $\Xi_c^{'+}$ and Ξ_c^0 presumably complete the SU(3) sextet whose other members are the Σ_c^{++} , Σ_c^+ , Σ_c^0 , and Ω_c^0 ; see Fig. 3 in the Note on Charmed Baryons just before the Λ_c^+ Listings. The quantum numbers given above come from this presumption but have not been measured.

$\Xi_c^{'+}$ MASS

The mass is obtained from the mass-difference measurement that follows.

VALUE (MeV)	DOCUMENT ID
2575.6 ± 3.1 OUR FIT	

$\Xi_c^{'+} - \Xi_c^+$ MASS DIFFERENCE

VALUE (MeV)	EVTS	DOCUMENT ID	TECN	COMMENT
107.8 ± 3.0 OUR FIT				
107.8 ± 1.7 ± 2.5	25	JESSOP 99	CLE2	$e^+ e^- \approx \Upsilon(4S)$

$\Xi_c^{'+}$ DECAY MODES

The $\Xi_c^{'+} - \Xi_c^+$ mass difference is too small for any strong decay to occur.

Mode	Fraction (Γ_i/Γ)
Γ_1 $\Xi_c^+ \gamma$	seen

$\Xi_c^{'+}$ REFERENCES

JESSOP 99	PRL 82 492	C.P. Jessop <i>et al.</i>	(CLEO Collab.)
-----------	------------	---------------------------	----------------

$$\Xi_c^{'0}$$

$$I(J^P) = \frac{1}{2}(\frac{1}{2}^+) \text{ Status: } ***$$

See the note in the Listing for the $\Xi_c^{'+}$, above.

$\Xi_c^{'0}$ MASS

The mass is obtained from the mass-difference measurement that follows.

VALUE (MeV)	DOCUMENT ID
2577.9 ± 2.9 OUR FIT	

$\Xi_c^{'0} - \Xi_c^0$ MASS DIFFERENCE

VALUE (MeV)	EVTS	DOCUMENT ID	TECN	COMMENT
107.0 ± 2.9 OUR FIT				
107.0 ± 1.4 ± 2.5	28	JESSOP 99	CLE2	$e^+ e^- \approx \Upsilon(4S)$

$\Xi_c^{'0}$ DECAY MODES

The $\Xi_c^{'0} - \Xi_c^0$ mass difference is too small for any strong decay to occur.

Mode	Fraction (Γ_i/Γ)
Γ_1 $\Xi_c^0 \gamma$	seen

$\Xi_c^{'0}$ REFERENCES

JESSOP 99	PRL 82 492	C.P. Jessop <i>et al.</i>	(CLEO Collab.)
-----------	------------	---------------------------	----------------

See key on page 405

Baryon Particle Listings

$\Xi_c(2645)$, $\Xi_c(2790)$, $\Xi_c(2815)$

 $\Xi_c(2645)$

$$I(J^P) = \frac{1}{2}(\frac{3}{2}^+) \text{ Status: } ***$$

A narrow peak seen in the $\Xi_c \pi$ mass spectrum. The natural assignment is that this is the $J^P = 3/2^+$ excitation of the Ξ_c in the same SU(4) multiplet as the $\Delta(1232)$, but the quantum numbers have not been measured.

 $\Xi_c(2645)$ MASSES

The masses are obtained from the mass-difference measurements that follow.

 $\Xi_c(2645)^+$ MASS

VALUE (MeV)	EVTS	DOCUMENT ID	TECN	COMMENT
2645.9\pm0.5\pm0.6 OUR FIT				Error includes scale factor of 1.1.

2645.6\pm0.2\pm0.6\pm0.8	578 \pm 32	LESIAK	08	BELL $e^+e^- \approx \Upsilon(4S)$
--	--------------	--------	----	------------------------------------

 $\Xi_c(2645)^0$ MASS

VALUE (MeV)	EVTS	DOCUMENT ID	TECN	COMMENT
2645.9\pm0.5 OUR FIT				

2645.7\pm0.2\pm0.6\pm0.7	611 \pm 32	LESIAK	08	BELL $e^+e^- \approx \Upsilon(4S)$
--	--------------	--------	----	------------------------------------

 $\Xi_c(2645) - \Xi_c$ MASS DIFFERENCES **$m_{\Xi_c(2645)^+} - m_{\Xi_c^0}$**

VALUE (MeV)	EVTS	DOCUMENT ID	TECN	COMMENT
175.0\pm0.8\pm0.6 OUR FIT				Error includes scale factor of 1.2.

175.6\pm1.4 OUR AVERAGE				Error includes scale factor of 1.7.
177.1 \pm 0.5 \pm 1.1	47	FRABETTI	98B	E687 γ Be, $\bar{E}_\gamma = 220$ GeV
174.3 \pm 0.5 \pm 1.0	34	GIBBONS	96	CLE2 $e^+e^- \approx \Upsilon(4S)$

 $m_{\Xi_c(2645)^0} - m_{\Xi_c^+}$

VALUE (MeV)	EVTS	DOCUMENT ID	TECN	COMMENT
178.1\pm0.6 OUR FIT				
178.2\pm0.5\pm1.0	55	AVERY	95	CLE2 $e^+e^- \approx \Upsilon(4S)$

 $\Xi_c(2645)^+ - \Xi_c(2645)^0$ MASS DIFFERENCE **$m_{\Xi_c(2645)^+} - m_{\Xi_c(2645)^0}$**

VALUE (MeV)	DOCUMENT ID	TECN	COMMENT
0.0\pm0.5 OUR FIT			
-0.1\pm0.3\pm0.6	LESIAK	08	BELL ≈ 600 evts each

 $\Xi_c(2645)$ WIDTHS **$\Xi_c(2645)^+$ WIDTH**

VALUE (MeV)	CL%	DOCUMENT ID	TECN	COMMENT
<3.1	90	GIBBONS	96	CLE2 $e^+e^- \approx \Upsilon(4S)$

 $\Xi_c(2645)^0$ WIDTH

VALUE (MeV)	CL%	EVTS	DOCUMENT ID	TECN	COMMENT
<5.5	90	55	AVERY	95	CLE2 $e^+e^- \approx \Upsilon(4S)$

 $\Xi_c(2645)$ DECAY MODES

$\Xi_c \pi$ is the only strong decay allowed to a Ξ_c resonance having this mass.

Mode	Fraction (Γ_i/Γ)
Γ_1 $\Xi_c^0 \pi^+$	seen
Γ_2 $\Xi_c^+ \pi^-$	seen

 $\Xi_c(2645)$ REFERENCES

LESIAK	08	PL B665 9	T. Lesiak et al.	(BELLE Collab.)
FRABETTI	98B	PL B426 403	PL Frabetti et al.	(FNAL E687 Collab.)
GIBBONS	96	PRL 77 310	L.K. Gibbons et al.	(CLEO Collab.)
AVERY	95	PRL 75 4364	P. Avery et al.	(CLEO Collab.)

 $\Xi_c(2790)$

$$I(J^P) = \frac{1}{2}(\frac{1}{2}^-) \text{ Status: } ***$$

A peak seen in the $\Xi_c' \pi$ mass spectrum. The simplest assignment, based on the mass, width, and decay mode, is that this belongs in the same SU(4) multiplet as the $\Lambda(1405)$ and the $\Lambda_c(2595)^+$, but the spin and parity have not been measured.

 $\Xi_c(2790)$ MASSES

The masses are obtained from the mass-difference measurements that follow.

 $\Xi_c(2790)^+$ MASS

VALUE (MeV)	DOCUMENT ID
2789.1\pm3.2 OUR FIT	

 $\Xi_c(2790)^0$ MASS

VALUE (MeV)	DOCUMENT ID
2791.8\pm3.3 OUR FIT	

 $\Xi_c(2790) - \Xi_c$ MASS DIFFERENCES **$m_{\Xi_c(2790)^+} - m_{\Xi_c^0}$**

VALUE (MeV)	EVTS	DOCUMENT ID	TECN	COMMENT
318.2\pm3.2 OUR FIT				
318.2\pm1.3\pm2.9	18	CSORNA	01	CLEO $e^+e^- \approx \Upsilon(4S)$

 $m_{\Xi_c(2790)^0} - m_{\Xi_c^+}$

VALUE (MeV)	EVTS	DOCUMENT ID	TECN	COMMENT
324.0\pm3.3 OUR FIT				
324.0\pm1.3\pm3.0	14	CSORNA	01	CLEO $e^+e^- \approx \Upsilon(4S)$

 $\Xi_c(2790)$ WIDTHS **$\Xi_c(2790)^+$ WIDTH**

VALUE (MeV)	CL%	DOCUMENT ID	TECN	COMMENT
<15	90	CSORNA	01	CLEO $e^+e^- \approx \Upsilon(4S)$

 $\Xi_c(2790)^0$ WIDTH

VALUE (MeV)	CL%	DOCUMENT ID	TECN	COMMENT
<12	90	CSORNA	01	CLEO $e^+e^- \approx \Upsilon(4S)$

 $\Xi_c(2790)$ DECAY MODES

Mode	Fraction (Γ_i/Γ)
Γ_1 $\Xi_c' \pi$	seen

 $\Xi_c(2790)$ REFERENCES

CSORNA	01	PRL 86 4243	S.E. Csorna et al.	(CLEO Collab.)
--------	----	-------------	--------------------	----------------

 $\Xi_c(2815)$

$$I(J^P) = \frac{1}{2}(\frac{3}{2}^-) \text{ Status: } ***$$

A narrow peak seen in the $\Xi_c \pi \pi$ mass spectrum. The simplest assignment is that this belongs to the same SU(4) multiplet as the $\Lambda(1520)$ and the $\Lambda_c(2625)$, but the spin and parity have not been measured.

 $\Xi_c(2815)$ MASSES

The masses are obtained from the mass-difference measurements that follow.

 $\Xi_c(2815)^+$ MASS

VALUE (MeV)	EVTS	DOCUMENT ID	TECN	COMMENT
2816.6\pm0.9 OUR FIT				
2817.0\pm1.2\pm0.7\pm0.8	73 \pm 10	LESIAK	08	BELL $e^+e^- \approx \Upsilon(4S)$

 $\Xi_c(2815)^0$ MASS

VALUE (MeV)	EVTS	DOCUMENT ID	TECN	COMMENT
2819.6\pm1.2 OUR FIT				
2820.4\pm1.4\pm0.9\pm1.0	48 \pm 8	LESIAK	08	BELL $e^+e^- \approx \Upsilon(4S)$

 $\Xi_c(2815) - \Xi_c$ MASS DIFFERENCES **$m_{\Xi_c(2815)^+} - m_{\Xi_c^+}$**

VALUE (MeV)	EVTS	DOCUMENT ID	TECN	COMMENT
348.8\pm0.9 OUR FIT				
348.6\pm0.6\pm1.0	20	ALEXANDER	99B	CLE2 $e^+e^- \approx \Upsilon(4S)$

Baryon Particle Listings

 $\Xi_c(2815), \Xi_c(2930), \Xi_c(2980)$ $m_{\Xi_c(2815)^0} - m_{\Xi_c^0}$

VALUE (MeV)	EVTS	DOCUMENT ID	TECN	COMMENT
348.7 ± 1.2 OUR FIT				
347.2 ± 0.7 ± 2.0	9	ALEXANDER 99B	CLE2	$e^+e^- \approx \Upsilon(4S)$

 $\Xi_c(2815)^+ - \Xi_c(2815)^0$ MASS DIFFERENCE $m_{\Xi_c(2815)^+} - m_{\Xi_c(2815)^0}$

VALUE (MeV)	DOCUMENT ID	TECN	COMMENT
-3.1 ± 1.3 OUR FIT			
-3.4 ± 1.9 ± 0.9	LESIAK 08	BELL	73 & 48 events

 $\Xi_c(2815)$ WIDTHS $\Xi_c(2815)^+$ WIDTH

VALUE (MeV)	CL%	DOCUMENT ID	TECN	COMMENT
<3.5	90	ALEXANDER 99B	CLE2	$e^+e^- \approx \Upsilon(4S)$

 $\Xi_c(2815)^0$ WIDTH

VALUE (MeV)	CL%	DOCUMENT ID	TECN	COMMENT
<6.5	90	ALEXANDER 99B	CLE2	$e^+e^- \approx \Upsilon(4S)$

 $\Xi_c(2815)$ DECAY MODES

The $\Xi_c \pi \pi$ modes are consistent with being entirely via $\Xi_c(2645) \pi$.

Mode	Fraction (Γ_i/Γ)
$\Gamma_1 \Xi_c^+ \pi^+ \pi^-$	seen
$\Gamma_2 \Xi_c^0 \pi^+ \pi^-$	seen

 $\Xi_c(2815)$ REFERENCES

LESIAK 08	PL B665 9	T. Lesiak <i>et al.</i>	(BELLE Collab.)
ALEXANDER 99B	PRL 83 3390	J.P. Alexander <i>et al.</i>	(CLEO Collab.)

 $\Xi_c(2930)$

$I(J^P) = ?(??)$ Status: *

OMITTED FROM SUMMARY TABLE

A peak seen in the $\Lambda_c^+ K^-$ mass projection of $B^- \rightarrow \Lambda_c^+ \bar{\Lambda}_c^- K^-$ events.

 $\Xi_c(2930)$ MASS

VALUE (MeV)	EVTS	DOCUMENT ID	TECN	COMMENT
2931 ± 3 ± 5	≈ 34	AUBERT 08H	BABR	$\Upsilon(4S) \rightarrow B \bar{B}$

 $\Xi_c(2930)$ WIDTH

VALUE (MeV)	EVTS	DOCUMENT ID	TECN	COMMENT
36 ± 7 ± 11	≈ 34	AUBERT 08H	BABR	$\Upsilon(4S) \rightarrow B \bar{B}$

 $\Xi_c(2930)$ REFERENCES

AUBERT 08H	PR D77 031101R	B. Aubert <i>et al.</i>	(BABAR Collab.)
------------	----------------	-------------------------	-----------------

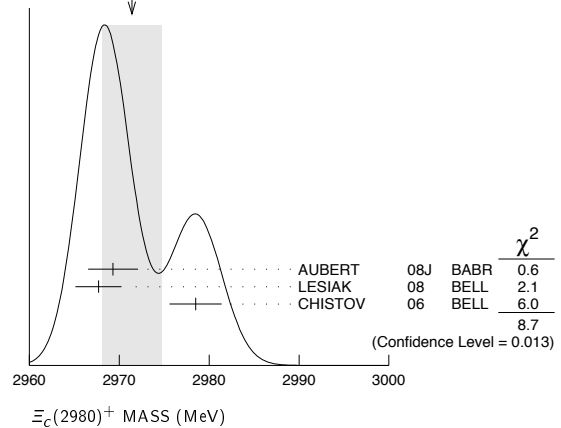
 $\Xi_c(2980)$

$I(J^P) = \frac{1}{2}(??)$ Status: ***

 $\Xi_c(2980)$ MASSES $\Xi_c(2980)^+$ MASS

VALUE (MeV)	EVTS	DOCUMENT ID	TECN	COMMENT
2971.4 ± 3.3 OUR AVERAGE				Error includes scale factor of 2.1. See the ideogram below.
2969.3 ± 2.2 ± 1.7	756 ± 206	AUBERT 08J	BABR	$e^+e^- \approx 10.58$ GeV
2967.7 ± 2.3 ± 1.1 ± 1.2	78 ± 13	LESIAK 08	BELL	$e^+e^- \approx \Upsilon(4S)$
2978.5 ± 2.1 ± 2.0	405 ± 51	CHISTOV 06	BELL	$e^+e^- \approx \Upsilon(4S)$

WEIGHTED AVERAGE
2971.4 ± 3.3 (Error scaled by 2.1)

 $\Xi_c(2980)^0$ MASS

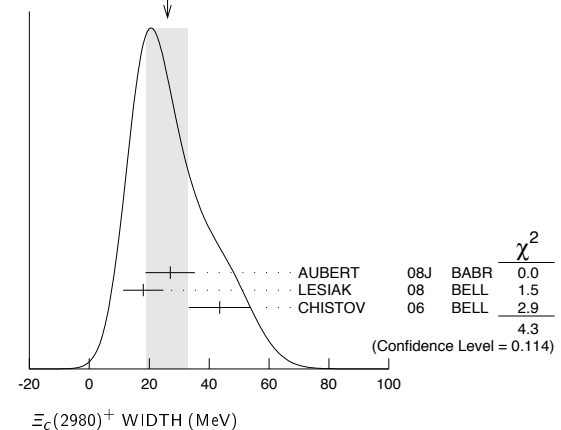
The evidence is statistically weaker for this charge state.

VALUE (MeV)	EVTS	DOCUMENT ID	TECN	COMMENT
2968.0 ± 2.6 OUR AVERAGE				Error includes scale factor of 1.2.
2972.9 ± 4.4 ± 1.6	67 ± 44	AUBERT 08J	BABR	$e^+e^- \approx 10.58$ GeV
2965.7 ± 2.4 ± 1.1 ± 1.2	57 ± 13	LESIAK 08	BELL	$e^+e^- \approx \Upsilon(4S)$
2977.1 ± 8.8 ± 3.5	42 ± 24	CHISTOV 06	BELL	$e^+e^- \approx \Upsilon(4S)$

 $\Xi_c(2980)$ WIDTHS $\Xi_c(2980)^+$ WIDTH

VALUE (MeV)	EVTS	DOCUMENT ID	TECN	COMMENT
26 ± 7 OUR AVERAGE				Error includes scale factor of 1.5. See the ideogram below.
27 ± 8 ± 2	756 ± 206	AUBERT 08J	BABR	$e^+e^- \approx 10.58$ GeV
18 ± 6 ± 3	78 ± 13	LESIAK 08	BELL	$e^+e^- \approx \Upsilon(4S)$
43.5 ± 7.5 ± 7.0	405 ± 51	CHISTOV 06	BELL	$e^+e^- \approx \Upsilon(4S)$

WEIGHTED AVERAGE
26 ± 7 (Error scaled by 1.5)

 $\Xi_c(2980)^0$ WIDTH

VALUE (MeV)	EVTS	DOCUMENT ID	TECN	COMMENT
20 ± 7 OUR AVERAGE				Error includes scale factor of 1.3.
31 ± 7 ± 8	67 ± 44	AUBERT 08J	BABR	$e^+e^- \approx 10.58$ GeV
15 ± 6 ± 3	57 ± 13	LESIAK 08	BELL	$e^+e^- \approx \Upsilon(4S)$

 $\Xi_c(2980)$ DECAY MODES

Mode	Fraction (Γ_i/Γ)
$\Gamma_1 \Lambda_c^+ \bar{K} \pi$	seen
$\Gamma_2 \Sigma_c(2455) \bar{K}$	seen
$\Gamma_3 \Lambda_c^+ \bar{K}$	not seen
$\Gamma_4 \Xi_c 2\pi$	seen
$\Gamma_5 \Xi_c(2645) \pi$	seen

See key on page 405

Baryon Particle Listings

 $\Xi_c(2980), \Xi_c(3055), \Xi_c(3080), \Xi_c(3123), \Omega_c^0$ $\Xi_c(2980)$ BRANCHING RATIOS

$\Gamma(\Lambda_c^+ \bar{K} \pi) / \Gamma_{\text{total}}$	DOCUMENT ID	TECN	COMMENT	Γ_1 / Γ
seen	AUBERT 08J	BABR	$e^+ e^- \approx \Upsilon(4S)$	
seen	CHISTOV 06	BELL	$e^+ e^- \approx \Upsilon(4S)$	
$\Gamma(\Sigma_c(2455) \bar{K}) / \Gamma(\Lambda_c^+ \bar{K} \pi)$				
VALUE	DOCUMENT ID	TECN	COMMENT	Γ_2 / Γ_1
$0.55 \pm 0.07 \pm 0.13$	AUBERT 08J	BABR	$e^+ e^- \approx \Upsilon(4S)$	
$\Gamma(\Xi_c(2645) \pi) / \Gamma_{\text{total}}$				
VALUE	DOCUMENT ID	TECN	COMMENT	Γ_5 / Γ
seen	LESIAK 08	BELL	$e^+ e^- \approx \Upsilon(4S)$	

 $\Xi_c(2980)$ REFERENCES

AUBERT 08J	PR D77 012002	B. Aubert <i>et al.</i>	(BABAR Collab.)
LESIAK 08	PL B665 9	T. Lesiak <i>et al.</i>	(BELLE Collab.)
CHISTOV 06	PRL 97 162001	R. Chistov <i>et al.</i>	(BELLE Collab.)

 $\Xi_c(3055)$ $I(J^P) = ?(??)$ Status: **

OMITTED FROM SUMMARY TABLE

A peak in the $\Sigma_c(2455)^{++} K^- \rightarrow \Lambda_c^+ K^- \pi^+$ mass spectrum with a claimed significance of 6.4 standard deviations. $\Xi_c(3055)$ MASSES

$\Xi_c(3055)^+$ MASS	VALUE (MeV)	EVTs	DOCUMENT ID	TECN	COMMENT
$3054.2 \pm 1.2 \pm 0.5$	218 ± 95	AUBERT 08J	BABR	$e^+ e^- \approx 10.58$ GeV	

 $\Xi_c(3055)$ WIDTHS

$\Xi_c(3055)^+$ WIDTH	VALUE (MeV)	EVTs	DOCUMENT ID	TECN	COMMENT
$17 \pm 6 \pm 11$	218 ± 95	AUBERT 08J	BABR	$e^+ e^- \approx 10.58$ GeV	

 $\Xi_c(3055)$ REFERENCES

AUBERT 08J	PR D77 012002	B. Aubert <i>et al.</i>	(BABAR Collab.)
------------	---------------	-------------------------	-----------------

 $\Xi_c(3080)$ $I(J^P) = \frac{1}{2}(??)$ Status: ***A narrow peak seen in the $\Lambda_c^+ K^- \pi^+$ and $\Lambda_c^+ K_S^0 \pi^-$ mass spectra. $\Xi_c(3080)$ MASSES

$\Xi_c(3080)^+$ MASS	VALUE (MeV)	EVTs	DOCUMENT ID	TECN	COMMENT
3077.0 ± 0.4 OUR AVERAGE					
$3077.0 \pm 0.4 \pm 0.2$	403 ± 60	AUBERT 08J	BABR	$e^+ e^- \approx 10.58$ GeV	
$3076.7 \pm 0.9 \pm 0.5$	326 ± 40	CHISTOV 06	BELL	$e^+ e^- \approx \Upsilon(4S)$	

 $\Xi_c(3080)^0$ MASS

$\Xi_c(3080)^0$ MASS	VALUE (MeV)	EVTs	DOCUMENT ID	TECN	COMMENT
3079.9 ± 1.4 OUR AVERAGE					Error includes scale factor of 1.3.
$3079.3 \pm 1.1 \pm 0.2$	90 ± 27	AUBERT 08J	BABR	$e^+ e^- \approx 10.58$ GeV	
$3082.8 \pm 1.8 \pm 1.5$	67 ± 20	CHISTOV 06	BELL	$e^+ e^- \approx \Upsilon(4S)$	

 $\Xi_c(3080)$ WIDTHS

$\Xi_c(3080)^+$ WIDTH	VALUE (MeV)	EVTs	DOCUMENT ID	TECN	COMMENT
5.8 ± 1.0 OUR AVERAGE					
$5.5 \pm 1.3 \pm 0.6$	403 ± 60	AUBERT 08J	BABR	$e^+ e^- \approx 10.58$ GeV	
$6.2 \pm 1.2 \pm 0.8$	326 ± 40	CHISTOV 06	BELL	$e^+ e^- \approx \Upsilon(4S)$	

 $\Xi_c(3080)^0$ WIDTH

$\Xi_c(3080)^0$ WIDTH	VALUE (MeV)	EVTs	DOCUMENT ID	TECN	COMMENT
5.6 ± 2.2 OUR AVERAGE					
$5.9 \pm 2.3 \pm 1.5$	90 ± 27	AUBERT 08J	BABR	$e^+ e^- \approx 10.58$ GeV	
$5.2 \pm 3.1 \pm 1.8$	67 ± 20	CHISTOV 06	BELL	$e^+ e^- \approx \Upsilon(4S)$	

 $\Xi_c(3080)$ DECAY MODES

Mode	Fraction (Γ_i / Γ)
$\Gamma_1 \Lambda_c^+ \bar{K} \pi$	seen
$\Gamma_2 \Sigma_c(2455) \bar{K}$	seen
$\Gamma_3 \Sigma_c(2455) \bar{K} + \Sigma_c(2520) \bar{K}$	seen
$\Gamma_4 \Lambda_c^+ \bar{K}$	not seen
$\Gamma_5 \Lambda_c^+ \bar{K} \pi^+ \pi^-$	not seen

 $\Xi_c(3080)$ BRANCHING RATIOS

$\Gamma(\Sigma_c(2455) \bar{K}) / \Gamma(\Lambda_c^+ \bar{K} \pi)$	VALUE	DOCUMENT ID	TECN	COMMENT	Γ_2 / Γ_1
0.45 ± 0.06 OUR AVERAGE					
$0.45 \pm 0.05 \pm 0.05$	AUBERT 08J	BABR	in $\Lambda_c^+ K^- \pi^+$		
$0.44 \pm 0.12 \pm 0.07$	AUBERT 08J	BABR	in $\Lambda_c^+ K_S^0 \pi^-$		
$[\Gamma(\Sigma_c(2455) \bar{K}) + \Gamma(\Sigma_c(2520) \bar{K})] / \Gamma(\Lambda_c^+ \bar{K} \pi)$					
VALUE	DOCUMENT ID	TECN	COMMENT	Γ_3 / Γ_1	
0.89 ± 0.12 OUR AVERAGE					
$0.95 \pm 0.14 \pm 0.06$	AUBERT 08J	BABR	in $\Lambda_c^+ K^- \pi^+$		
$0.78 \pm 0.21 \pm 0.05$	AUBERT 08J	BABR	in $\Lambda_c^+ K_S^0 \pi^-$		

 $\Xi_c(3080)$ REFERENCES

AUBERT 08J	PR D77 012002	B. Aubert <i>et al.</i>	(BABAR Collab.)
CHISTOV 06	PRL 97 162001	R. Chistov <i>et al.</i>	(BELLE Collab.)

 $\Xi_c(3123)$ $I(J^P) = ?(??)$ Status: *

OMITTED FROM SUMMARY TABLE

A peak in the $\Sigma_c(2520)^{++} K^- \rightarrow \Lambda_c^+ K^- \pi^+$ mass spectrum with a significance of 3.6 standard deviations. $\Xi_c(3123)$ MASSES

$\Xi_c(3123)^+$ MASS	VALUE (MeV)	EVTs	DOCUMENT ID	TECN	COMMENT
$3122.9 \pm 1.3 \pm 0.3$	101 ± 35	AUBERT 08J	BABR	$e^+ e^- \approx 10.58$ GeV	

 $\Xi_c(3123)$ WIDTHS

$\Xi_c(3123)^+$ WIDTH	VALUE (MeV)	EVTs	DOCUMENT ID	TECN	COMMENT
$4.4 \pm 3.4 \pm 1.7$	101 ± 35	AUBERT 08J	BABR	$e^+ e^- \approx 10.58$ GeV	

 $\Xi_c(3123)$ REFERENCES

AUBERT 08J	PR D77 012002	B. Aubert <i>et al.</i>	(BABAR Collab.)
------------	---------------	-------------------------	-----------------

 Ω_c^0 $I(J^P) = 0(\frac{1}{2}^+)$ Status: ***The quantum numbers have not been measured, but are simply assigned in accord with the quark model, in which the Ω_c^0 is the ssc ground state. Ω_c^0 MASS

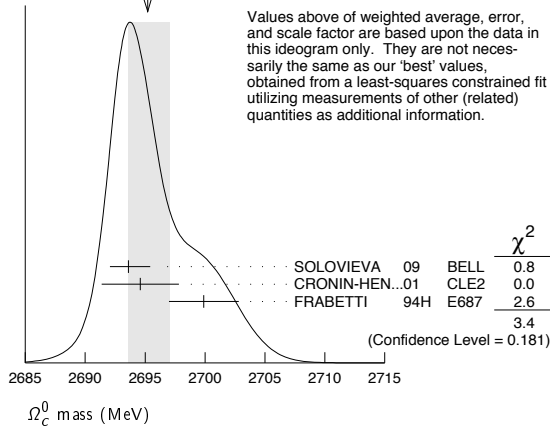
Ω_c^0 MASS	VALUE (MeV)	EVTs	DOCUMENT ID	TECN	COMMENT
2695.2 ± 1.7 OUR FIT					Error includes scale factor of 1.3.
2695.2 ± 1.8 OUR AVERAGE					Error includes scale factor of 1.3. See the ideogram below.
$2693.6 \pm 0.3 \pm 1.8$	725 ± 45	SOLOVIEVA 09	BELL	$\Omega^- \pi^+$ in $e^+ e^- \rightarrow \Upsilon(4S)$	
$2694.6 \pm 2.6 \pm 1.9$	40	¹ CRONIN-HEN.01	CLE2	$e^+ e^- \approx 10.6$ GeV	
$2699.9 \pm 1.5 \pm 2.5$	42	² FRABETTI 94H	E687	γ Be, $\bar{E}_\gamma = 221$ GeV	
• • • We do not use the following data for averages, fits, limits, etc. • • •					
$2705.9 \pm 3.3 \pm 2.0$	10	³ FRABETTI 93	E687	γ Be, $\bar{E}_\gamma = 221$ GeV	
$2719.0 \pm 7.0 \pm 2.5$	11	⁴ ALBRECHT 92H	ARG	$e^+ e^- \approx 10.6$ GeV	
2740 ± 20	3	BIAGI 85B	SPEC	Σ^- Be 135 GeV/c	

Baryon Particle Listings

 $\Omega_c^0, \Omega_c(2770)^0$

- ¹ CRONIN-HENNESSY 01 sees 40.4 ± 9.0 events in a sum over five channels.
² FRABETTI 94H claims a signal of 42.5 ± 8.8 $\Sigma^+ K^- K^- \pi^+$ events. The background is about 24 events.
³ FRABETTI 93 claims a signal of 10.3 ± 3.9 $\Omega^- \pi^+$ events above a background of 5.8 events.
⁴ ALBRECHT 92H claims a signal of 11.5 ± 4.3 $\Xi^- K^- \pi^+ \pi^+$ events. The background is about 5 events.

WEIGHTED AVERAGE
 2695.2+1.8-1.6 (Error scaled by 1.3)



Values above of weighted average, error, and scale factor are based upon the data in this ideogram only. They are not necessarily the same as our 'best' values, obtained from a least-squares constrained fit utilizing measurements of other (related) quantities as additional information.

 Ω_c^0 MEAN LIFE

VALUE (10^{-15} s)	EVTS	DOCUMENT ID	TECN	COMMENT
69 ± 12 OUR AVERAGE				
$72 \pm 11 \pm 11$	64	LINK	03c	FOCS $\Omega^- \pi^+, \Xi^- K^- \pi^+ \pi^+$
55^{+13+18}_{-11-23}	86	ADAMOVICH 95B	WA89	$\Omega^- \pi^- \pi^+ \pi^+, \Xi^- K^- \pi^+ \pi^+$
$86^{+27}_{-20} \pm 28$	25	FRABETTI 95D	E687	$\Sigma^+ K^- K^- \pi^+$

 Ω_c^0 DECAY MODES

No absolute branching fractions have been measured.

Mode	Fraction (Γ_i/Γ)
Γ_1 $\Sigma^+ K^- K^- \pi^+$	seen
Γ_2 $\Xi^0 K^- \pi^+$	seen
Γ_3 $\Xi^- K^- \pi^+ \pi^+$	seen
Γ_4 $\Omega^- e^+ \nu_e$	seen
Γ_5 $\Omega^- \pi^+$	seen
Γ_6 $\Omega^- \pi^+ \pi^0$	seen
Γ_7 $\Omega^- \pi^- \pi^+ \pi^+$	seen

 Ω_c^0 BRANCHING RATIOS

$\Gamma(\Sigma^+ K^- K^- \pi^+)/\Gamma_{\text{total}}$	Γ_1/Γ			
VALUE	EVTS	DOCUMENT ID	TECN	COMMENT
seen	42	FRABETTI 94H	E687	γ Be, $\bar{E}_\gamma = 221$ GeV

$\Gamma(\Sigma^+ K^- K^- \pi^+)/\Gamma(\Omega^- \pi^+)$	Γ_1/Γ_5			
VALUE	CL%	DOCUMENT ID	TECN	COMMENT
< 4.8	90	CRONIN-HEN..01	CLE2	$e^+ e^- \approx 10.6$ GeV

$\Gamma(\Xi^0 K^- \pi^+)/\Gamma(\Omega^- \pi^+)$	Γ_2/Γ_5			
VALUE	EVTS	DOCUMENT ID	TECN	COMMENT
$4.0 \pm 2.5 \pm 0.4$	9	CRONIN-HEN..01	CLE2	$e^+ e^- \approx 10.6$ GeV

$\Gamma(\Xi^- K^- \pi^+ \pi^+)/\Gamma_{\text{total}}$	Γ_3/Γ			
VALUE	EVTS	DOCUMENT ID	TECN	COMMENT
seen	11	ALBRECHT 92H	ARG	$e^+ e^- \approx 10.6$ GeV
seen	3	BIAGI 85B	SPEC	Σ^- Be 135 GeV/c

$\Gamma(\Xi^- K^- \pi^+ \pi^+)/\Gamma(\Omega^- \pi^+)$	Γ_3/Γ_5				
VALUE	CL%	EVTS	DOCUMENT ID	TECN	COMMENT
$0.46 \pm 0.13 \pm 0.03$	45	12	AUBERT 07AH	BABR	$e^+ e^- \approx 7(45)$
$1.6 \pm 1.1 \pm 0.4$	7		CRONIN-HEN..01	CLE2	$e^+ e^- \approx 10.6$ GeV
< 2.8	90		FRABETTI 93	E687	γ Be, $\bar{E}_\gamma = 221$ GeV

$\Gamma(\Omega^- \pi^+)/\Gamma(\Omega^- e^+ \nu_e)$	Γ_5/Γ_4			
VALUE	EVTS	DOCUMENT ID	TECN	COMMENT
$0.41 \pm 0.19 \pm 0.04$	11	AMMAR 02	CLE2	$e^+ e^- \approx 7(45)$

$\Gamma(\Omega^- \pi^- \pi^0)/\Gamma(\Omega^- \pi^+)$	Γ_6/Γ_5				
VALUE	EVTS	DOCUMENT ID	TECN	COMMENT	
$1.27 \pm 0.31 \pm 0.11$	64	15	AUBERT 07AH	BABR	$e^+ e^- \approx 7(45)$
$> > >$	We do not use the following data for averages, fits, limits, etc. $> > >$				
$4.2 \pm 2.2 \pm 0.9$	12	CRONIN-HEN..01	CLE2	$e^+ e^- \approx 10.6$ GeV	

$\Gamma(\Omega^- \pi^- \pi^+ \pi^+)/\Gamma(\Omega^- \pi^+)$	Γ_7/Γ_5					
VALUE	CL%	EVTS	DOCUMENT ID	TECN	COMMENT	
$0.28 \pm 0.09 \pm 0.01$		25	8	AUBERT 07AH	BABR	$e^+ e^- \approx 7(45)$
< 0.56	90	CRONIN-HEN..01			CLE2	$e^+ e^- \approx 10.6$ GeV
seen			ADAMOVICH 95B	WA89	Σ^- 340 GeV	
< 1.6	90		FRABETTI 93	E687	γ Be, $\bar{E}_\gamma = 221$ GeV	

 Ω_c^0 REFERENCES

SOLOVIEVA 09	PL B672 1	E. Solovieva et al.	(BELLE Collab.)
AUBERT 07AH	PRL 99 062001	B. Aubert et al.	(BABAR Collab.)
LINK 03C	PL B561 41	J.M. Link et al.	(FNAL FOCUS Collab.)
AMMAR 02	PRL 89 171803	R. Ammar et al.	(CLEO Collab.)
CRONIN-HEN..01	PRL 86 3730	D. Cronin-Hennessy et al.	(CLEO Collab.)
ADAMOVICH 95B	PL B358 151	M.I. Adamovich et al.	(CERN WA89 Collab.)
FRABETTI 95D	PL B357 678	P.L. Frabetti et al.	(FNAL E687 Collab.)
FRABETTI 94H	PL B338 106	P.L. Frabetti et al.	(FNAL E687 Collab.)
FRABETTI 93	PL B300 190	P.L. Frabetti et al.	(FNAL E687 Collab.)
ALBRECHT 92H	PL B288 367	H. Albrecht et al.	(ARGUS Collab.)
BIAGI 85B	ZPHY C28 175	S.F. Biagi et al.	(CERN WA62 Collab.)

 $\Omega_c(2770)^0$

$$I(J^P) = 0(\frac{3}{2}^+) \text{ Status: } ** *$$

The natural assignment is that this goes with the $\Sigma_c(2520)$ and $\Xi_c(2645)$ to complete the lowest mass $J^P = \frac{3}{2}^+$ SU(3) sextet, part of the SU(4) 20-plet that includes the $\Delta(1232)$. But J and P have not been measured.

 $\Omega_c(2770)^0$ MASS

The mass is obtained from the mass-difference measurement that follows.

VALUE (MeV)	DOCUMENT ID
2765.9 ± 2.0 OUR FIT	Error includes scale factor of 1.2.

 $\Omega_c(2770)^0 - \Omega_c^0$ MASS DIFFERENCE

VALUE (MeV)	EVTS	DOCUMENT ID	TECN	COMMENT
$70.7^{+0.8}_{-0.9}$ OUR FIT				
$70.7^{+0.8}_{-1.0}$ OUR AVERAGE				
$70.7 \pm 0.9^{+0.1}_{-0.9}$	54	9	SOLOVIEVA 09	BELL $\Omega_c^0 \gamma$ in $e^+ e^- \rightarrow 7(45)$
$70.8 \pm 1.0 \pm 1.1$	105	22	AUBERT, BE 06i	BABR $e^+ e^- \approx 7(45)$

 $\Omega_c(2770)^0$ DECAY MODES

The $\Omega_c(2770)^0 - \Omega_c^0$ mass difference is too small for any strong decay to occur.

Mode	Fraction (Γ_i/Γ)
Γ_1 $\Omega_c^0 \gamma$	presumably 100%

 $\Omega_c(2770)^0$ REFERENCES

SOLOVIEVA 09	PL B672 1	E. Solovieva et al.	(BELLE Collab.)
AUBERT, BE 06i	PRL 97 232001	B. Aubert et al.	(BABAR Collab.)

See key on page 405

Baryon Particle Listings

Ξ_{cc}^+

DOUBLY CHARMED BARYONS
(C = +2)
 $\Xi_{cc}^{++} = ucc, \Xi_{cc}^+ = dcc, \Omega_{cc}^+ = scc$

Ξ_{cc}^+

$I(J^P) = ?(??)$ Status: *

OMITTED FROM SUMMARY TABLE

This would presumably be an isospin-1/2 particle, a $ccu \Xi_{cc}^{++}$ and a $ccd \Xi_{cc}^+$. However, opposed to the evidence cited below, the BABAR experiment has found no evidence for a Ξ_{cc}^+ in a search in $\Lambda_c^+ K^- \pi^+$ and $\Xi_c^0 \pi^+$ modes, and no evidence of a Ξ_{cc}^{++} in $\Lambda_c^+ K^- \pi^+ \pi^+$ and $\Xi_c^0 \pi^+ \pi^+$ modes (AUBERT,B 06D). Nor has the BELLE experiment found any evidence for a Ξ_{cc}^+ in the $\Lambda_c^+ K^- \pi^+$ mode (CHISTOV 06).

Ξ_{cc}^+ MASS

VALUE (MeV)	EVTS	DOCUMENT ID	TECN	COMMENT
3518.9 ± 0.9 OUR AVERAGE				
3518 ± 3	6	¹ OCHERASHVI..05	SELX	Σ^- nucleus ≈ 600 GeV
3519 ± 1	16	² MATTSON 02	SELX	Σ^- nucleus ≈ 600 GeV

¹ OCHERASHVILI 05 claims "an excess of 5.62 events over ... 1.38 ± 0.13 events" for a significance of 4.8 σ in $pD^+ K^-$ events.

² MATTSON 02 claims "an excess of 15.9 events over an expected background of 6.1 ± 0.5 events, a statistical significance of 6.3 σ " in the $\Lambda_c^+ K^- \pi^+$ invariant-mass spectrum.

The probability that the peak is a fluctuation increases from 1.0 × 10⁻⁶ to 1.1 × 10⁻⁴ when the number of bins searched is considered.

Ξ_{cc}^+ MEAN LIFE

VALUE (10 ⁻¹⁵ s)	CL%	DOCUMENT ID	TECN	COMMENT
<33	90	MATTSON 02	SELX	Σ^- nucleus, ≈ 600 GeV

Ξ_{cc}^+ DECAY MODES

Mode	Γ_1	Γ_2
$\Lambda_c^+ K^- \pi^+$		
$pD^+ K^-$		

$\Gamma(pD^+ K^-)/\Gamma(\Lambda_c^+ K^- \pi^+)$				Γ_2/Γ_1
VALUE	EVTS	DOCUMENT ID	TECN	COMMENT
0.36 ± 0.21	6	OCHERASHVI..05	SELX	Σ^- ≈ 600 GeV

Ξ_{cc}^+ REFERENCES

AUBERT,B 06D	PR D74 011103R	B. Aubert <i>et al.</i>	(BABAR Collab.)
CHISTOV 06	PRL 97 162001	R. Chistov <i>et al.</i>	(BELLE Collab.)
OCHERASHVI..05	PL B628 18	A. Ocherashvili <i>et al.</i>	(FNAL SELEX Collab.)
MATTSON 02	PRL 89 112001	M. Mattson <i>et al.</i>	(FNAL SELEX Collab.)

Baryon Particle Listings

 Λ_b^0

BOTTOM BARYONS ($B = -1$)

$$\Lambda_b^0 = udb, \Xi_b^0 = usb, \Xi_b^- = dsb, \Omega_b^- = sss$$

 Λ_b^0

$$I(J^P) = 0(\frac{1}{2}^+) \text{ Status: } ***$$

In the quark model, a Λ_b^0 is an isospin-0 udb state. The lowest Λ_b^0 ought to have $J^P = 1/2^+$. None of $I, J,$ or P have actually been measured.

 Λ_b^0 MASS

VALUE (MeV)	EVTS	DOCUMENT ID	TECN	COMMENT
5620.2 ± 1.6	OUR AVERAGE			
5619.7 ± 1.2 ± 1.2		¹ ACOSTA	06 CDF	$p\bar{p}$ at 1.96 TeV
5621 ± 4 ± 3		² ABE	97B CDF	$p\bar{p}$ at 1.8 TeV
5668 ± 16 ± 8	4	³ ABREU	96N DLPH	$e^+e^- \rightarrow Z$
5614 ± 21 ± 4	4	³ BUSKULIC	96L ALEP	$e^+e^- \rightarrow Z$
not seen		⁴ ABE	93B CDF	Sup. by ABE 97B
5640 ± 50 ± 30	16	⁵ ALBAJAR	91E UA1	$p\bar{p}$ 630 GeV
5640 $^{+100}_{-210}$	52	BARI	91 SFM	$\Lambda_b^0 \rightarrow pD^0\pi^-$
5650 $^{+150}_{-200}$	90	BARI	91 SFM	$\Lambda_b^0 \rightarrow \Lambda_c^+ \pi^+ \pi^- \pi^-$

- • • We do not use the following data for averages, fits, limits, etc. • • •
- ¹ Uses exclusively reconstructed final states containing a $J/\psi \rightarrow \mu^+ \mu^-$ decays.
- ² ABE 97B observed 38 events with a background of 18 ± 1.6 events in the mass range 5.60–5.65 GeV/ c^2 , a significance of > 3.4 standard deviations.
- ³ Uses 4 fully reconstructed Λ_b events.
- ⁴ ABE 93B states that, based on the signal claimed by ALBAJAR 91E, CDF should have found $30 \pm 23 \Lambda_b^0 \rightarrow J/\psi(1S)\Lambda$ events. Instead, CDF found not more than 2 events.
- ⁵ ALBAJAR 91E claims 16 ± 5 events above a background of 9 ± 1 events, a significance of about 5 standard deviations.

 $m_{\Lambda_b} - m_{B^0}$

VALUE (MeV)	DOCUMENT ID	TECN	COMMENT
339.2 ± 1.4 ± 0.1	⁶ ACOSTA	06 CDF	$p\bar{p}$ at 1.96 TeV

- ⁶ Uses exclusively reconstructed final states containing a $J/\psi \rightarrow \mu^+ \mu^-$ decays.

 Λ_b^0 MEAN LIFE

See b -baryon Admixture section for data on b -baryon mean life average over species of b -baryon particles.

"OUR EVALUATION" is an average using rescaled values of the data listed below. The average and rescaling were performed by the Heavy Flavor Averaging Group (HFAG) and are described at <http://www.slac.stanford.edu/xorg/hfag/>. The averaging/rescaling procedure takes into account correlations between the measurements and asymmetric lifetime errors.

VALUE (10^{-12} s)	EVTS	DOCUMENT ID	TECN	COMMENT
1.391 $^{+0.038}_{-0.037}$	OUR EVALUATION			
1.401 ± 0.046 ± 0.035		⁷ AALTONEN	10B CDF	$p\bar{p}$ at 1.96 TeV
1.218 $^{+0.130}_{-0.115}$ ± 0.042		⁸ ABAZOV	07S D0	$p\bar{p}$ at 1.96 TeV
1.290 $^{+0.119+0.087}_{-0.110-0.091}$		⁹ ABAZOV	07U D0	$p\bar{p}$ at 1.96 TeV
1.593 $^{+0.083}_{-0.078}$ ± 0.033		⁸ ABULENCIA	07A CDF	$p\bar{p}$ at 1.96 TeV
1.11 $^{+0.19}_{-0.18}$ ± 0.05		¹⁰ ABREU	99W DLPH	$e^+e^- \rightarrow Z$
1.29 $^{+0.24}_{-0.22}$ ± 0.06		¹⁰ ACKERSTAFF	98G OPAL	$e^+e^- \rightarrow Z$
1.21 ± 0.11		¹⁰ BARATE	98D ALEP	$e^+e^- \rightarrow Z$
1.32 ± 0.15 ± 0.07		¹¹ ABE	96M CDF	$p\bar{p}$ at 1.8 TeV
• • • We do not use the following data for averages, fits, limits, etc. • • •				
1.22 $^{+0.22}_{-0.18}$ ± 0.04		⁸ ABAZOV	05C D0	Repl. by ABAZOV 07S
1.19 $^{+0.21}_{-0.18}$ $^{+0.07}_{-0.08}$		ABREU	96D DLPH	Repl. by ABREU 99W
1.14 $^{+0.22}_{-0.19}$ ± 0.07	69	AKERS	95K OPAL	Repl. by ACKERSTAFF 98G
1.02 $^{+0.23}_{-0.18}$ ± 0.06	44	BUSKULIC	95L ALEP	Repl. by BARATE 98D

- ⁷ Measured mean life using fully reconstructed $\Lambda_b^0 \rightarrow \Lambda_c^+ \pi^-$ decays.
- ⁸ Measured mean life using fully reconstructed $\Lambda_b^0 \rightarrow J/\psi \Lambda$ decays.
- ⁹ Measured using semileptonic decays $\Lambda_b^0 \rightarrow \Lambda_c^+ \mu \nu X$ and $\Lambda_c^+ \rightarrow K_S^0 p$.
- ¹⁰ Measured using $\Lambda_c \ell^-$ and $\Lambda \ell^+ \ell^-$.
- ¹¹ Excess $\Lambda_c \ell^-$, decay lengths.

 $\tau_{\Lambda_b^0}/\tau_{B^0}$ MEAN LIFE RATIO $\tau_{\Lambda_b^0}/\tau_{B^0}$ (direct measurements)

VALUE	DOCUMENT ID	TECN	COMMENT
0.99 ± 0.10	OUR AVERAGE		Error includes scale factor of 2.0.
0.811 $^{+0.096}_{-0.087}$ ± 0.034	^{12,13} ABAZOV	07S D0	$p\bar{p}$ at 1.96 TeV
1.041 ± 0.057	¹⁴ ABULENCIA	07A CDF	$p\bar{p}$ at 1.96 TeV
• • • We do not use the following data for averages, fits, limits, etc. • • •			
0.87 $^{+0.17}_{-0.14}$ ± 0.03	¹⁴ ABAZOV	05C D0	Repl. by ABAZOV 07S

¹² Uses fully reconstructed $\Lambda_b \rightarrow J/\psi \Lambda$ decays.

¹³ Uses $B^0 \rightarrow J/\psi K_S^0$ decays for denominator.

¹⁴ Measured mean life ratio using fully reconstructed decays.

 Λ_b^0 DECAY MODES

The branching fractions $B(b\text{-baryon} \rightarrow \Lambda \ell^- \bar{\nu}_\ell \text{ anything})$ and $B(\Lambda_b^0 \rightarrow \Lambda_c^+ \ell^- \bar{\nu}_\ell \text{ anything})$ are not pure measurements because the underlying measured products of these with $B(b \rightarrow b\text{-baryon})$ were used to determine $B(b \rightarrow b\text{-baryon})$, as described in the note "Production and Decay of b -Flavored Hadrons."

For inclusive branching fractions, e.g., $\Lambda_b \rightarrow \bar{\Lambda}_c \text{ anything}$, the values usually are multiplicities, not branching fractions. They can be greater than one.

Mode	Fraction (Γ_i/Γ)	Confidence level
Γ_1 $J/\psi(1S)\Lambda \times B(b \rightarrow \Lambda_b^0)$	(4.7 ± 2.3) × 10 ⁻⁵	
Γ_2 $pD^0\pi^-$		
Γ_3 $\Lambda_c^+ \pi^-$	(8.8 ± 3.2) × 10 ⁻³	
Γ_4 $\Lambda_c^+ a_1(1260)^-$	seen	
Γ_5 $\Lambda_c^+ \pi^+ \pi^- \pi^-$		
Γ_6 $\Lambda K^0 2\pi^+ 2\pi^-$		
Γ_7 $\Lambda_c^+ \ell^- \bar{\nu}_\ell \text{ anything}$	[a] (10.7 ± 3.2) %	
Γ_8 $\Lambda_c^+ \ell^- \bar{\nu}_\ell$	(5.0 $^{+1.9}_{-1.4}$) %	
Γ_9 $\Lambda_c^+ \pi^+ \pi^- \ell^- \bar{\nu}_\ell$	(5.6 ± 3.1) %	
Γ_{10} $\Lambda_c(2595)^+ \ell^- \bar{\nu}_\ell$	(6.3 $^{+4.0}_{-3.1}$) × 10 ⁻³	
Γ_{11} $\Lambda_c(2625)^+ \ell^- \bar{\nu}_\ell$	(1.1 $^{+0.6}_{-0.4}$) %	
Γ_{12} $\Sigma_c(2455)^0 \pi^+ \ell^- \bar{\nu}_\ell$		
Γ_{13} $\Sigma_c(2455)^{++} \pi^- \ell^- \bar{\nu}_\ell$		
Γ_{14} $p h^-$	[b] < 2.3 × 10 ⁻⁵	90%
Γ_{15} $p \pi^-$	(3.8 ± 1.3) × 10 ⁻⁶	
Γ_{16} $p K^-$	(6.0 ± 1.9) × 10 ⁻⁶	
Γ_{17} $\Lambda \gamma$	< 1.3 × 10 ⁻³	90%

[a] Not a pure measurement. See note at head of Λ_b^0 Decay Modes.

[b] Here h^- means π^- or K^- .

 Λ_b^0 BRANCHING RATIOS $\Gamma(J/\psi(1S)\Lambda \times B(b \rightarrow \Lambda_b^0))/\Gamma_{\text{total}}$ Γ_1/Γ

VALUE (units 10 ⁻⁴)	EVTS	DOCUMENT ID	TECN	COMMENT
0.47 ± 0.23 ± 0.02		¹⁵ ABE	97B CDF	$p\bar{p}$ at 1.8 TeV
• • • We do not use the following data for averages, fits, limits, etc. • • •				
18 ± 6 ± 9		¹⁶ ALBAJAR	91E UA1	$p\bar{p}$ at 630 GeV
¹⁵ ABE 97B reports $[B(\Lambda_b^0 \rightarrow J/\psi \Lambda) \times B(b \rightarrow \Lambda_b^0)] / [B(B^0 \rightarrow J/\psi K_S^0) \times B(b \rightarrow B^0)] = 0.27 \pm 0.12 \pm 0.05$. We multiply by our best value $B(B^0 \rightarrow J/\psi K_S^0) \times B(b \rightarrow B^0) = (1.74 \pm 0.08) \times 10^{-4}$. Our first error is their experiments's error and our second error is the systematic error from using our best value.				

 $\Gamma(pD^0\pi^-)/\Gamma_{\text{total}}$ Γ_2/Γ

VALUE	EVTS	DOCUMENT ID	TECN	COMMENT
• • • We do not use the following data for averages, fits, limits, etc. • • •				
seen	52	BARI	91 SFM	$D^0 \rightarrow K^- \pi^+$
seen		BASILE	81 SFM	$D^0 \rightarrow K^- \pi^+$

 $\Gamma(\Lambda_c^+ \pi^-)/\Gamma_{\text{total}}$ Γ_3/Γ

VALUE (units 10 ⁻³)	EVTS	DOCUMENT ID	TECN	COMMENT
8.8 ± 2.8 ± 1.5		¹⁶ ABULENCIA	07B CDF	$p\bar{p}$ at 1.96 TeV
• • • We do not use the following data for averages, fits, limits, etc. • • •				
seen	3	ABREU	96N DLPH	$\Lambda_c^+ \rightarrow p K^- \pi^+$
seen	4	BUSKULIC	96L ALEP	$\Lambda_c^+ \rightarrow p K^- \pi^+$, $p K^0, \Lambda \pi^+ \pi^+ \pi^-$

¹⁶ The result is obtained from $(f_{\text{baryon}}/f_d) (B(\Lambda_b^0 \rightarrow \Lambda_c^+ \pi^-)/B(\bar{B}^0 \rightarrow D^+ \pi^-)) = 0.82 \pm 0.08 \pm 0.11 \pm 0.22$, assuming $f_{\text{baryon}}/f_d = 0.25 \pm 0.04$ and $B(\bar{B}^0 \rightarrow D^+ \pi^-) = (2.68 \pm 0.13) \times 10^{-3}$.

$\Gamma(\Lambda_c^+ a_1(1260)^-)/\Gamma_{\text{total}}$					Γ_4/Γ
VALUE	EVTs	DOCUMENT ID	TECN	COMMENT	
seen	1	ABREU	96N	DLPH $\Lambda_c^+ \rightarrow p K^- \pi^+, a_1^- \rightarrow \rho^0 \pi^- \rightarrow \pi^+ \pi^- \pi^-$	

$\Gamma(\Lambda_c^+ \pi^+ \pi^- \pi^-)/\Gamma_{\text{total}}$					Γ_5/Γ
VALUE	EVTs	DOCUMENT ID	TECN	COMMENT	
••• We do not use the following data for averages, fits, limits, etc. •••					
seen	90	BARI	91	SFM $\Lambda_c^+ \rightarrow p K^- \pi^+$	

$\Gamma(\Lambda K^0 2\pi^+ 2\pi^-)/\Gamma_{\text{total}}$					Γ_6/Γ
VALUE	EVTs	DOCUMENT ID	TECN	COMMENT	
••• We do not use the following data for averages, fits, limits, etc. •••					
seen	4	17 ARENTON	86	FMP5 $\Lambda K_S^0 2\pi^+ 2\pi^-$	
17 See the footnote to the ARENTON 86 mass value.					

$\Gamma(\Lambda_c^+ \ell^- \bar{\nu}_\ell \text{ anything})/\Gamma_{\text{total}}$					Γ_7/Γ
VALUE	EVTs	DOCUMENT ID	TECN	COMMENT	
The values and averages in this section serve only to show what values result if one assumes our $B(b \rightarrow b\text{-baryon})$. They cannot be thought of as measurements since the underlying product branching fractions were also used to determine $B(b \rightarrow b\text{-baryon})$ as described in the note on "Production and Decay of b -Flavored Hadrons."					

VALUE	EVTs	DOCUMENT ID	TECN	COMMENT	
0.107 ± 0.032 OUR AVERAGE					
0.101 ± 0.018 ± 0.026		18 BARATE	98D	ALEP $e^+ e^- \rightarrow Z$	
0.14 $\begin{smallmatrix} +0.05 \\ -0.04 \end{smallmatrix} \pm 0.04$	29	19 ABREU	95S	DLPH $e^+ e^- \rightarrow Z$	
••• We do not use the following data for averages, fits, limits, etc. •••					
0.089 ± 0.022 ± 0.023	55	20 BUSKULIC	95L	ALEP Repl. by BARATE 98D	
0.18 ± 0.07 ± 0.05	21	21 BUSKULIC	92E	ALEP $\Lambda_c^+ \rightarrow p K^- \pi^+$	

18 BARATE 98D reports $[\Gamma(\Lambda_b^0 \rightarrow \Lambda_c^+ \ell^- \bar{\nu}_\ell \text{ anything})/\Gamma_{\text{total}}] \times [B(\bar{B} \rightarrow b\text{-baryon})] = 0.0086 \pm 0.0007 \pm 0.0014$ which we divide by our best value $B(\bar{B} \rightarrow b\text{-baryon}) = (8.5 \pm 2.2) \times 10^{-2}$. Our first error is their experiment's error and our second error is the systematic error from using our best value. Measured using $\Lambda_c \ell^-$ and $\Lambda \ell^+ \ell^-$.

19 ABREU 95S reports $[\Gamma(\Lambda_b^0 \rightarrow \Lambda_c^+ \ell^- \bar{\nu}_\ell \text{ anything})/\Gamma_{\text{total}}] \times [B(\bar{B} \rightarrow b\text{-baryon})] = 0.0118 \pm 0.0026 \pm \begin{smallmatrix} +0.0031 \\ -0.0021 \end{smallmatrix}$ which we divide by our best value $B(\bar{B} \rightarrow b\text{-baryon}) = (8.5 \pm 2.2) \times 10^{-2}$. Our first error is their experiment's error and our second error is the systematic error from using our best value.

20 BUSKULIC 95L reports $[\Gamma(\Lambda_b^0 \rightarrow \Lambda_c^+ \ell^- \bar{\nu}_\ell \text{ anything})/\Gamma_{\text{total}}] \times [B(\bar{B} \rightarrow b\text{-baryon})] = 0.00755 \pm 0.0014 \pm 0.0012$ which we divide by our best value $B(\bar{B} \rightarrow b\text{-baryon}) = (8.5 \pm 2.2) \times 10^{-2}$. Our first error is their experiment's error and our second error is the systematic error from using our best value.

21 BUSKULIC 92E reports $[\Gamma(\Lambda_b^0 \rightarrow \Lambda_c^+ \ell^- \bar{\nu}_\ell \text{ anything})/\Gamma_{\text{total}}] \times [B(\bar{B} \rightarrow b\text{-baryon})] = 0.015 \pm 0.0035 \pm 0.0045$ which we divide by our best value $B(\bar{B} \rightarrow b\text{-baryon}) = (8.5 \pm 2.2) \times 10^{-2}$. Our first error is their experiment's error and our second error is the systematic error from using our best value. Superseded by BUSKULIC 95L.

$\Gamma(\Lambda_c^+ \ell^- \bar{\nu}_\ell)/\Gamma_{\text{total}}$					Γ_8/Γ
VALUE		DOCUMENT ID	TECN	COMMENT	
0.050 ± 0.011 + 0.016 -0.008 - 0.012		22 ABDALLAH	04A	DLPH $e^+ e^- \rightarrow Z^0$	
22 Derived from a combined likelihood and event rate fit to the distribution of the $\ln \mu$ -wide variable and using HQET. The slope of the form factor is measured to be $\rho^2 = 2.03 \pm 0.46 \pm \begin{smallmatrix} +0.72 \\ -1.00 \end{smallmatrix}$.					

$\Gamma(\Lambda_c^+ \ell^- \bar{\nu}_\ell)/\Gamma(\Lambda_c^+ \pi^-)$					Γ_8/Γ_3
VALUE		DOCUMENT ID	TECN	COMMENT	
16.6 ± 3.0 + 2.8 -3.6		AALTONEN	09E	CDF $p\bar{p}$ at 1.96 TeV	

$\Gamma(\Lambda_c^+ \pi^+ \pi^- \ell^- \bar{\nu}_\ell)/\Gamma_{\text{total}}$					Γ_9/Γ
VALUE		DOCUMENT ID	TECN	COMMENT	
0.056 ± 0.031 -0.030		23 ABDALLAH	04A	DLPH $e^+ e^- \rightarrow Z^0$	
23 Derived from the fraction of $\Gamma(\Lambda_b^0 \rightarrow \Lambda_c^+ \ell^- \bar{\nu}_\ell) / (\Gamma(\Lambda_b^0 \rightarrow \Lambda_c^+ \ell^- \bar{\nu}_\ell) + \Gamma(\Lambda_b^0 \rightarrow \Lambda_c^+ \pi^+ \pi^- \ell^- \bar{\nu}_\ell)) = 0.47 \pm \begin{smallmatrix} +0.10 + 0.07 \\ -0.08 - 0.06 \end{smallmatrix}$.					

$\Gamma(\Lambda_c^+ \ell^- \bar{\nu}_\ell) / [\Gamma(\Lambda_c^+ \ell^- \bar{\nu}_\ell) + \Gamma(\Lambda_c^+ \pi^+ \pi^- \ell^- \bar{\nu}_\ell)]$					$\Gamma_8/(\Gamma_8 + \Gamma_9)$
VALUE		DOCUMENT ID	TECN	COMMENT	
0.47 ± 0.10 + 0.07 -0.08 - 0.06		ABDALLAH	04A	DLPH $e^+ e^- \rightarrow Z^0$	

$\Gamma(\Lambda_c(2595)^+ \ell^- \bar{\nu}_\ell)/\Gamma(\Lambda_c^+ \ell^- \bar{\nu}_\ell)$					Γ_{10}/Γ_8
VALUE		DOCUMENT ID	TECN	COMMENT	
0.126 ± 0.033 + 0.047 -0.038		AALTONEN	09E	CDF $p\bar{p}$ at 1.96 TeV	

$\Gamma(\Lambda_c(2625)^+ \ell^- \bar{\nu}_\ell)/\Gamma(\Lambda_c^+ \ell^- \bar{\nu}_\ell)$					Γ_{11}/Γ_8
VALUE		DOCUMENT ID	TECN	COMMENT	
0.210 ± 0.042 + 0.071 -0.050		AALTONEN	09E	CDF $p\bar{p}$ at 1.96 TeV	

$[\frac{1}{2}\Gamma(\Sigma_c(2455)^0 \pi^+ \ell^- \bar{\nu}_\ell) + \frac{1}{2}\Gamma(\Sigma_c(2455)^{++} \pi^- \ell^- \bar{\nu}_\ell)]/\Gamma(\Lambda_c^+ \ell^- \bar{\nu}_\ell)$ $(\frac{1}{2}\Gamma_{12} + \frac{1}{2}\Gamma_{13})/\Gamma_8$				
VALUE		DOCUMENT ID	TECN	COMMENT
0.054 ± 0.022 + 0.021 -0.018		AALTONEN	09E	CDF $p\bar{p}$ at 1.96 TeV

$\Gamma(\rho h^-)/\Gamma_{\text{total}}$					Γ_{14}/Γ
VALUE	CL%	DOCUMENT ID	TECN	COMMENT	
< 2.3 × 10⁻⁵	90	24 ACOSTA	05o	CDF $p\bar{p}$ at 1.96 TeV	
24 Assumes $f_{\Lambda} / f_{\Delta} = 0.25$, and equal momentum distribution for Λ_b and B mesons.					

$\Gamma(\rho \pi^-)/\Gamma_{\text{total}}$					Γ_{15}/Γ
VALUE (units 10 ⁻⁶)	CL%	DOCUMENT ID	TECN	COMMENT	
3.8 ± 0.8 ± 1.0		25 AALTONEN	09c	CDF $p\bar{p}$ at 1.96 TeV	
••• We do not use the following data for averages, fits, limits, etc. •••					
< 50	90	26 BUSKULIC	96v	ALEP $e^+ e^- \rightarrow Z$	

25 AALTONEN 09c reports $[\Gamma(\Lambda_b^0 \rightarrow \rho \pi^-)/\Gamma_{\text{total}}] / [B(B^0 \rightarrow K^+ \pi^-)] \times [B(\bar{B} \rightarrow b\text{-baryon})] / [B(\bar{B} \rightarrow B^0)] = 0.042 \pm 0.007 \pm 0.006$ which we multiply or divide by our best values $B(B^0 \rightarrow K^+ \pi^-) = (1.94 \pm 0.06) \times 10^{-5}$, $B(\bar{B} \rightarrow b\text{-baryon}) = (8.5 \pm 2.2) \times 10^{-2}$, $B(\bar{B} \rightarrow B^0) = (40.1 \pm 1.3) \times 10^{-2}$. Our first error is their experiment's error and our second error is the systematic error from using our best values.

$\Gamma(\rho K^-)/\Gamma_{\text{total}}$					Γ_{16}/Γ
VALUE (units 10 ⁻⁶)	CL%	DOCUMENT ID	TECN	COMMENT	
6.0 ± 1.1 ± 1.6		27 AALTONEN	09c	CDF $p\bar{p}$ at 1.96 TeV	
••• We do not use the following data for averages, fits, limits, etc. •••					
< 360	90	28 ADAM	96D	DLPH $e^+ e^- \rightarrow Z$	
< 50	90	29 BUSKULIC	96v	ALEP $e^+ e^- \rightarrow Z$	

27 AALTONEN 09c reports $[\Gamma(\Lambda_b^0 \rightarrow \rho K^-)/\Gamma_{\text{total}}] / [B(B^0 \rightarrow K^+ \pi^-)] \times [B(\bar{B} \rightarrow b\text{-baryon})] / [B(\bar{B} \rightarrow B^0)] = 0.066 \pm 0.009 \pm 0.008$ which we multiply or divide by our best values $B(B^0 \rightarrow K^+ \pi^-) = (1.94 \pm 0.06) \times 10^{-5}$, $B(\bar{B} \rightarrow b\text{-baryon}) = (8.5 \pm 2.2) \times 10^{-2}$, $B(\bar{B} \rightarrow B^0) = (40.1 \pm 1.3) \times 10^{-2}$. Our first error is their experiment's error and our second error is the systematic error from using our best values.

28 ADAM 96D assumes $f_{B^0} = f_{B^-} = 0.39$ and $f_{B_s} = 0.12$.

$\Gamma(\Lambda_7)/\Gamma_{\text{total}}$					Γ_{17}/Γ
VALUE	CL%	DOCUMENT ID	TECN	COMMENT	
< 1.3 × 10⁻³	90	ACOSTA	02G	CDF $p\bar{p}$ at 1.8 TeV	

 Λ_b^0 REFERENCES

AALTONEN	10B	PRL 104 102002	T. Aaltonen et al.	(CDF Collab.)
AALTONEN	09C	PRL 103 031801	T. Aaltonen et al.	(CDF Collab.)
AALTONEN	09E	PR D79 032001	T. Aaltonen et al.	(CDF Collab.)
ABAZOV	07S	PRL 99 142001	V.M. Abazov et al.	(DO Collab.)
ABAZOV	07U	PRL 99 182001	V.M. Abazov et al.	(DO Collab.)
ABULENCIA	07A	PRL 98 122001	A. Abulencia et al.	(FNAL CDF Collab.)
ABULENCIA	07B	PRL 98 122002	A. Abulencia et al.	(FNAL CDF Collab.)
ACOSTA	06	PRL 96 202001	D. Acosta et al.	(CDF Collab.)
ABAZOV	05C	PRL 94 102001	V.M. Abazov et al.	(DO Collab.)
ACOSTA	05O	PR D72 051104R	D. Acosta et al.	(CDF Collab.)
ABDALLAH	04A	PL B585 63	J. Abdallah et al.	(DELPHI Collab.)
ACOSTA	02G	PR D66 112002	D. Acosta et al.	(CDF Collab.)
ABREU	99W	EPJ C10 185	P. Abreu et al.	(DELPHI Collab.)
ACKERSTAFF	98D	PL B426 161	K. Ackerstaff et al.	(OPAL Collab.)
BARATE	98D	EPJ C2 197	R. Barate et al.	(ALEPH Collab.)
ABE	97B	PR D55 1142	F. Abe et al.	(CDF Collab.)
ABE	96M	PRL 77 1439	F. Abe et al.	(CDF Collab.)
ABREU	96D	ZPHY C71 199	P. Abreu et al.	(DELPHI Collab.)
ABREU	96N	PL B374 351	P. Abreu et al.	(DELPHI Collab.)
ADAM	96D	ZPHY C72 207	W. Adam et al.	(DELPHI Collab.)
BUSKULIC	96L	PL B380 442	D. Buskulic et al.	(ALEPH Collab.)
BUSKULIC	96V	PL B384 471	D. Buskulic et al.	(ALEPH Collab.)
PDG	96	PR D54 1	R. M. Barnett et al.	
ABREU	95S	ZPHY C68 375	P. Abreu et al.	(DELPHI Collab.)
AKERS	95K	PL B353 402	R. Akers et al.	(OPAL Collab.)
BUSKULIC	95L	PL B357 685	D. Buskulic et al.	(ALEPH Collab.)
ABE	93B	PR D47 R2639	F. Abe et al.	(CDF Collab.)
BUSKULIC	92E	PL B234 145	D. Buskulic et al.	(ALEPH Collab.)
ALBAJAR	91E	PL B273 540	C. Albajar et al.	(UA1 Collab.)
BARI	91	NC 104A 1787	G. Bari et al.	(CERN R422 Collab.)
ARENTON	86	NP B274 707	M.W. Arenton et al.	(ARIZ, NDAM, VAND)
BASILE	81	LNLC 31 97	M. Basile et al.	(CERN R415 Collab.)

Baryon Particle Listings

$\Sigma_b, \Sigma_b^*, \Xi_b^0, \Xi_b^-$

Σ_b

$I(J^P) = 1(\frac{1}{2}^+)$ Status: ***
I, J, P need confirmation.

In the quark model $\Sigma_b^+, \Sigma_b^0, \Sigma_b^-$ are an isotriplet (*uub, udb, ddb*) state. The lowest Σ_b ought to have $J^P = 1/2^+$. None of I, J, or P have actually been measured.

Σ_b MASS

Σ_b^+ MASS

VALUE (MeV)	DOCUMENT ID	TECN	COMMENT
5807.8 ± 2.7 OUR FIT			
5807.8 ^{+2.0} _{-2.2} ± 1.7	¹ AALTONEN	07k	CDF $p\bar{p}$ at 1.96 TeV

Σ_b^- MASS

VALUE (MeV)	DOCUMENT ID	TECN	COMMENT
5815.2 ± 2.0 OUR FIT			
5815.2 ± 1.0 ± 1.7	¹ AALTONEN	07k	CDF $p\bar{p}$ at 1.96 TeV

¹ Observed four $\Lambda_b^0 \pi^\pm$ resonances in the fully reconstructed decay mode $\Lambda_b^0 \rightarrow \Lambda_c^+ \pi^-$, where $\Lambda_c^+ \rightarrow p K^- \pi^+$.

Σ_b DECAY MODES

Mode	Fraction (Γ_i/Γ)
$\Gamma_1 \Lambda_b^0 \pi$	dominant

Σ_b BRANCHING RATIOS

$\Gamma(\Lambda_b^0 \pi)/\Gamma_{total}$	DOCUMENT ID	TECN	COMMENT	Γ_1/Γ
dominant	AALTONEN	07k	CDF $p\bar{p}$ at 1.96 TeV	

Σ_b REFERENCES

AALTONEN 07k PRL 99 202001 T. Aaltonen et al. (CDF Collab.)

Σ_b^*

$I(J^P) = 1(\frac{3}{2}^+)$ Status: ***
I, J, P need confirmation.

I, J, P need confirmation. Quantum numbers shown are quark-model predictions.

Σ_b^* MASS

Assumes $m_{\Sigma_b^{*+}} - m_{\Sigma_b^+} = m_{\Sigma_b^{*-}} - m_{\Sigma_b^-}$

Σ_b^{*+} MASS

VALUE (MeV)	DOCUMENT ID
5829.0 ± 3.4 OUR FIT	

Σ_b^{*-} MASS

VALUE (MeV)	DOCUMENT ID
5836.4 ± 2.8 OUR FIT	

$m_{\Sigma_b^*} - m_{\Sigma_b}$

VALUE (MeV)	DOCUMENT ID	TECN	COMMENT
21.2 ± 2.0 ± 0.4			
21.2 ^{+2.0} _{-1.9} ± 0.3	¹ AALTONEN	07k	CDF $p\bar{p}$ at 1.96 TeV

¹ Observed four $\Lambda_b^0 \pi^\pm$ resonances in the fully reconstructed decay mode $\Lambda_b^0 \rightarrow \Lambda_c^+ \pi^-$, where $\Lambda_c^+ \rightarrow p K^- \pi^+$. Assumes $m_{\Sigma_b^{*+}} - m_{\Sigma_b^+} = m_{\Sigma_b^{*-}} - m_{\Sigma_b^-}$

Σ_b^* DECAY MODES

Mode	Fraction (Γ_i/Γ)
$\Gamma_1 \Lambda_b^0 \pi$	dominant

Σ_b^* BRANCHING RATIOS

$\Gamma(\Lambda_b^0 \pi)/\Gamma_{total}$	DOCUMENT ID	TECN	COMMENT	Γ_1/Γ
dominant	AALTONEN	07k	CDF $p\bar{p}$ at 1.96 TeV	

Σ_b^* REFERENCES

AALTONEN 07k PRL 99 202001 T. Aaltonen et al. (CDF Collab.)

Ξ_b^0, Ξ_b^-

$I(J^P) = \frac{1}{2}(\frac{1}{2}^+)$ Status: ***
I, J, P need confirmation.

In the quark model, Ξ_b^0 and Ξ_b^- are an isodoublet (*usb, dsb*) state; the lowest Ξ_b^0 and Ξ_b^- ought to have $J^P = 1/2^+$. None of I, J, or P have actually been measured.

Ξ_b MASSES

Ξ_b^- MASS

VALUE (MeV)	DOCUMENT ID	TECN	COMMENT
5790.5 ± 2.7 OUR AVERAGE			
5790.9 ± 2.6 ± 0.8	¹ AALTONEN	09AP	CDF $p\bar{p}$ at 1.96 TeV
5774 ± 11 ± 15	² ABAZOV	07k	D0 $p\bar{p}$ at 1.96 TeV
••• We do not use the following data for averages, fits, limits, etc. •••			
5792.9 ± 2.5 ± 1.7	³ AALTONEN	07A	CDF Repl. by AALTONEN 09AP
¹ Measured in $\Xi_b^- \rightarrow J/\psi \Xi^-$ decays with 66 ± 14 candidates.			
² Observed in $\Xi_b^- \rightarrow J/\psi \Xi^-$ decays with 15.2 ± 4.4 ± 1.9 ± 0.4 candidates, a significance of 5.5 sigma.			
³ Observed in $\Xi_b^- \rightarrow J/\psi \Xi^-$ decays with 17.5 ± 4.3 candidates, a significance of 7.7 sigma.			

Ξ_b^- MEAN LIFE

VALUE (10^{-12} s)	DOCUMENT ID	TECN	COMMENT
1.56^{+0.27}_{-0.25} ± 0.02			
1.56 ± 0.25 ± 0.02	⁴ AALTONEN	09AP	CDF $p\bar{p}$ at 1.96 TeV
⁴ Measured in $\Xi_b^- \rightarrow J/\psi \Xi^-$ decays with 66 ± 14 candidates.			

Ξ_b MEAN LIFE

“OUR EVALUATION” is an average using rescaled values of the data listed below. The average and rescaling were performed by the Heavy Flavor Averaging Group (HFAG) and are described at <http://www.slac.stanford.edu/xorg/hfag/>. The averaging/rescaling procedure takes into account correlations between the measurements and asymmetric lifetime errors.

VALUE (10^{-12} s)	EVTS	DOCUMENT ID	TECN	COMMENT
1.49^{+0.19}_{-0.18} OUR EVALUATION				
1.56 ^{+0.27} _{-0.25} ± 0.02	⁵	AALTONEN	09AP	CDF $p\bar{p}$ at 1.96 TeV
1.48 ^{+0.40} _{-0.31} ± 0.12	⁶	ABDALLAH	05c	DLPH $e^+ e^- \rightarrow Z^0$
1.35 ^{+0.37} _{-0.28} ± 0.15	⁷	BUSKULIC	96T	ALEP $e^+ e^- \rightarrow Z$
••• We do not use the following data for averages, fits, limits, etc. •••				
1.5 ^{+0.7} _{-0.4} ± 0.3	⁸	ABREU	95v	DLPH Repl. by ABDALLAH 05c
⁵ Measured in $\Xi_b^- \rightarrow J/\psi \Xi^-$ decays with 66 ± 14 candidates.				
⁶ Used the decay length of Ξ^- accompanied by a lepton of the same sign.				
⁷ Excess $\Xi^- \ell^-$, impact parameters.				
⁸ Excess $\Xi^- \ell^-$, decay lengths.				

Ξ_b DECAY MODES

Mode	Fraction (Γ_i/Γ)	Scale factor
$\Gamma_1 \Xi_b^- \rightarrow \Xi^- \ell^- \bar{\nu}_\ell X \times B(\bar{b} \rightarrow \Xi_b^-)$	(3.9 ± 1.2) × 10 ⁻⁴	1.4
$\Gamma_2 \Xi_b^- \rightarrow J/\psi \Xi^- \times B(b \rightarrow \Xi_b^-)$	(8 ± 4) × 10 ⁻⁶	

Ξ_b BRANCHING RATIOS

$\Gamma(\Xi^- \ell^- \bar{\nu}_\ell X \times B(\bar{b} \rightarrow \Xi_b^-))/\Gamma_{total}$	DOCUMENT ID	TECN	COMMENT	Γ_1/Γ
3.9 ± 1.2 OUR AVERAGE			Error includes scale factor of 1.4.	
3.0 ± 1.0 ± 0.3	ABDALLAH	05c	DLPH $e^+ e^- \rightarrow Z^0$	
5.4 ± 1.1 ± 0.8	BUSKULIC	96T	ALEP Excess $\Xi^- \ell^-$ over $\Xi^- \ell^+$	
••• We do not use the following data for averages, fits, limits, etc. •••				
5.9 ± 2.1 ± 1.0	ABREU	95v	DLPH Repl. by ABDALLAH 05c	

$\Gamma(J/\psi \Xi^- \times B(b \rightarrow \Xi_b^-))/\Gamma_{total}$	DOCUMENT ID	TECN	COMMENT	Γ_2/Γ
0.08 ± 0.04 OUR AVERAGE				
0.08 ^{+0.02} _{-0.01} ± 0.04	⁹ AALTONEN	09AP	CDF $p\bar{p}$ at 1.96 TeV	
0.13 ± 0.06 ± 0.06	¹⁰ ABAZOV	07k	D0 $p\bar{p}$ at 1.96 TeV	

See key on page 405

Baryon Particle Listings

 $\Xi_b^0, \Xi_b^-, \Omega_b^-, b$ -baryon ADMIXTURE ($\Lambda_b, \Xi_b, \Sigma_b, \Omega_b$)

⁹AALTONEN 09AP reports $[\Gamma(\Xi_b^- \rightarrow J/\psi \Xi^- \times B(b \rightarrow \Xi_b^-))/\Gamma_{\text{total}}] / [B(\Lambda_b^0 \rightarrow J/\psi(1S)\Lambda \times B(b \rightarrow \Lambda_b^0))] = 0.167 \pm 0.037 \pm 0.025 \pm 0.012$ which we multiply by our best value $B(\Lambda_b^0 \rightarrow J/\psi(1S)\Lambda \times B(b \rightarrow \Lambda_b^0)) = (4.7 \pm 2.3) \times 10^{-5}$. Our first error is their experiment's error and our second error is the systematic error from using our best value.

¹⁰ABAZOV 07K reports $[\Gamma(\Xi_b^- \rightarrow J/\psi \Xi^- \times B(b \rightarrow \Xi_b^-))/\Gamma_{\text{total}}] / [B(\Lambda_b^0 \rightarrow J/\psi(1S)\Lambda \times B(b \rightarrow \Lambda_b^0))] = 0.28 \pm 0.09 \pm 0.09 \pm 0.08$ which we multiply by our best value $B(\Lambda_b^0 \rightarrow J/\psi(1S)\Lambda \times B(b \rightarrow \Lambda_b^0)) = (4.7 \pm 2.3) \times 10^{-5}$. Our first error is their experiment's error and our second error is the systematic error from using our best value.

 Ξ_b REFERENCES

AALTONEN	09AP	PR D80 072003	T. Aaltonen et al.	(CDF Collab.)
AALTONEN	07A	PRL 99 052002	T. Aaltonen et al.	(CDF Collab.)
ABAZOV	07K	PRL 99 052001	V.M. Abazov et al.	(D0 Collab.)
ABDALLAH	05C	EPL C44 299	J. Abdallah et al.	(DELPHI Collab.)
BUSKULIC	90T	PL B384 449	D. Buskulic et al.	(ALEPH Collab.)
ABREU	95V	ZPHY C68 541	P. Abreu et al.	(DELPHI Collab.)

 Ω_b^-

$I(J^P) = 0(\frac{1}{2}^+)$ Status: ***
I, J, P need confirmation.

In the quark model Ω_b^- is *ssb* ground state. None of its quantum numbers has been measured.

 Ω_b^- MASS

VALUE (MeV)	DOCUMENT ID	TECN	COMMENT
6071 ± 40 OUR AVERAGE	Error includes scale factor of 6.2.		
6054.4 ± 6.8 ± 0.9	¹ AALTONEN	09AP CDF	$p\bar{p}$ at 1.96 TeV
6165 ± 10 ± 13	² ABAZOV	08AL D0	$p\bar{p}$ at 1.96 TeV

¹ Observed in $\Omega_b^- \rightarrow J/\psi \Omega^-$ decays with 16 ± 6 candidates, a significance of 5.5 sigma from a combined mass-lifetime fit.

² Observed in $\Omega_b^- \rightarrow J/\psi \Omega^-$ decays with $17.8 \pm 4.9 \pm 0.8$ candidates, a significance of 5.4 sigma.

 Ω_b^- MEAN LIFE

VALUE (10^{-12} s)	DOCUMENT ID	TECN	COMMENT
1.13 ± 0.53 ± 0.40 OUR AVERAGE			
	³ AALTONEN	09AP CDF	$p\bar{p}$ at 1.96 TeV

³ Observed in $\Omega_b^- \rightarrow J/\psi \Omega^-$ decays with 16 ± 6 candidates, a significance of 5.5 sigma from a combined mass-lifetime fit.

 Ω_b^- DECAY MODES

Mode	Fraction (Γ_i/Γ)
Γ_1 $J/\psi \Omega^- \times B(b \rightarrow \Omega_b)$	$(2.4 \pm 1.2) \times 10^{-6}$

 Ω_b^- BRANCHING RATIOS

$\Gamma(J/\psi \Omega^- \times B(b \rightarrow \Omega_b))/\Gamma_{\text{total}}$	Γ_1/Γ
0.024 ± 0.012 OUR AVERAGE	
$0.021 \pm 0.008 \pm 0.010$	⁴ AALTONEN 09AP CDF $p\bar{p}$ at 1.96 TeV
$0.065 \pm 0.029 \pm 0.035$ $-0.032 - 0.033$	⁵ ABAZOV 08AL D0 $p\bar{p}$ at 1.96 TeV

⁴AALTONEN 09AP reports $[\Gamma(\Omega_b^- \rightarrow J/\psi \Omega^- \times B(b \rightarrow \Omega_b))/\Gamma_{\text{total}}] / [B(\Lambda_b^0 \rightarrow J/\psi(1S)\Lambda \times B(b \rightarrow \Lambda_b^0))] = 0.045 \pm 0.017 \pm 0.012 \pm 0.004$ which we multiply by our best value $B(\Lambda_b^0 \rightarrow J/\psi(1S)\Lambda \times B(b \rightarrow \Lambda_b^0)) = (4.7 \pm 2.3) \times 10^{-5}$. Our first error is their experiment's error and our second error is the systematic error from using our best value.

⁵ABAZOV 08AL reports $[\Gamma(\Omega_b^- \rightarrow J/\psi \Omega^- \times B(b \rightarrow \Omega_b))/\Gamma_{\text{total}}] / [B(\Xi_b^- \rightarrow J/\psi \Xi^- \times B(b \rightarrow \Xi_b^-))] = 0.80 \pm 0.32 \pm 0.34 \pm 0.22$ which we multiply by our best value $B(\Xi_b^- \rightarrow J/\psi \Xi^- \times B(b \rightarrow \Xi_b^-)) = (8 \pm 4) \times 10^{-6}$. Our first error is their experiment's error and our second error is the systematic error from using our best value.

 Ω_b^- REFERENCES

AALTONEN	09AP	PR D80 072003	T. Aaltonen et al.	(CDF Collab.)
ABAZOV	08AL	PRL 101 232002	V.M. Abazov et al.	(D0 Collab.)

 b -baryon ADMIXTURE ($\Lambda_b, \Xi_b, \Sigma_b, \Omega_b$) b -baryon ADMIXTURE MEAN LIFE

Each measurement of the b -baryon mean life is an average over an admixture of various b -baryons which decay weakly. Different techniques emphasize different admixtures of produced particles, which could result in a different b -baryon mean life. More b -baryon flavor specific channels are not included in the measurement.

"OUR EVALUATION" is an average using rescaled values of the data listed below. The average and rescaling were performed by the Heavy Flavor Averaging Group (HFAG) and are described at <http://www.slac.stanford.edu/xorg/hfag/>. The averaging/rescaling procedure takes into account correlations between the measurements and asymmetric lifetime errors.

VALUE (10^{-12} s)	EVTS	DOCUMENT ID	TECN	COMMENT
1.345 ± 0.032 OUR EVALUATION				
$1.401 \pm 0.046 \pm 0.035$	¹	AALTONEN	10B CDF	$p\bar{p}$ at 1.96 TeV
$1.218 \pm 0.130 \pm 0.115 \pm 0.042$	²	ABAZOV	07S D0	$p\bar{p}$ at 1.96 TeV
$1.290 \pm 0.119 \pm 0.087 \pm 0.110 \pm 0.091$	³	ABAZOV	07U D0	$p\bar{p}$ at 1.96 TeV
$1.593 \pm 0.083 \pm 0.078 \pm 0.033$	²	ABULENCIA	07A CDF	$p\bar{p}$ at 1.96 TeV
$1.16 \pm 0.20 \pm 0.08$	⁴	ABREU	99W DLPH	$e^+ e^- \rightarrow Z$
$1.19 \pm 0.14 \pm 0.07$	⁵	ABREU	99W DLPH	$e^+ e^- \rightarrow Z$
$1.11 \pm 0.19 \pm 0.18 \pm 0.05$	⁶	ABREU	99W DLPH	$e^+ e^- \rightarrow Z$
$1.29 \pm 0.24 \pm 0.22 \pm 0.06$	⁶	ACKERSTAFF	98G OPAL	$e^+ e^- \rightarrow Z$
$1.20 \pm 0.08 \pm 0.06$	⁷	BARATE	98D ALEP	$e^+ e^- \rightarrow Z$
1.21 ± 0.11	⁷	BARATE	98D ALEP	$e^+ e^- \rightarrow Z$
$1.32 \pm 0.15 \pm 0.07$	⁸	ABE	96M CDF	$p\bar{p}$ at 1.8 TeV
$1.10 \pm 0.19 \pm 0.17 \pm 0.09$	⁶	ABREU	96D DLPH	$e^+ e^- \rightarrow Z$
$1.16 \pm 0.11 \pm 0.06$	⁶	AKERS	96 OPAL	$e^+ e^- \rightarrow Z$
••• We do not use the following data for averages, fits, limits, etc. •••				
$1.22 \pm 0.22 \pm 0.18 \pm 0.04$	²	ABAZOV	05c D0	Repl. by ABAZOV 07s
$1.14 \pm 0.08 \pm 0.04$	⁹	ABREU	99W DLPH	$e^+ e^- \rightarrow Z$
$1.46 \pm 0.22 \pm 0.07 \pm 0.21 \pm 0.09$		ABREU	96D DLPH	Repl. by ABREU 99w
$1.27 \pm 0.35 \pm 0.29 \pm 0.09$		ABREU	95S DLPH	Repl. by ABREU 99w
$1.05 \pm 0.12 \pm 0.11 \pm 0.09$	290	BUSKULIC	95L ALEP	Repl. by BARATE 98d
$1.04 \pm 0.48 \pm 0.38 \pm 0.10$	11	¹⁰ ABREU	93F DLPH	Excess $\Lambda \mu^-$, decay lengths
$1.05 \pm 0.23 \pm 0.20 \pm 0.08$	157	¹¹ AKERS	93 OPAL	Excess $\Lambda \ell^-$, decay lengths
$1.12 \pm 0.32 \pm 0.29 \pm 0.16$	101	¹² BUSKULIC	92I ALEP	Excess $\Lambda \ell^-$, impact parameters

- Measured mean life using fully reconstructed $\Lambda_b^0 \rightarrow \Lambda_c^+ \pi^-$ decays.
- Measured mean life using fully reconstructed $\Lambda_b^0 \rightarrow J/\psi \Lambda$ decays.
- Measured using semileptonic decays $\Lambda_b(0) \rightarrow \Lambda_c^+ \mu \nu X, \Lambda_c^+ \rightarrow K_S^0 p$.
- Measured using $\Lambda \ell^-$ decay length.
- Measured using $p \ell^-$ decay length.
- Measured using $\Lambda_c \ell^-$ and $\Lambda \ell^+ \ell^-$.
- Measured using the excess of $\Lambda \ell^-$, lepton impact parameter.
- Measured using $\Lambda_c \ell^-$.
- This ABREU 99w result is the combined result of the $\Lambda \ell^-$, $p \ell^-$, and excess $\Lambda \mu^-$ impact parameter measurements.
- ABREU 93f superseded by ABREU 96d.
- AKERS 93 superseded by AKERS 96.
- BUSKULIC 92i superseded by BUSKULIC 95L.

 b -baryon ADMIXTURE DECAY MODES ($\Lambda_b, \Xi_b, \Sigma_b, \Omega_b$)

These branching fractions are actually an average over weakly decaying b -baryons weighted by their production rates in Z decay (or high-energy $p\bar{p}$), branching ratios, and detection efficiencies. They scale with the LEP b -baryon production fraction $B(b \rightarrow b\text{-baryon})$ and are evaluated for our value $B(b \rightarrow b\text{-baryon}) = (9.2 \pm 1.8)\%$.

The branching fractions $B(b\text{-baryon} \rightarrow \Lambda \ell^- \bar{\nu}_\ell \text{ anything})$ and $B(\Lambda_b^0 \rightarrow \Lambda_c^+ \ell^- \bar{\nu}_\ell \text{ anything})$ are not pure measurements because the underlying measured products of these with $B(b \rightarrow b\text{-baryon})$ were used to determine $B(b \rightarrow b\text{-baryon})$, as described in the note "Production and Decay of b -Flavored Hadrons."

For inclusive branching fractions, e.g., $B \rightarrow D^\pm \text{ anything}$, the values usually are multiplicities, not branching fractions. They can be greater than one.

Baryon Particle Listings

 b -baryon ADMIXTURE ($\Lambda_b, \Xi_b, \Sigma_b, \Omega_b$)

Mode	Fraction (Γ_i/Γ)
Γ_1 $p\mu^- \bar{\nu}$ anything	$(5.8^{+2.6}_{-2.4})\%$
Γ_2 $p\ell \bar{\nu}_\ell$ anything	$(5.6 \pm 1.7)\%$
Γ_3 p anything	$(69 \pm 27)\%$
Γ_4 $\Lambda \ell^- \bar{\nu}_\ell$ anything	$(3.7 \pm 1.0)\%$
Γ_5 $\Lambda \ell^+ \nu_\ell$ anything	
Γ_6 Λ anything	
Γ_7 $\Lambda_c^+ \ell^- \bar{\nu}_\ell$ anything	
Γ_8 $\Lambda/\bar{\Lambda}$ anything	$(39 \pm 11)\%$
Γ_9 $\Xi^- \ell^- \bar{\nu}_\ell$ anything	$(6.5 \pm 2.2) \times 10^{-3}$

 b -baryon ADMIXTURE ($\Lambda_b, \Xi_b, \Sigma_b, \Omega_b$) BRANCHING RATIOS

$\Gamma(p\mu^- \bar{\nu} \text{ anything})/\Gamma_{\text{total}}$	Γ_1/Γ			
VALUE	EVTS	DOCUMENT ID	TECN	COMMENT
$0.058^{+0.022}_{-0.016} \pm 0.015$	125	13 ABREU	95s	DLPH $e^+ e^- \rightarrow Z$

¹³ABREU 95s reports $[\Gamma(b\text{-baryon} \rightarrow p\mu^- \bar{\nu} \text{ anything})/\Gamma_{\text{total}}] \times [B(\bar{b} \rightarrow b\text{-baryon})] = 0.0049 \pm 0.0011^{+0.0015}_{-0.0011}$ which we divide by our best value $B(\bar{b} \rightarrow b\text{-baryon}) = (8.5 \pm 2.2) \times 10^{-2}$. Our first error is their experiment's error and our second error is the systematic error from using our best value.

$\Gamma(p\ell \bar{\nu}_\ell \text{ anything})/\Gamma_{\text{total}}$	Γ_2/Γ		
VALUE	DOCUMENT ID	TECN	COMMENT
$0.056 \pm 0.009 \pm 0.014$	14 BARATE	98v	ALEP $e^+ e^- \rightarrow Z$

¹⁴BARATE 98v reports $[\Gamma(b\text{-baryon} \rightarrow p\ell \bar{\nu}_\ell \text{ anything})/\Gamma_{\text{total}}] \times [B(\bar{b} \rightarrow b\text{-baryon})] = (4.72 \pm 0.66 \pm 0.44) \times 10^{-3}$ which we divide by our best value $B(\bar{b} \rightarrow b\text{-baryon}) = (8.5 \pm 2.2) \times 10^{-2}$. Our first error is their experiment's error and our second error is the systematic error from using our best value.

$\Gamma(p\ell \bar{\nu}_\ell \text{ anything})/\Gamma(p \text{ anything})$	Γ_2/Γ_3		
VALUE	DOCUMENT ID	TECN	COMMENT
$0.080 \pm 0.012 \pm 0.014$	BARATE	98v	ALEP $e^+ e^- \rightarrow Z$

$\Gamma(\Lambda \ell^- \bar{\nu}_\ell \text{ anything})/\Gamma_{\text{total}}$	Γ_4/Γ			
VALUE	EVTS	DOCUMENT ID	TECN	COMMENT
0.037 ± 0.010 OUR AVERAGE				
$0.038 \pm 0.005 \pm 0.010$		15 BARATE	98d	ALEP $e^+ e^- \rightarrow Z$
$0.034 \pm 0.004 \pm 0.009$		16 AKERS	96	OPAL Excess of $\Lambda \ell^-$ over $\Lambda \ell^+$
$0.035 \pm 0.008 \pm 0.009$	262	17 ABREU	95s	DLPH Excess of $\Lambda \ell^-$ over $\Lambda \ell^+$
$0.072 \pm 0.014 \pm 0.019$	290	18 BUSKULIC	95L	ALEP Excess of $\Lambda \ell^-$ over $\Lambda \ell^+$

• • • We do not use the following data for averages, fits, limits, etc. • • •
seen

¹⁵BARATE 98d reports $[\Gamma(b\text{-baryon} \rightarrow \Lambda \ell^- \bar{\nu}_\ell \text{ anything})/\Gamma_{\text{total}}] \times [B(\bar{b} \rightarrow b\text{-baryon})] = 0.00326 \pm 0.00016 \pm 0.00039$ which we divide by our best value $B(\bar{b} \rightarrow b\text{-baryon}) = (8.5 \pm 2.2) \times 10^{-2}$. Our first error is their experiment's error and our second error is the systematic error from using our best value. Measured using the excess of $\Lambda \ell^-$, lepton impact parameter.

¹⁶AKERS 96 reports $[\Gamma(b\text{-baryon} \rightarrow \Lambda \ell^- \bar{\nu}_\ell \text{ anything})/\Gamma_{\text{total}}] \times [B(\bar{b} \rightarrow b\text{-baryon})] = 0.00291 \pm 0.00023 \pm 0.00025$ which we divide by our best value $B(\bar{b} \rightarrow b\text{-baryon}) = (8.5 \pm 2.2) \times 10^{-2}$. Our first error is their experiment's error and our second error is the systematic error from using our best value.

¹⁷ABREU 95s reports $[\Gamma(b\text{-baryon} \rightarrow \Lambda \ell^- \bar{\nu}_\ell \text{ anything})/\Gamma_{\text{total}}] \times [B(\bar{b} \rightarrow b\text{-baryon})] = 0.0030 \pm 0.0006 \pm 0.0004$ which we divide by our best value $B(\bar{b} \rightarrow b\text{-baryon}) = (8.5 \pm 2.2) \times 10^{-2}$. Our first error is their experiment's error and our second error is the systematic error from using our best value.

¹⁸BUSKULIC 95L reports $[\Gamma(b\text{-baryon} \rightarrow \Lambda \ell^- \bar{\nu}_\ell \text{ anything})/\Gamma_{\text{total}}] \times [B(\bar{b} \rightarrow b\text{-baryon})] = 0.0061 \pm 0.0006 \pm 0.0010$ which we divide by our best value $B(\bar{b} \rightarrow b\text{-baryon}) = (8.5 \pm 2.2) \times 10^{-2}$. Our first error is their experiment's error and our second error is the systematic error from using our best value.

¹⁹AKERS 93 superseded by AKERS 96.

²⁰BUSKULIC 92i reports $[\Gamma(b\text{-baryon} \rightarrow \Lambda \ell^- \bar{\nu}_\ell \text{ anything})/\Gamma_{\text{total}}] \times [B(\bar{b} \rightarrow b\text{-baryon})] = 0.0070 \pm 0.0010 \pm 0.0018$ which we divide by our best value $B(\bar{b} \rightarrow b\text{-baryon}) = (8.5 \pm 2.2) \times 10^{-2}$. Our first error is their experiment's error and our second error is the systematic error from using our best value. Superseded by BUSKULIC 95L.

 $\Gamma(\Lambda \ell^+ \nu_\ell \text{ anything})/\Gamma(\Lambda \text{ anything})$ Γ_5/Γ_6

VALUE	DOCUMENT ID	TECN	COMMENT
$0.080 \pm 0.012 \pm 0.008$	ABBIENDI	99L	OPAL $e^+ e^- \rightarrow Z$
• • • We do not use the following data for averages, fits, limits, etc. • • •			
$0.070 \pm 0.012 \pm 0.007$	ACKERSTAFF	97N	OPAL Repl. by ABBIENDI 99L

 $\Gamma(\Lambda/\bar{\Lambda} \text{ anything})/\Gamma_{\text{total}}$ Γ_8/Γ

VALUE	DOCUMENT ID	TECN	COMMENT
0.39 ± 0.11 OUR AVERAGE			
$0.41 \pm 0.06 \pm 0.11$	21 ABBIENDI	99L	OPAL $e^+ e^- \rightarrow Z$
$0.26^{+0.15}_{-0.09} \pm 0.07$	22 ABREU	95c	DLPH $e^+ e^- \rightarrow Z$

• • • We do not use the following data for averages, fits, limits, etc. • • •
²³ACKERSTAFF 97N reports $[\Gamma(b\text{-baryon} \rightarrow \Lambda/\bar{\Lambda} \text{ anything})/\Gamma_{\text{total}}] \times [B(\bar{b} \rightarrow b\text{-baryon})] = 0.035 \pm 0.0032 \pm 0.0035$ which we divide by our best value $B(\bar{b} \rightarrow b\text{-baryon}) = (8.5 \pm 2.2) \times 10^{-2}$. Our first error is their experiment's error and our second error is the systematic error from using our best value.

²¹ABBIENDI 99L reports $[\Gamma(b\text{-baryon} \rightarrow \Lambda/\bar{\Lambda} \text{ anything})/\Gamma_{\text{total}}] \times [B(\bar{b} \rightarrow b\text{-baryon})] = 0.035 \pm 0.0032 \pm 0.0035$ which we divide by our best value $B(\bar{b} \rightarrow b\text{-baryon}) = (8.5 \pm 2.2) \times 10^{-2}$. Our first error is their experiment's error and our second error is the systematic error from using our best value.

²²ABREU 95c reports $0.28^{+0.17}_{-0.12}$ from a measurement of $[\Gamma(b\text{-baryon} \rightarrow \Lambda/\bar{\Lambda} \text{ anything})/\Gamma_{\text{total}}] \times [B(\bar{b} \rightarrow b\text{-baryon})]$ assuming $B(\bar{b} \rightarrow b\text{-baryon}) = 0.08 \pm 0.02$, which we rescale to our best value $B(\bar{b} \rightarrow b\text{-baryon}) = (8.5 \pm 2.2) \times 10^{-2}$. Our first error is their experiment's error and our second error is the systematic error from using our best value.

²³ACKERSTAFF 97N reports $[\Gamma(b\text{-baryon} \rightarrow \Lambda/\bar{\Lambda} \text{ anything})/\Gamma_{\text{total}}] \times [B(\bar{b} \rightarrow b\text{-baryon})] = 0.0393 \pm 0.0046 \pm 0.0037$ which we divide by our best value $B(\bar{b} \rightarrow b\text{-baryon}) = (8.5 \pm 2.2) \times 10^{-2}$. Our first error is their experiment's error and our second error is the systematic error from using our best value.

 $\Gamma(\Xi^- \ell^- \bar{\nu}_\ell \text{ anything})/\Gamma_{\text{total}}$ Γ_9/Γ

VALUE	DOCUMENT ID	TECN	COMMENT
0.0065 ± 0.0022 OUR AVERAGE			
$0.0064 \pm 0.0016 \pm 0.0016$	24 BUSKULIC	96T	ALEP Excess $\Xi^- \ell^-$ over $\Xi^- \ell^+$
$0.0069 \pm 0.0027 \pm 0.0018$	25 ABREU	95v	DLPH Excess $\Xi^- \ell^-$ over $\Xi^- \ell^+$

²⁴BUSKULIC 96T reports $[\Gamma(b\text{-baryon} \rightarrow \Xi^- \ell^- \bar{\nu}_\ell \text{ anything})/\Gamma_{\text{total}}] \times [B(\bar{b} \rightarrow b\text{-baryon})] = 0.00054 \pm 0.00011 \pm 0.00008$ which we divide by our best value $B(\bar{b} \rightarrow b\text{-baryon}) = (8.5 \pm 2.2) \times 10^{-2}$. Our first error is their experiment's error and our second error is the systematic error from using our best value.

²⁵ABREU 95v reports $[\Gamma(b\text{-baryon} \rightarrow \Xi^- \ell^- \bar{\nu}_\ell \text{ anything})/\Gamma_{\text{total}}] \times [B(\bar{b} \rightarrow b\text{-baryon})] = 0.00059 \pm 0.00021 \pm 0.0001$ which we divide by our best value $B(\bar{b} \rightarrow b\text{-baryon}) = (8.5 \pm 2.2) \times 10^{-2}$. Our first error is their experiment's error and our second error is the systematic error from using our best value.

 b -baryon ADMIXTURE ($\Lambda_b, \Xi_b, \Sigma_b, \Omega_b$) REFERENCES

AALTONEN	10B	PRL 104 102002	T. Aaltonen <i>et al.</i>	(CDF Collab.)
ABAZOV	07S	PRL 99 142001	V.M. Abazov <i>et al.</i>	(DO Collab.)
ABAZOV	07U	PRL 99 182001	V.M. Abazov <i>et al.</i>	(DO Collab.)
ABULENCIA	07A	PRL 98 122001	A. Abulencia <i>et al.</i>	(FNAL CDF Collab.)
ABAZOV	05C	PRL 94 102001	V.M. Abazov <i>et al.</i>	(DO Collab.)
ABBIENDI	99L	EPJ C9 1	G. Abbiendi <i>et al.</i>	(OPAL Collab.)
ABREU	99W	EPJ C10 185	P. Abreu <i>et al.</i>	(DELPHI Collab.)
ACKERSTAFF	98D	PL B426 161	K. Ackerstaff <i>et al.</i>	(OPAL Collab.)
BARATE	98D	EPJ C2 197	R. Barate <i>et al.</i>	(ALEPH Collab.)
BARATE	98V	EPJ C5 205	R. Barate <i>et al.</i>	(ALEPH Collab.)
ACKERSTAFF	97N	ZPHY C74 423	K. Ackerstaff <i>et al.</i>	(OPAL Collab.)
ABE	96M	PRL 77 1439	F. Abe <i>et al.</i>	(CDF Collab.)
ABREU	96D	ZPHY C71 119	P. Abreu <i>et al.</i>	(DELPHI Collab.)
AKERS	96	ZPHY C69 195	R. Akers <i>et al.</i>	(OPAL Collab.)
BUSKULIC	96T	PL B384 449	D. Buskulic <i>et al.</i>	(ALEPH Collab.)
ABREU	95C	PL B347 447	P. Abreu <i>et al.</i>	(DELPHI Collab.)
ABREU	95S	ZPHY C68 375	P. Abreu <i>et al.</i>	(DELPHI Collab.)
ABREU	95V	ZPHY C68 541	P. Abreu <i>et al.</i>	(DELPHI Collab.)
BUSKULIC	95L	PL B357 685	D. Buskulic <i>et al.</i>	(ALEPH Collab.)
ABREU	93F	PL B311 379	P. Abreu <i>et al.</i>	(DELPHI Collab.)
AKERS	93	PL B316 435	R. Akers <i>et al.</i>	(OPAL Collab.)
BUSKULIC	92I	PL B297 449	D. Buskulic <i>et al.</i>	(ALEPH Collab.)

MISCELLANEOUS SEARCHES

Magnetic Monopole Searches	1285
Supersymmetric Particle Searches	1292
Technicolor	1340
Quark and Lepton Compositeness	1347
Extra Dimensions	1354
WIMPs and Other Particle Searches	1365

Notes in the Search Listings

Magnetic Monopoles (new)	1285
Supersymmetry (rev.)	1292
I. Theory (rev.)	1292
II. Experiment (rev.)	1309
Dynamical Electroweak Symmetry Breaking (rev.)	1340
Searches for Quark and Lepton Compositeness	1347
Extra Dimensions	1354
WIMPs and Other Particle Searches	1365

SEARCHES IN OTHER SECTIONS

Higgs Bosons — H^0 and H^\pm	448
Heavy Bosons Other than Higgs Bosons	480
Leptoquarks	490
Axions (A^0) and Other Very Light Bosons	496
Heavy Charged Lepton Searches	553
Double- β Decay	562
Heavy Neutral Leptons, Searches for	577
b' (Fourth Generation) Quark	612
Free Quark Searches	613



**SEARCHES FOR
MONOPOLES,
SUPERSYMMETRY,
TECHNICOLOR,
COMPOSITENESS,
EXTRA DIMENSIONS, etc.**

Magnetic Monopole Searches

MAGNETIC MONOPOLES

Written in September 2009 by D. Milstead (Stockholm Univ.) and E.J. Weinberg (Columbia Univ.).

The symmetry between electric and magnetic fields in the sourcefree Maxwell's equations naturally suggests that electric charges might have magnetic counterparts, known as magnetic monopoles. Although the greatest interest has been in the supermassive monopoles that are a firm prediction of all grand unified theories, one cannot exclude the possibility of lighter monopoles, even though there is at present no strong theoretical motivation for these.

In either case, the magnetic charge is constrained by a quantization condition first found by Dirac [1]. Consider a monopole with magnetic charge Q_M and a Coulomb magnetic field

$$\mathbf{B} = \frac{Q_M}{4\pi} \frac{\hat{\mathbf{r}}}{r^2}. \quad (1)$$

Any vector potential \mathbf{A} whose curl is equal to \mathbf{B} must be singular along some line running from the origin to spatial infinity. This Dirac string singularity could potentially be detected through the extra phase that the wavefunction of a particle with electric charge Q_E would acquire if it moved along a loop encircling the string. For the string to be unobservable, this phase must be a multiple of 2π . Requiring that this be the case for any pair of electric and magnetic charges gives the condition that all charges be integer multiples of minimum charges Q_E^{\min} and Q_M^{\min} obeying

$$Q_E^{\min} Q_M^{\min} = 2\pi. \quad (2)$$

(For monopoles which also carry an electric charge, called dyons, the quantization conditions on their electric charges can be modified. However, the constraints on magnetic charges, as well as those on all purely electric particles, will be unchanged.)

Another way to understand this result is to note that the conserved orbital angular momentum of a point electric charge moving in the field of a magnetic monopole has an additional component, with

$$\mathbf{L} = m\mathbf{r} \times \mathbf{v} - 4\pi Q_E Q_M \hat{\mathbf{r}} \quad (3)$$

Requiring the radial component of \mathbf{L} to be quantized in half-integer units yields Eq. (2).

If there are unbroken gauge symmetries in addition to the U(1) of electromagnetism, the above analysis must be modified [2,3]. For example, a monopole could have both a

U(1) magnetic charge and a color magnetic charge. The latter could combine with the color charge of a quark to give an additional contribution to the phase factor associated with a loop around the Dirac string, so that the U(1) charge could be the Dirac charge $Q_M^D \equiv 2\pi/e$, the result that would be obtained by substituting the electron charge into Eq. (2). On the other hand, for monopoles without color-magnetic charge, one would simply insert the quark electric charges into Eq. (2) and conclude that Q_M must be a multiple of $6\pi/e$.

The prediction of GUT monopoles arises from the work of 't Hooft [4] and Polyakov [5], who showed that certain spontaneously broken gauge theories have nonsingular classical solutions that lead to magnetic monopoles in the quantum theory. The simplest example occurs in a theory where the vacuum expectation value of a triplet Higgs field ϕ breaks an SU(2) gauge symmetry down to the U(1) of electromagnetism and gives a mass M_V to two of the gauge bosons. In order to have finite energy, ϕ must approach a vacuum value at infinity. However, there is a continuous family of possible vacua, since the scalar field potential determines only the magnitude v of $\langle\phi\rangle$, but not its orientation in the internal SU(2) space. In the monopole solution, the direction of ϕ in internal space is correlated with the position in physical space; *i.e.*, $\phi^a \sim v\hat{r}^a$. The stability of the solution follows from the fact that this twisting Higgs field cannot be smoothly deformed to a spatially uniform vacuum configuration. Reducing the energetic cost of the spatial variation of ϕ requires a nonzero gauge potential, which turns out to yield the magnetic field corresponding to a charge $Q_M = 4\pi/e$. Numerical solution of the classical field equations shows that the mass of this monopole is

$$M_{\text{mon}} \sim \frac{4\pi M_V}{e^2}. \quad (4)$$

The essential ingredient here was the fact that the Higgs fields at spatial infinity could be arranged in a topologically nontrivial configuration. A discussion of the general conditions under which this is possible is beyond the scope of this review, so we restrict ourselves to the two phenomenologically most important cases.

The first is the electroweak theory, with SU(2) × U(1) broken to U(1). There are no topologically nontrivial configurations of the Higgs field, and hence no topologically stable monopole solutions.

The second is when any simple Lie group is broken to a subgroup with a U(1) factor, a case that includes all grand unified theories. The monopole mass is determined by the mass scale of the symmetry breaking that allows nontrivial topology. For example, an SU(5) model with

$$\text{SU}(5) \xrightarrow{M_X} \text{SU}(3) \times \text{SU}(2) \times \text{U}(1) \xrightarrow{M_W} \text{SU}(3) \times \text{U}(1) \quad (5)$$

has a monopole [6] with $Q_M = 2\pi/e$ and mass

$$M_{\text{mon}} \sim \frac{4\pi M_X}{g^2}, \quad (6)$$

Searches Particle Listings

Magnetic Monopole Searches

where g is the SU(5) gauge coupling. For a unification scale of 10^{16} GeV, these monopoles would have a mass $M_{\text{mon}} \sim 10^{17} - 10^{18}$ GeV.

In theories with several stages of symmetry breaking, monopoles of different mass scales can arise. In an SO(10) theory with

$$\text{SO}(10) \xrightarrow{M_1} \text{SU}(4) \times \text{SU}(2) \times \text{SU}(2) \xrightarrow{M_2} \text{SU}(3) \times \text{SU}(2) \times \text{U}(1) \quad (7)$$

there is monopole with $Q_M = 2\pi/e$ and mass $\sim 4\pi M_1/g^2$ and a much lighter monopole with $Q_M = 4\pi/e$ and mass $\sim 4\pi M_2/g^2$ [7].

The central core of a GUT monopole contains the fields of the superheavy gauge bosons that mediate baryon number violation, so one might expect that baryon number conservation could be violated in baryon-monopole scattering. The surprising feature, pointed out by Callan [8] and Rubakov [9], is that these processes are not suppressed by powers of the gauge boson mass. Instead, the cross-sections for catalysis processes such as $p + \text{monopole} \rightarrow e^+ + \pi^0 + \text{monopole}$ are essentially geometric; *i.e.*, $\sigma_{\Delta B} \beta \sim 10^{-27} \text{ cm}^2$, where $\beta = v/c$. Note, however, that intermediate mass monopoles arising at later stages of symmetry breakings, such as the doubly charged monopoles of the SO(10) theory, do not catalyze baryon number violation.

1. Production and Annihilation

GUT monopoles are far too massive to be produced in any foreseeable accelerator. However, they could have been produced in the early universe as topological defects arising via the Kibble mechanism [10] in a symmetry-breaking phase transition. Estimates of the initial monopole abundance, and of the degree to which it can be reduced by monopole-antimonopole annihilation, predict a present-day monopole abundance that exceeds by many orders of magnitude the astrophysical and experimental bounds described below [11]. Cosmological inflation and other proposed solutions to this primordial monopole problem generically lead to present-day abundances exponentially smaller than could be plausibly detected, although potentially observable abundances can be obtained in scenarios with carefully tuned parameters.

If monopoles light enough to be produced at colliders exist, one would expect that these could be produced by analogs of the electromagnetic processes that produce pairs of electrically charged particles. Because of the large size of the magnetic charge, this is a strong coupling problem for which perturbation theory cannot be trusted. Indeed, the problem of obtaining reliable quantitative estimates of the production cross-sections remains an open one, on which there is no clear consensus.

2. Astrophysical and Cosmological Bounds

If there were no galactic magnetic field, one would expect monopoles in the galaxy to have typical velocities of the order of $10^{-3}c$, comparable to the virial velocity in the galaxy (relevant if the monopoles cluster with the galaxy) and the peculiar velocity of the galaxy with respect to the CMB rest frame (relevant if the monopoles are not bound to the galaxy). This situation is modified by the existence of a galactic magnetic field $B \sim 3\mu\text{G}$. A monopole with the Dirac charge and mass M would be accelerated by this field to a velocity

$$v_{\text{mag}} \sim \begin{cases} 10^{-3}c \left(\frac{10^{17} \text{ GeV}}{M} \right)^{1/2}, & M \lesssim 10^{11} \text{ GeV} \\ c, & M \gtrsim 10^{11} \text{ GeV} \end{cases} \quad (8)$$

Accelerating these monopoles drains energy from the magnetic field. Parker [12] obtained an upper bound on the flux of monopoles in the galaxy by requiring that the rate of this energy loss be small compared to the time scale on which the galactic field can be regenerated. With reasonable choices for the astrophysical parameters (see Ref. 13 for details), this Parker bound is

$$F < \begin{cases} 10^{-15} \text{ cm}^{-2} \text{ sr}^{-1} \text{ sec}^{-1}, & M \lesssim 10^{17} \text{ GeV} \\ 10^{-15} \left(\frac{M}{10^{17} \text{ GeV}} \right) \text{ cm}^{-2} \text{ sr}^{-1} \text{ sec}^{-1}, & M \gtrsim 10^{17} \text{ GeV} \end{cases} \quad (9)$$

Applying similar arguments to an earlier seed field that was the progenitor of the current galactic field leads to a tighter bound [14],

$$F < \left[\frac{M}{10^{17} \text{ GeV}} + (3 \times 10^{-6}) \right] 10^{-16} \text{ cm}^{-2} \text{ sr}^{-1} \text{ sec}^{-1}. \quad (10)$$

Considering magnetic fields in galactic clusters gives a bound [15] which, although less secure, is about three orders of magnitude lower than the Parker bound.

A flux bound can also be inferred from the total mass of monopoles in the universe. If the monopole mass density is a fraction Ω_M of the critical density, and the monopoles were uniformly distributed throughout the universe, there would be a monopole flux

$$F_{\text{uniform}} = 1.3 \times 10^{-16} \Omega_M \left(\frac{10^{17} \text{ GeV}}{M} \right) \left(\frac{v}{10^{-3}c} \right) \text{ cm}^{-2} \text{ sr}^{-1} \text{ sec}^{-1}. \quad (11)$$

If we assume that $\Omega_M \sim 0.1$, this gives a stronger constraint than the Parker bound for $M \sim 10^{15}$ GeV. However, monopoles with masses $\sim 10^{17}$ GeV are not ejected by the galactic field and can be gravitationally bound to the galaxy. In this case their flux within the galaxy is increased by about five orders of magnitude for a given value of Ω_M , and the mass density bound only becomes stronger than the Parker bound for $M \sim 10^{18}$ GeV.

A much more stringent flux bound applies to GUT monopoles that catalyze baryon number violation. The essential idea is that compact astrophysical objects would capture monopoles at a rate proportional to the galactic flux. These monopoles would then catalyze proton decay, with the energy released

in the decay leading to an observable increase in the luminosity of the object. A variety of bounds, based on neutron stars [16–20], white dwarfs [21], and Jovian planets [22] have been obtained. These depend in the obvious manner on the catalysis cross section, but also on the details of the astrophysical scenarios; *e.g.*, on how much the accumulated density is reduced by monopole-antimonopole annihilation, and on whether monopoles accumulated in the progenitor star survive its collapse to a white dwarf or neutron star. The bounds obtained in this manner lie in the range

$$F\left(\frac{\sigma_{\Delta B}\beta}{10^{-27}\text{cm}^2}\right) \sim (10^{-18} - 10^{-29})\text{cm}^{-2}\text{sr}^{-1}\text{sec}^{-1}. \quad (12)$$

It is important to remember that not all GUT monopoles catalyze baryon number nonconservation. In particular, the intermediate mass monopoles that arise in some GUTs at later stages of symmetry-breaking are examples of theoretically motivated monopoles that are exempt from the bound of Eq. (12).

3. Searches for Magnetic Monopoles

To date there have been no confirmed observations of exotic particles possessing magnetic charge. Precision measurements of the properties of known particles have led to tight limits on the values of magnetic charge they may possess. Using the induction method (see below), the electron's magnetic charge has been found to be $Q_e^m < 10^{-24}Q_M^D$ [23] (where Q_M^D is the Dirac charge). Furthermore, measurements of the anomalous magnetic moment of the muon have been used to place a model dependent lower limit of 120 GeV on the monopole mass¹ [24]. Nevertheless, guided mainly by Dirac's argument and the predicted existence of monopoles from spontaneous symmetry breaking mechanisms, searches have been routinely made for monopoles produced at accelerators, in cosmic rays, and bound in matter [25]. Although the resultant limits from such searches are usually made under the assumption of a particle possessing only magnetic charge, most of the searches are also sensitive to dyons.

4. Search Techniques

Search strategies are determined by the expected interactions of monopoles as they pass through matter. These would give rise to a number of striking characteristic signatures. Since a complete description of monopole search techniques falls outside of the scope of this minireview, only the most common methods are described below. More comprehensive descriptions of search techniques can be found in Refs. [26,27].

The induction method exploits the long-ranged electromagnetic interaction of the monopole with the quantum state of a superconducting ring which would lead to a monopole which passes through such a ring inducing a permanent current. The induction technique typically uses Superconducting Quantum

Interference Devices (SQUID) technology for detection and is employed for searches for monopoles in cosmic rays and matter. Another approach is to exploit the electromagnetic energy loss of monopoles. Monopoles with Dirac charge would typically lose energy at a rate which is several thousand times larger than that expected from particles possessing the elementary electric charge. Consequently, scintillators, gas chambers and nuclear track detectors (NTDs) have been used in cosmic ray and collider experiments. A further approach, which has been used at colliders, is to search for particles describing a non-helical path in a magnetic field.

5. Searches for Monopoles Bound in Matter

Monopoles have been sought in a range of bulk materials which it is assumed would have absorbed incident cosmic ray monopoles over a long exposure time of order million years. Materials which have been studied include moon rock, meteorites, manganese modules, and sea water [28]. A stringent upper limit on the monopoles per nucleon ratio of $\sim 10^{-29}$ has been obtained [28].

6. Searches in Cosmic Rays

Direct searches for monopoles in cosmic rays refer to those experiments in which the passage of the monopole is measured by an active detector. Catalysis processes in which GUT monopoles could induce nucleon decay are discussed in the next section. To interpret the results of these searches, the cross section for the catalysis process is either set to zero [29–31] or assigned a modest value (1mb) [32]. Searches which explicitly exploit the expected catalysed decays are discussed in the next section.

Although early cosmic ray searches using the induction technique [33] and NTDs [34] observed monopole candidates, none of these apparent observations have been confirmed. Recent experiments have typically employed large scale detectors. The MACRO experiment at the Gran Sasso underground laboratory comprised three different types of detector: liquid scintillator, limited stream tubes, and NTDs, which provided a total acceptance of $\sim 10000\text{m}^2$ for an isotropic flux. As shown in Fig. 1, this experiment has so far provided the most extensive β -dependent flux limits for GUT monopoles with Dirac charge [32]. Also shown are limits from an experiment at the OHYA mine in Japan [29], which used a 2000m² array of NTDs.

In Fig. 1, upper flux limits are also shown as a function of mass for monopole speed $\beta > 0.05$. In addition to MACRO and OYHA flux limits, results from the SLIM [30] high-altitude experiment are shown. The SLIM experiment provided a good sensitivity to intermediate mass monopoles ($10^5 \lesssim M \lesssim 10^{12}$ GeV). The Radio Ice Cerenkov Experiment (RICE) at the South Pole have also provided flux limits of $\sim 10^{-18} \text{cm}^{-2}\text{s}^{-1}\text{sr}^{-1}$ (not shown) for intermediate mass monopoles [31]. This work was sensitive to ultrarelativistic monopoles ($10^7 \lesssim \gamma \lesssim 10^{12}$), and the

¹ Where no ambiguity is likely to arise, a reference to a monopole implies a particle possessing Dirac charge.

Searches Particle Listings

Magnetic Monopole Searches

limits were extracted assuming a monopole energy 10^{16} GeV. In addition to the aforementioned flux limits for monopoles with the Dirac charge, the OHYA experiment also presented limits for monopoles with charges up to $3Q_M^D$, as did the the SLIM experiment.

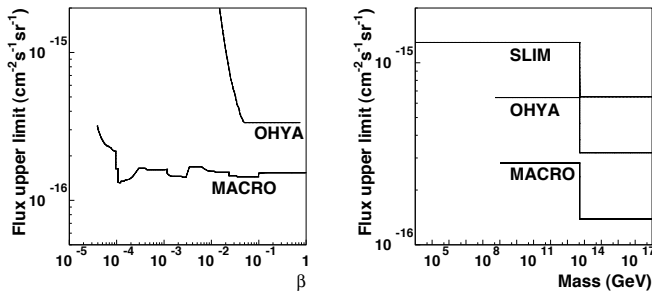


Figure 1: Upper flux limits for (a) GUT monopoles as a function of β (b) Monopoles as a function of mass for $\beta > 0.05$.

7. Searches via the Catalysis of Nucleon-Decay

Searches have also been performed for evidence of the catalysed decay of a nucleon, as predicted by the Callan-Rubakov mechanism. Searches have been made at a range of experiments which are sensitive to the induced nucleon decay of a passing monopole. For example, searches have been made with the Soudan [35] and Macro [36] experiments, using tracking detectors. Searches at Kamiokande [37], IMB [38] and the underwater Lake Baikal experiment [39] which exploit the Cerenkov effect have also been made. The resulting β -dependent flux limits from these experiments, which typically vary between $6 \times 10^{-17} - 9 \times 10^{-14} \text{cm}^{-2}\text{sr}^{-1}\text{s}^{-1}$ [25], are sensitive to the assumed values of the catalysis cross sections.

8. Searches at Colliders

Searches have been performed at hadron-hadron, electron-positron and lepton-hadron experiments. Collider searches can be broadly classed as being direct or indirect. In a direct search, evidence of the passage of a monopole through material, such as a charged particle track, is sought. In indirect searches, virtual monopole processes are assumed to influence the production rates of certain final states.

9. Direct Searches at Colliders

Collider experiments typically express their results in terms of upper limits on a production cross section and/or monopole mass. To calculate these limits, ansatzes are used to model the kinematics of monopole-antimonopole pair production processes since perturbative field theory cannot be used to calculate the rate and kinematic properties of produced monopoles. Limits therefore suffer from a degree of model-dependence, implying that a comparison between the results of different experiments can be problematic, in particular when this concerns excluded

mass regions. A conservative approach with as little model-dependence as possible is thus to present the upper cross-section limits as a function of one half the centre-of-mass energy of the collisions, as shown in Fig. 2 for recent results from high energy colliders.

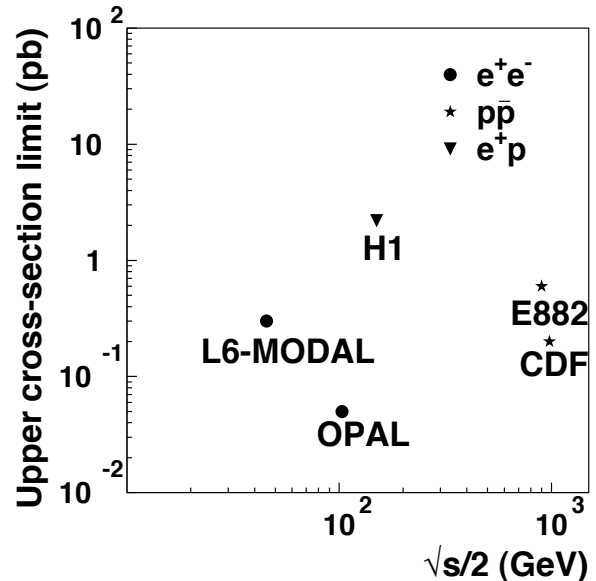


Figure 2: Upper limits on the production cross sections of monopoles from various collider-based experiments.

Searches for monopoles produced at the highest available energies in hadron-hadron collisions were made at the Tevatron by the CDF [40] and E882 [41] experiments. Complementary approaches were used; the CDF experiment used a dedicated time-of-flight system whereas the E882 experiment employed the induction technique to search for stopped monopoles in discarded detector material which had been part of the CDF and D0 detectors using periods of luminosity. Considered together, the searches provide a sensitivity to monopoles with charges between Q_M^D and $6Q_M^D$ and masses up to around 900 GeV. Earlier searches at the Tevatron, such as Ref. 42, used NTDs and were based on comparatively modest amounts of integrated luminosity. Lower energy hadron-hadron experiments have employed a variety of search techniques including plastic track detectors [43] and searches for trapped monopoles [44].

The only LEP-2 search was made by OPAL [45] which quoted cross section limits for the production of monopoles possessing masses up to around 103 GeV. At LEP-1, searches were made with NTDs deployed around an interaction region. This allowed a range of charges to be sought for masses up to ~ 45 GeV. The L6-MODAL experiment [46] gave limits for monopoles with charges in the range $0.9Q_M^D$ and $3.6Q_M^D$, whilst an earlier search by the MODAL experiment was sensitive to monopoles with charges as low as $0.1Q_M^D$ [47]. The deployment of NTDs around the beam interaction point was also used at earlier e^+e^- colliders such as KEK [48] and PETRA [49]. Searches at e^+e^- facilities have also been made for particles following non-helical trajectories [50,51].

There has so far been one search for monopole production in lepton-hadron scattering. Using the induction method, monopoles were sought which could have stopped in the aluminium beam pipe which had been used by the H1 experiment at HERA [52]. Cross section limits were set for monopoles with charges in the range $Q_M^D - 6Q_M^D$ for masses up to around 140 GeV.

10. Indirect Searches at Colliders

It has been proposed that virtual monopoles can mediate processes which give rise to multi-photon final-states [53,54]. Photon-based searches were made by the D0 [55] and L3 [56] experiments. The D0 work led to spin-dependent lower mass limits of between 610 and 1580 GeV, while L3 reported a lower mass limit of 510 GeV. However, it should be stressed that uncertainties on the theoretical calculations which were used to derive these limits are difficult to estimate.

References

1. P.A.M.Dirac, Proc. Roy. Soc. Lond. **A133**, 60 (1931).
2. F. Englert and P. Windey, Phys. Rev. **D14**, 2728 (1976).
3. P. Goddard, J. Nuyts, and D. I. Olive, Nucl. Phys. **B125**, 1 (1977).
4. G.'t Hooft, Nucl. Phys. **B79**, 276 (1974).
5. A.M. Polyakov, JETP Lett. **20**, 194 (1974) [Pisma Zh. Eksp. Teor. Fiz. **20**, 430 (1974)].
6. C.P. Dokos and T.N. Tomaras, Phys. Rev. **D21**, 2940 (1980).
7. G. Lazarides and Q. Shafi, Phys. Lett. **B94**, 149 (1980).
8. C.G. Callan, Phys. Rev. **D26**, 2058 (1982).
9. V.A. Rubakov, Nucl. Phys. **B203**, 311 (1982).
10. T.W.B. Kibble, J. Phys. **A9**, 1387 (1976).
11. J. Preskill, Phys. Rev. Lett. **43**, 1365 (1979).
12. E.N. Parker, Astrophys. J. **160**, 383 (1970).
13. M.S. Turner, E.N. Parker, and T.J. Bogdan, Phys. Rev. **D26**, 1296 (1982).
14. F.C. Adams *et al.*, Phys. Rev. Lett. **70**, 2511 (1993).
15. Y. Rephaeli and M.S. Turner, Phys. Lett. **B121**, 115 (1983).
16. E.W. Kolb, S.A. Colgate, and J.A. Harvey, Phys. Rev. Lett. **49**, 1373 (1982).
17. S. Dimopoulos, J. Preskill, and F. Wilczek, Phys. Lett. **B119**, 320 (1982).
18. K. Freese, M.S. Turner, and D.N. Schramm, Phys. Rev. Lett. **51**, 1625 (1983).
19. E.W. Kolb and M.S. Turner, Astrophys. J. **286**, 702 (1984).
20. J.A. Harvey, Nucl. Phys. **B236**, 255 (1984).
21. K. Freese and E. Krasteva, Phys. Rev. **D59**, 063007 (1999).
22. J. Arafune, M. Fukugita, and S. Yanagita, Phys. Rev. **D32**, 2586 (1985).
23. L.L. Vant-Hull, Phys. Rev. **173**, 1412 (1968).
24. S. Graf, A. Schaefer, and W. Greiner, Phys. Lett. **B262**, 463 (1991).
25. Review of Particle Physics 2010 (this *Review*), listing on *Searches for Magnetic Monopoles*.
26. G. Giacomelli and L. Patrizzii, arXiv:hep-ex/0506014.
27. M. Fairbairn *et al.*, Phys. Rept. **438**, 1 (2007).
28. J.M. Kovalik and J.L. Kirschvink, Phys. Rev. **A33**, 1183 (1986) ; H. Jeon and M. J. Longo, Phys. Rev. Lett. **75**, 1443 (1995) [Erratum-ibid. **76**, 159 (1996)].
29. S. Orito *et al.*, Phys. Rev. Lett. **66**, 1951 (1991).
30. S. Balestra *et al.*, Eur. Phys. J. **C55**, 57 (2008).
31. D.P. Hogan *et al.*, Phys. Rev. **D78**, 075031 (2008).
32. M. Ambrosio *et al.*, [MACRO Collab.], Eur. Phys. J. **C25**, 511 (2002).
33. B. Cabrera, Phys. Rev. Lett. **48**, 1378 (1982).
34. P.B. Price *et al.*, Phys. Rev. Lett. **35**, 487 (1975).
35. J.E. Bartelt *et al.*, Phys. Rev. **D36**, 1990 (1987) [Erratum-ibid. **D40**, 1701 (1989)].
36. M. Ambrosio *et al.*, Eur. Phys. J. C **26**, 163 (2002).
37. T. Kajita *et al.*, J. Phys. Soc. Jpn. **54** (1985) 4065.
38. R. Becker-Szendy *et al.*, Phys. Rev. **D49**, 2169 (1994).
39. V. A. Balkanov *et al.*, Prog. Part. Nucl. Phys. **40**, 391 (1998).
40. A. Abulencia *et al.*, [CDF Collab.], Phys. Rev. Lett. **96**, 201801 (2006).
41. G.R. Kalbfleisch *et al.*, Phys. Rev. **D69**, 052002 (2004).
42. P.B. Price, G.X. Ren, and K. Kinoshita, Phys. Rev. Lett. **59**, 2523 (1987).
43. B. Aubert *et al.*, Phys. Lett. **B120**, 465 (1983).
44. R.A. Carrigan, F.A. Nezrick, and B.P. Strauss, Phys. Rev. **D8**, 3717 (1973).
45. G. Abbiendi *et al.*, [OPAL Collab.], Phys. Lett. **B663**, 37 (2008).
46. J.L. Pinfold *et al.*, Phys. Lett. **B316**, 407 (1993).
47. K. Kinoshita *et al.*, Phys. Rev. **D46**, 881 (1992).
48. K. Kinoshita *et al.*, Phys. Lett. **B228**, 543 (1989).
49. P. Musset *et al.*, Phys. Lett. **B128**, 333 (1983).
50. T. Gentile *et al.*, [Cleo Collab.], Phys. Rev. **D35**, 1081 (1987).
51. W. Braunschweig *et al.*, [TASSO Collab.], Z. Phys. **C38**, 543 (1988).
52. A. Aktas *et al.*, [H1 Collab.], Eur. Phys. J. **C41**, 133 (2005).
53. A. De Rujula, Nucl. Phys. **B435**, 257 (1995).
54. I.F. Ginzburg and A. Schiller, Phys. Rev. **D60**, 075016 (1999).
55. B. Abbott *et al.*, [D0 Collab.], Phys. Rev. Lett. **81**, 524 (1998).
56. M. Acciarri *et al.*, [L3 Collab.], Phys. Lett. **B345**, 609 (1995).

Monopole Production Cross Section — Accelerator Searches

X-SECT (cm ²)	MASS (GeV)	CHG (e)	ENERGY (GeV)	BEAM	DOCUMENT ID	TECN
<5E-38	45-102	1	206	e ⁺ e ⁻	1 ABBIENDI 08	OPAL
<0.2E-36	200-700	1	1960	p \bar{p}	2 ABULENCIA 06K	CNTR
< 2.E-36		1	300	e ⁺ p	3,4 AKTAS 05A	INDU
< 0.2 E-36		2	300	e ⁺ p	3,4 AKTAS 05A	INDU
< 0.09E-36		3	300	e ⁺ p	3,4 AKTAS 05A	INDU
< 0.05E-36		≥ 6	300	e ⁺ p	3,4 AKTAS 05A	INDU
< 2.E-36		1	300	e ⁺ p	3,5 AKTAS 05A	INDU
< 0.2E-36		2	300	e ⁺ p	3,5 AKTAS 05A	INDU
< 0.07E-36		3	300	e ⁺ p	3,5 AKTAS 05A	INDU
< 0.06E-36		≥ 6	300	e ⁺ p	3,5 AKTAS 05A	INDU
< 0.6E-36	>265	1	1800	p \bar{p}	6 KALBFLEISCH 04	INDU
< 0.2E-36	>355	2	1800	p \bar{p}	6 KALBFLEISCH 04	INDU
< 0.07E-36	>410	3	1800	p \bar{p}	6 KALBFLEISCH 04	INDU

Searches Particle Listings

Magnetic Monopole Searches

Energy Range	Mass	SPIN	CHG	Beam	Document ID	TECN
< 0.2E-36	>375	6	1800	p \bar{p}	6 KALBFLEISCH 04	INDU
< 0.7E-36	>295	1	1800	p \bar{p}	7,8 KALBFLEISCH 00	INDU
< 7.8E-36	>260	2	1800	p \bar{p}	7,8 KALBFLEISCH 00	INDU
< 2.3E-36	>325	3	1800	p \bar{p}	7,9 KALBFLEISCH 00	INDU
< 0.11E-36	>420	6	1800	p \bar{p}	7,9 KALBFLEISCH 00	INDU
<0.65E-33	<3.3	≥ 2	11A	¹⁹⁷ Au	10 HE	97
<1.90E-33	<8.1	≥ 2	160A	²⁰⁸ Pb	10 HE	97
<3.E-37	<45.0	1.0	88-94	e ⁺ e ⁻	PINFOLD	93 PLAS
<3.E-37	<41.6	2.0	88-94	e ⁺ e ⁻	PINFOLD	93 PLAS
<7.E-35	<44.9	0.2-1.0	89-93	e ⁺ e ⁻	KINOSHITA	92 PLAS
<2.E-34	<85.0	≥ 0.5	1800	p \bar{p}	BERTANI	90 PLAS
<1.2E-33	<800	≥ 1	1800	p \bar{p}	PRICE	90 PLAS
<1.E-37	<29	1	50-61	e ⁺ e ⁻	KINOSHITA	89 PLAS
<1.E-37	<18	2	50-61	e ⁺ e ⁻	KINOSHITA	89 PLAS
<1.E-38	<17	<1	35	e ⁺ e ⁻	BRAUNSCHE... 88B	CNTR
<8.E-37	<24	1	50-52	e ⁺ e ⁻	KINOSHITA	88 PLAS
<1.3E-35	<22	2	50-52	e ⁺ e ⁻	KINOSHITA	88 PLAS
<9.E-37	<4	<0.15	10.6	e ⁺ e ⁻	GENTILE	87 CLEO
<3.E-32	<800	≥ 1	1800	p \bar{p}	PRICE	87 PLAS
<3.E-38	<3	<3	29	e ⁺ e ⁻	FRYBERGER	84 PLAS
<1.E-31	1,3	540	p \bar{p}	AUBERT	83B	PLAS
<4.E-38	<10	<6	34	e ⁺ e ⁻	MUSSET	83 PLAS
<8.E-36	<20		52	p \bar{p}	11 DELL	82 CNTR
<9.E-37	<30	<3	29	e ⁺ e ⁻	KINOSHITA	82 PLAS
<1.E-37	<20	<24	63	p \bar{p}	CARRIGAN	78 CNTR
<1.E-37	<30	<3	56	p \bar{p}	HOFFMANN	78 PLAS
			62	p \bar{p}	11 DELL	76 SPRK
<4.E-33			300	p	11 STEVENS	76B SPRK
<1.E-40	<5	<2	70	p	12 ZRELOV	76 CNTR
<2.E-30			300	n	11 BURKE	75 OSPK
<1.E-38			8	ν	13 CARRIGAN	75 HLBC
<5.E-43	<12	<10	400	p	EBERHARD	75B INDU
<2.E-36	<30	<3	60	p \bar{p}	GIACOMELLI	75 PLAS
<5.E-42	<13	<24	400	p	CARRIGAN	74 CNTR
<6.E-42	<12	<24	300	p	CARRIGAN	73 CNTR
<2.E-36		1	0.001	γ	12 BARTLETT	72 CNTR
<1.E-41	<5		70	p	GUREVICH	72 EMUL
<1.E-40	<3	<2	28	p	AMALDI	63 EMUL
<2.E-40	<3	<2	30	p	PURCELL	63 CNTR
<1.E-35	<3	<4	28	p	FIDECARO	61 CNTR
<2.E-35	<1	1	6	p	BRADNER	59 EMUL

- ¹ ABBIENDI 08 assume production of spin 1/2 monopoles with effective charge $g\beta$ ($n=1$), via $e^+e^- \rightarrow \gamma^* \rightarrow M\bar{M}$, so that the cross section is proportional to $(1 + \cos^2\theta)$. There is no χ information for such highly saturated tracks, so a parabolic track in the jet chamber is projected onto the xy plane. Charge per hit in the chamber produces a clean separation of signal and background.
- ² ABULENCIA 06k searches for high-ionizing signals in CDF central outer tracker and time-of-flight detector. For Drell-Yan $M\bar{M}$ production, the cross section limit implies $M > 360$ GeV at 95% CL.
- ³ AKTAS 05A model-dependent limits as a function of monopole mass shown for arbitrary mass of 60 GeV. Based on search for stopped monopoles in the H1 Al beam pipe.
- ⁴ AKTAS 05A limits with assumed elastic spin 0 monopole pair production.
- ⁵ AKTAS 05A limits with assumed inelastic spin 1/2 monopole pair production.
- ⁶ KALBFLEISCH 04 reports searches for stopped magnetic monopoles in Be, Al, and Pb samples obtained from discarded material from the upgrading of DØ and CDF. A large-aperture warm-bore cryogenic detector was used. The approach was an extension of the methods of KALBFLEISCH 00. Cross section results moderately model dependent; interpretation as a mass lower limit depends on possibly invalid perturbation expansion.
- ⁷ KALBFLEISCH 00 used an induction method to search for stopped monopoles in pieces of the DØ (FNAL) beryllium beam pipe and in extensions to the drift chamber aluminum support cylinder. Results are model dependent.
- ⁸ KALBFLEISCH 00 result is for aluminum.
- ⁹ KALBFLEISCH 00 result is for beryllium.
- ¹⁰ HE 97 used a lead target and barium phosphate glass detectors. Cross-section limits are well below those predicted via the Drell-Yan mechanism.
- ¹¹ Multiphoton events.
- ¹² Cherenkov radiation polarization.
- ¹³ Re-examines CERN neutrino experiments.

Monopole Production — Other Accelerator Searches

MASS (GeV)	CHG (g)	SPIN	ENERGY (GeV)	BEAM	DOCUMENT ID	TECN
> 610	≥ 1	0	1800	p \bar{p}	14 ABBOTT	98k D0
> 870	≥ 1	1/2	1800	p \bar{p}	14 ABBOTT	98k D0
>1580	≥ 1	1	1800	p \bar{p}	14 ABBOTT	98k D0
> 510			88-94	e ⁺ e ⁻	15 ACCIARRI	95c L3

- ¹⁴ ABBOTT 98k search for heavy pointlike Dirac monopoles via central production of a pair of photons with high transverse energies.
- ¹⁵ ACCIARRI 95c finds a limit $B(Z \rightarrow \gamma\gamma) < 0.8 \times 10^{-5}$ (which is possible via a monopole loop) at 95% CL and sets the mass limit via a cross section model.

Monopole Flux — Cosmic Ray Searches

"Caty" in the charge column indicates a search for monopole-catalyzed nucleon decay.

FLUX (cm ⁻² sr ⁻¹ s ⁻¹)	MASS (GeV)	CHG (g)	COMMENTS ($\beta = v/c$)	EVTs	DOCUMENT ID	TECN
<1.3E-15	1E4<M<5E13	1	$\beta > 0.05$	0	16 BALESTRA	08 PLAS
<0.65E-15	>5E13	1	$\beta > 0.05$	0	16 BALESTRA	08 PLAS

<1E-18	1	$\gamma > 1$	E8	0	17 HOGAN	08 RICE
<1.4E-16	1	1.1E-4 < β < 1		0	18 AMBROSIO	02b MCRO
<3E-16	Caty	1.1E-4 < β < 5E-3		0	19 AMBROSIO	02c MCRO
<1.5E-15	1	5E-3 < β < 0.99		0	20 AMBROSIO	02d MCRO
<1E-15	1	$1.1 \times 10^{-4} - 0.1$		0	21 AMBROSIO	97 MCRO
<5.6E-15	1	(0.18-3.0)E-3		0	22 AHLEN	94 MCRO
<2.7E-15	Caty	$\beta \sim 1 \times 10^{-3}$		0	23 BECKER-SZ...	94 IMB
<8.7E-15	1	>2.E-3		0	THRON	92 SOUD
<4.4E-12	1	all β		0	GARDNER	91 INDU
<7.2E-13	1	all β		0	HUBER	91 INDU
<3.7E-15	>E12	$\beta = 1.E-4$		0	24 ORITO	91 PLAS
<3.2E-16	>E10	$\beta > 0.05$		0	24 ORITO	91 PLAS
<3.2E-16	>E10-E12	2, 3		0	24 ORITO	91 PLAS
<3.8E-13	1	all β		0	BERMON	90 INDU
<5.E-16	Caty	$\beta < 1.E-3$		0	23 BEZRUKOV	90 CHER
<1.8E-14	1	$\beta > 1.1E-4$		0	25 BUCKLAND	90 HEPT
<1E-18	1	3.E-4 < β < 1.5E-3		0	26 GHOSH	90 MICA
<7.2E-13	1	all β		0	HUBER	90 INDU
<5.E-12	>E7	1 3.E-4 < β < 5.E-3		0	BARISH	87 CNTR
<1.E-13	Caty	1.E-5 < β < 1		0	23 BARTELT	87 SOUD
<1E-10	1	all β		0	EBISU	87 INDU
<2E-13	1	1.E-4 < β < 6.E-4		0	MASEK	87 HEPT
<2E-14	1	4.E-5 < β < 2.E-4		0	NA KAMURA	87 PLAS
<2E-14	1	1.E-3 < β < 1		0	NA KAMURA	87 PLAS
<5.E-14	1	9.E-4 < β < 1.E-2		0	SHEPKO	87 CNTR
<2E-13	1	4.E-4 < β < 1		0	TSUKAMOTO	87 CNTR
<5.E-14	1	all β		1	27 CAPLIN	86 INDU
<5.E-12	1			0	CROMAR	86 INDU
<1E-13	1	7.E-4 < β		0	HARA	86 CNTR
<7.E-11	1	all β		0	INCANDELA	86 INDU
<1E-18	1	4.E-4 < β < 1.E-3		0	26 PRICE	86 MICA
<5.E-12	1			0	BERMON	85 INDU
<6.E-12	1			0	CAPLIN	85 INDU
<6.E-10	1			0	EBISU	85 INDU
<3.E-15	Caty	5.E-5 $\leq \beta \leq 1.E-3$		0	23 KAJITA	85 KAMI
<2E-21	Caty	$\beta < 1.E-3$		0	23,28 KAJITA	85 KAMI
<3E-15	Caty	1.E-3 < β < 1.E-1		0	23 PARK	85B CNTR
<5.E-12	1	1.E-4 < β < 1		0	BATTISTONI	84 NUSX
<7E-12	1			0	INCANDELA	84 INDU
<7E-13	1	3.E-4 < β		0	25 KAJINO	84 CNTR
<2E-12	1	3.E-4 < β < 1.E-1		0	KAJINO	84B CNTR
<6E-13	1	5.E-4 < β < 1		0	KAWAGOE	84 CNTR
<2E-14	1	1.E-3 < β		0	23 KRISHNA...	84 CNTR
<4E-13	1	6.E-4 < β < 2.E-3		0	LISS	84 CNTR
<1E-16	1	3.E-4 < β < 1.E-3		0	26 PRICE	84 MICA
<1E-13	1	1.E-4 < β		0	PRICE	84B PLAS
<4E-13	1	6.E-4 < β < 2.E-3		0	TARLE	84 CNTR
	7				29 ANDERSON	83 EMUL
<4E-13	1	1.E-2 < β < 1.E-3		0	BARTELT	83B CNTR
<1E-12	1	7.E-3 < β < 1		0	BARWICK	83 PLAS
<3E-13	1	1.E-3 < β < 4.E-1		0	BONARELLI	83 CNTR
<3E-12	Caty	5.E-4 < β < 5.E-2		0	23 BOSETTI	83 CNTR
<4E-11	1			0	CABRERA	83 INDU
<5E-15	1	1.E-2 < β < 1		0	DOKE	83 PLAS
<8E-15	Caty	1.E-4 < β < 1.E-1		0	23 ERREDE	83 IMB
<5E-12	1	1.E-4 < β < 3.E-2		0	GROOM	83 CNTR
<2E-12	1	6.E-4 < β < 1		0	MASHIMO	83 CNTR
<1E-13	1	$\beta = 3.E-3$		0	ALEXEYEV	82 CNTR
<2E-12	1	7.E-3 < β < 6.E-1		0	BONARELLI	82 CNTR
6.E-10	1	all β		1	30 CABRERA	82 INDU
<2E-11	1	1.E-2 < β < 1.E-1		0	MASHIMO	82 CNTR
<2E-15		concentrator		0	BARTLETT	81 PLAS
<1E-13	>1	1.E-3 < β		0	KINOSHITA	81B PLAS
<5E-11	<E17	3.E-4 < β < 1.E-3		0	ULLMAN	81 CNTR
<2E-11		concentrator		0	BARTLETT	78 PLAS
1.E-1	>200	2		1	31 PRICE	75 PLAS
<2E-13	>2	>2		0	FLEISCHER	71 PLAS
<1E-19	>2	obsidian, mica		0	FLEISCHER	69c PLAS
<5E-15	<15	<3 concentrator		0	CARTHURS	66 ELEC
<2E-11	<1-3	concentrator		0	MALKUS	51 EMUL

- ¹⁶ BALESTRA 08 exposed of nuclear track detector modules totaling 400 m² for 4 years at the Chacaltaya Laboratory (5230 m) in search for intermediate-mass monopoles with $\beta > 0.05$. The analysis is mainly based on three CR39 modules. For $M > 5 \times 10^{13}$ GeV there can be upward-going monopoles as well, hence the flux limit is half that obtained for less massive monopoles. Previous experiments (e.g. MACRO and OHYA (ORITO 91)) had set limits only for $M > 1 \times 10^9$ GeV.
- ¹⁷ HOGAN 08 limit on relativistic monopoles is based on nonobservation of radio Cherenkov signals at the South Pole.
- ¹⁸ AMBROSIO 02b direct search final result for $m \geq 10^{17}$ GeV, based upon 4.2 to 9.5 years of running, depending upon the subsystem. Limit with CR39 track-etch detector extends the limit from $\beta=4 \times 10^{-5}$ (3.1×10^{-16} cm⁻²sr⁻¹s⁻¹) to $\beta=1 \times 10^{-4}$ (2.1×10^{-16} cm⁻²sr⁻¹s⁻¹). Limit curve in paper is piecewise continuous due to different detection techniques for different β ranges.
- ¹⁹ AMBROSIO 02c limit for catalysis of nucleon decay with catalysis cross section of ≈ 1 mb. The flux limit increases by ~ 3 at the higher β limit, and increases to 1×10^{-14} cm⁻²sr⁻¹s⁻¹ if the catalysis cross section is 0.01 mb. Based upon 71193 hr of data with the streamer detector, with an acceptance of 4250 m²sr.

- ²⁰ AMBROSIO 02d result for "more than two years of data." Ionization search using several subsystems. Limit curve as a function of β not given. Included in AMBROSIO 02b.
- ²¹ AMBROSIO 97 global MACRO 90%CL is 0.78×10^{-15} at $\beta=1.1 \times 10^{-4}$, goes through a minimum at 0.61×10^{-15} near $\beta=(1.1-2.7) \times 10^{-3}$, then rises to 0.84×10^{-15} at $\beta=0.1$. The global limit in this region is below the Parker bound at 10^{-15} . Less stringent limits are established for $4 \times 10^{-5} < \beta < 1 \times 10^{-4}$. Limits set by various triggers and different subdetectors are given in the paper. All limits assume a catalysis cross section smaller than a few mb.
- ²² AHLEN 94 limit for dyons extends down to $\beta=0.9E-4$ and a limit of $1.3E-14$ extends to $\beta = 0.8E-4$. Also see comment by PRICE 94 and reply of BARISH 94. One loophole in the AHLEN 94 result is that in the case of monopoles catalyzing nucleon decay, relativistic particles could veto the events. See AMBROSIO 97 for additional results.
- ²³ Catalysis of nucleon decay; sensitive to assumed catalysis cross section.
- ²⁴ ORITO 91 limits are functions of velocity. Lowest limits are given here.
- ²⁵ Used DKMPR mechanism and Penning effect.
- ²⁶ Assumes monopole attaches fermion nucleus.
- ²⁷ Limit from combining data of CAPLIN 86, BERMON 85, INCANDELA 84, and CABRERA 83. For a discussion of controversy about CAPLIN 86 observed event, see GUY 87. Also see SCHOUBEN 87.
- ²⁸ Based on lack of high-energy solar neutrinos from catalysis in the sun.
- ²⁹ Anomalous long-range α (^4He) tracks.
- ³⁰ CABRERA 82 candidate event has single Dirac charge within $\pm 5\%$.
- ³¹ ALVAREZ 75, FLEISCHER 75, and FRIEDLANDER 75 explain as fragmenting nucleus. EBERHARD 75 and ROSS 76 discuss conflict with other experiments. HAGSTROM 77 reinterprets as antinucleus. PRICE 78 reassesses.

REFERENCES FOR Magnetic Monopole Searches

ABBIENDI 08	PL B663 37	G. Abbiendi et al.	(OPAL Collab.)
BALESTRA 08	EPJ C55 57	S. Balestra et al.	(SLIM Collab.)
HOGAN 08	PR D78 075031	D.P. Hogan et al.	(KANS, NEBR, DELA)
ABULENCIA 06K	PRL 96 201801	A. Abulencia et al.	(CDF Collab.)
AKTAS 05A	EPJ C41 133	A. Aktas et al.	(HI Collab.)
KALBFLEISCH 04	PR D69 052002	G.R. Kalbfleisch et al.	(OKLA)
AMBROSIO 02B	EPJ C25 511	M. Ambrosio et al.	(MACRO Collab.)
AMBROSIO 02C	EPJ C26 163	M. Ambrosio et al.	(MACRO Collab.)
AMBROSIO 02D	ASP 18 27	M. Ambrosio et al.	(MACRO Collab.)
KALBFLEISCH 00	PRL 85 5292	G.R. Kalbfleisch et al.	(MACRO Collab.)
FREISE 99	PR D59 063007	K. Freese, E. Krasteva	(MACRO Collab.)
ABBOTT 98K	PRL 81 524	B. Abbott et al.	(D0 Collab.)
AMBROSIO 97	PL B406 249	M. Ambrosio et al.	(MACRO Collab.)
HE 97	PRL 79 1314	Y.D. He	(UCB)
ACCIARRI 95C	PL B345 609	M. Acciari et al.	(L3 Collab.)
JEON 95	PRL 75 1443	H. Jeon, M.J. Longo	(MICH)
Also	PRL 76 159 (erratum)	H. Jeon, M.J. Longo	(MICH)
AHLEN 94	PRL 72 608	S.P. Ahlen et al.	(MACRO Collab.)
BARISH 94	PRL 73 1306	B.C. Barish, G. Giacomelli, J.T. Hong	(CIT+)
BECKER-SZ... 94	PR D49 2169	R.A. Becker-Szendy et al.	(IMB Collab.)
PRICE 94	PRL 73 1305	P.B. Price	(IMB Collab.)
ADAMS 93	PRL 70 2511	F.C. Adams et al.	(MICH, FNAL)
PINFOLD 93	PL B316 407	J.L. Pinfold et al.	(ALBE, HARV, MONT+)
KINOSHITA 92	PR D46 R881	K. Kinoshita et al.	(HARV, BGNA, REHO)
THRON 92	PR D46 4846	J.L. Thron et al.	(SOUDAN-2 Collab.)
GARDNER 91	PR D44 622	R.D. Gardner et al.	(STAN)
HUBER 91	PR D44 636	M.E. Huber et al.	(STAN)
ORITO 91	PRL 66 1951	S. Orito et al.	(ICEPP, WASCR, NIHO, ICCR)
BERMON 90	PRL 64 839	S. Bermon et al.	(IBM, BNL)
BERTANI 90	EPL 12 613	M. Bertani et al.	(BGNA, INFN)
BEZRUKOV 90	SJNP 52 54	L.B. Bezrukov et al.	(INRM)
BUCKLAND 90	Translated from YAF 52 86	K.N. Buckland et al.	(UCSD)
GHOSH 90	EPL 12 25	D.C. Ghosh, S. Chatterjee	(JADA)
HUBER 90	PRL 64 835	M.E. Huber et al.	(STAN)
PRICE 90	PRL 65 149	P.B. Price, J. Giriu, K. Kinoshita	(UCB, HARV)
KINOSHITA 88	PR D228 543	K. Kinoshita et al.	(HARV, TISA, KEK+)
BRAUNSCH... 88B	ZPHY C38 543	R. Braunschweig et al.	(TASSO Collab.)
KINOSHITA 88	PRL 60 1610	K. Kinoshita et al.	(HARV, TISA, KEK+)
BARISH 87	PR D36 2641	B.C. Barish, G. Liu, C. Lane	(CIT)
BARTELT 87	PR D36 1990	J.E. Bartelt et al.	(Soudan Collab.)
Also	(erratum)	J.E. Bartelt et al.	(Soudan Collab.)
EBISU 87	PR D36 3359	T. Ebiisu, T. Watanabe	(KOBE)
Also	JPG 11 883	T. Ebiisu, T. Watanabe	(KOBE)
GENTILE 87	PR D35 1051	T. Gentile et al.	(CLEO Collab.)
GUY 87	NAT 325 463	J. Guy	(LOIC)
MASEK 87	PR D35 2758	G.E. Masek et al.	(UCSD)
NAKAMURA 87	PL B183 395	S. Nakamura et al.	(INUS, WASCR, NIHO)
PRICE 87	PR 59 2523	P.B. Price, R. Guoxiao, K. Kinoshita	(UCB, HARV)
SCHOUBEN 87	JPE 20 850	J.C. Schouben et al.	(LOIC)
SHEPKO 87	PR D35 2917	M.J. Shepko et al.	(TAMU)
TSUKAMOTO 87	EPL 3 39	T. Tsukamoto et al.	(ICRR)
CAPLIN 86	NAT 321 402	A.D. Caplin et al.	(LOIC)
Also	JPE 20 850	J.C. Schouben et al.	(LOIC)
Also	NAT 325 463	J. Guy	(LOIC)
CROMAR 86	PRL 56 2561	M.W. Cromar, A.F. Clark, F.R. Fickett	(NBS)
HARA 86	PRL 56 553	T. Hara et al.	(ICRR, KYOT, KEK, KOBE+)
INCANDELA 86	PR D34 2637	J. Incandela et al.	(CHIC, FNAL, MICH)
KOVALIK 86	PR A33 1183	J.M. Kovalik, J.L. Kirschvink	(CIT)
PRICE 86	PRL 56 1226	P.B. Price, M.H. Salamoun	(UCB)
ARAFUNE 85	PR D32 2586	J. Arafune, M. Fukugita, S. Yanagita	(ICRR, KYOTU+)
BERMON 85	PRL 55 1850	S. Bermon et al.	(IBM)
BRACCI 85B	NP B258 726	L. Bracci, G. Fiorentini, G. Mezzorani	(PISA+)
Also	LNC 42 123	L. Bracci, G. Fiorentini, G. Mezzorani	(PISA)
CAPLIN 85	NAT 317 234	A.D. Caplin et al.	(LOIC)
EBISU 85	JPG 11 883	T. Ebiisu, T. Watanabe	(KOBE)
KAJITA 85	JPSJ 54 4065	T. Kajita et al.	(ICRR, KEK, NIIG)
PARK 85B	NP B252 261	H.S. Park et al.	(IMB Collab.)
BATTISTONI 84	PL 133B 454	G. Battistoni et al.	(NUSEX Collab.)
FRYBERGER 84	PR D29 1524	D. Fryberger et al.	(SLAC, UCB)
HARVEY 84	NP B236 255	J.A. Harvey	(PRIN)
INCANDELA 84	PRL 53 2067	J. Incandela et al.	(CHIC, FNAL, MICH)
KAJINO 84B	JPG 10 447	F. Kajino et al.	(ICRR)
KAWAGOE 84	LNC 41 315	K. Kawagoe et al.	(TOKY)
KOLB 84	APJ 266 702	E.W. Kolb, M.S. Turner	(FNAL, CHIC)
KRISHNA... 84	PL 142B 99	M.R. Krishnaswamy et al.	(TATA, OSKC+)
LISS 84	PR D30 884	T.M. Liss, S.P. Ahlen, G. Tarle	(UCB, IND+)
PRICE 84	PRL 52 1265	P.B. Price et al.	(ROMA, UCB, IND+)
PRICE 84B	PL 140B 112	P.B. Price	(CERN)
TARLE 84	PRL 52 90	G. Tarle, S.P. Ahlen, T.M. Liss	(UCB, MICH+)
ANDERSON 83	PR D28 2308	S.N. Anderson et al.	(WASH)
ARAFUNE 83	PL 133B 380	J. Arafune, M. Fukugita	(ICRR, KYOTU)
AUBERT 83B	PL 120B 465	B. Aubert et al.	(CERN, LAPP)
BARTELT 83B	PRL 50 655	J.E. Bartelt et al.	(MIMN, ANL)
BARWICK 83	PR D28 2338	S.W. Barwick, K. Kinoshita, P.B. Price	(UCB)
BONARELLI 83	PL 126B 137	R. Bonarelli, P. Capiluppi, I. d'Annunzio	(BGNA)
BOSETTI 83	PL 133B 265	P.C. Bosetti et al.	(AAACH3, HAWA, TOKY)
CABRERA 83	PRL 51 1933	B. Cabrera et al.	(STAN)
DOKE 83	PL 129B 370	T. Doke et al.	(WASU, RIKK, TTAM, RIKEN)
ERREDE 83	PRL 51 245	S.M. Errede et al.	(IMB Collab.)
FREISE 83B	PRL 51 1625	K. Freese, M.S. Turner, D.N. Schramm	(CHIC)
GROOM 83	PRL 50 573	D.E. Groom et al.	(UTAH, STAN)
MASHIMO 83	PL 128B 327	T. Mashimo et al.	(ICEPP)
MIKHAILOV 83	PL 130B 331	V.F. Mikhailov	(KAZA)
MUSSET 83	PL 128B 333	P. Musset, M. Price, E. Lohrmann	(CERN, HAMB)
REPHELLI 83	PL 121B 115	V. Repphaeli, M.S. Turner	(CHIC)
SCHATTEN 83	PR D27 1525	K.H. Schatten	(NASA)
ALEXEYEV 82	LNC 35 413	E.M. Alexeev et al.	(INRM)
BONARELLI 82	PL 112B 100	R. Bonarelli et al.	(BGNA)
CABRERA 82	PRL 48 1378	B. Cabrera	(STAN)
DELL 82	NP B209 45	G.F. Dell et al.	(BNL, ADEL, ROMA)
DIMPOULOS... 82	PL 119B 320	S. Dimopoulos, J. Preskill, F. Wilczek	(HARV+)
KINOSHITA 82	PRL 48 77	K. Kinoshita, P.B. Price, D. Fryberger	(UCB+)
KOLB 82	PRL 49 1373	E.W. Kolb, S.A. Colgate, J.A. Harvey	(LASL, PRIN)
MASHIMO 82	JPSJ 51 3067	T. Mashimo, K. Kawagoe, M. Koshiba	(INUS)
SALPETER 82	PRL 49 1114	E.E. Salpeter, S.L. Shapiro, I. Wasserman	(CORN)
TURNER 82	PR D26 2196	M.S. Turner, E.N. Parker, T.J. Bogdan	(CHIC)
BARTLETT 81	PR D24 612	D.P. Bartlett et al.	(COLO, GSC)
KINOSHITA 81B	PR D24 1707	K. Kinoshita, P.B. Price	(UCB)
ULLMAN 81	PRL 47 289	J.D. Ullman	(LEHM, BNL)
CARRIGAN 80	NAT 288 348	R.A. Carrigan	(FNAL)
BRODERICK 79	PR D19 1046	J.J. Broderick et al.	(VPI)
BARTLETT 78	PR D18 2253	D.F. Bartlett, D. Soo, M.G. White	(COLO, PRIN)
CARRIGAN 78	PR D17 1754	R.A. Carrigan, B.P. Strauss, G. Giacomelli	(FNAL+)
HOFFMANN 78	LNC 23 357	H. Hoffmann et al.	(CERN, ROMA)
PRICE 78	PR D18 1382	P.B. Price et al.	(UCB, HOUS)
HAGSTROM 77	PR 38 729	R. Hagstrom	(LBL)
CARRIGAN 77	PR D13 1823	R.A. Carrigan, F.A. Zeznick, B.P. Strauss	(FNAL)

Monopole Flux — Astrophysics

FLUX ($\text{cm}^{-2}\text{sr}^{-1}\text{s}^{-1}$)	MASS (GeV)	CHG (g)	COMMENTS ($\beta = v/c$)	EVTS	DOCUMENT ID	TECN
<1.3E-20			faint white dwarf	0	32 FREESE 99	ASTR
<1.E-16	E17	1	galactic field	0	33 ADAMS 93	COSM
<1.E-23			Jovian planets	0	32 ARAFUNE 85	ASTR
<1.E-16	E15	0	solar trapping	0	BRACCI 85B	ASTR
<1.E-18	1	0	32 HARVEY 84	COSM		
<3.E-23			neutron stars	0	KOLB 84	ASTR
<7.E-22		0	pulsars	0	32 FREESE 83B	ASTR
<1.E-18	<E18	1	intergalactic field	0	32 REPHAELI 83	COSM
<1.E-23		0	neutron stars	0	32 DIMOPOULOS...	COSM
<5.E-22		0	neutron stars	0	32 KOLB 82	COSM
<5.E-15	>E21		galactic halo	0	SALPETER 82	COSM
<1.E-12	E19	1	$\beta = 3-3.E-3$	0	34 TURNER 82	COSM
<1.E-16	1	1	galactic field	0	PARKER 70	COSM

- ³² Catalysis of nucleon decay.
- ³³ ADAMS 93 limit based on "survival and growth of a small galactic seed field" is $10^{-16} (m/10^{17} \text{ GeV}) \text{ cm}^{-2} \text{sr}^{-1}$. Above 10^{17} GeV , limit $10^{-16} (10^{17} \text{ GeV}/m) \text{ cm}^{-2} \text{sr}^{-1}$ (from requirement that monopole density does not overclose the universe) is more stringent.
- ³⁴ Re-evaluates PARKER 70 limit for GUT monopoles.

Monopole Density — Matter Searches

DENSITY	CHG (g)	MATERIAL	EVTS	DOCUMENT ID	TECN
<6.9E-6/gram	>1/3	Meteorites and other	0	JEON 95	INDU
<2.E-7/gram	>0.6	Fe ore	0	35 EBISU 87	INDU
<4.E-6/gram	>0.5	deep schist	0	KOVALIK 86	INDU
<1.6E-6/gram	>0.5	manganese nodules	0	36 KOVALIK 86	INDU
<1.3E-6/gram	>0.5	seawater	0	KOVALIK 86	INDU
>1.E+14/gram	>1/3	iron aerosols	>1	MIKHAILOV 83	SPEC
<6.E-4/gram		air, seawater	0	CARRIGAN 76	CNTR
<5.E-1/gram	>0.04	11 materials	0	CABRERA 75	INDU
<2.E-4/gram	>0.05	moon rock	0	ROSS 73	INDU
<6.E-7/gram	<140	seawater	0	KOLM 71	CNTR
<1.E-2/gram	<120	manganese nodules	0	FLEISCHER 69	PLAS
<1.E-4/gram	>0	manganese	0	FLEISCHER 69B	PLAS
<2.E-3/gram	<1-3	magnetite, meteor	0	GOTO 63	EMUL
<2.E-2/gram		meteorite	0	PETUKHOV 63	CNTR

- ³⁵ Mass $1 \times 10^{14} - 1 \times 10^{17} \text{ GeV}$.
- ³⁶ KOVALIK 86 examined 498 kg of schist from two sites which exhibited clear minearalogic evidence of having been buried at least 20 km deep and held below the Curie temperature.

Monopole Density — Astrophysics

DENSITY	CHG (g)	MATERIAL	EVTS	DOCUMENT ID	TECN
<1.E-9/gram	1	sun, catalysis	0	37 ARAFUNE 83	COSM
<6.E-33/nuc1	1	moon wake	0	SCHATTEN 83	ELEC
<2.E-28/nuc1	0	earth heat	0	CARRIGAN 80	COSM
<2.E-4/prot	42cm	absorption	0	BRODERICK 79	COSM
<2.E-13/m3		moon wake	0	SCHATTEN 70	ELEC

- ³⁷ Catalysis of nucleon decay.

Searches Particle Listings

Magnetic Monopole Searches, Supersymmetric Particle Searches

DELL	76	LNC 15 269	G.F. Dell <i>et al.</i>	(CERN, BNL, ROMA, ADEL)
ROSS	76	LBL-4665	R.R. Ross	(LBL)
STEVENS	76B	PR D14 2207	D.M. Stevens <i>et al.</i>	(VPI, BNL)
ZRELOV	76	CZJP B26 1306	V.P. Zrelov <i>et al.</i>	(JINR)
ALVAREZ	75	LBL-4260	L.W. Alvarez	(LBL)
BURKE	75	PL 60B 113	D.L. Burke <i>et al.</i>	(MICH)
CABRERA	75	Thesis	B. Cabrera	(STAN)
CARRIGAN	75	NP B91 279	R.A. Carrigan, F.A. Nezrick	(FNAL)
Also		PR D3 56	R.A. Carrigan, F.A. Nezrick	(FNAL)
EBERHARD	75	PR D11 3099	P.H. Eberhard <i>et al.</i>	(LBL, MPIM)
EBERHARD	75B	LBL-4289	P.H. Eberhard	(LBL)
FLEISCHER	75	PRL 35 1412	R.L. Fleischer, R.N.F. Walker	(GESC, WUSL)
FRIEDLANDER	75	PRL 35 1167	M.W. Friedlander	(WUSL)
GIACOMELLI	75	NC 28A 21	G. Giacomelli <i>et al.</i>	(BGNA, CERN, SACL+)
PRICE	75	PRL 35 487	P.B. Price <i>et al.</i>	(UCB, HOUS)
CARRIGAN	74	PR D10 3867	R.A. Carrigan, F.A. Nezrick, B.P. Strauss	(FNAL)
CARRIGAN	73	PR D8 3717	R.A. Carrigan, F.A. Nezrick, B.P. Strauss	(FNAL)
ROSS	73	PR D8 698	R.R. Ross <i>et al.</i>	(LBL, SLAC)
Also		PR D4 3260	P.H. Eberhard <i>et al.</i>	(LBL, SLAC)
Also		SCI 167 701	L.W. Alvarez <i>et al.</i>	(LBL, SLAC)
BARTLETT	72	PR D6 1817	D.F. Bartlett, M.D. Lahana	(COLO)
GUREVICH	72	PL 38B 549	I.I. Gurevich <i>et al.</i>	(KIAE, NOVO, SERP)
Also		JETP 34 917	L.M. Barkov, I.I. Gurevich, M.S. Zolotarev	(KIAE+)
Also		Translated from ZETF 61 1721.		
Also		PL 31B 394	I.I. Gurevich <i>et al.</i>	(KIAE, NOVO, SERP)
FLEISCHER	71	PR D4 24	R.L. Fleischer <i>et al.</i>	(GESC)
KOLM	71	PR D4 1285	H.H. Kolm, F. Villa, A. Odian	(MIT, SLAC)
PARKER	70	APJ 160 383	E.N. Parker	(CHIC)
SCHATTEN	70	PR D1 2245	K.H. Schatten	(NASA)
FLEISCHER	69	PR 177 2029	R.L. Fleischer <i>et al.</i>	(GESC, FSU)
FLEISCHER	69B	PR 184 1393	R.L. Fleischer <i>et al.</i>	(GESC, UNCS, GSCO)
FLEISCHER	69C	PR 184 1398	R.L. Fleischer, P.B. Price, R.T. Woods	(GESC)
Also		JAP 41 958	R.L. Fleischer <i>et al.</i>	(GESC)
CARITHERS	66	PR 149 1070	W.C.J. Carithers, R.J. Stefanski, R.K. Adair	(KIAE)
AMALDI	63	NC 28 773	E. Amaldi <i>et al.</i>	(ROMA, UCSD, CERN)
GOTO	63	PR 132 387	E. Goto, H.H. Kolm, K.W. Ford	(TOKY, MIT, BRAN)
PETUKHOV	63	NP 49 87	V.A. Petukhov, M.N. Yakimenko	(LEBD)
PURCELL	63	PR 129 2326	E.M. Purcell <i>et al.</i>	(HARV, BNL)
FIDECARO	61	NC 22 657	M. Fidecaro, G. Finocchiaro, G. Giacomelli	(CERN)
BRADNER	59	PR 114 603	H. Bradner, W.M. Isbell	(LBL)
MALKUS	51	PR 83 899	W.V.R. Malkus	(CHIC)

OTHER RELATED PAPERS

GROOM	86	PRPL 140 323	D.E. Groom	(UTAH)
Review				

Supersymmetric Particle Searches

SUPERSYMMETRY, PART I (THEORY)

Revised October 2009 by Howard E. Haber (UC Santa Cruz).

- I.1. Introduction
- I.2. Structure of the MSSM
 - I.2.1. Constraints on supersymmetric parameters
 - I.2.2. R-parity and the lightest supersymmetric particle
 - I.2.3. The goldstino and gravitino
 - I.2.4. Hidden sectors and the structure of supersymmetry-breaking
 - I.2.5. Supersymmetry and extra dimensions
 - I.2.6. Split-supersymmetry
- I.3. Parameters of the MSSM
 - I.3.1. The supersymmetry-conserving parameters
 - I.3.2. The supersymmetry-breaking parameters
 - I.3.3. MSSM-124
- I.4. The supersymmetric-particle spectrum
 - I.4.1. The charginos and neutralinos
 - I.4.2. The squarks, sleptons and sneutrinos
- I.5. The Higgs sector of the MSSM
 - I.5.1. The tree-level MSSM Higgs sector
 - I.5.2. The radiatively-corrected MSSM Higgs sector
- I.6. Restricting the MSSM parameter freedom
 - I.6.1. Bottom-up approach for constraining the MSSM parameters
 - I.6.2. Top-down approach for constraining the MSSM parameters
 - I.6.3. Anomaly-mediated supersymmetry-breaking
- I.7. The constrained MSSMs: mSUGRA, GMSB, and SGUTs
 - I.7.1. The minimal supergravity model

I.7.2. Gauge-mediated supersymmetry-breaking

I.7.3. Supersymmetric grand unification

I.8. Massive neutrinos in low-energy supersymmetry

I.8.1. The supersymmetric seesaw

I.8.2. R-parity-violating supersymmetry

I.9. Extensions beyond the MSSM

I.1. Introduction: Supersymmetry (SUSY) is a generalization of the space-time symmetries of quantum field theory that transforms fermions into bosons and vice versa. The existence of such a non-trivial extension of the Poincaré symmetry of ordinary quantum field theory was initially surprising, and its form is highly constrained by theoretical principles [1]. Supersymmetry also provides a framework for the unification of particle physics and gravity [2–5], which is governed by the Planck energy scale, $M_P \approx 10^{19}$ GeV (where the gravitational interactions become comparable in magnitude to the gauge interactions). In particular, it is possible that supersymmetry will ultimately explain the origin of the large hierarchy of energy scales from the W and Z masses to the Planck scale [6–10]. This is the so-called *gauge hierarchy*. The stability of the gauge hierarchy in the presence of radiative quantum corrections is not possible to maintain in the Standard Model, but can be maintained in supersymmetric theories.

If supersymmetry were an exact symmetry of nature, then particles and their superpartners (which differ in spin by half a unit) would be degenerate in mass. Since superpartners have not (yet) been observed, supersymmetry must be a broken symmetry. Nevertheless, the stability of the gauge hierarchy can still be maintained if the supersymmetry breaking is *soft* [11,12], and the corresponding supersymmetry-breaking mass parameters are no larger than a few TeV. In particular, soft-supersymmetry-breaking terms of the Lagrangian are either linear, quadratic, or cubic in the fields, with some restrictions elucidated in Ref. 11. The impact of such terms becomes negligible at energy scales much larger than the size of the supersymmetry-breaking masses. The most interesting theories of this type are theories of “low-energy” (or “weak-scale”) supersymmetry, where the effective scale of supersymmetry breaking is tied to the scale of electroweak symmetry breaking [7–10]. The latter is characterized by the Standard Model Higgs vacuum expectation value, $v \simeq 246$ GeV.

Although there are no unambiguous experimental results (at present) that require the existence of new physics at the TeV-scale, expectations of the latter are primarily based on three theoretical arguments. First, a *natural* explanation (*i.e.*, one that is stable with respect to quantum corrections) of the gauge hierarchy demands new physics at the TeV-scale [10]. Second, the unification of the three Standard Model gauge couplings at a very high energy close to the Planck scale is possible if new physics beyond the Standard Model (which modifies the running of the gauge couplings above the electroweak scale) is present. The minimal supersymmetric extension of

the Standard Model, where supersymmetric masses lie below a few TeV, provides simple example of successful gauge coupling unification [13]. Third, the existence of dark matter, which makes up approximately one quarter of the energy density of the universe, cannot be explained within the Standard Model of particle physics [14]. Remarkably, a stable weakly-interacting massive particle (WIMP) whose mass and interaction rate are governed by new physics associated with the TeV-scale can be consistent with the observed density of dark matter (this is the so-called *WIMP miracle*, which is reviewed in Ref. 15). The lightest supersymmetric particle is a promising (although not the unique) candidate for the dark matter [16,17]. Further aspects of dark matter can be found in Ref. 18.

I.2. Structure of the MSSM: The minimal supersymmetric extension of the Standard Model (MSSM) consists of taking the fields of the two-Higgs-doublet extension of the Standard Model and adding the corresponding supersymmetric partners [19,20]. The corresponding field content of the MSSM and their gauge quantum numbers are shown in Table 1. The electric charge $Q = T_3 + \frac{1}{2}Y$ is determined in terms of the third component of the weak isospin (T_3) and the U(1) hypercharge (Y).

Table 1: The fields of the MSSM and their $SU(3) \times SU(2) \times U(1)$ quantum numbers are listed. Only one generation of quarks and leptons is exhibited. For each lepton, quark, and Higgs super-multiplet, there is a corresponding anti-particle multiplet of charge-conjugated fermions and their associated scalar partners.

Field Content of the MSSM					
Super-Multiplets	Boson Fields	Fermionic Partners	SU(3)	SU(2)	U(1)
gluon/gluino	g	\tilde{g}	8	1	0
gauge/	W^\pm, W^0	$\tilde{W}^\pm, \tilde{W}^0$	1	3	0
gaugino	B	\tilde{B}	1	1	0
slepton/	$(\tilde{\nu}, \tilde{e}^-)_L$	$(\nu, e^-)_L$	1	2	-1
lepton	\tilde{e}_R^-	e_R^-	1	1	-2
squark/	$(\tilde{u}_L, \tilde{d}_L)$	$(u, d)_L$	3	2	1/3
quark	\tilde{u}_R	u_R	3	1	4/3
	\tilde{d}_R	d_R	3	1	-2/3
Higgs/	$(H_d^0, H_{\bar{d}}^-)$	$(\tilde{H}_d^0, \tilde{H}_{\bar{d}}^-)$	1	2	-1
higgsino	(H_u^+, H_u^0)	$(\tilde{H}_u^+, \tilde{H}_u^0)$	1	2	1

The gauge super-multiplets consist of the gluons and their *gluino* fermionic superpartners, and the $SU(2) \times U(1)$ gauge bosons and their *gaugino* fermionic superpartners. The Higgs multiplets consist of two complex doublets of Higgs fields, their *higgsino* fermionic superpartners, and the corresponding antiparticle fields. The matter super-multiplets consist of three generations of left-handed and right-handed quarks and lepton fields, their scalar superpartners (squark and slepton fields), and the corresponding antiparticle fields. The enlarged Higgs sector of the MSSM constitutes the minimal structure needed to guarantee the cancellation of anomalies from the introduction of

the higgsino superpartners. Moreover, without a second Higgs doublet, one cannot generate mass for both “up”-type and “down”-type quarks (and charged leptons) in a way consistent with the supersymmetry [21–23].

A general supersymmetric Lagrangian is determined by three functions of the superfields (composed of the fields of the super-multiplets): the superpotential, the Kähler potential, and the gauge kinetic-energy function [5]. For *renormalizable* globally supersymmetric theories, minimal forms for the latter two functions are required in order to generate canonical kinetic energy terms for all the fields. A renormalizable superpotential, which is at most cubic in the superfields, yields supersymmetric Yukawa couplings and mass terms. A combination of gauge invariance and supersymmetry produces couplings of gaugino fields to matter (or Higgs) fields and their corresponding superpartners. The (renormalizable) MSSM Lagrangian is then constructed by including all possible supersymmetric interaction terms (of dimension four or less) that satisfy $SU(3) \times SU(2) \times U(1)$ gauge invariance and $B-L$ conservation (where B = baryon number and L = lepton number). Finally, the most general soft-supersymmetry-breaking terms are added [11,12,24]. To generate nonzero neutrino masses, extra structure is needed as discussed in section I.8.

I.2.1. Constraints on supersymmetric parameters: If supersymmetry is associated with the origin of the electroweak scale, then the mass parameters introduced by the soft-supersymmetry-breaking must be generally on the order of 1 TeV or below [25] (although models have been proposed in which some supersymmetric particle masses can be larger, in the range of 1–10 TeV [26]). Some lower bounds on these parameters exist due to the absence of supersymmetric-particle production at current accelerators [27,28]. Additional constraints arise from limits on the contributions of virtual supersymmetric particle exchange to a variety of Standard Model processes [29–31].

For example, the Standard Model global fit to precision electroweak data is quite good [32]. If all supersymmetric particle masses are significantly heavier than m_Z (in practice, masses greater than 300 GeV are sufficient [33]), then the effects of the supersymmetric particles decouple in loop corrections to electroweak observables [34]. In this case, the Standard Model global fit to precision data, and the corresponding MSSM fit yield similar results. On the other hand, regions of parameter space with light supersymmetric particle masses (just above the present day experimental limits) can in some cases generate significant one-loop corrections, resulting in a slight improvement or worsening of the overall global fit to the electroweak data, depending on the choice of the MSSM parameters [35]. Thus, the precision electroweak data provide some constraints on the magnitude of the soft-supersymmetry-breaking terms.

There are a number of other low-energy measurements that are especially sensitive to the effects of new physics through virtual loops. For example, the virtual exchange of supersymmetric particles can contribute to the muon anomalous

Searches Particle Listings

Supersymmetric Particle Searches

magnetic moment, $a_\mu \equiv \frac{1}{2}(g-2)_\mu$ [36], and to the inclusive decay rate for $b \rightarrow s\gamma$. The Standard Model prediction for a_μ (where the hadronic contribution is determined from all e^+e^- data) exhibits a 3.2σ deviation from the experimentally observed value [37]. The rare decay $b \rightarrow s\gamma$ also provides a sensitive probe to the virtual effects of new physics beyond the Standard Model. Recent experimental measurements of $B \rightarrow X_s + \gamma$ by the BELLE collaboration [38] are in very good agreement with the theoretical predictions of Ref. 39. In both cases, supersymmetric corrections can contribute an observable shift from the Standard Model prediction in some regions of the MSSM parameter space [40,41]. The absence of a *significant* deviation in these and other B -physics observables from their Standard Model predictions places interesting constraints on the low-energy supersymmetry parameters [42].

There is some tension between the expectation that supersymmetry-breaking is associated with the electroweak symmetry-breaking scale and the non-observation of supersymmetric particles in present day collider experiments [43]. In particular, the experimental lower bound on squark and gluino masses is already three to four times larger than the masses of the W and Z bosons [27]. The non-observation at LEP [44] of the Higgs boson [whose mass depends indirectly on the top-squark mass via radiative corrections, cf. Eq. (11)] adds to this tension [45]. The separation of scales that govern electroweak symmetry and supersymmetry breaking is an example of the *little hierarchy problem* [46]. It appears that the Higgs vacuum expectation value must be fine-tuned at the percent level in the MSSM, although one can imagine model extensions in which the degree of fine-tuning is relaxed [47].

I.2.2. R-parity and the lightest supersymmetric particle: As a consequence of $B-L$ invariance, the MSSM possesses a multiplicative R-parity invariance, where $R = (-1)^{3(B-L)+2S}$ for a particle of spin S [48]. Note that this implies that all the ordinary Standard Model particles have even R parity, whereas the corresponding supersymmetric partners have odd R parity. The conservation of R parity in scattering and decay processes has a crucial impact on supersymmetric phenomenology. For example, starting from an initial state involving ordinary (R-even) particles, it follows that supersymmetric particles must be produced in pairs. In general, these particles are highly unstable and decay into lighter states. However, R-parity invariance also implies that the lightest supersymmetric particle (LSP) is absolutely stable, and must eventually be produced at the end of a decay chain initiated by the decay of a heavy unstable supersymmetric particle.

In order to be consistent with cosmological constraints, a stable LSP is almost certainly electrically and color neutral [49]. (There are some model circumstances in which a colored gluino LSP is allowed [50], but we do not consider this possibility further here.) Consequently, the LSP in an R-parity-conserving theory is weakly interacting with ordinary matter, *i.e.*, it behaves like a stable heavy neutrino and will escape collider detectors without being directly observed. Thus, the canonical

signature for conventional R-parity-conserving supersymmetric theories is missing (transverse) energy, due to the escape of the LSP. Moreover, as noted at the end of Section I, the LSP is a promising candidate for dark matter [16,17].

I.2.3. The goldstino and gravitino: In the MSSM, supersymmetry breaking is accomplished by including the most general renormalizable soft-supersymmetry-breaking terms consistent with the $SU(3) \times SU(2) \times U(1)$ gauge symmetry and R-parity invariance. These terms parameterize our ignorance of the fundamental mechanism of supersymmetry breaking. If supersymmetry breaking occurs spontaneously, then a massless Goldstone fermion called the *goldstino* ($\tilde{G}_{1/2}$) must exist. The goldstino would then be the LSP, and could play an important role in supersymmetric phenomenology [51]. However, the goldstino degrees of freedom are physical only in models of spontaneously-broken global supersymmetry. If supersymmetry is a local symmetry, then the theory must incorporate gravity; the resulting theory is called supergravity [52]. In models of spontaneously-broken supergravity, the goldstino is “absorbed” by the *gravitino* (\tilde{G}) [sometimes called $\tilde{g}_{3/2}$ in the older literature], the spin-3/2 superpartner of the graviton [53]. By this super-Higgs mechanism, the goldstino is removed from the physical spectrum and the gravitino acquires a mass ($m_{3/2}$). In processes with center-of-mass energy $E \gg m_{3/2}$, the goldstino–gravitino equivalence theorem [54] states that the interactions of the helicity $\pm\frac{1}{2}$ gravitino (whose properties approximate those of the goldstino) dominate those of the helicity $\pm\frac{3}{2}$ gravitino. The interactions of gravitinos with other light fields can be described by a low-energy effective Lagrangian that is determined by fundamental principles (see, *e.g.*, Ref. 55).

I.2.4. Hidden sectors and the structure of supersymmetry breaking [24]: It is very difficult (perhaps impossible) to construct a realistic model of spontaneously-broken low-energy supersymmetry where the supersymmetry breaking arises solely as a consequence of the interactions of the particles of the MSSM. A more viable scheme posits a theory consisting of at least two distinct sectors: a *hidden* sector consisting of particles that are completely neutral with respect to the Standard Model gauge group, and a *visible* sector consisting of the particles of the MSSM. There are no renormalizable tree-level interactions between particles of the visible and hidden sectors. Supersymmetry breaking is assumed to originate in the hidden sector, and its effects are transmitted to the MSSM by some mechanism (often involving the mediation by particles that comprise an additional *messenger* sector). Two theoretical scenarios have been examined in detail: gravity-mediated and gauge-mediated supersymmetry breaking.

Supergravity models provide a natural mechanism for transmitting the supersymmetry breaking of the hidden sector to the particle spectrum of the MSSM. In models of *gravity-mediated* supersymmetry breaking, gravity is the messenger of supersymmetry breaking [56–58]. More precisely, supersymmetry

breaking is mediated by effects of gravitational strength (suppressed by inverse powers of the Planck mass). In this scenario, the gravitino mass is of order the electroweak-symmetry-breaking scale, while its couplings are roughly gravitational in strength [2,59]. Such a gravitino typically plays no role in supersymmetric phenomenology at colliders (except perhaps indirectly in the case where the gravitino is the LSP [60]).

In *gauge-mediated* supersymmetry breaking, gauge forces transmit the supersymmetry breaking to the MSSM. A typical structure of such models involves a hidden sector where supersymmetry is broken, a messenger sector consisting of particles (messengers) with $SU(3) \times SU(2) \times U(1)$ quantum numbers, and the visible sector consisting of the fields of the MSSM [61–63]. The direct coupling of the messengers to the hidden sector generates a supersymmetry-breaking spectrum in the messenger sector. Finally, supersymmetry breaking is transmitted to the MSSM via the virtual exchange of the messengers. In models of *direct gauge mediation*, the hidden sector fields also carry Standard Model quantum numbers, and no separate messenger sector is required [64]. The gravitino mass in these models is typically in the eV range (although in some cases it can be as large as a GeV), which implies that \tilde{G} is the LSP. In particular, the gravitino is a potential dark matter candidate (for a recent review and guide to the literature, see Ref. 17). The couplings of the helicity $\pm\frac{1}{2}$ components of \tilde{G} to the particles of the MSSM (which approximate those of the goldstino, cf. Section I.2.3) are significantly stronger than gravitational strength and amenable to experimental collider analyses.

The concept of a hidden sector is more general than supersymmetry. *Hidden valley* models [65] posit the existence of a hidden sector of new particles and interactions that are very weakly coupled to particles of the Standard Model. The impact of a hidden valley on supersymmetric phenomenology at colliders can be profound if the LSP lies in the valley sector [66]. Standard supersymmetric particle search strategies will need to be reconsidered if such a scenario is realized in nature.

I.2.5. *Supersymmetry and extra dimensions:*

Approaches to supersymmetry breaking have also been developed in the context of theories in which the number of space dimensions is greater than three. In particular, a number of supersymmetry-breaking mechanisms have been proposed that are inherently extra-dimensional [67]. The size of the extra dimensions can be significantly larger than M_P^{-1} ; in some cases on the order of $(\text{TeV})^{-1}$ or even larger [68,69]. For example, in one approach, the fields of the MSSM live on some brane (a lower-dimensional manifold embedded in a higher-dimensional spacetime), while the sector of the theory that breaks supersymmetry lives on a second-separated brane. Two examples of this approach are anomaly-mediated supersymmetry breaking of Ref. 70, and gaugino-mediated supersymmetry breaking of Ref. 71; in both cases supersymmetry breaking is transmitted through fields that live in the bulk (the higher-dimensional space between the two branes). This setup has some features in common with both gravity-mediated and gauge-mediated

supersymmetry breaking (*e.g.*, a hidden and visible sector and messengers).

Alternatively, one can consider a higher-dimensional theory that is compactified to four spacetime dimensions. In this approach, supersymmetry is broken by boundary conditions on the compactified space that distinguish between fermions and bosons. This is the so-called Scherk-Schwarz mechanism [72]. The phenomenology of such models can be strikingly different from that of the usual MSSM [73]. All these extra-dimensional ideas clearly deserve further investigation, although they will not be discussed further here.

I.2.6. *Split-supersymmetry:* If supersymmetry is not connected with the origin of the electroweak scale, string theory suggests that supersymmetry still plays a significant role in Planck-scale physics. However, it may still be possible that some remnant of the superparticle spectrum survives down to the TeV-scale or below. This is the idea of *split-supersymmetry* [74], in which supersymmetric scalar partners of the quarks and leptons are significantly heavier (perhaps by many orders of magnitude) than 1 TeV, whereas the fermionic partners of the gauge and Higgs bosons have masses on the order of 1 TeV or below (presumably protected by some chiral symmetry). With the exception of a single light neutral scalar whose properties are indistinguishable from those of the Standard Model Higgs boson, all other Higgs bosons are also taken to be very heavy.

The supersymmetry breaking required to produce such a scenario would destabilize the gauge hierarchy. In particular, split-supersymmetry cannot provide a natural explanation for the existence of the light Standard-Model-like Higgs boson, whose mass lies orders below the mass scale of the heavy scalars. Nevertheless, models of split-supersymmetry can account for the dark matter (which is assumed to be the LSP) and gauge coupling unification. Thus, there is some motivation for pursuing the phenomenology of such approaches [75]. One notable difference from the usual MSSM phenomenology is the existence of a long-lived gluino [76].

I.3. *Parameters of the MSSM:* The parameters of the MSSM are conveniently described by considering separately the supersymmetry-conserving sector and the supersymmetry-breaking sector. A careful discussion of the conventions used in defining the tree-level MSSM parameters can be found in Ref. 77. For simplicity, consider first the case of one generation of quarks, leptons, and their scalar superpartners.

I.3.1. *The supersymmetric-conserving parameters:*

The parameters of the supersymmetry-conserving sector consist of: (i) gauge couplings: g_s , g , and g' , corresponding to the Standard Model gauge group $SU(3) \times SU(2) \times U(1)$ respectively; (ii) a supersymmetry-conserving higgsino mass parameter μ ; and (iii) Higgs-fermion Yukawa coupling constants: λ_u , λ_d , and λ_e (corresponding to the coupling of one generation of left- and right-handed quarks and leptons, and their superpartners

Searches Particle Listings

Supersymmetric Particle Searches

to the Higgs bosons and higgsinos). Because there is no right-handed neutrino (and its superpartner) in the MSSM as defined here, one cannot introduce a Yukawa coupling λ_ν .

I.3.2. The supersymmetric-breaking parameters:

The supersymmetry-breaking sector contains the following set of parameters: (i) gaugino Majorana masses M_3 , M_2 , and M_1 associated with the SU(3), SU(2), and U(1) subgroups of the Standard Model; (ii) five scalar squared-mass parameters for the squarks and sleptons, M_Q^2 , M_U^2 , M_D^2 , M_L^2 , and M_E^2 [corresponding to the five electroweak gauge multiplets, *i.e.*, superpartners of $(u, d)_L$, u_L^c , d_L^c , $(\nu, e^-)_L$, and e_L^c , where the superscript c indicates a charge-conjugated fermion and flavor indices are suppressed]; and (iii) Higgs-squark-squark and Higgs-slepton-slepton trilinear interaction terms, with coefficients $\lambda_u A_U$, $\lambda_d A_D$, and $\lambda_e A_E$ (which define the so-called “ A -parameters”). It is traditional to factor out the Yukawa couplings in the definition of the A -parameters (originally motivated by a simple class of gravity-mediated supersymmetry-breaking models [2,4]). If the A -parameters defined in this way are parametrically of the same order (or smaller) as compared to other supersymmetry-breaking mass parameters, then only the A -parameters of the third generation will be phenomenologically relevant.

Finally, we add: (iv) three scalar squared-mass parameters—two of which (m_1^2 and m_2^2) contribute to the diagonal Higgs squared-masses, given by $m_1^2 + |\mu|^2$ and $m_2^2 + |\mu|^2$, and a third which contributes to the off-diagonal Higgs squared-mass term, $m_{12}^2 \equiv B\mu$ (which defines the “ B -parameter”). The breaking of the electroweak symmetry SU(2)×U(1) to U(1)_{EM} is only possible after introducing the supersymmetry-breaking Higgs squared-mass parameters. Minimizing the resulting Higgs scalar potential, these three squared-mass parameters can be re-expressed in terms of the two Higgs vacuum expectation values, v_d and v_u (also called v_1 and v_2 , respectively, in the literature), and one physical Higgs mass. Here, v_d [v_u] is the vacuum expectation value of the neutral component of the Higgs field H_d [H_u] that couples exclusively to down-type (up-type) quarks and leptons. Note that $v_d^2 + v_u^2 = 4m_W^2/g^2 \simeq (246 \text{ GeV})^2$ is fixed by the W mass and the gauge coupling, whereas the ratio

$$\tan\beta = v_u/v_d \quad (1)$$

is a free parameter of the model. By convention, the Higgs field phases are chosen such that $0 \leq \beta \leq \pi/2$.

Note that supersymmetry-breaking mass terms for the fermionic superpartners of scalar fields and non-holomorphic trilinear scalar interactions (*i.e.*, interactions that mix scalar fields and their complex conjugates) have not been included above in the soft-supersymmetry-breaking sector. These terms can potentially destabilize the gauge hierarchy [11] in models with a gauge-singlet superfield. The latter is not present in the MSSM; hence as noted in Ref. 12, these so-called non-standard soft-supersymmetry-breaking terms are benign. However, the

coefficients of these terms (which have dimensions of mass) are expected to be significantly suppressed compared to the TeV-scale in a fundamental theory of supersymmetry-breaking. Consequently, we follow the usual approach and omit these terms from further consideration.

I.3.3. MSSM-124: The total number of independent physical parameters that define the MSSM (in its most general form) is quite large, primarily due to the soft-supersymmetry-breaking sector. In particular, in the case of three generations of quarks, leptons, and their superpartners, M_Q^2 , M_U^2 , M_D^2 , M_L^2 , and M_E^2 are hermitian 3×3 matrices, and A_U , A_D , and A_E are complex 3×3 matrices. In addition, M_1 , M_2 , M_3 , B , and μ are, in general, complex. Finally, as in the Standard Model, the Higgs-fermion Yukawa couplings, λ_f ($f = u, d$, and e), are complex 3×3 matrices that are related to the quark and lepton mass matrices via: $M_f = \lambda_f v_f / \sqrt{2}$, where $v_e \equiv v_d$ [with v_u and v_d as defined above Eq. (1)].

However, not all these parameters are physical. Some of the MSSM parameters can be eliminated by expressing interaction eigenstates in terms of the mass eigenstates, with an appropriate redefinition of the MSSM fields to remove unphysical degrees of freedom. The analysis of Ref. 78 shows that the MSSM possesses 124 independent parameters. Of these, 18 parameters correspond to Standard Model parameters (including the QCD vacuum angle θ_{QCD}), one corresponds to a Higgs sector parameter (the analogue of the Standard Model Higgs mass), and 105 are genuinely new parameters of the model. The latter include: five real parameters and three CP -violating phases in the gaugino/higgsino sector, 21 squark and slepton masses, 36 real mixing angles to define the squark and slepton mass eigenstates, and 40 CP -violating phases that can appear in squark and slepton interactions. The most general R-parity-conserving minimal supersymmetric extension of the Standard Model (without additional theoretical assumptions) will be denoted henceforth as MSSM-124 [79].

I.4. The supersymmetric-particle spectrum: Consider the sector of supersymmetric particles (*sparticles*) in the MSSM. The supersymmetric partners of the gauge and Higgs bosons are fermions, whose names are obtained by appending “ino” at the end of the corresponding Standard Model particle name. The gluino is the color-octet Majorana fermion partner of the gluon with mass $M_{\tilde{g}} = |M_3|$. The supersymmetric partners of the electroweak gauge and Higgs bosons (the gauginos and higgsinos) can mix. As a result, the physical states of definite mass are model-dependent linear combinations of the charged and neutral gauginos and higgsinos, called *charginos* and *neutralinos*, respectively. Like the gluino, the neutralinos are also Majorana fermions, which provide for some distinctive phenomenological signatures [80,81]. The supersymmetric partners of the quarks and leptons are spin-zero bosons: the *squarks*, charged *sleptons*, and *sneutrinos*, respectively. A complete set of Feynman rules for the sparticles of the MSSM can be found in Ref. 82. The MSSM Feynman rules also are

implicitly contained in a number of Feynman diagram and amplitude generation software packages (see *e.g.*, Refs. 83–85).

I.4.1. The charginos and neutralinos: The mixing of the charged gauginos (\widetilde{W}^\pm) and charged higgsinos (H_u^\pm and H_d^\pm) is described (at tree-level) by a 2×2 complex mass matrix [86–88]:

$$M_C \equiv \begin{pmatrix} M_2 & \frac{1}{\sqrt{2}}g v_u \\ \frac{1}{\sqrt{2}}g v_d & \mu \end{pmatrix}. \quad (2)$$

To determine the physical chargino states and their masses, one must perform a singular value decomposition [89,90] of the complex matrix M_C :

$$U^* M_C V^{-1} = \text{diag}(M_{\widetilde{\chi}_1^\pm}, M_{\widetilde{\chi}_2^\pm}), \quad (3)$$

where U and V are unitary matrices, and the right-hand side of Eq. (3) is the diagonal matrix of (non-negative) chargino masses. The physical chargino states are denoted by $\widetilde{\chi}_1^\pm$ and $\widetilde{\chi}_2^\pm$. These are linear combinations of the charged gaugino and higgsino states determined by the matrix elements of U and V [86–88]. The chargino masses correspond to the *singular values* [89] of M_C , *i.e.*, the positive square roots of the eigenvalues of $M_C^\dagger M_C$:

$$M_{\widetilde{\chi}_1^\pm, \widetilde{\chi}_2^\pm}^2 = \frac{1}{2} \left\{ |\mu|^2 + |M_2|^2 + 2m_W^2 \mp \left[(|\mu|^2 + |M_2|^2 + 2m_W^2)^2 - 4|\mu|^2|M_2|^2 - 4m_W^4 \sin^2 2\beta + 8m_W^2 \sin 2\beta \text{Re}(\mu M_2) \right]^{1/2} \right\}, \quad (4)$$

where the states are ordered such that $M_{\widetilde{\chi}_1^\pm} \leq M_{\widetilde{\chi}_2^\pm}$. It is convenient to choose a convention where $\tan\beta$ and M_2 are real and positive. Note that the relative phase of M_2 and μ is meaningful. (If CP -violating effects are neglected, then μ can be chosen real but may be either positive or negative.) The sign of μ is convention-dependent; the reader is warned that both sign conventions appear in the literature. The sign convention for μ in Eq. (2) is used by the LEP collaborations [27] in their plots of exclusion contours in the M_2 vs. μ plane derived from the non-observation of $e^+e^- \rightarrow \widetilde{\chi}_1^+ \widetilde{\chi}_1^-$.

The mixing of the neutral gauginos (\widetilde{B} and \widetilde{W}^0) and neutral higgsinos (\widetilde{H}_d^0 and \widetilde{H}_u^0) is described (at tree-level) by a 4×4 complex symmetric mass matrix [86,87,91,92]:

$$M_N \equiv \begin{pmatrix} M_1 & 0 & -\frac{1}{2}g'v_d & \frac{1}{2}g'v_u \\ 0 & M_2 & \frac{1}{2}g v_d & -\frac{1}{2}g v_u \\ -\frac{1}{2}g'v_d & \frac{1}{2}g v_d & 0 & -\mu \\ \frac{1}{2}g'v_u & -\frac{1}{2}g v_u & -\mu & 0 \end{pmatrix}. \quad (5)$$

To determine the physical neutralino states and their masses, one must perform a Takagi-diagonalization [89,90,93,94] of the complex symmetric matrix M_N :

$$W^T M_N W = \text{diag}(M_{\widetilde{\chi}_1^0}, M_{\widetilde{\chi}_2^0}, M_{\widetilde{\chi}_3^0}, M_{\widetilde{\chi}_4^0}), \quad (6)$$

where W is a unitary matrix and the right-hand side of Eq. (6) is the diagonal matrix of (non-negative) neutralino masses. The physical neutralino states are denoted by $\widetilde{\chi}_i^0$ ($i = 1, \dots, 4$), where

the states are ordered such that $M_{\widetilde{\chi}_1^0} \leq M_{\widetilde{\chi}_2^0} \leq M_{\widetilde{\chi}_3^0} \leq M_{\widetilde{\chi}_4^0}$. The $\widetilde{\chi}_i^0$ are the linear combinations of the neutral gaugino and higgsino states determined by the matrix elements of W (in Ref. 86, $W = N^{-1}$). The neutralino masses correspond to the singular values of M_N (*i.e.*, the positive square roots of the eigenvalues of $M_N^\dagger M_N$). Exact formulae for these masses can be found in Refs. [91] and [95]. A numerical algorithm for determining the mixing matrix W has been given by Ref. 96.

If a chargino or neutralino state approximates a particular gaugino or higgsino state, it is convenient to employ the corresponding nomenclature. Specifically, if M_1 and M_2 are small compared to m_Z and $|\mu|$, then the lightest neutralino $\widetilde{\chi}_1^0$ would be nearly a pure *photino*, $\widetilde{\gamma}$, the supersymmetric partner of the photon. If M_1 and m_Z are small compared to M_2 and $|\mu|$, then the lightest neutralino would be nearly a pure *binos*, \widetilde{B} , the supersymmetric partner of the weak hypercharge gauge boson. If M_2 and m_Z are small compared to M_1 and $|\mu|$, then the lightest chargino pair and neutralino would constitute a triplet of roughly mass-degenerate pure *winos*, \widetilde{W}^\pm , and \widetilde{W}_3^0 , the supersymmetric partners of the weak SU(2) gauge bosons. Finally, if $|\mu|$ and m_Z are small compared to M_1 and M_2 , then the lightest neutralino would be nearly a pure *higgsino*. Each of the above cases leads to a strikingly different phenomenology.

I.4.2. The squarks, sleptons and sneutrinos: For a given fermion f , there are two supersymmetric partners, \widetilde{f}_L and \widetilde{f}_R , which are scalar partners of the corresponding left- and right-handed fermion. (There is no $\widetilde{\nu}_R$ in the MSSM.) However, in general, \widetilde{f}_L and \widetilde{f}_R are not mass eigenstates, since there is \widetilde{f}_L - \widetilde{f}_R mixing. For three generations of squarks, one must in general diagonalize 6×6 matrices corresponding to the basis $(\widetilde{q}_{iL}, \widetilde{q}_{iR})$, where $i = 1, 2, 3$ are the generation labels. For simplicity, only the one-generation case is illustrated in detail below. (The effects of second and third generation squark mixing can be significant and is treated in Ref. 97.) Using the notation of the third family, the one-generation tree-level squark squared-mass matrix is given by [98]

$$M_F^2 = \begin{pmatrix} M_Q^2 + m_q^2 + L_q & m_q X_q^* \\ m_q X_q & M_R^2 + m_q^2 + R_q \end{pmatrix}, \quad (7)$$

where

$$X_q \equiv A_q - \mu^* (\cot\beta)^{2T_{3q}}, \quad (8)$$

and $T_{3q} = \frac{1}{2} [-\frac{1}{2}]$ for $q = t$ [b]. The diagonal squared masses are governed by soft-supersymmetry-breaking squared masses M_Q^2 and $M_R^2 \equiv M_D^2$ [M_U^2] for $q = t$ [b], the corresponding quark masses m_t [m_b], and electroweak correction terms:

$$L_q \equiv (T_{3q} - e_q \sin^2 \theta_W) m_Z^2 \cos 2\beta, \quad R_q \equiv e_q \sin^2 \theta_W m_Z^2 \cos 2\beta, \quad (9)$$

where $e_q = \frac{2}{3} [-\frac{1}{3}]$ for $q = t$ [b]. The off-diagonal squared squark masses are proportional to the corresponding quark masses and depend on $\tan\beta$ [Eq. (1)], the soft-supersymmetry-breaking A -parameters and the higgsino mass parameter μ . The signs of the A and μ parameters are convention-dependent;

Searches Particle Listings

Supersymmetric Particle Searches

other choices appear frequently in the literature. Due to the appearance of the *quark* mass in the off-diagonal element of the squark squared-mass matrix, one expects the $\tilde{q}_L\text{-}\tilde{q}_R$ mixing to be small, with the possible exception of the third generation, where mixing can be enhanced by factors of m_t and $m_b \tan \beta$.

In the case of third generation $\tilde{q}_L\text{-}\tilde{q}_R$ mixing, the mass eigenstates (usually denoted by \tilde{q}_1 and \tilde{q}_2 , with $m_{\tilde{q}_1} < m_{\tilde{q}_2}$) are determined by diagonalizing the 2×2 matrix M_F^2 given by Eq. (7). The corresponding squared masses and mixing angle are given by [98]:

$$m_{\tilde{q}_{1,2}}^2 = \frac{1}{2} \left[\text{Tr} M_F^2 \mp \sqrt{(\text{Tr} M_F^2)^2 - 4 \det M_F^2} \right],$$

$$\sin 2\theta_{\tilde{q}} = \frac{2m_q |X_q|}{m_{\tilde{q}_2}^2 - m_{\tilde{q}_1}^2}. \quad (10)$$

The one-generation results above also apply to the charged sleptons, with the obvious substitutions: $q \rightarrow \tau$ with $T_{3\tau} = -\frac{1}{2}$ and $e_\tau = -1$, and the replacement of the supersymmetry-breaking parameters: $M_Q^2 \rightarrow M_L^2$, $M_D^2 \rightarrow M_E^2$, and $A_q \rightarrow A_\tau$. For the neutral sleptons, $\tilde{\nu}_R$ does not exist in the MSSM, so $\tilde{\nu}_L$ is a mass eigenstate.

In the case of three generations, the supersymmetry-breaking scalar-squared masses [M_Q^2 , M_U^2 , M_D^2 , M_L^2 , and M_E^2] and the A -parameters that parameterize the Higgs couplings to up- and down-type squarks and charged sleptons (henceforth denoted by A_U , A_D , and A_E , respectively) are now 3×3 matrices as noted in Section I.3. The diagonalization of the 6×6 squark mass matrices yields $\tilde{f}_{iL}\text{-}\tilde{f}_{jR}$ mixing (for $i \neq j$). In practice, since the $\tilde{f}_L\text{-}\tilde{f}_R$ mixing is appreciable only for the third generation, this additional complication can often be neglected (although see Ref. 97 for examples in which the mixing between the second and third generations is relevant).

Radiative loop corrections will modify all tree-level results for masses quoted in this section. These corrections must be included in any precision study of supersymmetric phenomenology [99]. Beyond tree level, the definition of the supersymmetric parameters becomes convention-dependent. For example, one can define physical couplings or running couplings, which differ beyond the tree level. This provides a challenge to any effort that attempts to extract supersymmetric parameters from data. The supersymmetric parameter analysis (SPA) project proposed a set of conventions [100] based on a consistent set of conventions and input parameters. This work employs a consistent dimensional reduction scheme for the regularization of higher-order loop corrections in supersymmetric theories recently advocated in Ref. 101. More recently, the Supersymmetry Les Houches Accord (SLHA) [102] has been adopted, which establishes a set of conventions for specifying generic file structures for supersymmetric model specifications and input parameters, supersymmetric mass and coupling spectra, and decay tables. These provide a universal interface between spectrum calculation programs, decay packages, and high energy physics event generators. Ultimately, these efforts will facilitate

the reconstruction of the fundamental supersymmetric theory (and its breaking mechanism) from high-precision studies of supersymmetric phenomena at future colliders.

I.5. The Higgs sector of the MSSM: Next, consider the MSSM Higgs sector [22,23,103]. Despite the large number of potential CP -violating phases among the MSSM-124 parameters, the tree-level MSSM Higgs sector is automatically CP -conserving. That is, unphysical phases can be absorbed into the definition of the Higgs fields such that $\tan \beta$ is a real parameter (conventionally chosen to be positive). Consequently, the physical neutral Higgs scalars are CP eigenstates. The MSSM Higgs sector contains five physical spin-zero particles: a charged Higgs boson pair (H^\pm), two CP -even neutral Higgs bosons (denoted by h^0 and H^0 where $m_h < m_H$), and one CP -odd neutral Higgs boson (A^0).

I.5.1 The Tree-level MSSM Higgs sector: The properties of the Higgs sector are determined by the Higgs potential, which is made up of quadratic terms [whose squared-mass coefficients were specified above Eq. (1)] and quartic interaction terms governed by dimensionless couplings. The quartic interaction terms are manifestly supersymmetric at tree level (although these are modified by supersymmetry-breaking effects at the loop level). In general, the quartic couplings arise from two sources: (i) the supersymmetric generalization of the scalar potential (the so-called “ F -terms”), and (ii) interaction terms related by supersymmetry to the coupling of the scalar fields and the gauge fields, whose coefficients are proportional to the corresponding gauge couplings (the so-called “ D -terms”). In the MSSM, F -term contributions to the quartic couplings are absent (although such terms may be present in extensions of the MSSM, *e.g.*, models with Higgs singlets). As a result, the strengths of the MSSM quartic Higgs interactions are fixed in terms of the gauge couplings. Due to the resulting constraint on the form of the two-Higgs-doublet scalar potential, all the tree-level MSSM Higgs-sector parameters depend only on two quantities: $\tan \beta$ [defined in Eq. (1)] and one Higgs mass usually taken to be m_A . From these two quantities, one can predict the values of the remaining Higgs boson masses, an angle α (which measures the component of the original $Y = \pm 1$ Higgs doublet states in the physical CP -even neutral scalars), and the Higgs boson self-couplings.

I.5.2 The radiatively-corrected MSSM Higgs sector: When radiative corrections are incorporated, additional parameters of the supersymmetric model enter via virtual loops. The impact of these corrections can be significant [104]. For example, the tree-level MSSM-124 prediction for the upper bound of the lightest CP -even Higgs mass, $m_h \leq m_Z |\cos 2\beta| \leq m_Z$ [22,23], can be substantially modified when radiative corrections are included. The qualitative behavior of these radiative corrections can be most easily seen in the large top-squark mass limit, where in addition, both the splitting of the two diagonal entries and the two off-diagonal entries of the top-squark squared-mass matrix [Eq. (7)] are small in comparison to the average of the two top-squark squared masses,

$M_S^2 \equiv \frac{1}{2}(M_{t_1}^2 + M_{t_2}^2)$. In this case (assuming $m_A > m_Z$), the predicted upper bound for m_h (which reaches its maximum at large $\tan \beta$) is approximately given by

$$m_h^2 \lesssim m_Z^2 + \frac{3g^2 m_t^4}{8\pi^2 m_W^2} \left[\ln(M_S^2/m_t^2) + \frac{X_t^2}{M_S^2} \left(1 - \frac{X_t^2}{12M_S^2} \right) \right], \quad (11)$$

where $X_t \equiv A_t - \mu \cot \beta$ is the top-squark mixing factor [see Eq. (7)]. A more complete treatment of the radiative corrections [105] shows that Eq. (11) somewhat overestimates the true upper bound of m_h . These more refined computations, which incorporate renormalization group improvement and the leading two-loop contributions, yield $m_h \lesssim 135$ GeV (with an accuracy of a few GeV) for $m_t = 175$ GeV and $M_S \lesssim 2$ TeV [105]. This Higgs-mass upper bound can be relaxed somewhat in non-minimal extensions of the MSSM, as noted in Section I.9.

In addition, one-loop radiative corrections can introduce CP -violating effects in the Higgs sector, which depend on some of the CP -violating phases among the MSSM-124 parameters [106]. Although these effects are more model-dependent, they can have a non-trivial impact on the Higgs searches at future colliders. A summary of the current MSSM Higgs mass limits can be found in Ref. 44.

I.6. Restricting the MSSM parameter freedom: In Sections I.4 and I.5, we surveyed the parameters that comprise the MSSM-124. However, in its most general form, the MSSM-124 is not a phenomenologically-viable theory over most of its parameter space. This conclusion follows from the observation that a generic point in the MSSM-124 parameter space exhibits: (i) no conservation of the separate lepton numbers L_e , L_μ , and L_τ ; (ii) unsuppressed flavor-changing neutral currents (FCNC's); and (iii) new sources of CP violation that are inconsistent with the experimental bounds.

For example, the MSSM contains many new sources of CP violation [107]. In particular, some combinations of the complex phases of the gaugino-mass parameters, the A parameters, and μ must be less than on the order of 10^{-2} – 10^{-3} (for a supersymmetry-breaking scale of 100 GeV) to avoid generating electric dipole moments for the neutron, electron, and atoms in conflict with observed data [108–110]. The non-observation of FCNC's [29,30] places additional strong constraints on the off-diagonal matrix elements of the squark and slepton soft-supersymmetry-breaking squared masses and A -parameters (see Section I.3.3). As a result of the phenomenological deficiencies listed above, almost the entire MSSM-124 parameter space is ruled out! This theory is viable only at very special “exceptional” regions of the full parameter space.

The MSSM-124 is also theoretically incomplete as it provides no explanation for the origin of the supersymmetry-breaking parameters (and in particular, why these parameters should conform to the exceptional points of the parameter space mentioned above). Moreover, there is no understanding of the choice of parameters that leads to the breaking of the electroweak symmetry. What is needed ultimately is a fundamental theory of supersymmetry breaking (depending on far

fewer than 124 parameters), which would provide a rationale for a set of soft-supersymmetry-breaking terms that would be consistent with all phenomenological constraints.

I.6.1. Bottom-up approach for constraining the MSSM parameters: In the absence of a fundamental theory of supersymmetry breaking, there are two general approaches for reducing the parameter freedom of MSSM-124. In the low-energy approach, an attempt is made to elucidate the nature of the exceptional points in the MSSM-124 parameter space that are phenomenologically viable. Consider two possible scenarios (under the assumption that squark and slepton masses are not significantly larger than the scale of electroweak symmetry breaking). First, one can assume that M_Q^2 , M_U^2 , M_D^2 , M_L^2 , M_E^2 , and A_U , A_D , A_E are generation-independent (horizontal universality [8,78,111]). Alternatively, one can simply require that all the aforementioned matrices are flavor diagonal in a basis where the quark and lepton mass matrices are diagonal (flavor alignment [112]). In either case, L_e , L_μ , and L_τ are separately conserved, while tree-level FCNC's are automatically absent. In both cases, the number of free parameters characterizing the MSSM is substantially less than 124, although there is no obvious fundamental theoretical basis for either scenario. It has been argued that flavor alignment scenarios are disfavored [113] in light of the recent observation of D^0 – \bar{D}^0 mixing [114]. Thus, if squarks are discovered with masses below about 1–2 TeV, then one would expect the first two generations of squarks to be highly degenerate in mass.

I.6.2. Top-down approach for constraining the MSSM parameters: In the high-energy approach, one imposes a particular structure on the soft-supersymmetry-breaking terms at a common high-energy scale M_X (typically chosen to be the Planck scale, M_P , or the grand unification scale, M_{GUT}). Using the renormalization group equations, one can then derive the low-energy MSSM parameters relevant for collider physics. The initial conditions (at the appropriate high-energy scale) for the renormalization group equations depend on the mechanism by which supersymmetry breaking is communicated to the effective low energy theory. Examples of this scenario are provided by models of gravity-mediated and gauge-mediated supersymmetry breaking (see Section I.7). One bonus of such an approach is that one of the diagonal Higgs squared-mass parameters is typically driven negative by renormalization group evolution [115]. Thus, electroweak symmetry breaking is generated radiatively, and the resulting electroweak symmetry-breaking scale is intimately tied to the scale of low-energy supersymmetry breaking.

One prediction of the high-energy approach that arises in many grand unified supergravity models and gauge-mediated supersymmetry-breaking models is the unification of the (tree-level) gaugino mass parameters at some high-energy scale M_X :

$$M_1(M_X) = M_2(M_X) = M_3(M_X) = m_{1/2}. \quad (12)$$

Searches Particle Listings

Supersymmetric Particle Searches

Consequently, the effective low-energy gaugino mass parameters (at the electroweak scale) are related:

$$M_3 = (g_s^2/g^2)M_2 \simeq 3.5M_2, \quad M_1 = (5g'^2/3g^2)M_2 \simeq 0.5M_2. \quad (13)$$

In this case, the chargino and neutralino masses and mixing angles depend only on three unknown parameters: the gluino mass, μ , and $\tan\beta$. If in addition $|\mu| \gg M_1 \gtrsim m_Z$, then the lightest neutralino is nearly a pure bino, an assumption often made in supersymmetric particle searches at colliders.

Although Eqs. (12) and (13) are often assumed in many phenomenological studies, a truly model-independent approach would take the gaugino mass parameters, M_i , to be independent parameters to be determined by experiment. For example, although LEP data yields a lower bound of 46 GeV on the mass of the lightest neutralino [28], an exactly massless neutralino *cannot* be ruled out today in a model-independent analysis [116].

Certain subsets of squark and slepton mass parameters are also unified in some top-down approaches. However, in contrast to the analysis of the gaugino masses, the renormalization group evolution of the scalar masses may depend strongly on the unknown fundamental supersymmetry-breaking dynamics [117]. Such effects have generally been ignored (or assumed to be negligible) in the prediction of low-energy scalar masses.

Finally, we remark that in certain top-down approaches the unification of gaugino masses and scalar masses can be accidental. In particular, the energy scale where unification takes place is not directly related to any physical scale. This phenomenon has been called *mirage unification* and can occur in certain theories of fundamental supersymmetry-breaking [118].

I.6.3. Anomaly-mediated supersymmetry-breaking:

In some supergravity models, tree-level masses for the gauginos are absent. The gaugino mass parameters arise at one-loop and do not satisfy Eq. (13). In this case, one finds a model-independent contribution to the gaugino mass whose origin can be traced to the super-conformal (super-Weyl) anomaly, which is common to all supergravity models [70]. This approach is called *anomaly-mediated* supersymmetry breaking (AMSB). Eq. (13) is then replaced (in the one-loop approximation) by:

$$M_i \simeq \frac{b_i g_i^2}{16\pi^2} m_{3/2}, \quad (14)$$

where $m_{3/2}$ is the gravitino mass (assumed to be on the order of 1 TeV), and b_i are the coefficients of the MSSM gauge beta-functions corresponding to the corresponding U(1), SU(2), and SU(3) gauge groups: $(b_1, b_2, b_3) = (\frac{33}{5}, 1, -3)$. Eq. (14) yields $M_1 \simeq 2.8M_2$ and $M_3 \simeq -8.3M_2$, which implies that the lightest chargino pair and neutralino comprise a nearly mass-degenerate triplet of winos, $\widetilde{W}^\pm, \widetilde{W}^0$ (c.f. Table 1), over most of the MSSM parameter space. (For example, if $|\mu| \gg m_Z$, then Eq. (14) implies that $M_{\widetilde{\chi}_1^\pm} \simeq M_{\widetilde{\chi}_1^0} \simeq M_2$ [119].) The corresponding supersymmetric phenomenology differs significantly from the standard phenomenology based on Eq. (13), and is explored in detail in Ref. 120. Under certain theoretical assumptions on

the structure of the Kähler potential (the so-called sequestered form introduced in Ref. 70), anomaly-mediated supersymmetry breaking also generates (approximate) flavor-diagonal squark and slepton mass matrices. However, this yields negative squared-mass contributions for the sleptons in the MSSM. It may be possible to cure this fatal flaw in approaches beyond the minimal supersymmetric model [121]. Alternatively, one may conclude that anomaly-mediation is not the sole source of supersymmetry-breaking in the slepton sector.

I.7. The constrained MSSMs: mSUGRA, GMSB, and

SGUTs: In this Section, we examine a number of top-down theoretical frameworks that constrain the parameters of the general MSSM and yield predictions for the low-energy supersymmetric particle spectrum as a function of their input parameters. In particular, the structure of the soft-supersymmetry-breaking parameters must be consistent with the absence of significant FCNC's mediated by virtual supersymmetric particle exchange.

Of course, any of the theoretical assumptions described in this Section could be wrong and must eventually be tested experimentally. In practice, one anticipates that the measurements of low-energy supersymmetric parameters may eventually provide sufficient information to determine the organizing principle governing supersymmetry breaking and yield significant constraints on the values of the fundamental (high-energy) supersymmetric parameters. In particular, a number of sophisticated techniques have been recently developed for analyzing experimental data to test the viability of the particular supersymmetric framework and for measuring the fundamental model parameters and their uncertainties [122].

I.7.1. The minimal supergravity model: In the *minimal* supergravity (mSUGRA) framework [2–4], a form of the Kähler potential is employed that yields minimal kinetic energy terms for the MSSM fields [123]. As a result, the soft-supersymmetry-breaking parameters at the high-energy scale M_X take a particularly simple form in which the scalar squared masses and the A -parameters are flavor-diagonal and universal [57]:

$$\begin{aligned} M_Q^2(M_X) &= M_U^2(M_X) = M_D^2(M_X) = m_0^2 \mathbf{1}, \\ M_L^2(M_X) &= M_E^2(M_X) = m_0^2 \mathbf{1}, \\ m_1^2(M_X) &= m_2^2(M_X) = m_0^2, \\ A_U(M_X) &= A_D(M_X) = A_E(M_X) = A_0 \mathbf{1}, \end{aligned} \quad (15)$$

where $\mathbf{1}$ is a 3×3 identity matrix in generation space. Renormalization group evolution is then used to derive the values of the supersymmetric parameters at the low-energy (electroweak) scale. For example, to compute squark masses, one must use the *low-energy* values for M_Q^2 , M_U^2 , and M_D^2 in Eq. (7). Through the renormalization group running with boundary conditions specified in Eqs. (13) and (15), one can show that the low-energy values of M_Q^2 , M_U^2 , and M_D^2 depend primarily on m_0^2 and $m_{1/2}^2$. A number of useful approximate analytic

expressions for superpartner masses in terms of the mSUGRA parameters can be found in Ref. 124.

In the mSUGRA approach, the MSSM-124 parameter freedom has been significantly reduced. Typical mSUGRA models give low-energy values for the scalar mass parameters that satisfy $M_{\tilde{L}} \lesssim M_{\tilde{E}} < M_{\tilde{Q}} \approx M_{\tilde{U}} \approx M_{\tilde{D}}$, with the squark mass parameters somewhere between a factor of 1–3 larger than the slepton mass parameters (*e.g.*, see Ref. 124). More precisely, the low-energy values of the squark mass parameters of the first two generations are roughly degenerate, while $M_{\tilde{Q}_3}$ and $M_{\tilde{U}_3}$ are typically reduced by a factor of 1–3 from the values of the first- and second-generation squark mass parameters, because of renormalization effects due to the heavy top-quark mass.

As a result, one typically finds that four flavors of squarks (with two squark eigenstates per flavor) and \tilde{b}_R are nearly mass-degenerate. The \tilde{b}_L mass and the diagonal \tilde{t}_L and \tilde{t}_R masses are reduced compared to the common squark mass of the first two generations. In addition, there are six flavors of nearly mass-degenerate sleptons (with two slepton eigenstates per flavor for the charged sleptons and one per flavor for the sneutrinos); the sleptons are expected to be somewhat lighter than the mass-degenerate squarks. Finally, third-generation squark masses and tau-slepton masses are sensitive to the strength of the respective \tilde{f}_L - \tilde{f}_R mixing, as discussed below Eq. (7). If $\tan\beta \gg 1$, then the pattern of third-generation squark masses is somewhat altered, as discussed in Ref. 125.

In mSUGRA models, the LSP is typically the lightest neutralino, $\tilde{\chi}_1^0$, which is dominated by its bino component. In particular, one can reject those mSUGRA parameter regimes in which the LSP is a chargino or the $\tilde{\tau}_1$ (the lightest scalar superpartner of the τ -lepton). In general, if one imposes the constraints of supersymmetric particle searches and those of cosmology (say, by requiring the LSP to be a suitable dark matter candidate), one obtains significant restrictions to the mSUGRA parameter space [42,126].

One can count the number of independent parameters in the mSUGRA framework. In addition to 18 Standard Model parameters (excluding the Higgs mass), one must specify m_0 , $m_{1/2}$, A_0 , the Planck-scale values for μ and B -parameters (denoted by μ_0 and B_0), and the gravitino mass $m_{3/2}$. Without additional model assumptions, $m_{3/2}$ is independent of the parameters that govern the mass spectrum of the superpartners of the Standard Model [57]. In principle, A_0 , B_0 , μ_0 , and $m_{3/2}$ can be complex, although in the mSUGRA approach, these parameters are taken (arbitrarily) to be real. In the early literature, additional conditions were obtained by assuming a simplifying form for the hidden sector that provides the fundamental source of supersymmetry breaking. Two additional relations emerged among the mSUGRA parameters [123]: $B_0 = A_0 - m_0$ and $m_{3/2} = m_0$. Although these relations characterize a theory that was called minimal supergravity when first proposed, it is now more common to omit these extra constraints in defining the mSUGRA model. To accommodate this prevailing convention, we propose that the more constrained

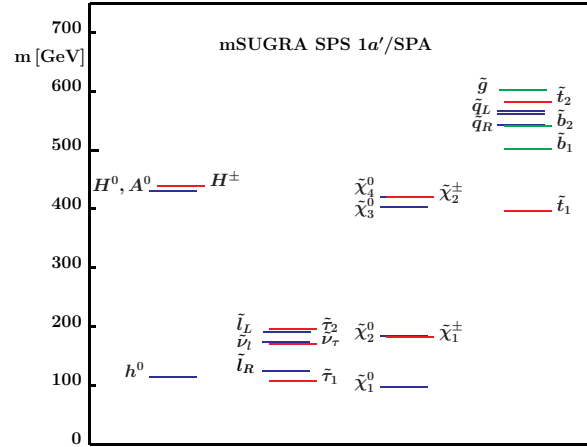


Figure 1: Mass spectrum of supersymmetric particles and Higgs bosons for the mSUGRA reference point SPS 1a'. The masses of the first and second generation squarks, sleptons, and sneutrinos are denoted collectively by \tilde{q} , $\tilde{\ell}$ and $\tilde{\nu}_\ell$, respectively. Taken from Ref. 100. Color version at end of book.

mSUGRA models, in which additional parameter relations are imposed, shall be designated as *more* minimal supergravity (mmSUGRA) models. Detailed studies of the phenomenology of various mmSUGRA models have been presented in Ref. 127.

As previously noted, renormalization group evolution is used to compute the low-energy values of the mSUGRA parameters, which then fixes all the parameters of the low-energy MSSM. In particular, the two Higgs vacuum expectation values (or equivalently, m_Z and $\tan\beta$) can be expressed as a function of the Planck-scale supergravity parameters. The simplest procedure is to remove μ_0 and B_0 in favor of m_Z and $\tan\beta$ [the sign of μ_0 , denoted $\text{sgn}(\mu_0)$ below, is not fixed in this process]. In this case, the MSSM spectrum and its interaction strengths are determined by five parameters:

$$m_0, A_0, m_{1/2}, \tan\beta, \text{ and } \text{sgn}(\mu_0), \quad (16)$$

in addition to the 18 parameters of the Standard Model. However, the mSUGRA approach is probably too simplistic. Theoretical considerations suggest that the universality of Planck-scale soft-supersymmetry-breaking parameters is not generic [128]. In particular, effective operators at the Planck scale exist that do not respect flavor universality, and it is difficult to find a theoretical principle that would forbid them.

In order to facilitate studies of supersymmetric phenomenology at colliders, it has been a valuable exercise to compile a set of benchmark supersymmetric parameters, from which supersymmetric spectra and couplings can be derived [129]. A compilation of benchmark mSUGRA points consistent with present data from particle physics and cosmology can be found in Ref. 130. One particular well-studied benchmark point, the so-called SPS 1a' reference point [100] (this is a slight modification of the SPS 1a point of Ref. 129, which incorporates the latest constraints from collider data and cosmology) has been

Searches Particle Listings

Supersymmetric Particle Searches

especially useful in experimental studies of supersymmetric phenomena at future colliders. In Fig. 1, the supersymmetric particle spectrum for the SPS 1a' reference point is exhibited. However, it is important to keep in mind that even within the mSUGRA framework, the resulting supersymmetric theory and its attendant phenomenology can be quite different from the SPS 1a' reference point.

I.7.2. Gauge-mediated supersymmetry breaking: In contrast to models of gravity-mediated supersymmetry breaking, the universality of the fundamental soft-supersymmetry-breaking squark and slepton squared-mass parameters is guaranteed in gauge-mediated supersymmetry breaking because the supersymmetry breaking is communicated to the sector of MSSM fields via gauge interactions [62,63]. In the minimal gauge-mediated supersymmetry-breaking (GMSB) approach, there is one effective mass scale, Λ , that determines all low-energy scalar and gaugino mass parameters through loop effects (while the resulting A parameters are suppressed). In order that the resulting superpartner masses be on the order of 1 TeV or less, one must have $\Lambda \sim 100$ TeV. The origin of the μ and B -parameters is quite model-dependent, and lies somewhat outside the ansatz of gauge-mediated supersymmetry breaking. The simplest models of this type are even more restrictive than mSUGRA, with two fewer degrees of freedom. Benchmark reference points for GMSB models have been proposed in Ref. 129 to facilitate collider studies.

The minimal GMSB is not a fully realized model. The sector of supersymmetry-breaking dynamics can be very complex, and no complete model of gauge-mediated supersymmetry yet exists that is both simple and compelling. However, advances in the theory of dynamical supersymmetry breaking (which exploit the existence of metastable supersymmetry-breaking vacua in broad classes of models [131]) have generated new ideas and opportunities for model building. As a result, simpler models of successful gauge mediation of supersymmetry breaking have been achieved with the potential for overcoming a number of long-standing theoretical challenges [132]. In addition, model-independent techniques that encompass all known gauge mediation models have been recently formulated [133]. These methods are well-suited for a comprehensive analysis [134] of the phenomenological profile of gauge-mediated supersymmetry breaking.

It was noted in Section I.2 that the gravitino is the LSP in GMSB models. Thus, in such models, the next-to-lightest supersymmetric particle (NLSP) plays a crucial role in the phenomenology of supersymmetric particle production and decay. Note that unlike the LSP, the NLSP can be charged. In GMSB models, the most likely candidates for the NLSP are $\tilde{\chi}_1^0$ and $\tilde{\tau}_R^\pm$. The NLSP will decay into its superpartner plus a gravitino (*e.g.*, $\tilde{\chi}_1^0 \rightarrow \gamma\tilde{G}$, $\tilde{\chi}_1^0 \rightarrow Z\tilde{G}$, or $\tilde{\tau}_R^\pm \rightarrow \tau^\pm\tilde{G}$), with lifetimes and branching ratios that depend on the model parameters.

Different choices for the identity of the NLSP and its decay rate lead to a variety of distinctive supersymmetric phenomenologies [63,135]. For example, a long-lived $\tilde{\chi}_1^0$ -NLSP

that decays outside collider detectors leads to supersymmetric decay chains with missing energy in association with leptons and/or hadronic jets (this case is indistinguishable from the standard phenomenology of the $\tilde{\chi}_1^0$ -LSP). On the other hand, if $\tilde{\chi}_1^0 \rightarrow \gamma\tilde{G}$ is the dominant decay mode, and the decay occurs inside the detector, then nearly *all* supersymmetric particle decay chains would contain a photon. In contrast, in the case of a $\tilde{\tau}_R^\pm$ -NLSP, the $\tilde{\tau}_R^\pm$ would either be long-lived or would decay inside the detector into a τ -lepton plus missing energy.

I.7.3. Supersymmetric grand unification: Finally, grand unification [136] can impose additional constraints on the MSSM parameters. As emphasized in Section I.1, it is striking that the $SU(3)\times SU(2)\times U(1)$ gauge couplings unify in models of supersymmetric grand unified theories (SGUTs) [8,74,137,138] with (some of) the supersymmetry-breaking parameters on the order of 1 TeV or below. Gauge coupling unification, which takes place at an energy scale on the order of 10^{16} GeV, is quite robust [139].

Given the low-energy values of the electroweak couplings $g(m_Z)$ and $g'(m_Z)$, one can predict $\alpha_s(m_Z)$ by using the MSSM renormalization group equations to extrapolate to higher energies, and by imposing the unification condition on the three gauge couplings at some high-energy scale, M_X . This procedure, which fixes M_X , can be successful (*i.e.*, three running couplings will meet at a single point) only for a unique value of $\alpha_s(m_Z)$. The extrapolation depends somewhat on the low-energy supersymmetric spectrum (so-called low-energy “threshold effects”), and on the SGUT spectrum (high-energy threshold effects), which can somewhat alter the evolution of couplings. A comparison of data with the expectations of SGUTs shows that the measured value of $\alpha_s(m_Z)$ is in good agreement with the predictions of supersymmetric grand unification for a reasonable choice of supersymmetric threshold corrections [140].

Additional SGUT predictions arise through the unification of the Higgs-fermion Yukawa couplings (λ_f). There is some evidence that $\lambda_b = \lambda_\tau$ is consistent with observed low-energy data [141], and an intriguing possibility that $\lambda_b = \lambda_\tau = \lambda_t$ may be phenomenologically viable [125,142] in the parameter regime where $\tan\beta \simeq m_t/m_b$.

I.8. Massive neutrinos in low-energy supersymmetry:

In the minimal Standard Model and its supersymmetric extension, there are no right-handed neutrinos, and Majorana mass terms for the left-handed neutrinos are absent. However, given the overwhelming evidence for neutrino masses and mixing [143,144], any viable model of fundamental particles must provide a mechanism for generating neutrino masses. In extended supersymmetric models, various mechanisms exist for producing massive neutrinos [145]. Although one can devise models for generating massive Dirac neutrinos [146], the most common approaches for incorporating neutrino masses are based on L -violating supersymmetric extensions of the MSSM, which generate massive Majorana neutrinos. Two classes of L -violating supersymmetric models will now be considered.

I.8.1. The supersymmetric seesaw: In this approach, one starts with an extended version of the Standard Model, which incorporates new structure that yields nonzero neutrino masses. Following the procedures of Sections I.2 and I.3, one then formulates a supersymmetric version of this extended Standard Model. For example, neutrino masses can be incorporated into the Standard Model by introducing $SU(3) \times SU(2) \times U(1)$ singlet right-handed neutrinos (ν_R) and super-heavy Majorana masses (typically on the order of a grand unified mass) for the ν_R . In addition, one must also include a standard Yukawa couplings between the lepton doublets, the Higgs doublet, and the ν_R . The Higgs vacuum expectation value then induces an off-diagonal ν_L - ν_R masses on the order of the electroweak scale. Diagonalizing the neutrino mass matrix (in the three-generation model) yields three superheavy neutrino states, and three very light neutrino states that are identified as the light neutrino states observed in nature. This is the seesaw mechanism [147]. The supersymmetric generalization of the seesaw model of neutrino masses is now easily constructed [148,149].

In the seesaw-extended Standard Model, lepton number is broken due to the presence of $\Delta L = 2$ terms in the Lagrangian (which include the Majorana mass terms for the light and superheavy neutrinos). Consequently, the seesaw-extended MSSM conserves R-parity. The supersymmetric analogue of the Majorana neutrino mass term in the sneutrino sector leads to sneutrino-antisneutrino mixing phenomena [149,150].

I.8.2. R-parity-violating supersymmetry: A second approach to incorporating massive neutrinos in supersymmetric models is to retain the minimal particle content of the MSSM but remove the assumption of R-parity invariance [151]. The most general R-parity-violating (RPV) theory involving the MSSM spectrum introduces many new parameters to both the supersymmetry-conserving and the supersymmetry-breaking sectors. Each new interaction term violates either B or L conservation. For example, consider new scalar-fermion Yukawa couplings derived from the following interactions:

$$(\lambda_L)_{pmn} \hat{L}_p \hat{L}_m \hat{E}_n^c + (\lambda'_L)_{pmn} \hat{L}_p \hat{Q}_m \hat{D}_n^c + (\lambda_B)_{pmn} \hat{U}_p^c \hat{D}_m^c \hat{D}_n^c, \quad (17)$$

where p , m , and n are generation indices, and gauge group indices are suppressed. In the notation above, \hat{Q} , \hat{U}^c , \hat{D}^c , \hat{L} , and \hat{E}^c respectively represent $(u, d)_L$, u_L^c , d_L^c , $(\nu, e^-)_L$, and e_L^c and the corresponding superpartners. The Yukawa interactions are obtained from Eq. (17) by taking all possible combinations involving two fermions and one scalar superpartner. Note that the term in Eq. (17) proportional to λ_B violates B , while the other two terms violate L . Even if all the terms of Eq. (17) are absent, there is one more possible supersymmetric source of R-parity violation. In the notation of Eq. (17), one can add a term of the form $(\mu_L)_p \hat{H}_u \hat{L}_p$, where \hat{H}_u represents the $Y = 1$ Higgs doublet and its higgsino superpartner. This term is the RPV generalization of the supersymmetry-conserving Higgs mass parameter μ of the MSSM, in which the $Y = -1$ Higgs/higgsino super-multiplet \hat{H}_d is replaced by the slepton/lepton super-multiplet \hat{L}_p . The RPV-parameters $(\mu_L)_p$ also violate L .

Phenomenological constraints derived from data on various low-energy B - and L -violating processes can be used to establish limits on each of the coefficients $(\lambda_L)_{pmn}$, $(\lambda'_L)_{pmn}$, and $(\lambda_B)_{pmn}$ taken one at a time [151,152]. If more than one coefficient is simultaneously non-zero, then the limits are, in general, more complicated [153]. All possible RPV terms cannot be simultaneously present and unsuppressed; otherwise the proton decay rate would be many orders of magnitude larger than the present experimental bound. One way to avoid proton decay is to impose B or L invariance (either one alone would suffice). Otherwise, one must accept the requirement that certain RPV coefficients must be extremely suppressed.

One particularly interesting class of RPV models is one in which B is conserved, but L is violated. It is possible to enforce baryon number conservation, while allowing for lepton-number-violating interactions by imposing a discrete \mathbf{Z}_3 baryon *triality* symmetry on the low-energy theory [154], in place of the standard \mathbf{Z}_2 R-parity. Since the distinction between the Higgs and matter super-multiplets is lost in RPV models, R-parity violation permits the mixing of sleptons and Higgs bosons, the mixing of neutrinos and neutralinos, and the mixing of charged leptons and charginos, leading to more complicated mass matrices and mass eigenstates than in the MSSM.

The supersymmetric phenomenology of the RPV models exhibits features that are quite distinct from that of the MSSM [151]. The LSP is no longer stable, which implies that not all supersymmetric decay chains must yield missing-energy events at colliders. Nevertheless, the loss of the missing-energy signature is often compensated by other striking signals (which depend on which R-parity-violating parameters are dominant). For example, supersymmetric particles in RPV models can be singly produced (in contrast to R-parity-conserving models where supersymmetric particles must be produced in pairs). The phenomenology of pair-produced supersymmetric particles is also modified in RPV models due to new decay chains not present in R-parity-conserving supersymmetry [151].

In RPV models with lepton number violation (these include low-energy supersymmetry models with baryon triality mentioned above), both $\Delta L = 1$ and $\Delta L = 2$ phenomena are allowed, leading to neutrino masses and mixing [155], neutrinoless double-beta decay [156], sneutrino-antisneutrino mixing [157], s -channel resonant production of sneutrinos in e^+e^- collisions [158] and charged sleptons in $p\bar{p}$ and pp collisions [159]. For example, Ref. 160 demonstrates how one can fit both the solar and atmospheric neutrino data in an RPV model where μ_L provides the dominant source of R-parity violation.

I.9. Extensions beyond the MSSM: Extensions of the MSSM have been proposed to solve a variety of theoretical problems. One such problem involves the μ parameter of the MSSM. Although μ is a supersymmetric-*preserving* parameter, it must be of order the supersymmetry-breaking scale to yield a consistent supersymmetric phenomenology. In the MSSM, one must devise a theoretical mechanism to guarantee that the

Searches Particle Listings

Supersymmetric Particle Searches

magnitude of μ is not larger than the TeV-scale (*e.g.*, in gravity-mediated supersymmetry, the Giudice-Masiero mechanism of Ref. 161 is the most cited explanation).

In extensions of the MSSM, new compelling solutions to the so-called μ -problem are possible. For example, one can replace μ by the vacuum expectation value of a new $SU(3) \times SU(2) \times U(1)$ singlet scalar field. In such a model, the Higgs sector of the MSSM is enlarged (and the corresponding fermionic higgsino superpartner is added). This is the so-called NMSSM (here, NM stands for non-minimal) [162]. There are some advantages to extending the model further by adding an additional $U(1)$ broken gauge symmetry [163] (which yields the USSM [94]).

Non-minimal extensions of the MSSM involving additional matter and/or Higgs super-multiplets can also yield a less restrictive bound on the mass of the lightest Higgs boson (as compared to the bound quoted in Section I.5.2). For example, MSSM-extended models consistent with gauge coupling unification can be constructed in which the upper limit on the lightest Higgs boson mass can be as high as 200–300 GeV [164] (a similar relaxation of the Higgs mass bound occurs in split supersymmetry [165] and extra-dimensional scenarios [166]).

Other MSSM extensions considered in the literature include an enlarged electroweak gauge group beyond $SU(2) \times U(1)$ [167]; and/or the addition of new, possibly exotic, matter super-multiplets (*e.g.*, new $U(1)$ gauge groups and a vector-like color triplet with electric charge $\frac{1}{3}e$ that appear as low-energy remnants in E_6 grand unification models [168]). A possible theoretical motivation for such new structures arises from the study of phenomenologically viable string theory ground states [169].

References

- R. Haag, J.T. Lopuszanski, and M. Sohnius, Nucl. Phys. **B88**, 257 (1975);
S.R. Coleman and J. Mandula, Phys. Rev. **159** (1967) 1251.
- H.P. Nilles, Phys. Reports **110**, 1 (1984).
- P. Nath, R. Arnowitt, and A.H. Chamseddine, *Applied $N = 1$ Supergravity* (World Scientific, Singapore, 1984).
- S.P. Martin, in *Perspectives on Supersymmetry II*, edited by G.L. Kane (World Scientific, Singapore, 2010) pp. 1–153; see <http://zippy.physics.niu.edu/primer.html> for the latest version and errata.
- S. Weinberg, *The Quantum Theory of Fields, Volume III: Supersymmetry* (Cambridge University Press, Cambridge, UK, 2000);
P. Binétruy, *Supersymmetry: Theory, Experiment, and Cosmology* (Oxford University Press, Oxford, UK, 2006).
- L. Maiani, in *Vector bosons and Higgs bosons in the Salam-Weinberg theory of weak and electromagnetic interactions, Proceedings of the 11th GIF Summer School on Particle Physics*, Gif-sur-Yvette, France, 3–7 September, 1979, edited by M. Davier *et al.*, (IN2P3, Paris, 1980) pp. 1–52.
- E. Witten, Nucl. Phys. **B188**, 513 (1981).
- S. Dimopoulos and H. Georgi, Nucl. Phys. **B193**, 150 (1981).
- N. Sakai, Z. Phys. **C11**, 153 (1981);
R.K. Kaul, Phys. Lett. **109B**, 19 (1982).
- L. Susskind, Phys. Reports **104**, 181 (1984).
- L. Girardello and M. Grisaru, Nucl. Phys. **B194**, 65 (1982).
- L.J. Hall and L. Randall, Phys. Rev. Lett. **65**, 2939 (1990);
I. Jack and D.R.T. Jones, Phys. Lett. **B457**, 101 (1999).
- For a review, see N. Polonsky, *Supersymmetry: Structure and phenomena. Extensions of the standard model*, Lect. Notes Phys. **M68**, 1 (2001).
- G. Bertone, D. Hooper, and J. Silk, Phys. Rept. **405**, 279 (2005).
- D. Hooper, “TASI 2008 Lectures on Dark Matter,” in *The Dawn of the LHC Era*, Proceedings of the 2008 Theoretical and Advanced Study Institute in Elementary Particle Physics, Boulder, Colorado, 2–27 June 2008, edited by Tao Han (World Scientific, Singapore, 2009).
- G. Jungman, M. Kamionkowski, and K. Griest, Phys. Reports **267**, 195 (1996);
K. Griest and M. Kamionkowski, Phys. Reports **333**, 167 (2000).
- F.D. Steffen, Eur. Phys. J. **C59**, 557 (2009).
- M. Drees and G. Gerbier, “Dark Matter,” in the section on Reviews, Tables, and Plots in this *Review*.
- H.E. Haber and G.L. Kane, Phys. Rept. **117**, 75 (1985).
- M. Drees, R. Godbole, and P. Roy, *Theory and Phenomenology of Sparticles* (World Scientific, Singapore, 2005);
H. Baer and X. Tata, *Weak scale supersymmetry: from superfields to scattering events* (Cambridge University Press, Cambridge, UK, 2006);
I.J.R. Aitchison, *Supersymmetry in particle physics: an elementary introduction* (Cambridge University Press, Cambridge, UK, 2007).
- P. Fayet, Nucl. Phys. **B78**, 14 (1974); *ibid.*, **B90**, 104 (1975).
- K. Inoue *et al.*, Prog. Theor. Phys. **67**, 1889 (1982) [erratum: **70**, 330 (1983)]; *ibid.*, **71**, 413 (1984);
R. Flores and M. Sher, Ann. Phys. (NY) **148**, 95 (1983).
- J.F. Gunion and H.E. Haber, Nucl. Phys. **B272**, 1 (1986) [erratum: **B402**, 567 (1993)].
- For an overview of the theory and models of the soft-supersymmetry-breaking Lagrangian, see D.J.H. Chung *et al.*, Phys. Rept. **407**, 1 (2005).
- See, *e.g.*, R. Barbieri and G.F. Giudice, Nucl. Phys. **B305**, 63 (1988);
G.W. Anderson and D.J. Castano, Phys. Lett. **B347**, 300 (1995); Phys. Rev. **D52**, 1693 (1995); Phys. Rev. **D53**, 2403 (1996);
J.L. Feng, K.T. Matchev, and T. Moroi, Phys. Rev. **D61**, 075005 (2000);
P. Athron and D.J. Miller, Phys. Rev. **D76**, 075010 (2007).
- S. Dimopoulos and G.F. Giudice, Phys. Lett. **B357**, 573 (1995);
A. Pomarol and D. Tommasini, Nucl. Phys. **B466**, 3 (1996);
A.G. Cohen, D.B. Kaplan, and A.E. Nelson, Phys. Lett. **B388**, 588 (1996);
J.L. Feng, K.T. Matchev, and T. Moroi, Phys. Rev. Lett. **84**, 2322 (2000).

27. L. Pape and D. Treille, *Prog. Part. Nucl. Phys.* **69**, 63 (2006).
28. J.-F. Grivaz, “Supersymmetry Part II (Experiment),” immediately following, in the section on Reviews, Tables, and Plots in this *Review*. See also *Particle Listings: Other Searches—Supersymmetric Particles* in this *Review*.
29. See, *e.g.*, F. Gabbiani *et al.*, *Nucl. Phys.* **B477**, 321 (1996); A. Masiero, and O. Vives, *New J. Phys.* **4**, 4.1 (2002).
30. For a recent review and references to the original literature, see: M.J. Ramsey-Musolf and S. Su, *Phys. Reports* **456**, 1 (2008).
31. W. Altmannshofer *et al.*, *Nucl. Phys.* **B830**, 17 (2010).
32. J. Erler and P. Langacker, “Electroweak Model and Constraints on New Physics,” in the section on Reviews, Tables, and Plots in this *Review*; The ALEPH, CDF, D0, DELPHI, L3, OPAL, SLD Collaborations, the LEP Electroweak Working Group, the Tevatron Electroweak Working Group, and the SLD Electroweak and Heavy Flavor groups, CERN-PH-EP/2009-023 (13 November, 2009); the most recent updated results can be found at lepewwg.web.cern.ch/LEPEWWG/.
33. P.H. Chankowski and S. Pokorski, in *Perspectives on Supersymmetry*, edited by G.L. Kane (World Scientific, Singapore, 1998) pp. 402–422.
34. A. Dobado, M.J. Herrero, and S. Penaranda, *Eur. Phys. J.* **C7**, 313 (1999); **C12**, 673 (2000); **C17**, 487 (2000).
35. J. Erler and D.M. Pierce, *Nucl. Phys.* **B526**, 53 (1998); G. Altarelli *et al.*, *JHEP* **0106**, 018 (2001); J.R. Ellis *et al.*, *JHEP* **0502**, 013 (2005); **0605**, 005 (2006); S. Heinemeyer, W. Hollik and G. Weiglein, *Phys. Rept.* **425**, 265 (2006).
36. For a review, see D. Stockinger, *J. Phys.* **G34**, R45 (2007).
37. A. Höcker and W.J. Marciano, “The Muon Anomalous Magnetic Moment,” in this *Review*; J.P. Miller, E. de Rafael, and B.L. Roberts, *Rept. Prog. Phys.* **70**, 795 (2007); M. Davier, *Chin. Phys.* **C33**, 1 (2009).
38. A. Limosani *et al.* [Belle Collab.], *Phys. Rev. Lett.* **103**, 241801 (2009).
39. M. Misiak *et al.*, *Phys. Rev. Lett.* **98**, 022002 (2007); T. Becher and M. Neubert, *Phys. Rev. Lett.* **98**, 022003 (2007).
40. See, *e.g.*, M. Ciuchini *et al.*, *Phys. Rev.* **D67**, 075016 (2003); T. Hurth, *Rev. Mod. Phys.* **75**, 1159 (2003).
41. T. Moroi, *Phys. Rev.* **D53**, 6565 (1996) [erratum: **D56**, 4424 (1997)]; Chattopadhyay U. Chattopadhyay and P. Nath, *Phys. Rev.* **D66**, 093001 (2002); S.P. Martin and J.D. Wells, *Phys. Rev.* **D67**, 015002 (2003).
42. J.R. Ellis *et al.*, *Phys. Lett.* **B653**, 292 (2007); J.R. Ellis *et al.*, *JHEP* **0708**, 083 (2007); S. Heinemeyer *et al.*, *JHEP* **0808**, 087 (2008).
43. L. Giusti, A. Romanino, and A. Strumia, *Nucl. Phys.* **B550**, 3 (1999); R. Barbieri and A. Strumia, Talk given at 4th Rencontres du Vietnam: International Conference on Physics at Extreme Energies (Particle Physics and Astrophysics), Hanoi, Vietnam, 19–25 July 2000, hep-ph/0007265.
44. A summary of the MSSM Higgs mass limits can be found in G. Bernardi, M. Carena, and T. Junk, “Higgs Bosons: Theory and Searches,” in “Particle Listings—Gauge and Higgs bosons” in this *Review*.
45. J.A. Casas, J.R. Espinosa, and I. Hidalgo, *JHEP* **0401**, 008 (2004); P. Batra *et al.*, *JHEP* **0406**, 032 (2004); R. Harnik *et al.*, *Phys. Rev.* **D70**, 015002 (2004); A. Birkedal, Z. Chacko, and M.K. Gaillard, *JHEP* **0410**, 036 (2004).
46. H.C. Cheng and I. Low, *JHEP* **0309**, 051 (2003); **0408**, 061 (2004).
47. For some recent examples, see, *e.g.*, R. Kitano and Y. Nomura, *Phys. Rev.* **D73**, 095004 (2006); R. Dermisek and J.F. Gunion, *Phys. Rev. Lett.* **95**, 041801 (2005); *Phys. Rev.* **D75**, 095019 (2007); *Phys. Rev.* **D76**, 095006 (2007); B. Bellazzini *et al.*, *Phys. Rev.* **D79**, 095003 (2009).
48. P. Fayet, *Phys. Lett.* **69B**, 489 (1977); G. Farrar and P. Fayet, *Phys. Lett.* **76B**, 575 (1978).
49. J. Ellis *et al.*, *Nucl. Phys.* **B238**, 453 (1984).
50. S. Raby, *Phys. Lett.* **B422**, 158 (1998); S. Raby and K. Tobe, *Nucl. Phys.* **B539**, 3 (1999); A. Mafi and S. Raby, *Phys. Rev.* **D62**, 035003 (2000).
51. P. Fayet, *Phys. Lett.* **84B**, 421 (1979); *Phys. Lett.* **86B**, 272 (1979).
52. P. van Nieuwenhuizen, *Phys. Reports* **68**, 189 (1981).
53. S. Deser and B. Zumino, *Phys. Rev. Lett.* **38**, 1433 (1977); E. Cremmer *et al.*, *Phys. Lett.* **79B**, 231 (1978).
54. R. Casalbuoni *et al.*, *Phys. Lett.* **B215**, 313 (1988); *Phys. Rev.* **D39**, 2281 (1989); A.L. Maroto and J.R. Pelaez, *Phys. Rev.* **D62**, 023518 (2000).
55. Z. Komargodski and N. Seiberg, *JHEP* **0909**, 066 (2009).
56. A.H. Chamseddine, R. Arnowitt, and P. Nath, *Phys. Rev. Lett.* **49**, 970 (1982); R. Barbieri, S. Ferrara, and C.A. Savoy, *Phys. Lett.* **119B**, 343 (1982); H.-P. Nilles, M. Srednicki, and D. Wyler, *Phys. Lett.* **120B**, 346 (1983); **124B**, 337 (1983) 337; E. Cremmer, P. Fayet, and L. Girardello, *Phys. Lett.* **122B**, 41 (1983); L. Ibáñez, *Nucl. Phys.* **B218**, 514 (1982); L. Alvarez-Gaumé, J. Polchinski, and M.B. Wise, *Nucl. Phys.* **B221**, 495 (1983).
57. L.J. Hall, J. Lykken, and S. Weinberg, *Phys. Rev.* **D27**, 2359 (1983).
58. S.K. Soni and H.A. Weldon, *Phys. Lett.* **126B**, 215 (1983); Y. Kawamura, H. Murayama, and M. Yamaguchi, *Phys. Rev.* **D51**, 1337 (1995).
59. A.B. Lahanas and D.V. Nanopoulos, *Phys. Reports* **145**, 1 (1987).
60. J.L. Feng, A. Rajaraman, and F. Takayama, *Phys. Rev. Lett.* **91**, 011302 (2003); *Phys. Rev.* **D68**, 063504 (2003); *Gen. Rel. Grav.* **36**, 2575 (2004).
61. M. Dine, W. Fischler, and M. Srednicki, *Nucl. Phys.* **B189**, 575 (1981);

Searches Particle Listings

Supersymmetric Particle Searches

- S. Dimopoulos and S. Raby, Nucl. Phys. **B192**, 353 (1982); **B219**, 479 (1983);
M. Dine and W. Fischler, Phys. Lett. **110B**, 227 (1982);
C. Nappi and B. Ovrut, Phys. Lett. **113B**, 175 (1982);
L. Alvarez-Gaumé, M. Claudson, and M. Wise, Nucl. Phys. **B207**, 96 (1982).
62. M. Dine and A.E. Nelson, Phys. Rev. **D48**, 1277 (1993);
M. Dine, A.E. Nelson, and Y. Shirman, Phys. Rev. **D51**, 1362 (1995);
M. Dine *et al.*, Phys. Rev. **D53**, 2658 (1996).
63. G.F. Giudice and R. Rattazzi, Phys. Reports **322**, 419 (1999).
64. E. Poppitz and S.P. Trivedi, Phys. Rev. **D55**, 5508 (1997);
H. Murayama, Phys. Rev. Lett. **79**, 18 (1997);
M.A. Luty and J. Terning, Phys. Rev. **D57**, 6799 (1998);
N. Arkani-Hamed, J. March-Russell and H. Murayama, Nucl. Phys. **B509**, 3 (1998);
K. Agashe, Phys. Lett. **B435**, 83 (1998);
C. Csaki, Y. Shirman and J. Terning, JHEP **0705**, 099 (2007);
M. Ibe and R. Kitano, Phys. Rev. **D77**, 075003 (2008).
65. M.J. Strassler and K. M. Zurek, Phys. Lett. **B651**, 374 (2007);
T. Han *et al.*, JHEP **0807**, 008 (2008).
66. M.J. Strassler, [arXiv:hep-ph/0607160](https://arxiv.org/abs/hep-ph/0607160);
K.M. Zurek, Phys. Rev. **D79**, 115002 (2009).
67. Pedagogical lectures describing such mechanisms can be found in: M. Quiros, in *Particle Physics and Cosmology: The Quest for Physics Beyond the Standard Model(s), Proceedings of the 2002 Theoretical Advanced Study Institute in Elementary Particle Physics (TASI 2002)*, edited by H.E. Haber and A.E. Nelson (World Scientific, Singapore, 2004) pp. 549–601;
C. Csaki, in *ibid.*, pp. 605–698.
68. See, *e.g.*, G.F. Giudice and J.D. Wells, “Extra Dimensions,” in the section on Reviews, Tables, and Plots in this *Review*.
69. These ideas are reviewed in: V.A. Rubakov, Phys. Usp. **44**, 871 (2001);
J. Hewett and M. Spiropulu, Ann. Rev. Nucl. Part. Sci. **52**, 397 (2002).
70. L. Randall and R. Sundrum, Nucl. Phys. **B557**, 79 (1999).
71. Z. Chacko, M.A. Luty, and E. Ponton, JHEP **0007**, 036 (2000);
D.E. Kaplan, G.D. Kribs, and M. Schmaltz, Phys. Rev. **D62**, 035010 (2000);
Z. Chacko *et al.*, JHEP **0001**, 003 (2000).
72. J. Scherk and J.H. Schwarz, Phys. Lett. **82B**, 60 (1979);
Nucl. Phys. **B153**, 61 (1979).
73. See, *e.g.*, R. Barbieri, L.J. Hall, and Y. Nomura, Phys. Rev. **D66**, 045025 (2002); Nucl. Phys. **B624**, 63 (2002).
74. N. Arkani-Hamed and S. Dimopoulos, JHEP **0506**, 073 (2005);
G.F. Giudice and A. Romanino, Nucl. Phys. **B699**, 65 (2004) [erratum: **B706**, 487 (2005)].
75. N. Arkani-Hamed *et al.*, Nucl. Phys. **B709**, 3 (2005);
W. Kilian *et al.*, Eur. Phys. J. **C39**, 229 (2005).
76. K. Cheung and W. Y. Keung, Phys. Rev. **D71**, 015015 (2005);
P. Gambino, G.F. Giudice, and P. Slavich, Nucl. Phys. **B726**, 35 (2005).
77. H.E. Haber, in *Recent Directions in Particle Theory, Proceedings of the 1992 Theoretical Advanced Study Institute in Particle Physics*, edited by J. Harvey and J. Polchinski (World Scientific, Singapore, 1993) pp. 589–686.
78. S. Dimopoulos and D. Sutter, Nucl. Phys. **B452**, 496 (1995);
D.W. Sutter, Stanford Ph. D. thesis, [hep-ph/9704390](https://arxiv.org/abs/hep-ph/9704390).
79. H.E. Haber, Nucl. Phys. B (Proc. Suppl.) **62A-C**, 469 (1998).
80. R.M. Barnett, J.F. Gunion, and H.E. Haber, Phys. Lett. **B315**, 349 (1993);
H. Baer, X. Tata, and J. Woodside, Phys. Rev. **D41**, 906 (1990).
81. S.M. Bilenky, E.Kh. Khristova, and N.P. Nedelcheva, Phys. Lett. **B161**, 397 (1985); Bulg. J. Phys. **13**, 283 (1986);
G. Moortgat-Pick and H. Fraas, Eur. Phys. J. **C25**, 189 (2002).
82. J. Rosiek, Phys. Rev. **D41**, 3464 (1990) [erratum: [hep-ph/9511250](https://arxiv.org/abs/hep-ph/9511250)]. The most recent corrected version of this manuscript can be found on the author’s webpage, www.fuw.edu.pl/~rosiek/physics/prd41.html.
83. J. Alwall *et al.*, JHEP **0709**, 028 (2007). The MadGraph homepage is located at madgraph.hep.uiuc.edu/.
84. T. Hahn, Comput. Phys. Commun. **140**, 418 (2001);
T. Hahn and C. Schappacher, Comput. Phys. Commun. **143**, 54 (2002). The FeynArts homepage is located at www.feynarts.de/.
85. A. Pukhov *et al.*, INP MSU report 98-41/542 ([arXiv:hep-ph/9908288](https://arxiv.org/abs/hep-ph/9908288));
E. Boos *et al.* [CompHEP Collaboration], Nucl. Instrum. Meth. A **534**, 250 (2004). The CompHEP homepage is located at <http://comphep.sinp.msu.ru>.
86. For further details, see *e.g.*, Appendix C of Ref. 19 and Appendix A of Ref. 23.
87. J.L. Kneur and G. Moultaka, Phys. Rev. **D59**, 015005 (1999).
88. S.Y. Choi *et al.*, Eur. Phys. J. **C14**, 535 (2000).
89. R.A. Horn and C.R. Johnson, *Matrix Analysis*, (Cambridge University Press, Cambridge, UK, 1985).
90. H.K. Dreiner, H.E. Haber, and S.P. Martin, [arXiv:0812.1594](https://arxiv.org/abs/0812.1594), Phys. Reports (2010) in press.
91. S.Y. Choi *et al.*, Eur. Phys. J. **C22**, 563 (2001); **C23**, 769 (2002).
92. G.J. Gounaris, C. Le Mouel, and P.I. Porfyriadis, Phys. Rev. **D65**, 035002 (2002);
G.J. Gounaris and C. Le Mouel, Phys. Rev. **D66**, 055007 (2002).
93. T. Takagi, Japan J. Math. **1**, 83 (1925).
94. S.Y. Choi *et al.*, Nucl. Phys. **B778**, 85 (2007).
95. M.M. El Kheishen, A.A. Aboshousha, and A.A. Shafik, Phys. Rev. **D45**, 4345 (1992);
M. Guchait, Z. Phys. **C57**, 157 (1993) [erratum: **C61**, 178 (1994)].
96. T. Hahn, preprint MPP-2006-85, [physics/0607103](https://arxiv.org/abs/physics/0607103).
97. K. Hikasa and M. Kobayashi, Phys. Rev. **D36**, 724 (1987);
F. Gabbiani and A. Masiero, Nucl. Phys. **B322**, 235

- (1989);
Ph. Brax and C.A. Savoy, Nucl. Phys. **B447**, 227 (1995).
98. J. Ellis and S. Rudaz, Phys. Lett. **128B**, 248 (1983);
F. Browning, D. Chang, and W.Y. Keung, Phys. Rev. **D64**, 015010 (2001);
A. Bartl *et al.*, Phys. Lett. **B573**, 153 (2003); Phys. Rev. **D70**, 035003 (2004).
99. D.M. Pierce *et al.*, Nucl. Phys. **B491**, 3 (1997).
100. J.A. Aguilar-Saavedra *et al.*, Eur. Phys. J. **C46**, 43 (2006).
101. D. Stockinger, JHEP **0503**, 076 (2005); Nucl. Phys. B (Proc. Suppl.) **160**, 250 (2006).
102. P. Skands *et al.*, JHEP **07** 036 (2004);
B.C. Allanach *et al.*, Comput. Phys. Commun. **180**, 8 (2009). The Supersymmetry Les Houches Accord homepage is located at home.fnal.gov/~skands/slha/.
103. J.F. Gunion *et al.*, *The Higgs Hunter's Guide* (Perseus Publishing, Cambridge, MA, 1990);
M. Carena and H.E. Haber, Prog. Part. Nucl. Phys. **50**, 63 (2003);
A. Djouadi, Phys. Reports **459**, 1 (2008).
104. H.E. Haber and R. Hempfling, Phys. Rev. Lett. **66**, 1815 (1991);
Y. Okada, M. Yamaguchi, and T. Yanagida, Prog. Theor. Phys. **85**, 1 (1991);
J. Ellis, G. Ridolfi, and F. Zwirner, Phys. Lett. **B257**, 83 (1991).
105. See, *e.g.*, G. Degross *et al.*, Eur. Phys. J. **C28**, 133 (2003);
B.C. Allanach *et al.*, JHEP **0409**, 044 (2004);
S.P. Martin, Phys. Rev. **D75**, 055005 (2007).
106. A. Pilaftsis and C.E.M. Wagner, Nucl. Phys. **B553**, 3 (1999);
D.A. Demir, Phys. Rev. **D60**, 055006 (1999);
S.Y. Choi, M. Drees, and J.S. Lee, Phys. Lett. **B481**, 57 (2000);
M. Carena *et al.*, Nucl. Phys. **B586**, 92 (2000); Phys. Lett. **B495**, 155 (2000); Nucl. Phys. **B625**, 345 (2002);
M. Frank *et al.*, JHEP **0702**, 047 (2007);
S. Heinemeyer *et al.*, Phys. Lett. **B652**, 300 (2007).
107. S. Khalil, Int. J. Mod. Phys. **A18**, 1697 (2003).
108. W. Fischler, S. Paban, and S. Thomas, Phys. Lett. **B289**, 373 (1992);
S.M. Barr, Int. J. Mod. Phys. **A8**, 209 (1993);
T. Ibrahim and P. Nath, Phys. Rev. **D58**, 111301 (1998) [erratum: **D60**, 099902 (1999)];
M. Brhlik, G.J. Good, and G.L. Kane, Phys. Rev. **D59**, 115004 (1999);
V.D. Barger *et al.*, Phys. Rev. **D64**, 056007 (2001);
S. Abel, S. Khalil, and O. Lebedev, Nucl. Phys. **B606**, 151 (2001);
K.A. Olive *et al.*, Phys. Rev. **D72**, 075001 (2005);
G.F. Giudice and A. Romanino, Phys. Lett. **B634**, 307 (2006).
109. A. Masiero and L. Silvestrini, in *Perspectives on Supersymmetry*, edited by G.L. Kane (World Scientific, Singapore, 1998) pp. 423–441.
110. M. Pospelov and A. Ritz, Annals Phys. **318**, 119 (2005).
111. H. Georgi, Phys. Lett. **169B**, 231 (1986);
L.J. Hall, V.A. Kostelecky, and S. Raby, Nucl. Phys. **B267**, 415 (1986).
112. Y. Nir and N. Seiberg, Phys. Lett. **B309**, 337 (1993);
S. Dimopoulos, G.F. Giudice, and N. Tetradis, Nucl. Phys. **B454**, 59 (1995);
G.F. Giudice *et al.*, JHEP **12**, 027 (1998);
J.L. Feng and T. Moroi, Phys. Rev. **D61**, 095004 (2000);
Y. Nir and G. Raz, Phys. Rev. **D66**, 035007 (2002).
113. M. Ciuchini *et al.*, Phys. Lett. **B655**, 162 (2007);
Y. Nir, JHEP **0705**, 102 (2007); and in Lectures given at 2nd Joint Fermilab-CERN Hadron Collider Physics Summer School, CERN, Geneva, Switzerland, 6–15 June 2007, [arXiv:0708.1872](https://arxiv.org/abs/0708.1872) [hep-ph].
114. B. Aubert *et al.* [BABAR Collab.], Phys. Rev. Lett. **98**, 211802 (2007);
M. Staric *et al.* [Belle Collab.], Phys. Rev. Lett. **98**, 211803 (2007).
115. L.E. Ibáñez and G.G. Ross, Phys. Lett. **B110**, 215 (1982).
116. H.K. Dreiner *et al.*, Eur. Phys. J. **C62**, 547 (2009).
117. A.G. Cohen, T.S. Roy, and M. Schmaltz, JHEP **0702**, 027 (2007).
118. M. Endo, M. Yamaguchi and K. Yoshioka, Phys. Rev. **D**, 015004 (2005);
K. Choi, K.S. Jeong and K-i. Okumura, JHEP **0509**, 039 (2005).
119. J.F. Gunion and H.E. Haber, Phys. Rev. **D37**, 2515 (1988);
S.Y. Choi, M. Drees, and B. Gaissmaier, Phys. Rev. **D70**, 014010 (2004).
120. J.L. Feng *et al.*, Phys. Rev. Lett. **83**, 1731 (1999);
T. Gherghetta, G.F. Giudice, and J.D. Wells, Nucl. Phys. **B559**, 27 (1999);
J.F. Gunion and S. Mrenna, Phys. Rev. **D62**, 015002 (2000).
121. For a number of recent attempts to resolve the tachyonic slepton problem, see *e.g.*, I. Jack, D.R.T. Jones, and R. Wild, Phys. Lett. **B535**, 193 (2002);
B. Murakami and J.D. Wells, Phys. Rev. **D68**, 035006 (2003);
R. Kitano, G.D. Kribs, and H. Murayama, Phys. Rev. **D70**, 035001 (2004);
R. Hodgson *et al.*, Nucl. Phys. **B728**, 192 (2005);
D.R.T. Jones and G.G. Ross, Phys. Lett. **B642**, 540 (2006).
122. B.C. Allanach *et al.*, JHEP **0708**, 023 (2007);
R. Lafaye *et al.*, Eur. Phys. J. **C54**, 617 (2008);
O. Buchmueller *et al.*, JHEP **0809**, 117 (2008);
O. Buchmueller *et al.*, Eur. Phys. J. **C64**, 391 (2009);
S.S. AbdusSalam *et al.*, Phys. Rev. **D80**, 035017 (2009);
S.S. AbdusSalam *et al.*, Phys. Rev. **D81**, 095012 (2010);
P. Bechtle *et al.*, Eur. Phys. J. **C66**, 215 (2010).
123. See, *e.g.*, A. Brignole, L.E. Ibanez, and C. Munoz, in *Perspectives on Supersymmetry II*, edited by G.L. Kane (World Scientific, Singapore, 2010) pp. 244–268.
124. M. Drees and S.P. Martin, in *Electroweak Symmetry Breaking and New Physics at the TeV Scale*, edited by T. Barklow *et al.* (World Scientific, Singapore, 1996) pp. 146–215.
125. M. Carena *et al.*, Nucl. Phys. **B426**, 269 (1994).
126. B.C. Allanach and C.G. Lester, Phys. Rev. **D73**, 015013 (2006);
J.R. Ellis *et al.*, Phys. Lett. **B565**, 176 (2003); Phys. Rev. **D69**, 095004 (2004);
H. Baer and C. Balazs, JCAP **0305**, 006 (2003).

Searches Particle Listings

Supersymmetric Particle Searches

127. J.R. Ellis *et al.*, Phys. Lett. **B573**, 162 (2003); Phys. Rev. **D70**, 055005 (2004).
128. L.E. Ibáñez and D. Lüst, Nucl. Phys. **B382**, 305 (1992); B. de Carlos, J.A. Casas, and C. Muñoz, Phys. Lett. **B299**, 234 (1993); V. Kaplunovsky and J. Louis, Phys. Lett. **B306**, 269 (1993); A. Brignole, L.E. Ibáñez, and C. Muñoz, Nucl. Phys. **B422**, 125 (1994) [erratum: **B436**, 747 (1995)].
129. B.C. Allanach *et al.*, Eur. Phys. J. **C25**, 113 (2002).
130. M. Battaglia *et al.*, Eur. Phys. J. **C33**, 273 (2004).
131. K. Intriligator, N. Seiberg, and D. Shih, JHEP **0604**, 021 (2006); **0707**, 017 (2007).
132. See, *e.g.*, M. Dine, J.L. Feng, and E. Silverstein, Phys. Rev. **D74**, 095012 (2006); H. Murayama and Y. Nomura, Phys. Rev. Lett. **98**, 151803 (2007); Phys. Rev. **D75**, 095011 (2007); R. Kitano, H. Ooguri, and Y. Ookouchi, Phys. Rev. **D75**, 045022 (2007); A. Delgado, G.F. Giudice, and P. Slavich, Phys. Lett. **B653**, 424 (2007); O. Aharony and N. Seiberg, JHEP **0702**, 054 (2007); C. Csaki, Y. Shirman, and J. Terning, JHEP **0705**, 099 (2007); N. Haba and N. Maru, Phys. Rev. **D76**, 115019 (2007).
133. P. Meade, N. Seiberg and D. Shih, Prog. Theor. Phys. Suppl. **177**, 143 (2009); M. Buican *et al.*, JHEP **0903**, 016 (2009).
134. A. Rajaraman *et al.*, Phys. Lett. **B678**, 367 (2009); L.M. Carpenter *et al.*, Phys. Rev. **D79**, 035002 (2009).
135. For a review and guide to the literature, see J.F. Gunion and H.E. Haber, in *Perspectives on Supersymmetry II*, edited by G.L. Kane (World Scientific, Singapore, 2010) pp. 420–445.
136. S. Raby, “Grand Unified Theories,” in the section on Reviews, Tables, and Plots in this *Review*.
137. M.B. Einhorn and D.R.T. Jones, Nucl. Phys. **B196**, 475 (1982).
138. For a review, see R.N. Mohapatra, in *Particle Physics 1999*, ICTP Summer School in Particle Physics, Trieste, Italy, 21 June–9 July, 1999, edited by G. Senjanovic and A.Yu. Smirnov (World Scientific, Singapore, 2000) pp. 336–394; W.J. Marciano and G. Senjanovic, Phys. Rev. **D25**, 3092 (1982).
139. D.M. Ghilencea and G.G. Ross, Nucl. Phys. **B606**, 101 (2001).
140. S. Pokorski, Acta Phys. Polon. **B30**, 1759 (1999).
141. H. Arason *et al.*, Phys. Rev. Lett. **67**, 2933 (1991); Phys. Rev. **D46**, 3945 (1992); V. Barger, M.S. Berger, and P. Ohmann, Phys. Rev. **D47**, 1093 (1993); M. Carena, S. Pokorski, and C.E.M. Wagner, Nucl. Phys. **B406**, 59 (1993); P. Langacker and N. Polonsky, Phys. Rev. **D49**, 1454 (1994).
142. M. Olechowski and S. Pokorski, Phys. Lett. **B214**, 393 (1988); B. Ananthanarayan, G. Lazarides, and Q. Shafi, Phys. Rev. **D44**, 1613 (1991); S. Dimopoulos, L.J. Hall, and S. Raby, Phys. Rev. Lett. **68**, 1984 (1992); L.J. Hall, R. Rattazzi, and U. Sarid, Phys. Rev. **D50**, 7048 (1994); R. Rattazzi and U. Sarid, Phys. Rev. **D53**, 1553 (1996).
143. For a review of the current status of neutrino masses and mixing, see: M.C. Gonzalez-Garcia and M. Maltoni, Phys. Reports **460**, 1 (2008); A. Strumia and F. Vissani, hep-ph/0606054.
144. See the section on neutrinos in “Particle Listings—Leptons” in this *Review*.
145. For a review of neutrino masses in supersymmetry, see B. Mukhopadhyaya, Proc. Indian National Science Academy **A70**, 239 (2004).
146. F. Borzumati and Y. Nomura, Phys. Rev. **D64**, 053005 (2001).
147. P. Minkowski, Phys. Lett. **67B**, 421 (1977); M. Gell-Mann, P. Ramond, and R. Slansky, in *Supergravity*, edited by D. Freedman and P. van Nieuwenhuizen (North Holland, Amsterdam, 1979) p. 315; T. Yanagida, in *Proceedings of the Workshop on Unified Theory and Baryon Number in the Universe*, edited by O. Sawada and A. Sugamoto (KEK, Tsukuba, Japan, 1979); R. Mohapatra and G. Senjanovic, Phys. Rev. Lett. **44**, 912 (1980); Phys. Rev. **D23**, 165 (1981).
148. J. Hisano *et al.*, Phys. Lett. **B357**, 579 (1995); J. Hisano *et al.*, Phys. Rev. **D53**, 2442 (1996); J.A. Casas and A. Ibarra, Nucl. Phys. **B618**, 171 (2001); J. Ellis *et al.*, Phys. Rev. **D66**, 115013 (2002); A. Masiero, S.K. Vempati, and O. Vives, New J. Phys. **6**, 202 (2004); E. Arganda *et al.*, Phys. Rev. **D71**, 035011 (2005); F.R. Joaquim and A. Rossi, Phys. Rev. Lett. **97**, 181801 (2006); J.R. Ellis and O. Lebedev, Phys. Lett. **B653**, 411 (2007).
149. Y. Grossman and H.E. Haber, Phys. Rev. Lett. **78**, 3438 (1997); A. Dedes, H.E. Haber, and J. Rosiek, JHEP **0711**, 059 (2007).
150. M. Hirsch, H.V. Klapdor-Kleingrothaus, and S.G. Kovalenko, Phys. Lett. **B398**, 311 (1997); L.J. Hall, T. Moroi, and H. Murayama, Phys. Lett. **B424**, 305 (1998); K. Choi, K. Hwang, and W.Y. Song, Phys. Rev. Lett. **88**, 141801 (2002); T. Honkavaara, K. Huitu, and S. Roy, Phys. Rev. **D73**, 055011 (2006).
151. For a review and references to the original literature, see M. Chemtob, Prog. Part. Nucl. Phys. **54**, 71 (2005); R. Barbier *et al.*, Phys. Rept. **420**, 1 (2005).
152. H. Dreiner, in *Perspectives on Supersymmetry II*, edited by G.L. Kane (World Scientific, Singapore, 2010) pp. 565–583.
153. B.C. Allanach, A. Dedes, and H.K. Dreiner, Phys. Rev. **D60**, 075014 (1999).
154. L.E. Ibáñez and G.G. Ross, Nucl. Phys. **B368**, 3 (1992); L.E. Ibáñez, Nucl. Phys. **B398**, 301 (1993).
155. For a review, see J.C. Romao, Nucl. Phys. Proc. Suppl. **81**, 231 (2000).
156. R.N. Mohapatra, Phys. Rev. **D34**, 3457 (1986); K.S. Babu and R.N. Mohapatra, Phys. Rev. Lett. **75**, 2276 (1995);

See key on page 405

- M. Hirsch, H.V. Klapdor-Kleingrothaus, and S.G. Kovalenko, Phys. Rev. Lett. **75**, 17 (1995); Phys. Rev. **D53**, 1329 (1996).
157. Y. Grossman and H.E. Haber, Phys. Rev. **D59**, 093008 (1999).
158. S. Dimopoulos and L.J. Hall, Phys. Lett. **B207**, 210 (1988);
J. Kalinowski *et al.*, Phys. Lett. **B406**, 314 (1997);
J. Erler, J.L. Feng, and N. Polonsky, Phys. Rev. Lett. **78**, 3063 (1997).
159. H.K. Dreiner, P. Richardson, and M.H. Seymour, Phys. Rev. **D63**, 055008 (2001).
160. See, *e.g.*, M. Hirsch *et al.*, Phys. Rev. **D62**, 113008 (2000) [erratum: **D65**, 119901 (2002)];
A. Abada, G. Bhattacharyya, and M. Losada, Phys. Rev. **D66**, 071701 (2002);
M.A. Diaz *et al.*, Phys. Rev. **D68**, 013009 (2003);
M. Hirsch and J.W.F. Valle, New J. Phys. **6**, 76 (2004).
161. G.F. Giudice and A. Masiero, Phys. Lett. **B206**, 480 (1988).
162. See, *e.g.*, U. Ellwanger, M. Rausch de Traubenberg, and C.A. Savoy, Nucl. Phys. **B492**, 21 (1997);
U. Ellwanger and C. Hugonie, Eur. J. Phys. **C25**, 297 (2002);;
U. Ellwanger, C. Hugonie and A.M. Teixeira, arXiv:0910.1785, and references contained therein.
163. M. Cvetič *et al.*, Phys. Rev. **D56**, 2861 (1997) [erratum: **D58**, 119905 (1998)].
164. J.R. Espinosa and M. Quiros, Phys. Rev. Lett. **81**, 516 (1998);
P. Batra *et al.*, JHEP **0402**, 043 (2004);
K.S. Babu, I. Gogoladze, and C. Kolda, hep-ph/0410085;
R. Barbieri *et al.*, Phys. Rev. **D75**, 035007 (2007).
165. N. Haba and N. Okada, Prog. Theor. Phys. **114**, 1057 (2006).
166. A. Birkedal, Z. Chacko, and Y. Nomura, Phys. Rev. **D71**, 015006 (2005).
167. J.L. Hewett and T.G. Rizzo, Phys. Reports **183**, 193 (1989).
168. S.F. King, S. Moretti, and R. Nevzorov, Phys. Lett. **B634**, 278 (2006); Phys. Rev. **D73**, 035009 (2006).
169. M. Cvetič and P. Langacker, Mod. Phys. Lett. **A11**, 1247 (1996);
K.R. Dienes, Phys. Reports **287**, 447 (1997).

SUPERSYMMETRY, PART II (EXPERIMENT)

Updated August, 2009 by J.-F. Grivaz (LAL - Orsay).

II.1. Introduction: Low-energy supersymmetry (SUSY) is probably the most extensively studied among the theories beyond the Standard Model (SM). Reasons are its success in solving some of the deficiencies of the SM, such as the stabilization of the Higgs boson mass or gauge coupling unification, while not being in contradiction with the precision electroweak measurements. If unbroken, SUSY would predict the existence of partners of the SM particles, differing by half a unit of spin, but otherwise sharing the same properties. Since no such particles have been observed with the same mass as their SM counterpart, SUSY is a broken symmetry. With an appropriate

choice of SUSY-breaking terms, denoted “soft,” and with superpartner masses at the TeV scale, the good properties of SUSY, such as those mentioned above, however, remain preserved.

SUSY and SM particles are distinguished by a multiplicative quantum number, R -parity, with $R = (-1)^{3(B-L)+2S}$ where B and L are the baryon and lepton numbers, and S is the spin. Therefore, SM particles have $R = 1$ while SUSY particles have $R = -1$. If R -parity is violated, the exchange of SUSY particles may lead to an unacceptably fast proton decay. It is therefore commonly assumed that R -parity is conserved. As a consequence, SUSY particles are produced in pairs, and a SUSY particle decays (possibly via a cascade) into SM particles accompanied by the lightest SUSY particle (LSP) which is stable. Cosmological constraints require that the LSP be neutral and colorless.

The first part of this review, by H.E. Haber, provides details of the theoretical aspects of supersymmetry, of the various SUSY-breaking schemes, and of the structure of the minimal supersymmetric extension of the Standard Model (MSSM), as well as an extensive set of references. The same notations and terminology are used in the following.

As will unfortunately appear in this review, no evidence for SUSY particle production has been found up to now. The search results are therefore presented in terms of production cross-section upper limits or of mass lower limits. In the following, all such limits are given at the 95% confidence level.

II.2. SUSY models: In the MSSM, every degree of freedom of the SM is balanced by a new one differing by half-a-unit of spin. There are, for instance, two scalar-quark weak eigenstates \tilde{q}_L and \tilde{q}_R , associated with the left and right chirality states of a given quark flavor. Two Higgs doublets are, however, needed, in contrast to the minimal Standard Model, in order to give masses to both up-type and down-type quarks, with vacuum expectation values v_2 and v_1 , the ratio of which is denoted $\tan\beta$. The SUSY partner weak eigenstates of the W^\pm and charged Higgs bosons mix to form the two chargino mass eigenstates $\tilde{\chi}_i^\pm$ ($i = 1, 2$). Similarly, there are four neutralinos $\tilde{\chi}_i^0$ ($i = 1, 4$) associated to the B , W^0 , and neutral Higgs bosons. Full details are given in H.E. Haber’s review.

The main phenomenological features of SUSY models arise from the choice of mechanism for SUSY-breaking mediation yielding the structure of the soft SUSY-breaking terms. There are more than one hundred such terms in the MSSM (masses, trilinear couplings, phases), and simplifying assumptions are necessary to bring this number to a more manageable level. Requiring no additional source of flavor-mixing and CP -violation than those present in the Cabibbo-Kobayashi-Maskawa matrix of the SM leaves only the gaugino mass terms M_1 , M_2 , and M_3 associated with the three-gauge groups of the SM, mass terms for the various slepton and squark fields, *e.g.*, $m_{\tilde{t}_R}$, and trilinear Higgs-squark-squark, and Higgs-slepton-slepton couplings such as A_t . The model is then fully specified with the addition of $\tan\beta$, of the supersymmetric Higgs-mixing-mass term μ , and of the mass of the CP -odd Higgs boson m_A .

Searches Particle Listings

Supersymmetric Particle Searches

By far the most widely studied models involve mediation by gravitational forces. In these supergravity models, the gravitino plays essentially no rôle in the phenomenology, unless it is the LSP. This possibility, which has not been addressed by experimental searches at colliders up to now except in terms of future prospects, is not considered in this review. In the minimal model of supergravity (mSUGRA), the number of free parameters is reduced to five: a universal gaugino mass $m_{1/2}$, a universal scalar mass m_0 , and a universal trilinear coupling A_0 , all defined at the scale of grand unification (GUT), $\tan\beta$, and the sign of μ . The low-energy parameters are obtained using the renormalization group equations (RGEs), which in particular fix the absolute value of μ through the requirement of electroweak symmetry-breaking at the appropriate scale. In most of the mSUGRA parameter space, the LSP, required to be neutral and colorless, turns out to be the lightest neutralino, $\tilde{\chi}_1^0$. For appropriate mSUGRA parameter choices and imposing R -parity conservation, this neutralino LSP has the right properties to form the dark matter of the universe. A slightly less constrained model has also been used, primarily at LEP, where μ and m_A are kept free. In such an approach, the mass parameters in the Higgs sector are not related to the universal sfermion mass m_0 , where “sfermion” stands for squark and slepton.

In contrast, the LSP is a very light gravitino \tilde{G} in models with gauge mediated SUSY-breaking (GMSB). The phenomenology depends on the nature of the next-to-lightest SUSY particle (NLSP), typically the lightest neutralino or the lightest stau, and on its lifetime. Another mediation mechanism which has been considered is via the super-conformal anomaly (AMSB, for anomaly mediation SUSY-breaking). In such models, the LSP is a wino \tilde{W}^0 , with a small mass splitting with the lightest chargino, so that the lifetime of that chargino may become phenomenologically relevant, possibly long enough for the chargino to behave like a stable charged particle. More recently, a model called “split SUSY,” which does not aim at solving the hierarchy problem, sets all scalar quark and lepton masses at a very high scale, such as the GUT scale, while keeping the gauginos at the TeV scale. As a result, the gluino, whose decay is mediated by squark exchange, becomes long-lived, which leads to unusual signatures.

II.3. Search strategies: Indirect constraints on SUSY particles can be obtained from cosmological considerations, primarily from the relic dark-matter density [1], from measurements of, or limits on, rare decays, mostly of B mesons [2], from the anomalous magnetic moment of the muon [3], or from precision electroweak observables [4]. These topics are not within the scope of this review. The most significant direct constraints on SUSY particles have been obtained at LEP and at the Tevatron. The large e^+e^- collider, LEP, was in operation at CERN from 1989 to 2000, first at and near the mass of the Z boson, 91.2 GeV, and progressively up to a center-of-mass energy of 209 GeV. Four detectors, ALEPH, DELPHI, L3, and OPAL, each collected a total of about 1 fb^{-1} of data. The Tevatron is

a $p\bar{p}$ collider located at Fermilab. After a first run at a center-of-mass energy of 1.8 TeV, which ended in 1996, and during which the CDF and $D\bar{O}$ detectors collected about 110 pb^{-1} of data each, both the accelerator complex and the detectors were substantially upgraded for Run II, which began in 2001. The center-of-mass energy was raised to 1.96 TeV, and the instantaneous luminosity reached the level of $3.5 \cdot 10^{32} \text{ cm}^{-2} \text{ s}^{-1}$ in the winter of 2009. By June 2009, over 6 fb^{-1} had been accumulated by each experiment.

The “canonical” SUSY scenario is an mSUGRA-inspired MSSM with R -parity conservation and a neutralino LSP. Since such an LSP is stable and weakly interacting, pair production of SUSY particles will lead to missing energy and momentum carried away by the LSPs resulting from the produced SUSY-particle decays. In scenarios other than the canonical one, the expected SUSY signatures may exhibit some additional, or even different features. In GMSB with a neutralino NLSP, for instance, photons are expected in addition to the missing energy carried away by the gravitino LSPs, arising from $\tilde{\chi}_1^0 \rightarrow \gamma\tilde{G}$ decays. But in GMSB again, a stau NLSP might have a lifetime long enough to appear stable in the detector, and therefore not to give rise to missing energy. If R -parity is not conserved, the LSP will decay into SM particles; increased lepton or jet multiplicities are hence expected, but missing energy will arise only from possible final state neutrinos.

In e^+e^- collisions, the missing energy can be directly inferred as $\sqrt{s}-E$, from the center-of-mass energy \sqrt{s} , and from the total energy E of the visible final state products. Similarly, the missing momentum is the opposite of the total momentum of those products. The situation is different in $p\bar{p}$ collisions where the center-of-mass energy of the colliding partons is not known. Only its probability density can be determined, by making use of universal parton distribution functions (PDFs) obtained from fits to a large set of experimental data, most prominently the proton structure functions measured at HERA. Since most of the beam remnants escape undetected in the beam pipe, only conservation of momentum in the plane transverse to the beam direction can be used, and canonical SUSY signals will be searched for in events exhibiting large missing *transverse* energy \cancel{E}_T .

All SUSY particles, except for the gluino, are produced in a democratic way in e^+e^- collisions via electroweak interactions. The search is therefore naturally directed toward the lightest ones, typically the NLSP, and the results are interpreted in a fairly model-independent way. Further specifying the model, various search results can be combined to obtain constraints on the model parameters. In $p\bar{p}$ collisions, the most copiously produced SUSY particles are expected to be the colored ones, namely squarks and gluinos. The pattern of lighter SUSY particles, however, plays a rôle in the interpretation of the search results, as it has an impact on the squark and gluino decay chains. A model, typically mSUGRA, is therefore needed to translate the search results into constraints on physically relevant quantities such as SUSY-particle masses. As will be

discussed later, the searches for squarks and gluinos in the canonical scenario suffer from large backgrounds, which renders competitive the searches for electroweak gauginos, in spite of lower-production cross sections, for parameter configurations such that multileptonic final states arising from the gaugino decays are enhanced. Searches in scenarios other than the canonical one call for specific strategies relying, for instance, on the observation of additional photons or stable particles.

II.4. Searches at LEP in the canonical scenario: At LEP, the production of SUSY particles via electroweak interactions is only suppressed, compared to similar SM processes, by the phase space reduction near the kinematic limit. This suppression is stronger for scalars (sleptons and squarks) than for charginos. In general, for a given process, only data collected at the highest LEP energies are relevant for the ultimate mass limits obtained, but it may happen for some specific processes that the cross section is strongly reduced by mixing effects, *e.g.*, for neutralinos with a small higgsino component, in which case the large integrated luminosity collected at lower energies provides additional sensitivity.

Sleptons: The simplest case is that of smuon pair production, which proceeds only via s -channel Z/γ^* exchange. In models with slepton and gaugino mass unification, the $\tilde{\mu}_R$ is expected to be lighter than the $\tilde{\mu}_L$. The search results are therefore interpreted under this assumption, which is conservative since the $\tilde{\mu}_R$ coupling to the Z is smaller than that of the $\tilde{\mu}_L$. Only one parameter is necessary to calculate the production cross section at the tree level, the smuon mass $m_{\tilde{\mu}_R}$. If the $\tilde{\mu}_R$ is the NLSP, its only decay mode is $\tilde{\mu}_R \rightarrow \mu\tilde{\chi}_1^0$, and its pair production therefore leads to a distinct final state consisting of two acoplanar muons with missing energy. (“Acoplanar” means that the difference in azimuth between the two muons is smaller than 180° , *i.e.*, the two muons are not back-to-back when projected onto a plane perpendicular to the beam axis.) The only significant background comes from $e^+e^- \rightarrow W^+W^- \rightarrow \mu^+\nu\mu^-\bar{\nu}$, which is well under control. The selection efficiency is very high, except when the $\tilde{\mu}_R-\tilde{\chi}_1^0$ mass difference is small, in which case the muons carry little momentum. A second parameter, the LSP mass $m_{\tilde{\chi}_1^0}$ is therefore needed to interpret the search results, as shown in Fig. 1 for the combination of the four LEP experiments [5]. In models with gaugino mass unification, it is expected that the second lightest neutralino $\tilde{\chi}_2^0$ will have a mass roughly twice that of the LSP, in which case the $\tilde{\mu}_R \rightarrow \mu\tilde{\chi}_2^0$ decay can compete with the direct decay into $\mu\tilde{\chi}_1^0$ for small $\tilde{\chi}_1^0$ masses. The impact of this effective efficiency reduction at low $\tilde{\chi}_1^0$ mass values can be seen in Fig. 1, for $\mu = -200$ GeV and $\tan\beta = 1.5$. Altogether, smuon masses below 95 to 99 GeV, depending on the $\tilde{\chi}_1^0$ mass, are excluded as long as the $\tilde{\mu}_R-\tilde{\chi}_1^0$ mass difference is larger than 5 GeV.

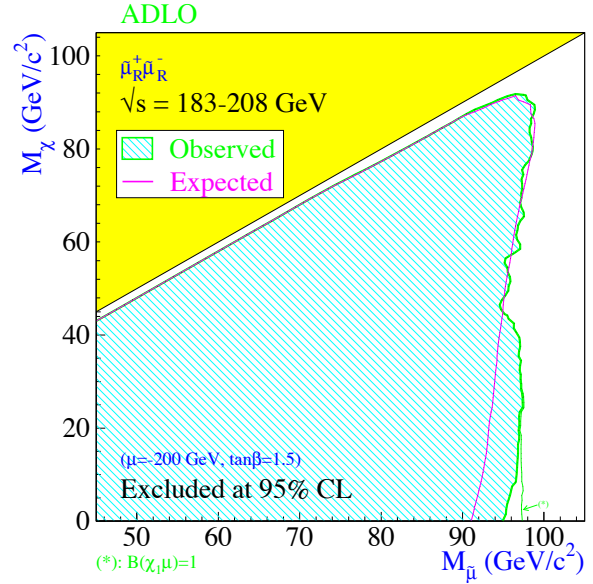


Figure 1: Region in the $(m_{\tilde{\mu}_R}, m_{\tilde{\chi}_1^0})$ plane excluded by the searches for smuons at LEP. Color version at end of book.

The case of staus is similar, except for the fact that the final taus further decay, and that the ultimate decay products are softer than the muons in the smuon case. The selection efficiency is therefore lower. An additional complication comes from the L - R mixing, which is expected to be non-negligible for large values of $\tan\beta$, and can reduce the coupling of the lightest stau to the Z . In the worst case where the stau does not couple to the Z , stau masses smaller than 86 to 95 GeV are excluded, depending on $m_{\tilde{\chi}_1^0}$, as long as the stau- $\tilde{\chi}_1^0$ mass difference is larger than 7 GeV [5].

For selectrons as for smuons, L - R mixing is expected to be negligible. But pair production receives an additional contribution from t -channel neutralino exchange, which tends to increase the production cross section. For $\mu = -200$ GeV and $\tan\beta = 1.5$, the \tilde{e}_R mass lower limit is 100 GeV for $m_{\tilde{\chi}_1^0} < 85$ GeV [5]. Furthermore, the t -channel exchange allows for associated $\tilde{e}_L\tilde{e}_R$ production. Assuming slepton and gaugino mass unification at the GUT scale, the \tilde{e}_L and \tilde{e}_R masses are related, with the former heavier by a few GeV. Associated production gives the viable signal of a single energetic electron in the case where the $\tilde{e}_R-\tilde{\chi}_1^0$ mass difference is too small to observe \tilde{e}_R pair production. This allows a lower limit of 73 GeV to be set on $m_{\tilde{e}_R}$, independent of the $\tilde{\chi}_1^0$ mass [6].

Indirect limits on the sneutrino mass can be derived from the slepton mass limits if slepton and gaugino mass unification is assumed. More generally, a $\tilde{\nu}$ LSP or NLSP mass limit of 45 GeV can be deduced from the measurement of the invisible Z width [7], for three mass degenerate sneutrinos.

Charginos and neutralinos: The masses and field content in the chargino sector depend on only three parameters: M_2 ,

Searches Particle Listings

Supersymmetric Particle Searches

μ and $\tan\beta$. The masses and field content in the neutralino sector depend on those same parameters, and, in addition, on M_1 . The latter is, however, related to M_2 assuming gaugino mass unification: $M_1 = (5/3)\tan^2\theta_W M_2 \sim 0.5M_2$. This assumption is made for the results presented below, unless explicitly specified. Traditionally, three regions are distinguished: “gaugino” if $M_2 \ll |\mu|$, “higgsino” if $|\mu| \ll M_2$, and mixed if M_2 and $|\mu|$ have similar values. In the gaugino region, the lighter chargino and second lightest neutralino masses are close to M_2 , the mass of the lightest neutralino is close to M_1 , while the heavier chargino and neutralinos all have masses close to $|\mu|$; this is the typical configuration encountered in mSUGRA. In the higgsino region, the lighter chargino and two lightest neutralino masses are close to $|\mu|$, so that the mass-splitting between the lightest chargino and neutralino tends to be small. In the following, “chargino” will stand for “lighter chargino.”

Chargino pair production proceeds via s -channel Z/γ^* and t -channel $\tilde{\nu}_e$ exchanges, with destructive interference. For chargino masses accessible at LEP energies, the decays are mediated by virtual W ($\tilde{\chi}^\pm \rightarrow W^{*\pm}\tilde{\chi}_1^0 \rightarrow f\bar{f}'\tilde{\chi}_1^0$) and sfermion ($\tilde{\chi}^\pm \rightarrow \tilde{f}^*\tilde{f}' \rightarrow f\bar{f}'\tilde{\chi}_1^0$) exchange. Two-body decays such as $\tilde{\chi}^\pm \rightarrow \ell^\pm\tilde{\nu}$ are occasionally kinematically allowed, in which case they are dominant. Similarly, neutralino pair or associated production proceeds via s -channel Z and t -channel \tilde{e} exchange, and $\tilde{\chi}_2^0$ decays are mediated by virtual Z and sfermion exchange. Here also, two-body decays such as $\tilde{\chi}_2^0 \rightarrow \nu\tilde{\nu}$ may have to be considered.

First, the case of heavy sfermions is addressed. Only s -channel exchange contributes to gaugino production, and the decays proceed via gauge boson exchange. For chargino pair production, the final states are therefore the same as those arising from W pairs, but for the addition of two LSPs. Selections have been designed for all-hadronic ($q\bar{q}'q\bar{q}'\tilde{\chi}_1^0\tilde{\chi}_1^0$), mixed ($q\bar{q}'\ell\nu\tilde{\chi}_1^0\tilde{\chi}_1^0$), and fully leptonic ($\ell\nu\ell\nu\tilde{\chi}_1^0\tilde{\chi}_1^0$) topologies. No excess over SM backgrounds, of which the largest comes from W -pair production, was observed. A scan over M_2 , μ , and $\tan\beta$ provided a robust chargino mass lower limit of 103 GeV for sneutrino masses larger than 200 GeV [8], except for very large values of M_2 ($\gtrsim 1$ TeV), in the so-called “deep higgsino” region, where the $\tilde{\chi}^\pm - \tilde{\chi}_1^0$ mass splitting is very small.

This limit is degraded for lower sneutrino masses for two reasons. First, the production cross section is reduced by the negative interference between the s - and t -channel exchanges. Second, two-body decays open up, which may reduce the selection efficiency. This is the case in particular in the so-called “corridor” where $m_{\tilde{\chi}^\pm} - m_{\tilde{\nu}}$ is smaller than a few GeV, so that the lepton from the $\tilde{\chi}^\pm \rightarrow \ell\tilde{\nu}$ decay is hardly visible. Neutralino-associated production ($e^+e^- \rightarrow \tilde{\chi}_1^0\tilde{\chi}_2^0$), for which the interference tends to be positive, can be used to mitigate those effects, and searches for acoplanar jets or leptons from $\tilde{\chi}_2^0 \rightarrow f\bar{f}\tilde{\chi}_1^0$ were devised, which did not reveal any excess over SM backgrounds. Chargino and neutralino production and decays now depend, however, on the detailed sfermion spectrum. To interpret the search results, squark and slepton

mass unification is therefore also assumed, so that the relevant phenomenology can be described with the addition of the single m_0 parameter. At this point, the results of neutralino searches can be combined with those for charginos into exclusion domains in the (M_2, μ) plane for selected values of $\tan\beta$ and m_0 .

The searches for neutralinos, however, lose their sensitivity when the two-body decay $\tilde{\chi}_2^0 \rightarrow \nu\tilde{\nu}$ opens up, which leads to an invisible final state. Slepton mass lower limits can provide useful constraints in that configuration. The reason is that the slepton and gaugino masses are related by the RGEs as $m_{\tilde{\ell}_R}^2 \simeq m_0^2 + 0.22M_2^2 - \sin^2\theta_W m_Z^2 \cos 2\beta$. For given values of $\tan\beta$ and m_0 , a lower limit on $m_{\tilde{\ell}_R}$ can therefore be translated into a lower limit on M_2 . In the end, the chargino-mass lower limit obtained in the simple case of heavy sfermions is only moderately degraded.

As indicated above, the chargino searches lose their sensitivity in the deep-higgsino region, because of too small a $\tilde{\chi}^\pm - \tilde{\chi}_1^0$ mass difference. In the most extreme case, the chargino becomes long-lived. Dedicated searches for charged massive stable particles were designed, which take advantage of the higher ionization of such particles. In less extreme cases, the soft final state products resemble those resulting from “two-photon” interactions. In such interactions, the beam electrons radiate quasi-real photons whose collision produces a low-mass system, while the incoming electrons escape undetected in the beam pipe. Chargino pair production can however be disentangled from that background when “tagged” by an energetic photon from initial state radiation ($e^+e^- \rightarrow \gamma\tilde{\chi}^+\tilde{\chi}^-$).

These various techniques allowed charginos with masses smaller than 92 GeV to be excluded in the canonical scenario with gaugino and sfermion mass unification [9].

The lightest neutralino: If the gaugino mass unification assumption is not made, there is no general mass limit from e^+e^- collisions for the lightest neutralino. A very light photino-like neutralino decouples from the Z , so that it cannot be pair produced via s -channel Z exchange, and production via t -channel selectron exchange can be rendered negligible for sufficiently heavy selectrons. The $e^+e^- \rightarrow \tilde{\chi}_1^0\tilde{\chi}_1^0\gamma$ channel provides a detectable final state that could be used in principle to infer constraints on the $\tilde{\chi}_1^0$ mass and couplings. However, it turns out that there is no sensitivity because of the overwhelming background from $e^+e^- \rightarrow \nu\bar{\nu}\gamma$.

With the assumption of gaugino mass unification, on the other hand, indirect mass limits can be derived, mostly from chargino pair production. In the case of heavy sfermions, the limit is 52 GeV at large $\tan\beta$, somewhat lower otherwise. If sfermions are allowed to be light, sfermion mass unification is used, and the limit at large $\tan\beta$ becomes 47 GeV. It is set by slepton searches in the corridor.

Higgs boson searches at LEP provide additional constraints at low $\tan\beta$. The analysis is rather involved, but can be summarized (and simplified) as follows. The mass of the lightest Higgs boson in the MSSM receives radiative corrections due to

the splitting between the top and stop masses. The stop mass depends on m_0 and M_3 , the latter being related by unification to M_2 . For given values of m_0 and $\tan\beta$, the mass lower limit on the Higgs boson translates into a lower limit on M_3 , hence on M_2 . These constraints are most effective at low m_0 and $\tan\beta$, where those from chargino searches are weakest.

The combination of chargino, slepton and Higgs boson searches provides the lower limit on $m_{\tilde{\chi}_1^0}$ as a function of $\tan\beta$ displayed in Fig. 2 [10]. The “absolute” lower limit is 47 GeV, obtained at large $\tan\beta$. In the more constrained mSUGRA scenario, where in particular μ is no longer a free parameter, a slightly tighter limit of 50 GeV is derived [11].

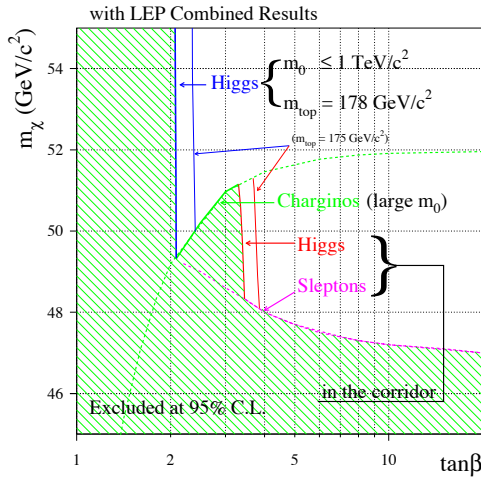


Figure 2: Lower mass limit for the lightest neutralino as a function of $\tan\beta$, inferred in the conventional scenario (with $M_1 \sim 0.5M_2$) from searches at LEP for charginos, sleptons, and neutral Higgs bosons.

Squarks: As will be seen later, the mass reach for squarks at the Tevatron extends well beyond the masses accessible at LEP. There are, however, configurations for which the Tevatron searches are not efficient, and for which useful information is still provided by LEP. This is particularly relevant in the stop sector because the lighter of the two mass eigenstates (hereafter simply denoted “stop” or \tilde{t}) may be substantially less massive than all other squarks. One reason is that, if squark masses are unified at the GUT scale, $m_{\tilde{t}_R}$ is driven at the electroweak scale to lower values than the other squark mass terms by the large top Yukawa coupling. Another reason is that the off-diagonal terms of the stop squared-mass matrix, which are proportional to m_t , are much larger than for the other squark species and enlarge the mass splitting.

At LEP energies, given the chargino mass limit which effectively forbids $\tilde{t} \rightarrow b\tilde{\chi}^+$, and as long as $m_{\tilde{t}} < m_W + m_b + m_{\tilde{\chi}_1^0}$, the main stop decay mode is expected to be $\tilde{t} \rightarrow c\tilde{\chi}_1^0$, which proceeds via flavor-changing loops. The stop lifetime may therefore be

long enough to compete with the hadronization time, a feature which has been included in the simulation programs. The final state arising from stop pair production followed by $\tilde{t} \rightarrow c\tilde{\chi}_1^0$ is a pair of acoplanar jets with missing energy. The mass limit obtained depends slightly on the amount of L - R mixing. In the worst case where the stop does not couple to the Z , stop masses from 96 to 99 GeV, depending on the $\tilde{\chi}_1^0$ mass, are excluded as long as $m_{\tilde{t}} - m_{\tilde{\chi}_1^0} - m_c > 5$ GeV [12]. Dedicated searches were performed in addition to cope with smaller mass differences. In particular, the creation of long-lived R -hadrons in the stop hadronization process was taken into account, as well as the specific interactions of those R -hadrons in the detector material. (R -hadrons are color-neutral exotic bound states, *e.g.*, formed from a squark and an antiquark.) In the end, a mass lower limit of 63 GeV was set for the top squark, irrespective of $m_{\tilde{t}} - m_{\tilde{\chi}_1^0}$ [13].

It has been pointed out that, for specific choices of parameters, the four-body decay mode $\tilde{t} \rightarrow bff'\tilde{\chi}_1^0$ could compete with $\tilde{t} \rightarrow c\tilde{\chi}_1^0$ [14]. A set of selections was designed to address this possibility, and the 63 GeV mass limit was found to hold, independent of the proportions of four-body and two-body decay modes [13]. Finally, if sneutrinos are sufficiently light for the $\tilde{t} \rightarrow b\tilde{\nu}$ three-body decay mode to be kinematically allowed, in which case it will be dominant, a stop mass lower limit of 96 GeV was obtained for sneutrino masses smaller than 86 GeV [12].

The lightest sbottom mass eigenstate, \tilde{b} , could also be light for large values of $\tan\beta$, which enhance the off-diagonal terms of the sbottom squared-mass matrix. The situation is simpler than for the stop, because the $\tilde{b} \rightarrow b\tilde{\chi}_1^0$ tree-level decay mode is expected to be dominant. Searches for acoplanar b -flavored jets were performed, leading to mass lower limits of about 95 GeV for a vanishing coupling of the sbottom to the Z [12].

II.5. Searches at LEP in non-canonical scenarios:

SUSY scenarios beyond the canonical one were also extensively studied at LEP.

GMSB: The phenomenology of GMSB, with an ultra-light gravitino LSP, depends essentially on the nature of the NLSP and on its lifetime.

In the case of a neutralino NLSP, the $\tilde{\chi}_1^0 \rightarrow \gamma\tilde{G}$ decay mode is expected to be dominant in the mass range accessible at LEP. The production of a pair of $\tilde{\chi}_1^0$ with short lifetime would therefore lead to acoplanar photons with missing energy. No excess was observed above the background from $e^+e^- \rightarrow (Z^*) \rightarrow \nu\bar{\nu}\gamma\gamma$ [15]. In typical GMSB models, the neutralino NLSP is bino-like. Pair production is thus mediated by t -channel selectron exchange. An exclusion domain in the $(m_{\tilde{e}_R}, m_{\tilde{\chi}_1^0})$ plane was therefore derived. The highest $\tilde{\chi}_1^0$ mass excluded is 102 GeV for light selectrons, and the interpretation of an anomalous $ee\gamma\gamma + \cancel{E}_T$ event observed by CDF in Run I of the Tevatron [16] in terms of pair production of selectrons with $\tilde{e} \rightarrow e\tilde{\chi}_1^0 \rightarrow e\gamma\tilde{G}$ is excluded. For non-prompt decays, searches for photons which do not point back to the primary vertex were

Searches Particle Listings

Supersymmetric Particle Searches

performed, while long neutralino lifetimes lead to a phenomenology similar to that of the canonical scenario. Combinations of the results of these and a number of other searches in various topologies expected within a minimal GMSB framework were performed, leading to an absolute neutralino NLSP mass limit of 54 GeV [17].

The other generic NLSP candidate in GMSB is a scalar tau, for some parameter configurations almost mass-degenerate with \tilde{e}_R and $\tilde{\mu}_R$. A stau NLSP decays according to $\tilde{\tau} \rightarrow \tau \tilde{G}$. For prompt decays, this is similar to a stau NLSP with a light $\tilde{\chi}_1^0$ in the canonical scenario. For long lifetimes, the stau will appear as a highly ionizing charged particle, for which searches have been designed as discussed for charginos in the deep-higgsino region. For intermediate lifetimes, dedicated selections for in-flight decays along charged particle tracks were devised. A combination of all these searches excluded a stau NLSP with mass below 87 GeV, irrespective of its lifetime [18].

AMSB: With a wino LSP, the mass difference between the chargino and the LSP is expected to be small, leading to topologies identical to those encountered in the deep higgsino region of the canonical scenario. The chargino mass lower limit of 92 GeV [9] also holds in the AMSB framework for large sfermion masses.

A gluino LSP: The possibility that the LSP be a light gluino has also been considered. Gluinos cannot be produced directly by e^+e^- annihilation, but they could be produced by gluon splitting, for instance in $e^+e^- \rightarrow Z \rightarrow q\bar{q}g^* \rightarrow q\bar{q}\tilde{g}\tilde{g}$, or in the decays of pair-produced squarks. Such gluinos would then hadronize into long-lived R -hadrons. Dedicated searches were performed [19], leading to the exclusion of a gluino LSP with mass smaller than 27 GeV.

R -parity violation: If R -parity is allowed to be violated, new terms appear in the superpotential that do not conserve the lepton or baryon number: $\lambda_{ijk}\hat{L}_i\hat{L}_j\hat{E}_k^c$, $\lambda'_{ijk}\hat{L}_i\hat{Q}_j\hat{D}_k^c$, $\lambda''_{ijk}\hat{U}_i^c\hat{D}_j^c\hat{D}_k^c$, where \hat{L} and \hat{Q} are lepton- and quark-doublet superfields, \hat{E}^c , \hat{D}^c and \hat{U}^c are lepton and quark singlet superfields, and i, j , and k are generation indices. These terms induce new couplings such that the LSP can decay to SM particles. For instance, a neutralino LSP could decay according to $\tilde{\chi}_1^0 \rightarrow e\mu\nu$ via a λ type coupling. With a λ'' coupling, a $\tilde{\chi}_1^0$ decay would lead to three hadronic jets. Since the simultaneous presence of different coupling types is strongly constrained, for instance by the lower limit on the proton lifetime, the assumption was made that only one of the R -parity-violating couplings is non-vanishing. It was also assumed that this coupling is sufficiently large for the R -parity-violating decays to take place close to the e^+e^- collision point ($< \sim 1$ cm) so that lifetime issues can be ignored.

Even with these simplifying assumptions, the number of possible final states arising from SUSY particle pair production is considerable. Nevertheless, all were considered at LEP, ranging from four leptons with missing energy for a λ coupling and $\tilde{\chi}_1^0$ pair production, now a process leaving a visible signature, to ten jets for a λ'' coupling and chargino pair production with

$\tilde{\chi}^\pm \rightarrow q\bar{q}\tilde{\chi}_1^0$. In the end, limits at least as constraining as in the canonical scenario were obtained [20].

Single production of a SUSY particle may also take place when R -parity is violated, with a production cross section now depending on the value of the λ coupling involved. The possibility of single, possibly resonant sneutrino production was investigated [21], and, in the absence of any signal, sneutrino mass lower limits extending almost to the full center-of-mass energy were established for sufficiently large values of the coupling.

II.6. Searches at HERA: The HERA $e^\pm p$ collider at DESY terminated its operation at the end of June 2007, after having delivered an integrated luminosity of ~ 0.5 fb $^{-1}$ at a center-of-mass energy of 320 GeV to each of the H1 and ZEUS experiments. Since ep collisions do not involve annihilation processes, only R -parity-violating resonant production of squarks could be investigated with good sensitivity. The production proceeds via a λ'_{j1} or λ'_{11k} coupling, with a cross section depending on the value of the R -parity-violating coupling involved. The produced squark can decay either directly with R -parity violation, or indirectly via a cascade leading to the LSP which in turn decays to SM particles (two jets and a neutrino or a charged lepton). Selections for these various topologies were combined to lead, within some mild model assumptions, to squark mass lower limits as high as 275 GeV for a λ' coupling of electromagnetic strength, *i.e.*, equal to 0.3 [22]. These results should be improved once the full HERA integrated luminosity is analyzed.

II.7. Searches at the Tevatron: Because of the much higher center-of-mass energy, the mass reach of the Tevatron for SUSY particles is expected to largely exceed the one achieved at LEP. In $p\bar{p}$ collisions, however, the effective parton-parton center-of-mass energy $\sqrt{\hat{s}}$ is only a fraction $\sqrt{x_1x_2}$ of the total center-of-mass energy \sqrt{s} , where x_1 and x_2 are the fractions of the p and \bar{p} momenta carried by the colliding partons. Because of the rapid decrease of the PDFs as a function of x , probing high $\sqrt{\hat{s}}$ values implies accumulating correspondingly large integrated luminosities.

Compared to the situation at LEP, the searches for SUSY in $p\bar{p}$ collisions are further complicated by the huge disparity between the cross sections of the processes of interest, currently of order 0.1 pb, and those of the SM backgrounds, *e.g.*, ~ 80 mb for the total inelastic cross section. Even for final states involving leptons, one has to cope with the $W \rightarrow \ell\nu$ and $Z \rightarrow \ell\ell$ backgrounds, with cross sections as large as ~ 2.6 nb and ~ 240 pb, respectively, per lepton flavor.

In the following, all results presented were obtained during Run II of the Tevatron collider, as they supersede those from Run I due to the higher center-of-mass energy and to integrated luminosities recorded already a factor fifty larger.

Squarks and gluinos: Colored SUSY particles are expected to be the most copiously produced in $p\bar{p}$ collisions. If $m_{\tilde{q}} \ll m_{\tilde{g}}$, $\tilde{q}\tilde{q}$ and, to a lesser extent, $\tilde{q}\tilde{q}$ pair productions are the dominant processes, and the search is performed in the $\tilde{q} \rightarrow q\tilde{\chi}_1^0$ decay

channel, which leads to a final state consisting of a pair of acoplanar jets. If $m_{\tilde{g}} \ll m_{\tilde{q}}$, gluino pair production dominates, and the decay channel considered is $\tilde{g} \rightarrow \tilde{q}^* \tilde{q} \rightarrow q\bar{q}\tilde{\chi}_1^0$, leading to a four-jet final state with \cancel{E}_T . Finally, if squark and gluino masses are similar, three-jet final states are expected to arise from $\tilde{q}\tilde{g}$ associated production. Soft jets from initial and final state radiation may increase these jet multiplicities. Cascade decays such as $\tilde{q} \rightarrow \tilde{\chi}^\pm q' \rightarrow \ell\nu q'\tilde{\chi}_1^0$, however, complicate the picture, and a specific model has to be used to assess their impact: both CDF and DØ revert to the mSUGRA framework to interpret their search results, in which case the ten SUSY partners of the five light quark flavors can be considered mass-degenerate for practical purposes.

Backgrounds to squark and gluino production arise from two types of sources: those with real \cancel{E}_T , such as $(W \rightarrow \ell\nu)+\text{jets}$, and those with fake \cancel{E}_T from jet-energy mismeasurements in standard multijet events produced by strong interaction. In the following, these backgrounds are denoted SM and QCD, respectively. Selection criteria were designed for each of the three relative mass configurations listed above, with at least two, at least three, and at least four energetic jets, and with large \cancel{E}_T . Backgrounds of the SM type are largely suppressed by vetoes on isolated leptons, except for $(Z \rightarrow \nu\nu)+\text{jets}$, which is irreducible, and the remaining contribution is determined from Monte Carlo simulations. In the QCD background, the distribution of missing transverse energy from jet mismeasurements peaks strongly at low values but, because of the huge multijet production cross section, significant contributions remain even at large \cancel{E}_T . A substantial reduction is obtained, however, by requiring that the \cancel{E}_T direction point away from the jets. While CDF estimates the remaining contribution from Monte Carlo simulations calibrated on control samples, DØ applies tighter selection criteria so that the QCD background is brought to a negligible level.

In the end, no excess was observed above expected backgrounds in the various selections, which translates into excluded domains in the $(m_{\tilde{g}}, m_{\tilde{q}})$ plane. Taking into account the large theoretical uncertainties on the signal production cross sections arising from the choice of PDFs, and of renormalization and factorization scales, lower limits of 379 and 308 GeV were published by DØ [23] for the squark and gluino masses, respectively, based on an integrated luminosity of 2.1 fb^{-1} . Along the $m_{\tilde{g}} = m_{\tilde{q}}$ line, the limit is 390 GeV. These results, derived for $\tan\beta = 3$, $A_0 = 0$, and $\mu < 0$, are valid for a large class of parameter sets at low $\tan\beta$. Similar results were obtained by the CDF collaboration, based on an integrated luminosity of 2.0 fb^{-1} [24], as shown in Fig. 3. Within the mSUGRA framework, these limits can be compared with those from slepton and chargino searches in e^+e^- collisions, as shown for CDF in Fig. 3 and for DØ in Fig. 4. The domain in the parameter space excluded at LEP is extended for simultaneously low values of m_0 and $m_{1/2}$.

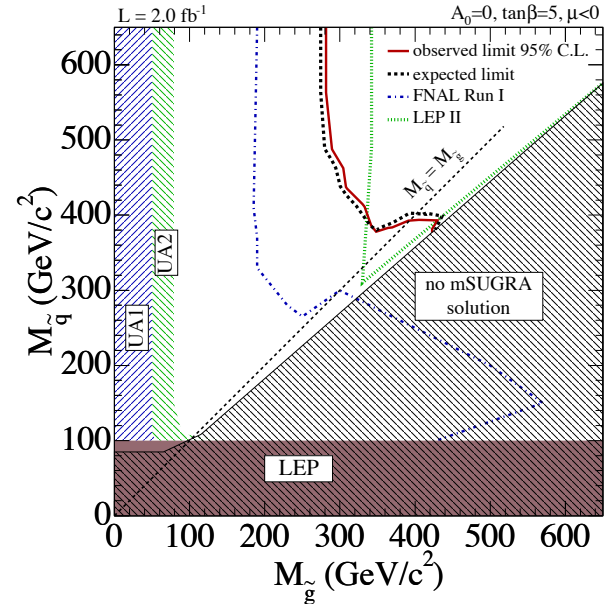


Figure 3: Region in the $(m_{\tilde{g}}, m_{\tilde{q}})$ plane excluded by CDF Run II and by earlier experiments. Color version at end of book.

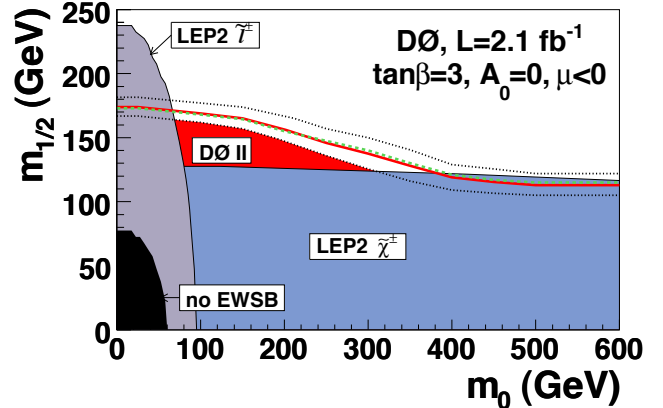


Figure 4: Region in the $(m_0, m_{1/2})$ plane excluded by the search for squarks and gluinos by DØ and by the searches for sleptons and charginos by the LEP experiments. The band at the edge of the excluded region represents the uncertainty associated with the scale and PDF choice, with the red curve corresponding to the nominal choice.

For larger values of $\tan\beta$, mass hierarchies such as $m_{\tilde{q}_L} > m_{\tilde{e}} \sim m_{\tilde{\mu}} > m_{\tilde{\chi}^\pm} > m_{\tilde{\tau}}$ are not uncommon, for which squark pair production leads to final states involving jets, τ s, and \cancel{E}_T . A dedicated search for these topologies was performed by DØ [25], which provides additional sensitivity for squark searches at larger values of $\tan\beta$.

Stop and sbottom: As explained earlier, a stop mass eigenstate could be much lighter than the other squarks. Dedicated searches were therefore performed by both CDF [26] and DØ [27] for stop pair production followed by $\tilde{t} \rightarrow c\tilde{\chi}_1^0$ decays. The final

Searches Particle Listings

Supersymmetric Particle Searches

state is a pair of acoplanar charm jets with \cancel{E}_T . Compared to the previous case of generic squarks, the cross section is much smaller because only one squark specie is produced. The mass range probed is, therefore, accordingly smaller. Consequently, the jets are softer and there is less \cancel{E}_T . A lifetime-based heavy-flavor tagging is used in the selection to mitigate the corresponding loss of sensitivity. The CDF analysis, based on an integrated luminosity of 2.6 fb^{-1} , excludes $m_{\tilde{t}} < 180 \text{ GeV}$ for $m_{\tilde{\chi}_1^0} = 95 \text{ GeV}$, as shown in Fig. 5. These stop searches at the Tevatron lose their sensitivity when the $\tilde{t}-\tilde{\chi}_1^0$ mass difference becomes smaller than $\sim 40 \text{ GeV}$, because of the \cancel{E}_T requirement applied to reduce the otherwise overwhelming QCD background, so that the LEP constraints remain relevant, although restricted to $m_{\tilde{t}} < 100 \text{ GeV}$.

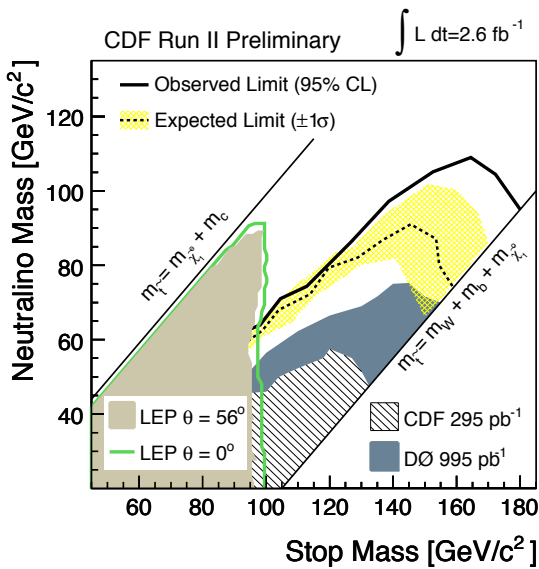


Figure 5: Region in the $(m_{\tilde{t}}, m_{\tilde{\chi}_1^0})$ plane excluded by CDF and by earlier experiments.

Similar searches were performed for sbottom pair production [28,29], with $\tilde{b} \rightarrow b\tilde{\chi}_1^0$. The sensitivity extends to higher masses than in the stop case because heavy-flavor tagging is more efficient for b than for c jets. The lower \tilde{b} mass limit set by DØ reaches 240 GeV for $m_{\tilde{\chi}_1^0} < 80 \text{ GeV}$, based on an integrated luminosity of 4.0 fb^{-1} . The CDF collaboration investigated the configuration where gluinos are lighter than all squark species except for the sbottom, thus decaying according to $\tilde{g} \rightarrow b\tilde{b}$, followed by $\tilde{b} \rightarrow b\tilde{\chi}_1^0$. The final state consists of four b jets with \cancel{E}_T . Gluino and sbottom mass lower limits reaching 350 and 325 GeV , respectively, were obtained for $m_{\tilde{\chi}_1^0} = 60 \text{ GeV}$, based on an integrated luminosity of 2.5 fb^{-1} [30].

Searches for stop pair production followed by $\tilde{t} \rightarrow b\ell\tilde{\nu}$ decays were also performed by CDF [31] and DØ [32], based on up to 3.1 fb^{-1} , to address the parameter configurations leading to light sneutrinos. Final states with two leptons, b jets and \cancel{E}_T were investigated. The largest stop mass excluded is 200 GeV for sneutrino masses up to 110 GeV [32]. The CDF collaboration also considered the possibility of a $\tilde{t} \rightarrow b\tilde{\chi}^+$ decay,

analyzing the same final-state topology, and derived limits in the $(m_{\tilde{t}}, m_{\tilde{\chi}_1^0})$ plane for various chargino masses and various branching fractions for the $\tilde{\chi}^+ \rightarrow \ell\nu\tilde{\chi}_1^0$ decay [33].

Finally, the possibility of a stop stable on the scale of the time needed to escape the detector was considered by the CDF collaboration [34]. The resulting R -hadron would behave as a slow-moving muon, and can be discriminated from the real muon background by comparing its momentum and its velocity, using a time-of-flight measurement. A mass lower limit of 250 GeV was obtained, based on an integrated luminosity of 1 fb^{-1} .

Charginos and neutralinos: Associated chargino-neutralino production, $p\bar{p} \rightarrow \tilde{\chi}^\pm\tilde{\chi}_2^0$, proceeds via s -channel W and t -channel squark exchange, with destructive interference. This process could provide a distinct trilepton+ \cancel{E}_T signal at the Tevatron if the branching ratios for leptonic decays ($\tilde{\chi}^\pm \rightarrow \ell^\pm\nu\tilde{\chi}_1^0$ and $\tilde{\chi}_2^0 \rightarrow \ell^+\ell^-\tilde{\chi}_1^0$) are sufficiently large. Since these decays are mediated by virtual vector boson or sfermion exchange, this condition will be satisfied if sleptons are sufficiently light. The search is nevertheless challenging because the final-state leptons carry little energy, and the production cross section is only a fraction of a picobarn.

In order to reduce the impact of lepton identification inefficiencies, and also to retain some sensitivity for final states involving τ s, only two leptons were required to be positively identified as electrons or muons, while for the third lepton only an isolated charged-track requirement was imposed. Series of analysis criteria involving requirements on the lepton and third-track isolation, on the amount of \cancel{E}_T , and on the absence of energetic jets were applied. The ultimate background arises from associated WZ production.

No significant excess over SM background expectation was observed by DØ [35] or CDF [36], based on 2.3 fb^{-1} and 3.2 fb^{-1} , respectively. These results were interpreted within the mSUGRA framework, with $\tan\beta = 3$, $A_0 = 0$, and $\mu > 0$, as shown in Fig. 6. The domain excluded at LEP is substantially extended. As an example, a chargino mass limit of 164 GeV is obtained for $m_0 = 60 \text{ GeV}$ [36]. The dependence of the exclusion range on $\tan\beta$ is discussed in [35]: for a chargino mass of 130 GeV , the exclusion holds for $\tan\beta \lesssim 10$. The gap in the exclusion domain visible in Fig. 6 is due to configurations where the $\tilde{\chi}_2^0 - \tilde{\ell}$ mass difference is very small, so that one of the final-state leptons cannot be detected. Searches for same sign lepton pairs can, however, be used in this configuration, as was shown in earlier DØ analyses [37]. The CDF collaboration also considered the same sign dilepton signature [38].

R -parity violation: A whole new phenomenology opens up if R -parity is not assumed to be conserved. The searches can be divided into two classes.

First, R -parity-conserving pair production of SUSY particles has been considered, with R -parity violation appearing only in the LSP decay at the end of the decay chains. The case of gaugino pair production, with a lepton-number-violating

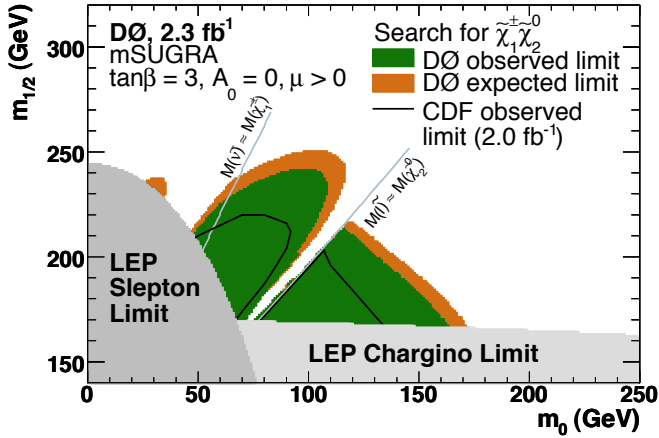


Figure 6: Regions in the $(m_0, m_{1/2})$ plane excluded by the $D\bar{O}$ search for trileptons and by the LEP experiments. Color version at end of book.

coupling of the λ type in the neutralino LSP decay, has been extensively studied. Four charged leptons are expected in the final state, with flavors depending on the generation indices in the λ_{ijk} coupling, and there is also some \cancel{E}_T from the two neutrinos. Searches have been performed by CDF [39] and $D\bar{O}$ [40] in the cases of λ_{121} and λ_{122} couplings, and by $D\bar{O}$ in the case of a λ_{133} coupling for which τ s appear in the final state. The chargino mass lower limits obtained by $D\bar{O}$ in the mSUGRA framework with $m_0 = 1$ TeV, $\tan\beta = 5$, and $\mu > 0$ are 231, 229, and 166 GeV for the λ_{121} , λ_{122} , and λ_{133} couplings, respectively, based on 360 pb^{-1} .

The CDF collaboration also searched for stop pair production, with $\tilde{t} \rightarrow b\tau$ decays mediated by a λ'_{333} coupling [41]. No such signal was observed in the topology where one τ decays into an electron or a muon and the other into hadrons, and a stop mass lower limit of 151 GeV was derived, based on 322 pb^{-1} .

The $D\bar{O}$ collaboration investigated the case of pair production of a neutralino LSP with a mass of a few GeV, followed by $\tilde{\chi}_1^0 \rightarrow \mu^+ \mu^- \nu$ decays via a λ_{i22} coupling [42]. The values of the coupling considered were such that the $\tilde{\chi}_1^0$ is long-lived, and the search was therefore directed toward dimuon vertices displaced from the main-interaction vertex. This search was motivated by anomalous dimuon events observed by the NuTeV collaboration in a neutrino experiment [43]. With no signal observed by $D\bar{O}$, such an explanation for those events has been ruled out.

Second, resonant slepton production could occur via a λ'_{i11} R -parity-violating coupling. The case of a λ'_{211} coupling was considered by $D\bar{O}$ [44], with R -parity-conserving decays of the resonantly produced slepton ($\tilde{\mu} \rightarrow \tilde{\chi}_i^0 \mu$ and $\tilde{\nu}_\mu \rightarrow \tilde{\chi}^\pm \mu$). The violation of R -parity is again manifest in the decay of the neutralino LSP into a muon or a neutrino + two jets. No excess

over background was observed, and an exclusion domain was placed in the $(m_{\tilde{\mu}}, \lambda'_{211})$ plane, the production cross section now depending on the value of λ'_{211} . For $\lambda'_{211} = 0.1$, a smuon mass lower limit of 363 GeV is obtained in mSUGRA with $\tan\beta = 5$, $A_0 = 0$ and $\mu < 0$, based on 380 pb^{-1} .

Resonant sneutrino production was also investigated in the case where the sneutrino decays via a λ type coupling, hence different from the coupling involved in the production. The decay channels considered were ee , $\mu\mu$, $\tau\tau$ and $e\mu$. Sneutrino mass limits were derived, dependent on the product of the λ' and λ couplings considered [45].

Other non-canonical scenarios: As discussed earlier, a neutralino or stau NLSP is expected in GMSB. SUSY-particle pair production, with cascade decays to a $\tilde{\chi}_1^0$ NLSP followed by $\tilde{\chi}_1^0 \rightarrow \gamma\tilde{G}$, has been investigated by both CDF [46] and $D\bar{O}$ [47] through inclusive searches for diphoton final states with large \cancel{E}_T . Backgrounds from photon misidentification or from fake \cancel{E}_T were determined from data, and no significant excess of events was observed. The results were interpreted in a benchmark GMSB model known as the ‘‘Snowmass slope SPS 8’’ [48]. (This model has one parameter, the effective SUSY-breaking scale Λ , with $N_5 = 1$ messenger, a messenger mass of 2Λ , $\tan\beta = 15$ and $\mu > 0$.) The CDF analysis, based on 2.6 fb^{-1} , sets a neutralino NLSP mass limit of 149 GeV.

The additional possibility of non-prompt $\tilde{\chi}_1^0$ decays was considered by CDF, taking advantage of the timing information provided by their calorimeter [49]. No signal of delayed photons was observed in 570 pb^{-1} , and an excluded domain in the $(m_{\tilde{\chi}_1^0}, \tau_{\tilde{\chi}_1^0})$ plane was derived, where $\tau_{\tilde{\chi}_1^0}$ is the $\tilde{\chi}_1^0$ lifetime, extending out to 101 GeV for $\tau_{\tilde{\chi}_1^0} = 5 \text{ ns}$.

The case of a long-lived stau NLSP was also investigated. Pair production would resemble a pair of slow-moving muons. The timing information of their muon system was used by $D\bar{O}$, and no excess of such anomalously slow muons was observed in 1.1 fb^{-1} [50]. However, the sensitivity of the search is not yet sufficient to set a stau mass lower limit. Long-lived charginos as in AMSB would lead to the same signature. The larger production cross section allowed a lower limit of 206 GeV to be set on the mass of such long-lived gaugino-like charginos.

Within the recently proposed model of split SUSY, gluinos are expected to acquire a substantial lifetime. After hadronization into a R -hadron, such a long-lived gluino produced in a $p\bar{p}$ collision could come to rest in a calorimeter, and decay during a later bunch crossing than that during which it was produced [51]. The main decay mode is expected to be $\tilde{g} \rightarrow g\tilde{\chi}_1^0$, with some competition from $\tilde{g} \rightarrow q\bar{q}\tilde{\chi}_1^0$. Such a late gluino decay would appear as a jet not pointing toward the detector center in an otherwise empty event. Such a possibility was considered by the $D\bar{O}$ collaboration. The main backgrounds, coming from showering cosmic muons and from muons belonging to the beam halo, were estimated from data, and no excess of such a topology was observed. Based on an integrated luminosity of 410 pb^{-1} , limits were set on the mass of such a gluino,

Searches Particle Listings

Supersymmetric Particle Searches

with some dependence on the lifetime, the decay-branching ratio, the $\tilde{\chi}_1^0$ mass, and the probability for a neutral R -hadron to convert into a charged one in the calorimeter [52]. For instance, for a lifetime smaller than three hours, a neutralino mass of 50 GeV, a conversion cross section of 3 mb, and a 100% branching ratio into $g\tilde{\chi}_1^0$, a mass limit of 270 GeV was obtained.

II.8. Conclusion: The masses of SUSY particles other than the gluino and the LSP have been constrained at LEP to be larger than ~ 100 GeV, essentially independent of any specific model. Within the MSSM with unification of gaugino and sfermion masses, an indirect lower limit of 47 GeV has been set by the LEP experiments for the mass of a neutralino LSP. The mass reach at the Tevatron is much larger than at LEP, but the results need to be interpreted in the context of specific models. Based on an integrated luminosity of 2 fb^{-1} , the current squark and gluino mass lower limits are 379 and 308 GeV, respectively, within the mSUGRA framework at low $\tan\beta$, and chargino masses up to 170 GeV are excluded for favorable choices of slepton masses. More than 6 fb^{-1} have already been accumulated at the Tevatron by spring 2009, and it is expected that the LHC will begin operation at a center-of-mass energy of 7 TeV in the winter 2009 – 2010, which will open a whole new window for SUSY searches.

References

- M. Drees and G. Gerbier, *Dark matter*, in this volume of the *Review*.
- Y. Kwon and G. Punzi, *Production and decay of b-flavored hadrons*, in this volume of the *Review*.
- A. Höcker and W.J. Marciano, *The muon anomalous moment*, in this volume of the *Review*.
- S. Heinemeyer, W. Hollik, and G. Weiglein, *Phys. Reports* **425**, 265 (2006).
- LEPSUSYWG, ALEPH, DELPHI, L3, and OPAL experiments, note LEPSUSYWG/04-01.1, <http://lepsusy.web.cern.ch/lepsusy/Welcme.html>.
- ALEPH Coll., *Phys. Lett.* **B544**, 73 (2002); L3 Coll., *Phys. Lett.* **B580**, 37 (2004).
- The ALEPH, DELPHI, L3, OPAL, SLD Collaborations, the LEP Electroweak Working Group, the SLD Electroweak and Heavy Flavours Groups, *Phys. Reports* **427**, 257 (2006).
- LEPSUSYWG, *ibid.*, note LEPSUSYWG/01-03.1.
- LEPSUSYWG, *ibid.*, note LEPSUSYWG/02-04.1.
- LEPSUSYWG, *ibid.*, note LEPSUSYWG/04-07.1.
- LEPSUSYWG, *ibid.*, note LEPSUSYWG/02-06.2.
- LEPSUSYWG, *ibid.*, note LEPSUSYWG/04-02.1.
- ALEPH Coll., *Phys. Lett.* **B537**, 5 (2002).
- C. Boehm, A. Djouadi, and Y. Mambrini, *Phys. Rev.* **D61**, 095006 (2000).
- LEPSUSYWG, *ibid.*, note LEPSUSYWG/04-09.1.
- CDF Coll., *Phys. Rev.* **D59**, 092002 (1999).
- ALEPH Coll., *Eur. Phys. J.* **C25**, 339 (2002); OPAL Coll., *Eur. Phys. J.* **C46**, 307 (2006).
- LEPSUSYWG, *ibid.*, note LEPSUSYWG/02-09.2.
- ALEPH Coll., *Eur. Phys. J.* **C31**, 327 (2003); DELPHI Coll., *Eur. Phys. J.* **C26**, 505 (2003).
- LEPSUSYWG, *ibid.*, note LEPSUSYWG/02-10.1; ALEPH Coll., *Eur. Phys. J.* **C31**, 1 (2003); DELPHI Coll., *Eur. Phys. J.* **C36**, 1 (2004); L3 Coll., *Phys. Lett.* **B524**, 65 (2002); OPAL Coll., *Eur. Phys. J.* **C33**, 149 (2004).
- ALEPH Coll., *Eur. Phys. J.* **C19**, 415 (2001) and *Eur. Phys. J.* **C25**, 1 (2002); DELPHI Coll., *Eur. Phys. J.* **C28**, 15 (2003); L3 Coll., *Phys. Lett.* **B414**, 373 (1997); OPAL Coll., *Eur. Phys. J.* **C13**, 553 (2000).
- H1 Coll., *Phys. Lett.* **B599**, 159 (2004); H1 Coll., *Eur. Phys. J.* **C36**, 425 (2004); ZEUS Coll., *Eur. Phys. J.* **C50**, 269 (2007).
- DØ Collab., *Phys. Lett.* **B660**, 449 (2008).
- CDF Collab., *Phys. Rev. Lett.* **102**, 121801 (2009).
- DØ Collab., *Search for squark production in events with jets, hadronically decaying tau leptons and missing transverse energy in $p\bar{p}$ collisions at $\sqrt{s}=1.96 \text{ TeV}$* , accepted for publication in *Phys. Lett. B*, [arXiv:0905.4086v1](https://arxiv.org/abs/0905.4086v1) [hep-ex].
- CDF Collab., *Search for scalar top decaying into $c + \tilde{\chi}^0$ in the MET+jets sample*, CDF-Note 9834.
- DØ Collab., *Phys. Lett.* **B665**, 1 (2008).
- CDF Collab., *Phys. Rev.* **D76**, 072010 (2007).
- DØ Collab., *Search for third generation leptoquarks and scalar bottom quarks in the $b\bar{b}$ plus missing energy topology in $p\bar{p}$ collisions at $\sqrt{s}=1.96 \text{ TeV}$* , DØ-Note 5931-CONF.
- CDF Collab., *Phys. Rev. Lett.* **102**, 221801 (2009).
- CDF Collab., *Search for the supersymmetric partner of the top quark in dilepton events produced in $p\bar{p}$ collisions at $\sqrt{s}=1.96 \text{ TeV}$* , CDF-Note 9775.
- DØ Collab., *Search for pair production of the supersymmetric partner of the top quark in the $t\bar{t} \rightarrow b\bar{b}e\mu\tilde{\nu}$ decay channel at DØ*, DØ-Note 5937-CONF.
- CDF Collab., *Search for Pair Production of Stop Quarks Mimicking Top Event Signatures*, CDF-Note 9439.
- CDF Collab., *Search for long-lived massive charged particles in 1.96 TeV $p\bar{p}$ collisions*, [arXiv:0902.1266v3](https://arxiv.org/abs/0902.1266v3) [hep-ex].
- DØ Collab., *Search for Associated Production of Charginos and Neutralinos in the Trilepton Final State using 2.3 fb^{-1} of Data*, accepted by *Phys. Lett. B*, [arXiv:0901.0646v1](https://arxiv.org/abs/0901.0646v1) [hep-ex].
- CDF Collab., *Update of the Unified Trilepton Search with 3.2 fb^{-1} of Data*, CDF-Note 9817.
- DØ Collab., *Search for the associated production of charginos and neutralinos in the like sign dimuon channel*, DØ-Note 5126-CONF.
- CDF Collab., *Phys. Rev. Lett.* **99**, 191806 (2007).
- CDF Collab., *Phys. Rev. Lett.* **98**, 131804 (2007).
- DØ Collab., *Phys. Lett.* **B638**, 441 (2006).
- CDF Collab., *Search for Pair Production of Scalar Top Quarks Decaying to a τ Lepton and a b Quark*, CDF-Note 7835.
- DØ Collab., *Phys. Rev. Lett.* **97**, 161802 (2006).
- NuTeV Collab., *Phys. Rev. Lett.* **87**, 041801 (2001).
- DØ Collab., *Phys. Rev. Lett.* **97**, 111801 (2006).

45. CDF Collab., Phys. Rev. Lett. **95**, 252001 (2005);
CDF Collab., Phys. Rev. Lett. **95**, 131801 (2005);
CDF Collab., Phys. Rev. Lett. **96**, 211802 (2006);
DØ Collab., *Search for tau sneutrino particles in the $e + \mu$ final state at DØ*, DØNote 5894-CONF.
46. CDF Collab., *Limits on Gauge-Mediated Supersymmetry-Breaking Models using Diphoton Events with Missing Transverse Energy at CDF II*, CDF-Note 9625.
47. DØ Collab., Phys. Rev. Lett. **659**, 856 (2008).
48. B.C. Allanach *et al.*, Eur. Phys. J. **C25**, 113 (2002).
49. CDF Collab., Phys. Rev. Lett. **99**, 121801 (2007).
50. DØ Collab., Phys. Rev. Lett. **102**, 161802 (2009).
51. A. Arvanitaki *et al.*, Phys. Rev. **D76**, 055007 (2007).
52. DØ Collab., Phys. Rev. Lett. **99**, 131801 (2007).

SUPERSYMMETRIC MODEL ASSUMPTIONS

The exclusion of particle masses within a mass range (m_1, m_2) will be denoted with the notation “none m_1 – m_2 ” in the VALUE column of the following Listings.

Most of the results shown below, unless stated otherwise, are based on the Minimal Supersymmetric Standard Model (MSSM), as described in the Note on Supersymmetry. Unless otherwise indicated, this includes the assumption of common gaugino and scalar masses at the scale of Grand Unification (GUT), and use of the resulting relations in the spectrum and decay branching ratios. It is also assumed that R -parity (R) is conserved. Unless otherwise indicated, the results also assume that:

- 1) The $\tilde{\chi}_1^0$ is the lightest supersymmetric particle (LSP)
- 2) $m_{\tilde{f}_L} = m_{\tilde{f}_R}$, where $\tilde{f}_{L,R}$ refer to the scalar partners of left- and right-handed fermions.

Limits involving different assumptions are identified in the Comments or in the Footnotes. We summarize here the notations used in this Chapter to characterize some of the most common deviations from the MSSM (for further details, see the Note on Supersymmetry).

Theories with R -parity violation (\tilde{R}) are characterized by a superpotential of the form: $\lambda_{ijk} L_i L_j e_k^c + \lambda'_{ijk} L_i Q_j d_k^c + \lambda''_{ijk} u_i^c d_j^c d_k^c$, where i, j, k are generation indices. The presence of any of these couplings is often identified in the following by the symbols $LL\bar{E}$, $LQ\bar{D}$, and UDD . Mass limits in the presence of \tilde{R} will often refer to “direct” and “indirect” decays. Direct refers to \tilde{R} decays of the particle in consideration. Indirect refers to cases where \tilde{R} appears in the decays of the LSP.

In several models, most notably in theories with so-called Gauge Mediated Supersymmetry Breaking (GMSB), the gravitino (\tilde{G}) is the LSP. It is usually much lighter than any other massive particle in the spectrum, and $m_{\tilde{G}}$ is then neglected in all decay processes involving gravitinos. In these scenarios, particles other than the neutralino are sometimes considered as the next-to-lightest supersymmetric particle (NLSP), and are assumed to decay to their even- R partner plus \tilde{G} . If the lifetime is short enough for the decay to take place within the detector, \tilde{G} is assumed to be undetected and to give rise to missing energy (\cancel{E}) or missing transverse energy (\cancel{E}_T) signatures.

When needed, specific assumptions on the eigenstate content of $\tilde{\chi}^0$ and $\tilde{\chi}^\pm$ states are indicated, using the notation $\tilde{\gamma}$ (photino), \tilde{H} (higgsino), \tilde{W} (wino), and \tilde{Z} (zino) to signal that the limit of pure states was used. The terms gaugino is also used, to generically indicate wino-like charginos and zino-like neutralinos.

$\tilde{\chi}_1^0$ (Lightest Neutralino) MASS LIMIT

$\tilde{\chi}_1^0$ is often assumed to be the lightest supersymmetric particle (LSP). See also the $\tilde{\chi}_2^0, \tilde{\chi}_3^0, \tilde{\chi}_4^0$ section below.

We have divided the $\tilde{\chi}_1^0$ listings below into five sections:

- 1) Accelerator limits for stable $\tilde{\chi}_1^0$,
- 2) Bounds on $\tilde{\chi}_1^0$ from dark matter searches,
- 3) Bounds on $\tilde{\chi}_1^0$ elastic cross sections from dark matter searches,
- 4) Other bounds on $\tilde{\chi}_1^0$ from astrophysics and cosmology, and
- 5) Bounds on unstable $\tilde{\chi}_1^0$.

Accelerator limits for stable $\tilde{\chi}_1^0$

Unless otherwise stated, results in this section assume spectra, production rates, decay modes, and branching ratios as evaluated in the MSSM, with gaugino and sfermion mass unification at the GUT scale. These papers generally study production of $\tilde{\chi}_i^0 \tilde{\chi}_j^0$ ($i \geq 1, j \geq 2$), $\tilde{\chi}_1^+ \tilde{\chi}_1^-$, and (in the case of hadronic collisions) $\tilde{\chi}_1^+ \tilde{\chi}_2^0$ pairs. The mass limits on $\tilde{\chi}_1^0$ are either direct, or follow indirectly from the constraints set by the non-observation of $\tilde{\chi}_1^\pm$ and $\tilde{\chi}_2^0$ states on the gaugino and higgsino MSSM parameters M_2 and μ . In some cases, information is used from the nonobservation of slepton decays.

Obsolete limits obtained from e^+e^- collisions up to $\sqrt{s}=184$ GeV have been removed from this compilation and can be found in the 2000 Edition (The European Physical Journal **C15** 1 (2000)) of this Review.

$$\Delta m = m_{\tilde{\chi}_2^0} - m_{\tilde{\chi}_1^0}$$

VALUE (GeV)	CL%	DOCUMENT ID	TECN	COMMENT
>40	95	1 ABBIENDI	04H OPAL	all $\tan\beta$, $\Delta m > 5$ GeV, $m_0 > 500$ GeV, $A_0 = 0$
>42.4	95	2 HEISTER	04 ALEP	all $\tan\beta$, all Δm , all m_0
>39.2	95	3 ABDALLAH	03M DLPH	all $\tan\beta$, $m_{\tilde{\nu}} > 500$ GeV
>46	95	4 ABDALLAH	03M DLPH	all $\tan\beta$, all Δm , all m_0
>32.5	95	5 ACCIARRI	00D L3	$\tan\beta > 0.7$, $\Delta m > 3$ GeV, all m_0
••• We do not use the following data for averages, fits, limits, etc. •••				
		6 DREINER	09 THEO	
		7 ABBOTT	98c D0	$p\bar{p} \rightarrow \tilde{\chi}_1^\pm \tilde{\chi}_2^0$
>41	95	8 ABE	98J CDF	$p\bar{p} \rightarrow \tilde{\chi}_1^\pm \tilde{\chi}_2^0$

1 ABBIENDI 04H search for charginos and neutralinos in events with acoplanar leptons+jets and multi-jet final states in the 192–209 GeV data, combined with the results on leptonic final states from ABBIENDI 04. The results hold for a scan over the parameter space covering the region $0 < M_2 < 5000$ GeV, $-1000 < \mu < 1000$ GeV and $\tan\beta$ from 1 to 40. This limit supersedes ABBIENDI 00H.

2 HEISTER 04 data collected up to 209 GeV. Updates earlier analysis of selections from HEISTER 02E, includes a new analysis of charginos and neutralinos decaying into stau and uses results on charginos with initial state radiation from HEISTER 02J. The limit is based on the direct search for charginos and neutralinos, the constraints from the slepton search and the Higgs mass limits from HEISTER 02 using a top mass of 175 GeV, interpreted in a framework with universal gaugino and sfermion masses. Assuming the mixing in the stau sector to be negligible, the limit improves to 43.1 GeV. Under the assumption of MSUGRA with unification of the Higgs and sfermion masses, the limit improves to 50 GeV, and reaches 53 GeV for $A_0 = 0$. These limits include and update the results of BARATE 01.

3 ABDALLAH 03M uses data from $\sqrt{s} = 192$ –208 GeV. A limit on the mass of $\tilde{\chi}_1^0$ is derived from direct searches for neutralinos combined with the chargino search. Neutralinos are searched in the production of $\tilde{\chi}_1^0 \tilde{\chi}_2^0, \tilde{\chi}_1^0 \tilde{\chi}_3^0$, as well as $\tilde{\chi}_2^0 \tilde{\chi}_3^0$ and $\tilde{\chi}_2^0 \tilde{\chi}_4^0$ giving rise to cascade decays, and $\tilde{\chi}_1^0 \tilde{\chi}_2^0$ and $\tilde{\chi}_1^0 \tilde{\chi}_3^0$, followed by the decay $\tilde{\chi}_2^0 \rightarrow \tilde{\tau}\tau$. The results hold for the parameter space defined by values of $M_2 < 1$ TeV, $|\mu| \leq 2$ TeV with the $\tilde{\chi}_1^0$ as LSP. The limit is obtained for $\tan\beta = 1$ and large m_0 , where $\tilde{\chi}_2^0 \tilde{\chi}_3^0$ and chargino pair production are important. If the constraint from Higgs searches is also imposed, the limit improves to 49.0 GeV in the M_h^{max} scenario with $m_t = 174.3$ GeV. These limits update the results of ABREU 00.

4 ABDALLAH 03M uses data from $\sqrt{s} = 192$ –208 GeV. An indirect limit on the mass of $\tilde{\chi}_1^0$ is derived by constraining the MSSM parameter space by the results from direct searches for neutralinos (including cascade decays and $\tilde{\tau}\tau$ final states), for charginos (for all Δm_\pm) and for sleptons, stop and sbottom. The results hold for the full parameter space defined by values of $M_2 < 1$ TeV, $|\mu| \leq 2$ TeV with the $\tilde{\chi}_1^0$ as LSP. Constraints from the Higgs search in the M_h^{max} scenario assuming $m_t = 174.3$ GeV are included. The limit is obtained for $\tan\beta \geq 5$ when stau mixing leads to mass degeneracy between $\tilde{\tau}_1$ and $\tilde{\chi}_1^0$ and the limit is based on $\tilde{\chi}_2^0$ production followed by its decay to $\tilde{\tau}_1\tau$. In the pathological scenario where m_0 and $|\mu|$ are large, so that the $\tilde{\chi}_2^0$ production cross section is negligible, and where there is mixing in the stau sector but not in stop nor

Searches Particle Listings

Supersymmetric Particle Searches

sbottom, the limit is based on charginos with soft decay products and an ISR photon. The limit then degrades to 39 GeV. See Figs 40–42 for the dependence of the limit on $\tan\beta$ and $m_{\tilde{\nu}}$. These limits update the results of ABREU 00w.

- 5 ACCIARRI 00d data collected at $\sqrt{s}=189$ GeV. The results hold over the full parameter space defined by $0.7 \leq \tan\beta \leq 60$, $0 \leq M_2 \leq 2$ TeV, $m_0 \leq 500$ GeV, $|\mu| \leq 2$ TeV. The minimum mass limit is reached for $\tan\beta=1$ and large m_0 . The results of slepton searches from ACCIARRI 99w are used to help set constraints in the region of small m_0 . The limit improves to 48 GeV for $m_0 \gtrsim 200$ GeV and $\tan\beta \gtrsim 10$. See their Figs. 6–8 for the $\tan\beta$ and m_0 dependence of the limits. Updates ACCIARRI 98f.
- 6 DREINER 09 show that in the general MSSM with non-universal gaugino masses there exists a model-independent laboratory bound on the mass of the lightest neutralino. An essentially massless $\tilde{\chi}_1^0$ is allowed by the experimental and observational data, imposing some constraints on other MSSM parameters, including M_2 , μ and the slepton and squark masses.
- 7 ABBOTT 98c searches for trilepton final states ($\ell=e,\mu$). See footnote to ABBOTT 98c in the Chargino Section for details on the assumptions. Assuming a negligible decay rate of $\tilde{\chi}_1^\pm$ and $\tilde{\chi}_2^0$ to quarks, they obtain $m_{\tilde{\chi}_2^0} \gtrsim 51$ GeV.
- 8 ABE 98j searches for trilepton final states ($\ell=e,\mu$). See footnote to ABE 98j in the Chargino Section for details on the assumptions. The quoted result corresponds to the best limit within the selected range of parameters, obtained for $m_{\tilde{q}} > m_{\tilde{g}}$, $\tan\beta=2$, and $\mu=-600$ GeV.

Bounds on $\tilde{\chi}_1^0$ from dark matter searches

These papers generally exclude regions in the $M_2 - \mu$ parameter plane assuming that $\tilde{\chi}_1^0$ is the dominant form of dark matter in the galactic halo. These limits are based on the lack of detection in laboratory experiments or by the absence of a signal in underground neutrino detectors. The latter signal is expected if $\tilde{\chi}_1^0$ accumulates in the Sun or the Earth and annihilates into high-energy $\nu\bar{\nu}$'s.

VALUE	DOCUMENT ID	TECN
••• We do not use the following data for averages, fits, limits, etc. •••		
1	ABBASI 09b	ICCB
2	ACHTERBERG 06	AMND
3	ACKERMANN 06	AMND
4	DEBOER 06	RVUE
5	DESAI 04	SKAM
5	AMBROSIO 99	MCR0
6	LOSECCO 95	RVUE
7	MORI 93	KAMI
8	BOTTINO 92	COSM
9	BOTTINO 91	RVUE
10	GELMINI 91	COSM
11	KAMIONKOWSKI 91	RVUE
12	MORI 91b	KAMI
13	OLIVE 88	COSM

none 4–15 GeV

- 1 ABBASI 09 is based on data collected during 104.3 effective days with the IceCube 22-string detector. They looked for interactions of ν_μ 's from neutralino annihilations in the Sun over a background of atmospheric neutrinos and set 90% CL limits on the muon flux. They also obtain limits on the spin dependent neutralino-proton cross section for neutralino masses in the range 25–5000 GeV.
- 2 ACHTERBERG 06 is based on data collected during 421.9 effective days with the AMANDA detector. They looked for interactions of ν_μ 's from the centre of the Earth over a background of atmospheric neutrinos and set 90% CL limits on the muon flux. Their limit is compared with the muon flux expected from neutralino annihilations into $W^+ W^-$ and $b\bar{b}$ at the centre of the Earth for MSSM parameters compatible with the relic dark matter density, see their Fig. 7.
- 3 ACKERMANN 06 is based on data collected during 143.7 days with the AMANDA-II detector. They looked for interactions of ν_μ 's from the Sun over a background of atmospheric neutrinos and set 90% CL limits on the muon flux. Their limit is compared with the muon flux expected from neutralino annihilations into $W^+ W^-$ in the Sun for SUSY model parameters compatible with the relic dark matter density, see their Fig. 3.
- 4 DEBOER 06 interpret an excess of diffuse Galactic gamma rays observed with the EGRET satellite as originating from π^0 decays from the annihilation of neutralinos into quark jets. They analyze the corresponding parameter space in a supergravity inspired MSSM model with radiative electroweak symmetry breaking, see their Fig. 3 for the preferred region in the $(m_0, m_{1/2})$ plane of a scenario with large $\tan\beta$.
- 5 AMBROSIO 99 and DESAI 04 set new neutrino flux limits which can be used to limit the parameter space in supersymmetric models based on neutralino annihilation in the Sun and the Earth.
- 6 LOSECCO 95 reanalyzed the IMB data and places lower limit on $m_{\tilde{\chi}_1^0}$ of 18 GeV if the LSP is a photino and 10 GeV if the LSP is a higgsino based on LSP annihilation in the sun producing high-energy neutrinos and the limits on neutrino fluxes from the IMB detector.
- 7 MORI 93 excludes some region in $M_2 - \mu$ parameter space depending on $\tan\beta$ and lightest scalar Higgs mass for neutralino dark matter $m_{\tilde{\chi}_1^0} > m_{H^\pm}$, using limits on ongoing muons produced by energetic neutrinos from neutralino annihilation in the Sun and the Earth.
- 8 BOTTINO 92 excludes some region $M_2 - \mu$ parameter space assuming that the lightest neutralino is the dark matter, using ongoing muons at Kamiokande, direct searches by Ge detectors, and by LEP experiments. The analysis includes top radiative corrections on Higgs parameters and employs two different hypotheses for nucleon-Higgs coupling. Effects of rescaling in the local neutralino density according to the neutralino relic abundance are taken into account.
- 9 BOTTINO 91 excluded a region in $M_2 - \mu$ plane using ongoing muon data from Kamioka experiment, assuming that the dark matter surrounding us is composed of neutralinos and that the Higgs boson is not too heavy.
- 10 GELMINI 91 exclude a region in $M_2 - \mu$ plane using dark matter searches.
- 11 KAMIONKOWSKI 91 excludes a region in the $M_2 - \mu$ plane using IMB limit on ongoing muons originated by energetic neutrinos from neutralino annihilation in the sun, assuming

that the dark matter is composed of neutralinos and that $m_{H_1^0} \lesssim 50$ GeV. See Fig. 8 in the paper.

- 12 MORI 91b exclude a part of the region in the $M_2 - \mu$ plane with $m_{\tilde{\chi}_1^0} \lesssim 80$ GeV using a limit on ongoing muons originated by energetic neutrinos from neutralino annihilation in the earth, assuming that the dark matter surrounding us is composed of neutralinos and that $m_{H_1^0} \lesssim 80$ GeV.
- 13 OLIVE 88 result assumes that photinos make up the dark matter in the galactic halo. Limit is based on annihilations in the sun and is due to an absence of high energy neutrinos detected in underground experiments. The limit is model dependent.

$\tilde{\chi}_1^0 - p$ elastic cross section

Experimental results on the $\tilde{\chi}_1^0 - p$ elastic cross section are evaluated at $m_{\tilde{\chi}_1^0} = 100$ GeV. The experimental results on the cross section are often mass dependent. Therefore, the mass and cross section results are also given where the limit is strongest, when appropriate. Results are quoted separately for spin-dependent interactions (based on an effective 4-Fermi Lagrangian of the form $\bar{\chi}\gamma^\mu\mu\gamma^5\chi\bar{q}\gamma_\mu\gamma^5q$) and spin-independent interactions ($\bar{\chi}\chi\bar{q}q$). For calculational details see GRIEST 88b, ELLIS 88d, BARBIERI 89c, DREES 93b, ARNOWITZ 96, BERGSTROM 96, and BAER 97 in addition to the theory papers listed in the Tables. For a description of the theoretical assumptions and experimental techniques underlying most of the listed papers, see the review on "Dark matter" in this "Review of Particle Physics," and references therein. Most of the following papers use galactic halo and nuclear interaction assumptions from (LEWIN 96).

Spin-dependent interactions

VALUE (pb)	CL%	DOCUMENT ID	TECN	COMMENT
••• We do not use the following data for averages, fits, limits, etc. •••				
< 0.3	90	1 ARCHAMBAU.09	PICA	F
< 0.8	90	2 LEBEDENKO 09a	ZEP3	Xe
< 1	90	3 ANGLE 08a	XE10	Xe
< 0.055		4 BEDNYAKOV 08	HDMS	Ge
< 0.33	90	5 BUHNKE 08	COUP	CF ₃ I
< 15	90	6 ALNER 07	ZEP2	Xe
< 0.17	90	7 LEE 07a	KIMS	Csl
< 5		8 AKERIB 06	CDMS	Ge
< 2		9 SHIMIZU 06a	CNTR	CaF ₂
< 0.4		10 ALNER 05	NAIA	Nal Spin Dep.
< 2		11 BARNABE-HE.05	PICA	C
< 1.4		12 GIRARD 05	SMP L	F, CI
2×10^{-11} to 1×10^{-4}		13 ELLIS 04	THEO	$\mu > 0$
< 16		14 GIULIANI 04	SIMP	F
< 0.8		15 AHMED 03	NAIA	Nal Spin Dep.
< 40		16 TAKEDA 03	BOLO	NaF Spin Dep.
< 10		17 ANGLÖHER 02	CRES	Saphire
8×10^{-7} to 2×10^{-5}		18 ELLIS 01c	THEO	$\tan\beta \leq 10$
< 3.8		19 BERNABE 00d	DAMA	Xe
< 15		20 COLLAR 00	SMP L	F
< 0.8		21 SPOONER 00	UKDM	Nal
< 4.8		21 BELL 99c	DAMA	F
< 100		22 OOTANI 99	BOLO	LiF
< 0.6		BERNABE 98c	DAMA	Xe
< 5		21 BERNABE 97	DAMA	F

- 1 The strongest limit is 0.16 pb and occurs at $m_\chi = 24$ GeV. The strongest limit for the scattering on neutrons is 2.6 pb, also at $m_\chi = 24$ GeV.
- 2 The strongest upper limit is 0.76 pb and occurs at $m_\chi \simeq 55$ GeV. The strongest limit on the neutron spin-dependent cross section is 0.01 pb, also at $m_\chi \simeq 55$ GeV (the same limit is achieved for $m_\chi = 100$ GeV).
- 3 The strongest limit is 0.6 pb and occurs at $m_\chi = 30$ GeV. The limit for scattering on neutrons is 0.01 pb at $m_\chi = 100$ GeV, and the strongest limit is 0.0045 pb at $m_\chi = 30$ GeV.
- 4 Limit applies to neutron elastic cross section.
- 5 The strongest upper limit is 0.25 pb and occurs at $m_\chi \simeq 40$ GeV.
- 6 The strongest upper limit is 14 pb and occurs at $m_\chi \simeq 65$ GeV. The limit on the neutron spin-dependent cross section is 0.08 pb at $m_\chi = 100$ GeV and the strongest limit for scattering on neutrons is 0.07 pb at $m_\chi = 65$ GeV.
- 7 The limit on the neutron spin-dependent cross section is 6 pb at $m_\chi = 100$ GeV.
- 8 The strongest upper limit is 4 pb and occurs at $m_\chi \simeq 60$ GeV. The limit on the neutron spin-dependent elastic cross section is 0.07 pb. This latter limit is improved in AHMED 09, where a limit of 0.02 pb is obtained at $m_\chi = 100$ GeV. The strongest limit in AHMED 09 is 0.018 pb and occurs at $m_\chi = 60$ GeV.
- 9 The strongest upper limit is 1.2 pb and occurs at $m_\chi \simeq 40$ GeV. The limit on the neutron spin-dependent cross section is 35 pb.
- 10 The strongest upper limit is 0.35 pb and occurs at $m_\chi \simeq 60$ GeV.
- 11 The strongest upper limit is 1.2 pb and occurs $m_\chi \simeq 30$ GeV.
- 12 The strongest upper limit is 1.2 pb and occurs $m_\chi \simeq 40$ GeV.
- 13 ELLIS 04 calculates the χp elastic scattering cross section in the framework of $N=1$ supergravity models with radiative breaking of the electroweak gauge symmetry, but without universal scalar masses. In the case of universal squark and slepton masses, but non-universal Higgs masses, the limit becomes 2×10^{-4} , see ELLIS 03e.
- 14 The strongest upper limit is 10 pb and occurs at $m_\chi \simeq 30$ GeV.
- 15 The strongest upper limit is 0.75 pb and occurs at $m_\chi \simeq 70$ GeV.

- 16 The strongest upper limit is 30 pb and occurs at $m_\chi \approx 20$ GeV.
- 17 The strongest upper limit is 8 pb and occurs at $m_\chi \approx 30$ GeV.
- 18 ELLIS 01c calculates the χ - p elastic scattering cross section in the framework of $N=1$ supergravity models with radiative breaking of the electroweak gauge symmetry. In models with nonuniversal Higgs masses, the upper limit to the cross section is 6×10^{-4} .
- 19 The strongest upper limit is 3 pb and occurs at $m_\chi \approx 60$ GeV. The limits are for inelastic scattering $\chi^0 + 129\text{Xe} \rightarrow \chi^0 + 129\text{Xe}^*$ (39.58 keV).
- 20 The strongest upper limit is 9 pb and occurs at $m_\chi \approx 30$ GeV.
- 21 The strongest upper limit is 4.4 pb and occurs at $m_\chi \approx 60$ GeV.
- 22 The strongest upper limit is about 35 pb and occurs at $m_\chi \approx 15$ GeV.

Spin-independent interactions

VALUE (pb)	CL%	DOCUMENT ID	TECN	COMMENT
●●● We do not use the following data for averages, fits, limits, etc. ●●●				
$< 5 \times 10^{-8}$		1 AHMED 09	CDMS	Ge
$< 7 \times 10^{-7}$	90	2 ANGLÖHER 09	CRES	CaWO ₄
3×10^{-10} to 3×10^{-8}	95	3 BUCHMUELLER... 09	THEO	
$< 1 \times 10^{-7}$	90	4 LEBEDENKO 09	ZEP3	Xe
$< 1 \times 10^{-7}$	90	5 ANGLE 08	XE10	Xe
$< 1 \times 10^{-6}$	90	6 BENETTI 08	WARP	Ar
$< 7.5 \times 10^{-7}$	90	6 ALNER 07A	ZEP2	Xe
$< 22 \times 10^{-7}$	90	7 LEE 07A	KIMS	Csl
$< 2 \times 10^{-7}$		8 AKERIB 06A	CDMS	Ge
$< 90 \times 10^{-7}$		9 LEE 06	KIMS	Csl
$< 5 \times 10^{-7}$		10 AKERIB 05	CDMS	Ge
$< 90 \times 10^{-7}$		ALNER 05	NAIA	Nal Spin Indep.
$< 12 \times 10^{-7}$		11 ALNER 05A	ZEPL	
$< 20 \times 10^{-7}$		12 ANGLÖHER 05	CRES	CaWO ₄
$< 14 \times 10^{-7}$		SANGLARD 05	EDEL	Ge
$< 4 \times 10^{-7}$		13 AKERIB 04	CDMS	Ge
2×10^{-11} to 8×10^{-6}	14,15	14,15 ELLIS 04	THEO	$\mu > 0$
$< 5 \times 10^{-8}$		16 PIERCE 04A	THEO	
$< 2 \times 10^{-5}$		17 AHMED 03	NAIA	Nal Spin Indep.
$< 3 \times 10^{-6}$		18 AKERIB 03	CDMS	Ge
2×10^{-13} to 2×10^{-7}		19 BAER 03A	THEO	
$< 1.4 \times 10^{-5}$		20 KLAPDOR-K... 03	HDMS	Ge
$< 6 \times 10^{-6}$		21 ABRAMS 02	CDMS	Ge
$< 1.4 \times 10^{-6}$		22 BENOIT 02	EDEL	Ge
1×10^{-12} to 7×10^{-6}		14 KIM 02B	THEO	
$< 3 \times 10^{-5}$		23 MORALES 02c	CSME	Ge
$< 1 \times 10^{-5}$		24 MORALES 02c	IGEX	Ge
$< 1 \times 10^{-6}$		BALTZ 01	THEO	
$< 3 \times 10^{-5}$		25 BAUDIS 01	HDMS	Ge
$< 4.5 \times 10^{-6}$		BENOIT 01	EDEL	Ge
$< 7 \times 10^{-6}$		26 BOTTINO 01	THEO	
$< 1 \times 10^{-8}$		27 CORSETTI 01	THEO	$\tan\beta \leq 25$
5×10^{-10} to 1.5×10^{-8}		28 ELLIS 01c	THEO	$\tan\beta \leq 10$
$< 4 \times 10^{-6}$		27 GOMEZ 01	THEO	
2×10^{-10} to 1×10^{-7}		27 LAHANAS 01	THEO	
$< 3 \times 10^{-6}$		ABUSAIIDI 00	CDMS	Ge, Si
$< 6 \times 10^{-7}$		29 ACCOMANDO 00	THEO	
2.5×10^{-9} to 3.5×10^{-8}		30 BERNABEI 00	DAMA	Nal
$< 1.5 \times 10^{-5}$		31 FENG 00	THEO	$\tan\beta=10$
$< 4 \times 10^{-5}$		MORALES 00	IGEX	Ge
$< 7 \times 10^{-6}$		SPOONER 00	UKDM	Nal
		BAUDIS 99	HDMS	⁷⁶ Ge
		32 BERNABEI 99	DAMA	Nal
		33 BERNABEI 98	DAMA	Nal
$< 7 \times 10^{-6}$		BERNABEI 98c	DAMA	Xe

- 1 AHMED 09 updates the results of AKERIB 06A. The strongest limit is 4.6×10^{-8} pb and occurs at $m_\chi = 60$ GeV.
- 2 The strongest upper limit is 4.8×10^{-7} pb and occurs at $m_\chi = 50$ GeV.
- 3 BUCHMUELLER 09 makes predictions for the spin-independent elastic cross section based on a frequentist approach to electroweak observables in the framework of $N = 1$ supergravity models with radiative breaking of the electroweak gauge symmetry.
- 4 The strongest upper limit is 8.1×10^{-8} pb and occurs at $m_\chi = 60$ GeV.
- 5 The strongest upper limit is 5.1×10^{-8} pb and occurs at $m_\chi \approx 30$ GeV. The values quoted here are based on the analysis performed in ANGLE 08 with the update from SORENSEN 09.
- 6 The strongest upper limit is 6.6×10^{-7} pb and occurs at $m_\chi \approx 65$ GeV.
- 7 The strongest upper limit is 1.9×10^{-7} pb and occurs at $m_\chi \approx 65$ GeV. Supersedes LEE 06.
- 8 AKERIB 06A updates the results of AKERIB 05. The strongest upper limit is 1.6×10^{-7} pb and occurs at $m_\chi \approx 60$ GeV.
- 9 The strongest upper limit is 8×10^{-6} pb and occurs at $m_\chi \approx 70$ GeV.
- 10 AKERIB 05 is incompatible with the DAMA most likely value. The strongest upper limit is 4×10^{-7} pb and occurs at $m_\chi \approx 60$ GeV.
- 11 The strongest upper limit is also close to 1.0×10^{-6} pb and occurs at $m_\chi \approx 70$ GeV. BENOIT 06 claim that the discrimination power of ZEPLIN-I measurement (ALNER 05A) is not reliable enough to obtain a limit better than 1×10^{-3} pb. However, SMITH 06 do not agree with the criticisms of BENOIT 06.
- 12 The strongest upper limit is also close to 1.4×10^{-6} pb and occurs at $m_\chi \approx 70$ GeV.

- 13 AKERIB 04 is incompatible with BERNABEI 00 most likely value, under the assumption of standard WIMP-halo interactions. The strongest upper limit is 4×10^{-7} pb and occurs at $m_\chi \approx 60$ GeV.
- 14 KIM 02 and ELLIS 04 calculate the χ - p elastic scattering cross section in the framework of $N=1$ supergravity models with radiative breaking of the electroweak gauge symmetry, but without universal scalar masses.
- 15 In the case of universal squark and slepton masses, but non-universal Higgs masses, the limit becomes 2×10^{-6} (2×10^{-11} when constraint from the BNL $g-2$ experiment are included), see ELLIS 03E. ELLIS 05 display the sensitivity of the elastic scattering cross section to the π -Nucleon Σ term.
- 16 PIERCE 04A calculates the χ - p elastic scattering cross section in the framework of models with very heavy scalar masses. See Fig. 2 of the paper.
- 17 The strongest upper limit is 1.8×10^{-5} pb and occurs at $m_\chi \approx 80$ GeV.
- 18 Under the assumption of standard WIMP-halo interactions, Akerib 03 is incompatible with BERNABEI 00 most likely value at the 99.98% CL. See Fig. 4.
- 19 BAER 03A calculates the χ - p elastic scattering cross section in several models including the framework of $N=1$ supergravity models with radiative breaking of the electroweak gauge symmetry.
- 20 The strongest upper limit is 7×10^{-6} pb and occurs at $m_\chi \approx 30$ GeV.
- 21 ABRAMS 02 is incompatible with the DAMA most likely value at the 99.9% CL. The strongest upper limit is 3×10^{-6} pb and occurs at $m_\chi \approx 30$ GeV.
- 22 BENOIT 02 excludes the central result of DAMA at the 99.8% CL.
- 23 The strongest upper limit is 2×10^{-5} pb and occurs at $m_\chi \approx 40$ GeV.
- 24 The strongest upper limit is 7×10^{-6} pb and occurs at $m_\chi \approx 46$ GeV.
- 25 The strongest upper limit is 1.8×10^{-5} pb and occurs at $m_\chi \approx 32$ GeV
- 26 BOTTINO 01 calculates the χ - p elastic scattering cross section in the framework of the following supersymmetric models: $N=1$ supergravity with the radiative breaking of the electroweak gauge symmetry, $N=1$ supergravity with nonuniversal scalar masses and an effective MSSM model at the electroweak scale.
- 27 Calculates the χ - p elastic scattering cross section in the framework of $N=1$ supergravity models with radiative breaking of the electroweak gauge symmetry.
- 28 ELLIS 01c calculates the χ - p elastic scattering cross section in the framework of $N=1$ supergravity models with radiative breaking of the electroweak gauge symmetry. ELLIS 02B find a range 2×10^{-8} - 1.5×10^{-7} at $\tan\beta=50$. In models with nonuniversal Higgs masses, the upper limit to the cross section is 4×10^{-7} .
- 29 ACCOMANDO 00 calculate the χ - p elastic scattering cross section in the framework of minimal $N=1$ supergravity models with radiative breaking of the electroweak gauge symmetry. The limit is relaxed by at least an order of magnitude when models with nonuniversal scalar masses are considered. A subset of the authors in ARNOWITT 02 updated the limit to $< 9 \times 10^{-8}$ ($\tan\beta < 55$).
- 30 BERNABEI 00 search for annual modulation of the WIMP signal. The data favor the hypothesis of annual modulation at 4σ and are consistent, for a particular model framework quoted there, with $m_{\chi^0}=44^{+12}_{-9}$ GeV and a spin-independent X^0 -proton cross section of $(5.4 \pm 1.0) \times 10^{-6}$ pb. See also BERNABEI 01 and BERNABEI 00c.
- 31 FENG 00 calculate the χ - p elastic scattering cross section in the framework of $N=1$ supergravity models with radiative breaking of the electroweak gauge symmetry with a particular emphasis on focus point models. At $\tan\beta=50$, the range is 8×10^{-8} - 4×10^{-7} .
- 32 BERNABEI 99 search for annual modulation of the WIMP signal. The data favor the hypothesis of annual modulation at 99.6%CL and are consistent, for the particular model framework considered there, with $m_{\chi^0}=59^{+17}_{-14}$ GeV and spin-independent X^0 -proton cross section of $(7.0^{+0.4}_{-1.2}) \times 10^{-6}$ pb (1 σ errors).
- 33 BERNABEI 98 search for annual modulation of the WIMP signal. The data are consistent, for the particular model framework considered there, with $m_{\chi^0}=59^{+36}_{-19}$ GeV and spin-independent X^0 -proton cross section of $(1.0^{+0.1}_{-0.4}) \times 10^{-5}$ pb (1 σ errors).

Other bounds on $\tilde{\chi}_1^0$ from astrophysics and cosmology

Most of these papers generally exclude regions in the $M_2 - \mu$ parameter plane by requiring that the $\tilde{\chi}_1^0$ contribution to the overall cosmological density is less than some maximal value to avoid overclosure of the Universe. Those not based on the cosmological density are indicated. Many of these papers also include LEP and/or other bounds.

VALUE	DOCUMENT ID	TECN	COMMENT
>46 GeV	1 ELLIS 00	RVUE	
●●● We do not use the following data for averages, fits, limits, etc. ●●●			
	2 BUCHMUELLER... 09	COSM	
	3 BUCHMUELLER... 08	COSM	
	4 ELLIS 08	COSM	
	5 ELLIS 07	COSM	
	4 BAER 05	COSM	
> 6 GeV	6,7 BELANGER 04	THEO	
	8 ELLIS 04B	COSM	
	9 PIERCE 04A	COSM	
	10 BAER 03C	COSM	
> 6 GeV	6 BOTTINO 03	COSM	
	10 CHATTOPAD...03	COSM	
	11 ELLIS 03	COSM	
	4 ELLIS 03B	COSM	
	10 ELLIS 03c	COSM	
> 18 GeV	6 HOOPER 03	COSM	$\Omega_\chi = 0.05-0.3$
	10 LAHANAS 03	COSM	
	12 BAER 02	COSM	
	13 ELLIS 02	COSM	
	14 LAHANAS 02	COSM	
	15 BARGER 01c	COSM	
	12 DJOUADI 01	COSM	
	16 ELLIS 01B	COSM	

Searches Particle Listings

Supersymmetric Particle Searches

	12	ROSZKOWSKI	01	COSM	
	11	BOEHM	00B	COSM	
	17	FENG	00	COSM	
	18	LAHANAS	00	COSM	
< 600 GeV	19	ELLIS	98B	COSM	
	20	EDSJO	97	COSM	Co-annihilation
	21	BAER	96	COSM	
	4	BEREZINSKY	95	COSM	
	22	FALK	95	COSM	CP-violating phases
	23	DREES	93	COSM	Minimal supergravity
	24	FALK	93	COSM	Sfermion mixing
	23	KELLEY	93	COSM	Minimal supergravity
	25	MIZUTA	93	COSM	Co-annihilation
	26	LOPEZ	92	COSM	Minimal supergravity, $m_0=A=0$
	27	MCDONALD	92	COSM	
	28	GRIEST	91	COSM	
	29	NOJIRI	91	COSM	Minimal supergravity
	30	OLIVE	91	COSM	
	31	ROSZKOWSKI	91	COSM	
	32	GRIEST	90	COSM	
	30	OLIVE	89	COSM	
none 100 eV - 15 GeV		SREDNICKI	88	COSM	$\tilde{\gamma}; m_{\tilde{\tau}}=100$ GeV
none 100 eV-5 GeV		ELLIS	84	COSM	$\tilde{\gamma}$; for $m_{\tilde{\tau}}=100$ GeV
		GOLDBERG	83	COSM	$\tilde{\gamma}$
	33	KRAUSS	83	COSM	$\tilde{\gamma}$
		VYSOTSKII	83	COSM	$\tilde{\gamma}$

- ELLIS 00 updates ELLIS 98. Uses LEP e^+e^- data at $\sqrt{s}=202$ and 204 GeV to improve bound on neutralino mass to 51 GeV when scalar mass universality is assumed and 46 GeV when Higgs mass universality is relaxed. Limits on $\tan\beta$ improve to > 2.7 ($\mu > 0$), > 2.2 ($\mu < 0$) when scalar mass universality is assumed and > 1.9 (both signs of μ) when Higgs mass universality is relaxed.
- BUCHMUELLER 09 places constraints on the SUSY parameter space in the framework of $N=1$ supergravity models with radiative breaking of the electroweak gauge symmetry using indirect experimental searches.
- BUCHMUELLER 08 places constraints on the SUSY parameter space in the framework of $N=1$ supergravity models with radiative breaking of the electroweak gauge symmetry using indirect experimental searches.
- Places constraints on the SUSY parameter space in the framework of $N=1$ supergravity models with radiative breaking of the electroweak gauge symmetry but non-Universal Higgs masses.
- ELLIS 07 places constraints on the SUSY parameter space in the framework of $N=1$ supergravity models with radiative breaking of the electroweak gauge symmetry with universality below the GUT scale.
- HOOPER 03, BOTTINO 03 (see also BOTTINO 03A and BOTTINO 04), and BELANGER 04 do not assume gaugino or scalar mass unification.
- Limit assumes a pseudo scalar mass < 200 GeV. For larger pseudo scalar masses, $m_\chi > 18(29)$ GeV for $\tan\beta = 50(10)$. Bounds from WMAP, $(g-2)_\mu$, $b \rightarrow s\gamma$, LEP.
- ELLIS 04b places constraints on the SUSY parameter space in the framework of $N=1$ supergravity models with radiative breaking of the electroweak gauge symmetry including supersymmetry breaking relations between A and B parameters. See also ELLIS 03d.
- PIERCE 04A places constraints on the SUSY parameter space in the framework of models with very heavy scalar masses.
- BAER 03, CHATTOPADHYAY 03, ELLIS 03c and LAHANAS 03 place constraints on the SUSY parameter space in the framework of $N=1$ supergravity models with radiative breaking of the electroweak gauge symmetry based on WMAP results for the cold dark matter density.
- BOEHM 00b and ELLIS 03 place constraints on the SUSY parameter space in the framework of minimal $N=1$ supergravity models with radiative breaking of the electroweak gauge symmetry. Includes the effect of $\chi\text{-}\tilde{t}$ co-annihilations.
- DJOUADI 01, ROSZKOWSKI 01, and BAER 02 place constraints on the SUSY parameter space in the framework of minimal $N=1$ supergravity models with radiative breaking of the electroweak gauge symmetry.
- ELLIS 02 places constraints on the soft supersymmetry breaking masses in the framework of minimal $N=1$ supergravity models with radiative breaking of the electroweak gauge symmetry.
- LAHANAS 02 places constraints on the SUSY parameter space in the framework of minimal $N=1$ supergravity models with radiative breaking of the electroweak gauge symmetry. Focuses on the role of pseudo-scalar Higgs exchange.
- BARGER 01c use the cosmic relic density inferred from recent CMB measurements to constrain the parameter space in the framework of minimal $N=1$ supergravity models with radiative breaking of the electroweak gauge symmetry.
- ELLIS 01b places constraints on the SUSY parameter space in the framework of minimal $N=1$ supergravity models with radiative breaking of the electroweak gauge symmetry. Focuses on models with large $\tan\beta$.
- FENG 00 explores cosmologically allowed regions of MSSM parameter space with multi-TeV masses.
- LAHANAS 00 use the new cosmological data which favor a cosmological constant and its implications on the relic density to constrain the parameter space in the framework of minimal $N=1$ supergravity models with radiative breaking of the electroweak gauge symmetry.
- ELLIS 98b assumes a universal scalar mass and radiative supersymmetry breaking with universal gaugino masses. The upper limit to the LSP mass is increased due to the inclusion of $\chi - \tilde{\tau}_R$ coannihilations.
- EDSJO 97 included all coannihilation processes between neutralinos and charginos for any neutralino mass and composition.
- Notes the location of the neutralino Z resonance and h resonance annihilation corridors in minimal supergravity models with radiative electroweak breaking.
- Mass of the bino (=LSP) is limited to $m_{\tilde{B}} \lesssim 350$ GeV for $m_t = 174$ GeV.
- DREES 93, KELLEY 93 compute the cosmic relic density of the LSP in the framework of minimal $N=1$ supergravity models with radiative breaking of the electroweak gauge symmetry.

- FALK 93 relax the upper limit to the LSP mass by considering sfermion mixing in the MSSM.
- MIZUTA 93 include coannihilations to compute the relic density of Higgsino dark matter.
- LOPEZ 92 calculate the relic LSP density in a minimal SUSY GUT model.
- MCDONALD 92 calculate the relic LSP density in the MSSM including exact tree-level annihilation cross sections for all two-body final states.
- GRIEST 91 improve relic density calculations to account for coannihilations, pole effects, and threshold effects.
- NOJIRI 91 uses minimal supergravity mass relations between squarks and sleptons to narrow cosmologically allowed parameter space.
- Mass of the bino (=LSP) is limited to $m_{\tilde{B}} \lesssim 350$ GeV for $m_t \leq 200$ GeV. Mass of the higgsino (=LSP) is limited to $m_{\tilde{H}} \lesssim 1$ TeV for $m_t \leq 200$ GeV.
- ROSZKOWSKI 91 calculates LSP relic density in mixed gaugino/higgsino region.
- Mass of the bino (=LSP) is limited to $m_{\tilde{B}} \lesssim 550$ GeV. Mass of the higgsino (=LSP) is limited to $m_{\tilde{H}} \lesssim 3.2$ TeV.
- KRAUSS 83 finds $m_{\tilde{\gamma}} \leq 30$ eV to 2.5 GeV. KRAUSS 83 takes into account the gravitino decay. Find that limits depend strongly on reheated temperature. For example a new allowed region $m_{\tilde{\gamma}} = 4\text{--}20$ MeV exists if $m_{\text{gravitino}} < 40$ TeV. See figure 2.

Unstable $\tilde{\chi}_1^0$ (Lightest Neutralino) MASS LIMIT

Unless otherwise stated, results in this section assume spectra and production rates as evaluated in the MSSM. Unless otherwise stated, the goldstino or gravitino mass $m_{\tilde{G}}$ is assumed to be negligible relative to all other masses. In the following, \tilde{G} is assumed to be undetected and to give rise to a missing energy (\cancel{E}) signature.

VALUE (GeV)	CL%	DOCUMENT ID	TECN	COMMENT
••• We do not use the following data for averages, fits, limits, etc. •••				
>149	95	1 AALTONEN	10 CDF	$p\bar{p} \rightarrow \tilde{\chi}\tilde{\chi}, \tilde{\chi}=\tilde{\chi}_2^0, \tilde{\chi}_1^\pm, \tilde{\chi}_1^0 \rightarrow \gamma\tilde{G}$, GMSB
		2 AALTONEN	08u CDF	$\tilde{\chi}_1^0 \rightarrow \gamma\tilde{G}$, GMSB
>125	95	3 ABAZOV	08F D0	$p\bar{p} \rightarrow \tilde{\chi}\tilde{\chi}, \tilde{\chi}=\tilde{\chi}_2^0, \tilde{\chi}_1^\pm, \tilde{\chi}_1^0 \rightarrow \gamma\tilde{G}$, GMSB
		4 ABAZOV	08x D0	$\tilde{\chi}_1^0 \rightarrow Z^0\tilde{G}$, GMSB
		5 ABULENCIA	07H CDF	$R, LL\bar{E}$
		6 ABAZOV	06D D0	$R, LL\bar{E}$
		7 ABAZOV	06P D0	R, λ_{122}
> 96.8	95	8 ABBIENDI	06B OPAL	$e^+e^- \rightarrow \tilde{B}\tilde{B}, (\tilde{B} \rightarrow \tilde{G}\gamma)$
		9 ABDALLAH	05B DLPH	$e^+e^- \rightarrow \tilde{G}\tilde{\chi}_1^0, (\tilde{\chi}_1^0 \rightarrow \tilde{G}\gamma)$
> 96	95	10 ABDALLAH	05B DLPH	$e^+e^- \rightarrow \tilde{B}\tilde{B}, (\tilde{B} \rightarrow \tilde{G}\gamma)$
> 93	95	11 ACOSTA	05E CDF	$p\bar{p} \rightarrow \tilde{\chi}\tilde{\chi}, \tilde{\chi}=\tilde{\chi}_2^0, \tilde{\chi}_1^\pm, \tilde{\chi}_1^0 \rightarrow \gamma\tilde{G}$, GMSB
		12 AKTAS	05 H1	$e^\pm p \rightarrow q\tilde{\chi}_1^0, \tilde{\chi}_1^0 \rightarrow \gamma\tilde{G}$, GMSB+ $R L Q\bar{D}$
		13 ABBIENDI	04N OPAL	$e^+e^- \rightarrow \gamma\gamma\tilde{E}$
> 66	95	14,15 ABDALLAH	04H DLPH	$AMS\bar{B}, \mu > 0$
> 38.0	95	16,17 ABDALLAH	04M DLPH	$R(\overline{UD}\bar{D})$
		18 ACHARD	04E L3	$e^+e^- \rightarrow \tilde{G}\tilde{\chi}_1^0, \tilde{\chi}_1^0 \rightarrow \tilde{G}\gamma$
> 99.5	95	19 ACHARD	04E L3	$e^+e^- \rightarrow \tilde{B}\tilde{B}, (\tilde{B} \rightarrow \tilde{G}\gamma)$
> 89		20 ABDALLAH	03D DLPH	$e^+e^- \rightarrow \tilde{\chi}_1^0\tilde{\chi}_1^0, \text{GMSB}, m(\tilde{G})=1\text{eV}$
		21 HEISTER	03C ALEP	$e^+e^- \rightarrow \tilde{B}\tilde{B}, (\tilde{B} \rightarrow \gamma\tilde{G})$
		22 HEISTER	03C ALEP	$e^+e^- \rightarrow \tilde{G}\tilde{\chi}_1^0, (\tilde{\chi}_1^0 \rightarrow \tilde{G}\gamma)$
> 39.9	95	23 ACHARD	02 L3	$R, MSUGRA$
> 92	95	24 HEISTER	02R ALEP	short lifetime
> 54	95	24 HEISTER	02R ALEP	any lifetime
> 85	95	25 ABBIENDI	01 OPAL	$e^+e^- \rightarrow \tilde{\chi}_1^0\tilde{\chi}_1^0, \text{GMSB}, \tan\beta=2$
> 76	95	25 ABBIENDI	01 OPAL	$e^+e^- \rightarrow \tilde{\chi}_1^0\tilde{\chi}_1^0, \text{GMSB}, \tan\beta=20$
> 32.5	95	26 ACCIARRI	01 L3	$R, \text{all } m_0, 0.7 \leq \tan\beta \leq 40$
		27 ADAMS	01 NTEV	$\tilde{\chi}^0 \rightarrow \mu\mu\nu, R, LL\bar{E}$
> 29	95	28 ABBIENDI	99T OPAL	$e^+e^- \rightarrow \tilde{\chi}_1^0\tilde{\chi}_1^0, R, m_0=500$ GeV, $\tan\beta > 1.2$
> 29	95	29 BARATE	99E ALEP	$R, LQ\bar{D}, \tan\beta=1.41, m_0=500$ GeV
		30 ABREU	98 DLPH	$e^+e^- \rightarrow \tilde{\chi}_1^0\tilde{\chi}_1^0, (\tilde{\chi}_1^0 \rightarrow \gamma\tilde{G})$
> 23	95	31 BARATE	98S ALEP	$R, LL\bar{E}$
		32 ELLIS	97 THEO	$e^+e^- \rightarrow \tilde{\chi}_1^0\tilde{\chi}_1^0, \tilde{\chi}_1^0 \rightarrow \gamma\tilde{G}$
		33 CABIBBO	81 COSM	

- AALTONEN 10 searched in 2.6 fb^{-1} of $p\bar{p}$ collisions at $\sqrt{s} = 1.96$ TeV for diphoton events with large E_T . They may originate from the production of $\tilde{\chi}^\pm$ in pairs or associated to a $\tilde{\chi}_2^0$, decaying into $\tilde{\chi}_1^0$ which itself decays in GMSB to $\gamma\tilde{G}$. There is no excess of events beyond expectation. An upper limit on the cross section is calculated in the GMSB model as a function of the $\tilde{\chi}_1^0$ mass and lifetime, see their Fig. 2. A limit is derived on the $\tilde{\chi}_1^0$ mass of 149 GeV for $\tau_{\tilde{\chi}_1^0} \ll 1$ ns, which improves the results of previous searches.
- AALTONEN 08u searched in 570 pb^{-1} of $p\bar{p}$ collisions at $\sqrt{s} = 1.96$ TeV for events that contain a time-delayed photon, at least one jet, and large E_T . The time-of-arrival is measured for each electromagnetic tower with a resolution of 0.50 ns. The number of observed events in the signal region is consistent with the background estimation. An upper limit on the cross section is derived as a function of the $\tilde{\chi}_1^0$ mass and lifetime, shown in their Fig. 24. The comparison with the NLO cross section for GMSB yields an exclusion of the $\tilde{\chi}_1^0$ mass as a function of its lifetime, see Fig. 25. See ABULENCIA 07P for a previous analysis of the same data set.

- ³ ABAZOV 08F looked in 1.1 fb^{-1} of $p\bar{p}$ collisions at $\sqrt{s} = 1.96 \text{ TeV}$ for diphoton events with large \cancel{E}_T . They may originate from the production of $\tilde{\chi}^\pm$ in pairs or associated to a $\tilde{\chi}_2^0$, decaying to a $\tilde{\chi}_1^0$ which itself decays promptly in GMSB to $\tilde{\chi}_1^0 \rightarrow \gamma \tilde{G}$. No significant excess was found compared to the background expectation. A limit is derived on the masses of SUSY particles in the GMSB framework for $M = 2\Lambda$, $N = 1$, $\tan\beta = 15$ and $\mu > 0$, see Figure 2. It also excludes $\Lambda < 91.5 \text{ TeV}$. Supersedes the results of ABAZOV 05A.
- ⁴ ABAZOV 08x searched in 1.1 fb^{-1} of $p\bar{p}$ collisions at $\sqrt{s} = 1.96 \text{ TeV}$ for an excess of events with electron pairs. Their vertex, reconstructed from the directions measured in the segmented electromagnetic calorimeter, is required to be away from the primary interaction point. Such delayed decays might be expected for a Higgsino-like $\tilde{\chi}_1^0$ in GMSB. No significant excess was found compared to the background expectation. Upper limits on the cross-section times branching ratio are extracted as a function of the lifetime for several ranges of dielectron invariant masses, see their Fig. 3.
- ⁵ ABULENCIA 07H searched in 346 pb^{-1} of $p\bar{p}$ collisions at $\sqrt{s} = 1.96 \text{ TeV}$ for events with at least three leptons (e or μ) from the decay of $\tilde{\chi}_1^0$ via $L\tilde{L}\tilde{E}$ couplings. The results are consistent with the hypothesis of no signal. Upper limits on the cross-section are extracted and a limit is derived in the framework of mSUGRA on the masses of $\tilde{\chi}_1^0$ and $\tilde{\chi}_1^\pm$, see e.g. their Fig. 3 and Tab. II.
- ⁶ ABAZOV 06d looked in 360 pb^{-1} of $p\bar{p}$ collisions at $\sqrt{s} = 1.96 \text{ TeV}$ for events with three leptons originating from the pair production of charginos and neutralinos, followed by R decays mediated by $L\tilde{L}\tilde{E}$ couplings. One coupling is assumed to be dominant at a time. No significant excess was found compared to the background expectation in the $e\ell$, $\mu\mu\ell$ nor $e\tau\tau$ ($\ell = e, \mu$) final states. Upper limits on the cross-section are extracted in a specific MSUGRA model and a MSSM model without unification of M_1 and M_2 at the GUT scale. A limit is derived on the masses of charginos and neutralinos for both scenarios assuming λ_{ijk} couplings such that the decay length is less than 1 cm, see their Table III and Fig. 4.
- ⁷ ABAZOV 06p looked in 380 pb^{-1} of $p\bar{p}$ collisions at $\sqrt{s} = 1.96 \text{ TeV}$ for events with at least 2 opposite sign isolated muons which might arise from the decays of neutralinos into $\mu\mu\nu$ via R couplings $L\tilde{L}\tilde{E}$. No events are observed in the decay region defined by a radius between 5 and 20 cm, in agreement with the SM expectation. Limits are set on the cross-section times branching ratio as a function of lifetime, shown in their Fig. 3. This limit excludes the SUSY interpretation of the NuTeV excess of dimuon events reported in ADAMS 01.
- ⁸ ABBIENDI 06b use 600 pb^{-1} of data from $\sqrt{s} = 189\text{--}209 \text{ GeV}$. They look for events with diphotons + \cancel{E} final states originating from prompt decays of pair-produced neutralinos in a GMSB scenario with $\tilde{\chi}_1^0$ NLSP. Limits on the cross-section are computed as a function of $m(\tilde{\chi}_1^0)$, see their Fig. 14. The limit on the $\tilde{\chi}_1^0$ mass is for a pure Bino state assuming a prompt decay, with lifetimes up to 10^{-9} s. Supersedes the results of ABBIENDI 04n.
- ⁹ ABDALLAH 05B use data from $\sqrt{s} = 180\text{--}209 \text{ GeV}$. They look for events with single photons + \cancel{E} final states. Limits are computed in the plane $(m(\tilde{G}), m(\tilde{\chi}_1^0))$, shown in their Fig. 9b for a pure Bino state in the GMSB framework and in Fig. 9c for a no-scale supergravity model. Supersedes the results of ABREU 00z.
- ¹⁰ ABDALLAH 05b use data from $\sqrt{s} = 130\text{--}209 \text{ GeV}$. They look for events with diphotons + \cancel{E} final states and single photons not pointing to the vertex, expected in GMSB when the $\tilde{\chi}_1^0$ is the NLSP. Limits are computed in the plane $(m(\tilde{G}), m(\tilde{\chi}_1^0))$, see their Fig. 10. The lower limit is derived on the $\tilde{\chi}_1^0$ mass for a pure Bino state assuming a prompt decay and $m_{\tilde{e}_R} = m_{\tilde{e}_L} = 2 m_{\tilde{\chi}_1^0}$. It improves to 100 GeV for $m_{\tilde{e}_R} = m_{\tilde{e}_L} = 1.1 m_{\tilde{\chi}_1^0}$. and the limit in the plane $(m(\tilde{\chi}_1^0), m(\tilde{e}_R))$ is shown in Fig. 10b. For long-lived neutralinos, cross-section limits are displayed in their Fig. 11. Supersedes the results of ABREU 00z.
- ¹¹ ACOSTA 05E looked in 202 pb^{-1} of $p\bar{p}$ collisions at $\sqrt{s}=1.96 \text{ TeV}$ for diphoton events with large \cancel{E}_T . They may originate from the production of $\tilde{\chi}^\pm$ in pairs or associated to a $\tilde{\chi}_2^0$, decaying to a $\tilde{\chi}_1^0$ which itself decays promptly in GMSB to $\gamma \tilde{G}$. No events are selected at large \cancel{E}_T compared to the background expectation. A limit is derived on the masses of SUSY particles in the GMSB framework for $M = 2\Lambda$, $N = 1$, $\tan\beta = 15$ and $\mu > 0$, see Figure 2. It also excludes $\Lambda < 69 \text{ TeV}$. Supersedes the results of ABE 99i.
- ¹² AKTAS 05 data collected at 319 GeV with 64.3 pb^{-1} of e^+p and 13.5 pb^{-1} of e^-p . They look for R resonant $\tilde{\chi}_1^0$ production via t -channel exchange of a \tilde{e} , followed by prompt GMSB decay of the $\tilde{\chi}_1^0$ to $\gamma \tilde{G}$. Upper limits at 95% on the cross section are derived, see their Figure 4, and compared to two example scenarios. In Figure 5, they display 95% exclusion limits in the plane of $M(\tilde{\chi}_1^0)$ versus $M(\tilde{e}_L) - M(\tilde{\chi}_1^0)$ for the two scenarios and several values of the χ' Yukawa coupling.
- ¹³ ABBIENDI 04n use data from $\sqrt{s} = 189\text{--}209 \text{ GeV}$, setting limits on $\sigma(e^+e^- \rightarrow XX) \times B^2(X \rightarrow Y\gamma)$, with Y invisible (see their Fig. 4). Limits on $\tilde{\chi}_1^0$ masses for a specific model are given. Supersedes the results of ABBIENDI, G 00d.
- ¹⁴ ABDALLAH 04H use data from LEP 1 and $\sqrt{s} = 192\text{--}208 \text{ GeV}$. They re-use results or re-analyze the data from ABDALLAH 03M to put limits on the parameter space of anomaly-mediated supersymmetry breaking (AMSB), which is scanned in the region $1 < m_{3/2} < 50 \text{ TeV}$, $0 < m_0 < 1000 \text{ GeV}$, $1.5 < \tan\beta < 35$, both signs of μ . The constraints are obtained from the searches for mass degenerate chargino and neutralino, for SM-like and invisible Higgs, for leptonically decaying charginos and from the limit on non-SM Z width of 3.2 MeV. The limit is for $m_t = 174.3 \text{ GeV}$ (see Table 2 for other m_t values).
- ¹⁵ The limit improves to 73 GeV for $\mu < 0$.
- ¹⁶ ABDALLAH 04M use data from $\sqrt{s} = 192\text{--}208 \text{ GeV}$ to derive limits on sparticle masses under the assumption of R with $L\tilde{L}\tilde{E}$ or $U\tilde{D}\tilde{D}$ couplings. The results are valid in the ranges $90 < m_0 < 500 \text{ GeV}$, $0.7 < \tan\beta < 30$, $-200 < \mu < 200 \text{ GeV}$, $0 < M_2 < 400 \text{ GeV}$. Supersedes the result of ABREU 01d and ABREU 00u.
- ¹⁷ The limit improves to 39.5 GeV for $L\tilde{L}\tilde{E}$ couplings.
- ¹⁸ ACHARD 04E use data from $\sqrt{s} = 189\text{--}209 \text{ GeV}$. They look for events with single photons + \cancel{E} final states. Limits are computed in the plane $(m(\tilde{G}), m(\tilde{\chi}_1^0))$, shown in their Fig. 8c for a no-scale supergravity model, excluding, e.g., Gravitino masses below 10^{-5} eV for neutralino masses below 172 GeV. Supersedes the results of ACCIARRI 99r.
- ¹⁹ ACHARD 04E use data from $\sqrt{s} = 189\text{--}209 \text{ GeV}$. They look for events with diphotons + \cancel{E} final states. Limits are computed in the plane $(m(\tilde{\chi}_1^0), m(\tilde{e}_R))$, see their Fig. 8d. The limit on the $\tilde{\chi}_1^0$ mass is for a pure Bino state assuming a prompt decay, with $m_{\tilde{e}_L} = 1.1 m_{\tilde{\chi}_1^0}$ and $m_{\tilde{e}_R} = 2.5 m_{\tilde{\chi}_1^0}$. Supersedes the results of ACCIARRI 99r.
- ²⁰ ABDALLAH 03D use data from $\sqrt{s} = 161\text{--}208 \text{ GeV}$. They look for 4-tau + \cancel{E} final states, expected in GMSB when the $\tilde{\tau}_1$ is the NLSP, and 4-lepton + \cancel{E} final states, expected in the co-NLSP scenario, and assuming a short-lived $\tilde{\chi}_1^0$ ($m(\tilde{G}) < 1 \text{ eV}$). Limits are computed in the plane $(m(\tilde{\tau}_1), m(\tilde{\chi}_1^0))$ from a scan of the GMSB parameters space, after combining these results with the search for slepton pair production from the same paper to cover prompt decays and for the case of $\tilde{\chi}_1^0$ NLSP from ABREU 00z. The limit above is reached for a single generation of messengers and when the $\tilde{\tau}_1$ is the NLSP. Stronger limits are obtained when more messenger generations are assumed or when the other sleptons are co-NLSP, see their Fig. 10. Supersedes the results of ABREU 01G.
- ²¹ HEISTER 03c use the data from $\sqrt{s} = 189\text{--}209 \text{ GeV}$ to search for $\gamma \cancel{E}_T$ final states with non-pointing photons and $\gamma \gamma \cancel{E}_T$ events. Interpreted in the framework of Minimal GMSB, a lower bound on the $\tilde{\chi}_1^0$ mass is obtained as function of its lifetime. For a laboratory lifetime of less than 3 ns, the limit at 95% CL is 98.8 GeV. For other lifetimes, see their Fig. 5. These results are interpreted in a more general GMSB framework in HEISTER 02r.
- ²² HEISTER 03c use the data from $\sqrt{s} = 189\text{--}209 \text{ GeV}$ to search for $\gamma \cancel{E}_T$ final states. They obtained an upper bound on the cross section for the process $e^+e^- \rightarrow \tilde{G} \tilde{\chi}_1^0$, followed by the prompt decay $\tilde{\chi}_1^0 \rightarrow \gamma \tilde{G}$, shown in their Fig. 4. These results supersede BARATE 98h.
- ²³ ACHARD 02 searches for the production of sparticles in the case of R prompt decays with $L\tilde{L}\tilde{E}$ or $U\tilde{D}\tilde{D}$ couplings at $\sqrt{s}=189\text{--}208 \text{ GeV}$. The search is performed for direct and indirect decays, assuming one coupling at a time to be nonzero. The MSUGRA limit results from a scan over the MSSM parameter space with the assumption of gaugino and scalar mass unification at the GUT scale, imposing simultaneously the exclusions from neutralino, chargino, sleptons, and squarks analyses. The limit holds for $U\tilde{D}\tilde{D}$ couplings and increases to 40.2 GeV for $L\tilde{L}\tilde{E}$ couplings. For L3 limits from $LQ\tilde{D}$ couplings, see ACCIARRI 01.
- ²⁴ HEISTER 02r search for signals of GMSB in the 189–209 GeV data. For the $\tilde{\chi}_1^0$ NLSP scenario, they looked for topologies consisting of $\gamma\gamma\cancel{E}$ or a single γ not pointing to the interaction vertex. For the $\tilde{\ell}$ NLSP case, the topologies consist of $\ell\ell\cancel{E}$ or $4\ell\cancel{E}$ (from $\tilde{\chi}_1^0 \tilde{\chi}_1^0$ production), including leptons with large impact parameters, kinks, or stable particles. Limits are derived from a scan over the GMSB parameters (see their Table 5 for the ranges). The limits are valid whichever is the NLSP. The absolute mass bound on the $\tilde{\chi}_1^0$ for any lifetime includes indirect limits from the chargino search, and from the slepton search HEISTER 02e performed within the MSUGRA framework. A bound for any NLSP and any lifetime of 77 GeV has also been derived by using the constraints from the neutral Higgs search in HEISTER 02. Limits on the universal SUSY mass scale Λ are also derived in the paper. Supersedes the results from BARATE 00c.
- ²⁵ ABBIENDI 01 looked for final states with $\gamma\gamma\cancel{E}$, $\ell\ell\cancel{E}$, with possibly additional activity and four leptons + \cancel{E} to search for prompt decays of $\tilde{\chi}_1^0$ or $\tilde{\ell}_1$ in GMSB. They derive limits in the plane $(m_{\tilde{\chi}_1^0}, m_{\tilde{\tau}_1})$, see Fig. 6, allowing either the $\tilde{\chi}_1^0$ or a $\tilde{\ell}_1$ to be the NLSP. Two scenarios are considered: $\tan\beta=2$ with the 3 sleptons degenerate in mass and $\tan\beta=20$ where the $\tilde{\tau}_1$ is lighter than the other sleptons. Data taken at $\sqrt{s}=189 \text{ GeV}$.
- ²⁶ ACCIARRI 01 searches for multi-lepton and/or multi-jet final states from R prompt decays with $L\tilde{L}\tilde{E}$, $LQ\tilde{D}$, or $U\tilde{D}\tilde{D}$ couplings at $\sqrt{s}=189 \text{ GeV}$. The search is performed for direct and indirect decays of neutralinos, charginos, and scalar leptons, with the $\tilde{\chi}_1^0$ or a $\tilde{\ell}$ as LSP and assuming one coupling to be nonzero at a time. Mass limits are derived using simultaneously the constraints from the neutralino, chargino, and slepton analyses; and the Z^0 width measurements from ACCIARRI 00c in a scan of the parameter space assuming MSUGRA with gaugino and scalar mass universality. Updates and supersedes the results from ACCIARRI 99i.
- ²⁷ ADAMS 01 looked for neutral particles with mass $> 2.2 \text{ GeV}$, produced by 900 GeV protons incident on a Beryllium oxide target and decaying through weak interactions into $\mu\mu$, μe , or $\mu\pi$ final states in the decay channel of the NuTeV detector (E815) at Fermilab. The number of observed events is $3\mu\mu$, $0\mu e$, and $0\mu\pi$ with an expected background of 0.069 ± 0.010 , 0.13 ± 0.02 , and 0.14 ± 0.02 , respectively. The $\mu\mu$ events are consistent with the R decay of a neutralino with mass around 5 GeV. However, they share several aspects with ν -interaction backgrounds. An upper limit on the differential production cross section of neutralinos in pp interactions as function of the decay length is given in Fig. 3.
- ²⁸ ABBIENDI 99t searches for the production of neutralinos in the case of R -parity violation with $L\tilde{L}\tilde{E}$, $LQ\tilde{D}$, or $U\tilde{D}\tilde{D}$ couplings using data from $\sqrt{s}=183 \text{ GeV}$. They investigate topologies with multiple leptons, jets plus leptons, or multiple jets, assuming one coupling at a time to be non-zero and giving rise to direct or indirect decays. Mixed decays (where one particle has a direct, the other an indirect decay) are also considered for the $U\tilde{D}\tilde{D}$ couplings. Upper limits on the cross section are derived which, combined with the constraint from the Z^0 width, allow to exclude regions in the M_2 versus μ plane for any coupling. Limits on the neutralino mass are obtained for non-zero $L\tilde{L}\tilde{E}$ couplings $> 10^{-5}$. The limit disappears for $\tan\beta < 1.2$ and it improves to 50 GeV for $\tan\beta > 20$.
- ²⁹ BARATE 99e looked for the decay of gauginos via R -violating couplings $LQ\tilde{D}$. The bound is significantly reduced for smaller values of m_0 . Data collected at $\sqrt{s}=130\text{--}172 \text{ GeV}$.
- ³⁰ ABREU 98 uses data at $\sqrt{s}=161$ and 172 GeV. Upper bounds on $\gamma\gamma\cancel{E}$ cross section are obtained. Similar limits on $\gamma\cancel{E}$ are also given, relevant for $e^+e^- \rightarrow \tilde{\chi}_1^0 \tilde{G}$ production.
- ³¹ BARATE 98s looked for the decay of gauginos via R -violating coupling $L\tilde{L}\tilde{E}$. The bound improves to 25 GeV if the chargino decays into neutralino which further decays into lepton pairs. Data collected at $\sqrt{s}=130\text{--}172 \text{ GeV}$.
- ³² ELLIS 97 reanalyzed the LEP 2 ($\sqrt{s}=161 \text{ GeV}$) limits of $\sigma(\gamma\gamma + E_{\text{miss}}) < 0.2 \text{ pb}$ to exclude $m_{\tilde{\chi}_1^0} < 63 \text{ GeV}$ if $m_{\tilde{e}_L} = m_{\tilde{e}_R} < 150 \text{ GeV}$ and $\tilde{\chi}_1^0$ decays to $\gamma \tilde{G}$ inside detector.
- ³³ CABIBBO 81 consider $\tilde{\gamma} \rightarrow \gamma$ goldstino. Photino must be either light enough ($< 30 \text{ eV}$) to satisfy cosmology bound, or heavy enough ($> 0.3 \text{ MeV}$) to have disappeared at early universe.

$\tilde{\chi}_2^0, \tilde{\chi}_3^0, \tilde{\chi}_4^0$ (Neutralinos) MASS LIMITS

Neutralinos are unknown mixtures of photinos, z-inos, and neutral higgsinos (the supersymmetric partners of photons and of Z and Higgs bosons). The limits here apply only to $\tilde{\chi}_2^0, \tilde{\chi}_3^0$, and $\tilde{\chi}_4^0$. $\tilde{\chi}_1^0$ is the lightest supersymmetric particle (LSP); see $\tilde{\chi}_1^0$ Mass Limits. It is not possible to quote rigorous mass limits because they are extremely model dependent; i.e. they depend on branching ratios of various $\tilde{\chi}^0$ decay

Searches Particle Listings

Supersymmetric Particle Searches

modes, on the masses of decay products ($\tilde{e}, \tilde{\gamma}, \tilde{q}, \tilde{g}$), and on the \tilde{e} mass exchanged in $e^+e^- \rightarrow \tilde{\chi}_i^0 \tilde{\chi}_j^0$. Limits arise either from direct searches, or from the MSSM constraints set on the gaugino and higgsino mass parameters M_2 and μ through searches for lighter charginos and neutralinos. Often limits are given as contour plots in the $m_{\tilde{\chi}_0^0} - m_{\tilde{e}}$ plane vs other parameters. When specific assumptions are made, e.g. the neutralino is a pure photino ($\tilde{\gamma}$), pure z-ino (\tilde{Z}), or pure neutral higgsino (\tilde{H}^0), the neutralinos will be labelled as such.

Limits obtained from e^+e^- collisions at energies up to 136 GeV, as well as other limits from different techniques, are now superseded and have not been included in this compilation. They can be found in the 1998 Edition (The European Physical Journal **C3** 1 (1998)) of this Review. $\Delta m = m_{\tilde{\chi}_2^0} - m_{\tilde{\chi}_1^0}$.

VALUE (GeV)	CL%	DOCUMENT ID	TECN	COMMENT
> 78	95	¹ ABBIENDI	04H OPAL	$\tilde{\chi}_2^0$, all $\tan\beta$, $\Delta m > 5$ GeV, $m_0 > 500$ GeV, $A_0 = 0$
> 62.4	95	² ABREU	00W DLPH	$\tilde{\chi}_2^0$, $1 \leq \tan\beta \leq 40$, all Δm , all m_0
> 99.9	95	² ABREU	00W DLPH	$\tilde{\chi}_3^0$, $1 \leq \tan\beta \leq 40$, all Δm , all m_0
> 116.0	95	² ABREU	00W DLPH	$\tilde{\chi}_4^0$, $1 \leq \tan\beta \leq 40$, all Δm , all m_0
• • • We do not use the following data for averages, fits, limits, etc. • • •				
		³ ABULENCIA	07N CDF	$\rho\bar{\rho} \rightarrow \tilde{\chi}_1^\pm \tilde{\chi}_2^0$
		⁴ ABDALLAH	05B DLPH	$e^+e^- \rightarrow \tilde{\chi}_2^0 \tilde{\chi}_2^0, (\tilde{\chi}_2^0 \rightarrow \tilde{\chi}_1^0 \gamma)$
		⁵ ACHARD	04E L3	$e^+e^- \rightarrow \tilde{\chi}_2^0 \tilde{\chi}_2^0, (\tilde{\chi}_2^0 \rightarrow \tilde{\chi}_1^0 \gamma)$
> 80.0	95	⁶ ACHARD	02 L3	$\tilde{\chi}_2^0, \tilde{R}$, MSUGRA
> 107.2	95	⁶ ACHARD	02 L3	$\tilde{\chi}_3^0, \tilde{R}$, MSUGRA
		⁷ ABREU	01B DLPH	$e^+e^- \rightarrow \tilde{\chi}_1^0 \tilde{\chi}_j^0$
> 68.0	95	⁸ ACCIARRI	01 L3	$\tilde{\chi}_2^0, \tilde{R}$, all m_0 , $0.7 \leq \tan\beta \leq 40$
> 99.0	95	⁸ ACCIARRI	01 L3	$\tilde{\chi}_3^0, \tilde{R}$, all m_0 , $0.7 \leq \tan\beta \leq 40$
> 50	95	⁹ ABREU	00U DLPH	$\tilde{\chi}_2^0, \tilde{R}$ ($LL\bar{E}$), all Δm , $1 \leq \tan\beta \leq 30$
		¹⁰ ABBIENDI	99F OPAL	$e^+e^- \rightarrow \tilde{\chi}_2^0 \tilde{\chi}_1^0$ ($\tilde{\chi}_2^0 \rightarrow \gamma \tilde{\chi}_1^0$)
		¹¹ ABBIENDI	99F OPAL	$e^+e^- \rightarrow \tilde{\chi}_2^0 \tilde{\chi}_2^0$ ($\tilde{\chi}_2^0 \rightarrow \gamma \tilde{\chi}_1^0$)
		¹² ABBOTT	98C D0	$\rho\bar{\rho} \rightarrow \tilde{\chi}_1^\pm \tilde{\chi}_2^0$
> 82.2	95	¹³ ABE	98J CDF	$\rho\bar{\rho} \rightarrow \tilde{\chi}_1^\pm \tilde{\chi}_2^0$
> 92	95	¹⁴ ACCIARRI	98F L3	$\tilde{H}_2^0, \tan\beta=1.41, M_2 < 500$ GeV
		¹⁵ ACCIARRI	98V L3	$e^+e^- \rightarrow \tilde{\chi}_2^0 \tilde{\chi}_{1,2}^0$ ($\tilde{\chi}_2^0 \rightarrow \gamma \tilde{\chi}_1^0$)
> 53	95	¹⁶ BARATE	98H ALEP	$e^+e^- \rightarrow \tilde{\gamma} \tilde{\gamma}$ ($\tilde{\gamma} \rightarrow \gamma \tilde{H}^0$)
> 74	95	¹⁷ BARATE	98J ALEP	$e^+e^- \rightarrow \tilde{\gamma} \tilde{\gamma}$ ($\tilde{\gamma} \rightarrow \gamma \tilde{H}^0$)
		¹⁸ ABACHI	96 D0	$\rho\bar{\rho} \rightarrow \tilde{\chi}_1^\pm \tilde{\chi}_2^0$
		¹⁹ ABE	96K CDF	$\rho\bar{\rho} \rightarrow \tilde{\chi}_1^\pm \tilde{\chi}_2^0$

¹ ABBIENDI 04H search for charginos and neutralinos in events with acoplanar leptons+jets and multi-jet final states in the 192–209 GeV data, combined with the results on leptonic final states from ABBIENDI 04. The results hold for a scan over the parameter space covering the region $0 < M_2 < 5000$ GeV, $-1000 < \mu < 1000$ GeV and $\tan\beta$ from 1 to 40. This limit supersedes ABBIENDI 00H.

² ABREU 00W combines data collected at $\sqrt{s}=189$ GeV with results from lower energies. The mass limit is obtained by constraining the MSSM parameter space with gaugino and stfermion mass universality at the GUT scale, using the results of negative direct searches for neutralinos (including cascade decays and $\tilde{\tau}\tau$ final states) from ABREU 01, for charginos from ABREU 00J and ABREU 00T (for all Δm_{\pm}), and for charged sleptons from ABREU 01B. The results hold for the full parameter space defined by all values of M_2 and $|\mu| \leq 2$ TeV with the $\tilde{\chi}_1^0$ as LSP.

³ ABULENCIA 07N searched in 1 fb^{-1} of $\rho\bar{\rho}$ collisions at $\sqrt{s} = 1.96$ TeV for events with two same sign leptons (e or μ) from the decay of $\tilde{\chi}_1^\pm \tilde{\chi}_2^0 X$ and large \cancel{E}_T . A slight excess of 13 events is observed over a SM background expectation of 7.8 ± 1.1 . However, the kinematic distributions do not show any anomalous deviation from expectations in any particular region of parameter space.

⁴ ABDALLAH 05B use data from $\sqrt{s} = 130\text{--}209$ GeV, looking for events with diphotons + \cancel{E} . Limits on the cross-section are computed in the plane $(m(\tilde{\chi}_2^0), m(\tilde{\chi}_1^0))$, see Fig. 12. Supersedes the results of ABREU 00Z.

⁵ ACHARD 04E use data from $\sqrt{s} = 189\text{--}209$ GeV, looking for events with diphotons + \cancel{E} . Limits are computed in the plane $(m(\tilde{\chi}_2^0), m(\tilde{e}_R))$, for $\Delta m > 10$ GeV, see Fig. 7. Supersedes the results of ACCIARRI 99R.

⁶ ACHARD 02 searches for the production of sparticles in the case of \tilde{R} prompt decays with $LL\bar{E}$ or UDD couplings at $\sqrt{s}=189\text{--}208$ GeV. The search is performed for direct and indirect decays, assuming one coupling at the time to be nonzero. The MSUGRA limit results from a scan over the MSSM parameter space with the assumption of gaugino and scalar mass unification at the GUT scale, imposing simultaneously the exclusions from neutralino, chargino, sleptons, and squarks analyses. The limit of $\tilde{\chi}_2^0$ holds for UDD couplings and increases to 84.0 GeV for $LL\bar{E}$ couplings. The same $\tilde{\chi}_3^0$ limit holds for both $LL\bar{E}$ and UDD couplings. For L3 limits from $LQ\bar{D}$ couplings, see ACCIARRI 01.

⁷ ABREU 01B used data from $\sqrt{s}=189$ GeV to search for the production of $\tilde{\chi}_i^0 \tilde{\chi}_j^0$. They looked for di-jet and di-lepton pairs with \cancel{E} for events from $\tilde{\chi}_i^0 \tilde{\chi}_j^0$ with the decay $\tilde{\chi}_j^0 \rightarrow f\bar{f} \tilde{\chi}_1^0$; multi-jet and multi-lepton pairs with or without additional photons to cover the cascade decays $\tilde{\chi}_j^0 \rightarrow f\bar{f} \tilde{\chi}_2^0$, followed by $\tilde{\chi}_j^0 \rightarrow \tilde{f}\tilde{f} \tilde{\chi}_1^0$ or $\tilde{\chi}_j^0 \rightarrow \gamma \tilde{\chi}_1^0$; multi-tau final states from $\tilde{\chi}_j^0 \rightarrow \tilde{\tau}\tau$ with $\tilde{\tau} \rightarrow \tau \tilde{\chi}_1^0$. See Figs. 9 and 10 for limits on the (μ, M_2) plane for $\tan\beta=1.0$ and different values of m_0 .

⁸ ACCIARRI 01 searches for multi-lepton and/or multi-jet final states from \tilde{R} prompt decays with $LL\bar{E}, LQ\bar{D}$, or UDD couplings at $\sqrt{s}=189$ GeV. The search is performed for direct and indirect decays of neutralinos, charginos, and scalar leptons, with the $\tilde{\chi}_1^0$ or a $\tilde{\ell}$ as LSP and assuming one coupling to be nonzero at a time. Mass limits are derived using simultaneously the constraints from the neutralino, chargino, and slepton analyses; and the Z^0 width measurements from ACCIARRI 00C in a scan of the parameter space assuming MSUGRA with gaugino and scalar mass universality. Updates and supersedes the results from ACCIARRI 99I.

⁹ ABREU 00U searches for the production of charginos and neutralinos in the case of R -parity violation with $LL\bar{E}$ couplings, using data from $\sqrt{s}=189$ GeV. They investigate topologies with multiple leptons or jets plus leptons, assuming one coupling to be nonzero at the time and giving rise to direct or indirect decays. Limits are obtained in the M_2 versus μ plane and a limit on the neutralino mass is derived from a scan over the parameters m_0 and $\tan\beta$.

¹⁰ ABBIENDI 99F looked for $\gamma\tilde{E}$ final states at $\sqrt{s}=183$ GeV. They obtained an upper bound on the cross section for the production $e^+e^- \rightarrow \tilde{\chi}_2^0 \tilde{\chi}_1^0$ followed by the prompt decay $\tilde{\chi}_2^0 \rightarrow \gamma \tilde{\chi}_1^0$ of 0.075–0.80 pb in the region $m_{\tilde{\chi}_2^0} + m_{\tilde{\chi}_1^0} > m_Z, m_{\tilde{\chi}_2^0} = 91\text{--}183$ GeV, and $\Delta m > 5$ GeV. See Fig. 7 for explicit limits in the $(m_{\tilde{\chi}_2^0}, m_{\tilde{\chi}_1^0})$ plane.

¹¹ ABBIENDI 99F looked for $\gamma\gamma\tilde{E}$ final states at $\sqrt{s}=183$ GeV. They obtained an upper bound on the cross section for the production $e^+e^- \rightarrow \tilde{\chi}_2^0 \tilde{\chi}_2^0$ followed by the prompt decay $\tilde{\chi}_2^0 \rightarrow \gamma \tilde{\chi}_1^0$ of 0.08–0.37 pb for $m_{\tilde{\chi}_2^0} = 45\text{--}81.5$ GeV, and $\Delta m > 5$ GeV. See Fig. 11 for explicit limits in the $(m_{\tilde{\chi}_2^0}, m_{\tilde{\chi}_1^0})$ plane.

¹² ABBOTT 98C searches for trilepton final states ($\ell=e, \mu$). See footnote to ABBOTT 98C in the Chargino Section for details on the assumptions. Assuming a negligible decay rate of $\tilde{\chi}_1^\pm$ and $\tilde{\chi}_2^0$ to quarks, they obtain $m_{\tilde{\chi}_2^0} \gtrsim 103$ GeV.

¹³ ABE 98J searches for trilepton final states ($\ell=e, \mu$). See footnote to ABE 98J in the Chargino Section for details on the assumptions. The quoted result for $m_{\tilde{\chi}_2^0}$ corresponds to the best limit within the selected range of parameters, obtained for $m_{\tilde{q}} > m_{\tilde{g}}, \tan\beta=2$, and $\mu=-600$ GeV.

¹⁴ ACCIARRI 98F is obtained from direct searches in the $e^+e^- \rightarrow \tilde{\chi}_{1,2}^0 \tilde{\chi}_2^0$ production channels, and indirectly from $\tilde{\chi}_1^\pm$ and $\tilde{\chi}_1^0$ searches within the MSSM. See footnote to ACCIARRI 98F in the Chargino Section for further details on the assumptions. Data taken at $\sqrt{s} = 130\text{--}172$ GeV.

¹⁵ ACCIARRI 98V looked for $\gamma(\gamma)\tilde{E}$ final states at $\sqrt{s}=183$ GeV. They obtained an upper bound on the cross section for the production $e^+e^- \rightarrow \tilde{\chi}_2^0 \tilde{\chi}_{1,2}^0$ followed by the prompt decay $\tilde{\chi}_2^0 \rightarrow \gamma \tilde{\chi}_1^0$. See Figs. 4a and 6a for explicit limits in the $(m_{\tilde{\chi}_2^0}, m_{\tilde{\chi}_1^0})$ plane.

¹⁶ BARATE 98H looked for $\gamma\gamma\tilde{E}$ final states at $\sqrt{s} = 161, 172$ GeV. They obtained an upper bound on the cross section for the production $e^+e^- \rightarrow \tilde{\chi}_2^0 \tilde{\chi}_2^0$ followed by the prompt decay $\tilde{\chi}_2^0 \rightarrow \gamma \tilde{\chi}_1^0$ of 0.4–0.8 pb for $m_{\tilde{\chi}_2^0} = 10\text{--}80$ GeV. The bound above is for the specific case of $\tilde{\chi}_1^0 = \tilde{H}^0$ and $\tilde{\chi}_2^0 = \tilde{\gamma}$ and $m_{\tilde{e}_R} = 100$ GeV. See Fig. 6 and 7 for explicit limits in the $(\tilde{\chi}_2^0, \tilde{\chi}_1^0)$ plane and in the $(\tilde{\chi}_2^0, \tilde{e}_R)$ plane.

¹⁷ BARATE 98J looked for $\gamma\gamma\tilde{E}$ final states at $\sqrt{s} = 161\text{--}183$ GeV. They obtained an upper bound on the cross section for the production $e^+e^- \rightarrow \tilde{\chi}_2^0 \tilde{\chi}_2^0$ followed by the prompt decay $\tilde{\chi}_2^0 \rightarrow \gamma \tilde{\chi}_1^0$ of 0.08–0.24 pb for $m_{\tilde{\chi}_2^0} < 91$ GeV. The bound above is for the specific case of $\tilde{\chi}_1^0 = \tilde{H}^0$ and $\tilde{\chi}_2^0 = \tilde{\gamma}$ and $m_{\tilde{e}_R} = 100$ GeV.

¹⁸ ABACHI 96 searches for 3-lepton final states. Efficiencies are calculated using mass relations and branching ratios in the Minimal Supergravity scenario. Results are presented as lower bounds on $\sigma(\tilde{\chi}_1^\pm \tilde{\chi}_2^0) \times \text{B}(\tilde{\chi}_1^\pm \rightarrow \ell\nu_{\tilde{\chi}_1^0}) \times \text{B}(\tilde{\chi}_2^0 \rightarrow \ell^+ \ell^- \tilde{\chi}_1^0)$ as a function of $m_{\tilde{\chi}_1^0}$. Limits range from 3.1 pb ($m_{\tilde{\chi}_1^0} = 45$ GeV) to 0.6 pb ($m_{\tilde{\chi}_1^0} = 100$ GeV).

¹⁹ ABE 96K looked for trilepton events from chargino-neutralino production. They obtained lower bounds on $m_{\tilde{\chi}_2^0}$ as a function of μ . The lower bounds are in the 45–50 GeV range for gaugino-dominant $\tilde{\chi}_2^0$ with negative μ , if $\tan\beta < 10$. See paper for more details of the assumptions.

$\tilde{\chi}_1^\pm, \tilde{\chi}_2^0$ (Charginos) MASS LIMITS

Charginos are unknown mixtures of w -inos and charged higgsinos (the supersymmetric partners of W and Higgs bosons). A lower mass limit for the lightest chargino ($\tilde{\chi}_1^\pm$) of approximately 45 GeV, independent of the field composition and of the decay mode, has been obtained by the LEP experiments from the analysis of the Z width and decays. These results, as well as other now superseded limits from e^+e^- collisions at energies below 136 GeV, and from hadronic collisions, can be found in the 1998 Edition (The European Physical Journal **C3** 1 (1998)) of this Review.

Unless otherwise stated, results in this section assume spectra, production rates, decay modes and branching ratios as evaluated in the MSSM, with gaugino and stfermion mass unification at the GUT scale. These papers generally study production of $\tilde{\chi}_1^0 \tilde{\chi}_2^0, \tilde{\chi}_1^\pm \tilde{\chi}_1^\mp$ and (in the case of hadronic collisions) $\tilde{\chi}_1^\pm \tilde{\chi}_2^0$ pairs, including the effects of cascade decays. The mass limits on $\tilde{\chi}_1^\pm$ are either direct, or follow indirectly from the constraints set by the non-observation of $\tilde{\chi}_2^0$ states on the gaugino and higgsino MSSM parameters M_2 and μ . For generic values of the MSSM parameters, limits from high-energy e^+e^- collisions coincide with the highest value of the mass allowed by phase-space, namely $m_{\tilde{\chi}_1^\pm} \lesssim \sqrt{s}/2$. The still unpublished combination of the results of the four LEP collaborations from the 2000 run of LEP 2 at \sqrt{s} up to $\simeq 209$ GeV yields a lower mass limit of 103.5 GeV valid for general MSSM models. The limits become however weaker in certain regions of the MSSM parameter space where the detection efficiencies or production cross sections are suppressed. For example, this may happen

See key on page 405

Searches Particle Listings

Supersymmetric Particle Searches

when: (i) the mass differences $\Delta m_{\pm} = m_{\tilde{\chi}_1^{\pm}} - m_{\tilde{\chi}_1^0}$ or $\Delta m_{\nu} = m_{\tilde{\chi}_1^{\pm}} - m_{\tilde{\nu}}$ are very small, and the detection efficiency is reduced; (ii) the electron sneutrino mass is small, and the $\tilde{\chi}_1^{\pm}$ production rate is suppressed due to a destructive interference between s and t channel exchange diagrams. The regions of MSSM parameter space where the following limits are valid are indicated in the comment lines or in the footnotes.

VALUE (GeV)	CL%	DOCUMENT ID	TECN	COMMENT
>101	95	1 ABBIENDI	04H OPAL	all $\tan\beta$, $\Delta m_{\pm} > 5$ GeV, $m_0 > 500$ GeV, $A_0 = 0$
> 89		2 ABBIENDI	03H OPAL	$0.5 \leq \Delta m_{\pm} \leq 5$ GeV, higgsino-like, $\tan\beta=1.5$
> 97.1	95	3 ABDALLAH	03M DLPH	$\tilde{\chi}_1^{\pm}$, $\Delta m_{\pm} \geq 3$ GeV, $m_{\tilde{\nu}} > m_{\tilde{\chi}^{\pm}}$
> 75	95	3 ABDALLAH	03M DLPH	$\tilde{\chi}_1^{\pm}$, higgsino, all $\Delta m_{\pm}, m_{\tilde{\nu}} > m_{\tilde{\chi}^{\pm}}$
> 70	95	3 ABDALLAH	03M DLPH	$\tilde{\chi}_1^{\pm}$, all Δm_{\pm} , $m_{\tilde{\nu}} > 500$ GeV, $M_2 \leq 2M_1 \leq 10M_2$
> 94	95	4 ABDALLAH	03M DLPH	$\tilde{\chi}_1^{\pm}$, $\tan\beta \leq 40$, $\Delta m_{\pm} > 3$ GeV, all m_0
> 88	95	5 HEISTER	02J ALEP	$\tilde{\chi}_1^{\pm}$, all Δm_{\pm} , large m_0
> 67.7	95	6 ACCIARRI	00D L3	$\tan\beta > 0.7$, all Δm_{\pm} , all m_0
> 69.4	95	7 ACCIARRI	00K L3	$e^+e^- \rightarrow \tilde{\chi}^{\pm}\tilde{\chi}^{\mp}$, all Δm_{\pm} , heavy scalars
• • • We do not use the following data for averages, fits, limits, etc. • • •				
>129	95	8 AALTONEN	09G CDF	$p\bar{p} \rightarrow \tilde{\chi}_1^{\pm}\tilde{\chi}_2^0$
>138	95	9 ABAZOV	09T D0	$p\bar{p} \rightarrow \tilde{\chi}_1^{\pm}\tilde{\chi}_2^0$
		10 AALTONEN	08AE CDF	$p\bar{p} \rightarrow \tilde{\chi}_1^{\pm}\tilde{\chi}_2^0$
		11 AALTONEN	08L CDF	$p\bar{p} \rightarrow \tilde{\chi}_1^{\pm}\tilde{\chi}_2^0$
>229	95	12 ABAZOV	08F D0	$p\bar{p} \rightarrow \tilde{\chi}\tilde{\chi}, \tilde{\chi}=\tilde{\chi}_2^0, \tilde{\chi}_1^{\pm}, \tilde{\chi}_1^0 \rightarrow \gamma\tilde{G}, \text{GMSB}$
		13 AALTONEN	07J CDF	$p\bar{p} \rightarrow \tilde{\chi}_1^{\pm}\tilde{\chi}_2^0$
		14 ABULENCIA	07H CDF	R, LLE
		15 ABULENCIA	07N CDF	$p\bar{p} \rightarrow \tilde{\chi}_1^{\pm}\tilde{\chi}_2^0$
		16 ABAZOV	06D D0	R, LLE
>195	95	17 ABAZOV	05A D0	$p\bar{p} \rightarrow \tilde{\chi}\tilde{\chi}, \tilde{\chi}=\tilde{\chi}_2^0, \tilde{\chi}_1^{\pm}, \tilde{\chi}_1^0 \rightarrow \gamma\tilde{G}, \text{GMSB}$
>167	95	18 ACOSTA	05E CDF	$p\bar{p} \rightarrow \tilde{\chi}\tilde{\chi}, \tilde{\chi}=\tilde{\chi}_2^0, \tilde{\chi}_1^{\pm}, \tilde{\chi}_1^0 \rightarrow \gamma\tilde{G}, \text{GMSB}$
> 66	95	19,20 ABDALLAH	04H DLPH	AMSB, $\mu > 0$
>102.5	95	21,22 ABDALLAH	04M DLPH	$R(UD\bar{D})$
>100		23 ABDALLAH	03D DLPH	$e^+e^- \rightarrow \tilde{\chi}_1^{\pm}\tilde{\chi}_1^{\mp} (\tilde{\chi}_1^{\pm} \rightarrow \tilde{\tau}_1\nu_{\tau}, \tilde{\tau}_1 \rightarrow \tau\tilde{G})$
>103		24 HEISTER	03G ALEP	R decays, $m_0 > 500$ GeV
>102.7	95	25 ACHARD	02 L3	R, MSUGRA
		26 GHODBANE	02 THEO	
> 94.3	95	27 ABREU	01C DLPH	$\tilde{\chi}^{\pm} \rightarrow \tau J$
> 93.8	95	28 ACCIARRI	01 L3	R , all m_0 , $0.7 \leq \tan\beta \leq 40$
>100	95	29 BARATE	01B ALEP	R decays, $m_0 > 500$ GeV
> 91.8	95	30 ABREU	00V DLPH	$e^+e^- \rightarrow \tilde{\chi}_1^{\pm}\tilde{\chi}_1^{\mp} (\tilde{\chi}_1^{\pm} \rightarrow \tilde{\tau}_1\nu_{\tau}, \tilde{\tau}_1 \rightarrow \tau\tilde{G})$
		31 CHO	00B THEO	EW analysis
> 76	95	32 ABBIENDI	99T OPAL	$R, m_0=500$ GeV
> 51	95	33 MALTONI	99B THEO	EW analysis, $\Delta m_{\pm} \sim 1$ GeV
> 81.5	95	34 ABE	98J CDF	$p\bar{p} \rightarrow \tilde{\chi}_1^{\pm}\tilde{\chi}_2^0$
		35 ACKERSTAFF	98K OPAL	$\tilde{\chi}^{\pm} \rightarrow \ell^{\pm}\tilde{E}$
> 65.7	95	36 ACKERSTAFF	98L OPAL	$\Delta m_{\pm} > 3$ GeV, $\Delta m_{\nu} > 2$ GeV
		37 ACKERSTAFF	98V OPAL	light gluino
		38 CARENA	97 THEO	$g_{\mu} = 2$
		39 KALINOWSKI	97 THEO	$W \rightarrow \tilde{\chi}_1^{\pm}\tilde{\chi}_1^0$
		40 ABE	96K CDF	$p\bar{p} \rightarrow \tilde{\chi}_1^{\pm}\tilde{\chi}_2^0$

1 ABBIENDI 04H search for charginos and neutralinos in events with acoplanar leptons+jets and multi-jet final states in the 192–209 GeV data, combined with the results on leptonic final states from ABBIENDI 04. The results hold for a scan over the parameter space covering the region $0 < M_2 \leq 5000$ GeV, $-1000 < \mu < 1000$ GeV and $\tan\beta$ from 1 to 40. This limit supersedes ABBIENDI 00h.

2 ABBIENDI 03H used e^+e^- data at $\sqrt{s} = 188\text{--}209$ GeV to search for chargino pair production in the case of small Δm_{\pm} . They select events with an energetic photon, large E and little hadronic or leptonic activity. The bound applies to higgsino-like charginos with zero lifetime and a 100% branching ratio $\tilde{\chi}_1^{\pm} \rightarrow \tilde{\chi}_1^0 W^*$. The mass limit for gaugino-like charginos, in case of non-universal gaugino masses, is of 92 GeV for $m_{\tilde{\nu}} = 1000$ GeV and is lowered to 74 GeV for $m_{\tilde{\nu}} \geq 100$ GeV. Limits in the plane $(m_{\tilde{\chi}_1^{\pm}}, \Delta m_{\pm})$ are shown in Fig. 7. Exclusion regions are also derived for the AMSB scenario in the $(m_{3/2}, \tan\beta)$ plane, see their Fig. 9.

3 ABDALLAH 03M searches for the production of charginos using data from $\sqrt{s} = 192$ to 208 GeV to investigate topologies with multiple leptons, jets plus leptons, multi-jets, or isolated photons. The first limit holds for $\tan\beta \geq 1$ and is obtained at $\Delta m_{\pm} = 3$ GeV in the higgsino region. For $\Delta m_{\pm} \geq 10$ (5) GeV and large m_0 , the limit improves to 102.7 (101.7) GeV. For the region of small Δm_{\pm} , all data from $\sqrt{s} = 130$ to 208 GeV are used to investigate final states with heavy stable charged particles, decay vertices inside the detector and soft topologies with a photon from initial state radiation. The second limit is obtained in the higgsino region, assuming gaugino mass universality at the GUT scale and $1 < \tan\beta < 50$. For the case of non-universality of gaugino masses, the parameter space is scanned in the domain $1 < \tan\beta < 50$ and, for $\Delta m_{\pm} < 3$ GeV, for

values of M_1, M_2 and μ such that $M_2 \leq 2M_1 \leq 10M_2$ and $|\mu| \geq M_2$. The third limit is obtained in the gaugino region. See Fig. 36 for the dependence of the low Δm_{\pm} limits on Δm_{\pm} . These limits include and update the results of ABREU 00j and ABREU 00t.

4 ABDALLAH 03M uses data from $\sqrt{s} = 192\text{--}208$ GeV to obtain limits in the framework of the MSSM with gaugino and sfermion mass universality at the GUT scale. An indirect limit on the mass of charginos is derived by constraining the MSSM parameter space by the results from direct searches for neutralinos (including cascade decays), for charginos and for sleptons. These limits are valid for values of $M_2 < 1$ TeV, $|\mu| \leq 2$ TeV with the $\tilde{\chi}_1^0$ as LSP. Constraints from the Higgs search in the M_h^{max} scenario assuming $m_t = 174.3$ GeV are included. The quoted limit applies if there is no mixing in the third family or when $m_{\tilde{\tau}_1} - m_{\tilde{\chi}_1^0} > 6$ GeV. If mixing is included the limit degrades to 90 GeV. See Fig. 43 for the mass limits as a function of $\tan\beta$. These limits update the results of ABREU 00w.

5 HEISTER 02J search for chargino production with small Δm_{\pm} in final states with a hard isolated initial state radiation photon and few low-momentum particles, using 189–208 GeV data. This search is sensitive in the intermediate Δm_{\pm} region. Combined with searches for \tilde{E} topologies and for stable charged particles, the above bound is obtained for m_0 larger than few hundred GeV, $1 < \tan\beta < 300$ and holds for any chargino field contents. For light scalars, the general limit reduces to the one from the Z^0 , but under the assumption of gaugino and sfermion mass unification the above bound is recovered. See Figs. 4–6 for the more general dependence of the limits on Δm_{\pm} . Updates BARATE 98x.

6 ACCIARRI 00D data collected at $\sqrt{s}=189$ GeV. The results hold over the full parameter space defined by $0.7 \leq \tan\beta \leq 60$, $0 \leq M_2 \leq 2$ TeV, $|\mu| \leq 2$ TeV $m_0 \leq 500$ GeV. The results of slepton searches from ACCIARRI 99w are used to help set constraints in the region of small m_0 . See their Figs. 5 for the $\tan\beta$ and M_2 dependence on the limits. See the text for the impact of a large $B(\tilde{\chi}^{\pm} \rightarrow \tau\tilde{\nu}_{\tau})$ on the result. The region of small Δm_{\pm} is excluded by the analysis of ACCIARRI 00k. Updates ACCIARRI 98f.

7 ACCIARRI 00k searches for the production of charginos with small Δm_{\pm} using data from $\sqrt{s}=189$ GeV. They investigate soft final states with a photon from initial state radiation. The results are combined with the limits on prompt decays from ACCIARRI 00D and from heavy stable charged particles from ACCIARRI 99L (see Heavy Charged Lepton Searches). The production and decay branching ratios are evaluated within the MSSM, assuming heavy sfermions. The parameter space is scanned in the domain $1 < \tan\beta < 50$, $0.3 < M_1/M_2 < 50$, and $0 < |\mu| < 2$ TeV. The limit is obtained in the higgsino region and improves to 78.6 GeV for gaugino-like charginos. The limit is unchanged for light scalar quarks. For light $\tilde{\tau}$ or $\tilde{\nu}_{\tau}$, the limit is unchanged in the gaugino-like region and is lowered by 0.8 GeV in the higgsino-like case. For light $\tilde{\mu}$ or $\tilde{\nu}_{\mu}$, the limit is unchanged in the higgsino-like region and is lowered by 0.9 GeV in the gaugino-like region. No direct mass limits are obtained for light \tilde{e} or $\tilde{\nu}_e$.

8 AALTONEN 09g searched in 976 pb^{-1} of $p\bar{p}$ collisions at $\sqrt{s} = 1.96$ TeV for events with trileptons ($\mu\mu\mu$ or $\mu\mu e$) with a low, 5 GeV, p_T threshold, and large E_T from the decay of $\tilde{\chi}_1^{\pm}\tilde{\chi}_2^0 X$. The selected number of events is consistent with the SM background expectation. The results are combined with the analysis of AALTONEN 07J to set a limit on the $\tilde{\chi}_1^{\pm}$ mass for a mSUGRA scenario with no slepton mixing.

9 ABAZOV 09t searched in 2.3 fb^{-1} of $p\bar{p}$ collisions at $\sqrt{s} = 1.96$ TeV for events with trileptons (e, μ or hadronically decaying τ) from the decay of $\tilde{\chi}_1^{\pm}\tilde{\chi}_2^0 X$ and large E_T . No evidence for a signal is observed. The data are used to constrain the cross section times branching ratio as a function of the $\tilde{\chi}_1^{\pm}$ mass under the assumption that $m_{\tilde{\chi}_1^{\pm}} = m_{\tilde{\chi}_2^0} = 2 m_{\tilde{\chi}_1^0}$, $\tan\beta = 3$, $\mu > 0$ and that the sleptons are heavier than the $\tilde{\chi}_1^{\pm}$, see their Fig. 8. A chargino lighter than 138 GeV is excluded in the “3l-max” scenario. Exclusion regions in the $(m_0, m_{1/2})$ plane are shown in their Fig. 9 for a mSUGRA scenario with $\tan\beta = 3$, $A_0 = 0$ and $\mu > 0$. The $\tan\beta$ dependence of this exclusion is illustrated in Fig. 10. Supersedes the results of ABAZOV 05u.

10 AALTONEN 08AE searched in 2.0 fb^{-1} of $p\bar{p}$ collisions at $\sqrt{s} = 1.96$ TeV for events with trileptons (e, μ or a charged isolated track from τ) from the decay of $p\bar{p} \rightarrow \tilde{\chi}_1^{\pm}\tilde{\chi}_2^0 X$ and large E_T . The selected number of events is consistent with the SM background expectation. The data are used to constrain the cross section times branching ratio as a function of the $\tilde{\chi}_1^{\pm}$ mass. Exclusion regions in the $(m_0, m_{1/2})$ plane are shown in their

Fig. 2 for a mSUGRA scenario. When the $\tilde{\chi}_1^{\pm}$ is nearly mass degenerate with the $\tilde{\tau}_1$ the leptons are too soft and no limit is obtained. For the case $m_0 = 60$ GeV a lower limit of 145 GeV on the chargino mass is obtained in this mSUGRA scenario.

11 AALTONEN 08L searched in 0.7 to 1.0 fb^{-1} of $p\bar{p}$ collisions at $\sqrt{s} = 1.96$ TeV for events with one high- p_T electron or muon and two additional leptons (e or μ) from the decay of $\tilde{\chi}_1^{\pm}\tilde{\chi}_2^0 X$. The selected number of events is consistent with the SM background expectation. The data are used to constrain the cross section times branching ratio as a function of the $\tilde{\chi}_1^{\pm}$ mass. The results are compared to three MSSM scenarios. An exclusion on chargino and neutralino production is only obtained in a scenario of no mixing between sleptons, yielding nearly equal branching ratios to all three lepton flavors. It amounts to $m_{\tilde{\chi}_1^{\pm}} > 151$ GeV, while the analysis is not sensitive to chargino

masses below about 110 GeV. The analyses have been combined with the analyses of AALTONEN 07J and ABULENCIA 07N. The observed limits for the combination are less stringent than the one obtained for the high- p_T analysis due to slight excesses in the other channels.

12 ABAZOV 08f looked in 1.1 fb^{-1} of $p\bar{p}$ collisions at $\sqrt{s} = 1.96$ TeV for diphoton events with large E_T . They may originate from the production of $\tilde{\chi}^{\pm}$ in pairs or associated to a $\tilde{\chi}_2^0$, decaying to a $\tilde{\chi}_1^0$ which itself decays promptly in $\text{GMSB to } \tilde{\chi}_1^0 \rightarrow \gamma\tilde{G}$. No significant excess was found compared to the background expectation. A limit is derived on the masses of SUSY particles in the GMSB framework for $M = 2\Lambda$, $N = 1$, $\tan\beta = 15$ and $\mu > 0$, see Figure 2. It also excludes $\Lambda < 91.5$ TeV. Supersedes the results of ABAZOV 05a.

13 AALTONEN 07J searched in 0.7 to 1.1 fb^{-1} of $p\bar{p}$ collisions at $\sqrt{s} = 1.96$ TeV for events with either two same sign leptons (e or μ) or trileptons from the decay of $\tilde{\chi}_1^{\pm}\tilde{\chi}_2^0 X$ and large E_T . The selected number of events is consistent with the SM background expectation. The data are used to constrain the cross section times branching ratio as a function of the $\tilde{\chi}_1^{\pm}$ mass. The results, shown in their Fig. 2, are compared to several MSSM scenarios. The strongest exclusion is in the case of no mixing between sleptons, yielding

Searches Particle Listings

Supersymmetric Particle Searches

- nearly equal branching ratios to all three lepton flavors, and amounting to $m_{\tilde{\chi}_1^\pm} > 129$ GeV. This analysis includes the same sign dilepton analysis of ABULENCIA 07N.
- 14 ABULENCIA 07H searched in 346 pb^{-1} of $p\bar{p}$ collisions at $\sqrt{s} = 1.96 \text{ TeV}$ for events with at least three leptons (e or μ) from the decay of $\tilde{\chi}_1^0$ via $LL\bar{E}$ couplings. The results are consistent with the hypothesis of no signal. Upper limits on the cross-section are extracted and a limit is derived in the framework of mSUGRA on the masses of $\tilde{\chi}_1^0$ and $\tilde{\chi}_1^\pm$, see e.g. their Fig. 3 and Tab. II.
- 15 ABULENCIA 07N searched in 1 fb^{-1} of $p\bar{p}$ collisions at $\sqrt{s} = 1.96 \text{ TeV}$ for events with two same sign leptons (e or μ) from the decay of $\tilde{\chi}_1^\pm \tilde{\chi}_1^0 X$ and large $E_{T\cancel{e}}$. A slight excess of 13 events is observed over a SM background expectation of 7.8 ± 1.1 . However, the kinematic distributions do not show any anomalous deviation from expectations in any particular region of parameter space.
- 16 ABAZOV 06d looked in 360 pb^{-1} of $p\bar{p}$ collisions at $\sqrt{s} = 1.96 \text{ TeV}$ for events with three leptons originating from the pair production of charginos and neutralinos, followed by R decays mediated by $LL\bar{E}$ couplings. One coupling is assumed to be dominant at a time. No significant excess was found compared to the background expectation in the $e\bar{e}l, \mu\bar{\mu}l$ nor $e\bar{e}\tau$ ($l = e, \mu$) final states. Upper limits on the cross-section are extracted in a specific MSUGRA model and a MSSM model without unification of M_1 and M_2 at the GUT scale. A limit is derived on the masses of charginos and neutralinos for both scenarios assuming λ_{ijk} couplings such that the decay length is less than 1 cm, see their Table III and Fig. 4.
- 17 ABAZOV 05a looked in 263 pb^{-1} of $p\bar{p}$ collisions at $\sqrt{s} = 1.96 \text{ TeV}$ for diphoton events with large $E_{T\cancel{e}}$. They may originate from the production of $\tilde{\chi}^\pm$ in pairs or associated to a $\tilde{\chi}_1^0$, decaying to a $\tilde{\chi}_1^0$ which itself decays promptly in GMSB to $\tilde{\chi}_1^0 \rightarrow \gamma\tilde{G}$. No significant excess was found at large $E_{T\cancel{e}}$ compared to the background expectation. A limit is derived on the masses of SUSY particles in the GMSB framework for $M = 2\Lambda$, $N = 1$, $\tan\beta = 15$ and $\mu > 0$, see Figure 2. It also excludes $\Lambda < 79.6 \text{ TeV}$. Very similar results are obtained for different choices of parameters, see their Table 2. Supersedes the results of ABBOTT 98.
- 18 ACOSTA 05e looked in 202 pb^{-1} of $p\bar{p}$ collisions at $\sqrt{s} = 1.96 \text{ TeV}$ for diphoton events with large $E_{T\cancel{e}}$. They may originate from the production of $\tilde{\chi}^\pm$ in pairs or associated to a $\tilde{\chi}_1^0$, decaying to a $\tilde{\chi}_1^0$ which itself decays promptly in GMSB to $\tilde{\chi}_1^0 \rightarrow \gamma\tilde{G}$. No events are selected at large $E_{T\cancel{e}}$ compared to the background expectation. A limit is derived on the masses of SUSY particles in the GMSB framework for $M = 2\Lambda$, $N = 1$, $\tan\beta = 15$ and $\mu > 0$, see Figure 2. It also excludes $\Lambda < 69 \text{ TeV}$. Supersedes the results of ABE 99i.
- 19 ABDALLAH 04h use data from LEP 1 and $\sqrt{s} = 192\text{--}208 \text{ GeV}$. They re-use results or re-analyze the data from ABDALLAH 03m to put limits on the parameter space of anomaly-mediated supersymmetry breaking (AMSB), which is scanned in the region $1 < m_{3/2} < 50 \text{ TeV}$, $0 < m_0 < 1000 \text{ GeV}$, $1.5 < \tan\beta < 35$, both signs of μ . The constraints are obtained from the searches for mass degenerate chargino and neutralino, for SM-like and invisible Higgs, for leptonically decaying charginos and from the limit on non-SM Z width of 3.2 MeV . The limit is for $m_{\tilde{t}_1} = 174.3 \text{ GeV}$ (see Table 2 for other $m_{\tilde{t}_1}$ values).
- 20 The limit improves to 73 GeV for $\mu < 0$.
- 21 ABDALLAH 04m use data from $\sqrt{s} = 192\text{--}208 \text{ GeV}$ to derive limits on sparticle masses under the assumption of R with $LL\bar{E}$ or UDD couplings. The results are valid in the ranges $90 < m_0 < 500 \text{ GeV}$, $0.7 < \tan\beta < 30$, $-200 < \mu < 200 \text{ GeV}$, $0 < M_2 < 400 \text{ GeV}$. Supersedes the result of ABREU 01d and ABREU 00u.
- 22 The limit improves to 103 GeV for $LL\bar{E}$ couplings.
- 23 ABDALLAH 03d use data from $\sqrt{s} = 183\text{--}208 \text{ GeV}$. They look for final states with two acoplanar leptons, expected in GMSB when the $\tilde{\tau}_1$ is the NLSP and assuming a short-lived $\tilde{\chi}_1^\pm$. Limits are obtained in the plane $(m(\tilde{\tau}), m(\tilde{\chi}_1^\pm))$ for different domains of $m(\tilde{G})$, after combining these results with the search for slepton pair production from the same paper. The limit above is valid if the $\tilde{\tau}_1$ is the NLSP for all values of $m(\tilde{G})$ provided $m(\tilde{\chi}_1^\pm) - m(\tilde{\tau}_1) \geq 0.3 \text{ GeV}$. For larger $m(\tilde{G}) > 100 \text{ eV}$ the limit improves to 102 GeV , see their Fig. 11. In the co-NLSP scenario, the limits are 96 and 102 GeV for all $m(\tilde{G})$ and $m(\tilde{G}) > 100 \text{ eV}$, respectively. Supersedes the results of ABREU 01g.
- 24 HEISTER 03g searches for the production of charginos prompt decays. In the case of R prompt decays with $LL\bar{E}$, $LQ\bar{D}$ or UDD couplings at $\sqrt{s} = 189\text{--}209 \text{ GeV}$. The search is performed for indirect decays, assuming one coupling at a time to be non-zero. The limit holds for $\tan\beta = 1.41$. Excluded regions in the (μ, M_2) plane are shown in their Fig. 3.
- 25 ACHARD 02 searches for the production of sparticles in the case of R prompt decays with $LL\bar{E}$ or UDD couplings at $\sqrt{s} = 189\text{--}208 \text{ GeV}$. The search is performed for direct and indirect decays, assuming one coupling at a time to be non-zero. The MSUGRA limit results from a scan over the MSSM parameter space with the assumption of gaugino and scalar mass unification at the GUT scale, imposing simultaneously the exclusions from neutralino, chargino, sleptons, and squarks analyses. The limit of $\tilde{\chi}_1^\pm$ holds for UDD couplings and increases to 103.0 GeV for $LL\bar{E}$ couplings. For L3 limits from $LQ\bar{D}$ couplings, see ACCIARRI 01.
- 26 GHODBANE 02 reanalyzes DELPHI data at $\sqrt{s} = 189 \text{ GeV}$ in the presence of complex phases for the MSSM parameters.
- 27 ABREU 01c looked for τ pairs with E at $\sqrt{s} = 183\text{--}189 \text{ GeV}$ to search for the associated production of charginos, followed by the decay $\tilde{\chi}^\pm \rightarrow \tau J$, J being an invisible massless particle. See Fig. 6 for the regions excluded in the (μ, M_2) plane.
- 28 ACCIARRI 01 searches for multi-lepton and/or multi-jet final states from R prompt decays with $LL\bar{E}$, $LQ\bar{D}$, or UDD couplings at $\sqrt{s} = 189 \text{ GeV}$. The search is performed for direct and indirect decays of neutralinos, charginos, and scalar leptons, with the $\tilde{\chi}_1^0$ or \tilde{l} as LSP and assuming one coupling to be non-zero at a time. Mass limits are derived using simultaneously the constraints from the neutralino, chargino, and slepton analyses; and the Z^0 width measurements from ACCIARRI 00c in a scan of the parameter space assuming MSUGRA with gaugino and scalar mass universality. Updates and supersedes the results from ACCIARRI 99i.
- 29 BARATE 01b searches for the production of charginos in the case of R prompt decays with $LL\bar{E}$, $LQ\bar{D}$, or UDD couplings at $\sqrt{s} = 189\text{--}202 \text{ GeV}$. The search is performed for indirect decays, assuming one coupling at a time to be non-zero. Updates BARATE 00h.
- 30 ABREU 00v use data from $\sqrt{s} = 183\text{--}189 \text{ GeV}$. They look for final states with two acoplanar leptons, expected in GMSB when the $\tilde{\tau}_1$ is the NLSP and assuming a short-lived $\tilde{\chi}_1^\pm$. Limits are obtained in the plane $(m(\tilde{\tau}), m(\tilde{\chi}_1^\pm))$ for different domains of $m(\tilde{G})$, after combining these results with the search for slepton pair production in the SUGRA
- framework from ABREU 01 to cover prompt decays and on stable particle searches from ABREU 00q. The limit above is valid for all values of $m_{\tilde{G}}$.
- 31 CHO 00b studied constraints on the MSSM spectrum from precision EW observables. Global fits favour charginos with masses at the lower bounds allowed by direct searches. Allowing for variations of the squark and slepton masses does not improve the fits.
- 32 ABBIENDI 99t searches for the production of neutralinos in the case of R -parity violation with $LL\bar{E}$, $LQ\bar{D}$, or UDD couplings using data from $\sqrt{s} = 183 \text{ GeV}$. They investigate topologies with multiple leptons, jets plus leptons, or multiple jets, assuming one coupling at the time to be non-zero and giving rise to direct or indirect decays. Mixed decays (where one particle has a direct, the other an indirect decay) are also considered for the UDD couplings. Upper limits on the cross section are derived which, combined with the constraint from the Z^0 width, allow to exclude regions in the M_2 versus μ plane for any coupling. Limits on the chargino mass are obtained for non-zero $LL\bar{E}$ couplings $> 10^{-5}$ and assuming decays via a W^* .
- 33 MALTONI 99b studied the effect of light chargino-neutralino to the electroweak precision data with a particular focus on the case where they are nearly degenerate ($\Delta m_{\pm} \sim 1 \text{ GeV}$) which is difficult to exclude from direct collider searches. The quoted limit is for higgsino-like case while the bound improves to 56 GeV for wino-like case. The values of the limits presented here are obtained in an update to MALTONI 99b, as described in MALTONI 00.
- 34 ABE 98t searches for trilepton final states ($l = e, \mu$). Efficiencies are calculated using mass relations in the Minimal Supergravity scenario, exploring the domain of parameter space defined by $1.1 < \tan\beta < 8$, $-1000 < \mu(\text{GeV}) < -200$, and $m_{\tilde{g}}/m_{\tilde{g}} = 1\text{--}2$. In this region $m_{\tilde{\chi}_1^\pm} \sim m_{\tilde{\chi}_2^0}$ and $m_{\tilde{\chi}_1^\pm} \sim 2m_{\tilde{\chi}_1^0}$. Results are presented in Fig. 1 as upper bounds on $\sigma(p\bar{p} \rightarrow \tilde{\chi}_1^\pm \tilde{\chi}_2^0) \times B(3\ell)$. Limits range from 0.8 pb ($m_{\tilde{\chi}_1^\pm} = 50 \text{ GeV}$) to 0.23 pb ($m_{\tilde{\chi}_1^\pm} = 100 \text{ GeV}$) at 95%CL. The gaugino mass unification hypothesis and the assumed mass relation between squarks and gluinos define the value of the leptonic branching ratios. The quoted result corresponds to the best limit within the selected range of parameters, obtained for $m_{\tilde{g}} > m_{\tilde{g}}$, $\tan\beta = 2$, and $\mu = -600 \text{ GeV}$. Mass limits for different values of $\tan\beta$ and μ are given in Fig. 2.
- 35 ACKERSTAFF 98k looked for dilepton+ $E_{T\cancel{e}}$ final states at $\sqrt{s} = 130\text{--}172 \text{ GeV}$. Limits on $\sigma(e^+e^- \rightarrow \tilde{\chi}_1^\pm \tilde{\chi}_1^0) \times B^2(\ell)$, with $B(\ell) = B(\chi^+ \rightarrow \ell^+ \nu_\ell \chi_1^0)$ ($B(\ell) = B(\chi^+ \rightarrow \ell^+ \tilde{\nu}_\ell)$), are given in Fig. 16 (Fig. 17).
- 36 ACKERSTAFF 98l limit is obtained for $0 < M_2 < 1500$, $|\mu| < 500$ and $\tan\beta > 1$, but remains valid outside this domain. The dependence on the trilinear-coupling parameter A is studied, and found negligible. The limit holds for the smallest value of m_0 consistent with scalar lepton constraints (ACKERSTAFF 97h) and for all values of m_0 where the condition $\Delta m_{\tilde{\nu}} > 2.0 \text{ GeV}$ is satisfied. $\Delta m_{\tilde{\nu}} > 10 \text{ GeV}$ if $\tilde{\chi}^\pm \rightarrow \ell \tilde{\nu}_\ell$. The limit improves to 84.5 GeV for $m_0 = 1 \text{ TeV}$. Data taken at $\sqrt{s} = 130\text{--}172 \text{ GeV}$.
- 37 ACKERSTAFF 98v excludes the light gluino with universal gaugino mass where charginos, neutralinos decay as $\tilde{\chi}_1^\pm, \tilde{\chi}_2^0 \rightarrow q\bar{q}\tilde{g}$ from total hadronic cross sections at $\sqrt{s} = 130\text{--}172 \text{ GeV}$. See paper for the case of nonuniversal gaugino mass.
- 38 CARENA 97 studied the constraints on chargino and sneutrino masses from muon $g-2$. The bound can be important for large $\tan\beta$.
- 39 KALINOWSKI 97 studies the constraints on the chargino-neutralino parameter space from limits on $\Gamma(W \rightarrow \tilde{\chi}_1^\pm \tilde{\chi}_1^0)$ achievable at LEP2. This is relevant when $\tilde{\chi}_1^\pm$ is "invisible", i.e., if $\tilde{\chi}_1^\pm$ dominantly decays into $\tilde{\nu}_\ell \ell^\pm$ with little energy for the lepton. Small otherwise allowed regions could be excluded.
- 40 ABE 96k looked for trilepton events from chargino-neutralino production. The bound on $m_{\tilde{\chi}_1^\pm}$ can reach up to 47 GeV for specific choices of parameters. The limits on the combined production cross section times 3-lepton branching ratios range between 1.4 and 0.4 pb , for $45 < m_{\tilde{\chi}_1^\pm}(\text{GeV}) < 100$. See the paper for more details on the parameter dependence of the results.

Long-lived $\tilde{\chi}^\pm$ (Chargino) MASS LIMITS

Limits on charginos which leave the detector before decaying.

VALUE (GeV)	CL%	DOCUMENT ID	TECN	COMMENT
>171	95	1 ABAZOV	09M D0	\tilde{H}
>102	95	2 ABBIENDI	03L OPAL	$m_{\tilde{\nu}_\tau} > 500 \text{ GeV}$
none 2-93.0	95	3 ABREU	00T DLPH	\tilde{H}^\pm or $m_{\tilde{\nu}_\tau} > m_{\tilde{\chi}_1^\pm}$

••• We do not use the following data for averages, fits, limits, etc. •••

> 83	95	4 BARATE	97k ALEP	
> 28.2	95	ADACHI	90c TOPZ	

1 ABAZOV 09M searched in 1.1 fb^{-1} of $p\bar{p}$ collisions at $\sqrt{s} = 1.96 \text{ TeV}$ for events with direct production of a pair of charged massive stable particles identified by their TOF. The number of the observed events is consistent with the predicted background. The data are used to constrain the production cross section as a function of the $\tilde{\chi}_1^\pm$ mass, see their Fig. 2. The quoted limit improves to 206 GeV for gaugino-like charginos.

2 ABBIENDI 03L used e^+e^- data at $\sqrt{s} = 130\text{--}209 \text{ GeV}$ to select events with two high momentum tracks with anomalous dE/dx . The excluded cross section is compared to the theoretical expectation as a function of the heavy particle mass in their Fig. 3. The bounds are valid for colorless fermions with lifetime longer than 10^{-6} s . Supersedes the results from ACKERSTAFF 98p.

3 ABREU 00T searches for the production of heavy stable charged particles, identified by their ionization or Cherenkov radiation, using data from $\sqrt{s} = 130$ to 189 GeV . These limits include and update the results of ABREU 98p.

4 BARATE 97k uses e^+e^- data collected at $\sqrt{s} = 130\text{--}172 \text{ GeV}$. Limit valid for $\tan\beta = \sqrt{2}$ and $m_{\tilde{\nu}_\tau} > 100 \text{ GeV}$. The limit improves to 86 GeV for $m_{\tilde{\nu}_\tau} > 250 \text{ GeV}$.

$\tilde{\nu}$ (Sneutrino) MASS LIMIT

The limits may depend on the number, $N(\tilde{\nu})$, of sneutrinos assumed to be degenerate in mass. Only $\tilde{\nu}_L$ (not $\tilde{\nu}_R$) is assumed to exist. It is possible that $\tilde{\nu}$ could be the lightest supersymmetric particle (LSP).

We report here, but do not include in the Listings, the limits obtained from the fit of the final results obtained by the LEP Collaborations on the invisible width of the Z boson ($\Delta\Gamma_{\text{inv.}} < 2.0$ MeV, LEP-SLC 06): $m_{\tilde{\nu}} > 43.7$ GeV ($N(\tilde{\nu})=1$) and $m_{\tilde{\nu}} > 44.7$ GeV ($N(\tilde{\nu})=3$).

VALUE (GeV)	CL%	DOCUMENT ID	TECN	COMMENT
> 94	95	1 ABDALLAH 03M	DLPH	$1 \leq \tan\beta \leq 40$, $m_{\tilde{e}_R} - m_{\tilde{\nu}} > 10$ GeV
> 84	95	2 HEISTER 02N	ALEP	$\tilde{\nu}_e$, any Δm
> 37.1	95	3 ADRIANI 93M	L3	$\Gamma(Z \rightarrow \text{invisible})$; $N(\tilde{\nu})=1$
> 41	95	4 DECAMP 92	ALEP	$\Gamma(Z \rightarrow \text{invisible})$; $N(\tilde{\nu})=3$
> 36	95	5 ABREU 91F	DLPH	$\Gamma(Z \rightarrow \text{invisible})$; $N(\tilde{\nu})=1$
> 31.2	95	5 ALEXANDER 91F	OPAL	$\Gamma(Z \rightarrow \text{invisible})$; $N(\tilde{\nu})=1$
• • • We do not use the following data for averages, fits, limits, etc. • • •				
		6 AALTONEN 09V	CDF	$p\bar{p} \rightarrow \tilde{\nu} \rightarrow \mu\mu, R, LQ\bar{D}$
		7 ABAZOV 08Q	D0	$\tilde{\nu}_\tau, R$
		8 SCHAEEL 07A	ALEP	$\tilde{\nu}_{\mu,\tau}, R, (s+t)$ -channel
		9 ABAZOV 06I	D0	R, λ'_{211}
		10 ABDALLAH 06C	DLPH	$\tilde{\nu}_\tau, R, (s+t)$ -channel
		11 ABULENCIA 06M	CDF	$\tilde{\nu}_\tau, R$
		12 ABULENCIA 05A	CDF	$p\bar{p} \rightarrow \tilde{\nu} \rightarrow ee, \mu\mu, R, LQ\bar{D}$
		13 ACOSTA 05R	CDF	$p\bar{p} \rightarrow \tilde{\nu} \rightarrow \tau\tau, R, LQ\bar{D}$
		14 ABBIENDI 04F	OPAL	$R, \tilde{\nu}_{e,\mu,\tau}$
> 95	95	15,16 ABDALLAH 04H	DLPH	AMSB, $\mu > 0$
> 98	95	17 ABDALLAH 04M	DLPH	$R(L\bar{L}\bar{E}), \tilde{\nu}_e$, indirect, $\Delta m > 5$ GeV
> 85	95	17 ABDALLAH 04M	DLPH	$R(L\bar{L}\bar{E}), \tilde{\nu}_\mu$, indirect, $\Delta m > 5$ GeV
> 85	95	17 ABDALLAH 04M	DLPH	$R(L\bar{L}\bar{E}), \tilde{\nu}_\tau$, indirect, $\Delta m > 5$ GeV
		18 ABDALLAH 03F	DLPH	$\tilde{\nu}_{\mu,\tau}, R, L\bar{L}\bar{E}$ decays
		19 ACOSTA 03E	CDF	$\tilde{\nu}_\tau, R, LQ\bar{D}$ production and $L\bar{L}\bar{E}$ decays
> 88	95	20 HEISTER 03G	ALEP	$\tilde{\nu}_e, R$ decays, $\mu = -200$ GeV, $\tan\beta=2$
> 65	95	20 HEISTER 03G	ALEP	$\tilde{\nu}_{\mu,\tau}, R$ decays
> 95	95	21 ABAZOV 02H	D0	R, λ'_{211}
> 95	95	22 ACHARD 02	L3	$\tilde{\nu}_e, R$ decays, $\mu = -200$ GeV, $\tan\beta = \sqrt{2}$
> 65	95	22 ACHARD 02	L3	$\tilde{\nu}_{\nu,\tau}, R$ decays
> 149	95	22 ACHARD 02	L3	$\tilde{\nu}_\tau, R$ decays, MSUGRA
		23 HEISTER 02F	ALEP	$e\gamma \rightarrow \tilde{\nu}_{\mu,\tau} \ell k, R, L\bar{L}\bar{E}$
none 100–264	95	24 ABBIENDI 00R	OPAL	$\tilde{\nu}_{\mu,\tau}, R, (s+t)$ -channel
none 100–200	95	25 ABBIENDI 00R	OPAL	$\tilde{\nu}_\tau, R, s$ -channel
		26 ABREU 00S	DLPH	$\tilde{\nu}_\tau, R, (s+t)$ -channel
		27 ACCIARRI 00P	L3	$\tilde{\nu}_{\mu,\tau}, R, s$ -channel
none 50–210	95	28 BARATE 00I	ALEP	Superseded by SCHAEEL 07A
none 50–210	95	29 BARATE 00I	ALEP	Superseded by SCHAEEL 07A
none 100–160	95	30 ABBIENDI 99	OPAL	$\tilde{\nu}_e, R, t$ -channel
$\neq m_Z$	95	31 ACCIARRI 97U	L3	$\tilde{\nu}_\tau, R, s$ -channel
none 125–180	95	31 ACCIARRI 97U	L3	$\tilde{\nu}_\tau, R, s$ -channel
		32 CARENA 97	THEO	$g_\mu - 2$
> 46.0	95	33 BUSKULIC 95E	ALEP	$N(\tilde{\nu})=1, \tilde{\nu} \rightarrow \nu\nu\ell\bar{\ell}'$
none 20–25000		34 BECK 94	COSM	Stable $\tilde{\nu}$, dark matter
< 600		35 FALK 94	COSM	$\tilde{\nu}$ LSP, cosmic abundance
none 3–90	90	36 SATO 91	KAMI	Stable $\tilde{\nu}_e$ or $\tilde{\nu}_\mu$, dark matter
none 4–90	90	36 SATO 91	KAMI	Stable $\tilde{\nu}_\tau$, dark matter

1 ABDALLAH 03M uses data from $\sqrt{s} = 192$ –208 GeV to obtain limits in the framework of the MSSM with gaugino and sfermion mass universality at the GUT scale. An indirect limit on the mass is derived by constraining the MSSM parameter space by the results from direct searches for neutralinos (including cascade decays) and for sleptons. These limits are valid for values of $M_2 < 1$ TeV, $|\mu| \leq 1$ TeV with the $\tilde{\chi}_1^0$ as LSP. The quoted limit is obtained when there is no mixing in the third family. See Fig. 43 for the mass limits as a function of $\tan\beta$. These limits update the results of ABREU 00W.

2 HEISTER 02N derives a bound on $m_{\tilde{\nu}_e}$ by exploiting the mass relation between the $\tilde{\nu}_e$ and \tilde{e} , based on the assumption of universal GUT scale gaugino and scalar masses $m_{1/2}$ and m_0 and the search described in the e section. In the MSUGRA framework with radiative electroweak symmetry breaking, the limit improves to $m_{\tilde{\nu}_e} > 130$ GeV, assuming a trilinear coupling $A_0=0$ at the GUT scale. See Figs. 5 and 7 for the dependence of the limits on $\tan\beta$.

3 ADRIANI 93M limit from $\Delta\Gamma(Z)(\text{invisible}) < 16.2$ MeV.

4 DECAMP 92 limit is from $\Gamma(\text{invisible})/\Gamma(\ell\ell) = 5.91 \pm 0.15$ ($N_\nu = 2.97 \pm 0.07$).

5 ALEXANDER 91F limit is for one species of $\tilde{\nu}$ and is derived from $\Gamma(\text{invisible, new})/\Gamma(\ell\ell) < 0.38$.

6 AALTONEN 09V searched in 2.3 fb $^{-1}$ of $p\bar{p}$ collisions at $\sqrt{s} = 1.96$ TeV for events with an oppositely charged pair originating from the R production of a sneutrino decaying to dimuons. A limit is derived on the cross section times branching ratio, B , of $\tilde{\nu} \rightarrow \mu\mu$ for several values of the coupling λ' , see their Fig. 3. For $\lambda'^2 B = 0.01$, the range 100 GeV $\leq m_{\tilde{\nu}} \leq 810$ GeV is excluded.

7 ABAZOV 08Q searched in 1.04 fb $^{-1}$ of $p\bar{p}$ collisions at $\sqrt{s} = 1.96$ TeV for an excess of events with oppositely charged $e\mu$ pairs. They might be expected in a SUSY model with R where a sneutrino is produced by $LQ\bar{D}$ couplings and decays via $L\bar{L}\bar{E}$ couplings, focusing on $\tilde{\nu}_\tau$, hence on the λ'_{311} and λ_{312} constants. No significant excess was found compared to the background expectation. Upper limits on the cross-section times branching ratio are extracted and displayed in their Fig. 2. Exclusion regions are determined for the $\tilde{\nu}_\tau$ mass as a function of both couplings, see their Fig. 3. As an indication, for $\tilde{\nu}_\tau$ masses of 100 GeV and $\lambda_{312} = 0.01$, values of $\lambda'_{311} \geq 1.6 \times 10^{-3}$ are excluded at the 95% C.L.

8 SCHAEEL 07A searches for the s - or t -channel exchange of sneutrinos in the case of R with $L\bar{L}\bar{E}$ couplings by studying di-lepton production at $\sqrt{s} = 189$ –209 GeV. Limits are obtained on the couplings as a function of the $\tilde{\nu}$ mass, see their Figs. 22–24. The results of this analysis are combined with BARATE 00I.

9 ABAZOV 06I looked in 380 pb $^{-1}$ of $p\bar{p}$ collisions at $\sqrt{s} = 1.96$ TeV for events with at least 2 muons and 2 jets for s -channel production of $\tilde{\mu}$ or $\tilde{\nu}$ and subsequent decay via R couplings $LQ\bar{D}$. The data are in agreement with the SM expectation. They set limits on resonant slepton production and derive exclusion contours on λ'_{211} in the mass plane of $\tilde{\ell}$ versus $\tilde{\chi}_1^0$ assuming a MSUGRA model with $\tan\beta = 5$, $\mu < 0$ and $A_0 = 0$, see their Fig. 3. For $\lambda'_{211} \geq 0.09$ slepton masses up to 358 GeV are excluded. Supersedes the results of ABAZOV 02H.

10 ABDALLAH 06C searches for anomalies in the production cross sections and forward-backward asymmetries of the $\ell^+ \ell^- (\gamma)$ final states ($\ell = e, \mu, \tau$) from 675 pb $^{-1}$ of $e^+ e^-$ data at $\sqrt{s} = 130$ –207 GeV. Limits are set on the s - and t -channel exchange of sneutrinos in the presence of R with $\lambda L\bar{L}\bar{E}$ couplings. For points between the energies at which data were taken, information is obtained from events in which a photon was radiated. Exclusion limits in the $(\lambda, m_{\tilde{\nu}})$ plane are given in Fig. 16. These limits include and update the results of ABREU 00S.

11 ABULENCIA 06M searched in 344 pb $^{-1}$ of $p\bar{p}$ collisions at $\sqrt{s} = 1.96$ TeV for an excess of events with oppositely charged $e\mu$ pairs. They might be expected in a SUSY model with R where a sneutrino is produced by $LQ\bar{D}$ couplings and decays via $L\bar{L}\bar{E}$ couplings, focusing on $\tilde{\nu}_\tau$, hence on the λ'_{311} and λ_{312} constants. No significant excess was found compared to the background expectation. Upper limits on the cross-section times branching ratio are extracted and exclusion regions determined for the $\tilde{\nu}_\tau$ mass as a function of both couplings, see their Fig. 3. As an indication, $\tilde{\nu}_\tau$ masses are excluded up to 300 GeV for $\lambda'_{311} \geq 0.01$ and $\lambda_{312} \geq 0.02$.

12 ABULENCIA 05A looked in ~ 200 pb $^{-1}$ of $p\bar{p}$ collisions at $\sqrt{s} = 1.96$ TeV for dimuon and dielectron events. They may originate from the R production of a sneutrino decaying to dileptons. No significant excess rate was found compared to the background expectation. A limit is derived on the cross section times branching ratio, B , of $\tilde{\nu} \rightarrow e e, \mu\mu$ of 25 fb at high mass, see their Figure 2. Sneutrino masses are excluded at 95% CL below 680, 620, 460 GeV ($e e$ channel) and 665, 590, 450 GeV ($\mu\mu$ channel) for a λ' coupling and branching ratio such that $\lambda'^2 B = 0.01, 0.005, 0.001$, respectively.

13 ACOSTA 05R looked in 195 pb $^{-1}$ of $p\bar{p}$ collisions at $\sqrt{s} = 1.96$ TeV for ditau events with one identified hadronic tau decay and one other tau decay. They may originate from the R production of a sneutrino decaying to $\tau\tau$. No significant excess rate was found compared to the background expectation, dominated by Drell-Yan. A limit is derived on the cross section times branching ratio, B , of $\tilde{\nu} \rightarrow \tau\tau$, see their Figure 3. Sneutrino masses below 377 GeV are excluded at 95% CL for a λ' coupling to $d\bar{d}$ and branching ratio such that $\lambda'^2 B = 0.01$.

14 ABBIENDI 04F use data from $\sqrt{s} = 189$ –209 GeV. They derive limits on sparticle masses under the assumption of R with $L\bar{L}\bar{E}$ or $LQ\bar{D}$ couplings. The results are valid for $\tan\beta = 1.5$, $\mu = -200$ GeV, and a BR for the decay given by CMSSM, assuming no sensitivity to other decays. Limits are quoted for $m_{\tilde{\chi}_1^0} = 60$ GeV and degrade for low-mass $\tilde{\chi}_1^0$. For $\tilde{\nu}_e$ the direct (indirect) limits with $L\bar{L}\bar{E}$ couplings are 89 (95) GeV and with $LQ\bar{D}$ they are 89 (88) GeV. For $\tilde{\nu}_{\mu,\tau}$ the direct (indirect) limits with $L\bar{L}\bar{E}$ couplings are 79 (81) GeV and with $LQ\bar{D}$ they are 74 (no limit) GeV. Supersedes the results of ABBIENDI 00I.

15 ABDALLAH 04H use data from LEP 1 and $\sqrt{s} = 192$ –208 GeV. They re-use results or re-analyze the data from ABDALLAH 03M to put limits on the parameter space of anomaly-mediated supersymmetry breaking (AMSB), which is scanned in the region $1 < m_{3/2} < 50$ TeV, $0 < m_0 < 1000$ GeV, $1.5 < \tan\beta < 35$, both signs of μ . The constraints are obtained from the searches for mass degenerate chargino and neutralino, for SM-like and invisible Higgs, for leptonically decaying charginos and from the limit on non-SM Z width of 3.2 MeV. The limit is for $m_t = 174.3$ GeV (see Table 2 for other m_t values).

16 The limit improves to 114 GeV for $\mu < 0$.

17 ABDALLAH 04M use data from $\sqrt{s} = 189$ –208 GeV. The results are valid for $\mu = -200$ GeV, $\tan\beta = 1.5$, $\Delta m > 5$ GeV and assuming a BR of 1 for the given decay. The limit quoted is for indirect decays using the neutralino constraint of 39.5 GeV, also derived in ABDALLAH 04M. For indirect decays the limit on $\tilde{\nu}_e$ decreases to 96 GeV if the constraint from the neutralino is not used and for direct decays it remains 96 GeV. For indirect decays the limit on $\tilde{\nu}_\mu$ decreases to 82 GeV if the constraint from the neutralino is not used and to 83 GeV for direct decays. For indirect decays the limit on $\tilde{\nu}_\tau$ decreases to 82 GeV if the constraint from the neutralino is not used and improves to 91 GeV for direct decays. Supersedes the results of ABREU 00U.

18 ABDALLAH 03F looked for events of the type $e^+ e^- \rightarrow \tilde{\nu} \rightarrow \tilde{\chi}_1^0 \nu, \tilde{\chi}_1^\pm \ell \bar{\ell}'$ followed by R decays of the $\tilde{\chi}_1^0$ via λ_{1j1} ($j = 2, 3$) couplings in the data at $\sqrt{s} = 183$ –208 GeV. From a scan over the SUGRA parameters, they derive upper limits on the λ_{1j1} couplings as a function of the sneutrino mass, see their Figs. 5–8.

19 ACOSTA 03E search for $e\mu, e\tau$ and $\mu\tau$ final states, and sets limits on the product of production cross-section and decay branching ratio for a $\tilde{\nu}$ in RPV models (see Fig. 3).

20 HEISTER 03G searches for the production of sneutrinos in the case of R prompt decays with $L\bar{L}\bar{E}, LQ\bar{D}$ or $U\bar{D}\bar{D}$ couplings at $\sqrt{s} = 189$ –209 GeV. The search is performed for direct and indirect decays, assuming one coupling at a time to be non-zero. The limit holds for indirect $\tilde{\nu}$ decays via $U\bar{D}\bar{D}$ couplings and $\Delta m > 10$ GeV. Stronger limits are reached for $(\tilde{\nu}_e, \tilde{\nu}_{\mu,\tau})$ for $L\bar{L}\bar{E}$ direct (100,90) GeV or indirect (98,89) GeV and for $LQ\bar{D}$ direct (–79) GeV or indirect (91,78) GeV couplings. For $L\bar{L}\bar{E}$ indirect decays, use is made of the bound $m(\tilde{\chi}_1^0) > 23$ GeV from BARATE 98S. Supersedes the results from BARATE 01B.

21 ABAZOV 02H looked in 94 pb $^{-1}$ of $p\bar{p}$ collisions at $\sqrt{s} = 1.8$ TeV for events with at least 2 muons and 2 jets for s -channel production of $\tilde{\mu}$ or $\tilde{\nu}$ and subsequent decay via R couplings $LQ\bar{D}$. A scan over the MSUGRA parameters is performed to exclude regions of the $(m_0, m_{1/2})$ plane, examples being shown in Fig. 2.

22 ACHARD 02 searches for the associated production of sneutrinos in the case of R prompt decays with $L\bar{L}\bar{E}$ or $U\bar{D}\bar{D}$ couplings at $\sqrt{s} = 189$ –208 GeV. The search is performed for direct and indirect decays, assuming one coupling at a time to be non-zero. The limit holds for direct decays via $L\bar{L}\bar{E}$ couplings. Stronger limits are reached for $(\tilde{\nu}_e, \tilde{\nu}_{\mu,\tau})$ for $L\bar{L}\bar{E}$ indirect (99,78) GeV and for $U\bar{D}\bar{D}$ direct or indirect (99,70) GeV decays. The MSUGRA limit results from a scan over the MSSM parameter space with the assumption of gaugino and scalar mass unification at the GUT scale, imposing simultaneously the exclusions from neutralino, chargino, sleptons, and squarks analyses. The limit holds for $U\bar{D}\bar{D}$ couplings and increases to 152.7 GeV for $L\bar{L}\bar{E}$ couplings.

Searches Particle Listings

Supersymmetric Particle Searches

- ²³ HEISTER 02F searched for single sneutrino production via $e\gamma \rightarrow \bar{\nu}_j \ell_k$ mediated by R $LL\bar{E}$ couplings, decaying directly or indirectly via a $\tilde{\chi}_1^0$ and assuming a single coupling to be nonzero at a time. Final states with three leptons and possible \cancel{E}_T due to neutrinos were selected in the 189–209 GeV data. Limits on the couplings λ_{1jk} as function of the sneutrino mass are shown in Figs. 10–14. The couplings λ_{232} and λ_{233} are not accessible and λ_{121} and λ_{131} are measured with better accuracy in sneutrino resonant production. For all tested couplings, except λ_{133} , the limits are significantly improved compared to the low-energy limits.
- ²⁴ ABBIENDI 00R studied the effect of s - and t -channel τ or μ sneutrino exchange in $e^+e^- \rightarrow e^+e^-$ at $\sqrt{s}=130$ –189 GeV, via the R -parity violating coupling $\lambda_{1j1}L_1L_1e_j^c$ ($i=2$ or 3). The limits quoted here hold for $\lambda_{1j1} > 0.13$, and supersede the results of ABBIENDI 99. See Fig. 11 for limits on $m_{\tilde{\nu}_\tau}$ versus coupling.
- ²⁵ ABBIENDI 00R studied the effect of s -channel τ sneutrino exchange in $e^+e^- \rightarrow \mu^+\mu^-$ at $\sqrt{s}=130$ –189 GeV, in presence of the R -parity violating couplings $\lambda_{1j3}L_1L_3e_j^c$ ($i=1$ and 2), with $\lambda_{131}=\lambda_{232}$. The limits quoted here hold for $\lambda_{131} > 0.09$, and supersede the results of ABBIENDI 99. See Fig. 12 for limits on $m_{\tilde{\nu}_\tau}$ versus coupling.
- ²⁶ ABREU 00s searches for anomalies in the production cross sections and forward-backward asymmetries of the $\ell^+\ell^-(\gamma)$ final states ($\ell=e,\mu,\tau$) from e^+e^- collisions at $\sqrt{s}=130$ –189 GeV. Limits are set on the s - and t -channel exchange of sneutrinos in the presence of R with $\lambda LL\bar{E}$ couplings. For points between the energies at which data were taken, information is obtained from events in which a photon was radiated. Exclusion limits in the $(\lambda, m_{\tilde{\nu}_\tau})$ plane are given in Fig. 5. These limits include and update the results of ABREU 99a.
- ²⁷ ACCIARRI 00P use the dilepton total cross sections and asymmetries at $\sqrt{s}=m_Z$ and $\sqrt{s}=130$ –189 GeV data to set limits on the effect of R $LL\bar{E}$ couplings giving rise to μ or τ sneutrino exchange. See their Fig. 5 for limits on the sneutrino mass versus couplings.
- ²⁸ BARATE 00I studied the effect of s -channel and t -channel τ or μ sneutrino exchange in $e^+e^- \rightarrow e^+e^-$ at $\sqrt{s}=130$ –183 GeV, via the R -parity violating coupling $\lambda_{1j1}L_1L_1e_j^c$ ($i=2$ or 3). The limits quoted here hold for $\lambda_{1j1} > 0.1$. See their Fig. 15 for limits as a function of the coupling.
- ²⁹ BARATE 00I studied the effect of s -channel τ sneutrino exchange in $e^+e^- \rightarrow \mu^+\mu^-$ at $\sqrt{s}=130$ –183 GeV, in presence of the R -parity violating coupling $\lambda_{1j3}L_1L_3e_j^c$ ($i=1$ and 2). The limits quoted here hold for $\sqrt{|\lambda_{131}\lambda_{232}|} > 0.2$. See their Fig. 16 for limits as a function of the coupling.
- ³⁰ ABBIENDI 99 studied the effect of t -channel electron sneutrino exchange in $e^+e^- \rightarrow \tau^+\tau^-$ at $\sqrt{s}=130$ –183 GeV, in presence of the R -parity violating couplings $\lambda_{131}L_1L_3e_1^c$. The limits quoted here hold for $\lambda_{131} > 0.6$.
- ³¹ ACCIARRI 97U studied the effect of the s -channel tau-sneutrino exchange in $e^+e^- \rightarrow e^+e^-$ at $\sqrt{s}=m_Z$ and $\sqrt{s}=130$ –172 GeV, via the R -parity violating coupling $\lambda_{131}L_1L_1e_1^c$. The limits quoted here hold for $\lambda_{131} > 0.05$. Similar limits were studied in $e^+e^- \rightarrow \mu^+\mu^-$ together with $\lambda_{232}L_2L_3e_2^c$ coupling.
- ³² CARENA 97 studied the constraints on chargino and sneutrino masses from muon $g-2$. The bound can be important for large $\tan\beta$.
- ³³ BUSKULIC 95E looked for $Z \rightarrow \bar{\nu}\nu$, where $\bar{\nu} \rightarrow \nu\chi_1^0$ and χ_1^0 decays via R -parity violating interactions into two leptons and a neutrino.
- ³⁴ BECK 94 limit can be inferred from limit on Dirac neutrino using $\sigma(\bar{\nu}) = 4\sigma(\nu)$. Also private communication with H.V. Klapdor-Kleingrothaus.
- ³⁵ FALK 94 puts an upper bound on $m_{\tilde{\nu}_\tau}$ when $\bar{\nu}$ is LSP by requiring its relic density does not overclose the Universe.
- ³⁶ SATO 91 search for high-energy neutrinos from the sun produced by annihilation of sneutrinos in the sun. Sneutrinos are assumed to be stable and to constitute dark matter in our galaxy. SATO 91 follow the analysis of NG 87, OLIVE 88, and GAISSER 86.

CHARGED SLEPTONS

This section contains limits on charged scalar leptons ($\tilde{\ell}$, with $\ell=e,\mu,\tau$). Studies of width and decays of the Z boson (use is made here of $\Delta\Gamma_{\text{inv}} < 2.0$ MeV, LEP 00) conclusively rule out $m_{\tilde{\ell}_R} < 40$ GeV (41 GeV for $\tilde{\ell}_L$), independently of decay modes, for each individual slepton. The limits improve to 43 GeV (43.5 GeV for $\tilde{\ell}_L$) assuming all 3 flavors to be degenerate. Limits on higher mass sleptons depend on model assumptions and on the mass splitting $\Delta m = m_{\tilde{\ell}_L} - m_{\tilde{\chi}_1^0}$. The mass and composition of $\tilde{\chi}_1^0$ may affect the slepton production rate in e^+e^- collisions through t -channel exchange diagrams. Production rates are also affected by the potentially large mixing angle of the lightest mass eigenstate $\tilde{\ell}_1 = \tilde{\ell}_R \sin\theta_\ell + \tilde{\ell}_L \cos\theta_\ell$. It is generally assumed that only $\tilde{\tau}$ may have significant mixing. The coupling to the Z vanishes for $\theta_\ell=0.82$. In the high-energy limit of e^+e^- collisions the interference between γ and Z exchange leads to a minimal cross section for $\theta_\ell=0.91$, a value which is sometimes used in the following entries relative to data taken at LEP2. When limits on $m_{\tilde{\ell}_R}$ are quoted, it is understood that limits on $m_{\tilde{\ell}_L}$ are usually at least as strong.

Possibly open decays involving gauginos other than $\tilde{\chi}_1^0$ will affect the detection efficiencies. Unless otherwise stated, the limits presented here result from the study of $\tilde{\ell}^+\tilde{\ell}^-$ production, with production rates and decay properties derived from the MSSM. Limits made obsolete by the recent analyses of e^+e^- collisions at high energies can be found in previous Editions of this Review.

For decays with final state gravitinos (\tilde{G}), $m_{\tilde{G}}$ is assumed to be negligible relative to all other masses.

$\tilde{\ell}$ (Selectron) MASS LIMIT

VALUE (GeV)	CL%	DOCUMENT ID	TECN	COMMENT
> 97.5		1 ABBIENDI 04	OPAL	$\tilde{e}_R, \Delta m > 11$ GeV, $ \mu > 100$ GeV, $\tan\beta=1.5$
> 94.4		2 ACHARD 04	L3	$\tilde{e}_R, \Delta m > 10$ GeV, $ \mu > 200$ GeV, $\tan\beta \geq 2$
> 71.3		2 ACHARD 04	L3	\tilde{e}_R , all Δm

none 30–94	95	3 ABDALLAH 03M	DLPH	$\Delta m > 15$ GeV, $\tilde{e}_R^+ \tilde{e}_R^-$
> 94	95	4 ABDALLAH 03M	DLPH	$\tilde{e}_R, 1 \leq \tan\beta \leq 40, \Delta m > 10$ GeV
> 95	95	5 HEISTER 02E	ALEP	$\Delta m > 15$ GeV, $\tilde{e}_R^+ \tilde{e}_R^-$
> 73	95	6 HEISTER 02N	ALEP	\tilde{e}_R , any Δm
> 107	95	6 HEISTER 02N	ALEP	\tilde{e}_L , any Δm
• • • We do not use the following data for averages, fits, limits, etc. • • •				
> 89	95	7 ABBIENDI 04F	OPAL	\tilde{R}, \tilde{e}_L
> 92	95	8 ABDALLAH 04M	DLPH	\tilde{R}, \tilde{e}_R , indirect, $\Delta m > 5$ GeV
> 93	95	9 HEISTER 03G	ALEP	\tilde{e}_R, \tilde{R} decays, $\mu=-200$ GeV, $\tan\beta=2$
> 69	95	10 ACHARD 02	L3	\tilde{e}_R, \tilde{R} decays, $\mu=-200$ GeV, $\tan\beta=\sqrt{2}$
> 92	95	11 BARATE 01	ALEP	$\Delta m > 10$ GeV, $\tilde{e}_R^+ \tilde{e}_R^-$
> 77	95	12 ABBIENDI 00J	OPAL	$\Delta m > 5$ GeV, $\tilde{e}_R^+ \tilde{e}_R^-$
> 83	95	13 ABREU 00U	DLPH	Superseded by ABDALLAH 04M
> 67	95	14 ABREU 00V	DLPH	$\tilde{e}_R \tilde{e}_R$ ($\tilde{e}_R \rightarrow e\tilde{G}$), $m_{\tilde{G}} > 10$ eV
> 85	95	15 BARATE 00G	ALEP	$\tilde{\ell}_R \rightarrow \ell\tilde{G}$, any $\tau(\tilde{\ell}_R)$
> 29.5	95	16 ACCIARRI 99I	L3	\tilde{e}_R, \tilde{R} , $\tan\beta \geq 2$
> 56	95	17 ACCIARRI 98F	L3	$\Delta m > 5$ GeV, $\tilde{e}_R^+ \tilde{e}_R^-$, $\tan\beta \geq 1.41$
> 77	95	18 BARATE 98K	ALEP	Any Δm , $\tilde{e}_R^+ \tilde{e}_R^-$, $\tilde{e}_R \rightarrow e\gamma\tilde{G}$
> 77	95	19 BREITWEG 98	ZEUS	$m_{\tilde{q}}=m_{\tilde{e}}$, $m(\tilde{\chi}_1^0)=40$ GeV
> 63	95	20 AID 96C	H1	$m_{\tilde{q}}=m_{\tilde{e}}$, $m_{\tilde{\chi}_1^0}=35$ GeV

¹ ABBIENDI 04 search for $\tilde{e}_R \tilde{e}_R$ production in acoplanar di-electron final states in the 183–208 GeV data. See Fig. 13 for the dependence of the limits on $m_{\tilde{\chi}_1^0}$ and for the limit at $\tan\beta=35$. This limit supersedes ABBIENDI 00G.

² ACHARD 04 search for $\tilde{e}_R \tilde{e}_L$ and $\tilde{e}_R \tilde{e}_R$ production in single- and acoplanar di-electron final states in the 192–209 GeV data. Absolute limits on $m_{\tilde{e}_R}$ are derived from a scan over the MSSM parameter space with universal GUT scale gaugino and scalar masses $m_{1/2}$ and m_0 , $1 \leq \tan\beta \leq 60$ and $-2 \leq \mu \leq 2$ TeV. See Fig. 4 for the dependence of the limits on $m_{\tilde{\chi}_1^0}$. This limit supersedes ACCIARRI 99W.

³ ABDALLAH 03M looked for acoplanar dielectron + \cancel{E} final states at $\sqrt{s}=189$ –208 GeV. The limit assumes $\mu=-200$ GeV and $\tan\beta=1.5$ in the calculation of the production cross section and $B(\tilde{e} \rightarrow e\tilde{\chi}_1^0)$. See Fig. 15 for limits in the $(m_{\tilde{e}_R}, m_{\tilde{\chi}_1^0})$ plane. These limits include and update the results of ABREU 01.

⁴ ABDALLAH 03M uses data from $\sqrt{s}=192$ –208 GeV to obtain limits in the framework of the MSSM with gaugino and sfermion mass universality at the LUT scale. An indirect limit on the mass is derived by constraining the MSSM parameter space by the results from direct searches for neutralinos (including cascade decays) and for sleptons. These limits are valid for values of $M_2 < 1$ TeV, $|\mu| \leq 1$ TeV with the $\tilde{\chi}_1^0$ as LSP. The quoted limit is obtained when there is no mixing in the third family. See Fig. 43 for the mass limits as a function of $\tan\beta$. These limits update the results of ABREU 00W.

⁵ HEISTER 02E looked for acoplanar dielectron + \cancel{E}_T final states from e^+e^- interactions between 183 and 209 GeV. The mass limit assumes $\mu < -200$ GeV and $\tan\beta=2$ for the production cross section and $B(\tilde{e} \rightarrow e\tilde{\chi}_1^0)=1$. See their Fig. 4 for the dependence of the limit on Δm . These limits include and update the results of BARATE 01.

⁶ HEISTER 02N search for $\tilde{e}_R \tilde{e}_L$ and $\tilde{e}_R \tilde{e}_R$ production in single- and acoplanar di-electron final states in the 183–208 GeV data. Absolute limits on $m_{\tilde{e}_R}$ are derived from a scan over the MSSM parameter space with universal GUT scale gaugino and scalar masses $m_{1/2}$ and m_0 , $1 \leq \tan\beta \leq 50$ and $-10 \leq \mu \leq 10$ TeV. The region of small $|\mu|$, where cascade decays are important, is covered by a search for $\tilde{\chi}_1^0 \tilde{\chi}_3^0$ in final states with leptons and possibly photons. Limits on $m_{\tilde{e}_L}$ are derived by exploiting the mass relation between the \tilde{e}_L and \tilde{e}_R , based on universal m_0 and $m_{1/2}$. When the constraint from the mass limit of the lightest Higgs from HEISTER 02 is included, the bounds improve to $m_{\tilde{e}_R} > 77(75)$ GeV and $m_{\tilde{e}_L} > 115(115)$ GeV for a top mass of 175(180) GeV. In the MSUGRA framework with radiative electroweak symmetry breaking, the limits improve further to $m_{\tilde{e}_R} > 95$ GeV and $m_{\tilde{e}_L} > 152$ GeV, assuming a trilinear coupling $A_0=0$ at the GUT scale. See Figs. 4, 5, 7 for the dependence of the limits on $\tan\beta$.

⁷ ABBIENDI 04F use data from $\sqrt{s}=189$ –209 GeV. They derive limits on sparticle masses under the assumption of R with $LL\bar{E}$ or $LQ\bar{D}$ couplings. The results are valid for $\tan\beta=1.5$, $\mu=-200$ GeV, with, in addition, $\Delta m \geq 5$ GeV for indirect decays via $LQ\bar{D}$. The limit quoted applies to direct decays via $LL\bar{E}$ or $LQ\bar{D}$ couplings. For indirect decays, the limits on the \tilde{e}_R mass are respectively 99 and 92 GeV for $LL\bar{E}$ and $LQ\bar{D}$ couplings and $m_{\tilde{\chi}_1^0}=10$ GeV and degrade slightly for larger $\tilde{\chi}_1^0$ mass. Supersedes the results of ABBIENDI 00.

⁸ ABDALLAH 04M use data from $\sqrt{s}=192$ –208 GeV to derive limits on sparticle masses under the assumption of R with $LL\bar{E}$ or $U\bar{D}\bar{D}$ couplings. The results are valid for $\mu=-200$ GeV, $\tan\beta=1.5$, $\Delta m > 5$ GeV and assuming a BR of 1 for the given decay. The limit quoted is for indirect $U\bar{D}\bar{D}$ decays using the neutralino constraint of 39.5 GeV for $LL\bar{E}$ and of 38.0 GeV for $U\bar{D}\bar{D}$ couplings, also derived in ABDALLAH 04M. For indirect decays via $LL\bar{E}$ the limit improves to 95 GeV if the constraint from the neutralino is used and to 94 GeV if it is not used. For indirect decays via $U\bar{D}\bar{D}$ couplings it remains unchanged when the neutralino constraint is not used. Supersedes the result of ABREU 00U.

⁹ HEISTER 03G searches for the production of selectrons in the case of R prompt decays with $LL\bar{E}$, $LQ\bar{D}$ or $U\bar{D}\bar{D}$ couplings at $\sqrt{s}=189$ –209 GeV. The search is performed for direct and indirect decays, assuming one coupling at a time to be non-zero. The limit holds for indirect decays mediated by $LQ\bar{D}$ couplings with $\Delta m > 10$ GeV. Limits are also given for $LL\bar{E}$ direct ($m_{\tilde{e}_R} > 96$ GeV) and indirect decays ($m_{\tilde{e}_R} > 96$ GeV for $m(\tilde{\chi}_1^0) > 23$ GeV from BARATE 98s) and for $U\bar{D}\bar{D}$ indirect decays ($m_{\tilde{e}_R} > 94$ GeV with $\Delta m > 10$ GeV). Supersedes the results from BARATE 01B.

¹⁰ ACHARD 02 searches for the production of selectrons in the case of R prompt decays with $LL\bar{E}$ or $U\bar{D}\bar{D}$ couplings at $\sqrt{s}=189$ –208 GeV. The search is performed for direct and indirect decays, assuming one coupling at a time to be non-zero. The limit holds for direct decays via $LL\bar{E}$ couplings. Stronger limits are reached for $LL\bar{E}$ indirect (79 GeV) and for $U\bar{D}\bar{D}$ direct or indirect (96 GeV) decays.

- ¹¹ BARATE 01 looked for acoplanar dielectron + \cancel{E}_T final states at 189 to 202 GeV. The limit assumes $\mu = -200$ GeV and $\tan\beta=2$ for the production cross section and 100% branching ratio for $\tilde{e} \rightarrow e\tilde{\chi}_1^0$. See their Fig. 1 for the dependence of the limit on Δm . These limits include and update the results of BARATE 99q.
- ¹² ABBIENDI 00j looked for acoplanar dielectron + \cancel{E}_T final states at $\sqrt{s}=161$ –183 GeV. The limit assumes $\mu < -100$ GeV and $\tan\beta=1.5$ for the production cross section and decay branching ratios, evaluated within the MSSM, and zero efficiency for decays other than $\tilde{e} \rightarrow e\tilde{\chi}_1^0$. See their Fig. 12 for the dependence of the limit on Δm and $\tan\beta$.
- ¹³ ABREU 00u studies decays induced by R -parity violating $LL\tilde{E}$ couplings, using data from $\sqrt{s}=189$ GeV. They investigate topologies with multiple leptons, assuming one coupling at the time to be nonzero and giving rise to indirect decays. The limits assume a neutralino mass limit of 30 GeV, also derived in ABREU 00u. Updates ABREU 00i.
- ¹⁴ ABREU 00v use data from $\sqrt{s}=130$ –189 GeV to search for tracks with large impact parameter or visible decay vertices. Limits are obtained as a function of $m_{\tilde{G}}$, from a scan of the GMSB parameter space, after combining these results with the search for slepton pair production in the SUGRA framework from ABREU 01 to cover prompt decays and on stable particle searches from ABREU 00q. For limits at different $m_{\tilde{G}}$, see their Fig. 12.
- ¹⁵ BARATE 00g combines the search for acoplanar dileptons, leptons with large impact parameters, kinks, and stable heavy-charged tracks, assuming 3 flavors of degenerate sleptons, produced in the schannel. Data collected at $\sqrt{s}=189$ GeV.
- ¹⁶ ACCIARRI 99i establish indirect limits on $m_{\tilde{e}_R}$ from the regions excluded in the M_2 versus m_0 plane by their chargino and neutralino searches at $\sqrt{s}=130$ –183 GeV. The situations where the $\tilde{\chi}_1^0$ is the LSP (indirect decays) and where a \tilde{e} is the LSP (direct decays) were both considered. The weakest limit, quoted above, comes from direct decays with $U\tilde{D}\tilde{D}$ couplings; $LL\tilde{E}$ couplings or indirect decays lead to a stronger limit.
- ¹⁷ ACCIARRI 98f looked for acoplanar dielectron+ \cancel{E}_T final states at $\sqrt{s}=130$ –172 GeV. The limit assumes $\mu = -200$ GeV, and zero efficiency for decays other than $\tilde{e}_R \rightarrow e\tilde{\chi}_1^0$. See their Fig. 6 for the dependence of the limit on Δm .
- ¹⁸ BARATE 98k looked for $e^+e^-\gamma\gamma + \cancel{E}$ final states at $\sqrt{s}=161$ –184 GeV. The limit assumes $\mu = -200$ GeV and $\tan\beta=2$ for the evaluation of the production cross section. See Fig. 4 for limits on the $(m_{\tilde{e}_R}, m_{\tilde{\chi}_1^0})$ plane and for the effect of cascade decays.
- ¹⁹ BREITWEG 98 used positron+jet events with missing energy and momentum to look for $e^+q \rightarrow \tilde{e}\tilde{q}$ via gaugino-like neutralino exchange with decays into $(e\tilde{\chi}_1^0)(q\tilde{\chi}_1^0)$. See paper for dependences in $m(\tilde{q})$, $m(\tilde{\chi}_1^0)$.
- ²⁰ AID 96c used positron+jet events with missing energy and momentum to look for $e^+q \rightarrow \tilde{e}\tilde{q}$ via neutralino exchange with decays into $(e\tilde{\chi}_1^0)(q\tilde{\chi}_1^0)$. See the paper for dependences on $m_{\tilde{q}}$, $m_{\tilde{\chi}_1^0}$.

 $\tilde{\mu}$ (Smuon) MASS LIMIT

VALUE (GeV)	CL%	DOCUMENT ID	TECN	COMMENT
>91.0		¹ ABBIENDI 04	OPAL	$\Delta m > 3$ GeV, $\tilde{\mu}_R^+ \tilde{\mu}_R^-$, $ \mu > 100$ GeV, $\tan\beta=1.5$
>86.7		² ACHARD 04	L3	$\Delta m > 10$ GeV, $\tilde{\mu}_R^+ \tilde{\mu}_R^-$, $ \mu > 200$ GeV, $\tan\beta \geq 2$
none 30–88	95	³ ABDALLAH 03M	DLPH	$\Delta m > 5$ GeV, $\tilde{\mu}_R^+ \tilde{\mu}_R^-$
>94	95	⁴ ABDALLAH 03M	DLPH	$\tilde{\mu}_R, 1 \leq \tan\beta \leq 40$, $\Delta m > 10$ GeV
>88	95	⁵ HEISTER 02E	ALEP	$\Delta m > 15$ GeV, $\tilde{\mu}_R^+ \tilde{\mu}_R^-$
• • • We do not use the following data for averages, fits, limits, etc. • • •				
>74	95	⁶ ABAZOV 06i	D0	$\tilde{R}, \lambda_{211}'$
>87	95	⁷ ABBIENDI 04F	OPAL	$\tilde{R}, \tilde{\mu}_L$
>81	95	⁸ ABDALLAH 04M	DLPH	$\tilde{R}, \tilde{\mu}_R$, indirect, $\Delta m > 5$ GeV
	95	⁹ HEISTER 03G	ALEP	$\tilde{\mu}_L, \tilde{R}$ decays
	95	¹⁰ ABAZOV 02H	D0	\tilde{R}, λ_{211}
>61	95	¹¹ ACHARD 02	L3	$\tilde{\mu}_R, \tilde{R}$ decays
>85	95	¹² BARATE 01	ALEP	$\Delta m > 10$ GeV, $\tilde{\mu}_R^+ \tilde{\mu}_R^-$
>65	95	¹³ ABBIENDI 00J	OPAL	$\Delta m > 2$ GeV, $\tilde{\mu}_R^+ \tilde{\mu}_R^-$
>80	95	¹⁴ ABREU 00V	DLPH	$\tilde{\mu}_R \tilde{\mu}_R (\tilde{\mu}_R \rightarrow \mu\tilde{G}), m_{\tilde{G}} > 8$ eV
>77	95	¹⁵ BARATE 98K	ALEP	Any $\Delta m, \tilde{\mu}_R^+ \tilde{\mu}_R^-, \tilde{\mu}_R \rightarrow \mu\gamma\tilde{G}$

¹ ABBIENDI 04 search for $\tilde{\mu}_R \tilde{\mu}_R$ production in acoplanar di-muon final states in the 183–208 GeV data. See Fig. 14 for the dependence of the limits on $m_{\tilde{\chi}_1^0}$ and for the

limit at $\tan\beta=35$. Under the assumption of 100% branching ratio for $\tilde{\mu}_R \rightarrow \mu\tilde{\chi}_1^0$, the limit improves to 94.0 GeV for $\Delta m > 4$ GeV. See Fig. 11 for the dependence of the limits on $m_{\tilde{\chi}_1^0}$ at several values of the branching ratio. This limit supersedes ABBIENDI 00g.

² ACHARD 04 search for $\tilde{\mu}_R \tilde{\mu}_R$ production in acoplanar di-muon final states in the 192–209 GeV data. Limits on $m_{\tilde{\mu}_R}$ are derived from a scan over the MSSM parameter space with universal GUT scale gaugino and scalar masses $m_{1/2}$ and m_0 , $1 \leq \tan\beta \leq 60$ and $-2 \leq \mu \leq 2$ TeV. See Fig. 4 for the dependence of the limits on $m_{\tilde{\chi}_1^0}$. This limit supersedes ACCIARRI 99w.

³ ABDALLAH 03M looked for acoplanar dimuon + \cancel{E} final states at $\sqrt{s}=189$ –208 GeV. The limit assumes $B(\tilde{\mu} \rightarrow \mu\tilde{\chi}_1^0) = 100\%$. See Fig. 16 for limits on the $(m_{\tilde{\mu}_R}, m_{\tilde{\chi}_1^0})$ plane. These limits include and update the results of ABREU 01.

⁴ ABDALLAH 03M uses data from $\sqrt{s}=192$ –208 GeV to obtain limits in the framework of the MSSM with gaugino and sfermion mass universality at the GUT scale. An indirect limit on the mass is derived by constraining the MSSM parameter space by the results from direct searches for neutralinos (including cascade decays) and for sleptons. These limits are valid for values of $M_2 < 1$ TeV, $|\mu| \leq 1$ TeV with the $\tilde{\chi}_1^0$ as LSP. The quoted limit is obtained when there is no mixing in the third family. See Fig. 43 for the mass limits as a function of $\tan\beta$. These limits update the results of ABREU 00w.

⁵ HEISTER 02E looked for acoplanar dimuon + \cancel{E}_T final states from e^+e^- interactions between 183 and 209 GeV. The mass limit assumes $B(\tilde{\mu} \rightarrow \mu\tilde{\chi}_1^0) = 1$. See their Fig. 4

for the dependence of the limit on Δm . These limits include and update the results of BARATE 01.

⁶ ABAZOV 06i looked in 380 pb⁻¹ of $p\bar{p}$ collisions at $\sqrt{s}=1.96$ TeV for events with at least 2 muons and 2 jets for s-channel production of $\tilde{\mu}$ or $\tilde{\nu}$ and subsequent decay via \tilde{R} couplings $LQ\tilde{D}$. The data are in agreement with the SM expectation. They set limits on resonant slepton production and derive exclusion contours on λ_{211}' in the mass plane of \tilde{e} versus $\tilde{\chi}_1^0$ assuming a MSUGRA model with $\tan\beta=5$, $\mu < 0$ and $A_0=0$, see their Fig. 3. For $\lambda_{211}' \geq 0.09$ slepton masses up to 358 GeV are excluded. Supersedes the results of ABÁZOV 02h.

⁷ ABBIENDI 04F use data from $\sqrt{s}=189$ –209 GeV. They derive limits on sparticle masses under the assumption of \tilde{R} with $LL\tilde{E}$ or $LQ\tilde{D}$ couplings. The results are valid for $\tan\beta=1.5$, $\mu = -200$ GeV, with, in addition, $\Delta m > 5$ GeV for indirect decays via $LQ\tilde{D}$. The limit quoted applies to direct decays with $LL\tilde{E}$ couplings and improves to 75 GeV for $LQ\tilde{D}$ couplings. The limits on the $\tilde{\mu}_R$ mass for indirect decays are respectively 94 and 87 GeV for $LL\tilde{E}$ and $LQ\tilde{D}$ couplings and $m_{\tilde{\chi}_1^0} = 10$ GeV. Supersedes the results of ABBIENDI 00.

⁸ ABDALLAH 04M use data from $\sqrt{s}=192$ –208 GeV to derive limits on sparticle masses under the assumption of \tilde{R} with $LL\tilde{E}$ or $U\tilde{D}\tilde{D}$ couplings. The results are valid for $\mu = -200$ GeV, $\tan\beta=1.5$, $\Delta m > 5$ GeV for the given decay. The limit quoted is for indirect $U\tilde{D}\tilde{D}$ decays using the neutralino constraint of 39.5 GeV for $LL\tilde{E}$ and of 38.0 GeV for $U\tilde{D}\tilde{D}$ couplings, also derived in ABDALLAH 04M. For indirect decays via $LL\tilde{E}$ the limit improves to 90 GeV if the constraint from the neutralino is used and remains at 87 GeV if it is not used. For indirect decays via $U\tilde{D}\tilde{D}$ couplings it degrades to 85 GeV when the neutralino constraint is not used. Supersedes the result of ABREU 00u.

⁹ HEISTER 03G searches for the production of smuons in the case of \tilde{R} prompt decays with $LL\tilde{E}$, $LQ\tilde{D}$ or $U\tilde{D}\tilde{D}$ couplings at $\sqrt{s}=189$ –209 GeV. The search is performed for direct and indirect decays, assuming one coupling at a time to be non-zero. The limit holds for direct decays mediated by \tilde{R} $LQ\tilde{D}$ couplings and improves to 90 GeV for indirect decays (for $\Delta m > 10$ GeV). Limits are also given for $LL\tilde{E}$ direct ($m_{\tilde{\mu}_R} > 87$ GeV) and indirect decays ($m_{\tilde{\mu}_R} > 96$ GeV for $m(\tilde{\chi}_1^0) > 23$ GeV from BARATE 98s) and for $U\tilde{D}\tilde{D}$ indirect decays ($m_{\tilde{\mu}_R} > 85$ GeV for $\Delta m > 10$ GeV). Supersedes the results from BARATE 01b.

¹⁰ ABÁZOV 02H looked in 94 pb⁻¹ of $p\bar{p}$ collisions at $\sqrt{s}=1.8$ TeV for events with at least 2 muons and 2 jets for s-channel production of $\tilde{\mu}$ or $\tilde{\nu}$ and subsequent decay via \tilde{R} couplings $LQ\tilde{D}$. A scan over the MSUGRA parameters is performed to exclude regions of the $(m_0, m_{1/2})$ plane, examples being shown in Fig. 2.

¹¹ ACHARD 02 searches for the production of smuons in the case of \tilde{R} prompt decays with $LL\tilde{E}$ or $U\tilde{D}\tilde{D}$ couplings at $\sqrt{s}=189$ –208 GeV. The search is performed for direct and indirect decays, assuming one coupling at a time to be nonzero. The limit holds for direct decays via $LL\tilde{E}$ couplings. Stronger limits are reached for $LL\tilde{E}$ indirect (87 GeV) and for $U\tilde{D}\tilde{D}$ direct or indirect (86 GeV) decays.

¹² BARATE 01 looked for acoplanar dimuon + \cancel{E}_T final states at 189 to 202 GeV. The limit assumes 100% branching ratio for $\tilde{\mu} \rightarrow \mu\tilde{\chi}_1^0$. See their Fig. 1 for the dependence of the limit on Δm . These limits include and update the results of BARATE 99q.

¹³ ABBIENDI 00j looked for acoplanar dimuon + \cancel{E}_T final states at $\sqrt{s}=161$ –183 GeV. The limit assumes $B(\tilde{\mu} \rightarrow \mu\tilde{\chi}_1^0) = 1$. Using decay branching ratios derived from the MSSM, a lower limit of 65 GeV is obtained for $\mu < -100$ GeV and $\tan\beta=1.5$. See their Figs. 10 and 13 for the dependence of the limit on the branching ratio and on Δm .

¹⁴ ABREU 00v use data from $\sqrt{s}=130$ –189 GeV to search for tracks with large impact parameter or visible decay vertices. Limits are obtained as function of $m_{\tilde{G}}$, after combining these results with the search for slepton pair production in the SUGRA framework from ABREU 01 to cover prompt decays and on stable particle searches from ABREU 00q. For limits at different $m_{\tilde{G}}$, see their Fig. 12.

¹⁵ BARATE 98k looked for $\mu^+\mu^-\gamma\gamma + \cancel{E}$ final states at $\sqrt{s}=161$ –184 GeV. See Fig. 4 for limits on the $(m_{\tilde{\mu}_R}, m_{\tilde{\chi}_1^0})$ plane and for the effect of cascade decays.

 $\tilde{\tau}$ (Stau) MASS LIMIT

VALUE (GeV)	CL%	DOCUMENT ID	TECN	COMMENT
>85.2		¹ ABBIENDI 04	OPAL	$\Delta m > 6$ GeV, $\theta_\tau = \pi/2$, $ \mu > 100$ GeV, $\tan\beta=1.5$
>78.3		² ACHARD 04	L3	$\Delta m > 15$ GeV, $\theta_\tau = \pi/2$, $ \mu > 200$ GeV, $\tan\beta \geq 2$
>81.9	95	³ ABDALLAH 03M	DLPH	$\Delta m > 15$ GeV, all θ_τ
none $m_\tau - 26.3$	95	³ ABDALLAH 03M	DLPH	$\Delta m > m_\tau$, all θ_τ
>79	95	⁴ HEISTER 02E	ALEP	$\Delta m > 15$ GeV, $\theta_\tau = \pi/2$
>76	95	⁴ HEISTER 02E	ALEP	$\Delta m > 15$ GeV, $\theta_\tau = 0.91$
• • • We do not use the following data for averages, fits, limits, etc. • • •				
>87.4	95	⁵ ABBIENDI 06B	OPAL	$\tilde{\tau}_R \rightarrow \tau\tilde{G}$, all $\tau(\tilde{\tau}_R)$
>74	95	⁶ ABBIENDI 04F	OPAL	$\tilde{R}, \tilde{\tau}_L$
>68	95	^{7,8} ABDALLAH 04H	DLPH	AMSB, $\mu > 0$
>90	95	⁹ ABDALLAH 04M	DLPH	$\tilde{R}, \tilde{\tau}_R$, indirect, $\Delta m > 5$ GeV
>82.5	95	¹⁰ ABDALLAH 03D	DLPH	$\tilde{\tau}_R \rightarrow \tau\tilde{G}$, all $\tau(\tilde{\tau}_R)$
>70	95	¹¹ HEISTER 03G	ALEP	$\tilde{\tau}_R, \tilde{R}$ decays
>61	95	¹² ACHARD 02	L3	$\tilde{\tau}_R, \tilde{R}$ decays
>77	95	¹³ HEISTER 02R	ALEP	τ_1 , any lifetime
>70	95	¹⁴ BARATE 01	ALEP	$\Delta m > 10$ GeV, $\theta_\tau = \pi/2$
>68	95	¹⁴ BARATE 01	ALEP	$\Delta m > 10$ GeV, $\theta_\tau = 0.91$
>64	95	¹⁵ ABBIENDI 00J	OPAL	$\Delta m > 10$ GeV, $\tilde{\tau}_R^+ \tilde{\tau}_R^-$
>84	95	¹⁶ ABREU 00V	DLPH	$\tilde{\tau}_R \tilde{\tau}_R (\tilde{\tau}_R \rightarrow \ell\tilde{G}), m_{\tilde{G}} > 9$ eV
>73	95	¹⁷ ABREU 00V	DLPH	$\tilde{\tau}_1 \tilde{\tau}_1 (\tilde{\tau}_1 \rightarrow \tau\tilde{G})$, all $\tau(\tilde{\tau}_1)$
>52	95	¹⁸ BARATE 98K	ALEP	Any $\Delta m, \theta_\tau = \pi/2, \tilde{\tau}_R \rightarrow \tau\gamma\tilde{G}$

¹ ABBIENDI 04 search for $\tilde{\tau}\tilde{\tau}$ production in acoplanar di-tau final states in the 183–208 GeV data. See Fig. 15 for the dependence of the limits on $m_{\tilde{\chi}_1^0}$ and for the limit

at $\tan\beta=35$. Under the assumption of 100% branching ratio for $\tilde{\tau}_R \rightarrow \tau\tilde{\chi}_1^0$, the limit improves to 89.8 GeV for $\Delta m > 8$ GeV. See Fig. 12 for the dependence of the limits on

Searches Particle Listings

Supersymmetric Particle Searches

- $m_{\tilde{\chi}_1^0}$ at several values of the branching ratio and for their dependence on $\theta_{\tilde{\tau}}$. This limit supersedes ABBIENDI 00g.
- ² ACHARD 04 search for $\tilde{\tau}\tilde{\tau}$ production in acoplanar di-tau final states in the 192–209 GeV data. Limits on $m_{\tilde{\tau}_R}$ are derived from a scan over the MSSM parameter space with universal GUT scale gaugino and scalar masses $m_{1/2}$ and m_0 , $1 \leq \tan\beta \leq 60$ and $-2 \leq \mu \leq 2$ TeV. See Fig. 4 for the dependence of the limits on $m_{\tilde{\chi}_1^0}$.
- ³ ABDALLAH 03M looked for acoplanar ditau + \cancel{E} final states at $\sqrt{s} = 130$ –208 GeV. A dedicated search was made for low mass $\tilde{\tau}$ s decoupling from the Z^0 . The limit assumes $B(\tilde{\tau} \rightarrow \tau\tilde{\chi}_1^0) = 100\%$. See Fig. 20 for limits on the $(m_{\tilde{\tau}_R}, m_{\tilde{\chi}_1^0})$ plane and as function of the $\tilde{\chi}_1^0$ mass and of the branching ratio. The limit in the low-mass region improves to 29.6 and 31.1 GeV for $\tilde{\tau}_R$ and $\tilde{\tau}_L$, respectively, at $\Delta m > m_{\tilde{\tau}}$. The limit in the high-mass region improves to 84.7 GeV for $\tilde{\tau}_R$ and $\Delta m > 15$ GeV. These limits include and update the results of ABREU 01.
- ⁴ HEISTER 02E looked for acoplanar ditau + \cancel{E}_T final states from e^+e^- interactions between 183 and 209 GeV. The mass limit assumes $B(\tilde{\tau} \rightarrow \tau\tilde{\chi}_1^0) = 1$. See their Fig. 4 for the dependence of the limit on Δm . These limits include and update the results of BARATE 01.
- ⁵ ABBIENDI 06B use 600 pb⁻¹ of data from $\sqrt{s} = 189$ –209 GeV. They look for events from pair-produced staus in a GMSB scenario with $\tilde{\tau}$ NLSP including prompt $\tilde{\tau}$ decays to ditau + \cancel{E} final states, large impact parameters, kinked tracks and heavy stable charged particles. Limits on the cross-section are computed as a function of $m(\tilde{\tau})$ and the lifetime, see their Fig. 7. The limit is compared to the $\sigma \cdot BR^2$ from a scan over the GMSB parameter space.
- ⁶ ABBIENDI 04F use data from $\sqrt{s} = 189$ –209 GeV. They derive limits on sparticle masses under the assumption of \tilde{R} with $LL\tilde{E}$ or $LQ\tilde{D}$ couplings. The results are valid for $\tan\beta = 1.5$, $\mu = -200$ GeV, with, in addition, $\Delta m > 5$ GeV for indirect decays via $LQ\tilde{D}$. The limit quoted applies to direct decays with $LL\tilde{E}$ couplings and improves to 75 GeV for $LQ\tilde{D}$ couplings. The limit on the $\tilde{\tau}_R$ mass for indirect decays is 92 GeV for $LL\tilde{E}$ couplings at $m_{\tilde{\chi}_1^0} = 10$ GeV and no exclusion is obtained for $LQ\tilde{D}$ couplings. Supersedes the results of ABBIENDI 00.
- ⁷ ABDALLAH 04H use data from LEP 1 and $\sqrt{s} = 192$ –208 GeV. They re-use results or re-analyze the data from ABDALLAH 03M to put limits on the parameter space of anomaly-mediated supersymmetry breaking (AMSB), which is scanned in the region $1 < m_{3/2} < 50$ TeV, $0 < m_0 < 1000$ GeV, $1.5 < \tan\beta < 35$, both signs of μ . The constraints are obtained from the searches for mass degenerate chargino and neutralino, for SM-like and invisible Higgs, for leptonically decaying charginos and from the limit on non-SM Z width of 3.2 MeV. The limit is for $m_t = 174.3$ GeV (see Table 2 for other m_t values).
- ⁸ The limit improves to 75 GeV for $\mu < 0$.
- ⁹ ABDALLAH 04M use data from $\sqrt{s} = 192$ –208 GeV to derive limits on sparticle masses under the assumption of \tilde{R} with $LL\tilde{E}$ couplings. The results are valid for $\mu = -200$ GeV, $\tan\beta = 1.5$, $\Delta m > 5$ GeV and assuming a BR of 1 for the given decay. The limit quoted is for indirect decays using the neutralino constraint of 39.5 GeV, also derived in ABDALLAH 04M. For indirect decays via $LL\tilde{E}$ the limit decreases to 86 GeV if the constraint from the neutralino is not used. Supersedes the result of ABREU 00u.
- ¹⁰ ABDALLAH 03D use data from $\sqrt{s} = 130$ –208 GeV to search for tracks with large impact parameter or visible decay vertices and for heavy charged stable particles. Limits are obtained as function of $m(\tilde{G})$, after combining these results with the search for slepton pair production in the SUGRA framework from ABDALLAH 03m to cover prompt decays. The above limit is reached for the stau decaying promptly, $m(\tilde{G}) < 6$ eV, and is computed for stau mixing yielding the minimal cross section. Stronger limits are obtained for longer lifetimes. See their Fig. 9. Supersedes the results of ABREU 01g.
- ¹¹ HEISTER 03g searches for the production of stau in the case of \tilde{R} prompt decays with $LL\tilde{E}$, $LQ\tilde{D}$ or UDD couplings at $\sqrt{s} = 189$ –209 GeV. The search is performed for direct and indirect decays, assuming one coupling at a time to be non-zero. The limit holds for indirect decays mediated by \tilde{R} UDD couplings with $\Delta m > 10$ GeV. Limits are also given for $LL\tilde{E}$ direct ($m_{\tilde{\tau}_R} > 87$ GeV) and indirect decays ($m_{\tilde{\tau}_R} > 95$ GeV for $m(\tilde{\chi}_1^0) > 23$ GeV from BARATE 98s) and for $LQ\tilde{D}$ indirect decays ($m_{\tilde{\tau}_R} > 76$ GeV). Supersedes the results from BARATE 01b.
- ¹² ACHARD 02 searches for the production of staus in the case of \tilde{R} prompt decays with $LL\tilde{E}$ or UDD couplings at $\sqrt{s} = 189$ –208 GeV. The search is performed for direct and indirect decays, assuming one coupling at a time to be non-zero. The limit holds for direct decays via $LL\tilde{E}$ couplings. Stronger limits are reached for $LL\tilde{E}$ indirect (86 GeV) and for UDD direct or indirect (75 GeV) decays.
- ¹³ HEISTER 02R search for signals of GMSB in the 189–209 GeV data. For the $\tilde{\chi}_1^0$ NLSP scenario, they looked for topologies consisting of $\gamma\gamma\cancel{E}$ or a single γ not pointing to the interaction vertex. For the $\tilde{\ell}$ NLSP case, the topologies consist of $\ell\ell\cancel{E}$, including leptons with large impact parameters, kinks, or stable particles. Limits are derived from a scan over the GMSB parameters (see their Table 5 for the ranges). The limit remains valid whichever is the NLSP. The absolute mass bound on the $\tilde{\chi}_1^0$ for any lifetime includes indirect limits from the slepton search HEISTER 02E performed within the MSUGRA framework. A bound for any NLSP and any lifetime of 77 GeV has also been derived by using the constraints from the neutral Higgs search in HEISTER 02. In the co-NLSP scenario, limits $m_{\tilde{\tau}_R} > 83$ GeV (neglecting t -channel exchange) and $m_{\tilde{\mu}_R} > 88$ GeV are obtained independent of the lifetime. Supersedes the results from BARATE 00g.
- ¹⁴ BARATE 01 looked for acoplanar ditau + \cancel{E}_T final states at 189 to 202 GeV. A slight excess (with 1.2% probability) of events is observed relative to the expected SM background. The limit assumes 100% branching ratio for $\tilde{\tau} \rightarrow \tau\tilde{\chi}_1^0$. See their Fig. 1 for the dependence of the limit on Δm . These limits include and update the results of BARATE 99a.
- ¹⁵ ABBIENDI 00j looked for acoplanar ditau + \cancel{E}_T final states at $\sqrt{s} = 161$ –183 GeV. The limit assumes $B(\tilde{\tau} \rightarrow \tau\tilde{\chi}_1^0) = 1$. Using decay branching ratios derived from the MSSM, a lower limit of 60 GeV at $\Delta m > 9$ GeV is obtained for $\mu < -100$ GeV and $\tan\beta = 1.5$. See their Figs. 11 and 14 for the dependence of the limit on the branching ratio and on Δm .
- ¹⁶ ABREU 00v use data from $\sqrt{s} = 130$ –189 GeV to search for tracks with large impact parameter or visible decay vertices. Limits are obtained as function of $m_{\tilde{G}}$, after combining these results with the search for slepton pair production in the SUGRA framework from ABREU 01 to cover prompt decays and on stable particle searches from ABREU 00q. The above limit assumes the degeneracy of stau and smuon. For limits at different $m_{\tilde{G}}$, see their Fig. 12.

- ¹⁷ ABREU 00v use data from $\sqrt{s} = 130$ –189 GeV to search for tracks with large impact parameter or visible decay vertices. Limits are obtained as function of $m_{\tilde{G}}$, after combining these results with the search for slepton pair production in the SUGRA framework from ABREU 01 to cover prompt decays and on stable particle searches from ABREU 00q. The above limit is reached for the stau mixing yielding the minimal cross section and decaying promptly. Stronger limits are obtained for longer lifetimes or for $\tilde{\tau}_R$; see their Fig. 11. For $10 \leq m_{\tilde{G}} \leq 310$ eV, the whole range $2 \leq m_{\tilde{\tau}_1} \leq 80$ GeV is excluded. Supersedes the results of ABREU 99c and ABREU 99f.
- ¹⁸ BARATE 98k looked for $\tau^+\tau^-\gamma\gamma + \cancel{E}$ final states at $\sqrt{s} = 161$ –184 GeV. See Fig. 4 for limits on the $(m_{\tilde{\tau}_R}, m_{\tilde{\chi}_1^0})$ plane and for the effect of cascade decays.

Degenerate Charged Sleptons

Unless stated otherwise in the comment lines or in the footnotes, the following limits assume 3 families of degenerate charged sleptons.

VALUE (GeV)	CL%	DOCUMENT ID	TECN	COMMENT
>93	95	¹ BARATE	01 ALEP	$\Delta m > 10$ GeV, $\tilde{\ell}_R^+ \tilde{\ell}_R^-$
>70	95	¹ BARATE	01 ALEP	all Δm , $\tilde{\ell}_R^+ \tilde{\ell}_R^-$
>91.9	95	² ABBIENDI	06B OPAL	$\tilde{\ell}_R \rightarrow \ell \tilde{G}$, all $\ell(\tilde{\ell}_R)$
>88	95	³ ABDALLAH	03D DLPH	$\tilde{\ell}_R \rightarrow \ell \tilde{G}$, all $\ell(\tilde{\ell}_R)$
>82.7	95	⁴ ACHARD	02 L3	$\tilde{\ell}_R, \tilde{R}$ decays, MSUGRA
>83	95	⁵ ABBIENDI	01 OPAL	$e^+e^- \rightarrow \tilde{\ell}_1 \tilde{\ell}_1$, GMSB, $\tan\beta=2$
		⁶ ABREU	01 DLPH	$\tilde{\ell} \rightarrow \ell \tilde{\chi}_1^0, \tilde{\chi}_2^0 \rightarrow \gamma \tilde{\chi}_1^0$, $\ell = e, \mu$
>68.8	95	⁷ ACCIARRI	01 L3	$\tilde{\ell}_R, \tilde{R}, 0.7 \leq \tan\beta \leq 40$
>84	95	^{8,9} ABREU	00V DLPH	$\tilde{\ell}_R \tilde{\ell}_R (\tilde{\ell}_R \rightarrow \ell \tilde{G}), m_{\tilde{G}} > 9$ eV

- ¹ BARATE 01 looked for acoplanar dilepton + \cancel{E}_T and single electron (for $\tilde{\ell}_R \tilde{\ell}_L$) final states at 189 to 202 GeV. The limit assumes $\mu = -200$ GeV and $\tan\beta = 2$ for the production cross section and decay branching ratios, evaluated within the MSSM, and zero efficiency for decays other than $\tilde{\ell} \rightarrow \ell \tilde{\chi}_1^0$. The slepton masses are determined from the GUT relations without stau mixing. See their Fig. 1 for the dependence of the limit on Δm .
- ² ABBIENDI 06B use 600 pb⁻¹ of data from $\sqrt{s} = 189$ –209 GeV. They look for events from pair-produced staus in a GMSB scenario with $\tilde{\ell}$ co-NLSP including prompt $\tilde{\ell}$ decays to dileptons + \cancel{E} final states, large impact parameters, kinked tracks and heavy stable charged particles. Limits on the cross-section are computed as a function of $m(\tilde{\ell})$ and the lifetime, see their Fig. 7. The limit is compared to the $\sigma \cdot BR^2$ from a scan over the GMSB parameter space. The highest mass limit is reached for $\tilde{\mu}_R$, from which the quoted mass limit is derived by subtracting $m_{\tilde{\tau}}$.
- ³ ABDALLAH 03D use data from $\sqrt{s} = 130$ –208 GeV to search for tracks with large impact parameter or visible decay vertices and for heavy charged stable particles. Limits are obtained as function of $m(\tilde{G})$, after combining these results with the search for slepton pair production in the SUGRA framework from ABDALLAH 03m to cover prompt decays. The above limit is reached for prompt decays and assumes the degeneracy of the sleptons. For limits at different $m(\tilde{G})$, see their Fig. 9. Supersedes the results of ABREU 01g.
- ⁴ ACHARD 02 searches for the production of sparticles in the case of \tilde{R} prompt decays with $LL\tilde{E}$ or UDD couplings at $\sqrt{s} = 189$ –208 GeV. The search is performed for direct and indirect decays, assuming one coupling at a time to be non-zero. The MSUGRA limit results from a scan over the MSSM parameter space with the assumption of gaugino and scalar mass unification at the GUT scale and no mixing in the slepton sector, imposing simultaneously the exclusions from neutralino, chargino, sleptons, and squarks analyses. The limit holds for $LL\tilde{E}$ couplings and increases to 88.7 GeV for UDD couplings. For L3 limits from $LQ\tilde{D}$ couplings, see ACCIARRI 01.
- ⁵ ABBIENDI 01 looked for final states with $\gamma\gamma\cancel{E}$, $\ell\ell\cancel{E}$, with possibly additional activity and four leptons + \cancel{E} to search for prompt decays of $\tilde{\chi}_1^0$ or $\tilde{\ell}_1$ in GMSB. They derive limits in the plane $(m_{\tilde{\chi}_1^0}, m_{\tilde{\tau}_1})$, see Fig. 6, allowing either the $\tilde{\chi}_1^0$ or a $\tilde{\ell}_1$ to be the NLSP. Two scenarios are considered: $\tan\beta = 2$ with the 3 sleptons degenerate in mass and $\tan\beta = 20$ where the $\tilde{\tau}_1$ is lighter than the other sleptons. Data taken at $\sqrt{s} = 189$ GeV. For $\tan\beta = 20$, the obtained limits are $m_{\tilde{\tau}_1} > 69$ GeV and $m_{\tilde{\mu}_1, \tilde{\nu}_1} > 88$ GeV.
- ⁶ ABREU 01 looked for acoplanar dilepton + diphoton + \cancel{E} final states from $\tilde{\ell}$ cascade decays at $\sqrt{s} = 130$ –189 GeV. See Fig. 9 for limits on the (μ, M_2) plane for $m_{\tilde{\ell}} = 80$ GeV, $\tan\beta = 1.0$, and assuming degeneracy of $\tilde{\mu}$ and \tilde{e} .
- ⁷ ACCIARRI 01 searches for multi-lepton and/or multi-jet final states from \tilde{R} prompt decays with $LL\tilde{E}$, $LQ\tilde{D}$, or UDD couplings at $\sqrt{s} = 189$ GeV. The search is performed for direct and indirect decays of neutralinos, charginos, and scalar leptons, with the $\tilde{\chi}_1^0$ or a $\tilde{\ell}$ as LSP and assuming one coupling to be non-zero at a time. Mass limits are derived using simultaneously the constraints from the neutralino, chargino, and slepton analyses; and the Z^0 width measurements from ACCIARRI 00c in a scan of the parameter space assuming MSUGRA with gaugino and scalar mass universality. Updates and supersedes the results from ACCIARRI 99i.
- ⁸ ABREU 00v use data from $\sqrt{s} = 130$ –189 GeV to search for tracks with large impact parameter or visible decay vertices. Limits are obtained as function of $m_{\tilde{G}}$, after combining these results with the search for slepton pair production in the SUGRA framework from ABREU 01 to cover prompt decays and on stable particle searches from ABREU 00q. For limits at different $m_{\tilde{G}}$, see their Fig. 12.
- ⁹ The above limit assumes the degeneracy of stau and smuon.

Long-lived $\tilde{\ell}$ (Slepton) MASS LIMIT

Limits on scalar leptons which leave detector before decaying. Limits from Z decays are independent of lepton flavor. Limits from continuum e^+e^- annihilation are also independent of flavor for smuons and staus. Selection limits from e^+e^- collisions in the continuum depend on MSSM parameters because of the additional neutralino exchange contribution.

VALUE (GeV)	CL%	DOCUMENT ID	TECN	COMMENT
>8	95	¹ ABBIENDI	03L OPAL	$\tilde{\mu}_R, \tilde{\tau}_R$
none 2–87.5	95	² ABREU	00Q DLPH	$\tilde{\mu}_R, \tilde{\tau}_R$
>81.2	95	³ ACCIARRI	99H L3	$\tilde{\mu}_R, \tilde{\tau}_R$
>81	95	⁴ BARATE	98K ALEP	$\tilde{\mu}_R, \tilde{\tau}_R$

See key on page 405

Searches Particle Listings

Supersymmetric Particle Searches

- ¹ ABBIENDI 03L used e^+e^- data at $\sqrt{s}=130\text{--}209$ GeV to select events with two high momentum tracks with anomalous dE/dx . The excluded cross section is compared to the theoretical expectation as a function of the heavy particle mass in their Fig. 3. The limit improves to 98.5 GeV for $\tilde{\mu}_L$ and $\tilde{\tau}_L$. The bounds are valid for colorless spin 0 particles with lifetimes longer than 10^{-6} s. Supersedes the results from ACKERSTAFF 98P.
- ² ABREU 00Q searches for the production of pairs of heavy, charged stable particles in e^+e^- annihilation at $\sqrt{s}=130\text{--}189$ GeV. The upper bound improves to 88 GeV for $\tilde{\mu}_L$, $\tilde{\tau}_L$. These limits include and update the results of ABREU 98P.
- ³ ACCIARRI 99H searched for production of pairs of back-to-back heavy charged particles at $\sqrt{s}=130\text{--}183$ GeV. The upper bound improves to 82.2 GeV for $\tilde{\mu}_L$, $\tilde{\tau}_L$.
- ⁴ The BARATE 98K mass limit improves to 82 GeV for $\tilde{\mu}_L$, $\tilde{\tau}_L$. Data collected at $\sqrt{s}=161\text{--}184$ GeV.

\tilde{q} (Squark) MASS LIMIT

For $m_{\tilde{q}} > 60\text{--}70$ GeV, it is expected that squarks would undergo a cascade decay via a number of neutralinos and/or charginos rather than undergo a direct decay to photinos as assumed by some papers. Limits obtained when direct decay is assumed are usually higher than limits when cascade decays are included.

Limits from e^+e^- collisions depend on the mixing angle of the lightest mass eigenstate $\tilde{q}_1 = q_R \sin\theta_q + \tilde{q}_L \cos\theta_q$. It is usually assumed that only the sbottom and stop squarks have non-trivial mixing angles (see the stop and sbottom sections). Here, unless otherwise noted, squarks are always taken to be either left/right degenerate, or purely of left or right type. Data from Z decays have set squark mass limits above 40 GeV, in the case of $\tilde{q} \rightarrow q\tilde{\chi}_1^0$ decays if $\Delta m = m_{\tilde{q}} - m_{\tilde{\chi}_1^0} \gtrsim 5$ GeV. For smaller values of Δm , current constraints on the invisible width of the Z ($\Delta\Gamma_{\text{inv}} < 2.0$ MeV, LEP 00) exclude $m_{\tilde{u}_{L,R}} < 44$ GeV, $m_{\tilde{d}_R} < 33$ GeV, $m_{\tilde{d}_L} < 44$ GeV and, assuming all squarks degenerate, $m_{\tilde{q}} < 45$ GeV.

Limits made obsolete by the most recent analyses of e^+e^- , $p\bar{p}$, and ep collisions can be found in previous Editions of this Review.

VALUE (GeV)	CL%	DOCUMENT ID	TECN	COMMENT
>392	95	1 AALTONEN 09s	CDF	jets+ E_T , $m_{\tilde{q}}=m_{\tilde{g}}$
>379	95	2 ABAZOV 08G	D0	jets+ E_T , $\tan\beta=3$, $\mu < 0$, $A_0=0$, any $m_{\tilde{g}}$
> 99.5		3 ACHARD 04	L3	$\Delta m > 10$ GeV, $e^+e^- \rightarrow \tilde{q}_{L,R}\tilde{q}_{L,R}$
> 97		3 ACHARD 04	L3	$\Delta m \geq 10$ GeV, $e^+e^- \rightarrow \tilde{q}_R\tilde{q}_R$
>138	95	4 ABBOTT 01D	D0	$\ell\ell$ +jets+ E_T , $\tan\beta < 10$, $m_0 < 300$ GeV, $\mu < 0$, $A_0=0$
>255	95	4 ABBOTT 01D	D0	$\tan\beta=2$, $m_{\tilde{g}}=m_{\tilde{q}}$, $\mu < 0$, $A_0=0$, $\ell\ell$ +jets+ E_T
> 97	95	5 BARATE 01	ALEP	$e^+e^- \rightarrow \tilde{q}\tilde{q}$, $\Delta m > 6$ GeV
>224	95	6 ABE 96D	CDF	$m_{\tilde{g}} \leq m_{\tilde{q}}$; with cascade decays, $\ell\ell$ +jets+ E_T
• • • We do not use the following data for averages, fits, limits, etc. • • •				
>490	95	7 ABAZOV 09s	D0	jets+ τ + E_T , $\tan\beta=15$, $\mu < 0$, $A_0=-2m_0$
>544	95	8 SCHAEEL 07A	ALEP	\tilde{d}_R, \tilde{R} , $\lambda=0.3$
>273	95	8 SCHAEEL 07A	ALEP	\tilde{s}_R, \tilde{R} , $\lambda=0.3$
>270	95	9 CHEKANOV 05A	ZEUS	$\tilde{q} \rightarrow \mu q, \tilde{R}, LQ\bar{D}$, $\lambda=0.3$
>275	95	9 CHEKANOV 05A	ZEUS	$\tilde{q} \rightarrow \tau q, \tilde{R}, LQ\bar{D}$, $\lambda=0.3$
>280		10 AKTAS 04D	H1	$e^\pm p \rightarrow \tilde{u}_L, \tilde{R}, LQ\bar{D}$
		10 AKTAS 04D	H1	$e^\pm p \rightarrow \tilde{d}_R, \tilde{R}, LQ\bar{D}$
>276	95	11 ADLOFF 03	H1	$e^\pm p \rightarrow \tilde{q}, \tilde{R}, LQ\bar{D}$
>260	95	12 CHEKANOV 03B	ZEUS	$\tilde{d} \rightarrow e^- u, \nu, d, \tilde{R}, LQ\bar{D}$, $\lambda > 0.1$
> 82.5	95	12 CHEKANOV 03B	ZEUS	$\tilde{u} \rightarrow e^+ d, \tilde{R}, LQ\bar{D}$, $\lambda > 0.1$
> 77	95	13 HEISTER 03G	ALEP	\tilde{u}_R, \tilde{R} decay
>240	95	13 HEISTER 03G	ALEP	\tilde{d}_R, \tilde{R} decay
		14 ABAZOV 02F	D0	$\tilde{q}, \tilde{R} \lambda_{2jk}$ indirect decays, $\tan\beta=2$, any $m_{\tilde{g}}$
>265	95	14 ABAZOV 02F	D0	$\tilde{q}, \tilde{R} \lambda'_{2jk}$ indirect decays, $\tan\beta=2$, $m_{\tilde{q}}=m_{\tilde{g}}$
none 80–121	95	15 ABAZOV 02G	D0	$p\bar{p} \rightarrow \tilde{g}\tilde{g}, \tilde{g}\tilde{q}$
none 80–158	95	16 ABBIENDI 02	OPAL	$e\gamma \rightarrow \tilde{u}_L, \tilde{R}, LQ\bar{D}$, $\lambda=0.3$
none 80–185	95	16 ABBIENDI 02	OPAL	$e\gamma \rightarrow \tilde{d}_R, \tilde{R}, LQ\bar{D}$, $\lambda=0.3$
none 80–196	95	17 ABBIENDI 02B	OPAL	$e\gamma \rightarrow \tilde{u}_L, \tilde{R}, LQ\bar{D}$, $\lambda=0.3$
> 79	95	17 ABBIENDI 02B	OPAL	$e\gamma \rightarrow \tilde{d}_R, \tilde{R}, LQ\bar{D}$, $\lambda=0.3$
> 55	95	18 ACHARD 02	L3	\tilde{u}_R, \tilde{R} decays
>263	95	18 ACHARD 02	L3	\tilde{d}_R, \tilde{R} decays
>258	95	19 CHEKANOV 02	ZEUS	$\tilde{u}_L \rightarrow \mu q, \tilde{R}, LQ\bar{D}$, $\lambda=0.3$
> 82	95	19 CHEKANOV 02	ZEUS	$\tilde{u}_L \rightarrow \tau q, \tilde{R}, LQ\bar{D}$, $\lambda=0.3$
> 68	95	20 BARATE 01B	ALEP	\tilde{u}_R, \tilde{R} decays
none 150–204	95	20 BARATE 01B	ALEP	\tilde{d}_R, \tilde{R} decays
>200	95	21 BREITWEG 01	ZEUS	$e^+p \rightarrow \tilde{d}_R, \tilde{R}, LQ\bar{D}$, $\lambda=0.3$
>180	95	22 ABBOTT 00C	D0	$\tilde{u}_L, \tilde{R}, \lambda'_{2jk}$ decays
>390	95	22 ABBOTT 00C	D0	$\tilde{d}_R, \tilde{R}, \lambda'_{2jk}$ decays
>148	95	23 ACCIARRI 00P	L3	$e^+e^- \rightarrow q\tilde{q}, \tilde{R}$, $\lambda=0.3$
>200	95	24 AFFOLDER 00K	CDF	$\tilde{d}_L, \tilde{R} \lambda'_{1j3}$ decays
	95	25 BARATE 00I	ALEP	Superseded by SCHAEEL 07A

none 150–269	95	26 BREITWEG 00E	ZEUS	$e^+p \rightarrow \tilde{u}_L, \tilde{R}, LQ\bar{D}$, $\lambda=0.3$
>240	95	27 ABBOTT 99	D0	$\tilde{q} \rightarrow \tilde{\chi}_2^0 X \rightarrow \tilde{\chi}_1^0 \gamma X$, $m_{\tilde{\chi}_2^0} - m_{\tilde{\chi}_1^0} > 20$ GeV
>320	95	27 ABBOTT 99	D0	$\tilde{q} \rightarrow \tilde{\chi}_1^0 X \rightarrow \tilde{G} \gamma X$
>243	95	28 ABBOTT 99K	D0	any $m_{\tilde{g}}, \tilde{R}$, $\tan\beta=2$, $\mu < 0$
>250	95	29 ABBOTT 99L	D0	$\tan\beta=2$, $\mu < 0$, $A=0$, jets+ E_T
>200	95	30 ABE 99M	CDF	$p\bar{p} \rightarrow \tilde{q}\tilde{q}, \tilde{R}$
none 80–134	95	31 ABREU 99G	DLPH	$e\gamma \rightarrow \tilde{u}_L, \tilde{R}, LQ\bar{D}$, $\lambda=0.3$
none 80–161	95	31 ABREU 99G	DLPH	$e\gamma \rightarrow \tilde{d}_R, \tilde{R}, LQ\bar{D}$, $\lambda=0.3$
>225	95	32 ABBOTT 98E	D0	$\tilde{u}_L, \tilde{R}, \lambda'_{1jk}$ decays
>204	95	32 ABBOTT 98E	D0	$\tilde{d}_R, \tilde{R}, \lambda'_{1jk}$ decays
> 79	95	32 ABBOTT 98E	D0	$\tilde{d}_L, \tilde{R}, \lambda'_{1jk}$ decays
>202	95	33 ABE 98S	CDF	$\tilde{u}_L, \tilde{R} \lambda'_{2jk}$ decays
>160	95	33 ABE 98S	CDF	$\tilde{d}_R, \tilde{R} \lambda'_{2jk}$ decays
>140	95	34 ACKERSTAFF 98V	OPAL	$e^+e^- \rightarrow q\tilde{q}, \tilde{R}$, $\lambda=0.3$
> 77	95	35 BREITWEG 98	ZEUS	$m_{\tilde{q}}=m_{\tilde{g}}$, $m(\tilde{\chi}_1^0)=40$ GeV
>216	95	36 DATTA 97	THEO	$\tilde{\nu}$'s lighter than $\tilde{\chi}_1^\pm, \tilde{\chi}_2^0$
none 130–573	95	37 DERRICK 97	ZEUS	$ep \rightarrow \tilde{q}, \tilde{q} \rightarrow \mu j$ or $\tau j, \tilde{R}$
none 190–650	95	38 HEWETT 97	THEO	$q\tilde{g} \rightarrow \tilde{q}, \tilde{q} \rightarrow q\tilde{g}$, with a light gluino
> 63	95	39 TEREKHOV 97	THEO	$q\tilde{g} \rightarrow q\tilde{g}, \tilde{q} \rightarrow q\tilde{g}$, with a light gluino
none 330–400	95	40 AID 96C	H1	$m_{\tilde{q}}=m_{\tilde{g}}$, $m_{\tilde{\chi}_1^0}=35$ GeV
>176	95	41 TEREKHOV 96	THEO	$u\tilde{g} \rightarrow \tilde{u}\tilde{g}, \tilde{u} \rightarrow u\tilde{g}$ with a light gluino
> 90	90	42 ABACHI 95C	D0	Any $m_{\tilde{g}} < 300$ GeV; with cascade decays
>100		43 ABE 95T	CDF	$\tilde{q} \rightarrow \tilde{\chi}_2^0 \rightarrow \tilde{\chi}_1^0 \gamma$
		44 ABE 92L	CDF	Any $m_{\tilde{g}} < 410$ GeV; with cascade decay
		45 ROY 92	RVUE	$p\bar{p} \rightarrow \tilde{q}\tilde{q}; \tilde{R}$
		46 NOJIRI 91	COSM	

- ¹ AALTONEN 09s searched in 2 fb^{-1} of $p\bar{p}$ collisions at $\sqrt{s}=1.96$ TeV for events with at least 2 jets and E_T . No evidence for a signal is observed. A limit is derived for a MSUGRA scenario in the $m_{\tilde{q}}$ versus $m_{\tilde{g}}$ plane, see their Fig. 2. For $m_{\tilde{g}} < 340$ GeV the bound increases to 400 GeV.
- ² ABAZOV 08G looked in 2.1 fb^{-1} of $p\bar{p}$ collisions at $\sqrt{s}=1.96$ TeV for events with acoplanar jets or multijets with large E_T . No significant excess was found compared to the background expectation. A limit is derived on the masses of squarks and gluinos for specific MSUGRA parameter values, see Figure 3. Similar results would be obtained for a large class of parameter sets. Supersedes the results of ABAZOV 06c.
- ³ ACHARD 04 search for the production of $\tilde{q}\tilde{q}$ of the first two generations in acoplanar di-jet final states in the 192–209 GeV data. Degeneracy of the squark masses is assumed either for both left and right squarks or for right squarks only, as well as $B(\tilde{q} \rightarrow q\tilde{\chi}_1^0) = 1$. See Fig. 7 for the dependence of the limits on $m_{\tilde{\chi}_1^0}$. This limit supersedes ACCIARRI 99v.
- ⁴ ABBOTT 01D looked in $\sim 108\text{ pb}^{-1}$ of $p\bar{p}$ collisions at $\sqrt{s}=1.8$ TeV for events with e, μ, τ , or $e\mu$ accompanied by at least 2 jets and E_T . Excluded regions are obtained in the MSUGRA framework from a scan over the parameters $0 < m_0 < 300$ GeV, $10 < m_{1/2} < 110$ GeV, and $1.2 < \tan\beta < 10$.
- ⁵ BARATE 01 looked for acoplanar dijets + E_T final states at 189 to 202 GeV. The limit assumes $B(\tilde{q} \rightarrow q\tilde{\chi}_1^0) = 1$, with $\Delta m = m_{\tilde{q}} - m_{\tilde{\chi}_1^0}$. It applies to $\tan\beta=4$, $\mu=-400$ GeV. See their Fig. 2 for the exclusion in the $(m_{\tilde{q}}, m_{\tilde{g}})$ plane. These limits include and update the results of BARATE 99q.
- ⁶ ABE 96D searched for production of gluinos and five degenerate squarks in final states containing a pair of leptons, two jets, and missing E_T . The two leptons arise from the semileptonic decays of charginos produced in the cascade decays. The limit is derived for fixed $\tan\beta=4.0$, $\mu=-400$ GeV, and $m_{H^\pm}=500$ GeV, and with the cascade decays of the squarks and gluinos calculated within the framework of the Minimal Supergravity scenario.
- ⁷ ABAZOV 09s looked in 0.96 fb^{-1} of $p\bar{p}$ collisions at $\sqrt{s}=1.96$ TeV for events with at least 2 jets, a tau decaying hadronically and E_T from the production $\tilde{q}_L\tilde{q}_R$, with the taus originating from the decay of a $\tilde{\chi}_2^0$ or $\tilde{\chi}_1^\pm$. The results were combined with ABAZOV 08G which searched for events with jets and E_T without requiring tau. No evidence for an excess over the SM expectation is observed. The excluded region is shown for an mSUGRA model in a plane of $m_{1/2}$ versus m_0 in the “tau corridor,” see their Figs. 5 and 6. The largest excluded squark mass in the corridor is 340 GeV for the tau analysis only and 410 GeV for the combined analysis.
- ⁸ SCHAEEL 07A studied the effect on hadronic cross sections and charge asymmetries of t-channel down-type squark exchange via R-parity violating couplings $LQ\bar{D}$ at $\sqrt{s}=189\text{--}209$ GeV. The limit here refers to the case $j=1, 2$ and holds for λ'_{1jk} of electromagnetic strength. The results of this analysis are combined with BARATE 00I.
- ⁹ CHEKANOV 05A search for lepton flavor violating processes $e^\pm p \rightarrow \ell X$, where $\ell = \mu$ or τ with high p_T , in 130 pb^{-1} at 300 and 318 GeV. Such final states may originate from LQD couplings with simultaneously non-zero λ'_{1jk} and λ'_{ijk} ($i=2$ or 3). The quoted mass bounds hold for a u -type squark, assume a λ' of electromagnetic strength and contributions from only direct squark decays. For d -type squarks the bounds are strengthened to 278 and 275 GeV for the μ and τ final states, respectively. Supersedes the results of CHEKANOV 02.
- ¹⁰ AKTAS 04D looked in 77.8 pb^{-1} of $e^\pm p$ collisions at $\sqrt{s}=319$ GeV for resonant production of \tilde{q} by R-parity violating $LQ\bar{D}$ couplings assuming that one of the λ' couplings dominates over all others. They consider final states with or without leptons and/or jets and/or p_T resulting from direct and indirect decays. They combine the channels to derive limits on λ'_{1j1} and λ'_{11k} as a function of the squark mass, see their Figs. 8 and 9, from a scan over the parameters $70 < M_2 < 350$ GeV, $-300 < \mu < 300$ GeV,

Searches Particle Listings

Supersymmetric Particle Searches

- $\tan\beta = 6$, for a fixed mass of 90 GeV for degenerate sleptons and an LSP mass > 30 GeV. The quoted limits refer to $\lambda' = 0.3$, with $U=u,c,t$ and $D=d,s,b$. Supersedes the results of ADLOFF 01b.
- 11 ADLOFF 03 looked for the s-channel production of squarks via R $LQ\bar{D}$ couplings in 117.2 pb^{-1} of e^+p data at $\sqrt{s} = 301$ and 319 GeV and of e^-p data at $\sqrt{s} = 319$ GeV. The comparison of the data with the SM differential cross section allows limits to be set on couplings for processes mediated through contact interactions. They obtain lower bounds on the value of $m_{\tilde{q}}/\lambda'$ of 710 GeV for the process $e^+\bar{\nu} \rightarrow \bar{d}^k$ (and charge conjugate), mediated by λ'_{11k} , and of 430 GeV for the process $e^+d \rightarrow \bar{u}^j$ (and charge conjugate), mediated by λ'_{1j1} .
- 12 CHEKANOV 03B used 131.5 pb^{-1} of e^+p and e^-p data taken at 300 and 318 GeV to look for narrow resonances in the $e q$ or νq final states. Such final states may originate from $LQ\bar{D}$ couplings with non-zero λ'_{1j1} (leading to \bar{u}_j) or λ'_{11k} (leading to \bar{d}_k). See their Fig. 8 and explanations in the text for limits. The quoted mass bound assumes that only direct squark decays contribute.
- 13 HEISTER 03c searches for the production of squarks in the case of R prompt decays with $\overline{UD\bar{D}}$ direct couplings at $\sqrt{s} = 189\text{--}209$ GeV.
- 14 ABAZOV 02F looked in 77.5 pb^{-1} of $p\bar{p}$ collisions at 1.8 TeV for events with $\geq 2\mu + \geq 4$ jets, originating from associated production of squarks followed by an indirect R decay (of the $\tilde{\chi}_1^0$) via $LQ\bar{D}$ couplings of the type λ'_{2jk} where $j=1,2$ and $k=1,2,3$. Bounds are obtained in the MSUGRA scenario by a scan in the range $0 \leq M_0 \leq 400$ GeV, $60 \leq m_{1/2} \leq 120$ GeV for fixed values $A_0=0$, $\mu < 0$, and $\tan\beta=2$ or 6 . The bounds are weaker for $\tan\beta=6$. See Figs. 2,3 for the exclusion contours in $m_{1/2}$ versus m_0 for $\tan\beta=2$ and 6 , respectively.
- 15 ABAZOV 02G search for associated production of gluinos and squarks in 92.7 pb^{-1} of $p\bar{p}$ collisions at $\sqrt{s}=1.8$ TeV, using events with one electron, ≥ 4 jets, and large \cancel{E}_T . The results are compared to a MSUGRA scenario with $\mu < 0$, $A_0=0$, and $\tan\beta=3$ and allow to exclude a region of the $(m_0, m_{1/2})$ shown in Fig. 11.
- 16 ABBIENDI 02 looked for events with an electron or neutrino and a jet in e^+e^- at 189 GeV. Squarks (or leptoquarks) could originate from a $LQ\bar{D}$ coupling of an electron with a quark from the fluctuation of a virtual photon. Limits on the couplings λ'_{1jk} as a function of the squark mass are shown in Figs. 8–9, assuming that only direct squark decays contribute.
- 17 ABBIENDI 02b looked for events with an electron or neutrino and a jet in e^+e^- at 189–209 GeV. Squarks (or leptoquarks) could originate from a $LQ\bar{D}$ coupling of an electron with a quark from the fluctuation of a virtual photon. Limits on the couplings λ'_{1jk} as a function of the squark mass are shown in Fig. 4, assuming that only direct squark decays contribute. The quoted limits are read off from Fig. 4. Supersedes the results of ABBIENDI 02.
- 18 ACHARD 02 searches for the production of squarks in the case of R prompt decays with $\overline{UD\bar{D}}$ couplings at $\sqrt{s}=189\text{--}208$ GeV. The search is performed for direct and indirect decays, assuming one coupling at the time to be nonzero. The limit holds for indirect decays. Stronger limits are reached for (\bar{u}_R, \bar{d}_R) direct (80,56) GeV and (\bar{u}_L, \bar{d}_L) direct or indirect (87,86) GeV decays.
- 19 CHEKANOV 02 search for lepton flavor violating processes $e^+p \rightarrow \ell X$, where $\ell = \mu$ or τ with high p_T , in 47.7 pb^{-1} of e^+p collisions at 300 GeV. Such final states may originate from $LQ\bar{D}$ couplings with simultaneously nonzero λ'_{1jk} and λ'_{ijk} ($i=2$ or 3). The quoted mass bound assumes that only direct squark decays contribute.
- 20 BARATE 01B searches for the production of squarks in the case of R prompt decays with \overline{LLE} indirect or $\overline{UD\bar{D}}$ direct couplings at $\sqrt{s}=189\text{--}202$ GeV. The limit holds for direct decays mediated by R $\overline{UD\bar{D}}$ couplings. Limits are also given for \overline{LLE} indirect decays ($m_{\bar{u}_R} > 90$ GeV and $m_{\bar{d}_R} > 89$ GeV). Supersedes the results from BARATE 00b.
- 21 BREITWEG 01 searches for squark production in 47.7 pb^{-1} of e^+p collisions, mediated by R couplings $LQ\bar{D}$ and leading to final states with $\bar{\nu}$ and ≥ 1 jet, complementing the e^+X final states of BREITWEG 00E. Limits are derived on $\lambda'\sqrt{\beta}$, where β is the branching fraction of the squarks into e^+q or $\bar{\nu}q$, as function of the squark mass, see their Fig. 15. The quoted mass limit assumes that only direct squark decays contribute.
- 22 ABBOTT 00c searched in $\sim 94 \text{ pb}^{-1}$ of $p\bar{p}$ collisions for events with $\mu\mu$ +jets, originating from associated production of leptoquarks. The results can be interpreted as limits on production of squarks followed by direct R decay via $\lambda'_{2jk}L_2Q_jd_k^c$ couplings. Bounds are obtained on the cross section for branching ratios of 1 and 1/2, see their Fig. 4. The former yields the limit on the \bar{u}_L . The latter is combined with the bound of ABBOTT 99i from the $\mu\nu$ +jets channel and of ABBOTT 98E and ABBOTT 98j from the $\nu\nu$ +jets channel to yield the limit on \bar{d}_R .
- 23 ACCIARRI 00P studied the effect on hadronic cross sections of t -channel down-type squark exchange via R -parity violating coupling $\lambda'_{1jk}L_1Q_jd_k^c$. The limit here refers to the case $j=1,2$, and holds for $\lambda'_{1jk}=0.3$. Data collected at $\sqrt{s}=130\text{--}189$ GeV, superseding the results of ACCIARRI 98j.
- 24 AFFOLDER 00k searched in $\sim 88 \text{ pb}^{-1}$ of $p\bar{p}$ collisions for events with 2–3 jets, at least one being b -tagged, large \cancel{E}_T and no high p_T leptons. Such $\nu\nu$ + b jets events would originate from associated production of squarks followed by direct R decay via $\lambda'_{1j3}L_1Q_jd_3^c$ couplings. Bounds are obtained on the production cross section assuming zero branching ratio to charged leptons.
- 25 BARATE 00i studied the effect on hadronic cross sections and charge asymmetries of t -channel down-type squark exchange via R -parity violating coupling $\lambda'_{1jk}L_1Q_jd_k^c$. The limit here refers to the case $j=1,2$, and holds for $\lambda'_{1jk}=0.3$. A 50 GeV limit is found for up-type squarks with $k=3$. Data collected at $\sqrt{s}=130\text{--}183$ GeV.
- 26 BREITWEG 00E searches for squark exchange in e^+p collisions, mediated by R couplings $LQ\bar{D}$ and leading to final states with an identified e^+ and ≥ 1 jet. The limit applies to up-type squarks of all generations, and assumes $B(\bar{q} \rightarrow qe)=1$.
- 27 ABBOTT 99 searched for $\gamma\cancel{E}_T + \geq 2$ jet final states, and set limits on $\sigma(p\bar{p} \rightarrow \bar{q}+X) \cdot B(\bar{q} \rightarrow \gamma\cancel{E}_T+X)$. The quoted limits correspond to $m_{\tilde{g}} \geq m_{\tilde{q}}$, with $B(\tilde{\chi}_2^0 \rightarrow \tilde{\chi}_1^0\gamma)=1$ and $B(\tilde{\chi}_1^0 \rightarrow \tilde{G}\gamma)=1$, respectively. They improve to 31.0 GeV (360 GeV in the case of $\gamma\tilde{G}$ decay) for $m_{\tilde{g}}=m_{\tilde{q}}$.
- 28 ABBOTT 99k uses events with an electron pair and four jets to search for the decay of the $\tilde{\chi}_1^0$ LSP via R $LQ\bar{D}$ couplings. The particle spectrum and decay branching ratios are taken in the framework of minimal supergravity. An excluded region at 95% CL is obtained in the $(m_0, m_{1/2})$ plane under the assumption that $A_0=0$, $\mu < 0$, $\tan\beta=2$ and any one of the couplings $\lambda'_{1jk} > 10^{-3}$ ($j=1,2$ and $k=1,2,3$) and from which the above limit is computed. For equal mass squarks and gluinos, the corresponding limit is 277 GeV. The results are essentially independent of A_0 , but the limit deteriorates rapidly with increasing $\tan\beta$ or $\mu > 0$.
- 29 ABBOTT 99L consider events with three or more jets and large \cancel{E}_T . Spectra and decay rates are evaluated in the framework of minimal Supergravity, assuming five flavors of degenerate squarks, and scanning the space of the universal gaugino ($m_{1/2}$) and scalar (m_0) masses. See their Figs. 2–3 for the dependence of the limit on the relative value of $m_{\tilde{q}}$ and $m_{\tilde{g}}$.
- 30 ABE 99m looked in 107 pb^{-1} of $p\bar{p}$ collisions at $\sqrt{s}=1.8$ TeV for events with like sign dileptons and two or more jets from the sequential decays $\bar{q} \rightarrow q\tilde{\chi}_1^0$ and $\tilde{\chi}_1^0 \rightarrow e q\bar{q}'$, assuming R coupling $L_1Q_jD_k^c$, with $j=2,3$ and $k=1,2,3$. They assume five degenerate squark flavors, $B(\bar{q} \rightarrow q\tilde{\chi}_1^0)=1$, $B(\tilde{\chi}_1^0 \rightarrow e q\bar{q}')=0.25$ for both e^+ and e^- , and $m_{\tilde{g}} \geq 200$ GeV. The limit is obtained for $m_{\tilde{\chi}_1^0} \geq m_{\tilde{q}}/2$ and improves for heavier gluinos or heavier $\tilde{\chi}_1^0$.
- 31 ABREU 99c looked for events with an electron or neutrino and a jet in e^+e^- at 183 GeV. Squarks (or leptoquarks) could originate from a $LQ\bar{D}$ coupling of an electron with a quark from the fluctuation of a virtual photon. Limits on the couplings λ'_{1jk} as a function of the squark mass are shown in Fig. 4, assuming that only direct squark decays contribute.
- 32 ABBOTT 98E searched in $\sim 115 \text{ pb}^{-1}$ of $p\bar{p}$ collisions for events with $e\nu$ +jets, originating from associated production of squarks followed by direct R decay via $\lambda'_{1jk}L_1Q_jd_k^c$ couplings. Bounds are obtained by combining these results with the previous bound of ABBOTT 97B from the ee +jets channel and with a reinterpretation of ABACHI 96b $\nu\nu$ +jets channel.
- 33 ABE 98s looked in $\sim 110 \text{ pb}^{-1}$ of $p\bar{p}$ collisions at $\sqrt{s}=1.8$ TeV for events with $\mu\mu$ +jets originating from associated production of squarks followed by direct R decay via $\lambda'_{2jk}L_2Q_jd_k^c$ couplings. Bounds are obtained on the production cross section times the square of the branching ratio, see Fig. 2. Mass limits result from the comparison with theoretical cross sections and branching ratio equal to 1 for \bar{u}_L and 1/2 for \bar{d}_R .
- 34 ACKERSTAFF 98v and ACCIARRI 98j studied the interference of t -channel squark (\bar{d}_R) exchange via R -parity violating $\lambda'_{1jk}L_1Q_jd_k^c$ coupling in $e^+e^- \rightarrow q\bar{q}$. The limit is for $\lambda'_{1jk}=0.3$. See paper for related limits on \bar{u}_L exchange. Data collected at $\sqrt{s}=130\text{--}172$ GeV.
- 35 BREITWEG 98 used positron+jet events with missing energy and momentum to look for $e^+q \rightarrow \bar{e}q$ via gaugino-like neutralino exchange with decays into $(e\tilde{\chi}_1^0)(q\tilde{\chi}_1^0)$. See paper for dependences in $m_{\tilde{e}}$, $m_{\tilde{\chi}_1^0}$.
- 36 DATTA 97 argues that the squark mass bound by ABACHI 95c can be weakened by 10–20 GeV if one relaxes the assumption of the universal scalar mass at the GUT-scale so that the $\tilde{\chi}_1^{\pm}, \tilde{\chi}_2^0$ in the squark cascade decays have dominant and invisible decays to $\bar{\nu}$.
- 37 DERRICK 97 looked for lepton-number violating final states via R -parity violating couplings $\lambda'_{ijk}L_iQ_jd_k$. When $\lambda'_{11k}\lambda'_{ijk} \neq 0$, the process $e u \rightarrow \bar{d}_k^* \rightarrow \ell_j u_j$ is possible. When $\lambda'_{1j1}\lambda'_{ijk} \neq 0$, the process $e\bar{\nu} \rightarrow \bar{u}_j^* \rightarrow \ell_j \bar{d}_k$ is possible. 100% branching fraction $\bar{q} \rightarrow \ell j$ is assumed. The limit quoted here corresponds to $\bar{t} \rightarrow \tau q$ decay, with $\lambda'=0.3$. For different channels, limits are slightly better. See Table 6 in their paper.
- 38 HEWETT 97 reanalyzed the limits on possible resonances in di-jet mode ($\bar{q} \rightarrow q\bar{q}$) from ALITTI 93 quoted in “Limits for Excited q (q^*) from Single Production,” ABE 96 in “SCALE LIMITS for Contact Interactions: $\Lambda(qqqq)$,” and unpublished CDF, $D\bar{0}$ bounds. The bound applies to the gluino mass of 5 GeV, and improves for lighter gluino. The analysis has gluinos in parton distribution function.
- 39 TEREKHOV 97 improved the analysis of TEREKHOV 96 by including di-jet angular distributions in the analysis.
- 40 AID 96c used positron+jet events with missing energy and momentum to look for $e^+q \rightarrow \bar{e}q$ via neutralino exchange with decays into $(e\tilde{\chi}_1^0)(q\tilde{\chi}_1^0)$. See the paper for dependences on $m_{\tilde{e}}$, $m_{\tilde{\chi}_1^0}$.
- 41 TEREKHOV 96 reanalyzed the limits on possible resonances in di-jet mode ($\bar{u} \rightarrow u\bar{g}$) from ABE 95N quoted in “MASS LIMITS for g_A (axigluon).” The bound applies only to the case with a light gluino.
- 42 ABACHI 95c assume five degenerate squark flavors with $m_{\tilde{q}_L} = m_{\tilde{q}_R}$. Sleptons are assumed to be heavier than squarks. The limits are derived for fixed $\tan\beta = 2.0$, $\mu = -250$ GeV, and $m_{H^\pm}=500$ GeV, and with the cascade decays of the squarks and gluinos calculated within the framework of the Minimal Supergravity scenario. The bounds are weakly sensitive to the three fixed parameters for a large fraction of parameter space. No limit is given for $m_{\tilde{g}}$ gluino > 547 GeV.
- 43 ABE 95t looked for a cascade decay of five degenerate squarks into $\tilde{\chi}_1^0$ which further decays into $\tilde{\chi}_1^0$ and a photon. No signal is observed. Limits vary widely depending on the choice of parameters. For $\mu = -40$ GeV, $\tan\beta = 1.5$, and heavy gluinos, the range $50 < m_{\tilde{q}} < 110$ (GeV) is excluded at 90% CL. See the paper for details.
- 44 ABE 92L assume five degenerate squark flavors and $m_{\tilde{q}_L} = m_{\tilde{q}_R}$. ABE 92L includes the effect of cascade decay, for a particular choice of parameters, $\mu = -250$ GeV, $\tan\beta = 2$. Results are weakly sensitive to these parameters over much of parameter space. No limit for $m_{\tilde{q}} \leq 50$ GeV (but other experiments rule out that region). Limits are 10–20 GeV higher if $B(\bar{q} \rightarrow q\bar{\gamma}) = 1$. Limit assumes GUT relations between gaugino masses and the gauge coupling; in particular that for $|\mu|$ not small, $m_{\tilde{\chi}_1^0} \approx m_{\tilde{g}}/6$. This last relation implies that as $m_{\tilde{g}}$ increases, the mass of $\tilde{\chi}_1^0$ will eventually exceed $m_{\tilde{q}}$ so that no decay is possible. Even before that occurs, the signal will disappear; in particular no bounds can be obtained for $m_{\tilde{g}} > 410$ GeV, $m_{H^\pm}=500$ GeV.

See key on page 405

Searches Particle Listings Supersymmetric Particle Searches

- ⁴⁵ ROY 92 reanalyzed CDF limits on di-lepton events to obtain limits on squark production in R -parity violating models. The 100% decay $\tilde{q} \rightarrow q\tilde{\chi}$ where $\tilde{\chi}$ is the LSP, and the LSP decays either into $\ell q\tilde{\nu}$ or $\ell\ell\tilde{\nu}$ is assumed.
- ⁴⁶ NOJIRI 91 argues that a heavy squark should be nearly degenerate with the gluino in minimal supergravity not to overclose the universe.

Long-lived \tilde{q} (Squark) MASS LIMIT

The following are bounds on long-lived scalar quarks, assumed to hadronise into hadrons with lifetime long enough to escape the detector prior to a possible decay. Limits may depend on the mixing angle of mass eigenstates: $\tilde{q}_1 = \tilde{q}_L \cos\theta_q + \tilde{q}_R \sin\theta_q$.

The coupling to the Z^0 boson vanishes for up-type squarks when $\theta_u=0.98$, and for down type squarks when $\theta_d=1.17$.

VALUE (GeV)	CL%	DOCUMENT ID	TECN	COMMENT
• • • We do not use the following data for averages, fits, limits, etc. • • •				
>249	95	1 AALTONEN 09Z	CDF	\tilde{t}
> 95	95	2 HEISTER 03H	ALEP	\tilde{u}
> 92	95	2 HEISTER 03H	ALEP	\tilde{d}
none 2–85	95	3 ABREU 98P	DLPH	\tilde{u}_L
none 2–81	95	3 ABREU 98P	DLPH	\tilde{u}_R
none 2–80	95	3 ABREU 98P	DLPH	\tilde{u} , $\theta_u=0.98$
none 2–83	95	3 ABREU 98P	DLPH	\tilde{d}_L
none 5–40	95	3 ABREU 98P	DLPH	\tilde{d}_R
none 5–38	95	3 ABREU 98P	DLPH	\tilde{d} , $\theta_d=1.17$

¹ AALTONEN 09Z searched in 1 fb^{-1} of $p\bar{p}$ collisions at $\sqrt{s} = 1.96 \text{ TeV}$ for events with direct production of a pair of charged massive stable particles identified by their TOF. No excess of events is observed over the expected background. The data are used to set a bound on the production cross section, and the result is compared with the pair production cross section of stable stops as a function of the \tilde{t} mass, see their Fig. 2.

² HEISTER 03H use e^+e^- data at and around the Z^0 peak to look for hadronizing stable squarks. Combining their results on searches for charged and neutral R -hadrons with JANOT 03, a lower limit of 15.7 GeV on the mass is obtained. Combining this further with the results of searches for tracks with anomalous ionization in data from 183 to 208 GeV yields the quoted bounds.

³ ABREU 98P assumes that 40% of the squarks will hadronise into a charged hadron, and 60% into a neutral hadron which deposits most of its energy in hadron calorimeter. Data collected at $\sqrt{s}=130\text{--}183 \text{ GeV}$.

\tilde{b} (Sbottom) MASS LIMIT

Limits in e^+e^- depend on the mixing angle of the mass eigenstate $\tilde{b}_1 = \tilde{b}_L \cos\theta_b + \tilde{b}_R \sin\theta_b$. Coupling to the Z vanishes for $\theta_b \sim 1.17$. As a consequence, no absolute constraint in the mass region $\lesssim 40 \text{ GeV}$ is available in the literature at this time from e^+e^- collisions. In the Listings below, we use $\Delta m = m_{\tilde{b}_1} - m_{\tilde{\chi}_1^0}$.

VALUE (GeV)	CL%	DOCUMENT ID	TECN	COMMENT
>193	95	1 AALTONEN 07E	CDF	$\tilde{b}_1 \rightarrow b\tilde{\chi}_1^0, m_{\tilde{\chi}_1^0}=40 \text{ GeV}$
none 35–222	95	2 ABAZOV 06R	D0	$\tilde{b} \rightarrow b\tilde{\chi}_1^0, m_{\tilde{\chi}_1^0}=50 \text{ GeV}$
>220	95	3 ABULENCIA 06i	CDF	$\tilde{g} \rightarrow \tilde{b}\tilde{b}, \Delta m > 6 \text{ GeV}, \tilde{b}_1 \rightarrow b\tilde{\chi}_1^0, m_{\tilde{\chi}_1^0} < 270 \text{ GeV}$
> 95		4 ACHARD 04	L3	$\tilde{b} \rightarrow b\tilde{\chi}_1^0, \theta_b=0, \Delta m > 15\text{--}25 \text{ GeV}$
> 81		4 ACHARD 04	L3	$\tilde{b} \rightarrow b\tilde{\chi}_1^0, \text{all } \theta_b, \Delta m > 15\text{--}25 \text{ GeV}$
> 7.5	95	5 JANOT 04	THEO	unstable $\tilde{b}_1, e^+e^- \rightarrow \text{hadrons}$
> 93	95	6 ABDALLAH 03M	DLPH	$\tilde{b} \rightarrow b\tilde{\chi}_1^0, \theta_b=0, \Delta m > 7 \text{ GeV}$
> 76	95	6 ABDALLAH 03M	DLPH	$\tilde{b} \rightarrow b\tilde{\chi}_1^0, \text{all } \theta_b, \Delta m > 7 \text{ GeV}$
> 85.1	95	7 ABBIENDI 02H	OPAL	$\tilde{b} \rightarrow b\tilde{\chi}_1^0, \text{all } \theta_b, \Delta m > 10 \text{ GeV},$ CDF
> 89	95	8 HEISTER 02K	ALEP	$\tilde{b} \rightarrow b\tilde{\chi}_1^0, \text{all } \theta_b, \Delta m > 8 \text{ GeV},$ CDF
none 3.5–4.5	95	9 SAVINOV 01	CLEO	\tilde{B} meson
none 80–145		10 AFFOLDER 00D	CDF	$\tilde{b} \rightarrow b\tilde{\chi}_1^0, m_{\tilde{\chi}_1^0} < 50 \text{ GeV}$
• • • We do not use the following data for averages, fits, limits, etc. • • •				
> 78	95	11 AALTONEN 09R	CDF	$\tilde{g} \rightarrow \tilde{b}\tilde{b}, \tilde{b} \rightarrow b\tilde{\chi}_1^0$
> 78	95	12 ABDALLAH 04M	DLPH	\tilde{R}, \tilde{b}_L , indirect, $\Delta m > 5 \text{ GeV}$
none 50–82	95	13 ABDALLAH 03C	DLPH	$\tilde{b} \rightarrow b\tilde{g}$, stable \tilde{g} , all $\theta_b,$ $\Delta m > 10 \text{ GeV}$
> 71.5	95	14 BERGER 03	THEO	\tilde{b}_L, \tilde{R} decay
> 27.4	95	15 HEISTER 03G	ALEP	$\tilde{b} \rightarrow b\tilde{g}$, stable \tilde{g} or \tilde{b}
> 48	95	16 HEISTER 03H	ALEP	$\tilde{b} \rightarrow b\tilde{g}$, stable \tilde{g} or \tilde{b}
		17 ACHARD 02	L3	\tilde{b}_1, \tilde{R} decays
		18 BAEK 02	THEO	
		19 BECHER 02	THEO	
		20 CHEUNG 02B	THEO	
		21 CHO 02	THEO	
none 52–115	95	22 BERGER 01	THEO	$p\bar{p} \rightarrow X+b\text{-quark}$
		23 ABBOTT 99F	D0	$\tilde{b} \rightarrow b\tilde{\chi}_1^0, m_{\tilde{\chi}_1^0} < 20 \text{ GeV}$

¹ AALTONEN 07E searched in 295 pb^{-1} of $p\bar{p}$ collisions at $\sqrt{s} = 1.96 \text{ TeV}$ for multijet events with large E_{Tj} . They request at least one heavy flavor-tagged jet and no identified leptons. The branching ratio $\tilde{b}_1 \rightarrow b\tilde{\chi}_1^0$ is assumed to be 100%. No significant excess was found compared to the background expectation. Upper limits on the cross-section are extracted and a limit is derived on the masses of sbottom versus $\tilde{\chi}_1^0$, see their Fig. 5.

² ABAZOV 06R looked in 310 pb^{-1} of $p\bar{p}$ collisions at $\sqrt{s} = 1.96 \text{ TeV}$ for events with 2 or 3 jets and large E_{Tj} with at least 1 b -tagged jet and a veto against isolated leptons.

No excess is observed relative to the SM background expectations. Limits are set on the sbottom pair production cross-section under the assumption that the only decay mode is into $b\tilde{\chi}_1^0$. Exclusion contours are derived in the plane of sbottom versus neutralino masses, shown in their Fig. 2. The observed limit is more constraining than the expected one due to a lack of events corresponding to large sbottom masses. Supersedes the results of ABBOTT 99F.

³ ABULENCIA 06i searched in 156 pb^{-1} of $p\bar{p}$ collisions at $\sqrt{s} = 1.96 \text{ TeV}$ for multijet events with large E_{Tj} . They request at least 2 b -tagged jets and no isolated leptons. They investigate the production of gluinos decaying into $\tilde{b}_1 b$ followed by $\tilde{b}_1 \rightarrow b\tilde{\chi}_1^0$. Both branching fractions are assumed to be 100% and the LSP mass to be 60 GeV. No significant excess was found compared to the background expectation. Upper limits on the cross-section are extracted and a limit is derived on the masses of sbottom and gluinos, see their Fig. 3.

⁴ ACHARD 04 search for the production of $b\tilde{b}$ in acoplanar b -tagged di-jet final states in the 192–209 GeV data. See Fig. 6 for the dependence of the limits on $m_{\tilde{\chi}_1^0}$. This limit supersedes ACCIARRI 99v.

⁵ JANOT 04 reanalyzes $e^+e^- \rightarrow \text{hadrons}$ total cross section data with $\sqrt{s} = 20\text{--}209 \text{ GeV}$ from PEP, PETRA, TRISTAN, SLC, and LEP and constrains the mass of \tilde{b}_1 assuming it decays quickly to hadrons.

⁶ ABDALLAH 03M looked for \tilde{b} pair production in events with acoplanar jets and E at $\sqrt{s} = 189\text{--}208 \text{ GeV}$. The limit improves to 87 (98) GeV for all θ_b ($\theta_b = 0$) for $\Delta m > 10 \text{ GeV}$. See Fig. 24 and Table 11 for other choices of Δm . These limits include and update the results of ABREU, P 00D.

⁷ ABBIENDI 02H search for events with two acoplanar jets and p_{Tj} in the 161–209 GeV data. The limit assumes 100% branching ratio and uses the exclusion at large Δm from CDF (AFFOLDER 00D). For $\theta_b=0$, the bound improves to $> 96.9 \text{ GeV}$. See Fig. 4 and Table 6 for the more general dependence on the limits on Δm . These results supersede ABBIENDI 99M.

⁸ HEISTER 02K search for bottom squarks in final states with acoplanar jets with b tagging, using 183–209 GeV data. The mass bound uses the CDF results from AFFOLDER 00D. See Fig. 5 for the more general dependence of the limits on Δm . Updates BARATE 01.

⁹ SAVINOV 01 use data taken at $\sqrt{s}=10.52 \text{ GeV}$, below the $B\bar{B}$ threshold. They look for events with a pair of leptons with opposite charge and a fully reconstructed hadronic D or D^* decay. These could originate from production of a light-sbottom hadron followed by $\tilde{B} \rightarrow D^{(*)} \ell^- \tilde{\nu}$, in case the $\tilde{\nu}$ is the LSP, or $\tilde{B} \rightarrow D^{(*)} \pi \ell^-$, in case of R . The mass range $3.5 \leq M(\tilde{B}) \leq 4.5 \text{ GeV}$ was explored, assuming 100% branching ratio for either of the decays. In the $\tilde{\nu}$ LSP scenario, the limit holds only for $M(\tilde{\nu})$ less than about 1 GeV and for the D^* decays it is reduced to the range 3.9–4.5 GeV. For the R decay, the whole range is excluded.

¹⁰ AFFOLDER 00D search for final states with 2 or 3 jets and E_{Tj} , one jet with a b tag. See their Fig. 3 for the mass exclusion in the $m_{\tilde{t}}, m_{\tilde{\chi}_1^0}$ plane.

¹¹ AALTONEN 09R searched in 2.5 fb^{-1} of $p\bar{p}$ collisions at $\sqrt{s} = 1.96 \text{ TeV}$ for events with at least 2 b -tagged jets and E_{Tj} , originating from the decay $\tilde{g} \rightarrow b\tilde{b}$ followed by $\tilde{b} \rightarrow b\tilde{\chi}_1^0$. Both decays are assumed to have 100% branching ratio. No significant deviation from the SM prediction is observed. An upper limit on the gluino pair production cross section is calculated as a function of the gluino mass, see their Fig. 2. A limit is derived in the $m_{\tilde{g}}$ versus $m_{\tilde{g}}$ plane which improves the results of previous searches, see their Fig. 3.

¹² ABDALLAH 04M use data from $\sqrt{s} = 192\text{--}208 \text{ GeV}$ to derive limits on sparticle masses under the assumption of R with $UD\bar{D}$ couplings. The results are valid for $\mu = -200 \text{ GeV}$, $\tan\beta = 1.5$, $\Delta m > 5 \text{ GeV}$ and assuming a BR of 1 for the given decay. The limit quoted is for indirect $UD\bar{D}$ decays using the neutralino constraint of 38.0 GeV, also derived in ABDALLAH 04M, and assumes no mixing. For indirect decays it remains at 78 GeV when the neutralino constraint is not used. Supersedes the result of ABREU 01b.

¹³ ABDALLAH 03C looked for events of the type $q\bar{q}R^\pm R^\pm, q\bar{q}R^\pm R^0, \text{ or } q\bar{q}R^0 R^0$ in e^+e^- interactions at $\sqrt{s} = 189\text{--}208 \text{ GeV}$. The R^\pm bound states are identified by anomalous dE/dx in the tracking chambers and the R^0 by missing energy due to their reduced energy loss in the calorimeters. Excluded mass regions in the $(m(\tilde{b}), m(\tilde{g}))$ plane for $m(\tilde{g}) > 2 \text{ GeV}$ are obtained for several values of the probability for the gluino to fragment into R^\pm or R^0 , as shown in their Fig. 19. The limit improves to 94 GeV for $\theta_b=0$.

¹⁴ BERGER 03 studies the constraints on a \tilde{b}_1 with mass in the 2.2–5.5 GeV region coming from radiative decays of $T(\text{nS})$ into sbottomonium. The constraints apply only if \tilde{b}_1 lives long enough to permit formation of the sbottomonium bound state. A small region of mass in the $m_{\tilde{b}_1} - m_{\tilde{g}}$ plane survives current experimental constraints from CLEO.

¹⁵ HEISTER 03G searches for the production of \tilde{b} pairs in the case of R prompt decays with $L\bar{L}E, LQ\bar{D}$ or $UD\bar{D}$ couplings at $\sqrt{s} = 189\text{--}209 \text{ GeV}$. The limit holds for indirect decays mediated by $R UD\bar{D}$ couplings. It improves to 90 GeV for indirect decays mediated by $R L\bar{L}E$ couplings and to 80 GeV for indirect decays mediated by $R LQ\bar{D}$ couplings. Supersedes the results from BARATE 01B.

¹⁶ HEISTER 03H use their results on bounds on stable squarks, on stable gluinos and on squarks decaying to a stable gluino from the same paper to derive a mass limit on \tilde{b} , see their Fig. 13. The limit for a long-lived \tilde{b}_1 is 92 GeV.

¹⁷ ACHARD 02 searches for the production of squarks in the case of R prompt decays with $UD\bar{D}$ couplings at $\sqrt{s}=189\text{--}208 \text{ GeV}$. The search is performed for direct and indirect decays, assuming one coupling at the time to be nonzero. The limit is computed for the minimal cross section and holds for indirect decays and reaches 55 GeV for direct decays.

¹⁸ BAEK 02 studies the constraints on a \tilde{b}_1 with mass in the 2.2–5.5 GeV region coming from precision measurements of Z^0 decays. It is noted that CP -violating couplings in the MSSM parameters relax the strong constraints otherwise derived from CP conservation.

¹⁹ BECHER 02 studies the constraints on a \tilde{b}_1 with mass in the 2.2–5.5 GeV region coming from radiative B meson decays, and sets limits on the off-diagonal flavor-changing couplings $q\bar{b}\tilde{g}$ ($q=d,s$).

²⁰ CHEUNG 02b studies the constraints on a \tilde{b}_1 with mass in the 2.2–5.5 GeV region and a gluino in the mass range 12–16 GeV, using precision measurements of Z^0 decays and e^+e^- annihilations at LEP2. Few detectable events are predicted in the LEP2 data for the model proposed by BERGER 01.

²¹ CHO 02 studies the constraints on a \tilde{b}_1 with mass in the 2.2–5.5 GeV region coming from precision measurements of Z^0 decays. Strong constraints are obtained for CP -conserving MSSM couplings.

Searches Particle Listings

Supersymmetric Particle Searches

²² BERGER 01 reanalyzed interpretation of Tevatron data on bottom-quark production. Argues that pair production of light gluinos ($m \sim 12\text{--}16$ GeV) with subsequent 2-body decay into a light sbottom ($m \sim 2\text{--}5.5$ GeV) and bottom can reconcile Tevatron data with predictions of perturbative QCD for the bottom production rate. The sbottom must either decay hadronically via a R -parity- and B -violating interaction, or be long-lived. Constraints on the mass spectrum are derived from the measurements of time-averaged $B^0\text{--}\bar{B}^0$ mixing.

²³ ABBOTT 99F looked for events with two jets, with or without an associated muon from b decay, and \cancel{E}_T . See Fig. 2 for the dependence of the limit on $m_{\tilde{\chi}_1^0}$. No limit for $m_{\tilde{\chi}_1^0} > 47$ GeV.

$\tilde{\tau}$ (Stop) MASS LIMIT

Limits depend on the decay mode. In e^+e^- collisions they also depend on the mixing angle of the mass eigenstate $\tilde{\tau}_1 = \tilde{\tau}_L \cos\theta_t + \tilde{\tau}_R \sin\theta_t$. The coupling to the Z vanishes when $\theta_t = 0.98$. In the Listings below, we use $\Delta m \equiv m_{\tilde{\tau}_1} - m_{\tilde{\chi}_1^0}$ or $\Delta m \equiv m_{\tilde{\tau}_1} - m_{\tilde{\nu}}$, depending on relevant decay mode. See also bounds in “ \tilde{q} (Squark) MASS LIMIT.” Limits made obsolete by the most recent analyses of e^+e^- and $p\bar{p}$ collisions can be found in previous Editions of this Review.

VALUE (GeV)	CL%	DOCUMENT ID	TECN	COMMENT
none 95–150	95	¹ ABAZOV 09D D0	D0	$\tilde{\tau} \rightarrow b\tilde{\nu}$
		² ABAZOV 08Z D0	D0	$\tilde{\tau} \rightarrow c\tilde{\chi}_1^0$, $m_c < \Delta m < m_{W+m_b}$
none 80–120	95	³ ABAZOV 04 D0	D0	$\tilde{\tau} \rightarrow b\ell\nu\tilde{\chi}_1^0$, $m_{\tilde{\chi}_1^0} = 50$ GeV
> 90		⁴ ACHARD 04 L3	L3	$\tilde{\tau} \rightarrow c\tilde{\chi}_1^0$, all θ_t , $\Delta m > 15\text{--}25$ GeV
> 93		⁴ ACHARD 04 L3	L3	$\tilde{b} \rightarrow b\tilde{\nu}$, all θ_t , $\Delta m > 15$ GeV
> 88		⁴ ACHARD 04 L3	L3	$\tilde{b} \rightarrow b\tau\tilde{\nu}$, all θ_t , $\Delta m > 15$ GeV
> 75	95	⁵ ABDALLAH 03M DLPH	DLPH	$\tilde{\tau} \rightarrow c\tilde{\chi}_1^0$, $\theta_t = 0$, $\Delta m > 2$ GeV
> 71	95	⁵ ABDALLAH 03M DLPH	DLPH	$\tilde{\tau} \rightarrow c\tilde{\chi}_1^0$, all θ_t , $\Delta m > 2$ GeV
> 96	95	⁵ ABDALLAH 03M DLPH	DLPH	$\tilde{\tau} \rightarrow c\tilde{\chi}_1^0$, $\theta_t = 0$, $\Delta m > 10$ GeV
> 92	95	⁵ ABDALLAH 03M DLPH	DLPH	$\tilde{\tau} \rightarrow c\tilde{\chi}_1^0$, all θ_t , $\Delta m > 10$ GeV
none 80–131	95	⁶ ACOSTA 03C CDF	CDF	$\tilde{\tau} \rightarrow b\tilde{\nu}$, $m_{\tilde{\nu}} \leq 63$ GeV
> 95.7	95	⁷ ABBIENDI 02H OPAL	OPAL	$c\tilde{\chi}_1^0$, all θ_t , $\Delta m > 10$ GeV
> 92.6	95	⁷ ABBIENDI 02H OPAL	OPAL	$b\tilde{\nu}$, all θ_t , $\Delta m > 10$ GeV
> 91.5	95	⁷ ABBIENDI 02H OPAL	OPAL	$b\tau\tilde{\nu}$, all θ_t , $\Delta m > 10$ GeV
> 63	95	⁸ HEISTER 02K ALEP	ALEP	any decay, any lifetime, all θ_t
> 92	95	⁸ HEISTER 02K ALEP	ALEP	$\tilde{\tau} \rightarrow c\tilde{\chi}_1^0$, all θ_t , $\Delta m > 8$ GeV, CDF
> 97	95	⁸ HEISTER 02K ALEP	ALEP	$\tilde{\tau} \rightarrow b\tilde{\nu}$, all θ_t , $\Delta m > 8$ GeV, DØ
> 78	95	⁸ HEISTER 02K ALEP	ALEP	$\tilde{\tau} \rightarrow b\tilde{\chi}_1^0 W^*$, all θ_t , $\Delta m > 8$ GeV
• • • We do not use the following data for averages, fits, limits, etc. • • •				
> 153	95	⁹ ABAZOV 09N D0	D0	$\tilde{\tau} \rightarrow b\tilde{\chi}_1^\pm$
> 185	95	¹⁰ AALTONEN 08Z CDF	CDF	$R, \tilde{\tau}_1 \rightarrow b\tau$
> 132	95	¹¹ ABAZOV 08 D0	D0	$\tilde{\tau} \rightarrow b\tilde{\nu}$, $m_{\tilde{\nu}} = 70$ GeV
none 80–134	95	¹² AALTONEN 07E CDF	CDF	$\tilde{\tau}_1 \rightarrow c\tilde{\chi}_1^0$, $m_{\tilde{\chi}_1^0} = 48$ GeV
> 77	95	¹³ ABAZOV 07B D0	D0	$\tilde{\tau} \rightarrow c\tilde{\chi}_1^0$, $m_{\tilde{\chi}_1^0} < 48$ GeV
> 77	95	¹⁴ CHEKANOV 07 ZEUS	ZEUS	$e^+p \rightarrow \tilde{\tau}_1, R, LQ\bar{D}$
> 77	95	¹⁵ ABBIENDI 04F OPAL	OPAL	R , direct, all θ_t
	95	¹⁶ ABDALLAH 04M DLPH	DLPH	R , indirect, all θ_t , $\Delta m > 5$ GeV
> 74.5	95	¹⁷ AKTAS 04B H1	H1	$R, \tilde{\tau}_1$
none 50–87	95	¹⁸ DAS 04 THEO	THEO	$\tilde{\tau}\tilde{\tau} \rightarrow b\ell\nu_\ell\chi^0\bar{b}q\bar{q}'\chi^0$, $m_{\tilde{\chi}_1^0} = 15$ GeV, no $\tilde{\tau} \rightarrow c\chi^0$, $\Delta m > 10$ GeV
> 71.5	95	¹⁹ ABDALLAH 03C DLPH	DLPH	$\tilde{\tau} \rightarrow c\tilde{g}$, stable \tilde{g} , all θ_t , $\Delta m > 10$ GeV
> 80	95	²⁰ CHAKRAB... 03 THEO	THEO	$p\bar{p} \rightarrow i\tilde{\nu}^*$, RPV
> 144	95	²¹ HEISTER 03G ALEP	ALEP	$\tilde{\tau}_L, R$ decay
> 77	95	²² HEISTER 03H ALEP	ALEP	$\tilde{\tau} \rightarrow c\tilde{g}$, stable \tilde{g} or $\tilde{\tau}$, all θ_t , all Δm
> 61	95	²³ ABAZOV 02C D0	D0	$\tilde{\tau} \rightarrow b\tilde{\nu}$, $m_{\tilde{\nu}} = 45$ GeV
none 68–119	95	²⁴ ACHARD 02 L3	L3	$\tilde{\tau}_1, R$ decays
none 84–120	95	²⁵ AFFOLDER 01B CDF	CDF	$t \rightarrow \tilde{\tau}\chi_1^0$
> 120	95	²⁶ ABREU 00I DLPH	DLPH	$R(LL\bar{E})$, $\theta_t = 0.98$, $\Delta m > 4$ GeV
none 9–24.4	95	²⁷ AFFOLDER 00D CDF	CDF	$\tilde{\tau} \rightarrow c\tilde{\chi}_1^0$, $m_{\tilde{\chi}_1^0} < 40$ GeV
> 138	95	²⁸ AFFOLDER 00G CDF	CDF	$\tilde{\tau}_1 \rightarrow b\tilde{\nu}$, $m_{\tilde{\nu}} < 45$
> 45	95	²⁹ ABE 99M CDF	CDF	$p\bar{p} \rightarrow \tilde{\tau}_1\tilde{\tau}_1, R$
none 11–41	95	³⁰ AID 96 H1	H1	$e p \rightarrow \tilde{\tau}, R$ decays
none 6.0–41.2	95	³¹ AID 96 H1	H1	$e p \rightarrow \tilde{\tau}, R, \cos\theta_t > 0.03$
none 5.0–46.0	95	³² CHO 96 RVUE	RVUE	$B^0\text{--}\bar{B}^0$ and $e, \theta_t = 0.98$, $\tan\beta < 2$
none 11.2–25.5	95	³³ BUSKULIC 95E ALEP	ALEP	$R(LL\bar{E})$, $\theta_t = 0.98$
	95	³³ AKERS 94K OPAL	OPAL	$\tilde{\tau} \rightarrow c\tilde{\chi}_1^0$, $\theta_t = 0$, $\Delta m > 2$ GeV
	95	³³ AKERS 94K OPAL	OPAL	$\tilde{\tau} \rightarrow c\tilde{\chi}_1^0$, $\theta_t = 0$, $\Delta m > 5$ GeV
	95	³³ AKERS 94K OPAL	OPAL	$\tilde{\tau} \rightarrow c\tilde{\chi}_1^0$, $\theta_t = 0.98$, $\Delta m > 2$ GeV

none 7.9–41.2 95 AKERS 94K OPAL $\tilde{\tau} \rightarrow c\tilde{\chi}_1^0$, $\theta_t = 0.98$, $\Delta m > 5$ GeV

none 7.6–28.0 95 ³⁴ SHIRAI 94 VNS $\tilde{\tau} \rightarrow c\tilde{\chi}_1^0$, any θ_t , $\Delta m > 10$ GeV

none 10–20 95 ³⁴ SHIRAI 94 VNS $\tilde{\tau} \rightarrow c\tilde{\chi}_1^0$, any θ_t , $\Delta m > 2.5$ GeV

¹ ABAZOV 09o looked in 1 fb^{-1} of $p\bar{p}$ collisions at $\sqrt{s} = 1.96$ TeV for events with two electrons or one electron and one muon and \cancel{E}_T originating from associated production $\tilde{\tau}\tilde{\tau}$, followed by the three-body decays $\tilde{\tau} \rightarrow b\ell\nu$. No evidence for an excess over the SM expectation is observed. The excluded region is shown in a plane of $m_{\tilde{\nu}}$ versus $m_{\tilde{\tau}}$, see their Fig. 3. The largest excluded $\tilde{\tau}$ mass is 175 GeV for a $\tilde{\nu}$ mass of 45 GeV, and the largest excluded $\tilde{\nu}$ mass is 96 GeV for a $\tilde{\tau}$ mass of 140 GeV. Supersedes the results of ABAZOV 08 and ABAZOV 02c.

² ABAZOV 08z looked in 995 pb^{-1} of $p\bar{p}$ collisions at $\sqrt{s} = 1.96$ TeV for events with exactly 2 jets, at least one being tagged as heavy quark, and \cancel{E}_T , originating from stop pair production. Branching ratios are assumed to be 100% for $\tilde{\tau}_1 \rightarrow c\tilde{\chi}_1^0$. No evidence for an excess over the SM expectation is observed. The excluded region is shown in a plane of $m_{\tilde{\tau}}$ versus $m_{\tilde{\chi}_1^0}$, see their Fig. 5. No limit can be obtained for $m_{\tilde{\chi}_1^0} > 70$ GeV. Supersedes the results of ABAZOV 07b.

³ ABAZOV 04 looked at 108.3 pb^{-1} of $p\bar{p}$ collisions at $\sqrt{s} = 1.8$ TeV for events with $e+\mu+\cancel{E}_T$ as signature for the 3- and 4-body decays of stop into $b\ell\nu\tilde{\chi}_1^0$ final states. For the $b\ell\nu$ channel they use the results from ABAZOV 02c. No significant excess is observed compared to the Standard Model expectation and limits are derived on the mass of $\tilde{\tau}_1$ for the 3- and 4-body decays in the $(m_{\tilde{\tau}}, m_{\tilde{\chi}_1^0})$ plane, see their Figure 4.

⁴ ACHARD 04 search in the 192–209 GeV data for the production of $\tilde{\tau}\tilde{\tau}$ in acoplanar dijet final states and, in case of $b\ell\nu$ ($b\tau\nu$) final states, two leptons (taus). The limits for $\theta_t = 0$ improve to 95, 96 and 93 GeV, respectively. All limits assume 100% branching ratio for the respective decay modes. See Fig. 6 for the dependence of the limits on $m_{\tilde{\chi}_1^0}$. These limits supersede ACCIARRI 99v.

⁵ ABDALLAH 03m looked for $\tilde{\tau}$ pair production in events with acoplanar jets and $\cancel{E} \approx \sqrt{s} = 189\text{--}208$ GeV. See Fig. 23 and Table 11 for other choices of Δm . These limits include and update the results of ABREU 00d.

⁶ ACOSTA 03c searched in 107 pb^{-1} of $p\bar{p}$ collisions at $\sqrt{s} = 1.8$ TeV for pair production of $\tilde{\tau}$ followed by the decay $\tilde{\tau} \rightarrow b\ell\nu$. They looked for events with two isolated leptons (e or μ), at least one jet and \cancel{E}_T . The excluded mass range is reduced for larger $m_{\tilde{\nu}}$, and no limit is set for $m_{\tilde{\nu}} > 88.4$ GeV (see Fig. 2).

⁷ ABBIENDI 02h looked for events with two acoplanar jets, \cancel{p}_T , and, in the case of $b\ell\nu$ final states, two leptons, in the 161–209 GeV data. The bound for $c\tilde{\chi}_1^0$ applies to the region where $\Delta m < m_{W+m_b}$, else the decay $\tilde{\tau}_1 \rightarrow b\tilde{\chi}_1^0 W^+$ becomes dominant. The limit for $b\ell\nu$ assumes equal branching ratios for the three lepton flavors and for $b\tau\nu$ 100% for this channel. For $\theta_t = 0$, the bounds improve to > 97.6 GeV ($c\tilde{\chi}_1^0$), > 96.0 GeV ($b\ell\nu$), and > 95.5 GeV ($b\tau\nu$). See Figs. 5–6 and Table 5 for the more general dependence of the limits on Δm . These results supersede ABBIENDI 99m.

⁸ HEISTER 02k search for top squarks in final states with jets (with/without b tagging or leptons) or long-lived hadrons, using 183–209 GeV data. The absolute mass bound is obtained by varying the branching ratio of $\tilde{\tau} \rightarrow c\tilde{\chi}_1^0$ and the lepton fraction in $\tilde{\tau} \rightarrow b\tilde{\chi}_1^0 \ell\bar{\ell}'$ decays. The mass bound for $\tilde{\tau} \rightarrow c\tilde{\chi}_1^0$ uses the CDF results from AFFOLDER 00d and for $\tilde{\tau} \rightarrow b\ell\nu$ the DØ results from ABAZOV 02c. See Figs. 2–5 for the more general dependence of the limits on Δm . Updates BARATE 01 and BARATE 00p.

⁹ ABAZOV 09n looked in 0.9 fb^{-1} of $p\bar{p}$ collisions at $\sqrt{s} = 1.96$ TeV for events with ≥ 3 jets, at least one being b -tagged, one electron or muon and \cancel{E}_T originating from associated production $\tilde{\tau}\tilde{\tau}$, with one $\tilde{\tau}$ decaying leptonically, the other hadronically. The branching ratios for $\tilde{\tau}_1 \rightarrow b\tilde{\chi}_1^\pm$ and $\tilde{\chi}_1^\pm \rightarrow \tilde{\chi}_1^0 W^\pm$ are assumed to be 100%. The separation from the dominant $t\bar{t}$ background is based on a multivariate likelihood discriminant analysis. The tested mass range is $130\text{ GeV} \leq m_{\tilde{\tau}_1} \leq 190\text{ GeV}$, $90\text{ GeV} \leq m_{\tilde{\chi}_1^\pm} \leq 150\text{ GeV}$ and $m_{\tilde{\chi}_1^0} = 50$ GeV fixed. The excluded cross section is a factor 2–13 larger than the theoretical expectation in the considered MSSM scenarios, see their Fig. 3.

¹⁰ AALTONEN 08z searched in 322 pb^{-1} of $p\bar{p}$ collisions at $\sqrt{s} = 1.96$ TeV for dijet events with a lepton (e or μ) and a hadronic τ decay produced via R -parity violating couplings $LQ\bar{D}$. No heavy flavour-tagged jets are requested. No significant excess was found compared to the background expectation. Upper limits on the cross-section times the square of the branching ratio $B(\tilde{\tau}_1 \rightarrow b\tau)$ are extracted, and a limit is derived on the stop mass assuming $B(\tilde{\tau}_1 \rightarrow b\tau) = 1$, see their Fig. 2. Supersedes the results of ACOSTA 04b.

¹¹ ABAZOV 08l looked at approximately 400 pb^{-1} of $p\bar{p}$ collisions at $\sqrt{s} = 1.96$ TeV for events with $b\bar{b}\ell\ell'\cancel{E}_T$ with $\ell\ell' = e^\pm\mu^\mp$ or $\ell\ell' = \mu^\pm\mu^\mp$, originating from associated production $\tilde{\tau}\tilde{\tau}$. Branching ratios are assumed to be 100% for both $\tilde{\chi}_1^\pm \rightarrow \ell\nu$ and $\tilde{\nu} \rightarrow \nu\tilde{\chi}_1^0$. No evidence for an excess over the SM expectation is observed. The excluded region is shown in a plane of $m_{\tilde{\nu}}$ versus $m_{\tilde{\tau}}$, see their Fig. 3.

¹² AALTONEN 07e searched in 295 pb^{-1} of $p\bar{p}$ collisions at $\sqrt{s} = 1.96$ TeV for multijet events with large \cancel{E}_T . They request at least one heavy flavor-tagged jet and no identified leptons. The branching ratio $\tilde{\tau}_1 \rightarrow c\tilde{\chi}_1^0$ is assumed to be 100%. No significant excess was found compared to the background expectation. Upper limits on the cross-section are extracted and a limit is derived on the masses of stop versus $\tilde{\chi}_1^0$, see their Fig. 4.

¹³ ABAZOV 07b looked in 360 pb^{-1} of $p\bar{p}$ collisions at $\sqrt{s} = 1.96$ TeV for events with a pair of acoplanar heavy-flavor jets with \cancel{E}_T . No excess is observed relative to the SM background expectations. Limits are set on the production of $\tilde{\tau}_1$ under the assumption that the only decay mode is into $c\tilde{\chi}_1^0$, see their Fig. 4 for the limit in the $(m_{\tilde{\tau}_1}, m_{\tilde{\chi}_1^0})$ plane. No limit can be obtained for $m_{\tilde{\chi}_1^0} > 54$ GeV. Supersedes the results of ABAZOV 04b.

¹⁴ CHEKANOV 07 search for the $LQ\bar{D}$ R -parity violating process $e^+p \rightarrow \tilde{\tau}_1$ in 65 pb^{-1} at 318 GeV. Final states may originate from $LQ\bar{D}$ couplings $\tilde{\tau} \rightarrow e^+d$ and from the R -parity conserving decay $\tilde{\tau} \rightarrow \tilde{\chi}^+b$, giving rise to $e + \text{jet}$, $e + \text{multi-jet}$, and $\nu + \text{multi-jet}$. The excluded region in an MSSM scenario is presented for λ_{131} as a function

- of the stop mass in Fig. 6. Other excluded regions in a more restricted mSUGRA model are shown in Fig. 7 and 8.
- 15 ABBIENDI 04F use data from $\sqrt{s} = 189\text{--}209$ GeV. They derive limits on the stop mass under the assumption of R with $LQ\bar{D}$ or $U\bar{D}\bar{D}$ couplings. The limit quoted applies to direct decays with $U\bar{D}\bar{D}$ couplings when the stop decouples from the Z^0 and improves to 88 GeV for $\theta_t = 0$. For $LQ\bar{D}$ couplings, the limit improves to 98 (100) GeV for λ'_{13k} or λ'_{23k} couplings and all θ_t ($\theta_t = 0$). For λ'_{33k} couplings it is 96 (98) GeV for all θ_t ($\theta_t = 0$). Supersedes the results of ABBIENDI 00.
- 16 ABDALLAH 04M use data from $\sqrt{s} = 192\text{--}208$ GeV to derive limits on sparticle masses under the assumption of R with LLE or $U\bar{D}\bar{D}$ couplings. The results are valid for $\mu = -200$ GeV, $\tan\beta = 1.5$, $\Delta m > 5$ GeV and assuming a BR of 1 for the given decay. The limit quoted is for decoupling of the stop from the Z^0 and indirect $U\bar{D}\bar{D}$ decays using the neutralino constraint of 39.5 GeV for LLE and of 38.0 GeV for $U\bar{D}\bar{D}$ couplings, also derived in ABDALLAH 04M. For no mixing (decoupling) and indirect decays via LLE the limit improves to 92 (87) GeV if the constraint from the neutralino is used and to 88 (81) GeV if it is not used. For indirect decays via $U\bar{D}\bar{D}$ couplings it improves to 87 GeV for no mixing and using the constraint from the neutralino, whereas it becomes 81 GeV (67) GeV for no mixing (decoupling) if the neutralino constraint is not used. Supersedes the result of ABREU 01d.
- 17 AKTAS 04B looked in 106 pb^{-1} of $e^\pm p$ collisions at $\sqrt{s} = 319$ GeV and 301 GeV for resonant production of \tilde{t}_1 by R -parity violating $LQ\bar{D}$ couplings with λ'_{131} , others being zero. They consider the decays $\tilde{t}_1 \rightarrow e^+ d$ and $\tilde{t}_1 \rightarrow W\bar{b}$ followed by $\bar{b} \rightarrow \bar{c} d$ and assume gauginos too heavy to participate in the decays. They combine the channels $j e \cancel{p}_T$, $j \mu \cancel{p}_T$, $j j \cancel{p}_T$ to derive limits in the plane $(m_{\tilde{t}_1}, \lambda'_{131})$, see their Fig. 5.
- 18 DAS 04 reanalyzes AFFOLDER 00G data and obtains constraints on $m_{\tilde{t}_1}$ as a function of $B(\tilde{t} \rightarrow b\ell\nu\chi^0) \times B(\tilde{t} \rightarrow b\bar{q}'\chi^0)$, $B(\tilde{t} \rightarrow c\chi^0)$ and m_{χ^0} . Bound weakens for larger $B(\tilde{t} \rightarrow c\chi^0)$ and m_{χ^0} .
- 19 ABDALLAH 03c looked for events of the type $q\bar{q}R^\pm R^\pm$, $q\bar{q}R^\pm R^0$ or $q\bar{q}R^0 R^0$ in e^+e^- interactions at $\sqrt{s} = 189\text{--}208$ GeV. The R^\pm bound states are identified by anomalous dE/dx in the tracking chambers and the R^0 by missing energy, due to their reduced energy loss in the calorimeters. Excluded mass regions in the $(m(\tilde{t}), m(\tilde{g}))$ plane for $m(\tilde{g}) > 2$ GeV are obtained for several values of the probability for the gluino to fragment into R^\pm or R^0 , as shown in their Fig. 18. The limit improves to 90 GeV for $\theta_t = 0$.
- 20 Theoretical analysis of $e^+e^- + 2$ jet final states from the RPV decay of $\tilde{t}\tilde{t}^*$ pairs produced in $p\bar{p}$ collisions at $\sqrt{s}=1.8$ TeV. 95%CL limits of 220 (165) GeV are derived for $B(\tilde{t} \rightarrow e q)=1$ (0.5).
- 21 HEISTER 03G searches for the production of \tilde{t} pairs in the case of R prompt decays with LLE , $LQ\bar{D}$ or $U\bar{D}\bar{D}$ couplings at $\sqrt{s} = 189\text{--}209$ GeV. The limit holds for indirect decays mediated by R $U\bar{D}\bar{D}$ couplings. It improves to 91 GeV for indirect decays mediated by R LLE couplings, to 97 GeV for direct (assuming $B(\tilde{t}_L \rightarrow q\tau) = 100\%$) and to 85 GeV for indirect decays mediated by R $LQ\bar{D}$ couplings. Supersedes the results from BARATE 01b.
- 22 HEISTER 03H use e^+e^- data from 183–208 GeV to look for the production of stop decaying into a c quark and a stable gluino hadronizing into charged or neutral R -hadrons. Combining these results with bounds on stable squarks and on a stable gluino LSP from the same paper yields the quoted limit. See their Fig. 13 for the dependence of the mass limit on the gluino mass and on θ_t .
- 23 ABAZOV 02c looked in 108.3pb^{-1} of $p\bar{p}$ collisions at $\sqrt{s}=1.8$ TeV for events with $e\mu\cancel{E}_T$, originating from associated production $\tilde{t}\tilde{t}$. Branching ratios are assumed to be 100%. The bound for the $b\ell\nu$ decay weakens for large $\tilde{\nu}$ mass (see Fig. 3), and no limit is set when $m_{\tilde{\nu}} > 85$ GeV. See Fig. 4 for the limits in case of decays to a real $\tilde{\chi}_1^\pm$, followed by $\tilde{\chi}_1^\pm \rightarrow \ell\tilde{\nu}$, as a function of $m_{\tilde{\chi}_1^\pm}$.
- 24 ACHARD 02 searches for the production of squarks in the case of R prompt decays with $U\bar{D}\bar{D}$ couplings at $\sqrt{s}=189\text{--}208$ GeV. The search is performed for direct and indirect decays, assuming one coupling at the time to be nonzero. The limit is computed for the minimal cross section and holds for both direct and indirect decays.
- 25 AFFOLDER 01B searches for decays of the top quark into stop and LSP, in $t\bar{t}$ events. Limits on the stop mass as a function of the LSP mass and of the decay branching ratio are shown in Fig. 3. They exclude branching ratios in excess of 45% for SLP masses up to 40 GeV.
- 26 ABREU 00i searches for the production of stop in the case of R -parity violation with LLE couplings, for which only indirect decays are allowed. They investigate topologies with jets plus leptons in data from $\sqrt{s}=183$ GeV. The lower bound on the stop mass assumes a neutralino mass limit of 27 GeV, also derived in ABREU 00i.
- 27 AFFOLDER 00D search for final states with 2 or 3 jets and \cancel{E}_T , one jet with a c tag. See their Fig. 2 for the mass exclusion in the $(m_{\tilde{t}_1}, m_{\tilde{\chi}_1^0})$ plane. The maximum excluded $m_{\tilde{t}_1}$ value is 119 GeV, for $m_{\tilde{\chi}_1^0} = 40$ GeV.
- 28 AFFOLDER 00G searches for $\tilde{t}_1\tilde{t}_1^*$ production, with $\tilde{t}_1 \rightarrow b\ell\nu$, leading to topologies with ≥ 1 isolated lepton (e or μ), \cancel{E}_T , and ≥ 2 jets with ≥ 1 tagged as b quark by a secondary vertex. See Fig. 4 for the excluded mass range as a function of $m_{\tilde{\nu}}$. Cross-section limits for $\tilde{t}_1\tilde{t}_1^*$, with $\tilde{t}_1 \rightarrow b\chi_1^\pm$ ($\chi_1^\pm \rightarrow \ell^\pm\nu\chi_1^0$), are given in Fig. 2.
- 29 ABE 99M looked in 107 pb^{-1} of $p\bar{p}$ collisions at $\sqrt{s}=1.8$ TeV for events with like sign dileptons and two or more jets from the sequential decays $\tilde{q} \rightarrow q\tilde{\chi}_1^0$ and $\tilde{\chi}_1^0 \rightarrow e q\bar{q}'$, assuming R coupling $L_1 Q_j D_k^c$, with $j=2,3$ and $k=1,2,3$. They assume $B(\tilde{t}_1 \rightarrow c\chi_1^0)=1$, $B(\tilde{\chi}_1^0 \rightarrow e q\bar{q}')=0.25$ for both e^+ and e^- , and $m_{\tilde{\chi}_1^0} \geq m_{\tilde{t}_1}/2$. The limit improves for heavier $\tilde{\chi}_1^0$.
- 30 AID 96 considers photoproduction of $\tilde{t}\tilde{t}$ pairs, with 100% R -parity violating decays of \tilde{t} to $e q$, with $q=d, s$, or b quarks.
- 31 AID 96 considers production and decay of \tilde{t} via the R -parity violating coupling $\lambda' L_1 Q_3 \bar{q}_1^c$.
- 32 CHO 96 studied the consistency among the $B^0\text{--}\bar{B}^0$ mixing, ϵ in $K^0\text{--}\bar{K}^0$ mixing, and the measurements of V_{cb} , V_{ub}/V_{cb} . For the range $25.5\text{ GeV} < m_{\tilde{t}_1} < m_Z/2$ left by

AKERS 94k for $\theta_t = 0.98$, and within the allowed range in $M_2\text{--}\mu$ parameter space from chargino, neutralino searches by ACCIARRI 95E, they found the scalar top contribution to $B^0\text{--}\bar{B}^0$ mixing and ϵ to be too large if $\tan\beta < 2$. For more on their assumptions, see the paper and their reference 10.

- 33 BUSKULIC 95E looked for $Z \rightarrow \tilde{t}\tilde{t}$, where $\tilde{t} \rightarrow c\chi_1^0$ and χ_1^0 decays via R -parity violating interactions into two leptons and a neutrino.
- 34 SHIRAI 94 bound assumes the cross section without the s -channel Z -exchange and the QCD correction, underestimating the cross section up to 20% and 30%, respectively. They assume $m_C=1.5$ GeV.

Heavy \tilde{g} (Gluino) MASS LIMIT

For $m_{\tilde{g}} > 60\text{--}70$ GeV, it is expected that gluinos would undergo a cascade decay via a number of neutralinos and/or charginos rather than undergo a direct decay to photinos as assumed by some papers. Limits obtained when direct decay is assumed are usually higher than limits when cascade decays are included. Limits made obsolete by the most recent analyses of $p\bar{p}$ collisions can be found in previous Editions of this Review.

VALUE (GeV)	CL%	DOCUMENT ID	TECN	COMMENT
>280	95	1 AALTONEN	09S CDF	$\text{jets} + \cancel{E}_T$, $\tan\beta=5$, $\mu < 0$, $A_0=0$, any $m_{\tilde{q}}$
>392	95	1 AALTONEN	09S CDF	$\text{jets} + \cancel{E}_T$, $\tan\beta=5$, $\mu < 0$, $A_0=0$, $m_{\tilde{q}}=m_{\tilde{g}}$
>308	95	2 ABAZOV	08G D0	$\text{jets} + \cancel{E}_T$, $\tan\beta=3$, $\mu < 0$, $A_0=0$, any $m_{\tilde{q}}$
>390	95	2 ABAZOV	08G D0	$\text{jets} + \cancel{E}_T$, $\tan\beta=3$, $\mu < 0$, $A_0=0$, $m_{\tilde{q}}=m_{\tilde{g}}$
>270	95	3 ABULENCIA	06I CDF	$\tilde{g} \rightarrow \bar{b}b$, $\Delta m > 6$ GeV, $\tilde{b}_1 \rightarrow b\tilde{\chi}_1^0$, $m_{\tilde{b}_1} < 220$ GeV
>195	95	4 AFFOLDER	02 CDF	$\text{jets} + \cancel{E}_T$, any $m_{\tilde{q}}$
>300	95	4 AFFOLDER	02 CDF	$\text{jets} + \cancel{E}_T$, $m_{\tilde{q}}=m_{\tilde{g}}$
>129	95	5 ABBOTT	01D D0	$\ell\ell + \text{jets} + \cancel{E}_T$, $\tan\beta < 10$, $m_0 < 300$ GeV, $\mu < 0$, $A_0=0$
>175	95	5 ABBOTT	01D D0	$\ell\ell + \text{jets} + \cancel{E}_T$, $\tan\beta=2$, large m_0 , $\mu < 0$, $A_0=0$
>255	95	5 ABBOTT	01D D0	$\ell\ell + \text{jets} + \cancel{E}_T$, $\tan\beta=2$, $m_{\tilde{g}}=m_{\tilde{q}}$, $\mu < 0$, $A_0=0$
>168	95	6 AFFOLDER	01J CDF	$\ell\ell + \text{jets} + \cancel{E}_T$, $\tan\beta=2$, $\mu = -800$ GeV, $m_{\tilde{q}} \gg m_{\tilde{g}}$
>221	95	6 AFFOLDER	01J CDF	$\ell\ell + \text{jets} + \cancel{E}_T$, $\tan\beta=2$, $\mu = -800$ GeV, $m_{\tilde{q}}=m_{\tilde{g}}$
>190	95	7 ABBOTT	99L D0	$\text{jets} + \cancel{E}_T$, $\tan\beta=2$, $\mu < 0$, $A=0$
>260	95	7 ABBOTT	99L D0	$\text{jets} + \cancel{E}_T$, $m_{\tilde{g}}=m_{\tilde{q}}$
>224	95	8 ABAZOV	02F D0	$R \lambda'_{2jk}$ indirect decays, $\tan\beta=2$, any $m_{\tilde{q}}$
>265	95	8 ABAZOV	02F D0	$R \lambda'_{2jk}$ indirect decays, $\tan\beta=2$, $m_{\tilde{q}}=m_{\tilde{g}}$
		9 ABAZOV	02G D0	$p\bar{p} \rightarrow \tilde{g}\tilde{g}, \tilde{g}\tilde{q}$
		10 CHEUNG	02B THEO	
		11 BERGER	01 THEO	$p\bar{p} \rightarrow X + b\text{-quark}$
>240	95	12 ABBOTT	99 D0	$\tilde{g} \rightarrow \tilde{\chi}_2^0 X \rightarrow \tilde{\chi}_1^0 \gamma X$, $m_{\tilde{\chi}_2^0} - m_{\tilde{\chi}_1^0} > 20$ GeV
>320	95	12 ABBOTT	99 D0	$\tilde{g} \rightarrow \tilde{\chi}_1^0 X \rightarrow \tilde{G} \gamma X$
>227	95	13 ABBOTT	99K D0	any $m_{\tilde{q}}$, R , $\tan\beta=2$, $\mu < 0$
>212	95	14 ABACHI	95C D0	$m_{\tilde{g}} \geq m_{\tilde{q}}$; with cascade decays
>144	95	14 ABACHI	95C D0	Any $m_{\tilde{q}}$; with cascade decays
		15 ABE	95T CDF	$\tilde{g} \rightarrow \tilde{\chi}_2^0 \rightarrow \tilde{\chi}_1^0 \gamma$
		16 HEBBEKER	93 RVUE	e^+e^- jet analyses
>218	90	17 ABE	92L CDF	$m_{\tilde{q}} \leq m_{\tilde{g}}$; with cascade decay
>100		18 ROY	92 RVUE	$p\bar{p} \rightarrow \tilde{g}\tilde{g}; R$
		19 NOJIRI	91 COSM	
none 4–53	90	20 ALBAJAR	87D UA1	Any $m_{\tilde{q}} > m_{\tilde{g}}$
none 4–75	90	20 ALBAJAR	87D UA1	$m_{\tilde{q}} = m_{\tilde{g}}$
none 16–58	90	21 ANSARI	87D UA2	$m_{\tilde{q}} \lesssim 100$ GeV

1 AALTONEN 09S searched in 2 fb^{-1} of $p\bar{p}$ collisions at $\sqrt{s} = 1.96$ TeV for events with at least 2 jets and \cancel{E}_T . No evidence for a signal is observed. A limit is derived for a mSUGRA scenario in the $m_{\tilde{q}}$ versus $m_{\tilde{g}}$ plane, see their Fig. 2.

2 ABAZOV 08G looked in 2.1 fb^{-1} of $p\bar{p}$ collisions at $\sqrt{s}=1.96$ TeV for events with acoplanar jets or multijets with large \cancel{E}_T . No significant excess was found compared to the background expectation. A limit is derived on the masses of squarks and gluinos for specific mSUGRA parameter values, see Figure 3. Similar results would be obtained for a large class of parameter sets. Supersedes the results of ABAZOV 06c.

3 ABULENCIA 06i searched in 156 pb^{-1} of $p\bar{p}$ collisions at $\sqrt{s} = 1.96$ TeV for multijet events with large \cancel{E}_T . They request at least 2 b -tagged jets and no isolated leptons. They investigate the production of gluinos decaying into $\tilde{b}_1 b$ followed by $\tilde{b}_1 \rightarrow b\tilde{\chi}_1^0$. Both branching fractions are assumed to be 100% and the LSP mass to be 60 GeV. No significant excess was found compared to the background expectation. Upper limits on the cross-section are extracted and a limit is derived on the masses of sbottom and gluinos, see their Fig. 3.

Searches Particle Listings

Supersymmetric Particle Searches

- 4 AFFOLDER 02 searched in $\sim 84 \text{ pb}^{-1}$ of $p\bar{p}$ collisions for events with ≥ 3 jets and \cancel{E}_T , arising from the production of gluinos and/or squarks. Limits are derived by scanning the parameter space, for $m_{\tilde{q}} \geq m_{\tilde{g}}$ in the framework of minimal Supergravity, assuming five flavors of degenerate squarks, and for $m_{\tilde{q}} < m_{\tilde{g}}$ in the framework of constrained MSSM, assuming conservatively four flavors of degenerate squarks. See Fig. 3 for the variation of the limit as function of the squark mass. Supersedes the results of ABE 97k.
- 5 ABBOTT 01D looked in $\sim 108 \text{ pb}^{-1}$ of $p\bar{p}$ collisions at $\sqrt{s}=1.8 \text{ TeV}$ for events with $e e$, $\mu\mu$, or $e\mu$ accompanied by at least 2 jets and \cancel{E}_T . Excluded regions are obtained in the MSUGRA framework from a scan over the parameters $0 < m_0 < 300 \text{ GeV}$, $10 < m_{1/2} < 110 \text{ GeV}$, and $1.2 < \tan\beta < 10$.
- 6 AFFOLDER 01J searched in $\sim 106 \text{ pb}^{-1}$ of $p\bar{p}$ collisions for events with 2 like-sign leptons (e or μ), ≥ 2 jets and \cancel{E}_T , expected to arise from the production of gluinos and/or squarks with cascade decays into $\tilde{\chi}^{\pm}$ or $\tilde{\chi}^0$. Spectra and decay rates are evaluated in the framework of minimal Supergravity, assuming five flavors of degenerate squarks and a pseudoscalar Higgs mass $m_A=500 \text{ GeV}$. The limits are derived for $\tan\beta=2$, $\mu=-800 \text{ GeV}$, and scanning over $m_{\tilde{g}}$ and $m_{\tilde{q}}$. See Fig. 2 for the variation of the limit as function of the squark mass. These limits supersede the results of ABE 96b.
- 7 ABBOTT 99L consider events with three or more jets and large \cancel{E}_T . Spectra and decay rates are evaluated in the framework of minimal Supergravity, assuming five flavors of degenerate squarks, and scanning the space of the universal gaugino ($m_{1/2}$) and scalar (m_0) masses. See their Figs. 2-3 for the dependence of the limit on the relative value of $m_{\tilde{q}}$ and $m_{\tilde{g}}$.
- 8 ABAZOV 02F looked in 77.5 pb^{-1} of $p\bar{p}$ collisions at 1.8 TeV for events with $\geq 2\mu + \geq 4$ jets, originating from associated production of squarks followed by an indirect R decay (of the $\tilde{\chi}_1^0$) via $LQ\bar{D}$ couplings of the type λ_{2jk} where $j=1,2$ and $k=1,2,3$. Bounds are obtained in the MSUGRA scenario by a scan in the range $0 \leq M_0 \leq 400 \text{ GeV}$, $60 \leq m_{1/2} \leq 120 \text{ GeV}$ for fixed values $A_0=0$, $\mu < 0$, and $\tan\beta=2$ or 6 . The bounds are weaker for $\tan\beta=6$. See Figs. 2,3 for the exclusion contours in $m_{1/2}$ versus m_0 for $\tan\beta=2$ and 6 , respectively.
- 9 ABAZOV 02G search for associated production of gluinos and squarks in 92.7 pb^{-1} of $p\bar{p}$ collisions at $\sqrt{s}=1.8 \text{ TeV}$, using events with one electron, ≥ 4 jets, and large \cancel{E}_T . The results are compared to a MSUGRA scenario with $\mu < 0$, $A_0=0$, and $\tan\beta=3$ and allow to exclude a region of the $(m_0, m_{1/2})$ shown in Fig. 11.
- 10 CHEUNG 02B studies the constraints on a \tilde{b}_1 with mass in the 2.2-5.5 GeV region and a gluino in the mass range 12-16 GeV, using precision measurements of Z^0 decays and e^+e^- annihilations at LEP2. Few detectable events are predicted in the LEP2 data for the model proposed by BERGER 01.
- 11 BERGER 01 reanalyzed interpretation of Tevatron data on bottom-quark production. Argues that pair production of light gluinos ($m \sim 12-16 \text{ GeV}$) with subsequent 2-body decay into a light sbottom ($m \sim 2-5.5 \text{ GeV}$) and bottom can reconcile Tevatron data with predictions of perturbative QCD for the bottom production rate. The sbottom must either decay hadronically via a R -parity- and B -violating interaction, or be long-lived.
- 12 ABBOTT 99 searched for $\gamma\cancel{E}_T + \geq 2$ jet final states, and set limits on $\sigma(p\bar{p} \rightarrow \tilde{g} + X) \cdot B(\tilde{g} \rightarrow \gamma\tilde{g} + X)$. The quoted limits correspond to $m_{\tilde{g}} \geq m_{\tilde{g}}$, with $B(\tilde{\chi}_2^0 \rightarrow \tilde{\chi}_1^0 \gamma)=1$ and $B(\tilde{\chi}_1^0 \rightarrow \tilde{G} \gamma)=1$, respectively. They improve to 310 GeV (360 GeV in the case of $\gamma\tilde{G}$ decay) for $m_{\tilde{g}}=m_{\tilde{q}}$.
- 13 ABBOTT 99k uses events with an electron pair and four jets to search for the decay of the $\tilde{\chi}_1^0$ LSP via $R LQ\bar{D}$ couplings. The particle spectrum and decay branching ratios are taken in the framework of minimal supergravity. An excluded region at 95% CL is obtained in the $(m_0, m_{1/2})$ plane under the assumption that $A_0=0$, $\mu < 0$, $\tan\beta=2$ and any one of the couplings $\lambda'_{jk} > 10^{-3}$ ($j=1,2$ and $k=1,2,3$) and from which the above limit is computed. For equal mass squarks and gluinos, the corresponding limit is 277 GeV. The results are essentially independent of A_0 , but the limit deteriorates rapidly with increasing $\tan\beta$ or $\mu > 0$.
- 14 ABACHI 95c assume five degenerate squark flavors with $m_{\tilde{q}} = m_{\tilde{q}}$. Sleptons are assumed to be heavier than squarks. The limits are derived for fixed $\tan\beta = 2.0$, $\mu = -250 \text{ GeV}$, and $m_{H^+} = 500 \text{ GeV}$, and with the cascade decays of the squarks and gluinos calculated within the framework of the Minimal Supergravity scenario. The bounds are weakly sensitive to the three fixed parameters for a large fraction of parameter space.
- 15 ABE 95T looked for a cascade decay of gluino into $\tilde{\chi}_2^0$ which further decays into $\tilde{\chi}_1^0$ and a photon. No signal is observed. Limits vary widely depending on the choice of parameters. For $\mu = -40 \text{ GeV}$, $\tan\beta = 1.5$, and heavy squarks, the range $50 < m_{\tilde{g}} < 140$ is excluded at 90% CL. See the paper for details.
- 16 HEBBEKER 93 combined jet analyses at various e^+e^- colliders. The 4-jet analyses at TRISTAN/LEP and the measured α_s at PEP/PETRA/TRISTAN/LEP are used. A constraint on effective number of quarks $N=6.3 \pm 1.1$ is obtained, which is compared to that with a light gluino, $N=8$.
- 17 ABE 92L bounds are based on similar assumptions as ABACHI 95c. Not sensitive to $m_{\text{gluino}} < 40 \text{ GeV}$ (but other experiments rule out that region).
- 18 ROY 92 reanalyzed CDF limits on di-lepton events to obtain limits on gluino production in R -parity violating models. The 100% decay $\tilde{g} \rightarrow q\bar{q}\tilde{\chi}$ where $\tilde{\chi}$ is the LSP, and the LSP decays either into $lq\bar{d}$ or $l\ell\bar{\nu}$ is assumed.
- 19 NOJIRI 91 argues that a heavy gluino should be nearly degenerate with squarks in minimal supergravity not to overclose the universe.
- 20 The limits of ALBAJAR 87D are from $p\bar{p} \rightarrow \tilde{g}\tilde{g}X$ ($\tilde{g} \rightarrow q\bar{q}\tilde{\gamma}$) and assume $m_{\tilde{q}} > m_{\tilde{g}}$. These limits apply for $m_{\tilde{\gamma}} \lesssim 20 \text{ GeV}$ and $\tau(\tilde{g}) < 10^{-10} \text{ s}$.
- 21 The limit of ANSARI 87D assumes $m_{\tilde{q}} > m_{\tilde{g}}$ and $m_{\tilde{\gamma}} \approx 0$.
- 1 ABAZOV 07L D0 long-lived \tilde{g}
- 2 BERGER 05 THEO hadron scattering data
- 3 ABDALLAH 03c DLPH $e^+e^- \rightarrow q\bar{q}\tilde{g}\tilde{g}$, stable \tilde{g}
- 4 ABDALLAH 03G DLPH QCD beta function
- 5 HEISTER 03 ALEP Color factors
- 6 HEISTER 03H ALEP $e^+e^- \rightarrow q\bar{q}\tilde{g}\tilde{g}$
- 7 JANOT 03 RVUE $\Delta\Gamma_{had} < 3.9 \text{ MeV}$
- 8 MAFI 00 THEO $p\bar{p} \rightarrow \text{jets} + \cancel{E}_T$
- 9 ALAVI-HARATI 99E KTEV $pN \rightarrow R^0$, with $R^0 \rightarrow \rho^0\tilde{\gamma}$ and $R^0 \rightarrow \pi^0\tilde{\gamma}$
- 10 BAER 99 RVUE Stable \tilde{g} hadrons
- 11 FANTI 99 NA48 $p\text{Be} \rightarrow R^0 \rightarrow \eta\tilde{\gamma}$
- 12 ACKERSTAFF 98V OPAL $e^+e^- \rightarrow \tilde{\chi}_1^+\tilde{\chi}_1^-$
- 13 ADAMS 97B KTEV $pN \rightarrow R^0 \rightarrow \rho^0\tilde{\gamma}$
- 14 ALBUQUERQUE 97 E761 $R^+(uud\tilde{g}) \rightarrow S^0(uds\tilde{g})\pi^+$, $X^-(ssd\tilde{g}) \rightarrow S^0\pi^-$
- 15 BARATE 97L ALEP Color factors
- 16 CSIKOR 99 RVUE β function, $Z \rightarrow \text{jets}$
- 17 DEGOUVEA 97 THEO $Z \rightarrow jjjj$
- 18 FARRAR 96 RVUE $R^0 \rightarrow \pi^0\tilde{\gamma}$
- 19 AKERS 95R OPAL Z decay into a long-lived $(\tilde{g}q\bar{q})^\pm$ quarkonia
- 20 CLAVELLI 95 RVUE quarkonia
- 21 CAKIR 94 RVUE $\Upsilon(1S) \rightarrow \gamma + \text{gluonium}$
- 22 LOPEZ 93C RVUE LEP
- 23 CLAVELLI 92 RVUE α_s running
- 24 ANTONIADIS 91 RVUE α_s running
- 25 ANTONIADIS 91 RVUE $pN \rightarrow \text{missing energy}$
- 26 NAKAMURA 89 SPEC $R-\Delta^{++}$
- 27 ARNOLD 87 EMUL $\pi^- (350 \text{ GeV})$. $\sigma \simeq A^1$
- 28 ARNOLD 87 EMUL $\pi^- (350 \text{ GeV})$. $\sigma \simeq A^{0.72}$
- 29 TUNTS 87 CUSB $\Upsilon(1S) \rightarrow \gamma + \text{gluonium}$
- 29 ALBRECHT 86C ARG $1 \times 10^{-11} \lesssim \tau \lesssim 1 \times 10^{-9} \text{ s}$
- 30 BADIER 86 BDMP $1 \times 10^{-10} < \tau < 1 \times 10^{-7} \text{ s}$
- 31 BARNETT 86 RVUE $p\bar{p} \rightarrow \text{gluino gluino gluon}$
- 32 VOLOSHIN 86 RVUE If (quasi) stable; $\tilde{g}uud$
- 33 COOPER... 85B BDMP For $m_{\tilde{q}}=300 \text{ GeV}$
- 33 COOPER... 85B BDMP For $m_{\tilde{q}} < 65 \text{ GeV}$
- 33 COOPER... 85B BDMP For $m_{\tilde{q}}=150 \text{ GeV}$
- 34 DAWSON 85 RVUE $\tau > 10^{-7} \text{ s}$
- 34 DAWSON 85 RVUE For $m_{\tilde{q}}=100 \text{ GeV}$
- 35 FARRAR 85 RVUE FNAL beam dump
- 36 GOLDMAN 85 RVUE Gluonium
- 37 HABER 85 RVUE
- 38 BALL 84 CALO
- 39 BRICK 84 RVUE
- 40 FARRAR 84 RVUE
- 41 BERGSMA 83C RVUE For $m_{\tilde{q}} < 100 \text{ GeV}$
- 42 CHANOWITZ 83 RVUE $\tilde{g}u\bar{d}, \tilde{g}uud$
- 43 KANE 82 RVUE Beam dump
- FARRAR 78 RVUE R-hadron
- 1 ABAZOV 07L looked in approximately 410 pb^{-1} of $p\bar{p}$ collisions at $\sqrt{s} = 1.96 \text{ TeV}$ for events with a long-lived gluino from split supersymmetry, decaying after stopping in the detector into $\tilde{g}\tilde{\chi}_1^0$ with lifetimes from 30 μs to 100 h. The signal signature is a largely empty event with a single large transverse energy deposit in the calorimeter. The main background is due to cosmic muons interacting in the calorimeter. The data agree with the estimated background and allow the authors to estimate a limit on the rate of an out-of-time monojet signal of a given energy. Assuming the branching ratios $\tilde{g} \rightarrow \tilde{g}\tilde{\chi}_1^0$ to be 100% the results can be translated to limits on the gluino cross section versus the gluino mass for fixed $\tilde{\chi}_1^0$ mass. After comparing to the expected gluino cross sections, the excluded region of gluino masses can be obtained, see examples in their Fig. 3.
- 2 BERGER 05 include the light gluino in proton PDF and perform global analysis of hadronic data. Effects on the running of α_s also included. Strong dependency on $\alpha_s(m_Z)$. Bound quoted for $\alpha_s(m_Z) = 0.118$.
- 3 ABDALLAH 03c looked for events of the type $q\bar{q}R^\pm R^\pm$, $q\bar{q}R^\pm R^0$ or $q\bar{q}R^0 R^0$ in e^+e^- interactions at 91.2 GeV collected in 1994. The R^\pm bound states are identified by anomalous dE/dx in the tracking chambers and the R^0 by missing energy, due to their reduced energy loss in the calorimeters. The upper value of the excluded range depends on the probability for the gluino to fragment into R^\pm or R^0 , see their Fig. 17. It improves to 23 GeV for 100% fragmentation to R^\pm .
- 4 ABDALLAH 03G used e^+e^- data at and around the Z^0 peak, above the Z^0 up to $\sqrt{s} = 202 \text{ GeV}$ and events from radiative return to cover the low energy region. They perform a direct measurement of the QCD beta-function from the means of fully inclusive event observables. Compared to the energy range, gluinos below 5 GeV can be considered massless and are firmly excluded by the measurement.
- 5 HEISTER 03 use e^+e^- data from 1994 and 1995 at and around the Z^0 peak to measure the 4-jet rate and angular correlations. The comparison with QCD NLO calculations allow $\alpha_s(M_Z)$ and the color factor ratios to be extracted and the results are in agreement with the expectations from QCD. The inclusion of a massless gluino in the beta functions yields $T_R / C_F = 0.15 \pm 0.06 \pm 0.06$ (expectation is $T_R / C_F = 3/8$), excluding a massless gluino at more than 95% CL. As no NLO calculations are available for massive gluinos, the earlier LO results from BARATE 97L for massive gluinos remain valid.
- 6 HEISTER 03H use e^+e^- data at and around the Z^0 peak to look for stable gluinos hadronizing into charged or neutral R-hadrons with arbitrary branching ratios. Combining these results with bounds on the Z^0 hadronic width from electroweak measurements (JANOT 03) to cover the low mass region the quoted lower limit on the mass of a long-lived gluino is obtained.

Long-lived/light \tilde{g} (Gluino) MASS LIMIT

Limits on light gluinos ($m_{\tilde{g}} < 5 \text{ GeV}$), or gluinos which leave the detector before decaying.

VALUE (GeV)	CL%	DOCUMENT ID	TECN	COMMENT
•••	•••	•••	•••	•••

••• We do not use the following data for averages, fits, limits, etc. •••

- 7 JANOT 03 excludes a light gluino from the upper limit on an additional contribution to the Z hadronic width. At higher confidence levels, $m_{\tilde{g}} > 5.3(4.2)$ GeV at $3\sigma(5\sigma)$ level.
- 8 MAFI 00 reanalyzed CDF data assuming a stable heavy gluino as the LSP, with model for R-hadron-nucleon scattering. Gluino masses between 35 GeV and 115 GeV are excluded based on the CDF Run I data. Combined with the analysis of BAER 99, this allows a LSP gluino mass between 25 and 35 GeV if the probability of fragmentation into charged R-hadron $P > 1/2$. The cosmological exclusion of such a gluino LSP are assumed to be avoided as in BAER 99. Gluino could be NLSP with $\tau_{\tilde{g}} \sim 100$ yrs, and decay to gluon gravitino.
- 9 ALAVI-HARATI 99E looked for R^0 bound states, yielding $\pi^+\pi^-$ or π^0 in the final state. The experiment is sensitive to values of $\Delta m = m_{R^0} - m_{\tilde{g}}$ larger than 280 MeV and 140 MeV for the two decay modes, respectively, and to R^0 mass and lifetime in the ranges 0.8–5 GeV and 10^{-10} – 10^{-3} s. The limits obtained depend on $B(R^0 \rightarrow \pi^+\pi^- \text{photon})$ and $B(R^0 \rightarrow \pi^0 \text{photon})$ on the value of $m_{R^0}/m_{\tilde{g}}$, and on the ratio of production rates $\sigma(R^0)/\sigma(K_L^0)$. See Figures in the paper for the excluded R^0 production rates as a function of Δm , R^0 mass and lifetime. Using the production rates expected from perturbative QCD, and assuming dominance of the above decay channels over the suitable phase space, R^0 masses in the range 0.8–5 GeV are excluded at 90%CL for a large fraction of the sensitive lifetime region. ALAVI-HARATI 99E updates and supersedes the results of ADA MS 97b.
- 10 BAER 99 set constraints on the existence of stable \tilde{g} hadrons, in the mass range $m_{\tilde{g}} > 3$ GeV. They argue that strong-interaction effects in the low-energy annihilation rates could leave small enough relic densities to evade cosmological constraints up to $m_{\tilde{g}} < 10$ TeV. They consider $\text{jet} + \cancel{E}_T$ as well as heavy-ionizing charged-particle signatures from production of stable \tilde{g} hadrons at LEP and Tevatron, developing modes for the energy loss of \tilde{g} hadrons inside the detectors. Results are obtained as a function of the fragmentation probability P of the \tilde{g} into a charged hadron. For $P < 1/2$, and for various energy-loss models, OPAL and CDF data exclude gluinos in the $3 < m_{\tilde{g}}(\text{GeV}) < 130$ mass range. For $P > 1/2$, gluinos are excluded in the mass ranges $3 < m_{\tilde{g}}(\text{GeV}) < 23$ and $50 < m_{\tilde{g}}(\text{GeV}) < 200$.
- 11 FANTI 99 looked for R^0 bound states yielding high $P_T \eta \rightarrow 3\pi^0$ decays. The experiment is sensitive to a region of R^0 mass and lifetime in the ranges of 1–5 GeV and 10^{-10} – 10^{-3} s. The limits obtained depend on $B(R^0 \rightarrow \eta\gamma)$, on the value of $m_{R^0}/m_{\tilde{g}}$, and on the ratio of production rates $\sigma(R^0)/\sigma(K_L^0)$. See Fig. 6–7 for the excluded production rates as a function of R^0 mass and lifetime.
- 12 ACKERSTAFF 98v excludes the light gluino with universal gaugino mass where charginos, neutralinos decay as $\tilde{\chi}_1^\pm, \tilde{\chi}_2^0 \rightarrow q\tilde{q}\tilde{g}$ from total hadronic cross sections at $\sqrt{s}=130$ –172 GeV. See paper for the case of nonuniversal gaugino mass.
- 13 ADA MS 97b looked for $\rho^0 \rightarrow \pi^+\pi^-$ as a signature of $R^0=(\tilde{g}\tilde{g})$ bound states. The experiment is sensitive to an R^0 mass range of 1.2–4.5 GeV and to a lifetime range of 10^{-10} – 10^{-3} sec. Precise limits depend on the assumed value of $m_{R^0}/m_{\tilde{g}}$. See Fig. 7 for the excluded mass and lifetime region.
- 14 ALBUQUERQUE 97 looked for weakly decaying baryon-like states which contain a light gluino, following the suggestions in FARRAR 96. See their Table 1 for limits on the production fraction. These limits exclude gluino masses in the range 100–600 MeV for the predicted lifetimes (FARRAR 96) and production rates, which are assumed to be comparable to those of strange or charmed baryons.
- 15 BARATE 97L studied the QCD color factors from four-jet angular correlations and the differential two-jet rate in Z decay. Limit obtained from the determination of $n_f = 4.24 \pm 0.29 \pm 1.15$, assuming $T_F/C_F=3/8$ and $C_A/C_F=9/4$.
- 16 CSIKOR 97 combined the α_s from $\sigma(e^+e^- \rightarrow \text{hadron})$, τ decay, and jet analysis in Z decay. They exclude a light gluino below 5 GeV at more than 99.7%CL.
- 17 DEGOUVEA 97 reanalyzed AKERS 95A data on Z decay into four jets to place constraints on a light stable gluino. The mass limit corresponds to the pole mass of 2.8 GeV. The analysis, however, is limited to the leading-order QCD calculation.
- 18 FARRAR 96 studied the possible $R^0=(\tilde{g}\tilde{g})$ component in Fermilab E799 experiment and used its bound $B(K_L^0 \rightarrow \pi^0\nu\bar{\nu}) \leq 5.8 \times 10^{-5}$ to place constraints on the combination of R^0 production cross section and its lifetime.
- 19 AKERS 95R looked for Z decay into $q\tilde{q}\tilde{g}\tilde{g}$, by searching for charged particles with dE/dx consistent with \tilde{g} fragmentation into a state $(\tilde{g}q\tilde{q})^\pm$ with lifetime $\tau > 10^{-7}$ sec. The fragmentation probability into a charged state is assumed to be 25%.
- 20 CLAVELLI 95 updates the analysis of CLAVELLI 93, based on a comparison of the hadronic widths of charmonium and bottomonium S-wave states. The analysis includes a parametrization of relativistic corrections. Claims that the presence of a light gluino improves agreement with the data by slowing down the running of α_s .
- 21 CAKIR 94 reanalyzed TUTS 87 and later unpublished data from CUSB to exclude pseudo-scalar gluinonium $\eta_{\tilde{g}}(\tilde{g}\tilde{g})$ of mass below 7 GeV. It was argued, however, that the perturbative QCD calculation of the branching fraction $\Upsilon \rightarrow \eta_{\tilde{g}}\gamma$ is unreliable for $m_{\eta_{\tilde{g}}} < 3$ GeV. The gluino mass is defined by $m_{\tilde{g}}=(m_{\eta_{\tilde{g}}})/2$. The limit holds for any gluino lifetime.
- 22 LOPEZ 93c uses combined restraint from the radiative symmetry breaking scenario within the minimal supergravity model, and the LEP bounds on the (M_2, μ) plane. Claims that the light gluino window is strongly disfavored.
- 23 CLAVELLI 92 claims that a light gluino mass around 4 GeV should exist to explain the discrepancy between α_s at LEP and at quarkonia (Υ), since a light gluino slows the running of the QCD coupling.
- 24 ANTONIADIS 91 argue that possible light gluinos (< 5 GeV) contradict the observed running of α_s between 5 GeV and m_Z . The significance is less than 2 s.d.
- 25 ANTONIADIS 91 interpret the search for missing energy events in 450 GeV/c pN collisions, AKESSON 91, in terms of light gluinos.
- 26 NAKAMURA 89 searched for a long-lived ($\tau \gtrsim 10^{-7}$ s) charge-(± 2) particle with mass $\lesssim 1.6$ GeV in proton-Pt interactions at 12 GeV and found that the yield is less than 10^{-8} times that of the pion. This excludes $R\text{-}\Delta^{++}$ (a $\tilde{g}uuu$ state) lighter than 1.6 GeV.
- 27 The limits assume $m_{\tilde{q}} = 100$ GeV. See their figure 3 for limits vs. $m_{\tilde{q}}$.
- 28 The gluino mass is defined by half the bound $\tilde{g}\tilde{g}$ mass. If zero gluino mass gives a $\tilde{g}\tilde{g}$ of mass about 1 GeV as suggested by various glueball mass estimates, then the low-mass bound can be replaced by zero. The high-mass bound is obtained by comparing the data with nonrelativistic potential-model estimates.
- 29 ALBRECHT 86c search for secondary decay vertices from $\chi_{b1}(1P) \rightarrow \tilde{g}\tilde{g}\tilde{g}$ where \tilde{g} 's make long-lived hadrons. See their figure 4 for excluded region in the $m_{\tilde{g}} - m_{\tilde{q}}$ and $m_{\tilde{g}} - m_{\tilde{q}}$ plane. The lower $m_{\tilde{g}}$ region below ~ 2 GeV may be sensitive to fragmentation effects. Remark that the \tilde{g} -hadron mass is expected to be ~ 1 GeV (glueball mass) in the zero \tilde{g} mass limit.
- 30 BADIER 86 looked for secondary decay vertices from long-lived \tilde{g} -hadrons produced at 300 GeV π^- beam dump. The quoted bound assumes \tilde{g} -hadron nucleon total cross section of $10\mu\text{b}$. See their figure 7 for excluded region in the $m_{\tilde{g}} - m_{\tilde{q}}$ plane for several assumed total cross-section values.
- 31 BARNETT 86 rule out light gluinos ($m = 3$ –5 GeV) by calculating the monojet rate from gluino gluino gluon events (and from gluino gluino events) and by using UA1 data from $p\bar{p}$ collisions at CERN.
- 32 VOLOSHIN 86 rules out stable gluino based on the cosmological argument that predicts too much hydrogen consisting of the charged stable hadron $\tilde{g}uud$. Quasi-stable ($\tau > 1 \times 10^{-7}$ s) light gluino of $m_{\tilde{g}} < 3$ GeV is also ruled out by nonobservation of the stable charged particles, $\tilde{g}uud$, in high energy hadron collisions.
- 33 COOPER-SARKAR 85B is BEBC beam-dump. Gluinos decaying in dump would yield $\tilde{\gamma}$'s in the detector giving neutral-current-like interactions. For $m_{\tilde{q}} > 330$ GeV, no limit is set.
- 34 DAWSON 85 first limit from neutral particle search. Second limit based on FNAL beam dump experiment.
- 35 FARRAR 85 points out that BALL 84 analysis applies only if the \tilde{g} 's decay before interacting, i.e. $m_{\tilde{q}} < 80m_{\tilde{g}}^{1.5}$. FARRAR 85 finds $m_{\tilde{g}} < 0.5$ not excluded for $m_{\tilde{q}} = 30$ –1000 GeV and $m_{\tilde{g}} < 1.0$ not excluded for $m_{\tilde{q}} = 100$ –500 GeV by BALL 84 experiment.
- 36 GOLDMAN 85 use nonobservation of a pseudoscalar $\tilde{g}\tilde{g}$ bound state in radiative ψ decay.
- 37 HABER 85 is based on survey of all previous searches sensitive to low mass \tilde{g} 's. Limit makes assumptions regarding the lifetime and electric charge of the lightest supersymmetric particle.
- 38 BALL 84 is FNAL beam dump experiment. Observed no interactions of $\tilde{\gamma}$ in the calorimeter, where $\tilde{\gamma}$'s are expected to come from pair-produced \tilde{g} 's. Search for long-lived $\tilde{\gamma}$ interacting in calorimeter 56m from target. Limit is for $m_{\tilde{q}} = 40$ GeV and production cross section proportional to $A^{0.72}$. BALL 84 find no \tilde{g} allowed below 4.1 GeV at CL = 90%. Their figure 1 shows dependence on $m_{\tilde{q}}$ and A. See also KANE 82.
- 39 BRICK 84 reanalyzed FNAL 147 GeV HBC data for $R\text{-}\Delta(1232)^{++}$ with $\tau > 10^{-9}$ s and $p_{\text{lab}} > 2$ GeV. Set CL = 90% upper limits 6.1, 4.4, and 29 microbarns in $p\bar{p}$, $\pi^+\pi^-$, K^+p collisions respectively. $R\text{-}\Delta^{++}$ is defined as being \tilde{g} and 3 up quarks. If mass = 1.2–1.5 GeV, then limits may be lower than theory predictions.
- 40 FARRAR 84 argues that $m_{\tilde{g}} < 100$ MeV is not ruled out if the lightest R-hadrons are long-lived. A long lifetime would occur if R-hadrons are lighter than $\tilde{\gamma}$'s or if $m_{\tilde{q}} > 100$ GeV.
- 41 BERGSMAN 83c is reanalysis of CERN-SPS beam-dump data. See their figure 1.
- 42 CHANOWITZ 83 find in bag-model that charged s-hadron exists which is stable against strong decay if $m_{\tilde{g}} < 1$ GeV. This is important since tracks from decay of neutral s-hadron cannot be reconstructed to primary vertex because of missed $\tilde{\gamma}$. Charged s-hadron leaves track from vertex.
- 43 KANE 82 inferred above \tilde{g} mass limit from retroactive analysis of hadronic collision and beam dump experiments. Limits valid if \tilde{g} decays inside detector.

LIGHT \tilde{G} (Gravitino) MASS LIMITS FROM COLLIDER EXPERIMENTS

The following are bounds on light ($\ll 1$ eV) gravitino indirectly inferred from its coupling to matter suppressed by the gravitino decay constant.

Unless otherwise stated, all limits assume that other supersymmetric particles besides the gravitino are too heavy to be produced. The gravitino is assumed to be undetected and to give rise to a missing energy (\cancel{E}) signature.

VALUE (eV)	CL%	DOCUMENT ID	TECN	COMMENT
••• Do not use the following data for averages, fits, limits, etc. •••				
$> 1.09 \times 10^{-5}$	95	1 ABDALLAH	05B DLPH	$e^+e^- \rightarrow \tilde{G}\tilde{G}\gamma$
$> 1.35 \times 10^{-5}$	95	2 ACHARD	04E L3	$e^+e^- \rightarrow \tilde{G}\tilde{G}\gamma$
$> 1.3 \times 10^{-5}$		3 HEISTER	03C ALEP	$e^+e^- \rightarrow \tilde{G}\tilde{G}\gamma$
$> 11.7 \times 10^{-6}$	95	4 ACOSTA	02H CDF	
$> 8.7 \times 10^{-6}$	95	5 ABBIENDI,G	00D OPAL	$e^+e^- \rightarrow \tilde{G}\tilde{G}\gamma$
$> 10.0 \times 10^{-6}$	95	6 ABREU	00Z DLPH	Superseded by ABDALLAH 05B
$> 11 \times 10^{-6}$	95	7 AFFOLDER	03J CDF	$p\bar{p} \rightarrow \tilde{G}\tilde{G} + \text{jet}$
$> 8.9 \times 10^{-6}$	95	6 ACCIARRI	99R L3	Superseded by ACHARD 04E
$> 7.9 \times 10^{-6}$	95	8 ACCIARRI	98J L3	$e^+e^- \rightarrow \tilde{G}\tilde{G}\gamma$
$> 8.3 \times 10^{-6}$	95	8 BARATE	98J ALEP	$e^+e^- \rightarrow \tilde{G}\tilde{G}\gamma$

- 1 ABDALLAH 05B use data from $\sqrt{s} = 180$ –208 GeV. They look for events with a single photon + \cancel{E} final states from which a cross section limit of $\sigma < 0.18$ pb at 208 GeV is obtained, allowing a limit on the mass to be set. Supersedes the results of ABREU 00Z.
- 2 ACHARD 04E use data from $\sqrt{s} = 189$ –209 GeV. They look for events with a single photon + \cancel{E} final states from which a limit on the Gravitino mass is set corresponding to $\sqrt{F} > 238$ GeV. Supersedes the results of ACCIARRI 99R.
- 3 HEISTER 03C use the data from $\sqrt{s} = 189$ –209 GeV to search for $\gamma\cancel{E}_T$ final states.
- 4 ACOSTA 02H looked in 87 pb $^{-1}$ of $p\bar{p}$ collisions at $\sqrt{s}=1.8$ TeV for events with a high- E_T photon and \cancel{E}_T . They compared the data with a GMSB model where the final state could arise from $q\tilde{q} \rightarrow \tilde{G}\tilde{G}\gamma$. Since the cross section for this process scales as $1/|F|^4$, a limit at 95% CL is derived on $|F|^{1/2} > 221$ GeV. A model independent limit for the above topology is also given in the paper.
- 5 ABBIENDI,G 00D searches for $\gamma\cancel{E}$ final states from $\sqrt{s}=189$ GeV.
- 6 ABREU 00Z, ACCIARRI 99R search for $\gamma\cancel{E}$ final states using data from $\sqrt{s}=189$ GeV.
- 7 AFFOLDER 00J searches for final states with an energetic jet (from quark or gluon) and large \cancel{E}_T from undetected gravitinos.

Searches Particle Listings

Supersymmetric Particle Searches

⁸ Searches for $\gamma\bar{\nu}$ final states at $\sqrt{s}=183$ GeV.

Supersymmetry Miscellaneous Results

Results that do not appear under other headings or that make nonminimal assumptions.

VALUE	DOCUMENT ID	TECN	COMMENT
• • •	We do not use the following data for averages, fits, limits, etc. • • •		
1	LOVE 08A	CLEO	$R, Y \rightarrow \mu\tau$
2	ABULENCIA 06P	CDF	$\ell\gamma\bar{\nu}_T, \ell\ell\gamma, \text{GMSB}$
3	ACOSTA 04E	CDF	
4	TCHIKILEV 04	ISTR	$K^- \rightarrow \pi^- \pi^0 P$
5	AFFOLDER 02D	CDF	$p\bar{p} \rightarrow \gamma b (\bar{\nu}_T)$
6	AFFOLDER 01H	CDF	$p\bar{p} \rightarrow \gamma\gamma X$
7	ABBOTT 00G	D0	$p\bar{p} \rightarrow 3\ell + \bar{\nu}_T, R, L\bar{L}\bar{E}$
8	ABREU,P 00C	DLPH	$e^+e^- \rightarrow \gamma + S/P$
9	ABACHI 97	D0	$\gamma\gamma X$
10	BARBER 84B	RVUE	
11	HOFFMAN 83	CNTR	$\pi p \rightarrow n(e^+e^-)$

- 1 LOVE 08A searched for decays of $Y(n)$ with $n = 1, 2, 3$ into $\mu\tau$ in 1.1, 1.3, 1.4 fb^{-1} , respectively, in the CLEO III detector at CESR. The signature is a muon with $\approx 97\%$ of the beam energy and an electron from the decay of τ . No evidence for lepton flavour violation is found and 95% CL limits on the branching ratio are estimated to be 6.0, 14.4 and 20.3×10^{-6} for $n = 1, 2, 3$, respectively.
- 2 ABULENCIA 06P searched in 305 pb^{-1} of $p\bar{p}$ collisions at $\sqrt{s} = 1.96$ TeV for an excess of events with $\ell\gamma\bar{\nu}_T$ and $\ell\ell\gamma$ ($\ell = e, \mu$). No significant excess was found compared to the background expectation. No events are found such as the $e\bar{e}\gamma\bar{\nu}_T$ event observed in ABE 99i.
- 3 ACOSTA 04E looked in 107 pb^{-1} of $p\bar{p}$ collisions at $\sqrt{s} = 1.8$ TeV for events with two same sign leptons without selection of other objects nor $\bar{\nu}_T$. No significant excess is observed compared to the Standard Model expectation and constraints are derived on the parameter space of MSUGRA models, see Figure 4.
- 4 Looked for the scalar partner of a goldstino in decays $K^- \rightarrow \pi^- \pi^0 P$ from a 25 GeV K^- beam produced at the IHEP 70 GeV proton synchrotron. The goldstino is assumed to be sufficiently long-lived to be invisible. A 90% CL upper limit on the decay branching ratio is set at $\sim 9.0 \times 10^{-6}$ for a goldstino mass range from 0 to 200 MeV, excluding the interval near $m(\pi^0)$, where the limit is $\sim 3.5 \times 10^{-5}$.
- 5 AFFOLDER 02D looked in 85 pb^{-1} of $p\bar{p}$ collisions at $\sqrt{s}=1.8$ TeV for events with a high- E_T photon, and a b -tagged jet with or without $\bar{\nu}_T$. They compared the data with models where the final state could arise from cascade decays of gluinos and/or squarks into $\bar{\chi}^\pm$ and $\bar{\chi}_2^0$ or direct associated production of $\bar{\chi}_2^0 \bar{\chi}_2^\pm$, followed by $\bar{\chi}_2^0 \rightarrow \gamma\bar{\chi}_1^0$ or a GMSB model where $\bar{\chi}_1^0 \rightarrow \gamma G$. It is concluded that the experimental sensitivity is insufficient to detect the associated production or the GMSB model, but some sensitivity may exist to the cascade decays. A model independent limit for the above topology is also given in the paper.
- 6 AFFOLDER 01H searches for $p\bar{p} \rightarrow \gamma\gamma X$ events, where the di-photon system originates from goldstino production, in 100 pb^{-1} of data. Upper limits on the cross section times branching ratio are shown as a function of the di-photon mass > 70 GeV in Fig. 5. Excluded regions are derived in the plane of the goldstino mass versus the supersymmetry breaking scale for two representative sets of parameter values, as shown in Figs. 6 and 7.
- 7 ABBOTT 00G searches for trilepton final states ($\ell=e, \mu$) with $\bar{\nu}_T$ from the indirect decay of gauginos via $L\bar{L}\bar{E}$ couplings. Efficiencies are computed for all possible production and decay modes of SUSY particles in the framework of the Minimal Supergravity scenario. See Figs. 1-4 for excluded regions in the $m_{1/2}$ versus m_0 plane.
- 8 ABREU,P 00C look for the CP -even (S) and CP -odd (P) scalar partners of the goldstino, expected to be produced in association with a photon. The S/P decay into two photons or into two gluons and both the tri-photon and the photon + two jets topologies are investigated. Upper limits on the production cross section are shown in Fig. 5 and the excluded regions in Fig. 6. Data collected at $\sqrt{s} = 189\text{--}202$ GeV.
- 9 ABACHI 97 searched for $p\bar{p} \rightarrow \gamma\gamma \bar{\nu}_T + X$ as supersymmetry signature. It can be caused by selectron, sneutrino, or neutralino production with a radiative decay of their decay products. They placed limits on cross sections.
- 10 BARBER 84B consider that $\bar{\mu}$ and \bar{e} may mix leading to $\mu \rightarrow e\bar{\gamma}\bar{\gamma}$. They discuss mass-mixing limits from decay dist. asym. in LBL-TRIUMF data and e^+ polarization in SIN data.
- 11 HOFFMAN 83 set CL = 90% limit $d\sigma/dt B(e^+e^-) < 3.5 \times 10^{-32} \text{ cm}^2/\text{GeV}^2$ for spin-1 partner of Goldstone fermions with $140 < m < 160$ MeV decaying $\rightarrow e^+e^-$ pair.

REFERENCES FOR Supersymmetric Particle Searches

AALTONEN 10	PRL 104 011801	T. Aaltonen et al.	(CDF Collab.)
AALTONEN 09G	PR D79 052004	T. Aaltonen et al.	(CDF Collab.)
AALTONEN 09R	PRL 102 221801	T. Aaltonen et al.	(CDF Collab.)
AALTONEN 09S	PRL 102 121801	T. Aaltonen et al.	(CDF Collab.)
AALTONEN 09V	PRL 102 091805	T. Aaltonen et al.	(CDF Collab.)
AALTONEN 09Z	PRL 103 021802	T. Aaltonen et al.	(CDF Collab.)
ABAZOV 09M	PRL 102 161802	V.M. Abazov et al.	(DO Collab.)
ABAZOV 09N	PL B674 4	V.M. Abazov et al.	(DO Collab.)
ABAZOV 09O	PL B675 289	V.M. Abazov et al.	(DO Collab.)
ABAZOV 09S	PL B680 24	V.M. Abazov et al.	(DO Collab.)
ABAZOV 09T	PL B680 34	V.M. Abazov et al.	(DO Collab.)
ABBASI 09	PR D79 102005	R. Abbasi et al.	(IceCube Collab.)
ABBASI 09B	PRL 102 201302	R. Abbasi et al.	(IceCube Collab.)
AHMED 09	PRL 102 011301	Z. Ahmed et al.	(CDMS Collab.)
ANGLOHER 09	ASP 31 270	G. Angloher et al.	(CRESS Collab.)
ARCHAMBAU... 09	PL B662 185	S. Archambault et al.	(PICASSO Collab.)
BUCHMUELL... 09	EPL C64 391	O. Buchmuller et al.	(LOIC, FNAL, CERN+)
DREINER 09	EPL C62 547	H. Dreiner et al.	
LEBEDENKO 09	PR D80 052010	V.N. Lebedenko et al.	(ZEPLIN-III Collab.)
LEBEDENKO 09A	PRL 103 151302	V.N. Lebedenko et al.	(ZEPLIN-III Collab.)
SORENSEN 09	NIM A601 339	P. Sorensen et al.	(XENON10 Collab.)
AALTONEN 08AE	PRL 101 251801	T. Aaltonen et al.	(CDF Collab.)
AALTONEN 08L	PR D77 052002	T. Aaltonen et al.	(CDF Collab.)
AALTONEN 08U	PR D78 032015	T. Aaltonen et al.	(CDF Collab.)
AALTONEN 08Z	PRL 101 071802	T. Aaltonen et al.	(CDF Collab.)
ABAZOV 08F	PL B659 500	V.M. Abazov et al.	(DO Collab.)
ABAZOV 08G	PL B659 856	V.M. Abazov et al.	(DO Collab.)
ABAZOV 08G	PL B660 449	V.M. Abazov et al.	(DO Collab.)

ABAZOV 08Q	PRL 100 241803	V.M. Abazov et al.	(DO Collab.)
ABAZOV 08X	PRL 101 111802	V.M. Abazov et al.	(DO Collab.)
ABAZOV 08Z	PL B665 1	V.M. Abazov et al.	(DO Collab.)
ANGLE 08	PRL 100 021303	J. Angle et al.	(XENON10 Collab.)
ANGLE 08A	PRL 101 091301	J. Angle et al.	(XENON10 Collab.)
BEDNYAKOV 08	PAN 71 111	V.A. Bednyakov, H.P. Klappdor-Kleingrothaus, I.V. Krivosheina	(XENON10 Collab.)
BENETTI 08	Translated 13	P. Benetti et al.	(WARP Collab.)
BUCHMUELL... 08	JHEP 0809 117	O. Buchmuller et al.	
BUHNKE 08	SCI 319 933	E. Behnke	(COUPE Collab.)
ELLIS 08	PR D78 075012	J. Ellis, K. Olive, P. Sandick	(CERN, MINN)
LOVE 08A	PRL 101 201601	W. Love et al.	(CLEO Collab.)
AALTONEN 07E	PR D76 072010	T. Aaltonen et al.	(CDF Collab.)
AALTONEN 07J	PRL 99 191806	T. Aaltonen et al.	(CDF Collab.)
ABAZOV 07B	PL B645 119	V.M. Abazov et al.	(DO Collab.)
ABAZOV 07L	PRL 99 131801	V.M. Abazov et al.	(DO Collab.)
ABULENCIA 07H	PRL 98 131804	A. Abulencia et al.	(CDF Collab.)
ABULENCIA 07N	PRL 98 221803	A. Abulencia et al.	(CDF Collab.)
ABULENCIA 07P	PRL 99 121801	A. Abulencia et al.	(CDF Collab.)
ALNER 07	PL B653 161	G.J. Alner et al.	(ZEPLIN-II Collab.)
ALNER 07A	ASP 28 287	G.J. Alner et al.	(ZEPLIN-II Collab.)
CHEKANOV 07	EPL C50 269	S. Chekanov et al.	(ZEUS Collab.)
ELLIS 07	JHEP 0706 079	J. Ellis, K. Olive, P. Sandick	(CERN, MINN)
LEE 07A	PRL 99 091301	H.S. Lee et al.	(KIMS Collab.)
SCHAEF 07A	EPL C49 411	S. Schael et al.	(ALEPH Collab.)
ABAZOV 06C	PL B638 119	V.M. Abazov et al.	(DO Collab.)
ABAZOV 06D	PL B638 441	V.M. Abazov et al.	(DO Collab.)
ABAZOV 06I	PRL 97 111801	V.M. Abazov et al.	(DO Collab.)
ABAZOV 06J	PRL 97 161802	V.M. Abazov et al.	(DO Collab.)
ABAZOV 06R	PRL 97 171806	V.M. Abazov et al.	(DO Collab.)
ABBIENDI 06B	EPL C46 307	G. Abbiendi et al.	(OPAL Collab.)
ABDALLAH 06C	EPL C45 589	J. Abdallah et al.	(DELPHI Collab.)
ABULENCIA 06I	PRL 96 171802	A. Abulencia et al.	(CDF Collab.)
ABULENCIA 06M	PRL 96 211802	A. Abulencia et al.	(CDF Collab.)
ABULENCIA 06P	PRL 97 031801	A. Abulencia et al.	(CDF Collab.)
ACHTERBERG 06	ASP 26 129	A. Achterberg et al.	(AMANDA Collab.)
ACKERMANN 06	ASP 24 459	M. Ackermann et al.	(AMANDA Collab.)
AKERIB 06	PR D73 011102R	D.S. Akerib et al.	(CDMS Collab.)
AKERIB 06A	PRL 96 011302	D.S. Akerib et al.	(CDMS Collab.)
BENOIT 06	PL B637 156	A. Benoit et al.	
DEBOER 06	PL B636 13	W. de Boer et al.	
LEE 06	PL B633 201	H.S. Lee et al.	(KIMS Collab.)
LEP-SLC 06	PRPL 427 257	ALEPH, DELPHI, L3, OPAL, SLD and working groups	
SHIMIZU 06A	PL B633 195	Y. Shimizu et al.	
SMITH 06	PL B642 567	N.J.T. Smith, A.S. Murphy, T.J. Summer	
ABAZOV 05A	PRL 94 041801	V.M. Abazov et al.	(DO Collab.)
ABAZOV 05U	PRL 95 151805	V.M. Abazov et al.	(DO Collab.)
ABDALLAH 05B	EPL C38 395	J. Abdallah et al.	(DELPHI Collab.)
ABULENCIA 05A	PRL 95 252001	A. Abulencia et al.	(CDF Collab.)
ACOSTA 05E	PR D71 031104R	D. Acosta et al.	(CDF Collab.)
ACOSTA 05R	PRL 95 131801	D. Acosta et al.	(CDF Collab.)
AKERIB 05	PR D72 052009	D.S. Akerib et al.	(CDMS Collab.)
AKTAS 05	PL B616 31	A. Aktas et al.	(HI Collab.)
ALNER 05	PL B616 17	G.J. Alner et al.	(UK Dark Matter Collab.)
ALNER 05A	ASP 23 444	G.J. Alner et al.	(UK Dark Matter Collab.)
ANGLOHER 05	ASP 23 325	G. Angloher et al.	(CRESS-II Collab.)
BAER 05	JHEP 0507 065	H. Baer et al.	(FSU, MSU, HAWA)
BARNABE-HE... 05	PL B624 186	M. Barnabe-Heider et al.	(PICASSO Collab.)
BERGER 05	PR D71 014007	E.L. Berger et al.	
CHEKANOV 05A	EPL C44 463	S. Chekanov et al.	(ZEUS Collab.)
ELLIS 05	PR D71 095007	J. Ellis et al.	
GIRARD 05	PL B621 233	T.A. Girard et al.	(SIMPLE Collab.)
SANGIARD 05	PR D71 122002	V. Sangiari et al.	(EDELWEISS Collab.)
ABAZOV 04B	PL B581 147	V.M. Abazov et al.	(DO Collab.)
ABAZOV 04B	PRL 93 011801	V.M. Abazov et al.	(DO Collab.)
ABBIENDI 04	EPL C32 453	G. Abbiendi et al.	(OPAL Collab.)
ABBIENDI 04F	EPL C33 149	G. Abbiendi et al.	(OPAL Collab.)
ABBIENDI 04H	EPL C35 1	G. Abbiendi et al.	(OPAL Collab.)
ABBIENDI 04N	PL B602 167	G. Abbiendi et al.	(OPAL Collab.)
ABDALLAH 04H	EPL C34 145	J. Abdallah et al.	(DELPHI Collab.)
ABDALLAH 04M	EPL C36 1	J. Abdallah et al.	(DELPHI Collab.)
Also	EPL C37 129 (erratum)	J. Abdallah et al.	(DELPHI Collab.)
ACHARD 04	PL B580 37	P. Achard et al.	(L3 Collab.)
ACHARD 04E	PL B587 16	P. Achard et al.	(L3 Collab.)
ACOSTA 04B	PRL 92 051803	D. Acosta et al.	(CDF Collab.)
ACOSTA 04E	PRL 93 061802	D. Acosta et al.	(CDF Collab.)
AKERIB 04	PRL 93 211301	D. Akerib et al.	(CDMSII Collab.)
AKTAS 04B	PL B599 159	A. Aktas et al.	(HI Collab.)
AKTAS 04D	EPL C36 425	A. Aktas et al.	(HI Collab.)
BELANGER 04	JHEP 0403 012	G. Belanger et al.	
BOTTINO 04	PR D69 037302	A. Bottino et al.	
DAS 04	PL B596 293	S.P. Das, A. Datta, M. Maitly	(Super-Kamiokande Collab.)
DESAI 04	PR D70 083523	S. Desai et al.	(Super-Kamiokande Collab.)
ELLIS 04	PR D69 015005	J. Ellis et al.	
ELLIS 04B	PR D70 055005	J. Ellis et al.	
GIULIANI 04	PL B588 151	F. Giuliani, T.A. Girard	
HEISTER 04	PL B583 247	A. Heister et al.	(ALEPH Collab.)
JANOT 04	PL B594 23	P. Janot	
PIERCE 04A	PR D70 075006	A. Pierce	
TCHIKILEV 04	PL B602 149	O.G. Tchikilev et al.	(ISTRA+ Coolab.)
ABBIENDI 03H	EPL C29 479	G. Abbiendi et al.	(OPAL Collab.)
ABBIENDI 03L	PL B572 8	G. Abbiendi et al.	(OPAL Collab.)
ABDALLAH 03C	EPL C26 505	J. Abdallah et al.	(DELPHI Collab.)
ABDALLAH 03D	EPL C27 153	J. Abdallah et al.	(DELPHI Collab.)
ABDALLAH 03F	EPL C28 15	J. Abdallah et al.	(DELPHI Collab.)
ABDALLAH 03G	EPL C29 285	J. Abdallah et al.	(DELPHI Collab.)
ABDALLAH 03M	EPL C31 421	J. Abdallah et al.	(DELPHI Collab.)
ACOSTA 03C	PRL 90 251801	D. Acosta et al.	(CDF Collab.)
ACOSTA 03E	PRL 91 171602	D. Acosta et al.	(CDF Collab.)
ADLOFF 03	PL B568 35	C. Adloff et al.	(HI Collab.)
AHMED 03	ASP 19 691	B. Ahmed et al.	(UK Dark Matter Collab.)
AKERIB 03	PR D68 082002	D. Akerib et al.	(CDMS Collab.)
BAER 03	JCAP 0305 006	H. Baer, C. Balazs	
BAER 03A	JCAP 0309 007	H. Baer et al.	
BERGER 03	PL B552 223	E. Berger et al.	
BOTTINO 03	PR D68 043506	A. Bottino et al.	
BOTTINO 03A	PR D67 063519	A. Bottino, N. Fornengo, S. Scopel	
CHAKRABARTI...	03	S. Chakrabarti, M. Guchait, N.K. Mondal	
CHATTOPAD... 03	PR D68 035005	U. Chattopadhyay, A. Corsetti, P. Nath	
CHEKANOV 03B	PR D68 052004	S. Chekanov et al.	(ZEUS Collab.)
ELLIS 03	ASP 18 395	J. Ellis, K.A. Olive, Y. Santoso	
ELLIS 03B	NP B652 259	J. Ellis et al.	
ELLIS 03C	PL B565 176	J. Ellis et al.	
ELLIS 03D	PL B573 162	J. Ellis et al.	
ELLIS 03E	PR D67 123502	J. Ellis et al.	
HEISTER 03	EPL C27 1	A. Heister et al.	(ALEPH Collab.)
HEISTER 03C	EPL C28 1	A. Heister et al.	(ALEPH Collab.)
HEISTER 03G	EPL C31 1	A. Heister et al.	(ALEPH Collab.)
HEISTER 03H	EPL C31 327	A. Heister et al.	(ALEPH Collab.)
HOOPER 03	PL B562 18	D. Hooper, T. Plehn	
JANOT 03	PL B564 183	P. Janot	
KLAPDOR-K... 03	ASP 18 525	H.V. Klappdor-Kleingrothaus et al.	

Searches Particle Listings

Supersymmetric Particle Searches, Technicolor

DECAMP	92	PRPL 216 253	D. Decamp <i>et al.</i>	(ALEPH Collab.)
LOPEZ	92	NP B370 445	J.L. Lopez, D.V. Nanopoulos, K.J. Yuan	(TAMU)
MCDONALD	92	PL B283 80	J. McDonald, K.A. Olive, M. Srednicki	(LISB+)
ROY	92	PL B283 270	D.P. Roy	(CERN)
ABREU	91F	NP B367 511	P. Abreu <i>et al.</i>	(DELPHI Collab.)
AKESSON	91	ZPHY C52 219	T. Akesson <i>et al.</i>	(HELIOS Collab.)
ALEXANDER	91F	ZPHY C52 175	G. Alexander <i>et al.</i>	(OPAL Collab.)
ANTONIADIS	91	PL B262 109	I. Antoniadis, J. Ellis, D.V. Nanopoulos	(EPOL+)
BOTTINO	91	PL B265 57	A. Bottino <i>et al.</i>	(TORI, INFN)
GELMINI	91	NP B351 623	G.B. Gelmini, P. Gondolo, E. Roulet	(UCLA, TRST)
GRIEST	91	PR D43 3191	K. Griest, D. Seckel	(CHIC, FNAL)
KAMIONKOW...	91	PR D44 3021	M. Kamionkowski	(Kamionkande Collab.)
MORI	91B	PL B270 89	M. Mori <i>et al.</i>	(KEK)
NOJIRI	91	PL B261 76	M.M. Nojiri	(MINN, UCSB)
OLIVE	91	NP B355 208	K.A. Olive, M. Srednicki	(MINN, UCSB)
ROSKOWSKI	91	PL B262 59	L. Roszkowski	(CERN)
SATO	91	PR D44 2220	N. Sato <i>et al.</i>	(Kamionkande Collab.)
ADACHI	90C	PL B244 352	I. Adachi <i>et al.</i>	(TOPAZ Collab.)
GRIEST	90	PR D41 3565	K. Griest, M. Kamionkowski, M.S. Turner	(UCB+)
BARBIERI	89C	NP B313 725	R. Barbieri, M. Frigeni, G. Giudice	(CERN)
NAKAMURA	89	PR D39 1261	T.T. Nakamura <i>et al.</i>	(KYOT, TMT/C)
OLIVE	89	PL B230 78	K.A. Olive, M. Srednicki	(MINN, UCSB)
ELLIS	88D	NP B307 883	J. Ellis, R. Flores	(CERN)
GRIEST	88B	PR D38 2357	K. Griest	(CERN)
OLIVE	88	PL B205 553	K.A. Olive, M. Srednicki	(MINN, UCSB)
SREDNICKI	88	NP B310 693	M. Srednicki, R. Watkins, K.A. Olive	(MINN, UCSB)
ALBAJAR	87D	PL B198 261	C. Albajar <i>et al.</i>	(UA1 Collab.)
ANSARI	87D	PL B195 613	R. Ansari <i>et al.</i>	(UA2 Collab.)
ARNOLD	87	PL B186 435	R.G. Arnold <i>et al.</i>	(BRUX, DUUC, LOUC+)
NG	87	PL B180 138	K.W. Ng, K.A. Olive, M. Srednicki	(MINN, UCSB)
TUTS	87	PL B186 233	P.M. Tuts <i>et al.</i>	(CERN)
ALBRECHT	86C	PL B178 360	H. Albrecht <i>et al.</i>	(ARGUS Collab.)
BADIER	86	ZPHY C31 21	J. Badier <i>et al.</i>	(NA3 Collab.)
BARNETT	86	NP B267 625	R.M. Barnett, H.E. Haber, G.L. Kane	(LBL, UCSB+)
GAISSER	86	PR D34 2206	T.K. Gaisser, G. Steigman, S. Tilav	(BART, DELA)
VOLOSHIN	86	SJNP 43 495	M.B. Voloshin, L.B. Okun	(ITEP)
		Translated from YAF 43 779		
COOPER...	85B	PL B160B 212	A.M. Cooper-Sarkar <i>et al.</i>	(WA66 Collab.)
DAWSON	85	PR D31 1581	S. Dawson, E. Eichten, C. Quigg	(LBL, FNAL)
FARRAR	85	PR L 55 895	G.R. Farrar	(RUTG)
GOLDMAN	85	Physica 15D 181	T. Goldman, H.E. Haber	(LANL, UCSB)
HABER	85	PRPL 117 75	H.E. Haber, G.L. Kane	(UCSC, MICH)
BALL	84	PRL 53 1314	R.C. Ball <i>et al.</i>	(MICH, FIRZ, OSU, FNAL+)
BARBER	84B	PL L39B 427	J.S. Barber, R.E. Shrock	(STON)
BRICK	84	PR D30 1134	D.H. Brick <i>et al.</i>	(BROW, CAVE, IIT+)
ELLIS	84	NP B238 453	J. Ellis <i>et al.</i>	(CERN)
FARRAR	84	PRL 53 1029	G.R. Farrar	(RUTG)
BERGSMAS	83C	PL L21B 429	F. Bergsma <i>et al.</i>	(CHARM Collab.)
CHANOWITZ	83	PL L26B 225	M.S. Chanowitz, S. Sharpe	(UCB, LBL)
GOLDBERG	83	PRL 50 1419	H. Goldberg	(NEAS)
HOFMAN	83	PR D28 1640	C.M. Hoffman <i>et al.</i>	(LANL, ARZS)
KRAUSS	83	NP B227 556	L.M. Krauss	(HARV)
VYSOTSKII	83	SJNP 37 948	M.I. Vysotsky	(ITEP)
		Translated from YAF 37 1597		
KANE	82	PL L12B 227	G.L. Kane, J.P. Leveille	(MICH)
CABBIBO	81	PL 105B 155	N. Cabibbo, G.R. Farrar, L. Maiani	(ROMA, RUTG)
FARRAR	78	PL 76B 575	G.R. Farrar, P. Fayet	(CIT)
Also		PL 79B 442	G.R. Farrar, P. Fayet	(CIT)

Table 1: Summary of the mass limits. Symbols are defined in the text.

Process	Excluded mass range	Decay channels	Ref.
$p\bar{p} \rightarrow \rho_T \rightarrow W\pi_T$	$170 < m_{\rho_T} < 215$ GeV and $80 < m_{\pi_T} < 115$ GeV for $M_V = 500$ GeV	$\rho_T \rightarrow W\pi_T$ $\pi_T^0 \rightarrow b\bar{b}$ $\pi_T^\pm \rightarrow b\bar{c}$	[19]
$p\bar{p} \rightarrow \omega_T \rightarrow \gamma\pi_T$	$140 < m_{\omega_T} < 290$ GeV for $m_{\pi_T} \approx m_{\omega_T}/3$ and $M_T = 100$ GeV	$\omega_T \rightarrow \gamma\pi_T$ $\pi_T^0 \rightarrow b\bar{b}$ $\pi_T^\pm \rightarrow b\bar{c}$	[20]
$p\bar{p} \rightarrow \omega_T/\rho_T$	$m_{\omega_T} = m_{\rho_T} < 203$ GeV for $m_{\omega_T} < m_{\pi_T} + m_W$ or $M_T > 200$ GeV	$\omega_T/\rho_T \rightarrow \ell^+\ell^-$	[21]
	$m_{\omega_T} = m_{\rho_T} < 280$ GeV for $m_{\omega_T} < m_{\pi_T} + m_W$ or $M_T > 500$ GeV	$\omega_T/\rho_T \rightarrow \ell^+\ell^-$	[22]
$e^+e^- \rightarrow \omega_T/\rho_T$	$90 < m_{\rho_T} < 206.7$ GeV $m_{\pi_T} < 79.8$ GeV	$\rho_T \rightarrow WW$, $W\pi_T$, $\pi_T\pi_T$, $\gamma\pi_T$, hadrons	[23]
$p\bar{p} \rightarrow \rho_{T8}$	$260 < m_{\rho_{T8}} < 480$ GeV	$\rho_{T8} \rightarrow q\bar{q}, gg$	[25]
$p\bar{p} \rightarrow \rho_{T8}$	$m_{\rho_{T8}} < 510$ GeV	$\pi_{LQ} \rightarrow c\nu$	[28]
$\rightarrow \pi_{LQ}\pi_{LQ}$	$m_{\rho_{T8}} < 600$ GeV	$\pi_{LQ} \rightarrow b\nu$	[28]
	$m_{\rho_{T8}} < 465$ GeV	$\pi_{LQ} \rightarrow \tau q$	[27]
$p\bar{p} \rightarrow g_t$	$0.3 < m_{g_t} < 0.6$ TeV for $0.3m_{g_t} < \Gamma < 0.7m_{g_t}$	$g_t \rightarrow b\bar{b}$	[35]
$p\bar{p} \rightarrow Z'$	$m_{Z'} < 480$ GeV for $\Gamma = 0.012m_{Z'}$ $m_{Z'} < 780$ GeV for $\Gamma = 0.04m_{Z'}$	$Z' \rightarrow t\bar{t}$	[36]

Technicolor

DYNAMICAL ELECTROWEAK SYMMETRY BREAKING

Revised August 2009 by R.S. Chivukula (Michigan State University), M. Narain (Brown University), and J. Womersley (STFC, Rutherford Appleton Laboratory).

In theories of dynamical electroweak symmetry breaking, the electroweak interactions are broken to electromagnetism by the vacuum expectation value of a fermion bilinear. These theories may thereby avoid the introduction of fundamental scalar particles, of which we have no examples in nature. In this note, we review the status of experimental searches for the particles predicted in technicolor, topcolor, and related models. The limits from these searches are summarized in Table 1.

I. Technicolor

The earliest models [1,2] of dynamical electroweak symmetry breaking [3] include a new asymptotically free non-abelian gauge theory (“technicolor”) and additional massless fermions (“technifermions”) transforming under a vectorial representation of the gauge group) which feel this new force. The global chiral symmetry of the fermions is spontaneously broken by the formation of a technifermion condensate, just as the approximate chiral $SU(2) \times SU(2)$ symmetry in QCD is broken down to $SU(2)$ isospin by the formation of a quark condensate. If the quantum numbers of the technifermions are chosen

correctly (*e.g.*, by choosing technifermions in the fundamental representation of an $SU(N)$ technicolor gauge group, with the left-handed technifermions being weak doublets and the right-handed ones weak singlets), this condensate can break the electroweak interactions down to electromagnetism.

The breaking of the global chiral symmetries implies the existence of Goldstone bosons, the “technipions” (π_T). Through the Higgs mechanism, three of the Goldstone bosons become the longitudinal components of the W and Z , and the weak gauge bosons acquire a mass proportional to the technipion decay constant (the analog of f_π in QCD). The quantum numbers and masses of any remaining technipions are model-dependent. There may be technipions which are colored (octets and triplets), as well as those carrying electroweak quantum numbers, and some color-singlet technipions are too light [4,3] unless additional sources of chiral-symmetry breaking are introduced. The next lightest technicolor resonances are expected to be the analogs of the vector mesons in QCD. The technivector mesons can also have color and electroweak quantum numbers and, for a theory with a small number of technifermions, are expected to have a mass in the TeV range [5].

While technicolor chiral-symmetry breaking can give mass to the W and Z particles, additional interactions must be introduced to produce the masses of the standard model

fermions. The most thoroughly studied mechanism for this invokes “extended technicolor” (ETC) gauge interactions [4,6]. In ETC, technicolor and flavor are embedded into a larger gauge group, which is broken at a sequence of mass scales down to the residual, exact technicolor gauge symmetry. The massive gauge bosons associated with this breaking mediate transitions between quarks/leptons and technifermions, giving rise to the couplings necessary to produce fermion masses. The ETC gauge bosons also mediate transitions among technifermions themselves, leading to interactions which can explicitly break unwanted chiral symmetries and raise the masses of any light technipions. The ETC interactions connecting technifermions to quarks/leptons also mediate technipion decays to ordinary fermion pairs. Since these interactions are responsible for fermion masses, one generally expects technipions to decay to the heaviest fermions kinematically allowed (though this need not hold in all models).

In addition to quark masses, ETC interactions must also give rise to quark mixing. One expects, therefore, that there are ETC interactions coupling quarks of the same charge from different generations. A stringent limit on these flavor-changing neutral current interactions comes from $K^0-\bar{K}^0$ mixing [4]. These force the scale of ETC breaking and the corresponding ETC gauge boson masses to be in the 100-1000 TeV range (at least insofar as ETC interactions of first two generations are concerned). To obtain quark and technipion masses that are large enough then requires an enhancement of the technifermion condensate over that expected naively by scaling from QCD. Such an enhancement can occur if the technicolor gauge coupling runs very slowly, or “walks” [7]. Some theories of walking technicolor incorporate many technifermions, implying that the technicolor scale and, in particular, the technivector mesons may be much lighter than 1 TeV [3,8]. It should also be noted that there is no reliable calculation of electroweak parameters in a walking technicolor theory, and the values of precisely measured electroweak quantities [9] cannot directly be used to constrain the models.† Recently, progress has been made in constructing a complete theory of fermion masses (including neutrino masses) in the context of extended technicolor [11].

In existing colliders, technivector mesons are dominantly produced when an off-shell standard model gauge boson “resonates” into a technivector meson with the same quantum numbers [12]. The technivector mesons may then decay, in analogy with $\rho \rightarrow \pi\pi$, to pairs of technipions. However, in walking technicolor the technipion masses may be increased to the point that the decay of a technirho to pairs of technipions is kinematically forbidden [8]. In this case the decay to a technipion and a longitudinally polarized weak boson (an “eaten” Goldstone boson) may be preferred, and the technivector meson

would be very narrow. Alternatively, the technivector may also decay, in analogy with the decay $\rho \rightarrow \pi\gamma$, to a technipion plus a photon, gluon, or transversely polarized weak gauge boson. Finally, in analogy with the decay $\rho \rightarrow e^+e^-$, the technivector meson may resonate back to an off-shell gluon or electroweak gauge boson, leading to a decay into a pair of leptons, quarks, or gluons.

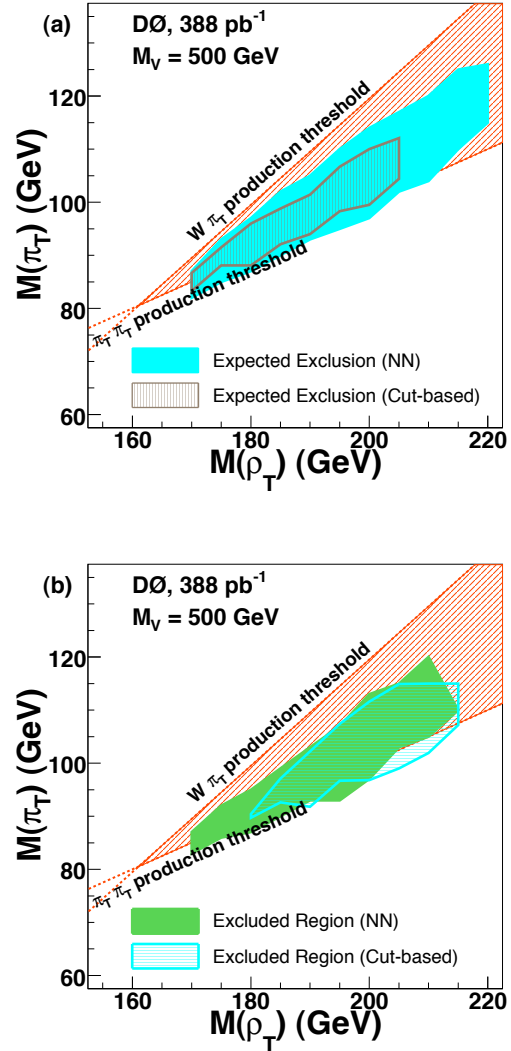


Figure 1: Search for a light technirho decaying to W^\pm and a π_T , and in which the π_T decays to two jets including at least one b quark [19]. Expected region of exclusion (a) and excluded region (b) at the 95% C.L. in the $M(\rho_T), M(\pi_T)$ plane for $\rho_T \rightarrow W\pi_T \rightarrow e\nu b\bar{b}(\bar{c})$ production with $M_V = 500$ GeV. Kinematic thresholds from $W\pi_T$ and $\pi_T\pi_T$ are shown on the figures. Color version at end of book.

† Indeed, it is possible that the spectrum of these theories is quite different from QCD – perhaps even a parity-doubled spectrum including light composite scalar states [10].

When comparing the various results presented in this review, one should be aware that the more recent analyses [18,19,21,23] make use of newer calculations [13] of technihadron production and decay, as implemented in PYTHIA [14]

Searches Particle Listings

Technicolor

version 6.126 and higher [15]. The results obtained with older cross section calculations are not generally directly comparable, and have only been listed in Table 1 when newer results are not available.

If the dominant decay mode of the technirho is $W_L\pi_T$, promising signal channels [16] are $\rho_T^\pm \rightarrow W^\pm\pi_T^0$ and $\rho_T^0 \rightarrow W^\pm\pi_T^\mp$. If we assume that the technipions decay to $b\bar{b}$ (neutral) and $b\bar{c}$ (charged), then both channels yield a signal of $W(\ell\nu) + 2$ jets, with one or more heavy flavor tags. The CDF collaboration carried out a search in this final state [17] based on Run I data and using PYTHIA version 6.1 for the signal simulation. Using 1.9 fb^{-1} of data from Run II, CDF [18] has shown a preliminary update of this analysis. The DØ [19] collaboration published an analysis based on 388 pb^{-1} of data from Run II and PYTHIA 6.22. The searches are sensitive to $\sigma \cdot B \gtrsim 4 \text{ pb}$ and DØ finds mass combinations up to $m_{\rho_T} = 215 \text{ GeV}$, $m_{\pi_T} = 115 \text{ GeV}$ to be excluded for certain values of the model parameters. The expected sensitivity and the region excluded at 95% C.L. by the DØ analysis for $M_V = 500 \text{ GeV}$ is shown in Fig. 1. For $M_V = 100 \text{ GeV}$, only a small region around $M(\rho_T) = 190 \text{ GeV}$ and $M(\pi_T) = 95 \text{ GeV}$ can be excluded. For an integrated luminosity of 2 fb^{-1} , the 5σ discovery reach is expected to extend to $m_{\rho_T} = 210 \text{ GeV}$ and $m_{\pi_T} = 110 \text{ GeV}$, while the 95% exclusion sensitivity will extend to $m_{\rho_T} = 250 \text{ GeV}$ and $m_{\pi_T} = 145 \text{ GeV}$.

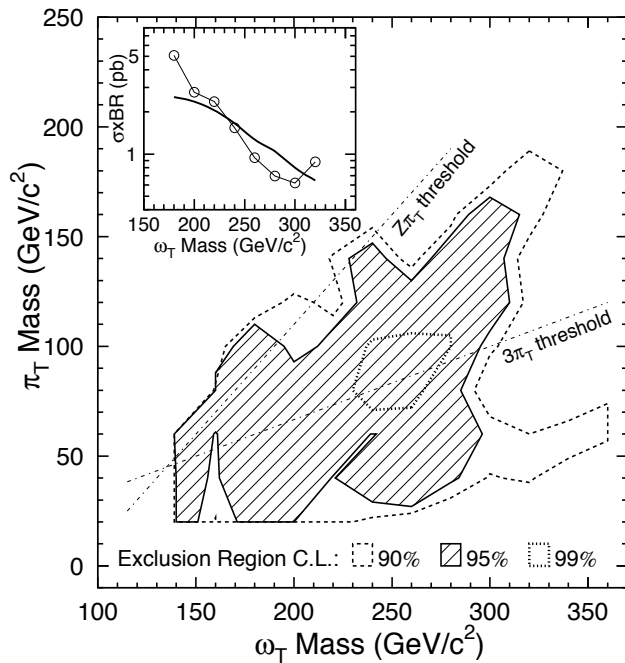


Figure 2: 95% CL exclusion region [20] for a light techniomuon decaying to γ and a π_T , and in which the π_T decays to two jets, including at least one b quark. (Inset: cross section limit for $m_{\pi_T} = 120 \text{ GeV}$.)

CDF also searched [20] in Run I for the process $\omega_T^0 \rightarrow \gamma\pi_T^0$, yielding a signal of a hard photon plus two jets, with one or more heavy flavor tags. The sensitivity to $\sigma \cdot B$ is of order 1 pb . The excluded region is shown in Fig. 2 and is roughly $140 < m_{\omega_T} < 290 \text{ GeV}$ at the 95% level, for $m_{\pi_T} \approx m_{\omega_T}/3$. The analysis assumes four technicolors, $Q_D = Q_U - 1 = \frac{1}{3}$ and $M_T = 100 \text{ GeV}/c^2$. Here Q_U and Q_D are the charges of the lightest technifermion doublet, and M_T is a dimensionful parameter, of order $100 \text{ GeV}/c^2$, which controls the rate of $\rho_T, \omega_T \rightarrow \gamma\pi_T$.

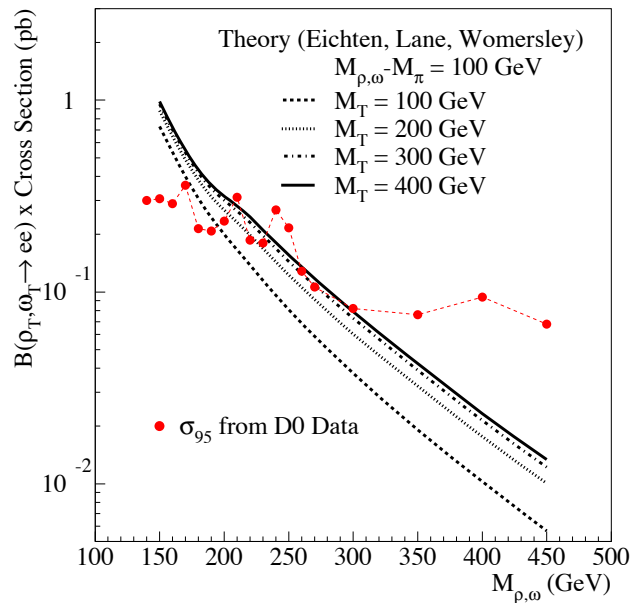


Figure 3: 95% CL cross-section limit [21] for a light techniomuon decaying to $\ell^+\ell^-$.

The DØ experiment has searched [21] for low-scale technicolor resonances ρ_T and ω_T decaying to dileptons, using an inclusive e^+e^- sample from Run I. In the search, the ρ_T and ω_T are assumed to be degenerate in mass. The absence of structure in the dilepton invariant mass distribution is then used to set limits. Masses $m_{\rho_T} = m_{\omega_T} \lesssim 200 \text{ GeV}$ are excluded, provided either $m_{\rho_T} < m_{\pi_T} + m_W$, or $M_T > 200 \text{ GeV}$ (as shown in Fig. 3). The CDF experiment also performed a similar search with 200 pb^{-1} of Run II data, and excluded equal $m_{\rho_T} = m_{\omega_T}$ masses below 280 GeV for $M_V = 500 \text{ GeV}$ and $m_{\rho_T} < m_{\pi_T} + m_W$ at 95% C.L. [22]. With 2 fb^{-1} of data, the sensitivity will extend to $m_{\rho_T} = m_{\omega_T} \approx 500 \text{ GeV}$.

DELPHI [23] has reported a search for technicolor production in 452 pb^{-1} of e^+e^- data taken between 192 and 208 GeV. The analysis combines searches for $e^+e^- \rightarrow \rho_T(\gamma)$ with $\rho_T \rightarrow W_L W_L$, $\rho_T \rightarrow \text{hadrons}$ ($\pi_T\pi_T$ or $q\bar{q}$), $\rho_T \rightarrow \pi_T\gamma$, and $e^+e^- \rightarrow \rho_T^* \rightarrow W_L\pi_T$ or $\pi_T\pi_T$. Technirho masses in the range $90 < m_{\rho_T} < 206.7 \text{ GeV}$ are excluded, while technipion masses $m_{\pi_T} < 79.8 \text{ GeV}$ are ruled out independent of the parameters of the technicolor model.

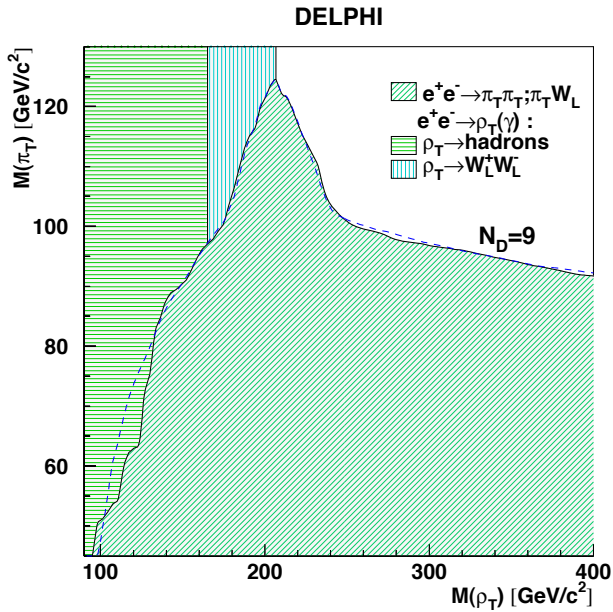


Figure 4: 95% CL exclusion region [23] in the technirho-technipion mass plane obtained from searches by the DELPHI collaboration at LEP 2, for nine technifermion doublets. The dashed line shows the expected limit for the 4-jet analysis. Color version at end of book.

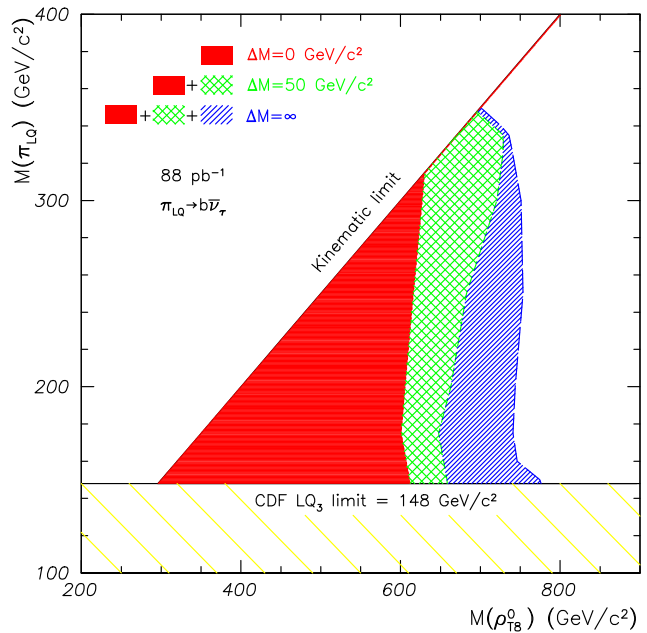


Figure 6: 95% CL exclusion region [28] in the technirho-technipion mass plane for pair produced technipions, with leptoquark couplings, decaying to $b\nu$. Color version at end of book.

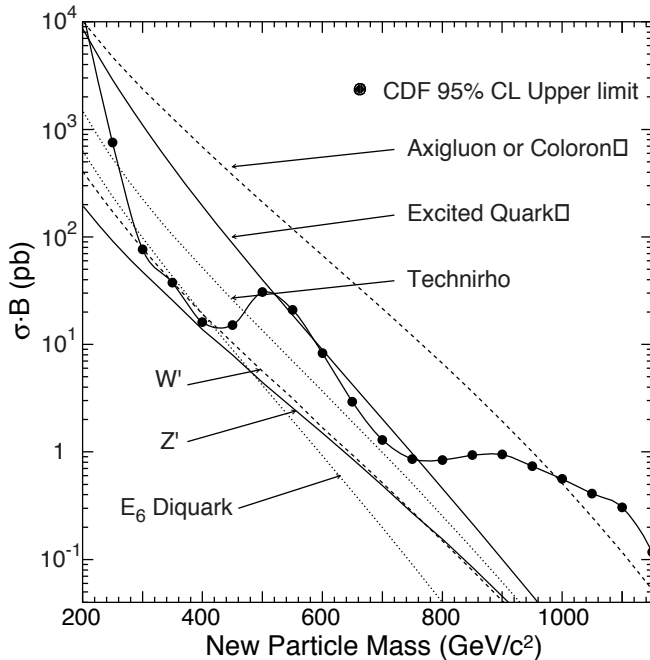


Figure 5: 95% CL Cross-section limits [25] for a technirho decaying to two jets at the Tevatron.

Searches have also been carried out at the Tevatron for colored technihadron resonances [24,25]. CDF has used a search for structure in the dijet invariant mass spectrum to set

limits on a color-octet technirho ρ_{T8} produced by an off-shell gluon, and decaying to two real quarks or gluons. As shown in Fig. 5, masses $260 < m_{\rho_{T8}} < 480$ GeV are excluded; in Run II the limits will improve to cover the whole mass range up to about 0.8 TeV [26].

The CDF second- and third-generation leptoquark searches (see Refs. [27,28]) have also been interpreted in terms of the complementary ρ_{T8} decay mode: $p\bar{p} \rightarrow \rho_{T8} \rightarrow \pi_{LQ}\pi_{LQ}$. Here π_{LQ} denotes a color-triplet technipion carrying both color and lepton number, assumed to decay to $b\nu$ or $c\nu$ [28], or to a τ plus a quark [27]. The searches exclude technirho masses $m_{\rho_{T8}}$ less than 510 GeV ($\pi_{LQ} \rightarrow c\nu$), 600 GeV ($\pi_{LQ} \rightarrow b\nu$), and 465 GeV ($\pi_{LQ} \rightarrow \tau q$) for technipion masses up to $m_{\rho_{T8}}/2$. Figure 6 shows the $\pi_{LQ} \rightarrow b\nu$ exclusion region. (Leptoquark masses $m_{\pi_{LQ}}$ less than 123 GeV ($c\nu$), 148 GeV ($b\nu$), and 99 GeV (τq) are already ruled out by standard continuum-production leptoquark searches).

Recently, it has been demonstrated that there is substantial uncertainty in the theoretical estimate of the ρ_{T8} production cross section at the Tevatron and that the cross section may be as much as an order of magnitude lower than the naive vector meson dominance estimate [29]. To establish the range of allowed masses, these limits will need to be redone with a reduced theoretical cross section.

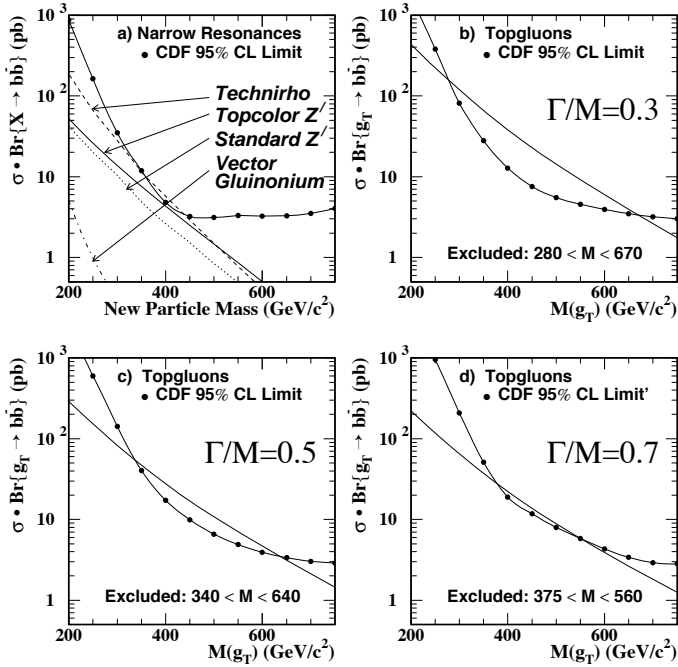


Figure 7: Tevatron limits [35] on new particles decaying to $b\bar{b}$: narrow resonances and topgluons for various widths.

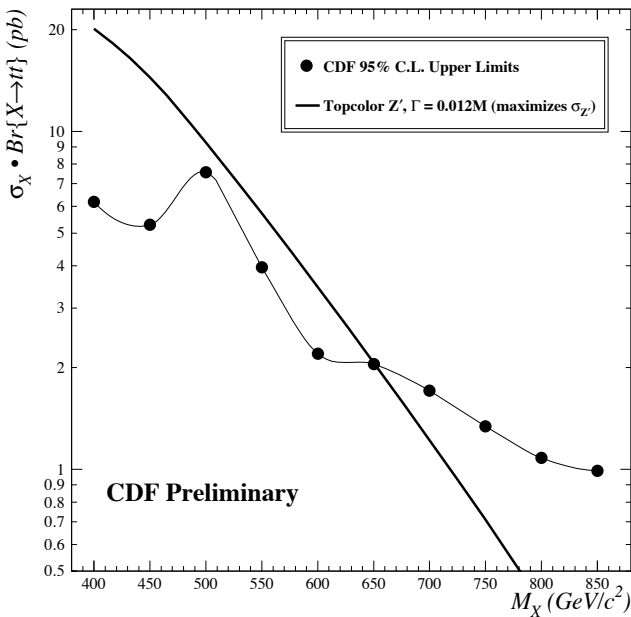


Figure 8: Cross-section limits for a narrow resonance decaying to $t\bar{t}$ [36] and expected cross section for a leptophobic topcolor Z' boson.

Within the context of the model in reference [13], both the ATLAS and CMS experiments have carried out sensitivity studies for observing technihadron production in proton-proton collisions at the LHC. A study of the process ρ_T and ω_T decaying to $\mu^+\mu^-$ by the ATLAS experiment [30] shows that

with about 1.5 (4.5) fb^{-1} of integrated luminosity at $\sqrt{s} = 14$ TeV, a 5σ discovery reach is possible for masses below 700 GeV (1 TeV). The CMS experiment has examined the sensitivity to ρ_T and its axial-vector partner, a_T production at $\sqrt{s} = 10$ TeV using the $\rho_T/a_T \rightarrow WZ \rightarrow ll\nu$ final state [31]. They conclude that it is possible to exclude masses up to 300 GeV with 450 pb^{-1} of data. For a 5σ discovery about 1 fb^{-1} or more of luminosity is needed. The discovery potential is expected to be enhanced when the LHC operates at the design energy of $\sqrt{s} = 14$ TeV.

II. Top Condensate, Higgsless, and Related Models

The top quark is much heavier than other fermions and must be more strongly coupled to the symmetry-breaking sector. It is natural to consider whether some or all of electroweak-symmetry breaking is due to a condensate of top quarks [3,32]. Top quark condensation alone, without additional fermions, seems to produce a top quark mass larger [33] than observed experimentally, and is therefore not favored. Topcolor-assisted technicolor [34] combines technicolor and top condensation. In addition to technicolor, which provides the bulk of electroweak symmetry breaking, top condensation and the top quark mass arise predominantly from “topcolor,” a new QCD-like interaction which couples strongly to the third generation of quarks. An additional, strong, U(1) interaction (giving rise to a topcolor Z') precludes the formation of a b -quark condensate.

CDF has searched [35] for the “topgluon,” a massive color-octet vector which couples preferentially to the third generation, in the mode $p\bar{p} \rightarrow g_t \rightarrow b\bar{b}$. The results are shown in Fig. 7. Topgluon masses from approximately 0.3 to 0.6 TeV are excluded at 95% confidence level, for topgluon widths in the range $0.3m_{g_t} < \Gamma < 0.7m_{g_t}$. Results have also been reported by CDF [36] on a search for narrow resonances in the $t\bar{t}$ invariant mass distribution. The cross section limit is shown in Fig. 8 and excludes a leptophobic topcolor Z' with masses less than 480 (780) GeV/c^2 , for the case where its width $\Gamma = 0.012(0.04)m_{Z'}$. (DØ has carried out a similar search, with greater sensitivity [37], but has not derived comparable Z' mass limits.) A broad topgluon could also be detected in the same final state, though no results are yet available. In Run II, the Tevatron [26] should be sensitive to topgluon and topcolor Z' masses up to of order 1 TeV in $b\bar{b}$ and $t\bar{t}$ final states. A detailed theoretical analysis of $B-\bar{B}$ mixing and light quark mass generation in top-color-assisted technicolor shows that, at least in some models, the topgluon and Z' boson masses must be greater than about 5 TeV [38].

The top quark seesaw model of electroweak symmetry breaking [39] is a variant of the original top condensate idea which reconciles top condensation with a lighter top quark mass. Such a model can easily be consistent with precision electroweak tests, either because the spectrum includes a light composite Higgs [40], or because additional interactions allow for a heavier Higgs [41]. Such theories may arise naturally from gauge fields propagating in compact extra spatial dimensions [42].

See key on page 405

A variant of topcolor-assisted technicolor is flavor-universal, in which the topcolor $SU(3)$ gauge bosons, called colorons, couple equally to all quarks [43]. Flavor-universal versions of the seesaw model [44] incorporating a gauged flavor symmetry are also possible. In these models *all* left-handed quarks (and possibly leptons as well) participate in electroweak-symmetry-breaking condensates with separate (one for each flavor) right-handed weak singlets, and the different fermion masses arise by adjusting the parameters which control the mixing of each fermion with the corresponding condensate.

A prediction of these flavor-universal models is the existence of new heavy gauge bosons, coupling to color or flavor, at relatively low mass scales. The absence of an excess of high- E_T jets in $D\bar{O}$ data [45] has been used to constrain strongly coupled flavor-universal colorons (massive color-octet bosons coupling to all quarks). A mass limit of between 0.8 and 3.5 TeV is set [46] depending on the coloron-gluon mixing angle. Precision electroweak measurements constrain [47] the masses of these new gauge bosons to be greater than 1–3 TeV in a variety of models, for strong couplings.

A new class [48] of composite Higgs model [49], dubbed “Little Higgs Theory,” has been developed which gives rise to naturally light Higgs bosons without supersymmetry [50]. Inspired by discretized versions of higher-dimensional gauge theory [51], these models are based on the chiral symmetries of “theory space.” The models involve extended gauge groups and novel gauge symmetry-breaking patterns [52]. The new chiral symmetries prevent large corrections to the Higgs boson mass, and allow the scale (Λ) of the underlying strong dynamics giving rise to the composite particles to be as large as 10 TeV. These models typically require new gauge bosons and fermions, and possibly additional composite scalars beyond the Higgs, in the TeV mass range [53].

Finally, “Higgsless” models [54] provide electroweak symmetry breaking, including unitarization of the scattering of longitudinal W and Z bosons, without employing a scalar Higgs boson. The most extensively studied models [55] are based on a five-dimensional $SU(2) \times SU(2) \times U(1)$ gauge theory in a slice of Anti-deSitter space, and electroweak symmetry breaking is encoded in the boundary conditions of the gauge fields. Using the AdS/CFT correspondence [56], these theories may be viewed as “dual” descriptions of walking technicolor theories [7]. In addition to a massless photon and near-standard W and Z bosons, the spectrum includes an infinite tower of additional massive vector bosons (the higher Kaluza-Klein or KK excitations), whose exchange is responsible for unitarizing longitudinal W and Z boson scattering [57]. Using deconstruction, it has been shown [58] that a Higgsless model whose fermions are localized (*i.e.*, derive their electroweak properties from a single site on the deconstructed lattice) cannot simultaneously satisfy unitarity bounds and precision electroweak constraints.

It has recently been proposed [59] that the size of corrections to electroweak processes in Higgsless models may be reduced by

considering delocalized fermions, *i.e.*, considering the effect of the distribution of the wavefunctions of ordinary fermions in the fifth dimension (corresponding, in the deconstruction language, to allowing the fermions to derive their electroweak properties from several sites on the lattice). It has been shown [60] that, in an arbitrary Higgsless model, if the probability distribution of the delocalized fermions is related to the W wavefunction (a condition called “ideal” delocalization), then deviations in precision electroweak parameters are minimized. Phenomenological limits on delocalized Higgsless models may be derived [61] from limits on the deviation of the triple-gauge boson (WWZ) vertices from the standard model, and current constraints allow for the lightest KK resonances (which tend to be fermiophobic in the case of ideal fermion delocalization) to have masses of only a few hundred GeV. Such resonances would have to be studied using WW scattering [62].

An alternative approach to “Higgsless” models, dubbed “holographic technicolor” [63], incorporates a generalized extra-dimensional framework and allows for arbitrary couplings of the vector mesons to the light fermions, resulting in a wide variety of potential signatures at the LHC [64].

Acknowledgments

We thank Tom Appelquist, Bogdan Dobrescu, Emilian Dudas, Robert Harris, Chris Hill, Greg Landsberg, Kenneth Lane, Bob Shrock, Elizabeth Simmons, and John Terning for help in the preparation of this article. *This work was supported in part by the Department of Energy under grant DE-FG02-91ER40676 and by the National Science Foundation under grant PHY-0354226.*

References

1. S. Weinberg, Phys. Rev. **D19**, 1277 (1979).
2. L. Susskind, Phys. Rev. **D20**, 2619 (1979).
3. For a recent reviews, see K. Lane, hep-ph/0202255; C.T. Hill, E.H. Simmons, Phys. Rept. **381**, 235 (2003); R. Shrock, hep-ph/0703050.
4. E. Eichten and K. Lane, Phys. Lett. **90B**, 125 (1980).
5. S. Dimopoulos, S. Raby, and G.L. Kane, Nucl. Phys. **B182**, 77 (1981).
6. S. Dimopoulos and L. Susskind, Nucl. Phys. **B155**, 237 (1979).
7. B. Holdom, Phys. Rev. **D24**, 1441 (1981) and Phys. Lett. **150B**, 301 (1985); K. Yamawaki, M. Bando, and K. Matumoto, Phys. Rev. Lett. **56**, 1335 (1986); T.W. Appelquist, D. Karabali, and L.C.R. Wijewardhana, Phys. Rev. Lett. **57**, 957 (1986); T. Appelquist and L.C.R. Wijewardhana, Phys. Rev. **D35**, 774 (1987) and Phys. Rev. **D36**, 568 (1987).
8. E. Eichten and K. Lane, Phys. Lett. **B222**, 274 (1989).
9. J. Erler and P. Langacker, “Electroweak Model and Constraints on New Physics,” in the section on Reviews, Tables, and Plots in this *Review*.
10. T. Appelquist, P. S. Rodrigues da Silva, and F. Sannino, Phys. Rev. **D60**, 116007 (1999).
11. T.W. Appelquist and R. Shrock, Phys. Lett. **B548**, 204 (2002) and Phys. Rev. Lett. **90**, 201801 (2003);

Searches Particle Listings

Technicolor

- T.W. Appelquist, M. Piai, and R. Shrock, Phys. Rev. **D69**, 015002 (2004);
T. Appelquist *et al.*, Phys. Rev. **D70**, 093010 (2004).
12. E. Eichten *et al.*, Rev. Mod. Phys. **56**, 579 (1984) and Phys. Rev. **D34**, 1547 (1986).
 13. K. Lane, Phys. Rev. **D60**, 075007 (1999);
K. Lane and S. Mrenna, Phys. Rev. **D67**, 115011 (2003);
see also K. Lane and A. Martin, arXiv:0907.3737.
 14. T. Sjostrand, Comp. Phys. Comm. **82**, 74 (1994).
 15. S. Mrenna, Technihadron production and decay at LEP2, Phys. Lett. **B461**, 352 (1999).
 16. E. Eichten, K. Lane, and J. Womersley, Phys. Lett. **B405**, 305 (1997).
 17. CDF Collaboration (T. Affolder *et al.*), Phys. Rev. Lett. **84**, 1110 (2000).
 18. CDF Collaboration, CDF/PUB/EXOTIC/PUBLIC/9302, April 2008; and arXiv:0808.0226v1.
 19. DØ Collaboration (V.M. Abazov *et al.*), Phys. Rev. **98**, 221801 (2007).
 20. CDF Collaboration (F. Abe *et al.*), Phys. Rev. Lett. **83**, 3124 (1999).
 21. DØ Collaboration (V.M. Abazov *et al.*), Phys. Rev. Lett. **87**, 061802 (2001).
 22. CDF Collaboration (A. Abulencia *et al.*), Phys. Rev. Lett. **95**, 252001 (2005).
 23. DELPHI Collaboration (J. Abdallah *et al.*), Eur. Phys. J. **C22**, 17 (2001).
 24. K. Lane and M.V. Ramana, Phys. Rev. **D44**, 2678 (1991).
 25. CDF Collaboration (F. Abe *et al.*), Phys. Rev. **D55**, R5263 (1997).
 26. K. Cheung and R.M. Harris, hep-ph/9610382.
 27. CDF Collaboration (F. Abe *et al.*), Phys. Rev. Lett. **82**, 3206 (1999).
 28. CDF Collaboration (T. Affolder *et al.*), Phys. Rev. Lett. **85**, 2056 (2000).
 29. A. Zerwekh and R. Rosenfeld, Phys. Lett. **B503**, 325 (2001);
R.S. Chivukula, *et al.*, Boston Univ. preprint BUHEP-01-19.
 30. ATLAS Collaboration, CERN-OPEN-2008-020, (2008).
 31. CMS Collaboration, CMS Physics Analysis Summary EXO-08-001 (2008).
 32. V.A. Miransky, M. Tanabashi, and K. Yamawaki, Phys. Lett. **221B**, 177 (1989), and Mod. Phys. Lett. **4**, 1043 (1989);
Y. Nambu, EFI-89-08 (1989);
W.J. Marciano, Phys. Rev. Lett. **62**, 2793 (1989).
 33. W.A. Bardeen, C.T. Hill, and M. Lindner, Phys. Rev. **D41**, 1647 (1990).
 34. C.T. Hill, Phys. Lett. **B345**, 483 (1995);
see also Phys. Lett. **266B**, 419 (1991).
 35. CDF Collaboration (F. Abe *et al.*), Phys. Rev. Lett. **82**, 2038 (1999).
 36. CDF Collaboration (F. Affolder *et al.*), Phys. Rev. Lett. **85**, 2062 (2000).
 37. D0 Collaboration (V. Abazov *et al.*), Phys. Rev. Lett. **87**, 231801 (2001).
 38. G. Burdman *et al.*, Phys. Lett. **B514**, 41 (2001).
 39. B.A. Dobrescu and C.T. Hill, Phys. Rev. Lett. **81**, 2634 (1998).
 40. R.S. Chivukula *et al.*, Phys. Rev. **D59**, 075003 (1999).
 41. H. Collins, A. Grant, and H. Georgi, Phys. Rev. **D61**, 055002 (2000).
 42. B.A. Dobrescu, Phys. Lett. **B461**, 99 (1999);
H.-C. Cheng, *et al.*, Nucl. Phys. **B589**, 249 (2000).
 43. E.H. Simmons, Nucl. Phys. **B324**, 315 (1989).
 44. G. Burdman and N. Evans, Phys. Rev. **D59**, 115005 (1999).
 45. DØ Collaboration (B. Abbott *et al.*), Phys. Rev. Lett. **82**, 2457 (1999).
 46. I. Bertram and E.H. Simmons, Phys. Lett. **B443**, 347 (1998).
 47. G. Burdman, R.S. Chivukula, and N. Evans, Phys. Rev. **D61**, 035009 (2000).
 48. N. Arkani-Hamed, A. G. Cohen, and H. Georgi, Phys. Lett. **B513**, 232 (2001).
 49. D.B. Kaplan and H. Georgi, Phys. Lett. **B136**, 183 (1984) and Phys. Lett. **B145**, 216 (1984);
T. Banks, Nucl. Phys. **B243**, 123 (1984);
D.B. Kaplan, H. Georgi, and S. Dimopoulos, Phys. Lett. **B136**, 187 (1984);
M.J. Dugan, H. Georgi, and D.B. Kaplan, Nucl. Phys. **B254**, 299 (1985).
 50. See also review by P. Igo-Kemenes, "Searches for Higgs Bosons," in the Boson Listings in this *Review*.
 51. N. Arkani-Hamed, A. G. Cohen, and H. Georgi, Phys. Rev. **D86**, 4757 (2001);
H. C. Cheng, C. T. Hill, and J. Wang, Phys. Rev. **D64**, 095003 (2001).
 52. M. Schmaltz and D. Tucker-Smith, Ann. Rev. Nucl. Part. Sci. **55**, 229 (2005).
 53. C. Csaki *et al.*, Phys. Rev. **D67**, 115002 (2003);
J. Hewett, F. Petriello, and T. Rizzo, JHEP **310**, 062 (2003);
T. Han *et al.*, Phys. Rev. **D67**, 095004 (2003);
Z. Han and W. Skiba, Phys. Rev. **D72**, 035005 (2005).
 54. C. Csaki *et al.*, Phys. Rev. **D69**, 055006 (2003).
 55. K. Agashe *et al.*, JHEP **0308**, 050 (2003);
C. Csaki *et al.*, Phys. Rev. Lett. **92**, 101802 (2004).
 56. J. Maldecena, Adv. Theor. Math. Phys. **2**, 231 (1998).
 57. R. S. Chivukula, D. Dicus, and H.-J. He, Phys. Lett. **B525**, 175 (2002).
 58. R. S. Chivukula *et al.*, Phys. Rev. **D71**, 035007 (2005).
 59. G. Cacciapaglia *et al.*, Phys. Rev. **D71**, 035015 (2005);
R. Foadi, S. Gopalkrishna, and C. Schmidt, Phys. Lett. **B606**, 157 (2005);
G. Cacciapaglia *et al.*, Phys. Rev. **D72**, 095018 (2005).
 60. R. S. Chivukula *et al.*, Phys. Rev. **D72**, 015008 (2005).
 61. R. S. Chivukula *et al.*, Phys. Rev. **D72**, 075012 (2005).
 62. A. Birkedal, K. Matchev, and M. Perelstein, Phys. Rev. Lett. **94**, 191803 (2005);
H.-J. He, *et al.*, arXiv:0708.2588.
 63. J. Hirn and V. Sanz Phys. Rev. Lett. **97**, 121803 (2006).
 64. J. Hirn, A. Martin, and V. Sanz, JHEP **0805**, 084 (2008) and Phys. Rev. **D78**, 075026 (2008).

**MASS LIMITS for Resonances
in Models of Dynamical Electroweak Symmetry Breaking**

VALUE (GeV)	CL%	DOCUMENT ID	TECN	COMMENT
>280	95	1 ABAZOV 07I 2 ABULENCIA 05A 3 CHEKANOV 02B	D0 CDF ZEUS	$\rho\bar{p} \rightarrow \rho_T/\omega_T \rightarrow W\pi_T$ $\rho_T \rightarrow e^+e^-, \mu^+\mu^-$ color octet techni- π
>207 none 90-206.7	95	4 ABAZOV 01B 5 ABDALLAH 01 6 AFFOLDER 00F	D0 DLPH CDF	$\rho_T \rightarrow e^+e^-$ $e^+e^- \rightarrow \rho_T$ color-singlet techni- ρ , $\rho_T \rightarrow W\pi_T, 2\pi_T$
>600	95	7 AFFOLDER 00k	CDF	color-octet techni- ρ , $\rho_{T8} \rightarrow 2\pi_{LQ}$
>480 none 350-440	95	8 AFFOLDER 00L 9 ABE 99F	CDF CDF	top-color Z' color-octet techni- ρ , $\rho_{T8} \rightarrow \bar{b}b$
>465	95	10 ABE 99H	CDF	color-octet techni- ρ , $\rho_{T8} \rightarrow 2\pi_{LQ}$
none 260-480	95	11 ABE 99N 12 ABE 97G	CDF CDF	techni- ω , $\omega_T \rightarrow \gamma\bar{b}b$ color-octet techni- ρ , $\rho_{T8} \rightarrow 2j\text{ets}$

- 1 ABAZOV 07I search for the vector techni-resonances (ρ_T, ω_T) decaying into $W\pi_T$ with $W \rightarrow e\nu$ and $\pi_T \rightarrow b\bar{b}$ or $b\bar{c}$. See their Fig. 2 for the exclusion plot in the $M_{\pi_T} - M_{\rho_T}$ plane.
- 2 ABULENCIA 05A search for resonances decaying to electron or muon pairs in $p\bar{p}$ collisions. at $\sqrt{s} = 1.96$ TeV. The limit assumes Technicolor-scale mass parameters $M_V = M_A = 500$ GeV.
- 3 CHEKANOV 02B search for color octet techni- π P decaying into dijets in ep collisions. See their Fig. 5 for the limit on $\sigma(ep \rightarrow ePX) \cdot B(P \rightarrow 2j)$.
- 4 ABAZOV 01B searches for vector techni-resonances (ρ_T, ω_T) decaying to e^+e^- . The limit assumes $M_{\rho_T} = M_{\omega_T} < M_{\pi_T} + M_W$.
- 5 The limit is independent of the π_T mass. See their Fig. 9 and Fig. 10 for the exclusion plot in the $M_{\rho_T} - M_{\pi_T}$ plane. ABDALLAH 01 limit on the techni- ρ mass is $M_{\rho_T} > 79.8$ GeV for $N_D=2$, assuming its point-like coupling to gauge bosons.
- 6 AFFOLDER 00F search for ρ_T decaying into $W\pi_T$ or $\pi_T\pi_T$ with $W \rightarrow \ell\nu$ and $\pi_T \rightarrow \bar{b}b, \bar{b}c$. See Fig. 1 in the above Note on "Dynamical Electroweak Symmetry Breaking" for the exclusion plot in the $M_{\rho_T} - M_{\pi_T}$ plane.
- 7 AFFOLDER 00k search for the ρ_{T8} decaying into $\pi_{LQ}\pi_{LQ}$ with $\pi_{LQ} \rightarrow b\nu$. For $\pi_{LQ} \rightarrow c\nu$, the limit is $M_{\rho_{T8}} > 510$ GeV. See their Fig. 2 and Fig. 3 for the exclusion plot in the $M_{\rho_{T8}} - M_{\pi_{LQ}}$ plane.
- 8 AFFOLDER 00L search for top-color Z'_{top} decaying into $\bar{t}t$. The quoted limit is for Z'_{top} with decay width $\Gamma = 0.012 M_{Z'}$. For $\Gamma = 0.04 M_{Z'}$, the limit becomes 780 GeV.
- 9 ABE 99F search for a new particle X decaying into $b\bar{b}$ in $p\bar{p}$ collisions at $E_{\text{cm}} = 1.8$ TeV. See Fig. 7 in the above Note on "Dynamical Electroweak Symmetry Breaking" for the upper limit on $\sigma(p\bar{p} \rightarrow X) \cdot B(X \rightarrow b\bar{b})$. ABE 99F also exclude top gluons of width $\Gamma = 0.3M$ in the mass interval $280 < M < 670$ GeV, of width $\Gamma = 0.5M$ in the mass interval $340 < M < 640$ GeV, and of width $\Gamma = 0.7M$ in the mass interval $375 < M < 560$ GeV.
- 10 ABE 99H search for the color-octet techni- ρ decaying into a pair of color-triplet technipions which subsequently decay into $\tau\tau$ jet. See Fig. 6 in the above Note on "Dynamical Electroweak Symmetry Breaking" for the exclusion plot in the $M_{\rho_{T8}} - M_{\pi_{LQ}}$ plane.
- 11 ABE 99N search for the techni- ω decaying into $\gamma\pi_T$. The technipion is assumed to decay $\pi_T \rightarrow b\bar{b}$. See Fig. 2 in the above Note on "Dynamical Electroweak Symmetry Breaking" for the exclusion plot in the $M_{\omega_T} - M_{\pi_T}$ plane.
- 12 ABE 97G search for a new particle X decaying into dijets in $p\bar{p}$ collisions at $E_{\text{cm}} = 1.8$ TeV. See Fig. 5 in the above Note on "Dynamical Electroweak Symmetry Breaking" for the upper limit on $\sigma(p\bar{p} \rightarrow X) \cdot B(X \rightarrow 2j)$.

REFERENCES FOR Technicolor

ABAZOV	07I	PRL 98 221801	V.M. Abazov et al.	(D0 Collab.)
ABULENCIA	05A	PRL 95 252001	A. Abulencia et al.	(CDF Collab.)
CHEKANOV	02B	PL B531 9	S. Chekanov et al.	(ZEUS Collab.)
ABAZOV	01B	PRL 87 061802	V.M. Abazov et al.	(D0 Collab.)
ABDALLAH	01	EPJ C22 17	J. Abdallah et al.	(DELPHI Collab.)
AFFOLDER	00F	PRL 84 1110	T. Affolder et al.	(CDF Collab.)
AFFOLDER	00k	PRL 85 2056	T. Affolder et al.	(CDF Collab.)
AFFOLDER	00L	PRL 85 2062	T. Affolder et al.	(CDF Collab.)
ABE	99F	PRL 82 2038	F. Abe et al.	(CDF Collab.)
ABE	99H	PRL 82 3206	F. Abe et al.	(CDF Collab.)
ABE	99N	PRL 83 3124	F. Abe et al.	(CDF Collab.)
ABE	97G	PR D55 R5263	F. Abe et al.	(CDF Collab.)

**Quark and Lepton Compositeness,
Searches for**

**SEARCHES FOR QUARK AND
LEPTON COMPOSITENESS**

Revised 2001 by K. Hagiwara (KEK), and K. Hikasa and M. Tanabashi (Tohoku University).

If quarks and leptons are made of constituents, then at the scale of constituent binding energies, there should appear new interactions among quarks and leptons. At energies much below the compositeness scale (Λ), these interactions are suppressed by inverse powers of Λ . The dominant effect should come from the lowest dimensional interactions with four fermions (contact terms), whose most general chirally invariant form reads [1]

$$L = \frac{g^2}{2\Lambda^2} \left[\eta_{LL} \bar{\psi}_L \gamma_\mu \psi_L \bar{\psi}_L \gamma^\mu \psi_L + \eta_{RR} \bar{\psi}_R \gamma_\mu \psi_R \bar{\psi}_R \gamma^\mu \psi_R + 2\eta_{LR} \bar{\psi}_L \gamma_\mu \psi_L \bar{\psi}_R \gamma^\mu \psi_R \right]. \quad (1)$$

Chiral invariance provides a natural explanation why quark and lepton masses are much smaller than their inverse size Λ . We may determine the scale Λ unambiguously by using the above form of the effective interactions; the conventional method [1] is to fix its scale by setting $g^2/4\pi = g^2(\Lambda)/4\pi = 1$ for the new strong interaction coupling and by setting the largest magnitude of the coefficients $\eta_{\alpha\beta}$ to be unity. In the following, we denote

$$\begin{aligned} \Lambda &= \Lambda_{LL}^\pm \quad \text{for } (\eta_{LL}, \eta_{RR}, \eta_{LR}) = (\pm 1, 0, 0), \\ \Lambda &= \Lambda_{RR}^\pm \quad \text{for } (\eta_{LL}, \eta_{RR}, \eta_{LR}) = (0, \pm 1, 0), \\ \Lambda &= \Lambda_{VV}^\pm \quad \text{for } (\eta_{LL}, \eta_{RR}, \eta_{LR}) = (\pm 1, \pm 1, \pm 1), \\ \Lambda &= \Lambda_{AA}^\pm \quad \text{for } (\eta_{LL}, \eta_{RR}, \eta_{LR}) = (\pm 1, \pm 1, \mp 1), \end{aligned} \quad (2)$$

as typical examples. Such interactions can arise by constituent interchange (when the fermions have common constituents, *e.g.*, for $ee \rightarrow ee$) and/or by exchange of the binding quanta (when ever binding quanta couple to constituents of both particles).

Another typical consequence of compositeness is the appearance of excited leptons and quarks (ℓ^* and q^*). Phenomenologically, an excited lepton is defined to be a heavy lepton which shares leptonic quantum number with one of the existing leptons (an excited quark is defined similarly). For example, an excited electron e^* is characterized by a nonzero transition-magnetic coupling with electrons. Smallness of the lepton mass and the success of QED prediction for $g=2$ suggest chirality conservation, *i.e.*, an excited lepton should not couple to both left- and right-handed components of the corresponding lepton.

Excited leptons may be classified by $SU(2) \times U(1)$ quantum numbers. Typical examples are:

1. Sequential type

$$\left(\begin{array}{c} \nu^* \\ \ell^* \end{array} \right)_L, \quad [\nu_R^*], \quad \ell_R^*.$$

ν_R^* is necessary unless ν^* has a Majorana mass.

Searches Particle Listings

Quark and Lepton Compositeness

2. Mirror type

$$[\nu_L^*], \quad \ell_L^*, \quad \begin{pmatrix} \nu^* \\ \ell^* \end{pmatrix}_R.$$

3. Homodoublet type

$$\begin{pmatrix} \nu^* \\ \ell^* \end{pmatrix}_L, \quad \begin{pmatrix} \nu^* \\ \ell^* \end{pmatrix}_R.$$

Similar classification can be made for excited quarks.

Excited fermions can be pair produced via their gauge couplings. The couplings of excited leptons with Z are listed in the following table (for notation see Eq. (1) in ‘‘Standard Model of Electroweak Interactions’’):

	Sequential type	Mirror type	Homodoublet type
V^{ℓ^*}	$-\frac{1}{2} + 2 \sin^2 \theta_W$	$-\frac{1}{2} + 2 \sin^2 \theta_W$	$-1 + 2 \sin^2 \theta_W$
A^{ℓ^*}	$-\frac{1}{2}$	$+\frac{1}{2}$	0
$V^{\nu_D^*}$	$+\frac{1}{2}$	$+\frac{1}{2}$	+1
$A^{\nu_D^*}$	$+\frac{1}{2}$	$-\frac{1}{2}$	0
$V^{\nu_M^*}$	0	0	—
$A^{\nu_M^*}$	+1	-1	—

Here ν_D^* (ν_M^*) stands for Dirac (Majorana) excited neutrino. The corresponding couplings of excited quarks can be easily obtained. Although form factor effects can be present for the gauge couplings at $q^2 \neq 0$, they are usually neglected.

In addition, transition magnetic type couplings with a gauge boson are expected. These couplings can be generally parameterized as follows:

$$\begin{aligned} \mathcal{L} = & \frac{\lambda_\gamma^{(f^*)}}{2m_{f^*}} \bar{f}^* \sigma^{\mu\nu} (\eta_L \frac{1-\gamma_5}{2} + \eta_R \frac{1+\gamma_5}{2}) f F_{\mu\nu} \\ & + \frac{\lambda_Z^{(f^*)}}{2m_{f^*}} \bar{f}^* \sigma^{\mu\nu} (\eta_L \frac{1-\gamma_5}{2} + \eta_R \frac{1+\gamma_5}{2}) f Z_{\mu\nu} \\ & + \frac{\lambda_W^{(\ell^*)}}{2m_{\ell^*}} g \bar{\ell}^* \sigma^{\mu\nu} \frac{1-\gamma_5}{2} \nu W_{\mu\nu} \\ & + \frac{\lambda_W^{(\nu^*)}}{2m_{\nu^*}} g \bar{\nu}^* \sigma^{\mu\nu} (\eta_L \frac{1-\gamma_5}{2} + \eta_R \frac{1+\gamma_5}{2}) \ell W_{\mu\nu}^\dagger \\ & + \text{h.c.}, \end{aligned} \quad (3)$$

where $g = e/\sin \theta_W$, $F_{\mu\nu} = \partial_\mu A_\nu - \partial_\nu A_\mu$ is the photon field strength, $Z_{\mu\nu} = \partial_\mu Z_\nu - \partial_\nu Z_\mu$, etc. The normalization of the coupling is chosen such that

$$\max(|\eta_L|, |\eta_R|) = 1.$$

Chirality conservation requires

$$\eta_L \eta_R = 0. \quad (4)$$

Some experimental analyses assume the relation $\eta_L = \eta_R = 1$, which violates chiral symmetry. We encode the results of such analyses if the crucial part of the cross section is proportional to the factor $\eta_L^2 + \eta_R^2$ and the limits can be reinterpreted as those for chirality conserving cases $(\eta_L, \eta_R) = (1, 0)$ or $(0, 1)$ after rescaling λ .

These couplings in Eq. (3) can arise from $SU(2) \times U(1)$ -invariant higher-dimensional interactions. A well-studied model is the interaction of homodoublet type ℓ^* with the Lagrangian [2,3]

$$\mathcal{L} = \frac{1}{2\Lambda} \bar{L}^* \sigma^{\mu\nu} (g f \frac{\tau_a}{2} W_{\mu\nu}^a + g' f' Y B_{\mu\nu}) \frac{1-\gamma_5}{2} L + \text{h.c.}, \quad (5)$$

where L denotes the lepton doublet (ν, ℓ) , Λ is the compositeness scale, g, g' are $SU(2)$ and $U(1)_Y$ gauge couplings, and $W_{\mu\nu}^a$ and $B_{\mu\nu}$ are the field strengths for $SU(2)$ and $U(1)_Y$ gauge fields. The same interaction occurs for mirror-type excited leptons. For sequential-type excited leptons, the ℓ^* and ν^* couplings become unrelated, and the couplings receive the extra suppression of $(250 \text{ GeV})/\Lambda$ or m_{L^*}/Λ . In any case, these couplings satisfy the relation

$$\lambda_W = -\sqrt{2} \sin^2 \theta_W (\lambda_Z \cot \theta_W + \lambda_\gamma). \quad (6)$$

Additional coupling with gluons is possible for excited quarks:

$$\begin{aligned} \mathcal{L} = & \frac{1}{2\Lambda} \bar{Q}^* \sigma^{\mu\nu} (g_s f_s \frac{\lambda_a}{2} G_{\mu\nu}^a + g f \frac{\tau_a}{2} W_{\mu\nu}^a + g' f' Y B_{\mu\nu}) \\ & \times \frac{1-\gamma_5}{2} Q + \text{h.c.}, \end{aligned} \quad (7)$$

where Q denotes a quark doublet, g_s is the QCD gauge coupling, and $G_{\mu\nu}^a$ the gluon field strength.

It should be noted that the electromagnetic radiative decay of ℓ^* (ν^*) is forbidden if $f = -f'$ ($f = f'$). These two possibilities ($f = f'$ and $f = -f'$) are investigated in many analyses of the LEP experiments above the Z pole.

Several different conventions are used by LEP experiments on Z pole to express the transition magnetic couplings. To facilitate comparison, we re-express these in terms of λ_Z and λ_γ using the following relations and taking $\sin^2 \theta_W = 0.23$. We assume chiral couplings, *i.e.*, $|c| = |d|$ in the notation of Ref. 2.

1. ALEPH (charged lepton and neutrino)

$$\lambda_Z^{\text{ALEPH}} = \frac{1}{2} \lambda_Z \quad (1990 \text{ papers}) \quad (8a)$$

$$\frac{2c}{\Lambda} = \frac{\lambda_Z}{m_{\ell^*} [\text{or } m_{\nu^*}]} \quad (\text{for } |c| = |d|) \quad (8b)$$

2. ALEPH (quark)

$$\lambda_u^{\text{ALEPH}} = \frac{\sin \theta_W \cos \theta_W}{\sqrt{\frac{1}{4} - \frac{2}{3} \sin^2 \theta_W + \frac{8}{9} \sin^4 \theta_W}} \lambda_Z = 1.11 \lambda_Z \quad (9)$$

3. L3 and DELPHI (charged lepton)

$$\lambda^{\text{L3}} = \lambda_Z^{\text{DELPHI}} = -\frac{\sqrt{2}}{\cot \theta_W - \tan \theta_W} \lambda_Z = -1.10 \lambda_Z \quad (10)$$

4. L3 (neutrino)

$$f_{\nu}^{L3} = \sqrt{2}\lambda_Z \quad (11)$$

5. OPAL (charged lepton)

$$\frac{f^{\text{OPAL}}}{\Lambda} = -\frac{2}{\cot\theta_W - \tan\theta_W} \frac{\lambda_Z}{m_{\ell^*}} = -1.56 \frac{\lambda_Z}{m_{\ell^*}} \quad (12)$$

6. OPAL (quark)

$$\frac{f^{\text{OPAL}c}}{\Lambda} = \frac{\lambda_Z}{2m_{q^*}} \quad (\text{for } |c| = |d|) \quad (13)$$

7. DELPHI (charged lepton)

$$\lambda_{\gamma}^{\text{DELPHI}} = -\frac{1}{\sqrt{2}} \lambda_{\gamma} \quad (14)$$

If leptons are made of color triplet and antitriplet constituents, we may expect their color-octet partners. Transitions between the octet leptons (ℓ_8) and the ordinary lepton (ℓ) may take place via the dimension-five interactions

$$\mathcal{L} = \frac{1}{2\Lambda} \sum_{\ell} \left\{ \bar{\ell}_8^{\alpha} g_S F_{\mu\nu}^{\alpha} \sigma^{\mu\nu} (\eta_L \ell_L + \eta_R \ell_R) + h.c. \right\} \quad (15)$$

where the summation is over charged leptons and neutrinos. The leptonic chiral invariance implies $\eta_L \eta_R = 0$ as before.

References

1. E.J. Eichten, K.D. Lane, and M.E. Peskin, Phys. Rev. Lett. **50**, 811 (1983).
2. K. Hagiwara, S. Komamiya, and D. Zeppenfeld, Z. Phys. **C29**, 115 (1985).
3. N. Cabibbo, L. Maiani, and Y. Srivastava, Phys. Lett. **139B**, 459 (1984).

SCALE LIMITS for Contact Interactions: $\Lambda(eeee)$

Limits are for Λ_{LL}^{\pm} only. For other cases, see each reference.

$\Lambda_{LL}^+(\text{TeV})$	$\Lambda_{LL}^-(\text{TeV})$	CL%	DOCUMENT ID	TECN	COMMENT
>8.3	>10.3	95	¹ BOURILKOV 01	RVUE	$E_{\text{cm}} = 192\text{--}208$ GeV
••• We do not use the following data for averages, fits, limits, etc. •••					
>4.5	>7.0	95	² SCHAEEL 07A	ALEP	$E_{\text{cm}} = 189\text{--}209$ GeV
>5.3	>6.8	95	ABDALLAH 06c	DLPH	$E_{\text{cm}} = 130\text{--}207$ GeV
>4.7	>6.1	95	³ ABBIENDI 04G	OPAL	$E_{\text{cm}} = 130\text{--}207$ GeV
>3.8	>5.6	95	ABBIENDI 00R	OPAL	$E_{\text{cm}} = 189$ GeV
>4.4	>5.4	95	ABREU 00s	DLPH	$E_{\text{cm}} = 183\text{--}189$ GeV
>4.3	>4.9	95	ACCIARRI 00P	L3	$E_{\text{cm}} = 130\text{--}189$ GeV
>3.5	>3.2	95	BARATE 00i	ALEP	Superseded by SCHAEEL 07A
>6.0	>7.7	95	⁴ BOURILKOV 00	RVUE	$E_{\text{cm}} = 183\text{--}189$ GeV
>3.1	>3.8	95	ABBIENDI 99	OPAL	$E_{\text{cm}} = 130\text{--}136, 161\text{--}172, 183$ GeV
>2.2	>2.8	95	ABREU 99A	DLPH	$E_{\text{cm}} = 130\text{--}172$ GeV
>2.7	>2.4	95	ACCIARRI 98J	L3	$E_{\text{cm}} = 130\text{--}172$ GeV
>3.0	>2.5	95	ACKERSTAFF 98V	OPAL	$E_{\text{cm}} = 130\text{--}172$ GeV

¹A combined analysis of the data from ALEPH, DELPHI, L3, and OPAL.

²SCHAEEL 07A limits are from $R_c, Q_{FB}^{\text{depl}}$, and hadronic cross section measurements.

³ABBIENDI 04G limits are from $e^+e^- \rightarrow e^+e^-$ cross section at $\sqrt{s} = 130\text{--}207$ GeV.

⁴A combined analysis of the data from ALEPH, L3, and OPAL.

SCALE LIMITS for Contact Interactions: $\Lambda(ee\mu\mu)$

Limits are for Λ_{LL}^{\pm} only. For other cases, see each reference.

$\Lambda_{LL}^+(\text{TeV})$	$\Lambda_{LL}^-(\text{TeV})$	CL%	DOCUMENT ID	TECN	COMMENT
>6.6	>9.5	95	⁵ SCHAEEL 07A	ALEP	$E_{\text{cm}} = 189\text{--}209$ GeV
>8.5	>3.8	95	ACCIARRI 00P	L3	$E_{\text{cm}} = 130\text{--}189$ GeV

••• We do not use the following data for averages, fits, limits, etc. •••

>7.3	>7.6	95	ABDALLAH 06c	DLPH	$E_{\text{cm}} = 130\text{--}207$ GeV
>8.1	>7.3	95	⁶ ABBIENDI 04G	OPAL	$E_{\text{cm}} = 130\text{--}207$ GeV
>7.3	>4.6	95	ABBIENDI 00R	OPAL	$E_{\text{cm}} = 189$ GeV
>6.6	>6.3	95	ABREU 00s	DLPH	$E_{\text{cm}} = 183\text{--}189$ GeV
>4.0	>4.7	95	BARATE 00i	ALEP	Superseded by SCHAEEL 07A
>4.5	>4.3	95	ABBIENDI 99	OPAL	$E_{\text{cm}} = 130\text{--}136, 161\text{--}172, 183$ GeV
>3.4	>2.7	95	ABREU 99A	DLPH	$E_{\text{cm}} = 130\text{--}172$ GeV
>3.6	>2.4	95	ACCIARRI 98J	L3	$E_{\text{cm}} = 130\text{--}172$ GeV
>2.9	>3.4	95	ACKERSTAFF 98V	OPAL	$E_{\text{cm}} = 130\text{--}172$ GeV
>3.1	>2.0	95	MIURA 98	VNS	$E_{\text{cm}} = 57.77$ GeV

⁵SCHAEEL 07A limits are from $R_c, Q_{FB}^{\text{depl}}$, and hadronic cross section measurements.

⁶ABBIENDI 04G limits are from $e^+e^- \rightarrow \mu\mu$ cross section at $\sqrt{s} = 130\text{--}207$ GeV.

SCALE LIMITS for Contact Interactions: $\Lambda(e\tau\tau)$

Limits are for Λ_{LL}^{\pm} only. For other cases, see each reference.

$\Lambda_{LL}^+(\text{TeV})$	$\Lambda_{LL}^-(\text{TeV})$	CL%	DOCUMENT ID	TECN	COMMENT
>7.9	>5.8	95	⁷ SCHAEEL 07A	ALEP	$E_{\text{cm}} = 189\text{--}209$ GeV
>7.9	>4.6	95	ABDALLAH 06c	DLPH	$E_{\text{cm}} = 130\text{--}207$ GeV
>4.9	>7.2	95	⁸ ABBIENDI 04G	OPAL	$E_{\text{cm}} = 130\text{--}207$ GeV
••• We do not use the following data for averages, fits, limits, etc. •••					
>3.9	>6.5	95	ABBIENDI 00R	OPAL	$E_{\text{cm}} = 189$ GeV
>5.2	>5.4	95	ABREU 00s	DLPH	$E_{\text{cm}} = 183\text{--}189$ GeV
>5.4	>4.7	95	ACCIARRI 00P	L3	$E_{\text{cm}} = 130\text{--}189$ GeV
>3.9	>3.7	95	BARATE 00i	ALEP	Superseded by SCHAEEL 07A
>3.8	>4.0	95	ABBIENDI 99	OPAL	$E_{\text{cm}} = 130\text{--}136, 161\text{--}172, 183$ GeV
>2.8	>2.6	95	ABREU 99A	DLPH	$E_{\text{cm}} = 130\text{--}172$ GeV
>2.4	>2.8	95	ACCIARRI 98J	L3	$E_{\text{cm}} = 130\text{--}172$ GeV
>2.3	>3.7	95	ACKERSTAFF 98V	OPAL	$E_{\text{cm}} = 130\text{--}172$ GeV

⁷SCHAEEL 07A limits are from $R_c, Q_{FB}^{\text{depl}}$, and hadronic cross section measurements.

⁸ABBIENDI 04G limits are from $e^+e^- \rightarrow \tau\tau$ cross section at $\sqrt{s} = 130\text{--}207$ GeV.

SCALE LIMITS for Contact Interactions: $\Lambda(\ell\ell\ell\ell)$

Lepton universality assumed. Limits are for Λ_{LL}^{\pm} only. For other cases, see each reference.

$\Lambda_{LL}^+(\text{TeV})$	$\Lambda_{LL}^-(\text{TeV})$	CL%	DOCUMENT ID	TECN	COMMENT
>7.9	>10.3	95	⁹ SCHAEEL 07A	ALEP	$E_{\text{cm}} = 189\text{--}209$ GeV
>9.1	>8.2	95	ABDALLAH 06c	DLPH	$E_{\text{cm}} = 130\text{--}207$ GeV
••• We do not use the following data for averages, fits, limits, etc. •••					
>7.7	>9.5	95	¹⁰ ABBIENDI 04G	OPAL	$E_{\text{cm}} = 130\text{--}207$ GeV
			¹¹ BABICH 03	RVUE	
>6.4	>7.2	95	ABBIENDI 00R	OPAL	$E_{\text{cm}} = 189$ GeV
>7.3	>7.8	95	ABREU 00s	DLPH	$E_{\text{cm}} = 183\text{--}189$ GeV
>9.0	>5.2	95	ACCIARRI 00P	L3	$E_{\text{cm}} = 130\text{--}189$ GeV
>5.3	>5.5	95	BARATE 00i	ALEP	Superseded by SCHAEEL 07A
>5.2	>5.3	95	ABBIENDI 99	OPAL	$E_{\text{cm}} = 130\text{--}136, 161\text{--}172, 183$ GeV
>4.4	>4.2	95	ABREU 99A	DLPH	$E_{\text{cm}} = 130\text{--}172$ GeV
>4.0	>3.1	95	¹² ACCIARRI 98J	L3	$E_{\text{cm}} = 130\text{--}172$ GeV
>3.4	>4.4	95	ACKERSTAFF 98V	OPAL	$E_{\text{cm}} = 130\text{--}172$ GeV

⁹SCHAEEL 07A limits are from $R_c, Q_{FB}^{\text{depl}}$, and hadronic cross section measurements.

¹⁰ABBIENDI 04G limits are from $e^+e^- \rightarrow \ell^+\ell^-$ cross section at $\sqrt{s} = 130\text{--}207$ GeV.

¹¹BABICH 03 obtain a bound $-0.175 \text{ TeV}^{-2} < 1/\Lambda_{LL}^2 < 0.095 \text{ TeV}^{-2}$ (95%CL) in a model independent analysis allowing all of $\Lambda_{LL}, \Lambda_{LR}, \Lambda_{RL}, \Lambda_{RR}$ to coexist.

¹²From $e^+e^- \rightarrow e^+e^-, \mu^+\mu^-,$ and $\tau^+\tau^-$.

SCALE LIMITS for Contact Interactions: $\Lambda(eqqq)$

Limits are for Λ_{LL}^{\pm} only. For other cases, see each reference.

$\Lambda_{LL}^+(\text{TeV})$	$\Lambda_{LL}^-(\text{TeV})$	CL%	DOCUMENT ID	TECN	COMMENT
> 8.4	>10.2	95	¹³ ABDALLAH 09	DLPH	($eebb$)
> 9.4	>5.6	95	¹⁴ SCHAEEL 07A	ALEP	($eecc$)
> 9.4	>4.9	95	¹³ SCHAEEL 07A	ALEP	($eebb$)
>23.3	>12.5	95	¹⁵ CHEUNG 01B	RVUE	($eeuu$)
>11.1	>26.4	95	¹⁵ CHEUNG 01B	RVUE	($eedd$)
••• We do not use the following data for averages, fits, limits, etc. •••					
>12.9	>7.2	95	¹⁶ SCHAEEL 07A	ALEP	($eeqq$)
> 3.7	>5.9	95	¹⁷ ABULENCIA 06L	CDF	($eeqq$)
> 8.2	>3.7	95	¹⁸ ABBIENDI 04G	OPAL	($eeqq$)
> 5.9	>9.1	95	¹⁸ ABBIENDI 04G	OPAL	($eeuu$)
> 8.6	>5.5	95	¹⁸ ABBIENDI 04G	OPAL	($eedd$)
> 2.7	>1.7	95	CHEKANOV 04B	ZEUS	($eeqq$)
> 2.8	>1.6	95	¹⁹ ADLOFF 03	H1	($eeqq$)
> 2.7	>2.7	95	²⁰ ACHARD 02J	L3	($ee\tau c$)
> 5.5	>3.1	95	²¹ ABBIENDI 00R	OPAL	($eeqq$)
> 4.9	>6.1	95	²¹ ABBIENDI 00R	OPAL	($eeuu$)
> 5.7	>4.5	95	²¹ ABBIENDI 00R	OPAL	($eedd$)
> 4.2	>2.8	95	²² ACCIARRI 00P	L3	($eeqq$)

Searches Particle Listings

Quark and Lepton Compositeness

> 2.4	>1.3	95	23	ADLOFF	00	H1	($eeqq$)
> 5.4	>6.2	95	24	BARATE	00i	ALEP	Superseded by SCHAEEL 07A
> 5.6	>4.9	95	25	BARATE	00i	ALEP	Superseded by SCHAEEL 07A
			26	BREITWEG	00b	ZEUS	
> 4.4	>2.8	95	27	ABBIENDI	99	OPAL	($eeqq$)
> 4.0	>4.8	95	28	ABBIENDI	99	OPAL	($eebb$)
> 3.3	>4.2	95	29	ABBOTT	99d	D0	($eeqq$)
> 2.4	>2.8	95	30	ABREU	99A	DLPH	($eeqq$) (d or s quark)
> 4.4	>3.9	95	30	ABREU	99A	DLPH	($eebb$)
> 1.0	>2.4	95	30	ABREU	99A	DLPH	($eeuu$)
> 1.0	>2.1	95	30	ABREU	99A	DLPH	($eecc$)
> 4.0	>3.4	95	31	ZARNECKI	99	RVUE	($eedd$)
> 4.3	>5.6	95	31	ZARNECKI	99	RVUE	($eeuu$)
> 3.0	>2.1	95	32	ACCIARRI	98j	L3	($eeqq$)
> 3.4	>2.2	95	33	ACKERSTAFF	98v	OPAL	($eeqq$)
> 4.0	>2.8	95	34	ACKERSTAFF	98v	OPAL	($eebb$)
> 9.3	>12.0	95	35	BARGER	98E	RVUE	($eeuu$)
> 8.8	>11.9	95	35	BARGER	98E	RVUE	($eedd$)

¹³ ABDALLAH 09 and SCHAEEL 07A limits are from R_b , A_{FB}^b .

¹⁴ SCHAEEL 07A limits are from R_c , Q_{FB}^{depl} , and hadronic cross section measurements.

¹⁵ CHEUNG 01B is an update of BARGER 98E.

¹⁶ SCHAEEL 07A limit assumes quark flavor universality of the contact interactions.

¹⁷ ABULENCIA 06L limits are from $p\bar{p}$ collisions at $\sqrt{s} = 1.96$ TeV.

¹⁸ ABBIENDI 04G limits are from $e^+e^- \rightarrow q\bar{q}$ cross section at $\sqrt{s} = 130$ –207 GeV.

¹⁹ ADLOFF 03 limits are from the $d\sigma/dQ^2$ measurement of $e^\pm p \rightarrow e^\pm X$.

²⁰ ACHARD 02i limit is from the bound on the $e^+e^- \rightarrow t\bar{t}$ cross section. $\Lambda_{LL} = \Lambda_{LR} = \Lambda_{RR}$ and $m_t = 175$ GeV are assumed.

²¹ ABBIENDI 00R limits are from $e^+e^- \rightarrow q\bar{q}$ cross section at $\sqrt{s} = 130$ –189 GeV.

²² ACCIARRI 00P limit is from $e^+e^- \rightarrow q\bar{q}$ cross section at $\sqrt{s} = 130$ –189 GeV.

²³ ADLOFF 00 limits are from the Q^2 spectrum measurement of $e^+p \rightarrow e^+X$.

²⁴ BARATE 00i limits are from $e^+e^- \rightarrow q\bar{q}$ cross section and jet-charge asymmetry at 130–183 GeV.

²⁵ BARATE 00i limits are from R_b and jet-charge asymmetry at 130–183 GeV.

²⁶ BREITWEG 00B limits are from Q^2 spectrum measurement of e^+p collisions. See their Table 3 for the limits of various models.

²⁷ ABBIENDI 99 limits are from $e^+e^- \rightarrow q\bar{q}$ cross section at 130–136, 161–172, 183 GeV.

²⁸ ABBIENDI 99 limits are from R_b at 130–136, 161–172, 183 GeV.

²⁹ ABBOTT 99d limits are from e^+e^- mass distribution in $p\bar{p} \rightarrow e^+e^-X$ at $E_{cm} = 1.8$ TeV.

³⁰ ABREU 99A limits are from flavor-tagged $e^+e^- \rightarrow q\bar{q}$ cross section at 130–172 GeV.

³¹ ZARNECKI 99 use data from HERA, LEP, Tevatron, and various low-energy experiments.

³² ACCIARRI 98j limits are from $e^+e^- \rightarrow q\bar{q}$ cross section at $E_{cm} = 130$ –172 GeV.

³³ ACKERSTAFF 98v limits are from $e^+e^- \rightarrow q\bar{q}$ at $E_{cm} = 130$ –172 GeV.

³⁴ ACKERSTAFF 98v limits are from R_b measurements at $E_{cm} = 130$ –172 GeV.

³⁵ BARGER 98E use data from HERA, LEP, Tevatron, and various low-energy experiments.

SCALE LIMITS for Contact Interactions: $\Lambda(\mu\mu qq)$

$\Lambda_{LL}^+(\text{TeV})$	$\Lambda_{LL}^-(\text{TeV})$	CL%	DOCUMENT ID	TECN	COMMENT
> 2.9	> 4.2	95	36	ABE	97T CDF ($\mu\mu qq$) (isosinglet)
••• We do not use the following data for averages, fits, limits, etc. •••					
> 1.4	> 1.6	95	ABE	92B CDF ($\mu\mu qq$) (isosinglet)	
³⁶ ABE 97T limits are from $\mu^+\mu^-$ mass distribution in $p\bar{p} \rightarrow \mu^+\mu^-X$ at $E_{cm} = 1.8$ TeV.					

SCALE LIMITS for Contact Interactions: $\Lambda(\ell\nu\ell\nu)$

VALUE (TeV)	CL%	DOCUMENT ID	TECN	COMMENT
> 3.10	90	37	JODIDIO	86 SPEC $\Lambda_{LR}^\pm(\nu_\mu\nu_e\mu e)$
••• We do not use the following data for averages, fits, limits, etc. •••				
> 3.8		38	DIAZCRUZ	94 RVUE $\Lambda_{LL}^+(\tau\nu_\tau e\nu_e)$
> 8.1		38	DIAZCRUZ	94 RVUE $\Lambda_{LL}^-(\tau\nu_\tau e\nu_e)$
> 4.1		39	DIAZCRUZ	94 RVUE $\Lambda_{LL}^+(\tau\nu_\tau\mu\nu_\mu)$
> 6.5		39	DIAZCRUZ	94 RVUE $\Lambda_{LL}^-(\tau\nu_\tau\mu\nu_\mu)$
³⁷ JODIDIO 86 limit is from $\mu^+ \rightarrow \bar{\nu}_\mu e^+ \nu_e$. Chirality invariant interactions $L = (g^2/\Lambda^2)$ [$\eta_{LL}(\bar{\nu}_\mu L \gamma^\alpha \mu_L)(\bar{e} L \gamma^\alpha \nu_e L) + \eta_{LR}(\bar{\nu}_\mu L \gamma^\alpha \nu_e L)(\bar{e} R \gamma^\alpha \mu_R)$] with $g^2/4\pi = 1$ and $(\eta_{LL}, \eta_{LR}) = (0, \pm 1)$ are taken. No limits are given for Λ_{LL}^\pm with $(\eta_{LL}, \eta_{LR}) = (\pm 1, 0)$. For more general constraints with right-handed neutrinos and chirality nonconserving contact interactions, see their text.				
³⁸ DIAZCRUZ 94 limits are from $\Gamma(\tau \rightarrow e\nu\nu)$ and assume flavor-dependent contact interactions with $\Lambda(\tau\nu_\tau e\nu_e) \ll \Lambda(\mu\nu_\mu e\nu_e)$.				
³⁹ DIAZCRUZ 94 limits are from $\Gamma(\tau \rightarrow \mu\nu\nu)$ and assume flavor-dependent contact interactions with $\Lambda(\tau\nu_\tau\mu\nu_\mu) \ll \Lambda(\mu\nu_\mu e\nu_e)$.				

SCALE LIMITS for Contact Interactions: $\Lambda(e\nu qq)$

VALUE (TeV)	CL%	DOCUMENT ID	TECN
> 2.81	95	40	AFFOLDER 01i CDF

⁴⁰ AFFOLDER 00i bound is for a scalar interaction $\bar{q}_R q_L \bar{\nu}_e \ell_L$.

SCALE LIMITS for Contact Interactions: $\Lambda(qqqq)$

Limits are for Λ_{LL}^\pm with color-singlet isoscalar exchanges among u_L 's and d_L 's only, unless otherwise noted. See EICHTEN 84 for details.

VALUE (TeV)	CL%	DOCUMENT ID	TECN	COMMENT
> 2.96	95	41	ABAZOV	09AE D0 $p\bar{p} \rightarrow$ dijet, angl. Λ_{LL}^+
••• We do not use the following data for averages, fits, limits, etc. •••				
> 2.0	95	42	ABBOTT	00E D0 H_T distribution; Λ_{LL}^+
> 2.7	95	43	ABBOTT	99C D0 $p\bar{p} \rightarrow$ dijet mass. Λ_{LL}^+
> 2.1	95	44	ABBOTT	98G D0 $p\bar{p} \rightarrow$ dijet angl. Λ_{LL}^+
		45	BERTRAM	98 RVUE $p\bar{p} \rightarrow$ dijet mass

⁴¹ ABAZOV 09AE also obtain $\Lambda_{LL}^- > 2.96$ TeV.

⁴² The quoted limit for ABBOTT 00E is from H_T distribution in $p\bar{p}$ collisions at $E_{cm} = 1.8$ TeV. CTEQ4M PDF and $\mu = E_T^{\text{max}}$ are assumed. For limits with different assumptions, see their Tables 2 and 3. All quarks are assumed composite.

⁴³ The quoted limit is from inclusive dijet mass spectrum in $p\bar{p}$ collisions at $E_{cm} = 1.8$ TeV. ABBOTT 99C also obtain $\Lambda_{LL}^- > 2.4$ TeV. All quarks are assumed composite.

⁴⁴ ABBOTT 98G limit is from dijet angular distribution in $p\bar{p}$ collisions at $E_{cm} = 1.8$ TeV. All quarks are assumed composite.

⁴⁵ BERTRAM 98 obtain limit on the scale of color-octet axial-vector flavor-universal contact interactions: $\Lambda_{A8} > 2.1$ TeV. They also obtain a limit $\Lambda_{V8} > 2.4$ TeV on a color-octet flavor-universal vectorial contact interaction.

SCALE LIMITS for Contact Interactions: $\Lambda(\nu\nu qq)$

Limits are for Λ_{LL}^\pm only. For other cases, see each reference.

$\Lambda_{LL}^+(\text{TeV})$	$\Lambda_{LL}^-(\text{TeV})$	CL%	DOCUMENT ID	TECN	COMMENT
> 5.0	> 5.4	95	46	MCFARLAND 98	CCFR νN scattering

⁴⁶ MCFARLAND 98 assumed a flavor universal interaction. Neutrinos were mostly of muon type.

MASS LIMITS for Excited $e(e^*)$

Most e^+e^- experiments assume one-photon or Z exchange. The limits from some e^+e^- experiments which depend on λ have assumed transition couplings which are chirality violating ($\eta_L = \eta_R$). However they can be interpreted as limits for chirality-conserving interactions after multiplying the coupling value λ by $\sqrt{2}$; see Note.

Excited leptons have the same quantum numbers as other ortholeptons. See also the searches for ortholeptons in the "Searches for Heavy Leptons" section.

Limits for Excited $e(e^*)$ from Pair Production

These limits are obtained from $e^+e^- \rightarrow e^+e^*e^-$ and thus rely only on the (electroweak) charge of e^* . Form factor effects are ignored unless noted. For the case of limits from Z decay, the e^* coupling is assumed to be of sequential type. Possible t -channel contribution from transition magnetic coupling is neglected. All limits assume a dominant $e^* \rightarrow e\gamma$ decay except the limits from $\Gamma(Z)$.

For limits prior to 1987, see our 1992 edition (Physical Review **D45** S1 (1992)).

VALUE (GeV)	CL%	DOCUMENT ID	TECN	COMMENT
> 103.2	95	47	ABBIENDI	02G OPAL $e^+e^- \rightarrow e^*e^*$ Homodoublet type
••• We do not use the following data for averages, fits, limits, etc. •••				
> 102.8	95	48	ACHARD	03B L3 $e^+e^- \rightarrow e^*e^*$ Homodoublet type
> 100.0	95	49	ACCIARRI	01D L3 $e^+e^- \rightarrow e^*e^*$ Homodoublet type
> 91.3	95	50	ABBIENDI	00i OPAL $e^+e^- \rightarrow e^*e^*$ Homodoublet type
> 94.2	95	51	ACCIARRI	00E L3 $e^+e^- \rightarrow e^*e^*$ Homodoublet type
> 90.7	95	52	ABREU	99o DLPH Homodoublet type
> 85.0	95	53	ACKERSTAFF	98C OPAL $e^+e^- \rightarrow e^*e^*$ Homodoublet type
		54	BARATE	98U ALEP $Z \rightarrow e^*e^*$
> 79.6	95	55,56	ABREU	97B DLPH $e^+e^- \rightarrow e^*e^*$ Homodoublet type
> 77.9	95	55,57	ABREU	97B DLPH $e^+e^- \rightarrow e^*e^*$ Sequential type
> 79.7	95	55	ACCIARRI	97G L3 $e^+e^- \rightarrow e^*e^*$ Sequential type

⁴⁷ From e^+e^- collisions at $\sqrt{s} = 183$ –209 GeV. $f = f'$ is assumed.

⁴⁸ From e^+e^- collisions at $\sqrt{s} = 189$ –209 GeV. $f = f'$ is assumed. ACHARD 03B also obtain limit for $f = -f'$: $m_{e^*} > 96.6$ GeV.

⁴⁹ From e^+e^- collisions at $\sqrt{s} = 192$ –202 GeV. $f = f'$ is assumed. ACCIARRI 01D also obtain limit for $f = -f'$: $m_{e^*} > 93.4$ GeV.

⁵⁰ From e^+e^- collisions at $\sqrt{s} = 161$ –183 GeV. $f = f'$ is assumed. ABBIENDI 00i also obtain limit for $f = -f'$ ($e^* \rightarrow \nu W$): $m_{e^*} > 86.0$ GeV.

⁵¹ From e^+e^- collisions at $\sqrt{s} = 189$ GeV. $f = f'$ is assumed. ACCIARRI 00E also obtain limit for $f = -f'$ ($e^* \rightarrow \nu W$): $m_{e^*} > 92.6$ GeV.

⁵² From e^+e^- collisions at $\sqrt{s} = 183$ GeV. $f = f'$ is assumed. ABREU 99o also obtain limit for $f = -f'$ ($e^* \rightarrow \nu W$): $m_{e^*} > 81.3$ GeV.

⁵³ From e^+e^- collisions at $\sqrt{s} = 170$ –172 GeV. ACKERSTAFF 98C also obtain limit from $e^* \rightarrow \nu W$ decay mode: $m_{e^*} > 81.3$ GeV.

See key on page 405

Searches Particle Listings Quark and Lepton Compositeness

⁵⁴ BARATE 98U obtain limits on the form factor. See their Fig. 14 for limits in mass-form factor plane.

⁵⁵ From e^+e^- collisions at $\sqrt{s}=161$ GeV.

⁵⁶ ABREU 97B also obtain limit from charged current decay mode $e^* \rightarrow \nu W$, $m_{e^*} > 70.9$ GeV.

⁵⁷ ABREU 97B also obtain limit from charged current decay mode $e^* \rightarrow \nu W$, $m_{e^*} > 44.6$ GeV.

Limits for Excited e (e^*) from Single Production

These limits are from $e^+e^- \rightarrow e^*e$, $W \rightarrow e^*\nu$, or $ep \rightarrow e^*X$ and depend on transition magnetic coupling between e and e^* . All limits assume $e^* \rightarrow e\gamma$ decay except as noted. Limits from LEP, UA2, and H1 are for chiral coupling, whereas all other limits are for nonchiral coupling, $\eta_L = \eta_R = 1$. In most papers, the limit is expressed in the form of an excluded region in the $\lambda-m_{e^*}$ plane. See the original papers.

For limits prior to 1987, see our 1992 edition (Physical Review **D45** S1 (1992)).

VALUE (GeV)	CL%	DOCUMENT ID	TECN	COMMENT
>272	95	⁵⁸ AARON 08A	H1	$ep \rightarrow e^*X$
• • • We do not use the following data for averages, fits, limits, etc. • • •				
>209	95	⁵⁹ ABAZOV 08H	D0	$p\bar{p} \rightarrow e^*e$
>206	95	⁶⁰ ACOSTA 05B	CDF	$p\bar{p} \rightarrow e^*X$
>208	95	⁶¹ ACHARD 03B	L3	$e^+e^- \rightarrow ee^*$
>205	95	⁶² ABBIENDI 02G	OPAL	$e^+e^- \rightarrow ee^*$
>255	95	⁶³ ADLOFF 02B	H1	$ep \rightarrow e^*X$
>228	95	⁶⁴ CHEKANOV 02D	ZEUS	$ep \rightarrow e^*X$
>202		⁶⁵ ACCIARRI 01D	L3	$e^+e^- \rightarrow ee^*$
		⁶⁶ ABBIENDI 00I	OPAL	$e^+e^- \rightarrow ee^*$
		⁶⁷ ACCIARRI 00E	L3	$e^+e^- \rightarrow ee^*$
>223	95	⁶⁸ ADLOFF 00E	H1	$ep \rightarrow e^*X$
		⁶⁹ ABREU 99O	DLPH	$e^+e^- \rightarrow ee^*$
none 20–170	95	⁷⁰ ACCIARRI 98T	L3	$e\gamma \rightarrow e^* \rightarrow e\gamma$
		⁷¹ ACKERSTAFF 98C	OPAL	$e^+e^- \rightarrow ee^*$
		⁷² BARATE 98U	ALEP	$e^+e^- \rightarrow ee^*$
		^{73,74} ABREU 97B	DLPH	$e^+e^- \rightarrow ee^*$
		^{73,75} ACCIARRI 97G	L3	$e^+e^- \rightarrow ee^*$
		⁷⁶ ACKERSTAFF 97	OPAL	$e^+e^- \rightarrow ee^*$
		⁷⁷ ADLOFF 97	H1	Lepton-flavor violation
none 30–200	95	⁷⁸ BREITWEG 97C	ZEUS	$ep \rightarrow e^*X$

⁵⁸ AARON 08A search for single e^* production in ep collisions with the decays $e^* \rightarrow e\gamma$, eZ , νW . The quoted limit assumes $f = f' = \Lambda/m_{e^*}$. See their Fig. 3 and Fig. 4 for the exclusion plots in the mass-coupling plane.

⁵⁹ ABAZOV 08H search for single e^* production in $p\bar{p}$ collisions with the decays $e^* \rightarrow e\gamma$. The e^* production is assumed to be described by an effective four-fermion interaction. See their Fig. 5 for the exclusion plot in the mass-coupling plane.

⁶⁰ ACOSTA 05B search for single e^* production in $p\bar{p}$ collisions with the decays $e^* \rightarrow e\gamma$. $f = f' = \Lambda/m_{e^*}$ is assumed for the e^* coupling. See their Fig. 3 for the exclusion limit in the mass-coupling plane.

⁶¹ ACHARD 03B result is from e^+e^- collisions at $\sqrt{s} = 189$ –209 GeV. See their Fig. 4 for the exclusion plot in the mass-coupling plane.

⁶² ABBIENDI 02G result is from e^+e^- collisions at $\sqrt{s} = 183$ –209 GeV. $f = f' = \Lambda/m_{e^*}$ is assumed for e^* coupling. See their Fig. 4c for the exclusion limit in the mass-coupling plane.

⁶³ ADLOFF 02B search for single e^* production in ep collisions with the decays $e^* \rightarrow e\gamma$, eZ , νW . $f = f' = \Lambda/m_{e^*}$ is assumed for the e^* coupling. See their Fig. 3 for the exclusion plot in the mass-coupling plane.

⁶⁴ CHEKANOV 02D search for single e^* production in ep collisions with the decays $e^* \rightarrow e\gamma$, eZ , νW . $f = f' = \Lambda/m_{e^*}$ is assumed for the e^* coupling. See their Fig. 5a for the exclusion plot in the mass-coupling plane.

⁶⁵ ACCIARRI 01D result is from e^+e^- collisions at $\sqrt{s} = 192$ –202 GeV. $f = f' = \Lambda/m_{e^*}$ is assumed for the e^* coupling. See their Fig. 4 for limits in the mass-coupling plane.

⁶⁶ ABBIENDI 00I result is from e^+e^- collisions at $\sqrt{s} = 161$ –183 GeV. See their Fig. 7 for limits in mass-coupling plane.

⁶⁷ ACCIARRI 00E result is from e^+e^- collisions at $\sqrt{s} = 189$ GeV. See their Fig. 3 for limits in mass-coupling plane.

⁶⁸ ADLOFF 00E search for single e^* production in ep collisions with the decays $e^* \rightarrow e\gamma$, eZ , νW . $f = f' = \Lambda/m_{e^*}$ is assumed for the e^* coupling. See their Fig. 9 for the exclusion plot in the mass-coupling plane.

⁶⁹ ABREU 99O result is from e^+e^- collisions at $\sqrt{s} = 183$ GeV. See their Figs. 4 and 5 for the exclusion limit in the mass-coupling plane.

⁷⁰ ACCIARRI 98T search for single e^* production in quasi-real Compton scattering. The limit is for $|\lambda| > 1.0 \times 10^{-1}$ and non-chiral coupling of e^* . See their Fig. 7 for the exclusion plot in the mass-coupling plane.

⁷¹ ACKERSTAFF 98C from e^+e^- collisions at $\sqrt{s} = 170$ –172 GeV. See their Fig. 11 for the exclusion limit in the mass-coupling plane.

⁷² BARATE 98U is from e^+e^- collision at $\sqrt{s} = M_Z$. See their Fig. 12 for limits in mass-coupling plane.

⁷³ From e^+e^- collisions at $\sqrt{s} = 161$ GeV.

⁷⁴ See Fig. 4a and Fig. 5a of ABREU 97B for the exclusion limit in the mass-coupling plane.

⁷⁵ See Fig. 2 and Fig. 3 of ACCIARRI 97G for the exclusion limit in the mass-coupling plane.

⁷⁶ ACKERSTAFF 97 result is from e^+e^- collisions at $\sqrt{s} = 161$ GeV. See their Fig. 3 for the exclusion limit in the mass-coupling plane.

⁷⁷ ADLOFF 97 search for single e^* production in ep collisions with the decays $e^* \rightarrow e\gamma$, eZ , νW . See their Fig. 4 for the rejection limits on the product of the production cross section and the branching ratio into a specific decay channel.

⁷⁸ BREITWEG 97C search for single e^* production in ep collisions with the decays $e^* \rightarrow e\gamma$, eZ , νW . $f = f' = 2\Lambda/m_{e^*}$ is assumed for the e^* coupling. See their Fig. 9 for the exclusion plot in the mass-coupling plane.

Limits for Excited e (e^*) from $e^+e^- \rightarrow \gamma\gamma$

These limits are derived from indirect effects due to e^* exchange in the t channel and depend on transition magnetic coupling between e and e^* . All limits are for $\lambda_\gamma = 1$. All limits except ABE 89J and ACHARD 02D are for nonchiral coupling with $\eta_L = \eta_R = 1$. We choose the chiral coupling limit as the best limit and list it in the Summary Table.

For limits prior to 1987, see our 1992 edition (Physical Review **D45** S1 (1992)).

VALUE (GeV)	CL%	DOCUMENT ID	TECN	COMMENT
>310	95	ACHARD 02D	L3	$\sqrt{s} = 192$ –209 GeV
• • • We do not use the following data for averages, fits, limits, etc. • • •				
>356	95	⁷⁹ ABDALLAH 04N	DLPH	$\sqrt{s} = 161$ –208 GeV
>311	95	ABREU 00A	DLPH	$\sqrt{s} = 189$ –202 GeV
>283	95	⁸⁰ ACCIARRI 00G	L3	$\sqrt{s} = 183$ –189 GeV
>306	95	ABBIENDI 99P	OPAL	$\sqrt{s} = 189$ GeV
>231	95	ABREU 98J	DLPH	$\sqrt{s} = 130$ –183 GeV
>194	95	ACKERSTAFF 98	OPAL	$\sqrt{s} = 130$ –172 GeV
>227	95	ACKERSTAFF 98B	OPAL	$\sqrt{s} = 183$ GeV
>250	95	BARATE 98J	ALEP	$\sqrt{s} = 183$ GeV
>160	95	⁸¹ BARATE 98U	ALEP	

⁷⁹ ABDALLAH 04N also obtain a limit on the excited electron mass with e^* chiral coupling, $m_{e^*} > 295$ GeV at 95% CL.

⁸⁰ ACCIARRI 00G also obtain a limit on e^* with chiral coupling, $m_{e^*} > 213$ GeV.

⁸¹ BARATE 98U is from e^+e^- collision at $\sqrt{s} = M_Z$. See their Fig. 5 for limits in mass-coupling plane.

Indirect Limits for Excited e (e^*)

These limits make use of loop effects involving e^* and are therefore subject to theoretical uncertainty.

VALUE (GeV)	DOCUMENT ID	TECN	COMMENT
• • • We do not use the following data for averages, fits, limits, etc. • • •			
	⁸² DORENBOSCH 89	CHRM	$\bar{\nu}_\mu e \rightarrow \bar{\nu}_\mu e$ and $\nu_\mu e \rightarrow \nu_\mu e$
	⁸³ GRIFOLS 86	THEO	$\nu_\mu e \rightarrow \nu_\mu e$
	⁸⁴ RENARD 82	THEO	$g=2$ of electron

⁸² DORENBOSCH 89 obtain the limit $\lambda_\gamma^2 \Lambda_{\text{cut}}^2 / m_{e^*}^2 < 2.6$ (95% CL), where Λ_{cut} is the cutoff scale, based on the one-loop calculation by GRIFOLS 86. If one assumes that $\Lambda_{\text{cut}} = 1$ TeV and $\lambda_\gamma = 1$, one obtains $m_{e^*} > 620$ GeV. However, one generally expects $\lambda_\gamma \approx m_{e^*} / \Lambda_{\text{cut}}$ in composite models.

⁸³ GRIFOLS 86 uses $\nu_\mu e \rightarrow \nu_\mu e$ and $\bar{\nu}_\mu e \rightarrow \bar{\nu}_\mu e$ data from CHARM Collaboration to derive mass limits which depend on the scale of compositeness.

⁸⁴ RENARD 82 derived from $g=2$ data limits on mass and couplings of e^* and μ^* . See figures 2 and 3 of the paper.

MASS LIMITS FOR EXCITED μ (μ^*)

Limits for Excited μ (μ^*) from Pair Production

These limits are obtained from $e^+e^- \rightarrow \mu^+\mu^*$ and thus rely only on the (electroweak) charge of μ^* . Form factor effects are ignored unless noted. For the case of limits from Z decay, the μ^* coupling is assumed to be of sequential type. All limits assume a dominant $\mu^* \rightarrow \mu\gamma$ decay except the limits from $\Gamma(Z)$.

For limits prior to 1987, see our 1992 edition (Physical Review **D45** S1 (1992)).

VALUE (GeV)	CL%	DOCUMENT ID	TECN	COMMENT
>103.2	95	⁸⁵ ABBIENDI 02G	OPAL	$e^+e^- \rightarrow \mu^*\mu^*$ Homodoublet type
• • • We do not use the following data for averages, fits, limits, etc. • • •				
>102.8	95	⁸⁶ ACHARD 03B	L3	$e^+e^- \rightarrow \mu^*\mu^*$ Homodoublet type
>100.2	95	⁸⁷ ACCIARRI 01D	L3	$e^+e^- \rightarrow \mu^*\mu^*$ Homodoublet type
> 91.3	95	⁸⁸ ABBIENDI 00I	OPAL	$e^+e^- \rightarrow \mu^*\mu^*$ Homodoublet type
> 94.2	95	⁸⁹ ACCIARRI 00E	L3	$e^+e^- \rightarrow \mu^*\mu^*$ Homodoublet type
> 90.7	95	⁹⁰ ABREU 99O	DLPH	Homodoublet type
> 85.3	95	⁹¹ ACKERSTAFF 98C	OPAL	$e^+e^- \rightarrow \mu^*\mu^*$ Homodoublet type
		⁹² BARATE 98U	ALEP	$Z \rightarrow \mu^*\mu^*$
> 79.6	95	^{93,94} ABREU 97B	DLPH	$e^+e^- \rightarrow \mu^*\mu^*$ Homodoublet type
> 78.4	95	^{93,95} ABREU 97B	DLPH	$e^+e^- \rightarrow \mu^*\mu^*$ Sequential type
> 79.9	95	⁹³ ACCIARRI 97G	L3	$e^+e^- \rightarrow \mu^*\mu^*$ Sequential type

⁸⁵ From e^+e^- collisions at $\sqrt{s} = 183$ –209 GeV. $f = f'$ is assumed.

⁸⁶ From e^+e^- collisions at $\sqrt{s} = 189$ –209 GeV. $f = f'$ is assumed. ACHARD 03B also obtain limit for $f = -f'$: $m_{\mu^*} > 96.6$ GeV.

⁸⁷ From e^+e^- collisions at $\sqrt{s} = 192$ –202 GeV. $f = f'$ is assumed. ACCIARRI 01D also obtain limit for $f = -f'$: $m_{\mu^*} > 93.4$ GeV.

⁸⁸ From e^+e^- collisions at $\sqrt{s} = 161$ –183 GeV. $f = f'$ is assumed. ABBIENDI 00I also obtain limit for $f = -f'$ ($\mu^* \rightarrow \nu W$): $m_{\mu^*} > 86.0$ GeV.

⁸⁹ From e^+e^- collisions at $\sqrt{s} = 189$ GeV. $f = f'$ is assumed. ACCIARRI 00E also obtain limit for $f = -f'$ ($\mu^* \rightarrow \nu W$): $m_{\mu^*} > 92.6$ GeV.

⁹⁰ From e^+e^- collisions at $\sqrt{s} = 183$ GeV. $f = f'$ is assumed. ABREU 99O also obtain limit for $f = -f'$ ($\mu^* \rightarrow \nu W$): $m_{\mu^*} > 81.3$ GeV.

⁹¹ From e^+e^- collisions at $\sqrt{s} = 170$ –172 GeV. ACKERSTAFF 98C also obtain limit from $\mu^* \rightarrow \nu W$ decay mode: $m_{\mu^*} > 81.3$ GeV.

⁹² BARATE 98U obtain limits on the form factor. See their Fig. 14 for limits in mass-form factor plane.

Searches Particle Listings

Quark and Lepton Compositeness

⁹³ From e^+e^- collisions at $\sqrt{s}=161$ GeV.

⁹⁴ ABREU 97B also obtain limit from charged current decay mode $\mu^* \rightarrow \nu W, m_{\mu^*} > 70.9$ GeV.

⁹⁵ ABREU 97B also obtain limit from charged current decay mode $\mu^* \rightarrow \nu W, m_{\mu^*} > 44.6$ GeV.

Limits for Excited μ (μ^*) from Single Production

These limits are from $e^+e^- \rightarrow \mu^*\mu$ and depend on transition magnetic coupling between μ and μ^* . All limits assume $\mu^* \rightarrow \mu\gamma$ decay. Limits from LEP are for chiral coupling, whereas all other limits are for nonchiral coupling, $\eta_L = \eta_R = 1$. In most papers, the limit is expressed in the form of an excluded region in the $\lambda - m_{\mu^*}$ plane. See the original papers.

For limits prior to 1987, see our 1992 edition (Physical Review **D45** S1 (1992)).

VALUE (GeV)	CL%	DOCUMENT ID	TECN	COMMENT
>221	95	⁹⁶ ABULENCIA,A 06B	CDF	$p\bar{p} \rightarrow \mu\mu^*, \mu^* \rightarrow \mu\gamma$
• • • We do not use the following data for averages, fits, limits, etc. • • •				
	95	⁹⁷ ABAZOV 06E	D0	$p\bar{p} \rightarrow \mu\mu^*$
>180	95	⁹⁸ ACHARD 03B	L3	$e^+e^- \rightarrow \mu\mu^*$
>190	95	⁹⁹ ABBIENDI 02G	OPAL	$e^+e^- \rightarrow \mu\mu^*$
>178	95	¹⁰⁰ ACCIARRI 01D	L3	$e^+e^- \rightarrow \mu\mu^*$
		¹⁰¹ ABBIENDI 00I	OPAL	$e^+e^- \rightarrow \mu\mu^*$
		¹⁰² ACCIARRI 00E	L3	$e^+e^- \rightarrow \mu\mu^*$
		¹⁰³ ABREU 99O	DLPH	$e^+e^- \rightarrow \mu\mu^*$
		¹⁰⁴ ACKERSTAFF 98C	OPAL	$e^+e^- \rightarrow \mu\mu^*$
		¹⁰⁵ BARATE 98U	ALEP	$Z \rightarrow \mu\mu^*$

⁹⁶ $f = f' = \Lambda/m_{\mu^*}$ is assumed for the μ^* coupling. See their Fig.4 for the exclusion limit in the mass-coupling plane. ABULENCIA,A 06B also obtain m_{μ^*} limit in the contact interaction model with $\Lambda = m_{\mu^*}, m_{\mu^*} > 696$ GeV.

⁹⁷ ABAZOV 06E assume $\mu\mu^*$ production via four-fermion contact interaction $(4\pi/\Lambda^2)(\bar{q}_L \gamma^\mu q_L)(\bar{\mu}_L^* \gamma_\mu \mu)$. The obtained limit is $m_{\mu^*} > 618$ GeV ($m_{\mu^*} > 688$ GeV) for $\Lambda = 1$ TeV ($\Lambda = m_{\mu^*}$).

⁹⁸ ACHARD 03B result is from e^+e^- collisions at $\sqrt{s} = 189-209$ GeV. $f = f' = \Lambda/m_{\mu^*}$ is assumed. See their Fig. 4 for the exclusion plot in the mass-coupling plane.

⁹⁹ ABBIENDI 02G result is from e^+e^- collisions at $\sqrt{s} = 183-209$ GeV. $f = f' = \Lambda/m_{\mu^*}$ is assumed for μ^* coupling. See their Fig. 4c for the exclusion limit in the mass-coupling plane.

¹⁰⁰ ACCIARRI 01D result is from e^+e^- collisions at $\sqrt{s} = 192-202$ GeV. $f = f' = \Lambda/m_{\mu^*}$ is assumed for the μ^* coupling. See their Fig. 4 for limits in the mass-coupling plane.

¹⁰¹ ABBIENDI 00I result is from e^+e^- collisions at $\sqrt{s}=161-183$ GeV. See their Fig. 7 for limits in mass-coupling plane.

¹⁰² ACCIARRI 00E result is from e^+e^- collisions at $\sqrt{s}=189$ GeV. See their Fig. 3 for limits in mass-coupling plane.

¹⁰³ ABREU 99O result is from e^+e^- collisions at $\sqrt{s}=183$ GeV. See their Figs. 4 and 5 for the exclusion limit in the mass-coupling plane.

¹⁰⁴ ACKERSTAFF 98C from e^+e^- collisions at $\sqrt{s}=170-172$ GeV. See their Fig. 11 for the exclusion limit in the mass-coupling plane.

¹⁰⁵ BARATE 98U obtain limits on the $Z\mu\mu^*$ coupling. See their Fig. 12 for limits in mass-coupling plane

Indirect Limits for Excited μ (μ^*)

These limits make use of loop effects involving μ^* and are therefore subject to theoretical uncertainty.

VALUE (GeV)	DOCUMENT ID	TECN	COMMENT
• • • We do not use the following data for averages, fits, limits, etc. • • •			
	¹⁰⁶ RENARD 82	THEO	$g-2$ of muon

¹⁰⁶ RENARD 82 derived from $g-2$ data limits on mass and couplings of e^* and μ^* . See figures 2 and 3 of the paper.

MASS LIMITS for Excited τ (τ^*)

Limits for Excited τ (τ^*) from Pair Production

These limits are obtained from $e^+e^- \rightarrow \tau^*\tau^*$ and thus rely only on the (electroweak) charge of τ^* . Form factor effects are ignored unless noted. For the case of limits from Z decay, the τ^* coupling is assumed to be of sequential type. All limits assume a dominant $\tau^* \rightarrow \tau\gamma$ decay except the limits from $\Gamma(Z)$.

For limits prior to 1987, see our 1992 edition (Physical Review **D45** S1 (1992)).

VALUE (GeV)	CL%	DOCUMENT ID	TECN	COMMENT
>103.2	95	¹⁰⁷ ABBIENDI 02G	OPAL	$e^+e^- \rightarrow \tau^*\tau^*$ Homodoublet type
• • • We do not use the following data for averages, fits, limits, etc. • • •				
>102.8	95	¹⁰⁸ ACHARD 03B	L3	$e^+e^- \rightarrow \tau^*\tau^*$ Homodoublet type
> 99.8	95	¹⁰⁹ ACCIARRI 01D	L3	$e^+e^- \rightarrow \tau^*\tau^*$ Homodoublet type
> 91.2	95	¹¹⁰ ABBIENDI 00I	OPAL	$e^+e^- \rightarrow \tau^*\tau^*$ Homodoublet type
> 94.2	95	¹¹¹ ACCIARRI 00E	L3	$e^+e^- \rightarrow \tau^*\tau^*$ Homodoublet type
> 89.7	95	¹¹² ABREU 99O	DLPH	Homodoublet type
> 84.6	95	¹¹³ ACKERSTAFF 98C	OPAL	$e^+e^- \rightarrow \tau^*\tau^*$ Homodoublet type
		¹¹⁴ BARATE 98U	ALEP	$Z \rightarrow \tau^*\tau^*$
> 79.4	95	^{115,116} ABREU 97B	DLPH	$e^+e^- \rightarrow \tau^*\tau^*$ Homodoublet type
> 77.4	95	^{115,117} ABREU 97B	DLPH	$e^+e^- \rightarrow \tau^*\tau^*$ Sequential type
> 79.3	95	¹¹⁵ ACCIARRI 97G	L3	$e^+e^- \rightarrow \tau^*\tau^*$ Sequential type

¹⁰⁷ From e^+e^- collisions at $\sqrt{s} = 183-209$ GeV. $f = f'$ is assumed.

¹⁰⁸ From e^+e^- collisions at $\sqrt{s} = 189-209$ GeV. $f = f'$ is assumed. ACHARD 03B also obtain limit for $f = -f'$: $m_{\tau^*} > 96.6$ GeV.

¹⁰⁹ From e^+e^- collisions at $\sqrt{s} = 192-202$ GeV. $f = f'$ is assumed. ACCIARRI 01D also obtain limit for $f = -f'$: $m_{\tau^*} > 93.4$ GeV.

¹¹⁰ From e^+e^- collisions at $\sqrt{s}=161-183$ GeV. $f = f'$ is assumed. ABBIENDI 00I also obtain limit for $f = -f'$ ($\tau^* \rightarrow \nu W$): $m_{\tau^*} > 86.0$ GeV.

¹¹¹ From e^+e^- collisions at $\sqrt{s}=189$ GeV. $f = f'$ is assumed. ACCIARRI 00E also obtain limit for $f = -f'$ ($\tau^* \rightarrow \nu W$): $m_{\tau^*} > 92.6$ GeV.

¹¹² From e^+e^- collisions at $\sqrt{s}=183$ GeV. $f = f'$ is assumed. ABREU 99O also obtain limit for $f = -f'$ ($\tau^* \rightarrow \nu W$): $m_{\tau^*} > 81.3$ GeV.

¹¹³ From e^+e^- collisions at $\sqrt{s}=170-172$ GeV. ACKERSTAFF 98C also obtain limit from $\tau^* \rightarrow \nu W$ decay mode: $m_{\tau^*} > 81.3$ GeV.

¹¹⁴ BARATE 98U obtain limits on the form factor. See their Fig. 14 for limits in mass-form factor plane.

¹¹⁵ From e^+e^- collisions at $\sqrt{s}=161$ GeV.

¹¹⁶ ABREU 97B also obtain limit from charged current decay mode $\tau^* \rightarrow \nu W, m_{\tau^*} > 70.9$ GeV.

¹¹⁷ ABREU 97B also obtain limit from charged current decay mode $\tau^* \rightarrow \nu W, m_{\tau^*} > 44.6$ GeV.

Limits for Excited τ (τ^*) from Single Production

These limits are from $e^+e^- \rightarrow \tau^*\tau$ and depend on transition magnetic coupling between τ and τ^* . All limits assume $\tau^* \rightarrow \tau\gamma$ decay. Limits from LEP are for chiral coupling, whereas all other limits are for nonchiral coupling, $\eta_L = \eta_R = 1$. In most papers, the limit is expressed in the form of an excluded region in the $\lambda - m_{\tau^*}$ plane. See the original papers.

VALUE (GeV)	CL%	DOCUMENT ID	TECN	COMMENT
>185	95	¹¹⁸ ABBIENDI 02G	OPAL	$e^+e^- \rightarrow \tau\tau^*$
• • • We do not use the following data for averages, fits, limits, etc. • • •				
>180	95	¹¹⁹ ACHARD 03B	L3	$e^+e^- \rightarrow \tau\tau^*$
>173	95	¹²⁰ ACCIARRI 01D	L3	$e^+e^- \rightarrow \tau\tau^*$
		¹²¹ ABBIENDI 00I	OPAL	$e^+e^- \rightarrow \tau\tau^*$
		¹²² ACCIARRI 00E	L3	$e^+e^- \rightarrow \tau\tau^*$
		¹²³ ABREU 99O	DLPH	$e^+e^- \rightarrow \tau\tau^*$
		¹²⁴ ACKERSTAFF 98C	OPAL	$e^+e^- \rightarrow \tau\tau^*$
		¹²⁵ BARATE 98U	ALEP	$Z \rightarrow \tau\tau^*$

¹¹⁸ ABBIENDI 02G result is from e^+e^- collisions at $\sqrt{s} = 183-209$ GeV. $f = f' = \Lambda/m_{\tau^*}$ is assumed for τ^* coupling. See their Fig. 4c for the exclusion limit in the mass-coupling plane.

¹¹⁹ ACHARD 03B result is from e^+e^- collisions at $\sqrt{s} = 189-209$ GeV. $f = f' = \Lambda/m_{\tau^*}$ is assumed. See their Fig. 4 for the exclusion plot in the mass-coupling plane.

¹²⁰ ACCIARRI 01D result is from e^+e^- collisions at $\sqrt{s} = 192-202$ GeV. $f = f' = \Lambda/m_{\tau^*}$ is assumed for the τ^* coupling. See their Fig. 4 for limits in the mass-coupling plane.

¹²¹ ABBIENDI 00I result is from e^+e^- collisions at $\sqrt{s}=161-183$ GeV. See their Fig. 7 for limits in mass-coupling plane.

¹²² ACCIARRI 00E result is from e^+e^- collisions at $\sqrt{s}=189$ GeV. See their Fig. 3 for limits in mass-coupling plane.

¹²³ ABREU 99O result is from e^+e^- collisions at $\sqrt{s}=183$ GeV. See their Figs. 4 and 5 for the exclusion limit in the mass-coupling plane.

¹²⁴ ACKERSTAFF 98C from e^+e^- collisions at $\sqrt{s}=170-172$ GeV. See their Fig. 11 for the exclusion limit in the mass-coupling plane.

¹²⁵ BARATE 98U obtain limits on the $Z\tau\tau^*$ coupling. See their Fig. 12 for limits in mass-coupling plane

MASS LIMITS for Excited Neutrino (ν^*)

Limits for Excited ν (ν^*) from Pair Production

These limits are obtained from $e^+e^- \rightarrow \nu^*\nu^*$ and thus rely only on the (electroweak) charge of ν^* . Form factor effects are ignored unless noted. The ν^* coupling is assumed to be of sequential type unless otherwise noted. All limits assume a dominant $\nu^* \rightarrow \nu\gamma$ decay except the limits from $\Gamma(Z)$.

VALUE (GeV)	CL%	DOCUMENT ID	TECN	COMMENT
>102.6	95	¹²⁶ ACHARD 03B	L3	$e^+e^- \rightarrow \nu^*\nu^*$ Homodoublet type
• • • We do not use the following data for averages, fits, limits, etc. • • •				
> 99.4	95	¹²⁷ ABBIENDI 04N	OPAL	
> 91.2	95	¹²⁸ ACCIARRI 01D	L3	$e^+e^- \rightarrow \nu^*\nu^*$ Homodoublet type
		¹²⁹ ABBIENDI 00I	OPAL	$e^+e^- \rightarrow \nu^*\nu^*$ Homodoublet type
		¹³⁰ ABBIENDI,G 00D	OPAL	
> 94.1	95	¹³¹ ACCIARRI 00E	L3	$e^+e^- \rightarrow \nu^*\nu^*$ Homodoublet type
		¹³² ABBIENDI 99F	OPAL	
> 90.0	95	¹³³ ABREU 99O	DLPH	Homodoublet type
> 84.9	95	¹³⁴ ACKERSTAFF 98C	OPAL	$e^+e^- \rightarrow \nu^*\nu^*$ Homodoublet type
		¹³⁵ BARATE 98U	ALEP	$Z \rightarrow \nu^*\nu^*$
> 77.6	95	^{136,137} ABREU 97B	DLPH	$e^+e^- \rightarrow \nu^*\nu^*$ Homodoublet type
> 64.4	95	^{136,138} ABREU 97B	DLPH	$e^+e^- \rightarrow \nu^*\nu^*$ Sequential type
> 71.2	95	^{136,139} ACCIARRI 97G	L3	$e^+e^- \rightarrow \nu^*\nu^*$ Sequential type

See key on page 405

Searches Particle Listings

Quark and Lepton Compositeness

- 126 From e^+e^- collisions at $\sqrt{s} = 189\text{--}209$ GeV. $f = -f'$ is assumed. ACHARD 03b also obtain limit for $f = f'$: $m_{\nu_e^*} > 101.7$ GeV, $m_{\nu_\mu^*} > 101.8$ GeV, and $m_{\nu_\tau^*} > 92.9$ GeV. See their Fig. 4 for the exclusion plot in the mass-coupling plane.
- 127 From e^+e^- collisions at $\sqrt{s} = 192\text{--}209$ GeV, ABBIENDI 04N obtain limit on $\sigma(e^+e^- \rightarrow \nu^*\nu^*) B^2(\nu^* \rightarrow \nu\gamma)$. See their Fig. 2. The limit ranges from 20 to 45fb for $m_{\nu^*} > 45$ GeV.
- 128 From e^+e^- collisions at $\sqrt{s} = 192\text{--}202$ GeV. $f = -f'$ is assumed. ACCIARRI 01d also obtain limit for $f = -f'$: $m_{\nu_e^*} > 99.1$ GeV, $m_{\nu_\mu^*} > 99.3$ GeV, $m_{\nu_\tau^*} > 90.5$ GeV.
- 129 From e^+e^- collisions at $\sqrt{s} = 161\text{--}183$ GeV. $f = -f'$ (photonic decay) is assumed. ABBIENDI 00i also obtain limit for $f = f'$ ($\nu^* \rightarrow \ell W$): $m_{\nu_e^*} > 91.1$ GeV, $m_{\nu_\mu^*} > 91.1$ GeV, $m_{\nu_\tau^*} > 83.1$ GeV.
- 130 From e^+e^- collisions at $\sqrt{s} = 189$ GeV. ABBIENDI,G 00d obtain limit on $\sigma(e^+e^- \rightarrow \nu^*\nu^*)B(\nu^* \rightarrow \nu\gamma)^2$. See their Fig. 14. The limit ranges from 50 to 80 fb for $\sqrt{s}/2 = 95$ GeV $> m_{\nu^*} > 45$ GeV.
- 131 From e^+e^- collisions at $\sqrt{s} = 189$ GeV. $f = -f'$ (photonic decay) is assumed. ACCIARRI 00E also obtain limit for $f = f'$ ($\nu^* \rightarrow \ell W$): $m_{\nu_e^*} > 93.9$ GeV, $m_{\nu_\mu^*} > 94.0$ GeV, $m_{\nu_\tau^*} > 91.5$ GeV.
- 132 From e^+e^- collisions at $\sqrt{s} = 130\text{--}183$ GeV, ABBIENDI 99F obtain limit on $\sigma(e^+e^- \rightarrow \nu^*\nu^*) B(\nu^* \rightarrow \nu\gamma)^2$. See their Fig. 13. The limit ranges from 0.094 to 0.14 pb for $\sqrt{s}/2 > m_{\nu^*} > 45$ GeV.
- 133 From e^+e^- collisions at $\sqrt{s} = 183$ GeV. $f = -f'$ is assumed. ABREU 99o also obtain limit for $f = f'$: $m_{\nu_e^*} > 87.3$ GeV, $m_{\nu_\mu^*} > 88.0$ GeV, $m_{\nu_\tau^*} > 81.0$ GeV.
- 134 From e^+e^- collisions at $\sqrt{s} = 170\text{--}172$ GeV. ACKERSTAFF 98c also obtain limit from charged decay modes: $m_{\nu_e^*} > 84.1$ GeV, $m_{\nu_\mu^*} > 83.9$ GeV, and $m_{\nu_\tau^*} > 79.4$ GeV.
- 135 BARATE 98u obtain limits on the form factor. See their Fig. 14 for limits in mass-form factor plane.
- 136 From e^+e^- collisions at $\sqrt{s} = 161$ GeV.
- 137 ABREU 97b also obtain limits from charged current decay modes, $m_{\nu^*} > 56.4$ GeV.
- 138 ABREU 97b also obtain limits from charged current decay modes, $m_{\nu^*} > 44.9$ GeV.
- 139 ACCIARRI 97G also obtain limits from charged current decay mode $\nu_e^* \rightarrow e W$, $m_{\nu^*} > 64.5$ GeV.

Limits for Excited ν (ν^*) from Single Production

These limits are from $e^+e^- \rightarrow \nu\nu^*$, $Z \rightarrow \nu\nu^*$, or $ep \rightarrow \nu^*X$ and depend on transition magnetic coupling between ν/e and ν^* . Assumptions about ν^* decay mode are given in footnotes.

VALUE (GeV)	CL%	DOCUMENT ID	TECN	COMMENT
>213	95	140 AARON	08 H1	$ep \rightarrow \nu^*X$
••• We do not use the following data for averages, fits, limits, etc. •••				
>190	95	141 ACHARD	03B L3	$e^+e^- \rightarrow \nu\nu^*$
none 50–150	95	142 ADLOFF	02 H1	$ep \rightarrow \nu^*X$
>158	95	143 CHEKANOV	02D ZEUS	$ep \rightarrow \nu^*X$
>171	95	144 ACCIARRI	01D L3	$e^+e^- \rightarrow \nu\nu^*$
		145 ABBIENDI	00I OPAL	$e^+e^- \rightarrow \nu\nu^*$
		146 ABBIENDI,G	00D OPAL	
		147 ACCIARRI	00E L3	$e^+e^- \rightarrow \nu\nu^*$
>114	95	148 ADLOFF	00E H1	$ep \rightarrow \nu^*X$
		149 ABBIENDI	99F OPAL	
		150 ABREU	99o DLPH	$e^+e^- \rightarrow \nu\nu^*$
		151 ACKERSTAFF	98c OPAL	$e^+e^- \rightarrow \nu^*\nu^*$ Homodoublet type
		152 BARATE	98u ALEP	$Z \rightarrow \nu\nu^*$

- 140 AARON 08 search for single ν^* production in ep collisions with the decays $\nu^* \rightarrow \nu\gamma$, νZ , eW . The quoted limit assumes $f = -f' = \Lambda/m_{\nu^*}$. See their Fig. 3 and Fig. 4 for the exclusion plots in the mass-coupling plane.
- 141 ACHARD 03b result is from e^+e^- collisions at $\sqrt{s} = 189\text{--}209$ GeV. The quoted limit is for ν_e^* . $f = -f' = \Lambda/m_{\nu^*}$ is assumed. See their Fig. 4 for the exclusion plot in the mass-coupling plane.
- 142 ADLOFF 02 search for single ν^* production in ep collisions with the decays $\nu^* \rightarrow \nu\gamma$, νZ , eW . The quoted limit assumes $f = -f' = \Lambda/m_{\nu^*}$. See their Fig. 1 for the exclusion plots in the mass-coupling plane.
- 143 CHEKANOV 02d search for single ν^* production in ep collisions with the decays $\nu^* \rightarrow \nu\gamma$, νZ , eW . $f = -f' = \Lambda/m_{\nu^*}$ is assumed for the e^* coupling. CHEKANOV 02d also obtain limit for $f = f' = \Lambda/m_{\nu^*}$: $m_{\nu^*} > 135$ GeV. See their Fig. 5c and Fig. 5d for the exclusion plot in the mass-coupling plane.
- 144 ACCIARRI 01D search for $\nu\nu^*$ production in e^+e^- collisions at $\sqrt{s} = 192\text{--}202$ GeV with decays $\nu^* \rightarrow \nu\gamma$, $\nu^* \rightarrow eW$. $f = -f' = \Lambda/m_{\nu^*}$ is assumed for the ν^* coupling. See their Fig. 4 for limits in the mass-coupling plane.
- 145 ABBIENDI 00i result is from e^+e^- collisions at $\sqrt{s} = 161\text{--}183$ GeV. See their Fig. 7 for limits in mass-coupling plane.
- 146 From e^+e^- collisions at $\sqrt{s} = 189$ GeV. ABBIENDI,G 00d obtain limit on $\sigma(e^+e^- \rightarrow \nu^*\nu^*)B(\nu^* \rightarrow \nu\gamma)^2$. See their Fig. 11.
- 147 ACCIARRI 00E result is from e^+e^- collisions at $\sqrt{s} = 189$ GeV. See their Fig. 3 for limits in mass-coupling plane.
- 148 ADLOFF 00E search for single ν^* production in ep collisions with the decays $\nu^* \rightarrow \nu\gamma$, νZ , eW . The quoted limit assumes $f = -f' = \Lambda/m_{\nu^*}$. See their Fig. 10 for the exclusion plot in the mass-coupling plane.
- 149 From e^+e^- collisions at $\sqrt{s} = 130\text{--}183$ GeV, ABBIENDI 99F obtain limit on $\sigma(e^+e^- \rightarrow \nu^*\nu^*) B(\nu^* \rightarrow \nu\gamma)$. See their Fig. 8.

- 150 ABREU 99o result is from e^+e^- collisions at $\sqrt{s} = 183$ GeV. See their Figs. 4 and 5 for the exclusion limit in the mass-coupling plane.
- 151 ACKERSTAFF 98c from e^+e^- collisions at $\sqrt{s} = 170\text{--}172$ GeV. See their Fig. 11 for the exclusion limit in the mass-coupling plane.
- 152 BARATE 98u obtain limits on the $Z\nu\nu^*$ coupling. See their Fig. 13 for limits in mass-coupling plane

MASS LIMITS for Excited q (q^*)

Limits for Excited q (q^*) from Pair Production

These limits are obtained from $e^+e^- \rightarrow q^*\bar{q}^*$ and thus rely only on the (electroweak) charge of the q^* . Form factor effects are ignored unless noted. Assumptions about the q^* decay are given in the comments and footnotes.

VALUE (GeV)	CL%	DOCUMENT ID	TECN	COMMENT
>45.6	95	153 ADRIANI	93M L3	u or d type, $Z \rightarrow q^*q^*$
••• We do not use the following data for averages, fits, limits, etc. •••				
		154 BARATE	98U ALEP	$Z \rightarrow q^*q^*$
		155 ADRIANI	92F L3	$Z \rightarrow q^*q^*$
>41.7	95	156 BARDADIN...	92 RVUE	u -type, $\Gamma(Z)$
>44.7	95	156 BARDADIN...	92 RVUE	d -type, $\Gamma(Z)$
>40.6	95	157 DECA MP	92 ALEP	u -type, $\Gamma(Z)$
>44.2	95	157 DECA MP	92 ALEP	d -type, $\Gamma(Z)$
>45	95	158 DECA MP	92 ALEP	u or d type, $Z \rightarrow q^*q^*$
>45	95	157 ABREU	91F DLPH	u -type, $\Gamma(Z)$
>45	95	157 ABREU	91F DLPH	d -type, $\Gamma(Z)$

- 153 ADRIANI 93M limit is valid for $B(q^* \rightarrow qg) > 0.25$ (0.17) for up (down) type.
- 154 BARATE 98u obtain limits on the form factor. See their Fig. 16 for limits in mass-form factor plane.
- 155 ADRIANI 92F search for $Z \rightarrow q^*\bar{q}^*$ followed with $q^* \rightarrow q\gamma$ decays and give the limit $\sigma_Z \cdot B(Z \rightarrow q^*\bar{q}^*) \cdot B^2(q^* \rightarrow q\gamma) < 2$ pb at 95%CL. Assuming five flavors of degenerate q^* of homodoublet type, $B(q^* \rightarrow q\gamma) < 4\%$ is obtained for $m_{q^*} < 45$ GeV.
- 156 BARDADIN-OTWINOWSKA 92 limit based on $\Delta\Gamma(Z) < 36$ MeV.
- 157 These limits are independent of decay modes.
- 158 Limit is for $B(q^* \rightarrow qg) + B(q^* \rightarrow q\gamma) = 1$.

Limits for Excited q (q^*) from Single Production

These limits are from $e^+e^- \rightarrow q^*\bar{q}$ or $p\bar{p} \rightarrow q^*X$ and depend on transition magnetic couplings between q and q^* . Assumptions about q^* decay mode are given in the footnotes and comments.

VALUE (GeV)	CL%	DOCUMENT ID	TECN	COMMENT
>775	95	159 ABAZOV	04c D0	$p\bar{p} \rightarrow q^*X, q^* \rightarrow qg$
none 200–520 and 580–760	95	160 ABE	97G CDF	$p\bar{p} \rightarrow q^*X, q^* \rightarrow 2$ jets
none 80–570	95	161 ABE	95N CDF	$p\bar{p} \rightarrow q^*X, q^* \rightarrow qg, qW$
••• We do not use the following data for averages, fits, limits, etc. •••				
>510	95	162 ABAZOV	06F D0	$p\bar{p} \rightarrow q^*X, q^* \rightarrow qZ$
>205	95	163 CHEKANOV	02D ZEUS	$ep \rightarrow q^*X$
>188	95	164 ADLOFF	00E H1	$ep \rightarrow q^*X$
		165 ABREU	99o DLPH	$e^+e^- \rightarrow q^*q^*$
		166 BARATE	98u ALEP	$Z \rightarrow qq^*$

- 159 ABAZOV 04c assume $f_s = f = f' = \Lambda/m_{q^*}$.
- 160 ABE 97G search for new particle decaying to dijets.
- 161 ABE 95N assume a degenerate u^* and d^* with $f_s = f = f' = \Lambda/m_{q^*}$. See their Fig. 4 for the excluded region in $m_{q^*} - f$ plane.
- 162 ABAZOV 06f assume q^* production via qg fusion and via contact interactions. The quoted limit is for $\Lambda = m_{q^*}$.
- 163 CHEKANOV 02d search for single q^* production in ep collisions with the decays $q^* \rightarrow q\gamma, qZ, qW$. $f_s = 0$ and $f = f' = \Lambda/m_{q^*}$ is assumed for the q^* coupling. See their Fig. 5b for the exclusion plot in the mass-coupling plane.
- 164 ADLOFF 00E search for single q^* production in ep collisions with the decays $q^* \rightarrow q\gamma, qZ, qW$. $f_s = 0$ and $f = f' = \Lambda/m_{q^*}$ is assumed for the q^* coupling. See their Fig. 11 for the exclusion plot in the mass-coupling plane.
- 165 ABREU 99o result is from e^+e^- collisions at $\sqrt{s} = 183$ GeV. See their Fig. 6 for the exclusion limit in the mass-coupling plane.
- 166 BARATE 98u obtain limits on the Zqq^* coupling. See their Fig. 16 for limits in mass-coupling plane

MASS LIMITS for Color Sextet Quarks (q_6)

VALUE (GeV)	CL%	DOCUMENT ID	TECN	COMMENT
>84	95	167 ABE	89D CDF	$p\bar{p} \rightarrow q_6\bar{q}_6$

- 167 ABE 89D look for pair production of unit-charged particles which leave the detector before decaying. In the above limit the color sextet quark is assumed to fragment into a unit-charged or neutral hadron with equal probability and to have long enough lifetime not to decay within the detector. A limit of 121 GeV is obtained for a color decuplet.

MASS LIMITS for Color Octet Charged Leptons (ℓ_8)

$\lambda \equiv m_{\ell_8}/\Lambda$

VALUE (GeV)	CL%	DOCUMENT ID	TECN	COMMENT
>86	95	168 ABE	89D CDF	Stable ℓ_8 : $p\bar{p} \rightarrow \ell_8\bar{\ell}_8$

Searches Particle Listings

Quark and Lepton Compositeness, Extra Dimensions

- • • We do not use the following data for averages, fits, limits, etc. • • •
- | | | | | | |
|---------------|-----|-----|-----|----|--|
| | 169 | ABT | 93 | H1 | $e_g: e p \rightarrow e_g X$ |
| none 3.0–30.3 | 95 | 170 | KIM | 90 | AMY $e_g: e^+ e^- \rightarrow e e + \text{jets}$ |
| none 3.5–30.3 | 95 | 170 | KIM | 90 | AMY $\mu_g: e^+ e^- \rightarrow \mu \mu + \text{jets}$ |
| | | 171 | KIM | 90 | AMY $e_g: e^+ e^- \rightarrow g g; R$ |
- 168 ABE 89D look for pair production of unit-charged particles which leave the detector before decaying. In the above limit the color octet lepton is assumed to fragment into a unit-charged or neutral hadron with equal probability and to have long enough lifetime not to decay within the detector. The limit improves to 99 GeV if it always fragments into a unit-charged hadron.
- 169 ABT 93 search for e_g production via e -gluon fusion in ep collisions with $e_g \rightarrow eg$. See their Fig. 3 for exclusion plot in the $m_{e_g} - \Lambda$ plane for $m_{e_g} = 35\text{--}220$ GeV.
- 170 KIM 90 is at $E_{cm} = 50\text{--}60.8$ GeV. The same assumptions as in BARTEL 87B are used.
- 171 KIM 90 result $(m_{e_g} \Lambda_M)^{1/2} > 178.4$ GeV (95%CL, $\alpha_s = 0.16$ used) is subject to the same restriction as for BARTEL 85K.

MASS LIMITS for Color Octet Neutrinos (ν_g)

VALUE (GeV)	CL%	DOCUMENT ID	TECN	COMMENT
$\lambda \equiv m_{\nu_g} / \Lambda$				
• • • We do not use the following data for averages, fits, limits, etc. • • •				
none 3.8–29.8	95	173	KIM	90 AMY $\nu_g: e^+ e^- \rightarrow \text{acoplanar jets}$
none 9–21.9	95	174	BARTEL	87B JADE $\nu_g: e^+ e^- \rightarrow \text{acoplanar jets}$
172				
BARGER 89				used ABE 89B limit for events with large missing transverse momentum. Two-body decay $\nu_g \rightarrow \nu g$ is assumed.
173				
KIM 90				is at $E_{cm} = 50\text{--}60.8$ GeV. The same assumptions as in BARTEL 87B are used.
174				
BARTEL 87B				is at $E_{cm} = 46.3\text{--}46.78$ GeV. The limit assumes the ν_g pair production cross section to be eight times larger than that of the corresponding heavy neutrino pair production. This assumption is not valid in general for the weak couplings, and the limit can be sensitive to its $SU(2)_L \times U(1)_Y$ quantum numbers.

MASS LIMITS for W_g (Color Octet W Boson)

VALUE (GeV)	DOCUMENT ID	TECN	COMMENT
• • • We do not use the following data for averages, fits, limits, etc. • • •			
175			
ALBAJAR 89			give $\sigma(W_g \rightarrow W + \text{jet}) / \sigma(W) < 0.019$ (90% CL) for $m_{W_g} > 220$ GeV.

REFERENCES FOR Searches for Quark and Lepton Compositeness

ABAZOV	09AE	PRL 103 191803	V.M. Abazov et al.	(D0 Collab.)
ABDALLAH	09	EPJ C60 1	J. Abdallah et al.	(DELPHI Collab.)
AARON	08	PL B663 382	F.D. Aaron et al.	(H1 Collab.)
AARON	08A	PL B666 131	F.D. Aaron et al.	(H1 Collab.)
ABAZOV	08H	PR D77 091102R	V.M. Abazov et al.	(D0 Collab.)
SCHAEEL	07A	EPJ C49 411	S. Schaeel et al.	(ALEPH Collab.)
ABAZOV	06E	PR D73 111102R	V.M. Abazov et al.	(D0 Collab.)
ABAZOV	06F	PR D74 011104R	V.M. Abazov et al.	(D0 Collab.)
ABDALLAH	06C	EPJ C45 589	J. Abdallah et al.	(DELPHI Collab.)
ABULENCIA	06L	PRL 96 211801	A. Abulencia et al.	(CDF Collab.)
ABULENCIA,A	06B	PRL 97 191802	A. Abulencia et al.	(CDF Collab.)
ACOSTA	05B	PRL 94 101802	D. Acosta et al.	(CDF Collab.)
ABAZOV	04C	PR D69 111101R	V.M. Abazov et al.	(D0 Collab.)
ABBIENDI	04G	EPJ C33 173	G. Abbiendi et al.	(OPAL Collab.)
ABBIENDI	04N	PL B602 167	G. Abbiendi et al.	(OPAL Collab.)
ABDALLAH	04N	EPJ C37 405	J. Abdallah et al.	(DELPHI Collab.)
CHEKANOV	04B	PL B591 23	S. Chekanov et al.	(ZEUS Collab.)
ACHARD	03B	PL B568 23	P. Achard et al.	(L3 Collab.)
ADLOFF	03	PL B568 35	C. Adloff et al.	(H1 Collab.)
BABICH	03	EPJ C29 103	A.A. Babich et al.	(CDF Collab.)
ABBIENDI	02G	PL B544 57	G. Abbiendi et al.	(OPAL Collab.)
ACHARD	02D	PL B531 28	P. Achard et al.	(L3 Collab.)
ACHARD	02J	PL B549 290	P. Achard et al.	(L3 Collab.)
ADLOFF	02	PL B525 9	C. Adloff et al.	(H1 Collab.)
ADLOFF	02B	PL B548 35	C. Adloff et al.	(H1 Collab.)
CHEKANOV	02D	PL B549 32	S. Chekanov et al.	(ZEUS Collab.)
ACCIARRI	01D	PL B502 37	M. Acciari et al.	(L3 Collab.)
AFFOLDER	01I	PRL 87 231803	T. Affolder et al.	(CDF Collab.)
BOURLIKOV	01	PR D64 071701	D. Bourlikov	(CDF Collab.)
CHEUNG	01B	PL B517 167	K. Cheung	(OPAL Collab.)
ABBIENDI	00I	EPJ C14 73	G. Abbiendi et al.	(OPAL Collab.)
ABBIENDI	00R	EPJ C13 553	G. Abbiendi et al.	(OPAL Collab.)
ABBIENDI,G	00D	EPJ C18 253	G. Abbiendi et al.	(OPAL Collab.)
ABBOTT	00E	PR D62 031101	B. Abbott et al.	(D0 Collab.)
ABREU	00A	PL B491 67	P. Abreu et al.	(DELPHI Collab.)
ABREU	00S	PL B485 45	P. Abreu et al.	(DELPHI Collab.)
ACCIARRI	00E	PL B473 177	M. Acciari et al.	(L3 Collab.)
ACCIARRI	00G	PL B475 198	M. Acciari et al.	(L3 Collab.)
ACCIARRI	00P	PL B489 81	M. Acciari et al.	(L3 Collab.)
ADLOFF	00	PL B479 358	C. Adloff et al.	(H1 Collab.)
ADLOFF	00E	EPJ C17 567	C. Adloff et al.	(H1 Collab.)
AFFOLDER	00I	PR D62 012004	T. Affolder et al.	(CDF Collab.)
BARATE	00I	EPJ C12 183	R. Barate et al.	(ALEPH Collab.)
BOURLIKOV	00	PR D62 076005	D. Bourlikov	(ALEPH Collab.)
BREITWEG	00B	EPJ C14 239	J. Breitweg et al.	(ZEUS Collab.)
ABBIENDI	99	EPJ C6 1	G. Abbiendi et al.	(OPAL Collab.)
ABBIENDI	99F	EPJ C8 23	G. Abbiendi et al.	(OPAL Collab.)
ABBIENDI	99P	PL B465 303	G. Abbiendi et al.	(OPAL Collab.)
ABBOTT	99C	PRL 82 2457	B. Abbott et al.	(D0 Collab.)
ABBOTT	99D	PRL 82 4769	B. Abbott et al.	(D0 Collab.)
ABREU	99A	EPJ C11 383	P. Abreu et al.	(DELPHI Collab.)
ABREU	99O	EPJ C8 41	P. Abreu et al.	(DELPHI Collab.)
ZARNECKI	99	EPJ C11 539	A.F. Zarnecki	(D0 Collab.)
ABBOTT	98G	PRL 80 666	B. Abbott et al.	(D0 Collab.)
ABREU	98J	PL B433 429	P. Abreu et al.	(DELPHI Collab.)
ACCIARRI	98T	PL B433 163	M. Acciari et al.	(L3 Collab.)
ACCIARRI	98T	PL B439 183	M. Acciari et al.	(L3 Collab.)
ACKERSTAFF	98	EPJ C1 21	K. Ackerstaff et al.	(OPAL Collab.)

ACKERSTAFF	98C	EPJ C1 45	K. Ackerstaff et al.	(OPAL Collab.)
ACKERSTAFF	98V	EPJ C2 441	K. Ackerstaff et al.	(OPAL Collab.)
ACKER...K...	98B	PL B438 379	K. Ackerstaff et al.	(OPAL Collab.)
BARATE	98J	PL B429 201	R. Barate et al.	(ALEPH Collab.)
BARATE	98U	EPJ C4 571	R. Barate et al.	(ALEPH Collab.)
BARGER	98E	PR D57 391	V. Barger et al.	(CDF Collab.)
BERTRAM	98	PL B443 347	I. Bertram, E.H. Simmons	(CCFR/NuTeV Collab.)
MCFARLAND	98	EPJ C1 509	K.S. McFarland et al.	(VENUS Collab.)
MIURA	98	PR D57 5345	M. Miura et al.	(CDF Collab.)
ABE	97G	PR D55 R5263	F. Abe et al.	(CDF Collab.)
ABE	97T	PRL 79 2198	F. Abe et al.	(CDF Collab.)
ABREU	97B	PL B393 245	P. Abreu et al.	(DELPHI Collab.)
ACCIARRI	97G	PL B401 139	M. Acciari et al.	(L3 Collab.)
ACKERS TAFF	97	PL B391 197	K. Ackerstaff et al.	(OPAL Collab.)
ADLOFF	97	NP B483 44	C. Adloff et al.	(H1 Collab.)
BREITWEG	97C	ZPHY C76 631	J. Breitweg et al.	(ZEUS Collab.)
ABE	95N	PRL 74 3538	F. Abe et al.	(CDF Collab.)
DIAZCRUZ	94	PR D49 R2149	J.L. Diaz Cruz, O.A. Sampayo	(CINV)
ABT	93	NP B396 3	I. Abt et al.	(H1 Collab.)
ADRIANI	93M	PRPL 226 1	O. Adriani et al.	(L3 Collab.)
ABE	92B	PRL 68 1463	F. Abe et al.	(CDF Collab.)
ADRIANI	92F	PL B292 472	O. Adriani et al.	(L3 Collab.)
BARDADIN...	92	ZPHY C55 163	M. Bardadin-Otwinowska	(CLER)
DECAMP	92	PRPL 216 253	D. Decamp et al.	(ALEPH Collab.)
PDG	92	PR D45 51	K. Hikasa et al.	(KEK, LBL, BOST+)
ABREU	91F	NP B367 511	P. Abreu et al.	(DELPHI Collab.)
KIM	90	PL B240 243	G.N. Kim et al.	(AMY Collab.)
ABE	89B	PRL 62 1825	F. Abe et al.	(CDF Collab.)
ABE	89D	PRL 63 1447	F. Abe et al.	(CDF Collab.)
ABE	89J	ZPHY C45 175	K. Abe et al.	(VENUS Collab.)
ALBAJAR	89	ZPHY C44 15	C. Albarajar et al.	(UA1 Collab.)
BARGER	89	PL B220 464	V. Barger et al.	(WIS C, KEK)
DORENBOS...	89	ZPHY C41 567	J. Dorenbosch et al.	(CHARM Collab.)
BARTEL	87B	ZPHY C36 15	W. Bartel et al.	(JADE Collab.)
GRIFOLS	86	PL B68B 264	J.A. Grifols, S. Peris	(BARC)
JODIDIO	86	PR D34 1967	A. Jodidio et al.	(LBL, NWES, TRIU)
Also		PR D37 237 (erratum)	A. Jodidio et al.	(LBL, NWES, TRIU)
BARTEL	85K	PL B60B 337	W. Bartel et al.	(JADE Collab.)
EICHTEN	84	RMP 56 579	E. Eichten et al.	(FNAL, LBL, OSU)
ACCIARRI	82	PL B116B 264	F.M. Renard	(CERN)

Extra Dimensions

For explanation of terms used and discussion of significant model dependence of following limits, see the "Extra Dimensions" review. Footnotes describe originally quoted limit. n indicates the number of extra dimensions.

Limits not encoded here are summarized in the "Extra Dimensions" review.

EXTRA DIMENSIONS

Updated Sept. 2007 by G.F. Giudice (CERN) and J.D. Wells (MCTP/Michigan).

I Introduction

The idea of using extra spatial dimensions to unify different forces started in 1914 with Nordstöm, who proposed a 5-dimensional vector theory to simultaneously describe electromagnetism and a scalar version of gravity. After the invention of general relativity, in 1919 Kaluza noticed that the 5-dimensional generalization of Einstein theory can simultaneously describe gravitational and electromagnetic interactions. The role of gauge invariance and the physical meaning of the compactification of extra dimensions was elucidated by Klein. However, the Kaluza-Klein (KK) theory failed in its original purpose because of internal inconsistencies and was essentially abandoned until the advent of supergravity in the late 1970's. Higher-dimensional theories were reintroduced in physics to exploit the special properties that supergravity and superstring theories possess for particular values of spacetime dimensions. More recently it was realized [1,2] that extra dimensions with a fundamental scale of order TeV^{-1} could address the $M_W - M_{Pl}$ hierarchy problem and therefore have direct implications for collider experiments. Here we will review [3] the proposed scenarios with experimentally accessible extra dimensions.

II Gravity in Flat Extra Dimensions**II.1 Theoretical Setup**

Following Ref. 1, let us consider a D -dimensional spacetime with $D = 4 + \delta$, where δ is the number of extra spatial dimensions. The space is factorized into $R^4 \times M_\delta$ (meaning that the 4-dimensional part of the metric does not depend on extra-dimensional coordinates), where M_δ is a δ -dimensional compact space with finite volume V_δ . For concreteness, we will consider a δ -dimensional torus of radius R , for which $V_\delta = (2\pi R)^\delta$. Standard Model (SM) fields are assumed to be localized on a $(3+1)$ -dimensional subspace. This assumption can be realized in field theory, but it is most natural [4] in the setting of string theory, where gauge and matter fields can be confined to live on “branes” (for a review see Ref. 5). On the other hand, gravity, which according to general relativity is described by the spacetime geometry, extends to all D dimensions. The Einstein action takes the form

$$S_E = \frac{\bar{M}_D^{2+\delta}}{2} \int d^4x d^\delta y \sqrt{-\det g} \mathcal{R}(g), \quad (1)$$

where x and y describe ordinary and extra coordinates, respectively. The metric g , the scalar curvature \mathcal{R} , and the reduced Planck mass \bar{M}_D refer to the D -dimensional theory. The effective action for the 4-dimensional graviton is obtained by restricting the metric indices to 4 dimensions and by performing the integral in y . Because of the above-mentioned factorization hypothesis, the integral in y reduces to the volume V_δ , and therefore the 4-dimensional reduced Planck mass is given by

$$\bar{M}_{\text{Pl}}^2 = \bar{M}_D^{2+\delta} V_\delta = \bar{M}_D^{2+\delta} (2\pi R)^\delta, \quad (2)$$

where $\bar{M}_{\text{Pl}} = M_{\text{Pl}}/\sqrt{8\pi} = 2.4 \times 10^{18}$ GeV. The same formula can be obtained from Gauss’s law in extra dimensions [6]. Following ref. [7], we will consider $M_D = (2\pi)^\delta/(2+\delta)\bar{M}_D$ as the fundamental D -dimensional Planck mass.

The key assumption of Ref. 1 is that the hierarchy problem is solved because the truly fundamental scale of gravity M_D (and therefore the ultraviolet cut-off of field theory) lies around the TeV region. From Eq. (2) it follows that the correct value of \bar{M}_{Pl} can be obtained with a large value of RM_D . The inverse compactification radius is therefore given by

$$R^{-1} = M_D (M_D/\bar{M}_{\text{Pl}})^{2/\delta}, \quad (3)$$

which corresponds to 4×10^{-4} eV, 20 keV, 7 MeV for $M_D = 1$ TeV and $\delta = 2, 4, 6$, respectively. In this framework, gravity is weak because it is diluted in a large space ($R \gg M_D^{-1}$). Of course, a complete solution of the hierarchy problem would require a dynamical explanation for the radius stabilization at a large value.

A D -dimensional bosonic field can be expanded in Fourier modes in the extra coordinates

$$\phi(x, y) = \sum_{\vec{n}} \frac{\varphi^{(\vec{n})}(x)}{\sqrt{V_\delta}} \exp\left(i \frac{\vec{n} \cdot \vec{y}}{R}\right). \quad (4)$$

The sum is discrete because of the finite size of the compactified space. The fields $\varphi^{(\vec{n})}$ are called the n^{th} KK excitations (or modes) of ϕ , and correspond to particles propagating in 4 dimensions with masses $m_{(\vec{n})}^2 = |\vec{n}|^2/R^2 + m_0^2$, where m_0 is the mass of the zero mode. The D -dimensional graviton can then be recast as a tower of KK states with increasing mass. However, since R^{-1} in Eq. (3) is smaller than the typical energy resolution in collider experiments, the mass distribution of KK gravitons is practically continuous.

Although each KK graviton has a purely gravitational coupling suppressed by \bar{M}_{Pl}^{-1} , inclusive processes in which we sum over the large number of available gravitons have cross sections suppressed only by powers of M_D . Indeed, for scatterings with typical energy E , we expect $\sigma \sim E^\delta/M_D^{2+\delta}$, as evident from power-counting in D dimensions. Processes involving gravitons are therefore detectable in collider experiments if M_D is in the TeV region.

The astrophysical considerations described in Sec. II.6 set very stringent bounds on M_D for $\delta < 4$, in some cases even ruling out the possibility of observing any signal at the LHC. However, these bounds disappear if there are no KK gravitons lighter than about 100 MeV. Variations of the original model exist [8,9] in which the light KK gravitons receive small extra contributions to their masses, sufficient to evade the astrophysical bounds. Notice that collider experiments are nearly insensitive to such modifications of the infrared part of the KK graviton spectrum, since they mostly probe the heavy graviton modes. Therefore, in the context of these variations, it is important to test at colliders extra-dimensional gravity also for low values of δ , and even for $\delta = 1$ [9]. In addition to these direct experimental constraints, the proposal of gravity in flat extra dimensions has dramatic cosmological consequences and requires a rethinking of the thermal history of the universe for temperatures as low as the MeV scale.

II.2 Collider Signals in Linearized Gravity

By making a derivative expansion of Einstein gravity, one can construct an effective theory describing KK graviton interactions, which is valid for energies much smaller than M_D [7,10,11]. With the aid of this effective theory, it is possible to make predictions for graviton-emission processes at colliders. Since the produced gravitons interact with matter only with rates suppressed by inverse powers of \bar{M}_{Pl} , they will remain undetected leaving a “missing-energy” signature. Extra-dimensional gravitons have been searched for in the processes $e^+e^- \rightarrow \gamma + \cancel{E}$ and $e^+e^- \rightarrow Z + \cancel{E}$ at LEP, and $p\bar{p} \rightarrow \text{jet} + \cancel{E}_T$ and $p\bar{p} \rightarrow \gamma + \cancel{E}_T$ at the Tevatron. The combined LEP 95% CL limits are [12] $M_D > 1.60, 1.20, 0.94, 0.77, 0.66$ TeV for $\delta = 2, \dots, 6$ respectively. Experiments at the LHC will improve the sensitivity. However, the theoretical predictions for the graviton-emission rates should be applied with care to hadron machines. The effective theory results are valid only for center-of-mass energy of the parton collision much smaller than M_D .

Searches Particle Listings

Extra Dimensions

The effective theory under consideration also contains the full set of higher-dimensional operators, whose coefficients are, however, not calculable, because they depend on the ultra-violet properties of gravity. This is in contrast with graviton emission, which is a calculable process within the effective theory because it is linked to the infrared properties of gravity. The higher-dimensional operators are the analogue of the contact interactions described in ref. [13]. Of particular interest is the dimension-8 operator mediated by tree-level graviton exchange [7,11,14]

$$\mathcal{L}_{\text{int}} = \pm \frac{4\pi}{\Lambda_T^4} \mathcal{T}, \quad \mathcal{T} = \frac{1}{2} \left(T_{\mu\nu} T^{\mu\nu} - \frac{1}{\delta+2} T_\mu^\mu T_\nu^\nu \right), \quad (5)$$

where $T_{\mu\nu}$ is the energy momentum tensor. (There exist several alternate definitions in the literature for the cutoff in Eq. (5) including M_{TT} used in the Listings, where $M_{TT}^4 = (2/\pi)\Lambda_T^4$.) This operator gives anomalous contributions to many high-energy processes. The 95% CL limit from Bhabha scattering and diphoton production at LEP is [15] $\Lambda_T > 1.29$ (1.12) TeV for constructive (destructive) interference, corresponding to the \pm signs in Eq. (5). The analogous limit from Drell-Yan and diphotons at Tevatron is [16] $\Lambda_T > 1.43$ (1.27) TeV.

Graviton loops can be even more important than tree-level exchange, because they can generate operators of dimension lower than 8. For simple graviton loops, there is only one dimension-6 operator that can be generated (excluding Higgs fields in the external legs) [18,19],

$$\mathcal{L}_{\text{int}} = \pm \frac{4\pi}{\Lambda_T^2} \Upsilon, \quad \Upsilon = \frac{1}{2} \left(\sum_{f=q,\ell} \bar{f} \gamma_\mu \gamma_5 f \right)^2. \quad (6)$$

Here the sum extends over all quarks and leptons in the theory. The 95% CL combined LEP limit [20] from lepton-pair processes is $\Lambda_T > 17.2$ (15.1) TeV for constructive (destructive) interference, and $\Lambda_T > 15.3$ (11.5) TeV is obtained from $b\bar{b}$ production. Limits from graviton emission and effective operators cannot be compared in a model-independent way, unless one introduces some well-defined cutoff procedure (see, *e.g.*, Ref. 19).

II.3 The Transplanckian Regime

The use of linearized Einstein gravity, discussed in Sec. II.2, is valid for processes with typical center-of-mass energy $\sqrt{s} \ll M_D$. The physics at $\sqrt{s} \sim M_D$ can be described only with knowledge of the underlying quantum-gravity theory. Toy models have been used to mimic possible effects of string theory at colliders [21]. Once we access the transplanckian region $\sqrt{s} \gg M_D$, a semiclassical description of the scattering process becomes adequate. Indeed, in the transplanckian limit, the Schwarzschild radius for a colliding system with center-of-mass energy \sqrt{s} in $D = 4 + \delta$ dimensions,

$$R_S = \left[\frac{2^\delta \pi^{(\delta-3)/2}}{\delta+2} \Gamma\left(\frac{\delta+3}{2}\right) \frac{\sqrt{s}}{M_D^{\delta+2}} \right]^{1/(\delta+1)}, \quad (7)$$

is larger than the D -dimensional Planck length M_D^{-1} . Therefore, quantum-gravity effects are subleading with respect to classical gravitational effects (described by R_S).

If the impact parameter b of the process satisfies $b \gg R_S$, the transplanckian collision is determined by linear semiclassical gravitational scattering. The corresponding cross sections have been computed [22] in the eikonal approximation, valid in the limit of small deflection angle. The collider signal at the LHC is a dijet final state, with features characteristic of gravity in extra dimensions.

When $b < R_S$, we expect gravitational collapse and black-hole formation [23,24] (see Ref. 25 and references therein). The black-hole production cross section is estimated to be of order the geometric area $\sigma \sim \pi R_S^2$. This estimate has large uncertainties due, for instance, to the unknown amount of gravitational radiation emitted during collapse. Nevertheless, for M_D close to the weak scale, the black-hole production rate at the LHC is large. For example, the production cross section of 6 TeV black holes is about 10 pb, for $M_D = 1.5$ TeV. The produced black-hole emits thermal radiation with Hawking temperature $T_H = (\delta+1)/(4\pi R_S)$ until it reaches the Planck phase (where quantum-gravity effects become important). A black hole of initial mass M_{BH} completely evaporates with lifetime $\tau \sim M_{BH}^{(\delta+3)/(\delta+1)} / M_D^{2(\delta+2)/(\delta+1)}$, which typically is 10^{-26} – 10^{-27} s for $M_D = 1$ TeV. The black hole can be easily detected because it emits a significant fraction of visible (*i.e.*, non-gravitational) radiation, although the precise amount is not known in the general case of D dimensions. Computations exist [26] for the grey-body factors, which describe the distortion of the emitted radiation from pure black-body caused by the strong gravitational background field.

To trust the semiclassical approximation, the typical energy of the process has to be much larger than M_D . Given the present constraints on extra-dimensional gravity, it is clear that the maximum energy available at the LHC allows, at best, to only marginally access the transplanckian region. If gravitational scattering and black-hole production are observed at the LHC, it is likely that significant quantum-gravity (or string-theory) corrections will affect the semiclassical calculations or estimates. In the context of string theory, it is possible that the production of string-balls [27] dominates over black holes.

If M_D is around the TeV scale, transplanckian collisions would regularly occur in the interaction of high-energy cosmic rays with the earth's atmosphere and could be observed in present and future cosmic ray experiments [28,29].

II.4 Graviscalars

After compactification, the D -dimensional graviton contains KK towers of spin-2 gravitational states (as discussed above), of spin-1 “graviphoton” states, and of spin-0 “graviscalar” states. In most processes, the graviphotons and graviscalars are much less important than their spin-2 counterparts. A single graviscalar tower is coupled to SM fields through the trace of the energy momentum tensor. The resulting coupling is, however, very weak for SM particles with small masses.

Perhaps the most accessible probe of the graviscalars would be through their allowed mixing with the Higgs boson [30] in the induced curvature-Higgs term of the 4-dimensional action. This can be recast as a contribution to the decay width of the SM Higgs boson into an invisible channel. Although the invisible branching fraction is a free parameter of the theory, it is more likely to be important when the SM Higgs boson width is particularly narrow ($m_H \lesssim 140$ GeV). The collider phenomenology of invisibly decaying Higgs bosons investigated in the literature is applicable here (see Ref. 31 and references therein).

II.5 Tests of the Gravitational Force Law

The theoretical developments in gravity with large extra dimensions have further stimulated interest in experiments looking for possible deviations from the gravitational inverse-square law (for a review, see Ref. 32). Such deviations are usually parametrized by a modified Newtonian potential of the form

$$V(r) = -G_N \frac{m_1 m_2}{r} [1 + \alpha \exp(-r/\lambda)]. \quad (8)$$

The experimental limits on the parameters α and λ are summarized in Fig. 1, taken from Ref. 33.

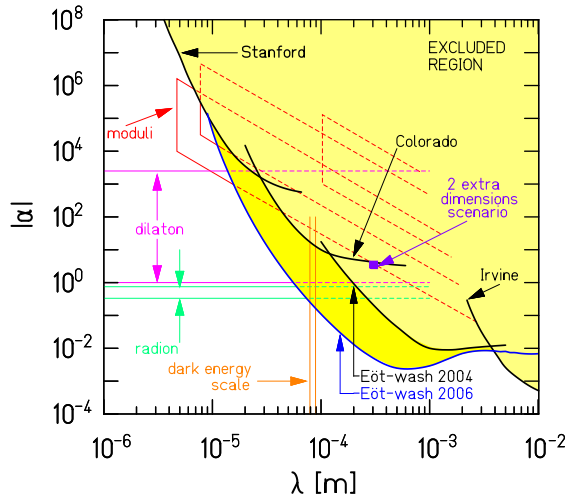


Figure 1: Experimental limits on α and λ of Eq. (8), which parametrize deviations from Newton’s law. From Ref. 33.

For gravity with δ extra dimensions, in the case of toroidal compactifications, the parameter α is given by $\alpha = 8 \delta/3$ and λ is the Compton wavelength of the first graviton Kaluza-Klein mode, equal to the radius R . From the results shown in Fig. 1, one finds $R < 37$ (44) μm at 95% CL for $\delta = 2$ (1) which, using Eq. (3), becomes $M_D > 3.6$ TeV for $\delta = 2$. This bound is weaker than the astrophysical bounds discussed in Sec. II.6, which actually exclude the occurrence of any visible signal in planned tests of Newton’s law. However, in the context of higher-dimensional theories, other particles like light gauge bosons, moduli or radions could mediate detectable modifications of Newton’s law, without running up against the astrophysical limits.

II.6 Astrophysical Bounds

Because of the existence of the light and weakly-coupled KK gravitons, gravity in extra dimensions is strongly constrained by several astrophysical considerations (see Ref. [34] and references therein). The requirement that KK gravitons do not carry away more than half of the energy emitted by the supernova SN1987A gives the bounds [35] $M_D > 14$ (1.6) TeV for $\delta = 2$ (3). KK gravitons produced by all supernovae in the universe lead to a diffuse γ ray background generated by graviton decays into photons. Measurements by the EGRET satellite imply [36] $M_D > 38$ (4.1) TeV for $\delta = 2$ (3). Most of the KK gravitons emitted by supernova remnants and neutron stars are gravitationally trapped. The gravitons forming this halo occasionally decay, emitting photons. Limits on γ rays from neutron-star sources imply [34] $M_D > 200$ (16) TeV for $\delta = 2$ (3). The decay products of the gravitons forming the halo can hit the surface of the neutron star, providing a heat source. The low measured luminosities of some pulsars imply [34] $M_D > 750$ (35) TeV for $\delta = 2$ (3). These bounds are valid only if the graviton KK mass spectrum below about 100 MeV is not modified by distortions of the compactification space (see Sec. II.1).

III Gravity in Warped Extra Dimensions

III.1 Theoretical Setup

In the proposal of Ref. 2, the M_W - M_{Pl} hierarchy is explained using an extra-dimensional analogy of the classical gravitational redshift in curved space, as we illustrate below. The setup consists of a 5-dimensional space in which the fifth dimension is compactified on S^1/Z_2 , *i.e.*, a circle projected into a segment by identifying points of the circle opposite with respect to a given diameter. Each end-point of the segment (the “fixed-points” of the orbifold projection) is the location of a 3-dimensional brane. The two branes have equal but opposite tensions. We will refer to the negative-tension brane as the infrared (IR) brane, where SM fields are assumed to be localized, and the positive-tension brane as the ultraviolet (UV) brane. The bulk cosmological constant is fine-tuned such that the effective cosmological constant in the 3-dimensional space exactly cancels.

The solution of the Einstein equation in vacuum gives the metric corresponding to the line element

$$ds^2 = \exp(-2k|y|) \eta_{\mu\nu} dx^\mu dx^\nu - dy^2. \quad (9)$$

Here y is the 5th coordinate, with the UV and IR branes located at $y = 0$ and $y = \pi R$, respectively; R is the compactification radius and k is the AdS curvature. The 4-dimensional metric in Eq. (9) is modified with respect to the flat Minkowski metric $\eta_{\mu\nu}$ by the factor $\exp(-2k|y|)$. This shows that the 5-dimensional space is not factorized, meaning that the 4-dimensional metric depends on the extra-dimensional coordinate y . This feature is key to the desired effect.

As is known from general relativity, the energy of a particle travelling through a gravitational field is redshifted by

Searches Particle Listings

Extra Dimensions

an amount proportional to $|g_{00}|^{-1/2}$, where g_{00} is the time-component of the metric. Analogously, energies (or masses) viewed on the IR brane ($y = \pi R$) are red-shifted with respect to their values at the UV brane ($y = 0$) by an amount equal to the warp factor $\exp(-\pi kR)$, as shown by Eq. (9):

$$m_{IR} = m_{UV} \exp(-\pi kR). \quad (10)$$

A mass $m_{UV} \sim \mathcal{O}(\overline{M}_{\text{Pl}})$ on the UV brane corresponds to a mass on the IR brane with a value $m_{IR} \sim \mathcal{O}(M_{\text{W}})$, if $R \simeq 12k^{-1}$. A radius moderately larger than the fundamental scale k is therefore sufficient to reproduce the large hierarchy between the Planck and Fermi scales. A simple and elegant mechanism to stabilize the radius exists [38], by adding a scalar particle with a bulk mass and different potential terms on the two branes.

The effective theory describing the interaction of the KK modes of the graviton is characterized by two mass parameters, which we take to be m_1 and Λ_π . Both are a warp-factor smaller than the UV scale, and therefore they are naturally of order the weak scale. The parameter m_1 is the mass of the first KK graviton mode, from which the mass m_n of the generic n^{th} mode is determined,

$$m_n = \frac{x_n}{x_1} m_1. \quad (11)$$

Here x_n is the n^{th} root of the Bessel function J_1 ($x_1 = 3.83$, $x_2 = 7.02$ and, for large n , $x_n = (n + 1/4)\pi$). The parameter Λ_π determines the strength of the coupling of the KK gravitons $h_{\mu\nu}^{(n)}$ with the energy momentum tensor $T_{\mu\nu}$,

$$\mathcal{L} = -\frac{T^{\mu\nu}}{\overline{M}_{\text{Pl}}} h_{\mu\nu}^{(0)} - \frac{T^{\mu\nu}}{\Lambda_\pi} \sum_{n=1}^{\infty} h_{\mu\nu}^{(n)}. \quad (12)$$

In the approach discussed in Sec. II.1, \overline{M}_{Pl} appears to us much larger than the weak scale because gravity is diluted in a large space. In the approach described in this section, the explanation lies instead in the non-trivial configuration of the gravitational field: the zero-mode graviton wavefunction is peaked around the UV brane and it has an exponentially small overlap with the IR brane where we live. The extra dimensions discussed in Sec. II.1 are large and “nearly flat;” the graviton excitations are very weakly coupled and have a mass gap that is negligibly small in collider experiments. Here, instead, the gravitons have a mass gap of \sim TeV size and become strongly-coupled at the weak scale.

III.2 Collider Signals

The KK excitations of the graviton, possibly being of order the TeV scale, are subject to experimental discovery at high-energy colliders. As discussed above, KK graviton production cross-sections and decay widths are set by the first KK mass m_1 and the graviton-matter interaction scale Λ_π . Some studies use m_1 and k as the independent parameters, and so it is helpful to keep in mind that the relationships between all of these parameters are

$$\frac{m_n}{\Lambda_\pi} = \frac{kx_n}{\overline{M}_{\text{Pl}}}, \quad \Lambda_\pi = \overline{M}_{\text{Pl}} \exp(-\pi kR), \quad (13)$$

where again x_n are the zeros of the J_1 Bessel function. Resonant and on-shell production of the n^{th} KK gravitons leads to characteristic peaks in the dilepton and diphoton invariant-mass spectra and it is probed at colliders for $\sqrt{s} \geq m_n$. Current limits from dimuon, dielectron, and diphoton channels at CDF and DØ give the 95% CL limits $\Lambda_\pi > 4.3(2.6)$ TeV for $m_1 = 500(700)$ GeV [16,17].

Contact interactions arising from integrating out heavy KK modes of the graviton generate the dimension-8 operator \mathcal{T} , analogous to the one in Eq. (5) in the flat extra dimensions case. Although searches for effects of these non-renormalizable operators cannot confirm directly the existence of a heavy spin-2 state, they nevertheless provide a good probe of the model [39,40].

Searches for direct production of KK excitations of the graviton and contact interactions induced by gravity in compact extra-dimensional warped space will continue at the LHC. With the large increase in energy, one expects prime regions of the parameter space up to $m_n, \Lambda_\pi \sim 10$ TeV [39] to be probed.

If SM states are in the AdS bulk, KK graviton phenomenology becomes much more model dependent. Present limits and future collider probes of the masses and interaction strengths of the KK gravitons to matter fields are significantly reduced [41] in some circumstances, and each specific model of SM fields in the AdS bulk should be analyzed on a case-by-case basis.

For warped metrics, black-hole production is analogous to the case discussed in Sec. II.3, as long the radius of the black hole is smaller than the AdS radius $1/k$, when the space is effectively flat. For heavier black holes, the production cross section is expected to grow with energy only as $\log^2 E$, saturating the Froissart bound [37].

III.3 The Radion

The size of the warped extra-dimensional space is controlled by the value of the radion, a scalar field corresponding to an overall dilatation of the extra coordinates. Stabilizing the radion is required for a viable theory, and known stabilization mechanisms often imply that the radion is less massive than the KK excitations of the graviton [38], thus making it perhaps the lightest beyond-the-SM particle in this scenario.

The coupling of the radion r to matter is $\mathcal{L} = -rT/\Lambda_\varphi$, where T is the trace of the energy momentum tensor and $\Lambda_\varphi = \sqrt{24}\Lambda_\pi$ is expected to be near the weak scale. The relative couplings of r to the SM fields are similar to, but not exactly the same as, those of the Higgs boson. The partial widths are generally smaller by a factor of v/Λ_φ compared to SM Higgs decay widths, where $v = 246$ GeV is the vacuum expectation value of the SM Higgs doublet. On the other hand, the trace anomaly that arises in the SM gauge groups by virtue of quantum effects enhances the couplings of the radion to gluons and photons over the naive v/Λ_φ rescaling of the Higgs couplings to these same particles. Thus, for example, one finds that the radion’s large coupling to gluons [30,43] enables a sizeable $gg \rightarrow r$ cross section even for Λ_φ large compared to m_{W} .

Another subtlety of the radion is its ability to mix with the Higgs boson through the curvature-scalar interaction [30],

$$S_{mix} = -\xi \int d^4x \sqrt{-\det g_{\text{ind}}} R(g_{\text{ind}}) H^+ H, \quad (14)$$

where g_{ind} is the four-dimensional induced metric. With $\xi \neq 0$, there is neither a pure Higgs boson nor pure radion mass eigenstate. Mixing between states enables decays of the heavier eigenstate into lighter eigenstates if kinematically allowed. Overall, the production cross sections, widths and relative branching fractions can all be affected significantly by the value of the mixing parameter ξ [30,42,43,44]. Despite the various permutations of couplings and branching fractions that the radion and the Higgs-radion mixed states can have into SM particles, the search strategies for these particles at high-energy colliders are similar to those of the SM Higgs boson.

IV Standard Model Fields in Flat Extra Dimensions

IV.1 TeV-Scale Compactification

Not only gravity, but also SM fields could live in an experimentally accessible higher-dimensional space [45]. This hypothesis could lead to unification of gauge couplings at a low scale [46]. In contrast with gravity, these extra dimensions must be at least as small as about TeV^{-1} in order to avoid incompatibility with experiment. The canonical extra-dimensional space of this type is a 5th dimension compactified on the interval S^1/Z_2 , where again the radius of the S^1 is denoted R , and the Z_2 symmetry identifies $y \leftrightarrow -y$ of the extra-dimensional coordinate. The two fixed points $y = 0$ and $y = \pi R$ define the end-points of the compactification interval.

Let us first consider the case in which gauge fields live in extra dimensions, while matter and Higgs fields are confined to a 3-brane. The masses M_n of the gauge-boson KK excitations are related to the masses M_0 of the zero-mode normal gauge bosons by

$$M_n^2 = M_0^2 + \frac{n^2}{R^2}. \quad (15)$$

The KK excitations of the vector bosons have couplings to matter a factor of $\sqrt{2}$ larger than the zero modes ($g_n = \sqrt{2}g$). Therefore, if the first KK excitation is $\sim \text{TeV}$, tree-level virtual effects of the KK gauge bosons can have a significant effect on precision electroweak observables and high-energy processes such as $e^+e^- \rightarrow f\bar{f}$. In this theory one expects that observables will be shifted with respect to their SM value by a fractional amount proportional to [47]

$$V = 2 \sum_n \left(\frac{g_n^2}{g^2} \right) \frac{M_Z^2 R^2}{n^2} \sim \frac{2}{3} \pi^2 M_Z^2 R^2. \quad (16)$$

More complicated compactifications lead to more complicated representations of V . A global fit to all relevant observables, including precision electroweak data, Tevatron, HERA and LEP2 results, shows that $R^{-1} \gtrsim 6.8 \text{ TeV}$ is required [48,49]. The LHC with 100 fb^{-1} integrated luminosity would be able to search nearly as high as $R^{-1} \sim 16 \text{ TeV}$ [48].

Fermions can also be promoted to live in the extra dimensions. Although fermions are vector-like in 5-dimension, chiral states in 4-dimensions can be obtained by using the Z_2 symmetry of the orbifold. An interesting possibility to explain the observed spectrum of quark and lepton masses is to assume that different fermions are localized in different points of the extra dimension. Their different overlap with the Higgs wavefunction can generate a hierarchical structure of Yukawa couplings [50], although there are strong bounds on the non-universal couplings of fermions to the KK gauge bosons from flavor-violating processes [51].

The case in which all SM particles uniformly propagate in the bulk of an extra-dimensional space is referred to as Universal Extra Dimensions (UED) [52]. The absence of a reference brane that breaks translation invariance in the extra dimensional direction implies extra-dimensional momentum conservation. After compactification and after inclusion of boundary terms at the fixed points, the conservation law preserves only a discrete Z_2 parity (called KK-parity). The KK-parity of the n^{th} KK mode of each particle is $(-1)^n$. Thus, in UED, the first KK excitations can only be pair-produced and their virtual effect comes only from loop corrections. Therefore the ability to search for and constrain parameter space is diminished. The result is that for one extra dimension the limit on R^{-1} is between 300 and 500 GeV depending on the Higgs mass [53].

Because of KK-parity conservation, the lightest KK state is stable. Thus, one interesting consequence of UED is the possibility of the lightest KK state comprising the dark matter. After including radiative corrections [54], it is found that the lightest KK state is the first excitation of the hypercharge gauge boson $B^{(1)}$. It can constitute the cold dark matter of the universe if its mass is approximately 600 GeV [55], well above current collider limits. The LHC should be able to probe UED up to $R^{-1} \sim 1.5 \text{ TeV}$ [56], and thus possibly confirm the UED dark matter scenario.

An interesting and ambitious approach is to use extra dimensions to explain the hierarchy problem through Higgs-gauge unification [57]. The SM Higgs doublet is interpreted as the extra-dimensional component of an extended gauge symmetry acting in more than four dimensions, and the weak scale is protected by the extra-dimensional gauge symmetry. There are several obstacles to make this proposal fully realistic, but ongoing research is trying to overcome them.

IV.2 Grand Unification in Extra Dimensions

Extra dimensions offer a simple and elegant way to break GUT symmetries [58] by appropriate field boundary conditions in compactifications on orbifolds. In this case the size of the relevant extra dimensions is much smaller than what has been considered so far, with compactification radii that are typically $\mathcal{O}(M_{\text{GUT}})$. This approach has several attractive features (for a review, see Ref. 59). The doublet-triplet splitting problem [60] is solved by projecting out the unwanted light Higgs triplet in the compactification. In the same way, one can eliminate

Searches Particle Listings

Extra Dimensions

the dangerous supersymmetric $d = 5$ proton-decay operators, or even forbid proton decay [61]. However, the prospects for proton-decay searches are not necessarily bleak. Because of the effect of the KK modes, the unification scale can be lowered to 10^{14} – 10^{15} GeV, enhancing the effect of $d = 6$ operators. The prediction for the proton lifetime is model-dependent.

V Standard Model Fields in Warped Extra Dimensions

V.1 Extra Dimensions and Strong Dynamics at the Weak Scale

In the original warped model of Ref. 2, all SM fields are confined on the IR brane, although to solve the hierarchy problem it is sufficient that only the Higgs field lives on the brane. The variation in which SM fermions and gauge bosons are bulk fields is interesting because it links warped extra dimensions to technicolor-like models with strong dynamics at the weak scale. This connection comes from the AdS/CFT correspondence [62], which relates the properties of AdS₅, 5-dimensional gravity with negative cosmological constant, to a strongly-coupled 4-dimensional conformal field theory (CFT). In the correspondence, the motion along the 5th dimension is interpreted as the renormalization-group flow of the 4-dimensional theory, with the UV brane playing the role of the Planck-mass cutoff and the IR brane as the breaking of the conformal invariance. Local gauge symmetries acting on the bulk of AdS₅ correspond to global symmetries of the 4-dimensional theory. The original warped model of Ref. 2 is then reinterpreted as an “almost CFT,” whose couplings run very slowly with the renormalization scale until the TeV scale is reached, where the theory develops a mass gap. In the variation in which SM fields, other than the Higgs, are promoted to the bulk, these fields correspond to elementary particles coupled to the CFT. Around the TeV scale the theory becomes strongly-interacting, producing a composite Higgs, which breaks electroweak symmetry. Notice the similarity with walking technicolor [63].

The most basic version of this theory is in conflict with electroweak precision measurements. To reduce the contribution to the ρ parameter, it is necessary to introduce an approximate global symmetry, a custodial $SU(2)$ under which the generators of $SU(2)_L$ transform as a triplet. Using the AdS/CFT correspondence, this requires the extension of the electroweak gauge symmetry to $SU(2)_L \times SU(2)_R \times U(1)$ in the bulk of the 5-dimensional theory [64]. Models along these lines have been constructed. The composite Higgs can be lighter than the strongly-interacting scale in models in which it is a pseudo-Goldstone boson [65]. Nevertheless, electroweak data provide strong constraints on such models.

When SM fermions are promoted to 5 dimensions, they become non-chiral and can acquire a bulk mass. The fermions are localized in different positions along the 5th dimension, with an exponential dependence on the value of the bulk mass (in units of the AdS curvature). Since the masses of the ordinary zero-mode SM fermions depend on their wavefunction overlap with the Higgs (localized on the IR brane), large hierarchies in

the mass spectrum of quarks and leptons can be obtained from order-unity variations of the bulk masses [66]. This mechanism can potentially explain the fermion mass pattern, and it can lead to new effects in flavor-changing processes, especially those involving the third-generation quarks [67]. The smallness of neutrino masses can also be explained, if right-handed neutrinos propagate in the bulk [68].

V.2 Higgsless Models

Extra dimensions offer new possibilities for breaking gauge symmetries. Even in the absence of physical scalars, electroweak symmetry can be broken by field boundary conditions on compactified spaces. The lightest KK modes of the gauge bosons corresponding to broken generators acquire masses equal to R^{-1} , the inverse of the compactification radius, now to be identified with M_W . In the ordinary 4-dimensional case, the SM without a Higgs boson violates unitarity at energies $E \sim 4\pi M_W/g \sim 1$ TeV. On the other hand, in extra dimensions, the breaking of unitarity in the longitudinal- W scattering amplitudes is delayed because of the contribution of the heavy KK gauge-boson modes [69]. The largest effect is obtained for one extra dimension, where the violation of unitarity occurs around $E \sim 12\pi^2 M_W/g \sim 10$ TeV. This is conceivably a large enough scale to render the strong dynamics, which is eventually responsible for unitarization, invisible to the processes measured by LEP experiments.

These Higgsless models, in their minimal version, are inconsistent with observations, because they predict new W gauge bosons with masses nM_W (with $n \geq 2$ integers) [70]. However, warping the 5th dimension has a double advantage [71]. The excited KK modes of the gauge bosons can all have masses in the TeV range, making them compatible with present collider limits. Also, by enlarging the bulk gauge symmetry to $SU(2)_L \times SU(2)_R \times U(1)$, one can obtain an approximate custodial symmetry, as described above, to tame tree-level corrections to ρ . If quarks and leptons are extended to the bulk, they can obtain masses through the electroweak-breaking effect on the boundaries. However at present, there is no model that reproduces the top quark mass and is totally consistent with electroweak data [72].

VI. Supersymmetry in Extra Dimensions

Extra dimensions have a natural home within string theory. Similarly, string theory and supersymmetry are closely connected, as the latter is implied by the former in most constructions. Coexistence between extra dimensions and supersymmetry is often considered a starting point for string model building. From a low-energy model-building point of view, perhaps the most compelling reason to introduce extra dimensions with supersymmetry lies in the mechanism of supersymmetry breaking.

When the field periodic boundary conditions on the compactified space are twisted using an R -symmetry, different zero modes for bosons and fermions are projected out and supersymmetry is broken. This is known as the Scherk-Schwarz

See key on page 405

mechanism of supersymmetry breaking [73]. In the simplest approach [74], a 5th dimension with $R^{-1} \sim 1$ TeV is introduced in which the non-chiral matter (gauge and Higgs multiplets) live. The chiral matter (quark and lepton multiplets) live on the three-dimensional spatial boundary. S^1/Z_2 compactification of the 5th dimension, which simultaneously employs the Scherk-Schwarz mechanism, generates masses for the bulk fields (gauginos and higgsinos) of order R^{-1} . Boundary states (squarks and sleptons) get mass from loop corrections, and are parametrically smaller in value. The right-handed slepton is expected to be the lightest supersymmetric particle (LSP), which being charged is not a good dark matter candidate. Thus, this theory likely requires R -parity violation in order to allow this charged LSP to decay and not cause cosmological problems.

By allowing all supersymmetric fields to propagate in the bulk of a $S^1/Z_2 \times Z'_2$ compactified space, it is possible to construct a model [75] taking advantage of the nonlocal breaking of supersymmetry. In this case, there are no quadratic divergences (except for a Fayet-Iliopoulos term [76]) and the Higgs mass is calculable. In the low-energy effective theory there is a single Higgs doublet, two superpartners for each SM particle, and the stop is the LSP, requiring a small amount of R -parity breaking.

Supersymmetry in warped space is also an interesting possibility. Again, one can consider [77] the case of chiral fields confined to our ordinary 3+1 dimensions, and gravity and gauge fields living in the 5-dimensional bulk space. Rather than being TeV^{-1} size, the 5th dimension is strongly warped to generate the supersymmetry-breaking scale. In this case, the tree-level mass of the gravitino is $\sim 10^{-3}$ eV and the masses of the gauginos are $\sim \text{TeV}$. The sleptons and squarks get mass at one loop from gauge interactions and thus are diagonal in flavor space, creating no additional FCNC problems. It has also been proposed [78] that an approximately supersymmetric Higgs sector confined on the IR brane could coexist with non-supersymmetric SM fields propagating in the bulk of the warped space.

In conclusion, we should reiterate that an important general consequence of extra dimensional theories is retained in supersymmetric extensions: KK excitations of the graviton and/or gauge fields are likely to be accessible at the LHC if the scale of compactification is directly related to solving the hierarchy problem. Any given extra-dimensional theory has many aspects to it, but the KK excitation spectrum is the most generic and most robust aspect of the idea to test in experiments.

References

1. N. Arkani-Hamed *et al.*, Phys. Lett. **B429**, 263 (1998).
2. L. Randall and R. Sundrum, Phys. Rev. Lett. **83**, 3370 (1999).
3. For other reviews, see V. A. Rubakov, Phys. Usp. **44**, 871 (2001);
J. Hewett and M. Spiropulu, Ann. Rev. Nucl. and Part. Sci. **52**, 397 (2002);
R. Rattazzi, *Proc. of Cargese School of Particle Physics and Cosmology*, Corsica, France, 4-16 Aug 2003;
- C. Csaki, hep-ph/0404096;
R. Sundrum, hep-th/0508134.
4. I. Antoniadis *et al.*, Phys. Lett. **B436**, 257 (1998).
5. J. Polchinski, "Lectures on D-branes," hep-th/9611050.
6. N. Arkani-Hamed *et al.*, Phys. Rev. **D59**, 086004 (1999).
7. G. F. Giudice *et al.*, Nucl. Phys. **B544**, 3 (1999).
8. N. Kaloper *et al.*, Phys. Rev. Lett. **85**, 928 (2000);
K. R. Dienes, Phys. Rev. Lett. **88**, 011601 (2002).
9. G. F. Giudice *et al.*, Nucl. Phys. **B706**, 455 (2005).
10. E. A. Mirabelli *et al.*, Phys. Rev. Lett. **82**, 2236 (1999).
11. T. Han *et al.*, Phys. Rev. **D59**, 105006 (1999).
12. LEP Exotica Working Group, LEP Exotica WG 2004-03.
13. K. Hagiwara *et al.*, "Searches for Quark and Lepton Compositeness," in this *Review*.
14. J. L. Hewett, Phys. Rev. Lett. **82**, 4765 (1999).
15. D. Bourilkov, hep-ex/0103039.
16. G. Landsberg, [D0 and CDF Collaboration], hep-ex/0412028.
17. V. M. Abazov *et al.*, [D0 Collaboration], Phys. Rev. Lett. **95**, 091801 (2005).
18. R. Contino *et al.*, JHEP **106**, 005 (2001).
19. G. F. Giudice and A. Strumia, Nucl. Phys. **B663**, 377 (2003).
20. LEP Working Group LEP2FF/02-03.
21. E. Dudas and J. Mourad, Nucl. Phys. **B575**, 3 (2000);
S. Cullen *et al.*, Phys. Rev. **D62**, 055012 (2000);
P. Burikham *et al.*, Phys. Rev. **D71**, 016005 (2005);
[Erratum-*ibid.*, **71**, 019905 (2005)].
22. G. F. Giudice *et al.*, Nucl. Phys. **B630**, 293 (2002).
23. S. B. Giddings and S. Thomas, Phys. Rev. **D65**, 056010 (2002).
24. S. Dimopoulos and G. Landsberg, Phys. Rev. Lett. **87**, 161602 (2001).
25. P. Kanti, Int. J. Mod. Phys. **A19**, 4899 (2004).
26. P. Kanti and J. March-Russell, Phys. Rev. **D66**, 024023 (2002);
Phys. Rev. **D67**, 104019 (2003).
27. S. Dimopoulos and R. Emparan, Phys. Lett. **B526**, 393 (2002).
28. J. L. Feng and A. D. Shapere, Phys. Rev. Lett. **88**, 021303 (2002).
29. R. Emparan *et al.*, Phys. Rev. **D65**, 064023 (2002).
30. G. F. Giudice *et al.*, Nucl. Phys. **B595**, 250 (2001).
31. D. Dominici, hep-ph/0503216.
32. E. G. Adelberger *et al.*, Ann. Rev. Nucl. and Part. Sci. **53**, 77 (2003).
33. D. J. Kapner *et al.*, Phys. Rev. Lett. **98**, 021101 (2007).
34. S. Hannestad and G. G. Raffelt, Phys. Rev. Lett. **88**, 071301 (2002).
35. C. Hanhart *et al.*, Phys. Lett. **B509**, 1 (2002).
36. S. Hannestad and G. Raffelt, Phys. Rev. Lett. **87**, 051301 (2001).
37. S. B. Giddings, Phys. Rev. **D67**, 126001 (2003).
38. W. D. Goldberger and M. B. Wise, Phys. Rev. Lett. **83**, 4922 (1999).
39. H. Davoudiasl *et al.*, Phys. Rev. Lett. **84**, 2080 (2000).
40. K. Cheung, hep-ph/0409028.

Searches Particle Listings

Extra Dimensions

41. H. Davoudiasl *et al.*, Phys. Rev. **D63**, 075004 (2001).
42. C. Csaki *et al.*, Phys. Rev. **D63**, 065002 (2001).
43. D. Dominici *et al.*, Nucl. Phys. **B671**, 243 (2003).
44. K. Cheung *et al.*, Phys. Rev. **D69**, 075011 (2004).
45. I. Antoniadis, Phys. Lett. **B246**, 377 (1990).
46. K. R. Dienes *et al.*, Phys. Lett. **B436**, 55 (1998);
K. R. Dienes *et al.*, Nucl. Phys. **B537**, 47 (1999).
47. T. G. Rizzo and J. D. Wells, Phys. Rev. **D61**, 016007 (2000).
48. K. Cheung and G. Landsberg, Phys. Rev. **D65**, 076003 (2002).
49. R. Barbieri *et al.*, Nucl. Phys. **B703**, 127 (2004).
50. N. Arkani-Hamed and M. Schmaltz, Phys. Rev. **D61**, 033005 (2000).
51. A. Delgado *et al.*, JHEP **0001**, 030 (2000).
52. T. Appelquist *et al.*, Phys. Rev. **D64**, 035002 (2001).
53. T. Appelquist and H. U. Yee, Phys. Rev. **D67**, 055002 (2003).
54. H. C. Cheng *et al.*, Phys. Rev. **D66**, 036005 (2002).
55. G. Servant and T. M. P. Tait, Nucl. Phys. **B650**, 391 (2003);
F. Burnell and G. D. Kribs, hep-ph/0509118;
K. Kong and K. T. Matchev, hep-ph/0509119.
56. H. C. Cheng *et al.*, Phys. Rev. **D66**, 056006 (2002).
57. N. S. Manton, Nucl. Phys. **B158**, 141 (1979).
58. Y. Kawamura, Prog. Theor. Phys. **105**, 999 (2001).
59. L. J. Hall and Y. Nomura, Annals Phys. **306**, 132 (2003).
60. S. Raby, "Grand Unified Theories," in this *Review*.
61. G. Altarelli and F. Feruglio, Phys. Lett. **B5111**, 257 (2001);
L. J. Hall and Y. Nomura, Phys. Rev. **D64**, 055003 (2001).
62. J. M. Maldacena, Adv. Theor. Math. Phys. **2**, 231 (1998) [Int. J. Theor. Phys. **38**, 1113 (1999)].
63. R.S. Chivukula *et al.*, "Technicolor," in this *Review*.
64. K. Agashe *et al.*, JHEP **0308**, 050 (2003).
65. K. Agashe *et al.*, Nucl. Phys. **B719**, 165 (2005).
66. T. Gherghetta and A. Pomarol, Nucl. Phys. **B586**, 141 (2000);
S. J. Huber and Q. Shafi, Phys. Lett. **B498**, 256 (2001).
67. K. Agashe *et al.*, Phys. Rev. **D71**, 016002 (2005).
68. Y. Grossman and M. Neubert, Phys. Lett. **B474**, 361 (2000).
69. R. S. Chivukula *et al.*, Phys. Lett. **B525**, 175 (2002).
70. C. Csaki *et al.*, Phys. Rev. **D69**, 055006 (2004).
71. C. Csaki *et al.*, Phys. Rev. Lett. **92**, 101802 (2004).
72. R. Barbieri *et al.*, Phys. Lett. **B591**, 141 (2004);
G. Cacciapaglia *et al.*, Phys. Rev. **D70**, 075014 (2004).
73. J. Scherk and J. H. Schwarz, Phys. Lett. **B82**, 60 (1979).
74. A. Pomarol and M. Quiros, Phys. Lett. **B438**, 255 (1998);
A. Delgado *et al.*, Phys. Rev. **D60**, 095008 (1999).
75. R. Barbieri *et al.*, Phys. Rev. **D63**, 105007 (2001).
76. D. M. Ghilencea *et al.*, Nucl. Phys. **B619**, 385 (2001).
77. T. Gherghetta and A. Pomarol, Nucl. Phys. **B602**, 3 (2001).
78. T. Gherghetta and A. Pomarol, Phys. Rev. **D67**, 085018 (2003).

Limits on R from Deviations in Gravitational Force Law

This section includes limits on the size of extra dimensions from deviations in the Newtonian ($1/r^2$) gravitational force law at short distances. Deviations are parametrized by a gravitational potential of the form $V = -(G m m'/r) [1 + \alpha \exp(-r/R)]$. For δ toroidal extra dimensions of equal size, $\alpha = 8\delta/3$. Quoted bounds are for $\delta = 2$ unless otherwise noted.

VALUE (μm)	CL%	DOCUMENT ID	COMMENT
		• • • We do not use the following data for averages, fits, limits, etc. • • •	
	95	1 MASUDA 09	Torsion pendulum
		2 GERACI 08	Microcantilever
		3 TRENKEL 08	Newton's constant
		4 DECCA 07A	Torsion oscillator
< 30	95	5 KAPNER 07	Torsion pendulum
< 47	95	6 TU 07	Torsion pendulum
		7 SMULLIN 05	Microcantilever
<130	95	8 HOYLE 04	Torsion pendulum
		9 CHIAVERINI 03	Microcantilever
< 200	95	10 LONG 03	Microcantilever
<190	95	11 HOYLE 01	Torsion pendulum
		12 HOSKINS 85	Torsion pendulum

1 MASUDA 09 obtain improved constraints on non-Newtonian forces with strengths $10^9 \lesssim |\alpha| \lesssim 10^{11}$ and length scales $R = 1.0\text{--}2.9 \mu\text{m}$. See their Fig. 3. This bound does not place limits on the size of extra flat dimensions.

2 GERACI 08 obtain improved constraints on non-Newtonian forces with strengths $|\alpha| > 14,000$ and length scales $R = 5\text{--}15 \mu\text{m}$. See their Fig. 9. This bound does not place limits on the size of extra flat dimensions.

3 TRENKEL 08 uses two independent measurements of Newton's constant G to constrain new forces with strength $|\alpha| \simeq 10^{-4}$ and length scales $R = 0.02\text{--}1 \text{ m}$. See their Fig. 1. This bound does not place limits on the size of extra flat dimensions.

4 DECCA 07A search for new forces and obtain bounds in the region with strengths $|\alpha| \simeq 10^{13}\text{--}10^{18}$ and length scales $R = 20\text{--}86 \text{ nm}$. See their Fig. 6. This bound does not place limits on the size of extra flat dimensions.

5 KAPNER 07 search for new forces, probing a range of $\alpha \simeq 10^{-3}\text{--}10^5$ and length scales $R \simeq 10\text{--}1000 \mu\text{m}$. For $\delta = 1$ the bound on R is $44 \mu\text{m}$. For $\delta = 2$, the bound is expressed in terms of M_* , here translated to a bound on the radius. See their Fig. 6 for details on the bound.

6 TU 07 search for new forces probing a range of $|\alpha| \simeq 10^{-1}\text{--}10^5$ and length scales $R \simeq 20\text{--}1000 \mu\text{m}$. For $\delta = 1$ the bound on R is $53 \mu\text{m}$. See their Fig. 3 for details on the bound.

7 SMULLIN 05 search for new forces, and obtain bounds in the region with strengths $\alpha \simeq 10^3\text{--}10^8$ and length scales $R = 6\text{--}20 \mu\text{m}$. See their Figs. 1 and 16 for details on the bound. This work does not place limits on the size of extra flat dimensions.

8 HOYLE 04 search for new forces, probing α down to 10^{-2} and distances down to $10 \mu\text{m}$. Quoted bound on R is for $\delta = 2$. For $\delta = 1$, bound goes to $160 \mu\text{m}$. See their Fig. 34 for details on the bound.

9 CHIAVERINI 03 search for new forces, probing α above 10^4 and λ down to $3 \mu\text{m}$, finding no signal. See their Fig. 4 for details on the bound. This bound does not place limits on the size of extra flat dimensions.

10 LONG 03 search for new forces, probing α down to 3, and distances down to about $10 \mu\text{m}$. See their Fig. 4 for details on the bound.

11 HOYLE 01 search for new forces, probing α down to 10^{-2} and distances down to $20 \mu\text{m}$. See their Fig. 4 for details on the bound. The quoted bound is for $\alpha \geq 3$.

12 HOSKINS 85 search for new forces, probing distances down to 4 mm . See their Fig. 13 for details on the bound. This bound does not place limits on the size of extra flat dimensions.

Limits on R from On-Shell Production of Gravitons: $\delta = 2$

This section includes limits on on-shell production of gravitons in collider and astrophysical processes. Bounds quoted are on R , the assumed common radius of the flat extra dimensions, for $\delta = 2$ extra dimensions. Studies often quote bounds in terms of derived parameter; experiments are actually sensitive to the masses of the KK gravitons: $m_{\vec{n}} = |\vec{n}|/R$. See the Review on "Extra Dimensions" for details. Bounds are given in μm for $\delta=2$.

VALUE (μm)	CL%	DOCUMENT ID	TECN	COMMENT
		• • • We do not use the following data for averages, fits, limits, etc. • • •		
< 245	95	13 AALTONEN 08AC	CDF	$p\bar{p} \rightarrow \gamma G, jG$
< 615	95	14 ABAZOV 08S	D0	$p\bar{p} \rightarrow \gamma G$
< 0.916	95	15 DAS 08		Supernova cooling
< 350	95	16 ABULENCIA,A 06	CDF	$p\bar{p} \rightarrow jG$
< 270	95	17 ABDALLAH 05B	DLPH	$e^+e^- \rightarrow \gamma G$
< 210	95	18 ACHARD 04E	L3	$e^+e^- \rightarrow \gamma G$
< 480	95	19 ACOSTA 04C	CDF	$p\bar{p} \rightarrow jG$
< 0.00038	95	20 CASSE 04		Neutron star γ sources
< 610	95	21 ABAZOV 03	D0	$p\bar{p} \rightarrow jG$
< 0.96	95	22 HANNESTAD 03		Supernova cooling
< 0.096	95	23 HANNESTAD 03		Diffuse γ background
< 0.051	95	24 HANNESTAD 03		Neutron star γ sources
< 0.00016	95	25 HANNESTAD 03		Neutron star heating
< 300	95	26 HEISTER 03C	ALEP	$e^+e^- \rightarrow \gamma G$
		27 FAIRBAIRN 01		Cosmology
< 0.66	95	28 HANHART 01		Supernova cooling
		29 CASSISI 00		Red giants
<1300	95	30 ACCIARRI 99S	L3	$e^+e^- \rightarrow ZG$

See key on page 405

Searches Particle Listings

Extra Dimensions

Limits on R from On-Shell Production of Gravitons: $\delta \geq 3$

This section includes limits similar to those in the previous section, but for $\delta = 3$ extra dimensions. Bounds are given in nm for $\delta = 3$. Entries are also shown for papers examining models with $\delta > 3$.

VALUE (nm)	CL%	DOCUMENT ID	TECN	COMMENT
< 2.8	95	13 AALTONEN	08AC CDF	$p\bar{p} \rightarrow \gamma G, jG$
< 4.56	95	14 ABAZOV	08S D0	$p\bar{p} \rightarrow \gamma G$
< 2.09	95	15 DAS	08	Supernova cooling
< 3.6	95	16 ABULENCIA,A	06 CDF	$p\bar{p} \rightarrow jG$
< 3.5	95	17 ABDALLAH	05B DLPH	$e^+e^- \rightarrow \gamma G$
< 2.9	95	18 ACHARD	04E L3	$e^+e^- \rightarrow \gamma G$
< 0.0042	95	19 ACOSTA	04C CDF	$\bar{p}p \rightarrow jG$
< 6.1	95	20 CASSE	04	Neutron star γ sources
< 1.14	95	21 ABAZOV	03 D0	$\bar{p}p \rightarrow jG$
< 0.025	95	22 HANNESTAD	03	Supernova cooling
< 0.11	95	23 HANNESTAD	03	Diffuse γ background
< 0.0026	95	24 HANNESTAD	03	Neutron star γ sources
< 3.9	95	25 HANNESTAD	03	Neutron star heating
< 0.8	95	26 HEISTER	03C ALEP	$e^+e^- \rightarrow \gamma G$
< 18	95	27 FAIRBAIRN	01	Cosmology
		28 HANHART	01	Supernova cooling
		29 CASSISI	00	Red giants
		30 ACCIARRI	99S L3	$e^+e^- \rightarrow ZG$
<p>13 AALTONEN 08AC search for $p\bar{p} \rightarrow \gamma G$ and $p\bar{p} \rightarrow jG$ at $\sqrt{s} = 1.96$ TeV with 2.0 fb⁻¹ and 1.1 fb⁻¹ respectively, in order to place bounds on the fundamental scale and size of the extra dimensions. See their Table III for limits on all $\delta \leq 6$.</p> <p>14 ABAZOV 08S search for $p\bar{p} \rightarrow \gamma G$, using 1 fb⁻¹ of data at $\sqrt{s} = 1.96$ TeV to place bounds on M_D for two to eight extra dimensions, from which these bounds on R are derived. See their paper for intermediate values of δ.</p> <p>15 DAS 08 obtain a limit on R from Kaluza-Klein graviton cooling of SN1987A due to plasmon-plasmon annihilation.</p> <p>16 ABULENCIA,A 06 search for $p\bar{p} \rightarrow jG$ using 368 pb⁻¹ of data at $\sqrt{s} = 1.96$ TeV. See their Table II for bounds for all $\delta \leq 6$.</p> <p>17 ABDALLAH 05B search for $e^+e^- \rightarrow \gamma G$ at $\sqrt{s} = 180$-209 GeV to place bounds on the size of extra dimensions and the fundamental scale. Limits for all $\delta \leq 6$ are given in their Table 6. These limits supersede those in ABREU 00Z.</p> <p>18 ACHARD 04E search for $e^+e^- \rightarrow \gamma G$ at $\sqrt{s} = 189$-209 GeV to place bounds on the size of extra dimensions and the fundamental scale. See their Table 8 for limits with $\delta \leq 8$. These limits supersede those in ACCIARRI 99R.</p> <p>19 ACOSTA 04C search for $\bar{p}p \rightarrow jG$ at $\sqrt{s} = 1.8$ TeV to place bounds on the size of extra dimensions and the fundamental scale. See their paper for bounds on $\delta = 4, 6$.</p> <p>20 CASSE 04 obtain a limit on R from the gamma-ray emission of point γ sources that arises from the photon decay of gravitons around newly born neutron stars, applying the technique of HANNESTAD 03 to neutron stars in the galactic bulge. Limits for all $\delta \leq 7$ are given in their Table I.</p> <p>21 ABAZOV 03 search for $p\bar{p} \rightarrow jG$ at $\sqrt{s} = 1.8$ TeV to place bounds on M_D for 2 to 7 extra dimensions, from which these bounds on R are derived. See their paper for bounds on intermediate values of δ. We quote results without the approximate NLO scaling introduced in the paper.</p> <p>22 HANNESTAD 03 obtain a limit on R from graviton cooling of supernova SN1987A. Limits for all $\delta \leq 7$ are given in their Tables V and VI.</p> <p>23 HANNESTAD 03 obtain a limit on R from gravitons emitted in supernovae and which subsequently decay, contaminating the diffuse cosmic γ background. Limits for all $\delta \leq 7$ are given in their Tables V and VI. These limits supersede those in HANNESTAD 02.</p> <p>24 HANNESTAD 03 obtain a limit on R from gravitons emitted in two recent supernovae and which subsequently decay, creating point γ sources. Limits for all $\delta \leq 7$ are given in their Tables V and VI. These limits are corrected in the published erratum.</p> <p>25 HANNESTAD 03 obtain a limit on R from the heating of old neutron stars by the surrounding cloud of trapped KK gravitons. Limits for all $\delta \leq 7$ are given in their Tables V and VI. These limits supersede those in HANNESTAD 02.</p> <p>26 HEISTER 03C use the process $e^+e^- \rightarrow \gamma G$ at $\sqrt{s} = 189$-209 GeV to place bounds on the size of extra dimensions and the scale of gravity. See their Table 4 for limits with $\delta \leq 6$ for derived limits on M_D.</p> <p>27 FAIRBAIRN 01 obtains bounds on R from over production of KK gravitons in the early universe. Bounds are quoted in paper in terms of fundamental scale of gravity. Bounds depend strongly on temperature of QCD phase transition and range from $R < 0.13 \mu\text{m}$ to $0.001 \mu\text{m}$ for $\delta=2$; bounds for $\delta=3,4$ can be derived from Table 1 in the paper.</p> <p>28 HANHART 01 obtain bounds on R from limits on graviton cooling of supernova SN1987A using numerical simulations of proto-neutron star neutrino emission.</p> <p>29 CASSISI 00 obtain rough bounds on M_D (and thus R) from red giant cooling for $\delta=2,3$. See their paper for details.</p> <p>30 ACCIARRI 99S search for $e^+e^- \rightarrow ZG$ at $\sqrt{s}=189$ GeV. Limits on the gravity scale are found in their Table 2, for $\delta \leq 4$.</p>				

Mass Limits on M_{TT}

This section includes limits on the cut-off mass scale, M_{TT} , of dimension-8 operators from KK graviton exchange in models of large extra dimensions. Ambiguities in the UV-divergent summation are absorbed into the parameter λ , which is taken to be $\lambda = \pm 1$ in the following analyses. Bounds for $\lambda = -1$ are shown in parenthesis after the bound for $\lambda = +1$, if appropriate. Different papers use slightly different definitions of the mass scale. The definition used here is related to another popular convention by $M_{TT}^2 = (2/\pi) \Lambda_{T,1}^2$, as discussed in the above Review on "Extra Dimensions."

VALUE (TeV)	CL%	DOCUMENT ID	TECN	COMMENT
> 1.48	95	31 ABAZOV	09AE D0	$p\bar{p} \rightarrow$ dijet, angular distrib.

> 1.45	95	32 ABAZOV	09D D0	$p\bar{p} \rightarrow e^+e^-, \gamma\gamma$	
> 1.1	(> 1.0)	95	33 SCHAEF	07A ALEP	$e^+e^- \rightarrow e^+e^-$
> 0.898	(> 0.998)	95	34 ABDALLAH	06C DLPH	$e^+e^- \rightarrow \ell^+\ell^-$
> 0.853	(> 0.939)	95	35 GERDES	06	$p\bar{p} \rightarrow e^+e^-, \gamma\gamma$
> 0.96	(> 0.93)	95	36 ABAZOV	05V D0	$p\bar{p} \rightarrow \mu^+\mu^-$
> 0.78	(> 0.79)	95	37 CHEKANOV	04B ZEUS	$e^{\pm}p \rightarrow e^{\pm}X$
> 0.805	(> 0.956)	95	38 ABBIENDI	03D OPAL	$e^+e^- \rightarrow \gamma\gamma$
> 0.7	(> 0.7)	95	39 ACHARD	03D L3	$e^{\pm}p \rightarrow ZZ$
> 0.82	(> 0.78)	95	40 ADLOFF	03 H1	$e^{\pm}p \rightarrow e^{\pm}X$
> 1.28	(> 1.25)	95	41 GIUDICE	03 RVUE	
>20.6	(> 15.7)	95	42 GIUDICE	03 RVUE	Dim-6 operators
> 0.80	(> 0.85)	95	43 HEISTER	03C ALEP	$e^+e^- \rightarrow \gamma\gamma$
> 0.84	(> 0.99)	95	44 ACHARD	02D L3	$e^+e^- \rightarrow \gamma\gamma$
> 1.2	(> 1.1)	95	45 ABBOTT	01 D0	$p\bar{p} \rightarrow e^+e^-, \gamma\gamma$
> 0.60	(> 0.63)	95	46 ABBIENDI	00R OPAL	$e^+e^- \rightarrow \mu^+\mu^-$
> 0.63	(> 0.50)	95	46 ABBIENDI	00R OPAL	$e^+e^- \rightarrow \tau^+\tau^-$
> 0.68	(> 0.61)	95	46 ABBIENDI	00R OPAL	$e^+e^- \rightarrow \mu^+\mu^-, \tau^+\tau^-$
			47 ABREU	00A DLPH	$e^+e^- \rightarrow \gamma\gamma$
> 0.680	(> 0.542)	95	48 ABREU	00S DLPH	$e^+e^- \rightarrow \mu^+\mu^-, \tau^+\tau^-$
> 15-28		99.7	49 CHANG	00B RVUE	Electroweak
> 0.98		95	50 CHEUNG	00 RVUE	$e^+e^- \rightarrow \gamma\gamma$
> 0.29-0.38		95	51 GRAESSER	00 RVUE	$(g-2)_\mu$
> 0.50-1.1		95	52 HAN	00 RVUE	Electroweak
> 2.0	(> 2.0)	95	53 MATHEWS	00 RVUE	$\bar{p}p \rightarrow jj$
> 1.0	(> 1.1)	95	54 MELE	00 RVUE	$e^+e^- \rightarrow VV$
			55 ABBIENDI	99P OPAL	
			56 ACCIARRI	99M L3	
			57 ACCIARRI	99S L3	
> 1.412	(> 1.077)	95	58 BOURILKOV	99S L3	$e^+e^- \rightarrow e^+e^-$
<p>31 ABAZOV 09AE use dijet angular distributions in 0.7 fb⁻¹ of data from $p\bar{p}$ collisions at $\sqrt{s} = 1.96$ TeV to place lower bounds on Λ_T (equivalent to their M_S), here converted to M_{TT}.</p> <p>32 ABAZOV 09D use 1.05 fb⁻¹ of data from $p\bar{p}$ collisions at $\sqrt{s} = 1.96$ TeV to place lower bounds on Λ_T (equivalent to their M_S), here converted to M_{TT}.</p> <p>33 SCHAEF 07A use e^+e^- collisions at $\sqrt{s} = 189$-209 GeV to place lower limits on Λ_T, here converted to limits on M_{TT}.</p> <p>34 ABDALLAH 06C use e^+e^- collisions at $\sqrt{s} \sim 130$-207 GeV to place lower limits on M_{TT}, which is equivalent to their definition of M_S. Bound shown includes all possible final state leptons, $\ell = e, \mu, \tau$. Bounds on individual leptonic final states can be found in their Table 31.</p> <p>35 GERDES 06 use 100 to 110 pb⁻¹ of data from $p\bar{p}$ collisions at $\sqrt{s} = 1.8$ TeV, as recorded by the CDF Collaboration during Run I of the Tevatron. Bound shown includes a K-factor of 1.3. Bounds on individual e^+e^- and $\gamma\gamma$ final states are found in their Table I.</p> <p>36 ABAZOV 05V use 246 pb⁻¹ of data from $p\bar{p}$ collisions at $\sqrt{s} = 1.96$ TeV to search for deviations in the differential cross section to $\mu^+\mu^-$ from graviton exchange.</p> <p>37 CHEKANOV 04B search for deviations in the differential cross section of $e^{\pm}p \rightarrow e^{\pm}X$ with 130 pb⁻¹ of combined data and Q^2 values up to 40,000 GeV² to place a bound on M_{TT}.</p> <p>38 ABBIENDI 03D use e^+e^- collisions at $\sqrt{s}=181$-209 GeV to place bounds on the ultraviolet scale M_{TT}, which is equivalent to their definition of M_S.</p> <p>39 ACHARD 03D look for deviations in the cross section for $e^+e^- \rightarrow ZZ$ from $\sqrt{s} = 200$-209 GeV to place a bound on M_{TT}.</p> <p>40 ADLOFF 03 search for deviations in the differential cross section of $e^{\pm}p \rightarrow e^{\pm}X$ at $\sqrt{s}=301$ and 319 GeV to place bounds on M_{TT}.</p> <p>41 GIUDICE 03 review existing experimental bounds on M_{TT} and derive a combined limit.</p> <p>42 GIUDICE 03 place bounds on Λ_6, the coefficient of the gravitationally-induced dimension-6 operator $(2\pi\lambda/\Lambda_6^2)(\sum \bar{T}_i\gamma_i^5\eta)(\sum \bar{T}_j\mu_j^5\eta)$, using data from a variety of experiments. Results are quoted for $\lambda=\pm 1$ and are independent of δ.</p> <p>43 HEISTER 03C use e^+e^- collisions at $\sqrt{s}=189$-209 GeV to place bounds on the scale of dim-8 gravitational interactions. Their M_S^{\pm} is equivalent to our M_{TT} with $\lambda=\pm 1$.</p> <p>44 ACHARD 02 search for s-channel graviton exchange effects in $e^+e^- \rightarrow \gamma\gamma$ at $E_{\text{cm}} = 192$-209 GeV.</p> <p>45 ABBOTT 01 search for variations in differential cross sections to e^+e^- and $\gamma\gamma$ final states at the Tevatron.</p> <p>46 ABBIENDI 00R uses e^+e^- collisions at $\sqrt{s} = 189$ GeV.</p> <p>47 ABREU 00A search for s-channel graviton exchange effects in $e^+e^- \rightarrow \gamma\gamma$ at $E_{\text{cm}} = 189$-202 GeV.</p> <p>48 ABREU 00S uses e^+e^- collisions at $\sqrt{s}=183$ and 189 GeV. Bounds on μ and τ individual final states given in paper.</p> <p>49 CHANG 00B derive 3σ limit on M_{TT} of (28,19,15) TeV for $\delta=(2,4,6)$ respectively assuming the presence of a torsional coupling in the gravitational action. Highly model dependent.</p> <p>50 CHEUNG 00 obtains limits from anomalous diphoton production at OPAL due to graviton exchange. Original limit for $\delta=4$. However, unknown UV theory renders δ dependence unreliable. Original paper works in HLZ convention.</p> <p>51 GRAESSER 00 obtains a bound from graviton contributions to $g-2$ of the muon through loops of 0.29 TeV for $\delta=2$ and 0.38 TeV for $\delta=4,6$. Limits scale as $\lambda^{1/2}$. However calculational scheme not well-defined without specification of high-scale theory. See the "Extra Dimensions Review."</p> <p>52 HAN 00 calculates corrections to gauge boson self-energies from KK graviton loops and constrain them using S and T. Bounds on M_{TT} range from 0.5 TeV ($\delta=6$) to 1.1 TeV ($\delta=2$); see text. Limits have strong dependence, $\lambda^{\delta+2}$, on unknown λ coefficient.</p> <p>53 MATHEWS 00 search for evidence of graviton exchange in CDF and D0 dijet production data. See their Table 2 for slightly stronger δ-dependent bounds. Limits expressed in terms of $\bar{M}_S^4 = M_{TT}^4/8$.</p> <p>54 MELE 00 obtains bound from KK graviton contributions to $e^+e^- \rightarrow VV$ ($V=\gamma,W,Z$) at LEP. Authors use Hewett conventions.</p>					

Searches Particle Listings

Extra Dimensions

- ⁵⁵ ABBIENDI 99P search for s -channel graviton exchange effects in $e^+e^- \rightarrow \gamma\gamma$ at $E_{\text{cm}}=189$ GeV. The limits $G_{\pm} > 660$ GeV and $G_{\pm} > 634$ GeV are obtained from combined $E_{\text{cm}}=183$ and 189 GeV data, where G_{\pm} is a scale related to the fundamental gravity scale.
- ⁵⁶ ACCIARRI 99M search for the reaction $e^+e^- \rightarrow \gamma G$ and s -channel graviton exchange effects in $e^+e^- \rightarrow \gamma\gamma, W^+W^-, ZZ, e^+e^-, \mu^+\mu^-, \tau^+\tau^-, q\bar{q}$ at $E_{\text{cm}}=183$ GeV. Limits on the gravity scale are listed in their Tables 1 and 2.
- ⁵⁷ ACCIARRI 99S search for the reaction $e^+e^- \rightarrow ZG$ and s -channel graviton exchange effects in $e^+e^- \rightarrow \gamma\gamma, W^+W^-, ZZ, e^+e^-, \mu^+\mu^-, \tau^+\tau^-, q\bar{q}$ at $E_{\text{cm}}=189$ GeV. Limits on the gravity scale are listed in their Tables 1 and 2.
- ⁵⁸ BOURILKOV 99 performs global analysis of LEP data on e^+e^- collisions at $\sqrt{s}=183$ and 189 GeV. Bound is on Λ_T .

Direct Limits on Gravitational or String Mass Scale

This section includes limits on the fundamental gravitational scale and/or the string scale from processes which depend directly on one or the other of these scales.

VALUE (TeV)	DOCUMENT ID	TECN	COMMENT
$> 1-2$	⁵⁹ ANCHORDOQI.02B	RVUE	Cosmic Rays
> 0.49	⁶⁰ ACCIARRI 00P	L3	$e^+e^- \rightarrow e^+e^-$
$> 1-2$	⁵⁹ ANCHORDOQI 02B	RVUE	Cosmic Rays
> 0.49	⁶⁰ ACCIARRI 00P	L3	$e^+e^- \rightarrow e^+e^-$
$> 1-2$	⁵⁹ ANCHORDOQI 02B	RVUE	Cosmic Rays
> 0.49	⁶⁰ ACCIARRI 00P	L3	$e^+e^- \rightarrow e^+e^-$

⁵⁹ ANCHORDOQI 02B derive bound on M_D from non-observation of black hole production in high-energy cosmic rays. Bound is stronger for larger δ , but depends sensitively on threshold for black hole production.

⁶⁰ ACCIARRI 00P uses e^+e^- collisions at $\sqrt{s}=183$ and 189 GeV. Bound on string scale M_S from massive string modes. M_S is defined in hep-ph/0001166 by $M_S(1/\pi)^{1/8} \alpha^{-1/4} = M$ where $(4\pi G)^{-1} = M^2 + 2R^2$.

Limits on $1/R = M_c$

This section includes limits on $1/R = M_c$, the compactification scale in models with TeV extra dimensions, due to exchange of Standard Model KK excitations. Bounds assume fermions are not in the bulk, unless stated otherwise. See the "Extra Dimensions" review for discussion of model dependence.

VALUE (TeV)	CL%	DOCUMENT ID	TECN	COMMENT
> 1.59	95	⁶¹ ABAZOV 09AE	D0	$p\bar{p} \rightarrow$ dijet, angular dist.
> 0.6	95	⁶² HAISCH 07	RVUE	$\bar{B} \rightarrow X_s \gamma$
> 0.6	90	⁶³ GOGOLADZE 06	RVUE	Electroweak
> 3.3	95	⁶⁴ CORNET 00	RVUE	Electroweak
$> 3.3-3.8$	95	⁶⁵ RIZZO 00	RVUE	Electroweak
> 1.59	95	⁶¹ ABAZOV 09AE	D0	$p\bar{p} \rightarrow$ dijet, angular dist.
> 0.6	95	⁶² HAISCH 07	RVUE	$\bar{B} \rightarrow X_s \gamma$
> 0.6	90	⁶³ GOGOLADZE 06	RVUE	Electroweak
> 3.3	95	⁶⁴ CORNET 00	RVUE	Electroweak
$> 3.3-3.8$	95	⁶⁵ RIZZO 00	RVUE	Electroweak

⁶¹ ABAZOV 09AE use dijet angular distributions in 0.7 fb^{-1} of data from $p\bar{p}$ collisions at $\sqrt{s}=1.96$ TeV to place a lower bound on the compactification scale.

⁶² HAISCH 07 use inclusive \bar{B} -meson decays to place a Higgs mass independent bound on the compactification scale $1/R$ in the minimal universal extra dimension model.

⁶³ GOGOLADZE 06 use electroweak precision observables to place a lower bound on the compactification scale in models with universal extra dimensions. Bound assumes a 115 GeV Higgs mass. See their Fig. 3 for the bound as a function of the Higgs mass.

⁶⁴ CORNET 00 translates a bound on the coefficient of the 4-fermion operator $(\bar{\ell}\gamma_\mu\tau^a\ell)(\bar{\ell}\gamma_\mu\tau^a\ell)$ derived by Hagiwara and Matsumoto into a limit on the mass scale of KK W bosons.

⁶⁵ RIZZO 00 obtains limits from global electroweak fits in models with a Higgs in the bulk (3.8 TeV) or on the standard brane (3.3 TeV).

Limits on Kaluza-Klein Gravitons in Warped Extra Dimensions

This section places limits on the mass of the first Kaluza-Klein (KK) excitation of the graviton in the warped extra dimension model of Randall and Sundrum. Experimental bounds depend strongly on the warp parameter, k . See the "Extra Dimensions" review for a full discussion.

VALUE	DOCUMENT ID	TECN	COMMENT
> 1.1	⁶⁶ AALTONEN 08s	CDF	$p\bar{p} \rightarrow G \rightarrow ZZ$
> 1.1	⁶⁷ ABAZOV 08J	D0	$p\bar{p} \rightarrow G \rightarrow e^+e^-, \gamma\gamma$
> 1.1	⁶⁸ AALTONEN 07G	CDF	$p\bar{p} \rightarrow G \rightarrow \gamma\gamma$
> 1.1	⁶⁹ AALTONEN 07H	CDF	$p\bar{p} \rightarrow G \rightarrow e\bar{e}$
> 1.1	⁷⁰ ABAZOV 05N	D0	$p\bar{p} \rightarrow G \rightarrow \ell\ell, \gamma\gamma$
> 1.1	⁷¹ ABULENCIA 05A	CDF	$p\bar{p} \rightarrow G \rightarrow \ell\bar{\ell}$
> 1.1	⁶⁶ AALTONEN 08s	CDF	$p\bar{p} \rightarrow G \rightarrow ZZ$
> 1.1	⁶⁷ ABAZOV 08J	D0	$p\bar{p} \rightarrow G \rightarrow e^+e^-, \gamma\gamma$
> 1.1	⁶⁸ AALTONEN 07G	CDF	$p\bar{p} \rightarrow G \rightarrow \gamma\gamma$
> 1.1	⁶⁹ AALTONEN 07H	CDF	$p\bar{p} \rightarrow G \rightarrow e\bar{e}$
> 1.1	⁷⁰ ABAZOV 05N	D0	$p\bar{p} \rightarrow G \rightarrow \ell\ell, \gamma\gamma$
> 1.1	⁷¹ ABULENCIA 05A	CDF	$p\bar{p} \rightarrow G \rightarrow \ell\bar{\ell}$
> 1.1	⁶⁶ AALTONEN 08s	CDF	$p\bar{p} \rightarrow G \rightarrow ZZ$
> 1.1	⁶⁷ ABAZOV 08J	D0	$p\bar{p} \rightarrow G \rightarrow e^+e^-, \gamma\gamma$
> 1.1	⁶⁸ AALTONEN 07G	CDF	$p\bar{p} \rightarrow G \rightarrow \gamma\gamma$
> 1.1	⁶⁹ AALTONEN 07H	CDF	$p\bar{p} \rightarrow G \rightarrow e\bar{e}$
> 1.1	⁷⁰ ABAZOV 05N	D0	$p\bar{p} \rightarrow G \rightarrow \ell\ell, \gamma\gamma$
> 1.1	⁷¹ ABULENCIA 05A	CDF	$p\bar{p} \rightarrow G \rightarrow \ell\bar{\ell}$

⁶⁶ AALTONEN 08s use $p\bar{p}$ collisions at $\sqrt{s}=1.96$ TeV to search for KK gravitons in warped extra dimensions. They search for graviton resonances decaying to four electrons via two Z bosons using 1.1 fb^{-1} of data. See their Fig. 8 for limits on $\sigma \cdot B(G \rightarrow ZZ)$ versus the graviton mass.

⁶⁷ ABAZOV 08J use $p\bar{p}$ collisions at $\sqrt{s}=1.96$ TeV to search for KK gravitons in warped extra dimensions. They search for graviton resonances decaying to electrons and photons using 1 fb^{-1} of data. For warp parameter values of k/\overline{M}_P between 0.01 and 0.1 the lower limit on the mass of the lightest excitation is between 300 and 900 GeV. See their Fig. 4 for more details.

⁶⁸ AALTONEN 07G use $p\bar{p}$ collisions at 1.96 TeV to search for KK gravitons in warped extra dimensions. They search for graviton resonances decaying to photons using 1.2 fb^{-1} of data. For warp parameter values of $k/\overline{M}_P = 0.1, 0.05,$ and 0.01 the bounds on the graviton mass are 850, 694, and 230 GeV, respectively. See their Fig. 3 for more details.

⁶⁹ AALTONEN 07H use $p\bar{p}$ collisions at 1.96 TeV to search for KK gravitons in warped extra dimensions. They search for graviton resonances decaying to electrons using 1.3 fb^{-1} of data. For a warp parameter value of $k/\overline{M}_P = 0.1$ the bound on the graviton mass is 807 GeV. See their Fig. 4 for more details. A combined analysis with the diphoton data of AALTONEN 07G yields for $k/\overline{M}_P = 0.1$ a graviton mass lower bound of 889 GeV.

- ⁷⁰ ABAZOV 05N use $p\bar{p}$ collisions at 1.96 TeV to search for KK gravitons in warped extra dimensions. They search for graviton resonances decaying to muons, electrons or photons, using 260 pb^{-1} of data. For warp parameter values of $k/\overline{M}_P = 0.1, 0.05,$ and $0.01,$ the bounds on the graviton mass are 785, 650 and 250 GeV respectively. See their Fig. 3 for more details.
- ⁷¹ ABULENCIA 05A use $p\bar{p}$ collisions at 1.96 TeV to search for KK gravitons in warped extra dimensions. They search for graviton resonances decaying to muons or electrons, using 200 pb^{-1} of data. For warp parameter values of $k/\overline{M}_P = 0.1, 0.05,$ and $0.01,$ the bounds on the graviton mass are 710, 510 and 170 GeV respectively.

Limits on Mass of Radion

This section includes limits on mass of radion, usually in context of Randall-Sundrum models. See the "Extra Dimension Review" for discussion of model dependence.

VALUE (GeV)	DOCUMENT ID	TECN	COMMENT
> 35	⁷² ABBIENDI 05	OPAL	$e^+e^- \rightarrow Z$ radion
> 120	⁷³ MAHANTA 00	00	$Z \rightarrow$ radion $\ell\bar{\ell}$
> 120	⁷⁴ MAHANTA 00b	00b	$p\bar{p} \rightarrow$ radion $\rightarrow \gamma\gamma$
> 35	⁷² ABBIENDI 05	OPAL	e^+e^- collisions at $\sqrt{s}=91$ GeV and $\sqrt{s}=189-209$ GeV to place bounds on the radion mass in the RS model. See their Fig. 5 for bounds that depend on the radion-Higgs mixing parameter ξ and on $\Lambda_{W^*} = \Lambda_\phi/\sqrt{6}$. No parameter-independent bound is obtained.
> 120	⁷³ MAHANTA 00	00	obtain bound on radion mass in the RS model. Bound is from Higgs boson search at LEP 1.
> 120	⁷⁴ MAHANTA 00b	00b	uses $p\bar{p}$ collisions at $\sqrt{s}=1.8$ TeV; production via gluon-gluon fusion. Authors assume a radion vacuum expectation value of 1 TeV.

REFERENCES FOR Extra Dimensions

ABAZOV 09AE	PRL 103 191803	V.M. Abazov et al.	(D0 Collab.)
ABAZOV 09D	PRL 102 051601	V.M. Abazov et al.	(D0 Collab.)
MASUDA 09	PRL 102 171101	M. Masuda, M. Sasaki	(ICRR)
AALTONEN 08AC	PRL 101 181602	T. Aaltonen et al.	(CDF Collab.)
AALTONEN 08S	PR D78 012008	T. Aaltonen et al.	(CDF Collab.)
ABAZOV 08J	PRL 100 091802	V.M. Abazov et al.	(D0 Collab.)
ABAZOV 08S	PRL 101 011601	V.M. Abazov et al.	(D0 Collab.)
DAS 08	PR D78 063011	P.K. Das, V.H.S. Kumar, P.K. Suresh	(STAN)
GERACI 08	PR D78 022002	A.A. Geraci et al.	(STAN)
TRENKEL 08	PR D77 122001	C. Trenkel	(CDF Collab.)
AALTONEN 07G	PRL 99 171801	T. Aaltonen et al.	(CDF Collab.)
AALTONEN 07H	PRL 99 171802	T. Aaltonen et al.	(CDF Collab.)
DECCA 07A	EPJ C51 963	R.S. Decca et al.	(CDF Collab.)
HAISCH 07	PR D76 034014	U. Haisch, A. Weiler	(CDF Collab.)
KAPNER 07	PRL 98 021101	D.J. Kapner et al.	(ALEPH Collab.)
SCHAEF 07A	EPJ C19 411	S. Schaefer et al.	(ALEPH Collab.)
TU 07	PRL 98 201101	L.-C. Tu et al.	(ALEPH Collab.)
ABDALLAH 06C	EPJ C45 589	J. Abdallah et al.	(DELPHI Collab.)
ABULENCIA 06	PRL 97 171802	A. Abulencia et al.	(CDF Collab.)
GERDES 06	PR D73 112008	D. Gerdes et al.	(CDF Collab.)
GOGOLADZE 06	PR D74 093012	I. Gogoladze, C. Macesanu	(CDF Collab.)
ABAZOV 05N	PRL 95 091801	V.M. Abazov et al.	(D0 Collab.)
ABAZOV 05V	PRL 95 161602	V.M. Abazov et al.	(D0 Collab.)
ABBIENDI 05	PL B609 20	G. Abbiendi et al.	(OPAL Collab.)
ABDALLAH 05B	EPJ C38 395	J. Abdallah et al.	(DELPHI Collab.)
ABULENCIA 05A	PRL 95 252001	A. Abulencia et al.	(CDF Collab.)
SMULLIN 05	PR D72 122001	S.J. Smullin et al.	(CDF Collab.)
ACHARD 04E	PL B587 16	P. Achard et al.	(L3 Collab.)
ACOSTA 04C	PRL 92 121802	D. Acosta et al.	(CDF Collab.)
CASSE 04	PRL 92 111102	M. Casse et al.	(CDF Collab.)
CHEKANOV 04B	PL B591 23	S. Chekanov et al.	(ZEUS Collab.)
HOYLE 04	PR D70 042004	C.D. Hoyle et al.	(WASH)
ABAZOV 03D	PRL 90 251802	V.M. Abazov et al.	(D0 Collab.)
ABBIENDI 03D	EPJ C26 331	G. Abbiendi et al.	(OPAL Collab.)
ACHARD 03D	PL B572 133	P. Achard et al.	(L3 Collab.)
ADLOFF 03	PL B568 35	C. Adloff et al.	(H1 Collab.)
CHIAVERINI 03	PRL 90 151101	J. Chilverini et al.	(H1 Collab.)
GIUDICE 03	NP B463 377	G.F. Giudice, A. Strumia	(H1 Collab.)
HANNENSTAD 03	PR D67 125008	S. Hannestad, G.G. Raffelt	(ALEPH Collab.)
Also	PR D69 029901(erratum)	S. Hannestad, G.G. Raffelt	(ALEPH Collab.)
HEISTER 03C	EPJ C28 1	A. Heister et al.	(ALEPH Collab.)
LONG 03	Nature 421 922	J.C. Long et al.	(L3 Collab.)
ACHARD 02	PL B524 65	P. Achard et al.	(L3 Collab.)
ACHARD 02B	PL B531 28	P. Achard et al.	(L3 Collab.)
ANCHORDOQI.02B	PR D66 103002	L. Anchordoqui et al.	(L3 Collab.)
HANNENSTAD 02	PRL 88 071301	S. Hannestad, G. Raffelt	(D0 Collab.)
ABBOTT 01	PRL 86 1156	B. Abbott et al.	(D0 Collab.)
FAIRBAIRN 01	PL B508 335	M. Fairbairn	(D0 Collab.)
HANBHART 01	PL B509 1	C. Hanhart et al.	(D0 Collab.)
HOYLE 01	PRL 86 1418	C.D. Hoyle et al.	(D0 Collab.)
ABBIENDI 00A	EPJ C13 553	G. Abbiendi et al.	(OPAL Collab.)
ABREU 00A	PL B491 67	P. Abreu et al.	(DELPHI Collab.)
ABREU 00S	PL B485 45	P. Abreu et al.	(DELPHI Collab.)
ABREU 00Z	EPJ C17 53	P. Abreu et al.	(DELPHI Collab.)
ACCIARRI 00P	PL B489 81	M. Acciari et al.	(L3 Collab.)
CASSISI 00	PL B481 323	S. Cassisi et al.	(L3 Collab.)
CHANG 00B	PRL 85 3765	L.N. Chang et al.	(L3 Collab.)
CHEUNG 00	PR D61 015005	K. Cheung	(L3 Collab.)
CORNET 00	PR D61 037701	F. Cornet, M. Relano, J. Rico	(L3 Collab.)
GRASSER 00	PR D61 074019	M.L. Graesser	(L3 Collab.)
HAN 00	PR D62 125018	T. Han, D. Marfatia, R.-J. Zhang	(L3 Collab.)
MAHANTA 00	PL B480 176	U. Mahanta, S. Rakshit	(L3 Collab.)
MAHANTA 00B	PL B483 196	U. Mahanta, A. Datta	(L3 Collab.)
MATHEWS 00	JHEP 0007 008	P. Mathews, S. Raychaudhuri, K. Sridhar	(L3 Collab.)
MELE 00	PR D61 117901	S. Mele, E. Sanchez	(L3 Collab.)
RIZZO 00	PR D61 016007	T.G. Rizzo, J.D. Wells	(L3 Collab.)
ABBIENDI 99P	PL B465 303	G. Abbiendi et al.	(OPAL Collab.)
ACCIARRI 99M	PL B464 135	M. Acciari et al.	(L3 Collab.)
ACCIARRI 99R	PL B470 268	M. Acciari et al.	(L3 Collab.)
ACCIARRI 99S	PL B470 281	M. Acciari et al.	(L3 Collab.)
BOURILKOV 99	JHEP 9908 0016	D. Bourilkov	(L3 Collab.)
HOSKINS 85	PR D32 3084	J.K. Hoskins et al.	(L3 Collab.)

WIMPs and Other Particles Searches for

OMITTED FROM SUMMARY TABLE

WIMPS AND OTHER PARTICLE SEARCHES

Revised March 2002 by K. Hikasa (Tohoku University).

We collect here those searches which do not appear in any of the above search categories. These are listed in the following order:

1. Galactic WIMP (weakly-interacting massive particle) searches
2. Concentration of stable particles in matter
3. Limits on neutral particle production at accelerators
4. Limits on jet-jet resonance in hadron collisions
5. Limits on charged particles in e^+e^- collisions
6. Limits on charged particles in hadron reactions
7. Limits on charged particles in cosmic rays

Note that searches appear in separate sections elsewhere for Higgs bosons (and technipions), other heavy bosons (including W_R, W', Z' , leptoquarks, axiguons), axions (including pseudo-Goldstone bosons, Majorons, familons), heavy leptons, heavy neutrinos, free quarks, monopoles, supersymmetric particles, and compositeness. We include specific WIMP searches in the appropriate sections when they yield limits on hypothetical particles such as supersymmetric particles, axions, massive neutrinos, monopoles, etc.

We omit papers on CHAMP's, millicharged particles, and other exotic particles. We no longer list for limits on tachyons and centauros. See our 1994 edition for these limits.

GALACTIC WIMP SEARCHES

Cross-Section Limits for Dark Matter Particles (X^0) on Nuclei

These limits are for weakly-interacting stable particles that may constitute the invisible mass in the galaxy. Unless otherwise noted, a local mass density of $0.3 \text{ GeV}/\text{cm}^3$ is assumed; see each paper for velocity distribution assumptions. In the papers the limit is given as a function of the X^0 mass. Here we list limits only for typical mass values of 20 GeV, 100 GeV, and 1 TeV. Specific limits on supersymmetric dark matter particles may be found in the Supersymmetry section.

For $m_{X^0} = 20 \text{ GeV}$

VALUE (nb)	CL%	DOCUMENT ID	TECN	COMMENT
• • • We do not use the following data for averages, fits, limits, etc. • • •				
		1 AHMED 09	CDMS Ge	
		2 ARCHAMBAU..09	PICA F	
		3 LEBEDENKO 09A	ZEP3 Xe	
		4 LIN 09	TEXN Ge	
		5 AALSETH 08	CGNT Ge	
		6 ANGLE 08A	XE10 Xe	
		7 ALNER 07	ZEP2 Xe	
		8 LEE 07A	KIMS Csl	
		9 AKERIB 06	CDMS $^{73}\text{Ge}, ^{29}\text{Si}$	
		10 SHIMIZU 06A	CNTR F (CaF_2)	
		11 ALNER 05	NAIA NaI	
		12 BARNABE-HE..05	PICA F (C_4F_{10})	
		13 BENOIT 05	EDEL ^{73}Ge	
		14 GIRARD 05	SMP L F (C_2ClF_5)	
		15 KLAPDOR-K... 05	HDMS ^{73}Ge (enriched)	
		16 MIUCHI 03	BOLO LiF	
		17 TAKEDA 03	BOLO NaF	
< 0.08	90	18 ANGLOHER 02	CRES Al	
		19 BENOIT 00	EDEL Ge	
< 0.04	95	20 KLIMENKO 98	CNTR ^{73}Ge , inel.	
< 0.8		ALESSAND... 96	CNTR O	
< 6		ALESSAND... 96	CNTR Te	
< 0.02	90	21 BELLI 96	CNTR ^{129}Xe , inel.	
		22 BELLI 96c	CNTR ^{129}Xe	

< 0.004	90	23 BERNABEI 96	CNTR Na
< 0.3	90	23 BERNABEI 96	CNTR I
< 0.2	95	24 SARSA 96	CNTR Na
< 0.015	90	25 SMITH 96	CNTR Na
< 0.05	95	26 GARCIA 95	CNTR Natural Ge
< 0.1	95	QUENBY 95	CNTR Na
< 90	90	27 SNOWDEN-... 95	MICA ^{16}O
< 4 $\times 10^3$	90	27 SNOWDEN-... 95	MICA ^{39}K
< 0.7	90	BACCI 92	CNTR Na
< 0.12	90	28 REUSSER 91	CNTR Natural Ge
< 0.06	95	CALDWELL 88	CNTR Natural Ge

- 1 AHMED 09 give $\sigma < 0.06 \text{ pb}$ (90% CL) for spin-dependent X^0 -neutron cross section.
- 2 ARCHAMBAULT 09 give $\sigma < 0.2 \text{ pb}$ (90% CL) for spin-dependent X^0 -proton cross section.
- 3 LEBEDENKO 09A give $\sigma < 4 (0.04) \text{ pb}$ (90% CL) for spin-dependent X^0 -proton (neutron) cross section.
- 4 See their Fig. 6(b) for limits on spin-dependent X^0 -neutron cross section for m_{X^0} between 2 and 10 GeV.
- 5 See their Fig. 2 for cross section limits for m_{X^0} between 4 and 10 GeV.
- 6 ANGLE 08A give $\sigma < 0.6 (0.007) \text{ pb}$ (90% CL) for spin-dependent X^0 -proton (neutron) cross section.
- 7 ALNER 07 give $\sigma < 100 (0.5) \text{ pb}$ (90% CL) for spin-dependent X^0 -proton (neutron) cross section.
- 8 LEE 07A give $\sigma < 1 (25) \text{ pb}$ (90% CL) for spin-dependent X^0 -proton (neutron) cross section.
- 9 AKERIB 06 give $\sigma < 20 (0.3) \text{ pb}$ (90% CL) for spin-dependent X^0 -proton (neutron) cross section. See also AKERIB 05.
- 10 SHIMIZU 06A give $\sigma < 2 (30) \text{ pb}$ (90% CL) for spin-dependent X^0 -proton (neutron) cross section.
- 11 ALNER 05 give $\sigma < 0.5 (60) \text{ pb}$ (90% CL) for spin-dependent X^0 -proton (neutron) cross section.
- 12 BARNABE-HEIDER 05 give $\sigma < 1.5 (20) \text{ pb}$ (90% CL) for spin-dependent X^0 -proton (neutron) cross section.
- 13 BENOIT 05 give $\sigma < 10 \text{ pb}$ (90% CL) for spin-dependent X^0 -neutron cross section.
- 14 GIRARD 05 give $\sigma < 1.5 \text{ pb}$ (90% CL) for spin-dependent X^0 -proton cross section.
- 15 KLAPDOR-KLEINGROTHAUS 05 give $\sigma < 4 \text{ pb}$ (90% CL) for spin-dependent X^0 -neutron cross section.
- 16 MIUCHI 03 give model-independent limit $\sigma < 35 \text{ pb}$ (90% CL) for spin-dependent X^0 -proton cross section.
- 17 TAKEDA 03 give model-independent limit $\sigma < 0.03 (0.6) \text{ nb}$ (90% CL) for spin-dependent X^0 -proton (neutron) cross section.
- 18 ANGLOHER 02 limit is for spin-dependent WIMP-Aluminum cross section.
- 19 BENOIT 00 find four event categories in Ge detectors and suggest that low-energy surface nuclear recoils can explain anomalous events reported by UKDMC and Saclay NaI experiments.
- 20 KLIMENKO 98 limit is for inelastic scattering $X^0 \text{ } ^{73}\text{Ge} \rightarrow X^0 \text{ } ^{73}\text{Ge}^* (13.26 \text{ keV})$.
- 21 BELLI 96 limit for inelastic scattering $X^0 \text{ } ^{129}\text{Xe} \rightarrow X^0 \text{ } ^{129}\text{Xe}^* (39.58 \text{ keV})$.
- 22 BELLI 96c use background subtraction and obtain $\sigma < 150 \text{ pb}$ ($< 1.5 \text{ fb}$) (90% CL) for spin-dependent (independent) X^0 -proton cross section. The confidence level is from R. Bernabei, private communication, May 20, 1999.
- 23 BERNABEI 96 use pulse shape discrimination to enhance the possible signal. The limit here is from R. Bernabei, private communication, September 19, 1997.
- 24 SARSA 96 search for annual modulation of WIMP signal. See SARSA 97 for details of the analysis. The limit here is from M.L. Sarsa, private communication, May 26, 1997.
- 25 SMITH 96 use pulse shape discrimination to enhance the possible signal. A dark matter density of 0.4 GeV cm^{-3} is assumed.
- 26 GARCIA 95 limit is from the event rate. A weaker limit is obtained from searches for diurnal and annual modulation.
- 27 SNOWDEN-IFFT 95 look for recoil tracks in an ancient mica crystal. Similar limits are also given for ^{27}Al and ^{28}Si . See COLLAR 96 and SNOWDEN-IFFT 96 for discussion on potential backgrounds.
- 28 REUSSER 91 limit here is changed from published (0.04) after reanalysis by authors. J.L. Vuilleumier, private communication, March 29, 1996.

For $m_{X^0} = 100 \text{ GeV}$

VALUE (nb)	CL%	DOCUMENT ID	TECN	COMMENT
• • • We do not use the following data for averages, fits, limits, etc. • • •				
		1 AHMED 09	CDMS Ge	
		2 ARCHAMBAU..09	PICA F	
		3 LEBEDENKO 09A	ZEP3 Xe	
		4 ANGLE 08A	XE10 Xe	
		5 BEDNYAKOV 08	RVUE Ge	
		6 ALNER 07	ZEP2 Xe	
		7 LEE 07A	KIMS Csl	
		8 MIUCHI 07	CNTR F (CF_4)	
		9 AKERIB 06	CDMS $^{73}\text{Ge}, ^{29}\text{Si}$	
		10 SHIMIZU 06A	CNTR F (CaF_2)	
		11 ALNER 05	NAIA NaI	
		12 BARNABE-HE..05	PICA F (C_4F_{10})	
		13 BENOIT 05	EDEL ^{73}Ge	
		14 GIRARD 05	SMP L F (C_2ClF_5)	
		15 GIULIANI 05	RVUE	
		16 GIULIANI 05A	RVUE	
		17 KLAPDOR-K... 05	HDMS ^{73}Ge (enriched)	
		18 GIULIANI 04	RVUE	
		19 GIULIANI 04A	RVUE	
		20 MIUCHI 03	BOLO LiF	
		21 MIUCHI 03	BOLO LiF	
		22 TAKEDA 03	BOLO NaF	
< 0.3	90	23 ANGLOHER 02	CRES Al	

Searches Particle Listings

WIMPs and Other Particle Searches

		24	BELLI	02	RVUE	
		25	BERNABEI	02c	DAMA	
		26	GREEN	02	RVUE	
		27	ULLIO	01	RVUE	
		28	BENOIT	00	EDEL	Ge
< 0.004	90	29	BERNABEI	00D		^{129}Xe , inel.
		30	AMBROSIO	99	MCRO	
		31	BRHLIK	99	RVUE	
< 0.008	95	32	KLIMENKO	98	CNTR	^{73}Ge , inel.
< 0.08	95	33	KLIMENKO	98	CNTR	^{73}Ge , inel.
< 4			ALESSAND...	96	CNTR	O
<25			ALESSAND...	96	CNTR	Te
< 0.006	90	34	BELLI	96	CNTR	^{129}Xe , inel.
		35	BELLI	96c	CNTR	^{129}Xe
< 0.001	90	36	BERNABEI	96	CNTR	Na
< 0.3	90	36	BERNABEI	96	CNTR	I
< 0.7	95	37	SARSA	96	CNTR	Na
< 0.03	90	38	SMITH	96	CNTR	Na
< 0.8	90	38	SMITH	96	CNTR	I
< 0.35	95	39	GARCIA	95	CNTR	Natural Ge
< 0.6	95		QUENBY	95	CNTR	Na
< 3	95		QUENBY	95	CNTR	I
< 1.5 $\times 10^2$	90	40	SNOWDEN...	95	MICA	^{16}O
< 4 $\times 10^2$	90	40	SNOWDEN...	95	MICA	^{39}K
< 0.08	90	41	BECK	94	CNTR	^{76}Ge
< 2.5	90		BACCI	92	CNTR	Na
< 3	90		BACCI	92	CNTR	I
< 0.9	90	42	REUSSER	91	CNTR	Natural Ge
< 0.7	95		CALDWELL	88	CNTR	Natural Ge

- 1 AHMED 09 give $\sigma < 0.02$ pb (90% CL) for spin-dependent X^0 -neutron cross section.
- 2 ARCHAMBAULT 09 give $\sigma < 0.4$ pb (90% CL) for spin-dependent X^0 -proton cross section.
- 3 LEBEDENKO 09A give $\sigma < 0.8$ (0.01) pb (90% CL) for spin-dependent X^0 -proton (neutron) cross section.
- 4 ANGLE 08A give $\sigma < 0.9$ (0.01) pb (90% CL) for spin-dependent X^0 -proton (neutron) cross section.
- 5 BEDNYAKOV 08 reanalyze KLAPDOR-KLEINGROTHAUS 05 and BAUDIS 01 data and give $\sigma < 0.05$ pb (90% CL) for spin-dependent X^0 -neutron cross section.
- 6 ALNER 07 give $\sigma < 15$ (0.08) pb (90% CL) for spin-dependent X^0 -proton (neutron) cross section.
- 7 LEE 07A give $\sigma < 0.2$ (6) pb (90% CL) for spin-dependent X^0 -proton (neutron) cross section.
- 8 MIUCHI 07 give $\sigma < 1 \times 10^4$ pb (90% CL) for spin-dependent X^0 -proton cross section with a direction-sensitive detector.
- 9 AKERIB 06 give $\sigma < 5$ (0.07) pb (90% CL) for spin-dependent X^0 -proton (neutron) cross section. See also AKERIB 05.
- 10 SHIMIZU 06A give $\sigma < 2$ (30) pb (90% CL) for spin-dependent X^0 -proton (neutron) cross section.
- 11 ALNER 05 give $\sigma < 0.3$ (10) pb (90% CL) for spin-dependent X^0 -proton (neutron) cross section.
- 12 BARNABE-HEIDER 05 give $\sigma < 2$ (30) pb (90% CL) for spin-dependent X^0 -proton (neutron) cross section.
- 13 BENOIT 05 give $\sigma < 100$ (0.7) pb (90% CL) for spin-dependent X^0 -proton (neutron) cross section.
- 14 GIRARD 05 give $\sigma < 1.5$ pb (90% CL) for spin-dependent X^0 -proton cross section.
- 15 GIULIANI 05 analyzes the spin-independent X^0 -nucleon cross section limits with both isoscalar and isovector couplings. See Figs. 3 and 4 for limits on the couplings.
- 16 GIULIANI 05A analyze available data and give combined limits $\sigma < 0.7$ (0.2) pb for spin-dependent X^0 -proton (neutron) cross section.
- 17 KLAPDOR-KLEINGROTHAUS 05 give $\sigma < 1.5$ pb (90% CL) for spin-dependent X^0 -neutron cross section.
- 18 GIULIANI 04 reanalyze COLLAR 00 data and give limits for spin-dependent X^0 -proton and neutron couplings.
- 19 GIULIANI 04A gives limits for spin-dependent X^0 -proton and neutron couplings from existing data.
- 20 MIUCHI 03 give model-independent limit for spin-dependent X^0 -proton and neutron cross sections. See their Fig. 5.
- 21 MIUCHI 03 give model-independent limit $\sigma < 35$ pb (90% CL) for spin-dependent X^0 -proton cross section.
- 22 TAKEDA 03 give model-independent limit $\sigma < 0.04$ (0.8) nb (90% CL) for spin-dependent X^0 -proton (neutron) cross section.
- 23 ANGLÖHER 02 limit is for spin-dependent WIMP-Aluminum cross section.
- 24 BELLI 02 discuss dependence of the extracted WIMP cross section on the assumptions of the galactic halo structure.
- 25 BERNABEI 02c analyze the DAMA data in the scenario in which X^0 scatters into a slightly heavier state as discussed by SMITH 01.
- 26 GREEN 02 discusses dependence of extracted WIMP cross section limits on the assumptions of the galactic halo structure.
- 27 ULLIO 01 disfavor the possibility that the BERNABEI 99 signal is due to spin-dependent WIMP coupling.
- 28 BENOIT 00 find four event categories in Ge detectors and suggest that low-energy surface nuclear recoils can explain anomalous events reported by UKDMC and Saclay NaI experiments.
- 29 BERNABEI 00D limit is for inelastic scattering $X^0 \ ^{129}\text{Xe} \rightarrow X^0 \ ^{129}\text{Xe}$ (39.58 keV).
- 30 AMBROSIO 99 search for ongoing moon events induced by neutrinos originating from WIMP annihilations in the Sun and Earth.
- 31 BRHLIK 99 discuss the effect of astrophysical uncertainties on the WIMP interpretation of the BERNABEI 99 signal.
- 32 KLIMENKO 98 limit is for inelastic scattering $X^0 \ ^{73}\text{Ge} \rightarrow X^0 \ ^{73}\text{Ge}^*$ (13.26 keV).
- 33 KLIMENKO 98 limit is for inelastic scattering $X^0 \ ^{73}\text{Ge} \rightarrow X^0 \ ^{73}\text{Ge}^*$ (66.73 keV).
- 34 BELLI 96 limit for inelastic scattering $X^0 \ ^{129}\text{Xe} \rightarrow X^0 \ ^{129}\text{Xe}^*$ (39.58 keV).

- 35 BELLI 96c use background subtraction and obtain $\sigma < 0.35$ pb (< 0.15 fb) (90% CL) for spin-dependent (independent) X^0 -proton cross section. The confidence level is from R. Bernabei, private communication, May 20, 1999.
- 36 BERNABEI 96 use pulse shape discrimination to enhance the possible signal. The limit here is from R. Bernabei, private communication, September 19, 1997.
- 37 SARSA 96 search for annual modulation of WIMP signal. See SARSA 97 for details of the analysis. The limit here is from M.L. Sarsa, private communication, May 26, 1997.
- 38 SMITH 96 use pulse shape discrimination to enhance the possible signal. A dark matter density of 0.4 GeV cm^{-3} is assumed.
- 39 GARCIA 95 limit is from the event rate. A weaker limit is obtained from searches for diurnal and annual modulation.
- 40 SNOWDEN-IFFT 95 look for recoil tracks in an ancient mica crystal. Similar limits are also given for ^{27}Al and ^{28}Si . See COLLAR 96 and SNOWDEN-IFFT 96 for discussion on potential backgrounds.
- 41 BECK 94 uses enriched ^{76}Ge (86% purity).
- 42 REUSSER 91 limit here is changed from published (0.3) after reanalysis by authors. J.L. Vuilleumier, private communication, March 29, 1996.

For $m_{X^0} = 1 \text{ TeV}$

VALUE (nb)	CL%	DOCUMENT ID	TECN	COMMENT
• • •				We do not use the following data for averages, fits, limits, etc. • • •
		1	ABBASI 09b	ICCB H, solar ν
		2	AHMED 09	CDMS Ge
		3	ARCHAMBAULT 09	PICA F
		4	LEBEDENKO 09A	ZEP3 Xe
		5	ANGLE 08A	XE10 Xe
		6	BEDNYAKOV 08	RVUE Ge
		7	ALNER 07	ZEP2 Xe
		8	LEE 07A	KIMS Csl
		9	MIUCHI 07	CNTR F (CF_4)
		10	AKERIB 06	CDMS ^{73}Ge , ^{29}Si
		11	ALNER 05	NAIA NaI
		12	BARNABE-HE.05	PICA F (C_4F_{10})
		13	BENOIT 05	EDEL ^{73}Ge
		14	GIRARD 05	SMP L F (C_2ClF_6)
		15	KLAPDOR-K...	05 HDMS ^{73}Ge (enriched)
		16	MIUCHI 03	BOLO LiF
		17	TAKEDA 03	BOLO NaF
< 3	90	18	ANGLÖHER 02	CRES Al
		19	BENOIT 00	EDEL Ge
		20	BERNABEI 99D	CNTR SIMP
		21	DERBIN 99	CNTR SIMP
< 0.06	95	22	KLIMENKO 98	CNTR ^{73}Ge , inel.
< 0.4	95	23	KLIMENKO 98	CNTR ^{73}Ge , inel.
< 40			ALESSAND... 96	CNTR O
<700			ALESSAND... 96	CNTR Te
< 0.05	90	24	BELLI 96	CNTR ^{129}Xe , inel.
< 1.5	90	25	BELLI 96	CNTR ^{129}Xe , inel.
		26	BELLI 96c	CNTR ^{129}Xe
< 0.01	90	27	BERNABEI 96	CNTR Na
< 9	90	27	BERNABEI 96	CNTR I
< 7	95	28	SARSA 96	CNTR Na
< 0.3	90	29	SMITH 96	CNTR Na
< 6	90	29	SMITH 96	CNTR I
< 6	95	30	GARCIA 95	CNTR Natural Ge
< 8	95		QUENBY 95	CNTR Na
< 50	95		QUENBY 95	CNTR I
< 7 $\times 10^2$	90	31	SNOWDEN...	95 MICA ^{16}O
< 1 $\times 10^3$	90	31	SNOWDEN...	95 MICA ^{39}K
< 0.8	90	32	BECK 94	CNTR ^{76}Ge
< 30	90		BACCI 92	CNTR Na
< 30	90		BACCI 92	CNTR I
< 15	90	33	REUSSER 91	CNTR Natural Ge
< 6	95		CALDWELL 88	CNTR Natural Ge

- 1 ABBASI 09b search for neutrinos produced by X^0 annihilation in the Sun and give $\sigma < 8.7 \times 10^{-4}$ (2.2×10^{-2}) pb (90% CL) for spin-dependent X^0 -proton cross section, if X^0 pairs annihilate to $W^+ W^- (b\bar{b})$.
- 2 AHMED 09 give $\sigma < 0.2$ pb (90% CL) for spin-dependent X^0 -neutron cross section.
- 3 ARCHAMBAULT 09 give $\sigma < 3$ pb (90% CL) for spin-dependent X^0 -proton cross section.
- 4 LEBEDENKO 09A give $\sigma < 6$ (0.1) pb (90% CL) for spin-dependent X^0 -proton (neutron) cross section.
- 5 ANGLE 08A give $\sigma < 8$ (0.1) pb (90% CL) for spin-dependent X^0 -proton (neutron) cross section.
- 6 BEDNYAKOV 08 reanalyze KLAPDOR-KLEINGROTHAUS 05 and BAUDIS 01 data and give $\sigma < 0.25$ pb (90% CL) for spin-dependent X^0 -neutron cross section.
- 7 ALNER 07 give $\sigma < 100$ (0.6) pb (90% CL) for spin-dependent X^0 -proton (neutron) cross section.
- 8 LEE 07A give $\sigma < 0.8$ (30) pb (90% CL) for spin-dependent X^0 -proton (neutron) cross section.
- 9 MIUCHI 07 give $\sigma < 4 \times 10^4$ pb (90% CL) for spin-dependent X^0 -proton cross section with a direction-sensitive detector.
- 10 AKERIB 06 give $\sigma < 30$ (0.5) pb (90% CL) for spin-dependent X^0 -proton (neutron) cross section. See also AKERIB 05.
- 11 ALNER 05 give $\sigma < 1.5$ (40) pb (90% CL) for spin-dependent X^0 -proton (neutron) cross section.
- 12 BARNABE-HEIDER 05 give $\sigma < 15$ (200) pb (90% CL) for spin-dependent X^0 -proton (neutron) cross section.

- ¹³ BENOIT 05 give $\sigma < 600$ (4) pb (90% CL) for spin-dependent X^0 -proton (neutron) cross section.
- ¹⁴ GIRARD 05 give $\sigma < 10$ pb (90% CL) for spin-dependent X^0 -proton cross section.
- ¹⁵ KLAPDOR-KLEINGROTHAUS 05 give $\sigma < 10$ pb (90% CL) for spin-dependent X^0 -neutron cross section.
- ¹⁶ MIUCHI 03 give model-independent limit $\sigma < 260$ pb (90% CL) for spin-dependent X^0 -proton cross section.
- ¹⁷ TAKEDA 03 give model-independent limit $\sigma < 0.15$ (4) nb (90% CL) for spin-dependent X^0 -proton (neutron) cross section.
- ¹⁸ ANGLÖHER 02 limit is for spin-dependent WIMP-Aluminum cross section.
- ¹⁹ BENOIT 00 find four event categories in Ge detectors and suggest that low-energy surface nuclear recoils can explain anomalous events reported by UKDMC and Saclay Nal experiments.
- ²⁰ BERNABEI 99p search for SIMPs (Strongly Interacting Massive Particles) in the mass range 10^3 - 10^{16} GeV. See their Fig. 3 for cross-section limits.
- ²¹ DERBIN 99 search for SIMPs (Strongly Interacting Massive Particles) in the mass range 10^2 - 10^{14} GeV. See their Fig. 3 for cross-section limits.
- ²² KLIMENKO 98 limit is for inelastic scattering $X^0 \text{ } ^{73}\text{Ge} \rightarrow X^0 \text{ } ^{73}\text{Ge}^*$ (13.26 keV).
- ²³ KLIMENKO 98 limit is for inelastic scattering $X^0 \text{ } ^{73}\text{Ge} \rightarrow X^0 \text{ } ^{73}\text{Ge}^*$ (66.73 keV).
- ²⁴ BELLI 96 limit for inelastic scattering $X^0 \text{ } ^{129}\text{Xe} \rightarrow X^0 \text{ } ^{129}\text{Xe}^*$ (39.58 keV).
- ²⁵ BELLI 96 limit for inelastic scattering $X^0 \text{ } ^{129}\text{Xe} \rightarrow X^0 \text{ } ^{129}\text{Xe}^*$ (236.14 keV).
- ²⁶ BELLI 96c use background subtraction and obtain $\sigma < 0.7$ pb (< 0.7 fb) (90% CL) for spin-dependent (independent) X^0 -proton cross section. The confidence level is from R. Bernabei, private communication, May 20, 1999.
- ²⁷ BERNABEI 96 use pulse shape discrimination to enhance the possible signal. The limit here is from R. Bernabei, private communication, September 19, 1997.
- ²⁸ SARSA 96 search for annual modulation of WIMP signal. See SARSA 97 for details of the analysis. The limit here is from M.L. Sarsa, private communication, May 26, 1997.
- ²⁹ SMITH 96 use pulse shape discrimination to enhance the possible signal. A dark matter density of 0.4 GeV cm^{-3} is assumed.
- ³⁰ GARCIA 95 limit is from the event rate. A weaker limit is obtained from searches for diurnal and annual modulation.
- ³¹ SNOWDEN-IFFT 95 look for recoil tracks in an ancient mica crystal. Similar limits are also given for ^{27}Al and ^{28}Si . See COLLAR 96 and SNOWDEN-IFFT 96 for discussion on potential backgrounds.
- ³² BECK 94 uses enriched ^{76}Ge (86% purity).
- ³³ REUSSER 91 limit here is changed from published (5) after reanalysis by authors. J.L. Vuilleumier, private communication, March 29, 1996.

CONCENTRATION OF STABLE PARTICLES IN MATTER

Concentration of Heavy (Charge +1) Stable Particles in Matter

VALUE	CL%	DOCUMENT ID	TECN	COMMENT
$< 4 \times 10^{-17}$	95	¹ YAMAGATA 93	SPEC	Deep sea water, $M=5-1600m_p$
$< 6 \times 10^{-15}$	95	² VERKERK 92	SPEC	Water, $M=10^5$ to 3×10^7 GeV
$< 7 \times 10^{-15}$	95	² VERKERK 92	SPEC	Water, $M=10^4$, 6×10^7 GeV
$< 9 \times 10^{-15}$	95	² VERKERK 92	SPEC	Water, $M=10^8$ GeV
$< 3 \times 10^{-23}$	90	³ HEMMICK 90	SPEC	Water, $M=1000m_p$
$< 2 \times 10^{-21}$	90	³ HEMMICK 90	SPEC	Water, $M=5000m_p$
$< 3 \times 10^{-20}$	90	³ HEMMICK 90	SPEC	Water, $M=10000m_p$
$< 1. \times 10^{-29}$		SMITH 82B	SPEC	Water, $M=30-400m_p$
$< 2. \times 10^{-28}$		SMITH 82B	SPEC	Water, $M=12-1000m_p$
$< 1. \times 10^{-14}$		SMITH 82B	SPEC	Water, $M > 1000m_p$
$< (0.2-1.) \times 10^{-21}$		SMITH 79	SPEC	Water, $M=6-350m_p$

- ¹ YAMAGATA 93 used deep sea water at 4000 m since the concentration is enhanced in deep sea due to gravity.
- ² VERKERK 92 looked for heavy isotopes in sea water and put a bound on concentration of stable charged massive particle in sea water. The above bound can be translated into a bound on charged dark matter particle (5×10^6 GeV), assuming the local density, $\rho=0.3 \text{ GeV/cm}^3$, and the mean velocity (v)=300 km/s.
- ³ See HEMMICK 90 Fig. 7 for other masses $100-10000 m_p$.

Concentration of Heavy Stable Particles Bound to Nuclei

VALUE	CL%	DOCUMENT ID	TECN	COMMENT
$< 1.2 \times 10^{-11}$	95	¹ JAVORSEK 01	SPEC	Au, $M=3 \text{ GeV}$
$< 6.9 \times 10^{-10}$	95	¹ JAVORSEK 01	SPEC	Au, $M=144 \text{ GeV}$
$< 1 \times 10^{-11}$	95	² JAVORSEK 01B	SPEC	Au, $M=188 \text{ GeV}$
$< 1 \times 10^{-8}$	95	² JAVORSEK 01B	SPEC	Au, $M=1669 \text{ GeV}$
$< 6 \times 10^{-9}$	95	² JAVORSEK 01B	SPEC	Fe, $M=188 \text{ GeV}$
$< 1 \times 10^{-8}$	95	² JAVORSEK 01B	SPEC	Fe, $M=647 \text{ GeV}$
$< 4 \times 10^{-20}$	90	³ HEMMICK 90	SPEC	C, $M=100m_p$
$< 8 \times 10^{-20}$	90	³ HEMMICK 90	SPEC	C, $M=1000m_p$
$< 2 \times 10^{-16}$	90	³ HEMMICK 90	SPEC	C, $M=10000m_p$
$< 6 \times 10^{-13}$	90	³ HEMMICK 90	SPEC	Li, $M=1000m_p$
$< 1 \times 10^{-11}$	90	³ HEMMICK 90	SPEC	Be, $M=1000m_p$
$< 6 \times 10^{-14}$	90	³ HEMMICK 90	SPEC	B, $M=1000m_p$
$< 4 \times 10^{-17}$	90	³ HEMMICK 90	SPEC	O, $M=1000m_p$
$< 4 \times 10^{-15}$	90	³ HEMMICK 90	SPEC	F, $M=1000m_p$
$< 1.5 \times 10^{-13}$ /nucleon	68	⁴ NORMAN 89	SPEC	$^{206}\text{Pb}X^-$
$< 1.2 \times 10^{-12}$ /nucleon	68	⁴ NORMAN 87	SPEC	$^{56,58}\text{Fe}X^-$

- ¹ JAVORSEK 01 search for (neutral) SIMPs (strongly interacting massive particles) bound to Au nuclei. Here M is the effective SIMP mass.
- ² JAVORSEK 01B search for (neutral) SIMPs (strongly interacting massive particles) bound to Au and Fe nuclei from various origins with exposures on the earth's surface, in a satellite, heavy ion collisions, etc. Here M is the mass of the anomalous nucleus. See also JAVORSEK 02.
- ³ See HEMMICK 90 Fig. 7 for other masses $100-10000 m_p$.
- ⁴ Bound valid up to $m_{X^-} \sim 100 \text{ TeV}$.

GENERAL NEW PHYSICS SEARCHES

This subsection lists some of the search experiments which look for general signatures characteristic of new physics, independent of the framework of a specific model.

VALUE	DOCUMENT ID	TECN	COMMENT
• • • We do not use the following data for averages, fits, limits, etc. • • •			
	¹ AALTONEN 09AF	CDF	$\ell\gamma b \cancel{E}_T$
	² AALTONEN 09G	CDF	$\ell\ell\ell \cancel{E}_T$
¹ AALTONEN 09AF search for $\ell\gamma b$ events with missing E_T in $p\bar{p}$ collisions at $E_{cm} = 1.96 \text{ TeV}$ with $L = 1.9 \text{ fb}^{-1}$. The observed events are compatible with Standard Model expectation including $t\bar{t}\gamma$ production.			
² AALTONEN 09G search for $\mu\mu\mu$ and $\mu\mu e$ events with missing E_T in $p\bar{p}$ collisions at $E_{cm} = 1.96 \text{ TeV}$ with $L = 976 \text{ pb}^{-1}$. The observed events are compatible with Standard Model expectation.			

LIMITS ON NEUTRAL PARTICLE PRODUCTION

Production Cross Section of Radiatively-Decaying Neutral Particle

VALUE (pb)	CL%	DOCUMENT ID	TECN	COMMENT
• • • We do not use the following data for averages, fits, limits, etc. • • •				
$< (0.043-0.17)$	95	¹ ABBIENDI 00D	OPAL	$e^+e^- \rightarrow X^0\gamma^0$, $X^0 \rightarrow \gamma^0\gamma$
$< (0.05-0.8)$	95	² ABBIENDI 00D	OPAL	$e^+e^- \rightarrow X^0X^0$, $X^0 \rightarrow \gamma^0\gamma$
$< (2.5-0.5)$	95	³ ACKERSTAFF 97B	OPAL	$e^+e^- \rightarrow X^0\gamma^0$, $X^0 \rightarrow \gamma^0\gamma$
$< (1.6-0.9)$	95	⁴ ACKERSTAFF 97B	OPAL	$e^+e^- \rightarrow X^0X^0$, $X^0 \rightarrow \gamma^0\gamma$

- ¹ ABBIENDI 00D associated production limit is for $m_{X^0} = 90-188 \text{ GeV}$, $m_{\gamma^0} = 0$ at $E_{cm} = 189 \text{ GeV}$. See also their Fig. 9.
- ² ABBIENDI 00D pair production limit is for $m_{X^0} = 45-94 \text{ GeV}$, $m_{\gamma^0} = 0$ at $E_{cm} = 189 \text{ GeV}$. See also their Fig. 12.
- ³ ACKERSTAFF 97B associated production limit is for $m_{X^0} = 80-160 \text{ GeV}$, $m_{\gamma^0} = 0$ from 10.0 pb^{-1} at $E_{cm} = 161 \text{ GeV}$. See their Fig. 3(a).
- ⁴ ACKERSTAFF 97B pair production limit is for $m_{X^0} = 40-80 \text{ GeV}$, $m_{\gamma^0} = 0$ from 10.0 pb^{-1} at $E_{cm} = 161 \text{ GeV}$. See their Fig. 3(b).

Heavy Particle Production Cross Section

VALUE (cm^2/N)	CL%	EVTS	DOCUMENT ID	TECN	COMMENT
• • • We do not use the following data for averages, fits, limits, etc. • • •					
$< 10^{-36}$ - 10^{-33}	90		¹ ADAMS 97B	KTEV	$m = 1.2-5 \text{ GeV}$
$< (4-0.3) \times 10^{-31}$	95		² GALLAS 95	TOF	$m = 0.5-20 \text{ GeV}$
$< 2 \times 10^{-36}$	90	0	³ AKESSON 91	CNTR	$m = 0-5 \text{ GeV}$
$< 2.5 \times 10^{-35}$		0	⁴ BADIÉ 86	BDMP	$\tau = (0.05-1.) \times 10^{-8} \text{ s}$
		0	⁵ GUSTAFSON 76	CNTR	$\tau > 10^{-7} \text{ s}$

- ¹ ADAMS 97B search for a hadron-like neutral particle produced in pN interactions, which decays into a ρ^0 and a weakly interacting massive particle. Upper limits are given for the ratio to K_S^0 production for the mass range $1.2-5 \text{ GeV}$ and lifetime $10^{-9}-10^{-4} \text{ s}$. See also our Light Gluino Section.
- ² GALLAS 95 limit is for a weakly interacting neutral particle produced in $800 \text{ GeV}/c \text{ } pN$ interactions decaying with a lifetime of $10^{-4}-10^{-8} \text{ s}$. See their Figs. 8 and 9. Similar limits are obtained for a stable particle with interaction cross section $10^{-29}-10^{-33} \text{ cm}^2$. See Fig. 10.
- ³ AKESSON 91 limit is for weakly interacting neutral long-lived particles produced in pN reaction at $450 \text{ GeV}/c$ performed at CERN SPS. Bourquin-Gaillard formula is used as the production model. The above limit is for $\tau > 10^{-7} \text{ s}$. For $\tau > 10^{-9} \text{ s}$, $\sigma < 10^{-30} \text{ cm}^2/\text{nucleon}$ is obtained.
- ⁴ BADIÉ 86 looked for long-lived particles at $300 \text{ GeV } \pi^-$ beam dump. The limit applies for nonstrongly interacting neutral or charged particles with $m > 2 \text{ GeV}$. The limit applies for particle modes, $\mu^+\pi^-$, $\mu^+\mu^-$, $\pi^+\pi^-X$, $\pi^+\pi^-\pi^\pm$ etc. See their figure 5 for the contours of limits in the mass- τ plane for each mode.
- ⁵ GUSTAFSON 76 is a 300 GeV FNAL experiment looking for heavy ($m > 2 \text{ GeV}$) long-lived neutral hadrons in the M4 neutral beam. The above typical value is for $m = 3 \text{ GeV}$ and assumes an interaction cross section of 1 mb . Values as a function of mass and interaction cross section are given in figure 2.

Production of New Penetrating Non- ν Like States in Beam Dump

VALUE	DOCUMENT ID	TECN	COMMENT
• • • We do not use the following data for averages, fits, limits, etc. • • •			
	¹ LOSECCO 81	CALO	28 GeV protons
¹ No excess neutral-current events leads to $\sigma(\text{production}) \times \sigma(\text{interaction}) \times \text{acceptance} < 2.26 \times 10^{-71} \text{ cm}^4/\text{nucleon}^2$ (CL = 90%) for light neutrals. Acceptance depends on models (0.1 to $4. \times 10^{-4}$).			

Searches Particle Listings

WIMPs and Other Particle Searches

LIMITS ON JET-JET RESONANCES

Heavy Particle Production Cross Section in $p\bar{p}$

Limits are for a particle decaying to two hadronic jets.

Units(pb)	CL%	Mass(GeV)	DOCUMENT ID	TECN	COMMENT
••• We do not use the following data for averages, fits, limits, etc. •••					
			1 ABE	99F CDF	1.8 TeV $p\bar{p} \rightarrow b\bar{b} + \text{anything}$
			2 ABE	97G CDF	1.8 TeV $p\bar{p} \rightarrow 2 \text{ jets}$
<2603	95	200	3 ABE	93G CDF	1.8 TeV $p\bar{p} \rightarrow 2 \text{ jets}$
< 44	95	400	3 ABE	93G CDF	1.8 TeV $p\bar{p} \rightarrow 2 \text{ jets}$
< 7	95	600	3 ABE	93G CDF	1.8 TeV $p\bar{p} \rightarrow 2 \text{ jets}$

1 ABE 99F search for narrow $b\bar{b}$ resonances in $p\bar{p}$ collisions at $E_{cm}=1.8$ TeV. Limits on $\sigma(p\bar{p} \rightarrow X + \text{anything}) \times B(X \rightarrow b\bar{b})$ in the range $3-10^3$ pb (95%CL) are given for $m_X=200-750$ GeV. See their Table I.

2 ABE 97G search for narrow dijet resonances in $p\bar{p}$ collisions with 106 pb^{-1} of data at $E_{cm} = 1.8$ TeV. Limits on $\sigma(p\bar{p} \rightarrow X + \text{anything}) \cdot B(X \rightarrow jj)$ in the range 10^4-10^{-1} pb (95%CL) are given for dijet mass $m=200-1150$ GeV with both jets having $|\eta| < 2.0$ and the dijet system having $|\cos\theta^*| < 0.67$. See their Table I for the list of limits. Supersedes ABE 93G.

3 ABE 93G gives cross section times branching ratio into light (d, u, s, c, b) quarks for $\Gamma = 0.02 M$. Their Table II gives limits for $M = 200-900$ GeV and $\Gamma = (0.02-0.2) M$.

LIMITS ON CHARGED PARTICLES IN e^+e^-

Heavy Particle Production Cross Section in e^+e^-

Ratio to $\sigma(e^+e^- \rightarrow \mu^+\mu^-)$ unless noted. See also entries in Free Quark Search and Magnetic Monopole Searches.

VALUE	CL%	EVTS	DOCUMENT ID	TECN	COMMENT
••• We do not use the following data for averages, fits, limits, etc. •••					
			1 ACKERSTAFF	98P OPAL	$Q=1,2/3, m=45-89.5$ GeV
			2 ABREU	97D DLPH	$Q=1,2/3, m=45-84$ GeV
<2 $\times 10^{-5}$	95		3 BARATE	97K ALEP	$Q=1, m=45-85$ GeV
<1 $\times 10^{-5}$	95		4 AKERS	95R OPAL	$Q=2, m=5-45$ GeV
<2 $\times 10^{-3}$	90		5 BUSKULIC	93C ALEP	$Q=1, m=32-72$ GeV
<(10 ⁻² -1)	95		6 ADACHI	90C TOPZ	$Q=1, m=1-16, 18-27$ GeV
<7 $\times 10^{-2}$	90		7 ADACHI	90E TOPZ	$Q=1, m=5-25$ GeV
<1.6 $\times 10^{-2}$	95	0	8 KINOSHITA	82 PLAS	$Q=3-180, m < 14.5$ GeV
<5.0 $\times 10^{-2}$	90	0	9 BARTEL	80 JADE	$Q=(3,4,5)/3$ 2-12 GeV

1 ACKERSTAFF 98P search for pair production of long-lived charged particles at E_{cm} between 130 and 183 GeV and give limits $\sigma < (0.05-0.2)$ pb (95%CL) for spin-0 and spin-1/2 particles with $m=45-89.5$ GeV, charge 1 and 2/3. The limit is translated to the cross section at $E_{cm}=183$ GeV with the s dependence described in the paper. See their Figs. 2-4.

2 ABREU 97D search for pair production of long-lived particles and give limits $\sigma < (0.4-2.3)$ pb (95%CL) for various center-of-mass energies $E_{cm}=130-136, 161,$ and 172 GeV, assuming an almost flat production distribution in $\cos\theta$.

3 BARATE 97K search for pair production of long-lived charged particles at $E_{cm} = 130, 136, 161,$ and 172 GeV and give limits $\sigma < (0.2-0.4)$ pb (95%CL) for spin-0 and spin-1/2 particles with $m=45-85$ GeV. The limit is translated to the cross section at $E_{cm}=172$ GeV with the E_{cm} dependence described in the paper. See their Figs. 2 and 3 for limits on $J = 1/2$ and $J = 0$ cases.

4 AKERS 95R is a CERN-LEP experiment with $W_{cm} \sim m_Z$. The limit is for the production of a stable particle in multihadron events normalized to $\sigma(e^+e^- \rightarrow \text{hadrons})$. Constant phase space distribution is assumed. See their Fig. 3 for bounds for $Q = \pm 2/3, \pm 4/3$.

5 BUSKULIC 93C is a CERN-LEP experiment with $W_{cm} = m_Z$. The limit is for a pair or single production of heavy particles with unusual ionization loss in TPC. See their Fig. 5 and Table 1.

6 ADACHI 90C is a KEK-TRISTAN experiment with $W_{cm} = 52-60$ GeV. The limit is for pair production of a scalar or spin-1/2 particle. See Figs. 3 and 4.

7 ADACHI 90E is KEK-TRISTAN experiment with $W_{cm} = 52-61.4$ GeV. The above limit is for inclusive production cross section normalized to $\sigma(e^+e^- \rightarrow \mu^+\mu^-) \cdot \beta(3-\beta^2)/2$, where $\beta = (1 - 4m^2/W_{cm}^2)^{1/2}$. See the paper for the assumption about the production mechanism.

8 KINOSHITA 82 is SLAC PEP experiment at $W_{cm} = 29$ GeV using lexan and ^{39}Cr plastic sheets sensitive to highly ionizing particles.

9 BARTEL 80 is DESY-PETRA experiment with $W_{cm} = 27-35$ GeV. Above limit is for inclusive pair production and ranges between $1. \times 10^{-1}$ and $1. \times 10^{-2}$ depending on mass and production momentum distributions. (See their figures 9, 10, 11).

Branching Fraction of Z^0 to a Pair of Stable Charged Heavy Fermions

VALUE	CL%	DOCUMENT ID	TECN	COMMENT
••• We do not use the following data for averages, fits, limits, etc. •••				
<5 $\times 10^{-6}$	95	1 AKERS	95R OPAL	$m=40.4-45.6$ GeV
<1 $\times 10^{-3}$	95	AKRAWY	90O OPAL	$m=29-40$ GeV

1 AKERS 95R give the 95% CL limit $\sigma(X\bar{X})/\sigma(\mu\mu) < 1.8 \times 10^{-4}$ for the pair production of singly- or doubly-charged stable particles. The limit applies for the mass range 40.4-45.6 GeV for X^\pm and < 45.6 GeV for $X^{\pm\pm}$. See the paper for bounds for $Q = \pm 2/3, \pm 4/3$.

LIMITS ON CHARGED PARTICLES IN HADRONIC REACTIONS

Heavy Particle Production Cross Section

VALUE (nb)	CL%	DOCUMENT ID	TECN	COMMENT
••• We do not use the following data for averages, fits, limits, etc. •••				
<1.0 $\times 10^{-5}$	95	1,2 AALTONEN	09Z CDF	$m > 100$ GeV, noncolored
<4.8 $\times 10^{-5}$	95	1,3 AALTONEN	09Z CDF	$m > 100$ GeV, colored
< 0.31-0.04 $\times 10^{-3}$	95	4 ABAZOV	09M D0	pair production
<0.19	95	5 AKTAS	04c H1	$m=3-10$ GeV
<0.05	95	6 ABE	92J CDF	$m=50-200$ GeV
<30-130		7 CARROLL	78 SPEC	$m=2-2.5$ GeV
<100		8 LEIPUNER	73 CNTR	$m=3-11$ GeV

1 AALTONEN 09Z search for long-lived charged particles in $p\bar{p}$ collisions at $E_{cm} = 1.96$ TeV with $L = 1.0 \text{ fb}^{-1}$. The limits are on production cross section for a particle of mass above 100 GeV in the region $|\eta| \lesssim 0.7, p_T > 40$ GeV, and $0.4 < \beta < 1.0$.

2 Limit for weakly interacting charge-1 particle.

3 Limit for up-quark like particle.

4 ABAZOV 09M search for pair production of long-lived charged particles in $p\bar{p}$ collisions at $E_{cm} = 1.96$ TeV with $L = 1.1 \text{ fb}^{-1}$. Limit on the cross section of $(0.31-0.04)$ pb (95%CL) is given for the mass range of 60-300 GeV, assuming the kinematics of stau pair production.

5 AKTAS 04c look for charged particle photoproduction at HERA with mean c.m. energy of 200 GeV.

6 ABE 92J look for pair production of unit-charged particles which leave detector before decaying. Limit shown here is for $m=50$ GeV. See their Fig. 5 for different charges and stronger limits for higher mass.

7 CARROLL 78 look for neutral, $S = -2$ dihyperon resonance in $pp \rightarrow 2K^+X$. Cross section varies within above limits over mass range and $p_{lab} = 5.1-5.9$ GeV/c.

8 LEIPUNER 73 is an NAL 300 GeV p experiment. Would have detected particles with lifetime greater than 200 ns.

Heavy Particle Production Differential Cross Section

VALUE (cm ² sr ⁻¹ GeV ⁻¹)	CL%	EVTS	DOCUMENT ID	TECN	CHG	COMMENT
••• We do not use the following data for averages, fits, limits, etc. •••						
<2.6 $\times 10^{-36}$	90	0	1 BALDIN	76 CNTR	-	$Q=1, m=2.1-9.4$ GeV
<2.2 $\times 10^{-33}$	90	0	2 ALBROW	75 SPEC	±	$Q=±1, m=4-15$ GeV
<1.1 $\times 10^{-33}$	90	0	2 ALBROW	75 SPEC	±	$Q=±2, m=6-27$ GeV
<8. $\times 10^{-35}$	90	0	3 JOVANOVI...	75 CNTR	±	$m=15-26$ GeV
<1.5 $\times 10^{-34}$	90	0	3 JOVANOVI...	75 CNTR	±	$Q=±2, m=3-10$ GeV
<6. $\times 10^{-35}$	90	0	3 JOVANOVI...	75 CNTR	±	$Q=±2, m=10-26$ GeV
<1. $\times 10^{-31}$	90	0	4 APPEL	74 CNTR	±	$m=3.2-7.2$ GeV
<5.8 $\times 10^{-34}$	90	0	5 ALPER	73 SPEC	±	$m=1.5-24$ GeV
<1.2 $\times 10^{-35}$	90	0	6 ANTIPOV	71B CNTR	-	$Q=-, m=2.2-2.8$
<2.4 $\times 10^{-35}$	90	0	7 ANTIPOV	71C CNTR	-	$Q=-, m=1.2-1.7, 2.1-4$
<2.4 $\times 10^{-35}$	90	0	BINON	69 CNTR	-	$Q=-, m=1-1.8$ GeV
<1.5 $\times 10^{-36}$	0		8 DORFAN	65 CNTR		Be target $m=3-7$ GeV
<3.0 $\times 10^{-36}$	0		8 DORFAN	65 CNTR		Fe target $m=3-7$ GeV

1 BALDIN 76 is a 70 GeV Serpukhov experiment. Value is per Al nucleus at $\theta = 0$. For other charges in range -0.5 to -3.0 , CL = 90% limit is $(2.6 \times 10^{-36})/|[\text{charge}]|$ for mass range $(2.1-9.4 \text{ GeV}) \times |[\text{charge}]|$. Assumes stable particle interacting with matter as do antiprotons.

2 ALBROW 75 is a CERN ISR experiment with $E_{cm} = 53$ GeV. $\theta = 40$ mr. See figure 5 for mass ranges up to 35 GeV.

3 JOVANOVI... 75 is a CERN ISR 26+26 and 15+15 GeV pp experiment. Figure 4 covers ranges $Q = 1/3$ to 2 and $m = 3$ to 26 GeV. Value is per GeV momentum.

4 APPEL 74 is NAL 300 GeV pW experiment. Studies forward production of heavy (up to 24 GeV) charged particles with momenta 24-200 GeV (-charge) and 40-150 GeV (+charge). Above typical value is for 75 GeV and is per GeV momentum per nucleon.

5 ALPER 73 is CERN ISR 26+26 GeV pp experiment. $p > 0.9$ GeV, $0.2 < \beta < 0.65$.

6 ANTIPOV 71B is from same 70 GeV p experiment as ANTIPOV 71C and BINON 69.

7 ANTIPOV 71C limit inferred from flux ratio. 70 GeV p experiment.

8 DORFAN 65 is a 30 GeV/c p experiment at BNL. Units are per GeV momentum per nucleus.

Long-Lived Heavy Particle Invariant Cross Section

VALUE (cm ² /GeV ² /N)	CL%	DOCUMENT ID	TECN	CHG	COMMENT
••• We do not use the following data for averages, fits, limits, etc. •••					
<5-700 $\times 10^{-35}$	90	1 BERNSTEIN	88 CNTR		
<5-700 $\times 10^{-37}$	90	1 BERNSTEIN	88 CNTR		
<2.5 $\times 10^{-36}$	90	2 THRON	85 CNTR	-	$Q=1, m=4-12$ GeV
<1. $\times 10^{-35}$	90	2 THRON	85 CNTR	+	$Q=1, m=4-12$ GeV
<6. $\times 10^{-33}$	90	3 ARMITAGE	79 SPEC		$m=1.87$ GeV
<1.5 $\times 10^{-33}$	90	3 ARMITAGE	79 SPEC		$m=1.5-3.0$ GeV
		4 BOZZOLI	79 CNTR	±	$Q = (2/3, 1, 4/3, 2)$
<1.1 $\times 10^{-37}$	90	5 CUTTS	78 CNTR		$m=4-10$ GeV
<3.0 $\times 10^{-37}$	90	6 VIDAL	78 CNTR		$m=4.5-6$ GeV

- ¹BERNSTEIN 88 limits apply at $x = 0.2$ and $p_T = 0$. Mass and lifetime dependence of limits are shown in the regions: $m = 1.5\text{--}7.5$ GeV and $\tau = 10^{-8}\text{--}2 \times 10^{-6}$ s. First number is for hadrons; second is for weakly interacting particles.
- ²THRON 85 is FNAL 400 GeV proton experiment. Mass determined from measured velocity and momentum. Limits are for $\tau > 3 \times 10^{-9}$ s.
- ³ARMITAGE 79 is CERN-ISR experiment at $E_{cm} = 53$ GeV. Value is for $x = 0.1$ and $p_T = 0.15$. Observed particles at $m = 1.87$ GeV are found all consistent with being antideuterons.
- ⁴BOZZOLI 79 is CERN-SPS 200 GeV pN experiment. Looks for particle with τ larger than 10^{-8} s. See their figure 11-18 for production cross-section upper limits vs mass.
- ⁵CUTTS 78 is p Be experiment at FNAL sensitive to particles of $\tau > 5 \times 10^{-8}$ s. Value is for $-0.3 < x < 0$ and $p_T = 0.175$.
- ⁶VIDAL 78 is FNAL 400 GeV proton experiment. Value is for $x = 0$ and $p_T = 0$. Puts lifetime limit of $< 5 \times 10^{-8}$ s on particle in this mass range.

Long-Lived Heavy Particle Production
 $(\sigma(\text{Heavy Particle}) / \sigma(\pi))$

VALUE	EVTS	DOCUMENT ID	TECN	CHG	COMMENT
$< 10^{-8}$	0	¹ NAKAMURA 89	SPEC	\pm	$Q = (-5/3, \pm 2)$
		² BUSSIERE 80	CNTR	\pm	$Q = (2/3, 1, 4/3, 2)$

- ¹NAKAMURA 89 is KEK experiment with 12 GeV protons on Pt target. The limit applies for mass $\lesssim 1.6$ GeV and lifetime $\gtrsim 10^{-7}$ s.
- ²BUSSIERE 80 is CERN-SPS experiment with 200-240 GeV protons on Be and Al target. See their figures 6 and 7 for cross-section ratio vs mass.

Production and Capture of Long-Lived Massive Particles

VALUE (10^{-36} cm ²)	EVTS	DOCUMENT ID	TECN	COMMENT
< 20 to 800	0	¹ ALEKSEEV 76	ELEC	$\tau = 5$ ms to 1 day
< 200 to 2000	0	¹ ALEKSEEV 76B	ELEC	$\tau = 100$ ms to 1 day
< 1.4 to 9	0	² FRANKEL 75	CNTR	$\tau = 50$ ms to 10 hours
< 0.1 to 9	0	³ FRANKEL 74	CNTR	$\tau = 1$ to 1000 hours

- ¹ALEKSEEV 76 and ALEKSEEV 76B are 61-70 GeV p Serpukhov experiment. Cross section is per Pb nucleus.
- ²FRANKEL 75 is extension of FRANKEL 74.
- ³FRANKEL 74 looks for particles produced in thick Al targets by 300-400 GeV/c protons.

Long-Lived Particle Search at Hadron Collisions

Limits are for cross section times branching ratio.

VALUE (pb/nucleon)	CL%	EVTS	DOCUMENT ID	TECN	COMMENT
< 2	90	0	¹ BADIER 86	BDMP	$\tau = (0.05\text{--}1) \times 10^{-8}$ s

- ¹BADIER 86 looked for long-lived particles at 300 GeV π^- beam dump. The limit applies for nonstrongly interacting neutral or charged particles with mass > 2 GeV. The limit applies for particle modes, $\mu^+ \pi^-$, $\mu^+ \mu^-$, $\pi^+ \pi^- X$, $\pi^+ \pi^- \pi^\pm$ etc. See their figure 5 for the contours of limits in the mass- τ plane for each mode.

Long-Lived Heavy Particle Cross Section

VALUE (pb/sr)	CL%	DOCUMENT ID	TECN	COMMENT
< 34	95	¹ RAM 94	SPEC	$1015 < m_{X^{++}} < 1085$ MeV
< 75	95	¹ RAM 94	SPEC	$920 < m_{X^{++}} < 1025$ MeV

- ¹RAM 94 search for a long-lived doubly-charged fermion X^{++} with mass between m_N and $m_{N+\pi}$ and baryon number +1 in the reaction $pp \rightarrow X^{++} + n$. No candidate is found. The limit is for the cross section at 15° scattering angle at 460 MeV incident energy and applies for $\tau(X^{++}) \gg 0.1$ μ s.

LIMITS ON CHARGED PARTICLES IN COSMIC RAYS

Heavy Particle Flux in Cosmic Rays

VALUE ($\text{cm}^{-2}\text{sr}^{-1}\text{s}^{-1}$)	CL%	EVTS	DOCUMENT ID	TECN	CHG	COMMENT
$\sim 6 \times 10^{-9}$		2	¹ SAITO 90			$Q \approx 14, m \approx 370 m_p$
$< 1.4 \times 10^{-12}$	90	0	² MINCER 85	CALO		$m \approx 1$ TeV
			³ SAKUYAMA 83B	PLAS		$m \approx 1$ TeV
$< 1.7 \times 10^{-11}$	99	0	⁴ BHAT 82	CC		
$< 1. \times 10^{-9}$	90	0	⁵ MARINI 82	CNTR	\pm	$Q = 1, m \sim 4.5 m_p$
$2. \times 10^{-9}$		3	⁶ YOCK 81	SPRK	\pm	$Q = 1, m \sim 4.5 m_p$
		3	⁶ YOCK 81	SPRK		Fractionally charged
3.0×10^{-9}		3	⁷ YOCK 80	SPRK		$m \sim 4.5 m_p$
$(4 \pm 1) \times 10^{-11}$		3	⁸ GOODMAN 79	ELEC		$m \geq 5$ GeV
$< 1.3 \times 10^{-9}$	90	0	⁸ BHAT 78	CNTR	\pm	$m > 1$ GeV
$< 1.0 \times 10^{-9}$		0	⁶ BRIATORE 76	ELEC		
$< 7. \times 10^{-10}$	90	0	⁶ YOCK 75	ELEC	\pm	$Q > 7e$ or $< -7e$
$> 6. \times 10^{-9}$		5	⁹ YOCK 74	CNTR		$m > 6$ GeV
$< 3.0 \times 10^{-8}$		0	⁰ DARDO 72	CNTR		
$< 1.5 \times 10^{-9}$		0	⁰ TONWAR 72	CNTR		$m > 10$ GeV
$< 3.0 \times 10^{-10}$		0	⁰ BJORNBOE 68	CNTR		$m > 5$ GeV
$< 5.0 \times 10^{-11}$	90	0	⁰ JONES 67	ELEC		$m = 5\text{--}15$ GeV

- ¹SAITO 90 candidates carry about 450 MeV/nucleon. Cannot be accounted for by conventional backgrounds. Consistent with strange quark matter hypothesis.
- ²MINCER 85 is high statistics study of calorimeter signals delayed by 20-200 ns. Calibration with AGS beam shows they can be accounted for by rare fluctuations in signals from low-energy hadrons in the shower. Claim that previous delayed signals including BJORNBOE 68, DARDO 72, BHAT 82, SAKUYAMA 83B below may be due to this fake effect.
- ³SAKUYAMA 83B analyzed 6000 extended air shower events. Increase of delayed particles and change of lateral distribution above 10^{17} eV may indicate production of very heavy parent at top of atmosphere.
- ⁴BHAT 82 observed 12 events with delay $> 2. \times 10^{-8}$ s and with more than 40 particles. 1 eV has good hadron shower. However all events are delayed in only one of two detectors in cloud chamber, and could not be due to strongly interacting massive particle.
- ⁵MARINI 82 applied PEP-counter for TOF. Above limit is for velocity = 0.54 of light. Limit is inconsistent with YOCK 80 YOCK 81 events if isotropic dependence on zenith angle is assumed.
- ⁶YOCK 81 saw another 3 events with $Q = \pm 1$ and m about $4.5 m_p$ as well as 2 events with $m > 5.3 m_p$, $Q = \pm 0.75 \pm 0.05$ and $m > 2.8 m_p$, $Q = \pm 0.70 \pm 0.05$ and 1 event with $m = (9.3 \pm 3) m_p$, $Q = \pm 0.89 \pm 0.06$ as possible heavy candidates.
- ⁷YOCK 80 events are with charge exactly or approximately equal to unity.
- ⁸BHAT 78 is at Kolar gold fields. Limit is for $\tau > 10^{-6}$ s.
- ⁹YOCK 74 events could be tritons.

Superheavy Particle (Quark Matter) Flux in Cosmic Rays

VALUE ($\text{cm}^{-2}\text{sr}^{-1}\text{s}^{-1}$)	CL%	EVTS	DOCUMENT ID	TECN	COMMENT
$< 5 \times 10^{-16}$	90		¹ AMBROSIO 00B	MCRO	$m > 5 \times 10^{14}$ GeV
$< 1.8 \times 10^{-12}$	90		² ASTONE 93	CNTR	$m \geq 1.5 \times 10^{-13}$ gram
$< 1.1 \times 10^{-14}$	90		³ AHLEN 92	MCRO	$10^{-10} < m < 0.1$ gram
$< 2.2 \times 10^{-14}$	90	0	⁴ NAKAMURA 91	PLAS	$m > 10^{11}$ GeV
$< 6.4 \times 10^{-16}$	90	0	⁵ ORITO 91	PLAS	$m > 10^{12}$ GeV
$< 2.0 \times 10^{-11}$	90		⁶ LIU 88	BOLO	$m > 1.5 \times 10^{-13}$ gram
$< 4.7 \times 10^{-12}$	90		⁷ BARISH 87	CNTR	$1.4 \times 10^8 < m < 10^{12}$ GeV
$< 3.2 \times 10^{-11}$	90	0	⁸ NAKAMURA 85	CNTR	$m > 1.5 \times 10^{-13}$ gram
$< 3.5 \times 10^{-11}$	90	0	⁹ ULLMAN 81	CNTR	Planck-mass 10^{19} GeV
$< 7. \times 10^{-11}$	90	0	⁹ ULLMAN 81	CNTR	$m \leq 10^{16}$ GeV

- ¹AMBROSIO 00B searched for quark matter ("nuclearites") in the velocity range $(10^{-5}\text{--}1)$ c. The listed limit is for 2×10^{-3} c.
- ²ASTONE 93 searched for quark matter ("nuclearites") in the velocity range $(10^{-3}\text{--}1)$ c. Their Table 1 gives a compilation of searches for nuclearites.
- ³AHLEN 92 searched for quark matter ("nuclearites"). The bound applies to velocity $< 2.5 \times 10^{-3}$ c. See their Fig. 3 for other velocity/c and heavier mass range.
- ⁴NAKAMURA 91 searched for quark matter in the velocity range $(4 \times 10^{-5}\text{--}1)$ c.
- ⁵ORITO 91 searched for quark matter. The limit is for the velocity range $(10^{-4}\text{--}10^{-3})$ c.
- ⁶LIU 88 searched for quark matter ("nuclearites") in the velocity range $(2.5 \times 10^{-3}\text{--}1)$ c. A less stringent limit of 5.8×10^{-11} applies for $(1\text{--}2.5) \times 10^{-3}$ c.
- ⁷BARISH 87 searched for quark matter ("nuclearites") in the velocity range $(2.7 \times 10^{-4}\text{--}5 \times 10^{-3})$ c.
- ⁸NAKAMURA 85 at KEK searched for quark-matter. These might be lumps of strange quark matter with roughly equal numbers of u, d, s quarks. These lumps or nuclearites were assumed to have velocity of $(10^{-4}\text{--}10^{-3})$ c.
- ⁹ULLMAN 81 is sensitive for heavy slow singly charge particle reaching earth with vertical velocity 100-350 km/s.

Highly Ionizing Particle Flux

VALUE ($\text{m}^{-2}\text{yr}^{-1}$)	CL%	EVTS	DOCUMENT ID	TECN	COMMENT
< 0.4	95	0	KINOSHITA 81B	PLAS	Z/β 30-100

REFERENCES FOR Searches for WIMPs and Other Particles

AALTONEN 09AF	PR D80 011102R	T. Aaltonen et al.	(CDF Collab.)
AALTONEN 09G	PR D79 052004	T. Aaltonen et al.	(CDF Collab.)
AALTONEN 09Z	PRL 103 021802	T. Aaltonen et al.	(CDF Collab.)
ABAZOV 09M	PRL 102 161802	V.M. Abazov et al.	(DO Collab.)
ABBASI 09B	PRL 102 201302	R. Abbasi et al.	(IceCube Collab.)
AHMED 09P	PRL 102 011301	Z. Ahmed et al.	(CDMS Collab.)
ARCHAMBAUD 09A	PL B682 185	S. Archambault et al.	(PICASSO Collab.)
LEBEDENKO 09A	PRL 103 151302	V.N. Lebedenko et al.	(ZEPLIN-III Collab.)
LIN 09P	PR D79 061101R	S.T. Lin et al.	(TEXONO Collab.)
AALSETH 08P	PRL 101 251301	C.E. Aalseth et al.	(CoGeNT Collab.)
ANGLE 08A	PRL 101 091301	J. Angle et al.	(XENON10 Collab.)
BEDNYAKOV 08B	PAN 71 111	V.A. Bednyakov, H.P. Klappdor-Kleingrothaus, I.V. Krivosheina	
	Translated from YAF 71 112.		
ALNER 07P	PL B653 161	G.J. Alner et al.	(ZEPLIN-II Collab.)
LEE 07A	PRL 99 091301	H.S. Lee et al.	(KIMS Collab.)
MIUCHI 07P	PL B654 58	K. Miuchi et al.	
AKERIB 06P	PR D73 01102R	D.S. Akerib et al.	(CDMS Collab.)
SHIMIZU 06A	PL B633 195	Y. Shimizu et al.	
AKERIB 05P	PR D72 052009	D.S. Akerib et al.	(CDMS Collab.)
ALNER 05P	PL B616 17	G.J. Alner et al.	(UK Dark Matter Collab.)
BARNABE-HELD 05P	PL B624 186	M. Barnabe-Heider et al.	(PICASSO Collab.)
BENOIT 05P	PL B616 25	A. Benoit et al.	(EDELWEISS Collab.)
GIRARD 05P	PL B621 233	T.A. Girard et al.	(SIMPLe Collab.)
GIULIANI 05P	PRL 95 101301	F. Giuliani	
GIULIANI 05A	PR D71 123503	F. Giuliani, T.A. Girard	
KLAPPDOR-K... 05P	PL B609 226	H.V. Klappdor-Kleingrothaus, I.V. Krivosheina, C. Tomei	
AKTAS 04C	EPJ C36 413	A. Aktas et al.	(HI Collab.)
GIULIANI 04P	PL B588 151	F. Giuliani, T.A. Girard	
GIULIANI 04A	PRL 93 161301	F. Giuliani	
MIUCHI 03P	ASP 19 135	K. Miuchi et al.	
TAKEDA 03P	PL B572 145	A. Takeda et al.	
ANGLOHER 02P	ASP 18 43	G. Angloher et al.	(CRESS T Collab.)
BELLI 02P	PR D66 043503	P. Belli et al.	
BERNABE 02C	EPJ C23 61	R. Bernabe et al.	(DAMA Collab.)
GREEN 02P	PR D66 083003	A.M. Green	

Searches Particle Listings

WIMPs and Other Particle Searches

JAVORSEK	02	PR D65 072003	D. Javorsek <i>et al.</i>		SAITO	90	PRL 65 2094	T. Saito <i>et al.</i>	(ICRR, KOBE)
BAUDIS	01	PR D63 022001	L. Baudis <i>et al.</i>	(Heidelberg-Moscow Collab.)	NAKAMURA	89	PR D39 1261	T.T. Nakamura <i>et al.</i>	(KYOT, TMTC)
JAVORSEK	01	PR D64 012005	D. Javorsek <i>et al.</i>		NORMAN	89	PR D39 2499	E.B. Norman <i>et al.</i>	(LBL)
JAVORSEK	01B	PRL 87 231804	D. Javorsek <i>et al.</i>		BERNSTEIN	88	PR D37 3103	R.M. Bernstein <i>et al.</i>	(STAN, WISC)
SMITH	01	PR D64 043502	D. Smith, N. Weiner		CALDWELL	88	PRL 61 510	D.O. Caldwell <i>et al.</i>	(UCSB, UCB, LBL)
ULLIO	01	JHEP 0107 044	P. Ullio, M. Kamionkowski, P. Vogel		LIU	88	PRL 61 271	G. Liu, B. Barish	(CIT)
ABBENDI	00D	EPJ C13 197	G. Abbiendi <i>et al.</i>	(OPAL Collab.)	BARISH	87	PR D36 2641	B.C. Barish, G. Liu, C. Lane	(LBL)
AMBROSIO	00B	EPJ C13 453	M. Ambrosio <i>et al.</i>	(MACRO Collab.)	NORMAN	87	PRL 56 1403	E.B. Norman, S.B. Gazes, D.A. Bennett	(UMD, GMAS, NSF)
BERNOIT	00	PL B479 8	A. Benoit <i>et al.</i>	(EDELWEISS Collab.)	BADIER	86	ZPHY C31 21	J. Badier <i>et al.</i>	(NA3 Collab.)
BERNABEI	00D	NJP 2 15	R. Bernabei <i>et al.</i>	(DAMA Collab.)	MINCER	85	PR D32 541	A. Mincer <i>et al.</i>	(KEK, INUS)
COLLAR	00	PRL 85 3083	J.J. Collar <i>et al.</i>	(SIMPLE Collab.)	NAKAMURA	85	PL 161B 417	K. Nakamura <i>et al.</i>	(YALE, FNAL, IOWA)
ABE	99F	PRL 82 2038	F. Abe <i>et al.</i>	(CDF Collab.)	THRON	85	PR D31 451	J.L. Thron <i>et al.</i>	(MEIS)
AMBROSIO	99	PR D60 082002	M. Ambrosio <i>et al.</i>	(Macro Collab.)	SAKUYAMA	83B	LCN 37 17	H. Sakuyama, N. Suzuki	(MEIS)
BERNABEI	99	PL B450 448	R. Bernabei <i>et al.</i>	(DAMA Collab.)	Also	LCN 36 389	H. Sakuyama, K. Watanabe	(MEIS)	
BERNABEI	99D	PRL 83 4918	R. Bernabei <i>et al.</i>	(DAMA Collab.)	Also	NC 78A 147	H. Sakuyama, K. Watanabe	(MEIS)	
BRHLIK	99	PL B464 303	M. Brhlik, L. Roszkowski		Also	NC 6C 371	H. Sakuyama, K. Watanabe	(MEIS)	
DERBIN	99	PAN 62 1886	A.V. Derbin <i>et al.</i>		BHAT	82	PR D25 2820	P.N. Bhat <i>et al.</i>	(TATA)
ACKERSTAFF	98P	Translated from YAF 62 2034	K. Ackerstaff <i>et al.</i>	(OPAL Collab.)	KINOSHITA	82	PRL 48 77	K. Kinoshita, P.B. Price, D. Fryberger	(UCB+)
KLIMENKO	98	JETPL 67 875	A.A. Klimenko <i>et al.</i>		MARINI	82	PR D26 1777	A. Marini <i>et al.</i>	(FRAS, LBL, NWES, STAN+)
ABE	97G	PR D55 R5263	F. Abe <i>et al.</i>	(CDF Collab.)	SMITH	82B	NP B206 333	P.F. Smith <i>et al.</i>	(RAL)
ABREU	97D	PL B396 315	P. Abreu <i>et al.</i>	(DELPHI Collab.)	KINOSHITA	81B	PR D24 1707	K. Kinoshita, P.B. Price	(UCB)
ACKERSTAFF	97B	PL B391 210	K. Ackerstaff <i>et al.</i>	(OPAL Collab.)	LOSECCO	81	PL 102B 209	J.M. LoSecco <i>et al.</i>	(MICH, PENN, BNL)
ADAMS	97B	PRL 79 4083	J. Adams <i>et al.</i>	(FNAL KTeV Collab.)	ULLMAN	81	PRL 47 289	J.D. Ullman	(LEHM, BNL)
BARATE	97K	PL B405 379	R. Barate <i>et al.</i>	(ALEPH Collab.)	YOCK	81	PR D23 1207	P.C.M. Yock	(AUCK)
SARSA	97	PR D56 1856	M.L. Sarsa <i>et al.</i>	(ZARA Collab.)	BARTEL	80	ZPHY C6 295	W. Bartel <i>et al.</i>	(JADE Collab.)
ALESSAND...	96	PL B384 316	A. Alessandrello <i>et al.</i>	(MILA, MILAI, SASSO Collab.)	BUSSIERE	80	NP B174 1	A. Bussiere <i>et al.</i>	(BGNA, SACL, LAPP)
BELLI	96	PL B387 222	P. Belli <i>et al.</i>	(DAMA Collab.)	YOCK	80	PR D22 61	P.C.M. Yock	(AUCK)
Also	PL B389 783 (erratum)	P. Belli <i>et al.</i>		(DAMA Collab.)	ARMITAGE	79	NP B150 87	J.C.M. Armitage <i>et al.</i>	(CERN, DARE, FOM+)
BELLI	96C	NC 19C 537	P. Belli <i>et al.</i>	(DAMA Collab.)	BOZZOLI	79	NP B159 363	W. Bozzoli <i>et al.</i>	(BGNA, LAPP, SACL+)
BERNABEI	96	PL B389 757	R. Bernabei <i>et al.</i>	(DAMA Collab.)	GOODMAN	79	PR D19 2572	J.A. Goodman <i>et al.</i>	(UMD)
COLLAR	96	PRL 76 331	J.J. Collar	(SUCU Collab.)	SMITH	79	NP B149 525	P.F. Smith, J.R.J. Bennett	(RHUL)
SARSA	96	PL B386 458	M.L. Sarsa <i>et al.</i>	(ZARA Collab.)	BHAT	78	PRAM 10 115	P.N. Bhat, P.V. Ramana Murthy	(TATA)
Also	PR D56 1856	M.L. Sarsa <i>et al.</i>		(ZARA Collab.)	CARROLL	78	PRL 41 777	A.S. Carroll <i>et al.</i>	(BNL, PRIN)
SMITH	96	PL B379 299	P.F. Smith <i>et al.</i>	(RAL, SHEF, LOIC+)	CUTTS	78	PRL 41 363	D. Cutts <i>et al.</i>	(BROW, FNAL, ILL, BARI+)
SNOWDEN...	96	PRL 76 332	D.P. Snowden-Hft, E.S. Freeman, P.B. Price	(UCB)	VIDAL	78	PL 77B 344	R.A. Vidal <i>et al.</i>	(COLU, FNAL, STON+)
AKERS	95R	ZPHY C67 203	R. Akers <i>et al.</i>	(OPAL Collab.)	ALEKSEEV	76	SJNP 22 531	G.D. Alekseev <i>et al.</i>	(JINR)
GALLAS	95	PR D52 6	E. Gallas <i>et al.</i>	(MSU, FNAL, MIT, FLOR)	ALEKSEEV	76B	SJNP 23 633	G.D. Alekseev <i>et al.</i>	(JINR)
GARCIA	95	PR D51 1458	E. Garcia <i>et al.</i>	(ZARA, SUCU, PNL)	BALDIN	76	SJNP 22 264	B.V. Baldin <i>et al.</i>	(JINR)
QUENBY	95	PL B351 70	J.J. Quenby <i>et al.</i>	(LOIC, RAL, SHEF+)	BRIATORE	76	NC 31A 553	L. Briatore <i>et al.</i>	(LCGT, FRAS, FREIB)
SNOWDEN...	95	PRL 74 4133	D.P. Snowden-Hft, E.S. Freeman, P.B. Price	(UCB)	GUSTAFSON	76	PRL 37 474	H.R. Gustafson <i>et al.</i>	(MICH)
Also	PRL 76 331	J.J. Collar		(SUCU Collab.)	ALBROW	75	NP B97 189	M.G. Albrow <i>et al.</i>	(CERN, DARE, FOM+)
Also	PRL 76 332	D.P. Snowden-Hft, E.S. Freeman, P.B. Price		(UCB)	FRANKEL	75	PR D12 2561	S. Frankel <i>et al.</i>	(PENN, FNAL)
BECK	94	PL B336 141	M. Beck <i>et al.</i>	(MPIH, KIAE, SASSO)	JOVANOVICH...	75	PL 56B 105	J.V. Jovanovich <i>et al.</i>	(MANI, AACH, CERN+)
RAM	94	PR D49 3120	S. Ram <i>et al.</i>	(TELA, TRIU)	YOCK	75	NP B86 216	P.C.M. Yock	(AUCK, SLAC)
ABE	93G	PRL 71 2542	F. Abe <i>et al.</i>	(CDF Collab.)	APPEL	74	PRL 32 428	J.A. Appel <i>et al.</i>	(COLU, FNAL)
ASTONE	93	PR D47 4770	P. Astone <i>et al.</i>	(ROMA, ROMA1, CATA, FRAS)	FRANKEL	74	PR D9 1932	S. Frankel <i>et al.</i>	(PENN, FNAL)
BUSKULIC	93C	PL B303 198	D. Buskulic <i>et al.</i>	(ALEPH Collab.)	YOCK	74	NP B76 175	P.C.M. Yock	(AUCK)
YAMAGATA	93	PR D47 1231	T. Yamagata, Y. Takamori, H. Utsunomiya	(KONAN)	ALPER	73	PL 46B 265	B. Alper <i>et al.</i>	(CERN, LVP, LUND, BOHR+)
ABE	92J	PR D46 R1889	F. Abe <i>et al.</i>	(CDF Collab.)	LEIPUNER	73	PRL 31 1226	L.B. Leipuner <i>et al.</i>	(BNL, YALE)
AHLEN	92	PRL 69 1860	S.P. Ahlen <i>et al.</i>	(MACRO Collab.)	DARDO	72	NC 9A 319	M. Dardo <i>et al.</i>	(TORI)
BACCI	92	PL B293 460	C. Bacci <i>et al.</i>	(Beijing-Roma-Saclay Collab.)	TONWAR	72	JPA 5 569	S.C. Tonwar, S. Naranan, B.V. Sreekantan	(TATA)
VERKERK	92	PRL 68 1116	P. Verkerk <i>et al.</i>	(ENSP, SACL, PAST)	ANTIPOV	71B	NP B31 235	Y.M. Antipov <i>et al.</i>	(SERP)
AKESSON	91	ZPHY C52 219	T. Akesson <i>et al.</i>	(HELIOS Collab.)	ANTIPOV	71C	PL 34B 164	Y.M. Antipov <i>et al.</i>	(SERP)
NAKAMURA	91	PL B263 529	S. Nakamura <i>et al.</i>		BINON	69	PL 30B 510	F.G. Binon <i>et al.</i>	(SERP)
ORITO	91	PRL 66 1951	S. Orito <i>et al.</i>	(ICEPP, WASCR, NIHO, ICRR)	BJORNBOE	68	NC B53 241	J. Bjornboe <i>et al.</i>	(BOHR, TATA, BERN+)
REUSSER	91	PL B255 143	D. Reusser <i>et al.</i>	(NEUC, CIT, PSI)	JONES	67	PR 164 1584	L.W. Jones	(MICH, WISC, LBL, UCLA, MINN+)
ADACHI	90C	PL B244 352	I. Adachi <i>et al.</i>	(TOPAZ Collab.)	DORFAN	65	PRL 14 999	D.E. Dorfman <i>et al.</i>	(COLU)
ADACHI	90E	PL B249 336	I. Adachi <i>et al.</i>	(TOPAZ Collab.)					
AKRAWY	90O	PL B252 290	M.Z. Akrawy <i>et al.</i>	(OPAL Collab.)					
HEMMICK	90	PR D41 2074	T.K. Hemmick <i>et al.</i>	(ROCH, MICH, OHIO+)					

INDEX

- A*, *a* meson resonances
- A*(1680) or [*now called* $\pi_2(1670)$] **35**, 702
 - A*(2100) [*now called* $\pi_2(2100)$] 726
 - a*₀(980) [*was* $\delta(980)$] **32**, 655
 - a*₀(1450) 687
 - a*₁(1260) [*was* *A*₁(1270) or *A*₁] **33**, 664
 - a*₁(1640) 699
 - a*₂(1320) [*was* *A*₂(1320)] **33**, 673
 - a*₂(1700) 713
 - A*₃ [*now called* $\pi_2(1670)$] **35**, 702
 - a*₄(2040) [*was* $\delta_4(2040)$] 724
 - a*₆(2450) [*was* $\delta_6(2450)$] 734
- Abbreviations used in Particle Listings 406
- Accelerator-induced radioactivity 343
- Accelerator parameters (colliders) 281
- Accelerator physics of colliders 277
- Acceptance-rejection method in Monte Carlo 361
- Activity, unit of, for radioactivity 341
- Age of the universe 102, 232
- Air showers (cosmic ray) 273
- Algorithms for Monte Carlo 362
- Amplitudes, Lorentz invariant 371
- Angular-diameter distance, *d*_A 232
- Anisotropy of cosmic microwave background radiation (CBR) 250, 261
- Anomalous *W/Z* Quartic Couplings 424
- Anomalous *ZZ* γ , *Z* $\gamma\gamma$, and *ZZV* couplings 445
- Argand diagram, definition 374
- Astronomical unit 102
- Astrophysics 230, 255
- Asymmetries of *Z*-boson decay 427
- Asymmetry formulae in Standard Model 128
- Atmospheric cosmic rays 270
- Atmospheric fluorescence 328
- Atmospheric pressure 101
- Atomic and nuclear properties of materials 108
- Atomic mass unit 101
- Atomic weights of elements 105
- Attenuation length for photons 294
- Authors and consultants 11
- Average hadron multiplicities in *e*⁺*e*⁻ annihilation events 387
- Averaging of data 14
- Avogadro number 101
- Axial vector couplings, *g*_V, *g*_A vector 126
- Axions as dark matter 230, 256
- Axion searches **26**, 496
- Axion searches, note on 496
- b*-baryon ADMIXTURE (*A*_{*b*}, Ξ_b , Σ_b , Ω_b) **85**, 1281
- b*-flavored hadrons, production and decay of, note on 877
- b*-hadron mixing and production fractions, note on 977
- b*₁(1235) [*was* *B*(1235)] **33**, 663
- b* (quarks) **30**, 595
- b*-quark fragmentation 220
- b'* quark (4th generation), searches for, **30**, 612
- b* \bar{b} mesons **66**, 1109
- B*⁰- \bar{B} ⁰ mixing, note on 973
- B* decay, *CP* violation in 154
- B* decays, hadronic, note on 882
- B* decays, rare, note on 882
- B*, bottom mesons
- Bottom mesons, HFAG activities 887
 - B* (bottom meson) **46**, 877
 - B*[±] (bottom meson) **47**, 887
 - B*⁰, \bar{B} ⁰ (bottom meson) **51**, 930
 - B*[±]/*B*⁰ ADMIXTURE **56**, 993
 - B*[±]/*B*⁰/*B*_s⁰/*b*-baryon ADMIXTURE **58**, 1007
 - B*^{*} **59**, 1029
 - B*_{*J*}^{*}(5732) 1029
 - B*_{*c*}[±] 1039
 - B*_{*d*} mixing studies, note on 975
 - B*_{*s*}⁰ **59**, 1031
 - B*_{*s*} mixing studies, note on 976
 - B*_{*s*}^{*} 1037
 - B*_{*sJ*}^{*}(5850) 1038
 - b* \bar{b} mesons **66**, 1109
- Baryogenesis 235
- Baryon decay parameters, note on 1146
- Baryon magnetic moments, note on 1201
- Baryon number conservation 89
- Baryon resonances, SU(3) classification of 187
- Baryonium candidates 735
- Baryons **73**, 1135
- Bottom (beauty) baryons **84**, 1278
 - Cascade baryons (Ξ baryons) **80**, 1241
 - Charmed baryons **81**, 1257
 - Dibaryons
 - (see p. VIII.118 in our 1992 edition, Phys. Rev. **D45**, Part II)
 - Exotic baryons (formerly *Z*^{*} resonances) 1199
 - Pentaquarks 1199
 - Hyperon baryons (Λ baryons) **77**, 1201
 - Hyperon baryons (Σ baryons) **78**, 1217
 - Nucleon resonances (Δ resonances) **76**, 1178
 - Nucleon resonances (*N* resonances) **74**, 1150
 - Nucleons **73**, 1135
 - Ω baryons **81**, 1254
- Baryons in quark model 187

- Baryons, stable **73**, 1135
 (see entries for p , n , Λ , Σ , Ξ , Ω , Λ_c , Ξ_c , Ω_c , Λ_b , and Ξ_b)
- Bayes' theorem 346
- Bayesian statistics 356
- Beam momentum, c.m. energy and momentum vs 371
- Beauty – see Bottom
- Bequerel, unit of radioactivity 341
- BEPC (China) collider parameters 281
- BEPC-II (China) collider parameters 281
- β decay, neutrinoless double, search for 562
- β -rays, from radioactive sources 345
- Bethe-Bloch equation 285
- Bias of an estimator 350
- Big-bang cosmology 230
- Binary pulsars 227
- Binomial distribution 347
- Binomial distribution, Monte Carlo algorithm for 362
- Binomial distribution, table of 348
- Birks' law 303
- Black holes 1354
- Bohr magneton 101
- Bohr radius 101
- Boiling points of cryogenic gases 108
- Boltzmann constant 101
- Booklet, Particle Physics, how to get 11
- Bosons **25**, 417
 (see individual entries for γ , W , Z , g , Axions, graviton, Higgs)
- Bottom baryons (Λ_b^0, Ξ_b) **84**, 1278
- Bottom, B^0 – \bar{B}^0 mixing, note on 973
- Bottom-changing neutral currents, tests for 89
- Bottom, charmed meson **60**, 1039
- Bottom mesons ($B, B^*, B_s, B_s^*, B_c^\pm$) **46**, 877
 Bottom mesons, note on HFAG activities 887
- Bottom quark (b) **30**, 595
- Bottom, strange mesons **59**, 1031
- Bottomonium system, level diagram 1109
- Bragg additivity 290
- Branes 1354
- Breit-Wigner
 distribution, Monte Carlo algorithm for 362
 resonance, definition 374
 vs pole parameters of N and Δ Resonances 1149
- Bremsstrahlung by electrons 291
- C (charge conjugation), tests of conservation 89
- c (quark) **30**, 594
- $c\bar{c}$ Region in e^+e^- Collisions, plot of 391
- c -quark fragmentation 220
- $c\bar{c}$ mesons **60**, 1040
- Cabibbo-Kobayashi-Maskawa mixing in B decay, note on 973
- Calorimetry 320
- Cascade baryons (Ξ baryons) **80**, 1241
- CBR—Cosmic background radiation (see CMB) 261
- Central limit theorem 348
- Cepheid variable stars 249
- CESR (Cornell) collider parameters 282
- CESR-C (Cornell) collider parameters 282
- Change of random variables 347
- Characteristic functions 347
- Charge conjugation (C) conservation 89
- Charge conservation 89
- Charge conservation and the Pauli exclusion principle, note on
 (see p. VI.10 in our 1992 edition, Phys. Rev. **D45**)
- Chargino searches 1324
- Charm-changing neutral currents, tests for 89
- Charm Dalitz analyses, note on 811
- Charm quark (c) **30**, 594
- Charmed baryons ($\Lambda_c^+, \Sigma_c, \Xi_c, \Omega_c^0$) **81**, 1259
- Charmed, bottom meson (B_c^\pm) **60**, 1039
- Charmed mesons (D, D^*, D_J) **40**, 803
- Charmed, strange mesons [D_s, D_s^*, D_{sJ}] **45**, 856
- Charmonium system, level diagram 1040
- Cherenkov detectors
 at accelerators 307
 differential 308
 ring imaging 308
 threshold 307
 tracking 307
 nonaccelerator
 atmospheric 329
 deep underground 330
- Cherenkov radiation 297
- χ^2 distribution 349
- χ^2 distribution, Monte Carlo algorithm for 362
- χ^2 distribution, table of 348
- χ_b and χ_c mesons
 $\chi_{b0}(1P)$ **66**, 1114
 $\chi_{b0}(2P)$ **67**, 1120
 $\chi_{b1}(1P)$ **66**, 1115
 $\chi_{b1}(2P)$ **67**, 1121
 $\chi_{b2}(1P)$ **67**, 1116
 $\chi_{b2}(2P)$ **67**, 1123
 $\chi_{c0}(1P)$ **62**, 1061
 $\chi_{c1}(1P)$ **62**, 1068
 $\chi_{c2}(1P)$ **63**, 1074
 $\chi_{c0,1,2}$ and $\psi(2S)$, branching ratios, note on 1060

- CKM mixing elements in B decay, note on 973
- Clebsch-Gordan coefficients 368
- c.m. energy and momentum vs beam momentum 371
- CMB–Cosmic microwave background 236, 261, 250
- Collaboration databases 19
- Collider parameters 281
- Colliders, accelerator physics of 277
- Color octet leptons **88**, 1353
- Color sextet quarks **88**, 1353
- Compensating calorimeters 321
- Compositeness, quark and lepton, searches **87**, 1347
- Compositeness, quark and lepton, searches, note on 1347
- Composition of the Universe 241
- Compton wavelength, electron 101
- Concordance cosmology 247
- Conditional probability density function 347
- Conference databases 18
- Confidence intervals 355
- Confidence intervals, frequentist 356
- Confidence intervals, Poisson 358
- Conservation laws 89
- Consistency of an estimator 350
- Cosmic microwave background 250
- Constrained fits, procedures for 15
- Consultants 12
- Conversion probability for photons to e^+e^- 294
- Correlation coefficient, definition 347
- Cosmic background radiation (CBR) temperature 102
- Cosmic ray(s) 269
- air showers 273
- ankle 274
- at surface of earth 270
- background in counters 341
- composition 269
- fluxes 270
- in atmosphere 270, 273
- knee 274
- primary spectra 269
- secondary neutrinos 272
- underground 271
- Cosmological constant Λ 102, 230, 246
- Cosmological density parameter, Ω 231
- Cosmological equation of state 231
- Cosmological mass density parameter 231
- Cosmological mass density parameter of vacuum (dark energy) . 231
- Cosmological parameters 246, 247
- Cosmology 230, 246, 255
- Coulomb scattering through small angles, multiple 290
- Coupling between matter and gravity 225
- Coupling unification 193
- Couplings, anomalous W/Z Quartic 424
- Couplings, anomalous $ZZ\gamma$, $Z\gamma\gamma$, and ZZV 445
- Couplings for photon, W , Z 126
- Couplings, note on the extraction of triple-gauge 422
- Covariance, definition 347
- Coverage 356
- CP , tests of conservation 89
- CP violation
- in B decay 154
- in K_L^0 decay 154
- in K_L^0 decays, note on 779
- in $K_S^0 \rightarrow 3\pi$ decays, note on 764
- overview 154
- CPT Invariance tests in neutral kaon decay 759
- CPT , tests of conservation 89
- Critical density in cosmology 102, 230
- Critical energy, electrons 292
- Critical energy, muons 296
- Cross sections and related quantities, plots of 385
- e^+e^- annihilation cross section near M_Z 392
- Fragmentation functions 215
- gamma production in $p\bar{p}$ interactions 385
- Jet production in pp and $\bar{p}p$ interactions 385
- νN and $\bar{\nu}N$ c.c. total cross section 393
- Nucleon structure functions 207
- Pseudorapidity distributions 386
- W and Z differential cross section 386
- Cross sections, Regge theory fits to total, table 394
- Cross sections, relations for 373, 376
- Cryogenic gases, boiling points 108
- Cumulative distribution function, definition 346
- Curie, unit of radioactivity 341
- d (quark) **30**, 590
- d functions 368
- $D^0-\bar{D}^0$ mixing, note on 820
- D -meson, Dalitz analyses, note on 811
- D mesons
- D^\pm **40**, 803
- D^0, \bar{D}^0 **41**, 819
- $D_1(2420)^0$ **44**, 852
- $D_1(2420)^\pm$ 852
- $D^*(2007)^0$ **44**, 849
- $D^*(2010)^\pm$ **44**, 850
- $D^*(2640)^\pm$ 855
- $D_2^*(2460)^0$ **44**, 853

- $D_2^*(2460)^\pm$ **44**, 854
 D_s^\pm [*was* F^\pm] **45**, 856
 $D_s^{*\pm}$ [*was* $F^{*\pm}$] **46**, 871
 $D_{s1}(2536)^\pm$ **46**, 874
 $D_{s2}(2573)$ **46**, 875
 $D_{sJ}^*(2860)^\pm$, 876
 $D_{sJ}(3040)^\pm$, 876
 D_s^+ Branching Fractions, note on 858
Dalitz analyses, D -meson, note on 811
Dalitz plot, relations for 372
DAΦNE (Frascati) collider parameters 281
Dark energy 231, 248
Dark energy equation of state parameter w 249
Dark energy parameter, Ω_N 231
Dark matter 238, 255, 247, 248
Dark matter detectors 335
 sub-Kelvin detectors 335
 table 335
Dark matter limits:
 Neutralinos mass limits 1323
 Sneutrino mass limits 1326
Dark matter, nonbaryonic 255
Data, averaging and fitting procedures 14
Data, selection and treatment 13
Databases, availability online 18
Databases, high-energy physics 18
Databases, particle physics 18
Day, sidereal 102
 dE/dx 285
Decay amplitudes (for hyperon decays)
 (see p. 286 in our 1982 edition, Phys. Lett. **111B**)
Decay constant, D_s^+ , note on 858
Decay constants of charged pseudoscalar mesons, note on 861
Decays, kinematics and phase space for 371
Deceleration parameter, q_0 231
Definitions for abbreviations used in Particle Listings 406
 δ -rays 288
 $\delta(980)$ [*now called* $a_0(980)$] **32**, 655
 $\delta_4(2040)$ [*now called* $a_4(2040)$] 724
 $\delta_6(2450)$ [*now called* $a_6(2450)$] 734
 Δ resonances (see also N and Δ resonances) **76**, 1178
 $\Delta B = 1$, weak-neutral currents, tests for 89
 $\Delta B = 2$, tests for 89
 $\Delta C = 1$, weak-neutral currents, tests for 89
 $\Delta C = 2$, tests for 89
 $\Delta I = 1/2$ rule for hyperon decays, test of
 (see p. 286 in our 1982 edition, Phys. Lett. **111B**)
 $\Delta S = 1$, weak-neutral currents, tests for 89
 $\Delta S = 2$, tests for 89
 $\Delta S = \Delta Q$ rule in K^0 decay, note on 785
 $\Delta S = \Delta Q$, tests of 89
 $\Delta T = 1$, weak-neutral currents, tests for 89
Density effect in energy loss rate 288
Density of materials, table 108
Density of matter, critical 102
Density of matter, local 102
Density parameter of the universe, Ω_0 102
Detector parameters 300
Deuteron mass 101
Deuteron structure function 208, 209
Dibaryons
 (see p. VIII.118 in our 1992 edition, Phys. Rev. **D45**, Part II)
Dielectric constant of gaseous elements, table 109
Dielectric suppression of bremsstrahlung 293
DIEHARD 361
Differential Cherenkov detectors 308
Dimensions, extra **88**, 1354
Directories, online, people, and organizations 18
Disk density 102
Distance-redshift relation 230, 246
Dose, radioactivity, unit of absorbed 342
Dose rate from gamma ray sources 343
Double- β Decay 562
 Double- β Decay, Limits from Neutrinoless, note on 562
Double- β decay, neutrinoless, search for 562
Drift Chambers 311
Drift velocities of electrons in liquids 323
Durham databases 18
Dynamical electroweak symmetry breaking 1340
 e (electron) **27**, 515
 e (natural log base) 101
 Charge conservation and the Pauli exclusion principle, note on
 (see p. VI.10 in our 1992 edition, Phys. Rev. **D45**)
 e^+e^- average multiplicity, plot of 389
 $E(1420)$ [*now called* $f_1(1420)$] **34**, 684
Earth equatorial radius 102
Earth mass 102
Education databases 19
Efficiency of an estimator 350
Electric charge (Q) conservation 89
Electrical resistivity of elements, table 109
Electromagnetic
 calorimeters 320
 interactions of N and Δ baryons (review) 1150
 penguin decays, note on 883

relations	110	$\eta_2(1645)$	700
shower detectors, energy resolution	320	$\eta_2(1870)$	719
showers, lateral distribution	295	$\eta'(958)$	32 , 648
showers, longitudinal distribution	294	$\eta_b(1S)$	1110
Electron	27 , 515	$\eta_c(1S)$	60 , 1040
and photon interactions in matter	291	$\eta_c(2S)$	1081
charge	101	Excitation energy	287
critical energy	292	Excited lepton searches	87 , 1350
cyclotron frequency/field	101	Exotic baryons (formerly Z^* resonances)	, 1199
mass	101, 27	Pentaquarks	1199
radius, classical	101	(sic p. VIII.58 in our 1992 edition, Phys. Rev. D45 , Part II)	
volt	101	Exotic meson resonances	1131
Electron drift velocities in liquids	323	Expansion of the Universe	231
Electronic structure of the elements	106	Expectation value, definition	346
Electroweak interactions, Standard Model of	126	Experiment databases	19
Elements, electronic structure of	106	Experimental issues in $B^0-\bar{B}^0$ mixing, note on	974
Elements, ionization energies of	106	Experimental tests of gravitational theory	225
Elements, periodic table of	105	Extensions to the cosmological standard model	248
Energy and momentum (c.m.) vs beam momentum	371	Extra Dimensions	88 , 1354
Energy density / Boltzmann constant	102	$f_{D^+}, f_{D_s^+}, f_{K^-}, f_{\pi^-}$ decay constants	861
Energy density of CBR	102	F, f meson resonances	
Energy density of relativistic particles	102	F^\pm [<i>now called</i> D_s^\pm]	45 , 856
Energy loss		$F^{*\pm}$ [<i>now called</i> $D_s^{*\pm}$]	46 , 871
by electrons	291	$f_0(600)$ [<i>was</i> $\epsilon(1200)$]	31 , 630
(fractional) for electrons and positrons in lead	291	$f_0(980)$ [<i>was</i> $S(975)$ or S^*]	32 , 652
rate for charged particles	286	$f_0(1370)$	33 , 676
rate for muons at high energies	296	$f_0(1500)$	34 , 691
rate, form factor corrections	287	$f_0(1710)$ [<i>was</i> $\theta(1690)$]	35 , 714
rate in compounds	289	$f_0(2020)$	723
rate, restricted	289	$f_0(2100)$	726
Entropy density	235	$f_0(2200)$	730
Entropy density / Boltzmann constant	102	$f_1(1285)$	33 , 669
$\epsilon(1200)$ [<i>now called</i> $f_0(600)$]	31 , 630	$f_1(1420)$ [<i>was</i> $E(1420)$]	34 , 684
$\epsilon(2150)$ [<i>now called</i> $f_2(2150)$]	726	$f_1(1420)$, note on	680
$\epsilon(2300)$ [<i>now called</i> $f_4(2300)$]	732	$f_1(1510)$	694
ϵ (permittivity)	101, 109, 110	$f_1(1510)$, note on	680
ϵ_0 (permittivity of free space)	101, 110	$f_2(1270)$	33 , 666
$\hat{\epsilon}_1, \hat{\epsilon}_2, \hat{\epsilon}_3$ electroweak variables	138–139	$f_2(1430)$	687
Error function	348	$f_2(1565)$	697
Error procedure for masses and widths of meson resonances	789	$f_2(1640)$	700
Errors, treatment of	14	$f_2(1810)$	718
Estimator	350	$f_2(1910)$	721
η meson	31 , 625	$f_2(1950)$	722
$\eta(1295)$	33 , 672	$f_2(2010)$ [<i>was</i> $g_T(2010)$]	36 , 723
$\eta(1405)$ [<i>was</i> $\iota(1440)$]	34 , 680	$f_2(2150)$ [<i>was</i> $\epsilon(2150)$]	726
$\eta(1440)$, note on	680	$f_2(2300)$ [<i>was</i> $g_T'(2300)$]	36 , 732
$\eta(1760)$	716	$f_2(2340)$ [<i>was</i> $g_T''(2340)$]	36 , 733
$\eta(2225)$	731		

Greek letters are alphabetized by their English-language spelling. Bold page numbers signify entries in the Particle Properties Summary Tables.

$f'_2(1525)$ [<i>was</i> $f'(1525)$]	34, 694	Gamma distribution, Monte Carlo algorithm for	362
$f_4(2050)$ [<i>was</i> $h(2030)$]	36 , 724	Gamma distribution, table of	348
$f_4(2300)$ [<i>was</i> $\epsilon(2300)$]	732	Gas-filled detectors	308
$f_6(2510)$ [<i>was</i> $r(2510)$]	734	electron drift velocity	309
$f_J(2220)$ [<i>was</i> $\xi(2220)$]	730	gas properties	309
F_2 structure function, plots	207	high rate effects	311
Familon searches	508	mobility of ions	310
Fermi coupling constant	101	Townsend coefficient	309
Fermi plateau	288	Gauge bosons	25 , 417
Feynman's x variable	373	(see individual entries for γ , W , Z , g , Axions, graviton, Higgs)	
Field equations, electromagnetic	110	Gauge couplings	126
Fine structure constant	101	Gaussian confidence intervals	357
Fit to Z electroweak measurements	426	Gaussian confidence intervals close to physical boundary	359
Fits to data	14	Gaussian distribution, Monte Carlo algorithm for	362
Flatness of Universe	102	Gaussian distribution, Multivariate	348
Flavor-changing neutral currents, tests for	89	Gaussian ellipsoid	349
Fluorescence, atmospheric	328	Gluino searches	87 , 1335
Fly's Eye	274, 328	gluon, g	25 , 417
Forbidden states in quark model	112	Gluonium candidates	1131
Force, Lorentz	110	Goldstone boson searches	508
Form factors, $K_{\ell 3}$, note on	753	Grand unified theories	193
Form factors, $\pi \rightarrow \ell\nu\gamma$ and $K \rightarrow \ell\nu\gamma$, note on	620	Gravitational	
Fourth generation (b') searches	30 , 612	acceleration g	101
Fractional energy loss for electrons and positrons in lead	291	constant G_N	101, 102
Fragmentation functions	215	field in the strong field regime, dynamical tests	226
Fragmentation, heavy-quark	220	field in the weak field regime, dynamical tests	226
Fragmentation in e^+e^- annihilation	215	lensing	237, 252
Fragmentation, longitudinal	217	theory, experimental tests of	225
Fragmentation models	217	graviton	418
Free quark searches	30 , 613	Gravitons	1354
Frequentist statistics	356	Gravity in extra dimensions	1354
Friedmann-Lemaître equations	230	Gray, unit of absorbed dose of radiation	341
Further States	735	GUTs	193
g (gluon)	25 , 417	$h(2030)$ [<i>now called</i> $f_4(2050)$]	36 , 724
$g(1690)$ [<i>now called</i> $\rho_3(1690)$]	35 , 705	$h_1(1170)$ [<i>was</i> $H(1190)$]	33 , 663
$g_T(2010)$ [<i>now called</i> $f_2(2010)$]	36 , 723	$h_1(1380)$	679
$g'_T(2300)$ [<i>now called</i> $f_2(2300)$]	36 , 732	$h_1(1595)$	698
$g''_T(2340)$ [<i>now called</i> $f_2(2340)$]	36 , 733	$h_c(1P)$	1073
g_V, g_A vector, axial vector couplings	126	Hadron (average) multiplicities in e^+e^- annihilation events	387
Galaxy clustering	251	Hadronic	
Galaxy power spectrum	251	calorimeters	321
γ (Euler constant)	101	flavor conservation	89
γ (photon)	25 , 417	shower detectors	321
γp and γd cross sections, plots of	401	Half-lives of commonly used radioactive nuclides	345
gamma production in $p\bar{p}$ interactions	385	Halo density	102
γ -rays, from radioactive sources	345	Harrison-Zel'dovich effect	246
Gamma distribution	349	Heavy boson searches	26 , 480

Heavy lepton searches	29, 553	$J/\psi(1S)$ or $\psi(1S)$	60, 1044
Heavy-Neutral Leptons, Searches for	29, 577	K^+p , K^+n , and K^+d cross sections, plots of	400
Heavy particle searches	1368	K^-p , K^-n , and K^-d cross sections, plots of	399
Heavy-quark fragmentation	220	K stable mesons (see meson resonances below)	
HERA (DESY) collider parameters	284	K^\pm	36, 740
Hierarchy problem	1292, 1354	K^0, \bar{K}^0	37, 758
Higgs boson in Standard Model	126, 136, 448	K_L^0	37, 766
Higgs boson mass in electroweak analyses	136–138	K_S^0	37, 762
Higgs, M_H , constraints on	136–138	K stable mesons, notes therein	
Higgs production in e^+e^- annihilation, cross-section formula	378	K_L^0 CP -violation parameters, fits for, note on	779
Higgs searches	26, 448	K decay, CPT invariance tests in neutral	759
Higgs searches, note on	448	K^0 decay, note on $\Delta S = \Delta Q$ rule in	785
History of measurements, discussion	16	K_L^0 decay, CP violation in	154
Hubble constant (expansion rate)	102	$K_{\ell 3}$ form factors, note on	753
Hubble constant H_0	246	K^\pm mass, note on	740
Hubble expansion	231	K rare decay, note on	742
Hyperon baryons (see Λ and Σ baryons)	77, 1201	$K \rightarrow \ell\nu\gamma$ form factors, note on	620
Hyperon decays, nonleptonic decay amplitudes		$K \rightarrow 3\pi$ Dalitz plot parameters, note on	752
(see p. 286 in our 1982 edition, Phys. Lett. 111B)		$K_S^0 \rightarrow 3\pi$ decay, note on CP violation in	764
Hyperon decays, test of $\Delta I = 1/2$ rule for		K, K^* meson resonances	
(see p. 286 in our 1982 edition, Phys. Lett. 111B)		$K(1460)$ [<i>was</i> $K(1400)$]	796
Hyperon radiative decays, note on	1242	$K(1630)$	796
ID particle codes for Monte Carlos	364	$K(1830)$	800
Ideograms, criteria for presentation	15	$K(3100)$	802
Illustrative key to the Particle Listings	405	$K^*(892)$	38, 788
Imaging Cherenkov detectors	307	$K^*(892)$ mass and mass differences, note on	789
Impedance, relations for	111	$K^*(1410)$	39, 792
Importance sampling in Monte Carlo calculations	361	$K^*(1680)$ [<i>was</i> $K^*(1790)$]	39, 797
Inclusive hadronic reactions	378	$K_0^*(1430)$ [<i>was</i> $\kappa(1350)$]	39, 793
Inclusive reactions, kinematics for	373	$K_0^*(1950)$	800
Inconsistent data, treatment of	15	$K_1(1270)$ [<i>was</i> $Q(1280)$ or Q_1]	38, 790
Independence of random variables	347	$K_1(1400)$ [<i>was</i> $Q(1400)$ or Q_2]	39, 792
Inflation of early universe	235, 246	$K_1(1650)$	797
Information horizon	233	$K_2(1580)$ [<i>was</i> $L(1580)$]	796
Inorganic scintillators	304	$K_2(1770)$ [<i>was</i> $L(1770)$]	39, 797
Inorganic scintillator parameters	303	$K_2(1820)$	39, 799
International System (SI) units	104	$K_2(2250)$ [<i>was</i> $K(2250)$]	801
INTERNET address for comments	11	$K_2^*(1430)$ [<i>was</i> $K^*(1430)$]	39, 794
Introduction	11	$K_2^*(1980)$	800
Inverse transform method in Monte Carlo	361	$K_3(2320)$ [<i>was</i> $K(2320)$]	801
Ionization energies of the elements	106	$K_3^*(1780)$ [<i>was</i> $K^*(1780)$]	39, 798
Ionization energy loss at minimum, table	108	$K_4(2500)$ [<i>was</i> $K(2500)$]	802
Ionization yields for charged particles	290	$K_4^*(2045)$ [<i>was</i> $K^*(2060)$]	39, 800
$\iota(1440)$ [<i>now called</i> $\eta(1405)$]	34, 680	$K_5^*(2380)$	802
Jansky	102	$K_{\ell 3}$ form factors, note on	753
Jet production in pp and $\bar{p}p$ interactions, plot of	385	Kaluza-Klein states	1354
Journals	18	Kaon (see also K)	36, 740

- Kaon decay, *CPT* invariance tests in neutral 759
- Kaon rare decay, note on 742
- $\kappa(1350)$ [*now called* $K_0^*(1430)$] **39**, 793
- KEKB collider parameters 283
- Key to the Particle Listings 405
- Kinematics, decays, and scattering 371
- Knock-on electrons, energetic 288
- Kobayashi-Maskawa (Cabibbo-) mixing matrix 146
- $L(1580)$ [*now called* $K_2(1580)$] 796
- $L(1770)$ [*now called* $K_2(1770)$] **39**, 797
- Lagrangian, standard electroweak 126
- Λ , cosmological constant 102, 230, 246
- Λ CDM (cold dark matter with dark energy) 247
- Λ **77**, 1201
- Λ and Σ baryons **77**, 1201
- Listings, Λ baryons 1201
- Listings, Σ baryons 1217
- Status of (review) 1204
- Λp cross section, plot of 401
- Λ_b^0 1278
- Λ_c^+ **81**, 1259
- Λ_c^+ branching fractions, note on 1260
- $\Lambda_c(2595)^+$ **82**, 1265
- $\Lambda_c(2625)^+$ **82**, 1266
- $\Lambda_c(2765)^+$ 1267
- $\Lambda_c(2880)^+$ 1267
- Lagged-Fibonacci-based random number generator 361
- Landau-Pomeranchuk-Migdal (LPM) effect 293
- Large-scale structure of the Universe 237
- Least squares 351
- Least squares with nonindependent data 351
- LEP (CERN) collider parameters 282
- Lepton conservation, tests of 89
- Lepton family number conservation 89
- Lepton (heavy) searches **29**, 553
- Lepton mixing, neutrinos (massive) and, search for **29**, 567
- Lepton, quark compositeness searches **87**, 1347
- Lepton, quark substructure searches **87**, 1347
- Leptons **27**, 515
- (see individual entries for e , μ , τ , and neutrino properties)
- Leptons, weak interactions of quarks and 126, 137
- Leptoquark quantum numbers, note on 490
- Leptoquark searches 492
- Lethal dose from penetrating ionizing radiation 342
- LHC (CERN) collider parameters 284
- Lifetimes of b -flavored hadrons, note on 877
- Light boson searches 496
- Light neutrino types, number of **29**, 561
- Light neutrino types from collider expts., number of, note on 561
- Light, speed of 101
- Light year 102
- Lineshape of Z boson 426
- Liquid ionization chambers, free electron drift velocity 323
- Listings, Full, keys to reading 405
- Local group velocity relative to CBR 102
- Longitudinal fragmentation 217
- Longitudinal structure function, plots of 212
- Lorentz force 110
- Lorentz invariant amplitudes 371
- Lorentz transformations of four-vectors 371
- Low-noise electronics 318
- Low-radioactivity background techniques 338
- cosmic rays 339
- cosmogenic 339
- environmental 338
- neutrons 339
- radioimpurities 338
- radon 339
- Luminosity conversion 102
- Luminosity distance d_L 232
- Ly α forest 236
- Magnetic moments, baryon, note on 1201
- Magnetic Monopole Searches **87**, 1285
- Magnetic Monopoles, note on 1285
- Majoron searches 508
- Mandelstam variables 373
- Marginal probability density function 346
- Mass attenuation coefficient for photons 294
- Mass density parameter, Ω_m 247, 252
- Massive neutrinos and lepton mixing, search for **29**, 567
- Materials, atomic and nuclear properties of 108
- Matter, passage of particles through 285
- Maximum energy transfer to e^- 287
- Maximum likelihood 351
- Maxwell equations 110
- Mean energy loss rate in H₂ liquid, He gas, C, Al, Fe, Sn, and
- Pb, plots 287
- Mean excitation energy 287
- Mean range in H₂ liquid, He gas, C, Fe, Pb, plots 287
- Median, definition 346
- Meson multiplets in quark model 184
- Mesons **31**, 619
- $b\bar{b}$ mesons **66**, 1109
- Bottom, charmed mesons **60**, 1039

- Bottom mesons **46**, 877
- Bottom, strange mesons **59**, 1031
- $c\bar{c}$ mesons **60**, 1040
- Charmed, bottom meson **60**, 1039
- Charmed mesons **60**, 1040
- Charmed, strange mesons **45**, 856
- Exotic mesons 1131
- Nonstrange mesons **31**, 619
- Strange mesons **36**, 740
- Mesons, stable **31**, 619
(see individual entries for π , η , K , D , D_s , B , and B_s)
- Metric prefixes, commonly used 104
- Michel parameter ρ **27**, 550
- Micro-pattern gas detectors (MPDG) 312
gas electron multiplier (GEM) 312
micro-mesh gaseous structure (MicroMegas) 312
micro-strip gas chamber 313
- Microwave background 236
- Minimum ionization 287
- Minimum ionization loss, table 108
- MIP (minimum ionizing particle) 287
- Mistag probabilities in $B^0-\bar{B}^0$ mixing, note on 974
- Mixing angle, weak ($\sin^2\theta_W$) 101, 126, 136
- Mixing, $B^0-\bar{B}^0$, note on 973
- Mixing, $D^0-\bar{D}^0$, note on 820
- Mixing studies, B_d , note on 975
- Mixing studies, B_s , note on 976
- Molar volume 101
- Molière radius 295
- Momenta, measurement of, in a magnetic field 325
- Momentum — c.m. energy and momentum
vs beam momentum 371
- Momentum transfer, minimum and maximum 371
- Monopole searches **87**, 1285
Monopole searches, note on 1285
- Monte Carlo particle numbering scheme 364
- Monte Carlo techniques 361
- $\overline{\text{MS}}$ renormalization scheme (Standard Model) 126
- μ (muon) **27**, 516
- $\mu \rightarrow e$ conversion 520
- μ_0 (permeability of free space) 101, 110
- Multibody decay kinematics 372
- Multiple Coulomb scattering through small angles 290
- Multiplets, meson in quark model 184
- Multiplets, SU(n) 370
- Multiplicities, average in e^+e^- interactions, table of 387
- Multiplicity, average in e^+e^- interactions, plot of 389
- Multiplicity, average in pp and $\bar{p}p$ interactions, plot of 389
- Multivariate Gaussian distribution 348
- Multivariate Gaussian distribution, table of 348
- Multi-wire proportional chamber (see also MWPC) 310
- Muon **27**, 516
anomalous magnetic moment, note on 517
critical energy 296
decay parameters, note on 521
energy loss rate at high energies 296
g-2 517
range/energy in rock 271
- MWPC, Multi-wire proportional chamber 310
drift chambers 311
maximum wire tension 311
wire stability 311
- n (neutron) **73**, 1143
- n -body differential cross sections 373
- n -body phase space 371
- $n - \bar{n}$ oscillations 1145
- N and Δ resonances **74**, 1149
Breit-Wigner vs pole parameters of 1149
Electromagnetic interactions (review) 1150
Listings, Δ resonances 1178
Listings, N resonances 1149
Status of (review) 1149
- N^* resonances (see N and Δ resonances) **74**, 1149
- Names, hadrons 13, 112
- Neutral-current parameters, values for 137
- Neutralino as dark matter 230
- Neutralino searches 1323
- Neutrino(s) **27**, 515
from cosmic rays 272
mass, cosmological limit 251
mass, mixing, and oscillations, note on 164
masses 193
(massive) and lepton mixing, search for **29**, 567
mixing **29**, 567
oscillation searches **29**, 567
properties **29**, 554
solar, review 164
types (light), number of **29**, 561
types (light) from collider experiments, number of, note on 561
- Neutrino detectors (deep, large, enclosed volume) 330
heavy water 331
liquid scintillator 330
table of detectors 330
water-filled 331

Neutrino Telescopes	332	$\omega(1420)$	34 , 686
astrophysical neutrinos	333	$\omega(1650)$	35 , 701
ice	332	$\omega_3(1670)$	35 , 702
sea water	332	Opposite-side tag in $B^0\text{--}\bar{B}^0$ mixing, note on	974
Neutrinoless double- β decay, search for	562	Optical theorem	374
Neutrino mass density parameter, Ω_ν	246	Organic scintillators	303
Neutron	73 , 1143	Organization of Particle Listings and Summary Tables	11
Neutrons at accelerators	342	Oscillation analyses in $B^0\text{--}\bar{B}^0$ mixing, note on	974
Neutrons, from radioactive sources	345	Oscillation parameters, three-flavor, note	571
Newtonian gravitational constant G_N	102	Other particle searches	1365
Nomenclature for hadrons	13, 112	Other particle searches, note on	1365
Nonbaryonic dark matter	241	P (parity), tests of conservation	89
Non- $q\bar{q}$ candidates	1131	p (proton)	73 , 1135
Normal distribution	348	$pp, \bar{p}p$ average multiplicity, plot of	389
Normal distribution, table of	348	pp jet production	385
Neutrino Mixing	29 , 567	pp, pn , and pd cross sections, plots of	396, 397
Neutrino Properties	29 , 554	$\bar{p}p$	
νN and $\bar{\nu}N$ cross sections, plot of		average multiplicity, plot of	389
(see p. III.75 in our 1992 edition, Phys. Rev. D45 , Part II)		gamma production	385
Nuclear collision length, table	108	jet production	385
Nuclear interaction length, table	108	$\bar{p}n$, and $\bar{p}d$ cross sections, plots of	396, 397
Nuclear magneton	101	pseudorapidity	386
Nuclear (and atomic) properties of materials	108	Parameter estimation	350
Nucleon decay	193	Parity of $q\bar{q}$ states	184
Nucleon resonances (see N and Δ resonances)	74 , 1149	Parsec	102
Nucleon structure functions, plots of	207	Partial-wave expansion of scattering amplitude	374
Nuclides, radioactive, commonly used	345	Particle detectors	300
Number density of baryons	102	Particle detectors for non-accelerator physics	328
Number density of CBR photons	102	Particle ID numbers for Monte Carlo	364
Numbering scheme for particles in Monte Carlo	364	Particle Listings, key to reading	405
Occupational radiation dose, U.S. maximum permissible	342	Particle Listings, organization of	11
Omega baryons (Ω baryons)	81 , 1254	Particle nomenclature	13, 112
Ω^- resonances	1255	Particle Physics Booklet, how to get	11
Ω^-	81 , 1254	Particle symbol style conventions	112
Ω_c^0	1275	Parton distributions	204
Ω , cosmological density parameter	231	Passage of particles through matter	285
Ω_b , baryon mass density	252	Pauli exclusion principle, charge conservation, note on	
Ω_{dm} , dark matter density	247, 248	(see p. VI.10 in our 1992 edition, Phys. Rev. D45)	
Ω_i , density parameter for i th matter constituent	246	Penguin decays, electromagnetic, note on	883
Ω_Λ , scaled cosmological constant	102, 231	Periodic table of the elements	105
Ω_m , mass density parameter	102, 231, 247, 252	Permeability μ_0 of free space	101, 110
Ω_ν , neutrino mass density parameter	246	Permittivity ϵ_0 of free space	101, 110
$\Omega_m + \Omega_\Lambda$	102	Phase space, Lorentz invariant	371
Ω_{tot} , total energy density of Universe	102, 253	Phase space, relations for	371
Ω_Q , quintessence (dark) energy density	248, 249	$\phi(1020)$	32 , 656
Ω_v , vacuum energy parameter	231	$\phi(1680)$	35 , 704
$\omega(782)$	32 , 643	$\phi_3(1850)$ [<i>was</i> $X(1850)$]	36 , 719
		Photino searches	1319

Greek letters are alphabetized by their English-language spelling. Bold page numbers signify entries in the Particle Properties Summary Tables.

Photon	25 , 417	ψ mesons	
and electron interactions with matter	291	$\psi(1S) = J/\psi(1S)$	60 , 1044
attenuation length	294	$\psi(2S)$	63 , 1082
collection efficiency, scintillators	303	$\psi(2S)$ and $\chi_{c0,1,1}$, branching ratios, note on	1060
coupling	126	$\psi(3770)$	64 , 1094
cross section in carbon and lead, contributions to	293	$X(3945)$	1101
pair production cross section	292	$\psi(4040)$	65 , 1102
to e^+e^- conversion probability	294	$\psi(4160)$	65 , 1103
total cross sections (C and Pb)	293	$\psi(4415)$	66 , 1107
Physical constants, table of	101	Pulsars, binary	227
Physical region, for confidence intervals	359	$Q(1280)$ or Q_1 [<i>now called</i> $K_1(1270)$]	38 , 790
π , value of	101	$Q(1400)$ or Q_2 [<i>now called</i> $K_1(1400)$]	39 , 792
$\pi^\pm p$ and $\pi^\pm d$ cross sections, plots of	398	and structure functions	202
$\pi \rightarrow \ell\nu\gamma$ form factors, note on	620	Quintessence (general dark energy of Universe)	248, 249
π mesons		Quantum mechanics in $B^0-\bar{B}^0$ mixing, note on	973
π^\pm	31 , 619	Quantum numbers in quark model	184
π^0	31 , 623	Quarks	30 , 583
$\pi(1300)$	33 , 672	and lepton compositeness searches	87 , 1347
$\pi(1800)$	716	and lepton substructure searches	87 , 1347
$\pi_1(1400)$	679	current masses of	126, 583
$\pi_1(1600)$	698	fragmentation in e^+e^- annihilation, heavy	220
$\pi_2(1670)$ [<i>was</i> $A(1680)$ or A_3]	35 , 702	and leptons, weak interactions of	126, 137
$\pi_2(2100)$ [<i>was</i> $A(2100)$]	726	mass, note on	583
Pion	31 , 619	model	184
Planck constant	101	model assignments	184
Planck mass	102	model, dynamical ingredients	190
Plasma energy	285	properties of	184
Plastic scintillators	303	Quark searches, free	30 , 613
Poisson distribution	347	Quark searches, note on	613
Poisson distribution, Monte Carlo algorithm for	362	R function, e^+e^- collisions, plot of	390
Poisson distribution, table of	348	$r(2510)$ [<i>now called</i> $f_6(2510)$]	734
Potentials, electromagnetic	110	Rad, unit of absorbed dose of radiation	341
Prefixes, metric, commonly used	104	Radiation	
Primary spectra, cosmic rays	269	Cherenkov	297
Probability	346	damage in Silicon detectors	318
Probability density function, definition	346	-dominated epoch	234
Production and spectroscopy of b -flavored hadrons, note on	878	length	291
Propagation of errors	353	length, approximate algorithm	291
Properties (atomic and nuclear) of materials	108	length of materials, table	108
Proton (see p)	73 , 1135	lethal dose from	342
Proton cyclotron frequency/field	101	weighting factor	341
Proton decay	193	Radiative corrections in Standard Model	126
Proton mass	73 , 101	Radiative decays, hyperons, note on	1242
Proton structure function	201	Radiative loss by muons	296
Proton structure function, plots	207, 210	Radioactive sources, commonly used	345
Pseudorapidity distribution in $\bar{p}p$ interactions, plot of	386	Radioactivity	
Pseudorapidity η , defined	373	and radiation protection	341
Pseudoscalar mesons, decay constants of charged, note on	861		

- at accelerators 343
- natural annual background 341
- unit of absorbed dose 341
- unit of activity 341
- Radioactivity, low-radioactivity background techniques 338
- cosmic rays 339
- cosmogenic 339
- environmental 338
- neutrons 339
- radioimpurities 338
- radon 339
- Radon, as component of natural background radioactivity 341
- Random angle, Monte Carlo algorithm for sine and cosine of 362
- Random number generators 361
- RANLUX 361
- Rapidity 373
- Rare B decays, note on 882
- Redshift 230
- Refractive index of materials, table 108
- Regge theory fits to total cross sections, table 394
- Re-ionization of the Universe 250
- Relativistic kinematics 371
- Relativistic rise 288
- Relativistic transformation of electromagnetic fields 110
- Renormalization in Standard Model 126
- Representations, $SU(n)$ 370
- Resistive plate chambers 316
- Resistivity, electrical, of elements, table 109
- Resistivity of metals 111
- Resistivity, relations for 111
- Resonance, Breit-Wigner form and Argand plot for 374
- Resonances (see Mesons and Baryons)
- Restricted energy loss rate, charged particles 289
- RHIC (Brookhaven) collider parameters 284
- ρ mesons
- $\rho(770)$ **31**, 637
- $\rho(770)$, note on 637
- $\rho(1450)$ **34**, 688
- $\rho(1450)$ and $\rho(1770)$, note on 709
- $\rho(1700)$ **35**, 709
- $\rho(1900)$ 720
- $\rho(2150)$ 728
- $\rho_3(1690)$ [*was* $g(1690)$] **35**, 705
- $\rho_3(1990)$ 723
- $\rho_3(2250)$ 731
- $\rho_5(2350)$ 733
- ρ parameter of electroweak interactions 137
- ρ parameter in electroweak analyses (Standard Model) 138
- ρ_c , critical density 102
- Ring-Imaging Cherenkov detectors 308
- Robertson-Walker metric 230
- Robustness of an estimator 350
- RPC (Resistive Plate Chambers) 316
- Rounding errors, treatment of 16
- Rydberg energy 101
- s (quark) **30**, 590
- S, T, U electroweak variables 138, 139
- $S = +1$ baryons (formerly Z^* baryons) 1199
- Pentaquarks 1199
- (see p. VIII.58 in our 1992 edition, Phys. Rev. **D45**, Part II)
- $S(975)$ or S^* [*now called* $f_0(980)$] **32**, 652
- S-matrix approach to Z lineshape 426
- S-matrix for two-body scattering 371
- Sachs-Wolfe effect 250
- Same-side tag in $B^0-\bar{B}^0$ mixing, note on 974
- Scalar mesons, note on 630
- Scale factor, definition of 14
- Scaled cosmological constant, Ω_Λ 102, 231
- Scaled Hubble constant 102, 231
- Schwarzschild radius of the Earth 102
- Schwarzschild radius of the Sun 102
- Scintillator parameters 303
- Sea-level cosmic ray fluxes 269
- Searches:
- Axion searches **26**, 496
- Baryonium candidates 735
- Chargino searches 1324
- Color octet leptons **88**, 1353
- Color sextet quarks **88**, 1353
- Compositeness, quark and lepton, searches **87**, 1347
- Excited lepton searches **87**, 1350
- Familon searches 508
- Fourth generation (b') searches **30**, 612
- Free quark searches **30**, 613
- Glino searches **87**, 1335
- Gluonium candidates 1131
- Goldstone boson searches 508
- Heavy boson searches **26**, 480
- Heavy lepton searches **29**, 553
- Heavy particle searches 1368
- Higgs searches **26**, 448
- Lepton (heavy) searches **29**, 553
- Lepton mixing, neutrinos (massive) and, search for **29**, 567
- Lepton, quark compositeness searches **87**, 1347
- Lepton, quark substructure searches **87**, 1347

Leptoquark searches	492	Silicon detectors, radiation damage	318
Light boson searches	26 , 496	Silicon particle detectors	316
Light neutrino types, number of	29 , 561	Silicon photodiodes	316
Magnetic Monopoles	87 , 1285	Silicon strip detectors	316
Majoron searches	508	$\sin^2 \theta_W$, weak-mixing angle	101, 126, 136
Massive neutrinos and lepton mixing, searches	29 , 567	Slepton searches	1326
Monopole searches	87 , 1285	Sloan Digital Sky Survey (SDSS)	251
Neutralino searches	1323	Sneutrino searches	1326
Neutrino oscillation searches	29 , 567	Solar	
Neutrino, solar, experiments	164	equatorial radius	102
Neutrino types, number of	29 , 561	luminosity	102
Neutrinoless double- β decay searches	562	mass	102
Neutrinos (massive) and lepton mixing, search for	29 , 567	ν experiments	164
Non- $q\bar{q}$ candidates	1131	radius in galaxy	102
Other particle searches	1365	velocity in galaxy	102
Photino searches	1319	velocity with respect to CBR	102
Quark and lepton compositeness searches	87 , 1347	Solenoidal collider detector magnets	323
Quark and lepton substructure searches	87 , 1347	Sources, radioactive, commonly used	345
Quark searches, free	30 , 613	Specific heats of elements, table	109
Slepton searches	1326	Spectroscopy of b -flavored hadrons, note on	878
Sneutrino searches	1326	Speed of light	102
Squark searches	1331	Spherical harmonics	368
Solar ν experiments	164	Spin-dependent structure functions	213
Substructure, quark and lepton, searches	87 , 1347	Squark searches	1331
Supersymmetric partner searches	87 , 1292	Standard cosmological model	247
Technicolor, review of	1340	Standard Model of electroweak interactions	126
Techniparticle searches	87 , 1340	Standard Model predictions in $B^0-\bar{B}^0$ mixing, note on	973
Technipion searches	26 , 478	Standard particle numbering for Monte Carlos	364
Vector meson candidates	735	Statistical procedures	14
W' searches, note on	480	Statistical significance in $B^0-\bar{B}^0$ mixing, note on	974
Weak gauge boson searches	26 , 480	Statistics	350
Z' searches, note on	483	Stefan-Boltzmann constant	101
Selection and treatment of data	13	Stopping power	286
Shower detector energy resolution	320	Stopping power for heavy-charged projectiles	285
Showers, electromagnetic, lateral distribution of	295	Strange baryons	77 , 1201
Showers, electromagnetic, longitudinal distribution of	294	Strange, bottom meson	59 , 1031
SI units, complete set	104	Strange, charmed mesons	45 , 856
Sidereal day	102	Strange mesons	36 , 740
Sidereal year	102	Strange quark (s)	30 , 590
Sievert, unit of radiation dose equivalent	341	Strangeness-changing neutral currents, tests for	89
σ, R function, e^+e^- collisions, plot of	390	Structure functions	201
Σ baryons (see also Λ and Σ baryons)	78 , 1217	Student's t distribution	349
Σ^+	78 , 1217	Student's t distribution, Monte Carlo algorithm for	362
Σ^0	78 , 1219	Student's t distribution, table of	348
Σ^-	79 , 1220	SU(2) \times U(1)	126
$\Sigma(1670)$, note on	1227	SU(3) classification of baryon resonances	187
$\Sigma_c(2455)$	82 , 1268	SU(3), generators of transformations	369
$\Sigma_c(2520)$	1268	SU(3) isoscalar factors	369

Greek letters are alphabetized by their English-language spelling. Bold page numbers signify entries in the Particle Properties Summary Tables.

- SU(3) multiplets (representations) 187
 SU(3) representation matrices 369
 SU(6) multiplets 188
 SU(n) multiplets 370
 Substructure, quark and lepton, searches **87**, 1347
 Substructure, quark and lepton, searches, note on 1347
 Summary Tables, organization of 11
 Sunyaev-Zel'dovich effect 246
 Superconducting solenoidal magnet 323
 Supernovae, Type Ia and Type II supernovae 249
 Supersymmetric partner searches **87**, 1292
 Supersymmetry, electroweak analyses of 138
 Superweak model of CP violation 779
 Survival probability, relations for 371
 Symmetry breaking 193, 126
 Synchrotron radiation 111
 Systematic errors, treatment of 14

 t (quark) **30**, 596
 T (time reversal), tests of conservation 89
 Tags in $B^0-\bar{B}^0$ mixing, note on 974
 τ lepton **27**, 525
 τ branching fractions, note on 529
 τ -decay parameters, note on 548
 τ polarization in Z decay 427
 Technicolor, electroweak analyses of 138
 Technicolor, review of 1340
 Techniparticle searches **87**, 1340
 Technipion searches **26**, 478
 Temperature of CBR 102
 TEVATRON (Fermilab) collider parameters 284
 Thermal conductivity of elements, table 109
 Thermal expansion coefficients of elements, table 109
 Thermal history of the Universe 233
 $\theta(1690)$ [*now called* $f_0(1710)$] **35**, 714
 θ_W , weak-mixing angle 101, 126, 136
 Thomson cross section 101
 Three-body decay kinematics 371
 Three-body phase space 371
 Threshold Cherenkov detectors 307
 Time-projection chambers (TPC) 313
 Time-projection chambers (TPC) (non-accelerator) 334
 Top-changing neutral currents, tests for 89
 Top quark (t) **30**, 596
 Top quark, note on 596
 Top quark mass from electroweak analyses 134
 Toroidal collider detector magnets 325
 Total cross sections, table of fit parameters 394
 Total cross sections, summary plot 395
 Total energy density of Universe, Ω_{tot} 253
 Total lepton number conservation 89
 TPC, Time-projection chambers 313
 TPC, Time-projection chambers (non-accelerator) 334
 Tracking Cherenkov detectors 307
 Transformation of electromagnetic fields, relativistic 110
 Transition radiation 297
 Transition radiation detectors (TRD) 315
 Triangles, unitarity, note on 146
 Triple gauge couplings, note on the extraction of 422
 Tropical year 102
 Two-body decay kinematics 371
 Two-body differential cross sections 371
 Two-body partial decay rate 371
 Two-body scattering kinematics 371
 Two-photon processes in e^+e^- annihilation 377

 u (quark) **30**, 590
 Ultra-high-energy cosmic rays 274
 Underground cosmic rays 271
 Unified atomic mass unit 101
 Unified theories, grand 193
 Uniform distribution, table of 348
 Units and conversion factors 101
 Units, electromagnetic 110
 Units, SI, complete set 104
 Universe
 age of 102, 230, 232, 253
 baryon density of 102, 241
 composition 232, 241
 cosmological properties of 230
 cosmological structure 234
 critical density of 102
 curvature of 231
 density fluctuations 237
 density parameter of 102
 entropy density 235
 (Hubble) expansion of 230, 246
 large-scale structure of 232, 237
 mass-energy 255
 Universe (cont.)
 matter-dominated 236
 phase transitions 235
 radiation content at early times 234
 thermodynamic equilibrium 234
 thermal history of 233
 Υ states, width determinations of, note on 1109

$\Upsilon(1S)$	66 , 1110	Ξ baryons	80 , 1241
$\Upsilon(2S)$	67 , 1117	Ξ resonances, note on	1246
$\Upsilon(3S)$	68 , 1124	Ξ^0	80 , 1241
$\Upsilon(4S)$	68 , 1127	Ξ^-	80 , 1243
$\Upsilon(10860)$	68 , 1129	Ξ_b^0, Ξ_b^-	1280
$\Upsilon(11020)$	68 , 1130	Ξ_c^+	83 , 1270
V_{cb} and V_{ub} CKM Matrix Elements	1014	Ξ_c^0	83 , 1271
V_{cb} and V_{ub} determination of, note on	1014	$\Xi_c'^+$	83 , 1272
V_{ud}, V_{us} determination of, note on	771	$\Xi_c'^0$	83 , 1272
$V_{ud}, V_{us}, V_{ub}, V_{cb}, V_{cd}, V_{cs}, V_{cb}, V_{td}, V_{ts}, V_{tb}$	146	$\Xi_c(2645)$	84 , 1273
Vacuum energy parameter, Ω_v	231	$\Xi_c(2790)$	84 , 1273
Variance, definition	346	$\Xi_c(2815)$	84 , 1273
Vector meson candidates	735	$\xi(2220)$ [<i>now called</i> $f_J(2220)$]	730
W (gauge boson)	25 , 418	Year, sidereal	102
W -boson mass, note on	418	Year, tropical	102
W boson, mass, width, branching ratios, and coupling to fermions	25 , 101, 127, 134, 136	Young diagrams (tableaux)	370
W^\pm : Triple gauge couplings, note on the extraction of	422	Young's modulus of solid elements, table	109
W and Z differential cross section	386	Yukawa coupling unification	193
w , dark energy equation of state parameter	231, 249	Z : Anomalous $ZZ\gamma$, $Z\gamma\gamma$, and ZZV couplings	445
W' searches, note on	480	Z (gauge boson)	25 , 426
WMAP, NASA's Wilkinson Microwave Anisotropy Probe	250	Z boson, note on	426
Weak boson searches	26 , 480	Z boson, mass, width, branching ratios, and coupling to fermions	25 , 101, 127, 134, 136, 483
Weak neutral currents, tests for ($\Delta B = 1, \Delta C = 1, \Delta S = 1, \Delta T = 1$)	89	Z decay to heavy flavors	429
Weinberg angle ($\sin^2 \theta_W$)	101, 126	Z width, plot	392
Width determinations of Υ states, note on	1109	Z' searches, note on	483
Width of W and Z bosons	134	Z^* resonances (KN system)	, 1199
Wien displacement law constant	101	Pentaquarks	1199
WIMPs (also see dark matter limits)	256		
WIMPs and other particle searches, note on	1365		
Wire chambers	308		
xF_3 structure function, plots of	211		
x variable (of Feynman's)	373		
X mesons			
$X(1850)$ [<i>now called</i> $\phi_3(1850)$]	36 , 719		
$X(3872)$	65 , 1099		
$X(3940)$	1101		
$X(3945)$	1101		
$X(4050)^\pm$	1103		
$X(4140)$	1103		
$X(4160)$	1104		
$X(4250)^\pm$	1105		
$X(4260)$	65 , 1105		
$X(4350)$	1106		
$X(4360)$	1107		
$X(4430)^\pm$	1108		
$X(4660)$	1108		

COLOR FIGURES

Quantum Chromodynamics (Figure 9.1)	1391
Electroweak model and constraints on new physics (Figure 10.2)	1391
Electroweak model and constraints on new physics (Figure 10.3)	1392
Electroweak model and constraints on new physics (Figure 10.4)	1392
CKM quark-mixing matrix (Figure 11.2)	1393
CP violation in meson decays (Figure 12.3)	1393
Neutrino mass, mixing, and oscillations (Figure 13.3)	1394
Neutrino mass, mixing, and oscillations (Figure 13.6)	1394
Neutrino mass, mixing, and oscillations (Figure 13.10)	1395
Neutrino mass, mixing, and oscillations (Figure 13.11)	1396
Structure functions (Figure 16.4)	1396
Big-Bang cosmology (Figure 19.2)	1397
Big-Bang nucleosynthesis (Figure 20.1)	1397
Cosmic microwave background (Figure 23.2)	1398
Cosmic microwave background (Figure 23.3)	1398
Cosmic microwave background (Figure 23.4)	1399
Cosmic Rays (Figure 24.1)	1399
Cosmic Rays (Figure 24.8)	1400
Particle detectors at accelerators (Figure 28.23)	1400
Particle detectors for non-accelerator physics (Figure 29.5)	1401
Radioactivity and radiation protection (Figure 30.2)	1401
Radioactivity and radiation protection (Figure 30.5)	1402
Radioactivity and radiation protection (Figure 30.6)	1402
Jet Production in pp and $\bar{p}p$ Interactions (Figure 41.1)	1403
Direct γ Production in $\bar{p}p$ Interactions (Figure 41.2)	1403
Plots of cross sections and related quantities (Figure 41.6)	1404
Plots of cross sections and related quantities (Figure 41.7)	1405
Plots of cross sections and related quantities (Figure 41.10)	1406
The Mass and Width of the W boson (Figure 1)	1407
The Mass and Width of the W boson (Figure 2)	1407
Searches for Higgs Bosons (Figure 1)	1408
Searches for Higgs Bosons (Figure 2)	1408
Searches for Higgs Bosons (Figure 5)	1409
Searches for Higgs Bosons (Figure 6)	1409
Searches for Higgs Bosons (Figure 7)	1410
Searches for Higgs Bosons (Figure 8)	1410
Searches for Higgs Bosons (Figure 9)	1411
Searches for Higgs Bosons (Figure 10)	1411
Searches for Higgs Bosons (Figure 11)	1412
Searches for Higgs Bosons (Figure 12)	1412
Searches for Higgs Bosons (Figure 13)	1413
Searches for Higgs Bosons (Figure 14)	1413
W' -boson searches (Figure 1)	1414
Leptoquarks (Figure 1)	1414
CP Violation in K_L Decays (Figure 1)	1415
CP Violation in K_L Decays (Figure 2)	1415
$D^0-\bar{D}^0$ Mixing (Figure 1)	1416
$D^0-\bar{D}^0$ Mixing (Figure 2)	1416
$B^0-\bar{B}^0$ Mixing (Figure 2)	1417
V_{cb} and V_{ub} CKM Matrix Elements (Figure 1)	1418
V_{cb} and V_{ub} CKM Matrix Elements (Figure 2)	1418
Supersymmetry, Part I (Theory, Figure 1)	1419
Supersymmetry, Part II (Experiment, Figure 1)	1419
Supersymmetry, Part II (Experiment, Figure 3)	1420
Supersymmetry, Part II (Experiment, Figure 6)	1420
Dynamical Electroweak Symmetry Breaking (Figure 1)	1421
Dynamical Electroweak Symmetry Breaking (Figure 4)	1422
Dynamical Electroweak Symmetry Breaking (Figure 6)	1422

Quantum Chromodynamics (p. 121)

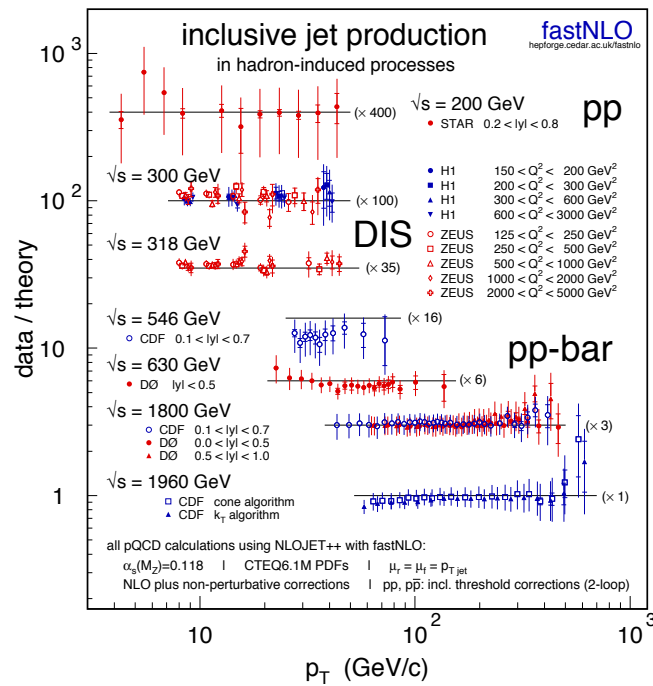


Figure 9.1: A compilation of data-over-theory ratios for inclusive jet cross sections as a function of jet transverse momentum (p_T), measured in different hadron-induced processes at different center-of-mass energies; from Ref. 156, including some updates [157]. The various ratios are scaled by arbitrary numbers (indicated between parentheses) for better readability of the plot. The theoretical predictions have been obtained at NLO accuracy, for parameter choices (coupling constant, PDFs, renormalization, and factorization scales) as indicated at the bottom of the figure.

Electroweak model and constraints on new physics (p. 137)

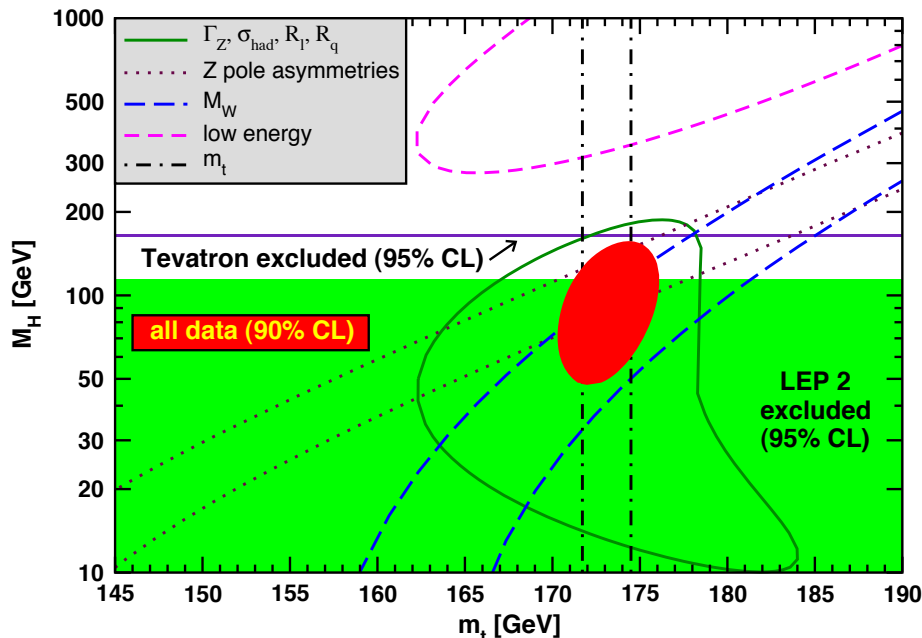


Figure 10.2: One-standard-deviation (39.35%) uncertainties in M_H as a function of m_t for various inputs, and the 90% CL region ($\Delta\chi^2 = 4.605$) allowed by all data. $\alpha_s(M_Z) = 0.1183$ is assumed except for the fits including the Z lineshape or low energy data. The direct lower limit from LEP 2 and the excluded window from the Tevatron [221] (both at the 95% CL) are also shown.

Electroweak model and constraints on new physics (p. 137)

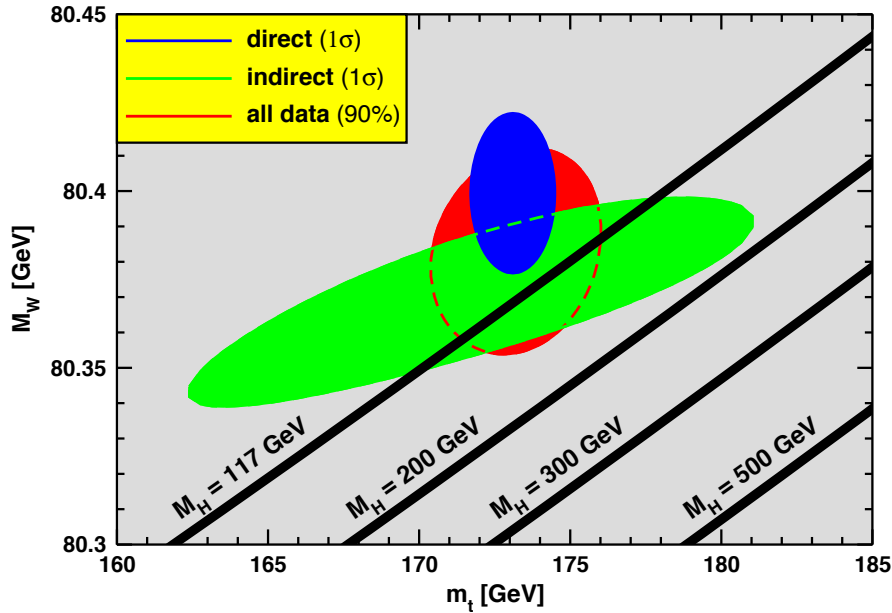


Figure 10.3: One-standard-deviation (39.35%) region in M_W as a function of m_t for the direct and indirect data, and the 90% CL region ($\Delta\chi^2 = 4.605$) allowed by all data. The SM prediction as a function of M_H is also indicated. The widths of the M_H bands reflect the theoretical uncertainty from $\alpha(M_Z)$.

Electroweak model and constraints on new physics (p. 139)

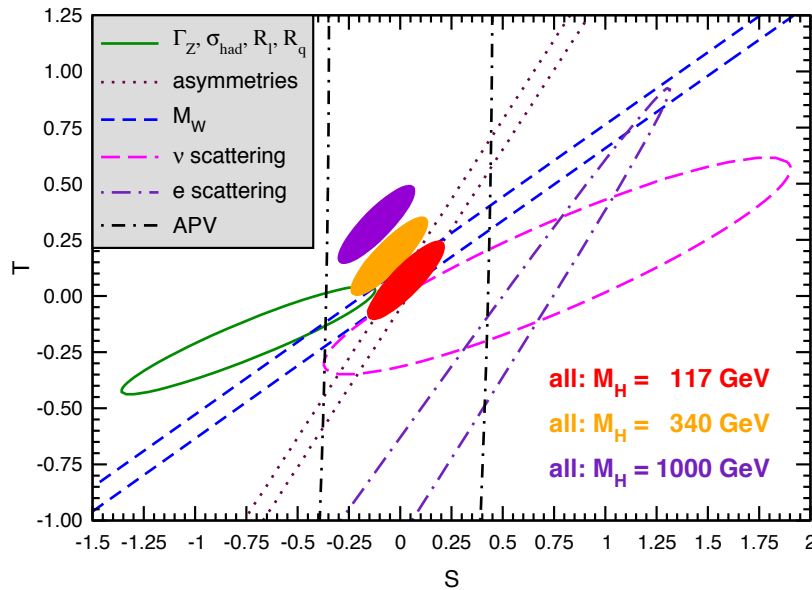


Figure 10.4: 1σ constraints (39.35%) on S and T from various inputs combined with M_Z . S and T represent the contributions of new physics only. (Uncertainties from m_t are included in the errors.) The contours assume $M_H = 117$ GeV, except for the central and upper 90% CL contours allowed by all data, which are for $M_H = 340$ GeV and 1000 GeV, respectively. Data sets not involving M_W are insensitive to U . Due to higher order effects, however, $U = 0$ has to be assumed in all fits. α_s is constrained using the τ lifetime as additional input in all fits. Because this has changed significantly since the 2008 edition of this *Review* (see the discussion in Sec. 10.5), the strongly α_s -dependent solid (green) contour from Z lineshape and cross-section measurements has moved significantly towards negative S and T . The long-dashed (magenta) contour from ν scattering has moved closer towards the global averages (see Sec. 10.3). The long-dash-dotted (indigo) contour from polarized e scattering [123,125] is the upper tip of an elongated ellipse centered at around $S = -15$ and $T = -21$. At first sight it looks as if it is deviating strongly but it is off by only 1.8σ . This illusion arises because $\Delta\chi^2 > 0.8$ everywhere on the visible part of the contour.

CKM quark-mixing matrix (p. 151)

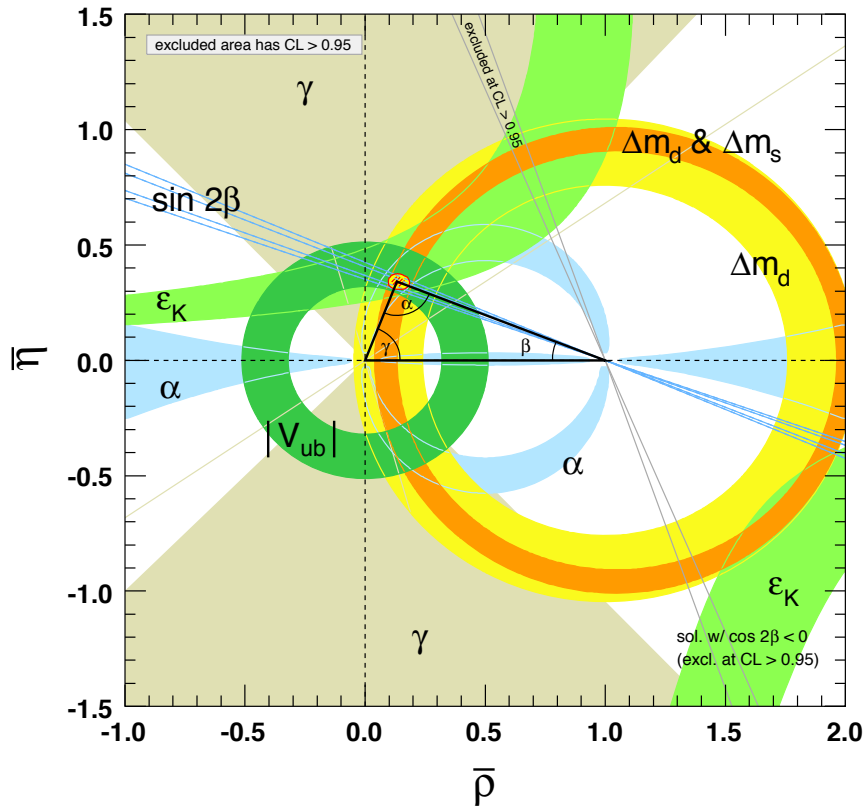


Figure 11.2: Constraints on the $\bar{\rho}, \bar{\eta}$ plane. The shaded areas have 95% CL.

CP violation in meson decays (p. 161)

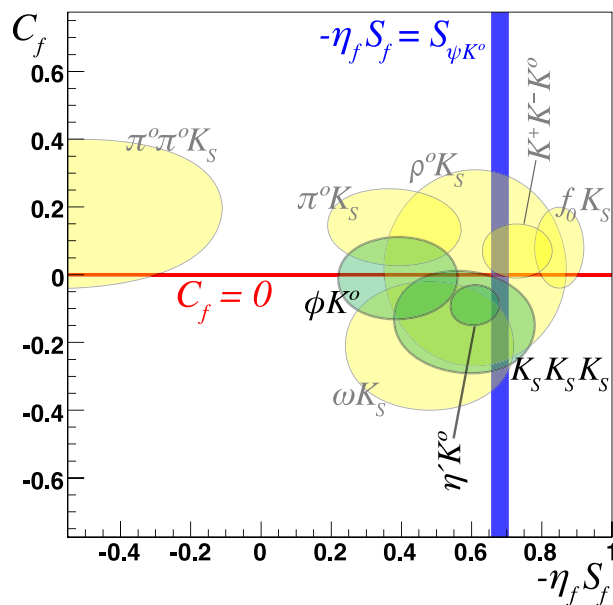


Figure 12.3: Summary of the results [21] of time-dependent analyses of $b \rightarrow q\bar{q}s$ decays, which are potentially sensitive to new physics. Subdominant corrections are expected to be smallest for the modes shown in green (darker). Results for final states including K^0 mesons combine CP -conjugate K_S and K_L measurements. The final state $K^+K^-K^0$ is not a CP eigenstate; the mixture of CP -even and CP -odd components is taken into account in obtaining an effective value for $\eta_f S_f$. Correlations between C_f and S_f are included when available.

Neutrino mass, mixing, and oscillations (p. 174)

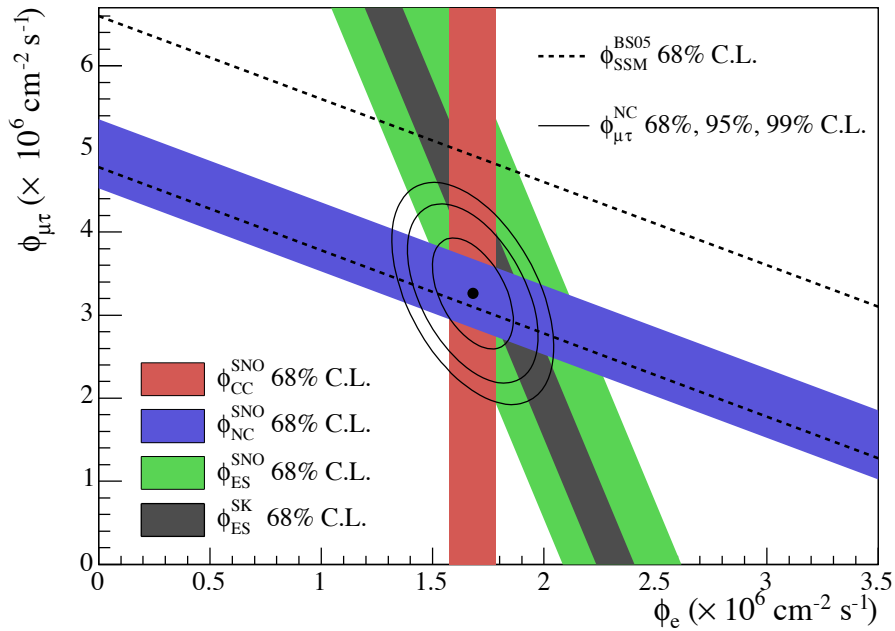


Figure 13.3: Fluxes of ^8B solar neutrinos, $\phi(\nu_e)$, and $\phi(\nu_\mu \text{ or } \tau)$, deduced from the SNO's CC, ES, and NC results of the salt phase measurement [94]. The Super-Kamiokande ES flux is from Ref. 99. The BS05(OP) standard solar model prediction [86] is also shown. The bands represent the 1σ error. The contours show the 68%, 95%, and 99% joint probability for $\phi(\nu_e)$ and $\phi(\nu_\mu \text{ or } \tau)$. The figure is from Ref. 94.

Neutrino mass, mixing, and oscillations (p. 176)

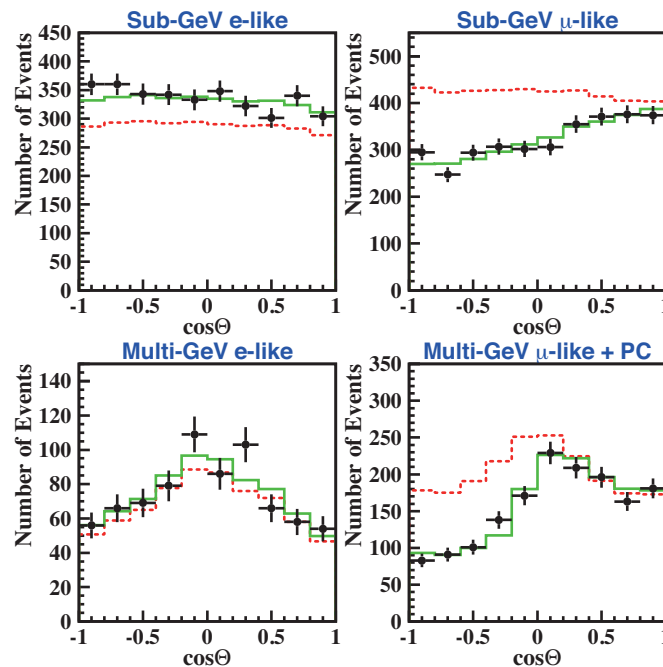


Figure 13.6: The zenith angle distributions for fully contained 1-ring e -like and μ -like events with visible energy < 1.33 GeV (sub-GeV) and > 1.33 GeV (multi-GeV). For multi-GeV μ -like events, a combined distribution with partially contained (PC) events is shown. The dotted histograms show the non-oscillated Monte Carlo events, and the solid histograms show the best-fit expectations for $\nu_\mu \leftrightarrow \nu_\tau$ oscillations. (This figure is provided by the Super-Kamiokande Collaboration.)

Neutrino mass, mixing, and oscillations (p. 178)

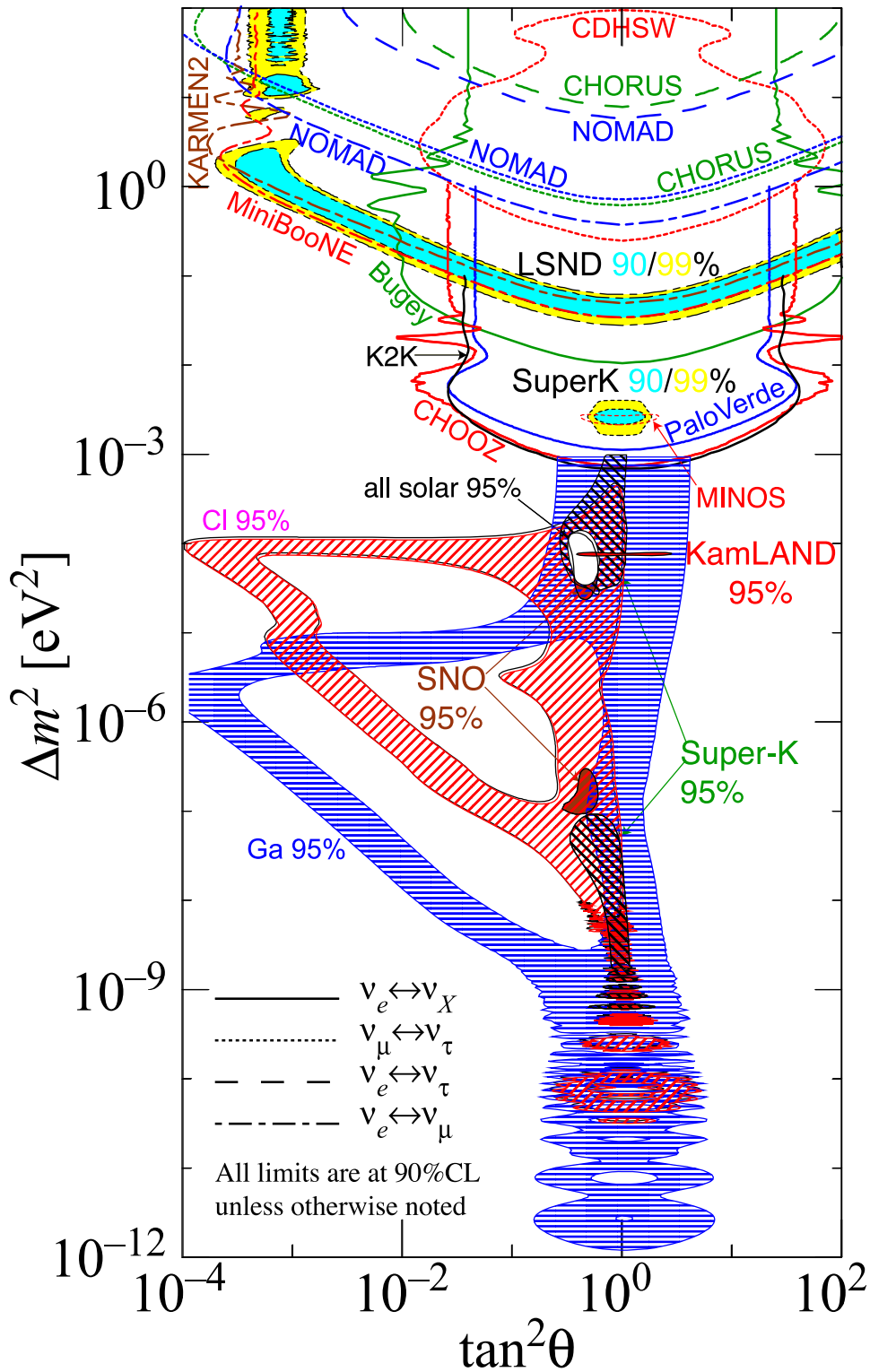


Figure 13.10: The regions of squared-mass splitting and mixing angle favored or excluded by various experiments. The figure was contributed by H. Murayama (University of California, Berkeley, and IPMU, University of Tokyo). References to the data used in the figure can be found at <http://hitoshi.berkeley.edu/neutrino>.

Neutrino mass, mixing, and oscillations (p. 181)

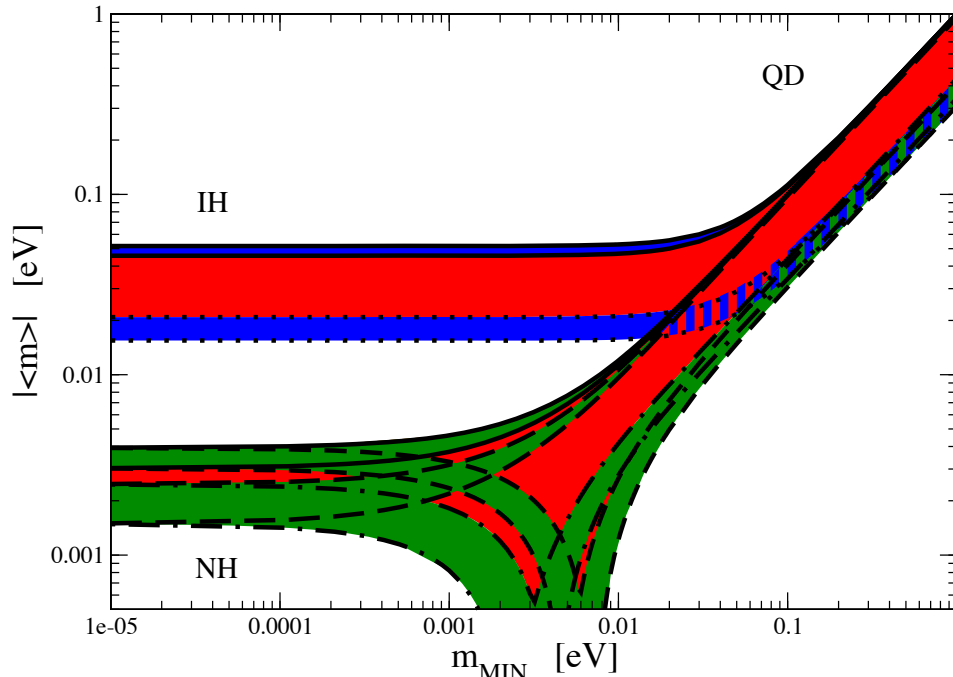


Figure 13.11: The effective Majorana mass $\langle m \rangle$ (including a 2σ uncertainty) as a function of $\min(m_j)$. The figure is obtained using the best fit values and 1σ errors of Δm_{21}^2 , $\sin^2 \theta_{12}$, and $|\Delta m_{31}^2| \cong |\Delta m_{32}^2|$ from Ref. 112, fixed $\sin^2 \theta_{13} = 0.01$ and $\delta = 0$. The phases $\alpha_{21,31}$ are varied in the interval $[0, \pi]$. The predictions for the NH, IH and QD spectra are indicated. The black lines determine the ranges of values of $\langle m \rangle$ for the different pairs of CP conserving values of $\alpha_{21,31}$: $(\alpha_{21}, \alpha_{31}) = (0, 0)$ solid, $(0, \pi)$ long dashed, $(\pi, 0)$ dash-dotted, (π, π) short dashed, lines. The red regions correspond to at least one of the phases $\alpha_{21,31}$ and $(\alpha_{31} - \alpha_{21})$ having a CP violating value. (Update by S. Pascoli of a figure from the last article quoted in Ref. 127.)

Structure functions (p. 204)

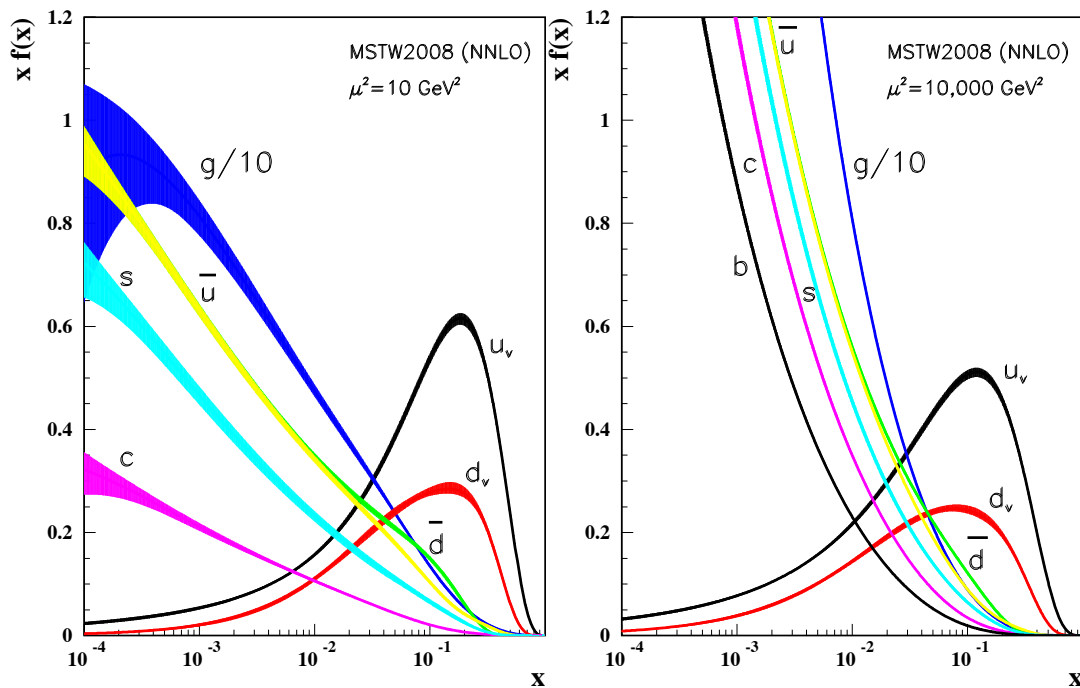


Figure 16.4: Distributions of x times the unpolarized parton distributions $f(x)$ (where $f = u_v, d_v, \bar{u}, \bar{d}, s, c, b, g$) and their associated uncertainties using the NNLO MSTW2008 parameterization [13] at a scale $\mu^2 = 10 \text{ GeV}^2$ and $\mu^2 = 10,000 \text{ GeV}^2$.

Big-Bang cosmology (p. 233)

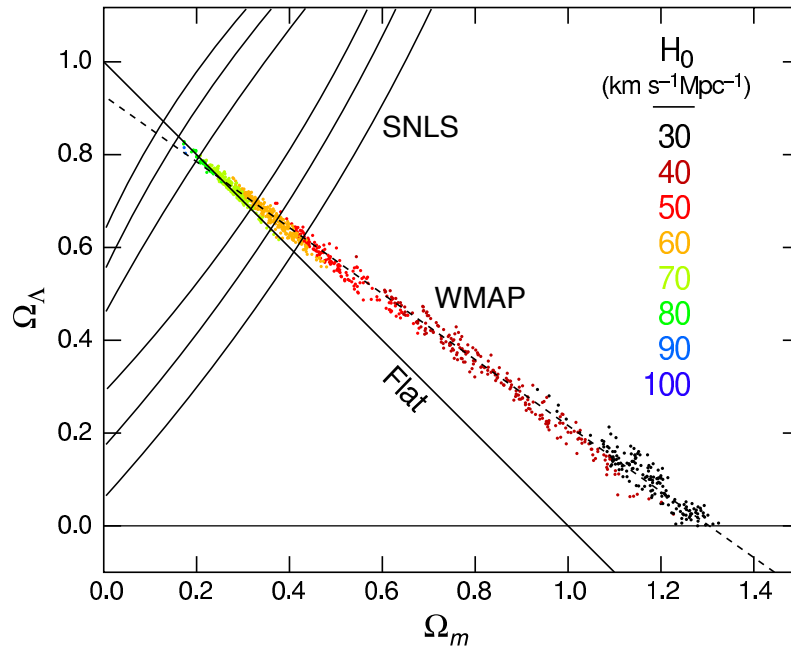


Figure 19.2: Likelihood-based probability densities on the plane Ω_Λ (*i.e.*, Ω_v assuming $w = -1$) vs Ω_m . The colored Monte-Carlo points derive from WMAP [32] and show that the CMB alone requires a flat universe $\Omega_v + \Omega_m \simeq 1$ if the Hubble constant is not too high. The SNe Ia results [33] very nearly constrain the orthogonal combination $\Omega_v - \Omega_m$. The intersection of these constraints is the most direct (but far from the only) piece of evidence favoring a flat model with $\Omega_m \simeq 0.25$.

Big-Bang nucleosynthesis (p. 241)

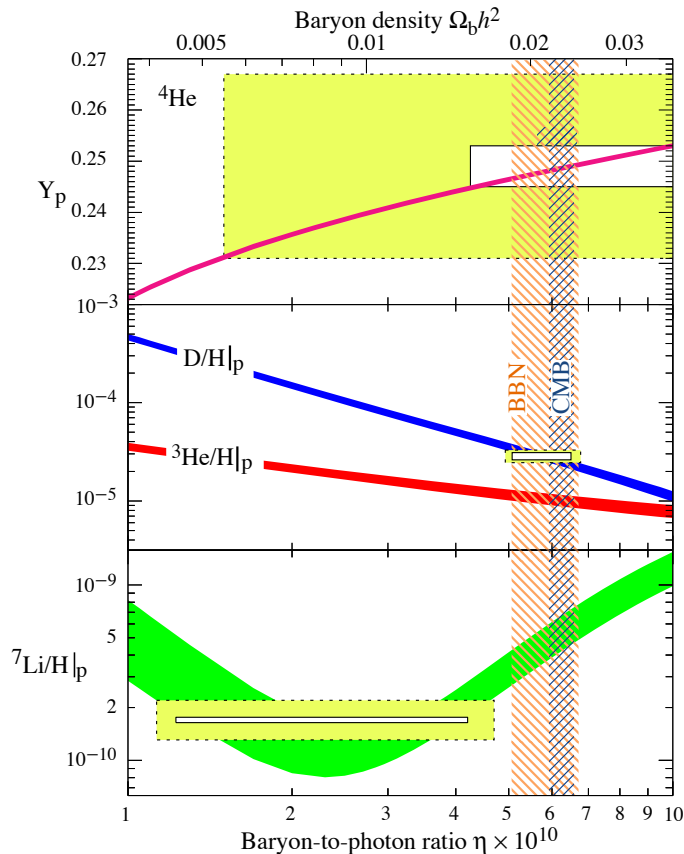


Figure 20.1: The abundances of ${}^4\text{He}$, D , ${}^3\text{He}$, and ${}^7\text{Li}$ as predicted by the standard model of Big-Bang nucleosynthesis [11] – the bands show the 95% CL range. Boxes indicate the observed light element abundances (smaller boxes: $\pm 2\sigma$ statistical errors; larger boxes: $\pm 2\sigma$ statistical and systematic errors). The narrow vertical band indicates the CMB measure of the cosmic baryon density, while the wider band indicates the BBN concordance range (both at 95% CL).

Cosmic microwave background (p. 264)

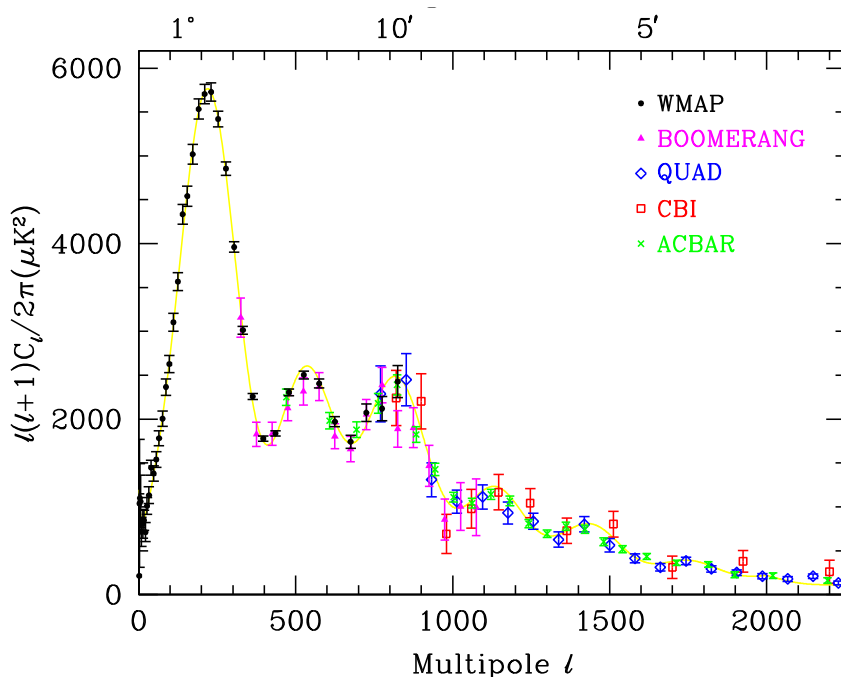


Figure 23.2: Band-power estimates from the *WMAP*, *BOOMERANG*, *QUAD*, *CBI*, and *ACBAR* experiments. Some of the low- ℓ and high- ℓ band-powers which have large error bars have been omitted. Note also that the widths of the ℓ -bands varies between experiments and have not been plotted. This figure represent only a selection of available experimental results, with some other data-sets being of similar quality. The multipole axis here is linear, so the Sachs-Wolfe plateau is hard to see. However, the acoustic peaks and damping region are very clearly observed, with no need for a theoretical curve to guide the eye; the curve plotted is a best-fit model from *WMAP* 5-year plus other CMB data.

Cosmic microwave background (p. 265)

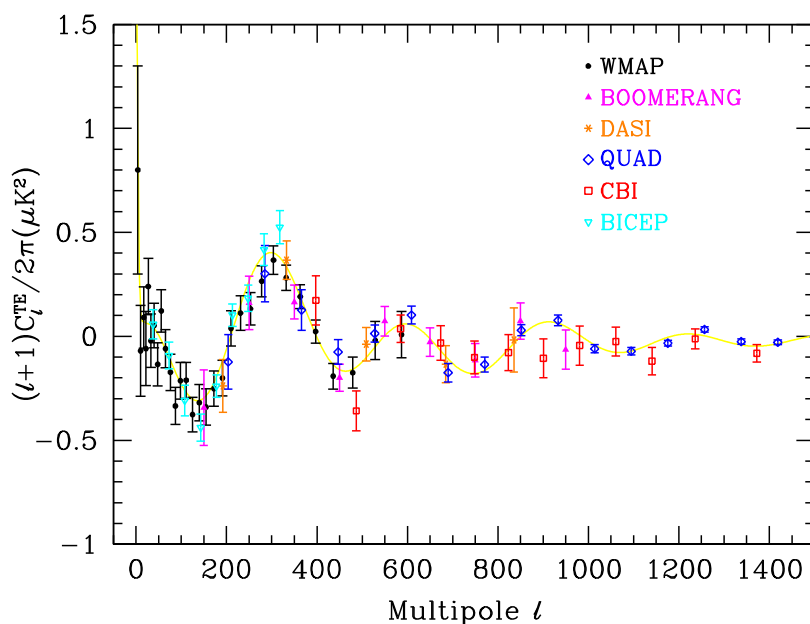


Figure 23.3: Cross power spectrum of the temperature anisotropies and E-mode polarization signal from *WMAP* [47], together with estimates from *BOOMERANG*, *DASI*, *QUAD*, *CBI* and *BICEP*, several of which extend to higher ℓ . Note that the widths of the bands have been suppressed for clarity, but that in some cases they are almost as wide as the features in the power spectrum. Also note that the y -axis here is not multiplied by the additional ℓ , which helps to show both the large and small angular scale features.

Cosmic microwave background (p. 265)

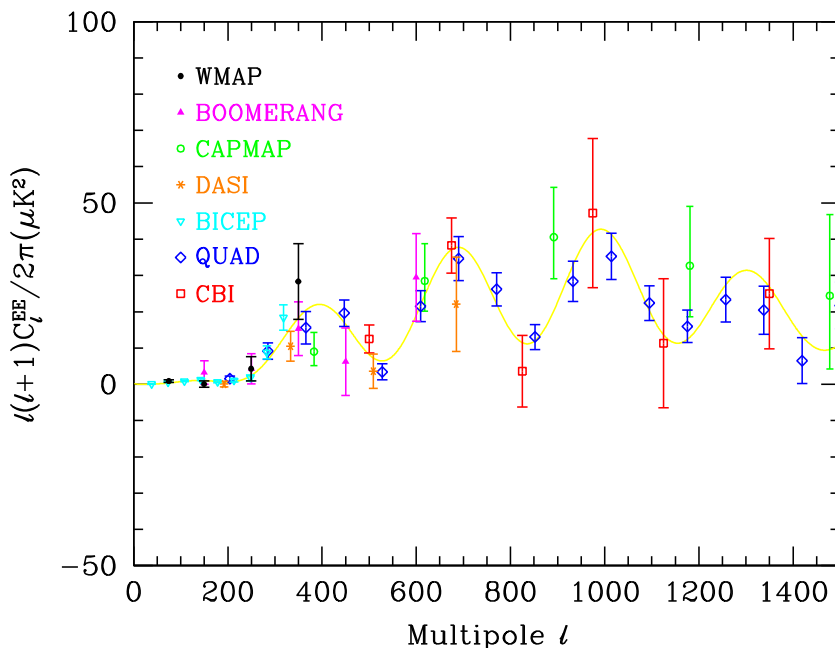


Figure 23.4: Power spectrum of E-mode polarization from several different experiments, plotted along with a theoretical model which fits *WMAP* plus other CMB data.

Cosmic Rays (p. 269)

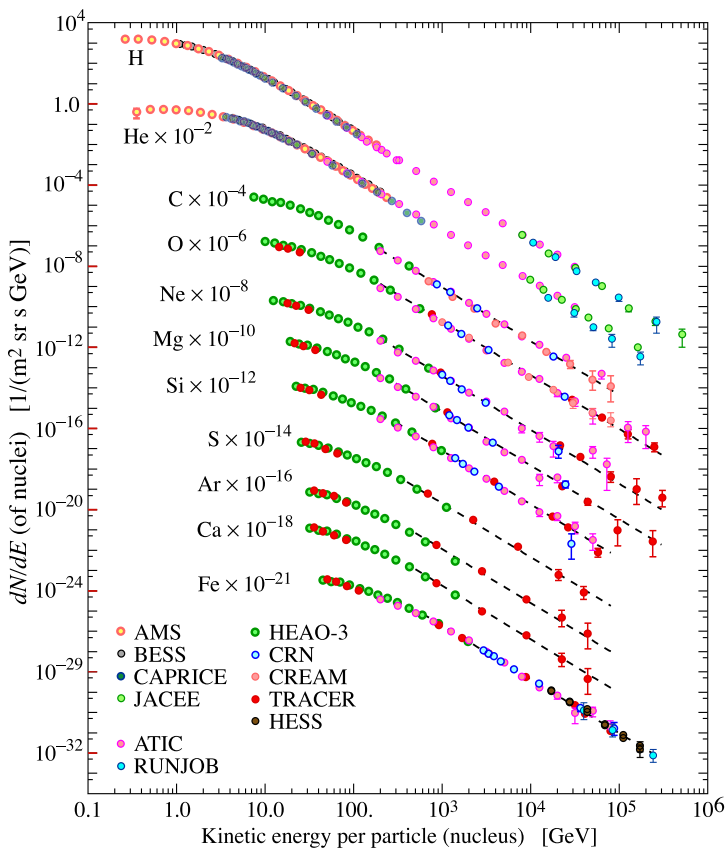


Figure 24.1: Major components of the primary cosmic radiation from Refs. [1–12]. The figure was created by P. Boyle and D. Muller.

Cosmic Rays (p. 273)

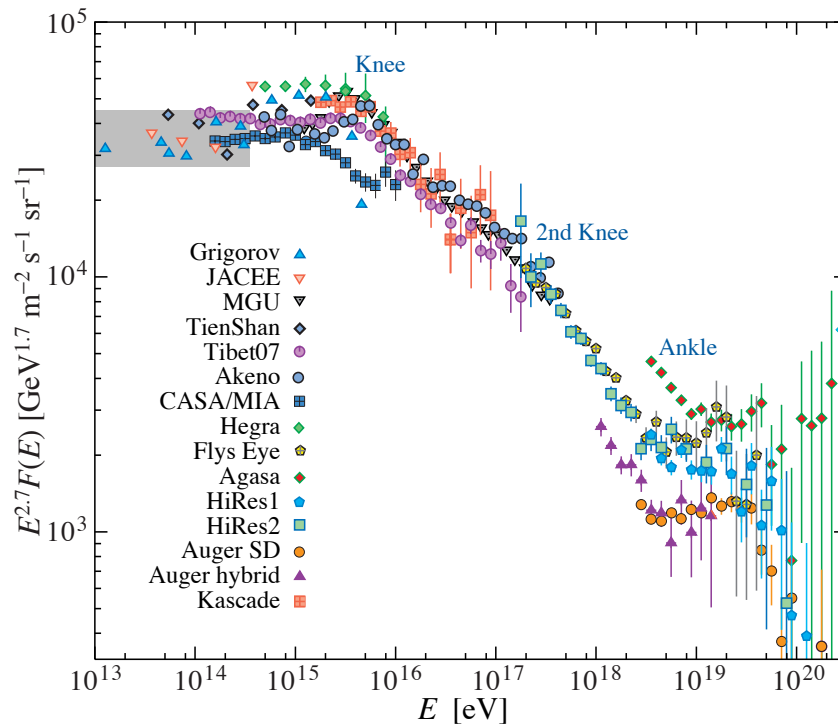


Figure 24.8: The all-particle spectrum from air shower measurements. The shaded area shows the range of the the direct cosmic ray spectrum measurements.

Particle detectors at accelerators (p. 323)

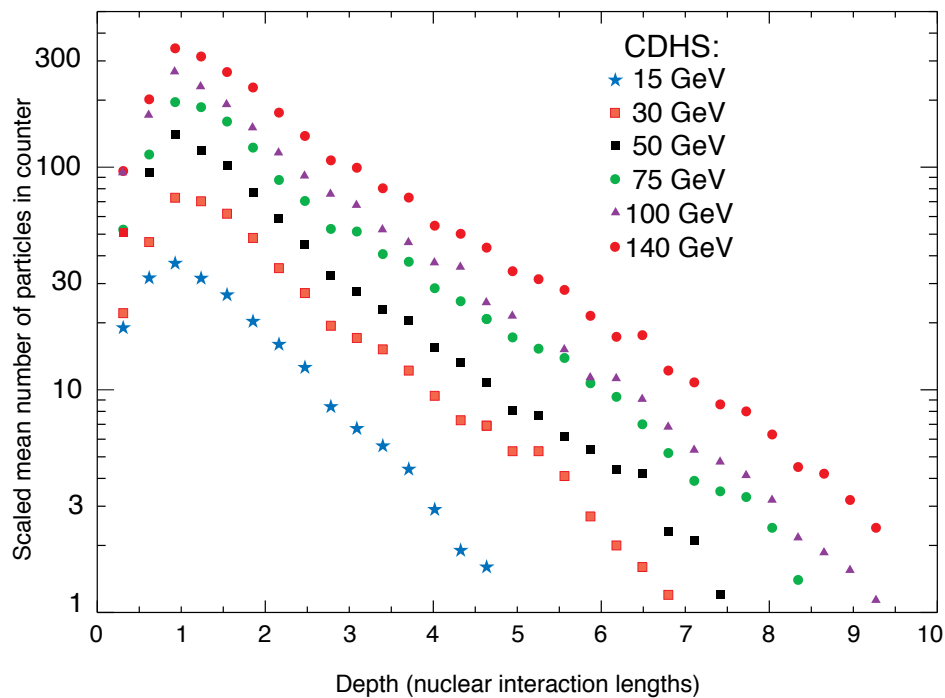


Figure 28.23: Mean profiles of π^+ (mostly) induced cascades in the CDHS neutrino detector [137].

Particle detectors for non-accelerator physics (p. 333)

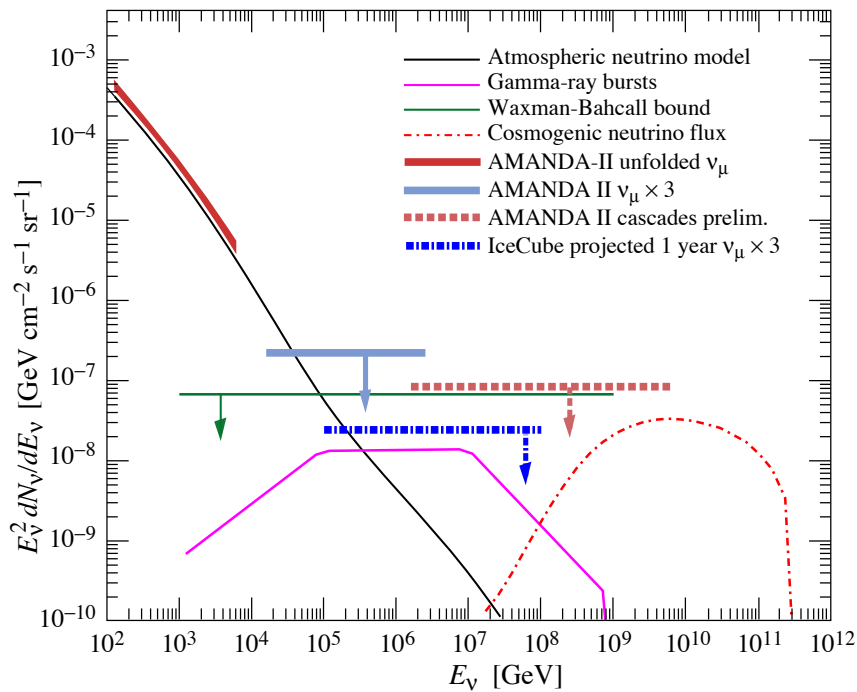


Figure 29.5: Measured atmospheric neutrino fluxes above 100 GeV are shown together with a few generic models for astrophysical neutrinos and some limits.

Radioactivity and radiation protection (p. 342)

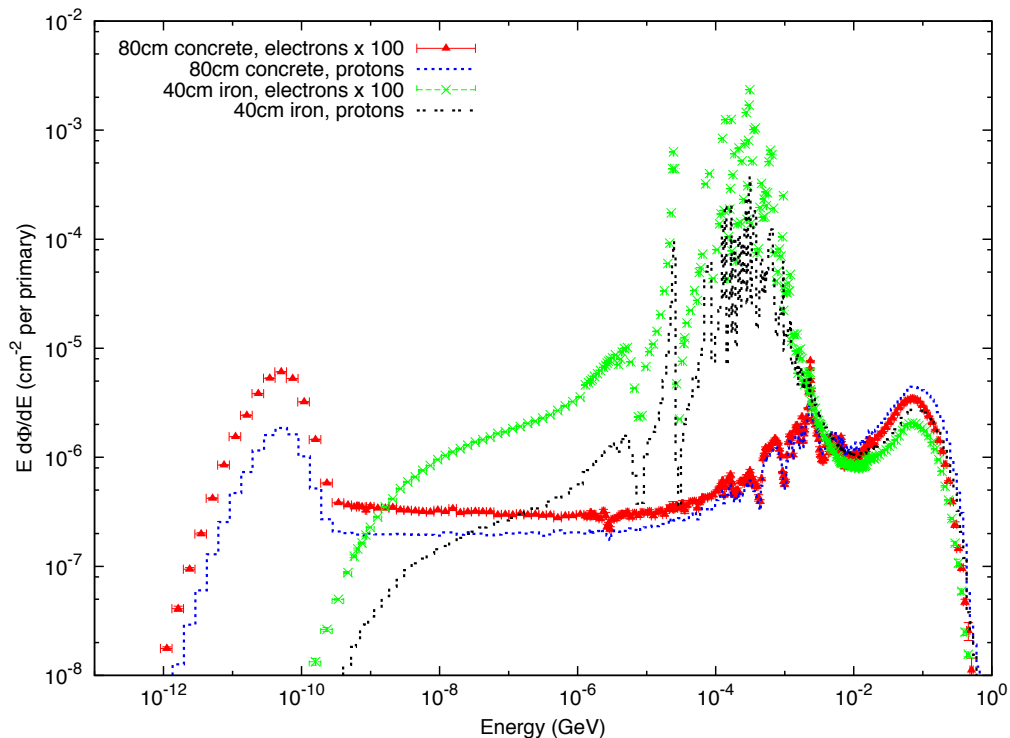


Figure 30.2: Neutron energy spectra calculated with the FLUKA code [6,7] from 25 GeV proton and electron beams on a thick copper target. Spectra are evaluated at 90° to the beam direction behind 80 cm of concrete or 40 cm of iron. All spectra are normalized per beam particle. In addition, spectra for electron beam are multiplied by a factor of 100.

Radioactivity and radiation protection (p. 343)

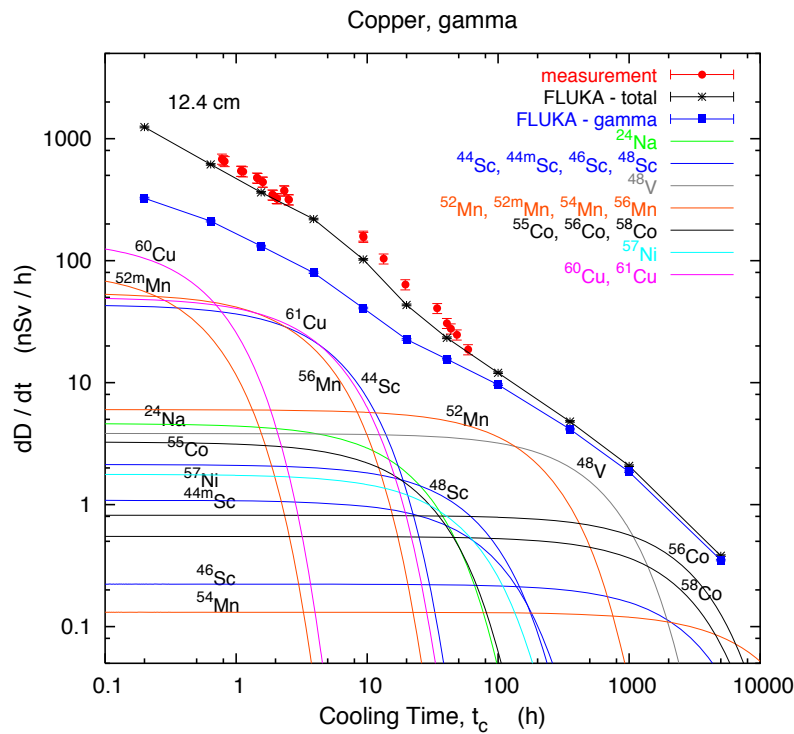


Figure 30.5: Contribution of individual gamma-emitting nuclides to the total dose rate at 12.4 cm distance to an activated copper sample [12].

Radioactivity and radiation protection (p. 344)

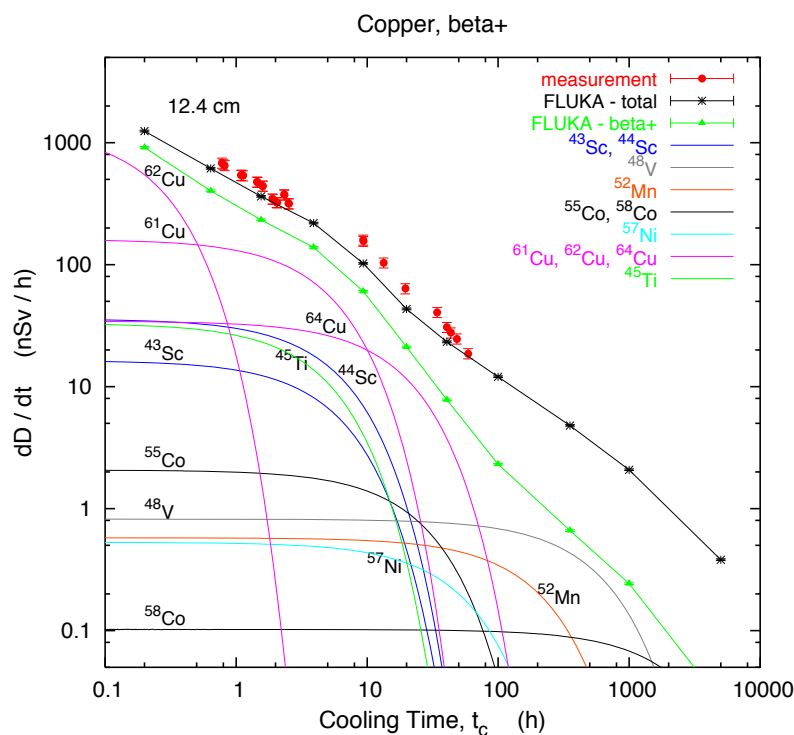


Figure 30.6: Contribution of individual positron-emitting nuclides to the total dose rate at 12.4 cm distance to an activated copper sample [12].

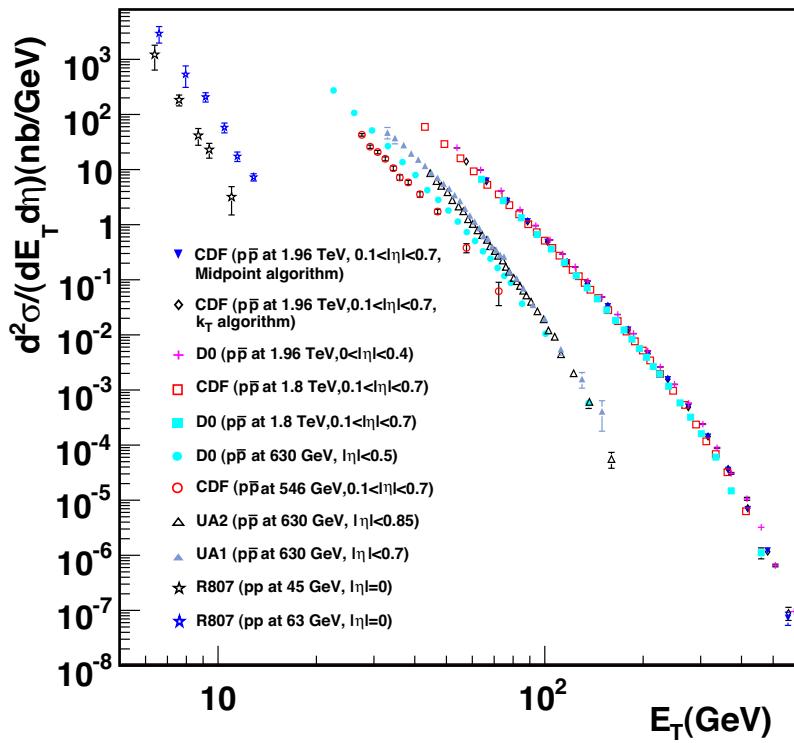
Jet Production in pp and $p\bar{p}$ Interactions (p. 385)

Figure 41.1: Inclusive differential jet cross sections plotted as a function of the jet transverse energy. The CDF and D0 measurements use a cone algorithm of radius 0.7 for all results shown except for the CDF measurements at 1.96 TeV which also use k_T with a D parameter of 0.7 and midpoint algorithms. The cone/ k_T results should be similar if $R_{cone} = D$. UA1 (UA2) uses a non-iterative cone algorithm with a radius of 1.0 (1.3). Recent NLO QCD predictions (such as CTEQ6M) provide a good description of the CDF and D0 jet cross sections, Rept. on Prog. in Phys. **70**, 89 (2007). Comparisons with the older cross sections are more difficult due to the nature of the jet algorithms used. **CDF**: Phys. Rev. **D75**, 092006 (2007), Phys. Rev. **D64**, 032001 (2001), Phys. Rev. Lett. **70**, 1376 (1993); **D0**: Phys. Rev. **D64**, 032003 (2001); **UA2**: Phys. Lett. **B257**, 232 (1991); **UA1**: Phys. Lett. **B172**, 461 (1986); **R807**: Phys. Lett. **B123**, 133 (1983). (Courtesy of J. Huston, Michigan State University, 2010)

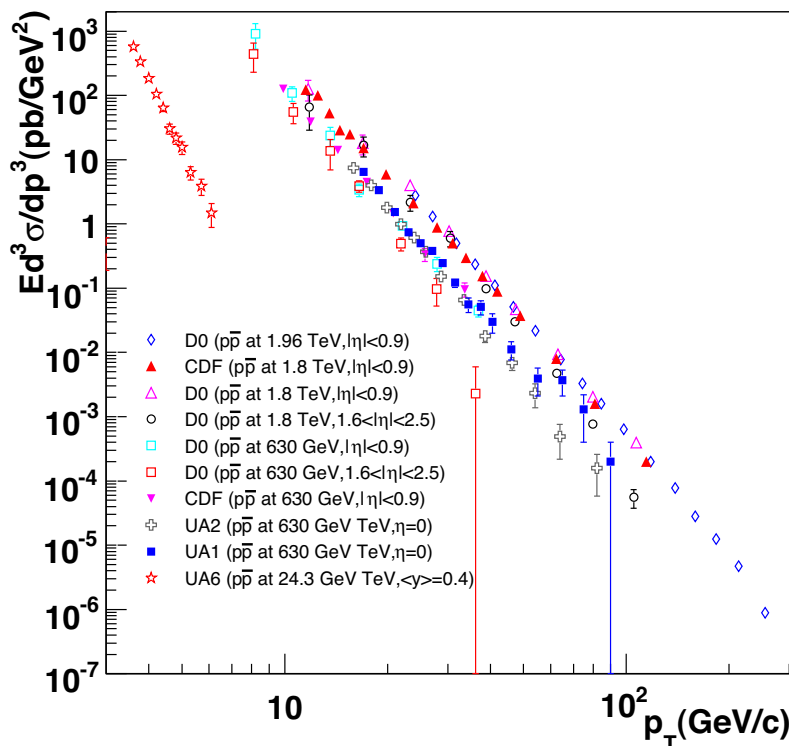
Direct γ Production in $p\bar{p}$ Interactions (p. 385)

Figure 41.2: Isolated photon cross sections plotted as a function of the photon transverse momentum. The errors are either statistical only (CDF, D0 (1.96 TeV), UA1, UA2, UA6) or uncorrelated (D0 1.8 TeV, 630 GeV). The data are generally in good agreement with NLO QCD predictions, albeit with a tendency for the data to be above (below) the theory for lower (large) transverse momenta, Phys. Rev. **D59**, 074007 (1999). **D0**: Phys. Lett. **B639**, 151 (2006), Phys. Rev. Lett. **87**, 251805 (2001); **CDF**: Phys. Rev. **D65**, 112003 (2002); **UA6**: Phys. Lett. **B206**, 163 (1988); **UA1**: Phys. Lett. **B209**, 385 (1988); **UA2**: Phys. Lett. **B288**, 386 (1992). (Courtesy of J. Huston, Michigan State University, 2007)

Plots of cross sections and related quantities (p. 390)

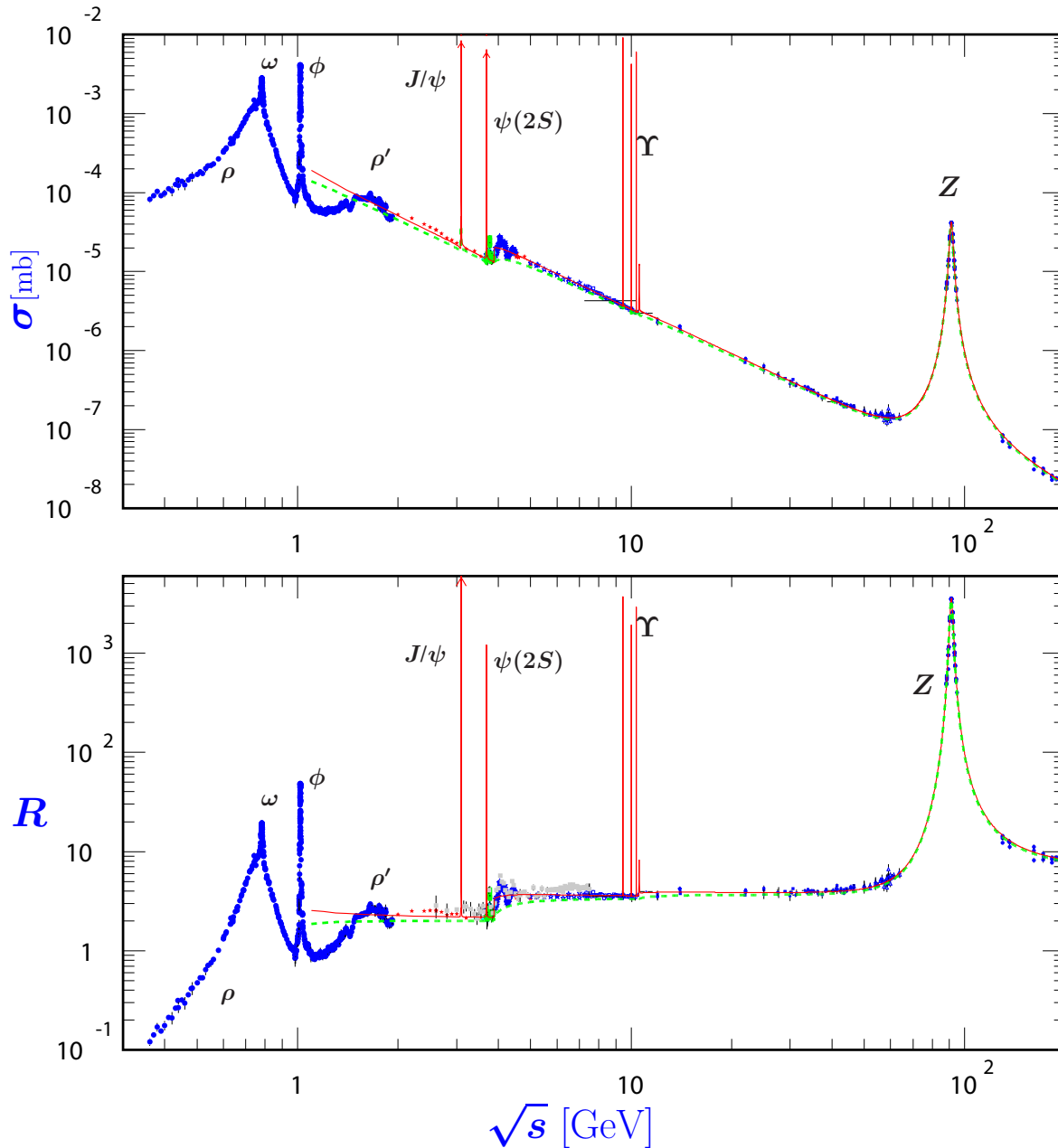
 σ and R in e^+e^- Collisions

Figure 41.6: World data on the total cross section of $e^+e^- \rightarrow \text{hadrons}$ and the ratio $R(s) = \sigma(e^+e^- \rightarrow \text{hadrons}, s) / \sigma(e^+e^- \rightarrow \mu^+\mu^-, s)$. $\sigma(e^+e^- \rightarrow \text{hadrons}, s)$ is the experimental cross section corrected for initial state radiation and electron-positron vertex loops, $\sigma(e^+e^- \rightarrow \mu^+\mu^-, s) = 4\pi\alpha^2(s)/3s$. Data errors are total below 2 GeV and statistical above 2 GeV. The curves are an educative guide: the broken one (green) is a naive quark-parton model prediction, and the solid one (red) is 3-loop pQCD prediction (see “Quantum Chromodynamics” section of this *Review*, Eq. (9.7) or, for more details, K. G. Chetyrkin *et al.*, Nucl. Phys. **B586**, 56 (2000) (Erratum *ibid.* **B634**, 413 (2002)). Breit-Wigner parameterizations of J/ψ , $\psi(2S)$, and $\Upsilon(nS)$, $n = 1, 2, 3, 4$ are also shown. The full list of references to the original data and the details of the R ratio extraction from them can be found in [arXiv:hep-ph/0312114]. Corresponding computer-readable data files are available at <http://pdg.lbl.gov/current/xsect/>. (Courtesy of the COMPAS (Protvino) and HEPDATA (Durham) Groups, May 2010.)

Plots of cross sections and related quantities (p. 391)

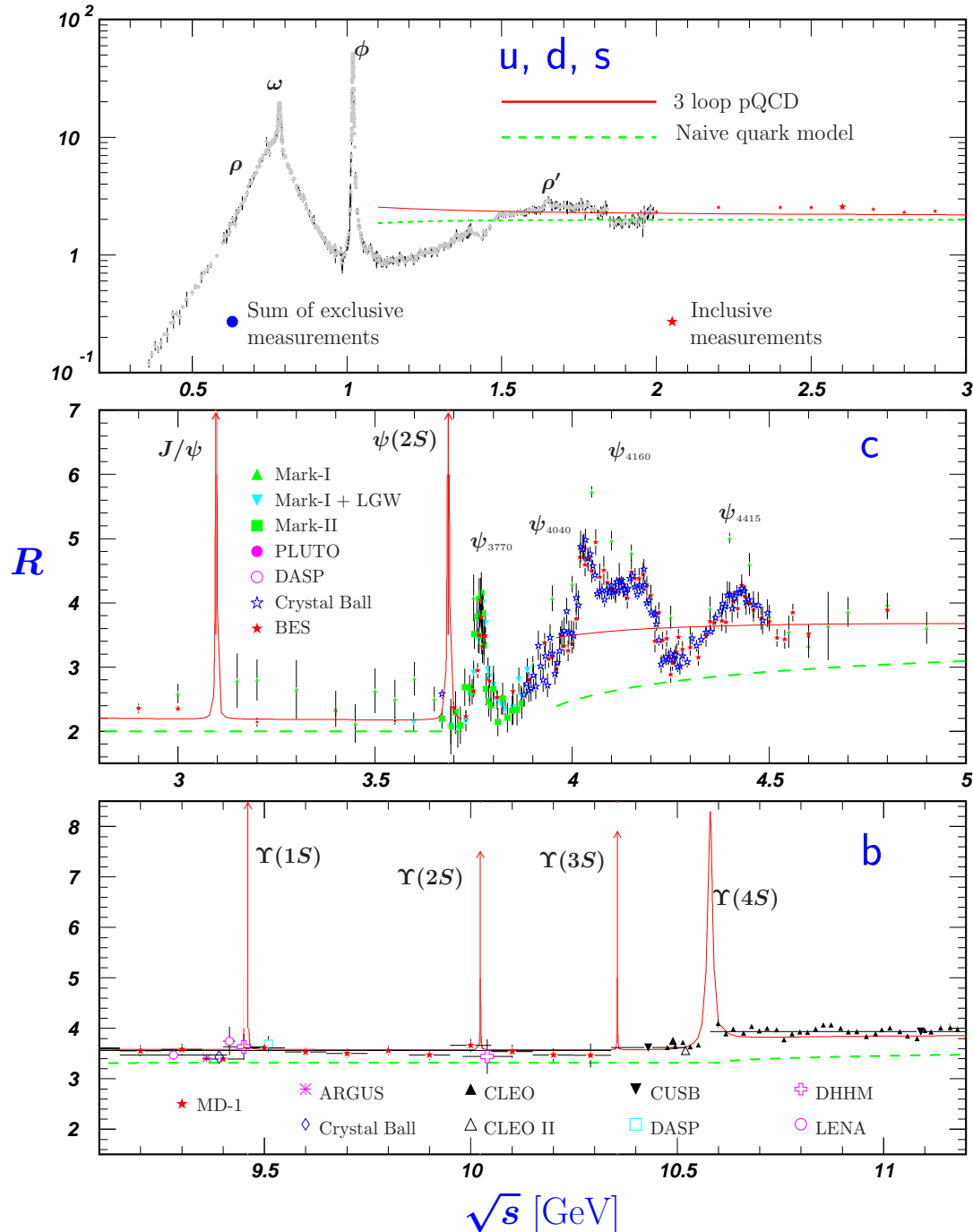
 R in Light-Flavor, Charm, and Beauty Threshold Regions

Figure 41.7: R in the light-flavor, charm, and beauty threshold regions. Data errors are total below 2 GeV and statistical above 2 GeV. The curves are the same as in Fig. 41.6. **Note:** CLEO data above $\Upsilon(4S)$ were not fully corrected for radiative effects, and we retain them on the plot only for illustrative purposes with a normalization factor of 0.8. The full list of references to the original data and the details of the R ratio extraction from them can be found in [arXiv:hep-ph/0312114]. The computer-readable data are available at <http://pdg.lbl.gov/current/xsect/>. (Courtesy of the COMPAS (Protvino) and HEPDATA (Durham) Groups, May 2010.)

Plots of cross sections and related quantities (p. 395)

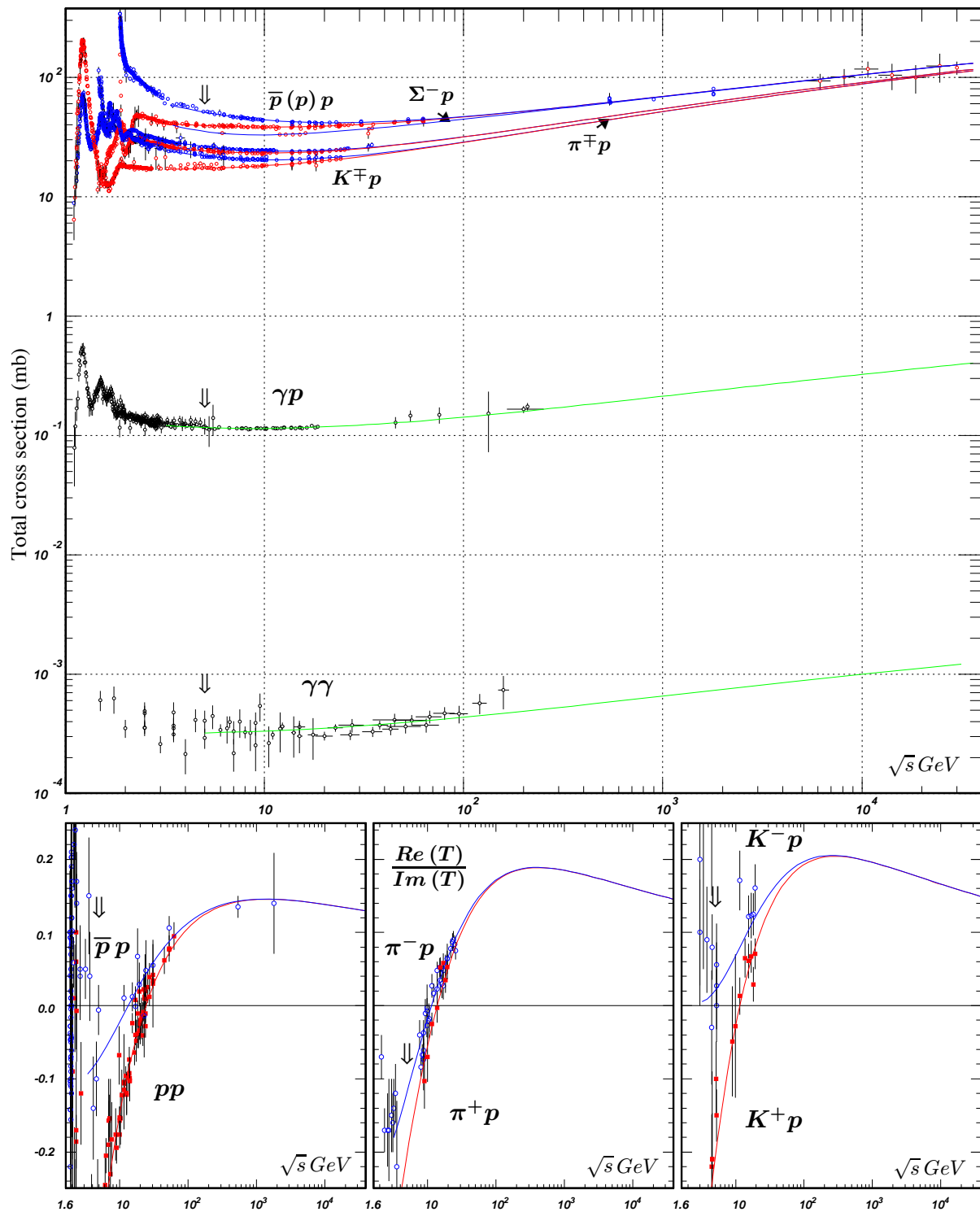
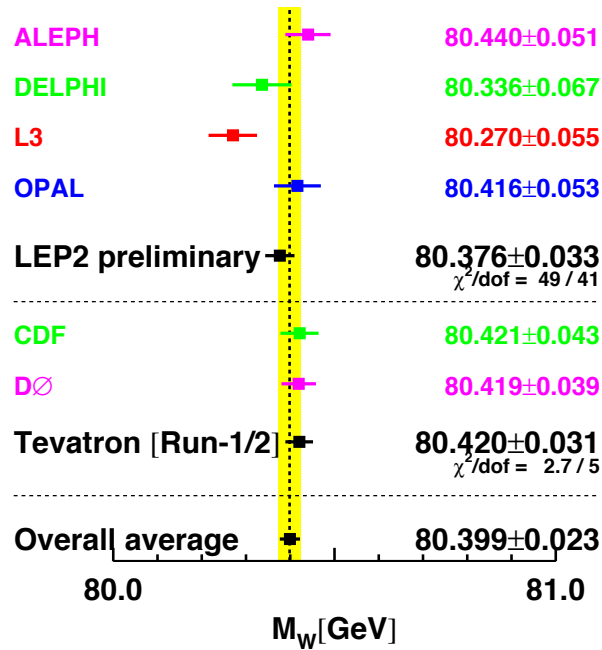
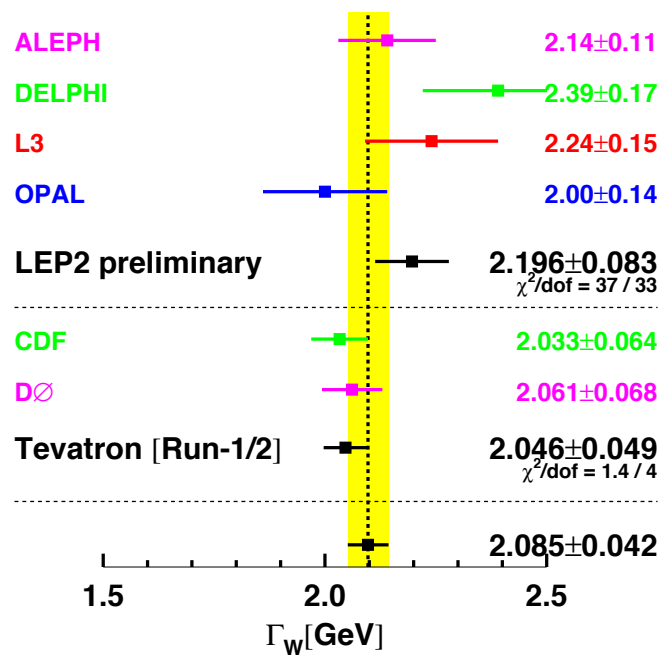


Figure 41.10: Summary of hadronic, γp , and $\gamma\gamma$ total cross sections, and ratio of the real to imaginary parts of the forward hadronic amplitudes. Corresponding computer-readable data files may be found at <http://pdg.lbl.gov/current/xsect/>. (Courtesy of the COMPAS group, IHEP, Protvino, August 2005)

The Mass and Width of the W boson (p. 418)Figure 1: Measurements of the W -boson mass by the LEP and Tevatron experiments.The Mass and Width of the W boson (p. 419)Figure 2: Measurements of the W -boson width by the LEP and Tevatron experiments.

Searches for Higgs Bosons (p. 450)

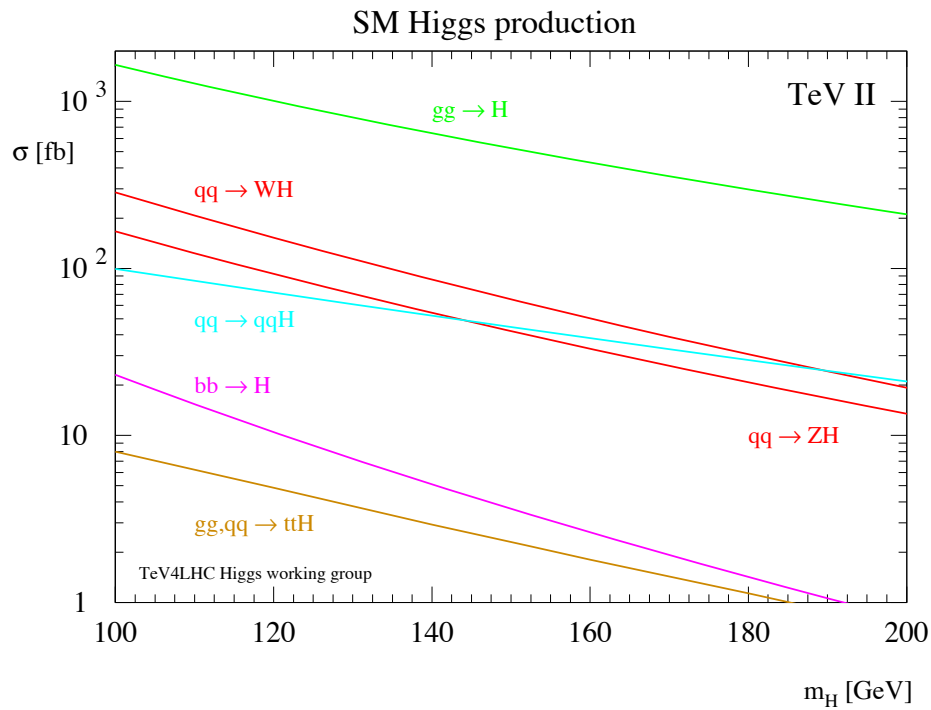


Figure 1: SM Higgs boson production cross sections for $p\bar{p}$ collisions at 1.96 TeV, from Ref. [29] and references therein.

Searches for Higgs Bosons (p. 450)

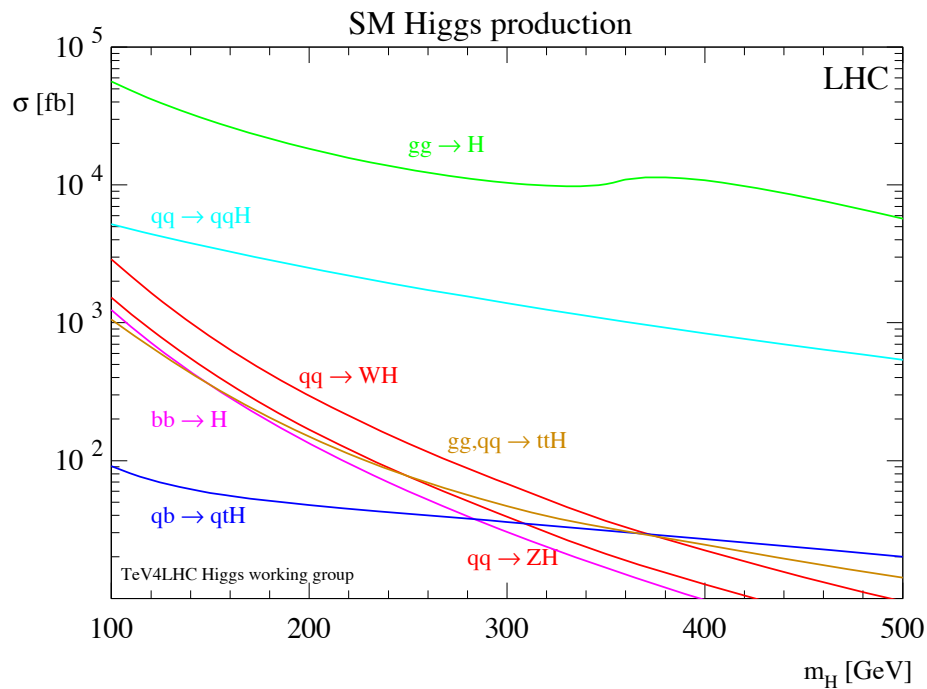


Figure 2: SM Higgs boson production cross sections for pp collisions at 14 TeV [29].

Searches for Higgs Bosons (p. 451)

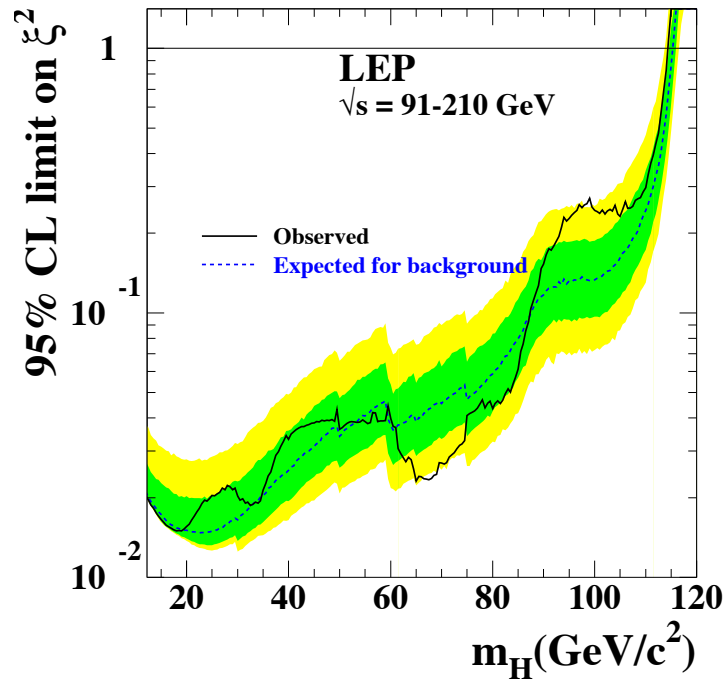


Figure 5: The 95% confidence level upper bound on the ratio $\xi^2 = (g_{HZZ}/g_{HZZ}^{\text{SM}})^2$ [17]. The solid line indicates the observed limit, and the dashed line indicates the median limit expected in the absence of a Higgs boson signal. The dark and light shaded bands around the expected limit line correspond to the 68% and 95% probability bands, indicating the range of statistical fluctuations of the expected outcomes. The horizontal line corresponds to the Standard Model coupling. Standard Model Higgs boson decay branching fractions are assumed.

Searches for Higgs Bosons (p. 453)

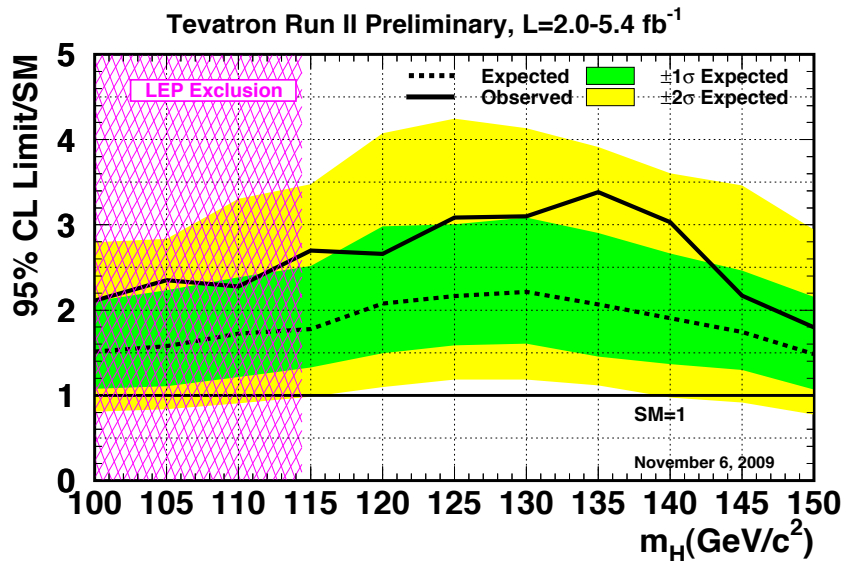


Figure 6: Upper bound on the SM Higgs boson cross section obtained by combining CDF and DØ search results, as a function of the mass of the Higgs boson sought [78]. The limits are shown as a multiple of the SM cross section. The ratios of the different production and decay modes are assumed to be as predicted by the SM. The solid curve is the observed upper bound, and the dashed black curve is the median expected upper bound assuming no signal is present. The shaded bands show the 68% and 95% probability bands around the expected upper bound.

Searches for Higgs Bosons (p. 454)

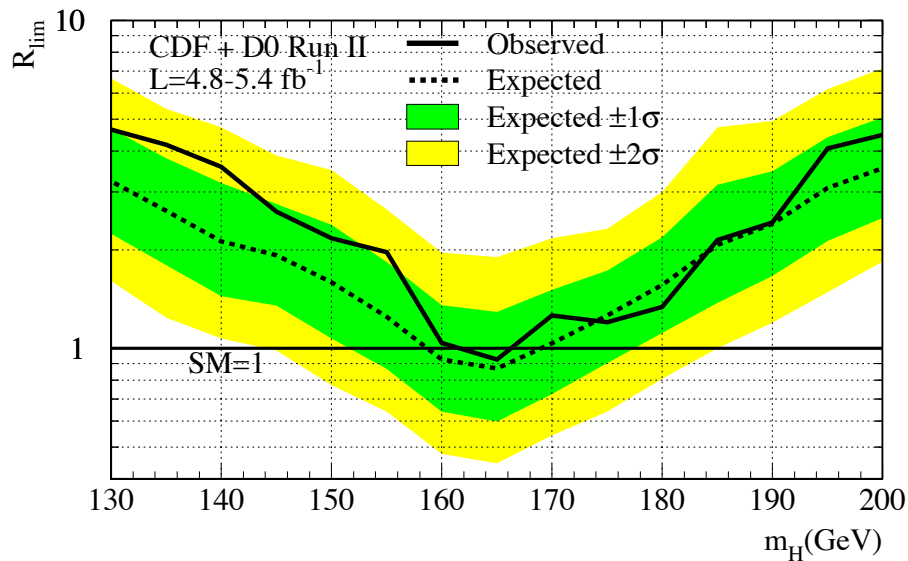


Figure 7: Upper bound on the SM Higgs boson cross section obtained by combining CDF and D0 search results in the $H \rightarrow W^+W^-$ decay mode, as a function of the mass of the Higgs boson sought [19]. The limits are shown as a multiple of the SM cross section. The ratios of the different production and decay modes are assumed to be as predicted by the SM. The solid curve shows the observed upper bound, the dashed black curve shows the median expected upper bound assuming no signal is present. The shaded bands show the 68% and 95% probability bands around the expected upper bound.

Searches for Higgs Bosons (p. 454)

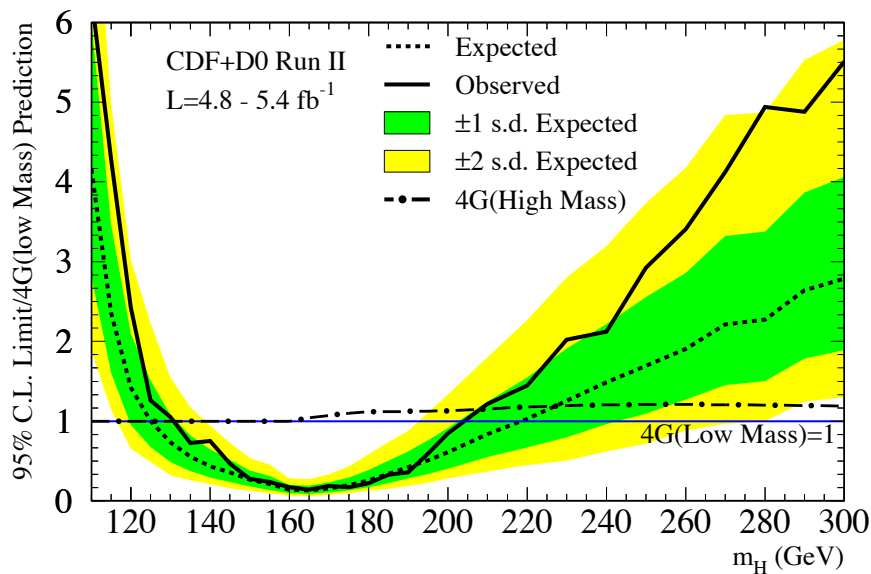


Figure 8: Upper bound on the Higgs boson cross section of the 4th generation sequential model obtained by combining CDF and D0 search results in the $H \rightarrow W^+W^-$ decay mode, as a function of the mass of the Higgs boson sought [87]. The limits are shown as a multiple of the cross section obtained in this extended model. The solid curve shows the observed upper bound, the dashed black curve shows the median expected upper bound assuming no signal is present, and the colored bands show the 68% and 95% probability bands around the expected upper bound.

Searches for Higgs Bosons (p. 458)

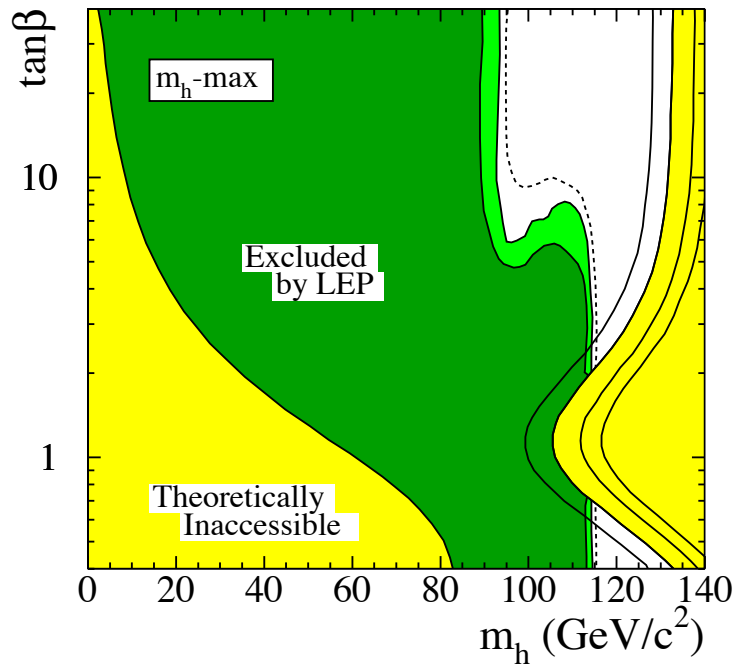


Figure 9: The MSSM exclusion contours, at 95% C.L. (light-green) and 99.7% CL (dark-green), obtained by LEP for the *CPC* m_h -max benchmark scenario, with $m_t = 174.3$ GeV. The figure shows the excluded and theoretically inaccessible regions in the $(m_h, \tan\beta)$ projection. The upper edge of the theoretically allowed region is sensitive to the top quark mass; it is indicated, from left to right, for $m_t = 169.3, 174.3, 179.3$ and 183.0 GeV. The dashed lines indicate the boundaries of the regions which are expected to be excluded on the basis of Monte Carlo simulations with no signal (from Ref. [18]).

Searches for Higgs Bosons (p. 459)

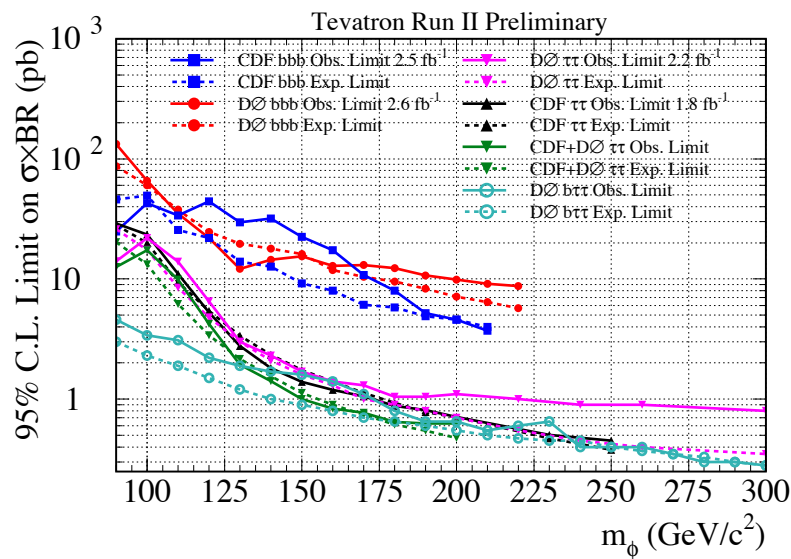


Figure 10: The 95% C.L. limits on $\sigma(b\bar{b}\phi) \times \text{BR}(\phi \rightarrow b\bar{b})$ and $\sigma(\phi + X) \times \text{BR}(\phi \rightarrow \tau^+\tau^-)$ from the Tevatron collaborations. The $D\bar{O}$ limit on $\sigma(b\bar{b}\phi) \times \text{BR}(\phi \rightarrow \tau^+\tau^-)$ and the Tevatron combined limit on $\sigma(\phi + X) \times \text{BR}(\phi \rightarrow \tau^+\tau^-)$ are also shown. The observed limits are indicated with solid lines, and the expected limits are indicated with dashed lines. The limits are to be compared with the sum of signal predictions for Higgs bosons with similar masses. The decay widths of the Higgs bosons are assumed to be much smaller than the experimental resolution.

Searches for Higgs Bosons (p. 460)

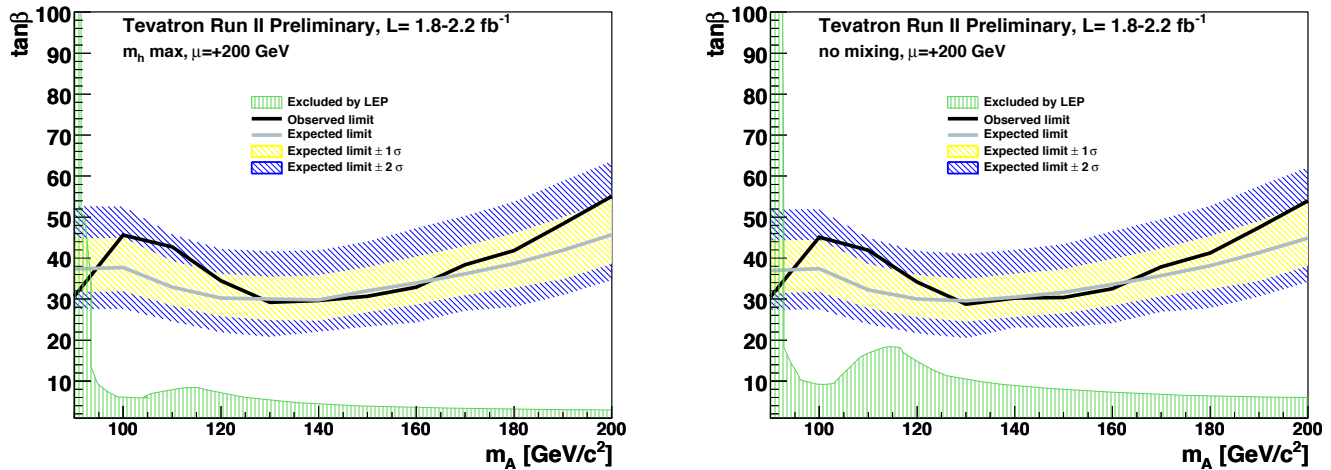


Figure 11: The 95% C.L. MSSM exclusion contours obtained by a combination of the CDF and DØ searches for $H \rightarrow \tau^+\tau^-$ in the m_h -max (left) and *no-mixing* (right) benchmark scenarios, both with $\mu = 200$ GeV, projected onto the $(m_A, \tan\beta)$ plane [147]. The regions above the solid black line are excluded, and the shaded and hatched bands centered on the lighter line show the distributions of expected exclusions in the absence of a signal. Also shown are the regions excluded by LEP searches [18], assuming a top quark mass of 174.3 GeV. The Tevatron results are not sensitive to the precise value of the top quark mass.

Searches for Higgs Bosons (p. 462)

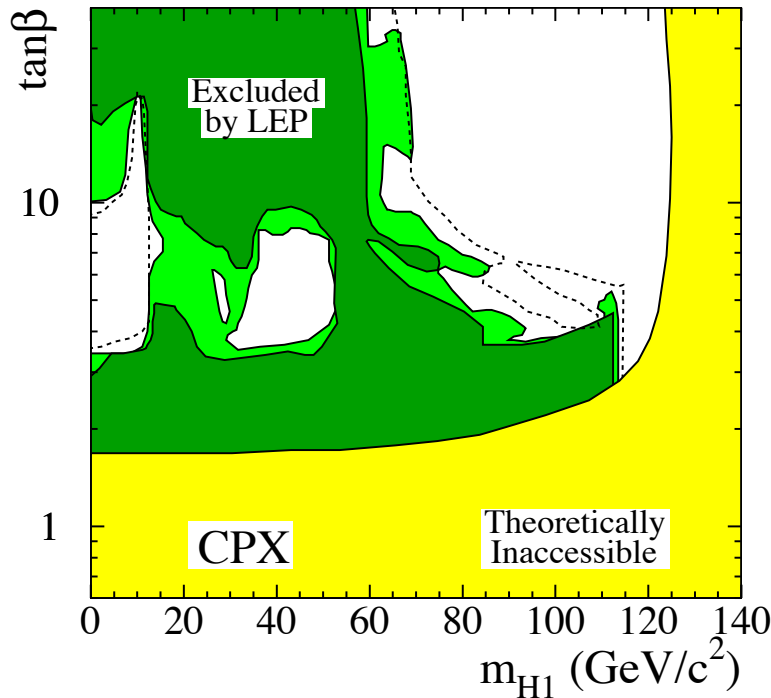


Figure 12: The MSSM exclusion contours, at the 95% C.L. (light-green) and the 99.7% CL (dark-green), obtained by LEP for the CPX scenario defined in the text. Here, $m_t = 174.3$ GeV. The figure shows the excluded and theoretically inaccessible regions in the $(m_{H_1}, \tan\beta)$ projection. The dashed lines indicate the boundary of the region which is expected to be excluded at the 95% C.L. in the absence of a signal.

Searches for Higgs Bosons (p. 463)

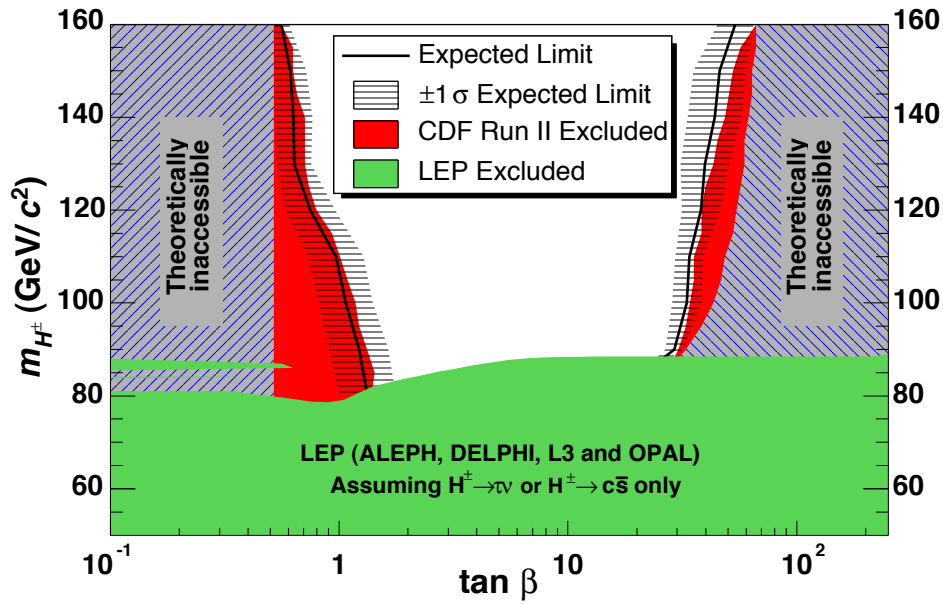


Figure 13: Summary of the 95% C.L. exclusions in the $(m_{H^\pm}, \tan \beta)$ plane obtained by LEP [195] and CDF [214]. The benchmark scenario parameters used to interpret the CDF results are very close to those of the m_h^{\max} scenario, and m_t is assumed to be 175 GeV. The full lines indicate the median limits expected in the absence of a H^\pm signal, and the horizontal hatching represents the $\pm 1\sigma$ bands about this expectation.

Searches for Higgs Bosons (p. 464)

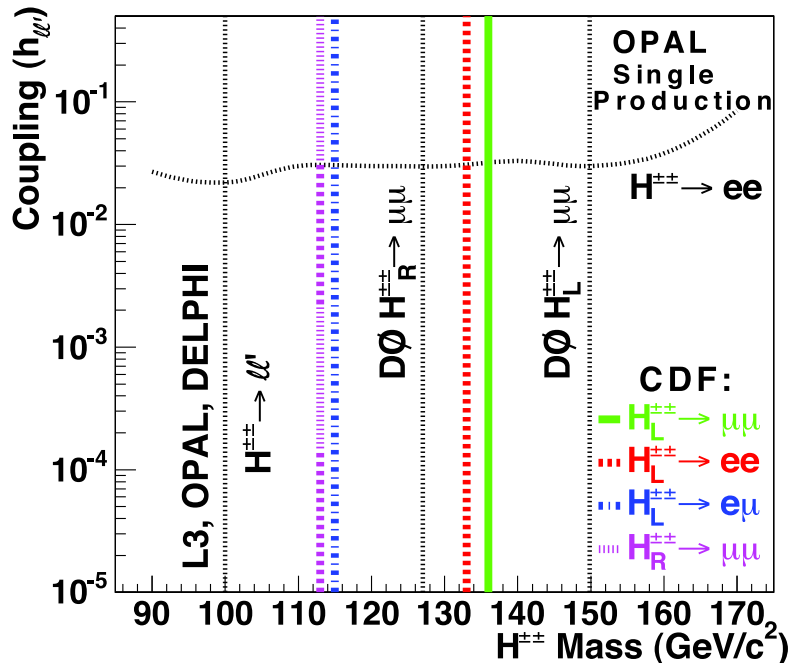


Figure 14: The 95% C.L. exclusion limits on the masses and couplings to leptons of right- and left-handed doubly-charged Higgs bosons, obtained by LEP and Tevatron experiments (from Ref. [223]).

W' -boson searches (p. 481)

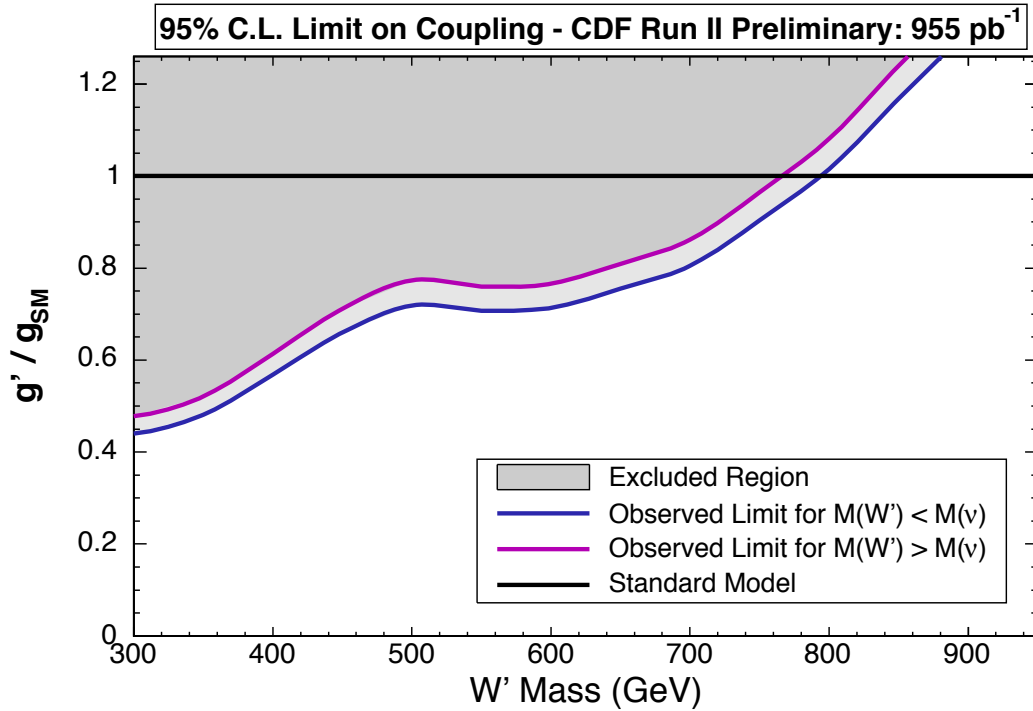


Figure 1: 95% CL exclusion limit from CDF [17] in the gauge coupling versus $M_{W'}$ plane, using the $t\bar{b}$ and $\bar{t}b$ final states.

Leptoquarks (p. 491)

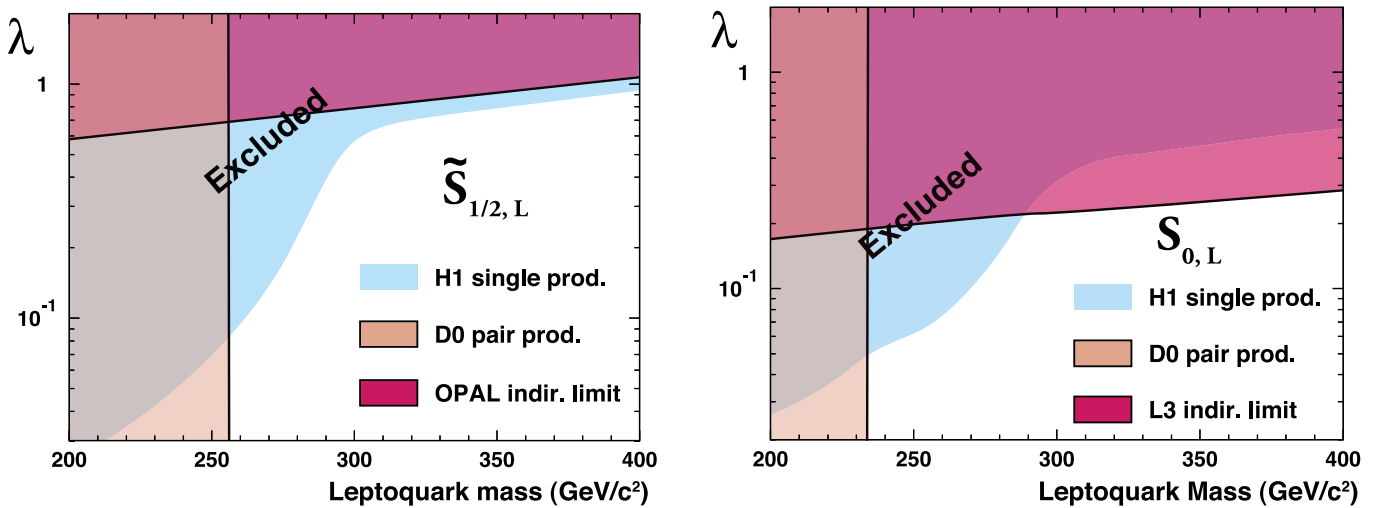


Figure 1: Limits on two typical first-generation scalar leptoquark states in the mass-coupling plane. The upper figure is for a weak-isodoublet, weak-hypercharge $7/6$, $3B + L = 0$ leptoquark state, while the lower figure for a weak-isosinglet, weak-hypercharge $-1/3$, $3B + L = 2$ state.

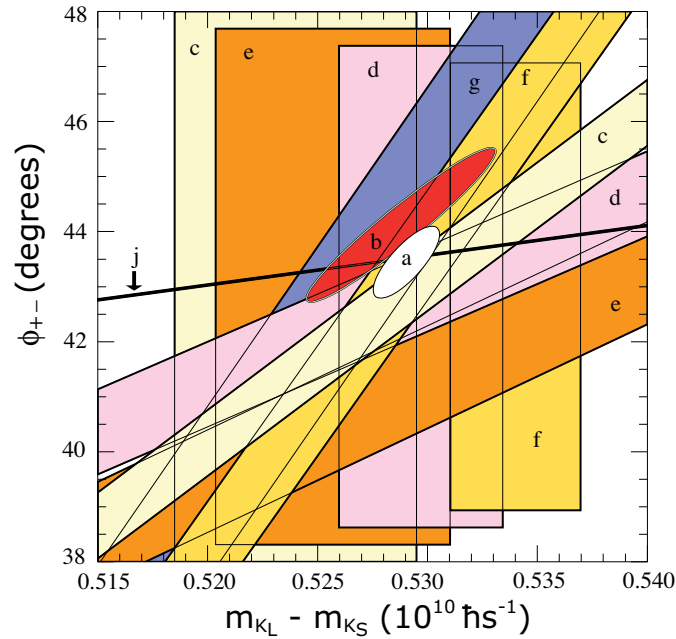
CP Violation in K_L Decays (p. 780)

Figure 1: ϕ_{+-} vs Δm for experiments which do not assume CPT invariance. Δm measurements appear as vertical bands spanning $\Delta m \pm 1\sigma$, cut near the top and bottom to aid the eye. Most ϕ_{+-} measurements appear as diagonal bands spanning $\phi_{+-} \pm \sigma_\phi$. Data are labeled by letters: “b”–FNAL KTeV, “c”–CERN CPLEAR, “d”–FNAL E773, “e”–FNAL E731, “f”–CERN, “g”–CERN NA31, and are cited in Table 1. The narrow band “j” shows ϕ_{SW} . The ellipse “a” shows the $\chi^2 = 1$ contour of the fit result.

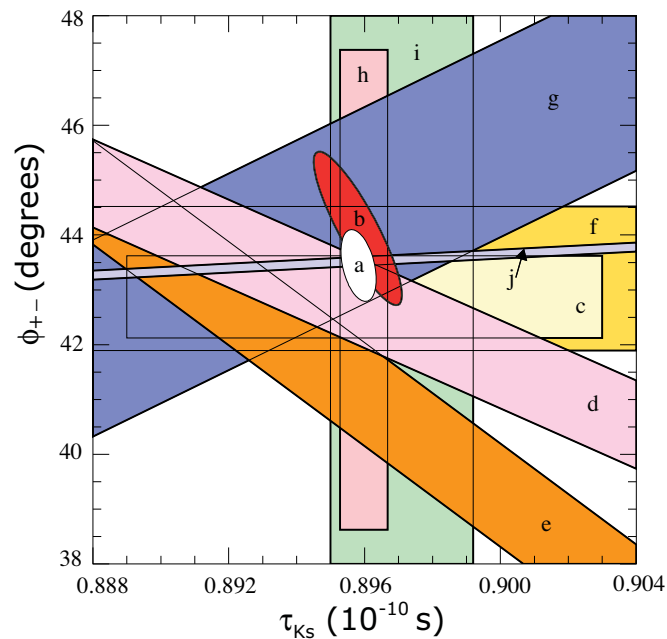
CP Violation in K_L Decays (p. 781)

Figure 2: ϕ_{+-} vs τ_S . τ_S measurements appear as vertical bands spanning $\tau_S \pm 1\sigma$, some of which are cut near the top and bottom to aid the eye. Most ϕ_{+-} measurements appear as diagonal or horizontal bands spanning $\phi_{+-} \pm \sigma_\phi$. Data are labeled by letters: “b”–FNAL KTeV, “c”–CERN CPLEAR, “d”–FNAL E773, “e”–FNAL E731, “f”–CERN, “g”–CERN NA31, “h”–CERN NA48, “i”–CERN NA31, and are cited in Table 1. The narrow band “j” shows ϕ_{SW} . The ellipse “a” shows the fit result’s $\chi^2 = 1$ contour.

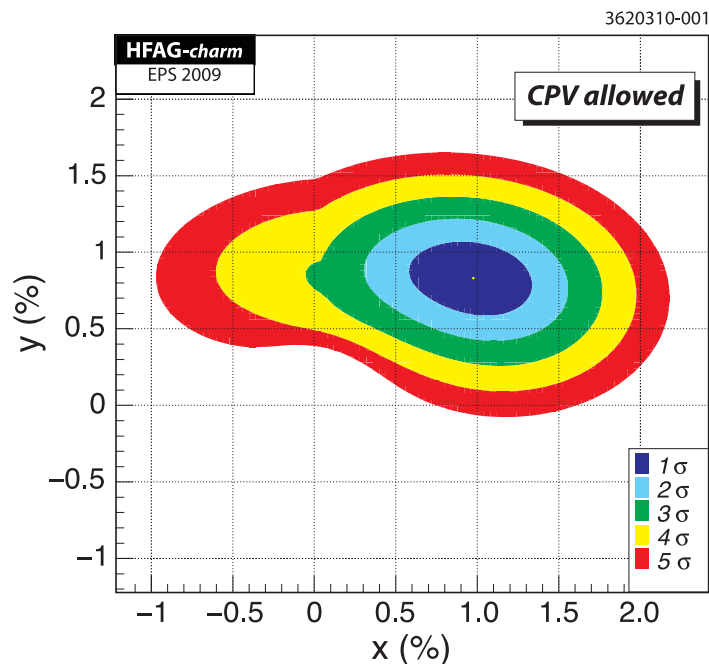
$D^0-\bar{D}^0$ Mixing (p. 825)

Figure 1: Two-dimensional 1σ - 5σ contours for (x, y) from measurements of $D^0 \rightarrow K^{(*)}\ell\nu$, h^+h^- , $K^+\pi^-$, $K^+\pi^-\pi^0$, $K^+\pi^-\pi^+\pi^-$, $K_S^0\pi^+\pi^-$, and $K_S^0K^+K^-$ decays, and double-tagged branching fractions measured at the $\psi(3770)$ resonance (from HFAG [10]).

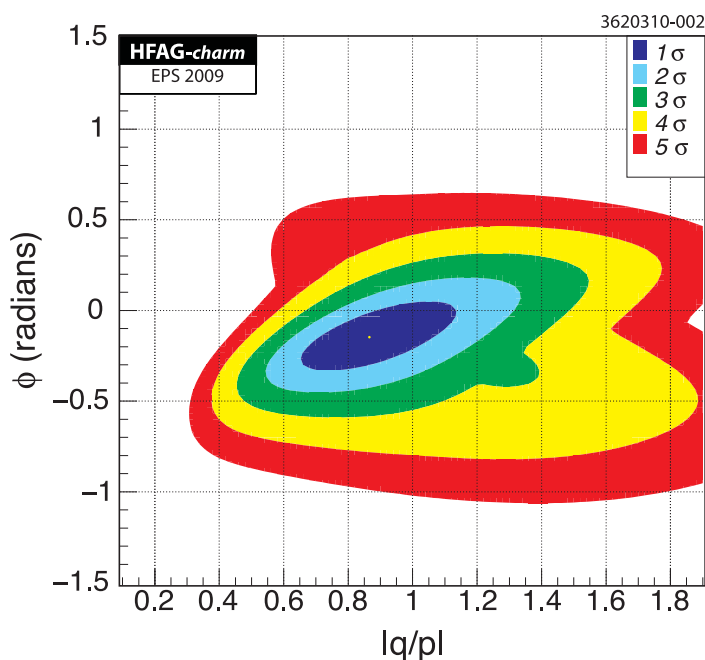
 $D^0-\bar{D}^0$ Mixing (p. 825)

Figure 2: Two-dimensional 1σ - 5σ contours for $(|q/p|, \text{Arg}(q/p))$ from measurements of $D^0 \rightarrow K^{(*)}\ell\nu$, h^+h^- , $K^+\pi^-$, $K^+\pi^-\pi^0$, $K^+\pi^-\pi^+\pi^-$, $K_S^0\pi^+\pi^-$, and $K_S^0K^+K^-$ decays, and double-tagged branching fractions measured at the $\psi(3770)$ resonance (from HFAG [10]).

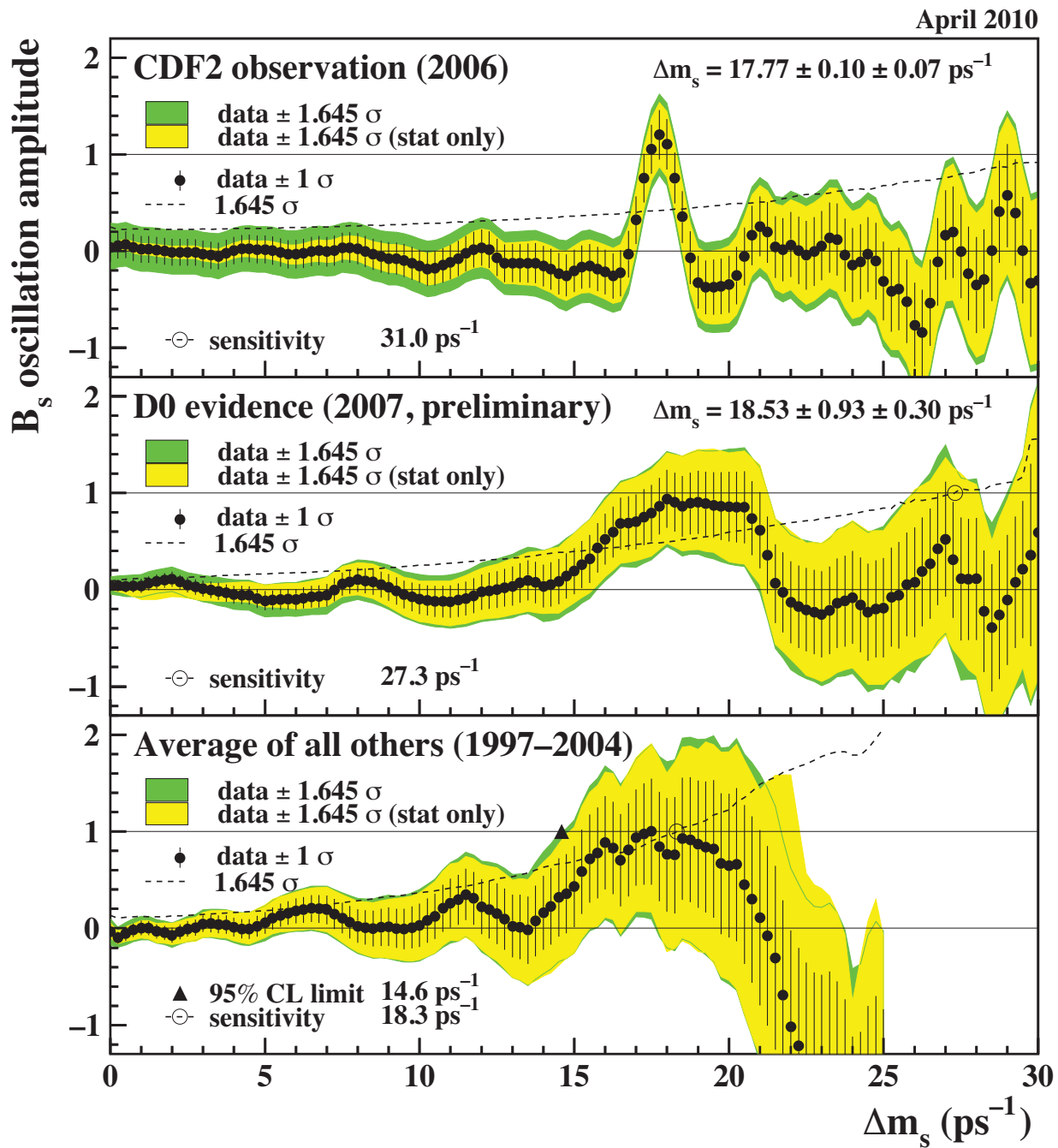
$B^0-\bar{B}^0$ Mixing (p. 976)

Figure 2: Combined measurements of the B_s^0 oscillation amplitude as a function of Δm_s . Top: CDF result based on Run II data, published in 2006 [19]. Middle: Average of all preliminary $D\bar{O}$ results available at the end of 2007 [21]. Bottom: Average of all other results (mainly from LEP and SLD) published between 1997 and 2004. All measurements are dominated by statistical uncertainties. Neighboring points are statistically correlated.

V_{cb} and V_{ub} CKM Matrix Elements (p. 1016)

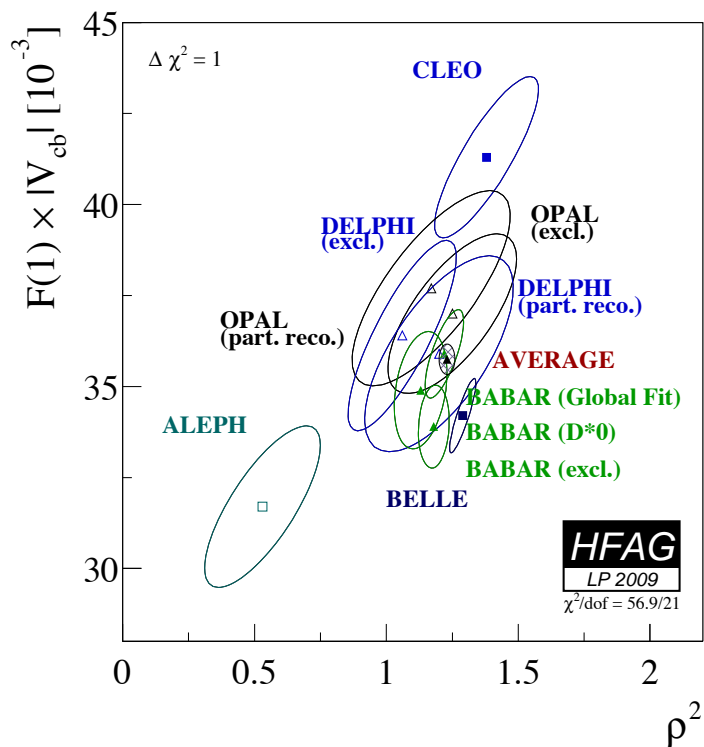


Figure 1: Measurements of $|V_{cb}|F(1)$ vs. $\rho_{A_1}^2$ are shown as $\Delta\chi^2 = 1$ ellipses.

V_{cb} and V_{ub} CKM Matrix Elements (p. 1017)

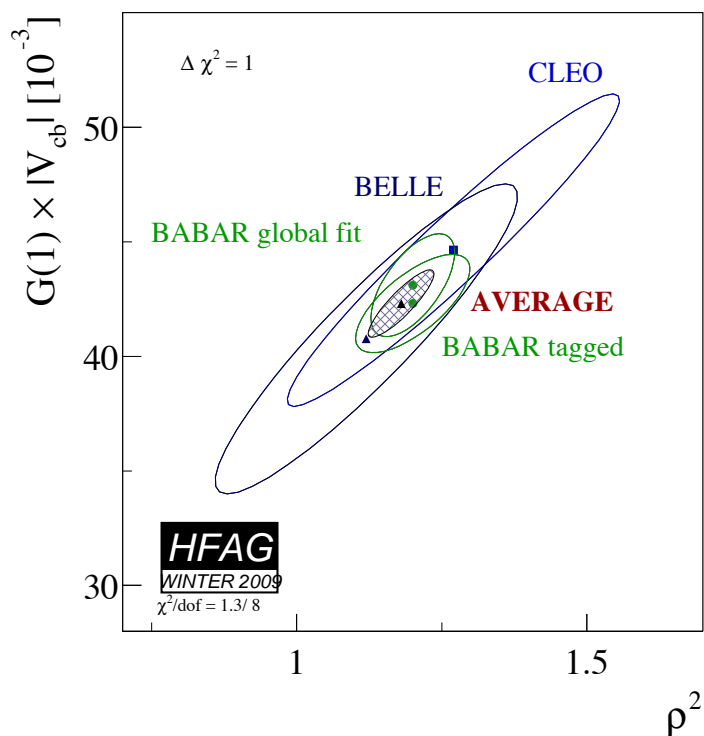


Figure 2: Measurements of $|V_{cb}|G(1)$ vs. ρ^2 are shown as $\Delta\chi^2 = 1$ ellipses.

Supersymmetry, Part I (Theory) (p. 1301)

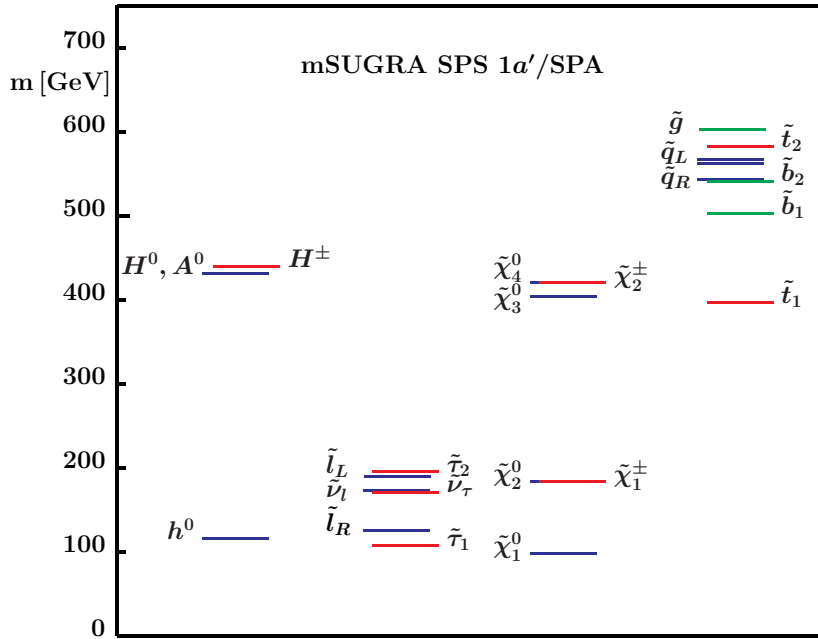


Figure 1: Mass spectrum of supersymmetric particles and Higgs bosons for the mSUGRA reference point SPS 1a'. The masses of the first and second generation squarks, sleptons, and sneutrinos are denoted collectively by \tilde{q} , $\tilde{\ell}$ and $\tilde{\nu}_\ell$, respectively. Taken from Ref. 100.

Supersymmetry, Part II (Experiment) (p. 1311)

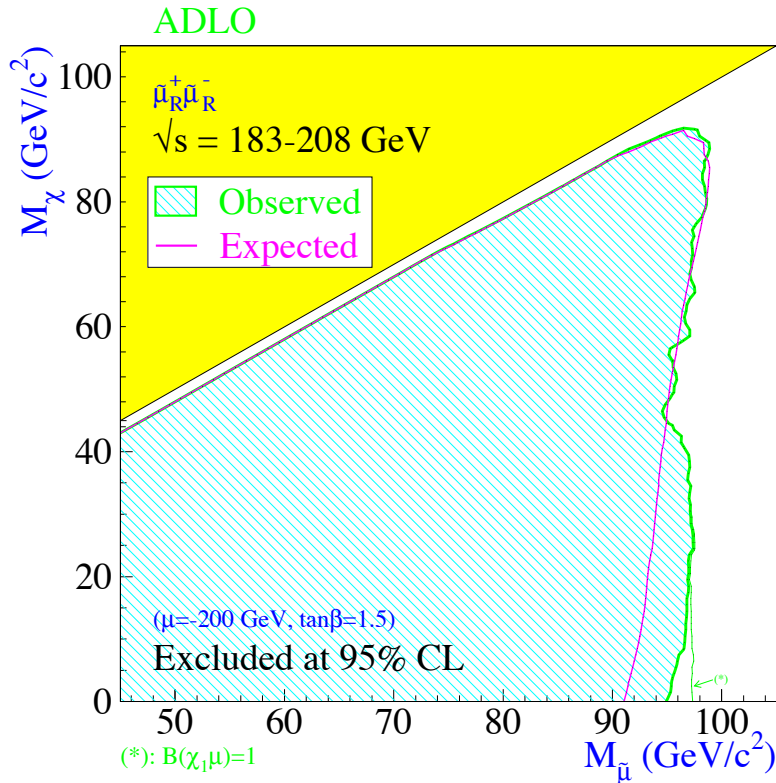


Figure 1: Region in the $(m_{\tilde{\mu}_R}, m_{\tilde{\chi}_1^0})$ plane excluded by the searches for smuons at LEP.

Supersymmetry, Part II (Experiment) (p. 1315)

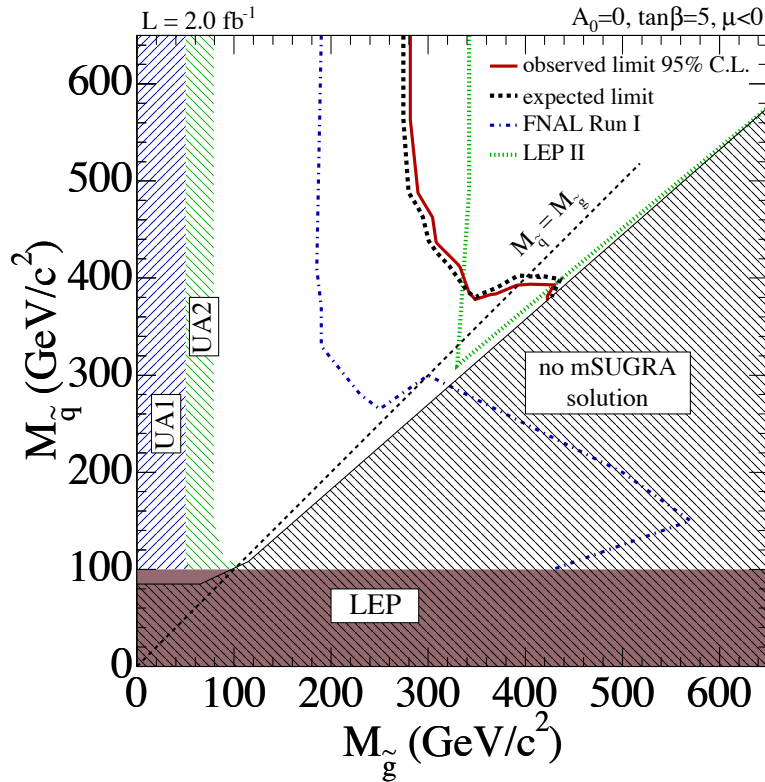


Figure 3: Region in the $(m_{\tilde{g}}, m_{\tilde{q}})$ plane excluded by CDF Run II and by earlier experiments.

Supersymmetry, Part II (Experiment) (p. 1317)

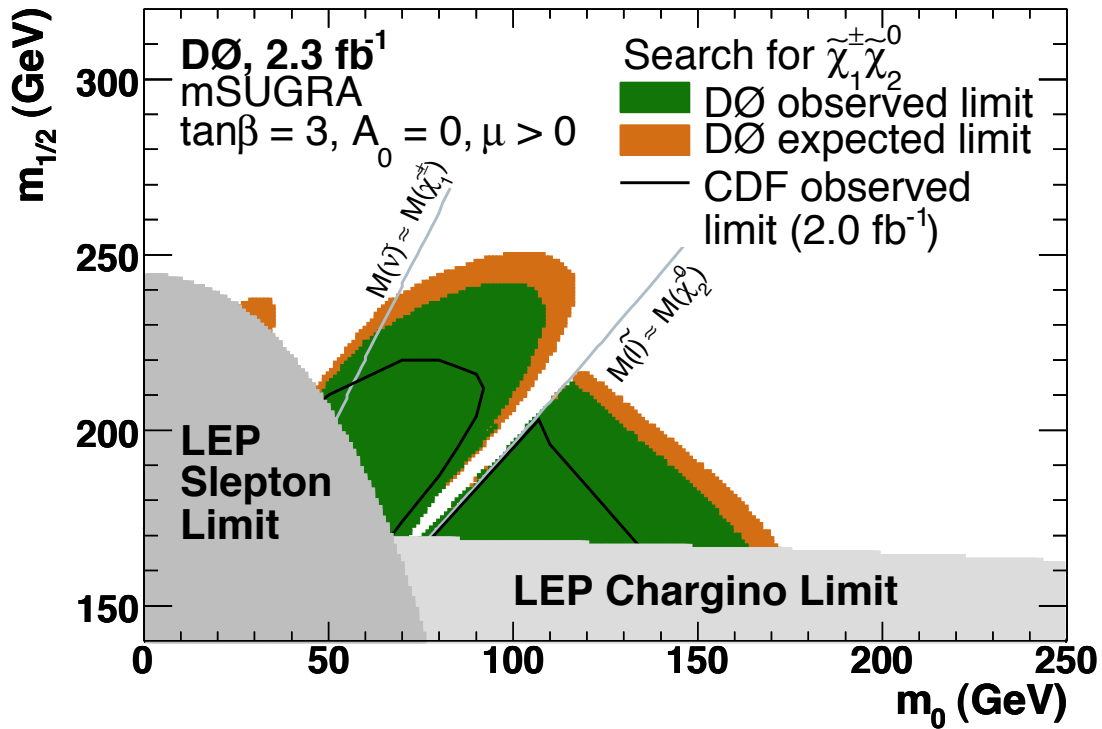


Figure 6: Regions in the $(m_0, m_{1/2})$ plane excluded by the $D\bar{0}$ search for tripletons and by the LEP experiments.

Dynamical Electroweak Symmetry Breaking (p. 1341)

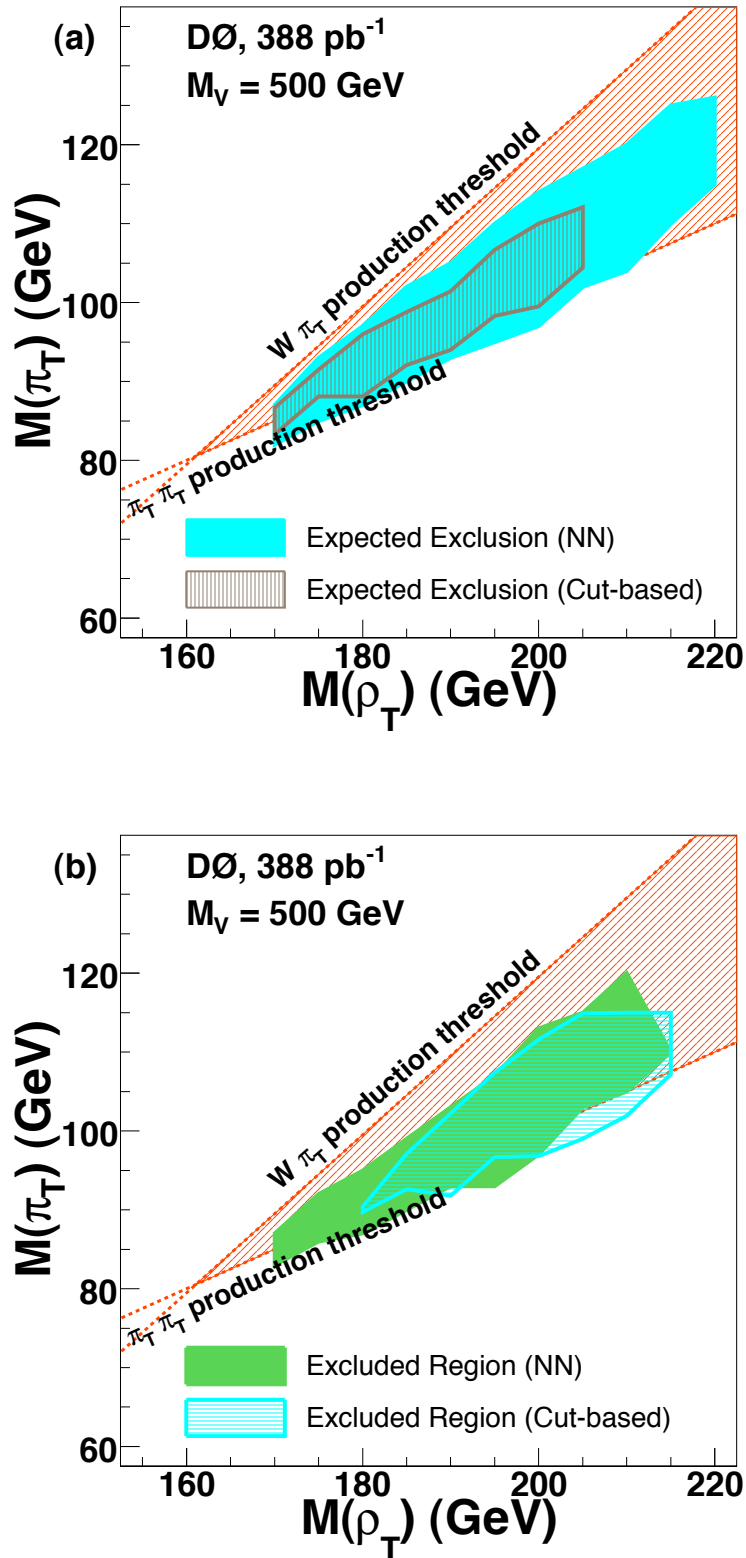


Figure 1: Search for a light technirho decaying to W^\pm and a π_T , and in which the π_T decays to two jets including at least one b quark [19]. Expected region of exclusion (a) and excluded region (b) at the 95% C.L. in the $M(\rho_T), M(\pi_T)$ plane for $\rho_T \rightarrow W\pi_T \rightarrow e\nu b\bar{b}(\bar{c})$ production with $M_V = 500 \text{ GeV}$. Kinematic thresholds from $W\pi_T$ and $\pi_T\pi_T$ are shown on the figures.

Dynamical Electroweak Symmetry Breaking (p. 1343)

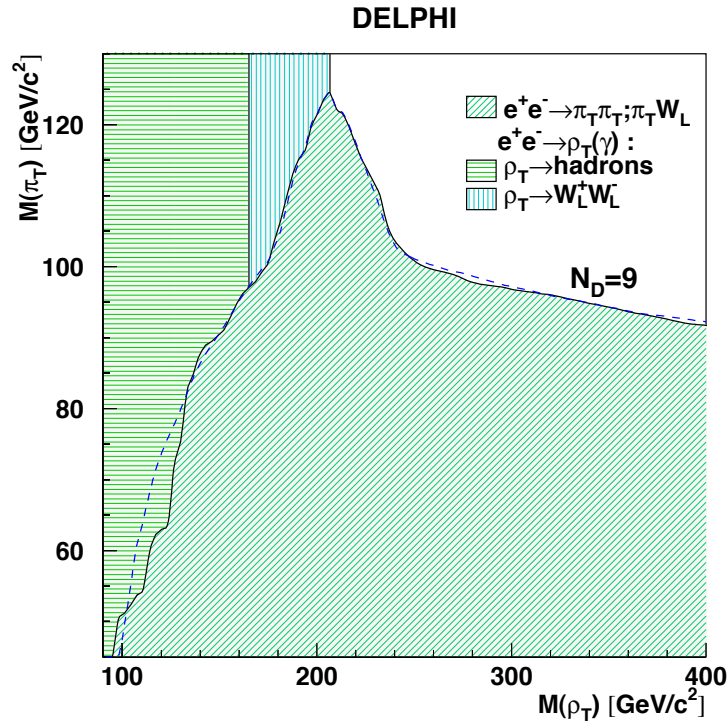


Figure 4: 95% CL exclusion region [23] in the technirho-technipion mass plane obtained from searches by the DELPHI collaboration at LEP 2, for nine technifermion doublets. The dashed line shows the expected limit for the 4-jet analysis.

Dynamical Electroweak Symmetry Breaking (p. 1343)

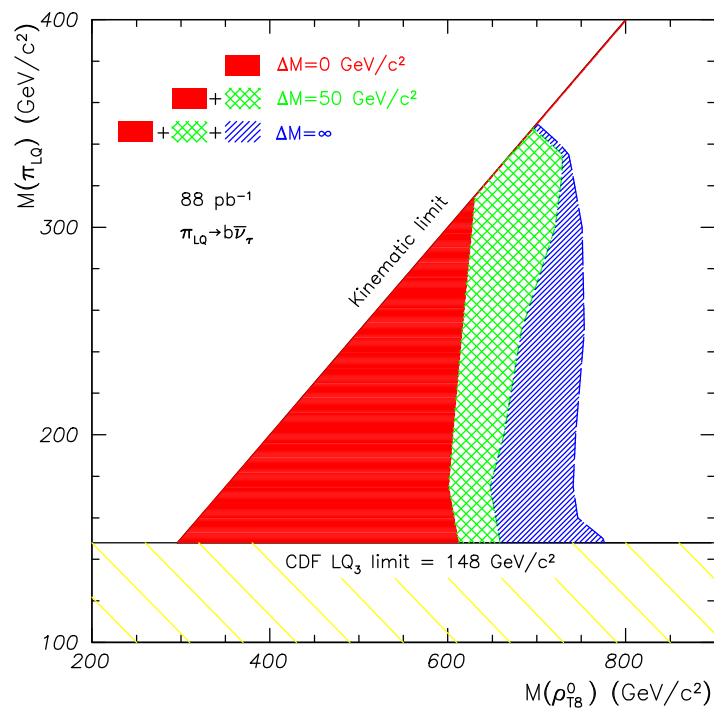


Figure 6: 95% CL exclusion region [28] in the technirho-technipion mass plane for pair produced technipions, with leptoquark couplings, decaying to $b\nu$.